Canadian Journal of Chemistry

Issued by THE NATIONAL RESEARCH COUNCIL OF CANADA

VOLUME 42 JANUARY 1964 NUMBER 1

Can. J. Chem. Downloaded from www.nrcresearchpress.com by 210.87.254.42 on 09/05/12
For personal use only.

THE REACTION OF HYDROGEN ATOMS WITH KETENE[1]

NICK DEMCHUK[2] AND H. GESSER
Parker Chemical Laboratory, University of Manitoba, Winnipeg, Manitoba

Received July 22, 1963

ABSTRACT

The gas-phase reaction of atomic hydrogen with ketene has been investigated over a temperature range of −130° to 232° C using a low-pressure, fast-flow system. In most cases methane, carbon monoxide, and ethane were the major products, but trace amounts of glyoxal were also detected. Above −96° C. considerable evidence exists for the occurrence of a chain reaction carried by HCO radicals. The surface reaction at −196° C produced methane and glyoxal predominantly with only a minor amount of carbon monoxide.

INTRODUCTION

Photochemical studies of ketene by a number of investigators (1–9) have revealed that the most probable primary step over a wide range of wavelengths was the rupture of the C—C bond with the formation of methylene radicals and carbon monoxide. The methylene radicals, either in the $^3\Sigma^-_g$ state or in the $^1A_1$ state, reacted rapidly with the excess ketene molecules and with any other appropriate species that happened to be present in the system.

Gesser and Steacie (10) made a thorough investigation of the photolysis of ketene in the presence of hydrogen over the temperature range of −40° to 207° C at a wavelength of 2700 Å. The major products were carbon monoxide, ethylene, and ethane, but at higher temperatures traces of methyl ethyl ketone were detected and a considerable amount of methane was also formed. The mechanism most consistent with their results was:

$$CH_2CO + h\nu \rightarrow CH_2 + CO \quad [1]$$

$$CH_2 + CH_2CO \rightarrow C_2H_4 + CO \quad [2]$$

$$CH_2 + H_2 \rightarrow CH_3 + H \quad [3]$$

$$H + CH_2CO \rightarrow CH_3 + CO \quad [4]$$

$$CH_3 + CH_3 \rightarrow C_2H_6 \quad [5]$$

$$CH_3 + H_2 \rightarrow CH_4 + H \quad [6]$$

From an Arrhenius plot the value of E_6 was calculated to be 10.2±0.5 kcal/mole, a result in good agreement with previous work.

[1]*Presented at the Photochemistry Symposium, University of Rochester, Rochester, New York, U.S.A. March, 1963.*

[2]*Holder of an Imperial Oil Graduate Research Fellowship.*

The reactions in the above scheme had been well established previously except reaction [4], which was first suggested by Knox, Norrish, and Porter (11). If this reaction was part of the actual mechanism then, in a flow-system study of the reactions of hydrogen atoms with ketene, at high ketene flow rates all hydrogen atoms would be scavenged to form carbon monoxide and methyl radicals. The latter may recombine to form ethane and the amount of carbon monoxide produced would be a good measure of the hydrogen atom concentration in the system. At high temperatures methane should also appear due to reaction [6] and there would be a good possibility that a chain mechanism might occur with hydrogen atoms as chain carriers. The present investigation was undertaken in an attempt to check the validity of the above arguments.

Reaction [3] has been thoroughly investigated recently by Bell and Kistiakowsky (20) and is postulated to pass through an intermediate excited state as follows:

$$CH_2 + H_2 \rightarrow CH_4^* \qquad [3a]$$

$$CH_4^* + W \rightarrow CH_4 + W \qquad [3b]$$

$$CH_4^* \rightarrow CH_3 + H, \qquad [3c]$$

where W is a third body. However, under the low pressure conditions of the following experiments the pressure quenching of the excited state would be expected to be very small and the overall reaction could be represented by [3].

EXPERIMENTAL

Apparatus and Methods

The apparatus consisted of a conventional fast-flow, low-pressure system. Hydrogen from a high pressure cylinder was passed through a reducing valve into a copper furnace maintained at 410° C. It was then further purified by passage through a trap cooled to −196° C. An Edward's high vacuum needle valve (type OSIC) was used to maintain the flow of hydrogen to the discharge tube at the rate of 1530 μmoles/min where it was partially dissociated into atoms by microwaves which were generated by a Raytheon Manufacturing Company Microtherm (Model CMD 7) unit. The discharge tube consisted of a 20-cm length of 19 mm (O.D.) quartz tubing which was internally cooled by means of a water condenser.

A 500-cc spherical bulb served as the reaction vessel in most high temperature experiments. For low temperature work the reaction vessel consisted of a U-shaped cylindrical tube as shown in Fig. 1. Its diameter was 30 mm (O.D.) and it was 18 cm long. The reaction temperature was determined by a sheathed thermocouple projecting into the reaction zone and the pressure was measured by a McLeod gauge. For experiments above room temperature the reaction vessel was surrounded by an appropriately shaped furnace. Low-temperature experiments were conducted in the cylindrical vessel only because it was designed for easy insertion into a Dewar flask containing the coolant at the required temperature. In some cases, the reaction vessel walls were poisoned with $Na_2HPO_4.10H_2O$.

All condensable reaction products were frozen out in a large trap maintained at −196° C with liquid nitrogen. Non-condensable gases, other than H_2, were trapped and collected as previously described (12).

In all cases the hydrogen pressure in the reaction vessel was maintained at 1.05 mm Hg. Under these conditions the hydrogen atom flow rate was found to be 47 μmoles/min as estimated by using CCl_4 as a scavenger (14). This value was kept approximately constant during each series of experiments by adjusting the power output of the microwave generator.

Condensable reaction products were separated in the conventional manner by means of a Le Roy still. The "pure" components were pumped into a gas burette where they were quantitatively measured from P.V.T. measurements. The identity of all components was established by vapor pressure data and infrared analysis. Ethylene in the C_2 fraction was determined by hydrogenation over a nickel–kieselguhr catalyst maintained at 100±1° C (13).

Non-condensable reaction products were desorbed from the silica gel trap at 170° C and were pumped into the gas burette. The amount of CO in the CH_4 was determined by oxidation in a CuO furnace at 210° C (13).

Materials

Commercial grade hydrogen was obtained from the Linde Company and was claimed to be 99.5% pure with oxygen, water vapor, and oil being the main impurities. Spectrograde carbon tetrachloride was purchased from the Eastman-Kodak Company. It was degassed three times by bulb-to-bulb distillation and

Can. J. Chem. Downloaded from www.nrcresearchpress.com by 210.87.254.42 on 09/05/12
For personal use only.

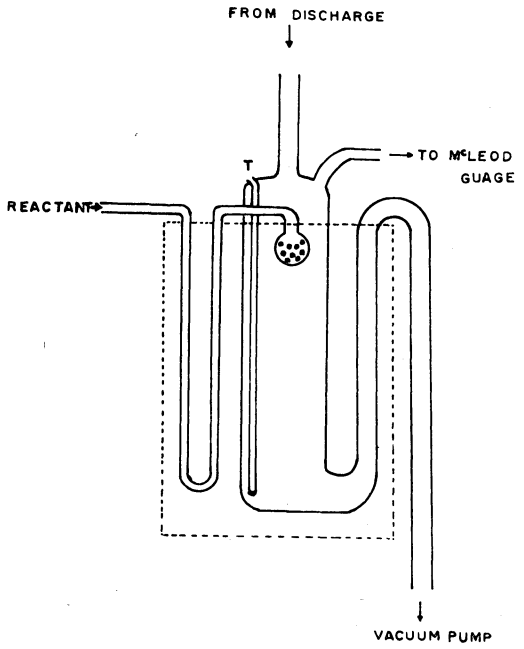

FIG. 1. Diagram of reaction vessel.

was used without any further purification. Ketene was prepared by the pyrolysis of commercial acetic anhydride at 500° C (15). It was degassed at the temperature of liquid oxygen, and distilled from a trap maintained at −125° C into a conical bulb where it was stored in liquid nitrogen.

RESULTS

The reaction of hydrogen atoms with ketene was examined over the temperature range of −196° to 232° C in two different reaction vessels. In the experiments conducted at −196° C the ketene was frozen onto the sides of a poisoned cylindrical reaction vessel and hydrogen atoms were then passed over it. In this case CH_4 and glyoxal were the main products but some CO was also produced (see Table I). The glyoxal was qualitatively

TABLE I

Yields of products in the surface reaction of hydrogen atoms with ketene at −196° C in a poisoned, cylindrical reaction vessel

Duration of experiment (minutes)	Ketene adsorbed (moles × 10^6)	Products (μmoles/min)			Ratio $\left(\frac{2(HCO)_2 + CO}{CH_4}\right)$
		CO	CH_4	$(HCO)_2$	
5.0	185	1.5	12.5	5	0.92
3.0	167	5.0	19.0		

identified by its infrared absorption spectrum but its quantitative determination was difficult owing to its low vapor pressure at room temperature. Only in one case was a quantitative estimate made. At all other temperatures only trace amounts of it were found. At −196° C twice the yield of glyoxal added to the CO produced was approximately equal to the yield of CH_4 and thus there was some indication of a material balance.

At −130±5° C it was possible to study the gas-phase reaction between hydrogen

Can. J. Chem. Downloaded from www.nrcresearchpress.com by 210.87.254.42 on 09/05/12
For personal use only.

TABLE II

Yields of products in the reaction of hydrogen atoms with ketene

Conditions	Duration of experiment (minutes)	Ketene flow (moles × 10^6/min)	Products (μmoles/min) CO	CH_4	C_2H_6	Ratio $\left(\frac{2C_2H_6 + CH_4}{CO}\right)$
−130±5° C	3.0	37.0	21.7	14.5	3.0	0.95
Poisoned,	2.0	74.0	27.5	19.0	3.0	0.91
cylindrical	1.0	145.0	44.0	30.0	3.1	0.82
reaction vessel	1.0	176.0	45.0	30.0	3.0	0.81
−96±2° C	2.0	28.1	26.0	23.9	—	0.92
Poisoned,	2.0	70.1	37.6	31.0	trace	0.83
cylindrical	1.5	115.5	41.4	30.2	1.9	0.82
reaction vessel	1.0	163.4	58.9	54.9	3.3	1.04
−78±2° C	3.0	24.7	20.5	18.5	—	0.90
Poisoned,	3.0	43.0	41.8	30.6	1.4	0.80
cylindrical	3.0	53.0	37.2	33.2	2.5	1.03
reaction vessel	2.0	78.0	43.0	35.1	2.6	0.94
	1.5	99.0	81.5	71.5	5.0	1.00
	1.0	132.0	108.5	106.0	4.0	1.05
72±2° C	5.0	19.0	14.0	14.0	—	1.00
Unpoisoned,	4.0	29.0	25.3	23.8	1.9	1.09
spherical	2.0	58.0	52.0	44.0	6.3	1.09
reaction vessel	1.5	89.0	64.0	54.0	12.5	1.19
	1.0	155.0	138.5	79.0	33.0	1.05
232±2° C	3.0	20.0	15.0	14.0	—	0.93
Unpoisoned,	2.0	58.0	46.0	29.0	5.0	0.85
spherical	1.5	95.0	70.0	57.0	12.0	1.16
reaction vessel	1.0	140.0	99.0	64.0	19.0	1.03
232±2° C	5.0	31.0	31.0	26.0	2.4	0.99
Poisoned,	3.0	46.5	46.0	32.0	6.6	0.98
spherical	2.0	85.0	76.5	25.7	25.1	0.99
reaction vessel	1.5	148.0	135.0	30.0	52.5	1.00
232±2° C	3.0	21.0	19.0	18.0	—	0.95
Poisoned,	2.0	55.0	49.0	21.5	10.0	0.85
cylindrical	1.5	86.5	57.6	20.0	21.0	1.08
reaction vessel	1.0	113.0	80.0	23.5	28.0	1.00

NOTE: 1. A dash signifies that no product was detected.
2. "Trace" signifies that the product yield was less than one μmole/min.
3. The ethane was found to contain 10% ethylene.

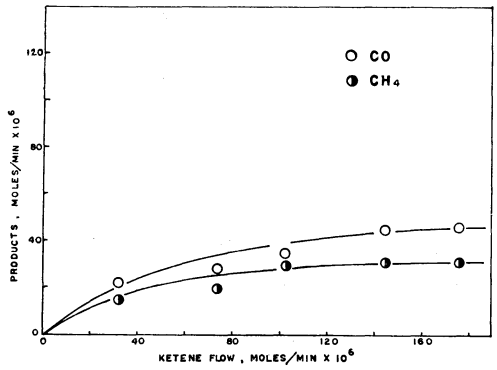

FIG. 2. Yields of products versus ketene flow rate in the reaction of hydrogen atoms with ketene at −130±5° C in a cylindrical, poisoned reaction vessel.

Can. J. Chem. Downloaded from www.nrcresearchpress.com by 210.87.254.42 on 09/05/12
For personal use only.

atoms and ketene because at this temperature the ketene vapor pressure is less than 1.0 mm Hg. A number of experiments were performed to determine the variation of the rates of formation of products with the flow rate of ketene and the results are listed in Table II. The main products were CO and CH_4 in this case along with a small amount of ethane. Figure 2 shows that the CO production levels off at the hydrogen atom concentration in the system (47 μmoles/min) while the methane production also levels off but at a smaller value. Only trace amounts of glyoxal were found.

Results obtained at $-96\pm2°$ C have been plotted in Fig. 3. Examination of this figure shows that at low ketene flow rates the behavior is about identical with that obtained in the previous set of experiments. However, at higher ketene flow rates a chain reaction is obviously initiated and a greater amount of ketene reacts than is possible if hydrogen atoms produced in the discharge were the only reactive species. This effect is even more pronounced at $-78°$ C (Fig. 4) where at high ketene flow rates all the ketene that is

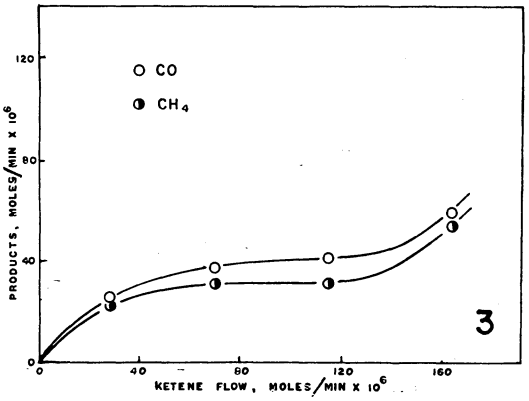

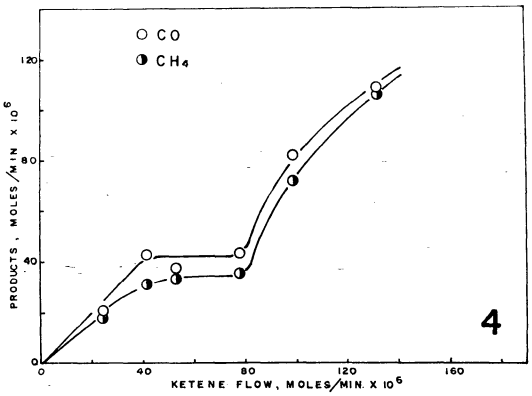

FIG. 3. Yields of products versus ketene flow rate in the reaction of hydrogen atoms with ketene at $-96\pm2°$ C in a cylindrical, poisoned reaction vessel.
FIG. 4. Yields of products versus ketene flow rate in the reaction of hydrogen atoms with ketene at $-78\pm2°$ C in a cylindrical, poisoned reaction vessel.

introduced into the reaction vessel is completely reacted. In both of these cases, only small amounts of ethane and glyoxal were detected.

The results for the same reaction at $72\pm2°$ C in an unpoisoned spherical reaction vessel are plotted in Fig. 5. At this temperature the most significant change is the appearance of considerable amounts of ethane, expecially at high ketene flow rates. Also, it is quite evident that a chain reaction is occurring. The ratio $(2C_2H_6+CH_4)/CO$, an indication of material balance, is in most cases approximately equal to one. The fact that this ratio is less than unity in some instances was probably due to the formation of a trace amount of free carbon which was deposited on the sides of the reaction vessel during the reaction. The formation of trace amounts of glyoxal can possibly account for the fact that the ratio exceeds unity at other times. This behavior is quite similar to that observed at $232\pm2°$ C.

Figure 6, in comparison to Fig. 5, shows the effect of poisoning the reaction vessel with $Na_2HPO_4.10H_2O$. The methane production is decreased considerably and seems to level off while the ethane yield increases. This seems to indicate that methane is in part formed by a heterogeneous surface reaction which is competitive with a reaction by which ethane is produced. The same behavior was obtained in a poisoned cylindrical reaction vessel indicating that the shape of the reaction vessel has very little effect on the reaction.

Can. J. Chem. Downloaded from www.nrcresearchpress.com by 210.87.254.42 on 09/05/12
For personal use only.

In blank experiments at 232° C in which hydrogen atoms were not generated, no thermal decomposition of the ketene was observed. Also, at 232° C and at −196° C the reaction of hydrogen atoms with carbon monoxide did not produce detectable amounts of glyoxal in a time comparable to that used in the above experiments.

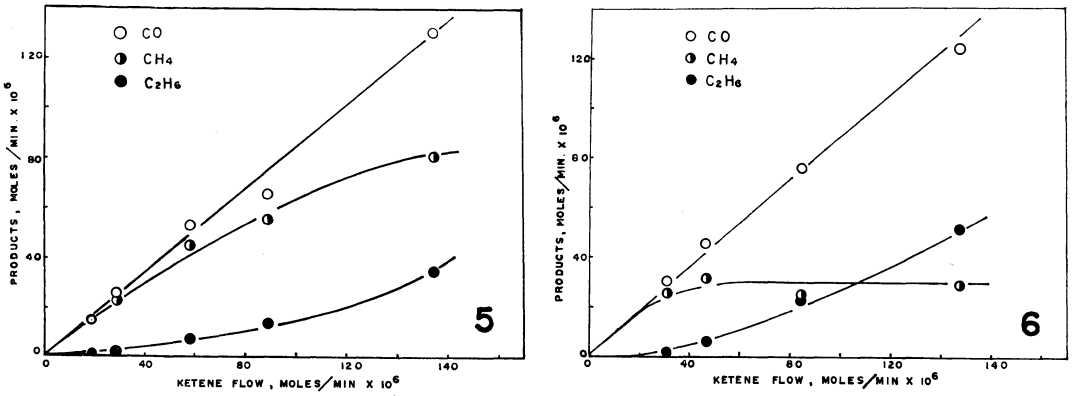

FIG. 5. Yields of products versus ketene flow rate in the reaction of hydrogen atoms with ketene at 72±2° C in a spherical, unpoisoned reaction vessel.
FIG. 6. Yields of products versus ketene flow rate in the reaction of hydrogen atoms with ketene at 232±2° C in a spherical, poisoned reaction vessel.

Finally, a few experiments were performed using hydrogen gas diluted with helium to see whether molecular hydrogen really entered into the reaction scheme. In such experiments, the flowing gas contained only about 18.5% hydrogen. Upon passage through a discharge this system gave a hydrogen atom flow rate of 13 μmoles/min, although it was difficult to keep this value constant. Introduction of ketene into such a system at 232±2° C resulted in the production of carbon monoxide as the main product with the yield varying from 11 to 25 μmoles/min. This shows that the chain reaction had been quenched

TABLE III
Reaction of hydrogen atoms with ketene in the presence of helium

Conditions	Duration of experiment	Ketene flow (μmoles/min)	Products (μmoles/min) CO	CH_4	C_2H_6
232 ± 2° C	3.0	65.0	16.8	—	Trace
	3.0	104.0	11.4	—	Trace
	1.0	140.0	25.6	—	3.7
	1.0	206.0	21.5	—	3.5
−196° C (Surface reaction)	5.0	110.0 (adsorbed)	5.06	—	—

NOTE: He flow rate = 694 μmoles/min.
H_2 flow rate = 129 μmoles/min.
H atom flow rate = 13 μmoles/min.
Pressure in reaction vessel = 1.05 mm Hg.
Cylindrical, poisoned reaction vessel.

and that hydrogen was indeed participating in the chain (see Table III). No methane was found and only a small amount of ethane was produced along with trace amounts of glyoxal. In a similar manner one experiment was conducted at −196° C using the H_2–He

Can. J. Chem. Downloaded from www.nrcresearchpress.com by 210.87.254.42 on 09/05/12
For personal use only.

mixture in the flow system. Here again methane was completely eliminated and carbon monoxide became the main product along with a trace of glyoxal. This series of experiments has thus shown that molecular hydrogen is necessary for the formation of methane and for the propagation of chain processes, which were observed in the pure hydrogen system.

DISCUSSION

A list of some of the most probable reactions occurring during the reaction of hydrogen atoms with ketene is as follows:

$$H + CH_2CO \rightarrow CH_2—CHO^* \quad [7]$$

or

$$H + CH_2CO \rightarrow CH_3—CO^* \quad [8]$$

$$H + CH_2—CHO^* \rightarrow CH_3 + HCO \quad [9]$$

or

$$H + CH_3—CO^* \rightarrow CH_4 + CO \quad [10]$$

$$\left.\begin{matrix} CH_2—CHO^* + H_2 \\ CH_3—CO^* + H_2 \end{matrix}\right] \rightarrow CH_4 + HCO \quad [11]$$

$$2HCO \rightarrow (HCO)_2 \quad [12]$$

or

$$2HCO \rightarrow H_2 + 2CO \quad [13]$$

$$HCO + CH_2CO \rightarrow CH_2—CHO^* + CO \quad [14]$$

or

$$HCO + CH_2CO \rightarrow CH_3—CO^* + CO \quad [15]$$

$$2CH_3CO^* \rightarrow C_2H_6 + 2CO \quad [16]$$

$$2CH_2CHO^* \rightarrow C_2H_4 + (HCO)_2 \quad [17]$$

$$CH_3—CO^* \rightarrow CH_3 + CO \quad [18]$$

$$CH_2—CHO^* \rightarrow CH_2 + HCO \quad [19]$$

$$HCO \rightarrow H + CO \quad [20]$$

$$CH_2 + H_2 \rightarrow CH_3 + H \quad [21]$$

$$CH_3 + H + W \rightarrow CH_4 + W \quad [22]$$

$$CH_3 + HCO + W \rightarrow CH_4 + CO + W \quad [23]$$

$$CH_3 + H_2 \rightarrow CH_4 + H \quad [24]$$

$$CH_3 + CH_3 \rightarrow C_2H_6 \quad [25]$$

At all temperatures the most probable primary step is an addition of the hydrogen atom to the olefinic double bond of ketene with the production of an excited radical. However, this addition could take place on either carbon. The rupture of one of the double bonds requires about 65 kcal/mole of energy but the formation of a C—H bond is exothermic by approximately 80 kcal/mole and as a result either radical will have at least 15 kcal/mole of excess energy. Since there was no evidence of any C_2 fraction at $-196°$ C, reactions [9], [16], and [17] must be eliminated as possible secondary steps. However, glyoxal formation seems to point to the presence of HCO radicals. Consequently, reaction [11]

Can. J. Chem. Downloaded from www.nrcresearchpress.com by 210.87.254.42 on 09/05/12
For personal use only.

is favored over [9] and [10] as the secondary step. This is followed by [12] in which two HCO radicals recombine on a surface to form glyoxal. Reaction [13] is postulated to occur to explain the small amount of CO at this low temperature. Also, reaction [11] is favored over [9] and [10] by the observation that dilution of the molecular hydrogen stream with helium reduces methane production to nil.

At $-130\pm5°$ C the same scheme could be postulated except that now reaction [13] predominates over [12] because there are fewer third body collisions in the gas phase. The fact that CO production levels off at the hydrogen atom concentration is another factor favoring the elimination of reactions [9] and [10] since these would require two hydrogen atoms for every molecule of CO produced. The trace amounts of ethane observed at this temperature may be due to reaction [16]. Such a mechanism for ethane formation is favored over that involving reactions [18] and [25] because reaction [18] is endothermic and would not be expected to occur at such low temperatures. This is also true for reaction [19].

A chain reaction must be postulated to explain the results at $-96°$ C at very high ketene flow rates. This can best be done by assuming that the HCO radicals act as the chain carriers, owing to the fact that the temperature is now high enough for reaction [14] to occur. This is supported by the fact that HCO radicals have been postulated as chain carriers in the photolysis of formaldehyde (16) and acetaldehyde (17). This effect is even more predominant at $-78°$ C with the chain reaction now being initiated at even lower ketene pressures.

The appearance of considerable quantities of ethane at higher temperatures (72°, 232° C) necessitates the presence of methyl radicals in the system. These could be most readily formed by the decomposition of the CH_3—CO* radical at these temperatures as postulated by Trost, Darwent, and Steacie (18) in their study of the reaction of hydrogen atoms with acetaldehyde. However, the production of such large quantities of ethane as have been observed in our experiments at high ketene flow rates would require that most of these radicals decompose and hence the chain reaction resulting from step [11] would cease. This would cause a leveling off in the CO production at high ketene flow rates. No such effect is observed in any of the high temperature plots. Also, hydrogen atoms produced by reaction [24] could not serve as the major chain carriers in the reaction sequence [8], [18], [24] because in such a case CH_4 and CO would be produced in approximately equal amounts with very little C_2H_6. Consequently, it must be assumed that even at high temperatures the HCO radical produced by reaction [11] is still responsible for the chain except that at these temperatures it is very probable that it does decompose according to reaction [20] and initiates a chain "carried" by hydrogen atoms. Also it must be postulated that methyl radicals are formed by an entirely different process, namely, the dissociation of the CH_2—CHO radical (reaction [19]) followed by the reaction of methylene radicals with the excess hydrogen in the system as postulated by Rosenblum (6), and Gesser and Steacie (10). In this way the chain reaction could still be propagated by HCO radicals. It is this fact that favors reaction [7] over reaction [8] as the primary step. The formation of methane could be accounted for by surface reactions such as [22] and [23] in agreement with the fact that a poisoned surface decreases the methane production and reaction [25] probably becomes more prominent.

ACKNOWLEDGMENTS

Grateful acknowledgment is made to the Petroleum Research Fund and the National Research Council for financial support of this work.

Can. J. Chem. Downloaded from www.nrcresearchpress.com by 210.87.254.42 on 09/05/12
For personal use only.

REFERENCES

1. R. G. W. NORRISH *et al.* J. Chem. Soc. 1533 (1938).
2. T. G. PEARSON *et al.* J. Chem. Soc. 409 (1938).
3. R. G. W. NORRISH and G. PORTER. Discussions Faraday Soc. **2**, 97 (1947).
4. W. F. ROSS and G. B. KISTIAKOWSKY. J. Am. Chem. Soc. **56**, 1112 (1934).
5. G. B. KISTIAKOWSKY and N. W. ROSENBERG. J. Am. Chem. Soc. **72**, 321 (1950).
6. C. ROSENBLUM. J. Am. Chem. Soc. **63**, 3322 (1941).
7. M. VANPEE and F. GRARD. Bull. Soc. Chem. Belg. **60**, 208 (1957).
8. A. N. STRACHAN and W. A. N. NOYES, JR. J. Am. Chem. Soc. **76**, 3258 (1954).
9. J. CHANMUGAM and M. BURTON. J. Am. Chem. Soc. **78**, 509 (1956).
10. H. GESSER and E. W. R. STEACIE. Can. J. Chem. **34**, 113 (1956).
11. K. KNOX, R. G. W. NORRISH, and G. PORTER. J. Chem. Soc. 1477 (1952).
12. NICK DEMCHUK and H. GESSER. Can. J. Chem. **41**, 1645 (1963).
13. F. B. MARCOTTE and K. O. KUTSCHKE. Laboratory procedures in microgasanalysis. University of Rochester. 1952.
14. J. E. VANCE and W. C. BAUMAN. J. Chem. Phys. **6**, 811 (1938).
15. G. J. FISHER *et al.* J. Org. Chem. **18**, 1055 (1953).
16. E. W. R. STEACIE. Atomic and free radical reactions. 2nd ed. Reinhold, New York. 1954.
17. W. L. HADEN, JR. and O. K. RICE. J. Chem. Phys. **10**, 455 (1942).
18. W. R. TROST, B. DEB. DARWENT, and E. W. R. STEACIE. J. Chem. Phys. **16**, 353 (1948).
19. C. E. H. BAWN and J. MILSTED. Trans. Faraday Soc. **35**, 889 (1939).
20. J. A. BELL and G. B. KISTIAKOWSKY. J. Am. Chem. Soc. **84**, 3417 (1962).

Can. J. Chem. Downloaded from www.nrcresearchpress.com by 210.87.254.42 on 09/05/12
For personal use only.

Can. J. Chem. Downloaded from www.nrcresearchpress.com by 210.87.254.105 on 09/05/12
For personal use only.

CONDENSATION OF ALICYCLIC KETONES WITH UREA AND THIOUREA

A. F. McKay, C. Podesva,[1] E. J. Tarlton, and J.-M. Billy[2]
L. G. Ryan Research Laboratories of Monsanto Canada Limited, LaSalle, Quebec[3]
Received August 2, 1963

ABSTRACT

The previous assignment of a cis conformation to cyclohexyl 2-carbamylcyclohexylamine, which was prepared by the condensation of urea with cyclohexanone, has been confirmed by equilibration in the presence of potassium *t*-butoxide. The failure of 4-*t*-butylcyclohexyl 2-carbamyl-4-*t*-butylcyclohexylamine to equilibrate under the same conditions is discussed in relation to its structure. 1,2,3,4,5,6,7,8-Octahydroacridine was prepared by the condensation of 2,2′-methylene-bis-cyclohexanone with urea.

The product from the condensation of cyclohexanone with urea in alkaline medium was assigned (1) structure I on the basis of its analysis, infrared spectrum, and hydrogenation to cyclohexyl 2-carbamylcyclohexylamine (II). Later Scarborough and Gould

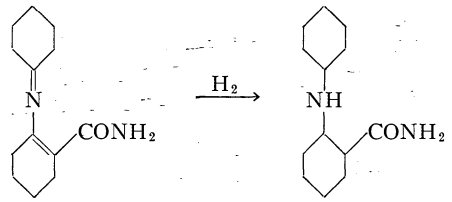

I II

(2) reported an improved procedure for the preparation of compound I. During the present investigation a new process (cf. Experimental) was developed which gives high yields of this condensation product. The latter procedure was used in the preparation of the compounds listed in Table I. Cyclohexylidene 2-thiocarbamylcyclohex-1-enylamine was prepared from the condensation of cyclohexanone with thiourea. The infrared and ultraviolet absorption bands listed in Tables II and III respectively show that these condensation products have the same general structure. If the imino nitrogen in structure I is assumed to be equivalent to carbon for calculating the ultraviolet absorption maximum then the calculated (3) value of 308 mμ is in good agreement with the observed value of 305 mμ (Table III).

Cyclohexylidene 2-carbamylcyclohex-1-enylamine (I) was considered (1) to be formed by the carbamylation of an enamine intermediate and the reaction sequence may be represented as follows:

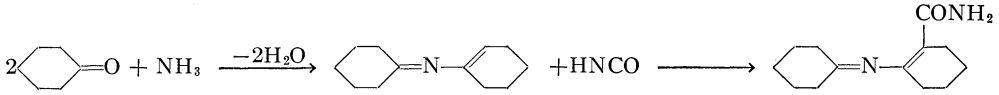

The previous (1) scheme showed the addition of HNCO to 1-aminocyclohexene instead of cyclohexylidene cyclohex-1-enylamine. Isocyanic acid would be expected to add more readily to the latter compound because of its closer structural relationship to typical

[1]*Present address: Delmar Chemicals Limited, Montreal, Que.*
[2]*Present address: Ogilvy Flour Mills Co. Ltd., Montreal, Que.*
[3]*Contribution No. 40.*

Can. J. Chem. Downloaded from www.nrcresearchpress.com by 210.87.254.105 on 09/05/12
For personal use only.

TABLE I

Alicyclic ketone – urea and – thiourea condensation products

Compound	M.p., °C (dec)	Yield, %	Formula	Carbon %		Hydrogen %		Nitrogen %	
				Calc.	Found	Calc.	Found	Calc.	Found
Cyclopentylidene 2-carbamylcyclopent-1-enylamine	237–238*,†	11	$C_{11}H_{16}N_2O$	68.71	68.69	8.39	8.39	14.58	14.95
4-Methylcyclohexylidene 2-carbamyl-4-methylcyclohex-1-enylamine	207‡	70§	$C_{15}H_{24}N_2O$	72.54	72.39	9.74	9.50	11.28	11.29
4-*t*-Butylcyclohexylidene 2-carbamyl-4-*t*-butylcyclohex-1-enylamine	274–275†	47‖	$C_{21}H_{36}N_2O$	75.86	76.12	10.91	11.08	8.42	8.44
Cyclohexylidene 2-thiocarbamylcyclohex-1-enylamine	218–222‡	87‖	$C_{13}H_{20}N_2S$	66.05	65.80	8.53	8.37	11.85	11.54¶
4-Methylcyclohexylidene 2-thiocarbamyl-4-methylcyclohex-1-enylamine	257–258‡	40‖	$C_{15}H_{24}N_2S$	68.13	68.05	9.15	9.42	10.59	10.61**

*Melting points vary with rate of heating. Decomposition points as high as 246° have been recorded for this compound in evacuated tubes.
†Crystallized from ethanol.
‡From aqueous methanol.
§Method A.
‖Method B.
¶Sulphur, Calc.: 13.57%. Found: 13.70%.
**Sulphur, Calc.: 12.12%. Found: 12.19%.

TABLE II

Infrared absorption band (cm^{-1}) assignments*

Compound	Stretching modes		Bending modes
	N—H	C=O	N—H
Cyclopentylidene 2-carbamylcyclopent-1-enylamine	3260	1610	1545
Cyclohexylidene 2-carbamylcyclohex-1-enylamine	3280, 3160	1625	1525
4-Methylcyclohexylidene 2-carbamyl-4-methylcyclohex-1-enylamine	3390, 3260	1620	1512
4-*t*-Butylcyclohexylidene 2-carbamyl-4-*t*-butylcyclohex-1-enylamine	3300, 3235, 3180	1615	1607, 1518
Cyclopentyl 2-carbamylcyclopentylamine hydrochloride	3325, 3125	1662	1580
Cyclohexyl 2-carbamylcyclohexylamine (m.p. 128°)	3325, 3260, 3140	1665	1580
Cyclohexyl 2-carbamylcyclohexylamine (m.p. 75–95°)	3445, 3340, 3280, 3195	1680	1610
4-Methylcyclohexyl 2-carbamyl-4-methylcyclohexylamine hydrochloride	3320, 3140	1663	1605
4-*t*-Butylcyclohexyl 2-carbamyl-4-*t*-butylcyclohexylamine	3275, 3100	1655	1580
Cyclohexyl 2-carbamylcyclohexylnitrosamine (m.p. 167°)	3425, 3325, 3215	1680	1625
Cyclohexyl 2-carbamylcyclohexylnitrosamine (m.p. 158°)	3380, 3200	1666, 1685	1632

*Infrared spectra were determined on Nujol mulls of the crystalline compounds. A Perkin–Elmer model 21 spectrometer was used.

TABLE III
Ultraviolet absorption*

Compound	λ_{max} (mμ)	ϵ_{max}
Cyclopentylidene 2-carbamylcyclopent-1-enylamine	306.5	6350
	220	End absorption
Cyclohexylidene 2-carbamylcyclohex-1-enylamine	305	6720
	220	End absorption
4-Methylcyclohexylidene 2-carbamyl-4-methylcyclohex-1-enylamine	305	6350
	220	End absorption
4-*t*-Butylcyclohexylidene 2-carbamyl-4-*t*-butylcyclohex-1-enylamine	306	2000
Cyclohexylidene 2-thiocarbamylcyclohex-1-enylamine	377	1800
	279.5	4950
	215	End absorption

*The ultraviolet spectra were determined on ethanolic solutions of the compounds with a Beckman DK–1 recording spectrophotometer.

enamines. Some evidence in support of the prior condensation of two more equivalents of cyclohexanone with ammonia is provided by the following observation.

An attempt to form a carbamyl derivative of 2,2′-methylene-bis-cyclohexanone under the conditions used for the preparation of cyclohexylidene 2-carbamylcyclohex-1-enylamine gave the known (4, 5) 1,2,3,4,5,6,7,8-octahydroacridine (III). This new method

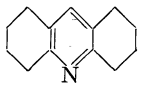

III

of producing *sym*-octahydroacridine involves condensation with ammonia and then oxidative aromatization.

The previous assignment (1) of a cis configuration to cyclohexyl 2-carbamylcyclohexylamine (IV*a* $\rightleftharpoons$ IV*b*) was confirmed by its equilibration in the presence of potassium tertiary butoxide. The equilibration product containing the trans epimer (V*a* $\rightleftharpoons$ V*b*) melted at 95° and on nitrosation gave a nitrosamine melting at 158°. The nitrosamine from the cis epimer (IV*a* $\rightleftharpoons$ IV*b*) melted at 167°. Infrared spectra of the epimeric cyclohexyl 2-carbamylcyclohexylamines and their N-nitroso derivatives also show distinct differences (see Table II).

Several attempts to equilibrate 4-*t*-butylcyclohexyl 2-carbamyl-4-*t*-butylcyclohexylamine were unsuccessful. The original compound was recovered in good yields in each experiment. Thus 4-*t*-butylcyclohexyl 2-carbamyl-4-*t*-butylcyclohexylamine must possess conformation VI*a* (cis 1*a*, 2*e*/cis 2*e*, 4*e*) or VI*b* (trans 1*e*, 2*e*/cis 2*e*, 4*e*). This conformation VI*a* would be formed by cis addition of hydrogen at the less hindered approach to the double bond. This conformation with the carbamyl group equatorial is stabilized by the 4-*t*-butyl group which prevents the ring from flipping over into the conformation with the carbamyl group axial and the amino substituent equatorial. Conformation VI*b* with all substituents equatorial could account also for the stability of the 4-*t*-butyl compound. Formation of conformation VI*b* can be explained by the migration of a double bond prior to hydrogenation. Actually the hydrogenation of cyclohexylidene 2-carbamylcyclohex-1-enylamine proceeded at a much more rapid rate than the hydrogenation of its 4-*t*-butyl derivative. The former compound absorbed two mole equivalents of hydrogen in 2 hours while 4-*t*-butylcyclohexylidene 2-carbamyl-4-*t*-butylcyclohex-1-enylamine absorbed one mole equivalent of hydrogen in 1 hour and then required an additional 20 hours to absorb a further 0.6 mole equivalents.

Can. J. Chem. Downloaded from www.nrcresearchpress.com by 210.87.254.105 on 09/05/12
For personal use only.

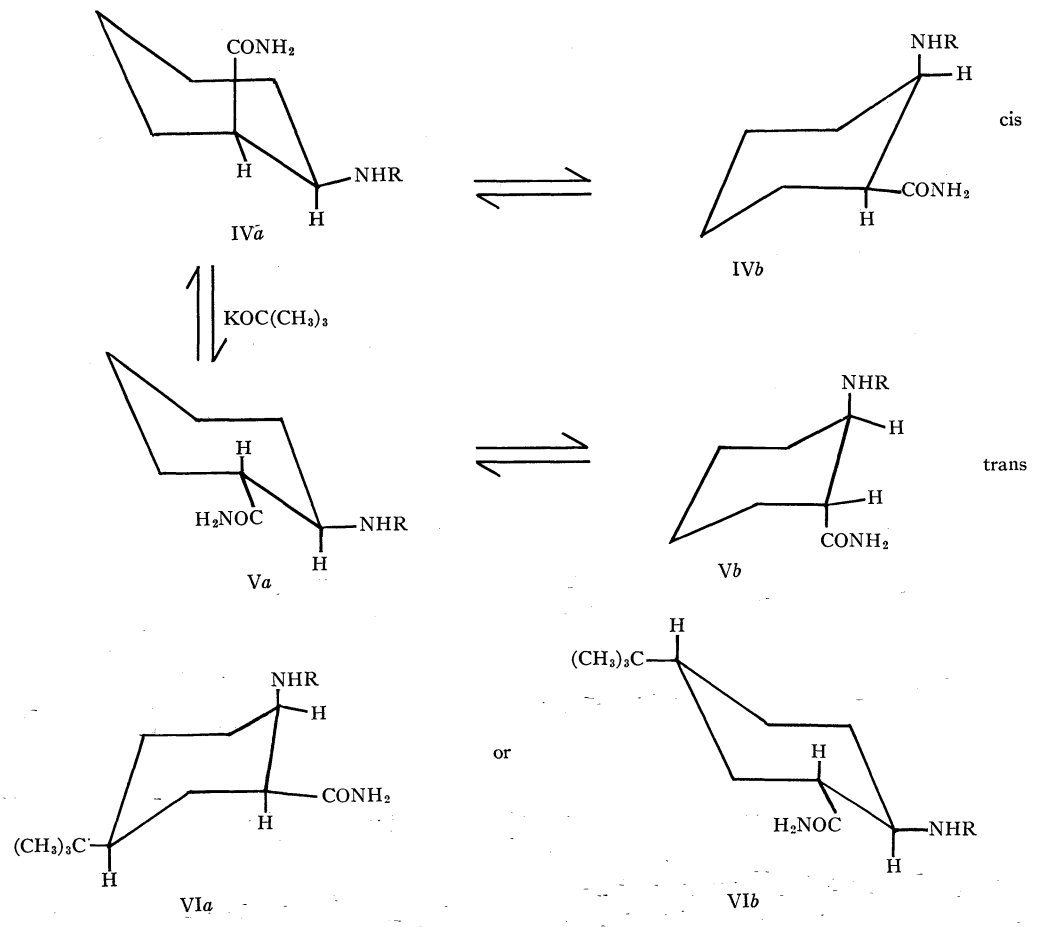

R = cyclohexyl or 4-*t*-butylcyclohexyl.

Cyclopentyl 2-carboxylcyclopentylamine was prepared by hydrolysis of the hydrogenation product from cyclopentylidene 2-carbamylcyclopent-1-enylamine. Attempts to prepare cyclopentyl 2-carboxylcyclopentylamine by other routes were unsuccessful. After heating cyanocyclopent-1-ene and cyclopentylamine in glacial acetic acid at 113° for 19 hours, the reagents were recovered unchanged. Heating an aqueous solution of cyclopentylamine and cyclopent-1-enylcarboxylic acid in a sealed tube at 155° for 48 hours gave mainly N-cyclopentyl cyclopent-1-enylcarboxamide (m.p. 141.5°).

EXPERIMENTAL*

4-t-Butylcyclohexanone

4-*t*-Butylcyclohexanone (m.p. 42°) was prepared in 75% yield from 4-*t*-butylcyclohexanol by the procedure described (6) for the conversion of menthol to menthone. The product was purified by distillation at 95–97° at 3 mm; m.p. 47°; oxime m.p. 137° (lit. (7) 137.5–138.5°).

Reaction of Alicyclic Ketones with Urea and Thiourea

The compounds listed in Table I were prepared by one of the following procedures.

**All melting points are uncorrected. Microanalyses were determined by Dr. C. Daessle, Montreal, Quebec.*

Can. J. Chem. Downloaded from www.nrcresearchpress.com by 210.87.254.105 on 09/05/12
For personal use only.

Method A.—Cyclohexanone (19.6 g, 0.2 mole) and urea (24 g, 0.4 mole) in *o*-xylene (20 ml) were heated at reflux for 40 minutes. Water was distilled azeotropically and it was collected in a Barrat trap. The reaction was cooled and water (50 ml) and benzene (25 ml) were added. The precipitate (m.p. 199–205°) was recovered by filtration, yield 19.9 g (90%). Recrystallization from 46% aqueous ethanol (175 ml) gave pure cyclohexylidene 2-carbamylcyclohex-1-enylamine (m.p. 224–225°), yield 13.8 g. A mixed melting point determination with a known sample gave no depression.

Method B.—Cyclohexanone (19.6 g, 0.2 mole) and urea (24 g, 0.4 mole) in a solution of *o*-xylene (20 ml) and dimethylformamide (75 ml) were heated under reflux for 2.6 hours. During the reaction period water was collected azeotropically in a Barrat trap. The solution was evaporated *in vacuo* to one-half of its original volume and the residual solution was diluted with water (150 ml). The product (m.p. 215°) was collected by filtration, yield 18.5 g (84%). Recrystallization from 45% aqueous ethanol (270 ml) gave pure product (m.p. 225–226°), yield 15.2 g. A mixed melting point determination with a sample of product from method A showed no depression.

Cyclohexyl 2-Carbamylcyclohexylamine Hydrochloride and Free Base

The hydrochloride (m.p. 276°) and free base (m.p. 128°) of this compound were prepared as previously described (1).

Cyclohexyl 2-Carbamylcyclohexylnitrosamine

Cyclohexyl 2-carbamylcyclohexylamine hydrochloride (0.4 g, 0.0015 mole) in aqueous hydrochloric acid (5 drops of concentrated hydrochloric acid in 25 ml water) was treated with an aqueous solution of sodium nitrite (1 g sodium nitrite in 5 ml water). This solution was allowed to stand at room temperature for 24 hours. Crystals (m.p. 162–165°) gradually separated from the solution, yield 0.14 g (36%). One recrystallization from aqueous ethanol raised the melting point to 165–167°. Anal. Calc. for $C_{13}H_{23}N_3O_2$: C, 61.63; H, 9.15; N, 16.59. Found: C, 61.44; H, 9.00; N, 16.55.

Equilibration of Cyclohexyl 2-Carbamylcyclohexylamine

Cyclohexyl 2-carbamylcyclohexylamine (1 g, 0.004 mole) in 20 moles of potassium *t*-butoxide solution (1.3 g of metallic potassium in 33 ml *t*-butanol) was heated under reflux for 1 hour. At the end of the reaction period the solution was diluted with 7 volumes of water and exhaustively extracted with chloroform. Evaporation of the chloroform extract *in vacuo* gave an oil which crystallized into needle-like crystals (m.p. 94–95°) on standing, yield 1 g (100%). Several recrystallizations of the product from ethyl acetate gave crystals with melting ranges varying between 75° and 90°. Anal. Calc. for $C_{13}H_{24}N_2O$: C, 69.60; H, 10.78; N, 12.49. Found: C, 69.45; H, 11.00; N, 12.21. This experiment was repeated several times with the same results.

Nitrosation of Equilibration Product from Cyclohexyl 2-Carbamylcyclohexylamine

To a solution of this equilibration product (1.9 g, 0.008 mole) in water (40 ml) containing concentrated hydrochloric acid (1.7 g, 0.017 mole) was added a solution of sodium nitrite (1.25 g, 0.017 mole) in water. After standing overnight at room temperature crystals (m.p. 156–158°) of the nitrosamine separated, yield 0.71 g (33%). Two recrystallizations from aqueous ethanol raised the melting point to a constant value of 158°. Anal. Calc. for $C_{13}H_{23}N_3O_2$: C, 61.63; H, 9.15; N, 16.59. Found: C, 61.61; H, 9.33; N, 16.94. The melting point of this epimeric nitrosamine was depressed on admixture with a sample of the nitrosamine (m.p. 167°) which was prepared from cyclohexyl 2-carbamylcyclohexylamine melting at 128° (*vide supra*).

4-t-Butylcyclohexyl 2-Carbamyl-4-t-butylcyclohexylamine

A solution of 4-*t*-butylcyclohexylidene 2-carbamyl-4-*t*-butylcyclohex-1-enylamine (2 g, 0.006 mole) in absolute ethanol (150 ml) containing concentrated hydrochloric acid (0.6 g) and platinum oxide (0.1 g) catalyst was hydrogenated at room temperature. The first mole equivalent of hydrogen was absorbed very rapidly and then hydrogenation proceeded very slowly. After 20.5 hours only 1.6 mole equivalent of hydrogen was absorbed. The reaction mixture was filtered and the filtrate was evaporated to dryness *in vacuo*. The amorphous residue was dissolved in water and the solution made alkaline with 5% aqueous sodium hydroxide solution. A white precipitate separated from solution. This mixture was extracted with chloroform and the chloroform extract was evaporated to dryness *in vacuo*. The residue (m.p. 189°) weighed 0.8 g (41% yield). Four recrystallizations from ethyl acetate raised the melting point to 194°. Anal. Calc. for $C_{21}H_{40}N_2O$: C, 74.94; H, 11.98; N, 8.33. Found: C, 75.04; H, 12.02; N, 8.10.

Attempt to Epimerize 4-t-Butylcyclohexyl 2-Carbamyl-4-t-butylcyclohexylamine

Several attempts to epimerize 4-*t*-butylcyclohexyl 2-carbamyl-4-*t*-butylcyclohexylamine (m.p. 194°) under the conditions employed for the equilibration of cyclohexyl 2-carbamylcyclohexylamine gave almost quantitative recoveries of unchanged starting material.

4-Methylcyclohexyl 2-Carbamyl-4-methylcyclohexylamine Hydrochloride

4-Methylcyclohexylidene 2-carbamyl-4-methylcyclohex-1-enylamine (6 g, 0.024 mole) in absolute ethanol (250 ml) containing concentrated hydrochloric acid (2.04 ml) and 109 mg of platinum oxide was hydrogenated at ambient temperature and pressure. Approximately two mole equivalents of hydrogen were absorbed in 35 minutes. The catalyst was removed by filtration and the filtrate was evaporated to a volume

Can. J. Chem. Downloaded from www.nrcresearchpress.com by 210.87.254.105 on 09/05/12
For personal use only.

of 25 ml *in vacuo*. After the residual solution was treated with ether (75 ml) and a few drops of concentrated hydrochloric acid, a crystalline precipitate (m.p. 216–217°) was obtained, yield 4.9 g (70%). A sample (1 g) was purified by several crystallizations from ethanol–ether solution, yield 0.41 g. The final melting point was 223–224°. Anal. Calc. for $C_{15}H_{29}ClN_2O$: C, 62.36; H, 10.12; Cl, 12.28; N, 9.70. Found: C, 62.00; H, 10.04; Cl, 12.68; N, 9.61.

A portion (1 g, 0.003 mole) of this hydrochloride salt in 15 ml of water was treated with excess aqueous sodium hydroxide solution. The resulting alkaline mixture was extracted with chloroform and the chloroform extract was dried over anhydrous sodium sulphate. Evaporation of chloroform solution gave 0.8 g (93%) of solid (m.p. 108–109°). One recrystallization from ether–pentane solution raised the melting point of 4-methylcyclohexyl 2-carbamyl-4-methylcyclohexylamine to 114–115°. Anal. Calc. for $C_{15}H_{28}N_2O$: C, 71.37; H, 11.18; N, 11.10. Found: C, 71.51; H, 11.00; N, 11.47.

Cyclopentyl 2-Carbamylcyclopentylamine Hydrochloride

Cyclopentyl 2-carbamylcyclopentylamine hydrochloride (m.p. 210–211°) was prepared in 61% yield by the hydrogenation of cyclopentylidene 2-carbamylcyclopent-1-enylamine under the conditions described for the preparation of 4-methylcyclohexyl 2-carbamyl-4-methylcyclohexylamine hydrochloride. Two recrystallizations from ethanol–ether solution raised the melting point to 223–224°. Anal. Calc. for $C_{11}H_{21}ClN_2O$: C, 56.76; H, 9.09; Cl, 15.24; N, 12.04. Found: C, 57.02; H, 9.02; Cl, 15.23; N, 12.04.

Cyclopentyl 2-Carboxylcyclopentylamine Hydrochloride

A solution of cyclopentyl 2-carbamylcyclopentylamine hydrochloride (0.2 g, 0.001 mole) in concentrated hydrochloric acid (5 ml) was heated on a steam bath for 1 hour. The solution was evaporated to dryness *in vacuo* and the residue was dissolved in methanol (6 ml). On addition of ether (15 ml) to the methanolic solution a precipitate (40 mg) of ammonium chloride was obtained. The filtrate was evaporated to dryness and the residual oil readily crystallized (m.p. 165–170°), yield 0.2 g (99.6%). One recrystallization from methanol–ether solution raised the melting point to 180.5–181°. Anal. Calc. for $C_{11}H_{20}ClNO_2$: C, 56.52; H, 8.63; Cl, 15.17; N, 5.99. Found: C, 56.55; H, 8.57; Cl, 15.33; N, 6.25.

Cyanocyclopent-1-ene

Cyanocyclopent-1-ene (b.p. 70° at 20 mm, n_D^{23} 1.46978) was prepared in 62% yield by the method of Wheeler and Lerner (8).

Cyclopent-1-enecarboxylic Acid

Cyanocyclopent-1-ene was converted in 63% yield into cyclopent-1-enecarboxylic acid (m.p. 121–122°; lit. (8) 121°) by the procedure of Wheeler and Lerner (8).

Cyclopentylamine

A solution of cyclopentanone (67.2 g, 0.8 mole) and hydroxylamine hydrochloride (69.5 g, 1 mole) in water (120 ml) was treated with an aqueous solution of sodium carbonate (53 g sodium carbonate in 130 ml water). After stirring for 30 minutes, the crystalline cyclopentanone oxime (m.p. 56.5–57.5°)was recovered by filtration, yield 53 g (67%).

The oxime (30 g, 0.3 mole) in absolute ethanol (700 ml) was treated with small portions of sodium metal (100 g). This mixture was refluxed for 12 hours until all the sodium disappeared. The viscous syrup was treated with an equal volume of water and the solution was exhaustively extracted with ether. After the ether extract was acidified with dry hydrogen chloride, it was evaporated to dryness. The residue was treated with 15% aqueous sodium hydroxide solution and this solution was extracted with ether. The ether was removed by fractional distillation through a Widmer column and the residual amine was fractionated in a spinning band column. Cyclopentylamine (b.p. 106–108°, n_D^{25} 1.44691; lit. (9) b.p. 106–108°, n_D^{25} 1.4478) was obtained in 47% yield.

Attempts to Prepare Cyclopentyl 2-Cyanocyclopentylamine

A solution of cyanocyclopent-1-ene (0.94 g, 0.001 mole) and cyclopentylamine (0.86 g, 0.001 mole) in glacial acetic acid (3 ml) was heated at 113° for 19 hours. The dark solution was made alkaline with 15% aqueous sodium hydroxide solution (20 ml) and extracted with ether. Washing the ether phase with 10% hydrochloric acid gave 1.12 g (91%) of cyclopentylamine hydrochloride (m.p. 200–202°).

The ether phase was washed with aqueous sodium bicarbonate solution and water and dried over anhydrous sodium sulphate. Evaporation of the ether solution gave 0.88 g (94%) of unchanged cyanocyclopent-1-ene.

The results were the same after the above reagents were heated for 22 hours at 113°.

Attempt to Prepare Cyclopentyl 2-Carboxycyclopentylamine

A solution of cyclopentylamine (2.34 g, 0.027 mole) and cyclopent-1-enylcarboxylic acid (1 g, 0.009 mole) in water (5 ml) was heated in a sealed tube at 155° for 48 hours. The resulting mixture was extracted with ether and the ether extract was washed with 10% hydrochloric acid and water. The ether extract on evaporation gave a solid which melted at 80–95°, yield 0.6 g (37%). Two recrystallizations from aqueous ethanol raised the melting point to 141–141.5°. This compound was identified as N-cyclopentyl cyclopent-1-enylcarboxamide by analysis and its infrared spectrum. Anal. Calc. for $C_{11}H_{17}NO$: C, 73.69; H, 9.56. Found:

Can. J. Chem. Downloaded from www.nrcresearchpress.com by 210.87.254.105 on 09/05/12
For personal use only.

C, 73.48; H, 9.47. Infrared spectrum of the solid in Nujol mull showed absorption bands at 1328, 1604, 1620, 1641, and 3330 cm^{-1}.

A mixture of oil and cyclopentylamine hydrochloride was obtained from the acidic aqueous washings of the ether extract. The crystals (m.p. 199–200°) were identified as cyclopentylamine hydrochloride by a mixed melting point determination, yield 0.4 g. Attempts to purify the remaining dark brown oil were unsuccessful. It did not have the properties expected for cyclopentyl 2-carboxycyclopentylamine.

2,2′-Methylene-bis-cyclohexanone

A modification of the procedure described by Wick and Becke (10) was used for the preparation of 2,2′-methylene-bis-cyclohexanone.

Cyclohexanone (98 g, 1 mole), dimethylamine hydrochloride (18 g, 0.2 mole), and 30% formalin (20 g, 0.2 mole) were mixed and heated gradually on an oil bath. An exothermic reaction occurred at a bath temperature of 120° and the reaction was allowed to proceed without further heating. After the reaction had subsided, the product was cooled to room temperature and 20% aqueous sodium hydroxide solution (45 g) was added. After thorough agitation, the organic layer was separated and the water and unreacted cyclohexanone were removed by distillation. When the distillation temperature reached 155°, the residue was refluxed until the reflux temperature reached 162° after which the residue was distilled *in vacuo*. The main fraction (b.p. 168–170° at 5 mm, yield 38.3 g) was refractionated in a spinning band column. The first fraction (b.p. 120° at 0.05 mm, yield 9.7 g) remained an oil while the second fraction (b.p. 104° at 0.02 mm) crystallized (m.p. 52°; lit. (11) 58°), yield 15 g (36%). Anal. Calc. for $C_{13}H_{20}O_2$: C, 74.96; H, 9.68. Found: C, 74.34; H, 9.39.

1,2,3,4,5,6,7,8-Octahydroacridine

A solution of 2,2′-methylene-bis-cyclohexanone (2 g, 0.02 mole) and urea (2 g, 0.03 mole) in dimethylformamide (15 ml) – xylene (5 ml) solution was heated under reflux until no more water separated in the Barrat trap. The reaction mixture was diluted with water and extracted with chloroform. The chloroform extract was evaporated to dryness and the residual oil was dissolved in methanol, diluted with an equal volume of water, and acidified with concentrated hydrochloric acid. The solution was extracted with ether and the aqueous phase was made alkaline with aqueous sodium hydroxide solution. The alkaline solution was exhaustively extracted with chloroform and the chloroform extract was evaporated *in vacuo*. The residual oil was dissolved in a small amount of ethyl acetate and the solution was filtered. Evaporation of the filtrate to dryness gave an oil which crystallized at room temperature, yield 1.75 g (97%). This crude product melted at 50°. It was dissolved in benzene and the benzene solution was passed through a column of neutral alumina. Evaporation of the benzene eluate *in vacuo* gave 1.2 g of crystals melting at 65–68°. These crystals were sublimed *in vacuo* and the sublimate melted at 69–71° (lit. (4, 5) 69° and 73.4–74°). Anal. Calc. for $C_{13}H_{17}N$: C, 83.37; H, 9.15; N, 7.48. Found: C, 83.65; H, 9.01; N, 7.19.

Ultraviolet absorption spectrum in ethanol gave λ_{max} 216, 222, 272, 276.5, 281, 285, and 290 mμ with $\epsilon_{max} \times 10^{-3}$ 6.3, 4.5, 4.3, 6.5, 7.8, 7.1, and 5.6 respectively.

A picrate (m.p. 195°) was prepared in 94% yield in the usual manner from a methanolic solution of the free base. Two crystallizations from ethanol raised the melting point to 200° with dec. (lit. (5) m.p. 200–201.5°). Anal. Calc. for $C_{19}H_{20}N_4O_7$: C, 54.80; H, 4.84; N, 13.46. Found: C, 54.96; H, 4.96; N, 13.31.

The hydrochloride (m.p. 201–202°) was prepared in 98% yield by passing dry hydrogen chloride through an ether solution of the free base. Anal. Calc. for $C_{13}H_{18}ClN$: C, 69.79; H, 8.10; Cl, 15.85; N, 6.26. Found: C, 69.83; H, 7.46; Cl, 15.79; N, 6.31.

REFERENCES

1. A. F. McKay, E. J. Tarlton, and C. Podesva. J. Org. Chem. **26**, 76 (1961).
2. H. C. Scarborough and W. A. Gould. J. Org. Chem. **26**, 3720 (1961).
3. L. F. Fieser and M. Fieser. Steroids. Reinhold Publishing Corp., New York. 1959. pp. 17–19.
4. J. von Braun, A. Petzold, and A. Schultheiss. Ber. **56**, 1347 (1933).
5. H. Adkins and H. L. Coonradt. J. Am. Chem. Soc. **63**, 1563 (1941).
6. H. Gilman and A. H. Blatt. Org. Syntheses. Coll. Vol. 1. 2nd ed. 1941. p. 340.
7. E. K. Harvill, C. W. Roberts, and R. M. Herbst. J. Org. Chem. **15**, 58 (1950).
8. O. H. Wheeler and I. Lerner. J. Am. Chem. Soc. **78**, 63 (1950).
9. J. R. Corrigan, M. J. Sullivan, H. W. Bishop, and A. W. Ruddy. J. Am. Chem. Soc. **75**, 6258 (1953).
10. Ger. Patent No. 1,109,675 (June (1961)).
11. J. Cologne. Bull. Soc. Chim. (France), 250 (1955).

Can. J. Chem. Downloaded from www.nrcresearchpress.com by 210.87.254.105 on 09/05/12
For personal use only.

ON THIOSEMICARBAZONE–COPPER (I) COMPLEXES. PART IV[1]

B. A. GINGRAS AND A. F. SIRIANNI
Division of Applied Chemistry, National Research Council, Ottawa, Canada

Received August 8, 1963

ABSTRACT

The structure of thiosemicarbazone–copper (I) complexes has been studied further and new data have been obtained. The most probable structure has the metal linearly coordinated to a sulphur atom of a thiosemicarbazone molecule and a nitrogen atom of a second molecu e. The diamagnetism of the complexes can be accounted for by a copper–copper interaction. Molecular weights of two typical complexes have been measured by a vapor pressure lowering method in benzene. The complexes were found to associate in this solvent but appeared as dimers at infinite dilution.

Can. J. Chem. Downloaded from www.nrcresearchpress.com by 210.87.254.42 on 09/05/12
For personal use only.

In earlier publications we have reported the preparation of some thiosemicarbazone–copper (I) complexes (1, 2) and discussed their possible structures (2). A number of polymeric structures in which the metal was tetrahedrally coordinated were considered but eventually rejected on the ground of steric strain. Other possibilities involved linearly coordinated copper, also in a polymer.

Many attempts to determine molecular weights of these complexes by the cryoscopic and ebullioscopic methods failed because of their extremely low solubility in suitable solvents. However, using a considerably more sensitive method (vapor pressure lowering) and working at low concentrations, we have now been able to measure molecular weights of two typical copper complexes: *o*-fluoro- (I*a*) and *m*-fluoro- (I*b*) benzaldehyde thiosemicarbazone – copper (I). These were chosen because they can be recrystallized from acetone and, therefore, were particularly pure specimens.

This paper reviews various data obtained earlier and along with the molecular weight observed in benzene, a more probable structure (I) is suggested for these complexes.

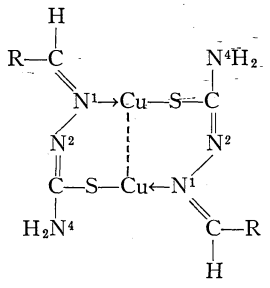

(I)

(I*a*) R = *o*-FC_6H_4— (I*b*) R = *m*-FC_6H_4—

EXPERIMENTAL

Molecular weight determinations were made using milligram quantities of solute and about 10 milliliters of benzene which was previously dried and distilled over calcium hydride. The complexes were recrystallized from acetone to constant melting point and were freed of volatiles by evacuation at room temperature prior to use. The solute was dispersed in the solvent by ultrasonic irradiation for 3 minutes using a 40-kc circo ultrasonic generator. The solutions were shaken periodically and allowed to equilibrate overnight at room temperature before measurements were taken, with a Mechrolab vapor pressure osmometer model 301, to

[1]*Presented at the forty-sixth annual meeting of the Chemical Institute of Canada, Toronto, Ontario, June 1963. Issued as N.R.C. No. 7623.*

determine vapor pressure lowering at 37° C. The instrument was calibrated with benzil solutions over a similar concentration range used for the copper complexes. The operating procedure of the "osmometer" and the calculation of the apparent molecular weights were carried out as described elsewhere (3).

RESULTS AND DISCUSSION

The variation of the apparent molecular weight with solute concentration (g solute/100 g solvent) is shown in Fig. 1. The closed and open circles were obtained for the meta and

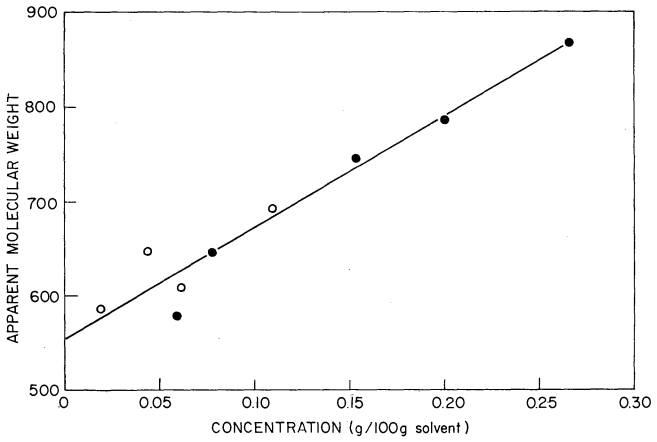

FIG. 1.

ortho isomers respectively. The latter isomer appeared to be less soluble and attempts were not made to carry out measurements over a much wider concentration range. The apparent molecular weight increases with solute concentration, indicating association in benzene. A straight line drawn through the experimental points extrapolated to infinite dilution indicates a molecular weight about twice the value of the monomer. These results suggest that the materials exist in the dimeric form, at least in very dilute solutions.

It was shown in Part II (2) that the complexes are in a 1:1 ratio (1 thiosemicarbazone to 1 copper) and are diamagnetic and that the metal is linked to the sulphur atom. The importance of the N^2 hydrogen atom was also stressed. Indeed, it has been shown that in cases where the N^2 atom was substituted with a methyl group, the resulting 2-methyl thiosemicarbazones failed to form complexes (2). It was suggested in this report that copper was coordinated to the N^4 atom on the ground that 4,4-dimethyl thiosemicarbazones formed 2:1 complexes and thus behaved in a different manner than the original thiosemicarbazones. However, it was found later that 4,4-dimethyl derivatives also formed 1:1 complexes, so that the argument no longer holds and it is now believed that copper is coordinated to the N^1 atom as in (I). This agrees with other findings that thiosemicarbazide and its derivatives form metallic complexes in which the metal is coordinated to the N^1 atom (4, 5, 6, 7, 8). Furthermore, there is little doubt that in the case of dithiosemicarbazone–copper (II) and nickel (II) complexes, coordination is also through the N^1 atom (9, 10).

Copper (I) is a d^{10} ion and to undergo linear coordination, one electron has to be promoted from the $3d$ orbital to the $4s$. A covalent bond would then be formed with an electron from the sulphur atom filling the $4s$ orbital. One $4p$ orbital would be filled by a doublet from the N^1 atom, resulting in sp hybridization, thence, linearly coordinated copper (I). This leaves the $3d$ orbitals with one unpaired electron and since the complexes are diamagnetic, a copper–copper bond is suggested. Atomic models of such a structure

Can. J. Chem. Downloaded from www.nrcresearchpress.com by 210.87.254.42 on 09/05/12
For personal use only.

show that the copper atoms lie so close to each other that they can actually be linked, resulting in two strainless six-membered rings.

Complexes having copper–copper bonds are not too common but in the last few years, a number of reports have been published in which this possibility exists. For instance, the diamagnetism of bis-diazoaminobenzene–copper (II) is explained by a copper–copper bond (11). It is interesting to note that this complex is dimeric. The corresponding complex with copper (I) is also dimeric and X-ray analyses indicate that the metal is linearly coordinated. The possibility of Cu–Cu bonding in this compound has been considered (12) since the distance between copper atoms is 2.45 Å, shorter than that in metallic copper (2.56 Å), and that in cupric acetate (2.64 Å) where a Cu–Cu interaction is known to occur (13). Coates and Parkin suggest the possibility of Cu–Cu bonds in ethynyl–copper (I) complexes with tertiary phosphines where the distance between copper atoms is 2.45 Å (14). A copper–copper interaction would also contribute to the insolubility of the compounds as pointed out by Frasson *et al.* (15) for the dimethylglyoxime complexes of various metals.

The association with increasing concentration in benzene solution may be due to further coordination of a metal atom to a sulphur atom of another dimeric molecule, resulting in a tetramer or even a hexamer by coordination of two metal atoms to two sulphur atoms. Further coordination of metals to sulphur atoms of other molecules is known to occur in the complexes of dialkyldithiocarbamates with the univalent coinage metals, e.g. silver (I) (hexamer), copper (I) (tetramer), and gold (I) (dimer) (16). The crystal structure of these complexes has been studied by Hesse (17), who discussed the degree of polymerity with respect to several factors including the tendency of the metal atoms to coordinate with more than two sulphur atoms. It is interesting to note that similarly to the thiosemicarbazone–copper (I) complexes discussed in this work, the dithiocarbamate–gold (I) complexes have a linear metal–sulphur coordination, are dimeric, and the possibility of metal–metal interactions exists (17).

It is realized that the interaction between copper atoms in thiosemicarbazone–copper (I) complexes may be rather weak and the dimeric structure is broken down by merely dissolving the complexes in dimethyl sulphoxide. Molecular weight determinations by the cryoscopic method in dimethyl sulphoxide showed the complexes to be monomers, which is likely due to dissociation of the dimer followed by coordination of the solvent around the copper atoms; this will be the subject of a subsequent publication.

REFERENCES

1. B. A. GINGRAS, R. W. HORNAL, and C. H. BAYLEY. Can. J. Chem. **38**, 712 (1960).
2. B. A. GINGRAS, R. L. SOMORJAI, and C. H. BAYLEY. Can. J. Chem. **39**, 973 (1961).
3. A. F. SIRIANNI, J. M. G. COWIE, and I. E. PUDDINGTON. Can. J. Chem. **40**, 957 (1961).
4. K. A. JENSEN. Z. Anorg. Allgem. Chem. **221**, 6 (1934).
5. K. A. JENSEN. Z. Anorg. Allgem. Chem. **221**, 11 (1934).
6. K. A. JENSEN and E. RANCKE-MADSEN. Z. Anorg. Allgem. Chem. **219**, 243 (1934).
7. K. A. JENSEN and E. RANCKE-MADSEN. Z. Anorg. Allgem. Chem. **227**, 25 (1936).
8. M. NARDELLI and I. CHIERICI. Ric. Sci. **30**, 276 (1960).
9. B. A. GINGRAS, T. SUPRUNCHUK, and C. H. BAYLEY. Can. J. Chem. **40**, 1053 (1962).
10. G. BAHR. Z. Anorg. Allgem. Chem. **268**, 351 (1952).
11. C. M. HARRIS and R. L. MARTIN. Proc. Chem. Soc. **259** (1958).
12. I. D. BROWN and J. D. DUNITZ. Acta Cryst. **14**, 480 (1961).
13. J. N. VAN NIEKERK and F. R. L. SCHOENING. Acta Cryst. **6**, 227 (1953).
14. G. E. COATES and C. PARKIN. J. Inorg. Nucl. Chem. **22**, 59 (1961).
15. E. FRASSON, R. ZANNETTI, R. BARDI, S. BEZZI, and G. GIACOMETTI. The chemistry of the co-ordination compounds; a symposium. *Edited by* H. Taube and A. G. Maddock. Pergamon Press. 1958. p. 452.
16. S. AKERSTROM. Arkiv Kemi, **14**, 387 (1959).
17. R. HESSE. Advances in the chemistry of the co-ordination compounds. *Edited by* S. Kirschner. Macmillan, New York. 1961. p. 314.

Can. J. Chem. Downloaded from www.nrcresearchpress.com by 210.87.254.42 on 09/05/12
For personal use only.

SYNTHESIS OF METHYL 4-ACETAMIDO-4-DEOXY-L-ERYTHROFURANOSIDE:* A SUGAR WITH NITROGEN IN A FIVE-MEMBERED RING

W. A. SZAREK AND J. K. N. JONES
Department of Chemistry, Queen's University, Kingston, Ontario
Received July 31, 1963

ABSTRACT

The synthesis of methyl 4-acetamido-4-deoxy-L-erythrofuranoside from D-ribose is described. The structural features that are believed to be necessary for the replacement of the ring oxygen of sugars by nitrogen are discussed.

Can. J. Chem. Downloaded from www.nrcresearchpress.com by 210.87.254.42 on 09/05/12
For personal use only.

The replacement of the ring oxygen of sugars by nitrogen has been achieved recently by a number of investigators. In this laboratory 5-acetamido-5-deoxy-L-arabinopyranose* and 5-acetamido-5-deoxy-D-xylopyranose have been synthesized from L-arabinose and D-xylose, respectively (1, 2). The same compounds have been obtained independently by Hanessian and Haskell (3). The latter compound has also been synthesized by a somewhat different route by Paulsen in Germany (4). In that work the compound was named 5-acetamido-5-deoxy-D-xylopiperidinose. Chemical Abstracts recommended the nomenclature used in the present paper.

All of the work cited above involved the introduction of nitrogen into pyranose rings. The present publication describes the synthesis of methyl 4-acetamido-4-deoxy-L-erythrofuranoside, a sugar derivative with nitrogen as the hetero atom in a five-membered ring.

1-Amino-1-deoxy-D-ribitol was prepared from D-ribose by the reductive alkylation of ammonia method of Kagan *et al.* (5) and purified through the crystalline salicylidene Schiff base. *N*-Acetylation of the pure 1-amino-1-deoxy-D-ribitol with aqueous acetic anhydride then gave 1-acetamido-1-deoxy-D-ribitol (I) (6).

Schwarz (7) has shown that the oxidation of mannitol, dulcitol, and sorbitol with a limited quantity of sodium metaperiodate involved preferential attack on threo-glycol groups (i.e., "trans"-glycol groups on the Fischer convention). These results suggested that sodium metaperiodate would oxidize 1-acetamido-1-deoxy-D-ribitol (I) initially between C-4 and C-5, and that a large excess of the ribitol derivative would diminish further oxidation of the initial fission product. Consequently, 1 mole of 1-acetamido-1-deoxy-D-ribitol was oxidized with 0.1 mole of sodium metaperiodate. Under these conditions 81% of the 1-acetamido-1-deoxy-D-ribitol which was oxidized underwent oxidation between C-4 and C-5 as determined by the production of formaldehyde. Clearly, in the major carbohydrate moiety produced in the oxidation, there existed the possibility of formation of a nitrogen-containing furanose ring by ring closure of the terminal aldehyde group on to the nitrogen atom of the amide group.

A large proportion of unreacted 1-acetamido-1-deoxy-D-ribitol was removed by crystallization, and the residual colorless syrup from the periodate oxidation was treated with methanolic hydrogen chloride. Chromatographic examination of the syrupy product indicated that in addition to 1-acetamido-1-deoxy-D-ribitol one major component and two minor components were present. The major component was separated and obtained as a yellow syrup which was a mixture of two compounds. These were separated by

**Nomenclature used by Chemical Abstracts.*

partition between chloroform and water. The chloroform phase yielded a small amount of a pale yellow syrup, the infrared spectrum of which showed carbonyl absorption at 1737 cm^{-1}, but no absorption attributable to OH, NH, or the amide linkage. The identity of this material is as yet unknown. From the water phase there was obtained a clear colorless syrup which gave absorptions in the infrared corresponding to OH and N—Ac, but no absorption attributable to NH. The compound, on periodate oxidation in unbuffered aqueous solution, consumed periodate (1 mole) very rapidly but did not liberate any formic acid even after 48 hours. These results are consistent with the structure proposed for methyl 4-acetamido-4-deoxy-L-erythrofuranoside (II).

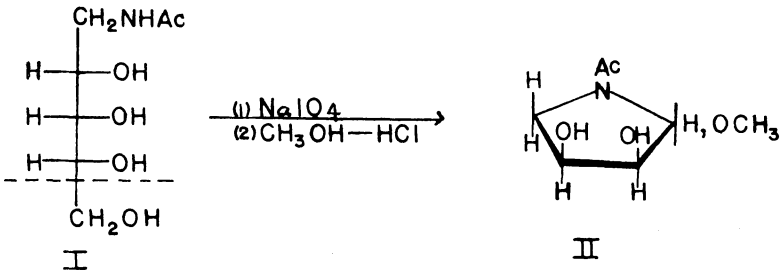

I II

Compound II gave a syrupy di-*O*-acetyl derivative which on gas–liquid chromatographic analysis gave a single symmetrical peak (see Fig. 1).

The proton magnetic resonance spectrum of methyl 4-acetamido-4-deoxy-L-erythrofuranoside is presented in Fig. 2. The spectrum contains two doublets at 5.09 and 5.00 p.p.m. in the general region characteristic of anomeric hydrogens (8, 9). In addition there are two peaks at 3.46 and 3.42 p.p.m. which may be assigned to the methoxyl protons (10), and peaks at 2.16 and 2.13 p.p.m. which may be assigned to the protons of the *N*-acetyl group (10). The n.m.r. spectrum can be interpreted in two ways. The substance may be an approximately 1:1 mixture of α- and β-anomers. Alternatively, the *N*-acetyl group might display restricted rotation, with the rotational isomers showing different chemical shifts for the substituents at C-1. These two possibilities are being investigated.

The preparation of the acyclic 2-pentuloses 5-acetamido-5-deoxy-D-*threo*-pentulose and 5-acetamido-5-deoxy-L-*erythro*-pentulose by the microbiological oxidation of 1-acetamido-1-deoxy-D-arabinitol and 1-acetamido-1-deoxy-D-ribitol, respectively, has been reported from this laboratory (6). These compounds were obtained as crystalline solids. Significantly, the formation of a five-membered ring involving the nitrogen atom was not observed. In the present work each of these ketoses was heated in a dilute acid solution in order to achieve a possible formation of a nitrogen-containing furanose ring. In both cases paper chromatography indicated the presence only of the original ketose sugar. These results suggest that a terminal aldehyde group is required for the formation of a nitrogen-containing furanose ring. An aldehyde group is believed also to be a necessary structural feature for the introduction of nitrogen into a pyranose ring on the basis of some results of Jones and Turner (11). These workers treated 6-acetamido-6-deoxy-D-*arabino*-hexulose with methanolic hydrogen chloride in the cold and at reflux temperature. A mixture of the α- and β-glycofuranosides of the ketose rather than a nitrogen-containing pyranose ring was obtained under both sets of conditions. Very recently Whistler and co-workers (12) reported that methanolysis of 5-amino-5-deoxy-1,2-*O*-isopropylidene-β-L-idofuranose gave methyl 5-amino-5-deoxy-α,β-L-idofuranoside, but no six-membered

Can. J. Chem. Downloaded from www.nrcresearchpress.com by 210.87.254.42 on 09/05/12
For personal use only.

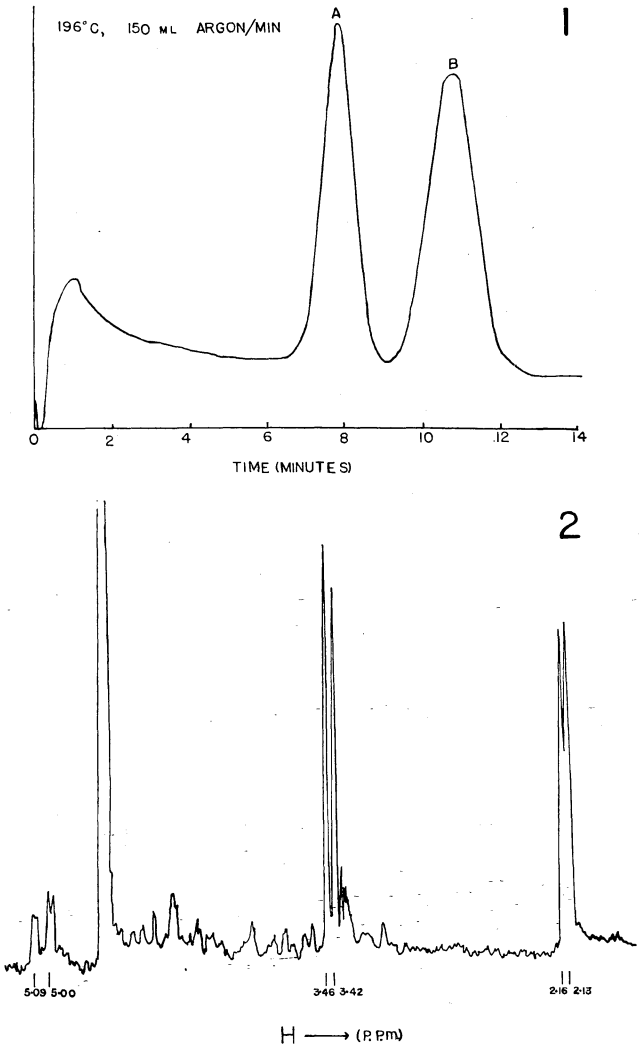

FIG. 1. Gas–liquid chromatogram of (A) methyl 4-acetamido-4-deoxy-2,3-di-*O*-acetyl-L-erythrofuranoside and (B) penta-*O*-acetyl-D-arabinitol.

FIG. 2. N.m.r. spectrum of methyl 4-acetamido-4-deoxy-L-erythrofuranoside measured at 60 Mc/s in deuterium oxide, with tetramethylsilane as an external reference.

nitrogen-containing ring compound was obtained. It appears, therefore, that the requisite structural features for the replacement of the ring oxygen of sugars by nitrogen are an aldehyde group and a *N*-acetyl group on a primary carbon atom.

EXPERIMENTAL

Solutions were concentrated under reduced pressure below 40° with a rotating vacuum-type evaporator. Melting points were determined on a Fisher–Johns melting point apparatus. Optical rotations were measured at 23±3° with a Hilger Standard Polarimeter. Infrared spectra were measured with a Perkin–Elmer Model 21 spectrophotometer. The n.m.r. spectrum was determined at 60 Mc/s with a Varian A-60 n.m.r. spectrometer using an approximately 10% by weight solution of the compound in deuterium oxide; tetramethylsilane was used as an external standard. Paper chromatography was carried out by the descending

Can. J. Chem. Downloaded from www.nrcresearchpress.com by 210.87.254.42 on 09/05/12
For personal use only.

method at room temperature on Whatman No. 1 filter paper; the solvent system was butan-1-ol:ethanol: water, 3:1:1 (v/v). Sugars were detected on paper chromatograms by the following spray reagents: (*i*) alkaline silver nitrate (13); (*ii*) *p*-anisidine hydrochloride (14); (*iii*) sodium metaperiodate – potassium permanganate (15). Rates of movement of the sugars on paper chromatograms are given relative to that of rhamnose (R_{rh}). The gas–liquid chromatographic analysis was carried out using a Pye Argon Chromatograph fitted with an ionization detector (80 μc radium D) and employing straight glass columns (117×0.5 cm I.D.). The column consisted of 38 cm of an intimate mixture of (*a*) 1 part of 20% w/w butanediol succinate polyester on 60–80 mesh Chromosorb W, (*b*) 0.7 part of 20% w/w methylated Damson Gum (OMe 40%) on 60–80 mesh Chromosorb W, placed on top of 79 cm of methyl silicone rubber gum SE-30, 1% w/w, on 60 plus mesh glass beads.

1-Acetamido-1-deoxy-D-ribitol

1-Amino-1-deoxy-D-ribitol was prepared by the reductive alkylation of ammonia method of Kagan *et al.* (5) in which D-ribose (100 g) was dissolved in liquid ammonia and hydrogenated with Raney Nickel catalyst at 1600 p.s.i. at 85° for 4 hours. The crude product was purified through the crystalline salicylidene Schiff base. The purified salicylidene derivative (67.4 g) was suspended in a mixture of 500 ml of water and 45 ml of concentrated hydrochloric acid, and the mixture was heated on a water bath for 15 minutes with vigorous stirring. After being cooled to room temeprature the reaction mixture was extracted three times with 100-ml portions of methylene chloride. The aqueous phase was evaporated to dryness, the residual 1-amino-1-deoxy-D-ribitol hydrochloride was dissolved in 1 l. of water and the solution was passed through a column of Amberlite IRA 400 (OH form) anion exchange resin (900 ml). The eluate was evaporated to dryness under reduced pressure to yield a light brown syrup (37.6 g). This material was dissolved in water (250 ml) and treated with acetic anhydride (37.3 ml). The solution was allowed to stand for 20 minutes with occasional shaking, then evaporated to dryness under reduced pressure to leave a syrup (46.2 g) which crystallized when left standing. Two recrystallizations of this material from methanol–ether gave white needles (27.1 g) which melted at 90–91° and had $[\alpha]_D = -24.5°$ (*c*, 3.14 in water) and R_{rh} 0.88 (spray *i*). Jones *et al.* (6) report m.p. 91.5–92°, $[\alpha]_D = -24°$ and R_{rh} 0.89 (butan-1-ol:ethanol:water, 3:1:1) for 1-acetamido-1-deoxy-D-ribitol.

Periodate Oxidation of 1-Acetamido-1-deoxy-D-ribitol

Preliminary Experiment

1-Acetamido-1-deoxy-D-ribitol (0.0268 g) (1.4×10^{-4} mole) was dissolved in water (12.5 ml), mixed with an equal volume of an aqueous solution of sodium metaperiodate (0.0030 g) (1.4×10^{-5} mole), and left to stand at room temperature. After 30 minutes the solution gave a negative test for periodate. Formaldehyde was then estimated by the chromotropic acid method (16); 0.081 mole formaldehyde per mole 1-acetamido-1-deoxy-D-ribitol had been produced.

Preparative Experiment

1-Acetamido-1-deoxy-D-ribitol (26.45 g) was dissolved in water (270 ml), mixed with an equal volume of a solution of sodium metaperiodate (2.93 g), and left to stand at room temperature for 30 minutes. The solution was then deionized by passing it through a column of Amberlite IR 120 (H form) cation exchange resin (40 ml) and then a column of Duolite A 4 (OH form) anion exchange resin (40 ml). The eluate and washings were then evaporated to dryness under reduced pressure to leave a colorless syrup. This material was taken up in methanol–ether, seeded with a crystal of 1-acetamido-1-deoxy-D-ribitol and set aside in a refrigerator. The crystalline 1-acetamido-1-deoxy-D-ribitol which separated was removed by filtration and washed with methanol. The filtrate and washings were evaporated to dryness under reduced pressure to yield a clear colorless syrup (7.25 g) which was examined on paper chromatograms. Spray *i* showed the presence of components at R_{rh} 0.88 (1-acetamido-1-deoxy-D-ribitol) and 1.13. The latter spot was also detected with spray *ii*.

Reaction with Methanolic Hydrogen Chloride

The clear colorless syrup (7.25 g) obtained above was dissolved in methanolic hydrogen chloride (1.2%, 60 ml) and allowed to stand at room temperature for 2 hours. The solution was then neutralized with silver carbonate and filtered. The clear solution was evaporated under reduced pressure to yield a syrupy product (7.06 g) which was examined on paper chromatograms. Spray *ii* showed one intense spot, R_{rh} 1.7, and two faint spots, R_{rh} 1.3 and 2.0. Spray *i* showed an additional component with R_{rh} 0.88 which was unchanged 1-acetamido-1-deoxy-D-ribitol.

The component having R_{rh} 1.7 was separated on a cellulose column (54×4.5 cm) with butan-1-ol half-saturated with water as the irigant and obtained as a pale yellow syrup (1.6 g). The infrared spectrum of this material in chloroform showed strong absorption at 3375 cm^{-1} attributable to OH, weak absorption at 1735 cm^{-1}, and strong absorption at 1640 cm^{-1} owing to N—Ac, but no absorption due to NH. The syrupy product was partitioned between chloroform and water. The chloroform phase yielded a pale yellow syrup (0.04 g), the infrared spectrum of which in chloroform showed absorption at 1737 cm^{-1}, but no absorption attributable to OH, NH, or the amide linkage. From the water phase there was obtained a clear colorless syrup. This syrup, methyl 4-acetamido-4-deoxy-L-erythrofuranoside, gave a strong absorption in the infrared in chloroform at 3375 cm^{-1} attributable to OH, and strong absorption at 1640 cm^{-1} owing to N—Ac, but no

Can. J. Chem. Downloaded from www.nrcresearchpress.com by 210.87.254.42 on 09/05/12
For personal use only.

absorption due to NH. The compound showed up on paper only faintly with the alkaline silver nitrate spray reagent (*i*), but an intense spot appeared within a few seconds with spray *iii*.

Periodate Oxidation of Methyl 4-Acetamido-4-deoxy-L-erythrofuranoside

Methyl 4-acetamido-4-deoxy L-erythrofuranoside (0.0173 g) was dissolved in water containing 0.3 *M* sodium metaperiodate solution (1 ml). The total volume was made up to 25 ml with additional water. A blank experiment was carried out at the same time. The oxidation was carried out in the dark and at room temperature. Formic acid yield and periodate uptake were determined in the usual fashion (17). After 0.38 hour 0.98 mole periodate per mole methyl 4-acetamido-4-deoxy-L-erythrofuranoside had been consumed and no formic acid had been liberated. The same results were obtained after 48 hours.

Methyl 4-Acetamido-4-deoxy-2,3-di-O-acetyl-L-erythrofuranoside

Methyl 4-acetamido-4-deoxy-L-erythrofuranoside (0.200 g) was dissolved in dry pyridine (1.5 ml), the solution cooled at 0°, and treated with acetic anhydride (0.5 ml). The solution was allowed to stand at room temperature for 24 hours. The di-*O*-acetyl derivative isolated in the usual manner was a syrup (0.258 g, 88%). The infrared spectrum in chloroform showed strong absorption at 1745 cm^{-1} attributable to the carbonyl group of an *O*-acetyl group, and strong absorption at 1660 cm^{-1} owing to N—Ac, but no absorption attributable to NH or OH. When subjected to gas–liquid chromatographic analysis, the acetate gave a single symmetrical peak (Fig. 1) with a retention time of 0.72 relative to penta-*O*-acetyl-D-arabinitol (=1.00). The acetate was readily purified by vacuum distillation to yield a clear, colorless syrup, $[\alpha]_D = -9°$ (*c*, 3.09 in chloroform containing 0.75% ethanol). Calc. for $C_{11}H_{17}O_6N$: C, 51.0; H, 6.6; N, 5.4; OCH_3, 12.0%. Found: C, 50.5; H, 6.8; N, 5.1; OCH_3, 10.8%.

Treatment of 5-Acetamido-5-deoxy-D-threo-pentulose and 5-Acetamido-5-deoxy-L-erythro-pentulose with Dilute Acid

To a 2% aqueous solution (1 ml) of each compound was added glacial acetic acid (0.1 ml). The solutions were heated at 80° for 1.5 hours and examined on paper chromatograms. In each case sprays *i*, *ii*, and *iii* showed the presence of only one component the R_{rh} value of which was the same as that quoted by Jones *et al.* (6) for the original ketose sugar.

ACKNOWLEDGMENTS

The authors thank the National Research Council for a grant (N.R.C.T-19) which made this work possible, and for a scholarship (to W. A. S.). They also wish to thank Dr. D. G. M. Diaper of the Royal Military College for the use of an autoclave, Mr. H. G. Jones of Queen's University for the gas chromatographic analysis, and Dr. S. Wolfe for helpful suggestions.

REFERENCES

1. J. K. N. Jones and J. C. Turner. J. Chem. Soc. 4699 (1962).
2. J. K. N. Jones and W. A. Szarek. Can. J. Chem. **41**, 636 (1963).
3. S. Hanessian and T. H. Haskell. Abstr. Papers Am. Chem. Soc. **144**, 19C (1963); J. Org. Chem. **28**, 2604 (1963).
4. H. Paulsen. Angew. Chem. **74**, 901 (1962).
5. F. Kagan, M. A. Rebenstorf, and R. V. Heinzelman. J. Am. Chem. Soc. **79**, 3541 (1957).
6. J. K. N. Jones, M. B. Perry, and J. C. Turner. Can. J. Chem. **40**, 503 (1962).
7. J. C. P. Schwarz. J. Chem. Soc. 276 (1957).
8. R. U. Lemieux, R. K. Kullnig, H. J. Bernstein, and W. G. Schneider. J. Am. Chem. Soc. **80**, 6098 (1958).
9. J. M. Van der Veen. J. Org. Chem. **28**, 564 (1963).
10. L. M. Jackman. Applications of nuclear magnetic resonance spectroscopy in organic chemistry. Pergamon Press, London. 1959. pp. 55–56.
11. J. K. N. Jones and J. C. Turner. Unpublished results.
12. R. E. Gramera, R. M. Bruce, S. Hirase, and R. L. Whistler. J. Org. Chem. **28**, 1401 (1963).
13. W. E. Trevelyan, D. P. Proctor, and J. S. Harrison. Nature, **166**, 444 (1950).
14. L. Hough, J. K. N. Jones, and W. H. Wadman. J. Chem. Soc. 1702 (1950).
15. R. U. Lemieux and H. F. Bauer. Anal. Chem. **26**, 920 (1954).
16. J. F. O'Dea and R. A. Gibbons. Biochem. J. **55**, 580 (1953).
17. G. Neumüller and E. Vasseur. Arkiv. Kemi, **5**, 235 (1953).

Can. J. Chem. Downloaded from www.nrcresearchpress.com by 210.87.254.42 on 09/05/12
For personal use only.

1,1′-SPIROBIINDANES[1]

L. R. C. Barclay and Ralph A. Chapman[2]
Department of Chemistry, Mount Allison University, Sackville, New Brunswick
Received June 24, 1963

ABSTRACT

The product from both the acid-catalyzed cyclodehydration of 4-methyl-4-phenyl-2-pentanone (I*a*) described by Hoffman (1) and by Barnes and co-worker (2) and the reaction of the saturated cyclic dimer of α-methylstyrene with aluminum chloride reported by Adams and co-workers (3) was shown to be 3,3,3′,3′-tetramethyl-1,1′-spirobiindane (IX*a*) by Curtis (4). A mechanism is postulated to explain the formation of the 1,1′-spirobiindane system. The reactions of several polyalkylindenes with α-methylstyrene and triphenylcarbinol were investigated. Several new polyalkyl-1,1′-spirobiindanes and a new polyalkylindene[1,2-*a*]indene were produced. Two of the 1,1′-spirobiindanes investigated were synthesized by unequivocal methods.

Can. J. Chem. Downloaded from www.nrcresearchpress.com by 210.87.254.40 on 09/05/12
For personal use only.

In 1929 Hoffman (1) reported the formation of a hydrocarbon from the treatment of 4-methyl-4-phenyl-2-pentanone (I*a*) with anhydrous zinc chloride at 180°. Later Barnes and co-worker (2) observed the formation of a hydrocarbon in low yield from refluxing 4-methyl-4-(*p*-tolyl)-2-pentanone (I*b*) with 50% sulphuric acid. Relating their work to that of Hoffman, they proposed after a thorough study that the compound he obtained was 4*b*,9,9,10,10-pentamethyl-4*b*,9,9*a*,10-tetrahydroindeno[1,2-]indene (VI*a*) and postulated the mechanism illustrated in Chart I to explain its formation.

Barnes and co-worker proposed that the beta-aryl ketone (I*a*) can undergo two simultaneous reactions. It can eliminate acetone by acid cleavage to yield the protonated α-methylstyrene (II*a*) and it can undergo cyclodehydration to yield the 1,1,3-trimethylindene (IV*a*). The carbonium ion II*a* then attacks the indene (IV*a*) at carbon 2 so as to produce the new carbonium ion (V), which alkylates the adjacent benzene ring to produce VI*a*.

In 1959 Adams and co-workers (3) reported the formation of (VI*a*) by the treatment of the saturated cyclic dimer of α-methylstyrene (1-phenyl-1,3,3-trimethylindane) with aluminum chloride at 180°. The mechanism proposed involved the formation of protonated α-methylstyrene (II*a*) and indene (IV*a*) from the indane by acid cleavage. These were postulated to react as illustrated in Chart I.

More recently Curtis (4) demonstrated by nuclear magnetic resonance (n.m.r.) studies that the product obtained by all these workers was not the polyalkylindeno[1,2-*a*]indene (VI*a*) but really the 3,3,3′,3′-tetramethyl-1,1′-spirobiindane (IX*a*). He later substantiated this (5) by carrying out a number of interconversions of the 1,1′-spirobiindanes.

In the light of this evidence, the mechanisms of the above reactions became of interest since those postulated by Barnes and Adams could not account for the formation of IX*a*. However, it is interesting to note that in the mechanisms proposed by these workers, two reactants, the indene (IV*a*) and the carbonium ion (II*a*), are present. The following new mechanism for the formation of (IX*a*), illustrated in Chart II, is proposed.* An equilibrium can be set up in the acid medium between the endocyclic form of the 1,1,3-trimethylindene (IV*a*) and the exocyclic form (VII*a*) ($R_1 = R_2 = H$). (The 1,1,3-trimethylindene could form as illustrated in Chart I or could be added as one of the starting

[1]*Presented in part before the Division of Petroleum Chemistry, Symposium on Aromatic Compounds at the 142nd meeting of the American Chemical Society, Atlantic City, September 1962.*
[2]*Recipient of a National Research Council Studentship.*
**This mechanism has also been independently proposed by R. A. Barnes, private communication.*

CHART I

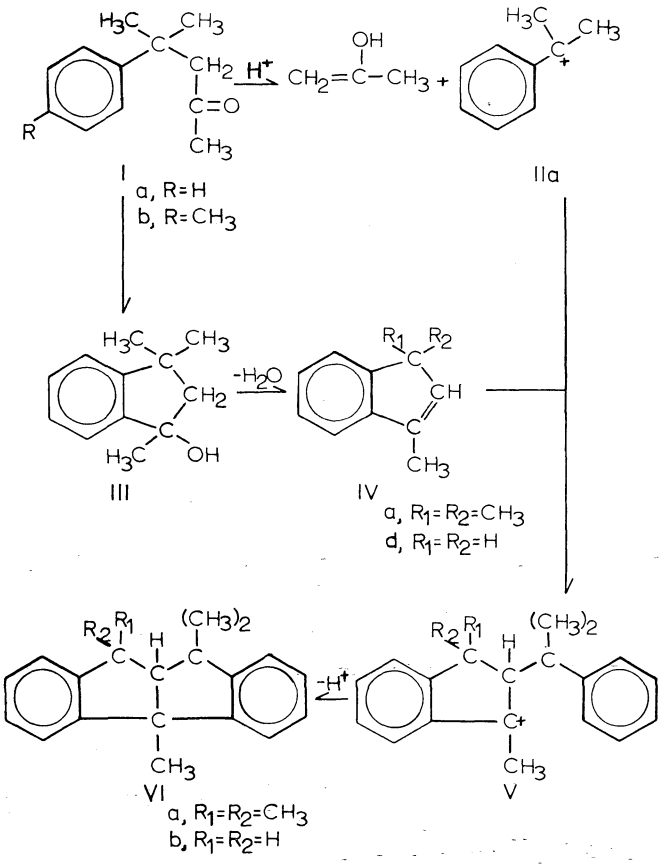

reagents.) This equilibrium is expected to favor the endocyclic form. However, the relatively bulky protonated α-methylstyrene (either formed as shown in Chart I or added as α-methylstyrene) can alkylate the exocyclic form more readily than the hindered endocyclic form. When alkylation occurs, it causes a continual shift in the endocyclic–exocyclic equilibrium because of removal of the exocyclic form as the new carbonium ion (VIII). This carbonium ion has the charge suitably situated to alkylate the second aromatic ring producing the 3,3,3′,3′-tetramethyl-1,1′-spirobiindane (IX*a*).

To substantiate the above mechanism we found that the indene (IV*a*) reacted with α-methylstyrene in sulphuric acid to produce the 1,1′-spirobiindane (IX*a*) in 54% yield. The product has identical physical properties to that prepared by Barnes and Adams. The n.m.r. spectrum of the compound (Fig. 1) was interesting. It showed a complicated multiplet integrating for 8 aromatic protons, a singlet at 7.72 p.p.m. for the 4 methylene protons, and a doublet at 8.61 and 8.65 p.p.m. corresponding to 12 methyl protons. The aromatic proton multiplet was divided into two signals one with maximum intensity at 2.89 p.p.m. (corresponding to 6 protons) and another at 3.30 p.p.m. (corresponding to 2 protons). The examination of a molecular model helped to clarify several points about the spectrum. A possible explanation of the two groups of partially resolved multiplets in the aromatic proton signal is based on the fact that the conformation of the molecule places

Can. J. Chem. Downloaded from www.nrcresearchpress.com by 210.87.254.40 on 09/05/12
For personal use only.

CHART II

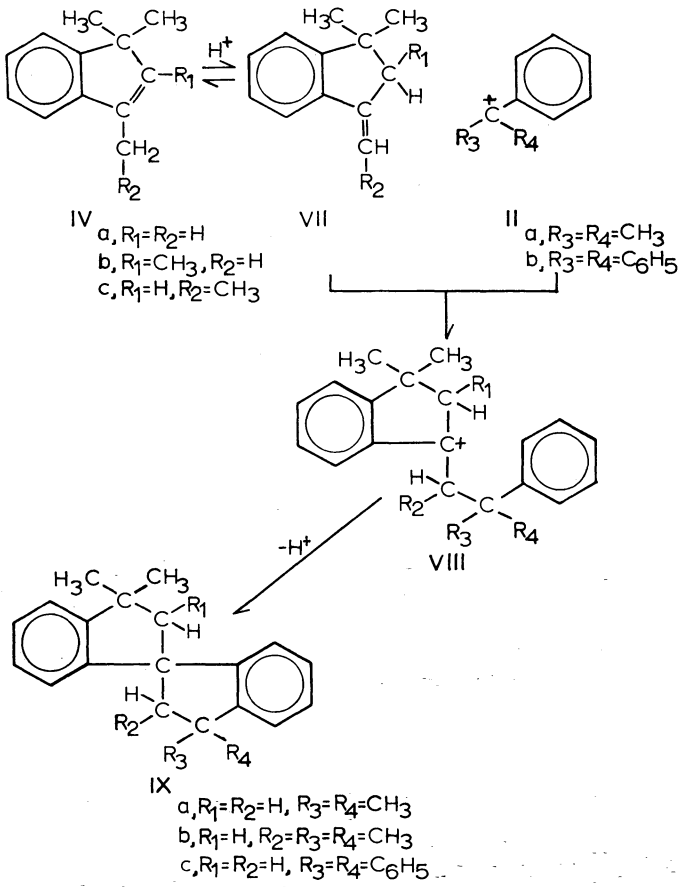

the two aromatic rings nearly at right angles to one another and reasonably close together. In such a situation the proton on carbon 7 (and 7′) would lie in a position more or less over the plane of the ring to which it was not directly attached. Thus it would be shielded and would resonate at higher field than the other aromatic protons, that is, near 3.30 p.p.m.

The fact that the methyl proton resonance is a doublet can be attributed to the fact that one of the methyl groups of each of the *gem* dimethyl systems on carbons 3 and 3′ lies in the plane of the aromatic ring to which it is less closely attached while the remaining methyl group lies slightly above the plane of the ring to which it is more closely attached. In such a situation, the group in the plane of the ring would be expected to be deshielded relative to the other group and thus resonate at slightly lower field.

On closer examination of the proposed reaction mechanism, it is obvious that any effect which tends to stabilize the endocyclic form of the indene would tend to prevent the formation of the 1,1′-spirobiindane system while any effect which tends to stabilize the exocyclic form would have the opposite effect.

With the former effect in mind, 1,1,2,3-tetramethylindene (IV*b*) was prepared. In such a system the methyl group on carbon 2 should tend to stabilize the double bond in the endocyclic form and one would expect less 1,1′-spirobiindane to form in a reaction of this indene with α-methylstyrene than was produced under similar conditions with

Can. J. Chem. Downloaded from www.nrcresearchpress.com by 210.87.254.40 on 09/05/12
For personal use only.

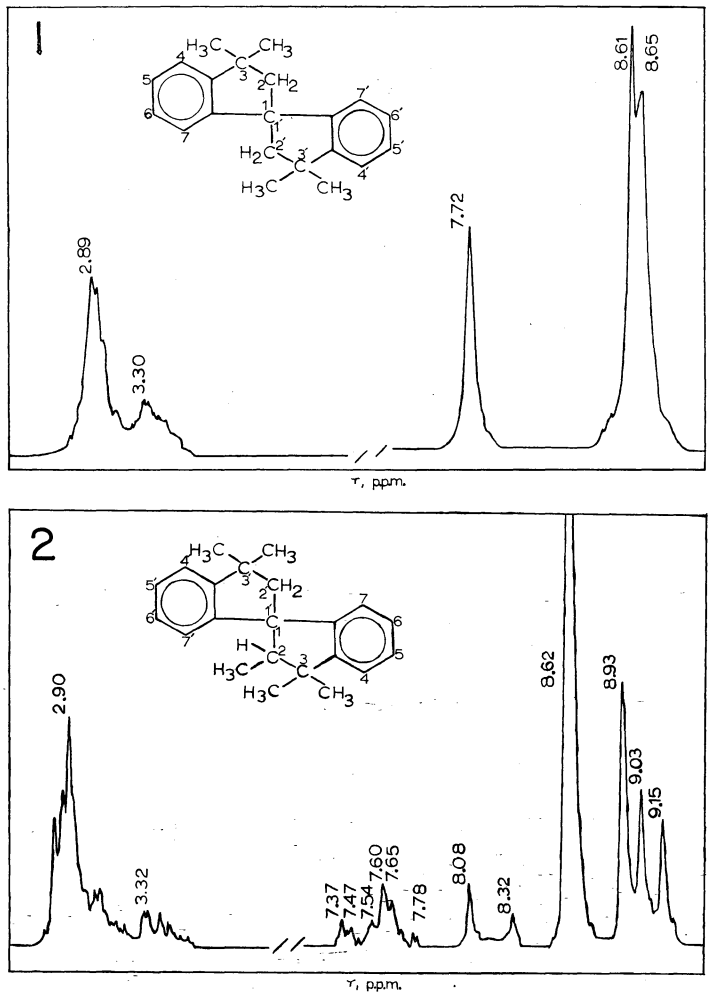

FIG. 1. Nuclear magnetic resonance spectrum of 3,3,3′,3′-tetramethyl-1,1′-spirobiindane.
FIG. 2. Nuclear magnetic resonance spectrum of 2,3,3,3′,3′-pentamethyl-1,1′-spirobiindane.

1,1,3-trimethylindene and α-methylstyrene. When the indene (IV*b*) and α-methylstyrene were reacted with sulphuric acid at −5° none of the 2,3,3,3′,3′-pentamethyl-1,1′-spirobiindane (IX*b*) was produced. The only high molecular weight compound formed was the saturated cyclic dimer of α-methylstyrene which under the conditions used does not react further to produce (IX*a*).

In order to test the stabilizing effect of an additional methyl group on the exocyclic form of an indene, 3,3-dimethyl-1-ethylindene (IV*c*) was prepared. In such a compound the exocyclic form would be expected to be more stable than in 1,1,3-trimethylindene. Reaction of the indene (IV*c*) with α-methylstyrene in sulphuric acid produced a colorless crystalline solid (m.p. 118–119°) in 67% yield. The ultraviolet spectrum gave bands at 2730 Å (log ϵ = 3.33), 2660 Å (log ϵ = 3.29), and 2590 Å (log ϵ = 3.08). The infrared spectrum gave a doublet in the 1385–1365 cm^{-1} region attributed to the *t*-butyl skeleton and two strong bands at 765 and 750 cm^{-1} attributed to *o*-disubstituted aromatics. The

Can. J. Chem. Downloaded from www.nrcresearchpress.com by 210.87.254.40 on 09/05/12
For personal use only.

mass spectrum showed a parent mass of 290. The analytical results agreed with the formula $C_{22}H_{26}$. This evidence indicated the compound was the 2,3,3,3′,3′-pentamethyl-1,1′-spirobiindane (IX*b*). The n.m.r. spectrum (Fig. 2) was complex but confirmed this. The eight aromatic protons absorbed as a complex multiplet with maximum intensities of the two separate branches at 2.90 and 3.32 p.p.m. respectively. The signals at 3.32 p.p.m. were again attributed to the shielding effect on the protons at carbons 7 and 7′ causing them to resonate at higher fields as they did in compound (IX*a*). An AB type quartet at 7.37, 7.60, 8.08, and 8.32 p.p.m. was attributed to the methylene protons of carbon 2′. These protons are not equivalent because of the interaction of one of them with the methyl group on carbon 2 which actually lies very close to it. A quartet at 7.47, 7.54, 7.65, and 7.78 p.p.m. was attributed to the methine proton on carbon 2. The quartet is a result of its spin–spin coupling with the protons of the methyl group and thus represents the methine proton's contribution to the AB_3 system. A doublet at 9.03 and 9.15 p.p.m. was attributed to the methyl protons attached to carbon 2. It formed the remainder of the AB_3 system. The singlet at 8.93 p.p.m. was attributed to one of the methyl groups on carbon 3 which appears at higher field than the other because of the shielding effect of the methyl group on the adjacent carbon 2. The singlet at 8.62 p.p.m. was attributed to the protons of the remaining three methyl groups on carbon 3 and 3′. It is interesting to note that this is not resolved as a doublet as was observed for IX*a* perhaps, because the signal of the three methyl protons on carbon 3′ that lie in the plane of the non-adjacent aromatic ring is only half as intense as that of the six methyl protons on carbons 3 and 3′ out of the plane of the adjacent aromatic rings, and is thus not resolved from the larger signal considering that the shift for two such groups in compound (IX*a*) was only 0.04 p.p.m.

Positive evidence in favor of the proposed mechanism is given by the non-reactivity of 1,1,2,3-tetramethylindene (IV*b*) with α-methylstyrene, and the fact that 3,3-dimethyl-1-ethylindene (IV*c*), in a reaction similar to the one in which compound (IX*a*) was produced from 1,1,3-trimethylindene (IV*a*) and α-methylstyrene, gave the expected product (IX*b*) in higher yield.

Several questions arise concerning the generality of these reactions. It was desirable to determine if an unhindered endocyclic form of an indene (Chart I, IV*d*) would alkylate even if an exocyclic form could exist. If the reaction producing the spirobiindanes is a general one, other suitable olefins and other alkylating agents (besides α-methylstyrene) should enter into the reaction. In attempts to investigate the generality of these reactions, further work was undertaken as described below.

The reaction of 1-methylindene with α-methylstyrene in sulphuric acid yielded a colorless liquid in 50% yield. The ultraviolet spectrum of this product gave bands at 2730 Å (log ϵ = 3.22), 2660 Å (log ϵ = 3.25), and 2600 Å (log ϵ = 3.06). The infrared spectrum gave a doublet at 1390 and 1385 cm^{-1} attributed to the *t*-butyl skeleton, as well as a strong band at 760 cm^{-1} indicating *o*-disubstituted aromatics. The analytical results agreed with a formula $C_{19}H_{20}$ which was substantiated by the mass spectrum which indicated a parent mass of 248. The n.m.r. spectrum (Fig. 3) consisted of a multiplet of maximum intensity at 2.91 p.p.m. corresponding to 8 protons, a series of 10 signals between 6.70 and 7.66 p.p.m. integrating for 3 protons and three singlets at 8.39, 8.62, and 9.05 p.p.m. corresponding to 3 protons each. On the basis of this spectrum, the compound was apparently not a 1,1′-spirobiindane but the 4*b*,9,9-trimethyl-4*b*,9,9*a*,10-tetrahydroindeno[1,2-*a*]indene (VI*b*). This product would form if the protonated α-methylstyrene (II*a*) alkylated the 1-methylindene (IV*d*) at carbon 2 and subsequent reaction

Can. J. Chem. Downloaded from www.nrcresearchpress.com by 210.87.254.40 on 09/05/12
For personal use only.

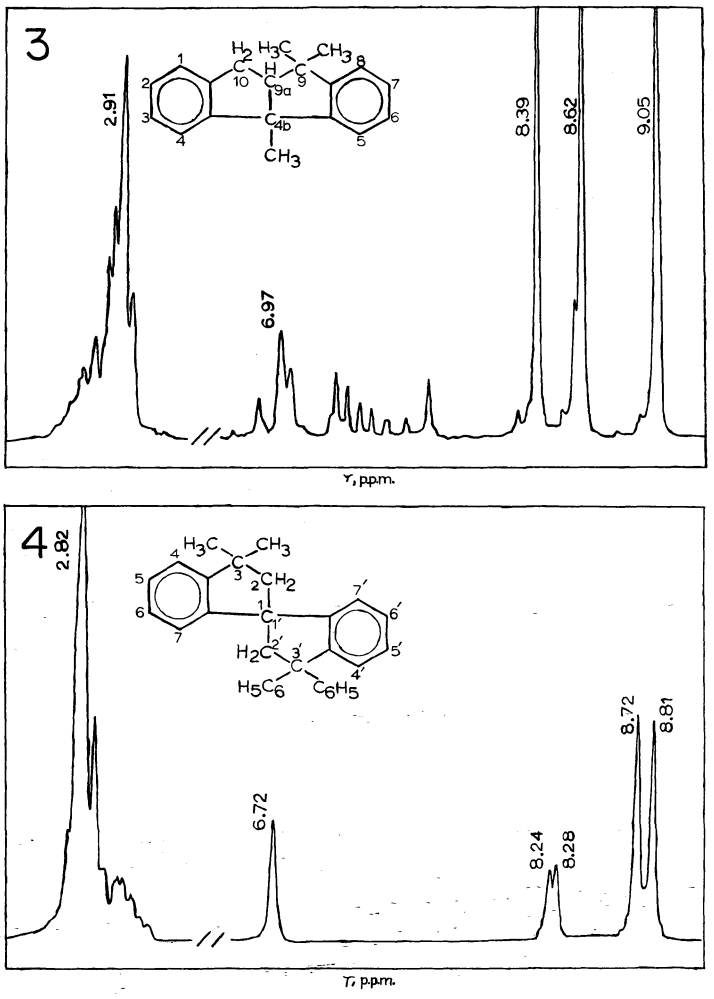

FIG. 3. Nuclear magnetic resonance spectrum of 4*b*,9,9-trimethyl-4*b*,9,9*a*,10-tetrahydroindene[1,2-*a*] indene.

FIG. 4. Nuclear magnetic resonance spectrum of 3,3-dimethyl-3′,3′-diphenyl-1,1′-spirobiindane.

followed the mechanism outlined in Chart I. The multiple signal in the n.m.r. between 6.70 and 7.66 p.p.m. was attributed to an ABC or ABX system consisting of the methine proton on carbon 9*a* and the methylene protons on carbon 10. The singlet at 8.39 p.p.m. was apparently due to one of the methyl groups on carbon 9, which, because of its position relative to the two aromatic rings, is deshielded. The singlet at 8.62 p.p.m. was then attributed to the other methyl group on carbon 9 while that at 9.05 p.p.m. was associated with the protons of the group on carbon 4*b* which, because of the type of fusion along the carbon 4*b* to carbon 9*a* bond, lie well away from either of the aromatic rings and thus resonate at higher field.

The product from the reaction of 1,1,3-trimethylindene (IV*a*) with triphenylcarbinol in sulphuric acid was a crystalline solid, m.p. 171–173° (41% yield). The ultraviolet spectrum gave bands at 2733 Å (log ϵ = 3.19), 2663 Å (log ϵ = 3.31), and a slight inflection at 2610 Å (log ϵ = 3.21). The infrared spectrum gave strong bands at 768, 755, and

Can. J. Chem. Downloaded from www.nrcresearchpress.com by 210.87.254.40 on 09/05/12
For personal use only.

Can. J. Chem. Downloaded from www.nrcresearchpress.com by 210.87.254.40 on 09/05/12
For personal use only.

702 cm^{-1} indicative of both *o*-disubstituted and monosubstituted aromatics. The mass spectrum showed a parent mass of 400. This was substantiated by an analytical result which agreed with the molecular formula $C_{31}H_{28}$. This evidence suggested the compound was the expected 3,3-dimethyl-3′,3′-diphenyl-1,1′-spirobiindane (IX*c*). This was substantiated by the n.m.r. spectrum (Fig. 4) which gave an 18 proton multiplet at 2.82 p.p.m. A singlet at 6.72 p.p.m. integrating for 2 protons was attributed to the methylene protons on carbon 2′ which are deshielded by the adjacent aromatic ring attached to carbon 3′. A doublet at 8.24 and 8.28 p.p.m. integrated for 2 protons and was attributed to the methylene protons on carbon 2. The two methyl groups on carbon 3 gave signals at 8.72 and 8.81 p.p.m. respectively. The chemical shift of one of the methyl groups to lower field is attributed to that methyl group being in the plane of an aromatic ring as it was in compound IX*a*. The fact that the shift is greater in this case than was observed for compound IX*a* is attributed to the fact that a buttressing effect of the two bulky phenyl groups on carbon 3′ causes the other aromatic ring attached to that carbon to approach the methyl group on carbon 3 more closely than in compound IX*a* with the result that it is significantly more shielded.

As proof of the structures of two of the compounds prepared, namely, the 3,3,3′,3′-tetramethyl (IX*a*) and the 2,3,3,3′,3′-pentamethyl-1,1′-spirobiindane (IX*b*), these compounds were synthesized by unequivocal methods as outlined in Chart III.

The synthesis of (IX*a*) was realized by first treating benzene with phorone (XIII) in

CHART III

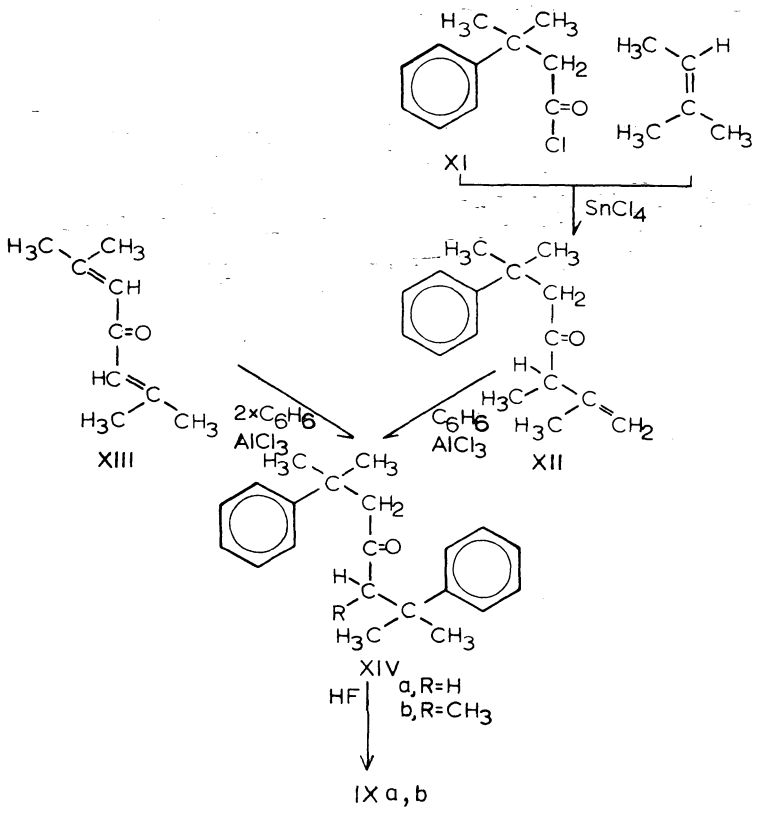

the presence of aluminum chloride to produce the 2,6-dimethyl-2,6-diphenyl-4-heptanone (XIV*a*) reported by Colonge and Pichat (6) in 70% yield. This compound had the expected n.m.r. spectra. Cyclization of this ketone with anhydrous hydrogen fluoride yielded (IX*a*) in 78% yield.

The synthesis of the 2,3,3,3′,3′-pentamethyl-compound (IX*b*) was carried out by first treating 3-methyl-3-phenylbutanoyl chloride (XI) with 2-methyl-2-butene and stannic chloride to yield 2,3,6-trimethyl-6-phenyl-1-heptene-4-one (XII). Reaction of this with benzene and aluminum chloride furnished 2,3,6-trimethyl-2,6-diphenyl-4-heptanone (XIV*b*). Treatment of this ketone with hydrogen fluoride yielded (IX*b*) identical with the (IX*b*) from the reaction of 3,3-dimethyl-1-ethylindene with α-methylstyrene.

EXPERIMENTAL

Apparatus and Methods

The ultraviolet spectra were recorded on a Beckman DK-2 ratio recording spectrophotometer using spectro grade cyclohexane as solvent. The infrared spectra were recorded on a Perkin–Elmer Model 137 "Infracord" spectrophotometer. Gas–liquid chromatography analyses were carried out on a Perkin–Elmer 154-D vapor fractometer or on an F & M Model 500 programmed temperature gas chromatograph equipped with a dual column attachment. Small samples of pure compounds were obtained by repetitive chromatography of a mixture followed by collection of pure components. The mass spectrometer analyses were done at an independent laboratory. Nuclear magnetic resonance spectra were recorded at the National Research Council, Halifax, Nova Scotia, on a Varian A-60 spectrometer using tetramethylsilane as internal standard and carbon tetrachloride as solvent. Melting points were determined on a Fischer–Johns melting point apparatus equipped with a microscope or on a Thomas–Hoover "Unimelt" capillary melting point apparatus. Reactions with anhydrous hydrogen fluoride were carried out in a 12-in. stainless steel MD test tube reactor equipped with stainless steel gaskets made by Autoclave Engineers Inc. Ultimate analyses were determined by Dr. E. Thommen, Basel, Switzerland and Dr. C. Daessle, Montreal.

*Preparation of 1,1,3-Trimethylindene (IV*a*)*

Benzene (800 ml) and aluminum chloride (360 g) were mixed at room temperature. Mesityl oxide (200 ml) was added dropwise to the stirred mixture over 45 minutes without external cooling. After 4 hours at room temperature, the mixture was hydrolyzed on ice. The organic material was separated and the aqueous layer was extracted with benzene. The combined organic layer and benzene extract were washed with 10% sodium carbonate, water, and dried over sodium sulphate. The solvent was distilled and the residue was further distilled *in vacuo* yielding 14.08 g of 1,1,3-trimethylindene, b.p. 50° at 0.65 mm, n_D^{25} = 1.5346 (literature (7), n_D^{25} = 1.5346), and 40.37 g of 4-methyl-4-phenyl-2-pentanone, b.p. 78–81° at 0.85 mm. Gas–liquid chromatography of the two products on an 8 ft silicone gum rubber column showed they were pure.

*3,3,3′,3′-Tetramethyl-1,1′-spirobiindane (IX*a*)*

The procedure for preparing IX*a* was essentially that of Barnes (2) except that phenyldimethylcarbinol was replaced by α-methylstyrene. The sulphuric acid catalyzed reaction between 1,1,3-trimethylindene (5 g, 0.031 mole) and α-methylstyrene (3.6 g, 0.031 mole) yielded 5.5 g of crude solid shown to be 81% compound IX*a* (a 54% yield) and 19% the saturated cyclic dimer of α-methylstyrene by gas–liquid chromatography.

The compound IX*a*, after recrystallization from methanol, had a melting point of 133–134° (literature (1) 133–134°). The ultraviolet spectrum gave bands at 2730 Å (log ε = 3.12), 2660 Å (log ε = 3.05), and 2595 Å (log ε = 2.99). This compound proved to be identical, by mixed melting point and infrared spectra, with the hydrocarbon prepared directly from 4-methyl-4-phenyl-2-pentanone according to the procedure of Hoffman (1). The infrared spectrum was identical with that reported by Adams and co-workers (3). The n.m.r. spectrum gave an 8-proton multiplet at 2.89 and 3.30 p.p.m., a 4-proton singlet at 7.72 p.p.m., and a 12-proton doublet at 8.61 and 8.65 p.p.m. The mass spectrum showed a parent mass of 276.

*Preparation of 1,1,2,3-Tetramethylindene (IV*b*)*

(a) Preparation of 3,4-Dimethyl-3-pentene-2-one

Acetyl chloride (55.75 g, 0.71 mole) and 2-methyl-2-butene, b.p. 38–41° (76.6 g, 1.09 mole), were reacted with anhydrous stannic chloride (7.1 g) according to the procedure of Colonge (8). The olefin and the acid chloride were cooled in ice and salt and the stannic chloride was added dropwise while the temperature was maintained below 0°. The mixture was then allowed to warm slowly to room temperature and finally was heated at 60–80° for 2 hours and allowed to cool slowly.

After hydrolysis on ice, extraction with ether, and washing the ether extract free of acid and drying, the solvent was distilled. Distillation of the residual liquid yielded 41.14 g of colorless liquid, b.p. 148–150°

Can. J. Chem. Downloaded from www.nrcresearchpress.com by 210.87.254.40 on 09/05/12
For personal use only.

(with the evolution of a great deal of hydrogen chloride) $n_D^{14} = 1.4491$ (literature (8), $n_D^{14} = 1.4506$). Gas–liquid chromatography showed a 99% pure product.

(b) Preparation of 1,1,2,3-Tetramethylindene

Twenty-eight grams (0.25 mole) of 3,4-dimethyl-3-pentene-2-one was cooled below 0° and hydrogen chloride (10 g) 0.27 mole, was bubbled in, thus forming the 4-chloro-3,4-dimethyl-2-pentanone. This was added dropwise to a stirred mixture of benzene (100 ml, 1.15 mole) and aluminum chloride (50 g, 0.37 mole) while the temperature was maintained at 0–10°. After it was stirred for an additional 3 hours in the cold, the mixture was hydrolyzed on ice and hydrochloric acid. The organic layer was separated, washed free of acid, and dried over sodium sulphate. Distillation yielded 19.96 g of 1,1,2,3-tetramethylindene, b.p. 76–82° at 1.6 mm, $n_D^{25} = 1.5384$ (literature (9), $n_D^{25} = 1.5431$.

Reaction of 1,1,2,3-Tetramethylindene with α-Methylstyrene

The 1,1,2,3-tetramethylindene (5.30 g, 0.031 mole) and α-methylstyrene (3.6 g, 0.031 mole) were cooled to −5° in ice and salt. Sulphuric acid (41 ml) was added dropwise with vigorous stirring as described above. After the procedure was repeated as for 1,1,3-trimethylindene, distillation of the solvent yielded 3.66 g of viscous liquid. Gas–liquid chromatography showed it to be mostly the saturated cyclic dimer of α-methylstyrene with no higher boiling material.

Preparation of 3,3-Dimethyl-1-ethylindene (IVc)

(a) 3,3-Dimethyl-1-indanone

3-Methyl-3-phenylbutanoic acid, prepared by the alkylation of benzene with 3-methyl-2-butenoic acid (10), had a melting point of 55–57° (literature (11), m.p. 58–59°). This acid was converted to 3,3-dimethyl-1-indanone according to the procedure of Koelsch and Le Clair (11).

(b) Preparation of 3,3-Dimethyl-1-ethylindene

A Grignard reagent was prepared from 4.86 g (0.045 mole) of ethyl bromide and 0.72 g (0.032 mole) of magnesium in 30 ml of anhydrous ethyl ether. Crude 3,3-dimethyl-1-indanone (from part *a*) (4.31 g, 0.026 mole) in 15 ml of ether was added to the reagent over 45 minutes while the temperature was maintained at 0–5°. The mixture was then refluxed for 2 hours and hydrolyzed on ice. The crude product isolated by extraction with ether was refluxed for 2 hours with 10% aqueous oxalic acid and the oil obtained by ether extraction was chromatographed from petroleum ether on alumina. The first fraction from the alumina column yielded 1.71 g of an oil which was mainly the desired indene according to the similarity of its ultraviolet and infrared spectra with those of 1,1,3-trimethylindene. There was a slight contamination with the starting ketone as shown by a weak band for carbonyl absorption at 1700 cm^{-1}.

2,3,3,3′,3′-Pentamethyl-1,1′-spirobiindane (IXb)

The 3,3-dimethyl-1-ethylindene (0.50 g, 0.0029 mole) and α-methylstyrene (0.34 g, 0.0029 mole) were cooled to −15° and sulphuric acid (5.0 g) was added as described before. Distillation of the solvent after completion of the reaction and extraction with petroleum ether yielded 0.52 g of solid. Gas–liquid chromatography indicated that the major component (90%) was not compound IX*a* but a higher boiling one. The solid was fractionally sublimed *in vacuo*. Recrystallization of the fractions from absolute ethanol yielded colorless crystals, m.p. 118–119°. The ultraviolet spectrum gave bands at 2730 Å ($\log \epsilon = 3.33$), 2660 Å ($\log \epsilon = 3.29$), and 2590 Å ($\log \epsilon = 3.08$). The infrared spectrum gave a doublet in the 1385–1365 cm^{-1} region attributed to the *t*-butyl structure and two bands of equal intensity at 765 and 750 cm^{-1} attributed to *o*-disubstituted aromatics. The n.m.r. spectrum showed an 8-proton multiplet with maximum intensities at 2.90 and 3.32 p.p.m., a 2-proton quartet at 7.37, 7.60, 8.08, and 8.32 p.p.m., a single proton quartet at 7.47, 7.54, 7.65, and 7.78 p.p.m., a 3-proton singlet at 8.93 p.p.m., a 3-proton doublet at 9.03 and 9.15 p.p.m., and a 9-proton singlet at 8.62 p.p.m. The mass spectrum indicated a parent mass of 290. Analysis—Found: C, 90.30, 90.38; H, 9.31, 9.29. Calculated for $C_{22}H_{26}$: C, 90.98; H, 9.02.

4b,9,9-Trimethyl-4b,9,9a,10-tetrahydroindeno-[1,2a]-indene (VIb)

The 1-methylindene was prepared following the procedure of Stoermer and Laage (12) using the modification of Parham and co-workers (13). The product distilled at 84° at 11 mm, $n_D^{25} = 1.5630$ (literature (13), b.p. 76–78° at 11 mm, $n_D^{25} = 1.5587$) yielding 7.63 g of 1-methylindene.

The 1-methylindene (0.78 g, 0.006 mole) and the α-methylstyrene (0.71 g, 0.006 mole) were reacted with sulphuric acid as described above to yield 0.66 g of viscous liquid. Gas–liquid chromatography on a silicone grease column showed it to be 12% the saturated cyclic dimer of α-methylstyrene and 62% a compound which was not IX*a*. An attempt to separate the major component by molecular distillation was unsuccessful. Small samples were then repeatedly chromatographed on the F & M Model 500 and the compound collected as a colorless liquid. The ultraviolet spectrum gave bands at 2730 Å ($\log \epsilon = 3.22$), 2660 Å ($\log \epsilon = 3.25$), and 2600 Å ($\log \epsilon = 3.06$). The infrared spectrum gave a doublet at 1390 and 1385 cm^{-1} characteristic of a *t*-butyl group and also showed a strong band at 760 cm^{-1} for *o*-disubstituted aromatics. The mass spectrum showed a parent mass of 248. The n.m.r. spectrum gave an 8-proton multiplet at 2.91 p.p.m., a complex 3-proton 10-band ABC or ABX multiplet between 6.70 and 7.66 p.p.m., and three

Can. J. Chem. Downloaded from www.nrcresearchpress.com by 210.87.254.40 on 09/05/12
For personal use only.

3-proton singlets at 8.39, 8.62, and 9.05 p.p.m. Analysis—Found: C, 91.07, 90.92; H, 8.11, 8.07. Calculated for $C_{19}H_{20}$: C, 91.54; H, 8.46.

3,3-Dimethyl-3',3'-diphenyl-1,1'-spirobiindane (IXc)

The 1,1,3-trimethylindene (1.0 g, 0.006 mole) and triphenylcarbinol (1.56 g, 0.006 mole) were reacted with 8 ml of sulphuric acid as described above. After 2 hours' stirring the temperature had risen to 10°. The mixture was extracted with benzene after standing overnight at room temperature. Subsequent washing, drying, and distillation of the solvent yielded 1.0 g (41% yield) of solid. The solid was chromatographed from benzene on alumina to yield a thick oil which crystallized on treatment with acetone. Recrystallization from acetone yielded colorless crystals, m.p. 171–173°. The ultraviolet spectrum gave bands at 2733 Å (log ϵ = 3.19), 2663 Å (log ϵ = 3.31), and an inflection at 2610 Å (log ϵ = 3.21). The infrared spectrum showed strong bands at 768, 755, and 702 cm^{-1} apparently due to both *o*-disubstituted and monosubstituted aromatics. The mass spectrum showed a parent mass of 400. The n.m.r. spectrum showed an 18-proton multiplet at 2.82 p.p.m., a 2-proton singlet at 6.72 p.p.m., a 2-proton doublet at 8.24 and 8.28 p.p.m., and two 6-proton singlets at 8.72 and 8.81 p.p.m. Analysis—Found: C, 92.83, 92.90; H, 7.08, 7.20. Calculated for $C_{31}H_{28}$: C, 92.95; H, 7.04.

Synthesis of 3,3,3',3'-Tetramethyl-1,1'-spirobiindane (IXa)

(a) Preparation of 2,6-Dimethyl-2,6-diphenyl-4-heptanone (XIVa)

Benzene (64 g, 0.82 mole) and aluminum chloride (26.0 g, 0.27 mole) were cooled to 15–20°. Phorone (27.6 g, 0.20 mole) was added with stirring over 45 minutes at 15–20°. The mixture was stirred for 4 hours and allowed to stand for 43 hours at room temperature. After hydrolysis on ice, extraction, drying, and distillation of the solvent, the residue was distilled to yield 41.5 g of the desired ketone, b.p. 158–160° at 0.45 mm, n_D^{19} = 1.5462 (literature (6), n_D^{17} = 1.5465). The infrared spectrum indicated a monosubstituted aromatic ketone. The carbonyl absorption appeared at 1700 cm^{-1} and two strong bands at 700 cm^{-1} and 830 cm^{-1} were attributed to a monosubstituted aromatic. The ultraviolet spectrum gave bands at 2640 Å (log ϵ = 2.70), 2585 Å (log ϵ = 2.77), and 2535 Å (log ϵ = 2.71). The n.m.r. spectrum gave a 10-proton singlet at 2.95 p.p.m., a 4-proton singlet at 7.73 p.p.m., and a 12-proton singlet at 8.76 p.p.m.

(b) Reaction of 2,6-Dimethyl-2,6-diphenyl-4-heptanone with Hydrogen Fluoride

The hydrogen fluoride (10.0 g) was condensed in the cold reactor tube. The ketone (9.11 g, 0.031 mole) was added rapidly. The tube was sealed and stirred for 24 hours. It was then cooled and opened. The contents were solid. Petroleum ether was added to dissolve the solid. The ether extract was washed free of acid with water and dried. Distillation of the solvent yielded 7.35 g of solid. Gas–liquid chromatography on a 2-m silicone grease column indicated the solid was 89% compound IX*a* (75% yield). Recrystallization from methanol gave colorless needles, m.p. 135–136°. A mixed melting point and infrared spectrum showed this product to be identical with IX*a* produced from 1,1,3-trimethylindene and α-methylstyrene.

Synthesis of 2,3,3,3',3'-Pentamethyl-1,1'-spirobiindane (IXb)

(a) Preparation of 2,3,6-Trimethyl-6-phenyl-1-heptene-4-one (XII)

Ten grams (0.051 mole) of 3-methyl-3-phenylbutanoyl chloride and 2-methyl-2-butene (4.68 g, 0.068 mole) were cooled below −5°. Anhydrous stannic chloride (1.5 g) was added dropwise with stirring while the temperature was maintained below 0°. The mixture was then allowed to warm slowly to room temperature. After 7 hours, the reaction was hydrolyzed on ice. After extraction with benzene, washing, drying, and distilling the solvent, the residual liquid distilled at 120° at 1.8 mm yielding 6.88 g of a colorless liquid. Gas–liquid chromatography indicated two components which were found by infrared and ultraviolet spectra to be the two isomeric olefins possible. The infrared spectrum of the major component showed carbonyl absorption at 1700 cm^{-1} and a strong band at 900 cm^{-1} attributed to out-of-plane deformations of the protons of the terminal methylene group of XII. The ultraviolet spectrum of this component showed fine structure in the absorption at 2640, 2585, and 2525 Å typical of a substituted (non-conjugated) aromatic compound. On the other hand, the ultraviolet spectrum of the minor component separated on the chromatograph showed a broad band at 2400–2420 Å, presumably indicative of the conjugated isomer of XII.

(b) Preparation of 2,3,6-Trimethyl-2,6-diphenyl-4-heptanone (XIVb)

Benzene (4.68 g, 0.06 mole) and aluminum chloride (2.66 g, 0.020 mole) were mixed and cooled to 5–10°. The 2,3,6-trimethyl-6-phenyl-1-heptene-4-one (3.44 g, 0.015 mole) was added over 30 minutes while the temperature was maintained by cooling. The mixture was allowed to warm slowly to room temperature. Gas–liquid chromatography of an aliquot after 3 hours indicated little starting olefin. The mixture was hydrolyzed at once on ice. After the usual extraction and subsequent treatment, the residue distilled at 172–174° at 0.8 mm to yield 2 g of a viscous yellow oil, n_D^{17} = 1.5460. The product showed strong carbonyl absorption at 1700 cm^{-1}, lacked the olefinic proton absorption of the starting material at 900 cm^{-1}, and was generally very similar to the spectrum of 2,6-dimethyl-2,6-diphenyl-4-heptanone. Analysis—Found: C, 86.35; H, 9.35. Calculated for $C_{22}H_{28}O$: C, 85.66; H, 9.12.

(c) Reaction of 2,3,6-Trimethyl-2,6-diphenyl-4-heptanone with Hydrogen Fluoride

The hydrogen fluoride (10 g) was condensed in the cooled reactor. The ketone (1.0 g, 0.003 mole), dissolved

Can. J. Chem. Downloaded from www.nrcresearchpress.com by 210.87.254.40 on 09/05/12
For personal use only.

in 6 ml of carbon tetrachloride, was added rapidly. The tube was sealed, stirred for 1 hour, and allowed to stand for 8 hours at room temperature. After the reactor was cooled and opened in the usual way, the contents were poured on ice. Subsequent treatment yielded 0.90 g of solid. Gas–liquid chromatography of this on an 8-ft silicone gum rubber column showed four components with the major one having a retention time identical with that of a sample of IX*b*. Recrystallization from ethanol yielded a colorless crystalline solid, m.p. 116–119°. A mixed melting point with a sample of IX*b* from the reaction of 3,3-dimethyl-1-ethylindene with α-methylstyrene showed no depression. The infrared spectra of the two samples were identical.

ACKNOWLEDGMENTS

The authors wish to thank Dr. G. McInnes of the National Research Council, Halifax, Nova Scotia, for recording the n.m.r. spectra. Financial assistance from the National Research Council is gratefully acknowledged.

REFERENCES

1. A. Hoffman. J. Am. Chem. Soc. **51**, 2542 (1929).
2. R. A. Barnes and B. D. Beitchman. J. Am. Chem. Soc. **76**, 5430 (1954).
3. L. M. Adams, R. L. Lee, and F. T. Wadsworth. J. Org. Chem. **24**, 1186 (1959).
4. R. F. Curtis. Chem. Ind. (London), 928 (1960).
5. R. F. Curtis. J. Chem. Soc. 418 (1962).
6. J. Colonge and L. Pichat. Bull. Soc. Chim. France, **16**, 421 (1949).
7. J. Colonge and P. Garnier. Bull. Soc. Chim. France, 5e Sér. **15**, 436 (1948).
8. J. Colonge and K. Mostafavi. Bull. Soc. Chim. France, **6**, 335 (1939); Chem. Abstr. **33**, 3758 (1939).
9. J. Colonge and L. Pichat. Bull. Soc. Chim. France, **15**, 177 (1949).
10. E. Bergmann, H. Taubadel, and H. Weiss. Ber. **64**, 1493 (1931).
11. C. F. Koelsch and C. D. LeClaire. J. Org. Chem. **6**, 516 (1941).
12. R. Stoermer and E. Laage. Ber. **50**, 981 (1917).
13. W. E. Parham, H. E. Ruff, and P. Swartzentraher. J. Am. Chem. Soc. **78**, 1440 (1956).

Can. J. Chem. Downloaded from www.nrcresearchpress.com by 210.87.254.40 on 09/05/12
For personal use only.

Can. J. Chem. Downloaded from www.nrcresearchpress.com by 210.87.254.105 on 09/05/12
For personal use only.

CONTRIBUTION TO THE INFRARED SPECTRA OF ORGANOSULPHUR COMPOUNDS[1]

C. N. R. RAO[2]
Department of Inorganic and Physical Chemistry, Indian Institute of Science, Bangalore-12, India

AND

R. VENKATARAGHAVAN[3] AND T. R. KASTURI
Department of Organic Chemistry, Indian Institute of Science, Bangalore-12, India

Received August 6, 1963

ABSTRACT

Infrared spectra of various types of organosulphur compounds have been examined and group frequencies arising from C—S, S—S, N—S, O—S, and C=S stretching vibrations have been assigned and discussed. The C—S bands of thioketals and S—S bands of tri- and tetra-sulphides show splittings due to vibrational coupling. The O—S and N—S stretching frequencies are found around 890 and 820 cm^{-1} respectively, values which are much higher than the C—S stretching frequencies. Potassium alkyl xanthates exhibit the asymmetric and symmetric stretching frequencies of the CS_2^- ion. The splitting of C—O and C=S stretching bands in dialkyl dixanthogens have been interpreted in terms of the Fermi interaction with the combination tone of C—S and S—S stretching vibrations and with the overtone of S—S stretching vibrations respectively. The relative intensity of the C=S stretching bands in a few derivatives show marked dependence on the electronegativities of the elements directly linked to the thiocarbonyl group. It is found that the earlier assignments of the "—N—C=S bands" due to mixed vibrations in thioamide type derivatives have been found to be well justified on the basis of the recent normal coordinate treatment. Another band tentatively designated as the "—N—C=S IV band" has been assigned for these derivatives in the region 850–680 cm^{-1}. Examination of the spectra of a number of thioamide type derivatives has shown no evidence for the presence of thiol tautomers. All of them exist as thiones exhibiting characteristic N—H absorption and "—N—C=S bands".

INTRODUCTION

Infrared spectra of organosulphur compounds have been recently reviewed by Bellamy (1). The uncertainty regarding the assignment of C=S stretching frequency in the literature has been examined by Rao and Venkataraghavan (2), who have carried out detailed correlations and have distinguished two groups of thiocarbonyl derivatives: the first group, where the thiocarbonyl group is linked to atoms such as carbon, sulphur, oxygen, and chlorine; and the second group, where the thiocarbonyl group is linked to one or two nitrogen atoms. An unambiguous assignment of the C=S stretching frequency seems to be possible only when the C=S group is attached to atoms other than nitrogen. Strong vibrational coupling is operative in the case of nitrogen-containing thiocarbonyl derivatives and three bands seem to consistently appear in the regions 1397–1570 cm^{-1}, 1260–1420 cm^{-1}, 940–1140 cm^{-1} due to mixed vibrations ("—N—C=S bands"). In this communication we have reported and discussed the assignments of infrared group frequencies

[1]*Material taken from the Ph.D. thesis of R. Venkataraghavan submitted to the Indian Institute of Science under the guidance of C. N. R. Rao.*

[2]*To whom all the correspondence should be addressed. Present address: Department of Chemistry, Indian Institute of Technology, Kanpur, India.*

[3]*University Grants Commission Junior Research Fellow in the Department of Organic Chemistry. Presently in the Pure Chemistry Division, National Research Council of Canada, Ottawa, Canada.*

associated with the C—S, S—S, O—S, N—S, and C=S stretching vibrations in several types of organosulphur compounds. We have also discussed the "—N—C=S bands" in the light of the results of the normal coordinate treatment.

EXPERIMENTAL

Preparation of Compounds

Ethylene-thioketals of (i) 3,20-dioxo-4-oxa-5α-pregnane, (ii) cholestane-3-one, and (iii) methyl *i*-butyl ketone were prepared by the methods described in the literature (3–5). The general method consists in treating a solution of the corresponding ketone in ethane-1,2-dithiol with borontrifluoro-ethereate. Compounds (i) and (ii) are solids melting at 237–239° C and 146–147° C respectively. The last one is a liquid boiling at 72–73° C at 1.5 mm. Dialkyl dixanthogens were obtained by the oxidation of the corresponding potassium alkyl xanthates with iodine (5, 6). Potassium alkyl xanthates were prepared by the addition of carbon disulphide to the corresponding potassium alkoxide at 0° C. Isoperthiocyanic acid was prepared by the decomposition of thiocyanic acid (7). The hydrochloride of 3,5-diimino-1,2,4-dithiazoline was prepared by the oxidation of dithiobiuret (8). Piperidine mono- and di-sulphides were prepared by the reaction of sulphur dichloride and sulphur monochloride respectively with piperidine in petroleum ether solution (9). The two sulphides were purified by crystallization from alcohol and obtained as needle-shaped crystals melting at 74° C and 64° C respectively. Piperidine tri- and tetra-sulphides were prepared by dissolving piperidine and sulphur in benzene and treating with lead oxide at 0° C and 50° C respectively and were purified by recrystallization from absolute alcohol solution (9). Piperidine trisulphide is a crystalline solid melting at 74° C and the tetrasulphide is an amorphous solid melting at 78° C. Dimethoxy disulphide and tetraethyl dithiodiamine were kindly given to us by Professor A. R. V. Murthy.

Thiofenchone was prepared by refluxing fenchone with phosphorus pentasulphide in heptane. *n*-Butyl-dithioacetate was prepared starting from acetonitrile and *n*-butylmercaptan (10). Thiatriazolinethiones were prepared by the reaction of carbon disulphide with azide ion and further esterification (11). Thiohydrazides were prepared by the reaction of hydrazine with the corresponding thioacids (12). Thiourethanes were prepared by refluxing isothiocyanates with ethyl alcohol (13). All the other compounds used in this study were commercially available.

Spectra

Infrared spectra were recorded employing Perkin–Elmer, Model 221 and Grubb–Parsons double-beam spectrometers fitted with NaCl and KBr prisms. Some of the spectra were also recorded with a Perkin–Elmer 137B spectrometer. The samples were in the form of solutions in CCl_4 and $CHCl_3$ or solids dispersed in Nujol mulls or KBr pellets.

RESULTS AND DISCUSSION

C—S Stretching Frequency

The C—S stretching vibration has been assigned to a weak band in the region 700–600 cm^{-1} (14). We have examined the infrared spectra of several alkyl thiocyanates (I) and have found

R—S—C≡N

I

weak to medium intensity bands in the region 772–622 cm^{-1}. In these compounds one should probably expect the C—S—C asymmetric and symmetric stretching vibrations instead of C—S stretching vibrations. In fact we observe two bands in all these compounds in the 772–622 cm^{-1} region, possibly due to the asymmetric and symmetric stretching vibrations. Infrared spectra of thioketals show broad bands with several maxima in the region 745–650 cm^{-1}, probably due to vibrational coupling in the thioketal unit (II), just as in ketals (15). Dialkyl dixanthogens (III) show the C—S stretching between 690 and

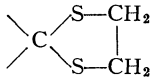

II

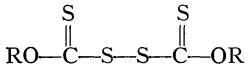

III

Can. J. Chem. Downloaded from www.nrcresearchpress.com by 210.87.254.105 on 09/05/12
For personal use only.

685 cm^{-1}. 1,2,4-Dithiazoline derivatives (IV) have been found to show at least two

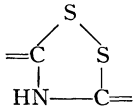

IV

bands in the range 635–602 cm^{-1} which may be due to C—S stretching vibrations.

S—S Stretching Frequency

The S—S linkage generally gives rise to a weak stretching band in the range 500–400 cm^{-1} (14). We have examined the infrared spectra of several compounds containing S—S bonds and the results are summarized below.

Compound	Band position, cm^{-1}
Dialkyl dixanthogens (III)	510–505
$H_{10}C_5N—(S)_n—NC_5H_{10}$ (n = 2, 3, 4)	448–418
Dithiazolines (IV)	440–418

It is interesting to find that dipiperidine tri- and tetra-sulphides show multiplicity in the bands, probably due to vibrational coupling.

O—S and N—S Stretching Frequencies

The S—O stretching frequency has been observed as a strong band around 900 cm^{-1} in the spectra of sulphonic acids (16) and around 860 cm^{-1} in sulphinic acids (17). In sulphonic acid esters this band appears around 780 cm^{-1} (16, 18). In covalent sulphites the in-phase and out-of-phase S—O stretching frequencies have been assigned in the regions 720–690 and 760–730 cm^{-1} (16). In dimethyl sulphate, the S—O stretching absorptions are found at 752 and 875 cm^{-1} (16). We have examined the infrared spectrum of the disulphide, $H_3CO—S—S—OCH_3$ and find the O—S stretching frequency as a strong band at 890 cm^{-1}.

The N—S stretching vibration has been assigned in several sulphonamide derivatives. In methane sulphonamides this appears as a medium intensity band in the region 912–866 cm^{-1} (19). In N-methyl-*p*-tolyl sulphonamides the N—S stretching frequency has been assigned at 839 cm^{-1} (20). In N,N′-disubstituted-N-benzenesulphonyl and N-methanesulphonyl formamidine derivatives the N—S stretching band appears between 906 and 828 cm^{-1} (21). Dipiperidine mono-, di-, tri-, and tetra-sulphides exhibit an intense band around 830 cm^{-1} probably due to the N—S stretching vibration. The compound $(C_2H_5)_2—N—S—S—N—(C_2H_5)_2$ shows the N—S stretching band at 807 cm^{-1}.

C=S Stretching Frequency

Rao and Venkataraghavan (2) have recently assigned the C=S stretching frequency to the region 1225–1025 cm^{-1} in thiocarbonyl derivatives where the C=S group is linked to elements other than nitrogen. We have now examined the infrared spectra of a few potassium alkyl xanthates and dialkyl dixanthogens (III) in detail. In potassium alkyl xanthates (V), we should have the limiting case of the dependence of the C=S stretching frequency on the double bond character of the thiocarbonyl linkage just as in the case of the carboxylate anion. One should therefore expect to find the asymmetric and symmetric CS_2^- stretching frequencies. We have tentatively assigned a medium intensity band in

Can. J. Chem. Downloaded from www.nrcresearchpress.com by 210.87.254.105 on 09/05/12
For personal use only.

the range 1060–1045 cm^{-1} to the asymmetric stretching vibration and a weak band between 833–819 cm^{-1} to the symmetric stretching vibration. The asymmetric stretching bands show splitting in solid state probably due to crystal field effects. The C—O stretching frequency in potassium alkyl xanthates is considerably reduced (1186–1140 cm^{-1}) compared to that in dialkyl dixanthogens (~1260 cm^{-1}). These results are hard to understand since one would expect an increase in C—O frequency due to the different canonical structures V*a*, V*b*, and V*c* of the xanthate ion. It is not clear whether we should again reverse the assignments of C—O and C=S stretching frequencies in dialkyl dixanthogens (22). Although the arguments regarding the relationship between double bond character

V*a*

V*b*

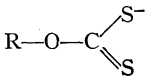

V*c*

and C—O and C=S group frequencies favor the low frequency assignment (1045–1010 cm^{-1}) to C—O and high frequency assignment (1270–1255 cm^{-1}) to C=S as reported by Shankaranarayana and Patel (23), it would still be very difficult to accept such a low frequency for C—O stretching in structures of this type where one would expect "contiguous" C—O bands (24).

The C—O and C=S stretching bands in dialkyl dixanthogens (III) show considerable splitting. On closer examination, we find that this may be due to Fermi interaction. The combination tone of C—S (690–685 cm^{-1}) and S—S (510–505 cm^{-1}) stretching vibrations seems to interact with the C—O stretching vibration (1270–1255 cm^{-1}), while the overtone of the S—S stretching frequency seems to interact with the C=S stretching vibration (1045–1010 cm^{-1}).

We have studied the relative intensities of the C=S bands in a few thiocarbonyl derivatives where the C=S stretching vibration is highly localized and the results are summarized below. In general, it appears that the C=S stretching band intensity varies fairly markedly with the electronegativity of the elements directly linked to the thiocarbonyl group.

Compound	*X*	*Y*	ϵ^{a}_{max}	$\Delta\nu^{a}_{\frac{1}{2}}$ cm^{-1}	Intensity ratio*
Thiofenchone	C	C	140	26	1
n-Butyl-dithioacetate	C	S	1538	21	7
Ethylenetrithiocarbonate	S	S	5350	21	16
Diisopropyldixanthogen	O	S	3890	46	54

*With respect to thiofenchone taken as unity.

"—*N*—*C*=*S Bands*"

Rao and Venkataraghavan (2) assigned three —N—C=S bands due to mixed vibrations in the regions 1395–1570 cm^{-1}, 1270–1420 cm^{-1}, 940–1140 cm^{-1} in thiocarbonyl derivatives where the C=S group is linked to one or two nitrogen atoms and pointed out the need for normal coordinate treatment to establish the nature of the mixed vibrations responsible for the —N—C=S bands. Recently, Suzuki (25) has carried out extensive normal coordinate calculations of thioformamide, thioacetamide, N-methylthioformamide, and N-methylthioacetamide. It is heartening to find adequate correlations between the

Can. J. Chem. Downloaded from www.nrcresearchpress.com by 210.87.254.105 on 09/05/12
For personal use only.

Can. J. Chem. Downloaded from www.nrcresearchpress.com by 210.87.254.105 on 09/05/12
For personal use only.

—N—C=S bands suggested by Rao and Venkataraghavan and the assignments of Suzuki. All primary thioamides show a band around 1620 cm^{-1} which is completely due to the NH_2 deformation vibration. In primary thioamide derivatives, —N—C=S I band is mostly due to C—N stretching. In thiourea, it is probably due to N—C—N asymmetric stretching. In secondary thioamides, NH deformation and C—N stretching constitute the —N—C=S I band. The —N—C=S II band in primary thioamides is due to a mixed vibration involving CH deformation, C—N stretching, C—C stretching, NH_2 bending, and C=S stretching, depending on the nature of the compound. Thus, in thioformamide the band at 1325 cm^{-1} is due to CH deformation and C—N stretching and in thioacetamide the band at 1306 cm^{-1} has been shown to have contributions from NH_2 bending, C—C stretching, and C=S stretching (25). In thiourea this band may be mostly due to N—C—N symmetric stretching vibration. In secondary thioamides, —N—C=S II band is mostly due to C—N stretching, NH deformation, and CH deformation. Thus, in N-methylthioformamide, the band at 1297 cm^{-1} has contributions from CH deformation, NH deformation, and C—N stretching. In N-methylthioacetamide CH_3—C deformation, C—N stretching, and NH deformation contribute to the —N—C=S II band (25). In primary thioamides and in thiourea itself, the —N—C=S III band is due to C=S stretching and NH_2 bending. The —N—C=S III band in secondary thioamides involve contributions from C—N stretching, C=S stretching, and CH_3 bending. Suzuki's studies (25) indicate that in addition to the —N—C=S I, II, and III bands all the nitrogen containing thiocarbonyl derivatives also show a band in the region 850–680 cm^{-1} due to a mixed vibration involving considerable contribution from C=S stretching. This band may be tentatively designated as the —N—C=S IV band. The description of the —N—C=S IV bands for some of the derivatives are shown below. On closer examination, we find that many of the derivatives studied earlier by us (2) also show absorption in the region 900–670 cm^{-1} probably due to the —N—C=S IV band.

Compound	Band position, cm^{-1}	Assignment (25)
Thioformamide	843	$\nu_{C=S} + \nu_{NH_2}$
Thioacetamide	718	$\nu_{C=S} + \nu_{CC}$
N-Methylthioformamide	868	$\nu_{C=S} + \nu_{CN}$
N-Methylthioacetamide	690	$\nu_{C=S} + \nu_{CC}$
Thiourea*	732	$\nu_{C=S} + \nu_{NH_2}$

*Our assignment.

We have looked into the spectra of several other nitrogen containing thiocarbonyl derivatives and the assignments of the —N—C=S bands are summarized below. In the

case of thiourethanes (VI), one of the —N—C=S bands in the region 1507–1492 cm^{-1}

Compound	Number of derivatives	Band position, cm^{-1} —N—C=S I	—N—C=S II	—N—C=S III
Thiohydrazides	8	1545–1495	1325–1300	1050–1010
Thiatriazolinethiones	4	1495–1440	1340–1315	943–916
Thiourethanes	5	1507–1492	1341–1304	1134–1130
Isoperthiocyanic acid	1	1508	1307	1005
*2-Mercapto-1,2,4-triazole (27)	1	1502	1274	985

*Data taken from the reference indicated.

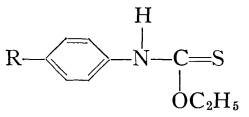

VI

seems to show slight dependence of its position on the electrical property of the para substituent. This may probably be due to the dependence of the Ph—N stretching vibration on the nature of the para substituent, since the transmission of electrical effects is through the Ph—N bond.

Thione–Thiol Tautomerism in Thioamides

Thione–thiol tautomerism (VII–VIII) has been suggested to occur in many thioamide

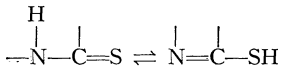

VII VIII

type derivatives based on the fact that many of them give rise to S-alkyl and N-alkyl derivatives depending on reaction conditions. But infrared evidence clearly shows that most of these derivatives exist only as the thiones (VII). During the course of our investigations, we have examined the infrared spectra of several of these derivatives, such as thiosemicarbazides, thiohydrazides, thiourethanes, 5-mercaptotetrazoles, 2- and 2,5-di-mercaptothiazoles, 5-mercapto-1,2,3,4-thiatriazoles, and 2-mercaptobenzthiazole and all these derivatives fail to show the S—H stretching frequency. Instead, they show N—H absorption and the —N—C=S bands. We have never come across a system which shows evidence for the mercapto structure VIII. Apparently, the proton always tends to go to the more electronegative nitrogen in such derivatives. The fact that one can prepare both S-alkyl and N-alkyl derivatives under suitable conditions is satisfactorily explained on the basis of proton transfer in these highly hydrogen bonded systems as suggested by Bellamy and Williams (26).

ACKNOWLEDGMENTS

The authors' thanks are due to Professor D. K. Banerjee and Professor M. R. A. Rao for their interest and to Professor A. R. V. Murthy for kindly giving some of the compounds studied by us.

Can. J. Chem. Downloaded from www.nrcresearchpress.com by 210.87.254.105 on 09/05/12
For personal use only.

REFERENCES

1. L. J. BELLAMY. The infrared spectra of organosulphur compounds. *In* Organic sulphur compounds. Pergamon Press, New York. 1961.
2. C. N. R. RAO and R. VENKATARAGHAVAN. Spectrochim. Acta, **18**, 541 (1962).
3. G. R. PETTIT, T. R. KASTURI, B. GREEN, and J. C. KNIGHT. J. Org. Chem. **26**, 4773 (1961).
4. L. F. FIESER. J. Am. Chem. Soc. **76**, 1945 (1954).
5. L. S. FOSTER. Preparation of xanthates and thiocarbonates. Technical Paper No. 2. Dept. of Mining and Metallurgy Research, University of Utah. 1927.
6. C. C. DEWITT and E. E. ROPER. J. Am. Chem. Soc. **54**, 445 (1932).
7. WOHLER. Ann. Physik. **69**, 273 (1821).
8. P. W. PREISLER and M. M. BATEMAN. J. Am. Chem. Soc. **69**, 2632 (1947).
9. K. SHARADA. Ph.D. Thesis, Indian Institute of Science. 1961.
10. C. S. MARVEL, P. DE RADZITZKY, and J. J. BRADER. J. Am. Chem. Soc. **77**, 5997 (1955).
11. E. LIEBER, E. OFTEDAHL, and C. N. R. RAO. J. Org. Chem. **28**, 194 (1963).
12. E. LIEBER, C. N. R. RAO, and R. C. ORLOWSKI. Can. J. Chem. **41**, 926 (1963).
13. C. N. R. RAO and R. VENKATARAGHAVAN. Tetrahedron, **18**, 531 (1962).
14. L. J. BELLAMY. The infrared spectra of complex molecules. Methuen, London. 1958.
15. E. D. BERGMANN and S. PINCHAS. Rev. trav. chim. **71**, 161 (1952).
16. S. DETONI and D. HADZI. Spectrochim. Acta, 601 (1957).
17. S. DETONI and D. HADZI. J. Chem. Soc. 3163 (1955).
18. N. S. HAM, A. N. HAMBLEY, and R. H. LEBY. Aust. J. Chem. **13**, 443 (1960).
19. A. R. KATRITZKY and R. A. JONES. J. Chem. Soc. 4497 (1960).
20. D. HADZI. J. Chem. Soc. 847 (1959).
21. G. TOSOLINI. Chem. Ber. **94**, 2731 (1961).
22. L. H. LITTLE, G. W. POLING, and J. LEJA. Can. J. Chem. **39**, 745 (1961).
23. M. L. SHANKARANARAYANA and C. C. PATEL. Can. J. Chem. **39**, 1633 (1961).
24. H. W. THOMPSON and P. TORKINGTON. J. Chem. Soc. 640 (1945).
25. I. SUZUKI. Bull. Chem. Soc. Japan, **35**, 1286, 1449, 1456 (1962).
26. L. J. BELLAMY and R. L. WILLIAMS. Proc. Roy. Soc. A, **257**, 98 (1960).
27. L. H. LITTLE and R. H. OTTEWILL. Can. J. Chem. **40**, 2110 (1962).

Can. J. Chem. Downloaded from www.nrcresearchpress.com by 210.87.254.105 on 09/05/12
For personal use only.

CONTRIBUTION TO THE INFRARED SPECTRA OF FIVE-MEMBERED N- AND N,S-HETEROCYCLIC COMPOUNDS[1]

C. N. R. RAO[2]
Department of Inorganic and Physical Chemistry, Indian Institute of Science, Bangalore-12, India

AND

R. VENKATARAGHAVAN[3]
Department of Organic Chemistry, Indian Institute of Science, Bangalore-12, India

Received August 6, 1963

ABSTRACT

Infrared spectra of 5-membered N- and N,S-heterocyclic derivatives such as triazoles, tetrazoles, thiazoles, thiadiazoles, thiatriazoles, and dithiazoles have been examined and empirical assignments have been made. The spectra of the two dithiazolidine derivatives, isoperthiocyanic acid and oxidation product of dithiobiuret, have been studied in detail. Assignments for benzthiazole derivatives are reported. The CH out-of-plane deformation bands of benzene rings fused to five-membered heterocyclic rings have been found to be in the region 760–740 cm^{-1}, characteristic of four adjacent benzenoid hydrogen atoms.

INTRODUCTION

Since the calculation of the normal vibrations of heterocyclic derivatives is rather tedious, the interpretation of the infrared spectra depends mainly on empirical correlations. Katritzky (1) has recently reviewed the infrared spectra of heteroaromatic compounds and classified the vibrations in terms of the ring-stretching, ring-breathing, CH in-plane deformation, and CH out-of-plane deformation modes. We have now examined the infrared spectra of several five-membered nitrogen- and nitrogen,sulphur-heterocyclic compounds in the light of Katritzky's review.

EXPERIMENTAL

Preparation of Compounds

The 1,2,3-triazole derivatives were prepared by the methods described by Lieber *et al.* (2, 3). The tetrazole derivatives were commercially available. All the thiazole derivatives were commercially available. The 1,2,3- and 1,2,4-thiadiazole derivatives were prepared by following the procedures described in the literature (4, 5). The thiatriazole derivatives were synthesized following the procedure described by Lieber *et al.* (6–8). Isoperthiocyanic acid was prepared by the decomposition of thiocyanic acid (9). The hydrochloride of 3,5-diimino-1,2,4-dithiazoline was prepared by the oxidation of dithiobiuret (10). Many of the benzthiazole derivatives were commercially available and some were synthesized in the laboratory following standard procedures.

Spectra

Infrared spectra were recorded employing Perkin–Elmer models 221 and 137B spectrometers fitted with NaCl prisms. The samples were in the form of solutions in $CHCl_3$ or solids dispersed in Nujol mulls or KBr pellets.

RESULTS AND DISCUSSION

Five-membered N-Heterocyclic Derivatives

The assignments for the first two five-membered nitrogen heterocyclic compounds,

[1]*Material taken from the Ph.D. thesis of R. Venkataraghavan submitted to the Indian Institute of Science under the guidance of C. N. R. Rao.*

[2]*To whom all the correspondence should be addressed. Present address: Department of Chemistry, Indian Institute of Technology, Kanpur, India.*

[3]*University Grants Commission Junior Research Fellow in the Department of Organic Chemistry. Presently in the Pure Chemistry Division, National Research Council of Canada, Ottawa, Canada.*

Can. J. Chem. Downloaded from www.nrcresearchpress.com by 210.87.254.5 on 09/05/12
For personal use only.

pyrrole (I) and imidazole (II), have been made by Katritzky (1). Making use of the infrared data of a few 1,2,3-triazole derivatives (III) reported by Hartzel and Benson (11),

I II

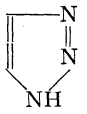

III

Katritzky (1) has assigned the ring-stretching frequencies around 1520, 1450, and 1410 cm^{-1}. We have examined the infrared spectra of several 1,2,3-vicinal-triazole derivatives, particularly in the region 1400–600 cm^{-1} and find that the following bands appear consistently in all of them: 1290–1150, 1130–1105, 1090–1010, 1000–900, and 850–700 cm^{-1}. The bands in the regions 1290–1105, 1090–900, and 850–700 cm^{-1} may be assigned to the CH in-plane deformation, ring-breathing, and CH out-of-plane deformation vibrations respectively. It should be mentioned, however, that assignments are difficult to make in many derivatives since they possess phenyl groups. We have examined the spectra of a few tetrazole derivatives (IV) and the following assignments may be made. The bands

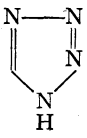

IV

in the region 1640–1335 cm^{-1} may be due to the ring-stretching vibrations. The CH in-plane deformations occur in the region 1300–1110 cm^{-1}. The bands in the region 1095–900 and 810–715 cm^{-1} may be assigned to the ring-breathing and CH out-of-plane deformation vibrations respectively.

All the important characteristic vibrations of the five-membered N-heterocyclic derivatives have been summarized in Table I. It may be seen that the regions of absorption are very similar in all of them and infrared spectroscopy will not be of much use in qualitative analysis particularly in differentiating these compounds. The data only indicate what one should expect in the spectra of such five-membered N-heterocyclic derivatives. Further, it is not possible to assign C=N and N=N frequencies since these systems are aromatic in nature.

Examination of the spectra of the five-membered N-heterocyclic compounds in the N—H stretching region shows that pyrrole derivatives (12) exhibit the highest stretching frequency (~3488 cm^{-1}). The reported spectra of imidazoles (13) and triazoles (11) are all in the condensed phase and the N—H stretching absorption in both these kinds of derivatives appears around 3100 cm^{-1}. We have examined the spectra of tetrazoles in very dilute solution and find N—H stretching absorption around 3145 cm^{-1}. It is interesting to see that the N—H stretching frequency in tetrazoles is considerably lower than in pyrroles. This is what one would expect considering that the tetrazole ring is much more electronegative than pyrrole. Tetrazole is indeed an acid (pK_a = 4.89).

Can. J. Chem. Downloaded from www.nrcresearchpress.com by 210.87.254.5 on 09/05/12
For personal use only.

Can. J. Chem. Downloaded from www.nrcresearchpress.com by 210.87.254.5 on 09/05/12
For personal use only.

TABLE I

Important characteristic vibrations of some 5-membered N-heterocyclic derivatives

Compound	n*	Band positions, cm^{-1}								
		Ring-skeletal				Ring-breathing and CH in-plane deformations				CH out-of-plane deformations
Pyrrole (1)†	1	1530	1467	1384	1237	1144	1076	1046	1015	838 768
Substituted pyrroles (12)	39	~1565	~1500	?†	~1250	~1140	~1060	~1030	~990	850 720
Imidazoles‡ (13)	2	~1550	~1490	~1325†	~1260	~1140	~1060	—	~940	~840 ~760
Triazoles‡ (11)	4	~1520	~1450	~1410	~1250	~1100		~1050	~990	850–700 —
Substituted triazoles	8	—	—	—§	1290–1150	1130–1105		1090–1010	1000–900	— —
Tetrazoles	4	1640–1615	1450–1410	1400–1335	1300–1260	1200–1110		1095–1035	990–900	810–715 —

*Number of compounds studied.
†Assignments by Katritzky (1).
‡Data were taken from the reference indicated.
§Data not available in this region due to interference from benzene ring absorptions.

Five-membered N,S-Heterocyclic Derivatives

The simplest member of this group of derivatives is thiazole (V) and the characteristic frequencies of thiazole derivatives have been assigned by Katritzky (1) and Taurins,

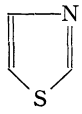

V

Fenyes, and Jones (14). We have examined the spectra of 2-substituted amino-thiazoles, thiazoline derivatives (VI), and thiazolidine derivatives (VII) and find that the assign-

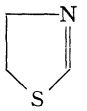

VI

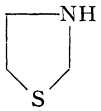

VII

ments are very much similar to those in simple thiazole derivatives. All the assignments are summarized in Table II. We have examined the spectra of derivatives of 1,2,3-, 1,2,4-, and 1,3,4-thiadiazoles (VIII, IX, and X respectively) and have made the relevant

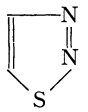

VIII

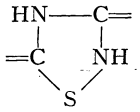

IX

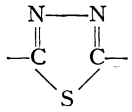

X

assignments (Table II). The regions of absorption are similar in all these derivatives.

Recently, the existence of 1,2,3,4-thiatriazole ring system (XI) has been established by Lieber *et al.* (8, 15). We have examined the spectra of 5-(substituted)-amino-1,2,3,4-

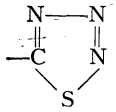

XI

thiatriazoles (XII), 5-(substituted)mercapto-1,2,3,4-thiatriazoles (XIII), 4-substituted-1,2,3,4-thiatriazoline-5-thiones (XIV), salts of 1,2,3,4-thiatriazoline-5-thiones (XV), and 5-(substituted)phenyl-1,2,3,4-thiatriazoles (XVI) and find that all of them show similar

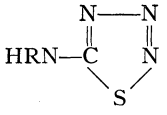

XII

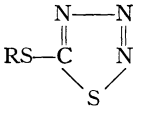

XIII

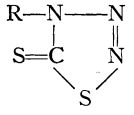

XIV

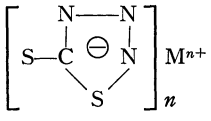

XV

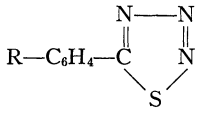

XVI

Can. J. Chem. Downloaded from www.nrcresearchpress.com by 210.87.254.5 on 09/05/12
For personal use only.

Can. J. Chem. Downloaded from www.nrcresearchpress.com by 210.87.254.5 on 09/05/12
For personal use only.

TABLE II

Important characteristic vibrations of some 5-membered N,S-heterocyclic derivatives

Compound	n*	Band positions, cm^{-1}												
		Ring-skeletal			Ring-breathing and CH in-plane deformations						CH out-of-plane deformations			
Thiazole (1, 14)	1	1615	1485	1385	1320	1240	1120	1075	1040	935	880	860	800	720
Methylthiazoles (14)	5	~1610	~1500	~1380	~1310	~1240	1160–1120	1095–1035		995–935	875–840		830–640	
Aminothiazoles† (27)	2	~1615	1538–1480	1404–1355	1333–1275	~1200	—	—	—	—¶	—	—	—	—¶
Thiazolines† (27)	4	1610–1580	1540–1430	~1360	1318–1304	1270–1200	1185–1100	—	—	—¶	—	—	—	—¶
Thiazolidine-2-thione§	1	—	1515, 1456, 1439	1379	1300	1258 1208	1166	1090	1053 1042	1003	854	—	—	—
2,4-Dioxothiazolidine†,‖ (27)	1	—	—	1340	1314	1229	1195, 1164	—	—	—¶	—	—	—	—¶
1,2,3-Thiadiazoles	10	1560–1475	—	1350–‡ 1280	—	1265–1200	1190–1175	1150–950			910–890	—	705–670	
1,2,4-Thiadiazoles	4	1587–1558	1548–1529 1504–1488	—	—	1270–1215	1185–1170	1160–1080	~1050	1030–1020	860–795		742–727	
1,3,4-Thiadiazoles†,§ (28)	6	—	1435–1415	—	1320–1265	1230–1165	1135–1120	—	—	975–935	907–875		—	
5-Aminothiatriazoles	14	1610–1560	1539–1404	1395–1318	1300–1270	1235–1210	1122–1090	1060–1030		962–930	911–889		—	
5-Substituted mercaptothiatriazoles	7	1610–1560	—	—	1300–1260	1238–1222	1105–1080	1025–1004			923–880		—	
4-Substituted thiatriazoline-§ 5-thiones	3	1610–1560	—	—	1320–1297	1226–1215	1100–1080	1030–1000			912–900		—	
Salts of thiatriazoline-5-§ thiones	6	1610–1560	—	—	1311–1275	1232–1185	1090–1033	—			925–900		—	
5-Substituted phenylthiatriazoles	4	1610–1540	1427–1403	—	1300–1270	—	1120–1100	1080–1030			930–910		—	

*Number of compounds studied.
†Data were taken from the reference indicated.
‡May be due to CH in-plane deformation.
§"—N—C=S bands" (29) are not listed.
‖The bands at 1742 and 1656 cm^{-1} are assigned to the free and hydrogen bonded carbonyl groups respectively.
¶Data are not available in this region.

characteristic vibrations of the heterocycle. The relevant assignments are shown in Table II. The frequencies characteristic of the 1,2,3,4-thiatriazole ring system have been useful in distinguishing this structure from other alternatives proposed earlier (16 (*a*, *b*)).

Isoperthiocyanic acid, $C_2H_2N_2S_3$, which is prepared by the decomposition of thiocyanic acid has been assigned various structures (XVII, XVIII, XIX) in the literature (17).

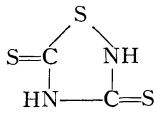

XVII

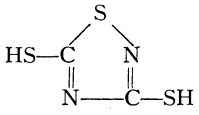

XVIII

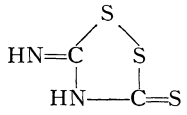

XIX

Recently, based on chemical and X-ray evidence (18, 19), the 1,2,4-dithiazoline structure (XIX) has been established. We have studied the infrared spectra of isoperthiocyanic acid and its silver and barium salts and the relevant assignments are given below: 3175 ν_{N-H} (not present in salts), 1631 $\nu_{C=N}$, 1508 —N—C=S I, 1372 and 1325 ring-stretching, 1307—N—C=S II, 1144, 1082, and 1036 ring-skeletal, 1005—NC=S III, 630 ring-breathing or deformation, 600 ν_{C-S}, and 418 ν_{S-S}. The results further confirm the 5-imino-1,2,4-dithiazolidine-3-thione structure (XIX) for isoperthiocyanic acid. Another 1,2,4-dithiazoline derivative, whose structure has been established as XX (20), is produced

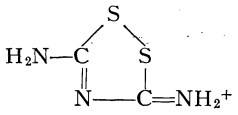

XX

by the peroxide oxidation of dithiobiuret. The tentative infrared assignments for this compound are shown below: 3333 and 3205 ν_{NH_2}, 2933 (triplet) $\nu_{NH_2}{}^+$, 1675 and 1639 $\nu_{C=N}$ and δ_{NH_2}, 1515, 1464, and 1372 ring-stretching, 1311 ν_{C-N}, 1046 ring-skeletal, 630 ring-breathing or deformation, 600 ν_{C-S}, and 418 ν_{S-S}.

The characteristic vibrations of the five-membered N,S-heterocyclic derivatives summarized in Table II are all found to be similar. Just as in the case of the five-membered N-heterocyclic derivatives, infrared data may not be of great value in qualitative analysis and since most of these derivatives are aromatic in nature it is difficult to assign characteristic ring N=N or C=N frequencies.

Benzene Ring Fused to a Five-membered Heterocyclic Ring

O'Sullivan (21) has studied the infrared spectra of several heterocyclic molecules possessing a benzene ring fused to a five-membered ring and has assigned the characteristic bands of such compounds. We have examined the infrared spectra of several benzthiazole derivatives (XXI) and the assignments are shown below: 1608–1580, 1577–1500, 1456–1440, and 1380–1340 cm^{-1}, ring-stretching vibrations; 1320–850 cm^{-1}, a number (~10)

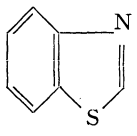

XXI

Can. J. Chem. Downloaded from www.nrcresearchpress.com by 210.87.254.5 on 09/05/12
For personal use only.

of bands due to the CH in-plane deformation, ring-breathing, and ring-skeletal vibrations. It is not possible to assign the C=N frequency in these conjugated systems.

O'Sullivan (22) has pointed out that the out-of-plane CH deformations of benzene rings fused to five-membered rings are found in the region 770–730 cm^{-1} characteristic of *o*-disubstituted benzenes (four adjacent hydrogen atoms). We have found that all the 2-substituted benzthiazole derivatives show a band around 750 cm^{-1} due to CH out-of-plane deformation. Examination of the data in the literature shows that fluorene (XXII) (23), carbazole (XXIII) (23), 3-substituted indoles (XXIV) (24, 25), thionaphthene (XXV) (26), and benzoxazoles (XXVI) (27) show a band in the region 760–740 cm^{-1}

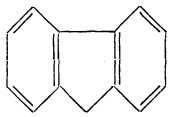

XXII

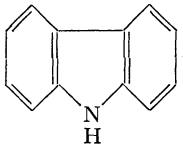

XXIII

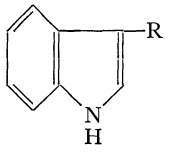

XXIV

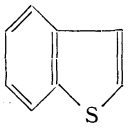

XXV

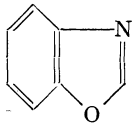

XXVI

characteristic of four adjacent benzenoid hydrogen atoms.

REFERENCES

1. A. R. KATRITZKY. Quart. Revs. **13**, 353 (1959).
2. E. LIEBER, T. S. CHAO, and C. N. R. RAO. J. Org. Chem. **22**, 654 (1957).
3. E. LIEBER, T. S. CHAO, and C. N. R. RAO. Can. J. Chem. **37**, 118 (1959).
4. E. LIEBER, N. CALVANICO, and C. N. R. RAO. J. Org. Chem. **28**, 257 (1963).
5. K. S. SURESH and C. N. R. RAO. J. Ind. Chem. Soc. **37**, 581 (1960).
6. E. LIEBER, C. N. PILLAI, and R. D. HITES. Can. J. Chem. **35**, 832 (1957).
7. E. LIEBER and J. RAMACHANDRAN. Can. J. Chem. **37**, 101 (1959).
8. E. LIEBER, E. OFTEDAHL, and C. N. R. RAO. J. Org. Chem. **28**, 194 (1963).
9. WOHLER. Ann. Physik. **69**, 273 (1821).
10. P. W. PREISLER and M. M. BATEMAN. J. Am. Chem. Soc. **69**, 2632 (1947).
11. L. W. HARTZEL and F. R. BENSON. J. Am. Chem. Soc. **76**, 667 (1954).
12. U. EISNER and R. L. ERSKINE. J. Chem. Soc. 971 (1958).
13. D. GARFINKEL and J. T. EDSALL. J. Am. Chem. Soc. **80**, 3807 (1958).
14. A. TAURINS, J. G. E. FENYES, and R. N. JONES. Can. J. Chem. **35**, 423 (1957).
15. E. LIEBER, C. N. PILLAI, J. RAMACHANDRAN, and R. D. HITES. J. Org. Chem. **22**, 1750 (1957).
16. (*a*) G. B. L. SMITH, F. WILCOXON, and A. W. BROWNE. J. Am. Chem. Soc. **45**, 2604 (1923).
(*b*) E. OLIVERI-MANDALA. Gazz. Chim. Ital. **52**, II, 139 (1922).
17. L. L. BAMBAS. *In* The chemistry of heterocyclic compounds: Five-membered heterocyclic compounds with nitrogen and sulfur or nitrogen, sulfur and oxygen (except thiazole). Interscience, New York. 1952.
18. A. SRINIVASAN, T. R. KASTURI, and C. N. R. RAO. Unpublished results.
19. A. HORDVIK. Acta Chem. Scand. **15**, 1186 (1961).
20. O. FOSS and O. TJOMSLAND. Acta Chem. Scand. **12**, 1799 (1958).
21. D. G. O'SULLIVAN. J. Chem. Soc. 3278 (1960).
22. D. G. O'SULLIVAN. Spectrochim. Acta, **16**, 762 (1960).
23. C. G. CANNON and G. B. B. M. SUTHERLAND. Spectrochim. Acta, **4**, 373 (1951).
24. J. B. BROWN, H. B. HENBEST, and E. R. H. JONES. J. Chem. Soc. 3172 (1952).
25. F. MILLICH and E. E. BECKER. J. Org. Chem. **23**, 1096 (1958).
26. P. LAMBERT and J. LECOMTE. Compt. rend. **208**, 1148 (1939).
27. H. M. RANDALL, R. G. FOWLER, N. FUSON, and J. R. DANGL. Infrared determination of organic structures. Van Nostrand Co. Inc., New York. 1949.
28. G. D. THORN. Can. J. Chem. **38**, 1439 (1960).
29. C. N. R. RAO and R. VENKATARAGHAVAN. Spectrochim. Acta, **18**, 541 (1962).

Can. J. Chem. Downloaded from www.nrcresearchpress.com by 210.87.254.5 on 09/05/12
For personal use only.

SOME REACTIONS OF CHROMIUM TETRAFLUORIDE

H. C. Clark and Y. N. Sadana
Department of Chemistry, University of British Columbia, Vancouver, British Columbia
Received July 31, 1963

ABSTRACT

The preparation of chromium tetrafluoride reported by von Wartenberg has been repeated, and some physical and chemical properties have been studied. Chromium tetrafluoride is surprisingly inert and does not react with ammonia, sulphur di- or tri-oxide, pyridine, halogen fluorides, or selenium tetrafluoride at ordinary temperatures. In boiling bromine trifluoride or selenium tetrafluoride, chromium tetrafluoride is reduced to lower fluorides, while a refluxing mixture of bromine tri- and penta-fluorides converts CrF_4 to $CrOF_3.0.25BrF_3$. Chromium (IV) fluoride complexes of the types $ACrF_5$ (A = K, Rb, or Cs) and A_2CrF_6 (A = K or Cs) have been prepared and their magnetic moments and lattice constants have been determined.

INTRODUCTION

The +4 oxidation state is uncommon for chromium; known simple compounds are tetra-*tert*-butoxychromium (IV) (1), the tetrafluoride CrF_4 (2), the corresponding bromide and chloride, $CrBr_4$ and $CrCl_4$, and the compound CrO_2 (3). In the latter case, the presence of Cr (IV) has recently been questioned (4) and it has been suggested that it is a Cr (III) – Cr (VI) compound, $(CrO)_2CrO_4$. The tetrabromide and tetrachloride appear to exist only in the vapor state. Von Wartenberg (2) prepared the tetrafluoride and small amounts of the pentafluoride by the direct fluorination of chromium metal, chromium (III) chloride, or fluoride at 300–350°, and very briefly described some of the properties of CrF_4. The only other reports on fluoride compounds of chromium (IV) have been concerned (5, 6) with the complexes M_2CrF_6 (M = K, Rb, or Cs). Hence, as Sharpe (7) has pointed out, there has been a need for more detailed study of chromium tetrafluoride and its derivatives, and following a similar investigation of vanadium tetrafluoride (8), we have now examined some properties of chromium tetrafluoride.

EXPERIMENTAL

Reactions were carried out in all-glass vacuum systems with taps replaced by combinations of capillary constrictions and break-seals. Reactions involving highly active fluorides (e.g. BrF_3, BrF_5) were performed in silica reaction vessels. All systems were baked out under vacuum before use to ensure the complete removal of moisture.

Magnetic susceptibilities were measured with a Gouy balance equipped with a cryostat which has been described previously (9). X-Ray powder photographs were taken on a G.E. unit with a camera of 14.4 cm diameter, using filtered Cu K_α radiation. Samples were sealed in 0.5 mm diameter, thin-walled capillaries (Pantak Ltd.) to avoid their decomposition by atmospheric moisture.

Fluorine was estimated by distillation as hydrogen fluoride from sulphuric acid at 130–135°, followed by precipitation as lead chlorofluoride, and the determination was then completed volumetrically. Other elements were determined by standard methods.

Preparation of Chromium Tetrafluoride

Chromium tetrafluoride was prepared by direct fluorination of powdered chromium metal at 300°–350° in a nickel apparatus described previously (8). Prior to fluorination, hydrogen was passed over the heated metal in an attempt to remove any oxide impurity. As fluorination proceeded, a mixture of chromyl fluoride and chromium pentafluoride condensed in the first of the series of traps connected to the nickel reactor, while a dark green solid mass of the tetrafluoride condensed at the reactor exit. Green chromium trifluoride remained in the nickel boat in the reactor. The tetrafluoride was removed under nitrogen and stored. The best conditions for fluorination involved a temperature of 350° and a moderate fluorine flow-rate. At higher temperatures or higher flow-rates, the reaction was sufficiently exothermic to cause fluorination and destruction of the nickel reactor.

Can. J. Chem. Downloaded from www.nrcresearchpress.com by 210.87.254.6 on 09/05/12
For personal use only.

Properties of Chromium Tetrafluoride

Chromium tetrafluoride is a very dark greenish-black solid, which, on exposure to moisture in the atmosphere, rapidly acquires a brown coating due to hydrolysis. It was hydrolyzed very rapidly in water but was insoluble in a wide range of organic solvents. Calc. for CrF_4: Cr, 40.63; F, 59.37. Found: Cr, 40.52; F, 59.63%. The magnetic moment at 294° K, with θ correction (Curie–Weiss law), was 3.02 B.m., the temperature dependence of the magnetic susceptibility of CrF_4 being shown in Table I. X-ray powder photographs of the tetrafluoride as prepared showed no diffraction lines, nor were any lines observed for samples which had been aged *in vacuo* at 80–100° for several days.

When chromium tetrafluoride was heated in a glass tube *in vacuo* at 100°, sublimation occurred and a bluish deposit was slowly formed on the cooler parts of the tube. At 150°, the rate of sublimation was more rapid, and after 15–20 hours at this temperature, the entire sample had sublimed.

Chemical Reactions with Chromium Tetrafluoride

(i) Dry ammonia was condensed in excess on to a sample of chromium tetrafluoride in an all-glass vacuum system. There were no signs of reaction with the liquid ammonia, and the residue after removal of ammonia was chromium tetrafluoride. Calc. for CrF_4: Cr, 40.63. Found: Cr, 39.8%.

(ii) In similar experiments, dry sulphur dioxide and sulphur trioxide were condensed on to separate samples of the tetrafluoride. In each case, after removal of the oxide, the residue was the original tetrafluoride.

(iii) Bromine trifluoride was condensed on to a weighed sample of chromium tetrafluoride in a silica reaction vessel, and was allowed to melt in contact with the tetrafluoride at atmospheric pressure. No reaction occurred and after the complete removal of bromine trifluoride at 100° *in vacuo*, the residue was unchanged tetrafluoride. Calc. for CrF_4: Cr, 40.63. Found: Cr, 40.55%.

(iv) A weighed sample of chromium tetrafluoride was refluxed with bromine trifluoride (b.p. 125.8°) in a silica reaction vessel for 20 minutes, at atmospheric pressure. The green residue left after removal of the trifluoride *in vacuo* at 120°, was shown to be $CrF_3.0.5BrF_3$. Calc. for $CrF_3.0.5BrF_3$: Cr, 29.4; equiv. wt. 25.0. Found: Cr, 30.0; equiv. wt. 25.5. The equivalent weight was calculated from the observed normality of an aqueous solution of known concentration of the sample, which had been passed through a Dowex-50 cation-exchange resin column. The molar susceptibility at 294° K was 6583×10^{-6} c.g.s. units, which gave a magnetic moment $\mu_{eff} = 3.96$ B.m., corresponding to three unpaired electrons.

(v) No reaction was observed between samples of chromium tetrafluoride and chlorine trifluoride (b.p. 12°), bromine pentafluoride (b.p. 40°), or iodine pentafluoride (b.p. 101°), either at room temperature or at the boiling points of the halogen fluorides. The residue from each experiment was identified analytically as chromium tetrafluoride.

(vi) A sample of chromium tetrafluoride was refluxed with a mixture of bromine tri- and penta-fluorides in a silica reaction vessel. A deep-red solution formed which, after removal of the bromine fluorides *in vacuo* at 100° gave a reddish solid, identified as $CrOF_3.0.25BrF_3$. Calc. for $CrOF_3.0.25BrF_3$: Cr, 32.71. Found: Cr, 32.9%. Magnetic measurements at 294° K gave a molar susceptibility of 1710×10^{-6} c.g.s. units and $\mu_{eff} = 2.01$ B.m., corresponding to one unpaired electron.

(vii) Although selenium tetrafluoride did not react with a sample of chromium tetrafluoride at room temperature, a reaction occurred on refluxing the mixture at atmospheric pressure (b.p. of SeF_4 106°) for 15 minutes. Removal of volatile material at 25° *in vacuo* left a heterogeneous solid. When the residue was heated at 80–90° to remove selenium tetrafluoride completely, the vapor of selenium tetrafluoride swept out of the residue a light buff-colored powder and left in the silica reaction vessel a pink solid. Analyses of the latter corresponded surprisingly well to $CrF_2.SeF_4$. Calc. for $CrF_2.SeF_4$: Cr, 21.24; F, 46.75. Found: Cr, 22.00; F, 47.50%. The molar susceptibility at 294° K was $11{,}900\times10^{-6}$ c.g.s. units giving μ_{eff} a value of 5.34 B.m. The buff-colored product which was much less susceptible to hydrolysis, corresponded in composition to $CrF_3.SeF_4$. Calc. for $CrF_3.SeF_4$: Cr, 19.7; F, 50.4. Found: Cr, 19.7; F, 50.0%.

Pentafluorochromium (IV) Complexes

(i) A mixture of chromium tetrafluoride and potassium chloride in a 1:1 molar ratio was heated in liquid bromine trifluoride. In different experiments, the excess trifluoride was distilled off *in vacuo* either (*a*) at 100°, or (*b*) at 160°. The product from method (*a*) was identified as $KCrF_5.0.5BrF_3$. Calc. for $KCrF_5.0.5BrF_3$: Cr, 20.43; F, 48.50. Found: Cr, 20.00; F, 49.10%. Magnetic measurements were made over the temperature range 98–294° K, as shown in Table I, giving a value for μ_{eff} at 294° of 3.22 B.m. (Curie law). The X-ray powder pattern was indexed on a tetragonal lattice with $a = 9.168$ Å, and $c = 13.49$ Å. The product from method (*b*) (removal of BrF_3 at 160°) was $KCrF_5$. Calc. for $KCrF_5$: Cr, 27.9; F, 51.0. Found: Cr, 26.0; F, 49.5%. The molar susceptibility at 294° K was 4193×10^{-6} c.g.s. units, giving μ_{eff} a value, without θ correction, of 3.16 B.m. The X-ray powder pattern was indexed on a hexagonal unit cell with $a = 8.739$ Å, and $c = 5.226$ Å.

(ii) Rubidium chloride and chromium tetrafluoride in a 1:1 molar ratio were heated in liquid bromine trifluoride, and the excess trifluoride was removed *in vacuo* at 160°. The product was $RbCrF_5$. Calc. for $RbCrF_5$: Cr, 22.4; F, 40.7. Found: Cr, 21.5; F, 40.7%. The variation of the molar susceptibility over the 98–294° K range is shown in Table I, and the value of μ_{eff} at 294° was 3.14 B.m. The X-ray pattern was indexed on the basis of a hexagonal lattice with $a = 6.985$ Å and $c = 12.12$ Å.

Can. J. Chem. Downloaded from www.nrcresearchpress.com by 210.87.254.6 on 09/05/12
For personal use only.

TABLE I

CrF_4			$KCrF_5.0.5BrF_3$		
T, °K	$\chi_M(\times10^6)$ c.g.s. units	μ_{eff}	T, °K	$\chi_M(\times10^6)$ c.g.s. units	μ_{eff}
123	5849	3.02	98	8830	3.56
148	5319	3.04	123	8063	3.63
170	4983	3.12	148	7182	3.63
198	4217	3.02	171	6485	3.62
220	3994	3.04	198	5847	3.62
245	3746	3.06	226	5474	3.67
294	3127	3.02	253	5040	3.67
	$\theta = -70°$		294	4485	3.67
				$\theta = -80°$	
$RbCrF_5$			$K_2CrF_6.0.5BrF_3$		
T, °K	$\chi_M(\times10^6)$ c.g.s. units	μ_{eff}	T, °K	$\chi_M(\times10^6)$ c.g.s. units	μ_{eff}
73	9550	2.84	123	6699	3.51
118	7245	2.96	143	6209	3.52
157	5935	3.01	173	5542	3.52
188	5234	3.04	199	5045	3.51
197	4841	2.99	223	4789	3.55
202	4754	2.99	248	4498	3.57
246	4228	3.08	294	3954	3.56
265	3987	3.09			
294	3918	3.14			
	$\theta = -32°$			$\theta = -105°$	

(iii) In a similar manner, chromium tetrafluoride and cesium bromide (1:1 molar ratio) were reacted with refluxing bromine trifluoride, the excess trifluoride then being removed at 160°, to give $CsCrF_5$. Calc. for $CsCrF_5$: Cr, 18.55; F, 33.95. Found: Cr, 18.00; F, 32.80%. The molar susceptibility at 294° was 4044×10^{-6} c.g.s. units giving a value of 3.09 B.m. for μ_{eff}. The X-ray powder pattern was indexed on the basis of a cubic lattice with $a = 8.107$ Å.

Hexafluorochromium (IV) Complexes

(i) The reaction of potassium chloride and chromium tetrafluoride in a 2:1 molar ratio, in bromine trifluoride solution gave, after removal of the trifluoride at 100°, the product $K_2CrF_6.0.5BrF_3$. Calc. for $K_2CrF_6.0.5BrF_3$: Cr, 16.62; F, 45.56. Found: Cr, 16.30; F, 46.93%. Magnetic measurements over the range 123–294° K, as shown in Table I, gave (θ correction applied) μ_{eff} at 294° K a value of 3.56 B.m. The X-ray powder pattern was indexed on a tetragonal lattice with $a = 4.339$ Å and $c = 5.500$ Å.

Samples of $K_2CrF_6.0.5BrF_3$ were heated *in vacuo* in sealed Pyrex tubes at 120° for 240 hours. The products gave X-ray powder patterns which could be indexed on a cubic lattice with $a = 8.104$ Å.

(ii) Chromium tetrafluoride and cesium chloride in bromine trifluoride solution gave, in a similar manner, the adduct $Cs_2CrF_6.0.5BrF_3$. Calc. for $Cs_2CrF_6.0.5BrF_3$: Cr, 10.40; F, 28.50. Found: Cr, 10.65; F, 28.10%. The molar susceptibility at 294° K was 4144×10^{-6} c.g.s. units giving μ_{eff} a value of 3.14 B.m. The X-ray powder pattern was indexed in terms of a cubic lattice with $a = 8.916$ Å. The indices of all the observed reflections were either even or odd indicating that the lattice was face-centered.

A sample of $Cs_2CrF_6.0.5BrF_3$, after being heated at 135° *in vacuo* for 72 hours, was converted to Cs_2CrF_6. Calc. for Cs_2CrF_6: Cr, 12.04. Found: Cr, 12.20%. The X-ray powder pattern was identical with that of $Cs_2CrF_6.0.5BrF_3$.

Potassium Pentafluoromanganese (IV)

A sample of $KMnF_5$ was prepared by the action of bromine trifluoride on potassium permanganate (10), and the X-ray powder pattern was indexed on a hexagonal unit cell with $a = 11.44$ Å and $c = 8.208$ Å.

DISCUSSION

The direct fluorination of chromium metal unfortunately gives a mixture, which is difficult to separate completely, of chromium tri-, tetra-, and penta-fluorides, as well as some chromyl fluoride. The formation of the latter, which cannot readily be separated from the pentafluoride, could be reduced but not prevented even by a prior high temperature reduction of the metal with hydrogen. These preparative difficulties have delayed study of the tetrafluoride, and particularly of the pentafluoride.

Can. J. Chem. Downloaded from www.nrcresearchpress.com by 210.87.254.6 on 09/05/12
For personal use only.

Chromium tetrafluoride, which is intermediate in volatility between the involatile trifluoride, and appreciably volatile pentafluoride, condenses as a dark-green, glassy solid. On exposure to air, it immediately is coated with a brown oxide layer, and this is presumably responsible for the cinnamon color reported for the tetrafluoride by von Wartenberg (2). Chromium tetrafluoride can be stored indefinitely *in vacuo* in well-dried Pyrex or silica vessels. In agreement with von Wartenberg, we have been unable to obtain samples of the tetrafluoride which would give X-ray diffraction lines, and the compound is probably amorphous. It can be sublimed *in vacuo* at ca. 150° and the steel-blue color of the vapor reported by von Wartenberg was particularly noticed during a fluorination of chromium metal in a silica vessel.

The volatility of chromium tetrafluoride, and in fact its general physical characteristics, are similar to those of titanium and vanadium tetrafluoride. To account for the anomalous properties of titanium tetrafluoride, Hückel (11) has suggested a chain-like structure, formed from condensed TiF_6 octahedra, in which each Ti atom has coordination number six. A similar structure has been proposed (8) for vanadium tetrafluoride, and may well occur in chromium tetrafluoride also. A coordination number of six for chromium in many of these chromium (IV) fluoro-compounds is supported by their magnetic properties which are discussed below. It should also be noted that the volatility and magnetic moment of chromium tetrafluoride are not consistent with formulations such as $CrF_5.CrF_3$ and $CrF_6.2CrF_3$, similar to those proposed (4) for CrO_2.

Chemically, chromium tetrafluoride is surprisingly inert, and does not react with ammonia, sulphur dioxide, sulphur trioxide, or pyridine. Thus chromium (IV) seems to differ markedly from chromium (III), which very readily forms coordination compounds. The tetrafluoride is, however, very rapidly hydrolyzed by water according to the equation

$$3Cr^{4+} \rightarrow CrO_4^{2-} + 2Cr^{3+},$$

as suggested by von Wartenberg (2).

The reactions of chromium tetrafluoride with reactive covalent fluorides, such as the halogen fluorides and selenium tetrafluoride, were investigated to see whether adduct formation or oxidation to a higher fluoride of chromium occurred. The tetrafluoride does not react with iodine or bromine pentafluorides, either at room temperature or at their boiling points, nor does it react with chlorine trifluoride at its boiling point of 12°. With bromine trifluoride, no reaction occurred at room temperature, but with refluxing bromine trifluoride, the green product was identified as $CrF_3.0.5BrF_3$. The reaction therefore differs from that of TiF_4 or VF_4 with bromine trifluoride. Titanium tetrafluoride forms (12) a very unstable adduct, $TiF_4.2BrF_3$, while vanadium tetrafluoride is oxidized (8) to the pentafluoride. It seems highly unlikely that chromium tetrafluoride can oxidize bromine trifluoride, and the more reasonable explanation would involve the thermal decomposition of the tetrafluoride to the trifluoride. This is consistent with the exothermic nature of this decomposition (13)

$$CrF_4 \rightarrow CrF_3 + \tfrac{1}{2}F_2, \Delta H = +22 \text{ kcal mole}^{-1}.$$

Whether the formula $CrF_3.0.5BrF_3$ represents true adduct formation, or just incomplete removal of the bromine trifluoride has not been determined. Certainly the experimental results indicate that vigorous conditions were generally necessary for the complete removal of BrF_3 from these chromium compounds.

As a more vigorous oxidizing agent than bromine trifluoride itself, a mixture of bromine tri- and penta-fluorides was refluxed with chromium tetrafluoride. A red solid was isolated from the solution, and was shown to be $CrOF_3.0.25BrF_3$, the oxygen presumably resulting

Can. J. Chem. Downloaded from www.nrcresearchpress.com by 210.87.254.6 on 09/05/12
For personal use only.

from attack of the silica container. The magnetic moment of 2.01 B.m. at 23° corresponds to one unpaired electron and confirms the presence of chromium (V). A similar product was apparently obtained by Sharpe and Woolf (10), and in both their study and ours, attempts to remove completely the bromine trifluoride to give pure $CrOF_3$ caused decomposition. Further attempts to obtain $CrOF_3$ will be described in a later paper.

Selenium tetrafluoride does not react with chromium tetrafluoride at room temperature, but reaction occurred with refluxing selenium tetrafluoride. The results suggested that two products were obtained, $CrF_3.SeF_4$ and $CrF_2.SeF_4$. The reduction to chromium (III) and formation of an adduct $CrF_3.SeF_4$ is not unexpected for SeF_4. For example, the adduct $PdF_3.SeF_4$ on heating yields PdF_2 (14). In other cases, reduction does not occur and stable adducts are formed. Thus, vanadium tetrafluoride gives (8) the 1:1 adduct, $VF_4.SeF_4$. On the other hand, the apparent reduction of chromium (IV) to chromium (II) in $CrF_2.SeF_4$ is remarkable. The magnetic moment of 5.34 B.m. at 23° almost certainly indicates chromium (II) with four unpaired electrons, since there is no reason to suppose from all other magnetic measurements on chromium-fluorine compounds, that such a value would arise from three unpaired electrons with a very large orbital contribution to the moment. Further work on this interesting reaction will clearly be worthwhile.

Complex fluorides of chromium (IV) of the type $ACrF_5$ (where A = K, Rb, or Cs) have now been prepared for the first time, and some of their properties are shown in Table II. The X-ray evidence clearly showed the absence of free potassium fluoride, so

TABLE II

Complex fluorides of chromium (IV) of the $ACrF_5$ type, and $KMnF_5$

Compound	Magnetic moment (B.m.) (Curie law)	Crystal system	Lattice constants (Å)
$KCrF_5.0.5BrF_3$	3.22	Tetragonal	$a = 9.168$ $c = 13.49$
$KCrF_5$	3.16	Hexagonal	$a = 8.739$ $c = 5.226$
$RbCrF_5$	3.14	Hexagonal	$a = 6.985$ $c = 12.12$
$CsCrF_5$	3.09	Cubic	$a = 8.107$
$KMnF_5$	—	Hexagonal	$a = 11.45$ $c = 8.208$

that the formulae suggest the presence of the unusual penta-coordinate state. However, all evidence indicates that penta-coordination is usually avoided in the solid state, and structure determinations of various complexes of the type A_nMX_5 have revealed that in every case coordination numbers four or six have been attained. Thus Cs_2CoCl_5 contains (15) tetrahedral $CoCl_4^-$ and Cl^- ions, while Tl_2AlF_5 has been shown (16) to contain infinite chains of AlF_6^{3-} octahedra, each of which has two shared corners. In general for A_nMX_5 complexes, structural examination shows that M actually has a coordination of four if its oxidation state is +2, and if in a +3 state, octahedral coordination is observed. The most closely related case to the $ACrF_5$ complexes is that of $KMnF_5$ (10), but its structure has not yet been determined. On the basis of the close similarity of its infrared spectrum to that of K_2MnF_6, it has been suggested (17) that both complexes contain MnF_6 units. Likewise, it can reasonably be expected that these $ACrF_5$ complexes in fact contain CrF_6^{2-} octahedral units, each of which would share two corners with neighboring octahedra to maintain the observed stoichiometry.

Chromium (IV) complexes of the type A_2CrF_6 have been reported previously (5, 6).

Can. J. Chem. Downloaded from www.nrcresearchpress.com by 210.87.254.6 on 09/05/12
For personal use only.

Bode and Voss (6) found that the salts A_2CrF_6 (A = K, Rb) exist in hexagonal and cubic modifications, while Cs_2CrF_6 was found only in the cubic form. We have prepared K_2CrF_6 and Cs_2CrF_6 by a different method employing bromine trifluoride as fluorinating agent and solvent and it is of interest to compare the results. Table III indicates the products

TABLE III

Chromium (IV) complexes of the A_2MF_6 type

Compound	Bode and Voss (6)	Present investigation
K_2CrF_6	Cubic a = 8.15 Å Hexagonal a = 5.69, c = 9.34 Å	Cubic a = 8.104 Å
$K_2CrF_6.0.5BrF_3$	—	Tetragonal a = 4.339 c = 5.500 Å
Rb_2CrF_6	Cubic a = 8.506 Hexagonal a = 5.94, c = 9.67 Å	—
Cs_2CrF_6	Cubic a = 9.004 Å	Cubic a = 8.916 Å
$Cs_2CrF_6.0.5BrF_3$	—	Cubic a = 8.916 Å

obtained and their unit cell dimensions. That the potassium and cesium salts in this present study were first obtained containing half a mole of solvating bromine trifluoride is, of course, just a result of the preparative method employed. However, it is clear that the presence of this BrF_3 causes distortion of the structure only for the potassium salt. For the cesium salt, the much larger cation presumably outweighs any distortion due to the bromine trifluoride in the crystal lattice. The values reported by Bode and Voss for the cubic modifications of K_2CrF_6 and Cs_2CrF_6 are higher than our values. Their preparations always contained excess alkali metal fluoride not discernible in the X-ray patterns, and this may be responsible for the slightly higher lattice constants. It is also of interest that the bromine trifluoride method of preparation leads only to the cubic form (i.e. high temperature form) of K_2CrF_6.

The magnetic properties of these chromium (IV) compounds described in Table I and in the experimental section are worth some discussion. Firstly, high values of θ are observed in many instances. As has been discussed (8) for vanadium tetrafluoride and some of its derivatives, such values may well arise from antiferromagnetic interactions, and similar arguments can clearly be applied for the Cr (IV) compounds. It is also clear that corrections for θ yield moments greater than the spin-only value (2.83 B.m.) for Cr (IV), and some spin–orbit interaction is therefore likely. This latter may also, of course, itself produce the large values of θ. Some conclusions regarding the stereochemistry about the chromium atoms in these compounds may be reached on the basis of the observance of a large orbital contribution to the magnetic moment.

The Cr^{4+} ion has a $^3F_2$ ground state which, in the presence of an octahedral field about the Cr^{4+} ion, is split (18) into two triplets and a singlet level, one triplet being the lowest and the singlet the highest energy level. For a Cr^{4+} ion in a tetrahedral environment, the splitting of the $^3F_2$ ground state is again into two triplets and a singlet, but in this case the singlet lies lowest (i.e. the Stark pattern is inverted). Only if a triplet lies lowest is there likely to be large spin–orbit interaction. The fact that our results indicate that there may be large spin–orbit interaction in CrF_4 and Cr (IV) fluoride compounds strongly suggests that, in all these cases, there is an octahedral field of fluoride ions about the Cr^{4+} ion.

Similar arguments also apply for D spectroscopic states. The Stark pattern for a D state has a low-lying triplet in the octahedral case and a low-lying doublet in the tetrahedral

Can. J. Chem. Downloaded from www.nrcresearchpress.com by 210.87.254.6 on 09/05/12
For personal use only.

case. A large spin–orbit interaction and a magnetic moment appreciably higher than the spin-only value can therefore only be expected for an octahedral environment. The observed (8) moments of VF_4 (in which V^{4+} has a D ground state) and related V (IV) compounds are all much higher than the spin-only values, suggesting the presence of octahedral coordination. The magnetic properties of Cr (IV) and V (IV) fluorides are thus consistent with an octahedral environment for the central metal atoms in these compounds.

Finally, it is now possible to compare briefly the tetrafluorides of titanium, vanadium, chromium, and manganese, although for MnF_4 (19) little detailed information is yet available. As shown in Table IV, there appears to be some increase in volatility in passing

TABLE IV

Tetrafluorides of titanium, vanadium, chromium, and manganese

	Color	Volatility	μ_{eff} (294° K) B.m.	$\theta(0°)$
TiF_4	White	760 mm at 284°	Diamag	Zero
VF_4	Lime-green	Subl. 100–120° *in vacuo* with disproportionation	2.17	198
CrF_4	Green-black	Subl. 150° *in vacuo*	3.02	70
MnF_4	Blue	(Volatile)	3.83	10

from TiF_4 to MnF_4 although precise vapor pressure measurements are lacking. It seems probable that TiF_4, VF, and CrF_4 have structures based on condensed octahedral MF_6 units and it may be that there is a tendency towards the formation of more discrete MF_4 molecules in passing towards MnF_4. There is also a remarkably regular decrease (*a*) in the deviation of the magnetic moment from the spin-only value, and (*b*) in the values of θ (Weiss constant) in passing from TiF_4 to MnF_4. Further structural information is necessary to interpret this although it may again indicate an increasing tendency to form molecular tetrafluorides.

ACKNOWLEDGMENTS

The financial support of the U.S. Office of Naval Research is gratefully acknowledged, and also the award of a National Research Council Studentship to Y.N.S.

REFERENCES

1. N. Hagihara and H. Yamazaki. J. Am. Chem. Soc. **81**, 3160 (1959).
2. H. von Wartenberg. Z. Anorg. Chem. **247**, 135 (1941).
3. A. Maus. Ann. Physik. **9**, 127 (1827).
4. I. Lebanov. Neorganischeskei Khimi (Engl. Transl.), **1**, 240 (1956).
5. E. Huss and W. Klemm. Z. Anorg. Chem. **262**, 25 (1950).
6. H. Bode and E. Voss. Z. Anorg. Chem. **286**, 136 (1956).
7. A. G. Sharpe. Advances in fluorine chemistry. Vol. 1. Butterworths, London. 1959.
8. R. G. Cavell and H. C. Clark. J. Chem. Soc. 2692 (1962).
9. H. C. Clark and R. J. O'Brien. Can. J. Chem. **39**, 1030 (1961).
10. A. G. Sharpe and A. A. Woolf. J. Chem. Soc. 798 (1951).
11. W. Hückel. Structural chemistry of inorganic compounds. (Engl. Transl.), Vol. 2. Elsevier, Amsterdam. 1951. pp. 470–474.
12. A. G. Sharpe. J. Chem. Soc. 2907 (1950).
13. R. G. Cavell and H. C. Clark. Unpublished results.
14. N. Bartlett and J. W. Quail. J. Chem. Soc. 3728 (1961).
15. H. H. Powell and A. F. Wells. J. Chem. Soc. 359 (1935).
16. C. Bossett. Z. Anorg. Chem. **235**, 139 (1937).
17. R. D. Peacock and D. W. A. Sharp. J. Chem. Soc. 2762 (1959).
18. W. G. Penney and E. Schlapp. Phys. Rev. **43**, 486 (1933).
19. R. Hoppe, W. Dahne, and W. Klemm. Naturwiss. **48**, 429 (1961).

Can. J. Chem. Downloaded from www.nrcresearchpress.com by 210.87.254.6 on 09/05/12
For personal use only.

INFRARED SPECTRA AND CRYSTALLINE PHASE TRANSITIONS OF AMMONIUM NITRATE

A. THÉORÊT AND C. SANDORFY
Département de chimie, Université de Montréal, Montréal, Québec
Received June 4, 1963

ABSTRACT

The infrared spectra of solid crystalline films of ammonium nitrate were measured at temperatures ranging between the melting point (169° C) and liquid air temperature (−190° C). Four different spectra were obtained which are shown to belong to phase I, II, IV, and (very probably) VII. Phases III and V were not encountered; only transitions I ⇄ II (125° C), II ⇄ IV (50° C), and IV ⇄ VII (−60° C) were observed. A spectrum measured at −190° C after rapid cooling is shown to correspond to a mixture of phases IV and VII. The symmetry properties of the different phases are discussed in relation with their infrared spectra.

Can. J. Chem. Downloaded from www.nrcresearchpress.com by 210.87.254.5 on 09/05/12
For personal use only.

INTRODUCTION

Ammonium nitrate has seven known crystalline modifications. These are the following.

Phase I	cubic	169°–125° C
Phase II	tetragonal	125°–84.5° C
Phase III	orthorhombic	84.5°–32° C
Phase IV	orthorhombic	32° to −16° C
Phase V	tetragonal	below −16° C
Phase VI		above 169° C, at pressures higher than 9000 kg/cm²
Phase VII		below −170° C

The related crystal structures and thermal properties were examined by Hendricks, Posnjak, and Kracek (1); West (2); Crenshaw and Ritter (3); Meerman (4); Jaffray (5); Goodwin and Whetstone (6); Hocart and Mathieu-Sicaud (7); Stephenson, Bentz, and Stevenson (8); Shinnaka (9); Amoros, Alonso, and Canut (10); and others. Volfkovich, Rubinchik, and Kozhin (11) re-examined all the phase transitions of ammonium nitrate and discovered the existence of phase VII. Disregarding phase VI, which was outside the reach of the experimental techniques used by the latter authors (and by the present ones), the following statements can be made.

1. The transition at 125° C (I ⇄ II) is easy to observe and does not lead to complications.

2. The occurrence of the transition at 84.5° C is highly dependent upon sample size and the speed of variation of temperature. Phase III is often missed and instead the transition II ⇄ IV occurs at 50° C.

3. Under certain circumstances the transition at −16° C is also missed, in which case an alternative transition is observed at around −60° C instead. Meerman (3) interpreted this phenomenon as a retardation of the transition IV ⇄ V. We shall examine this point later.

The infrared spectra of crystalline ammonium nitrate were studied by Keller and Halford (12); and then, under better resolution, by Newman and Halford (13, 14). The Raman spectra of phase IV were measured by Couture and Mathieu (15) and by Penot, Poulet, and Mathieu (16).

Since the occurrence of certain phases seems to depend on the way the samples are

prepared and since an appreciable number of new data became available after the original infrared work of Keller, Newman, and Halford was done, it seemed to us indicated to have a new look at the problem.

The present study was made on sublimed crystalline films and we attempted to measure the infrared spectra of all six phases of the same sample. As will be seen, however, only four different spectra were obtained.

EXPERIMENTAL

"Fisher Certified Reagent" ammonium nitrate was used. It was sublimed onto a silver chloride plate at 105° C under 0.1 mm Hg vacuum. In order to ascertain whether any exchange of ions occurred between the film and the AgCl plate (as it did with an NaCl plate), we repeated the experiments using Eastman-Kodak "IRTRAN II" plates. We obtained identical spectra.

A Perkin–Elmer model 21 spectrometer was used with a sodium chloride prism, supplemented in the 3 μ region with a Perkin–Elmer model 112 instrument with a lithium fluoride prism. The low-temperature cell has been described previously (17). Temperature was measured by a copper–constantan thermocouple introduced into a cavity made in the material of the silicon O-ring separating two silver chloride plates, onto one of which the film of ammonium nitrate had been deposited. The plates were pressed together between two copper rings inside of which heating wires were placed. Liquid air, liquid nitrogen + alcohol, and dry ice + alcohol were used as coolants.

RESULTS

Figure 1 gives the four different spectra which were obtained and Table I lists the observed frequency values. Figure 2 gives the spectrum measured at −190° C after rapid cooling.

DISCUSSION

Under T_d symmetry for NH_4^+ and D_{3h} for NO_3^- there would be the following fundamental vibrations.

Type	Description
ν_1' A_1	NH_4^+ sym. stretch, IR forbidden
ν_2' E	NH_4^+ sym. deformation, IR forbidden
ν_3' T	NH_4^+ asym. stretch
ν_4' T	NH_4^+ asym. deformation
ν_1 A_1'	NO_3^- sym. stretch, IR forbidden
ν_2 A_2''	NO_3^- out-of-plane deformation
ν_3 E′	NO_3^- asym. stretch
ν_4 E′	NO_3^- in-plane deformation

Our spectrum of phase IV of NH_4NO_3 is quite similar to the one of Newman and Halford (13). Phase IV has space group V_h^{13} (*Pmmn*) with two molecules per unit cell (2) and the site symmetries of both ions are C_{2v} (13). The strong bands at 3260 cm^{-1} and 1435 cm^{-1} are easily assigned to ν_3' and ν_4' respectively which are infrared active under T_d symmetry. ν_1' and ν_2' were found at 3130 cm^{-1} and 1656 cm^{-1} in the Raman spectrum by Penot, Poulet, and Mathieu (16). One may expect that these bands will at least weakly appear in the infrared under C_{2v} site symmetry but this does not seem to be the case. One may be tempted to assign the shoulder at 3070 cm^{-1} to ν_1' but Wagner and Hornig (18), who examined the spectra of crystalline ammonium chloride and bromide, gave strong reasons for believing that this band belongs actually to $\nu_2'+\nu_4'$ whose intensity is boosted by Fermi-resonance with ν_3'. It is equally difficult to assign the weak band at 1756 cm^{-1} to ν_2', its frequency being too high. It might belong to the combination $\nu_1+\nu_4$ of the nitrate ion or to a combination of ν_4' with a lattice mode. The argument concerning the ammonium-ion fundamentals has been critically reviewed by Mathieu and Poulet (19).

Can. J. Chem. Downloaded from www.nrcresearchpress.com by 210.87.254.5 on 09/05/12
For personal use only.

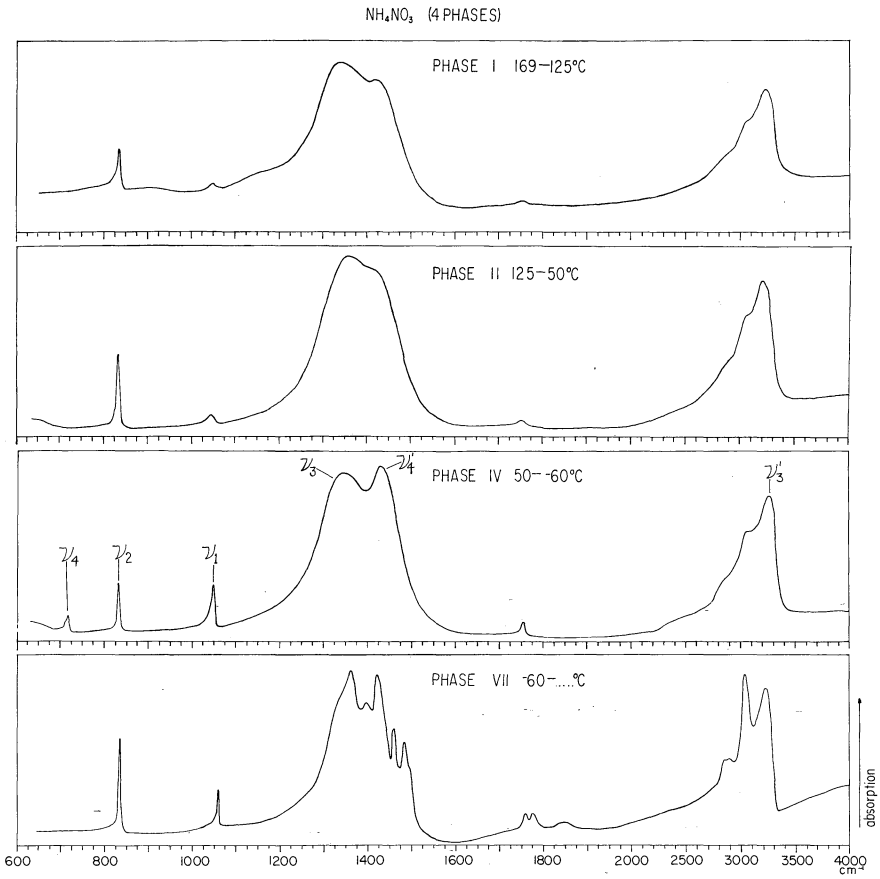

FIG. 1. The infrared spectra of solid crystalline films of ammonium nitrate: phases I, II, IV, and VII.

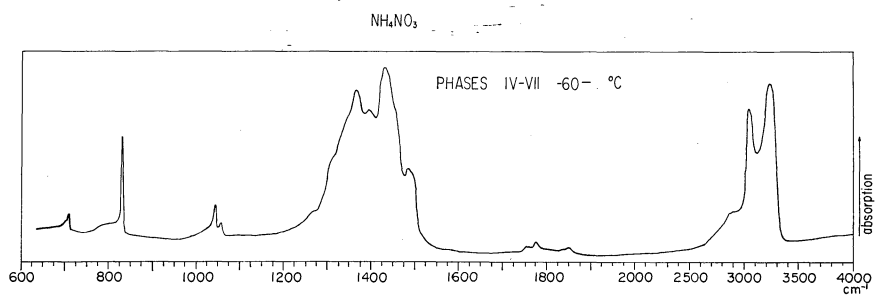

FIG. 2. The infrared spectrum of a solid crystalline film of ammonium nitrate rapidly cooled down to −190° C.

Nothing emerged from the present work that would elucidate these assignments further. We mention, however, that (i) the true intensity of the band at 3070 cm^{-1} may be much lower than its apparent intensity since it is highly overlapped by the much stronger ν_3' band and, (ii) that its intensity increases gradually with increasing departure from T_d symmetry in the order of phases I → II → IV → VII (Fig. 1). This seems to add some weight to its assignment to ν_1'. All we may conclude, however, is that there is no sure

Can. J. Chem. Downloaded from www.nrcresearchpress.com by 210.87.254.5 on 09/05/12
For personal use only.

TABLE I

Observed frequencies in the infrared spectra of phases I, II, IV, and VII of ammonium nitrate

	Phase I (169–125° C) cubic	Phase II (125–50° C) tetragonal	Phase IV (50– –60° C) orthorhombic	Phase VII (−60–. . .) unknown
ν_3'	3230	3230	3260	3230
$(\nu_2' + \nu_4')$	3070	3070	3070	3040
$2\nu_4'$	2880	2880	2880	2900 2860
$(\nu_1 + \nu_2)$				1850
$(\nu_1 + \nu_4)$	1755	1755	1756	1780 1760
$(\nu_2 + \nu_4)$				1495 sh.
ν_4'	1420	1415	1435	1485 1461 (see text) 1422
$2\nu_4$				1397
ν_3	1337	1365	1348	1363 1340 sh.
ν_1	1047	1047	1046	1060
ν_2	832	832	830	833
ν_4			715 713 sh.	

evidence for the presence of ν_1' and ν_2' in the infrared spectrum of phase IV and that the spectrum is compatible with space group V_h^{13} and C_{2v} site symmetry but it does not prove it.

There does not seem to be any such argument concerning the assignment of the frequencies of the nitrate ion. The observed frequencies are listed in Table I.

The spectra of phase I and phase II are very similar to each other (see ref. 12), the main difference being a 28 cm^{-1} shift in the frequency of ν_3. According to Hendricks, Posnjak, and Kracek (1) phase II is tetragonal with space group C_{4v}^2 ($P4bm$) and two molecules in the unit cell: a finding confirmed by Amoros, Alonso, and Canut (10), who suggested, however, that for the metastable state below 84.5° C the space group may be different. Phase I according to the former authors is cubic with only one molecule per unit cell. The site symmetries compatible with C_{4v}^2 are C_{2v} or C_4, much lower than any site symmetry compatible with a cubic structure. In view of this fact the great similarity between the two spectra is astonishing. ν_1 is present as a weak band in both spectra at 1047 cm^{-1} in violation of the selection rules applying to cubic symmetry, though it may be due to some residual phase IV. ν_4 is absent, but it is hard to draw any conclusions from this since, as will be seen below, it is also absent (or very weak) in the spectrum of phase VII whose symmetry is obviously much lower.*

In spite of all our efforts we were not able to obtain phase III. Even when cooling was as slow as 1° C per minute only the II $\rightleftarrows$ IV transition was observed at 50° C. Working with single crystals Newman and Halford (13) were able to measure the spectrum of phase III,

**The referee pointed out that "...the high temperature cubic phases of many crystals show orientational disorder. In that case the X-ray symmetry is a long range average symmetry and the appearance of ν_1 does not necessarily conflict with the X-ray structure." The authors wish to thank the referee for this and other helpful comments.*

Can. J. Chem. Downloaded from www.nrcresearchpress.com by 210.87.254.5 on 09/05/12
For personal use only.

and found it to be very similar to that of phase IV. According to Goodwin and Whetstone phase III has space group V_h^{16} (*Pbnm*) with four molecules per unit cel](6).

Phase V proved equally as elusive as phase III in our experiments on films. Instead of obtaining a transition at −16° C and another at about −170° C, we only obtained one at −60° C. The spectrum we obtained on slow cooling (1° C per minute) is the last one in Fig. 1; it remained unchanged down to −190° C. In this spectrum ν_3' (3230 cm^{-1}) is still strong and broad but the intensity of the band at 3040 cm^{-1} increases considerably and its apparent intensity is higher than that of ν_3'. At 2840 cm^{-1} $2\nu_4'$ is split into two components. The weaker but broad band observed at 1850 cm^{-1} may be $\nu_1+\nu_2$ or a combination involving a lattice mode. The band near 1756 cm^{-1} in phase IV is split into two components at 1760 cm^{-1} and 1780 cm^{-1} respectively. The 1400 cm^{-1} region is complicated because of the near coincidence of the triply degenerate deformation vibration, ν_4', of NH_4^+ and the doubly degenerate stretching, ν_3, of NO_3^-. Including shoulders we are able to distinguish seven bands in this part of the spectrum, some of which may be due to combinations of ν_3 with lattice modes. The observed splittings indicate a remarkable lowering of the site symmetry of the NH_4^+ and NO_3^- ions. Probably even more splitting would be found under higher resolution. Unfortunately, the crystal structure of this phase is not known.

We suggest that this spectrum (the last one in Fig. 1) belongs to phase VII, first obtained by Volfkovich, Rubinchik, and Kozhin (11), and that the transition occurring at −60° C is a IV ⇄ VII transition.

It may be argued that what we observed at −60° C is actually a retardation of the transition IV ⇄ V; but this view can be countered with the following consideration. Volfkovich, Rubinchik, and Kozhin (11) observed that when they "quenched" ammonium nitrate with liquid nitrogen they obtained a mixture of phases IV and VII. Now, after rapid cooling to −190° C we obtained the spectrum shown in Fig. 2. It is easily recognizable as being essentially a superposition of the spectra of phases IV and VII given in Fig. 1. When thick films were used this spectrum became practically identical with the one measured from 1200 to 700 cm^{-1} by Newman and Halford at −160° C for powdered NH_4NO_3.

To sum up, working with films, we have obtained the spectra of phases I, II, IV, and in all probability VII of ammonium nitrate.

We acknowledge financial support from the National Research Council of Canada. We are indebted to Mr. David Davies for correcting the English of our manuscript.

REFERENCES

1. S. B. HENDRICKS, E. POSNJAK, and F. C. KRACEK. J. Am. Chem. Soc. **54**, 2766 (1932).
2. C. D. WEST. J. Am. Chem. Soc. **54**, 2256 (1932).
3. J. L. CRENSHAW and J. RITTER. Z. Physik. Chem. (Leipzig), Pt. B, **16**, 143 (1932).
4. P. G. MEERMAN. Rec. Trav. Chim. **60**, 363 (1941).
5. J. JAFFRAY. Compt. Rend. **224**, 1346 (1947).
6. T. H. GOODWIN and J. WHETSTONE. J. Chem. Soc. 1455 (1947).
7. R. HOCART and A. MATHIEU-SICAUD. Discussions Faraday Soc. **5**, 237 (1949).
8. C. C. STEPHENSON, D. R. BENTZ, and D. A. STEVENSON. J. Am. Chem. Soc. **77**, 2161 (1955).
9. Y. SHINNAKA. J. Phys. Soc. Japan, **11**, 393 (1956).
10. J. L. AMOROS, P. ALONSO, and M. L. CANUT. Publ. Dept. Crist. Mineral. (Madrid), **4**, 30 (1958).
11. S. I. VOLFKOVICH, S. M. RUBINCHIK, and V. M. KOZHIN. Bull. Acad. Sci. USSR, Div. Chem. Sci. 209. 1954.
12. W. E. KELLER and R. S. HALFORD. J. Chem. Phys. **17**, 26 (1949).
13. R. NEWMAN and R. S. HALFORD. J. Chem. Phys. **18**, 1276 (1950).
14. R. NEWMAN and R. S. HALFORD. J. Chem. Phys. **18**, 1291 (1950).
15. L. COUTURE and J. P. MATHIEU. J. Phys. Radium, **10**, 145 (1949).

Can. J. Chem. Downloaded from www.nrcresearchpress.com by 210.87.254.5 on 09/05/12
For personal use only.

16. D. PENOT, H. POULET, and J. P. MATHIEU. Compt. Rend. **243**, 1303 (1956).
17. A. CABANA and C. SANDORFY. Spectrochim. Acta, **18**, 843 (1962).
18. E. L. WAGNER and D. F. HORNIG. J. Chem. Phys. **18**, 296, 305 (1950).
19. J. P. MATHIEU and H. POULET. Spectrochim. Acta, **16**, 696 (1960).

Can. J. Chem. Downloaded from www.nrcresearchpress.com by 210.87.254.5 on 09/05/12
For personal use only.

REACTION OF ANHYDROSEPEDONIN WITH ALKALI

SYNTHESIS OF A DEGRADATION PRODUCT AND SOME RELATED DIMETHYLHYDROXYBENZOIC ACIDS[1]

P. V. DIVEKAR[2] AND L. C. VINING[3]

Prairie Regional Laboratory, National Research Council, Saskatoon, Saskatchewan

Received August 9, 1963

ABSTRACT

Two products have been isolated from the reaction of anhydrosepedonin with alkali and identified as 3-hydroxy-5-methyl benzoic acid and 3,4-dimethyl-5-hydroxybenzoic acid. The structure of the latter compound was established by unambiguous synthesis. In the course of this work the remaining *o*- and *m*-hydroxybenzoic acids derived from *o*-xylene were also prepared.

Can. J. Chem. Downloaded from www.nrcresearchpress.com by 210.87.254.6 on 09/05/12
For personal use only.

Sepedonin, a metabolic product of the fungus *Sepedonium chrysospermum*, was first isolated as the anhydro derivative by Divekar and Raistrick (1). From its chemical properties these authors suspected that their product might be a substituted tropolone, several examples of which are already known among the secondary metabolites of fungi. Subsequent studies in this laboratory have shown that treatment of anhydrosepedonin with alkali under conditions expected to cause rearrangement of a tropolone to a benzoic acid derivative (2) affords a small amount of product with the properties of a phenolic acid.

Difficulty was encountered in obtaining sufficient material from the reaction mixture for adequate purification and characterization of the components. However, analytical and spectroscopic evidence suggested the presence of a dimethyl *o*- or *m*-hydroxybenzoic acid. Attempts to synthesize these compounds were therefore begun. Subsequently paper chromatographic examination showed the product to be a mixture of phenolic acid and tropolone derivatives. Partition chromatography on a cellulose column allowed two of the former to be separated and isolated in a pure form. These compounds had similar ultraviolet and infrared spectra and differed only in the number of C-methyl substituents. The simpler of the two was identified by comparison with a synthetic specimen as 3-hydroxy-5-methylbenzoic acid (I).

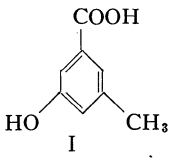

I

On biogenetic grounds it was considered likely that the two methyl substituents of the second compound were vicinal. It was compared with the isomeric dimethylhydroxybenzoic acids synthesized by the routes outlined (III–IX, XI–XVII) and found to be indistinguishable from 3,4-dimethyl-5-hydroxybenzoic acid. The derived acetates and methyl ethers of the two compounds were also identical. The acid has previously been known as a degradation product of camphor, resulting from the action of warm sulphuric acid on dicamphorylic acid (3). The orientation of the substituents was established at

[1]*Issued as N.R.C. No. 7603.*

[2]*National Research Council Postdoctoral Fellow 1957–1959. Present address: Microbiology Department, Defence Research Laboratory, Kanpur, U.P., India.*

[3]*Present address: Atlantic Regional Laboratory, National Research Council, Halifax, Nova Scotia.*

that time by decarboxylation to 2,3-xylenol, and by oxidation of the methyl ether to 6-methoxy-2-methylterephthalic acid, but does not appear to have been confirmed by synthesis.

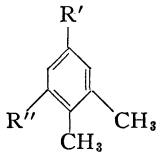

	R′ =	R″ =		R′ =	R″ =
II	NO_2	NO_2	XII	NO_2	CN
III	NH_2	NO_2	XIII	NO_2	COOH
IV	CN	NO_2	XIV	NO_2	$COOCH_3$
V	COOH	NO_2	XV	NH_2	$COOCH_3$
VI	$COOCH_3$	NO_2	XVI	OH	$COOCH_3$
VII	$COOCH_3$	NH_2	XVII	OH	COOH
VIII	$COOCH_3$	OH	XVIII	$OCOCH_3$	COOH
IX	COOH	OH	XIX	$CONH_2$	NO_2
X	COOH	$OCOCH_3$	XX	NO_2	$CONH_2$
XI	NO_2	NH_2			

The synthetic route used in the present work employed *o*-xylene as starting material. Nitration under suitable conditions gave mainly the dinitro derivatives in which each of the nitro groups can be selectively reduced to give the corresponding nitroxylidines. From these substances a series of *o*- and *m*-hydroxybenzoic acids containing two vicinal methyl substituents may be conveniently prepared by replacement of the amino and nitro with carboxyl and hydroxyl groups, respectively.

The three dimethylsalicylic acids derived from *o*-xylene were also prepared by other methods. 3,4-Dimethylsalicylic acid (XXXII), which has not been previously described, was obtained in good yield by carbonation (4) of 2,3-xylenol. When this reaction was applied to 3,4-xylenol, 4,5-dimethylsalicylic acid (XXXV) was the sole product. Earlier workers (4, 5) have observed a similar result which is evidently due to steric factors. Use of 3,4-xylenol in the Tiemann–Riemer reaction, on the other hand, is reported (6) to yield a mixture of 4,5- and 5,6-dimethylsalicylaldehydes (XXXVI and XXXI) which can be oxidized to the corresponding acids by fusion with alkali. Separation of the two aldehydes is difficult and Hunsberger and co-workers (5) in attempting to repeat Clayton's synthesis were able to obtain only one of them in pure condition. This was presumed to be the 5,6-derivative since 4,5-dimethylsalicylaldehyde was prepared by an alternative route and proved to be different. We have found, as did Auwers (7), that the main product from the Tiemann–Riemer reaction on 3,4-xylenol is the cyclohexadienone (XXXVII). Only a small amount of the mixture of aldehydes was obtained but these were separated

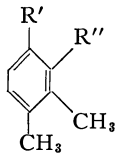

	R′ =	R″ =		R′ =	R″ =
XXI	NO_2	NO_2	XXVIII	OH	$COOCH_3$
XXII	NO_2	NH_2	XXIX	OH	COOH
XXIII	NO_2	CN	XXX	$OCOCH_3$	COOH
XXIV	NO_2	$CONH_2$	XXXI	OH	CHO
XXV	NO_2	COOH	XXXII	COOH	OH
XXVI	NO_2	$COOCH_3$	XXXIII	COOH	$OCOCH_3$
XXVII	NH_2	$COOCH_3$	XXXIV	$COOCH_3$	OH

Can. J. Chem. Downloaded from www.nrcresearchpress.com by 210.87.254.6 on 09/05/12
For personal use only.

and each obtained in a pure form. Oxidation of one of them gave 4,5-dimethylsalicylic acid in good yield. The other under more vigorous conditions afforded a little 5,6-dimethylsalicylic acid, the identity of which was established by comparison with a sample synthesized from 3-amino-4-nitro-*o*-xylene (XXII–XXIX).

Isolation of the two related hydroxybenzoic acids from the action of alkali on anhydrosepedonin provides strong evidence that this compound has a tropolone structure. It is, moreover, of interest that such a tropolone would have hydroxyl and carbon substitution at the same positions on the ring as found in stipitatonic acid, a tropolone derivative isolated from *Penicillium stipitatum* (8). Since anhydrosepedonin has a molecular formula $C_{11}H_{10}O_4$, one oxygen and two carbon atoms remain to be accounted for.

EXPERIMENTAL

Alkaline Degradation of Anhydrosepedonin

To anhydrosepedonin (100 mg), dissolved in *N* potassium hydroxide (0.25 ml) in a nickel crucible, pellets of potassium hydroxide (2 g) were added. The crucible was covered and placed for 5 minutes in a Woods metal bath preheated to 250°. After it had cooled, the reaction mixture was dissolved in water (10 ml), acidified carefully with concentrated HCl, while being stirred in an ice bath, and extracted with four portions (25 ml) of ether. The extracts were dried over anhydrous sodium sulphate and evaporated to dryness. The residue (70 mg) was heated in high vacuum at 160° C for 12 hours and the white sublimate (13 mg) collected. Paper chromatography using *sec*-butanol – 10% aqueous ammonia (4:1) showed two main components, R_f's 0.55 and 0.64, which gave orange-colored zones when the paper was sprayed with an aqueous solution of Fast Bordeaux Salt (9).

Similar fusions carried out at higher and lower temperatures, and for different periods of time, gave lower yields of the mixture of these two products.

The combined product (95 mg) from a number of experiments was dissolved in a small amount (1 ml) of the upper phase from an equilibrated mixture of *n*-butanol – toluene – 3% aqueous ammonia (5:1:3) and applied to a column (15 in. × ¾ in. diam.) of cellulose powder through which 1 liter of the upper phase of the solvent mixture had already been passed. The column was developed with the same solvent and 3 ml fractions collected. The desired compounds were located by paper chromatography of eluate fractions. Appropriate solutions were pooled and evaporated to dryness.

Fractions 34–42 gave on sublimation at 25×10^{-6} mm Hg and 95° C colorless needles (11 mg) m.p., 211–212° C. Found: C, 65.16; H, 6.01. Neutralization equivalent in 80% ethanol, 174. Calc. for $C_9H_{10}O_3$: C, 65.05; H, 6.07%. Mol. wt. 166. This substance was indistinguishable in R_f values, color reactions, and absorption spectra from a specimen of 3,4-dimethyl-5-hydroxybenzoic acid (IX), and no depression of melting point resulted from admixture of the two compounds. It was esterified in ethereal solution at 4° C for 30 minutes with diazomethane. The product was sublimed at 70° C in high vacuum and crystallized from petroleum ether (b.p. 60–80°) as colorless cubes, m.p. 153.5°. Found: C, 66.63; H, 6.76; OCH_3, 16.43; CCH_3, 23.82%. Saponification equivalent 185. Calc. for $C_{10}H_{12}O_3$: C, 66.65; H, 6.71; 1-OCH_3, 17.2; 2C—CH_3, 16.67%. Mol. wt. 180. A mixed melting point with methyl 3,4-dimethyl-5-hydroxybenzoate (VIII) caused no depression and the ultraviolet and infrared absorption spectra of the two substances were indistinguishable.

Fractions 55–80 gave on sublimation at 110° and 25×10^{-6} mm Hg colorless needles, m.p. 217° C. Found: C, 63.39; H, 5.22%. Neutralization equivalent in 80% ethanol, 155. Calc. for $C_8H_8O_3$: C, 63.15; H, 5.30. Mol. wt. 152. This substance had the same R_f values, color reactions, and absorption spectra as an authentic specimen of 3-hydroxy-5-methylbenzoic acid (I), m.p. 217° C. A mixed melting point also gave 217° C. Each compound was converted with diazomethane to the same methyl ester, m.p. 94°. Found for the product from anhydrosepedonin: C, 65.12; H, 6.18; C—CH_3, 9.6%. Calc. for $C_9H_{10}O_3$: C, 65.05; H, 6.07; 1C—CH_3, 9.04%.

2,3-Dimethyl-5-nitrobenzonitrile (XII)

o-Xylene was nitrated and the products separated by the procedure of Crossley and Renouf (10). Reduction of 3,5-dinitro-*o*-xylene (II) with 4 equivalents of stannous chloride in ethanolic hydrogen chloride (11) gave mainly 3-amino-5-nitro-*o*-xylene (XI) which, when purified by chromatography on alumina and crystallized from ethanol or benzene, had m.p. 113° C. This product (19.3 g) was dissolved by warming in concentrated sulphuric acid (35 ml) and water (175 ml) added. The solution was cooled rapidly with stirring and the fine suspension diazotized at 0° C with sodium nitrite (8.83 g) in water (40 ml). The diazonium salt was neutralized with calcium carbonate and the filtered solution added to a well-stirred mixture of toluene (100 ml) and potassium cuprocyanide (100 ml water, 20 g cuprous cyanide, and 40 g potassium cyanide) at 10° C (12). The temperature was allowed to rise to ambient and the mixture stirred vigorously at 60° C

Can. J. Chem. Downloaded from www.nrcresearchpress.com by 210.87.254.6 on 09/05/12
For personal use only.

until gas evolution ceased. The toluene layer was separated and extraction of the product from the aqueous phase completed with ether (3 × 100 ml). The combined extracts were washed successively with 4 *N* hydrochloric acid, *N* sodium hydroxide, and water, dried, and evaporated to dryness. The crude product was purified by chromatography on alumina and crystallized from ethanol as needles (10.6 g), m.p. 131–131.5° C, $\lambda\lambda_{max}^{KBr}$ 4.44, 6.54, 7.36 μ. Found: C, 61.37; H, 4.45; N, 16.13%. Calc. for $C_9H_8O_2N_2$: C, 61.36; H, 4.58; N, 15.90%.

3,4-Dimethyl-5-nitrobenzonitrile (IV)

5-Amino-3-nitro-*o*-xylene (III) was obtained from 3,5-dinitro-*o*-xylene by reduction with ammonium polysulphide as described by Noelting and Thesmar (13), or more simply with sodium hydrogen sulphide (14). It was separated from (XI) by fractional crystallization of the crude product from 4 *N* hydrochloric acid. The free base crystallized from ethanol as orange-red prisms, m.p. 69–71° C. The product (14 g) was diazotized and reacted with potassium cuprocyanide as above to give the nitrile as needles (7.6 g), m.p. 118.5–121° C, $\lambda\lambda_{max}^{KBr}$ 4.43, 6.52, 7.36 μ. Found: C, 61.31; H, 4.55; N, 16.08%.

2,3-Dimethyl-6-nitrobenzonitrile (XXIII)

3-Amino-4-nitro-*o*-xylene (XXII), prepared from 3,4-dinitro-*o*-xylene by the method of Burton and Kenner (15) was obtained as orange prisms, m.p. 120° C. The amine (14 g) was diazotized and treated with potassium cuprocyanide as in the preceding experiments to give the nitrile as needles (9.0 g), m.p. 111° C, $\lambda\lambda_{max}^{KBr}$ 4.46, 6.52, 7.41 μ. Found: C, 61.40; H, 4.54; N, 15.73%.

Hydrolysis of Nitriles

2,3-Dimethyl-5-nitrobenzonitrile (9.3 g) and 3,4-dimethyl-5-nitrobenzonitrile (7.0 g) were each hydrolyzed by heating in 100% phosphoric acid (50 ml) at a bath temperature of 150° C for 2 hours. The reaction mixture, which had set to a crystalline mass was diluted with water and filtered. The residue was separated into neutral and acidic fractions by distribution between chloroform and 5% sodium carbonate solution. Acidification of the aqueous layer yielded a crystalline product which was recrystallized from aqueous ethanol. The yield of 2,3-dimethyl-5-nitrobenzoic acid (XIII), m.p. 199–200° C, $\lambda\lambda_{max}^{KBr}$ 5.90, 6.58, 7.40μ, was 6.39 g. Found: C, 55.39; H, 4.68; N, 7.10%. Calc. for $C_9H_9O_4N$: C, 55.38; H, 4.65; N, 7.18%. The yield of 3,4-dimethyl-5-nitrobenzoic acid (V), m.p. 205–205.5° C, $\lambda\lambda_{max}^{KBr}$ 5.86, 6.50, 7.35 μ, was 5.0 g. Found: C, 55.46; H, 4.62; N, 7.11%.

The chloroform layers were evaporated and the products purified by sublimation in high vacuum followed by crystallization from ethanol. 2,3-Dimethyl-5-nitrobenzamide (XX) was obtained as needles (2.87 g) m.p. 198–199° C, $\lambda\lambda_{max}^{KBr}$ 2.88, 3.01, 3.11, 6.04, 6.17, 6.55, 7.45 μ. Found: C, 55.44; H, 5.06; N, 14.48%. Calc. for $C_9H_{10}O_3N_2$: C, 55.66; H, 5.19; N, 14.43%. 3,4-Dimethyl-5-nitrobenzamide (XIX) was obtained as prisms (2.15 g), m.p. 185–186° C, $\lambda\lambda_{max}^{KBr}$ 2.87, 3.14, 5.94, 6.15, 6.53, 7.46 μ. Found: C, 55.56; H, 5.06; N, 14.36%.

Attempts to hydrolyze 2,3-dimethyl-6-nitrobenzonitrile with phosphoric acid under these conditions caused extensive decarboxylation of the acid formed. Other vigorous methods of hydrolysis were similarly unsuccessful in converting the nitrile directly to the acid. The reaction was carried out in two steps. The nitrile (1.82 g) was heated for 3 hours at a bath temperature of 160° C in a mixture of glacial acetic acid (15 ml), sulphuric acid (15 ml), and water (15 ml). The cooled solution was diluted with water and the product extracted into chloroform. The residue from evaporation of the extract crystallized from ethanol as prisms (1.55 g), m.p. 182.5–183.5° C, $\lambda\lambda_{max}^{KBr}$ 2.96, 3.12, 6.03, 6.58, 7.40 μ of 2,3-dimethyl-6-nitrobenzamide (XXIV). Found: C, 55.66; H, 5.19; N, 14.43%.

2,3-Dimethyl-6-nitrobenzoic Acid (XXV)

2,3-Dimethyl-6-nitrobenzamide (1.83 g) was dissolved in 25% (v/v) aqueous sulphuric acid at a bath temperature of 160° C. Sodium nitrite (1.30 g) in water (25 ml) was then added slowly through a narrow funnel reaching to the bottom of the solution (16). On cooling, the reaction mixture deposited long needles (1.64 g), m.p. 175.5°, $\lambda\lambda_{max}^{KBr}$ 5.90, 6.58, 7.39 μ, after recrystallization from aqueous ethanol. Found: C, 55.38; H, 4.65; N, 7.18%.

Methyl Dimethylnitrobenzoates

The acids, suspended in ether, were each treated with excess of an ethereal solution of diazomethane, crystallized from aqueous ethanol and sublimed in high vacuum to give the following compounds.

(*a*) Methyl 2,3-dimethyl-5-nitrobenzoate (XIV), m.p. 76–76.5° C, $\lambda\lambda_{max}^{KBr}$ 5.80, 6.59, 7.45 μ. Found: C, 57.54; H, 5.43; N, 6.82%. Calc. for $C_{10}H_{11}O_4N$: C, 57.41; H, 5.30; N, 6.70%.

(*b*) Methyl 3,4-dimethyl-5-nitrobenzoate (VI), m.p. 59–60° C, $\lambda\lambda_{max}^{KBr}$ 5.82, 6.51, 7.39 μ. Found: C, 57.31; H, 5.26; N, 6.67%.

(*c*) Methyl 2,3-dimethyl-6-nitrobenzoate (XXVI), m.p. 86.5–87.5° C, $\lambda\lambda_{max}^{KBr}$ 5.77, 6.58, 7.43 μ. Found: C, 57.4; H, 5.30; N, 6.75%.

Methyl Aminodimethylbenzoates

The nitrobenzoates were each dissolved in 2.5% (w/v) methanolic hydrogen chloride and reduced with

Can. J. Chem. Downloaded from www.nrcresearchpress.com by 210.87.254.6 on 09/05/12
For personal use only.

hydrogen over palladium on charcoal catalyst at atmospheric pressure and room temperature. After hydrogen uptake ceased the filtered reaction mixtures were concentrated to a small volume under reduced pressure and neutralized with sodium bicarbonate solution. The product was extracted into ether and the dried ethereal solution evaporated to give three compounds.

(*a*) Methyl-5-amino-2,3-dimethylbenzoate (XV) as needles, m.p. 72°, $\lambda\lambda_{max}^{CHCl_3}$ 2.90, 2.96, 5.84, 6.17 μ, after crystallization from benzene – petroleum ether (b.p. 60–80° C). Found: C, 66.94; H, 7.23; N, 7.90%. Calc. for $C_{10}H_{13}O_2N$: C, 67.02; H, 7.31; N, 7.82%.

(*b*) Methyl-5-amino-3,4-dimethylbenzoate (VII), as fine needles, m.p. 80.5° C, $\lambda\lambda_{max}^{CHCl_3}$ 2.87, 2.94, 5.88, 6.17 μ after crystallization from benzene – petroleum ether (b.p. 60–80° C). Found: C, 66.99; H, 7.27; N, 7.97%.

(*c*) Methyl-5,6-dimethylanthranilate (XXVII) as a liquid $n_D^{25°\ C}$ 1.5626, $\lambda\lambda_{max}^{CHCl_3}$ 2.86, 2.94, 5.87, 6.19 μ after distillation *in vacuo*. Found: C, 67.12; H, 7.40; N, 7.65%.

Methyl Dimethylhydroxybenzoates

The aminobenzoates (1–2 g) suspended in *N* sulphuric acid (25 ml) were each diazotized at 0° C under vigorous stirring by the dropwise addition of a solution of sodium nitrite (0.41 g) in water (5 ml). Urea was added to destroy excess nitrite and the solution added slowly to a boiling solution of copper sulphate (100 g) in water (100 ml). The reaction mixture was then diluted with two volumes of water, cooled, and extracted with ether. The ether was washed with sodium bicarbonate solution, dried, and evaporated to give three compounds.

(*a*) Methyl-2,3-dimethyl-5-hydroxybenzoate (XVI) as prisms, m.p. 104–105° C, $\lambda\lambda_{max}^{CHCl_3}$ 2.79, 5.83 μ after crystallization from benzene – petroleum ether (b.p. 60–80° C) (yield 77%). Found: C, 66.80; H, 6.72%. Calc. for $C_{10}H_{12}O_3$: C, 66.65; H, 6.71%.

(*b*) Methyl-3,4-dimethyl-5-hydroxybenzoate (VIII), m.p. 153.5°, $\lambda\lambda_{max}^{CHCl_3}$ 2.79, 5.85 μ after crystallization from benzene followed by sublimation in vacuum (yield 92%). Found: C, 66.81; H, 6.78%.

(*c*) Methyl-5,6-dimethylsalicylate (XXVIII) as needles, m.p. 26–27° C, $\lambda\lambda_{max}^{CHCl_3}$ 3.23–4.17, 5.78 (w), 6.00 (s) μ, by spontaneous crystallization of liquid obtained when the crude product was distilled in vacuum (yield 94%). Found: C, 66.81; H, 6.81%. The absorption maximum at 5.78 μ did not disappear on dilution of the chloroform solution and was present at the same intensity in a sample purified by saponification, recrystallization of the acid to constant melting point (147.5–148° C) and re-esterification with diazomethane.

Dimethylhydroxybenzoic Acids

The esters were each saponified by heating with *N* potassium hydroxide at 50° C for 5 hours to give three compounds.

(*a*) 2,3-Dimethyl-5-hydroxybenzoic acid (XVII), $\lambda\lambda_{max}^{CHCl_3}$ 2.79, 3.20–4.21, 5.83 μ after crystallization from benzene followed by sublimation in high vacuum. The sample melted and resolidified at 189–190° C, and gave a second m.p. at 196–197.5° C. Found: C, 65.06; H, 6.02%. Calc. for $C_9H_{10}O_3$: C, 65.05; H, 6.07%.

(*b*) 3,4-Dimethyl-5-hydroxybenzoic acid (IX), m.p. 212° C, $\lambda\lambda_{max}^{CHCl_3}$ 2.77, 3.32–4.27, 5.86 μ after crystallization from benzene followed by sublimation in high vacuum. Found: C, 65.11; H, 6.06%.

(*c*) 5,6-Dimethylsalicylic acid (XXIX), m.p. 147.5–148°, $\lambda\lambda_{max}^{CHCl_3}$ 2.86–4.27, 6.03 μ, after sublimation in high vacuum. Found: C, 65.09; H, 6.11%.

Acetoxydimethylbenzoic Acids

The hydroxy acids were acetylated by heating with acetic anhydride and anhydrous sodium acetate on a steam bath for 3 hours. Excess acetic anhydride was decomposed with ice. The product was separated and recrystallized from aqueous ethanol to give four compounds.

(*a*) 5-Acetoxy-2,3-dimethylbenzoic acid (XVIII) as needles, m.p. 162.5–163° C. Found: C, 63.35; H, 5.93%. Calc. for $C_{11}H_{12}O_4$: C, 63.45; H, 5.81%.

(*b*) 5-Acetoxy-3,4-dimethylbenzoic acid (X) as needles, m.p. 162–163° C. Found: C, 63.35; H, 5.84%.

(*c*) Acetyl-5,6-dimethylsalicylic acid (XXX) as plates, m.p. 138–140° C. Found: C, 63.18; H, 5.79%.

(*d*) Acetyl-3,4-dimethylsalicylic acid (XXXIII) as needles, m.p. 143–145° C. Found: 63.21; H, 5.82%.

3,4-Dimethylsalicylic Acid (XXXII)

Kolbe–Schmitt carbonation of 2,3-xylenol (6.1 g) by the Marassé procedure (4) yielded a product which, after sublimation in high vacuum and crystallization from water, gave needles, m.p. 200–202° C, $\lambda\lambda_{max}^{CHCl_3}$ 2.86–4.17, 6.06 μ. Found: C, 65.05; H, 6.24%.

Methyl-3,4-dimethylsalicylate (XXXIV)

3,4-Dimethylsalicylic acid in ether was treated with a slight excess of ethereal diazomethane. The product, purified by sublimation in high vacuum, had m.p. 49.5° C. Found: C, 66.53; H, 6.77%.

Tiemann–Riemer Reaction with 3,4-Xylenol

The reaction was carried out according to the directions of Clayton (6). The main product separated from the steam distillate as long needles, m.p. 97° C (18% yield). Auwers (7) reported m.p. 102–103° C for 4-dichloromethyl-3,4-dimethylcyclohexa-2,5-dienone. Found: C, 52.45; H, 5.02; Cl, 33.91%. Calc. for $C_9H_{10}OCl_2$: C, 52.70; H, 4.91; Cl, 34.57%.

Can. J. Chem. Downloaded from www.nrcresearchpress.com by 210.87.254.6 on 09/05/12
For personal use only.

The material regenerated from the bisulphite derivative was crystallized from petroleum ether (b.p. 60–80° C) in 4% yield and the crystals sorted mechanically into two groups.

(*a*) Pale yellow needles, m.p. 67.5°, $\lambda\lambda_{max}^{CHCl_3}$ 2.8–3.7, 6.10 μ after several recrystallizations from petroleum ether and methanol. Found: C, 71.95; H, 6.76%. Calc. for $C_9H_{10}O_2$: C, 71.98; H, 6.71%. Clayton reported m.p. 72° for 5,6-dimethylsalicylaldehyde (XXXI).

(*b*) Colorless plates, m.p. 69.5–70° C, $\lambda\lambda_{max}^{CHCl_3}$ 2.8–3.7, 6.04 μ after several recrystallizations from petroleum ether. Found: C, 72.13; H, 6.84%. Clayton reported m.p. 71° for 4,5-dimethylsalicylaldehyde (XXXVI).

Oxidation of Dimethylsalicylaldehydes

When the plates, m.p. 69.5–70° C, were heated in a fusion mixture of sodium hydroxide – potassium hydroxide at 180° C for 1.5 hours (6) an acid, m.p. 202° C, was obtained in 84% yield. This was indistinguishable from the 4,5-dimethylsalicylic acid (XXXV), isolated as the sole product after carbonation of 3,4-xylenol (4).

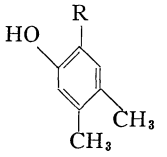

XXXV R = COOH
XXXVI R = CHO

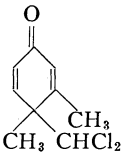

XXXVII

Oxidation of the needles, m.p. 67.5° C under the same conditions, gave only unchanged starting material. More vigorous conditions (210° and 4 hours) gave a small yield (1%) of an acid, m.p. 146° C, separated from unreacted aldehyde by solubility in sodium bicarbonate solution, followed by fractional crystallization from aqueous ethanol. This product was spectroscopically indistinguishable from and did not depress the melting point of a sample of 5,6-dimethylsalicylic acid synthesized from 3-amino-4-nitro-*o*-xylene. Attempts to improve the yield by increasing the temperature and reaction time, or by using the procedure of Pearl (17) were not successful.

ACKNOWLEDGMENTS

The authors wish to express their sincere appreciation to Professor H. Raistrick for his continued interest and helpful advice. They are also indebted to Dr. Guy Talbot for the gift of an authentic sample of 3-hydroxy-5-methylbenzoic acid, and to Miss M. J. A. Gates for competent technical assistance. Microanalyses were performed by Mr. E. Mazurek.

REFERENCES

1. P. V. Divekar. Ph.D. Thesis, University of London. 1956.
2. T. Nozoe. Fortschr. Chem. Org. Naturstoffe, **13**, 232 (1956).
3. W. H. Perkin. J. Chem. Soc. **75**, 179 (1899).
4. O. Baine, G. F. Adamson, J. W. Barton, J. L. Fitch, D. R. Swayampati, and H. Jeskey. J. Org. Chem. **19**, 510 (1954).
5. I. M. Hunsberger, D. Lednicer, H. S. Gutowsky, D. L. Bunker, and P. Taussig. J. Am. Chem. Soc. **77**, 2466 (1955).
6. A. Clayton. J. Chem. Soc. **97**, 1388 (1910).
7. K. Auwers. Ber. **32**, 3598 (1899).
8. W. Segal. J. Chem. Soc. 2847 (1959).
9. I. A. Pearl and P. F. McCoy. Anal. Chem. **32**, 1407 (1960).
10. A. W. Crossley and N. Renouf. J. Chem. Soc. **95**, 201 (1909).
11. A. W. Crossley and G. H. Wren. J. Chem. Soc. **99**, 2341 (1911).
12. H. T. Clark and R. R. Read. Organic Syntheses. Collective Vol. I. 2nd ed. John Wiley & Sons, Inc., New York. p. 514.
13. E. Noelting and G. Thesmar. Ber. **35**, 628 (1902).
14. K. Brand. J. Prakt. Chem. **74**, 449 (1906).
15. H. Burton and J. Kenner. J. Chem. Soc. **119**, 1047 (1921).
16. L. Gattermann. Ber. **32**, 1116 (1899).
17. I. A. Pearl. Org. Synth. **30**, 101 (1950).

Can. J. Chem. Downloaded from www.nrcresearchpress.com by 210.87.254.6 on 09/05/12
For personal use only.

THE CHEMISTRY OF APIOSE. PART I[1]

D. T. WILLIAMS AND J. K. N. JONES
Department of Chemistry, Queen's University, Kingston, Ontario
Received August 27, 1963

ABSTRACT

D-Apiose, D-xylose, and 2-*O*-methyl D-xylose have been identified as components of polysaccharides of *Zostera marina* L.

D-Apiose has been synthesized by a new procedure which clarifies the stereochemistry at C_3 of the D-apiose molecules and which gives a new general method for the synthesis of branched chain sugar alcohols.

INTRODUCTION

D-Apiose has been found in the seaweed *Posidonia australis* L. (1). It also occurs in trace amounts in many plants (2, 3). Bell pointed out that its rate of movement on chromatograms and color reactions might lead to its confusion with rhamnose, a very common constituent of many plant materials. As a result of discussion with Dr. D. J. Bell, it was decided to test the hypothesis that D-apiose might be a constituent of plants of the family Potomagoneacae.

RESULTS

One of the seaweeds most readily available to us (apart from *Posidonia australis* L.) was *Zostera marina* L. After hydrolysis of this plant, D-apiose, D-xylose, and 2-*O*-methyl D-xylose were isolated and characterized. A third sugar tentatively identified as an *O*-methyl apiose was also isolated in small quantity. This is the first time that 2-*O*-methyl D-xylose has been encountered in a seaweed. A polysaccharide composed of D-apiose and D-xylose in the ratio of approximately one to one and an unidentified uronic acid were also isolated from *Posidonia australis* L.

In order to identify the D-apiose, attempts were made to synthesize the D- and L- forms by procedures described in the literature (5, 6). As these methods gave poor yields in our hands, a new synthesis was devised which has the advantage that it will enable us to solve the problem of the stereochemistry at C_3 of the D-apiose molecule in apiin. This problem was first discussed by Bell (1). The method of synthesis yielded a branched chain sugar alcohol as an intermediate (cf. Schaffer (6)).

In this synthesis di-*O*-isopropylidene *aldehydo* L-arabinose (7) was treated with formaldehyde and sodium hydroxide in aqueous solution when the branched chain sugar alcohol (I) was produced (cf. ref. 6). Cautious hydrolysis with dilute acetic acid removed one *O*-isopropylidene residue from (I) and the product (II*a*) purified via its crystalline acetate (II*b*), on oxidation with periodate, yielded *O*-isopropylidene D-apiose (III), the stereochemistry of which is fixed at C_3 yielding (III*a*), not (III*b*), which possesses transfused five-membered rings. The product (III) after hydrolysis yielded D-apiose which was characterized as its benzylphenylhydrazone. The periodate oxidation of this hydrazone and of methyl apioside have been examined. Attempts to synthesize D-apiose via 2,3-di-*O*-benzyl 3,4-*O*-isopropylidene *aldehydo* L-arabinose were unsuccessful.

It is of interest that D- and L-apiose gave di-*O*-isopropylidene derivatives which were not identical, presumably because of the formation of isomers of the type IV and V.

[1]*Abstracted from the M.Sc. thesis of D. T. Williams.*

Can. J. Chem. Downloaded from www.nrcresearchpress.com by 210.87.254.6 on 09/05/12
For personal use only.

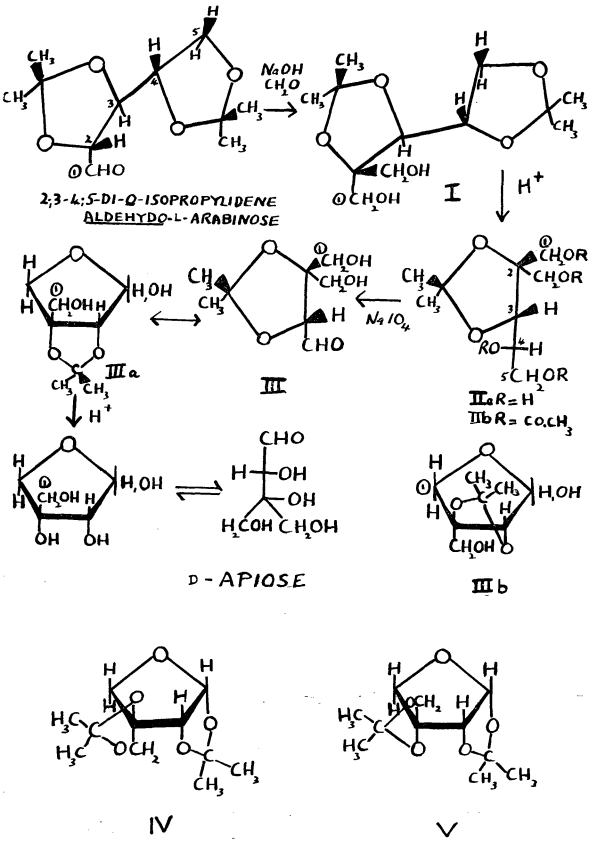

EXPERIMENTAL

The general experimental details and paper chromatography procedures have been described previously (8).

Isolation of D-*apiose and 2-O-methyl* D-*xylose from Zostera marina L.*

The seaweed (air dried, 500 g) was extracted in a Waring blender with (*a*) methanol (1 l.), (*b*) butan-1-ol saturated with water (1 l.), and (*c*) water saturated with butan-1-ol (1 l.), according to the procedure described to us by Dr. E. E. Percival (personal communication). These extracts contained colored material and amino acids but no D-apiose-containing material was present. The residue was divided into two equal parts. The first portion was hydrolyzed with *N* sulphuric acid at 70° for 4 hours. After filtration the cooled solution was neutralized ($BaCO_3$), filtered, and the filtrate was concentrated to a syrup (2 g). Paper chromatographic examination of the material showed the presence of apiose (mainly), plus trace amounts of sugars tentatively identified as xylose and glucose and (or) galactose. The second part (A) was extracted with cold 2% sodium hydroxide solution (2×500 ml) and the combined extracts were dialyzed for 4 days. Concentration of the solution gave a green residue (2.5 g), a small portion of which, after hydrolysis with 2 *N* sulphuric acid for 5 hours at 100°, showed only apiose and xylose in the approximate ratio 1:1 on chromatographic examination. Later work has shown that higher yields of polysaccharide are obtained if the seaweed is first given a treatment with ice-cold *N* hydrochloric acid before the alkaline extraction procedure (4). After alkaline extraction of the second portion (A), the insoluble residue, which still contained apiose, was hydrolyzed using the procedure described for the hydrolysis of the first portion of seaweed. The resulting reducing sugars were combined with those from the first hydrolysis, and the whole was fractionated on a cellulose column (9) using butan-1-ol half saturated with water as effluent. There resulted D-apiose (2.3 g), with R_{RH} 0.85; 2-*O*-methyl D-xylose, with R_{RH} 1.43, and *O*-methyl apiose (?) with R_{RH} 1.43 (solvent A).

D-Apiose was characterized as its *N*-benzyl *N*-phenylhydrazone (10) (1.4 g from 0.8 g D-apiose), which had m.p. 137–139° and $[\alpha]_D$ −68° (*c*, 1.3 pyridine) after recrystallization from chloroform. Analysis: Calc. for $C_{18}H_{22}O_4N_2$: C, 65.4; H, 6.7; N, 8.5%. Found: C, 65.3; H, 6.8; N, 8.6%. It was also characterized as

Can. J. Chem. Downloaded from www.nrcresearchpress.com by 210.87.254.6 on 09/05/12
For personal use only.

apiose 2,5-dichlorophenylosazone of m.p. 189–190°, not depressed on admixture with an authentic sample prepared from L-apiose by the method of Schaffer (6). On periodate oxidation D-apiose *N*-benzyl *N*-phenylhydrazone consumed 1.95 moles of periodate and yielded 1.06 moles of acid and 1.05 moles of formaldehyde per mole in 14 hours (constant values). During the oxidation pale yellow crystals of glyoxal *N*-benzyl *N*-phenylhydrazone were precipitated. They had m.p. 93° after recrystallization from methanol–water. Analysis: Calc. for $C_{15}H_{14}ON_2$: C, 75.6; H, 5.9; N, 11.8%. Found: C, 75.4; H, 5.7; N, 12.0%.

The 2-*O*-methyl D-xylose fraction crystallized and the recrystallized sugar (4 mg) had m.p. 132–133° not depressed on admixture with an authentic specimen (11). It yielded xylose on demethylation with boron trichloride (12) and the reduced acetylated product was indistinguishable from 1,3,4,5-tri-*O*-acetyl 2-*O*-methyl D-xylitol by gas–liquid chromatographic analysis.

The methylated apiose (?) fraction (10 mg) was admixed with 2-*O*-methyl D-xylose. Because of the small amount of sugar available it was not possible to characterize it completely. The fraction on demethylation (12) (boron trichloride) yielded apiose and xylose which were detected chromatographically (solvent A).

Synthesis of D-*apiose*

*4-C-Hydroxymethyl-1,2-3,4-di-O-isopropylidene 2,3-*D*-erythropentitol*

2,3-4,5-Di-*O*-isopropylidene *aldehydo*-L-arabinose (from 25 g of the corresponding diethyl dithioacetal) (7) was dissolved in ethanol (300 ml), and formaldehyde (20 ml of a 37% solution) and sodium hydroxide (12 g in ethanol) were added. After 5 days at ambient temperatures the solution was neutralized (formic acid) and evaporated to dryness. The residue was extracted with chloroform and the extracts were counter-extracted with an equal volume of water. The chloroform solution was dried and then concentrated to a syrup (12.5 g) which was taken up in ether and the solution was extracted with an equal volume of water. The ethereal solution was dried and evaporated to a syrup which crystallized. The product 4-*C*-(hydroxymethyl)-1,2–3,4-di-*O*-isopropylidene 2,3-D-*erythro*-pentitol had m.p. 91–92° and $[\alpha]_D$ +14° (*c*, 2.0 in methanol). Yields varied from 12 to 36%. Analysis: Calc. for $C_{12}H_{22}O_6$: C, 55.0; H, 8.4%. Found: C, 54.9; H, 8.2%.

*4-C-(Hydroxymethyl)-3,4-O-isopropylidene 2,3-*D*-erythropentitol*

The crystalline di-*O*-isopropylidene derivative (above, 2.0 g) was hydrolyzed with 65% acetic acid for 18 hours at room temperature. The reaction mixture was diluted with cold water (200 ml), neutralized ($BaCO_3$), filtered, and the filtrate was evaporated to dryness. The residue was extracted with acetone; the extracts were evaporated to a syrup which was again extracted with acetone. The extracts on concentration yielded a syrup (1.4 g) which, on extraction with ether, yielded some (200 mg) starting material. The overall yield of crude product was 79%. It was purified by acetylating it (1.2 g) in acetic anhydride (3 ml)–pyridine (3 ml) mixture. After 16 hours at room temperature and 1 hour at 60°, the acetate was isolated in chloroform solution in the usual way. The product crystallized and was recrystallized from ethanol. It had m.p. 82° and $[\alpha]_D$ −22° (*c*, 2.0 in ethanol). Analysis: Calc. for the tetraacetate $C_{17}H_{26}O_{10}$: C, 52.3; H, 6.7%. Found: C, 52.1; H, 6.6%.

De-*O*-acetylation was achieved by the Zemplen procedure (13). The tetraacetate (1.1 g) yielded a syrup (500 mg) which had $[\alpha]_D$ 0° (*c*, 1.1 in acetone).

2,3-O-Isopropylidene D-*Apiose*

The above *O*-isopropylidene pentitol derivative (485 mg) was dissolved in water (25 ml) and oxidized with sodium metaperiodate (500 mg) in water (25 ml). After 1 hour at room temperature, (a trial experiment (formaldehyde determination) had shown that reaction was complete in this time) ethylene glycol was added to the solution. After 1 hour water (25 ml) was added and the solution was continuously extracted with chloroform. Concentration of the extracts yielded a syrup (390 mg) which had $[\alpha]_D$ −35° (*c*, 0.87 in methanol). Analysis: Calc. for $C_8H_{14}O_5$: C, 50.5; H, 7.4%. Found: C, 50.8; H, 7.6%.

D-*Apiose N-benzyl N-phenylhydrazone*

2,3-*O*-Isopropylidene D-apiose (350 mg) was hydrolyzed in *N* sulphuric acid (5 ml) at 70° for 4 hours. The product was isolated after the solution had been neutralized ($BaCO_3$) and treated with a solution of *N*-benzyl *N*-phenylhydrazine (1 g) in ethanol (10 ml) at ambient temperatures. After 18 hours the product (300 mg) was isolated (10) and recrystallized from chloroform. It had m.p. 138–139° not depressed on admixture with an authentic specimen, and $[\alpha]_D$ −29° (*c*, 1.1 in methanol). Analysis: Calc. for $C_{18}H_{22}O_4N_2$: C, 65.4; H, 6.7; N, 8.5%. Found: C, 65.35; H, 6.4; N, 8.2%.

*Methyl-*D-*apiosides*

D-Apiose (500 mg) was heated under reflux with methanolic hydrogen chloride (50 ml, 1%) for 16 hours. The acid was neutralized (Ag_2CO_3) and the filtered solution was evaporated to a syrup (510 mg) which contained at least two components of R_{RH} 1.41 and R_{RH} 1.32. The syrup was fractionated on a cellulose column and yielded one syrupy component which appeared to be chromatographically pure. It had R_{RH} 1.41 solvent (A) and $[\alpha]_D$ −101° (*c*, 1.3 in methanol). On periodate oxidation it yielded 1 mole of acid and consumed 2 moles of periodate per mole. The fraction of R_{RH} 1.32 was not obtained pure. In addition a small quantity of a third component of R_{RH} 1.30 previously undetected was also noted.

Can. J. Chem. Downloaded from www.nrcresearchpress.com by 210.87.254.6 on 09/05/12
For personal use only.

Di-O-isopropylidene D-*apiose*

D-Apiose (150 mg) was shaken with dry acetone (60 ml) containing concentrated sulphuric acid (3 ml) for 5 hours. The acid was neutralized (Na_2CO_3) and the product, isolated as a syrup (180 mg), crystallized. The crystals were recrystallized (40 mg) and had m.p. 80–82° $[\alpha]_D$ +58° (*c*, 1.17 in ethanol). Bell (1) gives m.p. 81–83° and $[\alpha]_D$ +55.6° (*c*, 1.35 in ethanol). On hydrolysis with dilute acid the product regenerated D-apiose with $[\alpha]_D$ +7.6° (*c*, 0.7 in water).

Di-O-isopropylidene L-*apiose*

L-Apiose (250 mg) was concentrated to the di-*O*-isopropylidene derivative by the procedure described above. The product crystallized; it could not be purified by recrystallization but could be purified by sublimation. It had m.p. 56–58° and $[\alpha]_D$ −16° (*c* 1.14 in ethanol). It depressed the melting point of the D-isomer and its infrared spectrum was different from that of the D-isomer.

ACKNOWLEDGMENTS

The authors thank the National Research Council for a grant (NRC T-19) and the Ontario Research Foundation for financial assistance. We also thank Dr. R. Lewin of La Jolla, California, Miss E. M. Wollaston, and Dr. H. B. S. Womersley of the Department of Botany, University of Adelaide, South Australia, for gifts of seaweed.

REFERENCES

1. D. J. Bell, F. A. Isherwood, and N. E. Hardwick. J. Chem. Soc. 3702 (1954).
2. C. S. Hudson. Advances in carbohydrate chemistry. **4**, 57 (1949).
3. J. S. D. Bacon. Personal communication.
4. R. Hulyalkar and J. K. N. Jones. Unpublished results.
5. P. A. J. Gorin and A. S. Perlin. Can. J. Chem. **36**, 480 (1958).
6. R. Schaffer. J. Am. Chem. Soc. **81**, 5452 (1959).
7. J. English and P. H. Griswold. J. Am. Chem. Soc. **67**, 2039 (1945).
8. J. W. Bird and J. K. N. Jones. Can. J. Chem. **41**, 1878 (1963).
9. L. Hough, J. K. N. Jones, and W. H. Wadman. J. Chem. Soc. 1702 (1950).
10. E. Vongerichten and F. Müller. Ber. **39**, 235 (1906).
11. G. T. Robertson and T. H. Speedie. J. Chem. Soc. 824 (1934).
12. S. Allen, T. G. Bonner, E. J. Bourne, and N. M. Saville. Chem. Ind. (London), 630 (1958).
13. G. Zemplen. Ber. **59**, 1254 (1926).

Can. J. Chem. Downloaded from www.nrcresearchpress.com by 210.87.254.6 on 09/05/12
For personal use only.

RAPID ANALYSIS OF STRONTIUM AND RUBIDIUM IN MINERALS

A. A. MILLS
Department of Chemistry, Dalhousie University, Halifax, Nova Scotia
Received August 22, 1963

ABSTRACT

Methods are described for the rapid analysis of strontium and rubidium in micas and alkali feldspars by emission spectrography. The elements are determined in a common matrix, excess barium carbonate acting as buffer and internal standard. The techniques are applicable to the analysis of 5–500 p.p.m. strontium in the minerals, with relative deviations of ±5–8%. Semiquantitative results are obtained for 100–1500 p.p.m. rubidium in the same materials. These methods have also been successfully applied to the analysis of strontium and rubidium in certain whole rocks. Results obtained with the standard granite G-1 and standard diabase W-1 show satisfactory agreement with the recommended values.

Can. J. Chem. Downloaded from www.nrcresearchpress.com by 210.87.254.6 on 09/05/12
For personal use only.

INTRODUCTION

One method for the determination of geological age depends upon the decay of the naturally occurring radioactive nuclide rubidium-87 to strontium-87 (1). Whether this technique is applicable to a given rock or mineral depends upon the ratio of rubidium to total strontium in the sample, its age, and the accuracy desired. A comparatively high concentration of rubidium accompanied by a minimum of common strontium (which tends to mask the radiogenic strontium-87) is required. Micas (especially biotite and muscovite) and alkali feldspars have proved to be the most generally useful minerals for the dating of igneous rocks by the rubidium–strontium method.

A complete age determination, involving isotope dilution, ion exchange separation, and solid-source mass spectrometry, is time-consuming and expensive. A rapid method was therefore sought (2) which would indicate whether a given sample contained a suitable ratio of rubidium to strontium. An analysis yielding absolute quantities, rather than the ratio of the elements, was preferred to allow calculation of optimum 'spike' concentrations in any subsequent isotope dilution assay (3). The concentration of strontium was the more critical of the two determinations.

CHOICE OF TECHNIQUE

Method

A simple, rapid, sensitive technique necessitating minimum sample preparation was required. A method based on emission spectrography was therefore selected, relevant descriptions in the literature employing flame (4–6), arc (7–11), or spark (12) excitation of solid or liquid samples. Direct excitation of the powdered material at the anode of a d-c. arc was chosen as the technique to be developed.

Matrix Effects and Internal Standard

A notorious cause of inaccuracy in spectrographic analysis is the effect of a varying matrix (11). Turekian, Gast, and Kulp (10) showed that for the analysis of strontium in silicate rocks this effect may be minimized by the addition of an equal weight of calcium carbonate to the sample. The strontium content was then obtained from the Sr 4607/Ca 4578 intensity ratio, the calcium content of the original silicate being known from a previous analysis.

The basis of the present method was to mix the sample with an excess of barium carbonate; this acted as spectroscopic buffer, flux, and internal standard (11, 13, 14). Barium carbonate was preferred to the calcium salt for the following reasons:

(*i*) Traces of barium in the original samples would make a negligible contribution to the total barium in the mixture. The concentration of barium may therefore be considered constant, and comparatively weak lines in the spectrum of this element paired with sensitive lines of strontium and rubidium. Barium would be expected to be an excellent internal standard for strontium, less ideal for rubidium (11). 'Moving-plate' runs (11) and the experimental results confirmed this.

(*ii*) Barium carbonate gave a better burn than calcium carbonate, an observation previously reported by Marks and Potter (15). Adding an equal weight of graphite powder to the mix still further improved the steadiness of the arc.

(*iii*) Strontium was present in commercially available* spectrographic grades of both calcium and barium carbonate, but the latter contained less of this impurity.

A preliminary series of experiments confirmed that barium carbonate exhibited a buffering action comparable to that of calcium carbonate. A mixture of 1:1:2 by weight of sample, barium carbonate, and powdered graphite showed no matrix effect to over twice the range in concentrations of alumina, silica, potassium, and magnesium found in natural micas and alkali feldspars. A disadvantage was that bands due to molecular emission produced a heavy background in parts of the spectrum.

Systematic Error and Concentration Standards

Another possible cause of inaccuracy in spectrographic analysis is in the values assigned to the standards used to construct working curves. In the present work, standards were derived from selected samples analyzed by an isotope dilution technique (16) thought to be accurate to within ± 2–3% (2, 17).

EXPERIMENTAL

Sample Preparation

Clean, unweathered rock specimens were crushed in a roller crusher and sifted through nylon bolting cloth (18). The 40–80 mesh fraction was washed with deionized water to remove dust, then dried at 80° C.

Minerals were separated in a Frantz Isodynamic Separator; first arranged vertically to rapidly effect a coarse separation, and then sloped to the optimum angle. Three or four passages, monitored by optical microscopic examination of the products, were normally sufficient to yield one constituent in $>98\%$ purity. Selected minerals were carefully washed and dried. Samples (50–100 mg) were taken for spectrographic analysis, and reduced to a fine powder by vibrating for 2 minutes in a tool-steel micro ball-mill.

A stock mix was prepared from 1 g barium carbonate (J.M. 92) intimately ground with 2 g graphite powder (J.M. 9). Three parts by weight of this stock mix were combined in a plastic vial with one part by weight of the powdered mineral, and vibrated in the micro mill to give a uniform 1:1:2 mixture of sample, barium carbonate, and graphite. A mixture was stored in the plastic vial until required, 80 mg being adequate for the preparation of four electrodes.

Spectrography

Anodes were turned from graphite rod (J.M. 4B) to the dimensions shown in Fig. 1, the cavity holding about 15 mg of sample mix. Cathodes were of carbon rod, sharpened to a blunt point.

The following parameters were common to all determinations.

Spectrograph:	Hilger fully automatic large quartz-glass spectrograph, Littrow type.
Optics:	That part of the arc selected by a diaphragm was imaged on the collimating lens of the spectrograph, ensuring uniform illumination of the slit.
Rotating sector:	6-step, 2:1 transmission ratio.
Slit:	0.01 mm.
Arc length:	9 mm.
Potential drop across arc:	250 v on open circuit, falling to 50 v when operating.

**Johnson, Matthey and Co. Ltd., 73–83 Hatton Garden, London, E.C.1.*

Can. J. Chem. Downloaded from www.nrcresearchpress.com by 210.87.254.6 on 09/05/12
For personal use only.

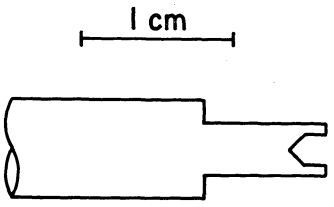

FIG. 1. Graphite anode.

Number of analyses: Normally in duplicate.
Photometer: Hilger non-recording microphotometer.

Plates were calibrated by the self-calibration method (11) on a plotting board of Seidel function (19) against intensity (sector steps). Relative intensities were read off from the straight line plots at Seidel function = 10, correction for background being made where required.

Strontium in Micas

Plates: Ilford ordinary.
Current: 5.7 amp.
Shutter: Opened just after striking arc. Average burning time 80 seconds.
Lines: Sr (I) 4607.3, Ba (I) 4700.4.
Correction for background was required.

It has been mentioned above that the barium carbonate contained strontium as an impurity. This was found by the addition method (11) to be equal to 8 p.p.m. strontium, and this quantity was therefore subtracted in all analyses for this element.

The resultant working curve is shown in Fig. 2: the range covered is from 5–100 p.p.m. strontium. The relative deviation was ±8% for single determinations in the 50 p.p.m. region. Analyses were normally carried out in duplicate, giving an error of the mean of ±6% at the 68% confidence level.

Strontium in Alkali Feldspars

Plates, current, and shutter as above.
Lines: Sr (II) 4077.7, Ba (II) 4166.0.
Correction for background not required.

The resultant working curve is shown in Fig. 3, being usable from 15–500 p.p.m. strontium. Precision at the 68% confidence level was ±5% for single determinations in the 100 p.p.m. region, equivalent to ±4% for duplicate analyses.

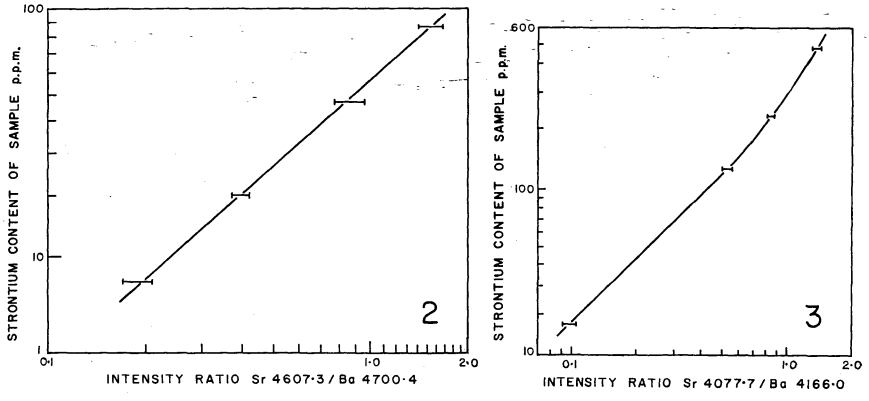

FIG. 2. Working curve for the determination of strontium in micas.
FIG. 3. Working curve for the determination of strontium in alkali feldspars.

Rubidium in Micas and Feldspars

Plates: Kodak I.R.E.R.
Current: 3.5 amp.
Shutter: Opened just before striking arc. Average burning time 2 minutes.
Lines: Rb (I) 7800.2, Ba (I) 7780.4.
Correction for background was required.

Can. J. Chem. Downloaded from www.nrcresearchpress.com by 210.87.254.6 on 09/05/12
For personal use only.

The resultant working curves are shown in Fig. 4, the range covered being from 100–1500 p.p.m. rubidium. The dispersion was assumed to follow a log-normal distribution (11), with the geometric mean of a set of analyses providing the best estimate of the correct value. The upper and lower 68% confidence limits were given by 3/2 G and 2/3 G respectively, where G represents the geometric mean.

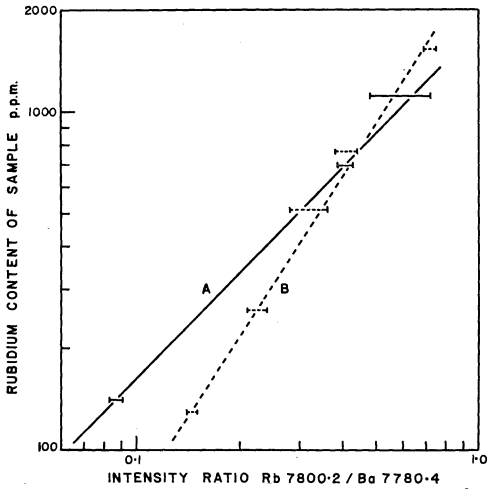

FIG. 4. Working curves for the determination of rubidium in: curve A, micas; curve B, alkali feldspars.

DISCUSSION

Strontium

In order to measure the very low concentrations of strontium sometimes found in biotites it was necessary to employ the most sensitive line in the spectrum of this element at 4607.3 Å. This atom line was paired with a barium-atom line at 4700.4 Å. Both lines lay in a region of comparatively high background ascribed to BaO molecular emission (20), and correction for this was required.

The greater concentrations of strontium associated with alkali feldspars permitted the use of the less intense ion line at 4077.7 Å, which was paired with a barium-ion line at 4166.0 Å. Correction for background was then unnecessary, provided registration of the cyanogen band spectrum was minimized. Self-absorption became apparent in the Sr 4077.7 line above 150 p.p.m., as shown by the deviation from linearity of the working curve above this concentration (Fig. 3). The slopes of the linear portions of the working curves were close to the expected value of 45° (11). A satisfactory degree of precision is indicated by relative deviations of ±5–8% for single determinations.

Rubidium

It was desirable to determine rubidium in the same sample mix, although this could not be expected to be as precise as a technique employing another alkali metal as internal standard.

The emission spectrum of rubidium contains four intense lines; two in the blue at 4201.8 and 4215.6 Å, and two in the red at 7800.2 and 7947.6 Å. The short-wavelength lines were not applicable because of the possibility of interference from Fe 4202.0 and Sr 4215.5 respectively. Use of a red line was therefore obligatory, although both are known to be very susceptible to self-absorption. Rb 7800.2 was chosen because the weaker Rb 7947.6 line lay in a region of heavy background.

Can. J. Chem. Downloaded from www.nrcresearchpress.com by 210.87.254.6 on 09/05/12
For personal use only.

Linear calibration curves were obtained (Fig. 4), although the precision was insufficient to preclude the presence of some self-absorption. The use of a barium carbonate matrix as an internal standard for rubidium is much less satisfactory than for strontium, but the accuracy was sufficient for the required purpose.

ANALYSIS OF STANDARDS G-1 AND W-1

The strontium contents of the standard granite G-1 and standard diabase W-1 (21) were determined by the method given for strontium in feldspars. The rubidium content of granite G-1 was also determined. The results are shown in Table I. The 'recommended' values are those of Fleischer and Stevens (22), the lower concentrations being derived from isotope dilution and neutron activation analyses, whilst inclusion of earlier spectrographic determinations gave the higher average. The results obtained in this work agree well with the lower recommended value in each case.

TABLE I

Analysis of standards G-1 and W-1

	Strontium, p.p.m.			Rubidium, p.p.m.		
Sample	Experimental results	Arithmetic mean	Recommended value	Experimental results	Geometric mean	Recommended value
G-1	258 250 250	253	250 or 280	195 210 255 160 230 270	217	220
W-1	166 182 179	176	175 or 220	Below detection limit	—	22

ACKNOWLEDGMENTS

I thank Mrs. N. Garton for the experimental work and Drs. B. J. Giletti and C. M. L. Bowler for their advice. The work was conducted at Oxford University as part of the geological age and isotopes research programme being carried out under the direction of Professor L. R. Wager, with support from the Department of Scientific and Industrial Research and the Overseas Geological Surveys, London.

REFERENCES

1. K. Rankama. Isotope geology. Pergamon Press Ltd., London. 1954. p. 332.
2. R. St. J. Lambert and A. A. Mills. Ann. N.Y. Acad. Sci. **91**, 378 (1961).
3. G. L. Davis and L. T. Aldrich. Bull. Geol. Soc. Am. **64**, 379 (1953).
4. A.-G. Hybbinette. Svensk. Kem. Tidskr. **55**, 151 (1943).
5. H. T. Odum. Ph.D. Thesis, Yale University. 1950.
6. J. Medek and F. Valeška. Spectrochim. Acta. Special issue 1957, being the Proc. Colloq. Spectroscopicum Intern. VI. p. 67.
7. V. M. Goldschmidt, H. Bauer, and H. Witte. Nachr. Ges. Wiss. Göttingen. Math.-Physik. Kl. **1**, 39 (1935).
8. L. H. Ahrens and L. G. Gorfinkle. Am. J. Sci. **249**, 451 (1951).
9. J. L. Kulp, K. Turekian, and D. W. Boyd. Bull. Geol. Soc. Am. **63**, 701 (1952).
10. K. K. Turekian, P. W. Gast, and J. L. Kulp. Spectrochim. Acta, **9**, 40 (1957).
11. L. H. Ahrens and S. R. Taylor. Spectrochemical analysis. 2nd ed. Addison-Wesley Pub. Co. Inc., Reading, Mass. 1961.
12. R. J. Grabowski and R. C. Unice. Anal. Chem. **30**, 1374 (1958).
13. A. Kvalheim. J. Opt. Soc. Am. **37**, 585 (1947).
14. J. E. Hawley and G. Macdonald. Geochim. Cosmochim. Acta, **10**, 197 (1956).

Can. J. Chem. Downloaded from www.nrcresearchpress.com by 210.87.254.6 on 09/05/12
For personal use only.

15. G. W. MARKS and E. V. POTTER. U.S. Bur. Mines Rept. Invest. 1949. p. 4461.
16. B. J. GILETTI, S. MOORBATH, and R. ST. J. LAMBERT. Quart. J. Geol. Soc. London. **117**, 233 (1961).
17. J. L. KULP, L. E. LONG, C. E. GIFFEN, A. A. MILLS, R. ST. J. LAMBERT, B. J. GILETTI, and R. K. WEBSTER. Nature, **185**, 495 (1960).
18. A. A. SMALES and L. R. WAGER. Methods in geochemistry. Interscience, London. 1960. Chap. 2.
19. H. KAISER. Spectrochim. Acta, **2**, 1 (1941).
20. R. W. B. PEARSE and A. G. GAYDON. The identification of molecular spectra. Chapman & Hall, London. 1941. p. 57.
21. L. H. AHRENS and M. FLEISCHER. U.S. Geol. Surv. Bull. 1113, p. 83 (1960).
22. M. FLEISCHER and R. E. STEVENS. Geochim. Cosmochim. Acta, **26**, 525 (1962).

Downloaded from www.nrcresearchpress.com by 210.87.254.6 on 09/05/12
For personal use only.

Can. J. Chem. Downloaded from www.nrcresearchpress.com by 210.87.254.105 on 09/05/12
For personal use only.

PHOTOCHEMICAL TRANSFORMATIONS OF DIENES

I. THE PHOTOLYSIS OF 3-ALKOXYCHOLESTA-3,5-DIENES

GEORGE JUST AND CLIFFORD C. LEZNOFF[1,2]
Department of Chemistry, McGill University, Montreal, Quebec

Received August 16, 1963

ABSTRACT

The photolysis of 3-alkoxycholesta-3,5-dienes in an alcohol has been found to result in a stereospecific addition of the alcohol to the Δ^3 double bond with formation of β,γ-unsaturated ketals. On silica gel, the non-cyclic β,γ-unsaturated ketals gave cholest-5-en-3-one.

As part of an investigation of the photoinduced transformations of heteroannular dienes, an ethanolic solution of 3-ethoxycholesta-3,5-diene (1) (I) was irradiated with a high-pressure mercury lamp. The reaction was very fast as evidenced by the disappearance of the chromophore at 239 mμ. Evaporation and purification by chromatography on alumina resulted in a 60% yield of a crystalline compound (II), $C_{31}H_{54}O_2$, m.p. 49–50°. Treatment with acid resulted in the formation of cholest-4-en-3-one (VIII). Chromatography of II on silica gel gave cholest-5-en-3-one (IV).

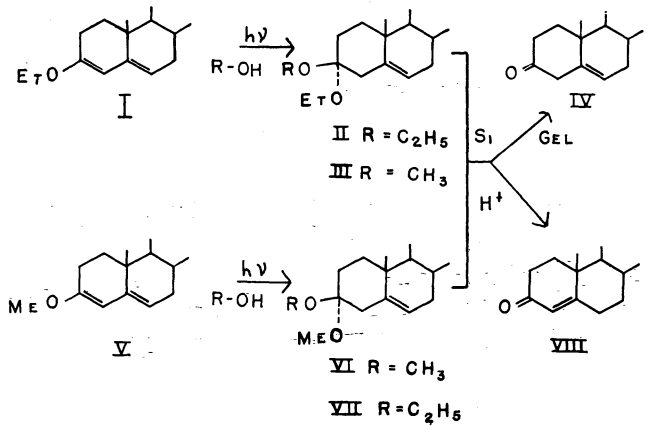

FIG. 1.

These results, in accord with the infrared (Fig. 2) and nuclear magnetic resonance (n.m.r.) data (Table I), indicated that the photoproduct was 3,3-diethoxycholest-5-ene (II). The structure was confirmed by synthesis in which cholest-5-ene-3-one was reacted with absolute ethanol in the presence of malonic acid (2).

Similarly, photolysis of 3-methoxycholesta-3,5-diene (V) in methanol gave 3,3-dimethoxycholest-5-ene (VI) in 50–60% yield, identical in all respects with a synthetic sample (2).

When 3,3-diethoxycholest-5-ene was recrystallized from methanol, a new compound

[1]*From a thesis to be presented to the Graduate Faculty, McGill University, in partial fulfillment of the requirements for the Ph.D. degree.*

[2]*Holder of a National Research Council of Canada Bursary, 1961–62, and National Research Council of Canada Studentships, 1962–64.*

TABLE I

Nuclear magnetic resonance data of photolysis products II, III, VI, and VII
(T.M.S. = 0, chemical shifts in p.p.m.)

Compound	Methylene group at C_4 singlet	3α-MeO singlet	3β-MeO singlet	3α-EtO quartet center	3β-EtO quartet center	Vinyl proton at C_6 singlet
3,3-Diethoxycholest-5-ene	2.25	—	—	3.40_5	3.33	5.25
3,3-Dimethoxycholest-5-ene	2.23	3.12_5	3.04_5	—	—	5.25
3α-Ethoxy-3β-methoxycholest-5-ene	2.25	—	3.05_5	3.44	—	5.25
3β-Ethoxy-3α-methoxycholest-5-ene	2.25	3.15	—	—	3.33	5.25

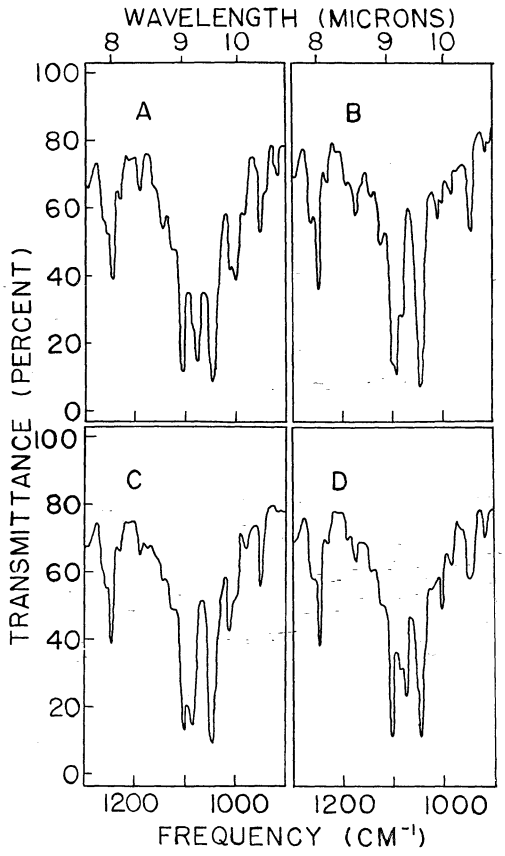

FIG. 2. The infrared spectra of (A) 3,3-diethoxycholest-5-ene; (B) 3,3-dimethoxycholest-5-ene; (C) 3α-ethoxy-3β-methoxycholest-5-ene; (D) 3β-ethoxy-3α-methoxycholest-5-ene.

(III), $C_{30}H_{52}O_2$, m.p. 105–106°, was obtained. The infrared spectrum (Fig. 2) showed strong absorption in the ether region and the n.m.r. spectrum showed the presence of one methoxy group, a singlet, and of one ethoxy group, a quartet (Table I), as well as a vinyl proton. The C_4 methylene group of these ketals at 2.25 p.p.m. is easily recognized and consistent with the structural assignments.

Since 3,3-dimethoxycholest-5-ene gives two distinct, unsplit signals for the two methoxy groups, compound III is a 3-ethoxy-3-methoxycholest-5-ene, in which one ethoxy group has been exchanged specifically for one methoxy group.

Can. J. Chem. Downloaded from www.nrcresearchpress.com by 210.87.254.105 on 09/05/12
For personal use only.

It is a well-known fact (4, 5, 7) that in solvolytic reactions of the cholesteryl type, the Δ^5 double bond participates to give a homoallylic carbonium ion and that the incoming group attaches itself at the 3β position in a stereospecific manner. It hence seems reasonable to assume that in this exchange reaction, the Δ^5 double bond assists preferentially the departure of the 3β substituent and that the resulting dialkoxy compound is 3α-ethoxy-3β-methoxycholest-5-ene (III).

It was fortuitous that compound III was obtained in the pure state since a more detailed investigation of the exchange reaction of 3,3-diethoxy and 3,3-dimethoxycholest-5-ene in methanol and ethanol respectively revealed that the 3α-alkoxy group also exchanges. The rate of exchange of the 3β substituent is twice that of the 3α substituent.

In order to obtain some insight into the mechanism of the photolysis reaction, 3-methoxycholesta-3,5-diene (V) was photolyzed in absolute ethanol. The main product (VII) of the reaction, obtained in 60% yield, was isomeric with compound (III), obtained by the methanolysis of II. Nuclear magnetic resonance (Table I) showed the presence of one methoxy and one ethoxy groups. The chemical shifts of the methoxy and ethoxy groups coincide with one of the methoxy and ethoxy groups in VI and II. On silica gel, VII gave cholest-4-ene-3-one and cholest-5-ene-3-one. The compound is, hence, assigned the structure 3β-ethoxy-3α-methoxycholest-5-ene (VII).

When 3-ethoxycholesta-3,5-diene (I) was photolyzed in methanol, 3,3-dimethoxycholest-5-ene (VI) was obtained. Obviously, the solvolysis exchange reaction was rapid. However, when the reaction was repeated in the presence of a small amount of pyridine, 3α-ethoxy-3β-methoxycholest-5-ene (III) was obtained. The product was identical with the methanolysis product of 3,3-diethoxycholest-5-ene (II). The n.m.r. of the crude photolysis product revealed that the reaction was not completely stereospecific, but that 5–10% of the isomeric mixed ketal (VII) was present.

It should be noted that n.m.r. and infrared spectra were taken on all crude photolysis products, in order to ensure that no isomerizations occurred during chromatography and crystallization.

The n.m.r. and infrared spectra were very characteristic for photolysis products II, III, VI, and VII, and resulted in unambiguous identification (Table I and Fig. 2).

If the assignment of stereochemistry of the epimeric mixed ketals is correct, the chemical shifts of the 3α- and 3β-methoxy groups are 3.12_5 and 3.04 p.p.m. and of the 3α- and 3β-ethoxy groups are 3.40_5 and 3.33 p.p.m. respectively. The methoxy groups give signals which appear as singlets while the ethoxy groups give signals which appear as quartets.

All of these results are consistent with the intermediacy of the carbonium ion C, formed either directly by interaction of a photoexcited species with solvent, or indirectly by sequence A → B → C.

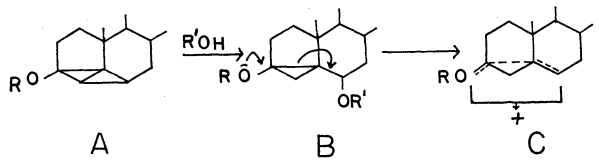

A similar sequence has been proposed some time ago by Dauben and Willey (8) to explain the photolysis of cholesta-3,5-diene (8, 9) in which an intermediate of type A (OR = H) was isolated. We were not able to isolate an intermediate of this nature, using the conditions described (8). In particular, the n.m.r. of the photolysis product (pentane, He atmosphere) did not show any peaks characteristic of alkoxy groups. Further work to determine the mechanism of the reaction is being carried out.

Can. J. Chem. Downloaded from www.nrcresearchpress.com by 210.87.254.105 on 09/05/12
For personal use only.

Can. J. Chem. Downloaded from www.nrcresearchpress.com by 210.87.254.105 on 09/05/12
For personal use only.

EXPERIMENTAL

The melting points were determined on a Kofler microscope hot-stage and are corrected. The analyses were carried out by Dr. C. Daesslé, Montreal. The infrared spectra were determined on a Perkin–Elmer 421 grating spectrophotometer using 1 millimeter sodium chloride cells and carbon disulphide as solvent. The ultraviolet absorptions spectra were measured by means of a Beckman recording spectrophotometer Model DK1. Nuclear magnetic resonance spectra were recorded on a Varian H.R. 60 instrument at 60 megacycles using carbon tetrachloride as solvent and tetramethylsilane (0 c.p.s.) as an internal standard. Optical rotations were performed with a Carl Zeiss automatic polarimeter using a 0.5-dm tube. All irradiations were performed with a Hanovia 450-watt lamp in a water-cooled immersion apparatus. Unless otherwise stated, Woelm alumina, activity II–III, was used for chromatography.

Irradiation of 3-Ethoxycholesta-3,5-diene (I) in Ethanol

A solution of 3.0 g of I, λ_{max}^{EtOH}, 239 mμ (ϵ 17,900), was irradiated until no absorption could be detected in the ultraviolet (1.5 hours). After evaporation, one-half of the crude material was chromatographed on silica gel (Davidson No. 923). Elution with hexane, hexane–benzene, and benzene–ether gave 0.5 g of crude cholest-5-ene-3-one (IV), m.p. 118–120°. Recrystallization from cyclohexane afforded 0.1 g of IV, m.p. 119–125°. The melting point was not depressed upon admixture of authentic IV (6*a*). The infrared spectra were superimposable.

The other half of the crude photolysis product was chromatographed on alumina. Elution with pentane gave crude 3,3-diethoxycholest-5-ene (II) in 60% yield. Several crystallizations from ethanol gave II, m.p. 49–50°, $[\alpha]_D$ −28.4° (*c*, 1.06 in chloroform). Calc. for $C_{31}H_{54}O_2$: C, 81.16; H, 11.87%. Found: C, 81.26; H, 11.96%.

Further elution with benzene gave 20% of cholest-4-en-3-one (VIII), m.p. 81–82° not depressed upon admixture of authentic (VIII). Infrared and ultraviolet spectroscopy further proved the identity of the two products.

Further elution with ether gave 25 mg of cholest-4-en-6β-ol-3-one (IX) (6*b*), m.p. 181–182°, λ_{max}^{EtOH}, 237 mμ (ϵ 12,800), ν_{CHCl_3} 3570 cm^{-1} (free O—H), 3380 cm^{-1} (hydrogen-bonded O—H), 1685 cm^{-1} (α,β-unsaturated ketone). The melting point was not depressed on admixture with authentic IX.

3,3-Diethoxycholest-5-ene (II) and 3,3-Dimethoxycholest-5-ene (VI)

Following the procedure described by Ueberwasser *et al.*, a solution of cholest-5-en-3-one (1.0 g) and 0.5 g of malonic acid in 60 ml absolute ethanol was stirred for 20 hours at 20–25°. The solution was worked up as described and the resulting oil chromatographed on alumina. Elution with pentane yielded 0.38 g of pure 3,3-diethoxycholest-5-ene (II), m.p. 48–49°, in 32% yield, identical (infrared, melting point, mixed melting point) with that obtained by photolysis.

Similarly, the reaction of cholest-5-en-3-one, 1.0 g, and 0.5 g of malonic acid in 60 ml of absolute methanol yielded 0.685 g of pure 3,3-dimethoxycholest-5-ene (VI), m.p. 96°, identical (infrared, melting point, and mixed melting point) with that obtained by photolysis.

3-Methoxycholesta-3,5-diene (V)

To cholest-4-en-3-one (10 g) and 10 ml of trimethylorthoformate in 50 ml of dioxane, was added two drops of concentrated sulphuric acid in 1.5 ml of dioxane and the mixture refluxed for 0.5 hours. Pyridine (0.25 ml) was then added and the solution evaporated to an oil which was covered with methanol and allowed to crystallize. Recrystallization from ether–methanol yielded 5.8 g of pure V, m.p. 67–68°, $[\alpha]_D$ −97.1 (*c*, 1.12 in pyridine), λ_{max}^{EtOH}, 239 mμ (ϵ 19,900). Calc. for $C_{28}H_{46}O$: C, 84.35; H, 11.63%. Found: C, 84.19; H, 11.97%.

Irradiation of 3-Methoxycholesta-3,5-diene (V) in Methanol

Irradiation of 0.5 g of V in 1800 ml of absolute methanol for 30 minutes yielded, after evaporation, 0.6 g of an oil. Chromatography on alumina and elution with pentane gave 200 mg of 3,3-dimethoxycholest-5-ene (VI), m.p. 93°. Recrystallization from acetonitrile–ether gave pure VI, m.p. 95.7–96.0°, $[\alpha]_D$ −35.5° (*c* 1.07 in chloroform), identical (infrared, melting point, and mixed melting point) with that described above. Calc. for $C_{29}H_{50}O_2$: C, 80.87; H, 11.70%. Found: C, 81.19; H, 11.82%.

Methanolysis of 3,3-Diethoxycholest-5-ene (II)

The crude irradiation product of 1.65 g of 3-ethoxycholesta-3,5-diene (I) in ethanol was chromatographed on alumina. The oily hexane eluate (0.90 g) was covered with methanol. After a few days, 0.36 g of 3α-ethoxy-3β-methoxycholest-5-ene (III), m.p. 88–91°, was obtained. Two recrystallizations from methanol raised the m.p. to 105–106°. Calc. for $C_{30}H_{52}O_2$: C, 81.02; H, 11.79%. Found: C, 80.70; H, 12.05%.

In a second run, 100 mg of pure 3,3-diethoxycholest-5-ene (II) was heated for 12 hours in methanol on a steam bath and the solvent allowed to evaporate. Crystallization of the reaction product from methanol gave 40 mg of III, m.p. 96–98°. The very characteristic infrared and n.m.r. spectra of the products, m.p. 96–98°, and m.p. 105–106°, were indistinguishable.

Cholest-4-en-3-one (VIII) from 3α-Ethoxy-3β-methoxycholest-5-ene (III)

When a 90-mg sample of III in carbon tetrachloride was taken to dryness on the steam bath, an oily

mixture was recovered. Chromatography on aluminum oxide and elution with hexane–benzene mixtures gave cholest-4-en-3-one (VIII), m.p. 81–82°. The melting point was not depressed on admixture of authentic (VIII). Comparison of the infrared spectra confirmed the identity of the two compounds.

Further elution with ether gave 25 mg of a crystalline material, which melted at 182–183° after recrystallization from hexane. The melting point was not depressed on admixture with the material obtained in the chromatogram of the photolysis product of I in ethanol and V in methanol.

Rate of Alcoholysis of the 3,3-Dialkoxycholest-5-enes

Ketals VI and II were heated under reflux with ethanol and methanol respectively. Aliquots were withdrawn periodically and their n.m.r. spectra recorded.

In the methanolysis of II the 3β-ethoxy group was replaced at a rate twice as fast as the 3α-ethoxy group. The 3β group was replaced after 10 hours, the 3α group after 20 hours.

When 3,3-diethoxycholest-5-ene in 55 ml of methanol plus two drops of pyridine was refluxed overnight, 3,3-dimethoxycholest-5-ene was obtained.

Irradiation of 3-Methoxycholesta-3,5-diene (V) in Absolute Ethanol

Irradiation of 2.0 g of V in 1800 ml of absolute ethanol for 3 hours gave 2.3 g of product, which, on chromatography on alumina, yielded 1.1 g of 3β-ethoxy-3α-methoxycholest-5-ene (VII). The n.m.r. spectrum of this material indicated the presence of some epimeric 3α-ethoxy-3β-methoxycholest-5-ene (III) in small amounts. Recrystallization from ethanol gave pure VII, m.p. 98–99°, $[\alpha]_D$ −32.3 (*c* 1.26 in chloroform). Calc. for $C_{30}H_{52}O_2$: C, 81.02; H, 11.79%. Found: C, 81.43; H, 12.07%.

Effect of Silica Gel on β,γ-Unsaturated Ketals

3β-Ethoxy-3α-methoxycholest-5-ene (70 mg) was chromatographed on 20 g of silica gel (Davidson No. 923). A mixture of cholest-4-en-3-one (VIII) and cholest-5-en-3-one (IV) was obtained as indicated by the infrared spectrum of the eluate, ν 1735 cm^{-1} (saturated ketone), 1690 cm^{-1} (α,β-unsaturated ketone).

Chromatography of pure cyclic diethylene ketal of cholest-5-ene-3-one (3) resulted in complete recovery of starting material.

Irradiation of 3-Ethoxycholesta-3,5-diene (I) in Methanol with Pyridine

Irradiation of 0.8 g of I in 1500 ml of methanol for 30 minutes and subsequent slow evaporation of the solvent resulted in the formation of 0.28 g of pure 3α-ethoxy-3β-methoxycholest-5-ene (III), m.p. 110–112°. Recrystallization from ether–methanol gave pure III, m.p. 112–113°, $[\alpha]_D$ −30.1 (*c* 1.13 in chloroform). The infrared and n.m.r. spectra further proved the identity of this material.

ACKNOWLEDGMENTS

We wish to thank the National Research Council and Bristol Laboratories for financial support and Dr. C. Stammer, Department of Chemistry, McGill University, for taking the n.m.r. spectra.

REFERENCES

1. E. Schwenk, G. Fleischer, and B. Whitman. J. Am. Chem. Soc. **60**, 1702 (1938).
2. H. Ueberwasser, K. Heusler, J. Kalvoda, C. Meystre, P. Wieland, G. Anner, and A. Wettstein. Helv. Chim. Acta, **34**, 344 (1963).
3. R. Antonucci, S. Bernstein, R. Littell, K. J. Sax, and J. H. Williams. J. Org. Chem. **17**, 1341 (1952).
4. W. Lwowski. Angew. Chem. **70**, 483 (1958).
5. M. Simonetta and S. Winstein. J. Am. Chem. Soc. **76**, 18 (1954).
6. L. F. Fieser and M. Fieser. Steroids. Reinhold Publishing Corp., New York, N.Y. 1959. (a) p. 50; (b) pp. 204–5.
7. J. H. Beynon, I. M. Heilbron, and F. S. Spring. J. Chem. Soc. 1459 (1937).
8. W. G. Dauben and F. G. Willey. Tetrahedron Letters, 893 (1962).
9. W. G. Dauben and J. A. Ross. J. Am. Chem. Soc. **81**, 6521 (1959).

Can. J. Chem. Downloaded from www.nrcresearchpress.com by 210.87.254.105 on 09/05/12
For personal use only.

INFRARED ABSORPTION OF SOLID PHOSPHINE

A. H. HARDIN AND K. B. HARVEY
Department of Chemistry, University of British Columbia, Vancouver, British Columbia
Received August 13, 1963

ABSTRACT

The infrared absorption of solid phosphine has been measured in the region of 4° K to 68° K. An hitherto unreported transition at about 10° K has been observed. Above this temperature the spectrum is characteristic of a disordered system; below 10° K the absorption arising from the symmetric vibrational modes exhibits a fine structure composed of sharp lines. The large number of lines attributed to ν_2 are interpreted as arising from inversion doubling, indicating a residual disorder in the system.

INTRODUCTION

The crystal structure of solid phosphine is as yet unknown but it has been shown that it undergoes a number of transitions at low temperatures (1). The present investigation was undertaken to study the changes in the infrared spectrum expected to accompany these transitions.

The data of Stephenson and Giauque (1) are summarized in Fig. 1, reproduced from

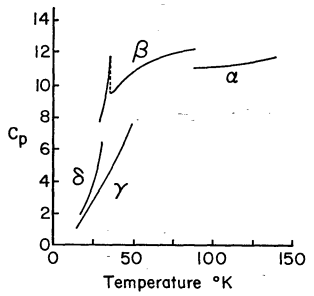

FIG. 1. Heat capacity of phosphine in cal/deg mole (from Stephenson and Giauque).

their paper. Three first-order transitions were observed at 30.29, 49.43, and 88.10° K and, in addition, they report a second-order transition in the region of 31–35° K. The transition from the α form to the β form (these designations are those of the present authors) at 88.10° K occurred rapidly and was readily observed. In contrast, the β to γ transition was an extremely slow one and Stephenson and Giauque found it necessary to hold the sample at 40° K for several days to obtain complete conversion. As a result, the β form could be readily supercooled to 30.29° K where a transition took place to the δ form. Stephenson and Giauque interpreted the heat capacity curves of the β and δ modifications as characteristic of the type associated with molecular rotation in the solid. Presumably the δ form is a disordered form of the γ phase.

The infrared spectrum of gaseous phosphine has been the subject of a number of investigations (2–6). McConaghie and Nielson (5) have partially analyzed the vibration–rotation spectrum in the region of the fundamentals and their structural data for the ground vibrational state are in good agreement with the microwave results (7, 8). The molecular parameters, as defined in Fig. 2, have the following values:

$$r = 1.42 \text{ Å}, h = 0.764 \text{ Å}, \alpha = 93°50', \text{ and } \beta = 57°30'.$$

Can. J. Chem. Downloaded from www.nrcresearchpress.com by 210.87.254.40 on 09/05/12
For personal use only.

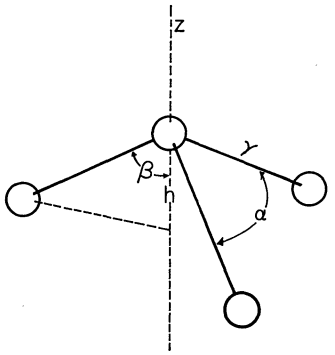

FIG. 2. Structural parameters of the PH_3 molecule.

The principal moments of inertia are

$$I_{xx} = 6.29\times10^{-40} \text{ g cm}^2 \text{ and } I_{zz} = 7.23\times10^{-40} \text{ g cm}^2,$$

so that phosphine is an oblate symmetric top.

It is also worth mentioning that no evidence has been obtained for inversion doubling in either the ground or first excited vibrational states of PH_3. This places upper limits on the splitting of 2×10^{-5} cm^{-1} in the ground state (8) and about 0.2 cm^{-1} for the first excited vibrational levels.

EXPERIMENTAL

The phosphine was prepared by adding PCl_3 dropwise to a vigorously stirred ethereal solution of $LiAlH_4$ under an inert atmosphere of nitrogen (9–11). A cold-finger at dry-ice temperature was used to prevent the ether from escaping the reaction vessel and the reaction products were trapped at 78° K. Separation of the PH_3 from P_2H_4, the other principle product, was accomplished by double distillation at 117° K (*n*-pentane slush) and the PH_3 produced was stored in the gaseous form. A slow reaction with stopcock grease was observed in the storage bulb, but this did not appear to introduce volatile impurities. As an added precaution, however, the phosphine was freshly distilled before each run. No impurities could be detected in the infrared spectrum of the gaseous phosphine. The latter was observed to explode on contact with air.

The low-temperature infrared absorption cell used in this work has been described previously (12). Temperatures intermediate between those attainable with liquid nitrogen and liquid helium were obtained by transferring quantities of helium just sufficient to maintain the desired temperature. It was found that the temperature of the copper block, in which the cesium iodide deposition plate is mounted, could be held to within ±3° K of the desired temperature by this method.

Spectroscopic measurements were carried out on a Perkin–Elmer 112G spectrometer with a modified source unit. Calibration was effected through established grating spectra and the reported frequencies are estimated to be accurate to within ±2 cm^{-1}. Spectral slit widths are indicated on the individual spectra.

RESULTS

The phosphine films investigated were deposited on the cesium iodide plate at about 65° K by admitting phosphine gas in short bursts. Spectra were recorded in the region of the fundamentals at a number of temperatures between 4° K and 65° K (approximately every 10 degrees), both while cooling and afterward during the warm-up. Several runs were made with deposits of different thicknesses and the results are summarized in Table I and Fig. 3. Attempts to deposit the PH_3 at temperatures above 88.10° K were unsuccessful because of the high vapor pressure of the solid so that we were unable to observe the spectrum of the α form. The high vapor pressure also limited the maximum annealing temperature to 65° K or 70° K.

At temperatures above 10° K the spectrum of each of the fundamentals consists of

Can. J. Chem. Downloaded from www.nrcresearchpress.com by 210.87.254.40 on 09/05/12
For personal use only.

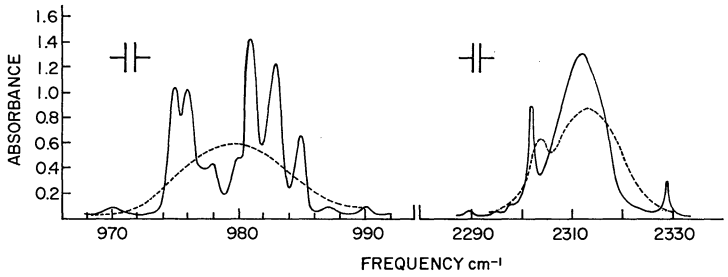

FIG. 3. Absorption spectrum of PH_3 in the 4.2 and 10.5 micron regions at 4° K (solid line) and 25° K (broken line).

TABLE I

Infrared absorption of phosphine (frequencies in cm^{-1})

Mode	Nielson, gas	This work		
		65° K	25° K	4° K
$\nu_1 a_1$	2322.9	2305 s	2304 s	2289 vw 2295 vw 2297 vw 2302 m 2329 w
$\nu_2 a_1$	992.0	981 s	979 s	970 vw 975 s 976 s 978 w 980 w 981 s 983 s 985 m 987 vw 990 vw
$\nu_3 e$	2327.7	2310 s	2314 s	2312 s
$\nu_4 e$	1122.4	1101 m	1097 m	1102 m

NOTE: s = strong, m = medium, w = weak, vw = very weak.

only a single absorption peak and, surprisingly, none of these peaks underwent any significant changes as the temperature was varied. It seems certain that under our conditions of deposition and rate of cooling we obtained the β form between 65° K and 30° K and the δ modification between 30° K and 10° K. Our results indicate therefore that no significant spectral changes accompany the first- and second-order transitions in this region.

On the other hand, the spectrum of the fundamental ν_2 underwent a marked change at about 10° K to give a series of 10, very sharp, closely spaced lines. The overlap of ν_1 and ν_3 introduces some confusion, but it seems likely that ν_1 also exhibits fine structure below 10° K, although not to the same extent as ν_2. Since the fine structure disappeared at 10° K on warm-up, it can be concluded that the transition producing these changes is a reversible one.

DISCUSSION

Assignments

The assignment of the absorption due to the symmetric bending mode ν_2 and the degenerate, asymmetric bending mode ν_4 is straightforward. Some confusion arises from

Can. J. Chem. Downloaded from www.nrcresearchpress.com by 210.87.254.40 on 09/05/12
For personal use only.

overlap of the other two fundamentals but, in the case of PH_3, intermolecular interactions in the solid would not be expected to result in a reversal of order of the frequencies of ν_1 and ν_3 so that we have assigned them in the same order as in the gas phase. At 4° K the problem is a more difficult one, but it is reasonable to assume that the fine structure in the 2300 cm^{-1} region is due to ν_1, which is of the same symmetry (a_1) as ν_2, the other mode giving rise to fine structure at this temperature. We have, therefore, assigned the single strong peak at 2312 cm^{-1} to ν_3. At the same time, the assumption that all of the remaining lines in this region are due to ν_1 must be treated with some reservation. Similarly, the strong absorption due to ν_3 may mask some of the ν_1 fine structure.

Frequency Shifts and Force Constants

All four fundamentals of phosphine shift downward in frequency as a result of condensation. This behavior is in contrast to that in crystalline ammonia (13) where the symmetric bending mode shifts upward in the crystal by over 100 cm^{-1}. It is unlikely therefore that hydrogen bonding, in the usual sense, plays any significant role in determining the crystal structure of phosphine. This conclusion is in agreement with the observed melting and boiling points of PH_3.

These relatively small downward shifts in crystalline PH_3 are reflected in the potential function, for internal vibrations. Assuming the coupling between the lattice vibrations and internal vibrations to be small, we may treat the internal problem separately and apply the same type of potential function as that used in the gas phase. We employed a simple valence–force potential function of the form

$$2V = k(\Delta r_1^2+\Delta r_2^2+\Delta r_3^2) + k_\delta(\Delta\alpha_1^2 +\Delta\alpha_2^2 +\Delta\alpha_3^2).$$

Since no corrections were made for anharmonicity, a more general potential function was unnecessary. The equations for the valence–force treatment of pyramidal XY_3 molecules have been derived by Lechner (14) and are tabulated by Herzberg (15). Since the frequencies of all four fundamentals are known in both the crystal and the gas it is possible to calculate two independent sets of values for k and k_δ in each case. Assuming the structural parameters to be the same as in the gas phase, the values listed in Table II are obtained.

TABLE II

Valence force constants for PH_3 (in units of 10^{-5} dynes/cm)

	From ν_1 and ν_2		From ν_3 and ν_4	
Gas	3.11	0.295	3.08	0.367
4° K	3.06	0.288	3.04	0.350

In view of the approximations involved, the agreement between the independent pairs of values is reasonable. At any rate there is little doubt that the stretching force constant k is about 1% smaller in the crystal as a result of crystal field perturbations, while the bending constant k_δ is about 3.5% smaller. In the case of ammonia the bending force constant was estimated by Hornig (13) to be about 5% larger in the crystal so that again we are led to the conclusion that hydrogen bonding is absent in crystalline PH_3.

Crystal Structure and the 10° K Transition

At temperatures above 10° K the lines assigned to ν_1, ν_2, ν_3, and ν_4 have band widths of approximately 7, 8, 15, and 17 cm^{-1} respectively; all far in excess of the spectral slit

Can. J. Chem. Downloaded from www.nrcresearchpress.com by 210.87.254.40 on 09/05/12
For personal use only.

width of the instrument. By absolute standards, these lines are not excessively broad for crystal spectra but the line widths are certainly far larger than the approximately 1 cm^{-1} line widths of the fine structure below 10° K. The latter are, in fact, of the same order as the resolution of the spectrometer.

We are led to conclude, then, that there is some degree of disorder in the β and δ forms right down to 10° K. This conclusion is in accord with the data of Stephenson and Giauque but it is surprising that no spectral changes accompany the transitions in the 30 to 35° K region. Furthermore, if as the calorimetric work indicated, the PH_3 molecules are executing rotational motion in the β and δ phases, a narrowing of the absorption peak would be expected as the temperature was lowered. We have been unable to detect any change in band width to confirm this. Such an effect might be masked, however, by the broadening due to additional disorder.

The transition at 10° K and the spectrum of the low temperature phase exhibit some interesting features. Since the transition is a reversible one and the β form is obtained on warming, the crystalline modification we observed at 4° K must also be metastable with respect to the γ form. Some degree of disorder might be expected then, even at 4° K. This is in accord with the broadness of the ν_3 and ν_4 absorption peaks (about 15 cm^{-1}) in the 4° K spectrum. On the other hand, the sharpness of the lines in the fine structure of the absorption due to ν_1 and ν_2 would indicate an ordered structure.

Apart from their sharpness, one must also account for the large number of lines in the ν_2 absorption band. Under a factor or unit cell group analysis, the number of absorption peaks arising from a single non-degenerate, internal vibrational mode may have a maximum value equal to the number of molecules in the unit cell. It is unlikely, however, that there are as many as 10 molecules in the unit cell of phosphine. A figure of two, four, or six seems more reasonable. Noting, in addition, that in the absorption assigned to ν_2 there are about twice as many components as there are in the ν_1 fine structure, one infers that some effect is giving rise to a doubling in the case of ν_2.

The effect observed is, in fact, consistent with inversion-doubling arising from the two equilibrium positions of the PH_3 molecule. In gaseous ammonia, for example, a splitting of some 35 cm^{-1} is observed for the $v_2 = 1$ level and 1 cm^{-1} for the $v_1 = 1$ level. On the other hand, the inversion doubling in gaseous phosphine is too small to be measured. It is clear, however, that the height of the barrier to inversion will be related to the magnitude of the bending force constant so that an increase in k_δ will decrease the magnitude of the splitting. This is observed in crystalline ammonia where the doubling is too small to be observed. In the case of phosphine, however, k_δ decreases on condensation so that the barrier to inversion will be lower than in the gas phase.

It is difficult to assign a specific value to the magnitude of the doubling in crystalline PH_3. On the basis of the two strong doublets (975, 976 cm^{-1} and 981, 983 cm^{-1}) the 10 peaks of the ν_2 absorption can be divided in two ways to give two sets of five lines differing by about 2 cm^{-1} or 6 cm^{-1}. Without single crystal spectra there is no criterion to decide which of these values is correct but the smaller one seems more reasonable. The ν_1 fine structure is of little value for comparison because of the overlap with ν_3.

ACKNOWLEDGMENTS

The authors are indebted to Mr. Rudolf Muehlchen for his assistance in the construction and maintenance of the apparatus. We wish also to acknowledge the financial assistance of the National Research Council of Canada and the University of British Columbia in carrying out this work.

Can. J. Chem. Downloaded from www.nrcresearchpress.com by 210.87.254.40 on 09/05/12
For personal use only.

RÉSUMÉ

On a mesuré l'absorption infrarouge de la phosphine crystalline entre 4° K et 68° K. Une nouvelle transition dans la région de 10° K a été observée. Aux températures plus élevées que 10° K, le spectre est caractéristique d'une système désordonnée; au-dessous de 10° K, l'absorption des vibrations symétriques a une structure composée de plusieurs lignes étraites. Dans le cas de ν_2 la multiplicité des lignes a été interprétée comme le résultat de deux positions d'équilibre occasionnées par l'inversion.

REFERENCES

1. C. C. Stephenson and W. F. Giauque. J. Chem. Phys. **5**, 149 (1937).
2. L. W. Fung and E. F. Barker. Phys. Rev. **45**, 238 (1934).
3. J. B. Howard. J. Chem. Phys. **3**, 207 (1935).
4. E. Lee and C. K. Wu. Trans. Faraday Soc. **35**, 1366 (1939).
5. V. M. McConaghie and H. H. Nielson. J. Chem. Phys. **21**, 1836 (1953).
6. D. C. McKean and P. N. Schatz. J. Chem. Phys. **24**, 316 (1956).
7. C. C. Loomis and M. W. P. Strandberg. Phys. Rev. **81**, 798 (1951).
8. M. H. Sirvetz and R. E. Weston. J. Chem. Phys. **21**, 898 (1953).
9. A. E. Finholt, A. C. Bond, and H. I. Schlesinger. J. Am. Chem. Soc. **69**, 1199 (47).
10. A. E. Finholt, A. C. Bond, K. E. Wilzbach, and H. I. Schlesinger. J. Am. Chem. Soc. **69**, 2692 (47).
11. E. Wiberg and G. Muller-Schiedmayer. Chem. Ber. **92**, 2372 (1959).
12. K. B. Harvey and J. F. Ogilvie. Can. J. Chem. **40**, 85 (1962).
13. F. P. Reding and D. F. Hornig. J. Chem. Phys. **19**, 594 (1951).
14. F. Lechner. Wien. Ber. **141**, 633 (1932).
15. G. Herzberg. Infrared and Raman spectra of polyatomic molecules. Van Nostrand, New York. 1945.

Can. J. Chem. Downloaded from www.nrcresearchpress.com by 210.87.254.40 on 09/05/12
For personal use only.

STEADY-STATE THEORY OF ADSORPTION PSEUDOCAPACITANCE IN ELECTROCHEMICAL RADICAL–ION REACTIONS

B. E. CONWAY AND E. GILEADI[1]
Department of Chemistry, University of Ottawa, Ottawa, Canada
Received July 24, 1963

ABSTRACT

The theory of adsorption pseudocapacity behavior is developed for a sequence of electrochemical reactions involving an ion discharge step which produces an adsorbed radical, followed by an "ion–atom" recombination reaction with or without desorption of the product of this step. The adsorption pseudocapacity behavior is deduced analytically particularly for the steady-state case and distinguished from the results obtained for assumed quasi-equilibrium in the ion discharge step when the succeeding step is rate-controlling. The effect of variation of the relative values of the rate constants of the discharge and of succeeding steps is investigated. It is shown that the capacity-potential behavior is sensitively dependent on the ratio of these rate constants, particularly for the case of adsorption isotherms involving a large value for the "heterogeneity parameter", r, defining the variation of energy of adsorption of the intermediates with coverage. Under the latter conditions, limiting coverages of the electrode by the adsorbed species are reached with increasing potential, depending on the relative values of the rate constants and the value of r.

1. INTRODUCTION

Most electrochemical reactions not involving simple metal–ion redox reactions proceed by two or more consecutive steps. Under these circumstances, adsorbed intermediates are involved, the surface concentrations of which are usually potential dependent. Since Faradaic charge is involved in the formation of the layer of intermediates, the potential dependence of the coverage leads to an adsorption pseudocapacitance (1, 2).[2] The importance of studies of charging curves was already recognized by Bowden and Rideal (3) with regard to the ionic double-layer and the method was developed by Slygin and Frumkin (4–6) for the study of H atom adsorption in the hydrogen evolution reaction; at about the same time, Butler and Drever (7) used this method for the study of oxide films and Pearson and Butler (8) examined electrochemical hydrogen adsorption at the platinum metals by means of charging curves. Studies of charging curves and the corresponding adsorption pseudocapacitance can provide an important method, complementary to direct kinetic current–potential studies, for elucidation of electrode reaction mechanisms. Much contemporary interest in electrochemical kinetics centers around the study of charging curves and the measurement of electrode capacitance, but further work is required in the interpretation of such data.

In a previously published paper (9), we have shown how studies of the dependence of adsorption pseudocapacitance upon potential can lead to information on the type of isotherm governing the adsorption of reaction intermediates, and to information about the potential dependence of coverage by such intermediates in two or multistep electrochemical reactions. In another paper (10), we have shown how these theoretical considerations can be applied to the elucidation of the adsorption behavior of intermediates involved in electrochemical decarboxylation reactions reported elsewhere (11–13).

[1]*Present address: John Harrison Laboratory, University of Pennsylvania, Philadelphia.*

[2]*The term pseudo-capacitance was introduced by Grahame (1) to distinguish the capacitance arising from adsorption of intermediates (and diffusion effects) from the strictly "non-Faradaic" capacitance associated with the dependence of ionic and electron charge in the double-layer on potential. In the present case, the capacitance arises from a Faradaic discharge process across the ionic double-layer producing an adsorbed radical intermediate, the surface concentration of which varies with potential.*

Can. J. Chem. Downloaded from www.nrcresearchpress.com by 210.87.254.42 on 09/05/12
For personal use only.

Examples of reactions in which the desorption step is electrochemical (in distinction to heterogeneous chemical radical recombination or disproportionation) are the hydrogen evolution reaction under certain conditions and the formate decarboxylation reaction (11). The kinetic sequence of steps in these reactions may be written:

$$H_3O^+ + M + e \xrightarrow{k_1} MH^\cdot + H_2O + e \qquad I$$

followed by

$$MH^\cdot + H_3O^+ + e \xrightarrow{k_2} H_2 + H_2O + M, \qquad II$$

and in the anodic decarboxylation of formate ions

$$HCOO^- + M \xrightarrow{k_3} MHCOO^\cdot + e \qquad III$$

followed by

$$MHCOO^\cdot \xrightarrow{k_4} M + CO_2 + H^+ + e. \qquad IV$$

Analogous steps to I and II occur in the oxygen evolution reaction (9). Evidence has been given that the pathway I and II is the mechanism of the hydrogen evolution reaction from aqueous acids at a number of transition metals (14–17), while III–IV is the mechanism of formate decarboxylation at high anodic potentials (10–13). In the above reactions, the pseudocapacitance is associated with H$^\cdot$ adsorption in I–II and with HCOO$^\cdot$ adsorption in III–IV (10). We have chosen to examine the "radical-ion"[3] type of reaction sequence since this is the only one for which explicit steady-state analytical expressions can be obtained for the capacitance behavior.

The basis of previous calculations on adsorption pseudocapacitance (2, 9) has been the assumption of effective, or quasi-equilibrium, in an ion-discharge step in a sequence of electrochemical reactions, for which the following step was a rate-determining desorption or rearrangement process. The quasi-equilibrium assumption is the one often made in the kinetics of consecutive reactions, e.g. for certain solvolytic reactions in solution. Provided that one step is "rate-determining", it is usually not very important in homogeneous chemical reactions to what extent the equilibrium is disturbed in the pre-rate-determining step(s), and usually the extent of the disturbance of this equilibrium cannot be directly known unless independent knowledge of the rate constants of the individual steps is available. We shall show that in consecutive *electrochemical* reactions, the behavior of the adsorbed intermediates, as reflected in the potential-dependence of the pseudocapacitance, can be a sensitive measure of the extent of departure from equilibrium in the step prior to the rate-determining one. These conclusions will also affect the interpretation of the pseudocapacitance behavior in terms of the adsorption isotherm.

So long as effectively complete equilibrium in the ion discharge steps I or III is maintained, the pseudocapacitance can be directly calculated from the following abbreviated kinetic equations of the type given previously (9, 18):

$$[1] \qquad v_1 = k_1(1-\theta)C_{H^+} \exp\,[-\beta VF/RT] \exp\,-[\alpha r\theta/RT]$$

and

$$[2] \qquad v_{-1} = k_{-1}\,\theta \exp\,[(1-\beta)\,VF/RT] \exp\,[(1-\alpha)r\theta/RT]$$

for step I (or analogously for step III), where θ is the fractional surface coverage by the adsorbed intermediate, C_{H^+} is the reactant (H^+) ion concentration in the double layer,

[3]*The term is used here in a general sense similar to that of the term "atom-ion reaction" suggested by Parsons (18) for step II.*

Can. J. Chem. Downloaded from www.nrcresearchpress.com by 210.87.254.42 on 09/05/12
For personal use only.

V is the metal-solution potential difference, r the parameter defining the extent of linear (18–20) variation of the energy of adsorption with coverage (see footnote [4]) in a Temkin type of isotherm, and α and β are symmetry factors, where $\alpha = 1-\beta$. When double-layer ion distribution effects (21) are maintained constant, and for convenience at unit C_{H^+}, equations [1] and [2] give

$$-\frac{k'}{C} = \frac{dV}{d\theta} = \frac{RT}{F}\frac{d\ln[\theta/(1-\theta)]}{d\theta} + r/F \qquad [4a]$$

or

$$C = \frac{k'F}{RT}\frac{\theta(1-\theta)}{1+(r/RT)\theta(1-\theta)} \qquad [4b]$$

where k' is a geometrical and electrical constant giving the charge required to form a complete monolayer of adsorbed species. It must be emphasized that equation [4*a*] (or [4*b*]), which we have deduced previously (9), is an equilibrium equation for the general case of coverage-dependent energy of adsorption analogous to that deduced for *Langmuir* conditions (viz. $r = 0$) by Bockris and Kita (22) in their analysis of transients in metal deposition processes.

For the purposes of defining a rate-determining step in a sequence of reactions, it is usually sufficient that the rate constant for whatever step is rate-controlling is at least some 10 times smaller than that for other steps. In the cases considered above for rate-controlling desorption steps, this implies that steps I or III will have to be in quasi-equilibrium. For the purposes of purely kinetic studies (e.g. of the current–potential behavior), it will not be very important exactly to what extent these steps are in equilibrium provided the condition mentioned above regarding the relative values of k_1 and k_2, or k_3 and k_4 is satisfied.

It is the purpose of the theoretical calculations presented below, to show that the pseudocapacitance and coverage behavior is very sensitive to the relative values of the rate constants for the initial ion discharge and the subsequent electrochemical desorption steps. It will also be shown that the pseudocapacitance must preferably be derived from a *steady-state* equation relating θ to V rather than from a quasi-equilibrium type of equation which can normally be used as a satisfactory limiting approximation only in the analysis (e.g. see Bockris, ref. 23) of the kinetics of consecutive electrochemical reactions in terms of the Tafel slopes for the steady current–potential behavior.

2. NON-EQUILIBRIUM PSEUDOCAPACITY BEHAVIOR

(a) Introduction

We now consider the form of the C–V relationship in a case for which the assumption of quasi-equilibrium in the pre-rate-determining discharge step discussed above is no longer valid. We recall that when the standard free energy of activation of a given step in a consecutive reaction sequence is much larger than that of any other step, i.e. its specific rate constant is much smaller, the rate of the overall reaction will be governed by the rate constant for the slowest step, and all other steps prior to the rate-controlling step will effectively be in equilibrium. The fundamental requirement for the applicability of the quasi-equilibrium assumption in kinetics is, hence, that a rate-determining step will, unambiguously, exist. The rates of electrochemical reactions may, in general, depend on potential in different ways, so that, as the potential is changed, conditions may change from those where the quasi-equilibrium assumption is applicable to those where it is not.

For the purpose of discussing the kinetics of electrode reactions, we can usually assume

Can. J. Chem. Downloaded from www.nrcresearchpress.com by 210.87.254.42 on 09/05/12
For personal use only.

that a definite rate-determining step exists over a particular range of potentials studied, since (*a*) a relatively small difference in the standard free energies of activation of the various steps will generally be sufficient to make one of them rate-determining (thus if $\Delta G^{0\neq}$ for one step is 2.8 kcal mole^{-1} larger than that for another at the same metal-solution potential difference, the ratio of specific rate constants will be 10^2 at 25° C), and (*b*) the electrochemical rate constants for different steps will usually depend on potential to different extents (i.e., the Tafel slopes associated with these steps will be different) and the region of potential over which two steps can have comparable rates is strictly limited, as shown by Parsons (24). The arguments of Parsons apply, however, only to limiting Langmuir conditions, and we have shown elsewhere (9) that when a Temkin type of isotherm is applicable, several mechanisms may correspond to the same Tafel slope, i.e. the rates of different steps may vary with potential in the same way. Moreover, we shall show below that, while for the purpose of discussing electrode kinetics, a step may be considered rate-determining if its rate constant is, say, one or two orders of magnitude smaller than that for any other consecutive step, the ideal symmetrical shape of the C–V curve (9) may not be observed under certain circumstances (in particular when the heat of adsorption[4] varies excessively with coverage, i.e. $r/RT \gg 1$) unless the rate constant of the rate-determining step is *5 to 10 orders of magnitude* smaller than that for any other consecutive step in the given reaction sequence.

We shall proceed below to discuss a general anodic reaction sequence[5] such as III and IV occurring through an initial discharge step followed by a rate-controlling electrochemical desorption or an electrochemical recombination step, with a possible final desorption step which tends to be very fast, and not at equilibrium with respect to its products. The form of the dependence of pseudocapacity and coverage on potential will be evaluated first by means of a steady-state calculation (for non-equilibrium in the discharge step) assuming limiting Langmuir conditions for the adsorption of the intermediates and then using a general adsorption isotherm (including both Temkin and Langmuir terms), for various ratios of the specific rate constants of the initial discharge step and the following electrochemical desorption step. It is clear that a somewhat different set of equations will be obtained if a different sequence of consecutive electrochemical steps is considered.[6] Our *method* of treating the problem, as given below, will, however, be applicable in general. The present case serves both to exemplify this method and to demonstrate the much more limited applicability of the quasi-equilibrium assumption when calculations of C and θ, and their dependence on potential, are considered, than when the kinetics of the reaction steps themselves are considered.

(b) Limiting Langmuir Conditions (Non-equilibrium in the Discharge Step)

We consider the following general sequence of anodic reactions:

Ion discharge

$$\mathrm{M} + \mathrm{A}^- \underset{k_{-5}}{\overset{k_5}{\rightleftarrows}} \mathrm{MA} + \mathrm{e} \qquad \mathrm{V}$$

[4]*The variation of heat of adsorption and apparent standard free energy of adsorption with coverage has been discussed previously (9, 25) and it was assumed by Parsons (18) that the variation of these two quantities with coverage was the same; in the latter paper, however, the "free energy of adsorption" was regarded as varying with coverage, but it is clear that neither the free energy of adsorption (which is zero at equilibrium) nor the standard free energy of adsorption (which is a constant) can vary with coverage. It is, in fact, an apparent standard free energy of adsorption, calculated with respect to fractional surface coverages (rather than activities), which varies with coverage.*

[5]*While we have given I and II with III and IV as examples, the discussion henceforth will be a general one; the choice of an anodic reaction (such as III and IV) is purely for convenience in the mathematical development.*

[6]*In a forthcoming paper (30), it is intended to treat other reaction sequences. However, explicit analytical solutions for the relationship between the capacity and the potential cannot be obtained for these cases and digital computer calculations are required in order to obtain numerical solutions.*

Can. J. Chem. Downloaded from www.nrcresearchpress.com by 210.87.254.42 on 09/05/12
For personal use only.

Electrochemical radical-ion step

$$MA + A^- \xrightarrow{k_6} MB + e + C \qquad VI$$

Final desorption

$$2MB \xrightarrow{k_7} 2M + B_2 \qquad VII$$

We shall assume first that the rate constant for reaction VII is much greater than that for either of the previous steps, so that $\theta_B \ll \theta_A$ and $\theta_A \doteqdot \theta_T$, the total coverage by A and B, which we shall write for simplicity as θ. With this assumption, we can proceed to calculate the *steady-state* coverage by 'A' radicals, determined by the condition

$$d\theta_A/dt = 0.$$

The rates of the relevant reaction steps can be written in an abbreviated form as

[5] $$v_5 = k_5\,(1-\theta)\exp\,[\beta VF/RT] = a_5\,(1-\theta)$$

[6] $$v_{-5} = k_{-5}\,\theta\exp\,[-(1-\beta)\,VF/RT] = a_{-5}\,\theta$$

[7] $$v_6 = k_6\,\theta\exp\,[\beta VF/RT] = a_6\,\theta$$

where k_5, k_{-5}, and k_6 are the specific rate constants; the equations have been written[7] for unit concentrations in the double-layer and for conditions under which the diffuse layer configuration is regarded as invariant. The terms a_5, a_{-5}, and a_6 are the corresponding electrochemical rate constants. We shall also define the Tafel slope parameter b as $2RT/F$ (assuming here that all symmetry factors are equal to 0.5).

The steady-state requirement leads to

[8] $$d\theta/dt = v_5 - v_{-5} - v_6 = 0$$

hence

[9] $$a_5(1-\theta) - a_{-5}\theta - a_6\theta = 0$$

or

[10] $$\theta = a_5/(a_5+a_{-5}+a_6).$$

Differentiating with respect to V gives

[11] $$\frac{d\theta}{dV} = \frac{(a_5+a_{-5}+a_6)a_5/b - (a_5-a_{-5}+a_6)a_5/b}{(a_5+a_{-5}+a_6)^2}$$

$$= \frac{2a_{-5}a_5/b}{(a_5+a_{-5}+a_6)^2}.$$

The Langmuir pseudocapacity (i.e. for $r = 0$) is hence given as

[12] $$C_L = k'(d\theta/dV) = k'\,\frac{2a_{-5}a_5/b}{(a_5+a_{-5}+a_6)^2}$$

where k' is the charge required to form a complete monolayer on the surface, as defined above. Substituting for the 'a' values from equations [5] to [7], gives

[7] *We consider only the forward directions of the rate-determining steps VI and VII, since the pseudocapacitance will be shown to vary over an appreciable range of polarizations, much greater than the approximately 30 mv potential range (from the reversible potential for the overall process $2A^- \leftrightarrows B_2 + 2e$) for which the back reactions of VI and VII can be significant in the kinetics. Thus we consider the pseudocapacitance in the regions of Tafel polarization behavior.*

Can. J. Chem. Downloaded from www.nrcresearchpress.com by 210.87.254.42 on 09/05/12
For personal use only.

[13] $$C_L = k' \frac{2k_5k_{-5}/b}{[k_5 \exp(V/b)+k_{-5}\exp(-V/b)+k_6\exp(V/b)]^2}.$$

The maximum in capacity will occur at a potential V_m where the condition $dC_L/dV = 0$ is satisfied, that is when,

[14] $$\frac{dC_L}{dV} = \frac{2k'k_5k_{-5}}{b}\cdot\frac{d}{dV}(a_5+a_{-5}+a_6)^{-2} = 0.$$

Hence, V_m must satisfy the equation

[15] $$a_5-a_{-5}+a_6 = 0$$

so that

[16] $$(k_5+k_6)\exp(V_m/b) = k_{-5}\exp(-V_m/b)$$

or

[17] $$\exp(2V_m/b) = k_{-5}/(k_5+k_6).$$

Equation [17] defines the potential[8] V_m at which C_L will reach its maximum value.

Combining equations [12], [15], and [16], we obtain

[18] $$C_{L(max)} = \frac{k'k_5}{2bk_{-5}}\exp[2V_m/b] = \frac{k'}{2b}\times\frac{k_5}{k_5+k_6}.$$

Substituting the value[9] of b into this equation, gives

[19] $$C_{L(max)} = \frac{k'F}{4RT}\times\left(\frac{k_5}{k_5+k_6}\right).$$

Equations [13] and [19] are the general expressions for the Langmuir adsorption pseudo-capacity and its maximum value when a single intermediate is adsorbed on the surface of the electrode. If step VI is rate-determining, and for the particular condition $k_5, k_{-5} \gg k_6$

[20] $$C_L = \frac{k'F}{RT}\cdot\frac{k_5/k_{-5}\exp(VF/RT)}{[1+(k_5/k_{-5})\exp(VF/RT)]^2}$$

which is the quasi-equilibrium result; the corresponding maximum value for C_L under these conditions, is (cf. ref. 22),

[21] $$C_{L(max)} = k'F/4RT.$$

The constant k' has been defined above as the charge associated with formation of a monolayer of adsorbed intermediates per unit real surface area. Taking the number of sites per square centimeter, for example, as 10^{15}, we obtain

$$k' = 1.6 \times 10^2 \text{ microcoulomb cm}^{-2};$$

and

$$C_{L(max)} = 1.6 \times 10^3 \ \mu\text{f cm}^{-2}.$$

[8]*The potential considered here, and in all the calculations, is expressed on an arbitrary scale dependent on the value of K_5, as discussed previously (9).*

[9]*In the above derivation we have assumed $\beta = 0.5$ and defined accordingly $b = 2RT/F$. The limiting results (equations [20] and [21]) do not depend on this assumption, since the symmetry factor β cancels out between terms in β and $(1-\beta)$. This must be so since θ, and consequently its derivative C_L, are quantities defined by (quasi)-equilibrium conditions considered for this limiting case and cannot therefore depend on the form of the energy barrier. However, the steady state expression for C_L will still depend on β, although for convenience we have assumed the usual value of $\beta = \frac{1}{2}$.*

Can. J. Chem. Downloaded from www.nrcresearchpress.com by 210.87.254.42 on 09/05/12
For personal use only.

The numerical value of k' obviously depends on both the size and "electrochemical valency" of the adsorbate, and the geometry of the adsorbent surface involved. We shall arbitrarily use the value given above for k' for our general calculations, since the discussion and conclusions do not depend on this value.

The coverage θ_m at which C_L reaches its maximum value is obtained by substituting equation [15] into equation [10] giving

$$\theta_m = \frac{a_5}{a_5+a_{-5}+a_6} = \frac{a_5}{2(a_5+a_6)} = \frac{1}{2}\left(\frac{k_5}{k_5+k_6}\right). \quad [22]$$

When step VI is rate-determining, with the particular condition $k_5 \gg k_6$, $\theta_m = 0.5$. The resulting expressions in terms of the steady-state assumption are thus reduced to those that would be obtained using the quasi-equilibrium assumption when $k_5 \gg k_6$ and v_5 can be almost equal to v_{-5}. This is to be expected since the above inequality applies when step VI is *unambiguously* rate-determining, and this is also the requirement for the applicability of the quasi-equilibrium assumption.

Equation [13] can be written for $\beta = 0.5$ as

$$C_L = \frac{k'F}{RT}\cdot\frac{(k_5/k_{-5})\exp(VF/RT)}{\left[1+\left(\frac{k_5+k_6}{k_{-5}}\right)\exp(VF/RT)\right]^2}. \quad [23]$$

For steady-state, rather than quasi-equilibrium conditions, the maximum in the C–V plot occurs at a potential given from the steady-state "Langmuir" equation [23] as

$$V_m = (RT/F)\ln[k_{-5}/(k_5+k_6)] \quad [24]$$

where the corresponding value of C_L is

$$C_{L(max)} = \frac{k'F}{4RT}\left(\frac{k_5}{k_5+k_6}\right). \quad [25]$$

We have used equation [23] to calculate C_L as a function of V taking three values for the rate constant ratio k_6/k_5, which determines the relative "extent" to which the discharge step is not in true equilibrium. Results of these calculations are shown in Fig. 1, taking the quasi-equilibrium constant $K_5 = k_5/k_{-5}$ as 10^{-2} (cf. previous calculations by Conway and Gileadi (9); choice of other values for K_5 only shifts the C–V profiles along the potential axis without changing their shapes). The quasi-equilibrium assumption obviously corresponds in the limiting case to $k_6/k_5 = 0$. As the latter ratio is increased, the pseudocapacities corresponding to each potential decrease, and the maximum is shifted towards less anodic potentials (or, in general, to lower values of the over-potential). The shapes of the curves remain, however, unchanged. This can be demonstrated by normalizing the curves in Fig. 1, so that they all have the same maximum (this is done by multiplying each capacity value by a factor $(k_5+k_6)/k_5$ and shifting the curves parallel to one another along the potential axis so that all maxima will occur arbitrarily at the same potential). The capacity curves normalized in this manner are then found to be identical. The coverage vs. potential relationships[10] corresponding to the pseudocapacitance behavior shown in Fig. 1, are illustrated in Fig. 2.

In the case when limiting Langmuir behavior is assumed to prevail, the conditions for a given step to be rate-controlling are similar to those required in the discussion of the

[10]*Experimentally, the coverage–potential relationship can be obtained by integration of the capacity-potential profile (10) or directly from charging or discharging transients (4, 5, 6, 11, 12).*

Can. J. Chem. Downloaded from www.nrcresearchpress.com by 210.87.254.42 on 09/05/12
For personal use only.

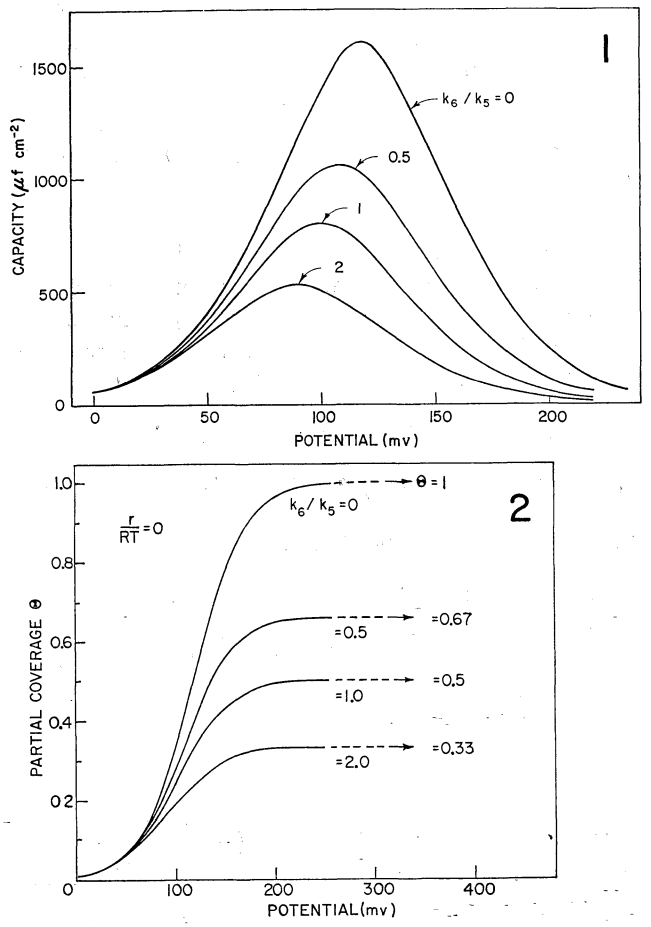

FIG. 1. Pseudocapacity–potential relationships calculated for Langmuir ($r = 0$) steady-state conditions for various values of the rate constant ratio k_6/k_5 equal to 0 (equilibrium case), 0.5, 1, and 2.

FIG. 2. Coverage–potential relations calculated for Langmuir ($r = 0$) steady-state conditions for various values of the rate constant ratio k_6/k_5 equal to 0 (equilibrium case), 0.5, 1, and 2. Note *limiting* coverages which are attained at high potentials.

electrode kinetics of the consecutive reactions involved. Thus when k_6/k_5 equals, say, 10^2 (which is a condition for the *discharge* step to be rate-determining),

$$C_{L(max)} = 0.01\ (k'F/4RT),$$

which is of the order of magnitude of the double-layer capacity, and, in addition, C_L will go from practically zero to its maximum and back to zero in a range of about 6 mv (cf. equation [24] and the argument above about the symmetrical form of the C–V curve for any value of k_6/k_5). Hence, when $k_6/k_5 = 10^2$ (as above), *no* significant pseudocapacity will be observed. Taking the other extreme case, when $k_6/k_5 = 10^{-2}$, $C_{L(max)}$ becomes equal to $0.99\ k'F/RT$ and the maximum occurs at a potential $V_m = 115$ mv if we take $k_{-5}/k_5 = 10^2$ (i.e., the equilibrium constant K_5 for the discharge step) as in our previous calculations (9). The maximum capacity thus obtained is 99% of the value deduced assuming complete quasi-equilibrium, and the potential range over which the

Can. J. Chem. Downloaded from www.nrcresearchpress.com by 210.87.254.42 on 09/05/12
For personal use only.

pseudocapacity is appreciable is only some 6 mV less than in the complete equilibrium case; thus, when $k_6/k_5 = 10^{-2}$, the quasi-equilibrium assumption may be considered valid for most practical purposes. It is important to emphasize, however, that these conclusions will apply only under limiting Langmuir conditions, as we now show below.

(c) A General Case (Combined Langmuir and Temkin Terms) for Non-equilibrium Conditions in the Discharge Step

(i) Pseudocapacitance Equations

We proceed now to calculate the total effective adsorption pseudocapacitance, using the steady-state treatment, i.e. without any limiting assumption regarding quasi-equilibrium but also now without any special assumption (Langmuir case) about the two-dimensional thermodynamic ideality of the ad-layer. We write the rate equations for reactions V and VI now as (see Conway and Gileadi (9), Parsons (18), and Thomas (26)):

$$[26] \qquad v_5 = k_5(1-\theta)\exp(-\alpha r\theta/RT)\exp(\beta VF/RT)$$

$$[27] \qquad v_{-5} = k_{-5}(\theta)\exp[(1-\alpha)r\theta/RT]\exp[-(1-\beta)VF/RT]$$

$$[28] \qquad v_6 = k_6\theta\exp[(1-\alpha)r\theta/RT]\exp(\beta VF/RT)$$

In the above equations, [26] to [28], the term r has the significance defined above introducing coverage-dependent terms arising in a dependence of energy of activation for the various steps upon coverage when a Temkin type of isotherm applies to the adsorption of the intermediates.

In the steady state $v_5 = v_{-5}+v_6$, hence

$$[29] \qquad k_5(1-\theta)\exp(-r\theta/2RT)\exp(VF/2RT) = k_{-5}\theta\exp(r\theta/2RT)\exp(-VF/2RT)+k_6\theta\exp(r\theta/2RT)\exp(VF/2RT)$$

where all symmetry factors have again been taken as equal to 0.5. Equation [29] can be rearranged to have the form

$$[30] \qquad k_5\left(\frac{1-\theta}{\theta}\right)\exp(-r\theta/RT) = \left[\frac{k_{-5}\exp(-VF/2RT)+k_6\exp(VF/2RT)}{\exp(VF/2RT)}\right] = k_6+k_{-5}\exp(-VF/RT).$$

Hence

$$[31] \qquad \left[k_5\left(\frac{1-\theta}{\theta}\right)\exp(-r\theta/RT)-k_6\right]/k_{-5} = \exp(-VF/RT)$$

and

$$[32] \qquad V = \frac{RT}{F}\ln\left[\frac{k_{-5}}{k_5\left(\frac{1-\theta}{\theta}\right)\exp(-r\theta/RT)-k_6}\right].$$

The total effective adsorption pseudocapacity can be obtained explicitly by differentiating the above equations; thus

$$[33] \qquad \frac{k'}{C} = \frac{dV}{d\theta} = -\frac{RT}{F}\frac{d}{d\theta}\ln\left[k_5\left(\frac{1-\theta}{\theta}\right)\exp(-r\theta/RT)-k_6\right]$$

or

Can. J. Chem. Downloaded from www.nrcresearchpress.com by 210.87.254.42 on 09/05/12
For personal use only.

$$[34] \qquad \frac{k'}{C} = \frac{(1-\theta)\theta r + RT}{F\theta^2} \times \frac{k_5 \exp(-r\theta/RT)}{\left[k_5\left(\frac{1-\theta}{\theta}\right)\exp(-r\theta/RT) - k_6\right]}$$

$$= \frac{(1-\theta)\theta r + RT}{F\theta^2} \times \frac{1}{[(1-\theta)/\theta] - (k_6/k_5)\exp(r\theta/RT)]}.$$

The total adsorption pseudocapacitance is hence related to the coverage in the most general case (subject only to the assumption that the apparent standard free energy of adsorption decreases linearly with coverage through the r terms) by the equation

$$[35] \qquad C = (k'F/RT)\left[\frac{\theta^2}{(1-\theta)\theta r/RT + 1}\right][(1-\theta)/\theta - (k_6/k_5)\exp(r\theta/RT)].$$

It is apparent that this equation has the correct form, since if we assume $k_6/k_5 = 0$, i.e. when the discharge step is, in the limiting case, at quasi-equilibrium, equation [34] becomes (see eq. [4*b*])

$$[4c] \qquad \frac{k'}{C} = \frac{r}{F} + \frac{RT}{F} \times \frac{1}{\theta(1-\theta)},$$

which is the expression obtained previously (9) using the quasi-equilibrium assumption and is equivalent to equation [4*a*] or [4*b*].

(ii) Attainment of Limiting Coverages

Frumkin (29) was the first to show that for the radical-ion type of mechanism in hydrogen evolution, a limiting coverage of H would be reached dependent on the relative values of the rate constants for the discharge and desorption steps but the pseudocapacitance was not investigated and the case was developed for implicit Langmuir conditions.

When $r = 0$ is substituted into equation [35] above,

$$[36] \qquad C_L = (k'F/RT)[(1-\theta)\theta - \theta^2 k_6/k_5].$$

The first term in the square bracket is the usual term obtained for the quasi-equilibrium assumption ($k_6/k_5 = 0$). When we take, for example, $k_6 = k_5$, the pseudocapacity becomes

$$[37] \qquad C_L = 2(k'F/RT)\,[(0.5-\theta)\theta],$$

which varies symmetrically with coverage between $\theta = 0$ and a *limiting* value of coverage $\theta = 0.5$ with $C_{L(max)} = k'F/8RT$, i.e. half the quasi-equilibrium maximum value. This result is to be expected since when $k_6 = k_5$ the coverage cannot rise above 0.5, and the value of $C_{L(max)}$ is exactly half the value obtained for the case when $k_6/k_5 = 0$ (quasi-equilibrium assumption). The limiting coverages attained under these conditions are shown in Fig. 2 for various values of k_6/k_5.

We may observe that equation [36] for the Langmuir pseudocapacitance C_L as a function of coverage is equivalent to equation [23], where C_L was expressed as a function of potential. While in the Langmuir case, the pseudocapacitance can be expressed as an explicit function of potential (equation [23]), we obtain it here as a special case of equation [35] in terms of coverage, since it is not possible in the general steady-state case to derive an equation analogous to [35] expressed explicitly in terms of potential; the same situation is encountered for the expression of the quasi-equilibrium pseudocapacitance as a function

Can. J. Chem. Downloaded from www.nrcresearchpress.com by 210.87.254.42 on 09/05/12
For personal use only.

of potential (9), where C as $f(V)$ must be calculated from an explicit $f(\theta)$ together with an equation giving θ as $f(V)$.

We presume that equation [35] relating the total effective adsorption pseudocapacity to coverage for the general case, applies only over the range of coverage where the resulting pseudocapacity is not negative, that is when

$$[38] \qquad (1-\theta)/\theta > k_6/k_5 \exp(r\theta/RT).$$

Hence, for the general case, the highest attainable coverage for given values of k_5/k_6 and r/RT is defined by the equation

$$[39] \qquad \theta/(1-\theta) \exp(r\theta/RT) = k_5/k_6.$$

The function on the left hand side of equation [39] is plotted in Fig. 3 against θ, for three

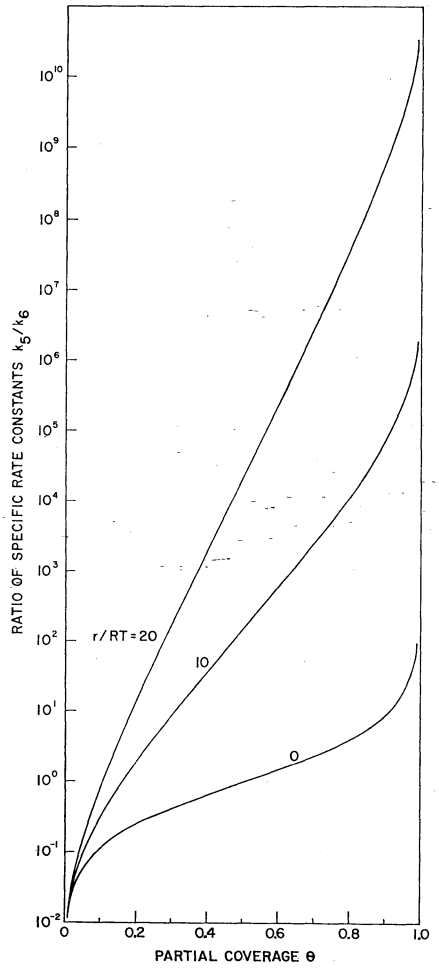

FIG. 3. The values of the ratio k_5/k_6 required for various limiting coverages to be attained at high potentials, calculated for three values of r/RT equal to 0 (Langmuir case), 10, and 20.

values of r/RT (0, 10, 20). The values of θ obtained from this graph constitute the various *limiting* coverages ($\theta < 1$) approached at high overpotentials for given values of the

Can. J. Chem. Downloaded from www.nrcresearchpress.com by 210.87.254.42 on 09/05/12
For personal use only.

parameters k_5, k_6, and r. As r/RT is increased, the ratio k_5/k_6 required for the limiting coverage to reach a given value increases rapidly, i.e. it becomes harder to realize a state of quasi-equilibrium (which obviously corresponds to a θ value approaching unity at sufficiently high overpotentials). Thus, for the limiting value of the coverage to be, for example, 0.9 with $r/RT = 20$ we require $k_5/k_6 = 6 \times 10^8$ corresponding to a difference of about 12 kcal mole^{-1} in the standard free energies of activation of the two consecutive steps. It must be recalled that these conclusions refer to the general type of mechanism shown in the scheme of reactions V, VI, and VII where an electrochemical "radical-ion" desorption step is rate-controlling.

(iii) Relation between Pseudocapacitance, Coverage, and Potential

We have used equation [35] to calculate the adsorption pseudocapacity for monovalent radicals as a function of coverage for different rate-constant ratios k_6/k_5 and two values of r/RT of 10 and 20. These results are shown in Figs. 4*a* and 4*b*. On the low coverage

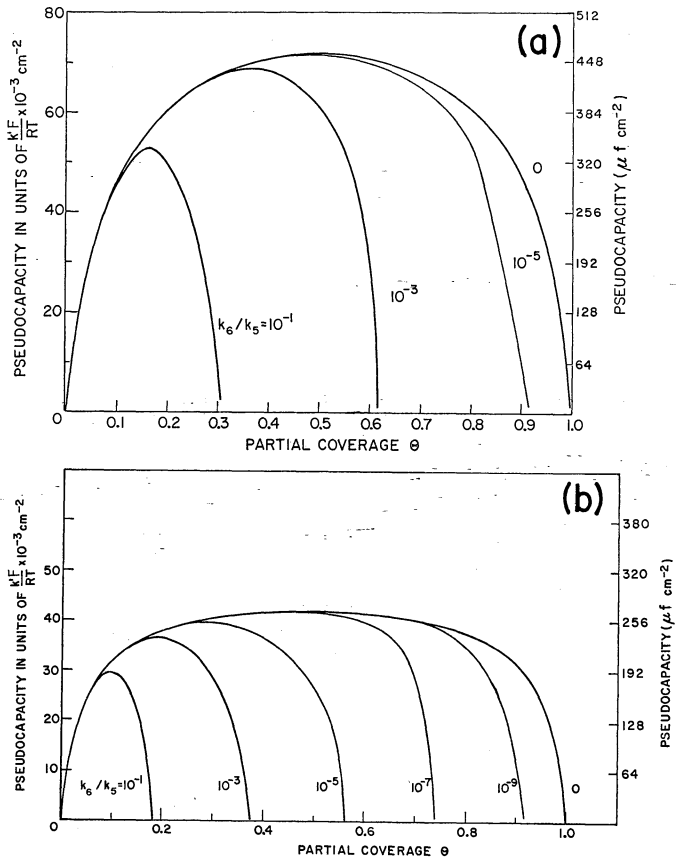

FIG. 4*a*. Adsorption pseudocapacitance as a function of coverage for various values of the rate constant ratio k_6/k_5 with $r/RT = 10$.

FIG. 4*b*. Adsorption pseudocapacitance as a function of coverage for various values of the rate constant ratio k_6/k_5 with $r/RT = 20$.

branch, the curves are almost identical with the one obtained for $k_6/k_5 = 0$ (the limiting quasi-equilibrium case), while on the high coverage side they deviate markedly from the quasi-equilibrium curve to an extent dependent on the values of r/RT and k_6/k_5.

Can. J. Chem. Downloaded from www.nrcresearchpress.com by 210.87.254.42 on 09/05/12
For personal use only.

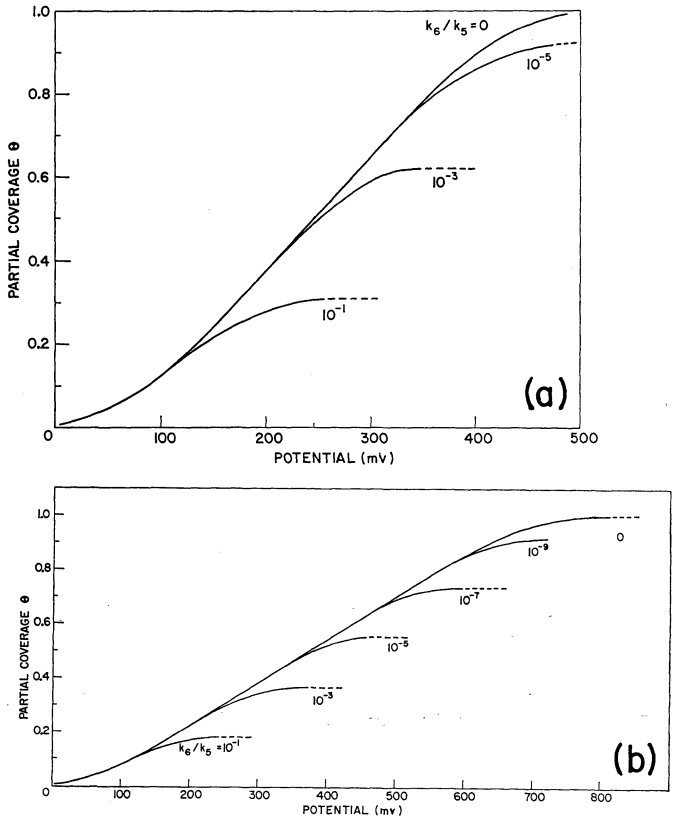

FIG. 5*a*. Coverage–potential relationships calculated for various values of the rate constant ratio k_6/k_5 with $r/RT = 10$ (compare Fig. 2).

FIG. 5*b*. Coverage–potential relationships calculated for various values of the rate constant ratio k_6/k_5 with $r/RT = 20$ (compare Fig. 2).

The corresponding variation of coverage with potential was calculated for the same values of r/RT and k_6/k_5, using equation [32], and is plotted in Figs. 5*a* and 5*b*. By combining equations [32] and [35], we can obtain numerically the dependence of pseudocapacity on potential, as shown in Figs. 6*a* and 6*b*. It is seen that for intermediate values of k_6/k_5, when this ratio is small enough for the discharge step to be considered practically at quasi-equilibrium for the purpose of discussing the kinetics of the reaction, the pseudocapacity will reach values comparable, but not identical, with those obtained for complete quasi-equilibrium for corresponding values of r, but the potential range over which the pseudocapacity will be appreciable will be greatly decreased.

It is clear from the above results, that while in many cases complete quasi-equilibrium may, without serious error, be assumed for the purpose of discussion of the current–potential behavior of the reactions considered, the relationship between the capacity and potential can, however, be quite different from that corresponding to quasi-equilibrium conditions, and is thus a more sensitive indication of the kinetic behavior in a sequence of consecutive reactions.

(d) Method of Application to Experimental Results

In a previous publication (10), we have proposed and applied a method by which the

Can. J. Chem. Downloaded from www.nrcresearchpress.com by 210.87.254.42 on 09/05/12
For personal use only.

Temkin parameter r and the roughness factor f of an electrode surface could be obtained from the shape of the experimental profile relating C to V. This calculation was carried out for the formate decomposition reaction assuming complete equilibrium in the initial formate ion discharge step but it is clear that such a procedure may be less applicable if k_6/k_5 were appreciably greater than zero, i.e. if the equilibrium in the initial ion discharge step were significantly disturbed. For the type of electrochemical reaction sequence considered here, a limiting coverage ($\theta < 1$) will be reached (equation [39]) and the pseudocapacity values will depend on k_6/k_5 as well as on r for given values of θ or V.

Experimental data can, in principle, be obtained for C from e.m.f. decay curves, from electronically differentiated charging curves (27), and from a.-c. impedance measurements (2). Corresponding coverage information can be obtained from charging curves and from integration of the $C-V$ relationship. At the present time, there are no data of sufficient precision to apply our calculations directly to experimental results for electrodes at which the mechanism considered here operates, although an atom–ion desorption mechanism is indicated in the hydrogen and oxygen evolution reactions at certain metals (14, 16, 17). However, we show below how the method may be applied to appropriate experimental results if information on surface coverage by intermediates and the associated pseudocapacity is available.

Apart from θ and V, three parameters are involved which determine C as $f(\theta, V)$, viz. r, f, and k_6/k_5. If the real surface area is known independently, e.g. from krypton B.E.T. adsorption measurements or from ionic double-layer capacity data, as used, for example, by Brodd and Hackerman (28), these deviations from quasi-equilibrium in the ion discharge step may be detected, and both r and k_6/k_5 can, in principle, be estimated, as shown below.

We consider the case of the atom-ion desorption type of mechanism for which both the relationship between C and V and the limiting coverage θ_{lim} could be obtained experimentally for an electrode, the surface area of which was known by the methods mentioned above. From the value of C at its maximum, $C_{\max}$, we can first estimate the value of the parameter r assuming, as a first approximation, that $k_6/k_5 = 0$ (cf. refs. 9 and 10). We note that the relationship in Fig. 6 indicates that $C_{\max}$, for a given value of r, will tend to decrease as k_6/k_5 increases, but this change of $C_{\max}$ does not become very large until k_6/k_5 is quite close to unity. Hence, the value obtained for r on the basis of the initial assumption that $k_6/k_5 = 0$ (equilibrium case) will tend to be too large[11] and would, in fact, constitute an upper limit for the estimate of r for the particular conditions involved.

In the light of the above discussion, it follows now that deviations from quasi-equilibrium conditions could be easily detected by considering the shape of the $C-V$ profile. Thus, we have shown previously (10) that the width ΔV_γ (in units of potential) of the $C-V$ profile at a value of $C = {}_\gamma C_{\max}$ (where γ is a fraction $0 < \gamma < 1$) is approximately linearly related to r when quasi-equilibrium conditions apply. We can use this relationship here to obtain an estimate of what would be the value of ΔV_γ (at, say, $\gamma = 0.5$) corresponding to the value of r estimated above from $C_{\max}$, if k_6/k_5 were, as a first approximation, zero. This quantity ΔV_γ could also be obtained experimentally from a $C-V$ profile; it is evident from Fig. 6 that ΔV_γ would be sensitively dependent on the kinetic parameter k_6/k_5 (much more so, for example, than the quantities $C_{\max}$ and the resulting r). Hence any departure from quasi-equilibrium conditions could readily be detected and

[11]*This conclusion follows from the fact, which we have discussed elsewhere (9), that C decreases with increasing r for a given value of θ or V in the equilibrium case. Some depression of C arises when* $k_6/k_5 \neq 0$ *and this would hence be counted as due to a higher apparent value of r.*

Can. J. Chem. Downloaded from www.nrcresearchpress.com by 210.87.254.42 on 09/05/12
For personal use only.

evaluated semiquantitatively by comparison of the experimentally determined ΔV_γ and that calculated from a value of r as estimated by the approximate procedure discussed above.

After the evaluation of r (or rather its upper limit), we can use equation [39] (cf. Fig. 3) to obtain k_6/k_5. Since the value of r used would be an upper limit, the corresponding calculated value for k_6/k_5 would be a lower limit.

A numerical example will help to clarify the use of the above procedure: let us consider the calculated profiles in Fig. 6*a* for $r/RT = 10$ and assume, for the purposes of this

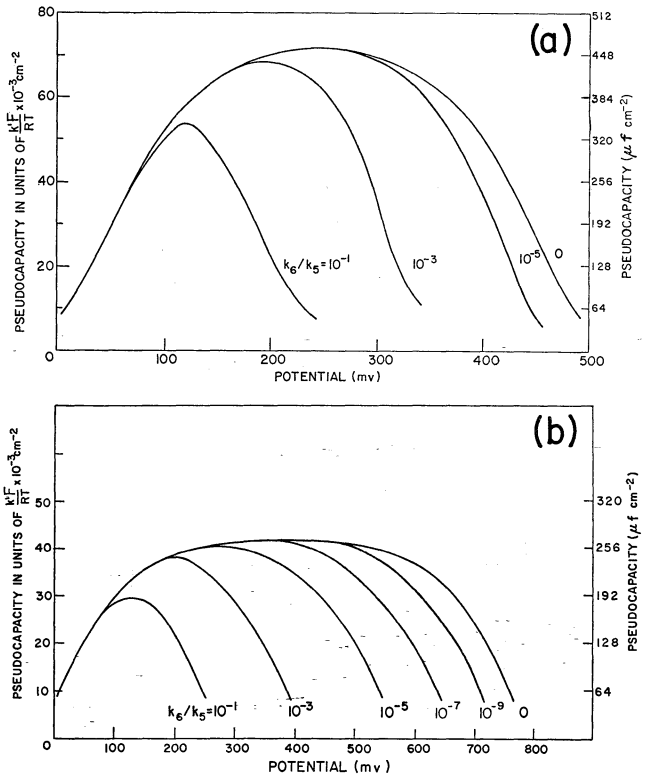

FIG. 6*a*. Adsorption pseudocapacitance as a function of potential for various values of the rate constant ratio k_6/k_5 with $r/RT = 10$.

FIG. 6*b*. Adsorption pseudocapacitance as a function of potential for various values of the rate constant ratio k_6/k_5 with $r/RT = 20$.

example, that a curve identical with that shown for $k_6/k_5 = 10^{-1}$ had been obtained experimentally. Assuming as the first approximation that $k_6/k_5 = 0$, a value of $r/RT = 15$ would be obtained. Using this value with the corresponding limiting coverage θ_{lim} (equation [35] and Fig. 3) which would arise with this mechanism, would give $k_6/k_5 = 2\times10^{-2}$. Also the experimental value of ΔV_γ ($\gamma = 0.5$) for this example would be approximately 0.12 v, while the theoretically expected value for $r/RT = 15$ and $k_6/k_5 = 0$ would be about 0.5 v; hence an appreciable deviation from quasi-equilibrium conditions would be directly evident.

A more accurate numerical evaluation of the parameters r and k_6/k_5 could be obtained from equations [35] and [39] if both $C_{\max}$ and θ_{lim} were experimentally available. Thus, in

Can. J. Chem. Downloaded from www.nrcresearchpress.com by 210.87.254.42 on 09/05/12
For personal use only.

equation [35] let C be equal to C_{max}, so that θ will be the value of the coverage at a potential corresponding to the maximum in the curve relating C to V (for example, obtained by integrating an experimental $C-V$ curve (10) up to that potential). With C and θ numerically known, equation [35] would have the two required parameters (r and k_6/k_5) as unknowns. Similarly, equation [39]—in which θ is the limiting coverage attained at high overpotentials —has the same two unknowns, so that r and k_6/k_5 could be evaluated numerically between these two equations, from experimental data for C_{max} and θ_{lim}.

(e) Conclusions

We may conclude that the adsorption pseudocapacity function appears to be much more sensitive to the various assumptions made in deriving the rate equations than the resulting overall current–potential behavior. Thus, while the pre-exponential terms in θ can be neglected (cf. 18, 26) with respect to the exponential terms when the $V - \ln i$ relationship is considered at intermediate coverage, this is hardly ever justified for the purpose of calculating the total effective adsorption pseudocapacitance.

Secondly, we observe that a step which, without serious error, could be considered *kinetically* at quasi-equilibrium, may nevertheless give rise to very different pseudocapacity behavior from that corresponding to complete equilibrium ($k_6/k_5 = 0$) in the primary discharge step when the steady-state treatment is applied. This effect is greater, the greater is the value of the parameter r defining the variation of energy of adsorption of the intermediate A (in reactions V and VI) with coverage.

Finally, we recall that the actual form of the variation of heat of adsorption with coverage (i.e. when the heat of adsorption is proportional to θ^n and $n \neq 1$) does not affect the observed kinetic parameters (as shown previously (9)), but qualitatively affects the form of the dependence of pseudocapacity and coverage on potential as shown elsewhere (10).

Can. J. Chem. Downloaded from www.nrcresearchpress.com by 210.87.254.42 on 09/05/12
For personal use only.

ACKNOWLEDGMENTS

Grateful acknowledgment is made to the Defence Research Board, Department of National Defence, for support of this work on Grant No. 5480–12. One of us (E. G.) acknowledges the award of an N.R.C. scholarship held during the execution of part of this work.

REFERENCES

1. D. C. GRAHAME. J. Electrochem. Soc. **99**, 370*C* (1952).
2. A. EUCKEN and B. WEBLUS. Z. Elektrochem. **55**, 114 (1951).
3. F. P. BOWDEN and E. K. RIDEAL. Proc. Roy. Soc. (London), Ser. A, **120**, 59, 80 (1928).
4. A. SLYGIN and A. N. FRUMKIN. Acta Physicochim. URSS, **3**, 791 (1935).
5. A. SLYGIN and A. N. FRUMKIN. Acta Physicochim. URSS, **4**, 991 (1936).
6. A. SLYGIN and A. N. FRUMKIN. Acta Physicochim. URSS, **5**, 819 (1936).
7. J. A. V. BUTLER and B. J. DREVER. Trans. Faraday Soc. **32**, 427 (1936).
8. J. O. PEARSON and J. A. V. BUTLER. Trans. Faraday Soc. **34**, 1163 (1938).
9. B. E. CONWAY and E. GILEADI. Trans. Faraday Soc. **58**, 2493 (1962).
10. B. E. CONWAY, E. GILEADI, and M. DZIECIUCH. Electrochim. Acta, **8**, 143 (1962).
11. B. E. CONWAY and M. DZIECIUCH. Can. J. Chem. **41**, 21 (1963).
12. B. E. CONWAY and M. DZIECIUCH. Can. J. Chem. **41**, 38 (1963).
13. B. E. CONWAY and M. DZIECIUCH. Can. J. Chem. **41**, 55 (1963).
14. J. P. HOARE and S. SCHULDINER. J. Phys. Chem. **62**, 229 (1958).
15. J. O'M. BOCKRIS and A. M. AZZAM. Trans. Faraday Soc. **48**, 145 (1952).
16. B. E. CONWAY and J. O'M. BOCKRIS. J. Chem. Phys. **26**, 533 (1957).
17. B. E. CONWAY and J. O'M. BOCKRIS. Can. J. Chem. **35**, 1124 (1957).
18. R. PARSONS. Trans. Faraday Soc. **54**, 1053 (1958).
19. M. BOUDART. J. Am. Chem. Soc. **74**, 3566 (1952).
20. M. I. TEMKIN. Zh. Fiz. Khim. **15**, 296 (1941).
21. A. N. FRUMKIN. Z. Phys. Chem. (Leipzig), A, **164**, 121 (1933).

22. J. O'M. BOCKRIS and H. KITA. J. Electrochem. Soc. **108**, 676 (1961).
23. J. O'M. BOCKRIS. Modern aspects of electrochemistry. Vol. I. Academic Press, New York. 1954. Chap. IV.
24. R. PARSONS. J. Chim. Phys. **49**, C82 (1952).
25. E. BLOMGREN and J. O'M. BOCKRIS. J. Phys. Chem. **63**, 1475 (1959).
26. J. G. N. THOMAS. Trans. Faraday Soc. **57**, 1603 (1961).
27. H. A. KOZLOWSKA and B. E. CONWAY. J. Electroanal. Chem. In press (1963).
28. J. BRODD and N. HACKERMAN. J. Electrochem. Soc. **104**, 704 (1957).
29. A. N. FRUMKIN. Acta Physicochim. URSS, **7**, 475 (1937).
30. E. GILEADI and B. E. CONWAY. J. Chem. Phys. In press (December, 1963).

Downloaded from www.nrcresearchpress.com by 210.87.254.42 on 09/05/12
For personal use only.

GUM JEOL: THE STRUCTURE OF THE DEGRADED GUM DERIVED FROM IT

A. K. Bhattacharyya and C. V. N. Rao
The Department of Macromolecules, Indian Association for the Cultivation of Science, Calcutta-32, India
Received May 15, 1963

ABSTRACT

Gum Jeol has been shown to be composed of residues of D-galactose, L-arabinose, and D-galacturonic acid. On mild acid hydrolysis the gum gave an aldobiouronic acid, viz. 3-*O*-(D-galactopyranosyl uronic acid)-D-galactopyranose. Hydrolysis of the fully methylated degraded gum yielded 2,3,4,6-tetra-(3 moles); 2,3,4-tri-(2 moles); 2,4-di-(1 mole); and 2-*O*-methyl-D-galactose (1 mole) in the neutral fraction of the hydrolyzate. The reduced acidic fraction yielded 2,3,4-tri-(2 moles) and 2,4-di-*O*-methyl-D-galactose (2 moles). Based on these results a partial structure of the degraded gum has been proposed, the additional evidence of which was deduced from periodate oxidation studies of the degraded gum.

Can. J. Chem. Downloaded from www.nrcresearchpress.com by 210.87.254.5 on 09/05/12
For personal use only.

The sample of the Jeol gum (*Odina wodier, Roxb*) investigated was obtained as an exudate from the plants commonly known in Bengal as "Jeol trees" (1, 2). The gum was investigated by Mukherjee *et al.* (3), who reported arabinose, galactose, and galacturonic acid as constituent units. An aldobiouronic acid has also been isolated and identified. In the present work a beginning has been made on a study of the detailed molecular architecture of the repeating unit of the degraded gum.

The gum examined had been purified by repeated precipitation by ethanol from an aqueous solution and alkaline solution was avoided to protect from deesterification. Even after taking this precaution the methoxyl content (0.51%) was found to be very low and was therefore not considered to have any structural significance. A purified sample of the gum had an equivalent weight, 1150 (by titration with alkali) and uronic anhydride (4) 14.5% (uronic anhydride content for a polysaccharide of equivalent weight 1150 should be 15.3%). The pentosan content (5) of the gum was 21.7%. On complete hydrolysis, the gum yielded L-arabinose and D-galactose in the neutral hydrolyzate; these were characterized by isolating the crystalline sugars. Hydrolysis and quantitative estimation (6) of the sugars showed them to be present as arabinose 19.5% and galactose 63.7%.

The gum was hydrolyzed under milder conditions (0.1 *N* sulphuric acid) and the acidic fraction was separated from the neutral one by ion exchange resin and was found to be a mixture. The aldobiouronic acid was isolated in a homogeneous state from the mixture. Methyl ester methyl glycoside of the aldobiouronic acid, on reduction with lithium aluminum hydride and subsequent hydrolysis, yielded galactose, showing that the aldobiouronic acid is composed of galactose and galacturonic acid residues. The structure of the aldobiouronic acid was finally established to be 3-*O*-(D-galactopyranosyl uronic acid)-D-galactopyranose, by methylation, reduction, and remethylation of the acid and subsequent identification of the methyl sugars, viz., 2,3,4,6-tetra-*O*-methyl-D-galactose and 2,4,6-tri-*O*-methyl-D-galactose, liberated on hydrolysis. The structure of the aldobiouronic acid obtained is in agreement with the one deduced by Mukherjee *et al.* (3).

As the natural gums are highly complex in their molecular architecture, these are generally degraded to relatively stable and smaller molecules, by removing some sugar residues connected by labile linkages, for structural investigation. Autohydrolysis is one of the convenient processes for such degradations.

Can. J. Chem. Downloaded from www.nrcresearchpress.com by 210.87.254.5 on 09/05/12
For personal use only.

In order to isolate the degraded gum, the gum was subjected to autohydrolysis, the course of which was followed by examining the supernatant liquid chromatographically. In the earlier stages of hydrolysis arabinose was detected, then arabinose and an oligosaccharide, and after 25 hours, galactose started appearing. The hydrolysis was stopped at this stage and the degraded gum was precipitated by pouring the solution into ethanol. The isolated degraded gum had $[\alpha]_D^{32}$ $-2°$, equivalent weight 920, and uronic anhydride 18.54% (corresponding to a calculated equivalent weight 950), and on hydrolysis yielded galactose and a trace of arabinose. The amount of anhydro galactose was estimated to be 76.5%. Jeolic acid (degraded gum) was converted to its fully methylated derivative by treatment with dimethylsulphate and alkali (7, 8) and methyl iodide and silver oxide (9) successively. The fully methylated polysaccharide was subjected to methanolysis under conditions known to effect no cleavage of aldobiouronic acid. The methyl ester was hydrolyzed with barium hydroxide solution (10) and the acidic fraction was separated from the neutral one by absorbing the former on Dowex-1-X4 anion exchange resin (11). The neutral glycosides were converted to the corresponding mixture of methyl sugars which were separated and identified as 2,3,4,6-tetra-*O*-methyl-D-galactose (3 moles), 2,3,4-tri-*O*-methyl-D-galactose (2 moles), 2,4-di-*O*-methyl-D-galactose (1 mole), and 2-*O*-methyl-D-galactose (1 mole). The acid portion was displaced from the resin column and was shown to be 3-*O*-(2,3,4-tri-*O*-methyl-D-galactopyranosyl uronic acid)-2,4-di-*O*-methyl-D-galactose (2 moles) since reduction (12, 13) of the methyl ester methyl glycoside and subsequent hydrolysis afforded two methyl sugars, viz., 2,3,4-tri-*O*-methyl-D-galactose and 2,4-di-*O*-methyl-D-galactose in an equimolecular proportion. The length of the repeating unit, which contains two uronic acid residues, is calculated to be 11 anhydro hexose units. From the above results a structure for the repeating unit of the degraded gum can be deduced.

Demonstration of the presence of only 2,3,4-tri-*O*-methyl-D-galactose in the trimethyl fraction indicates that the backbone chain is composed of $1 \rightarrow 6$ linked galactose residues. Some of the galactose residues in the main chain are linked through C_1, C_3, and C_6 and some through C_1, C_3, C_4, and C_6 as indicated by the presence of 2,4-di-*O*- and 2-*O*-methyl-D-galactose respectively in the neutral fraction of the hydrolyzate. It is evident that tetramethyl galactose originated from the non-reducing ends. The number of branch points (3) are equal to the number of non-reducing end groups (3), as required by the theory. Besides these considerations, the aldobiouronic acid (2 moles per repeating unit) is to be accommodated. From the structure of the aldobiouronic acid it is evident that the galactose moiety of it is joined through C_1 and C_6 in the main chain with single unit side chain of the galacturonic acid linked to C_3 of this galactose residue. Two such units are present per repeating unit of the degraded gum. The simplest structure, which can accommodate all the above facts, is as follows:

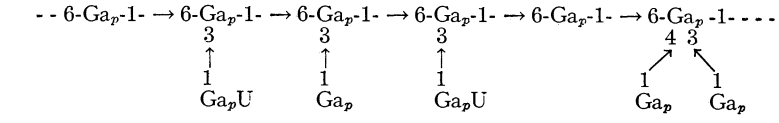

(Ga_p represents galactopyranose residues and Ga_pU represents galactopyranosyl uronic acid residue.)

The possibility of linking one galactopyranosyl uronic acid unit and one galactopyranose unit to the same galactose unit of the main chain is ruled out because of the failure to isolate a monomethyl galactose from the hydrolyzate of the reduced aldobiouronic acid obtained from the methylated degraded gum. It should be pointed out that at

the present state of our knowledge it is not possible to determine the exact sequence of the different sugar units in the repeating unit of the degraded gum.

The negative rotation of the degraded gum as well as its methylated derivative shows that the majority of the glycosidic linkages are of β-type.

Further support for the proposed structure of the repeating unit of the degraded gum was obtained from the periodate oxidation of the degraded gum. The uronic acid residues, when present in the polysaccharide molecules as non-reducing end units, undergo over-oxidation. However, by using periodic acid instead of sodium metaperiodate the over-oxidation during the reaction can be controlled (13, 14, 15). The periodic acid oxidation data show that each anhydro hexose unit consumed 1.20 moles of the oxidant after 25 hours liberating 0.67 mole of formic acid. Considering the fact that a non-reducing hexopyranose unit (which may be a galactopyranose or galactopyranosyl uronic acid unit) and $1 \rightarrow 6$ linked hexopyranose unit of the back bone chain consume 2 moles of periodic acid liberating 1 mole of formic acid and that hexopyranose units linked through C_1, C_3, and C_6 or C_1, C_3, C_4, and C_6 cannot react with periodic acid, the consumption of the oxidant and the liberation of formic acid per hexopyranose unit, assuming the above structure, work out to be 1.27 and 0.64 moles respectively.

The periodate-oxidized degraded gum after reduction with sodium borohydride (16) followed by usual treatments was precipitated by ethanol. The percentage weight of galactose (as anhydro sugar) unattacked by periodate was found to be 32.4%. This result is in good agreement with the calculated value (35.7% assuming the above structure).

EXPERIMENTAL

All specific rotations are equilibrium values. Unless otherwise stated, all evaporations were carried out *in vacuo* at 30–40°. Whatman No. 1 filter papers were used for paper partition chromatography. The solvent mixtures (v/v) used for partition chromatography for sugars and their derivatives were:

(A) ethyl acetate:pyridine:water (8:2:1),
(B) *n*-butanol:acetic acid:water (4:1:5), upper layer,
(C) *n*-butanol:ethanol:water (40:11:19),
(D) *n*-butanol:ethanol:water (5:1:4), upper layer,
(E) methyl ethyl ketone – water azeotrope,
(F) ethyl acetate:acetic acid:water (9:2:2),
(G) ethyl acetate:acetic acid:water (3:1:3), upper layer.

The spray reagents used were:

(*a*) aniline hydrogen oxalate (saturated aq. solution),
(*b*) *p*-anisidine hydrochloride (3% solution in *n*-butanol),
(*c*) aniline hydrogen phthalate.

Isolation and Purification of the Gum

The crude gum (140 g) was allowed to swell in water (700 ml) and the viscous solution formed was vigorously stirred for 6 hours at room temperature. The brown viscous solution was filtered through fine cloth and then passed through Cepa-supercentrifuge for further clarification. The solution was slowly added to acidified (pH 4–5) ethanol (2 l.) when a white amorphous precipitate was formed. This was filtered and triturated with absolute ethanol and dry ether. The product after second purification as above was dried *in vacuo* at 40°; yield 48 g.

The figures given below are mean values from a series of analyses carried out with two separately prepared batches; no significant differences in the properties were observed between the two preparations: moisture 8.8%; ash 0.79%; $[\alpha]_D$ −44° (*c*, 0.5 in 4% aqueous sodium hydroxide solution); equivalent weight by acidimetry, 1150; anhydro uronic acid, 14.5%; pentosan content, 21.7% (calc. from the amount of furfuraldehyde evolved under standard conditions (17), account being taken of the furfuraldehyde yielded by the uronic acid residues); nitrogen, nil; methoxyl, 0.51%. The gum on complete hydrolysis followed by deionization with Amberlite IR-120(H) and Amberlite IR-400(OH) yielded a neutral sirup, which contained D-galactose and L-arabinose. The mixture was separated and the sugars were isolated in their crystalline states. L-Arabinose, m.p. and mixed m.p. 153–154°, $[\alpha]_D^{30}$ +108° (*c*, 1.05 in water) and D-galactose, m.p. and mixed m.p. 163–164°, $[\alpha]_D^{30}$ +84° (*c*, 1 in water). The gum (102.6 mg) was hydrolyzed and the neutral sugars were estimated (6) quantitatively using D-ribose as reference sugar. The percentages of galactose and arabinose, as anhydro sugars, were 63.7 and 19.5 respectively.

Can. J. Chem. Downloaded from www.nrcresearchpress.com by 210.87.254.5 on 09/05/12
For personal use only.

Isolation and Characterization of the Aldobiouronic Acid

The gum (10 g) was heated on a boiling water bath with 0.1 *N* sulphuric acid (250 ml) for 60 hours. After neutralization and usual treatments, the acid fraction was separated from the neutral one by Dowex 1-X4 resin. The resulting acid mixture containing aldobio- and aldotrio-uronic acid was separated on a cellulose column and the aldobiouronic acid was obtained in a homogeneous state (equiv. wt. 340). The methyl ester methyl glycoside of the aldobiouronic acid on reduction with lithium aluminum hydride followed by hydrolysis yielded D-galactose, which was characterized through crystalline *p*-nitroaniline derivative m.p. and mixed m.p. 216–217°, lit. 217–218° (18); $[\alpha]_D^{30}$ −244° (in dry pyridine).

The methyl ester methyl glycoside of the methylated aldobiouronic acid was reduced with lithium aluminum hydride in dry ether and remethylated to yield a fully methylated disaccharide. Found: —OCH_3, 54.1%. Calc. $C_{20}H_{38}O_{11}$: —OCH_3, 54.6%. This, on hydrolysis, gave a mixture of two methyl sugars which were separated on filter sheets and were identified as 2,3,4,6-tetra-*O*-methyl-D-galactose and 2,4,6-tri-*O*-methyl-D-galactose through their crystalline aniline derivatives. N-Phenyl-2,3,4,6-tetra-*O*-methyl-D-galactosylamine, m.p. and mixed m.p. 186–188°, lit. 187° (18), $[\alpha]_D^{30}$ +40° (*c*, 0.5 in acetone), lit. +39° (19). N-Phenyl-2,4,6-tri-*O*-methyl-D-galactosylamine, m.p. and mixed m.p. 173–175°, lit. 175° (20) $[\alpha]_D^{30}$ +36° (*c*, 0.9 in acetone), lit. +38° (21).

Autohydrolysis of the Purified Gum and Isolation of the Degraded Gum

An aqueous solution of the gum acid (1 g, 10%) was heated on a boiling water bath. Paper chromatographic examination of the solution, using solvents A and G, at regular intervals of time, after removal of the precipitated polysaccharide by ethanol, showed that arabinose started splitting off in the beginning, and then arabinose and an oligosaccharide (R_{gal} 1.36 in solvent G). After 25 hours, galactose appeared in the hydrolyzate. A 10% aqueous solution of the gum acid (20 g) was subjected to autohydrolysis for 25 hours as stated above and the solution was filtered, concentrated to half its volume, and was poured into ethanol. The precipitated polysaccharide was washed with hot ethanol and dry ether and finally dried to give a white amorphous powder; $[\alpha]_D^{32}$ −2° (*c*, 1.2 in water); equiv. wt. (by acidimetry) 920; anhydrouronic acid 18.54% and moisture 9.5%. Paper chromatographic examination of the neutral sugars liberated on complete hydrolysis of the degraded gum indicated the presence of galactose and a trace amount of arabinose. Galactose was estimated, as anhydrosugar, to be 76.5% in the hydrolyzate.

Methylation of the Degraded Gum (7, 8)

The degraded gum (10 g) was methylated by treatment first with methylsulphate and alkali in an atmosphere of nitrogen and then with methyl iodide and silver oxide to yield a fully methylated derivative showing no hydroxyl absorption band in the infrared spectrum, $[\alpha]_D^{32}$ −30° (*c*, 1.05 in chloroform); —OCH_3 41.5%; yield 6.5 g.

Methanolysis and Separation and Identification of the Neutral Sugars of the Methylated Degraded Gum

A solution of the methylated degraded gum (1.5 g) in 2.5% dry methanolic hydrogen chloride (50 ml) was refluxed for 16 hours (till constant optical rotation). The solution was neutralized, filtered, and evaporated to a sirup which was heated with 2% aqueous barium hydroxide solution (30 ml) for 4 hours at 80°. The resulting solution was neutralized by passing carbon dioxide gas; then it was filtered and passed through a column of Amberlite IR 120(H) and the acidic portion was absorbed on a column of Dowex 1-X4 (bicarbonate form) resin. The column was thoroughly washed with water (5 l.) and the neutral solution was concentrated and hydrolyzed with *N* sulphuric acid for 12 hours (constant optical rotation). The solution after neutralization, filtration, and deionization, was evaporated to give a sirup (656 mg). On paper chromatographic examination of the sirup using solvents C and D four methyl sugars, viz. 2,3,4,6-tetra-, 2,3,4-tri-, 2,4-di-, and 2-*O*-methyl-D-galactose, were found to be present in it.

The sirup (ca. 600 mg) was separated on a cellulose column (22) (75×3.5 cm) using solvent E (23) as eluants to give five fractions. The following table shows the different fractions obtained by column chromatography.

TABLE I

Fraction No.	Tube No.	Methyl sugars	Yield (mg)
1	30–38	2,3,4,6-Tetra-*O*-methyl-D-galactose	238
2	39–43	Mixture of 2,3,4,6-tetra-*O*-methyl-D-galactose and 2,3,4-tri-*O*-methyl-D-galactose and traces of methyl arabinose	32
3	44–64	2,3,4-Tri-*O*-methyl-D-galactose	158
4	80–102	2,4-Di-*O*-methyl-D-galactose	76
5	121–133	2-*O*-Methyl-D-galactose	64

Can. J. Chem. Downloaded from www.nrcresearchpress.com by 210.87.254.5 on 09/05/12
For personal use only.

Fraction 1

The sirup (238 mg) had $[\alpha]_D^{31}$ +110° (*c*, 1 in water) lit. +109.5 (24) and —OCH_3 51.9% and was chromatographically homogeneous. The sugar was identified as 2,3,4,6-tetra-*O*-methyl-D-galactose by conversion into the anilide derivative, m.p. and mixed m.p. 187–189°, lit. 187° (18), $[\alpha]_D^{30}$ +40° (*c*, 0.5 in acetone) lit. +39° (19).

Fraction 2

The sirup (32 mg) on paper chromatography using solvents C and D separated into spots corresponding to 2,3,4,6-tetra- and 2,3,4-tri-*O*-methyl-D-galactose with a trace of methyl arabinose. Demethylation (25) gave galactose and a trace of arabinose.

Fraction 3

The chromatographically pure sirup (158 mg) had $[\alpha]_D^{30}$ +108° (*c*, 0.8 in water) lit. +114° (26). Found: —OCH_3, 41.1%. Calc. for $C_9H_{18}O_6$: —OCH_3, 41.8%. Demethylation gave only galactose. The sugar was identified as 2,3,4-tri-*O*-methyl-D-galactose through its aniline derivative which was crystallized (27) from acetone – petroleum ether, m.p. and mixed m.p. 162–163°, lit. 166° (27), $[\alpha]_D^{30}$ +41° (*c*, 0.9 in methanol) lit. +43° (28).

Fraction 4

This component (78 mg) was obtained as chromatographically pure solid and had $[\alpha]_D^{30}$ +82° (*c*, 1 in water) lit. +85° (29). Found: —OCH_3, 28.8%. Calc. for $C_8H_{16}O_6$: —OCH_3, 29.8%. The solid was crystallized from a small volume of ethanol, m.p. and mixed m.p. (with 2,4-di-*O*-methyl-D-galactose) 101–102° lit. 103° (28). It was further characterized as 2,4-di-*O*-methyl-D-galactose through its crystalline anilide, which on repeated crystallization from ethanol, had m.p. and mixed m.p. 217–218°, lit. 216° (29).

Fraction 5

The chromatographically pure sirup (64 mg) had $[\alpha]_D^{30}$ +78° (*c*, 0.6 in water) lit. +80° (30). Found: —OCH_2, 16.7%. Calc. for $C_7H_{14}O_6$: —OCH_3, 16.0%. On trituration with dry ether the sirup yielded a solid which on crystallization from glacial acetic acid showed m.p. and mixed m.p. (with 2-*O*-methyl-D-galactose) 142–144°, lit. 145–148° (26). It was further confirmed by conversion to N-phenyl-2-*O*-methyl-D-galactosylamine which after repeated crystallization from acetone – petroleum ether, had m.p. 159–161°; when mixed with an authentic sample of m.p. 163–164°, the melting point was 161–162°, lit. 165° (26).

A small quantity of the mixture was separated quantitatively by paper chromatography and the amount of each methyl sugar was estimated by alkaline hypoiodite method (31). The results were confirmed by duplicate experiments and were as follows: 2,3,4,6-tetra-*O*-methyl-D-galactose, 43.84%; 2,3,4-tri-*O*-methyl-D-galactose, 29.82%; 2,4-di-*O*-methyl-D-galactose, 13.39%; and 2-*O*-methyl-D-galactose, 12.95%.

Examination of the Acidic Fraction

The acidic fraction was displaced from the resin column in the usual way $[\alpha]_D^{32}$ +54° → +62° (*c*, 1.05 in chloroform); equiv. wt. 420. The methyl ester methyl glycoside of the methyl aldobiouronic acid was reduced with lithium aluminum hydride and then hydrolyzed to yield a mixture of methyl sugars. The mixture was separated on filter papers and the sugars obtained in equimolecular proportion were identified as 2,3,4-tri- and 2,4-di-*O*-methyl-D-galactose through their crystalline anilides. N-Phenyl-2,3,4-tri-*O*-methyl-D-galactosylamine, m.p. and mixed m.p. 164–166°, $[\alpha]_D^{31}$ +38° (*c*, 0.95 in acetone). N-Phenyl-2,4-di-*O*-methyl-D-galactosylamine, m.p. and mixed m.p. 218–219°.

Periodate Oxidation of the Degraded Gum

The degraded gum (118.5 mg) was dispersed in water (50 ml) and oxidized by shaking with 0.2 *M* periodic acid (50 ml) in dark at 15°. The liberated formic acid (after correcting for the titratable acidity of the gum) and the amount of periodic acid consumed during the reaction were estimated in the usual way (32) at regular intervals of time. The liberation of formic acid became constant after 25 hours, corresponding to 0.67 mole of formic acid per anhydro hexose residue and the periodate uptake became constant after 25 hours, corresponding to 1.20 moles of the oxidant per anhydro hexose unit.

The periodate-oxidized gum (114.4 mg) was neutralized with barium hydroxide and filtered, and to the clear solution sodium borohydride (200 mg) was added, and kept overnight at room temperature. The solution was acidified with acetic acid and then subjected to dialysis in running water to remove inorganic ions (5 days). The solution was concentrated (5 ml) and poured into ethanol. The amorphous white precipitate obtained was recovered at the centrifuge, triturated, and dried *in vacuo* at 40° (76 mg). The periodate-oxidized reduced polysaccharide (30 mg) was hydrolyzed with 2 *N* sulphuric acid and the percentage of galactose unattacked by periodate was estimated using D-ribose as reference sugar to be 32.4%.

ACKNOWLEDGMENT

The authors are thankful to Dr. P. Bagchi, Director, Research, East India Pharmaceutical Works Ltd., Calcutta, for suggesting the problem and his valuable advice and interest in the work reported in this paper.

Can. J. Chem. Downloaded from www.nrcresearchpress.com by 210.87.254.5 on 09/05/12
For personal use only.

REFERENCES

1. L. R. KIRTIKAR, B. D. BASU, and an I.C.S. Officer. Indian medicinal plants, Part I. S. N. Basu. Allahabad (India). 1918. pp. 664–666.
2. SIR J. D. HOOKER. The flora of British India. Vol. II. L. Reeves & Co., Ashford, Kent, London. 1894. p. 29.
3. S. MUKHERJEE and P. K. DHAR. J. Sci. & Industr. Res. **18B**, 219 (1959).
4. C. DOREE. The method of cellulose chemistry. 2nd ed. Chapman and Hall Ltd., London. 1947. p. 391.
5. C. DOREE. The method of cellulose chemistry. 2nd ed. Chapman and Hall Ltd., London. 1947. p. 381.
6. E. L. HIRST and J. K. N. JONES. J. Chem. Soc. 1659 (1949).
7. E. L. FALCONER and G. A. ADAMS. Can. J. Chem. **34**, 338 (1956).
8. G. A. ADAMS. Can. J. Chem. **36**, 755 (1958).
9. T. PURDIE and J. C. IRVINE. J. Chem. Soc. **83**, 1021 (1903).
10. G. G. S. DUTTON and F. SMITH. J. Am. Chem. Soc. **78**, 2505, 3744 (1956).
11. A product of Dow Chemical Company, Midland, Mich.
12. M. ABDEL-AKHER and F. SMITH. Nature, **166**, 1037 (1950).
13. F. SMITH. J. Chem. Soc. 2646 (1951).
14. E. L. HIRST, J. K. N. JONES, and W. O. JONES. J. Chem. Soc. 1880 (1939).
15. P. A. LEVANE and L. C. KREIDER. J. Biol. Chem., **120**, 591 (1937).
16. M. ABDEL-AKHER, J. K. HAMILTON, R. MONTGOMERY, and F. SMITH. J. Am. Chem. Soc. **74**, 4970 (1952).
17. F. W. NORRIS and C. E. RESCH. Biochem. J. **29**, 1590 (1935).
18. A. K. MUKHERJEE, D. CHOWDHURY, and P. BAGCHI. Can. J. Chem. **39**, 1408 (1961).
19. P. ANDREW, L. HOUGH, and J. K. N. JONES. J. Am. Chem. Soc. **74**, 4029 (1952).
20. J. K. N. JONES. J. Chem. Soc. 3141 (1949).
21. E. L. HIRST and J. K. N. JONES. J. Chem. Soc. 1482 (1939).
22. L. HOUGH, J. K. N. JONES, and W. H. WADMAN. J. Chem. Soc. 2511 (1949).
23. L. BOGGS, L. S. CUENDET, I. ERHENTHAL, R. KOCH, and F. SMITH. Nature, **166**, 520 (1950).
24. J. C. IRVINE and A. CAMERON. J. Chem. Soc. **85**, 1071 (1904).
25. L. HOUGH, J. K. N. JONES, and W. H. WADMAN. J. Chem. Soc. 1702 (1950).
26. D. MCCREATH, F. SMITH, E. G. COX, and A. I. WAGSTAFF. J. Chem. Soc. 387 (1939).
27. M. ABDEL-AKHER, F. SMITH, and D. R. SPRIESTERSBACH. J. Chem. Soc. 3637 (1952).
28. F. SMITH. J. Chem. Soc. 1724 (1939).
29. P. ANDREWS, L. HOUGH, and J. K. N. JONES. J. Chem. Soc. 806 (1954).
30. E. L. HIRST and J. K. N. JONES. J. Chem. Soc. 506 (1946).
31. E. L. HIRST, L. HOUGH, and J. K. N. JONES. J. Chem. Soc. 928 (1949).
32. P. FLEURY and J. LANGE. J. Pharm. Chim. (8), **17**, 107 (1933).

Can. J. Chem. Downloaded from www.nrcresearchpress.com by 210.87.254.5 on 09/05/12
For personal use only.

THE SYNTHESIS OF AROYL METHYL KETONES AS LIGNIN MODEL SUBSTANCES

J. M. Pepper and Maitreyi Saha
Department of Chemistry, University of Saskatchewan, Saskatoon, Saskatchewan
Received August 9, 1963

ABSTRACT

A series of aroyl methyl ketones ($ArCOCOCH_3$ in which Ar was phenyl, *p*-hydroxyphenyl, *p*-methoxyphenyl, 4-hydroxy-3-methoxyphenyl, 3,4-dimethoxyphenyl, 4-hydroxy-3,5-dimethoxyphenyl, and 3,4,5-trimethoxyphenyl) has been prepared by the oxidation, using selenium dioxide, of the correspondingly substituted benzyl methyl ketones.

INTRODUCTION

Two diketones, vanilloyl methyl ketone (IV) and syringoyl methyl ketone (VI), have been isolated from the products obtained by the acid-catalyzed solvolysis of wood or isolated lignins (1, 2). The characterization of such derivatives has contributed to the present knowledge of the chemical structure of lignin. They serve, too, as interesting model substances for lignin research. The reported syntheses of IV by Brickman, Hawkins,

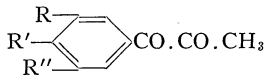

I R = R′ = R″ = H
II R = R″ = H, R′ = HO
III R = R″ = H, R′ = CH_3O
IV R = CH_3O, R′ = HO, R″ = H
V R = R′ = CH_3O, R″ = H
VI R = R″ = CH_3O, R′ = HO
VII R = R′ = R″ = CH_3O

and Hibbert (3) and of VI by Kulka, Hawkins, and Hibbert (4) involve many steps and low overall yields. An investigation was made to find a more suitable mode of synthesis of such aroyl methyl ketones in order that a sufficient amount might be obtained for an extended study of their properties and chemical reactions.

The method that was investigated involved the synthesis of ketones of the formulae $ArCOCH_2CH_3$ and $ArCH_2COCH_3$ and their subsequent oxidation, using selenium dioxide, to the corresponding α-diketones. The latter route was shown to be preferable and compounds IV and VI were obtained with little difficulty. The method was then extended to include the synthesis of five other related diketones (I, II, III, V, VII), only one of which (I) had been made previously by this method.

RESULTS AND DISCUSSION

Initially, monoketones of the formula $ArCOCH_2CH_3$ were prepared by the silver oxide oxidation of the corresponding alcohols, $ArCH(OH)CH_2CH_3$, which had been synthesized from the aryl aldehyde and ethyl magnesium bromide. Following the method of Roberti, York, and MacGregor (5), the required 1-(4-hydroxy-3-methoxyphenyl)-1-propanol was prepared in 68% yield. Similarly, but using tetrahydrofuran instead of diethyl ether, syringaldehyde was converted to 1-(4-hydroxy-3,5-dimethoxyphenyl)-1-propanol in 52% yield. Both compounds gave the characteristic color reaction with quinone monochloroimide which is indicative of a *p*-hydroxybenzyl alcoholic group (6, 7).

The oxidation of the alcohol to the corresponding keto compound using silver oxide

Can. J. Chem. Downloaded from www.nrcresearchpress.com by 210.87.254.6 on 09/05/12
For personal use only.

had been shown by Pearl (8) to proceed readily in the case of 1-(4-hydroxy-3-methoxyphenyl)-1-propanol in 89% yield. Initially some difficulty was experienced in repeating these results, especially in crystallization of the syrupy product. This was overcome partly by increasing the reaction time from 1½ hours to 5 hours and using freshly generated sulphur dioxide. Under these conditions, the highly viscous product solidified slowly and could be recrystallized from petroleum ether to yield the required ketone (propiovanillone) in 50.5% yield. 1-(4-Hydroxy-3,5-dimethoxyphenyl)-1-propanone (propiosyringone) was prepared by the same method. This product solidified readily and could be recrystallized to give the required ketone in 40.3% yield. Subsequently it was found that the synthesis and oxidation of monoketones of the formula $ArCH_2COCH_3$ gave better yields of the required α-diketones and attention was directed, therefore, to the synthesis using this route.

The synthesis of monoketones of the formula, $ArCH_2COCH_3$, was based on the procedure reported by Kulka and Hibbert (9) and outlined as follows:

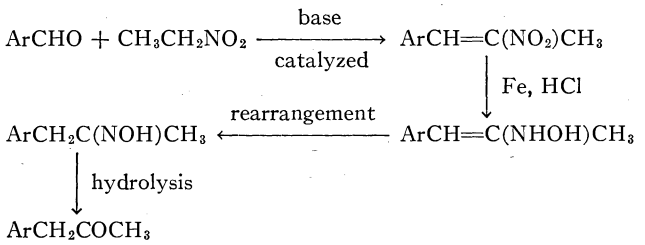

No difficulty was encountered in the condensation of vanillin with nitroethane using the methylamine hydrochloride – sodium carbonate method, but the similar reaction using syringaldehyde gave yields of product which varied widely from run to run. A more successful condensation was achieved using the method reported by Kaufmann (10) in which the methylamine hydrochloride was replaced by aqueous ethylamine. The condensation of other substituted benzaldehydes was then effected using one or other of these methods. The yields of the resulting 1-aryl-2-nitro-1-propenes are given in Table I.

TABLE I

Percentage yields of $ArCH=C(NO_2)CH_3$

Aldehyde	Methylamine method (9)	Ethylamine method (10)
p-Hydroxybenzaldehyde	49	65
Anisaldehyde	—	76
Vanillin	72	—
Veratraldehyde	—	76
Syringaldehyde	52	56
3,4,5-Trimethoxybenzaldehyde	66	52

The conversion of the 1-aryl-2-nitro-1-propenes to the substituted benzyl methyl ketones offered no difficulty. Purification of the monoketones was effected through the formation of the sodium bisulphite addition product. The yields are given in Table II.

It had been reported by Wegmann and Dahn (11) that benzyl methyl ketone could be oxidized, using selenium dioxide in dioxane, to the corresponding benzoyl methyl ketone. Since it was found possible to readily duplicate these results, attention was directed to this method as a means of synthesis of the required α-diketones from the correspondingly

Can. J. Chem. Downloaded from www.nrcresearchpress.com by 210.87.254.6 on 09/05/12
For personal use only.

TABLE II
Percentage yields of $ArCH_2COCH_3$ and $ArCOCOCH_3$

Ar—	$ArCH{=}C(NO_2)CH_3$ to $ArCH_2COCH_3$	$ArCH_2COCH_3$ to $ArCOCOCH_3$
Phenyl		60
p-Hydroxyphenyl	66	44
p-Methoxyphenyl	73	33
4-Hydroxy-3-methoxyphenyl	78	32
3,4-Dimethoxyphenyl	76	34
4-Hydroxy-3,5-dimethoxyphenyl	63	11
3,4,5-Trimethoxyphenyl	89	38

substituted benzyl methyl ketones. The conversion of 4-hydroxy-3-methoxybenzyl methyl ketone to 4-hydroxy-3-methoxybenzoyl methyl ketone was chosen as a typical system with which to study the optimum conditions for oxidation and the most satisfactory procedure for the isolation and purification of the product.

Using, initially, the conditions reported by Wegmann and Dahn (11), the oxidation was carried out for 4 hours in dioxane at reflux temperature. The resulting crude reaction product was studied by gas–liquid chromatography using a 6-ft, 1/4-in., 15% Apiezon N on Fluoropak column at 220° C. Three well-separated peaks, with retention times of 4.0, 5.5, and 6.8 minutes, indicated the presence of three compounds in this product. By comparison with authentic samples the peaks were shown to correspond to vanillin, unchanged 4-hydroxy-3-methoxybenzyl methyl ketone, and the required vanilloyl methyl ketone* respectively. Since approximately 65% of the eluted material was the α-diketone, this method of synthesis warranted a more detailed investigation to determine the optimum conditions for a maximum yield of vanilloyl methyl ketone.

An equimolar ratio of selenium dioxide to the monoketone was adopted and a study made of the effect of varying the time of oxidation, at reflux temperatures, and the nature of the solvent system. Reaction times of 4, 8, 12, 18, and 24 hours gave rise to the diketone in yields which represented percentage relative abundances of 32, 46, 64, 64, and 64 respectively. Having, therefore, chosen 12 hours as the most suitable reaction time, a similar study was made of the effect of the solvent system. For dimethyl sulphoxide, dioxane, tetrahydrofuran, acetic acid, acetic anhydride, and ethanol the percentage relative abundances were 75, 65, 53, 36, a trace, and zero respectively. For simplicity, dioxane was chosen as the solvent system for all subsequent oxidations.

Two separate methods of isolation and purification of the required vanilloyl methyl ketone were investigated. In the first instance, a study was made of the separation of the nickel glyoxime salt and its subsequent decomposition with dilute sulphuric acid to liberate the free diketone (4). The second method involved a column chromatographic separation of the crude oxidation product and was found to be more successful. Silica gel was used as the column packing and petroleum ether (b.p. 40–60°) followed by petroleum ether containing 5% diethyl ether, effected the elution of the vanilloyl methyl ketone. Using these conditions of oxidation and isolation, seven substituted benzyl methyl ketones were oxidized successfully to the corresponding α-diketones. The yields are given in Table II.

On hydrolysis of the precipitated nickel glyoxime salt of vanilloyl methyl ketone, a white precipitate separated. This compound was characterized as vanillic acid. Further

The donation of an authentic sample of vanilloyl methyl ketone by Dr. J. A. F. Gardner, Superintendent, Forest Products Laboratory, Vancouver, B.C., was much appreciated.

Can. J. Chem. Downloaded from www.nrcresearchpress.com by 210.87.254.6 on 09/05/12
For personal use only.

tests showed that the vanillic acid did not arise as a product of this hydrolysis or by oxidation of any vanillin that may have been present but rather that it was produced directly by oxidation of either the 4-hydroxy-3-methoxybenzyl methyl ketone or the vanilloyl methyl ketone. In subsequent syntheses involving the oxidation of *p*-methoxybenzyl methyl ketone and of 3,4,5-trimethoxybenzyl methyl ketone the two corresponding acids, anisic acid and 3,4,5-trimethoxybenzoic acid, were isolated and characterized. The mechanism of formation of these acids was not determined. A closer examination of a probable oxidation by air or peroxides in the dioxane must be made before a benzyl–acyl bond cleavage can be attributed to the action of selenium dioxide under these conditions.

The electronic absorption spectrum of each of the substituted benzoyl methyl ketones was determined using ethanol as the solvent. Table III records the λ_{max} and log ϵ_{max} for each diketone. The reported spectral bands of benzil and diacetyl are included for comparison.

TABLE III

Electronic absorption spectra of $ArCOCOCH_3$

Ar =	λ_{max}	log ϵ_{max}
1. Phenyl	255	4.36
2. *p*-Hydroxyphenyl	296	4.06
	225	3.82
3. *p*-Methoxyphenyl	294	4.00
	223	3.81
4. 4-Hydroxy-3-methoxyphenyl	320	4.93
	291 (sh)	—
	235	4.86
5. 3,4-Dimethoxyphenyl	317	3.64
	284 (sh)	3.50
	235	3.55
6. 4-Hydroxy-3,5-dimethoxyphenyl	326	4.02
7. 3,4,5-Trimethoxyphenyl	295	3.74
Benzil (ArCOCOAr)	259	4.31
	370	1.89
Diacetyl ($CH_3COCOCH_3$)	435	1.30

The spectral data recorded in Table III are in general agreement with the theory regarding the effect of ring substituents on the absorption spectra of aromatic compounds.

EXPERIMENTAL

All melting points are uncorrected. Ultraviolet spectra were measured using a Cary Model 14 spectrometer. Infrared spectra were determined using a Perkin–Elmer Model 21 spectrometer with sodium chloride optics. Gas–liquid chromatography was performed using a Beckman GC-2 chromatograph with a thermal conductivity detector unit. This machine had been modified by placing the injection system as close as possible to one end of the column and by modifying it to make it more comparable electronically to the GC-2A.

Synthesis of 1-Aryl-1-propanones

(i) 1-(4-Hydroxy-3-methoxyphenyl)-1-propanone

1-(4-Hydroxy-3-methoxyphenyl)-1-propanol was prepared according to the method of Roberti, York, and MacGregor (5) and then oxidized, using silver oxide, to 1-(4-hydroxy-3-methoxyphenyl)-1-propanone as described by Pearl (8). For the latter step it was found necessary to increase the time of reflux to 5 hours and to use freshly prepared sulphur dioxide otherwise no crystalline product was obtained. Under the modified conditions, the crude oily product solidified on standing and was recrystallized from petroleum ether (30–60°) to yield colorless needle-shaped crystals, m.p. 59–60; reported m.p. 61–62 (8). Calc. for $C_{10}H_{12}O_3$: OCH_3, 17.22%. Found: OCH_3, 17.10%.

(ii) 1-(4-Hydroxy-3,5-dimethoxyphenyl)-1-propanone

Synthesis of 1-(4-hydroxy-3,5-dimethoxyphenyl)-1-propanol.—Syringaldehyde (10 g) was dissolved in dry

Can. J. Chem. Downloaded from www.nrcresearchpress.com by 210.87.254.6 on 09/05/12
For personal use only.

tetrahydrofuran (150 ml) and the solution treated with another solution of ethyl magnesium bromide (prepared from ethyl bromide (42 g) and magnesium (10 g)). The resulting oily product crystallized on standing, yield 6.1 g (52.3%). Recrystallization from benzene gave white crystals, m.p. 94–95°; reported m.p. 98° (12). Calc. for $C_{11}H_{16}O_4$: C, 62.25; H, 7.61; OCH_3, 29.3%. Found: C, 62.40; H, 7.48; OCH_3, 29.0%.

Oxidation of 1-(4-hydroxy-3,5-dimethoxyphenyl)-1-propanol.—1-(4-Hydroxy-3,5-dimethoxyphenyl)-1-propanol (3.0 g) was treated with sodium hydroxide (7 g) and silver nitrate (8 g) and a similar procedure followed to that used for the oxidation of 1-(4-hydroxy-3-methoxyphenyl)-1-propanol. The yield of crude product was 1.2 g (40.3%). Recrystallization from aqueous ethanol gave white crystals, m.p. 108–109°; reported m.p. 109–110° (4).

Synthesis of 1-Aryl-2-propanones

2-Nitro-1-aryl-1-propenes

The experimental details are given for the preparation of a typical compound. Other compounds of the same series but differing in the ring substituent pattern were prepared by a similar procedure. The necessary data for each such individual synthesis are recorded in Table IV.

(i) Using the method of Kulka and Hibbert (9).—Vanillin (6 g) was dissolved in ethanol (10 ml) and to the solution, nitroethane (3 ml), methylamine hydrochloride (0.2 g), and sodium carbonate (0.016 g) were added. After 2 days at room temperature in the dark, the reaction mixture was cooled to 0°, the yellow needle-like crystals removed by filtration, washed with dilute sulphuric acid and with water, and dried. The yield was 5.9 g (71.5%). After recrystallization from a mixture of ethanol and ether the 2-nitro-1-(4-hydroxy-3-methoxyphenyl)-1-propene melted at 101–102°; reported m.p. 101–102° (9).

In Table IV are the experimental data for the similar condensations of *p*-hydroxybenzaldehyde, syringaldehyde, and 3,4,5-trimethoxybenzaldehyde.

(ii) Using the method of Kaufmann (10).—Veratraldehyde (15 g) was added to nitroethane (8 ml) and 20 drops of aqueous (75%) ethylamine added to the mixture. An initial turbidity slowly disappeared and a yellow oil separated which crystallized on standing. After 8 days, the crystals were removed by filtration and dried. The yield was 15.2 g (75.5%). After recrystallization from ethanol the 2-nitro-1-(3,4-dimethoxyphenyl)-1-propene melted at 73° (10).

In Table IV are the experimental data for the similar condensations of syringaldehyde, *p*-hydroxybenzaldehyde, and anisaldehyde.

1-Aryl-2-propanones

The experimental details are given for the preparation of a typical compound. All other compounds were prepared by a similar procedure, the necessary data for which are recorded in Table V.

(i) Using the method of Kulka and Hibbert (9).—2-Nitro-1-(4-hydroxy-3-methoxyphenyl)-1-propene (20 g) was dissolved in hot ethanol (200 ml) and hot water (500 ml), iron powder (40 g), ferric chloride (1.6 g), and concentrated hydrochloric acid added. The reaction mixture was refluxed, with stirring, for 6 hours and then concentrated to half the volume by removal of ethanol. The precipitated black iron oxide was filtered and washed with hot water. The combined filtrate and washings were extracted with benzene. From this extract was obtained an oil which was distilled to yield a clear, yellow product of 1-(4-hydroxy-3-methoxyphenyl)-2-propanone (13.4 g) (77.7%), b.p. 125° at 0.45 mm; reported b.p. 115° at 0.15 mm (9).

In Table V are the experimental data for the similar reduction and subsequent hydrolysis of the five other 2-nitro-1-aryl-1-propenes.

Synthesis of Aroyl Methyl Ketones

Vanilloyl Methyl Ketone

Selenium dioxide (2.4 g, 0.02 mole) was dissolved in dioxane (12 ml) and water (2 ml). 1-(4-Hydroxy-3-methoxyphenyl)-2-propanone (3 g, 0.02 mole) was added and the mixture refluxed for 12 hours. Initially the reaction mixture became red in color but gradually metallic selenium precipitated as a black powder. The selenium was removed by filtration and the dioxane and water removed by distillation. The residue, a dark brown tarry material, was distilled to give a clear yellow oil weighing 2.1 g, b.p. 115° at 0.6 mm. This product only partially crystallized.

(i) Purification of vanilloyl methyl ketone via the nickel glyoxime salt method.—From 3 g of the crude reaction product, prepared as above, the nickel glyoxime salt of the α-diketone was precipitated according to the method of Kulka, Hawkins, and Hibbert (4). The yield was 1.32 g. To hydrolyze this salt, it was added to 12 *N* sulphuric acid (400 ml), and the mixture was allowed to stand at room temperature for 24 hours and then at 40° for 4 hours. During hydrolysis a white precipitate separated (see below) which was removed by filtration. The filtrate was extracted with benzene in a continuous liquid–liquid extractor, the extract dried over anhydrous sodium sulphate and sodium bicarbonate, and concentrated to remove the excess benzene. A further slight precipitation of the white solid occurred during the concentration and it was removed by filtration. The residual oil was purified by fractional crystallization from benzene to give vanilloyl methyl ketone (0.55 g, 7%), m.p. 65–69°; reported m.p. 70–71° (9).

The white solid that precipitated during the hydrolysis was recrystallized from aqueous ethanol and characterized as vanillic acid on the basis of the following evidence: m.p. 204°, reported m.p. 207°; no melting

Can. J. Chem. Downloaded from www.nrcresearchpress.com by 210.87.254.6 on 09/05/12
For personal use only.

Can. J. Chem. Downloaded from www.nrcresearchpress.com by 210.87.254.6 on 09/05/12
For personal use only.

TABLE IV

The preparation of 2-nitro-1-aryl-1-propenes

Aldehyde	Aldehyde, g	Ethanol, ml	$C_2H_5NO_2$, ml	CH_3NH_3Cl, g	Na_2CO_3, g	$C_2H_5NH_2$ (75%), drops	2-Nitro-1-aryl-1-propene			
							g	Yield, %	M.p., °C	Reported m.p., °C
p-Hydroxybenzaldehyde	5	15	3.0	0.2	0.015		3.6	49	128–129	*
Vanillin	6	10	3.0	0.2	0.016		5.9	72	101–102	101–102 (9)
Syringaldehyde	9	25	4.5	0.3	0.024		6.1	52	101–102	103–104 (9)
3,4,5-Trimethoxybenzaldehyde	2	10	1.0	0.1	0.020		1.7	66	95–96	95 (13)
p-Hydroxybenzaldehyde	5	15	3.0			9	4.8	65	128–129	
Anisaldehyde	15	10	7.5			15	16.2	76	42–43	†
Veratraldehyde	15		8.0			20	15.2	76	73	73 (10)
Syringaldehyde	5	10	3.0			8	3.7	56	102–103	103–104 (9)

*Fine, needle-shaped orange crystals, recrystallized from methanol–water.
†Calc. for $C_{10}H_{11}O_3N$: C, 62.16; H, 5.74%. Found: C, 61.80; H, 5.88%.

Can. J. Chem. Downloaded from www.nrcresearchpress.com by 210.87.254.6 on 09/05/12
For personal use only.

TABLE V

The preparation of 1-aryl-2-propanones

$ArCH{=}C(NO_2)CH_3$ Ar =	Weight, g	Ethanol ml	Water ml	Fe powder g	12*N* HCl ml	$FeCl_3$ g	1-Aryl-2-propanone g	Yield, %	Found	Reported
p-Hydroxyphenyl	4	50	150	10	5	0.4	2.2	66	b.p. 140° at 0.08 mm	m.p. 35° (14)
p-Methoxyphenyl	10	150	350	20	10	0.8	6.2	73	b.p. 110° at 0.2 mm	b.p. 150° at 20 mm (15)
4-Hydroxy-3-methoxyphenyl	20	200	500	40	20	1.6	13.4	78	b.p. 125° at 0.45 mm	b.p. 115° at 0.15 mm (9)
3,4-Dimethoxyphenyl	10	150	350	20	10	0.8	6.6	76	b.p. 122° at 0.6 mm	b.p. 118° at 0.2 mm (16)
4-Hydroxy-3,5-dimethoxyphenyl	4.7	50	150	10	5	0.32	2.6	63	m.p. 67–68°	m.p. 68–69° (9)
3,4,5-Trimethoxyphenyl	2.8	25	120	5	2.5	0.06	2.2	89	m.p. 66–67°	*

*Recrystallized from diethyl ether to give white crystals. Calc. for $C_{12}H_{16}O_4$: C, 64.27; H, 7.19%. Found: C, 64.03; H, 7.35%.

TABLE VI

The preparation of aroyl methyl ketones

$ArCH_2COCH_3$, Ar =	Weight, g	Selenium dioxide, g	Dioxane:water, ml:ml	Aroyl methyl ketones g	Yield, %	Found	Reported
Phenyl	20	16	100:20	13.1	60	b.p. 110° at 10 mm	b.p. 102° at 12 mm (11)
p-Hydroxyphenyl	3.5	2.5	15:3	1.5	44	m.p. 92–93°	m.p. 92–93.5° (17)
p-Methoxyphenyl	3.5	2.3	15:3	1.2	33	m.p. 44–45°	m.p. 46° (18)
4-Hydroxy-3-methoxyphenyl	2.0	1.1	10:2	0.7	32	m.p. 70–71°	m.p. 70–71° (3)
3,4-Dimethoxyphenyl	3.0	1.6	15:3	1.1	34	m.p. 67–68°	m.p. 69–70° (16)
4-Hydroxy-3,5-dimethoxyphenyl	2.0	0.9	10:3	0.25	11.4	m.p. 78–79°	m.p. 80–81° (4)
3,4,5-Trimethoxyphenyl	3.0	1.4	15:3	1.2	37.6	m.p. 65–66°	*

*Recrystallized from petroleum ether as yellow crystals. Calc. for $C_{12}H_{14}O_5$: C, 60.50; H, 5.92%. Found: C, 60.51; H, 6.01%.

point depression with an authentic sample; identical infrared spectrum with that of an authentic sample; and by analysis. Calc. for $C_8H_8O_4$: C, 57.1; H, 4.76; OCH_3, 18.4%. Found: C, 57.13; H, 4.92; OCH_3, 18.27%.

(ii) Purification of vanilloyl methyl ketone via the column chromatography method.—A chromatographic column (2 in.×30 in.) was half filled with dry petroleum ether (b.p. 40–60°) and silica gel (200 g) was added slowly with constant stirring. During this addition the petroleum ether was slowly drawn off from the bottom and the loss replaced through the top. When an air-bubble-free, well-packed column was obtained, the petroleum ether was drawn off until a 0.5-cm layer of solvent remained above the column packing. The crude oxidation product (2.0 g) was dissolved in a minimum amount of diethyl ether and placed on the top of the column. Elution with petroleum ether (40–60°) resulted in the slow separation of a yellow band. After the passage of 2 liters of the eluant, the band had moved one-third the length of the column. At this stage 5% diethyl ether was added to petroleum ether and 1.5 liters of this mixed solvent eluted the band completely. Evaporation of the solvent left yellow crystals of vanilloyl methyl ketone (0.92 g, 33%). After recrystallization from ethanol–water the melting point was 70–71°; reported m.p. 70–71° (9). The quinoxaline derivative melted at 160–161°; reported m.p. 162–163° (3).

In a similar manner six other aroyl methyl ketones were synthesized and isolated. The experimental data are given in Table VI.

ACKNOWLEDGMENT

Financial assistance from the National Research Council is gratefully acknowledged.

REFERENCES

1. F. E. Brauns. The chemistry of lignin. Academic Press Inc., New York. 1952. Chap. XV.
2. F. E. Brauns and D. A. Brauns. The chemistry of lignin. Supplement volume. Academic Press Inc., New York. 1960. Chap. XV.
3. L. Brickman, W. L. Hawkins, and H. Hibbert. J. Am. Chem. Soc. **62**, 2149 (1940).
4. M. Kulka, W. L. Hawkins, and H. Hibbert. J. Am. Chem. Soc. **63**, 2371 (1941).
5. P. C. Roberti, R. F. York, and W. S. MacGregor. J. Am. Chem. Soc., **72**, 5760 (1950).
6. J. Gierer. Acta Chem. Scand. **8**, 1319 (1954).
7. J. Gierer. Ber. **89**, 257 (1956).
8. I. A. Pearl. J. Am. Chem. Soc. **78**, 4433 (1956).
9. M. Kulka and H. Hibbert. J. Am. Chem. Soc. **65**, 1180 (1943).
10. H. Kaufmann. Ber. **52**, 1431 (1919).
11. J. Wegmann and H. Dahn. Helv. Chim. Acta, **29**, 1247 (1946).
12. H. Richtzenhain. Ber. **81**, 260 (1948).
13. P. Hey. Quart. J. and Year Book of Pharmacy, **20**, 129 (1947).
14. E. L. Brazidic. Bull. Soc. Chim. **31**, 255 (1922).
15. G. D. Goodall and R. D. Haworth. J. Chem. Soc. 2486 (1930).
16. A. M. Eastham, H. E. Fisher, M. Kulka, and H. Hibbert. J. Am. Chem. Soc. **66**, 26 (1944).
17. K. Kratzl and W. Schweers. Ber. **89**, 186 (1956).
18. W. Brosche. Ber. **40**, 740 (1907).

Can. J. Chem. Downloaded from www.nrcresearchpress.com by 210.87.254.6 on 09/05/12
For personal use only.

THEORETICAL STUDIES ON THE ELECTRONIC SPECTRA OF SUBSTITUTED AROMATIC MOLECULES

PART II. SEMIEMPIRICAL SELF-CONSISTENT FIELD CALCULATIONS ON ANILINE

J. E. Bloor, P. N. Daykin, and P. Boltwood

British Columbia Research Council, University of British Columbia, Vancouver, British Columbia

Received July 15, 1963

ABSTRACT

The results of 14 calculations on the aniline molecule using different choices of parameters within the framework of the semiempirical SCFMO method have been carried out using an automatic Fortran 1A program written for an I.B.M. 1620 computer. It has been shown that the approximation of using the valence state ionization potential as a measure of the core integral of a heteroatomic substituent underestimates the amount of electron transfer between substituent AO and the benzene MO's. By adjusting this core integral empirically or by using a variable electronegativity MO approach it has been found possible to obtain, for the same set of parameters, agreement between experiment and theory for: the first two electronic transitions in the vapor state (4.23–4.38 ev and 5.22–5.41 ev), the change in ionization potential relative to benzene (AI = 1.54 ev), and the electron density para to the amino group (ρ_4^{π} = 1.059). It was not found possible to calculate values for the π-electron dipole moment and oscillator strengths which agreed, for any reasonable choice of parameters, with experimental values.

Can. J. Chem. Downloaded from www.nrcresearchpress.com by 210.87.254.6 on 09/05/12
For personal use only.

The semiempirical Self Consistent Field Molecular Orbital (SCFMO) theory as formulated by Pariser and Parr and Pople (1–4) is known to give calculated transition energies in fairly good agreement with those obtained experimentally for hydrocarbons. The reliability of the method for molecules with polar substituents in cases other than the replacement of a ring carbon atom by a nitrogen atom (5–9) have not been very thoroughly tested. We have therefore carried out a number of calculations on the SCFMO's of aniline using different approximations for the calculation of repulsion integrals and core integrals to try to obtain some insight as to the sensitivity of the SCFMO method to the values used for the basic parameters of the theory.

METHODS OF CALCULATION

The details of the approximations introduced by Pople and Pariser and Parr into the closed shell Hartree Fock method (9) in order to make it feasible to carry out calculations on conjugated systems have been described elsewhere many times (1–8) and only a summary necessary for the discussion will be given here. If the molecular orbitals (MO's) are expressed as linear combinations of atomic orbitals (AO's) ϕ_p [1],

$$\psi_i = \sum_{p}^{N\pi} C_{ip}\phi_p \qquad [1]$$

then the one-electron Hartree Fock problem for closed shell π-electron systems reduces to a matrix having elements [2] and [3].

$$F_{pq} = H_{pq}{}^{c} - \tfrac{1}{2}P_{pq}\gamma_{pq}, \quad p \neq q \qquad [2]$$

$$F_{pp} = H_{pp}{}^{c} + \sum_{q} P_{pq}\gamma_{pq} - \tfrac{1}{2}P_{pp}\gamma_{pp}, \qquad [3]$$

where P_{pq} is an element of the bond order matrix [4]

[4] $$P_{pq} = 2\sum_{i}^{N_{occ}} C_{ip}C_{iq};$$

the sum extending only over the occupied MO's N_{occ}. The eigenvectors C_{ip} and the orbital energies E_i are determined by the secular equation [5]:

[5] $$\sum_{p}^{N\pi} C_{ip}F_{pq} = E_iC_{iq}.$$

Since the eigenvectors used in [4] must also satisfy [5] some form of iterative procedure must be adopted. The numerical process used in the I.B.M. 1620 Fortran 1A program constructed for this investigation is described in the appendix. The process provides virtual as well as occupied MO coefficients and energies.

The central problem of assigning semiempirical values to the core terms $H_{pq}{}^{c}$ and atomic repulsion integrals γ_{pq} is discussed below.

Calculation of Core Matrix Elements

The off-diagonal elements $H_{pq}{}^{c}$ in [2] are very difficult to calculate theoretically so we have followed the common practice of treating them as empirical parameters β_{p-q} which have a value within the range -2.0 to -3.0 ev for the core where p and q are adjacent atoms contributing π-electrons. All other elements $H_{pq}{}^{c}$ are then neglected.

The diagonal elements $H_{pp}{}^{c}$ may be expanded as in [6]:

[6] $$H_{pp}{}^{c}(i) = \int \phi_p(i)\left|T_{(i)} + \sum_{q\neq p} U_q{}^{n_{q+}}(i) + \sum_{S} U_S(i) + \sum_{p} U_p{}^{n_{p+}}(i)\right|\phi_p(i)dv.$$

Where $U_q{}^{n_{q+}}$ represents the potential due to the core of atom q (with the n electrons contributing to the π-electron system removed) U_S represents the potential due to an atom S which does not contribute π-electrons to the system under consideration. T is the kinetic energy operator. The Goeppert–Mayer–Sklar approximation (10) [7] is utilized for the evaluation of the contribution of $(T+U_p{}^{n_{p+}})$

[7] $$\int\phi_p(i)|T(i)+U_p{}^{n+}(i)|\phi_p(i)dv = E_p = -I_p{}^{(n-1)+}$$

where $I_p{}^{(n-1)+}$ is the ionization potential of atom p in the appropriate valence state calculated using valence state tables (11).

The core terms in the first summation in [6] can be written in terms of a potential due to a neutral atom $U_q{}^{0}$ and a correction term allowing for the repulsion of the π-electrons contributed by that atom. Thus for an atom q contributing n π-electrons to

[8] $$U_q{}^{n+}(i) = U_q{}^{0}(i) - \sum_{j\neq i}^{n}\int\frac{\phi_q{}^{2}(j)}{r_{ij}}dv_{ij}$$

[9] $$H_{pp}{}^{c} = -I_p{}^{(n-1)+} - \sum_{p\neq q}(U_q{}^{0}{:}pp + n_q\gamma_{pq}) - \sum_{S} U_S{:}pp$$

the system we can write [8]. Then for the diagonal element $H_{pp}{}^{c}$ we can write [9]. The terms $U_S{:}pp$ and $U_q{}^{0}{:}pp$ are penetration integrals for neutral atoms following the convention that

$$U_S{:}pp = -\int U_s(i)\phi_p{}^{2}(i)dv(i).$$

The presence of the summation term over the number (n_r) of π-electrons contributed by atom r when $n_r > 1$ has led to some confusion in the literature (12). For example in the early work by Dewar and Paolini (13) it appears that only the repulsion of one

Can. J. Chem. Downloaded from www.nrcresearchpress.com by 210.87.254.6 on 09/05/12
For personal use only.

π-electron was included. In the case of Brown and Heffernan's work on pyrrole (8) the repulsion term for only one π-electron was included but then the penetration integrals for the nitrogen were calculated using an effective nuclear charge corresponding to N^+ rather than the neutral atom. In some of the more recent work (14–15) not enough data has been included to decide which approximation has been used. In the present work the core integral for the nitrogen (N^{2+}) has been approximated to that of a neutral nitrogen corrected by the repulsion of two π-electrons. The penetration integrals for nitrogen, carbon, and hydrogen have then been neglected. Some justification for this procedure has been given in the case of aniline by Peradejordi (17), who has shown that the penetration integrals, to be included in the core term of the nitrogen, add up to the same value as those for the carbon atoms. Leaving them out is tantamount to adjusting the energy zero of the orbitals and will not affect either the excited state energies or the charge distribution, although, as discussed later, this omission does alter the absolute value of the orbital energies.

Calculation of Repulsion Integrals

The calculation of the repulsion integrals γ_{pq} defined by [10],

$$\gamma_{pq} = \int \phi_p(i)\phi_p^*(i)(1/r_{12})\phi_q(2)\phi_q^*(2)dv_1dv_2, \qquad [10]$$

is probably the part of the theory which is at present the least satisfactory. It was shown by Pariser and Parr (1, 2) that if the values calculated theoretically using Slater orbitals are used then the calculated excited states even for hydrocarbons turn out to be far too high. They therefore proposed a method of calculating them empirically using data obtained from atomic spectra. For the one-center integrals γ_{pp} they proposed [11],

$$\gamma_{pp} = I_p - A_p, \qquad [11]$$

where I_p is the ionization potential of atom p in the valence state appropriate to the particular molecule under consideration and A_p is the electron affinity for the same valence state. For the two-center integrals γ_{pq} ($r_{pq} \geqslant 2.8$ Å) they proposed the formulae [12] and [13] based on treating the π-electronic charge distribution as charged spheres so giving [12] and [13] where Z_p is the Slater effective nuclear charge for atom p.

$$\gamma_{pq}(r) = \frac{7.1975}{r}\left\{\left[1+\left(\frac{R_p-R_q}{2r_{pq}}\right)^2\right]^{-\frac{1}{2}}+\left[1+\left(\frac{R_p+R_q}{2r_{pq}}\right)^2\right]^{-\frac{1}{2}}\right\} \qquad [12]$$

$$R_p = (4.597/Z_p). \qquad [13]$$

For distances shorter than 2.8 Å an extrapolation procedure [14] was adopted.

$$\gamma_{pq} = \tfrac{1}{2}[\gamma_{pp}+\gamma_{qq}]-ar-br^2 \qquad [14]$$

where a and b are found by using the values calculated from [12] for $r = 2.80$ Å and $r = 3.7$ Å. This method of calculating repulsion integrals has been adopted in the great majority of semiempirical SCF calculations published up to date. However it is clear from the work of Pariser (1) and the more recent work of Lykos (17) that even for hydrocarbons this method of calculating the two-center repulsion integrals is not suitable for calculations on excited states. To obtain satisfactory results for polyacene hydrocarbons it is necessary (1, 18, 19) to construct an empirical $\gamma_{pq}{}^r/r_{pq}$ curve from values obtained for benzene by equating the theoretical excited state energies to the experimental values. This curve can then be extended to greater r_{pq} values using either the values calculated from Slater orbitals or by using equation [14]. If [14] is used it should be noted that for

Can. J. Chem. Downloaded from www.nrcresearchpress.com by 210.87.254.6 on 09/05/12
For personal use only.

values >4.0 Å, the value obtained is very insensitive to the nature of p and q and the repulsion integral becomes independent of the nature of atoms p and q, and depends only on the distance r_{pq}.

An alternative to the Pariser–Parr formulation for the calculation of repulsion integrals, which has been used quite successfully in calculating the excited states of polyacene hydrocarbons (20), is that proposed by Mataga (6). In this method the one-center integrals are evaluated from [11] or by the Paolini approximation [18] discussed below. The two-center integrals are assumed to be of the form [15–16]:

$$\gamma_{pq}(r) = \frac{14.397}{a_{pq}+r_{pq}} \text{ ev}, \qquad [15]$$

$$a_{pq} = \frac{28.794}{(\gamma_{pp}+\gamma_{qq})} \text{ ev}. \qquad [16]$$

This method has been used apparently successfully on calculations described elsewhere (21) and was used as the starting point in many of the earlier calculations described below. It, however, has been found to be unsatisfactory (21) in cases where the substituent attached to the benzene ring ions is polyatomic (e.g. —HC, $=CH_2$, —C≡N, and $—NO_2$).

The Variable Electronegativity Method

As will be reported elsewhere, the simple SCF methods described above were found to be unsatisfactory for molecules where there was an uneven charge distribution due to the presence of more than one hetero atom in the molecule, e.g. in nitrobenzene and *p*-nitroaniline. The chief source of this error appears to lie in the choice of I_p which is assumed to be independent of the environment of atom p in the molecule. It has recently (8) been suggested that an improvement over the simple SCF method may be obtained by assuming both I_p and γ_{pp} to be dependent on the charge distribution at atom p in the particular molecule under consideration. We have therefore carried out two calculations using this method in the case of aniline. The dependency of I_p and γ_{pp} on the charge density P_{pp} is formulated in terms of the Slater effective nuclear charge Z_p which is related to the π-electron density P_{pp} by [17],

$$Z_p = N_p+K_1^p+K_2^pP_{pp}, \qquad [17]$$

where N_p is the atomic number of atom p, K_1 is a constant incorporating the constant part of Z_p due to the σ bonds and the lone pairs, and K_2 is a constant equal to -0.35 for atoms in the first row of the periodic table.

The one-center integrals were calculated from Z_p using the relationship [18] suggested by Paolini (7):

$$\gamma_{pp} = 3.294Z_p. \qquad [18]$$

The two-center integrals γ_{pq} were either found from the Mataga approximation [15] using the π_{pp} obtained from [18] at each iteration or, since their variation is quite small, they were kept constant after being calculated at the first iteration. The elements I_{pp} were calculated from the parabolic relationship [19],

$$I_{pp} = K_2Z_p^2+K_3Z_p+K_4, \qquad [19]$$

where K_2, K_3, and K_4 were constants obtained by fitting the Z values for an isoelectronic series calculated from valence state tables (11) and correcting for the valency of the atom

Can. J. Chem. Downloaded from www.nrcresearchpress.com by 210.87.254.6 on 09/05/12
For personal use only.

using the method suggested by Brown (8). The final values of the repulsion integrals provided by the SCF calculation were used in the configuration interaction calculations described below.

Calculation of Excited State Energies

The excited states of a molecule, e.g., Ψ_I can be expressed as a linear combination [20] of individual configurations ψ_i^k in which an electron has been excited from MO ψ_i into MO ψ_k. The mixing coefficients $A_I^{(ik)}$ and the excitation energies are obtained by diagonalizing a configuration interaction matrix with elements given by [21]. In [21] E_i is the orbital energy of the SCFMO ψ_i. $\langle ik|jl\rangle$ and $\langle ij|kl\rangle$ are molecular repulsion integrals defined by [22]. For the two lowest excited excitation energies of aniline it was found necessary to include only the configurations involving excitations from the two highest occupied MO's to the lowest unoccupied MO's.

The oscillator strength f_I of the Ith excited state of energy E_I was calculated using [23] where $Q_{0\to I}$ is the transition moment (1). The π-electron dipole moment of the ground state was calculated using [24].

[20] $$\Psi_I = \sum A_I^{(ik)} \psi_i^k$$

[21] $$({}^1\psi_i^k|H|{}^1\psi_j^l) = \delta_{ij}\delta_{kl}(E_k - E_i) + 2\langle ik|jl\rangle - \langle ij|kl\rangle$$

[22] $$\langle ik|jl\rangle = \sum_p \sum_q C_{ip}C_{kp}C_{jq}C_{mq}\gamma_{pq}$$

[23] $$f_I = 8.753\times 10^{-2} Q_{0\to I}^2 E_I. \quad (Q_{0\to I} = \int \Psi_0 e\mathbf{r}\Psi_I dv)$$

where L_{xp} L_{yp} L_{zp} are the co-ordinates of atom p, and Z_p is the number of electrons contributed by atom p to the π-electron system.

[24] $$\mu^\pi = 4.8\left[\left\{\sum_j^{x,y,z}\left[\sum_p^{N\pi} L_{jp}(z_p - p_{pp})\right]^2\right\}^{\frac{1}{2}}\right]$$

EXPERIMENTAL DETERMINATION OF TRANSITION ENERGIES

The primary purpose of this investigation was to obtain a set, or sets, of parameters which gave calculated transition energies fairly close to the observed ones for aniline so that these parameters for the amino nitrogen in aniline could be used in interpreting the spectra of other aromatic amino compounds. Since, for monosubstituted benzenes, the actual changes in the transition energies of the parent molecule on substitution are quite small (e.g. the change in the transition energies of the first and second transitions of benzene on substituting one hydrogen for a dimethylamino group, which is one of the strongest electron donating groups, are only 0.76 and 1.1 ev respectively (measurements in iso-octane solution)), it is necessary to obtain accurate experimental results. We have therefore re-examined the spectra of aniline in the vapor state using a Cary 14 spectrophotometer. As previously reported by Matsen (22) the first transition contains a large number of vibronic lines. The 0–0 transition is located at 34,130 cm^{-1} (4.23 ev) and the line of maximum intensity, corresponding to the Frank–Condon transition, is at 35,340 cm^{-1} (4.38 ev). Fine structure was also observed for the second transition and is reported apparently for the first time. The fine structure consisted of a shoulder at 42,100 cm^{-1} (5.22 ev), a well-defined peak at 42,510 cm^{-1}, a shoulder at 43,100 cm^{-1}, a pronounced peak at 43,670 cm^{-1} (5.41 ev), and two ill-defined shoulders at 44,200 cm^{-1} and 44,640 cm^{-1}. Because of the small number of bands observed no vibrational analysis was

Can. J. Chem. Downloaded from www.nrcresearchpress.com by 210.87.254.6 on 09/05/12
For personal use only.

attempted and the 0–0 transition was arbitrarily taken to be at the first shoulder, i.e., at 5.22 ev.

The theoretical calculations of the transition energies are based on virtual orbitals obtained from a solution of the Schroedinger equation using parameters dependent on the ground state physical dimensions. Consequently an exact correspondence between the experimental 0–0 transition energies and the theoretical transition energies should not be expected since the latter correspond to a Frank–Condon transition to a hypothetical excited state possessing the same dimensions as the ground state. We have therefore assumed that a satisfactory theoretical transition energy should be greater than the observed 0–0 transition energy and probably less than the experimentally observed line of maximum intensity. Thus in the case of aniline a satisfactory calculation would give the first transition between 4.23 ev and 4.38 ev and the second transition between 5.22 ev and 5.41 ev.

DISCUSSION AND RESULTS

The results of 14 calculations using the methods described above are summarized in Tables I and II. In these calculations the parameters were not varied entirely syste-

TABLE I

Parameters and transition energies for aniline

Calc No.	I_{N^+}	Parameters, in ev (NN/NN)	β_{C-N}	Transition energies (ev) and oscillator strength (f) E_1*	f_1*	E_2†	f_2†	E_3	f_3	E_4	f_4
1	29.14	14.36‡	−2.0	4.85	.006	5.96	.025	6.93	1.15	6.90	1.22
2	23.0	14.36‡	−2.5	4.24	.077	5.16	.240	6.26	.81	6.6	.80
3	23.5	14.36‡	−2.5	4.34	.070	5.25	.400	6.34	.89	6.58	.84
4	24.38	14.36‡	−2.5	4.49	.057	5.39	.336	6.61	.89	6.49	.85
5	24.38	14.36‡	−2.0	4.54	.021	5.36	.314	6.35	.86	6.56	.71
6	24.38	12.74‡	−2.5	4.68	.036	5.63	.194	6.76	1.12	6.76	.99
7	28.16	15.92‡	−2.59	4.71	.030	5.738	.139	6.80	1.169	6.80	1.03
8	25.0	15.92‡	−2.59	4.35	.069	5.30	.378	6.70	1.031	6.61	.800
9	24.38	15.92‡	−2.75	4.23	.080	5.25	.45	6.70	1.042	6.61	.752
10	24.38	15.92‡	−2.50	4.23	.070	5.20	.42	6.68	.982	6.56	.75
11	24.38	15.92‡	−2.00	4.21	.040	4.96	.42	6.48	.641	6.00	.74
12	25.00	14.36§	−2.50	4.32	.070	5.36	.341	6.28	1.32	6.08	.773
13	24.38	12.98‖	−2.50	4.64	.030	5.59	.24	6.68	1.35	6.64	.962
14	24.72	13.03‖	−2.50	4.50	.050	5.21	.16	6.49	1.17	6.41	.878

*Exp. values 4.23–4.38 ev, f = 0.03.
†Exp. values 5.22–5.41 ev, f = 0.17.
‡Mataga approx. [11] for γ_{pq}.
§Pariser–Parr method for γ_{CN} [12–14].
‖Variable electronegativity method.

matically but were largely based on values reported in the literature for calculations on amino compounds. The starting point in the calculations was the rigid set of rules suggested by Pariser and Parr (2, 4) for choosing the parameters I_{N^+}, γ_{NN}, and γ_{CN} while the γ_{C-C} value was chosen by reference to the benzene spectrum (1). β_{C-N} was then regarded as an empirical parameter. As will be discussed in detail below such a procedure did not give satisfactory results since it underestimated the amount of electron transfer from the amino nitrogen to the benzene ring. Agreement with experiment can be achieved by treating I_{N^+} as an empirical parameter, as suggested by McWeeny for calculations on pyridine type compounds (5). However the introduction of two empirical elements I_{N^+} and β_{C-N} has considerably reduced the fundamental significance of the approach. It is known from calculations using the simple Huckel LCAO method with two similar empirically chosen parameters α and β that it is possible to adjust these values to fit almost

Can. J. Chem. Downloaded from www.nrcresearchpress.com by 210.87.254.6 on 09/05/12
For personal use only.

TABLE II

Calculated dipole moments, changes in ionization potential and charge densities in aniline

Calc No.	μ^π (Debyes)	$-E_4$ ev	ΔI*	ρ_4^π	ρ_2^π	$(\Delta\rho_2^\pi/\Delta\rho_4^\pi)$
1	0.566	10.245	0.18	1.014	1.026	2.17
2	2.805	8.562	1.86	1.057	1.090	2.90
3	2.361	8.761	1.62	1.052	1.084	2.80
4	1.975	9.086	1.43	1.045	1.074	2.64
5	1.421	9.265	1.16	1.032	1.052	2.60
6	1.356	9.54	0.88	1.036	1.063	2.42
7	1.394	9.71	0.71	1.032	1.060	2.22
8	2.525	8.84	1.58	1.055	1.092	2.63
9	3.135	8.600	1.82	1.065	1.107	2.74
10	2.700	8.650	1.77	1.058	1.095	2.71
11	2.078	8.725	1.69	1.044	1.071	2.73
12	2.093	9.80	1.79	1.036	1.091	1.72
13	1.578	9.729	0.69	1.026	1.045	2.50
14	1.874	10.16	1.06	1.029	1.062	1.937

*Experimental quantities: $\mu^\pi = 1.02$ D, $\Delta I = 1.54$ ev, $\rho_4^\pi = 1.059$.

any set of experimental data. The situation was somewhat improved by using the VESCF method of obtaining I_{N^+}. In this method I_{N^+} is allowed to vary with the Slater effective nuclear charge according to [19]. The procedure described by equations [17] and [19] may be regarded as taking into consideration correlation effects between the two π-electrons on the nitrogen and between the nitrogen π-electrons and the carbon π-electrons. As P_{pp} increases the effective Z_p decreases so lowering the effective "electropositivity" of the nitrogen nucleus resulting in a lower value of $H_{pp}{}^c$.

When these calculations were started it was hoped that some information about the valence state of the amino nitrogen would be obtained by comparing the calculated and experimental results of the various physical quantities discussed below. There is a considerable body of evidence from infrared spectroscopy (24, 25), microwave absorption (26), and structural determinations (27, 28, 29) that the bonds about an amino group are not planar even in an amide such as formamide, where considerable conjugation between the amine group and the electron attracting carbonyl group is to be expected. The valence state of the nitrogen lone pair in the planar configuration would be that of a $2p$ π-electron and in the pyramidal configuration it would be sp^3. This difference in the valence state would be expected to be reflected both in the I_{N^+} value and the β_{C-N} value. Thus I_{N^+} $(\pi) = 28.17$ ev and I_{N^+} $(sp^3) = 33.3$ ev (11). If we assume the resonance integral β_{C-N} to be proportional to the overlap integral S_{C-N} we would expect β_{C-N} for sp^3 nitrogen to be only 0.61 of β_{C-N} for sp^2 nitrogen at $r = 1.36$ Å. Since, however, we have only been able to obtain agreement between experiment and theory by taking I_{N^+} much lower than either of the two values obtained from valence state tables it has not been possible to come to any conclusion regarding this problem.

The results of the calculations treating NH_2 as a monatomic substituent contributing two π-electrons to the system, are set out in Table I. In calc. 1, I_{N^+} was obtained using valence state tables (11), γ_{NN} was obtained using [11], and the two-center γ_{pq} were calculated using the Mataga approximation [15, 16]. For β_{C-N} an empirical value of -2.0 ev was chosen as being compatible with other work on substituted benzenes (21).

The calculated excitation energies (columns 5–12, Table I) were found to be much too high and were more like the values expected for a weakly interacting substituent such as Cl or OH rather than for the supposedly strongly interacting NH_2 group. In calc. 2 the

Can. J. Chem. Downloaded from www.nrcresearchpress.com by 210.87.254.6 on 09/05/12
For personal use only.

I_{N^+} value was dropped considerably to 23.0 ev and β_{C-N} was raised to -2.50 ev. This causes the value for the second excited state to be lowered outside the satisfactory limits. Raising I_{N^+} by 0.5 ev (calc. 3) now gives quite good agreement between experiment and theory. Since a value of I_{N^+} used in calc. 3 is quite close to that suggested by McEwen (23) for an amino nitrogen in nitramine (NH_2NO_2) (i.e., 24.38 ev) calculations using this value and $\beta_{C-N} = -2.5$ ev (calc. 4) and $\beta_{C-N} = -2.0$ ev (calc. 5) were carried out. The value of the first excited state now has become rather higher than the experimental value. To make a fairer comparison with McEwen's work however a calculation was carried using the same value for γ_{NN} as used by McEwen (calc. 6). The result was a considerable increase in the transition energies of both the first two excited states placing the energies well outside our criteria for a satisfactory calculation.

Calculations 4, 6, and 10 in which the only variation is the value of γ_{NN} show the appreciable sensitivity of the SCF method to the values used for the repulsion integrals. Previous workers have tended to ignore this factor (30), although it is of course implicit in Pariser's (1) work since he was unable to fit experimental values of the benzene transitions without choosing his γ_{CC} values very carefully.

In earlier calculations on aniline using equations [1–13] for the calculations of γ_{pq}, Peradejordi (16, 21) found the values $I_{N^+} = 28.16$, $\gamma_{NN} = 15.92$ ev, and $\beta_{C-N} = -2.59$ ev to be quite suitable parameters for aniline. Calculation no. 7 utilized these parameters but used the Mataga method [14–15] for determining the two-center integrals. It can be seen that again the calculation cannot be regarded as satisfactory since the transition energies are much higher than our limits for a satisfactory calculation.

The I_{N^+} was then reduced to 25.0 ev (calc. 8) and then to 24.38 ev (calcs. 9–11). In calcs. 9–11 I_{N^+} was kept constant but β_{C-N} was decreased gradually through the values -2.0, -2.5, and -2.75 ev. These last three calculations show that although the first transition energy is very insensitive to β_{C-N} the second transition energy is lowered in energy as β_{C-N} decreases. This rather unexpected increase in transition energy with decrease in the resonance integral β_{C-N} is apparently due to the increase in the energy of the second lowest unoccupied MO (E_6) as β_{C-N} is increased, due to the term F_{17} (as defined in equation [2]) in [25] for the orbital energy E_i which outweighs the increase in energy of E_4. In a molecule where the interaction of the substituent X is not as great as in

$$[25] \qquad E_i = \sum_{p}^{N\pi} \sum_{q}^{N\pi} C_{ip} C_{iq} F_{pq}$$

aniline an increase in β_{C-X} would raise the energy of the highest interacting occupied MO more than any of the unoccupied MO's so that increase in β_{C-X} would result in a lowering of transition energy. However, in the case of aniline the mixing of the substituent AO with the benzene MO's is so great that it is no longer correct to relate any of the aniline MO's with those of the parent benzene.

Calculations 1–11 have been carried out using the Mataga approximation for γ_{pq}. In calc. 12 we have used values for γ_{cc} obtained from an empirical curve of $\gamma_{cc}{}^r$ against the C—C distance r obtained by equating the calculated transition energies for benzene to the experimental values quoted by Pariser (1). The γ_{CN} values were then obtained using equations [12–14]. The results using $I_{N^+} = 25.0$ ev, i.e. a value much lower than that usually proposed for amino nitrogen, were in satisfactory agreement with experiment for the transition energies. Since the empirical lowering of I_{N^+}, until agreement with experiment is found, is not a very satisfactory procedure, and since calculations on other mono- and di-substituted benzenes (21) had also demonstrated deficiencies of the simple

Can. J. Chem. Downloaded from www.nrcresearchpress.com by 210.87.254.6 on 09/05/12
For personal use only.

SCF method calculations were next carried out using the VESCF method. In calc. 13 the Mataga method was used to calculate the γ_{pq} values and both the γ_{pp} values and the γ_{pq} values were allowed to change with the charge density according to equations [15–16] and [18]. The final result for I_{N^+} and γ_{NN} are recorded in Table I (calc. 13) together with the excitation energies. It is seen that both I_{N^+} and γ_{NN} are quite close to those suggested by McEwen for amino nitrogen but much lower than the values usually used. However the excitation energies are considerably higher than the experimental values. In carrying out this calculation it was noted that the final off-diagonal γ_{pq} values of the repulsion integrals (R matrix) differed only slightly from the starting values so that variation of these off-diagonal elements at each iteration seems an unnecessary refinement. In calc. 14, therefore, only the diagonal elements of the R matrix were varied. However, the calculation differed from calc. 13 in that the off-diagonal elements of the R matrix were those obtained as in calc. 12 for γ_{c-c} and equations [13–15] were used for the γ_{CN} values. It can be seen from Table I that the agreement between experiment and theory for the energy of second transition is very good but for the first transition the energy is a trifle high. Relative to the approximations used in the theory however the results cannot be described as poor.

As far as the transition energies of the third and fourth transitions are concerned it is not possible to say very much. They appear at greater energies than 6.0 ev but the absorption curves given by Klevens and Platt (32) reveal only a very broad absorption from which it is impossible to infer a 0–0 transition energy of even a clear cut maximum. However, the value 6.3 ev has often been quoted in the literature and it can be seen from Table I that the theory, whatever the parameters used, does predict two transitions of high intensity in the region 6.2–6.8 ev.

Although the oscillator strengths of the first two transitions are known for aniline in solution, namely 0.03 for the first transition and 0.17 for the second, agreement between theory and experiment should not be expected since even for benzene, where the repulsion integrals were adjusted to give a good fit for the energy levels, the calculated oscillator strengths of the first two allowed transitions are much too high. (Calc. $f = 2.215$, exp. $f = 0.74$.) Similar discrepancies between experimental and calculated results have been reported for other polyacene hydrocarbons (1). High results may therefore be expected for the calculated oscillator strengths of aniline but the questions of whether an appropriate correction factor to the calculated f values can be applied (e.g. Baba (33) has suggested 0.3) and if so what is its magnitude can only be answered when more calculations and more experimental data on oscillator strengths (preferably in the vapor state) are made available. From the results of Table I however it can be seen that the calculated f values are not very sensitive to variation in parameters and that the ratio of f_{II}/f_I is usually a factor of two higher than the experimental value ($f_{II}/f_I = 5.4$). More calculations on other molecules using the same methods are required to find out whether this factor is specific to aniline or whether it can be carried over to other monosubstituted benzenes.

Calculation of π-Electron Dipole Moments

It is usual for π-electron dipole moments calculated by the Hückel theory to be rather higher than those estimated from experimentally determined dipole moments but it has been claimed that the SCF theory and the VESCF theory (8) will produce more realistic values. We have tabulated the calculated dipole moments of the π-electrons (μ^π) in column 2 of Table II. To compare these values with the experimentally determined

Can. J. Chem. Downloaded from www.nrcresearchpress.com by 210.87.254.6 on 09/05/12
For personal use only.

value it is necessary to adjust the latter for the dipole moment of the N—H bonds, any moment due to other σ bonds and for the spatial distribution of the hydrogen, the lone pair and the phenyl ring about the amino nitrogen.

To do this we have accepted the arguments of Everard and Sutton (34) which lead to a π-electron dipole moment of 1.02 D. This value is based on a μ (N—H) bond moment of 1.31 D and a tetrahedral distribution of bonds about the nitrogen.*

The results of the theoretical calculations of μ^π given in Table II show that in general the calculated contribution of the electrons to the total dipole moment is too high compared with the estimate obtained by experiment. However, it is clear that μ^π is very sensitive to the parameters used in the calculations. Thus, in reducing β_{C-N} from -2.75 ev (calc. 8) to -2.0 ev (calc. 11) we have lowered μ^π to one-third of its original value while changing I_{N^+} from 23.0 ev (calc. 2) to 23.5 ev (calc. 3) decreases μ^π by 16% and increasing I_{N^+} further to 24.38 ev decreases μ^π by 30%. The calculation using the VESCF method (calc. 14) has also quite a high value for μ^π which is no better than the ordinary SCF method for parameters which give good values for excited state energies. The calculations (1, 7, 13) which have low μ^π values are calculations using (except for calc. 13 which is a VESCF calculation) high I_{N^+} values and which give high transition energies and a small lowering of the ionization potential compared to benzene. With the exception of the last two (calc. 1 and 7) discussed above, all the μ^π values are much higher than those experimentally estimated. One must therefore conclude that it is not possible to choose parameters to obtain good agreement between theoretically calculated and experimentally estimated μ^π electron dipole moments and at the same time obtain agreement between theory and experiment for other quantities.

Charge Densities and Bond Orders

There is unfortunately, as yet, no reliable experimental method of obtaining data which are directly comparable with the elements of the charge density matrix, the elements of which are given by [4]. It has been suggested (35) that C^{13} nuclear magnetic resonance chemical shifts may be related to π-electron densities. Such a relationship appears to be obeyed by both alternant and non-alternant hydrocarbons. The linear relationship [27] has been obtained (36) by using hydrocarbons (C_6H_6, C_7H_{7+}, C_5H_{5-}) of known π-electron density (ρ^π) and the C^{13} chemical shift δ_C (p.p.m.)

$$\rho^\pi = (\delta_C/160)+1. \qquad [27]$$

The electron density at all the carbon atoms in a monosubstituted aromatic hydrocarbon can in principle be obtained if the δ_C values could be measured and [27] is assumed applicable to such compounds. Unfortunately, as pointed out by Spiesecke and Schneider (35), magnetic anisotropic effects play an important part in determining the chemical shift of both the carbon atom to which a substituent is attached and the neighboring one. For aniline therefore we only obtain reliable experimental values for ρ_4^π and ρ_3^π. Moreover (35) ρ_3^π in insensitive to the nature of the substituent on the C_1 atom. Using the experimental value for $\delta_C = 9.5$ (rel. to benzene) (35) for the C_4 atom in [27] we arrive at the value $\rho_4^\pi = 1.0594$. We can either relate this directly to that calculated by an SCF calculation or,

**There are many other estimates of μ^π to be found in the literature. They mostly lie within the range of 1.0–1.6 D. The main exception is a value of 0.7 D quoted by Fischer (14 and 41). This value, however, is probably subject to rather a large degree of uncertainty because it is based on a comparison of the dipole moments of alkyl amines and alkyl anilines, both ring and N-substituted, and no attempt is made to consider changes in bond angles and sigma bond moments in the various compounds.*

Can. J. Chem. Downloaded from www.nrcresearchpress.com by 210.87.254.6 on 09/05/12
For personal use only.

since in these calculations we have not taken into consideration any direct field effect or any inductive effect transmitted by the sigma electrons, we can attempt (38) to split the chemical shift into two contributions by an empirical method using standard substituent constants such as σ_I and σ_R suggested by Taft (37). Since, however, it seems likely (38) that the predominant factor determining the C^{13} chemical shift in the para position is a π-electron effect we have directly related ρ_4^π to the calculated π-electron density, therefore neglecting any sigma electron inductive effect or any direct electrostatic (field) effects.

Comparison of the experimental value for ρ_4^π with the theoretical values in column 5 of Table II shows that quite a number of calculations give ρ_4^π values quite close to 1.059. The calculations which disagree are those which quite clearly are underestimating the electron transfer from the NH_2 group to the ring (calc. 1, 7, and 13). For values of I^+_N in the region of 23–25 ev the calculated ρ_4^π values are not sensitive with change of I^+_N. Therefore, although ρ_4^π can be used to select parameters of the right order which, considering the many approximations in the semiempirical π-electron theory used here, is perhaps all that can be expected, it is not very reliable for pinpointing the best I^+_N value. The VESCF calculation (14) gives a ρ_4^π value of 1.029 predicting an electron transfer to the C_4 atom only one-half of that estimated experimentally.

The ratio ρ_2^π/ρ_4^π is of interest. No quantitative experimental estimation of this value is available but it is now generally accepted that the ortho position in a monosubstituted benzene C_6H_5X, where X is an electron donating group, is much more sensitive to electrophilic reagents than the para position. The Hückel theory tends to give a much lower value for this ratio than the SCF method so one can make the tentative conclusion that the SCF method of calculating electron densities is more in accord with experiment than the Hückel theory. The bond orders ρ_{pq} of aniline have also been calculated. Unfortunately there do not appear to be any experimental determinations of bond distances with which to compare the bond orders. All values of the parameters give ρ_{pq} values which correspond to a marked lowering of the bond order of the C_1—C_2 and C_1—C_6 bonds, where the amine group is attached to the C_1, while the C_2—C_3 and C_3—C_4 bond orders are relatively little changed. It would be of very great interest to have available accurate bond distance measurements, preferably in the vapor state, for C_6H_5X, where X is a fairly strong electron donating agent, to see whether the prediction of a longer C_1—C_2 bond is fulfilled experimentally.

Ionization Potential

Assuming Koopman's theorem to be correct for polar molecules (9) we can relate the ionization potential of a molecule to the energy of the highest occupied MO. However, the absolute value of energy of this MO is determined by the values of the parameters used for the kinetic energy and potential energy of the core and if constant factors (e.g. the penetration integrals and many integrals due to the sigma electrons) relating to these are omitted from the diagonal elements of the F matrix they will alter the absolute values of the orbital energies but not their relative values. In comparing calculated orbital energies with experimental energies then it is very important to use relative values. In Table II column 4 we report the difference between the orbital energies of the highest occupied MO's of benzene and aniline, the benzene energies being calculated using [28].

[28] $$E_3 = -I_C+\beta_{C-C}+\tfrac{1}{6}(3\gamma_{11}-2\gamma_{12}-\gamma_{14})$$

Can. J. Chem. Downloaded from www.nrcresearchpress.com by 210.87.254.6 on 09/05/12
For personal use only.

These values should be compared with the experimental difference of (9.24 ev -7.7 ev) = 1.54 ev.

From the results of Table II it can be seen that the calculated ionization potential difference ΔI is quite sensitive to the parameters used but that a number of calculations give a reasonably correct value (e.g. calc. 3, 8, 11, 12). It can be seen that calculations which give poor agreement for other properties (calc. 1, 6, 7, 13) also give poor values for ΔI. Calculations 6, 9, 10, 11 indicate that ΔI is not very sensitive to change in β_{C-N} although it is probable that this condition would not be found in cases where the electron interaction between substituent and ring are not so great. In general it does appear that ΔI values could be used as a guide in choosing parameters for substituents. The effect of changes in electron distribution of the ion $(C_6H_5NH_2)^+$ making use of the method formulated by Roothaan (39) for open shells and applied to hydrocarbons by Hoyland and Goodman (18) is under investigation in order to test the validity of Koopman's theorem for polar molecules.

COMPARISON WITH PREVIOUS CALCULATIONS

Prior to the work reported here there have been three semiempirical SCF calculations reported for aniline (14, 16, 40). No details of the work of Peradejordi have yet been published so comment will be restricted to the calculations by Peacock (40) and Fischer (14). In reference 40 the first two transition energies were both given as being at 4.3 ev. These should be discussed in conjunction with the values calculated for the excited states of the parent molecule benzene using the same values for the γ_{CC} repulsion integrals (5), these were found to be at 4.90 ev and 5.66 ev. Thus the relative change of the first transition energy corresponds well to the experimental value ($\Delta\epsilon$ exp. = .67 ev, $\Delta\epsilon$ calc. = 0.6 ev) while the effect of the amino group on the second transition is considerably overestimated (calc. 1.36 ev, exp. 1.0 ev). Since the calculation predicts that the first two transitions are completely superimposed on each other whereas they are observed to be quite separate then it would appear to be inadvisable to use Peacock's parameters, especially the repulsion integrals, in calculations designed to aid in assigning bands of unknown origin. No data were given on the ionization potential and charge densities. In the other SCF calculation on aniline (14) the parameters β_{CC} and γ_{CC} were chosen to fit the transition energies of benzene and the I_C and I_{N^+} value was obtained by reference to the ionization potential of benzene and ethylamine respectively. The remaining parameter β_{C-N} was then calculated in terms of the other parameters and found to be -1.452 ev, i.e., rather lower than the range used in the present calculations. The first two transition energies were calculated to be at 4.7 ev ($f = 0.15$) and 5.58 ev ($f = 0.19$), the ionization potential relative to benzene was calculated as 1.05 ev and ρ_4^π was found to be 1.015. Comparison of these results with the corresponding experimental ones (Tables I and II) indicate that the parameters used underestimate considerably the interaction of the amino group with the benzene ring. However, the calculated dipole moment $\mu^\pi = 0.78$ D compares very favorably with that estimated experimentally ($\mu^\pi = 0.7$ D) by a different procedure (41) from that used in the present work. It is because of the difficulties in extracting a reliable μ^π from the experimental dipole moment that we prefer to use transition energies, ionization potentials, and charge densities as criteria for selecting parameter values in semiempirical calculations. Unfortunately, for polar molecules, there are available very few experimental measurements of these properties, and of bond lengths, which are free from environmental effects, such as crystal forces and solvent effects. Such results, which can be used to compare with theoretical calculations, are badly needed.

Can. J. Chem. Downloaded from www.nrcresearchpress.com by 210.87.254.6 on 09/05/12
For personal use only.

CONCLUSIONS

The main conclusions of the present work may be summarized as:

1. The Pariser–Parr method described in [12–14] for calculating two-center repulsion integrals does not give values which may be used in calculations of transition energies of monosubstituted benzenes. However, satisfactory results can be obtained if the γ_{CC} values are obtained by equating the observed transition energies to the corresponding theoretical expressions for benzene and then calculating the repulsion integrals involving the hetero atoms by means of the Pariser–Parr formulation.
2. Two-center repulsion integrals for monosubstituted benzenes C_6H_5X where X is a monatomic substituent can be calculated satisfactorily for both γ_{CC} and γ_{C-X} if the Mataga approximation [14, 15] is used.
3. The usual method of obtaining the core integral I_X in C_6H_5X from valence state ionization potentials yields a value which when used in the Pariser–Parr–Pople SCF method for calculating physical properties yields results which indicate considerable underestimation of the interaction between the benzene MO's and the substituent X.
4. If I_X is treated as an empirical parameter then a value can be found which, when used in the simple SCF method and applied to aniline, yields values for the first two transition energies: the ionization potential, relative to that of benzene (i.e. ΔI), and the charge density at the para position (ρ_4^π), which are in good agreement with experimental values. On the other hand it has not been possible to find parameters which would also give satisfactory agreement between calculated oscillator strengths and the μ_4^π electron dipole moment and the values obtained from experimental data which would also give satisfactory results for the other physical properties.
5. Parameters suitable for use in simple SCF calculations for compounds using an amino type nitrogen are $I_{N^+} = 25.0$ ev, $\beta_{C-N} = -2.5$ ev, and $\gamma_{NN} = 14.36$ ev.
6. The undesirable feature of treating I_{N^+} as an empirical parameter can be avoided by using the VESCF method devised by R. D. Brown (8). However, even here, the results for the transition energies are barely within the admittedly rather stringent requirements for a satisfactory calculation as defined above and the amount of charge transfer between the substituent and ring appears to be only about a half of that required to give satisfactory results for ρ_4^π and ΔI.

Further work is in progress by one of us (J. E. B.) in an attempt to improve the agreement between theory and experiment for the physical properties of conjugated systems containing hetero atoms. Preliminary results indicate that an improvement in the choice of I_X is achieved by taking into consideration the shielding of the effective nuclear charge acting on the π-electrons caused by polarization of the σ bonds attached to the atom X.

ACKNOWLEDGMENTS

The financial aid given by the National Research Council of Canada and the British Columbia Research Council is gratefully acknowledged. Thanks are extended to the staff, particularly Mr. W. Dettwiler, of the Computing Center of the University of British Columbia, for their cooperation and help in preparing and running the computer programs for the IBM 1620.

APPENDIX: COMPUTER SOLUTION OF MOLECULAR SCF EQUATIONS

A program has been constructed for completely automatic solution of the restricted molecular SCF problem for π-electron spectra. Because the available computer, an IBM

Can. J. Chem. Downloaded from www.nrcresearchpress.com by 210.87.254.6 on 09/05/12
For personal use only.

1620, is comparatively slow, some thought was given to developing a procedure which would economize in computing time. Those time-saving procedures likely to be of general use are reported in this note.

The self-consistent field problem may be expressed in the following condensed form:

$$P_{rs} = \sum_{i}^{m} C_{ri}\tilde{C}_{is} \qquad [1]$$

$$F_{pq} = H_{pq}+G_{pq}(P_{rs}) \qquad [2]$$

$$\sum_{p,\,q}^{n} \tilde{C}_{ip}F_{pq}C_{qk} = E_i\delta_{ik} \qquad [3]$$

In [1] the sum extends over the $m < n$ eigenvectors, C_{ri}, representing the occupied orbitals. If the eigenvectors are arranged in sequence corresponding to an ascending order of the corresponding eigenvalues E_i, then the occupied orbitals are designated by a set of integers $(i_1, i_2, \ldots i_m)$. For the ground state of the molecule the occupied orbitals are represented by the first m ordered eigenvectors.

The eigenvalue problem (3) can be solved rapidly with the Jacobi method (42) in which a unitary transformation **C** which diagonalizes **F** is constructed. The matrix **C** so obtained is used in [1] and the sequence [1, 2, 3] repeated until self-consistency, as judged by some suitable criterion, is reached.

The process is elementary from a purely mathematical viewpoint, but some modifications in it can reduce substantially the required computing time. First, the **C** matrix used in [1] to construct the bond order matrix **P** can also be used in [3] to partially diagonalize H:

$$\tilde{\mathbf{C}}\mathbf{F}\mathbf{C} = \mathbf{F}_1.$$

This step requires about half of the time consumed by the Jacobi method to achieve the same degree of diagonalization. At this point the off-diagonal elements of $\mathbf{F}_1$ can be examined. If the greatest is less than some tolerance, t, which may be some chosen fraction of the largest diagonal element of **F**, then self-consistency has been obtained; otherwise the diagonalization is continued by the Jacobi method. (The above step is omitted on the first iteration because an accurately orthornormal **C** matrix is not usually available; instead **F** is diagonalized directly by the Jacobi method to the tolerance t.) Second, there is little merit in continuing the Jacobi process, in any one iteration, until the tolerance t has been reached, because **F** itself is constructed from an approximate matrix **C**. Instead, the Jacobi process should be terminated when the off-diagonal elements of $\mathbf{F}_1$ have been reduced to a fraction k, which appears to be 0.3 on the basis of the number of iterations required for average size molecules. Further economy in computing time could undoubtedly be realized by treating k as a variable whose value is related to the degree of self-consistency currently obtained. Third, the rate of convergence can be increased, substantially in favorable cases, by making use of Aitken's acceleration (43). The most convenient function to accelerate is the bond order matrix **P**. If $\mathbf{P}_1$, $\mathbf{P}_2$, $\mathbf{P}_3$ are three successive estimates of **P**,

$$\begin{aligned} \boldsymbol{\Delta}_1 &= \mathbf{P}_2-\mathbf{P}_1, \\ \boldsymbol{\Delta}_2 &= \mathbf{P}_3-\mathbf{P}_2, \\ \boldsymbol{\delta} &= \boldsymbol{\Delta}_2-\boldsymbol{\Delta}_1; \end{aligned}$$

then an estimate of the limit **P** of the sequence is

$$P_{ik} = P_{3ik}-(\Delta_{2ik})^2/\delta_{ik}.$$

Can. J. Chem. Downloaded from www.nrcresearchpress.com by 210.87.254.6 on 09/05/12
For personal use only.

Since the computation, once started, is outside the control of the program user, it is essential to include some automatic restriction on the acceleration. The acceleration is convergent in a broad sense provided

$$|\Delta_{2ik}| < |\Delta_{1ik}|.$$

However, consideration of a few well chosen examples will show that this condition is not stringent enough to prevent "wild" estimates of **P** from occurring. A more stringent convergence condition,

$$|\Delta_{2ik}| < |\delta_{ik}|,$$

has been written into the program. Acceleration can be elected beforehand by the program user for any suitable subsequence of the sequence of iterations, but its implementation is automatically subject to this convergence condition.

After the SCF problem for the ground state has been solved, the automatic calculation of π-electron excited states by configuration interaction is straightforward.

A typical calculation for aniline required eight iterations and a computing time of 35 minutes to give a bond order matrix self-consistent to the fourth significant figure. The computing times compare favorably with the times reported by Amos (34) for some hydrocarbons, using the method of steepest descents with a Mercury computer, whose basic multiplication speed is about 30 times that of the I.B.M. 1620.

Can. J. Chem. Downloaded from www.nrcresearchpress.com by 210.87.254.6 on 09/05/12
For personal use only.

REFERENCES

1. R. PARISER. J. Chem. Phys. **24**, 250 (1956).
2. R. PARISER and R. G. PARR. J. Chem. Phys. **24**, 466, 767 (1953).
3. J. A. POPLE. Proc. Phys. Soc. (London), A, **68**, 81 (1955).
4. H. C. LONGUET HIGGINS. Advances in chemical physics. Vol. 1. Interscience Publishers, Inc., New York. 1958. p. 239.
5. R. MCWEENY and T. E. PEACOCK. Proc. Phys. Soc. (London), A, **70**, 41 (1957).
6. N. MATAGA and K. NISHIMOTO. Z. Physik. Chem. (Frankfurt, A. M.) **13**, 140 (1957).
7. L. PAOLINI. Nuovo Cimento, **4**, 410 (1956).
8. R. D. BROWN and M. L. HEFFERNAN. Aust. J. Chem. **12**, 319, 330, 543, 544 (1959).
9. J. C. SLATER. Quantum theory of molecules and solids. Vol. 1. McGraw-Hill Co., New York. 1963.
10. M. GOEPPERT-MAYER and A. L. SKLAR. J. Chem. Phys. **6**, 645 (1938).
11. J. HINZE and H. H. JAFFE. J. Am. Chem. Soc. **84**, 640 (1962).
12. R. L. MILLER, P. G. LYKOS, and H. N. SCHMEISING. J. Am. Chem. Soc. **85** (1963).
13. M. J. S. DEWAR and L. PAOLINI. Trans. Faraday Soc. **53**, 261 (1957).
14. I. FISCHER-HJALMERS. Ark. Fys. **21**, 123 (1962).
15. M. SUARD, G. BERTHIER, and B. PULLMAN. Biochim. and Biophys. Acta, **52**, 254 (1961).
16. F. PERADEJORDI. Calcul des fonctions d'onde moleculair. CNRS, Paris. 1958. p. 247.
17. P. LYKOS. J. Chem. Phys. **35**, 1249 (1961).
18. J. R. HOYLAND and L. GOODMAN. J. Chem. Phys. **36**, 12 (1962).
19. J. E. BLOOR and N. BREARLEY. Unpublished work.
20. N. MATAGA, K. NISHIMOTO, and S. MATAGA. Bull. Chem. Soc. Japan, **32**, 395 (1959).
21. J. E. BLOOR and F. PERADEJORDI. Theoret. Chem. Acta (Berl), **1**, 83 (1962) and unpublished work.
22. N. GINSBURG and F. A. MATSEN. J. Chem. Phys. **12**, 167 (1945).
23. K. L. MCEWEN. J. Chem. Phys. **34**, 547 (1961).
24. S. F. MASON. J. Chem. Soc. 3619 (1958).
25. P. J. KRUEGER. Nature, **194**, 4833 (1962). Can. J. Chem. **40**, 2300 (1962).
26. T. J. BHATTACHARYGA. Ind. J. Phys. **36**, 33 (1962).
27. D. J. MILLEN, G. TOPPING, and D. R. LIDE, JR. J. Mol. Spectroscopy, **8**, 153 (1962).
28. C. C. COSTAIN and J. M. DOWLING. J. Chem. Phys. **32**, 158 (1960).
29. B. BAK. Advances in molecular spectroscopy. *Edited by* A. Mangini. Pergamon, New York. 1962. p. 3.
30. B. J. MCCLELLAND. Trans. Faraday Soc. **57**, 2073 (1961).
31. J. E. BLOOR. Data presented at the Hylleras Symposium, Florida, 1963. To be published. Rev. Mod. Phys. 1963.
32. H. B. KLEVENS and J. R. PLATT. Survey of vacuum ultraviolet spectra laboratory of molecular structure and spectra. University of Chicago. 1954.
33. H. BABA. Bull. Chem. Soc. Japan, **34**, 76 (1961).
34. K. B. EVERARD and L. E. SUTTON. J. Chem. Soc. 2821, 2826 (1951).
35. H. SPIESECKE and W. G. SCHNEIDER. J. Chem. Phys. **35**, 731 (1961).
36. H. SPIESECKE and W. G. SCHNEIDER. Tetrahedron Letters, 468 (1961).

37. R. W. TAFT, JR. J. Phys. Chem. **64**, 1805 (1960).
38. J. E. BLOOR. Unpublished work.
39. C. C. J. ROOTHAAN. Rev. Mod. Phys. **32**, 179 (1960).
40. T. E. PEACOCK. Mol. Phys. **3**, 453 (1952).
41. I. FISCHER. Ark. Fys. **5**, 377 (1952).
42. A. RALSTON and H. S. WILF. Mathematical methods for digital computers. Wiley, New York. 1959.
43. A. C. AITKEN. Proc. Roy. Soc. Edin. **46**, 289 (1925); **63**, 52 (1949).
44. A. T. AMOS. Mol. Phys. **5**, 91 (1962).

Can. J. Chem. Downloaded from www.nrcresearchpress.com by 210.87.254.6 on 09/05/12
For personal use only.

Can. J. Chem. Downloaded from www.nrcresearchpress.com by 210.87.254.42 on 09/05/12
For personal use only.

THE STRUCTURE AND STEREOCHEMISTRY OF ATISINE[1]

D. DVORNIK[2] AND O. E. EDWARDS
Division of Pure Chemistry, National Research Council, Ottawa, Canada

Received August 9, 1963

ABSTRACT

A stereospecific hydration of the exocyclic methylene group of a derivative of the alkaloid atisine has been observed. The product was used to degrade the alkaloid to a tetracyclic phenol. This enabled rigorous proof of the structure and relative and absolute stereochemistry of atisine and related alkaloids. A detailed explanation of the abnormal basic strength and the isomerization of atisine is given. Long-range influence of polar groups on the basic strength of derivatives of the alkaloid is reported.

When the investigations described herein were undertaken a structure (I) had been suggested by Wiesner and co-workers for the aconite alkaloid atisine (1) on the basis of the dehydrogenation and oxidation evidence of Jacobs and colleagues (2) and analogy to the structures assigned to the very similar Garrya alkaloids (1,3). Further evidence was later produced in support of this structure (4–7) but rigorous proof of the skeleton and location of the functional groups was lacking and the stereochemistry was unknown.

We now amplify our preliminary report (8) on work which led to proof that structure I is correct and that the stereochemistry of atisine is correctly represented by II (9, 10, 11).[3]

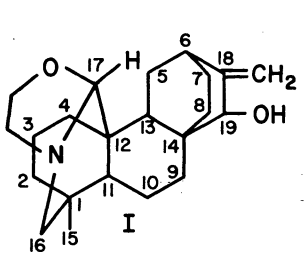

I

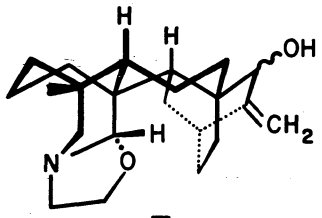

II

The initial object of this investigation was to prove by systematic degradation the environment of the allyl alcohol system in atisine. The starting material chosen was the very useful azomethine alcohol III prepared from atisine as described earlier (6).[4] It was found that in 10% aqueous hydrochloric acid III was converted to a mixture of two azomethine ketones, IV and the product of stereospecific hydration of the terminal

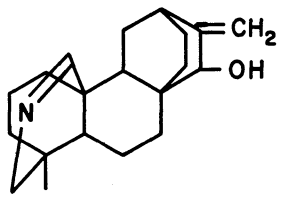

III

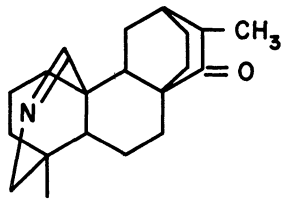

IV

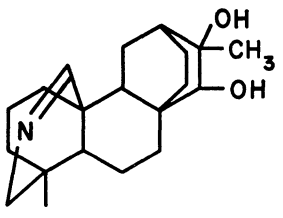

V

[1]*Issued as N.R.C. No. 7635.*
[2]*National Research Council Postdoctoral Fellow, 1955–57. Present address: Department of Biochemistry, Ayerst Research Laboratories, Montreal, Quebec.*
[3]*The numbering system is based on that suggested for pimarane by Klyne (6).*
[4]*This azomethine alcohol was also obtained as an oxidation product of atisine by Pelletier and Jacobs (7).*

methylene, the azomethine diol V. The isomerization of the allyl alcohol system to a methyl ketone under the influence of acid was observed by Jacobs and Huebner (12). Later Djerassi and co-workers (13) reported a similar transformation of the allyl alcohol system in garryfoline (VI) and Dreiding and Hartman showed the generality of the reaction [5] using simple models (14).

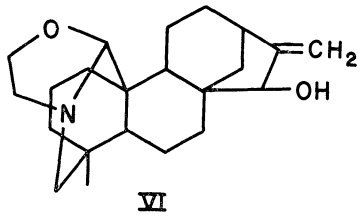

VI

The higher melting azomethine ketone IV had been isolated from the products of thermal decomposition of atisine in the presence of nickel on alumina (12) and of selenium (15). Pyrolysis of atisine hydrochloride (5*a*) gave a mixture of the two azomethine ketones which had been obtained from the action of acid on III. The formation of comparable amounts of the two ketones reflects a high degree of symmetry about the allyl alcohol system consonant with its presence on a bicyclo[2,2,2]octane.[6]

The hydration to the diol is a new reaction for this type of allyl alcohol. The maximum conversion to this compound was 54%. This could only be realized by successive separation of the diol from the mixture of methyl ketones and unrearranged allyl alcohol and recycling of the latter. If this was not done the diol was slowly converted to methyl ketones, with consequent reduction of the final yield.

The next step in the degradation sequence was reduction of the azomethine double bond in diol V. This was accomplished with sodium borohydride, or preferably, by catalytic hydrogenation. The resulting secondary aminodiol was acetylated and the diacetate selectively hydrolyzed to the *N*-acetyl diol VII (R = H). Sodium dichromate in acetic acid rapidly oxidized VII (R = H) to a mixture of the ketol VIII and the keto acid IX.

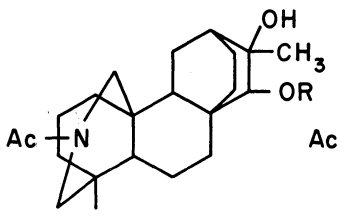

VII

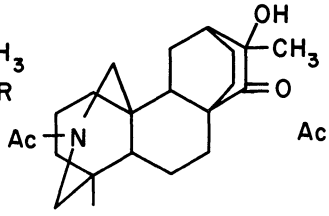

VIII

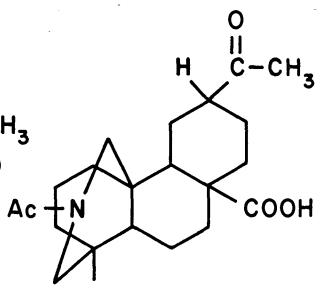

IX

Cleavage of VIII with lead tetraacetate also gave IX. The best method of preparation of IX, however, was by oxidation of VIII with the Kiliani reagent (16). This reaction probably proceeds by the illustrated mechanism.

[5]*It has been reported, without experimental details, that veatchine does not isomerize under comparable conditions and an explanation based on intermediacy of a non-classical ion in the garryfoline case advanced to account for this (3). It is very unlikely that such ions are important in the other cases of the rearrangement, since the charge can be delocalized by the vicinal hydroxyl; hence this warrants further investigation.*

[6]*The lower degree of symmetry of the bicyclo[3,2,1]octane system of the Garrya alkaloids (e.g. VI) is manifested in the formation of only one isomer in the parallel reaction (13).*

Can. J. Chem. Downloaded from www.nrcresearchpress.com by 210.87.254.42 on 09/05/12
For personal use only.

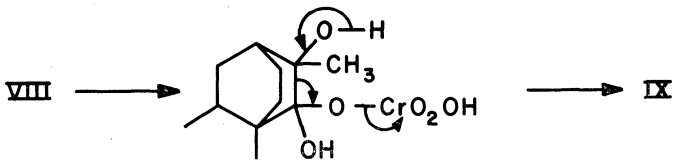

Trifluoroperacetic acid (17) oxidized IX to the acetoxy acid (X,R = $OCOCH_3$), which was then hydrolyzed to the hydroxy acid (X,R = OH). In the presence of traces of mineral acid the latter very readily lactonized to XI. The hydroxy acid was rapidly oxidized by sodium dichromate in acetic acid to the keto acid XII (R = H).

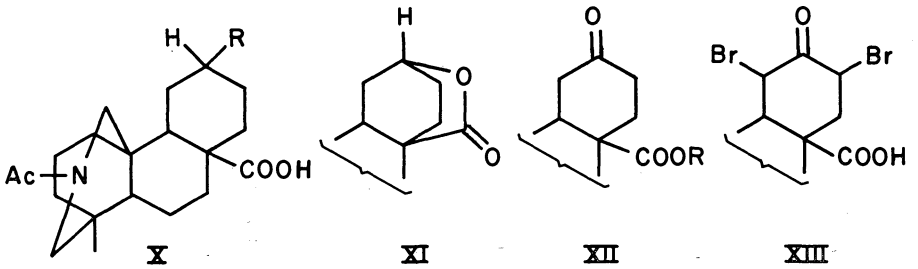

With two moles of bromine in dry acetic acid containing hydrogen bromide, XII (R = H) was converted to a dibromoketo acid. After 42 hours' contact with the hydrogen bromide we expected by analogy with steroidal ketones (18) that this would be predominantly XIII. However, no crystalline dibromo derivative was obtained from XII or its methyl ester. When the dibromoketo acid was treated with collidine at reflux temperature it was converted into a mixture of products. These were separated into acidic, phenolic, and neutral components. One neutral and one phenolic product crystallized.

The neutral substance proved to be a γ-lactone ketone (ν_{max} 1639, 1734, and 1796 cm^{-1}). The frequency of the ketone carbonyl is unusually high for a cyclohexanone with axial electronegative substituent on the α-carbon (19). However, we formulate this on grounds of its analysis and origin as XIV or XV. The bromoketone mixture must have contained

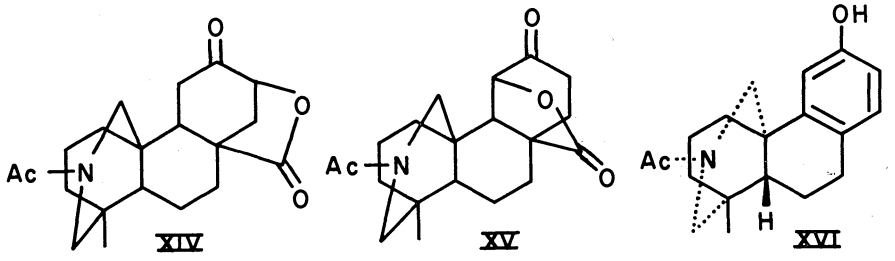

some monobromoketone, the bromine of which was displaced by the carboxylate anion to give the lactone. The lactone size proves a 1,4 relation between the carbon carrying the carboxyl and the carbonyl carbon, a fact consistent with, but not proving, ring *C* in atisine to be six-membered.

The phenol XVI, formed in around 8% yield had an ultraviolet spectrum with λ_{max} 282 mμ (log ϵ 2100), which shifted to λ_{max} 300 mμ in alkali. Its infrared absorption spectrum had a band at 828 cm^{-1} (nujol mull), a position characteristic of 3,4-disubstituted phenols

Can. J. Chem. Downloaded from www.nrcresearchpress.com by 210.87.254.42 on 09/05/12
For personal use only.

Can. J. Chem. Downloaded from www.nrcresearchpress.com by 210.87.254.42 on 09/05/12
For personal use only.

(20). Hence, barring the unlikely event of skeletal rearrangement during the dehydrobromination step, this proves ring *C* to be six-membered and, coupled with the evidence from the γ-lactone formation, establishes the presence of a bicyclo[2,2,2]octane system in atisine.

The location of the exocyclic methylene group on the bicyclooctane follows from the formation of the acetate of a secondary alcohol (X,R = $OCOH_3$) in the Baeyer–Villiger oxidation.[7] The chemistry of the closely related *Delphinium* alkaloid ajaconine (10) and the transformations of the heterocyclic ring of atisine (11) supported the rest of the skeletal assignment shown in I. Proof of the structure was completed by synthesis of the enantiomer of *N*-acetylphenol XVI from podocarpic acid (9). Independent proof of the structure comes from the synthesis of DL-kaurene (22) since the *Garrya* alkaloids have been related to L-kaurene (23) and to atisine (24).

The stereochemistry of atisine as designated by II is assigned on the basis of the following evidence. The *trans A*:*B* fusion is proved by the chemistry of ajaconine (10), which had been related to atisine, and by the synthesis of the mirror image of phenol XVI from podocarpic acid. An anti coupling of rings *A* and *C* is demanded by the chemistry of ajaconine (10,25) and in addition provides a satisfying explanation of the high basic strength of atisine and its isomerization by base into isoatisine (see below).

With the ring fusion established our earlier tentative conclusion (8) about which branch of the bicyclooctane system carried the allyl alcohol system was made rigorous. The argument follows.

The hydroxyl must be on C-8 or C-19. Inspection of Courtauld molecular models of the atisine skeleton (see XVII) showed that a hydrogen on C-19 oriented toward the hetero ring is in strong non-bonded interaction with one hydrogen on C-17. Clearly if the atisine

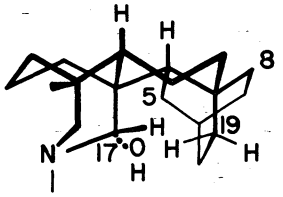

XVII

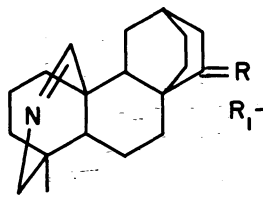

XVIII

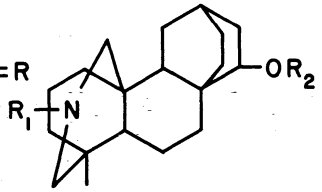

XIX

hydroxyl were on C-19 it would have to be oriented away from the hetero ring since the 19-epimeric alcohol, if it were capable of existence, would be extremely hindered. To test this point the azomethine ketone XVIII (R = O) (6) was reduced with sodium borohydride. Comparable amounts of two epimeric secondary amino-alcohols XIX (R_1= R_2=H) were produced.[8] Both could be readily acetylated to the *O*,*N*-diacetates, and the ester function in both diacetates was easily hydrolyzed. This result was consistent only with the oxygen function of the alkaloid being on C-8.

Another piece of evidence which led us to the same conclusion (8) came from the oxazolidine XX (6), with a double bond in the branch of the bicyclooctane system which originally carried the allyl alcohol system.[9] The repulsive interaction of the C-17 and C-19

[7]*Subsequent work by Pelletier (21) in which 6-isopropyl-1-methylphenanthrene was obtained by dehydrogenation of an atisine derivative is consistent with this assignment, although the isopropyl group could conceivably have arisen by rearrangement of a n-propyl group.*

[8]*One of these proved identical with the amino alcohol obtained by borohydride reduction of the C_{19}-azomethine alcohol described earlier (6). Since almost exclusively this one epimer was formed in the degradative sequence from atisine, its hydroxyl must have the same configuration as was originally present in the alkaloid.*

[9]*The double bond arose from Wolff–Kishner reduction of an α-acetoxy ketone, derived by acetylation and osmium tetroxide – periodate oxidation of the allyl alcohol system of III (6).*

hydrogens discussed below (see XVII) is a large factor in determining the high basic strength of the oxazolidines and carbinolamines with the oxygen on C-17. Had the double bond in XX been between C-18 and C-19, this interaction would have been absent (see XXI) and the base would have been weaker than atisine and the corresponding carbinolamines. Actually XX has the same extremely high basic strength as its saturated

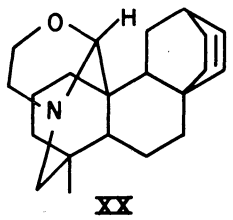

XX

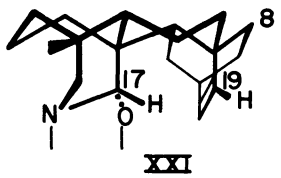

XXI

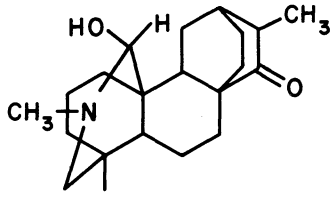

XXII

analogue; hence the double bond is in the branch *trans* to the hetero ring.

A similar argument can be used relative to the keto carbinolamine XXII derived from the methiodide of azomethine ketone IV. This is an extremely strong base. Had the carbonyl been on C-19, the 17–19 hydrogen interaction would have been absent, and the base would have been much weaker.

Wiesner and Edwards (3) used pK_a evidence to assign the allyl alcohol function to the *trans* branch of the bicyclooctane system of the *Garrya* alkaloids. Subsequently Pelletier produced similar evidence for atisine derivatives (21).

The absolute stereochemistry designated by II was first suggested on the basis of comparison of the molecular rotation of phenol XVI with that of similar phenolic diterpenes (8, 10). Further molecular rotational and rotatory dispersion information on ajaconine derivatives substantiated this conclusion (10) as did rotatory dispersion studies of the *Garrya* alkaloids and phyllocladene group of diterpenes (23). Rigorous proof of the antipodal character relative to the common resin acids was finally provided by the mirror image relation of phenol XVI and the molecule of this structure synthesized from podocarpic acid (9).

The structure of atisine is thus defined in every respect but the configuration of the 8-hydroxyl. Solo and Pelletier (26) and Whalley (27) advanced the argument that the hydroxyl had the configuration shown in XXIII since this compound was less strongly adsorbed on alumina than its 8-epimer. They attribute this to the possibility of simultaneous *cis* adsorption of the hydroxyl and acetamido group in the case of the epimer. This is tenuous since the nature of the adsorption process is not clearly defined.[10] Our evidence bearing on this point which might lead to the same conclusion is the fact that the diol

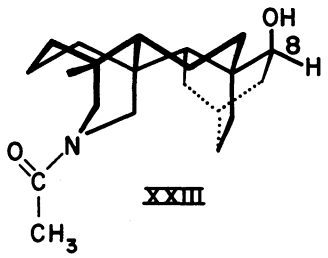

XXIII

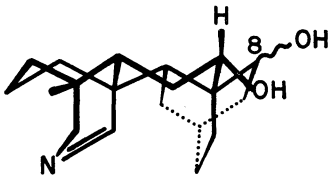

XXIV

[10]*See for example the conclusions of Pines regarding adsorption in alumina pores (28). It was found necessary to postulate simultaneous trans catalytic action of the alumina to account for some eliminations.*

Can. J. Chem. Downloaded from www.nrcresearchpress.com by 210.87.254.42 on 09/05/12
For personal use only.

XXIV derived from ajaconine failed to give *p*-nitrobenzylidene derivative (29).[11] However, a comparative study of the 8-epimers in this reaction is needed before a firm conclusion can be reached.[12]

A number of interesting chemical points were uncovered in the course of this work.

(*a*) The hydration of the allyl alcohol system of III is stereospecific despite the high symmetry of the bicyclooctane system. Strong evidence for the *trans* relation of the two hydroxyl groups in the resulting diol is provided by the very low rate of lead tetraacetate cleavage of VII[13] ($k_2 = 3.3\times10^{-2}$ l. mole^{-1} sec^{-1}) and by its failure to give an isopropylidene

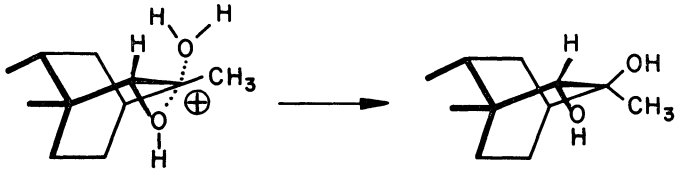

XXV

derivative. This stereochemistry could result from hydroxyl participation shielding one side of the carbonium ion formed by protonation of the double bond (as in XXV) or, in the extreme, formation of the epoxide as an intermediate in the reaction. The acetate of III gave very little if any diol when treated at room temperature with 7.5% sulphuric acid in 60% acetic acid. This is probably the result of proton capture by the nearby carbonyl instead of by the less basic double bond.

(*b*) The lactonization of hydroxy acid X(R = OH) is much more facile than that of simple *cis* 4-hydroxycyclohexane carboxylic acids (32). Much lactone was formed when the acid was liberated from its sodium salt, extracted into methylene chloride, and recovered by distillation of the solvent. It appears possible that traces of mineral acid carried over from the extraction catalyzed the reaction since the amount of lactone formed varied in apparently identical runs. The unique factors responsible for the unusual reactivity are the relief of the carboxyl vs. 5βH and 18βH interactions and the 6αH:17H interactions in going from chair to boat conformation of ring *C* (XXVI → XXVII) as the transition state for lactone formation develops.[14]

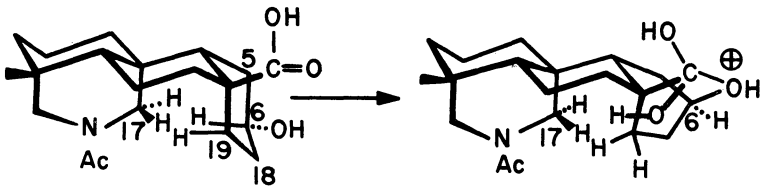

XXVI XXVII

(*c*) A phenomenon somewhat related to that described in (*b*) is the remarkable ease of alkaline hydrolysis of the bisnorketo ester XII (R = CH_3). The ester hydrolyzes as readily as that of a carboxyl group on a primary or secondary carbon. Carbomethoxy

[11] *Unpublished observations by Dr. D. Dvornik.*

[12] *Photolysis of the nitrite esters of the epimeric alcohols XIX (*R_1 = Ac, R_2 = H*) failed to give the oximino alcohols, which it was hoped would distinguish between the hydroxyl configurations. We warmly thank Dr. K. K. Purushothaman for these experiments.*

[13] *The angle between cis hydroxyls on a bicyclo[2,2,2]octane system is less than 10° (30). Even ditertiary glycols with similar geometry have values of* k_2 *around* 3×10^5 *l. mole*$^{-1}$ *sec*$^{-1}$ *(31).*

[14] *This is offset in part by development of a* 5αH:17H *interaction.*

Can. J. Chem. Downloaded from www.nrcresearchpress.com by 210.87.254.42 on 09/05/12
For personal use only.

groups on fully substituted carbon require prolonged heating with alkali under sealed tube conditions for hydrolysis (33). The boat form of ring *C* in XII is favored by absence of the 1,4 bowsprit interaction and by the absence of the 1,3-diaxial interactions of the carbomethoxyl group and the 5β and 18β hydrogens present in the chair form. Hence this conformation is present in sufficient concentration that the ketone carbonyl can markedly accelerate the hydrolysis as shown. A similar accelerated hydrolysis of the ester of a

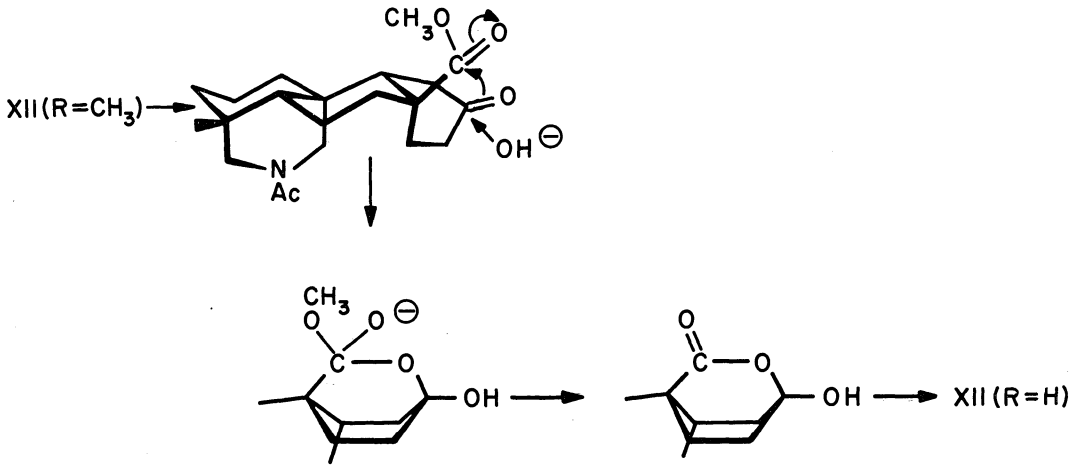

triterpene keto-acid was observed by Djerassi and Lipmann (34) and of keto and aldehydo aromatic esters by Bender and Silver (35) and Newman and Hishida (36).

(*d*) The basic strength of various azomethines prepared in this and related work varied with the substituents present on the bicyclooctane system. The pertinent data are summarized in Table I.

TABLE I

Base	pK_a'*	pK_a†
XVIII R = H_2	5.2	–
XVIII R = H,OH	5.3	+0.1
XVIII R = O	4.6	−0.6
III	5.0	−0.2
III acetate	4.8	−0.4
IV	4.6	−0.6

*In 95% ethanol.
†Difference from the pK_a' of XVIII (R = H_2).

It seems very unlikely that the C-8 substituent would significantly affect the steric environment of the nitrogen. We hence conclude that the pK_a differences are the result of electrical effects operating over the long distance (ca. 5.6 Å) between the nitrogen and C-8. The largest effect was observed in the 8-ketones. This may be ascribed to the orientation of the carbonyl dipole with the positive end facing the nitrogen, thus opposing the charging of the latter by protonation. Comparable effects on basic strength at shorter range have been observed for other diterpenoid alkaloids (37) and Roberts and Moreland (38) have reported a trans-spatial effect of polar groups on the strength of carboxylic acids.

The general conception that steric hindrance of C-17 accounts for the extremely high basic strength of atisine and for its base-catalyzed isomerization into isoatisine was enunciated some time ago (3, 39). However, the detailed explanation of these phenomena

Can. J. Chem. Downloaded from www.nrcresearchpress.com by 210.87.254.42 on 09/05/12
For personal use only.

has been the subject of some controversy (6, 10, 40). We now present a full account of our analysis of the steric factors involved.

There are only two conformations of ring *E* with an oxygen substituent on C-17 which need be considered (see also refs. 27, 40). These are illustrated in XXVIII and XXIX for

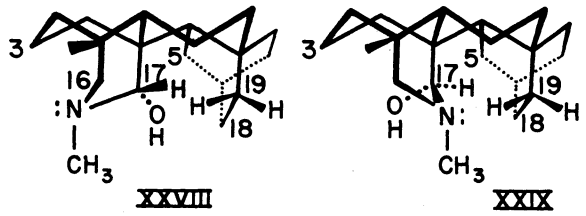

XXVIII XXIX

the *N*-methyl carbinolamines, which have the same properties as atisine itself. Using space-filling Courtauld molecular models the relative stability of these conformational isomers could be deduced. Since the interactions of the unshared pair of electrons on the nitrogen with the nearest hydrogen should be nearly the same for the two conformations, the serious repulsive hydrogen interactions determining their relative stability are:

for XXVIII (*a*) 17-oxygen:5αH,
(*b*) 17H:19H,
for XXIX (*a*) 17-oxygen:3αH,
(*b*) 16H:3αH,
(*c*) 17H:18H,
(*d*) 17H:19H,
(*e*) 17H:5αH.

We conclude that XXVIII is the stable conformational isomer.[15] In view of the above destabilizing interactions, the cause of the high basic strength of atisine and the analogous *N*-methyl carbinolamines is the relief of the 17:19 hydrogen interactions and the 17-oxygen:5αH interaction (10, 41) in going from the bases to the immonium salt form.

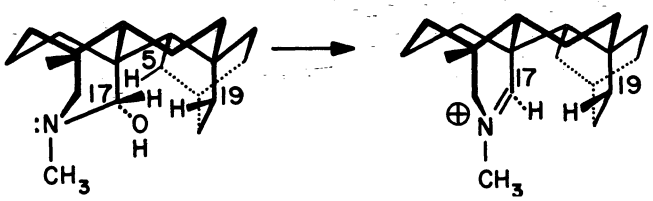

The pK_a of atisine is greater than 12 (5*a*, 39). Even if it is as high as 12.5 the concentration of the ionic form in a 1 *M* solution in methanol containing 1 *N* NaOH is negligible (ca. $3\times10^{-2}M$). Isoatisine (pK_a' 10) will be even less ionized, hence in considering the equilibrium of the two bases only the oxazolidine forms need be considered.[16] Under the above conditions the equilibrium lies nearly 90% in the isoatisine side (42); hence ΔF (isomeriz.) = -1.3 kcal/mole. The major difference between the two isomers is the replacement of a 17-oxygen:5α-hydrogen repulsive interaction by a 17H:5αH repulsion. The difference between the interactions of two 1,3 diaxial hydrogens and that of 1,3 diaxial hydrogen and hydroxyl is 0.4 to 0.5 kcal/mole (43, 44). But in the atisine series the 17-hydrogen and 5α-hydrogen are forced closer than the sum of the van der Waals radii and this compression is even more exaggerated for the 17-oxygenated case. Since the

[15]*Solo and Pelletier concluded that the two conformers have nearly equal stability (40).*
[16]*This is contrary to the argument of Solo and Pelletier (40).*

Can. J. Chem. Downloaded from www.nrcresearchpress.com by 210.87.254.42 on 09/05/12
For personal use only.

interacting atoms are thus in a region where the repulsion vs. distance curve rises steeply, the energy difference between the H:H and H:OH interactions will be magnified and may easily be as large at the 1.3 kcal/mole required to account for the position of the atisine–isoatisine equilibrium.[17]

EXPERIMENTAL

Rotations were of absolute ethanol solutions. Infrared spectra are of nujol mulls unless otherwise specified. Ultraviolet spectra are of solutions in 95% ethanol. The pK_a' values cited are the pH at half titration of solutions in the solvent specified using a glass electrode – calomel electrode pair. Alumina for chromatography was Woelm brand (neutral), with activity expressed on the Brockman scale.

Action of Acid on Azomethine Alcohol III

A solution of 1.44 g of the unsaturated azomethine alcohol III (6) in 20 ml of 10% hydrochloric acid was left at room temperature for 18½ hours. The solution was extracted with chloroform, and the chloroform back-washed with 3 *N* sulphuric acid. The combined aqueous layers were made strongly alkaline and extracted with chloroform. The recovered base crystallized from benzene giving 555 mg, m.p. 230–250°. The benzene-soluble material was treated again with 10% hydrochloric acid for 19 hours giving 216 mg of the benzene-insoluble crystals, m.p. 230–250°. A further recycling of the benzene-soluble fraction yielded 63 mg more crystals. The total yield of crude diol was 834 mg.

The benzene-soluble product was adsorbed on a 15-fold weight of alumina activity 1. Benzene and 1:1 benzene–ether eluted azomethine ketones, which crystallized from pentane.

Azomethine Diol V

The crude diol was recrystallized by solution in methanol, addition of benzene, then removal of the methanol by boiling until crystallization commenced. It had m.p. 264°, $[\alpha]_D$ +3° (*c*, 0.89), and ν_{max} ($CHCl_3$) 3600, 1651 cm^{-1}. Found: C, 75.48; H, 9.66. Calc. for $C_{20}H_{31}NO_2$: C, 75.67; H, 9.84. A solution of the azomethine diol in 10% hydrochloric acid was left at room temperature for three days. Thirty percent was converted to a mixture of methyl ketones (see below) with ν_{max} ($CHCl_3$) 1710 and 1650 cm^{-1}.

Methyl Ketones IV

The least soluble methyl ketone crystallized as prisms from a pentane solution of the readily eluted fractions. After repeated recrystallization from hexane this melted at 143.5–144.5, $[\alpha]_D$ −7° (*c*, 1.76) and had ν_{max} 1708 and 1651 cm^{-1}. Found: C, 80.13; H, 9.69. Calc. for $C_{20}H_{29}ON$: C, 80.22, H, 9.76. The ketone did not depress the melting point of the azomethine ketone, m.p. 141°, from pyrolysis of atisine hydrochloride (5*a*). If formed a methiodide when treated at room temperature with methyl iodide in ether. This crystallized as rectangular plates from methanol which became brown and amorphous at 340°. This has ν_{max} 1715 and 1677 cm^{-1}. Found: C, 57.20; H, 7.28. Calc. for $C_{21}H_{32}ONI$: C, 57.15; H, 7.31.

The more soluble methyl ketone crystallized from pentane. After several recrystallizations it melted at 93–99°, $[\alpha]_D^{26}$ −13° (*c*, 1.53), and had ν_{max} 1716 and 1650 cm^{-1}. Found: C, 80.17; H, 9.67. Calc. for $C_{20}H_{29}NO$: C, 80.22; H, 9.76. This was a mixture since it gave a methiodide separable by recrystallization from methanol–acetone into rectangular plates which became amorphous around 325° (crude methiodide of the 145° ketone) and needles m.p. 285–295°. The methiodide of the low melting point ketone from pyrolysis of atisine hydrochloride likewise gave less soluble plates (no true melting point, becoming amorphous at 330°) and needles, m.p. 290°. The latter had ν_{max} 1710 cm^{-1} and 1685 cm^{-1}.

O,N-Diacetate VII (R = Ac)

The azomethine double bond of the diol V could be reduced slowly by sodium borohydride in aqueous methanol. The product was hard to extract from water, hence the following catalytic reduction was preferable.

Azomethine diol V (880 mg) in 12 ml of acetic acid was reduced in the presence of platinum from 115 mg of Adams' platinum oxide. The hydrogen uptake in 4 hours was 61.6 ml at N.T.P. (1 molar equivalent). The catalyst was removed by filtration and the bulk of the acetic acid removed under reduced pressure. Fifteen milliliters of 1:1 mixture of acetic anhydride and pyridine was then added. After 7 hours at room temperature the reagents were removed under reduced pressure. Methanol was added to react with residual anhydride. After 10 minutes this was removed under reduced pressure, the product dissolved in methylene chloride, then the solution extracted successively with dilute sulphuric acid and dilute sodium carbonate solution. The 1.1 g of froth recovered from the methylene chloride crystallized readily from methanol. The first crop (1.0 g) melted at 206–215°. After two recrystallization from acetone this melted at 212–214° and had $[\alpha]_D$ 0° (*c*, 1.17), ν_{max} 3280, 1735, and 1620 cm^{-1}. Found: C, 71.36; H, 9.21. Calc. for $C_{24}H_{37}O_4N$: C, 71.43; H, 9.24.

[17]*Solo and Pelletier overlooked the extra compression (40). Furthermore, they argued that it is the oxazolidine ring in atisine which, by restricting rotation of* C-17 *increases the total steric hindrance relative to isoatisine. They consider this to be the major source of the energy difference between the two isomers. This explanation is invalidated by the fact that the N-methylcarbinolamine XXVIII (11) and the methiodide of III (see experimental part) are converted to the isomeric carbinolamines under the conditions of the atisine rearrangement.*

Can. J. Chem. Downloaded from www.nrcresearchpress.com by 210.87.254.42 on 09/05/12
For personal use only.

N-Acetyl Diol VII (R = H)

A solution of 966 mg of *O,N*-diacetate VII (R = Ac) and 600 mg of potassium hydroxide in 10 ml of methanol and 3 ml of water was left at room temperature for 5 hours. The solvent was removed under reduced pressure, the residue taken up in water, and the product extracted into chloroform. The froth remaining after evaporation of the chloroform was dissolved in acetone and ether added, giving 846 mg of crystals. These showed three melting points depending on crystallization conditions; 161–164°, 176–179.5°, and 205°. Sometimes the transition from a lower melting to a higher melting form took place after partial melting. $[\alpha]_D$ −17° (*c*, 1.38), ν_{max} ($CHCl_3$) 3580, 3380, and 1623 cm^{-1}. Found: C, 73.06; H, 9.74. Calc. for $C_{22}H_{35}O_3N$: C, 73.09; H, 9.76.

A solution of 51.5 mg of the *N*-acetyl diol in 10 ml of acetic acid containing 0.061 mole/liter of lead tetraacetate was titrated at intervals. One molar equivalent of reagent was consumed in approximately 9 hours but the uptake continued. After 68 hours 2.74 moles had been used. The bimolecular rate constant for the uptake of the first mole was 3.3×10^{-2} l. $mole^{-1}$ sec^{-1}.

In an attempt to form an isopropylidene derivative 46 mg of the *N*-acetyl diol was dissolved in 10 ml of dry acetone containing 81 mg of *p*-toluenesulphonic acid monohydrate. After 17 hours at room temperature 3 ml of 5% sodium carbonate solution was added, then the solution taken to small volume under reduced pressure. Chloroform extracted 56 mg of material which crystallized from acetone–ether to give 28 mg of pure and 10 mg of cruder starting material.

N-Acetyl Ketol VIII

To a solution of 106 mg of *N*-acetyl diol VII (R = H) in 2 ml of acetic acid was added quickly a solution of 61 mg of sodium dichromate dihydrate in 2 ml of acetic acid. After 1 hour at room temperature the excess dichromate was reduced with sodium hydrogen sulphite and the acetic acid removed under reduced pressure. The residue was taken up in dilute sulphuric acid, the organic matter extracted into methylene chloride, then this solution was washed twice with dilute sodium carbonate solution. The methylene chloride layers yielded 89 mg of neutral material and the carbonate solutions after acidification and extraction gave 16 mg of acid. The neutral fraction crystallized from acetone. After three recrystallizations from this solvent it melted at 226° and had $[\alpha]_D$ −30° (*c*, 1.24) and ν_{max} 3360, 1729, and 1626 cm^{-1}. Found: C, 73.63; H, 9.02. Calc. for $C_{22}H_{33}O_3N$: C, 73.50; H, 9.25.

N-Acetyl Keto Acid IX

(*a*) 2 ml of Kiliani chromic acid mixture (16) was added to a cold solution of 180 mg of *N*-acetyldiol VII (R = H) in 1 ml of acetic acid. A gum precipitated, which slowly dissolved after addition of 1 ml of acetic acid and stirring. After a total reaction time of 15 minutes sodium hydrogen sulphite solution was added until the solution was green. After further dilution with water, the mixture was thoroughly extracted with chloroform. The chloroform extracts were extracted twice with sodium carbonate solution, dried, and evaporated, yielding 27 mg of *N*-acetyl ketol VIII. The sodium carbonate solutions yielded 150 mg of acid. The latter crystallized from aqueous acetone giving 120 mg of hexagonal plates, m.p. 207–218°. After recrystallization from aqueous acetone and drying at 100° it melted at 218° and had $[\alpha]_D$ +19° (*c*, 1.32), ν_{max} 1705, 1693 cm^{-1}. Found: C, 69.99; H, 8.70. Calc. for $C_{22}H_{33}O_4N$: C, 70.37; H, 8.86.

(*b*) A solution of 15 mg of the *N*-acetylketol VIII in 10 ml of 0.054 *M* lead tetraacetate in 90% acetic acid – 10% water consumed 1 molar equivalent of the reagent after approximately 15 hours at room temperature. The resulting keto acid crystallized from acetone as six-sided plates, m.p. 214°. This did not depress the melting point of the keto acid described in (*a*).

Acetoxy Acid X (R = OAc)

To a solution of 735 mg of the methylketo acid IX in 12 ml of 1:1 chloroform – methylene chloride mixture (dry alcohol-free) was added 700 mg of anhydrous disodium hydrogen phosphate followed by 2 ml of a trifluoroperacetic acid solution (prepared from 0.2 ml of 98% hydrogen peroxide, 0.8 ml of trifluoroacetic anhydride, and 2 ml of methylene chloride). The suspension was refluxed for 15 minutes. After cooling, a solution of sodium hydrogen sulphite was added and the mixture vigorously shaken. The layers were separated, and the aqueous solution extracted three times with chloroform. The product crystallized readily from acetone, giving 673 mg of acid, m.p. 309° (decomp.). The material in the mother liquor was treated again with trifluoroperacetic acid as above, and a further 42 mg of crystalline acid obtained, m.p. 302°. Recrystallization from methanol did not raise the melting point above 309°. It had ν_{max} 1725 cm^{-1} (OAc). 1711 cm^{-1} (COOH), 1605 cm^{-1} (amide); $[\alpha]_D$ −21° (*c*, 0.68). Found: C, 67.37; H, 8.39. Calc. for $C_{22}H_{33}O_5N$: C, 67.49; H, 8.50.

Hydroxy Acid X (R = OH)

Acetoxy acid X (R = OAc) (900 mg) in solution in 20 cc of 50% aqueous methanol containing 800 mg of potassium hydroxide was left for 4½ hours at room temperature. The bulk of the solvent was removed under reduced pressure, the residue diluted with water and acidified. The hydroxy acid was extracted into chloroform, and this solution washed with water. The product recovered from the chloroform crystallized readily from acetone, giving 737 mg, m.p. 195°. The mother liquor contained mainly lactone (see below). The hydroxy acid, after recrystallization from methanol had m.p. 201–203°, $[\alpha]_D$ −5° (*c*, 1.4); ν_{max} 3160, 1709,

Can. J. Chem. Downloaded from www.nrcresearchpress.com by 210.87.254.42 on 09/05/12
For personal use only.

1619 cm^{-1}. Found: C, 68.62; H, 8.83. Calc. for $C_{20}H_{31}O_4N$: C, 68.74; H, 8.94. In apparently identical runs the proportion of lactone produced was as high as 60%. A solution of 20 mg of the hydroxy acid in 2 ml of methanol containing 0.1 ml of 6 *N* sulphuric acid was maintained at 50° for ½ hour. The product gave 18 mg of lactone, m.p. 167°.

δ-Lactone XI

The lactone formed from the hydroxy acid X (R = OH) as described above melted at 167° after recrystallization from acetone–ether. It had $[\alpha]_D$ −53° (*c*, 1.6); ν_{max} 1740 cm^{-1} (δ-lactone), 1640 cm^{-1} (amide). Found: C, 72.76; H, 8.75. Calc. for $C_{20}H_{29}O_3N$: C, 72.47; H, 8.82. The lactone (56 mg) after hydrolysis at room temperature for 2 hours in an 8% solution of potassium hydroxide in methanol gave 35 mg of pure hydroxy acid X (R = OH).

Bisnorketo Acid XII

A solution of 155 mg of bisnorhydroxy acid X (R = OH) in 4 ml of acetic acid was prepared. To this was added 0.5 ml-portions of a solution of 61 mg of chromium trioxide in 5 ml of acetic acid and 1 ml of water. As each portion was reduced the next was added. After addition of 4 ml of the chromic acid solution (in 3 hours) excess oxidant persisted for ¾ hour. After addition of sodium hydrogen sulphite to reduce the excess reagent, the solution was taken to dryness under reduced pressure. The residue was dissolved in methanol, 1 drop of 6 *N* sulphuric acid added, then left at 40° for 15 minutes. The methanol was removed under reduced pressure, then the product separated into 27 mg of neutral and 125 mg of acidic materials. The acid fraction crystallized from acetone giving 101 mg of keto acid, m.p. 245–255°. Recrystallization failed to raise the melting point, hence the acid was reoxidized with chromium trioxide in acetic acid. The acid then softened at 255° and melted at 266°. Further recrystallization from methanol–acetone mixtures raised the melting point to 268° with $[\alpha]_D$ −35° (*c*, 1.83) and λ_{max} 280 mμ (ε 21), λ_{min} 260 mμ (ε 16). It had ν_{max} 1711 and 1602 cm^{-1}.

The methyl ester of the keto acid prepared using diazomethane was not obtained crystalline. It had ν_{max} ($CHCl_3$) 1720 and 1632 cm^{-1}.

Dibromoketo Acid XII and its Dehydrobromination

To 67 mg of bisnorketo acid XII in 1 ml of dry acetic acid was added 0.05 ml of acetic acid containing 3.8 mg of hydrogen bromide. Over a period of 20 minutes 0.6 ml of a solution of bromine in acetic acid (64 mg Br_2) was added with stirring. A small amount of oil separated. After addition of a further 0.05 ml of the hydrogen bromide solution the reaction mixture was left in the dark at room temperature for 42 hours. The solvent was then removed under reduced pressure near room temperature, the residue taken up in chloroform, and this solution washed thoroughly with water. The chloroform solution on evaporation left 109 mg of froth which would not crystallize.

The bromo acid was dissolved in 3.5 ml of dry collidine and the solution refluxed under nitrogen for 1 hour. The bulk of the collidine was removed under reduced pressure, then the residue dissolved in chloroform. The solution was extracted twice with 2 *N* sulphuric acid, then twice with dilute sodium hydroxide in a nitrogen atmosphere. The chloroform gave 60 mg of neutral product (trace of collidine). The sodium hydroxide solution was adjusted to pH 8 and extracted with chloroform, yielding 7.5 mg of phenol. The aqueous layer was then acidified and extracted, giving a few milligrams of acid.

Keto-γ-lactone XIV or XV

The neutral fraction crystallized readily from concentrated acetone solution giving 17 mg, m.p. 270°. After two recrystallizations from methanol–acetone this separated as hexagonal plates with m.p. 275°, $[\alpha]_D^{24}$ −25° (*c*, 0.65). It had only end absorption in the ultraviolet and ν_{max} 1796, 1734, and 1639 cm^{-1}. Found: C, 69.62; H, 7.75. Calc. for $C_{20}H_{27}NO_4$: C, 69.54; H, 7.88.

Phenol XVI

The phenolic fraction crystallized from acetone, giving 4.8 mg, m.p. 272–275°. This was combined with material from other runs and recrystallized twice giving tiny prisms with m.p. 277–279°, $[\alpha]_D^{24}$ −105±9° (*c*, 0.35). It had λ_{min} 250 mμ (ε 450); λ_{max} 282 mμ (ε 2100). In alkaline ethanol the spectrum shifted to λ_{min} 270 mμ, λ_{max} 300 mμ. It had ν_{max} 828 (3,4-disubstituted phenol), 1586, and 1638 cm^{-1}. Found: C, 76.07; H, 8.25. Calc. for $C_{19}H_{25}NO_2$: C, 76.22; H, 8.42.

Methiodide of III and its Isomerization

The azomethine alcohol III (230 mg) was dissolved in 15 ml of 1:1 ether–benzene mixture. After addition of 0.8 ml of freshly distilled methyl iodide the mixture was left 2 hours at room temperature. The crystalline methiodide was collected by filtration, giving 386 mg, m.p. 250°. After one recrystallization from methanol–acetone combination it melted at 254° and had $[\alpha]_D^{26}$ −14° (*c*, 1.65), pK_a' greater than 12 (95% ethanol) and ν_{max} 3370, 1684, 1653, and 898 cm^{-1}. Found: C, 57.09; H, 7.20. Calc. for $C_{21}H_{32}INO$: C, 57.15; H, 7.31.

The methiodide (232 mg) was dissolved in 7 ml of methanol containing 400 mg of potassium hydroxide. The solution was refluxed for 3 hours, then the solvent removed under reduced pressure. The residue was dissolved in water and extracted with benzene giving 189 mg of pale yellow gum. This was converted to its iodide by careful titration with hydriodic acid in methanol. The crystalline *iso*methiodide was recrystallized

Can. J. Chem. Downloaded from www.nrcresearchpress.com by 210.87.254.42 on 09/05/12
For personal use only.

twice from acetone containing a little methanol; m.p. 246° (partially liquefied when placed on the hot stage at 220°, resolidified), $[\alpha]_D^{26}$ −13° (*c*, 1.74); pK_a' 10.6 (95% ethanol), ν_{max} 3380, 1696, 1634, 895 cm^{-1}. Found: C, 56.56; H, 7.24; Calc. for $C_{21}H_{32}INO$: C, 57.15; H, 7.31.

C_{19}-Secondary Amino Alcohol (XIX, $R_1 = R_2 = H$)

To a solution of 67 mg (0.23 m*M*) of the C_{19}-azomethine alcohol XVIII (R = H, OH) (6) in 4 ml of 80% aqueous methanol 250 mg of sodium borohydride were added. After being kept for 6 hours at room temperature, the solution was evaporated to dryness under reduced pressure, water was added, and the base extracted with ether. Evaporation of the solvent gave 54 mg (80%) of the crude dihydro derivative, which crystallized spontaneously on spraying with ether. After three recrystallizations from acetone–hexane and sublimation at 160–165° at 0.5 mμ it melted at 158–161°. $[\alpha]_D^{26}$ −49±2° (*c*, 0.84), $[M]_D$ −141±6°. Found: C, 78.63; H, 10.67. Calc. for $C_{19}H_{31}NO$ (289.45): C, 78.84; H, 10.80. ν_{max} 3425, 3320, 3180 cm^{-1}.

Acetylation of the C_{19}-Secondary Amino Alcohol (XIX, $R_1 = R_2 = H$)

A solution of 59 mg (0.20 m*M*) of the C_{19}-secondary amino alcohol in 3 ml of a mixture of pyridine and acetic anhydride (1:1) was kept at 40° for 5 hours. The residue obtained on evaporation to dryness under reduced pressure was distributed between ether and 3 *N* aqueous sodium carbonate solution. The ethereal phase was washed with 6 *N* aqueous sulphuric acid and water respectively. Evaporation of the solvent gave 71 mg (93%) of the crude diacetate, which after three recrystallizations from acetone–hexane melted at 175.5–177°; $[\alpha]_D^{26}$ −55±1° (*c*, 0.80); $[M]_D$ −205±4°. Found: C, 74.10; H, 9.37. Calc. for $C_{23}H_{35}NO_3$ (373.52): C, 73.95; H, 9.45. ν_{max} (CCl_4) 1742, 1247 cm^{-1} (OAc), 1648 cm^{-1} (>N—CO).

Sodium Borohydride Reduction of the C_{19}-Azomethine Ketone XVIII (R = O)

To a solution of 88 mg (0.31 m*M*) of the C_{19} azomethine ketone in 5 ml of 80% aqueous methanol 250 mg of sodium borohydride was added, the mixture being kept at room temperature for 3½ hours. The solution was evaporated to dryness under reduced pressure, water was added, and the solution extracted with ether. Evaporation of the solvent gave 68 mg (76%) of a product which crystallized partially on spraying with ether. After three recrystallizations from aqueous acetone the 8-epi secondary amino alcohol XIX ($R_1 = R_2 = H$) (26 mg) melted at 181.5–182.5°. $[\alpha]_D^{26}$ +1.2° (*c*, 0.83), $[M]_D$ +3.5°. Found: C, 78.98; H, 10.70. Calc. for $C_{19}H_{31}NO$ (289.45): C, 78.84; H, 10.80. ν_{max} 3330, 3280 cm^{-1} (—OH and >NH).

The combined mother liquors were dissolved in a pyridine – acetic anhydride mixture (1:1) and kept at room temperature for 92 hours. The solution was evaporated to dryness under reduced pressure, and the residue distributed between ether and 3 *N* aqueous sodium carbonate solution. The ethereal phase was then washed with 6 *N* aqueous sulphuric acid and water respectively. The residue after evaporating the solvent crystallized spontaneously. After three recrystallizations from acetone–hexane the product ($[\alpha]_D^{25}$ −49±2° (*c*, 0.90); $[M]_D$ −183±7°) showed no melting point depression (174–176°) with a sample of the diacetate obtained by reduction and acetylation of XVIII (R = H, OH). In addition the infrared spectra (carbon tetrachloride solution) of both compounds were superimposable.

Acetylation of the 8-epi Alcohol (XIX, $R_1 = R_2 = H$)

A solution of 30 mg (0.11 m*M*) of the 8-epi C_{19} alcohol (XIX, $R_1 = R_2 = H$) in 3 ml of a mixture of pyridine and acetic anhydride (1:1) was kept at room temperature for 90 hours. The solution was evaporated to dryness under reduced pressure and the residue dissolved in Et_2O. The ethereal solution was shaken with 3 *N* aqueous sodium carbonate solution, 6 *N* aqueous sulphuric acid, and water respectively. Evaporation of the solvent gave 38.5 mg (97%) of a *n*-pentane-soluble colorless oil. After passage through a column of neutral aluminum oxide (1:35, activity 1) from which it was eluted with benzene, this had $[\alpha]_D^{25.5}$ −14±1° (*c*, 1.25), $[M]_D$ −52±4°; ν_{max} (CCl_4) 1737 cm^{-1}, 1249 cm^{-1} (OAc), 1648 cm^{-1} (>N—CO). Except for a missing shoulder at 1150 cm^{-1} the I.R. spectrum was superimposable on that of the normal analogue.

Hydrolysis of the 8-epi O,N-Diacetate (XIX, $R_1 = R_2 = Ac$)

25 mg (0.067 m*M*) of the 8-epi *O,N*-diacetate was refluxed for 30 minutes with 2 ml of 70% aqueous methanol containing 5% of potassium hydroxide. The methanol was partially removed *in vacuo*, water was added, and the solution extracted with methylene chloride. Removal of the solvent gave 21 mg of an oily product, which crystallized on being sprayed with ether. After two recrystallizations from acetone–hexane the product melted at 191–192.5; $[\alpha]_D^{25}$ −14.5±1° (*c*, 0.90); $[M]_D$ −48±3°. Found: C, 76.15; H, 9.95, Calc. for $C_{21}H_{33}O_2N$ (331.48): C, 76.09; H, 10.03. On reacetylation the oily product had $[\alpha]_D^{23}$ −12±1° (*c*, 1.67); $[M]_D$ −45±4°. The ΔM_D for acetylation of the 8-epi hydroxyl is hence near 0°.

Hydrolysis of the O,N-Diacetate (XIX, $R_1 = R_2 = Ac$)

By the same procedure as mentioned above, XIX ($R_1 = R_2 = Ac$) gave an oily product with $[\alpha]_D^{24}$ −37±1°; $[M]_D$ −122±3°. The ΔM_D for acetylation of the *normal* 8-hydroxyl is hence −83°.

Can. J. Chem. Downloaded from www.nrcresearchpress.com by 210.87.254.42 on 09/05/12
For personal use only.

ACKNOWLEDGMENTS

We are grateful to Mr. H. Seguin for the analyses, Mr. M. Lesage for pK_a determinations and Mr. R. Lauzon for the infrared spectra.

REFERENCES

1. K. Wiesner, R. Armstrong, M. F. Bartlett, and J. A. Edwards. Chem.Ind. (London), 132 (1954).
2. W. A. Jacobs. J. Org. Chem. **16**, 1593 (1951).
3. K. Wiesner and J. A. Edwards. Experientia, **11**, 255 (1955).
4. S. W. Pelletier and W. A. Jacobs. J. Am. Chem. Soc. **76**, 4496 (1954).
5. (*a*) O. E. Edwards and T. Singh. Can. J. Chem. **32**, 465 (1954); (*b*) Can. J. Chem. **33**, 448 (1955).
6. D. Dvornik and O. E. Edwards. Can. J. Chem. **35**, 860 (1957).
7. S. W. Pelletier and W. A. Jacobs. J. Am. Chem. Soc. **78**, 4139, 4144 (1956).
8. D. Dvornik and O. E. Edwards. Chem. Ind. (London), 623 (1958).
9. J. W. ApSimon and O. E. Edwards. Can. J. Chem. **40**, 896 (1962).
10. D. Dvornik and O. E. Edwards. Tetrahedron, **14**, 54 (1961). Errata, Tetrahedron, **16**, 283 (1961).
11. J. W. ApSimon, O. E. Edwards, and R. Howe. Can. J. Chem. **40**, 630 (1962).
12. C. F. Huebner and W. A. Jacobs. J. Biol. Chem. **170**, 515 (1947).
13. C. Djerassi, C. R. Smith, A. E. Lippmann, S. K. Figdor, and J. Herran. J. Am. Chem. Soc. **77**, 4801, 6633 (1955).
14. A. S. Dreiding and J. A. Hartman. J. Am. Chem. Soc. **78**, 1216 (1956).
15. M. F. Bartlett, J. Edwards, W. I. Taylor, and K. Wiesner. Chem. Ind. (London), 323 (1953).
16. H. Kiliani and B. Merk. Ber. **34**, 3562 (1901).
17. W. D. Emmons and G. B. Lucas. J. Am. Chem. Soc. **77**, 2287 (1955).
18. C. W. P. Crowe, R. M. Evans, G. F. H. Gruman, and A. G. Long. J. Chem. Soc. 4351 (1956).
19. R. N. Jones, D. A. Ramsay, F. Herling, and K. Dobriner. J. Am. Chem. Soc. **74**, 2828 (1952).
20. L. J. Bellamy. The infrared spectra of complex molecules. John Wiley and Sons, Inc., New York. 1960. p. 78.
21. S. W. Pelletier. Chem. Ind. (London), 1116 (1958).
22. R. A. Bell, R. E. Ireland, and R. A. Partyka. J. Org. Chem. **27**, 3741 (1962).
23. H. Vorbrüggen and C. Djerassi. J. Am. Chem. Soc. **84**, 2990 (1962).
24. S. W. Pelletier. J. Am. Chem. Soc. **82**, 2398 (1960).
25. A. J. Solo and S. W. Pelletier. Chem. Ind. (London), 1108 (1960).
26. S. W. Pelletier. Tetrahedron, **14**, 76 (1961).
27. W. B. Whalley. Tetrahedron, **18**, 43 (1962).
28. K. Watanabe, C. N. Pillai, and H. Pines. J. Am. Chem. Soc. **84**, 3934 (1962).
29. H. M. Walborsky and D. F. Loncrini. J. Am. Chem. Soc. **76**, 5396 (1954).
30. R. B. Turner, W. R. Meador, and R. E. Winkler. J. Am. Chem. Soc. **79**, 4116 (1957).
31. R. Criegee, E. Buchner, and W. Walther. Ber. **73**, 571 (1940).
32. N. R. Campbell and J. H. Hunt. J. Chem. Soc. 1379 (1950).
33. I. R. Sherwood and W. F. Short. J. Chem. Soc. 1006 (1938).
34. C. Djerassi and A. E. Lippmann. J. Am. Chem. Soc. **77**, 1825 (1955).
35. M. Bender and M. S. Silver. J. Am. Chem. Soc. **84**, 4589 (1962).
36. M. S. Newman and S. Hishida. J. Am. Chem. Soc. **84**, 3582 (1962).
37. O. E. Edwards. Chem. Can. 40 (1961).
38. J. D. Roberts and W. T. Moreland. J. Am. Chem. Soc. **75**, 2167 (1953).
39. S. W. Pelletier and W. A. Jacobs. Chem. Ind. (London), 1385 (1955).
40. A. J. Solo and S. W. Pelletier. Proc. Chem. Soc. 14 (1961).
41. N. J. Leonard, K. Conrow, and R. R. Sauer. J. Am. Chem. Soc. **80**, 5185 (1958).
42. W. A. Jacobs and L. C. Craig. J. Biol. Chem. **147**, 567 (1943).
43. S. J. Angyal, P. A. J. Gorin, and M. Pitman. Proc. Chem. Soc. 337 (1962).
44. E. L. Eliel and R. S. Rao. J. Am. Chem. Soc. **79**, 5992 (1957).

Can. J. Chem. Downloaded from www.nrcresearchpress.com by 210.87.254.42 on 09/05/12
For personal use only.

COMPOUNDS OF THE TYPE M_5X_2: DETERMINATION OF THE SPACE GROUP OF PENTA NICKEL DIARSENIDE (Ni_5As_2) USING VAPOR-GROWN SINGLE CRYSTALS[1]

G. S. SAINI,[2] L. D. CALVERT, AND J. B. TAYLOR
Division of Applied Chemistry, National Research Council, Ottawa, Canada
Received July 30, 1963

ABSTRACT

Single crystals of Ni_5As_2 have been grown by vapor transport reactions involving the use of either bromine or iodine. Crystals and whiskers have also been grown in the absence of halogen. In neither case did the maximum dimensions of the crystals exceed 0.5 mm. Ni_5As_2 is hexagonal with space group $P6_322$: $a = 6.81$, $c = 12.48$ Å.

INTRODUCTION

There are many references in the literature to compounds having the general formula M_5X_2. This particular study has been confined to cases where M is a transition metal and X is either a pnigogen, a chalcogen, silicon, boron, carbon, or germanium. Crystallographic information is not available for all of the known compounds, e.g. Pt_5Sb_2 (1), Pd_5Te_2 (2), Pd_5Se_2 (2), and Pd_5P_2 (3) are reported to exist but the crystal symmetry is not known. In other cases, the lattice parameters and space group are known but the exact composition is not always certain. When analysis is reported the stoichiometry is found to fall within the range $M_{5.30}X_2$ to $M_{4.77}X_2$. The known compounds fall into three crystal classes but there is, at present, no necessary reason to regard the compounds in each system as isostructural. The data found in a literature survey are summarized below. All cell parameters are in Ångström units.

Tetragonal	Ti_5Sb_2 (4)	As Ti_2Sb C 38 type	$a = 4.01$; $c = 14.5$
	Ni_5Sb_2 (5)	As Ni_2Sb	$a = 5.80$; $c = 6.01$
	Cu_5As_2 (6)	Tentative indexing	$a = 7.48$; $c = 7.12$
	$Ni_{12}P_5$ (7)	$I4/m$ (C_{4h}^5)	$a = 8.646$; $c = 5.070$
Monoclinic	Pd_5B_2 (8)	$C2/c$	$a = 12.786$; $b = 4.955$; $c = 5.472$; $\beta = 97° 2'$
	Mn_5C_2 (9)	$C2/c$	$a = 5.086$; $b = 4.573$; $c = 11.66$; $\beta = 97° 45'$
Hexagonal	$Mn_{2.65}Ge$ (10)	($B8_2$?)	$a = 7.18$; $c = 13.08$
Hexagonal or trigonal	Ni_5As_2 (11)		$a = 6.815$; $c = 12.498$ (for $Ni_{4.77}As_2$)
Trigonal	Ni_5Si_2 (12, 14)		$a = 6.670$; $c = 12.267$ (in equilibrium with Ni_2Si)
Hexagonal	Ni_5P_2 (13)		$a = 13.220$; $c = 24.632$

It is interesting to note that in the case of the first two members of the tetragonal group the 5:2c ompounds have the same structure as the respective 2:1 phases. In fact Welsbach, Nowotny, and Kohl wrote Ti_5Sb_2 as Ti_2 [$Ti_{0.15}$ $Sb_{0.85}$]. Although the cell parameters for Ni_5Si_2 and Ni_5P_2 were based on single-crystal studies, no details, other than those given above, were published. The powder pattern of Ni_5Si_2 published by Osawa and Okamoto (14) is probably unreliable. The symmetry and the lattice parameters for Ni_5As_2 and

[1]*Issued as N.R.C. 7657.*
[2]*Postdoctoral Fellow.*

Can. J. Chem. Downloaded from www.nrcresearchpress.com by 210.87.254.5 on 09/05/12
For personal use only.

$Mn_{2.65}Ge$ were obtained by powder methods. In addition to the latter compound, the pattern of $Mn_{2.5}Ge$ was reported but was not indexed.

The present series of investigations has been directed towards an examination of structural similarities among these 5:2 compounds and this paper describes the preparation of single crystals of Ni_5As_2, derivation of a definite space group, and modification of the indexed powder pattern published earlier.

Many 5:2 compounds have incongruent melting points but Ni_5As_2 is an exception in that it melts congruently at 998° (15). Thus it would be theoretically possible to grow single crystals of Ni_5As_2 by freezing a liquid of stoichiometric composition. However, the crystals used in this study were prepared by a halide vapor transport reaction of the type reported by Brixner (16) and Nitsche, Bölsterli, and Lichtensteiger (17), which may be represented as follows:

$$Ni_5As_{2(s)} + \text{halogen}_{(g)} \rightleftharpoons Ni(\text{halide})_{(g)} + As_{(g)}.$$

There is a possibility that this method is generally applicable to the preparation of single crystals of all 5:2 compounds whereas preparation of a phase with an incongruent melting point from a liquid of carefully controlled composition by the method of zone leveling (18) is difficult in practice and requires detailed knowledge of the liquidus curve.

PREPARATIVE—EXPERIMENTAL

The nickel was supplied as sponge by Johnson Matthey and Co. and contained less than 0.8 p.p.m. total impurities as Fe, Cu, Si, and Mg. The sponge was completely reduced in hydrogen at 600° C prior to use. Arsenic was obtained from Cominco and had a purity of 99.999% as determined by spectrographic methods. This material was fractionally sublimed *in vacuo* at 450° C to remove carbon and oxide contaminants which are not recorded in the spectrographic analysis. Other chemicals employed were laboratory reagent grade. The bromine was vacuum sublimed from a source at −80° C to a receiver at −196° C before it was finally distilled into the reaction tube.

The tube furnace used was 62 cm long and 4 cm inside diameter. A center-tapped winding of "Kanthal" resistance tape was used. This was fed with two variable transformers to provide independent heating zones. No temperature control was used but the equilibrium temperature attained by the furnace on a given voltage supply was sufficiently constant for these experiments. The furnace operated horizontally and the ends were closed with tightly packed quartz wool plugs. The tubes in which the transport reactions occurred were made of clear quartz, 35 cm long, 2.0 cm diameter, with a 0.2-cm wall. Two chromel vs. alumel thermocouples were attached to the tubes to record "hot" and "cold" zone temperatures. The tubes were fitted with thin wire spiders which supported them away from the walls of the furnace. This method of support is distinctly preferable to the alternative of allowing the tube to lie on the inside wall of the furnace.

Three alternative methods of loading the tube were used. (1) A previously prepared polycrystalline sample of Ni_5As_2 was placed in the tube at one end. (2) A mixture of nickel and arsenic powders in the atomic proportion 5:2 was placed at one end of the tube. (3) Arsenic was placed at one end of the tube and nickel powder at the other end. The correct 5:2 atomic proportions were still maintained.

Either iodine or bromine was used in the transport reaction. The former was added as crystals and the bromine was distilled into the tube on a high vacuum system. The tube was cooled in liquid nitrogen and evacuated to 10^{-4} mm Hg prior to being sealed off. It was supported horizontally in the furnace, as described earlier, with the cold end at 650° C and the hot end containing the Ni_5As_2 or the Ni at 750° C.

One tube was also prepared which contained polycrystalline Ni_5As_2 at one end but into which no halogen was introduced. The tube was sealed at a pressure of 10^{-5} mm Hg and heated so that the Ni_5As_2 was at 800° C and the other end at 550° C.

RESULTS

In the experiments described, with the exception of the last case in which no halogen was used, there was an appreciable transport of material from the hot end towards the cooler end of the tube and clusters of crystals with a metallic luster were observed on the walls after a period of 3 days. The same results were obtained for each method of loading the tube and for concentrations of iodine or bromine of 0.03 mg per cc or 5 mg per cc. The majority of the crystals grew close to the initial charge and Debye–Sherrer photographs confirmed that these were Ni_5As_2. Large lustrous black flakes of NiI_2 were observed

Can. J. Chem. Downloaded from www.nrcresearchpress.com by 210.87.254.5 on 09/05/12
For personal use only.

at the cooler end of the tube in the case of iodide transport. In one iodide transport experiment, dark green crystals of NiO grew at the hottest end of the tube. With the exception of these two compounds (and the elements composing the starting materials) no other phase besides Ni_5As_2 was ever observed. Many of the Ni_5As_2 crystalline samples contained NiI_2 and the content of the impurity increased as the iodine concentration in the tube was raised.

The experiment using no halogen was performed after NiO was obtained in one transport tube. The part played by oxyhalides and even by oxygen itself in the transport reactions is at present open to conjecture. No bulk transport was observed in this tube but the polycrystalline Ni_5As_2 was found to have completely changed in appearance. Its surface had become covered with a variety of crystal growths which on X-ray powder examination proved to be composed entirely of the Ni_5As_2 phase.

CRYSTALLOGRAPHY

The most common habits of the Ni_5As_2 crystals grown with low pressure iodine transport were pyramidally terminated needles, rectangular based pyramids, and multifaceted beads. On X-ray examination, selected crystals were found generally to be imperfect multiple crystals with some apparently twinned. A few of the needles were found to be perfect. The overall maximum dimension of any crystal did not exceed 0.5 mm. In the case of crystals grown in the absence of halogen there were large numbers of multifaceted beads and flat hexagonal plates. Occurring less frequently were dendritic blades and whiskers about 1 mm long. The growth in this case appeared to have taken place upwards out of the substrate since the whiskers carried small fragments of the substrate polycrystalline material along their length.

Three crystals grown by iodine transport reactions were examined on a precession camera using zirconium-filtered molybdenum radiation. Zones recorded were $h0*l$, $\bar{h}2h*l$, $h1*l$, $hk*0$, and $hk*1$ and the only systematic absences were $00*l$ where l is odd.

The crystals were hexagonal, diffraction symbol $6/mmm\ P6_3..$, which uniquely determines the space group as $P6_322(D_6^6)$. The average observed unit cell dimensions were $a = 6.81 \pm 0.02$, $c = 12.48 \pm 0.02$ Å, $c/a = 1.833$, $D_x = 8.80$ for Ni_5As_2 (F.W. = 443.39), $V = 502$ Å^3, $Z = 6$.

The axial lengths are shorter than those recorded by Heyding and Calvert for $Ni_{4.77}As_2$ and as the lattice is reported to contract with increasing arsenic concentration it must be concluded that the crystals examined in this work were even richer in arsenic. The exact composition was never determined. The space group $P6_322$ modifies the aspect symbol previously suggested on the basis of the indexed powder photograph and requires that all indices of the type $h0*l$ be considered in indexing the powder pattern.

Examination of the intensities of reflections on the single crystal photographs indicates that one extra index should be added to the previous indexing of the line at $d = 1.96$ Å. The previous line in the powder pattern at $d = 2.01$ Å can be uniquely indexed as 11*5. Since the intensities of 30*0 and 11*5 are very similar on the single crystal photographs the indexing of the line at $d = 1.96$ Å should include 30*0.

The complete indexing of the two strong lines is as follows:

I_{obs}	$hk*l$	d_{obs}	d_{calc}
100	11*5	2.01	2.02
100	21*3	1.96	1.969
	30*0		1.967
	10*6		1.964

Can. J. Chem. Downloaded from www.nrcresearchpress.com by 210.87.254.5 on 09/05/12
For personal use only.

ACKNOWLEDGMENTS

The authors are indebted to Mr. G. J. G. Despault who grew the crystals and to Miss M. McLellan who obtained the Debye–Scherrer patterns.

REFERENCES

1. K. Friedrich and A. Leroux. Metallurgie, **6**, 1 (1909).
2. F. Grønvold and E. Røst. Acta Chem. Scand. **10**, 1620 (1956).
3. G. Wiehage, F. Weibke, and W. Biltz. Z. Anorg. Chem. **228**, 357 (1936).
4. H. Auer-Welsbach, H. Nowotny, and A. Kohl. Monatsh. Chem. **89**, 154 (1958).
5. U. Fürst and F. Halla. Z. Physik. Chem. B **40**, 285 (1938).
6. R. D. Heyding and G. J. G. Despault. Can. J. Chem. **38**, 2477 (1960).
7. S. Rundquist and E. Larsson. Acta Chem. Scand. **13**, 551 (1959).
8. E. Stenberg. Acta Chem. Scand. **15**, 861 (1961).
9. K. Kuo and L. E. Persson. J. Iron Steel Inst. **178**, 39 (1954).
10. T. Ohoyama. J. Phys. Soc. Japan, **15**, 1995 (1961).
11. R. D. Heyding and L. D. Calvert. Can. J. Chem. **35**, 1205 (1957).
12. G. Pilström. Acta Chem. Scand. **15**, 893 (1961).
13. S. Rundquist. Arkiv. Kemi, **20**, 67 (1962).
14. A. Osawa and M. Okamoto. Sci. Repts. Tohoku. Univ. First Ser. **27**, 331 (1939).
15. M. Hansen. Constitution of binary alloys. 2nd ed. McGraw-Hill. 1958.
16. L. H. Brixner. J. Inor. Nucl. Chem. **24**, 257 (1962).
17. R. Nitsche, H. V. Bölsterli, and M. Lichtensteiger. J. Phys. Chem. Solids, **21**, 199 (1961).
18. D. R. Mason and J. S. Cook. J. Appl. Phys. **32**, 475 (1961).

Can. J. Chem. Downloaded from www.nrcresearchpress.com by 210.87.254.5 on 09/05/12
For personal use only.

THE STRUCTURES OF TWO NEW ALKALOIDS: CHASMACONITINE AND CHASMANTHININE[1]

O. ACHMATOWICZ, JR.[2] AND LÉO MARION
Division of Pure Chemistry, National Research Council, Ottawa, Canada
Received August 28, 1963

ABSTRACT

A re-examination of the root of *Aconitum chasmanthum* Stapf has shown that it contains several alkaloids. Of these, besides indaconitine, the presence of which had been reported long ago, four new alkaloids have been isolated: base A ($C_{26}H_{43}O_6N$), base B ($C_{25}H_{41}O_6N$), chasmaconitine ($C_{34}H_{47}O_9N$), and chasmanthinine ($C_{36}H_{49}O_9N$). Chasmaconitine gives rise to bikhaconine on hydrolysis, and has been shown by conversion to delphinine to be N-ethyl-N-desmethyl-delphinine. Chasmanthinine is also hydrolyzable to bikhaconine. Whereas in chasmaconitine bikhaconine is esterified with acetic and benzoic acid, in chasmanthinine it is esterified with acetic and *trans*-cinnamic acid. The complete structures and absolute configurations of both bases are derived.

Can. J. Chem. Downloaded from www.nrcresearchpress.com by 210.87.254.42 on 09/05/12
For personal use only.

The Indian plant *Aconitum chasmanthum* Stapf was examined many years ago by Dunstan and Andrews (1), who isolated from it the alkaloid indaconitine ($C_{34}H_{47}O_{10}N$). To study the structure of this alkaloid (2) a quantity of the root of this plant was obtained from India.[3]

A careful examination of the methanolic extract of the root has shown that it contains several alkaloids, and five of these have now been isolated in crystalline and pure form (single spots in thin layer chromatography). The five alkaloids are the following: base A, $C_{26}H_{43}O_6N$, m.p. 105–107°; base B, $C_{25}H_{41}O_6N$, m.p. 90–91°, which is the major component of the mixture; base C, $C_{34}H_{47}O_9N$, m.p. 181–182°, also obtained in a low-melting form, m.p. 165–167°; base D, $C_{36}H_{49}O_9N$, m.p. 160–161°; and base E, $C_{34}H_{47}O_{10}N$, m.p. 189–191°. The first two alkaloids came mostly from the strong bases fraction while the remaining three were present in the fraction containing the weak bases (cf. Experimental).

Base E has been identified with indaconitine (II, R = C_2H_5, R_1 = OH, R_2 = C_6H_5) by direct comparison. In this paper we report work concerned with the establishment of the structures of bases C and D which we propose to designate as chasmaconitine and chasmanthinine respectively.

Chasmaconitine ($C_{34}H_{47}O_9N$), according to its infrared absorption spectrum, contains one free hydroxyl (3470 cm^{-1}), an aromatic ring (1600 cm^{-1}), ester carbonyls (strong band at 1718 cm^{-1}), and an acetate (1275 cm^{-1}). The n.m.r. spectrum of the base shows that it contains four methoxyls (δ 3.53, 3.28, 3.27, 3.16), one N-ethyl group (triplet centered at δ 1.08), and one acetoxy group (δ 1.27), and that the aromatic group is monosubstituted (signals corresponding to five aromatic protons at δ 7.35–8.20). The spectroscopic evidence, therefore, indicates that chasmaconitine is a diester of benzoic acid and acetic acid with an alkamine ($C_{25}H_{41}O_7N$) containing four methoxyl groups.

This is confirmed by the hydrolysis of chasmaconitine with alkali which produces benzoic acid, acetic acid, and an amorphous alkamine which on treatment with acetic

[1]*Issued as N.R.C. No. 7656.*
[2]*National Research Council of Canada Postdoctoral Fellow.*
[3]*Obtained through the courtesy of Mr. K. L. Handa, Regional Research Laboratory, Jammu, India, to whom we express our most cordial thanks. In two lots of the root, the major alkaloid was indaconitine. In this particular lot, however, the quantity of indaconitine was appreciably smaller.*

anhydride and *p*-toluenesulphonic acid, gave a derivative, $C_{31}H_{47}O_{10}N$, crystallizing as needles, m.p. 149–150°, or prisms, m.p. 159–161°, $[\alpha]_D$ −7.8°. This product proved to be identical in every way with an authentic sample (3) of triacetylbikhaconine I (melting point, that of the mixture, infrared and n.m.r. spectra, and mobility in thin-layer chromatography, as well as optical rotation). Hence the alkamine is bikhaconine and,

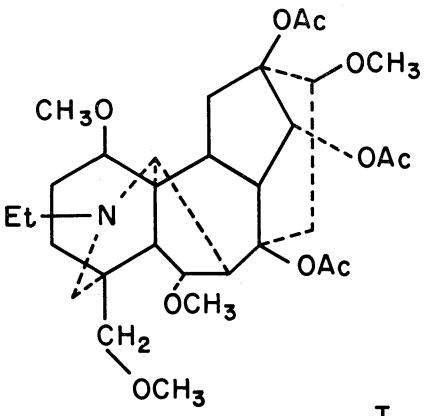

I

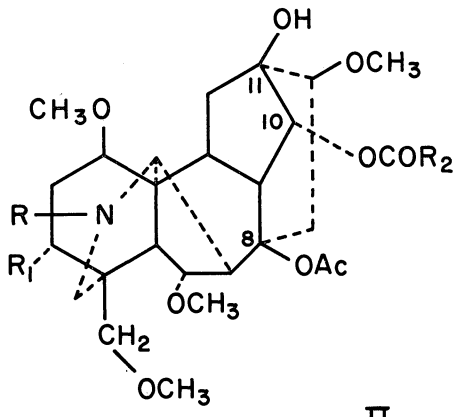

II

consequently, chasmaconitine should be identical with deoxyindaconitine, i.e. N-ethyl-N-desmethyl-delphinine (II, R = Et, R_1 = H, R_2 = C_6H_5). It has the same empirical formula and its properties (m.p. 181–182°, $[\alpha]_D^{25}$ +10.3°) are similar to those previously reported for deoxyindaconitine (m.p. 175–180°, $[\alpha]_D^{25}$ +14°). The infrared spectra of the two, however, showed some very slight differences, but the identity was confirmed in the following manner.

The imino-ethyl group of chasmaconitine was removed by oxidation with potassium permanganate in acetone–water solution at room temperature.[4] N-Desethylchasmaconitine, m.p. 161–164°, showed no triplet at δ 1.08 in its n.m.r. spectrum. That the removal of the ethyl group was the only effect of the oxidation was proved by the reconversion of a small quantity of the N-desethyl-base into chasmaconitine by the action of ethyl iodide. An analogous reaction with methyl iodide gave rise to a product which was identical with delphinine (II, R = CH_3, R_1 = H, R_2 = C_6H_5) in every respect (melting point, that of the mixture, infrared spectrum, and mobility in thin-layer chromatography). Consequently chasmaconitine has structure II (R = Et, R_1 = H, R_2 = C_6H_5). It is probable that the slight differences in properties of deoxyindaconitine (cf. ref. 2) are due to the presence of a small quantity of a compound arising in the course of the catalytic hydrogenation of anhydroindaconitine by elimination of the allylic methoxyl. A similar side reaction has been observed in the catalytic hydrogenation of the anhydropseudaconitine (3).

In the n.m.r. spectrum of chasmaconitine, the signal of the three protons of the acetoxy group occurs as a singlet at δ 1.27, which is at much higher field than normal. This shift of the signal to unusually high field has been observed previously in the n.m.r. spectra of aconitine, indaconitine, pseudaconitine, delphinine, and bikhaconitine and is due to the fact that the protons of the acetoxy group come within the shielding range of the aromatic nucleus, the anisotropic effect of which causes the shift (4). Consequently, the orientation

[4]*This oxidative dealkylation procedure will be fully described in a forthcoming paper.*

Can. J. Chem. Downloaded from www.nrcresearchpress.com by 210.87.254.42 on 09/05/12
For personal use only.

of the two ester groups in chasmaconitine is exactly the same as in aconitine and delphinine. In fact, the conversion of chasmaconitine into delphinine by the simple replacement of its N-ethyl group by an N-methyl not only confirms this, but proves that the absolute configuration is the same for both alkaloids (6).

Chasmanthinine (base D) ($C_{36}H_{49}O_9N$) has an empirical formula that contains C_2H_2 more than that of chasmaconitine. The R_F values of the two bases are very close, although different. The infrared spectrum of chasmanthinine, like that of chasmaconitine, shows the presence in the alkaloid of a hydroxyl (3440 cm^{-1}), of two ester carbonyl groups (1725 and shoulder at 1715 cm^{-1}), of an aromatic ring (1578 cm^{-1}) which is monosubstituted (765, 710 cm^{-1}) and of an acetate ester (1277 cm^{-1}). It differs in containing a sharp band at 1643 cm^{-1} indicative of an isolated double bond, and another band at 980 cm^{-1}, characteristic of a trans double bond.

The presence of an isolated double bond is also shown by the n.m.r. spectrum of chasmanthinine, which contains an AB type quartet (δ 6.42, 7.72, J_{AB} = 16 c.p.s.) corresponding to two protons characteristic of trans olefines. It further contained signals corresponding to five aromatic protons (δ 7.43), to four methoxyls (δ 3.50, 3.27, 3.24, 3.19), to an N-ethyl group (triplet at δ 1.08), and an acetoxy group (δ 1.77).

Consequently, the spectroscopic evidence indicates the presence in chasmanthinine of the features characterizing chasmaconitine, but shows the presence of an additional double bond in the former.

Hydrolysis of chasmanthinine with alkali gave rise to an alkamine isolated as its triacetate, $[\alpha]_D$ −7.9°, m.p. 159–161°, identical in every respect with bikhaconine triacetate, to acetic acid (not isolated), and to a crystalline acid which was not benzoic acid. The acid melted at 137–139°, either alone or in admixture with an authentic sample of *trans*-cinnamic acid. The identity of the acid was confirmed by comparison of its X-ray powder diagram with that of the authentic sample which was exactly alike.

The isolation of the cinnamic acid accounts for the additional C_2H_2 present in chasmanthinine and for the trans olefinic bond. Consequently, the structure of chasmanthinine (II, R = Et, R_1 = H, R_2 = $CH{:}CHC_6H_5$) is the same as that of chasmaconitine except that the benzoyl group of the latter is replaced by a *trans*-cinnamoyl group. That the aromatic ester group occupies the same position as in chasmaconitine follows from the n.m.r. evidence.

Just like the n.m.r. spectrum of pseudaconitine, delphinine, and bikhaconitine (4), the spectrum of chasmanthinine contains a doublet at δ 4.80, $J \sim 4.5$ c.p.s. corresponding to a single proton split by a single neighboring proton. This signal must be attributable to a proton attached to the carbon carrying the aromatic ester group (cf. ref. 4). Because the alkamine derived from chasmanthinine is identical with bikhaconine, it can be concluded that the cinnamic ester group must be located at C_{10} (formula II) since, of the three possible positions for esterification (C_8, C_{10}, C_{11}), that is the only carbon that would carry a proton accompanied by a single neighboring proton.

The signal for the acetoxy protons in the n.m.r. spectrum of chasmanthinine occurs at δ 1.77, which is at higher field than the normal signal (5) but is at lower field than the corresponding signal in chasmaconitine (δ 1.27) and of a number of other aconite alkaloids previously examined (4). It is possible to see from an examination of scale models that in chasmaconitine as in aconitine the acetoxy group stands very close to the plane of the benzene ring of the aromatic ester group and is subject to its anisotropic action which causes the shift. In chasmanthinine, which is esterified with cinnamic acid, the benzene ring is further away from the acetoxy group which, however, is close to the double bond.

Can. J. Chem. Downloaded from www.nrcresearchpress.com by 210.87.254.42 on 09/05/12
For personal use only.

Hence the smaller shift (δ 1.77) in the acetoxy protons signal must be due to the anisotropy of the double bond, which is not as strong as that of the aromatic ring. It can, therefore, be concluded that the location and the orientation of the two ester groups in chasmanthinine is exactly the same as in chasmaconitine and delphinine.

Since chasmaconitine has been shown to have the same absolute configuration as delphinine, and since both chasmaconitine and chasmanthinine are hydrolyzed to bikhaconine, it follows that chasmanthinine also has the same absolute configuration as delphinine.

Chasmanthinine is the first alkaloid reported in the highly oxygenated diterpenoid series that is esterified with cinnamic acid. In all the bases of the aconitine type so far studied the alkamine is esterified with acetic acid and one or the other of the following acids: benzoic, veratric, or anisic acid.

EXPERIMENTAL

All the infrared absorption spectra were measured on a Perkin–Elmer double beam spectrophotometer model 21B and unless otherwise mentioned, in a Nujol mull. The n.m.r. spectra were obtained on a Varian A-60 instrument.

Separation of Alkaloids

The dried, ground root of *Aconitum chasmanthum* Stapf (1.36 kg) was extracted by percolation with methanol and the extract evaporated under reduced pressure. The residue was dissolved in 3% hydrochloric acid, and the filtered acid solution extracted with methylene dichloride to remove the neutral and acid material (26.5 g).

Sodium carbonate was added to the aqueous solution (to pH 8), which was again extracted with methylene dichloride (extract 2). The aqueous solution was then made strongly basic with sodium hydroxide (pH 12) and extracted further with methylene dichloride (extract 3).

Extract 3 on evaporation left a residue of crude strong bases (22 g). Extract 2 was evaporated to dryness and the residue dissolved in ether. The ether solution was filtered to remove the insoluble material and the filtrate evaporated to dryness. The residue consisted of the crude weak bases (80 g).

The Strong Bases

The residue from extract 3 (22 g) was dissolved in hot benzene (200 ml) and the insoluble material (4.2 g) was filtered off. The benzene solution was passed through a column of alumina and the eluate evaporated. It left a residual yellowish oil (16.1 g) which partially crystallized. Two crystallizations from *n*-hexane yielded base B (10.6 g), m.p. 90–91°, $[\alpha]_D^{25}$ +23.6° (*c*, 2.5 in EtOH). Found: C, 66.31; H, 9.09; N, 3.14. Calc. for $C_{25}H_{41}O_6N$: C, 66.49; H, 9.15; N, 3.10%; ν 3460, 3365, 3260 cm^{-1}.

The mother liquor from the crystallization of base B was evaporated to dryness. It left a gum (5.4 g) which thin-layer chromatography showed to be a mixture of some base B and another component (base A). Chromatography on alumina (grade III) failed to effect a clean separation but gave a fraction enriched in base A. Separation was effected on this fraction by the use of thin-layer chromatography on a preparative scale. The mixture of bases A and B (136 mg) was adsorbed on silica gel spread on two plates (40×40 cm) and developed with cyclohexane–diethylamine (9:1). The strip of silica gel containing base A was eluted with chloroform–methanol (20:1) and the eluate evaporated. There was left a residue (118 mg) which was dissolved in benzene and chromatographed on alumina.[5] The base obtained (112 mg) crystallized immediately and consisted of pure base A. After two recrystallizations from *n*-hexane, it consisted of clumps of colorless prisms, m.p. 105–107°, $[\alpha]_D^{25}$ +19.2° (*c*, 2.4 in EtOH). Found: C, 67.32; H, 9.07; N, 2.96. Calc. for $C_{26}H_{33}O_6N$: C, 67.06; H, 9.31; N, 3.01%; ν 3420 cm^{-1}.

The Weak Bases

The crude weak bases (80 g) were dissolved in chloroform (500 ml) and shaken with three portions (1000 ml) of a buffer solution consisting of disodium orthophosphate (290 g) and citric acid (90 g) dissolved in water (4 l.) and adjusted to pH 5.4. Each portion of buffer solution extract was back extracted with chloroform (200 ml). The combined aqueous extract was made basic with alkali and extracted with chloroform. This last chloroform extract, after drying and evaporation, left a residual white foam (10 g) which thin-layer chromatography showed to consist mostly of base A and base B together with small quantities of other components.

The first chloroform solution (which had been extracted with buffer solution) was dried and evaporated to dryness. The gummy residue (70 g) was dissolved in benzene and chromatographed on a column (6×40 cm) of alumina (grade IV, 1000 g). The column was eluted first with benzene–chloroform (4:1), then a 1:1

[5]*In all cases of column chromatography, Woelm alumina was used as the adsorbent.*

Can. J. Chem. Downloaded from www.nrcresearchpress.com by 210.87.254.42 on 09/05/12
For personal use only.

mixture, afterwards with chloroform, and finally with chloroform–methanol (9:1). The eluate was collected in fractions of 500 ml.

Indaconitine

Fractions 1–4 (benzene–chloroform 4:1) left on evaporation a residue (36.1 g) which crystallized on contact with ether. Recrystallization from ether gave colorless crystals (6.2 g), m.p. 189–191°, undepressed by admixture with an authentic sample of indaconitine. The identity was confirmed by comparison of the infrared and n.m.r. spectra of both the isolated base and the authentic sample.

Fractions 5–8 (benzene–chloroform 1:1) afforded a further quantity of crude indaconitine (20.1 g).

Chasmaconitine

The mother liquors from the crystallization of indaconitine were combined and evaporated to dryness. The gummy residue (29.9 g) was dissolved in benzene–*n*-hexane (1:1), chromatographed on alumina (grade IV, 300 g), and eluted with benzene collected in 300-ml fractions. Fractions 4–7 (1200 ml) yielded an alkaloid which appeared homogeneous in thin-layer chromatography. This alkaloid (4.01 g), for which the name chasmaconitine is proposed, was crystallized from *n*-hexane from which it separated as colorless prisms, m.p. 181–182° (decomp.). When chasmaconitine was rapidly recrystallized from ether it formed fine needles, m.p. 165–167°. Either form could be obtained by cross-seeding, $[\alpha]_D^{25}$ +10.3° (*c*, 1.26 in EtOH). Found: C, 66.59; H, 7.67; N, 2.36. Calc. for $C_{34}H_{47}O_9N$: C, 66.54; H, 7.72; N, 2.28%.

Chasmanthinine

Fraction 8 (373 mg) obtained from the chromatogram that yielded chasmaconitine was rechromatographed over alumina (grade IV, 7 g). Fractions 1–7 (eluted with benzene–hexane 1:1, 80 ml, and with benzene, 60 ml) contained mainly the new base chasmanthinine (thin-layer chromatography). The residue after evaporation of the eluate (237 mg) was dissolved in methylene dichloride and adsorbed on preparative scale thin-layer chromatography plates. The chromatogram was developed on the plates with cyclohexane–diethylamine (9:1) and the strips of silica gel containing chasmanthinine were eluted with chloroform–methanol (9:1). The filtered eluate was evaporated and the residue dissolved in benzene and passed through a column of alumina. The benzene solution was evaporated and the residue (215 mg) crystallized twice from *n*-hexane and once from ether from which chasmanthinine separated as colorless needles, m.p. 160–161° (decomp.), $[\alpha]_D^{25}$ +9.6° (*c*, 1.09 in EtOH). Found: C, 67.48; H, 7.51; N, 2.31. Calc. for $C_{36}H_{49}O_9N$: C, 67.58; H, 7.72; N, 2.19%.

Hydrolysis of Chasmaconitine

Chasmaconitine (200 mg) was refluxed in 3% methanolic sodium hydroxide (20 ml) for 1 hour. The methanol was evaporated under reduced pressure, water was added, and the mixture extracted with chloroform. After drying and evaporation the extract left a basic gummy residue (148 mg) which, in the infrared, showed no carbonyl absorption.

The alkaline aqueous solution was acidified with dilute sulphuric acid and thoroughly extracted with ether. The ether extract on evaporation yielded a white solid (39 mg) which, after two crystallizations from water, consisted of colorless needles (20 mg), m.p. 123° either alone or in admixture with benzoic acid.

Triacetylbikhaconine

The alkamine formed in the hydrolysis of chasmaconitine and obtained as a gummy residue (148 mg) could not be induced to crystallize. It was heated with acetic anhydride (3 ml) and *p*-toluenesulphonic acid (100 mg) on a steam bath for 1 hour. The reaction mixture was poured onto cracked ice, made basic with sodium carbonate, and extracted with chloroform. Evaporation of the dried extract left a solid which was dissolved in benzene and passed through a column of alumina. The benzene eluate was evaporated to dryness and the crystalline residue (192 mg) recrystallized from *n*-hexane from which it separated as colorless needles, m.p. 149–150°. Needles are obtained if the crystallization is rapid, but from a more dilute solution when the crystallization is slow, colorless prisms, m.p. 159–161°, separate, $[\alpha]_D^{25}$ −7.8° (*c*, 2.5 in EtOH). The melting point of the prisms was not depressed when mixed with an authentic sample of triacetylbikhaconine, m.p. 159–161° (3). The identity was confirmed by comparison of the infrared absorption spectra which were superimposable.

N-Desethylchasmaconitine

Chasmaconitine (248 mg) was dissolved in acetone (35 ml) and a solution of potassium permanganate (248 mg) in acetone (35 ml) and water (35 ml) was added rapidly. The reaction mixture was stirred for 10 minutes, the excess permanganate decomposed with sulphurous acid and the filtered solution evaporated under reduced pressure to about one-third of its volume to remove the acetone. The aqueous solution was alkalized with sodium carbonate and extracted four times with chloroform. Evaporation of the dried chloroform extract left a residue which was dissolved in 1% sulphuric acid (10 ml) and the solution extracted with benzene to remove neutral products. The aqueous solution was alkalized with sodium carbonate and again extracted with chloroform. This last extract when evaporated to dryness left a foam (226 mg) which was dissolved in benzene and chromatographed an alumina (grade IV). Elution of the column with *n*-hexane–benzene 1:1 (fractions 1–2) yielded unchanged chasmaconitine (111 mg). Further elution with a mixture of

Can. J. Chem. Downloaded from www.nrcresearchpress.com by 210.87.254.42 on 09/05/12
For personal use only.

benzene and methylene dichloride (fractions 3–7) yielded the expected secondary base (92 mg) which gave one spot only in thin-layer chromatography. The secondary base crystallized from ether as colorless needles, m.p. 161–164.5°, $[\alpha]_D^{25}$ +25.7° (*c*, 1.4 in EtOH). Found: C, 65.76; H, 7.72. Calc. for $C_{32}H_{43}O_9N$: C, 65.62; H, 7.40%. Its n.m.r. spectrum did not contain the triplet characteristic of the ethyl group.

Treatment of the N-desethyl base (30 mg) dissolved in ether–methanol (1:1, 6 ml) with excess ethyl iodide and finely powdered potassium carbonate converted the base back to chasmaconitine, m.p. 180–182° either alone or in admixture with the starting material. The identity was also confirmed by comparison of the infrared absorption spectra.

N-Methyl-N-desethylchasmaconitine (Delphinine)

N-Desethylchasmaconitine (100 mg) was dissolved in ether–methanol (1:1, 10 ml) and an excess methyl iodide was added to the solution together with finely powdered potassium carbonate. The reaction mixture was refluxed for 1 hour and the solvent distilled off. Water was added to the residue and the solution was extracted with chloroform. The extract on evaporation left a foam which was dissolved in benzene and chromatographed on alumina. The benzene eluate was evaporated to dryness; it left a residue which crystallized on contact with ether (96 mg). The product, after two recrystallizations from ether, consisted of colorless prisms, m.p. 187–189° (decomp.), $[\alpha]_D$ +26.0° (*c*, 1.45 in EtOH). The melting point was not depressed by admixture with an authentic sample of delphinine, and the infrared absorption spectra were superimposable. Further, the product and delphinine had the same mobility on a chromatoplate.

Hydrolysis of Chasmanthinine

Chasmanthinine (101 mg) was refluxed with 3% methanolic sodium hydroxide (20 ml) for 1 hour. The methanol was evaporated under reduced pressure, water added, and the mixture extracted with chloroform. The dried extract on evaporation left a gum (92 mg) which did not show any carbonyl absorption in the infrared.

The aqueous solution, which had been extracted with chloroform, was acidified with dilute sulphuric acid and extracted with ether. Evaporation of the extract left a yellowish crystalline residue (22 mg), which, after two crystallizations from aqueous ethanol, consisted of colorless prisms (12 mg), m.p. 137–139°, not depressed in admixture with *trans*-cinnamic acid. The X-ray powder diagrams of both the acid from the hydrolysis and the authentic sample were identical.

The gummy alkamine (92 mg) was heated with acetic anhydride (3 ml) and *p*-toluenesulphonic acid (100 mg) on a steam bath for 1 hour. The mixture was poured into ice water, alkalized with sodium carbonate, and extracted with chloroform. The extract was dried and evaporated; it left a solid residue which was dissolved in benzene and passed through a column of alumina. The benzene eluate, on evaporation, left a crystalline product (90 mg) which, after crystallization from *n*-hexane, consisted of colorless prisms, m.p. 158–161°, $[\alpha]_D^{25}$ −7.9° (*c*, 1.2 in EtOH). This acetylated product proved to be identical with triacetylbikhaconine by comparison of melting point, that of the mixture with an authentic sample, infrared and n.m.r. spectra.

ACKNOWLEDGMENTS

We wish to express our thanks to Mr. A. Knoll who prepared the crude alkaloid extract, to Mr. R. Lauzon who measured the infrared spectra, to Mr. M. Lesage for the n.m.r. spectra, and to Mr. H. Séguin for the microanalyses.

REFERENCES

1. W. R. Dunstan and A. E. Andrews. J. Chem. Soc. **87**, 1620 (1905).
2. R. E. Gilman and L. Marion. Tetrahedron Letters, No. 20, 923 (1962).
3. Y. Tsuda and L. Marion. Can. J. Chem. **41**, 3055 (1963).
4. Y. Tsuda and L. Marion. Can. J. Chem. **41**, 1634 (1963).
5. L. M. Jackman. Applications of n.m.r. spectroscopy in organic chemistry. Pergamon Press. 1959. p. 57.
6. Y. Tsuda and L. Marion. Can. J. Chem. **41**, 1485 (1963).

Can. J. Chem. Downloaded from www.nrcresearchpress.com by 210.87.254.42 on 09/05/12
For personal use only.

Can. J. Chem. Downloaded from www.nrcresearchpress.com by 210.87.254.40 on 09/05/12
For personal use only.

NOTES

STEREOCHEMICAL CONFIGURATION OF SOME PHTHALIDEISOQUINOLINE ALKALOIDS

S. Safe and R. Y. Moir

A study of the proton magnetic resonance spectra of adlumine (I), corlumine (I), bicuculline (II), hydrastine (III), and narcotine (IV) (I) shows that adlumine has the configuration A (or its mirror image), and that the four other alkaloids have configuration B (or its mirror image).

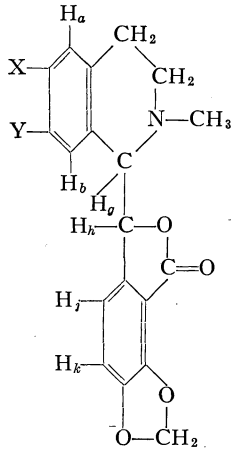

I X = Y = OCH_3
II X, Y = $-OCH_2O-$

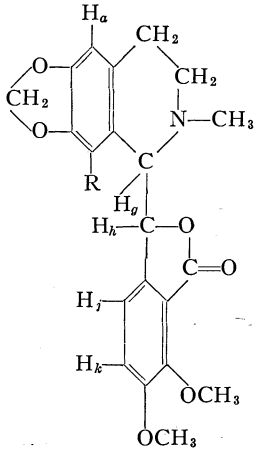

III R = H_b
IV R = OCH_3

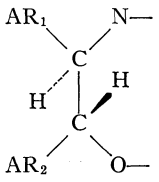

A

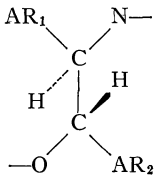

B

Since conformations with low steric interactions exist for both A and B when the tetrahydropyridine ring is a half-chair, the phthalide moiety is equatorial, and the asymmetric carbons are in a staggered conformation, it seems certain that conformations having these structural features will predominate greatly. Furthermore, the conformations A1 and B1, having H_g and H_h antiparallel, show large interactions and can contribute only slightly to the total population. This is borne out by the low coupling constant of these hydrogens (3.4–4.3 cycles per second). Thus only conformations A2 and A3, and B2 and B3, need be considered in the first approximation, and indeed a consideration of the minor conformations does not alter the following argument.

A proton in the region above or below an aromatic ring is magnetically shielded by the "supercurrent" in the ring (2, 3, 4). In configuration A, neither of the conformations A2 or A3 allows H_j to enter the shielding region of the benzene ring of the isoquinoline portion, but in configuration B, the conformation B2 places H_j well into the shielding region of one aromatic ring, while the other conformation B3 places H_b in a similar position with respect to the other aromatic ring. Thus structures might be assigned to the stereoisomers adlumine and corlumine on the basis of the relative shielding of H_j or of H_b; in the event,

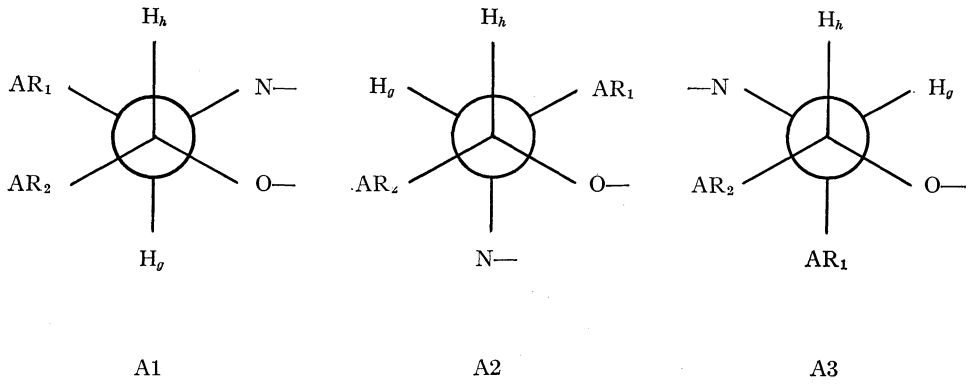

A1 A2 A3

Staggered conformations of configuration A.

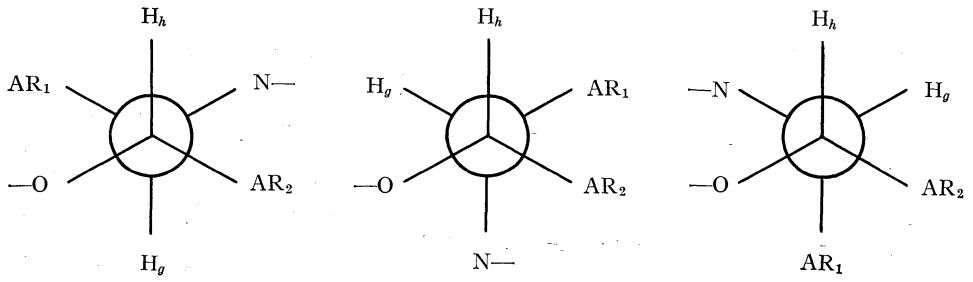

B1 B2 B3

Staggered conformations of configuration B.

only the effect on H_j could be used since the signal from H_b could not be distinguished with certainty from that of H_a.

In Table I are reported the mid-band frequencies of the relevant hydrogens, measured in deuterochloroform solutions containing tetramethylsilane as the internal standard at 60 megacycles per second on the Varian A-60 spectrometer.

TABLE I

Proton magnetic resonance frequencies

Alkaloid	H_j	H_k	H_a(?)	H_b(?)
Adlumine	431.5	412.5	384	404
Corlumine	374.5	416.5	386	397
Bicuculline	380	415.5	390	395
Hydrastine	390	425.5	394	384
Narcotine	364.5	418.5	378	—

Values are in cycles per second downfield from the standard, higher values representing lower shielding. The values for H_j and H_k of adlumine have been corrected for the quantum mechanical mixing of the states.

Can. J. Chem. Downloaded from www.nrcresearchpress.com by 210.87.254.40 on 09/05/12
For personal use only.

The signals from H_j and H_k were identified with certainty by their characteristic ortho-splitting constant of 7.9–8.3 cycles per second; they could be distinguished from each other since that from H_j suffered a further splitting of 0.8 cycles per second due to the presence of H_h. A similar phenomenon has been observed in this laboratory with a series of phthalides.

It is clear that the configurations given are correct, bicuculline acting as a link in the argument connecting corlumine, hydrastine, and narcotine. The large increase in the shielding of H_j in narcotine, compared to that in hydrastine, adds to the strength of the argument, since with narcotine (but not with hydrastine) the conformation B3 is blocked by the interaction of the R group and the phthalide group; thus the conformation B2, in which H_j is shielded, is occupied a much greater part of the time than with hydrastine.

Robinson (5) felt that hydrastine and narcotine have different configurations (from considerations based on optical rotations, conformational effects being ignored). From Table I, this could only mean that hydrastine should have configuration A, contrary to our conclusions. One would then have to say that the change observed in the frequency for H_j in going from adlumine to hydrastine was due to inductive and resonance effects from the change in substituents, that these effects were large, and that they acted in the opposite direction upon the signal for H_k. But these effects would be expected to be small and in the same direction, as indeed they were for H_k, and for H_a and H_b in the corresponding change from corlumine to bicuculline. Fortunately, other work of Robinson gives decisive support to our structure B for hydrastine, and *a fortiori* to the structures suggested for the other alkaloids. Synthetic hydrastine-*a* was shown to be the racemate of natural hydrastine (6). Aminohydrastine-*a* was easily converted to hydrastine-*a* by the same reactions that coupled the aromatic rings in aminohydrastine-*b*, the other racemic stereoisomer (7). A study of models shows that the ring coupling is easy for configuration A, but would involve tremendous distortion for configuration B. Hence the natural alkaloid, belonging to the series in which coupling did not occur, must be B.

Proton magnetic resonance assignments for hydrastine (8), and for corlumine and bicuculline (9), have been published previously. After the first submission of this note, there appeared the determination by another method of the absolute configuration of hydrastine by Ohta, Tani, and Moruzumi (10). Our work agrees with theirs.

We wish to express our gratitude to Dr. R. H. Manske, whose gift of adlumine, corlumine, and bicuculline made the work possible.

1. J. Stanek and R. H. F. Manske. The alkaloids. *Edited by* R. H. Manske and H. L. Holmes. Vol. IV. Academic Press, New York. 1954. p. 167.
2. J. A. Pople. J. Chem. Phys. **24**, 1111 (1956).
3. J. S. Waugh and R. W. Fessenden. J. Am. Chem. Soc. **79**, 846 (1957).
4. J. B. Hyne. J. Am. Chem. Soc. **81**, 6058 (1959).
5. M. A. Marshall, F. L. Pyman, and R. Robinson. J. Chem. Soc. 1315 (1934).
6. R. D. Haworth, A. R. Pinder, and R. Robinson. Nature, **165**, 529 (1950).
7. E. Hope, F. L. Pyman, F. G. P. Remfry, and R. Robinson. J. Chem. Soc. 236 (1931).
8. N. S. Bhacca, L. F. Johnson, and J. N. Schoolery. NMR Spectra Catalog, Varian Associates, 1962. Spectrum No. 347.
9. O. F. Edwards and K. L. Handa. Can. J. Chem. **39**, 1801 (1961).
10. M. Ohta, H. Tani, and S. Moruzumi. Tetrahedron Letters, 859 (1963).

Received July 15, 1963.
Department of Chemistry,
Queen's University,
Kingston, Ontario.

Can. J. Chem. Downloaded from www.nrcresearchpress.com by 210.87.254.40 on 09/05/12
For personal use only.

THE SYNTHESIS OF GLUCOAPPARIN

M. H. Benn

First isolated, from *Cleome spinosa* Jacq., by Kjaer and Gmelin (1), glucoapparin (V) is a mustard oil glucoside apparently widely distributed in plants of the family Capparidaceae (2). It is the progenitor of methyl isothiocyanate, the simplest mustard oil, in these plants. We wish to report here the first synthesis of glucoapparin, achieved by the general route developed by us for the synthesis of mustard oil glucosides and already illustrated by the synthesis of glucotropaeolin (3).

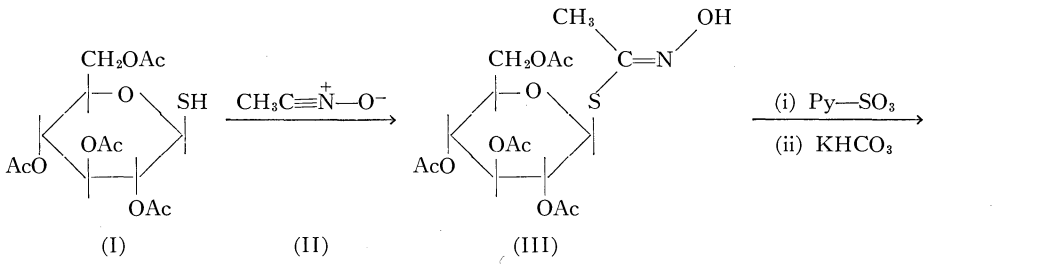

(I) (II) (III)

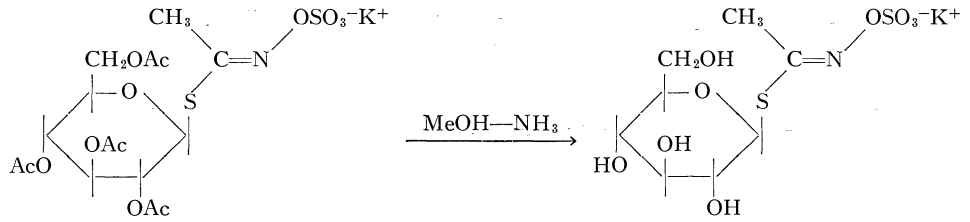

(IV) (V)

2,3,4,6-Tetra-O-acetyl-β-D-glucopyranosylthiol (I) was added to acetonitrile oxide (II), generated in situ from 1-chloroacetaldoxime, to form S-2′,3′,4′,6′-tetra-O-acetyl-β-D-glucopyranosyl methylthiohydroximate (tetraacetylproglucoapparin) (III). Sulphonation of this compound with pyridine – sulphur trioxide complex and isolation of the product as the potassium salt yielded tetraacetylglucoapparin (IV). Deacetylation of the tetraacetate with methanolic ammonia produced crystalline glucoapparin (V). Both the synthetic glucoapparin and its tetraacetate were identical with specimens of natural origin.

EXPERIMENTAL

Tetra-O-acetylproglucoapparin (III)

Acetaldoxime (3.0 g) was dissolved in chloroform (20 ml), the solution cooled to 0° in ice–salt and a slow stream of chlorine bubbled through the solution for 20 minutes. Removal of the solvent under reduced pressure (bath ⩾ 40°) left a pale blue oil containing a little colorless crystalline material. The total product was added in dry ether (30 ml) to a solution of tetraacetylglucosylthiol (1.00 g) in dry ether (130 ml). Triethylamine (8 g) in ether (10 ml) was added to the gently stirred reaction mixture. After 30 minutes at room temperature, the reaction mixture was poured into ice cold, ca. 1 *N* aqueous sulphuric acid. The ether layer was separated, the aqueous layer re-extracted with ether (1 × 50 ml) and the combined, dried ($MgSO_4$) ether extracts evaporated to small volume. The suspension of crystals was stored at 0° overnight and then filtered. Concentration of the mother liquors gave more product, total yield 1.02 g., m.p. 158–162°. Recrystallization from ethanol gave pure tetra-*O*-acetylproglucoapparin as colorless needles, m.p. 163–164°, $[\alpha]_D^{23}$ −16.8° (*c*, 2 in $CHCl_3$). Found: C, 45.94; H, 5.82; N, 3.66; S, 7.86. $C_{16}H_{23}NO_{10}S$ requires C, 45.60; H, 5.50; N, 3.34; S, 7.61%.

Can. J. Chem. Downloaded from www.nrcresearchpress.com by 210.87.254.6 on 09/05/12
For personal use only.

Tetra-O-acetylglucoapparin (IV)

Pyridine – sulphur trioxide complex (447 mg) was added to a solution of tetraacetylproglucoapparin (522 mg) in dry pyridine (6 ml). The reaction mixture stirred at room temperature for 20 hours, then poured into water (15 ml) containing potassium bicarbonate (675 mg). When effervescence had ceased the clear solution was freeze-dried and the amorphous residue rapidly extracted with boiling 95% aqueous ethanol* (3 × 30 ml). The combined, filtered extracts which rapidly deposited crystalline solid were stored overnight at 0°, then filtered to yield crude tetra-*O*-acetylglucoapparin (422 mg). Recrystallization from aqueous ethanol* gave the pure compound, m.p. 215–217° (*d*), $[\alpha]_D^{22}$ −29° (*c*, 2 in H_2O). Lit. (2) m.p. 209–210°; $[\alpha]_D^{25}$ −31° (*c*, 1.8 in H_2O). The infrared spectrum, in KBr disk, was identical with that of an authentic specimen of tetraacetylglucoapparin.

Glucoapparin (V)

Tetraacetylglucoapparin (100 mg) was dissolved in methanol (10 ml) saturated with ammonia. The solution was kept at room temperature for 18 hours, then evaporated under reduced pressure (bath ⩾ 40°), to yield a crystalline residue. Recrystallization was best achieved by dissolving this material in a few drops of water and then adding ethanol until the solution became turbid. Glucoapparin separated as tiny needles (51 mg), m.p. 207–209° (*d*), $[\alpha]_D^{22}$ −28° (*c*, 1.9 in H_2O). Lit. (2) m.p. 208–210° (*d*), $[\alpha]^{25}_D$ −31° (*c*, 2.2 in H_2O). The infrared spectrum of the synthetic material was superimposable upon that of an authentic specimen of the natural product. The synthetic material was homogeneous when examined by paper chromatography (4) on Whatman No. 1 paper in *n*-butanol – acetic acid – water (4:1:5), top phase, ascending, giving a single spot R_F 0.09, as did the natural product.

ACKNOWLEDGMENTS

We thank Professor Anders Kjaer for the gift of authentic specimens of glucoapparin and its tetraacetate. We are also grateful to the National Research Council for financial support of this work.

1. A. KJAER and R. GMELIN. Acta Chem. Scand. **10**, 325 (1956).
2. A. KJAER. Fortschr. Chem. Org. Naturstoffe, **18**, 122 (1960).
3. M. H. BENN. Can. J. Chem. To be published.
4. O. E. SCHULTZ and R. GMELIN. Z. Naturforsch. **8b**, 151 (1953).

RECEIVED AUGUST 28, 1963.
DEPARTMENT OF CHEMISTRY,
UNIVERSITY OF ALBERTA IN CALGARY,
CALGARY, ALBERTA.

**When aqueous methanol was used for the extraction of tetraacetylglucoapparin deacetylation occurred. Similarly, in our hands, attempted recrystallization of the tetraacetate from methanol gave pure, crystalline glucoapparin.*

THE POSSIBLE USE OF ^{14}C-LABELED *N*-ETHYLMALEIMIDE FOR THE ESTIMATION OF SULPHYDRYL GROUPS

C. C. LEE AND E. R. SAMUELS[1]

In earlier communications (1, 2), we have reported that under certain conditions of hydrolysis whereby the peptide bonds of the glutathione-*N*-ethylmaleimide adduct were cleaved, some L-cysteine-*N*-ethylmaleimide adduct (I) was recovered after the hydrolysis. These findings suggested that if a protein labeled with ^{35}S were allowed to react with *N*-ethylmaleimide (NEM) and then hydrolyzed, any sulphydryl groups originally present in cysteine residues would give rise to ^{35}S-labeled I whose activity could be a measure of the original sulphydryl content. Alternatively, ^{14}C-labeled NEM may be used to treat an ordinary protein. After hydrolysis, the activity of the recovered I-^{14}C would also be a measure of the amount of sulphydryl groups originally present in the protein. If the total

[1]*Holder of a Province of Saskatchewan Graduate Research Scholarship, 1961–62.*

Can. J. Chem. Downloaded from www.nrcresearchpress.com by 210.87.254.6 on 09/05/12
For personal use only.

Tetra-O-acetylglucoapparin (IV)

Pyridine – sulphur trioxide complex (447 mg) was added to a solution of tetraacetylproglucoapparin (522 mg) in dry pyridine (6 ml). The reaction mixture stirred at room temperature for 20 hours, then poured into water (15 ml) containing potassium bicarbonate (675 mg). When effervescence had ceased the clear solution was freeze-dried and the amorphous residue rapidly extracted with boiling 95% aqueous ethanol* (3 × 30 ml). The combined, filtered extracts which rapidly deposited crystalline solid were stored overnight at 0°, then filtered to yield crude tetra-*O*-acetylglucoapparin (422 mg). Recrystallization from aqueous ethanol* gave the pure compound, m.p. 215–217° (*d*), $[\alpha]_D^{22}$ −29° (*c*, 2 in H_2O). Lit. (2) m.p. 209–210°; $[\alpha]_D^{25}$ −31° (*c*, 1.8 in H_2O). The infrared spectrum, in KBr disk, was identical with that of an authentic specimen of tetraacetylglucoapparin.

Glucoapparin (V)

Tetraacetylglucoapparin (100 mg) was dissolved in methanol (10 ml) saturated with ammonia. The solution was kept at room temperature for 18 hours, then evaporated under reduced pressure (bath ⩾ 40°), to yield a crystalline residue. Recrystallization was best achieved by dissolving this material in a few drops of water and then adding ethanol until the solution became turbid. Glucoapparin separated as tiny needles (51 mg), m.p. 207–209° (*d*), $[\alpha]_D^{22}$ −28° (*c*, 1.9 in H_2O). Lit. (2) m.p. 208–210° (*d*), $[\alpha]^{25}_D$ −31° (*c*, 2.2 in H_2O). The infrared spectrum of the synthetic material was superimposable upon that of an authentic specimen of the natural product. The synthetic material was homogeneous when examined by paper chromatography (4) on Whatman No. 1 paper in *n*-butanol – acetic acid – water (4:1:5), top phase, ascending, giving a single spot R_F 0.09, as did the natural product.

ACKNOWLEDGMENTS

We thank Professor Anders Kjaer for the gift of authentic specimens of glucoapparin and its tetraacetate. We are also grateful to the National Research Council for financial support of this work.

1. A. KJAER and R. GMELIN. Acta Chem. Scand. **10**, 325 (1956).
2. A. KJAER. Fortschr. Chem. Org. Naturstoffe, **18**, 122 (1960).
3. M. H. BENN. Can. J. Chem. To be published.
4. O. E. SCHULTZ and R. GMELIN. Z. Naturforsch. **8b**, 151 (1953).

RECEIVED AUGUST 28, 1963.
DEPARTMENT OF CHEMISTRY,
UNIVERSITY OF ALBERTA IN CALGARY,
CALGARY, ALBERTA.

**When aqueous methanol was used for the extraction of tetraacetylglucoapparin deacetylation occurred. Similarly, in our hands, attempted recrystallization of the tetraacetate from methanol gave pure, crystalline glucoapparin.*

THE POSSIBLE USE OF ^{14}C-LABELED *N*-ETHYLMALEIMIDE FOR THE ESTIMATION OF SULPHYDRYL GROUPS

C. C. LEE AND E. R. SAMUELS[1]

In earlier communications (1, 2), we have reported that under certain conditions of hydrolysis whereby the peptide bonds of the glutathione-*N*-ethylmaleimide adduct were cleaved, some L-cysteine-*N*-ethylmaleimide adduct (I) was recovered after the hydrolysis. These findings suggested that if a protein labeled with ^{35}S were allowed to react with *N*-ethylmaleimide (NEM) and then hydrolyzed, any sulphydryl groups originally present in cysteine residues would give rise to ^{35}S-labeled I whose activity could be a measure of the original sulphydryl content. Alternatively, ^{14}C-labeled NEM may be used to treat an ordinary protein. After hydrolysis, the activity of the recovered I-^{14}C would also be a measure of the amount of sulphydryl groups originally present in the protein. If the total

[1]*Holder of a Province of Saskatchewan Graduate Research Scholarship, 1961–62.*

Can. J. Chem. Downloaded from www.nrcresearchpress.com by 210.87.254.5 on 09/05/12
For personal use only.

activity of the recovered ^{14}C- or ^{35}S-labeled I were to be used for a quantitative determination of sulphydryl content, either the recovery of I must be complete, or the fraction of I recovered must be constant. Since hydrolytic cleavage of the imide bonds of I should give rise to *S*-succinyl-L-cysteine (II), it is to be expected that under conditions of protein hydrolysis, some decomposition of I to II would occur. The extent of this decomposition was studied by subjecting I-^{14}C to various hydrolytic treatments.

Adduct I-^{14}C, prepared (1) from the reaction of L-cysteine with *N*-ethylmaleimide-1-^{14}C, showed a single active spot on paper chromatography. It is, however, of interest to point out that Dr. R. Tkachuk (3) of the Grain Research Laboratory, Winnipeg, has found that I may be resolved into two components by means of resin ion exchange columns. Possibly, the two components may be diastereoisomers as addition of L-cysteine to NEM creates a second asymmetric carbon. After I-^{14}C was subjected to hydrolytic treatment, two active spots corresponding to I-^{14}C and II-^{14}C were obtained. Typical results on the effect of hydrolysis temperature on the recovery of I-^{14}C are shown in Fig. 1. It can be

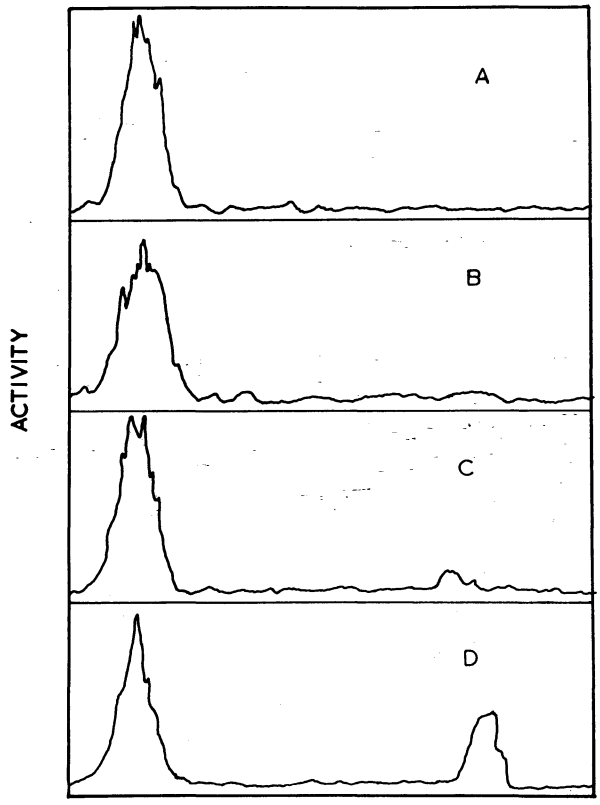

FIG. 1. Effect of temperature of hydrolysis on the decomposition L-cysteine-NEM-^{14}C adduct as measured by a Nuclear-Chicago Actigraph II chromatogram scanner. *A*, *B*, *C*, *D* are chromatograms of the adduct before hydrolysis and after hydrolysis at 75–78° C, 100–103° C, and 110–113° C, respectively, in 6 *N* hydrochloric acid for 18 hours.

seen that decomposition of I-^{14}C to II-^{14}C increased with increasing temperature of hydrolysis. As reported earlier (2), the recovery of I-^{14}C after hydrolysis at 100–103° C for 18 hours was fairly constant at $81 \pm 1\%$.

Can. J. Chem. Downloaded from www.nrcresearchpress.com by 210.87.254.5 on 09/05/12
For personal use only.

Conversion of I to II is apparently dependent on both reaction temperature and reaction time during acid hydrolysis. Moore and Ward (4) have reported the presence of II in paper chromatograms of the acid hydrolyzate of NEM-treated wool keratin, indicating that there was some decomposition of I to II during hydrolysis in 5 *N* hydrochloric acid at 125° C for 5 hours. Extensive destruction of I has resulted after prolonged hydrolysis. Thus Blemenfeld and Perlmann (5) found 84% destruction of I after hydrolysis at 110° C for 66 hours, while Tkachuk (3) observed complete decomposition of I to II on hydrolysis at 120° C for 60 hours. However, since our results indicated a constancy in the fraction of I recoverable after hydrolysis under a fixed set of conditions, the relative activity of I-^{14}C recovered after hydrolysis of a sulphydryl-bearing substance, which had been treated with NEM-^{14}C, should be directly related to the sulphydryl content of that substance.

To establish the applicability of this radiochemical method for the estimation of sulphydryls, tests were carried out using NEM-^{14}C on solutions of reduced glutathione or L-cysteine hydrochloride of known concentrations. The results are given in Table I. It

TABLE I

Data from experiments with glutathione or L-cysteine solutions of known concentration

Compound	Concentration, m*M*	Activity of I-^{14}C,* c.p.m.	Activity ratio†
Glutathione	0.20	45	0.23
	0.50	101	0.53
	0.70	130	0.69
	1.00	189	1.00
Cysteine	1.00	187	0.99

*Each value is the average of at least duplicate experiments.
†Relative to 1.00 m*M* glutathione as 1.00.

was realized that because the specific activity of the NEM-^{14}C available was quite low and because only a very small aliquot of the total hydrolyzate was chromatographed each time, it was more accurate to compare the relative activities of the chromatogram spots rather than attempt to calculate the total activity present in each hydrolyzate. As can be seen from Table I, the activity ratios obtained are in good agreement with expectation from the known sulphydryl concentrations of the glutathione and L-cysteine solutions.

Tests with NEM-^{14}C on compounds of known sulphydryl content have also been extended to include trials with thiolated gelatin. The results are summarized in Table II.

TABLE II

Data from experiments with thiolated gelatin

Trial	Specific activity of NEM-^{14}C, μc/mg	Reactants		Activity of I-^{14}C,* c.p.m.
		NEM-^{14}C, mmoles	Gelatin-SH, mmoles	
I	0.4	0.04	0.007	70
		0.04	0.014	137
II	1.0	0.04	0.007	180
		0.04	0.014	354

*Each value is the average of at least duplicate experiments.

Can. J. Chem. Downloaded from www.nrcresearchpress.com by 210.87.254.5 on 09/05/12
For personal use only.

From the observed activities of the chromatogram spots corresponding to I-^{14}C, it can be seen that a 2-fold increase in the amount of thiolated gelatin resulted in activity ratios of 137/70 and 354/180, or 1.96 and 1.97, respcetively, for the two trials. Moreover, an increase of 2.5-fold in the specific activity of the NEM-^{14}C increased the observed activities by factors of 180/70 and 354/137, or 2.57 and 2.58, respectively. These results are again in good agreement with expectation.

The results outlined in this communication indicate that the radiochemical approach to the determination of minute concentrations of sulphydryls is quite feasible, particularly if NEM-^{14}C of higher specific activity could be used. As already pointed out, the experimental conditions must be controlled so that a constant fraction of adduct I-^{14}C will be recovered after hydrolysis. It is, of course, also possible to use the activity of the recovered ^{14}C-labeled *S*-succinyl-L-cysteine (II-^{14}C) as a measure of sulphydryl groups provided the conditions of hydrolysis are so chosen as to convert I-^{14}C to II-^{14}C completely.

EXPERIMENTAL

N-Ethylmaleimide (NEM), *N*-ethylmaleimide-1-^{14}C (NEM-^{14}C), and thiolated gelatin (14 SH groups per molecular weight of 100,000) were obtained from Schwarz BioResearch Inc., Mount Vernon, New York. The L-cysteine-NEM-^{14}C adduct (I-^{14}C) was prepared according to the procedure previously reported from this laboratory (1). Paper chromatographic separation of I-^{14}C in the various hydrolyzates has also been previously described (1, 2).

Hydrolysis of Adduct I-^{14}C

Ten milligram samples of adduct I-^{14}C were each hydrolyzed by heating under reflux in 2.5 ml of 6 *N* hydrochloric acid for 18 hours at 75–78° C, 100–103° C, or 110–113° C, using heated glycerine baths. Each hydrolyzate was filtered and made up to 5.0 ml for use in subsequent paper chromatographic analyses.

Experiments with Glutathione and with L-*Cysteine*

To 10 ml of 0.20, 0.50, 0.70, or 1.00 m*M* solution of reduced glutathione were added 10 ml of a 2.00 m*M* solution of NEM-^{14}C containing 2.0 μc of activity. The resulting solution was allowed to stand overnight at room temperature and then evaporated almost to dryness on a steam bath under reduced pressure. The residue was transferred to a 10 ml flask with 3.0 ml of 6 *N* hydrochloric acid and hydrolyzed by heating under reflux at 100–103° C for 18 hours. A 1.0 m*M* solution of L-cysteine hydrochloride was similarly treated with NEM-^{14}C and hydrolyzed.

Experiments with Thiolated Gelatin

A 10-ml aqueous solution of 5.0 mg (0.04 mmoles) of NEM-^{14}C containing 2.0 or 5.0 μc of activity was added to 25 or 50 ml of a thiolated gelatin solution (2.0 g thiolated gelatin per liter of water). After standing overnight, the resulting solution was concentrated to a small volume under reduced pressure and then hydrolyzed in 4.0 ml of 6 *N* hydrochloric acid at 100–103° C for 18 hours.

ACKNOWLEDGMENT

Financial support given by the National Research Council of Canada and by the Saskatchewan Agricultural Research Foundation is gratefully acknowledged.

1. C. C. Lee and E. R. Samuels. Can. J. Chem. **39**, 1152 (1961).
2. C. C. Lee and E. R. Samuels. Can. J. Chem. **40**, 1040 (1962).
3. R. Tkachuk. Private communications.
4. J. E. Moore and W. H. Ward. J. Am. Chem. Soc. **78**, 2414 (1956).
5. O. O. Blumenfeld and G. E. Perlmann. J. Biol. Chem. **236**, 2472 (1961).

Received August 28, 1963.
Department of Chemistry,
University of Saskatchewan,
Saskatoon, Saskatchewan.

Can. J. Chem. Downloaded from www.nrcresearchpress.com by 210.87.254.5 on 09/05/12
For personal use only.

THE KINETICS OF REACTION BETWEEN L-CYSTEINE HYDROCHLORIDE AND SOME MALEIMIDES

C. C. LEE AND E. R. SAMUELS[1]

Work in this laboratory (1, 2) on a possible radiochemical method of estimating sulphydryls in proteins involving the addition of the sulphydryl to *N*-ethylmaleimide (NEM) suggested that it may be of interest to investigate the kinetics of this addition reaction. In work based on the U.V. absorption of NEM at 300 mμ, Roberts and Rouser (3) and Alexander (4) have reported that an excess of NEM reacts rapidly with sulphydryls in buffered solutions and have made use of this fact as basis of a quantitative determination of sulphydryls. Also utilizing the absorption at 300 mμ, Gregory (5) has followed the rate of reaction of NEM with sulphydryls as well as the stability of NEM at various pH values. Although no reaction order or rate constants were worked out, it was found that sulphydryls react with NEM faster in neutral than in acidic media and that a slow hydrolysis of NEM occurs in basic medium (5). In the present study, these findings were confirmed and extended, and, besides the reaction of L-cysteine hydrochloride (I) with NEM, reactions of I with maleimide (M) and with *N*-phenylmaleimide (NPM) were examined.

Because NPM is insoluble in water, its reaction with I was studied in 99.75% ethanol – 0.25% water. The reactions with M or NEM were studied both in aqueous solution and in 99.75% ethanol. The kinetics were followed spectrophotometrically. Since equal initial concentrations of the two reactants were used in all cases, for a second order reaction, $1/(a-x) = kt+C$, where $(a-x)$ is the concentration of the reactants at time t. Plots of the reciprocals of the concentrations of M, NEM, or NPM at time t vs. t gave straight lines from which the specific rate constants were obtained.

To study the effect of pH on the rate of reaction between NEM and I, water adjusted to a desired pH with either hydrochloric acid or sodium hydroxide solution was used as solvent. The results are shown in Table I. The reactions of M, NEM, or NPM with I,

TABLE I

Effect of pH on the second order specific rate constant for the reaction between L-cysteine hydrochloride and NEM at room temperature

pH of aqueous solvent	1.0	2.0	3.0	4.0	5.0	6.0	7.0	8.0	9.0	10.0
Initial pH of reaction mixture*	1.0	1.9	2.8	3.0	3.1	3.2	3.3	3.3	3.3	3.4
k (l. mole^{-1}sec^{-1})	0.015	0.076	0.160	0.273	0.305	0.313	0.305	0.305	0.328	0.398

*Initially containing 1.0 m*M* L-cysteine hydrochloride and 1.0 m*M* NEM.

in aqueous or 99.75% ethanolic solution, were followed at 25, 35, and 45° C. From the straight line plots of log k vs. the reciprocals of absolute temperature, the Arrhenius activation energies were obtained from which the enthalpies and entropies of activation, $\Delta H^{\ddagger}$ and $\Delta S^{\ddagger}$, were calculated (6). The results are summarized in Table II.

The addition of sulphydryls to double bonds has been discussed in terms of polar or free radical mechanisms (7). The dependency of the rates on pH and the fact that reactions in water are faster than in ethanol indicate that the present cases likely have a polar

[1]*Holder of a Province of Saskatchewan Graduate Research Scholarship, 1961–62.*

TABLE II

Specific rate constants and activation parameters for the reactions of M, NEM, or NPM with L-cysteine hydrochloride

Solvent	Maleimide	10^3k (l. mole^{-1}sec^{-1}) 25°	35°	45°	$\Delta H^{\ddagger}$ (kcal mole^{-1})	$\Delta S^{\ddagger}$ (cal mole^{-1} deg^{-1})
Water	M	120	210	360	9.8	−29.8
"	NEM	196	350	670	11.0	−25.1
99.75% ethanol	M	0.42	0.93	1.28	10.7	−33.5
"	NEM	1.25	2.16	3.12	8.0	−40.5
"	NPM	4.40	6.67	8.33	5.3	−47.0

rather than a free radical mechanism. Actually, the effect of pH is so pronounced that when L-cysteine free base instead of the hydrochloride (I) was used as reactant in aqueous medium, reaction with M or NEM was too fast for kinetic measurement (complete in less than 2 minutes). Similarly, reactions of M or NEM with I in phosphate buffers of pH 5.4, 6.0, or 6.6 also reached completion in less than 2 minutes. All the results thus suggest the probability of a rate-determining nucleophilic addition of the thiol or thiolate ion to the double bond of the maleimides. This is in accord with expectation as the electron-withdrawing effects of the carbonyl groups adjacent to the double bond would enhance the possibility of nucleophilic attack. In aqueous solution of low pH, formation of thiolate ions would be suppressed, hence retarding the reaction rate. The highly negative entropies of activation are also consistent with a rate-determining addition, as the transition state leading to the addition product would be much more restricted in freedom and randomness than the initial reactants.

EXPERIMENTAL

For reactions in aqueous medium, a 2.00 m*M* solution of M or NEM was added to an equal volume of 2.00 m*M* L-cysteine hydrochloride (I). The initial concentration of each reactant in the reaction mixture was thus 1.00 m*M*. At various time intervals, the concentration of M or NEM remaining was determined spectrophotometrically.

For reactions in ethanolic medium, 2.00 m*M* solution of I was made up by first dissolving I in a small amount of water and then diluting the solution with absolute ethanol. This was added to an equal volume of 2.00 m*M* M, NEM, or NPM in absolute ethanol. The final solvent composition was 99.75% ethanol – 0.25% water by volume.

A Cary recording U.V. spectrophotometer was used to draw all the spectra. The concentration of M or NEM in aqueous medium was measured by the absorbance at 277 mμ or 300 mμ, respectively. In ethanolic medium, concentrations of M, NEM, and NPM were determined, respectively, at 275 mμ, 294 mμ, and 308 mμ. These correspond to the wavelengths of maximum absorption of the maleimides in either aqueous or ethanolic solution. The adducts formed between L-cysteine and M, NEM, or NPM (8, 9) were also examined spectrophotometrically. The L-cysteine-NEM and L-cysteine-NPM adducts show no appreciable U.V. absorption in the region of interest. Thus in the reaction of NEM or NPM with I, λ_{max} for NEM or NPM remained unchanged and the absorbance at λ_{max} decreases as the reaction proceeds according to expectation. On the other hand, in the course of the reaction of M with I, there was a progressive shift of λ_{max} of the reaction mixture from 275 or 277 mμ towards shorter wavelengths because of interference by an appreciable absorption by the L-cysteine-M adduct in the U.V. region under study. Nevertheless, Beer's law was still obeyed and the concentration of M in the reaction mixtures was measured at 275 or 277 mμ, although these wavelengths no longer corresponded to maximum absorption.

ACKNOWLEDGMENT

The financial support given by the National Research Council of Canada is gratefully acknowledged.

1. C. C. LEE and E. R. SAMUELS. Can. J. Chem. **40**, 1040 (1962).
2. C. C. LEE and E. R. SAMUELS. Can. J. Chem. This issue.
3. E. ROBERTS and G. ROUSER. Anal. Chem. **30**, 1291 (1958).
4. N. M. ALEXANDER. Anal. Chem. **30**, 1292 (1958).

5. J. D. GREGORY. J. Am. Chem. Soc. **77**, 3922 (1955).
6. J. F. BUNNETT. Technique of organic chemistry. Vol. VIII. Part I. *Edited by* S. L. Friess, E. S. Lewis, and A. Weissberger. Interscience Publishers, New York. 1961. pp. 199–202.
7. W. A. PRYOR. Mechanism of sulphur reactions. McGraw-Hill, New York. 1962. pp. 71–93.
8. C. C. LEE and E. R. SAMUELS. Can. J. Chem. **39**, 1152 (1961).
9. C. C. LEE and L. M. REYNOLDS. Cereal Chem. **39**, 427 (1962).

RECEIVED AUGUST 28, 1963.
DEPARTMENT OF CHEMISTRY,
UNIVERSITY OF SASKATCHEWAN,
SASKATOON, SASKATCHEWAN.

THE PHOTOCHEMICAL ADDITION OF CYCLOHEXENE TO DIACETYL AND ETHYL PYRUVATE[1]

P. W. JOLLY AND P. DE MAYO

The photochemical addition of cyclohexene to saturated ketones (1) and a β-diketone (acetylacetone) (2) has, so far as products are concerned, been investigated. The present brief study was undertaken to ascertain if, in non-enolized α-dicarbonyl derivatives, specific addition would take place at one carbonyl group leaving the other available for chemical transformation such as cyclization.

The reaction of cyclohexene with diacetyl under mercury or tungsten light proceeded as expected (3, 4), the structure of the ketol (II) being demonstrated by periodate cleavage and characterization of the fission products. Compound (II) was probably a mixture of stereoisomers. The accompanying pinacol (5, 6, 7) (I) was recognized by the infrared spectrum, but the n.m.r. spectrum was particularly informative: this showed sharp singlets at τ 8.84 (3H), 7.76 (3H), and 5.54 (1H) for the CH_3—C—O, CH_3CO—, and hydroxyl protons, respectively. By-products formed in the irradiation were acetylcyclohexane and bicyclohexenyl.

Similar reaction of cyclohexene with ethyl pyruvate gave the stereoisomeric hydroxy-ester (III, R = Et) mixture expected.[2] Separation of the two stereoisomers was achieved by gas–liquid chromatography (g.l.c.) and the separated esters hydrolyzed to the corresponding crystalline acids (III, R = H).

Treatment of the hydroxy-ester mixture (III, R = Et) with *p*-toluene sulphonic acid in refluxing acetic acid gave a mixture of neutral and acidic products. From the neutral material, which from infrared spectra consisted of a mixture of hydroxylated and unsaturated lactones, a single crystalline hydroxy-lactone was isolated (IV) in about 10% yield. The presence of the hydroxyl and carbonyl groups was attested to by the infrared spectrum. The n.m.r. spectrum showed a singlet (3H) at τ 8.58 (CH_3—C—O) and a multiplet (1H) at τ 5.58 (methine hydrogen on carbon bearing oxygen).

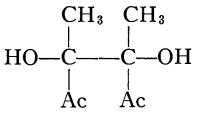

(I)

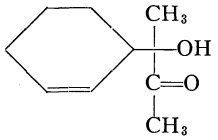

(II)

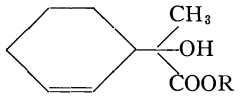

(III)

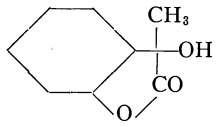

(IV)

[1]*Photochemical Syntheses Part 8.*
[2]*The suggestion that such a process occurs in the irradiation of pyruvic acid in dioxan solution has since been made (8), but without the isolation of any product.*

5. J. D. GREGORY. J. Am. Chem. Soc. **77**, 3922 (1955).
6. J. F. BUNNETT. Technique of organic chemistry. Vol. VIII. Part I. *Edited by* S. L. Friess, E. S. Lewis, and A. Weissberger. Interscience Publishers, New York. 1961. pp. 199–202.
7. W. A. PRYOR. Mechanism of sulphur reactions. McGraw-Hill, New York. 1962. pp. 71–93.
8. C. C. LEE and E. R. SAMUELS. Can. J. Chem. **39**, 1152 (1961).
9. C. C. LEE and L. M. REYNOLDS. Cereal Chem. **39**, 427 (1962).

RECEIVED AUGUST 28, 1963.
DEPARTMENT OF CHEMISTRY,
UNIVERSITY OF SASKATCHEWAN,
SASKATOON, SASKATCHEWAN.

Can. J. Chem. Downloaded from www.nrcresearchpress.com by 210.87.254.5 on 09/05/12
For personal use only.

THE PHOTOCHEMICAL ADDITION OF CYCLOHEXENE TO DIACETYL AND ETHYL PYRUVATE[1]

P. W. JOLLY AND P. DE MAYO

The photochemical addition of cyclohexene to saturated ketones (1) and a β-diketone (acetylacetone) (2) has, so far as products are concerned, been investigated. The present brief study was undertaken to ascertain if, in non-enolized α-dicarbonyl derivatives, specific addition would take place at one carbonyl group leaving the other available for chemical transformation such as cyclization.

The reaction of cyclohexene with diacetyl under mercury or tungsten light proceeded as expected (3, 4), the structure of the ketol (II) being demonstrated by periodate cleavage and characterization of the fission products. Compound (II) was probably a mixture of stereoisomers. The accompanying pinacol (5, 6, 7) (I) was recognized by the infrared spectrum, but the n.m.r. spectrum was particularly informative: this showed sharp singlets at τ 8.84 (3H), 7.76 (3H), and 5.54 (1H) for the CH_3—C—O, CH_3CO—, and hydroxyl protons, respectively. By-products formed in the irradiation were acetylcyclohexane and bicyclohexenyl.

Similar reaction of cyclohexene with ethyl pyruvate gave the stereoisomeric hydroxy-ester (III, R = Et) mixture expected.[2] Separation of the two stereoisomers was achieved by gas–liquid chromatography (g.l.c.) and the separated esters hydrolyzed to the corresponding crystalline acids (III, R = H).

Treatment of the hydroxy-ester mixture (III, R = Et) with *p*-toluene sulphonic acid in refluxing acetic acid gave a mixture of neutral and acidic products. From the neutral material, which from infrared spectra consisted of a mixture of hydroxylated and unsaturated lactones, a single crystalline hydroxy-lactone was isolated (IV) in about 10% yield. The presence of the hydroxyl and carbonyl groups was attested to by the infrared spectrum. The n.m.r. spectrum showed a singlet (3H) at τ 8.58 (CH_3—C—O) and a multiplet (1H) at τ 5.58 (methine hydrogen on carbon bearing oxygen).

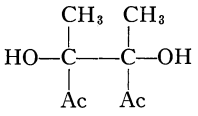

(I)

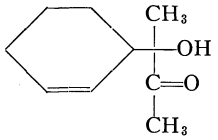

(II)

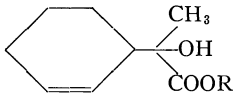

(III)

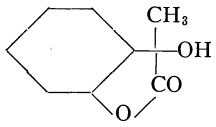

(IV)

[1]*Photochemical Syntheses Part 8.*
[2]*The suggestion that such a process occurs in the irradiation of pyruvic acid in dioxan solution has since been made (8), but without the isolation of any product.*

The decay of excited singlets of α-dicarbonyl compounds, it is well known, may proceed through triplets, that of diacetyl being well documented (see, for instance ref. 9). Since the present activation of diacetyl may be achieved with light from a tungsten lamp it may be presumed that $n \rightarrow \pi^*$ excitation is involved. This is followed by intersystem crossing and hydrogen abstraction by the resultant triplet (from the cyclohexene) to give the ketyl (V). The subsequent reactions of the ketyl are unexceptional. There is inferential evidence that the direct irradiation of ethyl pyruvate also gives, by intersystem crossing, a triplet state (10). The present observations indicate this triplet will also abstract hydrogen from cyclohexene to give a ketyl.

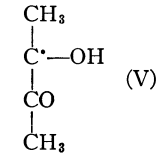

(V)

EXPERIMENTAL

Reagents were fractionated in a 40-in. spinning band column and their purity confirmed by g.l.c. The columns used were diethyleneglycol succinate (DEGS) and Carbowax.

Diacetyl–Cyclohexene Irradiation

Diacetyl (4 g) and cyclohexene (150 ml) were irradiated for 150 minutes in a quartz immersion apparatus with a Hanovia CH3 (80 w) lamp (quartz envelope). After this time the absorption at 450–500 mμ disappeared. The products from four such irradiations were combined and fractionated. The fraction with b.p. 62–66°/4 mm was crystallized from ether – light petroleum (1.3 g) to give the pinacol (1) m.p. 95–96° (literature (4), m.p. 95–96°). Calc. for $C_8H_{14}O_4$: C, 55.16; H, 8.10. Found: C, 55.36; H, 7.97%. Passage of the pinacol through a DEGS column at 175° resulted in its conversion to diacetyl, n_D^{23} 1.3929, identical in infrared spectrum and retention time with an authentic specimen.

The fraction collected between 44–49°/4 mm (1.4 g) consisted mainly of acetylcyclohexane. A pure specimen was isolated by g.l.c., n_D^{25} 1.4468, and was identical in infrared spectrum with an authentic specimen. It was characterized as the semicarbazone m.p. 172–173°.

The fraction of b.p. 50–80°/4 mm (including the mother liquors of the pinacol) consisted essentially of bicyclohexenyl (7 g), n_D^{25} 1.5056, identified by retention time and infrared spectrum with an authentic specimen.

The material distilling at 90–92°/3.5 mm (8.4 g) consisted of the ketol (II) contaminated by a small amount of bicyclohexenyl. Redistillation gave the ketol, n_D^{24} 1.4851. Calc. for $C_{10}H_{16}O_2$: C, 71.39; H, 9.59. Found: C, 71.42; H, 9.40%. The semicarbazone had m.p. 195–197°. Calc. for $C_{11}H_{19}O_2N_3$: C, 58.64; H, 8.5; N, 18.65. Found: C, 58.37; H, 8.78; N, 18.75%. Cleavage of the ketol (51 mg) with periodic acid resulted in the uptake of 1 atom of oxygen. The product (37 mg) was heated with *N* hydrochloric acid and then converted to the 2,4-dinitrophenylhydrazone in the usual way. Crystallized from ethanol – ethyl acetate the product had m.p. 200–202° undepressed on admixture with an authentic specimen of the derivative of acetylcyclohexene.

In a similar experiment steam distillation of the reaction mixture after cleavage gave acetic acid characterized as the *p*-bromophenacyl derivative, m.p. and mixed m.p. 83–84°.

Irradiation of diacetyl (2 g) in cyclohexene (150 ml) with an external 500 w T.D. Tungsten lamp in Pyrex apparatus gave a similar mixture.

Ethyl Pyruvate–Cyclohexene Irradiation

Ethyl pyruvate (4 g) in cyclohexene (150 ml) was irradiated for 7.5 hours with a Hanovia CH3 lamp in a Pyrex well acting as a cutoff below ~280 mμ, after which time the absorption at ca. 320 mμ was barely detectable. The product from two such irradiations was fractionally distilled. The material of b.p. 64–66°/0.2 mm (5.0 g) was collected and consisted of about 80% of mixed hydroxy esters. The pure esters were separated by g.l.c. on a preparative DEGS column (10 ft × 1/2 in. 20%) to give keto-ester A, n_D^{25} 1.4698. Calc. for $C_{11}H_{18}O_3$: C, 66.64; H, 9.15. Found: C, 66.41; H, 8.78%, and keto-ester B, n_D^{25} 1.4706. Found: C, 66.82; H, 9.18%.

Hydrolysis of the esters at room temperature (*N* NaOH; 2 hours) and acidification gave the corresponding acids: keto-acid A, m.p. 78–79°, from ether – light petroleum). Calc. for $C_9H_{14}O_3$: C, 63.51; H, 8.29. Found: C, 63.48; H, 8.38%. The *p*-bromophenacyl derivative (from aqueous ethanol) had m.p. 95–96. Calc. for $C_{17}H_{19}O_4Br$: C, 55.60; H, 5.17. Found: C, 55.77; H, 5.19%. keto-acid B, m.p. 110–111° (from ether – light petroleum). Found: C, 63.2; H, 8.25%.

Can. J. Chem. Downloaded from www.nrcresearchpress.com by 210.87.254.5 on 09/05/12
For personal use only.

Formation of Hydroxy-lactone (IV)

The mixed esters (1.4 g) in acetic acid (25 ml) were refluxed with *p*-toluene sulphonic acid (800 mg) for 18 hours. The acetic acid was removed *in vacuo* below 40° and after addition of water to the residue it was extracted with ether. Evaporation of the ether gave an oil (800 mg) from which acidic material was removed by extraction of an ethereal solution with sodium carbonate to give a neutral residue (400 mg). This was separated on a Carbowax column at 200°. The largest peak was collected (25%) and the material crystallized from ether – light petroleum to give the hydroxy-lactone, m.p. 113° (IV), described below. Infrared spectroscopy indicated that the remaining fractions were unsaturated or hydroxy-lactones.

Continuous ether extraction of the original aqueous phase for 24 hours gave material (390 mg) which, after extraction in ethereal solution with small amounts of aqueous sodium carbonate, gave a crystalline neutral product (IV) (180 mg), m.p. 112–113°, ν_{max} 3550, 1780 cm^{-1}. Calc. for $C_9H_{14}O_3$: C, 63.57; H, 8.29. Found: C, 63.70; H, 8.34%.

This work was supported by the U.S.A.F. under grant (AF-AFOSR-61-6).

1. P. DE MAYO, J. B. STOTHERS, and W. TEMPLETON. Can. J. Chem. **39**, 488 (1961).
2. P. DE MAYO and H. TAKESHITA. Can. J. Chem. **41**, 440 (1963).
3. P. DE MAYO and A. STOESSL. Can. J. Chem. **40**, 57 (1962).
4. F. RAMIREZ, N. RAMANTHAN, and N. B. DESAI. J. Am. Chem. Soc. **84**, 1317 (1962).
5. H. L. J. BACKSTRÖM and K. SANDROS. Acta Chem. Scand. **12**, 823 (1958).
6. E. J. BOWEN and A. T. HORTON. J. Chem. Soc. 1505 (1934).
7. W. D. COHEN. Chem. Weekblad, **13**, 590 (1916).
8. P. A. LEERMAKERS and G. F. VESLEY. J. Org. Chem. **28**, 1160 (1963).
9. G. N. LEWIS and M. KASHA. J. Am. Chem. Soc. **66**, 2100 (1944).
10. G. S. HAMMOND, P. A. LEERMAKERS, and N. J. TURRO. J. Am. Chem. Soc. **83**, 2395 (1961).

RECEIVED AUGUST 23, 1963.
DEPARTMENT OF CHEMISTRY,
UNIVERSITY OF WESTERN ONTARIO,
LONDON, ONTARIO.

Can. J. Chem. Downloaded from www.nrcresearchpress.com by 210.87.254.5 on 09/05/12
For personal use only.

SOME CHEMISTRY OF HETERATISINE[1]

O. E. EDWARDS AND C. FERRARI[2]

The minor alkaloid heteratisine from *Aconitum heterophyllum* is of special interest as the only base from aconite and delphinium species known to contain a lactone ring. A recent note outlines the determination of its structure by X-ray crystallography[3] (1). Simultaneous with this determination a number of simple transformation products of the alkaloid were prepared. A study of the physical properties of these enabled recognition of the environment of most of the functional groups of the alkaloid, but fell short of permitting unambiguous assignment of total structure. This evidence is now shown to be completely consistent with the assigned structure.

The early work of Jacobs and Craig on heteratisine (2) demonstrated the presence of a lactone ring, a methoxyl group, an N-alkyl group (presumed to be methyl), and two hydroxyl groups (Zerewitinoff). No easily reduced double bond was found, hence if none is present the empirical formula $C_{22}H_{33}NO_5$ corresponds to a 6-ring structure.

The present work showed that only one hydroxyl of heteratisine was readily acetylated, and that chromium trioxide in acetic acid oxidized the same hydroxyl giving a keto base. The alkaloid hence contains one secondary and probably one tertiary hydroxyl group. Chromium trioxide pyridine complex oxidized heteratisine to a keto-lactam $C_{22}H_{29}NO_6$, thus showing the presence of a methylene group attached to nitrogen. In the infrared spectra of chloroform solutions of the keto-base and keto-lactam, the lactone carbonyl

[1]*Issued as N.R.C. No. 7630.*
[2]*National Research Council Postdoctoral Fellow 1961–63.*
[3]*We are grateful to Dr. M. Przybylska for informing us of her conclusions prior to publication.*

Formation of Hydroxy-lactone (IV)

The mixed esters (1.4 g) in acetic acid (25 ml) were refluxed with *p*-toluene sulphonic acid (800 mg) for 18 hours. The acetic acid was removed *in vacuo* below 40° and after addition of water to the residue it was extracted with ether. Evaporation of the ether gave an oil (800 mg) from which acidic material was removed by extraction of an ethereal solution with sodium carbonate to give a neutral residue (400 mg). This was separated on a Carbowax column at 200°. The largest peak was collected (25%) and the material crystallized from ether – light petroleum to give the hydroxy-lactone, m.p. 113° (IV), described below. Infrared spectroscopy indicated that the remaining fractions were unsaturated or hydroxy-lactones.

Continuous ether extraction of the original aqueous phase for 24 hours gave material (390 mg) which, after extraction in ethereal solution with small amounts of aqueous sodium carbonate, gave a crystalline neutral product (IV) (180 mg), m.p. 112–113°, ν_{max} 3550, 1780 cm^{-1}. Calc. for $C_9H_{14}O_3$: C, 63.57; H, 8.29. Found: C, 63.70; H, 8.34%.

This work was supported by the U.S.A.F. under grant (AF-AFOSR-61-6).

1. P. DE MAYO, J. B. STOTHERS, and W. TEMPLETON. Can. J. Chem. **39**, 488 (1961).
2. P. DE MAYO and H. TAKESHITA. Can. J. Chem. **41**, 440 (1963).
3. P. DE MAYO and A. STOESSL. Can. J. Chem. **40**, 57 (1962).
4. F. RAMIREZ, N. RAMANTHAN, and N. B. DESAI. J. Am. Chem. Soc. **84**, 1317 (1962).
5. H. L. J. BACKSTRÖM and K. SANDROS. Acta Chem. Scand. **12**, 823 (1958).
6. E. J. BOWEN and A. T. HORTON. J. Chem. Soc. 1505 (1934).
7. W. D. COHEN. Chem. Weekblad, **13**, 590 (1916).
8. P. A. LEERMAKERS and G. F. VESLEY. J. Org. Chem. **28**, 1160 (1963).
9. G. N. LEWIS and M. KASHA. J. Am. Chem. Soc. **66**, 2100 (1944).
10. G. S. HAMMOND, P. A. LEERMAKERS, and N. J. TURRO. J. Am. Chem. Soc. **83**, 2395 (1961).

RECEIVED AUGUST 23, 1963.
DEPARTMENT OF CHEMISTRY,
UNIVERSITY OF WESTERN ONTARIO,
LONDON, ONTARIO.

Can. J. Chem. Downloaded from www.nrcresearchpress.com by 210.87.254.42 on 09/05/12
For personal use only.

SOME CHEMISTRY OF HETERATISINE[1]

O. E. EDWARDS AND C. FERRARI[2]

The minor alkaloid heteratisine from *Aconitum heterophyllum* is of special interest as the only base from aconite and delphinium species known to contain a lactone ring. A recent note outlines the determination of its structure by X-ray crystallography[3] (1). Simultaneous with this determination a number of simple transformation products of the alkaloid were prepared. A study of the physical properties of these enabled recognition of the environment of most of the functional groups of the alkaloid, but fell short of permitting unambiguous assignment of total structure. This evidence is now shown to be completely consistent with the assigned structure.

The early work of Jacobs and Craig on heteratisine (2) demonstrated the presence of a lactone ring, a methoxyl group, an N-alkyl group (presumed to be methyl), and two hydroxyl groups (Zerewitinoff). No easily reduced double bond was found, hence if none is present the empirical formula $C_{22}H_{33}NO_5$ corresponds to a 6-ring structure.

The present work showed that only one hydroxyl of heteratisine was readily acetylated, and that chromium trioxide in acetic acid oxidized the same hydroxyl giving a keto base. The alkaloid hence contains one secondary and probably one tertiary hydroxyl group. Chromium trioxide pyridine complex oxidized heteratisine to a keto-lactam $C_{22}H_{29}NO_6$, thus showing the presence of a methylene group attached to nitrogen. In the infrared spectra of chloroform solutions of the keto-base and keto-lactam, the lactone carbonyl

[1]*Issued as N.R.C. No. 7630.*
[2]*National Research Council Postdoctoral Fellow 1961–63.*
[3]*We are grateful to Dr. M. Przybylska for informing us of her conclusions prior to publication.*

absorbed at 1735 cm^{-1} (δ-lactone) and the ketone carbonyl absorbed above 1725 cm^{-1}. In mull spectra of various derivatives the carbonyl absorbed near 1750 cm^{-1}. The secondary hydroxyl of the alkaloid thus appeared to be on a 5-membered ring.

The pK_a of the keto-base (6.6) was two units below that of heteratisine (8.6). This dramatic difference is characteristic of the hydroxyl to carbonyl transformations when the oxygen is on rings A or B of diterpenoid alkaloids (3, 4, 5), and is identical with that for delpheline which has a 6-hydroxyl.

Potassium permanganate in acetone converted heteratisine monoacetate to a complex mixture from which a lactam and a N-desethyl lactam could be isolated. The analysis of the latter and the absence from its spectrum of the characteristic 3-hydrogen triplet which appears near $\delta = 1$ in the n.m.r. spectra of the bases and $\delta = 1.2$ in that of the lactam proved the N-alkyl group to the ethyl.

An unsplit methyl group resonated at $\delta = 1$ in the n.m.r. spectrum of heteratisine and at slightly higher field in that of the keto base and O-acetate. However, the methyl was deshielded markedly in the keto-lactam, resonating at $\delta = 1.25$. The evidence about the hetero ring was thus consistent with the presence of the usual ring A arrangement of the diterpenoid alkaloids:

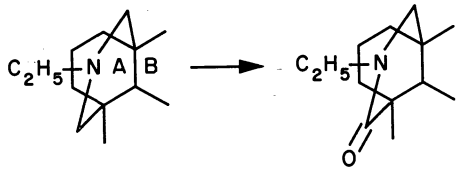

That the lactone ring and the hydroxyl groups were isolated from one another was demonstrated by the inertness to lead tetraacetate of the tetrahydroxy base produced by lithium aluminum hydride reduction of heteratisine.

The above evidence is consistent with structure I deduced in the X-ray crystallographic study. The remaining structural information obtained in this work was derived by analysis of the n.m.r. spectra of heteratisine and its transformation products. For economy of presentation this will be described using structure I. The chemical shift assignments that could be made with confidence are noted on the formulae:

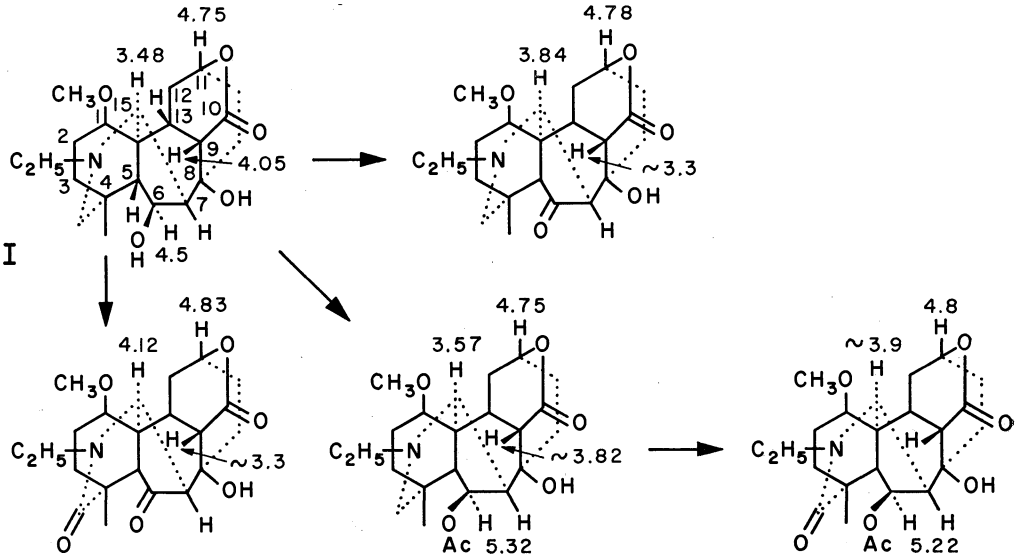

Can. J. Chem. Downloaded from www.nrcresearchpress.com by 210.87.254.42 on 09/05/12
For personal use only.

Can. J. Chem. Downloaded from www.nrcresearchpress.com by 210.87.254.42 on 09/05/12
For personal use only.

The 11-hydrogen gave a very broad (~20 c.p.s.) signal, relatively invariant in chemical shift as the nitrogen and secondary hydroxyl functions were modified. The chemical shift corresponded to tertiary hydrogen on carbon carrying an acyloxy group. The width of the signal suggested coupling with three or more α-hydrogens. The 15-hydrogen signal was always a doublet (J = 2 c.p.s.). The downfield shift on lactam formation identified this as due to a tertiary hydrogen on carbon carrying the nitrogen, and the multiplicity indicated at least one α-hydrogen. The 6-hydrogen gave a rather complex signal in the base and lactam, shifting downfield and becoming a doublet with J = 6.5 c.p.s. on acetylation and disappearing when the secondary hydroxyl group became a ketone. Thus at least one α-hydrogen was again present. A fourth low field hydrogen could be assigned to the carbon carrying the lactone carbonyl (C-9) or the methoxyl group (C-1). It was a doublet (J = 7 c.p.s.) and was strongly shielded by the ketone carbonyl. The possibility that this hydrogen was adjacent to and coupled with the 6-hydrogen, since the splitting of the doublet in each case was nearly the same, was discounted by spin-decoupling experiments. It was found that the 6-hydrogen was coupled with a hydrogen 161 c.p.s. upfield (hence probably tertiary) and the other was coupled with a hydrogen 91 c.p.s. upfield (again probably tertiary).* On the basis of I this signal corresponds unambiguously to the 9-hydrogen.

Two points, the negligible coupling of the 5- and 6-hydrogens ($\theta \simeq 90°$) and the marked shielding of the 9-hydrogen by the carbonyl on C-6, are beautifully accounted for by formula I.

The perfect correspondence of all the above properties with those expected for the X-ray structure I leaves no doubt about its correctness.

An attempt to test the structure by elimination of the 8-hydroxyl to give an analogue of the very characteristic pyroderivatives of pseudaconitine (6) and delphinine (7) was made. The major component of the resulting mixture proved so unstable, however, that no useful information was obtained from it.

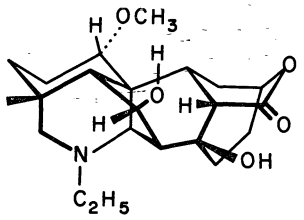

II

Evidence is available that the absolute stereochemistry of heteratisine is correctly represented by I and II. The 6-hydroxyl of heteratisine has the same relative configuration as that of delpheline, whose absolute stereochemistry is known (8, 9, 10). The ΔM_D on oxidation of this hydroxyl in delpheline derivatives is large and negative (−200° to −670°) (11). Since the ΔM_D on oxidation of the 6-hydroxyl of heteratisine is −370°, the absolute stereochemistry is undoubtedly the same as delpheline and all other known diterpenoid alkaloids.

A chair form of ring A has been illustrated in II although the X-ray study showed this ring to be a boat in the crystals of the hydrobromide. Two factors stabilize the boat conformation in the salt: (*a*) hydrogen bonding between the proton on the nitrogen and

We are grateful to Dr. L. Hall, University of Ottawa, who obtained the spin-decoupled spectra.

the 1-oxygen; (*b*) repulsive interaction of the 1-methoxyl and the 12-β hydrogen in the chair conformation of ring A which destabilizes this relative to the boat. Whether or not factor (*b*) is enough to make the boat or a half-boat conformation stable in the case of the free base is not certain.

The biogenesis of heteratisine must involve a Baeyer–Villiger type oxidation of a precursor having the commonly occurring lycoctonine skeleton and a 10-carbonyl group.

EXPERIMENTAL

Heteratisine

A solution of the total alkaloids of *Aconitum heterophyllum* in dilute sulphuric acid was adjusted to pH 8 using sodium carbonate, then extracted with benzene. The "weak" bases which were recovered from the benzene extracts crystallized in part from methanol solution. The colorless prisms melted at 267–268° (lit. m.p. 267°) and had $[\alpha]_D$ +29° (*c*, 1.55 in $CHCl_3$), ν_{max}^{Nujol} 3380, 1741 cm^{-1}. Found: C, 67.63; H, 8.41. Calc. for $C_{22}H_{33}O_5N$: C, 67.47; H, 8.50. The perchlorate of heteratisine crystallized as needles, m.p. 252–256° (dec.). Found: C, 53.90; H, 6.46. Calc. for $C_{22}H_{34}ClNO_9$: C, 53.70; H, 6.96. The pK_a' of the base (pH at half titration of the hydrochloride in 50% aqueous ethanol) was 8.6.

Heteratisine Monoacetate

Heteratisine (100 mg) was dissolved in 1 ml of pyridine, and 1 ml of acetic anhydride was added. The solution was left at room temperature overnight and then taken to dryness under reduced pressure. The crystalline residue was dissolved in boiling cyclohexane and when it was cooled 90 mg of white crystals separated, m.p. 155–165°. A second recrystallization from the same solvent raised the melting point to 161–166°. The compound retained solvent and before analysis had to be dried 9 hours at 120°, *in vacuo*. Heteratisine monoacetate sublimed at 145° at 10^{-4} mm, m.p. 161.5–167°. It had ν_{max}^{Nujol} 3430, (tertiary OH), 1738 (δ-lactone), and 1707 cm^{-1} (O-acetyl); pK_a' 7.8 (in 50% ethanol); $[\alpha]_D$ +16° (*c*, 1.66 in $CHCl_3$). Found: C, 66.10, 65.89; H, 8.01, 7.99; N, 3.35. Calc. for $C_{21}H_{35}O_6N$: C, 66.49; H, 8.14; N, 3.23.

N-Desethyl Lactam Acetate and Lactam Acetate

Heteratisine monoacetate (250 mg) was dissolved in 25 ml of acetone, at room temperature. A few drops of acetic acid was added followed by small amounts of finely ground potassium permanganate until the color was permanent for 30 minutes. The small excess was reduced with a few drops of alcohol, and the solution filtered through a bed of diatomaceous earth. The manganese dioxide was thoroughly washed with acetone, and the solution taken to dryness. The oily residue was dissolved in hot methanol and, when it was cooled, 50 mg of colorless platelets of N-desethyl lactam acetate were obtained, m.p. 268–272°. Recrystallization raised the melting point to 271–274°. This gave only one spot on thin-layer chromatography (TLC). It had ν_{max}^{Nujol} 3190 (OH and NH), 1737 (lactone), 1727 (O-acetyl), and 1647 cm^{-1} (lactam). Found: C, 62.80; H, 6.97; N, 3.47. Calc. for $C_{22}H_{29}O_7N$: C, 62.99; H, 6.97; N, 3.34.

The mother liquors of the first crystallization were taken to dryness, and chromatographed on a column of grade IV neutral alumina. Elution with benzene–chloroform 1:1 gave two fractions, the second of which was mainly the above N-desethyl lactam. The first fraction was dissolved in hot methanol; when it had been cooled 40 mg of colorless crystals of the lactam acetate appeared, m.p. 282–286°. A second recrystallization gave m.p. 286–288°. TLC showed only one spot. ν_{max}^{Nujol} 3380 (tertiary OH), 1732 (lactone and O-acetyl), and 1623 cm^{-1} (lactam). Found: C, 64.57; H, 7.42; N, 3.15. Calc. for $C_{24}H_{33}O_7N$: C, 64.41; H, 7.47; N, 3.13. Further elution of the column with 1% methanol in chloroform gave another crystalline fraction that was shown by TLC to be a mixture. This was not investigated further.

N-Desethyl Lactam

N-Desethyl lactam acetate (80 mg) was dissolved in 10 ml of methanol. One milliliter of 10% aqueous solution of sodium hydroxide was added, and the whole boiled 1 hour under reflux. Water was added and the methanol evaporated under reduced pressure. The remaining solution was acidified with sulphuric acid and extracted with chloroform. Evaporation of the extract left an oily residue that crystallized from methanol. TLC showed impurities that could not be removed by crystallization. The product was therefore chromatographed on a large silica gel plate. The main band was scraped off and extracted, giving approximately 50 mg of N-desethyl lactam. Crystallization from methanol gave colorless crystals melting at 266–269°. It had ν_{max}^{Nujol} 1733 (lactone) and 1630 cm^{-1} (lactam) and several peaks above 3000 cm^{-1}. Found: C, 63.66; H, 7.51. Calc. for $C_{20}H_{27}O_6N$: C, 63.64; H, 7.21. (Sample dried 48 hours at 120°.)

Dehydroheteratisine

Heteratisine (200 mg) was dissolved in 4.5 ml of acetic acid, and a suspension of 155 mg of chromium trioxide in 6 ml of acetic acid was added. The mixture was left 50 minutes at room temperature, with occasional shaking. It was then diluted with 3 *N* sulphuric acid and the excess chromic acid reduced with sulphur dioxide. The resulting green solution was extracted with methylene chloride and the extracts discarded. The remaining solution was made alkaline with solid sodium carbonate and then extracted with

Can. J. Chem. Downloaded from www.nrcresearchpress.com by 210.87.254.42 on 09/05/12
For personal use only.

methylene chloride. The extracts were taken to dryness, giving approximately 200 mg of slightly brown froth. This was shown by TLC to be mainly one product, with a small amount of starting material. The mixture failed to crystallize, so it was chromatographed on large silica gel plates, using chloroform–*n*-hexane–diethylamine (10:10:3) as developing solvent. The main band was scraped off and extracted. This afforded 140 mg of keto-base, that again failed to crystallize. It was then dissolved in methanol and a dilute solution of perchloric acid in methanol added until the pH was near 5. The perchlorate which separated immediately as a gel was dissolved by boiling and addition of more solvent. When the solution had been cooled, bulky white needles formed. These were collected and again crystallized from methanol–water, m.p. 266–269.5°. Weight: 85 mg. This had ν_{max}^{Nujol} 3390 (tertiary OH), 1750 (cyclopentanone), and 1715 cm^{-1} (lactone). Found: C, 53.88; H, 6.68; N, 2.98. Calc. for $C_{22}H_{31}O_5N.HClO_4$ ($C_{22}H_{32}ClNO_9$): C, 53.92; H, 6.58; N, 2.85. The free base finally crystallized from cyclohexane, m.p. 135–139°. A second recrystallization gave m.p. 130–135°; pK_a' 6.6 (in 50% ethanol); $[\alpha]_D$ −66° (*c*, 1.42 in $CHCl_3$). Found: C, 67.76; H, 7.93; N, 3.81. Calc. for $C_{22}H_{31}O_5N$: C, 67.84; H, 8.02; N, 3.60. The ultraviolet spectrum of dehydroheteratisine perchlorate only showed a very small peak at 302 mμ, $\epsilon \simeq 30$ unchanged on addition of sodium hydroxide.

Keto Lactam

Heteratisine (100 mg) was dissolved in 1.5 ml of pyridine, and the suspension of the complex from 80 mg of chromium trioxide in 2 ml of pyridine was added. The suspension was left overnight at room temperature, diluted with 3 *N* sulphuric acid, and the excess chromic acid reduced with sulphur dioxide. A base-neutral separation gave a basic fraction that was shown using TLC to be dehydroheteratisine. The neutral fraction (55 mg) contained two main components. Crystallization of this mixture from methanol gave colorless crystals, m.p. 268–275°. A second recrystallization gave m.p. 270–274°. The compound had ν_{max}^{Nujol} 3480 (tertiary OH); 1748 (cyclopentanone); 1735 (lactone); and 1635 cm^{-1} (lactam). Found: C, 65.46; H, 7.41; N, 3.38. Calc. for $C_{22}H_{29}O_6N$: C, 65.49; H, 7.25; N, 3.47.

Dehydration of Heteratisine with $POCl_3$–Pyridine

A solution of 100 mg of alkaloid in 3 ml of pyridine was cooled to 0°. One milliliter of phosphorus oxychloride was added dropwise during 15 minutes, and the resulting solution left 1 hour at room temperature. It was then slowly poured over ice, made alkaline with solid sodium carbonate, and extracted with methylene chloride. On evaporation to dryness under reduced pressure the solution turned purple, possibly due to oxidation. A thin layer chromatogram showed one main component that was separated on a preparative plate. The n.m.r. spectrum of this fraction showed possibly one olefinic proton, but a new TLC revealed that the compound had decomposed giving a complex mixture.

1. M. Przybylska. Can. J. Chem. **41**, 2911 (1963).
2. W. A. Jacobs and L. C. Craig. J. Biol. Chem. **143**, 605 (1942).
3. H. Mayer and L. Marion. Can. J. Chem. **37**, 856 (1959).
4. R. C. Cookson and M. E. Trevitt. J. Chem. Soc. 2689 (1956).
5. O. E. Edwards. Chem. Can. 40 (1961).
6. Y. Tsuda and L. Marion. Can. J. Chem. **41**, 1485 (1963).
7. K. Wiesner, D. L. Simmons, and R. H. Wightman. Tetrahedron Letters, No. 15, 23 (1960).
8. M. Carmack, J. P. Ferris, J. Harvey, Jr., P. L. Magat, E. W. Martin, and D. W. Mayo. J. Am. Chem. Soc. **80**, 497 (1958).
9. O. E. Edwards, L. Marion, and K. H. Palmer. Can. J. Chem. **36**, 1097 (1958).
10. M. Przybylska and L. Marion. Can. J. Chem. **37**, 1843 (1959).
11. R. C. Cookson and M. E. Trevitt. J. Chem. Soc. 3121 (1956).

Received September 16, 1963.
Division of Pure Chemistry,
National Research Council,
Ottawa, Canada.

Can. J. Chem. Downloaded from www.nrcresearchpress.com by 210.87.254.42 on 09/05/12
For personal use only.

N-SULPHONYLIMINO ESTERS

Bernard Loev and Minerva F. Kormendy

Orthoaminobenzenesulphonamide (I*a*) and orthoaminobenzylsulphonamide (I*b*) cyclize readily on heating with an orthoester to give, respectively, the six-membered benzothiadiazinedioxide (II*a*) (1) and the seven-membered benzothiadiazepinedioxide (II*b*) (2).

methylene chloride. The extracts were taken to dryness, giving approximately 200 mg of slightly brown froth. This was shown by TLC to be mainly one product, with a small amount of starting material. The mixture failed to crystallize, so it was chromatographed on large silica gel plates, using chloroform–*n*-hexane–diethylamine (10:10:3) as developing solvent. The main band was scraped off and extracted. This afforded 140 mg of keto-base, that again failed to crystallize. It was then dissolved in methanol and a dilute solution of perchloric acid in methanol added until the pH was near 5. The perchlorate which separated immediately as a gel was dissolved by boiling and addition of more solvent. When the solution had been cooled, bulky white needles formed. These were collected and again crystallized from methanol–water, m.p. 266–269.5°. Weight: 85 mg. This had ν_{max}^{Nujol} 3390 (tertiary OH), 1750 (cyclopentanone), and 1715 cm^{-1} (lactone). Found: C, 53.88; H, 6.68; N, 2.98. Calc. for $C_{22}H_{31}O_5N.HClO_4$ ($C_{22}H_{32}ClNO_9$): C, 53.92; H, 6.58; N, 2.85. The free base finally crystallized from cyclohexane, m.p. 135–139°. A second recrystallization gave m.p. 130–135°; pK_a' 6.6 (in 50% ethanol); $[\alpha]_D$ −66° (*c*, 1.42 in $CHCl_3$). Found: C, 67.76; H, 7.93; N, 3.81. Calc. for $C_{22}H_{31}O_5N$: C, 67.84; H, 8.02; N, 3.60. The ultraviolet spectrum of dehydroheteratisine perchlorate only showed a very small peak at 302 mμ, $\epsilon \simeq 30$ unchanged on addition of sodium hydroxide.

Keto Lactam

Heteratisine (100 mg) was dissolved in 1.5 ml of pyridine, and the suspension of the complex from 80 mg of chromium trioxide in 2 ml of pyridine was added. The suspension was left overnight at room temperature, diluted with 3 *N* sulphuric acid, and the excess chromic acid reduced with sulphur dioxide. A base-neutral separation gave a basic fraction that was shown using TLC to be dehydroheteratisine. The neutral fraction (55 mg) contained two main components. Crystallization of this mixture from methanol gave colorless crystals, m.p. 268–275°. A second recrystallization gave m.p. 270–274°. The compound had ν_{max}^{Nujol} 3480 (tertiary OH); 1748 (cyclopentanone); 1735 (lactone); and 1635 cm^{-1} (lactam). Found: C, 65.46; H, 7.41; N, 3.38. Calc. for $C_{22}H_{29}O_6N$: C, 65.49; H, 7.25; N, 3.47.

Dehydration of Heteratisine with $POCl_3$–Pyridine

A solution of 100 mg of alkaloid in 3 ml of pyridine was cooled to 0°. One milliliter of phosphorus oxychloride was added dropwise during 15 minutes, and the resulting solution left 1 hour at room temperature. It was then slowly poured over ice, made alkaline with solid sodium carbonate, and extracted with methylene chloride. On evaporation to dryness under reduced pressure the solution turned purple, possibly due to oxidation. A thin layer chromatogram showed one main component that was separated on a preparative plate. The n.m.r. spectrum of this fraction showed possibly one olefinic proton, but a new TLC revealed that the compound had decomposed giving a complex mixture.

1. M. Przybylska. Can. J. Chem. **41**, 2911 (1963).
2. W. A. Jacobs and L. C. Craig. J. Biol. Chem. **143**, 605 (1942).
3. H. Mayer and L. Marion. Can. J. Chem. **37**, 856 (1959).
4. R. C. Cookson and M. E. Trevitt. J. Chem. Soc. 2689 (1956).
5. O. E. Edwards. Chem. Can. 40 (1961).
6. Y. Tsuda and L. Marion. Can. J. Chem. **41**, 1485 (1963).
7. K. Wiesner, D. L. Simmons, and R. H. Wightman. Tetrahedron Letters, No. 15, 23 (1960).
8. M. Carmack, J. P. Ferris, J. Harvey, Jr., P. L. Magat, E. W. Martin, and D. W. Mayo. J. Am. Chem. Soc. **80**, 497 (1958).
9. O. E. Edwards, L. Marion, and K. H. Palmer. Can. J. Chem. **36**, 1097 (1958).
10. M. Przybylska and L. Marion. Can. J. Chem. **37**, 1843 (1959).
11. R. C. Cookson and M. E. Trevitt. J. Chem. Soc. 3121 (1956).

Received September 16, 1963.
Division of Pure Chemistry,
National Research Council,
Ottawa, Canada.

Can. J. Chem. Downloaded from www.nrcresearchpress.com by 210.87.254.6 on 09/05/12
For personal use only.

N-SULPHONYLIMINO ESTERS

Bernard Loev and Minerva F. Kormendy

Orthoaminobenzenesulphonamide (I*a*) and orthoaminobenzylsulphonamide (I*b*) cyclize readily on heating with an orthoester to give, respectively, the six-membered benzothiadiazinedioxide (II*a*) (1) and the seven-membered benzothiadiazepinedioxide (II*b*) (2).

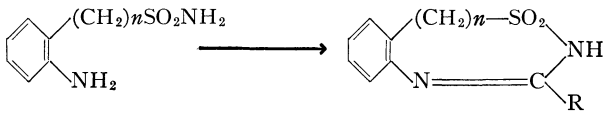

I
a, $n = 0$
b, $n = 1$
c, $n = 2$

II
a, $n = 0$
b, $n = 1$
c, $n = 2$

Under the same or modified conditions, orthoaminophenethylsulphonamide (I*c*) (3) has been found to give only the uncyclized products shown below, rather than the eight-membered analogue (II*c*).

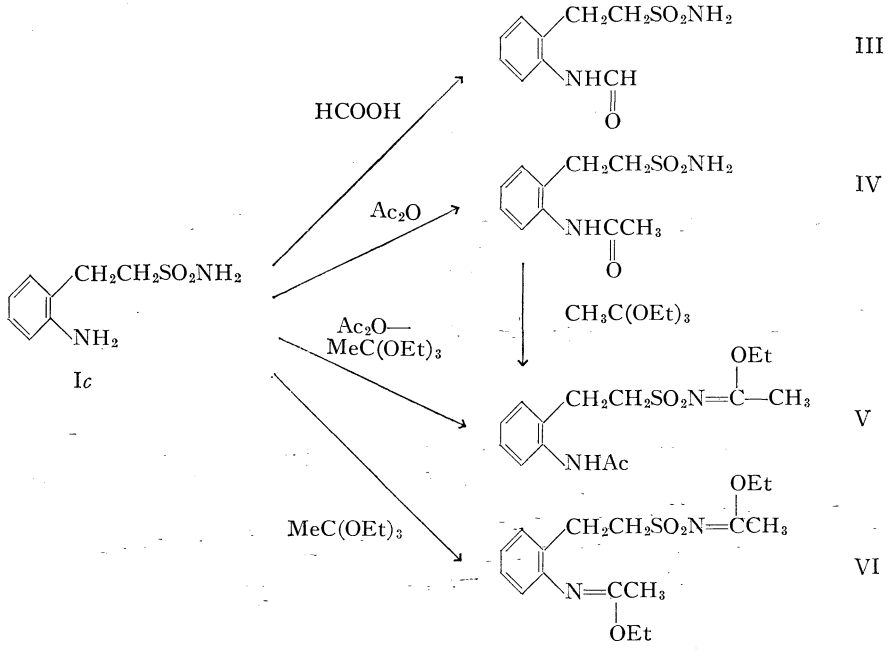

Iminoesters prepared by the reaction of aromatic amines with orthoesters are well known (1, 4); however, there are few examples of *sulphonyl*iminoesters. N-Sulphonylacetimidic and benzimidic acid esters were first described by Barber in 1943 (5); he prepared them by the reaction of a sulphonyl chloride with an iminoester. The utility of this

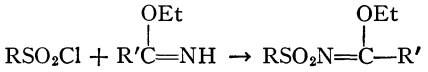

method may be gauged by the fact that subsequent workers (6) report that changes in experimental technique led to "greatly improved (to 25–30% total) yields". In another reference to such compounds, a small amount of VII was isolated as a by-product in the reaction of acetobromogalactose with the silver salt of *p*-toluenesulphonamide (7). This same compound has now been prepared in 80% yield simply by heating the sulphonamide and the orthoester.

Can. J. Chem. Downloaded from www.nrcresearchpress.com by 210.87.254.6 on 09/05/12
For personal use only.

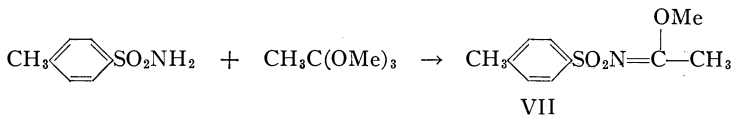

VII

Recently, Novello *et al.* (8), observed the formation of a sulphonyliminoester during the synthesis of 6-chloro-7-sulphamyl-1,2,4-benzothiadiazine-1,1-dioxide by reaction of 5-chloro-2,4-disulphamylaniline with ethyl orthoformate.

EXPERIMENTAL[1]

o-Formamido-β-phenethylsulphonamide (III)

A solution of 2.0 g (0.001 mole) of *o*-amino-β-phenethylsulphonamide (3) in 20 ml of 98–100% formic acid was refluxed for 18 hours. The solution was concentrated, *in vacuo*, to give a thick oily residue which crystallized on contact with ethanol. It was recrystallized from ethanol and from isopropanol to give 0.75 g of white solid, m.p. 122–124°. Anal. Calc. for $C_9H_{12}N_2O_3S$: C, 47.45; H, 5.27; N, 12.30. Found: C, 47.50; H, 5.38; N, 12.30.

o-Acetamido-β-phenethylsulphonamide (IV)

Four grams (0.002 mole) of *o*-amino-β-phenethylsulphonamide (3) was treated with 20 ml of acetic anhydride. There was some heat evolution and the solid dissolved momentarily and another solid separated. This material was recrystallized from ethanol to give 2.6 g of white crystalline solid, m.p. 158–160°. Anal. Calc. for $C_{10}H_{14}N_2O_3S$: C, 49.57; H, 5.82; N, 11.56. Found: C, 49.85; H, 5.93; N, 11.62.

N-(1-Ethoxyethylene)-o-acetamido-β-phenethylsulphonamide (V)

To 4.0 g (0.02 mole) of *o*-amino-β-phenethylsulphonamide (3) was added 20 ml of acetic anhydride; the solid dissolved completely with heat evolution. To this solution was then added 20 ml of ethyl orthoacetate, and the mixture was refluxed for 18 hours. The solution was concentrated *in vacuo* to give a residual oil which slowly solidified. The solid was recrystallized from a mixture of ethylacetate and hexane to give 2.6 g of white solid, m.p. 97–98°. Anal. Calc. for $C_{14}H_{20}N_2O_4S$: C, 53.93; H, 6.42; N, 8.98. Found: C, 53.99; H, 6.29; N, 9.29.

A sample of IV, on being heated with ethyl orthoacetate, gave a product identical with V.

N-(1-Ethoxyethylidene)-2-(1-ethoxyethylidene-amino)-phenethylsulphonamide (VI)

A mixture of 1.0 g (0.005 mole) of *o*-amino-β-phenethylsulphonamide in 10 ml of triethyl orthoacetate was heated to reflux; slowly all the solid dissolved. Reflux was continued for 3 hours. The solution was concentrated *in vacuo* to give a residual oil which slowly solidified. This solid was recrystallized from petroleum ether to give 0.6 g of N-(1-ethoxyethylidene)-2-(1-ethoxyethylidene amino)-phenethylsulphonamide, m.p. 45–46°. Anal. Calc. for $C_{16}H_{24}N_2SO_4$: C, 56.45; H, 7.11; N, 8.22. Found: C, 56.68; H, 7.28; N, 8.15.

Methyl N-(p-toluenesulphonyl)-iminoacetate (VII)

A mixture of 8.5 g (0.05 mole) of *p*-toluenesulphonamide and 15 ml of trimethyl orthoacetate was heated to reflux. Slowly the solid dissolved; heating was continued for 3 hours. The resulting solution was concentrated *in vacuo* and the residue crystallized. The solid (80% yield) was recrystallized from cyclohexane; white crystalline solid, m.p. 73–74°. (Lit. (7) m.p. 74–75°.)

1. J. H. Freeman and E. C. Wagner. J. Org. Chem. **16**, 815 (1951).
2. W. Beil and A. Hoeppener. Ger. Patent No. 1,111,199 (1961).
3. B. Loev and M. F. Kormendy. In preparation.
4. R. M. Roberts. J. Am. Chem. Soc. **71**, 3848 (1949).
5. H. J. Barber. J. Chem. Soc. 101 (1943).
6. S. J. Angyal and W. K. Warburton. Australian J. Sci. Res. **4A**, 93 (1951). Chem. Abstr. **45**, 7041*c* (1951). Schering. Ger. Patent Nos. 833,810 and 833,811 (1952).
7. B. Helferich, K. H. Schmidt, and D. Nachtsheim. Ann. **605**, 182 (1957).
8. F. C. Novello *et al.* J. Org. Chem. **25**, 970 (1960).

Received August 21, 1963.
Research and Development Division,
Smith Kline and French Laboratories,
Philadelphia, Pennsylvania.

[1]*All melting points corrected. Analyses were performed by Miss Margaret Carroll and her staff of these laboratories.*

Can. J. Chem. Downloaded from www.nrcresearchpress.com by 210.87.254.6 on 09/05/12
For personal use only.

SYNTHESIS OF BISNAPHTHOXAZOLES[1]

CHARANJIT RAI AND JOHN B. BRAUNWARTH

The usefulness of polyphosphoric acid as an effective condensing agent for intra- and inter-molecular condensations has been extensively demonstrated. Hein, Alheim, and Leavitt (1) extended its application to the benzoxazole synthesis and to similar related reactions (2). Several workers (3, 4, 5) reported the synthesis of heterocyclic compounds in improved yields by conducting the cyclizations in the polyphosphoric acid medium. The present study was undertaken to investigate whether polyphosphoric acid would successfully catalyze the intermolecular condensation of 1-amino-2 naphthol with diabasic acids, to give a new series of heterocyclic compounds, bisnaphth-(1,2)-oxazoles, which were needed for our studies.

Bis[2-naphth(1,2)oxazolyl]alkanes were readily prepared by the polyphosphoric acid catalyzed reaction of 1-amino-2-naphthol hydrochloride and dicarboxylic acids. The yields of α,ω-bis[2-naphth(1,2)oxazolyl]alkanes varied from 22 to 92% of the theory. It was observed that as the connecting alkylene chain length was increased, the preparation of the compounds became easier and in some cases the yields were higher.

The condensation reaction involving terephthalic acid and fumaric acid required higher temperatures (175° to 220°). Thus 1,4-bis[2-naphth(1,2)oxazolyl]benzene was prepared by conducting the reaction at 200° in 30% yield, whereas trans-1,2-bis[2-naphth(1,2)oxazolyl]ethylene was prepared at 175° in 35% yield.

The reaction of 3,3′-thiodipropionic acid and 1-amino-2-naphthol hydrochloride gave 2,2′-bis[2-naphth(1,2)-oxazolyl]diethyl sulphide in 22% yield. The reaction was catalyzed by polyphosphoric acid.

EXPERIMENTAL

The procedure for the syntheses of bis[2-naphth(1,2)oxazolyl]alkanes is described below. The data on the preparation, yields, melting points, and analysis are summarized in Table I. All melting points reported here are uncorrected. Commercially available polyphosphoric acid, also known as phospholeum, obtained from Monsanto Chemical Company, was used in this work.

Preparation of α,ω-Bis[2-naphth(1,2)oxazolyl]alkanes

1-Amino-2-naphthol hydrochloride (0.026 mole) was mixed with dicarboxylic acid, or its anhydride (.013 mole) and the mixture was poured into well-stirred polyphosphoric acid (approximately 75 ml) contained in a three-necked flask at room temperature. The reaction mixture was heated at 130° to 200° C for 1 to 2 hours. The α,ω-bis[2-naphth(1,2)oxazolyl]alkanes were isolated by pouring the cooled reaction mixture on ice. The precipitate was filtered, washed with water, then dilute sodium bicarbonate solution and water, and dried in a vacuum desiccator. The crude product was recrystallized from ethanol or dioxane until a constant melting point was obtained.

Preparation of 1,4-Bis[naphth(1,2)oxazolyl]benzene

A mixture of 1-amino-2-naphthol hydrochloride (0.05 mole) and terephthalic acid (0.025 mole) was added to polyphosphoric acid (100 ml) at 80° C. The reaction mixture was heated at 175° to 220° C for 2 hours. The product was isolated according to the procedure described for α,ω-bis[2-naphth(1,2)oxazolyl]alkanes. The compound was recrystallized from a mixture of methanol and benzene.

Preparation of 2,2′-Bis-[2-naphth(1,2)oxazolyl]diethyl sulphide

This compound was prepared by reacting 1-amino-2-naphthol hydrochloride (0.026 mole) with 3,3′-thiodipropionic acid (0.013 mole) in polyphosphoric (75 ml) at 130° C. The reaction was complete in less than an hour and the product was worked up by the normal procedure described earlier.

[1]*Presented in part at the 140th National Meeting of the American Chemical Society, Chicago, Ill., September 8, 1961.*

Can. J. Chem. Downloaded from www.nrcresearchpress.com by 210.87.254.40 on 09/05/12
For personal use only.

Can. J. Chem. Downloaded from www.nrcresearchpress.com by 210.87.254.40 on 09/05/12
For personal use only.

TABLE I

α,ω[2-Naphth(1,2)oxazolyl]alkanes and related compounds

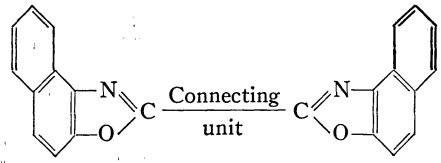

Acid	Connecting unit	Crude yield, %	M.p., °C	Formula	Found C	Found H	Found N	Calc. C	Calc. H	Calc. N
Succinic	$(CH_2)_2$	53	190	$C_{24}H_{16}O_2N_2$	78.9	4.5	7.6	79.1	4.4	7.7
Adipic	$(CH_2)_4$	40	155	$C_{26}H_{20}O_2N_2$	79.5	5.3	7.1	79.6	5.1	7.1
Glutaric	$(CH_2)_5$	87	81–82	$C_{27}H_{22}O_2N_2$	79.4	6.0	6.7	79.8	5.5	6.9
Suberic	$(CH_2)_6$	65	137	$C_{28}H_{24}O_2N_2$	79.8	6.0	6.5	80.0	5.8	6.7
Azelaic	$(CH_2)_7$	92	89–90	$C_{29}H_{26}O_2N_2$	79.4	6.3	6.2	80.1	6.0	6.5
Sebacic	$(CH_2)_8$	28	112.5	$C_{30}H_{28}O_2N_2$	80.1	6.3	6.3	80.3	6.3	6.3
Terephthalic	C_6H_4	30	294–95	$C_{28}H_{16}O_2N_2$	82.2	4.2	6.8	81.6	3.9	6.8
Fumaric	CH=CH	35	161–62	$C_{24}H_{14}O_2N_2$	79.3	4.1	7.8	79.6	3.9	7.7
Thiodipropionic	$CH_2CH_2SCH_2CH_2$	22	150	$C_{26}H_{20}O_2N_2S$	73.4	4.9	6.6	73.6	4.8	6.6

1. D. W. HEIN, R. J. ALHEIM, and J. J. LEAVITT. J. Am. Chem. Soc. **79**, 427 (1957).
2. M. A. PHILLIPS. J. Chem. Soc. 2398 (1928).
3. C. RAI and J. B. BRAUNWARTH. J. Org. Chem. **26**, 3434 (1961).
4. W. RIED and J. PATSCHORKE. Ann. **599**, 44 (1956).
5. E. NYILAS and J. L. PINTER. J. Am. Chem. Soc. **82**, 609 (1960).

ACKNOWLEDGMENT

We wish to thank Mr. A. J. Ackerman and his associates for the elemental analyses.

RECEIVED MARCH 29, 1963.
THE PURE OIL COMPANY,
RESEARCH CENTER,
CRYSTAL LAKE, ILLINOIS.

Can. J. Chem. Downloaded from www.nrcresearchpress.com by 210.87.254.40 on 09/05/12
For personal use only.

THE ACTIVITY PRODUCT OF FERRIC HYDROXIDE BY TURBIDIMETRY

R. F. PLATFORD

Electrometrically determined values for the activity product of ferric hydroxide vary from $10^{-35.5}$ to $10^{-38.7}$ (1,2,3,4) and show changes with aging of the precipitate (5). Turbidimetry has been used by other workers (6) in the study of complex formation and was used in the present work to detect the initial appearance of the precipitate produced by adding hydroxyl ions to solutions of ferric salts. Knowledge of initial ferric-ion activity and hydroxyl-ion activity at the point of initial precipitation allowed the calculation of an activity product for the reaction $Fe^{+++} + 3OH^- \rightarrow Fe(OH)_3$.

EXPERIMENTAL

Reagents

All chemicals used were reagent grade or better. Solutions of ferric salts were prepared (*a*) from $FeCl_3 . 6H_2O$, (*b*) from $FeNH_4(SO_4)_2 . 12H_2O$, and (*c*) by dissolving A.R. iron wire in HCl and oxidizing it with hydrogen peroxide. All solutions thus prepared contained sufficient HCl (usually 0.01 *N*) to prevent precipitation of $Fe(OH)_3$.

Instruments

A Radiometer pH meter 4 with glass electrode and saturated calomel reference electrode was used for pH measurements. The instrument was standardized before and after each run using 0.05 *M* potassium tetroxalate (pH 1.68 at 25° C) and 0.05 *M* potassium acid phthalate (pH 4.01 at 25° C).

Light scattering measurements were made with a Brice-Phoenix Universal 1000 Series light scattering photometer using a semioctagonal cell (7). The light scattering by a solution was calculated from the expression:

$$\tau = A(I_S)/h(I_T)$$

where:

τ = turbidity of solution in meters^{-1},
A = a constant related to the geometry of the instrument and equal to 9.85 for the light of 436 mμ wavelength used in these measurements,
I_S = intensity of light scattered at right angles to an incident beam,
I_T = intensity of light transmitted through the solution,
h = thickness of scattering solution in meters seen by photometer measuring I_S, i.e., width of incident beam.

In a typical experiment 100 ml of ferric solution in the scattering cell was stirred magnetically and standard NaOH or NH_4OH was added from a semimicro burette. The pH was measured after each addition and the temperature of the liquid in the scattering cell was controlled at 25±0.3° C by means of water circulated through a thin hollow plate atop the magnetic stirrer. Following each pH measurement the cell was transferred to the photometer and I_S/I_T was measured. Increases in I_S/I_T (indicating precipitation of $Fe(OH)_3$) were accepted only when it was possible to repeat the readings after the solution was restirred. The induction period for precipitate formation was short compared to the time for reagent addition.

1. D. W. HEIN, R. J. ALHEIM, and J. J. LEAVITT. J. Am. Chem. Soc. **79**, 427 (1957).
2. M. A. PHILLIPS. J. Chem. Soc. 2398 (1928).
3. C. RAI and J. B. BRAUNWARTH. J. Org. Chem. **26**, 3434 (1961).
4. W. RIED and J. PATSCHORKE. Ann. **599**, 44 (1956).
5. E. NYILAS and J. L. PINTER. J. Am. Chem. Soc. **82**, 609 (1960).

ACKNOWLEDGMENT

We wish to thank Mr. A. J. Ackerman and his associates for the elemental analyses.

RECEIVED MARCH 29, 1963.
THE PURE OIL COMPANY,
RESEARCH CENTER,
CRYSTAL LAKE, ILLINOIS.

Can. J. Chem. Downloaded from www.nrcresearchpress.com by 210.87.254.105 on 09/05/12
For personal use only.

THE ACTIVITY PRODUCT OF FERRIC HYDROXIDE BY TURBIDIMETRY

R. F. PLATFORD

Electrometrically determined values for the activity product of ferric hydroxide vary from $10^{-35.5}$ to $10^{-38.7}$ (1,2,3,4) and show changes with aging of the precipitate (5). Turbidimetry has been used by other workers (6) in the study of complex formation and was used in the present work to detect the initial appearance of the precipitate produced by adding hydroxyl ions to solutions of ferric salts. Knowledge of initial ferric-ion activity and hydroxyl-ion activity at the point of initial precipitation allowed the calculation of an activity product for the reaction $Fe^{+++}+3OH^- \rightarrow Fe(OH)_3$.

EXPERIMENTAL

Reagents

All chemicals used were reagent grade or better. Solutions of ferric salts were prepared (*a*) from $FeCl_3.6H_2O$, (*b*) from $FeNH_4(SO_4)_2.12H_2O$, and (*c*) by dissolving A.R. iron wire in HCl and oxidizing it with hydrogen peroxide. All solutions thus prepared contained sufficient HCl (usually 0.01 *N*) to prevent precipitation of $Fe(OH)_3$.

Instruments

A Radiometer pH meter 4 with glass electrode and saturated calomel reference electrode was used for pH measurements. The instrument was standardized before and after each run using 0.05 *M* potassium tetroxalate (pH 1.68 at 25° C) and 0.05 *M* potassium acid phthalate (pH 4.01 at 25° C).

Light scattering measurements were made with a Brice-Phoenix Universal 1000 Series light scattering photometer using a semioctagonal cell (7). The light scattering by a solution was calculated from the expression:

$$\tau = A(I_S)/h(I_T)$$

where:

τ = turbidity of solution in meters^{-1},
A = a constant related to the geometry of the instrument and equal to 9.85 for the light of 436 mμ wavelength used in these measurements,
I_S = intensity of light scattered at right angles to an incident beam,
I_T = intensity of light transmitted through the solution,
h = thickness of scattering solution in meters seen by photometer measuring I_S, i.e., width of incident beam.

In a typical experiment 100 ml of ferric solution in the scattering cell was stirred magnetically and standard NaOH or NH_4OH was added from a semimicro burette. The pH was measured after each addition and the temperature of the liquid in the scattering cell was controlled at 25±0.3° C by means of water circulated through a thin hollow plate atop the magnetic stirrer. Following each pH measurement the cell was transferred to the photometer and I_S/I_T was measured. Increases in I_S/I_T (indicating precipitation of $Fe(OH)_3$) were accepted only when it was possible to repeat the readings after the solution was restirred. The induction period for precipitate formation was short compared to the time for reagent addition.

RESULTS AND DISCUSSION

Plots of τ vs. pH were made for a series of solutions of varying initial ferric ion concentration $[Fe^{+++}]_0$, and typical results are shown in Fig. 1. The initial break in each curve was taken as the onset of formation of colloidal $Fe(OH)_3$. No attempt was made to remove suspended matter initially present in the solution as it was found to have no effect on the

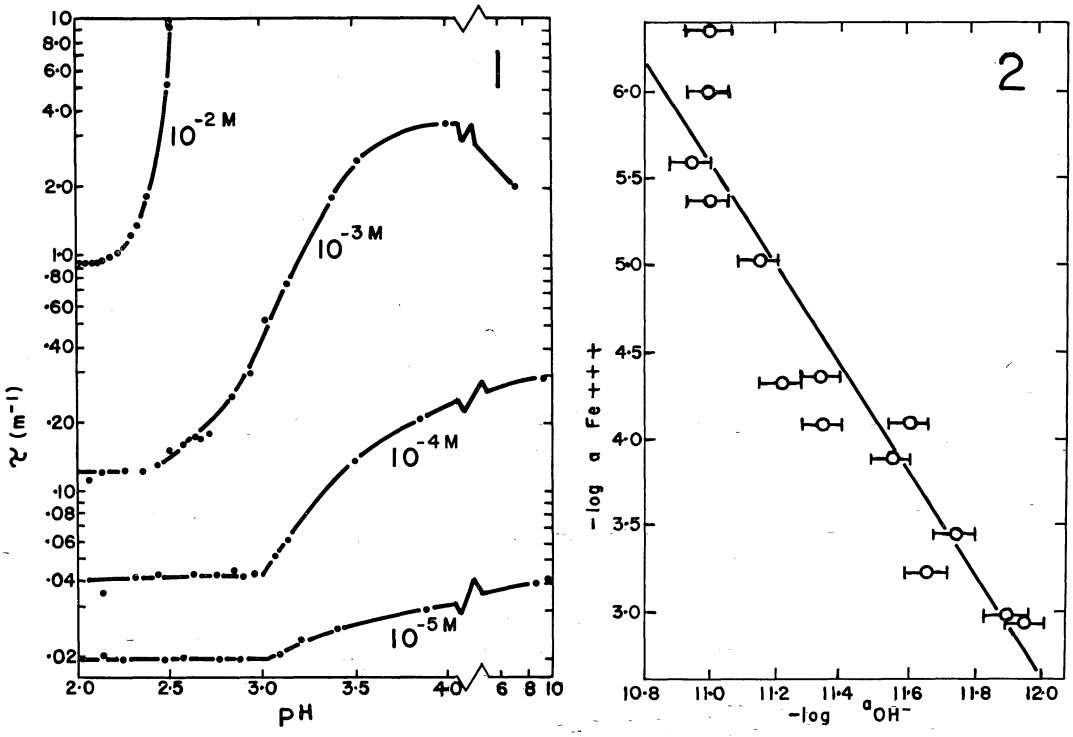

FIG. 1. Turbidity of solutions of ferric salts as a function of pH.
FIG. 2. Hydroxyl ion activity vs. ferric ion activity at point of initial precipitation.

overall results. It was unnecessary to correct for the color caused by the ferric ions in solution. The activity $a_{Fe^{+++}}$ was assumed to equal $[Fe^{+++}]_0\, fF$ where f was calculated from Kielland's expression for individual activity coefficients (8) and F was the fraction of "free" Fe^{+++} not bound to OH^-, Cl^-, or $SO_4^=$(9,10,11). Since association constants for possible complexes were not known at all ionic strengths employed, some interpolation was necessary in the evaluation of F. It was assumed that $-\log a_{OH^-} = 14.00 - pH$. The data are summarized in Table I and plotted in Fig. 2. The activity product, calculated from Fig. 2, is $10^{-38.6\pm0.4}$ at 25° C.

In spite of the questionable use of "individual" activity coefficients the method described gave reasonably constant values for $a_{Fe^{+++}} \times a^3_{OH^-}$ over a thousandfold range of $a_{Fe^{+++}}$. This indicated that the "free" Fe^{+++} was participating in the process:

$$Fe^{+++} + 3OH^- \rightarrow Fe(OH)_3$$

although the processes:

$$FeOH^{++} + 2OH^- \rightarrow Fe(OH)_3$$

and

$$Fe(OH)_2^+ + OH^- \rightarrow Fe(OH)_3$$

were presumably occurring simultaneously.

Can. J. Chem. Downloaded from www.nrcresearchpress.com by 210.87.254.105 on 09/05/12
For personal use only.

TABLE I

pH for initial precipitation of Fe^{+++} by NaOH

$-\log [Fe^{+++}]_0$	$[Cl^-]$	$FeCl^{++}$ $FeCl_2^+$ $FeSO_4^+$ (%)	$FeOH^{++}$ $Fe(OH)_2^+$ (%)	"Free" $F_{Fe^{+++}}$ (%)	μ	$-\log a_{Fe^{+++}}$	pH
5.00	0.10	25	50	25	0.10	6.35	3.00
5.00	0.01	15	65	20	0.01	6.05	3.00
4.57	0.01	15	65	20	0.01	5.62	3.05
4.10	0.01	5	70	25	0.01	5.05	2.85
4.00	0.10	25	50	25	0.10	5.35	2.99
3.68	0.01	10	45	45	0.01	4.38	2.65
3.52	0.01	5	60	35	0.01	4.32	2.78
3.19	0.01	10	40	50	0.01	3.84	2.45
3.00	0.10	45	10	45	0.10	4.10	2.40
3.00*	0.10	45	20	35	0.06	4.10	2.63
2.77	0.01	15	25	60	0.02	3.45	2.27
2.02	0.05	30	10	60	0.08	2.94	2.05
2.00*	0.13	50	10	40	0.10	3.15	2.34
2.00	0.07	35	10	55	0.09	2.98	2.10

*Precipitate with NH_4OH.

The events occurring at the point of initial precipitation of $Fe(OH)_3$ are not well known (5) and the complexity of the solutions treated here, and the assumptions made, limit this method as a means of measuring activity products. Because of the variation of K_w with temperature an error of 0.3° C in the temperature of the solution will lead to an error of $\pm 10^{0.01}$ in a_{OH^-} and a resultant error in K_{sp} of $Fe(OH)_3$ of $\pm 10^{0.03}$.

The author is grateful to Dr. D. E. Ryan of Dalhousie University for helpful criticism.

Received April 4, 1963.
Fisheries Research Board of Canada,
Atlantic Oceanographic Group,
Bedford Institute of Oceanography,
Dartmouth, Nova Scotia.

1. P. A. Kriukoff. Z. Electrochem. **38**, 975 (1934).
2. U. R. Evans and M. J. Pryor. J. Chem. Soc. 157 (1949).
3. N. V. Aksel'rud and Ya. A. Fialkoff. Ukr. Khim. Zhur. **16**, 288 (1950); Chem. Abstr. **49**, 9360 d (1955).
4. G. Biederman and P. Shindler. Acta Chem. Scand. **11**, 731 (1957).
5. R. M. Garrels. *In* Researches in oceanography. John Wiley and Sons, New York. 1959. p. 29.
6. E. Matijevič, K. G. Mathai, R. H. Ottewill, and M. Kerker. J. Phys. Chem. **65**, 826 (1961).
7. B. A. Brice, M. Halwer, and R. Speiser. J. Opt. Soc. Am. **40**, 768 (1950).
8. J. Kielland. J. Am. Chem. Soc. **59**, 1675 (1937).
9. E. Rabinowitch and W. H. Stockmayer. J. Am. Chem. Soc. **64**, 335 (1942).
10. B. O. Hedstrom. Arkiv. Kemi, **6**, 1 (1952); Chem. Abstr. **47**, 11938 i (1953).
11. C. W. Davies. Ion association. Butterworths, London. 1962.

A MODIFIED SYNTHESIS OF TETRAPHENYLCYCLOBUTADIENE PALLADIUM HALIDES

P. M. Maitlis and M. L. Games

In view of the current interest in the properties and reactions of tetraphenylcyclobutadiene–metal complexes, in particular those of palladium (B, X = halogen), we wish to describe a simplification of the original preparation of (A)[1] and also the preparation

Can. J. Chem. Downloaded from www.nrcresearchpress.com by 210.87.254.105 on 09/05/12
For personal use only.

TABLE I

pH for initial precipitation of Fe^{+++} by NaOH

$-\log [Fe^{+++}]_0$	$[Cl^-]$	$FeCl^{++}$ $FeCl_2^+$ $FeSO_4^+$ (%)	$FeOH^{++}$ $Fe(OH)_2^+$ (%)	"Free" $F_{Fe^{+++}}$ (%)	μ	$-\log a_{Fe^{+++}}$	pH
5.00	0.10	25	50	25	0.10	6.35	3.00
5.00	0.01	15	65	20	0.01	6.05	3.00
4.57	0.01	15	65	20	0.01	5.62	3.05
4.10	0.01	5	70	25	0.01	5.05	2.85
4.00	0.10	25	50	25	0.10	5.35	2.99
3.68	0.01	10	45	45	0.01	4.38	2.65
3.52	0.01	5	60	35	0.01	4.32	2.78
3.19	0.01	10	40	50	0.01	3.84	2.45
3.00	0.10	45	10	45	0.10	4.10	2.40
3.00*	0.10	45	20	35	0.06	4.10	2.63
2.77	0.01	15	25	60	0.02	3.45	2.27
2.02	0.05	30	10	60	0.08	2.94	2.05
2.00*	0.13	50	10	40	0.10	3.15	2.34
2.00	0.07	35	10	55	0.09	2.98	2.10

*Precipitate with NH_4OH.

The events occurring at the point of initial precipitation of $Fe(OH)_3$ are not well known (5) and the complexity of the solutions treated here, and the assumptions made, limit this method as a means of measuring activity products. Because of the variation of K_w with temperature an error of 0.3° C in the temperature of the solution will lead to an error of $\pm 10^{0.01}$ in a_{OH^-} and a resultant error in K_{sp} of $Fe(OH)_3$ of $\pm 10^{0.03}$.

The author is grateful to Dr. D. E. Ryan of Dalhousie University for helpful criticism.

Received April 4, 1963.
Fisheries Research Board of Canada,
Atlantic Oceanographic Group,
Bedford Institute of Oceanography,
Dartmouth, Nova Scotia.

1. P. A. Kriukoff. Z. Electrochem. **38**, 975 (1934).
2. U. R. Evans and M. J. Pryor. J. Chem. Soc. 157 (1949).
3. N. V. Aksel'rud and Ya. A. Fialkoff. Ukr. Khim. Zhur. **16**, 288 (1950); Chem. Abstr. **49**, 9360 d (1955).
4. G. Biederman and P. Shindler. Acta Chem. Scand. **11**, 731 (1957).
5. R. M. Garrels. *In* Researches in oceanography. John Wiley and Sons, New York. 1959. p. 29.
6. E. Matijevič, K. G. Mathai, R. H. Ottewill, and M. Kerker. J. Phys. Chem. **65**, 826 (1961).
7. B. A. Brice, M. Halwer, and R. Speiser. J. Opt. Soc. Am. **40**, 768 (1950).
8. J. Kielland. J. Am. Chem. Soc. **59**, 1675 (1937).
9. E. Rabinowitch and W. H. Stockmayer. J. Am. Chem. Soc. **64**, 335 (1942).
10. B. O. Hedstrom. Arkiv. Kemi, **6**, 1 (1952); Chem. Abstr. **47**, 11938 i (1953).
11. C. W. Davies. Ion association. Butterworths, London. 1962.

A MODIFIED SYNTHESIS OF TETRAPHENYLCYCLOBUTADIENE PALLADIUM HALIDES

P. M. Maitlis and M. L. Games

In view of the current interest in the properties and reactions of tetraphenylcyclobutadiene–metal complexes, in particular those of palladium (B, X = halogen), we wish to describe a simplification of the original preparation of (A)[1] and also the preparation

Can. J. Chem. Downloaded from www.nrcresearchpress.com by 210.87.254.5 on 09/05/12
For personal use only.

of the bromide and iodide of (B; X = Br, I). The modification entails reaction of sodium (or ammonium) chloropalladite with tolan (diphenylacetylene) in aqueous ethanol and avoids the necessity of preparing bis(benzonitrile) palladium chloride.* Further, the yield of (A) using sodium chloropalladite is rather better (92%) than that obtained with the benzonitrile complex (83%).

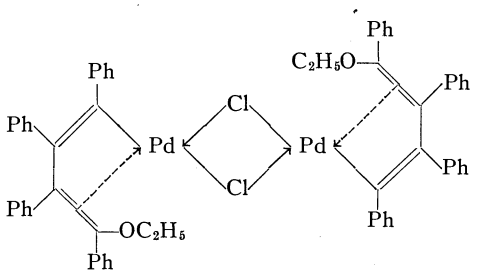

A

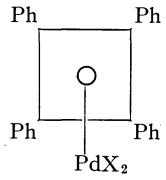

B

The conversion of complex A into tetraphenylcyclobutadiene palladium chloride (B, X = Cl) has already been noted (1); (A) can also be converted into the bromide (B, X = Br) using anhydrous hydrogen bromide (82% yield) and, less conveniently, with aqueous hydriodic acid, into the iodide (B, X = I) (50% yield). In the case of the bromide, particularly, appreciable amounts of hexaphenylbenzene were also sometimes formed. This was removed by boiling the mixture with benzene. The halides also tend to crystallize with solvent (chloroform or dichloromethane) of crystallization; these solvents were also removed on boiling of the mixtures with benzene or cyclohexane. Drying under high vacuum at 100° did not suffice.

Attempts were also made to use other palladium complexes to prepare (A); it was found that $[(\pi\text{-allyl})PdCl]_2$, $[(C_4H_9)_3P \cdot PdCl_2]_2$, and (dipyridyl)$PdCl_2$ were ineffective under normal conditions. The ligands in these complexes are presumably too firmly bound to be replaceable by acetylenes.

It was possible to prepare tetraphenylcyclobutadiene palladium bromide (B, X = Br) directly from tolan and palladium chloride in ethanol and hydrobromic acid. The yields under the best conditions, 4 hours refluxing, were much poorer than for the two-step reaction, and the product, while having the correct infrared spectrum, gave very high palladium analyses. In addition, a 41% yield of desoxybenzoin was obtained. More vigorous conditions (17 hours refluxing) gave poorer yields, while milder conditions (3 days at 25°) gave low yields of complexes A and B (infrared spectra). Use of hydrochloric instead of hydrobromic acid gave analogous results.

The formation of desoxybenzoin (none was formed in the absence of palladium salts, in the absence of acid, or in reactions at 25°) by hydration of tolan parallels the interesting recent discovery of a similar mercuric perchlorate catalyzed reaction (3). It therefore appears that palladium salts can react with tolan in at least two different ways, either to oligomerize it to (A), (B), or hexaphenylbenzene (1), depending on conditions, or to hydrate it to desoxybenzoin.

**Although numerous references (2) in the literature claim high yields for the preparation of this complex, we find that it is never possible to dissolve all of a given sample of palladium chloride (99.98% pure) in benzonitrile, thus resulting in low conversions. Addition of a solvent does not appear to improve the yield.*

Can. J. Chem. Downloaded from www.nrcresearchpress.com by 210.87.254.5 on 09/05/12
For personal use only.

EXPERIMENTAL

All melting points were carried out in evacuated capillaries and are uncorrected.

Complex A

Sodium chloride (2.5 g; 42.7 mmoles) and palladium chloride (3.75 g; 21.1 mmoles) were dissolved in hot water (25 ml) and filtered into a solution of tolan (8.25 g; 46.4 mmoles) in ethanol (95%; 130 ml). The solution was stirred at 25° for 1 hour, then filtered to give small yellow-brown crystals (8.22 g). The mother liquors were evaporated to small volume (<50 ml) on a rotary evaporator at 40° and gave a further crop of crystals of crude complex A (3.49 g). When the combined solids had been dissolved in dichloromethane and filtered, sodium chloride (1.17 g) was recovered. The filtrate gave the purified complex A (10.54 g; 92%). This was twice recrystallized from dichloromethane solution by addition of ethanol to give orange-red prisms, m.p. 181° (decomp.). The material had an infrared spectrum identical with that of the material prepared previously (1) and analyzed correctly. Calc. for $(C_{30}H_{25}OPdCl)_X$: Pd, 19.6%. Found: Pd, 19.7%. No desoxybenzoin was formed in this reaction.

Tetraphenylcyclobutadiene Palladium Bromide (B, X = Br)

Anhydrous hydrogen bromide was passed for 20 minutes into a solution of complex A (10.0 g) in chloroform (210 ml). Some complex B (solvated) crystallized out and the remainder was precipitated with light petroleum (b.p. 30–60°) to give crude (solvated) tetraphenylcyclobutadiene palladium bromide (10.4 g). Chloroform of crystallization and hexaphenylbenzene were removed by boiling the crude product with benzene (100 ml) for 30 minutes. Filtration gave pure tetraphenylcyclobutadiene palladium bromide (9.4 g, 82%). An analytical sample was prepared by dissolving the complex in dichloromethane saturated with hydrogen bromide; then the solution was filtered and allowed to crystallize. After removal of dichloromethane of crystallization by boiling with benzene and vacuum-drying, the compound analyzed correctly. Calc. for $C_{28}H_{20}PdBr_2$: Pd, 17.1%. Found: Pd, 17.1%. The infrared spectrum (KBr disk) of this complex was identical with that of tetraphenylcyclobutadiene nickel bromide (1) and tetraphenylcyclobutadiene palladium chloride (1) in the region measured (2–16 μ). The bromide (B, X = Br) had m.p. 347–348° (decomp.), the chloride (B, X = Cl) m.p. 297–298° (decomp.).

Tetraphenylcyclobutadiene Palladium Iodide (B, X = I)

Because of the expense of anhydrous hydrogen iodide the following method was used.

Complex A (5.0 g, 9.2 mmoles) dissolved in chloroform (50 ml) was refluxed with aqueous hydriodic acid (47%; 25 ml) for 17 hours. Filtration gave black needles (3.97 g) which, after being boiled with cyclohexane, gave the pure solvent-free iodide (B, X = I; 3.31 g; 50%) m.p. 287–290° (decomp.). Calc. for $C_{18}H_{20}PdI_2$: Pd, 14.9%. Found: Pd, 14.7%. The infrared spectrum was again identical with those of the bromide and chloride above.

Reaction of Tolan with Palladium Chloride in Aqueous Ethanolic Hydrobromic Acid

A solution of palladium chloride (1.78 g; 10 mmoles) in aqueous hydrobromic acid (48%; 5 ml) and ethanol (20 ml) was added to a solution of tolan (3.56 g; 20 mmoles) in ethanol (175 ml) and refluxed for 4 hours. Filtration gave crude tetraphenylcyclobutadiene palladium bromide (3.32 g). Calc. for $C_{28}H_{20}PdBr_2$: Pd, 17.1%. Found: Pd, 20.22, 20.87%, identified by infrared spectrum. The filtrate was evaporated to dryness, boiled with light petroleum (b.p. 100–120°), filtered, and concentrated to give desoxybenzoin (1.6 g, 41%), which was recrystallized from carbon tetrachloride, m.p. 54–55°, unchanged on admixture of a synthetic sample (4), m.p. 54–55°. The infrared spectra of the two samples were identical.

Longer periods of refluxing gave the same products in poorer yields. Reaction at 25° for 3 days gave poor yields of complex B (X = Br) containing large amounts of hexaphenylbenzene and complex A, even when a large excess of hydrobromic acid was used. No desoxybenzoin could be detected in this last reaction.

The authors thank the National Research Council of Canada and the Research Corporation of New York for supporting this work.

1. A. T. Blomquist and P. M. Maitlis. J. Am. Chem. Soc. **84**, 2329 (1962). L. Malatesta *et al.* Angew. Chem. **72**, 34 (1960).
2. J. R. Doyle, P. E. Slade, and H. B. Jonassen. Inorg. Synth. **V**, 218 (1960).
3. W. L. Budde and R. E. Dessy. Chem. Ind. 735 (1960).
4. J. Wislicenus and A. Blank. Ann. **248**, 5 (1888).

Received September 5, 1963.
Department of Chemistry,
McMaster University,
Hamilton, Ontario.

Can. J. Chem. Downloaded from www.nrcresearchpress.com by 210.87.254.5 on 09/05/12
For personal use only.

THE ISOBARIC BOILING POINTS OF THE SYSTEM: ACETIC ACID – CHLOROFORM – WATER AT A PRESSURE OF 760 mm Hg

A. N. CAMPBELL AND J. M. T. M. GIESKES

Can. J. Chem. Downloaded from www.nrcresearchpress.com by 210.87.254.40 on 09/05/12
For personal use only.

In previous papers where complete bibliographies are given, Campbell, Kartzmark, and Gieskes (1) have studied the isothermal vapor pressures at 25° C, and Campbell and Kartzmark (2) the critical phenomena of the system acetic acid – chloroform – water. It seemed a desirable sequel to the above work to determine the isobaric boiling points under one atmosphere pressure. Little discussion is necessary since the boiling point diagram is largely a consequence of the vapor pressure diagram. Further work is proceeding on the dielectric constants and heats of mixing of this system.

EXPERIMENTAL

Pressure was controlled with an accuracy of ±0.02 mm, by means of a two-stage barostat of the type described by Campbell and Dulmage (3). For the study of the liquid–vapor equilibria of the acetic acid – chloroform system, we used the equilibrium still of Scatchard, Raymond, and Gillman (4). This still, however, was found not to be satisfactory for the ternary mixtures, because in these mixtures the distillates usually separate into two layers so that no proper equilibrium can be established. For this purpose, therefore, we used the apparatus of Reinders and de Minjer (5); instead of their bell stirrer, we introduced a Scatchard pump. Nevertheless, the accuracy of this apparatus is not high and the boiling temperatures of the ternary system are not more accurate than ±0.5° C. The corresponding accuracy with the Scatchard still is ±0.1° C. Analyses were carried out by the method described by Campbell, Kartzmark, and Gieskes (1). Temperatures were measured with a double junction copper–constantan thermocouple and a precision potentiometer with an accuracy of ±0.1° C. The materials were purified by the methods described by Campbell, Kartzmark, and Gieskes (1).

RESULTS

Acetic Acid – Chloroform

TABLE I

Boiling points of acetic acid – chloroform mixtures at P = 760 mm

Liquid wt. % HAc	Vapor wt. % HAc	Boiling point, ° C
0.0	0.0	61.4
1.2	0.2	61.5
9.1	1.6	63.3
32.5	6.9	69.8
35.2	7.6	71.0
57.0	18.0	81.5
58.5	17.6	81.8
78.6	32.9	93.5
82.0	39.2	96.8
91.0	63.9	106.0
98.6	87.0	113.7
99.0	97.4	117.0
100.0	100.0	118.1

When the above figures are plotted in the usual way, the simplest type of boiling point diagram is obtained, without maximum or minimum; in other words, complete separation of chloroform and acetic acid is possible by fractional distillation.

Acetic Acid – Chloroform – Water

Since the vapor phase from ternary mixtures almost always separates into two layers on liquefaction, the analytical figures for vapor composition are unreliable and therefore we do not reproduce data for vapor composition. The boiling point data are reported in Table II. The experiments were carried out in series, starting with a mixture of given composition. The removal of condensed vapor phase caused the composition of the system as a whole to change, so that each set gives an indication of the course of progressive distillation.

TABLE II

Boiling points of mixtures of acetic acid, chloroform, and water, P = 760 mm

Series No.	Wt. % HAc	Wt. % H_2O	Boiling point	Series No.	Wt. % HAc	Wt. % H_2O	Boiling point
1	56.0	37.1	78.2	6	69.9	21.5	86.8
	56.6	36.9	80.2		71.0	22.1	89.3
	58.3	36.2	83.5		72.7	21.9	91.2
	58.3	37.1	86.6				
				7	78.4	9.4	90.1
2	57.9	29.9	76.2		79.1	9.9	91.1
	59.1	29.6	78.7		80.0	9.8	92.1
	61.7	30.2	83.3				
	62.3	30.8	84.9	8	88.0	3.4	101.3
	63.2	31.0	85.1		88.8	3.8	102.2
					89.4	3.9	103.0
3	53.6	21.1	66.4		90.2	4.1	104.3
	54.2	21.0	66.8				
	54.9	20.8	67.0	9	47.3	5.5	69.8
	55.2	21.1	67.4		48.1	5.0	69.8
	56.1	21.5	68.2				
				10	61.3	16.0	73.1
4	53.1	14.2	66.8		62.3	16.1	74.7
	54.2	14.3	67.7				
	55.0	14.6	68.2				
	56.9	15.5	68.9				
	57.8	15.5	69.8				
5	71.2	6.0	83.9				
	72.2	5.8	84.6				
	73.1	6.0	85.2				

DISCUSSION

The isobaric behavior of the system: acetic acid – chloroform is what would be expected from the previous isothermal work (1, 2), where it is shown that, provided that due allowance is made for the fact that acetic acid is dimerized, the behavior is ideal. Figure 1 has been constructed for the ternary system from the known data and the data of this paper to give a graphical representation of the equilibria and relative liquid and vapor compositions. The isothermal sections (consolute solutions) are taken from Brancker, Hunter, and Nash (6) and from Campbell and Kartzmark (2). We have not attempted to find the ternary minimum boiling point, if it exists, because it must be very close to the minimum in the binary system, chloroform–water (5), and the accuracy of our apparatus was not sufficient to detect it. Figure 2 represents diagrammatically the distillation paths, derived from the data of Table II. The form of the distillation paths is what would be expected. Reinders and de Minjer (7) discuss in detail the several possible types of distillation path diagrams. The present system shows some similarity to their Fig. 3, with the difference that in the present case a miscibility gap exists. Systems of the latter type are discussed by Haase (8).

Can. J. Chem. Downloaded from www.nrcresearchpress.com by 210.87.254.40 on 09/05/12
For personal use only.

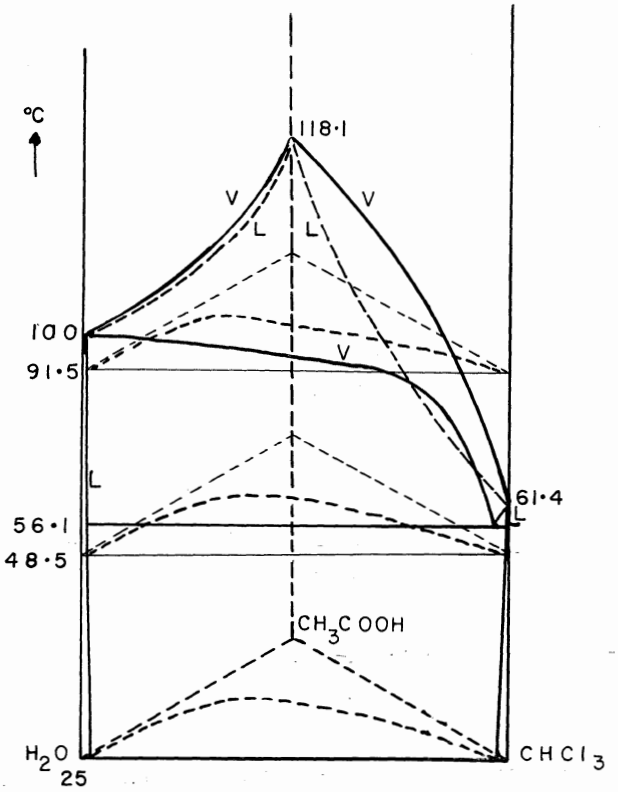

FIG. 1.

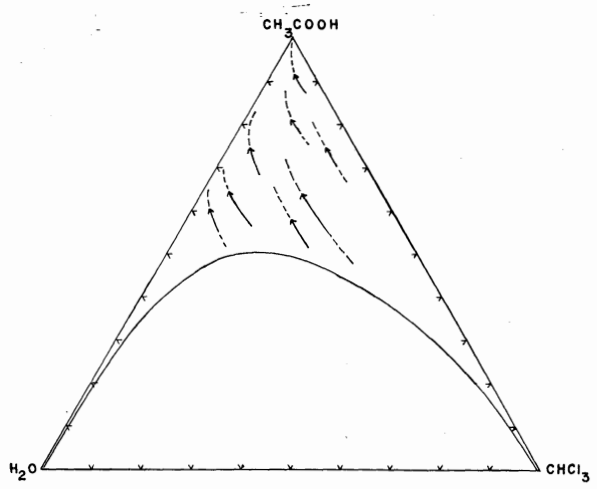

FIG. 2.

Can. J. Chem. Downloaded from www.nrcresearchpress.com by 210.87.254.40 on 09/05/12
For personal use only.

1. A. N. CAMPBELL, E. M. KARTZMARK, and J. M. T. M. GIESKES. Can. J. Chem. **41**, 407 (1963).
2. A. N. CAMPBELL and E. M. KARTZMARK. Can. J. Chem. **41**, 1088 (1963).
3. A. N. CAMPBELL and W. J. DULMAGE. J. Am. Chem. Soc. **70**, 1723 (1948).
4. G. SCATCHARD, C. L. RAYMOND, and H. H. GILMAN. J. Am. Chem. Soc. **60**, 1275 (1938).
5. W. REINDERS and C. H. DE MINJER. Rec. Trav. Chim. **66**, 573 (1947).
6. A. B. BRANCKER, T. G. HUNTER, and A. W. NASH. J. Phys. Chem. **44**, 683 (1940).
7. W. REINDERS and C. H. DE MINJER. Rec. Trav. Chim. **59**, 207 (1940).
8. R. HAASE. Z. Naturforsch. **5a**, 109 (1950).

RECEIVED AUGUST 6, 1963.
DEPARTMENT OF CHEMISTRY,
UNIVERSITY OF MANITOBA,
WINNIPEG, MANITOBA.

Can. J. Chem. Downloaded from www.nrcresearchpress.com by 210.87.254.40 on 09/05/12
For personal use only.

Δ^{11}-STEROIDS

P. ZIEGLER AND A. A. AMOS

During attempts at introduction of a Δ^{11} double bond into some steroids, we had occasion to prepare 3,20-dioxo-12α-tosyloxypregnane. This compound has previously been reported as having m.p. 130–132° (1, 2), 120–125° (3), 129–131° (4), but has otherwise not been characterized satisfactorily. In this laboratory, 3,20-dioxo-12α-hydroxypregnane was treated with *p*-tosyl chloride to yield 90% of crystalline material which, after purification, had m.p. 155–156.5°. Elemental analyses and ultraviolet absorption data indicated that our compound is authentic 3,20-dioxo-12α-tosyloxypregnane. The discrepancy in melting point might be due to polymorphism, which is known (3) to occur in this particular series of steroids. The steroid tosylate was then converted to 3,20-dioxo-12α-tosyloxypregnane bis-ethylene ketal, a crystalline compound which gave correct analyses and exhibited the expected ultraviolet absorption data (ϵ = 12,900 at 224 mμ in isooctane). This compound, obtained in the form of an amorphous solid, has been reported (4) to have ϵ = 25,120 at 225 mμ in ethanol.

Dehydrotosylation of 3,20-dioxo-12α-tosyloxypregnane to 3,20-dioxo-Δ^{11}-pregnene has been effected (1) by refluxing with collidine, but the yields of product were low (32%). A more recently developed procedure (2, 3, 4), consisting of dehydrotosylation by chromatography through a column of activated alumina, gave much improved yields (70–85%). In order to carry out this conversion on a larger scale, it seemed desirable to find an alternative method which would avoid chromatography and, at the same time, provide adequate yields. It has now been found that this can be accomplished (50–60% yield) by dehydrotosylating in N-methylpyrrolidone containing a small amount of water and 10% potassium acetate. It seems that this reaction proceeds readily in a slightly basic medium of high dielectric constant.

EXPERIMENTAL

3,20-Dioxo-12α-tosyloxypregnane

3,20-Dioxo-12α-hydroxypregnane (4 g), m.p. 182.5–184.5° and $[\alpha]_D^{25}$ +135.8° (*c*, 0.41, ethanol), was dissolved in dry pyridine (8 ml). After addition of *p*-tosyl chloride (4.5 g) the mixture was kept at 37° for 5 days. By that time the solution had turned brown and long crystals of pyridine hydrochloride had deposited. The solution was then cooled to 0°, the excess reagent was destroyed by addition of water (1 ml) and the mixture was poured into dilute hydrochloric acid. The products were extracted with ether, the solvent extract was washed with dilute acid, then with water until neutral. After it was dried over sodium sulphate, filtered, and evaporated, there remained 5.72 g of residue which crystallized from ether–hexane. In two crops, 5.17 g (89%) of crystals, m.p. 148–153°, were obtained. Three further recrystallizations from ether–hexane provided the analytical specimen, m.p. 155–156.5° (decomp. at 160°), $[\alpha]_D^{25}$ +66.1° (*c*, 0.61, ethanol), $\lambda_{max}^{isooctane}$ 224 mμ (ϵ 12,020). Calculated for $C_{28}H_{38}O_5S$: C, 69.10; H, 7.87; S, 6.59. Found: C, 69.14; H, 7.84; S, 6.43.

1. A. N. CAMPBELL, E. M. KARTZMARK, and J. M. T. M. GIESKES. Can. J. Chem. **41**, 407 (1963).
2. A. N. CAMPBELL and E. M. KARTZMARK. Can. J. Chem. **41**, 1088 (1963).
3. A. N. CAMPBELL and W. J. DULMAGE. J. Am. Chem. Soc. **70**, 1723 (1948).
4. G. SCATCHARD, C. L. RAYMOND, and H. H. GILMAN. J. Am. Chem. Soc. **60**, 1275 (1938).
5. W. REINDERS and C. H. DE MINJER. Rec. Trav. Chim. **66**, 573 (1947).
6. A. B. BRANCKER, T. G. HUNTER, and A. W. NASH. J. Phys. Chem. **44**, 683 (1940).
7. W. REINDERS and C. H. DE MINJER. Rec. Trav. Chim. **59**, 207 (1940).
8. R. HAASE. Z. Naturforsch. **5a**, 109 (1950).

RECEIVED AUGUST 6, 1963.
DEPARTMENT OF CHEMISTRY,
UNIVERSITY OF MANITOBA,
WINNIPEG, MANITOBA.

Can. J. Chem. Downloaded from www.nrcresearchpress.com by 210.87.254.40 on 09/05/12
For personal use only.

Δ^{11}-STEROIDS

P. ZIEGLER AND A. A. AMOS

During attempts at introduction of a Δ^{11} double bond into some steroids, we had occasion to prepare 3,20-dioxo-12α-tosyloxypregnane. This compound has previously been reported as having m.p. 130–132° (1, 2), 120–125° (3), 129–131° (4), but has otherwise not been characterized satisfactorily. In this laboratory, 3,20-dioxo-12α-hydroxypregnane was treated with *p*-tosyl chloride to yield 90% of crystalline material which, after purification, had m.p. 155–156.5°. Elemental analyses and ultraviolet absorption data indicated that our compound is authentic 3,20-dioxo-12α-tosyloxypregnane. The discrepancy in melting point might be due to polymorphism, which is known (3) to occur in this particular series of steroids. The steroid tosylate was then converted to 3,20-dioxo-12α-tosyloxypregnane bis-ethylene ketal, a crystalline compound which gave correct analyses and exhibited the expected ultraviolet absorption data (ϵ = 12,900 at 224 mμ in isooctane). This compound, obtained in the form of an amorphous solid, has been reported (4) to have ϵ = 25,120 at 225 mμ in ethanol.

Dehydrotosylation of 3,20-dioxo-12α-tosyloxypregnane to 3,20-dioxo-Δ^{11}-pregnene has been effected (1) by refluxing with collidine, but the yields of product were low (32%). A more recently developed procedure (2, 3, 4), consisting of dehydrotosylation by chromatography through a column of activated alumina, gave much improved yields (70–85%). In order to carry out this conversion on a larger scale, it seemed desirable to find an alternative method which would avoid chromatography and, at the same time, provide adequate yields. It has now been found that this can be accomplished (50–60% yield) by dehydrotosylating in N-methylpyrrolidone containing a small amount of water and 10% potassium acetate. It seems that this reaction proceeds readily in a slightly basic medium of high dielectric constant.

EXPERIMENTAL

3,20-Dioxo-12α-tosyloxypregnane

3,20-Dioxo-12α-hydroxypregnane (4 g), m.p. 182.5–184.5° and $[\alpha]_D^{25}$ +135.8° (*c*, 0.41, ethanol), was dissolved in dry pyridine (8 ml). After addition of *p*-tosyl chloride (4.5 g) the mixture was kept at 37° for 5 days. By that time the solution had turned brown and long crystals of pyridine hydrochloride had deposited. The solution was then cooled to 0°, the excess reagent was destroyed by addition of water (1 ml) and the mixture was poured into dilute hydrochloric acid. The products were extracted with ether, the solvent extract was washed with dilute acid, then with water until neutral. After it was dried over sodium sulphate, filtered, and evaporated, there remained 5.72 g of residue which crystallized from ether–hexane. In two crops, 5.17 g (89%) of crystals, m.p. 148–153°, were obtained. Three further recrystallizations from ether–hexane provided the analytical specimen, m.p. 155–156.5° (decomp. at 160°), $[\alpha]_D^{25}$ +66.1° (*c*, 0.61, ethanol), $\lambda_{max}^{isooctane}$ 224 mμ (ϵ 12,020). Calculated for $C_{28}H_{38}O_5S$: C, 69.10; H, 7.87; S, 6.59. Found: C, 69.14; H, 7.84; S, 6.43.

3,20-Dioxo-12α-tosyloxypregnane Bis-ethylene Ketal

3,20-Dioxo-12α-tosyloxypregnane (10 g) and *p*-toluenesulphonic acid (0.35 g) were stirred and refluxed for 7 hours in benzene (160 ml) and ethyleneglycol (30 ml). A Dean–Stark trap was used to separate the water formed. The mixture was cooled, neutralized with sodium bicarbonate, and diluted with water; the benzene extract was separated, then washed with water, dried, and evaporated. The residue (12.5 g) crystallized from ether to provide 9.3 g (85%) of ketal, m.p. 148–150° (decomp.). Repeated recrystallizations from ether gave the pure compound, m.p. 150° with decomp. (the melting point depends on the rate of heating), $[\alpha]_D^{25}$ +66.4° (*c*, 0.76, ethanol), and $\lambda_{max}^{isooctane}$ 224 mμ (ε 12,900). Calculated for $C_{32}H_{46}O_7S$: C, 66.87; H, 8.07; S, 5.58. Found: C, 67.03; H, 8.12; S, 5.49. This compound has been described (4) to be amorphous with $\lambda_{max}^{ethanol}$ 225 mμ (ε 25,120).

3,20-Dioxo-Δ¹¹-pregnene

Potassium acetate (3.75 g), water (1.25 ml), and N-methylpyrrolidone (37.5 ml) were stirred and heated to 110°. After addition of 3,20-dioxo-12α-tosyloxypregnane (5 g), the temperature was kept at 115–120° for 3.5 hours. The reaction mixture was then poured into water, the products were extracted with ether, the solvent extract was washed, dried, and evaporated. The residue crystallized from ether–hexane to yield, in two crops, 1.77 g (55%) of material, m.p. 130–133°. Two recrystallizations gave the pure compound, m.p. 138.5–140° and $[\alpha]_D^{25}$ +94.0° (*c*, 0.424, ethanol).

When 3,20-dioxo-Δ¹¹-pregnene was dissolved in methanol containing traces of mineral acid, the corresponding 3-dimethylketal precipitated as white crystals. Repeated recrystallization from ether gave m.p. 137–139° and $[\alpha]_D^{26}$ +89.0° (*c*, 0.551, chloroform). Calculated for $C_{23}H_{36}O_3$: C, 76.62; H, 10.04; O, 13.31. Found: C, 76.45; H, 10.04; O, 13.49.

1. J. van Euw and T. Reichstein. Helv. Chim. Acta, **29**, 654 (1946).
2. A. Ruff and T. Reichstein. Helv. Chim. Acta, **34**, 70 (1951).
3. G. Just and Ch. R. Engel. J. Org. Chem. **23**, 12 (1958).
4. Ch. R. Engel and S. F. Papadopoulos. J. Org. Chem. **26**, 2868 (1961).

Received July 30, 1963.
Research and Development Laboratories,
Canada Packers Limited,
Toronto 9, Ontario.

Can. J. Chem. Downloaded from www.nrcresearchpress.com by 210.87.254.40 on 09/05/12
For personal use only.

REACTIONS OF BENZYLIDENETRIPHENYLPHOSPHORANE WITH SOME DICARBONYL COMPOUNDS

J. Parrick

The reactions of Wittig reagents with certain dicarbonyl compounds is of proved synthetic utility (1). We have found that the reaction of benzylidenetriphenylphosphorane (I) with some 1,2-dicarbonyl compounds gave 2-benzylidene ketones, even when 2 molar equivalents of the phosphorane were used.

Phosphorane (I) reacted with phenanthraquinone to give 9,10-dihydro-9-benzylidene-10-oxophenanthrene but no reaction was observed with anthraquinone, and only intractable tars were obtained with diacetyl, *p*-benzoquinone, and 1,2- and 1,4-naphthoquinone. A mixture of what was assumed to be the two geometrically isomeric 1,2,3-triphenylprop-1-en-3-ones was obtained from benzil.

The reaction of Wittig reagents with compounds having a carbonyl group in a heterocyclic ring has been little investigated. Isatin was found to react readily with 1 molar equivalent of benzylidenetriphenylphosphosphorane to give 3-benzylidene oxindole, the same as that prepared from oxindole and benzaldehyde. Thus, the two reactions give the same pure stereoisomer. Reduction of 3-benzylidene oxindole with lithium aluminum hydride gave 3-benzylindole.

3,20-Dioxo-12α-tosyloxypregnane Bis-ethylene Ketal

3,20-Dioxo-12α-tosyloxypregnane (10 g) and *p*-toluenesulphonic acid (0.35 g) were stirred and refluxed for 7 hours in benzene (160 ml) and ethyleneglycol (30 ml). A Dean–Stark trap was used to separate the water formed. The mixture was cooled, neutralized with sodium bicarbonate, and diluted with water; the benzene extract was separated, then washed with water, dried, and evaporated. The residue (12.5 g) crystallized from ether to provide 9.3 g (85%) of ketal, m.p. 148–150° (decomp.). Repeated recrystallizations from ether gave the pure compound, m.p. 150° with decomp. (the melting point depends on the rate of heating), $[\alpha]_D^{25}$ +66.4° (*c*, 0.76, ethanol), and $\lambda_{max}^{isooctane}$ 224 mμ (ε 12,900). Calculated for $C_{32}H_{46}O_7S$: C, 66.87; H, 8.07; S, 5.58. Found: C, 67.03; H, 8.12; S, 5.49. This compound has been described (4) to be amorphous with $\lambda_{max}^{ethanol}$ 225 mμ (ε 25,120).

3,20-Dioxo-Δ¹¹-pregnene

Potassium acetate (3.75 g), water (1.25 ml), and N-methylpyrrolidone (37.5 ml) were stirred and heated to 110°. After addition of 3,20-dioxo-12α-tosyloxypregnane (5 g), the temperature was kept at 115–120° for 3.5 hours. The reaction mixture was then poured into water, the products were extracted with ether, the solvent extract was washed, dried, and evaporated. The residue crystallized from ether–hexane to yield, in two crops, 1.77 g (55%) of material, m.p. 130–133°. Two recrystallizations gave the pure compound, m.p. 138.5–140° and $[\alpha]_D^{25}$ +94.0° (*c*, 0.424, ethanol).

When 3,20-dioxo-Δ¹¹-pregnene was dissolved in methanol containing traces of mineral acid, the corresponding 3-dimethylketal precipitated as white crystals. Repeated recrystallization from ether gave m.p. 137–139° and $[\alpha]_D^{26}$ +89.0° (*c*, 0.551, chloroform). Calculated for $C_{23}H_{36}O_3$: C, 76.62; H, 10.04; O, 13.31. Found: C, 76.45; H, 10.04; O, 13.49.

1. J. van Euw and T. Reichstein. Helv. Chim. Acta, **29**, 654 (1946).
2. A. Ruff and T. Reichstein. Helv. Chim. Acta, **34**, 70 (1951).
3. G. Just and Ch. R. Engel. J. Org. Chem. **23**, 12 (1958).
4. Ch. R. Engel and S. F. Papadopoulos. J. Org. Chem. **26**, 2868 (1961).

Received July 30, 1963.
Research and Development Laboratories,
Canada Packers Limited,
Toronto 9, Ontario.

Can. J. Chem. Downloaded from www.nrcresearchpress.com by 210.87.254.42 on 09/05/12
For personal use only.

REACTIONS OF BENZYLIDENETRIPHENYLPHOSPHORANE WITH SOME DICARBONYL COMPOUNDS

J. Parrick

The reactions of Wittig reagents with certain dicarbonyl compounds is of proved synthetic utility (1). We have found that the reaction of benzylidenetriphenylphosphorane (I) with some 1,2-dicarbonyl compounds gave 2-benzylidene ketones, even when 2 molar equivalents of the phosphorane were used.

Phosphorane (I) reacted with phenanthraquinone to give 9,10-dihydro-9-benzylidene-10-oxophenanthrene but no reaction was observed with anthraquinone, and only intractable tars were obtained with diacetyl, *p*-benzoquinone, and 1,2- and 1,4-naphthoquinone. A mixture of what was assumed to be the two geometrically isomeric 1,2,3-triphenylprop-1-en-3-ones was obtained from benzil.

The reaction of Wittig reagents with compounds having a carbonyl group in a heterocyclic ring has been little investigated. Isatin was found to react readily with 1 molar equivalent of benzylidenetriphenylphosphosphorane to give 3-benzylidene oxindole, the same as that prepared from oxindole and benzaldehyde. Thus, the two reactions give the same pure stereoisomer. Reduction of 3-benzylidene oxindole with lithium aluminum hydride gave 3-benzylindole.

EXPERIMENTAL

The reactions were performed in apparatus which was thoroughly purged with dry nitrogen.

Benzylidenetriphenylphosphorane (I)

An ethanolic solution was prepared as described by Trippett (2).

9,10-Dihydro-9-benzylidene-10-oxophenanthrene

Addition of a hot benzene solution (200 ml) of phenanthraquinone (2.08 g, 0.01 mole) to a warm (0.4 *M*) ethanolic solution of phosphorane (I) (0.023 mole) gave a red solution, which was allowed to stand at room temperature for 1 day and then boiled under reflux for 5 hours. The solvent was distilled off and the residue extracted with hot petroleum ether (b.p. 60–80°). The extract deposited triphenylphosphine oxide on cooling and, after filtration, the mother liquor yielded 9,10-dihydro-9-benzylidene-10-oxophenanthrene on evaporation. Crystallization from a large volume of ethanol yielded colorless prisms, m.p. 146–147° (1.3 g, 46%). λC_6H_{12} 229, 248, 280, 320, 352, 370 mμ, log ε 4.33, 4.4, 4.11, 3.94, 3.91, 3.42, 3.51. Carbonyl stretching frequency: 1628 cm^{-1}. (Found: C, 89.1; H, 5.25. $C_{21}H_{14}O$ requires C, 89.4; H, 5.5%.)

1,2,3-Triphenylprop-1-en-3-one

A hot ethanolic solution of benzil (2.1 g, 0.01 mole) was added to the ethanolic phosphorane solution (I) (0.02 mole) and the red solution boiled under reflux for 6 hours. Isolation by the procedure described above afforded a pale yellow solid (1.8 g). Fractional crystallization from ethanol gave a less soluble fraction as colorless needles (0.9 g, 32%), m.p. 98–99°. Carbonyl stretching frequency: 1649 cm^{-1}. (Found: C, 88.7; H, 5.7. $C_{21}H_{16}O$ requires C, 88.8; H, 5.6%.) The more soluble fraction deposited as colorless prisms (0.4 g), m.p. 89–90°. Carbonyl stretching frequency: 1666 cm^{-1}. (Found: C, 89.0; H, 6.0%.)

3-Benzylidene Oxindole

Addition of a hot ethanolic solution of isatin (2.94 g, 0.02 mole) to the ethanolic phosphorane (I) (0.02 mole) gave a deep red solution, but the color faded after 2 hours with the formation of bright yellow needles of 3-benzylidene oxindole (78%), m.p. 177–178°. (Found: C, 81.0; H, 4.9. Calc. for $C_{15}H_{11}NO$: C, 81.5; H, 5.0%.) The compound prepared from oxindole and benzaldehyde had m.p. 176–177° (lit. m.p. 176° (3)), and showed no depression of melting point on admixture with the first specimen.

3-Benzylindole

Reduction of 3-benzylidene oxindole with lithium aluminum hydride in ether at room temperature gave 3-benzylindole, m.p. 106–108° (lit. m.p. 107° (4)).

1. G. Wittig, H. Eggers, and P. Duffner. Ann. **619**, 10 (1958). K. Dimroth and G. Pohl. Angew. Chem. **73**, 436 (1961).
2. S. Trippett. Advances in organic chemistry. Vol. I. Interscience Publishers Ltd., London. 1960. p. 83.
3. A. Wahl and P. Bagard. Compt. Rend. **149**, 132 (1909).
4. E. F. Pratt and L. W. Botimer. J. Am. Chem. Soc. **79**, 5248 (1957).

Received August 22, 1963.
Department of Chemistry and Metallurgy,
Rutherford College of Technology,
Newcastle-upon-Tyne, England.

THE OPTICAL ROTATION OF CERTAIN DERIVATIVES OF ASPIDOSPERMIDINE

Stewart McLean

During the study of the structure of aspidocarpine (I*a*) (1) it was observed that the specific rotation of this alkaloid (+140°) was of the same order of magnitude as that of aspidospermine (I*d*) (−93°) but of opposite sign. This immediately suggested an antipodal relationship between the two alkaloids, which were suspected to differ in the aromatic part of the molecule only; such an observation would have had important biogenetic implications. However, conversion of I*a* to a degradation product IV, which retained all of the asymmetric centers present in I*a* and which was identical in every respect, including

Can. J. Chem. Downloaded from www.nrcresearchpress.com by 210.87.254.42 on 09/05/12
For personal use only.

EXPERIMENTAL

The reactions were performed in apparatus which was thoroughly purged with dry nitrogen.

Benzylidenetriphenylphosphorane (I)

An ethanolic solution was prepared as described by Trippett (2).

9,10-Dihydro-9-benzylidene-10-oxophenanthrene

Addition of a hot benzene solution (200 ml) of phenanthraquinone (2.08 g, 0.01 mole) to a warm (0.4 *M*) ethanolic solution of phosphorane (I) (0.023 mole) gave a red solution, which was allowed to stand at room temperature for 1 day and then boiled under reflux for 5 hours. The solvent was distilled off and the residue extracted with hot petroleum ether (b.p. 60–80°). The extract deposited triphenylphosphine oxide on cooling and, after filtration, the mother liquor yielded 9,10-dihydro-9-benzylidene-10-oxophenanthrene on evaporation. Crystallization from a large volume of ethanol yielded colorless prisms, m.p. 146–147° (1.3 g, 46%). λC_6H_{12} 229, 248, 280, 320, 352, 370 mμ, log ε 4.33, 4.4, 4.11, 3.94, 3.91, 3.42, 3.51. Carbonyl stretching frequency: 1628 cm^{-1}. (Found: C, 89.1; H, 5.25. $C_{21}H_{14}O$ requires C, 89.4; H, 5.5%.)

1,2,3-Triphenylprop-1-en-3-one

A hot ethanolic solution of benzil (2.1 g, 0.01 mole) was added to the ethanolic phosphorane solution (I) (0.02 mole) and the red solution boiled under reflux for 6 hours. Isolation by the procedure described above afforded a pale yellow solid (1.8 g). Fractional crystallization from ethanol gave a less soluble fraction as colorless needles (0.9 g, 32%), m.p. 98–99°. Carbonyl stretching frequency: 1649 cm^{-1}. (Found: C, 88.7; H, 5.7. $C_{21}H_{16}O$ requires C, 88.8; H, 5.6%.) The more soluble fraction deposited as colorless prisms (0.4 g), m.p. 89–90°. Carbonyl stretching frequency: 1666 cm^{-1}. (Found: C, 89.0; H, 6.0%.)

3-Benzylidene Oxindole

Addition of a hot ethanolic solution of isatin (2.94 g, 0.02 mole) to the ethanolic phosphorane (I) (0.02 mole) gave a deep red solution, but the color faded after 2 hours with the formation of bright yellow needles of 3-benzylidene oxindole (78%), m.p. 177–178°. (Found: C, 81.0; H, 4.9. Calc. for $C_{15}H_{11}NO$: C, 81.5; H, 5.0%.) The compound prepared from oxindole and benzaldehyde had m.p. 176–177° (lit. m.p. 176° (3)), and showed no depression of melting point on admixture with the first specimen.

3-Benzylindole

Reduction of 3-benzylidene oxindole with lithium aluminum hydride in ether at room temperature gave 3-benzylindole, m.p. 106–108° (lit. m.p. 107° (4)).

1. G. Wittig, H. Eggers, and P. Duffner. Ann. **619**, 10 (1958). K. Dimroth and G. Pohl. Angew. Chem. **73**, 436 (1961).
2. S. Trippett. Advances in organic chemistry. Vol. I. Interscience Publishers Ltd., London. 1960. p. 83.
3. A. Wahl and P. Bagard. Compt. Rend. **149**, 132 (1909).
4. E. F. Pratt and L. W. Botimer. J. Am. Chem. Soc. **79**, 5248 (1957).

Received August 22, 1963.
Department of Chemistry and Metallurgy,
Rutherford College of Technology,
Newcastle-upon-Tyne, England.

THE OPTICAL ROTATION OF CERTAIN DERIVATIVES OF ASPIDOSPERMIDINE

Stewart McLean

During the study of the structure of aspidocarpine (I*a*) (1) it was observed that the specific rotation of this alkaloid (+140°) was of the same order of magnitude as that of aspidospermine (I*d*) (−93°) but of opposite sign. This immediately suggested an antipodal relationship between the two alkaloids, which were suspected to differ in the aromatic part of the molecule only; such an observation would have had important biogenetic implications. However, conversion of I*a* to a degradation product IV, which retained all of the asymmetric centers present in I*a* and which was identical in every respect, including

Can. J. Chem. Downloaded from www.nrcresearchpress.com by 210.87.254.105 on 09/05/12
For personal use only.

optical rotation, with that obtained by degradation of I*d*, proved that both alkaloids possessed the same structure in the saturated part of the molecule and had the same absolute configuration. A different reason had then to be found for the difference in optical rotation between the two alkaloids.*

A further examination of a series of derivatives of these alkaloids brought to light three significant differences between those N(1)-acyl derivatives with an OH group at C-17 and those with an OMe group at this position: the former show the hydrogen-bonded carbonyl near 1635 cm^{-1} in the infrared while the corresponding absorption is near 1660 cm^{-1} in the latter; the phenolic alkaloids show the C-2 proton at about 5.9 τ in the n.m.r. while the methoxy analogues show this signal near 5.5 τ (1, 2, 3); optical rotations of the phenolic alkaloids have large positive values whereas the O-methyl derivatives have large negative values. Values recorded for a number of derivatives prepared in the present study are listed in the table and compared with values recorded elsewhere for alkaloids which retain the aspidospermidine (4) skeleton. Comparison shows that the phenomenon is quite general; pyrifolidine (2) has, of course, a completely antipodal relationship. In fact the changes in optical rotation are also reflected in alkaloids in which the saturated part of the molecule has been modified, although it is not surprising to find, with molecules in which an extra asymmetric center has been introduced (II, III), that the values for the rotations no longer match the earlier pattern completely.

Conversion of an N-acyl-17-hydroxyaspidospermidine to its 17-acetoxy derivative produces a shift in rotation in the same direction as does conversion to a 17-methoxy derivative, but the effect is less pronounced (I*l*, *m*, *n*). N-Deacylation has a similar effect, and now the nature at the substituent at C-17, has little influence on the rotation (I*o*, *p*, *q*).

It is reasonable to consider it likely that these three parallel effects, i.e. shifts in the infrared, n.m.r., and specific rotation, have a common cause; that is to say, the presence or absence of a hydrogen-bonded acyl group, a feature that readily accounts for the change in the infrared spectrum, also leads to the possibility of other more subtle differences in the molecular environment and these are reflected in the n.m.r. spectrum and the optical rotation. It is, however, difficult to relate cause and effect in a detailed way. The unlikely possibility that changes in the conformation of ring C are involved can be disposed of since, although the *position* of the C-2 proton signal in the two series is different, its *pattern* is the same and shows the C-2 proton signal split by two vicinal protons with identical orientations with respect to the C-2 proton in both series (J values are approximately 6 and 11 c.p.s.) (5).

The effect observed must, therefore, be directly related to changes in the orientation of the N-acyl group. The n.m.r. differences would then arise from the different amount of diamagnetic shielding produced at the C-2 proton by the acyl carbonyl in two different conformations.†‡ The differences in optical rotation can then be traced to a conformational asymmetry (8) effect of the acyl group. It seems possible that the effect may be simply conformational or it may be that the contribution of the asymmetric center at C-2 is also influenced by a variation in the polarizability (8) of the C—N bond depending on whether or not the N-acyl group is hydrogen-bonded. It any event the system does not appear to be amenable to explicit analysis on the basis of available data and perhaps

**Ironically, an alkaloid belonging to the antipodal series was soon reported when it was shown that pyrifolidine is the enantiomer of O-methylaspidocarpine (Ib) (2). (The structures shown do not necessarily indicate the true absolute configurations.)*

†It is, however, difficult to see from models that the sense of this change is in the direction anticipated (6).

‡It is significant that Anet has recently reported a detailed n.m.r. study of strychnospermine in which he demonstrates that the N-acetyl group has a high conformational stability (7).

Can. J. Chem. Downloaded from www.nrcresearchpress.com by 210.87.254.105 on 09/05/12
For personal use only.

the most significant point at present is that a fairly small change in a molecule at a position well removed from an asymmetric center can have a large influence on the optical activity.

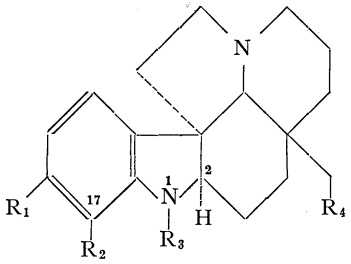

I

	R_1 =	R_2 =	R_3 =	R_4 =	
a	OMe	OH	Ac	CH_3	Aspidocarpine
b	OMe	OMe	Ac	CH_3	
c	H	OH	Ac	CH_3	
d	H	OMe	Ac	CH_3	Aspidospermine
e	OH	OH	Ac	CH_3	O-Demethylaspidocarpine
f	H	OMe	EtCO	CH_3	Palosine
g	H	OMe	HCO	CH_3	Vallesine
h	OMe	OH	EtCO	CH_3	Aspidolimine
i	H	OMe	Ac	CO_2Me	Cylindrocarpidine
j	H	OMe	PhCH=CHCO	CO_2Me	Cylindrocarpine
k	H	OH	EtCO	CH_2OH	Limaspermine
l	OMe	OAc	Ac	CH_3	
m	OAc	OAc	Ac	CH_3	
n	H	OAc	Ac	CH_3	
o	OMe	OMe	H	CH_3	
p	H	OH	H	CH_3	
q	H	OMe	H	CH_3	

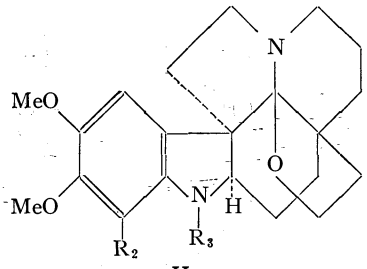

II

	R_2 =	R_3 =
a	OH	Ac
b	OMe	Ac
c	OH	EtCO
d	OMe	EtCO

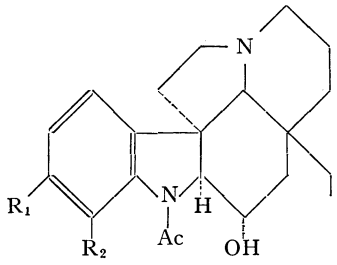

III

Can. J. Chem. Downloaded from www.nrcresearchpress.com by 210.87.254.105 on 09/05/12
For personal use only.

	R_1 =	R_2 =	
a	H	OH	Spegazzinine
b	H	OMe	
c	OH	OH	Spegazzinidine
d	OMe	OMe	

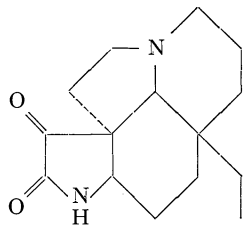

IV

Compound		R_1	R_3	R_4	R_2 = OH $[\alpha]_D$	R_2 = OMe $[\alpha]_D$	Reference
I	*a, b*	OMe	Ac	CH_3	+140°	−94°	(1)
	c, d	H	Ac	CH_3	+132°*	−93°	(9)
	e	OH	Ac	CH_3	+125		(1, 10)
	f	H	EtCO	CH_3		−86°	(11)
	g	H	HCO	CH_3		−91°†	(12)
	h	OMe	EtCO	CH_3	+133°		(13)
	i	H	Ac	CO_2Me		−122°	(2)
	j	H	PhCH=CHCO	CO_2Me		−181°	(14)
	k	H	EtCO	CH_2OH	+108°		(15)
II	*a, b*	—	Ac	—	+174°	+10°‡	(10, 16)
	c, d	—	EtCO	—	+164°	+9°‡	(10, 16)
III	*a, b*	H	—	—	+176°	−136°	(17)
	c	OH	—	—	+186°		(17)
	d	OMe	—	—		−156°	(17)
I	*o*	OMe	H	CH_3		−5°	(1)
	p, q	H	H	CH_3	+16°† +25°	+3°	(9, 17)
						R_2=OAc	
I	*l*	OMe	Ac	CH_3		−8°	(1)
	m	OAc	Ac	CH_3		+10°	(1)
	n	H	Ac	CH_3		+24°*	

*See experimental section.
†In EtOH.
‡In MeOH.
NOTE: All rotations are for $CHCl_3$ solutions unless otherwise indicated.

EXPERIMENTAL

O-Acetyl-O-demethylaspidospermine

Aspidospermine (Inland Alkaloid Co.) (0.616 g) was treated successively with hydrobromic acid and acetic anhydride by the method described for the preparation of O,O-diacetyl-O-demethylaspidocarpine (1). The isolation of the product was also the same as for the aspidocarpine derivative. The crude residue (0.550 g) was recrystallized from a mixture of hexane and acetone, and formed a product (0.478 g), m.p. 155–157°, which, on further recrystallization from the same solvent, was obtained as fine white rods, m.p. 157–158°, $[\alpha]_D^{25}$ +24.3° (*c*, 1.03; $CHCl_3$); infrared (chloroform), 1760(s), 1662(s) cm^{-1}.

Witkop (18) has obtained this compound, which he describes as birefringent prisms, m.p. 158–158.5° by a lightly different technique. His published spectral data correspond closely with the spectrum of our material.

O-Demethylaspidospermine

O-Acetyl-O-demethylaspidospermine (79 mg) was dissolved in methanol (5 ml) to which was added 20% aqueous sodium hydroxide (0.5 ml) and partial hydrolysis carried out in the manner described for the preparation of O-demethylaspidocarpine (1). The crude product (46 mg) was recrystallized with difficulty from hexane and obtained as white prisms, m.p. 120–131°. Anal. Calc. for $C_{21}H_{28}N_2O_2$: C, 74.08; H, 8.28.

Can. J. Chem. Downloaded from www.nrcresearchpress.com by 210.87.254.105 on 09/05/12
For personal use only.

Found: C, 74.23; H, 8.21. $[\alpha]_D^{25}$ +132° (*c*, 0.37; $CHCl_3$). Infrared ($CHCl_3$), 1634(s) cm^{-1}; no OH absorption apparent (compare with aspidocarpine (1); the spectrum is very similar to that of aspidocarpine, but the latter has an additional strong peak at 1080 cm^{-1}).

Witkop (18) has prepared this compound by a different technique, but he failed to obtain it crystalline. However, the infrared characteristics which he describes appear to confirm the identity of the two products.

ACKNOWLEDGMENT

The experimental part of this work was carried out during tenure of a postdoctoral fellowship at the National Research Council, Ottawa.

1. S. McLean, K. Palmer, and L. Marion. Can. J. Chem. **38**, 1547 (1960).
2. C. Djerassi, B. Gilbert, J. N. Shoolery, L. F. Johnson, and K. Biemann. Experientia, **17**, 162 (1961). C. Djerassi, A. A. P. G. Archer, T. George, B. Gilbert, and L. D. Antonaccio. Tetrahedron, **16**, 212 (1961).
3. S. McLean. Can. J. Chem. **38**, 2278 (1960).
4. K. Biemann, M. Spiteller-Friedmann, and G. Spiteller. J. Am. Chem. Soc. **85**, 631 (1963).
5. K. L. Williamson and W. S. Johnson. J. Am. Chem. Soc. **83**, 4623 (1961). F. A. L. Anet. J. Am. Chem. Soc. **84**, 1053 (1962).
6. L. M. Jackman. Application of nuclear resonance spectroscopy in organic chemistry. Pergamon Press, London. 1959. p. 124.
7. F. A. L. Anet. Can. J. Chem. **41**, 883 (1963).
8. J. H. Brewster. J. Am. Chem. Soc. **81**, 5475 (1959).
9. A. J. Ewins. J. Chem. Soc. **105**, 2738 (1914).
10. C. Ferrari, S. McLean, L. Marion, and K. Palmer. Can. J. Chem. **41**, 1531 (1963).
11. W. I. Taylor, N. Raab, H. Lehner, and J. Schmutz. Helv. Chim. Acta, **45**, 2260 (1962).
12. E. Schlittler and M. Rottenberg. Helv. Chim. Acta, **31**, 446 (1948).
13. M. Pinar and H. Schmid. Helv. Chim. Acta, **45**, 1283 (1962).
14. C. Djerassi, A. A. P. G. Archer, T. George, B. Gilbert, J. N. Shoolery, and L. F. Johnson. Experientia, **16**, 532 (1960).
15. M. Pinar, W. von Phillipsborn, W. Vetter, and H. Schmid. Helv. Chim. Acta, **45**, 2260 (1962).
16. C. Djerassi, L. D. Antonaccio, H. Budzikiewicz, J. M. Wilson, and B. Gilbert. Tetrahedron Letters, 1001 (1962).
17. O. O. Orazi, R. A. Corral, J. S. F. Holker, and C. Djerassi. J. Org. Chem. **21**, 979 (1956). C. Djerassi, H. W. Brewer, H. Budzikiewicz, O. O. Orazi, and R. A. Corral. J. Am. Chem. Soc. **84**, 3480 (1962).
18. B. Witkop and J. B. Patrick. J. Am. Chem. Soc. **76**, 5603 (1959).

Received August 26, 1963.
Department of Chemistry,
University of Toronto,
Toronto 5, Ontario.

Can. J. Chem. Downloaded from www.nrcresearchpress.com by 210.87.254.105 on 09/05/12
For personal use only.

ION–MOLECULE REACTIONS STUDIED BY TIME-OF-FLIGHT MASS SPECTROMETRY

Clifford W. Hand and Hanns von Weyssenhoff

Many reactions between ions and molecules in the gas phase have been studied during the last ten years; this field has been extensively reviewed by Lampe, Franklin, and Field (1), and by Talroze (2). The usual experimental method (1) of obtaining rate constants for such reactions has been to operate a mass spectrometer at relatively high pressure (10^{-4}–10^{-1} Torr.) in the source region. The primary ions (those formed by electron impact in the mass spectrometer) undergo reactive collisions with neutral species as they pass from their point of formation to the exit slit under the influence of the electric field. The average residence time of an ion in the high pressure source region can be calculated from a knowledge of the source geometry and the electric field; the rate constant for the reaction under investigation is then obtained from the residence time, the experimentally determined pressure, and the ion currents measured at the detector.

Found: C, 74.23; H, 8.21. $[\alpha]_D^{25}$ +132° (*c*, 0.37; $CHCl_3$). Infrared ($CHCl_3$), 1634(s) cm^{-1}; no OH absorption apparent (compare with aspidocarpine (1); the spectrum is very similar to that of aspidocarpine, but the latter has an additional strong peak at 1080 cm^{-1}).

Witkop (18) has prepared this compound by a different technique, but he failed to obtain it crystalline. However, the infrared characteristics which he describes appear to confirm the identity of the two products.

ACKNOWLEDGMENT

The experimental part of this work was carried out during tenure of a postdoctoral fellowship at the National Research Council, Ottawa.

1. S. McLean, K. Palmer, and L. Marion. Can. J. Chem. **38**, 1547 (1960).
2. C. Djerassi, B. Gilbert, J. N. Shoolery, L. F. Johnson, and K. Biemann. Experientia, **17**, 162 (1961). C. Djerassi, A. A. P. G. Archer, T. George, B. Gilbert, and L. D. Antonaccio. Tetrahedron, **16**, 212 (1961).
3. S. McLean. Can. J. Chem. **38**, 2278 (1960).
4. K. Biemann, M. Spiteller-Friedmann, and G. Spiteller. J. Am. Chem. Soc. **85**, 631 (1963).
5. K. L. Williamson and W. S. Johnson. J. Am. Chem. Soc. **83**, 4623 (1961). F. A. L. Anet. J. Am. Chem. Soc. **84**, 1053 (1962).
6. L. M. Jackman. Application of nuclear resonance spectroscopy in organic chemistry. Pergamon Press, London. 1959. p. 124.
7. F. A. L. Anet. Can. J. Chem. **41**, 883 (1963).
8. J. H. Brewster. J. Am. Chem. Soc. **81**, 5475 (1959).
9. A. J. Ewins. J. Chem. Soc. **105**, 2738 (1914).
10. C. Ferrari, S. McLean, L. Marion, and K. Palmer. Can. J. Chem. **41**, 1531 (1963).
11. W. I. Taylor, N. Raab, H. Lehner, and J. Schmutz. Helv. Chim. Acta, **45**, 2260 (1962).
12. E. Schlittler and M. Rottenberg. Helv. Chim. Acta, **31**, 446 (1948).
13. M. Pinar and H. Schmid. Helv. Chim. Acta, **45**, 1283 (1962).
14. C. Djerassi, A. A. P. G. Archer, T. George, B. Gilbert, J. N. Shoolery, and L. F. Johnson. Experientia, **16**, 532 (1960).
15. M. Pinar, W. von Phillipsborn, W. Vetter, and H. Schmid. Helv. Chim. Acta, **45**, 2260 (1962).
16. C. Djerassi, L. D. Antonaccio, H. Budzikiewicz, J. M. Wilson, and B. Gilbert. Tetrahedron Letters, 1001 (1962).
17. O. O. Orazi, R. A. Corral, J. S. F. Holker, and C. Djerassi. J. Org. Chem. **21**, 979 (1956). C. Djerassi, H. W. Brewer, H. Budzikiewicz, O. O. Orazi, and R. A. Corral. J. Am. Chem. Soc. **84**, 3480 (1962).
18. B. Witkop and J. B. Patrick. J. Am. Chem. Soc. **76**, 5603 (1959).

Received August 26, 1963.
Department of Chemistry,
University of Toronto,
Toronto 5, Ontario.

Can. J. Chem. Downloaded from www.nrcresearchpress.com by 210.87.254.40 on 09/05/12
For personal use only.

ION–MOLECULE REACTIONS STUDIED BY TIME-OF-FLIGHT MASS SPECTROMETRY

Clifford W. Hand and Hanns von Weyssenhoff

Many reactions between ions and molecules in the gas phase have been studied during the last ten years; this field has been extensively reviewed by Lampe, Franklin, and Field (1), and by Talroze (2). The usual experimental method (1) of obtaining rate constants for such reactions has been to operate a mass spectrometer at relatively high pressure (10^{-4}–10^{-1} Torr.) in the source region. The primary ions (those formed by electron impact in the mass spectrometer) undergo reactive collisions with neutral species as they pass from their point of formation to the exit slit under the influence of the electric field. The average residence time of an ion in the high pressure source region can be calculated from a knowledge of the source geometry and the electric field; the rate constant for the reaction under investigation is then obtained from the residence time, the experimentally determined pressure, and the ion currents measured at the detector.

Can. J. Chem. Downloaded from www.nrcresearchpress.com by 210.87.254.40 on 09/05/12
For personal use only.

We have developed a method in which time, rather than pressure or potential gradient, is the experimental variable. The basic instrument is a Bendix Model 14 time-of-flight mass spectrometer which has been modified as follows. *1.* A stainless steel box of dimensions 1.5 in.$\times$1.5 in$\times$0.240 in. was constructed around the ion source region, forming a reaction chamber with the short side parallel to the ion trajectories. The chamber is provided with a 0.1 in. diameter ion exit orifice, 0.030 in.$\times$0.200 in. electron beam entrance and exit slits, a 0.125 in. diameter gas inlet tube, and a 0.250 in. diameter orifice for pressure measurement. An auxilliary 6 in. diffusion pump was installed so that the source region could be differentially pumped. The instrument can be operated with up to 0.080 Torr. in the source region, while the pressure in the rest of the instrument remains less than 2×10^{-5} Torr. Pressures in the source region are measured with a McLeod gauge and (or) a Consolidated micromanometer. *2.* A delay circuit (available from the Bendix Corp. as the Time Lag Focus Modification) was provided to allow the introduction of a variable and accurately known delay between the ionizing electron pulse and the pulse which withdraws the ions for analysis. Thus primary ions formed in the electron beam react for a known time at thermal velocities in a field-free space.

To test the method we have reinvestigated the reaction $CH_4^+ + CH_4 = CH_5^+ + CH_3$. With the usual assumptions that competitive and consecutive reactions are negligible (3), that the ions CH_4^+ and CH_5^+ are collected by the detector with equal efficiency, and that these ions are lost at equal rates by neutralization at the walls and by flow out of the reaction chamber, the kinetic equation may be integrated to

$$\log_{10}(I_{16}+I_{17})/I_{16} = k[CH_4]t/2.303,$$

where I_m is the measured intensity of the ion current of mass m, k is the bimolecular rate constant, and t is the time.

Figure 1 shows a typical plot of $\log(I_{16}+I_{17})/I_{16}$ vs. time between formation and

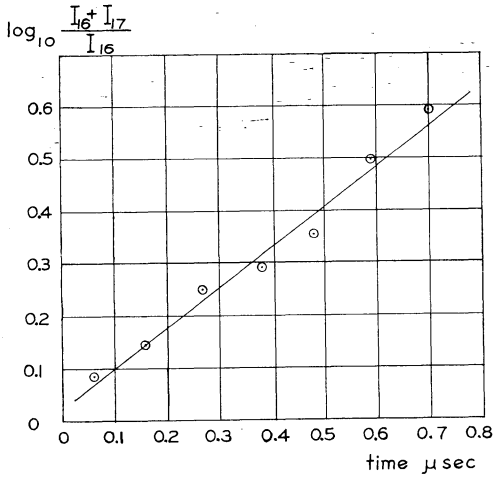

FIG. 1. $\log_{10}(I_{16}+I_{17})/I_{16}$ vs. time. Source pressure 0.049 Torr. $k = 10.3\times10^{-10}$ cc/molecule-sec.

analysis of the ions; the data were obtained at a source pressure of 0.049 Torr. and result in a rate constant of $k = 10.3\times10^{-10}$ cc/molecule-sec. Table I shows rate constants for this reaction determined at various pressures. The average value of the rate constant, 11×10^{-10} cc/molecule-sec, is in good agreement with the value $k = 8.9\times10^{-10}$ cc/molecule-sec, obtained by Franklin, Field, and Lampe (3), over a pressure range of 10^{-4}–10^{-2}

TABLE I

Pressure (Torr.$\times 10^3$)	k (cc/molecule-sec$\times 10^{10}$)
3.4	12.3
3.8	14.7
8	13.5
10	7.0
17	9.5
19	9.95
25	11.2
49	10.3
Average	11.1

Torr. Talroze (4), using a pulse technique similar to ours but with a conventional rather than a time-of-flight instrument, obtained $k = 11.6\times10^{-10}$ cc/molecule-sec over a pressure range 10^{-4}–10^{-3} Torr.

In view of the good agreement with the literature we feel that the method represents a valuable addition to the tools available for study of ion–molecule reactions.

1. F. W. Lampe, J. L. Franklin, and F. H. Field. Progress in reaction kinetics. Vol. 1. Pergamon Press, New York. 1961. p. 67.
2. V. I. Talroze. Pure Appl. Chem. **5**, 455 (1962).
3. F. H. Field, J. L. Franklin, and F. W. Lampe. J. Am. Chem. Soc. **79**, 2419 (1957).
4. V. I. Talroze. Izv. Akad. Nauk SSSR, Otd. Khim. Nauk, 1351 (1959); Chem. Abstr. **53**, 21184e (1959).

Received July 30, 1963.
Jet Propulsion Laboratory,
California Institute of Technology,
Pasadena, California, U.S.A.

A REMARK ON THE ULTRAVIOLET SPECTRUM OF CHRYSENE

P. Sauvageau and C. Sandorfy

It has been shown previously (1, 2, 3) by the measurement of low-temperature absorption spectra and fluorescence spectra of benzo[*a*]anthracene derivatives (1,2-benzanthracene in the old nomenclature) that in the case of this molecule the two longest wavelength electronic band systems (α and p according to Clar's nomenclature) overlap to a large extent so that the α-band system continues amongst or underneath the bands belonging to the p-band system.

The work of Jones and Spinner (4, 5) on anthracene, phenanthrene, and benzo[*c*]-phenanthrene (3,4-benzophenanthrene in the old nomenclature) did not yield similar results and it was suggested (3) that such a situation is likely to occur only with molecules intermediate between the "long field" and "round field" type (6) where the p-band system approached very closely but did not entirely overtake the α-band system. The lack of a good mirror-image relationship between the absorption and fluorescence spectra of chrysene (7) seemed to indicate that this molecule is of this type. We have therefore measured the absorption spectra at 83° K (in a 6:1 mixture of isopentane and 3-methylpentane) and the fluorescence spectra (in cyclohexane solution) of chrysene (Fig. 1),

Can. J. Chem. Downloaded from www.nrcresearchpress.com by 210.87.254.40 on 09/05/12
For personal use only.

TABLE I

Pressure (Torr.$\times 10^3$)	k (cc/molecule-sec$\times 10^{10}$)
3.4	12.3
3.8	14.7
8	13.5
10	7.0
17	9.5
19	9.95
25	11.2
49	10.3
Average	11.1

Torr. Talroze (4), using a pulse technique similar to ours but with a conventional rather than a time-of-flight instrument, obtained $k = 11.6\times10^{-10}$ cc/molecule-sec over a pressure range 10^{-4}–10^{-3} Torr.

In view of the good agreement with the literature we feel that the method represents a valuable addition to the tools available for study of ion–molecule reactions.

1. F. W. Lampe, J. L. Franklin, and F. H. Field. Progress in reaction kinetics. Vol. 1. Pergamon Press, New York. 1961. p. 67.
2. V. I. Talroze. Pure Appl. Chem. **5**, 455 (1962).
3. F. H. Field, J. L. Franklin, and F. W. Lampe. J. Am. Chem. Soc. **79**, 2419 (1957).
4. V. I. Talroze. Izv. Akad. Nauk SSSR, Otd. Khim. Nauk, 1351 (1959); Chem. Abstr. **53**, 21184e (1959).

Received July 30, 1963.
Jet Propulsion Laboratory,
California Institute of Technology,
Pasadena, California, U.S.A.

A REMARK ON THE ULTRAVIOLET SPECTRUM OF CHRYSENE

P. Sauvageau and C. Sandorfy

It has been shown previously (1, 2, 3) by the measurement of low-temperature absorption spectra and fluorescence spectra of benzo[*a*]anthracene derivatives (1,2-benzanthracene in the old nomenclature) that in the case of this molecule the two longest wavelength electronic band systems (α and p according to Clar's nomenclature) overlap to a large extent so that the α-band system continues amongst or underneath the bands belonging to the p-band system.

The work of Jones and Spinner (4, 5) on anthracene, phenanthrene, and benzo[*c*]-phenanthrene (3,4-benzophenanthrene in the old nomenclature) did not yield similar results and it was suggested (3) that such a situation is likely to occur only with molecules intermediate between the "long field" and "round field" type (6) where the p-band system approached very closely but did not entirely overtake the α-band system. The lack of a good mirror-image relationship between the absorption and fluorescence spectra of chrysene (7) seemed to indicate that this molecule is of this type. We have therefore measured the absorption spectra at 83° K (in a 6:1 mixture of isopentane and 3-methylpentane) and the fluorescence spectra (in cyclohexane solution) of chrysene (Fig. 1),

Can. J. Chem. Downloaded from www.nrcresearchpress.com by 210.87.254.5 on 09/05/12
For personal use only.

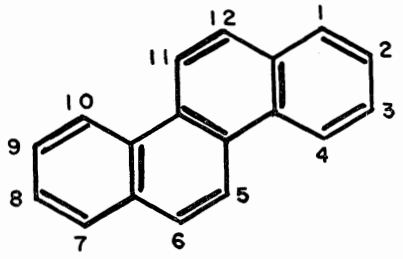

FIG. 1. The numbering of carbon atoms in the chrysene molecule.

5-methyl-, 6-methyl-, and 5,6-dimethyl-chrysene, samples of which were made available to us by Professor M. S. Newman of Ohio State University.

Only the results for 6-methylchrysene (Fig. 2) will be discussed here but the observations made on the other compounds were essentially the same.

1. The low-temperature absorption spectrum shows a somewhat improved resolution of the vibrational fine structure with respect to the room temperature spectrum but it does not give any significant new indications.

2. Taking the first apparent peak (of lowest and highest frequency respectively) for the 0–0 band in both the absorption of fluorescence spectra we find that they are shifted with respect to each other by 383 cm^{-1} for 6-methyl-, 144 cm^{-1} for 5-methyl-, and 407 cm^{-1} for 5,6-dimethyl-chrysene. Schoental and Scott (7) found 150 cm^{-1} for chrysene itself. These differences tend to be greater than for most other aromatic hydrocarbons.

3. The spacing between the main peaks is of the order of 1350 to 1400 cm^{-1} for the α- (and p-) band systems in absorption but only about 1150 to 1200 cm^{-1} in fluorescence where the bands are broader.

4. While the apparent spread of the weak α-band system is only about 2000 cm^{-1} in absorption, in fluorescence it is about 4000 cm^{-1} where four main peaks are observed

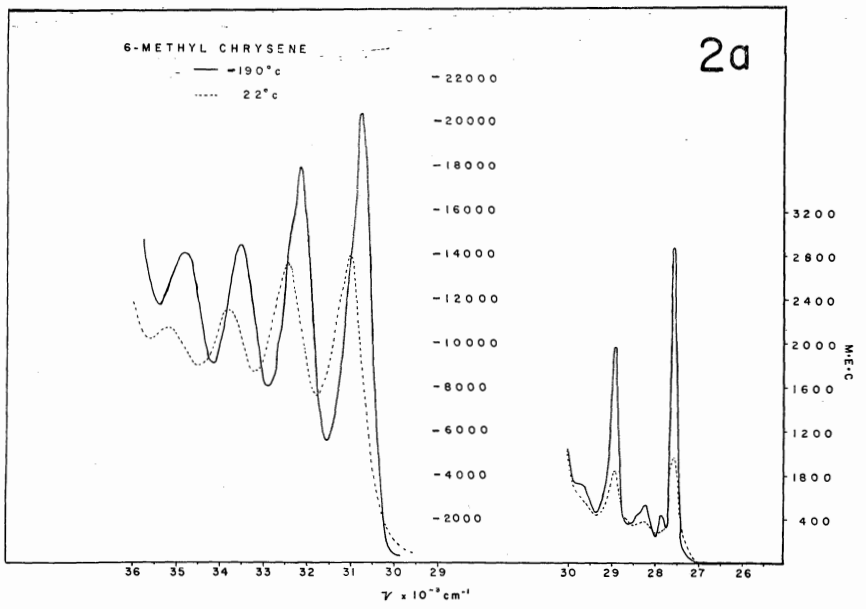

Can. J. Chem. Downloaded from www.nrcresearchpress.com by 210.87.254.5 on 09/05/12
For personal use only.

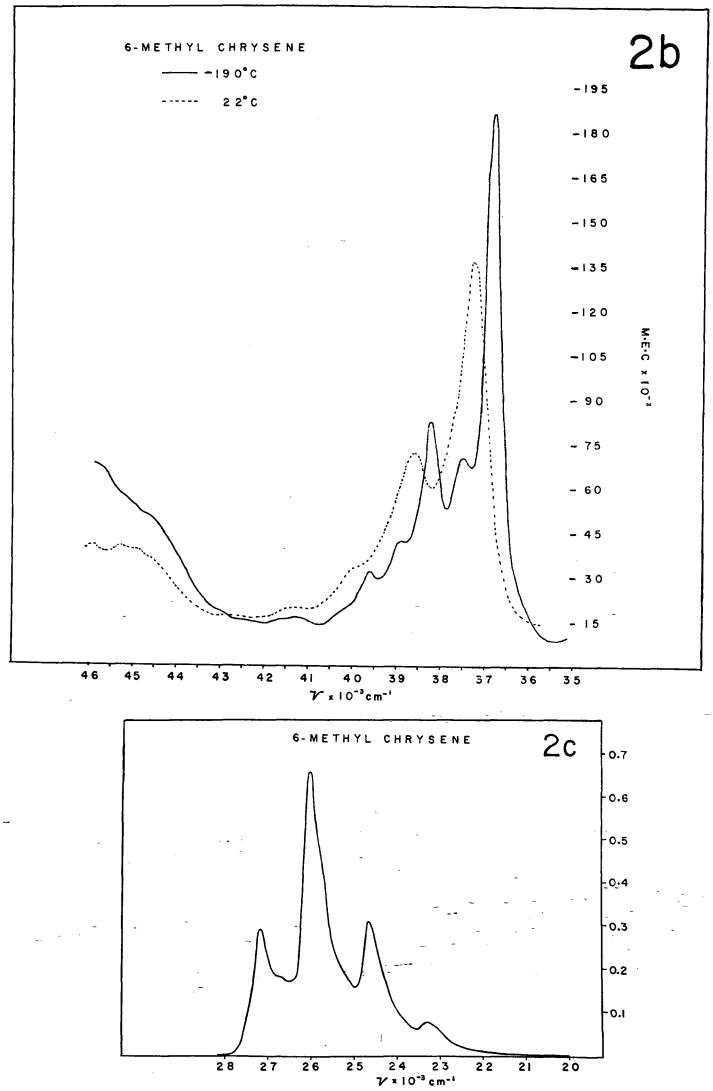

FIG. 2. (*a*) and (*b*) The ultraviolet absorption spectrum of 6-methylchrysene in a 6:1 mixture of isopentane and 3-methylpentane. Wave numbers against molecular extinction coefficients: - - - (*c*) The fluorescence spectrum of 6-methylchrysene at 21° C in cyclohexane solution. Wave numbers vs. arbitrary units.

against two in absorption. (For 6-methylchrysene the related wave numbers are, in cm^{-1}, fluorescence: 27196, 26042, 24661, 23256; absorption (−190° C): 27578, 28943.)

We conclude from these observations that, as expected, the case of chrysene is similar to that of benzo[*a*]anthracene inasmuch as the α- and p-band systems overlap to an appreciable extent, a part of the bands of the α-system being hidden below the bands of the p-band system. The extent of this overlapping is lesser, however, than in the case of benzo[*a*]anthracene. It may be concluded too that in the first excited singlet state the chrysene molecule differs more from its ground state than do most other aromatic molecules.

Experimental details and further references were given in paper (3).

Can. J. Chem. Downloaded from www.nrcresearchpress.com by 210.87.254.5 on 09/05/12
For personal use only.

Our sincere thanks are due to Professor M. S. Newman, who kindly provided us with the samples of the compounds whose spectra are discussed in this note.

We acknowledge financial support of the National Research Council of Canada and of the Petroleum Research Fund of the American Chemical Society.

1. C. SANDORFY and R. N. JONES. Can. J. Chem. **34**, 888 (1956).
2. R. N. JONES and C. SANDORFY. NRC (Natl. Res. Council) Can. Bull. 4 (1956).
3. J. L. PATENAUDE, P. SAUVAGEAU, and C. SANDORFY. Spectrochim. Acta, **18**, 241 (1962).
4. R. N. JONES and E. SPINNER. Spectrochim. Acta, **16**, 1060 (1960).
5. R. N. JONES and E. SPINNER. NRC (Natl. Res. Council) Can. Bull. 8 (1960).
6. H. C. LONGUET-HIGGINS, C. W. RECTOR, and J. R. PLATT. J. Chem. Phys. **18**, 1174 (1950).
7. R. SCHOENTAL and E. J. Y. SCOTT. J. Chem. Soc. 1683 (1949).

RECEIVED SEPTEMBER 13, 1963.
DÉPARTEMENT DE CHIMIE,
UNIVERSITÉ DE MONTRÉAL,
MONTRÉAL, QUÉBEC.

Can. J. Chem. Downloaded from www.nrcresearchpress.com by 210.87.254.5 on 09/05/12
For personal use only.

Can. J. Chem. Downloaded from www.nrcresearchpress.com by 210.87.254.105 on 09/05/12
For personal use only.

Canadian Journal of Chemistry

Issued by THE NATIONAL RESEARCH COUNCIL OF CANADA

VOLUME 42 FEBRUARY 1964 NUMBER 2

DOUBLE-MINIMUM POTENTIAL FOR INTRAMOLECULARLY HYDROGEN-BONDED PROTONS IN ORTHO-SUBSTITUTED ANILINES[1]

P. J. KRUEGER

Department of Chemistry, University of Alberta, Calgary, Alberta

Received August 12, 1963

ABSTRACT

The concentration and temperature-independent splitting of the first overtone NH_2 symmetric stretching band in 31 ortho-substituted anilines in which intramolecular hydrogen bonding is possible is interpreted in terms of a double-minimum potential for the hydrogen bonded proton. The intensity ratio of the doublet and the extent of the splitting is related to the basicity of the ortho-substituent, modified by the rigid geometrical restrictions of the intramolecular system. The absence of band splitting in the corresponding fundamental mode suggests that the secondary minimum lies in the vicinity of the $v = 2$ vibrational level. The antisymmetric mode appears to be less sensitive to perturbations.

Deuteration studies, the spectra of some *o*-substituted *N*-methyl anilines, and the first overtone bands of *N*-methyl aniline in very basic solvents support these views.

INTRODUCTION

Among the many contributions that have been made to our present understanding of the nature of hydrogen bonding (1, 2) there has recently been considerable support for the idea that the motion of the proton in an A—H···B system may be governed by a potential-energy function with two minima separated by a low barrier. This is represented schematically in Fig. 1(*a*) for a symmetrical hydrogen bond where the two minima have

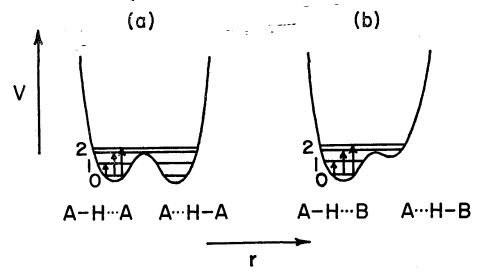

FIG. 1. Schematic representation of double-minimum potentials for hydrogen bonded protons where proton tunnelling (or a resonance splitting) occurs at the vibrational level $v = 2$. (*a*) Symmetric double-minimum potential. (*b*) Asymmetric double-minimum potential.

equal depth, and in Fig. 1(*b*) for the more common situation where the proton would always remain more firmly bonded to A than to B. Both sketches show the intermediate barrier height in the region of the $v = 2$ vibrational level. A potential system such as that in Fig. 1(*a*), where the minima are of sufficiently equal energy so that the lowest energy

[1]*Paper presented at the 46th Annual Conference of the Chemical Institute of Canada, Toronto, Ontario, June 6–8, 1963.*

levels of both are appreciably populated at room temperature, is applicable to tautomeric equilibria. This paper deals with unsymmetrical double-minimum potentials in some intramolecular systems.

Not only does the double-minimum concept have a sound theoretical basis (3, 4), but Bell and Barrow (5) presented the first experimental verification in 1959 by showing that the first and second overtone OH bands in ethanol and phenol in solvents of various proton-accepting abilities show a pair of solvent-dependent absorption bands. The observed spectra were held to arise from a potential energy function in which the second minimum lies in the region of the $v = 2$ vibrational level. It was shown that the height of the second potential minimum depends on the hydrogen bonding strength of the alcohol and on the acceptor strength of the solvent. In strongly basic solvents the higher overtones were characteristic of a broad potential well. Subsequent work by Bell and Barrow (6) showed that in phenol-*d* and *p*-nitrophenol-*d* the splitting of the fundamental OD stretching bands could be interpreted in terms of a second low-lying potential minimum and its effect on the $v = 0$ and $v = 1$ levels. For *p*-nitrophenol-*d* and very strong bases in non-dissociating solvents tautomeric equilibria between proton transferred and nonproton transferred species were found.

Pshenichnov and Sokolov (7) concluded independently that hydrogenic band splitting of the type observed could be interpreted in terms of quantum effects near the top of the barrier in double-minimum potential curves. Further, Bratoz and Hadzi (8) found that a potential energy surface with two minima for hydrogen bonded molecules occasionally played a significant part in the consistent interpretation of their spectra. On this basis doubling of the OH fundamental stretching band in the infrared spectra of carboxylic acids in pyridine solution has been ascribed to tunnelling of the proton between interacting double minima separated by a small barrier (9).

The detailed results of a general solution for the case of a proton moving in a potential field of two equal minima, given by Blinc and Hadzi (10), cover a wide range of physically possible parameters. The same authors have also described (11) the quantum-mechanical treatment of the case of two unequal minima, and interpreted the complex spectra in the OH stretching region for a number of ferroelectric compounds in the solid phase on the basis of proton tunnelling. By using the temperature dependence of resonance line widths in the proton magnetic resonance spectra of solid substances containing very short hydrogen bonds, Hadzi *et al.* (12, 13, 14) have demonstrated that the band splitting in infrared spectra is supported, and that the protons are either tunnelling between two minima of potential energy (e.g., in potassium hydrogen bis-*p*-nitrobenzoate) or that they are symmetrically situated midway between the electronegative atoms and are not moving appreciably (e.g., in potassium hydrogen bis-phenylacetate). The classification of the compounds investigated into these two categories could not be related simply to the length of the hydrogen bond; for compounds with an O···O distance of about 2.5 Å, where the potential barrier separating the minima should disappear and a flat single-bottomed type of curve should be attained, according to Reid's model (15), examples of both classes coexist.

There are obvious dangers inherent in the interpretation of experimentally observed doubling of hydrogenic stretching bands in infrared spectra of hydrogen bonded solids in terms of double-minimum potentials, as Somorjai and Hornig (16) have pointed out. They emphasize the necessity for obtaining sufficient experimental evidence, since it is well recognized that crystalline forces may play a large role in determining the potentials for hydrogen-bonded protons in the solid state (17).

Can. J. Chem. Downloaded from www.nrcresearchpress.com by 210.87.254.105 on 09/05/12
For personal use only.

Can. J. Chem. Downloaded from www.nrcresearchpress.com by 210.87.254.105 on 09/05/12
For personal use only.

In his review of the status of the double-minimum potential concept in interpreting experimental data Barrow (18) has shown that the relative heights of the potential minima can be correlated semiquantitatively with the pK_a values of the acids and bases involved.

To date there appears to have been no systematic study of infrared band splitting which may arise because of double-minimum potentials for intramolecularly hydrogen bonded protons, although Hambly (19) has suggested that the splitting of the first overtone symmetric NH_2 stretching vibration, first observed by Whetsel (20) for *o*-nitroaniline and *o*-phenylmethylsulphone in dilute CCl_4 solution, may arise from this phenomenon. Recent work in this laboratory has shown that a doubling of the first overtone symmetric NH_2 stretching band occurs in all ortho-substituted anilines where intramolecular NH···X hydrogen bonding is conceivable (21). No splitting is observed in the fundamental symmetric and antisymmetric NH_2 stretching bands in these compounds (22). The overtone data have now been amplified, and the suggestion is made that a second potential minimum lying at approximately the level $v = 2$, and with a low potential barrier, may indeed be responsible. The intramolecular hydrogen bond may actually be favorable for the experimental observation of this phenomenon because of the relatively fixed molecular geometry, and the absence of factors like the continuum of lattice vibrations which broaden each transition in the spectra of hydrogen bonded crystals (16). It is also well known that bands arising from intramolecularly hydrogen-bonded systems tend to be narrower than analogous intermolecularly hydrogen-bonded bands. Intramolecular systems may lead to more refined calculations on the nature of the potential function since the A—H···B distance is known. As Barrow (18) has pointed out, the lack of knowledge of the AB distance in intermolecular hydrogen bonds is a major obstacle in such calculations.

EXPERIMENTAL

The experimental details have been described for measurements in both the fundamental and overtone regions (21, 22). The compounds used were largely commercial materials purified by fractional distillation, recrystallization, or vacuum sublimation. A few were synthesized by standard methods described in the literature. Commercial spectroscopic quality solvents were employed. For spectra in the fundamental region the aniline concentrations were kept down below 0.01 *M*; in the first overtone region they were below 0.07 *M* in CCl_4. Overtone spectra in other solvents had to be obtained at higher concentrations. These are given in the captions to Figs. 5 and 6.

Table I lists the experimental data relevant to this discussion.

RESULTS AND DISCUSSION

The composite Fig. 2 shows the ν_{01} and ν_{02} NH_2 stretching band contours observed for:

(*a*) a typical *o*-substituted aniline with a small "inert" substituent (*o*-$CH_3C_6H_4NH_2$),

(*b*) a typical *m*- or *p*-substituted aniline (*m*-$BrC_6H_4NH_2$),

(*c*) a typical *o*-substituted aniline with a relatively weak NH····X bond (*o*-$IC_6H_4NH_2$),

(*d*) a typical *o*-substituted aniline with a moderately strong NH····X bond (*o*-$NO_2C_6H_4NH_2$), and

(*e*) a typical *o*-substituted aniline with a very strong NH····X bond (*o*-$COCH_3C_6H_4NH_2$).

The most significant feature is that although the resolution of a grating spectrophotometer (Beckman IR-7, slit width ~2 cm^{-1}) does not resolve either the symmetric or antisymmetric ν_{01} bands into components, the lower resolution of the near infrared quartz prism instrument (Beckman DK-1A) shows that the symmetric ν_{02} band is a doublet where the possibility of NH···X bonding exists, and that in general the separation

TABLE I

Doublet symmetric first overtone NH_2 stretching bands in *o*-substituted anilines with intramolecular NH···X bonds (measurements in dilute CCl_4 solution)

No.	Substituent(s)	Doublet separation (cm^{-1})	Absorbance ratio (low/high frequency component)
1	2-C_6H_5	33	9.3
2	2-OCH_3	46	16.8
3	2,5-di-OCH_3	46	12.8
4	2,5-di-OCH_2CH_3	46	14.0
5	2-OCH_2CH_3	47	16.8
6	2-CN	(47)[a]	—
7	2-F	52	12.4
8	2,6-di-$COOCH_3$	(52)[b]	—
9	2-Br	53 (49)[a]	1.9
10	2,6-di-NO_2	53	1.4
11	2,4-di-Br-6-Cl	(53)[b]	—
12	2,4-di-Cl	58	5.1
13	2,4,6-tri-Cl	58	5.7
14	2,4,6-tri-Br	61 (54)[b]	7.0
15	2,6-di-Cl-4-NO_2	61	3.3
16	2-I	67 (64)[a]	3.1
17	2-CF_3	67 (46)[c]	7.3
18	2-Cl	69 (44)[a]	5.7
19	2-SC_6H_5	(73)[d]	—
20	2-NH_2	98[e]	1.6
21	2-$SO_2CH_2CH_3$	104[d]	—
22	2-NO_2	106 (106)[f]	0.8
23	2-SO_2CH_3	(107)[f] (105)[d]	—
24	2-SCH_3	(107)[g]	—
25	2-SO_2-*i*-(C_3H_7)	(108)[d]	—
26	2,4-di-NO_2	120	0.8
27	2-$COOCH_3$	(154)[b]	—
28	2-$COOCH_2CH_3$	169 (160)[b]	0.4
29	2-COC_6H_5	(184)[b]	—
30	2-CHO	(232)[b]	—
31	2-$COCH_3$	254 (257)[b]	0.2

[a]Values from Hambly and O'Grady (23). Differences from present measurements may be due to methods employed to obtain positions of poorly resolved components. In this work the major band was reflected about the ordinate at the maximum and subtracted from the experimental curve to obtain the peak frequency and absorbance of the subsidiary band appearing as a shoulder.
[b]Values from Hambly and O'Grady (24).
[c]On the basis of deuteration studies Hambly and O'Grady (25) have proposed a repulsive interaction between the NH_2 and the adjacent CF_3 group. See text.
[d]Values from Hambly (19).
[e]Additional shoulder at 6603 cm^{-1} on high-frequency side of low-frequency component.
[f]Values from Whetsel (20).
[g]Values from Whetsel, Roberson, and Krell (26).

between the components increases and the apparent absorbance ratio (low-frequency component/high-frequency component) decreases dramatically as the NH···X interaction increases. The relationship between the doublet separation and the absorbance ratio is shown in Fig. 3, and appears to be asymptotic to both axes. As the NH···X interaction commences the intensity switches rapidly from one component into the other with only a slight increase in doublet separation. Infrared intensities are usually more sensitive to interaction effects than are vibrational frequencies. After the high frequency component predominates a further increase in the strength of the NH···X interaction alters the absorbance ratio little, but increases the doublet separation markedly.

Although the order in which the compounds are listed in Table I (increasing doublet separation) appears to be approximately that in which one would expect increasing hydrogen-bonding interaction between the NH_2 group and a single *o*-substituent, a precise correlation would have to take into account:

Can. J. Chem. Downloaded from www.nrcresearchpress.com by 210.87.254.105 on 09/05/12
For personal use only.

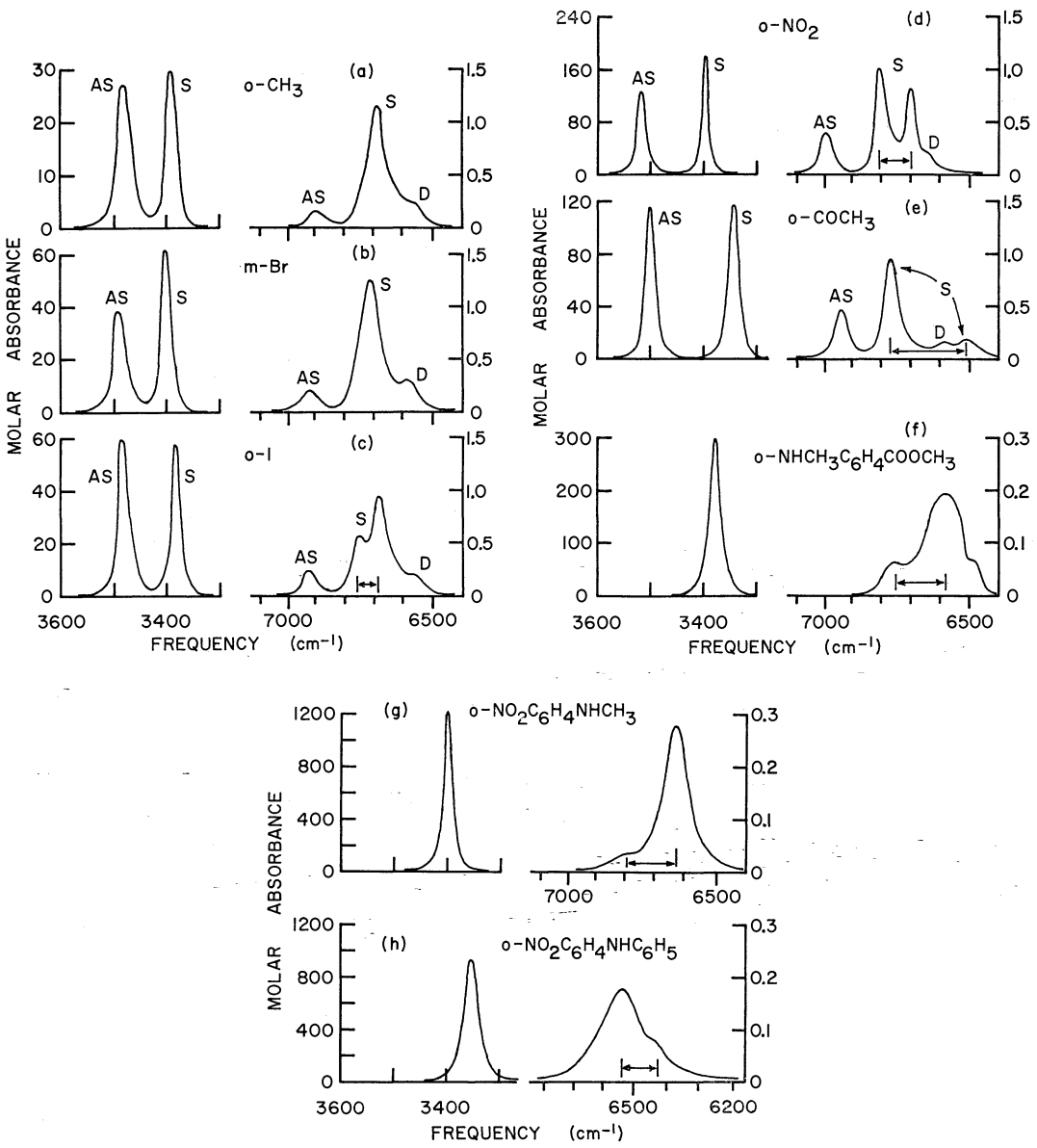

FIG. 2. Fundamental and first overtone NH bands for substituted anilines in CCl_4 solution. (*a*) *o*-Toluidine. (*b*) *m*-Bromoaniline. (*c*) *o*-Iodoaniline. (*d*) *o*-Nitroaniline. (*e*) *o*-Aminoacetophenone. (*f*) Methyl-*N*-methyl anthranilate. (*g*) *o*-Nitro-*N*-methylaniline. (*h*) *o*-Nitrodiphenylamine. AS = antisymmetric band; S = symmetric band; D = difference band.

(*a*) the acidity of the protons and the N—H distance as they reflect electronic effects of the substituent(s) through the aromatic ring system,

(*b*) the fixed NH···X geometry for each individual case (which may not be the optimum distance for hydrogen bonding, and may involve unusual angles), and

(*c*) other factors such as orbital–orbital repulsions (27), or other steric effects operating between adjacent groups.

Can. J. Chem. Downloaded from www.nrcresearchpress.com by 210.87.254.105 on 09/05/12
For personal use only.

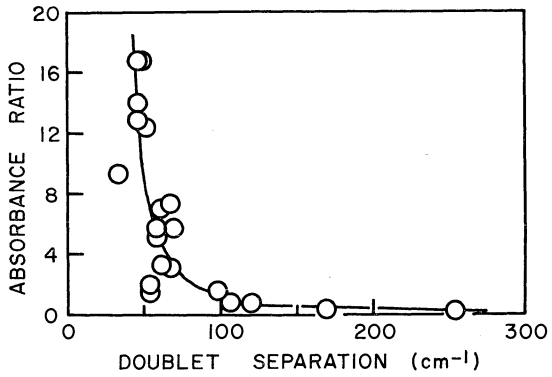

FIG. 3. Relationship of absorbance ratio in the first overtone symmetric mode doublet (low-frequency component/high-frequency component) to the doublet separation in *o*-substituted anilines.

Further, there are almost certainly factors operating in 2,6-disubstituted anilines which are not present in mono-2-substituted anilines. For example, Hambly and O'Grady (28) have shown on the basis of the failure to observe cis–trans isomerism of the NHD group in 2,4,6-trinitroaniline, a technique due to Moritz (29), that bilateral hydrogen bonding exists in this compound. Similar bilateral hydrogen bonding was suggested for 2,6-dicarbomethoxyaniline (24), and for 2,6-diiodo-4-methylaniline, but both the fundamental NH_2 stretching bands as well as the NH and ND bands of the NHD group in 2,6-dihalo-4-nitroanilines showed shoulders (23). Although Hambly and O'Grady suggest rotational isomerism with the NH_2 group rotated out of conjugation with the benzene ring because the two members of each of the stretching bands of the 2,6-dihalo-4-nitroanilines are respectively higher and lower than those of the corresponding 2,4,6-trihaloanilines, this may be band splitting observed in the fundamental region because of a secondary potential minimum in the $v = 1$ region in this particular compound. The effect of temperature on these spectra would probably decide between these two possibilities. With respect to twisting of the NH_2 group out of conjugation with the benzene ring, the work of Wepster (30) shows that even very bulky groups in the 2 and 6 positions do not appear to be capable of doing this.

A plot of the ν_{02} symmetric frequencies for a large number of *o*-, *m*-, and *p*-substituted anilines vs. the substituent σ values (see Fig. 3 of Ref. 21) shows that for weak proton acceptors like *o*-alkoxy groups the low-frequency component of the doublet lies close to the correlation line for *m*- and *p*-substituents while the high frequency component lies above it, but for substituents like 2-NH_2, 2-I, 2,4,6-tri-Br, 2-NO_2, 2,6-di-Cl-4-NO_2, and 2,4-di-NO_2 one component lies at a higher frequency and the other at a lower frequency than the general correlation. This suggests resonance separation of vibrational levels as a very likely cause of the doubling. Even if bilateral hydrogen bonding does not occur in all 2,6-di-*o*-substituted anilines both substituents would probably have a pronounced effect on the potential energy curves for the protons. A comparison of the symmetric ν_{02} band splitting for 2,6-dicarbomethoxyaniline (52 cm^{-1}) with that for methyl anthranilate (154 cm^{-1}), and the splitting for 2,6-dinitroaniline (53 cm^{-1}) with that for 2-nitroaniline (106 cm^{-1}) suggests that the intramolecular NH···O hydrogen bonds are weaker for bilaterally bonded NH_2 groups than they are if only one NH bond is involved (31).

In the overtone spectra a relatively weak absorption band is found in the approximate range 6560–6600 cm^{-1} for all anilines (band D in Fig. 2). This has tentatively been assigned

Can. J. Chem. Downloaded from www.nrcresearchpress.com by 210.87.254.105 on 09/05/12
For personal use only.

to a difference band involving the torsional vibration of the NH_2 group (23), although this may not prove to be entirely satisfactory. In ethyl anthranilate and *o*-aminoacetophenone the low-frequency component of the doublet is displaced downward sufficiently far as to overlap with the difference band, which led to early conclusions that the symmetric band was *single* in these compounds. With improved resolution the difference band and the low-frequency symmetric component can be resolved (Fig. 2(*e*)), the latter lying at a *lower* frequency than the difference band. This assignment is based on the solvent dependence of these frequencies; the low-frequency symmetric component shifts to higher frequency by 10–25 cm^{-1} on going from CCl_4 to $CHCl_3$, whereas the high-frequency component and the difference band lie at nearly the same positions respectively in these two solvents. Deuteration removes band D from this region of the spectrum (24).

The results of Whetsel (20) for *o*-nitroaniline and *o*-aminophenylmethylsulphone and the present measurements on ethyl anthranilate show that not only is the doublet separation decreased in the transition from CCl_4 to $CHCl_3$, but there is also a decrease in the relative intensity of the high frequency component. Both points strongly suggest that the intramolecular $HNH\cdots X$ interaction is weakened in $CHCl_3$ as might be expected because the H atom of chloroform complexes with the lone pair electrons of the amino N atom (32), thereby decreasing the acidity of the NH_2 protons as the sp^3 character of the N atom increases.

The basic criteria for a double-minimum potential for a hydrogen-bonded proton, with the second minimum at approximately the $v = 2$ level, appear to be as follows.

(1) No splitting of the ν_{01} hydrogenic stretching vibration, but a splitting of ν_{02}.
(2) A band splitting which is independent of concentration (to show that the effect originates in monomer species).
(3) An increase in the separation of the observed bands as the strength of the interaction increases.
(4) A strong dependence of the separation of the doublet on the mass of the hydrogen atom, i.e., a reduction on deuteration. Bell and Barrow (5, 6) have shown that the $v = 1$ or $v = 2$ level can be split only with a considerably stronger acid and base when deuterium rather than protium bonds are involved.
(5) A relative intensity in the doublet which is independent of isotopic substitution.
(6) A temperature-independent intensity ratio for the pair of bands since both transitions originate in the ground state.
(7) Second and higher overtones characteristic of a very broad potential well. It may not be valid to interpret changes in energy levels in terms of anharmonicity since the potential is no longer a sufficiently regular function. Overtones higher than the first should appear at frequencies very different from multiples of the fundamental frequency.
(8) A splitting which increases as the height of the intermediate barrier rises.

There appears to be sufficient evidence to substantiate a double-minimum potential for *o*-substituted anilines. Criterion (1) has already been discussed, and is illustrated in Fig. 2. The overtone splitting is these compounds is concentration independent. An examination of the order in which mono-*o*-substituted compounds appear in Table I in relation to an increase in the splitting shows that criterion (3) is met reasonably well, if one bears in mind the geometrical restrictions of intramolecular hydrogen bonds.

A sample of *N*,*N*-dideutero-*o*-nitroaniline, prepared by repeated equilibration with methanol-*d*, showed an antisymmetric ND_2 stretching band at 5263 cm^{-1}, and a symmetric ND_2 doublet at 5072 and 5039 cm^{-1} (separation 33 cm^{-1} as compared with 106 cm^{-1} in

Can. J. Chem. Downloaded from www.nrcresearchpress.com by 210.87.254.105 on 09/05/12
For personal use only.

the undeuterated compound). This pronounced importance of the mass of the particle in the tunnel effect is in agreement with item (4). Within experimental error, the absorbance ratio for the doublet was the same as that for *o*-nitroaniline, as required by criterion (5).

Temperature studies over the range 0–60° C for *o*-nitroaniline, *o*-iodoaniline, *o*-phenylenediamine, and ethyl anthranilate in CCl_4 solution led to no significant changes in intensity ratios for any of the pairs of bands, in agreement with item (6).

No second overtone spectra were obtained to test item (7), since the high aniline concentrations which are required (at the maximum convenient path length of 10 cm) introduce the possibility of intermolecular hydrogen bonding. Also, difficulties are sometimes encountered in the unambiguous assignment of these higher overtones. All knowledge about the height of the intermediate barrier in double-minimum potential systems is very speculative at the present, so that criterion (8) cannot be applied.*

The question which remains to be answered is the failure to observe splitting in the ν_{02} antisymmetric NH_2 stretching bands if the double-minimum potential is a valid interpretation for the symmetric mode splitting. It is known that these two modes respond differently to substitution effects, including *o*-substituents (21, 22). Applying a classical method of Kohlrausch (33), Wolff and Staschewski (34) have calculated how these two stretching modes in primary amines react as the HNH···X interaction increases, assuming that only one NH bond is weakened in this way, and that the other NH bond remains at a fixed strength (Fig. 4). Although this is clearly an approximation, there appears to

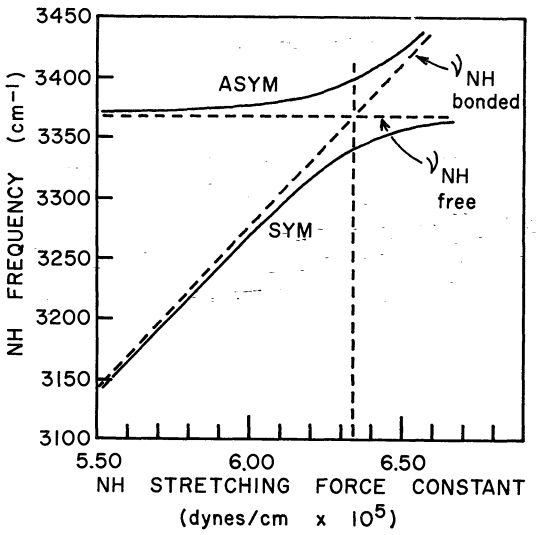

FIG. 4. Effect of HNH···X interaction on the NH_2 stretching frequencies, after Wolff and Staschewski (32). The broken vertical line corresponds to a completely "free" NH_2 group where both NH force constants are 6.34×10^5 dynes/cm. One of the force constants is kept at this value while the other is progressively reduced.

be little doubt that ν_{sym} is more sensitive to such interaction effects, which is reflected in larger frequency displacements. Thus the splitting of the levels for the antisymmetric mode in *o*-substituted anilines may be too small to be observed. It should be noted in this connection that even in cases where splitting of OH stretching bands has been

**The calculations of McKinney and Barrow (3) for an* OH···O *bond with an* O *to* O *distance of 2.8* Å *lead to a barrier height of 25 kcal/mole, with the secondary minimum lying 18 kcal/mole above the main minimum.*

Can. J. Chem. Downloaded from www.nrcresearchpress.com by 210.87.254.105 on 09/05/12
For personal use only.

observed and ascribed to double-minimum potentials, analogous doubling has not been observed for other OH vibrations, e.g. OH deformation (9).

In order to remove some of the ambiguities which the complex vibrational pattern of the NH_2 group may introduce, the methyl ester of *N*-methyl anthranilic acid, *o*-nitro-*N*-methylaniline, and *o*-nitro-diphenylamine were investigated. These spectra are shown in Fig. 2(*f*), (*g*), and (*h*) respectively. In all cases a single sharp fundamental NH stretching band is observed, whereas the first overtone band shows additional structure. For methyl-*N*-methyl anthranilate the ν_{01} band lies at 3382 cm^{-1} ($\Delta\nu_{\frac{1}{2}} = 27$ cm^{-1}). The fact that it is 71 cm^{-1} lower than the NH frequency in the methyl ester of *p*-aminobenzoic acid indicates the former is intramolecularly bonded. In the first overtone region an extremely weak pair of bands (6752 cm^{-1}, 6572 cm^{-1}, separation 180 cm^{-1}) is observed, with an unexplained low-frequency shoulder. *o*-Nitro-*N*-methylaniline is also known to exist exclusively with the CH_3 group trans to the NO_2 group, with a sharp intramolecularly bonded NH band at 3399 cm^{-1} (35, 29*b*) (present measurements located this band at 3401 cm^{-1}, $\Delta\nu_{\frac{1}{2}} = 19$ cm^{-1}) as compared with 3456 cm^{-1} in *p*-nitro-*N*-methylaniline (36). In the ν_{02} region this compound shows an NH overtone at 6625 cm^{-1} with a *high frequency* shoulder at 6792 cm^{-1}. For *o*-nitrodiphenylamine the fundamental NH band lies at 3354 cm^{-1} ($\Delta\nu_{\frac{1}{2}} = 33$ cm^{-1}), and the overtone region shows a band at 6536 cm^{-1} with a *low frequency* shoulder at 6423 cm^{-1}. If the secondary aromatic amines follow the same pattern as observed for the primary amines, i.e., the high frequency component becomes more intense as the intramolecular hydrogen bonding interaction increases, the overtone results for *o*-nitro-*N*-methylaniline and *o*-nitrodiphenylamine are consistent with the higher acidity of the latter. Also, the ν_{02} symmetric absorbance ratios for methyl-*N*-methyl anthranilate and *o*-nitro-*N*-methylaniline can be reconciled with greater intramolecular hydrogen bond strength in the six-membered chelate ring in the former compound.

Examination of Fig. 2 shows that the intensities of the fundamental bands increase on intramolecular hydrogen bond formation, whereas the first overtone bands become a little weaker. For the *N*-methylanilines the fundamentals are exceptionally intense, and the overtones very weak and broad. This behavior is well recognized in the spectra of hydrogen-bonded systems (p. 101, Ref. 2).

The possibility of overtone band splitting in some *o*-substituted anilines because of steric repulsion between substituents cannot be overlooked. Previous studies have shown that the symmetric ν_{02} band is plit in 2-*t*-Bu- and 2,5-di-*t*-Bu-aniline, but not in 2,4,6-tri-*t*-Bu-aniline where the NH_2 group has its symmetrical environment restored (21). Hambly and O'Grady (25) have demonstrated that rotational isomerism of the NHD group occurs in 2-*t*-Bu-anilines, as well as in 2-trifluoromethylaniline. Doubling of the NH bands of the NHD group is thus not a specific test for hydrogen bonding, but only for a difference in the environment of the two H atoms of the amino group. Since the separation between the symmetric and antisymmetric ν_{01} bands for 2-trifluoromethylaniline is smaller than that predicted by the modified Bellamy and Williams relationship (37), just as it is for 2,6-dimethylaniline, Hambly and O'Grady (23) ascribe the cis–trans isomerism of the NHD group in the former compound to a repulsive interaction.

Figures 5 and 6 show ν_{02} bands for *N*-methylaniline and aniline respectively in various solvents. These were obtained in an attempt to induce first overtone NH band splitting by means of intermolecular interaction with very basic solvents. For *N*-methylaniline the NH band appears to be symmetrical in CCl_4, toluene, and acetone (cf. the results for phenol in these solvents, where the proton donor is of sufficient strength to cause band splitting in the last two solvents, Ref. 5). In pyridine a shoulder appears at about 6557 cm^{-1},

Can. J. Chem. Downloaded from www.nrcresearchpress.com by 210.87.254.105 on 09/05/12
For personal use only.

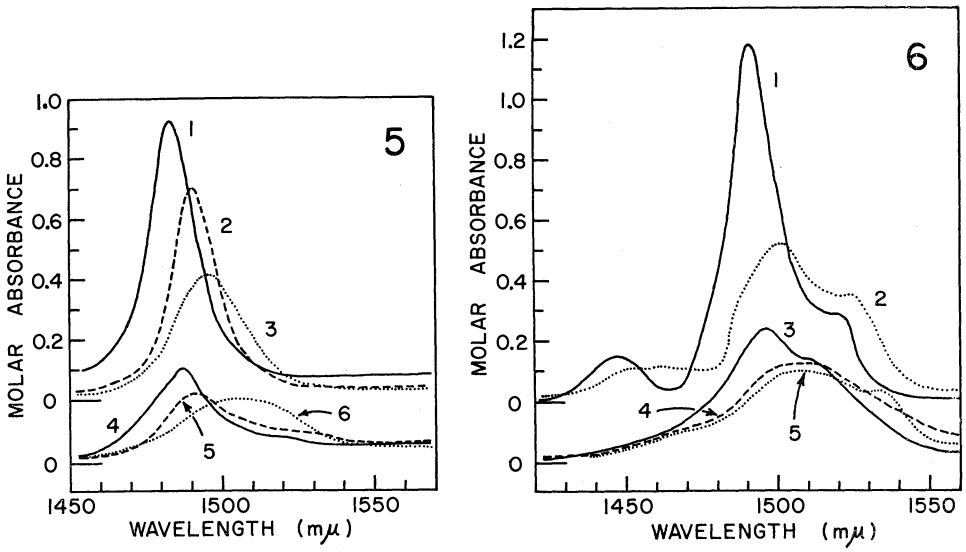

FIG. 5. First overtone NH bands of *N*-methylaniline in various solvents. The zero axis is displaced downward by 0.2 absorbance units for curves 4, 5, and 6. (1) Carbon tetrachloride (0.059 *M*). (2) Toluene (0.070 *M*). (3) Acetone (0.072 *M*). (4) Triethylamine (0.230 *M*). (5) Pyridine (0.234 *M*). (6) *N*,*N*-Dimethylformamide (0.072 *M*).

FIG. 6. First overtone NH_2 bands of aniline in various solvents. The zero axis is displaced downward by 0.2 absorbance units for curves 3, 4, and 5. (1) Carbon tetrachloride (0.058 *M*). (2) Acetone (0.101 *M*). (3) Triethylamine (0.173 *M*). (4) Pyridine (0.134 *M*). (5) *N*,*N*-Dimethylformamide (0.128 *M*).

displaced downward by 150 cm^{-1} from the main peak at 6707 cm^{-1}. In triethylamine a shoulder appears at 6623 cm^{-1}, down 102 cm^{-1} from the main peak at 6725 cm^{-1}. In dimethylformamide the very broad, flat-topped band centered at about 6638 cm^{-1} suggests unresolved bands. For the corresponding aniline spectra very broad bands are obtained, the envelopes involving the antisymmetric band and the difference band D as well. In acetone, triethylamine, pyridine, and dimethylformamide the main symmetric maximum appears doubled (this assumes that band D does not shift to shorter wavelength on going from CCl_4 to these basic solvents). In general, the NH bonds are not acidic enough to provide well-resolved symmetric ν_{02} doublets on intermolecular hydrogen bond formation.

ACKNOWLEDGMENTS

The financial assistance of the National Research Council is gratefully acknowledged. The author thanks Prof. H. Musso (Chemisches Institut der Universitaet Marburg/Lahn) for a sample of *o*-nitro-*N*-methylaniline.

REFERENCES

1. C. G. CANNON. Spectrochim. Acta, **10**, 341 (1958).
2. G. C. PIMENTEL and A. L. MCCLELLAN. The hydrogen bond. W. H. Freeman and Co., San Francisco. 1960.
3. P. C. MCKINNEY and G. M. BARROW. J. Chem. Phys. **31**, 294 (1959).
4. M. A. KOVNER and V. A. CHUENKOV. Izv. Akad. Nauk SSSR, **14**, 435 (1950).
5. C. L. BELL and G. M. BARROW. J. Chem. Phys. **31**, 300 (1959).
6. C. L. BELL and G. M. BARROW. J. Chem. Phys. **31**, 1158 (1959).
7. E. A. PSHENICHNOV and N. D. SOKOLOV. Opt. Spectr. **11**, 8 (1961).
8. S. BRATOZ and D. HADZI. J. Chem. Phys. **27**, 991 (1957).
9. D. HADZI. Z. Elektrochem. **62**, 1157 (1960).
10. R. BLINC and D. HADZI. *In* Hydrogen bonding. *Edited by* D. Hadzi. Pergamon Press, N.Y. 1959. p. 147.

Can. J. Chem. Downloaded from www.nrcresearchpress.com by 210.87.254.105 on 09/05/12
For personal use only.

11. R. BLINC and D. HADZI. Mol. Phys. **1**, 391 (1958).
12. R. BLINC, D. HADZI, and A. NOVAK. Z. Elektrochem. **64**, 567 (1960).
13. R. BLINC and D. HADZI. Spectrochim. Acta, **6**, 852 (1960).
14. D. HADZI and A. NOVAK. Infrared spectra of, and hydrogen bonding in, some acid salts of carboxylic acids. University of Ljubljana. 1960.
15. C. REID. J. Chem. Phys. **30**, 182 (1959).
16. R. L. SOMORJAI and D. F. HORNIG. J. Chem. Phys. **36**, 1980 (1962).
17. D. HADZI. J. Chem. Soc. 5128 (1962).
18. G. M. BARROW. Spectrochim. Acta, **16**, 799 (1960).
19. A. N. HAMBLY. Rev. Pure Appl. Chem. **11**, 212 (1961).
20. K. B. WHETSEL. Spectrochim. Acta, **17**, 614 (1961).
21. P. J. KRUEGER. Can. J. Chem. **41**, 363 (1963).
22. P. J. KRUEGER. Can. J. Chem. **40**, 2300 (1962).
23. A. N. HAMBLY and B. V. O'GRADY. Australian J. Chem. **15**, 626 (1962).
24. A. N. HAMBLY and B. V. O'GRADY. Australian J. Chem. **16**, 459 (1963).
25. A. N. HAMBLY and B. V. O'GRADY. Chem. Ind. 86 (1963).
26. K. B. WHETSEL, W. E. ROBERSON, and M. W. KRELL. Anal. Chem. **30**, 1598 (1958).
27. A. W. BAKER and W. W. KAEDING. J. Am. Chem. Soc. **81**, 5904 (1959).
28. A. N. HAMBLY and B. V. O'GRADY. Chem. Ind. 459 (1962).
29. A. G. MORITZ. (a) Spectrochim. Acta, **16**, 1176 (1960).
(b) Spectrochim. Acta, **18**, 671 (1962).
30. B. M. WEPSTER. *In* Steric effects in conjugated systems. *Edited by* G. W. Gray. Butterworths, London. 1958. p. 86.
31. V. C. FARMER and R. H. THOMSON. Spectrochim. Acta, **16**, 559 (1960).
32. A. G. MORITZ. Spectrochim. Acta, **17**, 365 (1961).
33. K. W. F. KOHLRAUSCH. Der Smekal-Raman Effect: Ergaenzungsband. J. Springer, Berlin. 1938.
34. H. WOLFF and D. STASCHEWSKI. Z. Elektrochem. **66**, 140 (1962).
35. H. MUSSO. Ber. **95**, 1722 (1962).
36. P. J. KRUEGER and H. W. THOMPSON. Proc. Roy. Soc. A, **243**, 143 (1957).
37. L. J. BELLAMY and R. L. WILLIAMS. Spectrochim. Acta, **9**, 341 (1957).

Can. J. Chem. Downloaded from www.nrcresearchpress.com by 210.87.254.105 on 09/05/12
For personal use only.

SUR LA DOUBLE ÉNOLISATION DE LA DIMÉTHYL-3,3 CYCLOHEXANONE

J. CHAMPAGNE,[1] H. FAVRE, D. VOCELLE,[2] ET MLLE I. ZBIKOWSKI

Département de chimie, Université de Montréal, Montréal, Québec

Reçu le 13 août 1963

RÉSUMÉ

On montre dans cet article, par l'étude des acétates énoliques et des ène-pyrrolidines de la diméthyl-3,3 cyclohexanone, par la mise en équilibre des diméthyl-3,3 et diméthyl-4,4 cyclohexènes et par l'oxydation nitrique de la diméthyl-3,3 cyclohexanone que l'énolisation de la diméthyl-3,3 cyclohexanone est double et qu'elle se fait de préférence dans la direction opposée aux groupes méthyles, le rapport entre les isomères formés étant de 3 à 1. De plus la diméthyl-4,4 cyclohexanedione-1,3 s'énolise aussi de préférence avec la double liaison C=C en 1,2 donc éloignée des groupes méthyles.

Can. J. Chem. Downloaded from www.nrcresearchpress.com by 210.87.254.6 on 09/05/12
For personal use only.

La diméthyl-3,3 cyclohexanone présente, selon la bibliographie, la particularité de ne réagir qu'en position 6, que l'on fasse agir le brome sur la cétone (1), l'acrylonitrile sur l'énamine correspondante (2) (méthode de Stork), le formiate d'éthyle (3) ou l'iodure de méthyle (4) sur le sel sodé de la cétone. Ceci peut être dû à deux causes: soit que l'énolisation ne se donne que vers la position 6 seulement pour donner l'énol, l'énamine, ou l'énolate, II*a*, II*b*, ou II*c* respectivement, soit que l'énolisation soit double pour donner les énols, énamines, et énolates II*a*, *b*, *c* et III*a*, *b*, *c*, un encombrement stérique empêchant la réaction de se faire ensuite en α du groupe *gem*-diméthyle. Nous avons voulu trancher cette question, en stabilisant la double liaison énolique par la formation d'un acétate énolique ou d'une énamine et en mettant en évidence la présence d'un ou de deux composés d'énolisation; pour fins de comparaison, nous avons mis à l'équilibre le diméthyl-4,4 cyclohexène (II*e*) et le diméthyl-3,3 cyclohexène (III*e*). Dans une discussion nous mettrons en parallèle les résultats ainsi obtenus, l'oxydation nitrique de la diméthyl-3,3 cyclohexanone et finalement l'énolisation de la diméthyl-4,4 cyclohexanedione-1,3.

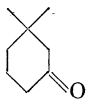

I

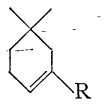

II*a*, R = —OH
II*b*, R = —NC_4H_8
II*c*, R = —O^-
II*d*, R = —$OCOCH_3$
II*e*, R = —H

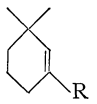

III*a*
III*b*
III*c*
III*d*
III*e*

Les acétates énoliques de la diméthyl-3,3 cyclohexanone

En faisant réagir la diméthyl-3,3 cyclohexanone (I) avec l'acétate d'isopropényle en présence d'acide sulfurique concentré, selon Dauben et ses collaborateurs (5), nous avons obtenu deux acétates énoliques, mis en évidence par chromatographie en phase gazeuse, dans le rapport de 62–38%. Ils se séparent facilement par chromatographie en phase gazeuse à l'échelle du gramme; l'acétate de diméthyl-5,5 cyclohexényle (II*d*) est identifié par son spectre de RMN: triplet à τ 5.1 p.p.m.; J 4 c.p.s.; l'acétate de diméthyl-3,3 cyclohexényle (III*d*) présente un singulet comme attendu, à τ 4.9. Les bandes caractéristiques

[1]*Boursier de l'Office de la Recherche Scientifique de la Province de Québec, 1959.*
[2]*Boursier de l'Office de la Recherche Scientifique de la Province de Québec, 1960.*

des acétates énoliques, dans l'infrarouge, sont à 1754 cm^{-1} et 1751 cm^{-1} pour II*d* et III*d* respectivement. Le spectra de RMN du mélange II*d*–III*d* permet d'établir que l'acétate II*d* représente 62% du mélange. Une corroboration chimique de ces résultats a été faite de la manière suivante: les acétates purs II*d* et III*d* ont été ozonolysés; les acides diméthyl-3,3 et diméthyl-2,2 adipiques VIII et IX respectivement obtenus ont été estérifiés par le diazométhane et les diesters caractérisés et dosés par CPG. Les diesters de référence ont été préparés à partir des acides VIII et IX qui sont connus (6) et que nous avons préparés par ozonolyse des acétates énoliques VI et VII issus respectivement de la diméthyl-4,4 et de la diméthyl-2,2 cyclohexanone IV et V. L'acétate énolique de la diméthyl-4,4 cyclohexanone (un seul est attendu) se forme sans difficultés; celui de la diméthyl-2,2 ne se forme pas complètement: il est toujours accompagné de la cétone de départ.

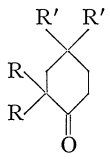

IV
V

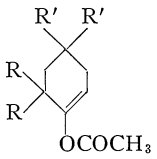

VI
VII

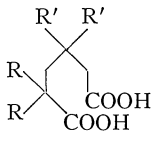

VIII
IX

R = H; R' = CH_3
R = CH_3; R' = H

Une autre manière de former des acétates énoliques est de traiter la cétone par de l'anhydride acétique et de l'acide perchlorique aqueux dans un mélange de tétrachlorure de carbone et de benzène (7, 8). Appliquée à la diméthyl-3,3 cyclohexanone cette méthode a conduit aux deux acétates énoliques II*d* et III*d*, dans un rapport de 73–27%, mais la réaction n'est pas complète, 12% de cétone de départ se retrouvant à côté des acétates énoliques.

Il nous a semblé intéressant de mettre en évidence les modes de contrôle ("cinétique et thermodynamique") de ces deux modes opératoires. A cet effet nous avons traité chaque acétate énolique pur II*d* et III*d* par l'acétate d'isopropényle et l'acide sulfurique; dans chaque cas l'acétate énolique est inchangé. Il n'y a pas de changement si l'on ajoute en plus de l'acétone. Lorsque l'acétate énolique III*d* est traité par l'acétate d'isopropényle et l'acide sulfurique en présence de diméthyl-3,3 cyclohexanone, l'acétate II*d* se forme, mais dans des proportions strictement équivalentes à la quantité de diméthyl-3,3 cyclohexanone présente dans le mélange. Nous tirons la conclusion que le contrôle est cinétique lorsque la cétone est traitée par l'acétate d'isopropényle et l'acide sulfurique concentré.

En revanche, lorsque l'acétate énolique III*d* est traité par de l'anhydride acétique et de l'acide perchlorique aqueux (78%) nous retrouvons 10% de diméthyl-3,3 cyclohexanone et 90% du mélange des acétates énoliques II*d* et III*d* dans les proportions de 75–25%, soit le mélange que l'on obtient à partir de la diméthyl-3,3 cyclohexanone elle-même. Nous tirons la conclusion que le contrôle est ici "thermodynamique".

Les ène-pyrrolidines de la diméthyl-3,3 cyclohexanone

L'action de la pyrrolidine sur la diméthyl-3,3 cyclohexanone a déjà été décrite par l'un de nous (2). Le produit brut a été ozonolysé, puis saponifié, et finalement traité par le diazométhane: la CPG a révélé les deux diesters méthyliques des acides diméthyl-3,3 et diméthyl-2,2 adipiques (VIII et IX). Du rapport 80–20% de ces diesters, nous concluons que les deux ène-pyrrolidines II*b* et III*b* se trouvaient présentes dans le mélange des énamines et qu'elles étaient dans ces proportions. Nous considérons, d'après Stork et ses collaborateurs (9), que les deux ène-pyrrolidines sont à l'équilibre.

Can. J. Chem. Downloaded from www.nrcresearchpress.com by 210.87.254.6 on 09/05/12
For personal use only.

Mise en équilibre des diméthyl-4,4 et 3,3 cyclohexènes

Nous avons déterminé la position d'équilibre des diméthyl-4,4 et diméthyl-3,3 cyclohexènes (II*e* et III*e*). En traitant chacun de ces composés par de l'acide *p*-toluène sulfonique dans de l'acide acétique glacial (10, 11) nous avons obtenu, par dosage en chromatographie en phase gazeuse, les résultats du Tableau I. Les mélanges d'isomérisation sont très complexes (cf. partie expérimentale): si nous admettons toutefois qu'au bout de 257 heures les hydrocarbures éthyléniques II*e* et III*e* sont à l'équilibre, bien qu'ils disparaissent progressivement au cours de l'isomérisation, nous obtenons un ΔF de −0.73–0.78 kcal/mole, le diméthyl-4,4 cyclohexène étant le plus stable. Turner,* par l'étude des chaleurs d'hydrogénation, a trouvé que le ΔH entre ces hydrocarbures est de 1.0 kcal/mole, le diméthyl-4,4 étant le plus stable également.

TABLEAU I

Isomérisation des diméthyl-4,4 et diméthyl-3,3 cyclohexènes

		Isomérisation du diméthyl-3,3 cyclohexène III*e*			Isomérisation du diméthyl-4,4 cyclohexène II*e*		
Durée (heures)		1	17	257	1	17	257
Pourcentage de diméthyl-3,3 et diméthyl-4,4 cyclohexènes, III*e* et II*e*, retrouvés		47.0	14.0	9.0	53.0	19.0	7
Composition du mélange en % de III*e* et II*e* retrouvés	III*e*	62	30	26	26	33	27
	II*e*	38	70	74	74	67	73

DISCUSSION ET COROLLAIRES

Les résultats précédents, rangés au Tableau II, montrent une prépondérance de composé à double liaison *loin* des groupes *gem*-diméthyles dans les mélanges d'acétates énoliques, d'ène-pyrrolidines et dans les diméthyl-4,4 et diméthyl-3,3 cyclohexènes à l'équilibre.

TABLEAU II

Pourcentages d'isomères d'énolisation de la diméthyl-3,3 cyclohexanone

	Isomères obtenus		
Composés	II	III	R =
Acétates énoliques (contrôle cinétique)	62%	38%	$-OCOCH_3$
Acétates énoliques (à l'équilibre)	73%	27%	$-OCOCH_3$
Ene-pyrrolidines (à l'équilibre)	80%	20%	$-NC_4H_8$
Enols de la diméthyl-3,3 cyclohexanone (par oxydation nitrique)	78%	22%	(—OH)

Turner et Garner (13) ont très bien résumé les arguments qui rendront une double liaison plus stable dans une position que dans l'autre dans des composés alicycliques: on ne peut encore trancher définitivement entre l'hyperconjugaison et les facteurs conformationnels. L'hyperconjugaison stabilisera plus le diméthyl-4,4 cyclohexène (deux groupes $—CH_2—$) que le diméthyl-3,3 cyclohexène (un seul groupe $—CH_2—$). Si l'on avance au

**Communication orale faite au 139ième Congrès de l'American Chemical Society (12).*

Can. J. Chem. Downloaded from www.nrcresearchpress.com by 210.87.254.6 on 09/05/12
For personal use only.

contraire les facteurs conformationnels seuls, la seule explication valable pour le moment (10) est que l'hydrogène en position 2 cause une interaction non liée défavorable avec le groupe méthyle quasi-équatorial (14) en position 3 (Fig. 1), défavorisant ainsi le diméthyl-3,3 cyclohexène par rapport au diméthyl-4,4 cyclohexène: dans cette dernière molécule les interactions créées par les groupes méthyles axial et équatorial en position 4 avec les hydrogènes en position 5, qui sont gauches dans une conformation demi-chaise (Fig. 2), sont moins dévaforables que l'interaction décrite pour le diméthyl-3,3 cyclohexène. Il est cependant très difficile de faire un choix entre les interactions non liées pour dire avec

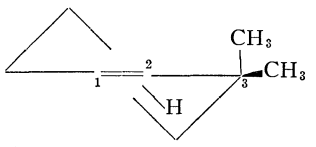

FIG. 1.

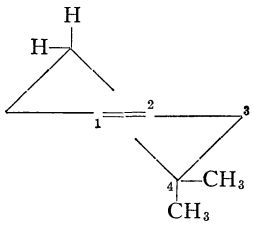

FIG. 2.

certitude que le diméthyl-4,4 cyclohexène est plus stable, par l'effet de ces seules interactions non liées, que le diméthyl-3,3 cyclohexène.

Pour ce qui est de la réactivité de ces doubles liaisons énolique et énaminique nous discuterons deux cas.

1. La cyanoéthylation des énamines II*b* et III*b*. Nous avons montré (2) qu'une seule cétone cyanoéthylée résulte de l'action de l'acrylonitrile sur le mélange de ces deux énamines: tout se passe comme si l'énamine II*b* réagissait seule pour donner la diméthyl-5,5 cyanoéthyl-2 cyclohexanone. Le refus de réagir de l'énamine III*b* peut être attribué à un encombrement stérique dû au groupe *gem*-diméthyle. Nous reviendrons sur la nature de cet encombrement stérique, qui a été mis en évidence par Conia et ses collaborateurs (15), dans une prochaine publication.

2. L'oxydation nitrique de la diméthyl-3,3 cyclohexanone. Nous l'avons conduite dans l'acide nitrique concentré bouillant et obtenu 70% des acides diméthyl-2,2 et diméthyl-3,3 adipiques (IX et VIII) dans le rapport de 22–78%, à côté des acides diméthyl-2,2, et diméthyl-3,3 glutariques (X et XI), de l'acide diméthyl-2,2 succinique (XII), et de l'acide diméthyl malonique (XIII). Tous ces acides ont été caractérisés en chromatographie en phase gazeuse, sous forme d'esters méthyliques. Nous avons vérifié que dans les mêmes conditions d'oxydation, la diméthyl-2,2 cyclohexanone (V) ne conduit qu'à quatre des diacides issus de la diméthyl-3,3 cyclohexanone, les diacides VIII et XI ne pouvant se former et la diméthyl-4,4 cyclohexanone ne conduit qu'à cinq des diacides de la diméthyl-3,3 cyclohexanone, le diacide IX ne pouvant se former.

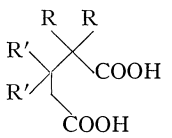

X, R = CH_3; R′ = H
XI, R = −H; R′ = $-CH_3$

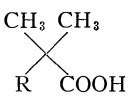

XII, R = $-CH_2COOH$
XIII, R = −COOH

On avance que l'oxydation nitrique se fait sur l'énol (ou les énols) correspondant à la cétone (16, 17, 18). Les énols de la diméthyl-3,3 cyclohexanone seraient ainsi formés dans

Can. J. Chem. Downloaded from www.nrcresearchpress.com by 210.87.254.6 on 09/05/12
For personal use only.

le rapport II*a*—78%/III*a*—22%, très voisin de celui que nous décrivons pour les acétates énoliques II*d*/III*d*, les ènes-pyrrolidines II*b*/III*b* et les diméthyl-4,4 et diméthyl-3,3 cyclohexènes à l'équilibre II*e*/III*e* (Tableau II). Il n'y aurait pas d'empêchement stérique du groupe *gem*-diméthyle dans l'oxydation nitrique.

Toutefois les travaux de van Asselt et van Krevelen (19, 20) sur l'oxydation nitrique à basse température, qui ne se fait qu'en présence d'acide nitreux et passe par des isonitroso cétones, montrent que l'oxydation sur l'énol est pour le moins un point de vue très simplifié. Selon eux, il faudrait admettre que les isonitroso cétones A et B (Fig. 3) se formeraient dans le rapport de 22–78% et qu'il se formerait encore d'autres nitroso cétones, par exemple C. Nous travaillons ici avec l'hypothèse que l'oxydation nitrique à température élevée est semblable à l'oxydation à basse température, ce qui n'est pas prouvé.

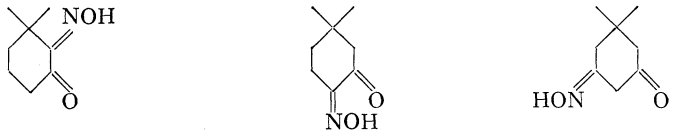

A B C

FIG. 3.

En définitive, pour prévoir l'isomère principal résultant de l'oxydation nitrique d'une cétone, il semble que l'on puisse continuer à dire que tout se passe comme si l'énol (ou les énols) étaient oxydés.

Nous décrivons maintenant un travail qui est un corollaire de ce que nous venons d'étudier et qui porte sur la diméthyl-4,4 cyclohexanedione-1,3 (XIV). Cette cétone peut conduire à deux céto-énols (XV, XVI, R = H), dans lesquels la double liaison énolique reflète la double énolisation de la diméthyl-3,3 cyclohexanone. Bien que nous ayons dans les céto-énols XV et XVI un groupe carbonyle qui doit certainement affecter la géométrie et les tensions internes de ces molécules, nous avons trouvé que la dicétone XIV s'énolise doublement et dans le rapport 35/65%—XV/XVI, donc dans le même sens que l'énolisation de la diméthyl-3,3 cyclohexanone, c'est-à-dire plus de double liaison loin des groupes méthyles. Nous avons montré ceci en stabilisant les céto-énols sous forme de céto-éthers XV to XVI (R = CH_3) par réaction avec le diazométhane; par le méthode maintenant classique de Frank et Hall (21), le mélange de ces céto-éthers a été réduit par l'hydrure de lithium et d'aluminium en diméthyl-4,4 et -6,6 cyclohexène-2 ones (XVIII et XVII),

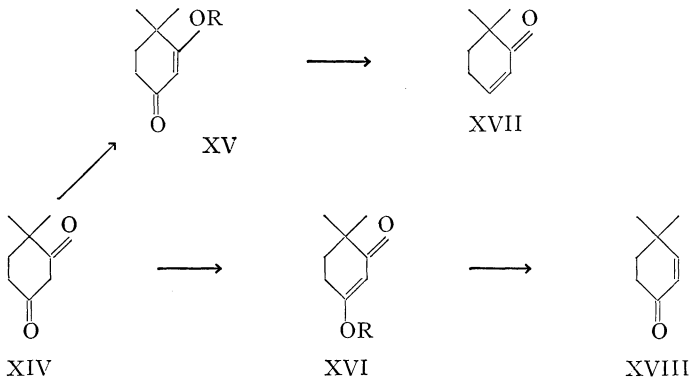

Can. J. Chem. Downloaded from www.nrcresearchpress.com by 210.87.254.6 on 09/05/12
For personal use only.

qui ont été réduites à leur tour en diméthyl-4,4 et -2,2 cyclohexanones (IV et V). Ce sont ces cétones saturées que nous avons dosées par chromatographie en phase gazeuse: nous avançons que leur rapport reflète le rapport des éthers céto-énoliques et ce rapport celui des céto-énols de la dicétone XIV, car nous admettons avec Tamm et ses collaborateurs (22) que le diazométhane réagit avec les céto-énols conformément à leurs vitesses de formation à partir de la dicétone.

La diméthyl-4,4 cyclohexanedione-1,3 (XIV) a été préparée selon la méthode classique (23) de cyclisation d'un méthyl-céto-ester; la séquence XIX → XX → XXI → XXII → XIV illustre cette synthèse. La dicétone XIV n'a pas donné une bonne analyse carbone–hydrogène, mais les céto-éthers correspondants l'ont fait. Leur preuve de structure découle essentiellement du fait de leur transformation en diméthyl-2,2 et diméthyl-4,4 cyclohexanones.

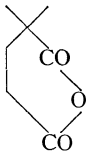

XIX

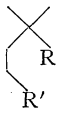

XX, R = COOEt; R′ = COOH
XXI, R = COOEt; R′ = COCl
XXIII, R = COOEt; R′ = $COCH_3$

PARTIE EXPERIMENTALE*

Les spectres infrarouges ont été déterminés à l'aide d'un spectrophotomètre Perkin–Elmer, modèle 21, double faisceau, prisme de chlorure de sodium.

Les analyses par chromatographie en phase gazeuse (CPG) ont été réalisées à l'aide d'un appareil "Kromo-Tog" de Burrell Corporation, modèle K–2, et les séparations préparatoires à l'aide d'un appareil "Prep/Partitioner" de Fisher, modèle 24. Sauf indications contraires, les colonnes sont en verre, diamètre intérieur 6 mm.

Les analyses élémentaires ont été effectuées par C. Daesslé, Organic Microanalyses, Montréal, et W. Manser, ingénieur, Herrliberg (Suisse).

Les spectres de résonance magnétique nucléaire (RMN), ont été pris avec un Spectromètre modèle A–60 de Varian. Les déplacements chimiques, τ, sont exprimés en parties par million (p.p.m.) du champs total. On utilise le tétraméthylsilane comme référence interne. Les constantes de couplage des spins J sont exprimées en cycles par seconde (c.p.s.).

1. Diméthyl-2,2, -3,3, et -4,4 cyclohexanones

Ces cétones ont été préparées par de nombreuses méthodes; nous décrivons brièvement ici les méthodes que nous avons mises en œuvre; elles permettent de préparer des cétones en grande quantité et d'une pureté de 99.6±0.2%, déterminée par CPG sur des colonnes de glycérol (20% sur brique), à température de 110°.

Diméthyl-2,2 cyclohexanone.—La méthode de Bailey et Madoff est très appropriée (24).

Diméthyl-3,3 cyclohexanone.—Pour préparer cette cétone à grande échelle nous recommandons la méthode suivante. Réduire le dimédon en diméthyl-3,3 cyclohexanol selon la méthode (25). Oxyder cet alcool: on prépare une solution de 210 g de bichromate de potassium dans 1100 ml d'eau à laquelle on ajoute, lentement, 254 ml d'acide sulfurique conc. Cette solution est ajoutée goutte à goutte à 203 g d'alcool en solution dans 417 ml d'acide acétique glacial. La température ne doit jamais dépasser 0°. On extrait par de l'éther et isole à la manière habituelle 191.2 g de cétone, p.é. 120–122° sous 142 mm (rendement de l'oxydation: 95.5%).

Diméthyl-4,4 cyclohexanone.—Cette cétone se prépare très bien, en grande quantité, par réduction catalytique sur palladium – carbonate de calcium selon (26) de la diméthyl-4,4 cyclohexène-2-one préparée selon (27). Elle fond à 38–40°. On donne p.f. 39–40° (28) et 38–41° (29).

2. Acétates énoliques

2.1. Acétates énoliques de la diméthyl-3,3 cyclohexanone (IId et IIId)

2.11. Méthode I (5)

18 ml d'acétate d'isopropényle et 0.08 ml d'acide sulfurique concentré sont ajoutés à 5.2 g de diméthyl-3,3 cyclohexanone. Le mélange est chauffé à reflux sous atmosphère d'azote pendant 1 heure, après quoi 6 ml

**Les p.f. ont été déterminés en tubes capillaires, à l'aide d'un thermomètre étalonné avec des composés purs de p.f. connus.*

Can. J. Chem. Downloaded from www.nrcresearchpress.com by 210.87.254.6 on 09/05/12
For personal use only.

de solvant sont distillés sous pression réduite à environ 400 mm en maintenant constamment une atmsophère d'azote dans le ballon. Le résidu refroidi est dissous dans l'éther et lavé successivement avec une solution glacée de NaOH 2% et de l'eau saturée de NaCl jusqu'à neutralité. La phase éthérée est séchée sur du Na_2SO_4 anhydre, l'éther est évaporé sous une colonne de Widmer et le résidu est distillé: p.é. 102–103° à 34 mm, $n_D^{26.5}$: 1.4498, rendement 90%.

La chromatographie en phase gazeuse sur une colonne de 2.5 mètres de polyester succinique de Craig, 20% sur Kromat FB, temp. 158°, débit 50 ml par min. He, indique la présence de deux acétates énoliques, III*d* et II*d*, dans des proportions de 38% et 62% respectivement; III*d* est élué avant II*d*: temps de rétention, 19.5 et 23 minutes. Une colonne de 2.5 mètres de Carbowax 20M, 20% sur Chromosorb P, temp. 154°, débit environ 50 ml par min. He, conduit au même résultat. L'analyse par RMN (tétrachlorure de carbone) indique la présence des deux composés: 38% de l'acétate III*d* et 62% de l'acétate II*d*.

Le mélange brut a été séparé en ses constituents II*d* et III*d* par chromatographie en phase gazeuse préparative. On injecte le mélange dans un appareil "Fisher Prep/Partitioner" modèle 24.

Les conditions utilisées sont les suivantes: (*a*) 4 colonnes de 50 cm chacune, chargées de Chromosorb P sur lequel est adsorbé 20% de Carbowax 20M. (*b*) Températures: colonnes, 142°; "flash evaporator", 230°; cellule, 200°. (*c*) Pression à l'entrée des colonnes: 18 livres par p.c., azote.

Après deux passages sur les colonnes, chacune des fractions recueillies est distillée et la chromatographie en phase gazeuse analytique indique l'homogénéité des échantillons.

Acétate de diméthyl-3,3 cyclohexényle (IIId).—Calculé pour $C_{10}H_{16}O_2$: C, 71.39; H, 9.58%. Trouvé: C, 71,60; H, 9.28%. Le spectre I.R. révèle des bandes à 1689 cm^{-1} et 1751 cm^{-1} (liquide pur); n_D^{23}: 1.4501. RMN: singulet, 5.1.

Acétate de diméthyl-5,5 cyclohexényle (IId).—Calculé pour $C_{10}H_{16}O_2$: C, 71.39; H, 9.58%. Trouvé: C, 71.15; H, 9.47%. Le spectre I.R. révèle des bandes à 1691 cm^{-1} et 1754 cm^{-1} (liquide pur); n_D^{23}: 1.4510. RMN: triplet, τ 4.9; J = 4 c.p.s.

2.12. Méthode II (8)

Une solution glacée de 6 ml d'anhydride acétique et 8 gouttes d'acide perchlorique 78% est ajoutée à une solution refroidie de 434 mg de diméthyl-3,3 cyclohexanone dans 80 ml de benzène et 30 ml de tétrachlorure de carbone. Le tout est agité à la température de la pièce pendant 4 heures et abandonné pour la nuit. On ajoute alors de l'eau glacée et du CCl_4 et la phase organique est lavée avec une solution de $NaHCO_3$ 5% et avec de l'eau saturée de NaCl, séchée sur le Na_2SO_4 anh. et les solvants sont distillés. Le résidu brut foncé est chromatographié en phase gazeuse comme en 2.11 (sur Carbowax 20M). La proportion des acétates énoliques est de 27% de l'acétate III*d* et 73% de l'acétate II*d*, et le mélange contient environ 12% de cétone de départ.

2.2. Acétate de diméthyl-6,6 cyclohexényle (VII)

A 2 g de la diméthyl-2,2 cyclohexanone on ajoute 9 ml d'acétate d'isopropényle et 0.04 ml d'acide sulfurique concentré. On isole comme rapporté en 2.11, après la distillation, un liquide incolore avec un rendement de 68%, p.é. environ 126° à 150 mm. La chromatographie en phase gazeuse sur polyester succinique de Craig semble indiquer la présence de 20% de cétone de départ. Le spectre I.R. a des bandes à 1707 cm^{-1} (cétone non réagie), 1755 et 1696 cm^{-1} (acétate énolique). Ce mélange n'a pas été analysé. Un temps de chauffage de 2 et 3 heures ne permet pas d'obtenir l'acétate exempt de cétone de départ.

2.3. Acétate de diméthyl-4,4 cyclohexényle (VI)

La diméthyl-4,4 cyclohexanone (4.91 g) est transformée en acétate énolique VI par la méthode rapportée en 2.11. On obtient 5.1 g d'un liquide incolore (78% du rendement théorique), p.é. 104–105° à 105 mm, $n_D^{26.5}$: 1.4512. Le spectre I.R. a des bandes à 1690 et 1748 cm^{-1} (liquide pur). Calculé pour $C_{10}H_{16}O_2$: C, 71.39; H, 9.58%. Trouvé: C, 71.72; H, 9.66.

3. Ozonolyse des acétates énoliques

3.1. Méthode générale

On dissout 1.6 g d'acétate énolique dans 75 ml d'éther de pétrole (p.é. 30–38°) exempt d'alcènes, on refroidit la solution dans un bain de glace sèche et d'acétone et on fait passer dans cette solution, en maintenant la réfrigération, un courant d'oxygène contenant environ 3% d'ozone jusqu'à obtention de la coloration bleue caractéristique d'un excès d'ozone (durée de l'opération: environ une heure et demie). On évapore alors l'éther de pétrole, en faisant passer un courant d'azote, sous un léger vide, et au résidu on ajoute 18 ml d'eau, 18 ml d'acétate d'éthyle, 18 ml d'acide acétique glacial, et 6 ml de peroxyde d'hydrogène à 30%. On agite pendant la nuit à la température ambiante. Les solvants sont évaporés en chauffant sous vide de 11 mm à une température ne dépassant pas 100°. On dissout le résidu brut dans de l'éther et on ajoute à cette solution refroidie, une solution éthérée de diazométhane jusqu'à coloration jaune persistante. L'éther est évaporé et le résidu chromatographié en phase gazeuse: colonne de 1 mètre, polyester succinique de Craig 15% sur Kromat FB; débit de l'éluant (hélium), environ 50 ml à la minute; température 162°. Dans ces conditions le diester méthylique de l'acide diméthyl-2,2 adipique est élué au bout de 10.5 minutes, celui de l'acide diméthyl-3,3 adipique au bout de 14.2 minutes.

Can. J. Chem. Downloaded from www.nrcresearchpress.com by 210.87.254.6 on 09/05/12
For personal use only.

3.2. Ozonolyse de l'acétate énolique IIId

Selon le mode général d'opération 3.1, 300 mg de l'acétate sont ozonolysés. La chromatographie en phase gazeuse du diester final ne donne qu'un pic, superposable à celui obtenu plus loin en 3.4.

3.3. Ozonolyse de l'acétate énolique IId

500 mg de l'acétate II*d* sont ozonolysés suivant le mode général d'opération 3.1. La chromatographie en phase gazeuse du diester final ne révèle qu'un pic, superposable à celui obtenu plus bas en 3.5.

3.4. Ozonolyse de l'acétate énolique VII

1.24 g de l'acétate énolique VII (préparé en 2.2 et contenant 20% de diméthyl-2,2 cyclohexanone) sont traités par l'ozone suivant le mode général 3.1. Après l'évaporation des solvants (suivant l'oxydation de l'ozonide) et un séchage sous vide, l'acide diméthyl-2,2 adipique ne se solidifie pas. Le p.f. rapporté est de 89–90° (6). L'acide brut est alors méthylé et la chromatographie en phase gazeuse du produit final indique un pic majeur (10.5 minutes d'élution) et une impureté de l'ordre de 5%.

3.5. Ozonolyse de l'acétate énolique VI

2.5 g de l'acétate de diméthyl-4,4 cyclohexényle, préparé en 2.3, sont ozonolysés suivant le mode général 3.1. Après l'évaporation des solvants qui suit l'oxydation par H_2O_2, le résidu est séché sous vide. Le diacide brut est recristallisé dans le chloroforme et l'éther de pétrole, p.f. 85.5–87° (litt. (6) 86–87°). L'acide diméthyl-3,3 adipique VIII est méthylé par le diazométhane et le diester ne fournit qu'un pic en chromatographie en phase gazeuse. (14.2 minutes d'élution).

4. Mises en équilibre des acétates énoliques de la diméthyl-3,3 cyclohexanone

4.1. Mise en équilibre de l'acétate de diméthyl-3,3 cyclohexényle IIId par un mélange anhydride acétique–acide perchlorique

Environ 150 mg de l'acétate énolique III*d* sont dissous dans 40 ml de benzène et 15 ml de CCl_4. A cette solution refroidie on ajoute une solution glacée de 3 ml d'anhydride acétique et 4 gouttes d'acide perchlorique 78%. Le mélange est ensuite traité de la même façon que lors de la préparation des acétates énoliques à partir de la diméthyl-3,3 cyclohexanone (voir plus haut, section 2.12). La chromatographie en phase gazeuse indique la présence d'environ 10% de diméthyl-3,3 cyclohexanone et 90% d'acétates énoliques dans un rapport de 25% de III*d* et 75% de II*d*.

4.2. Essai de mise en équilibre par l'acétate d'isopropényle – acide sulfurique

4.21. A partir de l'acétate de diméthyl-3,3 cyclohexényle IIId

A 600 mg de l'acétate de diméthyl-3,3 cyclohexényle (III*d*) on ajoute 2 ml d'acétate d'isopropényle et 0.01 ml d'acide sulfurique concentré et le mélange est chauffé à reflux pendant 75 minutes sous atmosphère d'azote, après quoi environ 30% du solvant est distillé sous pression légèrement réduite. Le produit est extrait de la même façon que lors de la préparation des acétates énoliques à partir de la diméthyl-3,3 cyclohexanone (voir plus haut, 2.11). La chromatographie en phase gazeuse indique que le composé de départ III*d* est resté inaltéré.

On a repris la même expérience en ajoutant 200 mg d'acétone au produit de départ mais ceci n'amène aucune isomérisation de l'acétate de départ.

4.22. A partir de l'acétate de diméthyl-5,5 cyclohexényle (IId)

600 mg de l'acétate énolique II*d* sont traités de la même façon que l'acétate III*d* (cf. 4.21). La chromatographie en phase gazeuse du produit final indique que c'est l'acétate de départ inchangé.

4.23. A partir de l'acétate énolique IIId en présence de la cétone I

Un mélange de 82 mg de diméthyl-3,3 cyclohexanone (I) et 132 mg d'acétate de diméthyl-3,3 cyclohexényle (III*d*) dans 1 ml d'acétate d'isopropényle et 0.005 ml de H_2SO_4 concentré, est traité suivant le même mode opératoire qu'à la section 4.21. La chromatographie en phase gazeuse du produit brut révèle la présence de 71.5% de l'acétate III*d* et 28.5% de l'acétate II*d*.

Ces pourcentages représentent: acétate III*d* = 132 mg au départ + 40.6 mg formés à partir de la cétone; et acétate II*d* = 68.7 mg formés à partir de la cétone. La cétone a donc engendré les acétates II*d*/III*d* dans le rapport 62.8/37.2. Nous concluons de ceci que l'acétate de départ III*d* ne s'est pas isomérisé et que la cétone a donné les acétates énoliques II*d*/III*d* comme en 2.11.

5. Oxydation nitrique des diméthyl-2,2, -3,3, et -4,4 cyclohexanones

La cétone (1.5 g) est ajoutée lentement à 6.0 ml d'acide nitrique concentré chauffé à reflux (30). Après l'addition on laisse refluer pendant 10 minutes puis on évapore l'acide nitrique en chauffant. Le résidu jaune, très visqueux, n'est pas purifié. On le dissout dans l'éther et on ajoute à cette solution refroidie, une solution éthérée de diazométhane jusqu'à ce que l'évolution d'azote cesse et la coloration jaune persiste. Le solvant est évaporé sur bain-marie et le produit brut est chromatographié en phase gazeuse, sur polyester succinique de Craig (15% sur Kromat FB, température 162°, hélium 50 ml par min.

Les acides diméthyl malonique (XIII), diméthyl-2,2 succinique (XII), diméthyl-3,3 glutarique (XI), et diméthyl-2,2 glutarique (X) ont été obtenus de la Maison Aldrich Chemical Co., Inc. Les diesters méthyliques correspondants ont été préparés en ajoutant une solution éthérée de diazométhane à une solution éthérée

Can. J. Chem. Downloaded from www.nrcresearchpress.com by 210.87.254.6 on 09/05/12
For personal use only.

TABLEAU III

Oxydation nitrique des cétones I, IV, et V

Cétone de départ	Diacides obtenus et temps de rétention (minutes) des diesters méthyliques correspondants					
	XIII 2.3	XII 3.8	XI 6.4	X 7.3	IX 10.5	VIII (diacides) 14.2 (minutes
I	+	+	+	+	22%	78%
IV	+	+	+	+		+
V	+	+		+	+	

de chacun des acides. Les esters des acides diméthyl-2,2 et -3,3 adipiques (IX et VIII) ont été préparés plus haut (cf. 3.4 et 3.5).

Les composants des mélanges indiqués au Tableau III ont été identifiés en faisant des mélanges avec les produits connus qui dans chaque cas, se superposent avec un des composants d'un mélange d'oxydation.

Seul le rapport des acides diméthyl-2,2 et -3,3 adipiques a été déterminé: il est de 22/78 (Tableau III). On remarque qu'à partir de la diméthyl-4,4 cyclohexanone, l'acide diméthyl-2,2 adipique (IX) ne se forme pas et à partir de la diméthyl-2,2 cyclohexanone, les acides diméthyl-3,3 adipique (VIII) et diméthyl-3,3 glutarique (XI) ne se forment pas. Nous n'avons pas dosé chaque constituant dans chaque mélange: en première approximation, en calculant simplement les surfaces de chaque pic, l'acide IX à partir de la cétone V, VIII à partir de IV, et les acides IX et VII à partir de I, représentent environ 70% du mélange brut.

6. Ozonolyse des ène-pyrrolidines IIIb et IIb

On effectue l'ozonolyse sur 1 g du mélange des énamines II*b* et III*b*. préparé selon (2) suivant la méthode générale 3.1. Après l'évaporation des solvants (qui suit l'oxydation par H_2O_2) le produit brut est saponifié en chauffant à reflux pendant 4 heures avec 20 ml de solution de NaOH 10%. Une forte odeur de pyrrolidine se dégage. La solution refroidie est acidifiée avec l'acide chlorhydrique concentré, jusqu'au bleu Congo, et on extrait avec de l'éther. La phase éthérée est lavée à l'eau saturée de NaCl et séchée sur le sulfate de sodium anhydre. Le solvant est évaporé et les acides bruts sont méthylés avec une solution éthérée de diazométhane. Après l'évaporation de l'éther, le résidu est chromatographié en phase gazeuse comme en 3.1: les deux diesters des acides IX et VIII sont présents dans un rapport de 20% et 80% respectivement.

7. Isomérisation des diméthyl-3,3 et diméthyl-4,4 cyclohexènes

7.1. Diméthyl-3,3 cyclohexène (IIIe)

On chauffe à l'ébullition à reflux pendant 20 heures, 2.2 g de diméthyl-2,2 cyclohexanol (31), 20 ml de toluène anhydre, et 1.0 g de sodium coupé en petits morceaux. On refroidit à 0°, enlève l'excès de sodium avec des pincettes, et ajoute 50 ml d'éther anhydre puis 3.3 g de sulfure de carbone fraîchement distillé; il n'y a pas de précipitation de sel sodé. On ajoute alors 6.3 g d'iodure de méthyle dans 20 ml de méthanol anhydre et chauffe à l'ébullition à reflux pendant 4 heures. Après refroidissement à 0°, on extrait par de l'éther et isole à la manière habituelle 6.9 g (rendement 81.2%) de xanthogénate, p.é. 102° sous 1.4 mm, $n_D^{26} = 1.5390$.

Le xanthogénate (6.9 g) est ajouté goutte à goutte dans un ballon de Claisen, contenant des anneaux de verre et chauffé à 270°. Le diméthyl-3,3 cyclohexène brut qui distille est redistillé: p.é. 113–114° sous 740 mm, $n_D^{21} = 1.4447$ (on donne (32): $n_D^{20} = 1.4426$). Cet hydrocarbure est homogène en chromatographie en phase gazeuse: colonne 5 mètres, 5 mm de diamètre interne, 35% de β,β'-oxydipropionitrile sur Kromat-FB, température 55°, hélium 40 ml par minute; temps d'élution: 32 minutes.

7.2. Diméthyl-4,4 cyclohexène (IIe)

Par la méthode 7.1 décrite plus haut, on transforme le diméthyl-4,4 cyclohexanol (27) en diméthyl-4,4 cyclohexène, p.é. 115° sous 740 mm. $n_D^{25} = 1.4383$, homogène en chromatographie en phase gazeuse (temps d'élution dans les conditions décrites en 7.1: 36 minutes). On donne (33): $n_D^{20} = 1.4414$; (34): $n_D^{20} = 1.4435$.

7.3. Isomérisation des diméthyl-3,3 et diméthyl-4,4 cyclohexènes (IIIe et IIe)

Ces deux hydrocarbures furent isomérisés selon la méthode de Cope (11).

Dans chaque cas, 360 à 390 mg de l'hydrocarbure en question furent dissous dans 10 ml d'acide acétique glacial en présence de 1.0 g d'acide *p*-toluène sulfonique. Le mélange fut porté à reflux sous une atmosphère d'azote pendant 1, 17, et 257 heures. A la fin du chauffage, les produits de la réaction sont extraits par de l'éther de pétrole. Cette solution est lavée par de l'eau, jusqu'à neutralité puis séchée. L'éther de pétrole est distillé (colonne de Widmer). L'analyse par chromatographie en phase gazeuse comme plus haut en 7.1, permit à la fois d'identifier les produits de réaction et de calculer les proportions relatives de chacun des deux isomères. Les résultats sont rapportés au Tableau I. L'isomérization des deux hydrocarbures donne naissance à un mélange fort complexe d'hydrocarbures (au moins 8) et d'acétates (au moins 4), comme le

Can. J. Chem. Downloaded from www.nrcresearchpress.com by 210.87.254.6 on 09/05/12
For personal use only.

montrent la chromatographie en phase gazeuse sur colonne de Ucon Polar (20% sur Kromat FB, 2.5 mètres, *T*: 85° pour les hydrocarbures et 137° pour les acétates) et la spectroscopie infrarouge.

8.1. Diméthyl-4,4 cyclohexanedione-1,3 (XIV)

L'anhydride diméthyl-2,2 glutarique, p.f. 38–40° (on donne (35) 38.5°), 5 g, est porté à l'ébullition à reflux dans 5 ml de méthanol. On reprend par de l'éther, extrait par une solution aqueuse de bicarbonate de sodium 10%, acidifie la solution aqueuse, extrait par de l'éther, sèche et évapore l'éther. On recueille, par distillation, 11.7 g de mono-ester XX, p.é. 120° sous 1.6 mm, $n_D^{24} = 1.4395$. Rendement 85.2%.

On agite pendant 15 heures, à température de la pièce, 16.5 g de mono-ester XX et 14.4 g de chlorure de thioyle (30% d'excès). Par distillation on obtient 17.4 g de chlorure d'acide XXI, p.é. 70° sous 1.2 mm; rendement 97%.

A une solution, refroidie à 0°, de bromure de méthyle magnésium (formée à partir de 4.5 g de magnésium, 30.0 g de bromure de méthyle liquide et 150 ml d'éther) on ajoute 19 g de chlorure de cadmium anhydre en l'espace de 20 minutes, puis on agite à température de la pièce durant 45 minutes. On évapore 100 ml d'éther, puis ajoute 150 ml de benzène anhydre. Le mélange est porté à l'ébullition à reflux. On interrompt le chauffage, ajoute aussi rapidement que possible 17.4 g du chlorure d'acide XXI dans 30 ml de benzène anhydre. On reprend l'ébullition durant 30 minutes, refroidit à 0° et ajoute lentement 150 ml d'acide sulfurique 0.15 *M* refroidi à 0°. On extrait par de l'éther, lave les solutions éthérées réunies par de l'eau, une solution de bicarbonate de sodium 10%, puis à l'eau saturée de chlorure de sodium. On distille les solvants, puis le céto-ester XXII, 11.3 g, p.é. 72° sous 2 mm, $n_D^{24} = 1.4347$; rendement 73%.

A 7 g de sodium pulvérisé, juste recouvert de xylène, on ajoute 2.6 ml de méthanol anhydre et 65 ml d'éther anhydre. On agite durant 12 heures à température ambiante. On ajoute ensuite 5.0 g du céto-ester XXII, puis reprend l'agitation durant 2 heures; on essore le précipité, on le lave avec de l'éther anhydre et le dissout, par petites portions, dans 100 ml acide chlorhydrique concentré – eau 1:1. On extrait par de l'éther, lave avec de l'eau saturée de chlorure de sodium, sèche, distille l'éther, et recueille 3.0 g de diméthyl-4,4 cyclohexanedione-1,3 (XIV), p.f. 105° après cristallisation dans de l'éther de pétrole; rendement 75%. Calculé pour $C_8H_{12}O_2$: C, 67.32; H, 8.37%. Trouvé: C, 68.54; H, 8.63%. Spectre infrarouge (Nujol): –OH, bande large 3400–2660 cm^{-1}, avec max. à 2620 et 2550 cm^{-1}; C=O, 1610 cm^{-1}; C=C 1535 cm^{-1} (36).

8.2. Ethers méthyliques céto-énoliques de la diméthyl-4,4 cyclohexanedione-1,3 (XV et XVI, R = $-CH_3$)

On ajoute à 2.2 g de dicétone XIV, en solution dans 100 ml d'éther anhydre, une solution de diazométhane jusqu'à coloration jaune persistante, puis en excès (26); on abandonne pendant 2 heures à température ambiante. On évapore l'éther, reprend par de l'éther pur, que l'on lave avec une solution aqueuse d'acide chlorhydrique 5% (rapidement), puis à l'eau, avec une solution aqueuse de bicarbonate de sodium 5% et enfin à l'eau. Après distillation de l'éther, le résidu est distillé: 2.05 g, p.é. 81° sous 2 mm, $n_D^{22} = 1.4969$; rendement 85%. Calculé pour $C_9H_{14}O_2$: C, 70.03; H, 9.05%. Trouvé: C, 70.10; H, 9.15%.

8.3. Double réduction des éthers céto-énoliques XV et XVI en diméthyl-2,2 et diméthyl-4,4 cyclohexanone

On suit fidèlement les indications données pour la réduction des éthers céto-énoliques de l'oxo-4 homocamphre en cétones α,β-éthyléniques par l'hydrure de lithium et d'aluminum, puis de ces cétones en cétones saturées en présence de palladium sur carbonate de calcium (26). C'est ainsi que 2.0 g des éthers céto-énoliques XV et XVI (R = CH_3) donnent 1.45 g des cétones XVII et XVIII, qui conduisent elles-mêmes à 1.10 g de diméthyl-2,2 et diméthyl-4,4 cyclohexanones en mélange. Par chromatographie en phase gazeuse (colonne de 2.5 mètres, 30% de graisse Apiezon sur cellite, 140°, hélium 65 ml par minute) nous avons montré, par la méthode du rehaussement des pics avec des cétones authentiques, la structure de ces cétones et nous les avons dosées: 65% de diméthyl-4,4 cyclohexanone et 35% de diméthyl-2,2 cyclohexanone, ±3%.

REMERCIEMENTS

Nous remercions vivement le Conseil National de Recherches du Canada d'une subvention de recherches (H. F.) et l'Office de la Recherche Scientifique de la province de Québec de bourses d'étude (J. C. et D. V.).

BIBLIOGRAPHIE

1. A. Brenner et H. Schinz. Helv. Chim. Acta, **35**, 1618 (1952).
2. F. Bruderlein, H. Bruderlein, H. Favre, R. Lapierre, et Y. Lefebvre. Can. J. Chem. **38**, 2085 (1960).
3. P. A. Plattner, F. T. Treadwell, et C. Scholz. Helv. Chim. Acta, **28**, 771 (1945).
4. A. W. Allen, R. P. A. Sneeden, et J. M. Wilson. J. Chem. Soc. 2186 (1959).
5. W. C. Dauben, R. A. Micheli, et J. F. Eastham. J. Am. Chem. Soc. **74**, 3854 (1952).
6. A. W. Crossley et N. Renouf. J. Chem. Soc. 1552 (1906).
7. B. Berkoz, E. P. Chavez, et C. Djerassi. J. Chem. Soc. 1363 (1962).
8. D. H. R. Barton, R. M. Evans, J. C. Hamlet, P. G. Jones, et T. Walker. J. Chem. Soc. 747 (1954).
9. G. Stork, A. Brizzolara, H. Landesman, J. Szmuszkovicz, et R. Terrell. J. Am. Chem. Soc. **85**, 207 (1963).
10. R. B. Turner, W. R. Meador, et R. E. Winkler. J. Am. Chem. Soc. **79**, 4122 (1957).

Can. J. Chem. Downloaded from www.nrcresearchpress.com by 210.87.254.6 on 09/05/12
For personal use only.

11. A. C. Cope, P. T. Moore, et W. R. Moore. J. Am. Chem. Soc. **82**, 1744 (1960).
12. R. B. Turner. Abstract of Papers, 139th Meeting, American Chemical Society. March 21–30, 1961. pp. 41–0.
13. R. B. Turner et R. H. Garner. J. Am. Chem. Soc. **80**, 1424 (1958).
14. D. H. R. Barton, R. P. Cookson, W. Klyne, et C. W. Shoppee. Chem. Ind. 21 (1954).
15. J. M. Conia. Record Chem. Progr. **24**, 43 (1963).
16. A. S. Dreiding. Chem. Ind. 1419 (1954).
17. H. M. E. Cardwell et A. E. H. Kilner. J. Chem. Soc. 2430 (1951).
18. G. Stork et R. K. Hill. J. Am. Chem. Soc. **79**, 495 (1957).
19. W. J. van Asselt et D. W. van Krevelen. Rec. Trav. Chim. **82**, 51 (1963).
20. W. J. van Asselt et D. W. van Krevelen. Rec. Trav. Chim. **82**, 438 (1963).
21. R. L. Frank et H. K. Hall, Jr. J. Am. Chem. Soc. **72**, 1645 (1950).
22. H. Mühle et Ch. Tamm. Helv. Chim. Acta, **46**, 268 (1963).
23. E. E. Blais et M. Maire. Bull. Soc. Chim. France, (4), **3**, 421 (1908).
24. W. J. Bailey et M. Madoff. J. Am. Chem. Soc. **76**, 2707 (1954).
25. T. Henshall. J. Soc. Chem. Ind. **62**, 127 (1943).
26. H. Favre, B. Marinier, et J. C. Richer. Can. J. Chem. **34**, 1329 (1956).
27. E. L. Eliel et C. A. Lukach. J. Am. Chem. Soc. **79**, 5986 (1957).
28. F. G. Bordwell et K. M. Wellman. J. Org. Chem. **28**, 1347 (1963).
29. E. B. Reid et T. E. Gomp. J. Org. Chem. **18**, 661 (1953).
30. J. F. Thorpe et G. A. R. Kon. Org. Syn. **5**, 9 (1925).
31. S. S. Nametkin et M. A. Volodina. J. Gen. Chem. **21**, 331 (1951).
32. H. C. Brown et G. Zweifel. J. Am. Chem. Soc. **83**, 2544 (1961).
33. H. Pines, F. J. Paulik, et V. N. Ipatieff. J. Am. Chem. Soc. **73**, 5738 (1951).
34. K. von Auwers et E. Lange. Ann. **409**, 149 (1915).
35. A. Béhal. Compt. Rend. **121**, 216 (1895).
36. L. J. Bellamy. The infrared spectra of complex molecules. 2nd ed. Methuen & Co. Ltd., London; John Wiley & Sons, Inc., New York. 1958. p. 142.

Can. J. Chem. Downloaded from www.nrcresearchpress.com by 210.87.254.6 on 09/05/12
For personal use only.

DIPHENYLMETHANE-3,3′-DICARBOXYLIC ACID

R. W. Beattie and R. H. F. Manske
Research Laboratory, Dominion Rubber Co. Ltd., Guelph, Ontario
Received August 27, 1963

ABSTRACT

The major condensation product of benzoic acid with formaldehyde in the presence of sulphuric acid was shown to be diphenylmethane-3,3′-dicarboxylic acid.

Can. J. Chem. Downloaded from www.nrcresearchpress.com by 210.87.254.42 on 09/05/12
For personal use only.

When benzoic acid is condensed with formaldehyde in the presence of sulphuric acid there is formed in small and variable yield a diphenylmethanedicarboxylic acid. Because the product is not identical with known diphenylmethanedicarboxylic acids and because of the predominantly meta directing nature of the carboxyl group Schöpff assigned the 3,3′-positions to the carboxyls (1).

We have had occasion to repeat the condensation of benzoic acid with formaldehyde and have succeeded in isolating the major condensation product in a pure form and in establishing its structure.

The pure acid melts at 270°* and this was oxidized to the corresponding benzophenone-dicarboxylic acid. The oxime of the methyl ester of the latter on Beckmann rearrangement yielded the dimethyl ester of 3,3′-dicarboxybenzanilide identical with a synthetic specimen and therefore the structural assignment of Schöpff is correct. The above benzanilide was also prepared as follows: *m*-aminobenzoic acid was reacted with *m*-toluoyl chloride under Schotten–Baumann conditions and the resulting *m*-tolu-3-carboxyanilide was oxidized with permanganate. Further proof of the structure of the dicarboxybenzanilide came from its hydrolysis to isophthalic acid.

EXPERIMENTAL

Dimethyl Diphenylmethane-3,3′-dicarboxylate

The mixture of acids as obtained by the procedure of Schöpff was esterified with methanol in the usual manner. Upon distillation there was obtained a first fraction of methyl benzoate followed by one boiling at 200–210° at 1.5 mm which constituted about one-third of the entire ester. There was considerable higher boiling material, evidently higher condensation products. The above middle fraction was a viscous oil which crystallized after many months standing at ambient temperature. Adhering oil was pressed out on filter paper and the ester then recrystallized from methanol; m.p. 64°. Found: C, 72.21, 72.31; H, 5.42, 5.56. $C_{17}H_{16}O_4$ requires: C, 71.83; H, 5.63.

The free *acid* obtained by alkaline hydrolysis, when recrystallized from methanol, melted at 270°. Found: C, 70.68, 70.76; H, 4.59, 4.87. Calc. for $C_{15}H_{12}O_4$: C, 70.31; H, 4.69.

Benzophenone-3,3′-dicarboxylic Acid

An alkaline solution of the above diphenylmethane-3,3′-dicarboxylic acid (5 g) was digested on the steam bath for several hours with potassium permanganate (5.35 g). The acid isolated by acidification, filtration, and drying (5.1 g) was recrystallized by adding isopropanol to the concentrated solution of it in dimethylformamide. The fine colorless crystals melted at 356°. Found: C, 66.83, 66.82; H, 3.93, 3.69. $C_{15}H_{10}O_5$ requires C, 66.66; H, 3.70.

Owing to the extremely low solubility of this acid in methanol its esterification with that solvent in excess required several days heating under reflux with a trace of sulphuric acid. The *dimethyl ester* crystallized from benzene in stout colorless prisms melting at 130°. Found: C, 68.72, 68.46; H, 4.68, 4.70. $C_{17}H_{14}O_5$ requires: C, 68.46; H, 4.70.

**All melting points are corrected.*

The *oxime* of the dimethyl ester, prepared by reaction with excess hydroxylamine hydrochloride and potassium acetate in methanol, was recrystallized from methanol; m.p. 130°. Found: C, 64.94; 64.64; H, 4.72, 4.79; N, 4.43, 4.41. $C_{17}H_{15}O_5N$ requires: C, 65.18; H, 4.79; N, 4.47.

When 2 g of this oxime was heated under reflux in 40 cc benzene with 2 g phosphorus pentachloride for 3 hours it was converted to dimethyl benzanilide-3,3′-dicarboxylate. The cooled benzene solution was washed with aqueous alkali and the solvent removed by evaporation. The residue (1.6 g) when recrystallized from methanol melted at 159° and this melting point was not depressed when the ester was admixed with that prepared as described below. Found: C, 65.42, 56.47; H, 4.82, 4.88; N, 4.44, 4.54. $C_{17}H_{15}O_5N$ requires: C, 65.18; H, 4.79; N, 4.47.

The acid, obtained by hydrolysis of the above ester, was recrystallized from dimethylformamide–water and then melted at 342°. This melting point was not depressed when the acid was admixed with the evidently less pure product (m.p. 333°) described below.

Further authentication of the above anilide was achieved by heating 1 gram of it for 50 hours in a mixture of 100 cc glycol and 13 cc concentrated hydrochloric acid. The reaction mixture was then rendered akaline with sodium hydroxide and most of the glycol removed by evaporation *in vacuo*. The residue was dissolved in water, the filtered solution acidified, and the precipitate recrystallized from aqueous ethanol. It then melted at 338–339° either alone or in admixture with an authentic specimen of isophthalic acid similarly recrystallized.

m-Tolu-3-carboxyanilide

The acid chloride prepared from 9 g of purified *m*-toluic acid and excess thionyl chloride was added to a cooled solution of 9 g *m*-aminobenzoic acid in 50 cc water containing 3 g sodium hydroxide; a 40% solution of sodium hydroxide was added in small portions to maintain constant alkalinity. A slight turbidity was removed by filtration and the filtrate diluted to 500 cc with hot water. The precipitate obtained upon acidification was separated by filtration and washed with a liter of boiling water. When dried it melted at 248° and when recrystallized either from ethanol, or from dimethylformamide-methanol it melted at 250°. Found: C, 70.30, 70.99; H, 5.20, 5.03. $C_{15}H_{13}O_3$ requires: C, 70.59; H, 5.10.

Dimethyl Benzanilide-3,3′-dicarboxylate

The above anilide (6.4 g) was suspended in 100 cc water to which had been added several pellets of sodium hydroxide. The hot solution was treated with powdered potassium permanganate until further oxidation was very slow (ca. 9.5 g). The mixture was filtered with the aid of 'filtercel' and the hot filtrate acidified. The washed and dried precipitate melted not quite sharply at 333°. This crude acid required 48 hours boiling under reflux with methanol and a trace of sulphuric acid to affect complete esterification. The *dimethyl ester* was crystallized first from benzene (m.p. 152–154°) and then from methanol; m.p. 158°.

REFERENCES

1. M. SCHÖPFF. Ber. **27**, 2321 (1894).

Can. J. Chem. Downloaded from www.nrcresearchpress.com by 210.87.254.42 on 09/05/12
For personal use only.

A STUDY OF MOLECULAR INTERACTIONS IN MOLECULAR BEAMS ISOLATED FROM THE EXHAUST OF SUPERSONIC NOZZLES

JOHN P. VALLEAU AND JACQUES M. DECKERS
Department of Chemistry, University of Toronto, Toronto, Ontario
Received June 12, 1963

ABSTRACT

In high density molecular beams, such as those isolated from supersonic nozzles, collisions between beam molecules may have an important effect on the beam behavior. This paper uses the classical kinetic theory to discuss the effect of these collisions on the intensities and velocity distributions in a beam. Initially, intensities are calculated assuming unchanging Maxwellian velocity distributions. However, the beam collisions will, in fact, alter the velocity distributions in a way that could be described as an "asymmetric cooling" of the beam; a start has been made on examining the effects of this phenomenon.

In the case of beams of mixed composition, the analysis indicates that an enrichment of the heavier component will take place as a result of collisions within the beam.

Formulae relating beam density profiles to the geometry of the beam-defining elements are also deduced. Numerical examples are worked out for an illustrative case in which the diameter of the beam diaphragms is 0.1 cm and the distance between them is 10 cm, assuming the beam to be isolated from the exhaust of a 7.5 mach expansion with a stagnation temperature of 300° K.

Can. J. Chem. Downloaded from www.nrcresearchpress.com by 210.87.254.40 on 09/05/12
For personal use only.

Section 1—Introduction

An ideal molecular beam could be described as a stream of molecules which move in rigorously parallel paths without undergoing collisions. However, all attempts to obtain molecular beams in the laboratory have yielded devices in which the beam molecules only approximate this behavior. In any beam, there are two reasons for molecular encounters: collisions with residual molecules in the environment and collisions among the molecules in the beam itself. The low background pressures achieved with modern large-capacity vacuum pumps have, however, reduced the number of collisions between beam and residual molecules to a very large extent.

Recently beam densities much higher than before have been achieved by isolating molecular beams from the core of the exhaust of small supersonic nozzles. The technique was originally suggested by Kantrowitz and Grey (1), and realized experimentally first by Kistiakowsky and Slichter (2) at Harvard University, and later by Becker *et al.* (3) in Germany (Marburg and Karlsruhe) and by groups at Princeton University (4) and at the University of Virginia (5). At the beam densities thus achieved the number of collisions between the beam molecules may affect the behavior of the molecular beam in a way that cannot be neglected. The purpose of the present paper is to discuss the effect of these collisions in the beam and in particular to make some estimate of the resulting variation of intensity and velocity distribution throughout the beam. Most measurements on "nozzle beams" have recorded the *total flux* at a *fixed* detection station. It will be shown that the flux at other positions in the beam can, as a result of collisions, differ significantly from the results of such measurements. The intensity profiles within the beam are also investigated.

It might be useful to point out that the variation of velocity distribution and density profiles as a function of the distance from the point of origin of the beam will have far-reaching influences on the beam experiments which are presently being carried out or

contemplated in various laboratories. Although surface-scattering experiments involving a single beam might not be too much affected provided all targets are mounted at exactly the same location and the beam is not too wide, the study of gas phase collisions and scatter will be especially sensitive to the detailed density distribution within the beam.

In section 2 beam formation is described, and the velocity distribution functions in the beam are discussed with reference to some assumptions basic to the later calculations. In the following section the purely geometrical factors affecting the behavior of molecular beams will be studied. We then go on to consider beams in which collisions may occur, examining first the central "core" region of a one component beam (section 4), and then the intensity profiles in the remaining peripheral region of the beam (section 5). Finally we make some remarks on beams composed of a mixture of heavy and light molecules.

Section 2—Formation of a Supersonic Beam

Only the experimental features relevant to the analysis will be given here, since a complete description of the method has appeared elsewhere (4).

As seen in Fig. 1 a converging nozzle exhausts into chamber I evacuated to a pressure

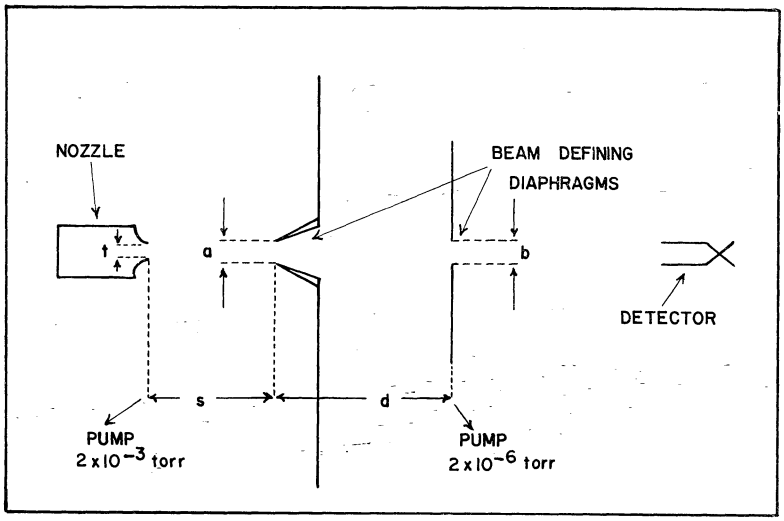

FIG. 1. Production of a "nozzle beam" (schematic).

of about 10^{-3} torr. Part of the core of the exhaust gases flows through a hole in the tip of a conical diaphragm into a second enclosure in which the pressure is maintained near 2×10^{-6} torr. In this enclosure is located a second diaphragm which further defines the molecular beam. The mean free path in the second chamber at those working pressures is larger than 10^3 cm, so the number of collisions between beam and background molecules is very small and might be neglected.

The fluid mechanical description of flow through nozzles may be found in adequate textbooks.* According to this the bulk mass velocity of a pure gas expanded through a nozzle will be

$$\bar{v} = \sqrt{\frac{2C_p(T_0-T)}{M}}, \qquad [2.1]$$

where the following symbols are used:

*For example, see ref. (6).

Can. J. Chem. Downloaded from www.nrcresearchpress.com by 210.87.254.40 on 09/05/12
For personal use only.

$\bar{v}$ is the bulk mass velocity or "beam velocity",
C_p is the specific heat per mole, at constant pressure,
M is the molecular weight,
T_0 is the temperature before expansion (stagnation temperature),
T is the temperature within the beam after expansion, with respect to an observer moving with the beam velocity $\bar{v}$.

The temperatures T_0, T will be related by

$$T_0/T = 1+[(\gamma-1)/2]\mathscr{M}^2 \qquad [2.2]$$

where $\mathscr{M}$ is the mach number of the gases expanded through the nozzle.

These equations assume isentropic flow and imply the retention, throughout the expansion, of a Boltzmann velocity distribution isotropic with respect to the local bulk velocity. We have adopted this Boltzmann distribution as a reasonable (and furthermore workable) basis for our calculations (cf. appendix 3). It must be admitted that this distribution will in fact be distorted, between the diaphragms, in two ways. The first concerns merely the spreading of the beam and leads, on a simple-minded view, to the distribution

$$f(v) \propto v^2 \exp\{-m(v-\bar{v})^2/2kT\}. \qquad [2.3]$$

The purely Maxwellian distribution we are using neglects,* in the words of Kantrowitz and Grey (1), "the influence of the random velocity on the probability of a molecule's getting through the slit, compared to the predominant effect of the mass flow velocity". The distortion is in fact not very great since most of the velocities $v \approx \bar{v}$, and it is smaller the higher the mach number of the beam. In any case it will become apparent from our analysis (section 4) that the beam's velocity distribution will be simultaneously subjected to a second, equally serious, distortion by collisions between the molecules. In view of this the above distribution [2.3] is not of special relevance. In section 4 we will consider how we may make some correction for the effect of collisions on the velocity distribution in the beam.

A beam is isolated from the expanded gas by two apertures, of diameters a and b, which are separated by a distance d. At the second aperture, no molecule in the beam will have a trajectory forming an angle with the beam axis greater than arctan (b/d). All smaller angles will, however, be present, and will result in the gradual spreading of the beam envelope. This "geometrical" effect will lead to no change in the *total* flux in the beam, of course, but only to a decrease of molecular density within the beam. At the same time, collisions will occur, and most such collisions will result in the removal from the beam of the colliding molecules. This leads to a decrease of total molecular flux in the beam, and thus results in a further reduction of the beam density.

It will be convenient to present some numerical examples in this paper. For this purpose we have chosen a sample beam of typical dimensions to which all illustrative examples will refer. This beam is defined by equal apertures $a = b = 0.1$ cm, separated by a distance $d = 10$ cm. The stagnation and beam temperatures will be taken as $T_0 = 300°$ K and $T = 15°$ K, respectively. The gas is assumed to be monatomic and ideal. The temperatures assumed are those of a mach 7.5 expansion.

Section 3—Geometrical Effects

We wish to calculate the molecular density at any point in the beam, and we consider in this section the purely geometrical effects. That is, we attempt to obtain the density

*We are grateful to R. P. Andres of Princeton University for raising this question.

Can. J. Chem. Downloaded from www.nrcresearchpress.com by 210.87.254.40 on 09/05/12
For personal use only.

in the absence of any collisions in the beam (for point particles, for example, or for photons).

This calculation is much simplified as a result of the following considerations. Suppose a particular molecule is moving with the beam velocity $\bar{v}$. If it is to remain in the beam after isolation by the two apertures, its *transverse* velocity, v_{tr}, must be less than $(b/d)\bar{v}$; i.e.

$$v_{tr} < \frac{b}{d}\bar{v} = \frac{b}{d}\mathscr{M}\sqrt{\frac{[C_p(\gamma-1)T]}{M}}. \qquad [3.1]$$

For most cases of interest this velocity is very small. In particular, $(b/d)\bar{v}$ is much less than the r.m.s. transverse velocity, $\sqrt{2(RT/M)}$, of the gas behind the apertures; for our "sample beam" ($(\gamma-1)C_p = 5R/3$, $\mathscr{M} = 7.5$)) we find a ratio of 0.068 for these quantities. Figure 2 shows a Boltzmann velocity distribution function, and indicates that even at

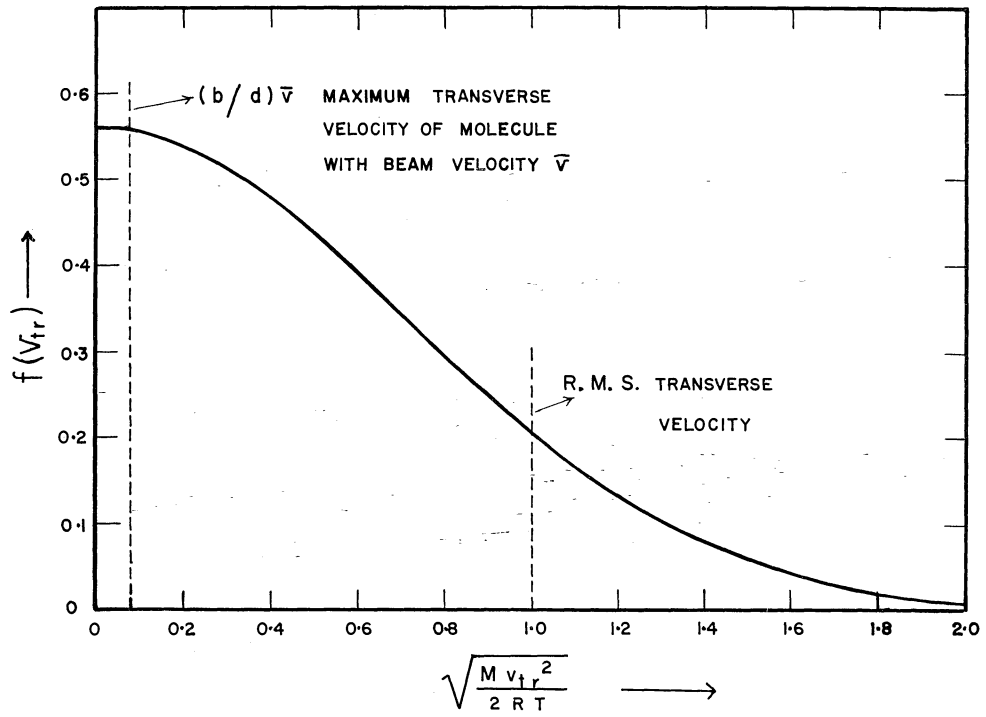

FIG. 2. A normalized Maxwell velocity distribution, showing the r.m.s. transverse velocity behind the apertures, and also the maximum transverse velocity of a molecule in the beam and travelling with the beam velocity $\bar{v}$ (for the sample beam).

the maximum value $(b/d)\bar{v}$ of v_{tr} the velocity probability is down only to 0.99_5 of its peak value. It is therefore a very fair approximation to take equal probabilities for all the (very small) transverse velocities attainable within the beam, and this approximation is the basis of the following calculations.

As shown in Fig. 3, the molecular beam consists of a central region, or "core", and a surrounding "off-core" or "peripheral" region. Points in the core "see" the whole of the first aperture. Since points in the first aperture are, according to the above approximation,

Can. J. Chem. Downloaded from www.nrcresearchpress.com by 210.87.254.40 on 09/05/12
For personal use only.

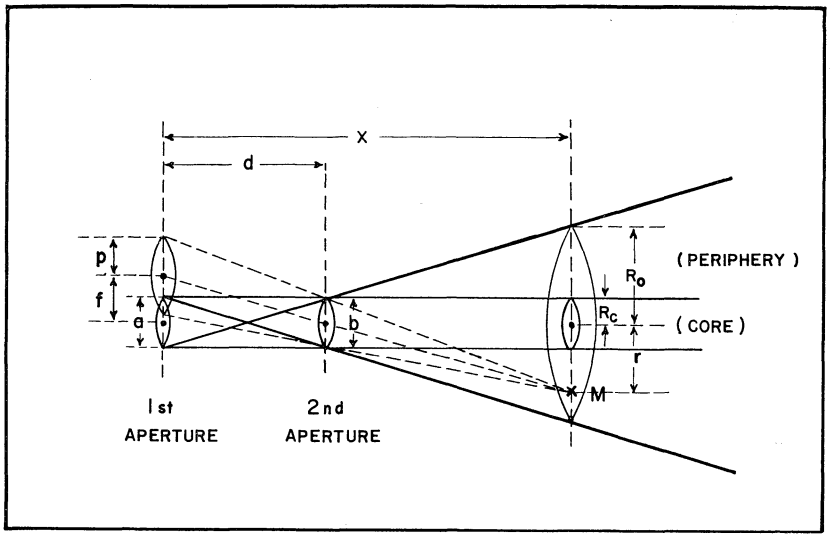

FIG. 3. Structure of the beam. Here $a = b = 2R_c$; if $a \neq b$, the core becomes conical.

regarded as isotropic point sources, the molecular density in the core will fall off according to the inverse square law:

$$n_c' = n_b d^2/x^2, \qquad [3.2]$$

$$dn_c'/dx = -2n_c'/x, \qquad [3.3]$$

where x is the distance, measured along the beam axis, from the first aperture, n_c' is the density in the core, and the prime refers to the calculations of this section, in which collisions are ignored; n_b is the value of the density in the second aperture. (Since the first aperture is finite, the above equations really involve the additional assumption that we may ignore the deviation from unity of the cosines of all angles less than arctan (b/d). For our sample beam, cos arctan (b/d) is 0.9999_5, and the approximation is entirely justified.)

According to the above, the intensity is uniform across the core of the beam at a given value of x; one may say that the intensity profile has a flat top. Turning now to points inside the beam, but at a distance r, greater than the radius of the core, from the beam axis, only a fraction $\sigma'(x,r)$ of the first aperture will be visible. The molecular density at this distance r will be related to that in the core by

$$n'/n_c' = \sigma'. \qquad [3.4]$$

In appendix 1, this ratio σ' has been evaluated as a function of x and r. It proves convenient to introduce the quantities R_c and R_o, which are respectively the radius of the core and that of the outer envelope of the beam. At a distance x from the first diaphragm $(x > d)$, these may be written

$$R_c = \frac{b}{2}\left(\frac{x}{d}\right) - \frac{a}{2}\left(\frac{x-d}{d}\right), \quad R_o = \frac{b}{2}\left(\frac{x}{d}\right) + \left(\frac{a}{2}\right)\left(\frac{x-d}{d}\right). \qquad [3.5]$$

Can. J. Chem. Downloaded from www.nrcresearchpress.com by 210.87.254.40 on 09/05/12
For personal use only.

When these quantities, along with [A.1.5], are introduced into [A.1.4], we find that

$$\sigma' = \frac{1}{\pi}\text{arc cos}\left(\frac{r^2-R_oR_c}{r(R_o-R_c)}\right)+\left(\frac{x}{x-d}\right)^2\left(\frac{b}{a}\right)^2\frac{1}{\pi}\text{arc cos}\left(\frac{r^2+R_oR_c}{r(R_o+R_c)}\right) - \frac{2}{\pi}\frac{\sqrt{(R_o^2-r^2)(r^2-R_c^2)}}{(R_o-R_c)^2}. \qquad [3.6]$$

We may describe the off-core values of r by the dimensionless quantity

$$\xi = (r-R_c)/(R_o-R_c); \qquad [3.7]$$

ξ ranges from zero at the edge of the core to unity at the outer edge of the beam.

In Fig. 4 is shown σ', for our sample beam, as a function of ξ for various values of x

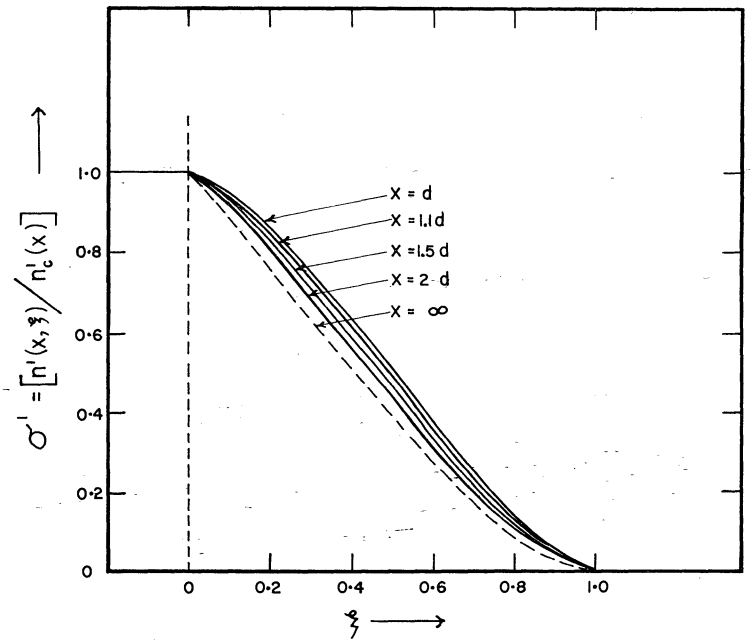

FIG. 4. Beam profiles, in the absence of collisions, for the sample beam: $a = b = 0.1\ d$.

from d to infinity. What seems remarkable is the consistency of this profile, which means that at constant ξ, the density falls off very closely as the inverse square of x. We shall later find this a helpful approximation (section 5).

At the second aperture there is no peripheral region (Fig. 3), and the beam flux is merely spread uniformly across the core of the beam. Considering points further along the beam ($x > d$), one could inquire into the distribution of the flux as a function of the distance, r, from the center of the beam. To do this one must evidently multiply the intensity profile (Fig. 4) by $2\pi r$. One then easily sees that, at least for a parallel beam, most of the flux very soon takes place through the peripheral region rather than through the core. We shall find that collisions in the beam will further increase the proportion of the flux appearing in the peripheral region. This is somewhat unfortunate, for one's estimates of collisional attenuation are apt to be rather better in the core than outside it. This migration

Can. J. Chem. Downloaded from www.nrcresearchpress.com by 210.87.254.40 on 09/05/12
For personal use only.

of the flux from the core to the periphery can be reduced by the use of a diverging beam, of course, and this may sometimes prove useful.

Section 4—Effect of Collisions on Density in the Core

Almost every molecule that collides with a similar molecule within the beam will be given a new trajectory which quickly carries it out of the beam (some further consideration of this statement will be found in appendix 2). Combining this collisional effect with the inverse square depletion [3.3], we obtain a corrected equation for attenuation of the core density:

$$dn_c/dx \equiv (1/\bar{v})(dn_c/dt) = -\lambda n_c^2/\bar{v} - 2n_c/x, \qquad [4.1]$$

where $\lambda n_c^2/2$ is the collision frequency in the core of the beam. If the velocity distribution functions are Maxwellian, the collision frequency may easily be calculated; this is done in appendix 3, where no allowance is made for the effect of the small transverse velocities. This result is

$$\lambda n^2/2 = 2n^2\rho^2\sqrt{(4\pi RT/M)}, \qquad [4.2]$$

where T is again the temperature within the beam, and where it has been assumed that the collision probability may be described in terms of a velocity-independent collision radius ρ. It has been found experimentally that ρ is strictly dependent on the relative velocity and it may prove necessary to take some account of this. On the other hand the relative velocities are, of course, mostly rather small in the molecular beams, so that we might expect ρ to be large, but not to vary greatly.

Equation [4.1] is easily solved when λ is independent of x; the result (cf. appendix 3) is

$$n_c = \frac{n_b d^2}{x^2\left\{1+\frac{\lambda n_b d(x-d)}{\bar{v}x}\right\}}, \qquad [4.3]$$

where n_b is again the density in the second aperture. According to this, the initial decrease in density is large, due to collisions; as the density gets smaller, however, the number of collisions quickly diminishes, and the attenuation approaches that of the inverse-square law. This is illustrated in Fig. 5, for two values of $\lambda n_b d/\bar{v} = \Lambda$. These values of Λ are not unrealistic. It appears that fluxes of about 5×10^{17} molecules cm^{-2} sec^{-1} can be achieved in nozzle beams (9). Taking this figure we find

$$\Lambda \equiv \frac{2\rho^2\sqrt{(4\pi RTM)}\times10^{18}\times d}{2C_p(T_o-T)} \doteq 2\times10^{13}\rho^2\sqrt{M},$$

where the final form applies to our sample beam. If we assign argon a collision radius of 15 Å, we find $\Lambda = 3$; the parameter Λ will be smaller for beams of higher mach number, however.

The above result [4.3] depends on the assumption that λ is independent of x. Unfortunately this is not the case. The complication arises in the following way. The beam is being depleted by collisions. Molecules moving rapidly relative to the mean motion of the beam are naturally most apt to collide; that is, the very slow and very fast molecules will be depleted more quickly than those moving with a velocity close to $\bar{v}$. This evidently corresponds to a "cooling" of the beam as it moves, but it also leads, as we shall see, to increasingly non-Maxwellian velocity distributions.

Can. J. Chem. Downloaded from www.nrcresearchpress.com by 210.87.254.40 on 09/05/12
For personal use only.

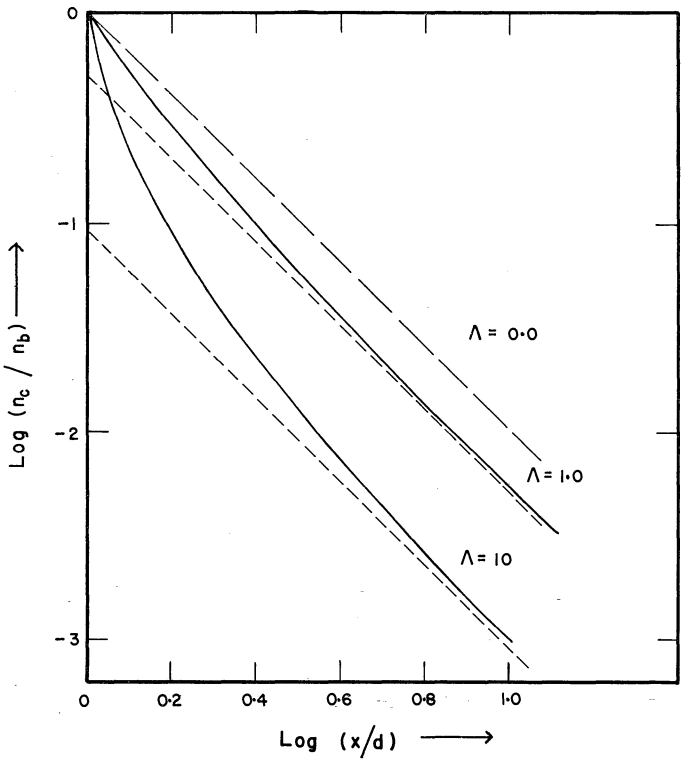

FIG. 5. Attenuation [4.3] of the core density, taking account of collisions, for two values of $\Lambda \equiv \lambda n_b d/\bar{v}$, along with the asymptotic inverse square laws.

We write an equation analogous to [4.1], but describing only the density $n_c f(v)$ of molecules with a particular velocity v:

$$\frac{d\, n_c f(v)}{dx} = -\frac{\lambda^*(v) n_c^2 f(v)}{v} - \frac{2 n_c f(v)}{x} \qquad [4.4]$$

In [4.4], $f(v)$ is the normalized probability of a molecule's having a velocity v; the integral $\lambda^*(v)$ is derived in appendix 3 [A.3.7]. Notice the denominator v in the collisional term of [4.]. Because of this, the *spatial* attenuation of the very slow molecules ($v \ll \bar{v}$) is greater than that of the very fast ($v \gg \bar{v}$). This is understandable, in that slower molecules remain a longer time in the high density part of the beam. It leads, of course, to an "acceleration" of the mean velocity of the beam and also to a skewed velocity distribution, having a long low-velocity wing. The existence of these effects can be seen in the curves published by Becker and Henkes (3(*c*)). It may be worth mentioning that the extent of the increase in the mean velocity, $\bar{v}$, is of course limited by the width (speaking loosely) of the thermal spread in the velocities. Detailed theoretical study of this effect has not been attempted here and further quantitative experiments are needed.

It is of interest, however, to make some estimate of how seriously this affects our result [4.3]. To do this we have examined the "cooling" effect of the collisions in an approximate way, ignoring the accompanying asymmetry: we suppose the velocity

Can. J. Chem. Downloaded from www.nrcresearchpress.com by 210.87.254.40 on 09/05/12
For personal use only.

distribution to remain Maxwellian. The approximations are discussed in appendix 3, where a set of differential equations for n_c and λ are derived and solved. The result is

$$n_c = \frac{n_b d^2}{x^2\left[1+\frac{(1+G)\,\lambda_b n_b d(x-d)}{\bar{v}x}\right]^{1/(1+G)}}. \qquad [4.5]$$

Here λ_b is the value of λ [4.2] at the second aperture. G is a constant, which may be chosen to give a rate of "cooling" close to that which a Boltzmann function would actually undergo (but which takes no account of the asymmetry that would simultaneously appear). This is discussed more fully in the appendix, and it is shown that a value $G = 0.29_3$ gives a reasonable account of the cooling effect in the molecular beams. Adopting this value, we may calculate by how much our new estimate [4.5] differs from [4.3]. The new result [4.5] may be regarded as a slightly better approximation, though the discrepancy will often be small, when compared with the total effect of the collisions as predicted by either. The two results are compared, in Fig. 6, for various beams, corresponding to $\Lambda_0 = \lambda_b n_b d/\bar{v} = 1.5$, 1, 0.75, and 0.5, as a function of position x in the beam. The discrepancy amounts, in these cases, to less than 10% at x equal infinity, and it is smaller for the useful parts of the beam ($x \sim 2d$).

Section 5—Effect of Collisions on Density outside the Core

The molecular density in the beam but outside the core varies both along the beam and in a radial direction. It could be described, knowing the density in the core, by a function σ:

$$\sigma(\xi,x) = n(x,\xi)/n_c(x) \qquad [5.1]$$

analogous to σ' [3.4]. Our task is to make some estimate of the form of σ, but this is not a simple problem.

It is easy to see qualitatively how σ will differ from σ'. The core density has been reduced below that in the absence of collisions, and this will be equally true for the density outside, but close to, the core. All paths leading to points near the outer envelope of the beam, on the other hand, pass only through low density regions, so that collisions will have had little effect; the density profile near the edge of the beam will therefore be very similar to that in the absence of collisions. It is thus evident that σ, when plotted against ξ, will be somewhat convex upwards for middle values of ξ, unlike the nearly linear σ'.

By noting that the total flux in the beam is attenuated only by collisions, it is possible to derive a somewhat complicated integral equation for $d\sigma/dr$; this equation has not been solved. Instead we write the following approximate equation

$$\left(\frac{dn}{dx}\right)_\xi = -\frac{\lambda n^2}{\bar{v}} + \frac{n}{n'}\left(\frac{dn'}{dx}\right)_\xi, \qquad [5.2]$$

where the subscripts signify that the differentials are to be taken along paths of constant ξ, and the primes once again signify the collision-free beams discussed in section 3. In [5.2], the first term describes the collisional depletion of the beam, in the same approximation as in [4.1]. The second term describes the convective contribution to $(dn/dx)_\xi$, but it

Can. J. Chem. Downloaded from www.nrcresearchpress.com by 210.87.254.40 on 09/05/12
For personal use only.

takes only partial account of the secondary effect of collisions on this convective contribution. This equation is derived in appendix 4, and the nature of the approximations is made more precise.

To solve [5.2], we set

$$n = Sn' \qquad [5.3]$$

when we obtain the new equation

$$\frac{1}{S^2}\left(\frac{dS}{dx}\right)_\xi = -\frac{\lambda n'}{\bar{v}}. \qquad [5.4]$$

To simplify the solution of this equation we introduce a further approximation. As mentioned at the end of section 3, the profile of σ' is remarkably unchanging as a function of x; this means that the attenuation of $n' = \sigma' n_c'$, at constant ξ, is very nearly that of n_c' only, [3.3]:

$$n_c' = n_b d^2/x^2 \qquad [5.5a]$$

or

$$\left(\frac{\partial n'}{\partial x}\right)_\xi \approx \sigma' \frac{\partial n_{c'}}{\partial x} = -\frac{2\sigma' n_c}{x}. \qquad [5.5b]$$

If this approximation is made, [5.4] is readily integrated; when it is combined with [5.3], [3.20], and [3.4] we obtain

$$n = \frac{\sigma' n_b d^2}{x^2\left[1+\sigma' \dfrac{\lambda n_b d(x-d)}{\bar{v}x}\right]} = n_c\sigma. \qquad [5.6]$$

We could also write, using [4.3],

$$\sigma = \sigma' \frac{\left[1+\Lambda\dfrac{x-d}{x}\right]}{\left[1+\sigma'\Lambda\dfrac{x-d}{x}\right]} \qquad [5.7]$$

showing that σ is everywhere greater than σ', as expected. The effect of collisions on the shape of σ is shown in Fig. 7, where the dimensions a, b, d are those of our sample beam, and $\Lambda = \lambda n_b d/\bar{v} = 1$.

This result, while approximate, has desirable characteristics. It correctly predicts $n = n'$ in the absence of collisions. It has the distortion from σ' which was expected, and it remains continuous at the edges of the beam and the core.

The effect of "beam cooling" could be allowed for as before, introducing a $(1+G)$ modification like that of [4.5].

Section 6—Mixture of Light and Heavy Gases

When expanding a solution of a heavy gas (argon) in a light gas (hydrogen), Becker and Henkes (3(*c*)) observed that the velocity of the heavy molecules was larger than that obtained in the expansion of the pure heavy gas. One pictures the heavy gas "carried along" by the much faster light molecules. This is only to say that during the expansion—i.e., while the gases are undergoing hydrodynamic flow—any average motion of one gas

Can. J. Chem. Downloaded from www.nrcresearchpress.com by 210.87.254.40 on 09/05/12
For personal use only.

Can. J. Chem. Downloaded from www.nrcresearchpress.com by 210.87.254.40 on 09/05/12
For personal use only.

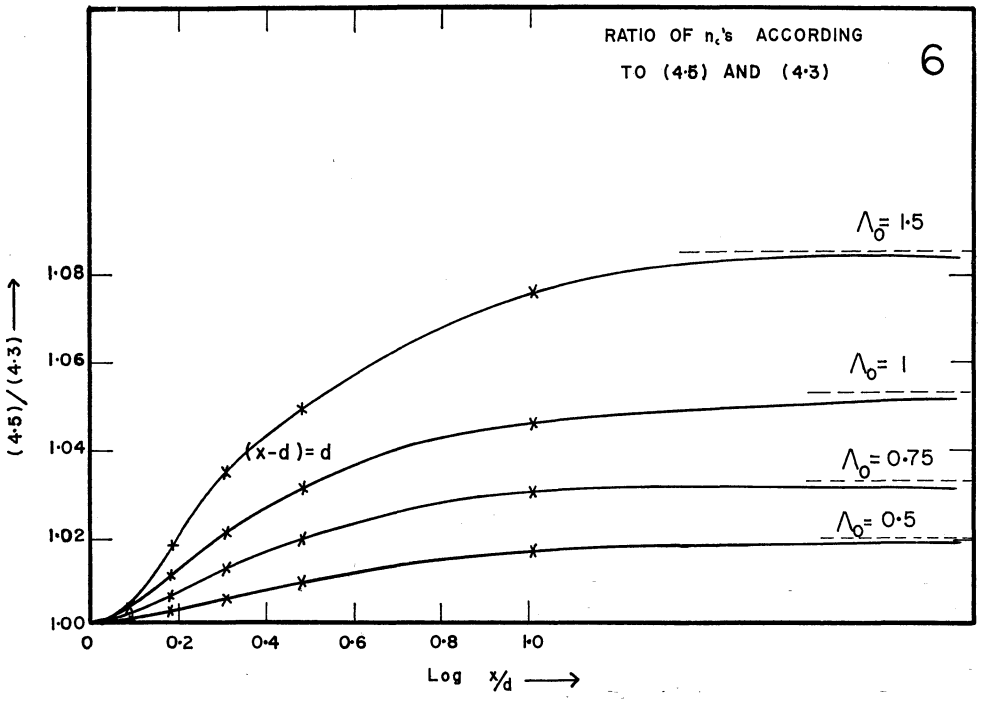

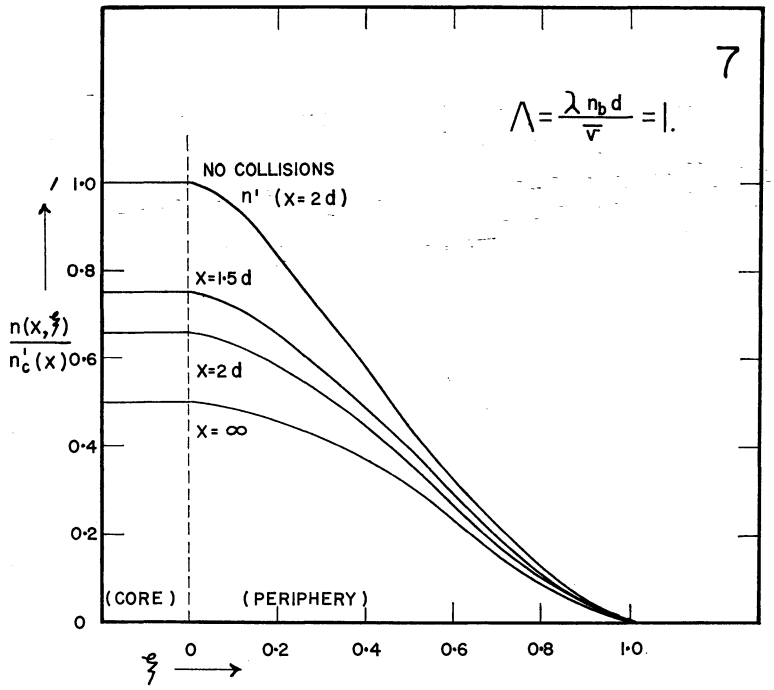

FIG. 6. Effect of the beam cooling; the figure shows the ratio of the densities according to [4.5] and [4.3], for several values of $\Lambda_0 = \lambda_b n_b d/\bar{v}$.

FIG. 7. Effect of collisions on the beam profiles. The number density, n, is compared with that in the core and in the absence of collisions, n_c'. (It is consistent with the approximation that the top curve, n', holds for all x in the absence of collisions. The actual small variation of σ' may be seen in Fig. 4.)

relative to the other must rapidly be dissipated. The same will be true of any temperature difference between the two gases. This appears to be in keeping with the physical model implied by the hydrodynamic description of flow through a nozzle (section 2 and ref. (6)).

We therefore assume that, as a good approximation, the two gases, immediately after expansion, share the same mean velocity $\bar{v}$ and the same temperature T within the beam. Then $\bar{v}$ and T will be related by [2.1] where C_p and M are replaced by $(X_1C_{p1}+X_2C_{p2})$ and $(X_1M_1+X_2M_2)$, X_1 and X_2 being the mole fractions of the two components. Evidently if $M_1 \gg M_2$ the resulting beam velocity will be greater than that for the pure heavy gas 1, but less than that for the light gas 2.

Becker, Bier, and Burghoff (3(*b*)) also reported that an almost pure argon beam was obtained from the originally dilute solution of argon in hydrogen. The relatively rapid disappearance of the light gas can again be ascribed partly to "geometrical" and partly to "collisional" effects. The geometrical effect (see Waterman and Stern (7)) may be explained as follows. If the two gases are described by the same temperature within the beam, the thermal velocities of the light molecules, including their transverse velocities, will be on the whole considerably greater than those of the heavy molecules. As a result the light gas will "spread", behind the diaphragms, much more rapidly than the heavy gas, and only a relatively small proportion of its molecules will have transverse velocities sufficiently small that they get through both apertures and into the beam.

In addition, however, one can see that the collisional attenuation of the light molecules will be much greater than that of the heavy, Nearly all collisions between molecules of equal weight lead (appendix 2) to the disappearance of both molecules from the beam. By contrast, the collision of a very light molecule with a very heavy molecule will be expected to lead to the departure of the light, while the path of the heavy molecule is scarcely altered. We can express this by a set of equations for the core densities, analogous to [4.1]:

$$dn_1/dx = -(\lambda_{11}n_1^2/\bar{v}) - (2n_1/x) \qquad [6.1]$$

$$dn_2/dx = -(\lambda_{12}n_1n_2/\bar{v}) - (\lambda_{22}n_2^2/\bar{v}) - (2n_2/x) \qquad [6.2]$$

where $M_1 \gg M_2$. The absence of a λ_{12} term from [6.1] (which is correct in the limit $M_1/M_2 \to \infty$) expresses the ineffectiveness, for the removal of the heavy molecules, of collisions with light molecules. The coefficients λ_{11}, λ_{12}, λ_{22} may be written [A.3.6]

$$\lambda_{11} = 4\rho_1^2\sqrt{(4\pi RT/M_1)},\ \lambda_{22} = 4\rho_2^2\sqrt{(4\pi RT/M_2)},$$

$$\lambda_{12} = (\rho_1+\rho_2)^2\sqrt{[2\pi RT(M_1+M_2)/M_1M_2]}.$$

We see that for $M_1 \gg M_2$, λ_{12} will certainly exceed λ_{11}; if the collision radii are well-behaved, λ_{22} will also be considerably greater than λ_{11}. The attenuation of the light gas will be correspondingly great.

The logarithmic decrements $(1/n_1)(dn_1/dx)$ and $(1/n_2)(dn_2/dx)$ are obtained on dividing [6.1] and [6.2] by n_1 and n_2 respectively. Figure 11 shows the ratio of the collisional contributions to these logarithmic decrements for various mole fractions: the curve has been drawn for the mass ratio $M_1/M_2 = 20$ (as for argon and hydrogen) and assumes equal collision radii. It can be seen that at low argon concentrations the collisional depletion of the hydrogen will be enormously more rapid than that of the argon. However, even in the limit of low hydrogen concentration ($X_2 \to 0$), the fractional decrease of the hydrogen remains considerably more rapid than that of the argon. It follows that an

Can. J. Chem. Downloaded from www.nrcresearchpress.com by 210.87.254.40 on 09/05/12
For personal use only.

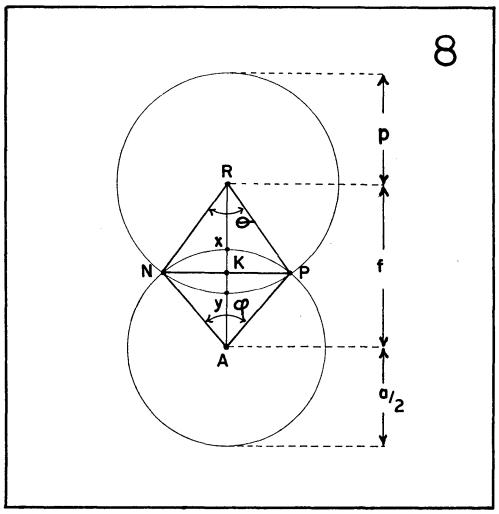

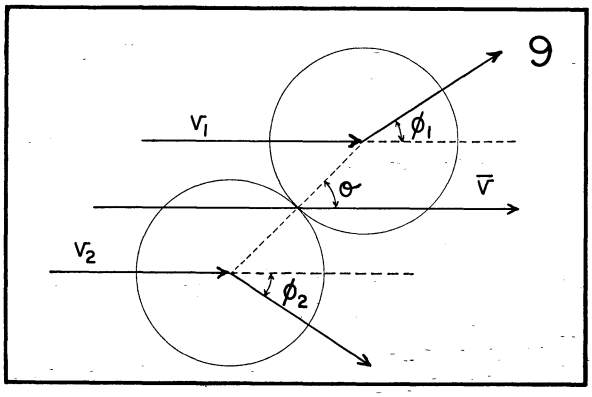

FIG. 8. Calculation of the fraction of the first aperture seen from a peripheral point M in the beam (cf. Fig. 3).

FIG. 9. Hypothetical collision discussed in appendix 2.

almost pure beam of a heavy gas could thus be obtained: no limit exists to the enrichment by collisions.

Equation [6.1] is exactly like [4.1] and has the same form of solution [4.3]; it is possible, using this result, to solve [6.2]. The "asymmetric cooling" effects will of course occur in the mixed beam. It is rather amusing that the light gas will thus be at first accelerated ahead of the heavy gas, but as the density of the light gas becomes small most of its collisions will begin to be with the heavy molecules—at this time the mean velocity of the light gas must return toward that of the heavy gas.

It is incidentally evident that for molecules of equal weight (so that a λ_{12} term will appear in [6.1]), the difference in collision radii will lead to a collisional depletion of the "larger" component. The relevant experiments on isolated beams have not been carried out. Immediately after expansion, nitrogen–ethylene mixtures show a separation in the *opposite* direction (Waterman and Stern (7)). This was ascribed to a perturbation of the isentropic expansion model of nozzle flow, such that the larger molecule acquires a larger mean velocity and a lower temperature in the beam.

Can. J. Chem. Downloaded from www.nrcresearchpress.com by 210.87.254.40 on 09/05/12
For personal use only.

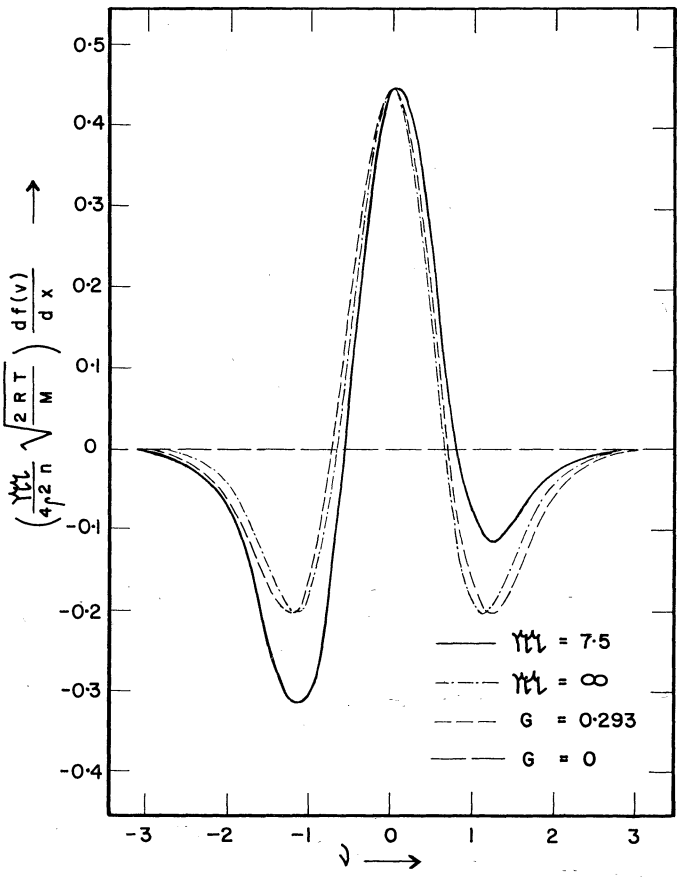

FIG. 10. "Asymmetric cooling". This shows the initial rate of the collisional distortion of a normalized Maxwellian velocity distribution (with $\mathcal{M} = 7.5$). The curve shows the cooling and accelerating effects, and also that the Maxwell distribution is destroyed. Also shown is the limit $\mathcal{M} = \infty$. The broken line shows the "cooling" approximation derived here ($G = 0.293$), in which the Maxwell distribution is retained but the temperature is allowed to diminish; the first approximation, [4.1], [4.3], (i.e. $G = 0$) is also shown by the dashed horizontal line.

Section 7—Conclusion

The calculations of this paper must be regarded as only a beginning of a classical kinetic theory of high density molecular beams. It is hoped that it provides a valuable qualitative description of some beam phenomena, and allows certain useful quantitative predictions. Less drastic assumptions can certainly be introduced, but the resulting equations will probably require numerical solution.

We have been especially interested in the effects of collisions within the beam, but have restricted our attention to the beam itself—i.e. to the region outside the second aperture. This was done to make the mathematical problems palatable, but it is, of course, precisely in the high density region behind the diaphragms that collisions will have their greatest effects in distorting the velocity distributions, reducing the beam density, and enriching the heavier gas of a mixture. The situation is much complicated by the fact that behind the first diaphragm, and to some extent between the diaphragms, there will also occur collisions which result in molecules *entering* the beam. That is to say that there exists,

Can. J. Chem. Downloaded from www.nrcresearchpress.com by 210.87.254.40 on 09/05/12
For personal use only.

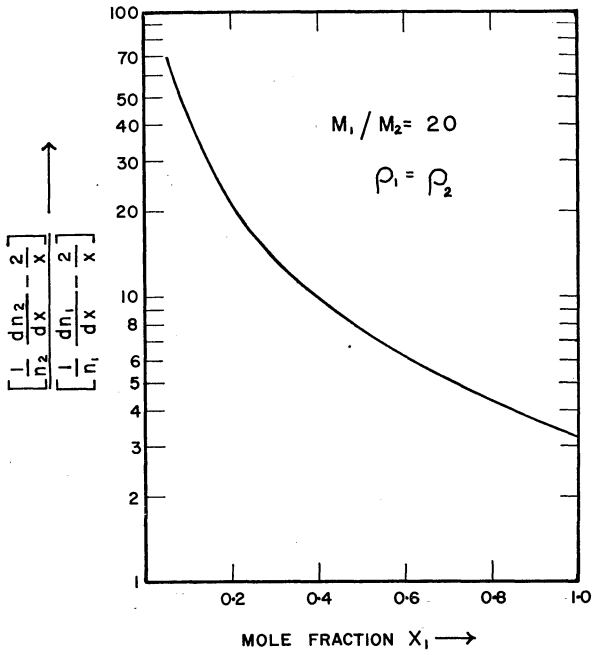

FIG. 11. Ratio of the collisional contributions to the logarithmic decrements of the light and the heavy gas in a mixed beam.

behind the diaphragms, a region not adequately described by either a hydrodynamic or a molecular collision treatment; we have shirked the study of this transition region.

It should be emphasized that, although the velocities with respect to laboratory coordinates may be very large, the relative velocities of molecules in the beam are small. Hence we may expect rather large values of the collisional radii.

The illustrations in the text have been for a sample beam of mach 7.5. For higher mach numbers it is easy to see that the approximations of section 3 and of appendix 2 slightly deteriorate, while the "Boltzmann" approximation to the beam cooling (section 4 and appendix 3) will improve.

Troitskii (8) has calculated that the mean free path in a beam having a velocity distribution uniform over a limited range Δv, is inversely proportional to this width Δv. This corresponds to the proportionality [A.3.6] of collision frequency to $\sqrt{(T/M)}$, found with the more realistic distribution assumed in this paper.

ACKNOWLEDGMENTS

The authors wish to thank Professor M. J. Dignam and Professor D. J. Le Roy, of this Department, for very valuable discussions. Some preliminary calculations were made while one of us (J. M. D.) was a research associate in Princeton University. He wishes to thank Professor R. M. Drake, Professor J. B. Fenn, and Professor M. Boudart for advice and discussion. Mr. Gordon Albright read the manuscript.

Acknowledgment for support of this research is made to the donors of "The Petroleum Research Fund", administered by the American Chemical Society, and to the National Research Council of Canada for a major equipment grant and for a grant in support of the molecular beam research. We are also grateful to the University of Toronto for special financial assistance with the molecular beam program.

Can. J. Chem. Downloaded from www.nrcresearchpress.com by 210.87.254.40 on 09/05/12
For personal use only.

REFERENCES

1. A. KANTROWITZ and J. GREY. Rev. Sci. Instr. **22**, 328 (1951).
2. G. B. KISTIAKOWSKY and W. P. SLICHTER. Rev. Sci. Instr. **22**, 333 (1951).
3. (*a*) E. W. BECKER and K. BIER. Z. Naturforsch. **9a**, 975 (1954).
   (*b*) E. W. BECKER, K. BIER, and H. BURGHOFF. Z. Naturforsch. **10a**, 565 (1955).
   (*c*) E. W. BECKER and W. HENKES. Z. Physik, **146**, 320 (1956).
4. (*a*) J. M. DECKERS and J. B. FENN. Rev. Sci. Instr. **34**, 96 (1963).
   (*b*) J. B. FENN and J. M. DECKERS. Proc. Third Intern. Symp. Rarefied Gas Dyn. Paris. 1962. To be published.
5. R. N. ZAPATA, H. M. PARKER, and J. H. BODINE. Proc. Second Intern. Symp. Rarefied Gas Dyn. Berkeley, Calif. 1960 (publ. 1961). p. 67.
6. A. H. SHAPIRO. The dynamics and thermodynamics of compressible flow. Vol. 1. Ronald Press, N.Y. 1953. Chap. 4.
7. P. C. WATERMAN and S. A. STERN. J. Chem. Phys. **31**, 405 (1959); S. A. STERN, P. C. WATERMAN, and T. F. SINCLAIR. J. Chem. Phys. **33**, 805 (1960).
8. V. S. TROITSKII. Zh. Eksperim. i Teor. Fiz. **14**, 389 (1961).
9. M. BOURGUIGNON, R. G. ALBRIGHT, R. L. LEROY, and J. M. DECKERS. To be published.

Can. J. Chem. Downloaded from www.nrcresearchpress.com by 210.87.254.40 on 09/05/12
For personal use only.

APPENDIX 1

Calculation of σ'

In Fig. 8, the smaller circle, of radius $a/2$, represents the first aperture, and the larger circle, of radius p, that portion of the first diaphragm, including part of the aperture, seen from a point M (Fig. 3). The circle of radius p is of course the projection, by the point M, of the second aperture.

The ratio of the overlap of the two circular surfaces to the area of the first aperture is equal to σ' [3.4], the ratio of the beam intensity at M to that in the core. We now calculate this ratio.

Referring to Fig. 8, we are interested in the area $N_y^x P$, which can evidently be written

$$\text{area } N_y^x P = \left(\frac{a}{2}\right)^2 \frac{\phi}{2} + p^2 \frac{\theta}{2} + f\left(\frac{a}{2}\right) \sin\frac{\phi}{2}. \qquad [A.1.1]$$

In triangle RNA,

$$\cos(\phi/2) = [f^2+(a/2)^2-p^2]/af = \sqrt{[1-\sin^2(\phi/2)]}, \qquad [A.1.2]$$

while

$$\cos\frac{\theta}{2} = \frac{RK}{p} = \frac{f-(a/2)\cos(\phi/2)}{p} = \frac{f}{p} - \frac{a}{2p}\left[\frac{f^2+(a/2)^2-p^2}{af}\right]. \qquad [A.1.3]$$

If we divide [A.1.1] by the area, $\pi(a/2)^2$, of the first aperture, we obtain σ', which we can write, introducing [A.1.2] and [A.1.3], as

$$\sigma' = \frac{1}{\pi}\arccos\left\{\frac{f^2+(a/2)^2-p^2}{af}\right\} + \frac{p^2}{\pi(a/2)^2}\arccos\left\{\frac{f}{p} - \frac{f^2+(a/2)^2-p^2}{2pf}\right\} - \frac{f}{\pi(a/2)}\sqrt{1-\left(\frac{f^2+(a/2)^2-p^2}{af}\right)^2} \qquad [A.1.4]$$

It is easy to see, in Fig. 3, that f and p are related to the position of the point M by

$$f = \left(\frac{d}{x-d}\right) r, \quad p = \left(\frac{x}{x-d}\right)\frac{b}{2}. \qquad [A.1.5]$$

The introduction of [A.1.5] and the definitions [3.5] transforms σ' [A.1.4] to the form [3.6] quoted in the text.

Can. J. Chem. Downloaded from www.nrcresearchpress.com by 210.87.254.40 on 09/05/12
For personal use only.

APPENDIX 2

Probability of Ineffective Collisions

Some of the collisions between beam molecules will be "ineffective", in the sense that they do not lead to the rapid removal from the beam of the colliding molecules. We could define the collision radii ρ ([4.2] and appendix 3) so that they described only effective collisions, but in that case ρ would depend on the beam geometry. If we regard ρ as a true molecular parameter, then we are agreeing to neglect the fact that a small number of collisions is not effective. It is interesting to make a rough estimate of the importance of such an assumption.

To do this we consider a simple and highly hypothetical case, of two hard spherical molecules of equal weight travelling, before collision, in paths parallel to the beam axis (Fig. 9). Suppose their velocities v_1, v_2 differ by $V = v_2 - v_1$ and that the line joining their centers forms an angle θ with the beam direction. It is easy to show that the trajectories of the two molecules after collision form, with the beam direction, angles ϕ_1, ϕ_2 given by:

$$\tan \phi_1 = (V \sin \theta \cos \theta)/(v_1 - V \cos^2 \theta), \qquad [A.2.1]$$

$$\tan \phi_2 = (V \sin \theta \cos \theta)/(v_2 - V \cos^2 \theta). \qquad [A.2.2]$$

The molecules will leave the beam unless these tangents are less than b/d—that is unless the molecules just graze ($\theta \approx \pi/2$) or collide head-on ($\theta \approx 0$). Characteristically, the denominators above will be near $\bar{v}$, the beam velocity, so that the condition for ineffective collisions is very roughly

$$\sin \theta \cos \theta < \frac{\bar{v}}{V}\left(\frac{b}{d}\right). \qquad [A.2.3]$$

A typical relative velocity V for a collision is $\sqrt{(2RT/M)}$. (This relative velocity gives, in fact, the maximum in the integrand of the one-dimensional collision integral.) Using this, and [3.1], we find, for a perfect gas,

$$\sin \theta \cos \theta < \frac{b}{d}\mathscr{M}\sqrt{\frac{5}{6}} \sim \frac{b}{d}\mathscr{M} \qquad [A.2.4]$$

For our example, $\mathscr{M} \sim 7.5$, $b/d = 0.01$, so $\sin \theta \cos \theta < 0.07$, roughly.

Regard the slow-moving molecule 1 as a circular target for molecule 2. An element of area in this target is given by

$$2\pi(2\rho)^2 \sin \theta \cos \theta \, d\theta,$$

where ρ is the radius of the spheres. Thus, the whole target area is

$$\int_0^{\pi/2} 8\pi\rho^2 \sin \theta \cos \theta \, d\theta = 4\pi\rho^2,$$

while that for ineffective collisions is approximately

$$\left\{\int_0^{\text{arc sin } 0.07} + \int_{\text{arc cos } 0.07}^{\pi/2}\right\} 8\pi\rho^2 \sin \theta \cos \theta \, d\theta \doteqdot 0.01(4\pi\rho^2).$$

The resulting error in our estimate, [4.1] [4.2], of the number of effective collisions thus appears, in the above case, to be around 1%. In addition, of course, molecules for which $\tan \phi$ is only slightly greater than (b/d) will remain in the beam some distance before escaping. Unlike the assumptions discussed in appendix 3, the present one deteriorates

for beams of low temperature and high mach number; this can be seen from [A.2.4], and is physically obvious.

APPENDIX 3

Collision Integrals and the "Cooling" of the Beam

Part I

We wish to calculate the frequency of collisions in the molecular beam. Suppose that n_I,n_J are the number densities of components I,J, having molecular weights M_I,M_J. We suppose that the collision probability may be described in terms of velocity-independent collision radii ρ_I,ρ_J, and we ignore the small transverse velocities within the beam, so that molecular velocities are regarded as parallel to $\bar{v}$, the mean motion of the beam.

Consider a molecule of component I having a velocity in dv_i at v_i; the number density of such a molecule is $n_I f_I(v_i)\, dv_i$, where $f_I(v_i)$ is a normalized one-dimensional velocity distribution.

Suppose that a J molecule of velocity v_j lies, with respect to the I molecule, in an element of solid angle dl, forming an angle θ with the molecular velocities. Then the speed of approach of the two molecules is $v = (v_i-v_j)\cos\theta$; this must be greater than zero if there is to be a collision:

$$v = (v_i-v_j)\cos\theta > 0. \qquad [A.3.1]$$

If they are to collide within a short time dt, the distance between their centers, r_{ij}, must fall in the range

$$(\rho_I+\rho_J) < r_{ij} < (\rho_I+\rho_J)+v\,dt, \qquad [A.3.2]$$

so that the element of volume available to such a J molecule is

$$(\rho_I+\rho_J)^2\, v\, dt\, dl. \qquad [A.3.3]$$

The probability of the configuration described, per unit volume, is therefore

$$(n_I f_I(v_i)dv_i)(n_J f_J(v_j)dv_j(\rho_I+\rho_J)^2\, v\, dt\, dl, \qquad [A.3.4]$$

where $v > 0$. The total rate of I,J collisions is therefore

$$\lambda_{IJ} n_I n_J = \oint_{(v_i-v_j)\cos\theta>0} \int\int n_I n_J f_I(v_i) f_J(v_j)(\rho_I+\rho_J)^2 (v_i-v_j)\cos\theta\, dl\, dv_i dv_j \qquad [A.3.5]$$

where the integration is carried over all directions of l, and may be taken over all values of v_i and v_j consistent with the indicated restriction, $(v_i-v_j)\cos\theta > 0$. If the velocity distributions f_I, f_J are Maxwellian,

$$f_I(v_i) = \sqrt{\left(\frac{M_I}{2\pi RT}\right)} \exp\left\{-\frac{M_I}{2RT}(v_i-\bar{v})^2\right\},$$

and are determined by the same temperature, [A.3.5] is easily integrated to give

$$\lambda_{IJ} n_I n_J = (\rho_I+\rho_J)^2 n_I n_J \sqrt{\left(\frac{2\pi RT(M_I+M_J)}{M_I M_J}\right)}. \qquad [A.3.6]$$

Where $I = J$, so that we consider collisions between like molecules, the above integral counts every collision twice; on the other hand, every such collision removes two I molecules from the beam, so that [A.3.6], with $I = J$, is the correct expression for λn^2 in [4.1] and [5.2].

Can. J. Chem. Downloaded from www.nrcresearchpress.com by 210.87.254.40 on 09/05/12
For personal use only.

Part 2

In [4.4] we are interested in the frequency of collisions involving molecules of a specified velocity $v_i = v$. The appropriate collision integral is like [A.3.5], but without integration over the velocity v_i. That is, the frequency of such collisions, per unit volume and time, is given by

$$(2\rho)^2 n^2 f(v_i) \oint\int_{(v_i-v_j)\cos\theta>0} f(v_j)(v_i-v_j)\cos\theta\, dl\, dv_j = \lambda^*(v) n^2 f(v_i), \qquad [A.3.7]$$

where the second form comes from comparison with [4.4], noting that

$$\frac{d}{dx}[nf(v_i)] = \frac{1}{v_i}\frac{d}{dt}[nf(v_i)]. \qquad [A.3.8]$$

This result could be used to investigate the distortion of the distribution functions in the beam. One might suppose that the changing distribution function $f(v_i)$ would at least approach a limiting form at large distances. One can see that this is not the case by first assuming it to be so, when we could set

$$0 = \frac{1}{f}\frac{df}{dx} = \frac{1}{nf}\frac{d(nf)}{dx} - \frac{1}{n}\frac{dn}{dx}$$
$$= -\frac{n\lambda^*}{v} + n\int\frac{\lambda^* f}{v}\,dv \qquad [A.3.9]$$

in which we have used the form [4.4]. It follows from [A.3.9] that λ^*/v is independent of the velocity v. Thus we would expect $d\lambda^*/dv$ to be independent of v in the postulated limiting case. It is not difficult, however, to show from [A.3.7] that

$$\frac{d\lambda^*}{dv} = -\pi(2\rho)^2\left\{\int_v^\infty f(v_j)dv_j - \int_0^v f(v_j)dv_j\right\} \qquad [A.3.10]$$

which cannot be independent of v for any non-trivial velocity distribution $f(v_j)$. We have proceeded no further with the general case.

Instead we consider the special case in which the velocity distribution functions are instantaneously Maxwellian, and of temperature T. Then [A.3.7] may be written

$$\lambda^*(v) = (2\rho)^2\sqrt{\left(\frac{2\pi RT}{M}\right)}\left[e^{-\nu^2} + 2|\nu|\int_0^{|\nu|} e^{-z^2}\,dz\right], \qquad [A.3.11]$$

where ν is the reduced velocity, relative to the beam velocity $\bar{v}$:

$$\nu = \sqrt{(M/2RT)}(v-\bar{v}). \qquad [A.3.12]$$

In Fig. 10 the solid line shows

$$\frac{\mathscr{M}}{4\rho^2}\sqrt{\left(\frac{2RT}{M}\right)}\left[\frac{\lambda^*}{v} - \frac{\lambda}{\bar{v}}\right] = \frac{\mathscr{M}}{4\rho^2 n}\sqrt{\left(\frac{2RT}{M}\right)}\left[\frac{df(v)}{dx}\right], \qquad [A.3.13]$$

as a function of ν, for the sample beam ($\mathscr{M} = 7.5$). This is a dimensionless form of the variation of the normalized velocity distribution function, and demonstrates the "asymmetric cooling" mentioned in the text; the high velocity wing ($\nu > 0$) of the normalized velocity distribution is reduced less than the low velocity wing ($\nu < 0$). The figure also shows [A.3.13] in the limit $\mathscr{M} \to \infty$; in this limit the asymmetry vanishes.

Can. J. Chem. Downloaded from www.nrcresearchpress.com by 210.87.254.40 on 09/05/12
For personal use only.

We wish to compare with the above calculation a mathematically tractable approximation. In this we assume that the distribution functions remain Maxwellian and of mean velocity $\bar{v}$, but we allow the temperature of the beam to change. We thus take some account of the cooling, but not of the acceleration, of the beam. Then, in view of the form

$$f(v) = \sqrt{\left(\frac{M}{2\pi RT}\right)} \exp\left\{\frac{-M(v-\bar{v})^2}{2RT}\right\} \qquad [A.3.14]$$

of the normalized velocity distribution, we can set

$$\frac{1}{4\rho^2 n}\frac{df(v)}{dx} = \frac{f(v)}{4\rho^2 n}(\nu^2 - \tfrac{1}{2})\frac{d\ln T}{dx}. \qquad [A.3.15]$$

Furthermore we restrict the temperature variation to the form

$$\frac{d\ln T}{dx} = -\frac{8\rho^2 n}{\bar{v}}\sqrt{\left(\frac{4\pi RT}{M}\right)}\, G, \qquad [A.3.16]$$

which defines the constant G. In order to fix the value of G, we make [A.3.15] coincide with [A.3.13] for molecules travelling at the beam velocity ($\nu = 0$); this gives $G = 1-(1/\sqrt{2}) = 0.293$. It should be noted that this result for G is independent of the temperature and mach number of the beam. The broken line in Fig. 10 shows the resulting value of [A.3.15] as a function of ν. Although this approximation takes no account of the asymmetry, it is certainly an improvement over the approximation of [4.1], [4.2], which corresponds to $G = 0$. The approximation improves for higher mach numbers.

It remains to determine the effect of the beam cooling [A.3.15], [A.3.16] on the density attenuation, dn_c/dx, in the core of the beam. We write again equations [4.1], [4.2]:

$$dn_c/dx = -(\lambda n_c^2/\bar{v}) - (2n_c/x) \qquad [A.3.17]$$

$$\lambda/\bar{v} = (4\rho^2/\bar{v})\sqrt{(4\pi RT/M)}. \qquad [A.3.18]$$

However, it follows from [A.3.16] that

$$\frac{d}{dx}\left(\frac{\lambda}{\bar{v}}\right) = \frac{\lambda}{2\bar{v}}\frac{d\ln T}{dx} = \left(\frac{\lambda}{\bar{v}}\right)^2 n_c G. \qquad [A.3.19]$$

We proceed to solve the set of equations [A.3.17], [A.3.19]. The latter may be integrated to give

$$\frac{\lambda}{\bar{v}} = \frac{(\lambda_b/\bar{v})}{1+(G\lambda_b/\bar{v})\int_d^x n_c\, dx} \qquad [A.3.20]$$

where λ_b is the value of λ at $x = d$, the second aperture. If this is put into [A.3.17] we obtain, making the substitution

$$n_c = S/x^2, \qquad [A.3.21]$$

$$\frac{d\ln S}{dx}\left[1+\frac{G\lambda_b}{\bar{v}}\int_d^x n_c\, dx\right] = -\frac{\lambda_b S}{\bar{v}x^2}. \qquad [A.3.22]$$

By differentiating this equation once more we can obtain

$$\frac{d^2\ln S}{dx^2} - (1+G)\left(\frac{d\ln S}{dx}\right)^2 + \frac{2}{x}\left(\frac{d\ln S}{dx}\right) = 0, \qquad [A.3.23]$$

Can. J. Chem. Downloaded from www.nrcresearchpress.com by 210.87.254.40 on 09/05/12
For personal use only.

which can be solved to give

$$S = \frac{n_b d^2}{\left\{1+(1+G)\,\frac{\lambda_b n_b d(x-d)}{\bar{v}x}\right\}^{1/1+G}}. \qquad [A.3.24]$$

This expression is combined with [A.3.21] at [4.5]; when $G = 0$ there is no cooling of the beam and [A.3.24] reduces to [4.3], a result which has also been obtained by a direct integration of [4.1].

APPENDIX 4

The Approximation [5.2]

Consider an element of volume δV, outside the core, defined by the ranges $\delta\xi$, δx, and $\delta\phi$, where ϕ describes rotation around the beam axis. Suppose that δV moves in the x-direction with beam velocity $\bar{v}$, but keeping ξ and ϕ fixed. The total number of molecules in δV changes in two ways: due to a collisional loss $-\lambda n^2$ cc^{-1} sec^{-1} (cf. [4.1]), and due to the flux, J_ξ of molecules through the $\delta x\delta\phi$ faces of δV. We may write this

$$\frac{d(n\delta V)}{dx} \equiv (\delta V)\frac{dn}{dx}+n\frac{d(\delta V)}{dx} = -\frac{\lambda n^2}{\bar{v}}-\frac{1}{\bar{v}}\left(\frac{\partial J_\xi}{\partial\xi}\delta\xi\right)\delta x\, r\,\delta\phi; \qquad [A.4.1]$$

$J_\xi(x,\xi)$ is the radial component of the molecular flux.

This equation is complete in the same approximation as [4.1]. The corresponding equation for the collision-free case (ξ3) is, in an obvious notation,

$$\frac{d(n'\delta V)}{dx} \equiv (\delta V)\frac{dn'}{dx}+n'\frac{d(\delta V)}{dx} = -\frac{1}{\bar{v}}\left(\frac{\partial J\xi'}{\partial\xi}\delta\xi\right)\delta x\, r\,\delta\phi. \qquad [A.4.2]$$

These equations [A.4.1,2] combine to give

$$\frac{1}{n}\frac{dn}{dx} = \frac{1}{n'}\frac{dn'}{dx}-\frac{\lambda n}{\bar{v}}-\frac{1}{\bar{v}}\left[\frac{1}{n}\frac{\partial J_\xi}{d\xi}-\frac{1}{n'}\frac{J\partial\xi'}{d\xi}\right]\frac{r\,\delta\xi\,\delta x\,\delta\phi}{\delta V}. \qquad [A.4.3]$$

Now in [5.2] the final term of this equation has been dropped. This clearly corresponds to assuming that the radial gradient of the flux J_ξ is proportional in all cases to the molecular density. If the direction and velocity of molecular flow were invariable, the approximation would become

$$\frac{1}{n}\frac{\partial n}{\partial\xi} = \frac{1}{n'}\frac{\partial n'}{\partial\xi}, \qquad [A.4.4]$$

a relation which agrees quite well with the derived beam profiles (cf. Fig. 7). However, we must expect that the flow pattern in the beam will in fact be affected by collisions, so that this agreement is not a valid justification of the approximation [5.2].

Can. J. Chem. Downloaded from www.nrcresearchpress.com by 210.87.254.40 on 09/05/12
For personal use only.

RELATION ENTRE LA DISSYMETRIE DES RAIES DE RESONANCE MAGNETIQUE NUCLEAIRE ET CERTAINS PARAMETRES STRUCTURAUX

PIERRE J. VAN TIGGELEN[1]
Laboratoire de Chimie Physique, Université de Louvain, Louvain, Belgique
Reçu le 27 mai 1963

ABSTRACT

We give here an equation describing the dissymmetry of nuclear magnetic resonance lines by means of the dipolar influence of the paramagnetic centers. In simple cases this equation coupled with the value of the second moment, will give us two structural parameters from spectra taken on powder samples.

1. INTRODUCTION

Certains auteurs ont déjà remarqué à plusieurs reprises que les spectres de poudres de substances paramagnétiques apparaissaient sous la forme de raies dissymétriques (1, 2, 3, 4, 5), du type schématisé à la Fig. 1. Cependant, à notre connaissance, aucun auteur

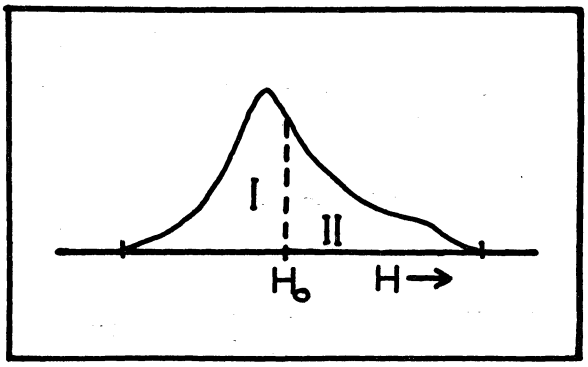

FIG. 1. Aspect d'un spectre dissymétrique.

n'a jusqu'à présent essayé d'exprimer cette dissymétrie en fonction de la structure des composés étudiés.

Nous nous proposons, dans cet article, de relier la dissymétrie des raies à des paramètres structuraux se rapportant aux centres paramagnétiques et ceci, par l'intermédiaire d'une fonction: le troisième moment. Cette grandeur dépend non seulement des distances séparant le centre paramagnétique du noyau en résonance mais encore de la valeur moyenne du moment magnétique du centre paramagnétique envisagé et, par conséquent, est fonction de la température et du champ magnétique directeur appliqué.

La détermination des distances interatomiques requiert un troisième moment précis qui peut être obtenu par la répétition de la mesure de cette grandeur.

Nous calculerons l'expression théorique du troisième moment sur la base d'une méthode statistique en moyennant les diverses fluctuations du champ à l'endroit du noyau en résonance.

2. INTERACTIONS ET CHAMPS AGISSANT SUR LE NOYAU

Avant d'exprimer le champ magnétique "vu" par le noyau, nous examinerons les interactions dont il faut tenir compte dans un cristal paramagnétique à structure figée.

[1]*Actuellement à l'Université Laval, Québec, Qué.*

Can. J. Chem. Downloaded from www.nrcresearchpress.com by 210.87.254.6 on 09/05/12
For personal use only.

L'hamiltonien du système $\mathscr{H}_{tot}$ peut s'écrire comme suit:

$$\mathscr{H}_{tot} = \mathscr{H}_{ZeN} + \mathscr{H}_{ZeP} + \mathscr{H}_{N} + \mathscr{H}_{PP} + \mathscr{H}_{E} + \mathscr{H}_{PN} + \mathscr{H}_{S} \qquad [1]$$

Ces sept termes sont représentés à la Fig. 2.

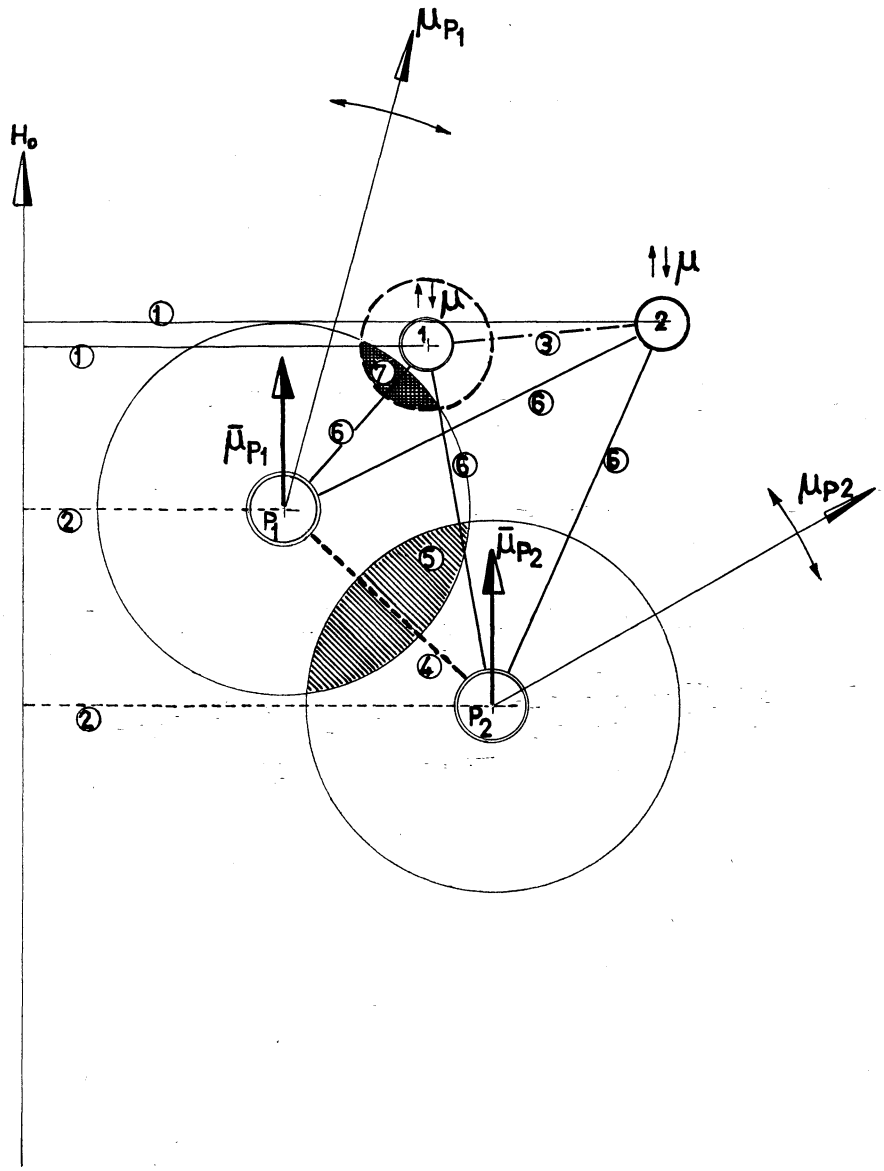

FIG. 2. Interactions auxquelles sont soumis les noyaux en résonance dans une substance paramagnétique: (1) interaction Zeeman nucléaire (H_0 – noyaux); (2) interaction Zeeman electronique (H_0–electron des centres para-magnétiques); (3) interaction spin–spin nucléaire (dipolaire–quadrupolaire); (4) interaction dipolaire entres les centres paramagnétiques; (5) interaction d'échange entre spins électroniques; (6) interaction dipolaire entre centre paramagnétique et noyau; (7) interaction de superéchange (couplage hyperfin de contact) entre le paramagnétique et le noyau.

Can. J. Chem. Downloaded from www.nrcresearchpress.com by 210.87.254.6 on 09/05/12
For personal use only.

Nous constatons donc qu'en plus des interactions Zeeman nucléaires ($\mathscr{H}_{\text{ZeN}}$) et électroniques ($\mathscr{H}_{\text{ZeP}}$) il y a lieu de tenir compte tout d'abord de l'interaction entre noyaux $\mathscr{H}_{\text{N}}$, soit dipolaire magnétique $\mathscr{H}_{\text{ND}}$, soit quadrupolaire électrique $\mathscr{H}_{\text{NQ}}$.

(*a*) L'interaction dipolaire magnétique nucléaire a été étudiée par Pake (6) dans le cas de deux noyaux i et j. Elle peut s'écrire:

$$\mathscr{H}_{\text{ND}} = \frac{\boldsymbol{\mu}_i\boldsymbol{\mu}_j}{r_{ij}^3} - 3\frac{(\boldsymbol{\mu}_i\mathbf{r}_{ij})(\boldsymbol{\mu}_j\mathbf{r}_{ij})}{r_{ij}^5}. \qquad [2]$$

Le résultat exprimé en unité de champ, est plus grand d'un facteur 3/2 pour des noyaux i et j semblables que pour des noyaux différents. Ceci provient de l'interaction "flip-flop" présente uniquement entre noyaux semblables.

(*b*) L'interaction quadrupolaire électrique $\mathscr{H}_{\text{NQ}}$ étudiée par Pound (7) apparait dans le cas d'interaction entre noyaux de nombre de spin I supérieur à $\frac{1}{2}$. Nous nous limiterons dans la suite aux noyaux $I = \frac{1}{2}$ et donc le terme $\mathscr{H}_{\text{NQ}}$ sera nul.

L'interaction dipolaire entre centres paramagnétiques $\mathscr{H}_{\text{PP}}$ n'aura pas d'influence directe sur le spectre de résonance nucléaire. Cependant, l'interaction dipolaire des centres paramagnétiques avec les noyaux $\mathscr{H}_{\text{PN}}$ sera influencée par $\mathscr{H}_{\text{PP}}$. En effet, $\mathscr{H}_{\text{PN}}$ devrait provoquer, par suite de la grandeur des moments magnétiques électroniques, une scission du spectre en $(2m_p+1)$ raies (si m_p désigne le nombre quantique magnétique total du centre paramagnétique) et, de cette manière, élargir considérablement le spectre. Dans la plupart des cas cependant, la réorientation rapide des moments des centres paramagnétiques μ'_p dans le champ (réorientation obtenue par l'échange de quanta d'énergie entre centres d'une part, entre centre et réseau d'autre part) donne au moment magnétique de l'ion une valeur moyenne $\bar{\mu}'_p$. Ce processus de réorientation est beaucoup plus rapide que le phénomène de résonance nucléaire et, par conséquent, le moment magnétique nucléaire "voit" une valeur moyenne de l'ion paramagnétique qui diffère de zéro par suite de l'écart de population entre les niveaux Zeeman électroniques. On peut, pour des températures pas trop faibles, estimer le moment magnétique $\bar{\mu}'_p$ sur la base d'une théorie classique du paramagnétisme. $\bar{\mu}'_p$ dépend de la température et du champ magnétique directeur appliqué.

Mais, à côté des interactions dipolaires entre centres paramagnétiques, il faut envisager l'interaction d'échange $\mathscr{H}_{\text{E}}$, responsable de la tendance des moments magnétiques à s'aligner parallèlement ou antiparallèlement les uns par rapport aux autres. Ces forces d'échange provoquent à la limite l'apparition des états ferro- et antiferro-magnétique. Cette interaction peut se représenter dans l'hamiltonien par une interaction scalaire:

$$\mathscr{H}_{\text{E}} = \sum_{k>p} A_{kp}\mathbf{S}_k\mathbf{S}_p \qquad [3]$$

où A_{kp} est la constante de couplage proportionnelle aux intégrales de recouvrement des fonctions d'onde des centres paramagnétiques p et k. Il est cependant possible de tenir compte de cette interaction d'échange en corrigeant le facteur $\bar{\mu}'_p$. Celui-ci, en effet, dépend de la température. En introduisant une température de Curie T_c dans l'expression de $\bar{\mu}'_p$ on aura donc, comme moment magnétique des centres paramagnétiques "vu" par les noyaux la valeur $\bar{\mu}_p$ qui résume à la fois l'influence des interactions $\mathscr{H}_{\text{ZeP}}$, $\mathscr{H}_{\text{PP}}$ et $\mathscr{H}_{\text{E}}$.

Ce moment magnétique moyen $\bar{\mu}_p$, localisé aux sites occupés par les centres paramagnétiques va provoquer une perturbation sur les noyaux en résonance. Cette interaction est représentée par $\mathscr{H}_{\text{PN}}$; il s'agit d'une interaction dipolaire entre $\bar{\mu}_p$ et les moments nucléaires μ_i. Cette interaction sera du même type que celle décrite par l'équation [2].

Can. J. Chem. Downloaded from www.nrcresearchpress.com by 210.87.254.6 on 09/05/12
For personal use only.

Mais, dans le calcul des niveaux d'énergie, il convient de remarquer que, pour le moment magnétique $\bar{\mu}_p$, la position parallèle au champ directeur H est seule permise et qu'il s'agit bien ici d'une interaction entre partenaires dissemblables (un noyau et un électron). Par conséquent, nous observerons un glissement de la position de résonance au lieu d'une scission de la raie, et le facteur numérique 3/2 n'apparait pas dans l'expression du champ résultant de cette interaction.

Il reste encore à considérer le dernier terme de l'hamiltonien total, c'est-à-dire $\mathcal{H}_S$ qui symbolise l'interaction de superéchange ou couplage hyperfin de contact. Cette interaction résulte de la non annulation de la fonction d'onde de l'électron responsable des propriétés paramagnétiques à l'endroit du noyau en résonance. Cette interaction est également de forme scalaire.

$\mathcal{H}_S = \sum_p A_{ip}\mathbf{I}_i\mathbf{S}_p$ où la constante A_{ip} est proportionnelle à la densité de probabilité de l'électron célibataire du paramagnétique p à l'emplacement du noyau i. Ce couplage a été introduit par Townes *et al.* (8) pour expliquer le "Knight shift" dans les métaux. Cette interaction joue également un role important dans des composés du type MnF_2 et $KMnF_3$, comme l'ont remarqué Shulman *et al.* (9, 10). Nous négligerons cependant ce couplage hyperfin car, en l'absence de liaison chimique entre le paramagnétique et le noyau, on peut supposer avec une bonne approximation que la fonction d'onde électronique s'annule à l'endroit du noyau en résonance. Shulman fait d'ailleurs la même approximation pour le proton dans le $CuF_2.2H_2O$ (11).

Dans l'étude de la dissymétrie de la raie, nous nous bornerons donc à l'effet des interactions dipolaires nucléaires et dipolaires électroniques statiques. Pour le système de noyaux en résonance, l'hamiltonien s'écrit sous la forme suivante où les interactions quadrupolaires nucléaires et de superéchange sont négligées:

$$\mathcal{H} = \mathcal{H}_{ZeN} + \mathcal{H}_{ND} + \mathcal{H}_{FN}. \qquad [5]$$

N. Bloembergen (12) a calculé les niveaux d'énergie d'un système à deux noyaux et plusieurs centres paramagnétiques ainsi que les transitions permises entre ces niveaux. Il a déterminé de cette manière la position et l'intensité des raies de résonance. Nous utiliserons le résultat de Bloembergen à la section 5 et nous verrons qu'il amène à une valeur du troisième moment identique à celle obtenue au moyen d'un raisonnement semi-classique. Nous pouvons donc supposer la simple additivité des effets dipolaires de sorte que chacune des perturbations $\mathcal{H}_{ND}$ et $\mathcal{H}_{FN}$ puisse être traitée comme si elle etait seule à influencer le spectre. Dans le cas de cristaux diamagnétiques, Pake (6) a étudié $\mathcal{H}_{ND}$ par un calcul quantique de perturbation. Le champ produit à l'endroit du noyau en résonance i par le noyau j s'écrit alors:

$$h_j = \pm k_{ij}\mu_j \cdot r_{ij}^{-3}(3\cos^2\theta_{ij} - 1) \qquad [6]$$

où le signe $\pm$ dépend de la position parallèle ou antiparallèle du spin j à H_0. $k = 1$ pour des noyaux diffèrents et $k = 3/2$ pour des noyaux semblables: la diffèrence représente la contribution de l'interaction "flip-flop" réalisable uniquement pour des noyaux identiques. μ_j désigne la valeur absolue de la projection suivant H_0 du moment magnétique du noyau j distant de r_{ij} du noyau i. θ_{ij} est l'angle entre la direction de H_0 et de r_{ij}. Pour plusieurs noyaux, le champ résultant en i sera:

$$H_j = \pm \sum_j h_j \qquad [7]$$

Can. J. Chem. Downloaded from www.nrcresearchpress.com by 210.87.254.6 on 09/05/12
For personal use only.

Un calcul classique de l'interaction $\mathscr{H}_{PN}$ donne pour le champ provoqué par les centres paramagnétiques la valeur de:

$$H_p = +\sum_p k_{ip}\bar{\mu}'_p \cdot R_{ip}^{-3}(3\cos^2\theta_{ip}-1) \qquad [8]$$

où

$$\bar{\mu}_p = \frac{\mu^2_p \cdot H_0}{3k(T-T_c)} \qquad [9]$$

expression où seul le signe + est permis et où le facteur k_{ip} vaut l'unité.

Nous aurons donc, à l'endroit du noyau en résonance i, à coté du champ directeur H_0, la contribution des centres paramagnétiques H_p et celle des autres noyaux, H_j:

$$H_i = H_0 + H_p + H_j. \qquad [10]$$

3. MOMENTS ET MOYENNES

La notion de moment permet de déterminer certaines grandeurs de la distribution spectrale et de les relier à des paramètres structuraux. Dans ce qui suit, nous exprimerons les moments en unité de champ. De façon générale, pour toute distribution spectrale $g(H)$, on peut définir deux types de moment: les moments centraux S_n rapportés au champ moyen H_m de la distribution, et les moments Σ_n rapportés au champ de résonance H_0 d'un noyau isolé, c'est-à-dire soustrait à toute interaction autre que celle du champ magnétique directeur H_0. Dans la plupart des cas, les deux types de moments coïncident par suite de l'égalité entre H_m et H_0. On notera les différents types de moment par les équations:

$$S_n = \langle (H-H_m)^n \rangle \qquad [11]$$

et

$$\Sigma_n = \langle (H-H_0)^n \rangle \qquad [12]$$

où n indique l'ordre du moment, H la variable du spectre enregistré et les crochets la moyenne effectuée en tenant compte de la fonction de distribution $g(H)$.

Ces expressions peuvent être appliquées aux spectres obtenus à l'enregistreur. Il existe entre ces types de moments des relations. Pour les moments d'ordre un: $S_1 = 0$ par définition de la grandeur H_m et $\Sigma_1 = H_m - H_0$, qui représente le glissement du centre de gravite de la distribution par rapport à H_0. Pour les moments d'ordre deux, où $\Sigma_2 = S_2 + \Sigma_1^2$, le second moment central S_2 indique la dispersion de la distribution. Enfin la relation entre les troisièmes moments s'écrit:

$$\Sigma_3 - S_3 = 3\Sigma_1\Sigma_2 - 2\Sigma_1^3. \qquad [13]$$

Ils mesurent la dissymétrie de la distribution spectrale.

A l'échelle nucléaire, au champ H du spectre correspond un champ instantané H_i à l'endroit du noyau i, champ tel que la condition de résonance est réalisée pour ce noyau. Le champ magnétique H_i à l'emplacement d'un noyau est le champ H_0 de l'électroaimant, modifié par les perturbations H_p et H_j dues aux interactions magnétiques dipolaires avec les centres paramagnétiques et d'autres moments nucléaires, respectivement. Ce champ H_i variera dans le temps pour un même site et les moyennes dans le temps seront par ailleurs différentes à priori d'un site à l'autre.

Dans le calcul des moments, nous aurons donc à prendre divers types de moyennes, les unes pour déterminer le champ moyen que connait un noyau, les autres pour déterminer le champ moyen règnant sur l'ensemble des sites non equivalents au point de vue de

Can. J. Chem. Downloaded from www.nrcresearchpress.com by 210.87.254.6 on 09/05/12
For personal use only.

l'entourage. Enfin, dans le cas des poudres, une troisième moyenne devra être faite pour tenir compte des différentes orientations des cristallites.

(a) Cas du monocristal

La moyenne à effectuer est double dans ce cas ci. Il s'agit de prendre tout d'abord la moyenne de $(H_i-H_0)^n$ sur le temps. On peut remarquer que calculer une moyenne sur le temps revient, conformément à l'hypothèse de Gibbs, à effectuer la moyenne d'ensemble à un moment donné. En effet, au même instant, les divers noyaux de type i répartis dans le monocristal sont soumis à tous les champs directeurs qu'un noyau i peut subir suite aux fluctuations du champ dans le temps. Dans la suite des calculs, cette moyenne sera symbolisée par une barre horizontale ne dépassant pas les crochets. La seconde moyenne est à prendre sur les noyaux de l'espèce en résonance, différents par leur position dans la maille de l'édifice cristallin. Elle sera représentés par des crochets entourant l'expression à moyenner. Le calcul de ces deux moyennes revient à scinder en deux parties la moyenne étendue à tous les noyaux du type étudié, contenus dans l'échantillon. Cependant, nous séparerons très nettement les deux moyennes.

(b) Cas des poudres

Ici les cristallites sont, en principe, orientés au hasard et de manière uniforme. L'angle que forme le champ directeur H_0 avec le vecteur liant les deux particules en interaction dipolaire, peut prendre toutes les valeurs. Il faut donc en plus moyenner sur la fonction angulaire. Ceci sera représenté par une barre horizontale débordant les crochets. Finalement, nous effectuerons les moyennes dans l'ordre suivant:

1. moyenne sur le temps,
2. moyenne sur les noyaux en des sites inéquivalents,
3. moyenne sur la fonction angulaire.

Les moments à l'échelle microscopique s'écriront donc:

pour un monocristal:	pour une poudre:
$S_n = \langle\overline{(H_i-H_m)^n}\rangle$ [14]	$\bar{S}_n = \overline{\langle(H_i-\bar{H}_m)^n\rangle}$ [16]
$\Sigma_n = \langle\overline{(H_i-H_0)^n}\rangle$ [15]	$\bar{\Sigma}_n = \overline{\langle(H_i-H_0)^n\rangle}$ [17]

où la valeur de H_i est donnée par [9]. De plus $H_m = \langle\bar{H}_i\rangle = H_0+\langle H_p\rangle$ [18] pour un monocristal et $\bar{H}_m = \overline{\langle\bar{H}_i\rangle} = H_0$ [19] pour une poudre. Par conséquent, pour des échantillons polycristallins, les deux types de moment $\bar{\Sigma}_n$ et $\bar{S}_n$ sont égaux. Par ailleurs, en l'absence de paramagnétiques, H_m et H_0 coincident même pour un monocristal ainsi que le signale également Kroon (1).

Le premier moment pour un monocristal vaut:

$$\frac{1}{N}\sum_i\sum_p \frac{\bar{\mu}_p}{R_{ip}^3}(3\cos^2\theta_{ip}-1) \qquad [20]$$

expression où la moyenne sur les sites inéquivalents est symbolisée par $1/N\sum_i$ et où la moyenne sur le temps est déjà inclue dans le facteur $\bar{\mu}_p$. Ce premier moment s'annule pour une poudre ainsi qu'en témoigne l'équation [19]. L'effet des centres paramagnétiques pour un échantillon polycristallin se fera donc uniquement sentir sur les moments d'ordre supérieur.

Can. J. Chem. Downloaded from www.nrcresearchpress.com by 210.87.254.6 on 09/05/12
For personal use only.

Des définitions [16] et [17] et des équations [9] et [19], le second moment d'une poudre s'exprimera par:

$$\bar{S}_2 = \bar{\Sigma}_2 = \overline{\langle H_p^2 \rangle} + \overline{\langle H_j^2 \rangle}.$$

Cette relation amène à un résultat semblable à celui de Van Vleck (13) une fois les moyennes effectuées.

Le résultat final pour $\bar{S}_2$ peut s'écrire:

$$S_2 = \frac{1}{N} \sum_i \left[\frac{4}{5} \sum_j k_{ij}^2 \mu_j^2 r_{ij}^{-6} + \frac{4}{5} \sum_p \bar{\mu}_p^2 R_{ip}^{-6} + \frac{2}{5} \sum_p \sum_{p' \neq p} \bar{\mu}_p \bar{\mu}_{p'} R_{ip}^{-3} R_{ip'}^{-3} (3 \cos^2 \lambda_{p\,ip'} - 1) \right] \quad [21]$$

Les deux derniers termes, qui représentent la contribution des centres paramagnétiques au second moment, sont équivalents aux équations [17] et [18] de Kroon (1) lorsqu'on y néglige l'effet d'anisotropie des cristallites qui, de toute façon, reste un effet fort difficile à déterminer quantitativement.

4. CALCUL DU TROISIEME MOMENT

Cette fonction caractérise la dissymétrie de la distribution; elle est donc nulle dans le cas des raies symétriques, par exemple pour des profils gaussiens et lorentziens, qui sont les plus fréquents en résonance. Par contre, dès que l'échantillon contient des centres paramagnétiques (paramagnétisme métallique, ions paramagnétiques), leur influence se marque sur le profil de la raie en provoquant une dissymétrie. Il est donc bien justifié d'utiliser le troisième moment pour chiffrer l'écart à la symétrie et, par là, l'influence du paramagnétisme.

Si, pour des monocristaux, le premier moment de type Σ est plus facile à utiliser (14), dans le cas d'une poudre polycristalline, l'annulation de $\bar{\Sigma}_1$ exige l'emploi des moments d'ordre supérieur et, entre autres, du moment d'ordre trois $\bar{S}_3$.

Celui-ci a pour expression générale, lorsqu'on utilise les définitions [16] et [17] et les équations [9] et [19]:

$$\bar{S}_3 = \bar{\Sigma}_3 = \overline{\langle H_p^3 \rangle} + 3\overline{\langle H_p \bar{H}_j^2 \rangle} \quad [22]$$

où, en remplacant H_p et H_j par leur valeur, il vient:

$$\bar{S}_3 = \overline{\frac{1}{N} \sum_i \left[\sum_p \bar{\mu}_p \cdot R_{ip}^{-3} (3 \cos^2 \theta_{ip} - 1) \right]^3} + \frac{3}{N} \overline{\sum_i \left[\sum_p \bar{\mu}_p R_{ip}^{-3} (3 \cos^2 \theta_{ip} - 1) \right] \cdot \left[\sum_j k_{ij}^2 \mu_j^2 r_{ij}^{-6} (3 \cos^2 \theta_{ij} - 1)^2 \right]}. \quad [23]$$

Pour évaluer ces moyennes sur les directions, nous remarquerons tout d'abord que le terme au cube peut se décomposer en:

$$\overline{\left(\sum_p A_p \right)^3} = \overline{\sum_p A_p^3} + 3\overline{\sum_p \sum_{p' \neq p} A_p^2 A_{p'}} + \overline{\sum_p \sum_{p' \neq p} \sum_{\substack{p'' \neq p' \\ \neq p}} A_p A_{p'} A_{p''}} \quad [24]$$

où A_p représente toute la fonction

$$\bar{\mu}_p R_{ip}^{-3} (3 \cos^2 \theta_{ip} - 1).$$

D'autre part le second terme de [23] s'écrit:

Can. J. Chem. Downloaded from www.nrcresearchpress.com by 210.87.254.6 on 09/05/12
For personal use only.

$$\overline{\sum_p A_p \sum_j B_j^2} = \sum_p \sum_j \overline{A_p B_j^2} \qquad [25]$$

où

$$B_j = k_{ij}\mu_j r_{ij}^{-3}(3\cos^2\theta_{ij}-1)$$

Pour effectuer la moyenne de ces diverses sommes, il suffit de prendre un terme caractéristique de chacune des sommes, d'en faire la moyenne et, enfin, de sommer les résultats obtenus.

Dans l'équation [25], la fonction angulaire,

$$(3\cos^2\theta_{ij}-1)^2(3\cos^2\theta_{ip}-1)$$

moyennée sur l'angle θ de 0 à π et sur l'angle φ de 0 à 2π amène au résultat

$$\frac{8}{35}(3\cos^2\lambda_{pij}-1)$$

où λ_{pij} représente l'angle entre les directions i–p et i–j.

Finalement le second terme de [23] se met sous la forme:

$$\frac{3}{N}\sum_i \sum_p \sum_j \overline{A_p B_j^2} = \frac{24}{35}\frac{1}{N}\sum_i \sum_p \sum_j \bar{\mu}_p k_{ij}^2 \mu_j^2 R_{ip}^{-3} r_{ij}^{-6}(3\cos^2\lambda_{pij}-1). \qquad [26]$$

La moyenne du cube de la somme s'effectue comme suit:

1. La moyenne sur un terme caractéristique de la simple somme en p du second membre de [24] devient après intégration sur θ_{ip}:

$$\overline{A_p^3} = \frac{16}{35}\bar{\mu}_p^3 R_{ip}^{-9}. \qquad [27]$$

2. La moyenne sur un terme caractéristique de la double somme en p et en p' se traite comme la moyenne sur le terme mixte $A_p B_j^2$. Après calcul on obtient un résultat similaire:

$$\overline{A_p^2 A_{p'}} = \frac{8}{35}\bar{\mu}_p^2 \cdot \bar{\mu}_{p'}(3\cos\lambda'-1) \qquad [28]$$

où λ' désigne l'angle entre les vecteurs i–p et i–p'.

3. Les termes $A_p A_{p'} A_{p''}$ font intervenir trois angles par rapport au champ magnétique H_0 et, pour effectuer la moyenne d'un terme caractéristique, nous utiliserons le système de référence comme indiqué à la Fig. 3. Dans le trièdre, nous plaçons le noyau i à l'origine des coordonnées, le vecteur ip suivant l'axe Z et le vecteur ip' dans le plan XOZ. Le vecteur ip'' est fixé par les constantes du réseau cristallin. La direction de H_0 est exprimée par la colatitude θ et la longitude φ mesurée par rapport à X. λ'' et λ''' représentent respectivement les angles entre ip et ip'', et entre ip' et ip''. χ est l'angle dièdre entre les plans ipp' et ipp''. λ', λ'', λ''' et κ sont des constantes de la structure cristalline du composé étudié.

Dans une telle représentation, les angles θ_{ip}, $\theta_{ip'}$ et $\theta_{ip''}$ deviennent, en fonction de φ et de θ:

$$\begin{cases} \cos\theta_{ip} = \cos\theta \\ \cos\theta_{ip'} = \cos\lambda'\cdot\cos\theta + \sin\lambda'\cdot\sin\theta\cdot\cos\varphi \\ \cos\theta_{ip''} = \cos\lambda''\cdot\cos\theta + \sin\lambda''\cdot\cos\kappa\cdot\sin\theta\cdot\cos\varphi + \sin\lambda''\cdot\sin\kappa\cdot\sin\theta\cdot\sin\varphi \end{cases} \qquad [29]$$

où

$$\cos\kappa = \frac{\cos\lambda''' - \cos\lambda'\cos\lambda''}{\sin\lambda'\sin\lambda''}.$$

Can. J. Chem. Downloaded from www.nrcresearchpress.com by 210.87.254.6 on 09/05/12
For personal use only.

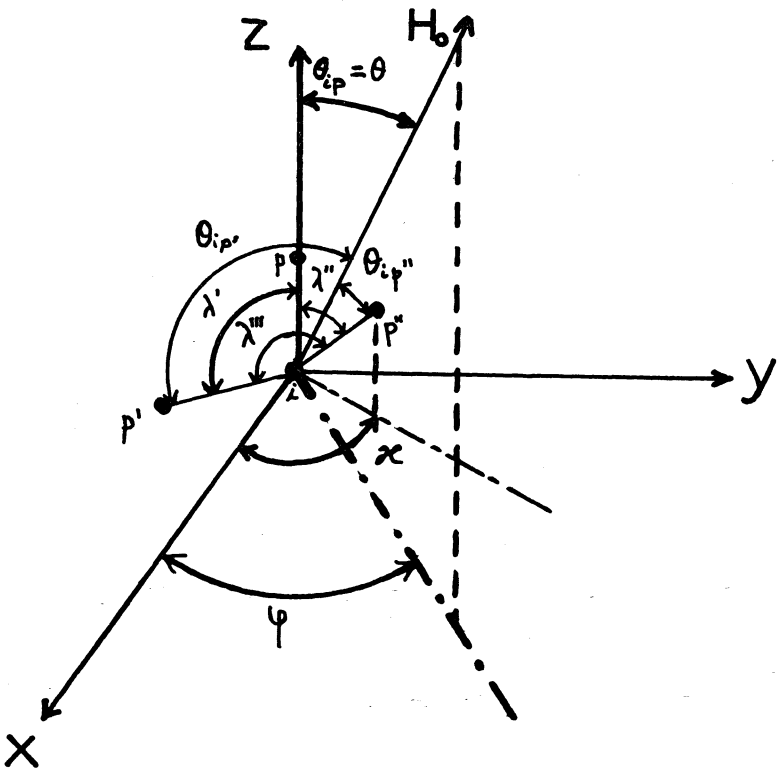

FIG. 3. Angles intervenant dans le calcul du troisième moment.

La partie angulaire de l'expression à moyenner $A_pA_{p'}A_{p''}$ peut se développer comme suit:

$$\bar{E} = 27\bar{E}_1-9\bar{E}_2-9\bar{E}_3-9\bar{E}_4+3\bar{E}_5+3\bar{E}_6+3\bar{E}_7-1. \qquad [30]$$

Les moyennes, après intégration en θ et en φ, donnent:

$$-9\bar{E}_2 = -\frac{3}{5}(2\cos^2\lambda'+1), \qquad +3\bar{E}_5 = +1$$

$$-9\bar{E}_3 = -\frac{3}{5}(2\cos^2\lambda''+1), \qquad +3\bar{E}_6 = +1$$

$$-9\bar{E}_4 = -\frac{3}{5}(2\cos^2\lambda'''+1), \qquad +3\bar{E}_7 = +1$$

et $$27E_1 = \frac{9}{35}(1+2\cos^2\lambda'+2\cos^2\lambda''+2\cos^2\lambda'''+8\cos\lambda'\cos\lambda''\cos\lambda''').$$

$\bar{E}$ s'écrit après simplification:

$$\frac{8}{35}[2-3(\cos^2\lambda'+\cos^2\lambda''+\cos^2\lambda''')+9\cos\lambda'\cos\lambda''\cos\lambda''']. \qquad [31]$$

En introduisant dans l'expression du troisième moment les équations [31, 26, 27, 28] il vient finalement:

Can. J. Chem. Downloaded from www.nrcresearchpress.com by 210.87.254.6 on 09/05/12
For personal use only.

$$\bar{S}_3 = \bar{\Sigma}_3 = \frac{1}{N}\sum_i \left[\frac{16}{35}\sum_p \bar{\mu}_p^3 R_{ip}^{-9} + \frac{24}{35}\sum_p \sum_{p'} \bar{\mu}_p^2 \bar{\mu}_{p'} R_{ip}^{-6} R_{ip'}^{-3}(3\cos^2\lambda' - 1)\right.$$

$$+\frac{8}{35}\sum_p \sum_{p'} \sum_{p''} \bar{\mu}_p \bar{\mu}_{p'} \bar{\mu}_{p''} R_{ip}^{-3} R_{ip'}^{-3} R_{ip''}^{-3}(2 - 3(\cos^2\lambda' + \cos^2\lambda'' + \cos^2\lambda''')$$

$$\left. +9\cos\lambda'\cos\lambda''\cos\lambda''') + \frac{24}{35}\sum_p \sum_j \bar{\mu}_p \mu_j^2 k_{ij}^2 R_{ip}^{-3} r_{ij}^{-6}(3\cos^2\lambda_{pij} - 1)\right] \quad [32]$$

Cette longue expression se simplifie considérablement dans le cas où un seul paramagnétique fait sentir son influence sur les noyaux. Les sommes en p se réduisent à un terme, de telle sorte que [32] devient:

$$\bar{S}_3 = \frac{1}{N}\sum_i \left[\frac{16}{35}\bar{\mu}_p^3 R_{ip}^{-9} + \frac{24}{35}\sum_j \bar{\mu}_p k_{ij}^2 \mu_j^2 R_{ip}^{-3} r_{ij}^{-6}(3\cos^2\lambda_{pij} - 1)\right]. \quad [33]$$

Pour une paire de noyaux identiques et équidistants du paramagnétique:

$$R = R_{1p} = R_{2p},\ \lambda = \lambda_{p12} = \lambda_{p21},\ k_{ij} = \frac{3}{2} \text{ et } \mu_j = \mu$$

si bien que le troisième moment sera pour une telle disposition:

$$\bar{S}_3 = \frac{16}{35}\frac{\bar{\mu}_p^3}{R^9} + \frac{54}{35}\frac{\bar{\mu}_p \mu^2}{r^6 R^3}(3\cos^2\lambda - 1) \quad [34]$$

Cette équation simplifiée est à rapprocher de l'équation suivante du second moment, valable dans les mêmes conditions:

$$\bar{S}_2 = \frac{9}{5}\frac{\mu^2}{r^6} + \frac{4\bar{\mu}_p^2}{5R^6}. \quad [35]$$

Pour fixer l'ordre de grandeur de $\bar{S}_3$, nous prendrons le cas d'un centre paramagnétique tel que l'ion Cu^{++}, placé dans un champ de 13,200 g à la température de 300° K. Le moment magnétique moyen de l'ion cuivre vaut alors 7.24 magnétons nucléaires ($K = 2.6$). Si cet ion est situé à 2.60 Å de deux protons distants de 1.60 Å, on trouve pour les second et troisième moments

$$\bar{S}_2 = \overline{\langle H_p^2\rangle} + \overline{\langle H_j^2\rangle} = 3.4 + 21.0 = 24.4g^2$$

$$\bar{S}_3 = \overline{\langle H_p^3\rangle} + 3\overline{\langle H_p H_j^2\rangle} = 4.1 - 29.2 = -25.1g^3.$$

Transformons l'équation [34] en exprimant $\bar{S}_3$ en fonction d'un paramètre K, qui représente le rapport du moment magnétique $\bar{\mu}_p$ du centre paramagnétique au moment μ du noyau. Pour la résonance du proton, il vient:

$$\bar{S}_3 = 8.03\cdot 10^{+71}\left[16\frac{K^3}{R^9} + 54\frac{K}{R^3 r^6}(3\cos^2\lambda - 1)\right]$$

A la Fig. 4, nous avons mis en graphique le troisième moment $\bar{S}_3$ en fonction de K pour différentes valeurs de R et de r.

	R	r	$\bar{S}_3$
I	2.60	1.56	$0.237\,K^3 - 12.5\,K$
II	2.60	1.60	$0.237\,K^3 - 11.2\,K$
III	3.00	1.56	$0.0650\,K^3 - 8.91\,K$
IV	3.00	1.60	$0.0650\,K^3 - 8.03\,K$

Can. J. Chem. Downloaded from www.nrcresearchpress.com by 210.87.254.6 on 09/05/12
For personal use only.

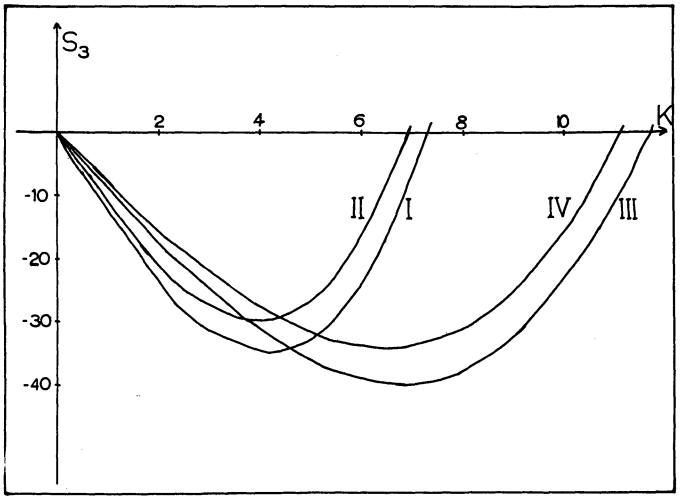

FIG. 4. Variation du troisième moment $\bar{S}_3$ en fonction du paramètre $K = \bar{\mu}_p/\mu$.

Remarquons toutefois que la dissymétrie d'une distribution reste une grandeur délicate à mesurer. L'erreur expérimentale à laquelle est soumis le troisième moment peut s'estimer comme suit.

Supposons la distribution de champ de la figure 1. Si $h = H - H_0$, de par la définition de S_3, nous aurons:

$$\bar{S}_3 = \frac{\int_{-\infty}^{+\infty} g(h)h^3 dh}{\int_{-\infty}^{+\infty} g(h)dh} = \bar{S}_{3II} - \bar{S}_{3I}$$

avec

$$\bar{S}_{3I} = \frac{\int_{-\infty}^{0} h^3 g(h)dh}{\int_{-\infty}^{+\infty} g(h)dh}$$

où $g(h)$ représente la fonction de normalisation et où l'indice I indique qu'il est question de l'aile à bas champ. La précision de la mesure sur l'aile I d'un spectre peut être de $\pm \bar{S}_{3I}/20$ et sur l'aile II, à haut champ, de $\pm \bar{S}_{3II}/20$. Et donc, la précision du troisième moment total sera exprimée par $\bar{S}_3 \pm (\bar{S}_{3I} + \bar{S}_{3II})/20$. De plus, si $\bar{S}_{2I} \sim \bar{S}_{2II} \sim \bar{S}_2/2$ et si $(\bar{S}_{2I})^{3/2} \sim \bar{S}_{3I}$, nous obtenons alors pour $\bar{S}_3$ une valeur précise à $\pm 5g^3$, dans le cas de l'exemple du paragraphe précédent. Or, l'ordre de grandeur de $\bar{S}_3$ est de $-30\ g^3$, comme nous l'avons vu plus haut. $\bar{S}_3$ est donc connu à $\pm 15\%$. On peut, par des mesures sur un plus grand nombre de spectres, préciser les valeurs de $\bar{S}_{3I}$ et de $\bar{S}_{3II}$ et, par là, diminuer l'erreur commise sur $\bar{S}_3$.

Par conséquent, en utilisant simultanément les valeurs de $\bar{S}_2$ et de $\bar{S}_3$, il est possible de déterminer deux paramètres structuraux si l'on enregistre, à *une* température et à *une* valeur du champ magnétique H_0, les spectres de résonance d'un noyau dans un échantillon à l'état de poudre.

Can. J. Chem. Downloaded from www.nrcresearchpress.com by 210.87.254.6 on 09/05/12
For personal use only.

5. CALCUL DE $\bar{S}_3$ À PARTIR DES RESULTATS QUANTIQUES

Au moyen d'un calcul de perturbation, N. Bloembergen (12) a déterminé la position et l'intensité des raies de résonance d'un système à deux protons entourés de plusieurs ions paramagnétiques.

Le spectre calculé comporte quatre raies (Fig. 5):

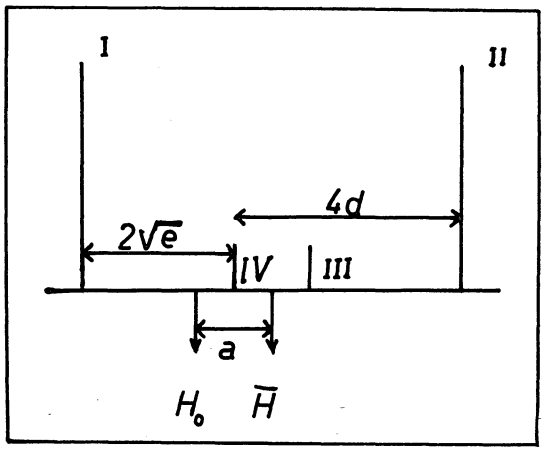

FIG. 5. Spectre de résonance nucléaire d'une paire isolée de protons soumis à l'interaction de plusieurs ions paramagnétiques.

	Position	Intensité
I	$H_1 = H_0 + a + 2d + \sqrt{e}$	$i_1 = \dfrac{(b - d - \sqrt{e})^2}{e - b\sqrt{e}}$
II	$H_2 = H_0 + a - 2d - \sqrt{e}$	
III	$H_3 = H_0 + a - 2d + \sqrt{e}$	$i_2 = \dfrac{(b - d + \sqrt{e})^2}{e + b\sqrt{e}}$
IV	$H_4 = H_0 + a + 2d - \sqrt{e}$	

[36]

Les positions des raies sont données en unité de champ et

$$a = \frac{1}{2}\left[\sum_p \bar{\mu}_p R_{1p}^{-3}(3\cos^2\theta_{1p} - 1) + \sum_p \bar{\mu}_p R_{2p}^{-3}(3\cos^2\theta_{2p} - 1)\right] = \frac{A+B}{2} \qquad [37]$$

$$b = \frac{1}{2}\left[\sum_p \bar{\mu}_p R_{1p}^{-3}(3\cos^2\theta_{1p} - 1) - \sum_p \bar{\mu}_p R_{2p}^{-3}(3\cos^2\theta_{2p} - 1)\right] = \frac{A-B}{2} \qquad [38]$$

$$H_{12} = 3d = \frac{3}{2}\mu r_{12}^{-3}(3\cos^2\theta_{12} - 1),\ e = b^2 + d^2,\ H_m = H_0 + a \qquad [39]$$

Les indices 1 et 2 concernent les deux protons de la paire et l'indice p se rapporte à l'ion paramagnétique p de l'entourage.

Calculons d'abord les seconds moments pour une orientation du monocristal:

$$S_2 = \sum_i p_i (H_i - H_m)^2$$

où i représente l'indice de la raie considérée et où p_i est le poids de cette raie.

I et II ont même poids: $p_1/2$ et $p_1 = i_1/(i_1 + i_2)$.

III et IV ont même poids: $p_2/2$ et $p_2 = 1 - p_1$.

Can. J. Chem. Downloaded from www.nrcresearchpress.com by 210.87.254.6 on 09/05/12
For personal use only.

Après calcul, il vient:

$$S_2 = 8dp_1\sqrt{e+4d^2+e-4d\sqrt{e}}$$

et $p_1 = (e^{1/2}+d)/2e^{1/2}$.

Enfin $S_2 = 9d^2+b^2$ [40]

A partir des relations: $\Sigma_2 = S_2+\Sigma_1^2$ et $\Sigma_1 = H_m-H_0 = a$ [41]

Σ_2 s'écrira donc:

$$9d^2+b^2+a^2 = 9d^2+\tfrac{1}{2}(A^2+B^2). \quad [42]$$

Nous pouvons maintenant passer au cas du second moment pour une poudre. En effet, le champ moyen de référence $\bar{H}_m$ est le même pour toutes les orientations et vaut H_0.

$$\bar{S}_2 = \bar{\Sigma}_2 = 9\overline{d^2}+\overline{b^2}+\overline{a^2} = 9\overline{d^2}+\frac{\overline{A^2}+\overline{B^2}}{2}$$

Cette expression donne un résultat identique à l'équation

$$\bar{S}_2 = \overline{\langle H_p^2\rangle}+\overline{\langle H_j^2\rangle}$$

pour une paire de protons entourés de plusieurs ions paramagnétiques.

D'après l'équation [13], Σ_3 s'écrit: $\Sigma_3 = S_3+3\Sigma_1\Sigma_2-2\Sigma_1^3$

Or, S_3 pour une orientation du monocristal est nulle.

Donc, en remplaçant Σ_1 et Σ_2 par les équations [42] et [41], il vient:

$$\Sigma_3 = 27d^2a+3b^2a+a^3$$

et, pour une poudre, après simplification, on obtient:

$$\bar{\Sigma}_3 = \bar{S}_3 = 3\overline{(3d)^2a}+\frac{\overline{A^3}+\overline{B^3}}{2}. \quad [43]$$

Ce qui peut s'écrire sous la forme suivante:

$$\bar{S}_3 = \overline{\langle H_p^3\rangle}+3\overline{\langle H_p\overline{H_j^2}\rangle} \quad [22]$$

car la somme est ici étendue à deux noyaux en résonance (protons).

L'expression du troisième moment d'un tel système est donc bien identique à celle calculée sur la base d'un résultat semi-classique.

Le facteur 3/2, qui exprime l'écart entre les raisonnements quantique et classique pour les interactions dipolaires entre partenaires semblables, intervient dans l'expression du second moment au carré. Cependant, pour les moments d'ordre n, la correction est, à priori, différente de $(3/2)^n$, ainsi que le signale Van Vleck (13). Ceci se vérifie bien dans l'expression du troisième moment. Le facteur 3/2 n'affecte en rien les termes en H_p^3 et H_p mais intéresse uniquement H_j^2 où la correction $(3/2)^2$ est présente sous forme de k_{ij}^2 dans les équations [32] et [33].

6. CONCLUSION

Le troisième moment $\bar{S}_3$ décrit la dissymétrie de la distribution spectrale. Cette dissymétrie est généralement imputable à la présence de centres paramagnétiques dans la substance étudiée.

Can. J. Chem. Downloaded from www.nrcresearchpress.com by 210.87.254.6 on 09/05/12
For personal use only.

Nous nous sommes bornés, ici, à voir l'influence sur le troisième moment de l'interaction dipolaire des noyaux ($I = \frac{1}{2}$) avec les centres paramagnétiques. Dans le cas d'un modèle simple, nous avons vu comment la mesure simultanée de $\tilde{S}_3$ et de $\tilde{S}_2$ pouvait déterminer deux paramètres structuraux R et r, à l'aide de spectres pris sur un échantillon polycristallin.

Il est possible d'étendre l'expression du troisième moment à des cas où l'interaction hyperfine $\mathscr{H}_S$ n'est plus négligeable. $\tilde{S}_3$, couplé aux autres moments ($\overline{\Sigma}$, et $\tilde{S}_2$), permettrait de distinguer les contributions au profil de la raie, des interactions dipolaires et des interactions hyperfines anisotropiques.

Le troisième moment pourrait également être appliqué au couplage de contact dans les métaux et dans les alliages où apparaissent aussi des raies dissymétriques (15).

Enfin, la dissymétrie pourrait mesurer le pourcentage de couplage quadrupolaire de second ordre dans le cas où celui-ci n'est plus négligeable (16).

REMERCIEMENTS

Je remercie tout particulièrement Monsieur le Professeur M. Van Meerssche pour l'intérêt qu'il a bien voulu porter à cette étude et j'exprime ma reconnaissance au Dr. D. J. Kroon pour les fructueuses discussions que nous avons eues ensemble.

Mes remerciements vont également au Fonds National de la Recherche Scientifique (Belgique) pour le mandat d'aspirant qu'il a bien voulu m'octroyer.

BIBLIOGRAPHIE

1. D. J. Kroon. Thèse, Amsterdam. 1960.
2. D. J. Kroon. Arch. Sci. (Geneva), 9e Colloq. Ampère, **13**, 392 (1960).
3. J. A. Ibers, C. Holm, et C. R. McAdam. Phys. Rev. **121**, 1620 (1961).
4. H. Nagasawa, et Y. Tomono. J. Phys. Soc. Japan, **16**, 123 (1961).
5. S. Yano, S. Sasaki, et T. Sidei. J. Phys. Soc. Japan, **12**, 227 (1958).
6. G. E. Pake. J. Chem. Phys. **16**, 327 (1948).
7. R. V. Pound. Phys. Rev. **79**, 685 (1950).
8. C. H. Townes, C. Herring, et W. D. Knight. Phys. Rev. **77**, 852 (1950).
9. R. G. Shulman et V. Jaccarino. Phys. Rev. **108**, 1219 (1957).
10. R. G. Shulman et K. Knox. Phys. Rev. **119**, 97 (1961).
11. R. G. Shulman. J. Chem. Phys. **35**, 1499 (1961).
12. N. Bloembergen. Physica, **16**, 95 (1950).
13. J. H. van Vleck. Phys. Rev. **74**, 1168 (1948).
14. P. J. Van Tiggelen, J. M. Dereppe, et M. Van Meerssche. J. Chim. Phys. **59**, 1042 (1962).
15. N. Bloembergen et T. J. Rowland. Acta Met. **1**, 731 (1953).
16. N. Bloembergen. Report of the Bristol Conference on Defects in Crystalline Solids. The Physical Society, London. 1954. p. 1.

Can. J. Chem. Downloaded from www.nrcresearchpress.com by 210.87.254.6 on 09/05/12
For personal use only.

L'EFFET RÉFLEXE DANS LE BICYCLO[3.2.1]OCTANEDIOL-2β,4β

J. G. DUROCHER[1] ET H. FAVRE
Département de Chimie de l'Université de Montréal, Montréal, Québec

Reçu le 4 juillet 1963

RÉSUMÉ

Les bicyclo[3.2.1]octanediols-2β,4β, -2α,4β et 2α,4α ont été préparés. Le diol diaxial -2β,4β a servi de substance molèle pour l'étude de l'effet de contrainte et de l'effet réflexe. Par l'étude du pont hydrogène interne de ce diol, il est confirmé que si l'on rapproche (effet de contrainte) les substituants diaxiaux sur les carbones 1 et 5 d'un cyclohexane, les substituants axiaux sur les carbones 2 et 4 s'écartent l'un de l'autre (effet réflexe).

En 1958, Sandris et Ourisson (1) signalaient un effet stérique, qu'ils appelaient *effet réflexe*, opérant dans un noyau cyclohexanique lorsque deux substituents axiaux subissent une contrainte. Deux groupes méthyles se repoussent: ils n'occupent pas, comme l'indique la Fig. 1, les positions *a*, mais les positions *a'*. En passant de *a* à *a'*, deux substituants

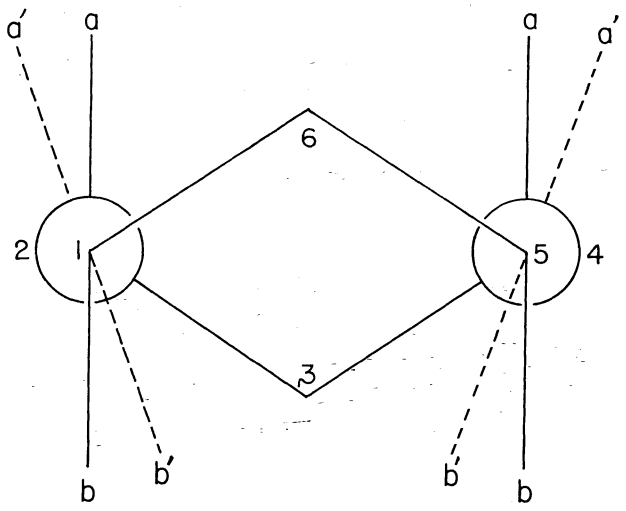

FIG. 1. Cyclohexane en projection de Newman et effet réflexe.

axiaux entraînent les substituants *b* qui se rapprochent l'un de l'autre pour occuper les positions *b'*: c'est l'effet réflexe, qui joue d'ailleurs dans deux sens, car si l'on rapproche les substituants *b* on écarte du même coup les substituants *a*. Les mouvements décrits sont facilement observables sur un modèle de Barton (2); la Fig. 1 les illustre. Si l'effet réflexe a été mis en évidence par les expériences d'Ourisson, il n'en reste pas moins que son aspect quantitatif est encore obscur. On peut en effet envisager que cet effet réflexe (stérique) est analogue à l'effet inductif (électronique); on sait que ce dernier diminue, pour finalement s'éteindre, à mesure que l'on s'éloigne du centre d'induction (3). On peut donc se poser la même question pour l'effet réflexe: quel est son ordre de grandeur à proximité des centres de contrainte, et ensuite, en fonction de la distance? On retrouve

[1]*Boursier du Conseil National de Recherches du Canada, 1960–1963.*

Can. J. Chem. Downloaded from www.nrcresearchpress.com by 210.87.254.6 on 09/05/12
For personal use only.

ainsi le problème plus général de la transmission conformationnelle soulevé par Barton (4, 5). Nos études sur les dérivés du bicyclo[3.2.1]octane, en particulier celles des diols (6, 7), nous ont amenés à entreprendre quelques travaux sur les déformations que subit un noyau cyclohexanique contraint en deux points et à approfondir les notions d'effet réflexe et de transmission conformationnelle.

Ce mémoire traite essentiellement du bicyclo[3.2.1]-octanediol-2β,4β (I), et accessoirement de ses isomères-2α,4β (II) et -2α,4α (III).

Nous envisageons le diol diaxial I (Fig. 2) comme un cyclohexanediol-1,3 *cis* diaxial

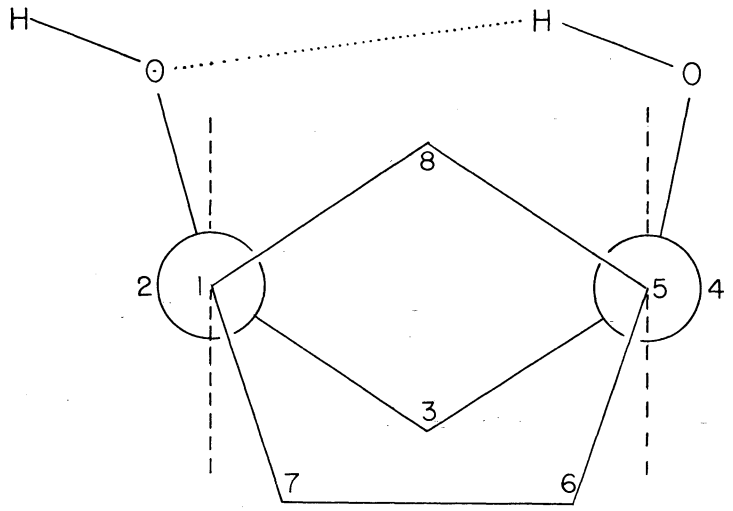

FIG. 2. Projection de Newman du bicyclo[3.2.1]octanediol-2β,4β.

idéal[2] (Fig. 1, a = OH, b = H, on néglige a', b') dans lequel la distance idéale de 2.51 Å H—H (= b—b) aurait été amenée à 1.54 Å, qui est la longueur de la liaison C_6—C_7 dans le diol I. On s'attend donc, par l'effet réflexe, à ce que les groupes OH soient plus éloignés l'un de l'autre dans le diol I que dans le cyclohexanediol-1,3 *cis* diaxial. La vérification en est aisée, car Kuhn (8) a montré que la différence ($\Delta\nu$, exprimé en cm^{-1}) entre les bandes infrarouges de vibration des groupes —OH libre et engagé dans un pont hydrogène intramoléculaire de nombreux diols est fonction de la longueur du pont hydrogène: plus ce dernier est court, plus le $\Delta\nu$ est grand. Nous avons trouvé que le $\Delta\nu$ du bicyclo[3.2.1]octanediol-2β,4β (I) est de 39 cm^{-1}, pour 76 cm^{-1} (8) pour le cyclohexanediol-1,3 *cis* (diaxial). Qualitativement donc nous sommes en mesure de confirmer l'effet réflexe d'Ourisson, puisque la diminution de $\Delta\nu$ en passant du diol non contraint (cyclohexanediol-1,3 *cis*) au diol contraint (diol I) correspond à un écartement des groupes —OH.

Un travail récent de Mühle et Tamm (10) corrobore nos résultats et justifie nos conclusions. Ces auteurs ont en effet observé une augmentation de $\Delta\nu$ en passant du cholestanediol-1α,3α ($\Delta\nu$ 87 cm^{-1}) au diméthyl-4,4 cholestanediol-1α,3α ($\Delta\nu$ 107 cm^{-1}), la répulsion entre les groupes méthyles β diaxiaux amenant par effet réflexe un rapprochement des groupes —OH diaxiaux en 1 et en 3.

[2]*La conformation du cyclohexanediol-1,3 cis diaxial idéal est représentée par la Fig. 1 (a = —OH, b = —H; on néglige a', b'). Des travaux récents (9, 10) indiquent toutefois qu'une certaine répulsion entre les groupes* —OH *fait que la forme (conformation réelle) est plutôt représentée par la Fig. 1 (a' = —OH, b' = —H; on néglige a, b); la grandeur de la déformation n'est pas connue.*

Can. J. Chem. Downloaded from www.nrcresearchpress.com by 210.87.254.6 on 09/05/12
For personal use only.

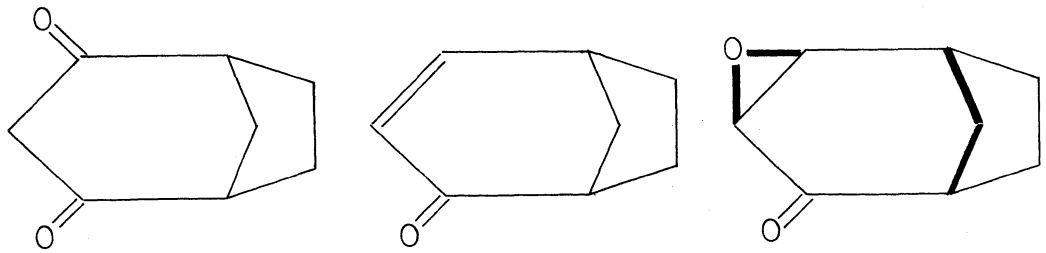

(IV) (V) (VI)

SYNTHÈSE DES TROIS BICYCLO[3.2.1]OCTANEDIOLS-2,4

Nous avons préparés les diols à partir: 1. de la bicyclo[3.2.1]octanedione-2,4 (IV), qui s'obtient facilement en faisant agir le diazométhane sur la norcamphoquinone et en hydrolysant l'éther céto-énolique obtenu, à l'image de la synthèse de l'oxo-4 homocamphre à partir de la camphoquinone (12, 13); 2. de l'époxyde 3β,4β de la bicyclo[3.2.1]octène-3 one-2, (VI) qui résulte de l'action du peroxyde d'hydrogène sur la cétone α,β-éthylénique correspondante (V).

Le diol diaxial résulte de la réduction de la β-dicétone IV par le nickel de Raney et le diol diéquatorial de la réduction par le sodium et l'éthanol de cette β-dicétone, à l'image des réductions de l'oxo-4 homocamphre (7). Le diol axial-équatorial s'obtient par réduction par l'hydrure de lithium et d'aluminium de l'époxyde-cétone VI (méthode de Tamm et de ses collaborateurs (10, 11). Dans les trois cas le diol pur a été obtenu par chromatographie sur alumine des diols bruts. D'une manière assez surprenante, dans ces chromatographies, nous avons toujours obtenu dans les fractions de tête un diol pur, que ce soit le diaxial (I), le diéquatorial (III), ou l'axial-équatorial (II); les trois diols n'ont donc pas de caractéristiques d'adsorption sur l'alumine bien marquées. La pureté de chaque diol a été établie en chromatographiant en phase gazeuse le diéther méthylique correspondant, que l'on obtient aisément en traitant le diol par le diazométhane en présence d'acide fluoroborique (14). Les temps de rétention des diéthers diaxial et diéquatorial sont identiques; ces deux diéthers sont élués après le diéther axial-équatorial. Nous n'avons ainsi pas pu doser chaque diol dans les mélanges bruts de réduction: nous ne pouvons que connaître le pourcentage de diol axial-équatorial qui se retrouve dans les 3 mélanges: 42% dans la réduction catalytique, 28% dans la réduction chimique de la dicétone et 90% dans la réduction de l'époxyde-cétone. Dans ce dernier cas les 10% qui restent sont nécessairement formés du diol diaxial, l'époxyde 3β,4β (VI) étant le seul formé au cours de l'époxydation.

Cette configuration 3β,4β a été déduite du fait que l'attaque du réactif doit so faire sur la face β, la plus dégagée de la cétone α,β-éthylénique V, celle qui n'est pas soumise à l'empêchement stérique causé par le pont C_6—C_7 diaxial. Ceci est conforme au travail récent de Mühle et Tamm (10), qui signalent que l'époxydation de la diméthyl-4,4 cholestène-1 one-3 (et même de la cholestène-1 one-3 (11)) se fait par la face α, non par la face β influencée par les groupes méthyles axiaux en 4 et 10. L'analogie entre le bicycle que nous décrivons et les stéroïdes se complète par le fait que l'oxydation périodique ne révèle pas de diol-1,2, mais elle s'arrête là, car dans la série stéroïde on obtient par réduction de l'époxyde-cétone principalement le diol-1,3 diaxial.

Can. J. Chem. Downloaded from www.nrcresearchpress.com by 210.87.254.6 on 09/05/12
For personal use only.

PREUVES DE CONFIGURATION DES DIOLS I, II ET III

Les preuves des configurations de ces diols sont les suivantes (voir Tableau I): dans l'*infrarouge* un seul des trois diols présente une bande OH libre et une bande OH associé,

TABLEAU I

Diol	Mode de préparation	Spectre IR ν —OH cm^{-1}	Résonance magnétique nucléaire*	Vitesses relatives d'oxydation chromique†
I Diaxial	Dicétone + H_2/NiRa	3615 (OH libre) 3576 (OH ass.) $\Delta\nu$ = 39 cm^{-1}	6.08 p.p.m. (2H) pic/unique	117.2
II Axial-équatorial	Epoxyde-cétone + $LiAlH_4$	3615 (OH libre)	5.94 p.p.m. (1H) pic/unique 5.55 p.p.m. (1H) multiplet	55.1
III Diéquatorial	Dicétone + Na/EtOH	3615 (OH libre)	6.05 p.p.m. (2H) multiplet	25.8

*Tétraméthylsilane, comme standard interne.
†*Tert*-butyl-4 cyclohexanol *trans* = 1.

d'après la méthode de Kuhn (8); ce ne peut être que le diaxial (I);[3] en *résonance magnétique nucléaire* (15) deux des diols présentent un type de proton H—C(OH), le troisième en a deux; les deux premiers doivent donc avoir un élément de symétrie qui rendra les deux protons identiques, le troisieme en est dépourvu: ce dernier composé est donc l'isomère axial-équatorial (II); des deux premiers diols l'un (I), est déjà connu par l'infrarouge (le diaxial), l'autre sera donc le diéquatorial (III); ces configurations sont confirmées *par oxydation chromique*, selon nos travaux antérieurs (6, 7) qui prévoyaient que le diol axial-équatorial devait s'oxyder plus rapidement que le diéquatorial, et le diaxial plus rapidement que l'axial-équatorial: c'est ce que nous observons en effet.

On peut envisager pour le bicyclo[3.2.1]octane deux conformations, chaise et bateau cyclohexanique, représentées respectivement par les formules des diols I–III et IA–IIIA. La conformation chaise est favorisée, en première approximation, par 7–10 kcal/mole (16). Il est donc évident que le diol diéquatorial chaise III n'aura pas tendance à passer au diol diaxial bateau IIIA, et aussi que le diol axial-équatorial chaise II ne gagnera rien à passer à la conformation diol axial-équatorial bateau IIA. Pour le diol diaxial chaise I $\rightleftarrows$ diéquatorial bateau IA, si la conformation diéquatoriale bateau IA était prédominante aucun des trois diols IA, II et III ne donnerait de pont hydrogène intramoléculaire. Ceci n'étant pas le cas, la conformation I doit exister de préférence à IA, ce qui est d'ailleurs confirmé par les vitesses d'oxydation chromique. A supposer que le diol bateau IIIA existât et que ce soit lui qui donnât le pont hydrogène intramoléculaire observé, sa vitesse d'oxydation chromique devrait être nettement plus élevée que celle du diol diéquatorial, supérieure à 4, de l'ordre de 25 au moins. Le triméthyl-1,8,8 bicyclo[3.2.1]octane diol-2,4 diaxial s'oxyde 25 fois plus rapidement que son isomère diéquatorial alors que l'interaction méthyle-hydroxyde diaxiale est 1–3 (7); l'on s'attendrait à ce qu'une interaction méthyle-hydroxyle diaxiale soit au moins aussi forte en 1–2 qu'en 1–3.

En définitive, les conformations I, II et III nous semblent tout à fait appropriées pour

[3]*Le triméthyl-1,8,8 bicyclo[3.2.1]octanediol-2β,4β n'a pas de pont hydrogène intramoléculaire, mesurable tout au moins dans l'infrarouge (7). C'est la raison pour laquelle nous avons dû préparer le diol diaxial I, dépourvu de groupes méthyles, pour étudier l'effet réflexe.*

Can. J. Chem. Downloaded from www.nrcresearchpress.com by 210.87.254.6 on 09/05/12
For personal use only.

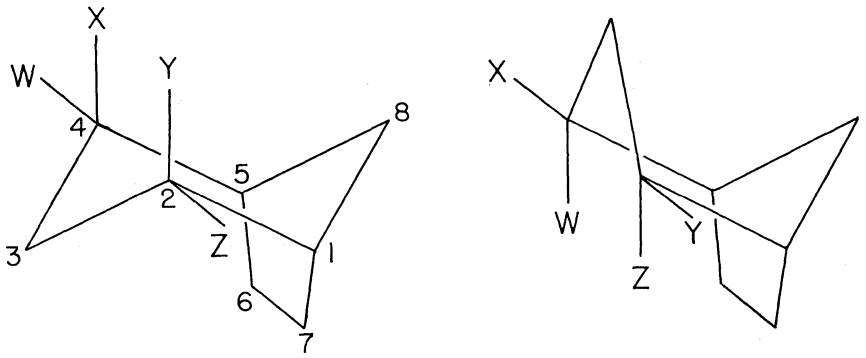

I	X = Y = −OH;	W = Z = −H	IA
II	X = Z = −OH;	W = Y = −H	IIA
III	W = Z = −OH;	X = Y = −H	IIIA

décrire ces diols. La conformation chaise cyclohexanique est d'ailleurs généralement acceptée pour les alcools de la série du bicyclo[3.2.1]octane (17, 18).

PARTIE EXPÉRIMENTALE[4]

1. Bicyclo[3.2.1]octanedione-2,4(IV)[5]

La norcamphoquinone préparée selon (19) est traitée par le diazométhane selon la méthode (12): 17.5 g donnent 11.5 g d'éther céto-énolique brut, liquide jaune qui est hydrolysé en β-dicétone IV selon la méthode (13), à la différence près que la dicétone est très soluble dans l'eau et qu'il faut l'extraire d'une manière continue au moyen d'un appareil de Kutscher-Steudel. On obtient ainsi 5 g de dicétone IV, p.f. 128–129°, après cristallisation dans le benzène et sublimation à 100° sous 1 mm. Calculé pour $C_8H_{10}O_2$: C, 69.54; H, 7.30%. Trouvé: C, 69.39; H, 7.24%. Le spectre infrarouge dans le nujol présente une bande forte à 2500 cm^{-1}: —OH à 1610 cm^{-1}: C=C et 1530 cm^{-1}: C=O. La dioxime fond à 182°. Calculé pour $C_8H_{12}O_2N_2$: C, 57.13; H, 7.19; N, 16.66%. Trouvé: C, 57.16; H, 7.22; N, 16.47%.

2. Bicyclo[3.2.1]octanediol-2β,4β (I)

On agite en atmosphère d'hydrogène 2 g de β-dicétone (IV) en solution dans 40 ml d'éthanol 95%, en présence de 2 g de nickel de Raney, à 20° et à la pression atmosphérique. Le nickel de Raney est préparé selon (7). En 10 heures, il y a absorption de 800 ml d'hydrogène (calculé 700 ml). Le catalyseur est éliminé par filtration; on le lave avec un peu de méthanol, évapore les filtrats réunis. Au résidu on ajoute 100 ml d'une solution aqueuse de NaOH 5%; on extrait cette solution par de l'éther, d'une manière continue, dans un appareil de Kutscher–Steudel, pendant 18 heures. L'évaporation de l'éther abondonne 2 g de diols bruts, que l'on dissout dans 200 ml de chloroforme et adsorbe sur 200 g d'alumine Woelm d'activité I. On élue ensuite par des portions de 200 ml de chloroforme. Les fractions 1 à 12 (477 mg) représentent le diol I pur, p.f. 265–267° après 6 cristallisations dans le benzène. Calculé pour $C_8H_{14}O_2$: C, 67.57; H, 9.92%. Trouvé: C, 67.46; H, 9.75%. Di-*p*-nitrobenzoate, p.f. 191–193° (EtOH). Calculé pour $C_{22}H_{20}O_8N_2$: C, 60.00; H, 4.58; N, 6.36%. Trouvé: C, 59.81; H, 4.43; N, 6.14%.

Les fractions 13 à 59 (chloroforme) (1.233 g) représentent des diols en mélange; on élue finalement par 200 ml de méthanol, fraction 60 (317 mg).

3. Bicyclo[3.2.1]octanediol-2α,4α (III)

A 671 mg de β-dicétone en solution dans 30 ml d'éthanol anhydre, on ajoute peu à peu 1.6 g de sodium coupé en petits morceaux. On agite à température de la pièce pendant 3 heures, on ajoute avec prudence 50 ml d'éthanol étendu d'eau (1:1) et évapore l'alcool à pression de 12 mm. La solution aqueuse résiduelle est extraite par de l'éther, d'une manière continue, pendant 18 heures. L'évaporation de l'éther abandonne 306 mg de diols bruts. Pour la chromatographie, on dissout 4 g de diols bruts dans 400 ml de chloroforme, on les adsorbe sur 400 g d'alumine Woelm d'activité I et élue par des portions de 400 ml de chloroforme. Les fractions 1 à 8 (460 mg) représentent le diol III pur, les fractions 9 à 30 (1.10 g) et la fraction 31 (éluée par du méthanol) (1.95 g) des diols en mélange que l'on rechromatographie sur 300 g d'alumine pour obtenir 138 mg (fractions 1 à 5) de diol III pur et 2.823 g de diols en mélange. Le diol III pur fond à 225–226°, après

[4]*Les points de fusion ont été déterminés en tubes capillaires, au moyen d'un thermomètre étalonné avec des substances pures de points de fusion connus. Les analyses sont de W. Manser, ing., Herrliberg (Suisse) et C. Daesslé, Organic Microanalyses, Montréal. Les chromatographies en phase gazeuse ont été réalisées au moyen d'un appareil, Kromo-Tog K–2, de Burrell Corporation.*

[5]*Nous devons la synthèse de cette dicétone à MM. J. Champagne et N. Dufort, candidats chimistes.*

Can. J. Chem. Downloaded from www.nrcresearchpress.com by 210.87.254.6 on 09/05/12
For personal use only.

cristallisation dans le benzène. Calculé pour $C_8H_{14}O_2$: C, 67.57; H, 9.92%. Trouvé: C, 67.42; H, 9.65%. Di-*p*-nitrobenzoate, p.f. 184–185°. Calculé pour $C_{22}H_{20}O_8N_2$: C, 60.00; H, 4.58; N, 6.36%. Trouvé: C, 59.84; H, 4.64; N, 6.16%.

4. Bicyclo[3.2.1]octène-3 one-2 (V)

Nous avons procédé de la manière suivante. La bicyclo[3.2.1]octanone-2, préparée selon (20), a été bromée selon (21) puis déshydrobromée selon la méthode (22); la cétone α,β-éthylénique brute a été purifiée par chromatographie en phase gazeuse, en utilisant un appareil Prep-Partitioner de Fisher (20% polyester succinique de Craig, sur brique, 185°, azote comme éluant). Le rendement en cétone pure est de 54% à partir de la cétone saturée: p. éb. 86° sous 12 mm: dinitro-2,4 phénylhydrazone, p.f. 139–140° (litt. 140.4–141.5° (23)).

5. Oxydo-3β,4β bicyclo[3.2.1]octanediol-2α,4β (II)

Nous avons adapté la méthode (24). Dans un bécher de 250 ml, muni d'un agitateur magnétique et placé dans un bain maintenu à 40°, on met 2.02 g de bicyclo[3,2,1]octène-3 one-2 (V) en solution dans 100 ml de méthanol aqueux 80%. On ajoute au compte-goutte, quelques gouttes de NaOH 1.5 *N* en solution dans du méthanol aqueux 80% pour que le pH, lu sur un pH-mètre, soit de 11.5. A l'aide d'une ampoule on ajoute, goutte à goutte, une solution de 10 ml de peroxyde d'hydrogène 30% dans 30 ml de méthanol. Pendant l'addition on maintient le pH du milieu réactionel en ajoutant au besoin quelques gouttes d'une solution de NaOH (0.2 *N*, méthanol–eau 8:2). L'addition terminée, on poursuit l'agitation et le chauffage à 40° pendant une heure en maintenant le pH constant par addition de la solution de NaOH 0.2 *N*. Puis on abandonne au réfrigérateur pendant une heure. On projette le tout sur 500 ml d'eau glacée saturée de NaCl. Le pH de l'eau est alors de 7, lu sur le pH-mètre. On extrait le produit à l'éther et on sèche le solution éthérée sur sulfate de sodium anhydre. On évapore l'éther sous vide. On reprend le résidu par du benzène qu'on évapore aussi sous vide pour éliminer les traces d'eau et de méthanol. On recueille un solide amorphe de 2.20 g, 90°–108°, après cristallisation dans l'éther de pétrole refroidi à −60°. Calculé pour $C_8H_{10}O_2$: C, 69.54; H, 7.30%. Trouvé: C, 69.29; H, 7.30%.

Le spectre infrarouge présente une bande forte à 1725 cm^{-1} (CCl_4).

6. Bicyclo[3.2.1]octanediol-2α,4β (II)

L'époxyde-cétone (336 mg) en solution dans 25 ml d'éther anhydre a été réduite par l'hydrure de lithium et d'aluminium, (2.0 g en suspension dans 50 ml d'éther anhydre), en chauffant à reflux pendant 3 heures. L'excès d'hydrure est détruit par de l'eau; on ajoute ensuite de l'eau (25 ml) et de l'acide chlorhydrique concentré (20 ml), extrait d'une manière continue par de l'éther pendant 18 heures. On recueille à la manière habituelle 333 mg de diols bruts. On chromatographie 2.1 g de ces diols bruts en les dissolvant dans 200 ml de chloroforme, sur 200 g d'alumine Woelm d'activité I. On élue par des portions de 200 ml de chloroforme. Les fractions 1 à 31 (1.328 g) représentent le diol II pur, p.f. 252–255° après 2 cristallisations dans le benzène. Calculé pour $C_8H_{14}O_2$: C, 67.57; H, 9.92%. Trouvé: C, 67.36; H, 9.88%. Di-*p*-nitrobenzoate, p.f. 161–163°. (EtOH). Calculé pour $C_{22}H_{20}O_8N_2$: C, 60.00; H, 4.58; N, 6.36%. Trouvé: C, 59.70; H, 4.61; N, 6.25%. Les fractions 31–36 de la chromatographie, éluées par du chloroforme contenant de 1 à 10% de méthanol (660 mg) représentent des diols en mélange.

L'oxydation des diols bruts par le periodate de sodium ne donne pas de composés de coupure (11).

7. Chromatographie en phase gazeuse des diéthers des diols I, II et III

Les diéthers correspondant aux diols se chromatographient bien, soit sur Tergitol, soit sur le polyester succinique de Craig.

Les diéthers des diols purs ou des mélanges de réduction ont été préparés selon la méthode (14) simplifiée. Un échantillon de 10 à 15 mg de diol(s) est dissous dans 1.5 à 2.0 ml de chloroforme. On refroidit à 0° dans un bain de glace, puis ajoute 5 à 6 ml de la solution de diazométhane dans le chlorure de méthylène. Puis on ajoute une goutte de la solution aqueuse d'acide fluoroborique 15 *N*. On continue d'ajouter de la solution de diazométhane dans le chlorure de méthylène jusqu'à coloration jaune persistante durant 30 secondes. On ajoute alors deux pastilles de KOH, du sulfate de sodium anhydre. On filtre. L'évaporation du solvant sous pression de 12 mm abandonne quelques gouttes de liquide jaune-brun, présentant une bande forte à 1097 cm^{-1} dans l'infrarouge (C—O—C) et aucune bande —OH. On chromatographie tel quel soit sur Tergitol (colonne 2.5 mètres, diamètre intérieur 6mm, 20% sur brique, 225°) soit sur polyester succinique de Craig (colonne 2.5 mètres, diamètre intérieur 6mm, 20% sur brique, 180°). Temps de rétention des diéthers issus des diols purs:

Tergitol: diéther de I et diéther de II: 20½ minutes;
diéther de II 17⅔ minutes.

Polyester succinique de Craig: diéther de I et diéther III 11 minutes;
diéther de II 9 minutes.

Les diols bruts de réduction ont donné, par cette méthode:

Réduction catalytique de la dicétone: 42% axial-équatorial;

Réduction chimique de la dicétone: 28% axial-équatorial;

Réduction de l'époxyde-cétone: 90% axial-équatorial.

Il n'est pas possible de séparer les diéthers des diols diaxial et diéquatorial par cette méthode.

Can. J. Chem. Downloaded from www.nrcresearchpress.com by 210.87.254.6 on 09/05/12
For personal use only.

8. Points de fusion des mélanges des diols et des di-p-nitrobenzoates

Tous les mélanges sont 1:1.
Diol I + diol II: 246–255° (dépression)
Diol I + diol III: 245–250° (pas de dépression)
Diol II + diol III: 238–241° (pas de dépression)
Di-*p*-nitrobenzoates de I + II: 141–149° (dépression)
Di-*p*-nitrobenzoates de I + III: 156–163° (dépression)
Di-*p*-nitrobenzoates de II + III: 144–150° (dépression)

9. Spectres infrarouges des diols I, II et III

Les spectres infrarouges des diols I, II et III ont été mesurés selon la méthode (8), dans la région de 3600 cm^{-1} au moyen d'un spectromètre Perkin Elmer, modèle 112; optique LiF; longueur de la cellule: 30.9 mm. Concentration des solutions 2.6×10^{-3} *M* (CCl_4). Les résultats sont rapportés au Tableau I.

10. Spectres de résonance magnétique nucléaire des diols I, II et III

Ils ont été mesurés au moyen d'un appareil Varian A60, dans la pyridine, selon les indications (15). Le tétraméthylsilane est pris comme système de référence. Les signaux caractéristiques sont rapportés au Tableau I.

11. Oxydations chromiques des diols I, II et III

Nous avons utilisé la technique déja décrite (25). La méthode de calcul a cependant été modifiée par le professeur Richer, qui la publiera bientôt *in extenso*. Nous rapporterons ici les données expérimentales: température 25°; système de référence, *tert*-butyl-4 cyclohexanol pour lequel *K* (litre $mole^{-1}$ sec^{-1}) = 2.502×10^{-3}. Les vitesses relatives pour le cyclohexanol et les diols I, II et III sont rapportées au Tableau I, la valeur de *K* pour le *tert*-butyl-4 cyclohexanol *trans* étant prise comme unité. Le détail des mesures apparaît au Tableau II.

TABLEAU II

Oxydation chromique des diols I, II et III

Diols	Essais	Concentrations molaires en CrO_3	Concentrations molaires des diols	*K*, litre $mole^{-1}sec^{-1}$	*K* Moyenne
I	1	4.076×10^{-4}	2.883×10^{-3}	296×10^{-3}	293×10^{-3}
	2	4.021×10^{-4}	3.007×10^{-3}	290×10^{-3}	
II	1	3.962×10^{-4}	2.937×10^{-3}	136×10^{-3}	
	2	3.855×10^{-4}	2.903×10^{-3}	133×10^{-3}	138×10^{-3}
	3	4.217×10^{-4}	2.889×10^{-3}	144×10^{-3}	
III	1	3.715×10^{-4}	2.920×10^{-3}	66×10^{-3}	67×10^{-3}
	2	3.654×10^{-4}	3.165×10^{-3}	68×10^{-3}	

REMERCIEMENTS

Nous remercions le Conseil National de Recherches du Canada pour une subvention de recherches (H. F.) et une bourse d'études (J. G. D.). Nous remercions également M. le professeur J. C. Richer et M. Cl. Gilardeau de l'aide apportée dans les mesures des vitesses d'oxydation chromique.

BIBLIOGRAPHIE

1. B. Waegell et G. Ourisson. Bull. Soc. Chim. France (5) 495 (1963).
2. D. H. R. Barton. Chem. Ind. 1136 (1956).
3. C. Sandorfy. Can. J. Chem. **33**, 1337 (1955).
4. D. H. R. Barton. *Dans* Conférences principales et conférences de sections, XIVe Congrès international de chimie pure et appliquée, Zurich, 21–27, VII, 1955. Birkhäuser Verlag, Basel und Stuttgart. 1955. p. 121.
5. D. H. R. Barton, F. McCapra, P. J. May, et F. Thudium. J. Chem. Soc. 1297 (1960).
6. H. Favre et J. C. Richer. Can. J. Chem. **37**, 411 (1959).
7. H. Favre et J. C. Richer. Can. J. Chem. **37**, 417 (1959).
8. L. P. Kuhn. J. Am. Chem. Soc. **74**, 2492 (1952).
9. S. Julia, D. Varech, Th. Bürer, et Hs. H. Günthard. Helv. Chim. Acta, **43**, 1623 (1960).
10. H. Mühle et Ch. Tamm. Helv. Chim. Acta, **46**, 268 (1963).
11. Ch. Tamm. Helv. Chim. Acta, **43**, 1700 (1960).
12. H. Rupe et F. Häfliger. Helv. Chim. Acta, **23**, 139 (1940).
13. H. Favre, B. Marinier, et J. C. Richer. Can. J. Chem. **34**, 1328 (1956).
14. M. Neeman, M. C. Caserio, J. D. Robert, et W. S. Johnson. Tetrahedron, **6**, 36 (1959).

Can. J. Chem. Downloaded from www.nrcresearchpress.com by 210.87.254.6 on 09/05/12
For personal use only.

15. H. FINEGOLD et H. KWART. J. Org. Chem. **27**, 2361 (1962).
16. A. A. YOUSSEF, M. E. BAUM, et H. M. WALBORSKY. J. Am. Chem. Soc. **81**, 4709 (1959).
17. H. M. WALBORSKY, M. E. BAUM, et A. A. YOUSSEF. J. Am. Chem. Soc. **83**, 988 (1961).
18. H. L. GOERING et M. F. SLOAN. J. Am. Chem. Soc. **83**, 1397 (1961).
19. K. ALDER, H. K. SCHAFER, H. ESSER, H. KRIEGER, et R. REUBKE. Ann. **593**, 23 (1955).
20. P. NEDENSKOV, H. HEIDE, et N. CLOUSON-KASS. Acta Chem. Scand. **16**, 247 (1962).
21. C. DJERASSI et C. R. SCHOLZ. J. Am. Chem. Soc. **70**, 417 (1948).
22. B. BERKOZ, E. P. CHAVEZ, et C. DJERASSI. J. Chem. Soc. 1323 (1962).
23. H. L. GOERING, R. W. GREINER, et M. F. SLOAN. J. Am. Chem. Soc. **83**, 1391 (1961).
24. J. ROMO, G. ROSENKRANZ, et C. DJERASSI. J. Am. Chem. Soc. **73**, 5489 (1951).
25. H. FAVRE, M. LEFEBVRE, et J. C. RICHER. Can. J. Chem. **37**, 403 (1959).

Can. J. Chem. Downloaded from www.nrcresearchpress.com by 210.87.254.6 on 09/05/12
For personal use only.

LES ACÉTATES ÉNOLIQUES DES DIMÉTHYL-6,6 ET DIMÉTHYL-7,7 DÉCALONES-2 CIS ET TRANS

H. Favre et A. J. Liston
Département de chimie, Université de Montréal, Montréal, Qué.
Reçu le 22 juillet 1963

RÉSUMÉ

Les quatre décalones mentionnées dans le titre conduisent chacune à deux acétates énoliques lorsqu'on les traite par l'acétate d'isopropényle et l'acide sulfurique concentré. Ces derniers ont été dosés et leurs structures déterminées. Des quatre décalones, seules les décalones cis donnent des acétates énoliques lorsque l'agent d'acétylation est un mélange d'anhydride acétique et d'acide perchlorique. La condensation des quatre décalones avec l'oxalate d'éthyle est également rapportée.

Nos études sur la stéréochimie des terpènes et des stéroides nous ont amenés à étudier le comportement chimique des décalones-2 cis et trans* pour préciser les facteurs stériques qui contrôlent l'énolisation et déterminer la façon dont un squelette alicyclique se modifie et se déforme sous les contraintes exercées par la présence d'une double liaison sur le cycle. Ce mémoire traite des acétates énoliques des diméthyl-6,6 et diméthyl-7,7 décalones-2 trans (I et II) et cis (III et IV) (1). Comme la triméthyl-7,7,10 décalone-2 cis (V) de Halsall et Thomas (2), que l'on doit tenir pour *nst* puisque la conformation *st* présente une interaction défavorable entre le groupe méthyle axial et l'embranchement décalinique; alors, la diméthyl-7,7 décalone-2 *cis* pour ces mêmes raisons doit être *nst*. Au contraire, la diméthyl-6,6 décalone-2 *cis* (III), doit être *st*, puisque c'est la conformation *nst* qui présente l'interaction défavorable entre le groupe méthyle axial et l'embranchement décalinique.†

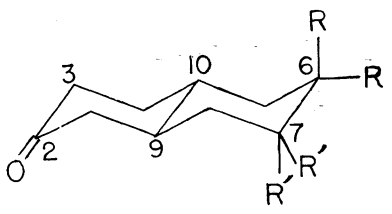

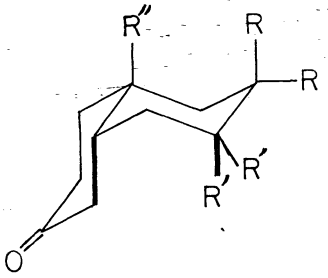

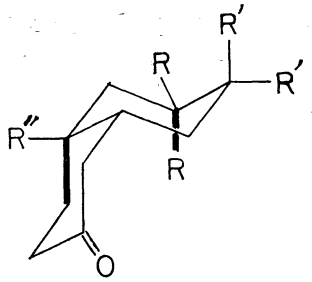

I R = —CH_3; R′ = —H
II R = H; R′ = —CH_3

III*st* R = —CH_3; R′ = R″ = —H
IV*st* R′ = —CH_3; R = R″ = —H
V*st* R″ = R′ = —CH_3; R = H
VI*st* R″ = —CH_3; R = R′ = —H
VII*st* R = R′ = R″ = —H

III*nst*
IV*nst*
V*nst*
VI*nst*
VII*nst*

**Dans ce mémoire le numérotage des décalones est indiqué à la formule I; celui des stéroïdes sera le numérotage officiel.*

†Le travail de Djerassi et de ses collaborateurs (3), qui permet de tirer la conclusion que la méthyl-10 décalone-2 cis (VI) est st, jette quelque doute sur la validité de l'argument thermodynamique (4) pour déterminer la conformation st–nst d'une décalone-2 cis. Jusqu'à preuve du contraire, nous considérerons que la diméthyl-6,6 décalone-2 cis est st, ou tout au moins un mélange des conformations st et nst dans lequel prédomine la conformation st; de même la diméthyl-7,7 décalone-2 cis sera nst, ou tout au moins un mélange st–nst dans lequel prédomine la conformation nst.

Préparation des acétates énoliques

En traitant les décalones trans I et II et cis III*st* et IV*nst* par l'acétate d'isopropényle en présence d'acide sulfurique concentré (5) nous avons obtenu dans chaque cas un mélange des deux acétates énoliques Δ^1 et Δ^2 correspondant à la double énolisation de la décalone, que nous avons dosés par chromatographie en phase gazeuse (Tableau I). La conversion

TABLEAU I

Pourcentages respectifs d'acétates énoliques obtenus à partir des décalones I, II, III*st*, et IV*nst*

Décalones de départ	Rapports des acétates énoliques formés Δ^1, Δ^2, et pourcentages de décalones de départ qui les accompagnent (C=O)								
	Méthode 1			Méthode 2			Méthode 3		
	Δ^1	Δ^2	C=O	Δ^1	Δ^2	C=O	Δ^1	Δ^2	C=O
I	36.7	63.2	0	0	0	100	0	0	100
II	33.8	66.2	0	0	0	100	0	0	100
III*st*	56.6	43.4	0	60.0	40.0	8	60.0	40.0	8
IV*nst*	59.0	41.0	0	74.0	26.0	6	74.0	26.0	6

Méthode 1: acétate d'isopropényle + acide sulfurique.
Méthode 2: anhydride acétique + acide perchlorique (24 heures, 25°).
Méthode 3: anhydride acétique + acide perchlorique sur les mélanges obtenus par la méthode 1 (36 heures, 25°).

en acétates énoliques est complète, comme l'indiquent l'infrarouge et la c.p.g. (chromatographies en phase gazeuse). Dans un cas, celui de la diméthyl-7,7 décalone-2 cis (IV*nst*) nous avons montré qu'il s'agissait bien des deux acétates énoliques correspondant à la décalone, en séparant le mélange par c.p.g. et en convertissant chaque acétate énolique en décalone de départ par l'hydroxyde de potassium méthanolique.

En traitant durant 24 heures les décalones cis III*st* et IV*nst* par l'anhydride acétique, en présence d'acide perchlorique aqueux, dans un mélange de tétrachlorure de carbone et de benzène (6, 7), nous avons obtenu dans les deux cas les acétates énoliques correspondants, que nous avons dosés par c.p.g., après avoir déterminé par infrarouge la teneur en décalone de départ qui se trouve présente dans les mélanges (Tableau I). Les décalones trans I et II ne donnent pas du tout les acétates énoliques attendus. L'un de nous ayant montré (8) que cette méthode donnait des acétates énoliques en équilibre, contrairement à la première méthode à l'acétate d'isopropényle qui est régie par un contrôle cinétique, nous avons soumis chacun des mélanges obtenus par contrôle cinétique aux conditions isomérisantes de la deuxième méthode, avec les résultats suivants pour un contact de 36 heures: dans la série trans, les mélanges d'acétates énoliques sont entièrement convertis en décalones; dans la série cis, les mélanges se mettent à l'équilibre et sont finalement semblables à ceux que l'on prépare directement à partir des décalones (voir Tableau I).

Preuves des structures des acétates énoliques

Il existe une preuve de structure absolue, illustrée par le Schéma 1, valable pour la série trans et pour la série cis, chacune prise séparément, fondée sur le principe suivant. La décalone trans I donne naissance à deux acétates énoliques VIII et IX trans, qui à leur tour engendrent deux composés de coupure XII et XIII trans. La décalone trans II, à son tour, engendre les acétates X et XI trans et les composés de coupure XIII et XIV trans en mélange. Les deux mélanges de composés de coupure, à partir de I et de II, contiennent donc un composé commun, qui ne peut être que XIII trans. Reconnaître et doser ce dernier dans les mélanges des composés de coupure permet donc sans ambiguité

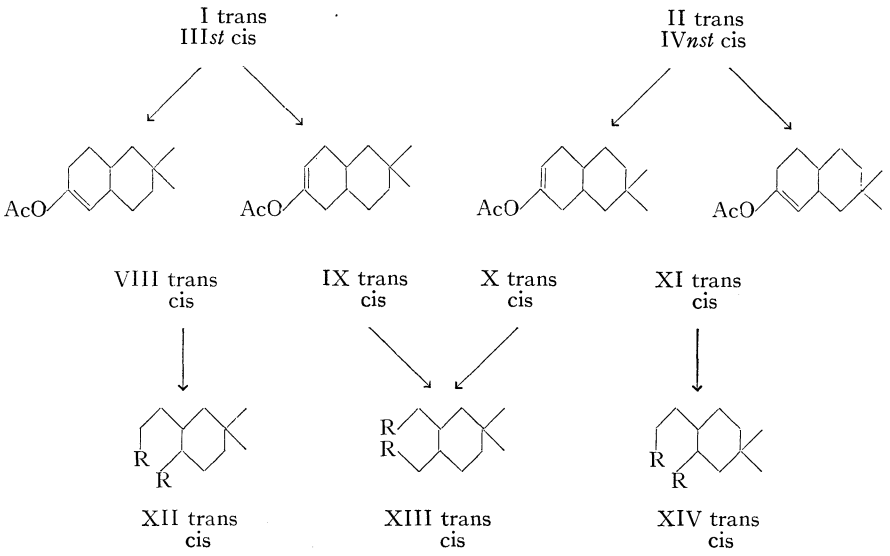

SCHÉMA 1. Preuves de structure des acétates énoliques issus des décalones I, II, III, et IV.

de déterminer les structures des acétates énoliques et finalement de doser ces derniers, si les proportions des composés de coupure reflètent celles des acétates énoliques. Le même raisonnement se fera dans la série cis, au départ des décalones *III*st et IV*nst*.

La c.p.g. semblait prometteuse pour résoudre facilement ce problème, puisque les mélanges binaires XII et XIII trans (et cis) et XIII et XIV trans (et cis) devaient donner un mélange ternaire dans lequel le composé commun XIII devait être facilement repérable à partir des temps de rétention des composés des mélanges binaires. Mise en œuvre cette méthode n'a pas donné des résultats définitifs. Nous avons d'abord choisi le type de composé de coupure le plus adapté à une analyse par c.p.g.: notre choix s'est arrêté sur les diéthers méthyliques XII, XIII, et XIV trans (et cis) (R = —CH_2OCH_3). On obtient aisément, et avec de bons rendements ces diéthers en ozonant les acétates énoliques, en réduisant les ozonides par l'hydrure de lithium et d'aluminium en diols XII, XIII, XIV trans (et cis) (R = —CH_2OH) et en éthérifiant ces derniers par la méthode de Williamson. Les mélanges binaires XII–XIII et XIII–XIV des diéthers des séries trans et cis montrent bien, en c.p.g., les deux pics attendus, suffisamment espacés pour permettre un dosage dans chaque cas (les résultats sont rapportés au Tableau II pour les diéthers issus des acétates énoliques en mélange préparés selon la méthode à l'acétate d'isopropényle).

TABLEAU II

Dosages des diéthers XII, XIII, et XIV issus des mélanges d'acétates énoliques résultant de l'action de l'acétate d'isopropényle sur les décalones I, II, III*st*, et IV*nst*

Acétates énoliques	Diéthers obtenus		
Δ^1 et Δ^2	XII	XIII	XIV (R = —CH_2OCH_3)
VIII et IX trans	30%	70%	
X et XI trans		72%	28%
VIII et IX cis	63.5%	36.5%	
X et XI cis		44%	56%

Les mélanges ternaires sont flous et mal définis en c.p.g., dans la série trans et dans la série cis: dans la série trans, nous pouvons en déduire que c'est le composé commun XIII trans qui prédomine dans chaque mélange binaire, d'où la conclusion que les acétates Δ^2 se forment en prépondérance à partir des décalones I et II; dans les mélanges binaires de la série cis, au contraire, le composé commun XIII cis est minoritaire, ce qui fait que les décalones III*st* et IV*nst* engendrent plus d'acétate Δ^1 que d'acétate Δ^2. Ces résultats cependant demandaient à être vérifiés d'une autre manière.

Dans la série trans, Schéma 2, en traitant les décalones I et II, sous forme de sel sodé, par

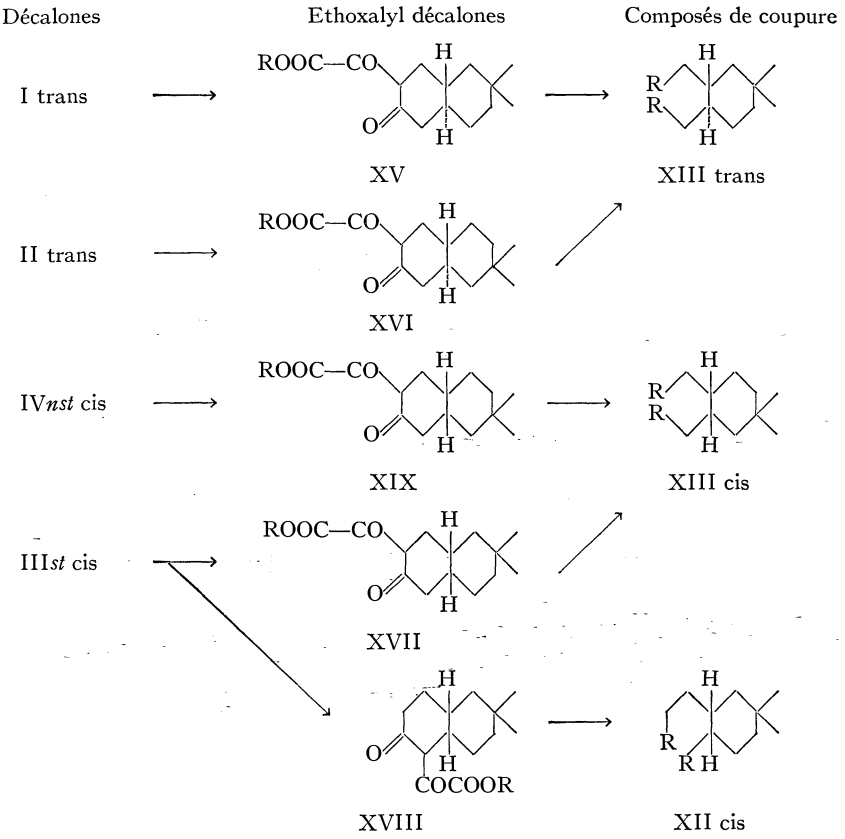

SCHÉMA 2. Ethoxalylation des décalones I, II, III, et IV et preuves de structure.

l'oxalate d'éthyle, puis en oxydant le composé de condensation par le permanganate de potassium, nous n'avons obtenu qu'un seul et même diacide de coupure, p.f. 154.5°, qui ne peut être que le diacide XIII trans (R = —COOH). Ce diacide a été estérifié par le diazométhane, le diester réduit par l'hydrure de lithium et d'aluminium en diol, le diol éthérifié par la méthode de Williamson en diéther XIII trans (R = —CH_2OCH_3). Par la méthode du rehaussement des pics en c.p.g. nous avons pu montrer que les mélanges binaires des diéthers XII–XIII et XIII–XIV trans contiennent bien en majorité le composé XIII trans, corroborant ainsi nos conclusions antérieures.

Dans la série cis, Schéma 2, nous avons procédé comme dans la série trans, soit éthoxalylation et oxydation permanganique. La diméthyl-7,7 décalone-2 cis (IV*nst*) conduit à

un acide bien cristallisé, p.f. 151.5°, que nous avons réduit en diol, puis éthérifié en diéther (XIII cis, R = —CH_2OCH_3). La diméthyl-6,6 décalone-2 cis (III*st*) conduit par les mêmes étapes, à un mélange de deux diéthers, nécessairement XII et XIII cis (R = —CH_2OCH_3). La c.p.g. montre que le diéther issu de la diméthyl-7,7 décalone-2 cis correspond, par superposition parfaite des pics, au diéther minoritaire issu de la diméthyl-6,6 décalone-2 cis, ce diéther doit donc être le diéther commun XIII cis, ce qui fait du diacide p.f. 151.5° le diacide XIII cis (R = —COOH). Par la méthode du rehaussement des pics, en c.p.g., il est facile de montrer que le diéther XIII cis est le diéther minoritaire dans les mélanges binaires XII–XIII cis et XIII–XIV cis issus des acétates énoliques en mélanges, d'où la conclusion que les acétates énoliques qui se forment en prépondérance, par la méthode à l'acétate d'isopropényle et par la méthode à l'anhydride acétique – acide perchlorique, sont bien, comme établi plus haut, VIII cis à partir de la décalone III*st* et XI cis à partir de la décalone IV*nst*.

Nous pouvons également tirer les conclusions suivantes: le groupe -COCOOR se fixe, dans les condensations avec l'oxalate d'éthyle, en position 3 des décalones trans I et II, pour donner XV et XVI respectivement (cf. Schéma 2), et de la décalone cis IV*nst* pour donner XIX. On obtient un mélange des deux composés de condensation XVII et XVIII à partir de la décalone cis III*st*, dans lequel l'isomère de substitution en position 1 (XVIII) prédomine (cf. Schéma 2).

DISCUSSION

Nos travaux mettent d'abord en évidence le parallélisme chimique évident dans la formation des acétates énoliques des décalones trans I et II et de la nor-19 androstanol-17β one-3 (9) par la méthode à l'acétate d'isopropényle, puisque dans chaque cas les deux acétates énoliques se forment, dans un rapport voisin de 2–1 avec prépondérance de double liaison éloignée des carbones de jonction. Ce parallélisme chimique doit être la conséquence directe de la superposabilité des décalones I et II et des anneaux A et B du stéroide en question et de la rigidité conformationnelle de ces anneaux condensés. Pour ce qui est de la série cis nos travaux indiquent qu'il n'y a que très peu de différence d'énergie entre les acétates Δ^1 et Δ^2 étudiés, et finalement entre les Δ^1, Δ^2, et Δ^3-octalines diméthylées en 6,6, dont l'ordre de stabilité serait $\Delta^3 > \Delta^1 > \Delta^2$ (XX > XXI > XXII) en première approximation, en négligeant le groupe —$OCOCH_3$.

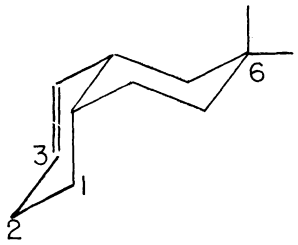

XX

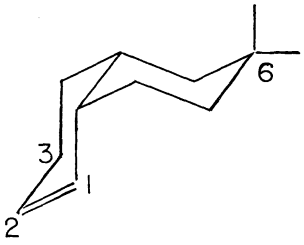

XXI

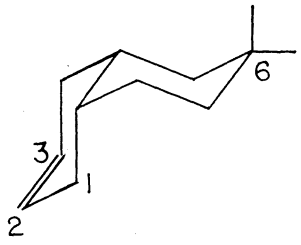

XXII

On sait que l'étude des ènes-pyrrolidines correspondant à la décalone-2 cis (VII) avait conduit Stork et ses collaborateurs (10) à signaler le peu de différence d'énergie entre les octalines Δ^1 et Δ^2. Il est aussi frappant de constater que la décalone III*st* ne donne pas plus d'acétate énolique Δ^1, comme les conclusions de Dreiding (11) le faisaient prévoir. Pour cet auteur, la différence très significative de comportement chimique, bromation

(12, 13, 14, 15), alkylation (16), et énolisation (5) entre la cholestanone et la coprostanone est due au fait que chez cette dernière l'introduction de la double liaison en position 3, 4 amène une décompression stérique notoire. Il faut toutefois tenir compte ici que nous ne pouvons comparer à priori la décalone III*st* et la coprostanone, et à plus forte raison la décalone IV*nst* et la coprostanone, car la présence du groupe méthyle en 10 doit certainement jouer un rôle à l'image de la série trans (6). Certainement d'autres expériences s'imposent pour comprendre l'influence du groupe méthyle angulaire et pour établir la distinction entre le comportement d'une décalone-2 cis *st* et *nst*: il est possible en effet que dans les décalones cis III*st* et IV*nst* le groupe méthyle axial ne soit pas suffisant pour assurer la stabilité conformationnelle *st* et *nst*.

Nos expériences infirment également, à notre avis, l'explication de Stork et Hill (17), qui, pour rendre compte de l'introduction du groupe —COCOOR dans la décalone-2 cis en position 3 seulement, ont avancé que l'état de transition étant volumineux dans une réaction de type Claisen, la réaction n'allait pas se faire du côté de l'embranchement décalinique (position 1) pour des raisons d'encombrement stérique. La réaction préférentielle de la décalone III*st* en position 1 et celle de la décalone IV*nst* en position 3 réfutent l'encombrement stérique comme facteur déterminant et font de la décalone-2 cis une décalone qui réagit dans sa conformation *nst*. Nos résultats sont encore trop fragmentaires pour pousser plus loin l'analyse dans ce domaine. Dans la série trans, les décalones I et II réagissent comme la décalone-2 trans (VII) elle-même, soit en position 3 (18).

Il est intéressant en revanche de souligner les différences marquées qui existent dans les mises en équilibre des acétates énoliques dans les séries cis et trans décaliniques, quand on n'a pas de méthyle angulaire. Si l'on considère l'équilibre décalone $\rightleftarrows$ acétates énoliques et le caractère semicyclique de la liaison C=O et cyclique de la liaison C=C, nous voyons qu'une décalone-2 cis s'accomodera mieux d'une double liaison cyclique qu'une décalone-2 trans: cette constatation prend son importance lorsqu'on considère le choix d'un réactif d'acétylation énolique.

PARTIE EXPÉRIMENTALE

Les p.f. ont été déterminés en tubes capillaires, au moyen d'un thermomètre étalonné avec des substances pures de p.f. connus. Les analyses sont de C. Daesslé, Organic Microanalyses, Montréal. Les c.p.g. ont été réalisées au moyen d'un appareil Kromo-Tog K-2 de Burrell Corporation. Les spectres infrarouges ont été mesurés sur un appareil Perkin–Elmer, modèle 21, prisme NaCl.

1. Acétates énoliques VIII, IX, X, et XI cis et trans

1.1. Méthode à l'acétate d'isopropényle

1.11. Méthode générale.—À 1.8 g de décalone on ajoute 8.0 ml d'acétate d'isopropényle et 0.02 ml d'acide sulfurique concentré. On chauffe à reflux, en atmosphère d'azote, pendant 1 heure, puis distille 3 ml de la solution en une demi-heure. On refroidit à 0°, reprend par 100 ml d'éther, lave la solution éthérée à 0° avec une solution aqueuse d'hydroxyde de sodium 0.5 *M* et avec de l'eau jusqu'à neutralité. On sèche sur sulfate de sodium anhydre, distille l'éther puis le résidu. Les acétates énoliques sont dosés en c.p.g. dans les conditions suivantes: colonne 2.5 mètres, température 195°, éluant hélium 60 ml par minute, 20% de polyester succinique de Craig sur brique.

1.12.—A partir de la diméthyl-6,6 décalone-2 cis 72% du mélange des deux acétates énoliques, Δ^1 (VIII cis) et Δ^2 (IX cis), p.éb. 98° sous 1 mm, $n_D^{27} = 1.4823$, spectre infrarouge: bandes à 1762 et 1690 cm^{-1}. Calculé pour $C_{14}H_{22}O_2$: C, 75.63; H, 9.96%. Trouvé: C, 75.42; H, 9.93%. En c.p.g.; il apparaît d'abord 43.4% d'acétate Δ^2 (IX cis) et ensuite 56.6% d'acétate Δ^1 (VIII cis), temps de rétention: (IX cis) 53.2 minutes, (VIII cis) 66.4 minutes.

1.13.—A partir de la diméthyl-7,7 décalone-2 cis, 94% du mélange des deux acétates énoliques Δ^1 (XI cis) et Δ^2 (X cis), p.éb. 106° sous 0.9–1.1 mm, $n_D^{22} = 1.4830$, spectre infrarouge, bandes à 1755 et 1692 cm^{-1}. Calculé pour $C_{14}H_{22}O_2$: C, 75.63; H, 9.96%. Trouvé: C, 75.56; H, 9.71%. En c.p.g. il apparaît d'abord 59.0% d'acétate Δ^1 (XI cis), puis 41.0% d'acétate Δ^2 (X cis), temps de rétention: (XI cis) 36.5 minutes, (X cis) 40 minutes. La cétone de départ a été regénérée des acétates énoliques de la façon suivante: 100 mg du mélange est dissout dans 20 ml de 2% d'hydroxide de potassium méthanolique, après 5 minutes on évapore

le solvent sous vide et on ajoute 30 ml d'éther et d'eau. La solution éthérée est lavée jusqu'à neutralité. On identifie la cétone par c.p.g. tel que décrit en 1.11 et par infrarouge, bande à 1715 cm^{-1}.

1.14.—La diméthyl-6,6 décalone-2 trans conduit à 89% du mélange des acétates énoliques Δ^1 et Δ^2, p.éb. 81.5° sous 0.48 mm, $n_D^{22} = 1.4758$; spectre infrarouge, bandes à 1752 et 1687 cm^{-1}. Calculé pour $C_{14}H_{22}O_2$: C, 75.63; H, 9.97%. Trouvé: C, 75.93; H, 9.74%. En c.p.g. il apparaît d'abord 63.2% d'acétate Δ^2 (IX trans) et ensuite 36.7% d'acétate Δ^1 (VIII trans), temps de rétention (IX trans) 42.2 minutes, (VIII trans) 49.2 minutes.

1.15.—La diméthyl-7,7 décalone-2 trans conduit à 89.2% du mélange des acétates énoliques Δ^1 et Δ^2, p.éb. 106° sous 1.2 mm, $n_D^{24} = 1.4903$; spectre infrarouge, bandes à 1763 et 1693 cm^{-1}. Calculé pour $C_{14}H_{22}O_2$: C, 75.63; H, 9.97%. Trouvé: C, 75.41; H, 10.24%. En c.p.g. il apparaît d'abord 33.8% d'acétate Δ^1 (XI trans) et ensuite 66.2% d'acétate Δ^2 (X trans): temps de rétention (XI trans) 56.2 minutes, (X trans) 62.0 minutes.

1.2. Méthode à l'anhydride acétique et acide perchlorique

Méthode générale.—On dissout 100 mg de décalone dans 16 ml de benzène anhydre et 6 ml de tétrachlorure de carbone anhydre; on y ajoute 1.2 ml d'anhydride acétique fraîchment distillé et 2 gouttes d'acide perchlorique – eau 75–25. On agite la solution pendant 24 heures à température de 25°. On ajoute alors 10 ml de tétrachlorure de carbone et 30.0 g de glace; on lave avec une solution aqueuse de bicarbonate de sodium 15%, puis avec une solution saturée de chlorure de sodium jusqu'à neutralité. On sèche sur sulfate de sodium anhydre et distille les solvents sous vide. Le résidu est analysé tel quel. Dans le série trans l'infrarouge n'indique pas d'acétates énoliques et la c.p.g. comme en 1.11 ne montre que la présence des décalones de départ. Dans la série cis, l'infrarouge montre la présence d'acétates énoliques (bandes à 1753 cm^{-1} et 1690 cm^{-1}) et de la décalone de départ (1715 cm^{-1}); le pourcentage de décalone est déterminé ainsi par l'infrarouge à partir de mélanges de proportions connues décalones – acétates énoliques; les résultats sont rapportés au Tableau I. Puis les acétates énoliques sont dosés par c.p.g. comme en 1.11, en faisant la correction pour la décalone présente dont le pic coincide avec celui d'un des acétates énoliques; les résultats sont rapportés au Tableau I.

1.3. Mise en équilibre des acétates énoliques

Méthode générale.—On dissout 100 mg des mélanges d'acétates énoliques préparés en 1.12, 1.13, 1.14, et 1.15 dans 16 ml de benzène et 6 ml de tétrachlorure de carbone anhydre; on y ajoute 1.2 ml d'anhydride acétique fraîchement distillé et 2 gouttes d'acide perchlorique – eau 75–25. On agite la solution pendant 36 heures à 25°. On isole les composés d'isomérisation comme en 1.2. Les résultats sont rapportés au Tableau I. Si l'on n'agite que 24 heures, dans la série trans, 85% environ des acétates énoliques sont déjà transformés en décalones. Au bout de 36 heures, l'isomérisation est totale.

2.1. Acide diméthyl-4,4 cyclohexane diacétique-1,2 cis (XIII cis, R = —COOH)

Selon la méthode de Cook et Lawrence (19), 5 g de diméthyl-7,7 décalone-2 cis (IV) et 5 g d'oxalate d'éthyle en mélange sont refroidis à −15°; on ajoute 16 ml d'éthanol anhydre dans lesquels on a fait réagir 0.8 g de sodium. Le tout est maintenu à −10° pendant 20 heures, puis traité par 20 ml d'acide sulfurique 3 *N*. On extrait à l'éther et obtient à la manière habituelle 5.8 g d'une huile jaune (diméthyl-7,7 éthoxalyl-3 décalone-2 cis brut) qui ne se cristallise pas et que l'on soumet immédiatement à l'oxydation permanganique.

L'oxalate brut (2.5 g) est mis en suspension dans 50 ml d'eau, à laquelle on ajoute une quantité suffisante de NaOH aqueux 10% pour obtenir un pH de 12. On ajoute ensuite une solution saturée de permanganate de potassium tant qu'il y a décoloration. Le tout est agité vivement et maintenu à 60° pendant 45 minutes. La solution à 60° est acidifiée par addition lente d'acide chlorhydrique concentré; le chauffage est maintenu jusqu'à ce que le dégagement de CO_2 cesse. On ajoute pendant la décarboxylation de la solution concentrée de permanganate de potassium de façon à garder la couleur pourpre. Après la décarboxylation on refroidit, détruit l'excès de permanganate de potassium et le bioxyde de manganèse par addition d'une solution saturée de $NaHSO_3$ et extrait la solution qu'on maintient à pH 2 par addition d'HCl, par trois portions d'éther, que l'on réunit, lave avec une solution saturée de NaCl, sèche sur sulfate de sodium anhydre; la distillation de l'éther abandonne un résidu huileux, de diacide diméthyl-4,4 cyclohexane diacétique-1,2 cis, p.f. 151.5° après ramollissement à 124°. Calculé pour $C_{12}H_{20}O_4$: C, 63.15; H, 8.77%. Trouvé: C, 63.14; H, 8.81%.

2.2. Acide diméthyl-4,4 cyclohexane diacétique-1,2 trans (XIII trans, R = —COOH)

2.21. A partir de la diméthyl-7,7 décalone-2 trans (II).—En suivant fidèlement le mode opératoire décrit en 2.1, 2.5 g de diméthyl-7,7 décalone-2 trans sont condensés avec l'oxalate d'éthyle, et l'ester dicétonique obtenu oxydé par le permanganate de potassium. On obtient 1.8 g (88%) de diacide brut, qui après recristallisation dans le mélange chloroforme – éther de pétrole fond à 154.5°. Calculé pour $C_{12}H_{20}O_4$: C, 63.15; H, 8.77. Trouvé: C, 63.34; H, 8.68%.

2.22. A partir de la diméthyl-6,6 décalone trans (I).—On obtient l'acide XIII trans décrit plus haut en 2.21, p.f. 154.5°, avec un rendement de 69% à partir de la décalone.

2.3. Diméthyl-4,4 bis-(hydroxy-2 éthyl)-1,2 cyclohexane cis (XIII cis, R = —CH_2OH)

On dissout 1.75 g du diacide XIII cis, p.f. 151.5°, obtenu en 2.1, dans 25 ml d'éther on ajoute une solution éthérée de diazométhane préparée selon (20), jusqu'à coloration jaune persistante et distille l'éther. Le

résidu (ester méthylique) est repris par 50 ml d'éther anhydre et ajouté goutte à goutte à une suspension de 2.5 g de lithium et d'aluminium dans 200 ml d'éther. On chauffe à reflux pendant 45 minutes, détruit l'excès d'hydrure par de l'eau, ajoute de l'acide chlorhydrique 3 *N*. Par extraction continue durant 6 heures par l'éther on épuise la phase aqueuse; on évapore l'éther et distille le résidu. On obtient le diméthyl-4,4 bis-(hydroxy-2 éthyl)-1,2 cyclohexane cis huile incolore, visqueuse, 1.2 g (76%), p.éb. 162° sous 0.9 mm. Calculé pour $C_{12}H_{24}O_2$: C, 71.96; H, 12.69%. Trouvé: C, 72.32; H, 12.45%.

2.4. Diméthyl-4,4 bis-(hydroxy-2 éthyl)-1,2 cyclohexane trans (XIII trans, R = —CH_2OH)

En suivant le mode opératoire décrit en 2.3, 1.2 g de diacide trans obtenu en 2.21 conduisent à 0.74 g (70%) de diol liquide, p.éb. 165° sous 0.8 mm. Calculé pour $C_{12}H_{24}O_2$: C, 71.98; H, 12.69%. Trouvé: C, 72.01; H, 12.38%.

2.5. Diméthyl-4,4 bis-(méthoxy-2 éthyl)-1,2 cyclohexane cis (XIII cis, R = —CH_2OCH_3)

On dissout 1.2 g du diol préparé en 2.3 dans 50 ml de toluène anhydre et ajoute 1.5 g de sodium métallique. On chauffe à reflux durant 4 heures et élimine l'excès de sodium après refroidissement. On ajoute alors 3.0 g d'iodure de méthyle et, en agitant, chauffe à reflux pendant 8 heures. On lave avec de l'eau pour enlever l'iodure de sodium, sèche la solution toluénique sur sulfate de sodium anhydre. On distille le toluène, puis sous 0.3 mm, le diéther qui passe à 82.5°, $n_D^{26} = 1.4562$, bande caractéristique R—O—R à 1117 cm^{-1} dans le spectre infrarouge. Calculé pour $C_{14}H_{28}O_2$: C, 73.68; H, 12.28%. Trouvé: C, 73.32; H, 12.26%.

2.6. Diméthyl-4,4 bis-(méthoxy-2 éthyl)-1,2 cyclohexane trans (XIII trans, R = —CH_2OCH_3)

En suivant le mode opératoire décrit en 2.5, 0.8 g de diol trans obtenu en 2.4 conduit à 0.69 g (76%) de diéther liquide, $n_D^{24.5} = 1.4566$, p.éb. 82.5° sous 0.3 mm; bande dans l'infrarouge à 1117 cm^{-1}. Calculé pour $C_{14}H_{28}O_2$: C, 73.68; H, 12.28%. Trouvé: C, 73.49; H, 12.14%.

2.7. Condensation de la décalone IIIst avec l'oxalate d'éthyle

On condense la décalone III*st* avec l'oxalate d'éthyle comme décrit plus haut en 2.1. On oxyde le mélange de condensation par le permanganate de potassium comme décrit plus haut en 2.1. On transforme les diacides en diesters méthyliques, puis en diols comme décrit plus haut en 2.3. On prépare les diéthers méthyliques comme décrit plus haut en 2.5. Les diéthers sont dosés en c.p.g. comme décrit plus loin en 3.0, avec les résultats suivants: diéther cis XIII 20%, diéther cis XIV 80%.

3.0. Ozonolyse des acétates énoliques et obtention des diéthers XII, XIII, et XIV cis et trans (R = —CH_2OCH_3)

On ozonolyse les mélanges des acétates énoliques (préparés en 1.12, 1.13, 1.14, et 1.15) en dissolvant 1.0 g de mélange dans 150 ml d'éther de pétrole (p.éb. 38–40°) et en faisant passer un courant d'oxygène chargé de 1.8% d'ozone dans la solution plongée dans un bain de CO_2–acétone jusqu'à coloration bleue persistante. On évapore ensuite l'éther de pétrole en faisant passer un courant d'azote dans l'appareil. Le résidu huileux est séché sous vide.

Les ozonides bruts sont dissous dans 100 ml d'éther anhydre; cette solution est ajoutée goutte à goutte à une suspension de 2.0 g d'hydrure de lithium et d'aluminium dans 200 ml d'éther anhydre. On chauffe à reflux durant 45 minutes, détruit l'excès d'hydrure par de l'eau, ajoute de l'acide chlorhydrique concentré jusqu'à disparition de tout précipité et extrait d'une manière continue à l'éther. En évaporant la solution éthérée on recueille le mélange de diols que l'on sèche sur P_2O_5 jusqu'à poids constant (rendement de 70–90%).

Pour la méthylation on procède selon les indications données en 2.5, plus haut. Les mélanges bruts cis sont chromatographiés (c.p.g.): colonne 2.5 mètres, 195°, 20% de polyester succinique de Craig sur brique, hélium 60 ml par minute. Les mélanges bruts trans sont chromatographiés sur une colonne de 1.5 mètre, 20% de Tergitol sur brique, 212°, hélium 50 ml par minute. Dans ces conditions les diéthers ont les temps de rétention suivants:

XIII trans pur (préparé en 2.5): 10 minutes, fluctue de 9 à 11 minutes, selon l'usure de la colonne.
XIII cis pur (préparé en 2.5): 15.8 et 19.2 minutes selon l'usure de la colonne.
XII et XIII trans: 9.1 et 10.0 minutes; XIII et XIV trans: 9.5 et 13.5 minutes.
XII et XIII cis: 21.8 et 19.2 minutes.
XIII et XIV cis: 15.8 et 16.9 minutes.

Les résultats sont rapportés au Tableau II. Les diéthers XIII cis et trans purs, préparés plus haut en 2.6 et 2.5, ont servi à l'analyse qualitative (méthode du rehaussement des pics) des mélanges binaires.

REMERCIEMENTS

Nous remercions le Conseil National de Recherches du Canada d'une subvention de recherches (H. F.).

BIBLIOGRAPHIE

1. H. Bruderlein, N. Dufort, H. Favre et A. Liston. Can. J. Chem. **41**, 2908 (1963).
2. T. G. Halsall et D. B. Thomas. J. Chem. Soc. 2431 (1956).
3. W. Moffitt, R. B. Woodward, A. Moscowitz, W. Klyne et C. Djerassi. J. Am. Chem. Soc. **83**, 4013 (1961).
4. W. Klyne. Experientia, **12**, 119 (1956).

5. W. G. DAUBEN, R. A. MICHELI et J. F. EASTHAM. J. Am. Chem. Soc. **74**, 3853 (1952).
6. B. BERKOZ, E. P. CHAVEZ et C. DJERASSI. J. Chem. Soc. 1363 (1962).
7. D. H. R. BARTON, R. M. EVANS, J. C. HAMLET, P. G. JONES et T. WALKER. J. Chem. Soc. 747 (1954).
8. J. CHAMPAGNE, H. FAVRE, D. VOCELLE et I. ZBIKOWSKI. Can. J. Chem. Sous presse.
9. R. VILLOTI, H. J. RINGOLD et C. DJERASSI. J. Am. Chem. Soc. **82**, 5693 (1960).
10. G. STORK, A. BRIZZOLARA, H. LANDESMAN, J. SZMUSZKOVICZ et R. TERRELL. J. Am. Chem. Soc. **85**, 207 (1963).
11. A. S. DREIDING. Chem. Ind. 1419 (1954).
12. A. BUTENANDT et A. WOLFF. Ber. **68**, 2091 (1935).
13. L. RUZICKA, P. A. PLATTNER et R. AESCHBACHER. Helv. Chim. Acta, **21**, 866 (1938).
14. G. ROSENKRANZ, S. KAUFMANN, J. PATAKI et C. DJERASSI. J. Am. Chem. Soc. **72**, 1046 (1950).
15. O. H. WHEELER et J. L. MATEOS. J. Org. Chem. **22**, 605 (1957).
16. Y. MAZUR et F. SONDHEIMER. J. Am. Chem. Soc. **80**, 5220 (1958).
17. G. STORK et R. K. HILL. J. Am. Chem. Soc. **79**, 495 (1957).
18. W. HÜCKEL et E. GOTH. Ber. **58**, 447 (1925).
19. J. W. COOK et C. A. LAWRENCE. J. Chem. Soc. 817 (1937).
20. A. VOGEL. Practical organic chemistry. Longmans, Green, London. 1959. p. 969.

ÉTUDE INFRAROUGE DES ACIDES FLUO- ET CHLORO-SULFURIQUES

RODRIGUE SAVOIE[1] ET PAUL A. GIGUÈRE
Département de Chimie, Université Laval, Québec, Qué.

Reçu le 13 août 1963

RÉSUMÉ

Les spectres d'absorption infrarouge entre 4000 et 150 cm^{-1} des acides fluosulfurique HSO_3F et chlorosulfurique HSO_3Cl à l'état solide, liquide, et gazeux montrent les douze vibrations fondamentales de ces molécules. De plus, ils révèlent l'existence de fortes liaisons hydrogène (quelque 6 kcal) qui conduisent à la formation de dimères cycliques, même dans la vapeur. Contrairement aux prévisions l'acide chlorosulfurique est plus fortement dimérisé que l'acide fluosulfurique. La rotation du groupe OH dans les molécules libres est empêchée par un seuil de potentiel à triple maximum d'environ 1.3 kcal. Le calcul des fonctions d'état à partir des présents résultats donne 71.4 cal deg^{-1} $mole^{-1}$ pour l'entropie standard de HSO_3F à 25° C, et 74.9 pour HSO_3Cl.

Les acides halosulfuriques sont beaucoup plus volatils que l'acide sulfurique parce que dans ce dernier les liaisons hydrogène (aussi de 6 kcal) relient toutes les molécules en un réseau à trois dimensions.

Le spectre moléculaire de l'acide fluosulfurique liquide a été étudié récemment par Gillespie et Robinson (1). Ces auteurs ont également repris le spectre Raman de l'acide chlorosulfurique qui avait fait l'objet de travaux antérieurs (2–4). Comme il n'existait pas de données sur les spectres de vibration de ces deux molécules à l'état libre, nous avons entrepis de mesurer leur absorption en infrarouge, aussi bien dans la vapeur que dans les phases condensées, et sur un intervalle de fréquence assez étendu pour observer toutes les fondamentales. Outre leur intérêt pour le calcul des fonctions d'état de ces molécules et d'autres analogues, en particulier H_2SO_4 (5), ces recherches ont fourni des précisions intéressantes et parfois inattendues sur la structure et l'association moléculaire par l'intermédiaire de liaisons hydrogène.

PARTIE EXPÉRIMENTALE

Pour l'acide fluosulfurique on a utilisé directement le produit commercial ("Technical Grade", Allied Chemical Co.). Le spectre montrait quelques faibles bandes dues à des impuretés ou à des produits de dissociation. En effet, cet acide tend à se dissocier suivant la réaction

$$HSO_3F = HF + SO_3,$$

et à s'hydrolyser

$$HSO_3F + H_2O = HF + H_2SO_4.$$

L'acide fluorhydrique ainsi formé peut ensuite attaquer le verre pour donner le composé volatil SiF_4 décelable en infrarouge par une forte bande à 1030 cm^{-1} (6). L'acide chlorosulfurique, un produit de la "British Drug Houses, Ltd.", titrant 99.5% au minimum, a été employé tel quel. Dans le spectre du liquide et du solide les bandes les plus fortes de H_2SO_4 provenant de l'hydrolyse étaient visibles. Dans la vapeur, par contre, on pouvait observer des concentrations appréciables, surtout à 60° C, de HCl grâce à la bande de vibration–rotation à 2886 cm^{-1} (7) ou encore aux bandes de rotation pure dans l'infrarouge lointain (8). L'autre produit de dissociation, SO_3, apparaissait dans le spectre d'absorption sous forme d'épaulement vers 525 cm^{-1} (9).

Les cellules d'absorption et les spectrophotomètres étaient les mêmes que précédemment (10), sauf pour l'étude des vapeurs dans l'infrarouge lointain (au-delà de 450 cm^{-1}) où il a fallu construire une cellule à double parcours pour augmenter l'absorption sans trop élever la température, et partant la dissociation. Cette cellule (Fig. 1) comprend deux miroirs concaves (*A* et *B*), diam. 9 cm, distance focale 20 cm, montés en opposition dans le tube d'absorption en Pyrex (*C*) au moyen d'une sorte de cage en tiges de Pyrex (*D*). Le petit miroir plan (*E*), de 14×18 mm, au centre de la cellule est aluminisé sur ses deux faces. A sa partie supérieure il se prolonge en une mince tige qui permet de le fixer à frottement (avec un manchon de Teflon) dans un petit tube de Pyrex scellé dans l'axe d'un bouchon à joint rodé 24/40 (*F*). Ce dernier est monté au

[1]*Boursier du Conseil National des Recherches.*

Can. J. Chem. Downloaded from www.nrcresearchpress.com by 210.87.254.42 on 09/05/12
For personal use only.

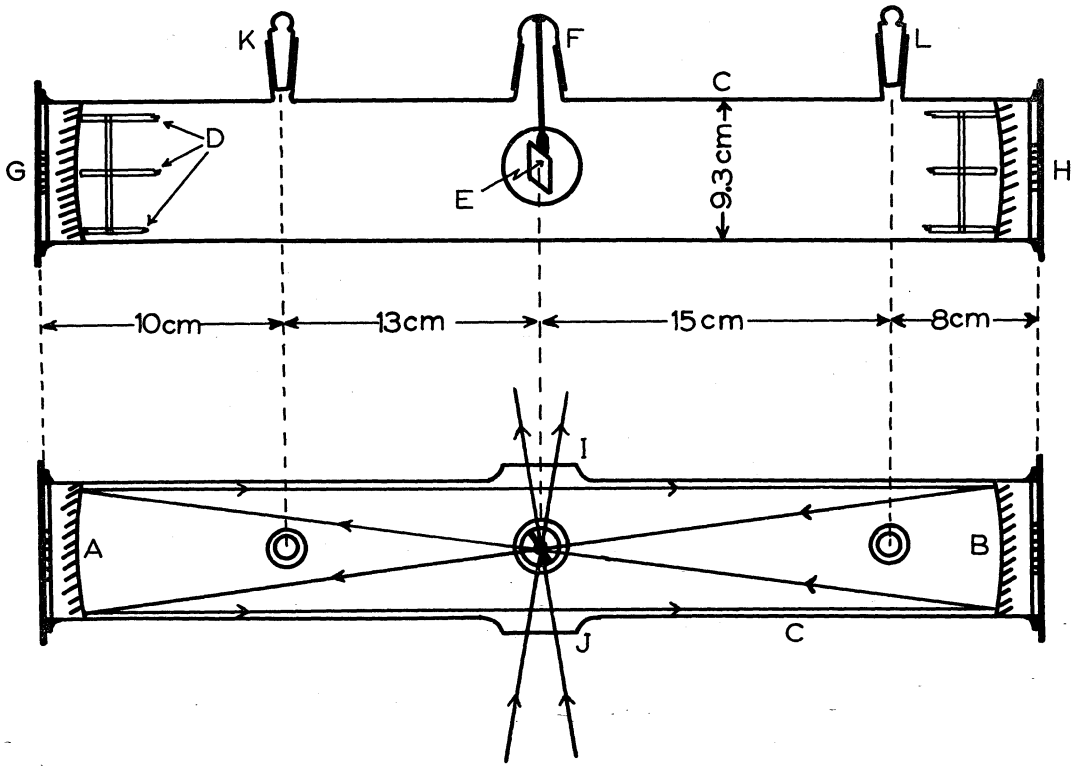

FIG. 1. Cellule à absorption pour le spectromètre infrarouge de Perkin–Elmer (*N*° 201-C).

centre de la cellule d'absorption, de sorte qu'une simple rotation permet d'orienter le faisceau lumineux. On réalise ainsi un parcours optique de quelque 92 cm, et la transmission peut atteindre jusqu'à 90% dans les conditions optima.

La cellule est fermée aux deux extrémités par des plaques d'aluminium (G et H) recouvertes de feuilles de Teflon et maintenues en place par trois tiges métalliques à l'extérieur. Deux ouvertures (*I* et *J*) de 50 mm de diamètre sont ménagées de chaque côté de la cellule pour le passage du faisceau infrarouge. Comme fenêtres on a utilisé, soit des films de Teflon, soit des disques de quartz cristallin. Enfin, deux tubulures (*K* et *L*) munies de joints rodés servent à introduire l'échantillon et à assécher la cellule d'absorption en y faisant circuler assez longtemps (environ une heure) un courant d'azote sec. Cette dernière précaution était d'une importance capitale dans le cas présent, non seulement parce que la vapeur d'eau absorbe fortement la radiation entre 400 et 150 cm^{-1}, mais encore à cause du caractère très hygroscopique des deux acides halosulfuriques. Effectivement, pour l'étude de l'acide fluosulfurique on enlevait les dernières traces d'humidité en introduisant d'abord une goutte d'acide chlorosulfurique qui absorbe très peu dans l'infrarouge au-delà de 400 cm^{-1}, du moins à température ordinaire. Lorsque nécessaire, la cellule pouvait être chauffée au moyen d'un enroulement de fil de résistance.

RÉSULTATS

Bien que la structure des deux molécules HSO_3F et HSO_3Cl n'ait pas encore été déterminée par une méthode directe, on peut sans hésitation la supposer du même type que celle de H_2SO_4 (11) ou encore SO_2F_2 (12) et SO_2Cl_2 (13). Selon l'orientation du groupe OH, diverses configurations sont possibles (Fig. 2), avec ou sans élément de symétrie. De toute façon une molécule XSO_3H quasi-tétraédrale doit avoir douze vibrations fondamentales, toutes actives en infrarouge.

Les spectres de HSO_3F

Les neuf bandes observées dans le spectre Raman de l'acide liquide se retrouvent

Can. J. Chem. Downloaded from www.nrcresearchpress.com by 210.87.254.42 on 09/05/12
For personal use only.

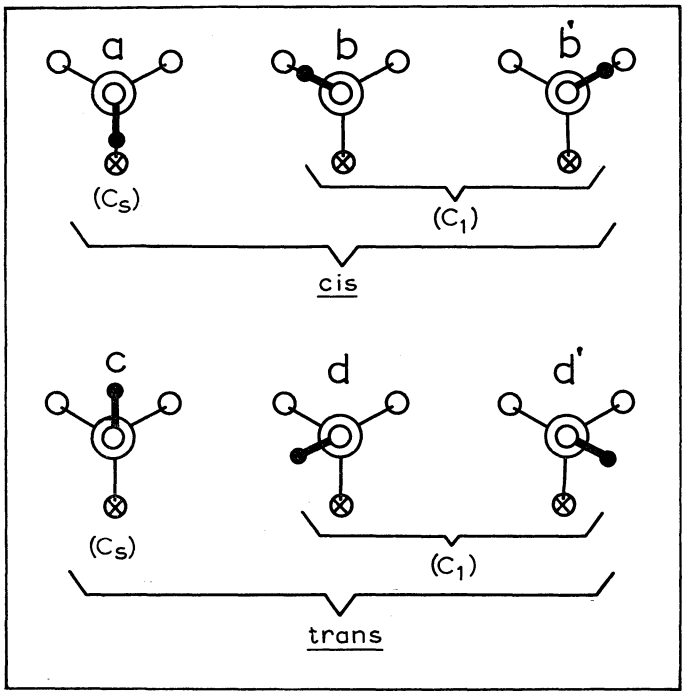

FIG. 2. Configurations possibles des molécules HSO_3X.

naturellement dans les présents spectres (Tableau I), avec en plus la bande de valence O—H à 3125 cm^{-1}, et un léger épaulement vers 650 cm^{-1} dû au mode de torsion ν_{12} du groupe OH. Ce dernier donne naissance à une bande beaucoup plus intense et plus nette dans le cristal (Fig. 3), sans doute parce que les variations de moment polaire qui l'accompagnent ne s'annulent pas, ou à peu près, comme dans le liquide. L'identification des diverses fondamentales par Gillespie et Robinson nous semble correcte, sauf pour ν_7, la fréquence de balancement de S—OH, qu'ils situent vers 560 cm^{-1} comme pour le balancement de S—O. La présente interprétation est cependant plus logique pour les raisons suivantes: (*a*) qualitativement on doit s'attendre à une fréquence de balancement moins élevée pour S—OH que pour S—O, vu la distance interatomique plus grande dans le premier cas; (*b*) la fréquence de balancement S—F (390 cm^{-1}) est dans le même rapport à la fréquence de balancement S—OH (409 cm^{-1}) dans la vapeur, que les vibrations de valence de ces deux groupes (896 et 955 cm^{-1}). D'ailleurs, ce rapport (0.94) est presque identique à la racine carrée du rapport des masses OH/F, ce qui est normal car les distances S—F et S—OH sont à peu près les mêmes dans ces molécules et d'autres analogues; (*c*) enfin, la fréquence 409 cm^{-1} a son équivalent à 407 cm^{-1} dans HSO_3Cl et à 412 cm^{-1} dans H_2SO_4 (5).

Les spectres de la vapeur (Fig. 4) révèlent des particularités intéressantes, entre autres quant à l'effet de la température sur l'intensité et le contour de certaines bandes. Ainsi la région des vibrations O—H montre deux types de bandes; l'une à 3600 cm^{-1}, avec branches *P*, *Q*, et *R*, et dont l'intensité croît avec la température; l'autre, de fréquence beaucoup plus basse, 3100 cm^{-1}, assez large, et dont l'intensité varie en sens inverse de la première avec la température. L'explication la plus obvie de ces résultats est que dans

Can. J. Chem. Downloaded from www.nrcresearchpress.com by 210.87.254.42 on 09/05/12
For personal use only.

TABLEAU I

Spectres de vibration de HSO_3F (Fréquences en cm^{-1})

Raman (1), liquide	Infrarouge: Solide	Infrarouge: Liquide	Infrarouge: Vapeur Assoc.	Infrarouge: Vapeur Libre	Description
—	2940	3125	3150 3050	3616 3602 3590	ν_1 (a') valence O—H
			2930		$2\nu_9$
	2560				?
		2450			$2\nu_2$
			2405		$\nu_2 + \nu_3$
	1970				$\nu_9 + \nu_{10}$
1445	1438 1425	1440	1450	1491 1480	ν_9 (a'') valence S—O
				1360 1352	$\nu_4 + \nu_8$
	1303				?
				1253	
1230	1250	1230	1243	1243 1233	ν_2 (a') valence S—O
				1162	
1178	1195	1170	(1160)	1150 1142	ν_3 (a') déformation S—O—H
				1035 1029	SiF_4
960	975 965	960	958	955	ν_4 (a') valence S—OH
	952				$\nu_{10} + \nu_{11}$
	885				?
				906	
850	829	837	844	896 887	ν_5 (a') valence S—F
				827	
				823 812	$2\nu_7$
	780				$2\nu_{11}$
560	568	(556)	(568)	568 556	ν_{10} (a'') balancement SO_2
555	543	554	(545)	556 545	ν_6 (a') déformation SO_2
			(525)		$2\nu_{12}$
				420	
405*	420	429		409 400	ν_7 (a') balancement SOH
391	(390)	(396)		(390)	ν_{11} (a'') torsion
				400	
—	399	385		390 380	ν_8 (a') balancement SF
				285	
—	667	(650)	(560)	275 260 245	ν_{12} (a'') torsion OH

*Notre interprétation.
( ) Fréquence incertaine.

la vapeur les molécules HSO_3F sont en partie associées par liaisons hydrogène formant des dimères cycliques comme dans le cas classique des acides carboxyliques. D'ailleurs, il apparaît à l'examen que la structure probable de la molécule HSO_3F se prête bien à ce genre d'association (Fig. 5). Nous discuterons plus loin des modalités de ce phénomène. Signalons ici qu'il permet de comprendre d'autres détails des spectres comme, par exemple, la bande de valence S—O (ν_2) dont les deux composantes à haute fréquence, 1491 et

Can. J. Chem. Downloaded from www.nrcresearchpress.com by 210.87.254.42 on 09/05/12
For personal use only.

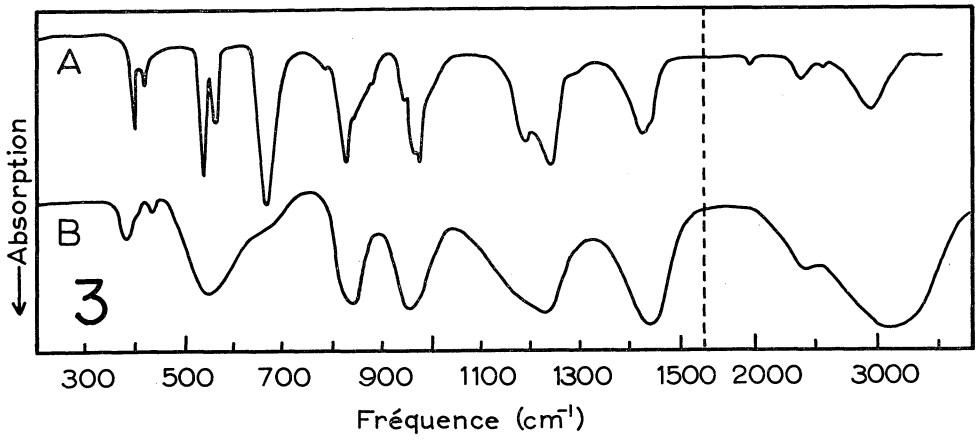

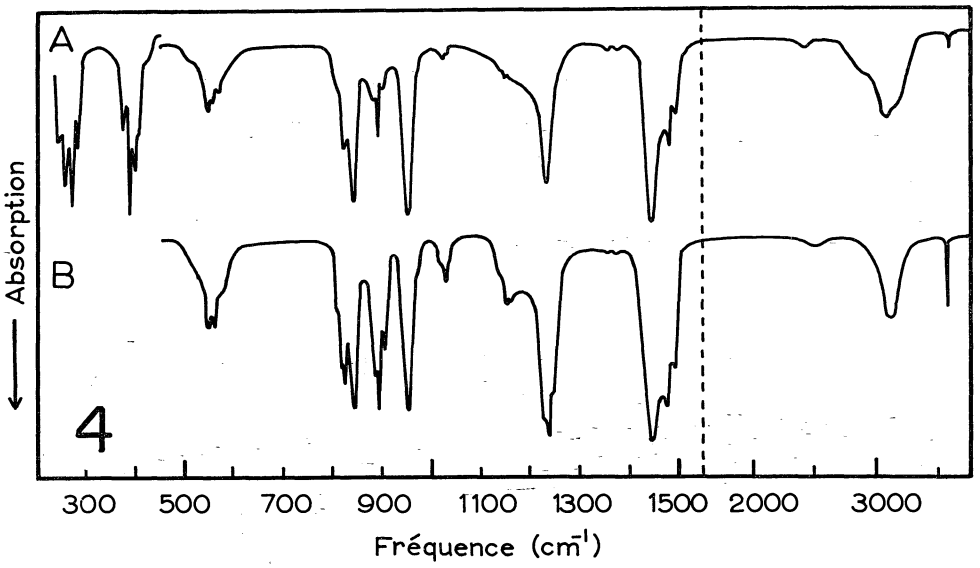

FIG. 3. Spectres infrarouges de HSO_3F à l'état solide (A) et liquide (B).
FIG. 4. Spectres infrarouges de la vapeur de HSO_3F à 25° C (A) et à 60° (B).

1480 cm^{-1}, augmentent d'intensité avec la température, contrairement à la troisième à 1450 cm^{-1}. Les deux premières doivent appartenir aux groupes S—O libres, et la dernière, aux groupes formant des liaisons hydrogène. On retrouve le même comportement pour les bandes S—F (ν_5) à 906–896–887 cm^{-1} et 844 cm^{-1} respectivement.

Enfin le mode de torsion interne du groupe OH, qui produit une bande à structure complexe vers 260 cm^{-1} dans la vapeur, apparaît à une fréquence beaucoup plus élevée, 550–650 cm^{-1}, dans les molécules dimères et les états condensés. On connaît plusieurs autres cas semblables.

Les spectres de HSO_3Cl

Pour diverses raisons les présents résultats pour l'acide chlorosulfurique (Tableau II) sont moins abondants que ceux de l'acide fluosulfurique. Ainsi, malgré plusieurs tentatives il n'a pas été possible d'obtenir le solide à l'état parfaitement cristallisé; d'où l'apparence

Can. J. Chem. Downloaded from www.nrcresearchpress.com by 210.87.254.42 on 09/05/12
For personal use only.

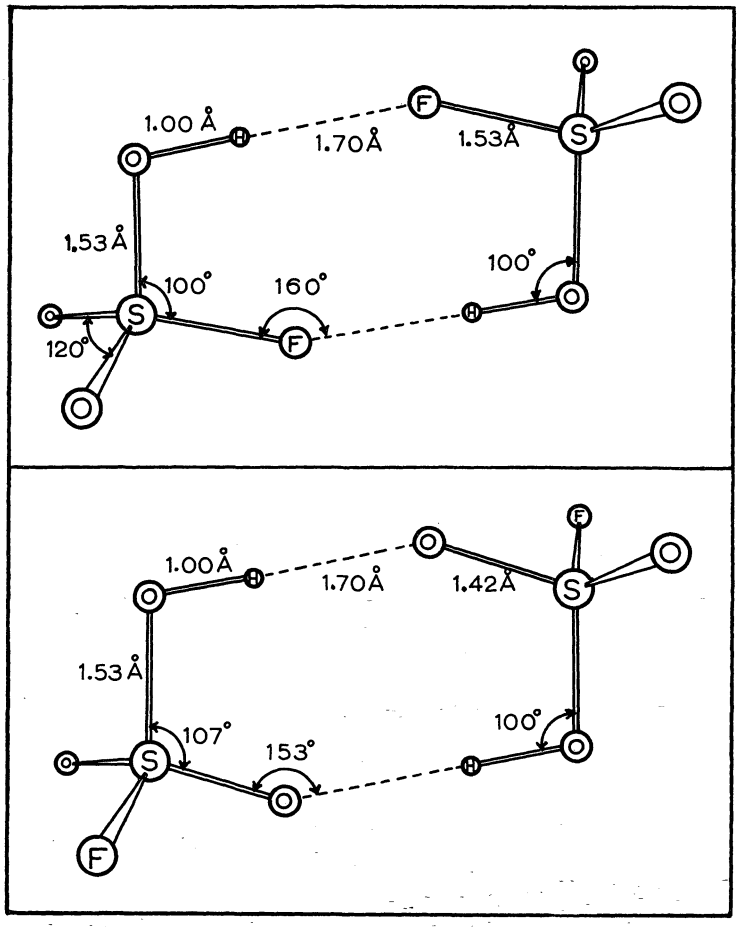

FIG. 5. Structures hypothétiques des dimères cycliques de HSO_3F.

plutôt diffuse des bandes (Fig. 6C). Du côté des basses fréquences, au delà de 250 cm^{-1}, l'absorption non sélective augmente rapidement dans le liquide aussi bien que dans le solide. Quant à la vapeur, l'association moléculaire y est si forte, même à 60°, que les vibrations des molécules HSO_3Cl libres sont à peine perceptibles. D'ailleurs à cette température la dissociation chimique devient assez importante pour que le spectre de rotation pure de HCl nuise à l'observation des vibrations de basse fréquence. Ainsi, la bande de balancement de S—Cl, à 200 cm^{-1} en Raman, n'a pu être aperçue en infrarouge.

Pour le reste, le spectre du liquide (Fig. 6B) ressemble de très près au spectre Raman, à l'exception de la bande à 413 cm^{-1} qui est beaucoup moins intense en infrarouge. Par conséquent on ne saurait l'attribuer à la vibration de valence S—Cl, tel que suggéré précédemment (1, 4). Elle doit plutôt appartenir au mode de balancement S—OH puisqu'on la retrouve à la même fréquence et avec la même intensité dans HSO_3F et dans H_2SO_4 (5). Quant à la vibration S—Cl, nous avons le choix entre les deux fortes bandes à 510 et 615 cm^{-1}. Cette dernière est à préférer car la bande correspondante en Raman est polarisée. D'ailleurs cette fréquence est assez rapprochée des valeurs 577 et 586 cm^{-1} dans SO_2Cl_2 selon la plus récente interprétation (14). Les deux bandes à 510 et 480 cm^{-1} pourraient convenir pour les modes de balancement et de déformation de SO_2, bien que

Can. J. Chem. Downloaded from www.nrcresearchpress.com by 210.87.254.42 on 09/05/12
For personal use only.

TABLEAU II

Spectres de vibration de HSO_3Cl (Fréquences en cm^{-1})

Raman (1, 4)	Infrarouge			Description
	Solide	Liquide	Vapeur	
			3587 }	ν_1 (a') valence O—H (libre)
			3569 }	
	2965	3100	3100	ν_1 (a') (assoc.)
			2886	HCl
	2394	(2440)		$2\nu_3$, H_2SO_4
			1410	
1396	1385	1400	1395	ν_9 (a'') valence S—O
			1380	
			(1230)	$2\nu_6$
1209	1165	1190	1196	ν_2 (a') valence S—O
			1166	ν_3 (a') déformation SOH
	975	970		H_2SO_4
916	925	925	913	ν_4 (a') valence S—OH (assoc.)
			862 }	
			852 }	ν_4 (libre)
			842 }	
623*	610	616	614	ν_5 (a') valence S—Cl
			525	SO_3
513	510	511	510	ν_{10} (a'') balancement SO_2
482	478	487	497	ν_6 (a') déformation SO_2
416*	420	413	407	ν_7 (a') balancement SOH
313	318	316	(315)	ν_{11} (a'') torsion
298	314			
	(650)	(650)	(650)	ν_{12} (a'') torsion OH
200	264	264	264	ν_8 (a') balancement SCl
			247 }	
			226 }	
			206 }	HCl (rotation)
			186 }	
			165 }	
			145 }	

*Notre interprétation.
( ) Fréquence incertaine.

ces fréquences soient notablement plus basses que dans HSO_3F. Aussi la présente interprétation n'est-elle pas définitive.

Signalons encore les particularités suivantes dans le spectre de la vapeur. Les trois pics vers 1400 cm^{-1} n'appartiennent pas à une seule bande (branches PQR), leur séparation étant trop grande, mais plutôt à deux bandes distinctes: celles des groupes S—O libres et S—O····H. Par contre, le faible triplet à 850 cm^{-1} doit être une bande fondamentale de la molécule HSO_3Cl libre, soit la bande de valence S—OH. Le décalage de quelque 60 cm^{-1} par rapport à la bande des dimères semble raisonnable par comparaison avec les acides carboxyliques et leurs dérivés fluorés (15). On a sans doute la même situation dans HSO_3F, mais alors la bande ν_4 des molécules libres est probablement cachée par la bande ν_5 à 900 cm^{-1}.

La structure des molécules HSO_3F et HSO_3Cl

La structure la plus probable pour les molécules des acides halosulfuriques permet diverses configurations selon l'orientation du groupe OH (Fig. 2). A ce sujet rien n'est connu avec certitude et on en est réduit à des hypothèses. Suivant que l'hydrogène est vis-à-vis d'un atome du groupe SO_2X ou entre deux de ces atomes, on aura des formes appelées ici cis- ou trans-. Etant donné le caractère électronégatif de l'oxygène et des halogènes la première alternative est la plus probable. Des trois formes cis- l'une (*a*)

Can. J. Chem. Downloaded from www.nrcresearchpress.com by 210.87.254.42 on 09/05/12
For personal use only.

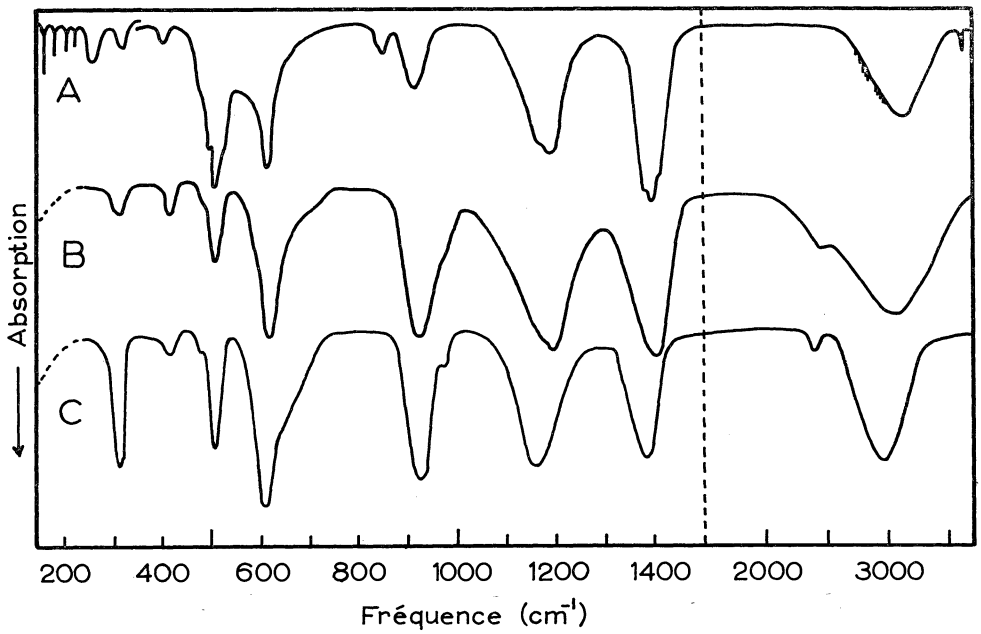

FIG. 6. Spectres d'absorption de HSO_3Cl en infrarouge: (A) gazeux à 60° C, (B) liquide à 25°, (C) solide à −185°.

possède un plan de symétrie C_s; les deux autres (b et b'), sans symétrie C_1, sont des énantiomorphes. Nous adopterons arbitrairement la première comme la plus stable, bien que les deux autres soient également possibles. En réalité, on doit avoir un mélange d'isomères; la structure complexe de certaines bandes dans la vapeur de HSO_3F est une indication en ce sens. Une étude plus détaillée de la structure de ces bandes, et en particulier des effets de la température fournirait des données utiles sur la stabilité relative de ces divers isomères. Le seuil de potentiel qui les sépare semble assez bas; environ 1.3 kcal d'après la fréquence de torsion $\nu_{12} = 275$ cm^{-1} (16). Cette valeur est un peu surprenante si l'on songe au caractère partiellement double de la liaison S—OH. Par ailleurs le fait que ce seuil soit triple contribue à abaisser notablement le maximum (par rapport à une molécule comme HNO_3, par exemple). De toute façon il s'agit ici d'une valeur moyenne puisque l'un des maxima (et aussi l'un des minima) doit être différent des deux autres.

Liaisons hydrogène et association moléculaire

La présence de fortes liaisons hydrogène dans les acides halosulfuriques était à prévoir, du moins dans les phases condensées. Les corrélations empiriques basées sur la fréquence de la vibration O—H dans les solides, ou encore sur le décalage de cette fréquence en passant de la molécule libre aux molécules associées (17, 18) indiquent des énergies de l'ordre de 6 kcal, et des distances O—H de 1.02 Å et O···O de 2.70 Å pour ces liaisons hydrogène. Par ailleurs, selon les mêmes critères, les liaisons hydrogène seraient un peu plus fortes dans HSO_3F que dans HSO_3Cl (Tableau III). Ceci est en accord avec la force relative des deux acides (19) et avec d'autres relations indirectes comme les fréquences caractéristiques du groupe S—OH (1). Etant donné les fortes liaisons hydrogène et les structures moléculaires favorables il n'est pas surprenant que ces deux acides soient associés en phase vapeur. Comme dans les acides carboxyliques on doit avoir surtout des dimères cycliques plutôt que des chaînes. Les paramètres indiqués ici (Fig. 5) sont basés

Can. J. Chem. Downloaded from www.nrcresearchpress.com by 210.87.254.42 on 09/05/12
For personal use only.

TABLEAU III

Propriétés physiques et association moléculaire des acides sulfuriques

	HSO_3F	HSO_3Cl
Valence O—H (décalage vapeur–cristal)	660 cm^{-1}	615 cm^{-1}
Valence O—H (décalage monomère–dimère)	550 cm^{-1} 450 cm^{-1}	475 cm^{-1}
Valence O—H (cristal)	2940 cm^{-1}	2965 cm^{-1}
Valence S—OH	970 cm^{-1}	925 cm^{-1}
Déformation SOH	1195 cm^{-1}	1165 cm^{-1}
Constante d'ionisation (25° C)	2.3×10^{-3}	9×10^{-4}
Point de fusion	−87.3° C	−80° C
Point d'ébullition	165.5° C	158° C

sur le modèle purement arbitraire de cycles plans. Une évaluation d'après l'intensité relative des bandes de valence O—H des molécules simples et doubles dans HSO_3F (Fig. 4) donne une enthalpie d'association de 11.5 kcal, environ le double de l'énergie de liaison mentionnée plus haut.

D'après ces considérations, on devrait trouver à peu près le même degré de dimérisation dans les deux acides à l'état de vapeur. Au contraire, les bandes de valence O—H révèlent une concentration relative de molécules libres HSO_3F aussi grande, sinon plus, à 25° C que celle de HSO_3Cl à 60°. Il est vrai que dans ce dernier cas la température plus élevée favorise la décomposition de l'acide, mais ce facteur est d'importance secondaire ici, comme on peut en juger par le peu d'intensité de la bande de vibration–rotation de HCl vers 2880 cm^{-1}. (Il n'existe malheureusement pas de données thermodynamiques sur la stabilité de ces deux acides; nos observations, purement qualitatives, confirment que l'acide fluosulfurique résiste mieux à la décomposition thermique que l'acide chlorosulfurique.)

Notons ici que le cas de HSO_3F est plus complexe que celui de HSO_3Cl. En effet, dans ce dernier composé les liaisons hydrogène sont toutes du même type, soit O—H···O, vu que l'atome de chlore ne participe pratiquement pas à ce phénomène. Au contraire dans HSO_3F, on peut imaginer trois sortes de dimères: (*i*) avec deux liaisons O—H···F, (*ii*) avec deux liaisons O—H···O, et enfin, (*iii*) avec une liaison de chaque sorte. Du simple point de vue statistique les trois possibilités sont dans les rapports 1:4:4 respectivement, mais il est clair que l'énergie de résonance n'est pas la même dans les trois cas. Ainsi le dimère asymétrique (*iii*) doit être moins stable que les deux autres. Quant à ceux-ci (Fig. 5), on ne peut dire ce qui l'emporte, de la plus grande électronégativité du fluor, ou de la stabilisation par résonance selon le schéma de Pauling (20),

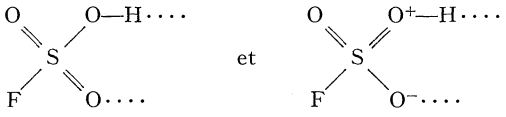

lequel ne s'applique pas aux liaisons O—H···F. Effectivement la bande de valence O—H des dimères dans la vapeur de HSO_3F à 25° C montre deux maxima à 3050 et 3150 cm^{-1} provenant sans doute de deux isomères différents. Le second, de moindre énergie, est à peu près disparu à 60°. Pour élucider cette question il faudrait compléter les données actuelles, soit par une étude à haute résolution de la région de 3 μ dans la vapeur à plusieurs températures et pressions, soit par l'étude de solutions dans un solvant approprié. Des mesures de densité de vapeur seraient également utiles, quoique d'exécution et d'interprétation difficiles à cause de la corrosion et de la décomposition thermique.

Can. J. Chem. Downloaded from www.nrcresearchpress.com by 210.87.254.42 on 09/05/12
For personal use only.

Il est instructif de comparer les acides halosulfuriques avec l'acide sulfurique du point de vue association moléculaire. Bien que leurs liaisons hydrogène soient de même énergie en première approximation, la différence entre leurs propriétés physiques est considérable. Ainsi l'acide sulfurique est beaucoup moins volatil (point d'ébullition évalué à 300° C) et plus visqueux que les acides halosulfuriques. L'explication réside dans la présence de deux protons par molécule dans l'acide sulfurique, ce qui conduit à un réseau de liaisons hydrogène à trois dimensions, comme c'est le cas pour H_2O. Au contraire, dans les acides halosulfuriques les molécules doubles (ou les chaînes?) ne sont retenues entre elles que par des forces de Van der Waals. A noter que les points d'ébullition de HSO_3F et HSO_3Cl sont dans l'ordre inverse de leur masse moléculaire; cependant il faut tenir compte ici de la décomposition thermique, sans doute importante à ces températures.

Les fonctions d'état du Tableau IV ont été calculées par les méthodes statistiques

TABLEAU IV

Paramètres de structure et fonctions d'état des acides halosulfuriques

Distances et angles	HSO_3F	HSO_3Cl
O—H	1.00 Å	1.00 Å
S=O	1.42 Å	1.43 Å
S—OH	1.53 Å	1.53 Å
S—X	1.53 Å	1.98 Å
∠ SO_2	120°	115°
∠ SOX	100°	105°
∠ SOH	100°	100°
Moments d'inertie		
I_A (g cm²)	161×10^{-40}	295×10^{-40}
I_B (g cm²)	165×10^{-40}	157×10^{-40}
I_C (g cm²)	166×10^{-40}	298×10^{-40}
I_{OH} (g cm²)	1.66×10^{-40}	1.66×10^{-40}
Seuil, V_0 (cal)	1320	1310
Fonctions d'état		
$C°$ (cal deg^{-1} mole^{-1})	17.64	18.95
$(H° - E°)/T$ "	12.14	13.21
$-(F° - E^0)/T$ "	59.25	61.73
$S°$ "	71.38	74.93

usuelles pour le gaz parfait, composé de molécules simples, à pression et température normales. Pour le calcul des moments d'inertie on a pris les distances et les angles les plus probables par analogie avec des molécules de structure connue comme H_2SO_4, SO_2F_2, et SO_2Cl_2.

SUMMARY

The infrared spectra of fluorosulphuric and chlorosulphuric acids were measured over the range 150–4000 cm^{-1} and in the three physical states. All 12 fundamental vibrations of both molecules were observed. Strong hydrogen bonds (some 6 kcal) lead to association through cyclic dimers in the vapor. The chloro-acid is more strongly associated than the fluoro-acid although the hydrogen bonds seem slightly stronger in the latter. Internal rotation of the OH group in the free molecules is hindered by a threefold barrier of about 1.3 kcal. Statistical calculations of the thermodynamic functions give 71.4 cal deg^{-1} mole^{-1} for the standard entropy of free HSO_3F molecules at 25° C, and 74.9 for HSO_3Cl.

Can. J. Chem. Downloaded from www.nrcresearchpress.com by 210.87.254.42 on 09/05/12
For personal use only.

These halosulphuric acids are much more volatile than sulphuric acid because in the latter the hydrogen bonds (also 6 kcal) form a three-dimensional network.

BIBLIOGRAPHIE

1. R. J. GILLESPIE et E. A. ROBINSON. Can. J. Chem. **40**, 644 (1962).
2. F. MATOSSI et H. ADERHOLD. Z. Physik, **68**, 683 (1931).
3. R. VOGEL-HÖGLER. Acta Phys. Austriaca, **1**, 323 (1948).
4. A. SIMON, H. KRIEGSMANN et H. DUTZ. Ber. **89**, 2378 (1956).
5. P. A. GIGUÈRE et R. SAVOIE. J. Am. Chem. Soc. **85**, 287 (1963).
6. E. A. JONES, J. S. KIRBY-SMITH, P. J. H. WOLTZ et A. H. NIELSEN. J. Chem. Phys. **19**, 242 (1951).
7. R. W. WOOD et G. H. DICKE. Phys. Rev. **35**, 1355 (1930).
8. M. CZERNY. Z. Physik, **34**, 227 (1925).
9. R. W. LOVEJOY, J. H. COLWELL, D. F. EGGERS et G. D. HALSEY, JR. J. Chem. Phys. **36**, 612 (1962).
10. R. SAVOIE et P. A. GIGUÈRE. Can. J. Chem. **40**, 991 (1962).
11. R. PASCARD. Compt. Rend. **240**, 2162 (1955).
12. D. R. LIDE, JR., D. E. MANN et R. M. FRISTROM. J. Chem. Phys. **26**, 734 (1957).
13. K. J. PALMER. J. Am. Chem. Soc. **60**, 2360 (1938).
14. G. R. HUNT et M. K. WILSON. Spectrochim. Acta, **18**, 959 (1962).
15. J. B. BARCELO et C. OTERO. Spectrochim. Acta, **18**, 1231 (1962).
16. K. S. PITZER et W. D. GWYNN. J. Chem. Phys. **10**, 428 (1942).
17. E. R. LIPPINCOTT et R. SCHROEDER. J. Chem. Phys. **23**, 1099 (1955).
18. K. NAKAMOTO, M. MARGOSHES et R. E. RUNDLE. J. Am. Chem. Soc. **77**, 6480 (1955).
19. J. BARR, R. J. GILLESPIE et E. A. ROBINSON. Can. J. Chem. **39**, 1266 (1961).
20. L. PAULING. The nature of the chemical bond. 3rd ed. Cornell University Press, Ithaca, N.Y. 1960.

Can. J. Chem. Downloaded from www.nrcresearchpress.com by 210.87.254.42 on 09/05/12
For personal use only.

SPECTROSCOPIC STUDIES OF ALCOHOLS

I. METHANOL-BASE ADDUCTS IN DILUTE CCl_4 SOLUTION

P. J. KRUEGER AND H. D. METTEE
Department of Chemistry, University of Alberta, Calgary, Alberta
Received September 17, 1963

ABSTRACT

The fundamental ν_{OH} shifts and association constants for methanol hydrogen bonded to some relatively weak proton acceptors (alkyl halides, aryl halides, aromatic hydrocarbons) are reported for standardized conditions in CCl_4 solution, and the data are compared with similar measurements involving some relatively strong bases (containing N or O acceptor atoms) under the same conditions. The general usefulness of hydrogenic frequency displacements of the donor species as a measure of the basicity of the acceptor species is questioned.

Can. J. Chem. Downloaded from www.nrcresearchpress.com by 210.87.254.105 on 09/05/12
For personal use only.

INTRODUCTION

In a recent experimental study of conformational equilibria in 2-haloethanols (following paper) it was necessary to have available for comparison the association constants and the fundamental ν_{OH} frequency displacements for ROH . . . base adducts involving covalently bound halogen atoms as proton acceptors. Although the chemical literature abounds with spectroscopic evaluations of hydrogen-bonded systems (1), most of them are for systems which involve hydrogen-bond energies of 3- kcal/mole or more, and which are associated with fundamental hydrogenic frequency displacements in excess of 100 cm^{-1}. Further, many of the reported measurements have been made with spectrophotometers offering poor resolution in the 3 μ region, or they apply to conditions other than those desired for our studies. Hence this series of measurements was made under carefully standardized conditions with a grating stectrophotometer, since the data desired were for weak intermolecular hydrogen bonds and small frequency shifts.

The measurements of Allerhand and Schleyer (2) show that, contrary to popular belief, ν_{OH} shifts encountered in hydrogen-bonded systems where a proton donor ROH interacts with a proton acceptor B in an "inert" solvent depend on the concentration of B. For the measurements described in this paper the concentration of B was, with few exceptions, held at 1.00 M in CCl_4.

While this work was in progress, Allerhand and Schleyer (3) reported the effect of quaternary ammonium halides on the OH stretching frequency of methanol, the magnitude of the shifts depending on the halide anion in the order of $Cl^- > F^- > Br^- > I^-$. Since, with the exception of the anomalous position of the fluoride ion, this order is the inverse of that found when *covalent* halides were used as proton acceptors (4), it was of interest to extend these measurements to more covalent halides with varying degrees of partial ionic character.

Methanol was chosen as the proton donor because the free methanol OH absorption band is known to be almost perfectly symmetrical (5).

EXPERIMENTAL

A Beckman IR-7 infrared spectrophotometer employing a NaCl foreprism and a 75 lines/mm grating blazed at 12 μ was used. The frequency calibration of this instrument has been described (6, 7). Measurements were made in the fourth grating order at a spectral slit width of 1.0 cm^{-1}. The entire optical path and the enclosed sample compartment was flushed with dry air partially freed from atmospheric CO_2. Matched 2.00-cm quartz ("Infrasil") absorption cells were used in double beam operation. The average cell temperature was 28° C.

n-Amyl fluoride was prepared by a method previously described (8). The other proton acceptors were commercial products purified by drying and fractional distillation. "Spectroquality" materials available were used directly; these included the solvent CCl_4 and the proton donor methanol.

Solutions of proton acceptors were made up to exactly 1.00 *M* concentration in CCl_4 in 50-ml volumetric flasks. Part of this solution was used to fill the reference cell, the rest of it was used to make up a sample beam solution containing 8.0 μl of methanol in 25 ml of solution (0.0079 *M*). The methanol was delivered with a screw-type micropipette. Some of the initial measurements were made on solutions made up on twice this scale to minimize pipetting errors. This was found to be unnecessary. The results reported are averages of three independent trials in most cases. During the course of the experimental work frequent "standard" solutions of methanol in CCl_4 (without base) were used to establish a peak absorbance of 0.882 ± 0.013 (average deviation from the mean). The association constants were based on the residual absorbance of the 'free" methanol peak in the presence of base.

RESULTS AND DISCUSSION

The frequency data and the derived association constants for hydrogen bond formation are collected in Table I. Figure 1 gives a comparative view of spectra obtained with weak bases (bonding to covalent halogen atoms or aromatic π-electrons), while Fig. 2 shows the experimental curves obtained in the presence of some stronger bases.

TABLE I

Frequency shifts and formation constants for methanol-base adducts in CCl_4 solution at ~28° C

	Base	ν_{OH}^{free} (cm^{-1})	ν_{OH}^{bonded} (cm^{-1})	ν_{OH} shift (cm^{-1})	K_{assoc}
1.	No base	3643.8*	—	—	—
2.	*n*-Amyl F†	3644	3626.5	17.5‡	1.5
3.	*n*-Butyl Cl	3649	3617.5	31.5‡	1.11
4.	*n*-Amyl Br	3644	3606	38‡	0.38
5.	*n*-Butyl Br	3644	3611	33‡	0.39
6.	*n*-Butyl I	3643.5	3599.5	45‡	0.28
7.	*t*-Butyl Cl	3644	3609	35	0.27
8.	*t*-Butyl Br	3643.5	3599.5	44	0.28
9.	Fluorobenzene	3644	3624	20	0.11
10.	Chlorobenzene	3643.5	3624.5	19	0.16
11.	Bromobenzene	3643	3620.5	22.5	0.15
12.	Iodobenzene	3641.5	3617.5	24	0.23
13.	Benzyl Cl	3641.5	3620	21.5	0.49
14.	Benzyl Br	3642.5	3610	32.5	0.59
15.	Benzene§	3644	3621	23	0.80
16.	Toluene	3643	3608.5	34.5	0.44
17.	*m*-Xylene	3643.5	3602	41.5	0.21
18.	Mesitylene	3643.5	3597	46.5	0.24
19.	Durene	3643.5	3590.5	53	0.45
20.	Hexamethylbenzene	3644	3574.5	69.5	~0.5
21.	Nitromethane	3640.5	3613	27.5	0.20
22.	Acetone	3643.5	3593.5	50	1.60
23.	Acetonitrile	3642.5	3560.5	82	1.22
24.	*p*-Dioxane	3643	3534.5	108.5	1.12
25.	N,N-Dimethylformamide	3643	3527.5	115.5	4.24
26.	Diethyl ether	3644.5	3505	140	1.16
27.	Pyridine	3644.5	(3504) broad	(140)	(3)
28.	Dimethylsulphoxide	3643	v. broad	—	7.6

*Allerhand and Schleyer (3) report the monomeric OH band in methanol at 3643 ± 2 cm^{-1}. The value determined in this work is the average of 20 independent measurements spread out over the period during which the other measurements were made. The maximum deviation from the mean was ± 0.4 cm^{-1}, which reflects in part the subjective error in locating the band center. The calibration procedure for the instrument has been described (6, 7).

†"Free" and "bonded" components determined by mathematical resolution of the experimentally observed asymmetric band, assuming a Lorentz shape for the components, and adjusting the band parameters to obtain the best fit. See Ref. (5) for previous application of this method.

‡Corresponding values reported by Schleyer and West (4) for *n*-BuF, Cl, Br, and I are 19, 37, 41, and 47 cm^{-1} respectively.

§Measurements based on 0.25 *M* benzene solution in CCl_4 because of high absorbance of benzene in this region.

Can. J. Chem. Downloaded from www.nrcresearchpress.com by 210.87.254.105 on 09/05/12
For personal use only.

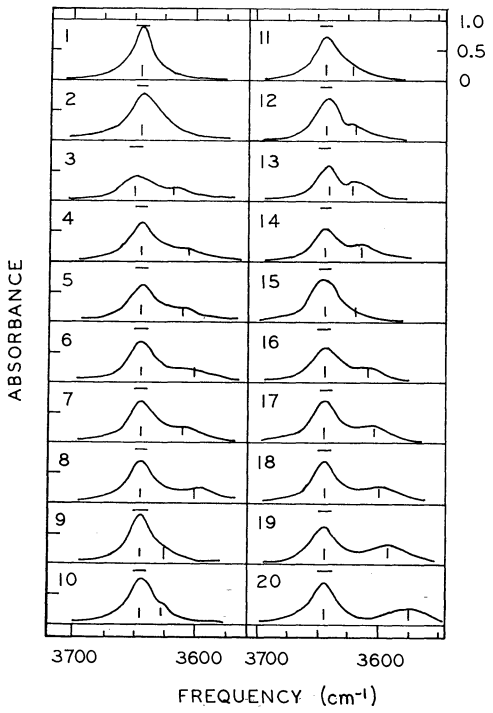

FIG. 1. "Free" and "bonded" methanol OH bands in the presence of covalent organic halides and aromatic hydrocarbons in CCl_4 solution. [Total methanol] = 0.0079 *M*. [Base] = 1.00 *M*. Spectra are numbered to refer to Table I.

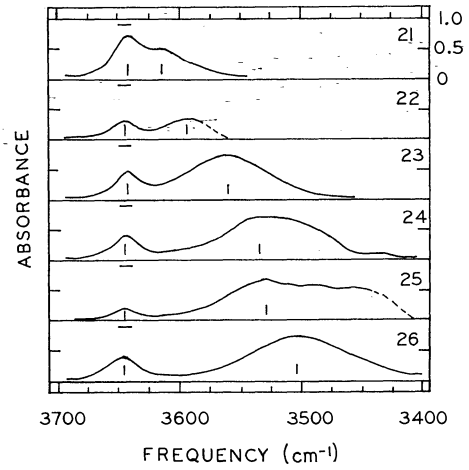

FIG. 2. "Free" and "bonded" methanol OH bands in the presence of bases containing O or N acceptor atoms. Conditions as in Fig. 1.

Table II summarizes trends in $\Delta\nu$ and K observed for variation of X on a given R group, and for variation of R on a given X group. Using the Taft σ^* parameter (9) for the group R in a covalent halide RX, the ionic character of the RX bond would be expected to increase in the order R = C_6H_5 < $C_6H_5CH_2$ < *n*-Bu < *t*-Bu (for a given X

Can. J. Chem. Downloaded from www.nrcresearchpress.com by 210.87.254.105 on 09/05/12
For personal use only.

TABLE II

Summary of $\Delta\nu$ and K trends for methanol adducts of weak bases in CCl_4 solution at ~28° C

Base	Trends
(*a*) For variation of X on a given R group:*	
C_6H_5X	$\Delta\nu$: F ≈ Cl < Br < I = benzene
	K: F < Cl ≈ Br < I < benzene
$C_6H_5CH_2X$	$\Delta\nu$: Cl < benzene < Br
	K: Cl < Br < benzene
n-Butyl X	$\Delta\nu$: (F <)Cl < Br < I
(*n*-Amyl)	K: (F >)Cl > Br > I
t-Butyl X	$\Delta\nu$: Cl < Br
	K: Cl ≈ Br
$R_4N^+X^-$†	$\Delta\nu$: $Cl^- > F^- > Br^- > I^-$
(*b*) For variation of R on a given X atom:	
RF	$\Delta\nu$: C_6H_5 > *n*-Am
	K: *n*-Am > C_6H_5
RCl	$\Delta\nu$: *t*-Bu > *n*-Bu = $C_6H_5CH_2$ > C_6H_5
	K: *n*-Bu > $C_6H_5CH_2$ > *t*-Bu > C_6H_5
RBr	$\Delta\nu$: *t*-Bu > *n*-Bu > $C_6H_5CH_2$ = C_6H_5
	K: $C_6H_5CH_2$ > *n*-Bu > *t*-Bu > C_6H_5
RI	$\Delta\nu$: *n*-Bu > C_6H_5
	K: *n*-Bu > C_6H_5
(*c*) For variation of R in aromatic systems:	
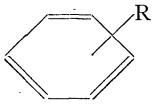	$\Delta\nu$: Benzene < toluene < *m*-xylene < mesitylene < durene < hexamethylbenzene
	K: Benzene ≫ toluene > *m*-xylene < mesitylene < durene < hexamethylbenzene(≈toluene)

*Bases in this section grouped and listed in the order of increasing negative charge on the X atom e.g. the Taft σ^* parameter (9) for R is +0.600, +0.215, −0.130, and −0.300 for C_6H_5, $C_6H_5CH_2$, *n*-Bu, and *t*-Bu respectively.

†Data from Ref. (3).

atom). As the ionic character of the halogen atom increases the ν_{OH} shift trend might be expected to revert to that observed for halide anions. Table II(*a*) shows that for the halides investigated the trend remains F < Cl < Br < I. A radical break in the order thus appears to exist as the halogen becomes completely ionized. For covalent halides the polarizability of the C—X bond may be a major factor in determining the ν_{OH} shift.

The methanol proton could conceivably bond to either the ring π-electrons or the halogen *n*-electrons in phenyl and benzyl halides, or be involved in equilibria involving both sites. For the halobenzene bases the order of increasing basicity deduced from $\Delta\nu$ and from K are identical, and in agreement with the conclusions of Olah *et al.* (10) and Josien and Sourisseau (11) based on frequency shifts. Josien and Sourisseau have indicated that in plots of ionization potential vs. $\Delta\nu$ for various proton donors with series of bases the data for C_6H_5Br and C_6H_5Cl do not correlate with the data for aromatic hydrocarbons. This would be consistent if the ionization potential of a halobenzene is due to the removal of a halogen non-bonding electron. Similar basic behavior differences have been noted by Caldow and Thompson (12) for HCN interaction with aromatic hydrocarbons and halogenated aromatics. These results suggest strongly that the proton is bonded to the halogen atom. On the basis of nuclear magnetic resonance shifts observed for the chloroform proton in chlorobenzene or bromobenzene solutions, Reeves and Schneider (13) had earlier allowed the possibility of some complexing to the π-electrons.

For the phenyl and benzyl halide bases the order of K is the same as $\Delta\nu_{OH}$, whereas for *n*-BuX bases the order of K is the reverse of the $\Delta\nu_{OH}$ trend. For halobenzenes other

Can. J. Chem. Downloaded from www.nrcresearchpress.com by 210.87.254.105 on 09/05/12
For personal use only.

physical measurements have also failed to lead to consistent basicity correlations. Thus, on the basis of solubilities of HCl in halobenzenes as determined from vapor pressure measurements Brown and Brady (14) found that the basicity of $C_6H_6 > C_6H_5F > C_6H_5Cl > C_6H_5Br > C_6H_5I$. On the other hand, assuming that lowering of ionization potential means increasing basicity of an aromatic, the results of Watanabe (15) show that the relative basicity order is $C_6H_5I > C_6H_5Br > C_6H_5Cl > C_6H_5F$.

Section (*b*) of Table II shows that, with the exception of the limited measurements with RF, the ν_{OH} shift increases as the ionic character of the C—X bond increases (for a given X atom). The same consistent behavior pattern is not observed for the corresponding K values.

The extensive early work on association constants for hydrogen-bonded systems has been summarized and analyzed (1). As stated earlier, most of the data apply to relatively strong hydrogen bonds. Some of the previous findings indicate that there exists a linear relationship between log K_{assoc} (or ΔF) and the frequency shift for strongly hydrogen-bonded systems.* Since the enthalpy and the entropy changes on hydrogen bond formation are related to the free energy change through the relationship $\Delta F = \Delta H - T\Delta S$, it follows that a linear dependence of ΔF on the frequency shift must mean that both ΔH and ΔS are also proportional to the frequency shift. This has been recognized and the linear ΔH vs. ΔS, ΔH vs. $\Delta\nu$, and ΔS vs. $\Delta\nu$ behavior has been demonstrated for certain systems. It thus appears that a decrease in enthalpy is counteracted by a decrease in entropy (more restricted configuration in the associated species), with the net result that K_{assoc} is not particularly sensitive to changes in hydrogen-bond strength.

Joesten and Drago (18) report that the monotonic ΔH vs. $\Delta\nu_{OH}$ relationship holds to ± 0.5 kcal/mole for adducts of phenol with nitrogen and oxygen donors ($\Delta H > 3$ kcal/mole); but that the log K vs. $\Delta\nu_{OH}$ relationship for the same system is limited to similar bases where no unusual entropy effects are observed. The review by Josien (19) suggests that there is no general correlation of the Badger–Bauer type (20) that will have widespread applicability, even if the same proton donor is used in conjunction with bases that differ only little.

For the data reported in this paper log K and $\Delta\nu$ do not correlate with sufficient precision to make the relationship useful, particularly when the high accuracy of frequency measurements is considered. No significant improvements in the correlation result when only closely related bases are used.

For aromatic hydrocarbons as bases (Table II (*c*)) the $\Delta\nu_{OH}$ shift increases with increasing methyl substitution, while K goes through a minimum for *m*-xylene in the series. It is tempting to suggest that this minimum is the result of two opposing factors:

(*i*) slight steric restriction in the approach of the angular CH_3OH molecule to the π-electron density because of methyl substitution, and

(*ii*) an increase in K as the number of electron-donating methyl groups increases.

Factor (*i*) would be absent for benzene itself, and may account for the observation that K for benzene as a base exceeds that for the other hydrocarbons. Factor (*ii*) rapidly overcomes (*i*), and is dominant beyond *m*-xylene in the series. Factor (*i*) presupposes that the OH bond will prefer to be perpendicular to the plane of the aromatic ring in the adduct. Reeves and Schneider (13) speculate that chloroform complexes with aromatic rings in this fashion. Solubility measurements of HCl in aromatic solvents (14) show that

**See for example the work of Grunwald and Coburn (16) on ethanol complexes of ethyl acetate and acetic anhydride, and of Aksnes and Gramstad (17) on the association of phenol with a large number of organophosphorous compounds.*

Can. J. Chem. Downloaded from www.nrcresearchpress.com by 210.87.254.105 on 09/05/12
For personal use only.

the order of increasing basicity is benzene < toluene < *m*-xylene < mesitylene. The difference in this order from that of the K's for methanol complexes may be in the absence of factor (*i*) for the HCl complexes because of the small spatial requirements of the proton donor.

The data reported in Table I for methanol complexes of bases containing O or N atoms as proton acceptors require little further comment. In general, the ν_{OH} shifts and the K's are larger than for methanol complexes formed with halogen atoms or π-electrons. Again a linear correlation between these quantities is absent. Nitromethane appears to be a poor proton acceptor, in agreement with some other spectroscopic studies of the nitro group (21).

More definite conclusions concerning the relationship of the ν_{OH} shift and the strength of the AOH. . .BY interaction could no doubt be drawn if complete thermodynamic data for these systems were available. However, the results described here provide further evidence to indicate that the decrease in ν_{OH} on hydrogen bond formation does not give a true picture of the overall strength of the hydrogen bond, since it only reflects the decrease in the OH stretching force constant, and neglects compensating changes in the A—OH, B—Y, and OH. . .B bonds, as Bernstein (22) has pointed out.

ACKNOWLEDGMENT

The financial assistance of the National Research Council is gratefully acknowledged.

REFERENCES

1. G. C. Pimentel and A. L. McClellan. The hydrogen bond. W. H. Freeman and Co., San Francisco. 1960. pp. 348–386.
2. A. Allerhand and P. von R. Schleyer. J. Am. Chem. Soc. **85**, 371 (1963).
3. A. Allerhand and P. von R. Schleyer. J. Am. Chem. Soc. **85**, 1233 (1963).
4. P. von R. Schleyer and R. West. J. Am. Chem. Soc. **81**, 3164 (1959).
5. M. Oki and H. Iwamura. Bull. Chem. Soc. Japan, **32**, 950 (1959).
6. P. J. Krueger. Appl. Opt. **1**, 443 (1962).
7. P. J. Krueger and G. H. Schulze. Rev. Sci. Instr. **34**, 88 (1963).
8. A. I. Vogel, J. Leicester, and W. A. T. Macey. Org. Syn. **36**, 40 (1956).
9. R. W. Taft, Jr. *In* Steric effects in organic chemistry. *Edited by* M. S. Newman. John Wiley and Sons, Inc., N.Y. 1956. p. 619.
10. G. A. Olah, S. J. Kuhn, and S. H. Flood. J. Am. Chem. Soc. **83**, 4581 (1961).
11. M. L. Josien and G. Sourisseau. *In* Hydrogen bonding. *Edited by* D. Hadzi. Pergamon Press, N.Y. 1959. p. 135.
12. G. L. Caldow and H. W. Thompson. Proc. Roy. Soc. A, **254**, 1 (1960).
13. L. W. Reeves and W. G. Schneider. Can. J. Chem. **35**, 251 (1957).
14. H. C. Brown and J. D. Brady. J. Am. Chem. Soc. **74**, 3570 (1952).
15. K. Watanabe. J. Chem. Phys. **26**, 542 (1957).
16. E. Grunwald and W. C. Coburn, Jr. J. Am. Chem. Soc. **80**, 1322 (1958).
17. G. Aksnes and T. Gramstad. Acta Chem. Scand. **14**, 1485 (1960).
18. M. D. Joesten and R. S. Drago. J. Am. Chem. Soc. **84**, 3817 (1962).
19. M. L. Josien. Pure Appl. Chem. **4**, 33 (1962).
20. R. M. Badger and S. H. Bauer. J. Chem. Phys. **5**, 839 (1937).
21. H. E. Ungnade, E. D. Loughran, and L. W. Kissinger. J. Phys. Chem. **66**, 2643 (1962). H. E. Ungnade and L. W. Kissinger. Tetrahedron, **19**, Suppl. 1, 121 (1963).
22. H. J. Bernstein. *Cited in* R. West, D. L. Powell, L. S. Whatley, M. K. T. Lee, and P. von R. Schleyer. J. Am. Chem. Soc. **84**, 3221 (1962).

Can. J. Chem. Downloaded from www.nrcresearchpress.com by 210.87.254.105 on 09/05/12
For personal use only.

Can. J. Chem. Downloaded from www.nrcresearchpress.com by 210.87.254.6 on 09/05/12
For personal use only.

PYROLYSIS STUDIES

X. RATES OF THE THERMAL DECOMPOSITION OF ortho-SUBSTITUTED ETHYL BENZOATES IN THE GAS PHASE[1,2]

GRANT GILL SMITH[3]
Department of Chemistry, Utah State University, Logan, Utah

AND

DAVID F. BROWN[4]
Department of Chemistry, Washington State University, Pullman, Washington

Received September 20, 1963

ABSTRACT

Eight ortho-substituted ethyl benzoates (with substituents varying from *o*-NH_2 to *o*-NO_2) have been partially pyrolyzed to ethylene and the corresponding benzoic acid. By gas chromatographic measurement of the amount of ethylene produced, the relative rates of the thermal decomposition of the various ethers have been determined. There are minor steric effects (primary or secondary) in the reaction and direct field influences are negligible. The varying reactivity, therefore, is attributed to changes in polar effects of the substituent. This reaction appears to be a useful method of determining, quantitatively, to a good first approximation, polar effects of ortho substituents.

The Hammett equation and its various modifications have proved useful in correlating reaction rates and equilibria with variations in structure at the *m* and *p* positions, but little success has been attained so far in applying it to ortho-substituted derivatives and obtaining σ values (1). The reasons for the deviations with ortho substituents are well known and are combined under the heading, proximity effects. These include primary and secondary steric effects, direct field interactions, hydrogen bonding, and, in condensed phase reactions, solvation of the reaction site, of the reagent, and of the ortho substituent (2).

Taft (3) has approached the problem of obtaining polar substituent constants for ortho substituents by applying a suggestion of Ingold (4) that steric hindrance and resonance effects in the transition state of both acidic and basic hydrolyses of esters were the same and formulated the equation

$$\sigma^\circ \equiv (1/2.48)[\log(k/k_0)_B - \log(k/k_0)_A].$$

This approach, however, requires data from two different reactions. Mammalis and Rydon (5) and more recently Charton (6) have suggested that constants for ortho substituents can be defined by reaction series in which the reaction site is not adjacent to the substituent but rather several atoms removed from the aromatic ring.

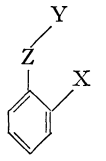

Z = —CH_2—CH_2—, —CH=CH—, —O—CH_2—

[1]*Paper IX: G. G. Smith, D. A. K. Jones, and R. Taylor. J. Org. Chem. In press. (1963).*

[2]*Acknowledgment is made to the donors of the Petroleum Research Fund administered by the American Chemical Society, and to the Air Force Office of Scientific Research, Grant No. AF-AFOSR 62-268, for partial support of this research.*

[3]*The author to whom inquiries should be addressed.*

[4]*Part of this study is abstracted from a thesis presented to the Graduate School, Washington State University, by David F. Brown in partial fulfillment of the requirements for the degree of Master of Science, August 1961.*

In the present vapor phase study of the thermal decomposition of alkyl benzoates, proximity complications have been eliminated or markedly reduced even though the reaction site is directly attached to the aromatic ring. Because the pyrolyses are carried out in the vapor phase, all solvent interactions are eliminated. Inasmuch as the reaction is unimolecular and intramolecular, primary steric effects are essentially precluded. Also, it is known that the pyrolysis of ethyl benzoates follows a σ° correlation (7) so resonance interactions between the substituent and the reaction site, including steric inhibition of resonance, are negligible. Hydrogen bonding can not occur with most substituents studied. The pyrolyses of esters are known to proceed via a cyclic transition state intermediate in which there is only a small amount of charge separation (8 (*a*, *b*)); therefore, there are no pole–pole or pole–dipole interactions and very likely only minor dipole–dipole interactions.

Eight ortho-substituted ethyl benzoates (with substituents varying from *o*-NH_2 to *o*-NO_2) have been pyrolyzed to ethylene and the corresponding benzoic acid in a static system under identical conditions in such a manner that not all of the ester decomposed. The relative rates for the thermal decomposition have been determined by gas chromatography and are given in Table I. The results reported earlier (7) for the meta and para

TABLE I

Relative rate data for the pyrolysis of *o*-, *m*-, and *p*-substituted ethyl benzoates at 515° C

Substituent	ortho	meta	para	*o*:*p* ratio	Infrared frequency cm^{-1} for *o*-substituted ester C=O	C—O
2,6-Me_2	0.88				1717	1243 (1213)
OMe	0.97	1.07	0.96	1.01	1719	1178
NH_2	0.98	1.01	0.86	1.14	1683	1163 (1155)
H	1.00	1.00	1.00	1.00	1714	1170
Me	1.09	1.08	1.03	1.06	1711	1162
OH	1.16	0.98	0.91	1.27	1669	1152 (1131)
Cl	1.34*	1.28	1.28	1.04	1725	1131
I	1.35	1.32	1.32	1.02	1721	1096
NO_2	1.61	1.50	1.42	1.13	1728	1069

*This value was obtained from the ratio of the absolute reaction rate data for ethyl *o*-chlorobenzoate and ethyl benzoate. Grateful acknowledgment is given to Dr. David A. K. Jones for determining these data. Decarboxylation is not sufficient to present a serious problem with these esters, therefore, studies could be made in a static reactor.

isomers are listed for comparison. Also included in the table are the frequencies of the C—O stretching in the 1100–1150 cm^{-1} region and the frequencies of the C=O stretching in the 1715 cm^{-1} region. At the temperatures necessary to cause the pyrolysis of ethyl benzoates, aromatic acids undergo decarboxylation. For this reason the absolute reaction rates are not readily determined by measuring the increase in pressure in a static reactor as reported from this laboratory on the studies of arylethyl acetates (8(*a*)), isopropyl benzoates (8(*c*)), and carbonates (8(*d*)). The present studies, however, were successfully made in a dynamic reactor, the design of which has been described (9).

This study is the first of a series on the pyrolyses of ortho-substituted benzoates in which the alkyl group is increased in size from ethyl, isopropyl, to *t*-butyl.

The most striking observation is that the *o*:*p* ratios for all but three of the substituents were in the range 1.00–1.06. To our knowledge, there is only one other similar reaction of σ° type reported (10) that does not show a marked difference in reactivity of the substituent in the ortho and para positions (3(*b*)). This demonstrates that the proximity effects for *o*-substituents are excluded in the pyrolysis of esters.

Can. J. Chem. Downloaded from www.nrcresearchpress.com by 210.87.254.6 on 09/05/12
For personal use only.

The three substituents that showed somewhat enhanced *o*:*p* ratios were NH_2 (1.14), OH (1.27), and NO_2 (1.13). Two of these (NH_2, OH) show hydrogen bonding in solution at room temperature as indicated by the occurrence of additional low frequencies of the C=O absorption in the infrared spectra (see Table I). This may explain the enhanced reactivity of these substituents in the ortho position, though bonding of this type will be much less important at high temperatures. Hydrogen bonding can help to stabilize the slight charge separation reported to occur in the transition state of this thermal decomposition reaction.

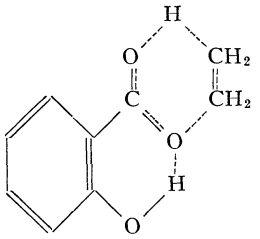

The nitro group, which has a strong —I and —R effect, would be expected to show an *o*:*p* ratio greater than 1.00 and greater than the *o*:*p* ratio for Cl and I. The size of the nitro group is considerable [$E_s = -0.75$] (3(*b*)) but there is little evidence that the slightly increased ortho reactivity is due to steric acceleration. Certainly the 2,6-dimethyl-substituted ester would be expected to show a marked difference in reactivity from the standard ethyl benzoate if steric effects were pertinent. The two groups reduce the rate only slightly ($k_{rel} = 0.88$). Bailey and Turek demonstrated that ethyl 2,4,6-trimethyl-benzoate could be pyrolyzed readily to the free acid and ethylene in 76% yield (11). This indicates very little steric hindrance or acceleration in this reaction as compared to many reactions run in the condensed phase such as in the esterification of 2,6-dimethylbenzoic acids (and the reverse, hydrolysis) where the rate is markedly affected by the presence of two ortho substituents (12).

Therefore, it is concluded that in the pyrolysis of ethyl benzoates the proximity effect appears to be minimal or non-existent, and changes in reactivity are primarily due to the changes in polar effects of the substituent. This reaction appears to be a useful method of determining, at least to a good first approximation, quantitative polar effects of ortho substituents. Such polar substituent values for ortho substituents will be reported in future papers.

EXPERIMENTAL

Ester Preparation

Esters were, in general, prepared from commercially available acids and ethanol, using either sulphuric acid or dry hydrogen chloride as a catalyst. *o*-Iodobenzoic acid was made using the method of Wachter (13) from anthranilic acid. Ethyl 2,6-dimethylbenzoate was prepared from 2,6-dimethylbromobenzene using a Grignard synthesis following the procedure outlined by Bailey and Turek (11). The esters were purified by careful fractionation, and the physical constants of the pure esters were found to agree with the best literature values.

Method of Pyrolysis

Each ester was pyrolyzed under identical conditions in such a manner that not all of the ester decomposed, otherwise a relative rate could not be determined. The extent of pyrolysis was determined by measuring the amount of ethylene produced using gas-phase chromatography and was found to be in the range of 50–60%. The details of the method have been described (9) as well as other applications (7).

A fixed volume of ester was injected into the hot zone of the reactor using a 10-μl syringe fitted with a Chaney adapter. The reactor was an 8-in. stainless tube inserted in the constant flow helium line leading to

Can. J. Chem. Downloaded from www.nrcresearchpress.com by 210.87.254.6 on 09/05/12
For personal use only.

the gas chromatograph. The temperature of the reactor was maintained by a well-lagged copper block surrounding the stainless steel tube. Although the temperature used was 515°, the time (0.7 second) that the ester was in the hot zone was not sufficient to cause complete pyrolysis.

The product from the pyrolysis and the unpyrolyzed ester were carried with the helium stream through an ice-cooled trap to remove the unpyrolyzed ester and the acid. The ethylene and carbon dioxide (produced by partial decarboxylation of the acid) were carried on through a 15-ft 40–60 mesh silica gel column maintained at 56°.

The amount of ethylene produced by a given ester was directly proportional to the rate of decomposition, as the stoichiometry of ester to olefin is one. Throughout the series studied the reaction temperature and time were held constant. The reference compound, ethyl benzoate, was pyrolyzed at regular intervals to check reproducibility. Triplicate or more runs were averaged to obtain mean values.

The relative rates are given in Table I. The results reported earlier for the meta and para isomers are listed for comparison (7).

Also included in Table I are the frequencies of the C—O stretching vibrations in the 1100–1150 cm^{-1} region and the frequency of the C=O stretching in the 1715 cm^{-1} region (measured in CS_2 solutions).

REFERENCES

1. J. HINE. Physical organic chemistry. 2nd ed. McGraw-Hill Book Company, Inc. 1962. p. 85.
2. (*a*) C. K. INGOLD. Structure and mechanism in organic chemistry. Cornell University Press. 1953. p. 256.
   (*b*) R. W. TAFT, JR. Steric effects in organic chemistry. *Edited by* M. S. Newman. John Wiley and Sons, Inc. 1955. p. 584.
3. (*a*) R. W. TAFT, JR. Steric effects in organic chemistry. *Edited by* M. S. Newman. John Wiley and Sons, Inc. 1955. p. 587; (*b*) p. 598.
4. C. K. INGOLD. J. Chem. Soc. 1032 (1930).
5. P. MAMMALIS and H. N. RYDON. J. Chem. Soc. 1049 (1955).
6. M. CHARTON. Can. J. Chem. **38**, 2493 (1960).
7. G. G. SMITH, D. A. K. JONES, and D. F. BROWN. J. Org. Chem. **28**, 403 (1963).
8. (*a*) G. G. SMITH, F. D. BAGLEY, and R. TAYLOR. J. Am. Chem. Soc. **83**, 3647 (1961).
   (*b*) G. G. SMITH, R. TAYLOR, and W. H. WETZEL. J. Am. Chem. Soc. **84**, 4817 (1962).
   (*c*) G. G. SMITH and D. A. K. JONES. Paper VIII. J. Org. Chem. **28**. In press (1963).
   (*d*) G. G. SMITH, D. A. K. JONES, and R. TAYLOR. J. Org. Chem. **28**, 85 (1963).
9. G. G. SMITH, W. H. WETZEL, and B. KOSTERS. Analyst, **86**, 480 (1961).
10. M. M. DAVIS and H. B. HETZER. J. Res. Nat. Bur. of Std. **60**, 569 (1958).
11. W. J. BAILEY and W. N. TUREK. J. Am. Oil Chemists' Soc. **33**, 317 (1956).
12. E. S. GOULD. Mechanism and structure in organic chemistry. Henry Holt and Co. 1959. p. 325.
13. W. WACHTER. Ber. **26**, 1744 (1893).

Can. J. Chem. Downloaded from www.nrcresearchpress.com by 210.87.254.6 on 09/05/12
For personal use only.

SPECTRAL AND CHEMICAL PROPERTIES OF β- AND γ-FUNCTIONAL SILANES

A. G. Brook and J. B. Pierce
Department of Chemistry, University of Toronto, Toronto, Ontario
Received June 28, 1963

ABSTRACT

The synthesis of β- and γ-hydroxy- and keto-silanes is described, together with that of their carbon analogues. Unlike the α-isomers. the hydroxysilanes do not rearrange to silyl ethers, and the ultraviolet spectra of the silyl ketones is essentially the same as those of the carbon analogues, and unlike that of α-silyl ketones. β-Silyl ketones have a carbonyl-stretching frequency midway between that of ordinary ketones and α-silyl ketones. These effects are discussed.

Can. J. Chem. Downloaded from www.nrcresearchpress.com by 210.87.254.40 on 09/05/12
For personal use only.

Previous studies from this laboratory have shown that organosilicon compounds having functional groups (OH, C=O) on the carbon atom adjacent (alpha) to silicon exhibit properties considerably different in behavior from those of their carbon analogues. Thus alpha-silyl ketones have anomalous infrared and ultraviolet spectra (1, 2), and both α-silyl ketones (3) and α-silyl carbinols (4, 5) (α-hydroxysilanes) undergo rearrangements unknown in carbon chemistry.

The ultraviolet spectra of benzoylsilanes are characterized by absorption in the visible region at about 403–417 mμ, so that all the compounds are bright yellow regardless of whether methyl (1), phenyl (1), hydroxyl (2), methoxyl (2), or halobenzyl (2) groups are attached to the silicon atom, whereas, in all cases the carbon analogues are colorless, absorbing at some 80–100 mμ's shorter wavelength. At the same time the infrared carbonyl stretching vibration of α-silyl ketones is at remarkably low frequency: 1618 cm^{-1} (6.18 μ) for benzoylsilanes (1, 2) and 1645 cm^{-1} (6.08 μ) for acetyl (1) or propionylsilanes, whereas the carbon analogues absorb at about 1686 cm^{-1} (5.93 μ) and 1715 cm^{-1} (5.83 μ) respectively. Again the position of the absorption band is rather insensitive to the nature of the groups attached to silicon (2).

It has been suggested that these anomalous spectral effects might be due to interaction of the unshared electrons of the oxygen atom of the carbonyl group with the unoccupied but accessible *d*-orbitals of silicon (1). Such interactions appear to be well established for oxygen attached directly to silicon (6). It might be anticipated that if such *n*–*d* interactions were associated with the anomalous spectra of α-silyl ketones (I), while little effect would be observed with β-ketosilanes (II) due to poor overlap, this type of interaction could also arise in a γ-ketosilane (III) in a suitable cyclic conformation.

While a number of carbon-functional silanes have been synthesized where the functional group is beta or gamma to the silicon atom (7(*a*)), no detailed investigation of their properties has been reported. Hence it appeared to be of interest to synthesize keto- and hydroxysilanes where the functional group was not next to silicon to see what effect position had on the infrared and ultraviolet absorption, and on the tendency of the compound to undergo rearrangement.

The ketones chosen were phenacyltriphenylsilane, a β-silyl ketone, and 1-triphenylsilyl-3-phenylpropan-3-one, a γ-silyl ketone, together with their carbon analogues, prepared to ensure absence of any unpredicted behavior. A by-product of one of the reactions also yielded what is believed to be 1,3-bis(triphenylsilyl)-5-phenylpentan-5-one, which is both

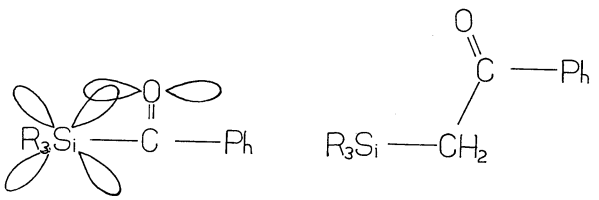

I

II

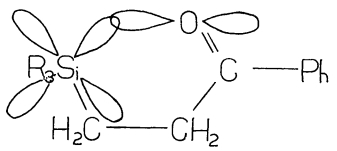

III

a γ and an ε ketone. The corresponding alcohols were also prepared to establish whether rearrangement to the isomeric silyl ethers occurred.

The spectral data for the various ketones are recorded in Table I.

TABLE I

Compound	Infrared carbonyl stretch, cm^{-1}	Ultraviolet (mμ) Benzoyl λ	Benzoyl ε	Phenyl λ	Phenyl ε	Carbonyl λ	Carbonyl ε
Ph_3SiCH_2COPh	1667	243	13,200	271	3120	310 (S)	328
Ph_3CCH_2COPh	1698	241	13,380	270 (S)	2070	323	95
$Ph_3SiCH_2CH_2COPh$	1692	242	12,200	270	1720	311 (S)	131
$Ph_3CCH_2CH_2COPh$	1692	235	15,500	270 (S)	1750	314 (S)	84
$Ph_3SiCOPh$	1618	258	15,500	—	—	403 (S)	264*
						417	300
Ph_3CCOPh	1692	253	11,600	293	782	329	299*
Ph_3CCOCH_3	1721			255	900	292	420
Ph_3CCOCH_2Ph	1721			253	1880		
				259	1530	300	404
$Ph_3Si—CH(CH_2—CH_2SiPh_3)—CH_2COPh$	1692			263	3610	314 (S)	117†
				270	2510		

*See reference 1.
†Ultraviolet spectrum run in $CHCl_3$ due to solubility problems.
S = Shoulder.

With respect to the infrared absorption, it is found that the characteristic carbonyl absorption at 1618 cm^{-1} of α-ketosilanes is raised to 1667 cm^{-1} in the β-ketosilane, and is still further raised to 1692 cm^{-1} in the γ-silyl ketones, the normal value for an alkyl phenyl ketone, as demonstrated by the results from the carbon analogues. This effect is typical of a simple inductive electron release from the relatively electropositive triphenylsilyl group to the carbonyl group, which diminishes as methylene groups are interposed between silicon and the electron-accepting group.

No anomalous ultraviolet absorption effects are observed for the β-, γ-, or ε-silyl ketones, as demonstrated by the similarity of their spectra to the appropriate carbon analogues. Thus only when the silicon atom is directly attached to the carbonyl group are anomalous

Can. J. Chem. Downloaded from www.nrcresearchpress.com by 210.87.254.40 on 09/05/12
For personal use only.

ultraviolet spectra obtained. While we wish to defer a detailed discussion of the interpretation of these absorption effects to a later paper, it seems obvious that some direct interaction between the carbonyl group and the silicon *d*-orbitals is occurring, probably involving contributions in the excited state from structures such as IV.

$$R_3SiCOPh \xrightarrow{h\nu} R_3Si^- = \overset{O^+}{\overset{|}{C}}—Ph$$

IV

West (7*b*) has recently interpreted these effects similarly in terms of resonance interaction between the silicon atom and the π orbitals of the carbonyl group, in which interaction with the π^* orbital is most important.

A characteristic of α-silyl carbinols is their ability to rearrange readily to the isomeric silyl ether under mild conditions (4). This has been shown to be an intramolecular reaction occurring with retention of configuration at silicon (8). It was of interest to establish whether β- or γ-silyl carbinols would rearrange similarly. Since the hydroxy compounds were readily available from the ketones, both 1-triphenylsilyl-2-phenylethan-2-ol and 1-triphenylsilyl-3-phenylpropan-3-ol were treated over several hours with sodium–potassium alloy in ether, conditions which, with α-silyl carbinols, would have been more than adequate to convert them to silyl ethers (4). However, in neither case was any evidence for isomerization observed and the starting materials were recovered in excess of 75%.

Hence it appears that β- and γ-functional silanes are devoid of the interesting physical or chemical properties that characterize alpha-hydroxy- or alpha-ketosilanes.

Synthesis of the β- and γ-silyl ketones and their carbon analogues presented some difficulties. The synthesis of the γ-silyl ketone, 1-triphenylsilyl-3-phenylpropan-3-one, followed closely the methods employed for the synthesis of α-silyl ketones (1, 2). Coupling of 3-phenylpropyllithium with triphenylchlorosilane gave 3-phenylpropyltriphenylsilane, which was dibrominated with N-bromosuccinimide and then hydrolyzed to the ketone with silver acetate and water. Alternatively, the compound was prepared in low yield by the photochemical-induced addition of benzaldehyde to vinyltriphenylsilane, using conditions previously described for the synthesis of 1-triphenylsilyl-butan-3-one (9).

A second major product was also isolated from this reaction. Although the structure was not rigorously proved, it seems reasonable from the infrared spectrum (1692 cm^{-1}), molecular weight determination, and analysis to ascribe to this compound the structure 1,3-bis(triphenylsilyl)-5-phenylpentane-5-one. Such a structure is reasonable from a radical reaction involving triphenylvinylsilane where the intermediate 1-triphenylsilyl-3-keto-3-phenylpropyl radical either abstracts hydrogen, giving 1-triphenylsilyl-3-phenylpropan-3-one, or attacks a second vinyltriphenylsilane molecule.

$$Ph_3SiCl + Li—(CH_2)_3Ph \rightarrow Ph_3Si—(CH_2)_3Ph \xrightarrow[(ii)\ AgOAc,\ H_2O]{(i)\ 2NBS} Ph_3Si—CH_2—CH_2—\overset{O}{\overset{\|}{C}}—Ph$$

$$Ph_3SiCH=CH_2 + HCOPh \rightarrow Ph_3Si—\overset{H}{\overset{|}{C}}—CH_2—\overset{O}{\overset{\|}{C}}—Ph \xrightarrow[\text{then } H\cdot]{Ph_3SiCH=CH_2} Ph_3Si—CH(CH_2—CH_2—SiPh_3)—CH_2—\overset{O}{\overset{\|}{C}}—Ph$$

(H· abstraction from the intermediate radical)

Can. J. Chem. Downloaded from www.nrcresearchpress.com by 210.87.254.40 on 09/05/12
For personal use only.

Can. J. Chem. Downloaded from www.nrcresearchpress.com by 210.87.254.40 on 09/05/12
For personal use only.

The β-silyl ketone, phenacyltriphenylsilane, was prepared by oxidation of 1-triphenylsilyl-2-phenylethan-2-ol, prepared by the method of Gilman *et al.* from triphenylsilyllithium and styrene oxide (10). Attempts to prepare the ketone following the methods described above for the γ-ketone failed.

Bromination with N-bromosuccinimide of 1-triphenylsilyl-2-phenylethane, prepared from 2-phenylethylmagnesium bromide and triphenylchlorosilane, gave the expected 1-triphenylsilyl-2-phenyl-2,2-dibromoethane. However, on some occasions, particularly with prolonged reflux, this compound spontaneously evolved hydrogen bromide, yielding instead 1-triphenylsilyl-2-bromo-2-phenylethene, characterized by carbon–carbon double bond absorption at 1587 cm^{-1}, and ultraviolet absorption at 260 mμ, ε 15,360, a position typical for an aryl-conjugated double bond with an alpha-bromine substituent (11). This result suggests that bromination followed by dehydrobromination occurred. Such behavior is not surprising for a β-bromosilane (12).

Attempts to hydrolyze 1-triphenylsilyl-2-phenyl-2,2-dibromoethane with silver acetate in the normal manner failed to yield any of the expected phenacyltriphenylsilane. Extensive silicon–carbon cleavage occurred, yielding triphenylsilanol and the only other material isolated appeared to be a mixture of α- and β-hydroxysilanes containing bromine, which could not be separated. Short refluxing of this material in ethanol gave low yields of 1-triphenylsilyl-2-bromo-2-phenylethene. These anomalous reactions have not been further investigated, but it is known from previous work that β-silyl halides frequently give rise to unusual reactions (7, 12).

The carbon analogues of the β- and γ-silyl ketones, viz. 1,1,1,3-tetraphenylpropan-3-one (13) and 1,1,1,4-tetraphenylbutan-4-one, were also synthesized by unambiguous routes, the latter not previously having been reported. Treatment of 3,3,3-triphenylpropionyl chloride with diphenylcadmium gave a good yield of 1,1,1,4-tetraphenylpropan-3-one, but attempts to convert the acid chloride to the phenyl ketone by Friedel–Crafts coupling with benzene using aluminum chloride gave only intramolecular cyclization to the previously reported 3,3-diphenylindanone (14).

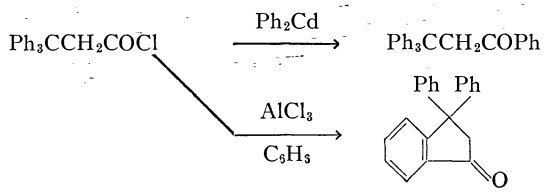

The ketone 1,1,1,4-tetraphenylbutan-4-one was prepared by a route similar to that used for the γ-silyl ketone. Triphenylmethylsodium was coupled with 3-phenylpropylbromide to yield 1,1,1,4-tetraphenylbutane. This hydrocarbon was dibrominated with N-bromosuccinimide and the bromide was hydrolyzed with silver trifluoroacetate and water.

$$Ph_3CNa + Br(CH_2)_3Ph \rightarrow Ph_3C(CH_2)_3Ph \xrightarrow[(ii)\ AgO{-}C{-}CF_3,\ H_2O]{(i)\ 2NBS} Ph_3CCH_2CH_2COPh$$

In addition, in the course of this work, two additional ketones were synthesized by exploratory reactions involving the coupling of triphenylmethylmagnesium bromide with acid chlorides. It was considered probable that the hindered ketones formed by this coupling reaction would not readily add a second mole of Grignard reagent as normally

occurs, and this was confirmed to some extent, although the yields of ketone were low and numerous other products accompanied the desired product. Thus 1,1,1-triphenylpropan-2-one (15) was prepared in low yield when trityl Grignard reagent was treated with acetyl chloride and 1,1,1,3-tetraphenylpropan-2-one was similarly prepared by reaction with phenylacetyl chloride.

$$Ph_3CMgI \xrightarrow{ClCOMe} Ph_3CCOMe$$

$$Ph_3CMgI \xrightarrow{ClCOCH_2Ph} Ph_3CCOCH_2Ph$$

EXPERIMENTAL

Reactions involving organometallics were carried out under a dry oxygen-free nitrogen atmosphere. Infrared spectra were determined in carbon tetrachloride on a Beckman IR5 instrument calibrated against polystyrene. Ultraviolet spectra were determined in 95% ethanol.

1-Triphenylsilyl-3-phenylpropan-3-one

A. From 1-Triphenylsilyl-3-phenylpropane

1-Triphenylsilyl-3-phenylpropane was prepared from triphenylchlorosilane and 3-phenylpropyllithium in 61% yield by the method of Gilman and Miles (16), m.p. 66.5–67.5° (reported 62.5–64°). Anal. Calc. for $C_{27}H_{26}Si$: C, 85.6; H, 6.92. Found: C, 84.7; H, 6.60.

Dibromination of 3.78 g (0.01 mole) of 1-triphenylsilyl-3-phenylpropane over 18 hours with 3.8 g (0.0215 mole) of N-bromosuccinimide in 100 ml of refluxing carbon tetrachloride, to which small lumps on benzoyl peroxide were added every 15 minutes over the first hour, gave, on cooling, 1.94 g (98%) of succinimide identified by mixed melting point. Removal of the carbon tetrachloride and crystallization from petroleum ether (b.p. 90–100°) gave 2.51 g (47%) of 1-triphenylsilyl-3,3-dibromo-3-phenylpropane, m.p. 111–113°.

Hydrolysis of 2.51 g (0.0047 mole) of the dibromide was accomplished by stirring its solution in 20 ml of benzene, 58 ml of acetone, and 2 ml of water with 1.57 g (0.0094 mole) of silver acetate for 22 hours in the dark at room temperature. After filtration of 1.69 g (96%) of silver bromide the solution was treated with water and extracted with benzene. After drying, and removal of the solvent under reduced pressure, the orange residue was recrystallized from ethanol to give 1.19 g (65%) of colorless 1-triphenylsilyl-3-phenylpropane-3-one, m.p. 84–84.5°. Anal. Calc. for $C_{27}H_{24}SiO$: C, 82.6; H, 6.16. Found: C, 82.2; H, 6.03.

B. From Vinyltriphenylsilane and Benzaldehyde

A solution of 5.3 g (0.05 mole) of benzaldehyde and 5.72 g (0.02 mole) of vinyltriphenylsilane and a trace of benzoyl peroxide in 75 ml of cyclohexane was irradiated with ultraviolet light from General Electric 40-watt Black Light fluorescent lamps, for a period of 2 weeks. After removal of the solvent, the residue was chromatographed on silica gel, using 50% benzene – petroleum ether (b.p. 90–100° C) and then benzene as eluants. The first fractions gave 3% of a high melting ketone (m.p. 189–191° C) after two recrystallizations from a 90–100° C petroleum ether – benzene mixture. This material is tentatively identified is 1,3-bis(triphenylsilyl)-5-phenylpentane-5-one. Anal. Calc. for $C_{47}H_{42}Si_2O$: C, 83.1; H, 6.23; mol. wt. 679. Found: C, 82.1; H, 6.28; mol. wt. (osmometer) 706.

The next fractions (benzene) yielded 1.0 g (12%) of 1-triphenylsilyl-3-phenylpropan-3-one, m.p. 84–84.5°, after crystallization from ethanol, shown to be identical with the material described above by mixed melting point.

Phenacyltriphenylsilane

A. To 2.0 g (0.0052 mole) of 1-triphenylsilyl-2-phenylethan-2-ol, prepared by the method of Gilman *et al.* (10), in 25 ml of ether and 20 ml of acetone was added over 45 minutes 3.8 ml of an oxidizing mixture made up from 25.80 g (0.25 mole) of 96% sulphuric acid and 16.67 g (0.167 mole) of chromium trioxide in water to a total volume of 100 ml. After it was stirred for 1 hour at room temperature, the reaction mixture was drowned in water, and was ether extracted. After drying and removal of the ether, an oily solid, smelling strongly of benzaldehyde, was obtained. Recrystallization from carbon tetrachloride removed 0.39 g (27%) of triphenylsilanol, m.p. 148–152°, identified by mixed melting point. Recrystallization from ethanol of the residue after removal of the carbon tetrachloride gave 0.52 g (27%) of phenacyltriphenylsilane, m.p. 89–91°. Anal. Calc. for $C_{26}H_{22}SiO$: C, 82.5; H, 5.86. Found: C, 82.5; H, 6.09.

B. Dibromination of 1-Triphenylsilyl-2-phenylethane

1-Triphenylsilyl-2-phenylethane, m.p. 147–149°, was prepared in 44% yield from 2-phenylethylmagnesium bromide and triphenylchlorosilane according to the method of Gilman and Miles (16); reported m.p. 146–147°.

A mixture of 5.0 g (0.018 mole) of 1-triphenylsilyl-2-phenylethane in 50 ml of carbon tetrachloride was refluxed with 4.87 g (0.0274 mole) of N-bromosuccinimide for 2 hours with periodic additions of small amounts of benzoyl peroxide. The bromination was distinctive in terms of the brown color which developed,

Can. J. Chem. Downloaded from www.nrcresearchpress.com by 210.87.254.40 on 09/05/12
For personal use only.

suggesting liberation of free bromine. After cooling and removal of 92% of succinimide, identified by mixed melting point, the solvent was removed under reduced pressure and the resulting oil was dissolved in cyclohexane and cooled to give 2.75 g (38%) of crude 1-triphenylsilyl-2,2-dibromo-2-phenylethane, m.p. 103–112°. Recrystallization from heptane raised the melting point to 115–117°. Anal. Calc. for $C_{26}H_{22}SiBr_2$: C, 59.8; H, 4.21. Found: C, 60.3; H, 4.23.

A variety of other compounds, whose identity has not been established, were isolated in low yield from the mother liquor.

Similar runs to the above gave on at least one occasion a vigorous evolution of HBr after about 2.5 hours reflux. Workup as above gave as the main product 2.0 g (32%) of 1-triphenylsilyl-2-bromo-2-phenylethene, m.p. 156.5–158° after recrystallization from benzene–petroleum ether (b.p. 90–100°). Anal. Calc. for $C_{26}H_{21}SiBr$: C, 70.7; H, 4.80. Found: C, 71.4; H, 4.92. Infrared ($CHCl_3$) 1587 cm^{-1}; ultraviolet λ_{max} 260.5, ϵ 15,360.

Hydrolysis of 1-Triphenylsilyl-2,2-dibromo-2-phenylethane

A mixture of 1.9 g (0.0036 mole) of the dibromo compound and 1.28 g (0.0077 mole) of silver acetate in 30 ml of acetone, 10 ml of benzene, and 1 ml of water was stirred for 18 hours. The insoluble silver salts were removed, water was added, and the material was extracted with ether. The ether layers were washed with water and dilute sodium bicarbonate and, after drying, the ether was removed. Recrystallization from heptane gave 0.46 g (46%) of triphenylsilanol, m.p. 150–152°, identified by mixed melting point, and 0.60 g of material melting 110–127°.

Recrystallization from heptane raised the melting range to 120–132°, but further recrystallization failed to alter the range. This material, which contains halogen, appeared to be a mixture of α- and β-hydroxy silanes based on the presence of two OH peaks at 3572 cm^{-1} (α) and 3636 cm^{-1} (β) in the infrared spectrum. If the material was refluxed in ethanol, about 50% of 1-triphenylsilyl-2-bromo-2-phenylethene, m.p. 154–157°, identified by mixed melting point with the material described above, could be isolated. None of the expected 1-phenacyltriphenylsilane was detected, and an infrared spectrum of the crude hydrolyzate showed no carbonyl absorption bands.

1-Triphenylsilyl-3-phenylpropan-3-ol

To a solution of 0.03 g (0.0007 mole) of lithium aluminum hydride in 25 ml of dry ether was added 1.0 g (0.0026 mole) of 1-triphenylsilyl-3-phenylpropan-3-one in 25 ml of ether. After stirring for 15 minutes at room temperature ethyl acetate was added and the mixture was then hydrolyzed. Removal of the ether from the ether layer gave 0.75 g (73%) of 1-triphenylsilyl-3-phenylpropan-3-ol, m.p. 80–80.5° after recrystallization from petroleum ether (b.p. 90–100°). Anal. Calc. for $C_{27}H_{26}SiO$: C, 82.2; H, 6.64. Found: C, 81.9; H, 6.35.

Attempted Isomerization of 1-Triphenylsilyl-3-phenylpropan-3-ol

To 0.30 g of the above carbinol in 5 ml of dry ether was added a drop of sodium–potassium alloy. Gas appeared to be evolved during the 4-hour reaction period. Workup by removal of the alloy and the solvent gave, after recrystallization, 0.24 g (80%) of recovered starting material, m.p. 80–81°.

Attempted Isomerization of 1-Triphenylsilyl-2-phenylethan-2-ol

To 0.56 g of the carbinol (10) in 5 ml of dry ether was added 1 drop of sodium–potassium alloy. A gas was slowly evolved. After occasional shaking over 4 hours the alloy was removed, the ether was removed under reduced pressure, and the resulting oil was crystallized from ethanol to give 0.42 g (75%) of recovered starting material, m.p. 134–137°.

1,1,1,3-Tetraphenylpropan-3-one

To 15.7 g (0.0347 mole) of 3,3,3-triphenylpropionyl chloride, prepared by the method of Hellerman (17), in 50 ml of dry benzene was added 0.0374 mole of diphenylcadmium (18) in benzene. The mixture was refluxed for 18 hours and then was drowned in ice and dilute hydrochloric acid and extracted with ether. After drying with sodium sulphate and removal of the ether, the residue was washed with petroleum ether (b.p. 90–100°) and the insoluble ketone was crystallized from ethanol – ethyl acetate to give 4.98 g (37%) of 1,1,1,3-tetraphenylpropan-3-one, m.p. 165–167°, Anal. Calc. for $C_{27}H_{22}O$: C, 89.4; H, 6.12. Found: C, 88.6; H, 6.12.

Attempted Synthesis of 1,1,1,3-Tetraphenylpropan-3-one by Friedel–Crafts Reaction

3,3-Diphenylindanone.—To a solution of 5.25 g (0.04 mole) of aluminum chloride in 40 ml of dry benzene was added 13.82 g (0.043 mole) of 3,3,3-triphenylpropionyl chloride in 20 ml of dry benzene. The mixture was heated carefully to near reflux, at which point a vigorous evolution of hydrogen chloride occurred. After 1 hour the reaction mixture was poured on ice and extracted with benzene. After removal of the solvent, recrystallization of the residue from ethanol gave 7.53 g (62%) of 3,3-diphenylindanone, m.p. 131–133°. Infrared of carbonyl, 1727 cm^{-1}. Reported (14) m.p. 130°. None of the expected product was obtained.

1,1,1,4-Tetraphenylbutane.—To 0.152 mole of triphenylmethylsodium in 1300 ml of ether, prepared from trityl chloride and sodium amalgam (19), was added 30.2 g (0.152 mole) of 1-phenyl-3-bromopropane in 100 ml of ether. The reaction mixture was stirred for 2 hours after addition was complete and then was hydrolyzed. The ether layers were dried, the ether was removed, and the residue was treated with hot

Can. J. Chem. Downloaded from www.nrcresearchpress.com by 210.87.254.40 on 09/05/12
For personal use only.

ethanol. An insoluble residue weighing 1.72 g (4.8%) of *p*-benzhydryltetraphenylmethane, "Gomberg's isomer" (20), was obtained, m.p. 215–220°, identified by mixed melting point with an authentic sample, m.p. 215–219°. The ethanol solution, on cooling, gave 25.5 g (59%) of 1,1,1,4-tetraphenylbutane, m.p. 92–93.5°. Anal. Calc. for $C_{28}H_{26}$: C, 92.4; H, 7.63. Found: C, 92.4; H, 7.37.

1,1,1,4-Tetraphenylbutan-4-one.—To 5.0 g (0.0138 mole) of 1,1,1,4-tetraphenylbutane in 100 ml of carbon tetrachloride was added 4.92 g (0.0276 mole) of N-bromosuccinimide. The mixture was refluxed for 18 hours, several small portions of benzoyl peroxide being added. Removal of the succinimide and then the solvent gave a dibromide which failed to crystallize and which therefore was hydrolyzed directly by treatment with 5.19 g (.0234 mole) of silver trifluoroacetate in 75 ml acetone and 2 ml of water over 18 hours. After removal of the silver bromide, water and ether were added and the ether layer was thoroughly washed with water and dilute sodium hydroxide. After removal of the ether the residue was chromatographed on silica gel, with benzene as eluant. The desired ketone was eluted, after the first 250 ml of solvent, as an oil which crystallized from ethanol to give 0.51 g (11%) of 1,1,1,4-tetraphenylbutan-4-one, m.p. 139–140.5°. Anal. Calc. for $C_{28}H_{24}O$: C, 89.3; H, 6.43. Found: C, 88.5; H, 6.17.

1,1,1-Triphenylpropan-2-one.—To 0.0495 mole of triphenylmethylmagnesium iodide, prepared by the method of Gilman and Zoellner (21), was added 4.3 g (0.055 mole) of acetyl chloride. The reaction mixture was stirred at 0° during the addition and for an additional half hour, and then was allowed to warm to room temperature. After hydrolysis with aqueous acid, the dried ether layers yielded 0.61 g (4.7%) of triphenylmethyl peroxide, m.p. 170–172°, identified by mixed melting point, and a dark residue which was chromatographed on silica gel using 50% benzene – petroleum ether as eluant. Isolated were: (*a*) 2.7 g (22%) of triphenylmethane, m.p. 91–93°, identified by mixed melting point with an authentic sample and after recrystallization from ethanol; (*b*) 2.37 g (17%) of 1,1,1-triphenylpropan-2-one (15), m.p. 138.5–140°. Anal. Calc. for $C_{18}H_{18}O$: C, 88.3; H, 6.34. Found: C, 87.8; H, 6.47.

1,1,1,3-Tetraphenylpropan-2-one.—To 7.70 g (0.0498 mole) of phenylacetyl chloride in 50 ml of benzene was added 0.0415 mole of triphenylmethylmagnesium iodide in 100 ml of benzene and 215 ml of ether. The mixture was maintained at −5° during addition and for an additional half hour and then was allowed to warm to room temperature. After hydrolysis with dilute aqueous acid the mixture was ether-extracted; from the extract precipitated 1.54 g (12%) of triphenylmethyl peroxide, m.p. 174–182°, identified by mixed melting point. After removal of the ether, the dark oily residue was chromatographed on silica gel using 50% benzene – petroleum ether as eluant. Obtained were (*a*) 2.94 g (29%) of triphenylmethane, m.p. 90–95°, identified by mixed melting point, (*b*) 1.87 g (12.5%) of 1,1,1,3-tetraphenylpropan-2-one, recrystallized from ethanol, m.p. 114–115°, and finally (*c*) 0.97 g (9%) of triphenylmethanol, m.p. 157–160°, identified by mixed melting point. Anal. Calc. for $C_{27}H_{22}O$: C, 89.5; H, 6.13. Found: C, 89.4; H, 6.25.

ACKNOWLEDGMENT

This research was supported in part by the National Research Council of Canada.

REFERENCES

1. A. G. Brook *et al.* J. Am. Chem. Soc. **82**, 5102 (1960).
2. A. G. Brook and G. J. D. Peddle. Can. J. Chem. In press.
3. A. G. Brook and N. V. Schwartz. J. Org. Chem. **27**, 2311 (1962).
4. A. G. Brook, C. M. Warner, and M. E. McGriskin. J. Am. Chem. Soc. **81**, 981 (1959).
5. A. G. Brook. J. Am. Chem. Soc. **80**, 1886 (1958).
6. R. West, L. S. Whatley, and K. J. Lake. J. Am. Chem. Soc. **83**, 761 (1961).
7. (*a*) C. Eaborn. Organosilicon compounds. Butterworths Scientific Publications, London. 1960.
   (*b*) D. F. Narnish and R. West. J. Am. Chem. Soc. In press.
8. A. G. Brook and C. M. Warner. Tetrahedron Letters, **18**, 821 (1962).
9. L. H. Sommer *et al.* J. Am. Chem. Soc. **76**, 1613 (1954).
10. H. Gilman, D. Aoki, and D. Wittenberg. J. Am. Chem. Soc. **81**, 1107 (1959).
11. E. A. Braude. *In* Determination of organic structures by physical methods. Academic Press, New York. 1955. p. 153.
12. L. H. Sommer, D. L. Bailey, and F. C. Whitmore. J. Am. Chem. Soc. **70**, 2869 (1948).
13. A. N. Nesmeyanov, I. F. Lutsenko, and I. M. Tumanova. Izv. Akad. Nauk SSSR, Otd. Khim. Nauk, 601 (1949).
14. C. Mavrea, C. Du Fraise, and P. M. Dean. Bull. Soc. Chim. France, **43**, 1367 (1928).
15. S. N. Danilov. Zh. Obshch. Khim. **18**, 2000 (1948).
16. H. Gilman and D. Miles. J. Org. Chem. **21**, 254 (1956).
17. L. Hellerman. J. Am. Chem. Soc. **49**, 1735 (1927).
18. D. Shirley. Organic reactions. Vol. VIII. J. Wiley and Sons, New York. 1954, p. 28.
19. Organic synthesis. Coll. Vol. II. J. Wiley and Sons, New York. 1943. p. 607.
20. M. Gomberg. Ber. **35**, 3918 (1902).
21. H. Gilman and E. A. Zoellner. J. Am. Chem. Soc. **51**, 3493 (1929).

Can. J. Chem. Downloaded from www.nrcresearchpress.com by 210.87.254.40 on 09/05/12
For personal use only.

Can. J. Chem. Downloaded from www.nrcresearchpress.com by 210.87.254.42 on 09/05/12
For personal use only.

THE RAMAN SPECTRA OF DEUTERATED METHYL LAURATES AND RELATED COMPOUNDS[1]

R. NORMAN JONES AND R. A. RIPLEY[2]
Division of Pure Chemistry, National Research Council of Canada, Ottawa
Received June 20, 1963

ABSTRACT

The Raman spectra of methyl laurate and five derivatives selectively deuterated in the terminal methyl group, the α-methylene group, and the carbomethoxy group have been examined in the liquid phase. Raman spectra of *n*-dodecane and *n*-dodecane-1,12-d_6 have also been determined. The spectra are compared with the infrared spectra, which have been reported previously, and are analyzed in terms of current views on the vibrations of compounds containing polymethylene chains.

Whereas the infrared spectra of the esters are dominated by absorption bands associated with the carbomethoxy group, this group has only a minor effect on the Raman spectrum; the implications of this in organic structural analysis are discussed.

INTRODUCTION

The Raman and infrared spectra of compounds containing methylene chains have been investigated extensively for solid phase systems, and the vibrations have been described in terms of models of increasing degrees of sophistication. The principal contributions prior to 1957 have been listed by Nielsen and Woollett (1), and the most detailed and recent analyses are by Tung Po Lin and Koenig (2), by Snyder and Schachtschneider (3, 4), and by Tasumi, Shimanouchi, and Miyazawa (5). It is generally assumed that the polymethylene chains pack in an all-trans conformation. If the end groups are identical, the compounds of even- and odd-chain length have C_{2h} or C_{2v} symmetry respectively, and if the chain is infinitely long, V_h symmetry is acquired. By the application of the appropriate selection rules, vibrational assignments have been made for most of the bands in both the infrared and Raman spectra of the *n*-alkanes and of polyethylene (loc. cit.).

As a result of vibrational coupling between successive methylene groups, "arrays" of bands are observed, which extend over defined regions of the spectrum. The array distribution pattern shown in Fig. 1 summarizes the vibrational assignments proposed several

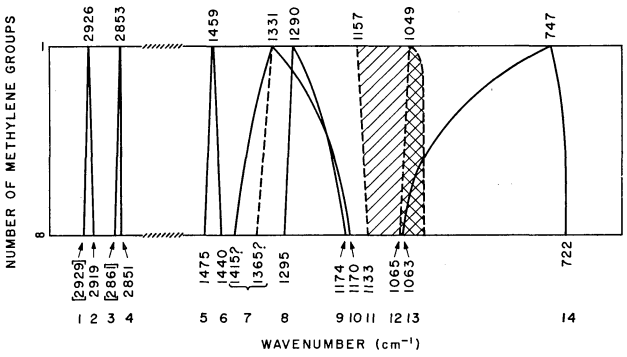

FIG. 1. Distribution of vibrational modes for an infinite polymethylene chain, according to Snyder and Schachtschneider (3, 4). The numbers 1–14 indicate the vibrations shown in Fig. 2.

[1]*Issued as N.R.C. No. 7622.*
[2]*National Research Council Postdoctoral Fellow, 1960–62.*

years ago by Sheppard and collaborators (6–8), as modified by the later measurements and normal co-ordinate calculations of Snyder and Schachtschneider for *n*-alkanes (3, 4). Within each array progressions of bands occur, the number increasing with the length of the chain. The relative intensities of consecutive bands in an array change progressively or alternatingly in accord with the selection rules for even or odd chain length. The peripheral bands usually have maximal or minimal infrared or Raman intensity, depending on the relevant selection rules. In the peripheral modes simple phase relationships usually exist between the vibrations of adjacent methylene units; these are illustrated in Fig. 2 for a section of an infinite methylene chain.* The array limits and symmetry characteristics are listed in Table I.

TABLE I

Characteristic vibrations of the infinite polymethylene chain

Band*	Position† (cm^{-1})	Symmetry‡	Activity§	Dipole change orientation‖	Description
1	(2929)¶	B_{1g}	R (dp)	—	Asym. C—H stretch
2	2919	B_{2u}	IR	y	Asym. C—H stretch
3	(2861)¶	A_g	R (p)	—	Sym. C—H stretch
4	2851	B_{3u}	IR	x	Sym. C—H stretch
5	1475	B_{3u}	IR	x	C—H scissor
6	1440	A_g	R (p)	—	C—H scissor
7	1415**	B_{2g}	R (dp)	—	C—H wag
8	1295	B_{3g}	R (dp)	—	C—H twist
9	1174	B_{1g}	R (dp)	—	C—H rock
10	1170	B_{1u}	IR	z	C—H wag
11	1133	A_g	R (p)	—	Skeletal stretch
12	1065	B_{2g}	R (dp)	—	Skeletal stretch
13	1063	A_u	—	—	C—H twist
14	722	B_{2u}	IR	x	C—H rock

*See Fig. 2.
†From measurements on crystalline polythene (ref. 3).
‡There is confusion in the literature concerning the selection of the symmetry axes. The symbols used here conform with those used in references 1 to 3. The z axis is the long axis of the molecule, the x axis lies in the plane of the carbon atoms, and the y axis is perpendicular to it. The symbols used by other investigators are summarized in reference 2.
§R (Raman active), p (polarized), dp (depolarized), IR (infrared active).
‖See ‡ above.
¶Calculated value.
**See text.

While the vibrational analysis of highly oriented crystalline systems has intrinsic interest in molecular spectroscopy and polymer chemistry, the organic chemist frequently encounters polymethylene chains under conditions that do not conform to the idealized state considered above. If the chain is attached to a more bulky molecule, it will not necessarily orient in the same manner as in *n*-alkanes. Even such simple derivatives as the *n*-alkanoic acids exhibit polymorphism with which is associated striking changes in the infrared spectra (9, 10), and the spectroscopic changes associated with polymorphism in triglycerides are even more profound (11). The transfer of vibrational assignments from *n*-alkane spectra to the spectra of more complex molecules containing polymethylene chains must be approached cautiously.

In the liquid state the chain will be subject to less highly directed interchain force

**These considerations do not apply to the C—C stretching modes, for which the array folds back upon itself on the low wavenumber side. There may also be minor departures for the arrays terminating at 1295 cm^{-1} and 722 cm^{-1} which extend these limits to 1310 and 719 cm^{-1} respectively (3, 4).*

Can. J. Chem. Downloaded from www.nrcresearchpress.com by 210.87.254.42 on 09/05/12
For personal use only.

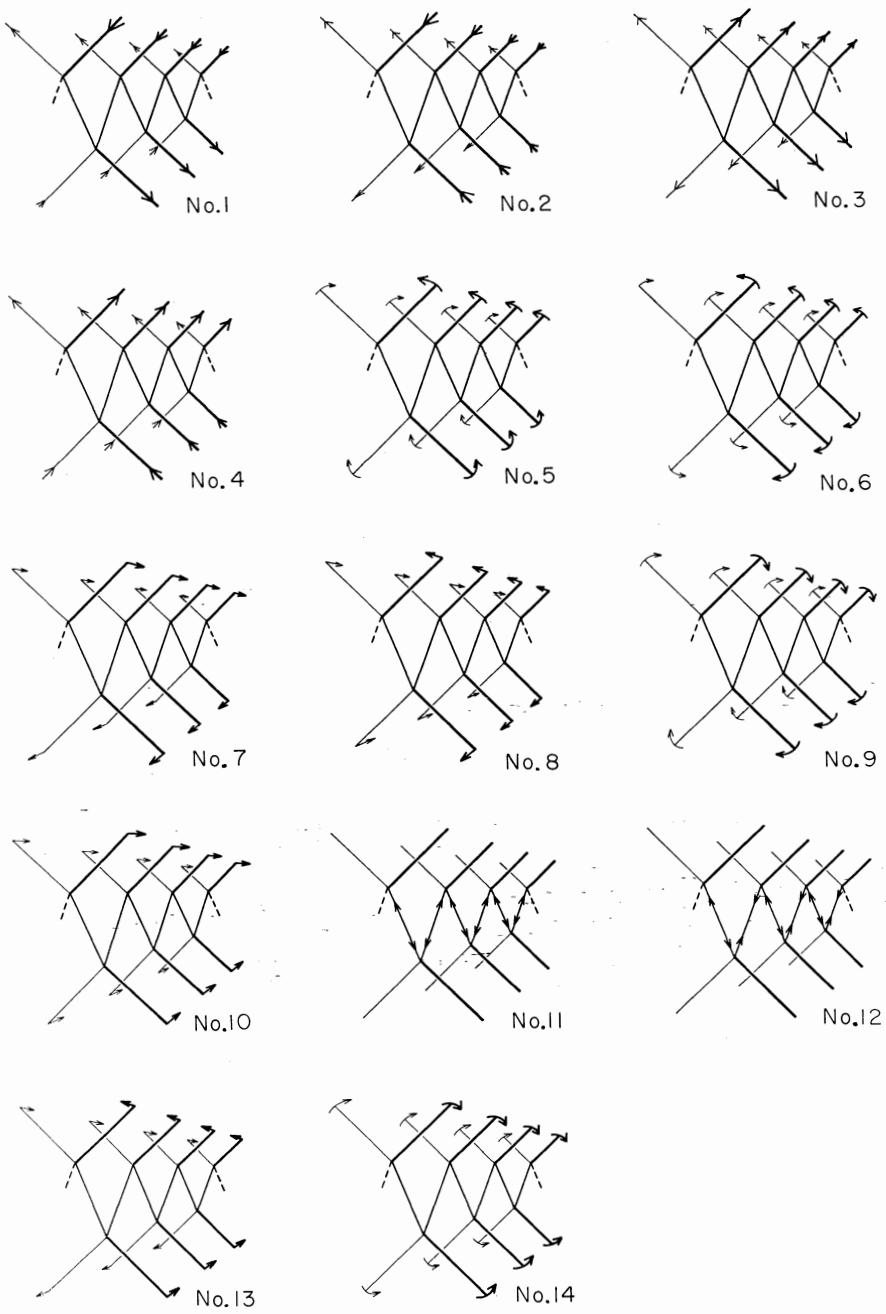

FIG. 2. Normal vibrations of an infinite polymethylene chain (the C—C bending vibrations are not included).

fields; the orientation will tend to randomize, and the vibrational frequencies, though less specific, should be more readily transferable among different types of compounds. Chain mobility in the liquid phase will permit nominal free rotation about C—C bonds, and bands characteristic of dimethylene units in gauche conformation may be observed (12, 13).

Can. J. Chem. Downloaded from www.nrcresearchpress.com by 210.87.254.42 on 09/05/12
For personal use only.

Thermodynamic considerations require that the trans linkages will predominate, and in general the gauche linkages will be randomly distributed along the chain. In some compounds, however, the statistical distribution of gauche-linked methylene groups in the chain may be determined by steric factors specific to the particular substance.*

In the liquid phase, it can be assumed that each trans-linked unit of the chain will vibrate approximately like an *n*-alkane methylene chain of the same length, and the vibrational frequencies will not be greatly affected by the nature of the terminal group, whether this be a gauche-linked methylene (I), a methyl group (II), or some other

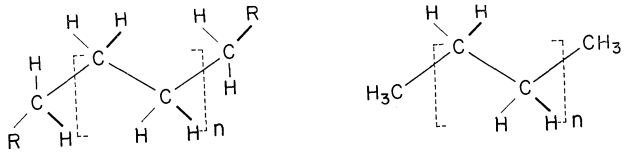

I II

terminating substituent. The total contribution of the methylene chain to the vibrational spectrum will be determined by the sum of the contributions of the trans-linked methylene chain units supplemented by the statistically weaker contributions from methylene groups in gauche conformations. Normally the contributions from gauche–gauche-linked trimethylene units will be statistically insignificant.†‡

Each trans-linked polymethylene chain section will contribute a set of bands to the vibrational pattern within each array, at positions determined by its chain length. The superposition of bands from chain units of different length will produce the broad band systems typical of polymethylene compounds in the liquid state. Within each array the major contributions will group around one or other of the peripheral regions, and will differ in the Raman and infrared spectra in accord with the selection rules applicable to the particular array. The sharpness or diffuseness of the band system will depend on the curvature of the array boundaries. Where these are narrow and steep (as for the scissoring modes Nos. 5 and 6 of Fig. 1) the envelopes will be sharp, and will be recognized as individual "bands".

Organic chemists will probably find it more useful to deal with the vibrational spectra of polymethylene compounds in these terms than in terms of isolated, oriented chains, and these considerations have prompted our interest in the spectra of the liquid phase systems. Previous publications from this laboratory have dealt with the infrared spectra of *n*-alkanes

Note, for example, that a terminal halogen atom may favor a gauche conformation for the adjacent methylene group in —$(CH_2)_n$—CH_2—X *(14).*

†*The chair form of cyclohexane provides an example of a molecule in which all the methylene groups are gauche linked, but the overall* D_{3h} *symmetry makes this unacceptable as a general case (15, 16).*

‡*The referee has noted that assuming a reasonable value of 0.5–0.8 kcal per mole for the energy difference between a pair of trans- and gauche-linked carbon atoms in a* C_4 *chain unit, it would be anticipated that a considerable number of gauche bonds will occur in the n-dodecane chain in the liquid state. While we recognize the validity of this argument, it must be kept in mind that the conversion of a C—C linkage near the center of the chain from trans to cis conformation will require considerable movement of the other trans-linked methylene groups of the molecule, and this will introduce an entropy term that will become increasingly important as the chain lengthens. The* B_{2u} *infrared active band at 721* cm^{-1} *requires the presence of a chain of at least four trans-linked methylene groups. The intensity of this band has been shown to increase linearly with the chain length for various types of polymethylene compounds, from which it can be inferred that, in the liquid state, such compounds exist predominantly in conformational sets in which at least four consecutive methylenes are trans linked.*

Considered in toto, both the Raman and infrared spectra of these compounds agree surprisingly well with the assignments based on the vibrational analysis of the all-trans methylene chain. The Raman band o near 1079 cm^{-1} *and the infrared triplet* ζ, η, *N near 1368, 1353, and 1340* cm^{-1} *are the only peaks that can be assigned with any degree of assurance to a non-trans conformation of methylene groups. Although this is conventionally regarded as "gauche" it may in fact be considerably distorted from the geometrical gauche configuration by interactions between neighboring non-bonded hydrogen atoms.*

Can. J. Chem. Downloaded from www.nrcresearchpress.com by 210.87.254.42 on 09/05/12
For personal use only.

in the liquid phase (17), and with the effect on the infrared spectrum of replacing one of the terminal methyl groups by a carbomethoxy group (18). In these investigations use has been made of selective deuteration and chlorination to distinguish the absorption of the main chain from that of the terminal substituents. It was also recognized that the α-methylene group adjacent to the carbomethoxy group is atypical, and esters specifically deuterated or chlorinated at this position were prepared.

The Raman spectra of a selection of these compounds (III–XI) have now been investigated; the object of this paper is to draw attention to the similarities and differences among these Raman and infrared spectra, and to consider the significance of these differences in evaluating the role of Raman spectroscopy in organic structural analysis.

III	CH_3—$(CH_2)_{10}$—CH_3	(X)*
IV	CD_3—$(CH_2)_{10}$—CD_3	(XII)
V	CH_3—$(CH_2)_9$—CH_2—$COOCH_3$	(II)
VI	CD_3—$(CH_2)_9$—CH_2—$COOCH_3$	(III)
VII	CH_3—$(CH_2)_9$—CD_2—$COOCH_3$	(IV)
VIII	CH_3—$(CH_2)_9$—CH_2—$COOCD_3$	(V)
IX	CD_3—$(CH_2)_9$—CD_2—$COOCH_3$	(VI)
X	CH_3—$(CH_2)_9$—CD_2—$COOCD_3$	(VIII)
XI	CD_3—$(CH_2)_9$—CD_2—$COOCD_3$	(IX)

EXPERIMENTAL

The compounds were provided by Isabelle and Leitch, and their preparation and characterization have been described previously (18, 19). The Raman spectra were measured on a Cary Model 81 Raman spectrophotometer using 4358 Å Hg irradiation, and capillary sample tubes of 1 mm internal diameter (20). Above 900 cm^{-1} the spectra were determined on solutions prepared by adding 1.5–2.0 millimoles of the compound to 0.25–0.3 millimoles of carbon tetrachloride; the spectra at lower wavenumbers were obtained on the pure liquid.† The wavenumber scale of the spectrometer was calibrated against the emission spectra of argon and neon, and a small systematic cam correction was applied; this nowhere exceeded 2 cm^{-1}. The band intensities were corrected for the spectral response of the photomultiplier tubes. The background slopes of the spectra were corrected by tangent constructions to the bases of the bands. The spectral slit width increased progressively from 4 cm^{-1} at 3000 cm^{-1} to 5 cm^{-1} at 459 cm^{-1}.

The band intensities were corrected for the mole fraction of carbon tetrachloride, and the peak height scattering coefficients relative to the CCl_4 band at 459 cm^{-1} were calculated, but these data are not considered accurate enough to warrant publication. The illustrative curves for the ester spectra have been normalized with respect to the peak height of the C=O stretching band at 1743 cm^{-1}, and since the intensity of this band is not likely to vary much in the series, it serves to put the spectra on a semiquantitative intensity basis adequate for comparison purposes.

Polarization data were obtained by the use of cylindrical Polaroid filters; the convergence errors of the source optical system were measured by the method of Rank and Kagarise (21) and corrections applied. The peak intensity depolarization ratios (ρ_{peak}) reported for the more highly polarized bands are averaged values for all the esters. The reproducibility of the band positions is ± 1 cm^{-1}, but various instrumental factors make it difficult to assess the absolute errors of these measurements. It is considered that these do not exceed ± 3 cm^{-1} and they will be discussed in more detail in a later publication dealing with the general aspects of the technique.

RESULTS AND DISCUSSION

The spectra are illustrated in Figs. 3–11, and the positions of the band maxima are reported in Tables II–IV. No comparisons are available for ester spectra, but the spectrum of *n*-dodecane agrees with the spectra published by earlier investigators (13, 22, 23).

**The structural formula numbers given in parenthesis provide cross reference to the paper on the infrared spectra (18).*

†To facilitate comparative discussion with the infrared spectra, band positions are expressed as wavenumbers, the displacement character of the Raman bands being implied, but not stated.

Can. J. Chem. Downloaded from www.nrcresearchpress.com by 210.87.254.42 on 09/05/12
For personal use only.

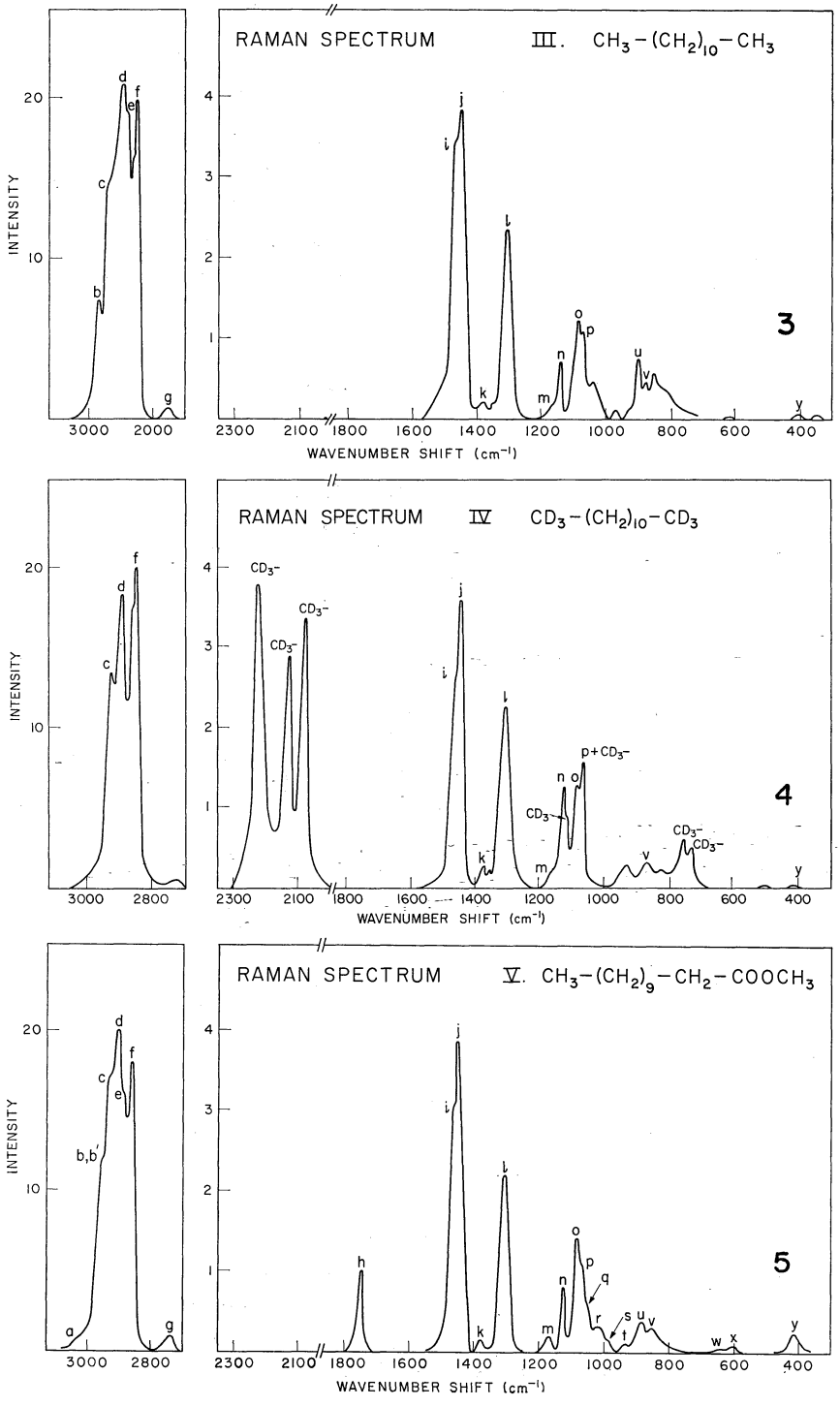

FIGS. 3–5.

Can. J. Chem. Downloaded from www.nrcresearchpress.com by 210.87.254.42 on 09/05/12
For personal use only.

Can. J. Chem. Downloaded from www.nrcresearchpress.com by 210.87.254.42 on 09/05/12
For personal use only.

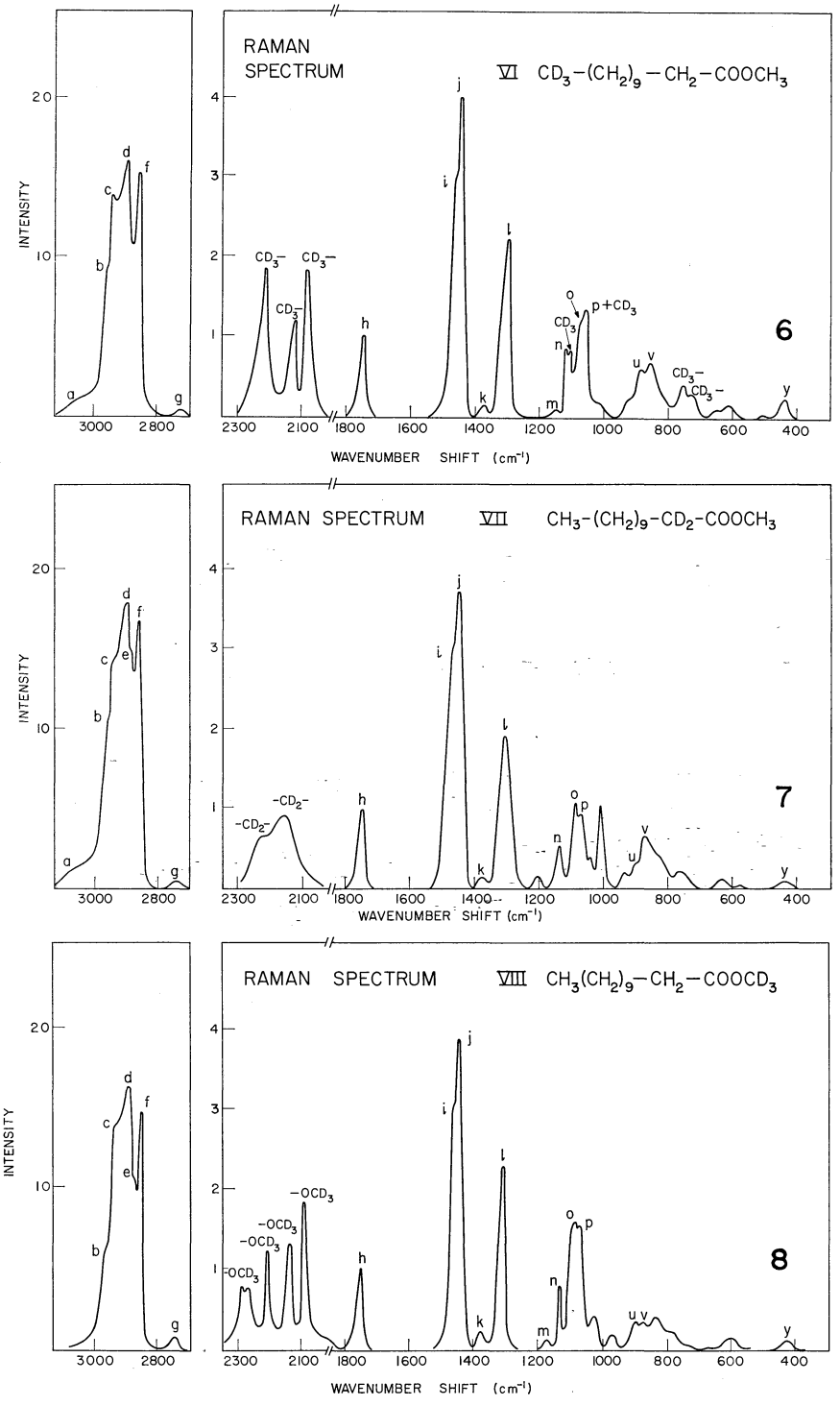

FIGS. 6–8.

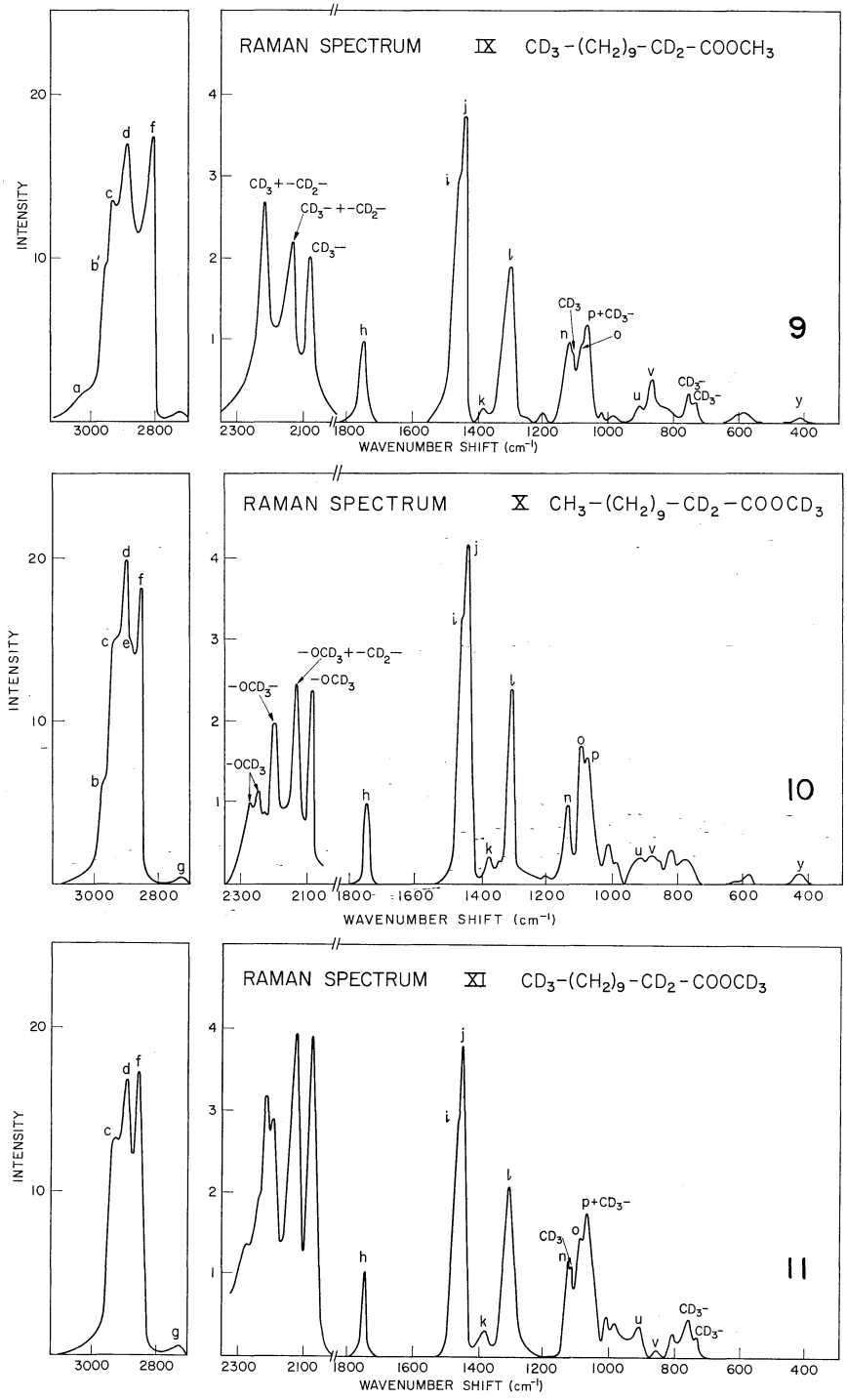

FIGS. 9–11.

Can. J. Chem. Downloaded from www.nrcresearchpress.com by 210.87.254.42 on 09/05/12
For personal use only.

TABLE II

Positions of Raman band maxima between (3100–2700 cm^{-1}) for methyl laurate and related compounds

Compound	Band maximum (cm^{-1})*								
	a	*b*	*b'*	*c*	*d*	*e*	—	*f*	*g*
III	—	2961	—	(2934)	2891	(2876)	(2858)	2849	2730
IV		—	—	2938	2893	—	(2862)	2851	2730
V	(3025†)	...(2948)...		(2928)	2893	(2876)	—	2850	2728
VI	(3025†)	(2950)	—	2929	2899	—	—	2852	2726
VII	(3025†)	...(2948)...		2933	2897	(2881)	—	2854	2730
VIII	—	(2956)	—	(2926)	2895	(2873)	—	2849	2730
IX	(3005†)	—	(2949)	2931	2895	—	—	2849	2730
X	—	(2958)	—	2929	2894	(2875)	—	2850	2730
XI	—	—	—	2927	2893	—	—	2850	2730
Polarization‡	—	—	—	—	p(w)	—	—	p(s)	—

*Inflections are indicated by parentheses.
†Broad band.
‡p(w), weakly polarized; p(s), strongly polarized.

Region 3100–2700 cm^{-1} (Bands a–g)

Structure characteristic of the methylene chain is best observed in the spectrum of the hexadeuterated dodecane (IV), shown in Fig. 4. The bands *c* and *f* at 2928 and 2851 cm^{-1} are obviously related to bands at 2926 and 2857 cm^{-1} in the infrared spectrum, but there is a strong additional Raman band *d* at 2891 cm^{-1}. A very weak infrared band near this position has been observed for *n*-alkanes of long chain length (17). A representative illustration of the polarized spectra is shown in Fig. 12; it indicates that band *f* is strongly polarized ($\rho_{peak} \sim 0.07$) and band *d* considerably less so ($\rho_{peak} \sim 0.4$).

The presence of a third strong band in this spectrum invalidates a simple explanation in terms of the two array patterns, each with one Raman and one infrared active edge, as suggested by Fig. 1. The positions of these array limits are in any case circumspect, since the array edges No. 1 and No. 3 are based only on normal coordinate calculations (4). For crystalline polyethylene Nielsen and Woollett (1) place the Raman active edges at 2883 and 2848 cm^{-1} respectively. This would reduce the symmetric array (Nos. 3–4) almost to a line, and reverse the direction of the antisymmetric array, putting the infrared active edge on the high wavenumber side. The identification of band *f* with the No. 3 array edge is consistent with the strong polarization of this band. Bernstein, however, regards bands *d* and *f* as resulting from Fermi resonance coupling between the No. 3 vibration and an overtone of the A_g scissoring mode (No. 6) (24), and Snyder and Schachtschneider speculate along similar lines (4). When these considerations are introduced, the commonly accepted assignment of the infrared band near 2850 cm^{-1} to a pure C—H stretching mode (No. 4) also becomes suspect. The same bands are clearly discerned in the spectra of the other compounds, and, in addition, all the compounds exhibit a weak Raman band *g* near 2730 cm^{-1} which may be a combination of No. 6 and No. 8 (A_g+B_{3g}), which is allowed.* A shoulder is observed at 2860 cm^{-1} in the Raman spectra of III and IV, but is not detected in the ester spectra.

Comparison of the Raman spectra of III and IV indicates that bands *b* and *e* of III at 2961 and 2876 cm^{-1} are associated with methyl vibrations and are assigned to antisymmetric and symmetric C—H stretching modes of the terminal methyl group. Band *e* is also present in the Raman spectra of V, VII, VIII, and X, but not in VI, IX, and XI.

**The forbidden Raman and infrared combination and overtone bands associated with V_h symmetry have been conveniently summarized by Cleveland (25).*

Can. J. Chem. Downloaded from www.nrcresearchpress.com by 210.87.254.42 on 09/05/12
For personal use only.

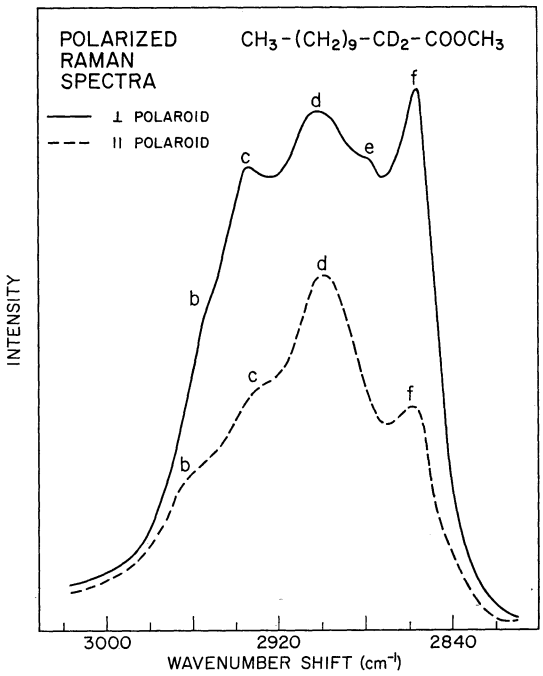

FIG. 12. Raman spectra of VII in the C—H stretching region obtained with polarized radiation. — Exciting radiation polarized transversely to the direction of observation. --- Exciting radiation polarized parallel. These curves are not corrected for convergence errors.

It disappears in the spectra measured through a parallel-oriented polarizer (Fig. 12), which suggests that it is strongly polarized, as expected for an A_1 vibration. Band *b* is displaced to 2956–2940 cm^{-1} in the ester spectra, and reduced to an inflection. Comparison among the ester spectra suggests that the carbomethoxy methyl contributes a weaker band (*b'*) at a lower wavenumber than the terminal methyl band *b*. Compounds containing —$COOCH_3$ also exhibit a prolongation of the —C—H stretching band envelope above 3000 cm^{-1}, suggestive of additional unresolved structure (band *a*). This is consistent with more clearly delineated structure in the infrared spectra.

Region 2300–2050 cm^{-1} (C—D Stretching Bands)

Compounds containing no deuterium exhibit no Raman bands in this region. The bands of the other compounds are presumed to involve C—D stretching motions and are listed in Table III. Bands associated with CD_3—, α—CD_2—, and —$COOCD_3$ are best illustrated in the spectra of IV, VII, and VIII respectively (Figs. 4, 7, 8).

The infrared and Raman spectra associated with CD_3— occur at the same positions within experimental error. In both spectra there are three bands, that at the highest wavenumber is depolarized and more intense than the other two. The two at lower wavenumber are both strongly polarized (ρ_{peak} ~0.1). The upper band is the antisymmetric C—D stretching vibration and the lower pair probably result from a Fermi resonance splitting of the symmetric mode. Bands associated with C—D deformation vibrations occur in the ranges 1115–1100 cm^{-1} and 1065–1054 cm^{-1} in both the infrared and Raman spectra (*vide infra*) and the overtone and combination bands of these vibrations will be suitably located to participate in the resonance. Similar splitting has been noted by Noether (26) in the Raman spectrum of $CD_3.OD$.

Can. J. Chem. Downloaded from www.nrcresearchpress.com by 210.87.254.42 on 09/05/12
For personal use only.

TABLE III

Positions of Raman band maxima between 2300 and 2050 cm^{-1} for compounds containing deuterium

	Band maximum (cm^{-1})*									
	$-OCD_3$	$-OCD_3$	$-CD_2-$	CD_3-	$-OCD_3$	$-OCD_3$	CD_3-	$-CD_2-$	$-OCD_3$	CD_3-
IV	—	—	—	2216	—	—	2124	—	—	2072
VI	—	—	—	2216	—	—	2121	—	—	2074
VII	—	—	2228	—	—	—	—	2144	—	—
VIII	2277	2252	—	—	2194	2126	—	—	2080	—
IX	—	—	—	2216	—	—	2126	—	—	2075
X	2266	2246	2230	—	2196	2125	—	—	2080	—
XI	2272	2246	—	2215	2196	...2124....		—	....2076....	
Polarization*	dp	dp	dp	dp	p(s)	p(s)	p(s)	p(s)	p(s)	p(s)

*dp, depolarized; p(s), strongly polarized.

Can. J. Chem. Downloaded from www.nrcresearchpress.com by 210.87.254.42 on 09/05/12
For personal use only.

The α-CD_2— group of VII produces two weak bands at 2228 and 2144 cm^{-1} the upper of which is depolarized (ρ_{peak} ~0.78) and the lower polarized (ρ_{peak} ~0.2). There is no evidence of the third weak band at 2312 cm^{-1} seen in the infrared spectrum. The upper and lower bands of the Raman active pair can be reasonably assigned to the antisymmetric and symmetric C—D stretching modes respectively.

As in the infrared spectra, the —$COOCD_3$ group of VIII yields a complex group of five bands at 2277, 2252, 2194, 2126, and 2075 cm^{-1} the lower three of which are very strongly polarized (ρ_{peak} ~0.1) and the two upper depolarized (ρ_{peak} ~0.8). Since the deuterium exchange in these compounds is not complete, some —$COOCD_2H$ could be present, and could conceivably account for the weaker bands at 2277 and 2252 cm^{-1}. Alternatively, splitting of the degeneracy of the asymmetric —OCD_3 stretching mode in a planar structure could explain the increase in the number of bands, as has been suggested to account for the analogous bands of —$COOCH_3$ at 2995 cm^{-1} and above (18, 27).

The Raman spectra of the compounds containing more than one deuterium-substituted group are consistent with simple additivity. The polarized spectrum of XI is shown in Fig. 13 and illustrates the polarization differences among these bands. In particular this

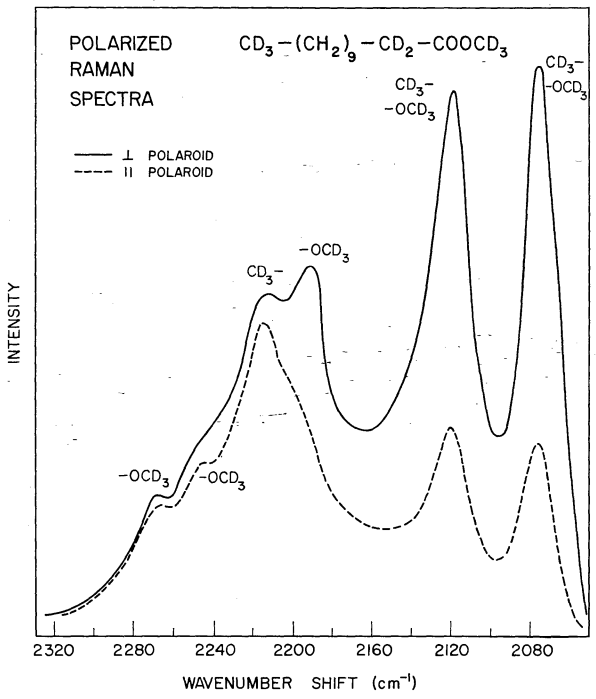

FIG. 13. Raman spectra of XI in the C—D stretching region. Experimental conditions as for Fig. 12.

diagram emphasizes the difference in the polarization characteristics of the CD_3— band at 2215 cm^{-1} and the —$COOCD_3$ band at 2196 cm^{-1}.

Region 1745–1740 cm^{-1} (Band h)

The C=O stretching band *h* in the ester spectra occurs in the range 1743–1740 cm^{-1}. It is strongly polarized (ρ_{peak} ~0.15) and relatively weaker in the Raman than the infrared spectra. The infrared band shifts appreciably from 1742 cm^{-1} to 1739 cm^{-1} on substitution

Can. J. Chem. Downloaded from www.nrcresearchpress.com by 210.87.254.42 on 09/05/12
For personal use only.

Can. J. Chem. Downloaded from www.nrcresearchpress.com by 210.87.254.42 on 09/05/12
For personal use only.

TABLE IV

Positions of Raman maxima below 2000 cm^{-1} for methyl laurate and related compounds

Compound	Band maximum (cm^{-1})*																			
	h	*i*	*j*	*k*	*l*	*m*	*n*	(CD_3—)	*o*	*p*	*u*	*v*	(CD_3—)	(CD_3—)	*y*	Other bands‡				
III	—	(1455)	1441	1371	1302	(1159)	1134	—	1081	1067	895	874	—	—	410 (1344)	1040	965	(920)	(811)	(620)	(360)
IV	—	(1455)	1440	1369	1303	(1152)	1122	(1113)	1079	1060†	—	865	751	729	(420)	1347	920	(820)	500		
V	1740	(1455)	1440	1368	1302	1160	1122	—	1079	(1064)	881	851	—	—	435	1030(*q*); 1014(*r*); (975(*s*)); 930(*t*) 650(*w*); 612(*x*) 350, 225					
VI	1741	(1455)	1442	1367	1303	1143	1116	1103	(1077)	1063†	886	855	751	732	435	(1025)	(930)	650	615	(510)	
VII	1743	(1455)	1441	1371	1303	—	1128	—	1082	1065	892	864	—	—	410	1005(*p*)	930	(830)	760	630	580
VIII	1742	(1455)	1440	1371	1301	1166	1124	—	1082	1068	896	871	—	—	420	1020	965	840	780	(720)	605
IX	1743	(1455)	1442	1372	1303	—	1122	(1112)	(1082)	1065†	902	863	750	730	(430)	1014	(826)	755	(602)	585	
X	1742	(1455)	1441	1370	1303	—	1127	—	1081	1064	894	870	—	—	410 (1342)	1002(*p*)	850	810	765	(635)	575
XI	1740	(1455)	1441	1368	1301	—	1119	1109	1081	1061†	905	850	752	730	—	1005(*p*)	905	805	750	(730)	
Polarization	p(s)	—	dp	dp(?)	(pw)	—	p(w)	—	p(w)	p(w)	—	—	dp or p(w)	dp or p(w)							

*Inflections are indicated by parentheses.
†Intensified by contribution from CD_3— group.
‡Some of these bands are weak and ill defined.

of —$COOCD_3$ for —$COOCH_3$. The failure to observe this displacement in the Raman spectra may not be significant, as the Raman bands are measured at a wider slit width and the determination of the exact peak position is less certain.

Region 1500–1290 cm^{-1} (Bands i–l)

Vibrations associated with the methylene scissoring array occur between 1475 and 1440 cm^{-1}; the infrared active peripheral mode No. 5 is observed at 1467 cm^{-1}, superimposed on methyl absorption (17, 18). This infrared band evelope is asymmetric, rising steeply on the high wavenumber side and falling less steeply to lower wavenumbers, where it shows evidence of partly resolved structure (cf. Fig. 9 of reference 17). The slow fall off may be due to contributions from less strongly infrared active modes within the scissoring array, and from scissoring modes of gauche-linked methylene units.* The Raman spectra of *n*-dodecane and the methyl laurates exhibit a strong band envelope with maximum near 1440 cm^{-1} (band *j*) and opposite skewness, rising sharply on the low wavenumber side and trailing at higher wavenumbers with an inflection (band *i*) near 1456 cm^{-1}. This pattern is consistent with the assignment of band *j* to the low wavenumber edge of the scissoring array, viz. the Raman active vibration No. 6 of Fig. 1, accompanied by diminishing contributions from other coupled scissoring modes of lesser Raman activity. It is to be noted, however, that the No. 6 vibration has A_g symmetry so that the Raman band should be polarized. In fact, the observed band can be polarized only slightly, if at all, the values obtained for ρ_{peak} range between 0.73 and 0.85. The inflection near 1456 cm^{-1} may be due in part to the antisymmetric C—H deformation vibration of the methyl group, but this cannot be the full explanation, since the band is retained with diminished intensity in the Raman spectra of IV, VI, and IX. Scissoring modes of methylene groups in gauche conformation may also be contributing.

In the infrared spectra of the methyl esters there is a prominent band at 1436 cm^{-1}, which is associated with the carbomethoxy group, and has been assigned to the symmetric C—H bending mode. There is no indication of any similar band in the Raman spectra, thus the spectra of V and VIII and of IX and X show no differences in this region. Assuming C_{3v} symmetry for the internal motions of the methyl group this band should be allowed in the Raman spectrum as well as in the infrared, and the failure to observe it will be further considered in the concluding part of this paper.

According to Nielsen and Woollett (1), the Raman active edge of the methylene wagging array occurs at 1415 cm^{-1} in polyethylene, but we have failed to observe any band near this position in these dodecane and ester spectra, nor is such a band recorded in the *n*-alkane spectra published by Mizushima and Shimanouchi (12, 13) or by Rea (23). It must therefore be extremely weak, and it is difficult to accept it as a Raman active fundamental. If the 1415 cm^{-1} band is rejected, the alternative would be to assign the Raman active (B_{2g}) edge of the wagging array to band *k*, which is observed at 1369 cm^{-1} in IV and in the range 1367–1373 cm^{-1} in the other spectra. Though measurement of the depolarization ratio was not practical, this band appears by inspection to be depolarized. A band at 1367 cm^{-1} in the infrared spectrum of polyethylene has been intensively investigated by Nielsen and Holland (28), who rejected its assignment to the B_{1u} infrared active wagging mode. We might note also that Snyder and Schachtschneider failed to observe any infrared components of the methylene wagging array of *n*-alkanes above the 1370's and we would prefer to regard the 1415 cm^{-1} location of the upper end of the wagging array as *sub judice* until more positive Raman evidence for the extension of this

**The gauche-linked methylene groups of cyclohexane have infrared active scissoring vibrations at 1453 cm^{-1} (15, 16).*

Can. J. Chem. Downloaded from www.nrcresearchpress.com by 210.87.254.42 on 09/05/12
For personal use only.

array above 1375 cm^{-1} is forthcoming. It is also relevant to note that the Raman spectra of III and IV are quite similar in the region of 1375 cm^{-1} and there is no indication of any contribution from the symmetric C—H deformation vibration of the terminal methyl groups of III, either as a distinctive group vibration, or in coupling with the wagging mode as is preferred by Snyder and Schachtschneider (3). Very weak and incompletely resolved structure between 1355 and 1340 cm^{-1} is observed in the Raman spectra of III, IV, and X which may be associated with wagging modes of gauche-linked methylene groups (cf. reference 28).

All the Raman spectra exhibit a strong largely depolarized band *l* at 1303–1301 cm^{-1} (ρ_{peak} ~0.7) which is identified with the high wavenumber edge of the twist–rock array. The peripheral band corresponds approximately with the pure twist mode No. 8 of Fig. 1. Snyder and Schachtschneider conclude from their normal coordinate analysis (4) that the arrays terminating at 1295–1175 cm^{-1} and 1063–722 cm^{-1} both involve combinations of rocking and twisting motions and, in good approximation, can be regarded as pure twisting modes at the high wavenumber edges and rocking modes at the low edges.* This constitutes the major departure of Snyder and Schachtschneider's analytical treatment from the vibrational patterns for polymethylene chains proposed by Sheppard (8), Krimm (29), Lin and Koenig (2), and other prior investigators.

Though the No. 8 twist vibration is forbidden in the infrared spectrum, a weak band at 1305–1300 cm^{-1} invariably appears in the infrared spectra of polymethylene compounds (17). Nielsen and Woollett assign this to the amorphous component of polyethylene, and, by inference, to a vibration of a gauche conformer. However, it always appears in the spectra of crystalline *n*-alkanes (12, 13) and could be a twist–rock vibration of a trans form arising under conditions where the selection rules break down.

Region 1290–1140 cm^{-1} (Band m)

The infrared spectrum of methyl laurate exhibits three strong absorption bands at 1245, 1196, and 1169 cm^{-1}. These are commonly designated "C—O stretching bands", but in fact involve coupled vibrational modes extending through the —CH_2—$COOCH_3$ "zone" of the molecule (18); they are the most characteristic feature of this structural unit in the whole infrared spectrum. The Raman spectrum of methyl laurate is singularly empty between 1290 and 1140 cm^{-1}. The esters V, VI, and VIII exhibit only a single weak band *m* between 1160 and 1140 cm^{-1}, which could be assigned to the Raman active B_{1g} rocking end of the twist–rock array (No. 9), though it is extremely weak. The esters VII, IX, and X, which contain a —CD_2— group possess a weak band at 1201–1190 cm^{-1}.

The failure to observe any Raman bands that can be specifically associated with the —CH_2—$COOCH_3$ structure in this region of the spectrum is one of the most notable distinctions between the Raman and infrared spectra of these esters. Since this structural unit has low symmetry the absence of these Raman bands does not result from the operation of selection rules and must stem from the low polarizability characteristics of the bonds involved.

Region 1140–1100 cm^{-1} (Band n)

A prominent, weakly polarized Raman band *n* (ρ_{peak} ~0.4) occurs at 1134 cm^{-1} in III, displaced to 1122 cm^{-1} in IV. In the esters containing the CH_3—$(CH_2)_9$— chain it occurs at 1127–1122 cm^{-1} and is displaced to lower wavenumber by a terminal CD_3—

**More precisely the pure twist vibration No. 8 occurs at 1295 cm^{-1} for a —$(CH_2)_{18}$ chain on the basis of Snyder and Schachtschneider's analysis, and the peripheral modes extend to 1310 cm^{-1} with a small rocking component. This rocking component reappears below 1295 cm^{-1} and becomes increasingly prominent at lower wavenumber. The low wavenumber edge is a pure No. 9 vibration.*

Can. J. Chem. Downloaded from www.nrcresearchpress.com by 210.87.254.42 on 09/05/12
For personal use only.

group. This is presumably the high wavenumber edge of the C—C skeletal array (No. 11 of Fig. 1) coupled weakly with terminal group vibrations.* In the infrared spectra, band S occurs in the same general region of the spectrum (18) and is displaced similarly to band *n* by change in the terminal group. In most of the compounds band S occurs some 8–10 cm^{-1} below band *n*. This is outside the experimental error; it is therefore not likely that the same vibration is involved though they may represent different modal combinations within the same array. The No. 11 skeletal vibration is infrared inactive though it may pick up infrared activity by coupling with the methyl rocking modes (4).

The esters VI, IX, and XI contain a terminal CD_3— group, and exhibit an additional weak band at 1109–1103 cm^{-1} which also occurs as an inflection in IV; it is presumably the antisymmetric C—D deformation mode and is also observed in the infrared spectra.

Region 1090–1050 cm^{-1} (Bands o, p)

n-Dodecane exhibits a moderately strong Raman band *o* at 1081 cm^{-1} and a weaker band *p* at 1067 cm^{-1}, both of which are slightly polarized (ρ_{peak} ~0.7); similar bands occur in the spectra of V, VII, VIII, and X. Deuteration of the terminal methyl group in IV, VI, and IX causes the relative intensities of the two peaks to invert. A band at the same position is observed in the liquid phase infrared spectra (17, 18). Band *o* does not occur in the Raman spectra of crystalline *n*-alkanes (12, 13), and Nielsen and Woollett (1) assign absorption at 1077 cm^{-1} in the infrared spectrum of polyethylene to the amorphous fraction, and attribute it to a C—C skeletal mode. If this band is a C—C skeletal mode associated with a gauche-linked chain, it constitutes the most prominent feature of the gauche conformer in the whole spectrum.

Band *p* is well recognized in the Raman spectra of polymethylene chains, and has been assigned by Nielsen and Woollett to a skeletal stretching vibration. In terms of Fig. 1 this would be the B_{2g} vibration, No. 12 of Fig. 2.† Snyder and Schachtschneider also locate the upper end of the second twist–rock array at 1063 cm^{-1}, but this vibration (No. 13 of Fig. 1) should be inactive in both the infrared and Raman spectra. The observed Raman band *p* is more probably the skeletal band, and the fact that band *p* is appreciably less polarized than band *n* supports Snyder and Schachtschneider's assignment of the higher frequency to the more symmetric A_g mode.

The intensification of the 1068 cm^{-1} band on replacement of the terminal CH_3— by CD_3— suggests the superposition by a CD_3— band.

Region Below 1050 cm^{-1} (Bands q–y)

The Raman spectra of these compounds are weak at the lower wavenumbers, and the band positions are variable. All show weak irregular structure between 1050 and 920 cm^{-1}. Compounds VII and XI possess a more prominent polarized band at 1005 cm^{-1} which could involve the —CD_2— group, though it is not observed in IX.

Most of the Raman spectra possess two bands in the ranges 909–883 and 875–859 cm^{-1} (bands *u* and *v*). Band *u* is consistent with Brown, Sheppard, and Simpson's identification of a Raman active band near 890 cm^{-1} in *n*-alkanes (7), which they assign to a C—C skeletal vibration coupled with a methyl rock. Band *u* is absent from the Raman spectrum of IV, supporting its association with a methyl group.‡ Band *v* is present in the spectrum

**In the Raman spectrum of CCl_3—$(CH_2)_9$—$COOCH_3$ this band occurs at 1106 cm^{-1}, which gives some indication of the extent to which it is displaced by coupling with the terminal methyl rocking vibration.*

†Note that Liang, Sutherland, and Krimm (30) and Nielsen and Woollett (1) assigned the peripheral vibrations of the C—C skeletal array of Fig. 1 in the reverse sequence, with the B_{2g} mode at the upper end and the A_g mode at the lower. Tasumi, Shimanouchi, and Miyazawa's assignments (5) agree with those of Snyder and Schachtschneider.

‡Absorption in the infrared at 875 and 845 cm^{-1} has been associated with the —$COOCH_3$ group (18). If these vibrations are Raman active they will complicate the interpretation of this region of the spectrum.

Can. J. Chem. Downloaded from www.nrcresearchpress.com by 210.87.254.42 on 09/05/12
For personal use only.

of IV, but is not seen in the Raman spectra of crystalline *n*-alkanes (12, 13), and Sheppard and Simpson have assigned it to a skeletal vibration involving gauche-linked methylene groups (6). These authors note a similar Raman band between 840 and 810 cm^{-1} for liquid *n*-alkanes, and this also is present in most of our spectra (band *w*). Bands *u*, *v*, and *w* should all be polarized (6) but they appear too weakly in our spectra to establish this.

Compounds containing a terminal CD_3— group all possess a pair of characteristic bands at 753 and 726 cm^{-1} which probably involve CD_3— rocking vibrations. The other compounds exhibit only weak ill-defined bands below 750 cm^{-1}. In most of the spectra there is some evidence of structure between 650 and 600 cm^{-1} and a better defined band is present in the range 430–400 cm^{-1}; this is presumably associated with a C—C—C bending mode. The rocking vibration (No. 14) which delineates the low wavenumber end of the lower twist–rock array at 719 cm^{-1} is not detected in the Raman spectra.

CONCLUSIONS

In Table V the assignments for both the infrared and the Raman bands of methyl laurate are summarized, and the characteristic vibrations of the deuterated substituent groups are listed in Table VI. Most details of the spectra can be rationally interpreted in terms of previous theoretical and experimental studies on simpler molecules, though some features call for comment since they have more general implications.

TABLE VI

Characteristic vibration frequencies associated with groups containing deuterium atoms

Infrared spectrum*		Raman spectrum	
Terminal CD_3— group			
2212	Asym. C—D stretch	2216	Asym. C—D stretch
2120\	Sym. C—D stretch split	2124\	Sym. C—D stretch split
2077/	by Fermi resonance	2074/	by Fermi resonance
1115	Asym. C—D bend	1109–1103	Asym. C—D bend
1054	Sym. C—D bend	1065 (?)	Sym. C—D bend?
		753	CD_3— rock?
		726	CD_3— rock?
684	CD_3— rock?		
656	CD_3— rock?		
(α)—CD_2— group			
2312	—		
2220	Asym. C—D stretch	2228	Asym. C—D stretch
2150	Sym. C—D stretch	2144	Sym. C—D stretch
1008 ?	—	1005 ?	—
—$COOCD_3$ group			
2272	—	2277	—
2250	—	2250	—
2195	—	2195	—
2125\	Sym. C—D stretch split	2125\	Sym. C—D stretch split
2080/	by Fermi resonance?	2080/	by Fermi resonance?
1087	Asym. C—D deformation?		

*See reference (17).

The intense Raman band *d* in the C—H stretching region is difficult to reconcile with a fundamental vibration, and suggests that the conventional analysis of this part of the spectrum in terms of antisymmetric and symmetric C—H stretching vibrations may be an oversimplification; Fermi resonance with overtones and combination tones of the scissoring deformation modes may play a larger part in these spectra than has generally been recognized. The almost complete depolarization of the Raman band *j* at 1440 cm^{-1} is

Can. J. Chem. Downloaded from www.nrcresearchpress.com by 210.87.254.42 on 09/05/12
For personal use only.

Can. J. Chem. Downloaded from www.nrcresearchpress.com by 210.87.254.42 on 09/05/12
For personal use only.

TABLE V

Summary of band assignments for methyl laurate

Infrared*					Raman					
Band	Position (cm^{-1})	Group	Symmetry	Mode	Band	Position (cm^{-1})	Polarization†	Group	Symmetry	Mode
					a	(3025)	—	$—COOCH_3$		asym. C—H stretch
A	(3020)	$—COOCH_3$		asym. C—H stretch						
B	2995	$—COOCH_3$		asym. C—H stretch						
α	2995	$—COOCH_3$		sym. C—H stretch			—	$—COOCH_3$		sym. C—H stretch
					b, *b'*	2950‡				
C	2950	$CH_3—$		asym. C—H stretch			—	$—CH_3$		asym. C—H stretch
					c	(2928)	—	$—(CH_2)_9—$	B_{1g}	asym. C—H stretch
D	2922	$—(CH_2)_9—$	B_{2u}	asym. C—H stretch						
					d	2893	p(w)	$—(CH_2)_9—$	—	Fermi res.§
					e	(2876)	p(s)?	$CH_3—$		sym. C—H stretch
E	(2870)	$CH_3—$		sym. C—H stretch						
F	2852	$—(CH_2)_9—$	B_{3u}	sym. C—H stretch	*f*	2850	p(s)	$—(CH_2)_9—$	A_g	sym. C—H stretch
					g	2730	—	$—(CH_2)_9$	—	Combination band§
G	1742	$—COOCH_3$		C=O stretch						
					h	1740	p(s)	$—COOCH_3$	—	C=O stretch
		$—(CH_2)_9—$	B_{3u}	C—H scissor						
H	1467	$CH_3—$		asym. C—H bend						
I	1458	$—COOCH_3$		asym. C—H bend				$CH_3—$		asym. C—H bend
					i	(1455)	—	$—(CH_2)_9—$(gauche)		C—H scissor
					j	1440	dp‖	$—(CH_2)_9—$	$A_g(\epsilon)$	C—H scissor
ϵ	1440	$—(CH_2)_9—$(gauche)		C—H scissor						
J	1436	$—COOCH_3$		sym. C—H bend						
K	1419	$—CH_2—COOCH_3$		CH_2 scissor						
L	1378	$CH_3—$		sym. C—H bend						
ζ	1368	$—(CH_2)_9—$		C—H twist or wag	*k*	1368	dp(?)	$—(CH_2)_9—$	B_{2g}(?)	C—H wag (?)
M	1362	$—CH_2—COOCH_3$		CH_2 wag						
η	1352	$—(CH_2)_9—$(gauche)		CH_2 wag (?)						
N	(1340)	$—(CH_2)_9—$(gauche)		CH_2 wag (?)						
O	(1305)	$—(CH_2)_9—$		CH_2 twist (or wag?)						
						1302	p(w)	$—(CH_2)_9—$	B_{3g}	C—H twist

Can. J. Chem. Downloaded from www.nrcresearchpress.com by 210.87.254.42 on 09/05/12
For personal use only.

Infrared*					Raman					
Band	Position (cm^{-1})	Group	Symmetry	Mode	Band	Position (cm^{-1})	Polarization†	Group	Symmetry	Mode
P	1245	$—CH_2—COOCH_3$		C—O skeletal coupled with CH_2 deformation						
Q	1196	$—CH_2—COOCH_3$		C—O skeletal coupled with CH_2 deformation						
R	1169	$—CH_2—COOCH_3$		C—O skeletal coupled with CH_2 deformation						
					m	1160	—	$—(CH_2)_9—$	B_{1g}(?)	C—H wag
					n	1122	p(w)	$—(CH_2)_9—$	A_g	C—C skeletal stretch coupled with end groups
S	1112	$—(CH_2)_9—$		C—C skeletal stretch coupled with end group						
					o	1079	p(w)	$—(CH_2)_9—$gauche		C—C skeletal stretch
T	1074	$—(CH_2)_9—$		C—C skeletal stretch						
					p	1064	p(w)	$—(CH_2)_9—$	B_{2g}	C—C skeletal stretch
U	1016	$—CH_2—COOCH_3$		C—O skeletal stretch coupled with CH_2 deformation						
					u	881	—	$—(CH_2)_9—$		C—C skeletal stretch coupled with end group
V	875	$—COOCH_3$		Methyl rock?	*v*	851	—	$—(CH_2)_9—$gauche		C—C skeletal stretch
W	845	$—COOCH_3$		Methyl rock?						
X	755	$—(CH_2)_9—$		C—H rock						
Y	721	$—(CH_2)_9—$	B_{2u}	C—H rock						
					y	435	—	$—(CH_2)_9—$		C—C—C bending

*Based on data in reference (18).
†p(w), weakly polarized; p(s), strongly polarized; dp, depolarized.
‡These bands were not separately resolved.
§For discussion of assignments see text.
‖See text.

unexpected, and is difficult to reconcile with the A_g edge of the methylene scissoring array to which other evidence points as the correct assignment of this band. The location of the high wavenumber edge of the B_{2g} wagging array in the 1415–1350 cm^{-1} range still remains to be positively established.

From the point of view of the organic chemist, the comparison of the Raman and infrared spectra of these compounds emphasizes that selection rules based on symmetry are inadequate to account for relative intensities in the two types of vibrational spectra. The introduction of strongly polarized bonds into an alicyclic or aliphatic molecule has a profound effect on the infrared spectrum, and, in the presence of such polar substituents, it becomes increasingly difficult to detect small changes in the purely hydrocarbon parts of the molecule (cf. Figs. 2, 3 of reference (31)). In the infrared spectrum of methyl laurate bands J, P, Q, and R are prominently associated with the carbomethoxy group, but they are not detected in the Raman spectrum. On the other hand we observe a Raman band profile extending from 1200 to 800 cm^{-1} which is characteristic of the aliphatic chain, and which is absent from the infrared spectrum or totally obscured by the strong absorption centered in the carbomethoxy group.

This distinction is a general one, thus it has been observed that the strongly infrared active "amide II" band of N-methyl acetamide is extremely weak in the Raman spectrum (32). Regions of the infrared spectra of carboxylic acids and of monosaccharides that are dominated by broad absorption bands associated with hydrogen bonds exhibit Raman structure characteristic of the alicyclic or aliphatic parts of the molecule because the hydroxyl vibrations are only weakly active. There are also indications that the Raman spectra of steroids are more sensitive than the infrared spectra to conformational and other stereochemical differences in the ring system for a similar reason.

In none of these cases is it plausible to attribute the weakness of the Raman bands to the operation of selection rules based on symmetry. In these complex compounds we are dealing with vibrating molecular systems that are grossly asymmetric, but they are systems in which the bonds are strongly polarized at their equilibrium lengths. The vibrational motions of the polar bonds will induce the large dipole moment changes required for intense infrared absorption, but the weak Raman scattering indicates that the change in the bond polarizabilities during the vibrations are small. This characteristic of polarized bonds was recognized by the early investigators of the Raman effect, and has been discussed in a more theoretical context by Placzek (33), Volkenstein and Elyashevich (34), Edgell (35), and Shorygin (36), among others. Although early attempts were made to use this effect in the structural analysis of complex molecules (37, 38) it was not pursued and should be more extensively investigated.

When the current technical problems associated with the routine measurement of Raman spectra are overcome, the organic chemist will acquire structural information that he cannot now obtain from the infrared spectra alone. From the more fundamental work on small molecules, we know that neither the Raman nor the infrared spectrum can by itself provide a complete picture of the vibrating system. To do this, both techniques must be employed, and, at a more empirical level, the same is also true for more complex organic compounds.

ACKNOWLEDGMENTS

We are grateful for the opportunity of discussing certain aspects of these spectra with H. J. Bernstein and N. Sheppard.

Can. J. Chem. Downloaded from www.nrcresearchpress.com by 210.87.254.42 on 09/05/12
For personal use only.

Can. J. Chem. Downloaded from www.nrcresearchpress.com by 210.87.254.42 on 09/05/12
For personal use only.

REFERENCES

1. J. R. NIELSEN and A. H. WOOLLETT. J. Chem. Phys. **26**, 1391 (1957).
2. TUNG PO LIN and K. L. KOENIG. J. Mol. Spectr. **9**, 228 (1962).
3. R. G. SNYDER and J. H. SCHACHTSCHNEIDER. Spectrochim. Acta, **19**, 85 (1963).
4. J. H. SCHACHTSCHNEIDER and R. G. SNYDER. Spectrochim. Acta, **19**, 117 (1963).
5. M. TASUMI, T. SHIMANOUCHI, and T. MIYAZAWA. J. Mol. Spectr. **9**, 261 (1962).
6. N. SHEPPARD and D. M. SIMPSON. Quart. Rev. (London), **7**, 19 (1953).
7. J. K. BROWN, N. SHEPPARD, and D. M. SIMPSON. Phil. Trans. Roy. Soc. (London), A, **247**, 35 (1954).
8. N. SHEPPARD. Advances in spectroscopy. Vol. 1. *Edited by* H. W. Thompson. Interscience Publishers, Inc., New York, London. 1959. pp. 288–353.
9. R. G. SINCLAIR, A. F. MCKAY, and R. N. JONES. J. Am. Chem. Soc. **74**, 2570 (1952).
10. E. VON SYDOW. Acta Chem. Scand. **9**, 1119 (1955).
11. D. CHAPMAN. Chem. Rev. **62**, 433 (1962).
12. T. SHIMANOUCHI and S. MIZUSHIMA. Sci. Papers. Inst. Phys. Chem. Res. (Tokyo), **40**, 467 (1943).
13. S. MIZUSHIMA. Structure of molecules and internal rotation. Academic Press Inc., New York. 1954. pp. 103–111.
14. J. K. BROWN and N. SHEPPARD. Proc. Roy. Soc. (London), A, **231**, 555 (1954).
15. M. LARNAUDIE. J. Phys. Radium, **15**, 365 (1954).
16. J. LECOMTE. Handbuch der Physik. Vol. XXVI. Springer-Verlag, Berlin, Göttingen, Heidelberg. 1958. p. 467.
17. R. N. JONES. Spectrochim. Acta, **9**, 235 (1957).
18. R. N. JONES. Can. J. Chem. **40**, 301 (1962).
19. M. E. ISABELLE and L. C. LEITCH. Can. J. Chem. **36**, 440 (1958).
20. R. N. JONES, P. J. KREUGER, K. NOACK, J. J. ELLIOTT, R. A. RIPLEY, G. A. A. NONNENMACHER, and J. B. DIGIORGIO. Proc. Xth Colloquium Spectroscopicum Internationale. Spartan Books, Washington. 1963. pp. 461–486.
21. D. H. RANK and R. E. KAGARISE. J. Opt. Soc. Am. **40**, 89 (1950).
22. M. R. FENSKE, W. G. BRAUN, R. V. WIEGAND, D. QUIGGLE, R. H. MCCORMICK, and D. H. RANK. Anal. Chem. **19**, 700 (1947).
23. D. G. REA. American Petroleum Institute Research Project 44. Raman Spectrum No. 268.
24. H. J. BERNSTEIN. Personal communication.
25. F. F. CLEVELAND. Determination of organic structures by physical methods. Vol. 1. *Edited by* E. A. Braude and F. C. Nachod. Academic Press Inc., New York. 1955. p. 247.
26. H. D. NOETHER. J. Chem. Phys. **10**, 693 (1942).
27. J. K. WILMSHURST. J. Mol. Spectr. **1**, 201 (1957).
28. J. R. NIELSEN and R. F. HOLLAND. J. Mol. Spectr. **4**, 488 (1960).
29. S. KRIMM. Fortschr. Hochpolymer Forsch. **2**, 51 (1960).
30. C. Y. LIANG, G. B. B. M. SUTHERLAND, and S. KRIMM. J. Chem. Phys. **22**, 1468 (1954).
31. R. N. JONES and C. SANDORFY. *In* Technique of organic chemistry. Vol. IX. *Edited by* A. Weissberger. Interscience Publishers Inc., New York, London. 1956. p. 253.
32. R. LUMLEY JONES. Unpublished observation from this laboratory.
33. G. PLACZEK. Handbuch der Radiologie. Vol. VI, Pt. 2. Leipzig. 1934. p. 205.
34. M. W. VOLKENSTEIN and M. A. ELYASHEVICH. Dokl. Akad. Nauk SSSR. **43**, 55 (1944); Zh. Eksperim. i Teor. Fiz. **15**, 124 (1945).
35. W. F. EDGELL. J. Chem. Phys. **13**, 132 (1945).
36. P. P. SHORYGIN. Usp. Khim. **19**, 419 (1950). National Research Council of Canada Technical Translation No. TT-228.
37. R. SAMUEL and M. J. KHAN. Z. Physik, **84**, 87 (1933).
38. I. HANSEN-DAMASCHUN. Z. Physik Chem. B, **22**, 97 (1933).

SPECTROSCOPIC STUDIES OF ALCOHOLS

II. THE CONFORMATION OF 2-HALOETHANOLS IN CARBON TETRACHLORIDE SOLUTION*

P. J. KRUEGER AND H. D. METTEE
Department of Chemistry, University of Alberta, Calgary, Alberta
Received August 23, 1963

ABSTRACT

Of the five conformers predicted for 2-haloethanols, only two (halogen and OH trans and gauche) can be positively identified by high resolution infrared spectroscopy. From the temperature dependence of the relative intensities of the fundamental OH stretching bands of the trans and gauche forms of the compounds XCH_2CH_2OH, where X = F, Cl, Br, and I, the gauche conformers are shown to be energetically favored in dilute carbon tetrachloride solution, with enthalpy differences between the two conformers of 2.07 ± 0.53, 1.20 ± 0.09, 1.25 ± 0.08, and 0.81 ± 0.09 kcal/mole respectively. Equilibrium constants and the conformational free energy and entropy differences are reported. Inter- and intra-molecular OH. . .X hydrogen-bond interactions are found to be similar in that the enthalpy increases in the order X = I < Br < Cl < F, and is linearly related to a *decrease* in the fundamental OH band shift, in contrast to the Badger–Bauer relationship. The molecular and thermodynamic factors governing conformational equilibria involving intramolecular hydrogen bonds are discussed.

INTRODUCTION

Since 1936, when the thermodynamic properties of hydrocarbons calculated on the basis of restricted internal rotation about a single bond were first shown to be in agreement with the experimental values (1), a large amount of information has been accumulated about the nature of the potential minima which exist for those molecular conformations in which the bonds to the atoms on the axis of rotation have taken up a staggered orientation (2). As the barriers to rotation are usually relatively low, aliphatic hydrocarbons and their derivatives exhibit a high degree of conformational heterogeneity in the gaseous or liquid state. In the crystalline state such rotational freedom is lost, and the molecule is frozen in its most stable form. Much of the early work in this field involved halogenated ethanes.

Recently Kuhn, Luettke, and Mecke (3) showed that in 2-haloethanols in CCl_4 solution only two conformers (trans and gauche) could be identified by means of infrared spectra in the OH stretching region obtained with a prism spectrophotometer. The two gauche forms in the equilibria are mirror images and thus spectroscopically equivalent. The low frequency ν_{OH} component is assigned to the gauche forms.

[1] 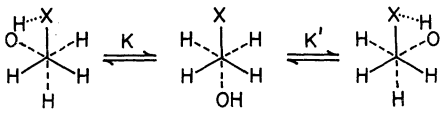

Number of molecules in each form:

N_g' N_t N_g''

Funck's general treatment of rotational isomerism in linear polymethylene chains $X—(CH_2)_n—Y$ (4) predicts nine rotational isomers for XCH_2CH_2OH, taking into

**Paper presented at the 46th Annual Conference of the Chemical Institute of Canada, Toronto, June 6–8, 1963.*

Can. J. Chem. Downloaded from www.nrcresearchpress.com by 210.87.254.105 on 09/05/12
For personal use only.

consideration rotation about C—C and C—O bonds. In four of these the OH group is in an identical environment with respect to the X atom as in one of the other five conformers because of the mirror-image relationship across the XCC plane, and hence a maximum of five conformers remain to be considered:

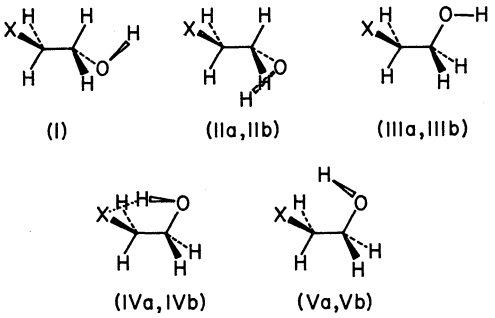

This work was begun with the object of checking whether the improved resolution of a grating spectrophotometer, together with temperature studies, would permit the identification of more than two conformers of XCH_2CH_2OH in dilute CCl_4 solution, where X = F, Cl, Br, and I. The temperature dependence of the infrared spectra should permit the determination of the enthalpy differences between the rotational isomers involved, and the effect of intramolecular hydrogen bonding on the equilibria. It was also of interest to compare the nature of intra- and inter-molecular hydrogen bonding of OH groups to covalently bound halogen atoms. A preliminary survey showed that the OH stretching vibration would be potentially the most useful band for the characterization of alcohol conformers.

EXPERIMENTAL

The spectra in the fundamental region were obtained with a Beckman IR-7 infrared spectrophotometer employing a NaCl foreprism and a 75 lines/mm grating in the fourth order. With a scanning speed of 6.4 cm^{-1} per minute, it was shown that bands obtained by scanning in the direction of decreasing frequency were identical in shape with those obtained by scanning in the conventional direction of increasing frequency. The frequency calibration of the instrument has been described (5). The frequencies reported by Kuhn, Luettke, and Mecke (3) are about 11.5 cm^{-1} lower than those found with our calibrated instrument. The calculated slit width in this region was approximately 0.7 cm^{-1} under the operating conditions. Higher resolution could be attained only at the expense of the signal-to-noise ratio, or by an unrealistic decrease in the scanning speed.

Double-beam operation was employed, using a pair of matched 2.00-cm fused quartz cells. Both the reference and the solution cell were jacketed with a closely fitting hollow brass block which was insulated from the spectrophotometer mounting and the rest of the sample compartment. Methylated spirits were circulated through the brass blocks, connected in parallel, from a Haake thermostat. For measurements below room temperature a dry ice – acetone mixture was used as a heat sink in conjunction with the thermostat. The entire spectrophotometer, including the sample compartment, was carefully purged with dry air to prevent condensation on the cell windows at low temperatures.

Temperatures were monitored during the course of a run by means of calibrated iron–constantan thermocouples inserted directly into the liquid in each of the two cells through Teflon stoppers in the filling ports. A Rubicon B-1 potentiometer, with a limit of error of ±1 microvolt in the low range, was used for the electromotive force measurements. The limiting factor in the temperature stabilization was the slight temperature rise experienced by the alcohol solution due to absorption of radiation. In general, temperatures are believed to be accurate to ±0.1° C above room temperature, and to ±0.2° C for those below room temperature.

Solutions were made up volumetrically with CCl_4 of spectroscopic quality, keeping concentrations below 0.006 *M* to avoid intermolecular hydrogen-bonding complications. The 2-iodoethanol was synthesized according to Norland and Hartmann (6) and 1-fluoropentane according to Vogel *et al.* (7); the others were commercial products which were carefully dried and purified by fractional distillation through a 23 theoretical-plate spinning band column. For the competitive inter- and intra-molecular OH . . . X studies both

Can. J. Chem. Downloaded from www.nrcresearchpress.com by 210.87.254.105 on 09/05/12
For personal use only.

the sample and reference solutions were 1.00 M with respect to RX′ and the sample solution was 0.005 M with respect to XCH_2CH_2OH.

Measurements in the first overtone region were made with a Beckman DK-1 spectrophotometer, using matched 10-cm quartz absorption cells held at 25.0±0.1° C, and alcohol concentrations below 0.05 M in CCl_4. Some error may be introduced into the overtone measurements because of the presence of a small amount of intermolecular hydrogen bonding, although no evidence of broad association peaks was found.

RESULTS AND DISCUSSION

Conformational Enthalpy Differences and Equilibrium Constants

The spectra obtained in the 3 μ region (Fig. 1) in the temperature range −20° C to

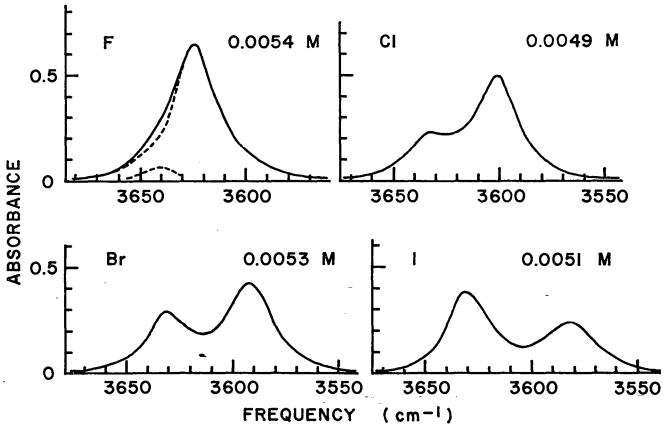

FIG. 1. The fundamental OH stretching bands of the trans and gauche conformers of 2-haloethanols in dilute CCl_4 solution. Path length = 2.00 cm.

+45° C exhibit only a partially resolved doublet for 2-chloro-, 2-bromo-, and 2-iodoethanol, of which the low frequency component is consistent with a hydrogen-bonded gauche form, and the high frequency component with a trans form having a "free" OH group. There is no evidence, such as pronounced band asymmetry, which would indicate further unresolved submaxima corresponding to other conformers.* For 2-fluoroethanol only one band showing pronounced asymmetry on the high frequency side is observed. By reflecting the low-frequency side of the band across the ordinate at the maximum and subtracting the mirror image from the observed envelope, the existence of a relatively weak trans component, which decreases as the temperature is lowered, can be established. The precision of this method is quite poor, but the components are too closely spaced (~15.5 cm^{-1}) and too wide (trans $\Delta\nu_{\frac{1}{2}}^{a}$ ~16 cm^{-1}; gauche $\Delta\nu_{\frac{1}{2}}^{a}$ ~24 cm^{-1}) to be resolved.

For 2-fluoroethanol a further broad component, of very low intensity, is found at about 3709 cm^{-1} at temperatures above 0° C only. It seems very doubtful whether such a high frequency can be assigned to an OH stretching band of an alcohol conformer. It is likely an overtone or a combination band.

The presence of only one distinguishable gauche-type conformer in these compounds implies that in the gauche orientation the hydrogen bonds are strong enough to hold the

**The contribution of conformers IIIa, IIIb, Va, and Vb (gauche with "free" OH groups) to the high frequency component or to its wings cannot be excluded completely. Since this contribution is probably small and cannot be estimated, this paper discusses the results in terms of trans conformers with "free" OH groups (I, IIa, and IIb) and gauche conformers with intramolecularly hydrogen-bonded OH groups (IVa and IVb). Although Mecke et al. (3) favor electrostatic interaction in these molecules as opposed to intramolecular hydrogen bonding, the data can be accommodated by the operational definition of the "hydrogen bond" as given by Pimentel and McClellan (25).*

Can. J. Chem. Downloaded from www.nrcresearchpress.com by 210.87.254.105 on 09/05/12
For personal use only.

hydrogen atom of the OH group in that position (of the three which arise due to restricted rotation about the C—O bond) where it is nearest the X atom. Spectral studies by Mizushima and by Edgell and Glockler (8) have demonstrated that substituted ethanes consistently assume trans and gauche forms rather than trans and cis types. The azimuthal angle in the gauche form may, however, be larger than 60° because of the oxygen–halogen repulsion due to electrical and steric factors. According to electron diffraction investigations of Bastiansen (9) the azimuthal angle in ethylene glycol and 2-chloroethanol appears to be 74°. This corresponds to an O to O distance of 2.96 Ångstroms in ethylene glycol, and an O to Cl distance of 3.17 Ångstroms in 2-chloroethanol. Similar investigations of Yamaha and Igarashi (10) led to angles of 75° in 2-chloroethanol and 60–70° in 2-fluoroethanol. They concluded that the latter compound was completely in the gauche form. The presence of only one distinguishable trans-type conformer suggests that in the trans orientation the OH group is so far removed from the halogen atom that the three potential minima governing rotation about the C—O bond are equivalent.

In the application of the Beer–Lambert absorption law to spectroscopic data involving an equilibrium like [1], the following expressions may be derived (11):

$$\ln (I_0/I)_t = E_t N_t l, \quad [2]$$

$$\ln (I_0/I)_g = E_g N_g l, \quad [3]$$

where I_0 and I are the intensities of incident and transmitted radiation respectively, E_t and E_g are the molecular extinction coefficients for the trans and gauche forms (at different frequencies), N_t and N_g are the numbers of molecules in the trans and gauche forms, and l is the path length. From these expressions

$$N_t/N_g = (E_g/E_t) \ln (I_0/I)_t/\ln (I_0/I)_g. \quad [4]$$

Experimental evaluation of (N_t/N_g) and hence the equilibrium constant is not usually possible by this method since E_g and E_t, the intrinsic molecular absorption coefficients for molecules known to be gauche and trans respectively, cannot be obtained, except perhaps by analogy with some model compounds.

If the number of molecules in one of the gauche forms involved in equilibrium [1] is N_g', and the number of molecules in the mirror-image gauche form is N_g'', then

$$N_g = N_g' + N_g'' = (N_t/K) + K'N_t \quad [5]$$

since $K = (N_t/N_g')$ and $K' = (N_g''/N_t)$. From the reciprocal relationship of K and K' it follows that $N_g = (2N_t/K)$, or

$$K = (2N_t/N_g) = 2(E_g/E_t)\ (D_t/D_g), \quad [6]$$

where D_t and D_g are the absorbances at the trans and gauche band maxima respectively. Provided the assumption $E_t = E_g$ is made, the equilibrium constants at 28° C calculated from [6] are 0.20, 0.92, 1.36, and 3.22 for X = F, Cl, Br, and I respectively. If a Lorentz band shape is assumed for both the trans and the gauche bands, then band areas can be estimated from the analytical expression

$$A = 2.303\ (\pi/2)D(\Delta\nu_{\frac{1}{2}}^{a}) \quad [7]$$

using the approximate $\Delta\nu_{\frac{1}{2}}^{a}$ values in Table I.* The K values (28° C) obtained on this basis are 0.13, 0.96, 1.20, and 2.08 for X = F, Cl, Br, and I respectively.

**For 2-fluoroethanol these band widths were obtained from the components established by graphical resolution. For the other alcohols the band widths reported in this table were obtained by doubling $\frac{1}{2}\Delta\nu_{\frac{1}{2}}^{a}$ as measured to the ordinate at the apparent band maximum on that side of the band which is relatively free from overlap.*

Can. J. Chem. Downloaded from www.nrcresearchpress.com by 210.87.254.105 on 09/05/12
For personal use only.

If the reasonable assumption is made that (E_g/E_t) is relatively temperature independent over a small temperature range,* the van't Hoff equation is applicable in the following form:

$$[8] \qquad \log (D_t/D_g) = -\Delta H/(2.303\,RT) + [\Delta S/(2.303\,R) - \log (2E_g/E_t)]$$

where ΔH is the enthalpy difference between the conformational isomers, and ΔS is the corresponding entropy difference. From graphs of log (D_t/D_g) versus $1/T$ (Fig. 2), the

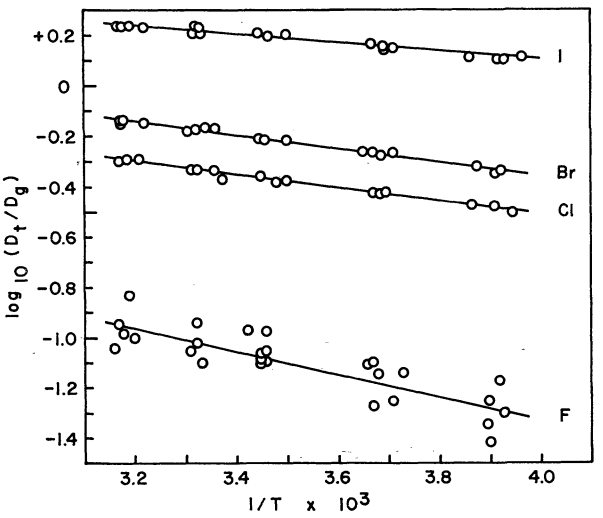

FIG. 2. The effect of temperature on the trans/gauche absorbance ratio in 2-haloethanols in dilute CCl_4 solution.

quantity ΔH can be obtained directly from the slope, and ΔS can be estimated if the assumption is made that $E_g = E_t$. This is certainly not true in intermolecular association, but is probably a better approximation in intramolecular association involving weak hydrogen bonds in five-membered rings. Baker and Kaeding (13) have argued that in the latter system the hydrogen bond may be largely an electrostatic effect, and that charge transfer phenomena, which are mainly responsible for increases in band intensity, are only of secondary importance in cases where highly bent hydrogen bonds to halogen atoms are involved. Table I includes the thermodynamic values obtained by a least squares analysis of the data on the basis of equation [8]. For the ΔH values 95% confidence limits are also given (18).

The conformational enthalpy difference increases in the order X = I < Br ≈ Cl < F, in all cases the gauche form having the greatest stability, as based on the decrease of the ratio D_t/D_g with decreasing temperature. This is in contrast to the qualitative deductions of Kuhn, Luettke, and Mecke (3), who suggest, on the basis of spectra at ambient temperature only, that in 2-bromoethanol the conformational energy difference must be nearly zero since $D_t \approx D_g$, and in 2-iodoethanol the trans form appears to be more stable since this is the only one of the compounds under consideration where $D_t > D_g$. However, it must be borne in mind that absorption band areas (A) should be compared rather than

*Over the small temperature range employed in this work the temperature dependence of the molar extinction coefficient of an absorption band arising in a given conformer is expected to be small. See, for example, the results reported by Lisitsa and Khalimonova (12) for CH stretching vibrations in a number of aromatic compounds.

Can. J. Chem. Downloaded from www.nrcresearchpress.com by 210.87.254.105 on 09/05/12
For personal use only.

TABLE I

Fundamental OH band parameters and thermodynamic properties of trans and gauche conformers of XCH_2CH_2OH in CCl_4 solution*

X =	$\sigma^*_{-CH_2X}$	Frequencies (cm^{-1})(~28° C) trans	gauche	($\nu_t - \nu_g$)†	Band widths (cm^{-1}) (~28° C) trans	gauche	$\Delta H^{28°}$ (kcal/mole)	$\Delta S^{28°}$ (e.u.)	$\Delta F^{28°}$ (kcal/mole)
F	+1.10	3639.7‡	3624.2‡	15.5	16	24	2.07±0.53§	3.6	0.98
Cl	+1.05	3634.6¶	3601.4¶	33.2	24	23	1.20±0.09	3.9‖	0.04
Br	+1.00	3631.9	3593.2	38.7	23	26	1.25±0.08	4.7	−0.17
I	+0.85	3629.3	3582.7	46.6	20	31	0.81±0.09	5.1	−0.72

*The frequencies, band widths, and absorbance ratios reported are for measurements close to 28° C to simplify the table. The form of the equilibrium is: gauche ⇌ trans; $K = 2[\text{trans}]/[\text{gauche}]$.

†Shifts for XCH_2CH_2OH observed by Schleyer and West (14): 12, 32, 38, and 46 cm^{-1} for F, Cl, Br, and I respectively. Corresponding intermolecular shifts for MeOH...*n*-BuX bonding (14): 19, 37, 41, and 47 cm^{-1} respectively for above X order.

‡Reported by Oki and Iwamura (15) at 3634.6 and 3620.9 cm^{-1}.

§The large 95% confidence limits for the ΔH value for 2-fluoroethanol are due to the low precision of the graphical resolution of the doublet.

¶Reported by Josien and Pineau (16) at 3623±5 cm^{-1} and 3597±4 cm^{-1}.

‖Using an optical method involving the relative intensities of the C—Cl stretching frequencies at 669 cm^{-1} and 760 cm^{-1} in the gauche and trans forms respectively, as well as the intensity of the C—H stretching band at 2890 cm^{-1} common to both conformers, Mizushima *et al.* (17) found $\Delta S = 3.7 \pm 0.4$ e.u. for experimental measurements in the gas phase.

apparent peak absorbances, and in 2-iodoethanol the gauche band has a half-intensity width which is more than 50% greater than that of the trans band, so that $A_g \approx A_t$ within the experimental error of the area measurements. In view of the resolution difficulties it seems unwise to attempt to use estimated band areas in the ΔH determinations. Also, since changes in the relative widths of these trans and gauche bands with temperature are not pronounced, the rate of change of D_t/D_g with temperature should approximate to the corresponding rate of change of A_t/A_g, leading to correct ΔH values.

In the 1,2-dihaloethanes thermodynamic calculations, dipole moment, infrared, and Raman studies all show that the trans isomers are energetically favored in the gas phase, with increasing population of the gauche form in the liquid state and in solution due to solvent stabilization of the form having the largest dipole moment (11). Only one recent gas phase ΔH value for the 2-haloethanols appears to have been published. Mizushima *et al.* (19) report that the gauche form of 2-chloroethanol is more stable than the trans form by 0.95 kcal/mole. The corresponding ΔH value in CCl_4 solution obtained in this work is 1.20 kcal/mole, also showing stabilization of the more polar form of the molecule in solution, even by non-polar although highly polarizable CCl_4 molecules.

The enthalpy differences between the gauche and trans forms are undoubtedly determined by a number of factors, among which the most important would be:

(*a*) steric repulsion between the oxygen and the halogen atoms in the gauche form, which would increase in the order F < Cl < Br < I, and thus tend to make the trans form more stable;

(*b*) electrostatic repulsion between the oxygen and halogen atoms (or between the C—X and C—O dipoles), which would also favor the trans form; and

(*c*) OH...X hydrogen bond interaction, which would stabilize the gauche form.

According to Parker (20) the idea that the proton-acceptor in hydrogen-bond formation must be an element of small atomic radius and high electronegativity, although true for the strong hydrogen bonding to anions (as in the bonding of water to halide ions, where the strength increases in the order $I^- < Br^- < Cl^- < F^-$), cannot automatically be extended to the much weaker hydrogen bonding to covalently bound electronegative atoms. Further, there is a deficiency of information about intramolecular OH...X hydrogen bonds, where the restricting geometry of the system may affect (*c*), and perhaps

Can. J. Chem. Downloaded from www.nrcresearchpress.com by 210.87.254.105 on 09/05/12
For personal use only.

even change the order of X in the bond strength series and make it different from the intermolecular order. In the formation of intramolecular hydrogen bonds between OH groups and halogen atoms, increasing size of the halogen atom may favor the bond strength since the minimum OH. . . X distance is fixed by the system. On the basis of n.m.r. spectroscopy Allan and Reeves (21) suggest that the flourine atom is too small to lead to measurable stability of a cis-isomer in *o*-fluorophenol. Similarly, the ultraviolet spectra of the *B*-bands of *o*-fluorophenol (22) and *o*-fluorobenzoic acid (23) indicate the absence of strong intramolecular hydrogen bonds in these compounds. However, these examples are not strictly analogous to the gauche form of FCH_2CH_2OH since the benzene ring modifies the character of the F atom and the OH group.

Intra- vs. Inter-molecular OH. . . X Hydrogen Bonding and the ν_{OH} Shift

In intermolecular hydrogen bonding, the extent by which the OH stretching frequency of the "bonded" molecule is displaced from the corresponding frequency of the "free" molecule has long been accepted as an approximate measure of the strength of the hydrogen bond (24, 25). The application of the Badger–Bauer rule to intramolecular hydrogen bonds in the *o*-halophenols has been criticized by Baker and Kaeding (13) on the grounds of a repulsive interaction between the OH bonding orbital and the donated lone-pair orbital of the halogen in the cis form of the molecule, so that the ν_{OH} shift observed is not a measure of the net energy of the resultant bonds.* This may be a valid argument for a rigid aromatic molecule where the OH group is preferentially constrained to the plane of the ring by resonance, making such repulsive interaction in the cis form a maximum, but in the more flexible saturated 2-haloethanols this should be of minor importance. In fact, a quasi-gauche form of the molecule allows for a certain amount of adjustment of the OH. . . X distance to attain the maximum hydrogen bond strength permitted by the geometry of the system.

On the basis of a large number of measurements on the 1,2-halohydrin steroid systems of known conformation, Nickon (26) has pointed out that, in the absence of other disturbing factors, the halogens follow the sequence I > Br > Cl in their ability to decrease the fundamental OH stretching frequency, whereas they adopt the reverse order in their power to increase the C—OH stretching frequency. Since the relationship for the bonded ν_{OH} shift is the reverse of the electronegativity sequence, Nickon suggests that the perturbing action of a halogen atom must be governed not only by electronegativity effects, but also by the proximity and polarizability of the electrons on the halogen.

On the basis of frequency shift data for the bonding of methanol and phenol to *n*-butyl and cyclohexyl halides, Schleyer and West (27) concluded in 1959 that the intermolecular hydrogen bond strength decreased in the order I > Br > Cl > F. These authors further concluded that although the ν_{OH} shifts for the intramolecular bonds in *o*-halophenols and 2-haloethanols indicated the same order of hydrogen bond enthalpy, the data for these systems could not be interpreted unambiguously because the groups were rigidly held. Recently West *et al.* (28) have reversed their arguments on the basis of more complete thermodynamic studies of the phenol – cyclohexyl halide system, and have shown that the Badger–Bauer rule is invalid for this system.

Bernstein (29) has offered an explanation for the lack of general correlation of $\Delta\nu$ with ΔH. The enthalpy change measures the total interaction energy of the system AH. . . BY, i.e. the strength of the H. . . B bond compensated in part by A—H and B—Y weakening, whereas $\Delta\nu$ measures only the weakening of the A—H bond. For the same proton donor

They deduced the order of intramolecular OH . . . X bond strength in o-halophenols to be Cl > Br > F > I.

Can. J. Chem. Downloaded from www.nrcresearchpress.com by 210.87.254.105 on 09/05/12
For personal use only.

$\Delta\nu$ and $-\Delta H$ may correlate for minor changes in the proton acceptor (in Y), but not necessarily for changes of the acceptor atom B. In this connection it may be noted that Nickon (26) has observed an increase in C—OH frequencies in steroid 1,2-halohydrins in the order I < Br < Cl.

The extended work of Josien and her associates (30) clearly shows that although a linear "correlation zone" of increasing $-\Delta H$ with increasing $\Delta\nu$ exists for a series of hydroxylic proton donors bonded to various bases, it is by no means a precise relationship. Taken over a large range of $\Delta\nu$ (up to and exceeding 300 cm^{-1}) and up to enthalpies of 6 kcal/mole, the Bauer–Badger relationship is a very approximate one. For relatively low enthalpies and small frequency shifts, Josien's work shows that good linear enthalpy vs. $\Delta\nu$ relationships are obtained for the bonding of phenol and *p*-chlorophenol to cyclohexyl halides, but that the slope is *in opposition* to the Bauer–Badger correlation.

Figure 3 (*a*) shows a comparative plot of ΔH vs. $\Delta\nu$ for the intermolecularly hydrogen-

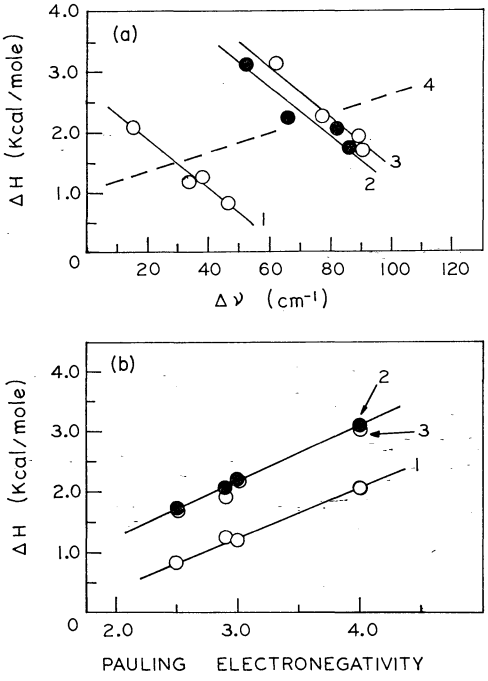

FIG. 3. (*a*) Enthalpy change vs. OH frequency shift correlations on OH ... X bond formation. (1) Intramolecular bonds in XCH_2CH_2OH. (2) Intermolecular phenol ... cyclohexyl X bonds (28). (3) Intermolecular *p*-chlorophenol ... cyclohexyl X bonds (30). (4) Broken line indicates approximate Bauer–Badger "correlation zone" taken from Fig. 19, p. 51, ref. 30. The scatter of points along this zone is sufficient to include the 12 points on this graph.
(*b*) Enthalpy change vs. Pauling electronegativity for X atom. Points have same significance as above.

bonded systems of phenol and *p*-chlorophenol with the cyclohexyl halides, as well as the present data for the intramolecular bonds in 2-haloethanols. All three correlations have identical slope; from this parallel behavior it is reasonable to conclude that the order of increasing intramolecular hydrogen bond strength in the 2-haloethanols is F > Cl > Br > I, this being the order established by West *et al.* (28) for intermolecular OH hydrogen bonds to halogens by a method not open to question. Figure 3 (*b*) confirms the parallelism of intra- and inter-molecular OH...X bonds, since both exhibit the same linear ΔH

Can. J. Chem. Downloaded from www.nrcresearchpress.com by 210.87.254.105 on 09/05/12
For personal use only.

dependence on the halogen electronegativity. It is interesting to note that both the intermolecular systems lie on the same line in this graph.

Becker (31) has discussed the Badger–Bauer relationship in the light of experimental data on a variety of alcohol complexes with strong bases, and reports only approximate behavior. In this context the work of Joesten and Drago (32) shows that the Bauer–Badger rule holds to ± 0.5 kcal/mole for adducts of phenol with nitrogen and oxygen donors, but here again $\Delta\nu$ values range from 144 to 553 cm^{-1}, with accompanying enthalpies from 3.2 to 9.2 kcal/mole. It appears that the prediction of hydrogen-bond enthalpies from frequency shifts is least reliable in the weak hydrogen bond range.

Figure 4 shows that in 2-haloethanols ν_t increases in an approximately linear manner

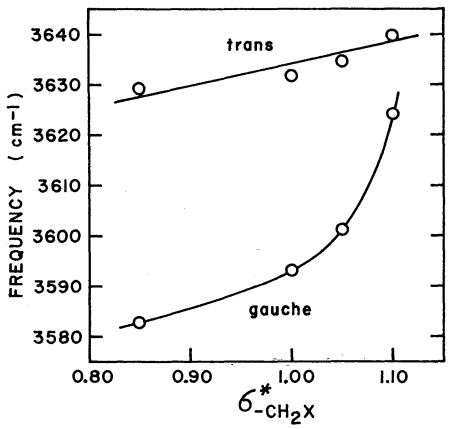

FIG. 4. The inductive effect of the halogen atom on ν_{OH} in the trans 2-haloethanols, and the frequency lowering due to hydrogen bonding in the gauche 2-haloethanols.

with the Taft inductive parameter σ^* of the substituent (33), whereas the ν_g behavior is non-linear. Bellamy's recent analysis (34) of group frequency shifts suggests that, in general, frequencies arising in groups well removed from the substituent in aliphatic systems follow the order of σ^* values, which measure the true inductive effect, but that where non-bonded interactions predominate the order of effectiveness of the substituent groups will more closely follow the order of the Pauling electronegativities since these include both inductive and polarizability effects. Figure 5 shows that ν_g is linearly related to the electronegativity of the X atom; as far as ν_t is concerned the frequency change is too small to distinguish this correlation from that with σ^*. Many group-frequency shifts are still poorly understood; in this series ν_t increases approximately linearly with increasing polarity of the OH group.

With increasing temperature, ν_{OH} for both the trans and gauche forms increases by approximately 0.8 cm^{-1} per 10° temperature rise, as shown in Fig. 6. This is probably related to the decreasing density of the solvent, which means that, on the average, the solvent molecules will be further removed from the solute molecules, and their influence will be reduced.

Rotational Entropy Differences

The review by Mizushima (2*a*) indicates that steric repulsion between movable groups is the major factor in determining the nature of the potential function hindering internal rotation, and that electrostatic interactions play a less significant role, except if hydrogen

Can. J. Chem. Downloaded from www.nrcresearchpress.com by 210.87.254.105 on 09/05/12
For personal use only.

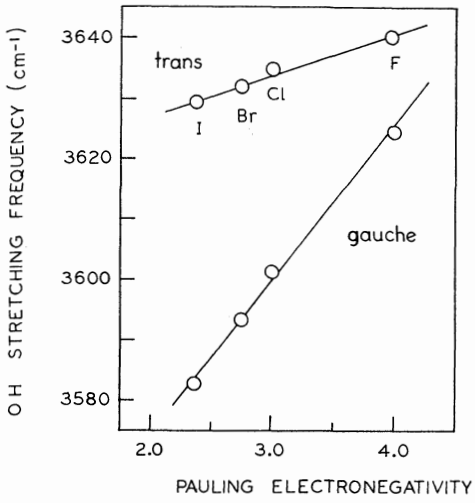

FIG. 5. The relationship of ν_{OH} in the trans and gauche XCH_2CH_2OH conformers to the Pauling electronegativity of the X atom.

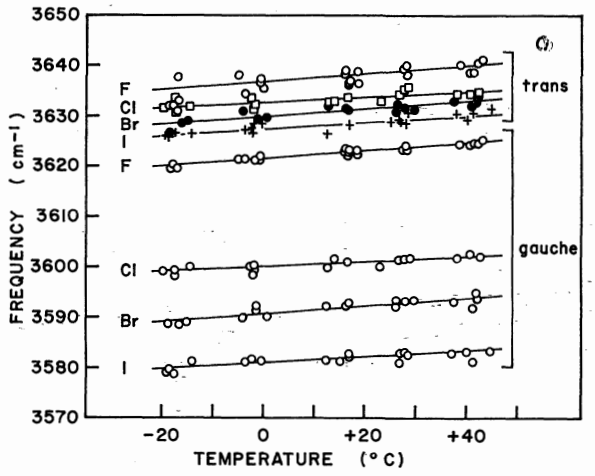

FIG. 6. The temperature dependence of the trans and gauche OH stretching frequencies in 2-haloethanols in dilute CCl_4 solution.

bonding is involved. In considering rotational isomerism in 2-haloethanols it is important to distinguish between the strength of the hydrogen bond and the population of the hydrogen-bonded conformation.

Jaffe (35) has pointed out that, in general, entropy changes in intermolecular hydrogen bond formation exceed those in intramolecular hydrogen-bond formation, and Mizushima (2(*b*)) has discussed the entropy differences of trans and gauche forms of 2-chloroethanol, which arise mainly from differences in the internal rotation about the C—C and C—O bonds. The calculated entropy differences arising from overall rotation and normal vibrations are less than 1/10th of the observed value (17). The fact that one of the conformers has a hydrogen bond is regarded as the main reason for the entropy difference. In the trans form rotation of the H atom about the C—O bond leads to three equivalent

Can. J. Chem. Downloaded from www.nrcresearchpress.com by 210.87.254.105 on 09/05/12
For personal use only.

stable positions, whereas in the gauche form this leads to one OH position which is much more stable than the other two, so that $S_g < S_t$. Further, the torsional oscillation frequency would be increased in the gauche form, also making the entropy of the gauche form smaller than that of the trans form. The ΔS values calculated in this work on the basis that $E_g = E_t$ increase as the strength of the intramolecular OH...X bond decreases. One factor which may lead to greater "ordering" of the system on hydrogen-bond formation in the series F < Cl < Br < I may be the increasing size of the halogen atom, which in the gauche conformation progressively comes closer to the hydroxyl proton, and may bind it more effectively during librational motion. The geometric factor involved in intramolecular hydrogen bonding shows up clearly here since the data of West *et al.* (28) on intramolecular OH...X bonds reveal the opposite ΔS order, i.e. largest for bonding to the strongest proton acceptor (F) since the optimum OH...F distance can be achieved. Solute–solvent interaction may also enter into the picture for the intramolecular hydrogen bonds, since the polarity of the OH bond depends on X and therefore the trans form may "order" the polarizable CCl_4 molecules in the vicinity in the series I < Br < Cl < F. The ΔS change on intramolecular hydrogen bond formation would be affected by such interaction in the trans conformer.

At present there is no information on the potential barriers to internal rotation in these molecules (36). It is possible that these barrier heights could be evaluated from the torsional frequencies in the far infrared region.

Competitive Inter- and Intra-molecular OH...X Bonding

Figure 7(*a*) shows the spectra of 2-iodoethanol (0.005 *M*) in the presence of a 1.00 *M* concentration of 1-iodobutane and 1-fluoropentane respectively in CCl_4 solution. Figure

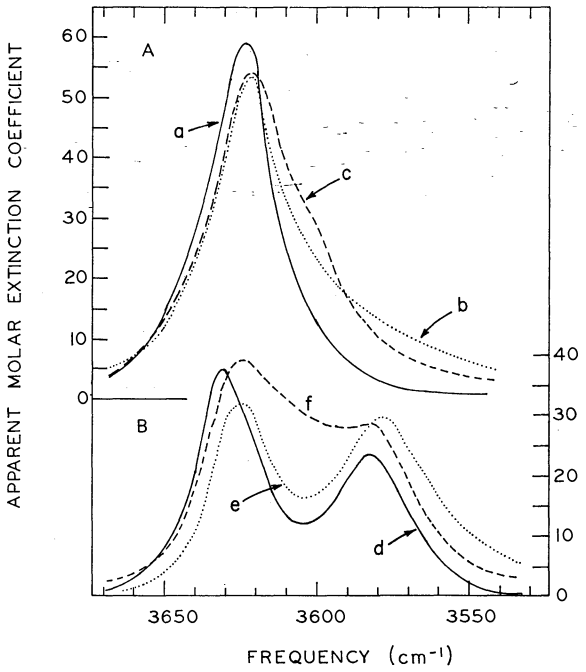

FIG. 7. Competitive inter- and intra-molecular OH ... X interactions. (*a*) FCH_2CH_2OH (0.005 *M*); (*b*) same as (*a*) but 1.00 *M* in *n*-BuI; (*c*) same as (*a*) but 1.00 *M* in *n*-AmF; (*d*) ICH_2CH_2OH (0.005 *M*); (*e*) same as (*d*) but 1.00 *M* in *n*-BuI; (*f*) same as (*d*) but 1.00 *M* in *n*-AmF.

Can. J. Chem. Downloaded from www.nrcresearchpress.com by 210.87.254.105 on 09/05/12
For personal use only.

7 (*b*) shows the effect of the same two alkyl halides on 2-fluoroethanol under the same conditions. In the competing equilibria

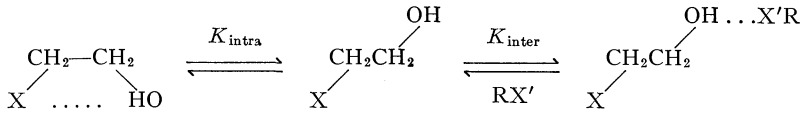

K_{intra} = 2[trans]/[gauche] and K_{inter} = [complex]/[trans][RX′]. Since K_{intra} = 2.08 for X = I and 0.13 for X = F, and K_{inter} = 0.28 for X′ = I and 1.5 for X′ = F (intermolecular methanol K values from preceding paper) it is easy to show that under the conditions of these experiments the ratio [complex]/[gauche] should be ≈1.5 for 1.00 *M* RF in 0.005 *M* ICH_2CH_2OH, and ≈0.02 for 1.00 *M* RI in 0.005 *M* FCH_2CH_2OH. Although these are only crude estimates, the experimental curves show that the intramolecular ICH_2CH_2OH equilibrium is upset more by intermolecular bonding to RF than is the intramolecular FCH_2CH_2OH equilibrium by the addition of either RF or RI. No band resolution was attempted, but in all cases the third component appears in the expected region of the spectrum. These studies provide further evidence that in this system covalently bound halogen atoms follow the order of electronegativity in their ability as proton acceptors.

First Overtone Measurements on 2-Haloethanols

In the first overtone OH stretching region trans/gauche doublets very similar to those shown in Fig. 1 are observed. The overtone band widths are increased with respect to the corresponding fundamental band widths by a factor of about 2.7. The overtone data are summarized in Table II, together with the calculated mechanical anharmonicities (x_e).

TABLE II

First overtone OH band parameters of trans and gauche conformers of XCH_2CH_2OH in CCl_4 solution

	Frequencies (cm^{-1}) (25° C)		Band widths (cm^{-1}) (25° C)		Mechanical anharmonicity (x_e)		
X =	trans	gauche	trans	gauche	trans	gauche	D_t/D_g (25° C)
F	7113	7079	38	57	0.0218	0.0224	0.15
Cl†	7097	7036	73	64*	0.0226	0.0222	0.53
Br	7096	7012	63	71	0.0221	0.0232	0.71
I	7086	6983	60	85	0.0227	0.0242	1.62

*2-Chloroethanol appears to be exceptional in that the gauche band width is less than the trans band width for both the fundamental and the first overtone vibrations.
†Piccolini and Winstein (37) have reported three components at 7101, 7072, and 7029 cm^{-1}.

It is seen that the x_e is constant for both conformations of all four compounds, having an average value of 0.0227±0.0015 (maximum deviation from the mean). These values are in agreement with those reported by Moccia and Thompson (38) for a large number of substituted phenols and aliphatic alcohols. The XCH_2CH_2OH trans and gauche enthalpy differences also correlate linearly with the overtone $\Delta\nu$ shifts.

The fundamental to first-overtone integrated intensity ratio (A_{01}/A_{02}) for a vibrational band is governed by both the mechanical and the electrical anharmonicity. Electrical anharmonicity in a diatomic molecule implies that the dipole moment (M) does not change linearly as the bond distance (r) is altered, but that M must be replaced by

[9] $$M = M_0 + M_1 r + M_2 r^2 + \ldots$$

Can. J. Chem. Downloaded from www.nrcresearchpress.com by 210.87.254.105 on 09/05/12
For personal use only.

If terms higher than quadratic are ignored, the quantity $B = M_2/M_1$ may be calculated according to Russell and Thompson (39), who showed that for a diatomic oscillator approximation with $x_e \ll 1$, both the methods of Dunham (40) and of Heaps and Herzberg (41) lead to the expression

$$[10] \qquad (A_{O2}/A_{O1}) = x_e\,(1-2B/ar_e)^2$$

where a is the constant in the Morse potential and r_e is the equilibrium OH bond length. As x_e is constant for both conformers in the 2-haloethanols, and changes in both a and r_e will be relatively small, differences in (A_{O2}/A_{O1}) must arise because of different B values for the two conformers.

Since, because of band overlapping, neither A_{O1} nor A_{O2} could be measured, they were estimated by using the peak absorbances and the approximate half-band widths (Tables I and II), on the assumption that both the fundamental and first overtone band envelopes conform to the Lorentz band shape. This has been shown to be a relatively satisfactory assumption for the fundamental OH band of methanol (42). The application of this method to our spectra of methanol in CCl_4 solution to obtain B led to a root of [10] which was within 5% of the value obtained by Moccia and Thompson (38) by rigorous methods, and which they supported by quantum mechanical calculations. Despite uncertainties in estimating r_e, there appears to be little doubt that for all four 2-haloethanols $|B_{trans}| > |B_{gauche}|$, the average values being 0.9 and 0.7 respectively. For NH bonds in secondary amines it has been shown (39) that the dipole moment change becomes more linear as the ionic character of the bond increases. For a completely ionic bond B should be zero. This concept is consistent with hydrogen bonding in the gauche form of the 2-haloethanols.

ACKNOWLEDGMENTS

The financial assistance of the National Research Council of Canada is gratefully acknowledged.

REFERENCES

1. J. D. Kemp and K. S. Pitzer. J. Chem. Phys. **4**, 749 (1936).
2. S. Mizushima. Structure of molecules and internal rotation. Academic Press, Inc., N.Y. 1954. (*a*) pp. 67–68. (*b*) pp. 61–63.
3. M. Kuhn, W. Luettke, and R. Mecke. Z. Anal. Chem. **170**, 106 (1959).
4. E. Funck. Z. Elektrochem. **62**, 901 (1958).
5. P. J. Krueger. Appl. Opt. **1**, 443 (1962).
6. W. E. Norland and P. J. Hartman. J. Am. Chem. Soc. **76**, 3227 (1954).
7. A. I. Vogel, J. Leicester, and W. A. T. Macey. Org. Syn. **36**, 40 (1956).
8. S. Mizushima, Y. Morino, and M. Takeda. J. Chem. Phys. **9**, 826 (1941). W. Edgell and G. Glockler. J. Chem. Phys. **9**, 375 (1941).
9. O. Bastiansen. Acta Chem. Scand. **3**, 415 (1949).
10. M. Yamaha. Bull. Chem. Soc. Japan, **29**, 865 (1956). M. Igarashi and M. Yamaha. Bull. Chem. Soc. Japan, **29**, 871 (1956).
11. E. L. Eliel. The stereochemistry of carbon compounds. McGraw-Hill, Inc., N.Y. 1962. pp. 129–133.
12. M. P. Lisitsa and I. N. Khalimonova. Opt. i Spektroskopiya. **11**, 332 (1961).
13. A. W. Baker and W. W. Kaeding. J. Am. Chem. Soc. **81**, 5904 (1959).
14. P. von R. Schleyer and R. West. J. Am. Chem. Soc. **81**, 3164 (1959).
15. M. Oki and H. Iwamura. Bull. Chem. Soc. Japan, **35**, 1744 (1962).
16. M. L. Josien and P. Pineau. Compt. rend. **250**, 2559 (1960).
17. S. Mizushima, T. Shimanouchi, K. Kuratani, and T. Miyazawa. J. Am. Chem. Soc. **74**, 1378 (1952).
18. F. S. Acton. Analysis of straight-line data. John Wiley and Sons, Inc., N.Y. 1959. Chap. 2.
19. S. Mizushima, T. Shimanouchi, T. Miyazawa, K. Abe, and M. Yasumi. J. Am. Chem. Soc. **19**, 1477 (1951).
20. A. J. Parker. Quart. Rev. **16**, 163 (1962).
21. E. A. Allan and L. W. Reeves. J. Phys. Chem. **66**, 613 (1962).
22. J. C. Dearden and W. F. Forbes. Can. J. Chem. **38**, 896 (1960).
23. W. F. Forbes, A. R. Knight, and D. L. Coffen. Can. J. Chem. **38**, 728 (1960).

Can. J. Chem. Downloaded from www.nrcresearchpress.com by 210.87.254.105 on 09/05/12
For personal use only.

24. R. M. BADGER and S. H. BAUER. J. Chem. Phys. **5**, 839 (1937).
25. G. C. PIMENTEL and A. L. MCCLELLAN. The hydrogen bond. W. H. Freeman and Co., San Francisco. 1960. Chap. 3.
26. A. NICKON. J. Am. Chem. Soc. **79**, 243 (1957).
27. P. VON R. SCHLEYER and R. WEST. J. Am. Chem. Soc. **81**, 3164 (1959).
28. R. WEST, D. L. POWELL, L. S. WHATLEY, M. K. T. LEE, and P. VON R. SCHLEYER. J. Am. Chem. Soc. **84**, 3221 (1962).
29. H. J. BERNSTEIN. *Cited in* R. West, D. L. Powell, L. S. Whatley, M. K. T. Lee, and P. von R. Schleyer. J. Am. Chem. Soc. **84**, 3221 (1962).
30. M. L. JOSIEN. Pure Appl. Chem. **4**, 33 (1962).
31. E. D. BECKER. Spectrochim. Acta, **17**, 436 (1961).
32. M. D. JOESTEN and R. S. DRAGO. J. Am. Chem. Soc. **84**, 3817 (1962).
33. R. W. TAFT, JR. *In* Steric effects in organic chemistry. *Edited by* M. S. Newman. John Wiley and Sons, Inc., N.Y. 1956. p. 619.
34. L. J. BELLAMY. *In* Proceedings of the Xth Colloquium Spectroscopicum Internationale. *Edited by* E. S. Lippincott and M. Margoshes. Spartan Books, Washington, D.C. 1963. p. 487.
35. H. H. JAFFE. J. Am. Chem. Soc. **79**, 2373 (1957).
36. E. B. WILSON. *In* Advances in chemical physics. Vol. 2. *Edited by* I. Prigogine. Interscience Publishers, Inc., N.Y. 1959. p. 367.
37. R. PICCOLINI and S. WINSTEIN. Tetrahedron Letters, No. 13, 4 (1959).
38. R. MOCCIA and H. W. THOMPSON. Proc. Roy. Soc. A, **243**, 154 (1957).
39. R. A. RUSSELL and H. W. THOMPSON. Proc. Roy. Soc. A, **234**, 318 (1956).
40. J. L. DUNHAM. Phys. Rev. **34**, 438 (1929); **35**, 1347 (1930).
41. H. S. HEAPS and G. HERZBERG. Z. Physik. **133**, 48 (1952).
42. M. OKI and H. IWAMURA. Bull. Chem. Soc. Japan, **32**, 950 (1959).

Can. J. Chem. Downloaded from www.nrcresearchpress.com by 210.87.254.105 on 09/05/12
For personal use only.

SPECTROSCOPIC STUDIES OF ALCOHOLS

III. FUNDAMENTAL OH STRETCHING BANDS OF 2,2-DI- AND 2,2,2-TRI-HALOETHANOLS

P. J. KRUEGER AND H. D. METTEE
Department of Chemistry, University of Alberta, Calgary, Alberta
Received August 23, 1963

Can. J. Chem. Downloaded from www.nrcresearchpress.com by 210.87.254.5 on 09/05/12
For personal use only.

ABSTRACT

The OH stretching region was examined for the compounds F_3CCH_2OH, Cl_2CHCH_2OH, Cl_3CCH_2OH, and Br_3CCH_2OH in dilute CCl_4 solution. The first two compounds exhibit temperature-dependent band asymmetry which is due to trans–gauche equilibria arising from rotation about the C—O bond, with relatively small populations in the trans forms. Enthalpy differences of 3.3 and 2.4 kcal/mole between the conformers were obtained for these two compounds respectively. Although symmetrical at lower temperatures, the band for Cl_3CCH_2OH shows the presence of a small amount of the trans conformer at temperatures above 45° C. These results are discussed in terms of intramolecular OH ... X hydrogen bond interaction, inductive effects, non-bonded interactions, O—H bond polarization, C—X bond polarizability, and the size of the halogen atoms in a geometrically constrained system.

INTRODUCTION

Recent work in this laboratory (1) has shown that 2-haloethanols in dilute CCl_4 solution exhibit an equilibrium between trans and gauche forms arising because of restricted rotation about the C—C bond. Thermodynamic studies have shown that the gauche form is more stable, and that the enthalpy difference (ΔH) between the two forms decreases in the order X = F > Cl ~ Br > I, whereas the frequency difference ($\nu_t - \nu_g$) increases in the order F < Cl < Br < I. The ΔH versus ($\nu_t - \nu_g$) behavior is linear, and parallels the behavior observed for intermolecular hydrogen bonding of phenol to cyclohexyl halides (2, 3) where it has been demonstrated that the OH frequency displacement does not measure the strength of hydrogen bond formation. Both the inter- and intra-molecular hydrogen bonding of OH groups to halogen atoms thus appears to disagree with the accepted Bauer–Badger relationship (4), but correlates with high precision in the opposite sense.

As an extension of this work some 2,2-di- and 2,2,2-tri-haloethanols have been examined under the same experimental conditions. On the basis of the measurements on FCH_2CH_2OH described in the preceding paper (1), it was expected that F_3CCH_2OH would be completely intramolecularly bonded. However, Cannon and Stace (5) have reported a "free" OH stretching band for trifluoroethanol in CCl_4 solution (3617 cm^{-1}), which persisted even in the pure liquid state (3628 cm^{-1}) and in dilute solution in perfluorocarbon (3644 cm^{-1}). Their interpretation did not support intramolecular OH...X bonding. Oki and Iwamura (6), working with a grating spectrophotometer and a spectral slit width of 1 cm^{-1}, found an OH band for F_3CCH_2OH in 0.003 *M* CCl_4 solution, which was asymmetric on the high frequency side, and interpreted it in terms of an unresolved doublet due to trans–gauche isomerism because of restricted rotation about the C—O bond. From mathematical resolution of the doublet (area of trans band/area of gauche band = 0.042) they concluded that trifluoroethanol was predominantly in the intramolecularly bonded gauche form. In some earlier work Haszeldine (7) had also considered intramolecular OH...X hydrogen bonding in primary and secondary haloalcohols, but his spectra, obtained with the poor resolving power of a NaCl prism, did not permit him to come to detailed conclusions about the nature of the "free" OH band. The recent work of Rao

and his associates (8, 9) on the acidity of the hydroxyl proton and the basicity of the hydroxyl oxygen, as deduced from solvent effect studies, together with the uncertainty in the interpretation of the OH absorption as described above, led to this investigation of a larger number of di- and tri-haloethanols at several temperatures.

EXPERIMENTAL

A Beckman IR-7 infrared spectrophotometer was employed under the conditions described previously (1). Alcohol concentrations were always below 0.006 *M*. A Lauda UltraKryostat UK 70 was used to regulate the temperature of the cells over the range 0–60° C. The haloethanols were all commercial materials purified by sublimation, recrystallization, or fractional distillation through a 23 theoretical-plate spinning band column. Analytical reagent grade CCl_4 was dried over P_2O_5 and distilled through a 50 theoretical-plate spinning band column.

RESULTS AND DISCUSSION

Figure 1 shows the nature of the OH bands obtained for F_3CCH_2OH, Cl_2CHCH_2OH,

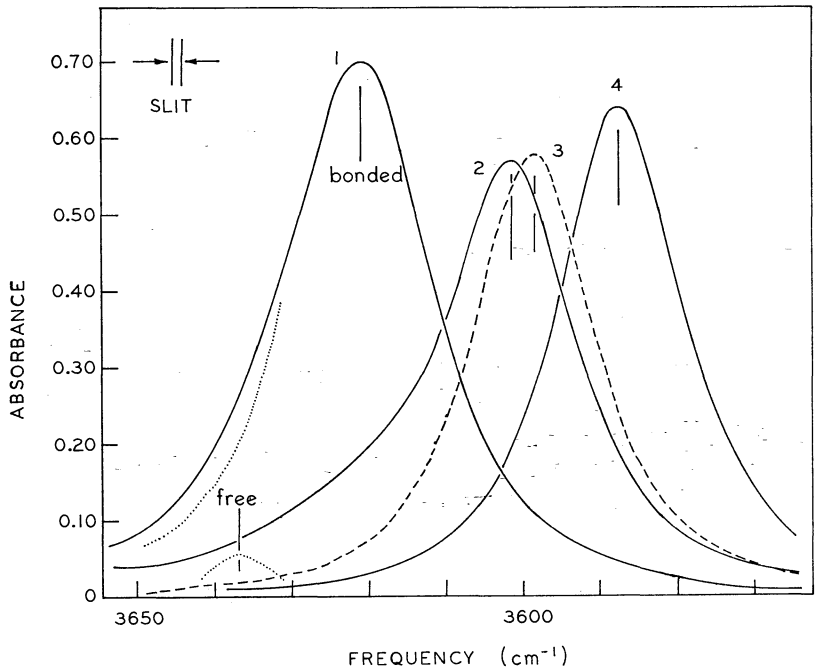

FIG. 1. Representative O—H stretching bands of di- and tri-haloethanols in CCl_4 solution. Path length = 2.00 cm.
(1) 2,2,2-Trifluoroethanol, 0.0030 *M*, t = 46° C. Dotted lines indicate residual "free" band obtained by reflection of the "bonded" band across the ordinate at the maximum.
(2) 2,2-Dichloroethanol, 0.0031 *M*, t = 48° C.
(3) 2,2,2-Trichloroethanol, 0.0022 *M*, t = 22° C.
(4) 2,2,2-Tribromoethanol, 0.0028 *M*, t = 27° C.

Cl_3CCH_2OH, and Br_3CCH_2OH in dilute CCl_4 solution. The band for Br_3CCH_2OH was found to be completely symmetrical over the temperature range investigated. The Cl_3CCH_2OH band was also symmetrical at lower temperatures, but exhibited slight asymmetry on the high frequency side at 45° C. On the other hand, F_3CCH_2OH and Cl_2CHCH_2OH show small but significant asymmetry on the high-frequency side over the entire temperature range investigated. By reflecting the major component of the

Can. J. Chem. Downloaded from www.nrcresearchpress.com by 210.87.254.5 on 09/05/12
For personal use only.

doublet about the ordinate at the maximum and subtracting the mirror image from the experimental spectrum, it can be demonstrated that the residual absorption causing asymmetry is due to a secondary band lying at higher frequency (example in Fig. 1). This method is satisfactory where the secondary component is relatively weak so that its contribution to the peak height of the principal band is negligible. The experimental data are summarized in Table I.

Examination of the frequency data shows that the major bands for all the di- and tri-haloethanols lie within 5 cm^{-1} of the corresponding values (ν_g) for the monohaloethanols. For trifluoroethanol the secondary band lies within 4 cm^{-1} of the corresponding value (ν_t) in FCH_2CH_2OH, while the secondary band for Cl_2CHCH_2OH differs from the corresponding value (ν_t) in $ClCH_2CH_2OH$ by the greatest amount, but even that is only 12 cm^{-1}. This frequency correspondence with the ν_t and ν_g bands respectively in the monohaloethanols indicates an equilibrium involving intramolecular OH...X hydrogen bonds,* with all molecules in the bonded form in Br_3CCH_2OH and Cl_3CCH_2OH (except at temperatures of 45° C or higher for the latter).

Considering rotation about both the C—C and the C—O bond, and staggering all bonds on the axes of rotation, the following equilibrium scheme can be formulated for 2,2-dichloroethanol (and other dihaloethanols):

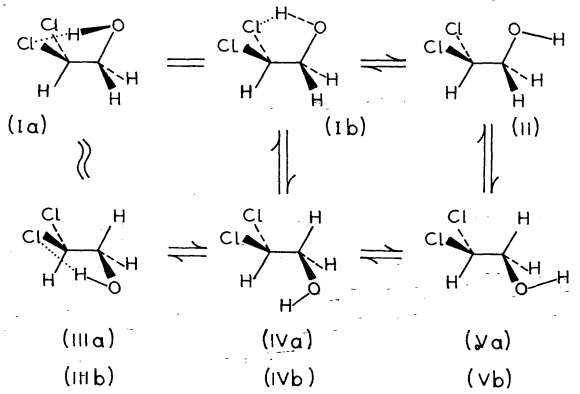

The low-frequency major component would be due to forms I*a* and III*a* (and their mirror images I*b* and III*b*). Conformer II would not be favored because both of the oxygen lone pair orbitals are directed toward chlorine atoms. The minor high frequency component must be due to the mirror image pairs IV*a*, IV*b* and V*a*, V*b*.

For 2,2,2-trihaloethanols only a very simple equilibrium is conceivable:

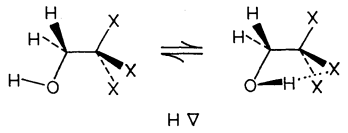

It should be noted that in 2,2-dihaloethanols the OH group always remains gauche to at least one halogen atom, whereas in 2,2,2-trihaloethanols the OH group is always gauche

**Intermolecular OH ... X or OH ... O bonding is ruled out because of the low alcohol concentrations used. No evidence of such interaction (broader concentration-dependent bands at reduced frequency) was found in any spectrum, even at 0° C.*

Can. J. Chem. Downloaded from www.nrcresearchpress.com by 210.87.254.5 on 09/05/12
For personal use only.

Can. J. Chem. Downloaded from www.nrcresearchpress.com by 210.87.254.5 on 09/05/12
For personal use only.

TABLE I

Fundamental OH band parameters and thermodynamic properties of X_2CHCH_2OH and X_3CCH_2OH in dilute CCl_4 solution*

Compound	Temp. (° C)	trans component†,‡ ν(cm^{-1})	gauche component ν(cm^{-1})	gauche component $\Delta\nu_{\frac{1}{2}}$(cm^{-1})	gauche component ϵ(cm^{2}mole^{-1})	$\nu_t-\nu_g$ (cm^{-1})	(D_g/D_t) (~25° C)	ΔH (kcal/mole)	ΔF (kcal/mole)	ΔS (e.u.)
FCH_2CH_2OH	28	3639.7	3624.2	24	‡	15.5	10.0	2.07	0.98	3.6
F_3CCH_2OH	3	3636	3617.5	22		19	31.7			
	20	3635§	3618.9¶	21	>140	16	13.8	3.32	1.12	7.5
	46	3637	3621.2	22		16	12.9			
	~60	3637	3622.8	23		14	13.0			
$ClCH_2CH_2OH$	28	3634.6	3601.4	23	‡	33.2	2.2	1.20	0.04	3.9
Cl_2CHCH_2OH	3	3623	3598.8	20		24	14.6			
	24	3623	3600.3‖	19	>105	23	11.3	2.48	1.00	5.0
	48	3624	3601.7	20		22	7.8			
Cl_3CCH_2OH	4	—	3597.3	18		—	0			
	22	—	3598.8**	19	132	—	0	—	—	—
	45	††	3600.0	18		—	(0)			
$BrCH_2CH_2OH$	28	3631.9	3593.2	26	‡	38.7	1.5	1.25	−0.17	4.7
Br_3CCH_2OH	3	—	3586.0	20		—	0			
	27	—	3587.5	19	114	—	0			
	46	—	3588.7	19		—	0			

*Some comparative measurements (1) on XCH_2CH_2OH compounds are included.
†The trans component in the di- and tri-haloethanols is too weak to permit determination of $\Delta\nu_{1/2}$.
‡Molar extinction coefficient cannot be determined because species cannot be obtained as pure conformer.
§Previously reported at 3636.2 cm^{-1} (6).
¶Previously reported at 3619.8 cm^{-1} (6) and at 3617 cm^{-1} (5).
‖Previously reported at 3600±4 cm^{-1} (10) with no indication of trans component.
**Previously reported at 3596±4 cm^{-1} (10).
††Slight asymmetry due to trans component at this temperature.

to two halogen atoms. The hydroxylic proton can get away from the gauche halogen(s) only by rotation about the C—O bond.

The temperature dependence of the relative absorbances of the two components of the doublet (D_t/D_g) shows that these are true equilibria; in both F_3CCH_2OH and Cl_2CHCH_2OH this ratio increases with increasing temperature.* From measurements at three different temperatures and plots of $\log_{10}(D_t/D_g)$ versus $1/T$, the enthalpy difference (ΔH) between bonded forms (I*a*, I*b*, III*a*, and III*b*) and non-bonded forms (II, IV*a*, IV*b*, V*a*, and V*b*) as well as the corresponding ΔS and ΔF values, can be determined (Fig. 2 and Table I).

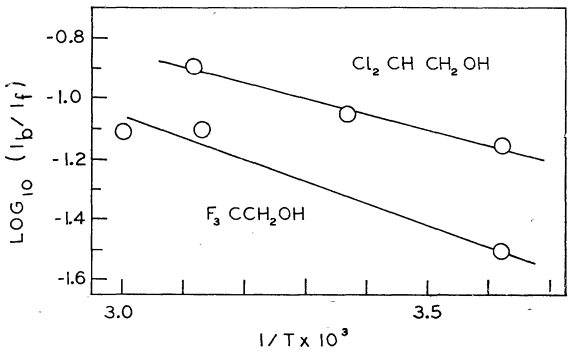

FIG. 2. The temperature dependence of the "free"/"bonded" OH absorbance ratio in 2,2-dichloroethanol and 2,2,2-trifluoroethanol in dilute CCl_4 solution.

The ΔH, ΔF, and ΔS values for the bonded $\rightleftharpoons$ free OH equilibrium in F_3CCH_2OH are uniformly much larger than the corresponding values for FCH_2CH_2OH, in harmony with the concept of stronger intramolecular OH...F bonding in the trifluoro compound. One of the contributing factors would be the increase in acidity of the alcohol, as revealed by the pK_a's (7). An increase in the effective positive charge on the hydroxyl H atom would make it more available for hydrogen bonding, assuming that the base strength of the acceptor remains the same. This may not be the case, since an F atom in an F_3C— group may have a smaller effective negative charge than an F atom in an FCH_2— group. Another factor which would favor the gauche form would be the repulsion between the oxygen atom lone pair orbitals and the F atoms, since in F_3CCH_2OH these orbitals are both approximately directed to an F atom when the OH bond takes up a staggered orientation with respect to the methylene CH bonds in the conformer where the OH is trans to the $-CF_3$ group. However, progressive substitution of fluorine on the same carbon atom is known to lead to C—F bond shortening (11). This would tend to reduce such repulsion. The overall interplay of such factors leads to a greater stability of the intramolecularly bonded form with respect to the free form of F_3CCH_2OH in comparison with FCH_2CH_2OH. Statistically the population of the intramolecularly bonded form is favored in F_3CCH_2OH in comparison with FCH_2CH_2OH. The intramolecular hydrogen bonds in Cl_2CHCH_2OH are also stronger than those in $ClCH_2CH_2OH$.

The fact that the unbonded OH peak disappears in the trihaloethanols in the order $F_3C- > Cl_3C- > Br_3C- = 0$ can be understood in terms of the following factors which override the OH...X hydrogen bonding order F > Cl > Br:

(*a*) Increasing size of the halogen atoms in the order F < Cl < Br, which makes it easier for OH...X bonds to form to the larger atoms in an intramolecular system.

**Here, and in the subsequent discussion, "trans" and "gauche" refer to the relative orientations of the OH group and the -CHX_2 or -CX_3 group respectively, and involve rotation about the C—O bond.*

Can. J. Chem. Downloaded from www.nrcresearchpress.com by 210.87.254.5 on 09/05/12
For personal use only.

(*b*) Halogen–halogen repulsion, which increases with the size of the halogen atoms, opening up the $—CX_3$ umbrella and bringing the X atoms nearer to the OH group. It is known that such angle deformations occur. (See, for example, the increasing XCX angle for CHF_3, $CHCl_3$, $CHBr_3$, and CHI_3, as given by Sutton (12).)

(*c*) Increasing polarizability of X in the order F < Cl < Br. As a result the repulsion between the X atoms and the oxygen lone pair orbitals (in the conformation where the hydroxyl proton is pointing away from the $—CX_3$ group) will increase in the order F < Cl < Br, favoring the hydrogen-bonded form in which the accessibility of X orbitals to the proton will also increase in the order F < Cl < Br. It appears therefore that in F_3CCH_2OH the presence of some unbonded molecules rests chiefly in the small size of the F atoms, which are held at a certain distance from the OH group.

The fact that the self-association constant of F_3CCH_2OH is less than that of ethanol, as reported by Rao *et al.* (8), can readily be interpreted in terms of the reduced basicity of the oxygen due to the electron-withdrawing trifluoromethyl group. Further, most of the OH groups are already tied up in intramolecular OH...F bonds and therefore not readily available for intermolecular association. However, as far as the proton-donating ability to good proton-acceptors is concerned, it is enhanced in F_3CCH_2OH, as Rao *et al.* (9) have shown on the basis of $n \rightarrow \pi^*$ blue shifts in ketones and nitro compounds when these are dissolved in trifluoroethanol.

Concerning half-band widths of ν_g, it is interesting to note that in all the di- and trihaloethanols investigated they are slightly less than for the corresponding monohaloethanols.

When conformational problems are investigated by infrared spectroscopy, an assumption must usually be made concerning the relative magnitudes of the intrinsic molar extinction coefficients (ϵ) (actually, the intrinsic integrated molar intensities) of bands arising in some functional group in the two conformers. Rarely can suitable model compounds be prepared which hold the molecule in a given conformer without perturbing the electron distribution in the group that is being studied. For Cl_3CCH_2OH and Br_3CCH_2OH ϵ_g values were found to be 132 and 114 cm^2 $mole^{-1}$ respectively, and for F_3CCH_2OH a value of >140 can be estimated. Since the band widths are roughly comparable, this indicates that the dipole moment changes involved during the OH stretching vibration increase in the order $OH...Br_3C— < OH...Cl_3C— < OH...F_3C—$, which is expected for increasing OH bond polarity due to the inductive effect, and for increasing strength of the OH...X bond.

Failure of ν_t for the trihaloethanols to correlate with the linear relationship established between ν_t for the monohaloethanols and the Taft σ^* values (1) is almost certainly due to non-bonded interactions between the X atoms and the oxygen atom, since in X_3CCH_2OH the O atom cannot rotate away from a halogen atom, i.e. molecules with "free" OH groups arise by rotation about the C—O bond. Non-bonded interactions have now been shown to play a very important role in determining frequencies (13).

ACKNOWLEDGMENTS

This research was supported financially by the National Research Council of Canada.

REFERENCES

1. P. J. Krueger and H. D. Mettee. Can. J. Chem. Paper II in this series. This issue.
2. M. L. Josien. Pure Appl. Chem. **4**, 33 (1962).
3. R. West, D. L. Powell, L. S. Whatley, M. K. T. Lee, and P. von R. Schleyer. J. Am. Chem. Soc. **84**, 3221 (1962).
4. R. M. Badger and S. H. Bauer. J. Chem. Phys. **5**, 839 (1937).

Can. J. Chem. Downloaded from www.nrcresearchpress.com by 210.87.254.5 on 09/05/12
For personal use only.

5. C. G. CANNON and B. C. STACE. Spectrochim. Acta, **13**, 253 (1958).
6. M. OKI and H. IWAMURA. Bull. Chem. Soc. Japan, **35**, 1744 (1962).
7. R. N. HASZELDINE. J. Chem. Soc. 1757 (1953).
8. B. D. NAGESWARA RAO, PUTCHA VENKATESWARLU, A. S. N. MURTHY, and C. N. R. RAO. Can. J. Chem. **40**, 387 (1962).
9. C. N. R. RAO, R. VENKATARAGHAVAN, K. R. BHASKAR, and A. BALASUBRAMANIAN. *In* Proceedings of the Xth Colloquium Spectroscopicum Internationale. Spartan Books, Washington, D.C. 1963. p. 505.
10. M. L. JOSIEN and P. PINEAU. Compt. rend. **250**, 2559 (1960).
11. D. PETERS. J. Chem. Phys. **38**, 561 (1963).
12. Tables of interatomic distances and configuration in molecules and ions. *Edited by* L.E. Sutton. The Chemical Society, London. 1958.
13. L. J. BELLAMY. *In* Proceedings of the Xth Colloquium Spectroscopicum Internationale. Spartan Books, Washington, D.C. 1963. p. 487.

Can. J. Chem. Downloaded from www.nrcresearchpress.com by 210.87.254.5 on 09/05/12
For personal use only.

SPECTROSCOPIC STUDIES OF ALCOHOLS

IV. CONFORMATIONAL HETEROGENEITY OF 1-PROPANOL IN DILUTE CCl_4 SOLUTION*

P. J. KRUEGER AND H. D. METTEE
Department of Chemistry, University of Alberta, Calgary, Alberta
Received August 23, 1963

Can. J. Chem. Downloaded from www.nrcresearchpress.com by 210.87.254.42 on 09/05/12
For personal use only.

ABSTRACT

High-resolution infrared spectroscopy indicates that the fundamental OH stretching band of 1-propanol in dilute CCl_4 solution is composed of three components caused by rotational isomerism about the C—C and C—O bonds. Although the conformer with the CH_3 and OH groups trans to each other is most heavily populated at room temperature, one of the two conformers having gauche CH_3 and OH groups is thermodynamically most stable. A conformational equilibrium scheme is postulated in which the most stable conformer has a methyl C—H interacting with one of the lone pairs of electrons on the oxygen atom.

INTRODUCTION

Recent studies in this laboratory have led to the spectroscopic evaluation of the enthalpy differences between the trans and the intramolecularly hydrogen-bonded gauche forms of some substituted alcohols of the type XCH_2CH_2OH, X_2CHCH_2OH, and X_3CCH_2OH in dilute CCl_4 solution (1). Of the 2,2,2-trihaloethanols examined, tribromoethanol was found to be exclusively intramolecularly bonded over the range 0–50° C. Trichloroethanol exhibited similar behavior at the lower temperatures, but a trace of "free" OH absorption appeared at 45° C. Trifluoroethanol showed temperature-dependent OH band asymmetry over the range 0–60° C, indicating a small but significant population of the conformer with the OH group directed away from the CF_3 group.

As an extension of this work, we have now investigated 1-propanol by means of high-resolution infrared spectroscopy, and have found three rotational isomers. Prior to this rotational isomerism was advanced to explain the *doublet* OH absorption observed for 1-propanol by Oki and Iwamura (2) in the fundamental region (CCl_4 solution), by Piccolini and Winstein (3) in the first overtone region (CCl_4 solution), and by Badger and Bauer (4) in the second overtone region (gas phase).

EXPERIMENTAL

The details of the instrumental procedure have been described (5, 6).

Reagent grade 1-propanol was dried over anhydrous sodium sulphate and fractionally distilled through a 23-plate spinning band column (b.p. 93.5° at 670 mm, n_D^{20} = 1.3849, lit. 1.38453). Commercial "spectrograde" CCl_4 was used.

RESULTS AND DISCUSSION

The fundamental OH stretching band observed exhibits three partially resolved components with temperature-dependent relative intensities. Figure 1 shows a representative spectrum, with the apparent band maxima at 3638.5 (I), 3632.5 (II), and 3626.7 cm^{-1} (III). The results of quantitative measurements of the changes in the relative absorbances of the peaks with temperature are illustrated in Fig. 2. The slopes of these plots permit the determination of the enthalpy differences between the different pairs of conformers that must exist in simultaneous equilibrium .This treatment suffers from the disadvantage

**A preliminary report of this work was presented at the 46th Annual Conference of the Chemical Institute of Canada, Toronto, June 6–8, 1963.*

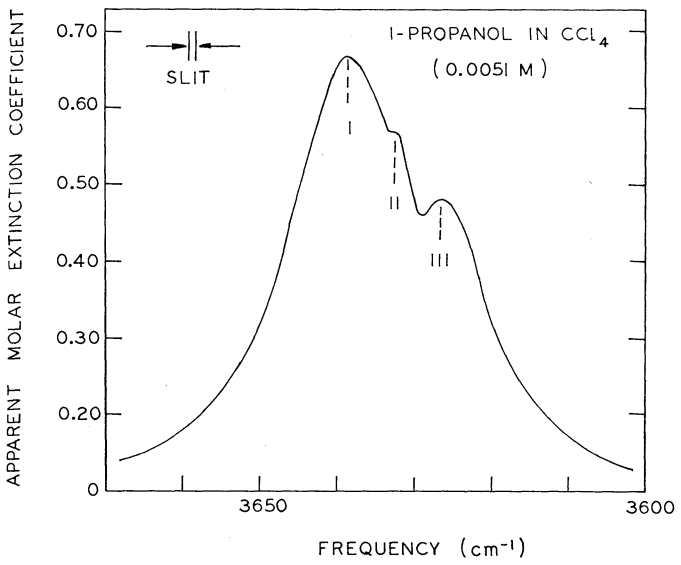

FIG. 1. Fundamental OH stretching bands for conformers of 1-propanol in dilute CCl_4 solution (0.0051 *M*). Path length = 2.00 cm. Temperature = 15° C.

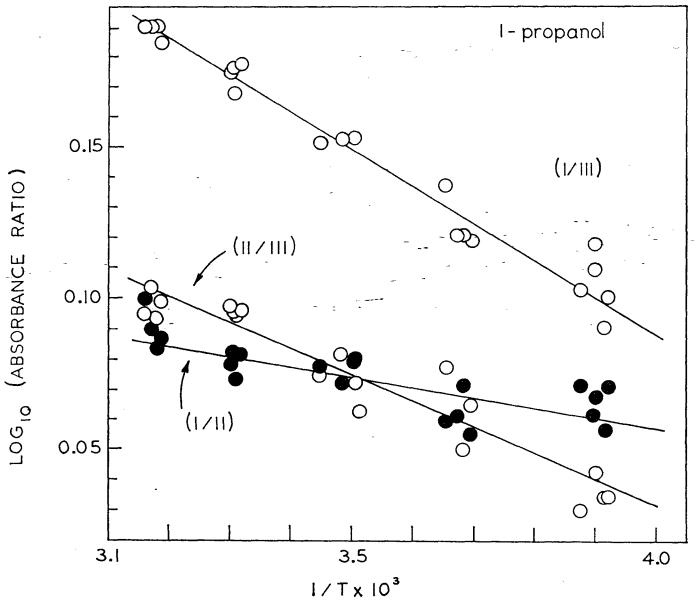

FIG. 2. Temperature dependence of relative absorbances of OH stretching band components in 1-propanol in dilute CCl_4 solution.

that the components of the band overlap badly and therefore make contributions to the peak absorbances of the neighboring band(s). If the assumption is made that the intrinsic molar extinction coefficient of the OH group is independent of its spatial orientation with respect to the CH_3 group, the thermodynamic quantities ΔS and ΔF can also be evaluated. This is a justified approximation since the effect of a hydrocarbon group on

Can. J. Chem. Downloaded from www.nrcresearchpress.com by 210.87.254.42 on 09/05/12
For personal use only.

the polarity of an OH bond due to non-bonded interactions must be small. The thermodynamic quantities are summarized in Table I.

TABLE I

Thermodynamic and spectral properties of 1-propanol in dilute CCl_4 solution

Equilibrium*	ΔH (kcal/mole)†	$\Delta S^{25°\,C}$ (e.u.)	$\Delta F^{25°\,C}$ (kcal/mole)	$\nu_{OH}^{15°\,C}$ shift (cm^{-1})‡
(1) III $\rightleftharpoons$ I	0.55	3.97	−0.63	5.8
(2) II $\rightleftharpoons$ I	0.16	2.28	−0.52	6.0
(3) III $\rightleftharpoons$ II	0.38	1.65	−0.49	11.8

*Components identified in Fig. 1 and in equilibrium scheme. A statistical factor of 2 is included in the calculations for the first two equilibria because there are two equivalent gauche forms for every trans form as far as rotation about the C—C bond is concerned. In the third equilibrium this factor is not required.
†Obtained by least squares fit of the data.
‡Apparent shifts due only to band overlapping. Temperature of 15° C selected for data in this column because of optimum resolution.

Despite the appreciable scatter of the experimental points in Fig. 2, the fact that $\Delta H_1 = \Delta H_2 + \Delta H_3$ (0.54 vs. 0.55 kcal/mole) confirms the validity of treating this system as a set of three simultaneous conformational equilibria. The data are consistent with the following scheme, which makes allowance for the nine conformers predicted by the general treatment of Funck (7). Rotation about both the C—C and the C—O bond is considered, and in each conformer the bonds to atoms on the axis of rotation are staggered.

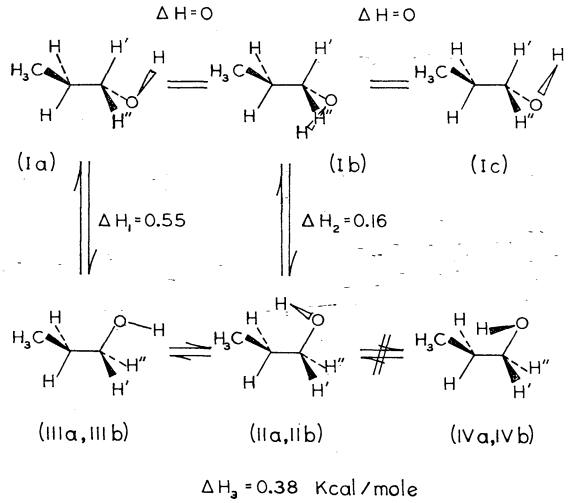

Conformers I*b* and I*c*, II*a* and II*b*, III*a* and III*b*, and IV*a* and IV*b* are mirror-image pairs and thus spectroscopically indistinguishable. The mirror plane passes through the three C atoms.

In (I*a*): O—H staggered re C—H′ and C—H″.
In (I*b*): C—H′ staggered re lone-pair oxygen orbitals.
In (I*c*): C—H″ staggered re lone-pair oxygen orbitals.
In (II): C—H′ staggered re lone-pair oxygen orbitals.
In (III): O—H staggered re C—H′ and C—H″ (one of the oxygen lone-pair orbitals directed toward a methyl H atom).
In (IV): attempted staggering of C—H″ re lone-pair oxygen orbitals (hydroxyl H atom interferes with CH_3 group).

Can. J. Chem. Downloaded from www.nrcresearchpress.com by 210.87.254.42 on 09/05/12
For personal use only.

The recent review of threefold potential barriers to rotation about single bonds by Wilson (8) indicates that unshared pairs of electrons on an axial atom appear to contribute little to these barriers. Thus, in methylamine with two NH bonds and one lone pair the barrier (1.94 kcal/mole) is about 2/3 that of ethane (2.7–3.0 kcal/mole), whereas in methanol with one OH bond and two lone pairs the barrier (1.07 kcal/mole) is about 1/3 the ethane value. However, staggering of the O—H with respect to the C—C and C—H bonds in the above conformers corresponds to staggering of the oxygen lone-pair orbitals with respect to the methylene C—H bonds.

The highest frequency component in the spectrum is assigned to form I where the CH_3 group cannot interfere with the trans OH group. Rotation about the C—O bond in this form, although involving a small barrier, would have a negligible effect on the energy so that I*a* is equivalent to the mirror-image pair I*b*, I*c*. If all three conformers absorb at the same frequency one might expect the high frequency component to be most intense. In III one of the oxygen lone-pair orbitals is directed toward a methyl H atom in close proximity. Form IV can be ruled out because the hydroxyl H atom interferes spatially with one of the methyl H atoms. Form II is relatively free from methyl interference with the hydroxyl proton, and neither of the oxygen lone-pair orbitals is directed toward the methyl group.

It is known that in the vapor phase the gauche form of 1-chloropropane is more stable than the trans form (9). Szasz (10) has suggested that the steric repulsive force between the CH_3 group and the chlorine atom has been overcome by an electrostatic attractive force between the chlorine atom (or the C—Cl bond) and the polarizable methyl group. Pentin and Tatevskii (11) have advanced a similar explanation. The azimuthal angle of $59\pm5°$ between the C—Cl and the C—CH_3 groups (12), compared with the 60° value for gauche C—H bonds in ethane, and with $71\pm5°$ estimated between the C—Cl bonds in 1,2-dichloroethane (13) agrees well with this concept. Since one of the methyl H atoms is directed toward the Cl atom and almost in direct contact (Fisher–Herschfelder model), conditions may be favorable for a CH. . .Cl interaction resembling weak hydrogen bonding.

On this basis the lowest frequency component in 1-propanol (most stable) is assigned to conformer III*a* and its mirror image III*b*, where a C—H of the methyl group could interact with one of the oxygen lone-pair orbitals (weak intramolecular CH. . .O hydrogen bonding). That leaves the intermediate component in the spectrum for the mirror-image pair II*a*, II*b*. The stretching frequency of a terminal OH group in a hydrogen-bonded ROH dimer or polymer is probably not very different from that of a ROH monomer (14). It is therefore difficult to make a prediction about the relative OH frequencies of II and III, particularly since the CH. . .O interaction is very weak.

Table I shows that for the reaction III→I (most stable form to highest energy form) the ΔS value is largest, corresponding to maximum disordering. This is expected, since I actually consists of three rotational isomers that are due to restricted rotation about the C—O band. Further, the torsional oscillation about the C—C bond is probably greatest in I. The reaction III→II corresponds to minimum disordering (smallest ΔS), whereas II→I corresponds to intermediate disordering (intermediate ΔS).

Pennington *et al.* (15) have investigated 1-propanethiol in the gas phase and have found the trans form more stable by 0.4 kcal/mole. Since steric interactions must be fairly similar to those in 1-chloropropane, this situation may be accounted for by the reduced attraction between the C—S bond and the methyl group. It is not known whether the gauche form of 1-propanethiol would be stabilized sufficiently by a solvent like CCl_4 to make it the most stable form in solution.

Can. J. Chem. Downloaded from www.nrcresearchpress.com by 210.87.254.42 on 09/05/12
For personal use only.

On the basis of photographic measurements of the temperature dependence of the relative intensities of four pairs of bands in the Raman spectra of liquid 1-propanol in the range 300–1500 cm^{-1} at 32° and −80° C, Berthelot (16) found an average $\Delta H = 820 \pm 180$ cal/mole, which he ascribes to the enthalpy difference between conformers which differ because of rotation about the C—C bond since the value is so similar to that obtained by Szasz *et al.* (17) for butane (785 ± 165 cal/mole). For 1-butanol Berthelot found $\Delta H = 670 \pm 190$ cal/mole, compared with 615 cal/mole reported for pentane (18). On the other hand Berthelot reports a higher value ($\Delta H = 1024 \pm 210$ cal/mole) for the enthalpy difference between rotational isomers in ethanol, where the rotation must be about the C—O bond. Undoubtedly these Raman values are affected by the strong intermolecular interaction in the pure liquid alcohols. Nevertheless the lower limit for 1-propanol ($820 - 180 = 640$ cal/mole) is reasonably close to the largest ΔH determined in this work (0.55 kcal/mole) for rotational isomerism involving only rotation about a C—C bond.

Recently Sutor (19) has summarized the available data on bond lengths and angles in crystals where "short" inter- and intra-molecular C. . .O distances exist, and has found considerable evidence for CH. . .O hydrogen bonds involving methylidyne groups, and probably also methylene and methyl groups. For systems involving CH_2 and CH_3 groups the CH. . .O angles range from 102° to 147°, with H . . .O distances between 2.07 and 2.77 Ångstroms. Assuming an azimuthal angle of 60°, our calculations show that in 1-propanol the CH. . .O angle is 94°, and the H. . .O distance is 2.6 Ångstroms. This distance is equal to the sum of the Van der Waals radii for an oxygen atom and a hydrogen atom (19). Although the CH. . .O angle is only slightly in excess of a right angle, the need for the H atom to be directed toward one of the lone-pair orbitals of the oxygen atom for most effective interaction cannot be overlooked.

The recent study of C—H groups as proton donors in intermolecular hydrogen bonds by Allerhand and Schleyer (20) shows that the proton-donating ability of the C—H group depends on the carbon hybridization ($sp > sp^2 > sp^3$), and increases with the number of adjacent electron-withdrawing groups. They conclude that a single electron-withdrawing group attached to a sp^3-hybridized carbon atom is not sufficient to make the hydrogens attached to such a carbon proton donors. Undoubtedly the favorable geometry is responsible for the detection of a weak intramolecular CH. . .O hydrogen bond in 1-propanol.

Can. J. Chem. Downloaded from www.nrcresearchpress.com by 210.87.254.42 on 09/05/12
For personal use only.

ACKNOWLEDGMENTS

The financial assistance of the National Research Council of Canada is gratefully acknowledged.

REFERENCES

1. P. J. KRUEGER and H. D. METTEE. Can. J. Chem. Paper III in this series. This issue.
2. M. OKI and H. IWAMURA. Bull. Chem. Soc. Japan, **32**, 950 (1959).
3. R. PICCOLINI and S. WINSTEIN. Tetrahedron Letters, No. 13, 4 (1959).
4. R. M. BADGER and S. H. BAUER. J. Chem. Phys. **4**, 711 (1936).
5. P. J. KRUEGER. Appl. Opt. **1**, 443 (1962).
6. P. J. KRUEGER and H. D. METTEE. Can. J. Chem. Paper II in this series. This issue.
7. E. FUNCK. Z. Elektrochem. **62**, 901 (1958).
8. E. B. WILSON. *In* Advances in chemical physics. Vol. II. *Edited by* I. Prigogine. Interscience, N.Y. 1959. p.367.
9. N. SHEPPARD. *In* Advances in spectroscopy. Vol. I. *Edited by* H. W. Thompson. Interscience, N.Y. 1959. p.288.
10. G. J. SZASZ. J. Chem. Phys. **23**, 2449 (1955).
11. Y. A. PENTIN and V. M. TATEVSKII. Dokl. Akad. Nauk SSSR, **108**, 290 (1956); see also Vestn. Mosk. Univ. **10**, Ser. Fiz. Mat. Estestv. Nauk No. 2, 63 (1955). (Chem. Abstr. **49**, 12963f (1955).)
12. Y. MORINO and K. KUCHITSU. J. Chem. Phys. **28**, 175 (1958).

13. J. AINSWORTH and J. KARLE. J. Chem. Phys. **20**, 425 (1952).
14. V. LIDDEL and E. D. BECKER. Spectrochim. Acta, **10**, 70 (1957).
15. R. E. PENNINGTON, D. W. SCOTT, H. L. FINKE, J. P. MCCULLOUGH, J. F. MESSERLY, I. A. HOSSENLOPP, and G. J. WADDINGTON. J. Am. Chem. Soc. **78**, 3266 (1956).
16. C. BERTHELOT. Compt. rend. 1481 (1950).
17. G. J. SZASZ, R. N. SHEPPARD, and D. H. RANK. J. Chem. Phys. **16**, 704, (1948).
18. S. MIZUSHIMA and H. OKAZAKI. J. Am. Chem. Soc. **71**, 3411 (1949).
19. D. J. SUTOR. J. Chem. Soc. 1105 (1963).
20. A. ALLERHAND and P. VON R. SCHLEYER. J. Am. Chem. Soc. **85**, 1715 (1963).

Can. J. Chem. Downloaded from www.nrcresearchpress.com by 210.87.254.42 on 09/05/12
For personal use only.

FLUORANTHENE STUDIES

E. H. Charlesworth and B. J. Blackburn
Department of Chemistry, University of Manitoba, Winnipeg, Manitoba
Received October 7, 1963

ABSTRACT

3-Acetamido- and 3-amino-fluoranthene are brominated in the 2-position. Two new fluoranthene compounds are reported: 2-bromo-3-acetamidofluoranthene and 2-bromofluoranthene. The theoretical implications of these results are discussed.

Can. J. Chem. Downloaded from www.nrcresearchpress.com by 210.87.254.40 on 09/05/12
For personal use only.

INTRODUCTION

Comparatively few disubstituted derivatives of fluoranthene* have been made by further reaction on monosubstituted derivatives and not too much is known regarding the directive influence of these substituents. It is known that, in general, compounds containing meta-directing groups in the 3-position undergo further substitution in the 9-position. 3-Bromofluoranthene on further bromination gives the 3,8-dibromo compound. On the basis of these data, Campbell and Keir (3) postulated in 1955, that a meta-directing group in ring A would direct to position 9 and an ortho–para directing group would direct to position 8. In the following year Kloetzel, King, and Menkes (4) showed that the above rule was over-simplified, as 3-acetamidofluoranthene was found to nitrate in the 2-position. They considered that the greater activating influence of the acetamido group activates the ring to which it is attached and substitution occurs in the same ring. It seemed desirable to study further examples of strongly activating directors such as the acetamido and amino groups under brominating conditions.

3-Acetamidofluoranthene (III) was brominated at room temperature in pyridine to give the 2-bromo-3-acetamido derivative (IV). Hydrolysis of IV in pyridine – methanol – sodium hydroxide gave 2-bromo-3-aminofluoranthene (II).

Attempts to establish the orientation of the bromine in IV by diazotization and a Sandmeyer reaction on 2-amino-3-acetamidofluoranthene (X) failed. The usual high sulphuric acid concentration required for diazotization of weak, insoluble amines of this type resulted in tar formation. This was due to the instability of the amine sulphate, as this salt, prepared in ether, decomposed when separated from the ether.

The 2-position of the bromine atom has been established in the following manner. If the two substituents are in the same ring, oxidation of IV would destroy this ring, whereas if the groups were in different rings, only the ring containing the amino group could be destroyed and a bromo-1-fluorenonecarboxylic acid would result. Oxidation with chromic anhydride in glacial acetic acid gave 1-fluorenonecarboxylic acid (V) identical with an authentic sample. That the bromine is in the 2-position in the A ring has been established through the 2-nitro-3-acetamido compound (VI) whose orientation was previously established by Kloetzel *et al.* (4). By hydrolysis and deamination of VI they obtained 2-nitrofluoranthene (VII) and by reduction 2-aminofluoranthene (VIII).

Attempted diazotization of VIII under the conventional high-acid concentration required for weak insoluble amines gave an unsatisfactory product. In this diazotization (and in the diazotization of I for practice) side reactions were largely avoided by isolation of the amine sulphate which was then dissolved in a concentrated sulphuric and acetic

**For excellent reviews of fluoranthene chemistry up to 1951, see references 1 and 2.*

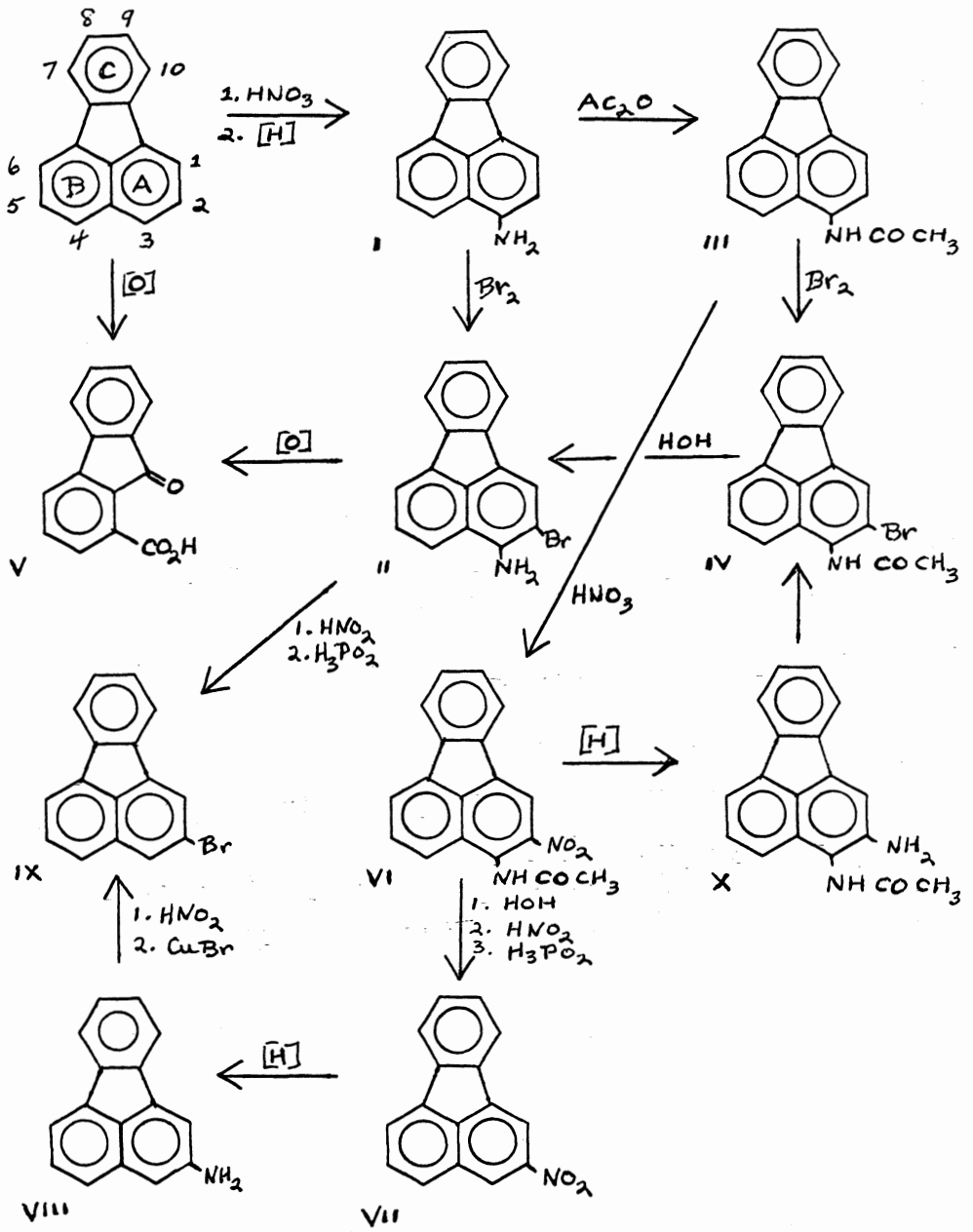

acid mixture and diluted for diazotization. This valuable method is fully described in the experimental preparation mentioned. A Sandmeyer reaction on the diazonium sulphate solution gave an authentic sample of 2-bromofluoranthene (IX). By deamination of II, IX is also obtained. Thus the orientation of the bromine in the original bromination has been established.

The direct bromination of 3-aminofluoranthene (I) is recorded in a German patent by Meyer and Falta (5), but they did not establish the orientation of the halogen. They

Can. J. Chem. Downloaded from www.nrcresearchpress.com by 210.87.254.40 on 09/05/12
For personal use only.

report a melting point of 166–167° C, but our purest product by their method melted at 152–158° C. Comparison of the nuclear magnetic resonance spectra indicates that this is an impure specimen of 2-bromo-3-aminofluoranthene which melts at 176–177° C. Thus direct bromination of 3-aminofluoranthene (II) occurs largely in the 2-position, but a purer product is obtained via the 3-acetamidofluoranthene (III).

These results substantiate those of Kloetzel *et al.* that an intensely activating substituent in fluoranthene causes further substitution in the same ring.

EXPERIMENTAL

3-Nitrofluoranthene was prepared by the method of Garascia, Fries, and Ching (6), reduced to 3-aminofluoranthene (I), and acetylated to the 3-acetamido derivative (III) by following the directions of Kloetzel, King, and Menkes (4).

2-Bromo-3-acetamidofluoranthene (IV)

Bromine (5 ml) was added, with stirring, to a solution of 3-acetamidofluoranthene (10.0 g) in technical grade pyridine (700 ml). The reaction was allowed to proceed at room temperature for 10 hours. The crude product was precipitated by addition of water (2 liters), filtered off, and washed successively with 10% aqueous solutions of sodium hydroxide and sodium bisulphite. The resulting material was placed in pyridine (200 ml) and heated to the boiling point. The insoluble material was filtered from the hot pyridine solution and discarded. The filtrate was treated with charcoal and then sufficient water was added to cause crystallization when the pyridine–water solution cooled. The 2-bromo-3-acetamidofluoranthene (7–8 g) was obtained as yellow flakes which melted at 266–267° C (decomp.). Found: N, 4.2; Br, 23.3; acetyl, 13.1%. Calc. for $C_{18}H_{12}NBrO$: N, 4.1; Br, 23.6; acetyl, 12.7%.

2-Bromo-3-aminofluoranthene (II)

The previous 2-bromo-3-acetamidofluoranthene (10.3 g) was hydrolyzed by heating under reflux for 12 hours in a solution of methanol (600 ml), pyridine (400 ml), and sodium hydroxide (30 g). A small amount of insoluble material was filtered off and discarded. The crude product was precipitated by dilution to 4 liters with water. The collected material was washed with water, dried, and dissolved in boiling pyridine. A small amount of insoluble material was filtered off and the filtrate was heated with charcoal. Sufficient water was added to cause crystallization when the solvent cooled. 2-Bromo-3-aminofluoranthene (7.2 g) was thus obtained as beautiful yellow needles, m.p. 176–177° C (decomp.). Found: N, 4.6; Br, 27.6%. Calc. for $C_{16}H_{10}NBr$: N, 4.7; Br, 27.0%.

Oxidation of 2-Bromo-3-aminofluoranthene

This was accomplished by heating 2-bromo-3-aminofluoranthene (2.0 g) under reflux for 5 hours with sodium dichromate (20 g) in glacial acetic acid (100 ml). This treatment caused evolution of bromine in gaseous form. The reaction mixture was poured into a solution of concentrated sulphuric acid (100 ml) in water (700 ml). The solid which precipitated was filtered off and heated in an aqueous solution of sodium carbonate. The insoluble material was filtered from the carbonate solution and discarded. The filtrate from the diluted reaction mixture was extracted with benzene. The benzene extract was in turn treated with carbonate solution, and the carbonate solutions combined. Acidification of the carbonate solution with sulphuric acid produced crude 1-fluorenonecarboxylic acid. The acid was dried and taken up in boiling *o*-xylene (100 ml). The acid was recovered by extraction with aqueous carbonate solution and acidified. Recrystallization from glacial acetic acid gave 1-fluorenonecarboxylic acid (0.53 g), m.p. 185–189° C. Admixture with an authentic sample prepared by oxidation of fluoranthene by the method of Fieser and Seligman (7) gave no depression in melting point. Comparison of the infrared spectra also proved the identity.

Treatment of the two samples of 1-fluorenonecarboxylic acid with *p*-nitrophenylhydrazine gave the same derivative as fine yellow-orange microcrystals which melted at 307–308° C and with no depression on mixing.

Preparation of 2-Bromofluoranthene (IX)

(a) from 2-Aminofluoranthene (VIII)

2-Nitrofluoranthene (VII) was made from 3-acetamidofluoranthene (III) as shown on the flow sheet according to the directions of Kloetzel *et al.* (4). Reduction of the nitro group gave 2-aminofluoranthene (VIII).

Crude 2-aminofluoranthene (2.0 g) was stirred in dry ether (170 ml) and the insoluble material filtered off. Concentrated sulphuric acid (1 ml) was added with stirring to the amine solution. The amine sulphate was filtered off, allowed to dry, and finely ground. The salt was dissolved in a vigorously stirred solution of concentrated sulphuric acid (75 ml) and glacial acetic acid (75 ml) with gentle warming. The solution was cooled and 150 g of ice and water were added rapidly with stirring to precipitate the amine salt in finely

Can. J. Chem. Downloaded from www.nrcresearchpress.com by 210.87.254.40 on 09/05/12
For personal use only.

divided condition. The salt was diazotized at 15–20° C by addition of sodium nitrite (1.6 g) in water (10 ml). The diazonium solution was poured, with stirring, into a solution of cuprous bromide (15 g) in 48% hydrobromic acid (70 ml) and water (30 ml). The mixture was heated slowly, with stirring, to 95° C. The cooled reaction mixture was diluted with water and the precipitate filtered off. The dried material was stirred with hot benzene and the insoluble material discarded. The aqueous filtrate from above was also extracted with benzene. The benzene extracts were combined and washed with an aqueous sodium hydroxide and sodium bisulphite solution. The benzene was then washed with concentrated sulphuric acid until further washing caused no visible change in the benzene solution. The benzene solution was now washed with an aqueous sodium carbonate solution, which was discarded. The benzene was removed by evaporation to dryness. Sublimation of the solid residue, at approximately 100° C under high vacuum, gave 2-bromofluoranthene (1.1 g) as a light yellow powder, m.p. 102–104° C. Found: C, 67.7; H, 3.39; Br, 27.3; N, 1.17%. Calc. for $C_{16}H_9Br$: C, 68.4; H, 3.23; Br, 28.4%. The analysis indicates some nitrogen containing impurity was present.

(b) Deamination of 2-Bromo-3-aminofluoranthene

Sodium nitrite (0.75 g) was added slowly with stirring to a solution of concentrated sulphuric acid and water (4.2 ml) at room temperature. The solution was then cooled to −5° C and finely ground 2-bromo-3-aminofluoranthene (1.16 g) was then added with vigorous stirring over a 15-minute period, the temperature being maintained at −5° C. Stirring was continued for another 45 minutes at this temperature. Then precooled 50% hypophosphorous acid (85 ml) was added to the stirred solution at such a rate that the temperature did not exceed 5° C. This took about 2½ hours. After 1 week, at 2–3° C, the reaction mixture was diluted with water to 1 liter. The precipitate was allowed to coagulate and then filtered off. The dried material was treated with benzene (250 ml) as previously described under (*a*). The sublimed pale yellow 2-bromofluoranthene (0.75 g) melted at 101–103° C. Found: C, 68.3; H, 3.32; Br, 28.8%. Calc. for $C_{16}H_9Br$: C, 68.4; H, 3.23; Br, 28.4%. A mixed melting point with sample (*a*) showed no depression.

ACKNOWLEDGMENTS

The authors are grateful to the National Research Council of Canada for grants which have aided in this research.

REFERENCES

1. S. H. Tucker and M. Whalley. Chem. Rev. **50**, 483 (1952).
2. Elsevier's Encyclopaedia of Organic Chemistry. Vol. 14. Elsevier Publishing Co., Amsterdam. 1940. p. 305. Vol. 14, Suppl. 1951. p. 54.
3. N. Campbell and N. H. Keir. J. Chem. Soc. 1233 (1955).
4. M. C. Kloetzel, W. King, and J. H. Menkes. J. Am. Chem. Soc. **78**, 1165 (1956).
5. K. Meyer and H. Falta. Ger. Patent No. 734,882. April, 1943. Chem. Abstr. 1252 (1944).
6. R. J. Garascia, E. F. Fries, and C. Ching. J. Org. Chem. **17**, 226 (1952).
7. L. F. Fieser and A. M. Seligman. J. Am. Chem. Soc. **57**, 2174 (1935).

Can. J. Chem. Downloaded from www.nrcresearchpress.com by 210.87.254.40 on 09/05/12
For personal use only.

THE REACTION OF CYCLOPENTANE VAPOR WITH Hg 6($^3P_1$) ATOMS AT ELEVATED TEMPERATURES: THE RECOMBINATION, DISPROPORTIONATION, AND DECOMPOSITION OF CYCLOPENTYL RADICALS[1,2,3]

HARRY E. GUNNING AND RICHARD L. STOCK
Department of Chemistry, University of Alberta, Edmonton, Alberta
Received September 23, 1963

ABSTRACT

The static reaction of Hg 6($^3P_1$) atoms with cyclopentane vapor (c-C_5H_{10}) has been studied with temperatures from 26 to 376°, at constant c-C_5H_{10} concentration and at low light intensities.

From 26 to 250°, the only important products are hydrogen, cyclopentene, and bicyclopentyl. Above 250° new products appearing are ethylene, biallyl, and allyl cyclopentane, together with smaller yields of propylene, ethane, propane, and methane. To 250°, the reaction can be explained in terms of a 5-step paraffinic sequence, involving initial C—H scission to form H atoms and cyclopentyl (c-C_5H_9) radicals. The Arrhenius plot of a function equal to k_{disp}/k_{comb} for c-C_5H_9 radicals showed that $E_{disp}-E_{comb} = 0$. Above 250° c-C_5H_9 radicals decompose into C_2H_4 and C_3H_5 radicals. The activation energy for this process was determined from a number of product functions to be 36.9±1.2 kcal/mole. Evidence was also found for scission of c-C_5H_9 into cyclopentene and H atoms, above ca. 300°.

A brief examination was also made of the thermal decomposition of c-C_5H_{10} up to 457° in a quartz reaction vessel. The substrate is unstable above 350° forming ethylene, propylene, cyclopentene, cyclopentadiene, and hydrogen. The rate data can be satisfactorily explained by two intramolecular decompositions of the substrate into (*a*) ethylene and propylene and (*b*) cyclopentene and hydrogen with the cyclopentene further dehydrogenating to cyclopentadiene. From the data $E_a = 49.6\pm2.0$ kcal/mole and $E_b = 44.0\pm2.0$ kcal/mole.

INTRODUCTION

The reaction of cyclopentane vapor with Hg 6($^3P_1$) atoms, at 30°, has been previously studied (1, 2, 3). It has been shown that the primary reaction involves exclusively C—H bond scission, resulting in the formation of cyclopentyl radicals (c-C_5H_9) and H atoms with a quantum efficiency of at least 80% (3). At this temperature the mechanism of the reaction is

$$c\text{-}C_5H_{10} + \text{Hg } 6(^3P_1) \rightarrow c\text{-}C_5H_9 + H + \text{Hg } 6(^1S_0) \quad [1]$$

$$H + c\text{-}C_5H_{10} \rightarrow H_2 + c\text{-}C_5H_9 \quad [2]$$

$$2(c\text{-}C_5H_9) \rightarrow c\text{-}C_5H_8 + c\text{-}C_5H_{10} \quad [3]$$

$$2(c\text{-}C_5H_9) \rightarrow c\text{-}C_{10}H_{18} \quad [4]$$

$$H + c\text{-}C_5H_8 \rightarrow c\text{-}C_5H_9, \quad [5]$$

and in the most recent study (3) of the reaction, it has been found that the quantum yields at zero extent of reaction ($\Phi°$) for the products, hydrogen, cyclopentene (c-C_5H_8), and bicyclopentyl (c-$C_{10}H_{18}$), are respectively 0.8, 0.4, and 0.4. It follows then from the mechanism and the quantum yield data that $k_4 = k_3$; in other words cyclopentyl radicals show equal rates for disproportionation and recombination. Furthermore, with increasing duration of exposure the cyclopentene level builds up, rendering step [5] more important

[1]*The partial support of this work by the National Research Council of Canada under grant No. NRC T-162 is gratefully acknowledged.*
[2]*From the Ph.D. thesis of R.L.S., Department of Chemistry, University of Alberta, Edmonton, January, 1961.*
[3]*A portion of this paper was presented at the XVIIIth International Congress of Pure and Applied Chemistry, Montreal, Aug. 6–12, 1961.*

Can. J. Chem. Downloaded from www.nrcresearchpress.com by 210.87.254.6 on 09/05/12
For personal use only.

and leading to a product stationary concentration in this product (2, 3). From the actual $(c\text{-}C_5H_8)/(c\text{-}C_5H_{10})$ ratio in the product stationary state, it has been estimated (3) that $k_5/k_2 \simeq 175$.

In view of the foregoing, the mercury-photosensitized decomposition of cyclopentane appeared to be a suitable system for studying the reactions of $c\text{-}C_5H_9$ radicals as a function of temperature. In this connection, previous studies (4, 5) on the behavior of $c\text{-}C_5H_9$ radicals, generated *in situ* by the abstractive attack of CD_3 radicals on $c\text{-}C_5H_{10}$, had shown that $c\text{-}C_5H_9$ is stable to ca. 250°, above which temperature thermolytic cleavage occurs largely via

$$c\text{-}C_5H_9 \rightarrow C_2H_4 + C_3H_5. \qquad [6]$$

In the present investigation the reaction of $c\text{-}C_5H_{10}$ with Hg $6(^3P_1)$ atoms has been examined in some detail over the temperature range from 26° to 375°—in the lower region of thermal instability of the substrate. Below ca. 250° the temperature coefficients of reactions associated with stable $c\text{-}C_5H_9$ radicals were studied, including the disproportionation and recombination processes. In addition activation energy data for the thermal decomposition of the $c\text{-}C_5H_9$ species were sought in the temperature range 250–375°. Finally the thermal decomposition of the substrate itself was briefly examined in the 351–457° region.

The details of the investigation follow.

EXPERIMENTAL

Cylindrical quartz reaction cells were used, 5 cm in diameter, 10 cm in length. The central stem of the cell connected to the high-vacuum manifold via a mercury U-valve, provided with a float valve in the arm on the manifold side. By raising the mercury level in the U-valve to a fixed mark, the cell could be isolated at constant volume from the remainder of the system. The furnace consisted of two brass cylinders, each 5.5 cm I.D. and 12.5 cm in length, wound with insulation and nichrome wire. The two sections were machined to fit around the cell as one unit, with Vycor 7910 ports at each end, opposite the cell windows. Iron–constantan thermocouples were installed close to each window. By mounting each furnace section on tracks parallel to the cylindrical axis of the cell, the two halves of the furnace could be united without altering the position of the cell. On the same tracks, the Hanovia, 87A45 mercury resonance source fitted into a lamp-housing, provided with a shutter on the cell side. Thereby the lamp-housing could be moved into a fixed position with respect to the incident window of the cell. The Vycor 7910 window attached to the furnace cut off radiation below 2200 Å, and thus the 1849 Å resonance line from the lamp was prevented from entering the cell.

Runs were carried out at a constant molar concentration of cyclopentane. Exactly 1120 μmole of substrate was measured in a gas burette, for each run, and transferred to the cell by immersing a small side-arm appendage of the cell stem in liquid nitrogen. This quantity of substrate, upon vaporization, provided a gas pressure of ca. 100 mm in the reaction cell at 25°. At the end of each run, liquid nitrogen was placed around the side arm, and the U-valve was opened. Non-condensable gases were transferred by a Toepler pump to a gas burette for measurement, after which the mole fraction of each component was determined by mass spectrometry.

For analysis of the condensable products, the section of the side arm, into which products and unreacted substrate had been condensed, was flame-cut from the cell, and inserted in a special crusher–preheater previously described (3). This unit could be connected in series with the H_2-carrier stream of the temperature-programmed gas chromatograph (G.L.C.) and complete vaporization of the condensables was assured by maintaining the unit at 150° (3). A by-pass system, downstream from the G.L.C., permitted trapping-out of any peak and removal for separate characterization. The molar, G.L.C. response factors, relative to $c\text{-}C_5H_{10}$, were determined directly for each product, with authentic samples, except for allyl cyclopentane. For this product, the response factor was obtained by interpolation on the linear plot of response factor vs. molecular weight for the naphthenes after Messner, Rosie, and Argabright (6).

The absorbed light intensity at 2537 Å was determined with propane as actinometer (7), taking $\Phi(H_2)$ for this reaction as 0.50 at propane pressures exceeding 40 mm. In our previous study (3) on the $c\text{-}C_5H_{10}$ reaction at 25°, it was shown that $\Phi(c\text{-}C_{10}H_{18})$ was invariant in exposure duration at 0.40 ± 0.01, on the basis of the propane standard (7). Hence the $\Phi(c\text{-}C_{10}H_{18})$ value at 25° was used as a secondary standard for the absorbed light intensity.

Can. J. Chem. Downloaded from www.nrcresearchpress.com by 210.87.254.6 on 09/05/12
For personal use only.

The cyclopentane used was Phillips, Research Grade (P.R.G.). Analysis by G.L.C. showed 0.051 mole %, cyclopentene as the only impurity. Repeated trap-to-trap distillation did not improve the purity. By check runs with an ultrapure c-C_5H_{10}, prepared by preparative G.L.C. (3), it was shown that the P.R.G. material gave identical rate data, when corrected for the small amount of c-C_5H_8 present in the starting material. The cyclopentene used was also P.R.G. material, containing, by G.L.C. analysis, 99.98 mole % of c-C_5H_8, with the impurities consisting of c-C_5H_{10} with traces of c-C_5H_6. The P.R.G. ethylene and propylene used were both further refined by several trap-to-trap distillations with retention of the middle fractions. Similar treatment was employed for further purifying the propane (Matheson, Instrument Grade). Bicyclopentyl was synthesized from cyclopentyl bromide by the Grignard route. A fraction, b.p. 181–183°, was taken which contained at least 99 mole % c-$C_{10}H_{18}$. The 1,5-hexadiene (biallyl) used for calibration was obtained from Matheson, Coleman, and Bell. G.L.C. analysis revealed hexenes as the only impurities.

RESULTS

The mercury-6($^3P_1$)-photosensitized decomposition of cyclopentane vapor was studied over the temperature range 26–376°. At several temperatures in this range, the reaction was examined as a function of duration of exposure (t), to determine the effect of t on the quantum yield ($\Phi(P)$) of each product (P), and to enable estimates to be made of $\Phi°(P)$—the $\Phi(P)$ values at $t = 0$. For the absorbed light intensity (I_a) at 2537 Å, propane actinometry gave $5.92 \pm 0.06 \times 10^{-7}$ einstein/minute. The I_a levels were repeatedly checked throughout the study by the primary propane standard, and by the measured rate of c-$C_{10}H_{18}$ formation, taking $\Phi(c\text{-}C_{10}H_{18}) = 0.40$, at 26° (3).

The significant products over all or part of the temperature region studied were hydrogen, ethylene, cyclopentene (c-C_5H_8), biallyl (C_6H_{10}), allyl cyclopentane (c-C_8H_{14}), bicyclopentyl (c-$C_{10}H_{18}$), methane, ethane, propylene, propane, cyclopentadiene (c-C_5H_6), and cyclopentyl cyclopentenes (c-$C_{10}H_{16}$).

In Figs. 1 and 2, the product yields in micromoles (μM), for runs with $t = 30$ minutes,

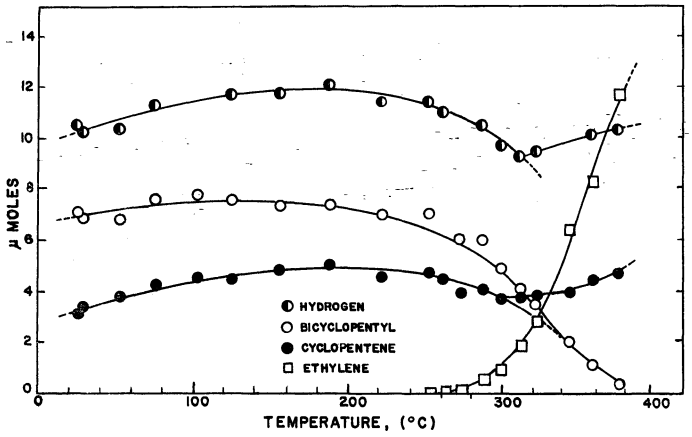

FIG. 1. Micromoles of major products formed for 30-minute runs as a function of cell temperature in the reaction of Hg 6($^3P_1$) atoms with P.R.G. cyclopentane.

are shown as a function of temperature for H_2, c-$C_{10}H_{18}$, c-C_5H_8, C_2H_4 (Fig. 1), and C_6H_{10}, c-C_8H_{14}, C_3H_6, C_2H_6 (Fig. 2). The mean quantum yields for the 12 products, as a function of exposure duration and reaction temperature are given as follows: H_2, C_2H_4, c-C_5H_8, C_6H_{10}, c-C_8H_{14}, c-$C_{10}H_{18}$ (Table I); CH_4, C_2H_6, C_3H_6, C_3H_8, c-C_5H_6, c-$C_{10}H_{16}$ (Table II). It is apparent from Figs. 1 and 2, and Tables I and II, that up to ca. 250°, the only important products are H_2, c-C_5H_8, and c-$C_{10}H_{18}$, as in the reaction at room temperature (3). Of the three minor products appearing below 250° (Table II), the most

Can. J. Chem. Downloaded from www.nrcresearchpress.com by 210.87.254.6 on 09/05/12
For personal use only.

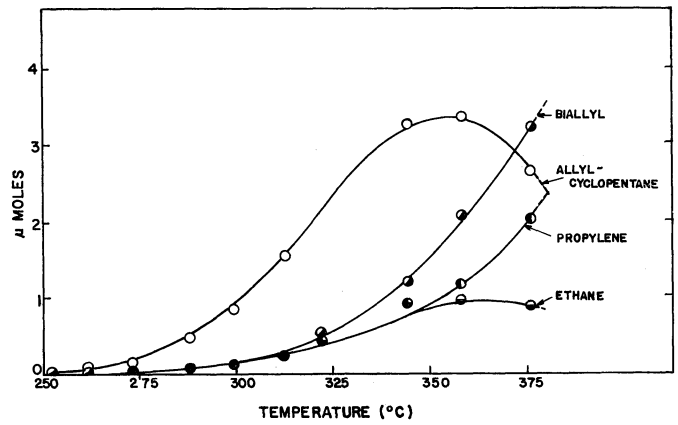

FIG. 2. Micromoles of minor products formed for 30-minute runs, as a function of cell temperature in the reaction of Hg $6(^3P_1)$ atoms with P.R.G. cyclopentane.

TABLE I

Quantum yields of the major products for runs of various duration as a function of the cell temperature in the reaction of Hg $6(^3P_1)$ atoms with P.R.G. cyclopentane

Run	Temp., °C	Time, minutes	Quantum yield A	B	C	D	E	F
139	26	30	0.59	—	0.180	—	—	0.400
153	29	30	0.58	—	0.192	—	—	0.390
141	51	30	0.66	—	0.243	—	—	0.472
155	53	30	0.58	—	0.216	—	—	0.384
143	76	30	0.63	—	0.241	—	—	0.428
145	103	30	0.56	—	0.257	—	—	0.437
147	125	30	0.67	—	0.250	—	—	0.426
149	156	30	0.66	—	0.270	—	—	0.412
151	189	30	0.68	—	0.284	—	—	0.416
150	222	30	0.63	—	0.256	—	—	0.392
148	252	30	0.64	0.0035	0.264	0.0010	0.0031	0.393
169	262	15	0.61	0.0055	0.304	0.0012	0.0059	0.424
168	261	30	0.62	0.0050	0.250	0.0010	0.0047	0.414
170	261	45	0.63	0.0054	0.244	0.0010	0.0044	0.450
146	273	30	0.54	0.0095	0.218	0.0015	0.0088	0.337
154	288	30	0.59	0.0290	0.228	0.0045	0.0270	0.336
167	299	15	0.67	0.030	0.308	0.0066	0.069	0.407
144	299	30	0.54	0.051	0.210	0.0069	0.047	0.273
166	299	45	0.54	0.052	0.217	0.0113	0.051	0.294
161	312	30	0.52	0.103	0.216	0.132	0.085	0.228
163	322	15	0.62	0.185	0.314	0.033	0.158	0.289
142	322	30	0.53	0.153	0.210	0.030	0.114	0.194
162	322	45	0.53	0.151	0.181	0.029	0.120	0.178
164	343	15	0.62	0.408	0.289	0.095	0.234	0.149
140	344	30	0.60	0.355	0.223	0.068	0.183	0.114
165	344	45	0.55	0.281	0.246	0.074	0.169	0.105
160	360	5	0.64	0.655	0.326	0.134	0.280	0.060
158	359	15	0.63	0.557	0.295	0.155	0.226	0.071
156	358	30	0.57	0.464	0.245	0.116	0.188	0.058
157	359	45	0.54	0.425	0.253	0.111	0.180	0.052
159	358	60	0.47	0.364	0.216	0.100	0.158	0.039
152	376	30	0.58	0.656	0.260	0.181	0.151	0.0052

NOTE: A = hydrogen; B = ethylene; C = cyclopentene; D = biallyl; C = allyl cyclopentane; F = bicyclopentyl.

Can. J. Chem. Downloaded from www.nrcresearchpress.com by 210.87.254.6 on 09/05/12
For personal use only.

TABLE II

Quantum yields of the minor products for runs of various duration as a function of the cell temperature in the reaction of Hg $6(^3P_1)$ atoms with P.R.G. cyclopentane

Run	Temp., °C	Time, minutes	Quantum yield G	H	J	K	L	M
139	26	30	—	—	—	—	0.002	0.007
153	29	30	—	—	—	—	—	0.010
141	51	30	—	—	—	—	—	0.014
155	53	30	—	—	—	—	0.0004	0.016
143	76	30	—	—	—	—	—	0.012
145	103	30	0.0003	—	—	—	—	0.012
147	125	30	0.0006	—	—	—	—	0.015
149	156	30	—	—	—	—	0.0005	0.012
151	189	30	0.0004	—	—	—	0.0010	0.017
150	222	30	0.0004	—	—	—	0.0015	0.016
148	252	30	0.0007	—	—	—	0.0012	0.021
169	262	15	0.0007	—	—	—	0.0012	0.015
168	261	30	0.0009	—	—	—	0.0022	0.021
170	261	45	0.0009	—	—	—	0.0025	0.028
146	273	30	0.0003	0.0011	0.0020	—	0.0010	0.020
154	288	30	0.0007	0.0030	0.0043	0.0006	0.0010	0.020
167	299	15	0.0016	0.0042	0.0018	0.0006	—	0.024
144	299	30	0.0004	0.0070	0.0064	0.0011	—	0.018
166	299	45	0.0018	0.0094	0.0076	0.0018	—	0.028
161	312	30	0.0007	0.0144	0.0137	0.0020	—	0.015
163	322	15	0.0049	0.0140	0.040	0.0012	—	0.014
142	322	30	0.0021	0.0240	0.024	0.0023	—	0.018
162	322	45	0.0030	0.0313	0.026	0.0039	—	0.013
164	343	15	0.0014	0.0280	0.050	0.0030	—	0.012
140	344	30	0.0046	0.050	0.050	0.0059	—	0.012
165	344	45	0.0056	0.055	0.050	0.0055	—	0.015
160	360	5	0.0024	0.0160	0.057	—	—	—
158	359	15	0.0030	0.046	0.073	0.0030	—	0.009
156	358	30	0.0053	0.054	0.067	0.0042	—	0.006
157	359	45	0.0075	0.067	0.072	0.0059	—	0.009
159	358	60	0.0060	0.072	0.071	0.0067	—	0.008
152	376	30	0.0045	0.051	0.113	0.0046	—	0.005

NOTE: G = methane; H = ethane; J = propylene; K = propane; L = cyclopentadiene; M = cyclopentyl cyclopentenes.

significant is the cyclopentyl cyclopentene isomers, previously observed in the reaction at 24° (3). It should be noted that *c*-$C_{10}H_{16}$ follows, within the experimental error, the same temperature trend as the major product, *c*-$C_{10}H_{18}$ (Table I), with the rate achieving a gentle maximum at ca. 260°. Cyclopentadiene is a very minor product with Φ values about an order of magnitude lower than Φ(*c*-$C_{10}H_{16}$). Below 250°, CH_4 is a trace product, never exceeding 0.1% of the H_2 product.

Above 250°, new products begin to appear in measurable yields. The first group, which were detected at 252°, consisted of C_2H_4, C_6H_{10}, and *c*-C_8H_{14} (Table I). In the 270–290° region, three further products emerged: C_3H_6, C_2H_6, and C_3H_8 (Table II). The exponential nature of the temperature profile of the C_2H_4 rate is clearly shown in Fig. 1. The corresponding rate vs. temperature graphs for *c*-C_8H_{14}, C_6H_{10}, C_3H_6, and C_2H_6 are displayed in Fig. 2. In both figures the rates are total yields per 30 minutes of exposure.

Thermal Decomposition of Cyclopentane

In order firmly to establish the upper temperature limit to which the photosensitized reaction could be studied, it was necessary to determine the temperature coefficient of

Can. J. Chem. Downloaded from www.nrcresearchpress.com by 210.87.254.6 on 09/05/12
For personal use only.

the thermal reaction. In the photosensitized runs, the longest exposure was 60 minutes, after 3 hours of equilibration at the reaction temperature. The thermal runs were therefore each performed for a period of 240 minutes, representing the maximum time of residence of the substrate in the reaction system for the photosensitization runs. In all, the thermolytic reaction was examined at five temperatures in the range 351–457°.

At the highest temperature studied, 457°, the major products, in order of decreasing importance, were C_3H_6, C_2H_4, c-C_5H_8, and c-C_5H_6. The minor products consisted of C_2H_6, CH_4, and C_3H_8. The results, expressed as μM of product formed in 240 minutes, are given for the five temperatures in Table III.

TABLE III

Rate of product formation as a function of temperature in the thermal decomposition of P.R.G. cyclopentane*

	Temp.				
° C:	351	378	401	429	457
Product			μM		
H_2	—	0.097	0.259	2.65	5.01
CH_4	—	—	—	0.0079	0.113
C_2H_6	—	—	—	0.0217	0.147
C_2H_4	—	0.224	0.716	4.50	14.5
C_3H_8	—	—	—	0.0152	0.073
C_3H_6	—	0.304	0.870	4.89	16.0
c-C_5H_8	0.08	0.160	0.306	1.36	3.06
c-C_5H_6	—	—	—	0.123	1.16

*Cyclopentane concentration = 5.60×10^{-3} mole/liter. Duration of runs = 240 minutes.

DISCUSSION

The Photosensitized Reaction from 26 to 250°

The salient features of the reaction in this temperature region are as follows.

(1) The significant products of the reaction remain qualitatively unchanged, with the major products being H_2, c-C_5H_8, and c-$C_{10}H_{18}$.

(2) The average rates, for 30-minute runs, for H_2 and c-C_5H_8 rise slightly with increasing temperature, passing through a shallow maximum at ca. 200° (cf. Fig. 1). The corresponding curve for c-$C_{10}H_{18}$ appears also to have a slight upward concavity, with the same rates at each end of the curve (Fig. 1).

(3) Comparison of the A, C, and F columns of Table I reveals that, within the experimental error, the following relation obtains:

$$[6a] \qquad \Phi(H_2) = \Phi(c\text{-}C_5H_8) + \Phi(c\text{-}C_{10}H_{18}),$$

as stoichiometrically required for (1) (above) to be valid.

It is apparent that the mechanism ([1] through [5] above) previously proposed (3) for the room-temperature reaction is operative over the entire temperature region (i.e. to 250°). From the steady-state treatment of this five-step sequence, one of the consequences is the relation

$$[7] \qquad K/\Phi(c\text{-}C_{10}H_{18}) - 1 = k_3/k_4$$

where K is the fractional efficiency of [1], that is, the quantum yield of the primary step. It follows from [7] that a plot of log $[K/\Phi(c\text{-}C_{10}H_{18})-1]$ vs. $1/T°_K$ should be linear, with

Can. J. Chem. Downloaded from www.nrcresearchpress.com by 210.87.254.6 on 09/05/12
For personal use only.

slope proportional to E_3-E_4, the difference in activation energy between the disproportionation and recombination reactions for c-C_5H_9 radicals. To calculate the L.H.S. of [7], K was taken as 0.8 from the previous study (3), and combined with the $\Phi(c\text{-}C_{10}H_{18})$ values in the F column of Table I. The results, presented in Fig. 3, yield a straight line

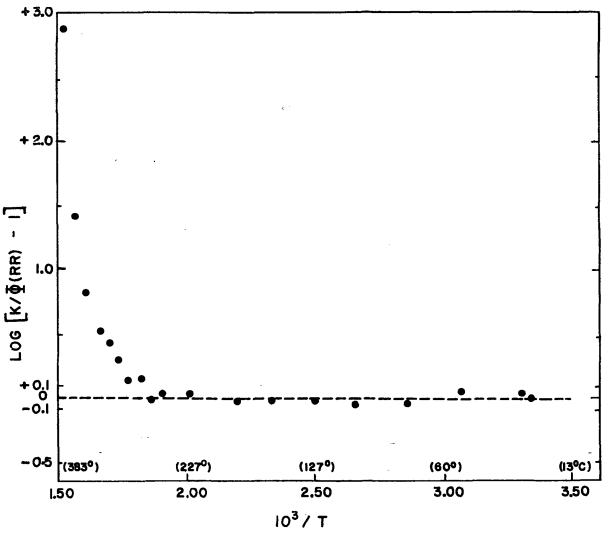

FIG. 3. Log $[K/\Phi(RR)-1]$ = log (k_{disp}/k_{comb}) for cyclopentyl radicals as a function of $1/T$ for runs of 30 minutes duration, in the reaction of Hg $6(^3P_1)$ atoms with P.R.G. cyclopentane.

of zero slope to ca. 250°, and therefore $E_3-E_4 = 0$, demonstrating that the disproportionation and recombination reactions have the same activation energies, presumably zero. A similar temperature behavior for the k_3/k_4 ratio has been found for ethyl, n-propyl, and isopropyl radicals (8–14).

Two factors contribute to the observed rise in $\Phi(c\text{-}C_5H_8)$ with temperature for the 30-minute run. At 26°, the product stationary concentration (P.S.C.) for c-C_5H_8 is reached after ca. 100 minutes of exposure. This period progressively shortens with rising temperature through an increase in the rate of diffusion, resulting in a larger c-C_5H_8 yield within the fixed time of irradiation. In addition the actual P.S.C. level of c-C_5H_8 moves upward with the temperature. This is a direct consequence of the mechanism which predicts for the P.S.C. of c-C_5H_8:

[8] $$(c\text{-}C_5H_8)_{SC} = k_2k_3(c\text{-}C_5H_{10})/k_4k_5.$$

Now, since $E_3 = E_4$ (Fig. 3), and $E_2 > E_5$, [8] will have a positive temperature coefficient at constant substrate concentration. The observed effect at constant exposure duration will be an enhanced c-C_5H_8 yield with increasing temperature.

The fact that $E_2 > E_5$ also accounts for the slight rise in $\Phi(H_2)$ with temperature, since increasing temperature will favor [2] over [5] and thus enhance $\Phi(H_2)$.

In the previous study (3) on the reaction at 24°, it was shown that $\Phi(c\text{-}C_{10}H_{18})$ was invariant in exposure time with a value of 0.40. Steady-state calculations for this quantity lead to the relation

[9] $$\Phi(c\text{-}C_{10}H_{18}) = Kr/(1+r)$$

where $r = k_4/k_3$, and thus since $r = 1$, K, the fractional primary efficiency is 0.8. Equation

Can. J. Chem. Downloaded from www.nrcresearchpress.com by 210.87.254.6 on 09/05/12
For personal use only.

[6] is of course a rearrangement of [7], the relation used to demonstrate (Fig. 3) that r has no temperature coefficient. Now if K is 0.8 rather than unity at 24°, owing to substrate reformation by recombination of the primary fragments,

$$H + c\text{-}C_5H_9 \rightarrow c\text{-}C_5H_{10} \qquad [10]$$

one would expect [10] to become less important with rising temperature through the increased rate of [2]. Any such changes in K with temperature would, through [9], be directly reflected in $\Phi(c\text{-}C_{10}H_{18})$. While there may be a slight increase in this quantity with temperature (Fig. 1, Table I), the small variation in $\Phi(c\text{-}C_{10}H_{18})$ could reasonably be included in the experimental error. It seems unlikely therefore that [10] is important in this system. That K appears to be less than unity more probably is due to our imprecise knowledge of the absolute $\Phi(H_2)$ values for the propane actinometer, used here to determine the absorbed light intensity (I_a). In this connection, a rather detailed study has recently been made in this laboratory (15), on the propane actinometer. The results would suggest that our estimates of I_a may be 20% higher than the true value. Under such conditions K would become 0.96.

The Photosensitized Reaction above 250°

At ca. 250° three new products appear: C_2H_4, C_6H_{10}, and $c\text{-}C_8H_{14}$ (Table I, Figs. 1 and 2). The products are readily explained by the sequence:

$$c\text{-}C_5H_9 \rightarrow C_2H_4 + C_3H_5 \qquad [6]$$

$$2C_3H_5 \rightarrow C_6H_{10} \qquad [11]$$

$$c\text{-}C_5H_9 + C_3H_5 \rightarrow c\text{-}C_8H_{14} \qquad [12]$$

in agreement with previous work on the thermolysis of $c\text{-}C_5H_9$ (4, 5). The exponential increase in the C_2H_4 rate above 250° is accompanied by a corresponding drop in the rate for $c\text{-}C_{10}H_{18}$ (Fig. 1, Table I). This is as expected, since [6] would depress the $c\text{-}C_5H_9$ level in the system, thus reducing $c\text{-}C_{10}H_{18}$ formation via the radical combination step [4]. The resonance-stabilized allyl radicals formed in [6] undergo exclusively radical combination reactions in the 250–270° region, i.e. [11] and [12], a fact consistent with a high activation energy for the abstractive process

$$C_3H_5 + c\text{-}C_5H_{10} \rightarrow C_3H_6 + c\text{-}C_5H_9. \qquad [13]$$

For E_{13}, Gordon, Smith, and McNesby (5) estimate 31.8±3.6 kcal/mole and their data indicate [13] to be important only above 450°. Actually C_3H_6 becomes detectable at 273°, with $\Phi(C_3H_6) = 0.002$ at $t = 30$ minutes (Table II). The rate rises slowly with temperature, reaching a maximum Φ of 0.11 at 376° (Table II), at which temperature thermolysis of the substrate is becoming appreciable (Table III). Examination of the Φ vs. t-runs in the J column of Table II indicates C_3H_6 to be truly a primary, if minor, product of the reaction. Since the rates for C_3H_6 and $c\text{-}C_8H_{14}$ vary independently with temperature, C_3H_6 cannot arise by disproportionation between $c\text{-}C_5H_9$ and C_3H_5. Likewise mutual disproportionation of C_3H_5 radicals is eliminated as a C_3H_6 source since allene was sought as a product and found absent. Accepting the conclusion (5) that [13] is significant only above 450°, there remains the reaction

$$H + C_3H_5 \rightarrow C_3H_6 \qquad [14]$$

to explain C_3H_6 formation. Now, with increasing temperature, the H atoms, formed at constant rate in [1], encounter an increasing C_3H_5 level through the steep rise in the rate of [6] with temperature, thus rendering [14] more important. On this basis, C_3H_6 formation

Can. J. Chem. Downloaded from www.nrcresearchpress.com by 210.87.254.6 on 09/05/12
For personal use only.

Can. J. Chem. Downloaded from www.nrcresearchpress.com by 210.87.254.6 on 09/05/12
For personal use only.

through [14], and C_6H_{10} formation through [11] should both be determined by the C_3H_5 level to a first approximation. The rate vs. temperature curves for the two products should therefore be similar, with the C_6H_{10} curve showing the steeper slope, since the rate here is proportional to $(C_3H_5)^2$. Inspection of Fig. 2 reveals that such is actually the case, thereby supporting [14] as the route to the C_3H_6 product.

Biallyl formation rises sharply and continuously with temperature (Fig. 2, Table I), as expected from the [6] and [11] sequence determining its rate of formation. In addition to [11] and [14], step [12] should also be favored by the increase in (C_3H_5) with temperature, dictated by the temperature dependence of [6]. However, any increase in the rate of [6] will simultaneously raise (C_3H_5) and depress $(c\text{-}C_5H_9)$. Thus it is not surprising that the $c\text{-}C_8H_{14}$ rate, which depends on (C_3H_5) $(c\text{-}C_5H_9)$ through [12], passes through a maximum (Fig. 2, Table I), and this occurs at ca. 350°. Ultimately, with increasing temperature, $(c\text{-}C_5H_9)$ should go to zero and the $c\text{-}C_8H_{14}$ should vanish. In fact $\Phi(c\text{-}C_8H_{14})$, at $t = 30$ (Table I), maximizes at 0.19 at 358°, and at 376° has only dropped to 0.15. Clearly it would be necessary to study the photosensitization reaction above 376°, where the substrate is thermally unstable (Table III), to find the temperature at which $(c\text{-}C_5H_9)$ is effectively zero. More specifically, the $c\text{-}C_{10}H_{18}$ rate through [4] is a direct monitor of $(c\text{-}C_5H_9)$. On this basis we estimate from Fig. 1 that $(c\text{-}C_5H_9)$ drops to zero at ca. 400°.

The minor products, C_2H_6 and C_3H_8, first detected at 273° and 288° respectively (Table II), presumably arise by addition of H atoms from [1] to the primary C_2H_4 and C_3H_6 products, followed by abstraction from the substrate:

$$H + C_2H_4 \rightarrow C_2H_5, \qquad [15]$$

$$C_2H_5 + c\text{-}C_5H_{10} \rightarrow C_2H_6 + c\text{-}C_5H_9, \qquad [16]$$

$$H + C_3H_6 \rightarrow C_3H_7, \qquad [17]$$

$$C_3H_7 + c\text{-}C_5H_{10} \rightarrow C_3H_8 + c\text{-}C_5H_9. \qquad [18]$$

Extrapolation of the Φ vs. t data at 358° (Table II) gives $\Phi°(C_3H_8) = 0.0015$, and $\Phi°(C_2H_6) = 0.005$, with zero being included for both $\Phi°$'s in the uncertainty range at $t = 0$. It is therefore concluded that both C_2H_6 and C_3H_8 are secondary products of the reaction.

The minor product, CH_4, is again mainly of secondary origin ($\Phi°(CH_4) = 0.0015$ at 358°, Table II). We attribute this product to the reaction (11, 12)

$$C_3H_7 \rightarrow C_2H_4 + CH_3 \qquad [19]$$

followed by

$$CH_3 + c\text{-}C_5H_{10} \rightarrow CH_4 + c\text{-}C_5H_9. \qquad [20]$$

Step [19] would reduce (C_3H_7), thus limiting C_3H_8 formation by [18]. Indeed $\Phi(C_3H_8)$ at $t = 30$ appears to maximize at 344° (Table II). Similarly at the higher temperature in the present range, (C_2H_5) should be reduced by

$$C_2H_5 \rightarrow C_2H_4 + H. \qquad [21]$$

From previous work (16), $E_{21} = 39.5$ kcal/mole. The effect of [21] on (C_2H_5) shows up in the C_2H_6 formation via [16]. Thus this rate flattens off above ca. 350° (Fig. 2, Table II).

Especial interest attaches to the temperature trends of the rates of H_2 and $c\text{-}C_5H_8$ formation. Both rates show similar behavior. Above 250° the rates decline slightly to shallow minima at ca. 300° (Fig. 1), and then begin gently to rise. With [3] the sole source of $c\text{-}C_5H_8$, the rate of this product should follow that of $c\text{-}C_{10}H_{18}$ to zero at ca. 300°, where

presumably (c-C_5H_9) becomes negligible. It follows that at ca. 300° and above a c-C_5H_8-forming reaction, other than [3], must come into play. In this connection McNesby and Gordon (17) studied the photolysis of a 1:1 mixture of acetone-d_6(Ad_6) and cyclopentane from 250 to 402°, thereby producing c-C_5H_9 by hydrogen abstraction from c-C_5H_{10} by CD_3 radicals. They found the hydrogen product of the reaction to be predominantly H_2 ($HD/H_2 = 0.04$), indicating that the H_2 must arise intramolecularly from c-C_5H_9:

$$c\text{-}C_5H_9 \rightarrow c\text{-}C_5H_7 + H_2. \qquad [22]$$

The fate of the c-C_5H_7 radicals was not discussed.

Our findings do not particularly support reaction [22], unless it is assumed that the c-C_5H_7 radicals, formed in [22], disappear almost exclusively by abstraction from the substrate to form c-C_5H_8. Here it is to be noted from Table II that $\Phi(C_{10}H_{16})$, which product likely forms by combination of c-C_5H_9 and c-C_5H_7 radicals (3), has a negative temperature coefficient above 300°, and the expected disproportionation product, c-C_5H_6, is not detectable above 288° (Table II). As the new source of c-C_5H_8 above ca. 300°, we postulate

$$c\text{-}C_5H_9 \rightarrow c\text{-}C_5H_8 + H. \qquad [23]$$

This reaction would explain the upturn in $\Phi(C_5H_8)$ above ca. 300° (Table I, Fig. 1), and also for the similar behavior (Table I, Fig. 1) of $\Phi(H_2)$, since [23] would increase the H-atom yield, thereby raising the rate of H_2 formation by [2]. The contribution which [23] makes to the observed $\Phi(c\text{-}C_5H_8)$ values can be estimated, at least at 350° from the Φ vs. t data in Table I. Thus from the data below 250°, where [3] and [4] are the respective sources of c-C_5H_8 and c-$C_{10}H_{18}$, it was found that $\Phi°(C_5H_8) = \Phi°(C_{10}H_{18})$. At 358°, direct extrapolation to $t = 0$, of the Φ vs. t data gives $\Phi°(C_5H_8) = 0.33$, and $\Phi°(C_{10}H_{18}) = 0.06$. Thus the $\Phi°$ for the c-C_5H_8 produced in [23] would be $0.33 - 0.06 = 0.27$.

Very recently Gordon (18) has re-examined the Ad_6–c-C_5H_{10} photolysis. Hydrogen and c-C_5H_8 were found as products, as well as those originating from [6]. He concludes that the formation of H_2 and c-C_5H_8 can best be explained by step [23], followed by [2], as in our system. From his temperature data he estimates E_{23} to be 28 kcal/mole.

The activation energy for reaction [6], the decomposition of c-C_5H_9 into C_2H_4 and C_3H_5, may be estimated from our data in several ways. Thus assuming that any of the primary C_2H_4 formed in [6] that is consumed during irradiation terminates as C_2H_6, we can calculate $\Phi(C_2H_4 + C_2H_6)$ at $t = 30$, ($\Phi(C_2)$), from Tables I and II. Now the total μM of products formed in 30 minutes of exposure (μM C_2) will be equal to $30\Phi(C_2)\ I_a$, when I_a is expressed in μeinstein/minute. In Fig. 4, log (μM C_2) is plotted against $1/T$. The plot is linear from 252° to 344°, and the best straight line gives $E_6 = 37.2$ kcal/ mole. Above 344°, a major fraction of the cyclopentyl radicals are decomposing by both [6] and [23], and under these conditions the exponential relation between rate of C_2 formation and temperature will no longer obtain.

Alternately E_6 can be calculated from a graph of $\log[\Phi°(C_2H_4)$ vs. $1/T$. To estimate $\Phi°(C_2H_4)$ from the data in Table I, extrapolation to $t = 0$ was used above 312°, and below this temperature the mean $\Phi(C_2H_4)$ values were used, since in this range $\Phi(C_2H_4)$ does not appear to depend on t. The Arrhenius plot is shown in Fig. 5 from which a value $E_6 = 36.2$ was obtained.

On the basis of the proposed mechanism several other relations can be used to determine E_6. Thus

$$\Phi°(C_2H_4)/[\Phi°(c\text{-}C_{10}H_{18})]^{\frac{1}{2}} = k_6/(I_a k_4)^{\frac{1}{2}}. \qquad [24]$$

Can. J. Chem. Downloaded from www.nrcresearchpress.com by 210.87.254.6 on 09/05/12
For personal use only.

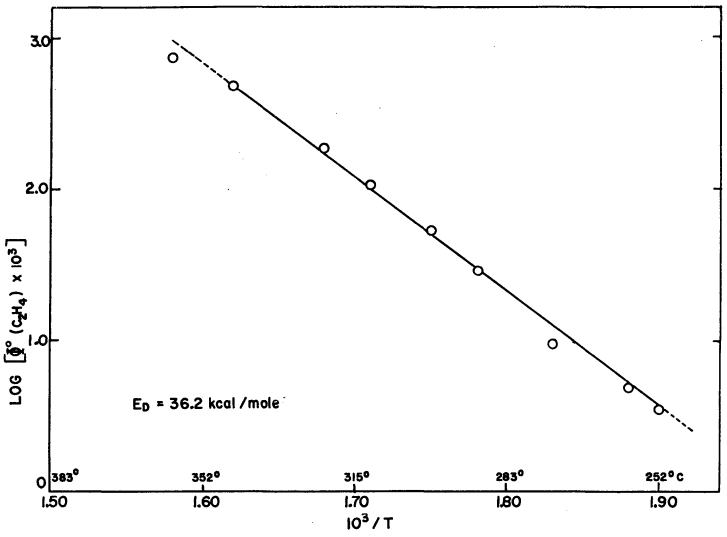

FIG. 4. Arrhenius plot for the decomposition of cyclopentyl radicals into ethylene and allyl radicals, using as monitor the total yield of C_2 products, in the reaction of Hg $6(^3P_1)$ atoms with P.R.G. cyclopentane.

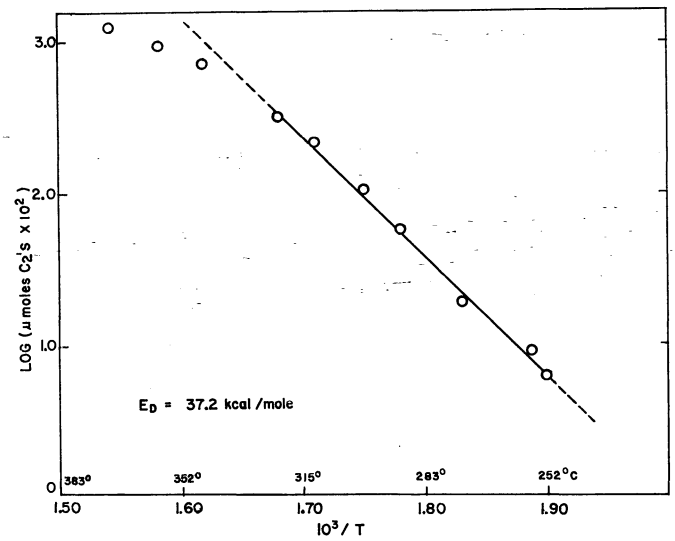

FIG. 5. Arrhenius plot for the decomposition of cyclopentyl radicals into ethylene and allyl radicals, using as monitor the primary quantum yield of ethylene formation, in the reaction of Hg $6(^3P_1)$ atoms with P.R.G. cyclopentane.

Since in the R.H.S. of [24] only k_6 is temperature-dependent, the plot log (L.H.S.) vs. $1/T$ should provide a value for E_6. A good straight line is obtained, from the slope of which $E_6 = 40.0$ kcal/mole. Again from the steady-state relations among the primary reactions, taking $K = 1$,

$$[25] \qquad \Phi^\circ(C_2H_4)/[1-\Phi^\circ(C_3H_6)-\Phi^\circ(C_6H_{10})-\Phi^\circ(c\text{-}C_8H_{14})]^{\frac{1}{2}} = k_6/[I_a(k_3+k_4)]^{\frac{1}{2}}$$

Can. J. Chem. Downloaded from www.nrcresearchpress.com by 210.87.254.6 on 09/05/12
For personal use only.

and

$$[26] \qquad \Phi^\circ(C_2H_4)/[1-\Phi^\circ(C_2H_4)+\Phi^\circ(C_6H_{10})]^{\frac{1}{2}} = k_6/[I_a(k_3+k_4)]^{\frac{1}{2}}.$$

The log (L.H.S.) vs. $1/T$ plots for [25] and [26] were both linear and the slopes gave E_6 values of 35.0 and 36.3 kcal/mole, respectively.

Combining the five independent values, we find $E_6 = 36.9 \pm 1.9$ kcal/mole (standard deviation). Since extrapolation to $t = 0$ may lead to large errors, it is likely that the E_6 value of 37.2 kcal/mole, obtained from Fig. 4, is the most reliable. Pertinently Gordon (18) has recently determined E_6 from the Ad_6–c-C_5H_{10} system, and obtains 37.7 kcal/mole, in satisfactory agreement with our findings.

Bywater and Steacie (19), for the reaction

$$n\text{-}C_4H_9 \rightarrow C_2H_4 + C_2H_5, \qquad [27]$$

found $E_{27} = 23$ kcal/mole. This reaction involves scission of a C—C single bond, and formation of one olefinic bond. On the other hand decomposition of c-C_5H_9 via [6] requires two C—C single bond ruptures, and the formation of two olefinic linkages. To a first approximation one would expect, therefore, that E_6 should be roughly twice E_{27} or 46 kcal/mole. The fact that E_6 is actually 9 kcal/mole lower than this estimate can be readily explained in terms of the resonance energy of the C_3H_5 radical, and any strain energy associated with the cyclic c-C_5H_9 structure.

In the mercury $6(^3P_1)$-photosensitized decomposition of saturated hydrocarbons, the C—H bond energy may be as much as 20–25 kcal/mole lower than the 112.7 kcal/mole available from the Hg $6(^3P_1)$ atom. Thus the primary process may lead to energy-rich alkyl radicals. Indeed Back (20) has seriously considered this possibility to explain certain aspects of the propane reaction. It is equally conceivable that in our system the primary reaction [1] may generate an energy-rich c-C_5H_9 radical. Now one would expect such hot species to decompose with a lower activation energy than thermalized radicals. It is therefore of considerable interest to find that our value for E_6 agrees very well with that obtained by Gordon (18) from a system in which c-C_5H_9 was generated by the abstractive attack of CD_3 on c-C_5H_{10}, a reaction which should not transfer excess energy to the resulting c-C_5H_9 radical.

The Thermal Decomposition of Cyclopentane Vapor

For the 351–457° range studied, the major products were C_2H_4, C_3H_6, H_2, c-C_5H_8, and c-C_5H_6 together with very minor yields of CH_4, C_2H_6, and C_3H_8 (Table III). It will further be noted (Table III) that C_2H_4 and C_3H_6 are produced in roughly equimolar yields, suggesting the unimolecular decomposition

$$c\text{-}C_5H_{10} \rightarrow C_2H_4 + C_3H_6. \qquad [28]$$

Alternately C—H cleavage would occur.

$$c\text{-}C_5H_{10} \rightarrow c\text{-}C_5H_9 + H, \qquad [29]$$

followed by [6], with C_3H_6 forming either by [13] or [14]. However, militating against the importance of [13], here, is the fact (4, 5, 17) that C_3H_5 does not appreciably abstract from c-C_5H_{10} below 450°. Also the virtual absence of C_2H_6 in our products (Table III) suggests a low H-atom level in the system, thereby rendering C_3H_6 formation through [14] improbable. Furthermore, no C_6H_{10} was found, again indicating the absence of C_3H_5 radicals. We conclude, therefore, that in our specific temperature range, reaction [28] is the main ring-cleavage process operative, in agreement with earlier workers [21–26]

Can. J. Chem. Downloaded from www.nrcresearchpress.com by 210.87.254.6 on 09/05/12
For personal use only.

who have used [28] to explain the c-C_5H_{10} thermolysis at much higher temperatures. In contrast, McNesby and Gordon (17) concluded that the reaction proceeded partly by [28] and partly by the free radical route. While our findings do not confirm their conclusions, the two studies are not completely comparable in that their work (17) was done above 500°.

If it is accepted that H atoms do not play an important role under our conditions, as discussed above, the c-C_5H_8 and c-C_5H_6 products must be attributed to intramolecular processes.

$$c\text{-}C_5H_{10} \rightarrow c\text{-}C_5H_8 + H_2 \qquad [30]$$

followed by further dehydrogenation of c-C_5H_8

$$c\text{-}C_5H_8 \rightarrow c\text{-}C_5H_6 + H_2. \qquad [31]$$

Now [31] and [32] would require that the H_2 yield be related to the amounts of c-C_5H_8 and c-C_5H_6 produced. From Table III, the ratio of H_2 found to that required by [30] and [31] varies from 0.6 to 0.98. The disparity is consistent with the experimental error and the incompleteness of the mechanism assumed. Insufficient data are available to discuss the origins of the minor products, CH_4, C_2H_6, and C_3H_8.

The activation energy for [28] can be estimated from the three Arrhenius plots log $[\mu M(C_2H_4)]$, log $[\mu M(C_3H_6)]$, and log $[\mu M(C_2H_4+C_3H_6)]$ all vs. $1/T$. The results give E_{28} values respectively of 50.4, 48.9, and 49.5 kcal/mole.

For reaction [30], the activation energy can be obtained by plotting log $[\mu M(c\text{-}C_5H_8) + \mu M(c\text{-}C_5H_6)]$ vs. $1/T$ on the assumption that c-C_5H_8 is the intermediate in the formation of c-C_5H_6, as indicated in [31]. For E_{30} we obtain 42.2 kcal/mole. Alternately we may plot log $[\mu M(H_2)-\mu M(c\text{-}C_5H_6)]$ vs. $1/T$. Here E_{30} is 46.4k cal/mole. Finally we may represent both the log $[\mu M(c\text{-}C_5H_8) + \mu M(c\text{-}C_5H_6)]$ and the log $[\mu M(H_2)-\mu M(c\text{-}C_5H_6)]$ points against $1/T$ on the same graph and put the best straight line through all points. Thereby we find $E_{30} = 43.7$ kcal/mole. Considering the paucity of the data and the inherent experimental error in the low temperature values for $\mu M(c\text{-}C_5H_8)$, we conclude E_{30} to be 44 ± 2 kcal/mole. For similar reasons we estimate E_{28} to lie within the range 49.6 ± 2 kcal/mole.

Finally it should be emphasized that in this brief ancillary study on the thermal decomposition of c-C_5H_{10} vapor, we may well be examining a reaction which is entirely heterogeneously catalyzed on the quartz surface of the reaction vessel.

REFERENCES

1. G. A. Allen, D. L. Kantro, and H. E. Gunning. J. Am. Chem. Soc. **72**, 3588 (1950).
2. P. W. Beck, D. V. Kniebes, and H. E. Gunning. J. Chem. Phys. **22**, 678 (1954).
3. R. L. Stock and H. E. Gunning. Can. J. Chem. **38**, 2295 (1960).
4. J. R. McNesby and A. S. Gordon. J. Am. Chem. Soc. **79**, 825 (1957).
5. A. S. Gordon, S. R. Smith, and J. R. McNesby. J. Am. Chem. Soc. **81**, 5059 (1959).
6. A. E. Messner, D. M. Rosie, and P. A. Argabright. Anal. Chem. **31**, 230 (1959).
7. S. Bywater and E. W. R. Steacie. J. Chem. Phys. **19**, 319 (1951).
8. C. A. Heller and A. S. Gordon. J. Phys. Chem. **60**, 1315 (1956).
9. E. J. Caule and E. W. R. Steacie. Can. J. Chem. **29**, 103 (1951).
10. Z. T. Casefort. U.S. Govt. Res. Rept. **31**, 409 (1959).
11. J. A. Kerr and A. F. Trotman-Dickenson. Trans. Faraday Soc. **55**, 572 (1959).
12. J. A. Kerr and A. F. Trotman-Dickenson. Trans. Faraday Soc. **55**, 921 (1959).
13. C. R. Masson. J. Am. Chem. Soc. **74**, 4731 (1952).
14. S. G. Whiteway and C. R. Masson. J. Chem. Phys. **25**, 233 (1956).
15. Y. Rousseau, O. P. Strausz, and H. E. Gunning. To be published.
16. S. Bywater and E. W. R. Steacie. J. Chem. Phys. **19**, 326 (1951).
17. J. R. McNesby and A. S. Gordon. J. Am. Chem. Soc. **79**, 4593 (1957).
18. A. S. Gordon. Private communication.
19. S. Bywater and E. W. R. Steacie. J. Chem. Phys. **19**, 172 (1951).

Can. J. Chem. Downloaded from www.nrcresearchpress.com by 210.87.254.6 on 09/05/12
For personal use only.

20. R. A. BACK. Can. J. Chem. **37**, 1834 (1959).
21. P. P. BORISON, E. M. SHAKHAZAROVA, and E. I. MARGOLIS. J. Gen. Chem. USSR, **4**, 1385 (1934).
22. F. E. FREY. Ind. Eng. Chem. **26**, 198 (1934).
23. B. A. KASANSKY and A. F. PLATE. Ber. **67**, 1023 (1934).
24. L. KÜCHLER. Z. Physik. Chem. B, **53**, 307 (1943).
25. F. O. RICE and M. T. MURPHY. J. Am. Chem. Soc. **64**, 996 (1942).
26. D. W. VANAS, N. M. LODGE, and W. D. WALTERS. J. Am. Chem. Soc. **74**, 451 (1952).

Can. J. Chem. Downloaded from www.nrcresearchpress.com by 210.87.254.6 on 09/05/12
For personal use only.

MOLD METABOLITES

2. THE STRUCTURE OF GRISEOVIRIDIN[1,2]

M. CATHERINE FALLONA, P. DE MAYO, T. C. MCMORRIS, T. MONEY, AND A. STOESSL

Department of Chemistry, University of Western Ontario, London, Ontario

Received August 21, 1963

ABSTRACT

By a combination of selectively reductive and hydrolytic processes the structure of perhydrodethiogriseoviridin diacetate, obtained by Raney nickel reduction of griseoviridin diacetate, has been shown to be that of a macrocyclic lactonic peptide (III). Other hydrolytic and degradative experiments have ascertained the points of attachment of the cysteine moiety and the disposition of the functional groups in the aminodecanoic acid. The remaining three carbon atoms have been shown to be part of an unusual dehydro amino acid fragment, and the totality of this and other evidence has defined the structure of griseoviridin as represented in (XXVII).

Can. J. Chem. Downloaded from www.nrcresearchpress.com by 210.87.254.105 on 09/05/12
For personal use only.

The antibiotic griseoviridin, isolated from cultures of a strain of *Streptomyces griseus* (16), has been the subject of studies by Ames, Bowman, and their collaborators (3, 4, 5) and by ourselves (1). The results of these investigations may be summarized as follows.

Griseoviridin, $C_{22}H_{27}O_7N_3S$,* on reduction with Raney nickel gave perhydrodethiogriseoviridin (2).† This on hydrolysis under various conditions gave 5-hydroxyhexanoic acid (1), two molecules of alanine (5), and ω-aminodecanoic acid, the latter representing a chain from which all the originally present functional groups had been stripped (5). All the carbon atoms in griseoviridin itself could, therefore, be accounted for in terms of four distinct moieties. These were (*a*) a C_6 fragment the structure of which had been shown (1) to be (I), (*b*) a C_3 alanine precursor which had been identified as D-cysteine (4), (*c*) a second C_3 alanine precursor concerning the nature of which no direct evidence was yet forthcoming, and (*d*) an unsaturated ω-aminodecanoic fragment required to contain, also, at least one of the hydroxylic functions present in griseoviridin itself. Another pertinent observation was the fact that griseoviridin contained but one C-methyl group, present in the C_6 fragment (1), and, therefore, that both the methyl groups present in the two molecules of alanine derived from perhydrodethiogriseoviridin were artefacts. Other significant results were recorded and will be referred to at the appropriate point. It may

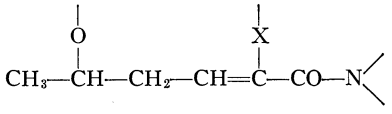

X = O, N, or S

(I)

be mentioned here that discussion of an important derivative of griseoviridin, namely its "hydrochloride," because it is not directly relevant to the structural elucidation of griseoviridin, will be deferred to the following paper.

[1]*Reference (1) is considered Part 1 in this series.*
[2]*A portion of the work here reported formed a preliminary communication (2).*

**The analytical figures did not permit selection of the number of hydrogen atoms to nearer than two; the final result awaited the structural clarification.*
†*This compound perhydrodethiogriseoviridin was originally termed octahydrodethiogriseoviridin, but has been renamed more appropriately. An authentic octahydro compound is referred to below.*

Since perhydrodethiogriseoviridin diacetate was obtainable from griseoviridin diacetate without the removal of any oxygen function and under mild conditions it seemed probable at the outset that this molecule contained the framework of carbon atoms originally present in griseoviridin. The relevant observation (4) that it was a neutral substance implied, considering the constituent functional groups, that the substance be cyclic, and be a lactone or, less likely, a diacylamide: the infrared spectrum (4) could be interpreted in either sense.

Perhydrodethiogriseoviridin diacetate prepared by Raney reduction of griseoviridin diacetate, and also by acetylation of perhydrodethiogriseoviridin (4) was hydrolyzed with dilute alkali at room temperature. Aside from the titrimetric requirements of the acetates one further equivalent of alkali was consumed. The product, which contained no acetyl group, was an acid and was characterized as the crystalline methyl ester. The latter consumed one equivalent of alkali on similar mild hydrolysis.

If the hydrolysis were that of a diacylimide, the functional groups revealed would necessarily be those of a carboxylic acid and an amide. In the case of a lactone a new hydroxyl function would be exposed. In any other circumstances an amino group would be released, and that this was not the case was shown by titration of the methyl ester with hydrochloric acid: no basic function could be detected. Acetylation of the ester gave an oily triacetate the nature of which was indicated by analytical data and also, persuasively, by the presence of three sharp closely spaced peaks (3H each) in the n.m.r. spectrum at τ 7.92, 7.94, and 7.96 for the three acetates. It was therefore to be concluded that perhydrodethiogriseoviridin diacetate was a lactone.

Three structures could then be written for the hydroxy acid corresponding to perhydrodethiogriseoviridin considering only, for the moment, the order of union of the four constituent moieties. These could be represented as in (II*a*, *b*, or *c*):

(II) (*a*) C_5—CO—Ala—Ala—NH—C_9—COOH,

(*b*) C_5—CO—Ala—NH—C_9—CO—Ala—OH,

(*c*) C_5—CO—NH—C_9—CO—Ala—Ala—OH.

In II*a* and II*c* the dipeptide alanylalanine was present whilst in II*b* and II*c* the terminal carboxyl was that of alanine. With these experimentally determinable features a solution was possible.

Milder acid hydrolysis of perhydrodethiogriseoviridin diacetate than had been previously used, afforded, after separation of the products by chromatography, alanylalanine isolated in crystalline form and further characterized by hydrolysis to alanine.

To distinguish between II*a* and II*c* advantage was taken of the selective reducing properties of lithium borohydride (6). Reduction of perhydrodethiogriseoviridin diacetate with this reagent, it was expected, would result in conversion of the lactonic carboxyl to primary alcohol and leave unaffected the remaining amide functions. The product obtained by this mode of reduction was hydrolyzed and the basified solution steam distilled. A volatile base was obtained, characterized as the crystalline 3,5-dinitrobenzoate, which behaved indistinguishably from *dl*-alaninol. Further, the active and racemic esters had identical infrared spectra. These observations allowed the rejection of (II*a*) as inappropriate, and required (II*c*) as the correct representation of the structure of the acid corresponding to perhydrodethiogriseoviridin.

Three hydroxyl groups were available as the site of lactonization. It will be shown later that, in parallel studies, it was ascertained that the two such functions in the C_{10} fragment

Can. J. Chem. Downloaded from www.nrcresearchpress.com by 210.87.254.105 on 09/05/12
For personal use only.

were not so involved, and that the C_6 hydroxyl provided the ethereal oxygen. With this anticipation perhydrodethiogriseoviridin could then be represented as (III).

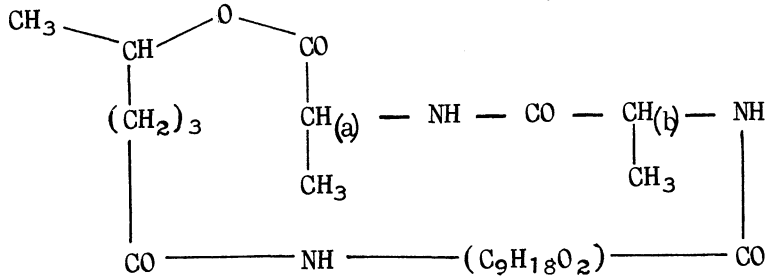

(III)

It was recorded previously (1) that (III), on alkaline hydrolysis gave, as expected, δ-caprolactone (IV). Hexahydrodeoxygriseoviridin, a reduction product of griseoviridin hydrochloride (see following paper), did not give (IV) on hydrolysis (1) and the same observation was later made with respect to hexahydrogriseoviridin diacetate. This suggested (1) that the atom 'X' in the representation (1) might be sulphur, and substance was added to this conception when it was observed that, whilst griseoviridin on treatment with perbenzoic acid gave an amorphous and uncharacterized "oxide" which did not show absorption bands in the infrared corresponding to those expected for sulphones, hexahydrodeoxygriseoviridin (1) and, later, hexahydrogriseoviridin diacetate gave such sulphones readily. The interpretation drawn from these observations was that hydrogenation or hydrogenolysis in the vicinity of the sulphur rendered it open to oxidative attack. Since, in the preparation of hexahydrodeoxygriseoviridin and hexahydrogriseoviridin diacetate, the unsaturation from the C_6 fragment was removed, as shown by the non-formation of crotonaldehyde after ozonolysis and distillation, the formulation (I, where X = S) would be acceptable. That this interpretation was, in fact, required was shown by the further observation that whereas, as has been mentioned, neither of the hexahydro-compounds gave (IV) on alkaline hydrolysis, the corresponding sulphones did so, together with one molecule of sulphur dioxide. This is readily explicable when it is recalled that the sulphur atom forms part of a cysteine moiety. The course of the base-catalyzed decomposition of the thio ether and sulphone may then be represented as in (V) and (VI). The obvious consequence of this mechanistic interpretation was that the alkaline hydrolysis of hexahydrogriseoviridin diacetate should produce the thiol (VII). By the process described in the experimental section this substance was isolated as a colorless oil which analyzed correctly. The n.m.r. spectrum with a doublet (3H) centered at τ 8.61 ($J \sim 6$ c.p.s.) showed the presence of a methyl attached to carbon bearing hydrogen. The infrared spectrum, beyond showing the obvious carbonyl absorption at 1735 cm^{-1}, revealed the presence of a thiol grouping with a weak band at 2570 cm^{-1}. The only element of structural ambiguity remaining—the point of attachment of the thiol grouping—was removed when it was noted that the pK_a of the hydroxy acid corresponding to (VII) was 3.76. This represented an increase in acidity over 5-hydroxyhexanoic acid or acetic acid comparable with that reported for thioglycollic acid (pK_a 3.67) (7).

In (V) the cysteine moiety represented was the precursor of either alanine (*a*) or

Can. J. Chem. Downloaded from www.nrcresearchpress.com by 210.87.254.105 on 09/05/12
For personal use only.

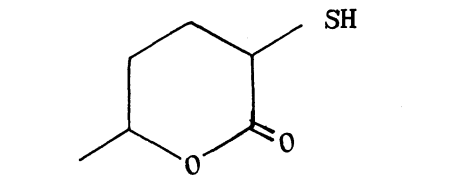

(VII)

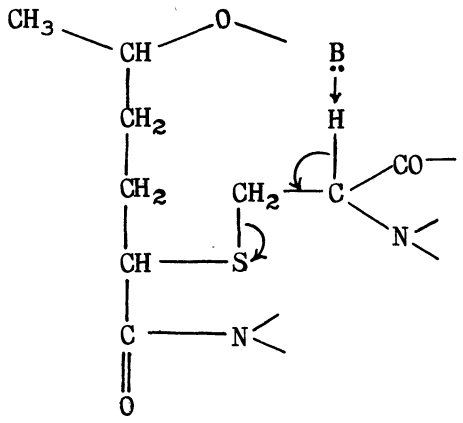

(V)

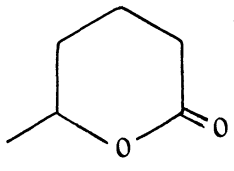

(IV)

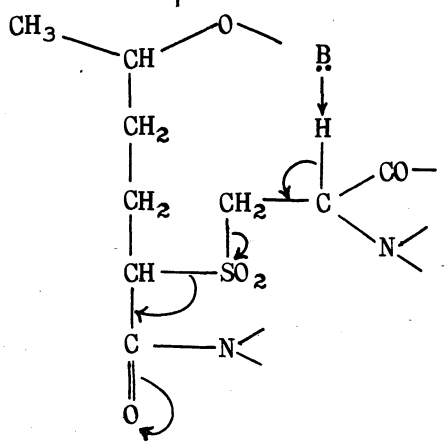

(VI)

alanine (*b*) in (III). In the first case, represented in (VIII), the cysteine carboxyl would be involved in lactone formation. In the alternative (IX), the other, as yet unspecified C_3 fragment, would be the precursor of alanine (*a*), the cysteine being that of alanine (*b*), with its carboxyl involved, consequently, in amide formation.

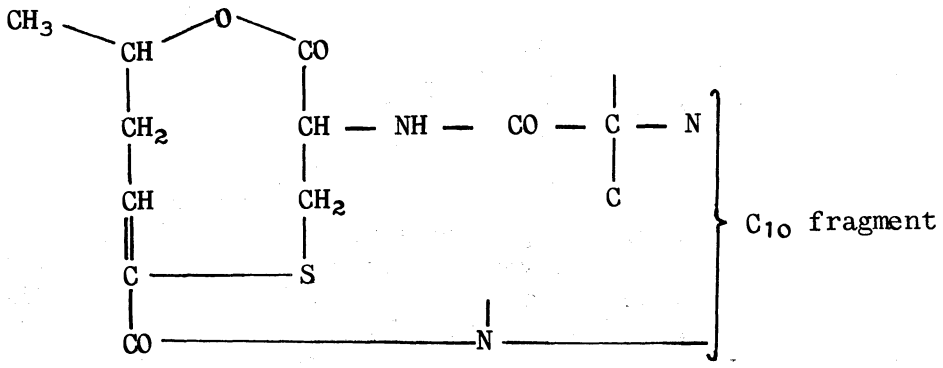

(VIII)

Can. J. Chem. Downloaded from www.nrcresearchpress.com by 210.87.254.105 on 09/05/12
For personal use only.

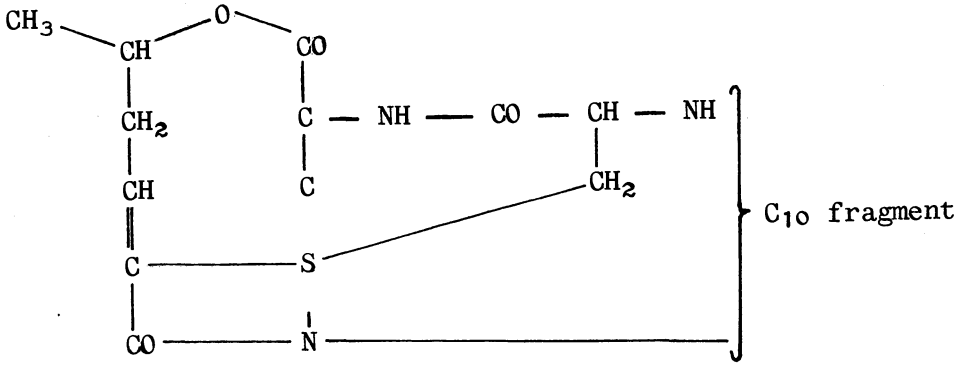

(IX)

In the event that (VIII) were correct, reduction of griseoviridin diacetate with lithium borohydride would, in reducing the lactone carbonyl specifically, be reducing the cysteine carboxyl. With (IX) the reverse situation would obtain. Since, however, it might cogently be argued that for the release of the sulphur from the C_6 fragment the unsaturation was a prerequisite, and that hydride reduction might, incidentally, remove this unsaturation, it was first shown that hexahydrogriseoviridin diacetate also gave cysteine on hydriodic acid – red phosphorus hydrolysis.

The decisive experiment could now be performed. Reduction of griseoviridin diacetate with lithium borohydride gave an oil in the infrared spectrum of which the amide carbonyl bands were unchanged in intensity, but in which the lactone carbonyl band was absent. Hydriodic acid – red phosphorus hydrolysis of this, followed by isolation of the amino acid fraction gave material which on paper chromatographic analysis showed the total absence of cysteine and cystine. Conditions were selected which would have revealed far smaller (less than 5%) amounts of the cystine obtained from the material not treated with lithium borohydride.

From these experiments it was concluded that alanine (*a*) was derived from cysteine and the part structure of griseoviridin could reasonably be expanded to that shown in (X).

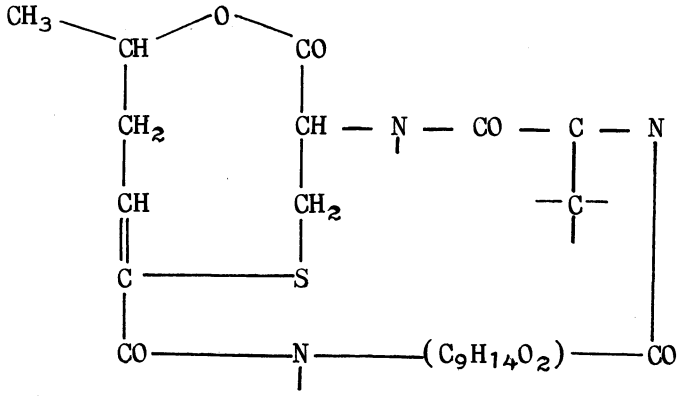

(X)

Can. J. Chem. Downloaded from www.nrcresearchpress.com by 210.87.254.105 on 09/05/12
For personal use only.

Although griseoviridin showed no well-defined high intensity absorption bands in the ultraviolet the intensity of the absorption between 200–225 mμ ($\epsilon \sim 39{,}000$), indicated that several chromophores must be absorbing in that region. One of these systems was contained in (X) and this, together with at least one other high-intensity band was removed upon hydrogenation to the hexahydro series leaving what was probably a single chromophore (λ_{max} 212 mμ; ϵ, 15,700). This, for reasons presented below, was to be attributed to the other C_3 fragment, so that a conjugated system of some kind was present in the aminodecanoic acid. Both a simple diene and an α,β-unsaturated amide could be entertained as possibilities for this chromophore, and a number of modes of distinguishing between these alternatives with varying degrees of finesse were considered. The simplest appeared the exposure of the molecule to reaction with maleic anhydride. In the event griseoviridin gave, with maleic anhydride in benzene solution, a crystalline adduct showing in the infrared spectrum the required anhydride bands.

Since reaction of a diene with maleic anhydride removes the dienic chromophore and adds only a single cis ethylene linkage, subtraction of the chromophore of an adduct from that of the starting material should reveal the nature of the chromophore removed by adduct formation. In the present instance such a check was necessary to ensure that no bond migration had occurred under the reaction condition prior to adduct formation. The difference spectrum is represented in Fig. 1, and is compatible with expectation.

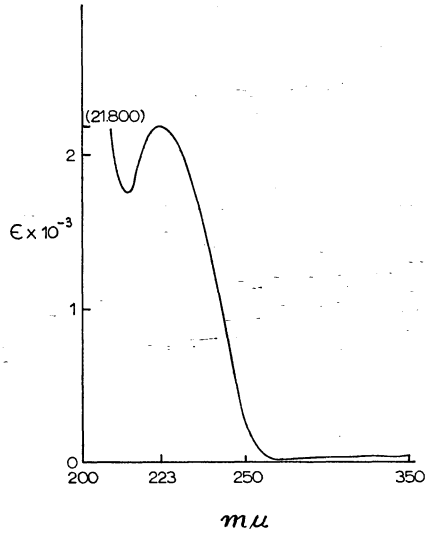

FIG. 1. Difference spectrum of griseoviridin diacetate and its maleic anhydride adduct.

Since the aminodecanoic acid moiety was now known to have four carbon atoms involved in a conjugated diene, and since it was further known that the hydroxyl groups were not vicinal (3) it seemed probable that one of these hydroxyl groups would be attached to a carbon atom adjacent to the dienic system, the probability being further increased by the fact that griseoviridin did not have the properties of a carbinolamine. An attempt to demonstrate this by forming an adduct of griseoviridin itself (instead of the diacetate) was partially successful in that the crude product after treatment with diazomethane showed the expected carboxylic and γ-lactone bands in the infrared spectrum, the lactone being formed by the internal attack of the vicinal hydroxyl on the anhydride. The product was, however, amorphous and intractable.

Can. J. Chem. Downloaded from www.nrcresearchpress.com by 210.87.254.105 on 09/05/12
For personal use only.

Can. J. Chem. Downloaded from www.nrcresearchpress.com by 210.87.254.105 on 09/05/12
For personal use only.

Griseoviridin lacked solubility in most solvents suitable for manganese dioxide allylic oxidation; it had however sufficient solubility in acetone for such to be attempted. By this means a crystalline dienone dehydrogriseoviridin, λ_{max} 277 mμ was obtained, further characterized as the crystalline acetate. The next object was the ascertaining of the spatial relationship of the second hydroxylic function with respect to the presently established five-carbon sequence. Since a vicinal position to the hydroxyl group was excluded a β- or vinylogous β-position seemed probable, and attempts were made to achieve β-elimination under mild conditions in dehydrogriseoviridin.

Addition of a small amount of alkali to an alcoholic solution of the dienone acetate produced, instantaneously, an absorption band in the ultraviolet at 415 mμ, moved to 355 mμ on acidification. The position of this absorption rendered interpretation somewhat uncertain since no distinction could be made between β- and vinylogous β-elimination. A preliminary removal of unsaturation from the dienone was therefore attempted. This was achieved in two ways.

Treatment of the dienone acetate very briefly (2 minutes) with activated zinc in acetic acid resulted in the complete disappearance of the long-wavelength-high intensity absorption band. Evidently electrons had been successfully transferred to the dienonic system, but the position of protonation was not revealed, it being possible mechanistically that the remaining ethylenic linkage be $\beta\gamma$ or $\gamma\delta$ to the carbonyl group. This subject will be returned to below.

This dihydrodehydrogriseoviridin acetate on treatment with alkali immediately produced, in alkaline solution an intense absorption at 387 mμ as shown in Fig. 2. This

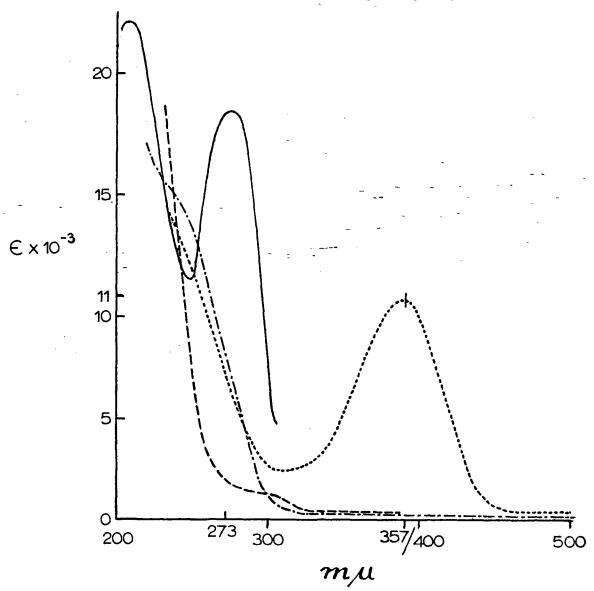

FIG. 2. Absorption spectrum of dehydrogriseoviridin (—), zinc – acetic acid reduction product before alkali treatment (- - -), after alkali treatment (· · ·), and after acidification of the alkali treated solution (·—·).

absorption was removed on acidification with acid but was reversibly generated. Isolation of the product gave an amorphous product which analyzed correctly for the loss of acetic acid, and whose infrared carbonyl absorption was clearly indicative of the loss of an acetoxyl group. Since in the zinc reduction product one ethylenic linkage had been

saturated, the possibility of vinylogous β-elimination could be clearly excluded, and the disposition and environment of seven contiguous carbon atoms in the ω-aminodecanoic acid be represented as in (XI) for griseoviridin, the further transformations being indicated in (XII)–(XIV). The loss of the acetoxyl was the surety of β-elimination in (XIV),

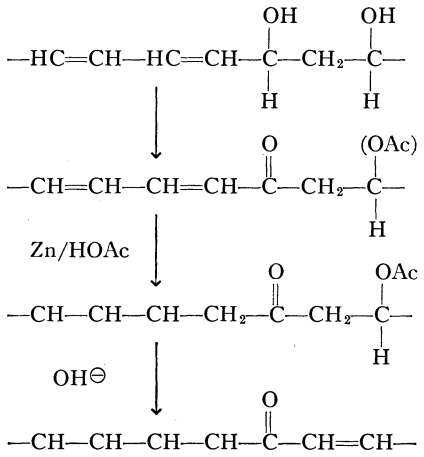

but the position of the absorption maximum in alkaline solution, and its reversibility, indicated the presence of an enolic system, and therefore of the participation of some other function. To simplify the interpretation a more saturated derivative than (XIII) was sought in which the putative β-elimination could be induced.

Hydrogenation of (XIII) resulted in saturation of the C_{10} ethylenic linkage and also of the C_6 unsaturation, to give a crystalline hexahydrogriseoviridin. The same crystalline substance was obtained by hydrogenation of (XII). Treatment of this substance having part structure (XV) with .05 *N* alkali for three seconds resulted in the ejection of the acetoxyl group. Acidification of the product with acetic acid and subsequent isolation gave a crystalline elimination product.

This substance showed absorption as represented in Fig. 3 and, since this was reversible, similarly contained an enolic system. The only group available for fulfilling this desired function was together with the unsaturated ketone produced by elimination, the terminal carboxyl; incorporation of this revealed the complex enolic function under discussion as that of a vinylogous β-ketoamide represented in (XVI). The rather longer wavelength of the enolate absorption maximum than perhaps expected is undoubtedly due to the cisoid disposition of the ethylenic linkage as required by the geometry of the molecule.

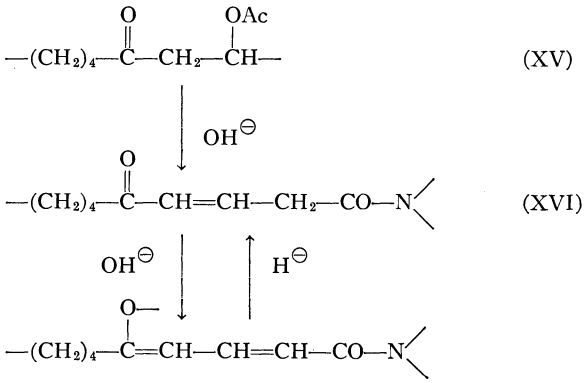

Can. J. Chem. Downloaded from www.nrcresearchpress.com by 210.87.254.105 on 09/05/12
For personal use only.

The incorporation of the chain of atoms represented by (XVI) into the framework of the ω-aminodecanoic acid led to a unique structure (XVII) for this fragment. However, it was realized that the disposition of these atoms in the chain were related, directly, only to one end, that of the carboxamide function, of the amino acid.

A consideration of the environment of the nitrogen atom at the other end of the chain suggested that, if the ethylenic linkages in the C_{10} and the C_6 fragments were cleaved by ozonolysis, quite mild acid hydrolysis would suffice to release glycine—an amino acid obtained by alkaline, but not by acid, hydrolysis of griseoviridin. This proved to be the case, and glycine was the only amino acid detected under the conditions used. Without

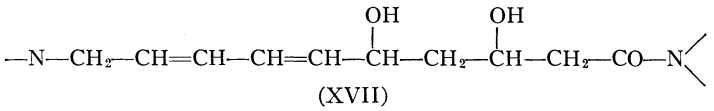

(XVII)

such prior ozonolysis no amino acids were revealed in the hydrolyzate by paper chromatography.

At this point it was of interest to subject the zinc reduction product, containing the part structure (XIII), to the same treatment to ascertain whether protonation of the carbanion (XVIII), produced by electron transfer from the zinc metal, was specific:

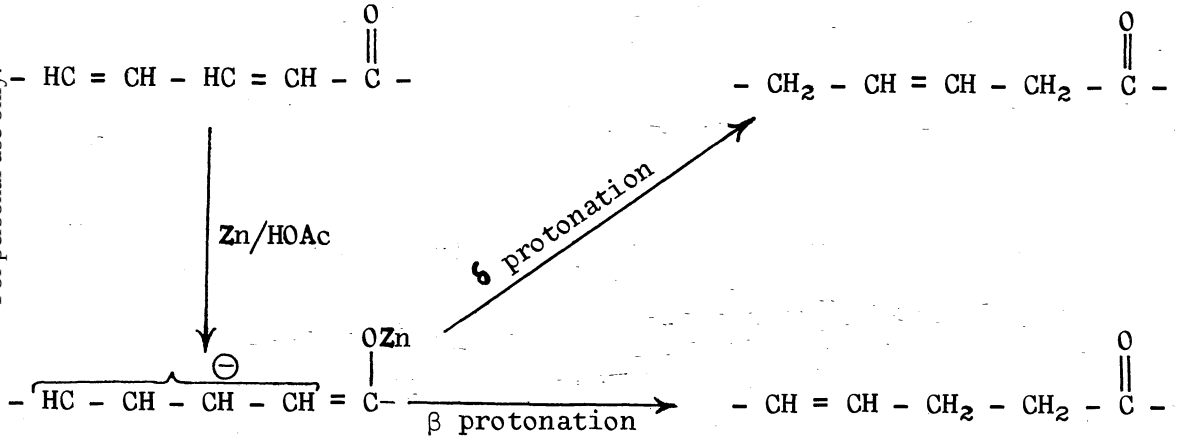

(XVIII)

Ozonolysis and mild acid hydrolysis in this case gave both glycine and β-alanine in roughly equal amounts, clearly indicating indiscriminate β and δ protonation.

At this point in our investigations the partial structure of griseoviridin (X) could be expanded to (XIX), and it was clear from this formulation why Bowman and his group obtained ω-aminodecanoic acid and an unidentified hydroxyaminodecanoic acid by Clemmensen reduction and hydrogenation–hydrolysis (5) respectively of perhydrodethiogriseoviridin. The hydroxyl groups were doubtless β-eliminated by activation of the appropriate protons by the terminal carboxamide function. Our attempts to induce such elimination with mild base were unsuccessful because under the general conditions necessary for such elimination, mild as they can be (8), the chromophore was destroyed and only a transitory formation of peaks of low intensity could be observed.

In the manipulations performed on the C_{10} fragment both hydroxylic functions had been transformed or affected without disturbance of the remote lactonic function. The

Can. J. Chem. Downloaded from www.nrcresearchpress.com by 210.87.254.105 on 09/05/12
For personal use only.

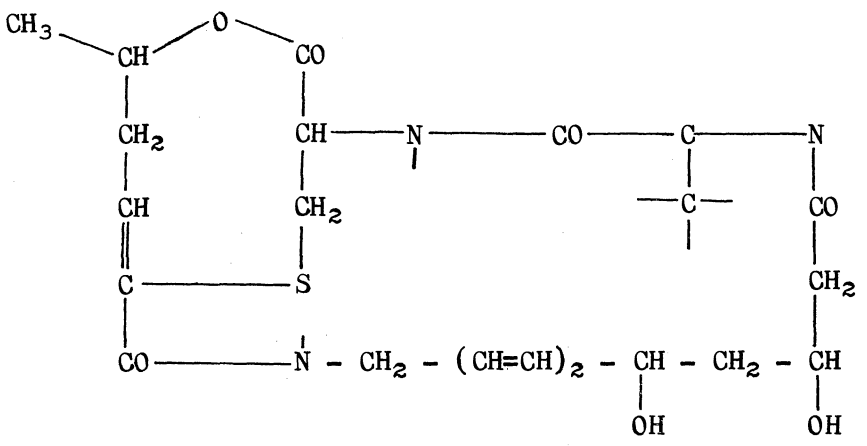

(XIX)

previous assumption made, in the determination of the structure of perhydrodethiogriseoviridin, that the ethereal oxygen of the lactone was that in the C_6 fragment could, therefore, be justified.

The final structural problem presented by griseoviridin was contained in the nature and arrangement of the three carbon atoms which appeared as alanine (*b*) in perhydrodethiogriseoviridin. It was not found possible to isolate these three atoms as one fragment in any form other than alanine, but a considerable amount of indirect evidence was forthcoming.

That this group of atoms contained unsaturation was known since it represented the residuum of ultraviolet absorption after saturation of the C_6 and C_{10} fragments in, for instance, hexahydrogriseoviridin diacetate. This unsaturation was resistant to further hydrogenation under the same condition, but conversion of the thioether to sulphone and subsequent hydrogenation in acetic acid over platinum oxide removed this unsaturation. The new substance perhydrogriseoviridin diacetate sulphone produced now contained an extra methyl group and on acid hydrolysis gave alanine. It appeared, therefore, that conditions of hydrogenation sufficiently severe to effect reduction also, directly or indirectly, effected hydrogenolysis.

Bands in the infrared spectrum at about 1600 cm^{-1} and 1500 cm^{-1} (Table I) were observed in all compounds which contained the C_3 unsaturation, which were absent in all compounds wherein such unsaturation had been removed, and which were therefore to be associated with this unsaturation.

These facts could be interpreted in terms of the part structure (XX*a*) which also explained in a simple manner the formation of glycine and formic acid (by β-addition and dealdolization) on alkaline hydrolysis of griseoviridin. The atom Y in (XX*a*) could not be hydrogen (as in XX*b*) because no spectral evidence for such a methylene group was obtainable—and such functions are readily detectable in the infrared and n.m.r. spectra—and no formaldehyde was produced on the ozonolysis of griseoviridin diacetate.

It was observed that in all substances which contained the C_3 unsaturation there was a sharp singlet (1 H) close to τ 1.9 in the n.m.r. spectra. This proton signal was to be

Can. J. Chem. Downloaded from www.nrcresearchpress.com by 210.87.254.105 on 09/05/12
For personal use only.

TABLE I

Absorption bands in the 1500–1600 cm^{-1} region of griseoviridin derivatives

Compound	Chloroform		Nujol	
1. Griseoviridin diacetate	1594	1494	1597	1499
2. Griseoviridin diacetate MA adduct	1594	1499	1600	1497
3. Hexahydrogriseoviridin diacetate	1589	1497	1607	1503
4. Hexahydrodeoxygriseoviridin	1600	1495	1592	1499
5. Hexahydrodehydrodeoxygriseoviridin sulphone	1597	1504	1590	1506
6. Dehydrogriseoviridin acetate	1597	1510	1592	1510
7. Hexahydrodehydrogriseoviridin acetate	1594	1508		
8. Elimination product (XVI) from 7	1592	1501		
9. Perhydrodethiogriseoviridin diacetate	—	—	—	—
10. Griseoviridin hydrochloride			1605	1504
11. Griseoviridin perchlorate			1608	1497
12. Octahydrodethiogriseoviridin			1600	1511
13. Perhydrogriseoviridin diacetate sulphone	—	—		

NOTE: A blank space indicates no determination made in that medium.

attributed to the proton in (XX*a*). Its position at very low field suggested that Y was an electron-withdrawing group, and that it was not the site of any proton. Bearing in mind the nature of hydrogenolysis of the C_3 fragment, which must be understood to proceed by hydrogenation, β-elimination, and further hydrogenation, then Y was required to be oxygen or nitrogen.

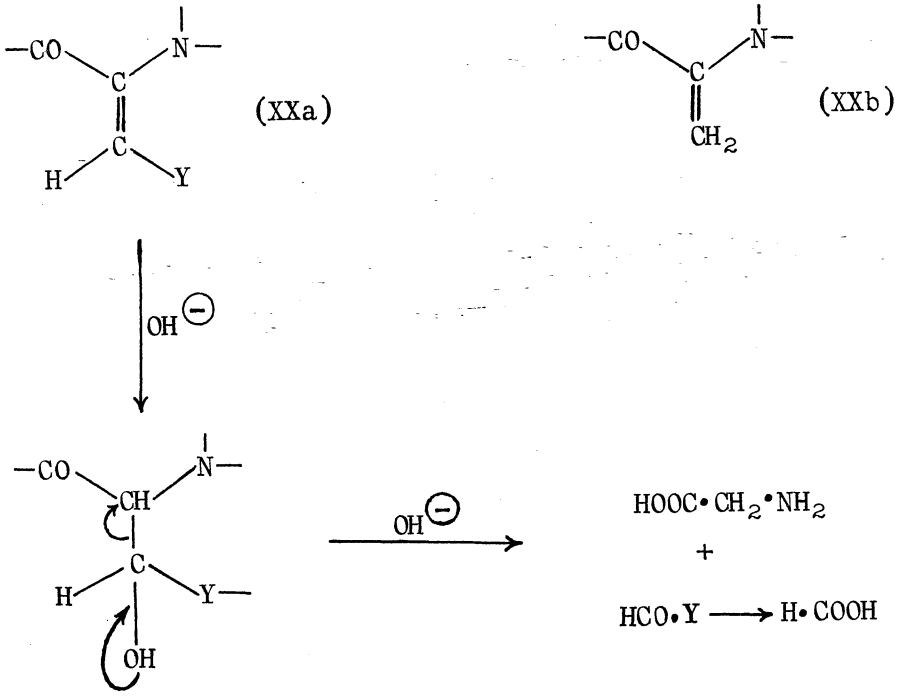

Support for the part-structure represented in (XX*a*) came from an unexpected source. The Raney desulphurization of griseoviridin diacetate gave an adequate yield of crystalline product, but purification was difficult and the final yield of pure perhydrodethiogriseoviridin diacetate was low. A careful examination of the mother liquors gave, after

Can. J. Chem. Downloaded from www.nrcresearchpress.com by 210.87.254.105 on 09/05/12
For personal use only.

tedious recrystallizations, a new substance which also had the requisite analysis for perhydrodethiogriseoviridin diacetate and which had an infrared spectrum virtually superposable on Bowman's substance. The melting point of the new substance, isoperhydrodethiogriseoviridin was close to that of perhydrodethiogriseoviridin diacetate, and the depression in mixed melting point though probably real was not impressive.

That these were, indeed, two substances was clearly shown by the large differences in specific rotation (84°) and by significant discrepancies in the n.m.r. spectra (Fig. 3). In

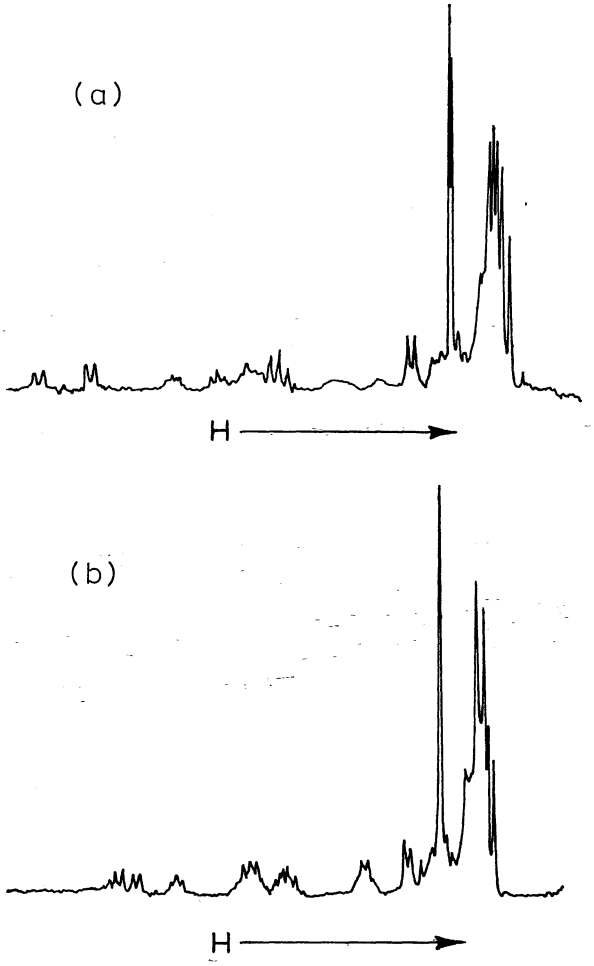

FIG. 3. Absorption spectrum of base eliminated compound (XVI) in neutral (—) and alkaline (···) solution.

particular divergencies were observed in the region where the methine hydrogen and amide hydrogen of the alanine moieties were displayed. These differences indicated alternative orientations of one of the alanine moieties and were explicable in terms of approach of the catalyst to either side of the ethylenic linkage in its final reduction stage:

Can. J. Chem. Downloaded from www.nrcresearchpress.com by 210.87.254.105 on 09/05/12
For personal use only.

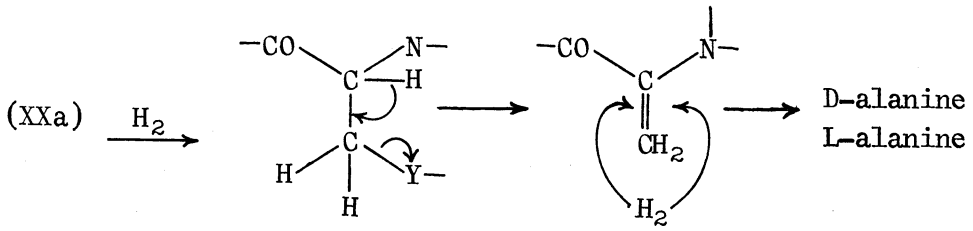

(XXb) (XXc)

Attempts to interrupt this sequence of hydrogenation–elimination–hydrogenation at an intermediate stage were unsuccessful. Using a weaker Raney catalyst (B.D.H. stabilized catalyst) under strictly defined conditions a substance octahydrodethiogriseoviridin (see footnote † on p. 371) was obtained which had lost the sulphur atom. All unsaturation appeared to have been removed with the exception of that contained in the C_3 fragment. Thus the compound exhibited high enol absorption in the ultraviolet spectrum and showed the appropriate bands at 1600 cm^{-1} and 1511 cm^{-1} in the infrared spectrum. On alkaline hydrolysis glycine, formic acid, and δ-caprolactone were obtained. However, attempted hydrogenation to the dihydro stage only (XXI) was unsuccessful: the substance took up two molecules of hydrogen with the formation of perhydrodethiogriseoviridin diacetate. Such behavior was not totally unexpected since the resistance of (XX*a*) to hydrogenation argued that this moiety was embedded in the molecular environment, whilst, in contrast (XX*c*) would be expected to be exposed.

The participation of nitrogen or oxygen in the function (XX*a*), it was recognized, would define the number of active hydrogen atoms present in griseoviridin diacetate which could at this stage be represented by (XXI). In principle any of the three nitrogen atoms,

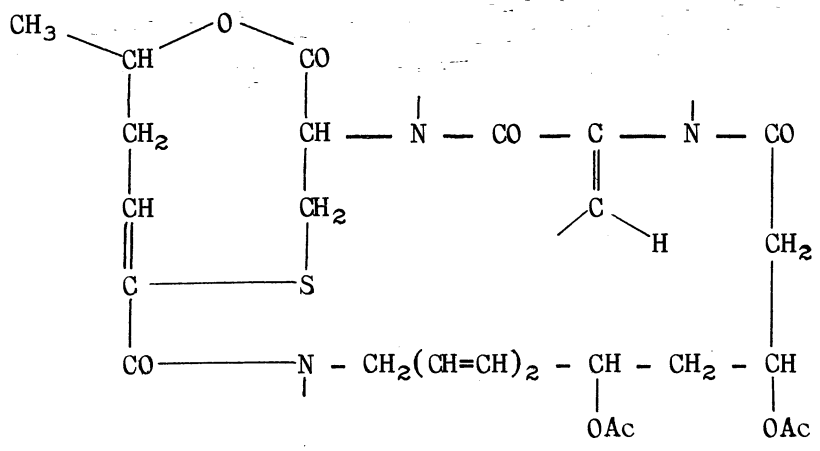

(XXI)

directly or through the lactim ether, could be involved, and if such were the case, as followed from the above discussion, then (XXI) should have two active hydrogen atoms

Can. J. Chem. Downloaded from www.nrcresearchpress.com by 210.87.254.105 on 09/05/12
For personal use only.

only, instead of the three expected for three secondary amides. The results are summarized in Table II. Modified Zerewitinoff (lithium aluminum hydride) estimation gave

TABLE II

Compound	Active hydrogen: method			Required
	Zerewitinoff*	Infrared†	N.m.r.‡	
Griseoviridin	3.9			4
Griseoviridin diacetate	2.2	2.14, 2.06	2.28	2
Hexahydrodeoxygriseoviridin	3.0			3
Hexahydrodeoxygriseoviridin acetate	2.2			2

*Modified procedure using lithium aluminum hydride.
†A standard, N-acetylcyclohexylamine was assumed to have one active hydrogen. A second standard, N-acetylbenzylamide, was calibrated against it and found to have 1.05 active hydrogen by comparison of the integrated areas at the same molecular concentration. No correction for slit width was made.
‡Deuterium exchange was effected by repeated evaporation from dioxan-D_2O, complete exchange being followed by intensity of the ND stretch in the infrared. The fully deuterated compound was assumed to have zero active hydrogen. The n.m.r. integration was referred to the τ 1.9 peak (one proton).

approximately four and two hydrogens for griseoviridin and its diacetate respectively. However, such determinations are not impeccably free from suspicion, and alternative methods were investigated for confirmation. In the first, the active hydrogen atoms in griseoviridin diacetate were exchanged with deuterium and the difference in the numbers of protons present estimated by integration in the appropriate areas with respect to the sharp singlet at τ 1.9. Again approximately two hydrogen atoms were detected. In the second procedure the NH stretch in the infrared was integrated directly,* with the same result.

Of the possibilities available two could be immediately dismissed (XXII*a* and XXII*b*) as requiring chemical behavior not consonant with that observed in griseoviridin. Amongst the various incompatibilities observed, the resistance of this unsaturated system to hydrogenation, and the similar resistance to moderately strong acid conditions (implied by such transformations as the formation of the hydrochloride) were particularly striking; the lability of such systems is well-known.

Similar arguments excluded all but two of the remaining possibilities. Of these the more superficially attractive was that represented in (XXIII). Much of the chemical evidence available could be interpreted in terms of (XXIII), and in addition a study of 4-carbethoxyoxazole (XXIV) as a model indicated that the vinyl hydrogen indeed appeared at approximately τ 1.9 and that a band in the infrared spectrum at 1590 ($CHCl_3$)

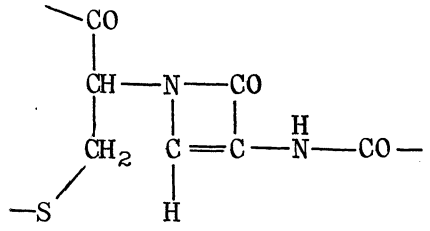

(XXIIa)

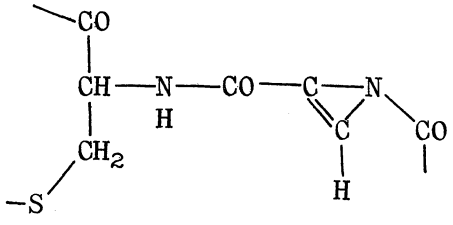

(XXIIb)

Such amide NH stretches appear to be remarkably independent of the nature of the substituents (9). As shown in the table a standard was taken, checked against a suitable model.

Can. J. Chem. Downloaded from www.nrcresearchpress.com by 210.87.254.105 on 09/05/12
For personal use only.

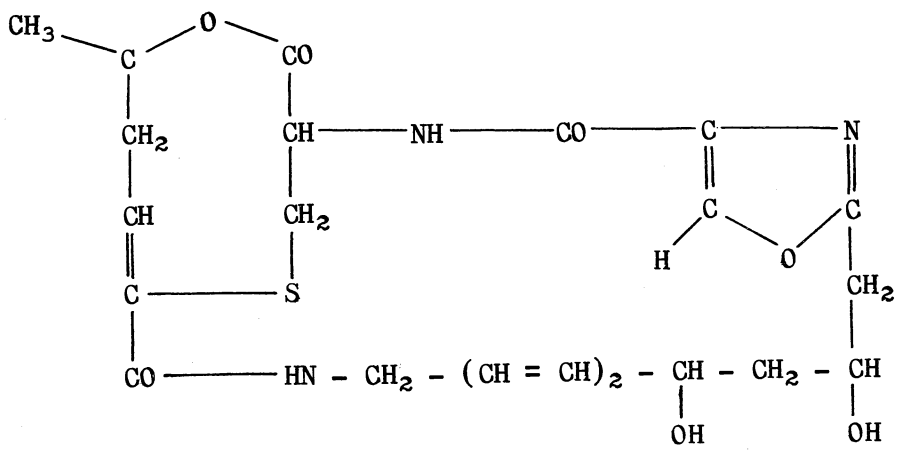

(XXIII)

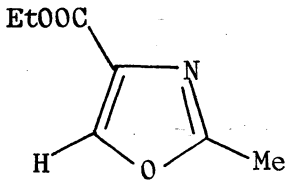

(XXIV)

was also observed, but the associated band at ca. 1500 was, significantly, absent. This formulation was rejected for the following reasons.

Although oxazoles are weak bases and (XXIV) would be expected to be even weaker, nevertheless it could be titrated in acetic acid solution when a pK_a of 3.3 was found. Under the same conditions a solution of griseoviridin diacetate was indistinguishable from the solvent.*

The presence of the unsaturated chromophore could be detected, as already discussed, both in the infrared and in the n.m.r. It was still present in the vinylogous β-keto amide from hexahydrodehydrogriseoviridin, which on the basis of (XXIII) was required to be represented as in (XXV). The behavior of this substance with dilute alkali is not compatible with (XXV) for which no such facile enolization as was noted could be expected. A similar observation could be made with regard to the ketone hexahydrodehydrodesoxygriseoviridin obtained from hexahydrodeoxygriseoviridin sulphone (1) which, in view of the nature of the hydrochloride, would be represented as (XXVI).

The most compelling evidence, however, devolved from the nature of the "hydrochloride" of griseoviridin (4). In this substance the unsaturated three-carbon unit remains intact whilst the nitrogen and carbon atoms required for oxazole formation could be demonstrated to be otherwise employed (see following paper).

**When left standing the 'perchlorate' separated out. As discussed in the following paper this slow process is a chemical reaction, and has no relevance to the present argument.*

Can. J. Chem. Downloaded from www.nrcresearchpress.com by 210.87.254.105 on 09/05/12
For personal use only.

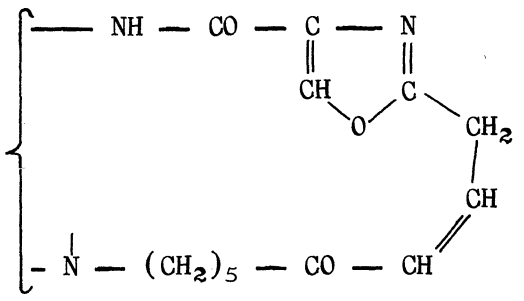

(XXV)

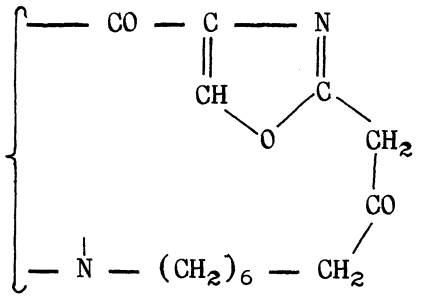

(XXVI)

For these reasons the formulation (XXIII) was rejected. Only one formulation remained which permitted the interpretation of the chemical and physical evidence; that is, (XXVII).

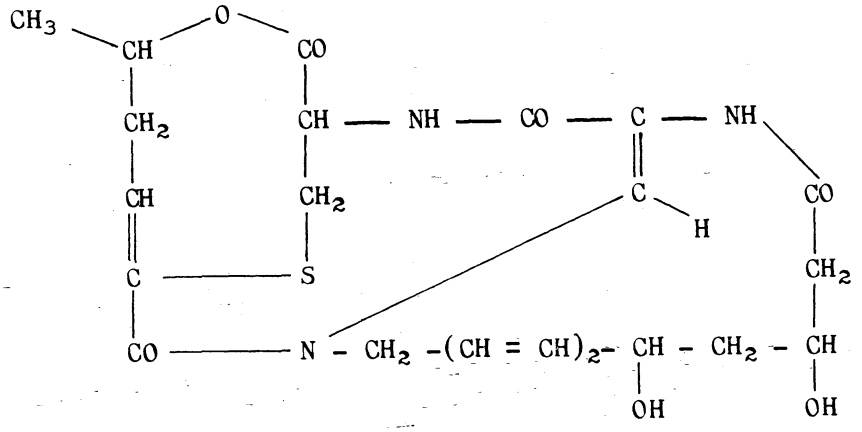

(XXVII)

With this representation a number of other facts noted during the study of this problem could be rationalized. It was apparent that the absorption of the unsaturated alanine (*b*) system was at shorter wavelengths than expected; inspection of models suggested this was attributable to the considerable distortion of this bridge and its pi system with respect to the *p* electron on the substituting nitrogen. The model also indicated, that the appropriate geometry of the diene for adduct formation was easily attained.

Although acid hydrolysis of griseoviridin and hexahydrodeoxygriseoviridin produced no alanine we had observed that alkaline hydrolysis of hexahydrodeoxygriseoviridin sulphone diacetate did lead to the formation of this amino acid. This must be interpreted as a reverse elimination (XXVIII, arrows) and the formation of a primary carbanion.

Whilst alkaline hydrolysis of griseoviridin followed by acidification gave about one-third mole of hydrogen sulphide (3) the alkaline solution did not contain sulphide ions since no precipitate was obtained with alkaline lead acetate. As presumed by Bowman the action of the alkali must be to produce a very acid-labile sulphur-containing moiety.

Can. J. Chem. Downloaded from www.nrcresearchpress.com by 210.87.254.105 on 09/05/12
For personal use only.

One possible explanation could be formation of the thioaldehyde (XXIX) by an elimination process,* the substance being stabilized as enolate until acidification.

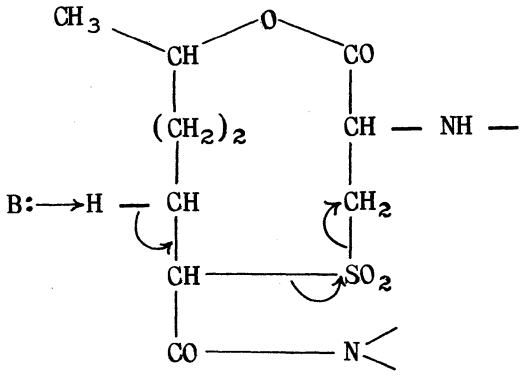

(XXVIII)

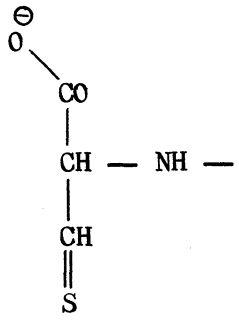

(XXIX)

A final observation requiring interpretation was that of Bowman (4) who noted that, whilst griseoviridin derivatives for the most part required ozonolysis followed by acid, alkali, or heat treatment for the release of crotonaldehyde, the product of oxidation of griseoviridin diacetate with perbenzoic acid (which was not a sulphone (1)) gave crotonaldehyde by simple acid hydrolysis. One interpretation is symbolized in the sequence (XXX).

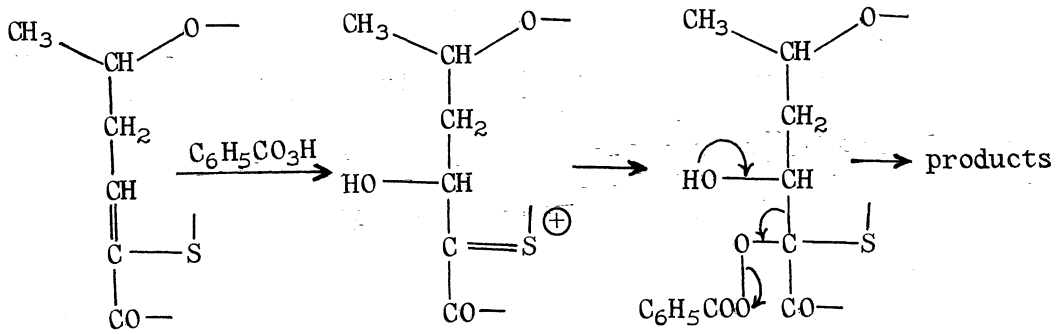

(XXX)

The structure represented by (XXVII) therefore appeared uniquely capable of allowing interpretation of the presently known chemistry of griseoviridin.

At the time of study griseoviridin appeared to have properties placing it in no known class of mold metabolites. The recent structural elucidation of its associated metabolite viridogrisein (17) (etamycin) (10) suggested some relationship to the ostreogrycin complex (11) from *streptomyces* wherein, also, two main groups of metabolites are found. One group consists of relatively simple lactonic peptides, having a general resemblance to etamycin, whilst the other group contains more complex structures which, although none

Reverse elimination would give an α-thiono acid for which identical comments would apply. No distinction is here implied, (XXIX) being selected merely illustratively.

Can. J. Chem. Downloaded from www.nrcresearchpress.com by 210.87.254.105 on 09/05/12
For personal use only.

have as yet been completely structurally elucidated, have a superficial resemblance to griseoviridin. They are at least lactonic peptides containing an unsaturated aliphatic acid, dehydro amino acids, and a long-chain, unsaturated ω-amino acid (12).

EXPERIMENTAL

Except where otherwise indicated melting points were taken on the Köfler hot stage, infrared spectra as Nujol mulls, and ultraviolet spectra in 95% ethanol. Light petroleum was that of boiling range 60–80°. Rotations were in chloroform unless otherwise stated.

Perhydro- and Isoperhydro-dethiogriseoviridin Diacetate

(*a*) Griseoviridin diacetate (4.5 g) was refluxed with Raney nickel as described by Ames *et al.* (4). The crude crystalline (from ethyl acetate) product (1.94 g) was crystallized twice from ethanol – ethyl acetate – light petroleum (0.8 g, m.p. 192–215°), then from chloroform – light petroleum and finally the original solvent mixture to give the pure diacetate m.p. 220–223°, $[\alpha]_D$ −55° (*c*, 1.7). A sample provided by Dr. Bowman had m.p. 216–217°, $[\alpha]_D$ −52° (*c*, 1.7), mixed m.p. 216–220°.

Concentration of the first ethyl acetate mother liquors gave material which was crystallized from chloroform – light petroleum, then from ethanol, and finally repeatedly from ethanol – ethyl acetate – light petroleum to give the isomeric diacetate m.p. 215–218°, $[\alpha]_D$ +30° (*c*, 2.3). The infrared spectrum of this substance was closely similar to that of the normal diacetate and the mixed melting point was depressed to ca. 200°. Calc. for $C_{26}H_{43}O_9N_3$: C, 57.65; H, 8.00; N, 7.76; O, 26.59%. Found: C, 57.75; H, 7.88; N, 7.82; O, 26.41%.

(*b*) Perhydrodethiogriseoviridin was prepared as described by Ames *et al.* (4). It had the melting point previously reported (190–192°) but had $[\alpha]_D$ −7° (*c*, 0.55; MeOH). The rotation $[\alpha]_D$ −32° previously reported may be attributed to the presence of a small amount of an impurity (responsible for a band at 1730 cm^{-1}) which was removed on repeated crystallization from chloroform–ethanol with little change in the melting point.

Acetylation of the diol (3.7 mg) with acetic anhydride and pyridine (1:1) at room temperature overnight gave after repeated crystallization from ethanol – ethyl acetate – light petroleum the diacetate, m.p. 223–225° undepressed on admixture with the normal diacetate.

Mild Alkaline Hydrolysis of Perhydrodethiogriseoviridin Diacetate

(*a*) The acetate on standing overnight with an excess of 0.1 *N* aqueous ethanolic sodium hydroxide consumed 3.13 equivalents of base. Under the same conditions the isomeric diacetate consumed 3.0 equivalents of base and perhydrodethiogriseoviridin 1.07 equivalents.

(*b*) Perhydrodethiogriseoviridin diacetate (300 mg) was hydrolyzed as described under (*a*). The mixture was neutralized with 0.1 *N* hydrochloric acid, freed from sodium ions by passage through Dowex 50W-X2 (H^+), and the acidic eluate evaporated to a glass under reduced pressure. After conversion to the ester with ethereal diazomethane the product was repeatedly crystallized from methanol – ethyl acetate when it had m.p. 125–127°. Calc. for $C_{23}H_{43}O_8N_7$: C, 56.44; H, 8.79; N, 8.59; O, 26.18, OMe (1), 6.34%. Found: C, 56.73; H, 8.51; N, 8.73; O, 26.45; OMe, 6.28%. On potentiometric titration with hydrochloric acid the substance in aqueous ethanolic solution was indistinguishable from the solvent.

The ester (44 mg) in pyridine (0.6 ml) containing acetic anhydride (0.3 ml) was allowed to stand at room temperature overnight. The triacetate was obtained as an oil. Calc. for $C_{29}H_{49}N_3O_{11}$: C, 56.57; H, 8.02; N, 6.82; 3 Ac, 21.0%. Found: C, 56.53; H, 8.20; N, 7.14; Ac, 20.1%.

The Isolation of Alaninol

Perhydrodethiogriseoviridin diacetate (51.3 mg) in dry tetrahydrofuran (50 ml) at 0° was treated with lithium borohydride (500 mg) in portions over 20 minutes. It was then stirred at room temperature under nitrogen for 18 hours. The mixture was then diluted with *n*-butanol (30 ml) and concentrated to ca. 20 ml under reduced pressure. *n*-Butanol (20 ml) saturated with water was then added and the mixture warmed to 60–75° for 20 minutes. The solid was filtered off and washed with several portions of hot butanol. After acidification with a few drops of 6 *N* hydrochloric acid, filtrate and washings were evaporated to dryness *in vacuo* at 100°. The product, in 6 *N* hydrochloric acid, was refluxed for 17 hours, the hydrolyzate evaporated to dryness under reduced pressure, and the residue rendered basic with 5% sodium carbonate solution. The mixture was then distilled under reduced pressure and the distillate neutralized with .01 *N* hydrochloric acid (6.15 ml; 0.67 equiv.). The volume was then reduced to 1.2 ml. Paper chromatography showed the presence of two weak and one intense ninhydrin-positive substances, the latter being indistinguishable from that of *dl*-alaninol in three different solvent systems.* The aqueous solution was basified with sodium hydrogen carbonate and 3,5-dinitrobenzoyl chloride (45 mg) was added. The mixture was shaken for 3 hours and the product isolated with ethyl acetate. The crystalline product melted from 195–235° and after repeated crystallization from ethyl acetate – methanol and aqueous acetone melted at 236–237°. Its infrared spectrum was superposable with that of the derivative described below from *dl*-alaninol.

**We wish to thank Dr. J. Walker (M.R.C. London) for a generous specimen of dl-alaninol.*

Can. J. Chem. Downloaded from www.nrcresearchpress.com by 210.87.254.105 on 09/05/12
For personal use only.

dl-Alaninol (19 mg) in water (5 ml) containing sodium hydrogen carbonate (500 mg) was shaken for 3 hours with 3,5-dinitrobenzoyl chloride (230 mg) and the product then isolated with ethyl acetate. Concentration gave a crystalline product which after recrystallization from aqueous acetone had m.p. 216–217°. Calc. for $C_{17}H_{18}O_{11}N_6$: C, 44.07; H, 2.83; N, 15.12%. Found: C, 44.07; H, 3.02; N, 15.19%.

Partial Hydrolysis of Perhydrodethiogriseoviridin Diacetate

The diacetate (210 mg) was refluxed in sulphuric acid (1.0 *N*; 50 ml) under nitrogen for 10 hours. The solution was then added to a Dowex 50W-X2 (H^+) column (10 g) and the material retained eluted with 3 *N* ammonia solution. The eluate was evaporated to dryness (79 mg) and on paper chromatographic examination (upper phase of *n*-BuOH – water – acetic acid, 4:5:1) revealed the presence of several ninhydrin-positive substances only two of which were intense and which corresponded to alanine (R_f 0.26) and alanylalanine (R_f 0.37).

The material, in the upper phase of the above solvent system (5 ml), was added to a "chromax" LKB paper column and eluted with the same solvent, the eluate being collected in 10-ml fractions. The contents of tubes 25–32 were evaporated and the residue (8 mg) crystallized from absolute ethanol when it had m.p. 268–272° (capillary) $[\alpha]_D \pm 0°$ (*c*, 0.6, H_2O). It was identical in melting point, mixed melting point, and infrared spectrum and in paper chromatographic behavior with authentic *dl*-alanylalanine. After hydrolysis in refluxing 6 *N* hydrochloric acid for 24 hours the product gave on paper chromatograms a single spot corresponding to alanine.

Hexahydrogriseoviridin Diacetate Sulphone

Hexahydrogriseoviridin diacetate (400 mg) (3) was dissolved in chloroform (65 ml) containing perbenzoic acid (ca. 400 mg) and allowed to stand at room temperature for 3 hours. Isolation of the product in the usual way (uptake 2 atoms of oxygen) gave the sulphone which was crystallized from chloroform–methanol, m.p. 215–225°. Calc. for $C_{26}H_{37}O_{11}N_3S$: C, 52.08; H, 6.22; N, 7.00; S, 5.35; C-Me (3), 7.5%. Found: C, 51.60; H, 6.31; N, 6.95; S, 5.03; C-Me, 6.63%.

Alkaline Hydrolysis of Hexahydrogriseoviridin Diacetate Sulphone

The sulphone (66.5 mg) in sodium hydroxide solution (4 *N*; 8 ml) was refluxed for 45 minutes. Ammonia (0.83 molecular equivalent (mol. eq.)) was evolved. Acidification of the cooled hydrolyzate liberated sulphur dioxide which was entrained in a stream of nitrogen and estimated by iodine titration: found, 0.52 mol. eq. The aqueous residue was distilled at constant volume until no further acid distilled (55 ml). The neutralized distillate was evaporated to dryness and treated with chromic acid solution (0.2 *N* chromic acid in 2 *N* sulphuric acid; 4 ml) and allowed to stand overnight. Excess oxidant was destroyed with sulphur dioxide and aqueous 2,4-dinitrophenylhydrazine sulphate added. The resultant precipitate was collected and crystallized from benzene to give the 2,4-dinitrophenylhydrazine of γ-acetobutyric acid, m.p. 136–137° undepressed on admixture with an authentic specimen.

In another, similar, experiment the acidified hydrolyzate was passed over a column of Dowex 50W-X2 (H^+) resin and the retained material on the washed column eluted with 6 *N* ammonia. After evaporation the residue was examined by paper chromatography. Two ninhydrin-positive substances, corresponding to glycine and alanine, were present.

Alkaline Hydrolysis of Hexahydrogriseoviridin Diacetate

The diacetate (259 mg) was refluxed in aqueous sodium hydroxide (4 *N*; 20 ml) for 1 hour. The solution was acidified with sulphuric acid (6 *N*; 40 ml) and continuously extracted with carbon tetrachloride for 24 hours. Evaporation of the carbon tetrachloride gave an oil (53 mg) which was injected onto a silicone Dow 710 column (20% stationary phase on firebrick, 10 ft × ¼ in.) the only peak eluted (retention time 30 minutes) being collected to give the thiol-lactone. Calc. for $C_6H_{10}O_2S$: C, 49.31; H, 6.90; S, 21.90; equiv. 146. Found: C, 49.14; H, 7.07; S, 21.66; equiv. 156. Titration in water gave pK_a 3.76.

Alkaline Hydrolysis of Hexahydrodeoxygriseoviridin Sulphone

The sulphone (1) (17.4 mg) was refluxed in aqueous sodium hydroxide (4 *N*; 2 ml) for 30 minutes. The liberated ammonia was entrained in nitrogen and titrated with .00667 *N* hydrochloric acid. Found: 0.94 mol. eq. volatile base.

The cooled hydrolyzate was acidified with 6 *N* hydrochloric acid (2 ml), warmed to 50°, and the liberated sulphur dioxide collected in ice-cold iodine solution (3 hours). Found: 0.95 mol. eq. sulphur dioxide. The nature and stoichiometry of the process was confirmed by titration of the acids formed (according to the equation $SO_2+I_2+2H_2O \rightarrow H_2SO_4 + 2HI$. Found 3.80 equiv. alkali consumed) and by a precipitate ($BaSO_4$) given with barium chloride.

After removal of the sulphur dioxide the hydrolyzate was distilled at constant volume. The distillate (30 ml) was warmed with .02 *N* sodium hydroxide (3 ml) and neutralized with standard hydrochloric acid (ca. 1 mol. eq. base consumed). Paper chromatography (propanol–ammonia 3:2) of the salts revealed the presence of formic acid (R_f .51; reduced silver nitrate) and 5-hydroxycaproic acid (R_f .65). A solution of chromic acid in 2 *N* sulphuric acid (0.4 *N*; 0.5 ml) was added and the mixture allowed to stand overnight. The excess oxidant was destroyed with sulphur dioxide and 2,4-dinitrophenylhydrazine (7 mg in 1 ml 10% sulphuric acid)

Can. J. Chem. Downloaded from www.nrcresearchpress.com by 210.87.254.105 on 09/05/12
For personal use only.

added. The precipitate was collected and crystallized from benzene to give the derivative of γ-acetobutyric acid melting point and mixed melting point 135–137°.

Reduction–Hydrolysis of Griseoviridin Diacetate and Hexahydrogriseoviridin Diacetate

(*a*) Griseoviridin diacetate (100 mg) in dry tetrahydrofuran (125 ml) was shaken for 18 hours under nitrogen with lithium borohydride (500 mg). *n*-Butanol was added to the mixture and the volume reduced to about 25 ml by evaporation under reduced pressure at 35°. A further quantity of water-saturated butanol (25 ml) was added and the mixture heated at 60° for 20 minutes. After filtration the filtrates were evaporated to dryness to give an oil (86 mg). The infrared spectrum of this material indicated that the ester had been reduced, but that the amide functions were unchanged.

The oil (300 mg, from several runs) was refluxed for 5 hours with hydriodic acid (15 ml; $d = 1.7$) containing red phosphorus (140 mg) (4). The filtered hydrolyzate was concentrated to small volume, diluted with water, and passed through a column of Amberlite IRA-400 (OH^-). The washed column was eluted with 10% aqueous acetic acid (400 ml) and the eluate evaporated to dryness under reduced pressure. A solution (A) of the product in 5% aqueous acetic acid (4 ml) was used for paper chromatography.

(*b*) A similar hydrolyzate was prepared directly from griseoviridin (510 mg), hydriodic acid (15 ml), and red phosphorus (105 mg) without prior lithium borohydride reduction (solution B).

(*c*) A similar hydrolyzate was prepared directly from hexahydrogriseoviridin diacetate (225 mg), hydriodic acid (15 ml), and red phosphorus (127 mg) (solution C).

Aliquots of the solutions and of those of authentic amino acids were chromatographed (*n*-BuOH–water–HOAc, 4:5:1) the chromatogram being developed with the ninhydrin reagent of Moffat and Lytle (13). Solutions B and C showed the presence of alanine, glycine, and cystine. Solution A showed the presence of alanine and glycine and no trace of cystine or cysteine could be detected even at vastly increased concentrations.

Griseoviridin Diacetate – Maleic Anhydride Adduct

Griseoviridin diacetate (503 mg) in benzene (10 ml) containing maleic anhydride (174 mg) was refluxed for 5 hours. The solvent and excess anhydride were removed under reduced pressure (80° at 0.2 mm), and the residue crystallized from ethyl acetate – light petroleum to give the adduct m.p. 266–269°, λ_{max} 209 mμ (ε, 27,000). The difference spectrum (Fig. 1) was determined directly by balancing equimolar solutions. Calc. for $C_{30}H_{33}O_{12}N_3S$: C, 54.62; H, 5.04; N, 6.37%. Found: C, 54.20; H, 5.23; N, 6.39%.

Attempted Diels–Alder Reaction with Griseoviridin

Griseoviridin (140 mg) was added to a melt of maleic anhydride (400 mg) and heated on the steam bath for 3 minutes. The yellow solution was cooled and diluted with ethyl acetate. The amorphous acidic precipitate was esterified with diazomethane and acetylated (acetic anhydride – pyridine). In solution ($CHCl_3$) there was a strong band at 1750 cm^{-1} with a pronounced shoulder at 1770 cm^{-1}.

Dehydrogriseoviridin

Griseoviridin (1 g) in acetone (400 ml) was stirred at room temperature with a slurry of active manganese dioxide (10 g) for 3 hours. Evaporation of the filtered solution gave the crystalline ketone, m.p. 245–248° (from ethanol), $\lambda\lambda_{max}$ 209, 277 mμ (ε, 25,300, 20,100). Calc. for $C_{22}H_{25}O_7N_3$: C, 55.55; H, 5.30; N, 8.84. Found: C, 55.63; H, 5.41; N, 8.33%. The dienone (13.6 mg) in methanol (5 ml) was treated with periodic acid (0.21 *M*; 0.5 ml). There was no uptake after 20 hours.

Acetylation of the ketone (50 mg) (acetic anhydride – pyridine at room temperature overnight) gave, after crystallization from methanol, the monoacetate, m.p. 238–241°, $\lambda\lambda_{max}$ 209, 277 mμ (ε, 28,000, 24,300). Calc. for $C_{24}H_{27}O_8N_3S$: C, 55.68; H, 5.26. Found: C, 55.49; H, 5.26.

Hexahydrodehydrogriseoviridin Acetate

Dehydrogriseoviridin acetate (120 mg) in ethanol (100 ml) was shaken over palladized charcoal (10%; 450 mg) for 4 hours. Repeated crystallization of the product from methanol gave the acetate, m.p. 173–175°, λ_{max} 214 mμ (ε, 20,400) in neutral solution. Calc. for $C_{24}H_{33}O_8N_3S$: C, 55.02; H, 6.35; N, 8.03; S, 6.12%. Found: C, 54.98; H, 5.95; N, 8.53; S, 6.12%.

Dihydrodehydrogriseoviridin Acetate

Dehydrogriseoviridin acetate (120 mg) in acetic acid (10 ml) was shaken with activated zinc dust (3 g) for 2 minutes. The filtered solution was evaporated, the residue taken up in ethyl acetate and washed with water. The product, a mixture of double-bond isomers, was precipitated as an amorphous colorless solid by addition of light petroleum to the ethyl acetate solution. λ_{max} 216 mμ (ε, 21,300) in neutral solution. Calc. for $C_{24}H_{29}O_8N_3S$: C, 55.48; H, 5.63; N, 8.09; S, 6.16; Ac(1), 8.28%. Found: C, 55.38; H, 5.72; N, 7.83; S, 5.91, Ac, 8.85%.

The zinc reduction product (100 mg) was hydrogenated in the manner described for dehydrogriseoviridin acetate and gave hexahydrodehydrogriseoviridin acetate identical in every respect with the material obtained by direct hydrogenation.

Can. J. Chem. Downloaded from www.nrcresearchpress.com by 210.87.254.105 on 09/05/12
For personal use only.

Base-catalyzed Elimination in the Zinc Reduction Product

To the zinc reduction product (105 mg) in ethanol (50 ml) was added 0.1 *N* sodium hydroxide solution (21 ml). After 20 seconds the resultant yellow solution was acidified with acetic acid and evaporated to dryness at 35° under reduced pressure. The residue was extracted with ethyl acetate, the organic phase washed with water, and the product precipitated as a colorless solid by addition of light petroleum. Calc. for $C_{22}H_{25}O_6N_3S$: C, 57.50; H, 5.44; N, 9.14; S, 6.96. Found: C, 57.16, 57.23; H, 5.71, 5.66; N, 9.02; S, 6.86%. An acetyl determination indicated the presence of less than 0.1 acetyl groups. The ultraviolet spectrum of this product is shown in Fig. 2.

Base-catalyzed Elimination in Hexahydrodehydrogriseoviridin Acetate

The acetate (26.0 mg) in ethanol (10 ml) was mixed with rapid stirring with 0.1 *N* sodium hydroxide solution (3 ml). It was then acidified with acetic acid (0.1 *N*; 7.5 ml). The time taken for neutralization was 3–5 seconds. The product was extracted into chloroform and the organic phase washed with water, EDTA (4 Na) solution, and water. After removal of the solvent the product crystallized from methanol and chloroform–methanol m.p. 264–267°. Calc. for $C_{22}H_{29}O_6N_3S$: C, 56.95; H, 6.25%. Found: C, 57.48; H, 6.88%. Repeated analyses gave variable but not improved figures. The compound had no maximum in the ultraviolet above 215 mμ (Fig. 4).

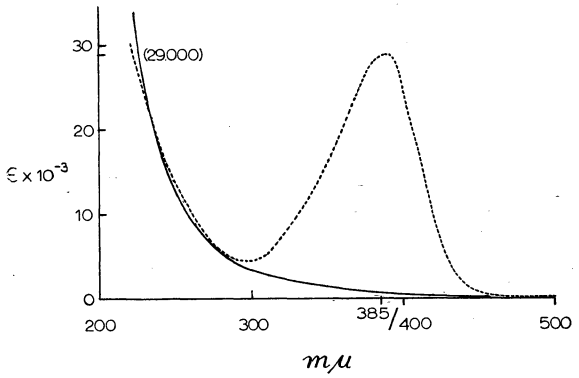

FIG. 4. N.m.r. spectra of (*a*) perhydro- and (*b*) isoperhydro-dethiogriseoviridin diacetate.

Ozonolysis–Hydrolysis of Griseoviridin Diacetate

Griseoviridin diacetate (506 mg) in ethyl acetate (30 ml) was treated with a stream of ozone for 75 minutes at −70°. Excess ozone was removed in a stream of oxygen and the solution evaporated at room temperature. The residue was heated on the steam bath with acetic acid (15 ml) and hydrogen peroxide (30%; 5 ml) for 90 minutes. The solution was concentrated under reduced pressure to about 3 ml, hydrochloric acid (*N*; 20 ml) added, and the mixture refluxed under nitrogen for 15 hours. The amino acid fraction was separated by ion-exchange on Dowex 50W-X2 (H^+) and on paper chromatography gave a single spot corresponding in R_f and color reaction to glycine.

The amino acid solution was rendered alkaline with *N* sodium hydroxide solution and shaken with benzoyl chloride (0.1 ml). After acidification benzoic acid was removed by filtration and extraction into chloroform. The residue from the aqueous layer was extracted with ethyl acetate and crystallized from ethyl acetate – light petroleum to give hippuric acid m.p. 183–190° undepressed on admixture with an authentic specimen.

Under identical conditions, but with omission of the ozonolytic step no trace of glycine could be detected by paper chromatography.

Ozonolysis–Hydrolysis of the Zinc Reduction Product

The substance (29 mg) in ethyl acetate (15 ml) was treated with ozonized oxygen for 1 hour. The solvent was removed under reduced pressure and the residue warmed on the water bath for 15 hours in acetic acid (10 ml) containing hydrogen peroxide (30%; 2 ml). After concentration under reduced pressure to ca. 0.5 ml hydrochloric acid (1 *N*; 10 ml) was added and the mixture refluxed for 1.5 hours. The amino acid fraction was isolated by Dowex 50W-X2 in the usual way. Paper chromatography of the product in hydrochloric acid (0.3 *N*; 1 ml) (upper phase of *n*-butanol:water:acetic acid, 4:5:1) using the polychromatic ninhydrin reagent of Moffat and Lytle (13) revealed the presence of glycine (R_f 0.17, orange brown) and β-alanine (R_f 0.25, blue-grey).

Alkaline Hydrolysis of Griseoviridin

Griseoviridin (120 mg) was refluxed under nitrogen for 1 hour with sodium hydroxide solution (4 *N*;

Can. J. Chem. Downloaded from www.nrcresearchpress.com by 210.87.254.105 on 09/05/12
For personal use only.

5 ml). The cooled hydrolyzate was adjusted to pH 8–9 with carbon dioxide, the solution diluted with water (15 ml) and benzoyl chloride added (0.3 ml), and the mixture shaken. The resultant solution was extracted with chloroform, ether, and ethyl acetate, and the extract discarded. The aqueous phase was acidified and continuously extracted with ether, the residue from removal of the ether being added to a column of silica gel. Elution with ether–benzene (1:1) gave hippuric acid which after crystallization from ether–ethanol had melting point and infrared spectrum identical with those of an authentic specimen, and gave no depression in melting point on admixture.

Perhydrogriseoviridin Diacetate Sulphone

Hexahydrogriseoviridin diacetate sulphone (210 mg) in acetic acid (75 ml) was hydrogenated for 16 hours over platinum oxide (400 mg). Evaporation of the filtered solution and crystallization from methanol gave the perhydro derivative, m.p. 221–229°. It showed only end absorption in the ultraviolet. Calc. for $C_{26}H_{41}O_{11}N_3S$: C, 51.74; H, 6.84; N, 6.96; S, 5.31; C-Me (4), 8.93. Found: C, 51.82; H, 6.83; N, 6.78; S, 5.05; C-Me, 9.94%.

Alkaline hydrolysis of the perhydro sulphone, in the manner described for hexahydrogriseoviridin diacetate sulphone gave a solution which on paper chromatographic examination showed the presence of alanine only. No trace of glycine, found in the hydrolysis of the less reduced derivative, could be detected.

Octahydrodethiogriseoviridin (see footnote† on p. 371)

Griseoviridin (1.03 g) in ethanol (100 ml) was refluxed with catalyst from six pellets of B.D.H. stabilized Raney nickel. Two further, similar, portions were added during the course of 6.5 hours. The catalyst was removed by filtration and washed with hot ethanol. Filtrate and washings were evaporated, the residue taken up in methanol and crystallized by the addition of methyl ethyl ketone. The crude product (240 mg) was repeatedly crystallized to give the octahydro compound, m.p. 168–169° (decomp.), $[\alpha]_D$ +4° (*c*, 0.92 MeOH). The compound had λ_{max} 212 mμ (ϵ, 14,200) unchanged by the addition of alkali. Calc. for $C_{22}H_{35}O_7N_3$: C, 58.26; H, 7.78; N, 9.27; C-Me(2), 6.6. Found: C, 58.00; H, 7.47; N, 9.35; S, 0.00; C-Me, 6.4%.

Hydrogenation of Octahydrodethiogriseoviridin (see footnote † on p. 371)

The compound (51 mg) was acetylated (acetic anhydride – pyridine) and the gummy product hydrogenated over Adam's catalyst (50 mg). Reaction was complete after 5 hours with the uptake of 1.8 mol. eq. hydrogen. The product was repeatedly crystallized from ethanol to give perhydrodethiogriseoviridin diacetate, m.p. 223–224°, $[\alpha]_D$ −50° (*c*, 0.88). Found: C, 57.77; H, 7.97; N, 7.63%.

Alkaline Hydrolysis of Octahydrodethiogriseoviridin

The substance (11.9 mg) was hydrolyzed in 4 *N* sodium hydroxide solution (2 ml) in the manner described for hexahydrodeoxygriseoviridin sulphone. No volatile base was evolved. After acidification with sulphuric acid (6 *N*; 2 ml) the solution was distilled at constant volume. The distillate (30 ml) consumed 1.1 equiv. alkali on rapid titration and a further 0.83 equiv. on warming with excess alkali and back titration. Paper chromatography of the distillate in the system propanol–ammonia (3:2) revealed the presence of two compounds indistinguishable in every respect (R_f; acidity towards indicator, coloration and time of development with silver nitrate) from 5-hydroxyhexanoic and formic acids respectively.

The salt mixture was oxidized with chromic acid (0.2 *N* in 1 *N* sulphuric acid; 1 ml) at 70° (ca. 1 hour) and after standing overnight at room temperature the excess oxidant was destroyed with sulphur dioxide. Addition of 2,4-dinitrophenylhydrazine (10 mg) in sulphuric acid (20%; 0.5 ml) and recrystallization of the precipitate from ethanol gave the derivative of 5-oxohexanoic acid, m.p. 143–145°.*

The distillation residue was diluted with water and passed through a column of Amberlite IR120 (H^+). After washing the column was eluted with ammonia. Paper chromatography of the evaporated eluate in 77% aqueous ethanol gave a number of ninhydrin-positive spots the two most intense corresponding to alanine and glycine. The presence of glycine was confirmed by the color with *o*-phthalaldehyde. After running on a single large sheet the band corresponding to glycine was cut out, the amino acid eluted and run in the two dimensional systems *n*-BuOH–water–ammonia (4:5:1)/*n*-BuOH – water – acetic acid (4:5:1) and *n*-BuOH – water – acetic acid (4:5:1)/77% ethanol. Glycine was again present.

Potentiometric Titration of Griseoviridin Diacetate

The diacetate (146 mg) in acetic acid (25 ml) was titrated with 0.109 *N* perchloric acid against a calomel electrode in saturated lithium chloride – acetic acid solution using a glass electrode. The titration curve was indistinguishable from that of the solvent. Urea and 2 methyl-4-carbethoxy-oxazole (15) gave end points with pK_a' 4.2 and 3.3 respectively.

ACKNOWLEDGMENTS

The authors wish to thank Dr. R. E. Bowman (Parke, Davis, London) for supplies of griseoviridin and helpful discussions, and Drs. L. Long and Q. Bartz (Parke, Davis,

**The mixture with the authentic derivative (m.p. 137–138°) reset after melting at ca. 135° and melted at 142–146°. The authentic derivative, m.p. 137–138°, was shown to be the unstable form by seeding a melt with a trace of material m.p. 143–146° when the higher melting point was observed. The literature melting point (14) is 143–145°.*

Can. J. Chem. Downloaded from www.nrcresearchpress.com by 210.87.254.105 on 09/05/12
For personal use only.

Detroit) for further supplies. They are indebted for financial support to the National Research Council (Canada) and the National Institutes of Health (Grants E-3317, AI 03317-03) U.S.A.

REFERENCES

1. P. DE MAYO and A. STOESSL. Can. J. Chem. **38**, 950 (1960).
2. M. C. FALLONA, T. C. MCMORRIS, P. DE MAYO, T. MONEY, and A. STOESSL. J. Am. Chem. Soc. **84**, 4162 (1962).
3. D. E. AMES, R. E. BOWMAN, J. F. CAVALLA, and D. D. EVANS. J. Chem. Soc. 4260 (1955).
4. D. E. AMES and R. E. BOWMAN. J. Chem. Soc. 4264 (1955).
5. D. E. AMES and R. E. BOWMAN. J. Chem. Soc. 2925 (1956).
6. W. KELLER-SCHIERLEIN, M. LJ. MIHAILOVIC, and V. PRELOG. Helv. Chim. Acta, **42**, 305 (1959).
7. H. C. BROWN, D. H. MCDANIEL, and O. HAEFLIGER. *In* Determination of organic structures by physical methods. *Edited by* E. A. Braude and F. C. Nachod. Vol. I. Academic Press Inc., New York, N.Y. 1955. p. 620.
8. A. C. COPE, R. K. BLY, E. P. BURROUGHS, O. J. CEDER, E. CIGANEK, B. T. GILLIS, R. F. PORTER, and H. E. JOHNSON. J. Am. Chem. Soc. **84**, 2170 (1962).
9. R. MOCCIA and H. W. THOMPSON. Spectrochim. Acta, **10**, 240 (1957).
10. J. C. SHEEHAN, H. G. ZACHU, and W. B. LAWSON. J. Am. Chem. Soc. **79**, 3933 (1957).
11. F. W. EASTWOOD, B. K. SNELL, and A. TODD. J. Chem. Soc. 2286 (1960).
12. A. TODD. Intern. Symp. Org. Chem. Nat. Products (I.U.P.A.C.) Brussels. 1962.
13. E. D. MOFFAT and R. I. LYTLE. Anal. Chem. **31**, 926 (1959).
14. A. ESCHENMOSER and A. FREY. Helv. Chim. Acta, **35**, 1660 (1952).
15. J. W. CORNFORTH and R. H. CORNFORTH. J. Chem. Soc. 96 (1947).
16. Q. R. BARTZ, J. STANDIFORD, J. D. MOLD, D. W. JOHANNESSEN, A. RYDER, A. MARETSKI, and T. H. HASKELL. *In* Antibiotics annual (1954–1955). Med. Ency. Inc., N.Y. 1955. pp. 777–783.

Can. J. Chem. Downloaded from www.nrcresearchpress.com by 210.87.254.105 on 09/05/12
For personal use only.

MOLD METABOLITES

3. THE STRUCTURE OF THE GRISEOVIRIDIN SALTS

M. CATHERINE FALLONA, P. DE MAYO, AND A. STOESSL
Department of Chemistry, University of Western Ontario, London, Ontario
Received August 21, 1963

ABSTRACT

The conversion of griseoviridin (I) into its hydrochloride and into its perchlorate has been shown to involve the ejection of one of the hydroxyl groups in (I) and the formation of an imino-lactone salt.

Can. J. Chem. Downloaded from www.nrcresearchpress.com by 210.87.254.40 on 09/05/12
For personal use only.

In the course of their characterization of, and preliminary studies on, griseoviridin, Bowman and his collaborators made the observation that although this substance was neutral, as judged by attempted titration with perchloric acid in acetic acid, it nevertheless under certain conditions gave crystalline salts (1–3). When heated with acetic anhydride and perchloric acid a substance designated a perchlorate diacetate was obtained, whilst using dioxan instead of acetic anhydride a simple perchlorate resulted. They also noted that griseoviridin dissolved rapidly in cold concentrated hydrochloric acid from which, by careful evaporation of the hydrochloric acid, a crystalline hydrochloride could be obtained, the analysis of which (2, 4) indicated that no loss of water had occurred in its genesis.

These salts differed from griseoviridin in having a lower intensity of ultraviolet absorption (Fig. 1) and, most importantly, they could now be titrated with alkali. Two titrable groups were disclosed ($pK_a' \sim 6.5$), one of which was the base hydrochloride, but on back titration only a single titrable group could be detected in this region. The second function at $pK_a' \sim 6.5$ was attributed to an enolic function because the perchlorate, after treating with hot water, gave a purple color with ferric chloride not given without preliminary heating. The significance of the potentiometric data was obscured by the fact that further reactions, such as hydrolysis, were undoubtedly proceeding under the titration conditions. This was clearly revealed in the case of the perchlorate which showed an ultraviolet absorption maximum at 218 mμ in water and at ca. 270 mμ in alkaline solution.

It was consequently difficult at the outset to be clear which physical properties were to be attributed to the salts themselves, and which to their decomposition products. Only one chemical transformation had been performed on the salts, in this case the hydrochloride, in which the chemical integrity of the reacting species seemed unequivocal. Ames and Bowman (2) found that hydrogenation of griseoviridin hydrochloride gave a substance which contained no chlorine and which was now neutral to titration with perchloric acid in acetic acid. At a later date this work was repeated (4) and the product, hexahydrodeoxygriseoviridin, was shown to differ from hexahydrogriseoviridin with respect to empirical formula, in the lack of one oxygen atom. Thus, whatever the nature of the basic function introduced through reaction with strong acid, it was removed irreversibly by hydrogenation; the deoxy compounds would not give salts under conditions adequate for griseoviridin.

With (I) proposed as a representation of the structure of griseoviridin (5), an interpretation of the facts concerning the salts was required if the validity of (I) was to be maintained.

A number of prerequisites were known for such salt formation. As mentioned, no salt could be obtained from hexahydrodeoxygriseoviridin indicating that the unsaturation in either the C_6 fragment or the aminodecanoic acid was required, or both. Then, since the maleic anhydride adduct (5) of griseoviridin diacetate also failed to give a salt with concentrated hydrochloric acid, the conclusion to be reached was that one of the ethylenic linkages in the aminodecanoic acid was essential, either in itself or because of some property to be associated with it. Further, the unsaturated C_3 fragment was clearly not involved in the salt formation since the singlet vinylic proton signal at low field ($\sim\tau$ 1.9) was still observable in the n.m.r. spectrum of the hydrochloride and of hexahydrodeoxygriseoviridin and its derivatives. Likewise the presence of the bands at ca. 1600 and 1500 cm^{-1} in the infrared spectrum (5) revealed that the unsaturation associated with this fragment was untouched in both series of compounds. In hydrolytic reactions the hydrochloride paralleled the behavior of griseoviridin (see Experimental). Finally, the unchanged situation of the C_6 unsaturation was confirmed by the obtention of crotonaldehyde by ozonolysis and distillation, and by the formation of acetaldehyde on base treatment of the hydrochloride. The formation of the basic function, therefore, involved an amide and some part of the C_{10} moiety encompassing at least one of the ethylenic linkages.

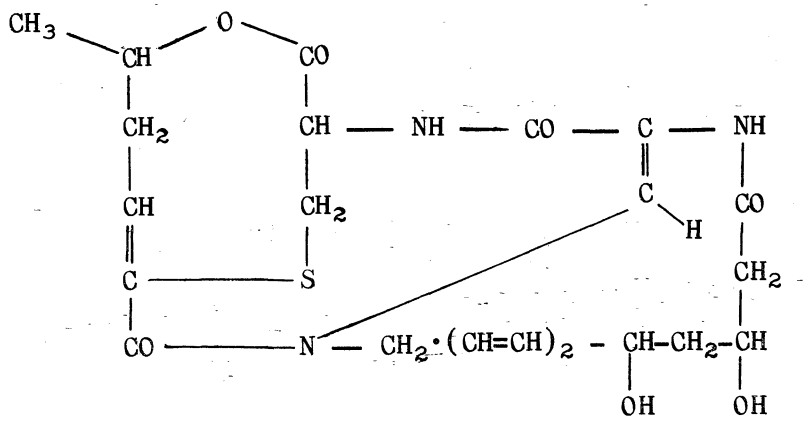

(I)

The decrease in the high-intensity ultraviolet absorption during hydrochloride formation noted by Bowman (2) has been mentioned. To ascertain more exactly the nature of the change, a plot of the difference curve between the absorption of griseoviridin and of its hydrochloride was constructed (Fig. 1). It was then apparent that concomitant with the decrease in absorption in the 220 mμ region a new absorption band had appeared at longer wave length. Furthermore, the chromophore removed from the 220 mμ region was not that of the diene (5) nor, since it was not apparently involved in the transformation, that of the C_6 fragment. It was, in fact, as closely as the errors inherent in such difference spectra would allow, the absorption associated with the unsaturated C_3 fragment and represented by, for instance, the absorption of hexahydrogriseoviridin diacetate; and this despite the fact that this particular arrangement of atoms, as concluded from infrared and n.m.r. spectra, had survived salt formation and subsequent hydrogenation intact.

Can. J. Chem. Downloaded from www.nrcresearchpress.com by 210.87.254.40 on 09/05/12
For personal use only.

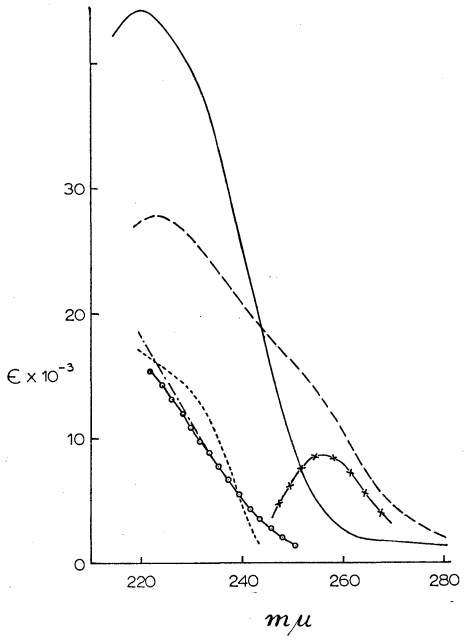

FIG. 1. Absorption spectrum of griseoviridin (—) and griseoviridin hydrochloride (– – –). The "disappearance" difference spectrum is given as (- - -), the "appearance" difference spectrum shown as (×—×). Hexahydrogriseoviridin and hexahydrodeoxygriseoviridin are (·—·) and (○—○).

The interpretation arrived at, compatible with these observations, was that the C_3 chromophore was extended in salt formation, but that in conversion to the hexahydrodeoxy series (the ultraviolet absorption of which was similar to that of hexahydrogriseoviridin diacetate) this extension of unsaturation was removed.

It was first assumed that the conversion of the salts to the hexahydrodeoxy series involved hydrogenolysis of an oxygen function, as suggested by the relevant analyses. Such supposition, it became evident, raised considerable interpretative difficulties. Careful preparation and analysis of the salts confirmed the empirical formula of the hydrochloride, but revealed that the perchlorate diacetate (I) was in fact a monoacetate. The fact was established, however, that the analytical values required that salt formation should not involve loss of water, and that where acetic acid was lost it was replaced by water. It was shown, also, that the acetate present in the perchlorate acetate was one originally present in griseoviridin diacetate by preparing the acetate perchlorate in propionic anhydride. Hydrolysis and paper chromatography showed no trace of propionate incorporation.

It was thus possible and necessary to presume that one of the oxygen atoms in the salts was present, simply as water of crystallization, water which, however, it was not possible to remove by prolonged drying. An observation relevant to this assumption was the fact that attempted repetitions of the perchlorate acetate preparation were subject to uncertainty until it was finally noted that traces of water were responsible for success. The addition of one equivalent of water (to the anhydride) after reaction resulted in spontaneous crystallization. With the assumption that one molecule of water (or acetic acid) was lost in salt formation, the necessity of postulating hydrogenolytic oxygen loss was removed.

Can. J. Chem. Downloaded from www.nrcresearchpress.com by 210.87.254.40 on 09/05/12
For personal use only.

During salt formation and the loss of an oxygen function, either the β or the δ oxygen could be the one ejected; the hydroxyl remaining was that present in hexahydrodeoxygriseoviridin. It had previously been shown that the sulphone of this substance could be oxidized to a ketone (4) which, whilst showing no long-wavelength absorption in neutral solution, in the presence of alkali exhibited a maximum at 298 mμ, which was reversibly formed in typical enolic fashion.

This clearly required that the β hydroxyl (in I) should be the one remaining. At this point sufficient data were available for unambiguous interpretation.

Protonation of the allylic hydroxyl group (or acetate) in the δ position followed by solvolysis would leave an allylic cationic charge which would be accessible to the non-bonded electrons of the aminodecanoic acid carbonyl oxygen.[1] Ether formation with participation of the nitrogen p electrons would complete the process. This sequence, shown in (II), would lead to (III) as a representation of the structure of the salts. Such a process is unexceptional and, in essentials, has adequate analogy (6, 7, 8).

The hydrogenation of allylic ethers leads frequently to carbon–oxygen bond fission. The product of such cleavage at the position '*a*' in (III) would be an amide of structure (IV, R = H) which would differ from hexahydrogriseoviridin diacetate (IV, R = OAc) only by the absence of one acetoxyl group. In Fig. 2 the infrared spectrum of hexahydro-

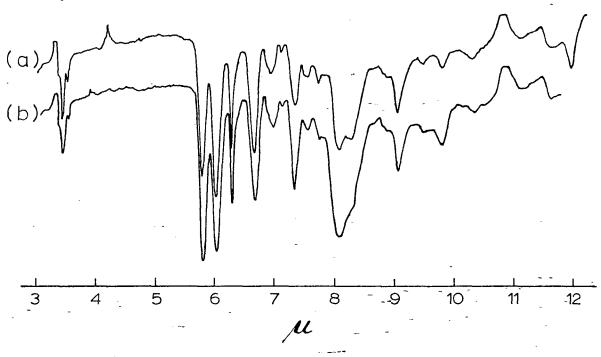

FIG. 2. Infrared spectra (*a*) of hexahydrodeoxygriseoviridin acetate and (*b*) hexahydrogriseoviridin acetate in equimolar solutions in chloroform.

griseoviridin diacetate and hexahydrodeoxygriseoviridin acetate are reproduced. With the exception of those frequencies associated with carbon–oxygen stretch the spectra are virtually identical.

The only impediment to the acceptance of this rationalization was the already mentioned persistent deviation of the analytical figures for the salts from those required by one molecule of water. Drying temperatures above 60° were not utilizable because of the decomposition which occurred over the prolonged periods necessary, so the retention of water under such condition by a salt was by no means inconceivable. However, the importance of this point did not allow of pious assumption.

Although the salts were not recoverable from pyridine solution, probably because of ready decomposition, no simple mechanism for the generation of water in this medium could be envisaged. Accordingly, Karl Fischer titration appeared to be an adequate tool for

[1]*If the stereochemistry of the diene is such as to give the maleic anhydride adduct (5) without geometrical inversion, then a study of models indicates that such inversion must occur in salt formation. Participation of the amide carbonyl in the solvolytic step is not thus possible.*

Can. J. Chem. Downloaded from www.nrcresearchpress.com by 210.87.254.40 on 09/05/12
For personal use only.

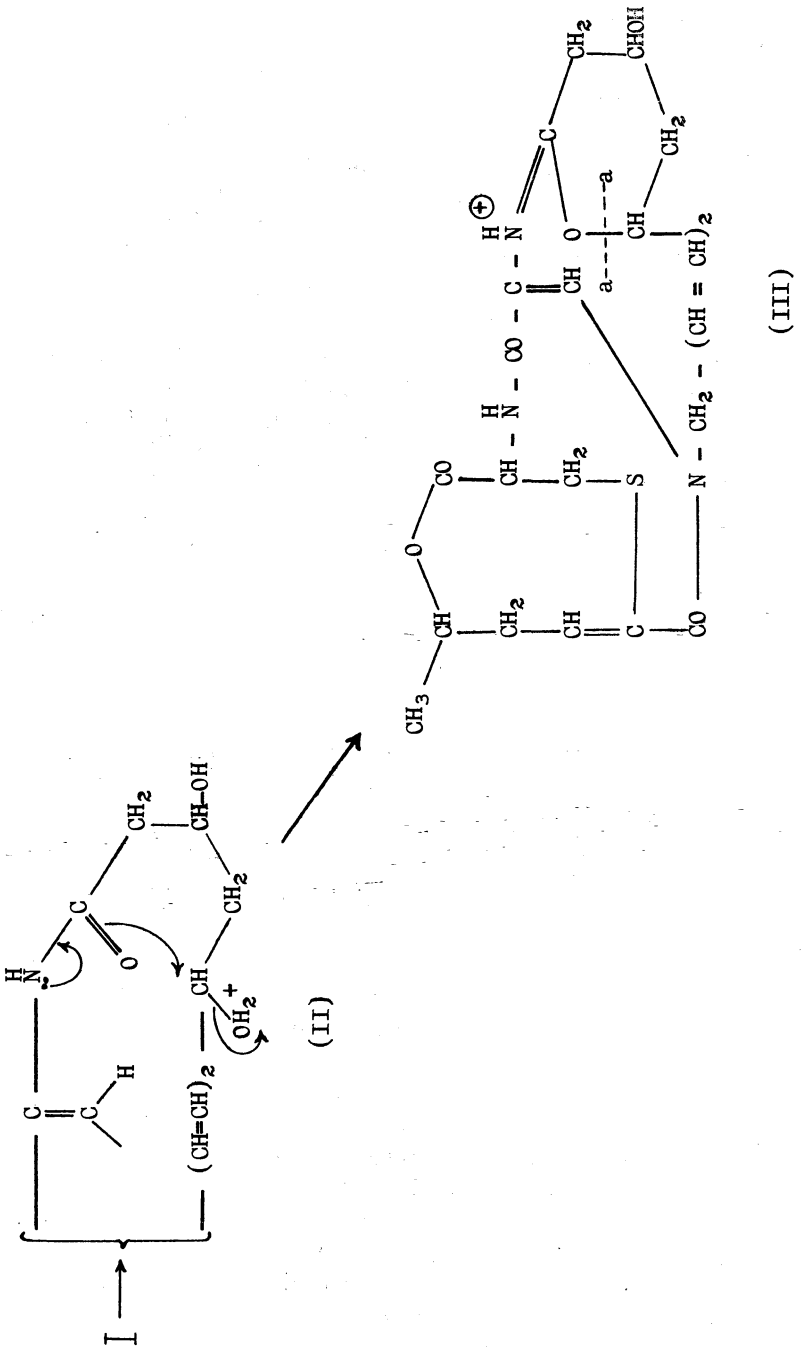

Can. J. Chem. Downloaded from www.nrcresearchpress.com by 210.87.254.40 on 09/05/12
For personal use only.

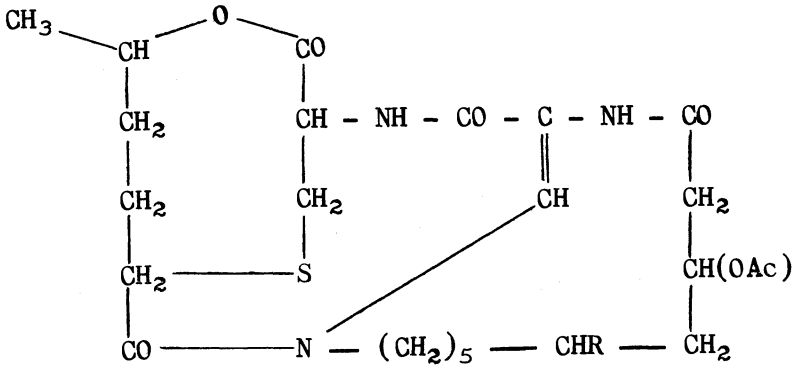

(IV)

water estimation in these circumstances. Titration with the reagent (see Experimental), in fact, revealed the presence of one molecule of water in the hydrochloride and in the monoacetate perchlorate.[2]

The last impediment to the acceptance of (III) was thus removed.

The enolic properties exhibited by the solutions of the hydrochloride in water after warming were not those, therefore, of the salt itself, but of some hydrolysis product. The aqueous hydrolysis of such imidate ethers had been studied and it appeared that an important mode of decomposition was formation of a carbinolamine followed by cleavage of the C—N bond. This is illustrated in the present instance by the process indicated in the part formula (V). Such a mode of reaction of an imino-lactone salt has ample analogy.[3] An opposite is the hydrolysis of the methyl benzimidate ion. The salt is stable in water for short periods, but on mild warming is converted to methyl benzoate and ammonium chloride (12).

The further transformation of (V) can only be interpreted tentatively. Two possibilities, at least, exist.

In the first, the vinylamine may be hydrolyzed to give (VI), whilst alternatively, water may add β to the amide carbonyl, followed by C—N bond cleavage in the carbinolamine to give the β-aldehydoamide (or tautomer) (VII). Both (VI) and (VII) may undergo further hydrolytic steps. Both could provide the requisite enolic system observed, but the evidence available does not justify further discussion.[4]

EXPERIMENTAL

(For general details see Part 2 (5))

Griseoviridin Hydrochloride

A solution of griseoviridin (200 mg) in methanol (10 ml) at 0° was saturated with hydrogen chloride over 1 hour. Evaporation under reduced pressure and crystallization from methanol–ether gave the hydrochloride identical in infrared spectrum with an authentic specimen (2).

[2]*A sample of the hydrochloride allowed to stand exposed to the atmosphere for 2 days contained approximately two molecules of water, but after redrying a figure of one molecule was again obtained.*

[3]*See, for example, the series of papers by McElvain (9) and many others including the hydrolysis of 2-cyclohexyliminotetrahydrofuran hydrobromide (10) and papers by Witkop (inter alia 11) on selective peptide cleavage.*

[4]*The phenylphenacyl derivative of the neutralized hydrochloride reported by Bowman may well be an enolate derivative. The analytical values reported (2) are in approximate agreement with this formulation.*

Can. J. Chem. Downloaded from www.nrcresearchpress.com by 210.87.254.40 on 09/05/12
For personal use only.

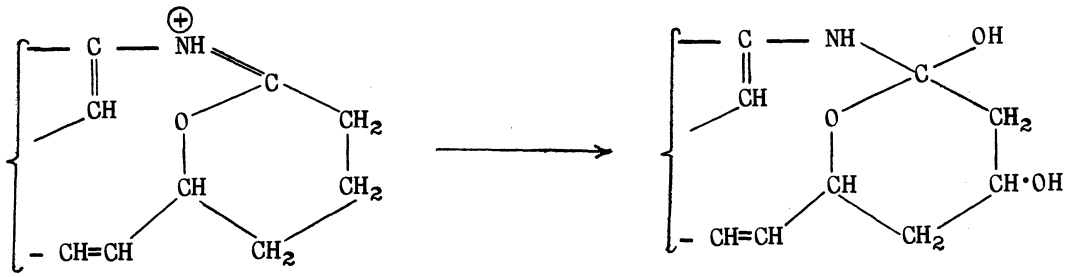

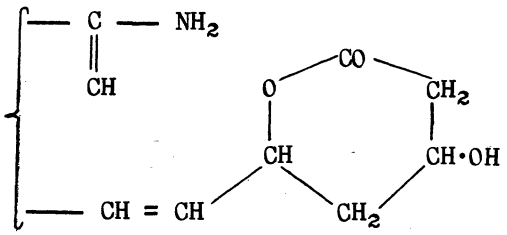

(V)

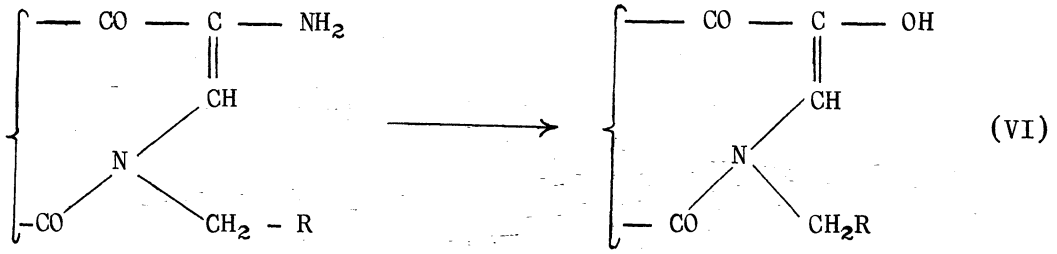

(VI)

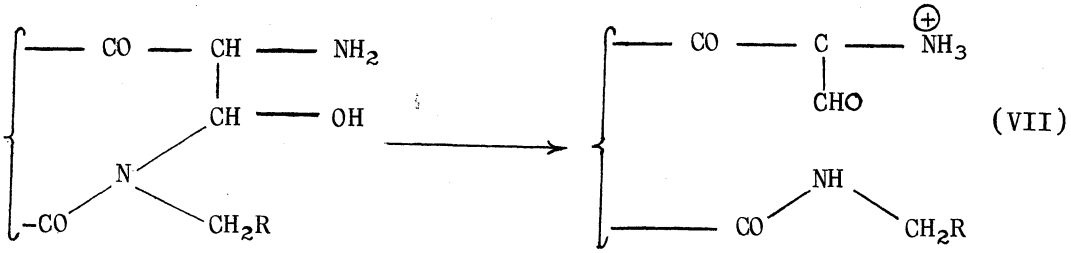

(VII)

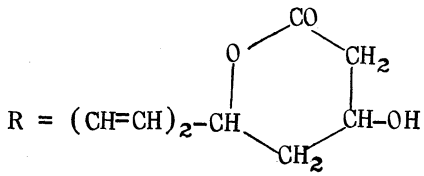

Can. J. Chem. Downloaded from www.nrcresearchpress.com by 210.87.254.40 on 09/05/12
For personal use only.

Alkaline Hydrolysis of Griseoviridin Hydrochloride

(*a*) The hydrochloride (245 mg) was hydrolyzed with 4*N* sodium hydroxide as described for griseoviridin (4). Acetaldehyde (isolated as the 2,4-dinitrophenylhydrazone (60 mg)), formic acid (0.64 molecular equivalent (mol. eq.)), and acetic acid (0.16 mol. eq.) were found.

(*b*) The hydrochloride (104 mg) was refluxed with barium hydroxide solution (0.46 *N*; 25 ml) for 4 hours. Ammonia (0.86 mol. eq.) was evolved. A 1-ml aliquot of the cooled hydrolyzate gave no sulphide reaction with alkaline lead acetate. A control indicated a positive response to 3×10^{-4} mmole. The barium carbonate precipitated (16 mg; 0.41 mol. eq.) was removed by filtration and the filtrate acidified. Hydrogen sulphide was immediately evolved in the cold. The solution was heated for 2 hours and the gases led into standard barium hydroxide by a stream of nitrogen. Barium carbonate (0.29 mol. eq.) was deposited and the filtrate was titrated with iodine: 0.33 mole H_2S had been absorbed. In a parallel experiment griseoviridin gave 0.97 mol. eq. ammonia and 0.47 mol. eq. carbon dioxide.

Griseoviridin Monoacetate Perchlorate

To griseoviridin (250 mg) in acetic acid – acetic anhydride (1:1, 2.5 ml) was added perchloric acid (70%; 0.1 ml), the solution kept at 55° for 30 minutes protected from the atmosphere, and then divided into two equal portions. To one of these water (0.12 ml) was added, whilst the other was protected from traces of water. On standing overnight, only the solution to which water had been added had deposited crystals (54 mg). These were collected, washed with acetic acid, and recrystallized from nitromethane–ether. After washing with ether, the crystals were dried at 97° under high vacuum for 3.5 hours and another 6 hours at 65°. Calc. for $C_{24}H_{28}O_{11}N_3SCl\cdot H_2O$: C, 46.48; H, 4.88; N, 6.78; S, 5.17; Cl, 5.72. Found: C, 45.94; H, 5.06; N, 6.33; S, 4.87; Cl, 5.47%.

The same compound was obtained from griseoviridin diacetate when the acetic anhydride – acetic acid mixture was replaced by propionic anhydride – propionic acid. Identity was established by ultraviolet and infrared spectroscopy and analysis. Found: C, 46.18; H, 5.05; N, 7.09; S, 5.38; Cl, 5.55%.

On acetyl determination (alkaline hydrolysis) the product liberated 1.42 mol. eq. volatile acid. Griseoviridin perchlorate (3) under the same conditions gave 0.18 mol. eq. volatile acid. Examination of the volatile acids by paper chromatography in three solvent systems revealed the presence of acetic and formic acids only, and no trace of propionic acid.

Estimation of Water of Crystallization (Karl Fischer Determinations)

The titrations were performed by the 'dead stop technique', using pyridine as solvent and standard water-in-methanol for back-titration (ref. 13 and references there cited).

		Calculated, %	Found, %
(1) Griseoviridin hydrochloride ($C_{22}H_{25}O_6N_3S\cdot HCl$)			
(*a*) Air-dried	($2\cdot H_2O$)	6.68	6.81
(*b*) Dried at 60°	($1\cdot H_2O$)	3.51	3.67[5]
(*c*) Sample (*b*) exposed to the atmosphere for 3 days		—	7.32
(*d*) Sample (*c*) redried		—	5.10
(2) Griseoviridin monoacetate perchlorate ($C_{24}H_{27}O_7N_3S\cdot HClO_4$)	($1\cdot H_2O$)	2.91	3.04

Titrations of Griseoviridin Salts

The compounds listed (ca. 0.02 mmole) were dissolved or suspended in water, sodium hydroxide (0.01 *N*; 10 ml) added, and the mixture left at room temperature overnight. The excess alkali was then titrated. Found (equivalent consumed in parentheses): griseoviridin hydrochloride (2.07); griseoviridin perchlorate (2.15); griseoviridin perchlorate acetate (3.21).

Hydrolysis–Hydrogenation of Griseoviridin Diacetate

The diacetate (250 mg) was dissolved in concentrated hydrochloric acid (1.0 ml). After evaporation under reduced pressure, the product was crystallized from methanol and methanol–ether. The product, for which a satisfactory carbon analysis could not be obtained, consumed 3.29 equivalents of alkali (see above) and gave an acetyl value of 1.15. Calc. for $C_{24}H_{28}O_7N_3Cl\cdot H_2O$: N, 7.56%; Cl, 6.38%. Found: N, 7.33; Cl, 6.00%. Hydrogenation of the salt (67 mg) over palladized charcoal (10%; 200 mg) in ethanol for 4 hours gave hexahydrodeoxygriseoviridin acetate identical in every respect with material obtained (4) by the acetylation of hexahydrodeoxygriseoviridin.

Hexahydrodeoxygriseoviridin

(*a*) The compound (43 mg) was dissolved in concentrated hydrochloric acid (0.5 ml). Evaporation and crystallization of the residue gave starting material (30 mg) identified by melting point and mixed melting point.

[5]*Average of two determinations.*

Can. J. Chem. Downloaded from www.nrcresearchpress.com by 210.87.254.40 on 09/05/12
For personal use only.

On hydrolysis in 0.46 *N* barium hydroxide, as described for griseoviridin hydrochloride, ammonia (0.99 mol. eq.) and carbon dioxide (0.81 mol. eq.) were liberated. No hydrogen sulphide was evolved on acidification.

Hydrolysis in 4 *N* sodium hydroxide, as described (4) for hexahydrodeoxygriseoviridin sulphone, gave ammonia (0.80 mol. eq.). Distillation of the acidified solution gave an oily lactone, which in paper-chromatographic behavior paralleled 2-mercapto-1,5-hexanolide (5), and formic acid.

In another comparable experiment the acidified hydrolyzate (from 318 mg hexahydrodeoxygriseoviridin) was distilled and the sodium salts of the volatile acid converted into the methyl esters by acidification and treatment with diazomethane in methanol–ether. The ether was distilled off and collected at −70°. Hydrolysis of the distillate, followed by reacidification and distillation, gave formic acid (0.18 mol. eq.) characterized by the melting point and infrared spectrum of the sodium salt.

ACKNOWLEDGMENTS

The authors are indebted to the National Research Council of Canada and the National Institute of Health (U.S. grant No. AI 03317-03) for financial support.

REFERENCES

1. D. E. Ames, R. E. Bowman, J. F. Cavalla, and D. D. Evans. J. Chem. Soc. 4260 (1955).
2. D. E. Ames and R. E. Bowman. J. Chem. Soc. 4264 (1955).
3. D. E. Ames and R. E. Bowman. J. Chem. Soc. 2925 (1956).
4. P. de Mayo and A. Stoessl. Can. J. Chem. **38**, 950 (1960).
5. M. C. Fallona, P. de Mayo, T. C. McMorris, T. Money, and A. Stoessl. Can. J. Chem. This issue.
6. R. R. Burford, F. R. Hewgill, and P. R. Jeffries. J. Chem. Soc. 2937 (1957).
7. B. G. Morin, B. G. Jackson, and E. H. Flynn. J. Am. Chem. Soc. **84**, 3400 (1962).
8. T. Wieland and V. Wintermeyer. Ber. **90**, 1721 (1957).
9. S. M. McElvain and J. W. Nelson. J. Am. Chem. Soc. **64**, 1825 (1942).
10. C. J. M. Stirling. J. Chem. Soc. 255 (1960).
11. A. Patchornik, W. B. Lawson, and B. Witkop. J. Am. Chem. Soc. **80**, 4748 (1958).
12. J. Stieglitz. Am. Chem. J. **39**, 29, 166, 402, 437, 586, 719 (1908); J. Am. Chem. Soc. **32**, 221 (1910); **34**, 1687 (1912); **35**, 1774 (1913).
13. J. Mitchell, Jr. Anal. Chem. **23**, 1069 (1951).

Can. J. Chem. Downloaded from www.nrcresearchpress.com by 210.87.254.40 on 09/05/12
For personal use only.

THE pH AND pD DEPENDENCE OF THE SPONTANEOUS AND MAGNESIUM-ION-CATALYZED DECARBOXYLATION OF OXALACETIC ACID

GEORGE W. KOSICKI AND STANISLAVA N. LIPOVAC[1]
Department of Chemistry, University of Windsor, Windsor, Ontario
Received March 15, 1963

ABSTRACT

Spectrophotometric studies of the spontaneous and magnesium-ion-catalyzed decarboxylation of oxalacetic acid in H_2O and D_2O have been carried out over a range of pH, pD, and magnesium ion concentrations.

The rate of decarboxylation of oxalacetic acid depends on the proposed equilibrium system between the acid anion and magnesium chelate under a variety of conditions.

The absorbancy indexes and the apparent equilibrium constant of the keto and enol forms of the magnesium chelate were estimated from a combination of the kinetic and spectral data.

INTRODUCTION

Oxalacetic acid has been shown to decompose to CO_2 and pyruvic acid spontaneously (1, 2, 3), and catalytically by the action of polyvalent cations (1, 4, 5) and enzymes (6). The catalysis by metal ions has served as a model for the enzymatic reaction (7,8). The kinetics of the spontaneous decarboxylation of oxalacetic acid in aqueous solution have been studied over a range of temperature and at varying degrees of dissociation (9,10). Steinberger and Westheimer (8) have proposed that the keto form of the acid decarboxylates by using the α,α-dimethyl substituted oxalacetic acid, in which only the keto form can exist. In this paper the decomposition was followed spectrophotometrically as a function of pH and pD. The results indicate that the keto form of the monoanion of oxalacetic acid is the predominant species leading to decarboxylation.

The decarboxylation of oxalacetic acid is also catalyzed by a variety of multivalent cations (11–14). Magnesium ion was found to have a low catalytic activity compared to other divalent metals, but still it involves a change of spectrum indicating the formation of a chelate. The results of the present study show a direct correlation between the rate of decarboxylation of oxalacetic acid and the magnesium ion concentration as a function of pH and pD. The range of optimal activity (pH 5 to 6) for the magnesium-ion-catalyzed reaction coincides with the range found for the enzymatic decarboxylation (11, 15, 16).

EXPERIMENTAL

The following materials were commercial preparations: oxalacetic acid (OAA) (Sigma Chemical Co.), $MgCl_2.6H_2O$ reagent grade, Tris(hydroxymethyl)aminomethane (Tris) was primary standard grade. The D_2O (99.78 atom % excess D) was purchased from the Atomic Energy Commission of Canada Limited, Ottawa.

Measurements of pH and pD of each reaction mixture were made at the end of the experiment with a Beckman Model G pH meter standardized with pH 7 buffer. When D_2O was used as a solvent the measurements were made with the same glass and calomel electrodes and the pD was calculated by adding 0.4 units to the observed meter reading (17). The buffer system used was a Tris–acetate mixture. To adjust the pH, 1 *M* basic Tris and 1 *M* acetic acid were mixed in the proper proportions. For the D_2O systems all the reagents were made up in D_2O.

Absorption spectra were measured with a Bausch and Lomb Spectronic 505 spectrophotometer. Rates of reaction were followed either in the Beckman DU spectrophotometer or on the Gilford Instrument Model 2000

[1]*Permanent address: Institute of Physical Chemistry, Faculty of Natural Sciences and Mathematics, University of Belgrad, Belgrad, Yugoslavia.*

Can. J. Chem. Downloaded from www.nrcresearchpress.com by 210.87.254.105 on 09/05/12
For personal use only.

absorbance recorder (Beckman monochromator). The temperature of the reaction cell was kept at 25.0±0.2° C by a water-cooled circulating bath.

Rate measurements were made at 25.0° C and followed over a period of 3 half-times for the spontaneous decarboxylation of oxalacetic acid, and followed to the end of the reaction for the magnesium-ion-catalyzed reaction. The observed rate constants were calculated graphically from the slopes of the first order plots and from the equation:

$$[1] \qquad k_{obs} = \frac{2.303}{t} \log \frac{A_0 - A_e}{A_t - A_e}$$

where A_0 is the absorbance at zero time, A_e is the absorbance at equilibrium, A_t is the absorbance at time t, t is the time in minutes and k_{obs} is the observed rate constant (minutes^{-1}).

RESULTS AND DISCUSSION

Spontaneous Decarboxylation

The observed first order rate constants for the spontaneous decarboxylation of oxalacetic acid measured at 255 mμ are plotted as a function of pH and pD in Fig. 1. The bell-shaped curve with a maximum of activity at pH 3.6 shows a shift to a higher pD value for the D_2O system of about 0.6 pH (pD) units. For the spontaneous decarboxylation of oxalacetic acid the buffer concentration definitely has an effect on the observed rate constant. Beyond a concentration of 0.7 M, however, further increases of buffer had no significant effect on the observed rate constant. For this reason the reactions were followed within the range of this plateau of buffer effect. At the optimal activities of decarboxylation, however, the deviations due to buffer effects are accentuated, and deviations from the first order plot are observed after a half-time of reactions. In the D_2O system from pD 6 to 8 the observed rates were corrected for initial ketonization.

The correspondence of the curve to the dissociation constants of oxalacetic acid of pK 2.5 and 4.37 (depending on ionic strength) indicates that the predominant species that decarboxylates is the monoanion:

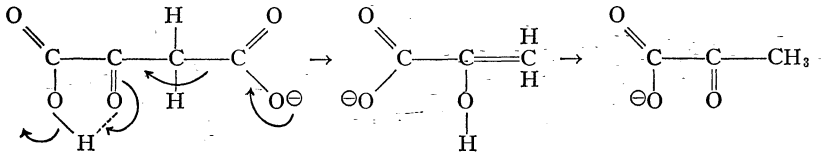

$+ CO_2$ [2]

At pH 3.6 the keto form of oxalacetic acid is the predominant species (18). When the maximum activity is reached at about pH 3.6 the first dissociation (pK_1 2.5) is virtually complete (19). The rate of the reaction begins to decrease as the pH increases to where the second carboxyl group starts to dissociate (pK_2 4.37) and reaches a minimum rate when the fully dissociated form is predominant. The anion of pyruvic acid with a pK of about 2.5 is the product at pH 3.6. The activity plot as a function of pH (Fig. 1) confirms the kinetic studies of Pedersen (9) and Gelles(9), who conclude that oxalacetic acid as the monoanion decarboxylates much faster than in the undissociated form (44 times).

The shift of the bell-shaped activity curve of 0.6 units in D_2O to higher pD values gives further and direct evidence that the monoanion is the predominant active species that decarboxylates (10). To obtain the same concentration of the active monoanion in D_2O a higher pD is required than the corresponding pH because oxalacetic acid is a weaker acid in D_2O than in H_2O.

Can. J. Chem. Downloaded from www.nrcresearchpress.com by 210.87.254.105 on 09/05/12
For personal use only.

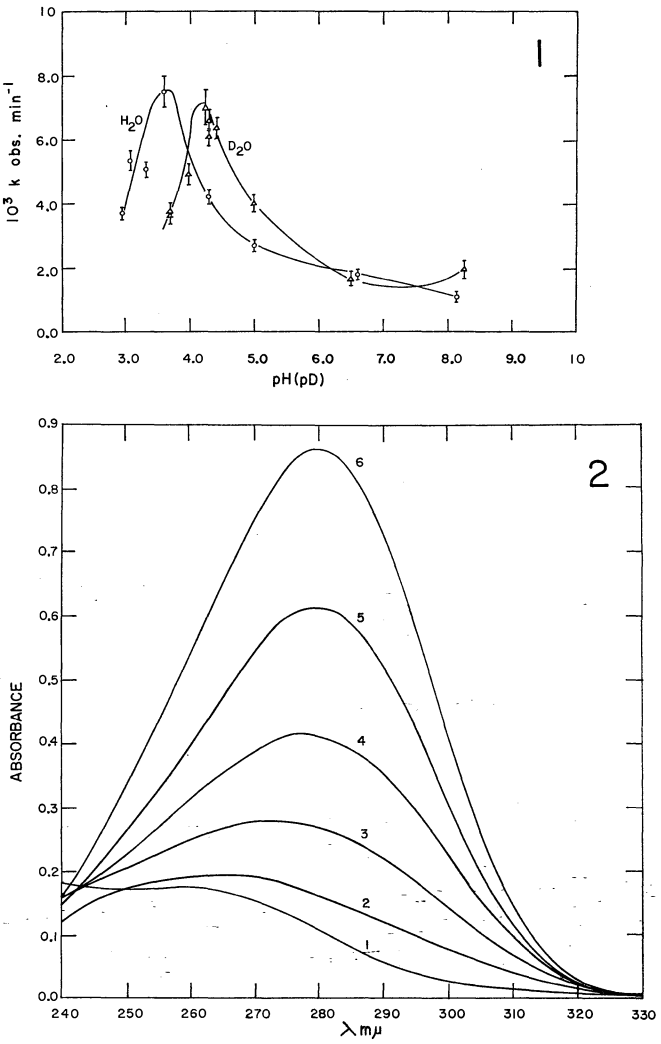

FIG. 1. Spontaneous decarboxylation of oxalacetic acid. Each cuvette (0.5 cm light path) contained $\sim 2\times10^{-4}$ *M* oxalacetic acid and 1.0 *M* Tris–acetate buffer of the appropriate pH made up in H_2O or D_2O. Solid oxalacetic acid was added last and its concentration measured immediately by its absorption at 255 mμ. The zero time absorbance was determined by extrapolation of the plot of absorbance versus time.

FIG. 2. The spectra of the magnesium chelate as a function of magnesium ion concentration. Solutions were prepared in 25 ml volumes adjusted to pH 7.40 ± 0.04 with Tris–acetate buffer 0.5 *M* and measured in 1.0-cm light path cuvettes within 2 minutes. The concentration of oxalacetic acid was 1.9×10^{-4} *M*. Magnesium chloride concentrations for the curves were: (1) 0.000, (2) 0.012, (3) 0.04, (4) 0.08, (5) 0.20, (6) 0.40 *M*, giving a molar ratio of Mg^{++}/OAA^{-} of 0, 64, 212, 424, 1060, 2120 respectively.

Magnesium Oxalacetic Acid Chelate

Addition of magnesium chloride to aqueous solutions of oxalacetic acid promotes decarboxylation of the acid, which can be measured by the changes in absorption. The changes in absorption are caused by the changes in the equilibrium concentration of the kinetically active keto and the spectrophotometrically active enol forms.

Each of the factors that affect the equilibrium, namely the concentration of the magnesium ion, pH, and ionic strength, or factors that are related to it, such as absorption,

Can. J. Chem. Downloaded from www.nrcresearchpress.com by 210.87.254.105 on 09/05/12
For personal use only.

observed rate constant of decarboxylation, overall association constant, and absorbing indexes will be discussed. The equilibrium itself will be treated in the 'General Discussion'.

(a) Absorption of the Chelate

The spectrum of oxalacetic acid (pH 7.4) as a function of magnesium ion concentration is plotted in Fig. 2, and indicates an increase in integral absorption and a shift of the 240–260 mμ plateau to a peak of absorption at 280 mμ, on the addition of magnesium ion. It appears from the high ratio of Mg^{++}/OAA (10^3) needed to form the complex that only a small fraction of the added magnesium chloride is effective in complexing with oxalacetic acid, probably because of the extensive hydration of the magnesium ion. The overall absorption of the complex in excess magnesium ion is also a function of pH (and pD).

Can. J. Chem. Downloaded from www.nrcresearchpress.com by 210.87.254.105 on 09/05/12
For personal use only.

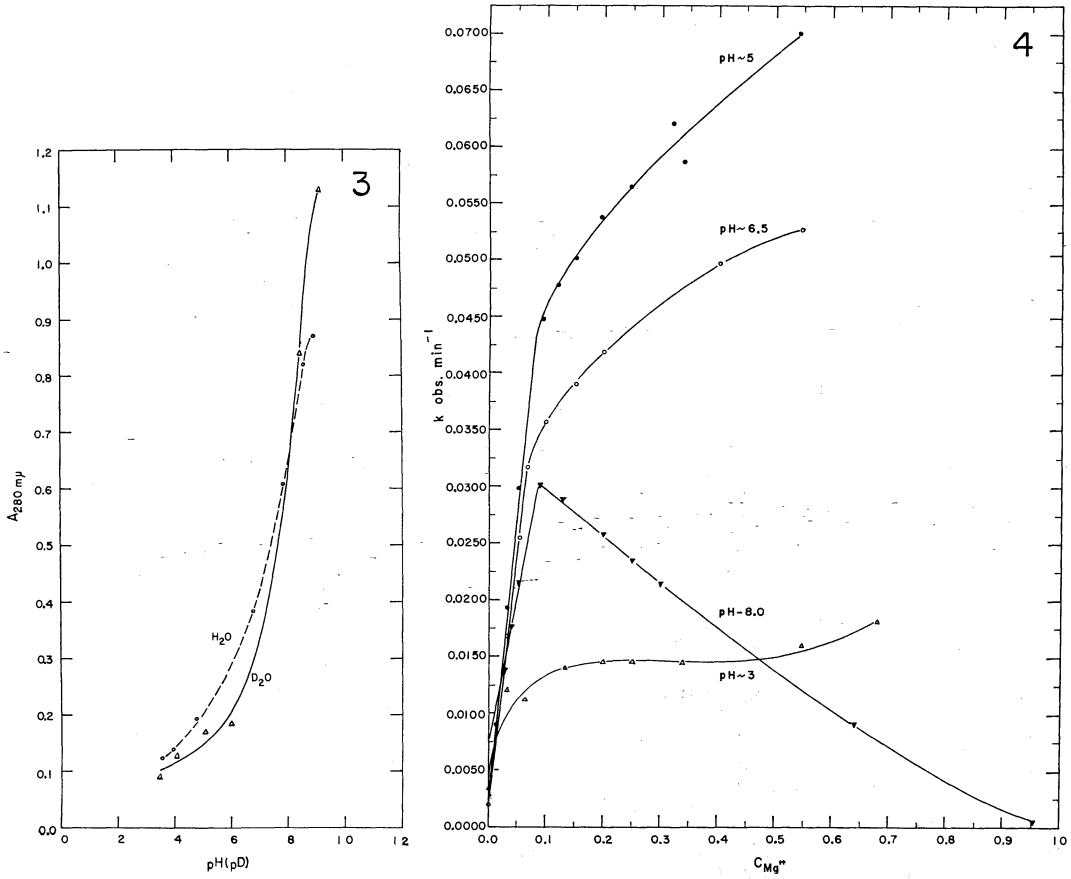

FIG. 3. The absorbance at 280 mμ of the magnesium chelate as function of pH and pD. For the H_2O system: solutions of 1.08×10^{-4} *M* oxalacetic acid, 0.2 *M* $MgCl_2$, and 0.1 *M* Tris–acetate buffer of the appropriate pH were made up to 25 ml in H_2O. Measurements were made within 1–1.5 minutes after each preparation in 1.0-cm light path cuvettes. For the D_2O system: $MgCl_2$, hydrated with heavy water, was prepared by partial dehydration at 98° C of the hexahydrate, dissolving it in D_2O, and repeating the process. Solutions of 1.14×10^{-4} *M* oxalacetic acid, 0.2 *M* $MgCl_2$, and 0.1 *M* Tris–acetate buffer of the appropriate pD were made up to 10 ml in D_2O and measured as above.

FIG. 4. The observed first order rate constant of decarboxylation as a function of magnesium ion concentration at various hydrogen ion concentrations (278 mμ). Each cuvette (0.5-cm light path) contained 0.5 *M* Tris–acetate buffers of the appropriate pH, $\sim2\times10^{-4}$ *M* oxalacetic acid, varying concentrations of $MgCl_2$ (expressed in molarity).

The absorption increases sharply in the region of pH 6 to 9 as shown in Fig. 3 as the concentration of the enol chelate increases. Other sets of measurements of the absorption at pH values up to 9.5 show no significant increase in the total absorption. Further increases of pH (and pD) caused precipitation of the system.

(b) Decarboxylation of the Chelate

The rate of decrease of absorption during the magnesium-ion-catalyzed decarboxylation of oxalacetic acid was measured spectrophotometrically (at 278 mμ for concentrations above 0.04 *M* $MgCl_2$ and at 255 mμ below 0.04 *M* $MgCl_2$). At magnesium ion concentrations below 0.1 *M* $MgCl_2$ (ratio of Mg^{++}/OAA of about 10^3), shown in Fig. 4, there is a linear relationship between the observed rare constant of decarboxylation and the magnesium ion concentration. In addition the rate becomes less dependent on pH as the concentration of magnesium ion decreases.

At concentrations of magnesium ion above 0.1 *M* $MgCl_2$ the reaction is strongly pH dependent (Fig. 4), with an apparent inhibition at pH 8.0 and stimulation at pH 5–6.5 as the $MgCl_2$ concentration is further increased. The depression and stimulation of the observed rate constants can be accounted for by the increase of ionic strength due to the excess magnesium chloride. The addition of KCl (equivalent to 0.25 *M* $MgCl_2$) to a system with optimal concentration of magnesium chloride (0.1 *M* $MgCl_2$) serves to increase the ionic strength and depress the observed rate constant at pH 8.0.

The observed first order rate constants for decarboxylation as a function of pH are plotted in Fig. 5, at varying concentrations of magnesium ion. For a given concentration of magnesium ion the ionic strength is constant. The bell-shaped activity curves show a maximum rate in the range of pH 5 to 6, with a convergence of k_{obs} (isokinetic point) at pH 7.4.

The rate of magnesium-ion-catalyzed decarboxylation was also measured in D_2O as a function of pD and magnesium ion concentration. The rate profile curve shows a shift to higher pD values (Fig. 6). The horizontal shift of the isokinetic point from pH 7.4 to pD 7.8 is evidence of the decreased dissociation constant of the α-C—D bond involved in the enolization of the magnesium oxalacetate complex. The spectrophotometric titration curve (Fig. 3) also indicates a similar shift of the equilibrium position between the keto and enol forms of the complex in D_2O.

(c) Absorbancy Index of the Chelate

The absorbancy index of the keto form of the magnesium-oxalacetate complex (a_K) in Tris–acetate buffer was calculated from kinetic and spectrophotometric measurements. On the basis of the kinetic experiments it is assumed:

(1) that the maximum concentration of the active species, the keto form of the magnesium oxalacetate complex (C_K), exists at pH 5.5, since the activity is maximal at pH 5.5 (Fig. 5).

(2) that the concentration of the active species is reduced to one-half its maximal concentration as the observed rate constant decreases to one-half of its maximal value as a function of pH. The average decrease to 50% activity was found to occur at pH 7.4 (isokinetic point) for magnesium ion concentrations above 0.1 *M* $MgCl_2$ (10^3 ratio of Mg^{++}/OAA).

On the basis of the spectrophotometric measurements (Fig. 3) made at greater than 1000-fold excess of magnesium ion as a function of pH, it is assumed:

(3) that the enol form of the magnesium oxalacetate complex predominates at pH 9.0.

Under such conditions, an approximate value for the apparent absorbancy index of the enol form of the magnesium oxalacetate complex (a_E) can be calculated to be 8.05×10^3

Can. J. Chem. Downloaded from www.nrcresearchpress.com by 210.87.254.105 on 09/05/12
For personal use only.

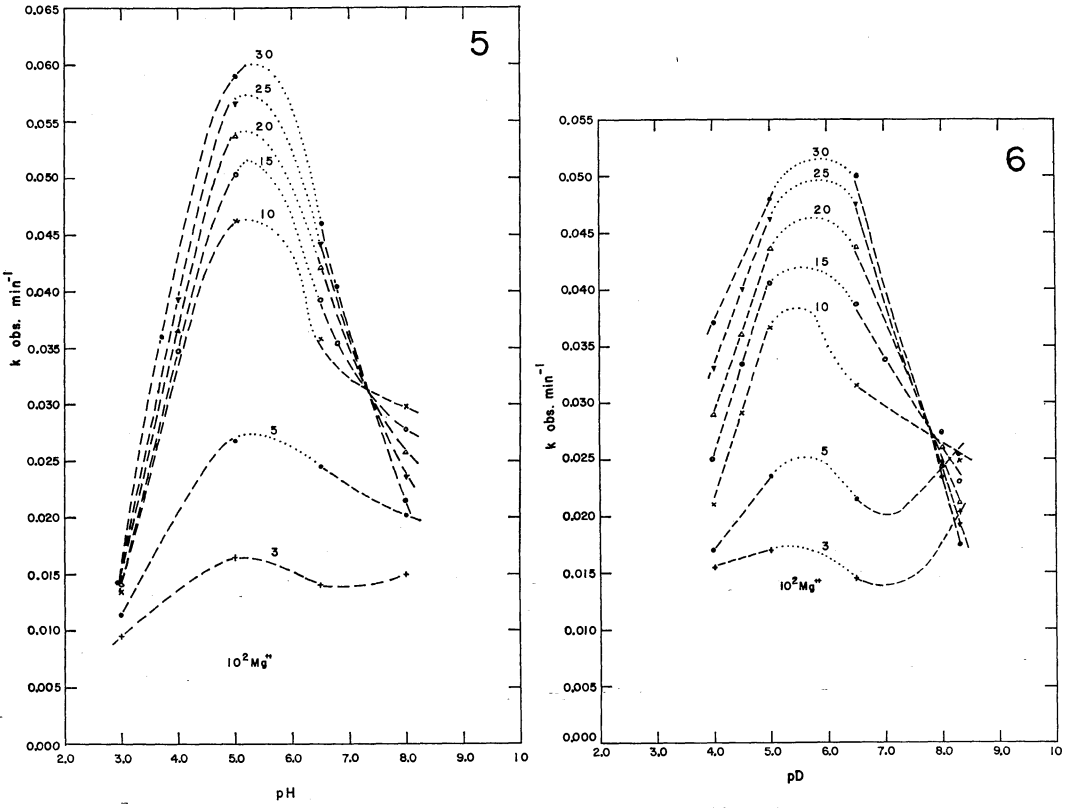

FIG. 5. The observed first order rate constant of decarboxylation as a function of pH at various magnesium ion concentrations (278 $m\mu$). Each cuvette (0.5-cm light path) contained 0.5 M Tris–acetate buffer of the appropriate pH, $\sim 2\times 10^{-4}$ M oxalacetic acid, varying concentrations of $MgCl_2$, 3, 5, 10, 15, 20, 25, 30 each $\times 10^{-2}$ M (see Fig. 4).

FIG. 6. The observed first order rate constant of decarboxylation as a function of pD and magnesium ion concentration (278 mμ). Each cuvette (0.5-cm light path) contained 0.3–0.5 M Tris–acetate buffer of the appropriate pD, $\sim 2\times 10^{-4}$ M oxalacetic acid, varying concentrations of $MgCl_2$, 3, 5, 10, 15, 20, 25, 30 each $\times 10^{-2}$ M.

(ionic strength conditions of Fig. 3). The absorbancy index for the keto form of the complex (a_K) can be then calculated from the following equations at pH $\geqslant$5.5, 1-cm light path:

[3] $$C_T = C_E + C_K = C_T' = C_E' + C_K'$$

[4] $$A_T = a_E c_E + a_K c_K$$

[5] $$A_T' = a_E c_E' + a_K c_K'$$

[6] $$C_K' = C_K/2$$

solving for a_K:

[7] $$a_K = \frac{a_E(A_T + C_T a_E - 2A_T')}{A_T + C_T a_E + 2A_T'}$$

where C_T is the total concentration of the complex and C_E and C_K are the concentrations of the enol and keto forms of the complex and A_T is the total absorbance at 280 mμ (pH 5.5). The primed numbers refer to the values at one-half maximal activity (pH 7.4).

Can. J. Chem. Downloaded from www.nrcresearchpress.com by 210.87.254.105 on 09/05/12
For personal use only.

From these equations the molar absorbancy index for a_K is 5.38×10^2 in H_2O. For the D_2O system a_E is 10^4 and a_K is 6.3×10^2.

The above assumptions are supported by other evidence. Calculations of the percentage of keto and enol forms of the complex as a function of pH (pD), using the above absorbancy indexes, show that at pH 7.4 (pD 7.8), which appears to be the pK for the keto–enol complex, there is a 1:1 ratio of the concentrations of the keto to enol complexes (Table I).

TABLE I

The keto–enol equilibrium of the magnesium chelate as a function of pH (pD)

pH	A_T 280 mμ	C_K %	C_E[a] %	C_E[b] %	pD	A_T 280 mμ	C_K %	C_E[a] %	C_E[b] %
5.5	.250	76	24		6.0	.190	89	11	
6.0	.290	71	29		7.0	.320	76	24	40
7.0	.410	56	44	46	7.8	.580	52	48	50
7.4	.490	50	50	50	8.0	.670	44	56	55
8.0	.680	23	77	58	9		0	100	
9		0	100						

[a]Approximate values calculated using equation [7] and spectrophotometric data from Fig. 3.
[b]Approximate values calculated using equation [18] and kinetic data from Figs. 5 and 7.

(d) Overall Association Constant of the Chelate

Further support for the assumptions in section (*c*) comes from the determination of the overall association constant for the magnesium oxalacetate complex at pH 7.4 in Tris–acetate buffer at constant ionic strength of 0.4. The calculations (20, 21) are based on the following equation (equation 8) where the magnesium ion concentration is much greater than the oxalacetate concentration and:

[8] $$\frac{C_{Mg^{++}}\,C_{OAA^{--}}}{A} = \frac{1}{K_C a_C} + \frac{C_{Mg^{++}}}{a_C}$$

where $C_{Mg^{++}}$ and $C_{OAA^{--}}$ are the concentrations of magnesium ion and the dianion of oxalacetic acid, A is the total absorbance at 280 mμ, a_C is the absorbancy index of the complex, and K_C is the overall association constant. The results are plotted in Fig. 7. Based on the overall absorbancy index of the complex at 3.85×10^3 and on the calculated absorbancy indexes for the keto and enol forms of the complex, the keto complex concentration at pH 7.4 is also found to be 51%.

The overall association constant (K_C) for the magnesium oxalacetic acid complex depends on pH and ionic strength as shown in Table II. The ionic strength was maintained at a fixed level by the addition of KCl for a given set of spectrophotometric measurements at varying magnesium ion concentrations and fixed concentrations of oxalacetic acid and hydrogen ion.

At pH 7.4 the association constant is almost independent of the ionic strength but at pH 6.7 and particularly at pH 8.0 there is a marked dependence of K_C, the value decreasing with higher ionic strength. This type of dependence of the K_C sensitivity on ionic strength seems to indicate that there are two distinct aspects of the equilibrium system affected by the ionic strength (cf. General Discussion).

GENERAL DISCUSSION

The changes in absorption observed during the magnesium-ion-catalyzed decarboxylation are caused by the changes in the equilibrium concentrations of the keto form of the

Can. J. Chem. Downloaded from www.nrcresearchpress.com by 210.87.254.105 on 09/05/12
For personal use only.

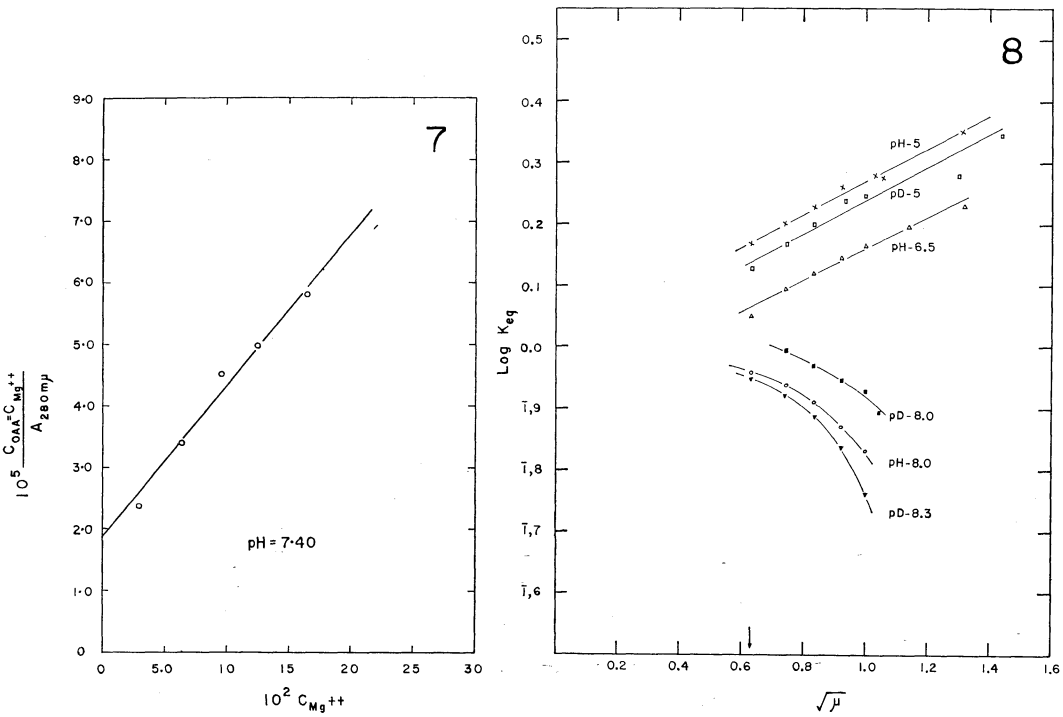

FIG. 7. Scott's plot (20) for the overall association constant for the magnesium chelate. Solutions of 8.66×10^{-5} *M* oxalacetic acid, varying concentrations of magnesium chloride, KCl to adjust the ionic strength to 0.4, and ~0.05 *M* Tris–acetate of the appropriate proportions to give a resultant pH of 7.40 ± 0.02 were made up to 50 ml H_2O. Measurements were made at 280 mμ 2 minutes after preparation of the solution in 1.0-cm light path cuvettes. For magnesium chloride concentrations of 3.20, 6.38, 9.57, 12.76, 16.74 each $\times 10^{-2}$ *M* the absorbancies at 280 mμ were 0.116, 0.163, 0.183, 0.222, 0.230 respectively.

FIG. 8. The keto–enol equilibrium of the magnesium chelate as a function of ionic strength, calculated from $K_{eq} = k_{obs}/k_1$ (18) at various ionic strengths. The arrow indicates the ionic strength which is equivalent to a ratio of Mg^{++}/OAA of 10^3.

TABLE II

Overall association constant of the magnesium chelate as a function of the ionic strength and pH

pH	Ionic strength	K_C, M^{-1}
8.0	0.2	43
	0.3	33
	0.4	18.5
	0.8	5.3
7.4	0.4	13
	0.6	10
	0.8	8.4
6.75	0.3	27.5
	0.6	11
	0.8	6.7

NOTE: The values were measured as described in the legend to Fig. 7.

Can. J. Chem. Downloaded from www.nrcresearchpress.com by 210.87.254.105 on 09/05/12
For personal use only.

magnesium oxalacetic acid chelate. A general equilibrium scheme can represent the system above pH 5.5 and show its pH and magnesium ion dependence.

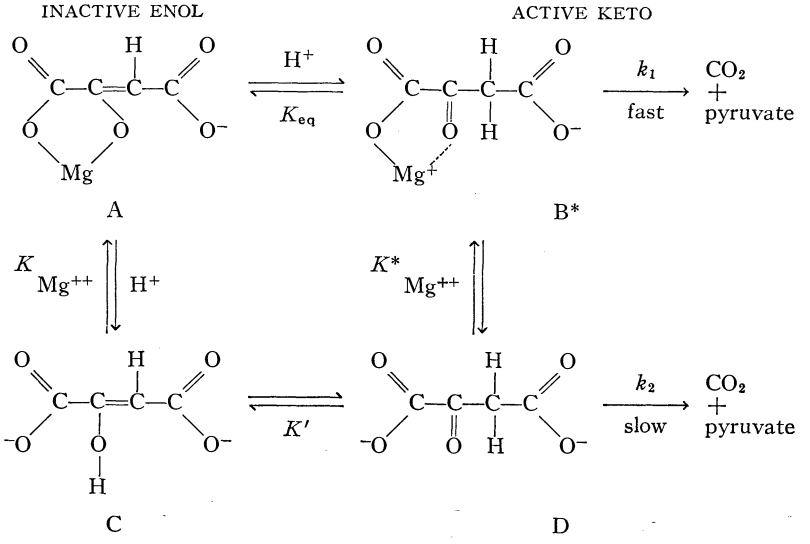

[9]

This equilibrium system can be considered under various conditions that displace the position of the equilibrium (indicated by heavy arrows) and so change the concentration of the active species [B*] and [D]. The apparent equilibrium constants are defined as:

$$K = \frac{[A]}{[Mg^{++}][C]}, \quad K_{eq} = \frac{[B^*]}{[A]}$$

and the equilibrium constants as:

$$K^* = \frac{[B^*]}{[Mg^{++}][D]} \text{ and } K' = \frac{[D]}{[C]}.$$

K' is constant in the pH range 5 to 10 (18). The overall association constant

$$K_C = \frac{[A][B^*][H^+]}{[Mg^{++}]^2[C][D]} = K^*K[H^+].$$

The rate of decarboxylation depends on the concentration of the active species.

[10] $$\text{Rate} = k_1[B^*] + k_2[D]$$

where $k_1 > k_2$.

Calculated values for K^* and K are reported in Table III for the isokinetic point.

TABLE III

The H_2O – OAA – Tris-acetate buffer system

$k_{obs} = k_1$	$K_{eq} = [B^*]/[A]^a$	K_C, M^{-1}	K^*, M^{-1b}	K, M^{-1b}
3.15×10^{-2}	1	10	4.8×10^4	0.5×10^4

NOTE: [a]Calculated from spectrophotometric measurements (Fig. 3).
[b]Calculated from $K_C = K^* K[H^+]$ and $K_{eq} = (K^*/K)K'$ where $[H^+] = 3.98\times10^{-8}$ (pH 7.4), $K' = 9.3$ (22) and ionic strength = 0.6.

Can. J. Chem. Downloaded from www.nrcresearchpress.com by 210.87.254.105 on 09/05/12
For personal use only.

(*i*) At low magnesium ion concentrations (e.g. 0.03 *M* $MgCl_2$) the k_{obs} becomes less dependent on pH changes (Fig. 5) since the concentration of D is more significant than that of B* and the C⇄ D equilibrium is H^+ independent:

$$\begin{array}{l} A \rightleftharpoons B^* \rightarrow CO_2 \\ \downarrow \quad \downarrow \\ C \rightleftharpoons D \rightarrow CO_2 \end{array} \quad . \qquad [11]$$

(*ii*) At the maximum rate (pH 5–6) the magnesium chelate exists predominantly as B*, the active keto form (Table I). For a given concentration of magnesium ion (e.g. 0.1 *M* $MgCl_2$), k_{obs} is at a maximum since the concentration of B* is at a maximum:

$$\begin{array}{l} A \rightarrow B^* \xrightarrow{k_1} CO_2 \\ \uparrow \quad \uparrow \\ C \rightleftharpoons D \xrightarrow{k_2} CO_2 \end{array} \quad . \qquad [12]$$

The k_{obs} depends on the pre-equilibrium concentration of the active forms of B* and D, which in turn depend on the magnesium ion concentration. Increasing the concentration of magnesium ion will increase the concentration of B* until the concentration of D is insignificant and so the k_2[D] term is negligible.

$$\text{Rate} = k_1[B^*]. \qquad [13]$$

In terms of the spectrophotometrically active species A:

$$\text{rate} = k_1K^*/K.\ K'[A], \qquad [14]$$

$$k_{obs} = k_1K^*/K.\ K' = k_1\ K_{eq} = k_1[B^*]/[A]. \qquad [15]$$

Addition of more $MgCl_2$ (pH 6.7) will not only increase the concentration of B* but will also increase ionic strength. Increasing the ionic strength depresses both the overall stability constant (Table II) and the A ⇌ B* dissociation (Fig. 8). The depressed dissociation, however, favors the kinetically active species B* and thus stimulates the rate of decarboxylation (equation 13).

(*iii*) An increase in the pH above 5.5 for a given high concentration of magnesium ion (e.g. 0.1 *M* $MgCl_2$) shifts the position of the pH dependent equilibrium A ⇌ B*. The observed rate constant is decreased because the concentration of the active form (B*) is diminished (see Table I and equation 13).

$$\begin{array}{l} A \leftarrow B \rightarrow CO_2 \\ \uparrow \quad \uparrow \\ C \rightleftharpoons D \end{array} \qquad [16]$$

(*iv*) Simultaneously with the decrease of k_{obs} with pH (section *iii*) the absorption at 280 mμ increases. The increased absorption is due to the increase of the concentration of form A, the highly absorbing enolic form of the metal chelate which does not decarboxylate. This dependence of the rate on pH is further evidence that it is the lower absorbing keto form of the chelate that is the active species in decarboxylation of oxalacetic acid.

(*v*) As the pH is increased to pH 8.0, high concentrations of magnesium chloride cause an apparent inhibition of the observed rate constant, i.e., k_{obs} increases up to a certain critical level (a ratio of Mg^{++}/OAA of 10^3) and then decreases on the addition of more magnesium chloride. Several combined factors may be involved in this behavior. A certain amount of magnesium ion promotes the reaction because it forms the 1:1 complex. As more $MgCl_2$ is added, increasing the ionic strength, the overall association constant decreases. The k_{obs} is also diminished since the concentration of the active form (B*) is decreased as reflected in the decrease of K_{eq} at pH 8.0 (section *viii*). The increase in ionic

Can. J. Chem. Downloaded from www.nrcresearchpress.com by 210.87.254.105 on 09/05/12
For personal use only.

strength, by addition of KCl to an optimal concentration of magnesium, shows that ionic strength increases do diminish k_{obs}.

At high pH the presence of OH^- changes the extent of hydration around the magnesium ion, which would then affect the Mg^{++} in its sensitivity to ionic strength, as well as in its effective positive charge, which promotes the decarboxylation. Davies (22) points out that cations are hydrated with a layer of water protecting them from the anion: M^+,H_2O,X^- but with hydroxides this probably changes to M^+,OH^-,H_2O so that the protective hydration is lost. Magnesium ion is a particularly highly hydrated ion and would be sensitive to pH changes. The K_C values at pH 8.0 are seen to be most sensitive to ionic strength changes. At this pH the effect of ionic strength changes is probably mostly on the state of hydration of the magnesium ion, changing its effective radius and charge. The effect is analogous to the addition of a different metal of the same group (24) which binds the ligand with a lower K_C and establishes a different K_{eq}.

(*vi*) At pH 7.4 there is a convergence of the observed rate constants (isokinetic point) such that k_{obs} is constant above a certain critical level of magnesium ion (Mg^{++}/OAA = 10^3). The data in Fig. 5 (pH 7.4) indicate that increases of magnesium chloride concentrations above 0.1 *M*, needed to form the 1:1 complex, cause no apparent inhibition of k_{obs} within the concentration range investigated. The p*K* of the keto–enol chelate equilibrium A $\rightleftarrows$ B* was also found to be about pH 7.4 by spectrophotometric titration of the chelate (Fig. 3). This means that at this pH, [A] = [B*] so that $k_{obs} = k_1$ (equation 15). The apparent equilibrium constant and the overall association constant are almost independent of ionic strength; the effect on the various equilibria may balance each other (see section *ix*).

(*vii*) At pH 3.0 increases of magnesium ion above a molar ratio of magnesium ion to oxalacetate of 10^3 have no effect on the observed rate constant in the range investigated. At this pH there was found an intensification of the absorption at 260 mμ but no shift of the peak to 280 mμ. This can be interpreted as the formation of the saturated monoligand complex, which has a slower rate of decarboxylation.

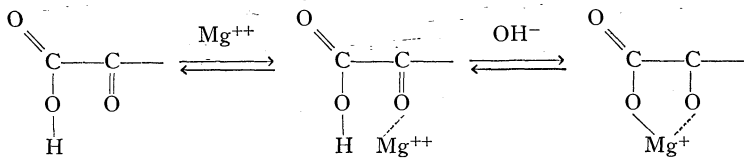

[17]

With increasing pH the observed rate constant increases are within the range of pH where the second carboxyl group of oxalacetic acid dissociates. By pH 5.5 the second carboxyl group is fully dissociated so that the bidentate chelate with magnesium ion can form and the observed rate constant is at a maximum.

(*viii*) The apparent keto–enol chelate equilibrium constant (K_{eq}) can be calculated from the scheme illustrated in equation (9); rearranging equation [15] to:

[18] $$K_{eq} = k_{obs}/k_1.$$

The calculated K_{eq} values at various pH (pD) values as a function of ionic strength are plotted in Fig. 8. The value of k_{obs} at the isokinetic point (pH 7.4) is used as k_1. These K_{eq} values determined from kinetic measurements compare favorably (Table I) to the K_{eq} values measured spectrophotometrically under similar conditions of ionic strength. Increase of the ionic strength (above 0.1 *M* $MgCl_2$) increases K_{eq} below pH 7.4 (pD 7.8)

Can. J. Chem. Downloaded from www.nrcresearchpress.com by 210.87.254.105 on 09/05/12
For personal use only.

but decreases K_{eq} above these values. This behavior of K_{eq} directly reflects the behavior of k_{obs} (equation 18).

(*ix*) The variation of the ionic strength sensitivity of K_{eq}, K_C, total absorption, and k_{obs} with pH changes gives indication that possibly two separate aspects of the equilibrium system are affected by ionic strength in different ways.

(*a*) In the acid range, increasing ionic strength diminishes the proton dissociation of the tautomeric equilibrium as indicated by the increase of K_{eq} favoring the active species B*. Although the increase of ionic strength also causes a decrease in K_C, the resulting effect on k_{obs} is balanced by the effect on K_{eq}.

(*b*) In the basic range, increasing ionic strength diminishes the positive charge of the less hydrated magnesium ion both in solution and in the chelate (see Section *v*) and decreases K_C and K_{eq}. The direction of the ionic strength effect on K_C supports the effect on K_{eq} and decreases [B*], resulting in a diminished k_{obs}.

(*x*) The decrease of the rate constant in D_2O at the isokinetic point, $k_{H_2O}/k_{D_2O} = 1.1$, is indicative of a secondary isotope rate effect. Such a secondary isotope effect might be expected in the keto form of the complex in which the two alpha hydrogens are replaced by deuterium. The fact that no primary isotope rate effect is observed is evidence that a C—D or O—D bond cleavage is not rate determining in the magnesium-ion-catalyzed decarboxylation of oxalacetic acid. This supports the mechanism in which the C—C bond cleavage is rate determining (16).

The nature of the shift of the isokinetic point in D_2O is further evidence that at the isokinetic point $k_{obs} = k_1$, since at pD 7.8 the ratio of [B*] to [A] is 1 (see equation 15). The general shift of the pD rate profile supports the explanation that whatever affects the equilibrium concentration of the active species B* affects the rate of the reaction.

(*xi*) It has been proposed (14) that the decrease in absorption observed when oxalacetate decarboxylates in the presence of metal ion is due to the ketonization of the enol–pyruvate complex which is the first product of decarboxylation. This interpretation was based on the assumption that the enol–pyruvate complex is a very strongly absorbing species compared to the oxalacetate complex, but no spectral evidence was presented for this assumption. The present calculations for the absorbancy indexes of the keto and enol magnesium complexes and for K_{eq}, which combine kinetic and spectral data, account for all the predominant absorption changes in the reaction without assuming a highly absorbing enol–pyruvate complex intermediate. The fast increase of absorption on the addition of magnesium ion to oxalacetate is interpreted as the fast formation of the more strongly absorbing magnesium oxalacetate complex. This fast formation was also observed for Al^{+++} (11), Cu^{++}, and Zn^{++} (14). The decrease of absorption during decarboxylation can be accounted for by the decrease in the concentration of the absorbing magnesium oxalacetate complex under various conditions of pH and magnesium ion concentration.

(*xii*) The magnesium-ion-catalyzed decarboxylation is analogous to the behavior of other metals, in its pH dependence to copper (10, 24), and in its inhibitory effect at higher concentrations to Pb^{++}, Cu^{++}, and La^{++} (4, 14).

Comparison of the effect of pH and pD on the rate of the magnesium-ion-catalyzed decarboxylation and the effect of pH and pD on the decarboxylation reaction catalyzed by oxalacetate carboxylase of *Micrococcus lysodeikticus* (15,16) shows that both systems have the same maximum of activity at about pH 5.5 and that both peaks are shifted to higher pD values in the D_2O systems (16). Other enzymes that decarboxylate oxalacetic acid also have certain common features in their mechanism. The malic enzyme (26) from

Can. J. Chem. Downloaded from www.nrcresearchpress.com by 210.87.254.105 on 09/05/12
For personal use only.

pigeon liver, which depends on manganese ion or magnesium ion, has a maximal activity at pH 4.5 to 5.0 and the enzyme from wheat germ has a maximal activity at pH 5.2. The oxalacetate carboxylase of chicken liver (27), which depends on inosine triphosphate, has a maximal activity at about pH 6.0. The oxalacetate decarboxylase of rat liver (28) with a maximal activity at pH 7.4 depends on magnesium ion and is inhibited by manganese ion. The inhibition of the magnesium-ion-catalyzed decarboxylation of oxalacetate at high concentration of magnesium ion above pH 7.4 is analogous to the behavior of phosphoenol pyruvate carboxylase (29) from spinach leaves in the formation of oxalacetate where, at 7.4, the reaction is stimulated by the magnesium ion concentrations up to 2×10^{-3} M magnesium chloride and inhibited above this concentration. The present results indicate a parallelism between the mechanism of the metal-ion-catalyzed and enzyme-catalyzed decarboxylation of oxalacetic acid.

ACKNOWLEDGMENTS

The authors wish to thank the National Research Council of Canada for financial support, Mr. P. A. Kelly, for mathematical assistance, and Doctors R. J. Thibert and K. G. Rutherford for their valuable discussions.

REFERENCES

1. H. A. KREBS. Biochem. J. **36**, 303 (1942).
2. S. OCHOA. J. Biol. Chem. **174**, 115 (1948).
3. F. LYNEN and H. SCHERER. Ann. Chem. **560**, 163 (1948).
4. J. F. SPECK. J. Biol. Chem. **178**, 315 (1949).
5. P. M. NOSSAL. Australian J. Exptl. Biol. Med. Sci. **27**, 143 (1949); **27**, 312 (1949).
6. L. O. KRAMPITZ and C. H. WERKMAN. Biochem. J. **35**, 595 (1941).
7. F. H. WESTHEIMER. Trans. N.Y. Acad. Sci. **18**, 15 (1955).
8. R. STEINBERGER and F. H. WESTHEIMER. J. Am. Chem. Soc. **71**, 4158 (1949); **73**, 429 (1951).
9. K. J. PEDERSEN. Acta Chem. Scand. **6**, 285 (1952).
10. E. GELLES. J. Chem. Soc. 4736 (1956).
11. A. KORNBERG, S. OCHOA, and A. MEHLER. J. Biol. Chem. **174**, 159 (1948).
12. E. GELLES. J. Inorg. and Nucl. Chem. **8**, 625 (1958).
13. E. GELLES and J. CLYTON. Trans. Faraday Soc. **52**, 353 (1956).
14. E. GELLES and R. W. HAY. Part (I). J. Chem. Soc. 3673 (1958). E. GELLES and A. SALAMA. Part (II). J. Chem. Soc. 3685 (1958).
15. D. HERBERT. Symp. Soc. Exptl. Biol. **4**, 52 (1951).
16. S. SELTZER, G. A. HAMILTON, and F. H. WESTHEIMER. J. Am. Chem. Soc. **81**, 4018 (1959).
17. R. LUMRY, E. L. SMITH, and R. R. GLANTZ. J. Am. Chem. Soc. **73**, 4330 (1951).
18. G. W. KOSICKI. Can. J. Chem. **40**, 1280 (1962).
19. K. J. PEDERSEN. Acta Chem. Scand. **6**, 243 (1952).
20. R. L. SCOTT. Rec. Trav. Chim. **75**, 787 (1956).
21. H. A. BENESI and J. HILDEBRAND. J. Am. Chem. Soc. **71**, 2703 (1949).
22. G. W. KOSICKI and S. N. LIPOVAC. XI Coll. Spect. Int. Belgrad, 1963.
23. C. W. DAVIES. Ion association. Butterworths, London. 1962. p. 84.
24. R. J. P. WILLIAMS. J. Chem. Soc. 3770 (1952).
25. P. NOSSAL. Nature, **163**, 405 (1949).
26. S. OCHOA. *In* Methods in Enzymology. Vol. I. *Edited by* S. P. Colowick and N. O. Kaplan. Academic Press Inc., N.Y. 1955. p. 739.
27. M. F. UTTER, K. KURAHASHI, and I. A. ROSE. J. Biol. Chem. **207**, 803 (1954).
28. L. M. CORWIN. J. Biol. Chem. **234**, 1338 (1959).
29. R. S. BANDURSKI and F. LIPMANN. J. Biol. Chem. **219**, 741 (1956).

Can. J. Chem. Downloaded from www.nrcresearchpress.com by 210.87.254.105 on 09/05/12
For personal use only.

ANTIMONY TETRAFLUORIDE MONOFLUOROSULPHATE: PREPARATION, PROPERTIES, AND STRUCTURE*

R. J. GILLESPIE AND R. A. ROTHENBURY
Department of Chemistry, McMaster University, Hamilton, Ontario
Received September 18, 1963

ABSTRACT

When antimony pentafluoride is refluxed with sulphur trioxide, a new compound with the composition $SbF_5.SO_3$ is formed together with sulphuryl fluoride, disulphuryl fluoride, and small amounts of the higher polysulphuryl fluorides. This compound is a colorless, very viscous liquid. From the chemical analysis, the F^{19} N.M.R. spectrum, and the Raman and infrared spectra of the liquid it was concluded that the compound is antimony tetrafluoride monofluorosulphate $SbF_4(SO_3F)$ and that it is highly polymerized in the liquid state by fluorosulphate bridges that can have either a cis or a trans orientation with respect to each other; the former occurring to a greater extent than the latter.

Can. J. Chem. Downloaded from www.nrcresearchpress.com by 210.87.254.40 on 09/05/12
For personal use only.

It has been reported that disulphuryl fluoride is formed when antimony pentafluoride is added dropwise to refluxing sulphur trioxide (1). The authors represented the reaction in the following manner:

$$2SbF_5 + 14SO_3 \rightarrow Sb_2O(SO_4)_4 + 5S_2O_5F_2.$$

We have found that when antimony pentafluoride (1 mole) is added slowly to refluxing sulphur trioxide (2 mole) and the resulting mixture distilled, unreacted sulphur trioxide, sulphuryl fluoride, disulphuryl fluoride, and small amounts of higher polysulphuryl fluorides were obtained, together with a relatively large amount of a colorless viscous liquid, with a boiling point of 227°. After distillation a white solid residue remained. When the reaction was repeated using considerable excess of sulphur trioxide, unreacted sulphur trioxide, disulphuryl fluoride, and some higher polysulphuryl fluorides were again obtained, but the viscous liquid was not obtained. A similar white solid residue remained behind. When heated in air at 1000° these solid residues afforded a mixture of Sb_2O_4 and Sb_2O_5. Analysis of the viscous liquid showed that it had the composition $SbF_5.SO_3$. During attempts to find a solvent for this substance it was found that it reacted with the common organic solvents and that it was insoluble in 1,2-dichloro-1,1,2,2-tetrafluoroethane (Freeon 114) and sulphur hexafluoride. It fumed in air and supercooled readily to give a glass-like solid.

The F^{19} nuclear magnetic resonance spectrum of the viscous liquid was determined at three temperatures (Table I); the three spectra were almost identical. The fluorine-on-antimony region is shown in Fig. 1; it consists of a pair of triplets *A* and *C* and a single line *B*. The relative areas of the peaks *A*:*B*:*C* were found to be 3.0:1.0:3.0. In the fluorine-on-sulphur part of the spectrum (Fig. 2) there are two main peaks *D* and *E* of relative areas 3.2:1.0 and four very small peaks *F*, *G*, *H*, and *I*. Peak *D* was at $+692\pm3$ c/second from an internal reference of SF_6. The chemical shift of the center of the triplet *A* (Fig. 1) with respect to the peak *D* (Fig. 2) was $+7729\pm28$ c/second.

The most obvious explanation for the two triplets in the fluorine-on-antimony region of the spectrum would be that the molecule contains pairs of fluorine atoms in the axial and

**Presented at the Symposium on Inorganic Fluorine Chemistry, Argonne National Laboratory, September 4–6, 1963.*

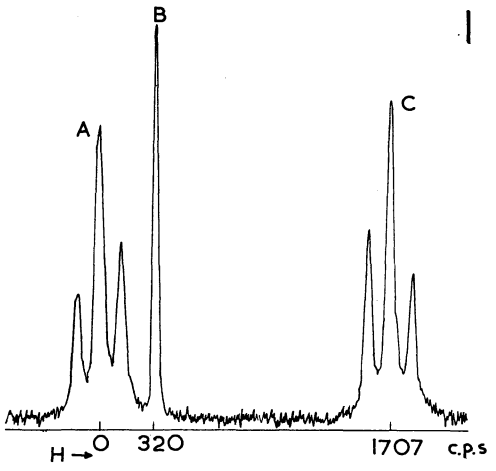

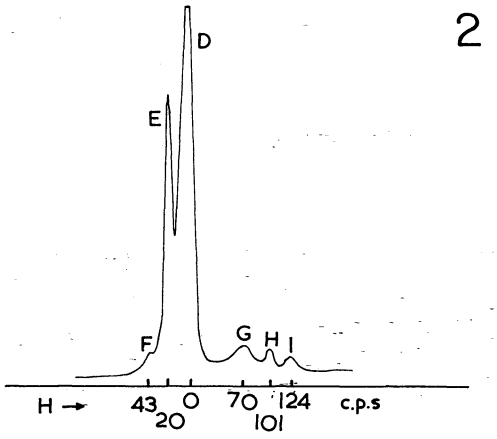

FIGS. 1 AND 2.

TABLE I

Chemical shifts and coupling constants for antimony tetrafluoride monofluorosulphate

Temperature (° C)	$J_{FF'}$(II)c/s	$\delta_{FF'}$(II)c/s	δ(III)*c/s
+50	125±4	1734±20	321±4
+25	128±3	1707±8	320±8
−37	125±2	1668±5	316±3

*Chemical shift from the center of the low field triplet due to II.

equatorial positions of a trigonal bipyramid molecule. However, this provides no explanation of the peak *B*, nor for the presence of more than one peak in the F^{19} on S region of the spectrum. The highly viscous nature of the liquid indicates extensive association or polymerization, as has been found in the case of antimony pentafluoride (2, 3). The observed spectrum is, however, not consistent with association by means of fluorine bridges

Can. J. Chem. Downloaded from www.nrcresearchpress.com by 210.87.254.40 on 09/05/12
For personal use only.

such as occur in liquid antimony pentafluoride, but only with association by means of fluorosulphate bridging groups (I). In such a polymeric chain the bridging fluorosulphate groups may be either cis or trans to each other. The fluorines in each cis unit of the polymer (II) would be expected to give an A_2X_2 spectrum of two triplets, while the four equivalent fluorines in each trans unit (III) of the polymer would be expected to give a single line, which we assume is *B*. Hence the polymers contain both cis and trans units in the ratio 6.0:1.0.

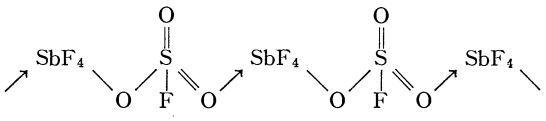

I

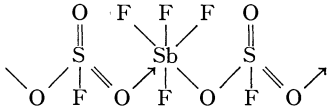

II

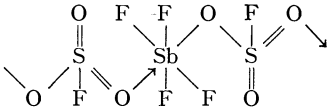

III

In any polymeric chain containing both cis and trans units a given fluorosulphate group can have one of three possible environments: the neighboring fluorosulphate groups can be both cis, both trans, or one cis and one trans. Since there is, on average, one trans unit for every six cis units, approximately 29% of the fluorosulphate groups would be expected to have cis–trans neighbors and approximately 2% to have trans–trans neighbors. Because of their appreciable overlap the areas of the peaks *D*, *E*, and *F* (Fig. 2) are difficult to measure accurately but they are in reasonable agreement with these predictions. Clearly peak *D* may be assigned to cis–cis fluorosulphate groups, *E* to cis–trans fluorosulphate groups, and *F* to trans–trans fluorosulphate groups. The small high-field peaks *G*, *H*, and *I* cannot be due to small amounts of the polysulphuryl fluorides since these give signals to low field of sulphuryl fluoride (5), which itself gives a peak at 360 c/second to low field of fluorosulphuric acid. They are assigned to terminal fluorosulphate groups; this assignment has been confirmed by more recent studies on solutions of $SbF_4.SO_3F$ in fluorosulphuric acid (6).

Further evidence in support of our interpretation of the n.m.r. spectrum is as follows: the coupling constant between the axial and equatorial fluorines in a cis unit of the polymer was found to be 128±3 c/second, which is close to the F–F coupling constant of 130 c/second for polymeric antimony pentafluoride (2, 3) and to the value of approximately 100 c/second found by Muetterties (4), and by the authors (3), for several SbF_5.base complexes. The chemical shift between the non-equivalent fluorines on antimony of 0.303 p.p.m. is also close to that of 0.260 p.p.m. found for antimony pentafluoride (3).

Since the peaks *G*, *H*, and *I* observed in the F^{19} on S region, and attributed to terminal fluorosulphate groups, are very small in comparison to *D* and *E*, attributed to the bridging

Can. J. Chem. Downloaded from www.nrcresearchpress.com by 210.87.254.40 on 09/05/12
For personal use only.

groups, it may be concluded that the average chain length is quite high, or that the polymers are mainly cyclic.

Two very small additional peaks were obtained in the spectrum of $SbF_4.SO_3F$ when the temperature was reduced to $-37°$; they occurred at 856 ± 9 c/second and 951 ± 10 c/second to high field of the center of triplet *A* (Fig. 1). They are probably due to the presence of a very small amount of antimony pentafluoride and presumably they do not appear at higher temperatures because of exchange processes. We assume that the two peaks are the X part of an AX_4 spectrum which would consist of a doublet and a quintet and that the quintet which would have only 1/4 of the intensity of the doublet is not resolved from the base-line noise. Such a spectrum could arise from an SbF_5 group occupying a terminal position in a polymeric chain (IV) and it would be expected to closely resemble the fluorine spectrum of an SbF_5.base complex. The observed fluorine–fluorine coupling constant of 95 c/second is in close agreement with values of approximately 100 c/second that have been found for various SbF_5.base complexes (3, 4). This SbF_5 could either be an impurity or it might possibly arise from the following self-dissociation process.

$$2SbF_4SO_3F = SbF_5 + SbF_3(SO_3F)_2.$$

However, no additional peaks were observed in the spectrum that could be attributed to $SbF_3(SO_3F)_2$ units in the polymer and we therefore believe that the SbF_5 was present as a very small impurity. From the areas of the peaks in the spectrum it was found that the amount of such impurity was less than 2 mole%. This amount of SbF_5 impurity could not have been detected by our analytical methods.

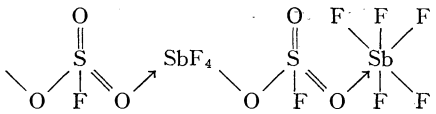

IV

Confirmation of the formulation of the compound as a fluorosulphate $SbF_4.SO_3F$ was obtained from a study of its infrared and Raman spectra. The lines observed in these spectra are listed in Table II. No lines are observed at frequencies higher than 750 cm^{-1}

TABLE II

Infrared and Raman spectra of antimony tetrafluoride monofluorosulphate

Raman	1430, 1080, 890, 695, 667, 654, 555, 425, 300, 270, 251, 200, 165, 143 cm^{-1}
I.R.	1400, 1216, 1020, 865, 670, 560

in the spectrum of antimony pentafluoride (7) thus the line observed at 890 cm^{-1} in the Raman spectrum and at 865 cm^{-1} in the infrared spectrum can be unambiguously assigned as an SF-stretching vibration. This vibration has frequencies of 848 and 885 cm^{-1} in SO_2F_2 (8), and 850 cm^{-1} in HSO_3F (9). The lines at 1430, 1216, and 1080 cm^{-1} may be assigned as SO stretching vibrations.

EXPERIMENTAL

Preparation of Antimony Tetrafluoride Monofluorosulphate

Antimony pentafluoride (47.3 g, 1.0 mole) was added slowly, with constant shaking, to refluxing sulphur trioxide (35.9 g, 2.1 mole). The main product was a mixture of a clear viscous liquid and a white solid, together with material which was obtained as a liquid-air trap condensate; the latter was identified as sulphuryl fluoride by its boiling point and its chemical shift in the F^{19} n.m.r. spectrum (b.p. $-53°$, $\delta(S_2O_5F_2)$ $+861 \pm 4$

Can. J. Chem. Downloaded from www.nrcresearchpress.com by 210.87.254.40 on 09/05/12
For personal use only.

c/second at −31° (3). Distillation of the mixture gave some more volatile material, which condensed in a liquid-air trap, a clear viscous liquid (45.7 g) b.p. 88° at 1.0 mm, and a white solid (8.2 g) (found: Sb, 62.6; F, 8.8; S, 4.7%), which when heated in air at 1000° for 7.5 hours afforded an off-white solid which was yellow when hot, and contained no fluorine or sulphur (found: Sb, 77.2; Sb_2O_4 requires: Sb, 79.2; Sb_2O_5 requires: Sb, 75.3%).

The liquid–air trap condensate contained a material which boiled below room temperature, and was identified as sulphuryl fluoride by its boiling point and its chemical shift in the F^{19} n.m.r. spectrum (b.p. −53°, $\delta(S_2O_5F_2)$ +861±4 c/seconds at −31° (3)) and a liquid which boiled above room temperature. This liquid was treated with 95% sulphuric acid to remove sulphur trioxide, and a sample distilled to afford a fraction, b.p. 51–62°, which has shown by means of its F^{19} n.m.r. spectrum to consist mainly of disulphuryl fluoride, plus a small amount of the trisulphuryl fluoride (5). The F^{19} n.m.r. spectrum of the residue was examined, and peaks were observed at −80, −109, −117, and −123 c/second from $S_2O_5F_2$ which could clearly be attributed to $S_3O_8F_2$, $S_4O_{11}F_2$, $S_5O_{14}F_2$, and $S_6O_{17}F_2$ respectively (5). A small unidentified peak was also observed at +366 c/second from $S_2O_5F_2$.

The clear viscous liquid (44.4 g) on distillation afforded a white solid residue (1.6 g) and a clear viscous distillate (36.5 g) (found: Sb, 40.6; F, 31.4; S, 10.3; $SbF_4(SO_3F)$ requires: Sb, 41.0; F, 32.0; S, 10.8%), b.p. 68° at 0.4 mm. The n.m.r. spectrum of this distillate is shown in Figs. 1 and 2.

Reaction of Antimony Pentafluoride with Excess Sulphur Trioxide

Antimony pentafluoride (32.2 g, 1.0 mole) was added slowly, with constant shaking, to refluxing sulphur trioxide (95.7 g, 8.1 mole) to afford a mixture of a clear liquid and a white solid. Distillation of the mixture gave 77.0 g of a distillate with b.p. 50°; further heating up to 360° at 1.0 mm yielded only a white solid residue (36.4 g) (found: Sb, 43.8; F, 11.7; S, 14.0%), which when heated in air at 1000° (12.5 hours) afforded a white solid which was yellow when hot, and contained no fluorine or sulphur (found: Sb, 78.8; Sb_2O_4 requires: Sb, 79.2; Sb_2O_5 requires: Sb, 75.3%).

The distillate was treated with 95% sulphuric acid to remove sulphur trioxide, and a sample distilled to afford pure disulphuryl fluoride, b.p. 50–51°, and a residue which the n.m.r. spectrum showed consisted of the higher sulphuryl fluorides (5).

Apparatus

The F^{19} n.m.r. spectra were obtained using a Varian high-resolution n.m.r. spectrometer and electromagnet at a frequency of 56.4 Mc and a field of 14,000 gauss. The infrared spectra were obtained with a Perkin–Elmer model 21 spectrometer using silver chloride cells and the Raman spectra were obtained with an apparatus that has been described previously (10).

ACKNOWLEDGMENT

We thank the Directorate of Chemical Sciences, United States Air Force Office of Scientific Research, and the Allied Chemical Company for financial assistance. We also thank Dr. K. Ramaswamy for obtaining some of the infrared and Raman spectra, and the Ozark Mahoning Co. for a gift of antimony pentafluoride.

REFERENCES

1. E. Hayek and W. Koller. Monatsh. Chem. **82**, 942 (1951).
2. C. J. Hoffman, B. E. Holder, and W. L. Jolly. J. Phys. Chem. **62**, 364 (1958).
3. R. J. Gillespie and R. A. Rothenbury. To be published.
4. E. L. Muetterties *In* Advances in the chemistry of the coordination compounds. *Edited by* Stanley Kirschner. MacMillan Co., N.Y. 1961. p. 513.
5. R. J. Gillespie, J. V. Oubridge, and E. A. Robinson. Proc. Chem. Soc. 428 (1961).
6. R. J. Gillespie, R. C. Thompson, and R. A. Rothenbury. To be published.
7. J. Gaunt and J. B. Ainscough. Spectrochim. Acta, **10**, 57 (1957).
8. R. J. Gillespie and E. A. Robinson. Can. J. Chem. **39**, 2171 (1961).
9. R. J. Gillespie and E. A. Robinson. Can. J. Chem. **40**, 644 (1962).
10. R. J. Gillespie and E. A. Robinson. Can. J. Chem. **39**, 2179 (1961).

Can. J. Chem. Downloaded from www.nrcresearchpress.com by 210.87.254.40 on 09/05/12
For personal use only.

THE SESQUITERPENE ALCOHOLS OF THE HEARTWOOD OF THUJA OCCIDENTALIS L.[1]

E. VON RUDLOFF AND G. V. NAIR[2]
National Research Council of Canada, Prairie Regional Laboratory, Saskatoon, Saskatchewan
Received September 27, 1963

ABSTRACT

γ-Eudesmol, a mixture of α- and β-eudesmol, and a new sesquiterpene diol, occidiol, were found to be minor components of the neutral extract of eastern white cedar heartwood. A tentative structure for occidiol is proposed. The biogenetic relationship between these compounds is discussed and a common precursor for the eudesmol and occidentalol series is suggested.

Can. J. Chem. Downloaded from www.nrcresearchpress.com by 210.87.254.42 on 09/05/12
For personal use only.

Nakatsuka and Hirose (1, 2) have isolated from the heartwood of eastern white cedar (*Thuja occidentalis* L.) the two sesquiterpene alcohols occidentalol (I) and occidol (II).

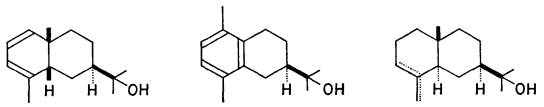

I II III

Nakazaki (3) has reported that in (+)-occidol the isopropanol group has the R-configuration (as shown). By conversion to the dihydro and tetrahydro derivatives and comparison with eudesmol (III) and its dihydro derivatives, occidentalol has been shown by von Rudloff and Erdtman (4) to have cis-fused rings. This was based on the reasonable assumption that the isopropanol group is in the equatorial position, i.e., as in the trans-fused eudesmane-type of compound (5). Recently, Mislow and Moscowitz (6) have presented arguments which indicate that the isopropanol group of occidentalol at C-7 has the R-configuration. This lends support to Nakazaki's view (3, 7) that occidentalol and occidol are biogenetically closely related.

In view of the unusual cis-fused ring system found in occidentalol and a possible biogenetic relationship with the eudesmols, it was of interest to determine the nature of the minor sesquiterpenoid constituents of the wood of eastern white cedar. Gas–liquid chromatography (G.L.C.; cf. also Refs. 4 and 8) showed that the wood extract from a mature tree from the Winnipeg district, Manitoba, contained mainly occidentalol (peak 1) and occidol (peak 6), three minor, and two trace constituents (see Table I). The three minor constituents (peaks 2, 3, and 5) were isolated in milligram amounts and were shown to be a mixture of γ-eudesmol and an unidentified compound, a mixture of α- and β-eudesmol, and a new sesquiterpene diol respectively.

Peak 2 had the retention time of α-cadinol and γ-eudesmol. Its infrared spectrum was similar in all respects to that of α-cadinol, when these were recorded as liquid films (8). The weak, but distinct, absorption bands near 1650 and 815 cm^{-1} are indicative of the trisubstituted double bond found in α-cadinol. However, the fraction of the oil of araucaria identified as α-cadinol by one of us (8) mainly on this basis was shown to be essentially γ-eudesmol by Bates and Hendrickson, who employed nuclear magnetic resonance (n.m.r.) spectroscopy and obtained dihydroeudesmol by hydrogenation of the material.

[1]*Issued as N.R.C. No. 7691.*
[2]*National Research Council of Canada Postdoctoral Fellow, 1958–1960.*

TABLE I

Sesquiterpenoid components of the wood of *Thuja occidentalis* L.

Peak	Compound	R.R.T.*	%
1	Occidentalol	0.92	36
2	γ-Eudesmol and unidentified	1.02	3
3	α- + β-Eudesmol	1.46	10
4	Unidentified	2.08	0.5
5	Diol	2.20	3
6	Occidol	6.0	46–47
7	Unidentified	6.5	0.5–1.0

*R.R.T. = relative retention time (cedrol = 1.00) on a 6 ft × 1/4 in. O.D. adipate polyester column.

Since insufficient amounts of peak 2 were isolated in this study to permit the recording of an n.m.r. spectrum, the component was hydrogenated over platinum catalyst. The product crystallized on standing and was found to be mainly dihydroeudesmol. Therefore, peak 2 must contain γ-eudesmol. However, rechromatography of peak 2 showed that it contained a second component, but this could not be isolated.

Peak 3 was obtained crystalline and a mixed melting point and comparison of infrared spectra and G.L.C. retention data confirmed that this was identical with the mixture of α- and β-eudesmol, which is the major constituent of the oil of araucaria (8). G.L.C. analysis also showed that the ratio of α- to β-isomer was nearly the same as that in oil, i.e., about 1 to 3.

Peak 5 was a viscous liquid, which appeared to decompose gradually under atmospheric conditions. The infrared spectrum of the freshly isolated material indicated it to be an unsaturated alcohol (strong bands at 3440, 2920, 1650, with a shoulder at 1670, 1382, and 1370 cm^{-1}, weaker ones at 3080, 3040, 1035, 915, 875, 850–825, and 750 cm^{-1}) which may have a terminal methylene and an isopropyl or isopropanol group and possibly a trisubstituted double bond. The molecular weight (236), obtained by mass spectroscopy,* and the elementary analysis agreed fairly well with $C_{15}H_{24}O_2$. The unsaturated character was confirmed by a strongly positive tetranitromethane test, as may also be deduced from the relatively high optical rotation ($[\alpha]_D^{23}$ −125.5°) and refractive index (n_D^{23} 1.5129). No characteristic ultraviolet spectrum was recorded. Thus, the compound appears to be a diol with at least two isolated double bonds. Hydrogenation over palladium catalyst gave a liquid dihydro product, the infrared spectrum of which no longer showed the peaks at 3080 and 875 cm^{-1}. Hydrogenation over platinum catalyst gave inconclusive results, possibly because hydrogenolysis took place. Dehydrogenation over palladium-on-charcoal at 250° C gave a high yield of guaiazulene, which was also obtained in very low yield when the total mixture of terpenes was distilled at temperatures above 150 to 160° C.

Most remarkable was the behavior of peak 5 towards dilute acids. Treatment with aqueous oxalic or methanolic sulphuric acid resulted in the formation of a ketol (strong I.R. bands at 3420 and 1710 cm^{-1}, weaker ones at 1643, 910, and 825 cm^{-1}). When this ketol was dehydrogenated over either selenium or palladium no guaiazulene was obtained, but a low yield of an aromatic hydrocarbon with the same retention time as eudalene was recorded by G.L.C. Dehydration of the ketol with pyridine-modified alumina reagent (10) gave mainly an unsaturated ketone (strong I.R. bands at 1740, 1693, 1633, and 1377 cm^{-1}). The ultraviolet absorption at 290 and 228 mμ confirmed α,β-conjugation.

The formation of guaiazulene from the parent diol and its acid-catalyzed rearrangement to a eudalene precursor are reminiscent of the behavior of germacrone (11). Further,

Kindly obtained by Prof. H. Erdtman, Royal Institute of Technology, Stockholm.

Can. J. Chem. Downloaded from www.nrcresearchpress.com by 210.87.254.42 on 09/05/12
For personal use only.

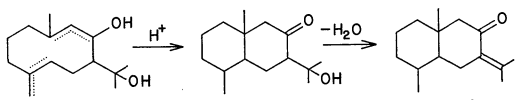

IV V VI

the above data can be reconciled with the properties of a diol having a 10-membered ring of type IV, which isomerizes to the ketol V under acidic conditions. Dehydration would produce the α,β-unsaturated ketone VI. The n.m.r. spectrum confirms the presence of an isopropanol group (singlet equivalent to 6 protons at 8.75), a trisubstituted double bond (triplet equivalent to 1 proton near 4.00) and two C-methyl groups. However, a complete interpretation of this spectrum was not possible. This may be due to some unusual properties of protons found in 10-membered rings. Also, the material isolated may be a mixture of double bond isomers. Further work to establish the structure more definitely will be carried out when the isolation of larger amounts of pure material has been achieved. The name "occidiol" is proposed for this component of the wood of *Thuja occidentalis* L.

Hendrickson (12) has discussed the stereochemical implications in sesquiterpene biogenesis and has shown that eudesmol may be formed from *trans*-farnesol via the 10-

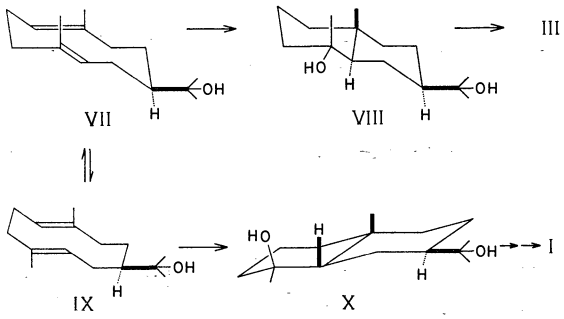

membered intermediate VII, which would form the precursor VIII by a concerted cyclization. This would then lead to α-, β-, and γ-eudesmol as described by Bates and Hendrickson (9). If the two methyl groups are aligned on opposite sides of the 10-membered ring (IX), then by the same mechanism the cis-fused precursor X would obtain, which would then lead to occidentalol, and further to occidol (3, 7). Such a scheme would result in the R-configuration of the isopropanol group at C-7 in both cases, and would predict the absolute configuration of occidentalol to be I.* Furthermore, a single oxidative step with perhaps a double bond isomerization would account for the formation of the diol in *Thuja occidentalis*.

EXPERIMENTAL

Melting points were determined on a Leitz hot-stage microscope. Infrared spectra were recorded with a Perkin–Elmer model 21 double beam spectrophotometer, liquids being mounted as films between sodium chloride plates and solids as KBr disks, unless otherwise indicated. Nuclear magnetic resonance spectra were obtained with a Varian A-60 spectrometer, using tetramethyl silane as internal standard. The G.L.C. columns and apparatus have been described previously (4, 8). Known compounds were identified by comparison of infrared spectra, G.L.C. retention data, and mixed melting point. All retention times (R.T.) were measured relative to cedrol (= 1.00).

Isolation of Sesquiterpenes

The milled heartwood (5.5 kg) of eastern white cedar (part of a mature tree from the Winnipeg district, Manitoba (4)) was extracted with acetone in a Soxhlet extractor for 36 hours. The solvent was removed under reduced pressure from the extract in a rotary evaporator at 40–50° C. The dark brown, viscous residue

See also H. Ziffer, I. T. Batterham, U. Weiss, and E. von Rudloff. Tetrahedron. In press (1963).

Can. J. Chem. Downloaded from www.nrcresearchpress.com by 210.87.254.42 on 09/05/12
For personal use only.

(313 g, 6.3%) was poured with stirring into ether (3 liters) and the insoluble precipitate was filtered off. The ethereal solution was shaken with several aliquots of aqueous potassium hydroxide solution (10%) to remove all acidic and phenolic components. After it was washed with water and dried over anhydrous sodium sulphate, the ether was moved by evaporation. The residue (195 g, 3.5%) was composed mainly of sesquiterpenoid compounds and G.L.C. analysis gave the composition shown in Table I.

Aliquots (20 mg) of the total neutral material were injected repeatedly onto the 6 ft × 1/4 in. adipate polyester column (160° C, flow rate 120 ml He/minute) and components 1, 2, 3, 5, and 6 were isolated practically pure. Components 1 and 5 were obtained crystalline (m.p. 94–96° and 66–69° C. respectively) and were found to be occidentalol and occidol.

γ-Eudesmol

Component 2, $[\alpha]_D$ −34.3° (*c*, 2.0, $CHCl_3$) was reinjected (0.5 μl) onto a 6 ft × 1/4 in. polyethylene glycol (Carbowax 20 M at 160° C) column, when two partially resolved peaks were recorded. In runs using more than 1–2 mg aliquots these merged into one single peak.

Component 2 (8.7 mg) was hydrogenated over reduced Adams catalyst with acetic acid as solvent; consumed: 0.70 ml H_2 at N.T.P.; required for 1 mole H_2 per mole: 0.85 ml. The product, after filtration, crystallized on standing; m.p. 78–82° C. G.L.C. analysis of this product gave, besides starting material, a peak corresponding in R.T. to dihydroeudesmol.

Eudesmol

Component 3 was also obtained crystalline; m.p. 81–84° C, $[\alpha]_D$ +33° ($CHCl_3$). Hydrogenation gave dihydroeudesmol, m.p. 81–83° C. G.L.C. analysis gave two partially resolved peaks (area ratio approximately 1:3) with the same R.T. of the mixture of α- and β-eudesmol, m.p. 82.0–83.5° C, isolated from the oil of araucaria (8).

Occidiol

Component 5 was obtained as a viscous liquid, b.p. (at 11 mm) 135–140° C (air bath); n_D^{23} 1.5129; $[\alpha_D]$ −125.5 (*c*, 2.3, $CHCl_3$). It did not form a crystalline nitrobenzoate or phenylurethane. Treatment with tetranitromethane in ethanol gave a strong yellow-brown color immediately. Found (for the freshly isolated material); C, 76.97; H, 9.93%; mol. wt. (by mass spectroscopy) 236. Caculated for $C_{15}H_{24}O_2$: C, 76.88; H, 9.46%; mol. wt. 236.34. Infrared spectrum: 3420(s), 3080(w), 3040(w), 2930(s), 1668(m), 1650(s), 1452(s), 1377(broad, s), 1197(s), 1125 (s), 1100 (s), 918(m), 878(m), 750(m) cm^{-1}. In chloroform solution there was also a strong band at 3620 cm^{-1}, and that at 886 was strong. The n.m.r. spectrum was recorded in $CDCl_3$ solution.

Dihydrooccidiol

Occidiol (7.4 mg) in ethanol (1 ml) was hydrogenated in a microhydrogenation apparatus over palladium-on-charcoal catalyst (2 mg). Hydrogen was absorbed rapidly during 10 minutes and much more slowly thereafter. Hydrogen consumed: 0.74 ml at N.T.P.; required for 1 mole H_2 per mole of diol: 0.71 ml. The solution was filtered and the solvent evaporated to give the sirupy dihydro diol. Infrared spectrum: 3440, 2940–2860, 1465, 1377, 1265(m), 1120, 950(m), 915(m), and 815(m) cm^{-1}.

Guaiazulene

Occidiol (15 mg) was mixed with palladium-on-charcoal catalyst (15 mg) and heated at 250° C for 30 minutes. The blue-black product was taken up in petrol (b.p. 60–66° C) and filtered, and the derived azulene was extracted with phosphoric acid (85%). Dilution with water liberated the azulene; trinitrobenzene adduct m.p. 162° C, picrate m.p. 120° C (lit. 121–122° C (13)). G.L.C. analysis gave a single peak having the same R.T. as guaiazulene.

Ketol

Occidiol (20 mg) in methanol (10 ml) and a few drops of dilute sulphuric acid (10%) were heated on a steam bath for 5 minutes, when a pink color developed. The product was extracted into ether and worked up to give a viscous residue. Infrared spectrum: 3420, 2930, 2700(w), 1710, 1643(w), 1463, 1378–1363, 1110, 1020(m), 910(m), 825(w) cm^{-1}. The same product was obtained when the diol was heated with aqueous oxalic acid.

The ketol (3 mg) was dehydrogenated as above and the colorless product was analyzed by G.L.C.; major peak with the same R.T. as eudalene, several smaller peaks in the eudesmene–eudesmane (selinane) range.

The ketol (10 mg) was heated with twice its weight pyridine-modified alumina (10) at 230° C for 15 minutes. A viscous product was obtained after extraction, filtration, and evaporation of solvent; infrared spectrum: 2960–2920, 1740, 1693, 1633, 1455, 1377, 1110(m), 877(w); λ_{max}^{EtOH} 290 mμ and inflexion near 228 mμ.

ACKNOWLEDGMENTS

We are grateful to Prof. H. Erdtman for his interest and for having obtained the mass spectrum of occidiol. Microanalyses and n.m.r. spectra were carried out by Mr. M.

Can. J. Chem. Downloaded from www.nrcresearchpress.com by 210.87.254.42 on 09/05/12
For personal use only.

Mazurek and infrared spectra by Miss I. Gaffney. The technical assistance of Mr. M. Granat is gratefully acknowledged.

REFERENCES

1. T. NAKATSUKA and Y. HIROSE. Bull. Agr. Chem. Soc. Japan, **20**, 215 (1956).
2. Y. HIROSE and T. NAKATSUKA. Bull. Agr. Chem. Soc. Japan, **23**, 143 (1959).
3. M. NAKAZAKI. Chem. Ind. 413 (1962).
4. E. VON RUDLOFF and H. ERDTMAN. Tetrahedron, **18**, 1315 (1962).
5. W. COCKER and T. B. H. MCMURRY. Tetrahedron, **8**, 181 (1960).
6. K. MISLOW and A. MOSCOWITZ. Tetrahedron Letters, No. 11, 699 (1963).
7. M. NAKAZAKI. Bull. Chem. Soc. Japan, **35**, 1387 (1962).
8. E. VON RUDLOFF. Chem. Ind. 743 (1962).
9. R. B. BATES and E. K. HENDRICKSON. Chem. Ind. 1759 (1962).
10. E. VON RUDLOFF. Can. J. Chem. **39**, 1860 (1961).
11. F. SORM. International Symposium Chemistry of Natural Products. Australia. 1960. p. 533.
12. J. B. HENDRICKSON. Tetrahedron, **7**, 82 (1959).
13. L. RUZICKA and A. J. HAAGEN-SMIT. Helv. Chim. Acta, **14**, 1104 (1931).

Can. J. Chem. Downloaded from www.nrcresearchpress.com by 210.87.254.42 on 09/05/12
For personal use only.

PORE STRUCTURES AND SURFACE AREAS OF HARDENED PORTLAND CEMENT PASTES BY NITROGEN ADSORPTION

R. Sh. Mikhail,[1] L. E. Copeland, and Stephen Brunauer
Portland Cement Association Research and Development Laboratories, Skokie, Illinois, U.S.A.
Received July 15, 1963

ABSTRACT

The investigations were performed on five hardened pastes of a type I (normal) portland cement, having initial weight ratios of water to cement of 0.35, 0.40, 0.50, 0.57, and 0.70, and hydrated for 12, 12, 12, 2½, and 2½ years, respectively. The percentage hydration ranged from 90 to 98%.

Nitrogen adsorption and desorption isotherms were determined for all pastes at the boiling point of nitrogen, from low pressures to almost the saturation pressure. The BET surface areas were calculated, and the pore space accessible to nitrogen was obtained by a slight extrapolation of the isotherms. In addition, pore structure analysis was made for three of the five pastes by the method of Cranston and Inkley.

The specific surface areas of the five pastes were also determined by water vapor adsorption, and the total porosity to water was measured. For every paste, the water areas and porosities were greater than the nitrogen areas and porosities.

The main conclusions from the results were as follows.

(1) There is a wide range of pore sizes in the pastes.

(2) Nitrogen is excluded from a part of the pore system by two mechanisms; some of the pores are too narrow and others have too narrow entrances to admit nitrogen.

(3) The hydraulic radius (the volume of the pore system divided by the surface area of the pore walls) for the system of small pores increases with increasing water to cement ratio.

(4) The hydraulic radius of the system of large pores also increases with increasing water to cement ratio, but the increase is smaller than for the small pores.

(5) The paste with water to cement ratio of 0.35 has enough pore space for complete hydration.

Some practical implications of the above conclusions are discussed.

INTRODUCTION

When portland cement is mixed with a limited amount of water, e.g., 0.5 of its own weight, and the paste is allowed to stand, it sets in a few hours and then continues hardening for months or even years. The hardened portland cement paste forms the matrix in which the grains of sand and pieces of coarse aggregate are embedded in concrete.

The hardened paste is not a compact solid mass but a porous material with a very large internal surface. The internal surface and the total porosity were first measured by Powers and Brownyard (1), using water vapor adsorption. Both water and nitrogen adsorption were employed later by others (2, 3). Powers and Brownyard demonstrated highly important correlations between such physical properties as specific surface area and porosity of the hardened paste on the one hand, and such vital engineering properties as strength, dimensional changes, permeability to water and freezing and thawing of water in the pore system, on the other. In the subsequent decade and a half, further work by Powers and many others has confirmed the validity and extended the scope of these correlations. During this period, much work has been done on the surface areas of hardened pastes but, as far as the authors know, a detailed study of the pore size distribution has not been made.

Nitrogen adsorption, in almost every instance, leads to a smaller specific surface area than water vapor adsorption. The smaller size and the strong dipole moment of the water molecule enable it to penetrate into pore spaces which are inaccessible to the larger

[1]*Present address: Chemistry Department, Faculty of Science, Ain Shams University, Cairo, Egypt, U.A.R.*

Can. J. Chem. Downloaded from www.nrcresearchpress.com by 210.87.254.5 on 09/05/12
For personal use only.

nonpolar nitrogen molecules. Kalousek was the first to point out the existence of spaces which may exercise such selectivity (4). The main constituent of hardened portland cement paste is a calcium silicate hydrate, called tobermorite gel (5). This gel is responsible for at least 80% of the specific surface area of fully hydrated portland cement, as measured by water adsorption. Tobermorite gel is a layer crystal, and Kalousek assumed that water could penetrate between the layers but nitrogen could not. However, later work has shown that water can not penetrate between the layers of strongly dried tobermorite gel, even when the gel is soaked in water (6). Thus, the difference between water and nitrogen adsorption is not a consequence of the layer structure of tobermorite gel.

The authors have undertaken the investigation of the pore structures of hardened portland cement pastes both by nitrogen and water vapor adsorption. Nitrogen has been used by many investigators for pore structure determinations (7, 8); consequently, the authors started with nitrogen. The results are given in the present paper. Although nitrogen determines only a part of the pore structure, important conclusions can still be drawn from the results. The determination of the complete pore structure by water vapor adsorption is now in progress.

EXPERIMENTAL

The hardened pastes were all prepared from a single type I (normal) portland cement, designated as 15754. The major constituents of this cement, as determined by X-ray diffraction analysis, are tricalcium silicate, 54.1%; β-dicalcium silicate, 26.0%; tricalcium aluminate, 6.5%; and tetracalcium aluminoferrite, 8.6%.

The pastes were prepared with initial weight ratios of water to cement, w_0/c, covering the range 0.35 to 0.70. They were placed in test tubes and covered with water. The test tube was then sealed and kept at 24±1° C until almost complete hydration was reached. The pastes with w_0/c values of 0.35, 0.40, 0.50, 0.57, and 0.70 were hydrated for 12, 12, 12, 2½, and 2½ years, respectively.

After a paste was removed from the test tube mold, the top and bottom half inch were cut off with a small diamond saw and discarded. The remainder was dried for 2 days in a vacuum-drying apparatus (9). It was then transferred to a carbon-dioxide-free controlled atmosphere cabinet and ground there to pass a U.S. standard 20-mesh screen. The part retained on a 50-mesh screen was used in the present work.

The ground specimens, in tared weighing bottles, were placed in the vacuum-drying apparatus and were dried to equilibrium at the vapor pressure of ice at −78° C (5×10^{-4} mm). A specimen was then transferred to the nitrogen adsorption system and outgassed overnight at room temperature, using a mercury diffusion pump backed by a mechanical oil pump. The adsorption data were obtained in a volumetric apparatus of the conventional type. Cylinder nitrogen (99% purity) was purified by passing over hot copper and drying by magnesium perchlorate. A nitrogen vapor pressure manometer was used to obtain the saturation pressure of nitrogen at the temperature of the experiment. Surface areas were calculated with a value of 16.2 Å² for the area of a nitrogen molecule. The porosity of the paste for nitrogen was determined by a very slight extrapolation of the adsorption isotherm.

Surface areas and porosities were also determined with water. The adsorption data were obtained gravimetrically in modified vacuum desiccators (10). A different relative pressure, in the range from 0.07 to 0.33, was maintained in each desiccator by means of a saturated salt solution. The value of 11.4 Å² was used for the molecular area of water (6). The total porosity of the paste to water was measured before the paste was dried. The surface of the saturated paste was wiped off with a slightly moist tissue paper, and the paste was weighed. Ignition and reweighing of the paste gave the total water content, combined and uncombined. Total water minus combined water gave the water in the pore system. The combined water was determined by the method of Copeland and Hayes (9). This involves drying the specimen as for the nitrogen or water vapor adsorption and igniting it. The combined water contents indicated percentage hydrations ranging from 90% for the paste with $w_0/c = 0.35$ to 98% for the paste with $w_0/c = 0.70$.

The densities of the saturated pastes were determined with a specific gravity balance.

RESULTS

1. Figure 1 represents the nitrogen adsorption isotherms near −195.8° C. The adsorbed volume is given in cubic centimeters of nitrogen at S.T.P. per gram of adsorbent; the abscissa is the relative pressure p/p_s, where p is the measured equilibrium pressure, and p_s is the vapor pressure of nitrogen at the temperature of the measurement. The abscissas

Can. J. Chem. Downloaded from www.nrcresearchpress.com by 210.87.254.5 on 09/05/12
For personal use only.

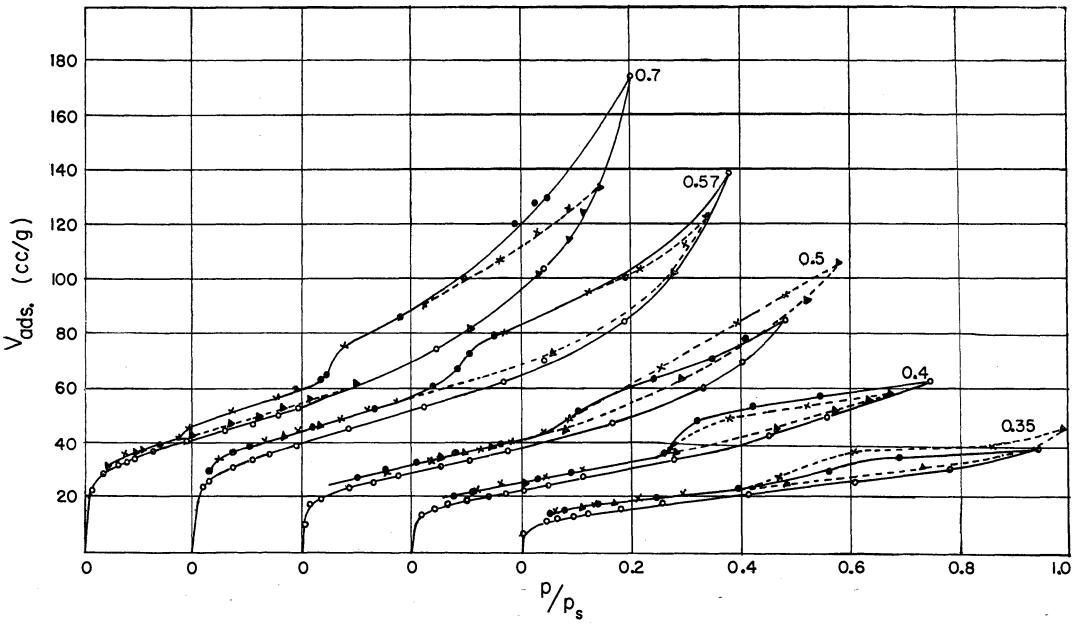

FIG. 1. Isotherms of nitrogen adsorption near the boiling point of nitrogen on hardened portland cement pastes.

are displaced for the different pastes, for clear representation. Two adsorption and two desorption isotherms were determined for each paste. The first adsorption isotherm is represented by empty circles, the first desorption isotherm by filled circles. In every instance, an open hysteresis loop was obtained down to low pressures. Then at some low pressure a second adsorption isotherm was started, represented by triangles in Fig. 1. The second adsorption isotherm, at lower relative pressures always coincided with the first desorption isotherm; which means that it indicated higher adsorption than the first adsorption isotherm. The second desorption isotherm, designated with crosses, formed a closed hysteresis loop with the second adsorption isotherm for four of the five pastes, the loop closing between $p/p_s = 0.41$ and 0.44. For the paste with $w_0/c = 0.7$, however, a double hysteresis loop was obtained. As Fig. 1 shows, the loop tended toward closing at $p/p_s = 0.44$, but it did not close completely until a p/p_s value slightly less than 0.2 was reached.

When the pastes were outgassed to remove nitrogen completely, both cycles of adsorption–desorption could be completely reproduced. It seems, therefore, that the adsorption of nitrogen itself causes a change in the pore structure. An expansion in the pore system is produced, which is not fully reversible; consequently, the hysteresis loop remains open in the first adsorption–desorption cycle. Subsequently, however, the structure remains stable, which is indicated by the closing of the hysteresis loop in the second cycle. At lower relative pressures, the first desorption, the second adsorption, and the second desorption isotherms coincide.

2. The pore structure was determined by the method of Cranston and Inkley (8). The determination involves three assumptions: (1) the pores are cylindrical capillaries with one end closed; (2) the amount of adsorbate in equilibrium with the gas phase is retained by the adsorbent by two mechanisms: (*a*) physical adsorption on the pore walls, and (*b*)

Can. J. Chem. Downloaded from www.nrcresearchpress.com by 210.87.254.5 on 09/05/12
For personal use only.

capillary condensation in the inner capillary volume; and (3) the multilayer thickness in the pores is the same as that on a flat surface. The first assumption will be discussed later. The second assumption may be stated in the form that the capillary radius is equal to the sum of the thickness of the multilayer adsorbed on the pore walls plus the radius calculated from the Kelvin equation.

From adsorption data of nitrogen on a variety of non-porous adsorbents, Cranston and Inkley deduced a so-called *t*-curve, a plot of the thickness of the adsorbed layer (v_{ads} in milliliters divided by the BET specific surface area) against the relative pressure. The pore volumes and surface areas corresponding to different pore diameters are calculated from the difference between the *t*-curve and the actual isotherm obtained for the porous adsorbent. The pore structure analysis can be made for both the adsorption and the desorption isotherm. Cranston and Inkley found that for most adsorbents the analysis of the adsorption isotherm gave more reliable results, as judged by the agreement between the cumulative surface area in the pore volumes and the BET area. The present authors have come to the same conclusion. The pore structures were determined for the 0.35, 0.50, and 0.70 paste. (Henceforth, the designation of 0.35 paste will be used for the paste with $w_0/c = 0.35$.) The adsorption isotherms gave cumulative pore areas in very good agreement with the BET areas, whereas the desorption isotherms did not. This can be seen by comparing column 3 with columns 4 and 5 in Table I. The BET area obtained

TABLE I

Specific surface areas of hardened pastes (in m^2 per g)

1	2	3	4	5	6	7
w_0/c	S_{H_2O}	S_{N_2}	S_{cum}^{ads}	S_{cum}^{des}	$S_{H_2O}-S_{N_2}$	$S_{N_2}-S_{cum}^{ads}$
0.35	208.0	56.7	53.1	56.0	151.3	3.6
0.40	202.6	79.4	—	—	123.2	—
0.50	194.6	97.3	95.0	108.9	97.3	2.3
0.57	193.8	132.2	—	—	61.6	—
0.70	199.6	139.5	136.0	184.6	60.1	3.5

by nitrogen adsorption is S_{N_2}, the cumulative areas in the pores, obtained from the adsorption and desorption isotherms are S_{cum}^{ads} and S_{cum}^{des}, respectively. In the analysis, the second adsorption isotherm was used. As was discussed earlier, a stable pore structure was obtained only in the second adsorption–desorption cycle.

Because of the poor agreement between S_{N_2} and S_{cum}^{des}, and because of other inconsistencies in the pore volume data based on the desorption isotherms, only the data obtained from the adsorption isotherms have been used. The Cranston–Inkley analysis starts with pores of 300 Å diameter and does not take larger pores in consideration. There is only a small surface in these larger pores, but there is a considerable volume, as will be seen. The surface in the larger pores is given in column 7 of Table I. These values may have a sizable error, because they represent small differences between two large numbers.

Table I, column 2, gives the BET surface areas obtained by water vapor adsorption. These values represent the total surface in the pores of the pastes (5). The values in column 3 represent the surface accessible to nitrogen molecules, and the values in column 6 represent the surface inaccessible to nitrogen molecules.

3. The pore structure analysis was kindly carried out by Dr. G. R. Lester of the Universal Oil Products Company, Research and Development Laboratories, Des Plaines, Illinois. The method he used was essentially that of Cranston and Inkley, with the

Can. J. Chem. Downloaded from www.nrcresearchpress.com by 210.87.254.5 on 09/05/12
For personal use only.

inclusion of a computer interpolation procedure. This interpolation is from point to point, rather than over the entire isotherm, so that if any deviation is introduced by the interpolation, it will be at a minimum in the neighborhood of each experimental point.

The results for the pore volume distributions are shown in Fig. 2. The curves are plots of $V(D)$, the pore volume in milliliters per gram of paste per Å, against D, the pore diameter in Å. There is a high point in the 0.7 paste curve at the smallest pores, which is not found for the two other pastes. It may be real, but more probably it is caused by a small error in a single isotherm point. Aside from this anomalous maximum, the maximum for the 0.7 paste is at 32.5 Å, and the same is true for the 0.5 paste. The maximum, i.e., the largest pore volume per Å for the paste, is at 22.5 Å for the 0.35 paste.

The cumulative pore volumes for the three pastes are given in Table II, column 4.

TABLE II

Pore volumes of hardened pastes (in ml per g)

1	2	3	4	5	6	7
w_0/c	V_{H_2O}	V_{N_2}	V_{cum}^{ads}	$V_{H_2O}-V_{N_2}$	$V_{N_2}-V_{cum}^{ads}$	ρ (g/ml)
0.35	0.1264	0.0748	0.0502	0.0516	0.0246	2.085
0.40	0.1776	0.1059	—	0.0717	—	2.040
0.50	0.2615	0.1792	0.1375	0.0823	0.0417	1.959
0.57	0.3110	0.2493	—	0.0617	—	1.856
0.70	0.4008	0.2758	0.1971	0.1250	0.0787	1.763

The total pore space accessible to nitrogen is given in column 3, and it is greater than v_{cum}^{ads} for each paste. This is because the Cranston–Inkley analysis does not take into account pores larger than 300 Å in diameter. The volume of nitrogen in pores larger than 300 Å is given in column 6 of Table II.

Table II, column 2, gives the porosity to water, which is the total porosity of the paste. Column 3 gives the pore space accessible to nitrogen, and column 5 that inaccessible to nitrogen. The table also contains, in column 7, the densities of the saturated pastes.

In the calculations of pore volumes, two approximations have been made: (1) the densities of nitrogen and water were assumed to be the same as those of the liquids; and (2) the effect of shrinkage of the pastes caused by drying was neglected. Even if some error is introduced by these approximations, it cannot affect any of the conclusions reached in this paper.

DISCUSSION

1. The shapes of the hysteresis loops in Fig. 1 come closest to those classified as type D loops by de Boer (11). He points out that such loops can be produced, for example, by a heterogeneous assembly of plate-like capillaries with a varying range of widths. Electron microscopic examination of hardened portland cement pastes (12) shows that tobermorite gel, which is largely responsible for the pore structure of the paste, consists of very thin sheets. Such sheets may well produce plate-like or slit-shaped pores. Type D hysteresis loops can also be produced by a heterogeneous assembly of capillaries with wide bodies having a varying range of narrow short necks (11). This may also fit the pastes investigated. It will be shown that many of the larger pores have narrow openings, but the present investigations did not reveal anything about the variation in lengths and widths of these openings.

De Boer has pointed out that for type D hysteresis loops, scanning is possible from any

Can. J. Chem. Downloaded from www.nrcresearchpress.com by 210.87.254.5 on 09/05/12
For personal use only.

point of the sloping desorption branch. This has been found to apply in the present investigations.

The question may be raised regarding the validity of a pore volume analysis based on the assumption of cylindrical pores to a system in which the pores are likely to be slit-shaped. Certainly caution must be applied in drawing quantitative conclusions, but the qualitative conclusions, as will be seen, are most helpful in supporting and extending quantitative conclusions drawn from other data. The cylindrical pore approximation has found useful application in many instances for solids widely differing in nature, even though there is probably no solid which contains only cylindrical pores.

2. When portland cement sets, the paste acquires a stable volume, which is approximately equal to the volume of the cement solids plus the volume of the water initially mixed with the cement, w_0. Thus, the total porosity of the paste is determined by the w_0/c ratio. The hydration products of portland cement have a larger specific volume than unhydrated portland cement; consequently, the total porosity decreases as the hydration progresses.

Powers (1, 13) divided the pore system into two types of pores. He reasoned that the hydration of a definite weight of a given cement was accompanied by the formation of a definite pore volume, and he called this the gel pore volume. He called the rest of the pores capillary pores. He visualized two overlapping pore systems, each having a wide pore size distribution, but he concluded that the average diameter of the capillary pore system was much greater than that of the gel pore system.

The measurements reported here can distinguish between smaller and larger pores but they can not distinguish between gel pores and capillary pores of equal sizes. There is a considerable advantage in distinguishing between a system of small pores and a system of large pores, regardless of their origin. Nuclei of hydration products can not grow into crystals in small pores. Water can not freeze in small pores for the same reason. Capillary condensation can not occur in small pores. For these reasons, as well as for others, the pore system will be divided into two parts: a system of small pores, designated as S pore system, and a system of large pores, designated as L pore system. These two systems are not identical with the gel pores and capillary pores of Powers, but they are similar to them. Most of the gel pores of Powers are S pores, and most of the capillary pores are L pores.

3. There is no sharp dividing line between the S and L pore systems. In Fig. 2, the pore volume distribution curves are continuous, and no bimodal distribution is indicated. The high point in the curve for the 0.7 paste at very small pore diameters is probably caused by an error in a single isotherm point. However, even if the dip is real, it signifies only a break in the distribution within the S pore system and not the division between the S and L pore systems. A small dip in the same curve, in the vicinity of 175 Å, is within the L pore region.

On the basis of the curves for the 0.7 and 0.5 pastes, an arbitrary but useful division between the pore systems could be made in the region of the sharp drop, somewhere between 60 and 80 Å. The division for the 0.35 paste, however, is around 40 Å. Thus the average diameter of the S pores in this paste is smaller than in the two other pastes. Further evidence for this will be presented later.

The curves of Fig. 2 represent only the pores accessible to nitrogen and not the total pore system but, as a comparison of columns 2 and 4 in Table II shows, about 40% of the total pore system for the 0.35 paste and about 50% for the two other pastes is represented by the curves of Fig. 2. Small and large pores are included for all three pastes.

Can. J. Chem. Downloaded from www.nrcresearchpress.com by 210.87.254.5 on 09/05/12
For personal use only.

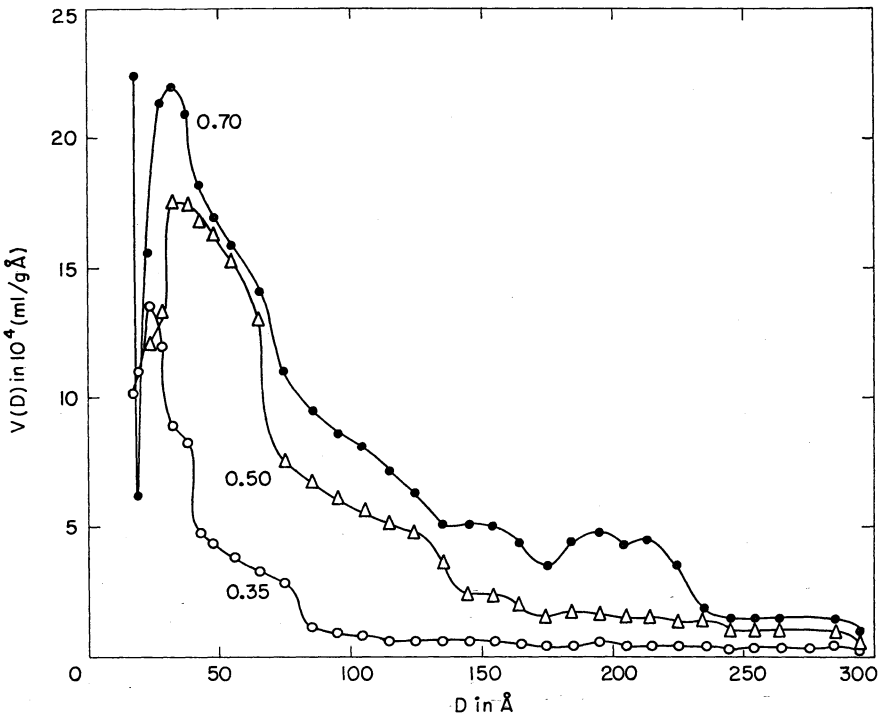

FIG. 2. Pore size distribution curves of hardened portland cement pastes.

Nevertheless, the question remains whether the "sample" is representative of the whole. This will be discussed later.

4. For pores of irregular or unknown shapes, an average radius called hydraulic radius can be calculated by dividing the volume of the pore system by its surface area. For a cylinder open at both ends, the hydraulic radius is one-fourth of the diameter, and for an open slit it is one-half of the width. The hydraulic radii for the five pastes are given in Table III. The values in columns 2, 3, 4, 5, and 6, designated as r_1, r_2, r_3, r_4, and r_5,

TABLE III

Hydraulic radii of pores (in Å)

1	2	3	4	5	6
w_0/c	Total pore system, r_1	Pores inaccessible to nitrogen, r_2	Pores accessible to nitrogen, r_3	Pores of the distribution curves, r_4	Largest pores, r_5
0.35	6.1	3.4	13.2	9.5	68
0.40	8.8	5.8	13.3	—	—
0.50	13.4	8.5	18.4	14.5	181
0.57	16.0	10.0	18.9	—	—
0.70	20.1	20.8	19.8	14.5	225

are V_{H_2O}/S_{H_2O}, $(V_{H_2O}-V_{N_2})/(S_{H_2O}-S_{N_2})$, V_{N_2}/S_{N_2}, $V_{cum}^{ads}/S_{cum}^{ads}$, and $(V_{N_2}-V_{cum}^{ads})/(S_{N_2}-S_{cum}^{ads})$, respectively.

(*a*) First it should be noted that r_4 is the same for the 0.5 and the 0.7 paste. Two materials having the same hydraulic radii may have widely differing pore size distribution,

Can. J. Chem. Downloaded from www.nrcresearchpress.com by 210.87.254.5 on 09/05/12
For personal use only.

but when the two materials are as similar as two pastes of the same portland cement, identity of hydraulic radii should imply at least a rough similarity of pore size distribution. This is actually so, as the two curves of Fig. 2 show. The maxima are at the same point; the sharp drops appear in the same region. The 0.35 paste curve, however, though in many respects similar to the two other curves, exhibits a shift toward smaller pore sizes. The value of r_4 for this paste is smaller than for the two others.

(*b*) For the 0.35 paste, the values of r_1, r_2, and r_3 are 6.1, 3.4, and 13.2 Å. This means that this paste possesses a large number of small pores inaccessible to nitrogen. If the pores are visualized as slits, the average width of the slits inaccessible to nitrogen is 2 r_2 or 6.8 Å; if the pores are visualized as cylinders, the average diameter is 4 r_2, or 13.6 Å. In either case, some of the pores are too narrow, and the others have too narrow entrances to permit access of nitrogen. It is important to note only that the hydraulic radius of the pore system accessible to nitrogen is about four times as large as that of the pore system inaccessible to nitrogen.

The situation is very different for the 0.7 paste. The values of r_1, r_2, and r_3 are 20.1, 20.8, and 19.8 Å, respectively. The hydraulic radius of the pores inaccessible to nitrogen is somewhat larger than that of the pores accessible to nitrogen, though this may be within experimental error. The exclusion of nitrogen from about half of the pore system must be a consequence of narrow entry ways to the pores. If there were a sizable fraction of pores into which nitrogen can not enter because of the small sizes of the pores, r_2 would be considerably smaller than r_3.

The conclusion from the last two paragraphs is that the small pores or *S* pores in the 0.7 paste have larger average diameters or widths than the small pores in the 0.35 paste. A comparison of columns 3 and 4 in Table III shows that the three other pastes are intermediate between these two. It was stated earlier that according to Powers (13) the gel pore system has a characteristic porosity. The present results show that the *S* pore system has no characteristic porosity valid for all w_0/c ratios of the same cement; on the contrary, the average widths or diameters of the *S* pores increase with increasing w_0/c ratio. However, the *S* pores can not be fully identified with the gel pores; consequently, the results do not disprove Powers' views.

Table III, column 3, shows that the hydraulic radius of the pore system inaccessible to nitrogen increases sixfold from the 0.35 paste to the 0.7 paste, and column 4 shows that the increase in the hydraulic radius of the pore system accessible to nitrogen is only about 50%. Especially slight is the increase in the hydraulic radius of the latter pore system from the 0.5 to the 0.7 paste; it is less than 8%. It follows, therefore, that the increase in the sizes of the *L* pores with increasing w_0/c ratio is considerably smaller than that of the *S* pores for these pastes.

The arguments advanced in this section (4*b*) are based solely on hydraulic radii. They assume nothing about the shapes of the pores, nor do they refer to the distribution curves of Fig. 2.

(*c*) It follows from the equality of r_1, r_2, and r_3 for the 0.7 paste that the distribution curve in Fig. 2 for this paste is probably representative for the entire pore system. This means that the distribution curve for water would not be very different from that of nitrogen, except that the ordinates would be roughly twice as large. The curves become less representative as one progresses to lower w_0/c ratios. The water distribution curves should show increasingly larger fractions of the total porosity at the small pore diameters.

5. A comparison of columns 3 and 6 in Table II shows that about one-fourth to one-third of the pore system accessible to nitrogen consists of pores larger in diameter than

Can. J. Chem. Downloaded from www.nrcresearchpress.com by 210.87.254.5 on 09/05/12
For personal use only.

the pores covered by the Cranston–Inkley analysis. The hydraulic radii of these largest pores, given in column 6, Table III, are questionable because of the uncertainty in $S_{N_2}-S_{cum}^{ads}$ (Table I, column 7) that was pointed out earlier. Nevertheless, they give a rough indication of the average diameters or widths of the pores.

The pores in Table II, column 6, for the 0.35 paste constitute 19.5% of the total porosity. In addition to these pores, a part of the pores shown in Fig. 2 belongs to the L pore system. One can estimate that the L pore system makes up at least one-fourth of the total porosity. This result has important implications.

According to Powers, for cement 15754 the weight of water in the gel pore system is 3.0 V_m, where V_m is the weight of water necessary to cover the surface with a monolayer of adsorbed water. It follows from this that for pastes with w_0/c ratios less than 0.38 there is not enough pore volume to accommodate the characteristic gel porosity at complete hydration; consequently, such pastes do not hydrate completely. Calculation gives 93% as the maximum hydration of the 0.35 paste.

It is possible that the pores of the S pore system are too narrow to permit growth of the nuclei of the hydration products, but this is not true of the L pores. The results cited above show that there is enough room in the L pore system of the 0.35 paste for complete hydration. This, in itself, would have little practical significance, because the hydration is so slow that it may take decades to reach even 93% hydration. It would have, however, great significance, if a way were found to accelerate the hydration process. The strength and dimensional stability of pastes possessing low porosities increase greatly with decreasing porosity. Thus, if the hydration could be accelerated, a marked improvement in concrete could be achieved. The authors consider this a distinct possibility.

Although there is enough room in the 0.35 paste for complete hydration, this may not be true of pastes with lower w_0/c ratios. Powers is doubtless correct in his view that the hydration of portland cement is accompanied by the formation of a gel pore system. The gel water content can not be as high as 3.0 V_m in all pastes of cement 15754. The 0.35 paste, if all the pores are assumed to be gel pores, has a gel water content of 2.46 V_m, and Powers cited a paste with a gel water content of 2.38 V_m (13). That paste had a w_0/c value of 0.235. If there is a minimum gel porosity, which is very likely, it necessarily leads to Powers' concept of a limiting w_0/c ratio, below which complete hydration can not occur.

6. There is another way of demonstrating the increase in the sizes of the S pores with increasing w_0/c ratio.

For adsorption on a plane surface, an average thickness can be defined for the adsorbed film, which is the volume of the adsorbed film divided by the surface area of the adsorbent. For nitrogen, the equation is

$$t = 15.47\ (v_{ads}/S_t) \qquad [1]$$

where the volume adsorbed is expressed in cc at S.T.P., S_t is in m^2 per g, and t in Å. A plot of v_{ads} against t is a straight line, the slope of which is 15.47 $/S_t$. The plot should be a straight line even for porous bodies at low relative pressures. It should remain a straight line until one of two things happens.* (*a*) Some of the narrowest pores become filled by multilayer adsorption. In this case, a part of the surface becomes unavailable for further adsorption, and the points of the plot should begin to drop below the straight line. (*b*) Capillary condensation starts in certain pores in addition to multilayer adsorption. In this case, the points of the plot should begin to deviate upward.

**We are greatly indebted to Professor J. H. de Boer for discussion of this point with one of the authors (R. Sh. M.).*

Can. J. Chem. Downloaded from www.nrcresearchpress.com by 210.87.254.5 on 09/05/12
For personal use only.

Figure 3 shows such v_{ads} vs. t plots for four of the five pastes. As stated earlier, Cranston and Inkley (8) plotted the thickness of the adsorbed film, t (the volume of the adsorbed film divided by the BET surface), against the relative pressure for the adsorption of nitrogen on a great variety of non-porous adsorbents. On the basis of these data, they drew an average "t-curve", which represents the adsorption of nitrogen on a plane surface. The points in Fig. 3 were obtained in the following manner. The values of v_{ads} were taken from the adsorption branches of the isotherms of Fig. 1, and the values of t were taken from the t-curve of Cranston and Inkley, by reading the value of t corresponding to the relative pressure of the particular isotherm point.

First it should be noted that at small values of relative pressure (or of t) the curves are straight lines. From the slopes of the straight lines, S_t was calculated for the pastes, and good agreement was obtained with the BET surface areas. This means that the t-curve of Cranston and Inkley gives a good representation of the average thickness of the nitrogen film adsorbed at low relative pressures on the pastes investigated.

The curve for the 0.35 paste deviates from the straight line already at a thickness of 4 Å. The downward deviation shows that an appreciable fraction of the pores, having hydraulic radii of 4 Å, are already filled with adsorbate. (If the pores are slits, the width of the slit is 8 Å). If the S pores in the four pastes would have the same size distribution, all four curves of Fig. 3 would show a downward deviation at the same point. Instead, the 0.4 paste shows a downward deviation at a considerably larger value of t, and the two other curves show upward deviations. The conclusion is that the S pores increase in width with increasing w_0/c ratio.

The 0.5 and 0.7 paste curves clearly indicate capillary condensation at p/p_s values between 0.4 and 0.5. This is an interesting way to detect the beginning of capillary condensation from an *adsorption* curve. Ordinarily, the closing of the hysteresis loop of the desorption isotherm is employed for the indication of the beginning of capillary condensation. As Fig. 1 shows, the hysteresis loops confirm the conclusions drawn from Fig. 3.

The fact that the downward deviation for the 0.4 paste comes only at a t value of about 9 Å indicates that the two effects discussed occurred already at smaller values of t, but they balanced each other. As the closing of the hysteresis loop shows, capillary condensation in this paste must also have occurred at a t value in the vicinity of 6 or 7 Å, but this was balanced by filling of pores by multilayer adsorption.

7. Figure 4 represents the variation of surface area with w_0/c. Curves I and II give the surface areas per gram of paste obtained by nitrogen and water vapor adsorption, respectively. The water areas are almost constant, as they should be for almost completely hydrated pastes, but the nitrogen areas increase with increasing w_0/c. The difference is more striking if the surface areas are plotted per cubic centimeter of paste. The water areas decrease, as curve IV shows, because there is less solid and more pore space per cubic centimeter of paste with increasing w_0/c. In spite of the fact that there is less adsorbing solid, the nitrogen areas increase with increasing w_0/c.

The explanation is that the major part of the surface area resides in the small pores of each paste. The nitrogen and water points for the 0.35 paste on curves III and IV are far apart because there are many pores in this paste that are too narrow to admit nitrogen. The widths of the small pores increase with increasing w_0/c; consequently, curves III and IV approach each other.

8. The main conclusions of the present investigations will now be summarized. They are partly definite and partly tentative conclusions. The tentative conclusions await

Can. J. Chem. Downloaded from www.nrcresearchpress.com by 210.87.254.5 on 09/05/12
For personal use only.

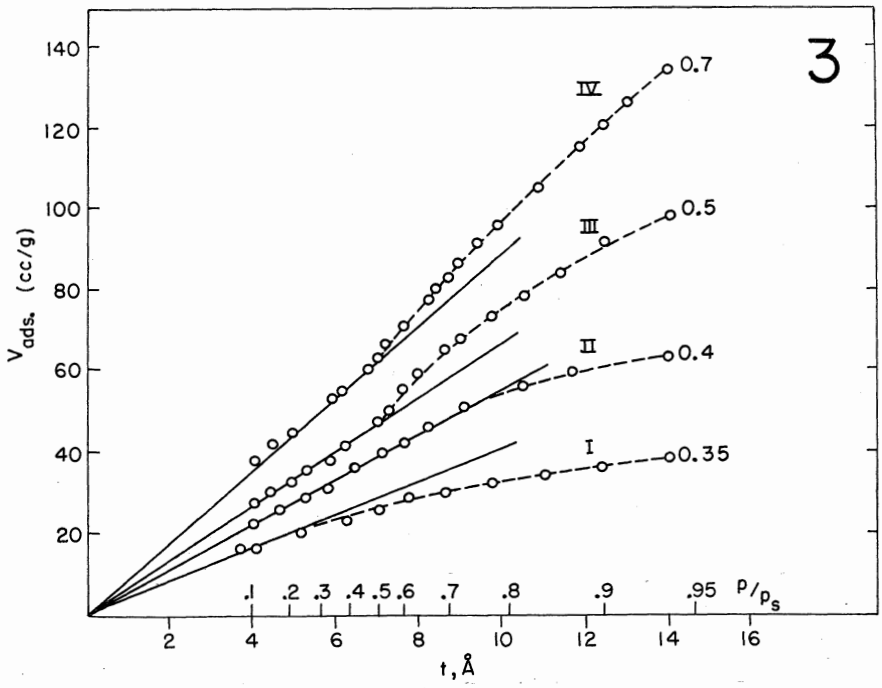

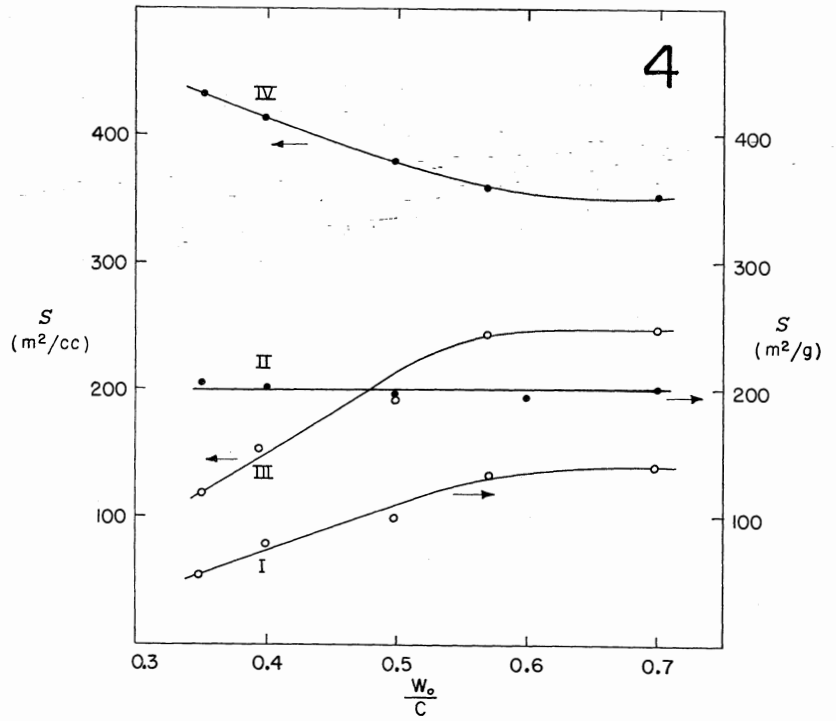

FIG. 3. Plots of v_{ads} vs. t for hardened portland cement pastes.
FIG. 4. Variation of specific surface area available to nitrogen and water with water:cement ratio.

Can. J. Chem. Downloaded from www.nrcresearchpress.com by 210.87.254.5 on 09/05/12
For personal use only.

confirmation or refutation by the work now in progress on the determination of the complete pore structure by water vapor adsorption and by other work in the future.

Definite Conclusions

(1) There is a wide range of pore sizes in almost fully hydrated portland cement pastes. There are pores in the 0.35 paste that have hydraulic radii of less than 3.4 Å, and there are pores in the 0.7 paste with hydraulic radii of greater than 200 Å.

(2) Nitrogen molecules are excluded from a part of the pore system by two mechanisms: some of the pores are too narrow and others have too narrow entrances to admit nitrogen.

(3) The system of small pores (the S pore system) increases in hydraulic radius with increasing w_0/c ratio.

(4) The system of large pores (the L pore system) also increases in hydraulic radius with increasing w_0/c ratio. The increase is smaller than the increase in the radii of the small pores for pastes in the w_0/c range 0.5 to 0.7.

(5) The L porosity of the 0.35 paste is greater than 25% of the total porosity. The hydration will not stop at 93% because of lack of room; there is enough room in the paste for complete hydration.

(6) If the gel porosity does reach a minimum short of zero, which is very probable, the minimum gel water content is less than 2.46 V_m.

Tentative Conclusions

(1) There is no bimodal distribution in the pore system, which would separate small pores and large pores. An arbitrary but useful separation may possibly be made at a hydraulic radius of about 15–20 Å for the 0.5 and 0.7 pastes and at 10 Å for the 0.35 paste.

(2) In the 0.7 paste, the small pores which exclude nitrogen because of their widths constitute a negligible fraction of the total porosity. Nitrogen is excluded because of narrow entrances to a part of the pore system.

(3) In pastes of lower w_0/c ratios than 0.35, hydration may stop and in pastes of very low w_0/c ratios, hydration will stop because of lack of room. However, it can not be predicted at what point hydration will stop because it is not known at present what is the minimum gel porosity that a paste can possess.

Can. J. Chem. Downloaded from www.nrcresearchpress.com by 210.87.254.5 on 09/05/12
For personal use only.

ACKNOWLEDGMENTS

The authors wish to express their gratitude to Dr. G. R. Lester of the Universal Oil Products Company, Research and Development Laboratories, Des Plaines, Illinois, for performing the Cranston–Inkley analysis. They also appreciate the help received from Messrs. R. A. Helmuth, C. H. Weise, and Donn Hathaway of the Portland Cement Association Research and Development Laboratories.

REFERENCES

1. T. C. Powers and T. L. Brownyard. Proc. Am. Concrete Institute, **43**, 101, 249, 469, 549, 669, 845, 933 (1946–47).
2. R. L. Blaine and H. J. Valis. J. Res. Nat. Bur. Std. **42**, 257 (1949).
3. L. F. Gleysteen and G. L. Kalousek. Proc. Am. Concrete Institute, **51**, 437 (1954–55).
4. G. L. Kalousek. Proc. Am. Concrete Institute, **51**, 233 (1954–55).
5. S. Brunauer. Am. Scientist, **50**, No. 1, 210 (March, 1962).
6. S. Brunauer, D. L. Kantro, and L. E. Copeland. J. Am. Chem. Soc. **80**, 761 (1958).
7. E. P. Barrett, L. G. Joyner, and P. P. Halenda. J. Am. Chem. Soc. **73**, 373 (1951).
8. R. W. Cranston and F. A. Inkley. Advances in catalysis. Vol. IX. Academic Press Inc., New York, N.Y. 1957. p. 143.
9. L. E. Copeland and J. C. Hayes. ASTM Bull. No. 194, 70 (1953).
10. D. L. Kantro, S. Brunauer, and C. H. Weise. Advances in chemistry series. Vol. 33. American Chemical Society, Washington, D.C. 1961. p. 199.

11. J. H. DE BOER. *In* The structure and properties of porous materials. *Edited by* D. H. Everett and F. S. Stone. Academic Press, Inc., New York. 1958. p. 68.
12. L. E. COPELAND and E. G. SCHULZ. Journal of the PCA Research and Development Laboratories. **4**, No. 1, 2 (1962).
13. T. C. POWERS. Proc. of Fourth Int. Symp. on Chem. of Cement. Volume II. Nat. Bur. of Standards Monograph No. 43. 1962. p. 577.

PCA R & D. Ser. 1001–1.

Can. J. Chem. Downloaded from www.nrcresearchpress.com by 210.87.254.5 on 09/05/12
For personal use only.

THE CHROMIC ACID OXIDATION OF ARYL TRIFLUOROMETHYL ALCOHOLS: ISOTOPE AND SUBSTITUENT EFFECTS[1]

ROSS STEWART AND DONALD G. LEE[2]
Department of Chemistry, University of British Columbia, Vancouver, British Columbia
Received September 3, 1963

ABSTRACT

The mechanism of the chromic acid oxidation of eight aryltrifluoromethylcarbinols has been studied in acetic acid solution. Electron-donating substituents accelerate the reaction and a good correlation of rate with σ^+ values has been found. The rho value is -1.01. Deuterium isotope effects for the oxidation of five of these compounds have been determined and the magnitude of the isotope effect has been found to correlate inversely with the ease of oxidation of the alcohol.

The results are interpreted in terms of a unimolecular decomposition of the chromate ester of the alcohol.

Can. J. Chem. Downloaded from www.nrcresearchpress.com by 210.87.254.40 on 09/05/12
For personal use only.

Previous work in this laboratory showed that unusually large kinetic isotope effects were observed when a group of aryl trifluoromethyl alcohols ($ArCDOHCF_3$) were oxidized to ketones by alkaline permanganate (1, 2). The values of k_H/k_D of 16:1 found at 25° are more than double those expected for complete loss of the C—H (D) stretching mode in the transition state (3, 4). Since proton tunnelling did not seem to be the dominant factor in these and related reactions the anomalous isotope effects have been tentatively attributed to alterations in the C—H bending modes in the transition state. It was of interest, then, to determine if the unusual isotope effects observed in the permanganate oxidation also occur in the oxidation of these alcohols by chromic acid. A "normal" isotope effect of 6.6 at 25° was found for the chromic acid oxidation of isopropyl-*d* alcohol, $(CH_3)_2CDOH$ (5).

A great deal of work has been done in elucidating the mechanism of chromic acid oxidation of alcohols, particularly by Westheimer (5–10), Roček (11, 12), and Kwart (13–15) and their colleagues.

The work of Westheimer and his group on the oxidation of isopropyl alcohol can be summarized as follows: (*a*) the reaction is acid catalyzed with the rate being proportional to the first (or in some cases a higher) power of the hydrogen ion concentration (or h_0), (*b*) the reaction is much faster in acetic acid solution than in mineral acids of the same H_0 value, (*c*) the transition state is a monochromium, not a dichromium, species, (*d*) the C—H bond at the carbinol carbon is broken in the rate-controlling step. Chromate esters of alcohols are known to exist under the reaction conditions and the following mechanism, in which such an ester decomposes by proton loss to any available base (probably a water molecule), was put forward.

$$R_2CHOH + HCrO_4^- + 2H^+ \rightleftharpoons R_2CHOCrO_3H_2^+ + H_2O$$

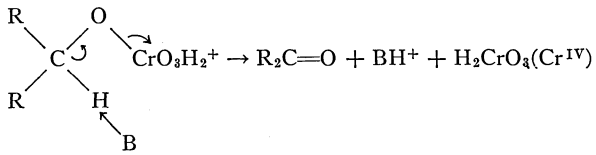

[1]*From part of the thesis presented by D. G. L. in partial fulfillment of the requirements for the Ph.D. degree, 1963.*
[2]*Present address: Camrose Lutheran College, Camrose, Alberta.*

Some elegant work on the induced oxidation of added substrates has traced the fate of the chromium (IV) intermediate formed in such reactions and which is eventually converted to chromium (III) (16, 17).

It has not proved possible to detect the participation of base in the rate-controlling step of the oxidation and this has led to other mechanisms being suggested. Furthermore, the Hammett reaction constant, rho, for the chromic acid oxidation of arylmethylcarbinols has a value of -1.01 (13) and this is not very easily reconciled with a rate-controlling proton abstraction from the α-carbon of the ester, even when the pre-equilibrium step is considered.

The effect of substituents on such a reaction has been elegantly illustrated by Buncel and Bourns (18) in their work on the decomposition of benzyl nitrate by ethoxide ions.

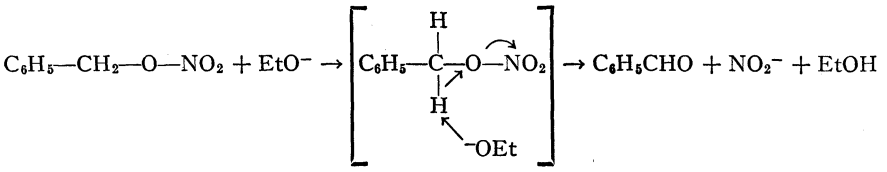

This reaction shows a deuterium isotope effect of 5.04 at 60° and a ^{15}N isotope effect of 1.0196 at 30° indicating that the carbon–hydrogen and the nitrogen–oxygen bonds are broken simultaneously in the course of the reaction. In this case it is evident that the hydrogen is being abstracted as a proton and the large positive rho value of $+3.40$ shows that the effect of substituents on the cleavage of the α-carbon–hydrogen bond is greater than on the more remote oxygen–nitrogen bond.

In subsequent papers in this series evidence will be presented in support of the idea that the chromate ester is a reactive intermediate which decomposes unimolecularly to products.

$$R_2CHOCrO_3H_2^+ \rightarrow R_2C{=}O + H_3CrO_3^+$$

The results presented herein are in accord with such a mechanism although they do not uniquely require it.

A unimolecular decomposition of the ester by an internal proton transfer has been previously suggested by Kwart and Francis (14) and the possibility of an internal hydride transfer has been noted by Littler (19). The relative merits of the cyclic and acyclic mechanisms have been discussed by Roček, Westheimer, Eschenmoser, Moldovanyi, and Schreiber (20) and by Stewart (21).

RESULTS AND DISCUSSION

The rates of oxidation of eight aryltrifluoromethylcarbinols have been determined at 25° in a 77.2% acetic acid solution containing 3.20 *M* perchloric acid. The deuterium isotope effects for five of these alcohols were also determined. The results are presented in Table I. A Hammett plot for both the protio and deuterio compounds is shown in Fig. 1. The σ^+ values were used since they gave a somewhat better correlation with the measured rate constants.

Attempts were made to determine the rates of oxidation of *p*-methoxyphenyltrifluoromethylcarbinol and β-naphthyltrifluoromethylcarbinol. Since the difference between σ and σ^+ values for the *p*-methoxy and the α-naphthyl group are greater than for any of the other groups they are most useful in differentiating between reactions which follow σ^+

Can. J. Chem. Downloaded from www.nrcresearchpress.com by 210.87.254.40 on 09/05/12
For personal use only.

TABLE I

Oxidation of fluoro alcohols in 77.2% acetic acid, 3.20 M $HClO_4$ ($H_0 = -2.82$), $T = 25°$ C, $[Cr^{VI}] = 1.79\times10^{-3}$ M

Alcohol	alc. ($M\times10^3$)	k_2 (l.moles^{-1} sec^{-1})	k_H/k_D
p-*t*-Butylphenyltrifluoromethylcarbinol	2.68	0.574	
	2.68	0.544	
p-Tolyltrifluoromethylcarbinol	2.68	0.534	
	2.68	0.537	
	2.68	0.564	
	2.68	0.540	
p-Tolyltrifluoromethylcarbinol-α-*d*	2.68	0.0727	7.40±0.20
	2.68	0.0740	
	2.68	0.0747	
	2.68	0.0706	
m-Tolyltrifluoromethylcarbinol	2.68	0.350	
	2.68	0.340	
Phenyltrifluoromethylcarbinol	2.68	0.259	
	2.68	0.250	
	15.3	0.258	
Phenyltrifluoromethylcarbinol-α-*d*	16.1	0.0310	8.53±0.15
	2.68	0.0294	
	2.68	0.0297	
p-Chlorophenyltrifluoromethylcarbinol	2.68	0.174	
	2.68	0.174	
m-Bromophenyltrifluoromethylcarbinol	2.68	0.119	
	2.68	0.106	
	2.68	0.110	
	2.68	0.109	
m-Bromophenyltrifluoromethylcarbinol-α-*d*	2.68	0.0117	9.80±0.20
	2.68	0.0111	
	20.8	0.0113	
m-Nitrophenyltrifluoromethyl carbinol	2.68	0.0494	
	2.68	0.0514	
	2.68	0.0484	
	14.06	0.0453	
	17.22	0.0444	
	15.96	0.0474	
m-Nitrophenyltrifluoromethylcarbinol-α-*d*	17.28	0.00360	12.20±.020
	18.69	0.00367	
3,5-Dinitrophenyltrifluoromethylcarbinol	17.65	0.0116	
	12.81	0.0118	
3,5-Dinitrophenyltrifluoromethylcarbinol-α-*d*	55.10	0.00100	12.93±0.78
	10.92	0.000834	

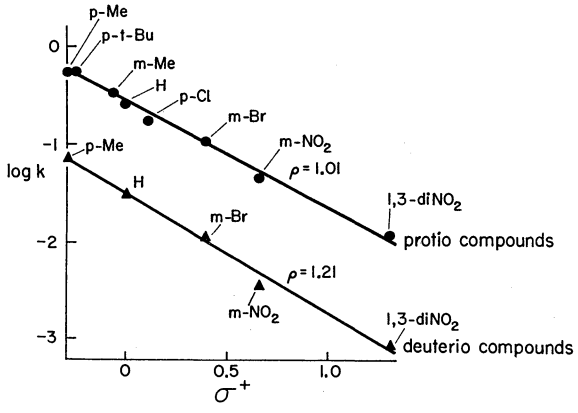

FIG. 1. A Hammett plot for the chromic acid oxidation of $ArCHOHCF_3$ and $ArCDOHCF_3$ in 77.2% acetic acid – 3.20 M perchloric acid.

Can. J. Chem. Downloaded from www.nrcresearchpress.com by 210.87.254.40 on 09/05/12
For personal use only.

values and those which follow σ values. Unfortunately both of these alcohols reduced chromium (VI) at a very fast rate in the medium used. This can be attributed to the oxidation of these compounds at sites other than the hydroxylated carbon since it was later found that both anisole and naphthalene were very rapidly oxidized under these conditions.

A rho value of -1.01 was calculated from the slope of the plot in Fig. 1. While other interpretations (6, 13) have been suggested for the negative rho values observed in the oxidation of alcohols by chromic acid the most direct explanation for any reaction exhibiting a negative ρ^+ value is that considerable positive charge is located on the α-carbon atom in the transition state. Further, the observation of very pronounced isotope effects demands that any proposed mechanism include as a rate-determining step, fission of the α-carbon–hydrogen bond.

The oxygen–hydrogen bond of the alcohol is probably not intact in the transition state (ethers are relatively inert to chromium (VI) (6)) nor being broken in the transition state (because of the positive solvent isotope effect observed in this reaction (6)). Westheimer's conclusion, then, that the chromate ester is a reactive intermediate in the oxidation, seems reasonable. The recent study by Roček, Westheimer, Eschenmoser, Moldovanyi, and Schreiber (20) of the chromic oxidation of a hindered alcohol lends further support to the ester being an intermediate in the oxidation. They found that the substrate isotope effect for the hindered alcohol vanished in concentrated acid, i.e. ester formation became rate controlling.

A unimolecular decomposition of the ester can be written in which the hydrogen is bonded in the transition state to both the alcoholic carbon atom and the oxygen atom attached to chromium.

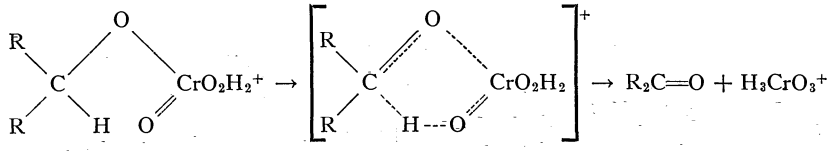

Kwart and Francis have written a similar transition state with the hydrogen being transferred as a proton (14). The question of electron flow in a cyclic transition state such as the above is a vexing one (22, 23) and we prefer to consider the conversion of ester to transition state in the following terms.

The transfer of electrons toward the chromium occurs by formation of carbon–hydrogen–oxygen bonds in the transition state as well as carbon–oxygen–chromium bonds, i.e. partly occupied orbitals are used to bind the transferred hydrogen to both carbon and oxygen in the transition state. The developing carbonyl group in the electron-deficient transition state will be stabilized by electron-donating substituents and this presumably accounts for the negative rho value. (See however Ref. 15.) Protonation of the chromate portion of the ester also increases the reaction rate. The conversion of ester to transition state is thus aided by the combined polarizing effects of an electron-donating aromatic ring and an electron-withdrawing metal cation.

An approximately linear relationship exists between the rates of oxidation of trifluoromethylcarbinols and the observed isotope effects. This relationship, which is illustrated in Fig. 2, fits in well with the suggestion, first made by Wiberg (3), that there should be a general correlation between rates and isotope effects within a group of analogous reactions, slow rates being accompanied by large isotope effects. Wiberg based his predictions on the

Can. J. Chem. Downloaded from www.nrcresearchpress.com by 210.87.254.40 on 09/05/12
For personal use only.

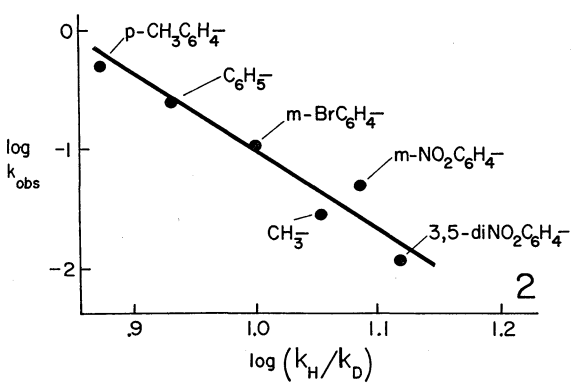

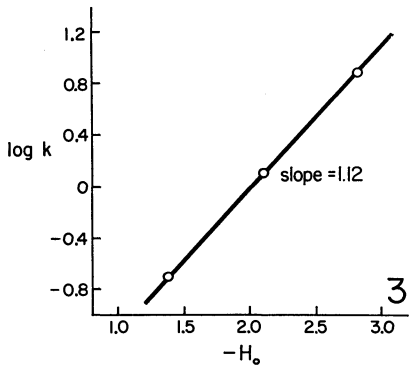

FIG. 2. The variation of isotope effect with rate constant for the chromic acid oxidation of $ArCHOHCF_3$.
FIG. 3. Variation of rate with acidity for the oxidation of phenyltrifluoromethylcarbinol in 77.2% acetic acid.

experimental observation that the isotope effects in the side-chain halogenation of para-substituted toluenes varied from 3.22 to 5.11 at 77°. Since the largest of these isotope effects is somewhat smaller than the maximum effect predicted from a consideration of zero-point energies of the carbon–hydrogen and carbon–deuterium bonds, the variation with rate was explained in terms of factors which could be related to C—H stretching frequencies (3, 24, 25).

In the present case, however, even the smallest isotope effect observed is larger than the maximal effect predicted from a consideration of carbon–hydrogen stretching frequencies. While it is not clear from the present results whether the large isotope effects are due to loss of bending frequencies in the transition state or to a tunnel effect it is interesting to note that a correlation between rate and isotope effect still exists. Such a correlation was not observed by Stewart and Van der Linden (1, 2) in the permanganate oxidation of these alcohols since the rho value for that reaction was almost zero. It does appear, however, that large isotope effects are intimately connected with the trifluoromethyl group or at least with the presence of strongly electron-withdrawing groups adjacent to the site of oxidation. (It should be pointed out here that in the chromic acid oxidation of fluorinated *aliphatic* alcohols a similar situation exists, i.e. the slower the oxidation rate (the more highly fluorinated the alcohol) the higher the isotope effect, with an important exception. 1,1,1,3,3,3-Hexafluoro-2-propanol is oxidized very slowly but its 2-deuterio derivative does not appear to show an anomalously large isotope effect (26).)

The rate of oxidation of phenyltrifluoromethylcarbinol was determined at three different acidities and was found to be linear with h_0 as indicated by the plot in Fig. 3. The acidity data reported in Table II were obtained by a comparative method using *p*-nitrodiphenylamine and 4-chloro-2-nitroaniline as indicators. (The pK_a's of these indicators were assumed to be −2.48 and −1.03 respectively (27).) This observed linearity with h_0, although based on three points only, is in accord with the rate law observed for the oxidation of isopropyl alcohol (9) and benzaldehyde (28) in acetic acid.

$$v = k[R_2CHOH][HCrO_4^-]h_0$$

The rho value observed for the oxidation of the aryltrifluoromethylcarbinols is also identical with the value observed for the corresponding oxidation of arylmethylcarbinols in acetic acid (13) and it is probable that they are oxidized via the same reaction path.

Can. J. Chem. Downloaded from www.nrcresearchpress.com by 210.87.254.40 on 09/05/12
For personal use only.

TABLE II

Variation in rate of oxidation of phenyltrifluoromethylcarbinol in 77.2% acetic acid with H_0

$HClO_4(M)$	H_0	k_2
3.20	−2.82	0.259
3.20	−2.82	0.250
3.20	−2.82	0.258
2.47	−2.12	0.0433
2.47	−2.12	0.0440
1.83	−1.40	0.0059
1.83	−1.40	0.0066

EXPERIMENTAL

Reagents

Many of the fluoro alcohols had previously been synthesized in this laboratory (2, 29). During the present investigation several of these compounds were resynthesized and good agreement with all the reported physical constants was found except in the case of *m*-nitrophenyltrifluoromethylcarbinol where the melting point was found to be 51–52° instead of the reported 47–48°. The preparation of other alcohols which were synthesized specially for this investigation are given below.

m-Tolyltrifluoromethylcarbinol

m-Bromotoluene (Eastman Organic Chemicals) (49 g, 0.286 mole) and magnesium (7 g, 0.286 mole) were converted to the Grignard reagent under anhydrous conditions. Then trifluoroacetic acid (10.5 g, 0.092 mole) in 25 ml of ether was added dropwise over a period of 2 hours. After refluxing for 1 hour the complex was decomposed in 10% sulphuric acid. The product (*m*-tolyltrifluoromethyl ketone) was extracted from the aqueous solution with ether, dried over anhydrous magnesium sulphate, and distilled. B.p. 58° at 8 mm. Yield: 8.5 g, 49%. ν_{max} (liq) 1717 cm^{-1} (C=O).

This ketone (6.0 g, 0.032 mole) was dissolved in 20 ml of dry ether and lithium aluminum hydride (0.38 g, 0.01 mole) in 20 ml of dry ether was added slowly under anhydrous conditions. After refluxing for 1 hour the complex was decomposed with dilute sulphuric acid and the product was extracted with ether, washed with water, and dried over anhydrous magnesium sulphate. Distillation yielded 3.5 g (57%) of *m*-tolyltrifluoromethylcarbinol. B.p. 95° at 14 mm. (Found: C, 57.0%; H, 3.6%. $C_9H_7OF_3$ requires: C, 57.4%; H, 3.7%.)

p-tert-Butylphenyltrifluoromethylcarbinol

Starting from *p-tert*-butylbromobenzene *p-tert*-butylphenyltrifluoromethylcarbinol (m.p. 75.0–75.5°) was prepared by the same procedure used to synthesize *m*-tolyltrifluoromethylcarbinol. (Found: C, 61.6%; H, 6.13%. $C_{12}H_{15}OF_3$ requires: C, 62.0%; H, 6.52%.)

β-Naphthyltrifluoromethylcarbinol

Magnesium (2.4 g, 0.1 mole) was placed in a flame-dried three-necked flask fitted with two dropping funnels, a reflux condenser, and a magnetic stirrer. Methyl iodide (0.5 g) dissolved in 10 ml of dry ether was added through the first funnel and after the reaction had started β-bromonaphthalene (13 g, 0.063 mole) dissolved in 50 ml of dry ether was added slowly. The mixture was refluxed for ½ hour after which 100 ml of dry ether was added. This was followed by the dropwise addition of trifluoroacetic acid (1.82, g 0.016 mole) dissolved in 20 ml of dry ether. After the addition was complete the solution was refluxed for 2 hours and then decomposed with cold dilute sulphuric acid, extracted with ether, and dried. The product (β-naphthyltrifluoromethyl ketone) was distilled under reduced pressure (b.p. 88° at 1.1 mm) and crystallized from low boiling petroleum ether. ν_{max} ($CHCl_3$) 1706 cm^{-1} (C=O). Yield: 5.0 g, 0.013 mole, 80%.

This ketone (2.5 g, 0.011 mole) was reduced with lithium aluminum hydride (0.25 g, 0.0066 mole), yielding, after recrystallization from petroleum ether, a fine white crystalline compound. M.p. 83–84°. A mixed melting point with naphthalene gave a depression of 20°. (Found: C, 63.4%; H, 3.64%. Required for $C_{12}H_9OF_3$: C, 63.76%; H, 4.01%.)

p-Chlorophenyltrifluoromethylcarbinol

Starting from 1-bromo-4-chlorobenzene *p*-chlorophenyltrifluoromethylcarbinol (b.p. 117–119° C at 22 mm) was prepared by the same procedure used to synthesize *m*-tolyltrifluoromethylcarbinol. (Found: C, 44.9%; H, 2.63%. Required for $C_8H_6OF_3Cl$: C, 45.6%; H, 2.87%.)

m-Nitrophenyltrifluoromethylcarbinol-α-d

m-Nitrophenyltrifluoromethyl ketone (29) was reduced with lithium diethoxyaluminodeuteride using the procedure developed by Brown and Tsukamoto (30). This produced a brown oil which distilled at 122° at

Can. J. Chem. Downloaded from www.nrcresearchpress.com by 210.87.254.40 on 09/05/12
For personal use only.

0.4 mm. This product was recrystallized several times from benzene and petroleum ether to give pale yellow crystals. M.p. 51.5–52.5°. (Found: C, 43.1%; H, 2.00%; N, 6.28%. Required for $C_8H_5DNO_3F_3$: C, 43.2%; H, 2.72%; N, 6.32%.)

3,5-Dinitrophenyltrifluoromethylcarbinol

Fuming nitric acid (sp. gr. 1.15) was added dropwise to a stirred solution of trifluoroacetophenone (Columbia Organic Chemicals) (38.4 g, 0.216 mole) in 150 ml of concentrated sulphuric acid. External cooling was applied to maintain a temperature of 60–80° during the addition. The mixture was then heated on a steam bath for 4 hours. This was followed by cooling and the addition of another 40 ml of fuming nitric acid. The mixture was again heated on a steam bath for 4 hours and finally at 130–150° for 4 hours. The reaction mixture was then poured into crushed ice and extracted with ether. The ethereal extract was dried over anhydrous magnesium sulphate and evaporated leaving a yellow oil which was distilled under reduced pressure. The distillation yielded 2 g forerun, 10.6 g *m*-nitrophenyltrifluoromethyl ketone (b.p. 90° at 0.95 mm) and 3,5-dinitrophenyltrifluoromethyl ketone (b.p. 120–127 at 0.95 mm) (32.4 g, 0.123 mole, 57%). ν_{max} (film) 1733 cm^{-1} (C=O). Hydrolysis of this compound with dilute sodium hydroxide yielded 3,5-dinitrobenzoic acid (m.p. 203–205°, lit. 204–205°).

Attempted recrystallization of the crude 3,5-dinitrophenyltrifluoromethyl ketone from most common solvents such as ether, petroleum ether, and chloroform yielded a stable white solid which showed no carbonyl band in the infrared, but exhibited peaks at 3490 and 3270 cm^{-1} (m.p. = 85.0–85.5°). It was concluded that this compound was 3,5-dinitrophenyltrifluoromethyl ketone hydrate. (Found: C, 32.52%; H, 2.13%; N, 9.22%. Required for $C_8H_5N_2O_6F_3$: C, 34.01%; H, 1.78%; N, 9.94%.) The analysis is hardly satisfactory, however, and despite the sharp melting point the compound may be impure. The N.M.R. spectra is consistent with the hydrate assignment as is the facile hydrolysis to 3,5-dinitrobenzoic acid which occurs in dilute sodium hydroxide.

Dehydration of 3,5-dinitrophenyltrifluoromethyl ketone hydrate by phosphorous pentoxide at 50° yielded the corresponding ketone (m.p. 77–78°). ν_{max} ($CHCl_3$) 1737 cm^{-1} (C=O). (Found: C, 35.8%; H, 1.28%; N, 10.27%. Required for $C_8H_3N_2O_5F_3$: C, 36.4%; H, 1.14%; N, 10.60%.)

Recrystallization of the crude 3,5-dinitrophenyltrifluoromethyl ketone from ethanol yielded a white crystalline compound (m.p. 70–71°) which showed no absorption in the carbonyl region of the infrared spectra nor any in the region from 3200 to 3500 cm^{-1}, where the hydrate absorbs. (Found: C, 29.85%; H, 1.53%; N, 10.96%; O, 26.35%; F, 0.00%; m.w. = 243.) This compound was resistant to basic hydrolysis and as yet its exact structure has not been determined.

3,5-Dinitrophenyltrifluoromethylcarbinol was prepared from crude 3,5-dinitrophenyltrifluoromethyl ketone by reduction with lithium tri-*t*-butoxyaluminohydride in diglyme (31). Distillation of the yellow oil which resulted from this reaction yielded 3,5-dinitrophenyltrifluoromethylcarbinol (b.p. 108–174° at 8 mm) (9.2 g, 63%). This product was further purified by recrystallization from carbon tetrachloride. The resulting fine white crystalline compound gave an infrared spectrum similar to *m*-nitrophenyltrifluoromethylcarbinol and a nuclear magnetic resonance spectrum consistent with the assumed structure (m.p. 76–77°). (Found: C, 36.16%; H, 1.72%; N, 10.54%. Required for $C_8H_3N_2O_5F_3$: C, 36.10%; H, 1.89%; N, 10.53%.)

3,5-Dinitrophenyltrifluoromethylcarbinol-α-d

This compound was prepared by the reduction of 3,5-dinitrophenyltrifluoromethyl ketone with lithium tri-*t*-butoxyaluminodeuteride as described above (m.p. 76.8°). (Found: C, 36.07%; H, 1.78%; N, 10.78%. Required for $C_8H_2DN_2O_5F_3$: C, 36.00%; H, 1.89%; N, 10.50%.) The nuclear magnetic resonance spectrum was also consistent with the assignment of this structure.

Kinetic Methods

Oxidation rates were obtained by following the disappearance of Cr^{VI}. A plot of the reciprocal of [Cr^{VI}] against time yielded the second-order rate constant directly.

Good straight line plots to at least 70% completion were obtained for all rate constants reported (Fig. 4).

Typical kinetic runs were carried out as follows: 50 ml of a 4.035×10^{-3} *M* acetic acid solution of phenyltrifluoromethylcarbinol was mixed with 20 ml of 71% perchloric acid and thermostated at 25.0±0.1° for 10 minutes. A fast-delivery pipette was then used to add 4.94 ml of 0.01361 *M* potassium dichromate to this solution and 4.92 ml aliquots were withdrawn at intervals. The aliquots were quenched by adding them to 15 ml of 5% sodium bicarbonate solution containing a large excess of potassium iodide. Two milliliters of 6 *M* sulphuric acid was added and the solution was set aside to develop for 3 minutes. The iodine formed was then titrated with standardized thiosulphate using Thyodene as an indicator.

The magnitude of the equilibrium constant in dilute aqueous solutions is such that the amount of chromium in the bichromate form is appreciable only at fairly high concentrations and Westheimer has observed that in dilute solutions (0.0005–0.005 *M*) the rate is proportional to the gross Cr^{VI} concentration (10). Although no further investigation of this equilibrium was conducted during the present work, an attempt to minimize any deviations arising from this effect was made by using concentrations of Cr^{VI} that were always lower than 0.005 *M* and in cases where rates were used for comparison purposes attempts were made to keep the Cr^{VI} concentration constant throughout the whole series.

Product Analysis

It is well known that chromic acid oxidizes most secondary alcohols smoothly to the corresponding ketones with little or no carbon–carbon bond fission (10; see, however, ref. 32). Since the concentration of

Can. J. Chem. Downloaded from www.nrcresearchpress.com by 210.87.254.40 on 09/05/12
For personal use only.

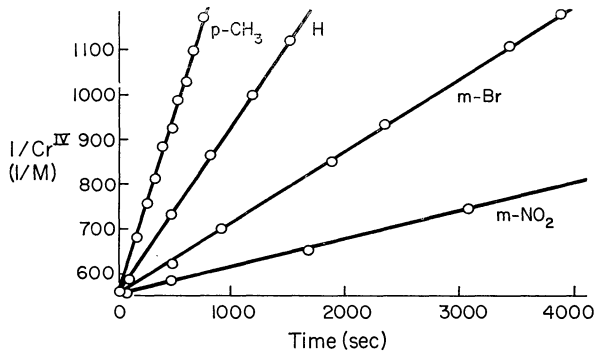

FIG. 4. Typical second-order rate plots for the oxidation of aryltrifluoromethylcarbinols in 77.2% acetic acid.

reactants was low in all of the kinetic experiments conducted in this investigation, it was found to be extremely difficult to isolate and identify the products of these reactions. However, when the concentrations of the reactants were increased to a preparative scale it was found that the aromatic alcohols gave almost quantitative yields of the corresponding ketones. The good second-order rate plots obtained also indicate that few side reactions are taking place.

ACKNOWLEDGMENT

The financial support of the National Research Council is gratefully acknowledged.

REFERENCES

1. R. STEWART and R. VAN DER LINDEN. Discussions Faraday Soc. **29**, 211 (1960).
2. R. STEWART and R. VAN DER LINDEN. Tetrahedron Letters, **2**, 28 (1960). See also R. STEWART and M. M. MOCEK. Can. J. Chem. **41**, 1160 (1963).
3. K. B. WIBERG. Chem. Rev. **55**, 713 (1955).
4. L. MELANDER. Isotope effects on reaction rates. Ronald Press, New York. 1960. pp. 21–22.
5. A. LEO and F. H. WESTHEIMER. J. Am. Chem. Soc. **74**, 4383 (1947).
6. R. BROWNELL, A. LEO, Y. W. CHANG, and F. H. WESTHEIMER. J. Am. Chem. Soc. **82**, 406 (1960).
7. G. T. E. GRAHAM and F. H. WESTHEIMER. J. Am. Chem. Soc. **80**, 3030 (1958).
8. F. HOLLOWAY, M. COHEN, and F. H. WESTHEIMER. J. Am. Chem. Soc. **73**, 65 (1951).
9. M. COHEN and F. H. WESTHEIMER. J. Am. Chem. Soc. **74**, 4387 (1952).
10. F. H. WESTHEIMER. Chem. Rev. **45**, 419 (1949).
11. J. ROČEK and J. KRUPICKA. Collection Czech. Chem. Comm. **23**, 2068 (1958).
12. J. ROČEK. Collection Czech. Chem. Comm. **25**, 1052 (1960).
13. H. KWART and P. S. FRANCIS. J. Am. Chem. Soc. **77**, 4709 (1955).
14. H. KWART and P. S. FRANCIS. J. Am. Chem. Soc. **81**, 2116 (1959).
15. H. KWART. Suomen Kemistilehti, A, **34**, 173 (1961).
16. W. WATANABE and F. H. WESTHEIMER. J. Chem. Phys. **17**, 61 (1949).
17. K. B. WIBERG and R. J. EVANS. Tetrahedron, **8**, 313 (1960).
18. E. BUNCEL and A. N. BOURNS. Can. J. Chem. **38**, 2457 (1960).
19. J. S. LITTLER. J. Chem. Soc. 2190 (1962).
20. J. ROČEK, F. H. WESTHEIMER, A. ESCHENMOSER, L. MOLDOVANYI, and J. SCHREIBER. Helv. Chim. Acta, **45**, 2554 (1962).
21. R. STEWART. Oxidation mechanisms: applications to organic chemistry. W. A. Benjamin, Inc., New York. 1963.
22. C. K. INGOLD. Structure and mechanism in organic chemistry. Cornell University Press, Ithaca, N.Y. 1953. p. 596.
23. C. G. SWAIN, R. F. W. BADER, R. M. ESTEVE, JR., and R. N. GRIFFIN. J. Am. Chem. Soc. **83**, 1951 (1961).
24. F. H. WESTHEIMER. Chem. Rev. **61**, 265 (1961).
25. E. R. THORNTON. J. Org. Chem. **27**, 1943 (1962).
26. D. G. LEE and R. STEWART. To be published.
27. M. A. PAUL and F. A. LONG. Chem. Rev. **57**, 1 (1957).
28. K. B. WIBERG and T. MILL. J. Am. Chem. Soc. **80**, 3022 (1958).
29. R. STEWART and R. VAN DER LINDEN. Can. J. Chem. **38**, 399 (1960).
30. H. C. BROWN and A. TSUKAMOTO. J. Am. Chem. Soc. **81**, 502 (1959).
31. H. C. BROWN and B. C. SUBBA RAO. J. Am. Chem. Soc. **80**, 5377 (1958).
32. J. HAMPTON, A. LEO, and F. H. WESTHEIMER. J. Am. Chem. Soc. **78**, 306 (1956).

Can. J. Chem. Downloaded from www.nrcresearchpress.com by 210.87.254.40 on 09/05/12
For personal use only.

PHOSPHONITRILIC COMPOUNDS

PART I. THE MECHANISM OF PHOSPHONITRILIC CHLORIDE POLYMERIZATION CAPACITANCE, CONDUCTANCE, AND ELECTRON-SPIN RESONANCE STUDIES[1]

H. R. Allcock and R. J. Best
Central Research Division, American Cyanamid Company, Stamford, Connecticut
Received September 11, 1963

ABSTRACT

Capacitance and conductance measurements were carried out with molten $(NPCl_2)_3$ and $[NP(OC_6H_5)_2]_3$ and dipole moments were determined in benzene solution. Attempts to detect free radicals in molten samples of the same compounds were unsuccessful. Evidence was obtained that homolytic or heterolytic phosphorus–nitrogen ring cleavage is not involved in the primary initiation process. The results favor, instead, a polymerization mechanism for $(NPCl_2)_3$ in which phosphorus–chlorine ionization is a preliminary step.

INTRODUCTION

Phosphonitrilic chloride trimer, $(NPCl_2)_3$, (I) and tetramer, $(NPCl_2)_4$, (II) polymerize at temperatures between 200 and 300° C to yield a series of higher polymers which include linear oils and elastomers, $(NPCl_2)_n$, (III) (1–11). The higher polymers produced by this process are believed to have molecular weights in excess of 100,000 (2).

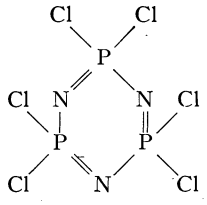

(I)

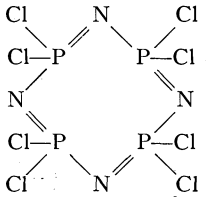

(II)

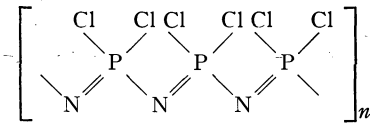

(III)

A similar behavior has been reported for phosphonitrilic fluorides and bromides (12–15). However, if phosphonitrilic chloride high polymer is heated above a temperature of 300 to 350° C, the material depolymerizes to low molecular weight oligomers which include the trimer (I) and tetramer (II). Under suitable conditions, a complete reversal of polymerization can be effected (5, 16, 17). By contrast, other phosphonitrilic compounds do not undergo polymerization–depolymerization reactions of this type (18). For example, the phenoxy derivative, $[NP(OC_6H_5)_2]_3$, does not polymerize to linear polymers at high temperatures and shows a high resistance to thermal degradation (19, 20).

Several authors have investigated the polymerization reactions of phosphonitrilic chlorides (4–10) but the different interpretations of the results have given rise to conflicting opinions concerning the reaction mechanism. In this paper, the polymerization mechanism is discussed in the light of capacitance, conductance, and electron-spin resonance experiments.

EXPERIMENTAL

Phosphonitrilic Chloride

Phosphonitrilic chloride trimer (Hooker Chemical Company) was recrystallized twice from reagent grade *n*-heptane and was then exhaustively dried in a vacuum oven at 60° C to give material having a melting

[1]*Presented at the Symposium on Inorganic Polymers held at the University of Western Ontario, September 4–6, 1963.*

Can. J. Chem. Downloaded from www.nrcresearchpress.com by 210.87.254.40 on 09/05/12
For personal use only.

point of 113–114° C. Subsequent purification was effected by sublimation to yield a product with a melting point of 114° C. Zone refining was also used to purify 55×0.7 cm columns of the material. After 17 passes using a Fisher zone refiner, the melting point was 114–114.5° C.

Phosphonitrilic Diphenoxide Trimer

The compound $[NP(OC_6H_5)_2]_3$ was prepared by a route similar to that reported previously (19, 20). A solution of sodium phenoxide in tetrahydrofuran (500 ml) was prepared from phenol (84.6 g) and sodium (20.7 g) in an atmosphere of dry argon. To this stirred solution was added a solution of phosphonitrilic chloride trimer (52.2 g) in tetrahydrofuran (500 ml). The mixture was then refluxed for 8 hours and was allowed to stand at 25° C for a total of 56 hours. Filtration of the mixture yielded sodium chloride (55 g); evaporation of the filtrate and precipitation of the residue from acetone into a large excess of water yielded 88.5 g of a material having a melting point of 106–109° C. The product was then recrystallized twice from *n*-heptane and *n*-heptane–benzene mixtures, and was exhaustively dried in a vacuum oven at 60° C to yield phosphonitrilic diphenoxide trimer (83.2 g, 93%), m.p. 112–112.5° C. Found: C, 62.32; H, 4.47; N, 6.04; P, 13.61%. $C_{36}H_{30}N_3P_3O_6$ requires: C, 62.5; H, 4.34; N, 6.07; P, 13.42%. The molecular weight by cryoscopy in naphthalene was 702, and by mass spectrometry was 693. (Theory = 693.)

Electron-Spin Resonance Measurements

Electron-spin resonance measurements were performed using a Varian V 4500 spectrometer with a modulation frequency of 100 kc. The samples were contained in quartz tubes (4 mm outside diameter), and were heated at temperatures up to 250° C using standard Varian accessories. Experiments were carried out with the samples either exposed to air or in vacuum.

Conductance and Capacitance Measurements

The bridge used for the capacitance and conductance measurements was based on a design by Cole (21). It consisted essentially of a Wheatstone bridge with a closely coupled pair of secondary transformer windings used as the ratio arms. Balancing was achieved by the use of a low-inductance Helipot and a switching arrangement to include any one of five accurate resistors on the measuring side. The capacitance was balanced with one of two General Radio standard variable capacitance boxes, No. 722 CC or No. 722 MD. The bridge was supplied with an a-c. signal from a Hewlett–Packard oscillator, No. 200CD/CDR, and the signal from the bridge was amplified by a Rohde and Schwarz tunable indicating amplifier, type UBM BN 12121/2, and was displayed on a Hickok oscilloscope, model 387R. The frequency range of this assembly was 50 c.p.s. to 400 kc, the conductance range was 5×10^{-10} to 5×10^{-3} mho cm, and the capacitance range was from 0 to 1100 $\mu\mu$f in two ranges.

The dielectric cells were Balsbaugh liquid sample holders, one with an interplate air capacitance of 51.790 $\mu\mu$f and the other with a capacitance of 18.48 $\mu\mu$f. The respective cell constants were 0.001710 and 0.004791. During the measurements the samples were in contact with the Monel electrodes and with the Pyrex glass of the cell. An atmosphere of dry argon was maintained above the sample throughout the experiments by passage of a slow stream of the gas (Linde) through a liquid-nitrogen cooled cold trap which contained dry silica gel, before passage through the dielectric cell. The exhaust gas was then passed through a second trap, and was released into the atmosphere through a mineral oil bubbler. Sublimation of $(NPCl_2)_3$ was noticeable at the higher temperatures, and sufficient vapor was present in the dry gas stream to cause test papers to indicate acidity. The cells were contained in an aluminum block which could be heated electrically up to a temperature of 360° C. During the measurements, the cell temperature was held to within ±0.5° C.

At the beginning of each experiment the crystalline material was placed in the cell and air was removed by a stream of argon. The temperature was then raised to the melting point. Capacitance and conductance measurements were taken at progressively increased temperatures, and also as the temperature was subsequently lowered. With $(NPCl_2)_3$, four successive experiments were performed with recrystallized and zone-refined starting material, different cells, and, in one case, after replacement of the Monel by platinum electrodes. Reproducible results were obtained from these runs. Dielectric constants were then calculated from the air capacitance, benzene capacitance, and the capacitance of the sample.

Dipole Moments

The dielectric constant values of the samples at 120° C over the frequency range 1 kc to 50 kc, were used to calculate dipole moments by the Onsager equation. The refractive indices were determined by comparison with a set of standard glass powders at temperatures from 110° C to 130° C. Densities were determined in a 10 ml graduated cylinder held at 120° C in an aluminum block.

Dielectric constant values were also determined for 4%, or less than 4%, solutions of the two compounds in benzene at 30° C and 70° C and at 1 kilocycle frequency. The refractive indices and weight fractions of the solutions were then used to calculate dipole moments by means of the Guggenheim equation.

RESULTS

Electron-Spin Resonance Measurements

No electron-spin resonance was observed for purified $(NPCl_2)_3$ and $[NP(OC_6H_5)_2]_3$ between 25° C and 250° C in air or in vacuum. Under the same conditions, radicals could

Can. J. Chem. Downloaded from www.nrcresearchpress.com by 210.87.254.40 on 09/05/12
For personal use only.

be detected readily in liquid sulphur, which also undergoes a ring-chain equilibrium (22). This indicated the absence of free-radical species in the molten phosphonitrilic compounds under these conditions.

However, samples of $[NPCl_2]_3$ which had been purified by recrystallization only gave spurious resonances below $g = 2$. These peaks were attributed to trace amounts of transition metals. Sublimed samples of $[NPCl_2]_3$ did not behave in this way.

Capacitance Measurements

(a) $(NPCl_2)_3$

The dielectric constant of $(NPCl_2)_3$ did not change as the temperature was raised from the melting point (114° C) to 203° C. (The small decrease in dielectric constant shown in Table I can be explained solely by thermal expansion of the liquid.) However, as the temperature was raised from 203° C to 253° C, through the temperature range where polymerization becomes important, the dielectric constant rose rapidly. When the temperature was maintained at 253° C, the dielectric constant continued to increase slowly with time. Moreover, the value continued to rise as the cell temperature was lowered to 202° C, by an extent which could not be explained by thermal contraction or by a time lag in the cooling of the reaction mixture. As the temperature was elevated initially from 114° to 253° C, the dielectric constant was independent of frequency from 1 to 100 Kc. However, during the period of continuous dielectric constant increase with time at 202° C, and on cooling to 164° C, the capacitance decreased slightly as the frequency was raised from 1 to 50 Kc.

TABLE I

Capacitance measurements for $(NPCl_2)_3$ and $[NP(OC_6H_5)_2]_3$

$(NPCl_2)_3$		$[NP(OC_6H_5)_2]_3$	
Temp., °C	Dielectric constant	Temp., °C	Dielectric constant
120	2.71±0.02	120	4.32
163	2.61	163	4.11
203	2.52	203.5	3.79
253	2.56–3.29*	252	3.55
202	3.92–4.05*	163	4.11
		139	4.17
		350	3.18
		120	4.35

*The dielectric constant rose continuously with time.

(b) $[NP(OC_6H_5)_2]_3$

The variation of dielectric constant with temperature for molten $[NP(OC_6H_5)_2]_3$ is also shown in Table I. Over a temperature range of 120° C to 350° C, a small decrease in dielectric constant occurred. This behavior was completely reversible when the temperature was lowered again, and could be accounted for entirely by the change in volume of the liquid due to thermal expansion and contraction.

Conductance Measurements

(a) $(NPCl_2)_3$

The variation of conductance with temperature for phosphonitrilic chloride trimer was complex, as shown by the data in Table II. The compound had a low conductance from 114° to 203° C, although above this temperature both the a-c. and d-c. conductance rose rapidly with temperature. At 253° C the conductance also showed a continuous increase

Can. J. Chem. Downloaded from www.nrcresearchpress.com by 210.87.254.40 on 09/05/12
For personal use only.

TABLE II

Conductance measurements (mho $cm^{-1} \times 10^{11}$) for $(NPCl_2)_3$ and $[NP(OC_6H_5)_2]_3$

$(NPCl_2)_3$		$[NP(OC_6H_5)_2]_3$	
Temp., °C	Conductance	Temp., °C	Conductance
120	1.7–0.1	120	1.5
163	1.7	165	3.5
203	33	203.5	4.3
253	6250*	252	17.7
202	2900*	163.5	4.8
		139	2.4
		350	316.0
		120	17.7

*The conductance rose continuously with time.

with time. The conductance fell slightly when the temperature was reduced to 202° C, but did not return to its original value at this temperature. Direct-current conductance measurements were taken simultaneously with the a-c. determinations and agreed satisfactorily with the a-c. values. The d-c. conductance decreased steadily when the current was maintained, a result which indicated a migration of charge carriers and a polarization at the electrodes.

(b) $[NP(OC_6H_5)_2]_3$

Conductance data for $[NP(OC_6H_5)_2]_3$ is also shown in Table II. Elevation of the temperature from 120° C to 252° C resulted in a small increase in conductance. This fivefold increase was approximately 400 times less than that observed with phosphonitrilic chloride trimer and was reversible when the sample was cooled. This behavior can probably be explained by increased solvation or ionic mobility at the higher temperatures. However, when the sample was heated to 350° C, about a 200-fold increase in conductance occurred. This increase was not completely reversible when the temperature was lowered to 120° C, and must be attributed to a decomposition at 350° C not connected with a polymerization process. Even so, the permanent increase in conductance at this temperature was considerably less than that observed with the chloro compound at 252° C.

Dipole Moments

The densities and refractive indices of the two compounds at 120° C were: $(NPCl_2)_3$, $d = 1.6891$, $n_D = 1.525$; $[NP(OC_6H_5)_2]_3$, $d = 1.2104$, $n_D = 1.564$. These values were used in conjunction with the dielectric constants to solve the Onsager equation for the dipole moment at this temperature. These values and the solution dipole moments are shown in Table III.

TABLE III

Dipole moments of $[NPCl_2)_3$ and $[NP(OC_6H_5)_2]_3$

Compound	Phase	Temp., °C	Dipole moment (D)
$(NPCl_2)_3$	Melt	120	0.98±0.2*
"	Benzene	70	0.92±0.1†
"	Benzene	30	0.83±0.1†
$[NP(OC_6H_5)_2]_3$	Melt	120	3.00*
"	Benzene	70	3.28†
"	Benzene	30	2.84†

*Onsager calculation.
†Guggenheim calculation.

Can. J. Chem. Downloaded from www.nrcresearchpress.com by 210.87.254.40 on 09/05/12
For personal use only.

DISCUSSION

An understanding of the polymerization and depolymerization reactions of phosphonitrilic halides must take into account the unique structural and bonding characteristics of this system. Phosphonitrilic chloride trimer, tetramer, and polymer have been studied by X-ray and electron diffraction (23–28). The trimer exists as an almost planar six-membered ring, the tetramer as a puckered eight-membered ring, and the polymer as a linear chain which is arranged in the form of a helix. Other homologues, such as the pentamer and higher oligomers, exist as puckered ring or chain structures (29). Structural determinations indicate that the N—P—N and P—N—P bond angles are not significantly different in the trimer, tetramer, and polymer (about 120°) (23–28). The N—P bond lengths are also similar in the three derivatives (about 1.6 Å) (23–28). It is probable therefore, that in the phosphonitrilic series, no marked steric advantage to the system occurs by polymerization or depolymerization. This contrasts markedly with other inorganic polymer systems such as organosiloxanes, borazoles, and silicon–nitrogen compounds, where the preferred steric arrangement of the six- or eight-membered ring thermodynamically favors these species relative to the higher polymers. Furthermore, the existence of $d\pi$–$p\pi$ bonding between the phosphorus and nitrogen atoms in these compounds (30, 31) implies that changes in ring or chain size and planarity do not appreciably influence the stability of the system.

Polymerization and depolymerization may be different aspects of the same thermal equilibration process. Heating of the lower oligomers or the higher polymers would result in the establishment of a statistical equilibrium to give a range of species with degrees of polymerization between 3 and about 1500. If such a mixture is heated at high temperature under conditions where the lower molecular weight species are volatilized and removed, more of these oligomers will be formed by equilibration of the system. Thus, in time, removal of the more volatile components will effect a general depolymerization. Some evidence has been reported in favor of such a process (5, 7, 8, 11, 17).

Two types of mechanism have been proposed for the polymerization of cyclic phosphonitrilic chlorides. Patat and co-workers (6–8) described the reaction as a free-radical polymerization, in which the initiation step included a ring opening, phosphorus–nitrogen bond cleavage into a diradical or a stabilized resonance form. The free-radical reaction was reported to occur both in the presence and absence of oxygen, and with or without solvents. Konecny and coworkers (9, 10) and Gimblett (18) suggested an ionic mechanism which involved prior dissociation of a chloride ion from phosphorus. In theory, phosphonitrilic chloride trimer or tetramer could undergo a number of simple, reversible bond cleavage reactions. These are summarized in Fig. 1.

Reaction (*a*) involves a thermally induced homolytic phosphorus–nitrogen bond cleavage to form a diradical. This species could either revert to the starting material or combine with the cyclic trimer or other diradicals to form polymeric chains. Reaction (*b*) involves a heterolytic cleavage of a phosphorus–nitrogen bond. Polymerization of such species could involve ionic addition reactions. Reaction (*c*) involves dissociation of a chloride ion from phosphorus (either thermally or under the influence of a cation) followed either by heterolytic phosphorus–nitrogen ring cleavage of the unstable species formed, or by attack of this species on the starting material. It was considered likely that the results of the present work might distinguish between these possible steps.

The two compounds, $(NPCl_2)_3$ and $[NP(OC_6H_5)_2]_3$, were chosen for the present study for several reasons. Firstly, $(NPCl_2)_3$ polymerizes thermally to linear high polymers while, under the same conditions, $[NP(OC_6H_5)_2]_3$ is completely unaffected. Secondly, the

Can. J. Chem. Downloaded from www.nrcresearchpress.com by 210.87.254.40 on 09/05/12
For personal use only.

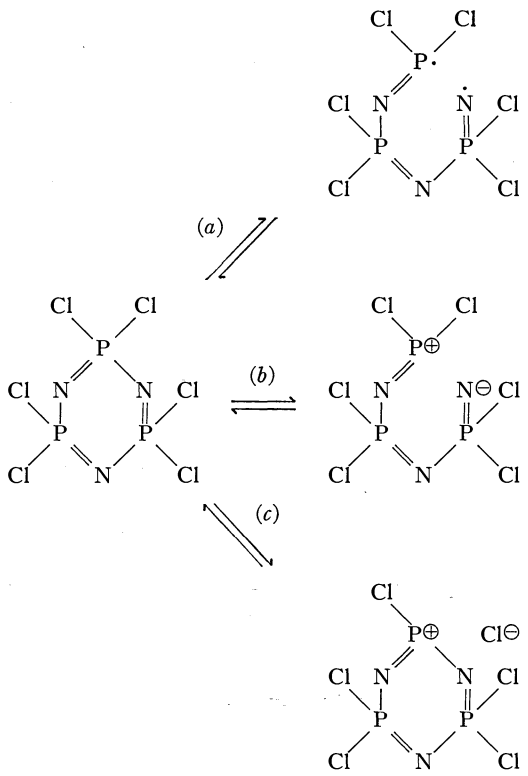

FIG. 1. Bond cleavage reactions of $(NPCl_2)_3$.

phosphorus–nitrogen bond strengths in the two compounds are expected to be similar, as indicated by the small shift in the phosphorus–nitrogen infrared absorption [$(NPCl_2)_3$, 1210 cm^{-1}; $[NP(OC_6H_5)_2]_3$, 1265 cm^{-1}]. This shift is indicative of a minor increase in π electron character within the phosphorus–nitrogen ring (29). The increase in P—N bond order is, however, less than for the compound $(NPF_2)_3$ (29). Thirdly, chlorine should ionize more readily than phenoxy from phosphorus.

It is of interest to compare the dipole moment values of $(NPCl_2)_3$ and $[NP(OC_2H_5)_2]_3$ shown in Table V. The low values for $(NPCl_2)_3$, (0.83–0.98 D) are consistent with the symmetry of the planar, cyclic structure in solution and in the melt. These values are somewhat higher than those reported for concentrated solutions in benzene (32). However, a surprisingly high value (about 3.0 D) was obtained for $[NP(OC_6H_5)_2]_3$ under the same conditions. This result indicates that the compound has a lower symmetry than does the chloride, and probably denotes that the phosphorus–nitrogen ring exists in a puckered form in this compound due to the steric crowding of the bulky phenoxy groups. The small increase of solution dipole moment with temperature for both compounds can be attributed to improved solvation at the higher temperature.

The failure to detect an electron-spin resonance spectrum in molten $(NPCl_2)_3$ and $[NP(OC_6H_5)_2]_3$ at temperatures where the polymerization of $(NPCl_2)_3$ takes place is an indication that a free-radical initiation (Fig. 1*a*) does not occur. The alternative explanation, that radicals are formed but are too labile to be detected, is considered unlikely. If this were the case, paramagnetic species should have been detected with $[NP(OC_6H_5)_2]_3$

Can. J. Chem. Downloaded from www.nrcresearchpress.com by 210.87.254.40 on 09/05/12
For personal use only.

where loss of radicals by polymerization cannot occur. Negative results of this type do not exclude the possibility of contributions from free-radical species, but the data provides strong evidence against a primary homolytic cleavage process.

Heterolytic cleavage of the phosphorus–nitrogen ring (Fig. 1*b*) would lead to the formation of dipolar species. If such species are present in appreciable concentrations, and do not polymerize rapidly, an increase in the capacitance of the system would be expected at higher temperatures. With $[NP(OC_6H_5)_2]_3$, no capacitance increase was detected between 120° C and 350° C. The evidence suggests that an initial heterolytic phosphorus–nitrogen ring cleavage is not involved in the polymerization of trimeric phosphonitrilic compounds within this temperature range.

The more complicated results obtained with $(NPCl_2)_3$ can be explained in terms of secondary processes. An irreversible rise in dielectric constant took place between 203° C and 253° C in the temperature range in which polymerization occurs. Furthermore, the dielectric constant rose continuously at constant temperature and continued to rise when the temperature was lowered to 202° C. A rough approximation of the rate of dielectric constant increase at 252° C and 202° C indicated that the activation energy of the process was about 19 kcal/mole. These results can be correlated with an increasing concentration of linear polymer. A decrease in molecular symmetry would accompany conversion of the cyclic trimer to linear polymers and would result in an increase in the polarizability of the system. Evidence in favor of this hypothesis was provided by the fact that, after the permanent dielectric constant increase had occurred, the capacitance was no longer independent of frequency. This small decrease in capacitance with increasing frequency was indicative of a slower relaxation process which would be expected for polarizable, polymeric species.

Eley and Willis (33) have recently reported the conductivity of crystalline $(NPCl_2)_3$, and suggested that the small conductance was due to ionization of chloride ions from phosphorus. If polymerization requires the prior ionization of a side-group from phosphorus, the conductance of molten $(NPCl_2)_3$ should increase with temperature. Furthermore, if polymerization is a slow step compared to ionization, the conductance increase with temperature should be reversible.

The compound $[NP(OC_6H_5)_2]_3$ was used as a control in these experiments also because thermal ionization of phenoxy from phosphorus was expected to be negligible below 250° C. As expected, the conductance of $[NP(OC_6H_5)_2]_3$ increased only slightly from 120° C to 252° C, and was completely reversible. The almost reversible conductance increase between 252° C and 350° C may be due to a small degree of phenoxy ionization.

The rising conductance of $(NPCl_2)_3$ with increasing temperature can be correlated with the polymerization process. The large, permanent conductance increase shown in Table III can similarly be attributed to the presence of polymer, although the fact that a part of the conductivity is reversible as the temperature is lowered suggests the presence of an ionization equilibrium. It is clear, however, that the increased conductance of $(NPCl_2)_3$ at higher temperature is due to some form of decomposition or release of charge-carrying species. If the assumption is made that chloride ion is one of the charge carriers, it is clear that the undissociated form is relatively stable at 253° C and the steady-state concentration of ionized species must be very low.

The results described suggest that a free-radical mechanism or one involving heterolytic phosphorus–nitrogen ring cleavage as *initial* steps are unlikely. The conductance data indicates that, for $(NPCl_2)_3$, ionization into charge-carrying species occurs concurrently with polymerization. Chloride ion is probably one of the charge-carriers, and an initial

Can. J. Chem. Downloaded from www.nrcresearchpress.com by 210.87.254.40 on 09/05/12
For personal use only.

step in the polymerization can be depicted as that shown in Fig. 1*c*. A description of subsequent steps beyond the initial ionization must be largely speculative. However, the results indicate that the polymerizing species have a high dielectric constant, a low relaxation frequency, and a permanently enhanced conductance. This evidence is consistent with the following initiation and chain-propagation steps.

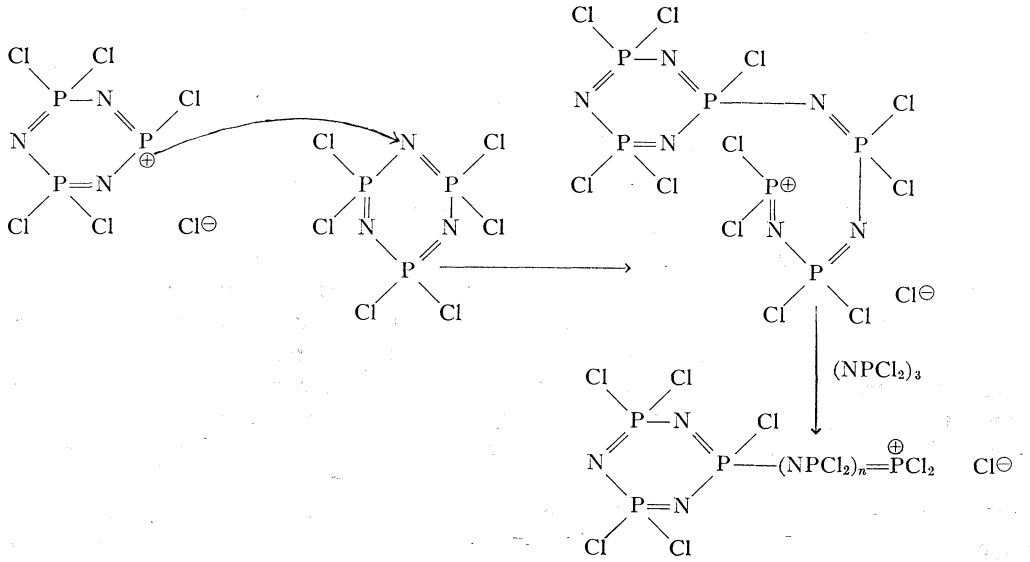

The mechanism depicted assumes an electrophilic attack by the P^+ unit on nitrogen without participation of chloride ion. This is consistent with the permanently increased conductivity during polymerization and with the enhanced dielectric constant, the latter due to the greater polarizability of the growing polymer chain.

This mechanism differs from the one suggested by Konecny *et al.* (10) in that phosphorus rather than nitrogen is assumed to be the electrophilic center of the initiating species. The greater electropositivity of phosphorus (34) is consistent with this interpretation. The mechanism proposed by Gimblett (18), in which chloride ion is consumed as an initiating unit, is inconsistent with the high conductivity observed for this system. The free-radical or Zwitterion mechanisms proposed by Patat and co-workers (6–8) can also be reinterpreted in terms of prior ionization of chloride ion from phosphorus.

This comparatively simple interpretation of the reaction is valid only for pure phosphonitrilic chloride in an inert reaction vessel. The accelerating effect of many impurities has been reported (9, 10, 17, 18) and, at high temperatures, reaction of phosphonitrilic chlorides with the glass walls of the reaction flask may occur. Impurities which function as chloride ion acceptors presumably catalyze the reaction by facilitating the initial ionization. A radiation-induced ionization probably occurs during the X-ray catalyzed, solid-state polymerization of $(NPCl_2)_3$ (35). Ionization of chloride ion from phosphorus is clearly responsible for many of the features of phosphonitrilic chloride polymerization, and also provides an explanation for the allied processes of chain-branching, cross-linking, and depolymerization.

ACKNOWLEDGMENTS

The authors wish to express their appreciation to Mrs. K. K. Mead, who obtained much of the conductance and capacitance data, and to Dr. W. G. Hodgson, who performed

Can. J. Chem. Downloaded from www.nrcresearchpress.com by 210.87.254.40 on 09/05/12
For personal use only.

the electron-spin resonance experiments. We also thank Dr. W. M. Thomas, Dr. R. A. Herrmann, and Dr. S. A. Giddings for their interest and suggestions, and Mr. D. G. Grabar for the refractive index determinations.

REFERENCES

1. L. F. Audrieth, R. Steinman, and A. D. F. Toy. Chem. Rev. **43**, 109 (1943).
2. R. A. Shaw, B. W. Fitzsimmons, and B. C. Smith. Chem. Rev. **62**, 247 (1962).
3. R. A. Shaw. J. Polymer Sci. **50**, 21 (1961).
4. O. Schmitz-Dumont. Angew. Chem. **52**, 498 (1939).
5. O. Schmitz-Dumont. Z. Elektrochem. **45**, 651 (1939).
6. F. Patat and F. Kollinsky. Makromol. Chem. **6**, 292 (1951).
7. F. Patat and K. Frombling. Monatsh. Chem. **86**, 718 (1955).
8. F. Patat and P. Derst. Angew. Chem. **71**, 105 (1959).
9. J. O. Konecny and C. M. Douglas. J. Polymer Sci. **36**, 195 (1959).
10. J. O. Konecny, C. M. Douglas, and M. Y. Gray. J. Polymer Sci. **42**, 383 (1960).
11. J. R. Soulen and M. S. Silverman. J. Polymer Sci. **A1**, 823 (1963).
12. A. C. Chapman, D. H. Paine, H. T. Searle, and D. R. Smith. J. Chem. Soc. 1825 (1961).
13. F. Seal and J. Langer. Z. Anorg. Allgem. Chem. **295**, 316 (1958).
14. N. E. Bean and R. A. Shaw. Chem. Ind. (London), 1189 (1960).
15. K. John and T. Moeller. J. Am. Chem. Soc. **82**, 2647 (1960).
16. H. N. Stokes. Am. Chem. J. **19**, 782 (1897).
17. F. G. R. Gimblett. Soc. Chem. Ind. (London), Monograph, **13**, 19 (1961).
18. F. G. R. Gimblett. J. Polymer Sci. **60**, S29 (1962).
19. B. W. Fitzsimmons and R. A. Shaw. Chem. Ind. (London), 109 (1961).
20. M. Yokoyama and F. Yamada. J. Chem. Soc. Japan, Ind. Chem. Sect. **66**, 613 (1963).
21. R. H. Cole. Private communication.
22. D. M. Gardner and G. K. Fraenkel. J. Am. Chem. Soc. **78**, 3279 (1956).
23. L. O. Brockway and W. M. Bright. J. Am. Chem. Soc. **65**, 1551 (1943).
24. A. Wilson and D. F. Carroll. J. Chem. Soc. 2548 (1960).
25. J. A. A. Ketelaar and T. A. DeVries. Rec. Trav. Chim. **58**, 1081 (1939).
26. R. Hazekamp, T. Migchelsen, and A. Vos. Acta Cryst. **15**, 539 (1962).
27. K. H. Meyer, W. Lotmar, and G. W. Pankow. Helv. Chim. Acta, **19**, 930 (1930).
28. E. Giglio, F. Pompa, and A. Ripiomonti. J. Polymer Sci. **59**, 293 (1962).
29. N. L. Paddock. Endeavour, 134, July (1960).
30. D. P. Craig and N. L. Paddock. J. Chem. Soc. 4118 (1962).
31. M. J. S. Dewar, E. A. C. Lucken, and M. A. Whitehead. J. Chem. Soc. 2423 (1960).
32. G. Corfield. J. Chem. Soc. 4258 (1962).
33. D. D. Eley and M. R. Willis. J. Chem. Soc. 1534 (1963).
34. J. R. Van Wazer. Phosphorus and its compounds. Interscience Publishers, Inc., New York. 1958. Chap. 2.
35. V. Caglioti, D. Cordischi, and A. Mele. Nature, 491 (1962).

Can. J. Chem. Downloaded from www.nrcresearchpress.com by 210.87.254.40 on 09/05/12
For personal use only.

STEROIDS

V. THE SYNTHESIS OF 4,4-DIMETHYL-3α,5-CYCLOCHOLESTAN-6-ONE (XI)[1]

GEORGE JUST AND KEITH ST. C. RICHARDSON[2]
Department of Chemistry, McGill University, Montreal, Que.
Received August 20, 1963

ABSTRACT

The synthesis of the title compound is described.

By analogy with cholesteryl derivatives, one of the expected products of the solvolysis of 4,4-dimethyl-cholesteryl tosylate should be 4,4-dimethyl-3α,5-cyclocholestan-6β-ol (II*a*) (1). Since the nature of this compound is disputed (2–4), we were interested in synthesizing it in an unambiguous fashion. This paper describes the synthesis of its immediate precursor, 4,4-dimethyl-3α,5-cyclocholestan-6-one (XI).

FLOWSHEET I

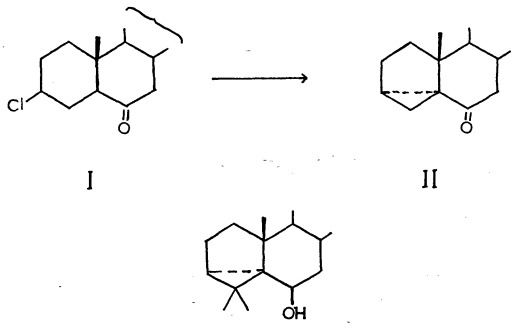

I II IIa

The parent compound, 3α,5-cyclocholestan-6-one (II) (5) had been synthesized by Windaus by the action of potassium hydroxide on 3β-chlorocholestan-6-one (I). Our first objective therefore was the preparation of a 4,4-dimethylsteroid bearing a carbonyl function at C_6. Nitration (6) and other methods (7–11) for introducing functional groups at the 6 position of the readily available 4,4-dimethylcholesteryl acetate (III) (12) did not result in the formation of the desired product. However, *cis*-hydroxylation with osmium tetroxide gave 4,4-dimethylcholestane-3β,5α,6α-triol acetate (IV*a*) in good yield. The stereochemistry is assigned in conformity with the "rule of rear-attack" (13) and is corroborated by the positive Cotton-effect (14) shown by the oxidation product of the triol monoacetate (IV*a*), 3β-acetoxy-4,4-dimethyl-5α-hydroxy-cholestan-6-one (V).

The 5α-hydroxy group was not removed by the action of zinc in acetic acid (15). However, treatment with calcium in liquid ammonia (16, 17), followed by alkaline hydrolysis of the reaction product, resulted in the formation of the desired 3β-hydroxy-4,4-dimethyl-cholestan-6-one (VII) in 40–45% yield. Its structure and stereochemistry follow from its

[1]*This paper forms a part of the Ph.D. thesis of K. St. C. Richardson, to be presented to the Faculty of Graduate Studies and Research, McGill University.*
[2]*Holder of Union Carbide Research Fellowship, 1961–62.*

Can. J. Chem. Downloaded from www.nrcresearchpress.com by 210.87.254.6 on 09/05/12
For personal use only.

FLOWSHEET II

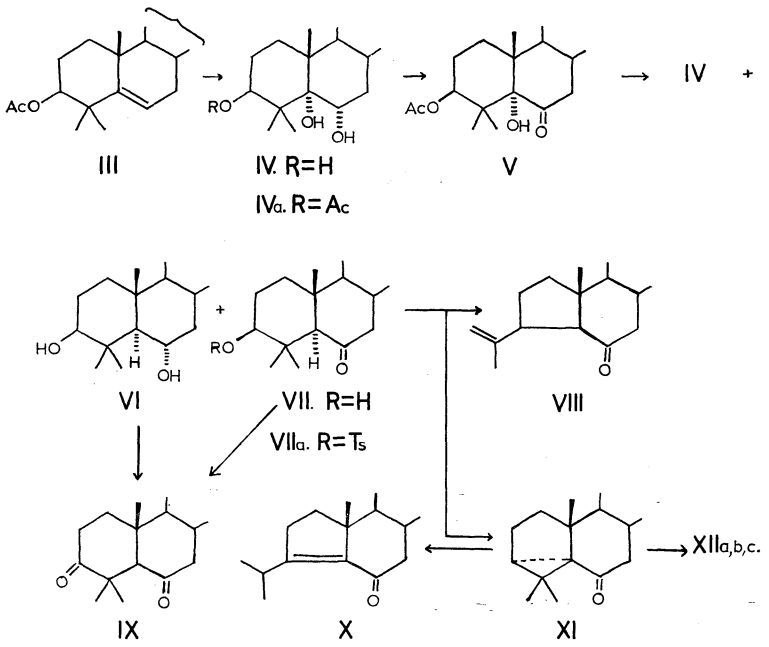

mode of formation, analysis, infrared spectrum (1708 cm^{-1}, 6-ketone) and optical rotatory dispersion curve (positive Cotton-effect), as well as the chemistry of the products derived from it. In the course of the calcium–ammonia reduction, there was obtained in addition to the 3-hydroxy-6-ketone VII, a diol VI, and a triol IV.

The structure of the diol VI was proved by conversion to 4,4-dimethylcholestane-3,6-dione (IX), also obtained by oxidation of VII. The stereochemistry of the hydroxyl group at C_6 is most probably α, since reductions of this type usually afford the thermodynamically more stable alcohols (18). Moreover, the magnitude of the rotatory power ($[M]_D$ 152°) is in agreement with the stereochemistry assigned[3]. Triol IV was shown to be identical with the hydrolysis product of IV*a* by melting point, mixed melting point, and comparison of their infrared spectra. Triol IV also exhibited the expected rotation[4], $[M]_D$ 97.8°.

Reaction of 4,4-dimethylcholestan-3β-ol-6-one (VII) with *p*-toluenesulphonyl chloride in pyridine gave the corresponding tosylate VII*a*. Treatment of the tosylate VII*a* with potassium *t*-butoxide for 3.5 hours afforded, after chromatography, two isomeric ketones XI, m.p. 107–108° and VIII, m.p. 116.5–118°. The latter ketone (VIII) was also obtained in 77% yield by treatment of tosylate VII*a* with potassium carbonate (19) in aqueous ethanol. Examination of the mother liquors of this reaction by infrared revealed the presence of ketone VIII only.

Ketone XI, $C_{29}H_{48}O$, absorbed in the ultraviolet at 203 mμ, ϵ4600 (20, 21) and in the infrared at 1696 cm^{-1}. This is indicative of a ketone in conjugation with a cyclopropane

[3]*Cholestane-3β-6α-diol, [M]D 154°; cholestane-3β-6β-diol, [M]D 52.7° (see ref. 5, p. 197).*
[4]*Cholestane-3β,5α,6α-triol, [M]D 88.5°; cholestane-3β,5α,6β-triol, [M]D 12.6° (see ref. 5, p. 192).*

Can. J. Chem. Downloaded from www.nrcresearchpress.com by 210.87.254.6 on 09/05/12
For personal use only.

ring (20–22). The nuclear magnetic resonance spectrum[5] reveals a poorly resolved multiplet centered at 0.19 p.p.m. (>C_3—H, cyclopropane) and thus confirms the structural assignment[6] (20).

Ketone VIII absorbed in the infrared at 1705 cm^{-1} (6-membered ketone) and at 3070, 1645, and 895 cm^{-1} (terminal methylene). There was no strong ultraviolet absorption above 215 mμ. The n.m.r. spectrum showed signals at 1.66 p.p.m. (3-H singlet, CH_3—C<) and 4.58 p.p.m. (2H, >C=CH_2). These data point to structure VIII, which is also plausible on mechanistic grounds.

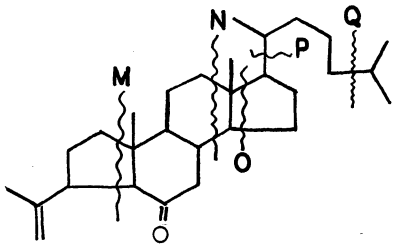

VIII

Mass Spectrometry Fragmentation Pattern

Mass spectrometry is also in accord with this structural assignment (24, 25). In particular, process M places the double bond in the environment of ring A. Furthermore, process M would be unlikely if the double bond were at any position other than the position assigned.

Ketone VIII is not a product of isomerization of the 3α,5-cycloketone XI. Prolonged treatment of XI under conditions of tosylate displacement did not effect isomerization to ketone VIII. The formation of ketones VIII and XI is hence best explained by postulating a duality of reaction paths depicted below.

In the presence of a large excess of strong base, reaction (ii) is favored, whereas, in a weakly basic medium the solvolytic reaction (i) predominates to the virtual exclusion of cyclopropane formation.

I-ketone XI seems to be stable to base, but very labile to acid. Thus, chromatography on Davison silica gel and elution with hexane–benzene afforded an oil, which absorbed in the infrared at 1677 and 1620 cm^{-1} (α,β-unsaturated ketone) and in the ultraviolet at λ_{max}^{EtOH} 253 mμ. Both absorption patterns are consistent with the product of isomerization X. Alterations and elimination reactions in the steroid molecule on anhydrous silica gel have been reported in the literature (26), but comparatively little is known about the particular mechanisms involved.

Finally, reduction of ketone XI with lithium aluminum hydride gave, after chromatography, a hydrocarbon mixture XII*a*, ($\lambda_{max}^{C_6H_{12}}$ 233 mμ and 252 mμ, with rising end absorption) and two unidentified alcohols XII*b* and XII*c* (infrared determined). One of

[5]*T.M.S. was taken as internal standard and is equal to zero.*

[6]*Recently Tadanier and Cole (23) used a series of complex signals between 0–0.83 p.p.m. to characterize some 3α,5-cyclo-6-substituted steroids.*

Can. J. Chem. Downloaded from www.nrcresearchpress.com by 210.87.254.6 on 09/05/12
For personal use only.

FLOWSHEET III

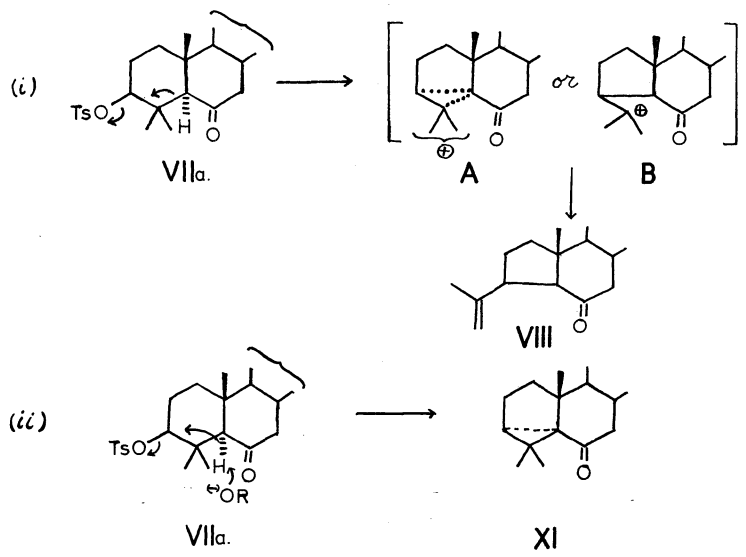

the latter alcohols could conceivably have the 3,5-cyclo structure. However, lack of an adequate supply of the starting ketone XI prevented a more detailed investigation of the products of reduction.

It might be pointed out that, whereas steroidal 6-ketones are reduced by lithium aluminum hydride in virtually quantitative yield to the 6β-hydroxy compound (27), 3,5-cyclocholestane-6-one is reduced to the 6α-alcohol (3*b*, 27, 28). A similar change in the stereochemistry of the reaction is also observed when 6-oxo and 3,5-cyclo-6-oxo steroids are submitted to a Grignard reaction (3*b*).

This "abnormal" stereochemistry of the lithium aluminum hydride reduction or Grignard addition to the *i*-ketones can best be explained by postulating an intermediate of type C, in which coordination of the carbonyl function with a Lewis acid (aluminum hydride, Grignard) leads to a homoallylic carbonium ion. The incoming nucleophile (hydride, Grignard, solvent in the case of solvolyses) attacks in the 6β-position, when R = H (formula C). However, with R = CH_3, it might be expected that attack might also take place at C_4, leading to more than one compound. Hence, this explains the multiplicity of products obtained above in the reduction of XI.

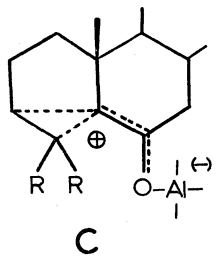

C

Can. J. Chem. Downloaded from www.nrcresearchpress.com by 210.87.254.6 on 09/05/12
For personal use only.

Can. J. Chem. Downloaded from www.nrcresearchpress.com by 210.87.254.6 on 09/05/12
For personal use only.

EXPERIMENTAL[7]

3β-Acetoxy-4,4-dimethylcholestane-5α,6α-diol (IVa)

A solution of 2.0 g (7.8 m mole) of osmium tetroxide in 94 ml of dry ether was poured into a solution of 2.5 g (5.6 m mole) of 4,4-dimethylcholest-5-en-3β-yl acetate (III), m.p. 136–137°, in 94 ml of dry ether (29). The reaction mixture was swirled briefly and set aside at room temperature for 7 days. The solvent was removed *in vacuo* at 25°. The dark residue was taken up in 340 ml of 70% aqueous ethanol, to which 0.99 g of sodium sulphite was added, and the mixture heated under reflux for 1 hour (30). The hot mixture was filtered through Celite and the filter-cake thoroughly washed with hot 80% aqueous ethanol. The volume was concentrated until partial crystallization was observed. Refrigeration overnight and filtration afforded 1.61 g (3.3 m mole) of colorless feathery needles, m.p. 186–189.5°. Crystallization of mother liquors gave an additional 713 mg (1.45 m mole) of IV*a*, m.p. 186–187.5°, for a total yield of 85%. Two recrystallizations for analysis raised the melting point to 190–191.5°, $[\alpha]_D^{23°}$ 35° (*c* 0.68). Anal. Calc. for $C_{31}H_{54}O_4$: C, 75.86; H, 11.0. Found: C, 75.64; H, 10.90. ν_{max} 3640 cm^{-1} (hydroxyl), 1735 cm^{-1} (acetate).

In a similar run, in which 3.5 ml of pyridine was added, the yield was not improved appreciably.

3β-Acetoxy-4,4-dimethyl-5α-hydroxycholestan-6-one (V)

Chromium trioxide (638 mg) in 6.38 ml of 90% aqueous acetic acid was added to a solution of 2.5 g (5.1 mmole) of the diol–acetate IV*a* in 180 ml of glacial acetic acid. The mixture was stirred continuously overnight at 25° C. Excess chromic acid was destroyed by addition of 3.5 ml of methanol, the entire mixture poured into 1 l. of ice water and the organic material extracted with ether. The ethereal solution was washed with dilute bicarbonate solution and with water; it was dried over magnesium sulphate and the solvent removed under reduced pressure. A colorless crystalline residue (2.42 g), m.p. 145–150°, was obtained. Recrystallization from ether–methanol afforded 2.04 g (82.2%) of needles, m.p. 158–160°. Three recrystallizations for analysis raised the melting point to 161–161.5°, $[\alpha]_D^{23°}$ −1.12 (*c* 0.73). Anal. Calc. for $C_{31}H_{52}O_4$: C, 76.18; H, 10.72. Found: C, 75.96; H, 10.59. ν_{max} 3650 cm^{-1} (5α-OH), 1735 cm^{-1} acetate) and 1710 cm^{-1} (C_6-ketone).

Treatment of V with Calcium – Liquid Ammonia

To 200 ml of liquid ammonia were added calcium turnings at −60°, until the solution became purple. A solution of 2 g (4.0 mmole) of the 5α-hydroxy ketone V in 15 ml of dry toluene was added to the stirred mixture, over a period of 6 minutes and the reaction allowed to proceed an additional 2 minutes. Bromobenzene (16 ml) was very cautiously added dropwise, followed in a similar manner by 50 ml of water. The temperature during the whole operation was maintained between −60° and −45°[8]. The excess ammonia was allowed to evaporate at room temperature. Concentrated hydrochloric acid was added with cooling, until the mixture was weakly acidic; the toluene layer was separated and the solvent removed *in vacuo*. Chloroform extraction gave a crimson product, the infrared analysis of which indicated partial hydrolysis of the 3β-acetate. Complete hydrolysis was subsequently effected by refluxing the residue overnight in 1.7 l. of 6% methanolic potassium hydroxide. The bulk of the solvent was distilled off and the remainder diluted with water. Ether extraction afforded 2.25 g of yellow viscous oil. The latter was combined with a similar oil (1.0 g, infrared analysis) obtained from a duplicate experiment run under identical conditions, and the whole chromatographed on alumina (Act. II–III).

Elution with benzene and benzene–ether (4:1) gave, after crystallization from ether–hexane, 4,4-dimethyl-3β-hydroxycholestan-6-one (VII), m.p. 173–175°, in 41.4% yield. Three recrystallizations for analysis raised the melting point to 175–175.5°, $[\alpha]_D^{23°}$ 8.4° (*c* 0.51). Anal. Calc. for $C_{29}H_{50}O_2$: C, 80.87; H, 11.70. Found: C, 80.53; H, 11.59. ν_{max} 3640 cm^{-1} (hydroxyl), 1708 cm^{-1} (>C=O).

The benzene–ether (1:1) eluates, after crystallization from methanol, gave 4,4-dimethylcholestane-3β,6α-diol (VI), m.p. 165–168° in 1.5% yield. Several crystallizations from ether–hexane for analysis raised the melting point to 167–168°, $[\alpha]_D^{23°}$ 35° (*c* 0.60). Anal. Calc. for $C_{29}H_{52}O_2H_2O$: C, 77.27; H, 12.08. Found: C, 77.71, H, 11.50[9]. $\nu_{max}^{CHCl_3}$ 3650 (hydroxyl), 3400 cm^{-1} (broad, hydrogen bonding).

A third crystalline product, 4,4-dimethylcholestane-3β,5α,6α-triol (IV), m.p. 208–210° C (20%), was

[7]*All rotations were taken in chloroform solutions on a Carl Zeiss Photoelectric Precision Polarimeter. Infrared (IR) spectra were determined with a Perkin–Elmer model 21 spectrophotometer. Unless otherwise stated, IR were taken in carbon tetrachloride solutions. Ultraviolet spectra were measured with a Beckmann spectrophotometer, model DK-1, except for i-ketone XI, which was measured on a Unicam, model SP500s. The commercially available aluminum oxide (Woelm) was used for chromatography. Microanalyses were carried out by Dr. C. Daessle, 5757 Decelles St., Montreal, Que., and by Dr. A. Bernhardt, Mulheim, Germany. Melting points were taken on a Kofler hot plate.*

[8]*In subsequent runs it was observed that maintaining the temperature well below −60° throughout the entire reaction period gave an optimum yield (46%) of the desired product VII.*

[9]*The diol VI proved quite hygroscopic and could have been analyzed as the monohydrate giving the calculated values in closer accord with the experimental values. $C_{29}H_{52}O_2.H_2O$: C, 77.27; H, 12.08.*

obtained directly from ether eluate. Recrystallization from ether–methanol for analysis did not alter the melting point, $[\alpha]_D^{23°}$ 21.8° (*c* 0.86). Anal. Calc. for $C_{29}H_{52}O_3$: C, 77.61; H, 11.68. Found: C, 76.53, 78.02; H, 11.49, 11.21. $\nu_{max}^{CHCl_3}$ 3640 cm^{-1} (hydroxyl), 3400 cm^{-1} (hydroxyl, broad hydrogen bonding).

4,4-Dimethyl-6-oxocholestan-3β-yl p-Toluenesulphonate (VIIa)

A solution of 1.06 g (2.4 mmole) of 4,4-dimethyl-6-oxocholestan-3β-ol (VII) and 1.06 g of *p*-toluenesulphonyl chloride in 45 ml of anhydrous pyridine was set aside at room temperature for 1 week. The mixture was poured into 550 ml of ice water and the tosylate extracted with previously chilled diethyl ether. The ethereal solution was washed successively with cold dilute hydrochloric acid, cold 5% sodium bicarbonate, and distilled water and finally with a saturated solution of sodium chloride. It was dried ($MgSO_4$) and the solvent removed *in vacuo*. A quantitative yield of tosylate VII*a*, m.p. 187–188.5° was obtained. Recrystallization from ether afforded 1.01 g (72.5%) of needles, m.p. 188–189°. Further crystallization of mother liquors gave an additional 159 mg (11.3%), melting also at 188–189°. Recrystallization for analysis afforded needles melting sharply at 189°, $[\alpha]_D^{23°}$ 6.9° (*c* 0.41). ν_{max} 1715 cm^{-1} (>C_6=O), 1345, 1190, 1180, 985, and 875 cm^{-1} (tosylate). $\lambda_{max}^{cyclohexane}$ 225 mμ, (ε 10,800). Anal. Calc. for $C_{36}H_{56}O_4S$: C, 73.92; H, 9.65; Found: C, 73.84; H, 10.02.

Treatment of VIIa with Potassium t-Butoxide

To a hot solution of 1.0 g (8.85 matom) of potassium in 100 ml of dry *t*-butanol was added, in one portion, a solution of 1.15 g (1.97 mmole) of VII*a* in 55 ml of dry *t*-butanol and the mixture heated under reflux for 3.5 hours. The cooled mixture was poured into 800 ml of ice water and the organic material extracted with ether. The ethereal solution was washed with cold dilute hydrochloric acid and with water; it was dried over magnesium sulphate and the solvent removed under reduced pressure. The recovered residual oil failed to crystallize.

Accordingly, the mixture was chromatographed on alumina (Act. II–III), effecting only partial separation of a single crystalline product (175 mg), the 3-isopropenyl-A-norcholestan-6-one (VIII). Recrystallization from ether–methanol gave 130 mg (18.2%) of colorless prisms, m.p. 115–117° C.

The remaining material was collected and rechromatographed on alumina (Act. II). Elution with hexane afforded 209 mg of 4,4-dimethyl-3α,5-cyclocholestan-6-one (XI). Crystallization from ether–methanol gave 132 mg (18.3%) of pure *i*-ketone, m.p. 104–107°. One portion of the hexane–benzene (95:5) eluate furnished 78 mg of a mixture of ketones VIII and XI (IR-spectra).

The remaining hexane–benzene eluates (95:5 and 4:1) gave 211 mg of crystalline material, m.p. 100–113°, exhibiting the same infrared spectral characteristics melting point and mixture melting point as an extra portion (57 mg) set aside from the first chromatogram and was not combined for rechromatography. The two identical portions were taken up together and crystallized from ether–methanol, furnishing 182 mg of VIII, m.p. 116–118°, for a total yield of 43.1%.

Repeated Potassium t-Butoxide Treatment of VIIa

To a hot solution of 181 mg (4.6 in atom) of freshly cut potassium in 40 ml of dry *t*-butanol was added dropwise and with stirring, a solution of 250 mg (0.43 mmole) of the tosylate VII*a* in 40 ml of dry *t*-butanol, over an extended period of time. The colorless reaction mixture was heated under reflux for 3 hours; it was cooled and poured into 250 ml of ice water. Ether extraction afforded 187 mg of an oily residue. Chromatography on alumina (Act. II) and elution with hexane afforded 77 mg of ketone XI (IR). One crystallization from ether–methanol gave 64 mg (31.5%)[10] of the pure product, m.p. 105–108°. Two recrystallizations for analysis raised the melting point to 107–108°, $[\alpha]_D^{23°}$ 35.4 (*c* 0.41). Anal. Calc. for $C_{29}H_{48}O$: C, 84.40; H, 11.72. Found: C, 84.36; H, 11.57. ν_{max} 1695 cm^{-1} (C_6-ketone in conjugation with a cyclopropane ring), 1308 cm^{-1} (31), 1025–1005 cm^{-1}, and 925 cm^{-1} (cyclopropane). λ_{max}^{EtOH} 203 mμ (ε 4650), (20). N.m.r. 0.19 p.p.m. (>C_3—H), 0.95 p.p.m. and 1.01 p.p.m. (C_4-*gem*dimethyl).[11]

Elution with hexane–benzene (5:1 and 2:1) gave, after four crystallizations from ether–methanol 20 mg (10.6%) of ketone VIII, m.p. 116.5–118°, $[\alpha]_D^{23°}$ −27.2° (*c* 0.41). Anal. Calc. for $C_{29}H_{48}O$: C, 84.40; H, 11.72. Found: C, 84.29; H, 11.89. ν_{max} 1705 cm^{-1} (>C_6=O), 3070, 1645, and 895 cm^{-1} (>C=CH_2). N.m.r. 1.66 p.p.m. (>C—CH_3), 4.58 p.p.m. (>C=CH_2) (32).

Solvolysis of VIIa in Aqueous Ethanol

To a refluxing solution of 150 mg (0.26 mmole) of tosylate VIIa in 100 ml of absolute ethanol was added 450 mg of potassium carbonate in 10 ml of water and 10 ml of absolute ethanol, and the colorless reaction mixture allowed to reflux overnight. The bulk of the solvent was distilled off and the remainder diluted with water. Ether extraction afforded 100 mg, (m.p. 113–115°) of ketone VIII. Recrystallization from ether–

[10]*Although the overall yield of the A-nor-ketone VIII and i-ketone XI appears less than it was before, the ultraviolet spectrum of the crude reaction product showed the presence of 75% content of i-ketone XI.*

[11]*Lehn and Ourisson (32) have attributed signals in the n.m.r. at 0.92 p.p.m. and 1.04 p.p.m. to the C_4-gemdimethyl groups in a 4,4-dimethyl-3-oxo triterpene derivative of the lupane series.*

Can. J. Chem. Downloaded from www.nrcresearchpress.com by 210.87.254.6 on 09/05/12
For personal use only.

methanol gave 65 mg (59%) of VIII, m.p. 115–116°. The mother liquors upon further crystallization furnished an additional 20 mg (18.5%), m.p. 115–116.5°, which did not depress upon admixture with an authentic sample. ν_{max} 1705 cm^{-1} ($>C_6{=}O$), 3070, 1645, and 895 cm^{-1} ($>C{=}CH_2$). Infrared analysis of subsequent mother liquors showed the presence of ketone VIII, only.

Lithium Aluminum Hydride Reduction of Ketone XI

Chromatographically pure 4,4-dimethyl-3α,5-cyclocholestan-6-one (XI, 145 mg) was treated with 800 mg of lithium aluminum hydride in 45 ml of dry ether at 25° (12). Excess hydride was destroyed by the dropwise addition of 1.7 ml of distilled water, followed in similar fashion by 1.5 ml of 10% sodium hydroxide solution. The solid inorganic material was filtered, the filter cake thoroughly washed with dry ether, and the filtrate evaporated to dryness under reduced pressure. Infrared analysis of the residue (146 mg), which resisted crystallization, established the complete reduction of the ketone. A portion of the residue (70 mg) was chromatographed on alumina (Act. II–III). Elution with hexane afforded 21 mg of a colorless oil XII*a*. No carbon–oxygen functions were observed in the infrared spectrum. $\lambda_{max}^{cyclohexane}$ 233 mμ and 252 mμ, with end absorption.

Hexane–benzene (95:5) eluted 14 mg of a crystalline product XII*b*, m.p. 92–96°. ν_{max} 3650 cm^{-1} (hydroxyl), 1033 cm^{-1}. Crystallization for analysis was unsuccessful.

Elution with hexane–benzene (9:1 and 2:1) gave 17 mg of a second crystalline product XII*c*, m.p. 105–107°. Two crystallizations from ether–methanol gave a few crystals and raised the melting point to 117–120°. $\nu_{max}^{CCl_4}$ 3665 cm^{-1} (hydroxyl), 1037 cm^{-1}.

Isomerization of Ketone X on Silica Gel

Mother liquors (78 mg) obtained from a previous crystallization of ketone XI were chromatographed on a column of Davison silica gel (commercial Grade No. 923). Elution with hexane–benzene afforded 24 mg of colorless oil, which failed to crystallize. $\nu_{max}^{CCl_4}$ 1677 and 1620 cm^{-1} (α,β-unsaturated ketone), 1740 cm^{-1} (unidentified weak shoulder).[12] λ_{max}^{EtOH} 253 mμ. The compound was formulated as XI from its infrared and ultraviolet data.

Further elution with benzene and benzene–ether (9:1 and 4:1) gave 44 mg of an intractable oil. $\nu_{max}^{CCl_4}$ 1740 cm^{-1}, 1696 cm^{-1}, 1675 cm^{-1}, and 1620 cm^{-1}. λ_{max}^{EtOH} 252 mμ and 236 mμ, with strong end absorption.

*Hydrolysis of 3β-Acetoxy-4,4-dimethylcholestane-5α,6α-diol (IV*a*)*

A solution of the diol acetate IV*a* (200 mg, 0.4 mmole) in 50 ml of 6% methanolic potassium hydroxide was heated under reflux overnight. Ether extraction afforded 176 mg of a crystalline product. Recrystallization from chloroform–ethanol gave 150 mg (75%) of the 3β,5α,6α-triol IV, m.p. 205–207°, which did not depress upon admixture with an authentic sample of IV obtained from the Ca–NH_3 reduction. The infrared spectra were essentially identical.

4,4-Dimethylcholestan-3,6-dione IX

A solution of 170 mg (0.4 mmole) of VI in 25 ml of glacial acetic acid was treated with 150 mg (15 mmole) of chromium trioxide in 1.5 ml of 90% aqueous acetic acid as described. Ether extraction afforded 163 mg of crystalline material. Recrystallization from chloroform–methanol gave only 50 mg of dione IX, m.p. 140–146°. Three successive crystallizations afforded less than 10 mg of needles, m.p. 149–151°. $\nu_{max}^{CCl_4}$ 1710 cm^{-1} (C_3 and C_6 ketones, double intensity). No hydroxyl bands were present in the infrared spectrum.

Treatment of VII with Chromium Trioxide

To a solution of 20 mg of VII in 5 ml of glacial acetic acid was added 0.2 ml (20 mg) of a solution of chromic trioxide in 90% aqueous acetic acid as described. The reaction followed the general procedure described above, affording 18 mg of a semicrystalline residue, which failed to crystallize. The infrared spectrum was identical with the crude residue obtained from chromic acid oxidation of VI.

ACKNOWLEDGMENTS

We wish to thank the National Research Council for generous financial support. We also wish to thank Mr. I. Wang of our laboratory for having taken the ultraviolet spectrum of the 3,5-cycloketone. We are indebted to Mr. J. Nicholson of the National Research Council, Ottawa, for the nuclear magnetic resonance spectra, Dr. R. Schaffer, American Oil Co., Whiting, Ind., for the mass spectrometry, and to Professor J.C. Richer of the University of Montreal for the ORD curves and to each for his very valuable interpretations.

[12]*It is interesting to note that when the tosylate VII*a *was treated with base as described above, and the reaction followed at intervals by infrared, the anomalous peak at 1740 cm^{-1} reached a maximum (medium to strong band) at 1.5 to 2 hours and gradually disappeared upon complete displacement of the tosyl group. Investigation of this anomalous band was not attempted.*

Can. J. Chem. Downloaded from www.nrcresearchpress.com by 210.87.254.6 on 09/05/12
For personal use only.

REFERENCES

1. (*a*) S. WINSTEIN and R. A. ADAMS. J. Am. Chem. Soc. **70**, 838 (1948).
   (*b*) S. WINSTEIN and E. M. KOSOWER. J. Am. Chem. Soc. **78**, 4347 (1956); **81**, 4399 (1959).
2. Y. M. Y. HADDED and G. H. R. SUMMEUS. J. Chem. Soc. 769 (1959).
3. (*a*) G. JUST, F. E. SHORTLAND, R. SNEEN, and S. WINSTEIN. C.I.C. meeting, Edmonton, Alta. 1962.
   (*b*) F. E. SHORTLAND. Ph.D. Thesis, McGill University, Montreal. 1963.
4. R. M. MORIARTY and E. S. WALLIS. J. Org. Chem. **24**, 1987 (1959).
5. L. FIESER and M. FIESER. Steroids. Reinhold Publishing Corp., New York. 1959. p. 315.
6. A. WINDAUS. Ber. **53**, 488 (1920).
7. W. D. EMMONS, A. S. PAGANO, and J. FREEMAN. J. Am. Chem. Soc. **76**, 3472 (1954).
8. R. TULL, R. E. JONES, S. A. ROBINSON, and M. TISHLER. J. Am. Chem. Soc. **77**, 196 (1955).
9. K. B. WIBERG and K. A. SAEGEBARTH. J. Am. Chem. Soc. **79**, 2822 (1957).
10. R. B. WOODWARD and F. V. BRUTCHER, JR. J. Am. Chem. Soc. **80**, 209 (1958).
11. J. F. EASTHAM, G. B. MILES, and C. A. KRAUTH. J. Am. Chem. Soc. **81**, 3114 (1959).
12. R. B. WOODWARD, A. A. PATCHETT, D. H. R. BARTON, D. A. J. IVES, and R. B. KELLY. J. Chem. Soc. 1131 (1957).
13. L. F. FIESER. Experientia, **6**, 312 (1950).
14. C. DJERASSI, O. HALPERN, V. HALPERN, O. SCHINDLER, and C. TAMM. Helv. Chim. Acta, **41**, 250 (1958).
15. R. B. WOODWARD, F. SONDHEIMER, D. TAUB, K. HEUSLER, and W. M. MCLAMORE. J. Am. Chem. Soc. **74**, 4223 (1952).
16. J. H. CHAPMAN, J. ELKS, C. H. PHILLIPS, and J. WYMAN. J. Chem. Soc. 4344 (1956).
17. A. J. BIRCH and H. SMITH. Quart. Rev. **12**, 17 (1958).
18. D. H. R. BARTON and C. H. ROBINSON. J. Chem. Soc. 3045 (1954).
19. N. F. BLAU and N. STUCKWISCH. J. Org. Chem. **27**, 371 (1962).
20. V. GEORGIAN, J. F. KERWIN, M. E. WOLF, and F. F. OWINGS. J. Am. Chem. Soc. **84**, 3594 (1962).
21. G. W. CANNON, A. A. SANTILLI, and P. SHENIAN. J. Am. Chem. Soc. **81**, 1660 (1959).
22. L. J. BELLAMY. The infrared spectra of complex molecules. John Wiley and Sons, Inc., New York. 1958. p. 138.
23. J. TADANIER and W. COLE. J. Org. Chem. **27**, 4610 (1962).
24. K. BIEMAN. Angew Chem. Intern. Ed. Engl. 106 (1962).
25. S. S. FRIEDLAND and M. J. O'NEAL JR. Anal. Chem. **31**, 169 (1959).
26. J. H. LINDFORD. Can. J. Biochem. Physiol. **34**, 1153 (1956).
27. C .W. SHOPPEE and G. H. R. SUMMERS. J. Chem. Soc. 3361 (1952).
28. A. F. WAGNER and E. S. WALLIS. J. Am. Chem. Soc. **72**, 1047 (1950).
29. N. L. WENDLER and D. TAUB. J. Am. Chem. Soc. **82**, 2836 (1960).
30. G. COOLEY, B. ELLIS, F. HARTLEY, and V. PETROW. J. Chem. Soc. 4377 (1955).
31. M. L. JOSIEN, N. FUSON, and A. S. CAREY. J. Am. Chem. Soc. **73**, 4445 (1951).
32. J. M. LEHN and G. OURISSON. Bull. Soc. Chim. France, 1137 (1962).

Can. J. Chem. Downloaded from www.nrcresearchpress.com by 210.87.254.6 on 09/05/12
For personal use only.

STEROIDS

VI. THE STEREOCHEMISTRY OF 4-ETHYL-4-METHYLCHOLEST-5-EN-3-ONE (II)[1]

GEORGE JUST AND KEITH ST. C. RICHARDSON[2]
Department of Chemistry, McGill University, Montreal, Que.
Received August 20, 1963

ABSTRACT

The stereochemistry of the title compound was determined.

Can. J. Chem. Downloaded from www.nrcresearchpress.com by 210.87.254.6 on 09/05/12
For personal use only.

In the course of the solvolysis of 4,4-dimethylcholesteryl tosylate, some 3,4-dimethylcholestane derivatives were isolated (1). It was shown (2) that their formation was probably due to a 1,3-diaxial interaction of the C_4- and C_{10}-methyl groups, resulting in deformation of the A-ring, since analogous 19-nor steroids give only the expected solvolysis products.

In order to establish whether the 4α or the 4β-methyl group migrated in this solvolysis, it was decided to prepare a 4-ethyl-4-methylcholesteryl derivative of known stereochemistry at C_4. The object of this paper is to describe the preparation and structure proof of such a compound.

Ethylation of 4-methylcholest-4-en-3-one (I) (3) with ethyl iodide and potassium *t*-butoxide in *t*-butanol resulted in the formation of a 70% yield of 4α-ethyl-4β-methylcholest-5-en-3-one (II), obtained by direct crystallization. In addition, small amounts of its isomer III were obtained with difficulty (see Experimental). Ultraviolet and infrared spectroscopy indicated the absence of conjugation in the two epimeric ketones.

FLOWSHEET I

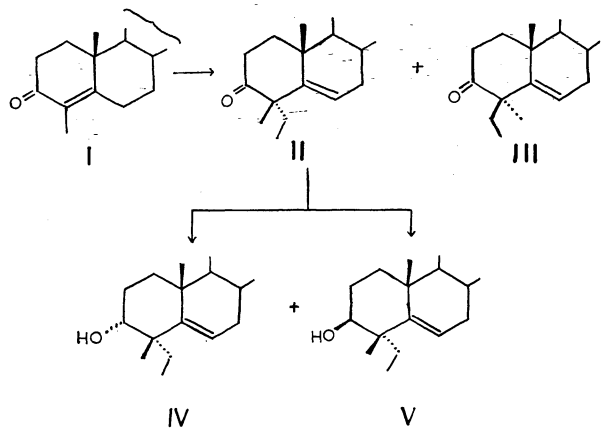

In order to prove the stereochemistry at C_4, a sample of 3α-hydroxy-4-ethyl-4-methylcholest-5-ene was required.

Reduction of ketone II with sodium borohydride in aqueous dimethyl formamide (4),

[1]*This paper forms a part of the Ph.D. thesis of K. St. C. Richardson, to be presented to the Faculty of Graduate Studies and Research, McGill University.*
[2]*Union Carbide Research Fellow 1961–62.*

followed by chromatography of the product gave, upon elution with hexane–benzene (2:1) and crystallization from ether–ethanol, the 3α-alcohol IV, in 17% yield. Elution with benzene ether afforded the 3β-epimer V in 67% yield. The stereochemistry of the alcohols was assigned by analogy with the reduction of the 4,4-dimethyl-3-oxo steroids (2), by their relative ease of elution on alumina (5), by their infrared spectral characteristics (6), and finally by the product derived from solvolysis of their respective mesylates[3].

When the ketone II was reduced with lithium aluminum hydride, the 3α-alcohol IV was obtained in 6% yield. In the corresponding 4,4-dimethyl series, lithium aluminum hydride reduction had resulted in the formation of more than 99% of 4,4-dimethylcholesterol (2).

FLOWSHEET II

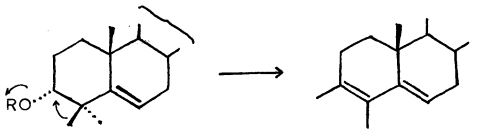

VI R=H VII

VIa R=Ts

In the 4,4-dimethylcholestene series, it had been shown that acetolysis of the 3α-tosylate VI*a* gave in virtually quantitative yield 3,4-dimethylcholesta-3,5-diene (VII) (1, 7). In that instance, there was no doubt that the reaction involved the migration of the 4β-(axial) methyl group to C_3 (see flowsheet II). A similar acetolysis should result in the formation of either 3-methyl-4-ethyl- or 3-ethyl-4-methylcholesta-3,5-diene from the 4β-methyl- or the 4β-ethyl-3α-alcohol respectively.

Two dienes VIII and XII were therefore prepared by reaction of the ethyl and methyl Grignard reagents with 4-methyl- and 4-ethylcholest-4-en-3-one (I and X) respectively. The latter ketone X was obtained by monoethylation (3) of cholestenone IX. The infrared and ultraviolet spectra of the two isomeric dienes were very similar. However, the melting point of the two dienes was depressed upon admixture.

Alcohol IV was treated with *p*-toluenesulphonyl chloride in pyridine at room and elevated temperatures for extended periods of time. No tosylate was formed in these attempts. Next, the alcohol IV was treated with phosphorus oxychloride in dry pyridine. There was obtained from this reaction a mixture of dienes, readily separable by chromatography. The diene XIII, m.p. 98–98.5°, $[\alpha]_D$ −35°, obtained in 21% yield, showed no absorption in the ultraviolet above 220 mμ. The structure of diene XIII was assigned by analogy with a similar product obtained on treatment of 4,4-dimethyl-cholest-5-en-3α-ol (VI) with thionyl chloride by Shoppee and Johnson (7). The structural assignment is confirmed by n.m.r. data, which exhibited a complex signal centered at 5.46 p.p.m. (3H, olefinic protons).

The second diene XII, m.p. 101–102°, was obtained in 26% yield (65% by UV) and was identical in all respects with the sample obtained by direct synthesis.

When the 3α-alcohol was treated with methanesulphonyl chloride in pyridine at 0°, an oily, unstable mesylate was obtained. Its infrared spectrum showed the lack of hydroxyl absorption. The ultraviolet spectrum gave no evidence for a conjugated chromophore.

[3]*A report on the solvolysis of 4α-ethyl-4β-methylcholest-5-en-3β-yl mesylate will appear in a future publication.*

Can. J. Chem. Downloaded from www.nrcresearchpress.com by 210.87.254.6 on 09/05/12
For personal use only.

FLOWSHEET III

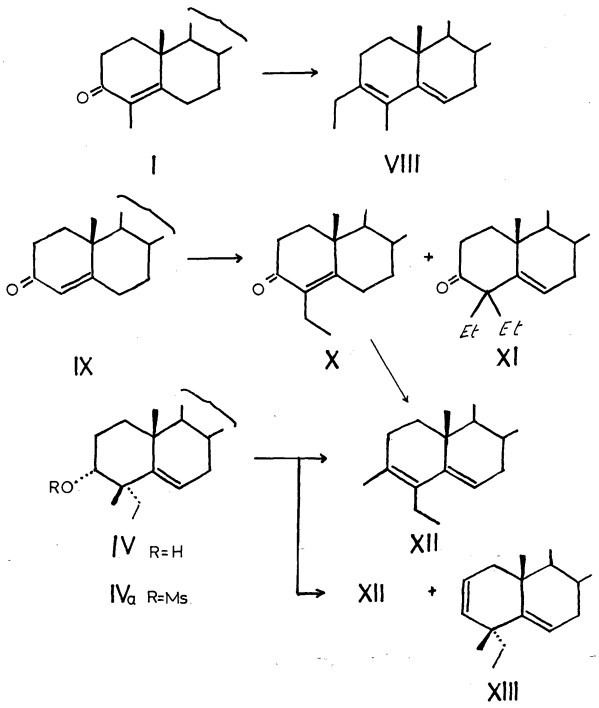

Solvolysis of the crude mesylate IV*a* in buffered glacial acetic acid gave a conjugated diene. Crystallization afforded 80% of pure 3-methyl-4-ethylcholesta-3,5-diene (XII), m.p. 100–102°, identical in all respects with the sample synthesized from 4-ethylcholestenone (X) and different from 3-ethyl-4-methylcholesta-3,5-diene (VIII). The infrared spectrum of the mother liquors of crystallization revealed only the presence of XII. The stereochemistry at C_4 is hence as depicted by ketone II.

This indicates that steric factors determine the entry of the alkylating agent (8–10). In the absence of steric hindrance, axial entry of the ethyl group (12, 13) would have been the preferred mode of the alkylation.

EXPERIMENTAL[4]

4α-Ethyl-4β-methylcholest-5-en-3-one (II)

A solution of 20g (50 mmole) of 4-methylcholestenone (I) (3), m.p. 101–104° C, λ_{max}^{EtOH} 250 mμ (ε 15,800) in 100 ml of dry *t*-butanol was treated with a solution of 6.3 g (160 matom) of potassium in 160 ml of dry *t*-butanol. To the vigorously stirred solution at 75° was added a solution of 20.3 ml (250 mmole) of ethyl iodide in 50 ml of dry *t*-butanol. The reaction mixture was heated under reflux for 1 hour; the bulk of the solvent was distilled off. The remainder was diluted with cold dilute hydrochloric acid and the organic material extracted with chloroform. The chloroform extract was washed successively with dilute hydrochloric acid, 5% sodium bicarbonate and water, and dried ($MgSO_4$) and the solvent removed under reduced pressure. The infrared spectrum of the yellow amorphous residue (22.5 g) showed carbonyl bands at 1710 cm^{-1} (saturated ketone) and at 1675 and 1610 cm^{-1} (unsaturated ketone). It contained approximately 10%

[4]*All rotations were taken in chloroform on a Carl Zeiss photoelectric precision polarimeter.*
Infrared spectra were taken in carbon tetrachloride solutions. Ultraviolet spectra were measured with a Beckman spectrophotometer, model DK-1.
Melting points were taken on a Kofler hot plate.
Microanalyses were carried out by Dr. C. Daessle, 5757 Decelles Street, Montreal, Quebec.
The commercially available aluminum oxide (Woelm) was used for chromatography.

Can. J. Chem. Downloaded from www.nrcresearchpress.com by 210.87.254.6 on 09/05/12
For personal use only.

of the starting Δ^4-ketone I, (λ_{max}^{EtOH} 250 mμ, ϵ 1550). Crystallization from chloroform–ethanol readily afforded 14.85 g (70%) of 4α-ethyl-4β-methylcholest-5-en-3-one (II), m.p. 158.5–160°. Recrystallization for analysis raised the melting point to 160–161°, $[\alpha]_D^{23°}$ 14.7° (*c* 0.33). Anal. Calc. for $C_{30}H_{50}O$: C, 84.44; H, 11.81. Found: C, 84.21; H, 11.83. ν_{max} 1710 cm^{-1} (C_3=O). The mother liquors were chromatographed on alumina (Act. II). Elution with hexane and hexane–benzene (19:1) gave 2.66 g (12.5%) of an intractable semicrystalline mixture of isomeric products II and III. Further elution with hexane–benzene (19:1 and 4:1) afforded 1.75 g (8.2%) of a more easily separable crystalline mixture, m.p. 131–137°. Six consecutive recrystallizations gave 140 mg of pure 4β-ethyl-4α-methylcholest-5-en-3-one (III), m.p. 153.5–154°; admixture of II resulted in depression of the melting point, $[\alpha]_D^{23°}$ 10.6° (*c* 1.08). Anal. Calc. for $C_{30}H_{50}O$: C, 84.44; H, 11.81; Found: C, 84.38; H, 11.70. The infrared spectra of II and III were essentially identical.

Benzene–ether (9:1) eluted 1.2 g (6%) of the starting material, (λ_{max}^{EtOH} 250 mμ, ν_{max} 1670 and 1610 cm^{-1}).

Sodium Borohydride Reduction of Ketone II

To a stirred solution of 4 g (9.4 mmole) of ketone II in 170 ml of redistilled N,N-dimethyl formamide (DMF) was added, dropwise, 4 g of sodium borohydride in 25 ml of water and 55 ml of DMF, at a rate which did not allow precipitation of the starting material. During the period of addition the temperature was maintained at 90–95°, thereafter at 100° for 3 hours, when bubbling ceased. The reaction mixture was then allowed to reflux overnight. The mixture was cooled and the excess hydride carefully destroyed with dilute hydrochloric acid. Water was added to ensure complete precipitation of the organic material. The latter was extracted with ether and the ethereal solution washed successively with cold dilute hydrochloric acid, twice with cold 5% sodium bicarbonate, and three times with water. It was dried ($MgSO_4$) and the solvent removed under reduced pressure, furnishing 4.06 g of a colorless semicrystalline residue.

Chromatography on alumina (Act. II) and elution with hexane–benzene (9:1 and 4:1) gave, after crystallization from chloroform–ethanol, 180 mg (4.5%) of the starting ketone II, m.p. 158–159°, $\nu_{max}^{CCl_4}$ 1710 cm^{-1}.

Elution with hexane–benzene (2:1) gave 800 mg of crystalline product, m.p. 139–144°. Crystallization from ether–ethanol yielded 610 mg (15.2%) of 4α-ethyl-4β-methylcholest-5-en-3α-ol (IV), m.p. 144–145°. The mother liquors gave an additional 70 mg (1.8%) of IV, m.p. 141–143°. Two crystallizations for analysis raised the melting point to 145–145.5°, $[\alpha]_D^{23°}$ −72.5° (*c* 0.85). Anal. Calc. for $C_{30}H_{52}O$: C, 84.03; H, 12.23. Found: C, 83.90; H, 12.32. ν_{max} 3640 cm^{-1} (C_3O—H), and 1080 cm^{-1} (C—O stretch) (13).

The benzene ether eluate (9:1) afforded 2.7 g (67%) of 4α-ethyl-4β-methylcholest-5-en-3β-ol (V), m.p. 120–122°. Crystallization for analysis raised the melting point to 123–123.5°; $[\alpha]_D^{23°}$ −61.5 (*c* 1.51). Anal. Calc. for $C_{30}H_{52}O$: C, 84.03; H, 12.23. Found: C, 84.28; H, 12.44. ν_{max} 3640 cm^{-1} (C_3O—H), 1050, 1040, and 1025 cm^{-1} (equatorial C—O stretch) (6).

Reduction of Ketone II with Lithium Aluminum Hydride

To a stirred suspension of lithium aluminum hydride (2.5 g) in 200 ml of anhydrous ether was added 6.2 g (14.5 mmole) of ketone II in 300 ml of anhydrous ether (14). Excess hydride was destroyed by the dropwise addition of water and 10% sodium hydroxide solution. Filtration of the inorganic solid and removal of the solvent under reduced pressure afforded 6.2 g of a colorless crystalline mixture, m.p. 110–112°, which could not be separated by fractional crystallization; 5.5 g of this mixture was hence chromatographed on alumina (Act. II). Crystallization from ether–ethanol of the hexane–benzene eluates gave 325 mg (5.3%) of 4α-ethyl-4β-methyl-cholest-5-en-3α-ol (IV), m.p. 143.5–145° C, and identified by melting point, mixed melting point, and infrared spectra with the product IV eluted with hexane–benzene from the sodium borohydride reduction. Crystallization of the mother liquors afforded an additional 56 mg (1%), m.p. 141–143°.

The benzene–ether eluate afforded, upon crystallization from ether methanol, alcohol V (2.75 g, 44.2%), m.p. 123–124°. Further recrystallization of mother liquors gave 31.8% of V, m.p. 121–123.5°. The alcohol was identified by the melting point, mixed melting point, and infrared spectra with the alcohol V similarly obtained from chromatography of the previous sodium borohydride reduction product.

4-Ethylcholest-4-en-3-one (X)

A solution of 3.3 g (78 matoms) of potassium and 10 g (26 mmole) of Δ^4-cholesten-3-one (IX), m.p. 82–83° (λ_{max}^{EtOH} 240 mμ, ϵ 16,600) in 450 ml of dry *t*-butanol was heated under reflux for 10 minutes. To the refluxing solution was added dropwise, over a period of 2 hours, a solution of 2.5 ml (31.2 mmole) of ethyl iodide in 200 ml of dry *t*-butanol. The reaction mixture was allowed to reflux an additional 30 minutes, the bulk of the solvent distilled off, and the remainder poured into 150 ml of dilute hydrochloric acid. Extraction with ether gave 10.01 g of yellow oil.

Chromatography on alumina (Act. II–III) and elution with hexane–benzene (19:1) gave 1.71 g (14.7%) of 4,4-diethylcholest-5-en-3-one (XI), m.p. 96–97°. Two crystallizations from ether–methanol for analysis raised the melting point to 96.5–97.5°, $[\alpha]_D^{23}$ 3° (*c* 0.81). Anal. Calc. for $C_{31}H_{52}O$: C, 84.48; H, 11.89. Found: C, 84.20; H, 11.75. $\nu_{max}^{CCl_4}$ 1705 cm^{-1}.

The hexane–benzene eluates (9:1 and 4:1) furnished, upon crystallization from ether–acetone, 2.55 g (24%) of 4-ethylcholest-4-en-3-one (X), m.p. 84–86°. Recrystallization from ether–acetone afforded 2.2 g of crystals, m.p. 87–88° C. Further crystallization for analysis did not raise the melting point, $[\alpha]_D^{23°}$ 93° (*c* 1.58). Anal. Calc. for $C_{29}H_{48}O$: C, 84.40; H, 11.72. Found: C, 84.66; H, 11.82. ν_{max} 1675 and 1610 cm^{-1} (α,β-unsat'd ketone). λ_{max}^{EtOH} 250 mμ (ϵ 17,700).

Can. J. Chem. Downloaded from www.nrcresearchpress.com by 210.87.254.6 on 09/05/12
For personal use only.

Further elution with hexane–benzene (1:1) afforded 1.58 g (17%) of the starting material, m.p. 79–81° (ν_{max} 1680 and 1620 cm^{-1}; λ_{max}^{EtOH} 240 mμ).

3-Methyl-4-ethylcholesta-3,5-diene (XII)

To 6 ml of an ethereal solution of methyl magnesium iodide formed from 350 mg of magnesium and 1.7 ml of methyl iodide was added at 0°, a solution of 100 mg (0.24 mmole) of 4-ethyl-cholestenone (X) in 8 ml of anhydrous ether (15). The temperature was gradually raised to the boiling point and the mixture heated under reflux overnight. Cold saturated ammonium chloride was added and the organic material extracted with ether. The ethereal solution was washed successively with cold dilute hydrochloric acid, with cold 5% sodium hydroxide, three times with water, and finally with a saturated sodium chloride solution; it was dried over magnesium sulphate and the solvent removed at reduced pressure. The residual oil exhibited three peaks in the ultraviolet spectrum ($\lambda_{max}^{cyclohexane}$ 283 mμ, 246 mμ, and 235 mμ), consonant with a mixture of heteroannular and homoannular dienes.

Accordingly, the residual oil (116 mg) was taken up in 200 ml of 95% aqueous ethanol, three drops of concentrated hydrochloric acid were added, and the mixture refluxed overnight. The ethanol was distilled off and 50 ml of water was added to the residue. Ether extraction of the organic material furnished 114 mg of crystalline product XII, which upon crystallization from ether–ethanol gave 86 mg (87.2%) of 3-methyl-4-ethylcholesta-3,5-diene (XII) as long needles, m.p. 101–103°. Two crystallizations for analysis raised the melting point to 102.5–103° C, $[\alpha]_D^{23°}$ −129° (*c* 0.32). Anal. Calc. for $C_{30}H_{50}$: C, 87.74; H, 12.27. Found: C, 87.79; H, 12.22. $\lambda_{max}^{cyclohexane}$ 237 mμ (ϵ 19,500), 244.5 mμ (ϵ 20,000), and 253 mμ (ϵ 12,800, inflection) (2,16,17).

3-Ethyl-4-methylcholesta-3,5-diene (VIII)

Ketone I (400 mg, 1 mmole) in 15 ml of anhydrous ether was reacted with ethereal ethyl magnesium iodide prepared from 1.2 g of magnesium and 8 ml (100 mmole) of ethyl iodide in 5 ml of ether as described above (15). Ether extraction of the acid isomerized product (400 mg) afforded, upon crystallization from ether–ethanol, 300 mg (73%) of 3-ethyl-4-methylcholesta-3,5-diene (VIII), m.p. 115–117.5°, as needles. Further crystallization of the mother liquors gave an additional 41 mg (10%), m.p. 117–118°. Recrystallization for analysis raised the melting point to 117.5–118°, $[\alpha]_D^{23°}$ −116° (*c* 0.36). Anal. Calc. for $C_{30}H_{50}$: C, 87.74; H, 12.27. Found: C, 87.55; H, 12.25. $\lambda_{max}^{cyclohexane}$ 237.5 mμ (ϵ 19,400), 245 mμ (ϵ 21,200), and 253 mμ (ϵ 13,400, inflection).

A mixture of diene XII, m.p. 102.5–103° and of diene VIII, m.p. 117.5–118°, melted at 100–104.5°.

Reaction of 4α-Ethyl-4β-methylcholest-5-en-3α-ol (IV) with Phosphorus Oxychloride

Ten milliliters of phosphorus oxychloride was added to a solution of 450 mg (1.0 mmole) of IV in 25 ml of dry pyridine at room temperature. The reaction mixture was kept at 40° for 12 hours. Infrared analysis of an aliquot indicated the presence of sizable amounts of starting material. The reaction mixture was, therefore, heated for an additional 24 hours at 60°, cooled, then carefully poured into 200 ml of ice water and extracted with ether. The ethereal solution was washed successively with dilute hydrochloric acid, 5% sodium bicarbonate, water, and finally a saturated solution of sodium chloride. It was dried over magnesium sulphate and the solvent removed at reduced pressure, affording 400 mg of yellow oil. The ultraviolet spectrum of the crude product showed the presence of about 65% of the conjugated diene XII ($\lambda_{max}^{cyclohexane}$ 244.5 mμ, ϵ 12,700).

Chromatography on alumina (Act. I) and elution with hexane afforded 104 mg of colorless oil. Crystallization from ether–ethanol gave 86 mg (20.9%) of leaflets, m.p. 95–97°, which depressed upon admixture with dienes VIII and XII. Recrystallization from the same mixed solvents gave a product melting sharply at 98–98.5°, $[\alpha]_D^{23}$ −35° (*c* 0.64)[5]. No absorption maxima above 220 mμ were recorded in the ultraviolet spectrum.

Further elution with hexane and hexane–benzene (19:1) afforded 124 mg of crystalline material, which, upon recrystallization from ether–ethanol, gave 101 mg (24.6%) of diene XII, m.p. 99.5–102°. Recrystallization gave sharply melting needles, m.p. 101–102°, which was depressed upon admixture with VIII, but not with the diene XII obtained by direct synthesis; $[\alpha]_D^{23°}$ −129° (*c* 0.37), $\lambda_{max}^{cyclohexane}$ 237 mμ (ϵ 18,800), 244.5 mμ (ϵ 19,600), and 253 mμ (ϵ 12,600 inflection).

4α-Ethyl-4β-methylcholest-5-en-3α-yl Methanesulphonate (IVa)

To a chilled solution of 200 mg (0.47 mmole) of alcohol IV in 2.5 ml of dry pyridine was added 1 ml of methanesulphonyl chloride and the mixture kept at 0° for 2 hours, with continuous stirring. The mixture was poured over crushed ice and extracted with ether after 30 minutes. The ethereal solution was washed successively with cold dilute hydrochloric acid, cold 5% sodium bicarbonate solution, water, and finally a saturated solution of sodium chloride. It was dried ($MgSO_4$) and the solvent removed under reduced pressure at 30°. A pale yellow crystalline residue IV*a* (293 mg) was obtained. The infrared spectrum showed medium to strong bands at 1415, 1385, 1340, 1180, 963, and 900 cm^{-1}, associated with the expected frequencies of

[5]*The non-absorbing diene XIII has been assigned on analogy with 4,4-dimethylcholesta-2,5-diene (m.p. 92–93° $[\alpha]_D$ −37°, rising ultraviolet end-absorption) obtained in the work of Shoppee and Johnson (7).*

Can. J. Chem. Downloaded from www.nrcresearchpress.com by 210.87.254.6 on 09/05/12
For personal use only.

a mesyl group. The ultraviolet spectrum exhibited no absorption maximum above 220 mμ. Owing to the extreme instability of the mesylate IV*a*, the product could not be recrystallized.

Acetolysis of Mesylate IVa

A stirred solution of the crude mesylate IV*a* (293 mg) and 100 mg of anhydrous sodium acetate in 40 ml of glacial acetic acid was heated at 60° for 5 hours. The reaction mixture was cooled, poured into 400 ml of ice water, and extracted with ether. The ethereal solution was worked up in the usual manner, yielding 190 mg of crystalline product XII. Recrystallization from ether–ethanol afforded 145 mg (80%) of needles, m.p. 98–100°. Two recrystallizations raised the m.p. to 100–102°, $[\alpha]_D^{23°}$ −130° (*c* 0.34). $\lambda_{max}^{cyclohexane}$ 237 mμ (ε 18,400), 244.5 mμ (ε 19,000), and 253 mμ (ε 12,200 inflection). The product upon admixture with diene VIII gave a depression of the mixture melting point, which was not observed with the authentic sample of XII. The infrared and ultraviolet spectra of the mother liquors revealed the presence of diene XII only.

ACKNOWLEDGMENTS

We wish to thank the National Research Council for generous financial support, and Dr. Stammer of this Department for taking the n.m.r. spectra.

REFERENCES

1. G. Just, F. E. Shortland, R. Sneen and S. Winstein. C.I.C. meeting, Edmonton, Alta. 1962.
2. G. Just and F. E. Shortland. Can. J. Chem. In press (1964).
3. N. Atwater. J. Am. Chem. Soc. **82**, 2847 (1960).
4. D. Taub, R. D. Hoffsommer, and N. L. Wendler. J. Am. Chem. Soc. **81**, 3291 (1959).
5. D. H. R. Barton. J. Chem. Soc. 1027 (1953).
6. I. L. Allsop, A. R. H. Cole, D. E. White, and R. S. Willix. J. Chem. Soc. 4868 (1956).
7. G. W. Shoppee and G. A. R. Johnson. J. Chem. Soc. 2684 (1962).
8. G. Stork and J. W. Schulenberg. J. Am. Chem. Soc. **78**, 250 (1956).
9. N. A. Rogers and J. A. Barltrop. Quart. Rev. **16**, 117 (1962).
10. M. E. Kuehne. J. Am. Chem. Soc. **83**, 1492 (1961).
11. R. E. Ireland and P. W. Schiess. J. Org. Chem. **28**, 6 (1963).
12. W. S. Johnson. Chem. Ind. 167 (1956).
13. J. H. Ringold and S. K. Malhota. J. Am. Chem. Soc. **84**, 3402 (1962).
14. R. B. Woodward, A. A. Patchett, D. H. R. Barton, D. A. J. Ives, and R. B. Kelly. J. Chem. Soc. 1131 (1957).
15. W. Bergmann and F. Hirschmann. J. Org. Chem. **4**, 40 (1939).
16. L. Dorfman. Chem. Rev. **53**, 47 (1953).
17. R. B. Woodward. J. Am. Chem. Soc. **64**, 72 (1942).

Can. J. Chem. Downloaded from www.nrcresearchpress.com by 210.87.254.6 on 09/05/12
For personal use only.

STEROIDS

VII. THE SOLVOLYSIS OF 4,4-DIMETHYL-17β-ACETOXY-ESTR-5-EN-3-YL *p*-TOLUENESULPHONATE[1, 2]

GEORGE JUST AND F. E. SHORTLAND[3, 4]
Department of Chemistry, McGill University, Montreal, Quebec
Received August 20, 1963

ABSTRACT

The solvolysis of the title compound resulted mainly in products of ring contraction. No product of methyl shift could be detected.

In the solvolysis of 4,4-dialkylcholesteryl *p*-toluenesulphonate (I), it had been noticed that 6–20% of the 3,4-dimethylcholestane derivatives II and III were formed (1, 2). To establish if these unexpected rearrangement products were due to a deformation of ring

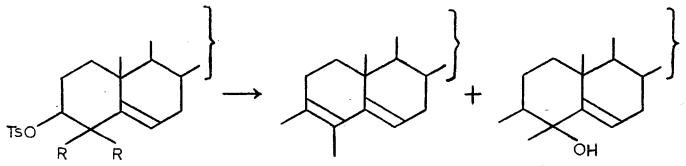

I R=CH_3 II III

A arising from the 1,3-diaxial interaction of the alkyl groups at C-4 and C-10, the solvolysis of 19-norsteroids was studied.

Starting Materials

A suitable intermediate for this investigation was the recently described 4,4-dimethyl-estr-5-en-17β-ol-3-one (IV)(3), which can be obtained by a 5-step reaction from estrone* (3, 4).

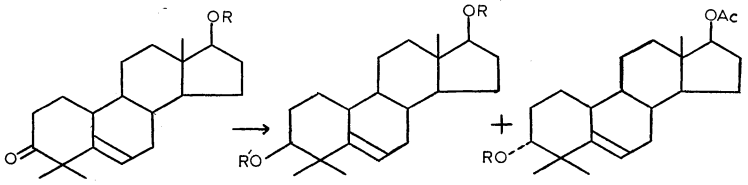

IV R=H V R'=H, R=Ac VI R=H

IVa R=Ac Va R'=Ts, R=Ac VIa R=Ts

Vb R'=R=H

[1]*Presented in part at the Meeting of the Chemical Institute of Canada, Edmonton, Alberta, June 1962.*
[2]*This investigation was supported by a National Research Council Grant.*
[3]*From the Ph.D. thesis presented to the Faculty of Graduate Studies, McGill University.*
[4]*Holder of a National Research Council of Canada Studentship, 1959–61.*
**We wish to thank Ayerst, McKenna, and Harrison for a generous gift of estrone.*

Can. J. Chem. Downloaded from www.nrcresearchpress.com by 210.87.254.5 on 09/05/12
For personal use only.

Acetylation of the 17β-alcohol IV gave 4,4-dimethyl-17β-acetoxyestr-5-en-3-one IV*a*, m.p. 135.5–136°, $[\alpha]_D$ −10.6°. The acetate IV*a* possessed infrared absorption maxima at 1707 cm^{-1} (ketone)and 1737 cm^{-1} (acetate) and the elemental analysis agreed well with the molecular formula $C_{22}H_{32}O_3$.

The reduction of 4,4-dimethyl-17β-acetoxyestr-5-en-3-one (IV*a*) using a slight excess of sodium borohydride in dimethyl formamide (5), followed by careful chromatography, resulted in the formation of very small amounts of 3α-alcohol VI, m.p. 144–147°, which was not depressed on admixture with the corresponding β-alcohol,* m.p. 184.5–185°. A comparison of infrared absorption curves in the 3400–3650 cm^{-1} region revealed small but constant differences between the two epimers. For example, with identical concentrations, 4,4-dimethyl-17β-acetoxyestr-5-en-3α-ol (VI) absorbed at 3642 cm^{-1} (CCl_4, hydroxyl) whilst 4,4-dimethyl-17β-acetoxyestr-5-en-3β-ol (V) possessed a maximum at 3635 cm^{-1} (CCl_4, hydroxyl).

The 3α-alcohol VI was reacted with *p*-toluenesulphonyl chloride for 12 days at room temperature to give 4,4-dimethyl-17β-acetoxyestr-5-en-3α-ol 3-*p*-toluenesulphonate (VI*a*) in 75% yield. Because of decomposition of the tosylate when reacted for longer periods, the reaction was interrupted before completion. An oily residue was isolated which still contained 25% unreacted starting alcohol VI.

Reduction using aluminum isopropoxide in isopropanol (6) resulted in hydrolysis of the 17-acetate group without reduction of the carbonyl function.

Solvolysis of 4,4-Dimethyl-17β-acetoxyestr-5-en-3β-ol 3-p-Toluenesulphonate

The acetolysis of 4,4-dimethyl-17β-acetoxyestr-5-en-3β-ol 3-*p*-toluenesulphonate (V*a*) was effected by maintaining a sodium acetate buffered glacial acetic acid solution of the sulphonate at 50° for 50 hours. The resulting oil was chromatographed on aluminum oxide. Hexane eluted 11% of a non-conjugated diene monoacetate VII, followed closely by 22% of a conjugated diene monoacetate VIII. Hexane–benzene mixtures gave 53% of a diacetate IX*a*.

Acetone–water solvolysis of 4,4-dimethyl-17β-acetoxyestr-5-en-3β-ol 3-*p*-toluenesulphonate (V*a*) was carried out at the reflux temperature for 20.5 hours using sodium

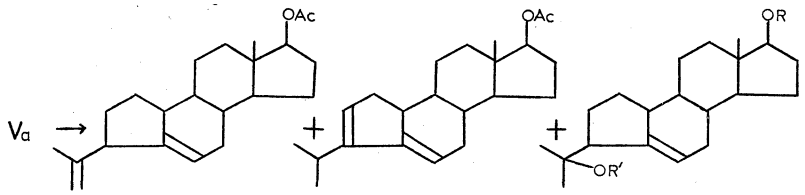

VII VIII IX R=Ac, R'=H

IXa R=R'=Ac

IXb R=R'=H

acetate buffer. The resulting oil was chromatographed on aluminum oxide. Hexane and hexane–benzene (95:5) eluted 20% of a non-conjugated diene monoacetate which was identical with the acetolysis diene VII. A conjugated diene monoacetate was next eluted in 7.5% yield and was found to have the same ultraviolet spectrum as the conjugated

**For the β-alcohol V, see the experimental section.*

Can. J. Chem. Downloaded from www.nrcresearchpress.com by 210.87.254.5 on 09/05/12
For personal use only.

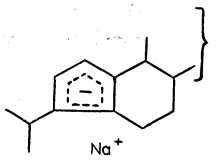

X

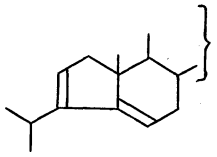

XI

diene VIII derived from the acetolysis. Continued elution with hexane–benzene (1:1 and 1:2) gave 66.5% of ring-contracted diol monoacetate IX.

Both ring-contracted dienes VII and VIII gave a water-soluble sodium salt on refluxing in methanolic sodium hydroxide. This behavior pointed to the formation of a cyclopentadienyl anion X. Under the same conditions the ring-contracted diol monoacetate IX quantitatively gave the diol IX*b*.

Diene monoacetate VII, derived from both solvolyses, did not absorb between 220 and 350 mμ and hence was not conjugated. Infrared analysis revealed, in particular, strong absorption at 3060, 1641, and 887 cm^{-1} (CCl_4) typical for an exomethylene double bond. The only structure compatible with the lack of significant absorption between 220 mμ and 350 mμ, the infrared evidence, and the formation of a cyclopentadienyl anion upon treatment with strong alkali, is that proposed in VII. As will be shown below, it is also compatible with the proposed mechanism of the solvolysis.

Diene monoacetate VIII exhibited a characteristic ultraviolet absorption pattern, λ_{max} 244 mμ (ϵ 9700), 252 mμ (10,000) and 262 mμ, inflection (6600), which was very similar to that assigned to the $\Delta^{2,5}$-diene XI, λ_{max} 244.5 mμ (ϵ 15,500), 252 mμ (16,600), and 261.5 mμ (10,400), encountered in the cholesterol series (1). This makes VIII the probable structure for this conjugated diene, although other formulations cannot be rigorously ruled out.

Hydrolysis of the diol monoacetate IX in 5% methanolic potassium hydroxide gave diol IX*b*, m.p. 168–168.5°, $[\alpha]_D$ −1.4°, for which the elemental analysis agreed with the empirical formula $C_{20}H_{32}O_2$. Reacetylation with acetic anhydride in pyridine for 16 hours at room temperature regenerated the diol monoacetate IX. This indicated that the unesterified alcohol was tertiary. Oxidation of IX with chromium trioxide in pyridine resulted in the recovery of unchanged starting material, further confirming the tertiary nature of the alcohol. A solution of the diol IX*b* in glacial acetic acid was hydrogenated using Adam's catalyst. One equivalent of hydrogen was absorbed. The resulting saturated alcohol XII was acetylated at room temperature, yielding a diol monoacetate XII*a* (ν^{CCl_4}, 3610 cm^{-1} hydroxyl and 1733 cm^{-1} acetate). The alcohol therefore did not suffer hydrogenolysis, a finding which was in direct contrast to results obtained in the cholesterol series (1).

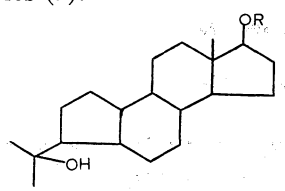

XII R=H

XIIa R=Ac

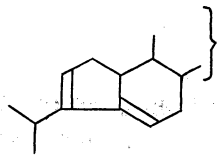

XIII

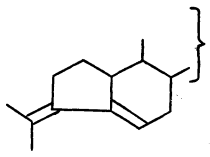

XIV

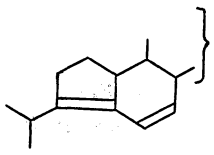

XV

Can. J. Chem. Downloaded from www.nrcresearchpress.com by 210.87.254.5 on 09/05/12
For personal use only.

The reaction of phosphorus oxychloride in pyridine on diol IX*b* resulted in the production of an oil which contained at least two dienes. Ultraviolet absorption analysis of the above oil revealed the following absorption maxima in cyclohexane: 244 mμ (ε 7800), 252 mμ (6700), and 262 mμ, inflection (5200). Comparison of ε-values with those obtained in the cholesterol series indicated the possible presence of approximately 40% of the $\Delta^{2,5}$-diene XIII. However, the relative ratios of ε-values were somewhat high between 240 mμ and 250 mμ, showing that some other diene similar to XIV (λ_{max} 250 mμ, ε 13,300) or XV (λ_{max} 243 mμ, ε 9250) might also have been formed. Substituted cyclopentadiene compounds have been shown (7) to absorb in the region of 243 mμ and could account for the enhanced ultraviolet absorption indicated. Too little material was available to investigate in detail the composition of this mixture.

Solvolysis of 4,4-Dimethyl-17β-acetoxyestr-5-en-3α-ol 3-p-Toluenesulphonate

The *p*-toluenesulphonate VI*a* was dissolved in glacial acetic acid, containing excess sodium acetate, and solvolyzed at 52° for 3 days. Examination of an aliquot showed that the reaction was not complete. Hence, the mixture was heated to reflux for 12 hours. A yellow oil was isolated which in addition to containing unchanged 4,4-dimethyl-17β-acetoxyestr-5-en-3α-ol (VI) also contained an olefinic acetate. The crude solvolysis oil possessed ultraviolet absorption maxima at 236 mμ (ε 11,000), 243 mμ (18,000), and 252 mμ, inflection (6930). A comparison of this absorption data with that obtained for 3,4-dimethylcholesta-3,5-diene (II), λ_{max} 236 mμ (ε 19,500), 243 mμ (19,900), and 252 mμ, inflection (12,800), indicated that the acetolysis of 4,4-dimethyl-17β-acetoxyestr-5-en-3α-ol 3-*p*-toluenesulphonate (VI*a*) produced 56% of methyl-shifted diene XVI. The absorption at 243 mμ is obviously elevated because of the presence of at least one more conjugated diene. As indicated previously, cyclopentadiene compounds absorb precisely in this range. Hence the presence of a cyclopentadiene contaminant cannot be ignored

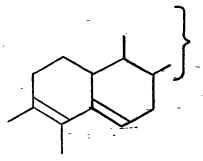

XVI

in accounting for the remaining acetolysis products. Since only small amounts of the 3α-epimer were available, the study was discontinued.

However unsatisfactory these results are with respect to the identification of the products, they show clearly that 3α-hydroxyestrene derivatives also give products of methyl shift, similar to those obtained in the cholesteryl series, and that they could easily be detected. It can therefore be concluded that no significant amount of methyl-shifted product was formed in the solvolysis of 4,4-dimethyl-17β-acetoxyestr-5-en-3β-ol 3-*p*-toluenesulphonate.

EXPERIMENTAL

(*a*) All melting points were corrected.
(*b*) The commercially available aluminum oxide (Woelm) was used for chromatography.
(*c*) All ether solutions were dried over anhydrous magnesium sulphate.

Acetylation of 4,4-Dimethylestr-5-en-17β-ol-3-one (3) (IV)

A solution of 1.215 g of the 17β-alcohol IV, m.p. 143.5–144.5°, in 10 ml of pyridine and 10 ml of acetic anhydride was allowed to stand overnight at room temperature. The pyridine solution was poured into iced

Can. J. Chem. Downloaded from www.nrcresearchpress.com by 210.87.254.5 on 09/05/12
For personal use only.

5% hydrochloric acid and extracted with ether. Washing with water, followed by drying and evaporation, gave 1.315 g of colorless residue, m.p. 131–132°. A single recrystallization from acetone–water raised the melting point to 133.5–134° (1.03 g). Two further recrystallizations gave pure 4,4-dimethyl-17β-acetoxyestr-5-en-3-one, m.p. 135.5-136°, $[\alpha]_D^{15}$ −10.6° (*c*, 0.946), ν^{CCl_4} 1707 cm^{-1} (carbonyl) and 1737 cm^{-1} (acetate). Anal. Calc. for $C_{22}H_{32}O_3$: C, 76.74; H, 9.30. Found: C, 76.29; H, 9.34.

Sodium Borohydride Reduction of 4,4-Dimethyl-17β-acetoxyestr-5-en-3-one (IVa)

A solution of 1.03 g of ketone IV*a*, m.p. 135.5–136°, in 25 ml of methanol was added to a solution of 119 mg of sodium borohydride in 10 ml of methanol and 2 ml of water. The mixture was stirred for 20 minutes at room temperature and diluted with 40 ml of water. Extraction with ether followed by washing with water, drying, and evaporation to dryness gave 1.06 g of colorless residue, m.p. 174–175°. Difficulty was experienced in obtaining a suitable recrystallizing solvent system.

The reduced product (1.06 g) was chromatographed on 35 g of aluminum oxide (activity II–III). Hexane–benzene (4:1) eluted 244 mg of colorless residue, melting range 174.5–182.5°. Rechromatography of this fraction gave 114 mg of the 3β-alcohol, m.p. 184–186°, which did not give a melting point depression with the main alcohol fractions.

Further elutions with hexane–benzene (4:1) gave 846 mg of pure alcohol V, m.p. 184.5–185.5°, ν^{CCl_4} 3655 cm^{-1} (hydroxyl) and 1735 cm^{-1} (acetate). Anal. Calc. for $C_{22}H_{34}O_3$: C, 76.25; H, 9.83. Found C, 76.50; H, 9.91.

Repeated chromatography of the initial fractions on aluminum oxide and silica gel failed to produce any detectable amounts of the α-epimer VI.

Hydrolysis of 4,4-Dimethyl-17β-acetoxyestr-5-en-3β-ol (V)

A solution of the 17β-acetate V (30 mg, m.p. 184.5–185°) in 5% methanolic potassium hydroxide (20 ml) was refluxed for 60 minutes. The reaction mixture was poured into cold water and extracted with ether. After it was washed with water and dried, the ether solution, on evaporation, yielded 32 mg of an oily residue. Recrystallization from aqueous methanol gave 19 mg of diol V*b*, m.p. 193.5–194.5°, $[\alpha]_D$ +8° (*c*, 1.32) (m.p. 192–194°, $[\alpha]_D$ +4°) (3).

Preparation of 4,4-Dimethyl-17β-acetoxyestr-5-en-3β-ol 3-p-Toluenesulphonate (Va)

To a solution of 620 mg of alcohol V, m.p. 184.5–185°, in 20 ml of pyridine was added 1.0 g of *p*-toluenesulphonyl chloride and the mixture allowed to stand at room temperature for 6 days. The pyridine solution was poured on crushed ice and the ether extract washed initially with iced 5% hydrochloric acid and finally with iced water. Drying followed by evaporation *in vacuo* gave 0.98 g of colorless tosylate V*a*, m.p. 134° dec., ν^{CCl_4} 1735 cm^{-1} (acetate), 1188 cm^{-1}, and 1178 cm^{-1} (tosylate); $\lambda_{max}^{ethanol}$ 225 mμ, ε 13,500.

Acetolysis of 4,4-Dimethyl-17β-acetoxyestr-5-en-3β-ol 3-p-Toluenesulphonate (Va)

A solution of 100 mg of toluenesulphonate V*a*, m.p. 134° dec., in 30 ml of glacial acetic acid was buffered with 75 mg of sodium acetate and maintained at 50° for 50 hours. The reaction mixture was poured into a large volume of iced water and extracted with ether. Washing was carried out with 5% sodium bicarbonate solution and water. The ethereal layer was finally dried and evaporated to dryness. A yellow oil (80 mg) resulted.

On chromatography, using 5 g of aluminum oxide (activity II–III), hexane eluted 9 mg (11%) of oil which failed to crystallize and possessed no characteristic ultraviolet absorption. The infrared analysis (CCl_4) revealed absorption at 1735 cm^{-1} (acetate), 3080 cm^{-1}, 1641 cm^{-1}, and 887 cm^{-1}, strong (exomethylene). The compound was assigned structure VII.

Further elution with hexane gave 17 mg (22%) of oil, $\lambda_{max}^{ethanol}$ 244 mμ, ε 14,550, 252 mμ, ε 15,840, 261 mμ, inflection, ε 13,200. The ultraviolet absorption pattern for this compound was very similar to that of diene XI in the cholesterol series and was assigned the structure VIII.

Hexane–benzene mixtures eluted initially 9 mg of oil followed by 32 mg of oily crystals, representing a total of 53%. Infrared analysis (CCl_4) indicated absorption in the region of 1735 cm^{-1}, broad, very strong (diacetate). Diacetate IX*a* possessed no characteristic ultraviolet absorption.

Solvolysis of 4,4-Dimethyl-17β-acetoxyestr-5-en-3β-ol 3-p-Toluenesulphonate (Va) in Aqueous Acetone

To a solution of 750 mg of tosylate V*a*, m.p. 134° dec., in 180 ml of acetone was added a solution of 400 mg of sodium acetate in 18 ml of water. The mixture was refluxed for 20.5 hours, then cooled and most of the acetone was evaporated *in vacuo*. The residual aqueous oily liquor was extracted with ether, the ethereal layer washed well with iced water, dried, and evaporated to dryness. The resulting oil (0.52 g) possessed no infrared absorption (CCl_4) in the region 1175–1190 cm^{-1}, indicating complete solvolysis.

The solvolysis oil was chromatographed on 25 g of aluminum oxide (activity II–III). Hexane and hexane–benzene (95:5) eluted 126 mg, 25% (second run 15%), of a colorless oil (VII) which failed to crystallize, ν^{CCl_4} 1732 cm^{-1} (acetate), 3060 cm^{-1} (double bond), and 887 cm^{-1}, strong and sharp (exomethylene). Hydroxyl absorption was absent. Ultraviolet analysis revealed no recognizable characteristics.

Hexane–benzene (95:5) eluted 35 mg, 7% (second run 8%), of an oily residue (VIII), ν^{CCl_4} 1735 cm^{-1} (acetate), $\lambda_{max}^{ethanol}$ 244 mμ, ε 9700, 252 mμ, ε 10,000, and 262 mμ (inflection), ε 6000. The ultraviolet absorption

Can. J. Chem. Downloaded from www.nrcresearchpress.com by 210.87.254.5 on 09/05/12
For personal use only.

pattern is typical for the assigned $\Delta^{2,5}$-diene XI, $\lambda_{max}^{cyclohexane}$ 244 mμ (ϵ 15,000), 252 mμ (16,300), and 262 mμ (10,700), encountered in the cholesteryl series.

Hexane–benzene (1:1 and 1:2) and benzene eluted 325 mg, 63% (second run 70%), of colorless oil (IX) which readily crystallized on moistening with methanol, m.p. 88–91°, ν^{CCl_4} 3630 cm^{-1} (hydroxyl), 1735 cm^{-1} (acetate), and 1670 cm^{-1} (double bond). Attempted recrystallization from the normal solvents failed to give good crystalline form. Alcohol IX was therefore characterized by its diol derivative IX*b* described below.

Reaction of Diene VII with 5% Methanolic Sodium Hydroxide

Diene VII (50 mg) was dissolved in 15 ml of 5% methanolic sodium hydroxide and gently refluxed for 60 minutes. The solution turned from a pale yellow coloration to an intense brown-red. On extraction of the solution with ether, followed by three water washes, most of the colored material transferred to the aqueous phase. The ether layer was dried and evaporated *in vacuo* to yield 30 mg of pale yellow oil.

The aqueous layer was acidified with a few drops of concentrated hydrochloric acid and re-extracted with ether. After washing with water, the ether layer was dried and evaporated to give 17 mg of oil, a total of 47 mg.

Reaction of Diene VIII with 5% Methanolic Sodium Hydroxide

Diene VIII (33 mg) was refluxed in 15 ml of 5% methanolic sodium hydroxide for 60 minutes and extracted as given in the previous experiment. The neutral ether extract gave 22 mg of oil whilst the acidified alkaline extract gave 9 mg of oil, totalling 31 mg overall.

Reaction of Alcohol IX with 5% Methanolic Sodium Hydroxide

Alcohol IX (295 mg, m.p. 88–91°) was refluxed in 30 ml of 5% methanolic sodium hydroxide for 60 minutes. The reaction mixture was cooled and most of the methanol removed *in vacuo*. Ether (300 ml) was added and the ether solution washed with water until neutral. It was then dried and the ethereal solution evaporated *in vacuo* to yield 294 mg of a colorless residue, m.p. 164–167°. Successive recrystallizations from methanol–water (1:1) gave 183 mg of pure diol IX*b*, m.p. 168–168.5°, $[\alpha]_D^{27}$ −1.41° (*c*, 0.71), ν^{CCl_4} 3620 cm^{-1} (hydroxyl), 3030 cm^{-1}, and 1662 cm^{-1} (double bond), 1154 cm^{-1} (tert. alcohol), 1052 cm^{-1} (sec. alcohol). Anal. Calc. for $C_{20}H_{32}O_2$: C, 78.93; H, 10.52. Found: C, 78.71; H, 10.48.

Acetylation of Ring-contracted Diol IXb

Diol IX*b* (53 mg, m.p. 168°) was dissolved in 2 ml of pyridine and 1 ml of acetic anhydride added. After standing overnight at room temperature, the reaction mixture was poured on iced 5% hydrochloric acid. Extraction with ether followed by aqueous washes, drying, and evaporation to dryness gave 64 mg of crystals, m.p. 85–86°. Mixed melting points with the original solvolysis alcohol–acetate IX gave no depression. A comparison of the infrared absorption curves obtained from the solvolysis acetate and the synthesized acetate, in both carbon disulphide and carbon tetrachloride, indicated no detectable difference.

Chromium Trioxide – Pyridine Oxidation of Ring-contracted Acetate IX (8)

Acetate IX (13 mg, m.p. 88–91°) was dissolved in 0.25 ml of pyridine and a solution of 25 mg of chromium trioxide in 0.25 ml of pyridine added. The reaction mixture was gently agitated for 30 minutes and then allowed to stand at room temperature overnight. After pouring on iced 5% hydrochloric acid, extraction with ether was carried out. Three water washes rendered the ethereal layer neutral. After drying, evaporation to dryness yielded an oily residue. A comparison of infrared curves showed no difference between that of the reaction product and the starting material.

Hydrogenation of Ring-contracted Diol IXb

A glacial acetic acid solution of diol IX*b* (9 mg, m.p. 168°) was hydrogenated at room temperature using Adam's catalyst. One equivalent of hydrogen was quickly taken up. The hydrogenation was continued for a further 3 hours without detectable hydrogen uptake. The hydrogenation mixture was diluted with ether and filtered. Numerous washings with 10% sodium bicarbonate solution, followed by water washes, rendered the ether layer neutral. After drying, the ether solution was evaporated *in vacuo* to give 8 mg of a colorless oil.

Without further examination, the hydrogenation product XII was dissolved in 2 ml of pyridine, 2 ml of acetic anhydride added, and the mixture was allowed to stand at room temperature overnight. The pyridine solution was added to iced 5% hydrochloric acid, extracted with ether and the extract washed well with water. When the solution was dried and evaporated to dryness, a pale yellow oil (XII*a*) resulted; ν^{CCl_4} 3610 cm^{-1} (hydroxyl) and 1733 cm^{-1} (acetate). It was not possible to detect any absorption due to unsaturation.

Reaction of Phosphorus Oxychloride – Pyridine with Ring-contracted Diol IXb

A solution of 5 mg of diol IX*b* in 1 ml of pyridine was treated with 0.5 ml of phosphorus oxychloride and allowed to stand overnight at room temperature. With cooling, a careful addition of ice was made and the whole extracted with ether. After water washing, the ether solution was dried and evaporated *in vacuo*. A pale yellow oil (5 mg) was obtained; ν^{CCl_4} 3030 cm^{-1} (double bond), $\lambda_{max}^{cyclohexane}$ 244.5 mμ, ϵ 7800; 252 mμ,

Can. J. Chem. Downloaded from www.nrcresearchpress.com by 210.87.254.5 on 09/05/12
For personal use only.

ϵ 6700 and 262 mμ (inflection), ϵ 5200. On the basis of ultraviolet absorption values obtained for the assigned $\Delta^{2,5}$-diene XI, $\lambda_{max}^{cyclohexane}$ 244.5 mμ (ϵ 15,500), 252 mμ (16,600), and 261.5 mμ (10,400), the presence of 41% of diene XIII is indicated.

Anhydrous Sodium Borohydride Reduction of 4,4-Dimethyl-17β-acetoxyestr-5-en-3-one (IVa)

Ketone IV*a*, m.p. 139° (2.263 g), was dissolved in anhydrous dimethyl formamide (b.p. 152–153°) and 0.390 g (1.5 equivalents) of sodium borohydride added. Refluxing was carried out for 20 minutes. The cooled reaction mixture was poured on 300 ml of iced water containing 10 ml of concentrated hydrochloric acid. Extraction with ether was carried out and the ether solution washed four times with water before drying *in vacuo*. The resulting colorless residue (2.27 g) was chromatographed on 100 g of silica gel (Davison).

Careful elution with benzene–ether (98:2) at first gave 31 mg of oil followed by 62 mg of crystalline 3α-alcohol VI, m.p. 141–147°. Further elution with the same solvent system gave 412 mg of colorless residue, m.p. 162.5–164°, followed by 286 mg, m.p. 167–169°.

Ether (100%) gave 1.50 g of colorless residue, m.p. 167–169°. A 5% methanolic potassium hydroxide hydrolysis of a representative sample taken from the latter fractions gave a diol, m.p. 185–187°. The diol did not give a melting point depression on admixture with an authentic sample of diol V*b* and the infrared absorption curves were superimposable.

Rechromatography of 300 mg of material, m.p. 162.5–164°, on 60 g of silica gel (Davison) yielded a further 28 mg of 3α-alcohol, m.p. 148–150°.

The low melting fractions of 3α-alcohol were combined (90 mg) and recrystallized repeatedly from methanol to give pure material, m.p. 144–147°; ν^{CCl_4} 3642 cm^{-1} (hydroxyl), 1733 cm^{-1} (acetate), 3050 cm^{-1}, and 1652 cm^{-1} (double bond). Anal. Calc. for $C_{22}H_{34}O_3$: C, 76.26; H, 9.86. Found C, 76.30; H, 9.73.

Comparison of 4,4-Dimethyl-17β-acetoxyestr-5-en-3α- and -3β -ols

Upon admixture, no melting point depression was observed. Infrared curves were recorded for both epimers on the Perkin–Elmer 421 spectrophotometer. An enlarged scale for the 3000–3600 cm^{-1} region was used. Extreme care was taken in using identical concentrations. 3α-Hydroxy: ν^{CCl_4} 3642 cm^{-1} (hydroxyl). 3β-Hydroxy: ν^{CCl_4} 3635 cm^{-1} (hydroxyl).

Preparation of 4,4-Dimethyl-17β-acetoxyestr-5-en-3α-ol 3-p-Toluenesulphonate (VIa)

The 3α-alcohol VI (86 mg, m.p. 144–147°) was dissolved in 8 ml of pyridine and 100 mg of *p*-toluenesulphonyl chloride added. After standing at room temperature for 12 days, the pyridine solution was poured on crushed ice. Extraction with ether was carried out followed by iced 5% hydrochloric acid and water washes. The ethereal layer was dried and evaporated *in vacuo*. A yellow oily solid (100 mg) resulted, ν^{CCl_4} 3640 cm^{-1} (hydroxyl), 3050 cm^{-1} (double bond), 1733 cm^{-1} (acetate), 1189 cm^{-1}, and 1180 cm^{-1} (tosylate); $\lambda_{max}^{ethanol}$ 224–225 mμ, ϵ 9000.

Acetolysis of 4,4-Dimethyl-17β-acetoxyestr-5-en-3α-ol 3-p-Toluenesulphonate (VIa)

Toluenesulphonate VI*a* (100 mg) was dissolved in 15 ml of glacial acetic acid and 100 mg of sodium acetate added. The reaction mixture was maintained at 52° for 3 days. Examination of an aliquot indicated incomplete reaction, hence the acetolysis was continued at reflux temperature overnight. On cooling, the solvolysis mixture was extracted with ether and the extract washed twice with water, four times with 10% sodium bicarbonate solution, three times with water, dried and evaporated to dryness to give 75 mg of yellow oil; ν^{CCl_4} 3640 cm^{-1} (hydroxyl), 3050 cm^{-1} (double bond), and 1733 cm^{-1} (acetate); $\lambda_{max}^{cyclohexane}$ 236 mμ (ϵ 11,000), 243 mμ (ϵ 18,000), and 252 mμ, inflection (ϵ 6930). On the basis of ultraviolet absorption data derived from methyl-shifted diene II ($\lambda_{max}^{cyclohexane}$ 236 mμ, ϵ 19,500; 243 mμ, ϵ 19,000; and 252 mμ, inflection, ϵ 12,800), the presence of 56% methyl-shifted diene XVI is indicated.

REFERENCES

1. G. Just, F. E. Shortland, R. Sneen, and S. Winstein. Abstracts of the C. I. C. Meeting, Edmonton, Alberta. June, 1962.
2. G. Just and K. St. C. Richardson. Can. J. Chem. In press.
3. A. Bowers and H. J. Ringold. J. Am. Chem. Soc. **81**, 424 (1959).
4. D. J. Marshall. Private communication. G. Papineau-Couture, E. M. Richardson, and G. A. Grant. Can. J. Res. **27B**, 902 (1949). A. L. Wilds and N. A. Nelson. J. Am. Chem. Soc. **75**, 5360, 5366 (1953). A. J. Birch. J. Chem. Soc. 367 (1950).
5. D. Taub, R. D. Hofsommer, and N. L. Wendler. J. Am. Chem. Soc. **81**, 3291 (1959).
6. W. J. Wilds. Organic reactions. Vol. 2. John Wiley and Sons, Inc., New York. 1944. Chap. 5.
7. A. Weissberger. Technique of organic chemistry. Vol. IX. Interscience Publishers, Inc., New York. 1956. p.656.
8. G. I. Poos, G. E. Arth, R. E. Beyler, and L. H. Sarett. J. Am. Chem. Soc. **75**, 422 (1953).

Can. J. Chem. Downloaded from www.nrcresearchpress.com by 210.87.254.5 on 09/05/12
For personal use only.

Can. J. Chem. Downloaded from www.nrcresearchpress.com by 210.87.254.6 on 09/05/12
For personal use only.

NOTES

ON THE EQUILIBRIUM ATTAINED BY ELECTROLYTIC SOLUTIONS UNDER IONIZING RADIATION*

J. R. COLEMAN

Henderson *et al.* (1) irradiated a number of redox systems in aqueous solution and measured the resulting potentials at a platinum electrode. They observed in each case a potential of 0.83–0.88 v referred to a hydrogen electrode in the same solution, or approximately 0.85–0.06 pH, referred to the normal hydrogen electrode.† These results were advanced in support of a suggestion by Dainton and Collinson (2) that aqueous solutions under prolonged irradiation might attain a steady state in which the reducing and oxidizing actions of irradiation products and (or) intermediates were equal and opposed. Dainton and Collinson called the potential corresponding to this state the equivalent redox potential (e.r.p.). It was subsequently pointed out (3–5) that Bockris and Oldfield (6) had found a very similar behavior and pH dependence while measuring potentials produced by H_2O_2 solutions at a platinum electrode, and it was shown by Feates and Knight (5) that the potentials observed by Henderson *et al.* could be reproduced by adding H_2O_2 to aqueous H_2SO_4. It was decided to repeat certain of these experiments, analyzing where possible for substances that might affect or determine the potential.

Dainton and Collinson's original estimate of the e.r.p. (0.94 v) was based on the work of Lefort (7) on nitrite and nitrate systems. A later investigation of the nitrite system (8) suggested the necessity of repeating this work.

EXPERIMENTAL

The apparatus and experimental procedures have been described by Henderson *et al.* The apparatus was modified to permit sampling by expulsion of aliquots of solution with inert gas during brief intermissions in irradiation. All experiments were carried out in N_2- or argon-saturated solution. X- and Co^{60} γ-radiation were used at dose rates of 4 to 6×10^{14} ev ml^{-1} sec^{-1}. All potentials are reported with respect to a hydrogen electrode in the same solution.

H_2O_2 was determined by titanium sulphate reagent (9) and NO_2^- by a variation of the Griess method (10). I_2 was determined by the optical density maximum at 460 mμ in aqueous solution. As I_2 and I_3^- have the same extinction coefficient at 465 mμ (11), measurements at 460 mμ give $(I_2+I_3^-)$ as I_2 with sufficient accuracy. Ferric and ceric ion were determined spectrophotometrically at 305 and 330 mμ, at 24° (12, 13).

RESULTS

Nitrite–Nitrate

Lefort reported that $NaNO_2$ and $NaNO_3$ in neutral unbuffered solution (10^{-3} *M*) reached on irradiation an equilibrium in which about 4×10^{-4} *M* NO_2^- and 6×10^{-4} *M* NO_3^- were present, and this, together with the E_0 of the HNO_2/NO_3^- couple, 0.94 v (14), led Dainton and Collinson to propose 0.95 v for the e.r.p. Lefort analyzed for NO_2^- by determining the I_2 produced in acidified solution by the reaction

$$HNO_2 + I^- + H^+ \rightarrow NO + \tfrac{1}{2}I_2 + H_2O$$

when excess KI was added. H_2O_2, subsequently demonstrated to be present by Schwarz and Allen (8), would also oxidize I^- to I_2 by

$$2H^+ + H_2O_2 + 2I^- \rightarrow I_2 + 2H_2O.$$

*Issued as D.R.C.L. Report No. 419.
†European sign convention.

Lefort's experiments were therefore repeated, analyzing for NO_2^- and H_2O_2 as in the experimental part above. Analysis disclosed that, beginning with either 10^{-3} *M* $NaNO_2$ or $NaNO_3$, only about 1.1×10^{-5} *M* NO_2^- was present finally, while H_2O_2 built up to a concentration of 1.75×10^{-4} *M*. As H_2O_2 is twice as efficient as NO_2^-, mole for mole, in oxidizing I^- to I_2, it was concluded that Lefort's results could be accounted for by the presence of H_2O_2, the final ratio NO_2^-/NO_3^- being 1:90 and not 4:6.

Iron and Cerium Sulphates

When solutions of $FeSO_4$ (5×10^{-4} *M*) or $Ce(SO_4)_2$ ($2–5\times10^{-4}$ *M*) in 0.5 *M* H_2SO_4 were irradiated, oxidation of Fe^{+2} and reduction of Ce^{+4} went to completion. While oxidation (or reduction) was proceeding, the observed potentials and Fe^{+2}/Fe^{+3} (or Ce^{+3}/Ce^{+4}) ratios determined by analysis were related by the Nernst equation, the potentials being the same as those of unirradiated solutions of the same composition. When irradiation was continued past the point of complete oxidation or reduction respectively, H_2O_2 began to be formed in detectible amount, and the potential drifted to final steady values in the range 0.86–0.88 v for iron (12 runs) and 0.82–0.88 v for cerium (five runs). Final potentials were quite steady in any one run but varied within the limits given in a series of runs. Similar results were obtained when $FeSO_4$ or $Ce(SO_4)_2$ in H_2SO_4 was titrated with H_2O_2 until an excess of H_2O_2 had been added. Potentials rose (with $FeSO_4$) or fell (with $Ce(SO_4)_2$), after each H_2O_2 addition, to constant values which were related by the Nernst equation to the new Fe^{+2}/Fe^{+3} or Ce^{+3}/Ce^{+4} level. After addition of excess H_2O_2 potentials drifted to final steady values in the same range (0.83–0.88 v).

H_2SO_4 Alone

The observation of Zalkind and Veselovsky (15) and Feates (16) was confirmed, that when H_2SO_4 (1.0 *M*) without added redox system was irradiated, the potential fell first to a hydrogen-like value and then rose to values constant in any one run but varying between runs from 0.81 to 0.87 v, H_2O_2 again being observed in amounts of the order of 10^{-4} *M*.

These final peroxide-like potentials, whether obtained by prolonged irradiation or by addition of excess H_2O_2 to $FeSO_4$ or $Ce(SO_4)_2$, were affected by the presence or absence of irradiation, fluctuating by 10—20 mv as it is cut off or resumed, but there is little doubt that in all these systems they are ascribable to H_2O_2 acting at the platinum electrode, perturbed to some extent by radiation and by Fe^{+3} or Ce^{+3} if present.

Iodide–Iodine

When solutions of KI or I_2 ($1–3\times10^{-4}$ *M*) in 1 *M* H_2SO_4 were irradiated, oxidation of I^- or reduction of I_2 was observed, a quasi steady state being reached from both sides in which about 85% of the iodine was in the oxidized form, I_2. This steady state persisted for about 24 hours and was followed by a slow further oxidation of I^- to I_2, proceeding for as long as it was possible to irradiate continuously (120 hours). A Nernst plot (v vs. log $I_2/(I^-)^2$) coincided with that obtained by oxidation of KI in H_2SO_4 with H_2O_2, or by electrolytic oxidation and reduction of KI–I_2 solution in H_2SO_4 at an auxiliary electrode. Extrapolation of the Nernst plot to log $I_2/(I^-)^2 = 0$ gave an E_0 of 0.620 v, in agreement with Riddiford's value (17) for I_2 (in solution)/I^-.

The potential was unaffected by momentary removal of the source, or by the presence of H_2O_2, which accumulated from the beginning of irradiation.

Corresponding to the steady-state I_2/I^- ratio a constant potential of 0.76–0.77 v was observed during irradiation, rising slowly as the oxidation of I^- resumed. If irradiation

Can. J. Chem. Downloaded from www.nrcresearchpress.com by 210.87.254.6 on 09/05/12
For personal use only.

was cut off during the steady-state period the accumulated H_2O_2 rapidly oxidized the remaining I^- to I_2, and in the presence of sufficient H_2O_2 a rapid oxidation of I_2 to IO_3^- set in, after an induction period of several hours. Parallelling these postirradiation changes, the potential rose from 0.76–0.77 v to about 0.85 v, and, after an arrest of several hours, climbed rapidly to 1.15 v, with the beginning of IO_3^- formation. When the system had once passed from the I_2–I^- to the I_2–IO_3^- domain, further irradiation led only to complete oxidation of the remaining I_2 to IO_3^-, which was stable to doses $>10^{21}$ ev ml^{-1}.

DISCUSSION

In the earlier work (1) a steady potential of about 0.85 v was obtained in a relatively short time (<24 hours) on irradiation of KI–I_2 solution in H_2SO_4. This potential would correspond to complete oxidation of I^- to I_2, and is in fact observed when H_2O_2 is added to I_2 in H_2SO_4, during the induction period preceding the oxidation of I_2 to IO_3^-. The H_2O_2–I_2 system behaves in this respect as does H_2O_2 with Fe^{+3} and Ce^{+3}. However, in the present work under continuous irradiation I^- is not oxidized to I_2 completely even after 120 hours. No explanation has been found for this discrepancy.

In all the systems studied except iodine, the final potentials reached after prolonged irradiation can be reproduced simply by adding H_2O_2 to the original solution. There is then, as Feates and Knight suggested (5), no need to invoke a radiation-produced steady-state potential as explanation. Further, in the presence of a redox couple which is electromotively active on platinum, the potential observed during oxidation or reduction of the couple by irradiation is that of the couple itself. That is, all values are ascribable to molecular products of irradiation.

Two phenomena do not fit into this scheme: (*i*) In several systems the final potentials are affected by the presence of irradiation, fluctuating by 10–20 mv as it is cut off or resumed. This has been ascribed to photosorptions (1). (*ii*) In the I_2–I^- system a temporary arrest occurs under irradiation at about the 85% level of oxidation. Allen (18) suggested that in air-saturated KI solutions H (through HO_2 formation) might reduce I_2 by

$$HO_2 + I_2 \rightarrow I^- + I + H^+ + O_2,$$

as well as oxidizing I^- by

$$HO_2 + H^+ + I^- \rightarrow H_2O_2 + \tfrac{1}{2}I_2.$$

In the present work, although solutions were originally O_2 free, the formation and decomposition of H_2O_2 could provide O_2 for HO_2 formation. Alternatively, H_2^+ might reduce I_2 by some such reaction as:

$$H_2^+ + I_2 \rightarrow I + I^- + 2H^+.$$

The first or third reaction above, working in opposition to the second, could account for this arrest. The accumulation of H_2O_2 under irradiation and consequent increase in rate of the ordinary dark reaction

$$2H^+ + 2I^- + H_2O_2 \rightarrow 2H_2O + I_2$$

will result in the subsequent observed displacement of the steady state towards 100% I_2.

ACKNOWLEDGMENTS

The author acknowledges the valuable assistance and encouragement given him by Dr. E. J. Casey, Dr. I. H. S. Henderson, Mr. Pierre Roberge, and Mr. Brendan Timmons.

Can. J. Chem. Downloaded from www.nrcresearchpress.com by 210.87.254.6 on 09/05/12
For personal use only.

1. I. H. S. HENDERSON, E. G. LOVERING, R. L. HAINES, and E. J. CASEY. Can. J. Chem. **37**, 164 (1959).
2. F. S. DAINTON and E. COLLINSON. Ann. Rev. Phys. Chem. **2**, 99 (1951).
3. G. H. CARTLEDGE. Nature, **186**, 370 (1960).
4. E. J. CASEY. Proceedings 2nd International Conf. on Batteries. Signals Research and Development Establishment, Christchurch, England. October, 1960.
5. F. S. FEATES and B. KNIGHT. Trans. Faraday Soc. **56**, 1680 (1960).
6. J. O. BOCKRIS and L. F. OLDFIELD. Trans. Faraday Soc. **51**, 249 (1955).
7. M. LEFORT. J. Chim. Phys. **47**, 776 (1950).
8. H. A. SCHWARZ and A. O. ALLEN. J. Am. Chem. Soc. **77**, 1324 (1955).
9. W. C. SCHUMB, C. N. SATTERFIELD, and R. L. WENTWORTH. Hydrogen peroxide. Reinhold Publishing Corporation, New York. 1955. p. 561.
10. F. D. SNELL and C. T. SNELL. Colorimetric methods of analysis. Vol. II. 3rd ed. D. Van Nostrand Co. Inc., New York. 1949. p. 805.
11. A. D. AWTREY and R. E. CONNICK. J. Am. Chem. Soc. **73**, 1842 (1951).
12. C. J. HOCHANADEL and J. A. GHORMLEY. J. Chem. Phys. **21**, 880 (1953).
13. N. MILLER and F. WILKINSON. Discussions Faraday Soc. No. 12, 50 (1952).
14. W. M. LATIMER. The oxidation states of the elements and their potentials in aqueous solutions. 2nd ed. Prentice-Hall Inc., New York. 1952.
15. Ts. I. ZALKIND and V. I. VESELOVSKY. Sb. Rabot po Radiatsionnoi Khim. Akad. Nauk SSSR. 1955. p. 66.
16. F. S. FEATES. Trans. Faraday Soc. **56**, 1671 (1960).
17. A. C. RIDDIFORD. Z. Elektrochem. **61**, 752 (1957).
18. A. O. ALLEN. The radiation chemistry of water and aqueous solutions. D. Van Nostrand Co. Inc., New York. 1961.

RECEIVED SEPTEMBER 23, 1963.
DEFENCE RESEARCH CHEMICAL LABORATORIES,
OTTAWA, CANADA.

Can. J. Chem. Downloaded from www.nrcresearchpress.com by 210.87.254.6 on 09/05/12
For personal use only.

SYNTHESIS OF 2- OR 4,6-DINITRO-*sec*-PENTYL PHENOLS

G. G. S. DUTTON, M. E. D. HILLMAN, AND J. G. MOFFATT

In previous papers we have reported the synthesis and characterization of dinitro-*n*-alkyl and iso-alkyl phenols (1–3), compounds which have insecticidal and selective herbicidal properties. In view of the known superiority of 2,4-dinitro-6-*sec*-butyl phenol compared to the *n*-isomer (4, 5) it was of interest to prepare the *sec*-pentyl derivatives for physiological tests which will be reported elsewhere.

The isomeric *sec*-pentyl phenols were prepared by reacting a carbonyl compound with a

TABLE I

Properties of alcohols and derived alkenes

	Alcohols ($C_{12}H_{18}O_2$)		Alkenes ($C_{12}H_{16}O$)		Nitrosyl chloride (9, 10) ($C_{12}H_{16}NO_2Cl$), melting point, °C
	Boiling point °C (mm)	n^{25}	Boiling point °C (mm)	n^{25}	
2-(2-Methoxyphenyl)-pentanol-2	85 (0.02)	1.5129	67 (0.4)	1.5229	93
2-(4-Methoxyphenyl)-pentanol-2	100 (0.05)	1.5308	70 (0.1)	1.5370	84
3-(2-Methoxyphenyl)-pentanol-3	76 (0.01)	1.5160	70 (0.03)	1.5220	97
3-(4-Methoxyphenyl)-pentanol-3 (12, 13)	87 (0.01)	1.5278	58 (0.03)	1.5310	79
2-(2-Methoxyphenyl)-3-methyl-butanol-2 (14)	68 (0.02)	1.5163	55 (0.1)	1.5204	—
2-(4-Methoxyphenyl)-3-methyl-butanol-2	107 (0.02)	1.5223	65 (0.1)	1.5310	—

1. I. H. S. HENDERSON, E. G. LOVERING, R. L. HAINES, and E. J. CASEY. Can. J. Chem. **37**, 164 (1959).
2. F. S. DAINTON and E. COLLINSON. Ann. Rev. Phys. Chem. **2**, 99 (1951).
3. G. H. CARTLEDGE. Nature, **186**, 370 (1960).
4. E. J. CASEY. Proceedings 2nd International Conf. on Batteries. Signals Research and Development Establishment, Christchurch, England. October, 1960.
5. F. S. FEATES and B. KNIGHT. Trans. Faraday Soc. **56**, 1680 (1960).
6. J. O. BOCKRIS and L. F. OLDFIELD. Trans. Faraday Soc. **51**, 249 (1955).
7. M. LEFORT. J. Chim. Phys. **47**, 776 (1950).
8. H. A. SCHWARZ and A. O. ALLEN. J. Am. Chem. Soc. **77**, 1324 (1955).
9. W. C. SCHUMB, C. N. SATTERFIELD, and R. L. WENTWORTH. Hydrogen peroxide. Reinhold Publishing Corporation, New York. 1955. p. 561.
10. F. D. SNELL and C. T. SNELL. Colorimetric methods of analysis. Vol. II. 3rd ed. D. Van Nostrand Co. Inc., New York. 1949. p. 805.
11. A. D. AWTREY and R. E. CONNICK. J. Am. Chem. Soc. **73**, 1842 (1951).
12. C. J. HOCHANADEL and J. A. GHORMLEY. J. Chem. Phys. **21**, 880 (1953).
13. N. MILLER and F. WILKINSON. Discussions Faraday Soc. No. 12, 50 (1952).
14. W. M. LATIMER. The oxidation states of the elements and their potentials in aqueous solutions. 2nd ed. Prentice-Hall Inc., New York. 1952.
15. Ts. I. ZALKIND and V. I. VESELOVSKY. Sb. Rabot po Radiatsionnoi Khim. Akad. Nauk SSSR. 1955. p. 66.
16. F. S. FEATES. Trans. Faraday Soc. **56**, 1671 (1960).
17. A. C. RIDDIFORD. Z. Elektrochem. **61**, 752 (1957).
18. A. O. ALLEN. The radiation chemistry of water and aqueous solutions. D. Van Nostrand Co. Inc., New York. 1961.

RECEIVED SEPTEMBER 23, 1963.
DEFENCE RESEARCH CHEMICAL LABORATORIES,
OTTAWA, CANADA.

Can. J. Chem. Downloaded from www.nrcresearchpress.com by 210.87.254.105 on 09/05/12
For personal use only.

SYNTHESIS OF 2- OR 4,6-DINITRO-*sec*-PENTYL PHENOLS

G. G. S. DUTTON, M. E. D. HILLMAN, AND J. G. MOFFATT

In previous papers we have reported the synthesis and characterization of dinitro-*n*-alkyl and iso-alkyl phenols (1–3), compounds which have insecticidal and selective herbicidal properties. In view of the known superiority of 2,4-dinitro-6-*sec*-butyl phenol compared to the *n*-isomer (4, 5) it was of interest to prepare the *sec*-pentyl derivatives for physiological tests which will be reported elsewhere.

The isomeric *sec*-pentyl phenols were prepared by reacting a carbonyl compound with a

TABLE I

Properties of alcohols and derived alkenes

	Alcohols ($C_{12}H_{18}O_2$)		Alkenes ($C_{12}H_{16}O$)		Nitrosyl chloride (9, 10) ($C_{12}H_{16}NO_2Cl$), melting point, °C
	Boiling point °C (mm)	n^{25}	Boiling point °C (mm)	n^{25}	
2-(2-Methoxyphenyl)-pentanol-2	85 (0.02)	1.5129	67 (0.4)	1.5229	93
2-(4-Methoxyphenyl)-pentanol-2	100 (0.05)	1.5308	70 (0.1)	1.5370	84
3-(2-Methoxyphenyl)-pentanol-3	76 (0.01)	1.5160	70 (0.03)	1.5220	97
3-(4-Methoxyphenyl)-pentanol-3 (12, 13)	87 (0.01)	1.5278	58 (0.03)	1.5310	79
2-(2-Methoxyphenyl)-3-methyl-butanol-2 (14)	68 (0.02)	1.5163	55 (0.1)	1.5204	—
2-(4-Methoxyphenyl)-3-methyl-butanol-2	107 (0.02)	1.5223	65 (0.1)	1.5310	—

TABLE II

Properties of alkylanisoles and their derivatives

	Alkylanisole ($C_{12}H_{18}O$)		Sulphonamide (11) $C_{12}H_{19}NO_3S$, melting point, °C
	Boiling point °C (mm)	n^{25}	
2-(2-Methoxyphenyl)-pentane	62 (0.3)	1.4980	60
2-(4-Methoxyphenyl)-pentane	68 (0.3)	1.4970	63
3-(2-Methoxyphenyl)-pentane	50 (0.01)	1.5010	—
3-(4-Methoxyphenyl)-pentane (13)	56 (0.02)	1.5030	107
2-(2-Methoxyphenyl)-2-methylbutane	58 (0.3)	1.5070	111
2-(4-Methoxyphenyl)-2-methylbutane	71 (0.5)	1.5011	104

TABLE III

Properties of alkylphenols and their derivatives

	Alkylphenol ($C_{11}H_{16}O$)		3,5-Dinitrobenzoate ($C_{18}H_{18}N_2O_6$), melting point, °C	Dinitro-alkylphenol ($C_{11}H_{14}N_2O_5$)	
	Boiling point °C (mm)	n^{25}		Boiling point °C (mm)	n^{25}
2-(2-Hydroxyphenyl)-pentane	65 (0.1)	1.5122	85	145 (0.05)	1.5686
2-(4-Hydroxyphenyl)-pentane (15)	84 (0.5)	1.5132	81	155 (0.1)	1.5624
3-(2-Hydroxyphenyl)-pentane	61 (0.1)	m.p. 64°	87	138 (0.01)	1.5668
3-(4-Hydroxyphenyl)-pentane	83 (0.3)	m.p. 72°	92	149 (0.03)	1.5664
2-(2-Hydroxyphenyl)-3-methylbutane	60 (0.25)	1.5157	72	140 (0.08)	1.5713
2-(4-Hydroxyphenyl)-3-methylbutane	110 (0.8)	m.p. 73°	109	155 (0.1)	1.5669

TABLE IV

Amine salts of dinitrophenols

	Piperidine ($C_{16}H_{25}N_3O_5$), m.p., °C	Morpholine ($C_{15}H_{23}N_3O_6$), m.p., °C	Cyclohexylamine ($C_{17}H_{27}N_3O_5$) m.p., °C
2-(2-Hydroxy-3,5-dinitrophenyl)-pentane	140	146	189
2-(4-Hydroxy-3,5-dinitrophenyl)-pentane	187	160	169
3-(2-Hydroxy-3,5-dinitrophenyl)-pentane	173	157	192
3-(4-Hydroxy-3,5-dinitrophenyl)-pentane	213	185	217
2-(2-Hydroxy-3,5-dinitrophenyl)-3-methylbutane	145	153	213 (decomp.)
2-(4-Hydroxy-3,5-dinitrophenyl)-3-methylbutane	199	170	217 (decomp.)

Grignard reagent (e.g. 4-methoxypropiophenone and ethyl magnesium bromide), dehydrating the carbinol (6), and hydrogenating the alkene. The 4-alkyl anisoles were demethylated using pyridine hydrobromide and acetic acid but this method failed with the 2-isomers which were accordingly reacted with hydriodic acid and phenol. Nitration of the phenols was done in acetic acid and each dinitrophenol was characterized by the preparation of crystalline salts with morphine, piperidine, and cyclohexylamine.

The dinitrophenols, their derivatives, and intermediates are listed in the tables. All the compounds reported are new except where noted and satisfactory analyses were obtained for all the compounds. These analyses together with experimental details of the preparations are available elsewhere (7, 8).

Can. J. Chem. Downloaded from www.nrcresearchpress.com by 210.87.254.105 on 09/05/12
For personal use only.

ACKNOWLEDGMENT

We are grateful to the National Research Council and the President's Research Fund (U.B.C.) for continued financial support.

1. G. G. S. DUTTON, T. I. BRIGGS, B. R. BROWN, and R. K. POWELL. Can. J. Chem. **31**, 837 (1953).
2. G. G. S. DUTTON, T. I. BRIGGS, and E. MERLER. Can. J. Chem. **31**, 1138 (1953).
3. G. G. S. DUTTON, T. I. BRIGGS, B. R. BROWN, and M. E. D. HILLMAN. Can. J. Chem. **31**, 685 (1953).
4. J. F. KAGY. J. Econ. Entomol. **34**, 660 (1941).
5. A. S. CRAFTS. Plant Physiol. **21**, 345 (1946).
6. H. W. DEAN and D. D. STARK. Ind. Eng. Chem. **12**, 486 (1920).
7. M. E. D. HILLMAN. M.Sc. Thesis, University of British Columbia, Vancouver, B.C. 1954.
8. J. G. MOFFATT. M.Sc. Thesis, University of British Columbia, Vancouver, B.C. 1954.
9. W. A. TILDEN and R. J. SHENSTONE. J. Chem. Soc. **31**, 554 (1877).
10. W. J. HICKINBOTTOM. Reactions of organic compounds. Longmans, Green and Co., New York. 1949. p. 19.
11. F. WILD. Characterization of organic compounds. University Press, Cambridge. 1947. p. 27.
12. P. L. COUTURIER. Ann. Chim. **10**, 559 (1938).
13. A. KLAGES. Ber. **37**, 3987 (1904).
14. W. M. LAUER and O. MOE. J. Am. Chem. Soc. **65**, 289 (1943).
15. R. C. HUSTON and I. A. KAYE. J. Am. Chem. Soc. **64**, 1576 (1942).

RECEIVED SEPTEMBER 30, 1963.
DEPARTMENT OF CHEMISTRY,
UNIVERSITY OF BRITISH COLUMBIA,
VANCOUVER 8, BRITISH COLUMBIA.

Can. J. Chem. Downloaded from www.nrcresearchpress.com by 210.87.254.105 on 09/05/12
For personal use only.

SYNTHESIS OF 2- OR 4,6-DINITRO-*sec*-HEXYL PHENOLS

G. G. S. DUTTON, M. E. D. HILLMAN, AND J. G. MOFFATT

The synthesis of dinitro-*sec*-pentyl phenols was reported in a recent note (1), and some corresponding *sec*-hexyl homologues are now described and characterized as their crystalline amine salts (2). These compounds are of interest because of the known herbicidal activity of 2,4-dinitro-6-*sec*-butyl phenol (3) and the physiological tests on these compounds will be reported elsewhere.

TABLE I

Properties of alcohols and alkenes

	Alcohols ($C_{13}H_{20}O_2$)		Alkenes ($C_{13}H_{18}O$)		Nitrosyl chloride ($C_{13}H_{18}NO_2Cl$), m.p.° C
	b.p.° C (0.01 mm)	n^{25}	b.p.° C (mm)	n^{25}	
2-(2-Methoxyphenyl)-hexanol-2	79	1.5095	64 (0.04)	1.5199	103
2-(4-Methoxyphenyl)-hexanol-2	68	1.5285	70 (0.01)	1.5329	86
3-(2-Methoxyphenyl)-hexanol-3 (6)	77	1.5163	80 (0.05)	1.5204	73
3-(4-Methoxyphenyl)-hexanol-3 (6)	84	1.5204	85 (0.4)	1.5260	67
2-(2-Methoxyphenyl)-3-methylpentanol-3	73	Partial dehydration	57 (0.04)	1.5170	—
2-(4-Methoxyphenyl)-3-methylpentanol-3	spontaneous dehydration		63 (0.04)	1.5260	—
2-(2-Methoxyphenyl)-4-methylpentanol-2	68	1.5260	59 (0.01)	1.5134	—
2-(2-Methoxyphenyl)-4-methylpentanol-2	63	1.5128	68 (0.04)	1.5290	104
3-(2-Methoxyphenyl)-2-methylpentanol-3	89	1.5175	70 (0.05)	1.5228	—
3-(4-Methoxyphenyl)-2-methylpentanol-3 (8)	82	1.5196	84 (0.1)	1.5240	—

ACKNOWLEDGMENT

We are grateful to the National Research Council and the President's Research Fund (U.B.C.) for continued financial support.

1. G. G. S. DUTTON, T. I. BRIGGS, B. R. BROWN, and R. K. POWELL. Can. J. Chem. **31**, 837 (1953).
2. G. G. S. DUTTON, T. I. BRIGGS, and E. MERLER. Can. J. Chem. **31**, 1138 (1953).
3. G. G. S. DUTTON, T. I. BRIGGS, B. R. BROWN, and M. E. D. HILLMAN. Can. J. Chem. **31**, 685 (1953).
4. J. F. KAGY. J. Econ. Entomol. **34**, 660 (1941).
5. A. S. CRAFTS. Plant Physiol. **21**, 345 (1946).
6. H. W. DEAN and D. D. STARK. Ind. Eng. Chem. **12**, 486 (1920).
7. M. E. D. HILLMAN. M.Sc. Thesis, University of British Columbia, Vancouver, B.C. 1954.
8. J. G. MOFFATT. M.Sc. Thesis, University of British Columbia, Vancouver, B.C. 1954.
9. W. A. TILDEN and R. J. SHENSTONE. J. Chem. Soc. **31**, 554 (1877).
10. W. J. HICKINBOTTOM. Reactions of organic compounds. Longmans, Green and Co., New York. 1949. p. 19.
11. F. WILD. Characterization of organic compounds. University Press, Cambridge. 1947. p. 27.
12. P. L. COUTURIER. Ann. Chim. **10**, 559 (1938).
13. A. KLAGES. Ber. **37**, 3987 (1904).
14. W. M. LAUER and O. MOE. J. Am. Chem. Soc. **65**, 289 (1943).
15. R. C. HUSTON and I. A. KAYE. J. Am. Chem. Soc. **64**, 1576 (1942).

RECEIVED SEPTEMBER 30, 1963.
DEPARTMENT OF CHEMISTRY,
UNIVERSITY OF BRITISH COLUMBIA,
VANCOUVER 8, BRITISH COLUMBIA.

Can. J. Chem. Downloaded from www.nrcresearchpress.com by 210.87.254.5 on 09/05/12
For personal use only.

SYNTHESIS OF 2- OR 4,6-DINITRO-*sec*-HEXYL PHENOLS

G. G. S. DUTTON, M. E. D. HILLMAN, AND J. G. MOFFATT

The synthesis of dinitro-*sec*-pentyl phenols was reported in a recent note (1), and some corresponding *sec*-hexyl homologues are now described and characterized as their crystalline amine salts (2). These compounds are of interest because of the known herbicidal activity of 2,4-dinitro-6-*sec*-butyl phenol (3) and the physiological tests on these compounds will be reported elsewhere.

TABLE I

Properties of alcohols and alkenes

	Alcohols ($C_{13}H_{20}O_2$)		Alkenes ($C_{13}H_{18}O$)		Nitrosyl chloride ($C_{13}H_{18}NO_2Cl$), m.p.° C
	b.p.° C (0.01 mm)	n^{25}	b.p.° C (mm)	n^{25}	
2-(2-Methoxyphenyl)-hexanol-2	79	1.5095	64 (0.04)	1.5199	103
2-(4-Methoxyphenyl)-hexanol-2	68	1.5285	70 (0.01)	1.5329	86
3-(2-Methoxyphenyl)-hexanol-3 (6)	77	1.5163	80 (0.05)	1.5204	73
3-(4-Methoxyphenyl)-hexanol-3 (6)	84	1.5204	85 (0.4)	1.5260	67
2-(2-Methoxyphenyl)-3-methylpentanol-3	73	Partial dehydration	57 (0.04)	1.5170	—
2-(4-Methoxyphenyl)-3-methylpentanol-3	spontaneous dehydration		63 (0.04)	1.5260	—
2-(2-Methoxyphenyl)-4-methylpentanol-2	68	1.5260	59 (0.01)	1.5134	—
2-(2-Methoxyphenyl)-4-methylpentanol-2	63	1.5128	68 (0.04)	1.5290	104
3-(2-Methoxyphenyl)-2-methylpentanol-3	89	1.5175	70 (0.05)	1.5228	—
3-(4-Methoxyphenyl)-2-methylpentanol-3 (8)	82	1.5196	84 (0.1)	1.5240	—

TABLE II

Properties of alkylanisoles and their sulphonamide derivatives

	Alkylanisole ($C_{13}H_{20}O$)		Sulphonamide ($C_{13}H_{21}NO_3S$), m.p.° C
	b.p.° C (mm)	n^{25}	
2-(2-Methoxyphenyl)-hexane	59 (0.02)	1.5045	—
2-(4-Methoxyphenyl)-hexane	60 (0.03)	1.5012	79
3-(2-Methoxyphenyl)-hexane (6)	58 (0.05)	1.5022	—
3-(4-Methoxyphenyl)-hexane (6, 7)	85 (0.1)	1.4968	82
2-(2-Methoxyphenyl)-3-methylpentane	52 (0.01)	1.5070	—
2-(4-Methoxyphenyl)-3-methylpentane	60 (0.03)	1.5060	100
2-(2-Methoxyphenyl)-4-methylpentane	54 (0.04)	1.4951	103
2-(4-Methoxyphenyl)-4-methylpentane	54 (0.04)	1.4930	92
3-(2-Methoxyphenyl)-2-methylpentane	56 (0.05)	1.5069	—
3-(4-Methoxyphenyl)-2-methylpentane (8)	74 (0.05)	1.5030	69

TABLE III

Properties of alkylphenols and their dinitro derivatives

	Alkylphenol ($C_{12}H_{18}O$)		3,5-Dinitrobenzoate ($C_{19}H_{20}N_2O_6$), m.p.° C	Dinitro-alkylphenol ($C_{12}H_{16}N_2O_5$)	
	b.p.° C (mm)	n^{25}		b.p.° C (mm)	n^{25}
2-(2-Hydroxyphenyl)-hexane	60 (0.01)	1.5160	94	145 (0.05)	1.5636
2-(4-Hydroxyphenyl)-hexane (9)	80 (0.05)	1.5110	92	160 (0.02)	1.5574
3-(2-Hydroxyphenyl)-hexane	55 (0.01)	1.5162	61	150 (0.1)	1.5631
3-(4-Hydroxyphenyl)-hexane (6, 7)	90 (0.03)	m.p. 49	82	155 (0.05)	1.5586
2-(2-Hydroxyphenyl)-3-methylpentane	53 (0.02)	1.5074	94	137 (0.05)	1.5520
2-(4-Hydroxyphenyl)-3-methylpentane (9)	87 (0.09)	1.5210	103	157 (0.03)	1.5648
2-(2-Hydroxyphenyl)-4-methylpentane	59 (0.03)	1.5077	95	142 (0.04)	1.5589
2-(4-Hydroxyphenyl)-4-methylpentane (9)	80 (0.1)	1.5082	93	147 (0.01)	1.5562
3-(2-Hydroxyphenyl)-2-methylpentane	75 (0.08)	1.5098	70	132 (0.1)	1.5710
3-(4-Hydroxyphenyl)-2-methylpentane (8)	75 (0.1)	m.p. 30	118 (8)	155 (0.05)	1.5620

TABLE IV

Amine salts of dinitrophenols

Salt of:	Piperidine ($C_{17}H_{27}N_3O_5$), m.p.° C	Morpholine ($C_{16}H_{25}N_3O_6$), m.p.° C	Cyclohexylamine ($C_{18}H_{29}N_3O_5$), m.p.° C
2-(2-Hydroxy-3,5-dinitrophenyl)-hexane	—	133	173
2-(4-Hydroxy-3,5-dinitrophenyl)-hexane	150	145	138
3-(2-Hydroxy-3,5-dinitrophenyl)-hexane	155	157	160
3-(4-Hydroxy-3,5-dinitrophenyl)-hexane	192	154	200
2-(2-Hydroxy-3,5-dinitrophenyl)-3-methylpentane	187	—	207
2-(4-Hydroxy-3,5-dinitrophyl)-3-methylpentane	160	113	163
2-(2-Hydroxy-3,5-dinitrophenyl)-4-methylpentane	136	144	193
2-(4-Hydroxy-3,5-dinitrophenyl)-4-methylpentane	186	168	165
3-(2-Hydroxy-3,5-dinitrophenyl)-2-methylpentane	177	166	179
3-(4-Hydroxy-3,5-dinitrophenyl)-2-methylpentane	158	182	216

Can. J. Chem. Downloaded from www.nrcresearchpress.com by 210.87.254.5 on 09/05/12
For personal use only.

As before (1), all compounds reported are new unless otherwise noted and satisfactory analyses were obtained for all compounds. These figures, together with experimental details, may be found elsewhere (4, 5).

ACKNOWLEDGMENT

We are indebted to the National Research Council of Canada and the Presidents' Research Fund (U.B.C.) for generous financial support.

1. G. G. S. Dutton, M. E. D. Hillman, and J. G. Moffatt. Can. J. Chem. In press (1964).
2. G. G. S. Dutton, T. I. Briggs, B. R. Brown, and M. E. D. Hillman. Can. J. Chem. **31**, 685 (1953).
3. A. S. Crafts. Plant. Physiol. **21**, 345 (1946).
4. M. E. D. Hillman. M. Sc. Thesis, University of British Columbia (1954).
5. J. G. Moffatt. M. Sc. Thesis, University of British Columbia (1954).
6. L. I. Smith, H. E. Ungnade, W. M. Lauer and R. M. Leekley. J. Am. Chem. Soc. **61**, 3079 (1939).
7. M. Rubin. J. Am. Chem. Soc. **66**, 2075 (1944).
8. R. C. Huston, R. L. Guile, D. L. Bailey, R. J. Curtis and M. T. Esterdahl. J. Am. Chem. Soc. **67**, 899 (1945).
9. R. C. Huston and I. A. Kaye. J. Am. Chem. Soc. **64**, 1576 (1942).

Received October 21, 1963.
Department of Chemistry,
University of British Columbia,
Vancouver 8, B.C.

Can. J. Chem. Downloaded from www.nrcresearchpress.com by 210.87.254.5 on 09/05/12
For personal use only.

A SIMPLE PREPARATION OF 5,6-DIHYDROXY-*N*-METHYLINDOLE

G. L. Mattok and R. A. Heacock

5,6-Dihydroxy-*N*-methylindole (III) has previously been obtained in crystalline form by the reduction of adrenochrome (II) (1, 2, 3); the rearrangement of epinochrome (4) and the rearrangement (accompanied by decarboxylation) of *N*-methyldopachrome (5).

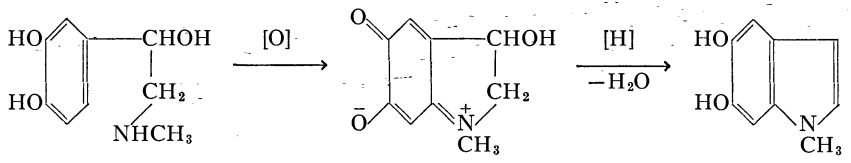

I II III

The present note describes an adaptation of the first of these methods to give a rapid and simple procedure for the preparation of (III). A solution of adrenochrome (II), prepared by oxidation of adrenaline (I) with buffered potassium ferricyanide (cf. 6), was reduced with excess ascorbic acid in the presence of ether. The use of a two-phase system ensured that (III) was extracted as soon as it was formed; thus preventing lowering of the yield by interaction of (III) with dehydroascorbic acid present in solution (7). The yields (based on adrenaline) obtained by this procedure (ca. 60%) are considerably better than those previously reported (ca. 30%) (cf. refs. 1–5).

EXPERIMENTAL

5,6-Dihydroxy-N-methylindole

Adrenaline bitartrate (2.5 g), in aqueous solution (25 ml), was oxidized by a solution of potassium ferricyanide (13 g) and sodium bicarbonate (4.2 g) in water (50 ml). After 5 minutes, peroxide-free ether

As before (1), all compounds reported are new unless otherwise noted and satisfactory analyses were obtained for all compounds. These figures, together with experimental details, may be found elsewhere (4, 5).

ACKNOWLEDGMENT

We are indebted to the National Research Council of Canada and the Presidents' Research Fund (U.B.C.) for generous financial support.

1. G. G. S. Dutton, M. E. D. Hillman, and J. G. Moffatt. Can. J. Chem. In press (1964).
2. G. G. S. Dutton, T. I. Briggs, B. R. Brown, and M. E. D. Hillman. Can. J. Chem. **31**, 685 (1953).
3. A. S. Crafts. Plant. Physiol. **21**, 345 (1946).
4. M. E. D. Hillman. M. Sc. Thesis, University of British Columbia (1954).
5. J. G. Moffatt. M. Sc. Thesis, University of British Columbia (1954).
6. L. I. Smith, H. E. Ungnade, W. M. Lauer and R. M. Leekley. J. Am. Chem. Soc. **61**, 3079 (1939).
7. M. Rubin. J. Am. Chem. Soc. **66**, 2075 (1944).
8. R. C. Huston, R. L. Guile, D. L. Bailey, R. J. Curtis and M. T. Esterdahl. J. Am. Chem. Soc. **67**, 899 (1945).
9. R. C. Huston and I. A. Kaye. J. Am. Chem. Soc. **64**, 1576 (1942).

Received October 21, 1963.
Department of Chemistry,
University of British Columbia,
Vancouver 8, B.C.

Can. J. Chem. Downloaded from www.nrcresearchpress.com by 210.87.254.42 on 09/05/12
For personal use only.

A SIMPLE PREPARATION OF 5,6-DIHYDROXY-*N*-METHYLINDOLE

G. L. Mattok and R. A. Heacock

5,6-Dihydroxy-*N*-methylindole (III) has previously been obtained in crystalline form by the reduction of adrenochrome (II) (1, 2, 3); the rearrangement of epinochrome (4) and the rearrangement (accompanied by decarboxylation) of *N*-methyldopachrome (5).

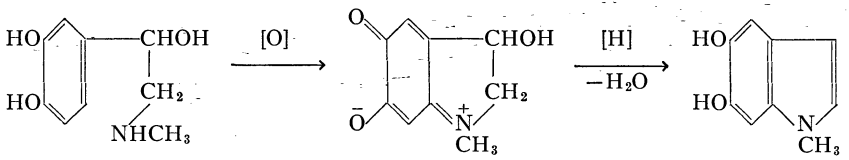

I II III

The present note describes an adaptation of the first of these methods to give a rapid and simple procedure for the preparation of (III). A solution of adrenochrome (II), prepared by oxidation of adrenaline (I) with buffered potassium ferricyanide (cf. 6), was reduced with excess ascorbic acid in the presence of ether. The use of a two-phase system ensured that (III) was extracted as soon as it was formed; thus preventing lowering of the yield by interaction of (III) with dehydroascorbic acid present in solution (7). The yields (based on adrenaline) obtained by this procedure (ca. 60%) are considerably better than those previously reported (ca. 30%) (cf. refs. 1–5).

EXPERIMENTAL

5,6-Dihydroxy-N-methylindole

Adrenaline bitartrate (2.5 g), in aqueous solution (25 ml), was oxidized by a solution of potassium ferricyanide (13 g) and sodium bicarbonate (4.2 g) in water (50 ml). After 5 minutes, peroxide-free ether

(150 ml) was added to the reaction mixture, followed by ascorbic acid (25 g). The system was shaken for several minutes until all the red color was discharged. The ether layer was separated, dried (Na_2SO_4), and concentrated, under nitrogen, to about 30 ml. Dry benzene (50 ml) was added and the solution concentrated under reduced pressure, at ca. 30°, (nitrogen "leak") to about 30 ml. This solution was then filtered and *n*-heptane (100 ml) added to the filtrate; a flocculent white precipitate was obtained, which was purified by dissolving in warm benzene (35°), reprecipitating with *n*-heptane giving 5,6-dihydroxy-*N*-methylindole (0.7 g; 57%) m.p. 131–132° in long colorless needles. Recrystallization of a sample from *n*-heptane raised the melting point to 133–134°. The melting points quoted for (III) in the literature range from 133° to 136° (refs. 1–6). However, the product obtained by the current procedure was sufficiently pure for most purposes.

ACKNOWLEDGMENTS

This investigation received financial support from the Department of National Health and Welfare (Ottawa) and the Government of Saskatchewan (Department of Public Health).

1. J. HARLEY-MASON. J. Chem. Soc. 1276 (1950).
2. R. A. HEACOCK and B. D. LAIDLAW. Nature, **182**, 526 (1958).
3. R. A. HEACOCK, M. E. MAHON, and B. D. SCOTT. Can. J. Chem. **39**, 231 (1961).
4. J. AUSTIN, J. D. CHANLEY, and H. SOBOTKA. J. Am. Chem. Soc. **73**, 5299 (1951).
5. J. D. BU'LOCK and J. HARLEY-MASON. J. Chem. Soc. 2248 (1951).
6. J. D. BU'LOCK and J. HARLEY-MASON. J. Chem. Soc. 712 (1951).
7. G. L. MATTOK and R. A. HEACOCK. Nature, **198**, 993 (1963).

RECEIVED SEPTEMBER 30, 1963.
PSYCHIATRIC RESEARCH UNIT.
UNIVERSITY HOSPITAL,
SASKATOON, SASKATCHEWAN.

Can. J. Chem. Downloaded from www.nrcresearchpress.com by 210.87.254.42 on 09/05/12
For personal use only.

A CONVENIENT PREPARATION OF TRYPTOPHOL

THOMAS NOGRADY AND TERRENCE W. DOYLE

Trytophol, 3-indolylethanol, is of considerable interest as an intermediate in indole chemistry. Its preparation in larger amounts is, however, not too convenient with the existing methods, and yields are sometimes poor.

Usually, it is prepared by the LAH reduction of ethyl 3-indolyl-acetate, in a near-quantitative yield. The ester, however, is rather difficult to obtain, through gramine, its methosulphate, indolylacetonitrile, and indolylacetic acid. This 6-step synthesis gives an overall yield of 59% only (cf. (1)).

The new procedure of Johnson and Crosby (2) makes indolylacetic acid available at a 90% yield, and from this acid tryptophol, in an overall yield of 79%, can be obtained. This method requires the use of a concentrated potassium hydroxide solution, and a heating period of 14–22 hours at 250° in an autoclave.

The reduction of ethyl indolylacetate suffers from the disadvantage that it has to be conducted at −20°, otherwise the reaction mixture becomes a tough gum which is impossible to stir.

In the method of Elderfield and Fischer (3) the indolylglyoxylyl chloride is obtained in one step from the indole, according to Speeter and Anthony (4). The chloride is then directly reduced by LAH in tetrahydrofuran at room temperature, and gives an overall yield of 74%. This elegant procedure, described for the 6-methoxy derivative, gave unsatisfactory yields and an impure product when applied to unsubstituted indolyl-3-glyoxylyl chloride.

(150 ml) was added to the reaction mixture, followed by ascorbic acid (25 g). The system was shaken for several minutes until all the red color was discharged. The ether layer was separated, dried (Na_2SO_4), and concentrated, under nitrogen, to about 30 ml. Dry benzene (50 ml) was added and the solution concentrated under reduced pressure, at ca. 30°, (nitrogen "leak") to about 30 ml. This solution was then filtered and *n*-heptane (100 ml) added to the filtrate; a flocculent white precipitate was obtained, which was purified by dissolving in warm benzene (35°), reprecipitating with *n*-heptane giving 5,6-dihydroxy-*N*-methylindole (0.7 g; 57%) m.p. 131–132° in long colorless needles. Recrystallization of a sample from *n*-heptane raised the melting point to 133–134°. The melting points quoted for (III) in the literature range from 133° to 136° (refs. 1–6). However, the product obtained by the current procedure was sufficiently pure for most purposes.

ACKNOWLEDGMENTS

This investigation received financial support from the Department of National Health and Welfare (Ottawa) and the Government of Saskatchewan (Department of Public Health).

1. J. HARLEY-MASON. J. Chem. Soc. 1276 (1950).
2. R. A. HEACOCK and B. D. LAIDLAW. Nature, **182**, 526 (1958).
3. R. A. HEACOCK, M. E. MAHON, and B. D. SCOTT. Can. J. Chem. **39**, 231 (1961).
4. J. AUSTIN, J. D. CHANLEY, and H. SOBOTKA. J. Am. Chem. Soc. **73**, 5299 (1951).
5. J. D. BU'LOCK and J. HARLEY-MASON. J. Chem. Soc. 2248 (1951).
6. J. D. BU'LOCK and J. HARLEY-MASON. J. Chem. Soc. 712 (1951).
7. G. L. MATTOK and R. A. HEACOCK. Nature, **198**, 993 (1963).

RECEIVED SEPTEMBER 30, 1963.
PSYCHIATRIC RESEARCH UNIT.
UNIVERSITY HOSPITAL,
SASKATOON, SASKATCHEWAN.

Can. J. Chem. Downloaded from www.nrcresearchpress.com by 210.87.254.5 on 09/05/12
For personal use only.

A CONVENIENT PREPARATION OF TRYPTOPHOL

THOMAS NOGRADY AND TERRENCE W. DOYLE

Trytophol, 3-indolylethanol, is of considerable interest as an intermediate in indole chemistry. Its preparation in larger amounts is, however, not too convenient with the existing methods, and yields are sometimes poor.

Usually, it is prepared by the LAH reduction of ethyl 3-indolyl-acetate, in a near-quantitative yield. The ester, however, is rather difficult to obtain, through gramine, its methosulphate, indolylacetonitrile, and indolylacetic acid. This 6-step synthesis gives an overall yield of 59% only (cf. (1)).

The new procedure of Johnson and Crosby (2) makes indolylacetic acid available at a 90% yield, and from this acid tryptophol, in an overall yield of 79%, can be obtained. This method requires the use of a concentrated potassium hydroxide solution, and a heating period of 14–22 hours at 250° in an autoclave.

The reduction of ethyl indolylacetate suffers from the disadvantage that it has to be conducted at −20°, otherwise the reaction mixture becomes a tough gum which is impossible to stir.

In the method of Elderfield and Fischer (3) the indolylglyoxylyl chloride is obtained in one step from the indole, according to Speeter and Anthony (4). The chloride is then directly reduced by LAH in tetrahydrofuran at room temperature, and gives an overall yield of 74%. This elegant procedure, described for the 6-methoxy derivative, gave unsatisfactory yields and an impure product when applied to unsubstituted indolyl-3-glyoxylyl chloride.

Therefore, we prepared ethyl 3-indolylglyoxylate from the chloride (4), by the action of ethanol, in the presence of triethylamine. The crude ester, obtained in a 95% yield and showing the melting point reported in the literature (5) was reduced with LAH in tetrahydrofuran to give tryptophol in a 95% yield. The overall yield from indole is therefore 85–86%.

EXPERIMENTAL

Melting points were taken in capillaries in a Gallenkamp aluminum block, and are corrected. Infrared spectra were determined in KBr disks on a Beckman IR8 grating instrument.

Ethyl 3-indolylglyoxylate

3-Indolylglyoxylyl chloride (4), 10.35 g (0.05 moles), was refluxed for 30 minutes in a mixture of 60 ml absolute ethanol and 5.30 g (7.2 ml, 0.052 moles) of triethylamine. The reaction mixture was chilled, and the crystals were filtered and washed with a little ethanol. Yield 7.60 g (70.0%), m.p. 186–187° (lit. m.p. 186°) (5).

The mother liquid was evaporated under reduced pressure, and the residue triturated with water. On filtration, an additional 2.70 g (25.0%) ester was obtained, m.p. 184–186°.

Infrared absorption (λ_{max}, μ): 3.11 (NH, vs), 3.37 (C—H, w), 5.87 (C=O, s), 6.20 (C=C, s), 7.95 (C—O, s).

3-Indolylethanol (Tryptophol)

Ethyl indolylglyoxylate (10.85 g (0.05 moles)) was refluxed for 2 hours with 6.6 g (0.175 moles) $LiAlH_4$ in 200 ml dry tetrahydrofuran, with mechanical stirring. We then added 20 ml water slowly while cooling the reaction mixture in ice water. The precipitate was filtered and washed several times with tetrahydrofuran, and the solvent evaporated after drying over Na_2SO_4. The white crystalline residue weighed 6.50 g (95.0%), m.p. 54–55°.

It can be recrystallized from benzene–petroleum ether, m.p. 56–58° (lit. m.p. 58–59° (6)).

Infrared absorption (λ_{max}, μ): 2.94 (NH, OH, vs), 3.40, 3.43, 3.50 (C—H, w), 6.20 (C=C, w), 9.52 (OH, s, broad).

ACKNOWLEDGMENT

This work was supported by Grant A-1333 of the National Research Council of Canada.

1. J. Thesing and F. Schülde. Chem. Ber. **85**, 324 (1952).
2. H. E. Johnson and D. G. Crosby. J. Org. Chem. **28**, 1246 (1963).
3. R. C. Elderfield and B. A. Fischer. J. Org. Chem. **23**, 949 (1958).
4. M. E. Speeter and W. C. Anthony. J. Am. Chem. Soc. **76**, 6208 (1954).
5. B. Oddo and A. Albanese. Gazz. Chim. Ital. **57**, 827 (1927).
6. T. Hoshino and K. Shimodaira. Ann. **520**, 19 (1935).

Received October 9, 1963.
Department of Chemistry,
Loyola College,
Montreal 28, Que.

H_0 ACIDITY FUNCTIONS FOR NITRIC AND PHOSPHORIC ACID SOLUTIONS CONTAINING ADDED SODIUM PERCHLORATE

Donald G. Lee and Ross Stewart

In connection with an investigation of the mechanism of the chromic acid oxidation of alcohols (1) we required the values of the Hammett acidity function, H_0, for nitric and phosphoric acid solutions containing equimolar amounts of sodium perchlorate and acid. The functions were determined by use of weak bases for indicators in the manner described by Paul and Long (2).

Can. J. Chem. Downloaded from www.nrcresearchpress.com by 210.87.254.5 on 09/05/12
For personal use only.

Therefore, we prepared ethyl 3-indolylglyoxylate from the chloride (4), by the action of ethanol, in the presence of triethylamine. The crude ester, obtained in a 95% yield and showing the melting point reported in the literature (5) was reduced with LAH in tetrahydrofuran to give tryptophol in a 95% yield. The overall yield from indole is therefore 85–86%.

EXPERIMENTAL

Melting points were taken in capillaries in a Gallenkamp aluminum block, and are corrected. Infrared spectra were determined in KBr disks on a Beckman IR8 grating instrument.

Ethyl 3-indolylglyoxylate

3-Indolylglyoxylyl chloride (4), 10.35 g (0.05 moles), was refluxed for 30 minutes in a mixture of 60 ml absolute ethanol and 5.30 g (7.2 ml, 0.052 moles) of triethylamine. The reaction mixture was chilled, and the crystals were filtered and washed with a little ethanol. Yield 7.60 g (70.0%), m.p. 186–187° (lit. m.p. 186°) (5).

The mother liquid was evaporated under reduced pressure, and the residue triturated with water. On filtration, an additional 2.70 g (25.0%) ester was obtained, m.p. 184–186°.

Infrared absorption (λ_{max}, μ): 3.11 (NH, vs), 3.37 (C—H, w), 5.87 (C=O, s), 6.20 (C=C, s), 7.95 (C—O, s).

3-Indolylethanol (Tryptophol)

Ethyl indolylglyoxylate (10.85 g (0.05 moles)) was refluxed for 2 hours with 6.6 g (0.175 moles) $LiAlH_4$ in 200 ml dry tetrahydrofuran, with mechanical stirring. We then added 20 ml water slowly while cooling the reaction mixture in ice water. The precipitate was filtered and washed several times with tetrahydrofuran, and the solvent evaporated after drying over Na_2SO_4. The white crystalline residue weighed 6.50 g (95.0%), m.p. 54–55°.

It can be recrystallized from benzene–petroleum ether, m.p. 56–58° (lit. m.p. 58–59° (6)).

Infrared absorption (λ_{max}, μ): 2.94 (NH, OH, vs), 3.40, 3.43, 3.50 (C—H, w), 6.20 (C=C, w), 9.52 (OH, s, broad).

ACKNOWLEDGMENT

This work was supported by Grant A-1333 of the National Research Council of Canada.

1. J. Thesing and F. Schülde. Chem. Ber. **85**, 324 (1952).
2. H. E. Johnson and D. G. Crosby. J. Org. Chem. **28**, 1246 (1963).
3. R. C. Elderfield and B. A. Fischer. J. Org. Chem. **23**, 949 (1958).
4. M. E. Speeter and W. C. Anthony. J. Am. Chem. Soc. **76**, 6208 (1954).
5. B. Oddo and A. Albanese. Gazz. Chim. Ital. **57**, 827 (1927).
6. T. Hoshino and K. Shimodaira. Ann. **520**, 19 (1935).

Received October 9, 1963.
Department of Chemistry,
Loyola College,
Montreal 28, Que.

H_0 ACIDITY FUNCTIONS FOR NITRIC AND PHOSPHORIC ACID SOLUTIONS CONTAINING ADDED SODIUM PERCHLORATE

Donald G. Lee and Ross Stewart

In connection with an investigation of the mechanism of the chromic acid oxidation of alcohols (1) we required the values of the Hammett acidity function, H_0, for nitric and phosphoric acid solutions containing equimolar amounts of sodium perchlorate and acid. The functions were determined by use of weak bases for indicators in the manner described by Paul and Long (2).

Can. J. Chem. Downloaded from www.nrcresearchpress.com by 210.87.254.6 on 09/05/12
For personal use only.

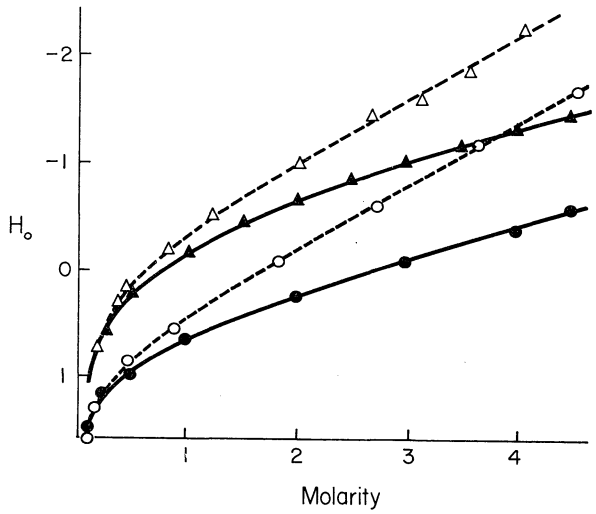

FIG. 1. Acidity functions for solutions of nitric acid ▲ and phosphoric acid ●, and for nitric acid – sodium perchlorate △ and phosphoric acid – sodium perchlorate. ○ All solutions are equimolar in acid and salt.

Figure 1 reveals that the functions obtained in dilute regions are identical with previously determined functions containing no added salt (2), the addition of small amounts of salt having very little effect on the acidity of these solutions. In more concentrated solutions, however, the addition of increasing amounts of salt results in a continuous increase in acidity as compared to solutions containing no added salt. This is in agreement with the work of Harbottle (3) and Paul (4), who have reported that the addition of varying amounts of sodium perchlorate to perchloric acid and hydrochloric acid solutions causes increases in the acidity of the media.

$-H_0$ is defined as

$$-H_0 = \log C_{H^+} + \log (f_{H^+}/f_{BH^+}) + \log f_B.$$

The more rapid increase in $-H_0$ as compared to C_{H^+} in acid solutions containing no added salt is due primarily to an increase in log (f_{H^+}/f_{BH^+}) as the acid concentration is raised. The additional effect of added sodium perchlorate is presumably due to a further increase in this term and probably an increase in the log f_B term since it is known that sodium perchlorate has a tendency to salt-out non-electrolytes (2, 4).

EXPERIMENTAL

The indicators used in this investigation (*p*-nitroaniline, *o*-nitroaniline, and 4-chloro-2-nitroaniline) were all obtained commercially and recrystallized from ethanol to constant melting points. The melting points were all found to agree favorably with the values reported in the literature (5).

Concentrated stock solutions containing equimolar ratios of either H_3PO_4 or HNO_3 and sodium perchlorate were prepared and then diluted to give a series of solutions of varying concentrations. Fifty microliters of an alcoholic solution of indicator was then added to a series of 5-ml volumetric flasks which were then filled to the mark with salt–acid solutions. The visible and ultraviolet spectral data were then obtained in the usual way using a Beckman DU Spectrophotometer, controlled to 25°±0.5° by means of thermospacers.

The data are shown in Tables I and II. In dilute solutions the H_0 determined from *p*-nitroaniline solutions was found to agree to within 0.03 units with pH measurements made with a glass electrode on a Beckman Model G pH meter.

Can. J. Chem. Downloaded from www.nrcresearchpress.com by 210.87.254.6 on 09/05/12
For personal use only.

TABLE I

Acidity of solutions containing a 1:1 molar ratio of H_3PO_4 to $NaClO_4$

Molarity	C_{BH^+}/C_B	H_0
(*a*) *p*-Nitroaniline, pK = 0.99, λ_{max} = 380 mμ		
0.0457	0.161	1.78
0.0914	0.286	1.53
0.183	0.525	1.27
0.457	1.415	0.84
0.914	3.39	0.46
1.83	11.82	−0.08
(*b*) *o*-Nitroaniline, pK = −0.20, λ_{max} = 412 mμ		
0.457	0.0823	0.84
0.730	0.175	0.57
0.914	0.216	0.46
1.83	0.802	−0.08
2.74	2.57	−0.60
3.66	9.30	−1.17
(*c*) 4-Chloro-2-nitroaniline, pK = −0.95, λ_{max} = 425 mμ		
1.83	0.130	−0.08
2.74	0.479	−0.60
3.66	1.630	−1.17
4.57	5.17	−1.66

TABLE II

Acidity of solutions containing a 1:1 molar ratio of HNO_3 to $NaClO_4$

Molarity	C_{BH^+}/C_B	H_0
(*a*) *p*-Nitroaniline, pK_a = 1.00, λ_{max} = 383 mμ		
0.0139	0.136	1.89
0.0232	0.198	1.68
0.0464	0.401	1.38
0.0928	0.870	1.06
0.186	1.97	0.705
0.371	5.05	0.297
0.464	6.81	0.167
(*b*) *o*-Nitroaniline, pK_a = −0.28, λ_{max} = 412 mμ		
0.0928	0.0460	1.060
0.1856	0.109	0.705
0.464	0.358	0.167
0.812	0.809	−0.20
1.218	1.74	−0.53
2.030	5.17	−1.00
2.676	14.40	−1.45
(*c*) 4-Chloro-2-nitroaniline,* pK_a = −0.98, λ_{max} = 429 mμ		
0.464	0.0605	0.167
0.812	0.150	−0.20
1.218	0.330	−0.53
1.338	0.415	−0.60
1.784	0.786	−0.87
2.03	1.12	−1.00
2.23	1.40	−1.16
2.44	2.27	−1.29
2.68	2.55	−1.45
3.12	4.44	−1.60
3.57	8.42	−1.85
4.06	21.7	−2.25

*For this indicator the optical density at this wavelength increased with time in the more concentrated acid solutions. Hence all readings were extrapolated to zero time.

Can. J. Chem. Downloaded from www.nrcresearchpress.com by 210.87.254.6 on 09/05/12
For personal use only.

1. R. STEWART and D. G. LEE. Can. J. Chem. This issue.
2. M. A. PAUL and F. A. LONG. Chem. Rev. **57**, 1 (1957).
3. G. HARBOTTLE. J. Am. Chem. Soc. **73**, 4024 (1951).
4. M. A. PAUL. J. Am. Chem. Soc. **76**, 3236 (1954).
5. L. P. HAMMETT and A. J. DEYRUP. J. Am. Chem. Soc. **54**, 2721 (1932).

RECEIVED SEPTEMBER 3, 1963.
DEPARTMENT OF CHEMISTRY,
UNIVERSITY OF BRITISH COLUMBIA,
VANCOUVER 8, B.C.

Can. J. Chem. Downloaded from www.nrcresearchpress.com by 210.87.254.6 on 09/05/12
For personal use only.

A QUEBRACHAMINE MODEL

ERNEST WENKERT,[1] SHEILA GARRATT, AND K. G. DAVE

Chemical studies, biogenetic considerations (1) and mass-spectrometric analysis (2) have led to the proposal of I as the structure of quebrachamine. While probably biogenetically related to the natural pentacyclic *Aspidosperma* bases (3), tetracyclic quebrachamine possesses an unusual nine-membered ring. This rare structural feature has now been incorporated in a synthetic model (II) by a method which, in principle, is applicable to the total synthesis of the indole alkaloid itself.

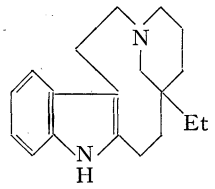

I

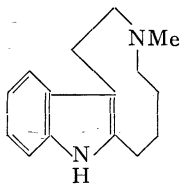

II

The first synthetic goal was the indolopyrrocoline system III. It was obtained in form of the lactam ester III*a* by the condensation of ethyl α-ketoglutarate with tryptamine. Alternatively, it was produced as the amine III*c* by the acid-catalyzed condensation of tryptamine and α-ketoglutaric acid, pyrolytic decarboxylation–dehydration, and lithium aluminum hydride reduction of the resultant lactam III*b*—a procedure published by Corsano and Algieri (4). The proton magnetic resonance spectrum of the base III*c* [a one-proton multiplet at 4.0–4.2 p.p.m. characteristic of C(3)—H] showed it to possess a cis-pyrrocoline configuration (5). An alternative synthesis of III*c*, via the intermediacy of IV and modelled after recorded reactions with tryptimides (6), failed in the crucial cyclization step.

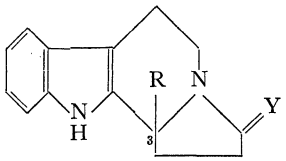

III*a*, R = CO_2Et, Y = O
b, R = H, Y = O
c, R = H, Y = H_2

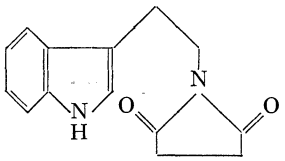

IV

Conversion of III*c* to its methiodide and treatment of the latter with lithium in liquid ammonia yielded the medium-sized ring, compound II (cf. 7).

[1]*Present address: Department of Chemistry, Indiana University, Bloomington, Indiana, U.S.A.*

1. R. STEWART and D. G. LEE. Can. J. Chem. This issue.
2. M. A. PAUL and F. A. LONG. Chem. Rev. **57**, 1 (1957).
3. G. HARBOTTLE. J. Am. Chem. Soc. **73**, 4024 (1951).
4. M. A. PAUL. J. Am. Chem. Soc. **76**, 3236 (1954).
5. L. P. HAMMETT and A. J. DEYRUP. J. Am. Chem. Soc. **54**, 2721 (1932).

RECEIVED SEPTEMBER 3, 1963.
DEPARTMENT OF CHEMISTRY,
UNIVERSITY OF BRITISH COLUMBIA,
VANCOUVER 8, B.C.

Can. J. Chem. Downloaded from www.nrcresearchpress.com by 210.87.254.6 on 09/05/12
For personal use only.

A QUEBRACHAMINE MODEL

ERNEST WENKERT,[1] SHEILA GARRATT, AND K. G. DAVE

Chemical studies, biogenetic considerations (1) and mass-spectrometric analysis (2) have led to the proposal of I as the structure of quebrachamine. While probably biogenetically related to the natural pentacyclic *Aspidosperma* bases (3), tetracyclic quebrachamine possesses an unusual nine-membered ring. This rare structural feature has now been incorporated in a synthetic model (II) by a method which, in principle, is applicable to the total synthesis of the indole alkaloid itself.

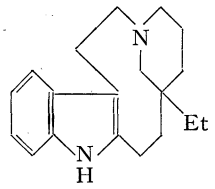

I

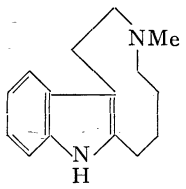

II

The first synthetic goal was the indolopyrrocoline system III. It was obtained in form of the lactam ester III*a* by the condensation of ethyl α-ketoglutarate with tryptamine. Alternatively, it was produced as the amine III*c* by the acid-catalyzed condensation of tryptamine and α-ketoglutaric acid, pyrolytic decarboxylation–dehydration, and lithium aluminum hydride reduction of the resultant lactam III*b*—a procedure published by Corsano and Algieri (4). The proton magnetic resonance spectrum of the base III*c* [a one-proton multiplet at 4.0–4.2 p.p.m. characteristic of C(3)—H] showed it to possess a cis-pyrrocoline configuration (5). An alternative synthesis of III*c*, via the intermediacy of IV and modelled after recorded reactions with tryptimides (6), failed in the crucial cyclization step.

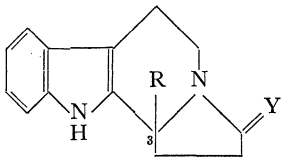

III*a*, R = CO_2Et, Y = O
b, R = H, Y = O
c, R = H, Y = H_2

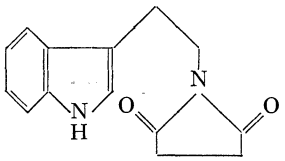

IV

Conversion of III*c* to its methiodide and treatment of the latter with lithium in liquid ammonia yielded the medium-sized ring, compound II (cf. 7).

[1]*Present address: Department of Chemistry, Indiana University, Bloomington, Indiana, U.S.A.*

EXPERIMENTAL

All melting points were observed on a Kofler microscope hot stage. Ultraviolet spectra were run on 95% ethanol solutions on a Cary model 12 spectrophotometer, while infrared spectra were obtained on a Perkin–Elmer infrared spectrophotometer. Proton magnetic resonance spectra were measured on deuterochloroform solutions with tetramethylsilane as internal standard on a Varian A-60 spectrometer (courtesy of the Department of Chemistry, Indiana University, Bloomington, Indiana, U.S.A.).

Lactam IIIa

A solution of 1.20 g of tryptamine hydrochloride and 1.00 g of ethyl α-ketoglutarate in 10 ml of ethanol was refluxed for 60 hours under nitrogen. Evaporation of the solvent left 0.88 g of crystalline residue whose recrystallization from methanol yielded colorless prisms of lactam ester III*a*, m.p. 225–226°; μ (Nujol) NH 3.00 (s), C=O 5.75 (s), 5.92 (s), C=C 6.30 (w); λ_{max} 223 mμ (log ϵ 4.60), 282 mμ (log ϵ 3.95), and 292 mμ (log ϵ 3.85); δ broad NH singlet 8.58 p.p.m., ester CH_2 quartet 4.25 p.p.m. (J = 7 c.p.s.), ester CH_3 triplet 1.29 p.p.m. (J = 7 c.p.s.). Anal. Calc. for $C_{17}H_{18}O_3N_2$: C, 68.45; H, 6.08. Found: C, 68.15; H, 6.02.

N-[β-(3-Indolyl)ethyl]succinimide (IV)

A suspension of an intimate mixture of 1.14 g of tryptamine and 0.70 g of succinic anhydride in 120 ml of benzene was refluxed for 5 hours. The cooled suspension was decanted and the solution extracted with 5% sodium hydroxide solution and with water. The solid residue from the decantation was dissolved in 5% sodium hydroxide solution and thereafter combined with the previous basic extract. The joint alkaline extracts were acidified with 5% hydrochloric acid and the resultant solid taken up in ethyl acetate. The organic solution was dried over anhydrous magnesium sulphate and evaporated under reduced pressure. Crystallization of the solid residue, 1.36 g, from ethyl acetate yielded N_b-succinoyl tryptamine, m.p. 138–139°. Anal. Calc. for $C_{14}H_{16}O_3N_2$: C, 64.58; H, 6.20; N, 10.77. Found: C, 64.77; H, 6.27; N, 10.62. An ether solution of an excess diazomethane was added to a solution of 82 mg of the amide acid in 10 ml of methanol and the mixture left standing for 30 minutes. Evaporation of the solvent and crystallization of the resultant solid, 85 mg, from methanol yielded colorless plates of the amide ester, m.p. 110–111°; μ (Nujol) NH 2.95 (s), 3.0–3.1 (m), C=O 5.80 (s), 6.03 (s); δ ester CH_3 singlet 3.62 p.p.m.

N_b-Succinoyl tryptamine, 1.44 g, was heated for 10 minutes at 200° under slightly reduced pressure. Crystallization of the dark brown reaction residue from methanol yielded the imide IV, m.p. 166–167°; μ (Nujol) NH 2.95 (s), C=O 5.60 (w), 5.85 (s); δ two succinoyl CH_2 singlet 2.58 p.p.m. Anal. Calc. for $C_{14}H_{14}O_2N_2$: C, 69.37; H, 5.82; N, 11.56. Found: C, 69.34; H, 5.92; N, 11.47.

Amine II

A solution of 188 mg of the amine III*c* and an excess of methyl iodide in 10 ml of ether was left standing for 8 hours. The resultant precipitate was filtered and dried. (Since this methiodide was exceedingly hygroscopic, its isolation had to be carried out rapidly.) The dried salt, 275 mg, was dissolved in 5 ml of absolute ethanol and 75 ml of liquid ammonia and enough lithium added to the stirring solution until the resultant blue color persisted for 1 hour. Then solid ammonium chloride was added, the ammonia allowed to evaporate, and the residue dissolved in water. Sodium hydroxide, 5%, was added and the aqueous solution extracted with ether. The extract was washed with water, dried over anhydrous magnesium sulphate, and evaporated under reduced pressure. Chromatography of the residue, 136 mg, on alumina and elution with 1:1 chloroform–benzene yielded 44 mg of crystals whose crystallizations from aqueous ethanol led to amine II, m.p. 128–130°; δ N—CH_3 singlet 2.38 p.p.m., no C—CH_3 present. Anal. Calc. for $C_{15}H_{20}N_2$: C, 78.89; H, 8.83; N, 12.27; C-alkyl, 0.00. Found: C, 78.70; H, 8.89; N, 12.28; C-alkyl, negative.

ACKNOWLEDGMENT

The authors are indebted to the U.S. Public Health Service for support of this work by grant MY-5815 and to Mr. L. Dorfman (Ciba Pharmaceutical Co., Summit, New Jersey, U.S.A.) for the C-alkyl determination.

1. H. Kny and B. Witkop. J. Org. Chem. **25**, 635 (1960).
2. K. Biemann and G. Spiteller. J. Am. Chem. Soc. **84**, 4578 (1962).
3. E. Wenkert. J. Am. Chem. Soc. **84**, 98 (1962).
4. S. Corsano and S. Algieri. Ann. Chim. **50**, 75 (1960).
5. E. Wenkert and B. Wickberg. J. Am. Chem. Soc. **84**, 4914 (1962).
6. J. Jost. Helv. Chim. Acta, **32**, 1297 (1949), and references contained therein.
7. E. Leete. J. Am. Chem. Soc. **82**, 6338 (1960).

Received September 30, 1963.
Department of Chemistry,
Iowa State University,
Ames, Iowa, U.S.A.

Can. J. Chem. Downloaded from www.nrcresearchpress.com by 210.87.254.6 on 09/05/12
For personal use only.

Canadian Journal of Chemistry

Issued by THE NATIONAL RESEARCH COUNCIL OF CANADA

VOLUME 42 MARCH 1964 NUMBER 3

TERPENOIDS

V. SENEGENIN: FUNCTIONAL GROUPS AND PART STRUCTURE

J. J. DUGAN, P. DE MAYO, AND A. N. STARRATT

Department of Chemistry, University of Western Ontario, London, Ontario

Received September 23, 1963

ABSTRACT

Senegenin, the sapogenin from *Polygala senega* has been shown to contain chlorine; it has the empirical formula $C_{30}H_{45}O_6Cl$. The oxygen atoms, contrary to earlier work, are contained in two carboxyl groups and two secondary hydroxyl groups. There is one isolated ethylenic linkage. The environment of the hydroxylic functions and one carboxyl group has been shown to be as in (XI).

Of the known triterpenoids of undetermined constitution remaining, senegenin has a claim to outstanding interest. Investigations directed to a study of the saponin of *Polygala senega* have spread over many years, but, as mentioned by Simonsen and Ross (1), such "investigations . . . have given rise to very divergent results". It is this confusion, and its present clarification, which exculpates us from a charge of literary proliferation in the presentation of incomplete work.

Although senega extract has been used medicinally for some time, chiefly as an expectorant (however, see ref. 2), the first results of chemical importance were obtained by Wedekind and Krecke (3). They isolated, by acid hydrolysis of the saponin, a product to which they assigned the formula $C_{26}H_{44}O_6$. It contained two hydroxyl groups, as indicated by the formation of a diacetate, and gave a dimethyl ester.

A more extensive study was later reported by Jacobs and Isler (4), who observed the presence of two crystalline sapogenins. That of lower solubility appeared to be senegenin, although the constants differed somewhat from those of Wedekind and Krecke: the diacetate, in particular, melted at a much higher temperature. The empirical formula $C_{30}H_{46}O_8$ or $C_{30}H_{44}O_8$ was proposed, and evidence for an isolated ethylenic linkage found in a weak tetranitromethane test. Titration with alkali indicated the presence of two carboxyl groups (again confirmed by the preparation of a non-crystalline dimethyl ester) and the presence of a lactone was inferred by the consumption of a third equivalent of alkali on heating. Senegenin could not be recovered from the acidified hydrolysis mixture.

The second sapogenin isolated from senega root by Jacobs and Isler was an acid, m.p. 257°, which appeared to have the empirical formula $C_{31}H_{50}O_6$ or $C_{31}H_{48}O_6$. This substance also gave a positive reaction with tetranitromethane, and was shown to give a diacetate. Hydrolysis revealed it to be the monoethyl ester of a dibasic acid. Both the sapogenins gave, on selenium dehydrogenation, the same substituted picene obtained previously from such triterpenoids as oleanolic acid, and shown to be (5) 1,8-dimethylpicene: results which strongly supported the supposition of Jacobs and Isler that they were dealing with a triterpenoid.

Can. J. Chem. Downloaded from www.nrcresearchpress.com by 210.87.254.105 on 09/05/12
For personal use only.

More recently senegenin has been the subject of study by Shamma and Reiff (6). The allocation of oxygen functions previously proposed (4) was accepted by these authors with the added qualification, because of the absence of an appropriate band for a γ-lactone, that the lactone be six (or more) membered. Confirmation of the presence of the double bond led them to assign the molecular formula $C_{30}H_{44}O_8$ to senegenin, an interpretation requiring that the substance be tetracyclic. Senegenin gave on lithium aluminum hydride reduction a product believed to be a hexaol from which a pentaacetate could be prepared. An important observation was that senegenin gave an isopropylidene derivative.

Senegenin consumed (6) 2 molecules of lead tetraacetate whereas the dimethyl ester consumed but 1 molecule. No crystalline or characterized compounds were, however, isolated from the cleavage. From their observations the conclusion was drawn that senegenin contained the grouping (I) which required it to be of a carbon skeleton different from that of the then known triterpenoids. It could, however, be incorporated into the carbon skeleton, recently established, of ceanothic acid (7) (II) and our interest in this substance led us to a study of senegenin.

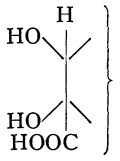

(I)

A number of triterpenoids have been reported as having been isolated for *Polygala* species. *Polygala tenuifolia* Willd. has been shown to contain (8, 9) an acid, tenuifolic acid, to which the empirical formula $C_{30}H_{44-46}O_8$ has been attributed: the same substance has been isolated from *Bredemeyera floribunda* Willd. A similar substance has been isolated from *Polygala senega* L. var. *latifolia* Torr. and Gray (10) which may, however, be identical with senegenin. From *Polygala paenea* Polonsky has isolated polygalacic acid (11) and shown it to have the structure (III) whilst very recently, after the completion of the work to be described, Tschesche and his collaborators have modified their original findings and presented (IV) (12) as the structure of bredemolic acid, a substance found together with tenuifolic acid. The relevance of this related work will become apparent in the sequel.

The isolation procedure of Jacobs and Isler was modified (see Experimental), the crude sapogenin, obtained from the hydrochloric acid hydrolysis of the prosapogenin, being acetylated directly. The material extracted with aqueous bicarbonate solution gave senegenin monoacetate.* Acid hydrolysis afforded senegenin (see Table I).

Our first endeavor was to confirm the nature of the functional groups. The ultraviolet absorption (λ_{max} 205 mμ, ϵ = 6900) suggested the presence of an isolated ethylenic linkage (4), but no indication whatsoever could be found for the presence of a vinylic proton (6) in the n.m.r. spectra of several derivatives. The double bond was, therefore, fully substituted.

The n.m.r. spectrum of dimethyl senegenin showed two singlets (3H each) at τ 6.29 and 6.41 in agreement with the presence of two carbomethoxyl groups. In addition there was absorption at τ 5.81 and 6.10 (1H each). Senegenin monoacetate dimethyl ester, obtained by brief exposure to mild acetylating conditions, had two bands at τ 5.74 (1H, multiplet) and 4.77 (1H, doublet) whilst in the diacetate both bands had moved

**Professor W. D. Ollis (Sheffield) has isolated senegenin in a similar manner, and we would like to present our sincere thanks for a gift of a generous sample.*

Can. J. Chem. Downloaded from www.nrcresearchpress.com by 210.87.254.105 on 09/05/12
For personal use only.

TABLE I

Compound	Present work	Jacobs and Isler (4)	Reiff (22)
Senegenin	M.p. 281–283°* $[\alpha]_D$+19° (EtOH)	290–292° $[\alpha]_D$+19° (EtOH)	280–283° $[\alpha]_D$+16° (EtOH)
Senegenin diacetate	M.p. 257–263° $[\alpha]_D$+29° (MeOH)	260–270°	225–230° $[\alpha]_D$+26° (EtOH)

*The melting point was determined on the Kofler block by placing the compound on the block about 15° below the melting point. This is the procedure indicated to us by Dr. S. W. Pelletier (Athens) as giving the recorded melting point on Dr. Jacob's samples. We are grateful to Dr. Pelletier for this information. Melting points determined on the block in the usual way were in the region 265–270° and varied with the rate of heating.

A direct comparison of the senegenin used in these experiments and that of Jacobs and Shamma has established identity in melting point, mixed melting point, infrared spectrum, and behavior on thin-layer chromatography. We are grateful to Professors Pelletier and Shamma for making the material available.

down field to τ 4.47 (1H, multiplet) and 4.68 (1H, doublet). These changes are those to be expected in the stepwise acetylation of two secondary hydroxyl groups. In confirmation, a diformate could be prepared by the action of formic acid. Further, since one of the methine hydrogens was a doublet, and senegenin dimethyl ester consumed one mole of periodic acid, the part structure (I) (6) must be rejected and replaced by (V), where $(HO)_b$ is the hydroxyl group acetylated first.

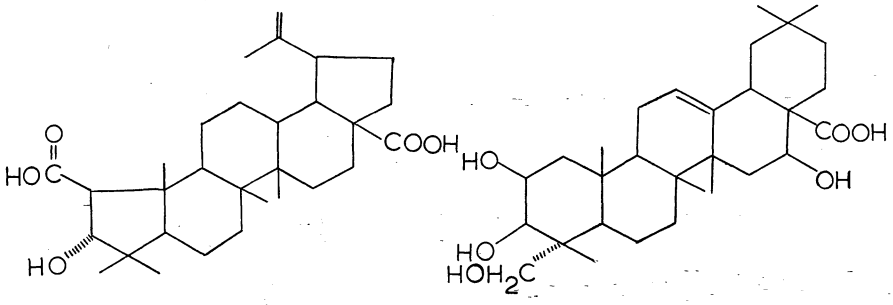

II

III

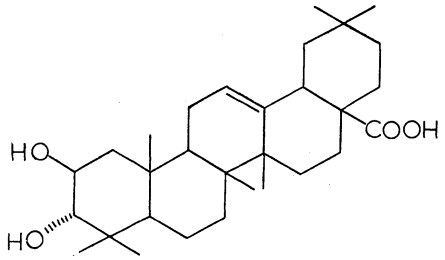

IV

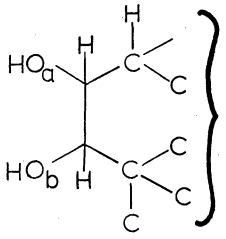

V

Six of the oxygen atoms in senegenin were thereby satisfactorily accounted for. The remaining two were those attributed by previous workers to a lactonic function essentially because of the consumption of an extra equivalent of alkali. This lactone was presumed to suffer ring change to a γ-lactone with perbenzoic acid (6) the exact nature of the

Can. J. Chem. Downloaded from www.nrcresearchpress.com by 210.87.254.105 on 09/05/12
For personal use only.

transformation being, however, unspecified. In an attempt to obtain direct spectral evidence for the lactone the sodium salt of senegenin was prepared and shown, by analysis, to be a disodium salt. However, the infrared spectrum of this salt showed no carbonyl absorption above 1550 cm^{-1} (carboxylate anion). The presence of a lactone in senegenin was, therefore, precluded.

The obstinate fact remained that one equivalent of alkali was consumed by senegenin, beyond the requirements of its carboxyl functions. Yet this potentially acidic function was generated from a non-carbonylic precursor. Whilst such a system, as an improbable grotesquerie, can be devised, the interpretive problem was considerably simplified when it was discovered that senegenin contained chlorine. The atomic weight of chlorine renders distinction from two oxygen atoms by carbon and hydrogen analysis alone a subtle one, and the presently proposed empirical formula, $C_{30}H_{45}O_6Cl$, has requirements close to the O_8 formula previously entertained.

For the further study of senegenin, and in particular for the investigation of the environment of the vicinal hydroxyl groups, the removal of the chlorine was required. This was achieved in two ways.

In the first, senegenin was refluxed in quinoline when de(hydrochloro)senegenin was obtained. This compound could also be obtained, under defined conditions, as the product of the alkali treatment of senegenin, the "extra" equivalent of alkali being consumed by the liberated hydrochloric acid. De(hydrochloro)senegenin was characterized as a diacetate and a dimethyl ester. From the ester a mono- and di-acetate were prepared. The ultraviolet absorption (see Experimental) showed the presence of a heteroannular diene. In the n.m.r. spectrum the de(hydrochloro)senegenin dimethyl ester showed the two bands (3H each) at τ 6.49 and 6.32 for the ester methyl groups and at 6.11 (doublet) and 5.92 (multiplet) for the continuing presence of the glycol system. There was also a band at 4.70 (1H) for a vinyl hydrogen. In addition it was still possible to prepare an isopropylidene derivative. Treatment of senegenin dimethyl ester with quinoline afforded a product identical with that obtained by the methylation of the product from senegenin. The molecular weight, 528, determined mass spectroscopically* further showed that only hydrogen chloride had been lost during the treatment with alkali or with quinoline.

De(hydrochloro)senegenin dimethyl ester was hydrogenated over platinum oxide, with the uptake of one molecule of hydrogen, to give a dihydro compound, termed isodechlorosenegenin dimethyl ester, showing end absorption (λ_{max} 199 mμ, ϵ = 6700) only, and which was characterized as a mono- and di-acetate. De(hydrochloro)senegenin, similarly, gave isodechlorosenegenin.

In the second method of eliminating the chlorine direct reduction of the monoacetate with lithium in liquid ammonia was employed; the product, dechlorosenegenin, was characterized as the diacetate.

A difference in the reactivity of the two carboxyl groups was noted when de(hydrochloro)senegenin dimethyl ester was heated for 2 hours in refluxing 5% alcoholic potassium hydroxide. The product proved to be a monomethyl ester. It has previously been observed in other triterpenoids (13, 14, 15, 16) that the presence of an appropriately situated oxygen function can greatly facilitate the hydrolysis of an otherwise very resistant ester. This observation suggested that the carbomethoxyl group which underwent hydrolysis should be placed as in (VI, R = Me), a part structure which already assumed a general familiarity, but a more direct demonstration of this relationship was required.

Oxidation of isodechlorosenegenin dimethyl ester with chromic acid in pyridine gave a

*We are grateful to Professor K. Biemann for this determination.

Can. J. Chem. Downloaded from www.nrcresearchpress.com by 210.87.254.105 on 09/05/12
For personal use only.

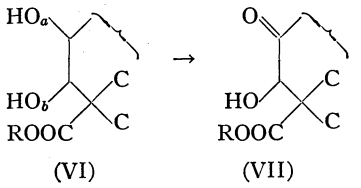

(VI) (VII)

ketol showing hydroxyl absorption at 3495 cm^{-1} in the infrared and a band in the n.m.r. spectrum at τ 5.51 moved to 4.57 on acetylation. This band was a singlet, and therefore it is hydroxyl (*a*) which has been oxidized to the ketone (as in (VII, R = Me)). Since

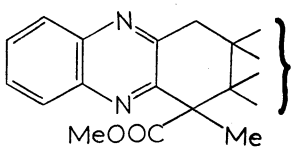

VIII

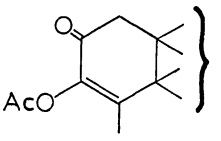

IX

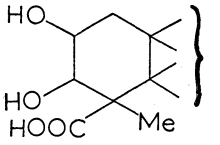

X

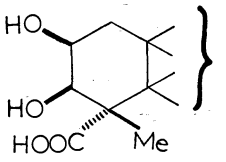

XI

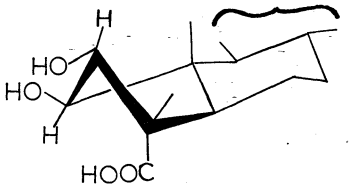

XII

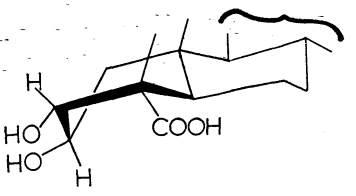

XIII

the carbonyl absorption of the keto-acetate was at 1728 cm^{-1} the possibility of a five-membered ring could not, at this stage, be dismissed. Attempts to hydrolyze the ester grouping in (VII, R = Me) were abortive, however, since the ketol underwent air-oxidation (17) and yielded no tractable product. (VII, R = Me) was converted by bismuth oxide (18) to the non-crystalline α-diketone characterized as the crystalline quinoxaline derivative (VIII).

An alternative approach to the establishment of the relationship of the hydroxyl and carboxyl functions was therefore sought. Isodechlorosenegenin dimethyl ester was converted to the monomethyl ester by alkaline hydrolysis. Oxidation with chromic acid in pyridine gave a gum. On warming in alkali, and acidification, a compound was obtained having the properties of a diosphenol and which had decarboxylated. It was characterized

Can. J. Chem. Downloaded from www.nrcresearchpress.com by 210.87.254.105 on 09/05/12
For personal use only.

as the crystalline acetyl derivative (IX) (λ_{max} 247 mμ).* Since this compound showed ν_{max} for the unsaturated ketone at 1675 cm^{-1} a six-membered (or larger) ring was indicated.

The decarboxylation, that of a β-keto acid, confirms the position of the carboxyl function and the presence of a singlet (3H) at τ 7.76 in the diosphenol acetate indicates the position of a methyl group at this point. The part structure (V) may thus be reasonably expanded to (X)—that is, the normal triterpenoid ring A carbon skeleton. No evidence is presently available for the presence of the C_{10} methyl group.

The carboxyl group must be placed at the 4α, equatorial, position since the resistance of 4β carboxylic ester groups to hydrolysis at this position is well known (for example, ref. 19). Of the four possible arrangements of the glycol one, 2α,3β, can be immediately dismissed since this would require a large trans diaxial coupling of the methine protons ($J \sim$ 8–10 c.p.s.) (20) whereas that observed is ~3.8 c.p.s. Of those remaining only the 2α, 3α, and 2β,3β would be expected to give an isopropylidene derivative easily (21).

Since in senegenin monoacetate the low field (τ 4.83) methine proton is the doublet it is the C_3 hydroxyl that acetylates first. If the arrangement were 2α,3α then this would require the preferential acetylation of an axial 3-hydroxyl group over the far less hindered equatorial 2-hydroxyl group. Since this cannot be accepted the remaining 2β,3β stereochemistry follows (XI), and is consistent with the preferred oxidation of the 2β hydroxyl. It will be noted that a 2β configuration of a hydroxyl group requires a 4α configuration of the carboxyl group since no evidence of lactonization under a variety of conditions has been observed. The structure of what is presumably ring A of senegenin is therefore identical with that observed in medicagenic acid (13).†

The above discussion requires that ring A be a chair, but the possibility of twist or boat forms requires consideration. Of the three remaining possible assignments of glycol stereochemistry rejected, two, namely 2α,3β and 2α,3α, should show no tendency to assume conformations other than chair and so remain unacceptable. The third, 2β,3α, because of the three 1:3 hydroxyl and methyl interactions (present also in (XI)) and because of two 1:3 hydroxyl–hydrogen interactions could invert into a boat or twist form of which (XII) and (XIII) represent extremes. Whilst this might account for acetonide formation and the order of acetylation and oxidation of the hydroxyl groups, in (XII) and (XIII) or all conformations in between the methine protons at C_2 and C_3 are essentially trans-diaxial. The coupling constant here, as in the 2α,3β chair form, would therefore be larger than that actually observed.

Since the hydrolysis of the saponin was effected by all previous workers using hydrochloric acid it seemed probable that the introduction of chlorine into the senegenin moiety took place at this point. Isolation and halogen analysis of the crude saponin indicated the total absence of chlorine. Analysis of the crude prosapogenin on the other hand indicated the presence of 1.57% chlorine not removed by repeated precipitation from ethanol. It is therefore at this stage that the halide is most probably introduced.

Tenuifolic acid, previously referred to (9), has two unassigned oxygen atoms in the formula proposed. On treatment with quinoline it is converted to anhydrotenuifolic acid which, although not a conjugated diene as in the case of de(hydrochloro)senegenin, has analytical figures closely corresponding. It is possible therefore that tenuifolic acid may also contain chlorine, as may other "O_8 substances" from *Polygala* species (10).

Such a sequence has been reported in the chemistry of medicagenic acid (13).

†*That dechlorosenegenin is not medicagenic acid has been shown by a comparison of the acids. We thank Dr. R. J. Morris (Nevada) for a generous specimen of medicagenic acid.*

Can. J. Chem. Downloaded from www.nrcresearchpress.com by 210.87.254.105 on 09/05/12
For personal use only.

Can. J. Chem. Downloaded from www.nrcresearchpress.com by 210.87.254.105 on 09/05/12
For personal use only.

EXPERIMENTAL*

Extraction of Ground Root of Polygala senega

The ground root (6 kg, supplied by S.B. Penick and Co.) was extracted in methanol for approximately 1 day, after which time the solvent was drained off. This was repeated three times and the combined extract was concentrated. The saponin was precipitated by the addition of ethanol and removed by filtration. Crude saponin (2 g) was dissolved in methanol and treated with activated charcoal. After filtration the solution was concentrated to one-third volume and the saponin precipitated with acetone. Analysis showed the absence of chlorine.

The saponin (156 g) was dissolved in alcohol–water (1:1; 480 ml) and warmed on the steam bath for 1 hour with concentrated hydrochloric acid (320 ml). The solution was cooled and the precipitated prosapogenin filtered off.

Upon standing, a crystalline material was slowly deposited from the concentrated saponin mother liquors, m.p. 183–186° (alcohol), $[\alpha]_D$ +67° (*c*, 1.21; water). This compound was identified as sucrose by mixed melting point and infrared spectrum.

Prosapogenin (1 g) was dissolved in alcohol and treated with activated charcoal. After filtration the solution was concentrated and the prosapogenin precipitated with water. This process was repeated six times (with omission of treatment with activated charcoal) at which time the mother liquors no longer gave a positive test for chloride ion. The dried material contained 1.57% chlorine.

Without drying, the total prosapogenin was further hydrolyzed by refluxing 6 hours in a mixture of alcohol (960 ml), water (320 ml), and concentrated hydrochloric acid (320 ml). The solution was cooled and the precipitate collected. The precipitate was extracted exhaustively with ether and the ether extract washed with water and concentrated to dryness.

Acetylation of the Crude Sapogenin Mixture

To the above ether crude extract in pyridine (100 ml) was added acetic anhydride (50 ml) and the solution allowed to stand at room temperature for 6 hours. After isolation the product was dissolved in ether and extracted with sodium bicarbonate solution (5%). After acidification with dilute hydrochloric acid, the acidic product was crystallized from ether–chloroform solution to yield a crude monoacetate (6.8 g). Additional crystalline material (1.6 g) was obtained as a second crop. Recrystallization from methanol–chloroform gave senegenin monoacetate, m.p. 209–211°, $[\alpha]_D$ +23° (*c*, 1.32), ν_{max} 1743, 1700 cm^{-1} (Nujol mull), λ_{max}^{MeOH} 205 mμ (ϵ 6400). Calc. for $C_{32}H_{47}O_7Cl$: C, 66.26; H, 8.18; Cl, 6.12%. Found: C, 66.05; H, 7.95; Cl, 6.01%. Methylation with diazomethane yielded a non-crystalline ester, ν_{max} 1722 cm^{-1}, n.m.r. bands at τ 9.13, 9.07, 8.97, 8.80, 8.64, 7.95, 6.43, 6.37, 5.78 (multiplet), 4.83 (doublet).

On one occasion, the material not extracted by bicarbonate solution was purified by filtration through silica gel. A crystalline product was obtained which was recrystallized from alcohol to give an acetate, m.p. 164–166°, $[\alpha]_D$ +25° (*c*, 1.10), λ_{max} 200 mμ (ϵ 5560), n.m.r. bands of methyl ester at τ 7.98, 6.41, 5.98 (quartet), 4.97 (doublet). Found: C, 70.74; H, 8.97%.

Hydrolysis of the latter acetate (100 mg) by refluxing 30 minutes under nitrogen in methanolic potassium hydroxide solution (5%; 10 ml) afforded, upon isolation, a substance recrystallized from aqueous alcohol to give a product, m.p. 214–217°, $[\alpha]_D$ +20° (*c*, 0.70; alcohol). Found: C, 71.09; H, 9.32%. This compares favorably with the dihydroxy dicarboxylic acid monoethyl ester isolated together with senegenin by Jacobs and Isler (4) and reported to have m.p. 215–218°, $[\alpha]_D$ +24.5° (alcohol). This compound was found to contain no chlorine.

Senegenin

The monoacetate (1.33 g), m.p. 209–211°, was refluxed for 1 hour with methanol (83 ml), water (6 ml), and concentrated hydrochloric acid (18 ml). Isolation of the product and recrystallization from aqueous alcohol gave a product (962 mg) further recrystallized from aqueous alcohol and acetone–water to yield senegenin, m.p. 265–267° (gas evolution) (see Table I), $[\alpha]_D$ +19° (*c*, 0.74; alcohol), ν_{max} 3400, 1700 cm^{-1} (Nujol mull), λ_{max} 205 mμ, (ϵ 6950). The dimethyl ester (glass) exhibited n.m.r. bands at τ 9.15, 9.09, 8.98, 8.85, 8.62, 6.41, 6.29, 6.10, and 5.81. Calc. for $C_{30}H_{45}O_6Cl$: O, 17.87; Cl, 6.60%. Found: O, 17.87; Cl, 6.56%.

Senegenin Diacetate

Acetylation of senegenin at room temperature for 46 hours (acetic anhydride – pyridine) gave senegenin diacetate, m.p. 257–263° (decomposition), $[\alpha]_D$ +29° (*c*, 1.09; methanol), ν_{max} 1736, 1698 cm^{-1}. Calc. for $C_{34}H_{49}O_8Cl$: C, 65.73; H, 7.95; Cl, 5.71%. Found: C, 65.94; H, 7.99; Cl, 5.90%. The non-crystalline methyl ester showed n.m.r. bands at τ 9.14, 9.05, 9.00, 8.87, 8.62, 8.06, 7.93, 6.40, 6.34, 4.68 (doublet), 4.48 (multiplet), and 6.77, 6.58.

Acetonide of Senegenin

Senegenin (48 mg) in acetone (10 ml) was shaken 70 hours with anhydrous copper sulphate. The solution was filtered and the solvent evaporated to give a product which was recrystallized from aqueous alcohol

**For general procedure, see part IV (23).*

to yield the acetonide of senegenin, m.p. 282–284°, (Reiff (22) reports m.p. 261–264°) $[\alpha]_D$ +28° (*c*, 0.93; methanol), ν_{max} 1697 cm^{-1} (Nujol mull). Calc. for $C_{33}H_{49}O_6Cl$: C, 68.64; H, 8.56%. Found: C, 68.86; H, 8.53%.

Sodium Salt of Senegenin

Senegenin was titrated with sodium hydroxide solution (*N*/100 in methanol:water (1:1)). The solvent was evaporated and the residue, dissolved in methanol, was precipitated with ether. The product, $[\alpha]_D$ +5° (*c*, 1.16; methanol), decomposed over a wide range starting at about 260° and showed ν_{max} 1550 cm^{-1} (KBr disk) (carboxylate group). No absorption attributable to a γ or δ lactone was detected between 1550 and 1800 cm^{-1}. Calc. for $C_{30}H_{43}O_6ClNa_2$: Na, 7.92%. Found: Na, 7.34%.

Dechlorination of Senegenin Monoacetate

Senegenin monoacetate (1.2 g) dissolved in anhydrous ether (200 ml) was added over a period of 5 minutes to a stirred solution of an excess of lithium metal in liquid ammonia (200 ml) cooled by immersion in a dry ice – acetone bath. Stirring was continued for 20 minutes and then ammonium chloride was added carefully until the disappearance of the blue color. The ammonia was allowed to evaporate, water added, and the mixture acidified with hydrochloric acid. Isolation of the product by ether extraction and crystallization from methanol afforded dechlorosenegenin (760 mg), m.p. 279–281, $[\alpha]_D$ −15° (*c*, 1.57, methanol). Calc. for $C_{30}H_{46}O_6$: C, 71.68; H, 9.22; O, 19.10%. Found: C, 71.48; H, 9.14; O, 18.58%. The compound was converted into the non-crystalline dimethyl ester with diazomethane and the molecular weight determined by mass spectroscopy. Mol. wt. calc. for $C_{32}H_{50}O_6$: 530.7. Found: 530.*

Dechlorosenegenin Diacetate

Dechlorosenegenin (57 mg) was acetylated (acetic anhydride – pyridine) by standing 3 days at room temperature. Isolation of the product and recrystallization from ether – light petroleum gave dechlorosenegenin diacetate (45 mg), m.p. 281–285°, $[\alpha]_D$ −2° (*c*, 1.61). Calc. for $C_{34}H_{50}O_8$: C, 69.59; H, 8.59%. Found: C, 69.76; H, 8.44%.

De(hydrochloro)senegenin

Senegenin (290 mg) was refluxed 3 hours in quinoline (6 ml; freshly distilled from zinc dust) under nitrogen. The reaction mixture was poured into dilute acid and extracted with ether. The ether extract was then extracted with sodium bicarbonate solution (5%) and the bicarbonate-soluble material isolated (180 mg). This gave a crystalline product (146 mg), found to be free of chlorine, from aqueous alcohol. Further recrystallization gave de(hydrochloro)senegenin, softened ~240°, m.p. 294–296° (gas evolution; evacuated capillary), $[\alpha]_D$ +80° (*c*, 0.75; methanol), ν_{max} 3320, 1697 cm^{-1} (Nujol mull). Calc. for $C_{30}H_{44}O_6.0.5H_2O$: C, 70.68; H, 8.90%. Found: C, 70.61; H, 8.67%.

De(hydrochloro)senegenin Diacetate

De(hydrochloro)senegenin (60 mg) in pyridine (2 ml) was treated overnight at room temperature with acetic anhydride (1 ml). After isolation, the product was placed on a silica gel column (Davison) and eluted with benzene–ether (4:1) to yield a crystalline product which when recrystallized from aqueous alcohol gave de(hydrochloro)senegenin diacetate, m.p. 215–218°, $[\alpha]_D$ +84° (*c*, 0.72; methanol). Calc. for $C_{34}H_{48}O_8.0.5H_2$: C, 68.77; H, 8.32%. Found: C, 68.61; H, 8.64%.

Dimethyl Ester of De(hydrochloro)senegenin

Dehydrochlorosenegenin (93 mg) was methylated with diazomethane and chromatographed on alumina (3 g; Woelm). Elution with benzene:ether (19:1) and recrystallization from alcohol gave the dimethyl ester of de(hydrochloro)senegenin, m.p. 228–231° (evacuated capillary), $[\alpha]_D$ +78° (*c*, 0.99), ν_{max} 3500, 1716 cm^{-1}, λ_{max} 243, 249, 256 mμ (ϵ = 13,200; 14,900; 11,800), n.m.r. bands at τ 9.22, 9.12, 8.97, 8.79, 8.65, 6.49, 6.32, 6.11 (doublet), 5.92 (multiplet), 4.70 (multiplet). Calc. for $C_{32}H_{48}O_6$: C, 72.69; H, 9.15%. Found: C, 72.11; H, 8.99%. Molecular weight determined by mass spectroscopy 528. Mol. wt. calc. for $C_{32}H_{48}O_6$: 528.7.

Treatment of Senegenin Dimethyl Ester with Quinoline

Senegenin dimethyl ester (53 mg) in quinoline (2.5 ml) was refluxed 0.5 hour under nitrogen. The mixture was poured into dilute sulphuric acid and extracted by ether. The ether extract was washed with dilute hydrochloric acid and then with sodium bicarbonate solution (5%). Removal of the ether gave a crude product (48 mg) which was chromatographed on alumina (2 g; Woelm). Elution with benzene:ether (9:1) afforded a substance recrystallized from alcohol and shown by ultraviolet and infrared spectra and mixed melting point to be identical with de(hydrochloro)senegenin dimethyl ester obtained above.

Acetylation of De(hydrochloro)senegenin Dimethyl Ester

The dimethyl ester of de(hydrochloro)senegenin (97 mg) in pyridine (2 ml) was treated overnight with acetic anhydride (1 ml). Upon isolation, the product was filtered through alumina (Merck). Benzene eluted a crystalline fraction recrystallized from alcohol to give the dimethyl ester of de(hydrochloro)senegenin

**We wish to thank Professor K. Biemann (M.I.T.) for this determination.*

Can. J. Chem. Downloaded from www.nrcresearchpress.com by 210.87.254.105 on 09/05/12
For personal use only.

diacetate, m.p. 179–181° (evacuated capillary), $[\alpha]_D$ +64° (*c*, 1.03), ν_{max} 1732 cm^{-1} ($CHCl_3$), n.m.r. bands at τ 9.21, 9.09, 8.94, 8.83, 8.69, 8.09, 7.96, 6.51, 6.37, 4.76 (broad composite band). Calc. for $C_{36}H_{52}O_8$: C, 70.55; H, 8.55%. Found: C, 70.49; H, 8.50%.

Elution with ether gave a product recrystallized from alcohol to yield the monoacetate of the dimethyl ester of de(hydrochloro)senegenin, m.p. 218–221° (evacuated capillary), $[\alpha]_D$ +75° (*c*, 1.02), ν_{max} 3500 1720 cm^{-1}, n.m.r. bands at τ 9.21, 9.07, 8.92, 8.87, 8.74, 7.95, 6.49, 6.42, 6.32, 5.98 (multiplet), 4.80 (composite band). Calc. for $C_{34}H_{50}O_7$: C, 71.55; H, 8.83%. Found: C, 71.25; H, 8.79%.

Acetonide of De(hydrochloro)senegenin

De(hydrochloro)senegenin (24 mg) was shaken 64 hours in acetone (6 ml) with anhydrous copper sulphate. Paper chromatography using Tschesche's mixture B (9) indicated reaction to be complete at this time. The copper sulphate was filtered off and the acetone evaporated to yield a product which upon recrystallization from alcohol gave the acetonide of de(hydrochloro)senegenin, m.p. 281–295° (gas evolution), $[\alpha]_D$ +89° (*c*, 0.64; methanol). Calc. for $C_{33}H_{48}O_6 . 0.5H_2O$: C, 72.07; H, 8.98%. Found: C, 72.52; H, 8.76%.

Dimethyl De(hydrochloro)senegenin Diformate

Senegenin (59 mg) was refluxed 4 hours with formic acid (15 ml; 97%). The formic acid was removed under reduced pressure on the steam bath and the residue filtered through silica gel with ether. The product furnished crystals from alcohol when methylated with diazomethane. The crude methyl ester was chromatographed on silica gel (1.5 g; Davison). Elution with benzene afforded crystalline fractions (41 mg) which were combined and recrystallized from alcohol to give the dimethyl ester diformate of de(hydrochloro)-senegenin, m.p. 235–240° (evacuated capillary), $[\alpha]_D$ +72° (*c*, 0.95), ν_{max} 1720 cm^{-1} (broad band), λ_{max}^{MeOH} 240, 248, 256 mμ, (ϵ 11,910; 13,850; 9440), n.m.r. bands at τ 6.34, 6.22, 1.82, 1.65. Calc. for $C_{34}H_{48}O_8$: C, 69.83; H, 8.27%. Found: C, 69.16; H, 8.39%.

Alkaline Hydrolysis of Senegenin Monoacetate

(*a*) Senegenin monoacetate (135 mg) was refluxed under nitrogen with methanolic potassium hydroxide solution (10 ml; 5%) for 15 minutes. Upon cooling, crystals of the potassium salt deposited on the surface of the flask. Isolation of the product after acidification and recrystallization from alcohol afforded senegenin showing no melting point depression on admixture with material obtained by acid hydrolysis of the monoacetate.

(*b*) Senegenin monoacetate (30 mg) was refluxed 24 hours under nitrogen with an aqueous alcoholic (1:3, water:ethanol) sodium hydroxide solution (10 ml; 5%). After acidification, isolation of the product, followed by methylation and recrystallization from alcohol, the dimethyl ester of de(hydrochloro)senegenin was obtained, m.p. 234–237° (evacuated capillary), which was undepressed on admixture with that obtained above and which exhibited identical behavior upon thin-layer chromatography.

Isodechlorosenegenin

Dehydrochlorosenegenin (28 mg) was hydrogenated in glacial acetic acid (5 ml) over platinum oxide catalyst for a period of 2.5 hours. Recrystallization of the product from aqueous alcohol gave isodechlorosenegenin, m.p. 289–292°, $[\alpha]_D$ +58° (*c*, 0.96; methanol), λ_{max} 199 mμ, (ϵ 6680). Calc. for $C_{30}H_{46}O_6 . 0.5H_2O$: C, 70.42; H, 9.26%. Found: C, 69.96; H, 9.22%.

Isodechlorosenegenin Dimethyl Ester

The dimethyl ester of dehydrochlorosenegenin (31 mg) in ethyl acetate was hydrogenated using palladium on charcoal (5%) catalyst. In 7 minutes 0.9 mole of hydrogen was absorbed. The product was recrystallized from alcohol to give the dihydro derivative, isodechlorosenegenin dimethyl ester, m.p. 221–223° (evacuated capillary), $[\alpha]_D$ +41° (*c*, 1.30), n.m.r. bands at τ 5.86 (multiplet), 6.05 (doublet), 6.29, 6.40 ($COCH_3$). Calc. for $C_{32}H_{50}O_6 . 0.5H_2O$: C, 71.20; H, 9.52%. Found: C, 71.41; H, 9.48%.

Acetylation of Isodechlorosenegenin Dimethyl Ester

Isodechlorosenegenin dimethyl ester (43 mg) in pyridine (2 ml) was treated with acetic anhydride (1 ml) for 6 hours. The product consisting of monoacetate together with some diacetate (see below) was separated by (silicic acid) thin-layer chromatography (3% methanol in chloroform). Recrystallization of the slower moving compound from methanol gave the monoacetate of isodechlorosenegenin dimethyl ester, m.p. 173–176°, $[\alpha]_D$ +33° (*c*, 1.15), ν_{max} 3490, 1720 cm^{-1}. Calc. for $C_{34}H_{52}O_7 . 0.5H_2O$: C, 70.19; H, 9.18%. Found: C, 70.55; H, 8.79%.

Isodechlorosenegenin dimethyl ester (74 mg) was allowed to react with acetic anhydride – pyridine for a period of 50 hours and yielded a product which was recrystallized from alcohol to give the dicaetate, m.p. 192–196° (evacuated capillary), $[\alpha]_D$ +53° (*c*, 0.96), ν_{max} 1725 cm^{-1}, n.m.r. bands at τ 8.04, 7.94, 6.39, 6.34, 4.66 (broad composite band) ($CDCl_3$). Calc. for $C_{36}H_{54}O_8$: C, 70.33; H, 8.85%. Found: C, 70.65; H, 8.77%.

De(hydrochloro)senegenin Monomethyl Ester

De(hydrochloro)senegenin dimethyl ester (34 mg) was refluxed for 2 hours under nitrogen with alcoholic potassium hydroxide solution (5%; 10 ml). The product was isolated by ether extraction after acidification

Can. J. Chem. Downloaded from www.nrcresearchpress.com by 210.87.254.105 on 09/05/12
For personal use only.

and dilution with water. The acid obtained was recrystallized from aqueous alcohol to give the de(hydrochloro)senegenin monomethyl ester, m.p. 249–252° (evacuated capillary; gas evolution), $[\alpha]_D$ +58° (*c*, 0.79; methanol). Calc. for $C_{31}H_{46}O_6.H_2O$: C, 69.89; H, 9.08%. Found: C, 70.38; H, 9.03%.

Remethylation of the monoacid (6 mg) gave a crystalline compound with identical infrared spectrum and behavior upon thin-layer chromatography (silica gel) as was observed with de(hydrochloro)senegenin dimethyl ester.

Periodic Acid Titration of Senegenin Dimethyl Ester

Senegenin dimethyl ester (36 mg), dissolved in methanol (8 ml) and water (1 ml), was titrated with periodic acid (1 ml; approx. 0.32 *N*). After 1.25 hours, the uptake of oxidant had ceased with consumption of 1 mole. The product was isolated but could not be induced to crystallize.

Dehydroisodechlorosenegenin Dimethyl Ester

Isodechlorosenegenin (109 mg) in pyridine (1.1 ml) was added to chromic anhydride (108 mg) in pyridine (1.1 ml) and let stand at room temperature for 10 hours. The reaction mixture was dissolved in alcohol and dilute hydrochloric acid, diluted with water, and extracted with ether to yield the crude ketol (92 mg). This was recrystallized from alcohol to give dehydroisodechlorosenegenin dimethyl ester, m.p. 186–188° (evacuated capillary), $[\alpha]_D$ +31° (*c*, 0.97), ν_{max} 3495, 1723 cm^{-1} (CCl_4), n.m.r. bands at τ 6.43, 6.27, 5.51. Calc. for $C_{32}H_{48}O_6$: C, 72.69; H, 9.15%. Found: C, 73.11; H, 9.03%.

The above ketol (20 mg) was acetylated (acetic anhydride – pyridine; room temperature) to give a non-crystalline acetate, ν_{max} 1758, 1728 cm^{-1} (CCl_4), n.m.r. bands at τ 7.95, 6.46, 6.32, 4.57 (singlet).

Diketone from Isodechlorosenegenin Dimethyl Ester

The above ketol (42 mg) was refluxed 10 hours under nitrogen in glacial acetic acid (4 ml) with bismuth oxide (53 mg). The solvent was evaporated and the residue dissolved in ether and dilute hydrochloric acid. The ether solution was washed, dried, and evaporated, yielding a crude product, which appeared as mainly one spot upon thin-layer chromatography. This crude, non-crystalline, diketone in absolute alcohol (3 ml) and acetic acid (0.5 ml) was refluxed 3 hours under nitrogen with *o*-phenylenediamine. The product was isolated by ether extraction and the ether was washed with dilute hydrochloric acid. Recrystallization from alcohol afforded the quinoxaline derivative, m.p. 260–263° (evacuated capillary), $[\alpha]_D$ +40° (*c*, 0.99), ν_{max} 1728 cm^{-1} (CCl_4), λ_{max} 238, 322, 312 (shoulder) (ϵ 34,300; 10,200; 7900). Calc. for $C_{38}H_{48}O_4N_2.0.5H_2O$: C, 75.34; H, 8.15; N, 4.63%. Found: C, 75.61; H, 8.44; N, 4.79%.

Isodechlorosenegenin Monomethyl Ester

Isodechlorosenegenin dimethyl ester (40 mg) was refluxed 2 hours under nitrogen with alcoholic potassium hydroxide solution (5%; 5 ml). The acidic material was isolated and recrystallized from aqueous alcohol to give isodechlorosenegenin monomethyl ester, m.p. 284–286° (evacuated capillary), $[\alpha]_D$ +57° (*c*, 1.09; methanol). Calc. for $C_{31}H_{48}O_6$: C, 72.06; H, 9.36; O, 18.58%. Found: C, 71.82; H, 9.20; O, 18.61%.

Nor-diosphenol Acetate

Isodechlorosenegenin monomethyl ester (80 mg) in pyridine (0.8 ml) was added to chromic anhydride (88 mg) in pyridine (0.8 ml) and let stand 9 hours at room temperature. The oxidation product (53 mg) was isolated as previously but could not be induced to crystallize. The gum was then refluxed 1 hour with methanolic potassium hydroxide (10%; 10 ml). The crude product (49 mg) was isolated and found to give a positive ferric chloride test. It exhibited ν_{max} 3460 (hydroxyl), 1725 (methyl ester and ketone), 1675 (unsaturated ketone), 1648 (double bond) cm^{-1} (CCl_4), λ_{max}^{MeOH} 279 mμ (ϵ 4600) (band showed characteristic change to higher wavelength upon addition of alkali). It was then acetylated (acetic anhydride – pyridine, overnight). The crude acetate was chromatographed on a column of silica gel (Davison). Elution with benzene:ether (19:1) afforded the crystalline nor-diosphenol acetate, m.p. 190–192° (evacuated capillary), $[\alpha]_D$ +83° (*c*, 0.85), ν_{max} 1752 (acetate), 1718 (methyl ester), 1674 (unsaturated ketone), 1640 (double bond) cm^{-1}, λ_{max}^{MeOH} 246 mμ (ϵ 9630). Calc. for $C_{32}H_{46}O_5$: C, 75.26; H, 9.08%. Found: C, 74.87; H, 9.08%.

ACKNOWLEDGMENTS

The support of the National Research Council is gratefully acknowledged. We also wish to thank Mr. R. E. Klinck for the determination of the n.m.r. spectra.

REFERENCES

1. J. Simonsen and W. C. J. Ross. *In* The terpenes. Vol. V. The University Press, Cambridge. 1957. p. 358.
2. E. M. Boyd and M. E. Palmer. Acta Pharmacol. Toxicol. **2**, 235 (1946).
3. E. Wedekind and R. Krecke. Chem. Ber. **57**, 1118 (1924).
4. W. A. Jacobs and O. Isler. J. Biol. Chem. **119**, 155 (1937).
5. L. Ruzicka and K. Hofmann. Helv. Chim. Acta, **20**, 1155 (1937).
6. M. Shamma and L. P. Rieff. Chem. Ind. (London), 1272 (1960).

Can. J. Chem. Downloaded from www.nrcresearchpress.com by 210.87.254.105 on 09/05/12
For personal use only.

7. P. DE MAYO and A. N. STARRATT. Can. J. Chem. **40**, 788 (1962).
8. T. Q. CHOU, J. H. CHU, and P. F. MEI. J. Am. Pharm. Assoc. Sci. Ed. **36**, 241 (1947).
9. R. TSCHESCHE and A. K. SEN GUPTA. Chem. Ber. **93**, 1903 (1960).
10. M. FUJITA and H. ITOKAWA. Chem. Pharm. Bull. (Tokyo), **9**, 1006 (1961).
11. J. RONDEST and J. POLONSKY. Bull. Soc. Chim. France, 1253 (1963).
12. R. TSCHESCHE, E. HENCKEL, and G. SNATZKE. Tetrahedron Letters, 613 (1963).
13. C. DJERASSI, D. B. THOMAS, A. L. LIVINGSTON, and C. R. THOMPSON. J. Am. Chem. Soc. **79**, 5292 (1957).
14. C. DJERASSI and H. G. MONSIMER. J. Am. Chem. Soc. **79**, 2901 (1957).
15. C. DJERASSI and A. E. LIPPMAN. J. Am. Chem. Soc. **77**, 1825 (1955).
16. A. F. THOMAS. Tetrahedron, **15**, 212 (1961).
17. P. R. ENSLIN, J. M. HUGO, K. B. NORTON, and D. E. A. RIVETT. J. Chem. Soc. 4779 (1960).
18. W. RIGBY. J. Chem. Soc. 793 (1951).
19. P. BILHAM, G. A. R. KON, and W. C. J. ROSS. J. Chem. Soc. 35 (1942).
20. R. U. LEMIEUX, R. N. KULLNIG, H. J. BERNSTEIN, and W. G. SCHNEIDER. J. Am. Chem. Soc. **79**, 1005 (1957).
21. N. L. WENDLER and H. L. SLATES. Chem. Ind. (London), 167 (1955).
22. L. P. REIFF. Ph.D. Thesis, Pennsylvania State University, Philadelphia, Penn. 1960.
23. P. DE MAYO, E. Y. SPENCER, and R. W. WHITE. Can. J. Chem. **41**, 2996 (1963).

Can. J. Chem. Downloaded from www.nrcresearchpress.com by 210.87.254.105 on 09/05/12
For personal use only.

NUCLEAR MAGNETIC RESONANCE STUDIES OF THE PROTONATION OF WEAK BASES IN FLUOROSULPHURIC ACID

III. METHYLBENZENES AND ANISOLE

T. Birchall and R. J. Gillespie
Department of Chemistry, McMaster University, Hamilton, Ontario

Received May 29, 1963

ABSTRACT

The proton magnetic resonance spectra of solutions of mesitylene, durene, pentamethylbenzene, hexamethylbenzene, *m*- and *p*-xylenes, and anisole have been studied in fluorosulphuric acid and protonation on the ring carbon atom established. Rates of proton exchange have been measured and activation energies calculated for the proton exchange process. Intermolecular exchange with the solvent is suggested as the most probable exchange process in all cases.

Can. J. Chem. Downloaded from www.nrcresearchpress.com by 210.87.254.42 on 09/05/12
For personal use only.

INTRODUCTION

The protonation and relative basicities of the various methylbenzenes has been discussed in a number of papers (1–5). It has been assumed that the proton adds to one carbon atom thereby forming an "aliphatic" CH_2 group as first suggested by Gold and Tye (2) in the case of anthracene. Definite evidence in support of this has been obtained from the n.m.r. spectra of the conjugate acids of a number of aromatic hydrocarbons obtained by dissolving the hydrocarbon in a strongly acidic medium such as $BF_3.H_2O/CF_3CO_2H$ or BF_3/HF (6). Although for pentamethylbenzene in BF_3/HF a rather broad line due to the CH_2 group was observed at room temperature; for hexamethylbenzene, mesitylene, and other weaker bases it was necessary to make measurements at low temperatures in order to observe the resonance of the CH_2 protons. This has been attributed to the exchange of the CH_2 protons by one or more of three processes.

(i) Exchange with the solvent HS

$$AH^+ + S^- = A + HS.$$

(ii) Intermolecular exchange between the aromatic hydrocarbon and its conjugate acid

$$A + AH^+ = AH^+ + A.$$

(iii) Intramolecular exchange of the proton between positions of equal proton affinity on the same carbonium ion, for example,

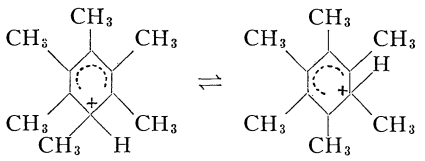

From the results of their studies of the protonation of aromatic hydrocarbons in HF/BF_3 MacLean and Mackor (7) have concluded that for hexamethylbenzene, durene, and prehnitene, exchange proceeds by (iii); for mesitylene, by (ii) and (i); and for *m*-xylene by (ii) alone, while for pentamethylbenzene, they observed no exchange.

We have made similar measurements of the spectra of aromatic hydrocarbons in solutions in fluorosulphuric acid at temperatures down to −90°. In contrast to MacLean and

Mackors' conclusions we find that the observed spectra may in all cases be interpreted in terms of exchange by (i).

EXPERIMENTAL

The bases were commercial samples; solids were recrystallized. The n.m.r. spectra run at high gain showed no peaks that could be attributed to impurities. Fluorosulphuric acid was distilled twice in a dry atmosphere before use. The solutions were prepared at the temperature of an acetone – dry ice mixture.

The n.m.r. spectra were recorded with a Varian H.R. 60 spectrometer equipped with a variable temperature probe and an integrator. Chemical shifts were measured from an external reference of tetramethylsilane using the audio side-band technique.

RESULTS AND DISCUSSION

Spectra of Hydrocarbon Conjugate Acids

For each of the hydrocarbons studied it was found that at sufficiently low temperatures and under sufficiently acid conditions the lifetime of the hydrocarbon conjugate acid is long enough for its n.m.r. spectrum to be observed.

Mesitylene

The spectrum of a 6.16 mole % (1.2 molar) solution of mesitylene in fluorosulphuric acid at −79° C is shown in Fig. 1. It consists of three peaks A, B, and C of relative areas 2.02:1.96:9.08. These three peaks must arise from the two aromatic protons A, the two methylene protons B, and the three methyl groups C respectively, indicating that protonation has occurred on one of the ring carbon atoms. Since the three methyl groups are no longer equivalent the methyl resonance actually consists of two overlapping peaks of relative areas 2:1. The spectra of other solutions with concentrations in the range 2–6 mole% were all quite similar. No signals were observed for any of the solutions that could be attributed to the unprotonated mesitylene, indicating that, under our experimental conditions, the protonation of mesitylene is essentially complete. This is of some interest since MacLean and Mackor's (7) n.m.r. spectrum of a 3.5 molar solution of mesitylene in anhydrous hydrogen fluoride saturated with boron trifluoride indicated that only 60% of the mesitylene was present in the protonated form, the remainder being present as the free base.

No fine structure due to spin–spin coupling was observed in our spectra. In HF solution MacLean and Mackor found that the para-methyl group signal was a triplet and they attributed this to spin–spin coupling with the methylene group although the expected quartet splitting of the methylene signal was not observed.

Durene

Four peaks A, B, C, and D are observed in the spectrum of a solution of durene in fluorosulphuric acid at low temperature (Fig. 2). These may be attributed to the CH and CH_2 groups and two non-equivalent methyl groups respectively. The relative areas were found to be A:B:C+D = 0.87:1.79:12.0 in agreement with the proposed assignment.

Pentamethylbenzene

Protonation of pentamethylbenzene occurs at the only unsubstituted ring position. The spectrum of a fluorosulphuric acid solution at −49° is shown in Fig. 3; it consists of four peaks A, B, C, and D of relative areas A:B:C:D = 1.77:3.14:6.09:6.00 which may be attributed to the CH_2, p-CH_3, o-CH_3, and m-CH_3 groups respectively.

Hexamethylbenzene

A solution of hexamethylbenzene (2.7 mole %) in fluorosulphuric acid was found to give at −85°, a spectrum consisting of five peaks of relative areas A:B:C:D:E =

Can. J. Chem. Downloaded from www.nrcresearchpress.com by 210.87.254.42 on 09/05/12
For personal use only.

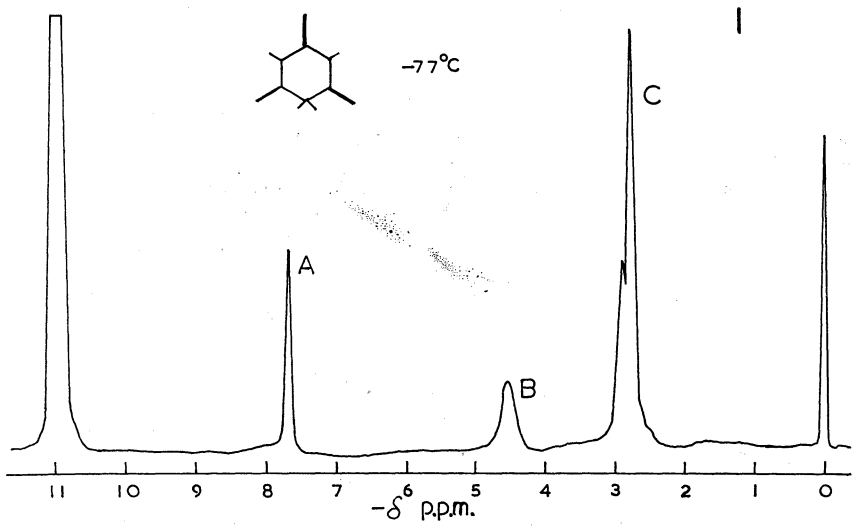

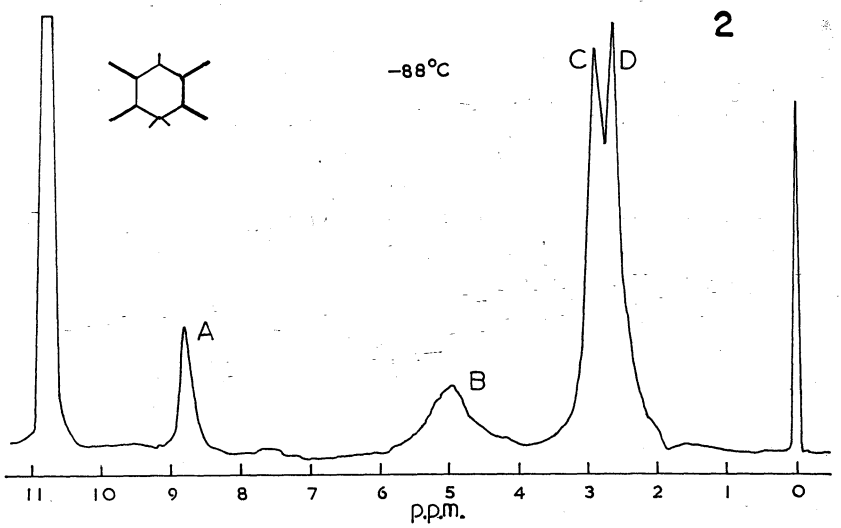

FIG. 1. Nuclear magnetic resonance spectrum of a solution of mesitylene (6.16 mole%) in fluorosulphuric acid.

FIG. 2. Nuclear magnetic resonance spectrum of a solution of durene (1.12 mole%) in fluorosulphuric acid.

0.99:3.06:6.13:6.35:3.00 which may be attributed to the HCCH$_3$, p-CH$_3$, o-CH$_3$, m-CH$_3$, and HCCH_3 groups respectively (Fig. 4*a*). Under favorable conditions E was observed as a poorly resolved doublet due to coupling with the single proton A (J = 5.8 c/s) but no corresponding splitting of peak A was observed. In HF/BF$_3$ solution MacLean and Mackor found J_{AE} = 6.7 c/s and also J_{AB} = 3.5 c/s and J_{AC} = 1 c/s (6, 7). We were unable to observe any fine structure other than the doublet E.

m-Xylene

Figure 5 shows the spectrum of a solution of *m*-xylene in 1.2 mole % SbF$_5$/HSO$_3$F at

Can. J. Chem. Downloaded from www.nrcresearchpress.com by 210.87.254.42 on 09/05/12
For personal use only.

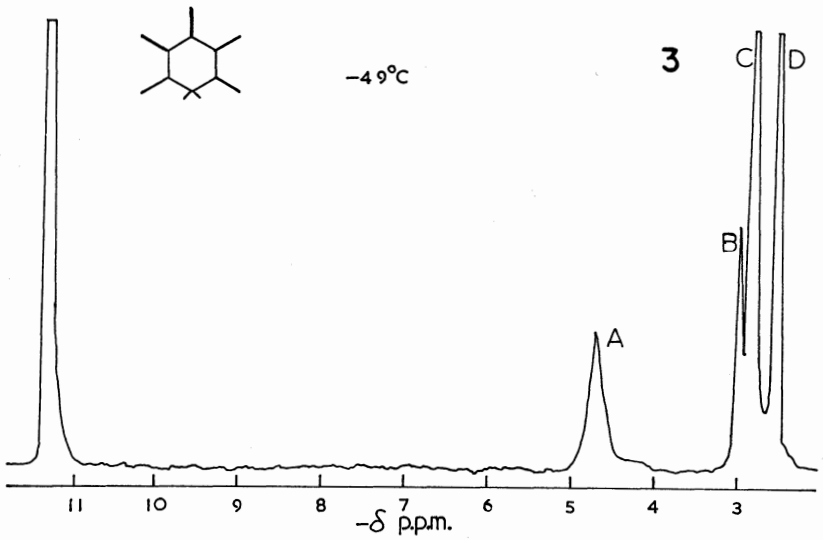

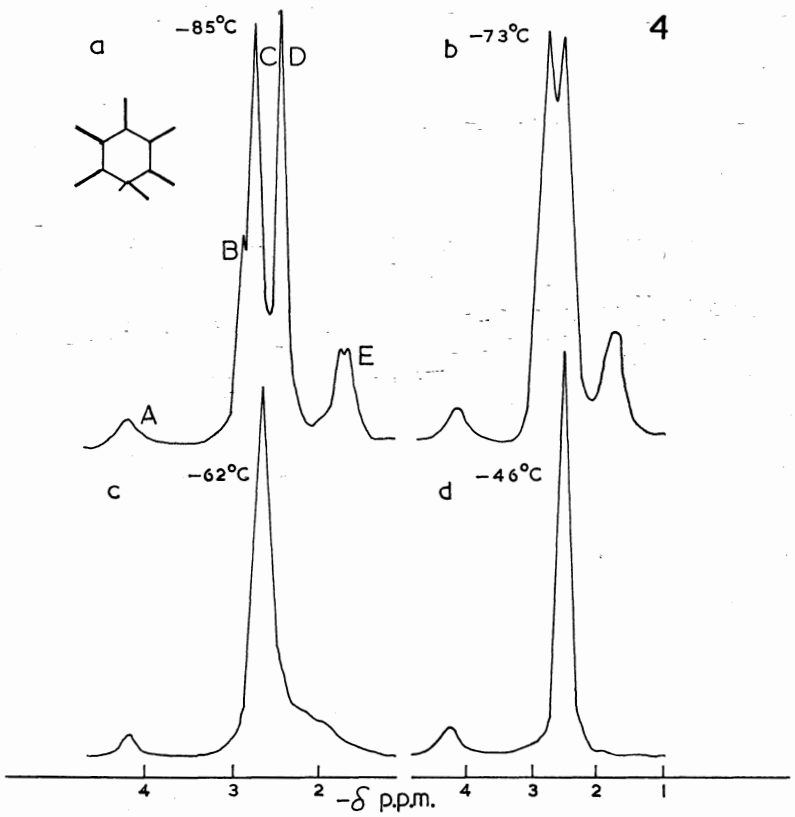

FIG. 3. Nuclear magnetic resonance spectrum of pentamethylbenzene (2.82 mole%) in fluorosulphuric acid. Peak A was recorded at a higher power level than peaks B, C, and D.

FIG. 4. Nuclear magnetic resonance spectra of a solution of hexamethylbenzene (2.7 mole%) in fluorosulphuric acid.

Can. J. Chem. Downloaded from www.nrcresearchpress.com by 210.87.254.42 on 09/05/12
For personal use only.

−50° C. The relative areas of the peaks were found to be A:B:C = 2.91:1.80:6.00. The spectrum is best explained by assuming protonation ortho to one methyl group and para to the other methyl group. The "doublet" C is due to the non-equivalent methyl groups and B arises from the methylene protons. The phenyl part of the spectrum A consists of a single peak due to the proton ortho to both methyl groups superimposed on an AB quartet arising from the other two ring protons. The unequal heights of the methyl peaks may be attributed to unresolved spin–spin coupling causing a greater broadening of one peak than the other.

p-Xylene

The much weaker base *p*-xylene was examined in a 13 mole% SbF_5/HSO_3F solution. At −63° C the lowest temperature at which a reasonable spectrum could be recorded due to the high viscosity of the solution, only two very broad lines were visible in the spectrum: one was due to the ring protons and the other to the methyl groups. From an integrated spectrum the relative areas of the two peaks were found to be 4.77:6.00, indicating that ring protonation had taken place.

Anisole

The spectrum of a solution of anisole in fluorosulphuric acid at 25° shown in Fig. 6*a* closely resembles that obtained in an organic solvent except that the spectrum is shifted 0.6 p.p.m. to lower field. Figures 6*b* and 6*c* show the effect of decreasing the temperature. A new peak appears at 4.4 p.p.m. below the tetramethylsilane reference which can be attributed to a methylene group formed by ring protonation. At 0° the lack of resolution in the phenyl spectrum indicates that exchange of the CH_2 protons with the solvent is still occurring but at −64° fine structure can be observed in the phenyl spectrum and as this does not change further at lower temperatures it is reasonable to suppose that exchange has become very slow. The spectrum is best explained by postulating protonation at the ring position para to the methoxy group as MacLean and Mackor have previously done in order to explain the results of their studies of HF solutions (7), and not on the oxygen atom as has been assumed to explain the results of ultraviolet spectroscopic measurements (8). Evidence for ring protonation has also been obtained recently in the cases of di- and tri-methoxybenzene (7, 9).

Rates of Proton Exchange

On increase of the temperature of the solutions the lifetime of the conjugate acid decreases and the spectrum changes correspondingly. The methyl spectrum collapses to a single line for all the solutes except pentamethylbenzene, which is the only one for which proton exchange does not lead to equivalence of the *o*-, *m*-, and *p*-CH_3 groups; the methylene (or $CH.CH_3$) and phenyl peaks broaden and eventually merge into the base line, and finally the solvent line broadens somewhat. The broadening of the solvent peak is especially noticeable when the concentration of the hydrocarbon is relatively large. The collapse of the methyl peaks of the conjugate acid of hexamethylbenzene with increasing rate of proton exchange is illustrated in Figs. 4*a–d*. The *o*-CH_3 group is the first to collapse since it has the smallest chemical shift and the methyl group on the site of protonation is the last since it has the largest chemical shift from the other methyl peaks.

These observations may be attributed to proton exchange by one or more of the processes (i), (ii), and (iii). The lifetime of the conjugate acid can be obtained from the widths of the CH and CH_2 (or $CH.CH_3$) signals. Under conditions where these signals can be observed the lifetime of the conjugate acid is large compared with the inverse of the separation of exchangeable sites and the condition for slow exchange may be applied.

Can. J. Chem. Downloaded from www.nrcresearchpress.com by 210.87.254.42 on 09/05/12
For personal use only.

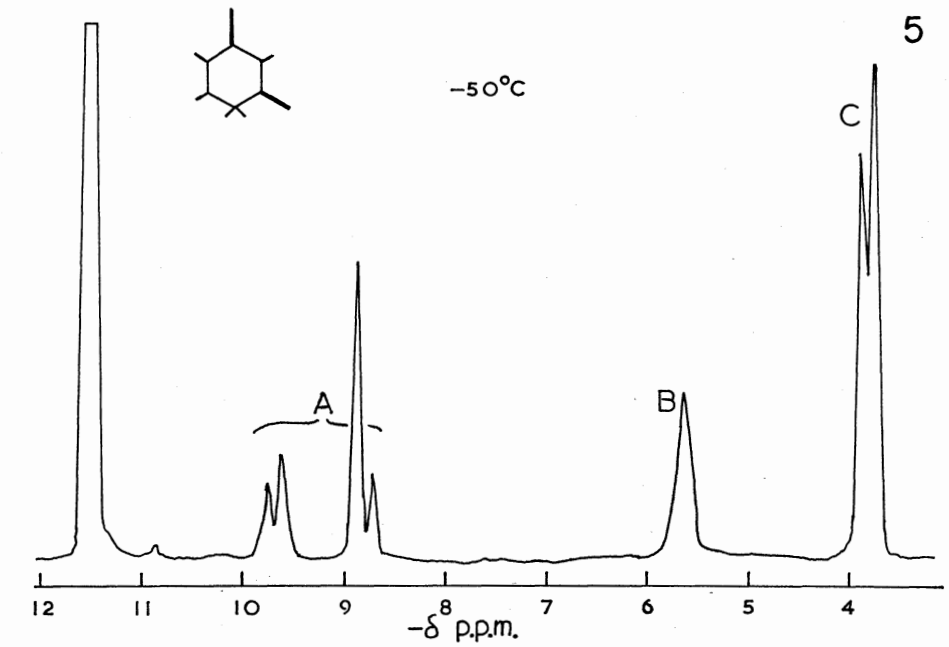

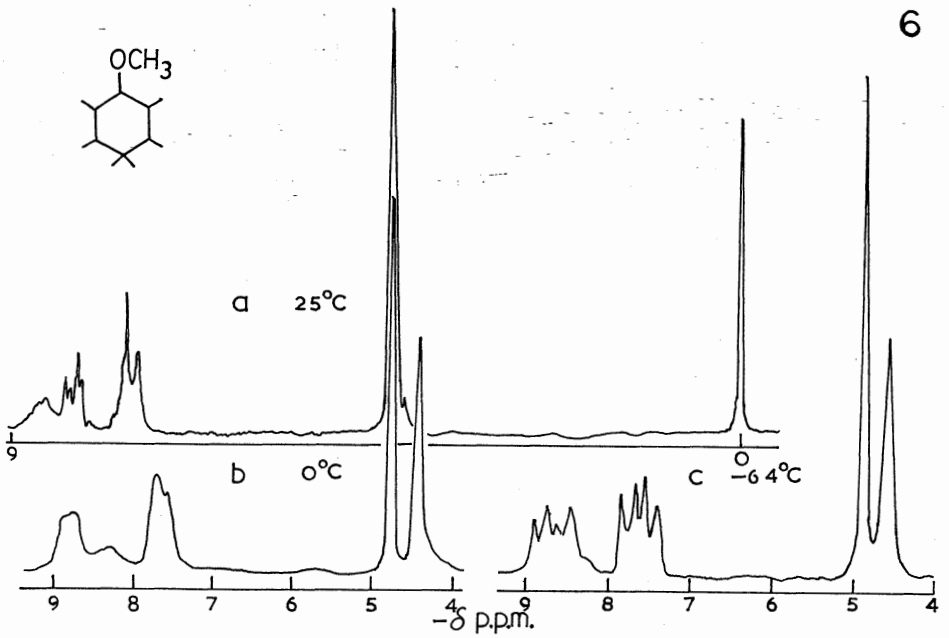

FIG. 5. Nuclear magnetic resonance spectrum of a solution of *m*-xylene (7.82 mole%) in fluorosulphuric acid containing 12 mole% antimony pentafluoride.
FIG. 6. Nuclear magnetic resonance spectra of a solution of anisole (4.12 mole%) in fluorosulphuric acid.

Can. J. Chem. Downloaded from www.nrcresearchpress.com by 210.87.254.42 on 09/05/12
For personal use only.

The relation between the lifetime of any particular proton in a hydrocarbon conjugate acid and the lifetime of the conjugate acid τ depends on the conditions under which exchange occurs and on the particular hydrocarbon under consideration. MacLean and Mackor (7) have dealt with the case when the concentration of the free base and of the conjugate acid are comparable. Under our conditions the concentration of free base is negligibly small. For the conjugate acid of mesitylene under these conditions exchange between the two proton sites *a* and *b* occurs by slow rate-determining loss of the proton to a solvent molecule followed by rapid addition of another proton from the solvent.

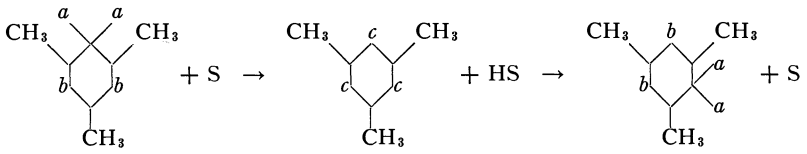

If τ_{as}^{-1} and τ_{ac}^{-1} are the probabilities that an *a* proton becomes an *S* proton or a *c* proton respectively then

$$\tau_{as}^{-1} = \tfrac{1}{2}\tau^{-1} \text{ and } \tau_{ac}^{-1} = \tfrac{1}{2}\tau^{-1}.$$

Since two-thirds of the *c* protons are rapidly reconverted to *b* protons

$$\tau_{ab}^{-1} = \tfrac{2}{3}\tau_{ac}^{-1} = \tfrac{1}{3}\tau^{-1}.$$

Hence

$$\tau_{CH_2}^{-1} = \tau_{ab}^{-1} + \tau_{as}^{-1} = \tfrac{5}{6}\tau^{-1}.$$

Now $\tau_{bc}^{-1} = \tau^{-1}$ and since one-third of the *c* protons are rapidly reconverted to *a* protons

$$\tau_{ba}^{-1} = \tfrac{1}{3}\tau_{bc}^{-1} = \tfrac{1}{3}\tau^{-1}.$$

Hence

$$\tau_{CH}^{-1} = \tau_{ba}^{-1} = \tfrac{1}{3}\tau^{-1}.$$

According to mechanism (ii) exchange between the protons sites *a* and *b* in the conjugate acid occurs by bimolecular reaction with the free base.

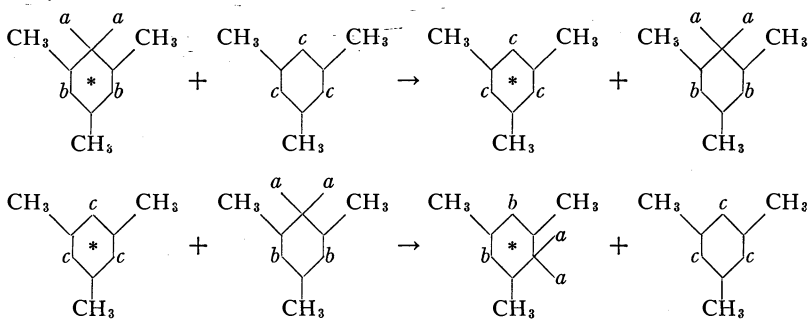

We have

$$\tau_{ac}^{-1} = \tfrac{1}{2}\tau^{-1} \text{ and } \tau_{bc}^{-1} = \tau^{-1}.$$

Since two-thirds of the *c* protons are rapidly reconverted to *b* protons and one-third to *a* protons

$$\tau_{ab}^{-1} = \tfrac{2}{3}\tau_{ac}^{-1} = \tfrac{1}{3}\tau^{-1} \text{ and } \tau_{ba}^{-1} = \tfrac{1}{3}\tau_{bc}^{-1} = \tfrac{1}{3}\tau^{-1}.$$

Hence

$$\tau_{CH_2}^{-1} = \tau_{CH}^{-1} = \tfrac{1}{3}\tau^{-1}.$$

Can. J. Chem. Downloaded from www.nrcresearchpress.com by 210.87.254.42 on 09/05/12
For personal use only.

The corresponding relations for other hydrocarbons may be derived similarly.

	Mechanism (i)		Mechanism (ii)
Mesitylene	$\tau_{CH_2}^{-1} = \frac{5}{6}\tau^{-1}$,	$\tau_{CH}^{-1} = \frac{1}{3}\tau^{-1}$	$\tau_{CH_2}^{-1} = \tau_{CH}^{-1} = \frac{1}{3}\tau^{-1}$
Durene	$\tau_{CH_2}^{-1} = \frac{3}{4}\tau^{-1}$,	$\tau_{CH}^{-1} = \frac{1}{2}\tau^{-1}$	$\tau_{CH_2}^{-1} = \frac{1}{4}\tau^{-1}$, $\tau_{CH}^{-1} = \frac{1}{2}\tau^{-1}$
Hexamethylbenzene	$\tau_{CH.CH_3}^{-1} = \tau^{-1}$		No broadening
Pentamethylbenzene	$\tau_{CH_2}^{-1} = \frac{1}{2}\tau^{-1}$		No broadening
m-Xylene	$\tau_{CH_2}^{-1} = \frac{3}{4}\tau^{-1}$		$\tau_{CH_2}^{-1} = \frac{1}{4}\tau^{-1}$

The width of the signal ($T_2'^{-1}$) from the protons at a site A is given by

$$T_2'^{-1} = T_2^{-1} + \tau_A^{-1},$$

where τ_A is the lifetime of the protons at A and T_2^{-1} is the natural line width in the absence of exchange. The first-order rate constant for proton loss by the conjugate acid is given by

$$k = \tau^{-1}.$$

In order to obtain a value for τ from the measured line widths it is necessary to know T_2. The CH and CH_2 line widths for mesitylene are plotted against the temperature in Fig. 7.

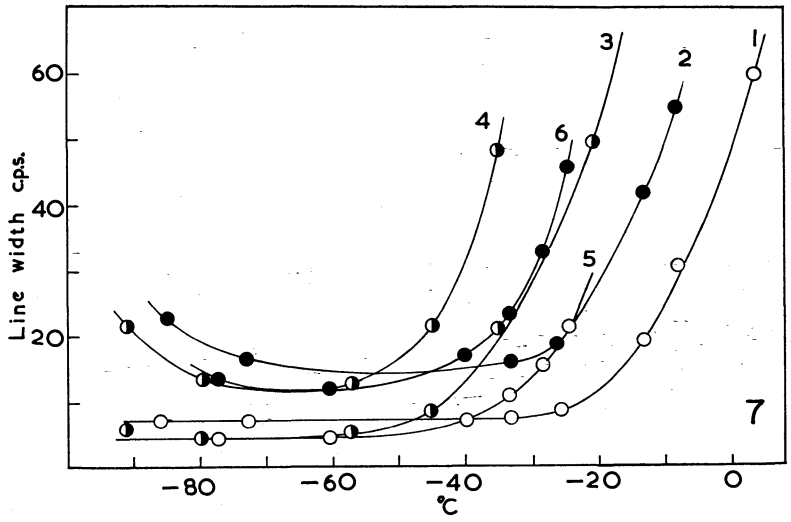

FIG. 7. Plots of line width against temperature for the CH and CH_2 peaks of solutions of mesitylene in fluorosulphuric acid.

CH	CH_2	Mole% mesitylene	Mole% SbF_5
1	2	5.79	4.29
3	4	6.16	—
5	6	3.59	—

They decrease with decreasing temperature and eventually reach a constant limiting value. It seems reasonable to assume that at these temperatures proton exchange is slow enough that it no longer affects these line widths and these limiting values were taken as a measure of the line width in the absence of exchange (T_2^{-1}). Values were obtained in a similar manner for the other hydrocarbons. At very low temperatures the CH_2 but not the CH line widths increase again somewhat. This may possibly be attributed to a decrease in the relaxation time as a consequence of an increase in η/T where η is the viscosity and T is the absolute temperature. The line width of the CH_2 peak is in all cases considerably

Can. J. Chem. Downloaded from www.nrcresearchpress.com by 210.87.254.42 on 09/05/12
For personal use only.

greater than that of the CH peak. This may be due to unresolved spin–spin coupling in the CH_2 signal or to the protons of the methylene group having a shorter relaxation time which might possibly be attributed to these protons being involved in rather strong hydrogen bonding with the solvent. The line widths of the CH and CH_2 peaks in SbF_5/HSO_3F solutions are greater than for solutions in HSO_3F alone, which is consistent with the greater viscosity of these solutions.

It is also clear from Fig. 7 that the line widths are dependent on the concentration of the hydrocarbon base. An increase in the concentration of hydrocarbon results in an increase in the CH and CH_2 line widths and a decrease in the temperature at which line broadening is first observed. Evidently the rate of proton exchange increases with increasing concentration of the hydrocarbon base. As the ionization of the hydrocarbon produces fluorosulphate ion which increases the basicity of the solvent we attribute this increase in exchange rate to an increase in the solvent basicity. A detailed comparison of the rates of proton exchange at −20° of all the compounds studied is given in Table I. The rate

TABLE I

Rate constants for proton exchange at −20°

Base	Base (mole%)	SbF_5 (mole %)	k (sec^{-1})
Mesitylene	1.93	—	96.9
	3.59	—	243.1
	3.71	—	276.5
	6.16	—	843.0
	5.79	4.29	53.7
Durene	1.12	—	1.06×10^5
	1.48	9.04	1.04×10^4
	1.74	4.42	3.44×10^4
Pentamethylbenzene	2.82*	—	200.0
	4.01	—	108.0
Hexamethylbenzene	2.73	—	9.8
	4.73	—	27.5
	5.67	—	38.9
	8.21	—	154.9
	2.85	4.42	†
m-Xylene	7.82	11.55	28.0

*This solution also contained 3.39 mole% potassium fluorosulphate.
†The rate of exchange was too slow to measure.

increases in every case with increase in the concentration of the hydrocarbon. Our suggestion that this may be attributed to the effect of the increased concentration of fluorosulphate ion resulting from the protonation of the hydrocarbon is confirmed by the effect of added fluorosulphate ion in increasing the rate in the case of pentamethylbenzene and the effect of added antimony pentafluoride in reducing the rate in the cases of mesitylene, durene, hexamethylbenzene, and *m*-xylene. In this respect our results differ substantially from those of MacLean and Mackor (7), who claim that the rate of proton exchange for hexamethylbenzene and prehnitene are independent of the concentration of the BF_3 in a BF_3/HF solvent and they concluded that in these cases exchange occurs by the intramolecular process (iii). We found, in fact, that the addition of antimony pentafluoride to a solution of hexamethylbenzene in fluorosulphuric acid increased the lifetime of the conjugate acid to such an extent that the CH peak did not broaden sufficiently even at 25° to enable a lifetime to be measured. These results clearly exclude the

Can. J. Chem. Downloaded from www.nrcresearchpress.com by 210.87.254.42 on 09/05/12
For personal use only.

possibility that (iii) is the only exchange process for any of the compounds that we have studied.

In the case of mesitylene we may note that mechanism (ii) predicts equal broadening for both the CH and CH_2 signals whereas mechanism (i) predicts a greater broadening for the CH_2 than the CH signal. Figure 7 shows that the CH_2 signal broadens more rapidly than the CH signal. Thus, in this case at least, mechanism (i) seems to be more important than (ii). Further evidence in favor of (i) is provided by the observation that the solvent peak broadens somewhat as the CH and CH_2 peaks broaden; some representative results are given in Table II. Because of the high concentration of the solvent in the

TABLE II

Dependence of the solvent line width on temperature

Base	Base (mole%)	Temp. (° C)	Solvent line width (c/s)
Hexamethylbenzene	4.73	−41	3.2
		− 4	5.4
	8.21	−69.5	1.8
		−25	4.5
Mesitylene	5.79	−26	4.6
	(4.29% SbF_5)	+ 4	9.2
	3.9	−77	2.2
		−24.5	4.4
Durene	1.34	−89	4.0
	(4.42% SbF_5)	−56	6.6

solutions the amount of broadening of the solvent peak is not great enough to enable exchange rates to be calculated with any accuracy but nevertheless our results clearly indicate that exchange cannot occur only by process (ii) because this does not involve the solvent. We conclude therefore that proton exchange occurs mainly via the solvent although one cannot entirely rule out the possibility that there might, in addition, be some exchange by (ii) and (iii) under suitable conditions.

The dependence of the rate of proton exchange on the temperature can be expressed by the Arrhenius equation

$$k = k_0 e^{-E/RT}.$$

Plots of log k against $1/T$ are shown in Fig. 8 for solutions of mesitylene in HSO_3F. We note that the rates obtained from both the CH and CH_2 line widths give reasonably straight and parallel lines; this provides some confirmation of the values chosen for T_2^{-1}.

Similar plots were made for the other bases, and the results are summarized in Table III. We note that except for pentamethylbenzene the activation energies fall in the range 13–15 kcal and are much higher than the values obtained by MacLean and Mackor for HF/BF_3 solutions which are in the range 7–8.5 kcal. This is possibly a reflection of the smaller basicity of our solvent media. However, there are other differences between our results and those of MacLean and Mackor that are difficult to explain. It seems remarkable, for example, that proton exchange involving the conjugate acid of hexamethylbenzene proceeds entirely by an intramolecular process in solution in hydrogen fluoride but predominantly, if not entirely, by intermolecular exchange with the solvent in solution in fluorosulphuric acid. Again, we find that in fluorosulphuric acid durene exchanges very much more rapidly than hexamethylbenzene, which is consistent with the relative

Can. J. Chem. Downloaded from www.nrcresearchpress.com by 210.87.254.42 on 09/05/12
For personal use only.

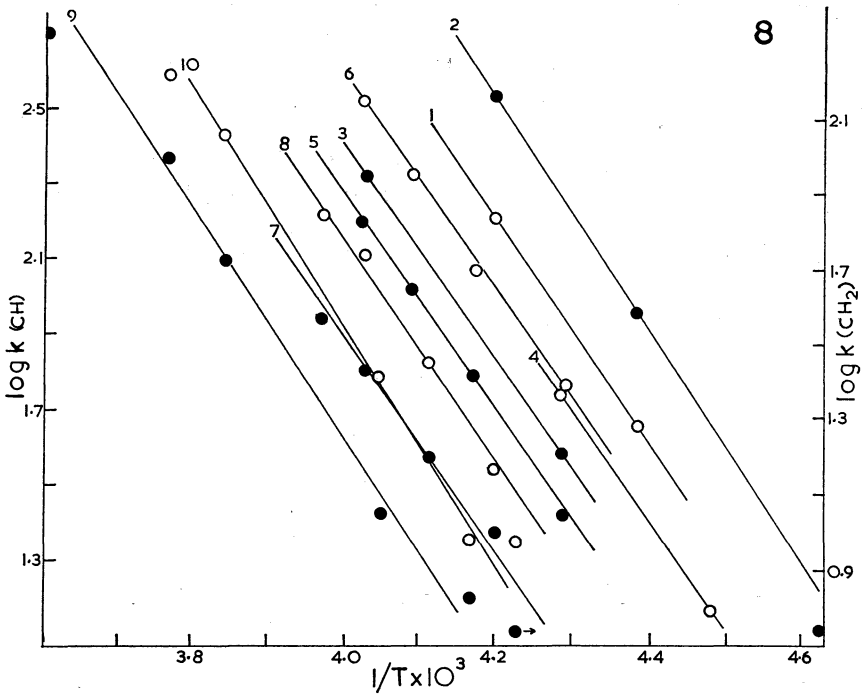

FIG. 8. Plots of log k against $1/T$ for solutions of mesitylene in fluorosulphuric acid.

CH ●	CH_2 ○	Mole% mesitylene	Mole% SbF_5
1	2	6.16	—
3	4	3.71	—
5	6	3.59	—
7	8	1.93	—
9	10	5.79	4.29

TABLE III

Activation energies (E) and frequency factors (k_0) for methylbenzenes in fluorosulphuric acid

Base	Base (mole%)	SbF_5 (mole%)	Log k_0	E (kcal/mole)
Mesitylene	1.93	—	13.72	13.6
	3.59	—	13.91	13.3
	3.71	—	13.82	13.2
	6.16	—	14.38	13.8
	5.79	4.29	13.89	14.1
Durene	1.12	—	17.92	14.9
	1.48	9.04	17.23	15.3
	1.74	4.42	16.20	13.5
Pentamethylbenzene	4.01	—	10.65	9.9
	2.82*	—	11.52	10.4
Hexamethylbenzene	2.73	—	12.95	13.7
	4.73	—	13.42	13.9
	5.67	—	14.51	15.0
	8.21	—	15.60	15.5
m-Xylene	7.82	11.55	13.72	14.2

*This solution also contained 3.39 mole% potassium fluorosulphate.

Can. J. Chem. Downloaded from www.nrcresearchpress.com by 210.87.254.42 on 09/05/12
For personal use only.

basicities of these compounds, whereas MacLean and Mackor obtained exchange rates in hydrogen fluoride that were almost the same under the same conditions.

ACKNOWLEDGMENT

We are grateful to the Directorate of Chemical Sciences, United States Air Force Office of Scientific Research, and the Petroleum Research Fund of the American Chemical Society for financial aid and to the Dow Chemical Company of Canada, Limited, for a Postgraduate Fellowship (to T. B.). We also thank Dr. E. L. Mackor for his very helpful comments on the manuscript.

REFERENCES

1. D. A. McCauley and A. P. Lien. J. Am. Chem. Soc. **73**, 2013 (1951).
2. V. Gold and F. L. Tye. J. Chem. Soc. 2172 (1952).
3. C. Reid. J. Am. Chem. Soc. **76**, 3264 (1954).
4. G. Dallinga, E. L. Mackor, and A. A. Verrijn Stuart. Mol. Phys. **1**, 123 (1958).
5. E. L. Mackor, A. Hofstra, and J. H. van der Waals. Trans. Faraday Soc. **54**, 66 (1958); **54**, 187 (1958).
6. C. MacLean and E. L. Mackor. Mol. Phys. **4**, 241 (1961).
7. C. MacLean and E. L. Mackor. Disc. Faraday Soc. **34**, 165 (1962).
8. E. M. Arnett and C. Y. Wu. J. Am. Chem. Soc. **82**, 5660 (1960).
9. A. J. Kresge and Y. Chiang. Proc. Chem. Soc. 81 (1961).

Can. J. Chem. Downloaded from www.nrcresearchpress.com by 210.87.254.42 on 09/05/12
For personal use only.

THE PREPARATION OF THE HYDROXYSKATOLES AND 5,6-DIHYDROXYSKATOLE[1]

R. A. HEACOCK AND O. HUTZINGER
The Psychiatric Research Unit, University Hospital, Saskatoon, Saskatchewan
Received September 16, 1963

ABSTRACT

A new procedure for the preparation of the hydroxyskatoles has been devised. 4-, 5-, 6-, and 7-benzyloxyindole-3-carboxaldehyde and 5,6-dibenzyloxyindole-3-carboxaldehyde have been prepared and give the corresponding benzyloxyskatoles on reduction with either $LiAlH_4$ or $NaBH_4$/Pd–C. The 4-, 5-, 6-, and 7-hydroxyskatoles and 5,6-dihydroxyskatole are readily obtained on catalytic debenzylation of the relevant benzyloxy compound. An alternative method for the preparation of the hydroxyskatoles involving hydrogenolysis of the benzyloxygramines is also described.

The possible structures of by-products obtained in some instances are discussed.

Can. J. Chem. Downloaded from www.nrcresearchpress.com by 210.87.254.6 on 09/05/12
For personal use only.

The sulphate ester of a hydroxyskatole, usually considered to be the 6-isomer, has been reported to be excreted in the urine in certain pathological conditions (1, 2) including some forms of mental illness (cf. reviews by Sprince (3) and Rodnight (4)). However, until relatively recently none of the hydroxyskatoles had been described in the literature. In 1956 Teuber and Staiger reported obtaining a substance described as 5-hydroxyskatole (VI: HO— = 5-HO—) by the oxidation of 3-methylindoline with potassium nitrosodisulphonate although no proof of structure or analytical data was given (5). In 1959, Horning *et al.* claimed, without giving any details of their experimental procedure, that 6-hydroxyskatole (VI: HO— = 6-HO—) could be obtained from 6-benzyloxyskatole (V: RO— = 6-$C_6H_5CH_2O$—); the benzyloxyskatole having been obtained by an application of the Fischer indole synthesis (2). 5-Hydroxyskatole (VI: HO— = 5-HO—) has been obtained by the hydrogenolysis of 5-benzyloxygramine (II: RO— = 5-$C_6H_5CH_2O$—) (Acheson and Hands (6), Marchand (7), and Heacock and Hutzinger (8)). The hydrogenation of 6-benzyloxygramine (II: RO— = 6-$C_6H_5CH_2O$—) was initially reported to give a mixture of 6-hydroxyskatole (VI: HO— = 6-HO—), 6-benzyloxyskatole (V: RO— = 6-$C_6H_5CH_2O$—), and unchanged starting material from which the pure hydroxy compound was apparently not isolated (9) although this has recently been accomplished (8). It has now been established that this reaction is of general applicability and that all four hydroxyskatoles can be obtained from the corresponding benzyloxgramine (cf. preliminary report (8)). The reaction conditions for optimum yields of the hydroxyskatoles (cf. VI) from the benzyloxygramines (cf. II) were determined by examining test samples of the reaction mixture chromatographically on formamide-treated paper (cf. 10). This technique also indicated the degree of by-product formation under any particular set of reaction conditions. No significant by-product formation was detected during the preparation of the 5- and 7-hydroxyskatoles by this procedure; however, it was impossible to prevent by-product formation during the synthesis of the 4- and 6-isomers. (The nature of these products will be discussed later.)

In view of the fact that high yields of the hydroxyskatoles could not always be obtained by the method described above, a new procedure has been developed. The synthesis of

[1]*This investigation was supported by grants from the Government of Saskatchewan (Department of Public Health) and the Department of National Health and Welfare (Ottawa).*

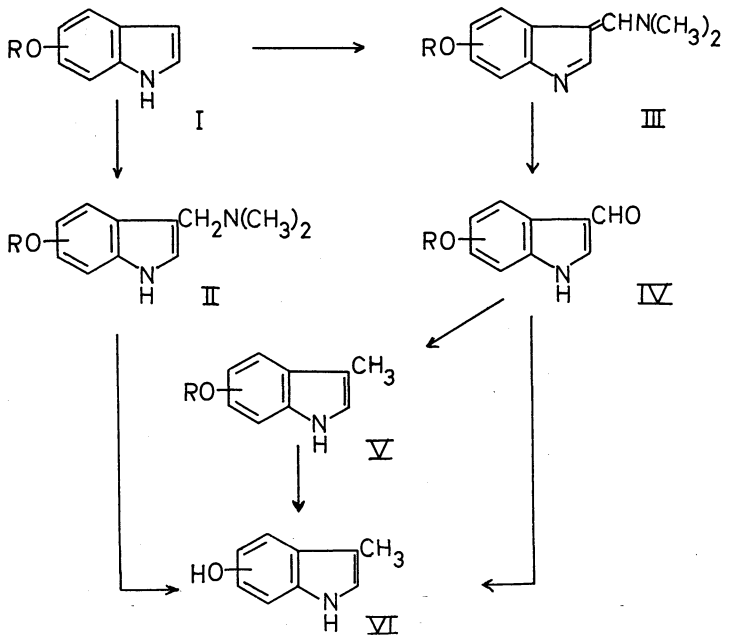

the 5- and 6-benzyloxindole-3-carboxaldehydes (IV: RO— = 5- and 6-$C_6H_5CH_2O$— respectively) (11, 12) by procedures similar to that described for the formylation of indole (13, 14) with phosphorus oxychloride and dimethylformamide has been described in the literature. The intermediate 3-dimethylaminomethyleneindolenine (cf. III) giving the indole-3-carboxaldehyde (cf. IV) derivative on treatment with alkali. This procedure has now been applied to the preparation of 4- and 7*-benzyloxyindole-3-carboxaldehydes (IV: RO— = 4- and 7-$C_6H_5CH_2O$— respectively). In all cases good yields of the aldehydes were obtained, and the crude products were usually sufficiently pure to be used in the next stage of the procedure.

In one instance, 4-benzyloxygramine (II: RO— = 4-$C_6H_5CH_2O$—) was obtained on reduction of the crude formylation product; this must have arisen from the reduction of the undecomposed intermediate 4-benzyloxy-3-dimethylaminomethyleneindolenine (III: RO— = 4-$C_6H_5CH_2O$—). Hydrogenation of (II: RO— = 4-$C_6H_5CH_2O$—) then gave 4-hydroxyskatole (VI: HO = 4-HO—). Usually the intermediate (III: RO— = 4-$C_6H_5CH_2O$—) would be decomposed by alkali to give 4-benzyloxyindole-3-carboxaldehyde (IV: RO— = 4-$C_6H_5CH_2O$—), which would give (VI: HO— = 4-HO—) on reduction and debenzylation.

In 1953 it was reported that skatole, and not the expected 3-hydroxymethylindole, was obtained, on reduction of indole-3-carboxaldehyde with lithium aluminum hydride (Leete and Marion (15) and Rossiter and Saxton (16)). The current investigation has shown that all the benzyloxyindole-3-carboxaldehydes (cf. IV) described above can be reduced to the corresponding benzyloxyskatoles (cf. V) by this procedure. However, in some cases (i.e. with 5- and 6-benzyloxyindole-3-carboxaldehyde) (IV: RO— = 5- and 6-$C_6H_5CH_2O$— respectively) significant amounts of unidentified by-products were formed

**Although 7-benzyloxyindole-3-carboxaldehyde is available commercially (L. Light and Co.; Regis Chemical Co.) as far as the authors are aware details of the preparation of this compound have not been reported in the literature.*

Can. J. Chem. Downloaded from www.nrcresearchpress.com by 210.87.254.6 on 09/05/12
For personal use only.

at the same time as the desired benzyloxyskatole and consequently the possible use of different reducing systems was investigated in these cases. It has been reported that 3-hydroxymethylindoles are obtained on reduction of indole-3-carboxaldehydes with sodium or lithium borohydride (17, 18, 19, 20). Recently, it has been demonstrated that the reducing power of sodium borohydride is markedly enhanced by the addition of a suitable precious metal catalyst and that functional groups not usually attacked by sodium borohydride are reduced by this system (21, 22, 23, 24). Good yields of 5- and 6-benzyloxyskatole (V: RO— = 5- and 6-$C_6H_5CH_2O$— respectively) have now been obtained by the reduction of the corresponding aldehydes with sodium borohydride and 10% Pd–C in boiling isopropanol. The corresponding 4- and 7-benzyloxyskatoles (V: RO— = 4- and 7-$C_6H_5CH_2O$— respectively) could be obtained satisfactorily by reduction of the aldehyde with lithium aluminum hydride in boiling tetrahydrofuran. The only benzyloxyskatole which had previously been fully described in the literature was the 5-isomer (V: RO— = 5-$C_6H_5CH_2O$—) (6), which was obtained by the action of zinc and sodium hydroxide on 5-benzyloxygramine (II: RO— = 5-$C_6H_5CH_2O$—) (cf. 25). The desired hydroxyskatoles were readily obtained by catalytic debenzylation of the corresponding benzyloxyskatole.

A by-product (VII) of unknown structure was invariably formed along with 4-hydroxyskatole on catalytic hydrogenation (Pd–C) of 4-benzyloxygramine. The presence of VII was indicated by the appearance of a second spot on paper chromatograms of the crude reaction mixtures. The unknown compound VII was also obtained on hydrogenation of 4-benzyloxyskatole and 4-hydroxyskatole, indicating that it was probably formed from the hydroxyskatole and not from either of the two possible precursors (i.e. 4-benzyloxyskatole or 4-benzyloxygramine). The formation of (VII) appeared to be facilitated if the hydrogenation was carried out in polar solvents (i.e. methanol). Elemental analysis and molecular weight determinations suggest that VII (a colorless crystalline solid, m.p. 205–206°) was a dihydrohydroxyskatole. However, it is probably not the corresponding indoline (i.e. 4-hydroxy-3-methylindoline), which might have been expected, in view of the well-known fact that indolines can be obtained by the hydrogenation of indoles (26), for the following reasons: (*a*) the ultraviolet absorption maximum of VII did not show the typical shift to higher frequency in acid solution expected for an indoline; (*b*) VII gave a pink-mauve color with Ehrlich's reagent (turning to a gray-blue overnight) and not the stable yellow color expected from an indoline; (*c*) VII does not appear to have any appreciable basic character and did not form a crystalline picrate, and (*d*) VII has a higher melting point than would have been expected for an indoline. The structure of the compound (VII), which may be a derivative of 4-hydroxyskatole, in which the benzene ring has been partially reduced, will be the subject of further investigations.

The hydrogenation of 6-benzyloxygramine or 6-benzyloxyskatole in ethyl acetate at $3\frac{1}{2}$ atmospheres pressure gave, besides the expected 6-hydroxyskatole, a smaller quantity of a second product (VIII). The formation of VIII, which gave a yellow color with Ehrlich's reagent, could be followed by paper chromatography. The compound (VIII) was probably 6-hydroxy-3-methylindoline for the following reasons: (*a*) the main ultraviolet absorption maximum showed the expected shift to shorter wavelengths in acid solution (i.e. 295 mμ → 279 mμ); (*b*) satisfactory microanalytical results; (*c*) the low melting point of VIII (it is a yellow oil at room temperature) is not inconsistent with its being an indoline; (*d*) catalytic dehydrogenation (Pd–C) gave 6-hydroxyskatole.

Under more vigorous hydrogenation conditions, 6-benzyloxygramine and 6-benzyloxyskatole, or their primary hydrogenation products 6-hydroxyskatole or 6-hydroxy-3-methylindoline (VIII), were converted into a new product (IX). The formation of IX

Can. J. Chem. Downloaded from www.nrcresearchpress.com by 210.87.254.6 on 09/05/12
For personal use only.

can be detected by paper chromatography (although IX did not react with Ehrlich's reagent, it could be detected by viewing of the chromatograms in short-wave ultraviolet light). Microanalytical and molecular weight data suggested that IX (a colorless crystalline solid, m.p. 194–195°) is a tetrahydro-6-hydroxyskatole. This compound is weakly basic in nature. The nitrogen atom must be involved in its chromophoric system since its single ultraviolet absorption maximum shifts from 285 mμ in neutral solution to 275 mμ in acid solution. Attempted catalytic dehydrogenation of IX was unsuccessful and the compound was recovered unchanged. Although more work will be needed to ascertain the structure of IX with certainty the evidence to date is not altogether incompatible with its being a 6-oxo-3-methyl-2,3,4,5,6,9-hexahydroindole (IX*a*), which probably exists mainly in the zwitterionic form (IX*b*). A similar product (the zwitterionic form (X) of

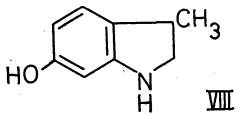

VIII

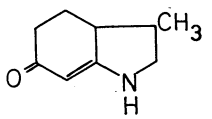

IX a

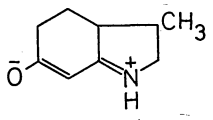

IX b

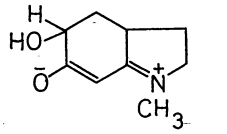

X

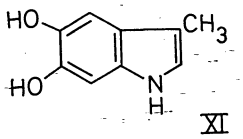

XI

which is depicted above) has previously been obtained, by Austin, Chanley, and Sobotka by the catalytic hydrogenation of 5,6-dihydroxy-*N*-methylindole (27).

5,6-Dihydroxyskatole (XI) previously obtained by the thermal decarboxylation of 5,6-dihydroxy-3-methylindole-2-carboxylic acid (28) was readily obtained by the hydrogenolysis of either 5,6-dibenzoyloxygramine or 5,6-dibenzyloxyskatole (this latter compound was prepared by the reduction of 5,6-dibenzyloxyindole-3-carboxaldehyde with sodium borohydride in the presence of a palladium–charcoal catalyst). The preparation of XI by the methods described above proceeded very readily with no detectable quantities of by-products being formed at the same time. The authors are unable to explain the claim by Acheson *et al.* that 5,6-dibenzyloxyskatole could not be debenzylated (29).

EXPERIMENTAL

All operations involving free hydroxyskatoles were carried out in an atmosphere of nitrogen. This is an important precaution to follow, otherwise yields are significantly reduced due to the formation of colored by-products, by air oxidation. The palladium-on-charcoal catalyst was added to the organic solvents in an atmosphere of nitrogen to prevent spontaneous ignition. The identity of compounds prepared by different procedures was established by mixed melting point determinations and by comparison of their infrared spectra, unless otherwise specified.

Can. J. Chem. Downloaded from www.nrcresearchpress.com by 210.87.254.6 on 09/05/12
For personal use only.

The silica gel (200/400 mesh size) used for column chromatography was obtained from L. Light and Co. The following indole compounds were available commercially: 5-benzyloxyindole (Aldrich Chem. Co.); 6-benzyloxyindole (L. Light and Co.); 4- and 7-benzyloxyindole, 5,6-dibenzyloxyindole, and 5-, 6- and 7-benzyloxygramine (Regis Chemical Co.). The light petroleum used throughout this investigation was B.D.H. AnalaR grade (b.p. 80–100°).

4-Hydroxyskatole

(A) From 4-Benzyloxygramine

A suspension of 4-benzyloxygramine (250 mg) prepared by the method of Stoll *et al.* (30) and 5% palladium–charcoal (100 mg) in ethyl acetate (100 ml) was shaken at room temperature in an atmosphere of hydrogen at 30 p.s.i. for 3 hours. After this time the reaction mixture was filtered and the colorless solid obtained after concentration of the filtrate was dissolved in benzene and adsorbed on a silica gel column. Elution of the column with benzene – ethyl acetate (49:1) gave a solid product, which, on recrystallization from benzene – light petroleum, gave 4-hydroxyskatole, m.p. 123°, in colorless prisms (16 mg; 12%). (Found: C, 73.64; H, 6.18; N, 9.34. Calc. for C_9H_9NO: C, 73.45; H, 6.16; N, 9.52%). Further elution of the column with benzene – ethyl acetate (44:6) gave a colorless solid, which, on recrystallization from benzene, afforded colorless prisms, m.p. 205–206°, of the substance (VII) (28 mg), which analyzed well for a dihydrohydroxyskatole. (Found: C, 72.25; H, 7.40; N, 9.12%; mol. wt. 147. Calc. for $C_9H_{11}NO$: C, 72.47; H, 7.43; N, 9.39%; mol. wt. 149.) The ultraviolet absorption spectrum was measured in (i) methanol (λ_{max}: 247 mμ with a shoulder at 275 mμ) and (ii) methanol containing 3% perchloric acid (70%) (λ_{max}: 269 mμ).

A solution of 4-hydroxyskatole (2 mg) in methanol (5 ml) containing a 10% palladium–charcoal catalyst (1 mg) was shaken at room temperature in an atmosphere of hydrogen at 50 p.s.i. for 10 hours. Paper chromatographic examinations of the products indicated* that all the 4-hydroxyskatole had been converted to the dihydro derivative (VII).

(B) From 4-Benzyloxyindole-3-carboxaldehyde

4-Benzyloxyindole-3-carboxaldehyde.—Phosphorus oxychloride (2.88 ml) was added to a stirred solution of dimethylformamide at 0° followed by 4-benzyloxyindole (1.9 g) in dimethylformamide (2 ml), the temperature being kept below 35° during the addition of the indole derivative. After the mixture had been stirred at 30–35° for 30 minutes a solution of sodium hydroxide (3.8 g) in water (10 ml) was added and the reaction mixture boiled for 10 minutes; pale yellow crystals of 4-benzyloxyindole-3-carboxaldehyde separated out during this period. After the mixture had been cooled, water (100 ml) was added and the crystalline product removed by filtration and washed with water several times. The crude product (1.95 g; 91%), m.p. 165°, was sufficiently pure for lithium aluminum hydride reduction.† A sample for analysis was twice recrystallized from 80% ethanol, giving pure 4-benzyloxyindole-3-carboxaldehyde in colorless prisms, m.p. 168°. (Found: C, 76.32; H, 5.38; N, 5.54. Calc. for $C_{16}H_{13}NO_2$: C, 76.47; H, 5.22; N, 5.57%.)

4-Benzyloxyskatole.—A stirred suspension of 4-benzyloxyindole-3-carboxaldehyde (0.5 g) and lithium aluminum hydride (0.16 g) in dry tetrahydrofuran (30 ml) was boiled under reflux in an atmosphere of nitrogen for 6 hours. The excess lithium aluminum hydride was decomposed by the cautious addition of moist ether; the reaction mixture was filtered, dried (Na_2SO_4), and evaporated to dryness. Recrystallization of the residue from benzene – light petroleum gave 4-benzyloxyskatole (0.44 g; 93%) in pale yellow needles, m.p. 83–84°. (Found: C, 80.97; H, 6.26; N, 6.01. Calc. for $C_{16}H_{15}NO$: C, 80.98; H, 6.37; N, 5.90%.)

4-Hydroxyskatole.—A solution of 4-benzyloxyskatole (0.44 g) in ethyl acetate (80 ml) containing a 5% palladium–charcoal catalyst (0.15 g) was shaken in an atmosphere of hydrogen at room temperature and under atmospheric pressure for 4 hours. After this time the hydrogenation mixture was filtered, and the residue obtained on concentration of the filtrate (a mixture of crude 4-hydroxyskatole and VII) was dissolved in benzene and adsorbed on a silica gel column. Elution of the column with benzene – ethyl acetate (49:1) and recrystallization of the product obtained from benzene – light petroleum gave 4-hydroxyskatole (73 mg; 27%) identical with the material obtained from the hydrogenolysis of 4-benzyloxygramine. Further elution of the column with benzene – ethyl acetate (44:6) gave VII (88 mg; 32%), after recrystallization from benzene.

5-Hydroxyskatole

(A) From 5-Benzyloxygramine

The preparation of 5-hydroxyskatole by the hydrogenolysis of 5-benzyloxygramine has been described in the literature. Melting points and yields given are 116°, 72% (6); 114–115°, 45% (7). In the current investigation with hydrogenation in methanolic solution at 50 p.s.i. (room temperature; 10% Pd–C catalyst) a 62% yield of 5-hydroxyskatole, m.p. 114°, was obtained.

**All paper chromatographic data are given at the end of the experimental section.*

†*In some early experiments the mixture was boiled for 2 minutes only and the bulk of the water was added before heating was begun. Anomalous results were obtained on reduction of some of these crude aldehyde preparations; lithium aluminum hydride gave various amounts of 4-benzyloxygramine probably formed by reduction of some unhydrolyzed indolenine intermediate present in the reaction mixture.*

Can. J. Chem. Downloaded from www.nrcresearchpress.com by 210.87.254.6 on 09/05/12
For personal use only.

(B) From 5-Benzyloxyindole-3-carboxaldehyde

5-Benzyloxyskatole.—A suspension of 5-benzyloxyindole-3-carboxaldehyde (1 g; prepared by the method of Young (12)), 10% palladium–charcoal (0.5 g) and sodium borohydride (2 g) in isopropanol (300 ml) was boiled under reflux, with stirring, for 2½ hours. After this time a further quantity of sodium borohydride (1 g) was added and the mixture was boiled under reflux for a further 2½ hours. The catalyst was then removed by filtration, water (100 ml) added to the filtrate, and most of the isopropanol removed by distillation under reduced pressure. The resulting aqueous solution was extracted with ether; the residue obtained on concentration of the dried (Na_2SO_4) ether extract was recrystallized from aqueous ethanol and gave 5-benzyloxyskatole (0.7 g; 74%) in colorless needles, m.p. 115–116°. (Found: C, 80.70; H, 6.50; N, 5.80. Calc. for $C_{16}H_{15}NO$: C, 80.98; H, 6.37; N, 5.90 %.) Acheson and Hands prepared this compound by a different route and report a melting point of 118° (6).

5-Hydroxyskatole.—A solution of 5-benzyloxyskatole (100 mg) in methanol (100 ml) containing 10% palladium–charcoal (50 mg) was shaken in an atmosphere of hydrogen at room temperature and under atmospheric pressure for 3 hours. 5-Hydroxyskatole (42 mg; 67.5%) was obtained on recrystallization of the residue obtained on concentration of the filtered hydrogenation mixture from benzene – light petroleum.

6-Hydroxyskatole

(A) From 6-Benzyloxygramine

A suspension of 6-benzyloxygramine (0.4 g) and 5% palladium–charcoal (0.2 g) in methanol (80 ml) was shaken in an atmosphere of hydrogen at 45 p.s.i. at room temperature for 2½ hours. The reaction mixture was filtered and the residue obtained on concentration of the filtrate was dissolved in benzene and adsorbed on a silica gel column. Elution with benzene – ethyl acetate (99:1) gave a white solid, which afforded 6-hydroxyskatole (63 mg; 30%) in colorless plates, m.p. 162° on recrystallization from benzene – light petroleum. (Found: C, 73.22; H, 6.24; N, 9.63. Calc. for C_9H_9NO: C, 73.45; H, 6.16; N, 9.52%.) Melting point recorded in the literature: 149–151° (2). Further elution of the column with benzene – ethyl acetate (97:3) gave a thick yellow oil (24 mg; 11%) (VIII). An analytical sample of VIII, probably 6-hydroxy-3-methylindoline, was obtained by distillation of a portion of this material in vacuum, b.p. 180° (bath temperature) at 2 mm. (Found: N, 9.35. Calc. for $C_9H_{11}NO$: N, 9.39%.) The ultraviolet absorption spectrum was measured in (i) methanol (λ_{max}: 295 mμ) and (ii) in methanol containing 3% perchloric acid (70%) (λ_{max}: 279 mμ and 223 mμ).

When the hydrogenation was carried out at 45° for 3 hours and at 50 p.s.i. a solid was obtained after removal of the catalyst and evaporation of the filtrate, which on recrystallization, firstly from ethyl acetate and secondly from benzene, gave colorless prisms of the tetrahydro-6-hydroxyskatole (IX), m.p. 194–195°. (Found: C, 71.54; H, 8.64; N, 9.01%; mol. wt. 156. Calc. for $C_9H_{13}NO$: C, 71.49; H, 8.67; N, 9.26%; mol. wt. 151.2.) The ultraviolet absorption spectrum was measured in (i) methanol (λ_{max}: 285 mμ) and (ii) methanol containing 3% perchloric acid (70%) (λ_{max}: 275 mμ).

(B) From 6-Benzyloxyindole-3-carboxaldehyde

6-Benzyloxyskatole.—A suspension of 6-benzyloxyindole-3-carboxaldehyde (2.5 g; prepared by the method of Young (12)), sodium borohydride (2.5 g) and 10% palladium–charcoal (1.2 g) in isopropanol (500 ml) was boiled under reflux for 5 hours. Crude 6-benzyloxyskatole (2.1 g; 89%) was obtained as a colorless solid on concentration of the reaction mixture to small bulk after filtration. An analytical sample was obtained by repeated recrystallization of a small quantity of the crude product from benzene. Colorless prisms: m.p. 148°. (Found: 81.10; H, 6.25; N, 5.65. Calc. for $C_{16}H_{15}NO$: C, 80.98; H, 6.37; N, 5.90%.)

6-Hydroxyskatole.—A solution of 6-benzyloxyskatole (1 g) in ethyl acetate (100 ml) containing 5% palladium–charcoal (0.3 g) was shaken in an atmosphere of hydrogen at room temperature and under atmospheric pressure for 8 hours. 6-Hydroxyskatole and the dihydro-hydroxyskatole were shown to be present by means of paper chromatography. The catalyst was removed by filtration, and the residue obtained on concentration of the filtrate was dissolved in benzene and separated into 6-hydroxyskatole (270 mg; 43.5%) and 6-hydroxy-3-methylindoline (VIII) (55 mg; 9%) by chromatography on a silica gel column by the procedure described above.

Dehydrogenation of 6-Hydroxy-3-methylindoline (VIII)

A solution of the 6-hydroxy-3-methylindoline (VIII) (2 mg) in xylene (3 ml) containing 10% palladium–charcoal (5 mg) was boiled under reflux for 5 hours whilst a stream of nitrogen was bubbled through the mixture. After this time the suspension was filtered and the solvent removed *in vacuo*; the residue obtained was recrystallized from benzene – light petroleum and gave a few crystals of 6-hydroxyskatole identical with an authentic specimen.

Attempted dehydration of IX by a similar procedure was not successful, the starting material being recovered in an essentially unchanged condition.

Methylation of 6-Hydroxyskatole

A solution of sodium methoxide in methanol (2.4 ml), prepared by dissolving sodium (1 g) in methanol (100 ml), was added to a solution of 6-hydroxyskatole (0.15 g) in methanol (10 ml) and the solvent removed *in vacuo*. Dimethyl sulphate (1 ml) in dry benzene (20 ml) was added to the crude sodio derivative and the

Can. J. Chem. Downloaded from www.nrcresearchpress.com by 210.87.254.6 on 09/05/12
For personal use only.

suspension stirred at 50° for 3 hours. After this time the reaction mixture was filtered, and the benzene solution shaken with 2 *N* sodium hydroxide solution and washed with water, dried (Na_2SO_4), and evaporated to dryness. Purification of the residue, firstly by sublimation in high vacuum (50° at 0.1 mm) and finally by recrystallization from light petroleum afforded 6-methoxyskatole, m.p. 125° in fine plates (Blaikie and Perkin prepared this compound by a different route but report the same melting point (31)).

7-Hydroxyskatole

(A) From 7-Benzyloxygramine

A suspension of 7-benzyloxygramine (250 mg) and 10% palladium–charcoal (125 mg) in a mixture of methanol (80 ml) and ethyl acetate (80 ml) was shaken in an atmosphere of hydrogen at room temperature and 55 p.s.i. for 5 hours. After it was treated as described above a waxy solid was obtained which was purified chromatographically on a silica gel column with adsorption from benzene – ethyl acetate (97:3). Recrystallization of the crude chromatographic product from light petroleum gave 7-hydroxyskatole (41 mg; 31%), m.p. 82.5° in colorless needles. (Found: C, 73.75; H, 6.43; N, 9.27. Calc. for C_9H_9NO: C, 73.45; H, 6.16; N, 9.52%.)

(B) From 7-Benzyloxyindole-3-carboxaldehyde

7-Benzyloxyindole-3-carboxaldehyde.—This compound was prepared in a fashion analogous to that described above for the synthesis of the corresponding 4-isomer. In this way 2.0 g (93.5%) of 7-benzyloxyindole-3-carboxyaldehyde, m.p. 158°, were obtained from 1.9 g of 7-benzyloxyindole. Recrystallization of a small sample for analysis from aqueous ethanol raised the melting point to 159° (melting point reported in the current catalogues of L. Light and Co. and the Regis Chemical Co., 157–159°). (Found: C, 76.57; H, 5.18; N, 5.65. Calc. for $C_{16}H_{13}NO_2$: C, 76.47; H, 5.22; N, 5.57%.)

7-Benzyloxyskatole.—A suspension of 7-benzyloxyindole-3-carboxaldehyde (0.9 g) and lithium aluminum hydride (0.3 g) in tetrahydrofuran (80 ml) was boiled under reflux for 30 minutes. After it was treated as described above for 4-benzyloxyskatole, 7-benzyloxyskatole (0.65 g; 77%) was obtained as a colorless oil which could be debenzylated satisfactorily without further purification. A small sample for microanalysis was purified by distillation in vacuum, b.p. 160° (bath temperature) at 0.2 mm. (Found: C, 81.22; H, 6.25; N, 6.09. Calc. for $C_{16}H_{15}NO$: C, 80.98; H, 6.37; N, 5.90%.)

7-Hydroxyskatole.—Hydrogenolytic debenzylation of 7-benzyloxyskatole (0.65 g) with 10% palladium–charcoal (0.3 g) in methanol (120 ml) (45 minutes; atmospheric pressure) gave 7-hydroxyskatole (180 mg; 44.5%).

5,6-Dihydroxyskatole

(A) From 5,6-Dibenzyloxygramine

A suspension of 5,6-dibenzyloxygramine (200 mg; prepared by the method of Schlossberger and Kuch (32, 33)) and 5% palladium–charcoal (120 mg) in ethyl acetate (80 ml) was shaken in a hydrogen atmosphere at room temperature and under atmospheric pressure for 3 hours. After filtration of the reaction mixture and concentration of the filtrate the residue was purified chromatographically on silica gel with adsorption from benzene and elution with benzene – ethyl acetate (49:1), followed by recrystallization from benzene – light petroleum. 5,6-Dihydroxyskatole was obtained in colorless prisms (18 mg; 38%) m.p. 151°. (Found: C, 66.00; H, 5.64. Calc. for $C_9H_9NO_2$: C, 66.24; H, 5.56%.) This compound had previously been prepared by a different route by Beer *et al.*, who reported a melting point of 152° (28).

(B) From 5,6-Dibenzyloxyindole-3-carboxaldehyde

5,6-Dibenzyloxyindole-3-carboxaldehyde.—5,6-Dibenzyloxyindole (0.7 g) in dimethylformamide (0.8 ml) was added to a well-cooled, stirred mixture of dimethylformamide (1 ml) and phosphorus oxychloride (0.325 g). A solution of sodium hydroxide (1.4 g) in water (3.8 ml) was added to the reaction mixture after it had been stirred at 30–35° for 30 minutes. The crude product obtained after the aqueous alkaline reaction mixture had been boiled for 10 minutes was recrystallized from 95% ethanol and gave 5,6-dibenzyloxyindole-3-carboxaldehyde, m.p. 195° in colorless fine plates (0.6 g; 79%). (Found: C, 76.98; H, 5.20; N, 4.23. Calc. for $C_{23}H_{19}NO_3$: C, 77.29; H, 5.36; N, 3.92%.)

5,6-Dibenzyloxyskatole.—A stirred suspension of 5,6-dibenzyloxyindole-3-carboxaldehyde (200 mg), 10% palladium–charcoal (100 mg), and sodium borohydride (200 mg) in isopropanol (20 ml) was boiled under reflux for 2 hours and the products worked up in a manner identical with that described above. Recrystallization of the crude product from benzene – light petroleum gave 5,6-dibenzyloxyskatole, m.p. 122° in colorless prisms (110 mg; 52%). (Found: C, 80.42; H, 6.27; N, 4.10. Calc. for $C_{23}H_{21}NO_2$: C, 80.44; H, 6.16; N, 4.08%.) Acheson *et al.* prepared this compound by a different route and quote m.p. 123° (29).

5,6-Dihydroxyskatole.—Debenzylation of 5,6-dibenzyloxyskatole (40 mg) in ethyl acetate (30 ml) with hydrogen in the presence of 5% palladium–charcoal (20 mg) gave 5,6-dihydroxyskatole (12 mg; 63%).

Paper Chromatography

Disks (diameter = 24 cm) of Whatman No. 1 paper were pretreated with formamide by the method previously described and radial development in a modified Kawerau apparatus was carried out with a benzene:chloroform (1:1) mixture containing 0.4% formamide (cf. (34)).

Can. J. Chem. Downloaded from www.nrcresearchpress.com by 210.87.254.6 on 09/05/12
For personal use only.

The benzyloxyindole-3-carboxaldehydes, which could be located on the developed chromatograms by the red- to orange-brown colors they gave with the 2,4-dinitrophenylhydrazine reagent, had the following R_f values in this system: 4-, 0.81; 5-, 0.75; 6-, 0.73; 7-, 0.88; and 5,6-di-, 1.0.

All these compounds could be detected by viewing the developed chromatograms in ultraviolet light. The 4-, 5-, and 7-benzyloxyindole-3-carboxaldehydes showed a distinct blue fluorescence and although the 6-benzyloxy- and 5,6-dibenzyloxy- derivatives did not fluoresce they could be located by the fact that they absorbed the ultraviolet light.

The benzyloxyskatoles, all of which gave blue or blue-green colors with Ehrlich's reagent, migrated to the solvent front under these conditions of chromatography. The hydroxyskatoles have previously been reported to have the following R_f's in this system 4-, 0.27; 5-, 0.21; 6-, 0.22; and 7-, 0.32 (10). 5,6-Dihydroxyskatole did not migrate at all in this solvent system.

The three products VII, VIII (i.e. 6-hydroxy-3-methylindoline), and IX had R_f's of 0.55, 0.34, and 0.32 respectively. They could be detected on the chromatograms by the fact that they all absorbed ultraviolet light. Compound VII gave a pink-mauve color with Ehrich's reagent, turning blue-gray overnight; 6-hydroxy-3-methylindoline (VIII) gave a yellow color with the Ehrlich's reagent.

REFERENCES

1. C. E. Dalgleish, W. Kelly, and E. C. Horning. Biochem. J. **70**, 13 P. (1958).
2. E. C. Horning, C. C. Sweeley, C. E. Dalgleish, and W. Kelly. Biochim. Biophys. Acta, **32**, 566 (1959).
3. H. Sprince. Clin. Chem. **7**, 203 (1961).
4. R. Rodnight. *In* International reviews of neurobiology. Vol.3. *Edited by* C. C. Pfeiffer and J. R. Smythies. Academic Press, New York. 1961. p. 251.
5. H. J. Teuber and G. Staiger. Chem. Ber. **89**, 489 (1956).
6. R. M. Acheson and A. R. Hands. J. Chem. Soc. 746 (1961).
7. B. Marchand. Chem. Ber. **95**, 577 (1962).
8. R. A. Heacock and O. Hutzinger. Experientia, **18**, 254 (1962).
9. R. M. Acheson and A. R. Hands. Biochim. Biophys. Acta, **51**, 579 (1961).
10. R. A. Heacock and M. E. Mahon. Can. J. Biochem. Physiol. **41**, 487 (1963).
11. A. S. F. Ash and W. R. Wragg. J. Chem. Soc. 3887 (1958).
12. E. H. P. Young. J. Chem. Soc. 3493 (1958).
13. F. T. Tyson and J. T. Shaw. J. Am. Chem. Soc. **74**, 2273 (1952).
14. G. F. Smith. J. Chem. Soc. 3842 (1954).
15. E. Leete and L. Marion. Can. J. Chem. **31**, 775 (1953).
16. E. D. Rossiter and J. E. Saxton. J. Chem. Soc. 3654 (1953).
17. E. Leete. J. Am. Chem. Soc. **81**, 6023 (1959).
18. J. Thesing. Chem. Ber. **87**, 692 (1954).
19. R. M. Silverstein, E. E. Ryskiewicz, and S. W. Chaikin. J. Am. Chem. Soc. **76**, 4485 (1954).
20. D. E. Ames, R. E. Bowman, D. D. Evans, and W. A. Jones. J. Chem. Soc. 1984 (1956).
21. T. Neilson, H. C. S. Wood, and A. G. Wylie. J. Chem. Soc. 371 (1962).
22. H. C. Brown and C. A. Brown. J. Am. Chem. Soc. **84**, 1495 (1962).
23. H. C. Brown and C. A. Brown. J. Am. Chem. Soc. **84**, 2827 (1962).
24. H. C. Brown and K. Sivasankaran. J. Am. Chem. Soc. **84**, 288 (1962).
25. A. P. Terent'ev, N. A. Dzbanovskii, and N. A. Favorskaya. Zh. Obshch. Khim. **23**, 2035 (1953); Chem. Abstr. **49**, 3124 (1955).
26. W. C. Sumpter and F. M. Miller. Heterocyclic compounds with indole and carbazole systems. Interscience Publishers, Inc., New York. 1954. p. 36.
27. J. Austin, J. D. Chanley, and H. Sobotka. J. Am. Chem. Soc. **73**, 5299 (1951).
28. R. J. S. Beer, L. McGrath, A. Robertson, and A. B. Woodier. J. Chem. Soc. 2061 (1949).
29. R. M. Acheson, A. R. Hands, and L. J. King. J. Chem. Soc. 1134 (1962).
30. A. Stoll, F. Troxler, J. Peyer, and A. Hofmann. Helv. Chim. Acta, **38**, 1432 (1955).
31. K. G. Blaike and W. H. Perkin. J. Chem. Soc. 296 (1924).
32. H. G. Schlossberger and H. Kuch. Z. Physiol. Chem. **328**, 284 (1962).
33. H. G. Schlossberger and H. Kuch. Ann. **662**, 132 (1963).
34. R. A. Heacock and M. E. Mahon. Can. J. Biochem. Physiol. **38**, 1500 (1960).

Can. J. Chem. Downloaded from www.nrcresearchpress.com by 210.87.254.6 on 09/05/12
For personal use only.

PHOTOLYSIS OF POLYMETHACRYLIC ACID IN AQUEOUS SOLUTIONS

C. H. CHOU* AND H. H. G. JELLINEK
Department of Chemistry, University of Windsor, Windsor, Ontario
Received October 2, 1963

ABSTRACT

The photolysis of polymethacrylic acid was studied in aqueous solutions as a function of pH, polymer concentration, polymer chain length, and small additions of electrolytes in the absence of oxygen with light of wavelength 2537 Å. The random chain scission constants decrease with increasing pH values. Small variations in polymer chain length and concentration and electrolyte concentration have no effect on the photolysis. Changes in the ultraviolet spectra with irradiation time are more pronounced at low pH values than higher ones. It is shown that the decrease in susceptibility to photolysis with increasing degree of ionization of the acid is not proportional to the decrease or increase of the number of COOH or COO^- groups respectively. It is rather due to the same causes—that is changes in ionic atmosphere—which make the polymer chains uncoil with increasing ionization.

Can. J. Chem. Downloaded from www.nrcresearchpress.com by 210.87.254.5 on 09/05/12
For personal use only.

The photodegradation of polymethacrylic acid was studied by Baxendale and Thomas (1). Their work was mainly concerned with the photolysis in the presence of hydrogen peroxide; however, a few experiments were also performed in its absence. Völker (2) made a study of polymethacrylic acid copolymers exposed to daylight under various conditions, but he did not carry out detailed rate measurements. He concluded that the changes in the extent and rate of degradation are a function of the degree of coiling of the chain molecules as a function of pH.

In the present work, rate measurements were performed as a function of pH, electrolyte, and polymer concentration and also of chain length. All irradiations were carried out with light of wavelength 2537 Å.

No appreciable change in rate constants was found in a region of pH values where the intrinsic viscosities rise very sharply.

EXPERIMENTAL

(a) Materials

All chemicals were of analytical reagent grade quality.

Methacrylic acid, obtained from Matheson, Coleman, and Bell, was polymerized in carefully purified dioxane, using 0.5% w/v benzoylperoxide as described by Eisenberg and Katchalsky (3). The polymerization was carried out under oxygen-free nitrogen at 25° C. The polymer was dissolved in methanol and precipitated with ether. This procedure was repeated three times. The polymer was then dried *in vacuo* at 100° C until constant weight was attained. Percentage conversion was about 10%. Three samples were prepared, which had the following intrinsic viscosities in 5×10^{-4} *M* HCl aqueous solutions: $[\eta]_I = 0.45$, $[\eta]_{II} = 0.42$, and $[\eta]_{III} = 0.25$. All intrinsic viscosities are expressed in $(g/100\ ml)^{-1}$; viscosities were measured at 25±0.05° C. These samples are referred to below as I, II, and III.

(b) Apparatus

The apparatus was similar to the one used previously (4) except for a few minor modifications: (1) The distance between the lamp (low pressure Hg lamp; over 90% of its light output is at $\lambda = 2537$ Å; current 30 ma; total output ca. 3×10^{18} to 5×10^{18} quanta/sec) and the incident surface of the cylindrical Ultrasil cell (4 cm i.d., length 3 cm) was 5.5 cm; (2) the polymer was degraded in absence of air by passing cylinder nitrogen through alkaline pyrogallol, water, and finally through a drying tower into the polymer solution. The reaction cell was located in a thermostated water bath kept at 25±0.05° C.

**National Research Council of Canada Postdoctoral Fellow.*

PROCEDURE AND RESULTS

(a) Influence of pH

As already pointed out above, all irradiations were carried out with ultraviolet light of wavelength $\lambda = 2537$ Å. Data for solutions of polymers I and II, indicating their initial intrinsic viscosities, pH values, and composition, is given in Table I. The polymer concentrations were in all cases within 2.5% of 0.200% w/v; calculations were, of course, made using the exact polymer concentrations in each case. It will be shown subsequently that the photolysis is independent of polymer concentration over a range of concentrations.

TABLE I

Intrinsic viscosities as a function of pH values
(Polymer concentration 0.200±0.005% w/v; temperature 25±0.05° C)

Solvent	Intrinsic viscosity $[\eta]_0$ before irradiation	pH	Remarks
1×10^{-1} *M* HCl	0.41	1.1	
1×10^{-2} *M* HCl	0.41	2.1	
2×10^{-3} *M* HCl	0.42	2.7	
1×10^{-3} *M* HCl	0.42	2.9	
5×10^{-4} *M* HCl	0.45	3.2	
1×10^{-5} *M* HCl	—	3.6	$[\eta]$ cannot be measured
Buffer A	0.41	4.4	
Buffer D_1	0.45	5.4	
Buffer D_2	1.45	5.6	
Buffer D_3	3.50	5.8	
Buffer C	3.65	6.0	
Buffer B	3.60	7.1	
5×10^{-2} *M* NaOH	—	9.7	$[\eta]$ cannot be measured
Distilled H_2O	—	3.5	$[\eta]$ cannot be measured

NOTE: The buffers were made up from mixtures of *M*/15 Na_2HPO_4 and *M*/15 KH_2PO_4.

Figure 1 shows $(1/[\eta]_t)-(1/[\eta]_0)$ values plotted against the irradiation time t for the polymer in the various HCl solutions and the distilled water solution. $[\eta]_t$ and $[\eta]_0$ are the intrinsic viscosities at time t and $t = 0$ of the irradiation process. The intrinsic viscosities were obtained by adjusting all solutions, except the 1×10^{-1} and 1×10^{-2} *M* HCl solutions, to 2×10^{-3} *M* HCl and diluting with 2×10^{-3} *M* HCl solution.

The irradiation results for the 5×10^{-2} *M* NaOH solutions are also shown in Fig. 1. After irradiation these solutions were adjusted to pH 2.0 by adding to 15 ml of the irradiated solution 1 ml of 1 *M* HCl. The intrinsic viscosities were then determined by diluting with 2×10^{-3} *M* HCl. It is shown below that the presence of *M*/15 NaCl has a negligible effect on intrinsic viscosities and rate of degradation.

Figure 2 gives $(1/[\eta]_t)-(1/[\eta]_0)$ values as a function of irradiation time for polymer I in the buffer solutions. In these instances, the intrinsic viscosities were obtained by diluting with the respective buffer solutions. This, of course, dilutes the polymer and the pH values change somewhat with dilution, as the buffers are not strong enough, and approach eventually the pH values of the pure buffer solutions.

Rate constants were derived from the slopes of the straight lines shown in Figs. 1 and 2, using the relationship:

$$(1/[\eta]_t)-(1/[\eta]_0) = kt \qquad [1]$$

where $[\eta]_t$ and $[\eta]_0$ are the intrinsic viscosities at time t and the beginning of the irradiation respectively.

Can. J. Chem. Downloaded from www.nrcresearchpress.com by 210.87.254.5 on 09/05/12
For personal use only.

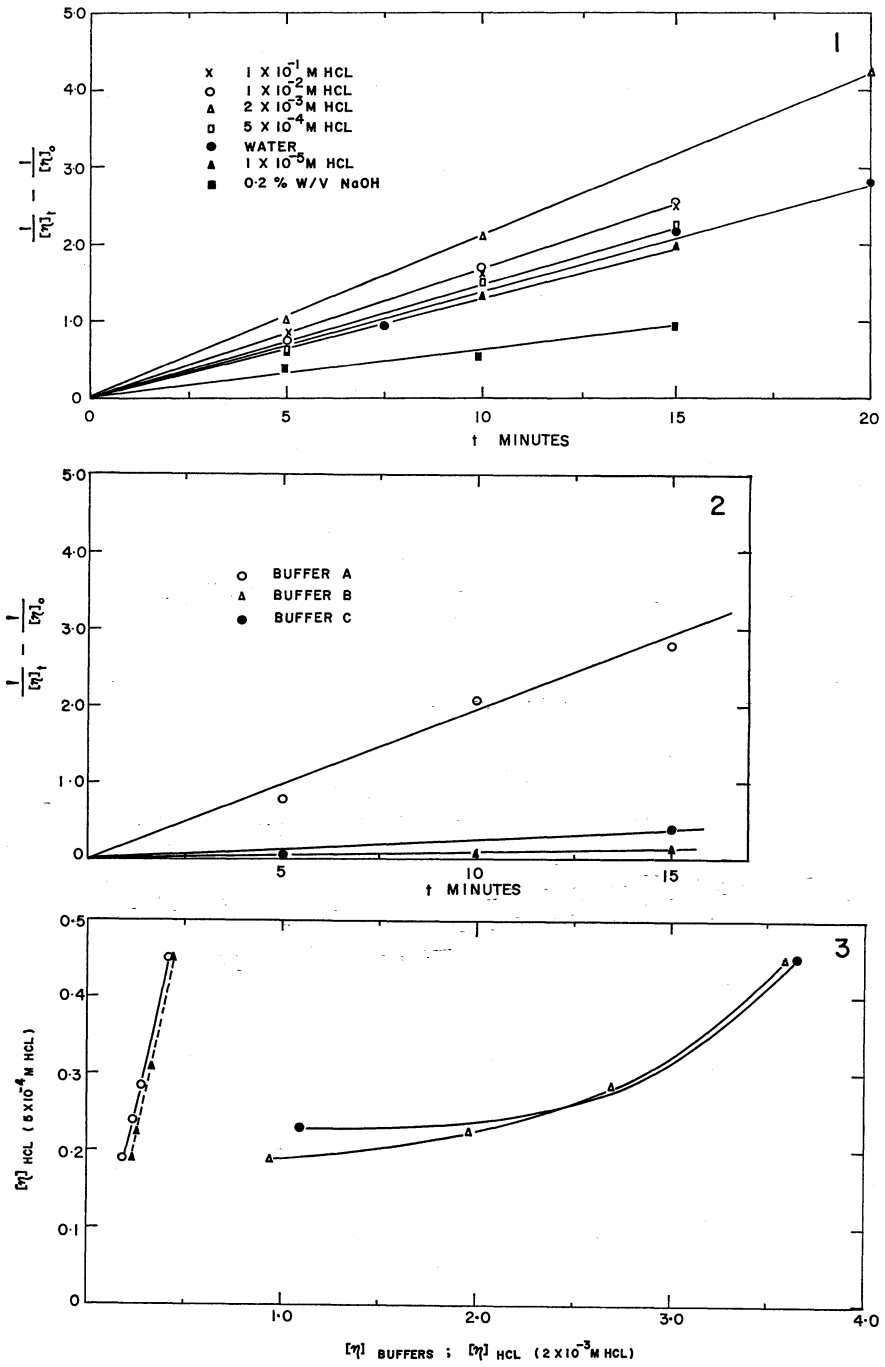

FIG. 1. $(1/[\eta]_t) - (1/[\eta]_0)$ versus irradiation time for polymethacrylic acid in various HCl solutions, distilled water, and 1×10^{-2} *M* NaOH. All solutions adjusted for viscosity measurements to 2×10^{-3} *M* HCl except 1×10^{-1} *M* and 1×10^{-2} *M* HCl (polymer samples I and III).

FIG. 2. $(1/[\eta]_t) - (1/[\eta]_0)$ versus irradiation time for polymethacrylic acid (sample I) in buffer solutions.

FIG. 3. Calibration curves (○ buffer A, △ buffer B, ● buffer C, ▲ 2×10^{-3} *M* HCl).

Can. J. Chem. Downloaded from www.nrcresearchpress.com by 210.87.254.5 on 09/05/12
For personal use only.

Can. J. Chem. Downloaded from www.nrcresearchpress.com by 210.87.254.5 on 09/05/12
For personal use only.

It is apparent that the degradation rate constants are not immediately comparable for the different types of solutions. In order to refer all rate constants to one reference solution, thus making the degrees of degradation and number of chain scissions comparable, the following procedure was adopted.

Irradiation was carried out in 5×10^{-4} *M* HCl solutions for various periods of time. Each irradiated solution was divided into four parts. One part was made 2×10^{-3} *M* with respect to HCl, to the other three parts, buffers A, B, and C were added respectively in such quantities that these solutions were equivalent with respect to buffer to those irradiated in previous experiments. In this way, calibration curves were obtained giving intrinsic viscosity values for the buffer solutions and the 5×10^{-4} *M* HCl solutions as a function of intrinsic viscosity values of the 2×10^{-3} *M* HCl solutions. Figure 3 shows these calibration curves. Calibration curves are not needed for the 1×10^{-1} *M* and 1×10^{-3} *M* HCl solutions as the intrinsic viscosities do not change with pH in this range.

5×10^{-4} *M* HCl solutions were chosen for obtaining calibration curves for the following reason. A polymer solution containing buffers A, B, or C plus 5×10^{-4} *M* HCl has a lower pH value than the respective polymer solution containing buffer only. However, by diluting buffer solutions also containing 5×10^{-4} *M* HCl with the buffer, a region is reached where the specific viscosity versus concentration curves coincide with those for the polymer solutions containing buffer only. If 2×10^{-3} *M* HCl had been used for irradiation, the region where solutions (buffer with and without HCl) show the same values would have been too dilute with respect to polymer to obtain intrinsic viscosity measurements. This is shown in Fig. 4.

Figure 5 shows $(1/[\eta]_t)-(1/[\eta]_0)$ values plotted against irradiation time for the buffer solutions referred to 2×10^{-3} *M* HCl.

Rate constants, referred to the 2×10^{-3} *M* HCl solutions are given in Table II; rate constants for the buffer solutions without reference to 2×10^{-3} *M* HCl are also indicated.

TABLE II

Degradation rate constants as a function of pH values
(Polymer concentrations 0.200±0.005% w/v, λ = 2537 Å, 25±0.05° C)

Solution irradiated	pH	Rate constant $min^{-1}\times$(g/100 ml)	Rate constant referred to 2×10^{-3} *M* HCl $min^{-1}\times$(g/100 ml)
1×10^{-1} *M* HCl	1.1	1.70×10^{-1}	1.70×10^{-1}
1×10^{-2} *M* HCl	2.1	1.70×10^{-1}	1.70×10^{-1}
2×10^{-3} *M* HCl	2.7	2.12×10^{-1}	2.12×10^{-1}
5×10^{-4} *M* HCl	3.2	1.64×10^{-1}	1.50×10^{-1}
Distilled water	3.5	—	1.40×10^{-1}
1×10^{-5} *M* HCl	3.6	—	1.32×10^{-1}
Buffer A	4.4	1.95×10^{-1}	1.30×10^{-1}
Buffer C	6.0	2.5×10^{-2}	0.90×10^{-1}
Buffer B	7.1	8.7×10^{-3}	0.78×10^{-1}
0.05 *M* NaOH	9.7	—	0.65×10^{-1}

(b) Influence of Polymer Chain Length

The rate constants for samples I ($[\eta] = 0.45$) and III ($[\eta] = 0.25$) are as follows:

(1) In 5×10^{-4} *M* HCl: $k_I = 1.64\times10^{-1}$ and $k_{III} = 1.55\times10^{-1}$.

(2) In buffer B (referred to 2×10^{-3} *M* HCl): $k_I = 0.78\times10^{-1}$ and $k_{III} = 0.77\times10^{-1}$.

There is no effect of polymer chain length on the rate of degradation.

Can. J. Chem. Downloaded from www.nrcresearchpress.com by 210.87.254.5 on 09/05/12
For personal use only.

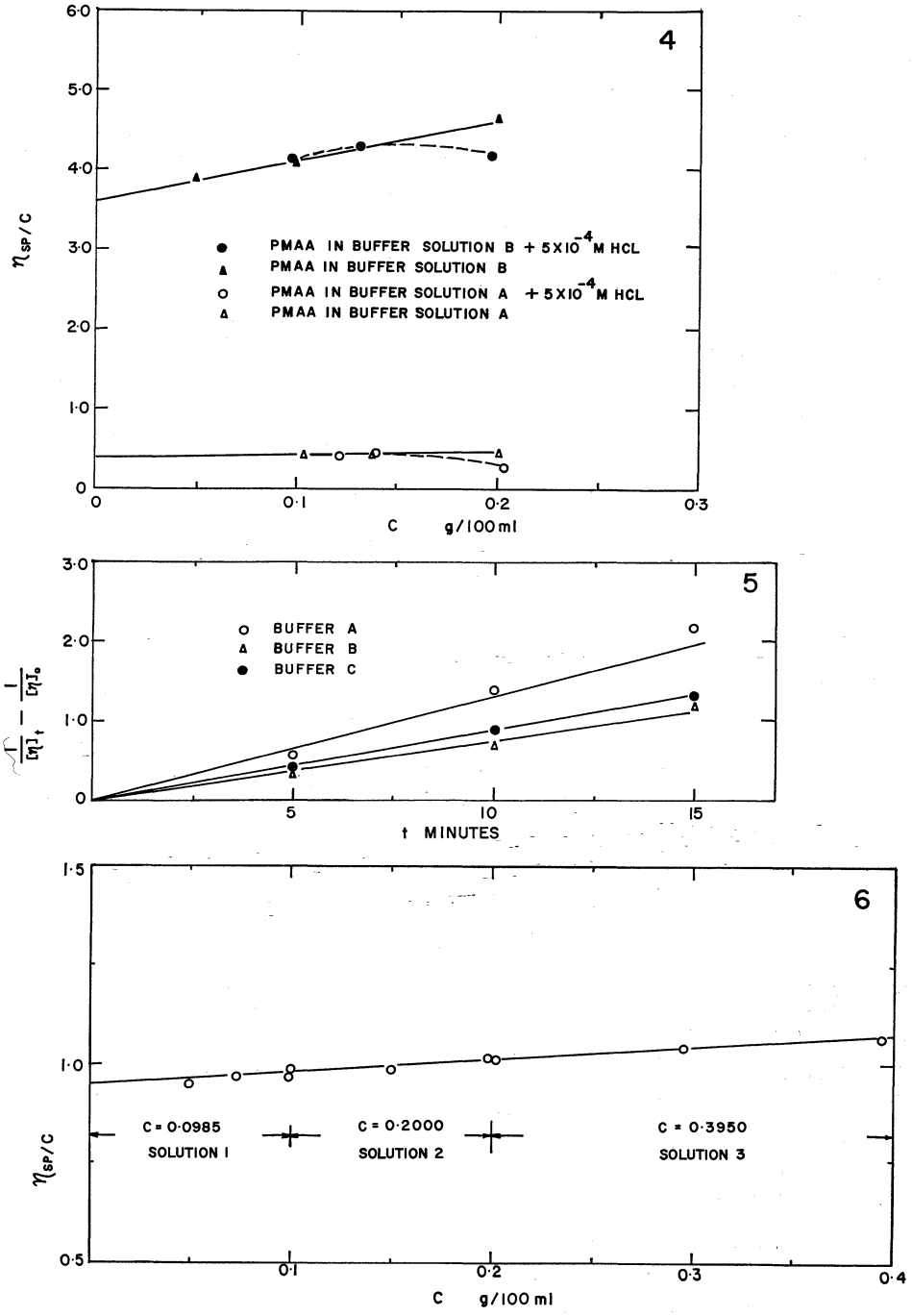

FIG. 4. Specific viscosities for buffers A and B with and without 5×10^{-4} *M* HCl.
FIG. 5. $(1/[\eta]_t)-(1/[\eta]_0)$ versus irradiation time for buffer solutions referred to 2×10^{-3} *M* HCl.
FIG. 6. Effect of polymer concentration on rate of degradation. Sample III irradiated for 10 minutes in each case. The same intrinsic viscosity is obtained irrespective of concentration.

(c) Influence of Polymer Concentration

Polymer solutions of sample III in buffer B were irradiated over a concentration range from 0.099 to 0.395% w/v for 10 minutes each. Figure 6 shows that the concentration has no effect on the rate.

(d) Influence of Electrolyte Concentration

A number of experiments were carried out on the effect of the addition of sodium chloride; sample III was irradiated for 10 minutes in each case. The results are given below:

	5×10^{-4} *M* HCl	5×10^{-4} *M* HCl + 1/15 *M* NaCl	Buffer B	Buffer B + 1/15 *M* NaCl
pH	3.1	3.1	7.15	7.15
$[\eta]_t$ = 10 minutes	0.17	0.17	0.90	0.90

Small additions of NaCl have no effect on the degradation rate.

(e) Ultraviolet Spectra

Ultraviolet spectra of the polymer in the various solutions have been determined for various stages of the irradiation process. In all cases the optical densities in 1-cm cells were measured. Figures 7 and 8, for example, show the spectra for 2×10^{-3} *M* HCl and buffer A solutions. The solutions were diluted 10 times before taking the spectra. The spectra in distilled water are of interest. Figure 9 shows these, including some longer irradiation periods. The extinctions first decrease and eventually increase again with a shift of the maximum absorption to shorter wavelengths for the water solutions. The spectrum for the monomer is given for comparison. In general, the spectra at higher pH values are not much different from those at lower pH values. The extinctions of the peak values of the absorption spectrum change much less with irradiation time at higher pH values than those at lower ones.

DISCUSSION

Figure 10 shows the intrinsic viscosities of the unirradiated solutions as a function of pH. It also shows the rate constants k referred to 2×10^{-3} *M* HCl. The optical densities of the unirradiated solutions were all similar except the value for the 2×10^{-3} *M* HCl solution, which was somewhat higher.

The fact that equation (1) is obeyed suggests a linear relationship between the intrinsic viscosity and polymer chain length, which does not agree with the relationship found by Eisenberg and Katchalsky (3) for polymethacrylic acid fractions measured in 2×10^{-3} *M* HCl solutions: $[\eta] = 6.16\times10^{-3} P^{0.5}$. However, Oth and Doty (7) have indicated that the relationship is dependent on the degree of ionization and the power to which P is raised varies according to them from 0.82 to 1.87 starting with a degree of ionization α of about 0.001 at pH 1.55 to $\alpha = 0.7$ at higher pH values. Baxendale and Thomas (1) found linear relationships between the number of chain scissions and irradiation time. Chain lengths were calculated from intrinsic viscosity values using Eisenberg and Katchalsky's relationship. However, their irradiation times were rather short.

It was shown in previous publications (5) that the rate constants for chain scission are directly proportional to the chain scission quantum yield for a random process, provided all other variables are kept constant. The relationship is as follows:

$$k = \phi_s \frac{(1-e^{-E})I_0}{n_0 l} \qquad [2]$$

Can. J. Chem. Downloaded from www.nrcresearchpress.com by 210.87.254.5 on 09/05/12
For personal use only.

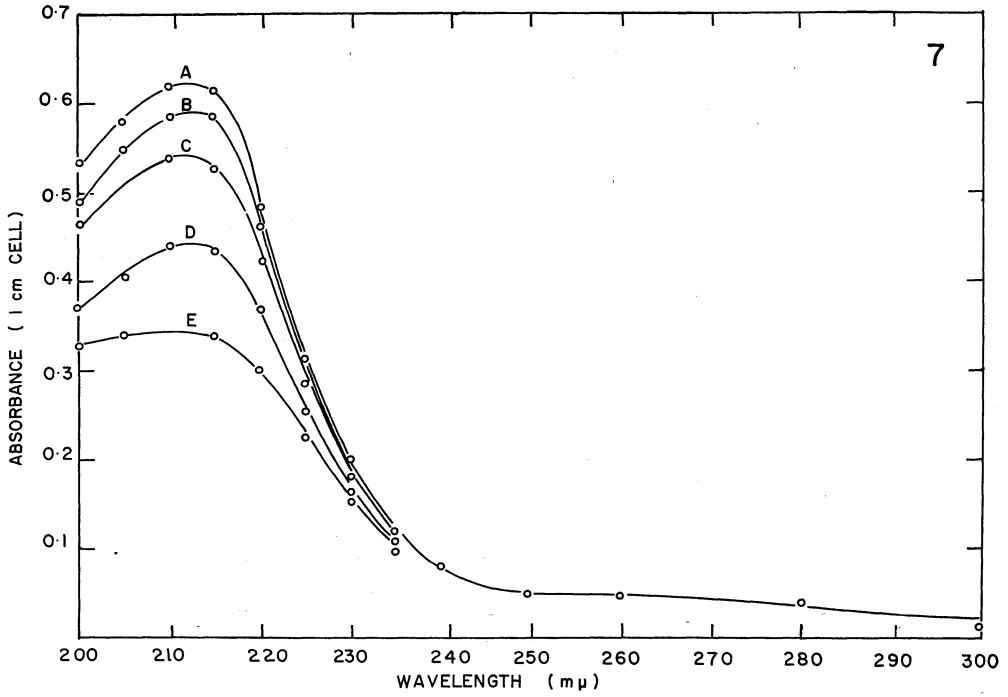

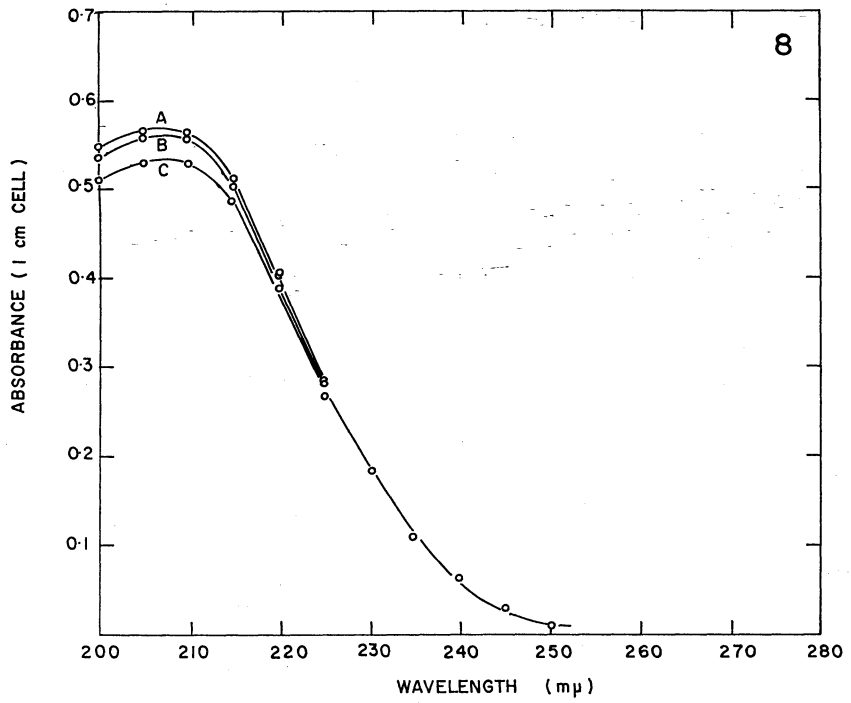

FIG. 7. Ultraviolet absorption spectra for various irradiation times in 2×10^{-3} *M* HCl: A, unexposed; B, 5 minutes; C, 10 minutes; D, 20 minutes; E, 50 minutes; diluted 10 times after exposure; $c = 0.0202\%$ w/v, sample I.

FIG. 8. Ultraviolet absorption spectra for various irradiation times in buffer (A): A, unexposed; B, 5 minutes; C, 15 minutes; diluted 10 times after exposure, $c = 0.0203$, sample III.

Can. J. Chem. Downloaded from www.nrcresearchpress.com by 210.87.254.5 on 09/05/12
For personal use only.

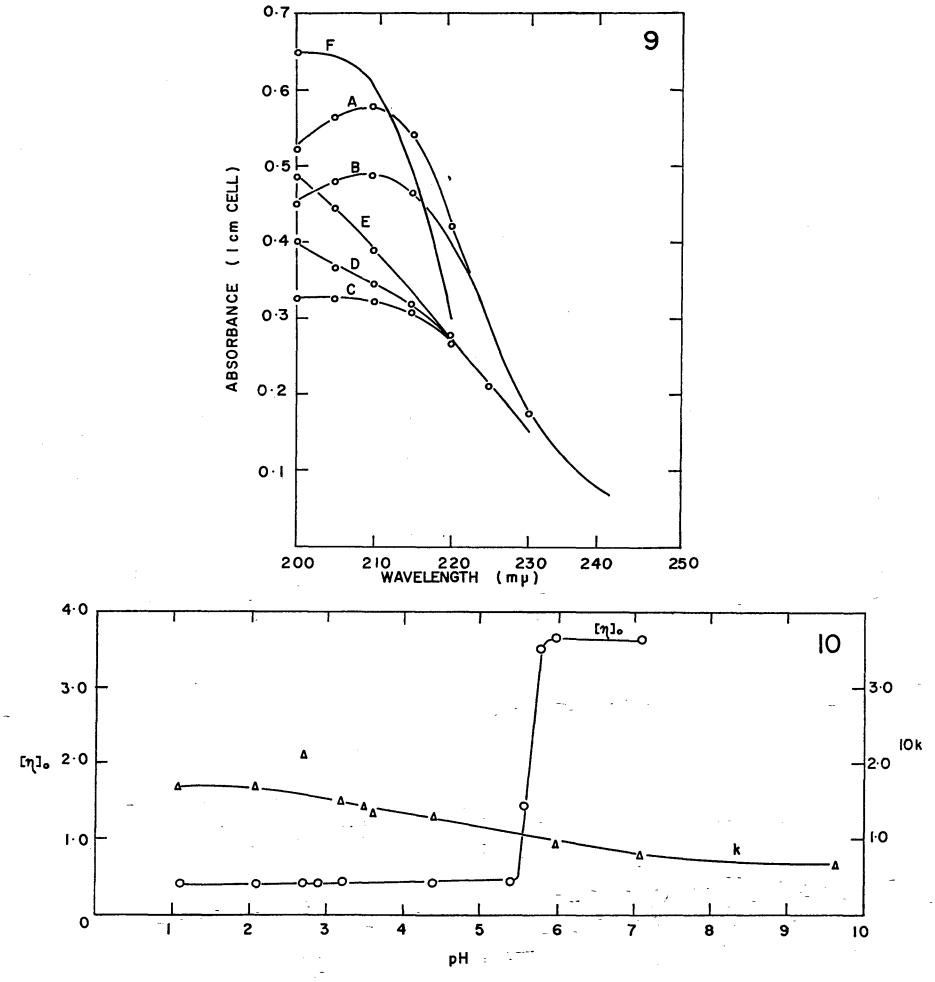

FIG. 9. Ultraviolet absorption spectra for various irradiation times in distilled water: A, unexposed; B, 15 minutes; C, 60 minutes; D, 2 hours; E, 3 hours; F, monomer; diluted 10 times after exposure, $c = 0.0203$ % w/v, sample I.

FIG. 10. Initial intrinsic viscosity $[\eta]_0$ as a function of pH and rate constants k referred to 2×10^{-3} M HCl as a function of pH.

where ϕ_s is the quantum yield for chain scission (number of main chain links broken for each quantum absorbed by the solution), E the optical density, I_0 the incident light intensity, n_0 the initial concentration of main chain links in the polymer solution, and l the length of the reaction cell. All these quantities were kept constant, hence k is a direct measure of the quantum yield.

It is apparent that the susceptibility of polymethacrylic acid to photolysis decreases with increasing pH values becoming practically constant at either end of the pH range. This means that the quantum yield for chain scission decreases with increasing degrees of ionization and also with increasing degrees of uncoiling (stretching) of the polymer chains.

If the rate of breaking main chain links were directly proportional to the number of

Can. J. Chem. Downloaded from www.nrcresearchpress.com by 210.87.254.5 on 09/05/12
For personal use only.

COOH groups and COO^- groups respectively, each having its individual rate constant, the following equations should hold:

$$s_1/[(1-\alpha)P_0] = k_1 t \quad \text{and} \quad s_2/\alpha P_0 = k_2 t$$

where s_1 and s_2 are the average numbers of chain scissions per original chain molecule of length P_0 due to COOH and COO^- groups, respectively, k_1 and k_2 are the corresponding rate constants, and α is the degree of ionization.

Further
$$(s_1+s_2)/P_0 = k_{exp}t = (1-\alpha)k_1 t + \alpha k_2 t$$
or
$$\alpha = (k_{exp}-k_1)/(k_2-k_1)\,. \qquad [4]$$

Our experiments indicate that $[\eta] \propto P$; hence the ratio given by equation [4] can be evaluated directly. k_1 represents the rate constant at the low end of the pH range and k_2 that at the high range, k_{exp} are the experimental rate constants between the two extremes. As a guide, the degrees of ionization α_k as a function of pH may be given from Katchalsky *et al.* (6) (see Fig. 8, ref. 6).

pH	3	4	5	6	7	8
α_k	0.01	0.04	0.1	0.25	0.5	0.8
α_{calc}	0.19	0.38	0.53	0.67	0.86	1.0

The degrees of ionization α_{calc} calculated from equation [4] are also given. The rate constants were read off the graph in Fig. 10: $k_1 = 1.70\times10^{-1}$ and $k_2 = 0.65\times10^{-1}$. In actual fact the rate constant for photolysis decreases much faster with increase in degree of ionization than predicted by the above assumption of direct proportionality of rate of breaking links and number of COOH or COO^- groups respectively.

The ratio of the root mean extension R_α/R_0 of the chains (R_α root mean extension at degree of ionization α, R_0 at $\alpha = 0$) as a function of the degree of ionization was calculated for a polymethacrylic acid fraction by Oth and Doty (7) (see Fig. 7, ref. 7). In our case the experimental photolysis rate constants decrease with increasing α; however, R_α/R_0 increases with α. Hence $1/k$ was plotted against α. A curve is obtained of a similar type as that for the plot R_α/R_0 versus α. As a matter of fact, if the values of R_α/R_0 as a function of α are chosen which were obtained from titration data by Oth and Doty and these values are plotted against the corresponding $1/k$ values, a straight line is obtained. Not much significance should be attached to any quantitative aspects of these relationships; however, it is clear that the photolysis is influenced by the same causes which are responsible for the stretching of the polymer chains as a function of pH or degree of ionization. In other words, the ionic atmosphere produced by even a very small amount of ionization of the polymethacrylic acid seems to have an appreciable effect on the susceptibility to photolysis. The corresponding α, $1/k$, and R_α/R_0 values, the latter taken from Oth and Doty's paper (Fig. 7, titration values, ref. 7) are given below:

α	0.01	0.04	0.1	0.25	0.5
R_α/R_0	1.3	2.5	5.0	6.8	11.0
$1/k$	6.7	7.7	9.1	10.5	12.5

However, it must not be forgotten that the rate of photolysis of fatty acids (8) seems to be influenced by pH, but systematic investigations do not appear to have been made.

Can. J. Chem. Downloaded from www.nrcresearchpress.com by 210.87.254.5 on 09/05/12
For personal use only.

Also decomposition products such as CO_2 and gaseous hydrocarbons have been observed during the photolysis of fatty acids. It is likely that such gases are also produced during the photolysis of polymethacrylic acid; even some monomer may be evolved.

The primary photolytic process consists probably of the absorption of a light quantum by the carboxylic groups which may then lead to production of COOH radicals and also to some random chain scissions, as indicated by Baxendale and Thomas (1),

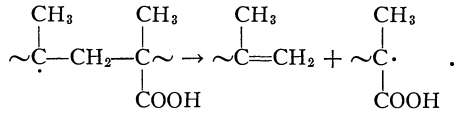

ACKNOWLEDGMENT

This work was made possible by a postdoctoral fellowship (C. H. Chou) and an equipment grant from the National Research Council of Canada.

REFERENCES

1. J. H. Baxendale and J. K. Thomas. Trans. Faraday Soc. **54**, 1515 (1958).
2. T. Völker. Makromol. Chem. **44**, 107 (1961).
3. H. Eisenberg and A. Katchalsky. J. Polymer Sci. **6**, 145 (1951).
4. H. H. G. Jellinek and I. J. Bastien. Can. J. Chem. **39**, 2056 (1961). H. H. G. Jellinek and W. A. Schlueter. J. Appl. Polymer Sci. **3**, 206 (1960).
5. H. H. G. Jellinek. Pure Appl. Chem. **4**, 419 (1962). H. H. G. Jellinek. J. Appl. Polymer Sci. **4**, 253 (1960).
6. A. Katchalsky, O. Kuenzle, and W. Kuhn. J. Polymer Sci. **5**, 283 (1950).
7. A. Oth and P. Doty. J. Phys. Chem. **56**, 43 (1952).
8. L. Farkas and O. H. Wansborough. Z. Physik. Chem. B, **18**, 124 (1932). K. Clusius and W. Schanzer. Ber. B, **75**, 1795 (1942).

Can. J. Chem. Downloaded from www.nrcresearchpress.com by 210.87.254.5 on 09/05/12
For personal use only.

THE BROMINATION AND HALOGENOMETHOXYLATION OF D-GLUCAL TRIACETATE[1]

R. U. LEMIEUX AND B. FRASER-REID
Department of Chemistry, University of Alberta, Edmonton, Alberta
Received September 19, 1963

ABSTRACT

The bromination of D-glucal triacetate gave a mixture of tri-*O*-acetyl-2-bromo-2-deoxyglycopyranosyl bromides containing about 60% and 30% of the compounds with the α-D-gluco and α-D-manno configurations, respectively. Reaction of the bromides with methanol in the presence of silver carbonate proceeded almost entirely with inversion of the reacting anomeric centers. Hydrogenolysis of the product of methanolysis gave methyl 2-deoxy-β-D-glucopyranoside. Reaction of D-glucal triacetate with either bromine, chlorine, or iodine in methanol containing silver acetate gave in each case about 60–65% and 35–40% yields of the corresponding methyl 2-deoxy-2-halogeno-α-D-mannopyranoside and -β-D-glucopyranoside triacetates. The mechanisms of the reactions are discussed.

Can. J. Chem. Downloaded from www.nrcresearchpress.com by 210.87.254.40 on 09/05/12
For personal use only.

In 1920, Fischer, Bergmann, and Schotte (1) reported the bromination of D-glucal triacetate and methanolysis of the product to form two crystalline compounds termed the "triacetyl methyl glucoside-2-bromohydrins I and II". These reactions were reinvestigated since it was apparent (2) that application of nuclear magnetic resonance spectroscopy would readily allow the establishment of the configurations of these and the related compounds. The β-D-configuration was established for the anomeric centers of the "bromohydrins I and II" by reduction of each with sodium amalgam to methyl 2-deoxy-β-D-glucopyranoside (1). Also, the stereochemistry of the direct preparation of methyl 2-deoxy-2-halogeno-D-glycopyranosides by halomethoxylation of D-glucal was of interest as an alternative synthetic route to 2-halogeno-glycosides and their various possible derivatives (3–5).

Three publications related to this present contribution appeared in the course of this investigation. Manolopoulos, Mednick, and Lichtin (6) offered a proof of the configurations of the 2-positions of the "bromohydrins I and II" based on the rates of the iodide-catalyzed deoxymercuration of the methyl 2-acetoxymercuri-2-deoxyglycosides obtained on the reaction of D-glucal triacetate with methanolic mercuric acetate. The brominolysis of the acetoxymercuri-glycosides was assumed to yield the bromohydrins of related configuration. It will be seen below that the assignments of configuration were indeed correct although Inglis, Schwarz, and McLaren (7) have more recently contended that the compound characterized [by Monolopoulos and co-workers (6)] as methyl 2-acetoxymercuri-2-deoxy-β-D-mannopyranoside triacetate in fact has the α-D-manno configuration. Agaki, Tejima, and Nakamira (8) deacetylated the "bromohydrin I" and converted the product to the 4,6-benzylidene derivative which, on treatment with sodium methoxide, gave the known methyl 2,3-anhydro-4,6-benzylidene-β-D-mannopyranoside. It was therefore concluded that "bromohydrin I" possessed the D-gluco configuration.

D-Glucal triacetate was brominated as described by Fischer, Bergmann, and Schotte (1) to provide a syrupy product, the NMR spectrum of which required 90% of the mixture to be two glycosyl bromides. The major component (II) gave a doublet in the NMR spectrum with a 3.5 c.p.s. spacing at 6.47 p.p.m. The other compound (III) produced a

[1]*This research is to constitute a portion of a thesis to be submitted by B. F.-R. in partial fulfillment of the requirements for the degree of Doctor of Philosophy.*

doublet at 6.65 p.p.m. with a spacing of 1.0 c.p.s. The general experience with NMR spectra (9) of acetylated glycosyl bromides clearly indicated that both these doublets because of their chemical shifts arose from anomeric hydrogens in equatorial orientation. Furthermore, the spacings indicated that compounds II and III possessed the α-D-gluco- and α-D-manno-configurations, respectively, since, in general, derivatives of α-D-glucopyranose and α-D-mannopyranose provide signals for the anomeric hydrogens with spacings of 3.0–3.6 c.p.s. and 1.0–1.5 c.p.s., respectively. As will be seen below, this conclusion was confirmed through characterization of the products formed on the methanolysis of the dibromides.

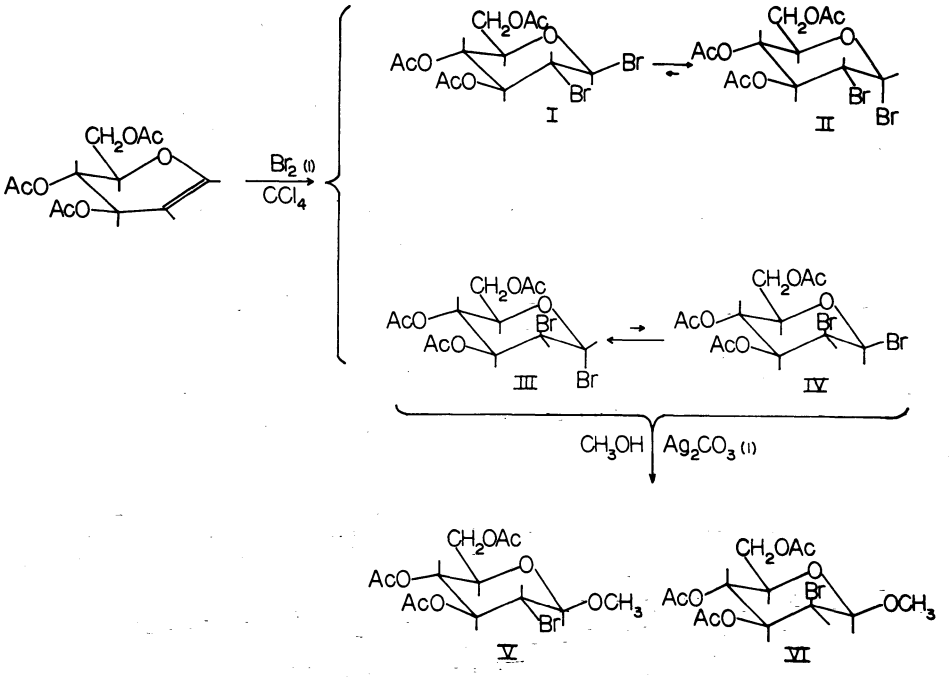

The formation of the 1,2-*trans*-α-D-manno dibromide (III) in about 30% yield is in accordance with the usual stereochemical route found in the halogenation of alkenes. However, the formation of the 1,2-*cis*-α-D-gluco dibromide (II) as the main product (about 60%) of the reaction is not a classical route of reaction. It is now well established that, in the absence of large axial substituents at the 3- or 5-positions, the thermodynamically stable anomer for glycopyranosyl halides is the anomer which has the halogen in axial orientation (10, 11). The dipole–dipole interaction responsible for this condition has been termed the "anomeric effect" and can provide a driving force of 1.5 to 2.0 kcal/mole (10). Therefore, it can be expected that, if formed, the β-D-gluco dibromide (I) would anomerize to II to an extent of 85 to 90%. The α-D-mannosyl bromide (III) would possess an even greater stability over that of its β-anomer (IV) since its formation from the β-anomer not only involves the driving force of the anomeric effect but also that derived from the interaction of vicinal bromine atoms in *gauche* relationship (12). Therefore, it can be concluded that the bromination of D-glucal triacetate gave an equilibrium mixture of the dibromides I–IV and judging from the NMR analysis for compounds II and III, the β-anomers I and IV are present to an extent of about 10%. The dibromide

Can. J. Chem. Downloaded from www.nrcresearchpress.com by 210.87.254.40 on 09/05/12
For personal use only.

II may have formed directly in the bromination reaction since it is conceivable that an initially formed 1,2-cyclic bromonium ion rearranged directly to the glucosyloxonium ion, which then accepted bromide to form the thermodynamically stable α-D-anomer (II). This conjecture seems eliminated by the observation that the bromomethoxylation of D-glucal triacetate gave only the β-D-gluco (V) and α-D-manno (VII) glycosides. It does not seem likely that the change in solvent from chloroform for the bromination to methanol for the bromomethoxylation would profoundly alter the courses of these mechanistically closely related reactions. Nevertheless, we were not able to demonstrate the anomerization reaction of I to II by following the bromination in the NMR spectrometer. Equilibration must have been achieved within about 15 seconds. It is possible that the bromination in the case of D-glucal triacetate is a rapidly reversible reaction and that the composition of the product reflects the relative stabilities of the four dibromides.

Reaction of the mixture of dibromides with methanol in the presence of silver carbonate gave a mixture of *O*-acetylated methyl 2-deoxy-2-bromoglycosides containing 80–85% of the β-anomers V and VI. As normally observed in the NMR spectra of methyl glycosides, the equatorial methoxyl groups of V and VI gave their signals at substantially lower field, 3.60 p.p.m. (see Fig. 1), than the axial methoxyl groups of the α-anomers,

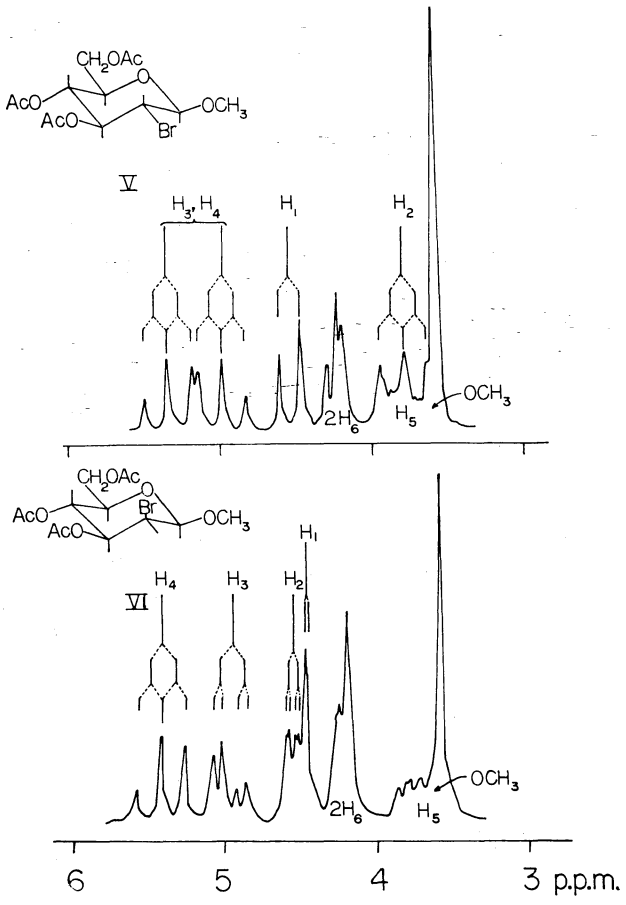

FIG. 1.

Can. J. Chem. Downloaded from www.nrcresearchpress.com by 210.87.254.40 on 09/05/12
For personal use only.

3.44 and 3.48 p.p.m. The intensities of the latter signals required the α-anomers to be formed in nearly equal amounts. Hydrogenolysis of the mixture followed by deacetylation and deionization readily gave a 69% yield of methyl 2-deoxy-β-D-glucopyranoside. It is therefore clear that the glycosyl bromides, I–IV, underwent reaction with near quantitative inversion of the anomeric centers—the normal stereochemical route of reaction for 1,2-*cis*-glycosyl halides. Evidently, there was no appreciable tendency for the axial 2-bromine to participate in the reaction of the 1,2-*trans*-bromide (III). The NMR spectrum of the reaction product clearly indicated a high content of methyl 2-bromo-2-deoxy-β-D-glucopyranoside triacetate (V). The spectrum of V as well as that for the β-D-manno isomer (VI) are shown in Fig. 1. The assignments shown in the spectrum for compound V obviously require the β-D-gluco configuration. The β-D-manno configuration of compound VI was apparent from the chemical shifts for the methoxy group and anomeric hydrogen as compared to those shown in Fig. 2 for the α-anomer (VII). The latter

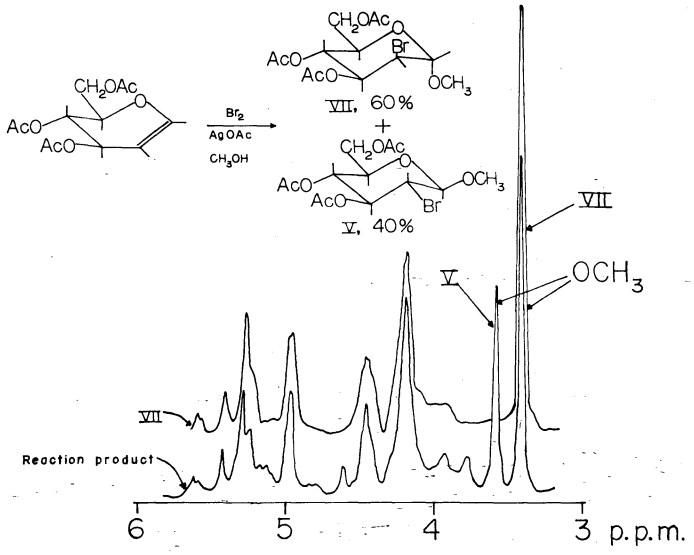

FIG. 2.

compound (VII) was the main product of the bromomethoxylation of D-glucal triacetate. Its configuration was apparent from the NMR spectrum shown in Fig. 2 and confirmed by hydrogenolysis followed by deacetylation to give methyl 2-deoxy-α-D-glucopyranoside. The bromomethoxylation of D-glucal triacetate is undoubtedly an irreversible process and it is of interest to note that, in contrast to the bromination reaction, the 1,2-diaxial-α-D-*manno*side (VII) was the main product (see Fig. 2).

The chloro- and iodo-methoxylation reactions followed virtually the same stereochemical routes as found for the bromomethoxylation. It was established that the "triacetyl methyl glucoside-2-chlorohydrin I," m.p. 149–150°, $[\alpha]_D$ +53°, reported by Fischer and co-workers (1) is methyl 2-chloro-2-deoxy-β-D-glucopyranoside triacetate (VIII). The α-D-manno isomer failed to crystallize. Treatment of VIII with titanium tetrachloride in chloroform (13) was shown to bring about anomerization to the α-D-isomer. The products formed on the iodomethoxylation of D-glucal triacetate have been reported (2). The preparation described here was found most convenient for the large scale preparation of the

Can. J. Chem. Downloaded from www.nrcresearchpress.com by 210.87.254.40 on 09/05/12
For personal use only.

methyl 2-deoxy-2-iodo-β-D-gluco- and α-D-manno-pyranoside triacetates for brominolysis (4, 5). It was found that the addition of a mole of collidine per mole of iodine raised the yield of the α-D-mannoside from 63% to 75–80% and this procedure is recommended for the preparation of this compound.

EXPERIMENTAL

All melting points were determined on a heating stage and are uncorrected. The nuclear magnetic resonance spectra were determined, unless otherwise stated, in chloroform with a Varian A60 spectrometer and the chemical shifts are reported in parts per million from tetramethylsilane used as an internal standard. Unless otherwise stated, the paper chromatograms were made on Whatman No. 1 paper. The zones were detected with the silver nitrate – sodium hydroxide (14) or the permanganate–periodate (15) reagents.

Bromination of D-*Glucal Triacetate*

D-Glucal triacetate (16) was brominated in chloroform as described by Fischer, Bergmann, and Schotte (1). The product was obtained as a colorless syrup in 95% yield. Two doublets for anomeric hydrogens were present in the NMR spectrum of the product at 6.65 p.p.m. (1 c.p.s. spacing) (III), and at 6.47 p.p.m. (3.5 c.p.s. spacing) (II). The relative intensities of these signals were 1:2, respectively. The total intensity of these two signals as compared to the total intensities of the other signals, except for acetyl, required the two compounds to make up more than 90% of the mixture.

Methanolysis of Compounds II and III

The dibromide mixture was reacted with methanol and silver carbonate as described by Fischer and co-workers (1). The NMR spectrum of the product showed three signals for methoxyl groups at 3.60, 3.48, and 3.44 p.p.m. with relative intensities of 10:1:1, respectively. A portion of the product, 150 mg, was dissolved in 15 ml of a 10:9:1 mixture of methanol, water, and triethylamine, respectively, and reacted with hydrogen in the presence of 5% palladium on charcoal. The hydrogen was taken up within a half hour. After 12 hours, the catalyst was removed by filtration and the bromide ion by stirring with an excess of basic Amberlite IRA-400 resin. Evaporation left a residue which readily crystallized from ethyl acetate in 69% yield (71 mg). The compound, m.p. 121–122° did not depress the melting point of an authentic sample of methyl 2-deoxy-β-D-glucopyranoside (2).

The product partially crystallized when dissolved in ethanol to yield compound V, m.p. 135–136°, $[\alpha]_D$ +46.0° (*c*, 2 in chloroform), in 26% yield. Reported for "triacetyl methyl glucoside-2-bromohydrin I" (1), m.p. 138°, $[\alpha]_D$ +50.4°. The NMR spectrum of V is reported in Fig. 2. Deacetylation of V in methanolic ammonia provided methyl 2-bromo-2-deoxy-β-D-glucopyranoside, m.p. 182–184°, $[\alpha]_D$ +0.9 (*c*, 2.4 in methanol). Fischer and co-workers (1) reported the constants, m.p. 179–180° and $[\alpha]_D$ +0.87° for this product.

The mother liquor from the isolation of V was deacetylated at room temperature in methanolic ammonia and the product was fractionated by preparative paper chromatography on Whatman 3MM paper using *n*-butanol–ethanol–water (5:1:4). The chromatogram showed five main components with R_f values of 0.14, 0.33, 0.49, 0.66, and 0.80. The central zone, R_f = 0.49, provided a substance which crystallized on acetylation with acetic anhydride and pyridine. The melting point of the compound (VI), 110–111°, and $[\alpha]_D$ −89.5° (*c*, 1.2 in chloroform) were similar to those reported by Fischer and co-workers (1) for their "triacetyl methyl glucoside-2-bromohydrin II", m.p. 115–116° $[\alpha]_D$ −92.0°. The NMR spectrum of VI is shown in Fig. 1. The R_f value of the product formed on the deacetylation of V was 0.66 and this spot was more intense than that for deacetylated VI in the above-mentioned preparative chromatogram.

Bromomethoxylation of D-*Glucal Triacetate*

D-Glucal triacetate, 10.0 g (37 mmoles), was dissolved in 250 ml of dry methanol containing 8.76 g (52 mmoles) of silver acetate. The mixture was cooled to 0° and 8.4 g (52 mmoles) of bromine was added over a period of 10 minutes with stirring. After an additional 20 minutes, the silver salts were removed by filtration and washed with methanol. The filtrate was evaporated *in vacuo* to a syrup which was taken up in chloroform. The chloroform solution was washed with aqueous sodium bicarbonate and sodium thiosulphate solutions. The dried solution was evaporated to a clear dry syrup. The NMR spectrum of the substance contained two signals for methoxyl groups of relative intensities 1:2 at 3.60 and 3.45 p.p.m., respectively (see Fig. 2).

The syrup was dissolved in ethanol and, on cooling, a 26% yield of the above described methyl 2-bromo-2-deoxy-β-D-glucopyranoside triacetate (V) was deposited. The methoxy group of this compound was found to give its signal at 3.60 p.p.m. A portion, 4 g, of the material in the mother liquor was deacetylated with methanolic ammonia and chromatographed on a cellulose column using *n*-butanol saturated with water. The first fraction, 670 ml of eluate, contained 1.45 g of material which was acetylated with acetic anhydride in pyridine. From the relative intensities of the signals for the methoxy groups, it was concluded that the product which gave a strong methoxy signal at 3.45 p.p.m. was methyl 2-bromo-2-deoxy-α-D-manno-pyranoside triacetate (VII) contaminated 14% by the β-D-gluco isomer (V). The specific rotation of the mixture was +31.2° in chloroform. Catalytic hydrogenolysis of 450 mg of VII using palladium on charcoal

Can. J. Chem. Downloaded from www.nrcresearchpress.com by 210.87.254.40 on 09/05/12
For personal use only.

in methanol containing triethylamine gave 118 mg (57% from VII) of methyl 2-deoxy-α-D-glucopyranoside, m.p. 90–91 (2).

Chloromethoxylation of D-*Glucal Triacetate and Characterization of the Product*

Chlorine was passed through a stirred solution of D-glucal triacetate, 5.00 g (18.5 mmoles) in 125 ml of dry methanol containing 4.35 g (26 mmoles) of silver acetate at 0° until an excess was present. The reaction mixture was then left for 20 minutes before the product was isolated by the procedure described above for the bromomethoxylation reaction. The NMR spectrum of the syrupy product showed the presence of two methyl glycosides as main products of the reaction. The signals for the methoxy groups at 3.60 and 3.45 p.p.m. were in the ratio 2:3, respectively. The NMR spectrum also showed a weak signal for methoxy group at 3.48 p.p.m.

On trituration with methanol, a 19% yield of material (VIII), m.p. 141–145°, was obtained. After two crystallizations from ethanol the material possessed physical constants, m.p. 149–150°, $[\alpha]_D = 53°$ (*c*, 1 in chloroform) and undoubtedly was identical with the "triacetyl methyl glucoside-2-chlorohydrin I" of same melting point and $[\alpha]_D$ +40.2° reported by Fischer and co-workers (1). Deacetylation gave a material (IX) of same melting point, 164–165°, and specific rotation in water, −12.9°, as reported (1) for this compound. The NMR spectrum of VIII was very similar to that for the bromine analogue V shown in Fig. 2 and therefore required the compound to be methyl 2-chloro-2-deoxy-β-D-glucopyranoside triacetate. The substance, 0.51 g, was treated with a refluxing solution of titanium tetrachloride, 0.86 g, in 15 ml of dry chloroform for 15 hours. The product, isolated in the usual manner (13), possessed a specific rotation of 104° in chloroform and its NMR spectrum required the presence of the starting material and a second methyl glycoside with the signal for the methoxy group at 3.48 p.p.m. in the relative amounts 1:2, respectively. The latter substance, undoubtedly methyl 2-chloro-2-deoxy-α-D-glucopyranoside triacetate, resisted crystallization.

The residue from the crystallization of VIII was deacetylated with methanolic ammonia to give a syrupy product, 2.26 g of which was fractionated on a cellulose column using *n*-butanol saturated with water. The first fraction contained 1.30 g of a substance with $R_f = 0.87$ (the R_f value for IX was 0.76) and its NMR spectrum, measured in deuterium oxide, had a doublet, 1.2 c.p.s. spacing at 5.03 p.p.m., assigned to the anomeric hydrogen and a quartet at 4.44 p.p.m. with spacings of 1.2 and 3.5 c.p.s. assigned to the 2-hydrogen of methyl 2-chloro-2-deoxy-α-D-mannopyranoside. The position of the signal for the methoxy group was at 3.50 p.p.m. Its tri-*O*-acetyl derivative (X) produced a signal at 3.45 p.p.m. for the methoxy group. Although the substance appeared virtually pure, $[\alpha]_D$ +45.2° (*c*, 1.7 in chloroform), it resisted crystallization.

Iodomethoxylation of D-*Glucal Triacetate and Characterization of the Product*

To 5 g (18 mmoles) of D-glucal triacetate in 125 ml methanol containing 4.35 g (26 mmoles) silver acetate cooled to 0°, was added iodine, 6.6 g (26 mmoles), during 5 minutes. The mixture was allowed to stand for a further 10 minutes.

The syrupy product was isolated in the manner already described. The NMR spectrum had signals for methoxy groups at 3.58 and 3.43 p.p.m. with relative intensities 3:5. The material was deacetylated by solution in a mixture of 45 ml water, 50 ml methanol, and 5 ml of triethylamine. After 5 hours the solvents were removed by evaporation and the residue was dissolved in methanol for decolorization using charcoal. The methanol was removed and the residue was dissolved with heating in 30 ml of ethanol. Within 1 hour, 2.01 g (36%) of the glucoside crystallized. After two recrystallizations from ethanol, the compound had the physical constants, m.p. 187–188°, $[\alpha]_D$ +3.8° (*c*, 3.9 in water). The reported values (2) for methyl-2-deoxy-2-iodo-β-D-glucopyranoside are 189–189.5° and +6.9° respectively. Acetylation in the usual manner using acetic anhydride and pyridine provided methyl 2-deoxy-2-iodo-β-D-glucopyranoside triacetate, m.p. 94–95°, $[\alpha]_D$ +61.1° (*c*, 2.03 in chloroform).

The mother liquors from the glucoside were dissolved in ethyl acetate, 20 ml, and nucleation with an authentic sample afforded 1.15 g (20%) of crystalline methyl 2-deoxy-2-iodo-α-D-mannopyranoside contaminated (about 15%) with the glucoside. The product was extracted twice with 15 ml of cold ethanol, and the combined ethanolic extracts (which were shown by nuclear magnetic resonance to be free from the glucoside) on evaporation and crystallization from ethyl acetate gave 0.95 g of the pure mannoside, m.p. 147–8°, $[\alpha]_D$ +48.8° (*c*, 1.0 in water). The reported values (2) are 145–146° and +49.6°, respectively.

The residue from the first crop of crystalline mannoside was dissolved in methanol and treated with charcoal. The clarified solution was evaporated to dryness and taken up in a minimum of ethyl acetate to provide a further 0.73 g of crystalline mannoside. The mother liquors from the second crop of crystals were eluted through a short column of silicic acid with methanol. The concentrated eluate afforded a further 0.32 g of mannoside. The total yield of methyl 2-deoxy-2-iodo-α-D-mannopyranoside was 2.00 g (36%). The crystalline residue from the above-mentioned extractions with cold ethanol was recrystallized from ethanol to yield 0.17 g of methyl 2-deoxy-2-iodo-β-D-glucopyranoside and thus raise the yield of this compound to 39%.

ACKNOWLEDGMENTS

The 60 Mc.p.s. nuclear magnetic resonance and infrared spectra were determined by R. N. Swindlehurst and Mrs. G. B. Conway. The research was supported by two National

Can. J. Chem. Downloaded from www.nrcresearchpress.com by 210.87.254.40 on 09/05/12
For personal use only.

Research Council of Canada Studentships to B. F.-R. and National Research Council of Canada grants-in-aid of research (T-172) to R. U. L.

REFERENCES

1. E. FISCHER, M. BERGMANN, and H. SCHOTTE. Ber. **53**, 509 (1920).
2. R. U. LEMIEUX and S. LEVINE. Can. J. Chem. **40**, 1926 (1962).
3. R. U. LEMIEUX and S. LEVINE. Can. J. Chem. In press.
4. R. U. LEMIEUX and B. FRASER-REID. Can. J. Chem. This issue.
5. R. U. LEMIEUX and B. FRASER-REID. Can. J. Chem. This issue.
6. P. T. MANOLOPOULOS, M. MEDNICK, and N. N. LICHTIN. J. Am. Chem. Soc. **84**, 2203 (1962).
7. G. R. INGLIS, J. C. P. SCHWARZ, and L. MCLAREN. J. Chem. Soc. 1014 (1962).
8. M. AKAGI, S. TEJIMA, and H. NAKAMURA. Yakugaku Zasshi. **82**, 1337 (1962).
9. R. U. LEMIEUX, R. K. KULLNIG, H. J. BERNSTEIN, and W. G. SCHNEIDER. J. Am. Chem. Soc. **81**, 6098 (1958).
10. R. U. LEMIEUX and N. J. CHÜ. Abstracts of Papers, 133rd National Meeting of the American Chemical Society. 1958. p. 31N.
11. J. T. EDWARD, P. F. MORAND, and I. PUSKAS. Can. J. Chem. **39**, 2069 (1961).
12. R. U. LEMIEUX and J. W. LOWN. Can. J. Chem. In press (1964).
13. E. PACSU. Ber. **61**, 1508 (1928).
14. W. G. TREVELYEN, D. P. PROCTOR, and J. S. HARRISON. Nature, **165**, 444 (1950).
15. R. U. LEMIEUX and H. F. BAUER. Anal. Chem. **26**, 920 (1954).
16. W. W. PIGMAN and H. S. ISBELL. J. Res. Natl. Bur. Std. **10**, 204 (1937).

Can. J. Chem. Downloaded from www.nrcresearchpress.com by 210.87.254.40 on 09/05/12
For personal use only.

THE BROMINOLYSIS OF CARBOHYDRATE IODIDES

I. ACETYLATED 6-DEOXY-6-IODO AND 2-DEOXY-2-IODO GLYCOSIDES[1]

R. U. LEMIEUX AND B. FRASER-REID
Department of Chemistry, University of Alberta, Edmonton, Alberta

Received September 19, 1963

ABSTRACT

Reaction of methyl 6-deoxy-6-iodo-α-D-glucopyranoside triacetate with an excess of bromine in glacial acetic acid, *N* in potassium acetate, gave a 1.1:1 mixture of the products resulting from replacement of the iodine by bromine and by acetoxy group, respectively. When 2 moles of silver acetate were present per mole of bromine, the reaction was much more rapid and only methyl α-D-glucopyranoside tetraacetate was formed. The brominolysis of methyl 2-deoxy-2-iodo-α-D-mannopyranoside triacetate proceeded at a useful rate only when catalyzed by silver acetate. The main product of the reaction appeared to be methyl 3-acetoxy-2-bromo-2-deoxy-α-D-*arabino*-hexopyranoside triacetate. The compound could be converted by way of sodium borohydride reduction to methyl 2-bromo-2-deoxy-α-D-altropyranoside and by way of zinc dust reduction to methyl 2-deoxy-α-D-*erythro*-hexopyranoside-3-ulose diacetate. About 20% of the reaction proceeded with migration of the methoxy group to the 2-position to yield 2-*O*-methyl-D-glucose tetraacetate. The mechanisms of these reactions are discussed.

The reaction of alkyl iodides with bromine was discovered by Geuther (1) and, in 1865, Friedel (2) observed that the addition of bromine to isopropyl iodide led to the formation of isopropyl bromide and propylene dibromide. Recently, Keefer and Andrews (3) showed that the substitution of iodine chloride for bromine led to the formation of isopropyl chloride and chloroiodopropane. This "halogenolysis" reaction of alkyl iodides was adapted by Viebock and Schwappach (4) for the determination of the volatile alkyl iodides in the classical Ziesel alkoxy group determination (5). The alkyl iodide is distilled into a receiver containing bromine and potassium acetate dissolved in acetic acid. The reaction is described in books of quantitative analysis as involving replacement of the iodine by bromine to form iodine bromide which is subsequently oxidized to iodate—the substance ultimately determined by iodometric titration (6–8).

It would be expected that the driving force for the halogenolysis of an alkyl iodide would originate in the oxidation of the iodine by the halogen and thus provide a better leaving group. In fact, it has long been known that compounds of the type RIX_2 can have existence, ever since Willgerodt (9) isolated phenyl iodine dichloride from the reaction of phenyl iodide with chlorine. However, iodine dihalides appear to have appreciable stability only in the aromatic series (10). Their analogues have been detected in the aliphatic series only at exceedingly low temperatures (4, 11). Thus, the stabilities of the iodine dihalide salts are reminiscent of those for aromatic and aliphatic diazonium salts. As will be seen below, their reaction properties are very similar. Viebock and Schwappach (4) postulated the formation of alkyl iodine dibromides as intermediates in the brominolysis of alkyl iodides.

The stereochemistry and mechanism of the halogenolysis reaction of alkyl iodides has received considerable attention. Corey and Wechter (12) examined the extent of inversion in the reaction of optically active 2-octyl iodide with chlorine and iodine chloride in a number of solvents. The 2-octyl chloride formed was isolated by distillation in 30 to 50% yield and its rotation was measured under standard conditions. The extent of

[1]*This research is to constitute a portion of a thesis to be submitted by B. Fraser-Reid in partial fulfillment of the requirements for the degree of Doctor of Philosophy.*

Can. J. Chem. Downloaded from www.nrcresearchpress.com by 210.87.254.6 on 09/05/12
For personal use only.

inversion with chlorine as the reagent was 1.5 to 2.3 times that of retention when inert, non-polar solvents were used (methylene chloride, ether, pentane, and ethyl acetate). The highest degree of inversion (10.25 times greater) occurred when a 3:1 mixture of methylene chloride and methanol, 4 *M* in hydrogen chloride, was used. In the absence of the hydrogen chloride, the extent of inversion was reduced to 5.8 times that of retention. In the presence of methanol, methyl 2-octyl ether was also formed.

Keefer and Andrews (3, 13) examined the kinetics of the reaction in carbon tetrachloride and concluded that the rate-controlling step involves attack by the halogen on a 1:1 complex (4, 14) of the alkyl iodide and the halogen. A direct nucleophilic attack on carbon by the halogen would then explain the inversions observed by Corey and Wechter (12). However, Keefer and Andrews (13) pointed out that the second molecule of halogen may make an electrophilic attack on a halogen of the complex. Thus, one can envisage the formation of a high-energy alkyl iodonium halide cation which presumably could rapidly decompose to a carbonium ion – iodine halide molecule pair. Nucleophilic attack on this pair by a nucleophile from the immediate environment could then account for the products of replacement. Increased solvent polarity would be expected to facilitate separation of the carbonium ion – iodine halide pair and the neighboring halide anion, and thus account for the increase in inversion noted with increasing polarity of the solvent (12). The departing iodine halide would be expected to help shield the carbonium ion from nucleophilic attack to produce products of retention.

The formation of a high-energy alkyl dihalide cationic intermediate is favored by the indiscriminate courses of reaction observed. First of all, it is to be noted that the substitution reaction is often the minor reaction. Instead, elimination can be the main course of reaction even in the absence of proton abstracting reagents (2). Also in line with carbonium ion formation is the fact that Meerwein–Wagner type rearrangement of the neopentyl to the *sec*-isobutyl carbon skeleton occurs when neopentyl iodide is treated with either bromine or chlorine (15). We were interested in the possibility of replacing the iodine of alkyl 2-deoxy-2-iodo-α-D-mannopyranoside triacetates by acetoxy and thus achieving a synthesis of α-D-glucopyranosides. This approach would be attractive since alkyl 2-deoxy-2-iodo-α-D-mannopyranosides are readily prepared (16). However, the iodide proved so highly resistant to nucleophilic attack on carbon that only elimination was obtained under a variety of solvolytic conditions. It was decided to examine the dark reaction of the iodide with bromine under the standard Viebock–Ziesel conditions used in methoxyl group determinations, namely, to react the iodide in the dark with bromine in glacial acetic acid, *N* in potassium acetate. In view of the relatively high concentration of acetate ion and polarity of the medium, it could be expected that the inversion mechanism would lead to replacement of the axial iodine atom by acetoxy group. The rate of the cleavage of the carbon–iodine bond could be conveniently followed by titration of the iodate content after various periods of time.

Although the rate of the reaction of simple alkyl iodides with bromine under the above conditions is extremely rapid, the methyl 2-deoxy-2-iodo-α-D-mannopyranoside triacetate (I) proved exceedingly resistant to reaction. In order to achieve reaction at a useful rate, silver acetate was added to the reaction medium. This procedure proved, in fact, to accelerate the reaction greatly and provided evidence that the rate-controlling stage in the brominolysis of an iodide involves the formation of a bromoiodonium cation. Inspection of the crude product by nuclear magnetic resonance showed the presence of at least five compounds (five different methoxy group signals). The major component (VI) produced

Can. J. Chem. Downloaded from www.nrcresearchpress.com by 210.87.254.6 on 09/05/12
For personal use only.

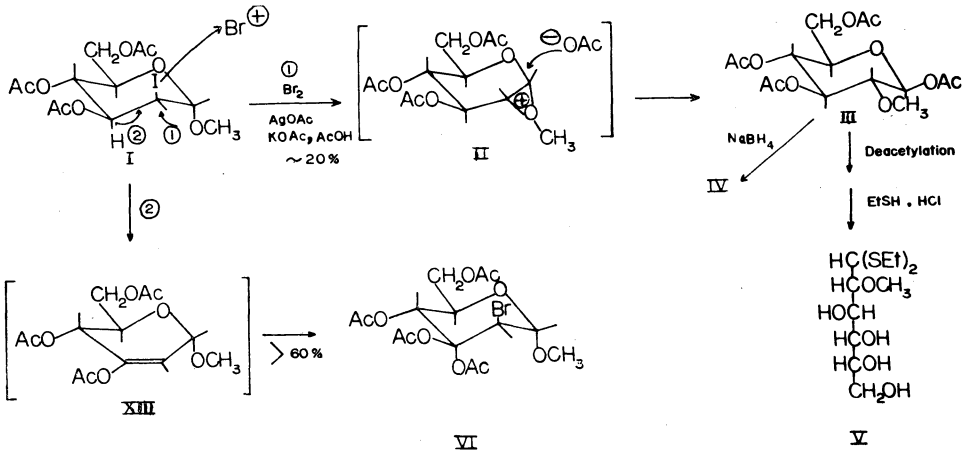

a signal for the methoxy group at 3.52 p.p.m. and constituted more than one-half of the product. Chromatography on dimethyl sulphoxide impregnated paper (17) showed the presence of at least 10 components, one of which was starting material.

The crude product was reduced and deacetylated with sodium borohydride. Column chromatography allowed the isolation of at least two of the five components. One of these substances (compound IV) represented about 20% of the product isolated from the borohydride reduction and appeared to be 2-*O*-methyl-D-glucitol when examined by periodate oxidation followed by paper chromatography (18). It was decided on this basis to examine the product of the brominolysis reaction for 2-*O*-methyl-D-glucose. The material was deacetylated with sodium methoxide in methanol and the resulting syrup was treated with ethanethiol and hydrochloric acid in the anticipation that the well-characterized and high-melting diethyl dithioacetal derivative of 2-*O*-methyl-D-glucose (V) could be isolated from the product of the mercaptolysis reaction. In fact, a crystalline product was readily isolated, which was identical with an authentic sample of 2-*O*-methyl-D-glucose diethyl dithioacetal (19). It is therefore clear that a course of the brominolysis reaction involved cleavage of the axial C_2–I bond, likely by way of a $[C_2—I—Br]^{\oplus}$ intermediate, with participation of the axial C_1-methoxy group, to lead to a 1,2-methoxonium ion (II). This ion would, of course, accept a nucleophile preferentially at the 1-position. Thus, one product of the reaction may be 2-*O*-methyl-β-D-glucopyranose tetraacetate (III). However, it is conceivable that the methoxonium ion is much less favorable than the glucosyloxonium ion. Thus, the latter ion may be an important intermediate in the reaction and its presence could lead to the formation of α- as well as β-anomer. It was not possible to obtain information on this matter. To our knowledge, this is the first example of a methoxy group migration in carbohydrate chemistry although Winstein and Ingraham (20) observed a methoxy migration in the silver ion assisted solvolysis of 2-methyl-2-methoxy-3-bromobutane. In both cases, the migration occurred because the intermediate ethylene oxonium ion was preferentially attacked at the center, which was originally bonded to the methoxyl group. The extent of the migration was at least 7.3% (the actual yield of 2-*O*-methyl-D-glucitol IV). However, judging from the intensities and sizes of the spots obtained in the chromatograms of the sodium borohydride – reduction product, compound IV and a second substance (compound VII) necessarily made up nearly all of the mixture. Also, only two methoxy group signals of appreciable intensity were present in

Can. J. Chem. Downloaded from www.nrcresearchpress.com by 210.87.254.6 on 09/05/12
For personal use only.

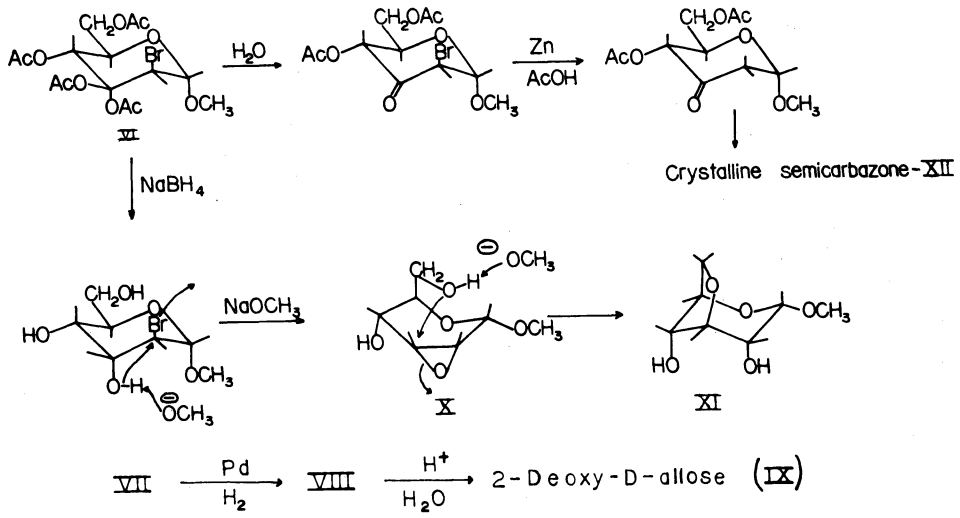

the NMR spectrum of the product. On these bases, it can be concluded that the migration represented about 20% of the course of the brominolysis reaction, and the sequence of reactions leading to compound VI about 60%.

Compound VII failed to crystallize. The substance contained bromine, appeared pure on chromatograms, and possessed (NMR) three acetyl groups per methoxyl group. Hydrogenolysis of the bromine provided a methyl 2-deoxyglycoside, different from either methyl 2-deoxy-α- or β-D-glucopyranoside but possessing the specific rotation reported for methyl 2-deoxy-α-D-allopyranoside (VIII) (21). Acid hydrolysis gave a 2-deoxy sugar found identical, by direct comparison, with 2-deoxy-D-allose (IX) (22). It was therefore evident that compound VII was a methyl 2-bromo-2-deoxy-D-hexopyranoside possessing either the *altro* or *allo* configuration. The D-*altro* configuration was established by treatment of VII with sodium methoxide to form methyl 3,6-anhydro-α-D-glucopyranoside (XI) (23). This conversion requires the intermediary formation of methyl 2,3-anhydro-α-D-allopyranoside (X), which undergoes oxide-ring migration (23) to form the 3,6-anhydro sugar.

It was therefore clearly apparent that the major product (VI) of the brominolysis of I was an acetylated derivative of methyl 2-bromo-2-deoxy-α-D-*erythro*-hexopyranoside-3-ulose. This compound appeared (NMR) to make up about 60% of the reaction product. In order to confirm the structure for VI, a sample of the crude product of brominolysis was reduced with zinc dust in acetic acid. The main component in the reaction mixture (paper chromatography) was converted by sodium borohydride reduction with simultaneous deacetylation to a substance with the same R_f and color reactions as the above-mentioned methyl 2-deoxy-α-D-allopyranoside (VIII). When the crude product of the zinc dust reaction was treated with semicarbazide, a crystalline product was deposited, which possessed the elementary composition and NMR spectrum expected for methyl 4,6-di-*O*-acetyl-2-deoxy-3-oxo-α-D-glucopyranoside semicarbazone (XII). It was therefore concluded that the main course of reaction in the brominolysis of I involved elimination to form the acetylated enol (XIII), which subsequently underwent acetoxybromination to form VI. The formation of the acetylated enol as an intermediate found support in the observation that brominolysis of cyclohexyl iodide, under the same conditions as used

Can. J. Chem. Downloaded from www.nrcresearchpress.com by 210.87.254.6 on 09/05/12
For personal use only.

above except that silver acetate was not added, led to the formation of a substantial amount of *trans*-2-acetoxycyclohexyl bromide (54.6%) along with cyclohexyl bromide, cyclohexyl acetate, and *trans*-cyclohexene dibromide.

In order to achieve a better insight into the essential mechanism of the brominolysis reaction, a number of experiments were conducted starting from methyl 6-deoxy-6-iodo-α-D-glucopyranoside triacetate (24). First of all, the compound was treated with a 5 mole excess of bromine (0.13 *M*) in *N* potassium acetate in acetic acid. After 7 hours, reaction was complete and the product was a 1.1:1 mixture of methyl 6-bromo-6-deoxy-α-D-glucopyranoside triacetate and methyl α-D-glucopyranoside tetraacetate. When the reaction mixture was diluted with the potassium acetate in acetic acid solution to provide an initial bromine concentration of 0.013 *M*, the reaction after 7 hours was only about 44% complete (determined from the relative intensities of the methoxy group signals in the NMR spectrum taken at 100 Mc.p.s.). The relative amounts of the 6-bromo and 6-acetoxy reaction products was now 0.4:1, respectively. The brominolysis reaction under these dilute conditions was complete after 43 hours and the reaction product was a 0.6:1 mixture of the 6-bromo to 6-acetoxy products, respectively. These experiments clearly show that the 6-bromide is to some extent formed by way of an attack by external bromine and (or) bromide on the reactive intermediate. The reaction was then conducted under these same conditions of dilution but in the presence of 2 moles of dissolved silver acetate per mole of bromine in order to exclude any possibility of the presence of bromide ion. The reaction product was analytically pure methyl α-D-glucopyranoside tetraacetate. In view of the fact that the brominolysis reaction is second order in bromine (3), the reduction in the extent of replacement by bromine on a 10-fold dilution of the reaction mixture was much less than expected unless the bromide is formed extensively by attack on the reactive intermediate by a bromide ion from the immediate environment. It is evident therefore that the retention mechanism is operative to an important extent in these reactions. Evidently, the iodine may be replaced by acetoxy with retention in the reactions conducted in the presence of silver acetate. The brominolysis of the 6-iodide under the same conditions as were used for the 2-iodide (I) gave an 0.82:1 ratio of the 6-bromo and 6-acetoxy products, respectively.

EXPERIMENTAL

All melting points were determined on a heating stage and are uncorrected. The nuclear magnetic resonance spectra were determined, unless otherwise stated, in chloroform with Varian A60 or HR100 spectrometers and the chemical shifts are reported in parts per million from tetramethylsilane used as an internal standard. Unless otherwise stated, the paper chromatograms were made on Whatman No. 1 paper and developed with the lighter phase of an *n*-butanol, ethanol, and water mixture (5:1:4) (25). The zones were detected with the silver nitrate – sodium hydroxide (26) or the permanganate–periodate (27) reagents.

Brominolysis of Methyl 2-Deoxy-2-iodo-α-D-mannopyranoside Triacetate (I)

The starting material was a 9:1 mixture (NMR determination) of methyl 2-deoxy-2-iodo-α-D-mannopyranoside (I) and methyl 2-deoxy-2-iodo-β-D-glucopyranoside triacetates. The mixture, 3.24 g (7.5 mmoles, 6.75 mmoles of I), was dissolved in 150 ml of a 10% solution of potassium acetate in acetic acid which contained 24.0 g (150 mmoles) of bromine. Silver acetate, 12.5 g (75 mmoles), was added and the reaction mixture was kept in the dark. Titration of the iodate showed the reaction to be complete after 6 hours at room temperature. The reaction was much slower, about 10% reaction in 1 week, in the absence of the silver acetate. After a 7-hour reaction time, 150 ml of a 25% aqueous solution of sodium acetate was added and the bromine was reduced by the addition of formic acid (4). The product was isolated by filtration to remove insoluble salts and extraction of the filtrate in the usual manner. The brown-colored syrupy product, 2.4 g, was examined by chromatography on dimethyl sulphoxide impregnated paper (17) and found to be a complex mixture containing at least 10 components. The product obviously underwent profound degradation on deacetylation in methanolic ammonia. For this reason, it was deacetylated under reductive conditions using sodium borohydride.

Can. J. Chem. Downloaded from www.nrcresearchpress.com by 210.87.254.6 on 09/05/12
For personal use only.

A. Reduction with Sodium Borohydride

The mixture, 5 g, was treated with an excess of sodium borohydride, 10 g, in aqueous methanol at room temperature for 7 hours. An excess of acetic acid was then added and the solution was reduced to dryness. Methanol was distilled several times from the residue to remove the boric acid and then dissolved in water and the sodium ion was removed by sulphonic acid resin in the acid form. The dark-colored, water-soluble product was found on paper chromatography to contain five main components, one of which, $R_f = 0.71$, was identical with the deacetylated starting material. The other components showed R_f values of 0.18, 0.30, 0.53, and 0.65 and were separated by chromatography on a cellulose column using a *n*-butanol – Skellysolve B (4:1) mixture for development. The components with R_f values of 0.30 and 0.65 (compounds IV and VII, respectively) were obtained in yields of 0.23 g and 1.03 g, respectively.

Characterization of compound IV.—The compound was acetylated and the product was found by nuclear magnetic resonance to contain five acetoxy groups per methoxy group. IV, 15.4 mg, in 50 ml of 0.02 *M* sodium metaperiodate consumed 3.28 moles of periodate per mole and liberated 2.2 moles of formic acid and 1.1 moles of formaldehyde per mole (28). A portion of the oxidized material was analyzed by paper chromatography and a canary yellow spot was revealed by the aniline phthalate reagent (29) with the $R_f = 0.78$ of 2-*O*-methyl glyceraldehyde (18). It was therefore concluded that IV was a 2-*O*-methyl hexitol. The parent compound 2-*O*-methyl-D-glucose was characterized as described further on.

Characterization of compound VII.—The major component, VII, R_f 0.65, obtained from the cellulose column chromatogram was acetylated. The NMR spectrum in chloroform showed the presence of three chemically shifted *O*-acetyl groups and one *O*-methyl group. Qualitative tests revealed the presence of bromine. Hydrogenolysis of VII, 320 mg, over 5% palladium on charcoal in 50 ml of 50% aqueous methanol containing 0.2 ml of triethylamine, afforded 110 mg of a substance with $[\alpha]_D = 146°$ (*c*, 1.2 in methanol), which on paper chromatography gave the color reaction with the *p*-anisidine hydrochloride spray reagent (30) found characteristic for methyl 2-deoxyhexosides. The latter, VIII, was neither methyl 2-deoxy-α- or -β-D-glucopyranoside as shown by comparison of their NMR spectra measured in deuterium oxide. The specific rotation of methyl 2-deoxy-α-D-allopyranoside is reported to be 144° (21). Hydrolysis of VII with cold normal sulphuric acid was complete after 4 hours (constant optical rotation). Neutralization of the acid with basic Amberlite IRA-400 followed by filtration and evaporation *in vacuo* gave a syrup which crystallized from ethanol. The melting point after four recrystallizations from ethanol was 135–6°, $[\alpha]_D$ 55.2° (*c*, 1 in water), and was not depressed when admixed with an authentic sample of 2-deoxy-D-allose kindly provided by Professor J. K. N. Jones. The reported constants are m.p. 133–5° and $[\alpha]_D$ 57.9±2 (22).

Treatment of VII, 150 mg, with 5 ml of 0.75 *N* sodium methoxide in methanol for 19 hours followed by neutralization of the base with sulphonic acid resin in the acid form, filtration, evaporation, and fractionation of the resulting mixture, 99 mg, on Whatman 3 MM paper afforded 9 mg of a compound, $R_f = 0.84$, which had an infrared spectrum identical with that for methyl 3,6-anhydro-α-D-glucopyranoside (XI) prepared from methyl 6-*O*-tosyl-α-D-glucopyranoside (31) by the method of Haworth and co-workers (23).

B. Reduction with Zinc Dust

To a well-stirred mixture of 6 ml water, 3 ml glacial acetic acid and 0.6 g zinc dust at 0°, a 5-ml portion of VI, 4.4 g, in 20 ml of glacial acetic acid was added. After 1 hour, 1.2 g zinc dust, 5 ml water, and a further 5-ml portion of the above solution were added to the reaction mixture. Addition of similar quantities of these substances was made twice during the succeeding 2 hours, after which the mixture was allowed to stand, with stirring, at room temperature for an additional 15 hours. Excess zinc dust and precipitated salts were removed by filtration and the filtrate was exhaustively extracted with chloroform. The chloroform phase, after being washed to neutrality with water, was dried and evaporated *in vacuo* to yield 2.71 g of a syrupy halogen-free product which, according to its infrared spectrum, did not contain an olefinic double bond but contained a ketonic carbonyl group as indicated by absorption at 1740 cm^{-1}. The product was readily deacetylated on standing for 2 hours in a mixture of methanol, water, and triethylamine (50:45:5). Paper chromatography of the deacetylated material showed a very intense spot (30) with $R_f = 0.57$. Sodium borohydride reduction of the deacetylated material, and isolation as described above, led to a product which, on paper chromatograms, had color reactions characteristic of a methyl 2-deoxyhexoside.

The material from the zinc dust reduction, 1.30 g, was dissolved in 5 ml of ethanol and water was added until a turbid solution resulted. Semicarbazide hydrochloride, 0.75 g, and 1.19 g anhydrous sodium acetate were then added. After the mixture had been allowed to stand at room temperature for 30 minutes crystals were deposited and after it was cooled at 0° for a further 2 hours, 0.40 g of crystalline material was isolated. After four recrystallizations from ethanol, the material had a melting point of 195–196°, $[\alpha]_D = +146°$ (*c*, 0.75 in pyridine). Calc. for $C_{12}H_{19}N_3O_7$: C, 45.43; H, 5.99; N, 13.25%. Found: C, 45.67; H, 5.88; N, 13.08%.

Identification of 2-O-Methyl-D-glucose

The product, 0.5 g, of the brominolysis reaction was treated with 5 ml of 0.05 *N* sodium methoxide in dry methanol for 30 minutes. The solution was then neutralized with sulphonic acid resin in the acid form, filtered, and evaporated to dryness *in vacuo*. The resulting syrup, 110 mg, was treated with a mixture of 0.5 ml ethanethiol and 0.5 ml concentrated hydrochloric acid at room temperature. After 15 hours, 5 ml

Can. J. Chem. Downloaded from www.nrcresearchpress.com by 210.87.254.6 on 09/05/12
For personal use only.

water was added to the cooled solution and the excess ethanethiol was removed. The solution was neutralized with basic ion exchange resin (Amberlite IRA-400). After filtration and evaporation the product was dissolved in ethyl ether to deposit 13.2 mg of material which after four recrystallizations from ethanol had a melting point of 157–158° and a specific rotation of −22.4° (*c*, 0.52 in pyridine). An authentic specimen of V was prepared from D-glucose diethyl dithioacetal by the method of Lieser and Leckzyck (19). The two compounds had identical melting points (which were undepressed on admixture), infrared spectra, and NMR spectra.

Brominolysis of Cyclohexyl Iodide

Cyclohexyl iodide, 3.20 g (15 mmoles), was treated with 100 ml of a 10% w/v solution of potassium acetate in acetic acid containing 33 g (200 mmoles) of bromine. After 7 hours, 100 ml of 25% aqueous sodium acetate was added and the excess bromine was reduced by the addition of formic acid. The mixture was extracted with chloroform and the chloroform solution was thoroughly neutralized by washing with aqueous sodium bicarbonate. The dried chloroform solution was evaporated to an oily residue. The material was subjected to gas–liquid partition chromatography on a silicone oil – Celite column using a temperature program over the range 50° to 225°. Four components were detected comprising 4.3, 6.7, 34.4, and 54.6% of the material which passed through the column. These components were identified by direct comparison of their retention times with those of authentic samples and found to be cyclohexyl bromide, cyclohexyl acetate, *trans*-cyclohexane dibromide, and *trans*-2-bromocyclohexyl acetate, respectively.

Brominolysis of Methyl 6-Deoxy-6-iodo-α-D-glucopyranoside Triacetate (XIV)

The reaction was performed under conditions essentially identical with those described above for the 2-iodomannoside. A solution of the product in ethanol readily deposited a crystalline compound (XV), m.p. 109–111°, $[\alpha]_D = +144.1°$ (*c*, 1 in pyridine). Although these constants are not exactly those reported (32) for methyl 6-bromo-6-deoxy-tri-*O*-acetyl-α-D-glucopyranoside, the NMR spectrum could leave no doubt about this identity. The major difference between its spectrum at 60 Mc.p.s. and that for methyl tetra-*O*-acetyl-α-D-glucopyranoside (XVI) was the chemical shift for the methylenic 6-hydrogens from 4.15 p.p.m. for the 6-acetate to 3.4 p.p.m. for the 6-bromide. In the case of the 6-iodide (XIV), the starting material, this signal appeared at 3.28 p.p.m. Furthermore, on hydrogenolysis of XV with palladium as catalyst, followed by deacetylation, a substance with the same R_f value as methyl 6-deoxy-α-D-glucopyranoside was obtained. The other product formed in the brominolysis was readily isolated by fractional crystallization and found by direct comparison to be methyl tetra-*O*-acetyl-α-D-glucopyranoside (XVI). The signals for the methoxyl groups in compounds XIV, XV, and XVI occurred at 3.5, 3.48, and 3.42 p.p.m. and were well resolved by the spectrometer operating at 100 Mc.p.s. The relative intensities of these signals in the spectrum of the above described reaction product showed the absence of starting material and the ratio of XV to XVI to be 0.82:1.

In another experiment, compound XIV, 215 mg (0.5 mmole), was reacted in the dark with 2.6 mmoles of bromine in 18.5 ml of 10% potassium acetate in acetic acid. Reaction was complete after 7 hours. The product, 163 mg, isolated in the usual manner, was found by nuclear magnetic resonance to comprise a mixture of XV and XVI in the ratio 1.1:1.0. When the reaction was performed at higher dilution using 185 ml of the 10% potassium acetate in acetic acid, the reaction was only 47% complete after 7 hours and the ratio of XV to XVI was 0.4 to 1. After 43 hours, the reaction was complete and the ratio of XV to XVI in the product was 0.6:1.

In an experiment identical with that described immediately above at high dilution except that 5 mmoles of silver acetate was added, the reaction was complete within 3 hours and the product was pure XVI.

ACKNOWLEDGMENTS

The 60 Mc.p.s. NMR and infrared spectra were determined by R. N. Swindlehurst and Mrs. G. B. Conway. The 100 Mc.p.s. NMR spectra were obtained by G. B. Bigam of this department. The research was supported by two National Research Council of Canada Studentships to B.F-R. and National Research Council of Canada grants-in-aid of research (T-172) to R.U.L.

REFERENCES

1. A. GEUTHER. Ann. **123**, 124 (1862).
2. C. FRIEDEL. Ann. **135**, 203 (1865).
3. R. M. KEEFER and L. J. ANDREWS. J. Am. Chem. Soc. **75**, 543 (1953).
4. F. VIEBOCK and A. SCHWAPPACH. Ber. **63**, 2818 (1930).
5. S. ZIESEL. Monatsh Chem. **6**, 989 (1885).
6. J. B. NIEDERL and V. NIEDERL. Micromethods of quantitative organic elementary analysis. John Wiley and Sons, Inc., New York. 1938. p. 192.
7. S. J. CLARK. Quantitative methods of organic microanalysis. Butterworths Scientific Publications. 1956. p. 161.

Can. J. Chem. Downloaded from www.nrcresearchpress.com by 210.87.254.6 on 09/05/12
For personal use only.

8. A. STEYERMARK. Quantitative organic microanalysis. 2nd ed. Academic Press, New York. 1961. p. 423.
9. C. WILLGERODT. Ber. **25**, 3494 (1892).
10. R. B. SANDIN. Chem. Rev. **32**, 249 (1943).
11. J. THIELE and H. HAAKH. Ann. **369**, 131 (1909).
12. E. J. COREY and W. J. WECHTER. J. Am. Chem. Soc. **76**, 6040 (1954).
13. R. M. KEEFER and L. J. ANDREWS. J. Am. Chem. Soc. **76**, 253 (1954).
14. R. M. KEEFER and L. J. ANDREWS. J. Am. Chem. Soc. **74**, 1891 (1952).
15. F. M. BERINGER and H. S. SCHULTZ. J. Am. Chem. Soc. **77**, 5533 (1955).
16. R. U. LEMIEUX and S. LEVINE. Can. J. Chem. To be published.
17. B. WICKBERG. Acta Chem. Scand. **12**, 615 (1958).
18. R. U. LEMIEUX and H. F. BAUER. Can. J. Chem. **31**, 814 (1953).
19. T. LIESER and E. LECKZYCK. Ann. **511**, 137 (1934).
20. S. WINSTEIN and L. L. INGRAHAM. J. Am. Chem. Soc. **74**, 1160 (1952).
21. G. N. RICHARDS and L. F. WIGGINS. J. Chem. Soc. 2442 (1953).
22. M. GUT and D. A. PRINS. Helv. Chim. Acta. **30**, 1223 (1947).
23. W. N. HAWORTH, L. N. OWEN, and F. SMITH. J. Chem. Soc. 88 (1941).
24. M. ZIEF and R. C. HOCKETT. J. Am. Chem. Soc. **67**, 1267 (1945).
25. E. L. HIRST and J. K. N. JONES. Disc. Faraday Soc. No. 7, 271 (1949).
26. W. E. TREVELYAN, D. P. PROCTOR, and J. S. HARRISON. Nature, **165**, 444 (1950).
27. R. U. LEMIEUX and H. F. BAUER. Anal. Chem. **26**, 920 (1954).
28. B. FRASER-REID, J. K. N. JONES, and M. B. PERRY. Can. J. Chem. **39**, 555 (1961).
29. S. M. PARTRIDGE. Nature, **164**, 443 (1949).
30. L. HOUGH, J. K. N. JONES, and W. H. WADMAN. J. Chem. Soc. 1702 (1950).
31. A. B. FOSTER, W. G. OVEREND, and M. STACEY. J. Chem. Soc. 3367 (1954).
32. B. HELFERICH and A. SCHNEIDMÜLLER. Ber. **60**, 2002 (1927).

Can. J. Chem. Downloaded from www.nrcresearchpress.com by 210.87.254.6 on 09/05/12
For personal use only.

Can. J. Chem. Downloaded from www.nrcresearchpress.com by 210.87.254.40 on 09/05/12
For personal use only.

THE BROMINOLYSIS OF CARBOHYDRATE IODIDES

II. A SYNTHETIC ROUTE TO 2,5-ANHYDROSUGARS[1]

R. U. LEMIEUX AND B. FRASER-REID
Department of Chemistry, University of Alberta, Edmonton, Alberta

Received September 19, 1963

ABSTRACT

Reaction of methyl 2-deoxy-2-iodo-β-D-glucopyranoside triacetate with a 20-fold excess of bromine and a 10-fold excess of silver acetate in a 10% solution of potassium acetate in acetic acid gave a near-quantitative yield of an equimolar mixture of the anomeric forms of 1,3,4,6-tetra-*O*-acetyl-2,5-anhydro-1-methoxy-D-mannose. Treatment of the mixture with methanolic hydrogen chloride gave the dimethylacetal of 2,5-anhydro-D-mannose (chitose).

In the first paper in this series (1), the halogenolysis of alkyl iodides was reviewed and the products formed on the brominolysis in the presence of silver acetate of methyl 6-deoxy-6-iodo-α-D-glucopyranoside triacetate and methyl 2-deoxy-2-iodo-α-D-mannopyranoside triacetate were described. This communication reports the formation of 1,3,4,6-tetra-*O*-acetyl-2,5-anhydro-1-methoxy-D-mannose on the brominolysis of methyl 2-deoxy-2-iodo-β-D-glucopyranoside triacetate (I).

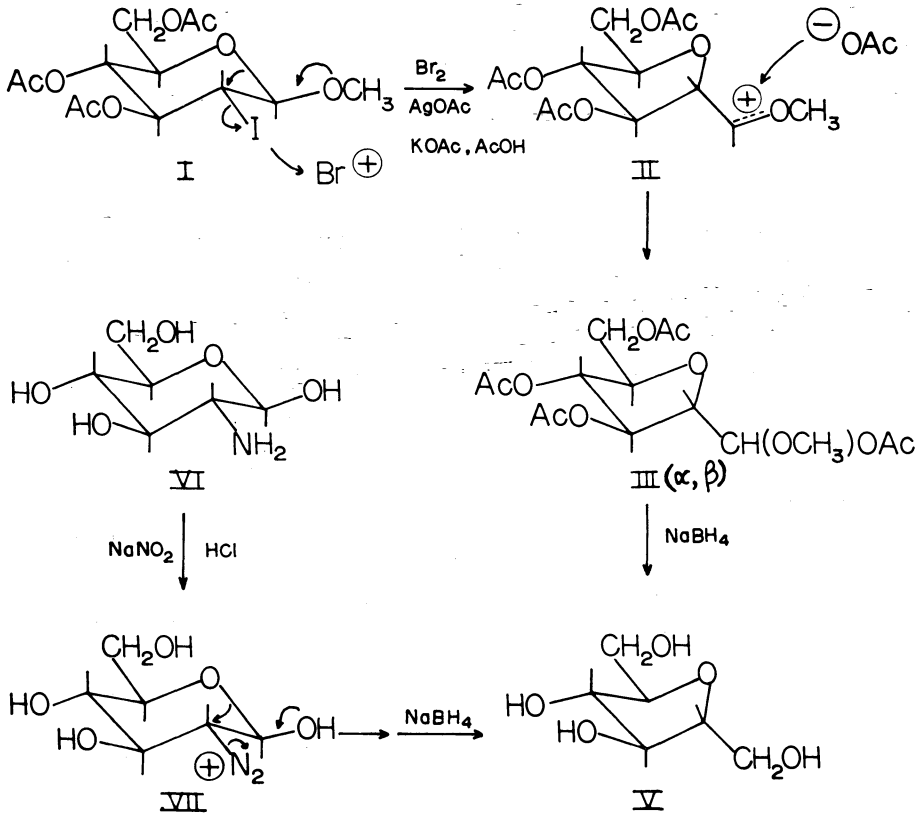

[1]*This research is to constitute a portion of a thesis to be submitted by B.F.-R. in partial fulfillment of the requirements for the degree of Doctor of Philosophy.*

Can. J. Chem. Downloaded from www.nrcresearchpress.com by 210.87.254.40 on 09/05/12
For personal use only.

Brominolysis of I in 10% potassium acetate in acetic acid containing silver acetate led to the formation in quantitative yield of an about equimolar mixture of two compounds. The compounds were separated by column partition chromatography using dimethyl sulphoxide on silicic acid as static phase (2). Nuclear magnetic resonance (NMR) spectroscopy clearly required the compounds to be diastereoisomers differing only in configuration at the anomeric center. The more dextrorotatory compound (IIIα) was assigned the α-configuration and the other (IIIβ) the β-configuration following the original basis for naming anomeric compounds derived from D-sugars (3). Except for the spacings of doublets arising from the anomeric hydrogen, the NMR spectra of the two compounds were virtually identical and required the presence of four acetyl groups per methoxyl group. For IIIα, the doublet was at 5.90 p.p.m. with a spacing of 5.0 c.p.s. In the case of IIIβ, the doublet was at 5.91 p.p.m. with a spacing of 5.8 c.p.s. Since both IIIα and IIIβ underwent profound and rapid degradation on attempted deacetylation with base, the compounds were deacetylated under reductive conditions using sodium borohydride. Although several compounds were formed, the main product of the reaction was a substance identified as 2,5-anhydro-D-mannitol (V) by direct comparison with a sample prepared by borohydride reduction of 2,5-anhydro-D-mannose obtained by nitrous acid deamination of D-glucosamine (VI) (4, 5). It was therefore clear that the brominolysis of I proceeded with participation of the ring-oxygen as is established for the deamination of D-glucosamine (6). The fact that about equimolar amounts of IIIα and IIIβ were formed indicates that the oxocarbonium ion II was a discrete reaction intermediate. This course of reaction further illustrates that the brominolyses of iodides proceed by way of highly reactive intermediates (1) which possess properties very similar to the diazonium salts (VII) formed as intermediates in the nitrous acid deaminations of primary amines (7).

The great ease for the formation of hydroxymethylfurfuraldehyde and related compounds on treatment of 2,5-anhydro-D-mannose with bases or aqueous acid is well known (8–10). It is of interest in this regard that treatment of the mixture of IIIα and IIIβ with methanolic hydrogen chloride readily gave the dimethyl acetal (IV). This type of compound is stable to bases and may prove useful as intermediates in the preparation of 2,5-anhydrosugars (11–13).

EXPERIMENTAL

The melting points, nuclear magnetic resonance spectra, and paper chromatograms were established as described in the previous paper of this series (1). The methyl 2-deoxy-2-iodo-β-D-glucopyranoside triacetate (I) was prepared by iodomethoxylation of D-glucal triacetate (14).

1,3,4,6-Tetra-O-acetyl-2,5-anhydro-1-methoxy-α- and -β-D-mannose (IIIα and IIIβ)

Methyl 2-deoxy-2-iodo-β-D-glucopyranoside triacetate (I), m.p. 94–95° (14), 3.24 g (7.5 mmoles), was dissolved in 150 ml of a 10% solution of potassium acetate in acetic acid which contained 24.0 g (150 mmoles) of bromine. In separate experiments, titration for iodate in the reaction mixture showed that the brominolysis of the iodine was extremely slow (10% reaction in 1 week). However, on the addition of 12.5 g (75 mmoles) of silver acetate, reaction in the dark as shown by the appearance of iodate was complete in 6 hours at room temperature. After a 7-hour reaction time, 150 ml of a 25% aqueous solution of sodium acetate was added and the bromine was reduced by the addition of formic acid. The product was isolated by filtration to remove precipitated solids followed by extraction with chloroform and evaporation in the usual manner (1). The dried colorless syrupy product, 2.48 g, was found by chromatography on dimethyl sulphoxide impregnated paper (15), using Skellysolve B as the developing phase, to contain two components. This composition was substantiated by a comparison of the NMR spectrum of the mixture with those of the two components obtained by preparative chromatography on a column of silicic acid impregnated with dimethyl sulphoxide (2) using a 15% mixture of diisopropyl ether in Skellysolve B as developing phase. The mixture, 853 mg, was added to 2.5 cm × 27.5 cm column and the first pure component (IIIβ), 261 mg, $[\alpha]_D$ +46.3° (*c*, 2.26 in chloroform) was isolated in the 1500 to 1600 ml fraction of eluate. The next 75 ml provided 350 mg of a mixture of the two components. Compound (IIIα), 161 mg, $[\alpha]_D$ +49.4° (*c*, 2.7 in chloroform) was obtained in the following 80 ml of eluate. Both the pure compounds gave NMR spectra with sharp signals for four

acetoxy groups and one methoxy group at 2.12 and 3.51 p.p.m., respectively. The spectra were almost identical in the range 4.0 to 5.7 p.p.m. and could readily be assigned to the presence in both compounds of two methylenic hydrogens of an acetoxymethyl group (4.26 p.p.m.), two hydrogens on secondary carbons bonded to ring-oxygen (4.0–4.4 p.p.m.) and two hydrogens bonded to secondary carbons each substituted by acetoxy groups (5.37 and 5.14 p.p.m.). In addition, both compounds gave a doublet of intensity 1 at low field. For compound IIIβ, the doublet was at 5.91 p.p.m. and had a spacing of 5.8 c.p.s. In the other compound (IIIα) the doublet center was at 5.90 p.p.m. and the spacing was 5.0 c.p.s. The relative intensities of these doublets in the spectrum of the mixture required IIIβ and IIIα to be present in about equal amounts.

2,5-Anhydro-D-mannose Dimethyl Acetal (IV)

On reacting the mixture of IIIα and IIIβ (0.410 g) formed in the brominolysis reaction with 15 ml of 2% methanolic hydrogen chloride for 7 hours, followed by isolation in the usual manner, the material was converted to a single substance, $R_f = 0.67$, which produced a strong color reaction with *p*-anisidine hydrochloride on paper chromatograms. The compound rapidly consumed 1 mole of periodate per mole in agreement with the assumption that the substance is the dimethylacetal (IV) of 2,5-anhydro-D-mannose (chitose). The compound was acetylated with acetic anhydride in pyridine and the product, $[\alpha]_D$ +41.7° (*c*, 1.39 in chloroform), produced signals in its NMR spectrum for acetoxy- and methoxy-group hydrogens of intensities in the ratio 3:2. A sharp doublet of intensity 1 was present at 3.54 p.p.m. with a spacing of 5.5 c.p.s.

2,5-Anhydro-D-Mannitol (V)

A. From D-glucosamine.—A sample of D-chitose was prepared according to the directions prescribed by Bera, Foster, and Stacey (5) starting from D-glucosamine hydrochloride. Reduction of the product with sodium borohydride as described below for the alternate preparation led to the isolation of a substance which on analysis by paper chromatography showed the presence of at least six components using the periodate–permanganate spray reagent. The main component, $R_f = 0.66$, was isolated by chromatography on a cellulose column using *n*-butanol as developing phase. The substance was acetylated using pyridine and acetic anhydride and isolated in the usual manner. The clear syrupy product was dissolved in chloroform and the solution was passed through a short column of silicic acid and the column was washed with chloroform. The chloroform was removed *in vacuo* to leave a syrup, $[\alpha]_D$ +27.3° (*c*, 4.2 in chloroform). The NMR spectrum showed three sharp signals at 4.83 (3- and 4-hydrogens), 5.75, and 1.88 (acetyl hydrogens) p.p.m. of relative intensities 2:6:12 as expected for tetra-*O*-acetyl-2,5-anhydro-D-mannitol should the signals for the six hydrogens at the 1-, 2-, 5-, and 6-positions show no chemical shift and occur at 5.75 p.p.m.

B. From the mixture of IIIα and IIIβ.—The mixture of IIIα and IIIβ from the brominolysis reaction, 4.10 g, was treated with an excess of sodium borohydride, 10 g, in aqueous methanol at room temperature for 7 hours. An excess of acetic acid was then added and the solution was reduced to dryness. Methanol was distilled several times from the residue to remove the boric acid. The product was dissolved in water and the sodium ion was removed by sulphonic acid resin in the acid form. Paper chromatographic examination of the residue obtained on evaporation *in vacuo* showed the presence of at least six components with the main zone at $R_f = 0.66$. The R_f values and relative intensities of the zones were the same as those observed above on chromatography of the product from the borohydride reduction of D-chitose. The main component was isolated on a cellulose column and acetylated and purified as described above. The product $[\alpha]_D$ +26.4° (*c*, 3.9 in chloroform) had the same NMR and infrared spectra as the above described tetra-*O*-acetyl-2,5-anhydro-D-mannitol.

ACKNOWLEDGMENTS

The 60 Mc.p.s. NMR and infrared spectra were determined by R. N. Swindlehurst and Mrs. G. B. Conway. The research was supported by two National Research Council of Canada Studentships to B. F-R. and National Research Council of Canada grants-in-aid of research (T-172) to R. U. L.

REFERENCES

1. R. U. Lemieux and B. Fraser-Reid. Can. J. Chem. This issue.
2. B. Lindberg and B. Wickberg. Arkiv. Kemi. **13**, 447 (1959).
3. C. S. Hudson. Advan. Carbohydrate Chem. **3**, 1 (1948).
4. P. A. Levene and F. B. La Forge. J. Biol. Chem. **21**, 351 (1915).
5. B. C. Bera, A. B. Foster, and M. Stacey. J. Chem. Soc. 4531 (1956).
6. S. Peat. Advan. Carbohydrate Chem. **2**, 37 (1946).
7. J. H. Ridd. Quarterly Rev. **15**, 418 (1961).
8. W. A. von Ekenstein and J. J. Blanksma. Ber. **43**, 2355 (1910).
9. W. N. Haworth and W. G. M. Jones. J. Chem. Soc. 667 (1949).
10. C. A. Decker and T. Hashizume. Arch. Biochem. Biophys. **78**. 348 (1958).
11. P. Slonimski, J. Defaye, J. Asselineau, and E. Lederer. Compt. Rend. **249**, 192 (1959).
12. W. N. Haworth, L. N. Owen, and F. Smith. J. Chem. Soc. 88 (1941).
13. C. Araki. J. Chem. Soc. Japan, **65**, 725 (1944).
14. R. U. Lemieux and B. Fraser-Reid. Can. J. Chem. This issue.
15. B. Wickberg. Acta Chem. Scand. **12**, 615 (1958).

Can. J. Chem. Downloaded from www.nrcresearchpress.com by 210.87.254.40 on 09/05/12
For personal use only.

KINETICS OF ETARD'S REACTION

PART III. EFFECT OF RING SUBSTITUTION

R. A. STAIRS

Department of Chemistry, Queen's University, Kingston, Ontario

Received September 27, 1963

ABSTRACT

The initial rates of reaction of a number of para- and meta-substituted toluenes with chromyl chloride in carbon tetrachloride solution have been measured and the results analyzed using Hammett's relation. The results are interpreted in terms of electrophilic attack by CrO_2Cl_2 molecules. The reaction appears to be marked by an unusually large effect of ring substitution on the entropy of activation. The mechanistic significance of this observation is discussed.

INTRODUCTION

Earlier papers in this series report the effects on the rate of reaction with CrO_2Cl_2 of varying number of phenyl substituents in methane (1), and of change of solvent (2). We have now measured the initial rates of the reaction of chromyl chloride with toluenes having para and meta methyl, fluoro, chloro, bromo, and nitro substituents at three temperatures.

EXPERIMENTAL

The method of measurement was by titration for Cr VI as previously described (1). The carbon tetrachloride solvent was Fisher Certified Reagent, used as purchased in small bottles. A portion was purified by treatment first with concentrated sulphuric acid and then with water, followed by drying over $CaCl_2$ and distillation through a short column, without perceptible improvement. The toluene and the substituted toluenes were Eastman or Fisher reagent grades, and were fractionally distilled before use, with the exception of *p*-nitrotoluene, which was recrystallized from ethanol.

All the experiments were carried out in subdued light, as it was found that the laboratory fluorescent lights had an easily noticeable effect on the rates, particularly of the slower reactions. Each reaction was carried out at a number of different initial concentrations of both reactants, and second-order rate constants were calculated from the initial rates. The constants were examined for trends that might suggest that any of the reactions were other than first order in each of the reactants. No such trends were found.

RESULTS

The rate constants recorded in Table I are averages of at least six runs each. In the

TABLE I

Summary of kinetic data

		k_t l. mole^{-1} sec^{-1}*		
Substituent	σ	at t = 1° C	25° C	40° C
p-Me	−0.18	1.23×10^{-4}	5.24×10^{-4}	1.51×10^{-3}
m-Me	−0.09	5.10×10^{-5}	4.28×10^{-4}	
H	0.00	1.04×10^{-5}	1.60×10^{-4}	3.93×10^{-4}
p-F	0.06	7.4×10^{-6}	9.70×10^{-5}	3.00×10^{-4}
p-Cl	0.23		6.45×10^{-5}	2.11×10^{-4}
p-Br	0.23		4.42×10^{-5}	2.05×10^{-4}
m-F	0.35		2.33×10^{-5}	
m-Br	0.38			6.68×10^{-5}
m-Cl	0.39		1.76×10^{-5}	
p-NO_2	0.78			2.23×10^{-5}

*Overall uncertainty in k is about 12%.

Can. J. Chem. Downloaded from www.nrcresearchpress.com by 210.87.254.105 on 09/05/12
For personal use only.

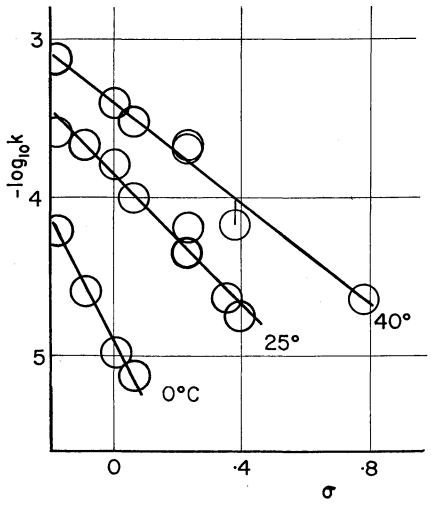

FIG. 1. Hammett plot for Etard's reaction. The common logarithm of the rate constant for each substituted toluene is plotted against the Hammett sigma for the substituent, at the three indicated temperatures. The constants for the two xylenes have been divided by two to allow for the fact that either methyl group may be attacked.

table are also noted the Hammett sigma values for each substituent (3). Figure 1 shows the same data, plotted as the common logarithm of the rate constant versus the corresponding values of σ, at three temperatures. The lines were fitted by the method of least squares, and the following constants were obtained:

(*a*) Hammett's ρ, -3.94 at 1° C, -2.06 at 25° C, -1.58 at 40° C, with overall standard deviation 0.15.

(*b*) Assuming that the enthalpy and entropy of activation are both independent of temperature, and writing H^σ for $d(\Delta H^\ddagger)/d\sigma$, etc., $H^\sigma = 25 \pm 1$ kcal; $S^\sigma = 72 \pm 10$ cal/deg; $F^\sigma{}_{298} = 2.81 \pm 0.20$ kcal. From the data of ref. (1) one may calculate for toluene $\Delta H^\ddagger = 14.3$ kcal; $\Delta S^\ddagger = -28$ cal/deg; $\Delta F^\ddagger{}_{298} = 22.6$ kcal.

The present data were also examined by the method of Bekkum, Verkade, and Wepster (4) as outlined by Wells (5) to determine whether direct resonance effects were present. There appeared to be no such effects, and $\Delta\Delta F_p$ values were zero within experimental error.

DISCUSSION

Leffler has pointed out (6) the dangers in interpreting Hammett ρ values obtained at a single temperature as criteria of mechanism. In the present case, it appears by extrapolation that ρ would change sign in the vicinity of 70° C, this being the approximate isokinetic temperature of this reaction series. The effect of substitution on the enthalpy of activation, represented here by $H^\sigma = 25$ kcal, however, is a clear indication of a substantial electron demand at the reaction site. This is clearly compatible with the known electrophilic nature of CrO_2Cl_2, and a fortiori of species such as CrO_2Cl^+ that have been invoked in proposed mechanisms (7, 8). The positive sign of the quantity S^σ is explained by what Brown has called the compensation law (9), i.e. the fact that a change in a reactant molecule that raises the enthalpy of activation by making the binding in the activated complex weaker would be expected to raise the entropy of activation for the same reason. Parallel changes in these two quantities have opposite effects on the rate,

Can. J. Chem. Downloaded from www.nrcresearchpress.com by 210.87.254.105 on 09/05/12
For personal use only.

and the degree of compensation depends on how close the experimental temperature is to the isokinetic temperature, which, if H^σ and S^σ are independent of temperature, is given by $\beta = H^\sigma/S^\sigma$, here about 340° K.

The rather large size of S^σ is probably explained by Wheeler's suggestion (10) that the reaction involves complex formation between CrO_2Cl_2 and the π-electrons of the ring. Electron-withdrawing substituents would reduce the strength of binding in such a complex, and if, as has been suggested earlier (1), this involvement of the ring persists in the activated complex there would be an additional positive contribution to S^σ.

Our earlier conclusion (2) that the formation of the activated complex does not involve a large change in polarity appears at first sight to be at variance with the foregoing discussion. However, it should be noted that the dipole moment of toluene presumably is in such a direction as to make the methyl group relatively positive. During the approach of the electrophilic attacking species, presumably CrO_2Cl_2, to the methyl group, this polarity will be reversed so that a fairly large movement of electrons can take place with only a moderate increase in dipole moment.

It is therefore proposed that the probable mode of reaction of chromyl chloride with toluene is as follows:
(The arrows and numbers in parentheses represent the dipole moments.)

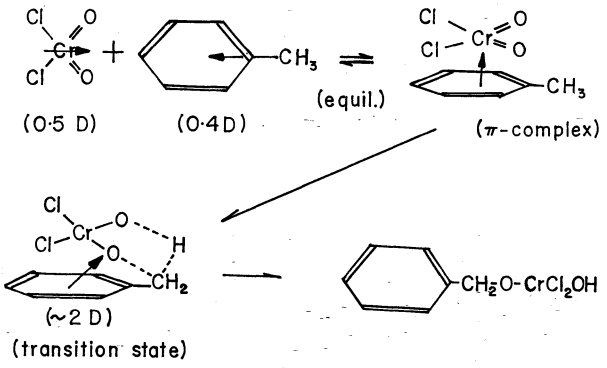

The above scheme accounts for only one of the two molecules of chromyl chloride involved in the stoichiometric reaction. It has usually been assumed (7) that the second molecule reacts with another hydrogen of the methyl group in a similar manner in a subsequent step. A recent paper from Nenitzescu's laboratory (11) reports that the two chromium atoms are not both reduced, one being still in oxidation state VI (a conclusion based on measurements of electron spin resonance absorption intensity), and suggests that the second step of the oxidation does not take place until the hydrolysis. The second molecule of chromyl chloride, it is suggested, is bound to the first in an unknown manner, perhaps as in the dichromate ion (though this requires the unusual coordination number of five for Cr VI). This disagrees with Wheeler's magnetic susceptibility measurement (10), which indicated that all the chromium was quadrivalent. However, both magnetic susceptibility, when not measured over a range of temperature and of field strength, and e.s.r. intensity are difficult to interpret, so this point must still be considered open to discussion. Since the reaction is first order in CrO_2Cl_2 (1), it is improbable that both molecules of chromyl chloride are involved in the transition state.

Can. J. Chem. Downloaded from www.nrcresearchpress.com by 210.87.254.105 on 09/05/12
For personal use only.

ACKNOWLEDGMENTS

The author wishes to acknowledge the assistance of Mr. D. Brock in making the measurements, a Summer Research Associateship from Queen's University, a grant from the National Research Council, and helpful discussions with Dr. E. Buncel. He is also grateful to the referee for pointing out the necessity of dividing the rate constants for the two xylenes by the statistical factor of two.

REFERENCES

1. R. A. STAIRS and J. W. BURNS. Can. J. Chem. **39**, 960 (1961).
2. R. A. STAIRS. Can. J. Chem. **40**, 1656 (1962).
3. L. P. HAMMETT. Physical organic chemistry. McGraw-Hill Book Co. Inc., New York. 1940.
4. H. VAN BEKKUM, P. E. V. VERKADE, and B. M. WEPSTER. Rec. Trav. Chim. **78**, 815 (1959).
5. P. R. WELLS. Chem. Rev. **63**, 171 (1963).
6. J. E. LEFFLER. J. Org. Chem. **20**, 1202 (1955).
7. W. H. HARTFORD and M. DARRIN. Chem. Rev. **58**, 1 (1958).
8. S. J. CRISTOL and K. R. EILAR. J. Am. Chem. Soc. **72**, 4353 (1950).
9. R. F. BROWN. J. Org. Chem. **27**, 3015 (1962).
10. O. H. WHEELER. Can. J. Chem. **38**, 2137 (1960).
11. I. NECSOIU, A. T. BALABAN, I. PASCARU, E. SLIAM, M. ELIAN, and C. D. NENITZESCU. Tetrahedron, **19**, 1133 (1963).

Can. J. Chem. Downloaded from www.nrcresearchpress.com by 210.87.254.105 on 09/05/12
For personal use only.

Can. J. Chem. Downloaded from www.nrcresearchpress.com by 210.87.254.42 on 09/05/12
For personal use only.

OXIDATION–REDUCTION POLYMERS

III. STANDARD OXIDATION POTENTIALS OF 2,5-DIHYDROXYDIPHENYL SULPHONES[1]

I. H. SPINNER, H. P. KASSERRA,[2] AND W. METANOMSKI
Department of Chemical Engineering and Applied Chemistry, University of Toronto, Toronto, Ontario
Received October 8, 1963

ABSTRACT

The preparation of two new sulphonyl derivatives of methoxy- and naphtha-hydroquinone as possible intermediate compounds in the synthesis of redox monomers is described. The standard oxidation potentials of these and other sulphonyl derivatives of hydroquinones were determined and compared with the values for similar compounds, reported previously (1).

In Part II (1) we have described the preparation of redox polymers containing repeating hydroquinone units joined through a sulphone bridge to a polystyrene chain.

Although 2,5-dihydroxydiphenyl sulphones were first synthesized by Hinsberg (2, 3) in 1894–1895, and in some cases their oxidized forms prepared, no systematic study of redox potentials of these and similar derivatives of hydro- and naphthahydro-quinones has been made. The sulphones whose redox potentials have been reported are *p*-toluene-sulphonyl, *p*-bromobenzenesulphonyl, and *d*-camphor-10-sulphonyl derivatives of 1,4-naphthahydroquinone (4, 5) and the *d*-camphor-10-sulphonyl derivative of 2,5-dimethyl-hydroquinone (4). The redox potentials of these compounds are 121, 125, 114, and 135 mv, respectively, higher than the potentials of the corresponding parent quinones.

Data previously obtained from potentiometric titrations (1) on intermediate and model compounds of redox polymers of the sulphone type showed the effect of various substituent

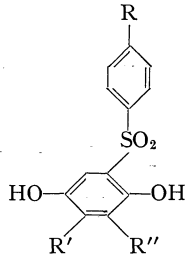

	R	R′	R″
I =	CH_2CH_2Br	OCH_3	H
III =	H	H	H
IV =	CH_3	H	H
V =	CH_2CH_2Br	H	CH_3

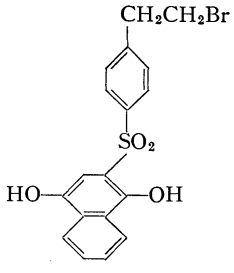

(II)

[1]*Taken in part from the thesis submitted by H. P. Kasserra to the School of Graduate Studies, University of Toronto, Toronto, in partial fulfillment of the requirements for the degree of Master of Applied Science in April, 1963.*

[2]*Present address: Du Pont of Canada Limited, Maitland, Ontario.*

groups on the standard oxidation potential (E_0) of the parent compound. The relative stability and reversibility of the compounds studied was also evaluated.

In our efforts to produce monomers and polymers of increased stability, two new sulphones derived from methoxy-*p*-benzoquinone and 1,4-naphthaquinone were synthesized. It was intended to have a $-CH_2CH_2Br$ side chain on the non-oxidizable benzene nucleus, which could be dehydrobrominated to a vinyl group (1, 6).

The addition of *p*-(β-bromoethyl)benzenesulphinic acid to methoxy-*p*-benzoquinone produced 2,5-dihydroxy-4-methoxy-4′-(β-bromoethyl)diphenyl sulphone (I). This compound was characterized by the preparation of diacetate and dibenzoate derivatives. Contrary to experience with toluquinone (1), only one isomer in a relatively high yield was isolated. Since in methoxy-*p*-benzoquinone the para position to the methoxy group is most reactive, the sulphinate ion would most probably react with quinone at this position. Therefore, the structure I has been assigned to the compound. Attempts to protect both hydroxyl groups by pyranylation, as in the schemes reported previously (1, 6), were not successful.

A second new sulphone, 2-[*p*-(β-bromoethyl)benzenesulphonyl]-1,4-naphthahydroquinone (II), was obtained through 1,4-addition of *p*-(β-bromoethyl)benzenesulphinic acid to 1,4-naphthaquinone. A diacetate derivative was prepared. Attempts to pyranylate the sulphone II resulted in the formation of a monopyranylated derivative. This behavior is in agreement with previously reported results for sulphones based on toluhydroquinone (1). The hydroxyl group which is in the ortho position to the sulphonyl group is sterically hindered because of the presence of a rigid naphthalene structure and does not react with 2,3-dihydropyran.

Attempts to add the same sulphinic acid to hydroxy-*p*-benzoquinone were not successful. This is in agreement with the original observation of Hinsberg (3), who, however, did not advance any explanation. A successful 1,4-addition to a quinone is usually accomplished by adding an aqueous suspension of the acid to a solution of the quinone and stirring the mixture for several hours. The hydroxy-*p*-benzoquinone decomposes very rapidly in water and a black polymeric material is formed before any other reaction can take place.

The solubility of *p*-(β-bromoethyl)benzenesulphinic acid in water is low. On the other hand, the presence of water was found essential for 1,4-addition to occur. The reaction did not take place in benzene or absolute ethanol. Water is primarily necessary for ionizing the sulphinic acid, the dissociation constant of which will be in the range 1×10^{-2} to 2×10^{-2} (7, 8). Even in an aqueous suspension there is enough sulphinic acid dissolved and dissociated for the reaction to go virtually to completion.

Two additional derivatives of unsubstituted hydroquinone, 2,5-dihydroxydiphenyl sulphone (III) and 2,5-dihydroxy-4′-methyldiphenyl sulphone (IV), were synthesized according to methods described in the literature (2, 9). 2,5-Dihydroxy-3-methyl-4′-(β-bromoethyl)diphenyl sulphone (V) described previously (1) has also been investigated.

The dihydroxy sulphones and their parent hydroquinones were potentiometrically titrated in 50% acetic acid (pH 1.2), unbuffered 80% acetic acid (pH 0.2), and 80% acetic acid buffered with sodium acetate (pH 2.0). The standard oxidation potentials (E_0) were essentially the same under these conditions. Representative examples of continuous and discontinuous titrations are shown in Table I. The parent hydroquinones are included for control and comparison purposes. The sulphones III and IV had to be titrated discontinuously. The decomposition of the oxidized form, as indicated by the potential decay index, was relatively slow in 80% acetic acid. This is also characteristic of other sulphones based on unsubstituted hydroquinone (1). The sulphones I and V, being

Can. J. Chem. Downloaded from www.nrcresearchpress.com by 210.87.254.42 on 09/05/12
For personal use only.

Can. J. Chem. Downloaded from www.nrcresearchpress.com by 210.87.254.42 on 09/05/12
For personal use only.

TABLE I

Potentiometric titrations
(Solvent: 80% acetic acid; oxidant: bromine in 80% acetic acid; temperature: 25.0° C)

No.	Compound	Oxidant	Average pH	E_0 (v)	ΔE_0* (mv)	E_i (mv)	Potential decay (mv/min)	Method
1	Methoxyhydroquinone†	0.04464 *N* Br_2	0.236	0.5925±0.0005‡		12.8	—	Continuous
2	Sulphone I	0.04414 *N* Br_2	0.259	0.724 ±0.003	132	10.0	—	Continuous
3	1,4-Naphthahydroquinone	0.04430 *N* Br_2	0.242	0.4689±0.0008§		12.8	—	Continuous
4	Sulphone II	0.04375 *N* Br_2	0.236	0.587 ±0.003	118	9.9	—	Continuous
5	Hydroquinone	0.04017 *N* Br_2	0.172	0.6974±0.0005‖		14.7	—	Continuous
6	Sulphone III¶	0.04116 *N* Br_2	0.246	0.740 ±0.007	43	9.0	0.87	Discontinuous
7	Sulphone IV**	0.04067 *N* Br_2	0.210	0.743 ±0.008	46	9.0	0.69	Discontinuous
8	Toluhydroquinone	0.04365 *N* Br_2	0.211	0.6413±0.0005††		13.7	—	Continuous
9	Sulphone V	0.04216 *N* Br_2	0.233	0.756 ±0.004	115	11.2	—	Continuous

NOTE: *The difference between E_0 of the compound and that of the parent hydroquinone.
†Prepared by the method of Dakin (15), m.p. 88.5–89° (previously reported 82–83° (15), 88–89° (16)).
‡Literature value: 0.594 v (conditions not specified) (10).
§Literature value: 0.470 v in 0.2 *N* HCl at 25° C (11).
‖Literature value: 0.697 v in 90% acetic acid at 24° C (12), 0.696 v in 50% acetic acid at 25° C (13).
¶Prepared by the method of Hinsberg (2), m.p. 196–197°.
**Prepared by the method of Walker (9), m.p. 212–213°.
††Literature value: 0.641 v in *N* HCl at 25° C (14).

derivatives of methoxy- and methyl-hydroquinone, respectively, could be titrated continuously and their oxidized forms were relatively stable to about 85% oxidation. The oxidized sulphone II (derivative of naphthahydroquinone) was even more stable and the characteristic sharp rise in potential was observed at the equivalence point. It has been noted that all the sulphones gave generally a lower index potential (E_1) than that calculated for a theoretical bivalent oxidation.

The effect of substitution on the standard oxidation potential is also indicated in Table I. The addition of the $-SO_2C_6H_4R$ group to the quinone caused an increase in potential, as expected. Considering the originally substituted quinones (methyl-, methoxy-, and naphtha-), this increase (ΔE_0) ranged from 115 to 132 mv. This range is nearly the same as that reported (114–135 mv) for other sulphonyl-substituted naphtha- and dimethyl-hydroquinones (4, 5).

The increase in potential for the sulphone V (3-methyl isomer) is higher than that for the 4-methyl isomer (ΔE_0 = 77–88 mv), reported previously (1). This fact agrees well with the earlier observation of Conant and Fieser (14, 17), who investigated isomeric disubstituted quinones (dichloro- and dimethoxy-).

The increase in potential on the addition of the $-SO_2C_6H_4R$ group to unsubstituted *p*-benzoquinone is relatively smaller. Table II confirms the conclusion arrived at previously

TABLE II

Standard oxidation potentials of $2,5\text{-}(OH)_2C_6H_3SO_2C_6H_4R$

R (para position)	ΔE_0* (mv)	Reference
H	43	
CH_3	46	
C_2H_5	66	(1)
C_2H_4Br	52–60	(1)
iso-C_3H_7	44	(1)

*The difference between E_0 of the compound and that of hydroquinone.

(1) that the group R in the para position to the sulphonyl group on the non-oxidizable benzenoid ring does not influence the E_0 of the compound to any great extent. A slight trend towards a larger increase appears with the lengthening of the side chain (ethyl, bromoethyl), whereas for methyl and symmetrical isopropyl groups ΔE_0 has practically the same value as that for the simplest sulphone III.

In the case of naphthahydroquinone derivatives, ΔE_0 for the sulphone II (R = CH_2CH_2Br) is nearly the same as that for the sulphone having R = CH_3 (121 mv) (4, 5).

Potentiometric titrations were also carried out in 50% aqueous dioxane. Standard oxidation potentials of both parent quinones and their sulphonyl derivatives were higher by a nearly constant value (23–29 mv) than those measured in aqueous acetic acid. The interpretation of these data is difficult because of the lack of knowledge of activity coefficients and liquid junction potential in such a system. It might be noted that a similar increase in E_0 is well known for quinones in alcoholic solutions (18).

EXPERIMENTAL*

p-(β-Bromoethyl)benzenesulphinic Acid

The preparation of this compound has been reported in Part I (6). Since all attempts to provide a sample suitable for microanalysis failed, additional derivatives were prepared.

**Melting points are corrected. All alcohol solutions are reported on a percentage by volume basis. Microanalyses were done by Galbraith Laboratories, Inc., Knoxville, Tennessee, and Micro-Tech Laboratories, Skokie, Illinois.*

Can. J. Chem. Downloaded from www.nrcresearchpress.com by 210.87.254.42 on 09/05/12
For personal use only.

Ferric *p*-(β-bromoethyl)benzenesulphinate was obtained on the addition of 15% ferric chloride solution to about 1% sulphinic acid in hot water (19). The light-orange precipitate was found insoluble in organic solvents and soluble in concentrated hydrochloric acid. It decomposed in alkaline solution. Anal. Calc. for $(C_8H_8BrO_2S)_3Fe$ (800.20): Fe, 6.98. Found: Fe, 7.05%.

Another derivative, C-[*p*-(β-bromoethyl)benzenesulphonyl]formamidine, was prepared according to a method of Farrar (20). Sodium sulphinate solution was first prepared by passing a hot aqueous solution of the sulphinic acid through a bed of Dowex 50W-X8 resin, converted to sodium form and maintained at 90–95° by means of an external hot water jacket. The addition of sodium cyanate to the effluent followed by acidification with acetic acid produced a white precipitate with the simultaneous evolution of carbon dioxide. Recrystallization from a large volume of water gave the product melting at 159–159.5° with decomposition. Anal. Calc. for $C_9H_{11}BrN_2O_2S$ (291.18): C, 37.12; H, 3.81; Br, 27.45; N, 9.62; S, 11.01. Found: C, 37.52; H, 3.72; Br, 27.11; N, 9.47; S, 10.88%.

2,5-Dihydroxy-4-methoxy-4′-(β-bromoethyl)diphenyl Sulphone (I)

A solution of methoxy-*p*-benzoquinone (13.3 g, 0.0964 mole) (prepared by the method of Ioffe and Sukhina (21), m.p. 144.5–145°) in dioxane (210 ml) was added dropwise to a suspension of *p*-(β-bromoethyl)benzenesulphinic acid (24 g, 0.0964 mole) in 1800 ml of water. The addition took about 4 hours and stirring was continued for an additional hour. The mixture was kept at 0–5°. The typical yellow color of quinone disappeared and the original fluffy white sulphinic acid particles changed gradually into heavy, sandy-colored particles of sulphone. Crystallization from 30% alcohol (3:1 ethanol–methanol), in the presence of a few milliliters of 6% stannous chloride in 6 *N* HCl as a reducing agent, gave a white powder (31 g, 85.5%) melting at 166.5–167°. Anal. Calc. for $C_{15}H_{15}BrO_5S$ (387.25): C, 46.52; H, 3.90; Br, 20.64; O, 20.66; S, 8.28; OCH_3, 8.01. Found: C, 46.79; H, 3.96; Br, 20.75; O, 20.44; S, 8.15; OCH_3, 8.19%. Infrared spectrum: 1148 (s) and 1267 (s) (—SO_2—) (22), 3390 (s) (—OH) cm^{-1}.

A derivative, 2,5-diacetoxy-4-methoxy-4′-(β-bromoethyl)diphenyl sulphone, was prepared by reacting the dihydroxysulphone I with acetic anhydride and a drop of concentrated sulphuric acid as a catalyst. Crystallization from 55% ethanol gave white crystals melting at 146.5–147°. Anal. Calc. for $C_{19}H_{19}BrO_7S$ (471.32): C, 48.42; H, 4.06; Br, 16.96; S, 6.80. Found: C, 48.74; H, 3.97; Br, 17.85; S, 6.98%.

Another derivative, 2,5-benzoxy-4-methoxy-4′-(β-bromoethyl)diphenyl sulphone, was prepared by reacting the dihydroxysulphone I with benzoyl chloride in dilute sodium hydroxide solution. Crystallization from 80% ethanol gave a white powder melting at 184–184.5°. Anal. Calc. for $C_{29}H_{23}BrO_7S$ (595.45): C, 58.50; H, 4.06; Br, 13.42; S, 5.38. Found: C, 58.56; H, 4.05; Br, 13.12; S, 5.32%.

2-[p-(β-Bromoethyl)benzenesulphonyl]-1,4-naphthahydroquinone (II)

A solution of 1,4-naphthaquinone (16 g, 0.101 mole) in 650 ml of ethanol was added dropwise to a suspension of *p*-(β-bromoethyl)benzenesulphinic acid (25 g, 0.100 mole) in 1500 ml of water. At the end of 3 hours, a gray, light precipitate settled, leaving the supernatant liquid clear and nearly colorless. The crude product was dissolved in 450 ml of cold dioxane, containing 10 ml of 6% stannous chloride solution, and precipitated by the addition of 1300 ml of water. A white powder (25 g, 61%) melted at 166–167° with decomposition to a red liquid. Anal. Calc. for $C_{18}H_{15}BrO_4S$ (407.28): C, 53.08; H, 3.71; Br, 19.62; S, 7.87. Found: C, 53.29; H, 3.35; Br, 19.62; S, 7.81%. Infrared spectrum: 1131 (s) and 1282 (s) (—SO_2—) (22), 3344 (s) (—OH) cm^{-1}.

A derivative, 2-[*p*-(β-bromoethyl)benzenesulphonyl]-1,4-diacetoxynaphthalene, was prepared. Crystallization from 33% ethanol gave a white product melting at 179.5–180.5°. Anal. Calc. for $C_{22}H_{19}BrO_6S$ (491.35): C, 53.77; H, 3.89; Br, 16.27; S, 6.53. Found: C, 53.71; H, 4.02; Br, 16.39; S, 6.61%.

Attempts to fully pyranylate this dihydroxysulphone failed. Only a monopyranylated derivative, 1-hydroxy-2-[*p*-(β-bromoethyl)benzenesulphonyl]-4-(2-tetrahydropyranyloxy)naphthalene, was obtained. The dihydroxysulphone II was dissolved in a large excess of 2,3-dihydropyran containing a drop of concentrated hydrochloric acid as a catalyst. The product precipitated on overnight shaking at room temperature. It was filtered, washed with 5% sodium hydroxide, and recrystallized from a dioxane–water mixture buffered to pH 7. A white product melted at 129–130°. Anal. Calc. for $C_{23}H_{23}BrO_5S$ (491.39): C, 56.21; H, 4.72; Br, 16.26; S, 6.53. Found: C, 56.28; H, 4.84; Br, 16.14; S, 6.46%.

Potentiometric Titrations

The assembly used as well as the techniques employed were similar to those described in the previous paper (1). The titration vessel and the calomel cell were placed in a constant temperature bath kept at 25±0.1° C. Another improvement was the use of a more accurate pH meter (Radiometer 4) permitting the measurement of pH to 0.001 unit. In titrations where unbuffered 80% acetic acid was used, the pH reading was taken after each potential reading. The cell potential was then corrected for any changes in pH.

ACKNOWLEDGMENTS

The financial assistance of the National Research Council of Canada and the Advisory Committee on Scientific Research, University of Toronto (to H. P. K.), and of the Ontario Research Foundation (to W. M.) is gratefully acknowledged.

Can. J. Chem. Downloaded from www.nrcresearchpress.com by 210.87.254.42 on 09/05/12
For personal use only.

REFERENCES

1. I. H. SPINNER, W. D. RAPER, and W. METANOMSKI. Can. J. Chem. **41**, 483 (1963).
2. O. HINSBERG. Ber. **27**, 3259 (1894).
3. O. HINSBERG. Ber. **28**, 1315 (1895).
4. D. E. KVALNES. J. Am. Chem. Soc. **56**, 670 (1934).
5. L. F. FIESER and M. FIESER. J. Am. Chem. Soc. **57**, 491 (1935).
6. I. H. SPINNER, J. YANNOPOULOS, and W. METANOMSKI. Can. J. Chem. **39**, 2529 (1961).
7. R. K. BURKHARD, D. E. SELLERS, F. DECOU, and J. L. LAMBERT. J. Org. Chem. **24**, 767 (1959).
8. T. P. FORREST and D. E. RYAN. Can. J. Chem. **36**, 1674 (1958).
9. J. J. WALKER. J. Chem. Soc. 630 (1945).
10. J. B. CONANT. Unpublished. (Quoted by L. F. FIESER. J. Am. Chem. Soc. **52**, 5223 (1930).)
11. V. K. LAMER and L. E. BAKER. J. Am. Chem. Soc. **44**, 1954 (1922).
12. I. H. UPDEGRAFF and H. G. CASSIDY. J. Am. Chem. Soc. **71**, 407 (1949).
13. K. WALLENFELS and W. MÖHLE. Ber. B, **76**, 924 (1943).
14. J. B. CONANT and L. F. FIESER. J. Am. Chem. Soc. **45**, 2194 (1923).
15. H. D. DAKIN. Am. Chem. J. **42**, 477 (1909).
16. C. D. LOGAN, R. M. HUSBAND, and C. B. PURVES. Can. J. Chem. **33**, 82 (1955).
17. J. B. CONANT and L. F. FIESER. J. Am. Chem. Soc. **46**, 1858 (1924).
18. J. B. CONANT and L. F. FIESER. J. Am. Chem. Soc. **44**, 2480 (1922).
19. S. KRISHNA and H. SINGH. J. Am. Chem. Soc. **50**, 792 (1928).
20. W. V. FARRAR. J. Chem. Soc. 3160 (1960).
21. I. S. IOFFE and A. F. SUKHINA. J. Gen. Chem. USSR (Eng. Transl.), **23**, 307 (1953).
22. K. C. SCHREIBER. Anal. Chem. **21**, 1168 (1948).

Can. J. Chem. Downloaded from www.nrcresearchpress.com by 210.87.254.42 on 09/05/12
For personal use only.

FATTY ACID COMPOSITION OF SOME CUCURBITACEAE SEED OILS[1]

MARY J. CHISHOLM AND C. Y. HOPKINS
Division of Pure Chemistry, National Research Council, Ottawa, Canada
Received October 15, 1963

ABSTRACT

Seed oils of nine species of Cucurbitaceae were analyzed by gas chromatography and other techniques. The oil of *Ecballium elaterium* yielded 22% of punicic acid; *Cucumis dipsaceus* and *Cucurbita ficifolia* had the ordinary palmitic–oleic–linoleic composition; a variety of *Momordica charantia* had 57% of α-eleostearic acid. Occurrence of punicic acid as the major acid of *Trichosanthes anguina* was confirmed. No evidence could be found for the existence of an isomer of linoleic acid in *Telfairia pedata* oil. The fatty acid composition was determined quantitatively for the above oils and for those of *Cucumis melo*, *Lagenaria siceraria*, and *Luffa cylindrica*. The 4-bromophenacyl esters of α-eleostearic and punicic acids were prepared.

Seed oils of the Cucurbitaceae family fall into two distinct groups, one having the ordinary palmitic–oleic–linoleic composition, the other having a considerable proportion of conjugated triene fatty acids in the glycerides. The first group includes the common cultivated cucurbits. The second or conjugated oil group consists of certain species of *Cucurbita*, *Momordica*, *Telfairia*, and *Trichosanthes*.

Nine species of the family were examined in the present work to ascertain or confirm the identity of the conjugated acids and to resolve certain anomalies in previous studies. *Ecballium elaterium*, *Cucumis dipsaceus*, and *Cucurbita ficifolia* had not been analyzed previously. The percentage composition of each oil was determined by gas–liquid chromatography (GLC) of the methyl esters, in conjunction with ultraviolet absorption analysis. The conjugated acids, when present in substantial amount, were isolated and purified by crystallization at low temperatures. They were identified by orthodox chemical methods.

RESULTS AND DISCUSSION

Preliminary data are shown in Table I. The high refractive indices of the first three oils indicate conjugated unsaturation and this was confirmed by their ultraviolet spectra and by isolation of conjugated triene fatty acids (see Table II). None of the oils had an absorption peak in the region of 233 mμ; thus they contained no appreciable amount of conjugated diene acid.

In the analysis of the methyl esters by GLC, neither myristic nor linolenic acid was observed, although these two acids had been reported in some species by earlier workers (11, 15, 16). The results suggest that seed oils of Cucurbitaceae contain little or no linolenic acid. No acids other than those shown in Table II were observed. The infrared spectra did not disclose any evidence of oxygenated acids and GLC analysis showed that C_{20} and C_{22} acids were absent.

There was evidently some loss of conjugated triene ester on the GLC column during the analysis. Accordingly, the content of conjugated triene was determined by ultraviolet absorption analysis and the amount of each non-conjugated acid was calculated as a percentage of the remainder.

[1]*Issued as N.R.C. No. 7735.*

Can. J. Chem. Downloaded from www.nrcresearchpress.com by 210.87.254.6 on 09/05/12
For personal use only.

TABLE I

Seed oils of Cucurbitaceae

Species	Oil in seed,* wt.%	Refractive index, 25°	Iodine value
Oils with conjugated unsaturation			
Ecballium elaterium A. Rich.	33.3	1.4880	—
Momordica charantia L. var. Long green monsoon	25.4	(1.4990)†	—
Trichosanthes anguina L.	29.1	1.4979	—
Oils with ordinary unsaturation			
Cucumis dipsaceus Ehrenb.	28.8	1.4742	139.0
Cucumis melo L.	29.8	1.4748	132.6
Cucurbita ficifolia Bouché	32.9	1.4722	121.8
Lagenaria siceraria Standl.	26.8‡	1.4741	134.3
Luffa cylindrica Roem.	20.1	1.4730	126.6
Telfairia pedata Hook	38.3§	1.4671	83.2

*By Soxhlet extraction, air-dry basis.
†At 37°; solid at 25°.
‡In kernel, 51.1%.
§In kernel, 61.0%.

TABLE II

Estimated fatty acid composition

Species	Fatty acid, wt. % of total acids				
	Conjugated trienoic	16:0*	18:0	18:1	18:2
Ecballium elaterium	22.2†	9	3	9	57
Momordica charantia	56.9‡	2	34	4	3
Trichosanthes anguina	42.8†	6	7	23	21
Cucumis dipsaceus	0.8	10	5	6	78
Cucumis melo	0.5	11	4	15	70
Cucurbita ficifolia	0.1	12	4	26	57
Lagenaria siceraria	0.3	14	3	7	76
Luffa cylindrica	0.2	13	6	15	66
Telfairia pedata	0.4	35	14	7	44

*The figures indicate chain length and number of double bonds.
†Punicic acid.
‡α-Eleostearic acid.

The conjugated triene esters gave rise to a broad composite peak in the C_{22} region. This peak undoubtedly represents a mixture of the original conjugated ester and one or more of its geometric isomers, produced by cis–trans isomerization on the column, as observed with methyl α-eleostearate by Morris, Holman, and Fontell (1).

Some degree of uniformity can be seen in the fatty acid composition of this group of oils. In seven of the nine species, in spite of the variation in individual acids, the sum of the unsaturated acids fell within the range 81–88% of the total acids. (The exceptions were *Momordica charantia* and *Telfairia pedata*.) This suggests that the unsaturated acids, both conjugated and non-conjugated, may arise from a common substrate.

From a taxonomic viewpoint, it is noted that all species of *Momordica* and *Trichosanthes* reported to date have conjugated oils (three species of each) and all species of *Citrullus*, *Cucumis*, and *Luffa* studies so far have non-conjugated oils (three, three, and four species). On the other hand, one species of *Telfairia* has a conjugated oil (2) and one has not. Similarly, two species of *Cucurbita* have an appreciable amount of conjugated fatty acid (3) while three species have a negligible amount.

Can. J. Chem. Downloaded from www.nrcresearchpress.com by 210.87.254.6 on 09/05/12
For personal use only.

Can. J. Chem. Downloaded from www.nrcresearchpress.com by 210.87.254.6 on 09/05/12
For personal use only.

Ecballium elaterium

Punicic acid was isolated from the oil of this seed and identified by its spectral absorption and by mixed melting point with an authentic sample. Punicic acid constituted 22% of the total fatty acids but the largest component was linoleic acid.

Momordica charantia

Occurrence of α-eleostearic acid as the major acid of *M. charantia* seed oil has been established (4, 5). The present sample, variety "Long green monsoon", had a noticeably higher content of α-eleostearic acid (57%) than that of the unnamed varieties reported previously (40–48%). This was reflected in the higher refractive index and higher melting point of the oil. The oil is unusual in composition, since the fatty acids consist almost entirely of α-eleostearic acid (57%) and stearic acid (34%). There is less than 5% each of palmitic, oleic, and linoleic acids.

Trichosanthes anguina

The major acid of *T. anguina* was reported to be an isomer of α-eleostearic acid (6, 7) and was identified unequivocally by Crombie and Jacklin in 1957 as punicic acid (8). However, in 1960, Chowdhury (9) re-examined the oil of this species and found the major component to be α-eleostearic acid; conclusive evidence of its identity was given. Our sample of this seed yielded punicic acid as the major component of the oil (43% of the total acids) and there was no evidence of α-eleostearic acid. It is possible that Chowdhury had an unusual variety of *T. anguina.*

The strong infrared band at 752 cm^{-1} appears to be characteristic of the cis,trans,cis grouping in punicic acid and was not observed in the spectrum of α-eleostearic acid (cis,trans,trans).

Telfairia pedata

An early report of the occurrence of an isomer of linoleic acid in *T. pedata* oil (10) was refuted by several authorities (11, 12). However, in view of the recent discovery of linoleic acid isomers in a seed oil (13, 14), *T. pedata* was re-examined. The infrared spectrum of the oil showed no evidence of trans unsaturation, thus ruling out the presence of geometric isomers. The total mixed acids were subjected to oxidative splitting and the fragments were identified by gas chromatography over a wide range of column temperatures. The expected acids, hexanoic, nonoic, and azelaic (from the oxidation of oleic and linoleic acids), were found in quantity. The major dienoic acid is, therefore, linoleic acid. Other fragments were few and very small in amount. It was judged from the GLC data that traces of valeric, heptanoic, and glutaric acids were produced. It is possible, therefore, that traces of isomers of linoleic acid were present but it is estimated that the amount of any one isomer would not exceed 1% of the total fatty acids.

T. pedata oil differs markedly in composition from other Cucurbitaceae oils, having a much higher content of saturated acids (49%). The major acid is linoleic (44%). The data confirm the earlier analyses by Smit and van Loon (11) and by Hilditch and Meara (15) except that linolenic acid was not present in our sample.

Other Species

The other species in this study had the ordinary palmitic–oleic–linoleic composition, with minor amounts of stearic acid and less than 1% of conjugated triene acid. No other fatty acids were detected and it is judged that any minor component acid that may be present does not exceed 0.5% of the total. All of the non-conjugated oils had a relatively

high content of octadecadienoic acid. The fatty acids of *Cucumis dipsaceus* oil contained 78% of linoleic acid, identified as its tetrahydroxy derivative, and it is presumed that the dienoic acid in the other species is also linoleic.

A high refractive index, reported earlier for *Cucumis melo* oil (16), suggested the presence of conjugated acids. However, the present sample had a normal refractive index and contained only 0.5% of conjugated acids.

EXPERIMENTAL

Seed of *Telfairia pedata* (oyster nut) was supplied and its identity was verified through the kindness of Dr. D. H. S. Horn. The other seeds were obtained from reliable commercial sources. Ultraviolet spectra were determined in cyclohexane solution with a Beckman DU spectrophotometer. Infrared spectra were determined in carbon disulphide in a Perkin–Elmer model 21 spectrophotometer with sodium chloride prism. Melting points were determined in capillary tubes and were corrected. The oils were obtained by Soxhlet extraction with petroleum ether (b.p. 30–60°) except where noted otherwise. Iodine values were determined by the Wijs method (30 minutes).

The oils were converted to methyl esters by transesterification in methanol with hydrogen chloride catalyst. The esters were examined by GLC and the composition was estimated by measuring the peak areas. The GLC analyses were made using a copper column at 185° and a thermal conductivity (thermistor) detector. The liquid phase was a diethylene glycol – succinic acid polyester. The average of three determinations for each oil is reported in Table II. A slightly different procedure was followed with oils containing much conjugated acid, as explained above.

Ecballium elaterium

The seeds were ground and extracted by stirring with petroleum ether at 25° and the solvent was removed in a current of nitrogen at 25–30°. The oil had ultraviolet absorption λ_{max} 266, 275, 287 mμ and absorptivity $E^{1\%}_{1\,cm}$ 382 at 275 mμ, equivalent to 22.2% of conjugated triene acid. The oil was hydrolyzed by refluxing under nitrogen for 30 minutes with aqueous 6% potassium hydroxide. The acids (8.5 g) were dissolved in 85 ml of acetone and cooled. Crystals were taken off at −10, −30, and −55°. Ultraviolet absorption analysis showed that the −30° fraction had 68% and the −55° fraction 23% of conjugated triene acid. The −55° fraction (3.65 g) was crystallized three times from pentane at −25°, yielding 0.41 g of punicic acid, m.p. 43.5–44°. After one crystallization from acetone it had m.p. 44.5–45.5°, alone and mixed with authentic punicic acid of m.p. 45.0–45.5°. The ultraviolet spectrum was the same as that of punicic acid, λ_{max} 265, 275, 287 mμ.

Momordica charantia

Seed of *M. charantia*, var. Long green monsoon (from Poona, India), was hulled and the kernel oil was extracted at 25°. The oil had λ_{max} 262, 272, 283 mμ and negligible absorption at 233 mμ. The absorptivity, $E^{1\%}_{1\,cm}$, was 1007 at 272 mμ, equivalent to 56.9% of conjugated triene acid, calculated as α-eleostearic. Infrared maxima were at 987 (vs) and 959 (w) cm^{-1}. The mixed fatty acids were crystallized fractionally from acetone at low temperatures. There was a large yield of crystals at 10°, mainly stearic acid. After one crystallization from ethanol it had melting point and mixed m.p. 68–69°. Conjugated triene acid was collected at −15°. After further crystallization from acetone it melted at 45.5–46.5°. It formed an adduct readily with maleic anhydride by the usual method (17). The adduct melted at 63.5–64.5°, alone and mixed with the maleic anhydride adduct of α-eleostearic acid.

Trichosanthes anguina

Seed of *T. anguina* (from Poona, India) yielded an oil having λ_{max} 265, 275, 287 mμ and $E^{1\%}_{1\,cm}$ 739 at 275 mμ, equivalent to 42.8% of conjugated triene fatty acid. Absorption at 233 mμ was negligible. Infrared maxima were at 982 (s) and 931 (s) cm^{-1} (cis,trans,cis-triene), also at 752 cm^{-1}. There were no absorption bands attributable to hydroxy, keto, or isolated trans unsaturated groupings.

Twenty grams of the oil was hydrolyzed and the mixed acids were crystallized from acetone. Saturated acids were removed at −15° and the conjugated acid (6.5 g) at −38°. The latter, after three crystallizations from pentane melted at 44.5–45.5°, alone and mixed with punicic acid from pomegranate seed oil.

4-Bromophenacyl Esters

A solution of 0.5 g of punicic acid in 20 ml of ethanol was treated with 2,4′-dibromoacetophenone by the method of Neish and Lemieux (18). The crude product (0.8 g) was crystallized from ethanol at 0°, giving 4-bromophenacyl punicate, m.p. 61–63°. The ester is unstable like the acid. Its identity was confirmed by hydrogenation to the saturated ester by means of Adams catalyst in ethyl ether. The product, 4-bromophenacyl stearate, melted at 88–89° after two crystallizations from ethanol. The melting point was unchanged in admixture with an authentic sample of m.p. 88.5–89.0° (lit., 90°).

Can. J. Chem. Downloaded from www.nrcresearchpress.com by 210.87.254.6 on 09/05/12
For personal use only.

α-Eleostearic acid was converted to its 4-bromophenacyl ester in the same way. The ester had m.p. 53–54° and was unstable. Anal. Calc. for $C_{26}H_{35}O_3Br$: C, 65.67; H, 7.42. Found: C, 65.33; H, 7.40.

Telfairia pedata

Oil from seed kernels of *T. pedata* (origin South Africa) was hydrolyzed and the mixed fatty acids were subjected to oxidative splitting by permanganate–periodate (19). The unchanged saturated acids were filtered off and esterified with methanol (A). The water-soluble monobasic and dibasic acids were extracted from the filtrate with ether in a continuous extractor. They were converted to methyl esters (B) by a method that avoids loss by evaporation of any component (20).

The A esters, examined by GLC at column temperatures of 140°, 160°, and 185°, gave peaks corresponding to palmitate and stearate. The B esters, examined at temperatures from 50° to 195°, gave major peaks corresponding to hexanoate, nonoate, and azelate. The minor peaks were very small. They indicated traces of valerate, heptanoate, and glutarate. There was no indication of other monobasic acids from C_3 to C_{15} inclusive, nor of dibasic acids from C_3 to C_{14} inclusive.

The infrared spectrum of *T. pedata* oil showed no absorption characteristic of a terminal double bond (ca. 910 cm^{-1}), nor of an αβ-unsaturated acid (ca. 1275 cm^{-1}).

Cucumis dipsaceus

The dienoic acid of the oil was identified as linoleic acid as follows. The mixed fatty acids (1.2 g) were oxidized by aqueous alkaline permanganate for 10 minutes at 10°. The solid product (0.92 g) was washed with hexane, then with ethyl acetate, and finally crystallized from ethanol, giving di-erythro-9,10,12,13-tetrahydroxystearic acid, m.p. 173–174°, alone and mixed with an authentic sample.

ACKNOWLEDGMENTS

The authors are indebted to Mr. R. Lauzon for determination of infrared spectra and to Mr. H. Seguin for microanalyses.

REFERENCES

1. L. J. Morris, R. T. Holman, and K. Fontell. J. Lipid Res. **1**, 412 (1960).
2. T. P. Hilditch and J. P. Riley. J. Soc. Chem. Ind. **65**, 74 (1946).
3. W. C. Ault, M. L. Swain, and L. C. Curtis. J. Am. Oil Chemists' Soc. **24**, 289 (1947).
4. J. P. Verma and J. S. Aggarwal. J. Indian Chem. Soc. **33**, 357 (1956).
5. C. Y. Hopkins and M. J. Chisholm. Can. J. Chem. **40**, 2078 (1962).
6. P. Soni and J. S. Aggarwal. J. Sci. Ind. Res. (India), **8B**, 150 (1949).
7. N. H. E. Ahlers and A. C. Dennison. Chem. Ind. (London), 603 (1954).
8. L. Crombie and A. G. Jacklin. J. Chem. Soc. 1632 (1957).
9. D. K. Chowdhury. Nahrung, **4**, No. 1, 17 (1960).
10. H. Thoms. Arch. Pharm. **238**, 48 (1900).
11. W. C. Smit and J. van Loon. Fettchem. Umschau, **43**, 71 (1936).
12. G. D. Goodall and R. D. Haworth. J. Chem. Soc. 399 (1936).
13. C. Y. Hopkins and M. J. Chisholm. Chem. Ind. (London), 2064 (1962).
14. M. J. Chisholm and C. Y. Hopkins. Can. J. Chem. **41**, 1888 (1963).
15. T. P. Hilditch and M. L. Meara. J. Soc. Chem. Ind. **63**, 112 (1944).
16. S. A. Ahmad and D. R. Dhingra. J. Indian Chem. Soc. **22**, 337 (1945).
17. C. Y. Hopkins and M. J. Chisholm. J. Chem. Soc. 573 (1962).
18. A. C. Neish and R. U. Lemieux. Can. J. Chem. **30**, 454 (1952).
19. R. U. Lemieux and E. von Rudloff. Can. J. Chem. **33**, 1701 (1955).
20. M. J. Chisholm and C. Y. Hopkins. Can. J. Chem. **38**, 805 (1960).

Can. J. Chem. Downloaded from www.nrcresearchpress.com by 210.87.254.6 on 09/05/12
For personal use only.

HINDERED CONFORMATIONAL ISOMERIZATION OF 9,10-DIHYDRO-9,9-DIMETHYL-10-METHYLENEANTHRACENES[1]

D. Y. Curtin, C. G. Carlson,[2] and C. G. McCarty[3]

Received September 18, 1963

ABSTRACT

While the n.m.r. spectrum of 10,10-dimethyl-9-methylene-9,10-dihydroanthracene (I) shows the geminal methyl group absorption as a sharp singlet the spectrum of the dibromo derivative, 10,10-dimethyl-9-dibromomethylene-9,10-dihydroanthracene (II) shows the methyl absorptions as two sharp well-separated peaks at room temperature which coalesce at 91°. 10,10-Dimethyl-9-phenylbromomethylene-9,10-dihydroanthracene (III), and the methyl ester (V) of IV show a broad geminal methyl spectrum at room temperature which separates to a doublet at lower temperatures and sharpens to a singlet at higher temperatures. Rate constants for the first-order processes responsible for the change in spectrum of II, III, and V have been calculated at the coalescence temperatures to be 57 (364° K), 35 (305° K), and 61 (300° K) sec^{-1}, respectively. The ΔH^{+}'s were used to extrapolate the rates to 305° to give values of 1, 40, and 100 sec^{-1}, respectively. The process being studied is inferred to be the equilibrium between two boat conformations of the center ring in the dihydroanthracene system, rapid interconversion leading to identical environments for the two methyl groups. A comparison with the geometrically similar *o,o'*-disubstituted biphenyl racemization gives support for this explanation. A number of compounds with a proton and one substituent on the methylene carbon atom of I (substituents: bromine, chlorine, phenyl, carboxy, carbomethoxy, phenylmercapto) and also 10,10-dimethyl-9-phenylcarbomethoxymethylene-9,10-dihydroanthracene (XII) showed a single methyl absorption at room temperature. The methyl spectrum of the mono bromo compound VI did not broaden at temperatures down to 246° K.

INTRODUCTION

In a continuation of a study of the reaction of vinyl halides with lithium reagents (1) 10,10-dimethyl-9-methylene-9,10-dihydroanthracene (I) and a number of its derivatives were prepared. Examination of the n.m.r. spectrum of the parent compound I at room

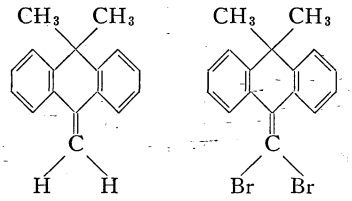

I II

temperature showed, not unexpectedly, a single absorption maximum due to the protons of the two methyl groups in the 10-position. The derived dibromomethylene compound II, however, showed absorption attributable to the two methyl groups as a well-separated pair of lines. Examination of molecular models suggests that the two compounds I and II might be expected to have a boat conformation as that preferred by the center ring. The situation is somewhat similar to that of 9,10-dihydroanthracene which has been shown to exist in a boat conformation in the crystalline state (2) and whose derivatives show

[1]*Taken from the Ph.D. theses of C. G. Carlson and C. G. McCarty submitted to the University of Illinois, 1963, available from University Microfilms, Ann Arbor, Michigan, U.S.A. Acknowledgment is made to the donors of the Petroleum Research Fund administered by the American Chemical Society for partial support of this work.*

[2]*Procter and Gamble Fellow, 1959–1960. Charles Pfizer Fellow, Summer, 1960.*

[3]*Roger Adams Fellow, 1959–1960. National Science Foundation Fellow, 1960–1961. Standard Oil of California Fellow, 1961–1962. Public Health Service Fellow, 1962–1963.*

Can. J. Chem. Downloaded from www.nrcresearchpress.com by 210.87.254.40 on 09/05/12
For personal use only.

chemical behavior which has been interpreted in terms of a preferred boat conformation for the ring system. In such a molecule as has been pointed out previously (3) the two methyl groups are non-equivalent, one being almost perpendicular to the plane which is approximately the plane of the ring system and the other methyl group nearly in that plane as is shown in Fig. 1.* These considerations suggested that the dibromide II, when

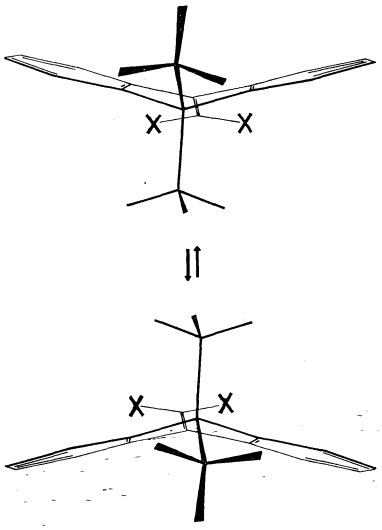

FIG. 1.

heated, might undergo a sufficiently rapid interconversion from one boat form to the other to average the magnetic environments of the methyl protons (4). Not only I and II but also a number of compounds (III–XII) with other substituents at the vinyl carbon atom have been submitted to examination with n.m.r. with results to be reported here.

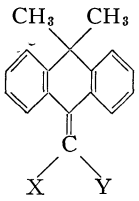

III, X = Br; Y = C_6H_5
IV, X = Br; Y = COOH
V, X = Br; Y = $COOCH_3$

VI, X = H; Y = Br
VII, X = H; Y = Cl
VIII, X = H; Y = C_6H_5
IX, X = H; Y = COOH
X, X = H; Y = $COOCH_3$
XI, X = H; Y = C_6H_5S
XII, X = C_6H_5; Y = $COOCH_3$

EXPERIMENTAL

Preparation of Materials

The preparation and structure determination of each of the compounds studied will be published elsewhere. Details are available in the Ph.D. thesis of C. G. Carlson (see footnote 1 of this paper).

Nuclear Magnetic Resonance Instrumentation and Procedure

The spectra were obtained by use of a Varian Associates high-resolution n.m.r. spectrometer with a Model V-K 3506 super stabilizer and a Model V-4311 RF probe for operation at 60 Mc. The Varian Model V-4340 variable temperature probe accessory and the Model V-4331-THR Dewar probe insert were used in the high- and low-temperature studies. The spectra were recorded by a modified Varian Model G-10 recorder.

**Beckett and Mulley (3) proposed that atoms or groups in these positions be designated "perp" and "lin", respectively. However, "axial" and "equatorial" appear to us to be sufficiently descriptive to make it unnecessary to introduce new terminology.*

Can. J. Chem. Downloaded from www.nrcresearchpress.com by 210.87.254.40 on 09/05/12
For personal use only.

Can. J. Chem. Downloaded from www.nrcresearchpress.com by 210.87.254.40 on 09/05/12
For personal use only.

Sample temperatures from −40° to +30° were achieved by means of a nichrome immersion heater placed in a 25-l. Dewar flask of liquid nitrogen with an exit tube connected to the variable temperature probe accessory. The power input to the immersion coil determined the rate of vaporization of the liquid nitrogen and, thus, the temperature of the insert. A flow of compressed air, heated by the coils in the probe accessory, was employed to provide sample temperatures from +30° to +120°. A copper–constantan thermocouple, calibrated against National Bureau of Standards thermometers over the range of −35° to +150°, and a Leeds and Northrup Model 8662 precision potentiometer were employed for determining temperatures of the samples.

Solutions were 6% in carbon tetrachloride. Tetramethylsilane was used as an internal standard. Pyrex glass tubes, 6½ inches in length and 5 mm o.d., were filled to 3½ inches with the solutions of the samples. Air was replaced with nitrogen and the tubes sealed.

High resolution n.m.r. spectra of the dihydroanthracenes II, III, and V were obtained at a series of temperatures from −40° to +120°. Each sample was studied at room temperature before and after the high- and low-temperature work in order to check on the chemical and thermal stability of the compounds and the reproducibility of the spectra. Sufficient time was allowed for equilibration of temperature at each setting. Temperature was monitored with the copper–constantan thermocouple immersed in a dummy sample tube of carbon tetrachloride until a constant temperature was obtained. The sample tube was then inserted, allowed to come to thermal equilibrium, and the spectra obtained. The dummy tube was then returned to the probe insert in order to detect any change in temperature. In no case did the temperature change more than ±0.1°.

From four to six spectra were obtained at each temperature. Some were recorded with increasing and some with decreasing linear sweep fields but all were recorded at the same applied R_F field, H_1, which was well below the minimum value giving R_F saturation. Variables such as spinning rate, recorder input level, and sweep rate were adjusted to give the best spectra and the smallest percentage error in the measurement of signal separation. Audiofrequency side bands of tetramethylsilane generated with a Hewlett–Packard Model 200 CD audio oscillator which was calibrated by a Hewlett–Packard Model 521C electronic counter were used to determine the chemical shift difference, $\delta\nu_e$, between the maxima of the lines of the methyl doublet. Of the four to six spectra recorded at each temperature, usually one and sometimes two would yield values well away from the others due presumably to non-linearity in the sweep. This left three to five values which could be used to obtain an average value of $\delta\nu_e$ at each temperature. The deviation from the average, in every case, was $\leqslant \pm 0.30$ c.p.s.

The coalescence point of the methyl doublet in spectra of II, III, and V was taken as that temperature at which the spectrum consisted of a single broad flat top peak. This point was closely bracketed by spectra obtained at slightly higher and lower temperatures. In this manner the true coalescence temperature of each compound was obtained to within about ±0.8°. The limiting maximum separation, $\delta\nu_\infty$, was found from graphs of $\delta\nu_e$ vs. temperature. This was felt to be accurate to within ±0.2 c.p.s. in each case.

Sample data are presented in Table I.*

TABLE I

Variation with temperature of the methyl spectrum of the dibromide II*

T (° C)	$\delta\nu_e$† (c.p.s.)	T (° C)	$\delta\nu_e$† (c.p.s.)
101	0	69.1	24.9±0.3 (3)
92.0	0	59.6	25.2±0.2 (4)
91.2	0	50.1	25.3±0.2 (3)
90.7	12.7 (1)	31.2	25.5±0.1 (5)
89.9	14.0±0.3 (3)	10.5	25.6±0.1 (4)
88.0	16.9±0.2 (3)	0.5	25.5±0.2 (5)
84.7	20.3±0.3 (4)	−8.7	25.5±0.3 (4)
78.5	22.9±0.2 (4)	−17.3	25.3±0.2 (5)
76.1	23.5±0.3 (4)	−29.2	25.6±0.2 (4)
T_{coal}	91.1±0.8°	k_1	56.9±0.4 sec^{-1}
$\delta\nu_\infty$	25.6±0.2 c.p.s.	$\Delta F^{\ddagger}$	18.6 kcal/mole

*All samples 6% (w/v) solutions in carbon tetrachloride.
†The range of values of $\delta\nu_e$ is indicated. The value in parentheses is the number of measurements averaged.

RESULTS

A study of the dibromide II showed that the twin methyl peaks found at room temperature coalesced to a single sharp peak at temperatures above 90°. It might be hoped that,

**Additional data and critical spectra are available in the theses referred to in footnote 1.*

conversely, the barrier to interconversion of the two boat conformations of the parent olefin I would be high enough so that at some temperature below room temperature the methyl singlet absorption could be observed to separate to a doublet. No change in the spectrum was observed down to −27°, however. Examination of the N.M.R. spectra of the series of compounds III–XII with various substituents attached to the methylene carbon atom showed that they fall into two distinct classes differing in the shape of the methyl proton spectrum. The first class (compounds III–V), containing one vinyl bromine atom and a second vinyl substituent showed methyl proton spectra which were broad but not separated into a doublet at room temperature. The methyl proton spectra of III and V separated to a doublet when the solutions were cooled to −27°, however. The second group of compounds VI–XII had the methyl absorption as a single peak. The mono bromo compound VI showed no significant broadening at temperatures down to −27°.

Of the methods available (5, 6, 7, 8, 9) for the calculation of rate constants of processes which lead to this type of change in the n.m.r. spectrum the method of Gutowsky and Holm (5, 11) was chosen in order to obtain a more detailed interpretation of the effect of temperature on the spectra of the dibromide II, the bromo phenyl compound III, and the bromo ester V. The maximum experimental separation, $\delta\nu_\infty$, and the coalescence temperature were measured and the rate constant, $k_1 = k_{-1}$, at the coalescence temperature was calculated using the following expression (4(*b*)) $k_1 = k_{-1} = \pi(\delta\nu_\infty)/\sqrt{2}$. From the equation (10) $k_1 = (kT_e/h)(-\Delta F^{\ddagger}/RT)$ was calculated the standard free energy of activation at the coalescence temperature for each of the compounds studied. These results are summarized in Table II.

TABLE II

Compound	Coalescence temperature (° K)	$\delta\nu_\infty$ (c.p.s.)	k_1 (sec^{-1})	$\Delta F^{\ddagger}$ (kcal/mole)
X = Y = Br (II)	364.4±0.5	25.6±0.2	56.9±0.4	18.6
X = Br, Y = C_6H_5 (III)	305.2±0.5	15.8±0.2	35.1±0.4	15.7
X = Br, Y = $COOCH_3$ (V)	300.3±0.5	27.6±0.2	61.3±0.5	15.1

Equations developed by Gutowsky and Holm (5) permit the calculation of the activation energy, E_a, for the boat–boat interconversion from the temperature dependence of the separation of the methyl peaks. Thus, from

$$\log_{10} 1/[2\pi\tau(\nu_A-\nu_B)] = \log_{10} A/[\pi(\nu_A-\nu_B)] - E_a/(2.30\,RT)$$

a plot of log $1/[2\pi\tau(\nu_A-\nu_B)]$ against $1/T$ gave a line from whose slope and intercept were evaluated E_a and the frequency factor, A, for the interconversion. The function log $1/[2\pi\tau(\nu_A-\nu_B)]$ was evaluated with the aid of the assumption that the signal widths are sufficiently small relative to the separation, $\nu_A-\nu_B$ so that $\tau(\nu_A-\nu_B)$ could be obtained (5) from the separation of the peaks at any temperature, $\delta\nu_e$ and the limiting separation approached at low temperatures, ν_∞, with the expression

$$\frac{\delta\nu_e}{\delta\nu_\infty} = \left[1 - \frac{1}{2\pi^2\tau^2(\nu_A-\nu_B)^2}\right]^{\frac{1}{2}}.$$

The results of this analysis of the data are presented in Table III with the designation Method A. A second method, Method B in Table III, which was both more rigorous and

Can. J. Chem. Downloaded from www.nrcresearchpress.com by 210.87.254.40 on 09/05/12
For personal use only.

TABLE III

	Method	Compound X = Y = Br(II)	X = Br, Y = C_6H_5(III)	X = Br Y = $COOCH_3$(V)
T_2 (sec)		0.13	0.10	0.11
E_a (kcal/mole)	A	15.1±0.2	14.8±0.3	15.0±0.3
	B	16.5±0.3	16.9±0.4	16.5±0.3
log A	A	10.8±0.2	12.2±0.1	12.7±0.2
	B	11.6±0.1	13.7±0.2	13.8±0.2
$k_{305.2°}$ (sec^{-1})	A	1.00±0.14	35.1±0.4	91.7±9.0
	B	0.69±0.11	35.1±0.4	95.5±10.0
$\Delta F^{\ddagger}_{305.2°}$ (kcal/mole)	A	17.9±0.1	15.7	15.1±0.1
	B	18.1±0.1	15.7	15.1±0.1
$\Delta H^{\ddagger}_{305.2°}$ (kcal/mole)	A	14.5±0.2	14.2±0.3	14.4±0.3
	B	15.9±0.3	16.3±0.4	15.9±0.3
$\Delta S^{\ddagger}_{305.2°}$ (e.u.)	A	−11.1±1.2	−5.0±1.0	−2.3±1.3
	B	−7.2±1.3	+2.0±1.3	+2.7±1.3

more laborious than that just described gave substantially the same results. In this method the nuclear relaxation time, T_2, is determined from the line width at half maximum under conditions of rapid exchange, together with graphical solutions (5, 11) of the equations relating $1/\tau(\nu_A-\nu_B)$ with $1/T_2(\nu_A-\nu_B)$ for different values of $\delta\nu_e/(\nu_A-\nu_B)$. Values of E_a and A and their probable errors were obtained by the method of least squares (12). The questionable assumption in method A that line widths are small relative to $(\nu_A-\nu_B)$ suggests that the E_a's obtained by method B are the more reliable.

TABLE IV

Effects of vinyl substituents on the rate of conformational isomerization of 9,10-dihydro-9,9-dimethyl-10-methyleneanthracene

Substituents at the vinyl carbon atom		Rate at 305° K (sec^{-1})	$\Delta H^{\ddagger}$(305°) (kcal/mole)	$T\Delta S^{\ddagger}$(305°) (kcal/mole)
X	Y			
Br	Br (II)	1	16	−2
Br	C_6H_5 (III)	40	16	+0.6
Br	$COOCH_3$ (V)	100	16	+0.8
H	Br (VI)	>1000*	—	—

*This estimate has been arrived at in the following way. Assuming a limiting separation of 15 c.p.s. at a temperature of −30° or lower gives a rate constant ($k_1 = \pi\delta\nu_{ac}/\sqrt{2}$) of 35 sec^{-1}. Extrapolation to 305° K with an estimated energy of activation of 9 kcal leads to a rate constant greater than 1000.

DISCUSSION

The results as summarized in Table IV show the rather considerable dependence of the rate of the reaction being followed on substituents on the vinyl carbon atom. The spread of rates for the three compounds for which quantitative data are available is only a factor of 100, however, and it will be noted that, unfortunately, $\Delta H^{\ddagger}$ is constant to within the limits of experimental error, the difference in rates being due principally to differences in the entropies of activation of the three compounds. In a case of this kind, as has been pointed out by Hammett (13), it is unclear whether the potential energies of activation parallel the free energies or the enthalpies (or either one). There does, however, appear

Can. J. Chem. Downloaded from www.nrcresearchpress.com by 210.87.254.40 on 09/05/12
For personal use only.

to be a relationship of the type which would be expected from potential energy considerations between the rates and effective steric requirements of the substituents as judged by examination of molecular models. A comparison of the present system with the optically active *o,o'*-disubstituted biphenyls is of particular interest in view of the striking similarity of the geometry of the planar transition state of the methylenedihydroanthracene isomerization with that for the racemization of the biphenyls (Fig. 2). Although there

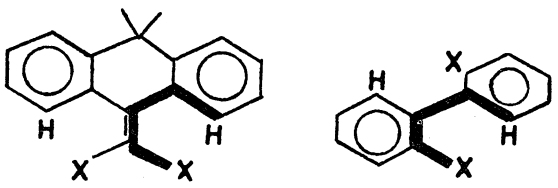

FIG. 2.

are minor differences in bond distances (for example, there is a C=C in one system instead of the C—C aromatic bond in the other) it is seen that the geometry is very similar and the same H—X interaction occurs twice in each transition state. There may, of course, be other important differences between the two systems such as any change in the resonance stabilization of either system resulting from a change in the overlap of the pi electron clouds of the two halves of the molecule in going from the non-planar initial state to the planar transition state. Nevertheless a comparison of the two systems is highly instructive, particularly because of the excellent discussion of the racemization of the *o,o'*-disubstituted biphenyls by Westheimer (14). This discussion applies to a large extent to the isomerization which is the subject of this paper. It is reassuring to note that the value of 17 kcal/mole estimated for the enthalpy of activation of the racemization of 2,2'-dibromo-4,4'-dicarboxybiphenyl is close to the value of 16 kcal for the isomerization of the dibromomethylene compound II. Also the order of effectiveness of substituents in interference with the attainment of the planar transition state, Br > COOH > H, is in agreement with the limited data available for the racemization of biphenyls (15).

Finally, the origin of the difference in chemical shift of the two methyl groups in the methylene derivatives II–V deserves comment. Inspection of models indicates that the position of the methyl groups with respect to the benzene ring currents differs sufficiently so that this ring current effect (16) should be a substantial factor in accounting for the observed differences of 16–28 c.p.s. (at 60 Mc). An estimation of the difference to be expected using the tables of Johnson and Bovey (17)* gives a value of 36 c.p.s. and suggests that the ring current effect may be the predominant or almost exclusive factor responsible for the separation.

REFERENCES

1. D. Y. CURTIN and W. H. RICHARDSON. J. Am. Chem. Soc. **81**, 4721 (1959).
2. W. G. FERRIER and J. IBALL. Chem. Ind. 1296 (1954).
3. A. H. BECKETT and B. A. MULLEY. Chem. Ind. 146 (1955).
4. J. A. POPLE, W. G. SCHNEIDER, and H. J. BERNSTEIN. High-resolution nuclear magnetic resonance. McGraw-Hill Book Co., Inc., New York. 1959. (*a*) p. 365 ff. (*b*) p. 223.
5. H. S. GUTOWSKY and C. H. HOLM. J. Chem. Phys. **25**, 1228 (1956).
6. E. GRUNWALD, A. LOEWENSTEIN, and S. MEIBOOM. J. Chem. Phys. **27**, 630 (1957).
7. L. H. PIETTE and W. A. ANDERSON. J. Chem. Phys. **30**, 899 (1959).
8. M. TAKEDA and E. O. STEJSKAL. J. Am. Chem. Soc. **82**, 25 (1960).

**We are indebted to Dr. G. v. D. Tiers for a copy of the tables referred to in this paper.*

Can. J. Chem. Downloaded from www.nrcresearchpress.com by 210.87.254.40 on 09/05/12
For personal use only.

9. M. T. ROGERS and J. C. WOODBREY. J. Phys. Chem. **66**, 540 (1962).
10. L. P. HAMMETT. Introduction to the study of physical chemistry. McGraw-Hill Book Co., New York. 1952. pp. 190–195.
11. C. H. HOLM. Ph.D. Thesis, University of Illinois, Chicago, Ill. 1955. p. 32.
12. W. J. YOUDEN. Statistical methods for chemists. John Wiley and Sons, Inc., New York. 1951. p. 40 ff.
13. L. P. HAMMETT. Physical Organic Chemistry. McGraw-Hill Book Co., New York. 1940. p. 118 ff.
14. F. H. WESTHEIMER. Steric effects in organic chemistry. *Edited by* M. S. Newman. John Wiley and Sons, Inc., New York, N. Y. 1956. p. 542 ff.
15. E. L. ELIEL. Stereochemistry of carbon compounds. McGraw-Hill Book Company, New York, N. Y. 1962. p. 160.
16. J. A. POPLE, W. G. SCHNEIDER, and H. J. BERNSTEIN. High-resolution nuclear magnetic resonance. McGraw-Hill Book Co., Inc., New York. 1959. pp 180–183.
17. C. E. JOHNSON and F. A. BOVEY. J. Chem. Phys. **29**, 1012 (1958).

Can. J. Chem. Downloaded from www.nrcresearchpress.com by 210.87.254.40 on 09/05/12
For personal use only.

ANTINEOPLASTIC AGENTS

X. N-BIS(2-FLUOROETHYL)AMINES[1,2]

GEORGE R. PETTIT AND ROBERT L. SMITH
Department of Chemistry, University of Maine, Orono, Maine

Received September 30, 1963

ABSTRACT

Successive conversion of N-bis(2-hydroxyethyl)-*p*-toluenesulphonamide (I*b*) to respective dimethanesulphonate and difluoro derivatives (II*a*, III*a*, and III*c*) was found to provide a convenient route to N-bis(2-fluoroethyl)amine. Reaction of N-bis(2-methanesulphonyloxyethyl)-*p*-toluenesulphonamide (III*a*) with limited quantities of potassium fluoride, in several protic solvents, was shown to yield N-(*p*-toluenesulphonyl)morpholine (IV). Utility of N-bis(2-fluoroethyl)amine as a precursor of fluoro-nitrogen mustards was illustrated by synthesis of two N-bis(2-fluoroethyl)benzylamines (IX*b* and X*a*). Application of an aluminum chloride – lithium aluminum hydride reagent for hydrogenolysis of carbon–fluorine bonds was also suggested.

Greater versatility in design of potential antineoplastic agents should be possible by utilizing predictable differences in the chemical reactivity expected for N-bis(2-fluoroethyl)amines, as compared to other N-bis(2-haloethyl)amines. For example, neighboring group displacement of halogen from a 2-fluoroethylamine should proceed substantially more slowly than with related 2-haloethylamines.[3] Intensive study of fluoro-nitrogen mustards might, therefore, lead to substances with more specific and prolonged antitumor activity.

Advantage might also be taken of the known ability of certain fluorine derivatives to inhibit the citric acid cycle (2, 3). The pronounced toxicity of fluoroacetic acid and several even-numbered linear homologs has been attributed to their eventual in vivo conversion to fluorocitric acid. Apparently, the odd-numbered homologs do not yield one of the necessary precursors, fluoroacetic acid, and are considerably less toxic. Fluorocitric acid, in turn, is believed to block the citric acid cycle during the tricarboxylic acid sequence. Although utilization of glycolytic products at this stage, by neoplastic tissue, appears less important than conversion to lactic acid, interruption of glycolysis during the citric acid cycle might be useful in control of certain neoplasms.

The above considerations and general paucity of information relating to synthesis and biological properties[4] of N-bis(2-fluoroethyl)amines has led to the present investigation. Syntheses of N-bis(2-fluoroethyl)-3,4-methylenedioxybenzylamine and N-bis(2-fluoroethyl)-3,4,5-trimethoxybenzylamine were first considered, as the corresponding chloro derivatives (5) gave encouraging results in the Dunning leukemia test system.

Synthesis of N-bis(2-fluoroethyl)amine (6) from 1-bromo-2-fluoroethane and ammonia illustrates the method employed for obtaining the two previously reported (6, 7) fluoro-nitrogen mustards. However, appropriate N-substitution of N-bis(2-fluoroethyl)amine was

[1]*Part IX. G. R. Pettit, D. S. Blonda, and E. C. Harrington. Can. J. Chem. 41, 2962 (1963).*

[2]*Abstracted in part from the Master of Science thesis submitted by R. L. Smith to the Graduate School, University of Maine, August, 1963.*

[3]*A proton magnetic resonance study of several N-bis(2-haloethyl)amines, in deuterium oxide, has indicated that the fluoro compounds undergo hydrolysis (see also ref. 1) and intermolecular condensation reactions at a markedly slower rate than, for example, the chloro derivatives. Details of this investigation will be reported by G. R. Pettit, J. A. Settepani, and R. A. Hill.*

[4]*Only one N-bis(2-fluoroethyl)amine appears in the comprehensive survey of alkylating agents prepared by R. B. Ross and colleagues (ref. 4). By contrast, over 2200 other nitrogen mustards are included in this valuable review.*

Can. J. Chem. Downloaded from www.nrcresearchpress.com by 210.87.254.40 on 09/05/12
For personal use only.

considered a more convenient approach to the required benzylamines and, in general, to fluoro-nitrogen mustards. Initially, N-bis(2-fluoroethyl)amine was prepared using the Childs procedure (6). When requirements for the amine increased, a more practical laboratory synthesis based on 2,2′-iminodiethanol (I) was undertaken.

A useful synthesis of N-bis(2-fluoroethyl)amine was eventually developed[5] employing the ready nucleophilic displacement of sulphonate esters by fluoride ion (12, 13). The bismethanesulphonate derivative (II*a*) of *p*-toluenesulphonamide I*b* was prepared, in cold pyridine solution (12), and allowed to react with excess anhydrous potassium fluoride. Treating the resulting N-bis(2-fluoroethyl)sulphonamide (III*a*) with hydrogen bromide (14), in glacial acetic acid, led to N-bis(2-fluoroethyl)amine (III*c*) hydrobromide. In this manner, substantial quantities (>50 g) of amine III*c* hydrobromide were routinely prepared. Similar transformation of methanesulphonamide II*b* to amine III*c* was less satisfactory.

Interestingly, an attempt to prepare the monofluoro derivative of sulphonate II*a* using almost equimolar quantities of ester (II*a*) and potassium fluoride, in diethylene glycol, gave N-(*p*-toluenesulphonyl)morpholine (IV) as major product. Repeating the reaction with formamide (13) as solvent led to a 72% yield of morpholine IV, while only unreacted sulphonamide II*a* was recovered when diglyme or dimethylformamide was used as solvent. These experiments suggest that potassium fluoride may first promote an exchange reaction (II*a* → V) between the sulphonate ester and protic solvent and then catalyze (15) intramolecular nucleophilic displacement (V → VI, see also ref. 16) of the second sulphonate group.[6]

Synthesis of the required benzylamines was initiated as described (5) for preparing the corresponding chloro analogs. Amine III*c* was easily converted to both 3,4-methylenedioxy- and 3,4,5-trimethoxy-benzamide derivatives (VII*a* and VIII*a*). Subjecting amide VII*a* to the aluminum chloride – lithium aluminum hydride reduction reaction, successfully used[1] (5) for obtaining N-bis(2-chloroethyl)benzylamines, unexpectedly caused nearly complete hydrogenolysis of the carbon–fluorine bond to yield N,N-diethyl-3,4-methylenedioxybenzylamine (IX*a*)[7] as major product. Subsequently, a reduction technique employing only lithium aluminum hydride was developed, using N,N-diethyl-3,4,5-trimethoxybenzamide (VIII*b*) as model substrate, and found suitable for reducing amides VII*a* and VIII*a* to N-bis(2-fluoroethyl)benzylamines IX*b* and X*a*.

Biological evaluation of the fluoro-nitrogen mustards has been undertaken by the Cancer Chemotherapy National Service Center (National Institutes of Health, U. S. Public Health Service). Initial biological studies have shown that amine III*c* is a very toxic compound. No animals survived when random-bred albino rats were treated with N-bis(2-fluoroethyl)amine hydrobromide at a dose of 3 mg/kg in saline (by the intraperitoneal route). While a dose of 0.6 mg/kg was tolerated, only two of three survived at 1 mg/kg. By analogous experimental methods, the maleic acid salt of N-bis(2-chloroethyl)-amine was tolerated at 100 mg/kg, N-bis(2-bromoethyl)amine hydrobromide at 4 mg/kg, and N-bis(2-iodoethyl)amine hydroiodide at 10 mg/kg. Interestingly, when similar animals bearing Walker 256 (subcutaneous) were treated (saline solution, intraperitoneally, beginning on the first day of tumor transplant) with the above nitrogen mustards,

[5]*The approach employed was selected from among a number of potentially valuable methods (ref. 8, 9, 10, and 11).*

[6]*The major side reaction during displacement of p-toluenesulphonate esters by potassium fluoride, in diethylene glycol, has been attributed to ether formation (12).*

[7]*The aluminum chloride – lithium aluminum hydride reagent, used in this experiment, may provide a mild and general method for hydrogenolysis of carbon–fluorine bonds. Complex metal hydrides do not readily affect the carbon–fluorine bond (cf. Hudlický, ref. 3 (p. 161) and ref. 17).*

Can. J. Chem. Downloaded from www.nrcresearchpress.com by 210.87.254.40 on 09/05/12
For personal use only.

tumor growth was inhibited; 40% by the fluoro mustard (0.6 mg/kg), completely by the chloro (22 mg/kg), completely by the bromo (4 mg/kg), and 88% by the iodo (6.5 mg/kg). Tumor growth was measured on the 10th day.

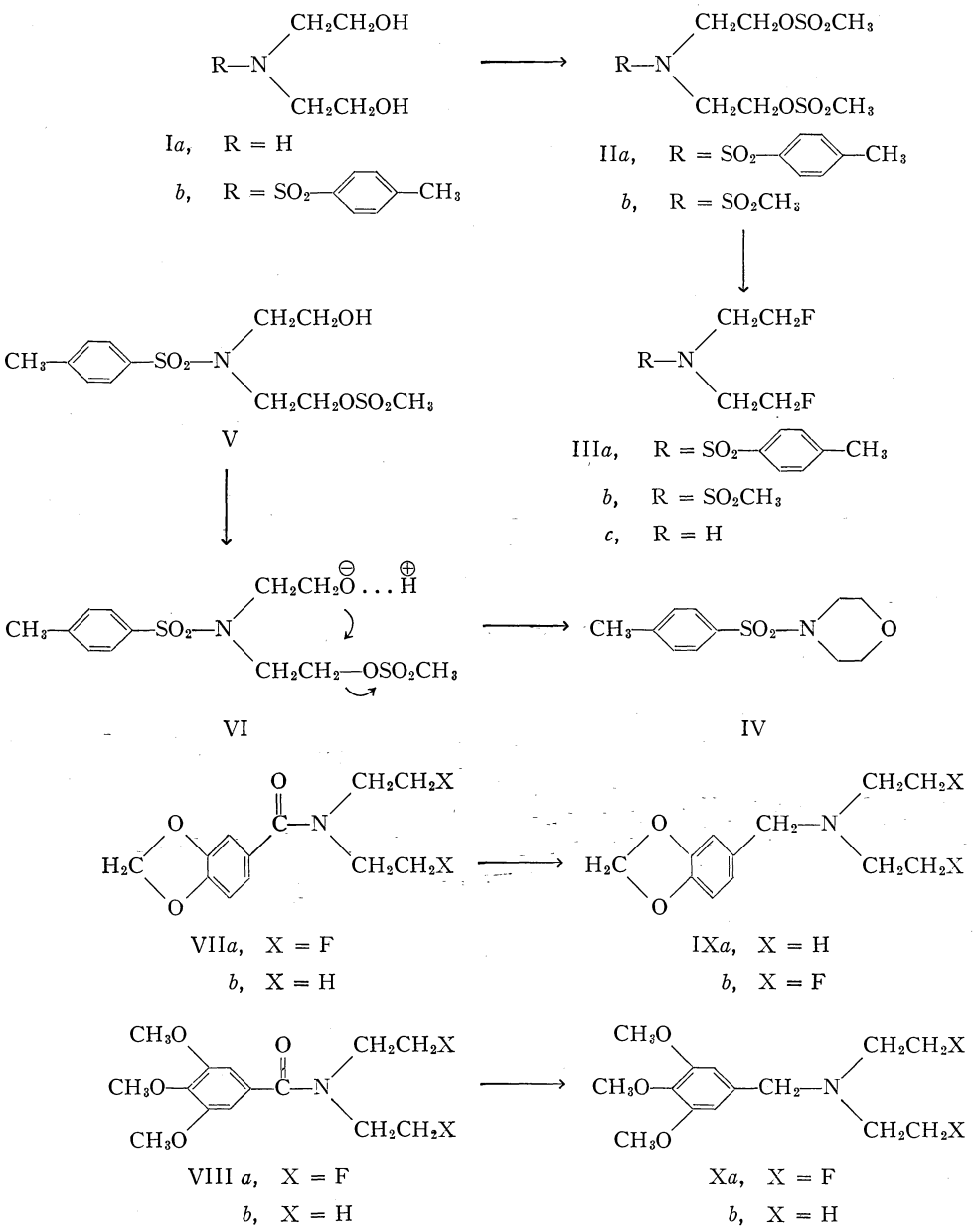

EXPERIMENTAL

Glass apparatus employed for preparation and subsequent reduction of the benzamides was previously dried at 120° C. Tetrahydrofuran used in the reduction procedure was heated at reflux over sodium for 4 hours and then distilled (from lithium aluminum hydride) into the reaction container. The formamide and dimethylformamide were both distilled *in vacuo* and stored over molecular sieve type 4-A. Potassium fluoride was dried in a vacuum oven at 165° for 24 hours. All solvent extracts were dried over magnesium sulphate.

Can. J. Chem. Downloaded from www.nrcresearchpress.com by 210.87.254.40 on 09/05/12
For personal use only.

Melting points were observed using a Kofler apparatus. Infrared spectral data was recorded by Dr. R. A. Hill of this laboratory. Microanalyses were provided by Dr. A. Bernhardt, Max-Planck Institute, Mülheim (Ruhr), Germany, and Drs. Weiler and Strauss, Oxford, England.

N-bis(2-methanesulphonyloxyethyl)-p-toluenesulphonamide (IIa)

Methanesulphonyl chloride (115 g) was added dropwise with stirring over a 5.5 hour period to a cold (ice bath) solution of N-bis(2-hydroxyethyl)-*p*-toluenesulphonamide (I*b*, 130 g, ref. 18) in dry pyridine (107 ml). The resulting pale yellow mixture was stirred with cooling for 1.5 hours and then allowed to stand 2.5 hours. After the mixture was washed with ice water and 6 *N* hydrochloric acid the residue was extracted with chloroform. The combined extract was washed successively with water, 6 *N* hydrochloric acid, and water. Following removal of solvent *in vacuo* and trituration with ether, the pale yellow residue solidified. Recrystallization from chloroform–benzene gave colorless crystals; yield, 136 g (66%), m.p. 58–62°. Four recrystallizations from benzene (Norit-A) afforded an analytical sample melting at 63–63.5°; ν_{max}^{KBr} 1355–1318 (broad), 1180–1154 (broad), 1015, 998, 980, 910, 820, and 720 cm^{-1}. Calc. for $C_{13}H_{21}NO_8S_3$: C, 37.58; H, 5.09; N, 3.37; S, 23.16%. Found: C, 37.30 to 41.68; H, 4.92 to 5.39; N, 3.08 to 3.19; S, 22.04 to 22.18%.

Three apparently pure analytical samples of sulphonamide II*a*, m.p. 63–64°, were prepared using different methods and submitted for elemental analysis. However, the product (II*a*) was generally accompanied by a tenacious impurity as evidenced by the above analytical data.

N-Bis(2-fluoroethyl)-p-toluenesulphonamide (IIIa)

A mixture of sulphonamide II*a* (18.0 g, 0.01 mole), anhydrous potassium fluoride (10.0 g, 0.17 mole) and diethylene glycol (180 ml) was stirred at 130–140° for 4.5 hours. The solution was cooled to room temperature and diluted with ice water (150 ml). The resulting mixture was extracted with chloroform and the extract was concentrated to a colorless oil, which crystallized upon trituration with ether. Recrystallization from benzene – ethyl ether yielded (4.0 g, 32%) colorless needles melting at 76–78°. Childs (6) reported a melting point of 79°. Four recrystallizations from ethyl ether (Norit-A) gave an analytical specimen melting at 79–79.4°; ν_{max}^{KBr} 1598, 1468, 1447, 1400, 1365, 1342–1330 (broad), 1293, 1172–1148 (broad), 1038, 937–922, 858, 720, and 700 cm^{-1}. Calc. for $C_{11}H_{15}F_2NO_2S$: C, 50.18; H, 5.74; F, 14.43; N, 5.32; S, 12.18%. Found: C, 50.40; H, 5.67; F, 14.29; N, 5.13; S, 12.36%.

N-Bis(2-methanesulphonyloxyethyl)methanesulphonamide (IIb)

Methanesulphonyl chloride (115 ml) was added (dropwise) over 1 hour to a cold (ice bath) solution composed of 2′,2′-iminodiethanol (52.6 g) and dry pyridine (160 ml). The resulting yellow suspension was stirred for 0.25 hours and then the solution was filtered. The solid phase was washed well with water, with 6 *N* hydrochloric acid (250 ml), and again with water. Following crystallization from acetone, the product (137 g, 81%), m.p. 110–112°, was recrystallized from chloroform to yield pale yellow needles melting at 114.5–115.5°; yield, 50.0 g (33%). Several recrystallizations from acetone raised the melting point to 117–118°; ν_{max}^{KBr} 1368–1320 (broad), 1176, 1148, 1135, 1020, 978, 900, 808, 778, 740, and 727 cm^{-1}. Calc. for $C_7H_{17}NO_8S_3$: C, 24.76; H, 5.05; N, 4.13; S, 28.34%. Found: C, 24.95; H, 4.97; N, 3.94; S, 27.98%.

N-Bis(2-fluoroethyl)methanesulphonamide (IIIb)

A mixture composed of anhydrous potassium fluoride (70.0 g, 1.2 mole), methanesulphonamide II*b* (10.0 g, 0.3 mole), and diethylene glycol (500 ml) was stirred and heated at 150–155° for 6 hours. As the reaction proceeded, the mixture began to gel and darken. After cooling, and dilution with cold water (750 ml), the mixture was extracted with chloroform. The extract was concentrated *in vacuo* to a brown oil and triturated with ethyl ether. Next, the waxy residue was extracted with benzene (50 ml) and the extract was treated with Norit-A. Following dilution with ethyl ether and cooling, two crystal crops were obtained: the first 5.9 g (10%), m.p. 42.5–45.5°, and the second 10.1 g (18%), m.p. 38–42°. Three recrystallizations of the higher melting specimen from carbon tetrachloride led to an analytical sample of colorless needles, m.p. 46.2–46.7°; ν_{max}^{KBr} 1346–1320 (broad), 1155–1144 (broad), 1012, 966, 922, 843, and 776 cm^{-1}. Calc. for $C_5H_{11}F_2NO_2S$: C, 32.08; H, 5.92; F, 20.03; N, 7.48; S, 17.13%. Found: C, 32.35; H, 5.72; F, 20.01; N, 7.73; S, 16.90%.

N-Bis(2-fluoroethyl)amine (IIIc) Hydrobromide

Procedure A

Toluenesulphonamide III*a* (1.32 g) was added to a solution of phenol (0.47 g) in anhydrous 3:7 hydrogen bromide – glacial acetic acid and the pale yellow solution was allowed to remain at room temperature for 13 hours. After dilution with ethyl ether (30 ml) the colorless crystalline hydrobromide weighed 0.25 g (26%) and melted at 186–188°. Increasing the reaction time to 2.5 or to 4 days afforded respectively 48 to 60% yields of amine III*c* hydrobromide.[8] Three recrystallizations from methanol – ethyl ether gave a pure sample, m.p. 187–189°; ν_{max}^{KBr} 3000–2900 (broad), 2760, 1563, 1455, 1422, 1273, 1058, 925, and 785 cm^{-1}. Calc. for $C_4H_{10}BrF_2N$: C, 25.28; H, 5.30; F, 19.99%. Found: C, 25.46; H, 5.23; F, 20.26%.

By mixture melting point determination and infrared spectral comparison in potassium bromide, the

[8]*Experiments conducted by T. P. Habif and M. Sciaraffa.*

Can. J. Chem. Downloaded from www.nrcresearchpress.com by 210.87.254.40 on 09/05/12
For personal use only.

hydrobromide salt was found to be identical with a specimen prepared from N-bis(2-fluoroethyl)amine hydrochloride (see below). Fluoro-nitrogen mustard III*c* was further characterized by conversion to *N-bis(2-fluoroethyl)-3,4,5-triiodobenzamide.* The amide was prepared (cf. VII*a*) using the amine corresponding to 4.2 g of N-bis(2-fluoroethyl)amine hydrobromide and 5.2 g of 3,4,5-triiodobenzoyl chloride (19). The crude pale yellow solid was recrystallized from benzene (Norit-A) to yield 2.9 g (49%) of colorless needles melting at 152–154.5°. Concentrating the mother liquor gave a second crop (0.2 g) melting at 151–153.5°. Several recrystallizations from benzene–hexane afforded an analytical specimen melting at 154–155° with sublimation from 150°, ν_{max}^{KBr} 1630 cm^{-1}. Calc. for $C_{11}H_{10}F_2I_3NO$: C, 22.35; H, 1.71; I, 64.42; N, 2.37%. Found: C, 22.56; H, 1.64; I, 64.22; N, 2.23%.

Procedure B

When the general cleavage reaction over a 13 hour period described in procedure A was applied to methanesulphonamide III*b* (3.7 g), the yield of N-bis(2-fluoroethyl)amine hydrobromide (0.3 g), m.p. 183–187°, was 8%. Two recrystallizations from methanol – ethyl ether led to a pure sample, m.p. 187–189°, which was identical with the hydrobromide obtained using procedure A. The identical composition of both products was established by infrared spectral comparison (in potassium bromide) and mixture melting point determination.

N-Bis(2-fluoroethyl)amine Hydrochloride

A specimen of N-bis(2-fluoroethyl)amine prepared as described by Childs (6) was converted to the hydrochloride derivative by D. S. Blonda of this laboratory. Three recrystallizations from methanol – ethyl ether gave an analytical sample melting at 202°; ν_{max}^{KBr} 2990–2970, 2730, 2460, 1590–1578 (broad), 1460, 1058, 936–922 (broad), cm^{-1}. Calc. for $C_4H_{10}ClF_2N$: C, 33.00; H, 6.92; Cl, 24.35%. Found: C, 33.02; H, 6.84; Cl, 24.16%.

N-(p-Toluenesulphonyl)morpholine (IV)

Approximately 60 ml of a solution prepared from anhydrous potassium fluoride (1.4 g, 0.024 mole) and formamide (75 ml) was added dropwise over a 0.25 hour period to a warm (90°) solution of *p*-toluenesulphonamide II*a* (9.1 g, 0.22 mole) in formamide (50 ml). Before addition of the remaining potassium fluoride solution, over 0.25 hour, stirring and heating at 120–125° were continued 4 hours. Heating was then continued at 120–125° for 3 hours. The solution was cooled to room temperature and poured into cold water (125 ml). Following extraction with benzene the combined extract was concentrated *in vacuo* to a colorless solid; yield, 3.8 g (71.5%), m.p. 144.5°. Recrystallization from methanol gave colorless needles melting at 148–149°. By mixture melting point determination and infrared spectral comparison in potassium bromide, the product was found to be identical with an authentic sample (16).

When the above experiment was repeated essentially as described using diethylene glycol as solvent the crude yield of *p*-toluenesulphonamide IV was 5.6 g, m.p. 142–143.5°. Recrystallization from methanol gave 0.43 g of colorless needles melting at 147–148.5°. However, when the reaction was repeated using the dimethyl ether of diethylene glycol or dimethylformamide as solvent only starting material (II*a*) was isolated.

N-Bis-ethyl-3,4-methylenedioxybenzylamine (IXa) Hydrochloride[9]

(a) From N-bis(2-fluoroethyl)-3,4-methylenedioxybenzamide (VIIa)

In a typical experiment N-bis(2-fluoroethyl)amine hydrobromide (5.7 g) was treated with 1.3 g of sodium hydroxide in water (25 ml). The corresponding amine was extracted with benzene and the combined extract was dried. Next, a solution of 3,4-methylenedioxybenzoyl chloride (2.6 g, ref. 5) in benzene (25 ml) was added over a 1 hour period with cooling (ice bath). Stirring was continued while the mixture was heated at reflux for 5 hours. After it was cooled to room temperature, N-bis(2-fluoroethyl)amine hydrochloride was collected and the colorless filtrate was concentrated to a deep straw-colored oil; yield, 3.45 g, ν_{max}^{pure} 1640 cm^{-1}. Several attempts to crystallize the crude oily amide were unsuccessful.

The N-bis(2-fluoroethyl)amide (VII*a*, 9.2 g) was reduced using a mixture of aluminum chloride (4.8 g) and lithium aluminum hydride (1.2 g) as described for preparation of N-bis(2-chloroethyl)-3,4-methylenedioxybenzylamine hydrochloride in a prior investigation (5). In this case, addition of excess ethyl ether – hydrogen chloride solution did not precipitate the hydrochloride. However, removing the solvent *in vacuo* led to 3.5 g of colorless crystalline amine (IX*a*) hydrochloride, m.p. 190–195°. Four recrystallizations from methanol – ethyl ether raised the melting point to 203–204°, with darkening from 198°.

(b) From N-bis-ethyl-3,4-methylenedioxybenzamide (VIIb)

Preparation (cf. ref. 20) and conversion of amide VII*b* (9.7 g) to the corresponding amine (2.1 g, decomp. 210–211° with darkening from 209°) was accomplished essentially as described in the preceding experiment. Calc. for $C_{12}H_{18}ClNO_2$: C, 59.13; H, 7.44; N, 5.76%. Found: C, 59.39; H, 7.30; N, 5.86%.

Amine IX*a* hydrochloride prepared by procedure (*a*) was found to be identical (infrared spectral comparison) with the specimen prepared by this method. A mixture of both products melted at 206–207° (darkening from 203°). However, elemental analysis of the product from procedure (*a*) indicated that this specimen still contained a small amount (1.44%) of fluorine.

[9]*These experiments were performed by D. S. Blonda.*

Can. J. Chem. Downloaded from www.nrcresearchpress.com by 210.87.254.40 on 09/05/12
For personal use only.

N-Bis-ethyl-3,4,5-trimethoxybenzylamine (Xb) Hydrochloride

A solution of N-bis-ethyl-3,4,5-trimethoxybenzamide (3.0 g, 0.011 mole (ref. 21)) in tetrahydrofuran (20 ml) was slowly (0.5 hour) added to a cold (ice bath) suspension of lithium aluminum hydride (0.24 g, 0.006 mole). The ice bath was removed and stirring was continued at room temperature for 24 hours. The reaction was conducted in a nitrogen atmosphere. After cautious addition of ethyl acetate, 95% ethanol, and water, the reaction mixture was concentrated *in vacuo* at 40–50°. The residual mixture was treated with 40% sodium hydroxide (20 ml) and extracted with benzene. Diluting the combined and dried extract with dry hydrogen chloride in ethyl ether gave 2.28 g (70.4%), m.p. 179.5–181°, of amine X*b* hydrochloride. Three recrystallizations from methanol – ethyl ether (Norit-A) led to a pure sample as colorless needles, m.p. 183–184°; ν_{max}^{KBr} 2920, 2600, 1590, 1512, 1470, 1428, 1335, 1260–1243 (broad), 1122, 1018, 860, and 780 cm^{-1}. Calc. for $C_{14}H_{24}ClNO_3$: C, 58.03; H, 8.35; N, 4.83%. Found: C, 58.30; H, 8.42; N, 4.93%.

N-Bis(2-fluoroethyl)-3,4-methylenedioxybenzylamine (IXb) Hydrochloride

Lithium aluminum hydride (0.5 g) was used to reduce N-bis(2-fluoroethyl)-3,4-methylenedioxybenzamide (VII*a*, 3.1 g) as described for preparation of diethyl amine X*b*. The crude hydrochloride was obtained as colorless crystals; yield, 1.73 g (52%), m.p. 176–178°. Four recrystallizations from methanol – ethyl ether led to an analytical specimen melting at 185° (sublimation at 150°), ν_{max}^{KBr} 2900, 2600–2500 (broad), 1510, 1494, 1445, 1255, 1140, 922, and 905 cm^{-1}. Calc. for $C_{12}H_{16}ClF_2NO_2$: C, 51.53; H, 5.77; N, 5.01%. Found: C, 51.42; H, 5.87; N, 4.88%.

N-Bis(2-fluoroethyl)-3,4,5-trimethoxybenzamide (VIIIa)

A 6.1 g sample of bis(2-fluoroethyl)amine hydrobromide was converted to the free base and allowed to react with 3,4,5-trimethoxybenzoyl chloride (3.5 g) in dry benzene (100 ml) as described for synthesis of amide VII*a*. The crude amide crystallized from benzene–hexane as colorless needles weighing 4.4 g (96%), m.p. 80.5–83.5°. Two recrystallizations from the same solvent afforded a pure sample melting at 83.7–84.5°, ν_{max}^{KBr} 1638 cm^{-1}. Calc. for $C_{14}H_{19}F_2NO_4$: C, 55.44; H, 6.31; F, 12.53; N, 4.61%. Found: C, 55.55; H, 6.36; F, 12.30; N, 4.56%.

N-Bis(2-fluoroethyl)-3,4,5-trimethoxybenzylamine (Xa) Hydrochloride

Lithium aluminum hydride (0.14 g) reduction of amide VIII*a* (2.0 g) was accomplished as described for preparation of amine X*b* hydrochloride. Recrystallizing the crude hydrochloride from methanol – ethyl ether (Norit-A) gave a first crop (0.75 g) melting at 132–134.5° and a second crop (0.14 g, total yield 41%) melting at 129.5–131.5°. Three recrystallizations of the higher melting specimen from the same solvent gave a pure sample of colorless platelets melting at 133.5–135°, ν_{max}^{KBr} 1589, 1510, 1468, 1422, 1335, 1258, 1172, and 965 cm^{-1}. Calc. for $C_{14}H_{22}ClF_2NO_3$: C, 51.62; H, 6.81; F, 11.66; N, 4.30%. Found: C, 51.75; H, 6.91; F, 11.44; N, 4.29%.

ACKNOWLEDGMENTS

This investigation was aided by Grants Number T-79C and T-79D from the American Cancer Society. We also wish to thank Dr. R. B. Ross for providing a summary of the N-bis(2-fluoroethyl)amine toxicity studies.

REFERENCES

1. W. C. J. Ross. Biological alkylating agents. Butterworth and Co. London. 1962. p. 105. V. G. Nemets and G. G. Tsybaeva. Tr. Leningr. Tekhnol. Inst. im. Lensoveta. **60**, 56 (1960). Chem. Abstr. **55**, 20943 (1961).
2. H. Busch. Biochemistry of the cancer cell. Academic Press, New York. 1962. p. 332.
3. M. Hudlicky. Chemistry of organic fluorine compounds. Macmillan Co., New York. 1962. p. 312. R. E. A. Dear and F. L. M. Pattison, J. Am. Chem. Soc. **85**, 622 (1963). F. H. Dean and F. L. M. Pattison, Can. J. Chem. **41**, 1833 (1963).
4. R. P. Bratzel, R. B. Ross, T. H. Goodridge, W. T. Huntress, M. T. Flather, and D. E. Johnson. Cancer Chemotherapy Rept. **26**, 1 (1963).
5. G. R. Pettit, M. F. Baumann, and K. N. Rangammal. J. Med. Pharm. Chem. **5**, 800 (1962).
6. A. F. Childs, L. J. Goldsworthy, G. F. Harding, F. E. King, A. W. Nineham, W. L. Norris, S. G. P. Plant, B. Selton, and A. L. L. Tompsett. J. Chem. Soc. 2174 (1948).
7. E. Wilson and M. Tishler, J. Am. Chem. Soc. **73**, 3635 (1951).
8. E. Forche. *In* Methoden der organischen Chemie. *Edited by* E. Müller. Georg Theime Co., Stuttgart. 1962. p. 1. Advances in fluorine chemistry. Vol. III. *Edited by* M. Stacey, J. C. Tatlow and A. G. Sharpe. Butterworth and Co. Ltd., London. 1963.
9. L. H. Knox, E. Velarde, S. Berger, D. Cuadriello, and A. D. Cross. Tetrahedron Letters, 1249 (1962). D. E. Ayer. Tetrahedron Letters, 1065 (1962).
10. P. Malatesta and B. D'atri. Ric. Sci. **22**, 1589 (1952); Chem. Abstr. **47**, 10478 (1953).
11. J. T. Maynard. J. Org. Chem. **28**, 112 (1963).
12. W. F. Edgell and L. Parts. J. Am. Chem. Soc. **77**, 4899 (1955).

Can. J. Chem. Downloaded from www.nrcresearchpress.com by 210.87.254.40 on 09/05/12
For personal use only.

13. F. L. M. PATTISON and J. E. MILLINGTON. Can. J. Chem. **34**, 757 (1956). A. I. TITOV, G. N. VEREMEEV, V. V. SMIRNOV, and O. D. SHAPILOV. Dokl. Akad. Nauk SSSR **113**, 358 (1957); Chem. Abstr. **51**, 14551 (1957).
14. G. R. PETTIT and R. E. KADUNCE. Can. J. Chem. **41**, 2695 (1963). S. SEARLES and S. NUKINA. Chem. Rev. **59**, 1077 (1959).
15. F. W. HOFFMANN. J. Org. Chem. **15**, 425 (1950). L. RAND, J. W. SWISHER, and C. J. CRONIN. J. Org. Chem. **27**, 3505 (1962).
16. J. KLOUBEK and A. MARHOUL. Coll. Czeck. Chem. Comm. **28**, 1016 (1963).
17. N. G. GAYLORD. Reduction with complex metal hydrides. Interscience Publishers, Inc., New York. 1956. p. 889. J. RUDINGER and M. FERLES. Hydrid lithno-hlinitý. Československé akademie véd., Prague. 1956. p. 475.
18. A. E. KRETOV and G. V. TIKNONOVA. Zh. Obschch. Khim. **28**, 2808 (1958).
19. C. KLEMME and J. HUNTER. J. Org. Chem. **5**, 508 (1940).
20. V. M. MICOVIC and M. Lj. MIHAILOVIC. J. Org. Chem. **18**, 1190 (1953).
21. E. T. MCCABE, W. F. BARTHEL, S. I. GERTLER, and S. A. HALL. J. Org. Chem. **19**, 493 (1954).

Can. J. Chem. Downloaded from www.nrcresearchpress.com by 210.87.254.40 on 09/05/12
For personal use only.

FRIEDEL–CRAFTS REARRANGEMENTS

II. REARRANGEMENTS DURING CYCLIALKYLATION OF ε-ARYL-SUBSTITUTED COMPOUNDS[1]

L. R. C. BARCLAY, B. A. GINN, AND C. E. MILLIGAN[2]
Department of Chemistry, Mount Allison University, Sackville, New Brunswick
Received October 3, 1963

ABSTRACT

Friedel–Crafts cyclialkylation of aromatics such as 1,1,4,4-tetramethyltetralin with 2,6-dichloro-2,6-dimethylheptane does not yield a benzsuberane as previously reported. Several 5-phenyl-substituted chlorides, alcohols, and olefins were synthesized for cyclialkylation studies. These included 2-chloro-2,6-dimethyl-6-phenylheptane (X*a*), 3-chloro-3,7-dimethyl-7-phenyloctane (X*b*), 2,6-dimethyl-6-phenyl-2-heptanol, 2,6-dimethyl-6-phenyl-2-hepten-4-one (XX), 2-chloro-6-methyl-6-phenylheptane, and 1-chloro-5-phenylpentane (XXIV). Cyclialkylation of X*a* (and the corresponding alcohol), X*b*, 2-chloro-6-methyl-6-phenylheptane, and XXIV produced alkyltetralins instead of benzsuberanes. Evidence is presented and discussed which indicates that the alkyltetralins form by rearrangements in the side chains of the aryl-substituted systems. The alternative mechanism involving rearrangement of a benzsuberane intermediate via a phenonium ion mechanism was unequivocally ruled out in at least one case—the cyclization of X*b*. Nuclear magnetic resonance evidence is presented and discussed for the structural assignments.

INTRODUCTION

In Part I (1), it was shown that the ortho-diquaternary aromatic hydrocarbon octamethyloctahydroanthracene (I) was stable under the usual Friedel–Crafts conditions. However, prolonged heating of I with aluminum chloride caused ring contraction involving a 1,2-aryl shift and a phenonium ion mechanism was favored to account for the rearrangement involving conversion of a tertiary to a secondary alkyl system.

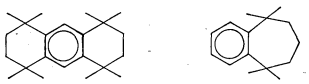

I II

The present investigation was initiated to study rearrangements in systems homologous to I. In this connection the polyalkyl benzsuberane (II) would be of particular interest. Such systems were reported by Colonge (2). However, we found at the outset that ortho-diquaternarybenzsuberane systems such as II could not be prepared by Friedel–Crafts cyclialkylations with appropriate dichlorides. Rearrangement products (alkyltetralins) formed instead. It was desirable to find if such rearrangements take place through intermediate formation of II followed by a 1,2-aryl shift, as proposed in the case of I, or whether the rearrangement takes place in the alkylating agent before ring closure. The former mechanism would conform to the phenonium ion mechanism proposed by Schmerling and co-workers (3) and by Roberts and co-workers (4) for the isomerization of *t*-pentylbenzene into 2-methyl-3-phenylbutane. The latter mechanism would be analogous to that proposed by Friedman and co-workers (5), who cited evidence indicating that (at least in the alkylation of para-xylene) the *t*-pentyl cation may isomerize to a secondary pentyl system, as opposed to isomerization taking place through the arylalkane.

[1]*Presented in part before the Chemical Institute of Canada, Organic Chemistry Symposium, McMaster University, August 1962, and the Division of Petroleum Chemistry, Symposium on Aromatic Compounds at the 142nd Meeting of the American Chemical Society, Atlantic City, September 1962.*
[2]*National Research Council Studentship holder.*

Can. J. Chem. Downloaded from www.nrcresearchpress.com by 210.87.254.40 on 09/05/12
For personal use only.

Can. J. Chem. Downloaded from www.nrcresearchpress.com by 210.87.254.40 on 09/05/12
For personal use only.

TABLE I

Cyclialkylation reactions

No.	Reactants (mole)	Catalyst (mole)	Solvent	Temp., °C	Time, hours	Products	% yield
1	1,1,4-4-Tetramethyltetralin (III) (0.03) + $CCl(CH_3)_2$—$(CH_2)_3$—$CCl(CH_3)_2$ (IV) (0.03)	$AlCl_3$ (0.006)	CS_2	0	6	V VI	60 12
2	1,1-Dimethyl-4-isopropyltetralin (VIII) (0.003) + $CCl(CH_3)_2$—$CH_2CH_2CCl(CH_3)_2$	AlCl (0.002)	CS_2	0	6	V VI	46 40
3	$C_6H_5(CH_3)_2(CH_2)_3CCl(CH_3)_2$ (0.017)	AlCl (0.017)	CS_2	−10	7	VIII	75
4	$C_6H_5C(CH_3)_2(CH_2)_3COH$—$(CH_3)_2$ (0.024)	HF (0.50)	CCl_4	10	1	VIII	100
5	$C_6H_5C(CH_3)_2(CH_2)_3CCl$—$(CH_3)CH_2CH_3$ (0.0079)	$AlCl_3$ (0.0079)	CS_2	0	1	IX	93.3
6(*a*)	$C_6H_5C(CH_3)_2CH_2CO$—$CH{=}C(CH_3)_2$ XX (0.0081)	$BF_3{:}O(C_2H_5)_2$ (15 ml)	CH_2Cl_2	Room temp.	23	No reaction	
6(*b*)	XX (0.0023)	HF (0.50)	CCl_4	Room temp.	24	No reaction	
6(*c*)	XX (0.0023)	PPA	None	100	7	1,1-Dimethylindanone	65.2
7	$C_6H_5C(CH_3)_2(CH_2)_3$—$CHClCH_3$ (0.0047)	$FeCl_3$ (0.0047)	CH_3NO_2	0	¾–2	Unreacted chloride + 1,1-dimethyl-4-ethyltetralin (XXIII)	
					4	XXIII	89.2
8(*a*)	$C_6H_5(CH_2)_5Cl$ (XXIV) (0.0055)	$AlCl_3$ (0.0055)	Pet. ether, (b.p. 60–80° C)	Reflux	1	1-Methyltetralin	80
8(*b*)	XXIV (0.0027)	$AlCl_3$ (0.0027)	Pet. ether, (b.p. 60–80° C)	0	0.5	1-Methyltetralin XXIV	2 98

In cases Nos. 3–8, the percentage yields were calculated from gas–liquid chromatographic analyses.

A number of synthetic phenyl-substituted chlorides, related olefins, and alcohols were selected for cyclialkylation–rearrangement studies. Polyalkyltetralins rather than benzsuberanes were the products of cyclization and evidence is provided in favor of rearrangement in the side chain before ring closure.

DISCUSSION OF RESULTS

The structure for Colonge's reported 1,1,5,5-tetramethylbenzsuberane (II) (2) from cyclialkylation of benzene with 2,6-dichloro-2,6-dimethylheptane (IV) was based upon a reported oxidation of II to *o*-phenylenediisobutyric acid anhydride with a melting point of 116°. However, this anhydride was recently synthesized by unambiguous routes (6, 7) and found to have a melting point of 98–99°. The structure offered for II is therefore open to question and an initial cyclialkylation study was made using the dichloride (IV). 1,1,4,4-Tetramethyltetralin (III) was selected as the substrate since it is cyclialkylated under mild conditions and does not lead to complex mixtures as is the case with benzene. This cyclialkylation of III (Table I, No. 1) yielded two hydrocarbons—a saturated hydrocarbon (60%) (V) from the solvent (CS_2) layer and an unsaturated hydrocarbon (12%) (VI) from the complex layer of the reaction. The unsaturated hydrocarbon was related to V by catalytic reduction of the olefinic double bond. These hydrocarbons were shown to have structures V and VI shown below by spectroscopic evidence and a classical synthesis. The ultraviolet spectrum of V was very similar to that of octamethyloctahydroanthracene (I) (1) (see Table II for ultraviolet spectra). The infrared spectrum of V (CS_2) showed a strong band at 11.2 microns attributed to 1,2,4,5-tetrasubstitution. Hydrocarbon VI displayed an ultraviolet spectrum (Table II) typical of compounds containing a double

TABLE II

Ultraviolet spectra

	λ_{max} (mμ)	ϵ
Octamethyloctahydroanthracene (I)	278, 270	1096, 955
Saturated hydrocarbon (V)	279.6, 271	1362, 1227
Unsaturated hydrocarbon (VI)	262 (broad)	14,725
1,1,4,4-Tetramethyltetralin (III)	271, 264, 257	398, 457, 324
1,1-Dimethyl-4-isopropyltetralin (XII*a*)	272.5, 265	269, 330
2,2,5,5-Tetramethyl-3,4-benzo-ϵ-caprolactol (7)	262 (broad)	237
1,1,4,4-Tetramethylbenzsuberane (XVIII)	271,* 267.7, 261.5	139, 188, 237
Benzsuberane (XXV)	271.5, 267.7, 264	261, 211, 280
1,1-Dimethyl-4-ethyltetralin	272, 264.5	328, 361
1-Methyltetralin (XXVIII)	273.2, 266	427, 431

*Shoulder.

bond conjugated with a benzene ring. Its infrared spectrum showed a strong band at 11.2 microns attributed to 1,2,4,5-tetrasubstitution and a strong band at 12.5 μ attributable to the out-of-plane deformation of an olefinic proton. The latter band disappeared upon catalytic reduction of VI. The compounds showed the expected nuclear magnetic resonance spectra. Hydrocarbon V exhibited a multiplet in the region of C—CH_3 absorption between 9.28 and 8.76 p.p.m. of intensity corresponding to 24 protons. A band at 8.36 corresponded to eight methylene protons and one at 7.59 was attributed to the two methine hydrogens. The two aromatic protons absorbed as a doublet at 3.07 and 2.91. The unsaturated hydrocarbon (VI) had a doublet at 8.80–8.73 p.p.m. corresponding to 24 methyl protons, a peak at 8.34 for four methylene protons, a doublet at 7.92–7.81 for the methylene adjacent to the conjugated double bond, a doublet at 4.42–4.34 attributed to the olefinic proton, and a band at 2.82 attributed to the two aromatic protons.

Can. J. Chem. Downloaded from www.nrcresearchpress.com by 210.87.254.40 on 09/05/12
For personal use only.

A classical synthesis confirmed the structures offered for V and VI (see Chart I). The previously reported 4,4-dimethyl-1-tetralone (VII) (8, 9) was converted to 1,1-dimethyl-4-isopropyltetralin (VIII). Cyclialkylation of VIII with 2,5-dichloro-2,5-dimethylhexane (Table I, No. 2) yielded a mixture of V and VI. These hydrocarbons were shown to be identical by mixed melting points and infrared spectra with the products formed in the cyclialkylation of 1,1,4,4-tetramethyltetralin with 2,6-dichloro-2,6-dimethylheptane (IV).

CHART I

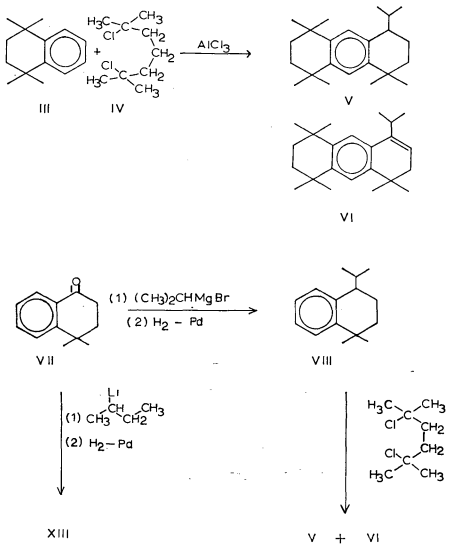

From the above results it seems unlikely that benzsuberanes can be prepared by Friedel–Crafts cyclialkylations with ditertiary halides. However, it was desirable to determine the mechanism whereby the rearrangement products (alkyltetralins) formed. Two distinct possibilities existed. Firstly, the ortho-diquaternarybenzsuberane system (i.e. II) could form as an intermediate in the reaction followed by rearrangement through a 1,2-phenyl shift as was demonstrated in the rearrangement of I (1). Secondly, the rearrangement could take place before cyclization, possibly in a phenyl-substituted chloride. A method of testing for both of these possibilities was worked out by cyclizations of 2-chloro-6-phenyl-2,6-dialkylheptanes (X*a* and *b*) (Chart II). A key intermediate in the synthesis of these chlorides was the ketone 6-methyl-6-phenyl-2-heptanone (IX) prepared by alkylation of benzene with 6-methyl-5-heptene-2-one. The ketone (IX) has been synthesized previously (10). Nevertheless it was desirable to establish the authenticity of our own sample by n.m.r. analysis. This ketone showed a singlet at 8.74 p.p.m. integrating for six protons and attributed to the *gem* dimethyls. A singlet at 8.13 of intensity corresponding to three protons was attributed to the methyl on the carbonyl carbon. A triplet at 7.93, 7.83, and 7.60 p.p.m. integrating for two protons was attributed to the methylene group adjacent to the carbonyl. The remaining four methylene hydrogens appeared in a multiplet with the prominent band at 8.57 p.p.m. The desired chlorides, 2-chloro-2,6-dimethyl-6-phenylheptane (X*a*) and 3-chloro-3,7-dimethyl-7-phenyloctane (X*b*), were synthesized from IX as outlined in Chart II.

The chloride X*a* provided a "control" to determine if cyclization of such a system would yield any benzsuberane (XI*a*). A rearrangement product (VIII) resulted as is discussed

Can. J. Chem. Downloaded from www.nrcresearchpress.com by 210.87.254.40 on 09/05/12
For personal use only.

CHART II

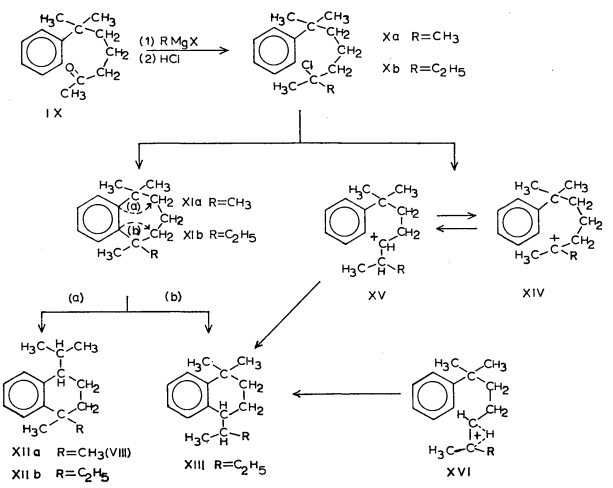

below. In the chloride X*b* the ethyl group is in effect a "label". *If* the rearrangement takes place through an ortho-diquaternary benzsuberane (XI*b*), the 1,2-aryl shift can take place by two routes "*a*" and "*b*". One would expect equal proportions of two tetralins from this mechanism—dimethylsecondarybutyltetralin (XIII) and isopropylmethylethyltetralin (XII*b*). The alternative mechanism for this rearrangement involves rearrangement in the side-chain by equilibration of the tertiary carbonium ion XIV with the secondary carbonium ion XV followed by cyclization of the latter (see Chart II). This latter mechanism would be expected to produce only one tetralin (XIII) from X*b*.

Friedel–Crafts cyclization of the chloride X*a* (Table I, No. 3) or hydrogen fluoride cyclization of the corresponding alcohol (Table I, No. 4) produced 1,1-dimethyl-4-isopropyltetralin (VIII) as the only cyclic product. This compound was found by ultraviolet, n.m.r., and infrared analyses to be identical with a synthetic sample of VIII. It was similarly identical with VIII recently prepared by Wood and co-workers (10). The n.m.r. spectrum of VIII provided a useful characterization (Fig. 1(*a*)). The six protons of the *gem* dimethyl group appeared as a singlet at 8.75 p.p.m. A four proton doublet at 8.28 and 8.31 p.p.m. was attributed to the four methylene protons. The characteristic feature of the spectrum was the appearance of two doublets at higher fields—8.93–9.03 and 9.19–9.31 p.p.m.—and attributed to the methyl protons of the isopropyl group. The two doublets indicate that the two methyls are non-equivalent. This is probably due to restricted rotation of the isopropyl grouping so that one of the methyls (Fig. 2, R_1) lies over the aromatic ring and is subjected to diamagnetic shielding which causes these protons to absorb at higher field than those of the more remote methyl (R_2). Hindered rotation in the isopropyl group of VIII was evident in a Stuart–Briegleb model.

Cyclization of 3-chloro-3,7-dimethyl-7-phenyloctane (X*b*) with aluminum chloride (Table I, No. 5) yielded 1,1-dimethyl-4-secondarybutyltetralin XIII(identity discussed below) rather than a mixture of tetralins XII*b* and XIII. This result rules out the phenonium ion mechanism (through XI*b*) to account for the rearrangement. Thus the rearrangement in this case must have taken place in the side chain, for example by the isomerization of XIV $\rightleftarrows$ XV.

The identity of XIII was established by comparison of the ultraviolet (Table II) and

Can. J. Chem. Downloaded from www.nrcresearchpress.com by 210.87.254.40 on 09/05/12
For personal use only.

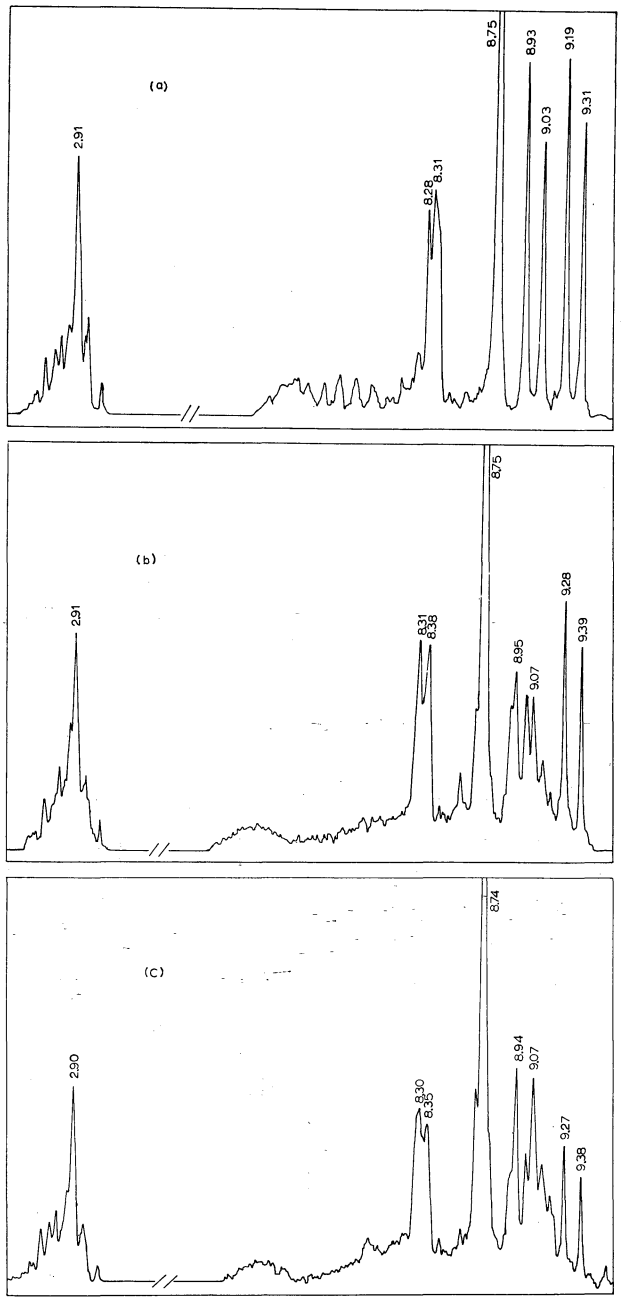

FIG. 1. Nuclear magnetic resonance spectra. (*a*) 1,1-Dimethyl-4-isopropyltetralin (VIII). (*b*) 1,1-Dimethyl-4-secondarybutyltetralin (XIII) from cyclization of (X*b*). (*c*) XIII synthetic.

infrared spectra with a synthetic sample prepared from 4,4-dimethyl-1-tetralone (VII) as is outlined on Chart I.

The n.m.r. spectra of XIII from the cyclization and also from the synthesis are shown in Fig. 1(*b*) and 1(*c*). The spectra were practically identical in the aromatic proton region

Can. J. Chem. Downloaded from www.nrcresearchpress.com by 210.87.254.40 on 09/05/12
For personal use only.

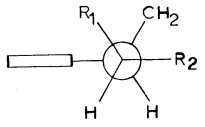

FIG. 2. (*a*) $R_1 = R_2 = CH_3$; (*b*) $R_1 = CH_3$, $R_2 = C_2H_5$; (*c*) $R_1 = C_2H_5$, $R_2 = CH_3$.

near 2.90 and in the doublet attributed to methylenes at 8.31–8.38 in Fig. 1(*b*) and 8.30–8.35 in Fig. 1(*c*). Both showed a six proton singlet at 8.75–8.74 attributed to the *gem* dimethyl grouping. The only significant difference in the spectra was in the intensities of the doublets at 9.39–9.28 (9.38–9.27) and 9.07–8.95 (9.07–8.94) in each. In the synthetic sample the high field doublet at 9.38–9.27 integrated for 1.4 protons. This might be taken to indicate that this sample consisted of approximately an equal amount of the two possible configurations in the conformations shown in Fig. 2(*b* and *c*). On the other hand, in the cyclization product the high-field doublet (Fig. 1(*b*)) integrated for 2.3 protons and indicates that this sample is enriched in configuration *b* (77%) which has the methyl group (R_1) over the field of the aromatic ring. If this speculation is correct, the cyclization of X*b* shows some stereospecificity. This would be expected if the cyclization takes place preferentially through a hydrogen bridged ion such as XVI (Chart II) since the phenyl group might be expected to approach the bridged ion (XVI) more easily on the side nearer the methyl rather than the ethyl group.

The mechanism established for the cyclization of X*a* and X*b* cannot be generalized to apply to other similar systems without unequivocal evidence. For example, Hart (11) found that cyclization of 2,5,5-trimethyl-6-phenyl-2-hexene (XVII) yielded some tetramethylbenzsuberane (XVIII) as well as 2,2-dimethyl-4-isopropyltetraline (XIX).

An attempt was made to synthesize a benzsuberane containing ortho-diquaternary carbons by cyclization of 2,6-dimethyl-6-phenyl-2-heptene-4-one (XX). Compound XX resisted cyclization (Table I, Nos. 6(*a*) and 6(*b*)). Vigorous conditions with polyphosphoric acid (No. 6(*c*) resulted in the formation of 4,4-dimethylindanone (XXII) (1). The carbonium ion (XXI) derived from XX could form XXII by a cyclization with elimination of isobutylene (Chart III).

CHART III

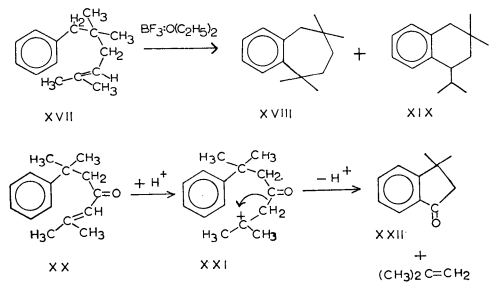

The failure of compounds X*a*, X*b*, and XX to cyclize to benzsuberanes can be attributed to strain in an ortho-diquaternarybenzsuberane system such as XI*a* or *b*. A Stuart–Briegleb model of the latter system showed very strong conformational interactions; for example, between the methyls and the ortho aromatic protons. An analogy can be made between XI*a* and derivatives of the strained aromatic system *o*-di-*t*-butylbenzene. For example, 4,5-benzo-3,3,6,6-tetramethyl-1-oxacycloheptene (which is isoelectronic with

Can. J. Chem. Downloaded from www.nrcresearchpress.com by 210.87.254.40 on 09/05/12
For personal use only.

XI*a*) and 2,2,5,5-tetramethyl-3,4-benzo-ϵ-caprolactol lack the usual vibrational fine structure in their ultraviolet spectra and this has been taken as evidence of strain (6, 7). On the other hand, the tetramethylbenzsuberane (XVIII) prepared by Hart showed some fine structure in its ultraviolet spectrum (see Table II) although it was not so well developed as in the tetralins or in benzsuberane itself.

Cyclization of the secondary chloride 2-chloro-6-methyl-6-phenylheptane under mild conditions also yielded a tetralin, 1,1-dimethyl-4-ethyltetralin (XXIII) instead of a benzsuberane (Table I, No. 7). The structure of XXIII was determined by a classical synthesis from 4,4-dimethyl-1-tetralone (VII) using the Grignard method similar to the synthesis of XII*a*.

In view of the above results on cyclialkylations of chlorides X*a*, X*b*, and 2-chloro-6-methyl-6-phenylheptane, it was desirable to reinvestigate the cyclialkylation of the primary chloride 1-chloro-5-phenylpentane (XXIV). The generally accepted view (12, 13) is that this chloride cyclizes to yield benzosuberane (XXV). Contrary to this we found that XXIV does not yield benzsuberane under conditions reported in the literature (Table I, No. 8(*a*)). It yielded instead the rearrangement product 1-methyltetralin (XXVIII). The ultraviolet spectrum of XXVIII was clearly distinguishable from that of a synthetic sample of benzsuberane (Table II). The structure of XXVIII was confirmed by its n.m.r. spectrum. The most important feature of this spectrum was a three-proton doublet at 8.69 and 8.80 p.p.m. for the methyl group on carbon one. The synthetic benzsuberane showed only methylene absorption and aromatic proton absorption as expected. The methylene absorption appeared in two multiplets—one near 8.24 p.p.m. and assigned to the protons on carbons 2, 3, and 4 and the other at 7.13–7.29 and assigned to the protons on carbons 1 and 5.

Cyclialkylation of 1-chloro-5-phenylpentane (XXIV) under milder conditions (Table I, No. 8(*b*)) resulted in recovery of 98% of XXIV and 2% of 1-methyltetralin. The absence of benzsuberane even at this stage of the reaction indicates that it is probably *not* an intermediate in the rearrangement. This reaction may therefore take place by rearrangement in the side chain through equilibration of XXVI and XXVII prior to cyclization (see Chart IV). Experiments are now underway to test this postulated mechanism by using a deuterium tracer in the side chain of XXIV.

CHART IV

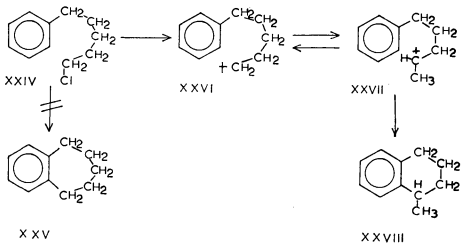

EXPERIMENTAL

The melting points were determined on a hot stage equipped with a microscope and are uncorrected. Ultraviolet spectra were recorded on a Beckman DK-2 spectrophotometer in spectrograde cyclohexane and infrared spectra on a Perkin–Elmer Model 137 Infracord. Reaction products were analyzed on a F & M Model 500 programmed temperature gas chromatograph equipped with a dual column attachment. The column packings contained silicone gum rubber. The percentage yields were determined by gas chromatography. Pure samples of liquid compounds for analyses were obtained by repetitive gas chromatography.

Can. J. Chem. Downloaded from www.nrcresearchpress.com by 210.87.254.40 on 09/05/12
For personal use only.

Nuclear magnetic resonance spectra were measured on a Varian A-60 in carbon tetrachloride solvent. Values are reported in p.p.m. relative to tetramethylsilane equals 10. Ultimate analyses were determined by Dr. E. Thommen, Basel, Switzerland.

Syntheses of Compounds for Cyclialkylation Studies

(a) 2,6-Dichloro-2,6-dimethylheptane (IV)

The dichloride (IV) was prepared from 2,6-dimethyl-5-hepten-2-ol according to the method of Colonge (2). It gave a melting point of 41–42° (lit. (2) 43°).

(b) 1,1,4,4-Tetramethyltetralin (III)

Hydrocarbon III was prepared by reacting benzene with 2,5-dichloro-2,5-dimethylhexane by a modification of the Bruson procedure (14). Gas–liquid chromatographic analysis indicated 98% purity.

(c) 2-Chloro-2,6-dimethyl-6-phenylheptane (Xa)

6-Methyl-6-phenyl-2-heptanone (IX) was prepared by a procedure similar to that reported by Wood and co-workers (10). The infrared spectrum of this ketone showed carbonyl absorption at 1700 cm^{-1} and bands attributed to monosubstitution at 770 and 704 cm^{-1}. The ketone (IX) was converted by the Grignard method into 2,6-dimethyl-6-phenyl-2-heptanol as previously reported (10). The purified alcohol gave $n_D^{23.3}$ 1.5034 (lit. (10) n_D^{20} 1.5034). The hydroxyl absorption appeared at 3250 cm^{-1}.

The chloride X*a* was prepared in 81.3% yield by the action of hydrogen chloride gas and concentrated hydrochloric acid (25 ml) on 2,6-dimethyl-6-phenyl-2-heptanol. Hydrogen chloride was bubbled into the alcohol (24.0 g) for 1.5 hours. The organic layer was then washed with sodium carbonate solution and water and dried over anhydrous calcium chloride. The crude product was vacuum distilled at 0.72 mm and 110° to yield 21.3 g of liquid (n_D^{20} 1.5041). The infrared spectrum of this compound showed no hydroxyl absorption.

(d) 3,7-Dimethyl-7-phenyl-3-octanol

The alcohol was prepared by the reaction of an ethyl Grignard with IX. The Grignard reagent, ethyl magnesium bromide, was prepared in the usual manner from 2.4 g (0.10 mole) of magnesium and 10.9 g (0.10 mole) of ethyl bromide. The ketone (13.9 g, 0.068 mole) was added slowly to the Grignard reagent in anhydrous ethyl ether and the solution was then refluxed for 6 hours and then allowed to stand overnight at room temperature. After the solution was worked up in the usual way, 14.5 g of crude liquid was obtained. The infrared spectrum showed strong hydroxyl absorption at 3250 cm^{-1} and no carbonyl absorption. Gas–liquid chromatography indicated 98.5% purity. This product was used directly without distillation for the synthesis of the chloride X*b* described below.

(e) 3-Chloro-3,7-dimethyl-7-phenyloctane (Xb)

The chloride X*b* was prepared by treating 3,7-dimethyl-7-phenyl-3-octanol (14.0 g, 0.060 mole) with 15 ml of concentrated hydrochloric acid for 15 hours. The organic layer was then washed with sodium carbonate solution and water and dried over anhydrous sodium sulphate. The ether was distilled and the crude liquid was vacuum distilled at 1.1 mm and 128–133° to yield 8.33 g of a compound, the infrared spectrum of which showed no hydroxyl absorption. Gas–liquid chromatographic analysis indicated the compound to be pure (n_D^{20} 1.5053).

(f) 2,6-Dimethyl-6-phenyl-2-hepten-4-one (XX)

Benzene (15.6 g, 0.200 mole) and aluminum chloride (36.0 g, 0.270 mole) were placed in a 200-ml three-necked flask and cooled to 10–15°. 2,6-Dimethyl-2,5-heptadien-4-one (27.6 g, 0.200 mole) was added to the above mixture over a period of 50 minutes maintaining the above temperature limits. The mixture was then allowed to come to room temperature and 2 hours later gas–liquid chromatography indicated that the phorone had been consumed. The infrared spectrum of the major component (28.4%) was typical of a monoalkyl benzene with bands at 772 and 703 cm^{-1}. A band at 1670 cm^{-1} indicated a conjugated carbonyl. This material was distilled at 1.3 mm and 117–122° (n_D^{20} 1.5268) and was assumed to be 2,6-dimethyl-6-phenyl-2-hepten-4-one.

Another component of longer retention time on the gas chromatograph was found to be 2,6-diphenyl-2,6-dimethyl-4-heptanone (15).

(g) 2-Chloro-6-methyl-6-phenylheptane

The secondary alcohol, 6-methyl-6-phenyl-2-heptanol, was prepared by the reduction of 6-methyl-6-phenyl-2-heptanone (IX) with lithium aluminum hydride. The lithium aluminum hydride (0.95 g, 0.025 mole) and anhydrous ethyl ether were placed in a 65-ml three-necked flask equipped with a mechanical stirrer, addition funnel, and reflux condenser. The ketone (5.00 g, 0.025 mole) was added slowly to produce gentle reflux, after which the mixture was refluxed for 4.5 hours. The mixture was cooled and the excess lithium aluminum hydride was decomposed first with methanol and then water. Dilute hydrochloric acid was then added to dissolve the precipitated hydroxides. The mixture was then extracted with ether and the ethereal extracts were washed with water and dried over sodium sulphate. Evaporation of the ether left 4.23 g of liquid, the infrared spectrum of which showed strong hydroxyl absorption at 3230 cm^{-1}, bands at 770 and 703 cm^{-1} for monosubstitution and no carbonyl absorption.

The chloride was prepared by heating 2.00 g (0.0098 mole) of 6-methyl-6-phenyl-2-heptanol with 10 ml of concentrated hydrochloric acid – zinc chloride reagent at 100° C for 20 minutes with stirring. The mixture

Can. J. Chem. Downloaded from www.nrcresearchpress.com by 210.87.254.40 on 09/05/12
For personal use only.

was then allowed to stand at room temperature for several hours. The organic layer was then separated, washed free of acid with water, and dried over sodium sulphate. The infrared spectrum of the product did not show hydroxyl absorption but still showed the bands at 770 and 703 cm^{-1} for a monosubstituted benzene.

(h) 1-Chloro-5-phenylpentane (XXIV)

The alcohol, 5-phenyl-1-pentanol, was prepared by lithium aluminum hydride reduction of 5-phenylpentanoic acid (Aldrich Chemical Co.). Lithium aluminum hydride (11.4 g, 0.330 mole) and anhydrous ethyl ether were refluxed for 2 hours to effect solution. 5-Phenylpentanoic acid (17.8 g, 0.100 mole) in ethyl ether was added over a period of 3 hours, a rate which promoted gentle refluxing. After one additional hour of refluxing, the solution was cooled in ice. Water was then cautiously added to decompose excess lithium aluminum hydride, after which 150 ml of 10% sulphuric acid was added. The organic layer was separated, washed with water, and dried over sodium sulphate. After distillation of the ether, the liquid residue was vacuum distilled at 1.4 mm pressure and 114–118° to yield 10.9 g (67%) of pure 5-phenyl-1-pentanol (n_D^{20} 1.5182, lit. (16) n_D^{21} 1.5170). The infrared spectrum of this compound showed no carbonyl absorption. There was strong hydroxyl absorption at 3200 cm^{-1}.

The chloride, 1-chloro-5-phenylpentane (XXIV), was prepared by heating 3.66 g (0.023 mole) of 5-phenyl-1-pentanol and 25 ml of concentrated hydrochloric acid – zinc chloride reagent for 2 days. The organic layer was then washed free of acid with sodium carbonate solution and then water and dried over sodium sulphate. The crude product was then vacuum distilled at 2.4 mm and 95–96° to yield 1.87 g of pure 1-chloro-5-phenylpentane ($n_D^{23.2}$ 1.5149). The infrared spectrum of the product showed no hydroxyl absorption and had a strong band at 670 cm^{-1} attributed to the carbon-to-chlorine linkage.

Procedures for Cyclialkylation Experiments

Cyclialkylations catalyzed by aluminum chloride and ferric chloride were carried out in a three-necked flask equipped with a mechanical stirrer and a condenser fitted with a calcium chloride drying tube. The catalyst was placed in a small Erlenmeyer flask attached to the reaction flask with flexible rubber tubing to permit convenient addition of catalyst. The reagent and solvent were placed in the flask and the mixture was cooled in an ice–salt bath. The catalyst was then added slowly with stirring to maintain the temperatures listed in Table I. The reactions were terminated by pouring the mixtures on to ice. The organic products were extracted with peroxide-free ethyl ether, the extracts washed free of acid with sodium carbonate solution then washed with water and dried over anhydrous sodium sulphate.

Reactions with anhydrous hydrogen fluoride were carried out in a 12-in. stainless steel MD test tube reactor (Autoclave Engineers Inc.). After addition of the reagents, the tube was sealed by using two-way valves and fittings. Mixing of the reaction mixture was effected by rotating the tube slowly on the shaft of an electric motor. The catalyst polyphosphoric acid was prepared from phosphoric acid and phosphorous pentoxide in the flask to be used for the reaction. The compound to be cyclized was quickly added to this catalyst with stirring. When boron fluoride – etherate was used, it was cooled to 0° with the solvent. The reagent was then added in the solvent to the cooled catalyst with stirring.

Details on the reactants and catalyst used, solvent, temperature, time, and percentage yields of products are outlined in Table I. Ultimate analyses are summarized in Table III below.

TABLE III

Ultimate analyses

Compound	Anal. calc.	Anal. found
V($C_{23}H_{36}$)	C, 88.39 H, 11.61	C, 88.65 H, 11.70
VI ($C_{23}H_{34}$)	C, 88.96 H, 11.04	C, 88.64, 88.79 H, 11.16, 11.24
VIII ($C_{15}H_{22}$)	C, 89.04 H, 10.96	C, 88.82, 88.97 H, 11.09, 11.07
XIII ($C_{16}H_{24}$)	C, 88.82 H, 11.18	C, 88.95, 89.05 H, 11.10, 11.07
Semicarbazone of IX ($C_{15}H_{23}N_3$), m.p. 118.5–120°	C, 68.93 H, 8.87 N, 16.08	C, 68.82, 68.87 H, 8.91, 8.90 N, 15.76, 15.79

Classical Syntheses of Hydrocarbons

(a) 4,4-Dimethyl-1-tetralone (VII)

The ketone (VII) was prepared by the method of Arnold and co-workers (8) by alkylation of benzene with α-methyl-valerolactone. However, our product proved to be a mixture which was difficult to purify. The method of Campbell and Cromwell (9) involving a Willgerodt–Kindler reaction on 4-methyl-4-phenyl-2-pentanone was more successful. This reaction yielded 4-methyl-4-phenylbutanoic acid (n_D^{25} 1.5182, lit. (9)

Can. J. Chem. Downloaded from www.nrcresearchpress.com by 210.87.254.40 on 09/05/12
For personal use only.

n_D^{25} 1.518; anilide, m.p. 115–116°, lit. (9) 116.5–117.5°). The latter was cyclized to 4,4-dimethyl-1-tetralone (VII) as reported (9). Vapor phase chromatography of VII indicated it was pure. The ultraviolet spectrum of VII had bands at 245 mμ, ϵ = 12,174; 285 mμ, ϵ = 1904; and 295 mμ, ϵ = 1492. The infrared spectrum showed carbonyl absorption at 1660 cm^{-1} and a strong band at 770 cm^{-1} attributed to *o*-disubstitution.

(b) 1,1-Dimethyl-4-isopropyltetralin (VIII)

The Grignard reagent, isopropyl magnesium bromide, was prepared from 7.13 g (0.058 mole) of isopropyl bromide and 1.41 g (0.058 mole) of magnesium in 50 ml of dry ethyl ether in an atmosphere of nitrogen. The Grignard reagent was cooled to −5° and 1,1-dimethyl-4-tetralone (5.0 g, 0.029 mole) in 50 ml of benzene was added over 1 hour. The reaction mixture was refluxed for 2½ hours. The product was hydrolyzed by pouring into aqueous ammonium chloride. Distillation of the solvent yielded a liquid residue which was shown to contain some starting ketone (42%) by gas–liquid chromatography. This crude product was freed of ketone by chromatography on alumina in petroleum ether. The first eluates yielded a hydrocarbon fraction (1.65 g) which showed a broad band in the ultraviolet spectrum near 260 mμ indicative of conjugation. The infrared spectrum showed a strong band at 757 cm^{-1} attributed to ortho-disubstitution and a band at 815 cm^{-1} assigned to an olefinic proton. This hydrocarbon was dissolved in methanol and reduced with hydrogen at 50 p.s.i. over palladium – calcium carbonate. The product 1,1-dimethyl-4-isopropyltetralin showed a strong band in the infrared at 760 cm^{-1} assigned to ortho-disubstitution. This compound proved to be identical with the cyclization product of 2-chloro-2,6-dimethyl-6-phenylheptane (X*a*) (Table I, No. 3) by infrared, ultraviolet (Table II), and nuclear magnetic resonance spectra (Fig. 1(*a*)).

(c) 1,1-Dimethyl-4-sec-butyltetralin (XIII)

4,4-Dimethyl-1-tetralone (4.33 g, 0.025 mole) and 50 ml of dry pentane were placed in a 200-ml three-necked flask equipped with graduated dropping funnel, nitrogen inlet, condenser, and calcium chloride drying tubes. Commercial *sec*-butyl lithium (19 ml of a 12.6% solution was added to the ketone with stirring at −5° C over 10 minutes. The reaction mixture was then allowed to stand for 24 hours and at the end of that time water was added to hydrolyze the alkyl lithium compounds. The organic layer was separated, washed with water, and dried over anhydrous sodium sulphate. The crude product showed hydroxyl absorption in the infrared spectrum and was heated with 10% oxalic acid for 18 hours to dehydrate the alcohol. After working up in the usual manner, the infrared spectrum of the product showed no hydroxyl absorption. Gas–liquid chromatography of the product after dehydration indicated that some starting ketone (39%) was still present. The product was freed of unreacted ketone by chromatography on alumina as in the previous experiment. There was obtained 2.0 g of hydrocarbon from the first eluates. This material was dissolved in methanol and hydrogenated at 60 p.s.i. over palladium calcium carbonate. After distillation of the methanol, the product was purified by repetitive gas–liquid chromatography. The infrared spectrum of the product had a strong band at 763 cm^{-1} attributed to ortho-disubstitution. The infrared and ultraviolet spectra of this hydrocarbon, 1,1-dimethyl-4-*sec*-butyltetralin, were identical with those of the cyclization product of 3-chloro-3,7-dimethyl-7-phenyloctane (X*b*) (see Table I, No. 5).

(d) 1,1,5,5,8,8-Hexamethyl-4-isopropyl-1,2,3,4,5,6,7,8-octahydroanthracene (V) and 1,1,5,5,8,8-Hexamethyl-4-isopropyl-1,2,5,6,7,8-hexahydroanthracene (VI)

1,1-Dimethyl-4-isopropyltetralin (VIII) (0.60 g, 0.003 mole) was alkylated in dry carbon disulphide solvent at 0° C with 0.55 g (0.003 mole) of 2,5-dichloro-2,5-dimethylhexane in the presence of 0.24 g (0.0018 mole) of aluminum chloride. After 6 hours reaction time, two layers were carefully separated by filtration and worked up separately to yield 0.43 g of white crystals from the carbon disulphide layer and 0.37 g of brownish white crystals from the solid complex layer. Recrystallizations from ethanol of the product from the solvent layer yielded crystals of m.p. 93.5–94.5° C. The mixed melting point of this compound with hydrocarbon V (Table I, No. 1) was 93.5–95° C. The infrared spectra of these two compounds in KBr pellets were identical. The product from the lower layer was recrystallized once from ethanol and sublimed to yield crystals of m.p. 122–124° C. The mixed melting point of this compound and hydrocarbon VI (Table I, No. 1) was 123–125° C. The infrared spectra of these two compounds in KBr pellets were identical.

(e) 1,1-Dimethyl-4-ethyltetralin

The Grignard reagent, ethyl magnesium iodide, was prepared in the usual manner from 2.68 g (0.017 mole) of ethyl iodide and 0.41 g (0.017 mole) of magnesium in 20 ml of anhydrous ethyl ether in an atmosphere of nitrogen. The Grignard reagent was cooled to 0° C and 4,4-dimethyl-1-tetralone (1.50 g, 0.0086 mole) in 20 ml of benzene was added over 20 minutes. The reaction mixture was then refluxed for 4.5 hours and at the end of that time it was worked up in the usual manner. The infrared spectrum of the crude product showed strong hydroxyl absorption. There was some carbonyl absorption indicative of some unreacted ketone. The crude product was then refluxed with aqueous oxalic acid for 21 hours to dehydrate the alcohol. The dehydrated product was chromatographed on alumina from petroleum ether to yield 0.88 g of hydrocarbon free of starting ketone. Gas–liquid chromatography indicated this material was pure.

This hydrocarbon was reduced in methanol over a palladium catalyst at 60 p.s.i. of hydrogen to yield pure 1,1-dimethyl-4-ethyltetralin. The hydrocarbon was further purified by repetitive gas–liquid chromatography. From infrared, ultraviolet, and n.m.r. spectra this compound was found to be identical with hydrocarbon XXIII produced by cyclization of 2-chloro-6-methyl-6-phenylheptane (Table I, No. 7).

Can. J. Chem. Downloaded from www.nrcresearchpress.com by 210.87.254.40 on 09/05/12
For personal use only.

(f) Benzsuberane

Benzsuberone was prepared by cyclization of 5-phenylvaleric acid (Adrich Chemical Co.) with polyphosphoric acid by the method of Muth and co-workers (17). The product was distilled at 3 mm, b.p. 122–123°, n_D^{20} 1.5659 (lit. (17) n_D^{20} 1.5642); λ_{max} 241 mμ, ϵ = 8382, λ_{max} 280 mμ, ϵ = 884. Carbonyl absorption appeared in the infrared at 1660 cm^{-1} and a strong band at 773 cm^{-1} was attributed to ortho-disubstitution. Benzsuberane was prepared by Clemmensen reduction of the above benzsuberone. The hydrocarbon was purified by gas–liquid chromatography for spectral analyses (Table II). The infrared band for ortho-disubstitution appeared at 754 cm^{-1}.

ACKNOWLEDGMENTS

This research was supported by grants from the National Research Council of Canada, the American Chemical Society (Petroleum Research Fund), Research Corporation (Frederick G. Cottrell grant), and Imperial Oil Limited.

We thank Dr. A. G. McInnes of the Atlantic Regional Laboratory, Halifax, Nova Scotia, for determining the nuclear magnetic resonance spectra. We thank Dr. T. F. Wood for a sample of 1,1-dimethyl-4-isopropyltetralin and Dr. H. Hart for a sample of 1,1,4,4-tetramethylbenzsuberane.

REFERENCES

1. L. R. C. Barclay, A. H. Gray, and C. E. Milligan. Can. J. Chem. **39**, 870 (1961).
2. J. Colonge and A. Lagier. Bull. Soc. Chim. France, **16**, 27 (1949).
3. L. Schmerling, R. W. Welch, and J. P. Luvisi. J. Am. Chem. Soc. **79**, 2636 (1957).
4. R. M. Roberts and Y. W. Han. Tetrahedron Letters, No. 6, 5 (1959). R. M. Roberts and D. Shiengthong. J. Am. Chem. Soc. **82**, 732 (1960). R. M. Roberts and Y. W. Han. J. Am. Chem. Soc. **85**, 1168 (1963).
5. B. S. Friedman, F. L. Morritz, C. J. Morrissey, and R. Koncos. J. Am. Chem. Soc. **80**, 5867 (1958).
6. L. R. C. Barclay, C. E. Milligan, and N. D. Hall. Can. J. Chem. **40**, 1664 (1962).
7. A. W. Burgstahler and M. O. Abdel-Rahman. J. Am. Chem. Soc. **85**, 173 (1963).
8. R. T. Arnold, J. T. Buckley, Jr., and J. Richter. J. Am. Chem. Soc. **69**, 2322 (1947).
9. R. D. Campbell and N. H. Cromwell. J. Am. Chem. Soc. **77**, 5169 (1955).
10. T. F. Wood, W. M. Easter, M. S. Carpenter, and J. Angiolini. J. Org. Chem. **28**, 2248 (1963).
11. H. Hart. Dept. of Chemistry, Michigan State University, Michigan. Private communication.
12. G. Baddeley and R. Williamson. J. Chem. Soc. 4647 (1956).
13. L. F. Fieser and M. Fieser. Advanced organic chemistry. Reinhold Publishing Corporation. 1961. p. 659.
14. H. A. Bruson and J. W. Kroeger. J. Am. Chem. Soc. **62**, 36 (1940).
15. L. R. C. Barclay and R. A. Chapman. Can. J. Chem. In press (1963).
16. L. J. Haynes, I. Heilbron, E. R. H. Jones, and F. Sondheimer. J. Chem. Soc. 1583 (1947).
17. C. W. Muth, D. O. Steiniger, and Z. B. Papanastassiou. J. Am. Chem. Soc. **77**, 1006 (1955).

Can. J. Chem. Downloaded from www.nrcresearchpress.com by 210.87.254.40 on 09/05/12
For personal use only.

Can. J. Chem. Downloaded from www.nrcresearchpress.com by 210.87.254.6 on 09/05/12
For personal use only.

TOTAL SYNTHESIS OF STEROIDAL DERIVATIVES

III. SYNTHESIS OF HYDROCHRYSENE ANALOGUES AND RELATED COMPOUNDS[1]

JAMES P. KUTNEY AND ARNOLD BY
Department of Chemistry, University of British Columbia, Vancouver, British Columbia

Received October 30, 1963

ABSTRACT

A synthetic sequence leading to the total synthesis of certain octahydrochrysene derivatives is described. The introduction of a ketonic function into ring B of these substances is also given and it is noted that these ketone intermediates allow entry into ring-B-modified steroidal analogues. The sequence indicates an interesting difference in the mode of reaction of cis–syn–cis and trans–anti–trans hydrochrysene analogues, which is undoubtedly due to the difference in the conformational structures of these compounds.

Recently we reported (1, 2) stereospecific syntheses leading to certain hydrochrysene analogues in both the trans–anti–trans and cis–syn–cis series. Having completed this phase of the investigation we then considered the introduction of functional groups into ring C of the hydrochrysene molecule (see I) to allow entry into intermediates where ring C had been opened. This goal was achieved in the trans–anti–trans series where a ketonic group was introduced at C_{12} (see I) by the use of the sterically large oxidant, namely *t*-butyl chromate (2). We would now like to present similar studies in the cis–syn–cis series which indicate a rather remarkable difference in reaction from that of the former series.

The ketone, I, synthesized previously (1) was reduced with lithium aluminum hydride to give a good yield of the cis–syn–cis alcohol, II. The assignment of the equatorial (8 α) hydroxyl group is well supported by previous work (3). The alcohol was acetylated by means of isopropenyl acetate and the corresponding acetate, III, was oxidized under

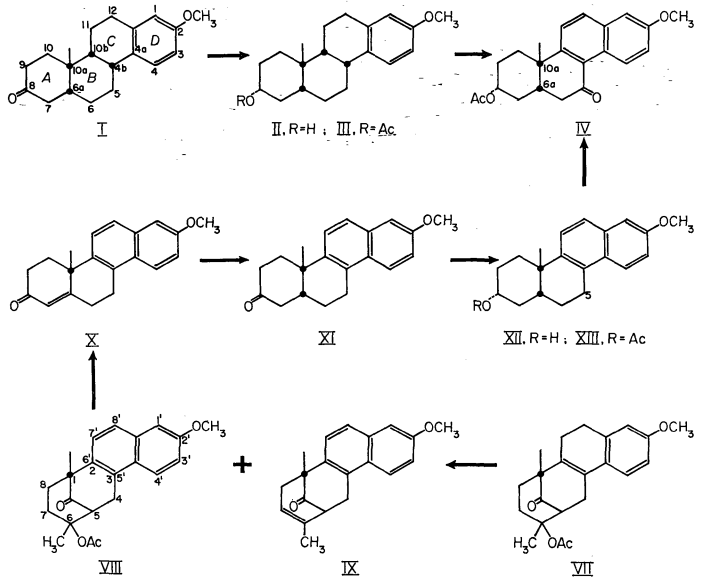

[1]*Presented, in part, at the Second International Symposium on the Chemistry of Natural Products, Prague, Czechoslovakia, August 27–September 2, 1962.*

conditions *identical* with those utilized for the preparation of the trans–anti–trans-2-methoxy-12-keto compound (2). To our surprise, the spectral properties of the reaction product suggested immediately that the expected cis–syn–cis-2-methoxy-12-keto compound was not being isolated. Indeed the data indicated that an aromatization of ring C had occurred and furthermore, on subsequent comparison with data already available from other work in our laboratory, established that the structure of this oxidation product was the octahydrochrysene analogue, IV. This latter substance had been synthesized by an unambiguous route for another purpose and its synthesis is presented below.

During the early course of our investigations it became apparent that the readily available keto acetate, VII (1) by virtue of its bridged structure, should provide an obvious access to octahydrochrysene derivatives possessing an aromatic C ring. It was clear that dehydrogenation studies may provide fruitful results since aromatization of ring C would take place rapidly but any further aromatization of the molecule must be preceded by bond fission at one of the bridged carbon atoms. Indeed when the keto acetate, VII, was treated with 10% palladium on carbon, it gave, in good yield, a new crystalline product. The spectral data provided strong evidence for the success of the dehydrogenation and was in complete agreement with the expected structure, VIII. In particular the ultraviolet spectrum was very informative here and showed the typical complicated spectrum of a naphthalenic chromophore (λ_{max} 231, 266, 277, 287, 307, ca. 315 (shoulder), 321, 330, and 335.5 mμ). Apart from the usual carbonyl absorption characteristic of the ketone and acetate functions in the infrared spectrum (5.84, 5.79 μ), the nuclear magnetic resonance (n.m.r.) spectrum of this substance also indicated some interesting features. For example, the C_1-methyl peak now occurred at 8.47 τ and the methoxyl signal at 6.10 τ represented a downfield shift when compared to the corresponding signals in the spectrum of the starting material. However, as would be expected, the signals for the methyl group at C_6 (8.32 τ) and for the acetate methyl group (8.0 τ) have not been effected to an appreciable extent. Furthermore the increase in the area under the aromatic signals indicated that aromatization of ring C had occurred. During the dehydrogenation reaction, some acetic acid was evolved and, as a minor product, an olefinic material was also isolated. This olefinic material was proved to be 1β,6-dimethyl-2,3-(2′-methoxy-6′,5′-naphtho)-$\Delta^{2,6}$-bicyclo[3.3.1]-nonadiene-9-one (IX) on the basis of the following evidence. The infrared spectrum of this olefin showed only ketonic function (5.84 μ) and the ultraviolet spectrum, which was superimposable on the spectrum of VIII, excluded any further skeletal degradation. The n.m.r. spectrum of this compound still retained the C_6-methyl signal at 8.32 τ but now also indicated a weak, broad absorption in the olefinic region (4.75 τ) due to the endocyclic olefinic proton. It is clear that the exocyclic olefin, which was also a possible product in this reaction, was not formed since it would not exhibit any signal at high field for the C_6-methyl group and would have an olefinic signal at higher field than observed in the above spectrum.

Having obtained the bridged intermediate with rings C and D aromatic, it was then desirable to convert this substance into the hydrochrysene skeleton. Consequently the keto acetate, VIII, was subjected to a retroaldol rearrangement (1) and the expected tetracyclic α,β-unsaturated ketone, X, was obtained in excellent yield. The success of the reaction was indicated by the appearance of a conjugated ketonic absorption in the infrared spectrum (6.04 μ) and also by the appearance of an additional chromophore (λ_{max} 236 mμ) in the ultraviolet spectrum. The n.m.r. spectrum of X now showed only *one* methyl signal at high field (8.37 τ) and a weak signal at 4.04 τ due to the olefinic proton.

In order to provide further desirable derivatives in this series, the unsaturated ketone,

Can. J. Chem. Downloaded from www.nrcresearchpress.com by 210.87.254.6 on 09/05/12
For personal use only.

X, was hydrogenated with 10% palladium on carbon in a benzene solution containing a trace of 48% hydrobromic acid. These reaction conditions are known to provide a ring A/B cis fusion in some related syn–cis series (1, 4) and it was felt that a similar situation may prevail here. The reduction product, XI, can, in fact, be assigned the A/B cis configuration since it was subsequently converted to the monoketone, IV, wherein the assignment of carbon atoms 6*a* and 10*a* can be made with certainty. The saturated ketone, XI, then reduced with lithium aluminum hydride to the saturated alcohol, XII, and this latter substance was acetylated by the use of isopropenyl acetate to provide a good yield of the crystalline acetate, XIII. This sequence completed the first phase of this investigation, namely the construction of hydrochrysene derivatives possessing aromatic rings C and D.

It was now necessary to consider the introduction of a carbonyl function at the benzylic position (C_5, see XIII) since this would allow entry into ring B—a desirable feature for other studies in our laboratory. For this purpose, three different reaction conditions were investigated: (1) a refluxing solution of *t*-butyl chromate in carbon tetrachloride and acetic anhydride, (2) a solution of chromium trioxide in aqueous acetic acid at room temperature, and (3) a refluxing solution of *t*-butyl chromate in carbon tetrachloride. The first set of conditions did not give the desired ketone, but instead some other oxidation products which were not investigated any further. The second method, similar to that used by Barnes and Beachem (5), gave only a 12% yield of the desired ketone and about 12% recovery of starting material, while the use of *t*-butyl chromate in carbon tetrachloride proved most satisfactory. Under optimum conditions, the latter oxidizing agent provided 30% of the desired ketone, IV, and allowed recovery of 19% of starting material. The infrared spectrum of the desired ketone showed the presence of a conjugated ketone and an acetate group (6.03, 5.79 μ) and the n.m.r. spectrum showed some interesting changes from that of the starting material, XIII. For instance, the angular methyl signal was shifted downfield to 8.63 τ and a considerable difference was noted in the aromatic region. In particular, a doublet corresponding to one proton was found at 0.78 τ and is suspected to be due to the C_4 aromatic hydrogen atom. It may be expected that this proton would be deshielded by virtue of its close proximity to the carbonyl oxygen at C_5. At this point, this sequence not only provided a good synthetic intermediate for the subsequent synthesis of ring B modified steroidal analogues but also allowed us to establish the structure of the oxidation product in the reaction of *t*-butyl chromate on the cis–syn–cis hydrochrysene analogue, III. This latter substance was identical in every respect with the monoketone, IV, from the above synthesis.

The formation of the monoketone, IV, from III is quite remarkable considering the fact that under *identical* conditions, the corresponding trans–anti–trans compound is converted to the expected ketonic substance. It is clear from numerous investigations in our laboratory, some of which are already published (2), that the introduction of a substituent at C_{12} always receives serious competition from the tertiary carbon designated as 4*b* since the latter, by virtue of its para relationship to the methoxyl group, is highly reactive. Indeed, as indicated previously (2), *t*-butyl chromate, which is an oxidizing agent possessing considerable bulk, is the only reagent which allows attack at C_{12} in preference to C_{4b} in the trans–anti–trans series. The isolation of IV indicates that this tertiary center (4*b*) in the cis–syn–cis series must be more accessible to attack even by *t*-butyl chromate than in the trans–anti–trans series. A study of molecular models of both series reveals information in support of this proposal. Consideration of the model for the trans–anti–trans series (XIV) shows the well-known rigid flat skeleton encountered in the steroid

Can. J. Chem. Downloaded from www.nrcresearchpress.com by 210.87.254.6 on 09/05/12
For personal use only.

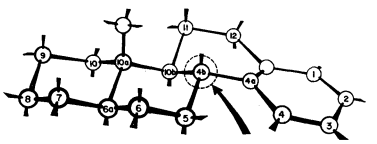

XIV

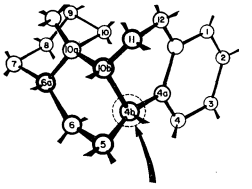

XV

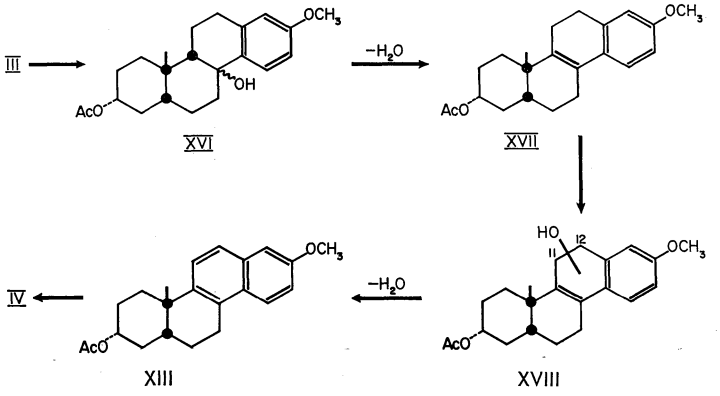

series and reveals that any attack at C_{4b} is hindered particularly by the angular methyl group at C_{10a} and by atoms in a 1:3 diaxial relationship to the hydrogen atom at C_{4b}. On the other hand, although the cis–syn–cis skeleton is considerably less rigid and several conformations become possible, it is clear that any of these conformations must possess a "bent" structure so that C_{4b} is now more accessible. Furthermore the angular methyl group does not hinder any approach of the attacking reagent, which must certainly approach from the "side" of the molecule possessing the flat, aromatic ring. To illustrate this point, one possible conformation is reproduced in XV.

A mechanism for the formation of IV is presented below although it must be emphasized that this is merely speculation and we do not have any experimental evidence in support of this mechanism.

We feel that the initial step involves formation of the tertiary alcohol XVI, which would be expected to dehydrate readily to XVII. This latter intermediate possessing an allylic carbon (C_{11}) and a benzylic carbon (C_{12}) could be oxidized at either one of these positions to provide XVIII, which would immediately aromatize to XIII. Subsequent oxidation of XIII then yields the final product, IV.

We hope to present, in forthcoming publications, the value of intermediates such as IV in the synthesis of certain novel steroidal analogues.

EXPERIMENTAL

All melting points were determined on a Fischer–Johns apparatus and are uncorrected. The ultraviolet spectra were recorded in 95% ethyl alcohol on a Cary 11 or 14 recording spectrophotometer. Infrared spectra were recorded as potassium bromide pellets on a Perkin–Elmer Model 21 spectrophotometer. The n.m.r. spectra were taken at 60 Mc/second on a Varian A 60 instrument. In all cases, tetramethylsilane was the internal standard with its signal set at 10.0 τ units and the positions of all the signals are given in the Tiers τ scale. Integration of areas under the signals was carried out and the number of protons corresponding to each signal is indicated in parentheses. Deuteriocholoroform was the solvent used in all cases. The analyses were performed by Dr. A. Bernhardt and his associates, Mulheim (Ruhr), Germany, and by Mrs. A. Aldridge, University of British Columbia.

Can. J. Chem. Downloaded from www.nrcresearchpress.com by 210.87.254.6 on 09/05/12
For personal use only.

Synthesis of cis–syn–cis-2-Methoxy-8α-hydroxy-10a-methyl-4b,5,6,6a,7,8,9,10,10a,10b,11,12-dodecahydrochrysene (II)

The saturated ketone, I (1.43 g) was dissolved in a mixture of benzene (20 ml) and dioxane (49 ml), and to this solution, anhydrous ethyl ether (98 ml) was added. A solution of lithium aluminum hydride (0.773 g) in anhydrous ethyl ether (19.5 ml) was added dropwise, over a 15-minute period, to the stirred refluxing mixture. After the addition was complete, the solution was refluxed for an additional hour after which time it was cooled and treated with ethyl acetate to decompose the excess hydride. The reaction mixture was made acidic by the addition of a solution of concentrated sulphuric acid (0.6 ml) in water (7 ml). Finally, the mixture was diluted with water and the organic layer was separated. The aqueous layer was extracted with ether and the combined ether extract was washed with a saturated solution of sodium bicarbonate, then with cold water, and finally dried over anhydrous magnesium sulphate. Removal of the drying agent and evaporation of the solvent *in vacuo* provided a slightly yellow gum (1.6 g). It was found that purification could not be successfully accomplished by recrystallization and the product was therefore chromatographed on alumina (40 g). Elution with benzene–chloroform (2:3) mixture gave the desired alcohol, II (1.11 g). Several recrystallizations from benzene – petroleum ether provided the analytical sample as colorless needles, m.p. 124–125°. Infrared: 2.93 μ; ultraviolet: λ_{max} 221 (log ϵ 3.88), 279 (log ϵ 3.31), and 287 mμ (log ϵ 3.31); λ_{min} 246 (log ϵ 2.46) and 285 mμ (log ϵ 3.23); n.m.r. signals: 8.90 τ (angular methyl, area = 3H), 6.25 τ (CH_3O—, area = 3H), broad signal ca. 6.43 τ (*H*—C—OH, area = 1H), multiplet centered at 3.15 τ (aromatic H, area = 3H). Found: C, 79.52; H, 9.32; O, 11.45. Calc. for $C_{20}H_{28}O_2$: C, 79.95; H, 9.39; O, 10.65.

Synthesis of cis–syn–cis-2-Methoxy-8α-acetoxy-10a-methyl-4b,5,6,6a,7,8,9,10,10a,10b,11,12-dodecahydrochrysene (III)

A solution of the saturated alcohol, II (1.822 g) in isopropenyl acetate (21 ml) and *p*-toluenesulphonic acid monohydrate (70 mg) was refluxed for 5 hours. The mixture was concentrated *in vacuo* and the residue was treated repeatedly with ether and water. The combined ether extract was washed with a saturated solution of sodium bicarbonate and then water. After drying over anhydrous magnesium sulphate, the solvent was removed to yield a crude gum (2.011 g). Recrystallization from benzene – petroleum ether gave colorless plates (1.404 g), m.p. 110°. Infrared: 5.81 μ; ultraviolet: λ_{max} 221 (log ϵ 3.89), 280 (log ϵ 3.29) and 287 mμ (log ϵ 3.29); λ_{min} 285 mμ (log ϵ 3.22); n.m.r. signals: 8.90 τ (angular methyl, area = 3H), 8.00 τ ($CH_3C(=O)$—, area = 3H), 6.27 τ (CH_3O—, area = 3H), broad multiplet centered at 5.22 τ (*H*—C—OAc, area = 1H), multiplet centered at 3.06 τ (aromatic H, area = 3H). Found: C, 77.22; H, 8.82; O, 14.21. Calc. for $C_{22}H_{30}O_3$: C, 77.15; H, 8.83; O, 14.02.

Oxidation of cis–syn–cis-2-Methoxy-8α-acetoxy-10a-methyl-4b,5,6,6a,7,8,9,10,10a,10b,11,12-dodecahydrochrysene

A solution of *t*-butyl chromate in carbon tetrachloride was prepared according to the procedure of Heusler and Wettstein (6) except that the final solution was concentrated to 600 ml instead of 1000 ml. Aliquots of this solution were then used for the various experiments.

The acetate, III (550 mg) was dissolved in dry carbon tetrachloride (17.5 ml) and to this solution, acetic anhydride (8.7 ml) and *t*-butyl chromate (17.5 ml, about 0.003 moles CrO_3 per milliliter) were added. The mixture was refluxed for 3 hours during which time a green precipitate gradually formed. The reaction mixture was cooled and a solution of oxalic acid (5 g) in water (35 ml) was added. This mixture was then stirred at room temperature for 2 hours. The resulting mixture was diluted with chloroform and water, and the layers were separated. The aqueous layer was extracted twice with chloroform, and the combined reddish chloroform extract was washed twice with cold water and three times with a solution of sodium carbonate (10 g) in a saturated aqueous solution of sodium bicarbonate (100 ml). The basic aqueous layer was extracted once with chloroform and this extract was added to the main chloroform extract. The pink aqueous basic layer was made acidic with concentrated sulphuric acid to yield a yellow solution which was then extracted with chloroform. After this extract was dried over anhydrous magnesium sulphate, the solvent was evaporated to yield a yellow acidic gum (16 mg).

The chloroform extract containing the neutral materials was washed several times with cold water and then dried over anhydrous magnesium sulphate. Removal of the solvent provided the main neutral product (0.578 g). This neutral material was taken up in benzene (5 ml) and chromatographed on deactivated alumina (30 g, approx. activity II–III). Elution with benzene gave in the initial fractions an orange gum (75 mg) which contained some starting material and the keto-acetate, IV. Further elution with benzene gave more of the keto-acetate, IV (108 mg). This latter fraction was crystallized from benzene – petroleum ether to provide pure IV, m.p. 143–144.5°. A comparison of this product (mixed melting point, infrared, ultraviolet, and n.m.r.) with the compound IV, prepared unambiguously via the octahydrochrysene series below, showed both of these to be identical.

Can. J. Chem. Downloaded from www.nrcresearchpress.com by 210.87.254.6 on 09/05/12
For personal use only.

Synthesis of 1β,6-Dimethyl-6-acetoxy-2,3-(2′-methoxy-6′,5′-naphtho)-Δ²-bicyclo[3.3.1]nonene-9-one (VIII)

The unsaturated keto-acetate, VII (1.0 g) was mixed and powdered with 10% palladium on carbon (0.75 g) in a 250-ml three-necked flask. The flask was then heated for 3 minutes at 230–235° with nitrogen passing over the mixture. Bubbling generally took place in the first 2 minutes and some acetic acid was evolved near the end of the heating period. After it was cooled to room temperature, the residue was treated with hot benzene, the catalyst filtered, and the solvent removed *in vacuo* to yield 0.94 g of a product. This material was dissolved in benzene (7 ml) and chromatographed on deactivated alumina (60 g, approx. activity II–III). Elution with 2:3 benzene – petroleum ether yielded first a solid material which, on two recrystallizations from benzene – petroleum ether gave an analytical sample of 1β,6-dimethyl-2,3-(2′-methoxy-6′,5′-naphtho)-$\Delta^{2,6}$-bicyclo[3.3.1]nonadiene-9-one (IX), m.p. 181.5°–182. Infrared: 5.84 μ; ultraviolet: λ_{max} 231 (log ε 4.76), 266 (log ε 3.77), 276 (log ε 3.76), 286 (log ε 3.57), 307 (log ε 3.02), broad shoulder at 315 (log ε 3.06), 320 (log ε 3.72), 329 (log ε 3.16), and 335 mμ (log ε 3.34); λ_{min} 261 (log ε 3.72), 271 (log ε 3.71), 284.5 (log ε 3.58), 303 (log ε 2.96), 310 (log ε 2.99), 325 (log ε 3.12), and 331 mμ (log ε 3.15); n.m.r. signals: 8.48 τ (angular methyl, area = 3H), quartet centered at 8.32 τ (CH_3—C=C, area = 3H), 6.12 τ (CH_3O—, area = 3H), broad signal centered at 4.75 τ (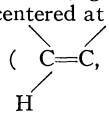 , area = 1H), multiplet centered at 2.47 τ (aromatic H, area = 5H). Found: C, 82.04; H, 7.10. Calc. for $C_{20}H_{20}O_2$: C, 82.15; H, 6.89.

Further elution with 3:2 benzene – petroleum ether gave the desired keto acetate, VIII (767 mg). Several recrystallizations from aqueous ethyl alcohol or benzene : petroleum ether gave colorless square plates, m.p. 185.5–186°. Infrared: 5.79 μ, 5.84 μ; ultraviolet: λ_{max} 231 (log ε 4.75), 266 (log ε 3.76), 277 (log ε 3.74), 287 (log ε 3.57), 307 (log ε 3.03), broad shoulder at 315 (log ε 3.09), 321 (log ε 3.25), 330 (log ε 3.18), and 335.5 mμ (log ε 3.36); λ_{min} 262 (log ε 3.72), 272 (log ε 3.69), 303 (log ε 2.97), 311 (log ε 3.00), 326 (log ε 3.14), and 331 mμ (log ε 3.18); n.m.r. signals: 8.47 τ (angular methyl, area = 3H), 8.32 τ (CH_3—C—OAc, area = 3H), 8.0 τ (CH_3—C(=O)—, area = 3H), 6.10 τ (CH_3O—, area = 3H), multiplet centered at 2.46 τ (aromatic H, area = 5H). Found: C, 74.89; H, 7.04. Calc. for $C_{22}H_{24}O_4$: C, 74.98; H, 6.86.

Synthesis of 2-Methoxy-8-keto-10a-methyl-5,6,8,9,10,10a-hexahydrochrysene (X)

The apparatus used in this experiment was set up exactly as in the tricyclic ketone preparation (1) in order to maintain anhydrous conditions and a nitrogen atmosphere at all times.

A 1-liter three-necked flask was charged with anhydrous methanol (318 ml) and then sodium (2.94 g) was added gradually in small pieces. After the sodium had reacted, the methoxide solution was cooled, and the entire apparatus evacuated until the solvent began to boil. Dry nitrogen was admitted, the system evacuated again, and the entire process repeated several times. To the stirred methoxide solution, a solution of the acetate, VIII (7.188 g) in dry benzene (81 ml) was added through a dropping funnel under a flow of escaping nitrogen. After the addition was complete, the system was evacuated, and dry nitrogen admitted to ensure complete removal of oxygen. The reaction mixture was then refluxed for 5 hours in this inert atmosphere. At the end of the reflux period, the solution was cooled in ice, glacial acetic acid (8.5 ml) was added, and the mixture was swirled for several minutes. Some water and benzene were added to the reaction flask, the layers were then separated, and the aqueous layer was extracted three times with benzene. The combined benzene extract was washed with a cold saturated solution of sodium chloride and then dried over anhydrous magnesium sulphate. Evaporation of the solvent *in vacuo* yielded a yellow crystalline product (5.808 g). Decoloration with Norite and three recrystallizations from benzene provided X, m.p. 198–199°. Infrared: 6.04 μ; ultraviolet: λ_{max} broad shoulder at 230 (log ε 4.83), 236 (log ε 4.86), broad shoulder at 262 (log ε 3.94), 274 (log ε 3.84), broad shoulder at 284 (log ε 3.65), 306 (log ε 3.05), broad shoulder at 314 (log ε 3.12); 319 (log ε 3.28), 327 (log ε 3.22), and 333.5 mμ (log ε 3.38); λ_{min} 270 (log ε 3.82), 301 (log ε 2.99), 308 (log ε 3.03), 324 (log ε 3.18), and 329 mμ (log ε 3.20); n.m.r. signals: 8.37 τ (angular methyl, area = 3H), 6.10 τ (CH_3O—, area = 3H), 4.04 τ (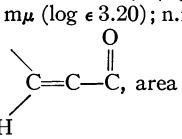 , area = 1H), multiplet centered at 2.43 τ (aromatic H, area = 5H). Found: C, 82.45; H, 6.68; O, 11.08. Calc. for $C_{20}H_{20}O_2$: C, 82.15; H, 6.89; O, 10.95.

Synthesis of cis-2-Methoxy-8-keto-10a-methyl-5,6,6a,7,8,9,10,10a-octahydrochrysene (XI)

A solution of the α,β-unsaturated ketone, X (1.39 g) in benzene (94 ml) was treated with 10% palladium on carbon (0.338 g) and three drops of 48% hydrobromic acid. This mixture was hydrogenated at room temperature and atmospheric pressure for 3½ hours, after which time 1 mole of hydrogen had been absorbed. The catalyst was removed by filtration and was then washed with hot benzene. After evaporation of the solvent *in vacuo*, a gum (1.497 g) was obtained. This gum was dissolved in benzene (15 ml) and chromatographed on deactivated alumina (80 g, approx. activity II–III). Elution with 1:2 benzene – petroleum ether provided a fraction (1.405 g) which crystallized from ethyl ether. Two further recrystallizations from

Can. J. Chem. Downloaded from www.nrcresearchpress.com by 210.87.254.6 on 09/05/12
For personal use only.

benzene – petroleum ether yield pure XI, as colorless plates, m.p. 155–155.5°. Infrared: 5.87 μ; ultraviolet: λ_{max} 229 (log ϵ 4.82), 255 (log ϵ 3.69), 266 (log ϵ 3.76), 276 (log ϵ 3.77), 286 (log ϵ 3.59), 307 (log ϵ 3.03), broad shoulder at 315 (log ϵ 3.11), 320 (log ϵ 3.28), 328 (log ϵ 3.21), and 335 mμ (log 3.38); λ_{min} 259 (log ϵ 3.67), 271 (log ϵ 3.71), 284 (log ϵ 3.59), 302 (log ϵ 2.94), 309 (log ϵ 3.01), 325 (log ϵ 3.17), and 331 mμ (log ϵ 3.20); n.m.r. signals: 8.63 τ (angular methyl, area = 3H), 6.15 τ (CH_3O—, area = 3H), multiplet centered at 2.56 τ (aromatic H, area = 5H). Found: C, 81.60; H, 7.45; O, 10.84. Calc. for $C_{20}H_{22}O_2$: C, 81.60; H, 7.53; O, 10.87.

Synthesis of cis-2-Methoxy-8α-hydroxy-10a-methyl-5,6,6a,7,8,9,10,10a-octahydrochrysene (XII)

The ketone, XI (3.75 g) was dissolved in dry benzene (60 ml) and then put into the dropping funnel which already contained dry dioxane (100 ml) and anhydrous ether (50 ml). This solution was added dropwise, over a period of 12 minutes, to a stirred refluxing solution of lithium aluminum hydride (2.14 g) in a mixture of dry dioxane (34 ml) and ether (150 ml). The reaction mixture was refluxed for a further 65 minutes and then cooled to 0°. The excess hydride was destroyed by careful addition of water and the resulting mixture was acidified with concentrated sulphuric acid (7.2 ml) diluted with water (84 ml). The organic layer was separated and the aqueous layer was extracted several times with benzene. The combined benzene extract was washed with cold water and then dried over magnesium sulphate. Removal of the solvent yielded the crude product (3.737 g). This material was purified by chromatography on deactivated alumina (260 g, approx. activity II–III). Elution with 1:1 benzene – petroleum ether provided a small amount of starting material and further elution with 3:2 chloroform–benzene yielded the desired alcohol, XII. After two recrystallizations from benzene – petroleum ether, the pure product was obtained as colorless needles, m.p. 150–150.5°. Infrared: 2.97 μ; ultraviolet: λ_{max} 228 (log ϵ 4.82), 254.5 (log ϵ 3.67), 266 (log ϵ 3.75), 276 (log ϵ 3.76), 287 (log ϵ 3.60), 307 (log ϵ 3.08), broad shoulder at 315 mμ (log ϵ 3.15), 321 (log ϵ 3.31), 329 (log ϵ 3.24), and 335.5 mμ (log ϵ 3.40); λ_{min} 252 (log ϵ 3.66), 259 (log ϵ 3.66), 271 (log ϵ 3.70), 284 (log ϵ 3.59), 302 (log ϵ 3.01), 310 (log ϵ 3.08), 325 (log ϵ 3.20), and 331 mμ (log ϵ 3.23); n.m.r. signals: 8.83 τ (angular methyl, area = 3H), multiplet centered at 6.50 τ (*H*—C(OH)—, area = 1H), 6.17 τ (CH_3O—, area = 3H), multiplet centered at 2.58 τ (aromatic H, area = 5H). Found: C, 80.82; H, 8.19; O, 10.63. Calc. for $C_{20}H_{24}O_2$: C, 81.04; H, 8.16; O, 10.80.

Synthesis of cis-2-Methoxy-8α-acetoxy-10a-methyl-5,6,6a,7,8,9,10,10a-octahydrochrysene (XIII)

The alcohol, XII, (4.672 g) was treated with *p*-toluenesulphonic acid monohydrate (156 mg) and isopropenyl acetate (80 ml) and the mixture was heated on a steam bath for 4½ hours. The reaction mixture was cooled to room temperature and pyridine (10 drops) was added. The solvent was evaporated on a steam bath *in vacuo* and the residue was dissolved by the addition of benzene and water. The layers were separated and the aqueous solution was extracted twice with benzene. The combined benzene extract was washed twice with cold water and then dried over anhydrous magnesium sulphate. Removal of the solvent on a steam bath *in vacuo* gave the crude acetate (5.34 g). After four recrystallizations from benzene – petroleum ether, the pure acetate, XIII, m.p. 158–159° was obtained. Infrared: 5.82 μ; ultraviolet: λ_{max} 228 (log ϵ 4.82), 254 (log ϵ 3.64), 266 (log ϵ 3.73), 276 (log ϵ 3.75), 287 (log ϵ 3.58), 308 (log ϵ 3.06), broad shoulder at 315 (log ϵ 3.11), 321 (log ϵ 3.29), 329 (log ϵ 3.22), and 335 mμ (log ϵ 3.40); λ_{min} 251 (log ϵ 3.63), 259 (log ϵ 3.63), 271 (log ϵ 3.68), 284 (log ϵ 3.56), 302 (log ϵ 2.92), 310 (log ϵ 2.99), 325 (log ϵ 3.18), and 331 mμ (log ϵ 3.21); n.m.r. signals: 8.78 τ (angular methyl, area = 3H), 8.13 τ (CH_3—C(=O)—O—, area = 3H), 6.17 τ (CH_3O—, area = 3H), broad signal centered at 5.21 τ (H—C(OAc)—, area = 1H), multiplet centered at 2.55 τ (aromatic H, area = 5H). Found: C, 78.12; H, 7.61; O, 14.40. Calc. for $C_{22}H_{26}O_3$: C, 78.01; H, 7.69; O, 14.20.

Synthesis of cis-2-Methoxy-8α-acetoxy-5-keto-10a-methyl-5,6,6a,7,8,9,10,10a-octahydrochrysene (IV)

(a) By Oxidation with t-Butyl Chromate

The methoxy-acetate, XII (250 mg) was dissolved in dry carbon tetrachloride (9 ml) and *t*-butyl chromate solution (3 ml, about 0.009 moles CrO_3) was added. The mixture was refluxed, with stirring, for 4½ hours after which time, the mixture was cooled to 0°, and treated with a solution of oxalic acid (0.9 g) in water (10 ml). The reaction mixture was then stirred, with a little cooling, for 2 hours. Chloroform and water were added and the layers were separated. The aqueous solution was extracted several times with chloroform and the combined organic extract was washed successively with cold water, a 1:1 mixture of saturated aqueous sodium bicarbonate and 1 *N* sodium carbonate solution and finally water. The carbonate solution was extracted once with chloroform, then acidified with concentrated sulphuric acid, and the resulting aqueous acidic layer was extracted with chloroform to yield, after removal of solvent, 6 mg of an acidic product.

The original organic layer and the chloroform extract of the carbonate layer were combined and washed with cold water until the washings were neutral to litmus. The organic layer was dried over anhydrous magnesium sulphate and, after removal of the solvent, provided a crude neutral product (186 mg). The

Can. J. Chem. Downloaded from www.nrcresearchpress.com by 210.87.254.6 on 09/05/12
For personal use only.

material was purified by chromatography on silica gel (12 g). Elution with 2:1 benzene – petroleum ether provided some starting material (48 mg, 19% recovery) and further elution with 3:1 benzene – petroleum ether yielded the desired ketone, IV (81 mg, 31% yield). After two recrystallizations from benzene – petroleum ether, a pure sample of IV was obtained, m.p. 143–144.5°. Infrared: 5.79 μ, 6.03 μ; ultraviolet: λ_{max} 220 (log ϵ 4.71), 247 (log ϵ 4.45), 316 (log ϵ 3.87), and broad shoulder at 348 mμ (log ϵ 3.61); λ_{min} 232 (log ϵ 4.28) and 278 mμ (log ϵ 3.35); n.m.r. signals: 8.63 τ (angular methyl, area = 3H), 8.13 τ (CH_3—$\overset{\overset{O}{\|}}{C}$—O—, area = 3H), 6.12 τ (CH_3O—, area = 3H), broad signal centered at 5.20 τ (H—$\overset{|}{C}$—OAc, area = 1H), multiplet centered at 2.52 τ (aromatic H, area = 4H), doublet centered at 0.78 τ (C_4 aromatic H, area = 1H). Found: C, 75.08; H, 6.93; O, 18.09. Calc. for $C_{22}H_{24}O_4$: C, 74.97; H, 6.86; O, 18.16.

(b) By Oxidation with Chromium Trioxide

The methoxy-acetate, XII (0.5 g) was dissolved in a mixture of glacial acetic acid (9.9 ml) and water (0.1 ml). A chromic acid solution (0.337 g CrO_3 in 0.63 ml 80% aqueous acetic acid) was added dropwise, over a period of 45 minutes, to the mixture kept at room temperature. The reaction mixture was stirred for a further 36 hours at room temperature, then 95% ethyl alcohol (15 ml) was added to destroy the excess chromic acid. Water and chloroform were then added and the layers separated. The aqueous solution was extracted several times with chloroform. The combined chloroform extract was washed twice with cold water, twice with saturated sodium bicarbonate solution, and then four times with a 1:1 saturated sodium bicarbonate – 1*N* sodium carbonate solution. The alkaline aqueous extracts were combined and extracted twice with chloroform. These chloroform extracts were combined with the original reddish-orange chloroform extract, washed with water, and then finally dried over anhydrous magnesium sulphate. Removal of the solvent *in vacuo* provided the crude neutral material (0.461 g). This material was dissolved in 3:2 benzene – petroleum ether (5 ml) and chromatographed on silica gel. Elution with benzene provided some starting material (59 mg, 12% recovery) and further elutions with the same eluant gave the desired ketone, IV (64 mg, 12% yield). This ketone was identical with that obtained from the *t*-butyl chromate oxidation.

ACKNOWLEDGMENTS

Financial aid from National Institutes of Health, Grant No. CY-5037, the National Research Council of Canada, and the President's Research Fund, University of British Columbia, is very gratefully acknowledged.

REFERENCES

1. J. P. Kutney, W. McCrae, and A. By. Can. J. Chem. **40**, 982 (1962).
2. J. P. Kutney, J. Winter, W. McCrae, and A. By. Can. J. Chem. **41**, 470 (1963).
3. W. S. Johnson, E. R. Rogier, J. Szmuszkovicz, H. I. Hadler, J. Ackerman, B. K. Bhattacharyya, B. M. Bloom, L. Stalmann, R. A. Clement, B. Bannister, and H. Wynberg. J. Am. Chem. Soc. **78**, 6289 (1956). P. W. Schiess, D. M. Bailey, and W. S. Johnson. Tetrahedron Letters, 549 (1963).
4. W. S. Johnson, J. Ackerman, J. F. Eastham, and H. A. DeWalt. J. Am. Chem. Soc. **78**, 6302 (1956).
5. R. A. Barnes and M. T. Beachem. J. Am. Chem. Soc. **77**, 5388 (1955).
6. K. Heusler and A. Wettstein. Helv. Chim. Acta, **35**, 284 (1952).

Can. J. Chem. Downloaded from www.nrcresearchpress.com by 210.87.254.6 on 09/05/12
For personal use only.

A GENERAL SYNTHESIS OF NUCLEOSIDE-5′ TRIPHOSPHATES[1]

J. G. MOFFATT
Syntex Institute for Molecular Biology, Palo Alto, California
Received August 15, 1963

ABSTRACT

The reaction between ribo- and deoxyribo-nucleoside-5′ phosphoromorpholidates and tributylammonium pyrophosphate in molecular sieve dried dimethyl sulphoxide has been found to give the nucleoside-5′ triphosphates in 81–84% yields. A convenient work-up of the triphosphates following ion exchange chromatography permits isolation of the triphosphates in overall yields of 73–80% as the pure sodium salts. A number of examples of the reaction are given.

Can. J. Chem. Downloaded from www.nrcresearchpress.com by 210.87.254.42 on 09/05/12
For personal use only.

Progress in biochemical research during recent years has clearly pointed out the unique importance of ribo- and deoxyribo-nucleoside-5′ triphosphates in biological systems. Thus, in addition to the well-known role of adenosine-5′ triphosphate (ATP) as the primary energy source in many systems, the nucleoside triphosphates also serve as direct precursors of both ribonucleic (1) and deoxyribonucleic (2) acids, and of nucleotide coenzymes (3). Certain triphosphates also act as rather poorly understood specific cofactors for certain biological transformations (4). This multiplicity of function of nucleoside triphosphates has led to a demand for efficient synthetic routes to the compounds, and a considerable effort has been made in this direction (5). The general method which has been most widely used to date consists of the reaction of a nucleoside-5′ phosphate with a large excess of inorganic orthophosphate in the presence of dicyclohexylcarbodiimide (6). This method was much improved when it was realized that the reaction could be conducted in anhydrous pyridine if the tributylamine salts of the various acidic components were used (7). This modification allowed the reaction to be run for the first time in a homogeneous system and also led to the selective formation of the nucleoside triphosphates in considerably higher yield than the other mixed products. In order to achieve a satisfactory yield, however, it was necessary to use at least 10 molar equivalents of orthophosphate. The presence of the resulting large excess of mixed inorganic polyphosphates formed during the reaction necessitated selective adsorption of the nucleotides on carbon followed by elution with ethanolic ammonia prior to ion exchange chromatography. Such a step frequently leads to considerable losses of the nucleotidic material and usually the final isolated yields are far below those present in the crude reaction. In spite of this, the simplicity of the method has made this the most widely used route to nucleoside triphosphates (8).

The development of a simple general method for the conversion of nucleoside-5′ phosphates into activated but insolable phosphoramidate (9), and in particular phosphoromorpholidate (10), derivatives (I) has opened the way to syntheses, in high yield, of nucleoside-5′ diphosphates (III, R′ = H) and nucleotide coenzymes (III, R′ = sugars, etc.) by their reaction with orthophosphate (II, R′ = H) or various phosphate monoesters (II, R′ = sugar, etc.) in anhydrous solvents (10, 11, 12).

In an earlier paper (10), the attempted extension of the above reactions to the direct synthesis of a nucleotide-5′ triphosphate through the reaction of adenosine-5′ phosphoromorpholidate (IV, R = OH, R′ = adenine) with tributylammonium pyrophosphate in

[1]*Contribution No. 3 from the Syntex Institute for Molecular Biology, Palo Alto, California.*

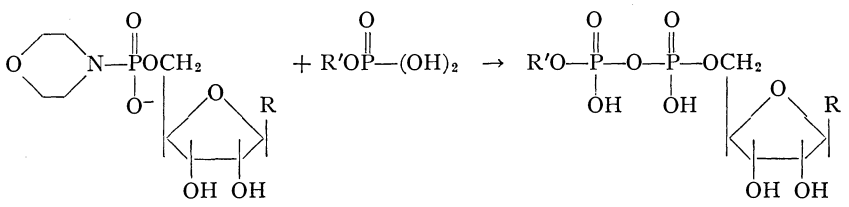

I II III

anhydrous pyridine was described. This reaction led rather rapidly to a moderate yield (57%) of adenosine-5′ triphosphate (V, R = OH, R′ = adenine) within 2 hours but on prolonged reaction this initial product disappeared and was converted into adenosine-5′ diphosphate, which was present in 76% yield after 24 hours. Further studies on this reaction (13) have shown it to be quite general, the rate of disappearance of the initially

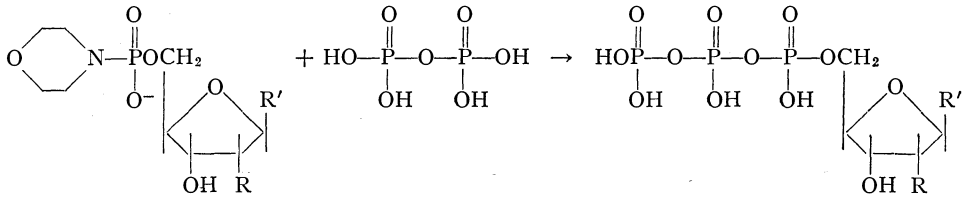

IV V

formed triphosphate being a function of the particular nucleotide under consideration (14).* It is, moreover, possible to conduct the reaction using only 3–4 molar equivalents of pyrosphosphate without appreciable formation of P^1,P^4-dinucleoside-5′ tetraphosphates (13). Since the excess pyrophosphate is not chemically activated, and hence remains substantially unchanged, it is possible to separate the resulting nucleotides by ion exchange chromatography without the necessity of charcoal absorption. Several other workers (15) have also studied the reaction of nucleoside-5′ phosphoramidates with pyrophosphate in a variety of solvents but only in a recent study by Ikehara and Ohtsuka (15(*d*)) has any mention been made of the disappearance of the initial products, and the final yields have not been sufficiently good to make this route superior to the carbodiimide reaction. Only in the work of Tanaka *et al.* (15(*b*)) was pure pyrophosphate free of large amounts of orthophosphate used, thus allowing a critical examination of the desired reaction.

It was of considerable importance to devise reaction conditions such that degradation of the initially formed triphosphates did not occur and this product could be isolated in high yield. As a result of another study in this laboratory (14), it was observed that while tributylammonium adenosine-5′ triphosphate was rapidly converted into a complex mixture of products in pyridine (10) it was virtually completely stable in a number of other anhydrous organic solvents. One such agent is dimethyl sulphoxide which offers particular interest in view of its high solvent power for nucleotides. Accordingly the reaction of deoxyadenosine-5′ phosphoromorpholidate (IV, R = H, R′ = adenine) with tributylammonium pyrophosphate was studied in dimethyl sulphoxide. Initially the two components were separately rendered anhydrous by coevaporation with pyridine and then mixed in distilled dimethyl sulphoxide. The reaction proceeded

**Verheyden and Moffatt will describe shortly a detailed study of the interesting decomposition of the nucleoside polyphosphates in certain anhydrous organic solvents.*

Can. J. Chem. Downloaded from www.nrcresearchpress.com by 210.87.254.42 on 09/05/12
For personal use only.

quite rapidly, the morpholidate having almost completely disappeared after 10 hours, and the product distribution remaining unchanged after 24 hours. The products were separated by ion exchange chromatography on a DEAE cellulose column in the bicarbonate form using a linear gradient of triethylammonium bicarbonate as eluant.* Under these conditions, the major product was indeed deoxyadenosine-5′ triphosphate (54%). Only small amounts (2% and 10% respectively) of deoxyadenosine-5′ phosphoromorpholidate and deoxyadenosine-5′ diphosphate were present but deoxyadenosine-5′ monophosphate comprised 34% of the total nucleotides. This picture was surprisingly reproducible under a variety of reaction conditions including further coevaporation of the final reaction mixture with pyridine and dropwise addition of the morpholidate. When, however, the dimethyl sulphoxide was dried by standing for several days with a molecular sieve† and then used in a similar reaction, the yield of deoxyadenosine-5′ triphosphate rose to 82% with only 6%, 7%, and 5% respectively of the unreacted morpholidate, monophosphate, and diphosphate. It appears, therefore, that, as was found earlier (10, 11) in experiments leading to the synthesis of nucleotide coenzymes in pyridine, it is essential to maintain conditions as anhydrous as possible to avoid simple hydrolysis of the morpholidate. It is interesting to note that when molecular sieve dried dimethyl sulphoxide was used the reaction becomes much slower, usually 48–72 hours being necessary for disappearance of nearly all the morpholidate.

Isolation of the product in a water-soluble, non-hygroscopic, solid form is readily accomplished by removal of excess triethylammonium bicarbonate by low temperature evaporation, and adding an excess of sodium iodide in acetone to a concentrated solution of the resulting triethylammonium salt of the nucleotide in methanol. Recoveries of the resulting sodium salt are generally excellent and the products as directly obtained are suitable for use in biochemical studies.

This general procedure has been used for the synthesis of all the normal deoxynucleoside-5′ triphosphates and also several ribonucleoside-5′ triphosphates. The results are summarized in Table I and it can be seen that in all cases the yield of pure isolated sodium

TABLE I

Product distribution of the various nucleoside polyphosphates

	% yields based on starting material				
Nucleoside	Morpholidate	$MonoPO_4$	$DiPO_4$	$TriPO_4$	Isolated Na salt of $TriPO_4$
Deoxyadenosine	6	7	5	82	73
Deoxycytidine	6	5	7	82	80
Deoxyguanosine	3	7	6	82	77
Thymidine	5	4	9	81	75
Cytidine	4	5	7	84	80
6-Azauridine	7	9	5	82	77

salt fell in the range 70–80% thus being much higher than those by any previous method. Several triphosphates have also been prepared from P^{32}-labeled ribo- and deoxyribonucleotides in connection with another problem which will be reported on at a later date (16).

It is our experience that it is very difficult to isolate nucleoside polyphosphates (particularly the tri- or higher phosphates) from columns in the chloride form without minor decomposition to the lower homologues. This does not appear to be a problem with the bicarbonate columns.

†*Type 10X obtained through the courtesy of the Linde Co., Los Angeles. More recently we have been informed by this company that type 4A might be the agent of choice for drying dimethyl sulphoxide.*

Can. J. Chem. Downloaded from www.nrcresearchpress.com by 210.87.254.42 on 09/05/12
For personal use only.

It is interesting to note the remarkable consistency of product distribution for the various reactions summarized in Table I. The small amount of diphosphate which invariably appears seems not to be due to the presence of orthophosphate in the reagent grade sodium pyrophosphate used in these experiments. Indeed measurement of the orthophosphate content by the method of Lowry and Lopez (17) shows that less than 0.1% of the total phosphorus is orthophosphate. It is particularly to be emphasized that in no case is there any contamination of the triphosphate peak by inorganic phosphates even without prior necessity of charcoal adsorption and elution. The combination of simplicity, high yield, and purity of the products clearly makes the procedure of unique value in the synthesis of nucleoside triphosphates. The efficient syntheses of nucleoside-5′ diphosphates previously reported using pyridine as the solvent (10) perhaps make the use of dimethyl sulphoxide unnecessary in these syntheses but an extension of the previous method to the direct synthesis of nucleoside-5′ tetraphosphates using tripolyphosphate will be described at a later date.

EXPERIMENTAL

Paper chromatography was conducted by the descending technique on Schleicher and Schuell No. 589 Orange Ribbon paper using the following solvent systems: solvent I, isobutyric acid : 1 *N* ammonium hydroxide : 0.1 *M* tetrasodium ethylenediamine tetraacetic acid (60:100:1.6); solvent II, *n*-propyl alcohol : ammonium hydroxide : water (6:3:1). R_f's of all pertinent compounds in solvent I are given in Table II

TABLE II

Compound	R_f in solvent I	Compound	R_f in solvent II
Deoxyadenosine-5′ phosphate	0.66	Thymidine-5′ phosphate	0.44
Deoxyadenosine-5′ diphosphate	0.53	Thymidine-5′ diphosphate	0.30
Deoxyadenosine-5′ triphosphate	0.41	Thymidine-5′ triphosphate	0.21
Deoxycytidine-5′ phosphate	0.55	Cytidine-5′ phosphate	0.43
Deoxycytidine-5′ diphosphate	0.40	Cytidine-5′ diphosphate	0.29
Deoxycytidine-5′ triphosphate	0.30	Cytidine-5′ triphosphate	0.21
Deoxyguanosine-5′ phosphate	0.36	6-Azauridine-5′ phosphate	0.24
Deoxyguanosine-5′ diphosphate	0.25	6-Azauridine-5′ diphosphate	0.16
Deoxyguanosine-5′ triphosphate	0.19	6-Azauridine-5′ triphosphate	0.12

with the exception of the morpholidates which decompose in this system. In all cases the disappearance of the morpholidate may be conveniently followed using solvent II in which they move far ahead of the corresponding monophosphates. Phosphorus-containing compounds were localized on paper chromatograms using the Hanes and Isherwood spray (18) followed by ultraviolet irradiation (19). Total phosphorus determinations were done by the method of King (20) and ultraviolet spectra were recorded on a Cary Model 15 spectrophotometer. Elemental analyses (other than for phosphorus) were obtained by Midwest Microlab Inc., Indianapolis, Indiana. All evaporations were done at approximately 1 mm pressure using a rotary-type evaporator in which the condensing bulb was cooled with circulating aqueous glycol at −10° to −20° C.

Deoxyadenosine-5′ phosphoromorpholidate (IV, R′ = adenine, R = H).—This material was prepared and isolated in 91% yield as its 4-morpholine N,N′-dicyclohexylcarboxamidinium salt by the general procedure previously reported (10). As directly obtained the chromatographically pure material (R_f 0.54 in solvent II) was a tetrahydrate (equivalent weight 776 by spectra) but after drying in 80° *in vacuo* the dihydrate was obtained. Calc. for $C_{31}H_{52}N_9O_7P \cdot 2H_2O$: C, 51.00; H, 7.73; N, 17.28. Found: C, 50.33; H, 8.23; N, 17.36.

Deoxyguanosine-5′ phosphoromorpholidate (IV, R′ = guanine, R = H).—Isolated as the tetrahydrate of its 4-morpholine N,N′-dicyclohexylcarboxamidinium salt in 95% yield by the usual procedure (10). R_f 0.35 in solvent II. Drying *in vacuo* at 80° gave the monohydrate. Calc. for $C_{31}H_{52}N_9O_8P \cdot H_2O$: C, 51.18; H, 7.48; N, 17.33. Found: C, 52.02; H, 8.23; N, 17.27.

6-Azauridine-5′ phosphoromorpholidate (IV, R′ = 6-azauracil, R = OH).—This material was obtained in the usual way (10) from 6-azauridine-5′ phosphate* and isolated in 89% yield as its chromatographically pure

**Prepared by phosphorylation of 2′,3′-O-isopropylidine 6-azauridine by the cyanoethyl phosphate method (see ref. (21)). Details will be published shortly.*

Can. J. Chem. Downloaded from www.nrcresearchpress.com by 210.87.254.42 on 09/05/12
For personal use only.

4-morpholine N,N′-dicyclohexylcarboxamidinium salt. R_f 0.36 in solvent II. Calc. for $C_{29}H_{50}N_7O_{10}P \cdot H_2O$: C, 49.38; H, 7.43; N, 13.90. Found: C, 49.04; H, 7.86; N, 14.08.

Nucleoside-5′ triphosphates. General procedure.—Reagent grade tetrasodium pyrophosphate $\cdot 10H_2O$ (1 mmole, 446 mg) is dissolved in water and passed through a column containing Dowex 50-W resin in the pyridine form (15 ml). The resin is then washed with water (30 ml) and the total effluent evaporated *in vacuo* to a volume of approximately 10 ml. Pyridine (30 ml) is then added followed by tri *n*-butylamine (1.0 ml, 4.2 mmoles). The resulting homogeneous solution is evaporated to a syrup and tendered anhydrous by four evaporations with 10-ml portions of pyridine (dried by distillation from, and stored over calcium hydride). The residual pyridine is then removed by two evaporations with 5-ml portions of calcium hydride dried benzene. Separately the 4-morpholine N,N′-dicyclohexylcarboxamidinium salt of the nucleoside-5′ phosphoromorpholidate (0.25 mmoles) is dried by two evaporations with 5-ml portions of pyridine followed by two evaporations of the residue with benzene (5 ml each). The pyrophosphate is then transferred onto the dried morpholidate with the aid of four 1.0-ml portions of dimethyl sulphoxide* which had been dried by distillation and storage for at least several days, over Linde Molecular Sieve Type 10X. The resulting clear solution is kept at room temperature for 2 to 4 days, the disappearance of the morpholidate being readily followed by chromatography in solvent II. Water (30 ml) is then added and the solution is directly applied to a 2×35-cm column of DEAE cellulose† in the bicarbonate form. The column is then washed with water until the optical density of the effluent falls to zero and the components are eluted using a linear gradient of triethylammonium bicarbonate. In each case the mixing vessel initially contains 1500 ml of water and the reservoir contains 1500 ml of 0.35–0.45 *M* triethylammonium bicarbonate depending upon the individual nucleotides being separated. In the cases of deoxyadenosine, thymidine, deoxycytidine, and cytidine-5′ triphosphate, 0.35 *M* salt is used while with deoxyguanosine and azauridine-5′ triphosphates 0.40 *M* and 0.45 *M* respectively are necessary. In each case four clearly separated ultraviolet-absorbing peaks are observed and the recovery of optical density is quantitative. The product distributions are shown in Table I. The pooled triphosphate peak is evaporated to dryness with a bath temperature of 30–35°, and all residual triethylammonium bicarbonate removed by four evaporations with 25-ml portions of methanol. The final residue is dissolved in approximately 5 ml of methanol and a 1 *M* solution of sodium iodide in acetone (6 equivalents relative to the nucleoside by spectra) is added followed by 75 ml of acetone. The precipitate is collected by centrifugation, washed three times with 30-ml portions of acetone, and dried overnight *in vacuo* over phosphorus pentoxide at room temperature. In each case the product is a white, freely water-soluble and non-hygroscopic powder which is chromatographically homogeneous in solvents I and II.

Deoxyadenosine-5′ triphosphate (V, R′ = adenine, R = H).—The final isolated yield of the tetrasodium salt hexahydrate was 73%. Calc. for $C_{10}H_{12}N_5O_{12}P_3Na_4 \cdot 3H_2O$: C, 18.97; H, 2.87; N, 11.06. Ratio of P:deoxyadenosine,‡ 3.0. Found: C, 19.06; H, 3.12; N, 10.91; P/dAdenosine, 3.12.

Deoxycytidine-5′ triphosphate (V, R′ = cytosine, R = H).—The tetrasodium salt monohydrate was isolated in 80% yield. Calc. for $C_9H_{12}N_3O_{13}P_3Na_4 \cdot H_2O$: N, 7.33; P/dCytidine, 3.0 Found: N, 7.29; P/dCytidine, 2.93.

Deoxyguanosine-5′ triphosphate (V, R′ = guanine, R = H).—The tetrasodium salt trihydrate was isolated in 77% yield. Calc. for $C_{10}H_{12}N_5O_{13}P_3Na_4 \cdot 3H_2O$: N, 10.79; P/dGuanosine, 3.0. Found: N, 10.78; P/dGuanosine, 2.90.

Thymidine-5′ triphosphate (V, R′ = thymine, R = H).—The tetrasodium salt dihydrate was isolated in 75% yield. Calc. for $C_{10}H_{13}N_2O_{14}P_3Na_4 \cdot 2H_2O$: N, 4.62; P/Thymidine, 3.00. Found: N, 4.65; P/Thymidine, 3.15.

Cytidine-5′ triphosphate (V, R′ = cytosine, R = OH).—The anhydrous tetrasodium salt was isolated in 80% yield. Calc. for $C_9H_{12}N_3O_{14}P_3Na_4$: N, 7.36; P/Cytidine, 3.00. Found: N, 7.30; P/Cytidine, 2.94.

6-Azauridine-5′ triphosphate (V, R′ = 6-azauracil, R = OH).—Isolated as the trisodium salt dihydrate in 77% yield. Calc. for $C_8H_{10}N_3O_{15}P_3Na_4 \cdot 2H_2O$: N, 7.11; P/Azauridine, 3.0. Found: N, 6.98; P/Azauracil, 3.12.

REFERENCES

1. (*a*) S. B. WEISS. Proc. Nat. Acad. Sci. **46**, 1020 (1960); (*b*) J. J. FURTH, J. HURWITZ, and M. ANDERS. J. Biol. Chem. **237**, 2611 (1962); (*c*) M. CHAMBERLIN and P. BERG. Proc. Nat. Acad. Sci. **48**, 81 (1962); (*d*) T. NAKAMOTO and S. B. WEISS. Proc. Nat. Acad. Sci. **48**, 880 (1962).
2. A. KORNBERG. Enzymatic synthesis of DNA. John Wiley & Sons, New York. 1961.
3. A. KORNBERG. Advan. Enzymol. **18**, 191 (1957).
4. (*a*) G. M. BROWN. J. Biol. Chem. **234**, 370 (1959); (*b*) D. NATHANS, G. VON EHRENSTEIN, R. MONRO, and F. LIPMANN. Federation Proc. **21**, 127 (1962) and references cited therein on the requirement for guanosine triphosphate in protein biosynthesis.
5. J. BADDILEY and N. A. HUGHES. Advan. Enzymol. **22**, 157 (1960).
6. H. G. KHORANA. J. Am. Chem. Soc. **76**, 3517 (1954) and many subsequent references in Ref. 5.
7. M. SMITH and H. G. KHORANA. J. Am. Chem. Soc. **80**, 1141 (1958).

*Generously provided by the Crown Zellerbach Corp., Camas, Wash.

†*Brown Co., Berlin, N.H.*

‡*Nucleoside content is determined spectrally.*

Can. J. Chem. Downloaded from www.nrcresearchpress.com by 210.87.254.42 on 09/05/12
For personal use only.

8. (*a*) M. IKEHARA, E. OHTSUKA, S. KITAGAWA, K. YAGI, and Y. TONOMURA. J. Am. Chem. Soc. **83**, 2679 (1961); (*b*) J. K. ROY, D. C. KVAM, J. L. DAHL, and R. E. PARKS. J. Biol. Chem. **236**, 1158 (1961); (*c*) H. K. SCHACHMAN, J. ALDER, C. M. RADDING, I. R. LEHMAN, and A. KORNBERG. J. Biol. Chem. **235**, 3242 (1960).
9. R. W. CHAMBERS and J. G. MOFFATT. J. Am. Chem. Soc. **80**, 3752 (1958).
10. J. G. MOFFATT and H. G. KHORANA. J. Am. Chem. Chem. Soc. **83**, 649 (1961).
11. (*a*) S. ROSEMAN, J. J. DISTLER, and J. G. MOFFATT. J. Am. Chem. Soc. **83**, 649 (1961); (*b*) J. G. MOFFATT and H. G. KHORANA. J. Am. Chem. Soc. **83**, 663 (1961); (*c*) N. K. KOTCHETKOV, E. I. BUDOWSKY, and V. N. SHIBAEV. Biochem. Biophys. Acta, **53**, 415 (1962).
12. (*a*) T. UEDA. Chem. Pharm. Bull. **8**, 464 (1960); (*b*) R. W. CHAMBERS. J. Am. Chem. Soc. **81**, 3032 (1959); (*c*) R. W. CHAMBERS, P. SHAPIRO, and V. KURKOV. J. Am. Chem. Soc. **82**, 970 (1960).
13. J. REISS and J. G. MOFFATT. In preparation.
14. D. L. VERHEYDEN, W. E. WEHRLI, and J. G. MOFFATT. Unpublished.
15. (*a*) D. KESSLER, B. MOSS, and R. W. CHAMBERS. Biochem. Biophys. Acta, **38**, 549 (1960); (*b*) K. TANAKA, M. HONJO, Y. SANNO, and H. MORIYAMA. Chem. Pharm. Bull. **10**, 220 (1962); (*c*) L. G. ANDRONOVA, Z. A. SHABAROVA, T. S. RYABOVA, and M. A. PROKOF'EV. Zh. Obshch. Khim. **31**, 3243 (1961); (*d*) M. IKEHARA and E. OHTUSUKA. Chem. Pharm. Bull. **10**, 997 (1962).
16. K. PFITZNER and J. G. MOFFATT. Unpublished results.
17. O. H. LOWRY and J. A. LOPEZ. J. Biol. Chem. **162**, 421 (1946).
18. C. S. HANES and F. A. ISHERWOOD. Nature, **164**, 1107 (1949).
19. R. S. BANDURSKI and B. AXELROD. J. Biol. Chem. **193**, 405 (1951).
20. E. J. KING. Biochem. J. **26**, 292 (1932).
21. G. M. TENER. J. Am. Chem. Soc. **83**, 159 (1961).

Can. J. Chem. Downloaded from www.nrcresearchpress.com by 210.87.254.42 on 09/05/12
For personal use only.

SYNTHESIS OF 5-ACETAMIDO SUBSTITUTED BARBITURATES

PRITAM SINGH AND LOUIS BERLINGUET
Department of Biochemistry, Faculty of Medicine, Laval University, Quebec, Quebec
Received July 26, 1963

ABSTRACT

A series of 22 5-acetamido and 5-amino barbituric acids as well as corresponding thiobarbiturates and N-methylated derivatives have been prepared for hypnotic activity evaluation. From comparative studies of their infrared spectra, various frequencies have been ascribed to the acetamido and amino groups at C-5 position. S-Alkylation resulted in the formation of unstable thioethers which hydrolyzed to give corresponding barbituric acids and mercaptans.

Can. J. Chem. Downloaded from www.nrcresearchpress.com by 210.87.254.40 on 09/05/12
For personal use only.

We were interested in preparing for biological evaluation, a new series of barbituric acids in which an amino group, free or acetylated, would be attached to carbon-5. A survey of the literature showed that of the many barbituric acids prepared, only a few have an amino group in the fifth position. These new compounds which we have prepared were obtained by condensing the alkylated acetamido malonic esters with urea or thiourea in the presence of sodium ethoxide. Tables I and II give the description of the various compounds prepared.

Some of these new barbiturates were methylated with dimethyl sulphate in alkaline solution.

With barbituric acids, N-methylated compounds were obtained as expected and isolated. They were characterized by distillation with soda lime. The methylamine thus formed was identified (1). The yields of N-methylated compounds were in the range of 40–60% (Table III).

With thiobarbituric acids, methylation can occur either on the nitrogen (N-1) or on the sulphur located on C-2. When 5,5-dialkylthiobarbiturates were methylated, N-methylation along with some methylation on the sulphur atom took place. However, it has been shown by Lee (2) that "5,5-dialkyl-2-alkyl-thiobarbituric acids are unstable substances evolving a strong thiol-like odor in air". It is not surprising, then, that we isolated, after the methylation of 5-acetamido-5-phenoxypropyl-2-thiobarbituric acid, 10% of the corresponding non-methylated 2-oxygen analogue and 40% of the N-methylated thiobarbiturate. 5-Acetamido-5-isobutyl thiobarbiturate gave, similarly, 45% of 5-acetamido-5-isobutyl barbituric acid.

The substitution of the sulphur atom by oxygen in these two attempts of methylation could only be explained by the labile nature of the intermediate methyl thioether formed at carbon-2.

To confirm this, sodium pentothal was refluxed in 95% ethanol with excess allyl bromide, and benzyl chloride. In both cases pentobarbital could be isolated in 68% yield.

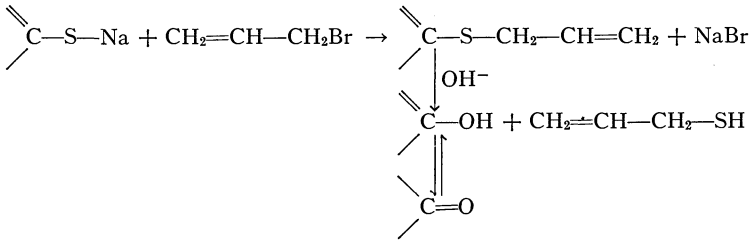

Can. J. Chem. Downloaded from www.nrcresearchpress.com by 210.87.254.40 on 09/05/12
For personal use only.

TABLE I

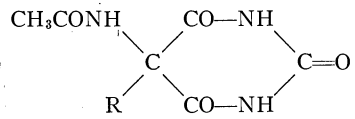

No. of compound	R	Yield (%)	M.p. (° C)	Cryst. solvent	Refluxing time (hours)	Formula	% N Calc.	% N Found
I	n-C_3H_7—	67	296	DMF–H_2O	18	$C_9H_{13}N_3O_4$	18.50	18.23
II	n-C_4H_9—	75	276	DMF–ethanol	6	$C_{10}H_{15}N_3O_4$	17.42	17.44
III	CH_2=CH—CH_2—	61	333 dec.	DMF–H_2O	3	$C_9H_{10}N_3O_4$	18.59	18.66
IV	CH_3 \ CH—CH_2— / CH_3	44	318	Ethanol	5	$C_{10}H_{15}N_3O_4$	17.42	17.43
V	$C_6H_5CH_2$—	60	318	DMF–H_2O	4	$C_{13}H_{13}N_3O_4$	15.27	15.15
VI	$C_6H_5O(CH_2)_3$—	70	275	DMF–ethanol	5	$C_{15}H_{17}N_3O_5$	13.16	13.16

The U.V. absorption for compound VI λ_{max} = 280, 274 mμ, ϵ_{max} = 3×10^2, 3.2×10^2.

TABLE II

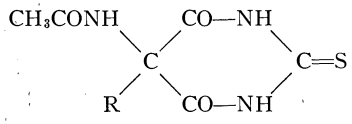

No. of compound	R	Yield (%)	M.p. (° C)	Cryst. solvent	Refluxing time (hours)	Formula	Nitrogen Calc.	Nitrogen Found	U.V. absorption λ_{max}(mμ)	U.V. absorption ϵ_{max} = $\times10^3$
VII	H—	65	284 dec.	Acetic acid	6	$C_6H_7N_3O_3S$	20.89	20.75	292	19
VIII	p-$OCH_3C_6H_4CH_2$—	68	237	Ethanol–H_2O	6	$C_{14}H_{15}N_3O_4S$	13.09	12.78	292	25
IX	$NCCH_2$—CH_2—	28	292	Dioxane	6	$C_9H_{10}N_4O_3S$	22.04	21.64	292	22
X	$C_6H_5CH_2$—	70	288 dec.	Ethanol	6	$C_{13}H_{13}N_3O_3S$	14.43	14.35	296, 240	26, 14
XI	CH_2=CH—CH_2—	66	244	Ethanol	3	$C_9H_{11}N_3O_3S$	17.42	17.54	292, 238	19, 12
XII	$(CH_3)_2$CH—CH_2—	60	269	Dioxane–benzene	6	$C_{10}H_{15}N_3O_3S$	16.34	16.31	294	23
XIII	$C_6H_5O(CH_2)_3$—	70	204	Ethanol	6	$C_{15}H_{17}N_3O_4S$	12.53	12.42	290, 236	27, 17

Can. J. Chem. Downloaded from www.nrcresearchpress.com by 210.87.254.40 on 09/05/12
For personal use only.

TABLE III

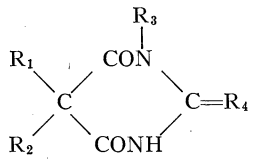

No. of compound	R_1	R_2	R_3	R_4	Yield (%)	M.p. (° C)	Cryst. solvent	Time	Formula	% C Calc.	% C Found	% H Calc.	% H Found	% N Calc.	% N Found	λ_{max}(mμ)	$\epsilon_{max} = \times 10^3$
XIV	CH_3CONH—	$C_6H_5CH_2$	CH_3	S	50	283	DMF–H_2O	30 min	$C_{14}H_{15}N_3O_3S$	55.00	54.50	4.90	4.52	13.77	13.70	264	18
XV	CH_3CONH	H	CH_3	S	60	251	Diox-C_6H_6	30 min	$C_7H_9N_3O_3S$	—	—	—	—	19.53	19.38	288	17
XVI	CH_3CONH	CH_2=CH—CH_2	CH_3	O	40	324	Diox-C_6H_6	30 min	$C_{10}H_{13}N_3O_4$	50.21	49.93	5.44	5.31	17.37	17.57	—	—
XVII	CH_3CONH	$C_6H_5O(CH_2)_3$—	CH_3	O	64	208	Diox-H_2O	30 min	$C_{16}H_{19}N_3O_5$	57.66	56.69	5.70	5.78	12.65	12.68	280, 274	2.6, 2.7
XVIII	CH_3CONH	$C_6H_5O(CH_2)_3$—	CH_3	S	45	233	DMF–ethanol	30 min	$C_{16}H_{19}N_3O_4S$	55.01	54.87	5.44	5.42	12.03	12.04	270	28
XIX	NH_2.HCl	C_6H_5—CH_2—	H	O	70	264	Dil. HCl	6 hr	$C_{11}H_{12}ClN_3O_3$	48.23	48.40	4.45	4.38	15.58	15.75	—	—
XX	NH_2.HCl	$C_6H_5O(CH_2)_3$—	H	O	30	262	Dil. HCl	18 hr	$C_{13}H_{16}ClN_3O_4$	49.76	49.86	5.10	4.93	13.42	13.57	280, 274	2.5, 2.8
XXI	NH_2.HCl	n-C_4H_9	H	O	45	255	Dil. HCl	16 hr	$C_8H_{14}ClN_3O_3$	40.76	40.57	5.94	5.96	17.83	17.64	—	—
XXII	NH_2	n-C_3H_7	H	O	51	207	DMF–H_2O	12 hr	$C_7H_{11}N_3O_3$	45.40	45.30	6.08	5.94	22.70	22.61	—	—

TABLE IV

Infrared absorptions in the range of 3400 cm^{-1} to 1450 cm^{-1}

Compound No.											
II	3375(s)	3200(s)	3100(s)	3000(m)	2875(m)	1770(s)	1740(s)	1710(s)	1645(s)	1530(s)	1460(m)
V	3375(s)	3225(m)	3125(s)	2890(m)	1750(s)	1715(s)	1660(s)	1540(s)	1500(m)	1450(m)	
VI	3400(s)	3200(sh)	3100(s)	2875(m)	1750–1710(s)	1650(s)	1600(s)	1545(s)	1500(m)	1460(s)	
XIX	3200(m)	3000(m)	2800(m)	1780(sh)	1750(s)	1720(s)	1555(m)	1545(m)	1490(m)	1450(m)	
XX	3200(s)	3010(s)	2800(s)	1780(s)	1750–1720(s)	1600(m)	1585(m)	1540(m)	1500(m)		
XXI	3200(s)	3150(s)	3100(s)	2975(s)	2800(s)	2675(m)	1760–1710(s)	1555(m)	1475(s)	1460(m)	

Hydrolysis of some 5-acetamido barbiturates with 4 *N* HCl gave the 5-amino hydrochloride barbiturates which are listed in Table III along with the N-methylated derivatives.

The hydrolysis of the 5-acetamido group to an amine hydrochloride results in the disappearance of absorptions at 3400 cm^{-1} (free N—H stretching mode), 1650 cm^{-1} (amide I band), 1365 cm^{-1} (amide II band), and 1298 cm^{-1} (amide III band) (Table IV). There is also the disappearance of the lowest of the first three carbonyl frequencies in the region 1800–1640 cm^{-1} (3). In the 5-aminohydrochloride compounds, new bands around 1585–1555 cm^{-1} and 1340 cm^{-1} are probably due to NH_3 deformation frequency and symmetric mode respectively. There is also some displacement towards lower frequencies of 3100 cm^{-1} and 2900 cm^{-1} to 3000 and 2800 cm^{-1} (VI, XX; V, XIX).

Pharmacology.—All these barbiturates (Tables I, II, and III) were tested on mice in dosage of 100 mg/kilogram, as their sodium salts. No hypnotic activity was found in any case. The replacement of an alkyl chain in position-5 by a free or acetylated amino group resulted in the loss of hypnotic activity.

EXPERIMENTAL

All the melting points reported are uncorrected and some of them depend on the rate of heating. The infrared spectra were recorded with a Beckman IR4 spectrophotometer using KBr pellets containing 0.5% by weight of sample and reported spectra are all calibrated. Ultraviolet spectra were all recorded with a Beckman DB Spectrophotometer using 95% ethanol as solvent. Analyses were performed by Dr. C. Daessle of Organic Microanalysis, Montreal.

The method used for preparing alkylated acetamido malonic esters was mainly that reported by Snyder (4) and Albertson (5) as reviewed by Cope (6). The criterion used for the completion of the reaction was its neutral reaction towards litmus. If, on vacuum evaporation, the compound solidified, it was filtered, washed with water, and dried before crystallization. However, if, on vacuum evaporation an oil was obtained, small amount of water was added and the oil extracted with benzene. The benzene solution was dried with anhydrous sodium sulphate and vacuum evaporated.

For the preparation of barbiturates, 1 mole of the alkylated acetamido malonic ester was refluxed with 2 moles of sodium dissolved in absolute ethanol and 1.5 mole of urea. The condenser carried a $CaCl_2$ tube. The amount of absolute alcohol was so adjusted that the reaction mixture always retained enough fluid to be refluxed and stirred. After the reaction was completed, the mixture was cooled and vacuum evaporated. The semisolid was brought into solution by adding water and the mixture was acidified with 10% HCl to precipitate the barbiturate.

Methylation with dimethyl sulphate consisted in dissolving 5 g of the barbituric acid in 75 ml of 4% NaOH solution and then adding an equimolar amount of dimethyl sulphate. The mixture was stirred at room temperature for 0.5 hour and then acidified with cold 10% HCl.

Hydrolysis of acetamido group was performed with 4 *N* HCl. The complete dissolution of the compound indicated completion of the reaction. The reaction mixture was filtered, evaporated, and crystallized from a minimum amount of dilute HCl.

Attempted S-Alkylation of 5-Ethyl-5-(1-methylbutyl)-2-thiobarbituric Acid

Sodium pentothal, 5 g (0.021 mole), was dissolved in ethyl alcohol (150 ml, 95%), and allyl bromide (15 ml, excess) was added to it. The mixture was refluxed for 3 hours and then evaporated. The solid residue was extracted with benzene and repeatedly crystallized from benzene – petrol ether (b.p. 35–75°) (six times) to yield 3.5 g of pentobarbital m.p. 130.5° (lit. 131°). An easier way to purify the compound is by adsorption chromatography on alumina (B.D.H.) using as eluant benzene – ethyl acetate (1:1 mixture) or ethyl acetate alone. The pentobarbital thus obtained gave negative Lassaigne's test for sulphur and gave superimposable ultraviolet and infrared spectra with an authentic sample obtained from commercial Nembutal by precipitation with dilute HCl and crystallization from benzene – petrol ether mixture. It also showed no depression in mixed melting point determination. Mol. wt. (Rast) 235 (theory, 226). Anal. Calc. for $C_{11}H_{18}N_2O_3$ (226): C, 58.40; H, 7.97; N, 12.39. Found: C, 58.64; H, 8.16; N, 12.40.

Similarly sodium pentothal, 1 g (0.004 mole), on refluxing with benzyl chloride (3 ml, excess), in ethyl alcohol (30 ml, 95%) for 16 hours, and vacuum evaporation gave 0.5 g of pentobarbital. The characteristic smell of benzyl mercaptan and allyl mercaptan in the above case was noted but no efforts were made to isolate them. The characterization of the pentobarbital was done according to the method described in the case of allyl bromide.

Can. J. Chem. Downloaded from www.nrcresearchpress.com by 210.87.254.40 on 09/05/12
For personal use only.

Preparation of 5-Acetamido-5-isobutylbarbituric Acid (IV) from 5-Acetamido-5-isobutyl-2-thiobarbituric Acid (XII)

To a solution of 5.2 g (0.02 mole) of XII in 75 ml of 4% caustic soda solution was added 2.52 g (0.02 mole) of dimethyl sulphate. The mixture was stirred at room temperature for half an hour and then acidified with 10% HCl. If the mixture was kept in the refrigerator overnight, 2 g of the crystals of IV were obtained. Crystallization from dioxane–H_2O gave the analytical sample, m.p. 318°. Lassaigne's test for sulphur was negative. Anal. Calc. for $C_{10}H_{15}N_3O_4$ (241): C, 49.79; H, 6.22; N, 17.42. Found: C, 49.85; H, 6.07; N, 17.38. Mixed melting point with the sample prepared by condensation of urea and 5-acetamido-5-isobutyl malonic ester showed no depression. The two compounds also gave identical infrared spectra.

ACKNOWLEDGMENTS

The authors are indebted to the Medical Research Council of Canada for a grant.

REFERENCES

1. R. C. A. C. Bonino. Rev. Asoc. Bioquim Arg. **17**, 157 (1952).
2. J. Lee. J. Am. Chem. Soc. **60**, 993 (1938).
3. W. C. Price, J. E. Bradley, P. D. B. Fraser, and J. P. Quillian. J. Pharm. Pharmacol. **6**, 522 (1954).
4. H. R. Snyder, J. P. Shekleton, and C. D. Lewis. J. Am. Chem. Soc. **67**, 310 (1945).
5. N. F. Albertson. J. Am. Chem. Soc. **68**, 450 (1946).
6. A. C. Cope, H. L. Holmes, and H. O. House. Org. Reactions, **9**, 107 (1957).

Can. J. Chem. Downloaded from www.nrcresearchpress.com by 210.87.254.40 on 09/05/12
For personal use only.

ISOTOPE EFFECTS IN METHYL RADICAL ABSTRACTION REACTIONS

MARK SALOMON
Department of Chemistry, University of Ottawa, Ottawa, Canada
Received October 18, 1963

ABSTRACT

The high k_H/k_D ratio found experimentally for methyl radical abstraction reactions is explained on the basis of classical rate theory. It is shown that if the bending frequencies in the activated complex approach zero, good agreement is found between experimental and calculated k_H/k_D values. For abstraction of H and D from hydrocarbons, both the tunneling and classical rate theories predict acceptable k_H/k_D values. Abstraction of H and D from H_2 and D_2, however, can best be explained on the basis of a classical process.

INTRODUCTION

The ratio of rate constants, k_H/k_D, for the abstraction of H and D from hydrocarbons by methyl radicals has been found to be higher than that calculated from classical rate theory when the bending frequencies of the RC—H bond is assumed to remain constant from the initial to final states (1–6). To explain these high values for k_H/k_D, several workers (1, 2) have proposed that the rates are largely determined by appreciable participation of a quantum mechanical tunneling process. The basis for the tunneling mechanism is the theory of Johnston and Rapp (3), who give the relation

$$k_H/k_D = 0.99 \exp(1580/RT). \qquad [1]$$

for methyl radical abstractions based on proton tunneling (2). This theory is attractive since it does predict the experimental values of k_H/k_D with a good degree of accuracy, but the theory does not explain the lower values of k_H/k_D found for methyl radical abstraction from H_2 and D_2. In Table I, the k_H/k_D values for various reactions are given together with the ratio of frequency factors, A_H/A_D, and the difference in activation energies, ΔE, found experimentally. It will now be shown that these observed values can be correlated with classical rate theory and that quantum mechanical tunneling need not be invoked.

CALCULATIONS

From absolute reaction rate theory (9), the ratio of rate constants is given by

$$\frac{k_H}{k_D} = \frac{\prod^{3n^{\neq}-7} \sinh \tfrac{1}{2}U_{i_D}^{\neq}}{\prod^{3n^{\neq}-7} \sinh \tfrac{1}{2}U_{i_H}^{\neq}} \frac{\prod^{3n-6} \sinh \tfrac{1}{2}U_{i_H}}{\prod^{3n-6} \sinh \tfrac{1}{2}U_{i_D}} \qquad [2]$$

where the products and ratios of molecular mass and moments of inertia are assumed to be unity and U_i is $h\nu_i/kT$. We now examine several cases for the isotopic dependence of frequencies in the initial and activated states. If we first make the assumption that the frequencies associated with the activated complex are isotopically independent, then two limiting cases are obtained from equation 2. The first is that cleavage of a C—H bond occurs and the bending frequencies do not change from the initial to the activated state, that is, the only isotopically dependent vibration is the C—H stretch, so that equation (2) can be simplified to

$$k_H/k_D = \exp \tfrac{1}{2}(U_H - U_D). \qquad [3]$$

Can. J. Chem. Downloaded from www.nrcresearchpress.com by 210.87.254.6 on 09/05/12
For personal use only.

The second case arises when the C—H bond undergoing cleavage is stretched significantly so that the bending frequencies approach zero in the activated state. If this bending frequency is assumed to be doubly degenerate, equation 2 reduces (10) to

$$\frac{k_H}{k_D} = \tfrac{1}{2} \exp \tfrac{1}{2} \sum (U_{1H} - U_{1D}). \quad [4]$$

A third case arises for the $CH_3 + H_2$ reaction when the frequencies in the activated complex are isotopically dependent. If the simple pseudo-three-atom model, the activated complex has the linear form $C \ldots H \ldots H_{(2)}$. In bending frequencies (which would be absent if the $H_{(2)}$ atom were sufficiently far away from the C atom in (CH_3·) are neglected, there are two vibrations which exist (11). The first is the asymmetric one which leads to reaction and need not be considered. The second is the symmetric vibration which will result in the movement of the central H atom. Replacement of the central atom with D will then change this frequency and the symmetric vibration is therefore isotopically dependent. For abstraction from methane, the activated complex has the form C. . .H. . .C and the symmetric vibration does not involve any motion of the central H atom. For abstraction from a hydrocarbon, the activated complex has the same general form as that for methane and the symmetric vibration is assumed not to involve any motion of the central H or D atom. Hence replacement by D will have no effect and this frequency can, in principle, be neglected for this case. For $CH_3 + H_2$ and $CH_3 + D_2$ then, the ratio of rate constants is, from equation 2,

$$\frac{k_H}{k_D} = \exp \tfrac{1}{2}(U_D^{\neq} - U_H^{\neq}) \exp \tfrac{1}{2}(U_H - U_D). \quad [5]$$

We can now calculate the isotope effect for the abstraction of H and D from hydrocarbons. When the C—H and C—D stretch vibrations in CH_4 and CD_4 are assumed to be 3020 and 2258 cm^{-1} respectively (12), then from equation 3,

$$\frac{k_H}{k_D} = \exp (1090/RT), \quad [6]$$

which is 2.2 at 200° C. If the C—H and C—D bending frequencies of 1306 and 996 cm^{-1} (12) are doubly degenerate, then from equation 4

$$k_H/k_D = 0.5 \exp 1977/RT, \quad [7]$$

which equals 4.1 at 200° C. Equation 7 predicts satisfactory k_H/k_D values (see Table I). There is some discrepancy, however, for the k_H/k_D values for abstraction from methane (1). This large discrepancy was explained by assuming that the potential energy barrier for abstraction from methane is higher than for ethane, propane, etc., and therefore results in a larger contribution from tunneling (1). The bond dissociation energy of methane is reported to be between 100 and 102 kcal $mole^{-1}$ (13, 14) and the corresponding value of the C—H bond energy for ethane is 98 kcal $mole^{-1}$ (14). If this difference between the C—H bond dissociation energies causes an increase in tunneling, then one would expect that proton tunneling for the reaction $CH_3 + H_2$ would be greater. This would follow from the bond dissociation energy of 103 kcal $mole^{-1}$ for H_2 (15) and also on steric grounds. The H_2 or D_2 molecule could approach the CH_3 radical more closely than a hydrocarbon molecule so that the width of the potential energy barrier would be decreased and the tunneling probability increased. The k_H/k_D ratio for abstraction from H_2 and D_2 is, however, 2.0 (7) and therefore precludes any significant tunneling.

Can. J. Chem. Downloaded from www.nrcresearchpress.com by 210.87.254.6 on 09/05/12
For personal use only.

TABLE I

Kinetic parameters for abstraction reactions

Reaction	ΔE (kcal mole^{-1})	A_H/A_D	k_H/k_D (200°)	Reference
$CH_3 + CH_4 \rightarrow CH_4 + CH_3$ $CD_3 + CD_4 \rightarrow CD_4 + CD_3$	3.5	8.91	8.1	5 1
$CD_3 + C_2H_6 \rightarrow CD_3H + C_2H_5$ $CD_3 + C_2D_6 \rightarrow CD_4 + C_2D_5$	1.5	1.0	4.95	4 4
$CD_3 + CH_3CD_3 \rightarrow CD_3H + CH_2CD_3$ $CD_3 + CH_3CD_3 \rightarrow CD_4 + CH_3CD_2$	1.9	0.72	4.95	4 4
$CD_3 + (CH_3)_3CH \rightarrow CD_3H + (CH_3)_3C$ $CD_3 + (CH_3)CD \rightarrow CD_4 + (CH_3)_3C$	1.6	0.8	4.4	2 2
$CD_3 + CH_3CH_2CH_3 \rightarrow CD_3 + CH_3CHCH_3$ $CD_3 + CH_3CD_2CH_3 \rightarrow CD_4 + CH_3CDCH_3$	1.4	1.04	4.5	2 6
$CH_3 + H_2 \rightarrow CH_4 + H$ $CH_3 + D_2 \rightarrow CH_3D + D$	1.7	0.41	2.0	7 7
$CF_3 + CHD_3 \rightarrow CF_3H + CD_3$ $CF_3 + CHD_3 \rightarrow CF_3D + CHD_2$	2.2	0.51	5.0	8 8

If the vibrations for H_2 and D_2 are taken as 4395 and 3118 cm^{-1} respectively (16), k_H/k_D is calculated to be 6.7 from equation 3. We have seen, however, that the symmetric vibration in the activated complex is isotopically dependent and equation 5 must be used to calculate k_H/k_D. In addition to this symmetric frequency, a doubly degenerate bending frequency may be generated in the activated complex if the approach of H_2 to CH_3 is close enough. These uncertainties prohibit a quantitative evaluation of the frequencies in the activated state, but their effect is clear. The "tighter" the activated complex, the smaller is the isotope effect. An activated complex which shows this behavior is that which arises during the electrochemical discharge of a proton (or a deuteron) from acid solution onto a mercury cathode. The sum of the frequencies for the activated complex Hg. . . H. . .O has been calculated by Conway and Salomon (17) and is 3550 cm^{-1}. It is also possible that the bonding in the activated state becomes tight enough to cause an inverse isotope effect, i.e. k_H/k_D is less than unity (11). Swain *et al.* (18) have found such a case for the decarboxylation of *p*-methylbenzoylacetic acid where $k_H/k_D = 0.85$.

CONCLUSION

It has been found that the k_H/k_D ratios found for methyl radical abstraction reactions can be explained on the basis of classical rate theory. There are several discrepancies noted in the literature and the main one is the k_H/k_D value obtained for abstraction from CH_4 and CD_4. There are also some minor differences in the predicted and experimental ratio of frequency factors. This can be attributed to experimental error, since an error of $\pm 2\%$ in the measurement of k_H/k_D can give large errors in A_H/A_D and in ΔE. The C—H bend has been treated as consisting of a single stretching and a doubly degenerate bending frequency. If the symmetric and asymmetric vibrations are taken into account, the effect would be to increase k_H/k_D still more. In the reactions considered, it is found that the theory of quantum mechanical tunneling need not be invoked to explain the observed isotope effects.

ACKNOWLEDGMENTS

The author wishes to thank Professors K. J. Laidler and B. E. Conway and Dr. M. Back for their interest in this work. Grateful acknowledgment is also made to the Sprague Electric Company for the award of a Fellowship.

Can. J. Chem. Downloaded from www.nrcresearchpress.com by 210.87.254.6 on 09/05/12
For personal use only.

REFERENCES

1. F. S. DAINTON, E. A. CREAK, and K. J. IVIN. Trans. Faraday Soc. **58**, 326 (1962).
2. W. JACKSON, J. R. MCNESBY, and B. DARWENT. J. Chem. Phys. **37**, 1610 (1962).
3. H. S. JOHNSTON and D. RAPP. J. Am. Chem. Soc. **83**, 1 (1961).
4. J. R. MCNESBY. J. Phys. Chem. **64**, 1671 (1960).
5. F. S. DAINTON, K. J. IVIN, and F. WILKINSON. Trans. Faraday Soc. **55**, 929 (1959).
6. W. M. JACKSON and J. R. MCNESBY. J. Am. Chem. Soc. **83**, 4891 (1961).
7. E. WHITTLE and E. W. R. STEACIE. J. Chem. Phys. **21**, 993 (1953).
8. T. E. SHARP and H. S. JOHNSTON. J. Chem. Phys. **37**, 1541 (1962).
9. S. GLASSTONE, K. J. LAIDLER, and H. EYRING. Theory of rate processes. McGraw-Hill, N.Y. 1941.
10. L. MELANDER. Isotope effects on reaction rates. Ronald Press, N.Y. 1960.
11. F. H. WESTHEIMER. Chem. Rev. **61**, 265 (1961).
12. G. HERZBERG. Infrared and raman spectra. Van Nostrand, N.Y. 1945.
13. E. W. R. STEACIE. Atomic and free radical reactions. Reinhold, N.Y. 1953.
14. T. L. COTTRELL. Strength of chemical bonds. Butterworths, London. 1958.
15. A. G. GAYDON. Dissociation energies and spectra of diatomic molecules. Chapman and Hall, London. 1953.
16. G. HERZBERG. Spectra of diatomic molecules. Van Nostrand, N.Y. 1950.
17. B. E. CONWAY and M. SALOMON. In press (1964).
18. C. G. SWAIN, R. F. W. BADER, R. M. ESTEVE, and R. N. GRIFFIN. J. Am. Chem. Soc. **83**, 1951 (1961).

Can. J. Chem. Downloaded from www.nrcresearchpress.com by 210.87.254.6 on 09/05/12
For personal use only.

SYNTHESIS OF THE 2,4-DI-*O*-METHYL TETROSES

G. G. S. DUTTON AND K. N. SLESSOR
Department of Chemistry, University of British Columbia, Vancouver, British Columbia
Received November 22, 1963

ABSTRACT

The four isomeric 2,4-di-*O*-methyl tetroses were prepared by periodate oxidation of known methylated sugars. 2,4-Di-*O*-methyl-D- and L-erythroses were prepared from 4,6-di-*O*-methyl-D-glucose and 3,5-di-*O*-methyl-L-arabinose respectively. 2,4-Di-*O*-methyl-D- and L-threoses were prepared from 3,5-di-*O*-methyl-D-xylose and 1,4,6-tri-*O*-methyl-L-sorbose.

The tetroses were characterized by their crystalline 2,4-dinitrophenylhydrazones. The R_F and R_G values of the free sugars were recorded in a variety of solvents including a silica gel thin-layer chromatography system.

Can. J. Chem. Downloaded from www.nrcresearchpress.com by 210.87.254.40 on 09/05/12
For personal use only.

In the structural investigation of *Virgillia oroboides* gum, Stephen (1) observed several chromatographically fast-running products obtained from periodate oxidations of partially methylated sugars. From consideration of the structure of the parent sugars, these compounds were assumed to be partially methylated tetroses. No attempt to isolate these products was made due to the small amount of material present. Periodate oxidation of partially methylated glucoses, obtained from hydrolysis of a methylated glucan (2), produced methylated reducing fragments, believed to be of the tetrose series. Had recognition of the structure of these fragments been possible by comparison with known compounds, the structural elucidation of the parent sugars would have been simplified. For this reason, the synthesis of reference compounds in the 2,4-di-*O*-methyl tetrose series was undertaken.

2,4-Di-*O*-methyl-D-erythrose was prepared by periodate oxidation of 4,6-di-*O*-methyl-D-glucitol. This hexitol was obtained by borohydride reduction of crystalline 4,6-di-*O*-methyl-D-glucose prepared by the method of Bell and Lorber (3). Its optical isomer, 2,4-di-*O*-methyl-L-erythrose was obtained by periodate oxidation of 3,5-di-*O*-methyl-L-arabinitol. The dimethyl pentitol was obtained by borohydride reduction of 3,5-di-*O*-methyl-L-arabinose (4).

Periodate oxidation of 3,5-di-*O*-methyl-D-xylitol yielded 2,4-di-*O*-methyl-D-threose which, upon purification, yielded a crystalline product. The pentitol was obtained from the known (5) 3,5-di-*O*-methyl-D-xylose by borohydride reduction. Periodate oxidation of the borohydride reduction product of 1,4,6-tri-*O*-methyl-L-sorbose yielded the isomeric 2,4-di-*O*-methyl-L-threose. Reduction of the known 1,4,6-tri-*O*-methyl-L-sorbose (6) may yield two hexitols (1,4,6-tri-*O*-methyl-L-sorbitol or 1,3,6-tri-*O*-methyl-D-glucitol and 1,4,6-tri-*O*-methyl-L-iditol or 1,3,6-tri-*O*-methyl-L-iditol). Examination of the reduction mixture by thin-layer chromatography indicated only one major product, the absolute structure of which remains unknown.

Incomplete periodate oxidation of reducing sugars has been reported (1) and was substantiated in this work. Periodate oxidation of the derived glycitol gave expected periodate uptakes for all the compounds studied. The resistance of 3-substituted aldoses to borohydride reduction has been reported (7). This effect has been attributed to steric hindrance of the borohydride as it approaches the 1,3 system. In the preparation of 3,5-di-*O*-methyl pentitols from the parent pentoses and 1,3,6-tri-*O*-methyl-glycitol from 1,4,6-tri-*O*-methyl-sorbose, borohydride reduction was not complete after 24 hours. If longer reduction times

Can. J. Chem. Downloaded from www.nrcresearchpress.com by 210.87.254.40 on 09/05/12
For personal use only.

were used, detectable amounts of degradation products were formed; these were, presumably, due to Lobry de Bruyn – van Ekenstein transformations. Reductions were carried out overnight and subsequent separation of the product from the unreduced material was effected by chromatography on a silica gel column using butanone–water azeotrope as the solvent.

The use of silica gel columns originated with Bell (8), who estimated the chain length of methylated polysaccharides by use of this method. Elution of the fully methylated sugars, formerly end groups, allowed estimation of the ratio of end group to backbone residues. With the advent of cellulose chromatography, the use of silica gel columns was neglected. In purifications, such as described in this paper, silica gel column chromatography offers comparable resolution in approximately one-fourth of the time. It should be noted that thin-layer chromatography is a fast, efficient method of analyzing methylated sugar fractions (9) obtained from either cellulose or silica gel columns.

Attempts to prepare crystalline derivatives of the glycitols were unsuccessful. Although some acetates and *p*-nitrobenzoates were prepared and shown to be homogeneous by thin-layer chromatography (10), crystallization could not be induced.

Paper chromatography of the tetroses in some solvents and on silica gel thin-layer chromatography indicated the existence of two modifications of the tetroses, which were inseparable by silica gel column chromatography. Upon standing for extended lengths of time (3 months), sirupy tetroses were observed to become more viscous. Infrared spectra of the viscous sirup in contrast with those of the more mobile sirup, showed reduction in the carbonyl stretching band at 1750 cm^{-1} and enhancement of the hydroxyl band at 3400 cm^{-1}, with respect to the more mobile sirup. The infrared spectrum of the crystalline 2,4-di-*O*-methyl-D-threose showed no carbonyl stretching band but contained a hydroxyl band which was split into two equal-intensity absorptions at 3375 and 3480 cm^{-1}. The anomalous optical rotation of the threose isomers (D, $-14.8°$; L, $-14.3°$) in methanol is attributed to the existence of two or more modifications present in the solution of the sirupy L-threose compound. Upon solution of the isomers in 1 *N* sulphuric acid, the rotations dropped to near-zero values with opposite signs. These results suggest that 2,4-di-*O*-methyl tetroses easily undergo dimerization to a compound of structure similar to that from 5-aldo-1,2,-*O*-isopropylidene-D-*xylo*-pentofuranose (11). The structure of the crystalline modification of 2,4-di-*O*-methyl-D-threose may therefore be of the following nature:

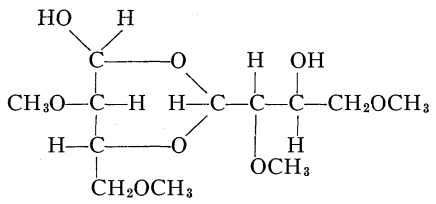

Thin-layer chromatography of the tetroses isolated as sirups contained appreciable quantities of modifications of this type. Because of the small amounts of product, molecular weight and nuclear magnetic resonance studies were not undertaken.

Acceptable analytical values were seldom obtained for the sirupy di-*O*-methyl tetroses presumably because of occluded solvent. No attempt was made to distil them because of the small amounts obtained and their volatility. Several different reagents were tried for characterizing the tetroses but only 2,4-dinitrophenylhydrazine gave satisfactory crystalline derivatives in all four cases. This reagent was used in neutral solution to give

the phenylhydrazone rather than the osazone. In retrospect the difficulty of making crystalline derivatives may be due to the equilibrium with a dimer.

Because the importance of the partially methylated tetroses lies in their chromatographic recognition, R_F and R_G values were recorded in a large number of solvent systems (Table I).

TABLE I

Physical properties of 2,4-di-*O*-methyl tetroses

	2,4-Di-*O*-methyl D-erythrose	2,4-Di-*O*-methyl L-erythrose	2,4-Di-*O*-methyl D-threose	2,4-Di-*O*-methyl L-threose
Melting point	Sirup	Sirup	114–116° (dimer?)	Sirup
$[\alpha]_D$ of free sugar	60.1° (*c*, 1.4 in MeOH)	−61.4° (*c*, 4.9 in MeOH)	−14.8° (*c*, 1.17 in MeOH) −9° (3 min) → + 0.9° (15 min) (*c*, 0.35 in 1 *N* H_2SO_4)	−14.3° (*c*, 5.7 in MeOH) −17° (5 min) → −3° (15 min) (*c*, 0.55 in 1 *N* H_2SO_4)
2,4-Dinitrophenylhydrazone melting point	105–106°	107–108°	148–149°	149–150°
Solvent system[1]				
Butanone Water Azeotrope	R_F 0.70, 0.64 R_G 0.86, 0.78	Silica gel T. L. C. R_F 0.62, 0.50	R_F 0.66, 0.57 R_G 0.89, 0.76	Silica gel T. L. C. R_F 0.65, 0.50
Ethyl acetate Pyridine Water (8:2:1)	R_F 0.77 R_G 0.92		R_F 0.81 R_G 0.96	
Butan-1-ol Ethanol Water (4:1:5) upper layer	R_F 0.82 R_G 0.96		R_F 0.84 R_G 0.98	
Ethyl acetate Acetic acid Formic acid Water (18:3:1:4)	R_F 0.80, 0.75 R_G 0.95, 0.88		R_F 0.86, 0.75 R_G 1.02, 0.88	

[1]Descending paper chromatography was carried out using Whatman No. 1 paper and R_G values are relative to 2,3,4,6-tetra-*O*-methyl-D-glucose. Sugars were detected by use of *p*-anisidine trichloracetate spray reagent. Optical isomers showed identical chromatographic patterns in all solvents. R_F and R_G values quoted for D-threose refer to the sirup before crystallization. The crystalline modification gave only the slower running component.

Ascending silica gel thin-layer chromatography was adopted for rapid examination of column fractions. Detection was achieved by use of 5% HNO_3 in H_2SO_4. Subsequent heating at 150° was sufficient for development.

In view of the apparent tendency of the 2,4-di-*O*-methyl-tetroses to dimerize and the consequent difficulty in obtaining them pure or securing crystalline derivatives in high yield these compounds cannot be recommended for characterization purposes. A knowledge of their chromatographic behavior will, however, be useful in analysis of complex mixtures of methylated sugars.

EXPERIMENTAL

Evaporations were carried out under reduced pressure at a bath temperature of 40–45° C. Optical rotations are equilibrium values measured on either a Bendix ETL-NPL Automatic Polarimeter (Type 143A) or a Rudolph Polarimeter (Model 219) at 21±2°. Melting points quoted are uncorrected. Periodate oxidation estimations were carried out by quenching oxidation aliquots in buffered arsenite and back-titrating with iodine.

Preparation of the Silica Gel Column

To silica gel (Fisher S-157, 200 g) that had been screened to pass through 60 mesh was added butanone–water azeotrope (500 ml) with stirring. The slurry was allowed to sit for 1 hour, with occasional stirring.

Can. J. Chem. Downloaded from www.nrcresearchpress.com by 210.87.254.40 on 09/05/12
For personal use only.

The mixture was then slurried into a column (3×36 cm), fitted with a fritted disc, and the silica was packed tightly by tapping the outside of the column until no further settling was apparent. A 1-cm layer of sand was then carefully placed on top of the silica gel.

The column was equilibrated by passing butanone–water azeotrope through the column for 2 days. At the end of this time the flow rate was constant at 1.8 ml per minute.

The movement of the solvent can be approximated with Sudan IV dye which shows an R_F of about 0.95 on thin-layer plates. If this is used as a marker, the front time for the column was about 1 hour.

Fractions from the column were analyzed by running samples on silica gel thin-layer plates using the same solvent system as that used on the column.

*4,6-Di-O-methyl-*D*-glucose*

4,6-Di-*O*-methyl-D-glucose was prepared by the method of Bell and Lorber (3). After recrystallization from ethyl acetate the constants were: m.p. 154–156° $[\alpha]_D$ 116° → 70.5° (*c*, 1.23 in H_2O). Lit. (3), m.p. 156–157°, $[\alpha]_D$ 108° → 65.7° (*c*, 4 in H_2O).

*4,6-Di-O-methyl-*D*-glucitol (1,3-Di-O-methyl-*L*-gulitol)*

4,6-Di-*O*-methyl-D-glucose (2.7 g) was dissolved in water (50 ml) and sodium borohydride (0.5 g) was added. The solution was neutralized with acetic acid after 18 hours, and evaporated to dryness. The resulting solid was treated with 3% HCl in methanol (3×15 ml) and evaporated to dryness. The residue was dissolved in water (25 ml) and the solution deionized with Amberlite IR-120 (H^+) and Duolite A-4 (OH^-). Evaporation of the resulting solution gave a non-reducing sirup (2.6 g), $[\alpha]_D$ 7° (*c*, 1.5 in $CHCl_3$).

*2,4-Di-O-methyl-*D*-erythrose*

4,6-Di-*O*-methyl-D-glucitol (524 mg, 2.5 mmoles) in water (25 ml) was added to 0.12 *M* sodium periodate (50 ml, 6 mmoles). The oxidation was complete in 25 minutes with an uptake of 2.03 moles of periodate per mole of hexitol. The solution was neutralized with washed barium carbonate, and diluted with an equal volume of methanol, filtered, and evaporated to give a mobile sirup which was purified by chromatography on a silica gel column (297 mg) $[\alpha]_D$ 60.1° (*c*, 1.4 in MeOH).

*2,4-Dinitrophenylhydrazone of 2,4-Di-O-methyl-*D*-erythrose*

2,4-Di-*O*-methyl-D-erythrose (100 mg) was dissolved in 100% ethanol (3 ml) and recrystallized 2,4-dinitrophenylhydrazine (110 mg) was added. The mixture was refluxed on a steam bath for 5 hours, evaporated to dryness, dissolved in ethyl acetate (10 ml), and petroleum ether (30–60°) (10 ml) was added to precipitate excess reagent. The mixture was filtered after 10 minutes, the filtrate evaporated to a sirup, dissolved in chloroform (2 ml), and applied to an alumina column (3×20 cm). Collection of the light yellow band eluted with chloroform afforded yellow-orange crystals melting at 102–103°. Subsequent recrystallization from ethyl acetate – petroleum ether (30–60°) gave crystals melting at 105–106°. Calculated for $C_{12}H_{16}O_7N_4$: N, 17.07; OCH_3, 18.90%. Found: N, 17.04; OCH_3, 19.23%.

*3,5-Di-O-methyl-*L*-arabinose*

3,5-Di-*O*-methyl-L-arabinose was obtained by the procedure of Hirst, Jones, and Williams (4). The sirup showed only one component (R_F 0.59) upon paper chromatography in butanone–water azeotrope and had $[\alpha]_D$ −36° (*c*, 6.7 in MeOH). Lit. (4), $[\alpha]_D$ −39° (25% aqueous acetic acid).

*3,5-Di-O-methyl-*L*-arabinonolactone*

3,5-Di-*O*-methyl-L-arabinose (75 mg) in water (4 ml) was treated with bromine (4 drops) and the mixture was left at room temperature overnight. Aeration, and treatment with silver carbonate followed by filtration, gave a solution which was passed through IR-120 (H^+), and evaporated to a sirup. Sublimation at 65–70° (0.05 mm) gave crystals of 3,5-di-*O*-methyl-L-arabinonolactone, m.p. 72–73°. Lit. (4), m.p. 73°.

*3,5-Di-O-methyl-*L*-arabinonamide*

3,5-Di-*O*-methyl-L-arabinonolactone (6 mg) was dissolved in methanol saturated with ammonia (1 ml) and the solution was left overnight at room temperature. The solution was evaporated to give crystals, which, after recrystallization from acetone, melted at 144°. Lit. (4), m.p. 144°.

*3,5-Di-O-methyl-*L*-arabinitol (1,3-Di-O-methyl-*L*-lyxitol)*

3,5-Di-*O*-methyl-L-arabinose (1.7 g) dissolved in water (30 ml) was treated with excess sodium borohydride (1 g) and left at room temperature overnight. The solution was worked up in the same manner as described for 4,6-di-*O*-methyl-D-glucitol. The sirup containing 3,5-di-*O*-methyl-L-arabinitol and 3,5-di-*O*-methyl-L-arabinose (ca. 9:1) was separated completely on the silica gel column. The arabinose (R_F 0.56 on T.L.C. same solvent) was found in the eluate, 175–300 ml after the dye marking the front. The arabinitol (R_F 0.40) was found in the 675–1000 ml fraction. Evaporation of the fraction containing arabinitol yielded a non-reducing sirup (1.4 g) $[\alpha]_D$ −7° (*c*, 5.8 in $CHCl_3$).

*2,4-Di-O-methyl-*L*-erythrose*

3,5-Di-*O*-methyl-L-arabinitol (527 mg, 2.93 mmoles) in water (200 ml) was treated with 0.08 *M* sodium periodate (50 ml). The oxidation was complete in 10 minutes and was worked up as described for its isomer.

Can. J. Chem. Downloaded from www.nrcresearchpress.com by 210.87.254.40 on 09/05/12
For personal use only.

The final periodate uptake was 1.04 moles per mole of pentitol. Purification on silica gel gave a colorless sirup (365 mg) $[\alpha]_D$ −61.4° (*c*, 4.85 in MeOH).

2,4-Dinitrophenylhydrazone of 2,4-di-O-methyl-L-erythrose

The hydrazone was prepared using the same quantities as those used in the preparation of its optical isomer. Upon recrystallization from ethyl acetate – petroleum ether (30–60°), it melted at 107–108°. Calculated for $C_{12}H_{16}O_7N_4$: N, 17.07; OCH_3, 18.90%. Found: N, 16.97; OCH_3, 19.08%.

1,2-Isopropylidene-D-xylofuranose

1,2-Isopropylidene-D-xylofuranose was prepared by the acid hydrolysis of 1,2:3,5-diisopropylidene-D-xylose. The product was recrystallized from ethyl acetate – petroleum ether (30–60°) (1:4) m.p. 67–69° $[\alpha]_D$ −21.9° (*c*, 3.15 in H_2O). Lit. (12), m.p. 41–43° $[\alpha]_D$ −19.0° (*c*, 2 in H_2O). Calculated for $C_9H_{14}O_5$: C, 50.52; H, 7.37%. Found: C, 50.68; H, 7.65%.

3,5-Di-O-methyl-1,2-isopropylidene-D-xylose

1,2-Isopropylidene-D-xylofuranose was methylated by the method of Kuhn *et al.* (13). The compound was isolated as a sirup, which was distilled under vacuum, and the fraction boiling at 80–82° (0.05 mm) was collected. The mobile liquid had a specific rotation $[\alpha]_D$ −57.3° (*c*, 5.2 in $CHCl_3$). Lit. (14), $[\alpha]_D$ −60° (*c*, 1.09 in $CHCl_3$).

3,5-Di-O-methyl-D-xylose

3,5-Di-*O*-methyl-1,2-isopropylidene-D-xylose (5 g) was dissolved in 25% aqueous acetic acid and heated on a steam bath for 5 hours after which time the optical rotation was constant. After evaporation a yellow sirup (2.1 g) remained which showed only one component (R_F 0.57) upon paper chromatography in butanone–water azeotrope, $[\alpha]_D$ 23.5° (*c*, 3.9 in H_2O). Lit. (14), $[\alpha]_D$ 25° (*c*, 1.13 in H_2O).

p-Bromophenylosazone of 3,5-Di-O-methyl-D-xylose

The osazone was prepared by the method of Applegarth, Dutton, and Tanaka (15). 3,5-Di-*O*-methyl-D-xylose (75 mg) and *p*-bromophenylhydrazine (280 mg) were dissolved in glacial acetic acid (4.3 ml). Water (2.2 ml) was added and the solution was heated 6 minutes on a steam bath and allowed to cool. After 2 hours at 5° the crystals were filtered and recrystallized from ethyl acetate – petroleum ether (30–60°) (1:7) m.p. 106.5–107.5°. Lit. (5), m.p. 107–108°.

3,5-Di-O-methyl-D-xylitol (1,3-Di-O-methyl-L-xylitol)

3,5-Di-*O*-methyl-D-xylose (390 mg) dissolved in water (15 ml) was treated with excess sodium borohydride (200 mg). The solution was left at room temperature overnight, and worked up in the manner described for the arabinitol. The sirup (330 mg) obtained showed no reducing properties $[\alpha]_D$ −5.4° (*c*, 6.6 in $CHCl_3$).

2,4-Di-O-methyl-D-threose

3,5-Di-*O*-methyl-D-xylitol (212 mg, 1.17 mmoles) in water (40 ml) was treated with 0.203 *M* periodic acid (10 ml). The oxidation was complete in 10 minutes and the final periodate uptake amounted to 0.91 moles per mole of pentitol. Workup was identical with that described earlier for the erythroses and a mobile sirup (124 mg) was obtained. Purification of this material on a silica gel column yielded crystalline (dimeric?) 2,4-di-*O*-methyl-D-threose. Recrystallization from ethyl acetate – petroleum ether (30–60°) (1:5) gave crystals melting at 114–116° $[\alpha]_D$ −14.8° (*c*, 1.17 in MeOH) showing no mutarotation after 24 hours. $[\alpha]_D$ −9° (3 min) → +0.9° (15 min) (*c*, 0.35 in 1 *N* H_2SO_4). Calculated for $C_6H_{12}O_4$: C, 48.64; H, 8.11; OCH_3, 41.89%. Found: C, 48.78; H, 8.22; OCH_3, 41.51%.

2,4-Dinitrophenylhydrazone of 2,4-di-O-methyl-D-threose

The hydrazone was prepared in the same manner and using the same quantities as for the 2,4-di-*O*-methyl erythroses. The derivative after recrystallization from ethyl acetate – petroleum ether melted at 148–149°. Calculated for $C_{12}H_{16}O_7N_4$: N, 17.07; OCH_3, 18.90%. Found: N, 17.26; OCH_3, 18.43%.

1,4,6-Tri-O-methyl-L-sorbose

1,4,6-Tri-*O*-methyl-L-sorbose was prepared by the method of Schlubach and Olters (6). The sirup showed only one component (R_F 0.72) upon paper chromatography in butanone–water azeotrope. $[\alpha]_D$ −1.85° → +3.16° (*c*, 7.2 in $CHCl_3$). Lit. (6), $[\alpha]_D$ 3.8° (*c*, 1.5 in $CHCl_3$).

Tri-O-methyl-hexitol (1,3,6-Tri-O-methyl-D-glucitol or 1,3,6-Tri-O-methyl-L-iditol)

1,4,6-Tri-*O*-methyl-L-sorbose (520 mg) in water (15 ml) was treated with excess sodium borohydride (1 g) and left overnight at room temperature. The methylated hexitols were isolated in the same manner as previously described. The resulting sirup showed only one major component (R_F 0.45) on silica gel thin-layer chromatography using butanone–water azeotrope. This component was isolated by chromatography on a silica gel column to give a sirup (280 mg) having a rotation $[\alpha]_D$ 5.6° (*c*, 1.5 in $CHCl_3$).

2,4-Di-O-methyl-L-threose

To the tri-*O*-methyl-hexitol (650 mg, 2.9 mmoles) dissolved in water (5 ml), 0.2 *M* sodium periodate (20 ml) was added. The oxidation was complete in 5 minutes with an uptake of 0.98 moles of periodate per

Can. J. Chem. Downloaded from www.nrcresearchpress.com by 210.87.254.40 on 09/05/12
For personal use only.

mole of hexitol. Recovery of the tetrose in the manner described above and subsequent purification on the silica gel column yielded a colorless sirup (370 mg) $[\alpha]_D$ −14.3° (*c*, 5.7 in MeOH). $[\alpha]_D$ −17° (5 min) → −3° (15 min) (*c*, 0.55 in 1 *N* H_2SO_4).

*2,4-Dinitrophenylhydrazone of 2,4-Di-O-methyl-*L*-threose*

The hydrazone was prepared using the same quantities as were used for preparing its optical isomer. The derivative, upon recrystallization from ethyl acetate – petroleum ether (30–60°), melted at 149–150°. Calculated for $C_{12}H_{16}O_7N_4$: N, 17.07; OCH_3, 18.90%. Found: N, 16.87; OCH_3, 19.16%.

ACKNOWLEDGMENTS

We are grateful to the National Research Council of Canada and the National Institute of Health (U. S. A.) for financial support and one of us (K. N. S.) thanks the Council for the award of a studentship. We are also indebted to Mr. A. Barlay and Mr. K. Gibney for technical assistance and to Mrs. A. Aldridge and Mrs. C. Jenkins for analyses.

REFERENCES

1. A. M. STEPHEN. J. Chem. Soc. 2030 (1962).
2. G. G. S. DUTTON and A. M. UNRAU. Can. J. Chem. **41**, 2439 (1963).
3. D. J. BELL and J. LORBER. J. Chem. Soc. 453 (1940).
4. E. L. HIRST, J. K. N. JONES, and E. WILLIAMS. J. Chem. Soc. 1062 (1947).
5. P. A. LEVENE and A. L. RAYMOND. J. Biol. Chem. **102**, 331 (1933).
6. H. H. SCHLUBACH and P. OLTERS. Ann. **550**, 140 (1942).
7. P. D. BRAGG and L. HOUGH. J. Chem. Soc. 4347 (1957).
8. D. J. BELL. J. Chem. Soc. 473 (1944).
9. G. W. HAY, B. A. LEWIS, and F. SMITH. J. Chromatog. **11**, 479 (1963).
10. M. E. TATE and C. T. BISHOP. Can. J. Chem. **40**, 1043 (1962).
11. R. SCHAFFER and H. S. ISBELL. J. Am. Chem. Soc. **79**, 3864 (1957).
12. O. SVANBERG and K. SJOBERG. Ber. **56**, 863 (1923).
13. R. KUHN, I. LOW, and N. TRISCHMAN. Ber. **90**, 203 (1957).
14. R. A. LAIDLAW. J. Chem. Soc. 2941 (1952).
15. D. A. APPLEGARTH, G. G. S. DUTTON, and Y. TANAKA. Can. J. Chem. **40**, 2177 (1962).

Can. J. Chem. Downloaded from www.nrcresearchpress.com by 210.87.254.40 on 09/05/12
For personal use only.

ARSENIDES OF THE TRANSITION METALS

VII. THE PALLADIUM–ARSENIC SYSTEM[1]

G. S. SAINI,[2] L. D. CALVERT, R. D. HEYDING,[3] J. B. TAYLOR
Division of Applied Chemistry, National Research Council, Ottawa, Canada
Received October 4, 1963

ABSTRACT

In the Pd–As system the existence of seven intermediate phases, $PdAs_2$, α-Pd_2As, β-Pd_2As, Pd_5As_2, $Pd_{2.65}As$, Pd_3As, and Pd_5As has been established by X-ray diffraction and thermal analysis. Single crystals of β-Pd_2As and $PdAs_2$ have been grown by slow cooling from a temperature above the liquidus and of Pd_3As and Pd_5As by halide vapor transport. $PdAs_2$ is cubic, C2 (pyrite) structure, space group $Pa3(T_h^6)$, $a = 5.983\pm0.001$ Å. α-Pd_2As (stable below 455° C) is monoclinic, $a = 9.24\pm0.01$ Å, $b = 8.47\pm0.01$ Å, $c = 10.45\pm0.01$ Å, $\beta = 94°$. β-Pd_2As (stable above 455° C) has the revised C22 (Fe_2P) structure, space group $P\bar{6}2m$ (D_{3h}^3), $a = 6.650\pm0.003$ Å, $c = 3.583\pm0.003$ Å, $c/a = 0.5388$. Pd_5As_2 displays a form of polytypism and shows trigonal as well as hexagonal symmetry with different c parameters. $Pd_{2.65}As$ decomposes peritectically and its structure is unknown. Pd_3As has tetragonal $D0_e$ (Fe_3P) structure, space group $I\bar{4}(S_4^2)$; redetermined lattice constants are $a = 9.974\pm0.002$ Å, $c = 4.822\pm0.002$ Å, $c/a = 0.4834$. Pd_5As is C-face centered monoclinic, $a = 5.51_4\pm0.01$ Å, $b = 7.72_5\pm0.01$ Å, $c = 8.42_7\pm0.01$ Å, and $\beta = 99°\pm5'$.

The literature on the Pd–As system is very scanty. To our knowledge there are no reports on the formation and structure of palladium arsenides except an early study of $PdAs_2$ by Thomassen (1), short reports on Pd_3As by Schubert (2), Heyding and Calvert (3), and a recent note on Pd_2As (high temperature phase) by Schubert (4). In order to establish the existence and composition of the intermediate phases and to characterize them, an investigation of this system by X-ray diffraction and thermal analysis has been undertaken in this laboratory.

EXPERIMENTAL

The palladium sponge was supplied by Engelhard Industries and had a purity of 99.99% as determined spectrographically. It was used without further purification. Arsenic (99.999% purity) was obtained from Cominco. It was fractionally sublimed *in vacuo* at 450° C to remove oxide contaminant not recorded in the spectrographic analysis. Calculated quantities (5 to 10 g total) of palladium and arsenic were sealed in quartz ampoules at 10^{-5} mm Hg and heated at 700° C for 24 hours. The reaction between palladium and arsenic being highly exothermic, all specimens were found to have melted after the initial reaction. The products were removed, crushed, and resealed in quartz ampoules for a series of annealing periods ranging from 2 months at 300° C to 7 days at 850° C. After each annealing period the specimens were quenched in water and Debye–Scherrer patterns obtained in 11.46 cm Norelco cameras using Ni-filtered Cu radiation. Powder photographs were also obtained on a Guinier–deWolff focussing camera with As_2O_3 as an internal standard. The intensities of the powder diffraction lines were obtained by comparison with a logarithmic interval density scale. Single crystal photographs were taken on a precession camera using zirconium-filtered molybdenum radiation. Densities were determined pycnometrically using water except in the cases of β-Pd_2As and Pd_5As where single crystals were large enough to be measured on a Berman torsion balance using toluene as the immersion fluid.

Thermal analyses were performed on 3 g samples using vacuum-sealed thin-walled quartz ampoules. Seventeen samples ranging in composition from 24.4 at.% As to 66.7 at.% As were studied.

Single crystals were prepared by techniques involving either growth from the melt or vapor growth by halide transport. In the first case, a previously prepared polycrystalline specimen of the requisite composition was vacuum sealed in a quartz ampoule leaving a minimum of void space. Single crystals were

[1]*Issued as N.R.C. No. 7728.*
[2]*Present address: Chemistry Department, Queen's University, Kingston, Ont.*
[3]*Postdoctoral Fellow.*

Can. J. Chem. Downloaded from www.nrcresearchpress.com by 210.87.254.42 on 09/05/12
For personal use only.

obtained on slow cooling of the specimen from a temperature above the liquidus by lowering the ampoule through a suitable temperature gradient in a vertical furnace.

In the halide vapor transport experiments, the general reaction was of the type

$$Pd_xAs_{y(s)} + \text{halogen}_{(g)} \rightleftharpoons Pd\ \text{halide}_{(g)} + As_{(g)}.$$

Experiments were conducted with chlorine, bromine, and iodine but, within the range of conditions used, only chlorine was found to give successful transport reactions. The reaction tube was made of clear quartz, 35 cm long, 2 cm in diameter with 0.2 cm wall. A polycrystalline charge of required composition was contained in a fused alumina boat situated at one end of this tube. After evacuation to 10^{-4} mm Hg, dry chlorine was distilled into the tube to give a concentration of about 0.03 mg Cl_2/cc. The tube was sealed off and supported horizontally in a two-zone furnace. Temperatures were recorded on two chromel vs. alumel thermocouples attached to each end of the reaction tube. Manipulation of the temperature of the charge material and of the temperature gradient along the tube enabled crystals to be grown. Details of the exact procedure followed in individual cases and the results obtained are given under the relevant subheadings in the next section.

RESULTS AND DISCUSSION

The Phase Diagram

The results of the phase analytical studies are embodied in the phase diagram (Fig. 1) and may be summarized as below.

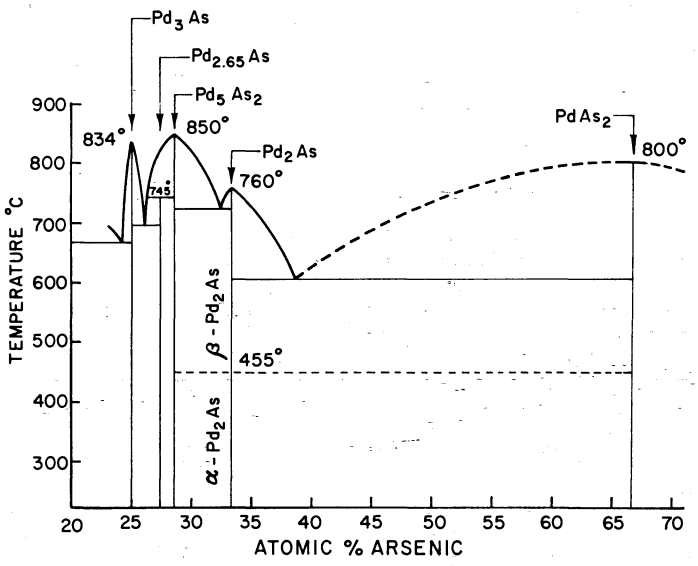

FIG. 1. Partial phase diagram of the system palladium–arsenic.

(i) In the Pd–As system, seven intermediate phases exist. They are Pd_5As, Pd_3As, $Pd_{2.65}As$, Pd_5As_2, α-Pd_2As, β-Pd_2As, and $PdAs_2$. (ii) The compound PdAs does not exist. This supports Thomassen's observation (1). (iii) The hexagonal β-Pd_2As phase transforms into the monoclinic α-Pd_2As phase when annealed at a temperature below 455° C. The transformation is extremely rapid and readily detectable on a thermal analysis cooling curve. (iv) $PdAs_2$, β-Pd_2As, Pd_5As_2, Pd_3As, and Pd_5As have congruent melting points whereas $Pd_{2.65}As$ undergoes peritectic decomposition above 745° C. (v) The formation of Pd_5As from the elements is very slow. The exact position of the liquidus curve in the region of Pd_5As was uncertain and results did not justify the inclusion of this portion of the phase diagram. The composition of this phase was deduced from the density and the unit cell volume as obtained by measurements on single crystals.

Can. J. Chem. Downloaded from www.nrcresearchpress.com by 210.87.254.42 on 09/05/12
For personal use only.

The $PdAs_2$ Phase

From a study of powder photographs Thomassen (1) reported that $PdAs_2$ has the C2 (pyrite) structure; space group $Pa3(T_h^6)$; $a = 5.982$ Å. Heyding and Calvert (3) confirmed these observations and reported $a = 5.983 \pm 0.001$ Å. During attempts to grow single crystals of Pd_2As by slow cooling of melts of compositions Pd_2As, $Pd_{1.8}As$, and $Pd_{1.6}As$, a few well-developed rectangular crystals were observed in the matrix of a broken ingot of $Pd_{1.6}As$. When examined on the precession camera, these crystals were found to be $PdAs_2$; $a = 5.98_7 \pm 0.01$ Å; $U = 214.6$ Å^3; $Z = 4$; F.W. = 256.22; $D_x = 7.93$ g.cm^{-3} and $D_m = 7.62$ g.cm^{-3}.

The x parameter for the As atoms in the position 8*c* of the space group $Pa3$ (T_h^6) was determined to be 0.382 ± 0.004 from the ratios of the intensities of the observed reflections, {321}/{123}; {631}/{136}; {641}/{146}; and {421}/{124}. This is in good agreement with the value 0.38 found by Thomassen (5) for $PtSb_2$. The shortest interatomic distances (a taken as 5.984 Å) are: Pd to 6As = 2.49 Å; As to 1As = 2.45 Å; As to 3Pd = 2.49 Å.

The α-Pd_2As Phase

The low temperature α-Pd_2As phase was obtained by annealing a specimen of stoichiometric composition at 450° C. Debye–Scherrer photographs indicated α-Pd_2As to be of a low symmetry. All efforts to grow single crystals of this phase failed. Photographs obtained with a Guinier focussing camera, using As_2O_3 as internal standard (Table I) were indexed by Ito's method and subsequently reduced to a monoclinic cell; $a = 9.24 \pm 0.01$ Å, $b = 8.47 \pm 0.01$ Å, $c = 10.45 \pm 0.01$ Å, $\beta = 94°$; diffraction symbol $12/m1P\ldots$;

TABLE I

Powder diffraction pattern of α-Pd_2As

Monoclinic; diffraction symbol $12/m1P\ldots$; $a = 9.24 \pm 0.01$ Å, $b = 8.47 \pm 0.01$ Å, $c = 10.45 \pm 0.01$ Å, $\beta = 94°$; Guinier focussing camera, diameter 11.46 cm; CuK_α radiation, $\lambda\alpha_1 = 1.5405$ Å; temp. 24° C; internal standard As_2O_3 ($a = 11.075_5$ Å); d values > 1.736; cutoff 35 Å

I/I_1	d_{obs}(Å)	d_{calc}(Å)	hkl	I/I_1	d_{obs}(Å)	d_{calc}(Å)	hkl
2.8	8.473	8.470	010	51	2.305	2.304	400
2.2	5.218	5.214	002			2.220	024
		5.244	111	100	2.216	2.217	401
0.7	4.705	4.680	$\bar{1}02$			2.217	$\bar{2}32$
0.9	4.606	4.608	200			2.154	$\bar{1}33$
1.8	4.435	4.440	012	100	2.149	2.153	313
		4.408	$\underline{1}02$			2.145	411
2.2	4.299	4.328	$\bar{2}01$	41	2.133	2.133	214
2.2	4.230	4.235	020			2.130	124
0.6	4.040	4.048	210	26	2.118	2.118	040
0.7	3.919	3.924	021			2.020	331
		3.910	$\underline{1}12$	26	2.017	2.019	$\underline{1}41$
3.5	3.565	3.579	$\bar{2}02$			2.014	$\bar{2}33$
		3.577	$\underline{1}21$	33	1.959	1.963	$\bar{3}32$
2.2	3.309	3.297	$\bar{2}12$			1.962	042
<0.6	3.259	3.287	022	3.5	1.942	1.946	233
3.5	3.219	3.216	013	21	1.917	1.915	034
11	3.081	3.072	300	13	1.865	1.862	403
26	2.887	2.893	301	17	1.817	1.818	$\underline{4}13$
		2.888	$\underline{3}10$			1.787	$\bar{1}43$
8.6	2.822	2.831	$\bar{3}11$	1.1	1.785	1.785	430
		2.823	030			1.784	$\bar{3}05$
64	2.601	2.607	004			1.739	$\bar{5}12$
		2.601	131	13	1.738	1.738	006
		2.366	$\underline{1}14$			1.737	234
51	2.352	2.365	$\bar{2}31$				
		2.340	$\bar{2}04$				

Can. J. Chem. Downloaded from www.nrcresearchpress.com by 210.87.254.42 on 09/05/12
For personal use only.

$U = 815.8$ Å^3; $Z = 18$; F.W. $= 287.71$; $D_x = 10.54$ g.cm^{-3}, and $D_m = 10.13$ g.cm^{-3}. The indexing was confirmed by using an I.B.M. digital computor.

It is to be noted that the indexing on a monoclinic cell is based on the presence of lines 3, 6, 10, and 11 in the powder pattern, which have been indexed as $\bar{1}02$, $\bar{2}01$, $\bar{2}02$, and 121, and $\bar{2}12$. In the absence of these lines the pattern can be indexed on an orthorhombic unit cell. However, careful consideration of all the available data indicates that these lines are unique to the α-Pd_2As phase and the assignment of the lower symmetry is regarded as essential.

The β-Pd_2As Phase

The high temperature Pd_2As phase is hexagonal with revised C22 (Fe_2P) structure; space group $P\bar{6}2m(D_{3h}^3)$; $a = 6.650\pm0.003$ Å, $c = 3.583\pm0.003$ Å, $c/a = 0.5388$; $U = 137.22$ Å^3; $Z = 3$; F.W. $= 287.71$; $D_x = 10.44$ g.cm^{-3}; $D_m = 10.33$ g.cm^{-3}.

Alloys with nominal compositions of $Pd_{2.0}As$ (two alloys, both single phase), $Pd_{2.1}As$ (one alloy, two phases β-Pd_2As + Pd_5As_2), and $Pd_{2.2}As$ (one alloy, two phases β-Pd_2As + Pd_5As_2) gave, for β-Pd_2As, lattice parameters which fell within the range of $a = 6.650\pm0.003$ Å, $c = 3.583\pm0.003$ Å, and $c/a = 0.5388\pm0.0007$ Å. A powder pattern of one $Pd_{2.0}As$ alloy indexed on the basis of $a = 6.651\pm0.002$ Å, $c = 3.582\pm0.002$ Å is listed in Table II. It was concluded from this that, at 700° C, β-Pd_2As has a negligible range of

TABLE II

Powder diffraction pattern of β-Pd_2As

Hexagonal; space group $P\bar{6}2m(D_{3h}^3)$; $a = 6.651\pm0.002$ Å, $c = 3.582\pm0.002$ Å, $c/a = 0.5386$; Ni-filtered Cu radiation, $\lambda\alpha_1 = 1.5405$ Å; Debye–Scherrer camera, diameter 11.46 cm; cutoff 20 Å; temp. 24° C

I/I_1	d_{obs}(Å)	d_{calc}(Å)	hkl	I/I_1	d_{obs}(Å)	d_{calc}(Å)	hkl
100	2.423	2.437	111	11	1.028	1.029	412
80	2.235	2.244	201	21	0.993	0.994	511
80	2.168	2.177	210	13	0.968	0.969	502
64	1.913	1.920	300	21	0.9301	0.9302	422
41	1.852	1.860	211	13	0.9226	0.9223	520
17	1.786	1.791	002	7	0.9155	0.9155	431
21	1.591	1.598	310	26	0.8957	0.8958	512
13	1.504	1.508	221			0.8955	004
21	1.455	1.459	311	17*	0.8927	0.8932	521
11	1.437	1.440	400	21	0.8857	0.8859	323
26	1.379	1.383	212	26	0.8530	0.8531	611
17	1.333	1.336	401	17	0.8371	0.8371	432
13	1.319	1.321	320	13	0.8313	0.8314	440
26	1.306	1.310	302	21*	0.8289	0.8290	503
13	1.254	1.257	410	13	0.8228	0.8229	530
80	1.238	1.240	321				700
13	1.191	1.192	312	26	0.8199	0.8200	522
11	1.185	1.186	411	8.6	0.8118	0.8116	304
11	1.150	1.152	500	26*	0.8097	0.8099	441
17	1.122	1.122	402	7	0.8045	0.8044	423
		1.124	113	17*	0.8018	0.8020	531
8.6	1.108	1.108	330				701
17	1.096	1.097	501	17	0.7886	0.7886	612
17	1.087	1.089	420			0.7884	224
13	1.062	1.063	322	21	0.7818	0.7819	513
13	1.034	1.035	510	41	0.7796	0.7796	621

*α_1 α_2 overlap.

composition on the metal-rich side. The homogeneity range on the arsenic-rich side of β-Pd_2As was not ascertained because the alloys rich in arsenic were not successfully quenched to give patterns of β-Pd_2As + $PdAs_2$. Invariably the patterns obtained were

Can. J. Chem. Downloaded from www.nrcresearchpress.com by 210.87.254.42 on 09/05/12
For personal use only.

α-Pd_2As + $PdAs_2$. Three other alloys with a nominal composition of $Pd_{2.0}As$ and showing only a single phase pattern gave lattice parameters which ranged from $a = 6.652 \pm 0.002$ Å, $c = 3.576 \pm 0.002$ Å to $a = 6.642 \pm 0.002$ Å and $c = 3.600 \pm 0.002$ Å. These alloys were prepared by reannealing of crushed powders, and spectrographic analysis of a representative alloy showed no extra impurities. The origin of this variation is not certain.

Single crystals of β-Pd_2As were obtained by slow cooling from a temperature above the liquidus at stoichiometric composition. Crystal fragments for the precession camera were selected from the broken ingot. The zones recorded were $h0l$, $h1l$, $hk0$, and $hk1$. No systematic extinctions were observed. The intensities of $hk0$ and $h0l$ reflections compared very well with those obtained by Rundqvist and Jellinek (6) for Ni_6Si_2B and Fe_2P. Cell parameters determined from single crystal photographs are $a = 6.64_5 \pm 0.015$ Å, $c = 3.58_0 \pm 0.01$ Å, and $c/a = 0.5388$.

These results, obtained both by single crystal and powder diffraction studies are to be compared with values of $a = 6.62$ Å and $c = 3.60$ Å reported by Schubert in a recent note (4).

The Pd_5As_2 Phase

The specimen with 28.6 at.% As (Pd_5As_2) was extremely malleable and difficult to powder. It gave a rather complex powder pattern which seemed to be of a low symmetry. The phase has been characterized crystallographically by powder and single-crystal studies. The results indicate that it displays a form of polytypism and shows trigonal as well as hexagonal symmetry with a number of different c parameters. Detailed results will form the subject of a later communication in connection with the compounds of the type M_5X_2.

The $Pd_{2.65}As$ Phase

The Debye–Scherrer patterns show the presence of a phase between the compositions Pd_5As_2 and Pd_3As. The photographs of well-annealed specimens with 27.03 at.% As ($Pd_{2.7}As$) showed traces of diffraction lines from the Pd_3As phase, whilst those of specimens with 27.78 at.% As ($Pd_{2.6}As$) showed traces of diffraction lines from Pd_5As_2 in addition to the characteristic lines of the $Pd_{2.65}As$ phase. The specimen containing 27.4 at.% As ($Pd_{2.65}As$), which gave a single phase pattern, was, therefore, taken as representative. The pattern seems to be of a low symmetry. The compound undergoes peritectic decomposition at 745° C. Unsuccessful attempts were made to prepare single crystals of this phase by vapor transport and by slow cooling of a specimen in the two-phase region close to the stoichiometric composition on the palladium rich side. The powder pattern has not been indexed but is recorded in Table III.

The Pd_3As Phase

This phase was first reported in a short note by Schubert (2) and subsequently by Heyding and Calvert (3). Schubert reported the cell parameters to be $a = 9.98_6$ Å and $c = 4.83_6$ Å. Heyding and Calvert gave $a = 9.95_1 \pm 0.01$ Å and $c = 4.81_7 \pm 0.01$ Å based on an indexing of low-angle reflections only. A completely indexed powder pattern is given in Table IV and parameters have been calculated from measurements in the back reflection region. Pd_3As is body-centered tetragonal with the $D0_e$ (Fe_3P) structure; space group $I\bar{4}(S_4^2)$; $a = 9.974 \pm 0.002$ Å, $c = 4.822 \pm 0.002$ Å, $c/a = 0.4834$; $U = 479.7$ Å^3; $Z = 8$; F.W. = 394.11; $D_x = 10.91$ g.cm^{-3}, and $D_m = 10.88$ g.cm^{-3}.

In one of a series of experiments to grow single crystals of α-Pd_2As by vapor transport, a polycrystalline charge of composition Pd_2As was used. The tube was maintained at a

Can. J. Chem. Downloaded from www.nrcresearchpress.com by 210.87.254.42 on 09/05/12
For personal use only.

TABLE III

Powder diffraction pattern of $Pd_{2.65}As$

Guinier focussing camera, diameter 11.46 cm; CuK_α radiation, $\lambda\alpha_1 = 1.5405$ Å; temp. 24° C; internal standard As_2O_3 ($a = 11.075_5$ Å); d values > 1.353; cutoff 35 Å

I/I_1	d_{obs}(Å)	I/I_1	d_{obs}(Å)	I/I_1	d_{obs}(Å)
2.2	5.468	51	2.351	5.5	1.6882
2.8	4.741	4.4	2.328	5.5	1.6356
2.2	4.407	51	2.202	2.2	1.5375
3.5	4.301	100	2.146	5.5	1.5086
3.5	4.251	100	2.121	4.4	1.4698
2.2	3.492	8.6	2.102	5.5	1.4208
4.4	3.018	4.4	2.014	8.6	1.4065
8.6	2.731	21	1.987	4.4	1.3937
2.2	2.583	4.4	1.969	5.5	1.3833
7	2.527	8.6	1.830	4.4	1.3719
13	2.434	8.6	1.822	11	1.3585
7	2.396	5.5	1.806	7	1.3531
64	2.369	21	1.7597		

uniform temperature of 450° C for 4 weeks. Needle-shaped crystals about 0.2 mm long and faceted beads about 0.03 mm across were found to have grown on the inside of the boat. Both types of crystals were examined by Debye–Scherrer photographs and were found to be Pd_3As. The beads were examined by the precession method. Measurements of the photographs gave $a = 9.96_3 \pm 0.01$ Å, $c = 4.82_9 \pm 0.01$ Å.

The Pd_5As Phase

The powder patterns of well-annealed polycrystalline samples, prepared by the usual methods, were unsatisfactory for analysis. Invariably they were not single phase and lines unique to Pd_5As were not sharp. Accordingly attempts were made to grow single crystals by chloride vapor transport using an annealed polycrystalline charge containing 17 at.% Pd. This material was known to contain some Pd_3As. No crystals were obtained. As the failure of the experiment could be attributed to the particularly low decomposition pressure of the arsenide used, the experiment was repeated by using a charge of composition $Pd_{2.7}As$, which was suspected to have a relatively higher arsenic decomposition pressure. The charge was maintained at 500° C and the opposite end of the tube at 650° C for 6 days. Well-formed platelike crystals with skewed faces and having sides up to 1 mm and thickness about 0.05 mm were observed on the walls of the tube towards the hotter end. In addition there were also some needle-shaped crystals. Photographs of both types of crystals in a Debye–Scherrer camera showed them to be Pd_5As. Selected platelike crystals were examined by the precession method. Pd_5As is face centered monoclinic; $a = 5.51_4 \pm 0.01$ Å, $b = 7.72_5 \pm 0.01$ Å, $c = 8.42_7 \pm 0.01$ Å, and $\beta = 99° \pm 5'$; $U = 354.5$ Å^3; $Z = 4$; F.W. 606.91; $D_x = 11.37$ g.cm^{-3}, and $D_m = 11.33$ g.cm^{-3}. The zones studied were $hk0$, $hk1$, $0kl$, $1kl$, $h0l$, and $h1l$. The b axis was taken as unique. The only absent reflections were hkl with $h + k = 2n + 1$. The diffraction symbol is $12/m1C$ . . . and the space group may be any of the three: $C2/m(C_{2h}^3)$, $Cm(C_s^3)$, and $C2(C_2^3)$. The platelike crystals had the monoclinic b axis lying along the long diagonal of the well-developed parallelogram-shaped 001 face.

In the case of one crystal, the zone $1kl$ had the number of reflections along the c^* direction doubled, apparently corresponding to a doubled c axis; the $0kl$ zone had the expected reflections. This could be explained if the crystal was assumed to be twinned by a 180° rotation around the [100] direction. Three different crystals were examined to confirm the basic cell.

Can. J. Chem. Downloaded from www.nrcresearchpress.com by 210.87.254.42 on 09/05/12
For personal use only.

TABLE IV

Powder diffraction pattern of Pd_3As

Tetragonal $D0_e$ (Fe_3P), $I\bar{4}(S_4^2)$; $a = 9.974 \pm 0.002$ Å, $c = 4.822 \pm 0.002$ Å. Ni-filtered Cu radiation, $\lambda_{\alpha_1} = 1.5405$ Å, Debye–Scherrer camera, diameter = 11.46 cm; cutoff 20 Å; temp. 24° C

I/I_1	d_{obs} (Å)	d_{calc} (Å)	h	k	l	I/I_1	d_{obs} (Å)	d_{calc} (Å)	h	k	l
33	2.70	2.74	3	0	1	33	0.935	0.937	10	3	1
64	2.37	2.40	3	2	1	41	0.920	0.922	10	0	2
41	2.32	2.35	3	3	0				8	6	2
64	2.26	2.28	1	1	2			0.921	8	7	1
51	2.21	2.23	4	2	0	33	0.9155	0.9164	7	1	4
100	2.14	2.16	4	1	1				5	5	4
51	1.97	1.99	2	2	2	33	0.9097	0.9107	3	2	5
41	1.94	1.96	5	1	0	33*	0.9074	0.9088	6	4	4
51	1.90	1.92	3	1	2	41	0.9050	0.9063	10	2	2
41	1.83	1.85	5	0	1			0.9057	9	6	1
			4	3	1	33*	0.9023	0.9030	11	1	0
33	1.72	1.73	5	2	1	26	0.8964	0.8981	9	2	3
20	1.70	1.71	5	3	0				7	6	3
33	1.57	1.58	6	2	0	64*	0.8950	0.8956	4	1	5
41	1.54	1.55	6	1	1	<11	0.8859	0.8870	7	3	4
20	1.505	1.512	2	1	3	41	0.8827	0.8833	8	5	3
20	1.472	1.482	5	4	1	41	0.8768	0.8772	11	2	1
20	1.438	1.447	3	0	3				10	5	1
33	1.415	1.421	6	3	1	41*	0.8743	0.8748	11	3	0
33	1.402	1.410	7	1	0				9	7	0
			5	5	0	<11	0.8676	0.8682	5	0	5
64	1.383	1.390	3	2	3				4	3	5
		1.383	6	4	0	33	0.8641	0.8645	10	4	2
41	1.360	1.367	7	0	1	20	0.8561	0.8568	9	4	3
51	1.333	1.339	4	1	3	41	0.8532	0.8538	8	2	4
51	1.312	1.320	6	2	2	33	0.8453	0.8457	11	1	2
		1.318	7	2	1	33	0.8390	0.8392	11	4	1
51	1.246	1.252	5	0	3	33	0.8350	0.8357	7	5	4
			4	3	3	51	0.8309	0.8313	6	1	5
		1.247	8	0	0			0.8312	12	0	0
51	1.229	1.235	6	5	1	11	0.8253	0.8254	11	5	0
64	1.213	1.217	7	1	2	11	0.8219	0.8223	11	3	2
			5	5	2				9	7	2
		1.214	5	2	3	20	0.8195	0.8199	5	4	5
41	1.204	1.210	8	2	0			0.8198	12	2	0
		1.206	0	0	4	51	0.8161	0.8163	12	1	1
64	1.195	1.200	6	4	2				9	8	1
		1.198	8	1	1	41	0.8129	0.8131	9	1	4
			7	4	1	41*	0.8105	0.8103	8	7	3
33	1.145	1.148	6	1	3	41	0.8087	0.8091	6	3	5
33	1.131	1.135	8	3	1	26	0.8057	0.8060	10	6	2
20	1.122	1.126	3	1	4			0.8056	10	7	1
11	1.113	1.115	8	4	0	26*	0.8039	0.8037	0	0	6
11	1.098	1.102	9	1	0	64	0.7997	0.7998	9	6	3
26	1.088	1.092	6	3	3	64	0.7981	0.7987	7	0	5
33	1.070	1.073	3	3	4			0.7985	1	1	6
33	1.063	1.066	7	0	3	20	0.7953	0.7953	12	3	1
33	1.058	1.061	4	2	4	41*	0.7933	0.7934	2	0	6
41	1.053	1.056	9	2	1	11	0.7921	0.7923	9	3	4
			7	6	1	64	0.7884	0.7886	7	2	5
33	1.040	1.043	7	2	3			0.7885	12	4	0
33	1.030	1.033	8	5	1	64	0.7855	0.7858	12	0	2
33	1.023	1.026	5	1	4			0.7854	11	6	1
41	0.998	1.000	6	5	3	64*	0.78354	0.78363	9	9	0
		0.997	10	0	0			0.78357	2	2	6
			8	6	0	51	0.78100	0.78096	11	5	2
20	0.989	0.991	9	4	1	80	0.78000	0.78002	11	2	3
20	0.983	0.985	5	3	4				10	5	3
33	0.977	0.978	10	2	0	51	0.77874	0.77883	10	8	0
33	0.955	0.958	6	2	4			0.77878	3	1	6
33	0.943	0.945	8	3	3	41	0.77622	0.77620	12	2	2
		0.943	2	1	5	33	0.77311	0.77307	7	7	4

*α_1 α_2 overlap.

Can. J. Chem. Downloaded from www.nrcresearchpress.com by 210.87.254.42 on 09/05/12
For personal use only.

Can. J. Chem. Downloaded from www.nrcresearchpress.com by 210.87.254.42 on 09/05/12
For personal use only.

The empirical formula for Pd_5As was deduced from its cell volume, space group, observed density, and the approximately known chemical composition. Powder photographs indicate that the composition lies between Pd_6As and Pd_3As. The allowed space groups $C2/m$, Cm, and $C2$ require that the atoms occur in multiples of 2. Using a value of 20.4 Å^3 for the atomic volume of As and 13.2 Å^3 for the Pd, based on the observed cell volumes in Pd_3As, Pd_2As, and $PdAs_2$, we find, for the formula Pd_5As, a calculated volume of 346 Å^3 for four molecules in the unit cell. This agrees well with the observed unit cell volume 354.5 Å^3. The calculated density, 11.37 g.cm^{-3}, for four formula units of Pd_5As in the unit cell, is in good agreement with the observed density 11.33 g.cm^{-3}. No other atomic ratio in the required range fitted the observed data.

The monoclinic cell of Pd_5As resembles the monoclinic cells of the compounds $Co_{17}Th_2$ and $Fe_{17}Th_2$, which are based on the well-known $D2_d$ ($CaZn_5$) structure (7). There is also a striking resemblance between the pseudo-orthorhombic cell, which it is possible to choose for Pd_5As, namely $a = 7.72$ Å. $b = 16.64$ Å, $c = 5.51$ Å, and $\beta = 90°25'$, and the orthorhombic cell of PBr_5 with $a = 8.3$ Å, $b = 16.9$ Å, and $c = 5.6$ Å.

Efforts to obtain a smooth Debye–Scherrer pattern by crushing the single crystals failed because of their extreme malleability and, as mentioned above, it was found difficult to obtain a diffraction pattern of the pure Pd_5As phase from a well-annealed polycrystalline material of nominal composition Pd_5As. Some lines unique to Pd_3As pattern were always observed in this pattern. The principal lines of the Pd_5As pattern recorded in Table V, therefore, were obtained by subtracting all lines unique to Pd_3As with the exception of the obviously superimposed reflections.

TABLE V

Partial powder diffraction pattern of Pd_5As

Monoclinic; diffraction symbol $12/m1C\ldots$; $a = 5.51_4 \pm 0.01$ Å, $b = 7.72_5 \pm 0.01$ Å, $c = 8.42_7 \pm 0.01$ Å, $\beta = 99° \pm 5'$; Ni-filtered Cu radiation, $\lambda\alpha_1 = 1.5405$ Å, Debye-Scherrer camera, diameter = 11.46 cm; cutoff 20 Å; temp. 24° C. Lines up to $\theta = 45°$ and observed $I/I_1 > 20$ only are included

I/I_1	d_{obs}(Å)	d_{calc}(Å)	h	k	l	I/I_1	d_{obs}(Å)	d_{calc}(Å)	h	k	l
20	2.44	2.46	2	0	$\bar{2}$	64	1.384	1.387	0	0	6
41	2.31	2.33	1	3	0			1.384	3	3	$\bar{3}$
100	2.24	2.25	0	2	3			1.381	1	5	2
80	2.219	2.229	1	1	3	41	1.316	1.320	2	4	$\bar{3}$
		2.225	2	2	0			1.316	3	1	$\bar{5}$
		2.222	2	2	$\bar{1}$			1.315	2	4	$\bar{4}$
51	2.108	2.116	2	0	$\bar{3}$	41	1.286	1.287	0	6	0
64	1.927	1.931	0	4	0			1.287	1	5	3
20	1.838	1.845	1	3	$\bar{3}$			1.284	4	2	0
		1.832	0	2	4	20	1.257	1.258	2	2	5
64	1.802	1.807	2	0	3			1.256	3	1	4
		1.799	1	1	$\bar{4}$	41	1.246	1.244	3	3	3
20	1.622	1.629	1	1	$\bar{5}$	51	1.1630	1.1639	2	6	0
		1.627	2	2	$\bar{4}$			1.1635	3	5	$\bar{2}$
20	1.454	1.458	3	3	$\bar{2}$			1.1632	2	6	$\bar{1}$
		1.453	1	5	1	51	1.1241	1.1250	3	5	$\bar{3}$
64	1.427	1.430	3	3	$\bar{1}$						
		1.426	2	4	$\bar{3}$						

ACKNOWLEDGMENTS

The authors are indebted to Mr. G. J. G. Despault, who prepared the samples; to Miss M. McLellan, who obtained the Debye–Scherrer patterns; and to Dr. F. R. Ahmed, who obtained the computor data relating to the α-Pd_2As phase.

NOTE ADDED IN PROOF: The paper by Ch. J. Raub and G. W. Webb (J. Less Common Metals, **5**, 271 (1963)) on the palladium–arsenic system has come to hand since submission of this manuscript. We have summarized Raub and Webb's results by plotting their thermal analysis points (triangles) together with ours (dots) in Fig. 2. Their inter-

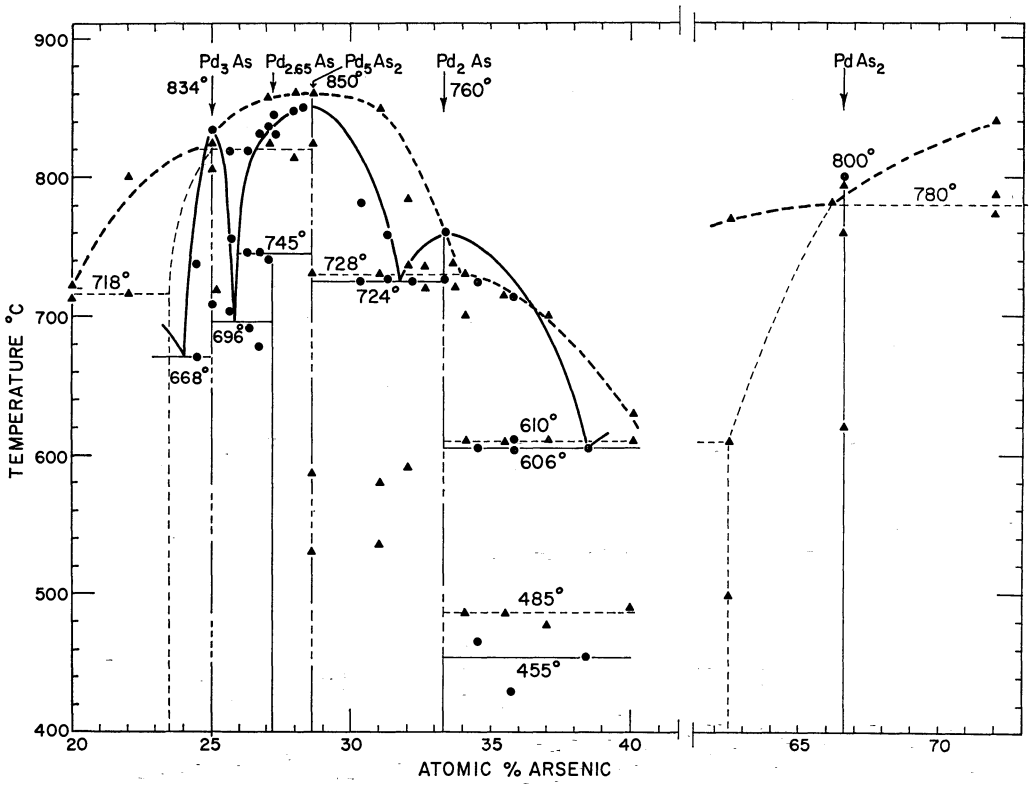

FIG. 2. Combined phase diagram for the system palladium–arsenic.

pretation is shown in dotted lines and ours in solid lines. There is a considerable measure of agreement in the actual observations but as the interpretations differ markedly, a few brief comments confined to the areas of significant difference appear necessary.

1. The phase tentatively designated Pd_7As by Raub and Webb is actually Pd_5As from our single crystal data.

2. Pd_3As is given by Raub and Webb as peritectically formed at 820° C. Since they did not detect the phase $Pd_{2.65}As$, their interpretation in this region is open to doubt. We did not obtain thermal data on samples of sufficiently low arsenic percentage to enable us to construct this area of the phase diagram with complete certainty.

3. Raub and Webb show Pd_2As being formed by a peritectic reaction 32° below the liquidus line. We have interpreted our results in terms of a congruent melting point 36° above the eutectic horizontal. Both interpretations are reasonably consistent with the observed data. We did grow crystals of β-Pd_2As (high temperature form) from a melt of stoichiometric composition, which would add support to the congruent melting interpretation.

Can. J. Chem. Downloaded from www.nrcresearchpress.com by 210.87.254.42 on 09/05/12
For personal use only.

REFERENCES

1. L. THOMASSEN. Z. Physik. Chem. B, **4**, 279 (1929).
2. K. SCHUBERT, S. BAHN, W. BURKHARDT, R. GOHLE, H. G. MEISSNER, M. POTZSCHKE, and E. STOLZ. Naturwiss. **13**, 303 (1960).
3. R. D. HEYDING and L. D. CALVERT. Can. J. Chem. **39**, 955 (1961).
4. K. SCHUBERT, K. FRANK, R. GOHLE, A. MALDONADO, H. G. MEISSNER, A. RAMAN, and W. ROSSTENTSCHER. Naturwiss. **50**, 41 (1963).
5. L. THOMASSEN. Z. Physik. Chem. **135**, 388 (1928); B **2**, 349 (1929).
6. S. RUNDQVIST and F. JELLINEK. Acta Chem. Scand. **13**, 425 (1959).
7. J. V. FLORIO, N. C. BAENZIGER, and R. E. RUNDLE. Acta Cryst. **9**, 367 (1956).

Can. J. Chem. Downloaded from www.nrcresearchpress.com by 210.87.254.42 on 09/05/12
For personal use only.

PREPARATION AND CHARACTERIZATION OF CRYSTALS OF MX- AND MX_2-TYPE ARSENIDES OF NIOBIUM AND TANTALUM[1]

G. S. SAINI,[2] L. D. CALVERT, AND J. B. TAYLOR
Division of Applied Chemistry, National Research Council, Ottawa, Canada
Received October 19, 1963

ABSTRACT

Phase analytical work on the systems niobium–arsenic and tantalum–arsenic has established the existence of mono- and di-arsenides as the only phases on the arsenic-rich side of the composition 50 atomic % As. Single crystals of these phases were grown by halide vapor transport reactions. The monoarsenides are tetragonal and isostructural. The lattice parameters of NbAs are $a = 3.453 \pm 0.002$ Å, $c = 11.672 \pm 0.005$ Å and of TaAs, $a = 3.436 \pm 0.002$ Å, $c = 11.644 \pm 0.005$ Å. The diarsenides are isostructural and have a C-face centered monoclinic cell with $a = 9.354 \pm 0.002$ Å, $b = 3.381 \pm 0.002$ Å, $c = 7.799 \pm 0.002$ Å, $\beta = 119°26' \pm 5'$ for $NbAs_2$ and $a = 9.350 \pm 0.002$ Å, $b = 3.388 \pm 0.002$ Å, $c = 7.760 \pm 0.002$ Å, $\beta = 119°45' \pm 5'$ for $TaAs_2$.

The literature contains very little information on the systems Nb–As and Ta–As with the exception of early preparative work by Heinerth and Biltz (1) which claimed the isolation of $NbAs_{1.8}$ and $TaAs_{1.4}$.

Recent work by Brixner (2) on the diselenides and ditellurides of niobium and tantalum led to the successful growth of single crystals by halide vapor transport. The concept of vapor transport reactions first introduced by Schäfer (3) has also been applied to growth of other chalcogenides by Nitsche, Bölsterli, and Lichtensteiger (4). Our studies of the systems Ni–As and Pd–As have included the growth of single crystals of Ni_5As_2, Pd_5As, and Pd_3As using vapor transport reactions (5). These techniques have now been applied to the growth of niobium and tantalum arsenide crystals and this paper describes the preliminary phase analytical study, the subsequent single crystal preparations, and the determination of the lattice parameters.

EXPERIMENTAL

1. Phase Analysis

Niobium and tantalum were obtained as powders from A. D. Mackey and Johnson Matthey respectively. Both the elements were better than 99.7% pure with respect to the other. Both materials also contained up to 500 p.p.m. of iron. They were used without further purification. Arsenic was supplied by Cominco as "high purity arsenic" with a claimed spectrographic analysis better than 99.999%. It was fractionally sublimed *in vacuo* at 450° C to reduce oxide contaminant not accounted for in the analysis.

A number of 5-g samples were prepared by reacting calculated quantities of niobium or tantalum with 50 to 75 atomic percent arsenic in evacuated quartz ampoules at 700° C for 3 weeks. After this initial reaction period the samples were quenched, ground, divided into three parts, and resealed in quartz. These samples were then subjected to annealing treatments at 500°, 750°, and 1000° C for periods up to 4 months. As required, samples were quenched in water and Debye–Scherrer patterns obtained on 11.46-cm Norelco cameras using Ni-filtered copper radiation.

This examination revealed that within the composition range under examination there were two phases present in each system. These phases occurred at compositions corresponding to MX and MX_2. The patterns obtained in the case of the niobium arsenides were remarkably similar to the corresponding tantalum arsenide patterns. However, the thermal stability of NbAs differed from that of TaAs in that the NbAs pattern was obtained for all alloys of stoichiometric composition regardless of the thermal treatment. Some samples were held at 1700° C for a period of minutes and then quenched in air. They did not melt

[1]*Issued as N.R.C. No. 7743.*
[2]*Present address: Department of Chemical Engineering Technology, Panjab University, Chandigarh-3, India.*

Can. J. Chem. Downloaded from www.nrcresearchpress.com by 210.87.254.42 on 09/05/12
For personal use only.

and still retained the NbAs structure. The TaAs samples, on the other hand, only showed the characteristic NbAs-type pattern when quenched from temperatures above 750° C. Below this temperature the pattern was of $TaAs_2$ together with a metal-rich phase. A somewhat similar metal-rich phase has also been observed in the Nb–As system and probably occurs at the composition Nb_3As but in contrast to the tantalum analogue it is unstable below 1000° C. Attempts to obtain good diffraction patterns or single crystals of these latter phases have not yet been successful so that no characterization is possible at this time.

2. Single Crystal Preparation

Growth of crystals from the melt was not attempted because of the high liquidus temperatures in this system. Direct growth from the vapor was not practicable either since there is no evidence that niobium and tantalum arsenides exist as molecular species in the vapor state. Halide vapor transport reactions using chlorine or bromine proved successful for growing small crystals of these arsenides. No transport was obtained with iodine. The general procedure has been described elsewhere (5) but in spite of a semiquantitative analysis given by Nitsche *et al.* concerning transport reactions in general, choice of temperatures for the charge and receiver is an empirical process because of lack of information on the thermodynamic functions involved. Accordingly the relevant parameters are recorded for each case although they may not define unique conditions necessary for crystal growth.

$NbAs_2$ and $TaAs_2$ crystals were grown in tubes 18 cm long and 1 cm bore using 0.25 mg/cc of chlorine or bromine. A charge of previously reacted polycrystalline diarsenide was held at 1000° C and the receiver end of the tube at 600 to 700° C. Lustrous black bladelike crystals grew at the cooler end, and after 2 days were about 3 mm long.

Experiments to grow NbAs and TaAs crystals using a charge of polycrystalline monoarsenide were unsuccessful. Previous experience with transport reactions in the palladium–arsenic system had indicated that the best results were always obtained when arsenic-rich phases were used as the charge material even when metal-rich crystals were required. Crystals of NbAs were finally grown from a charge of $NbAs_2$ using 0.2 mg/cc of bromine in the usual tube with the charge at 1000° C and the receiver at 760° C. After 20 hours the NbAs was obtained as small black polyhedra having a maximum dimension of 0.2 mm. These crystals were deposited at a temperature of about 850° C whilst further down the tube $NbAs_2$ blades appeared so that both phases were simultaneously present in the tube. Extension of the heating period resulted in complete disappearance of the monoarsenide phase. Parallel experiments in the tantalum system failed to yield TaAs crystals.

CRYSTALLOGRAPHY

The Monoarsenides

NbAs

Single crystals were examined on a precession camera using zirconium-filtered molybdenum radiation. The zones studied were $h0l$, $h1l$, $hk0$, $hk1$, and $hk2$. The only reflections present were hkl with $h + k + l = 2n$ and $00l$ with $l = 4n$. NbAs is tetragonal and the apparent observed symmetry is $4/mmm$ consistent with the space group $I4_122(D_4^{10})$. Cell parameters determined from the single crystal photographs are $a = 3.45 \pm 0.01$ Å, $c = 11.65 \pm 0.02$ Å. An indexed powder photograph obtained on an 11.46-cm Debye–Scherrer camera is given in Table I. The cell parameters obtained from this pattern are: $a = 3.453 \pm 0.002$ Å, $c = 11.672 \pm 0.005$ Å; from which we derive $c/a = 3.380$; $U = 139.2$ Å^3; $Z = 4$; F.W. = 167.83; $D_x = 8.01$ g cm^{-3}. The density measured on a Berman torsion balance using toluene as immersion fluid is 8.11 g cm^{-3}.

TaAs

An indexed powder photograph is given in Table II. TaAs is isostructural with NbAs; $a = 3.436 \pm 0.002$ Å, $c = 11.644 \pm 0.005$ Å, $c/a = 3.389$; $U = 137.5$ Å^3; $Z = 4$; F.W. = 255.87; $D_x = 12.36$ g cm^{-3}.

The monophosphides β-NbP and β-TaP were reported by Schönberg (6) as being $I4_122(D_6^{10})$ with 4Nb in 4(a) and 4P in 4(b). Rundqvist (7) suggests an alternative structure in the space group $I4_1(C_6^4)$ with 4Nb in 4(a), $z = 0$, and 4P in 4(a), $z = 0.42$. Rough estimates of our single crystal intensities are more consistent with Rundqvist's proposals than Schönberg's. Detailed structure factor calculations are required to resolve this point.

Can. J. Chem. Downloaded from www.nrcresearchpress.com by 210.87.254.42 on 09/05/12
For personal use only.

TABLE I

Powder diffraction pattern of NbAs
Tetragonal, space groups $I4_1$ or $I4_122$; $a = 3.453 \pm 0.002$ Å, $c = 11.672 \pm 0.005$ Å.
Ni filtered Cu radiation $\lambda\alpha_1 = 1.5405$ Å. Debye–Scherrer camera diameter = 11.46 cm;
cutoff 20 Å; temperature 24° C

I/I_1	d_{obs} (Å)	d_{calc} (Å)	h	k	l	I/I_1	d_{obs} (Å)	d_{calc} (Å)	h	k	l
17	3.29	3.31	1	0	1	21	0.9708	0.9726	0	0	12
21	2.88	2.92	0	0	4	11	0.9524	0.9516	3	1	6
51	2.55	2.52	1	0	3			0.9537	3	2	1
100	2.23	2.25	1	1	2	26	0.9459	0.9472	3	0	7
64	1.92	1.93	1	0	5	17	0.9352	0.9362	2	2	8
64	1.718	1.726	2	0	0	26	0.9289	0.9300	3	2	3
13	1.523	1.531	2	1	1	41	0.8853	0.8860	3	2	5
		1.521	1	1	6	13	0.8741	0.8745	2	1	11
41	1.495	1.501	1	0	7	26	0.8626	0.8632	4	0	0
26	1.479	1.486	2	0	4	26*	0.8599	0.8608	3	0	9
11	1.453	1.459	0	0	8	51	0.8469	0.8473	2	0	12
41	1.429	1.425	2	1	3	26	0.8444	0.8436	2	2	10
64	1.283	1.288	2	1	5	11	0.8349	0.8352	4	1	1
26	1.217	1.221	2	2	0	41*	0.8275	0.8277	4	0	4
11	1.210	1.214	1	0	9	33	0.8180	0.8187	4	1	3
5	1.142	1.145	3	0	1	41	0.8055	0.8061	3	3	2
51	1.131	1.133	2	1	7	100	0.7969	0.7978	3	1	10
8.5	1.121	1.126	2	2	4	41	0.7889	0.7889	1	1	14
13	1.111	1.114	2	0	8			0.7890	4	0	6
13	1.101	1.099	3	0	3	51*	0.7879	0.7883	4	1	5
64	1.070	1.073	3	1	2	13	0.7799	0.7801	3	0	11
41	1.051	1.053	1	1	10	13	0.7760	0.7760	2	1	13
26	1.030	1.032	3	0	5	51	0.7719	0.7721	4	2	0
41	0.9903	0.9931	2	1	9						

*α_1 α_2 overlap.

TABLE II

Powder diffraction pattern of TaAs
Tetragonal, space groups $I4_1$ or $I4_122$; $a = 3.436 \pm 0.002$ Å, $c = 11.644 \pm 0.005$ Å.
Ni filtered Cu radiation $\lambda\alpha_1 = 1.5405$ Å. Debye–Scherrer camera diameter = 11.46 cm;
cutoff 20 Å; temperature 24° C

I/I_1	d_{obs} (Å)	d_{calc} (Å)	h	k	l	I/I_1	d_{obs} (Å)	d_{calc} (Å)	h	k	l
21	3.27	3.29	1	0	1	4	1.010	1.011	1	0	11
17	2.97	2.91	0	0	4	13	0.988	0.989	2	1	9
35	2.56	2.57	1	0	3	8.6	0.9692	0.9700	0	0	12
100	2.23	2.24	1	1	2	15	0.9475	0.9480	3	1	6
45	1.92	1.93	1	0	5			0.9498	3	2	1
50	1.707	1.718	2	0	0	15	0.9420	0.9430	3	0	7
11	1.515	1.524	2	1	1	15	0.9321	0.9325	2	2	8
		1.516	1	1	6	26	0.9250	0.9255	3	2	3
20	1.494	1.497	1	0	7	41	0.8812	0.8819	3	2	5
20	1.476	1.479	2	0	4	5	0.8707	0.8715	2	1	11
3.5	1.450	1.455	0	0	8	30	0.8585	0.8590	4	0	0
40	1.425	1.429	2	1	3	21*	0.8567	0.8572	3	0	9
50	1.280	1.283	2	1	5	33	0.8445	0.8447	2	0	12
33	1.212	1.215	2	2	0	8.6	0.8308	0.8312	4	1	1
		1.211	1	0	9	26	0.8264	0.8268	3	2	7
4	1.137	1.139	3	0	1	21*	0.8241	0.8239	4	0	4
40	1.127	1.129	2	1	7	41	0.8145	0.8148	4	1	3
11	1.119	1.121	2	2	4	45	0.8020	0.8021	3	3	2
11	1.109	1.110	2	0	8	75	0.7944	0.7943	3	1	10
8	1.097	1.098	3	0	3	41	0.7867	0.7866	1	1	14
64	1.067	1.068	3	1	2	70*	0.7845	0.7846	4	1	5
51	1.049	1.050	1	1	10	5.3	0.7772	0.7771	3	0	11
21	1.026	1.027	3	0	5	20	0.7738	0.7736	2	1	13

*α_1 α_2 overlap.

Can. J. Chem. Downloaded from www.nrcresearchpress.com by 210.87.254.42 on 09/05/12
For personal use only.

The Diarsenides

$NbAs_2$

The bladelike crystals were examined by the precession method. The zones studied were $hk0$, $hk1$, $hk2$, $h0l$, $h1l$, and $0kl$. The b-axis was taken as unique. The only absent reflections were hkl with $h + k = 2n + 1$. $NbAs_2$ is monoclinic, diffraction symbol $12/m\ 1\ C\ldots$, and the space group may be any of the three $C2/m(C_{2h}^3)$, $Cm(C_s^3)$, and $C2(C_2^3)$. One crystal was found to be elongated along the b-axis with 001 as the large flat face. Not all crystals had this orientation. The cell parameters determined from the precession photographs are $a = 9.36_5 \pm 0.02$ Å, $b = 3.38_3 \pm 0.01$ Å, $c = 7.80_9 \pm 0.02$ Å, $\beta = 119.25' \pm 5'$. The indexed powder pattern in Table IV was obtained on a Guinier

TABLE III

Powder diffraction pattern of $NbAs_2$

Monoclinic; diffraction symbol $12/m\ 1\ C\ldots$; $a = 9.354 \pm 0.002$ Å; $b = 3.381 \pm 0.002$ Å, $c = 7.799 \pm 0.002$ Å, $\beta = 119°26' \pm 5'$; monochromatic CuK_α radiation $\lambda\alpha_1 = 1.5405$ Å; Guinier focussing camera, diameter 11.46 cm; temp. 24° C; internal standard As_2O_3 ($a = 11.075_5$ Å); low-angle cutoff 40 Å; high-angle cutoff 1.24 Å

I/I_1	d_{obs} (Å)	d_{calc} (Å)	h	k	l	I/I_1	d_{obs} (Å)	d_{calc} (Å)	h	k	l
7	6.78	6.79	0	0	$\bar{1}$	17	1.637	1.637	5	1	$\bar{2}$
26	4.64	4.64	2	0	$\bar{1}$	17	1.625	1.626	1	1	$\bar{4}$
7	4.070	4.073	2	0	0	7	1.597	1.596	5	1	$\bar{3}$
7	3.624	3.627	2	0	$\bar{2}$	7	1.588	1.589	2	2	$\bar{1}$
11	3.118	3.123	1	1	0			1.587	5	1	$\bar{1}$
5.5	3.064	3.065	1	1	$\bar{1}$	17	1.550	1.550	6	0	$\bar{2}$
100	2.653	2.654	1	1	1			1.550	3	1	2
41	2.590	2.593	2	0	$\bar{3}$	17	1.534	1.535	2	0	$\bar{5}$
51	2.549	2.550	1	1	$\bar{2}$			1.533	2	2	$\bar{2}$
33	2.319	2.320	4	0	$\bar{2}$	5.5	1.479	1.478	6	0	$\bar{1}$
51	2.284	2.286	3	1	$\bar{1}$	21	1.468	1.470	6	0	$\bar{4}$
		2.284	4	0	$\bar{1}$			1.468	5	1	0
51	2.262	2.264	0	0	3	5.5	1.4580	1.4588	4	0	2
41	2.218	2.218	3	1	$\bar{2}$	41	1.4154	1.4161	3	1	$\bar{5}$
80	2.118	2.118	4	0	$\bar{3}$			1.4161	2	2	$\bar{3}$
		2.118	3	1	0	33	1.3853	1.3862	1	1	$\bar{4}$
51	2.107	2.109	1	1	2	26	1.3665	1.3665	4	2	$\bar{2}$
51	2.037	2.037	4	0	0	26	1.3544	1.3547	0	2	3
41	2.021	2.023	1	1	$\bar{3}$	17	1.3466	1.3466	6	0	$\bar{5}$
51	1.968	1.968	3	1	$\bar{3}$	41	1.3208	1.3212	4	2	$\bar{3}$
17	1.942	1.943	2	0	$\bar{4}$	41	1.3017	1.3010	4	2	0
13	1.731	1.731	4	0	1	26	1.2755	1.2753	2	2	$\bar{4}$
51	1.691	1.691	0	2	0	26	1.2624	1.2624	2	0	$\bar{6}$
26	1.661	1.662	2	0	3	41	1.2428	1.2422	7	1	$\bar{3}$

focussing camera using As_2O_3 as internal standard. Parameters determined from this pattern are $a = 9.354 \pm 0.002°$, $b = 3.381 \pm 0.002$ Å, $c = 7.799 \pm 0.002$ Å, $\beta = 119°26' \pm 5'$; from which $U = 214.8$ Å^3; $Z = 4$; F.W. = 242.75; $D_x = 7.50$ g cm^{-3}. The density measured pycnometrically using water is 7.01 g cm^{-3}.

$TaAs_2$

The diarsenides of niobium and tantalum are isostructural. An indexed powder pattern of $TaAs_2$ is given in Table IV. $TaAs_2$ is monoclinic, diffraction symbol $12/m\ 1\ C\ldots$, $a = 9.350 \pm 0.002$ Å, $b = 3.388 \pm 0.002$ Å, $c = 7.760 \pm 0.002$ Å, $\beta = 119°45' \pm 5'$; $U = 213.4$ Å; $Z = 4$; F.W. = 330.79; $D_x = 10.29$ g cm^{-3}; and $D_m = 9.21$ g cm^{-3} (pycnometric).

The monoclinic diarsenides $NbAs_2$ and $TaAs_2$ represent a new structure type in binary pnictides systems. The structure differs from that of the monoclinic diarsenides of the cobalt family (8).

Can. J. Chem. Downloaded from www.nrcresearchpress.com by 210.87.254.42 on 09/05/12
For personal use only.

TABLE IV

Powder diffraction pattern of $TaAs_2$

Monoclinic; diffraction symbol $12/m\,1C\ldots$; $a = 9.350\pm0.002$ Å, $b = 3.388\pm0.002$ Å, $c = 7.760\pm0.002$ Å, $\beta = 119°45'\pm5'$; monochromatic CuK_α radiation $\lambda\alpha_1 = 1.5405$ Å; Guinier focussing camera, diameter 11.46 cm; temp. 24° C; internal standard As_2O_3 ($a = 11.075_5$ Å); low-angle cutoff 40 Å; high-angle cutoff 1.24 Å

I/I_1	d_{obs} (Å)	d_{calc} (Å)	h	k	l	I/I_1	d_{obs} (Å)	d_{calc} (Å)	h	k	l
8.6	6.727	6.737	0	0	$\bar{1}$	17	1.636	1.637	5	1	$\bar{2}$
41	4.633	4.640	2	0	$\bar{1}$	11	1.590	1.592	2	2	$\bar{1}$
11	4.059	4.059	2	0	0	7	1.549	1.549	6	0	$\bar{2}$
21	3.620	3.622	2	0	$\bar{2}$			1.547	6	0	$\bar{3}$
5.5	3.371	3.368	0	0	2	7	1.534	1.534	2	2	$\bar{2}$
21	3.123	3.126	1	1	0	7	1.526	1.525	2	0	$\bar{5}$
21	3.065	3.068	1	1	$\bar{1}$	7	1.468	1.469	6	0	$\bar{4}$
11	2.900	2.899	2	0	1	7	1.463	1.464	5	1	0
100	2.648	2.650	1	1	$\bar{1}$			1.463	2	2	1
26	2.580	2.582	2	0	$\bar{3}$	7	1.4493	1.4493	4	0	$\bar{2}$
26	2.540	2.547	1	1	$\bar{2}$	7	1.4152	1.4161	2	2	$\bar{3}$
17	2.320	2.320	4	0	$\bar{2}$	17	1.4110	1.4110	3	1	$\bar{5}$
41	2.282	2.286	3	1	$\bar{1}$	17	1.3778	1.3771	1	1	$\bar{4}$
		2.281	4	0	$\bar{1}$	7	1.3675	1.3679	4	2	$\bar{2}$
51	2.245	2.246	0	0	$\bar{3}$	7	1.3602	1.3599	4	2	$\bar{1}$
51	2.217	2.220	3	1	$\bar{2}$	33	1.3530	1.3530	6	0	0
80	2.113	2.116	4	0	$\bar{3}$			1.3523	0	2	$\bar{3}$
		2.114	3	1	0	13	1.3451	1.3451	6	0	$\bar{5}$
51	2.101	2.100	1	1	2	17	1.3225	1.3222	4	2	$\bar{3}$
41	2.029	2.030	4	0	0	17	1.3145	1.3139	5	1	1
41	2.015	2.016	1	1	$\bar{3}$	13	1.3070	1.3072	3	1	3
51	1.966	1.966	3	1	$\bar{3}$	17	1.3003	1.3004	4	2	0
21	1.933	1.932	2	0	$\bar{4}$	17	1.2743	1.2736	2	2	$\bar{4}$
7	1.721	1.721	4	0	1	7	1.2543	1.2539	2	0	$\bar{6}$
41	1.693	1.694	0	2	0	33	1.2410	1.2422	7	1	$\bar{3}$
17	1.649	1.649	2	0	3						

ACKNOWLEDGMENTS

The authors are indebted to Mr. G. J. G. Despault, who prepared the samples, and to Miss M. McLellan, who obtained the Debye–Scherrer patterns.

REFERENCES

1. E. Heinerth and W. Biltz. Z. Anorg. Chem. **198**, 175 (1931).
2. L. H. Brixner. J. Inorg. Nucl. Chem. **24**, 257 (1962).
3. H. Schäfer. Z. Anorg. Chem. **286**, 27, 42 (1956); **290**, 279 (1957); **291**, 221, 254 (1957).
4. R. Nitsche, H. V. Bölsterli, and M. Lichtensteiger. J. Phys. Chem. Solids, **21**, 199 (1961).
5. G. S. Saini, L. D. Calvert, and J. B. Taylor. Can. J. Chem. In press (1964).
6. N. Schönberg. Acta Chem. Scand. **8**, 226 (1954).
7. S. Rundqvist. Arkiv. Kemi, **20**, 67 (1962).
8. J. C. Quesnel and R. D. Heyding. Can. J. Chem. **40**, 814 (1962).

Can. J. Chem. Downloaded from www.nrcresearchpress.com by 210.87.254.42 on 09/05/12
For personal use only.

THE HEARTWOOD EXTRACTIVES OF PINUS RESINOSA AIT.[1]

A. SATO[2] AND E. VON RUDLOFF
National Research Council of Canada, Prairie Regional Laboratory, Saskatoon, Saskatchewan
Received October 10, 1963

ABSTRACT

The acetone extract of red pine heartwood was found to contain mainly pinosylvin monomethyl ether, oleic, linoleic, dehydroabietic, and isopimaric acids, and triglycerides of unsaturated fatty acids. Smaller amounts of pinosylvin, β-sitosteryl esters, and benzoic acid were isolated. Palmitic, palmitoleic, stearic, linoleic, pimaric, sandaracopimaric, abietic, neoabietic, vanillic, and three unidentified acids, as well as pinocembrin, vanillin, and eleven trace components were recorded by gas–liquid chromatography. A small amount of steam volatile oil, which may have taxonomic significance, was isolated. α-Pinene, β-pinene, myrcene, limonene, γ-terpinene, terpinolene, camphor, *cis*-*p*-menthan-8-ol, terpinen-4-ol, and α-terpineol were tentatively identified.

Besides glucose and xylose, the methanol extract contained polylignan fractions similar to those which had been isolated previously from jack pine.

The North American red pine, *Pinus resinosa* Ait., a member of the subgenera diploxylon, is a medium-to-large tree found from the Atlantic Coast to southeastern Manitoba. Its thick sapwood is readily penetrated by creosote and the wood is therefore used extensively for poles and piling (1). Lindstedt and Misiorny (2) have shown that the heartwood phenols consist mainly of pinosylvin monomethyl ether and, by paper chromatography, have demonstrated the presence of pinosylvin, two unknowns (E and F), but could not confirm the presence of pinocembrin or pinobanksin. Levitin (3) reported the amount of ether extract in the heartwood and sapwood, and recently (4) demonstrated that knots contain a higher amount of α- and β-pinene than the sap or heartwood. However, a complete analysis of the heartwood extractives of this pine does not appear to have been carried out.

Recently, we reported on the total analysis of the heartwood extractives of jack pine (*Pinus banksiana* Lamb.) (5). The same chromatographic techniques and countercurrent distribution have now been applied to a similar analysis of those of the red pine. Equally satisfactory results have been obtained, except for the analysis of the phenolic fraction. The fractionation scheme is summarized in Fig. 1. The neutral components were saponified and the resulting alcohols and free fatty acids were analyzed by thin-layer (TLC) and gas–liquid (GLC) chromatography. The quantitative data obtained for the fatty acids are shown in Table I, and from these it follows that the neutral fraction is composed mainly of triglycerides of oleic and linoleic acids and smaller amounts of stearic, linolenic, palmitic, palmitoleic, and the two minor unidentified acids also found in jack pine heartwood (5). The free acids were separated from the phenolic constituents by countercurrent distribution, and were analyzed by GLC (see Table I) after conversion to the methyl esters. The same resin acid esters were recorded as had been found in jack pine heartwood (5), but the amounts (see Table I) of each differed. Also, approximately 40% fatty acid esters were recorded, showing that, in red pine, free fatty acids were a major constituent. Isopimaric and dehydroabietic were the main resin acids. Steam distillation of the acid fraction gave a small amount of benzoic acid, just as was obtained from jack pine wood (5).

[1]*Presented at the 1st Canadian Wood Chemistry Symposium at Toronto, September 4–6, 1963. Issued as N.R.C. No. 7734.*
[2]*National Research Council of Canada Postdoctoral Fellow, 1961–1963. Present address: Department of Agricultural Chemistry, University of Kyoto, Kyoto, Japan.*

Can. J. Chem. Downloaded from www.nrcresearchpress.com by 210.87.254.105 on 09/05/12
For personal use only.

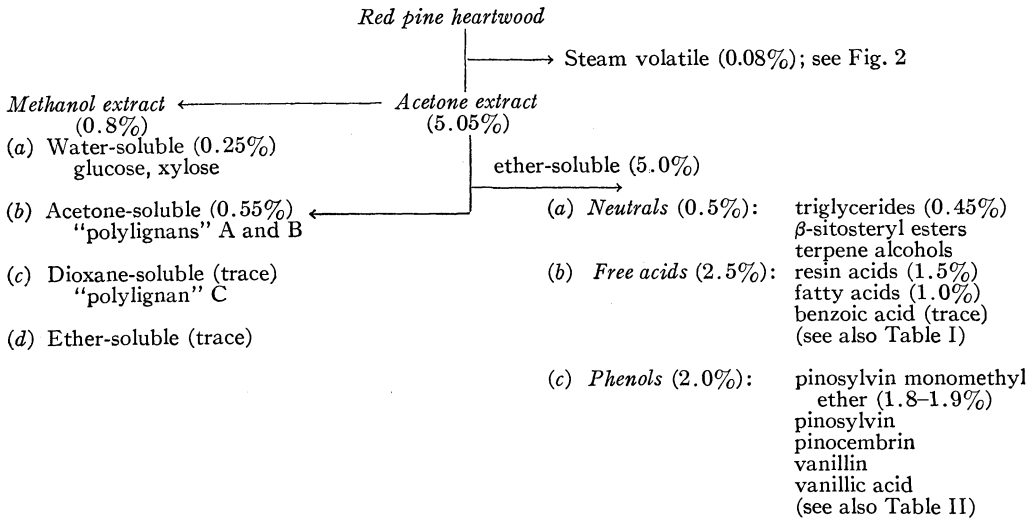

FIG. 1. Fractionation scheme for the heartwood extractives of red pine.

TABLE I

Composition (in percent) of the free and combined acid mixtures of red pine heartwood

Acid	Free	Combined
Palmitic	0.5	1
Palmitoleic	Trace	Trace
Stearic	Trace	10
Oleic	27	52.5
Linoleic	15	20
Linolenic	4	9
Arachidic } ? Palustric }	5	—
Lignoceric	—	—
Unknown A*	—	2.5
Unknown B*	—	5
Pimaric	2	—
Sandaracopimaric	1.5	—
Levopimaric	—	—
Isopimaric	13.5	—
Dehydroabietic	17.5	—
Abietic	10.5	—
Neoabietic	2.5	—

*Same relative retention times (RRT 0.53 and 0.73) as two unidentified components of the free acid mixture of jack pine (5).

Paper- or thin-layer chromatograms of the phenolic fraction streaked excessively and showed only the presence of pinosylvin monomethyl ether. This was the major constituent (at least 90%) of this fraction and crystalline pinosylvin monomethyl ether was isolated. TLC analysis of the mother liquors did not give useful data. Since Narasimhachari and von Rudloff (6) had shown that the methyl ethers of polyphenols, including flavonoids, may be separated by GLC, this method was investigated. However, Erdtman (7) as well as Lindstedt and co-workers (2, 8) have shown that in the heartwood of many pine species the monomethyl ethers of pinosylvin and flavanones may occur together with the parent polyphenol. Thus, GLC of the methylated phenol fraction could not be expected to give complete resolution of all components. Bentley *et al.* (9) have described successful

Can. J. Chem. Downloaded from www.nrcresearchpress.com by 210.87.254.105 on 09/05/12
For personal use only.

GLC of polyols and saccharides in the form of their trimethylsilyl (TMS) ethers. These ethers are relatively volatile, fairly stable, and resistant to oxidation (10). Using a 15% SE-52 silicone polymer column, good peaks and resolution were obtained for the TMS derivatives of vanillin, vanillic acid, ferulic acid, and the pinosylvins (see Table II), but conversion of flavanones was not quantitative and double peaks were frequently recorded. However, the technique permitted qualitative analysis and the presence of pinosylvin, pinocembrin, vanillin, vanillic acid, and several unidentified trace constituents (see experimental) in red pine heartwood were demonstrated. The derivative of pinobanksin was not recorded. On the other hand, vanillin, vanillic acid, and the unidentified compounds were not found in the phenolic fraction from Jack pine heartwood.

The volatile oil was obtained only in very low yield. (see Fig. 1), and the amounts available were insufficient for the isolation of individual components. The GLC chromatogram, obtained from a temperature-programmed run on a 6 ft polyethylene glycol column, is shown in Fig. 2. At least 33 different compounds appear to be present and of these α-

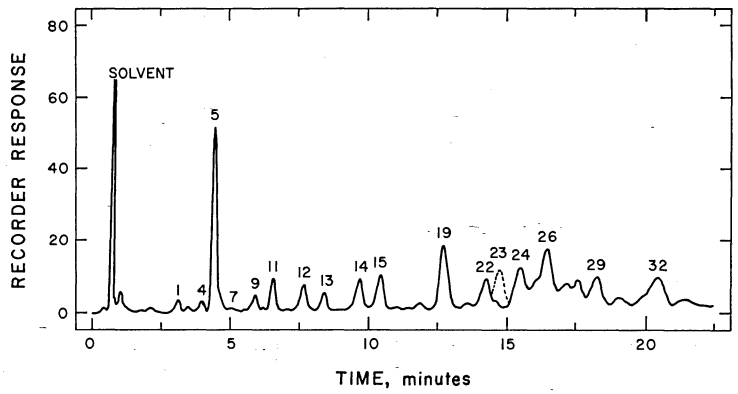

FIG. 2. Temperature-programmed chromatogram of the volatile oil from the heartwood of red pine as obtained on a 6 ft × 1/4 in. polyethylene glycol (Carbowax 20 M) column; 65 to 200° C, 120 ml helium/minute.

pinene (peak 4), β-pinene (peak 7), myrcene (peak 9), limonene (peak 11), γ-terpinene (peak 12), terpinolene (peak 13), camphor (peak 19), *cis*-*p*-menthan-8-ol (peak 22), terpinen-4-ol (peak 24), and α-terpineol (peak 26) were tentatively identified by retention characteristics. The major peak 5 does not appear to be a monoterpene (e.g. fenchene), since on Apiezon it had a considerably lower retention time than did these hydrocarbons. Peak 32 could be geraniol and peaks 14 and 15 are in the allo-ocimene range. When the oil was treated with diazomethane, peak 23 was recorded in significantly larger amounts (dotted lines in Fig. 2). This peak has the retention time of methyl benzoate. The chromatographic spectrum differs significantly from that of the oil of jack pine heartwood (5) and it appears likely that the volatile oil of pines may be used for taxonomic purposes. Swan (11) has recently applied this concept to a study of hybridization among West Coast pine species.

The methanol extract (see Fig. 1) was divided into water-soluble, acetone-soluble constituents, and a trace of ether-soluble material. The water-soluble portion was analyzed by paper chromatography and spots corresponding to glucose and xylose were detected. The acetone-soluble part was fractionated by precipitation from acetone or methanol

Can. J. Chem. Downloaded from www.nrcresearchpress.com by 210.87.254.105 on 09/05/12
For personal use only.

and three fractions having fairly sharp melting points were obtained. All had infrared spectra which were very similar to that of lariciresinol, and appeared to be similar to the polylignan fractions isolated from jack pine heartwood (5). Fraction A had m.p. 177–180° C, 10.6% methoxyl content, and a molecular weight of 1883. Fraction B melted at 164° C and fraction C at 145.5–150° C. During attempts to purify these fractions further it was noticed that the molecular weight increased. Thus, fraction A was found to have a molecular weight of 1790, which changed to 1883 upon re-precipitation. This was accompanied by a slight broadening of the melting point range, viz. from 178–180° C to 177–180° C. Nitrobenzene oxidation of these polylignan fractions gave mainly vanillin and some *p*-hydroxybenzaldehyde, showing that a guaiacyl residue is a typical feature of this group of compounds. Work is in progress to establish whether these compounds are true lignan polymers or rather simple lignin precursors, such as the guaiacyl glycerol dimers and trimers isolated by Freudenberg *et al.* (12, 13). In further work on the polylignans from Jack pine it was found that this group of compounds reacted with methanol during the extraction. This lends support to the surmise that a guaiacyl glycerol derivative is present, since the α-hydroxyl group of such compounds reacts readily with alcohols, phenols, and carbohydrates.

EXPERIMENTAL

Most of the experimental procedures and apparatus used were described previously (5). The wood was supplied by the Department of Mines and Natural Resources, Manitoba, and came from the Marchand district. The log was freed from bark and sapwood and milled in a hammer and a Wiley mill. The air-dried wood meal (3.0 kg) was extracted with acetone (10 liters) in a Soxhlet extractor for 30 to 36 hours. The solvent was removed by evaporation *in vacuo* in a rotary evaporator. The residual wood meal was similarly extracted with methanol or dioxane. Known crystalline compounds were identified by mixed melting point and comparison of infrared spectra.

Acetone Extract

The brown, viscous residue (152 g, 5.05%) from the acetone extraction was poured with stirring into ether (2 liters) and the small amount of precipitate (0.7 g) which formed was filtered off. The ethereal solution was extracted exhaustively with aqueous potassium hydroxide solution (5%) to remove all acids and phenols. After washing with water it was dried over sodium sulphate and the ether was removed to give the neutral constituents (15 g, 0.5%). The aqueous alkaline solution was acidified with dilute hydrochloric acid (10%) and extracted thoroughly with ether. The ethereal solution was dried and evaporated to dryness. The residual material (136 g, 4.5%) was resolved into free acids and free phenols by countercurrent distribution (5).

Neutrals

An aliquot (3 g) of the total neutral material was saponified and worked up in the usual manner to give the free alcohols (0.06 g) and acids (2.2 g). The latter were analyzed by GLC on a butanediol succinate (Craig) polyester column at 205° C and the results obtained are shown in Table I. The alcohols were analyzed by TLC when several terpenoid spots and a spot corresponding to β-sitosterol were recorded. The latter was obtained crystalline, m.p. 129–132° C, from the crude product by recrystallization from ethanol; the derived acetate had m.p. 122.5–124° C. Steam distillation of the filtrate gave a small amount of volatile product. Analysis by GLC (6 ft × 1/4 in. O.D.; 15% polyethylene glycol 20 M on Chromosorb W, 60–80 mesh) showed the presence of 10 peaks in the monoterpene range. The three major peaks (20 to 30% each) had the retention times of α-terpineol, terpinen-4-ol, and *cis*-*p*-menthan-8-ol respectively. These alcohols were presumably present in the free state, since they were also found in the steam volatile fraction (see below).

The aqueous residue from the above saponification was deionized with ion exchange resin and evaporated *in vacuo* to a viscous residue (0.8 g). This was acetylated and GLC analysis gave a single peak having the same retention time as triacetin.

Free Acids

An aliquot (5.0 g) of the total acids and phenols was subjected to countercurrent distribution (petrol, b.p. 40–60° C, and 75% aqueous ethanol saturated with each other, 20 transfers). Tubes 9 to 20 were combined to give the total free acids (3.0 g) and these were analyzed by GLC after conversion to the methyl esters. Since it was found that relatively large amounts of free fatty acids were present, the analyses were carried out on butanediol succinate polyester (at 205° C) as well as on the columns used previously for fractionation of the resin acid esters (5). The results obtained are summarized in Table I. Steam distillation of the free acid fraction gave a small amount of benzoic acid, m.p. 120–122° C.

Can. J. Chem. Downloaded from www.nrcresearchpress.com by 210.87.254.105 on 09/05/12
For personal use only.

Free Phenols

Tubes 1 to 8 from the above experiment were analyzed separately by TLC but the chromatograms streaked excessively. The material was therefore combined and crystallization from aqueous ethanol and benzene gave pinosylvin monomethyl ether m.p. 119.5–121° C, undepressed in admixture with authentic material. An aliquot (30 mg) of the residue from the mother liquor was dissolved in dry pyridine (0.1 ml) and to this was added hexamethyl disilazane (0.1 ml) and trimethyl chlorosilane (0.1 ml). The mixture was shaken for a few minutes, allowed to stand for 5 minutes, and aliquots (10 to 40 μl) of the supernatant liquid were injected into the GLC apparatus. The column (3 ft × 1/4 in. O.C., 15% SE-52 silicone polymer on Chromosorb W, 60–80 mesh) was maintained at 160°, 192°, or 242° C to determine the presence of low- and high-boiling phenol ethers. Reference compounds were similarly converted to the TMS derivatives and the relative retention times (RRT) obtained are shown in Table II. The major component in the TMS-treated

TABLE II

Relative retention times* of polyphenol and phenolic acid trimethylsilyl (TMS) derivatives on a 3 ft×1/4 in. O.D. SE-52 column

Compound	Temperature		
	160°	192°	242°
TMS-*p*-hydroxybenzaldehyde	0.46	—	—
Vanillin	0.57	—	—
TMS-vanillin†	*1.00*	0.48	—
Syringaldehyde	1.94	—	—
TMS-syringaldehyde	2.12	—	—
TMS-vanillic acid†	2.78	*1.00*	0.19
TMS-coniferyl alcohol		1.93	0.32
TMS-*p*-hydroxy cinnamic acid	—	2.02	0.34
TMS-ferulic acid	—	3.59	0.53
TMS caffeic acid	—	4.42	0.68
TMS-stearic acid	—	6.32	0.82
Pinosylvin monomethyl ether†	—	7.15	0.97
TMS-pinosylvin monomethyl ether†	—	7.30	*1.00*
TMS-pinosylvin†	—	—	1.10
Pinocembrin†	—	—	1.72
TMS-pinocembrin†	—	—	2.08
TMS-pinobanksin‡	—	—	2.42
TMS-xylose	—	—	0.17
TMS-sucrose	—	—	3.28
TMS-β-sitosterol	—	—	3.71

*Retention time of TMS-vanillin (at 160°), 6.5 minutes; of TMS-vanillic acid (at 192°), 5.7 minutes; and of TMS-pinosylvin monomethyl ether, 7.1 minutes.
†Found in red pine heartwood extractives.
‡Double peak.

phenol mixture was pinosylvin monomethyl ether and only small amounts of pinosylvin, pinocembrin, vanillin, and vanillic acid were recorded. In addition 11 trace components were recorded (RRT at 160° C 0.15; at 192° 0.53, 0.67, 1.08, 2.23, 2.98, 3.83, and 5.70; and at 242° 1.36, 2.68, and 2.89). Of these, the peak at RRT (at 242°) 1.36 may have been due to a resin acid. The presence of the relatively large amounts of pyridine in the injected aliquot resulted in a very large, tailing solvent peak, which tended to overlap (and distort) peaks of short retention times.

Column chromatography on silicic acid of the mother liquors gave a small fraction from which pinosylvin (m.p. 158.5–159.5° C) was obtained after recrystallization. None of the other components was obtained pure.

Steam-volatile Components

Fresh wood meal (100 g) was steam distilled for 2 hours and the distillate was taken up in ether. The ethereal solution was dried and the solvent carefully evaporated to give the volatile oil (0.08 g). The chromatogram obtained with a 5 μl aliquot on a 6 ft × 1/4 in. O.D. polyethylene glycol (Carbowax 20 M) column is shown in Fig. 2. The oil (10 μl) was treated with ethereal diazomethane solution. The chromatogram obtained with this product was similar to that obtained under the same conditions with the untreated oil, except that peak 23 was recorded in larger amounts (shown by the dotted lines in Fig. 2), and corresponded to methyl benzoate. Components were tentatively identified by comparison of RRT values with those of known compounds, using polyethylene glycol, Apiezon N, and polyester columns.

Ether-insoluble Material

TLC analysis of the ether-insoluble portion of the acetone extract (see above) gave two spots of R_f 0.00

Can. J. Chem. Downloaded from www.nrcresearchpress.com by 210.87.254.105 on 09/05/12
For personal use only.

and R_f 0.15 ($CHCl_3$:HOAc; 9:1 v/v), which was the same as obtained from the polylignan fractions found in the methanol extract.

Methanol Extract

The residual wood meal (1.2 kg) after acetone extraction was extracted with methanol (5 liters) for 36 hours. The brown, sirupy residue (10 g, 0.8%) obtained after evaporation of the solvent was extracted with hot water (300 ml). The water-soluble portion (3.5 g) was analyzed by paper chromatography (Whatman No. 1; pyridine–butanol–water, 3:3:1 v/v) and two spots corresponding in color (aniline phthalate spray reagent) and R_f values to glucose (R_f 0.16) and xylose (R_f 0.27) were obtained.

The water-insoluble portion (6.4 g) was triturated with hot acetone and the soluble portion was separated. The solvent was evaporated and the residue (6.1 g) was taken up in a few milliliters methanol and dispersed into 2-butanone (200 ml). The resulting precipitate (0.40 g) was filtered off and had m.p. 178–180° C; OCH_3, 12.9%; molecular weight (osmometric, in acetone) 1790. The material was dissolved in dioxane and dispersed into water to give a precipitate, fraction A, with m.p. 177–180° C, $[\alpha]_D$ +1.0° (*c*, 1, dioxane). Found: C, 62.62; H, 6.17; N, 0.51; OCH_3, 10.63%; molecular weight, 1883. After some weeks, the material was no longer completely soluble in acetone or dioxane. On addition of ether to the above filtrate (methanol–butanone solution) fraction B (0.32 g), m.p. 164° C, $[\alpha]_D$ approx. 0° (*c*, 0.5, dioxane) was obtained. This fraction gave a crystalline acetate of m.p. 143–144° C.

The acetone-insoluble portion (0.3 g) was taken up in dioxane and dispersed into ether. The precipitate (0.01 g), fraction C, had m.p. 145.5–150° C.

Fractions A, B, and C had infrared spectra which resembled that of lariciresinol closely.

Nitrobenzene Oxidation

The compound (0.1 g), 2 *N* sodium hydroxide solution (6 ml), and freshly distilled nitrobenzene (0.4 ml) were placed in a stainless steel cylinder of 10 ml capacity (14). The mixture was then heated at 180° C ± 2° in an autoclave for 2 hours with rocking. After being cooled, the reaction mixture was transferred and the excess nitrobenzene was removed by continuous extraction with ether. The aqueous layer was acidified with dilute sulphuric acid (to pH 3) and extracted with ether. After it was dried over anhydrous sodium sulphate, the solvent was evaporated. The residue was taken up in pyridine, converted to the trimethyl silyl derivative, and analyzed by GLC on the SE-52 column (see above).

ACKNOWLEDGMENTS

We wish to thank Mr. M. Kaye, Extension Forester, Manitoba Department of Mines and Natural Resources, Winnipeg, for procuring the red pine log, and Mr. M. Granat for technical assistance. The microanalyses were carried out by Mr. M. Mazurek and infrared spectra were recorded by Mr. W. C. Haid.

REFERENCES

1. Canadian Department of Forestry. Native trees of Canada. 6th ed. Queen's Printer, Ottawa. 1961. p. 14.
2. G. LINDSTEDT and A. MISIORNY. Acta Chem. Scand. **5**, 121 (1951).
3. N. LEVITIN. Pulp and Paper Magazine of Canada, **63**, 169 (1962).
4. N. LEVITIN. 1st Canadian Wood Chemistry Symposium, Toronto, September 4–6, 1963.
5. E. VON RUDLOFF and A. SATO. Can. J. Chem. **41**, 2165 (1963).
6. N. NARASIMHACHARI and E. VON RUDLOFF. Can. J. Chem. **40**, 1123 (1961).
7. H. ERDTMAN. *In* Perspectives in organic chemistry. *Edited by* A. Todd. Interscience Publishers, Inc., New York. 1956. p. 453.
8. G. LINDSTEDT. Acta Chem. Scand. **5**, 129 (1951).
9. R. BENTLEY, C. C. SWEELEY, M. MAKITA, and W. W. WELLS. Biochem. Biophys. Res. Commun. **11**, 14 (1963).
10. J. F. W. MCOMIE. Advan. Org. Chem. **3**, 191 (1963).
11. E. P. SWAN. Forest Products Laboratory, Vancouver. Private communication.
12. K. FREUDENBERG. Chem. Ber. **93**, 2138 (1960).
13. K. FREUDENBERG and H. TAUSEND. Chem. Ber. **96**, 2081 (1963).
14. J. M. PEPPER, M. MANOLOPOULO, and R. BURTON. Can. J. Chem. **40**, 1976 (1962).

Can. J. Chem. Downloaded from www.nrcresearchpress.com by 210.87.254.105 on 09/05/12
For personal use only.

THE THERMAL REVERSIBILITY OF THE MICHAEL REACTION

I. NITRILES[1]

C. F. H. ALLEN
Department of Chemistry, Rochester Institute of Technology, Rochester, New York

AND

G. P. HAPP
Kodak Research Laboratories, Eastman Kodak Co., Rochester, New York

Received August 12, 1963

ABSTRACT

Michael adducts of nitriles and α,β-unsaturated ketones have been found generally to undergo two or more kinds of thermal reversibility upon being heated to moderate temperatures. When the products are those from which the adduct was prepared, the dissociation is termed "normal," whereas the "abnormal" route gives an α,β-unsaturated nitrile and a methyl ketone. The scope and generality of the reversibility are described in three papers. The first deals with 31 ketonic nitriles, the second with nitroketones, and the last with diketones and acidic derivatives.

Allowing the materials to decompose thermally in the heated inlet of a mass spectrometer permits a direct study of thermal reaction mixtures and it affords data the interpretation of which gives an indication of the products present, many of which may not have been previously expected. Identification of products is confirmed by comparison of the mass spectra with those of reference compounds. Under favorable conditions, such products can be isolated from independent decomposition reactions and their identities further confirmed by classical chemical methods. Both operations have been done often enough to show the general application of the mass spectrometer for this purpose. Thus laborious laboratory separations may be avoided. In two instances the four major products from both paths were isolated, identified, and quantitatively determined.

Forty years ago, the senior author of this paper found that γ-benzoyl-α,β-diphenylbutyronitrile (I) (1), the adduct from benzyl cyanide and benzalacetophenone, dissociated on attempted distillation, and its components were identified in the distillate.

$$\begin{matrix} C_6H_5CHCH_2COC_6H_5 \\ | \\ C_6H_5CHCN \end{matrix} \rightleftarrows \begin{matrix} C_6H_5CH{=}CHCOC_6H_5 \\ + \\ C_6H_5CH_2CN \end{matrix}$$

I

Twenty years later, β,γ-diphenyl-γ-nitrobutyrophenone (II) was found to decompose when heated above its melting point; the products identified were benzalacetophenone, benzaldehyde, and nitric oxide (2).

$$\begin{matrix} C_6H_5CHCH_2COC_6H_5 \\ | \\ C_6H_5CHNO_2 \end{matrix} \rightarrow \begin{matrix} C_6H_5CH{=}CHCOC_6H_5 \\ + \\ C_6H_5CHO + NO + ? \end{matrix}$$

II

Although the reversibility of the Michael reaction in the presence of alkaline reagents is well known (3), there are very few recorded instances of the effect of heat upon the adducts. Those few described are all dicarbonyl compounds (see Part III). It seemed

[1]*Contribution No. 2254 from the Kodak Research Laboratories, Eastman Kodak Co., Rochester 50, New York, and the Department of Chemistry, Rochester Institute of Technology, Rochester 8, New York.*

Can. J. Chem. Downloaded from www.nrcresearchpress.com by 210.87.254.5 on 09/05/12
For personal use only.

advisable to postpone a study of the thermal reversibility of the Michael reaction until relatively simple but rapid qualitative and quantitative methods were available. Such tools have been employed in these Laboratories for some years in the form of the mass spectrometer and the gas chromatograph.

Summarizing the present work in three papers, it has been found that the thermal reversibility is dependent upon the number and kind of groups present. The degree of substitution, which has been varied from one to three aryl groups, has considerable effect. Cleavage, which is greatest and may occur in two ways when there are three aryl groups along the chain, is not detectable when there is but one such substituent; the results are intermediate with two aryls. In a given class, the nature of the functional groups is very important. For instance, 1,5-diketones (Part III) and delta ketonic nitriles (this paper) cleave the most easily and follow both paths; keto esters go both ways but less easily. γ-Nitroketones are thermally more stable; they can even be distilled with partial cleavage, which goes only one (normal) way. Cyano esters and diesters are relatively stable; the latter show slight decomposition, but not dissociation, on distillation. Ketonic acids are subject to a competing reaction—any Michael reversal is often undetectable by classical chemical methods.

The mass spectrometer is especially well suited for studying reaction mixtures from thermal decompositions because it furnishes mass numbers from which one can speculate usefully about the identity of the cleavage products, and which can provide positive identification when reference spectra are available. This paper discusses the behavior of nitriles, in particular, those of type I, of which a considerable variety are available.

Approximately 1 milligram of each substance studied was allowed to decompose in the glass and metal heated inlet (230°) system (9) of a mass spectrometer over a period of an hour while several spectra were recorded. Many of the reactions were rapid and there was little change in the spectral pattern during this time, indicating that an equilibrium state had been reached before making the first observation. The pattern changes during the hour were sufficient, however, to indicate that the spectra were those of mixtures. Careful measurement showed that the cracking patterns of the components, as identified, remained constant while the ratios of the several components changed with respect to each other during the period of observation. Factors such as rates of reaction, of volatilization, and of effusion through the leak, may account for the changes. For some slower decompositions, decrease in peak size for the original molecule was observed, accompanied by an increase in the pattern size of the products. Mass-spectral peaks which were judged to be probable parent peaks of undissociated molecule-ions formed the initial basis of speculation concerning the identity of components. Identifications were verified by subsequently comparing the entire spectral pattern with those of known reference compounds. Some of the identifications made by mass spectrometry were further confirmed by carrying out independent decompositions on a larger scale in the laboratory, followed by separation and identification by chemical means as well as by infrared and mass spectrometry.

The quantitative aspects of mass spectrometry are well known and might be applied to these studies. Since this work involved substances of widely different vapor pressures, it would have been necessary to establish the limits within which each substance would yield a linear relationship between amount present and peak intensity under the conditions of operation. The scope of the mass-spectrometric work was limited, therefore, to the qualitative identification of the reaction products, thereby establishing the modes of decomposition of the compounds studied. Once the identity of certain of the products was established by mass spectrometry, it was relatively simple to make quantitative

Can. J. Chem. Downloaded from www.nrcresearchpress.com by 210.87.254.5 on 09/05/12
For personal use only.

measurements on these components by gas chromatography on some of the reaction mixtures from decompositions carried out under laboratory conditions.

Both isomers of adduct I, when decomposed in the heated inlet of the mass spectrometer, yielded not only the expected chalcone and benzyl cyanide (1), but also α-phenylcinnamonitrile (III) and acetophenone, the products of a second mode of decomposition.

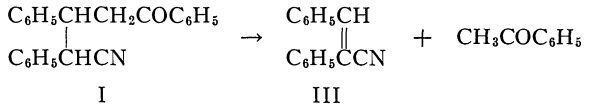

I III

The mass spectra also showed the presence of smaller amounts of other materials which we were unable to identify from the spectral peaks. There was no peak for the parent molecule-ion of either diastereomer of I. However, in a subsequent examination of the adducts, using an all-glass heated inlet to minimize thermal degradation, the mass spectra contained the peaks of the products plus the peaks of the undecomposed molecule, including a prominent peak at the mass of the parent molecule-ion. This finding shows that in the examination of these adducts under the original conditions, where no parent peaks of the adducts were found, the mass spectra represented only the reaction products.

Although the mass-spectrometric identifications were confirmed by comparison with reference spectra of known compounds, further proof was obtained to show that the adducts undergo thermal decomposition to yield the identical products. From an independent decomposition, carried out in the laboratory, the four reaction products were isolated and identified by classical methods.

In this paper the re-formation of the original components is called the "normal" reaction and the second mode of retrogression is termed "abnormal." Although presumably reversible, up to now it has not been possible to isolate any of the adduct I from the attempted Michael addition of these abnormal cleavage products, although from the infrared spectrum a small amount might be present.

It now became important to demonstrate the effect of the glass and metal surfaces of the mass spectrometer upon the reversibility of the Michael reaction at the temperature, 230°, of the heated inlet. Series of experiments in which the decompositions were carried out under several conditions in the laboratory were devised to clarify these and other points, using mainly adduct I. The amounts of benzyl cyanide and acetophenone were determined by gas chromatography, the total being taken as a measure of the retrogression. The results are collected in Table I. Quartz and steamed-out soft glass behaved essentially alike at 230°, giving the lowest value, which was used as the standard. At this temperature only normal dissociation occurred; but at 250° the abnormal reaction occurred. The latter was small in quartz, being only 1/10th that taking place in soft glass; hence it must be concluded that the abnormal retrogression is catalyzed to a much greater extent by the alkali present in the glass. This assumption is supported by the results in untreated soft glass at 250°; the normal reaction is of the same order, but the abnormal is doubled. This behavior also accounts for the failure to effect the synthesis of the Michael adduct from the products of the abnormal cleavage (the rate of the latter reaction must be greater than the rate of adduct formation). Retrogression in steamed-out Pyrex glass was, surprisingly, greater than that in soft glass, and approached that shown by metals (lead in the glass?). The metals tested were copper, stainless steel, Kovar alloy, and silver solder; all these are present in the heated inlet. The steel and Kovar were equal, but the silver solder was four times more effective. In the presence of copper, the

Can. J. Chem. Downloaded from www.nrcresearchpress.com by 210.87.254.5 on 09/05/12
For personal use only.

Can. J. Chem. Downloaded from www.nrcresearchpress.com by 210.87.254.5 on 09/05/12
For personal use only.

TABLE I

Reversal shown by δ-ketonic nitriles*, †

Substance	At 230° C, 20 minutes			At 250° C, 20 minutes			Footnotes
	Total, %	Normal, $\%C_6H_5CH_2CN$	Abnormal, $\%CH_3COC_6H_5$	Total, %	Normal, $\%C_6H_5CH_2CN$	Abnormal, $\%CH_3COC_6H_5$	
I, 109° Isomer	1.3	1.0	0.3	5.2	5.2		
I, 118° Isomer	7.2(*)	7.2					‡
I, 118° Isomer	7.5	7.5		17.6	11.5	6.1	§
I, 118° Isomer	10.1(*)	10.0	0.1				
I, 118° Isomer	11	11		18.0	10.9	7.1	¶
I, 118° Isomer	11	11		18.1	12.8	5.3	**
I, 118° Isomer	12.6	12.5	0.1	22.4	10.3	12.1	††
I, 118° Isomer	25.2	21	4.2				‡‡
4-Chloro derivative	29.9	29.5	0.4				
4-Chloro derivative	28.4	25.0	3.4				‖
4-Chloro derivative	32.8	32.5	0.3				§, §§
4-CH_3O derivative				18.8	18.0	0.8	
4-CH_3O derivative				11.5	11.5		
Ester, VI	26	$(CNCH_2CO_2CH_3)$ 12	14				§, ¶¶

*Steamed-out soft glass used except in runs indicated by (*).
†Gas chromatography data, ± 0.5%.
‡In quartz.
§Steamed-out soft glass only.
‖Steamed-out Pyrex glass.
¶Stainless steel.
**Kovar alloy.
††New, unwashed soft glass.
‡‡Silver solder.
§§Effect of doubling time, 40 min.
‖‖With a condenser.
¶¶At 195–215°.

retrogression started 20° lower and took only two-thirds as long to run to completion. Doubling the time of heating gave only 4% more products, while raising the temperature by 20° increased them by 2.5 times. The reversal could be made complete by allowing the volatile products (nitrile and ketone) to distill (Table II). Quite surprisingly, the lower-

TABLE II

Volatiles distilled, Pyrex glass; final bath temperature, 345°±5° C*

Adduct from:	Total, %	Normal nitrile, %	Abnormal ketone, %	Time, minutes	Decomp. began at ° C
Benzyl cyanide, 109° isomer (I)	99.6	94.5	5.1	19	270
Benzyl cyanide, 118° isomer (I)	100	56	44	24	259
Benzyl cyanide, 118° isomer (I) + copper	92	48	44	14	240
4-Chlorobenzyl cyanide (IV)	99	28	71	15	252†
Methyl cyano-acetate (VI)	84	36	48	20	196

*Values determined by gas chromatography.
†Acetophenone, the lowest-boiling component, distilled, upsetting the equilibrium.

melting form was much less (one-sixth at 230°, one-fourth at 250°) active. However, the relative proportion of volatile products on distillation was considerably different, the abnormal component (acetophenone) being considerably less. It is concluded from these experiments that the materials used in constructing the heated inlet of the mass spectrometer do affect the rate of the decomposition reactions of these Michael adducts. In all cases the qualitative mass-spectrometric identifications were substantiated.

The thermal decomposition of 22 delta ketonic nitriles were studied in like manner, by allowing them to decompose in the heated inlet of the mass spectrometer. All identifications were confirmed by comparison with reference spectra, and most were further substantiated by classical methods. In addition to the product identification listed in Table III, in many instances there were other products not identified by their peaks in the spectra.

The effect of substitution was determined in a few instances. Nitrile adducts bearing substituents (IV: X, Z = H; Y = 4-Cl, 4-CH_3O, 3-NO_2, 4-NO_2, 4-NH_2) were selected. They all decomposed both normally and abnormally. In the confirming independent laboratory decompositions, gas-chromatographic analysis of the products showed that there was more retrogression of the first two than of the unsubstituted adduct. One type of adduct (IV: X = CH_3O; Y, Z = H) gave only the normal products (benzyl cyanide and 4′-methoxychalcone) from the confirming laboratory decomposition at 250°, yet in the mass spectrometer it showed some evidence of a small amount of abnormal dissociation. The mass spectrum of the phenyl analogue (IV: X = C_6H_5; Y, Z = H) showed only normal retrogression. The pair of diastereomers (IV: X, Z = H; Y = 4-NO_2) decomposed so badly in a large-scale laboratory decomposition that no useful quantitative results were obtained by gas chromatography.

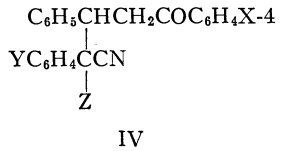

IV

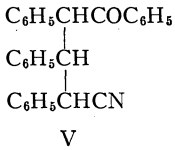

V

Can. J. Chem. Downloaded from www.nrcresearchpress.com by 210.87.254.5 on 09/05/12
For personal use only.

TABLE III

Thermal decomposition products identified by mass spectrometer and masses of parent ions, helpful in establishing identification

Substance	Products
I, Both diastereomers	(208) Chalcone; (205) α-phenylcinnamonitrile (I*a*); (120) acetophenone; (117) benzyl cyanide
IV, X, Z = H; Y = F	(223) 4-Fluoro-I*a*; (208) chalcone; (135) 4-fluorobenzyl cyanide; (120) acetophenone
IV, X, Z = H; Y = Cl	(239) 4-Chloro-I*a*; (208) chalcone; (151) 4-chlorobenzyl cyanide
IV, X, Z = H; Y = 4-CH_3O	(235) 4-Methoxy-I*a*; (208) chalcone; (147) 4-methoxybenzyl cyanide
IV, X, Z = H; Y = 3-NO_2	(250) 3-Nitro-I*a*; (208) chalcone; (162) 3-nitrobenzyl cyanide; (30) nitric oxide*
IV, X, Z = H; Y = 4-NO_2 (both diastereomers)	(250) 4-Nitro-I*a*; (208) chalcone; (162) 4-nitrobenzyl cyanide; (30) nitric oxide*
IV, X, Z = H; Y = 4-NH_2 (both diastereomers)	(220) 4-Amino-I*a*; (208) chalcone; (132) 4-aminobenzyl cyanide; (120) acetophenone
IV, X = CH_3O; Y = 4-NO_2; Z = H	(250) 4-Nitro-I*a*; (238) 4′-methoxychalcone; (162) 4-nitrobenzyl cyanide; (150) 4-methoxyacetophenone; (30) nitric oxide*
IV, X = CH_3O; Y, Z = H	(238) 4′-Methoxychalcone; (205) α-phenylcinnamonitrile; (150) 4-methoxyacetophenone; (117) benzyl cyanide
IV, X = C_6H_5; Y, Z = H	(284) 4-Phenylchalcone; (117) benzyl cyanide
Amides of type IV	
X = OCH_3; Y, Z = H	(238) 4′-Methoxychalcone; (135) phenylacetamide
X, Z = H; Y = 4-NO_2	(208) Chalcone; (137) unidentified
V	(284) Benzaldesoxybenzoin; (205) α-phenylcinnamonitrile; (117) benzyl cyanide
VI, X = H	(208) Chalcone; (187) methyl α-cyanocinnamate; (120) acetophenone
VI, X = Cl	(242) 4′-Chlorochalcone; (187) methyl α-cyanocinnamate; (154) 4-chloroacetophenone
VII	(249) UM;† (208) chalcone; (129) cinnamonitrile; (120) acetophenone
VIII	(173) UM
IX, Ar′ = C_6H_5	(235) UM; (208) chalcone
IX, Ar′ = mesityl	(257) UM; (250) benzalacetomesitylene
IV, X, Y = H; Z = Br (both diastereomers)	(208) Chalcone; (205) α-phenylcinnamonitrile; (117) benzyl cyanide
IV, X = H; Y = NO_2; Z = Br	(208) Chalcone; (162) 4-nitrobenzyl cyanide; (30) nitric oxide*
XI, Ar = H	(208) Chalcone; (205) α-phenylcinnamonitrile; (120) acetophenone; (117) benzyl cyanide
XI, Ar = 4-CH_3O	(235) 4-Methoxy-I*a*; (208) chalcone; (120) acetophenone
XI, Ar = F	(223) 4-Fluoro-I*a*; (208) chalcone; (135) 4-fluorobenzyl cyanide; (120) acetophenone
XII (three)	(132) Phenyl vinyl ketone

*Unconfirmed.
†Undecomposed molecule.

Both diastereomeric amides (adducts from *p*-nitrophenylacetamide) corresponding to IV (X, Z = H; Y = 4-NO_2; $CONH_2$ for CN) gave only normal retrogression as would be expected; this is due to the relative inactivity of the $CONH_2$ as compared to the CN in a Michael reaction.

From these very limited data it may be concluded that the nature of the addendum is the most important single factor in the thermal reversal. This conclusion is borne out by quantitatively observing the behavior of one of the methyl cyanoacetate adducts (VI) (4)—retrogression was 26% at a much lower temperature (195–215°) (Table I). The more highly substituted delta ketonic nitrile (V) (5) falls into line (5) since it gives both the normal products (benzaldesoxybenzoin and benzyl cyanide) and one abnormal product (α-phenylcinnamonitrile) in the mass spectrometer decomposition.

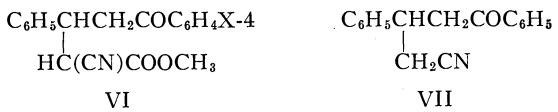

VI VII

Can. J. Chem. Downloaded from www.nrcresearchpress.com by 210.87.254.5 on 09/05/12
For personal use only.

In order to learn the effect of fewer substituents along the chain, other ketonic nitriles were examined. γ-Benzoyl-β-phenylbutyronitrile (VII) (3) gave a parent peak of the undecomposed compound, as well as the normal product (chalcone) formed by loss of acetonitrile, and the abnormal products, cinnamonitrile and acetophenone. γ-Benzoylbutyronitrile (VIII) (6), having no substituents, shows no retrogression at all; this is in agreement with the fact that it distills unchanged. The mass spectrum appeared to be consistent with the structure of the undecomposed molecule, containing a parent peak at *m*/e 173 and a fragment ion peak at *m*/e 119 from cleavage of the bond β to the carbonyl. The largest peak was at *m*/e 105, the $C_6H_5\,CO^+$ ion. Two gamma ketonic nitriles (IX) which cannot give abnormal products were also examined; undecomposed molecules and chalcones were

VIII IX

found. In none of these last instances could the nitrile be identified because of undetermined contributions to the useful mass-spectral peaks by other components.

Two diastereomeric bromo derivatives (IV: X, Y = H; Z = Br) were also examined. The unsaturated compounds (chalcone, α-phenylcinnamonitrile), formed by both types of retrogression, were found. Benzyl cyanide was also identified, but there was no evidence as to the fate of the bromine. From the decomposition of the nitro derivative (IV: X = H; Y = NO_2; Z = Br), chalcone and *p*-nitrobenzyl cyanide, formed by normal retrogression only, were found. There was evidence for the liberation of nitric oxide also, but there were no products of abnormal decomposition. The identification of nitric oxide could not be confirmed in the mass spectrometer because of other possible sources of an NO^+ ion.

The trimolecular products, which are usually formed in small amounts in the preparation of Michael adducts from chalcones and nitriles, from their infrared absorption in the solid state, are now known to exist in the form of highly substituted cyclohexanols (X) (7). They are easily reversible by heat. The open-chain form (XI) (XI: Ar = C_6H_5, 4-$CH_3OC_6H_4$, 4-FC_6H_4) is obviously a Michael adduct, and is likewise reversible. The laboratory experiments again confirmed the mass-spectrometric identifications (1). The

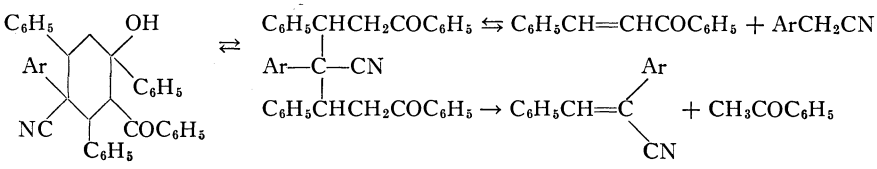

X XI

only recognizable decomposition product from three non-cyclic trimolecular molecules of the type XII (8) was phenyl vinyl ketone, a normal retrogression product.

XII $RR'C(CH_2CH_2COC_6H_5)_2$ R = CN, R′ = CN, $CONH_2$, $COOCH_3$

EXPERIMENTAL

Mass Spectrometry

The instrument was a 60° sector type, equipped with a 230° heated inlet system designed to accept readily samples of liquids or solids. The heated inlet (9) is constructed principally of Pyrex glass with some smaller exposed surfaces of stainless steel, Teflon, Kovar metal, silver solder, and platinum. Relatively large samples were introduced resulting, at least in some instances, in excess non-volatilized material, a condition which precludes quantitative treatment of the data.

Can. J. Chem. Downloaded from www.nrcresearchpress.com by 210.87.254.5 on 09/05/12
For personal use only.

Gas Chromatography

The gas-chromatographic separations were carried out in an 8 ft × 0.25 in. column packed with 25%, by weight, General Electric silicone gum rubber SE-30, on 80–100 mesh Celite 545. The column was thermostatted with boiling *p*-cymene and the flow rate was 50 ml of helium per minute. A Gow-Mac thermoconductivity cell, Model 9285, was used as the detector. The retention times observed were: methyl cyanoacetate, 2.23 minutes; acetophenone, 6.26 minutes; benzyl cyanide, 7.80 minutes; 4-chlorobenzyl cyanide, 18.8 minutes; 4-methoxybenzyl cyanide, 21.7 minutes; 4-methoxyacetophenone, 22.8 minutes.

Thermolyses

The specimens for gas chromatography were prepared as follows. One-gram samples of the adducts in vials were heated simultaneously in an oil bath at two temperatures (230°, 250°) for 20 minutes. Metal "catalysts" were included, as has been mentioned; the silver solder had the composition: 50% silver, 18% cadmium, 15.5% copper, and 10.5% zinc. The decomposition products were introduced into the chromatograph as ethyl acetate solutions; chalcone was not estimated since its amount would be equivalent to the benzyl cyanide.

The new soft-glass vials received a hot trisodium phosphate wash, followed by five rinses (in one instance, hydrochloric acid was used as a rinse, but the result was unchanged) and drying at 110°. Vials, steamed out for 10 minutes and dried at 110°, likewise gave a comparable result. In the instances in which all the volatiles were distilled, 5 g of adduct in a 25-ml Pyrex distilling flask was heated in an oil bath as long as distillate collected (Table I). The main features of the findings have already been mentioned.

Reagents and Chemical Reactions

The reagents used were Eastman chemicals except *p*-fluorobenzyl cyanide (10) and 4-aminobenzyl cyanide. The fluoro compound was quite acidic, requiring considerable sodium methoxide in the addition reaction before an alkaline test in moist litmus was obtained. Since Pschorr's procedure (11) (reduction of *p*-nitrobenzyl cyanide by tin and hydrochloric acid) gives a very pure aminonitrile in a high yield, this was followed. Selective catalytic reduction, using 10% palladium on charcoal, gave a very complex mixture.

Many of the adducts and reference compounds required in this and in the following papers were available from previous work. New 4-substituted-α-phenylcinnamonitriles were synthesized by the usual procedure using sodium methoxide, except for the 4-nitro, in which case Triton B was employed. For example, a mixture of 1.5 g of *p*-nitrobenzyl cyanide, 1 ml of benzaldehyde, and 10 ml of alcohol was heated to dissolve the solid, and five drops of Triton B were added. The initial magenta color quickly became greenish, the solvent boiled, and the solid product crystallized shortly. The yield was quantitative. The buff solid, m.p. 177–178°, was rinsed with methanol to remove most of the green color, and recrystallized from propyl alcohol.

The new delta ketonic nitriles of type I were prepared either in the continuous reactor (12), which gives more of the higher-melting isomer, or batchwise, using only a small amount of sodium methoxide as catalyst. The yield of crystalline mixed adduct was 85–87%; the sticky residue that did not crystallize appeared to be mainly the same adducts, according to infrared spectrometry. Only one of the two possible diastereomeric forms of the new adducts (IV: X, Z = H; 4-Y = F, Cl, OCH_3, 3-NO_2; Y, Z = H; X = C_6H_5) was isolated. Mixtures tended to oil out; the anisyl adduct crystallized readily from solutions if the latter were seeded with a little previously prepared sample. The 4-fluoro derivative did not separate from the oil for a month. Tedious fractional crystallizations from petroleum ether and also from methanol afforded no separation; in the previous instances it had been fortuitous with I, but very easy with IV (X, Z = H; Y = NO_2). The various crystalline fractions, which were mixtures of the diastereomeric forms, gave the correct elemental analyses. Since the differences were of degree rather than in kind, it was unnecessary to have both pure forms. A little trimolecular product (X) was separated during the first recrystallization of each of the adducts except the amino derivatives.

Both 4-amino adducts were obtained, however, one by addition and the other by selective catalytic reduction of the corresponding nitro adducts (13). The addition takes place (6 hours) at room temperature, after this mixture had been warmed enough to produce complete solution. Prolonged heating gives a complex mixture from which an impure amine can be isolated only with difficulty. In the catalytic reduction procedure, both adducts (m.p. 126° and 143°) gave 50% yields of the same amine, isomeric with the one produced on addition. The remainder of the product was an intractable yellow pitch. A solution of 32.5 g of nitro adduct in 370 ml of dioxane, containing 1 g of 10% palladium on charcoal, was shaken at room temperature and 60 p.s.i. of hydrogen until the theoretical amount was absorbed (24 hours). Most of the solvent was distilled. The residue was a sticky pitch in which a white solid had formed after 3 weeks. Methanol was added to facilitate manipulation, the solid was collected on a filter, and recrystallized.

The properties of the new substances are listed in Table IV.

All attempts to bring about formation of the Michael adducts (I) from the products of the abnormal dissociation (acetophenone and α-phenylcinnamonitrile) have so far been fruitless; conditions employed included changes in time, catalyst, and solvent. Either the cinnamonitrile, which crystallizes well from mixtures, or a sticky glue resulted. Occurrence of addition would have been indicated by the presence of the known adducts, detectable by infrared spectrometry, or the easily isolable trimolecular product (X),

Can. J. Chem. Downloaded from www.nrcresearchpress.com by 210.87.254.5 on 09/05/12
For personal use only.

TABLE IV

Properties of new substances

$C_6H_5CH{=}C(CN)—C_6H_4X$-4		α-(4X-Phenyl) cinnamonitriles	Analyses					
			Calc.			Found		
X	M.p., ° C	emp. formula	C	H	N	C	H	N
F	107*	$C_{15}H_{10}FN$	80.7	4.5	6.3	80.5	4.6	6.2
Cl	115–116†	$C_{15}H_{10}ClN$	75.2	4.2	14.8§	75.0	3.9	14.8§
NO_2	179–180‡	$C_{15}H_{10}N_2O_2$	72.0	4.0	11.2	72.0	3.9	11.6
CH_3O	96–97†	$C_{16}H_{13}NO$	81.7	5.5	6.0	82.0	5.5	5.6
Michael adducts (IV) Y = H								
C_6H_5	116‡	$C_{29}H_{23}NO$	86.8	5.7	3.5	87.1	5.6	3.1
4-F	94–95*	$C_{23}H_{18}FNO$	80.5	5.3	4.1	80.2	5.6	4.1
4-Cl	128–129*	$C_{23}H_{18}ClNO$	76.3	5.0	9.9§	76.2	4.9	9.8§
its DNPH	96	$C_{29}H_{22}ClN_5O_4$		6.5§	13.0		6.6§	12.8
4-CH_3O	124–125*	$C_{24}H_{21}NO_2$	81.1	5.9	3.9	81.0	5.9	3.6
3-NO_2	134–135‡	$C_{23}H_{18}N_2O_3$	74.6	4.9	7.6	74.9	4.8	7.3
4-NH_2‖	163‡, **	$C_{23}H_{20}N_2O$	81.2	5.9	8.2	80.8	6.0	8.6
4-NH_2¶	166‡, **	$C_{23}H_{20}N_2O$	81.2	5.9	8.2	80.8	5.6	8.3

*From methanol.
†From ethanol.
‡From propanol.
§% chlorine.
‖By reduction.
¶By addition.
**Mixed melting point, 141–143°.

or the known 2-oxo-1,2,3,4-tetrahydro-3,4,6-triphenylpyridine (1) which has a very brilliant blue fluorescence when exposed to ultraviolet light. The uncrystallizable glue from these attempts (as well as the residual oil from the normal preparation) always shows a blue fluorescence, but there was insufficient adduct to be isolated or detected by infrared spectrometry.

Tetrahydropyridine formation from delta ketonic nitriles under alkaline conditions (14) was successful with the latter only if they were not highly substituted. The triphenyl derivative (I), when treated in the same way, gives the trimolecular product (X) as previously determined (1) and now reconfirmed; the accompanying uncrystallizable portion does show a similar blue fluorescence.

ACKNOWLEDGMENT

The authors take pleasure in acknowledging the technical assistance of Dr. O. E. Schupp for the gas chromatography; of Mr. J. F. Stenberg and Mr. R. W. Ryan for the reactions under pressure; of Miss Thelma J. Davis and Mrs. L. C. Ketchum for the infrared determinations; of Mr. D. P. Maier for operation of the mass spectrometer; of Mr. D. F. Ketchum for the microanalyses; and of Dr. D. W. Stewart for many helpful suggestions.

REFERENCES

1. E. P. Kohler and C. F. H. Allen. J. Am. Chem. Soc. **46**, 1522 (1924).
2. C. F. H. Allen and C. V. Wilson. J. Org. Chem. **5**, 146 (1940).
3. E. D. Bergmann, D. Ginsberg, and R. Pappo. Org. Reactions, **10**, 179 (1959).
4. E. P. Kohler, A. Graustein, and D. H. Merrill. J. Am. Chem. Soc. **44**, 2536 (1922).
5. E. Knoevenagel and R. Weissgerber. Ber. **26**, 445 (1893).
6. C. F. H. Allen and W. L. Ball. J. Am. Chem. Soc. **59**, 686 (1937).
7. C. F. H. Allen, T. J. Davis, W. J. Humphlett, and D. W. Stewart. J. Org. Chem. **22**, 1291 (1957).
8. C. F. H. Allen and A. C. Bell. Can. J. Res. **11**, 40 (1934).
9. V. J. Caldecourt. Anal. Chem. **27**, 1670 (1955).
10. *From* Research Laboratorium Dr. C. Janssen, Beerse, Belgium.
11. R. Pschorr. Ber. **35**, 4403 (1902).
12. C. F. H. Allen, J. R. Byers, W. J. Humphlett, and D. D. Reynolds. J. Chem. Educ. **32**, 394 (1955).
13. C. F. H. Allen. J. Am. Chem. Soc. **47**, 1743 (1925).
14. A. D. Campbell and I. D. R. Stevens. J. Chem. Soc. 59, (1956).

Can. J. Chem. Downloaded from www.nrcresearchpress.com by 210.87.254.5 on 09/05/12
For personal use only.

THE THERMAL REVERSIBILITY OF THE MICHAEL REACTION

II. NITROKETONES AND RELATED COMPOUNDS[1]

C. F. H. ALLEN
Department of Chemistry, Rochester Institute of Technology, Rochester, New York

AND

G. P. HAPP
Kodak Research Laboratories, Eastman Kodak Co., Rochester, New York

Received August 12, 1963

ABSTRACT

In continuation of the study of the thermal reversibility of Michael adducts, 13 γ-nitroketones were examined in the mass spectrometer, using the inlet heated at 230°. The presence of furans was indicated, arising from the intact molecule. Such remotely related substances would never have been envisaged had not the mass spectrum been available. In contrast to the behavior of delta ketonic nitriles (Part I) only normal retrogression was found. There were many secondary products resulting from extensive decomposition of the expected nitro addend. Not all the products can be isolated by classical procedures, but their presence is predictable, and can be shown by the use of the mass spectrometer. Nine simple nitro- and bromonitro-ethylenes, sensitive to heat alone, were unexpectedly stable in the heated inlet of the mass spectrometer, but did give rise to very small amounts of decomposition products. Phenyl- and 1-naphthyl-nitromethanes, which decomposed completely, gave comparable types of products. Most of these nitro compounds have previously been thermally treated by classical methods.

The γ-nitroketones used in this work are analogous to the δ-ketonic nitriles described in the previous paper (1), and were prepared similarly. In their behavior they differ from the latter in that the expected addend bearing the nitro group was never found, on account of its susceptibility to further degradation.

$$\begin{array}{lcll} C_6H_5CH{=}CHCOC_6H_4X\text{-}4 & & C_6H_5CHCH_2COC_6H_4X\text{-}4 & C_6H_5CH{=}CHCOC_6H_4X\text{-}4 \\ + C_6H_5CH_2NO_2 & \rightarrow & C_6H_5\underset{|}{C}HNO_2 \quad I & \rightarrow \quad + C_6H_5CHO + NO + ? \end{array}$$

In the first chemical investigation 20 years ago (2) three products of the thermal decomposition of I (X = H) were recorded; these were chalcone, benzaldehyde, and nitric oxide. In a renewed chemical investigation, after removal of the benzaldehyde as the 2,4-dinitrophenylhydrazone, benzonitrile, which has a very similar odor, remained; it was identified by infrared and mass spectra. Benzonitrile is present (3.5%) in the more volatile fractions of the thermolysis; however, as the temperature was raised, considerable water appeared along with the nitrile, as though both had resulted from the decomposition of some intermediate product. The latter could be benzaldoxime, a trace of which was found by gas chromatography; it was identified in the mass spectra of several of the fractions. That the nitrile arises from benzaldoxime was confirmed by following the course of the thermal decomposition of the pure oxime at 230° in the heated inlet of the mass spectrometer. The benzaldoxime peaks decreased with time, while those of the benzonitrile were simultaneously increasing. A small amount of benzoic acid was also isolated from the distilled products from I (X = H); this was not surprising, since it could arise by oxidation of the aldehyde by the nitric oxide, or by hydrolysis of the nitrile. When

[1]*Contribution No. 2280 from the Kodak Research Laboratories, Eastman Kodak Co., Rochester 50, New York, and the Department of Chemistry, Rochester Institute of Technology, Rochester 8, New York.*

Can. J. Chem. Downloaded from www.nrcresearchpress.com by 210.87.254.42 on 09/05/12
For personal use only.

the decomposition of this adduct I was examined in the mass spectrometer, by allowing the compound to decompose in the heated inlet, a considerable variety of products were identified (Table I). The ratios of the components changed during the 1-hour observation

TABLE I

Thermal decomposition products identified by mass spectrometer and masses of parent ions, helpful in establishing identifications

Substances	Products
I, X = H, 2 isomers	(296) Triphenylfuran; (208) chalcone; (180) stilbene; (120) acetophenone; (106) benzaldehyde; (103) benzonitrile; (30) nitric oxide*
I, X = C_6H_5	(284) 4′-Phenylchalcone; (30) nitric oxide; many peaks unaccounted for
I, X = Cl	(330) 2-(4-Chlorophenyl)-4,5-diphenylfuran;† (242) 4′-chlorochalcone; (30) nitric oxide
I, X = Br	(375) 2-(4-Bromophenyl)-4,5-diphenylfuran;† (287) 4′-bromochalcone; (103) benzonitrile; (30) nitric oxide
γ-Br-I; X = Cl	(330) 2-(4-Chlorophenyl)-4,5-diphenylfuran;† (258) bromostilbene;† (242) 4′-chlorochalcone; (218) bromochlorostyrene†
γ-Br-I; X = Br	(374) 2-(4-Bromophenyl)-4,5-diphenylfuran;† (286) 4′-bromochalcone; (262) 1,2-dibromostyrene; (258) bromostilbene;† (30) nitric oxide
II	(220) Diphenylfuran; (132) phenyl vinyl ketone; (small 120) acetophenone; (30) nitric oxide
III	(208) Chalcone; (30) nitric oxide
γ-Br-II	(220) Diphenylfuran; (30) nitric oxide
γ-Br-I; X = H	(296) Triphenylfuran; (208) chalcone
γ-Br-I; X = Cl	(180) Stilbene
γ-Br-I; X = Br	(286) 4′-Bromochalcone;† (262) 1,2-dibromostyrene; (259) bromostilbene;† (30) nitric oxide
$C_6H_5CH_2NO_2$	(182) Bibenzyl; (121) benzaldoxime; (119) *o*-hydroxybenzonitrile;‡ (106) benzaldehyde; (103) benzonitrile; (30) nitric oxide; (78) benzene
1-$C_{10}H_7CH_2NO_2$	(282) Dinaphthylethane;† (169) 2-hydroxy-1-naphthonitrile;‡ (156) 1-naphthonitrile; (128) naphthalene; (30) nitric oxide
aci-Form	Same, plus (172) 1-naphthoic acid
β-Nitrostyrene	(149) UM;§ (102) phenylacetylene;† (30) nitric oxide
2,5-Dimethoxy-derivative	(209) UM; (30) nitric oxide
2,5-Dimethoxy-β-methyl derivative	(223) UM; (30) nitric oxide
β-Bromo-β-nitrostyrene	(262) 1,2-Dibromostyrene; (258) bromodiphenylethylene;† (228) UM; (30) nitric oxide
1,1-Diphenylethylenes:	
-2-nitro	(225) UM; (30) nitric oxide
4′-phenyl-2-nitro	(301) UM; (30) nitric oxide
2-bromo-2-nitro-	(338) 2,2-Dibromo-1,1-diphenylethylene; (332) tetraphenylethylene; (303) UM; (178) tolane; (30) nitric oxide
2,2-dibromo-	(338) UM; (178) tolane

*In all cases when nitric oxide is reported it could not be confirmed because of other possible sources of an NO^+ ion.
†Unconfirmed.
‡Confirmation is qualified because peaks are very small.
§Undecomposed molecule.

period, while the cracking patterns of the components remained constant in all of the spectra. All of the identifications tabulated were confirmed by comparison with reference spectra, of known compounds unless otherwise noted. Adduct I gave 2,3,5-triphenylfuran, stilbene, chalcone, and nitric oxide; which presumably arise from the intact adduct. The furan and chalcone were estimated by gas chromatography. Many of the smaller molecules may be attributed to the very heat-sensitive phenylnitromethane, formed by retrogression. In this and in all other instances where nitric oxide is reported, its presence could not be confirmed by a reference mass spectrum because of the alternate possible source of an NO^+ ion fragment from most nitro compounds. However, nitric oxide was identified chemically as a product of the independent laboratory decomposition reaction

Can. J. Chem. Downloaded from www.nrcresearchpress.com by 210.87.254.42 on 09/05/12
For personal use only.

of I. There was no definite indication of an abnormal dissociation, which would yield α-nitrostilbene and acetophenone. Both diastereomeric adducts behaved in a similar manner. γ-Bromo derivatives of I gave 3-bromo-2,4,5-triphenylfurans (2). At the time of the classical type of investigation the furan found was not even envisaged because of its seemingly remote relation to the bromonitro ketone; *it could have been predicted had a mass spectrometer been available*! The less highly arylated diphenyl-γ-nitroketone (II) (3) decomposed in the mass spectrometer inlet to yield diphenylfuran, vinyl phenyl ketone, nitric oxide, and a little acetophenone. Its isomer (III) gave chalcone and nitric oxide; none of the expected nitromethane was found, it being unstable under the experimental conditions.

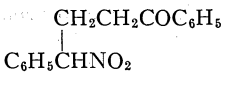

II

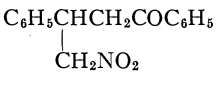

III

The γ-bromo derivative of II gave 2,5-diphenylfuran and nitric oxide. This is at variance with the chemical finding (3) that heat alone gives rise to 3-bromo-2,5-diphenylfuran. Two γ-bromo derivatives corresponding to I gave complex mixtures, among which the previously detected chalcones and nitric oxide predominated, but in each instance there was some triarylfuran.

With a view to further elucidating these results, phenylnitromethane itself was examined in the mass spectrometer. It decomposed in the heated inlet, yielding a mass spectrum consistent with a mixture containing bibenzyl (1,2-diphenyl ethane), benzaldoxime, benzaldehyde, benzonitrile, benzene, nitric oxide, and an unknown giving a very small peak at mass 119, but no stilbene. Benzaldehyde, dibenzhydroxamic acid, nitric oxide, and water have been previously reported as products of thermolysis (4). Since phenylnitromethane is an unstable liquid that is not easily purified, α-naphthylnitromethane, which can be crystallized to constant melting point, was next examined. After exposure in the mass spectrometer at 230°, the analytically pure compound gave a spectral pattern corresponding to a mixture of dinaphthylethane, α-naphthaldehyde, α-naphthonitrile, naphthalene, nitric oxide, and an unknown giving a very small peak at mass 169. The *aci*-form, which is an oil, gave all the same products, plus a little α-naphthoic acid; however, there appeared to be more of the unknown and naphthonitrile. There was no α-naphthaldoxime, but a separate examination of this substance in the mass spectrometer at 230° revealed such a rapid decomposition to the unknown (169) and nitrile that its absence was not surprising. These results are analogous to and correspond with those found with the phenylnitromethane. Since there was no dinaphthylstilbene, it may indicate that the stilbene found on heating the adduct I probably arises from the latter structure rather than from the phenylnitromethane.

In view of these complex results, all the nine nitro- and bromo-nitroethylenes, available from the previous work (3), were examined in the mass spectrometer. Rather surprisingly, they were all relatively stable under the prevailing conditions, each giving a peak corresponding to the molecular weight of the original undecomposed molecule, with very little nitric oxide; there were peaks that could be attributed to the respective phenylacetylenes, although these were not confirmed. The changing ratio of these peaks with respect to the parent peak of the undecomposed molecule was accepted as proof that these peaks represented reaction products. This is in agreement with the chemical evidence; β-nitrostyrene can be distilled with some decomposition (b.p. 250–260°) (5). β-Bromo-β-nitro-α,α-diphenylethylene also showed a peak at its molecular weight, but partially decomposed to

Can. J. Chem. Downloaded from www.nrcresearchpress.com by 210.87.254.42 on 09/05/12
For personal use only.

give some β,β-dibromo-α,α-diphenylethylene and tetraphenylethylene. β-Bromo-β-nitrostyrene showed the parent undecomposed molecule, plus 1,2-dibromostyrene and a monobromodiphenylethylene. β,β-Dibromo-α,α-diphenylethylene showed the parent molecule and tolane (diphenylacetylene). The latter and 1,2-dibromostyrene have been shown previously (2) by chemical methods.

DISCUSSION OF RESULTS

The formation of 2,3,5-triphenylfuran, which contains *all* the carbon atoms of the chalcone–phenylnitromethane adduct I indicates that it is not a retrogression product. In this instance, the yield of furan is low, whereas with the bromonitro ketones, the yield of bromofuran was very high; the difference is one of degree rather than kind. The adduct, either as such or in its *aci*-form, has lost nitrous acid, possibly to give the carbene (IV),[2] from which a hydride ion is removed under the prevailing oxidizing conditions. An alternate possibility, the direct displacement of nitrite ion by the free electron pair of the oxygen atom, seems less likely since the analogous cyano adduct (1) does not show a similar behavior, no furan being formed.[3]

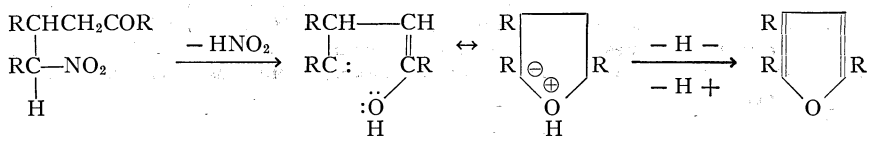

IV

In the retrogression to chalcone and arylnitromethane, the behavior of the arylnitromethane can be summarized as shown in Chart I.

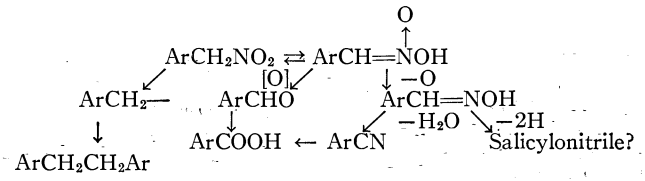

Chart I. Possible paths of decomposition of arylnitromethanes.

The unknown giving a peak of mass 119 could be benzonitrile oxide (6), benz[4,5]isoxazole (indoxazene), or its conversion product *o*-hydroxybenzonitrile (salicylonitrile) (7), all of molecular weight 119. The first two were excluded by comparison with mass spectra of authentic specimens. The unknown giving a peak at mass 169 could be a benzolog of any of the three; it is probably 2-hydroxy-1-naphthonitrile (8). Owing to the small size of the mass peaks, the identification of the hydroxynitriles (possible parent peaks at *m*/e119 and 169) is inconclusive; products corresponding to these molecular weights could not be isolated in the laboratory. The hydroxynitriles are probably formed as a result of the

[2]*The intermediate formation of a carbene, as proposed in an earlier paper (2), seems to have been overlooked by subsequent workers in the carbene field.*

[3]*The referee suggested an alternative mechanism, involving the beta-elimination of nitrous acid, and nucleophilic addition, followed by oxidation to the furan.*

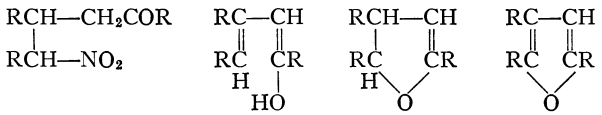

Can. J. Chem. Downloaded from www.nrcresearchpress.com by 210.87.254.42 on 09/05/12
For personal use only.

known easy cleavage (7) of an indoxazene; the latter undoubtedly arises by formation of an additional ring which results from a dehydrogenation under the prevailing oxidizing conditions.

EXPERIMENTAL

The substances used for the thermolyses and the reference compounds were on hand from previous work[4] or were prepared by methods given in the literature, e.g., phenylnitromethane (9), 1-naphthylnitromethane (10), *o*-hydroxybenzonitrile (7), and 2-hydroxy-1-naphthonitrile (8).

Both stereomeric forms of the adduct (I) gave the same products, when heated for 0.5 hour *in vacuo* at 214–286°. Water appeared at 238°, and much unchanged adduct distilled; even at atmospheric pressure a little adduct comes over. This indicates that the nitroketones are more stable thermally that the cyanoketones (delta ketonic nitriles (1)). The evolved gas is nitric oxide (colorless, turns brown in air). The distillate from 5 g of adduct was collected in fractions for examination by gas chromatography; the percentages of the components given are totals. The main products were benzaldehyde (52%) and chalcone (35%). Lesser products were 2,3,5-triphenylfuran (19%), benzonitrile (3.5%), benzaldoxime (a trace), and benzoic acid. The benzaldehyde, benzaldoxime, and benzonitrile were chromatographed as before (1), the retention times being 3.87, 9.02, and 4.18 minutes, respectively. The chalcone and triphenylfuran were chromatographed in a Barber–Colman Model 10 Gas Chromatograph, containing the Lovelock ionization detector, with radium sulphate as the ionizing source. The conditions of the separation were as follows: the column contained 5%, by weight, of General Electric SE-30 silicone gum rubber on 80–100 mesh, acid-washed Celite 545. The column was 5 ft long, and was operated at 200° C with a flow rate of approximately 50 ml/minute. The retention times of chalcone and triphenylfuran were 0.48, 2.23 minutes, respectively.

Mass spectrometry.—The mass spectrometer used was described previously (1). The peaks found in the mass spectra and their identification by comparison of the entire pattern, with known reference compounds, are summarized in Table I.

ACKNOWLEDGMENTS

We are pleased to have had the assistance of Dr. O. E. Schupp for the gas chromatography; of Dr. J. F. Tinker for valuable mechanistic discussions; of Mr. D. Maier for operation of the mass spectrometer; and of Dr. D. W. Stewart for many helpful discussions.

REFERENCES

1. C. F. H. Allen and G. P. Happ. Can. J. Chem. In press.
2. C. F. H. Allen and C. V. Wilson. J. Org. Chem. **5**, 146 (1940).
3. C. F. H. Allen and M. P. Bridgess. J. Am. Chem. Soc. **51**, 2151 (1929).
4. F. Heim. Ber. **43**, 3419 (1910).
5. B. Priebs. Ann. **225**, 339 (1884).
6. H. Wieland. Ber. **40**, 1671 (1907).
7. M. A. Conduché. Ann. Chim. 8e Sér. **13**, 48 (1908).
8. M. Passerini. Gazz. Chim. Ital. **56**, 125 (1926).
9. A. P. Black and F. H. Babers. Org. Syn. Coll. Vol. 2. 1934. p. 512.
10. W. Wislicenus and H. Wren. Ber. **38**, 502 (1905).

[4]*We are indebted to Dr. Paul Johnson, of the University of New Hampshire, for a chromatographically pure sample of bibenzyl; and to B. D. Wilson, C. V. Wilson, and D. M. Burness (of Eastman Kodak Company), for the indoxazene, benzonitrile oxide, and substituted β-nitrostyrenes, respectively.*

Can. J. Chem. Downloaded from www.nrcresearchpress.com by 210.87.254.42 on 09/05/12
For personal use only.

Can. J. Chem. Downloaded from www.nrcresearchpress.com by 210.87.254.105 on 09/05/12
For personal use only.

THE THERMAL REVERSIBILITY OF THE MICHAEL REACTION

III. 1,5-DIKETONES AND ADDUCTS BEARING ACIDIC GROUPS[1]

C. F. H. ALLEN

Department of Chemistry, Rochester Institute of Technology, Rochester, New York

AND

G. P. HAPP

Kodak Research Laboratories, Eastman Kodak Co., Rochester, New York

Received August 12, 1963

ABSTRACT

In this paper a number of known chemical facts obtained by classical methods are correlated with the mass spectra of compounds thermally decomposed in the heated inlet of the mass spectrometer. Of the 31 substances examined, 24 are dioxo compounds. Among them are the few and only Michael adducts previously known to undergo thermal reversal. Both normal and abnormal types of retrogression were found, but ketonic acids which could only regress normally, in a competing reaction, formed lactones by dehydration. A formally similar β-hydroxyketone dissociated both ways in a comparable manner. Esters were more stable than cyano ketones under the conditions employed.

In two previous communications mass-spectrometric studies of the thermal reversibility of Michael adducts from nitriles (1) and nitroketones (2) have been described. This paper deals with diketones, adducts bearing acidic groups, and related substances.

Diketones

Many 1,5-dicarbonyl compounds belong to a class of substances now recognized as Michael adducts. The earliest representatives of this group were benzaldiacetophenone (1,3-dibenzoyl-2-phenylpropane (I) (3), dibenzaltriacetophenone (2,4-diphenyl-1,3,5-tribenzoylpentane (II) (3), which exists in two diastereomeric forms, and benzamaron (III) (4). Upon distillation, the first two were reported to give chalcone (benzalacetophenone) and acetophenone (3), while benzamaron (III) was reported to show retrogression to desoxybenzoin and benzaldesoxybenzoin (IV) (4).

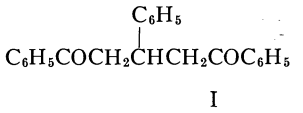

I

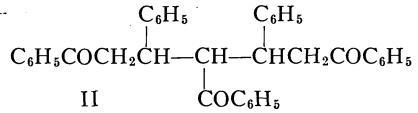

II

All mass-spectrometric identifications, unless otherwise noted, were established by comparison of the entire spectra of known reference compounds with those of the decomposition mixtures. Even for the compounds which appeared to decompose rapidly in the 230° heated inlet, the spectral changes during the period of observation showed changing ratios of components while the cracking pattern of each remained constant, lending further support to the identifications.

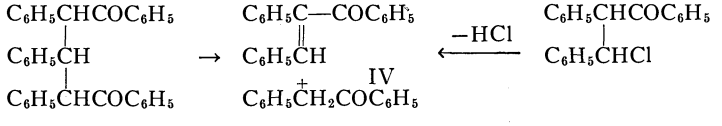

III IV V

[1]*Contribution No. 2293 from the Kodak Research Laboratories, Eastman Kodak Co., Rochester 50, New York, and the Department of Chemistry, Rochester Institute of Technology, Rochester 8, New York.*

As indicated in Table I, mass spectra obtained by thermal decomposition of these compounds in the heated spectrometer inlet showed spectral patterns of the same products that were reported in the earlier work (3, 4). A related adduct, β-chlorobenzyldesoxybenzoin (V) (5), yielded products identified by mass spectrometer as benzaldesoxybenzoin

TABLE I

Thermal decomposition products identified by mass spectrometer and masses of parent ions, helpful in establishing identification

Substances	Products
I	(208) Chalcone; (120) acetophenone
II	(208) Chalcone; (120) acetophenone
III	(284) Benzaldesoxybenzoin; (small 196) desoxybenzoin
V	(284) Benzaldesoxybenzoin; (180) stilbene
VI	(286) Benzhydrylacetophenone;* (208) chalcone
VIII (Ar = C_6H_5, n = 2)	(292) UM;† (208) chalcone; (168) benzalcyclopentanone;* (120) acetophenone; (84) cyclopentanone
VIII*a* (Ar = C_6H_5, n = 3)	(306) UM; (208) chalcone; (182) benzalcyclohexanone;* (120) acetophenone; (98) cyclohexanone
IX (X, Y = H)	(238) Methyl α-phenylcinnamate; (208) chalcone; (150) methyl phenylacetate; (120) acetophenone
IX*a* (X = CH_3O, Y = H)	(338) UM;† (238) methyl α-phenylcinnamate; 4′-methoxychalcone; (150) 4-methoxyacetophenone
IX*b* (X = CH_3O, Y = NO_2)	(238) 4′-Methoxychalcone; (208) chalcone; (195) methyl 4-nitrophenylacetate; (150) 4-methoxyacetophenone
X	(340) UM; (220) dimethyl benzalmalonate XII; (208) chalcone; (120) acetophenone
XI	(352) UM; (220) dimethyl benzalmalonate XII; (132) dimethyl malonate
XIII	(220) XII; (132) dimethyl malonate
XV	(336) UM; (262, 216) unidentified
XVI	(293) UM; (v. small 205) α-phenylcinnamonitrile; (135) not identified; (v.v. small 117) benzyl cyanide
XVII	(265) UM; (205 and 117 as in XVI); (104) unidentified
XVIII	(192) UM; (174) lactone XIX
XX*a*	(236) Lactone XXI; (208) chalcone
XX*b*	(278) Lactone XXI type; (250) 2′,4′,6′-trimethylchalcone
XXII	(220, 202) Acid and lactone corresponding to XX, XXI; (174) mesityl vinyl ketone
2-Acetoxybenzonitrile	(161) UM; (119) 2-hydroxybenzonitrile
XXIII	(312) Triphenylcrotonolactone XXIV; (284) β-phenylchalcone; (120) acetophenone
XXV*a*	(296) Triphenylfuran
XXV*b*	(375) 3-Bromo-2,4,5-triphenylfuran
XXIV	(312) UM; (284) β-phenylchalcone
XXVI	(284) β-Phenylchalcone; (182) benzophenone; (120) acetophenone
XXVII	(253, 238, 208) The three corresponding chalcones

*Reference compound not available.
†UM = undecomposed molecule.

(IV) and stilbene; the former is also obtained chemically by removing the elements of hydrogen chloride using alcoholic potassium acetate. Although stilbene has not been found in a chemical experiment, there is little doubt concerning its identification as a major product in the mass spectrometer inlet, where conditions are apparently more favorable for its production. While some stilbene might possibly be formed as a result of electron bombardment, at least a major part of it must have been formed thermally. In a subsequent study using an all-glass heated inlet, parent peaks at m/e 320 and 322 of V were present. During the 1-hour observation, their decay rate was noticeably different from that of the stilbene peaks, indicating that stilbene is present in the thermal reaction mixture.

Can. J. Chem. Downloaded from www.nrcresearchpress.com by 210.87.254.105 on 09/05/12
For personal use only.

More recently discovered members of the first series are 1,1,3-triphenyl-2,4-dibenzoylbutane (VI) (6) and an isomer of I, 1,3-dibenzoyl-1-phenylpropane (VII) (7). Products identified from the mass spectrum indicate that VI dissociates as shown here. The diketone VII, however,

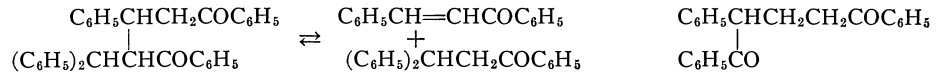

showed no appreciable thermal dissociation and the volatility of the substance was insufficient to yield a mass spectrum.

In his study of "semicyclic diketones" (VIII), Stobbe (8) observed that two of them distilled "partially decomposed" in two ways; in one (normal, see Part I (1)), the components were regenerated, but the other (abnormal) gave acetophenone and an arylideneketone. This was the first observed instance of an abnormal dissociation. In the present mass-spectrometric study of two members of the series (8, 9), the products which were identified indicated dissociation by both paths.

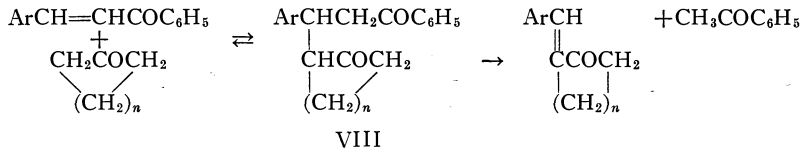

On distilling adducts from aliphatic aldehydes, Meerwein (10, 11) found that the components were regenerated (normal) except in two instances, which gave products from abnormal-type retrogression. These adducts were unavailable for mass spectral examination.

Esters

Michael adducts that are ketoesters (IX, IX*a*, IX*b* (12), X (13)) are much more thermally stable than cyanoketones (1). Mass peaks corresponding to the undecomposed molecule, as well as confirmed identification of products of both kinds of retrogression are found (Table I). It is concluded, as previously (1), from the very low intensity of the mass spectrum that the presence of a methoxy group in the para position of the chalcone residue greatly diminishes the tendency to dissociation (IX*a*, *b*).

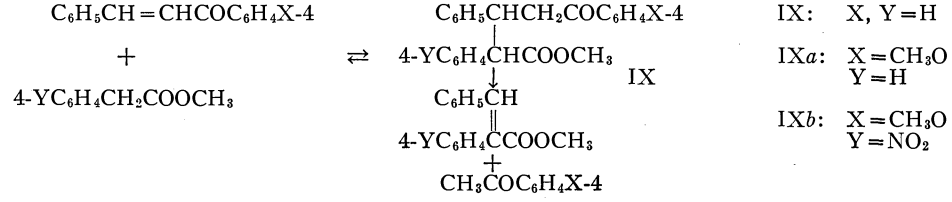

Polyesters such as methyl α,γ-dicarbomethoxy-β-phenylglutarate (XI) gave a mass spectrum showing the presence of the undecomposed molecule, plus dimethyl benzalmalonate (XII) and dimethyl malonate.

Can. J. Chem. Downloaded from www.nrcresearchpress.com by 210.87.254.105 on 09/05/12
For personal use only.

Its α-bromo derivative (XIII) also gave predominantly the ester (XII). It is noteworthy that there was no evidence for the formation of a lactone (XIV) through loss of methyl bromide, a type of reaction that is so easily brought about in the laboratory (12).

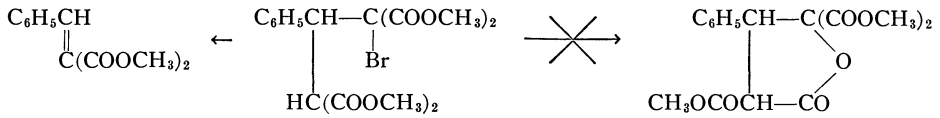

XII XIII XIV

Michael's ester adduct (XV) (14) is stated to distill with decomposition at atmospheric pressure; we have found that the loss is a very small carbonaceous residue. In the heated inlet of the mass spectrometer, this ester is very stable; it showed neither type of retrogression.

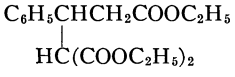

XV

Cyanoester and Acid

In contrast to cyanoketones, ethyl γ-cyano-β,γ-diphenylbutyrate (XVI) (15) appears to be considerably more stable to heat, for the temperature has to be raised to 345° before appreciable dissociation is achieved. In a previously heated sample, examined by gas chromatography, we found 11% of benzyl cyanide, 8.6% of ethyl cinnamate (both products of normal dissociation), 12% of α-phenylcinnamonitrile (the abnormal cleavage product), and 42% of unchanged ester. In the mass spectrometer (inlet heated at 230°) only a slight reversal would be expected. In agreement there were small spectral peaks representing undecomposed molecule and the possible retrogression products, both normal and abnormal; these were too small to establish a confirmation although the patterns were reasonably consistent with those of benzyl cyanide and α-phenylcinnamonitrile. A large peak at mass 135 was not identified; it was *not* phenylacetamide, with which a direct comparison was made.

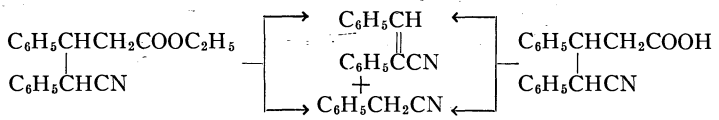

XVI XVII

When a sample of the corresponding acid (XVII) (16) was heated at 300° for 20 minutes, a trace of benzyl cyanide, but no styrene, was detected by gas chromatography. In the mass spectrometer, however, α-phenylcinnamonitrile and benzyl cyanide were indicated, with an unidentified peak at 104, which might have been from styrene, the known decarboxylation product of cinnamic acid. There was also some indication of undecomposed acid.

Ketonic Acids

Gamma and delta ketonic acids are known to be readily dehydrated to unsaturated lactones by classical methods; this type of reaction would compete with any retrogression. The only delta ketonic acid (XVIII) examined in the mass spectrometer was very stable, being comparable to γ-benzoylbutyronitrile (1); the formation of a lactone (XIX) was indicated.

Can. J. Chem. Downloaded from www.nrcresearchpress.com by 210.87.254.105 on 09/05/12
For personal use only.

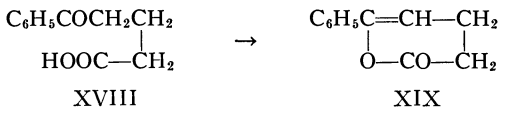

XVIII XIX

Gamma ketonic acids (XX) can be considered as Michael adducts formed by the addition of formic acid to α,β-unsaturated ketones. They can give only a normal retrogression to chalcones; this behavior, which cannot be readily realized by classical methods, was observed in the mass spectrometer. The expected formic acid undoubtedly decomposed to carbon dioxide and hydrogen. However, these acids can also cyclize by a loss of water to give the unsaturated crotonolactones (XXI), which were identified from the mass spectra; this reaction has also been demonstrated in the laboratory (17, 18).

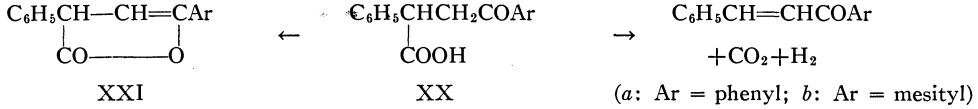

XXI XX (a: Ar = phenyl; b: Ar = mesityl)

The closely related (β-acetoxy-β-mesitylvinyl) acetic acid (XXII) (18) gave a mass spectrum indicating the presence of β-mesitoylpropionic acid plus the corresponding lactone and mesityl vinyl ketone. The keto acid could result from the enol formed by a cleavage in the

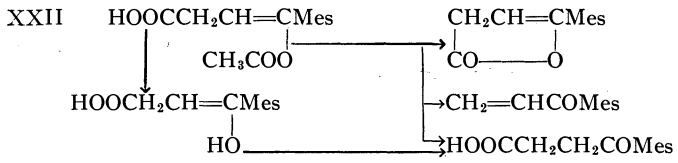

acetate, with elimination of ketene. This behavior is supported by that of 2-acetoxybenzonitrile, which, we have found, gives 2-hydroxybenzonitrile under the same conditions.

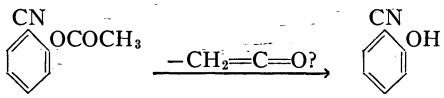

The formation of the chalcone from the γ-ketonic acids (XX) was postulated earlier as being due to the elimination of formic acid. It could equally well result from a decarbonylation of the unsaturated crotonolactone (XXI). That unsaturated lactones can be decarbonylated to α,β-unsaturated ketones was shown many years ago by Japp (19) in his study of the unsaturated 1,4-diketone, α,β-dibenzoylstyrene (XXIII). The latter was first isomerized to 1,1,3-triphenylcrotonolactone (XXIV) which was then decarbonylated (19) to β-phenylchalcone.

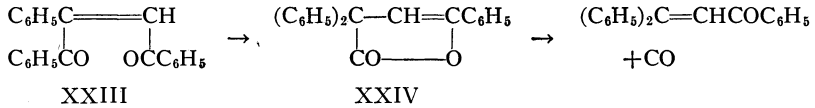

XXIII XXIV

These reactions were confirmed in the mass spectrometer, although the carbon monoxide was not identified.

Can. J. Chem. Downloaded from www.nrcresearchpress.com by 210.87.254.105 on 09/05/12
For personal use only.

In contrast, saturated 1,4-diketones, which have only a formal similarity to Michael adducts, give mass peaks that indicate they are dehydrated to furans in the mass spectrometer inlet just as they are by classical methods.

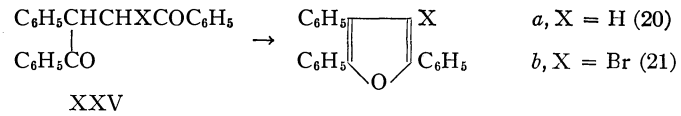

a, X = H (20)
b, X = Br (21)

Related Compounds

Finally, two other series that have a formal similarity to the foregoing will be considered briefly. The first (XXVI) is the chalcone-type adduct, phenacylodiphenylcarbinol, which may be regarded as having been formed by the addition of water. In the mass spectrometer heated inlet, it dissociated by both possible paths. The same cleavages are brought about by laboratory reagents (22).

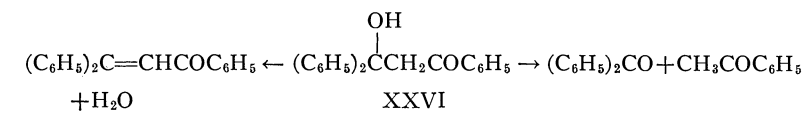

The loss of water corresponds to the normal retrogression shown by Michael adducts, whereas the alternate scission follows the abnormal path.

Finally, three Michael-type adducts (XXVII) (23), formed from β-morpholinoethylethanethiol and three chalcones, showed only normal dissociation as expected; the nonvolatile amine hydrochloride was not detected.

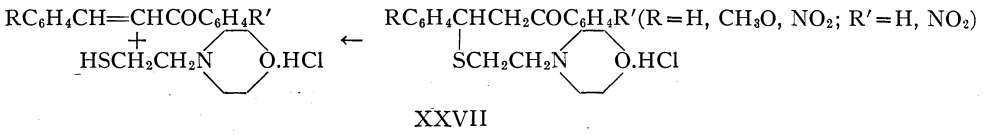

EXPERIMENTAL

The substances examined were available from previous work or were prepared by procedures already in the literature. The β-chlorobenzyldesoxybenzoin (V) was made by J. R. Byers, Jr. The acetoxybenzonitrile and salicylonitrile were readily obtained by published procedures (24). The crotonolactone (XXIV) was readily prepared in quantity by heating dibenzoylstyrene (19) but its subsequent conversion to the β-phenylchalcone was not very satisfactory; most of the lactone was recovered unchanged. This chalcone was obtained more easily by dehydration of the carbinol (XXVI) (22). In our hands, the yields of the acid (XVII) and of crystalline ester (XVI) were low, a large amount of a thick oil that had not crystallized in months being obtained.

Thermolyses.—When the ester (XVI) was heated in a Pyrex glass flask containing a "silver-solder catalyst," (1) there was no change until 300°, at which point a little volatile liquid condensed on the walls of the flask. No distillate appeared up to 345°; after 40 minutes, the now brown liquid was submitted to gas chromatography. In addition to the main components already mentioned, there were indications of a dozen others in very small amounts. The acid (XVII) was similarly heated at 300° for 20 minutes; it became brown. The residual solid, after recrystallization from acetic acid, melted at 226–227°. On treatment with alcoholic sodium hydroxide, followed by acid, a white solid, melting above 400°, was obtained. Since these were apparently not cleavage products they were not further investigated.

Gas Chromatography.—The samples were chromatographed on an 8-ft column of standard 6 mm O.D. glass containing 25%, by weight, of Dow Corning 200 silicone fluid on Celite (80–100 mesh) which had been previously washed with alcoholic potash and concentrated hydrochloric acid. The column was thermostated with boiling 1,2,4-trichlorobenzene (b.p. 218–219°). The detector was a Gow-Mac thermal conductivity cell, pretzel design, Model No. 9285. The carrier gas was helium at a flow rate of 50 ml per minute. The retention times were benzyl cyanide, 2.5 minutes; ethyl cinnamate, 8.9 minutes; α-phenylcinnamonitrile, 46.3 minutes; and the ester (XVI) approximately 103 minutes.

Can. J. Chem. Downloaded from www.nrcresearchpress.com by 210.87.254.105 on 09/05/12
For personal use only.

Mass Spectrometry.—The mass spectrometer and its operation have already been described (1). The peaks found in the mass spectra and their identification, by comparison of the entire pattern with known reference compounds, are summarized in Table I. Unless otherwise indicated, identifications were based upon comparisons of the complete spectral patterns with those of authentic reference compounds.

ACKNOWLEDGMENTS

We are pleased to have had the assistance of Dr. O. E. Schupp for the gas chromatography; of Miss Thelma J. Davis for the infrared spectrometry; of Mr. D. Maier for operation of the mass spectrometer; and of Dr. D. W. Stewart for many helpful suggestions.

REFERENCES

1. C. F. H. Allen and G. P. Happ. Can. J. Chem. In press.
2. C. F. H. Allen and G. P. Happ. Can. J. Chem. In press.
3. S. Kostanecki and G. Rossbach. Ber. **29**, 1488 (1896).
4. E. Knoevenagel and R. Weissgerber. Ber. **26**, 441 (1893).
5. A. Klages and E. Knoevenagel. Ber. **26**, 447 (1893).
6. E. P. Kohler and W. D. Peterson. J. Am. Chem. Soc. **55**, 1073 (1933).
7. C. F. H. Allen and W. E. Barker. J. Am. Chem. Soc. **54**, 736 (1932).
8. H. Stobbe. J. Prakt. Chem. **86**, 209 (especially pp. 214, 265) (1912).
9. C. F. H. Allen and H. R. Sallans. Can. J. Res. **9**, 574 (1933).
10. H. Meerwein. J. Prakt. Chem. **97**, 225 (1918).
11. H. Meerwein. Ber. **53**, 1829 (1920).
12. C. F. H. Allen, E. E. Massey, and R. V. V. Nicholls. J. Am. Chem. Soc. **59**, 679 (1937).
13. E. P. Kohler and J. B. Conant. J. Am. Chem. Soc. **39**, 1404 (1917).
14. A. Michael. Am. Chem. J. **9**, 112 (1887).
15. E. Erlenmeyer, Jr. Ber. **33**, 2006 (1900).
16. S. Avery and G. R. McDale. J. Am. Chem. Soc. **30**, 595 (1908).
17. R. Anschutz and W. F. Montfort. Ann. **284**, 1 (1895).
18. C. F. H. Allen, J. B. Normington, and C. V. Wilson. Can. J. Res. **11**, 382 (1934).
19. F. R. Japp and F. Klingemann. J. Chem. Soc. **57**, 662 (1890).
20. A. Smith. J. Chem. Soc. **57**, 649 (1890).
21. C. F. H. Allen and E. F. Herrmann. J. Am. Chem. Soc. **51**, 3591 (1929).
22. D. Vorländer, J. Osterburg, and O. Meye. Ber. **56B**, 1136 (1923).
23. W. J. Humphlett. Unpublished work.
24. V. Meyer. Ber. **26**, 1254 (1893).

Can. J. Chem. Downloaded from www.nrcresearchpress.com by 210.87.254.105 on 09/05/12
For personal use only.

Can. J. Chem. Downloaded from www.nrcresearchpress.com by 210.87.254.105 on 09/05/12
For personal use only.

THE STABILITY OF THIOCOMPLEXES AND SOLUBILITY PRODUCTS OF METAL SULPHIDES

I. CADMIUM SULPHIDE

J. STE-MARIE, A. E. TORMA, AND A. O. GÜBELI
Department of Chemistry, Laval University, Quebec, Quebec

Received October 8, 1963

Abstract

The nature and stability of cadmium sulphide complexes in aqueous solutions have been investigated. The total concentration of the metal in solution was determined at constant temperature and ionic strength, and at various pH values, by a radioactive tracer technique.

Introduction

This work is part of a programme of study on the formation of complexes. A first paper (1) dealt with silver sulphide.

From the modern theory of complex compounds we know that many insoluble metal compounds may be formed through coordination of the metal ion with various ligands. These coordinate bonds are similar to those of mono- and poly-nuclear complexes in solution. Thus, a solution in equilibrium with a precipitate usually contains a number of complex ions besides the simple metal ions (2–5).

EXPERIMENTAL PART

The classical solubility product is a physicochemical constant, independent of the complex formation. Accordingly its value does not necessarily indicate the true solubility of a solid.

The values given in the literature for the second dissociation constant of H_2S differ considerably among themselves (6). Therefore we have decided to redetermine the constants k_1 and k_2 at ionic strength $\mu = 1.0$ and 25° C by means of pH titrations and potentiometric determinations of pAg vs. pH (Fig. 1).

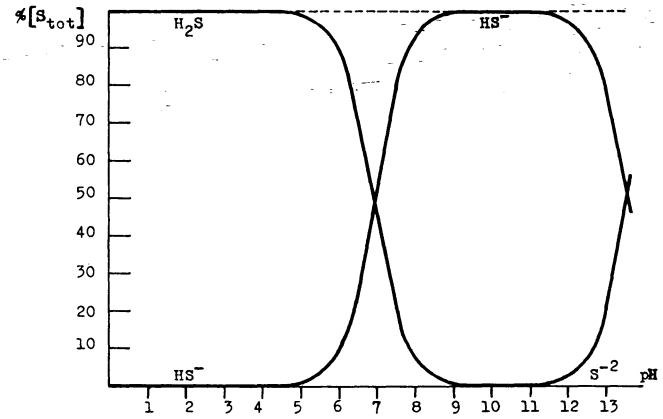

FIG. 1. Dissociated forms of H_2S.

$$[H_2S] \rightleftarrows [HS^-] + [H^+] \qquad pk_1 = 6.90 \pm 0.03 \qquad [1]$$

$$[HS^-] \rightleftarrows [S^{-2}] + [H^+] \qquad pk_2 = 13.48 \pm 0.16 \qquad [2]$$

The total concentration of metal in aqueous solution, $[M]_{tot}$, in presence of an excess of sulphide ion may

only be measured by means of a radioactive tracer. These measurements were carried out at constant temperature and ionic strength $\mu = 1.0$ with sodium perchlorate. Buffers were chosen to avoid complex formation with the metal ion. All reagents, even distilled water, were prepared in absence of oxygen. A scintillation detector was used for radioactive determinations.

The following reagents were added to pure oxygen-free water to obtain the desired concentrations of cadmium (7): $CdSO_4$, 0.01 M (added tracer Cd^{115}); $NaClO_4$, up to ionic strength $\mu = 1.0$; Na_2S, 0.021 M; HCl, 0.04 M (decomposing the excess of Na_2S); buffer solutions 0.001–0.1 M (pH 1 to 2, $HClO_4$; pH 3 to 6, acetic acid + sodium acetate; pH 7 to 8, imidazole; pH 8 to 9, triethanolamine; pH 9 to 10.5, monoethanolamine; pH 10 to 12, piperidine; pH 12 to 14, NaOH).

THEORETICAL PART

From the experimental results it appears that the following diagram gives the best description of the formation of complexes.

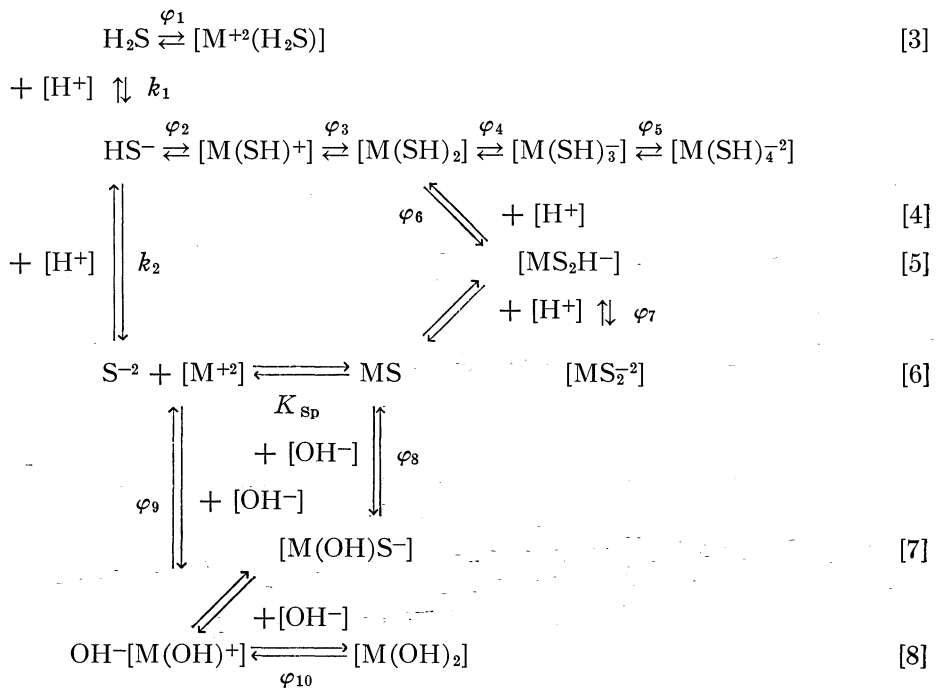

The values of φ, to be determined from the experimental curve, represent the following equilibria:

$$\frac{[M^{+2}(H_2S)]}{[M^{+2}][H^+]^2[S^{-2}]} = \varphi_1 \quad [9] \qquad \frac{[M(SH)^+]}{[M^{+2}][H^+][S^{-2}]} = \varphi_2 \quad [10]$$

$$\frac{[M(SH)_2]}{[M^{+2}][H^+]^2[S^{-2}]^2} = \varphi_3 \quad [11] \qquad \frac{[M(SH)_3^-]}{[M^{+2}][H^+]^3[S^{-2}]^3} = \varphi_4 \quad [12]$$

$$\frac{[M(SH)_4]}{[M^{+2}][H^+]^4[S^{-2}]^4} = \varphi_5 \quad [13] \qquad \frac{[MS_2H^-]}{[M^{+2}][H^+][S^{-2}]^2} = \varphi_6 \quad [14]$$

$$\frac{[MS_2^{-2}]}{[M^{+2}][S^{-2}]^2} = \varphi_7 \quad [15] \qquad \frac{[M(OH)S]}{[M^{+2}][OH^-][S^{-2}]} = \varphi_8 \quad [16]$$

$$\frac{[M(OH)^+]}{[M^{+2}][OH^-]} = \varphi_9 \quad [17] \qquad \frac{[M(OH)_2]}{[M^{+2}][OH^-]^2} = \varphi_{10} \quad [18]$$

Can. J. Chem. Downloaded from www.nrcresearchpress.com by 210.87.254.105 on 09/05/12
For personal use only.

From experimental determinations the following constants are known:

$$\frac{[H^+][HS^-]}{[H_2S]} = k_1, \qquad \frac{[H^+][S^{-2}]}{[HS^-]} = k_2, \tag{19}$$

$$[H^+][OH^-] = K_w, \text{ and } [M^{+2}][S^{-2}] = K_{sp}. \tag{20}$$

The $[S]_{tot}$ may be expressed by the following equation, when the sulphur, complexed with the small amounts of Cd in solution, is neglected:

$$[H_2S] + [HS^-] + [S^{-2}] = [S]_{tot} \tag{21}$$

and

$$[S^{-2}] = \frac{k_1k_2[S]_{tot}}{[H^+]^2 + k_1[H^+] + k_1k_2}. \tag{22}$$

$[S^{-2}]$ is a function of pH; as a function of $[S^{-2}]$, $[M^{+2}]$ is the same:

$$[M^{+2}] = \frac{K_{sp}}{[S]_{tot}}\left[\frac{[H^{+2}]}{k_1k_2} + \frac{[H^+]}{k_2} + 1\right] \tag{23}$$

We know that

$$[M^{+2}] + [M^{+2}(H_2S)] + [M(SH)^+] + [M(SH)_2] + [M(SH)_3^-] + [M(SH_4^{-2}] + [MS_2H^+] + [MS_2^{-2}] + [M(OH)S^-] + [M(OH)^+] + [M(OH)_2] = [M]_{tot} \tag{24}$$

and

$$[M^{+2}](1 + \varphi_1[H^+]^2[S^{-2}] + \varphi_2[H^+][S^{-2}] + \varphi_3[H^+]^2[S^{-2}]^2 + \varphi_4[H^+]^3[S^{-2}]^3 + \varphi_5[H^+]^4[S^{-2}]^4 + \varphi_6[H^+][S^{-2}]^2 + \varphi_7[S^{-2}]^2 + \varphi_8[OH^-][S^{-2}] + \varphi_9[OH^-] + \varphi_{10}[OH^-]^2) = [M]_{tot}. \tag{25}$$

Replacing

$$[M^{+2}] = \frac{K_{sp}}{[S^{-2}]} \text{ and } [OH^-] = \frac{K_w}{[H^+]}$$

we get

$$\frac{K_{sp}}{[S^{-2}]}\left(1 + \frac{\varphi_9K_w}{[H^+]} + \frac{\varphi_{10}K_w^2}{[H^+]^2} + [S^{-2}]\left[\varphi_1[H^+]^2 + \varphi_2[H^+] + \frac{\varphi_8K_w}{[H^+]}\right] + [S^{-2}]^2\left[\varphi_3[H^+]^2 + \varphi_6[H^+] + \varphi_7\right] + [S^{-2}]^3\left[\varphi_4[H^+]^3\right] + [S^{-2}]^4\left[\varphi_5[H^+]^4\right]\right) = [M]_{tot}. \tag{26}$$

In terms of pH the final equation becomes:

$$\frac{K_{sp}}{[S]_{tot}k_1k_2}\left[1 + \frac{K_w\varphi_9}{[H^+]} + \frac{K_w^2\varphi_{10}}{[H^+]^2}\right]\left[[H^+]^2 + k_1[H^+] + k_1k_2\right] + K_{sp}\left[\varphi_1[H^+]^2 + \varphi_2[H^+] + \frac{K_w\varphi_8}{[H^+]}\right] + K_{sp}[S]_{tot}k_1k_2\left[\frac{\varphi_3[H^+]^2 + \varphi_6[H^+] + \varphi_9}{[H^+]^2 + k_1[H^+] + k_1k_2}\right] + K_{sp}[S]_{tot}^2k_1^2k_2^2\left[\frac{\varphi_4[H^+]^3}{([H^+]^2 + k_1[H^+] + k_1k_2)^2}\right] + K_{sp}[S]_{tot}^3k_1^3k_2^3\left[\frac{\varphi_5[H^+]^4}{([H^+]^2 + k_1[H^+] + k_1k_2)^3}\right] = [M]_{tot}. \tag{27}$$

This takes into account all possible complexes in a fairly complex bivalent metal – sulphide system with a coordination number of four.

Can. J. Chem. Downloaded from www.nrcresearchpress.com by 210.87.254.105 on 09/05/12
For personal use only.

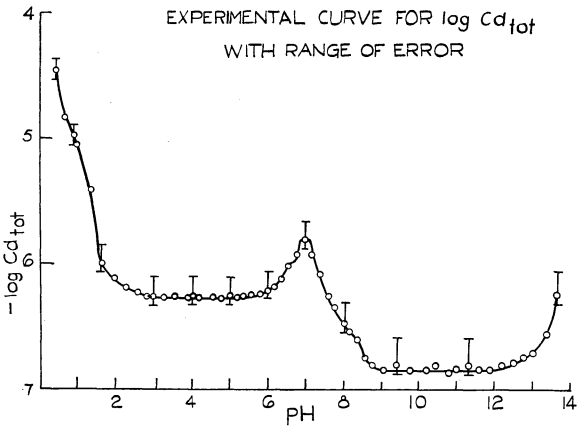

FIG. 2. Experimental curve for log Cd_{tot} with range of error.

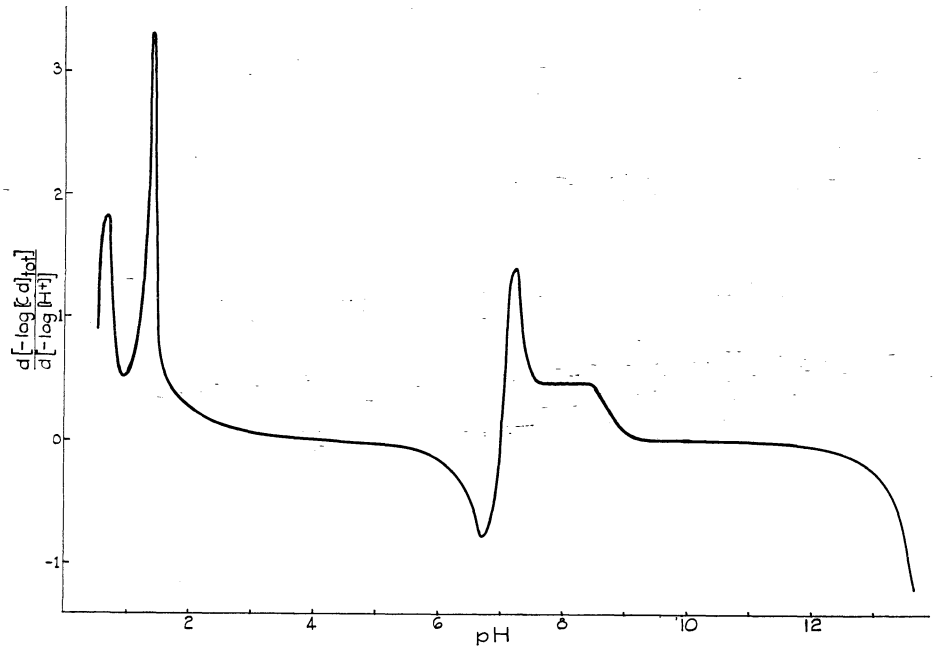

FIG. 3.

The experimental curve obtained from radioactivity measurements in equilibrated sulphide filtrates in presence of a known excess of sulphide ion is plotted vs. pH, i.e. $-\log [M]_{tot}$ vs. pH, and the experimental errors are calculated for each point of the curve (Fig. 2).

The first derivative of the experimental curve (Fig. 3) is used in the following treatment:

$$\frac{d(-\log [M]_{tot})}{d\text{pH}}.$$

Can. J. Chem. Downloaded from www.nrcresearchpress.com by 210.87.254.105 on 09/05/12
For personal use only.

Mathematically:

$$\frac{d(-\log [M]_{tot})}{d(-\log [H^+])} = \frac{-d[M]_{tot}}{[M]_{tot}} \frac{-[H^+]}{d[H^+]} = \frac{[H^+]}{[M]_{tot}} \frac{d[M]_{tot}}{d[H^+]}$$

giving

$$\frac{d[M]_{tot}}{d[H^+]} = \frac{[M]_{tot}}{[H^+]} \frac{d(-\log [M]_{tot})}{d(-\log [H^+])}. \qquad [28]$$

The second term in equation [28] is known from experimental results (Figs. 2 and 3). The first term of this equation is also the first derivative of equation [27] vs. pH.

$$\frac{d(-\log [M]_{tot})[M]_{tot}}{d(-\log [H^+])[H^+]} = \frac{d[M]_{tot}}{d[H^+]} = \frac{K_{sp}}{d[H^+]} d\Bigg[[S^{-2}]^{-1}\left(1 + \frac{\varphi_9 K_w}{[H^+]} + \frac{\varphi_{10} K_w^2}{[H^+]^2}\right)$$
$$+ \varphi_1[H^+]^2 + \varphi_2[H^+] + \frac{\varphi_8 K_w}{[H^+]} + [S^{-2}](\varphi_3[H^+]^2 + \varphi_6[H^+] + \varphi_7)$$
$$+ [S^{-2}]^2(\varphi_4[H^+]^3) + [S^{-2}]^3(\varphi_5[H^+]^4)\Bigg]. \qquad [29]$$

Equation [29] may be written as a function of φ_1 to φ_{10} with the coefficients f_0 to f_{10} as a function of pH.

$$\frac{d(-\log [M]_{tot}}{d(-\log [H^+])K_{sp}} \frac{[M]_{tot}}{[H^+]}$$
$$= f_0 + f_1\varphi_1 + f_2\varphi_2 + f_3\varphi_3 + f_5\varphi_5 + f_6\varphi_6 + f_7\varphi_7 + f_8\varphi_8 + f_9\varphi_9 + f_{10}\varphi_{10}. \qquad [30]$$

The values of f are as follows.

$$f_0 = \frac{2[H^+] + k_1}{k_1k_2[S]_{tot}} \qquad f_1 = 2[H^+] \qquad f_2 = 1$$

$$f_3 = \frac{([H^+] + 2k_2)k_1[H^+][S^{-2}]}{[H^+]^2 + k_1[H^+] + k_1k_2}$$

$$f_4 = \frac{(3k_1k_2 + k_1[H^+] - [H^+]^2)[H^+]^2[S^{-2}]^2}{[H^+]^2 + k_1[H^+] + k_1k_2}$$

$$f_5 = \frac{(4k_1k_2 + k_1[H^+] - 2[H^+]^2)[H^+]^3[S^{-2}]^3}{[H^+]^2 + k_1[H^+] + k_1k_2}$$

$$f_6 = \frac{-([H^+]^2 - k_1k_2)[S^{-2}]}{[H^+]^2 + k_1[H^+] + k_1k_2} \qquad f_7 = \frac{-(2[H^+] + k_1)[S^{-2}]}{[H^+]^2 + k_1[H^+] + k_1k_2}$$

$$f_8 = -\frac{K_w}{[H^+]^2} \qquad f_9 = \frac{([H^+]^2 - k_1k_2)K_w}{k_1k_2[S]_{tot}[H^+]^2} \qquad f_{10} = \frac{(2k_2 + [H^+])K_w^2}{k_1k_2[S]_{tot}[H^+]^3} \qquad [31]$$

Fitting ten experimental values of the pH into equation [30] and solving gives zero, or vanishing values for the constants φ_1, φ_6, φ_7, φ_8, and φ_{10}, which correspond to the following complexes: $[Cd(H_2S)^{+2}]$, $[CdHS_2^-]$, $[CdS_2^{-2}]$, $[Cd(OH)S^-]$, and $[Cd(OH)_2]$. For the other constants we get the following values:

$$\varphi_2 = 10^{21.03},\ \varphi_3 = 10^{41.57},\ \varphi_4 = 10^{56.93},\ \varphi_5 = 10^{72.77},\ \varphi_9 = 10^{17.76}. \qquad [32]$$

By adding one more equation the solubility product may be calculated:

$$K_{sp} = [Cd^{+2}][S^{-2}] = 10^{-25.76}. \qquad [33]$$

Can. J. Chem. Downloaded from www.nrcresearchpress.com by 210.87.254.105 on 09/05/12
For personal use only.

The thermodynamic constant given by Rossini (8) is $10^{-26.16}$. We used our experimental result for K_{sp} to calculate the constants for complex formation. The value of K_W in 1.0 N $NaClO_4$ was determined to be $10^{-14.0}$.

The constants for complex formation are as follows.

$$\frac{[Cd(HS)^+]}{[Cd^{+2}][HS^-]} = k_2\varphi_2 = K_1 = 10^{7.55\pm0.16} \quad [34]$$

$$\frac{[Cd(HS)_2]}{[Cd(HS)^+][HS^-]} = \frac{k_2\varphi_3}{\varphi_2} = K_2 = 10^{7.06\pm0.16} \quad [35]$$

$$\frac{[Cd(HS)_3^-]}{[Cd(HS)_2][HS^-]} = k_2\frac{\varphi_4}{\varphi_3} = K_3 = 10^{1.88\pm0.2} \quad [36]$$

$$\frac{[Cd(HS)_4^{-2}]}{[Cd(HS)_3^-][HS^-]} = k_2\frac{\varphi_5}{\varphi_4} = K_4 = 10^{2.36\pm0.2} \quad [37]$$

$$\frac{[Cd(OH)^+]}{[Cd^{+2}][OH^-]} = \varphi_9 = K_5 = 10^{17.76\pm0.16} \quad [38]$$

DISCUSSION OF RESULTS

As mentioned above, the solubility product of cadmium sulphide does not give an idea of the actual solubility, particularly in presence of an excess of sulphide.

Depending on pH, with the same concentration of $[S]_{tot}$, $\mu = 1.0$ and at constant temperature, we find the data shown in Fig. 4.

In strongly acidic media (pH 0.5 to 1.0) Cd^{+2} is predominant and no formation of $[Cd(H_2S)^{+2}]$ is noted. In this region the solubility product may be calculated by taking into account the formation of Cd^{+2} and $[Cd(HS)^+]$ complexes.

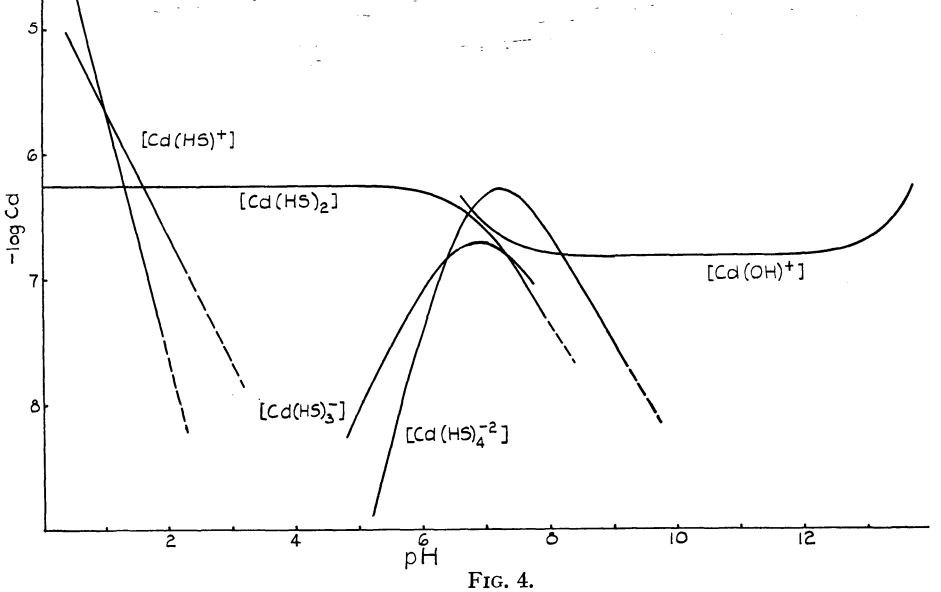

FIG. 4.

Can. J. Chem. Downloaded from www.nrcresearchpress.com by 210.87.254.105 on 09/05/12
For personal use only.

In acidic media (pH 1.0 to 3.0) $[Cd(HS)^+]$ is formed and is very stable, but as the concentration of HS^- increases rapidly other complexes become more important.

$[Cd(HS)_2]$ is also very stable and exists over a large pH range (pH 0 to 8.0). This complex is unaffected by pH. Equation [11] corresponds to the formation of $[Cd(HS)_2]$. With equation [20] and the modified form for this pH region of equation [22]:

$$[S^{-2}] = \frac{k_1 k_2 [S]_{tot}}{[H^+]^2}$$

we replace in equation [11] the factors of $[Cd^{+2}]$ and $[S^{-2}]$. We obtain $[Cd(HS)_2] = \varphi_3[Cd^{+2}][H^+]^2[S^{-2}]^2 = \varphi_3 K_{Sp}[H^+]^2[S^{-2}] = \varphi_3 K_{Sp}[S]_{tot} k_1 k_2$, which are constants.

The maximum solubility of cadmium sulphide is found at pH 6.89 where SH^- is present in the highest possible concentration. Now two complexes $[Cd(SH)_3^-]$ and $[Cd(SH)_4^{-2}]$ suddenly appear between pH 5.5 and 9.5.

These two complexes are not very stable and the first one may even be regarded as only an intermediate form. Other possible forms of thiocomplexes of cadmium do not exist.

In alkaline media only the hydroxy complex $[Cd(OH)^+]$ is present; its stability is high.

There are no data to be found in the literature on the stability of these thiocomplexes of cadmium.

ACKNOWLEDGMENT

The authors wish to express their sincere thanks to the National Research Council of Canada and to the Swiss National Foundation for generous grants.

REFERENCES

1. H. Züst. Ph.D. Thesis No. 2762, Swiss Federal Institute of Technology, Zurich, Switzerland; G. Schwarzenbach, O. Gübeli, und H. Züst. Chimia, **12**, 84 (1958).
2. I. Bjerrum. Ph. D. Thesis, Copenhagen, Denmark. 1941.
3. I. Leden. Svensk Kem. Tidskr. **64**, 249 (1952); Naturforsch. **8a**, 719 (1953); Acta Chem. Scand. **10**, 540 (1956).
4. I. C. Sullivan and I. C. Hindman. J. Am. Chem. Soc. **74**, 6091 (1952).
5. F. I. C. Rosotti and H. S. Rosotti. Acta Chem. Scand. **9**, 1166 (1955).
6. O. Konopik and O. Leberl. Monatsh. **80**, 781 (1949).
7. A. E. Torma. M. Sc. Thesis, Laval University, Quebec, Quebec. 1962.
8. F. D. Rossini. Natl. Bur. Std. (U.S.), Circ. No. 500. 1950.

Can. J. Chem. Downloaded from www.nrcresearchpress.com by 210.87.254.105 on 09/05/12
For personal use only.

RADIATION CHEMISTRY OF CYCLOHEXANE

VI. DILUTE SOLUTIONS OF CARBON TETRACHLORIDE AND CHLOROFORM IN CYCLOHEXANE[1]

J. A. STONE AND P. J. DYNE

Research Chemistry Branch, Atomic Energy of Canada Limited, Chalk River, Ontario

Received September 3, 1963

Can. J. Chem. Downloaded from www.nrcresearchpress.com by 210.87.254.6 on 09/05/12
For personal use only.

ABSTRACT

A study of the effect of the addition of small amounts (<3.5%) of the halogenated compounds CCl_4, $CHCl_3$, and $CDCl_3$ on the radiolysis of cyclohexane has shown that processes other than radical scavenging occur. At the lowest concentrations of solute that it was practical to employ (0.004 *M*) cyclohexyl radicals were scavenged without a corresponding reduction in the hydrogen yield. At higher solute concentrations $G(H_2)$ was reduced by a physical process which did not involve the scavenging of thermal hydrogen atoms but did lead to chemical reaction involving the solute.

INTRODUCTION

The addition of small amounts of solutes to saturated hydrocarbons can cause a spectacular decrease in the yields of radiolysis products derived solely from the hydrocarbon. Explanations for this have been offered in terms of the known physical or chemical properties of the solutes. Hardwick (1) has interpreted the effect of many organic solutes on the hydrogen yields in terms of hydrogen atom scavenging. Holroyd (2), using ethylene as solute, has observed products which are formed by the addition of free radicals to the olefinic double bond. On the other hand, Hamill (3) has suggested that electron attachment to the solute may play an important part in changing the yields of products derived from the hydrocarbon. Our own work (4) with dilute solutions of benzene in cyclohexane led us to the conclusion that the major interaction was non-chemical and that, in this case, a physical interaction such as electron attachment or energy transfer, was occurring.

An identification of the interaction mechanism is only possible through a complete product analysis (and only then in favorable cases). In this study, carbon tetrachloride and chloroform were chosen as solutes in the hope that, since they are not hydrocarbons, all products derived from them could be readily separated and identified. Since these solutes do not contain π-bonds, product analysis would not be complicated by polymer formation. The use of isotopically substituted chloroform, $CDCl_3$, enabled us to measure the extent of hydrogen abstraction from chloroform.

We find that the yields of the liquid products derived solely from the hydrocarbon are reduced as a result of free radical reactions involving both solute and solvent. The yield of hydrogen, however, is reduced by another mechanism which involves a physical interaction between the solute and a precursor of molecular hydrogen (an excited molecule or an electron). This mechanism, which does not involve the scavenging of thermal hydrogen atoms, produces other free radicals which take part in subsequent reactions leading to liquid products.

EXPERIMENTAL

Materials

Cyclohexane (Fisher Spectranalyzed), carbon tetrachloride (Fisher Reagent Grade), chloroform (Fisher Spectranalyzed), and deuterated chloroform (Merck) were used as received. The non-deuterated chloroform

[1]*Issued as A.E.C.L. No. 1891.*

was found to contain about 0.2% carbon tetrachloride. This amount was shown to have negligible effect on the product yields since addition of comparable amounts of carbon tetrachloride did not alter these yields in any of the mixtures in which chloroform was the solute. The deuterated chloroform contained about 0.01% carbon tetrachloride and, again, further addition caused no appreciable difference in product yields.

Preparation and Irradiation of Samples

The degassed 20 ml samples were prepared as described previously (5). Solutions were made up in bulk and pipetted out as required. Two Co^{60} irradiation facilities were used with dose rates of 1.40×10^{19} ev/liter minute and 3.94×10^{20} ev/liter minute in cyclohexane as determined by the Fricke dosimeter. The samples were irradiated at 22° C to a total dose of 4.7×10^{22} ev/liter unless otherwise stated.

Product Analysis

Mass spectrometry showed that over 99% of the gas non-condensible at −196° C was hydrogen. Other gases in this fraction were therefore neither identified nor measured. Hydrogen isotopic analyses were performed on a C.E.C. 21–610 mass spectrometer.

Hydrogen chloride was estimated by measuring photometrically the chloride ion produced (6). Twenty-milliliter samples were irradiated under vacuum in specially designed cells which were then opened under a measured volume of doubly distilled water. Mercuric thiocyanate was added. The chloride ion displaced the thiocyanate ion, which subsequently reacted with added ferric perchlorate. The absorption of the colored complex formed was measured photometrically at 460 mμ. None of the reactants or major products of radiolysis of the various solutions used was found to produce chloride ions by hydrolysis and it was therefore assumed that all these ions came from hydrogen chloride.

All liquid products were analyzed by a combination of gas–liquid chromatography and mass spectrometry. Quantitative analysis was by gas–liquid chromatography. The columns used were as follows: for cyclohexene, a 1/4 in. by 16 ft 20% 123 tris(2-cyanoethoxy) propane column at 55° C; for bicyclohexyl, hexachloroethane, cyclohexyl chloride, trichloromethylcyclohexane, and dichloromethylcyclohexane, a 1/4 in. by 12 ft, 0.1% Apiezon-L grease on glass beads column at 100° C; for chloroform and carbon tetrachloride, a 1/4 in. by 8 ft, 20% Carbowax 6000 column at 60° C. Standard solutions of the products were interspersed with the unknowns for calibration purposes. No pure samples of the chlorinated methylcyclohexanes were available and the comparable chlorinated toluenes were therefore used as standards. This is justified since the sensitivity of the Beckman hydrogen flame detector used is practically the same for benzene and cyclohexane.

Product identification was by mass spectral analysis of the individual products trapped from the chromatographic effluent.

RESULTS

(a) Cyclohexane/Carbon Tetrachloride Mixtures

The principal products obtained in the radiolysis of pure cyclohexane are hydrogen, cyclohexene, and bicyclohexyl (5). These products are also formed in mixtures of cyclohexane and carbon tetrachloride but in yields which decrease with increasing solute contration as shown in Fig. 1. Since carbon tetrachloride reacted extremely rapidly during radiolysis, [$G(-CCl_4) \sim 30$], the yields of products at carbon tetrachloride concentrations less than 0.05 M were obtained by extrapolating to zero dose the results obtained at doses from 2×10^{21} to 1×10^{22} ev/liter. Above 0.05 M solute concentration, this extrapolation was unnecessary and the values shown are for doses of 4.7×10^{22} ev/liter.

Also shown in Fig. 1 is the variation of the yield of hexachloroethane with carbon tetrachloride concentration. This product also disappeared extremely rapidly during radiolysis and all the points shown were obtained by extrapolation to zero dose. Even so, the points for the lower solute concentrations involved long extrapolations and so represent minimum values only.

Figure 2 shows the yields of chloroform and cyclohexyl chloride together with the G value for the disappearance of carbon tetrachloride, all as a function of solute concentration. Once again the values at the lower solute concentrations were obtained by extrapolation to zero dose. Above 0.1 M carbon tetrachloride, the measurements of $G(-CCl_4)$ involved small differences in chromatographic peak heights and so the accuracy becomes less with increasing concentration.

The yield of the only other major liquid product, trichloromethylcyclohexane, was,

Can. J. Chem. Downloaded from www.nrcresearchpress.com by 210.87.254.6 on 09/05/12
For personal use only.

Can. J. Chem. Downloaded from www.nrcresearchpress.com by 210.87.254.6 on 09/05/12
For personal use only.

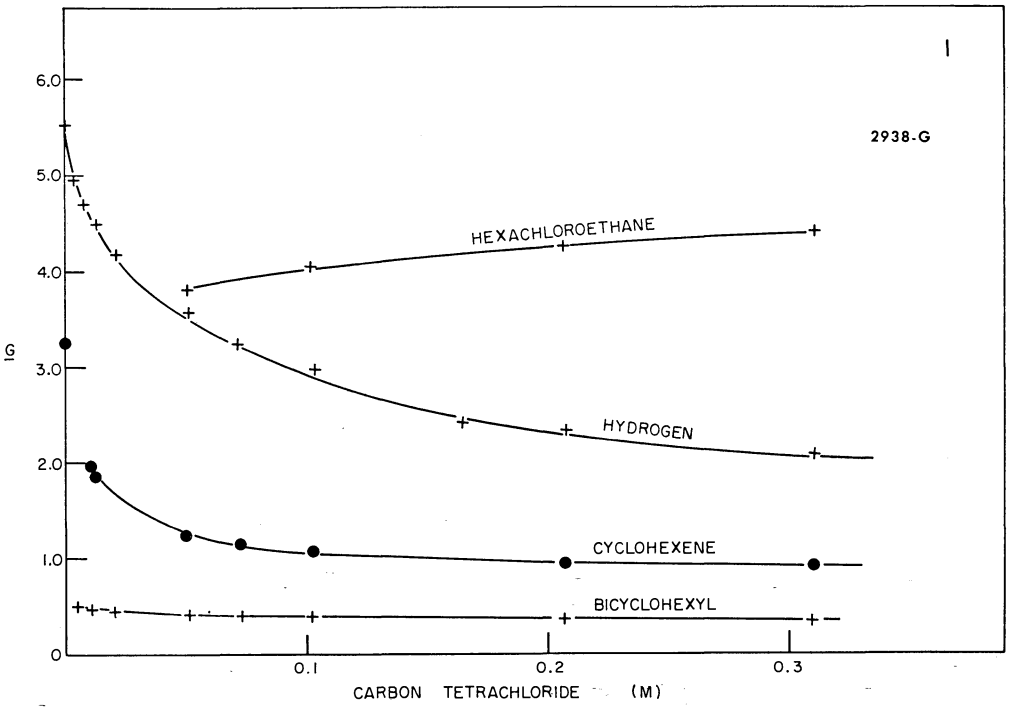

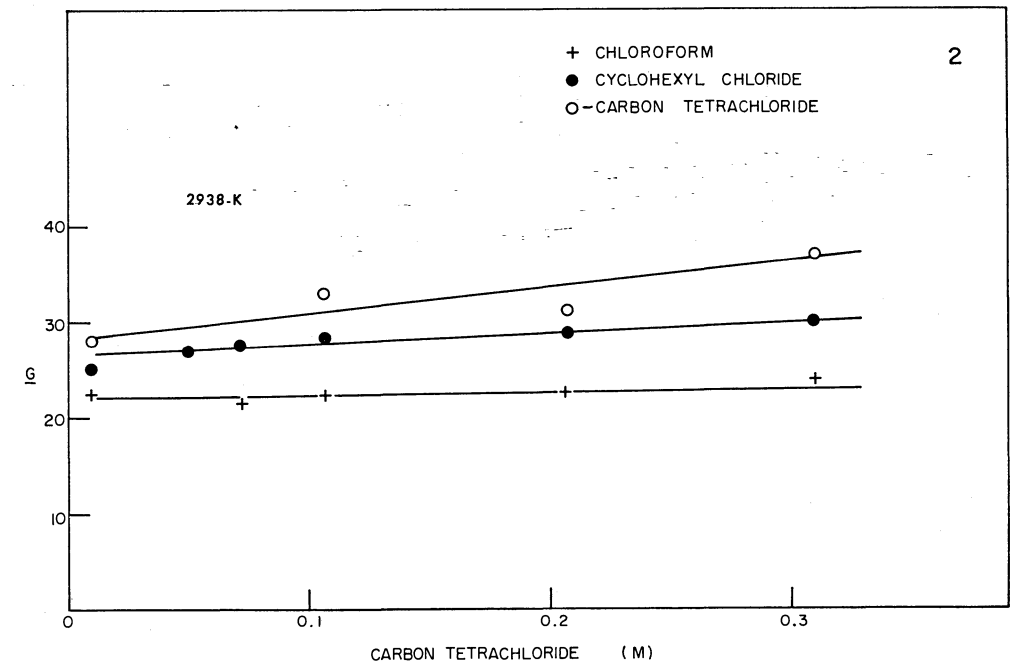

FIG. 1. G(hydrogen), G(cyclohexene), G(bicyclohexyl), and G(hexachloroethane) in C_6H_{12}/CCl_4 mixtures.
FIG. 2. G(cyclohexyl chloride), G(chloroform), and G(carbon tetrachloride) in C_6H_{12}/CCl_4 mixtures.

within experimental error, unchanged ($G = 0.65 \pm 0.03$) over the solute concentration range studied.

The yield of hydrogen chloride is shown in Fig. 3. There was no measurable variation in the yield with dose. While most of the carbon tetrachloride which reacts forms chloroform, this product also yields hydrogen chloride during radiolysis.

The yields of all products, with the exception of chloroform and cyclohexyl chloride, were invariant with dose rate. At 0.01 *M* carbon tetrachloride, *G*(chloroform) and *G*(cyclohexyl chloride) increased from values of around 23 at 3.94×10^{20} ev/liter minute to values of around 105 at 1.40×10^{19} ev/liter minute.

Cyclohexane/Chloroform Mixtures

Solutions of chloroform and deuterochloroform in cyclohexane were studied. At 0.01 *M* solute concentration, no variation of product yields with dose up to 4.7×10^{22} ev/liter was observed. Figure 4 shows that the decrease in $G(H_2)$ with increasing solute concentration is the same, within experimental error, for both solutes. For comparison, $G(H_2)$ in C_6H_{12}/CCl_4 solutions is shown. $G(H_2)$ decreases at the same rate for all three solutes up to about 0.04 *M*. Above this concentration, carbon tetrachloride is the most efficient in reducing the yield. In Figure 3, *G*(HCl) at different $CHCl_3$ concentrations is compared with *G*(HCl) at different CCl_4 concentrations. Up to 0.04 *M*, the values of *G*(HCl) are analogous to those for $G(H_2)$ in that, within experimental error, the yields are the same for both solutes. Above 0.04 *M*, the yield of HCl is greater with CCl_4 as solute. Deuterium chloride was not determined for the $C_6H_{12}/CDCl_3$ system but results similar to those for the $C_6H_{12}/CHCl_3$ system would be expected.

The variations in the yields of liquid products derived solely from cyclohexane are shown in Figs. 5 (cyclohexene) and 6 (bicyclohexyl) for both chloroform and deuterochloroform solutions and for carbon tetrachloride solutions. The yields of the chlorinated cyclohexanes (cyclohexyl chloride, dichloromethylcyclohexane, and trichloromethylcyclohexane) for the $C_6H_{12}/CHCl_3$ mixtures are shown in Fig. 7 whilst those for the corresponding compounds with $CDCl_3$ as solute are shown in Fig. 8. Trichloromethylcyclohexane was observed in such low yield ($G < 0.05$) in the latter system that its variation with solute concentration could not be determined with any accuracy. Monodeuteromethylene chloride ($CHDCl_2$) was identified and its yield was measured in the C_6H_{12}–$CDCl_3$ systems. Unfortunately, CH_2Cl_2 was not measured in the C_6H_{12}–$CHCl_3$ system.

DISCUSSION

In a previous paper (5) we showed that the yield of hydrogen in the radiolysis of pure cyclohexane is equivalent to the yields of liquid products, mainly cyclohexene and bicyclohexyl, which are formed from cyclohexane by loss of hydrogen. While, in the cases so far studied, solutes which reduce the hydrogen yield also reduce the yield of liquid products, it is not clearly established, if at all, whether these yield reductions are equivalent (4, 7).

In this discussion, we will show that at the lowest concentrations of the solutes, the total yield of liquid products is reduced to a much greater extent than the hydrogen yield. Further we will show that, while the products bicyclohexyl and cyclohexene may have, in part, a common precursor, there is a fraction of the cyclohexene yield which has another precursor. We will show that the large reduction in liquid product yields at low solute concentration is consistent with the scavenging of cyclohexyl radicals but that the reduction in hydrogen yield observed at higher concentrations is not explained by hydrogen

Can. J. Chem. Downloaded from www.nrcresearchpress.com by 210.87.254.6 on 09/05/12
For personal use only.

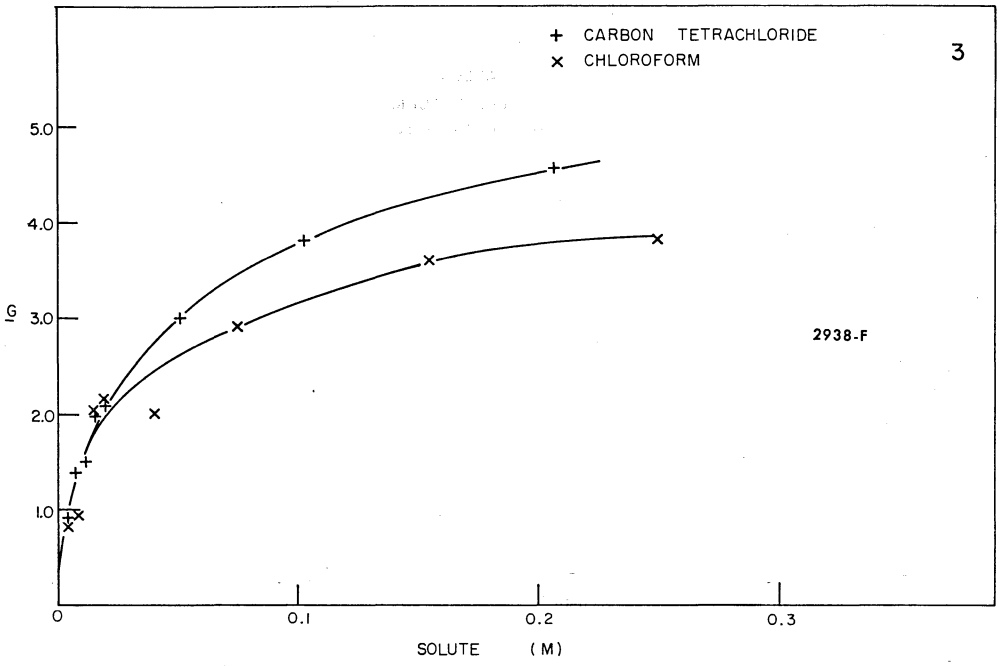

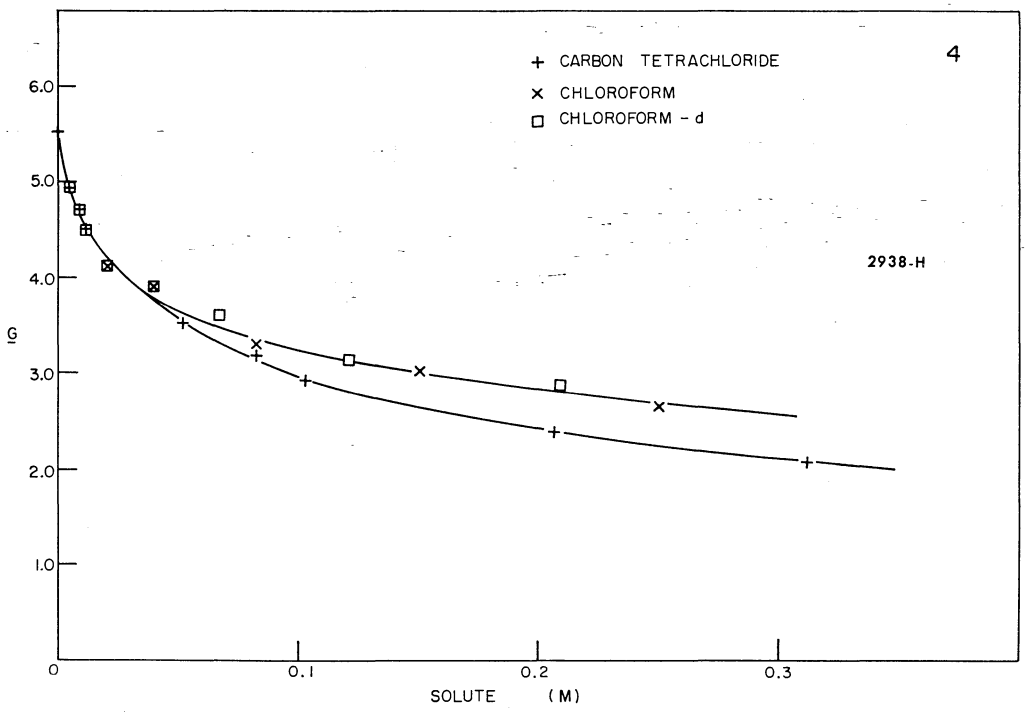

FIG. 3. G(hydrogen chloride) in C_6H_{12}/CCl_4 and $C_6H_{12}/CHCl_3$ mixtures.
FIG. 4. G(hydrogen) in C_6H_{12}/CCl_4, $C_6H_{12}/CHCl_3$, and $C_6H_{12}/CDCl_3$ mixtures.

Can. J. Chem. Downloaded from www.nrcresearchpress.com by 210.87.254.6 on 09/05/12
For personal use only.

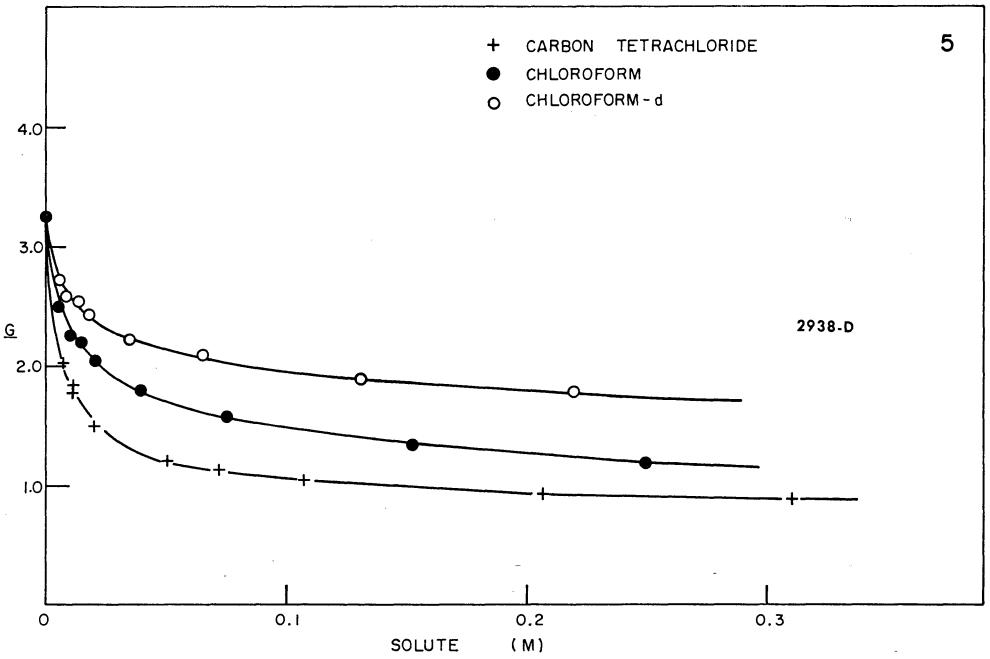

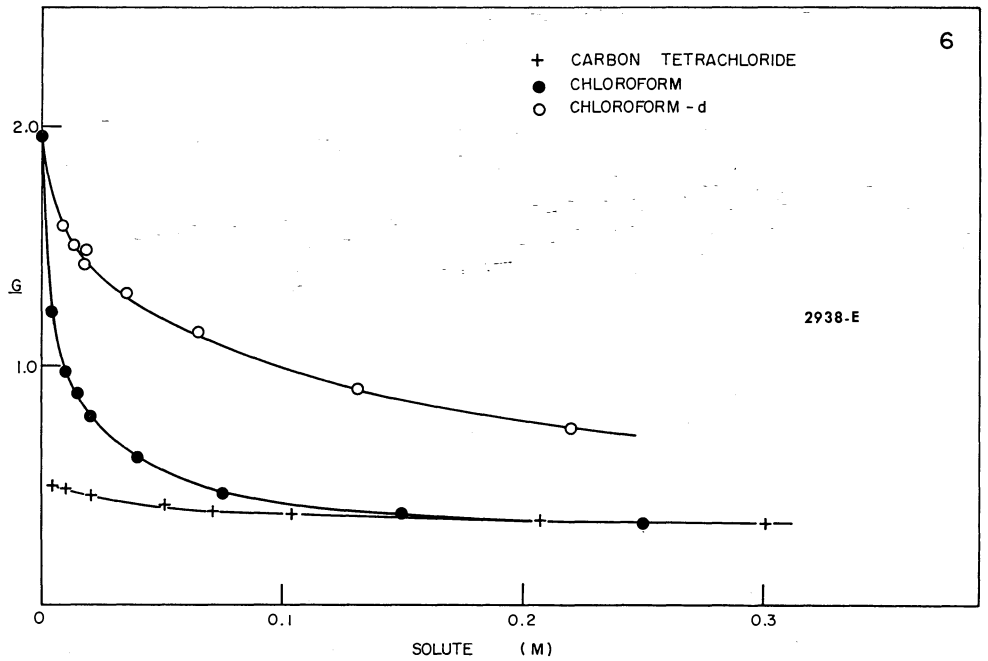

FIG. 5. G(cyclohexene) in C_6H_{12}/CCl_4, $C_6H_{12}/CHCl_3$, and $C_6H_{12}/CDCl_3$ mixtures.
FIG. 6. G(bicyclohexyl) in C_6H_{12}/CCl_4, $C_6H_{12}/CHCl_3$, and $C_6H_{12}/CDCl_3$ mixtures.

Can. J. Chem. Downloaded from www.nrcresearchpress.com by 210.87.254.6 on 09/05/12
For personal use only.

Can. J. Chem. Downloaded from www.nrcresearchpress.com by 210.87.254.6 on 09/05/12
For personal use only.

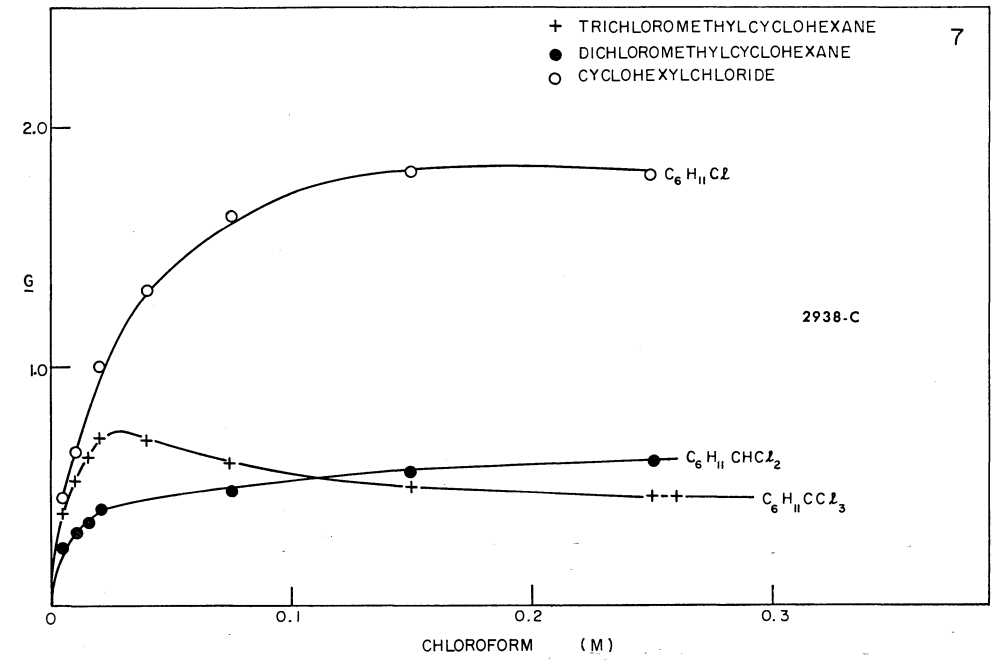

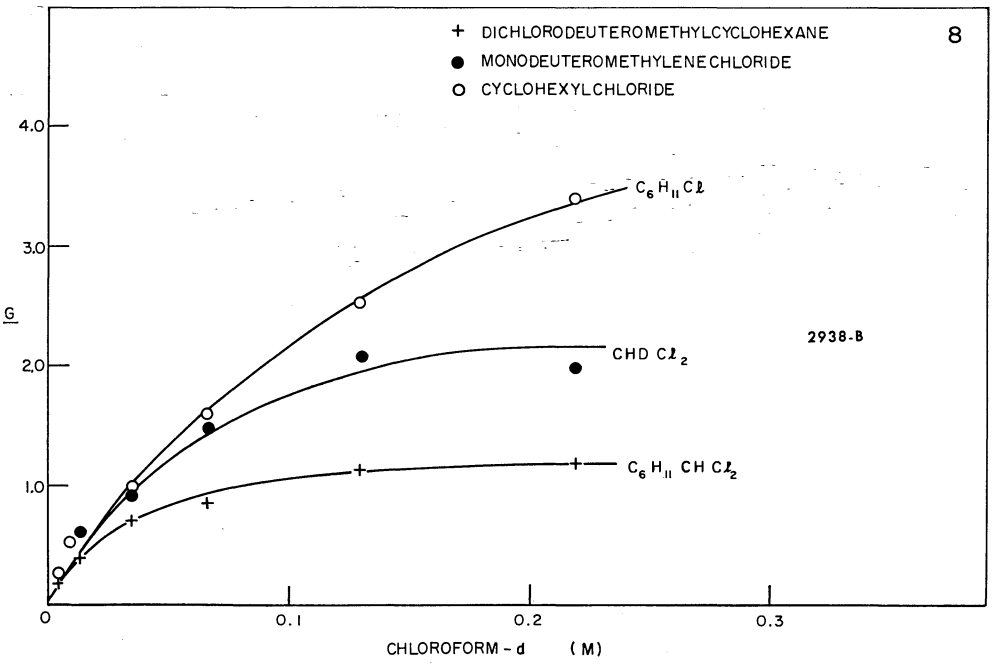

FIG. 7. Yields of chlorinated cyclohexanes in $C_6H_{12}/CHCl_3$ mixtures.
FIG. 8. Yields of chlorinated cyclohexanes and methylene chloride in $C_6H_{12}/CDCl_3$ mixtures.

atom scavenging. The decrease in hydrogen yield is consistent with one or more types of physical interaction (e.g. energy transfer or electron capture) between the solvent and the solute.

We have divided this section into two parts: (*a*) a discussion of the liquid products from the irradiation of pure cyclohexane, their mechanism of formation, and the mode of interaction of their precursors with added solute; (*b*) the hydrogen yield, its variation with added solute, and the evidence we have obtained against the scavenging of thermalized hydrogen atoms by the solutes used.

(a) Liquid Products

(i) Cyclohexane/Carbon Tetrachloride

The high G values for the products cyclohexyl chloride and chloroform show that a chain reaction is occurring. A non-branching, radical chain reaction leading to the same major products has been initiated in the C_6H_{12}/CCl_4 system by the thermal decomposition of *n*-heptanoyl peroxide (8). The propagation steps of the radical chain were

$$\cdot CCl_3 + C_6H_{12} \rightarrow CHCl_3 + \cdot C_6H_{11}, \quad [1]$$

$$\cdot C_6H_{11} + CCl_4 \rightarrow C_6H_{11}Cl + \cdot CCl_3. \quad [2]$$

Chain termination was mainly by dimerization of trichloromethyl radicals to give hexachloroethane

$$\cdot CCl_3 + \cdot CCl_3 \rightarrow C_2Cl_6. \quad [3]$$

The similarity of these results to those for the radiolysis leads to the conclusion that the radiolytic products, chloroform, cyclohexyl chloride, and hexachloroethane are formed by the same reaction sequence.

Other chain termination products are possible besides hexachloroethane (equations 4, 5, and 6).

$$\cdot C_6H_{11} + \cdot C_6H_{11} \rightarrow (C_6H_{11})_2, \quad [4]$$

$$\cdot C_6H_{11} + \cdot C_6H_{11} \rightarrow C_6H_{10} + C_6H_{12}, \quad [5]$$

$$\cdot C_6H_{11} + \cdot CCl_3 \rightarrow C_6H_{11} \cdot CCl_3. \quad [6]$$

All these products are found. However, as Hardwick [9] has suggested, some or all of the yields of bicyclohexyl and cyclohexene at high concentrations of solute might be due to the reactions of radicals formed together in the same solvent cage.*

The experiments performed at the lower dose rate show that while the chain termination is not a function of dose rate, the chain length is. This is characteristic of a non-branching chain with termination by dimerization of radicals. The number of radicals involved in the termination stage (or stages) must therefore be equal to the number of initiating radicals. Unfortunately, the yield of hexachloroethane could not be measured accurately at the lowest CCl_4 concentrations and so a summation of radicals is not possible in this region.

From several pieces of evidence, it is clear that at the lowest solute concentration the initiating species must be the cyclohexyl radical, (*a*) the yields of bicyclohexyl and cyclohexene are decreased considerably even at the lowest concentrations while the yield of hydrogen is still close to its initial value (e.g. at 0.01 M CCl_4, $\Delta G(H_2) = 0.55$ whereas ΔG(bicyclohexyl) = 1.45 and ΔG(cyclohexene) = 1.30). At this solute concentration G(hexachloroethane) > 3.0. The decrease in hydrogen yield is far too small to account

**Ion–molecule reactions, as described by Williams (10) and Kevan and Libby (11), are other possible explanations for the residual yields. No solute has so far been described which, in reasonably low concentration, will reduce the yields of bicyclohexyl and cyclohexene to zero. In every case, some limiting yield is reached at ~0.3 M solute concentration when further addition of solute has negligible effect. In the present case, we have no means of distinguishing between products formed in a cage reaction and those formed as a result of chain termination.*

Can. J. Chem. Downloaded from www.nrcresearchpress.com by 210.87.254.6 on 09/05/12
For personal use only.

Can. J. Chem. Downloaded from www.nrcresearchpress.com by 210.87.254.6 on 09/05/12
For personal use only.

for the total number of radical groups in the termination products. (*b*) the yields of all possible chain termination products (with the exception of cyclohexene at the lower CCl_4 concentrations) show only small variations with solute concentration. The chain propagation products, cyclohexyl chloride and chloroform show a similar behavior and have high yields even at the lowest solute concentration employed.

Since all (>95%) the cyclohexyl radicals are scavenged at the lowest CCl_4 concentration an important conclusion can be drawn from Fig. 1. It is not until ~0.07 *M* CCl_4 that the yield of cyclohexene attains its limiting value. Part of the yield (~1 *G* unit) of cyclohexene which can be inhibited by CCl_4 cannot therefore arise from the disproportionation of cyclohexyl radicals.

If cyclohexyl radicals do disproportionate to give cyclohexene and cyclohexane, then the yield of cyclohexene is composed of three parts.

(i) That due to the disproportionation of radicals (~1.3 *G* units)

(ii) The yield of ~1 *G* unit mentioned above. This could arise from the unimolecular decomposition of some form of excited cyclohexane molecule (12).

(iii) The yield that cannot be inhibited by added solute (~0.9 *G* units).

If, however, there is no contribution to cyclohexene formation by mechanism (i) only two processes are present, the reduction in *G*(cyclohexene) to its limiting value being due to the inhibition of process (ii).

(ii) Cyclohexane/Chloroform

From Figs. 5 and 6 it is seen that (*a*) CCl_4 is much more efficient in reducing the yields of liquid products than either $CHCl_3$ or $CDCl_3$, (*b*) $CHCl_3$ is more efficient than $CDCl_3$, and (*c*) no observable chain reaction occurs in either chloroform system. But, Fig. 4 shows that up to 0.04 *M*, all three solutes reduce $G(H_2)$ to the same extent while at higher concentrations, CCl_4 is more efficient, $CHCl_3$ and $CDCl_3$ having the same efficiency. In all cases, however, the decrease in yield of liquid products is greater than the decrease in hydrogen yield. The mechanism by which the liquid products are reduced in yield cannot therefore be directly related to or correlated with the mechanism by which the hydrogen yield is reduced.

In the $C_6H_{12}/CHCl_3$ system, *G*(bicyclohexyl) does not reach its limiting value until ~0.15 *M* $CHCl_3$. In the case of $C_6H_{12}/CDCl_3$, this limiting value is not attained at the maximum solute concentration employed (0.22 *M*). Neither $CHCl_3$ nor $CDCl_3$ is therefore as efficient a radical scavenger as CCl_4. This is in agreement with chain transfer constants derived from polymerization studies in $CHCl_3$ and CCl_4 as solvents (13). Chain transfer with CCl_4 is at least an order of magnitude greater than for transfer with $CHCl_3$.

Evidence that chloroform is acting in part as a radical scavenger is provided by the relative product distributions. Free radicals preferentially attack the C—H bond in $CHCl_3$. However, with $CDCl_3$, C—D bond cleavage is reduced by a factor of 10 or more and a significant increase in C—Cl bond cleavage occurs (14). Figures 7 and 8 show that more $C_6H_{11}Cl$ is produced in $C_6H_{12}/CDCl_3$ than in $C_6H_{12}/CHCl_3$ even though the decreases in bicyclohexyl yields suggest the reverse. Scavenging by $CHCl_3$ will produce cyclohexane as well as cyclohexyl chloride.*

**Reaction [7] is the reverse of reaction [1] and so these reactions should more accurately be written as an equilibrium*

$$\cdot C_6H_{11} + CHCl_3 \overset{7}{\rightleftharpoons} C_6H_{12} + \cdot CCl_3$$

Although $\cdot CCl_3$ radicals (which take part in the chain reaction in the C_6H_{12}/CCl_4 system) are produced they do not in this system lead to an observable chain since reaction [1] simply regenerates chloroform and a cyclohexyl radical. This equilibrium decreases the net probability of reaction [7] and therefore facilitates the competing reaction [8].

$$\cdot C_6H_{11} + CHCl_3 \rightarrow C_6H_{12} + \cdot CCl_3, \quad [7]$$

$$\rightarrow C_6H_{11}Cl + \cdot CHCl_2. \quad [8]$$

With $CDCl_3$ little $C_6H_{11}D$ will be produced and the main reaction will be

$$\cdot C_6H_{11} + CDCl_3 \rightarrow C_6H_{11}Cl + \cdot CDCl_2. \quad [9]$$

Reference to other products show this to be the case. In the $C_6H_{12}/CHCl_3$ system we also obtain $C_6H_{11}CCl_3$ and $C_6H_{11}CHCl_2$, presumably by radical–radical additions:

$$\cdot C_6H_{11} + \cdot CCl_3 \rightarrow C_6H_{11}CCl_3, \quad [10]$$

$$\cdot C_6H_{11} + \cdot CHCl_2 \rightarrow C_6H_{11}CHCl_2. \quad [11]$$

In the $C_6H_{12}/CDCl_3$ system, $G(C_6H_{11}CCl_3)$ was immeasurably small. A radical–radical reaction would produce the large yields of $C_6H_{11}CDCl_2$

$$\cdot C_6H_{11} + \cdot CDCl_2 \rightarrow C_6H_{11}CDCl_2. \quad [12]$$

$CHDCl_2$ would be produced by hydrogen abstraction from C_6H_{12}:

$$\cdot CDCl_2 + C_6H_{12} \rightarrow CHDCl_2 + \cdot C_6H_{11}. \quad [13]$$

The yields of cyclohexene and bicyclohexyl in the $C_6H_{12}/CHCl_3$ system confirm once again that part of the inhibitable yield of cyclohexene cannot have the same precursors, namely cyclohexyl radicals, as bicyclohexyl. From Figs. 5 and 6, it is seen that although G(bicyclohexyl) attains its limiting value at $\sim$0.07 M $CHCl_3$, G(cyclohexene) is still above the limiting value found in the C_6H_{12}/CCl_4 system.

The Increased Radical Yield in C_6H_{12}/CCl_4 Mixtures

In a previous paper (4), we showed that the number of molecules of cyclohexane which react to form products is greater in pure cyclohexane than in cyclohexane containing small amounts of benzene. We interpreted this in terms of a physical interaction between the benzene and some form of excited cyclohexane, the benzene dissipating the energy gained in this process without decomposition. When carbon tetrachloride is used as solute, the converse is the case, more chemical reaction occurring than in pure cyclohexane. This excess of chemical reaction is shown by comparing the number of radicals found in chain termination products ($C_6H_{11}CCl_3$ and C_2Cl_6) to the number missing as calculated from the decrease in the yields of liquid products formed from cyclohexane alone. This summation of radicals (which is possible only at high solute concentrations) is shown in Table I. Each product molecule has been equated to two radicals. Some cyclohexene may, however, be formed by a first order process.

$$C_6H_{12} \rightarrow C_6H_{10} + H_2. \quad [14]$$

The quenching of this reaction by carbon tetrachloride could, however, lead to radical formation.

The yield of hydrogen chloride also demonstrates that, far from acting as a non-sacrificial protector, carbon tetrachloride enhances radiolytic reaction. It is customary to

TABLE I

The yields of "excess" radicals and hydrogen chloride in C_6H_{12}/CCl_4 mixtures

CCl_4, M	$2[\Delta G$(cyclohexene) $+ \Delta G$(bicyclohexyl) $+ \Delta G$(cyclohexyl-hexene-1)]	$2[G(C_2Cl_6) + G(C_6H_{11}CCl_3)]$	G (excess radicals)	G (excess HCl)
0.1	8.20±0.3	9.30±0.5	1.10	1.20
0.2	8.46±0.3	9.70±0.5	1.24	1.32
0.3	8.58±0.3	9.98±0.5	1.40	1.40

Can. J. Chem. Downloaded from www.nrcresearchpress.com by 210.87.254.6 on 09/05/12
For personal use only.

associate a 1:1 correlation between ΔG(hydrogen) and the G value for the reaction of an inhibitor, i.e. for every molecule of cyclohexane which is "protected", or every hydrogen atom which is scavenged, one molecule of solute is directly involved. If the solute is designated S then for H atom scavenging $\Delta G(H_2) = G(HS)$, or, if S takes part in an energy transfer process, $\Delta G(H_2) = G(S^*)$. We find that at low concentrations of $CHCl_3$ and CCl_4, hydrogen chloride (which could be formed by hydrogen atom scavenging or by some form of energy transfer) is not equivalent to $\Delta G(H_2)$ but is much greater. Figure 9

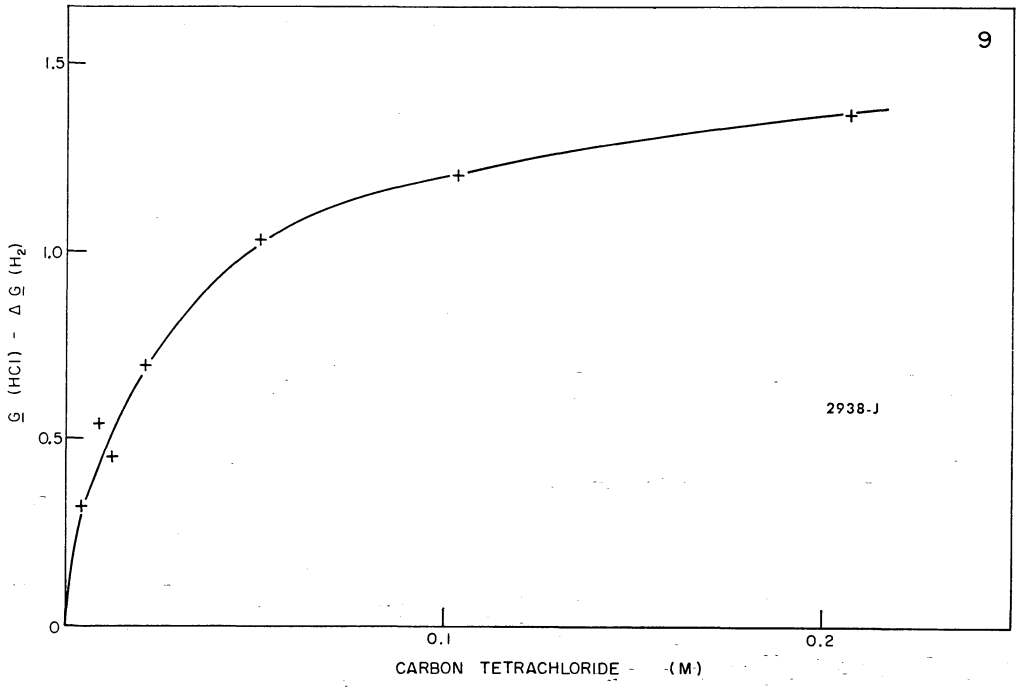

FIG. 9. The yield of hydrogen chloride that is in excess of that accounted for by the decrease in the yield of hydrogen (C_6H_{12}/CCl_4 mixtures).

shows that most of this excess HCl is produced at low solute concentration. The excess HCl formed at the highest solute concentrations is compared with G(excess radicals) in Table I.

The excess radicals are equivalent to the excess HCl. A sensitized decomposition must be occurring. Oster and Kallman (15) have suggested that a similar increase in radical production on the addition of carbon tetrachloride to benzene is due to an energy transfer mechanism. Molecules which, although excited by the incident radiation, do not normally yield products can hand on this excitation energy to the solute which then decomposes. A different interpretation for a similar phenomenon has been given by Nash and Hamill (16). They attribute the increase in $G(H_2)$ observed when hydrogen iodide is added to cyclohexane to an electron capture process.

(*b*) *Hydrogen*

We have shown that at low solute concentration, particularly in the case of CCl_4, cyclohexyl radicals can be scavenged without a corresponding large reduction in the hydrogen yield. It would be natural to assume that the decrease in hydrogen yield at

Can. J. Chem. Downloaded from www.nrcresearchpress.com by 210.87.254.6 on 09/05/12
For personal use only.

higher solute concentrations is due to hydrogen atom scavenging. Our results do not support such a mechanism.

It has been demonstrated that CCl_4, $CHCl_3$, and $CDCl_3$ scavenge cyclohexyl radicals with different efficiencies. The hydrogen yields in the various systems do not reflect the same differing efficiencies. In particular, at concentrations of less than 0.04 M all three solutes show the same efficiency in reducing $G(H_2)$. It is just in this region that the largest differences in the rates of cyclohexyl radical scavenging are observed. One would also expect a difference for the reaction of any other free radicals, including hydrogen atoms. We therefore conclude that the reduction in hydrogen yield cannot be due to a scavenging process.

Hardwick (17) has interpreted the action of halogenated compounds on the hydrogen yield from the radiolysis of *n*-hexane in terms of hydrogen atom scavenging. The difference in limiting hydrogen yield at the highest concentrations of $CHCl_3$ and CCl_4 employed is explained as due to hydrogen abstraction from chloroform, i.e. with $CHCl_3$ we can have

$$\cdot H + CHCl_3 \rightarrow HCl + \cdot CHCl_2, \quad [15]$$

$$\cdot H + CHCl_3 \rightarrow H_2 + \cdot CCl_3, \quad [16]$$

but for CCl_4 only reaction (17) is possible.

$$\cdot H + CCl_4 \rightarrow HCl + \cdot CCl_3. \quad [17]$$

The value quoted for k_{16}/k_{15} is 0.14. We find for the systems $C_6H_{12}/CHCl_3$ and $C_6H_{12}/CDCl_3$ that $\Delta G(H_2)$ is the same at any given solute concentration. Using the above ratio of rate constants we have calculated the values of $G(HD)$ to be expected for given values of $\Delta G(H_2)$ in the $C_6H_{12}/CDCl_3$ system. These are shown in Table II together with

TABLE II

The decrease in hydrogen yield and the yield of HD in the system C_6H_{12}–$CDCl_3$

$CDCl_3$, M	$G(H_2)$	$G(HD)$ (measured)	$\Delta G(H_2)$	$G(HD)$ (calculated)
0.01	4.66	0.0013	0.89	0.12
0.05	3.64	0.0027	1.91	0.27
0.31	2.57	0.012	2.98	0.42

the experimentally determined values. As was to be expected, no D_2 was produced at these low solute concentrations. The decrease in total hydrogen yield, $\Delta G(H_2)$ at the same concentrations, is also tabulated.

The very large difference between these two sets of results (~a factor of 50) argue against the above hypothesis and hence against the presence of thermalized hydrogen atoms in the system.

Since the ionization potential of CCl_4 is ~1.5 ev greater than that for cyclohexane, charge exchange from the ground state of $C_6H_{12}^+$ cannot occur. Ion–molecule reactions as a major source of the inhibitable hydrogen are ruled out for the same reason. The effect must therefore be due to either an electron capture process or some form of energy transfer.

Van Dusen and Hamill (17) suggest that dissociative electron attachment is an important process in the radiation chemistry of liquid systems containing components that can readily attach slow electrons at low pressures in the gas phase. CCl_4 and $CHCl_3$

Can. J. Chem. Downloaded from www.nrcresearchpress.com by 210.87.254.6 on 09/05/12
For personal use only.

are two such compounds. Lovelock (18) and Guarino, Ronayne, and Hamill (19), using different methods, showed that the affinity of CCl_4 for thermal electrons is greater than that of $CHCl_3$. Figure 4 shows that above 0.04 *M* solute, the relative decreases in hydrogen yield are as one would expect if thermal electron capture did occur. However, at low solute concentrations, both solutes decrease the hydrogen yield to the same extent and this is inconsistent with an electron capture mechanism.

From the results of experiments with very dilute solutions of iodine in cyclohexane, Schuler (20) suggested that solutes at low concentration can act as energy sinks and thus protect the solvent molecules although they may themselves decompose as a result of this absorption of energy. A similar conclusion was reached by us to explain the effect of dilute solutions of benzene on the radiolysis of cyclohexane (4). In the C_6H_{12}/CCl_4 system, any explanation for the decrease in the hydrogen yield must leave the total number of radicals unchanged. Both electron capture and energy transfer would do this if the participating CCl_4 molecules subsequently reacted. For example,

(i) energy transfer:

$$C_6H_{12}^* + CCl_4 \rightarrow C_6H_{12} + CCl_4^*, \quad [18]$$

$$CCl_4^* \rightarrow \cdot CCl_3 + \cdot Cl; \quad [19]$$

(ii) electron capture:

$$C_6H_{12} \rightarrow C_6H_{12}^+ + e, \quad [20]$$

$$e + CCl_4 \rightarrow CCl_4^- \rightarrow CCl_3 + Cl^-. \quad [21]$$

Recent work with hydrocarbons containing deuterated cyclohexane has also shown that explanations for reductions in $G(H_2)$ by added solutes must be formulated in terms of a non-chemical interaction (22).

From the complexity of the hydrogen yield curves (Fig. 4), it is not improbable that there is more than one mechanism operating to reduce the hydrogen yield.

REFERENCES

1. T. J. HARDWICK. J. Phys. Chem. **66**, 117 (1962).
2. R. A. HOLROYD. J. Am. Chem. Soc. **84**, 4000 (1962).
3. W. H. HAMILL. *In* Comparative effects of radiation. *Edited by* M. Burton, J. S. Kirby-Smith, and J. L. Magee. John Wiley and Sons, Inc., New York. 1960. p. 190.
4. J. A. STONE and P. J. DYNE. Radiation Res. **17**, 353 (1962).
5. P. J. DYNE and J. A. STONE. Can. J. Chem. **39**, 2381 (1961).
6. D. M. ZALL, D. FISHER, and M. Q. GARNER. Anal. Chem. **28**, 2381 (1961).
7. G. R. FREEMAN. J. Chem. Phys. **33**, 71 (1960).
8. D. F. DETAR and D. V. WELLS. J. Am. Chem. Soc. **82**, 5839 (1950).
9. T. J. HARDWICK. J. Phys. Chem. **64**, 1623 (1960).
10. T. F. WILLIAMS. Trans. Faraday Soc. **57**, 755 (1961).
11. L. KEVAN and W. F. LIBBY. J. Chem. Phys. **37**, 2496 (1962).
12. P. J. DYNE. J. Phys. Chem. **66**, 767 (1962).
13. C. WALLING. Free radicals in solution. John Wiley and Sons, Inc., New York. 1957. p. 97.
14. C. WALLING. Free radicals in solution. John Wiley and Sons, Inc., New York. 1957. p. 255.
15. G. K. OSTER and H. P. KALLMAN. Nature, **194**, 1033 (1962).
16. J. R. NASH and W. H. HAMILL. J. Phys. Chem. **66**, 1097 (1962).
17. T. J. HARDWICK. J. Phys. Chem. **66**, 2246 (1962).
18. W. VAN DUSEN and W. H. HAMILL. J. Am. Chem. Soc. **84**, 3648 (1962).
19. J. E. LOVELOCK. Nature, **189**, 729 (1961).
20. J. P. GUARINO, M. R. RONAYNE, and W. H. HAMILL. Radiation Res. **17**, 379 (1962).
21. R. H. SCHULER. J. Phys. Chem. **61**, 1472 (1957).
22. P. J. DYNE, D. R. SMITH, and J. DENHARTOG. Disc. Faraday Soc. (1963).

Can. J. Chem. Downloaded from www.nrcresearchpress.com by 210.87.254.6 on 09/05/12
For personal use only.

THE SOLUTION PROPERTIES OF SOME POLYOXYETHYLATED NONIONIC SUBSTANCES IN AQUEOUS AND IN NONAQUEOUS SOLVENTS[1]

A. F. SIRIANNI AND R. D. COLEMAN[2]
Division of Applied Chemistry, National Research Council, Ottawa, Canada
Received August 16, 1963

Can. J. Chem. Downloaded from www.nrcresearchpress.com by 210.87.254.40 on 09/05/12
For personal use only.

ABSTRACT

Unlike sorbitan and glycerol monostearates, alkylphenol derivatives of polyoxytheylene appear to be monodisperse in benzene when the solutions were examined by vapor pressure lowering. In addition, the existence of micelles was not detected by light-scattering measurements in benzene with a few representative samples. In agreement with light-scattering data, the number average micellar weight in water decreased with increasing number of ethylene oxide units per molecule. A difference of about a factor of 8 between weight and number average molecular weight appears to exist for materials of similar composition.

INTRODUCTION

Nonionic detergents which derive their hydrophilic properties from ethylene oxide interact in aqueous solutions forming micelles above a critical concentration. The number of monomers clustering together to form micelles is dependent on the temperature (1, 2) and to some extent on the homogeneity of the polyoxyethylene chain lengths (3).

Although a linear relationship appears to exist between aggregation number (n) and the reciprocal of the average number of ethylene oxide units for compounds containing more than 10 such units (4,5), the micellar weight of surfactants of lower solubility rises sharply in water with decreasing numbers of hydrophilic groups (6). Thus departures from linearity occur that became particularly apparent at high ethylene oxide ratios when a wide range of ethylene oxide content is examined. Large differences in micellar weights were found between cryoscopic (7) and light-scattering measurements (8) of commercial isooctylphenol derivatives of nine ethylene oxide units. Since evidence for the existence of differences in number ($\bar{M}_n$) and weight ($\bar{M}_w$) average molecular weight appeared for other nonionic surface active agents in nonaqueous solvents (9, 10), it was of considerable interest to assess the solution properties of some alkylphenol derivatives of ethylene oxide in both aqueous and nonaqueous media.

In the present communication a number of octylphenol – ethylene oxide adducts (Tritons) were examined wherein the number of ethylene oxide units varied from 3 to 30 with the hydrophobic constituent of the molecule remaining constant. Two nonylphenols, Triton N128 and DowFax 9N9, were examined in benzene by vapor pressure lowering. Triton N128, DowFax 9N9, and Triton X-45 were also examined in benzene by light-scattering measurements and some vapor pressure measurements were carried out with DowFax 9N9 in alcohol. A variety of polyoxyethylated alkylphenols with cloud points above 50° C were examined in water using a vapor pressure "Osmometer".

A lauryl alcohol derivative of 23 (poly)oxyethylene units (Brij 35)* in which non-equilibrium states were found in water by light-scattering measurements (11) was examined in water and in benzene at 37° C and in alcohol at 44°. Some measurements were

[1]*Issued as N.R.C. No. 7700.*
[2]*Present address, Atomic Energy of Canada, Chalk River, Ontario.*
**Obtained through the courtesy of Dr. Paul Becher, Atlas Chemical Industries, Inc.*

carried out with solutions of methoxy polyoxyethylene glycols (Carbowax 350 and 750) in water and in dioxane at 35°.

EXPERIMENTAL

The nonionic surface-active agents were of industrial origin. The liquid materials were centrifuged to separate out insoluble matter, evacuated at room temperature to remove volatiles, and then stored under vacuum.

Solutions examined in benzene and in alcohol by vapor pressure lowering measurements and by light-scattering measurements in benzene at 25° C for Triton N128, Triton X-45, and DowFax 9N9 were prepared as described previously (10).

The aqueous solutions were prepared with conductivity water which was stored in thoroughly conditioned polythene bottles, and measurements made with a Mechrolab Vapor Pressure "Osmometer" Model 301 at 37° C using a probe adapted for aqueous systems. The apparatus was calibrated with solutions of reagent grade urea, sucrose, and mannitol. One solution syringe was used to diminish concentration errors due to evaporation. The solutions were measured in the order of increasing concentration.

Owing to aggregation of the nonionic detergents and the rather low readings due to the high latent heat of vaporization of water, it was necessary to carry out the measurements over a wide range of concentrations. Readings close to the calibrated range at low concentrations were obtained with solutions containing about 4 to 28% surface-active agent (grams of solute/100 g water). The solutions were shaken periodically and they were allowed to equilibrate at room temperature overnight. Because of the low sensitivity observed with water the required time to reach equilibrium was established by trial and error. Reproducible measurements were obtained by the following procedure.

The syringe containing an aliquot portion of the solution was allowed to stand about 20 minutes in the apparatus to reach ambient temperature, after which the solution thermistor was rinsed 8–10 times, then a drop of solution was deposited on the bead. Readings were taken every minute for 6 minutes. Three or four sets of measurements were taken for each solution. The average value after 5 minutes was used in calculating the apparent molecular weight at finite concentrations. The molar constant was obtained from a calibration curve relating the variation of $\Delta R/C$ versus ΔR.

The solutions assessed by static vapor pressure measurements employing a sensitive differential mercury micromanometer were prepared with rigorously deaired conductivity water. The amount of water used for making up the solutions was measured in a calibrated capillary tube. The amounts of solvent and solute used were in the range of 1 to 10 mg and 30 to 90 mg respectively.

The measurements were carried out as described previously for the organic solvents (10).

The methoxy polyoxyethylene glycols (Carbowax 350 and 750) were assessed by static vapor pressure determinations in water and dioxane at 35° C. The apparatus was modified to prevent the alternate condensation and evaporation of solvent on the solution cell while measurements were being taken (12). Carbowax 350 was distilled and the fraction boiling at 163° C at 2 mm Hg pressure was used. Carbowax 750 was used as received; however, a small portion of the material was distilled in a Späte tube under reduced pressure and used in a few experiments. The distillate was further evacuated at room temperature to remove light ends.

Dioxane was redistilled from and stored over CaH_2. It was used after being thoroughly deaired. The amount of dioxane used was measured in a calibrated capillary tube as described for the preparation of the aqueous solutions.

RESULTS AND DISCUSSION

The variation of the apparent molecular weight with solute concentration for a group of polyoxyethylated octylphenols in benzene at about 37° C is indicated in Fig. 1. Curves 1, 2, 3, 4, 5, and 6 were obtained for Triton X-35, X-45, X-102, X-165, X-205, and X-305 respectively (see Table I). The crosses (×) were obtained with the differential mercury micromanometer and the other points with the "Osmometer". The agreement between these two techniques is acceptable. The observed and the estimated molecular weights based on the composition data supplied by the manufacturers are also in fairly good agreement. The molecular weight of Triton X-305 is about 20% lower than the estimated value. This could be due to a higher heterogeneity of the substance. With the possible exception of Triton X-35 the apparent molecular weight versus concentration curves indicate that the solutions are monodisperse in benzene. Some departures from "ideal" behavior are indicated for the substances containing more than 12 to 13 ethylene oxide units (E.O.) The deviation becomes more pronounced with increasing ethylene oxide content. This

Can. J. Chem. Downloaded from www.nrcresearchpress.com by 210.87.254.40 on 09/05/12
For personal use only.

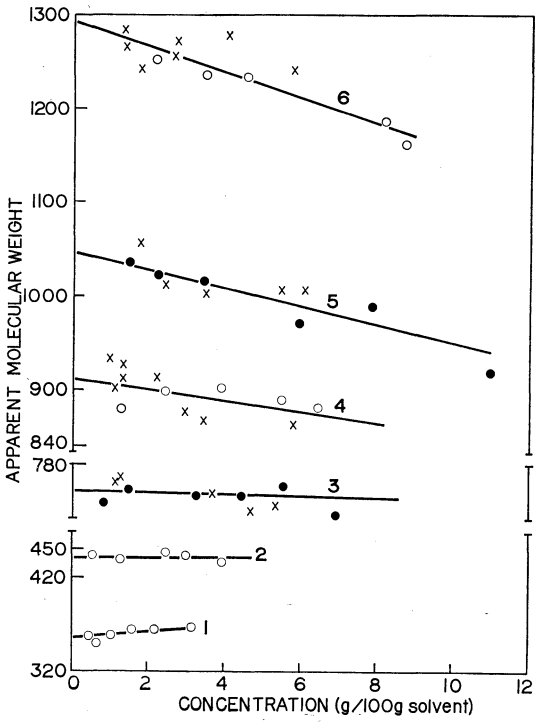

FIG. 1. Apparent molecular weight versus solute concentration for a series of polyoxyethylated octylphenols in benzene at about 37° C. Curve 1, Triton X-35; curve 2, Triton X-45; curve 3, Triton X-102; curve 4, Triton X-165; curve 5, Triton X-205; and curve 6, Triton X-305.

TABLE I

Summary of results indicated from vapor pressure measurements using the "Osmometer" on solutions of polyoxyethylated octyl- and nonyl-phenols in benzene at 37° C

	Av. No. E.O.	Mol. wt. estimated	Mol. wt. observed
Octylphenols			
Triton X-35	3	338	338
Triton X-45	5	426	442
Triton X-102	12–13	734–778	752
Triton X-165	16	910	910
Triton X-205	20	1086	1050
Triton X-305	30	1526	1290
Nonylphenols			
DowFax 9N9	9–10	616–660	655
Triton N128	12–13	748–792	770

suggests that polymer–solvent interaction increases with increased ethylene oxide units in benzene.

The results obtained for Triton N128 and DowFax 9N9 are summarized in Table II. The molecular weight of Triton N128 was about 10% higher at infinite dilution by static vapor pressure measurements than the value observed with the "Osmometer". The discrepancy between the two procedures was smaller in the case of DowFax 9N9. The differences are probably due to the different experimental conditions of the two procedures.

Can. J. Chem. Downloaded from www.nrcresearchpress.com by 210.87.254.40 on 09/05/12
For personal use only.

TABLE II

Molecular weights of Triton N128 in benzene and DowFax 9N9 in benzene and in alcohol by vapor pressure lowering measurements

Detergent	Solvent	% conc. range	Method	Mol. wt. indicated
Triton N-128	Benzene	1–10	"Osmometer"	770
		2–6	S.V.P.	860
DowFax 9N9	Benzene	1–7.5	"Osmometer"	655
	Benzene	2–6	S.V.P.	685
	Alcohol	1–8	"Osmometer"	630
	Alcohol	0.5–10.5	S.V.P.	660

While it is possible to work under very dry conditions under vacuum when employing the mercury micromanometer, it is impossible to do this when using the "Osmometer".

A slight negative deviation from Raoult's law was indicated for Triton N128. DowFax 9N9 behaved in an "ideal" way in benzene and in alcohol. Micelle formation with Triton N128, X-45, and DowFax 9N9 was not detected by light-scattering measurements in benzene at 25° C. This also suggests that benzene is a good solvent for these surface-active substances. The rise in apparent molecular weight with concentration for glyceryl and sorbitan monostearates in benzene (10) perhaps could be due to the influence of the lyophilic portion of the molecule which dimerizes in this solvent. The alcohol containing the same number of carbon atoms appears to be monodisperse. Since the hydrogen bond in carboxylic acids appears to be stronger than that in alcohols or in phenol, perhaps it has an influence on the solution properties of the esters. Association of polyoxyethylene glycol was not observed in benzene.

The variation of the apparent molecular weight with solute concentration for the octylphenol – and the nonylphenol – ethylene oxide adducts in water at 37° C using the "Osmometer" is shown in Fig. 2. The apparent $\bar{M}_n$ micellar weight and aggregation number (n) indicated for these substances are summarized in Table III. Curves 1, 2, 3, and 4 were obtained for Triton X-102, X-165, X-205, and X-305 respectively. Curves 5 and 6 represent the behavior of Triton N128 and DowFax 9N9 respectively. Each point in curve 5 is an average of three separate determinations conducted at different times at about the same concentration. The variation of the apparent molecular weight observed for each measurement lies within the vertical lines. The curves for the octylphenol series are of similar shape. As observed by ultracentrifugal measurements (3) over a narrower concentration range, the molecular weight above the critical micelle concentration (circa 0.01% for most members in distilled water) remains reasonably constant over a wide concentration range. With further solute concentration a decrease in apparent molecular weight occurred. A straight line through these experimental points, extrapolated to infinite dilution indicates a $\bar{M}_n$ micellar weight within 10% of that calculated from the results obtained at the lower concentrations. However, at the higher concentrations these solutions are very close to the gel range. Under these circumstances the extrapolation to zero concentration is of doubtful validity (13). The behavior of the nonylphenol – ethylene oxide adducts seems to be less dependent upon concentration. In every case, however, the micellar weight decreased with increasing number of ethylene oxide groups per molecule.

The lauryl alcohol derivative (Brij 35) behaved in much the same way as did the octylphenol series. The solutions were examined over a concentration range from about 5 to 23%. The apparent molecular weight of solutions of 5–10 weight% concentrations

Can. J. Chem. Downloaded from www.nrcresearchpress.com by 210.87.254.40 on 09/05/12
For personal use only.

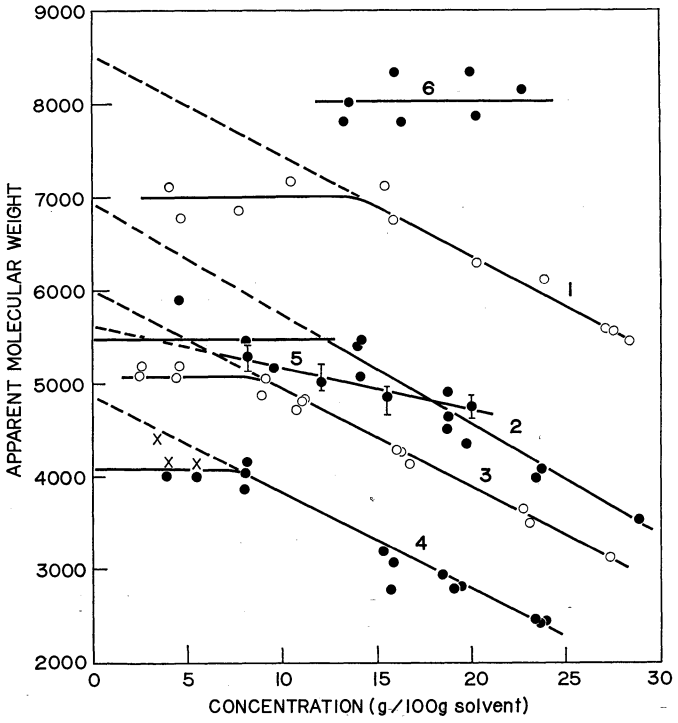

FIG. 2. Apparent molecular weight versus solute concentration for the octylphenol – and the nonylphenol – ethylene oxide adducts in water at 37° C. Curve 1, Triton X-102; curve 2, Triton X-165; curve 3, Triton X-205; curve 4, Triton X-305. (The ×'s were obtained by static vapor pressure lowering measurements.) Curve 5, Triton N-128; curve 6, DowFax 9N9.

TABLE III

The apparent $\bar{M}_n$ micellar weight and aggregation number (n) indicated from vapor pressure lowering measurements on aqueous solutions of polyoxyethylated nonionic detergents

	M_o benzene	No. E.O.	M_a	$\bar{M}_m$ calculated	n, calculated
Triton X-102	752	12.4	7000	7750	10.3
Triton X-165	910	16	5600	6500	7.1
Triton X-205	1050	19.2	5100	6170	5.9
Triton X-305	1290	24.7	4100	5370	4.2
Triton N128	770	12.5	5000	5800	7.5
DowFax 9N9	655	9.9	8000	8600	13
Brij. 35	1120	21.2	3800	4900	4.4

was about 3800±10%. It decreased to about 1800 at 20%. A value of 1120 was obtained when the substance was examined in alcohol over a concentration range of 1 to 10%. This is presumably the monomeric weight. Unlike DowFax 9N9, which behaved in an "ideal" way in alcohol over the same concentration region, Brij 35 showed a small discontinuity. The system was "ideal" from 1 to 4%. At about 5% the apparent molecular weight was 1020 and dropped to 960 at 10% concentration. These measurements fitted very closely a curve having a slight upward curvature and it converged to a value of 1120 at infinite dilution. The value calculated from the monomer composition is close to 1200. The solutions assessed in benzene with the "Osmometer" were concentration dependent

Can. J. Chem. Downloaded from www.nrcresearchpress.com by 210.87.254.40 on 09/05/12
For personal use only.

and the molecular weight at infinite dilution was in fairly good agreement with the value observed in alcohol.

The variation of the apparent molecular weight with solute concentration for the samples of methoxy polyoxyethylene glycol in water and in dioxane is shown in Fig. 3. Curves 1, 2,

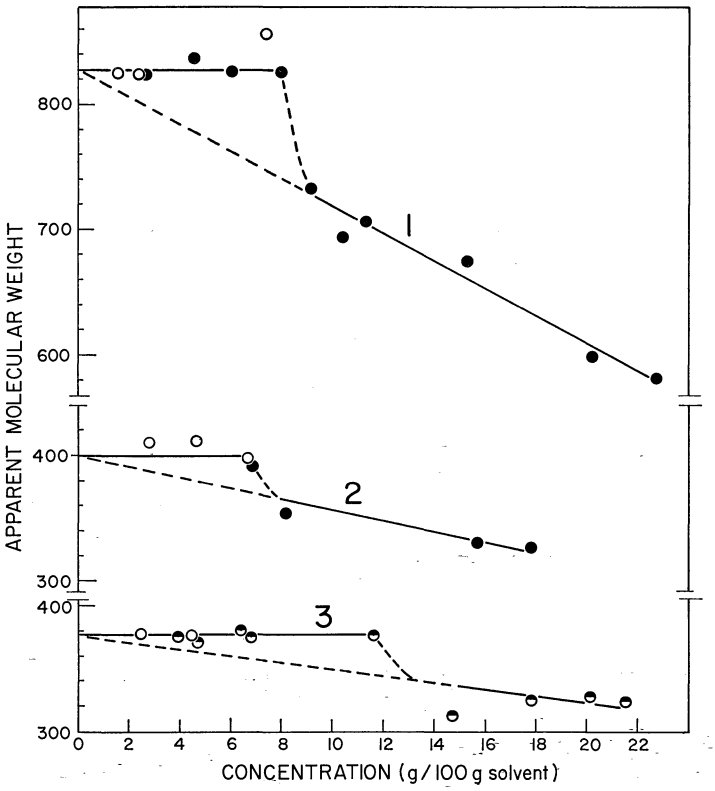

FIG. 3. Apparent molecular weight versus solute concentration for the samples of methoxy polyoxyethylene glycol in water and in dioxane (open circles) at about 35° C. Curve 1, Carbowax 750, curve 2, distilled fraction of Carbowax 750; and curve 3, Carbowax, 350.

and 3 were obtained for Carbowax 750, a distilled portion of the same material, and distilled Carbowax 350 respectively. The solutions behaved in an "ideal" fashion over a finite concentration range, then a sharp drop occurred in molecular weight. Subsequent determinations were dependent on concentration. However, a straight line joining these latter experimental points extrapolated to zero concentration yielded the same value for the molecular weight. The results obtained in dioxane (open circles) were in good agreement with those observed in water. It was not possible to cover a very wide concentration range with dioxane since the vapor pressure lowering was beyond the calibrated range of the apparatus.

The molecular weights of these nonionic substances are in reasonably close agreement with the value expected from the composition data supplied by the manufacturer. The reason for the break in the apparent molecular weight curves in aqueous systems even with the distilled materials is not too clear. It is quite possible that the polymer is not in a coiled configuration and, particularly, in the case of the octylphenol derivatives, the

Can. J. Chem. Downloaded from www.nrcresearchpress.com by 210.87.254.40 on 09/05/12
For personal use only.

micelles immobilize large quantities of water in addition to hydrogen bonding to the ether linkages. This immobilization gives rise to an abnormally high lowering of the vapor pressure owing to an increase in solute concentration; a lower apparent molecular weight results. If the surfactant were less soluble at the higher concentrations the vapor pressure of the solutions would remain virtually constant and a rise in apparent molecular weight would be observed.

The deviation could possibly be due to a slight amount of volatile precipitant sorbed on the polyoxyethylene chains. A similar phenomenon was observed previously with freshly prepared benzene solutions of a sample of polyvinyl acetate. When the solution was evaporated to dryness in a hard vacuum and a new solution was prepared under hermetically sealed conditions with fresh solvent, the effect disappeared and the molecular weight was dependent on concentration (14). Because the solution properties depend on delicately balanced lyophobic–lyophilic characteristics, small concentrations of extraneous materials can have an unexpectedly large influence.

Viscosity measurements on aqueous solutions of Carbowax 750 at 30° C indicated that the reduced viscosity increased slightly with concentration. At about 7% concentration, upward curvature became more pronounced. Although there was no evidence of a sharp break in the curve, it indicates that solvation contributes to the phenomenon. This agrees with previously reported work (15, 16).

The $\bar{M}_n$ micellar weight and aggregation number (n) for the lauryl alcohol derivative indicated by vapor pressure measurements in water is also shown in Table III. The aggregation numbers and the average number of ethylene oxide units in each substance was based on the molecular weight observed in benzene with the "Osmometer". The results suggest that considerable differences exist between $\bar{M}_n$ and $\bar{M}_w$ micellar weight in water for surface-active agents of similar composition. Owing to the negative temperature coefficient of solubility (1,2) these differences could be accentuated. The results observed by Gonick and McBain (7) support the molecular weights indicated from the colligative properties of the solutions.

It is quite possible that polydispersity of the micellar sizes, differences in molecular species, and the presence of soluble impurities could be contributing factors. The presence of electrolytes decreases $\bar{M}_n$ because of their contribution to the vapor pressure lowering but increases $\bar{M}_w$ by light-scattering measurements owing to probable "salting out" effects (4,5). Dust particles have very little effect on the colligative properties of the solutions, but these increased $\bar{M}_w$ by light-scattering measurements even after successive filtrations (17).

The variation of the aggregation number (n) with the reciprocal of the number of ethylene oxide units per mole of hydrophobe for the alkylphenols is shown in Fig. 4 by curve 1. The solid and open circles represent this property for the octyl- and nonyl-phenols respectively. Curve 2 indicates the concentration in which deviations from linearity occurred for the octylphenol series of surfactants. Although the data are too meager to attach too much significance to this, it could possibly indicate a transition in the properties of the solutions (18).

In good agreement with the $\bar{M}_w$ micellar weight obtained by light-scattering measurements (4,5), the $\bar{M}_n$ micellar weight indicated by curve 1 decreases with increasing ethylene oxide content. As found by Becher (4) the tendency to form large micelles decreases with increased solubility of the surfactant. Although most data obtained over a moderate range of ethylene oxide content can be fitted by a straight line which intercepts the 1/E.O. axis, it does not appear too unreasonable to fit a curved line over the same

Can. J. Chem. Downloaded from www.nrcresearchpress.com by 210.87.254.40 on 09/05/12
For personal use only.

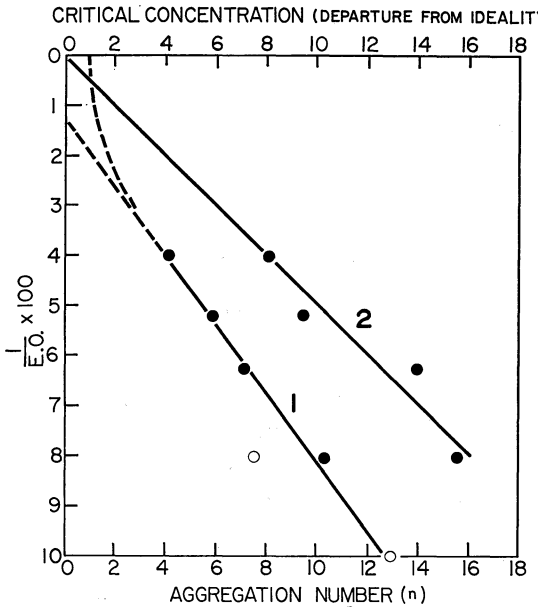

FIG. 4. Variation in the solution properties of alkyl phenols with ethylene oxide content of the surfactants. Curve 1, variation of the aggregation number (n) with the reciprocal of the number of ethylene oxide units in the compound. Curve 2, the concentration at which deviations from "ideality" occurred owing to an increase in vapor pressure lowering versus the reciprocal of the number of ethylene oxide units for the octylphenol series of surfactants.

experimental results which can be extrapolated to $n = 1$. Nonionic detergents consisting of alternating water-soluble and insoluble units of ethylene oxide and propylene oxide did not form micelles in water according to ultracentrifugal measurements (3). In agreement with this, solute aggregation was not indicated with the Carbowaxes in this work.

ACKNOWLEDGMENTS

The authors are indebted to Dr. I. E. Puddington for his interest and for the many valuable discussions concerning this work. We are grateful to Mr. P. E. Black for light-scattering measurements and to Dr. B. A. Gingras for purifying some of the materials.

REFERENCES

1. C. W. DWIGGINS, JR. and R. J. BOLEN. J. Phys. Chem. **65**, 1787 (1961).
2. R. R. BALMBRA, J. S. CLUNIE, J. M. CORKILL, and J. F. GOODMAN. Trans. Faraday Soc. **38**, 1661 (1962).
3. C. W. DWIGGINS, JR., R. J. BOLEN, and H. N. DUNNING. J. Phys. Chem. **64**, 1175 (1960).
4. P. BECHER. J. Colloid Sci. **16**, 49 (1961).
5. M. J. SCHICK, S. M. ATLAS, and F. R. EIRICH. J. Phys. Chem. **66**, 1326 (1962).
6. C. W. DWIGGINS, JR. and R. J. BOLEN. J. Phys. Chem. **66**, 574 (1962).
7. E. GONICK and J. W. MCBAIN. J. Am. Chem. Soc. **69**, 334 (1947).
8. A. M. MANKOWICH. J. Phys. Chem. **58**, 1027 (1954).
9. P. DEBYE and H. COLL. J. Colloid Sci. **17**, 220 (1962).
10. A. F. SIRIANNI, J. M. G. COWIE, and I. E. PUDDINGTON. Can. J. Chem. **40**, 957 (1962).
11. P. BECHER and N. K. CLIFTON. J. Colloid Sci. **14**, 519 (1959).
12. G. R. COTTEN, A. F. SIRIANNI, and I. E. PUDDINGTON. J. Polymer Sci. **32**, 115 (1958).
13. P. BECHER. Private communication.
14. A. F. SIRIANNI, R. TREMBLAY, and I. E. PUDDINGTON. Can. J. Chem. **36**, 543 (1958).
15. F. E. BAILEY, JR. and R. W. CALLARD. J. Appl. Polymer Sci. **1**, 56 (1959).
16. H. L. GREENWALD and G. L. BROWN. J. Phys. Chem. **58**, 825 (1954).
17. P. DEBYE and H. COLL. U.S. Dep. Comm. Office Tech. Serv. P. B. Rept. 146, 513 (1960).
18. J. M. CORKILL and K. W. HERRMAN. J. Phys. Chem. **67**, 934 (1963).

Can. J. Chem. Downloaded from www.nrcresearchpress.com by 210.87.254.40 on 09/05/12
For personal use only.

INFRARED AND RAMAN SPECTRA OF CYANURIC FLUORIDE

JAMES E. GRIFFITHS AND DONALD E. IRISH*
Bell Telephone Laboratories, Incorporated, Murray Hill, New Jersey
Received October 4, 1963

ABSTRACT

Infrared spectra (250–2000 cm^{-1}) and Raman displacements ($\Delta\nu$ = 100–1800 cm^{-1}) with qualitative polarization measurements are reported for cyanuric fluoride. All of the active fundamentals are assigned on the basis of a planar D_{3h} model: a_1' = 1496, 999, 642; e' = 1617, 1424, 1087, 576, 378; a_2'' = 817, 436; e'' = 743 and 226 cm^{-1}.

Can. J. Chem. Downloaded from www.nrcresearchpress.com by 210.87.254.6 on 09/05/12
For personal use only.

The infrared and Raman spectra of cyanuric fluoride, $C_3N_3F_3$, have not been discussed previously, although an infrared spectrum of the liquid has been published without comment (1) and an attempt to assign four of the strongest infrared bands was made (2). The infrared spectrum of the basic structural unit, cyanogen fluoride, however, has been reported (3, 4, 5) and the three fundamentals were assigned.

Since cyanuric fluoride is a reactive compound and a potentially useful starting material for a variety of chemical reactions, a knowledge of its vibrational spectrum is desirable. Furthermore, chemical evidence favors a planar structure for this compound, but there has been no physical evidence presented up to this time. In this work, the infrared and Raman spectra are analyzed in terms of a planar D_{3h} model and all of the active fundamentals are assigned.

EXPERIMENTAL

The cyanuric fluoride was purchased from the Hynes Chemical Research Co., Durham, N.C. The sample was purified by fractional condensation and vaporization *in vacuo* until its vapor pressure was 21.8±0.2 mm at 0° (calc., 21.7±0.4 mm^2) and its molecular weight was 135.0 (calc., 135.0). A nuclear magnetic resonance spectrum measured at 56.4 Mc in $CFCl_3$ and in CF_3COOH showed single F^{19} resonance lines at +1760 c.p.s. upfield from $CFCl_3$ and at −2591 c.p.s. downfield from CF_3COOH. Therefore, there were no detectable fluorine-containing impurities.

The infrared spectrum was examined in the vapor and liquid states from 250 to 2000 cm^{-1} using a Perkin–Elmer Model 421 spectrophotometer which was equipped with a medium-far infrared grating interchange. Raman displacements (from the 4358 Å Hg line) were recorded photoelectrically with a Cary Model 81 spectrophotometer and the liquid sample was contained in a 0.7×27 cm glass tube. A light trap was incorporated into the tube to remove any spurious reflections and a sodium nitrite filter removed almost all undesirable mercury excitation lines. Frequencies reported in Table I are expected to be accurate to ±2 cm^{-1} and the individual spectra are shown in Figs. 1 (IR) and 2 (R). Qualitative polarization data were also obtained although the spectra themselves are not shown.

DISCUSSION

Of the possible models for $C_3N_3F_3$ the chemical evidence (1, 6) favors a symmetric ring structure which is expected to be planar (D_{3h} point group). The reduced representation of internal motion is $3A_1' + 2A_2' + 5E' + 2A_2'' + 2E''$. The A_1' (polarized) and E'' (depolarized) species are Raman active only and the A_2'' species are active only in the infrared. The E' type vibrations are active in both (Raman depolarized); whereas the A_2' species are inactive in both. The A_1', A_2', and E' type modes are of the in-plane type, whereas the A_2'' and E'' species represent out-of-plane motions. Therefore, in the vapor state infrared spectra, the unresolved rotational structure in the parallel A_2'' type absorption bands is expected to produce band contours which are similar to simple P, Q, and R

**Permanent address: Department of Chemistry, University of Waterloo, Waterloo, Ontario.*

TABLE I

Vibrational assignment for cyanuric fluoride

Infrared*		Raman	Freq.	
Gas	Liquid	(liquid)	calc.	Assignment
—	—	226 dp	—	ν_{14} (e'')
—	—	244–252	256	$\nu_2-\nu_{13}$ (E'')
379 m	378 m	379 dp	—	ν_{10} (e')
436 w	437 vw	—	—	ν_{12} (a_2'')
—	—	458	452	$2\nu_{14}$ ($A_1'+E'$)
578 w	577 w	579 dp	—	ν_9 (e')
—	534 vvw	—	530	$\nu_6-\nu_8$ ($A_1'+A_2'+E'$)
606 vw	—	—	605	$\nu_{10}+\nu_{14}$ ($A_1''+A_2''+E''$)
—	640 vvw	—	—	impurity (?)
—	—	642 p	—	ν_3 (a_1')
—	743 w	743 dp	—	ν_{13} (e'')
810 s	—	—	—	P
817 s	817 s	—	—	Q ν_{11} (a_2'')
826 s	—	—	—	R
858 vvw	—	—	868	$\nu_3+\nu_{14}$ ($A_1'+E'$)
918 vvw	912 vvw	—	918	$\nu_1-\nu_9$ (E')
962 w	948 vw 967	967	969	$\nu_{13}+\nu_{14}$ ($A_1'+A_2'+E'$)
—	—	999 p	—	ν_2 (a_1')
	1020			
1035 w	1035 w	—	1043	$\nu_{11}+\nu_{14}$ (E')
	1045			
1081 s		—	—	P
1087 s	1087 s	1087 dp	—	Q ν_8 (e')
1093 s		—	—	R
1152 1158 w	1157 w	—	1156	$2\nu_9$ ($A_1'+E'$)
—	1187 vw	—	1179	$\nu_{12}+\nu_{13}$ (E')
1209 vw	1206 vw 1227 vw	—	1220	$\nu_3+\nu_9$ (E')
—	—	1230	1225	$\nu_2+\nu_{14}$ (E'')
1246 vw	1245 w	—	1238	$\nu_6-\nu_{10}$ ($A_1'+A_2'+E'$)
1278 vvw	1303 vw	—	—	Impurity (?)
1332 vvw	—	—	1321	$\nu_9+\nu_{13}$ ($A_1''+A_2''+E''$)
—	—	1354	1348	$\nu_{10}+\nu_{13}+\nu_{14}$ ($A_1'+A_2'+3E'$)
1367 w	—	—	—	P
1372 w	1377 msh	—	1378	Q $\nu_2+\nu_{10}$ (E')
1377 w	—	—	—	R
1394 msh	—	1392	1391	$\nu_6-\nu_{14}$ ($A_1''+A_2''+E''$)
1414 vs	—	—	—	P
1424 vs	1424 vs	1418 dp	—	Q ν_7 (e')
1432 vs	—	—	—	R
1463 m	1462 m	—	1459;1466	$\nu_3+\nu_{11}$ (A_2''); $\nu_8+\nu_{10}$ ($A_1''+A_2''+E''$)
—	1489 m	1482	1486	$2\nu_{13}$ ($A_1'+E'$)
—	—	1496 p	—	ν_1 (a_1')
1505 w	—	—	1514	$\nu_3+2\nu_{12}$ ($A_1'+E'$)
—	—	1554	1560	$\nu_{11}+\nu_{13}$ (E')
1581 vs	1577 vs	1573	1577	$\nu_2+\nu_9$ (E')
—	—	1594	1592	$2\nu_9+\nu_{12}$ ($A_2''+E''$)
			1599	$\nu_3+\nu_9+\nu_{10}$ ($A_1'+A_2'+E'$)
1617 vs	1617 vs	1622 dp	—	ν_6 (e')
1647 w	1641 s	—	1650	$\nu_7+\nu_{14}$ ($A_1''+A_2''+E''$)
1664 m	1666 m	—	1665	$\nu_8+\nu_9$ ($A_1'+A_2'+E'$)
—	—	1675	—	Hg
1725 w	—	—	—	P
1732 w	1727 w	1728	1729;1742	Q $\nu_3+\nu_8$ (E'); $\nu_2+\nu_{13}$ (E'')
1738 w	—	—	—	R
—	1755 m	—	1757	$\nu_9+\nu_{12}+\nu_{13}$ ($A_1'+A_2'+E'$)
—	—	1768	—	Hg
1805 w	1792 1809 w	—	1803	$\nu_7+\nu_{10}$ ($A_1'+A_2'+E'$)
1862 vvw	1870 vvw	—	1875	$\nu_1+\nu_{10}$ (E')

*v = very, s = strong, m = medium, w = weak, sh = shoulder, p = polarized, dp = depolarized.

Can. J. Chem. Downloaded from www.nrcresearchpress.com by 210.87.254.6 on 09/05/12
For personal use only.

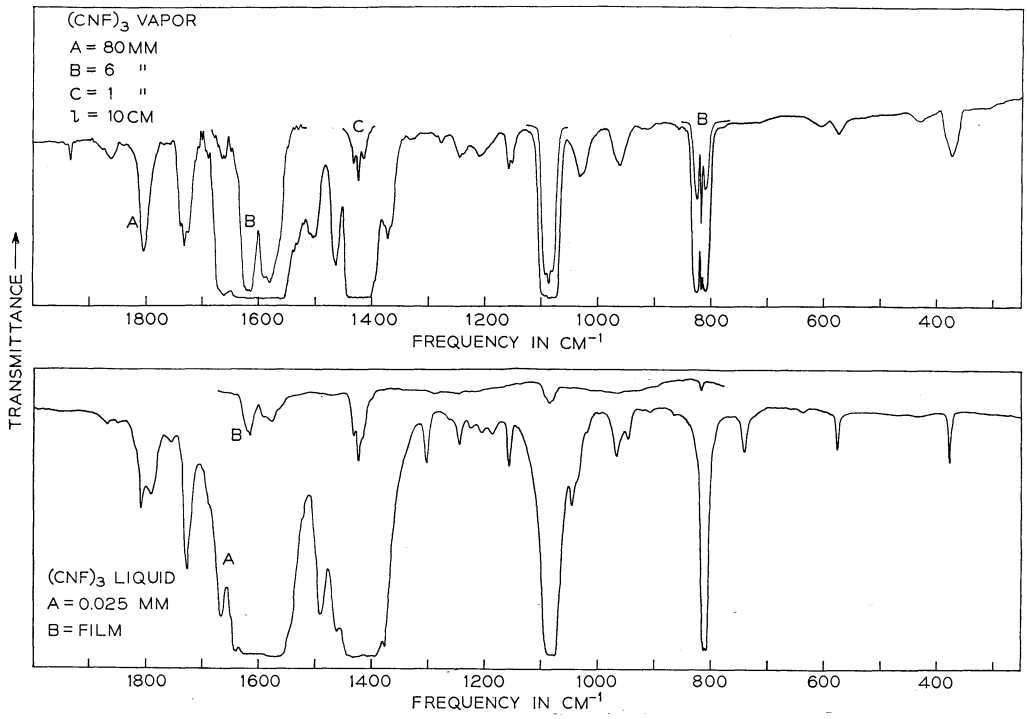

FIG. 1. Infrared spectra of cyanuric fluoride.

branches. Moreover, since I_A will likely be greater than I_B, the intensity of the observed Q branch will be more intense than that of the P or R branches (7). The fundamental frequencies are collected in Table II and the numbering system conforms to that of Herzberg.

VIBRATIONAL ASSIGNMENT

Three strong polarized bands at 1496, 999, and 642 cm^{-1} were observed in the Raman effect and are assigned to the three A_1' vibrations. The 1496 cm^{-1} band is assigned to the symmetric C–F stretching vibration. This leaves the two ring modes ν_2 and ν_3 for assignment to the bands at 999 and 642 cm^{-1}.

Two depolarized Raman lines, which are not observed in the gas phase infrared spectrum, are found at 743 and 226 cm^{-1}. These are assigned to the E'' type vibrations ν_{13} and ν_{14} and represent the C–F wagging and the out-of-plane ring modes respectively. The latter corresponds to the bands at 340 and 309 cm^{-1} in $C_3N_3H_3$ and $C_3N_3D_3$ respectively (8). The 226 cm^{-1} band is asymmetrical and a careful analysis shows the presence of a weak band whose center occurs at 244–253 cm^{-1}. This is assigned to $\nu_2-\nu_{13} = 256$ cm^{-1} (E''), and its comparable intensity relative to that of the sum band $\nu_2 + \nu_{13}$, might arise from a Fermi resonance with the $\nu_{14}(e'')$ fundamental.

The two infrared active but Raman inactive fundamentals of the A_2'' species occur at 817 and at 436 cm^{-1}. The first shows a well-defined PQR structure with a P–R separation of 16 cm^{-1}, but the contour of the second is poorly defined because of overlapping water vapor bands.

There remain the five fundamentals of the E' species to be assigned. Since these must be

Can. J. Chem. Downloaded from www.nrcresearchpress.com by 210.87.254.6 on 09/05/12
For personal use only.

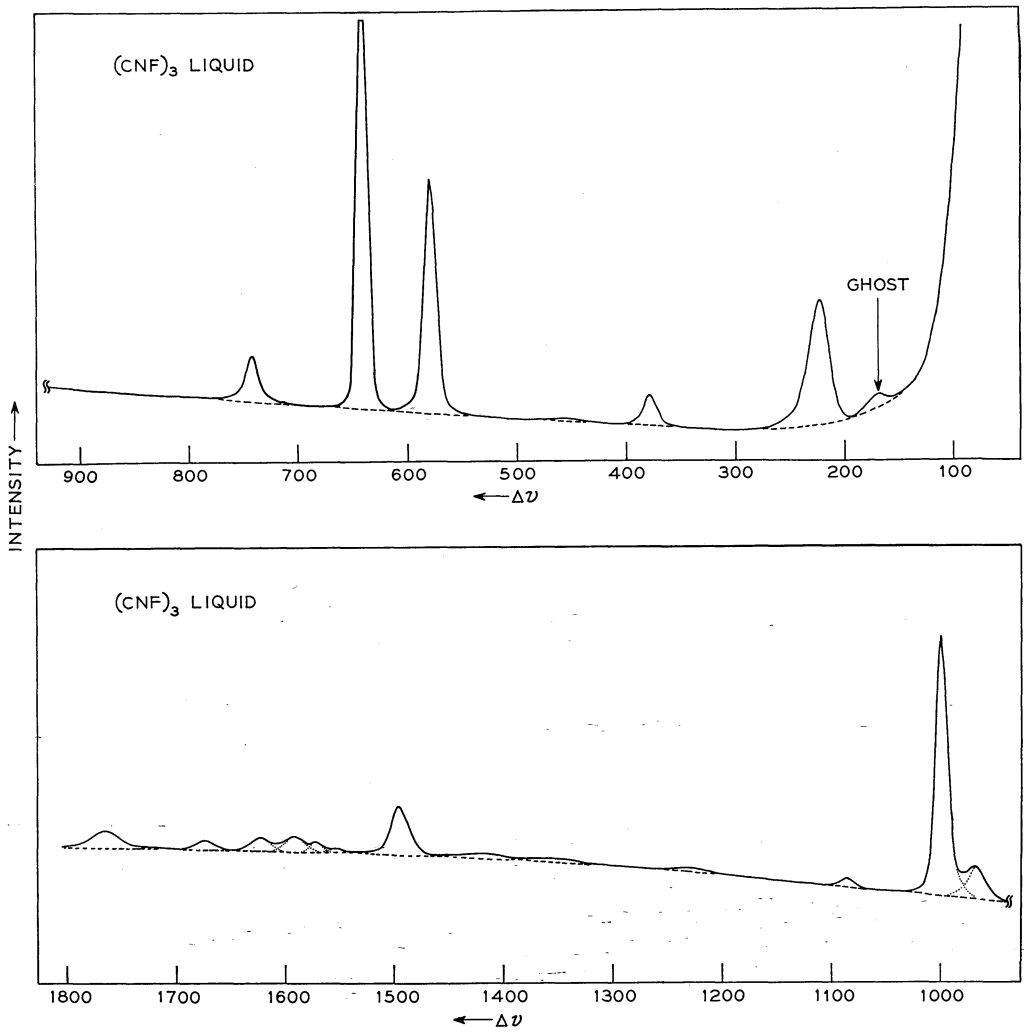

FIG. 2. Raman spectrum of cyanuric fluoride.

Raman and infrared active, the assignment of the bands at 1617, 1424, 1087, 578, and 378 cm^{-1} in the infrared (gas) and at 1622, 1418, 1087, 579, and 379 cm^{-1} in the Raman effect (liquid) is straightforward. The two highest frequencies represent the ring modes. The 1087 cm^{-1} band (strong in the infrared and weak in the Raman) obviously corresponds to the C–F stretching mode because of its proximity to the similar fundamental at 1078 cm^{-1} in FCN (5). There is no conclusive evidence for favoring the assignment of the 578 cm^{-1} band to the ring angle bend and the 378 cm^{-1} band to the C–F rocking mode (in-plane) over the opposite assignment. It does seem more likely, however, that the C–F rocking mode would be accompanied by a greater dipole moment change than in the case of the ring angle bending mode. Thus, the greater intensity of the 378 cm^{-1} band in the infrared when compared with the 578 cm^{-1} band supports the present assignment.

No information concerning the inactive fundamentals could be gleaned from the numerous combination and overtone bands. All but the very weak bands at 640 and 1303

Can. J. Chem. Downloaded from www.nrcresearchpress.com by 210.87.254.6 on 09/05/12
For personal use only.

TABLE II

Fundamental frequencies of cyanuric fluoride

ν	cm^{-1}	Species	Approximate vibration
1	1496	Raman	sym. C–F stretching
2	999	A_1' (pol.)	Ring breathing (C and N out of phase)
3	642		Ring breathing (all atoms in phase)
4	—	A_2'	C atom twist against N
5	—	Inactive	F atom twist against ring
6	1617	E'	Ring stretching
7	1424	Infrared	Ring stretching
8	1087	Raman (depol.)	C–F stretching
9	578		Ring angle bend
10	379		C–F rocking
11	817	A_2''	Out-of-plane ring mode (C and N out of phase)
12	436	Infrared	C–F wagging (F in phase)
13	743	E''	C–F wagging
14	226	Raman (depol.)	Out-of-plane ring mode

cm^{-1} could be explained in terms of the active fundamentals. These probably arise from unknown impurities.

Although the spectra are interpreted in terms of the planar D_{3h} model, there are two bands which at first seemed to contradict the interpretation. A very strong band at 1581 cm^{-1} in the infrared (1573 cm^{-1} in the Raman effect) could possibly arise if the molecule had a lower symmetry, thereby splitting the degeneracy of ν_6. On the other hand, the combination band $\nu_2 + \nu_9 = 1577$ cm^{-1} has the symmetry species (E') of ν_6 and occurs sufficiently close to ν_6 for its intensity to be greatly enhanced through a Fermi resonance interaction. The presence of a single F^{19} resonance in the nuclear magnetic resonance experiment is not proof of the planar structure either, for one could construct a structure of lower symmetry than D_{3h} in which the fluorine atoms were still equivalent. The fact that none of the other E' fundamentals appear to be split into doublets would favor the Fermi resonance interpretation offered above.

The second conflict with the D_{3h} model occurs with the ν_{13} (e'') mode which should be inactive in the infrared. It was not observed in the gas phase study (80 mm pressure) but it could be detected in the liquid phase spectrum. It can be argued, of course, that in the liquid phase the selection rules break down and, therefore, the ν_{13} fundamental might be observable. The problem can best be resolved by observing the infrared spectrum in the gas phase at elevated temperatures where the vapor pressure of the compound is higher, or by using a long path cell to see if $\nu_{13} = 743$ cm^{-1} is observable. The other point of interest is to see if $\nu_{14} = 224$ cm^{-1} (liquid phase) is present in the infrared spectrum. Nevertheless, the evidence presented in the paper strongly supports a planar structure for cyanuric fluoride.

ACKNOWLEDGMENTS

The authors are especially grateful to Miss D. M. Dodd and Mr. J. P. Luongo for the infrared spectra and to Mr. E. W. Anderson for the nuclear magnetic resonance data.

REFERENCES

1. D. W. Grisley, Jr., E. W. Gluesenkamp, and S. A. Heininger. J. Org. Chem. **23**, 1802 (1958).
2. F. Seel and K. Ballreich. Ber. **92**, 344 (1959).
3. E. E. Aynsley, R. E. Dodd, and R. Little. Proc. Chem. Soc. 265 (1959).

Can. J. Chem. Downloaded from www.nrcresearchpress.com by 210.87.254.6 on 09/05/12
For personal use only.

4. F. S. FAWCETT and R. D. LIPSCOMB. J. Am. Chem. Soc. **82**, 1509 (1960).
5. R. E. DODD and R. LITTLE. Spectrochim. Acta, **16**, 1083 (1960).
6. A. F. MAXWELL, J. S. FRY, and L. A. BIGELOW. J. Am. Chem. Soc. **80**, 548 (1958).
7. G. HERZBERG. Molecular spectra and molecular structure. Vol. II. D. Van Nostrand Co., Inc., Princeton, New Jersey. 1945. p. 421.
8. J. E. LANCASTER, R. F. STAMM, and N. B. COLTHUP. Spectrochim. Acta, **17**, 155 (1961).

Can. J. Chem. Downloaded from www.nrcresearchpress.com by 210.87.254.6 on 09/05/12
For personal use only.

Can. J. Chem. Downloaded from www.nrcresearchpress.com by 210.87.254.105 on 09/05/12
For personal use only.

NOTES

A NEW SYNTHESIS OF ARYLPYRROLES

C. F. H. ALLEN

In connection with a routine examination of certain Michael adducts of type I in the mass spectrometer (1), the oxime (II) of a delta ketonic nitrile (2) was included. Entirely unexpectedly, it showed large peaks at masses 322 and 295. These are assumed to be the parent ions of two pyrroles (III, IV), thermal products, which could be accounted for by assuming successive losses of the elements of water and of hydrogen cyanide from the oxime.

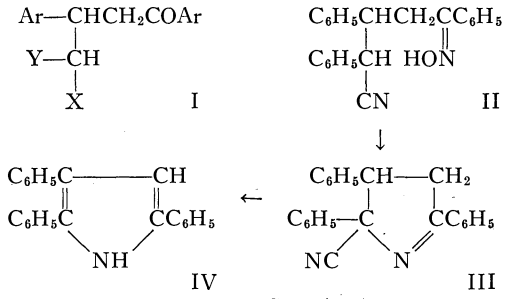

Upon comparison, the complete mass spectral pattern in the mixture spectrum was found to be identical with that of an authentic specimen of 2,4,5-triphenylpyrrole. The latter only was isolable by classical methods, and was identified in the usual way.

The oxime (V) of the nitroketone (I, Ar, Y = C_6H_5, X = NO_2) (3), in an analogous manner, loses the elements of water and of nitrous acid; in this instance there is no suggestion of a dihydro derivative corresponding to III, the triphenylpyrrole (IV) being the main product. Similarly, the oximes of a diarylnitroketone (I, Ar = C_6H_5, X = H, Y = NO_2) (4) and of γ-benzoylbutyronitrile (5) give 2,4-diphenyl- and 2-phenyl-pyrrole, respectively. The pyrroles were not only indicated and identified by the use of the mass spectrometer, but triphenylpyrrole was isolated by classical methods upon attempted distillation of the oximes (II, V).

These series of reactions constitute a new synthesis of arylpyrroles.

ACKNOWLEDGMENT

I am indebted to Mr. Glenn P. Happ for the mass spectral data and interpretation.

1. C. F. H. ALLEN and G. P. HAPP. Can. J. Chem. To be published.
2. E. P. KOHLER and C. F. H. ALLEN. J. Am. Chem. Soc. **46**, 1522 (1924).
3. E. P. KOHLER. J. Am. Chem. Soc. **46**, 1733 (1924).
4. E. P. KOHLER. J. Am. Chem. Soc. **38**, 892 (1916).
5. C. F. H. ALLEN and W. L. BALL. J. Am. Chem. Soc. **59**, 686 (1937).

RECEIVED AUGUST 9, 1963.
DEPARTMENT OF CHEMISTRY,
ROCHESTER INSTITUTE OF TECHNOLOGY,
11 PLYMOUTH AVENUE, SOUTH,
ROCHESTER, NEW YORK 14608.

THE SIGNS OF THE H′—C—H′ AND H′—C—O—H′ NUCLEAR MAGNETIC RESONANCE COUPLING CONSTANTS

F. HRUSKA,* T. SCHAEFER, AND C. A. REILLY

Buckingham and McLauchlan have recently shown that J_0(H′—H′) is definitely positive in *p*-nitrotoluene (1). It follows that $J(C^{13}—H)$ is also positive (1), thus vindicating the suggestion of Karplus (2). Then the work of Lauterbur and Kurland (3) shows that J(H′—C—C—H′) is positive, while the measurements of Anet (4) give J(H′—C—H′) as negative. Manatt *et al.* (5) have suggested that J(H′—P—C—H′) and J(H′—P—P—H′) are positive. From their data it follows that $J(P^{31}—H')$ is then also positive. However, Whitesides *et al.* (6) state that the latter coupling may be either positive or negative, which would mean that J(H′—P—C—H′) may be of either sign. Anderson, Freeman, and Reilly have shown that all the couplings in trivinylphosphine have the same sign (7). Presumably then, they are all positive, which means that $J(P^{31}—C—H')$ is positive. We show here that J(H′—C—H′) and J(H′—C—O—H′) are of opposite sign, an additional datum in the rapidly increasing knowledge of the signs of coupling constants.

2-Methyl-2-nitropropanediol-1,3 has magnetically nonequivalent methylene protons because the plane bisecting the HCH angle and perpendicular to the interproton axis is not a plane of symmetry of the molecule as a whole for any conformation (8, 9). Much of the shift is probably also due to differing conformer populations (9). In a saturated solution of this compound in water we find an AB quartet for the methylene protons with an AB shift of 0.23 p.p.m. and a magnitude of J(H′—C—H′) of 12.4 ± 0.2 c.p.s. No coupling to the hydroxyl protons was observed, no doubt as a result of rapid exchange of the latter protons with water molecules. A small broadening of the methyl and methylene protons indicated unresolved long-range couplings. A saturated solution of this compound in acetone gave rise to an ABC proton spectrum for the methylene and hydroxyl protons. The line widths were larger than in water solution indicating kinetic processes of some sort. A computer analysis by an iterative technique (10) yielded the parameters in Table I. The parameters with the vicinal couplings opposite in sign to the geminal

TABLE I

Chemical shifts relative to internal cyclohexane and proton coupling constants of 2-methyl-2-nitropropanediol-1,3 in acetone

Coupling constants (c.p.s.)	Chemical shift (p.p.m.)
$J(H'_A—C—H'_B) = \mp11.67\pm0.04$*	$H_A = -2.41$
$J(H'_A—C—O—H'_C) = \pm5.96\pm0.03$	$H_B = -2.57$
$J(H'_B—C—O—H'_C) = \pm5.80\pm0.08$	$H_C = -3.04$

*R.M.S. deviations.

one gave a better fit to the observed spectrum than when the signs were the same. This was true for both the frequencies and intensities of the observed and calculated lines. The discussion in the first paragraph above means that the geminal coupling is negative and the H′—C—O—H′ vicinal couplings are positive, just as for H′—C—C—H′ couplings.

The geminal coupling differs from that in water as a solvent. A similar situation is discussed by Snyder (11). The two vicinal couplings are almost equal within experimental

*N.R.C. Bursary Holder 1962–63.

Can. J. Chem. Downloaded from www.nrcresearchpress.com by 210.87.254.105 on 09/05/12
For personal use only.

error. It might appear that there is hydrogen-bonding to acetone; at any rate intramolecular hydrogen-bonding would appear to be absent (12). Temperature studies in a number of proton acceptors as well as in inert solvents are underway. It is hoped that these studies will yield information on the effect of the solvent on the geminal coupling, on the magnitude of the asymmetry shift (dependent on attaining sufficiently high temperatures in order to equalize conformational populations), on the magnitude of the cis and the trans vicinal couplings (dependent on attaining low enough temperatures), and on the magnitude of the hydrogen-bond shifts and enthalpies in the acceptor solvents.

EXPERIMENTAL

Proton magnetic resonance measurements were done on a Varian DP-60 high resolution N.M.R. spectrometer. Line separations were measured by the usual sideband technique using a Model 521 Hewlett–Packard Frequency Counter. The analysis was carried out on the IBM 7040 at the Shell Development Company.

ACKNOWLEDGMENTS

We are grateful to Dr. A. Unrau for a sample of 2-methyl-2-nitropropanediol-1,3. F. H. and T. S. thank the National Research Council for financial support.

1. A. D. Buckingham and K. A. McLauchlan. Proc. Chem. Soc. (London), 144 (1963).
2. M. Karplus. J. Am. Chem. Soc. **84**, 2458 (1962).
3. P. C. Lauterbur and R. J. Kurland. J. Am. Chem. Soc. **84**, 3405 (1962).
4. F. A. L. Anet. J. Am. Chem. Soc. **84**, 3767 (1962).
5. S. L. Manatt, F. L. Juvinall, and D. D. Elleman. J. Am. Chem. Soc. **85**, 2664 (1963).
6. G. M. Whitesides, J. L. Beauchamp, and J. D. Roberts. J. Am. Chem. Soc. **85**, 2665 (1963).
7. W. Anderson, R. Freeman, and C. A. Reilly. J. Chem. Phys. **39**, 1518 (1963).
8. J. S. Waugh and F. A. Cotton. J. Phys. Chem. **65**, 562 (1961).
9. H. S. Gutowsky. J. Chem. Phys. **37**, 2196 (1962).
10. J. D. Swalen and C. A. Reilly. J. Chem. Phys. **37**, 21 (1963).
11. E. I. Snyder. J. Am. Chem. Soc. **85**, 2624 (1963).
12. H. E. Ungnade and L. W. Kissinger. Tetrahedron, **19**, Suppl. 1, 121 (1963).

Received October 21, 1963.
Department of Chemistry,
University of Manitoba,
Winnipeg, Canada,
and
Shell Development Company,
Emeryville, California,
U.S.A.

THE REACTION OF N-BROMOSUCCINIMIDE WITH SOME ALKYL PYRIDINES

James P. Kutney, W. Cretney, T. Tabata, and M. Frank

In relation to another problem in our laboratory, it became necessary to prepare several bromoalkyl pyridines. Several methods are available for side chain halogenation in the pyridine series (1, 2) but, in general, these are not particularly attractive for the bromoalkyl series. It appeared that the most direct approach to this problem was to consider the reaction of N-bromosuccinimide (N.B.S.) with several alkyl pyridines. Previous work in the literature (3, 4) and our own experience with this reagent (5) encouraged further study.

When 4-ethylpyridine was reacted with N.B.S., it was found, as expected, that the nature of the reaction product was dependent on the relative amounts of brominating

Can. J. Chem. Downloaded from www.nrcresearchpress.com by 210.87.254.105 on 09/05/12
For personal use only.

error. It might appear that there is hydrogen-bonding to acetone; at any rate intramolecular hydrogen-bonding would appear to be absent (12). Temperature studies in a number of proton acceptors as well as in inert solvents are underway. It is hoped that these studies will yield information on the effect of the solvent on the geminal coupling, on the magnitude of the asymmetry shift (dependent on attaining sufficiently high temperatures in order to equalize conformational populations), on the magnitude of the cis and the trans vicinal couplings (dependent on attaining low enough temperatures), and on the magnitude of the hydrogen-bond shifts and enthalpies in the acceptor solvents.

EXPERIMENTAL

Proton magnetic resonance measurements were done on a Varian DP-60 high resolution N.M.R. spectrometer. Line separations were measured by the usual sideband technique using a Model 521 Hewlett–Packard Frequency Counter. The analysis was carried out on the IBM 7040 at the Shell Development Company.

ACKNOWLEDGMENTS

We are grateful to Dr. A. Unrau for a sample of 2-methyl-2-nitropropanediol-1,3. F. H. and T. S. thank the National Research Council for financial support.

1. A. D. Buckingham and K. A. McLauchlan. Proc. Chem. Soc. (London), 144 (1963).
2. M. Karplus. J. Am. Chem. Soc. **84**, 2458 (1962).
3. P. C. Lauterbur and R. J. Kurland. J. Am. Chem. Soc. **84**, 3405 (1962).
4. F. A. L. Anet. J. Am. Chem. Soc. **84**, 3767 (1962).
5. S. L. Manatt, F. L. Juvinall, and D. D. Elleman. J. Am. Chem. Soc. **85**, 2664 (1963).
6. G. M. Whitesides, J. L. Beauchamp, and J. D. Roberts. J. Am. Chem. Soc. **85**, 2665 (1963).
7. W. Anderson, R. Freeman, and C. A. Reilly. J. Chem. Phys. **39**, 1518 (1963).
8. J. S. Waugh and F. A. Cotton. J. Phys. Chem. **65**, 562 (1961).
9. H. S. Gutowsky. J. Chem. Phys. **37**, 2196 (1962).
10. J. D. Swalen and C. A. Reilly. J. Chem. Phys. **37**, 21 (1963).
11. E. I. Snyder. J. Am. Chem. Soc. **85**, 2624 (1963).
12. H. E. Ungnade and L. W. Kissinger. Tetrahedron, **19**, Suppl. 1, 121 (1963).

Received October 21, 1963.
Department of Chemistry,
University of Manitoba,
Winnipeg, Canada,
and
Shell Development Company,
Emeryville, California,
U.S.A.

THE REACTION OF N-BROMOSUCCINIMIDE WITH SOME ALKYL PYRIDINES

James P. Kutney, W. Cretney, T. Tabata, and M. Frank

In relation to another problem in our laboratory, it became necessary to prepare several bromoalkyl pyridines. Several methods are available for side chain halogenation in the pyridine series (1, 2) but, in general, these are not particularly attractive for the bromoalkyl series. It appeared that the most direct approach to this problem was to consider the reaction of N-bromosuccinimide (N.B.S.) with several alkyl pyridines. Previous work in the literature (3, 4) and our own experience with this reagent (5) encouraged further study.

When 4-ethylpyridine was reacted with N.B.S., it was found, as expected, that the nature of the reaction product was dependent on the relative amounts of brominating

Can. J. Chem. Downloaded from www.nrcresearchpress.com by 210.87.254.6 on 09/05/12
For personal use only.

agent which were used in the reaction. As previously reported (5) utilization of a 1:1 molar ratio of 4-ethylpyridine to N.B.S. provides 4-(1-bromoethyl) pyridine as the major product whereas subsequent work reported here reveals that a 2:1 ratio of N.B.S. to 4-ethylpyridine provides 4-(1,1-dibromoethyl) pyridine in good yield. In both instances isolation and characterization of the products was carried out on the crystalline hydrobromides (I and II) since it is well known that halogenoalkyl pyridines of this type are unstable as the parent bases. At this point of the investigation it was clear to us that N.B.S. does indeed provide a simple and attractive method for the preparation of bromoalkyl pyridines particularly of type II since the yield of II was always good (about 70%) on the numerous occasions which we had to prepare this compound.

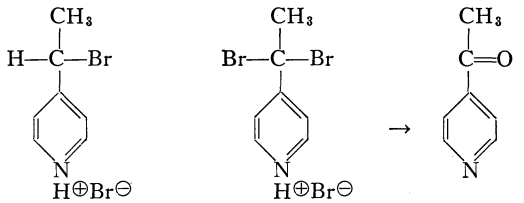

I II

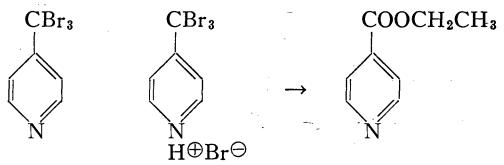

IV III

Our attention was then directed at the methyl pyridine compounds with particular interest in the 4-methylpyridine series, since brominated derivatives in this series were also desirable. Hasegawa (3) had already shown that 2-methylpyridine reacts with N.B.S. to yield mono- and di-bromomethylpyridines as the products. On this basis, there seemed little reason to suppose that similar results should not be obtained from the 4-methyl series. Consequently 4-methylpyridine was reacted with N.B.S. according to the published procedure, and the product isolated as the hydrobromide salt. Subsequent analysis on this substance revealed, however, that neither the mono- nor di-bromoethylpyridines was formed but that the fully brominated, 4-tribromomethylpyridine, was actually being isolated as its salt (III). The n.m.r. spectrum of this salt indicated only two sets of multiplets—one set centered at 1.54 τ and the other centered at 1.19 τ, as expected for the α and β protons of the pyridine ring. Furthermore, the areas under these signals were equal and therefore provided good evidence for structure III. This latter structure was further confirmed when the parent base (IV) could be obtained as a stable, crystalline substance which analyzed well for $C_6H_4NBr_3$. The n.m.r. spectrum of 4-tribromomethylpyridine, in complete agreement with the assigned structure, indicated two sets of multiplets centered at 2.23 τ and 1.34 τ. The set at higher field (2.23 τ) was resolved into four peaks whereas the lower field set was broad and poorly resolved thereby approximating a doublet. The broadening of the latter signals is probably due to the nitrogen atom. A final confirmation of structure IV for the N.B.S. product was obtained from hydrolysis of the hydrobromide, III, which provided isonicotinic acid isolated and characterized as the ethyl ester.

Can. J. Chem. Downloaded from www.nrcresearchpress.com by 210.87.254.6 on 09/05/12
For personal use only.

It must be emphasized at this point that although in all instances reported herein, the two sets of low field n.m.r. signals can be definitely assigned to α and β pairs of protons on the pyridine ring, it is not possible to assign with absolute certainty a particular set of signals to a particular pair of protons. It is clear that the bromoalkyl substituents at the γ position will have an appreciable, but unknown, effect on the chemical shift of the β protons.

These results indicated that 4-methylpyridine was more reactive toward the action of N.B.S. than 2-methylpyridine. To eliminate any doubt about this point we repeated the bromination of the 2-methyl compound under conditions *identical* with those used in the 4-methyl series and were able to confirm the results first reported by Hasegawa (3).

Finally, several attempts were made to brominate the methyl group in 3-methylpyridine under the above conditions but no bromo compounds could be obtained. On this basis it can be concluded that in the methylpyridine series, the rate of reactivity toward N.B.S. is 4-methyl > 2-methyl > 3-methyl.

Since 4-bromoalkylpyridines were readily available from the above work, a few preliminary experiments were carried out to determine whether some of these derivatives would be suitable intermediates for the preparation of pyridyl ketones which were desirable for another problem. Consequently, 4-(1,1-dibromoethyl) pyridine hydrobromide was reacted with aqueous sodium carbonate at the reflux temperature and, as expected, the product obtained in 41% yield was the known 4-acetylpyridine. The overall yield of 4-acetylpyridine from 4-ethylpyridine was 29% although it must be emphasized that sufficient experimentation was not carried out to develop optimum conditions for the alkaline hydrolysis of the brominated product. The overall yield in this two-step sequence could probably be improved and we feel that this approach does provide an attractive synthetic approach to pyridyl ketones.

EXPERIMENTAL

All melting points were determined on a Fischer–Johns apparatus and are uncorrected. The ultraviolet spectra were recorded in 95% ethyl alcohol on a Cary 11 recording spectrophotometer. Infrared spectra were recorded on a Perkin–Elmer model 21 spectrophotometer. The n.m.r. spectra were taken at 60 Mc/s on a Varian A60 instrument. The values are given in the Tiers τ scale with the signal of tetramethylsilane which was used as the internal standard, set at 10.0 τ units. Integration of areas under the signals was carried out in all cases and the number of protons is indicated in parentheses. The solvents used are indicated below. The analyses were performed by Dr. A. Bernhardt and his associates, Mulheim (Ruhr), Germany, and by Mrs. A. Aldridge, University of British Columbia.

4-(1,1-Dibromoethyl)-pyridine Hydrobromide (II)

A mixture of 4-ethylpyridine (6.5 g), N-bromosuccinimide (21.7 g), and benzoyl peroxide (1.0 g) in carbon tetrachloride (300 ml) was refluxed for 6 hours. The reaction mixture was allowed to stand at room temperature overnight, then filtered, and the filtrate was washed successively with 4% aqueous sodium hydroxide (100 ml), water (200 ml), 2% hydrobromic acid (50 ml), and finally dried over anhydrous magnesium sulphate. The carbon tetrachloride solution was then saturated with hydrogen bromide gas whereupon a white solid, mixed with an orange oil, separated. The solvent was carefully removed *in vacuo* at *room temperature* and the resulting paste was taken up in hot, absolute ethyl alcohol (50 ml). Upon cooling, the first crop (12.5 g) of product separated as long, white needles. A second crop (2.4 g) was obtained on further concentration of the solution. Several recrystallizations of a small portion of this product from ethyl alcohol – petroleum ether provided an analytical sample, m.p. 158–160° (with considerable decomposition); ultraviolet: λ_{max} 264 mμ (log ϵ 3.43), λ_{min} 249 mμ (log ϵ 3.37); n.m.r. signals ($CDCl_3$); intense singlet at 6.95 τ(CH_3—C, area = 3H), doublet centered at 1.56 τ(βH, area = 2H), doublet centered at 0.75 τ(αH, area = 2H). Found: C, 24.36; H, 2.54; N, 4.04; Br, 69.40. Calc. for $C_7H_8NBr_3$: C, 24.29; H, 2.33; N, 4.05; Br, 69.33.

4-Tribromomethylpyridine Hydrobromide (III)

A mixture of 4-methylpyridine (10 g), N-bromosuccinimide (44.3 g), and benzoyl peroxide (2.1 g) in carbon tetrachloride (300 ml) was refluxed with stirring. The reaction mixture darkened gradually until,

Can. J. Chem. Downloaded from www.nrcresearchpress.com by 210.87.254.6 on 09/05/12
For personal use only.

after about 1½ hours, a vigorous exothermic reaction occurred and was accompanied by considerable tarring. The external source of heat was removed until this vigorous reaction had subsided and then applied again so that the total reflux period was 3 hours. The hot reaction mixture was filtered and the tarry residue which remained was washed with hot carbon tetrachloride and ether. All the washings were combined with the main filtrate and this solution was then concentrated *in vacuo* at *room temperature.* The orange-red oil which remained was extracted in the manner described by Hasegawa (3) in order to separate any mono- and di-bromomethyl derivatives which may be present.

Consequently this orange-red oil was treated with 20% hydrobromic acid (40 ml) and then diluted with water to a total volume of 400 ml. A small amount (1.04 g) of yellow solid material which had separated was removed by filtration. The acidic aqueous solution was extracted repeatedly with ether. The ether extract was dried over anhydrous magnesium sulphate, the drying agent removed by filtration, and the ether solution was then saturated with hydrogen bromide. Removal of the solvent *in vacuo* at *room temperature* provided 3.10 g of a white solid.

The remaining aqueous acidic solution was made weakly alkaline by the addition of sodium carbonate and extracted again with ether. After the ether extract was dried over anhydrous magnesium sulphate and the drying agent removed, the ether solution was saturated with hydrogen bromide. The solvent was then removed *in vacuo* at room temperature to provide 4.34 g of white solid. It was established that the three different crops of solid material (total of 8.84 g) melted in the same range (180–205°) and did in fact represent the same substance. Several recrystallizations from absolute ethyl alcohol provided an analytical sample, m.p. 204–206° (with decomposition); ultraviolet: λ_{max} 268 mμ (log ε 3.64), λ_{min} 254.5 mμ (log ε 4.02); n.m.r. signals (D_2O–acetone 2:1); multiplets centered at 1.19 τ and 1.54 τ (α and β protons, area = 4H). Found: C, 17.69; H, 1.34; N, 3.31; Br, 77.60. Calc. for $C_6H_5NBr_4$: C, 17.54; H, 1.22; N, 3.41; Br, 77.59.

4-Tribromomethylpyridine (IV)

The hydrobromide (III) (700 mg) was treated with anhydrous ether (25 ml) and anhydrous ammonia gas was then passed into the mixture until it was basic. The inorganic residue was removed by filtration and the ether removed *in vacuo* at *room temperature.* A brown residue (448 mg) which remained was divided into two equal portions and worked up as follows.

One portion was crystallized several times from petroleum ether to afford IV as colorless needles, m.p. 71–72°; ultraviolet: λ_{max} 269 mμ (log ε 3.37), λ_{min} 262 mμ (log ε 3.32); n.m.r. signals (CCl_4); multiplets centered at 1.34 τ and 2.23 τ (α and β protons, area = 4H). Found: C, 21.84; H, 1.22; N, 3.97; Br, 73.01. Calc. for $C_6H_4NBr_3$: C, 21.82; H, 1.21; N, 4.24; Br, 72.72.

The other portion was treated with an alcoholic solution of picric acid and the picrate which formed was then recrystallized from ethyl alcohol to provide an analytical sample, m.p. 162.5°–167°. Found: C, 25.98; H, 1.50; N, 9.85; O, 20.14; Br, 43.12. Calc. for $C_{12}H_7N_4O_7Br_3$: C, 25.80; H, 1.25; N, 10.00; O, 20.00; Br, 42.80.

Hydrolysis of 4-Tribromomethylpyridine Hydrobromide

4-Tribromomethylpyridine hydrobromide (1.1 g) was treated with 30% aqueous sulphuric acid (70 ml) and the mixture refluxed for 8 hours. After this time, the mixture was allowed to stand overnight at room temperature whereupon a portion (2.10 g) of a solid material had crystallized from the solution. Subsequent infrared comparison etc. established that the material was unreacted starting material.

The sulphuric acid solution was concentrated *in vacuo* at 100–130° to a volume of 25 ml and this concentrate was then treated with ammonia gas until the mixture was just slightly acidic. At this point, the mixture was essentially a solid paste and this was washed repeatedly with ethyl alcohol. The alcohol extract was reduced in volume to about 20 ml, concentrated sulphuric acid (2 ml) was added, and the whole mixture refluxed for 4 hours. After this time, about one-half of the solvent was removed *in vacuo* and the mixture was poured on ice, treated with concentrated ammonium hydroxide until basic and finally extracted with ether. The ether extract was dried over anhydrous magnesium sulphate, the solvents were removed carefully, and the residual liquid distilled to provide 521 mg of a liquid distilling at 125–130° (bath temp)/16 mm. This liquid product proved to be identical in every respect (infrared, ultraviolet, n.m.r.) with an authentic sample of ethyl isonicotinate prepared from isonicotinic acid. n.m.r. signals ($CDCl_3$); triplet centered at 8.59 τ(CH_3—, area = 3H), quartet centered at 5.58 τ(—CH_2—, area = 2H), doublets centered at 1.24 τ and 2.14 τ (α and β protons, area = 4H).

4-Acetylpyridine

A stirred mixture of 4-(1,1-dibromoethyl) pyridine hydrobromide (6 g), sodium carbonate (9 g), and water (30 ml) was refluxed over a period of 4 hours. The cooled reaction mixture was diluted with water and then extracted with ether. The ether extract was dried over anhydrous magnesium sulphate, the solvent *carefully removed*, and the dark red oil which remained was distilled to provide the known (6, 7) 4-acetylpyridine (1 g). n.m.r. signals (neat liquid); two sets of multiplets centered at 1.19 τ and 2.29 τ (α and β protons, area = 4H), a single peak at 7.35 τ (CH_3CO—, area = 3H). A crystalline oxime was prepared and its melting point (155°) was in good agreement with the literature value (8), m.p. 157–159°.

Can. J. Chem. Downloaded from www.nrcresearchpress.com by 210.87.254.6 on 09/05/12
For personal use only.

ACKNOWLEDGMENT

Financial aid from the National Research Council of Canada is very gratefully acknowledged.

1. E. KLINGSBERG. Heterocyclic compounds, pyridine and its derivatives. Interscience Publishers Inc., New York. 1961. p. 360.
2. W. MATHES and H. SCHULY. Angew. Chem. Int. Edition, 144 (1963).
3. M. HASEGAWA. Pharm. Bull. Japan, **1**, 293 (1953).
4. J. HURST and D. G. WIBBERLEY. J. Chem. Soc. 119 (1962).
5. J. P. KUTNEY and T. TABATA. Can. J. Chem. **41**, 695 (1963).
6. H. G. KOLLOFF and J. H. HUNTER. J. Am. Chem. Soc. **63**, 490 (1941).
7. A. R. KATRITZKY. J. Chem. Soc. 2586 (1955).
8. M. V. RUBTSOV, E. S. NIKITSKAYA, and V. S. USOVSKAYA. Zh. Obshch. Khim. **25**, 2453 (1955); Chem. Abstr. **50**, 9401d (1956).

RECEIVED OCTOBER 15, 1963.
DEPARTMENT OF CHEMISTRY,
UNIVERSITY OF BRITISH COLUMBIA,
VANCOUVER 8, BRITISH COLUMBIA.

Can. J. Chem. Downloaded from www.nrcresearchpress.com by 210.87.254.6 on 09/05/12
For personal use only.

THE FLUORINATION OF CHROMIUM(VI) OXIDE AND POTASSIUM DICHROMATE

H. C. CLARK AND Y. N. SADANA

INTRODUCTION

The fluorination of metal oxides by bromine trifluoride frequently constitutes a useful method for the preparation of metal fluorides and oxyfluorides. However, considerable differences are observed in the ease with which such fluorinations occur. Some oxides (e.g. MgO, ZnO, MnO_2, Fe_2O_3) do not react or react only very slowly with bromine trifluoride. With other oxides (e.g. TiO_2, As_2O_3, SeO_2), complete replacement of the oxygen by fluorine occurs, together with oxidation of the metal to its highest state. In a few instances (e.g. V_2O_5), only partial replacement of oxygen takes place to give oxyfluorides. Chromium (VI) oxide is unique, in that reaction with bromine trifluoride (1) replaces two-thirds of the oxygen by fluorine and *reduction* of chromium occurs to Cr(V), the final product apparently being a thermally unstable addition compound of $CrOF_3$, with BrF_3. Also, it is interesting to notice the decreasing ease with which fluorination of the oxides occurs in the series TiO_2, V_2O_5, CrO_3, Fe_2O_3, although as yet no explanation can be given.

It seemed of interest to determine the ease and extent of fluorination of chromium(VI) oxide with other halogen fluorides, particularly bromine pentafluoride and chlorine trifluoride, since the higher fluorides CrF_5 and CrF_6, and an oxyfluoride such as $CrOF_4$ might well be formed. Since this work was completed, brief reports have appeared of the preparation by other methods of chromium hexafluoride (2), chromium pentafluoride, and chromium oxide tetrafluoride (3).

EXPERIMENTAL

The general manipulative and analytical techniques employed have been described elsewhere (4, 5); magnetic susceptibilities were determined with a Gouy magnetic balance (6), and X-ray powder photographs were taken on a General Electric unit with a camera of 14.4 cm diameter.

Reactions of Chromium(VI) Oxide

(i) With bromine trifluoride.—Excess bromine trifluoride was condensed onto a sample of chromium(VI) oxide in a silica vessel, and the reaction was allowed to take place at room temperature, with the evolution of gas and formation of a deep red solution. The excess bromine trifluoride was distilled off *in vacuo*, first

ACKNOWLEDGMENT

Financial aid from the National Research Council of Canada is very gratefully acknowledged.

1. E. KLINGSBERG. Heterocyclic compounds, pyridine and its derivatives. Interscience Publishers Inc., New York. 1961. p. 360.
2. W. MATHES and H. SCHULY. Angew. Chem. Int. Edition, 144 (1963).
3. M. HASEGAWA. Pharm. Bull. Japan, **1**, 293 (1953).
4. J. HURST and D. G. WIBBERLEY. J. Chem. Soc. 119 (1962).
5. J. P. KUTNEY and T. TABATA. Can. J. Chem. **41**, 695 (1963).
6. H. G. KOLLOFF and J. H. HUNTER. J. Am. Chem. Soc. **63**, 490 (1941).
7. A. R. KATRITZKY. J. Chem. Soc. 2586 (1955).
8. M. V. RUBTSOV, E. S. NIKITSKAYA, and V. S. USOVSKAYA. Zh. Obshch. Khim. **25**, 2453 (1955); Chem. Abstr. **50**, 9401d (1956).

RECEIVED OCTOBER 15, 1963.
DEPARTMENT OF CHEMISTRY,
UNIVERSITY OF BRITISH COLUMBIA,
VANCOUVER 8, BRITISH COLUMBIA.

Can. J. Chem. Downloaded from www.nrcresearchpress.com by 210.87.254.6 on 09/05/12
For personal use only.

THE FLUORINATION OF CHROMIUM(VI) OXIDE AND POTASSIUM DICHROMATE

H. C. CLARK AND Y. N. SADANA

INTRODUCTION

The fluorination of metal oxides by bromine trifluoride frequently constitutes a useful method for the preparation of metal fluorides and oxyfluorides. However, considerable differences are observed in the ease with which such fluorinations occur. Some oxides (e.g. MgO, ZnO, MnO_2, Fe_2O_3) do not react or react only very slowly with bromine trifluoride. With other oxides (e.g. TiO_2, As_2O_3, SeO_2), complete replacement of the oxygen by fluorine occurs, together with oxidation of the metal to its highest state. In a few instances (e.g. V_2O_5), only partial replacement of oxygen takes place to give oxyfluorides. Chromium (VI) oxide is unique, in that reaction with bromine trifluoride (1) replaces two-thirds of the oxygen by fluorine and *reduction* of chromium occurs to Cr(V), the final product apparently being a thermally unstable addition compound of $CrOF_3$, with BrF_3. Also, it is interesting to notice the decreasing ease with which fluorination of the oxides occurs in the series TiO_2, V_2O_5, CrO_3, Fe_2O_3, although as yet no explanation can be given.

It seemed of interest to determine the ease and extent of fluorination of chromium(VI) oxide with other halogen fluorides, particularly bromine pentafluoride and chlorine trifluoride, since the higher fluorides CrF_5 and CrF_6, and an oxyfluoride such as $CrOF_4$ might well be formed. Since this work was completed, brief reports have appeared of the preparation by other methods of chromium hexafluoride (2), chromium pentafluoride, and chromium oxide tetrafluoride (3).

EXPERIMENTAL

The general manipulative and analytical techniques employed have been described elsewhere (4, 5); magnetic susceptibilities were determined with a Gouy magnetic balance (6), and X-ray powder photographs were taken on a General Electric unit with a camera of 14.4 cm diameter.

Reactions of Chromium(VI) Oxide

(i) With bromine trifluoride.—Excess bromine trifluoride was condensed onto a sample of chromium(VI) oxide in a silica vessel, and the reaction was allowed to take place at room temperature, with the evolution of gas and formation of a deep red solution. The excess bromine trifluoride was distilled off *in vacuo*, first

at room temperature and then at 100°. Chemical analyses of the red residue showed the presence of bromine and indicated an approximate composition $CrOF_3.0.25BrF_3$. Calc. for $CrOF_3.0.25BrF_3$: Cr, 32.7; F, 44.8. Found: Cr, 33.4; F, 44.5%. The molar magnetic susceptibility was 1715×10^{-6} c.g.s. units at 25°, giving $\mu_{eff.}$ a value of 2.02 Bohr magnetons (B.M.) corresponding to one unpaired electron. In a second similar experiment, the product was heated to 120° for 24 hours in an attempt to complete the removal of bromine trifluoride. The final product was a light-green powder characterized as $CrF_3.BrF_3$. Calc. for $CrF_3.BrF_3$: Cr, 21.1; F, 47.2. Found: Cr. 21.6; F, 48.5%. The molar susceptibility at 25° was 5682×10^{-6} c.g.s. units giving a magnetic moment of 3.67 B.M.

(ii) With bromine pentafluoride.—Excess pentafluoride was allowed to react with the oxide at room temperature, and when effervescence had ceased, the pentafluoride was removed under vacuum, first at 25° and then at 80°, leaving a red powder, $CrOF_3.0.25BrF_5$ Calc. for $CrOF_3.0.25BrF_5$: Cr, 30.6; F, 47.9; Br, 11.9. Found: Cr, 30.6; F, 47.7, 48.5; Br, 13.3%. This product, which reacted more rapidly with glass than did the bromine trifluoride product, had a molar susceptibility at 25° of 1443×10^{-6} c.g.s. units and an effective magnetic moment of 1.85 B.M.

(iii) With chlorine trifluoride in the liquid phase.—The reaction of chlorine trifluoride with chromium(VI) oxide was carried out as in *(i)* and *(ii)* at 12° (b.p. of ClF_3), the excess trifluoride being removed finally at 50° *in vacuo*. The orange-red product gave analytical results in agreement with $CrOF_3.0.30ClF_3$. Calc. for $CrOF_3.0.30ClF_3$: Cr, 34.1; F, 48.6. Found: Cr, 34.2; F, 48.0%. From the molar susceptibility at 25°, of 1418×10^{-6} c.g.s. units, the effective magnetic moment was calculated to be 1.83 B.M.

(iv) With chlorine trifluoride in the vapor phase.—Chlorine trifluoride gas was passed over chromium(VI) oxide which was contained in a nickel boat inside a silica tube heated to 120°. A dull-red volatile solid was swept with the excess trifluoride into the first of a series of traps connected to the silica tube. The passage of trifluoride was continued until all the oxide had reacted. Analysis of the dense red product, after the removal of excess trifluoride, agreed with the composition $CrOF_3.0.30ClF_3$. Calc. for $CrOF_3.0.30ClF_3$: Cr, 34.1; F, 48.6. Found: Cr, 34.5; F, 49.5%. Magnetic measurements at 25° gave $\chi_M = 1308\times10^{-6}$ c.g.s. units, and $\mu_{eff.} = 1.76$ B.M. This product differed considerably in color from that obtained from the liquid phase reaction, but when heated *in vacuo* at 75°, a phase transformation occurred with a considerable increase in volume from the dense red solid to the orange-red product. Chemical analyses confirmed that the composition was unchanged.

Reactions of Potassium Dichromate

(i) With bromine trifluoride.—The reaction was allowed to take place in a silica reaction vessel as described previously (1). Removal of bromine trifluoride at 100° gave a product of composition $KCrOF_4.0.5BrF_3$. Calc. for $KCrOF_4.0.5BrF_3$: Cr, 20.7. Found: Cr, 19.9%. The molar susceptibility at 25° was 1265×10^{-6} c.g.s. units, and susceptibility measurements over the range 85–298° K gave a value of +4° for θ (Weiss constant), and hence $\mu_{eff.}$ at 25° C was 1.73 B.M. When a sample of $KCrOF_4.0.5BrF_2$ was heated *in vacuo* at 160°, pure $KCrOF_4$ was obtained as previously reported (1). Both $KCrOF_4.0.5BrF_3$ and $KCrOF_4$ gave the same X-ray powder photograph which was indexed on an orthorhombic lattice with $a = 13.24$, $b = 10.31$, and $c = 8.32$ Å.

(ii) With bromine pentafluoride.—Potassium dichromate reacted readily with bromine pentafluoride at room temperature to give, after removal of excess pentafluoride, a product of composition $KCrOF_4.0.5BrF_5$. Calc. for $KCrOF_4.0.5BrF_5$: Cr, 19.2; F, 45.6. Found: Cr, 19.0; F, 44.5%. The molar susceptibility at 25° was 1237×10^{-6} c.g.s. units and $\mu_{eff.}$ had a value of 1.75 B.M. The excess bromine pentafluoride could be removed at 160° *in vacuo* to give pure $KCrOF_4$, identified by means of its X-ray diffraction powder photograph.

(iii) With chlorine trifluoride.—Similarly, liquid chlorine trifluoride reacted readily with potassium dichromate to give $KCrOF_4$, identified by its X-ray powder pattern.

DISCUSSION

In an extension of the work of Sharpe and Woolf (1) it has now been shown that chromium(VI) oxide reacts vigorously with bromine trifluoride, bromine pentafluoride, and chlorine trifluoride at or below room temperature to give products containing chromium(V). Our results indicate that these products have the approximate composition $CrOF_3.0.25$ (halogen fluoride), but it is not possible to determine whether this represents adduct formation, or just incomplete removal of solvating halogen fluoride. All attempts to remove the halogen fluoride completely leaving pure $CrOF_3$ were unsuccessful, and resulted in the formation of lower fluorides of chromium. The reaction of chromium(VI) oxide with chlorine trifluoride vapor also gave a product of composition $CrOF_3.0.25ClF_3$. This was a dull-red solid, which on heating at 75° appeared to transform without change in composition to an orange, less dense product, similar to that obtained from the reaction with *liquid* chlorine trifluoride.

Can. J. Chem. Downloaded from www.nrcresearchpress.com by 210.87.254.6 on 09/05/12
For personal use only.

These chromium oxytrifluoride products fumed in air giving chromyl fluoride, and were hydrolyzed vigorously by water giving Cr^{3+} and CrO_4^{2-} ions, in solution. They reacted with glass, even under vacuum, presumably because of the liberation of small quantities of halogen fluoride. Attempts to obtain X-ray diffraction powder photographs were all unsuccessful since reaction with the capillary (either silica or pyrex) always caused the capillary to explode during the exposure.

The fluorination of chromium(VI) oxide can therefore be summarized as follows. Sulphur tetrafluoride (7), selenium tetrafluoride (8), and iodine pentafluoride (9) cause displacement of only one-third of the oxygen to form chromyl fluoride, CrO_2F_2. Bromine tri- and penta-fluoride and chlorine trifluoride, which are more vigorous fluorinating agents, displace two-thirds of the oxygen to give the unstable oxytrifluoride, $CrOF_3$. It is perhaps surprising that none of these strong fluorinating agents produces the oxytetrafluoride, $CrOF_4$, which has recently been obtained (3) as a minor product from the direct fluorination of chromium metal.

Potassium dichromate, on fluorination with bromine trifluoride or pentafluoride, or chlorine trifluoride, gave potassium oxytetrafluorochromium(V), which has been previously reported (1). Again therefore, even the most vigorous fluorinating agents failed to remove oxygen completely, and again reduction to chromium(V) occurred. The compound $KCrOF_4$ is readily hydrolyzed in air, and is decomposed in water.

$$3KCrOF_4 + 5H_2O \rightarrow 3KF + CrF_3 + 2H_2CrO_4 + 6HF$$

The value of the Weiss constant, θ, for $KCrOF_4$ is $+4°$, which is remarkably low, particularly in comparison with the high θ values of 120° observed (4) for complex fluorides of V^{4+}, which is isoelectronic with Cr^{5+}. Unfortunately, no comparison can yet be made with other complex fluorides of chromium(V), and it may be that the low θ value in $KCrOF_4$ is associated with the presence of oxygen in the molecule.

ACKNOWLEDGMENTS

The financial support of the U. S. Office of Naval Research is gratefully acknowledged, and also the award of a National Research Council of Canada Studentship to Y. N. S.

1. A. G. Sharpe and A. A. Woolf. J. Chem. Soc. 798 (1951).
2. O. Glemser, H. Roesky, and K. H. Hellberg. Angew. Chem. **75**, 346 (1963).
3. A. J. Edwards. Proc. Chem. Soc. 205 (1963).
4. R. G. Cavell and H. C. Clark. J. Chem. Soc. 2692 (1962).
5. H. C. Clark and Y. N. Sadana. Can. J. Chem. **42**, 50 (1964).
6. H. C. Clark and R. J. O'Brien. Can. J. Chem. **39**, 1030 (1961).
7. W. C. Smith. Angew. Chem. Intern. Ed. Engl. **1**, 467 (1962).
8. N. Bartlett and P. L. Robinson. J. Chem. Soc. 3549 (1961).
9. E. E. Aynsley, R. Nichols, and P. L. Robinson. J. Chem. Soc. 623 (1953).

Received October 22, 1963.
Department of Chemistry,
University of British Columbia,
Vancouver 8, British Columbia.

Can. J. Chem. Downloaded from www.nrcresearchpress.com by 210.87.254.6 on 09/05/12
For personal use only.

CHLOROMETHYL ACETATE

P. M. G. Bavin

Chloromethyl acetate has been shown to have limited value as an alkylating agent, reaction with sodium benzylate and potassiopyrrole giving benzyloxymethyl acetate (15%) (1) and N-pyrrylmethyl acetate (18%) (2), respectively. However, because methyl

These chromium oxytrifluoride products fumed in air giving chromyl fluoride, and were hydrolyzed vigorously by water giving Cr^{3+} and CrO_4^{2-} ions, in solution. They reacted with glass, even under vacuum, presumably because of the liberation of small quantities of halogen fluoride. Attempts to obtain X-ray diffraction powder photographs were all unsuccessful since reaction with the capillary (either silica or pyrex) always caused the capillary to explode during the exposure.

The fluorination of chromium(VI) oxide can therefore be summarized as follows. Sulphur tetrafluoride (7), selenium tetrafluoride (8), and iodine pentafluoride (9) cause displacement of only one-third of the oxygen to form chromyl fluoride, CrO_2F_2. Bromine tri- and penta-fluoride and chlorine trifluoride, which are more vigorous fluorinating agents, displace two-thirds of the oxygen to give the unstable oxytrifluoride, $CrOF_3$. It is perhaps surprising that none of these strong fluorinating agents produces the oxytetrafluoride, $CrOF_4$, which has recently been obtained (3) as a minor product from the direct fluorination of chromium metal.

Potassium dichromate, on fluorination with bromine trifluoride or pentafluoride, or chlorine trifluoride, gave potassium oxytetrafluorochromium(V), which has been previously reported (1). Again therefore, even the most vigorous fluorinating agents failed to remove oxygen completely, and again reduction to chromium(V) occurred. The compound $KCrOF_4$ is readily hydrolyzed in air, and is decomposed in water.

$$3KCrOF_4 + 5H_2O \rightarrow 3KF + CrF_3 + 2H_2CrO_4 + 6HF$$

The value of the Weiss constant, θ, for $KCrOF_4$ is $+4°$, which is remarkably low, particularly in comparison with the high θ values of 120° observed (4) for complex fluorides of V^{4+}, which is isoelectronic with Cr^{5+}. Unfortunately, no comparison can yet be made with other complex fluorides of chromium(V), and it may be that the low θ value in $KCrOF_4$ is associated with the presence of oxygen in the molecule.

ACKNOWLEDGMENTS

The financial support of the U. S. Office of Naval Research is gratefully acknowledged, and also the award of a National Research Council of Canada Studentship to Y. N. S.

1. A. G. Sharpe and A. A. Woolf. J. Chem. Soc. 798 (1951).
2. O. Glemser, H. Roesky, and K. H. Hellberg. Angew. Chem. **75**, 346 (1963).
3. A. J. Edwards. Proc. Chem. Soc. 205 (1963).
4. R. G. Cavell and H. C. Clark. J. Chem. Soc. 2692 (1962).
5. H. C. Clark and Y. N. Sadana. Can. J. Chem. **42**, 50 (1964).
6. H. C. Clark and R. J. O'Brien. Can. J. Chem. **39**, 1030 (1961).
7. W. C. Smith. Angew. Chem. Intern. Ed. Engl. **1**, 467 (1962).
8. N. Bartlett and P. L. Robinson. J. Chem. Soc. 3549 (1961).
9. E. E. Aynsley, R. Nichols, and P. L. Robinson. J. Chem. Soc. 623 (1953).

Received October 22, 1963.
Department of Chemistry,
University of British Columbia,
Vancouver 8, British Columbia.

CHLOROMETHYL ACETATE

P. M. G. Bavin

Chloromethyl acetate has been shown to have limited value as an alkylating agent, reaction with sodium benzylate and potassiopyrrole giving benzyloxymethyl acetate (15%) (1) and N-pyrrylmethyl acetate (18%) (2), respectively. However, because methyl

Can. J. Chem. Downloaded from www.nrcresearchpress.com by 210.87.254.42 on 09/05/12
For personal use only.

fluorene-9-carboxylate has shown exceptional reactivity (3) we examined its reaction with chloromethyl acetate. The major product, a sparingly soluble substance isolated in variable yield, proved to be I (4). The expected diester II was isolated in poor yield by chromatography. It seemed likely that the bis-fluorene I arose from α,α'-dichlorodimethyl ether and this was confirmed by both infrared spectroscopy and gas–liquid chromatographic analysis.

Although chloromethyl acetate has been used as a source of methylene for cellulose (5), in the Prins reaction (6) and in kinetic (7, 8) and mechanistic (9) studies, only Descude (10) amongst earlier workers seems to have noted the presence of α,α'-dichlorodimethyl ether. It has, however, been reported from the products of the reaction between benzoyl chloride and paraformaldehyde (11). We have now prepared and characterized pure chloromethyl acetate (see Experimental) from the reaction between paraformaldehyde and acetyl chloride (9). The dichlorodimethyl ether probably arises from water present in the paraformaldehyde, hydrolysis of part of the acetyl chloride liberating the necessary hydrogen chloride (c.f. the formation of α,α'-dichlorodimethyl ether from formaldehyde and hydrochloric and sulphuric acids (12)). Pure chloromethyl acetate is probably most easily prepared by photochlorination of methyl acetate (13, 14) since this method eliminates dichlorodimethyl ether as a likely contaminant.

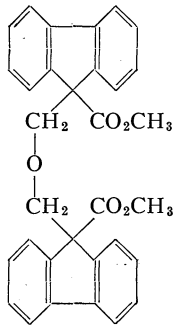

I

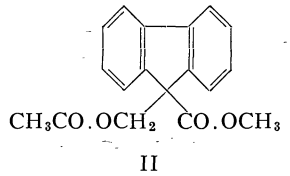

II

EXPERIMENTAL

Chloromethyl acetate was prepared as described by Ulich and Adams (9) and fractionated under slightly reduced pressure using a 20×0.75 in. column packed with glass helices and fitted with a liquid dividing head. The first distillation at a reflux ratio of 10 to 1 gave ester of 97% purity. Refractionation using a reflux ratio of 30 to 1 gave pure chloromethyl acetate (30–40%), b.p. 95° at 729 mm (9, 15, 16): n_D^{20} 1.4102 (lit. n_D^{20} 1.409, (8*a*). Found: C, 33.32; H, 4.64; Cl, 32.43. Calc. for $C_3H_5ClO_2$: C, 33.29; H, 4.64; Cl, 32.66%. The infrared spectrum of a capillary film showed the following absorption peaks (cm^{-1}): 717 (vs), 818 (s), 936 (w), 986 (w), 1050 (vs), 1102 (w), 1209 (vs), 1263 (m), 1291 (w), 1341 (m), 1374 (s), 1443 (s), 1715 (w), 1764 (vs).

Before each distillation the apparatus was cleaned and dried by boiling acetyl chloride in the still pot. Polyformaldehyde was always deposited during the initial distillation of chloromethyl acetate and may have arisen from decomposition of the ester. Although some samples of crude ester contained as little as 8% dichlorodimethyl ether, product distilled through a Claisen head contained up to 45% of the ether.

Analysis of chloromethyl acetate fractions was carried out by gas–liquid chromatography, employing a 6 ft tube packed with 20% silicone oil on Hyflo and maintained at 20°. The carrier gas was argon. α,α'-Dichloromethyl ether showed a retention time of 0.86 relative to chloromethyl acetate (1.00). These results were checked by infrared spectroscopy, using the absorption peak shown by the ether at 915 cm^{-1}.

ACKNOWLEDGMENTS

The author is indebted to Mr. J. Cross, Mr. M. Graham, and Miss E. V. Egginton for the analyses, and to Mr. B. J. Wood for technical assistance.

Can. J. Chem. Downloaded from www.nrcresearchpress.com by 210.87.254.42 on 09/05/12
For personal use only.

1. M. L. GUPTA, R. KAUSHAL, and S. S. DESHAPANDE. J. Indian Chem. Soc. **18**, 638 (1941).
2. M. S. TAGGART and G. H. RICHTER. J. Am. Chem. Soc. **56**, 1386 (1934).
3. P. M. G. BAVIN. Anal. Chem. **32**, 554 (1960).
4. P. M. G. BAVIN. Can. J. Chem. To be published.
5. F. C. WOOD. J. Soc. Chem. Ind. **50**, 411T (1931).
6. J. COLONGE and H. ROBERT. Bull. Soc. Chim. France, 463 (1960).
7. H. BÖHME, H. BEZZENBERGER, M. CLEMENT, A. DICK, E. NÜRNBERG, and W. SCHLEPHACK. Ann. **623**, 92 (1959).
8. E. EURANTO. (*a*) Ann. Univ. Turku. A, **I131**, 107 (1959); (*b*) Suomen Kemi, B, **29**, 144 (1956).
9. L. H. ULICH and R. ADAMS. J. Am. Chem. Soc. **43**, 660 (1921).
10. DESCUDE. Bull. Soc. Chim. France, 3rd ser. **27**, 867 (1902).
11. H. STAUDINGER and M. LÜTHY. Helv. **8**, 57 (1925).
12. S. R. BUC. Org. Syn. **36**, 1 (1956).
13. A. R. JONES and W. J. SKRABA. Science, **110**, 332 (1949).
14. R. N. RENAUD and L. C. LEITCH. Can. J. Chem. **39**, 261 (1961).
15. P. SCHLICHTA, J. K. INMAN, and H. J. LUCAS. J. Am. Chem. Soc. **77**, 3784 (1955).
16. A. BRUYLANTS, M. TITS, and R. DAUBY. Bull. Soc. Chim. Belges, **58**, 310 (1949).

RECEIVED OCTOBER 24, 1963.
SMITH KLINE AND FRENCH LABORATORIES LTD.,
WELWYN GARDEN CITY,
ENGLAND.

Can. J. Chem. Downloaded from www.nrcresearchpress.com by 210.87.254.42 on 09/05/12
For personal use only.

ÉTARD REACTION. IV. DEUTERIUM ISOTOPE EFFECT†

OWEN H. WHEELER

Evidence has been advanced (1) that the Étard oxidation of toluene with chromyl chloride proceeds by the rapid formation of a soluble π-complex, followed by the formation of the insoluble Étard complex. Stairs and Burns (2) carried out kinetic studies on this reaction which indicate that the insoluble complex is formed in two successive steps, each involving the replacement of one hydrogen atom. A consideration of the effect of solvent on the reaction (3) suggested that the activated complex is somewhat more polar than the starting materials. However, the reaction cannot be truly ionic since it is carried out in nonpolar solvents. In a recent study Gragerov and Ponomarchuk (4) found that, in the oxidation of α-monodeuterotoluene, the unreacted toluene and the benzaldehyde formed both contained an excess of deuterium. However, the reaction was carried out at reflux in carbon tetrachloride and much benzyl chloride was formed. This present study reports the oxidation of a mixture of toluene and α,α,α-trideuterotoluene with chromyl chloride in carbon disulphide at room temperature, under which conditions the minimum amount of chlorination occurs. Moreover, no complications arise as a result of the competition with hydrogen and deuterium in the same molecule (5).

EXPERIMENTAL

A mixture of distilled toluene (1.71 g) and α,α,α-trideuterotoluene (1.70 g) (Volk Radiochemical Co., 98%; infrared spectrum showed no C—D aromatic absorption (6)) in carbon disulphide (20 ml) was treated dropwise, with cooling to 0° in an ice bath, with distilled chromyl chloride (6.0 g, 0.55 equivalents) in carbon disulphide (10 ml) over 1/2 hour. The reaction was stirred at room temperature overnight and poured onto ice water containing sodium bisulphide. The organic phase was dried and most of the solvent removed through a 12 in. column packed with Fenske rings. The residue was fractionated through an 18 in. spinning-band column, giving toluene, b.p. 110–111°, 1.24 g (36%; 81% theory).

The deuterium analysis of the mixture before reaction was 16.60 atom%.

Deuterium analysis of recovered unreacted toluene was 24.40 atom%. If it is assumed that the reaction

†*For Part III, see Can. J. Chem. 38, 2137 (1960).*

1. M. L. GUPTA, R. KAUSHAL, and S. S. DESHAPANDE. J. Indian Chem. Soc. **18**, 638 (1941).
2. M. S. TAGGART and G. H. RICHTER. J. Am. Chem. Soc. **56**, 1386 (1934).
3. P. M. G. BAVIN. Anal. Chem. **32**, 554 (1960).
4. P. M. G. BAVIN. Can. J. Chem. To be published.
5. F. C. WOOD. J. Soc. Chem. Ind. **50**, 411T (1931).
6. J. COLONGE and H. ROBERT. Bull. Soc. Chim. France, 463 (1960).
7. H. BÖHME, H. BEZZENBERGER, M. CLEMENT, A. DICK, E. NÜRNBERG, and W. SCHLEPHACK. Ann. **623**, 92 (1959).
8. E. EURANTO. (*a*) Ann. Univ. Turku. A, **I131**, 107 (1959); (*b*) Suomen Kemi, B, **29**, 144 (1956).
9. L. H. ULICH and R. ADAMS. J. Am. Chem. Soc. **43**, 660 (1921).
10. DESCUDE. Bull. Soc. Chim. France, 3rd ser. **27**, 867 (1902).
11. H. STAUDINGER and M. LÜTHY. Helv. **8**, 57 (1925).
12. S. R. BUC. Org. Syn. **36**, 1 (1956).
13. A. R. JONES and W. J. SKRABA. Science, **110**, 332 (1949).
14. R. N. RENAUD and L. C. LEITCH. Can. J. Chem. **39**, 261 (1961).
15. P. SCHLICHTA, J. K. INMAN, and H. J. LUCAS. J. Am. Chem. Soc. **77**, 3784 (1955).
16. A. BRUYLANTS, M. TITS, and R. DAUBY. Bull. Soc. Chim. Belges, **58**, 310 (1949).

RECEIVED OCTOBER 24, 1963.
SMITH KLINE AND FRENCH LABORATORIES LTD.,
WELWYN GARDEN CITY,
ENGLAND.

Can. J. Chem. Downloaded from www.nrcresearchpress.com by 210.87.254.105 on 09/05/12
For personal use only.

ÉTARD REACTION. IV. DEUTERIUM ISOTOPE EFFECT†

OWEN H. WHEELER

Evidence has been advanced (1) that the Étard oxidation of toluene with chromyl chloride proceeds by the rapid formation of a soluble π-complex, followed by the formation of the insoluble Étard complex. Stairs and Burns (2) carried out kinetic studies on this reaction which indicate that the insoluble complex is formed in two successive steps, each involving the replacement of one hydrogen atom. A consideration of the effect of solvent on the reaction (3) suggested that the activated complex is somewhat more polar than the starting materials. However, the reaction cannot be truly ionic since it is carried out in nonpolar solvents. In a recent study Gragerov and Ponomarchuk (4) found that, in the oxidation of α-monodeuterotoluene, the unreacted toluene and the benzaldehyde formed both contained an excess of deuterium. However, the reaction was carried out at reflux in carbon tetrachloride and much benzyl chloride was formed. This present study reports the oxidation of a mixture of toluene and α,α,α-trideuterotoluene with chromyl chloride in carbon disulphide at room temperature, under which conditions the minimum amount of chlorination occurs. Moreover, no complications arise as a result of the competition with hydrogen and deuterium in the same molecule (5).

EXPERIMENTAL

A mixture of distilled toluene (1.71 g) and α,α,α-trideuterotoluene (1.70 g) (Volk Radiochemical Co., 98%; infrared spectrum showed no C—D aromatic absorption (6)) in carbon disulphide (20 ml) was treated dropwise, with cooling to 0° in an ice bath, with distilled chromyl chloride (6.0 g, 0.55 equivalents) in carbon disulphide (10 ml) over 1/2 hour. The reaction was stirred at room temperature overnight and poured onto ice water containing sodium bisulphide. The organic phase was dried and most of the solvent removed through a 12 in. column packed with Fenske rings. The residue was fractionated through an 18 in. spinning-band column, giving toluene, b.p. 110–111°, 1.24 g (36%; 81% theory).

The deuterium analysis of the mixture before reaction was 16.60 atom%.

Deuterium analysis of recovered unreacted toluene was 24.40 atom%. If it is assumed that the reaction

†*For Part III, see Can. J. Chem. 38, 2137 (1960).*

is first order in toluene (2), following Melander (7), then k_H/k_D = log (a_H/a^0_H/log (a_D/a^0_D), where a_H and a_D, and a^0_H and a^0_D are, respectively, the concentrations of unreacted toluene and deuterotoluene, and their initial concentrations. For 35% recovery k_H/k_D = 2.4. This value is approximate since the reaction is not strictly first order in toluene (2) and because of the error in measuring the yield of the reaction.

A second fraction, b.p. 150–155° (0.8 g), was treated with a solution of 2,4-dinitrophenylhydrazine in sulphuric acid and methanol and warmed to 50° for 10 minutes. The precipitate of benzaldehyde dinitrophenylhydrazone was chromatographed on alumina from benzene and recrystallized from ethyl acetate, m.p. 240–241° (lit. m.p. 238–239° (8)). The deuterium analysis was 0.2 atom%. It is not clear whether the exchange had taken place during workup or on formation of the derivative. The latter may be the case, since Gragerov and Ponomarchuk (4) report that the benzaldehyde recovered from the isolated Étard complex contains an excess of deuterium.

DISCUSSION

The maximum value k_H/k_D at 25° for carbon–hydrogen and carbon–deuterium bond breaking is 6.9 (7, 9). In many typical displacement reactions the observed value of k_H/k_D is much lower, although oxidation reactions in aqueous solution usually show high values for k_H/k_D (9). The value of this ratio in the present case indicates that the breaking of a carbon–hydrogen bond of the methyl group in toluene is the rate-determining step. This is in agreement with the suggestion that the replacement of the first hydrogen atom is the rate-determining step (2). A recent publication (10) indicates that the structure of the Étard complex is best represented by a formula (I) with tetra- and hexa-valent

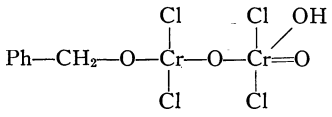

I

chromium, and that the second hydrogen atom is removed by the cyclic attack of the divalent oxygen atom of this complex. This mechanism is consistent with the above findings. The kinetic deuterium isotope effect does not distinguish between hydride ion and hydrogen atom transfer (9), although the former is the more probable (10).

ACKNOWLEDGMENTS

The deuterium analyses were kindly determined by Dr. A. P. Wolf and Dr. D. Christman of the Department of Chemistry, Brookhaven National Laboratory. This work was carried out under contract No. AT (40-1)-1833 of the U.S. Atomic Energy Commission with the University of Puerto Rico.

1. O. H. Wheeler. Can. J. Chem. **38**, 2137 (1960).
2. R. A. Stairs and J. W. Burns. Can. J. Chem. **39**, 960 (1961).
3. R. A. Stairs. Can. J. Chem. **40**, 1656 (1962).
4. I. P. Gragerov and M. P. Ponomarchuk. Zh. Obshch. Khim. **32**, 3568 (1962); J. Gen. Chem. USSR, **32**, 3501 (1962).
5. K. B. Wiberg and L. H. Slaugh. J. Am. Chem. Soc. **80**, 3033 (1958).
6. I. Turkevish, H. A. McKenzie, L. Friedman, and R. Spurr. J. Am. Chem. Soc. **71**, 4045 (1949); J. K. Wilmshurst and H. J. Bernstein. Can. J. Chem. **35**, 911 (1957).
7. L. Melander. Isotope effects on reaction rates. Ronald Press, New York. 1960. p. 48.
8. L. A. Jones and C. K. Hancock. J. Org. Chem. **25**, 226 (1960).
9. K. B. Wiberg. Chem. Rev. **55**, 713 (1955); *cf.* F. A. Westheimer. Chem. Rev. **61**, 265 (1961).
10. I. Necsoiu, A. T. Balaban, I. Pascaru, E. Sliam, M. Elian, and C. D. Nenitzescu. Tetrahedron, **19**, 1133 (1963).

Received October 11, 1963.
Puerto Rico Nuclear Center,
University of Puerto Rico,
Mayaguez, Puerto Rico.

Can. J. Chem. Downloaded from www.nrcresearchpress.com by 210.87.254.105 on 09/05/12
For personal use only.

THE EXTRACTION OF SCANDIUM BY MIXTURES OF OXINE AND NEUTRAL ORGANOPHOSPHORUS REAGENTS

P. G. MANNING[1] AND PRANOWO[2]

We have made a study of the two-phase liquid–liquid systems (Sc^{3+}–HCl–HX–TOPO–hexone and Sc^{3+}–HCl–HX–DBBP–hexone) at 25° C where HX is oxine, TOPO is trioctyl phosphine oxide, and DBBP is dibutyl butyl phosphonate. The experimental details, involving the use of "carrier-free" Sc^{46}, have been described in an earlier publication (1).

In 1.24×10^{-3} *M* HCl, scandium is present as the trivalent ion (2). When mixtures of oxine and the neutral extractants are used, the extraction stoichiometry may be formulated as

$$Sc_w^{3+} + nCl_w^- + (3-n)HX_o + mS_o = ScCl_nX_{3-n}S_{m_0} + (3-n)H_w^+,$$

where "w" and "o" designate water and organic phase species respectively, and S is the neutral organophosphorus extractant. The equilibrium constant is

$$[1] \qquad k = \frac{[ScCl_nX_{3-n}S_m]_0\,[H^+]^{3-n}}{[Sc^{3+}]\,[Cl^-]^n\,[HX^{3-n}]\,[S]^m}.$$

Since the distribution coefficient is, by definition,

$$[2] \qquad K = \frac{[Sc]_o}{[Sc]_w},$$

$$[3] \qquad \text{then } K = \frac{k[Cl^-]^n\,[HX]^{3-n}\,[S]^m}{[H^+]^{3-n}}.$$

It follows from equation (3) that a plot of log K against log [HX] has a slope of $3-n$, and from a plot of log K against log [S] we can estimate m.

That the reaction is synergic is evident from Fig. 1. The addition of 0.0050 *M* oxine to hexone solutions of TOPO or DBBP increases K by a factor of approximately 4. The extraction of Sc^{3+} by a 0.0050 *M* solution of oxine in hexone is small ($K < 10^{-4}$) by comparison, and can be ignored. The slopes of the plots indicate that $m = 2$. Also, when DBBP and TOPO are used individually, scandium extracts as the disolvate, in contrast to the lanthanides that extract as trisolvates (3, 4). The slopes of the plots of log K against log [HX], with [DBBP] = [TOPO] = 0.0010 *M*, show that $3-n = 2$, whence $n = 1$. The reaction stoichiometry is, therefore,

$$Sc_w^{3+} + Cl_w^- + 2HX_0 + 2S_0 = ScClX_2S_{2_0} + 2H_w^+.$$

The present extraction system differs from other synergic systems involving trivalent metals in that the supporting anion has replaced one of the chelating extractant molecules (1, 5, 6). Figures 1 and 2 show that TOPO and DBBP give similar synergic enhancements, whereas from a comparison of their electron donor properties, one would expect TOPO to be the more powerful synergistic agent. Experiments were then conducted with tributyl phosphate (TBP) to obtain further correlation between electron donor strength and degree

[1]*National Research Council of Canada Postdoctoral Fellow.*
[2]*Summer Student with Colombo Plan, at the Mines Branch, Department of Mines and Technical Surveys. 1963.*

Can. J. Chem. Downloaded from www.nrcresearchpress.com by 210.87.254.40 on 09/05/12
For personal use only.

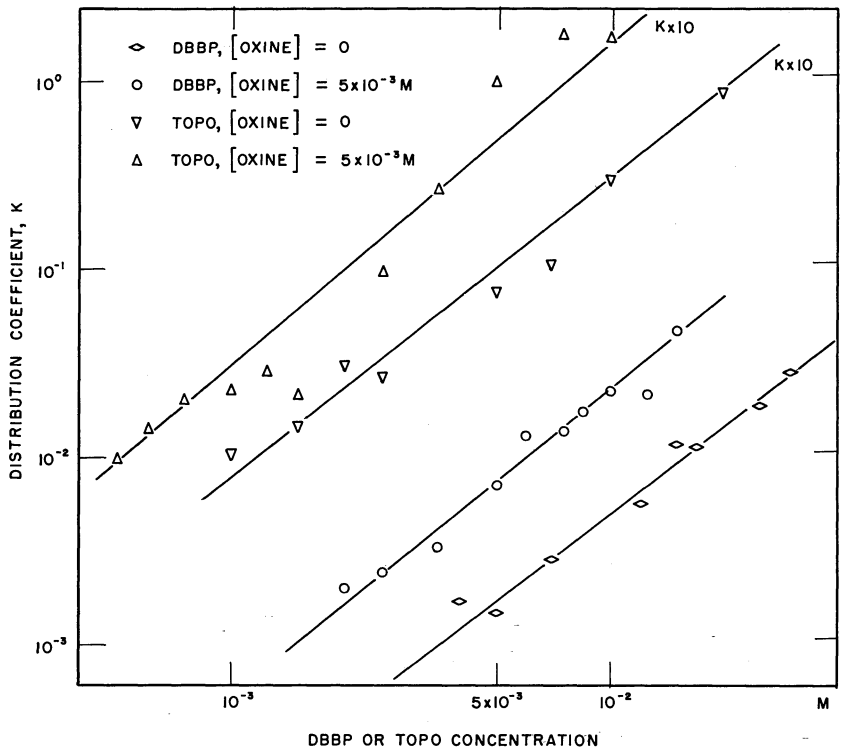

FIG. 1. Metal distribution coefficients as a function of DBBP and TOPO concentrations.

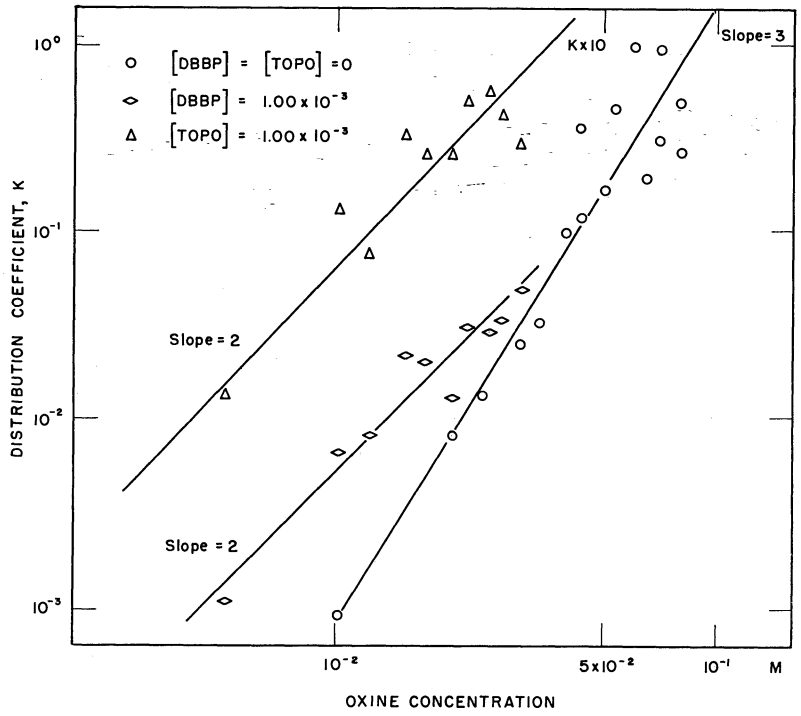

FIG. 2. Metal distribution coefficients as a function of oxine concentration.

Can. J. Chem. Downloaded from www.nrcresearchpress.com by 210.87.254.40 on 09/05/12
For personal use only.

of synergic enhancement. TBP, however, failed to produce a synergic reaction. It is possible, therefore, that steric hindrance is an important factor in the present system; the weakest electron donor (TBP) being unable to overcome steric hindrance to coordination. In the case of DBBP and TOPO, steric hindrance and extractive power are balanced.

It is interesting to note, in the Sc^{3+}–HNO_3–thenoyltrifluoroacetone(HTTA)–DBBP–toluene system, that, because of steric obstruction, the extractable complex is $Sc(TTA)_3$–$(DBBP)_1$ (1). In the present investigation, extraction occurs via the formation of the complex $ScClX_2S_2$. Clearly, more work is required on the mechanism of synergism.

1. P. G. MANNING. Can. J. Chem. **41**, 658 (1963).
2. A. D. PAUL. J. Phys. Chem. **66**, 1248 (1962).
3. E. HESFORD, E. E. JACKSON, and H. A. C. MCKAY. J. Inorg. Nucl. Chem. **9**, 279 (1959).
4. P. G. MANNING. Can. J. Chem. **40**, 1684 (1962).
5. T. V. HEALY. J. Inorg. Nucl. Chem. **19**, 314 (1961).
6. H. IRVING and D. N. EDGINGTON. J. Inorg. Nucl. Chem. **21**, 169 (1961).

RECEIVED AUGUST 7, 1963.
MINES BRANCH,
DEPARTMENT OF MINES AND TECHNICAL SURVEYS,
555 BOOTH STREET,
OTTAWA, CANADA.

Can. J. Chem. Downloaded from www.nrcresearchpress.com by 210.87.254.40 on 09/05/12
For personal use only.

VAPOR PRESSURE MEASUREMENTS ON THE SYSTEM D_2O–H_2O. ANALYSIS OF D_2O–H_2O MIXTURES[1]

M. MAZUREK AND A. S. PERLIN

The difference in vapor pressure between a solution and the pure solvent is readily measured as the steady-state temperature difference (heat of vaporization) by use of thermally sensitive resistors (thermistors) (1). This thermometric type of measurement is now shown to be suitable also for examining some vapor pressure characteristics of mixtures of deuterium oxide and water, i.e., of two miscible liquids having substantially different vapor pressures (2, 3).

A commercial model (Mechrolab Inc., Mountain View, California) of a modified (1) thermoelectric osmometer (4, 5), developed for estimation of molecular weight, was used in these experiments. The general procedure was that devised for molecular weight estimations with this instrument. The measurement chamber (at 37° C) was saturated with water vapor and a drop of water was applied to the reference thermistor. A drop of deuterium oxide, or of a given deuterium oxide – water mixture, was applied to the sample thermistor, and resistance readings (ΔR) were then noted at chosen time intervals. The vapor pressure difference between pure deuterium oxide and water was found to be rather large in terms of the range of the instrument, and measurement of the equilibration process occurring with this system was not satisfactory. Much more satisfactory resistance readings were obtained with solutions of deuterium oxide at intermediate concentrations in water (5–20% deuterium oxide).

As shown in Fig. 1, the vapor pressure equilibrium process observed under these conditions follows an exponential law, the plot of log ΔR vs. time being linear. It is clear from these data that the concentration of deuterium oxide in the mixture initially can be related

[1]*Issued as N.R.C. No. 7729.*

of synergic enhancement. TBP, however, failed to produce a synergic reaction. It is possible, therefore, that steric hindrance is an important factor in the present system; the weakest electron donor (TBP) being unable to overcome steric hindrance to coordination. In the case of DBBP and TOPO, steric hindrance and extractive power are balanced.

It is interesting to note, in the Sc^{3+}–HNO_3–thenoyltrifluoroacetone(HTTA)–DBBP–toluene system, that, because of steric obstruction, the extractable complex is $Sc(TTA)_3$–$(DBBP)_1$ (1). In the present investigation, extraction occurs via the formation of the complex $ScClX_2S_2$. Clearly, more work is required on the mechanism of synergism.

1. P. G. MANNING. Can. J. Chem. **41**, 658 (1963).
2. A. D. PAUL. J. Phys. Chem. **66**, 1248 (1962).
3. E. HESFORD, E. E. JACKSON, and H. A. C. MCKAY. J. Inorg. Nucl. Chem. **9**, 279 (1959).
4. P. G. MANNING. Can. J. Chem. **40**, 1684 (1962).
5. T. V. HEALY. J. Inorg. Nucl. Chem. **19**, 314 (1961).
6. H. IRVING and D. N. EDGINGTON. J. Inorg. Nucl. Chem. **21**, 169 (1961).

RECEIVED AUGUST 7, 1963.
MINES BRANCH,
DEPARTMENT OF MINES AND TECHNICAL SURVEYS,
555 BOOTH STREET,
OTTAWA, CANADA.

Can. J. Chem. Downloaded from www.nrcresearchpress.com by 210.87.254.40 on 09/05/12
For personal use only.

VAPOR PRESSURE MEASUREMENTS ON THE SYSTEM D_2O–H_2O. ANALYSIS OF D_2O–H_2O MIXTURES[1]

M. MAZUREK AND A. S. PERLIN

The difference in vapor pressure between a solution and the pure solvent is readily measured as the steady-state temperature difference (heat of vaporization) by use of thermally sensitive resistors (thermistors) (1). This thermometric type of measurement is now shown to be suitable also for examining some vapor pressure characteristics of mixtures of deuterium oxide and water, i.e., of two miscible liquids having substantially different vapor pressures (2, 3).

A commercial model (Mechrolab Inc., Mountain View, California) of a modified (1) thermoelectric osmometer (4, 5), developed for estimation of molecular weight, was used in these experiments. The general procedure was that devised for molecular weight estimations with this instrument. The measurement chamber (at 37° C) was saturated with water vapor and a drop of water was applied to the reference thermistor. A drop of deuterium oxide, or of a given deuterium oxide – water mixture, was applied to the sample thermistor, and resistance readings (ΔR) were then noted at chosen time intervals. The vapor pressure difference between pure deuterium oxide and water was found to be rather large in terms of the range of the instrument, and measurement of the equilibration process occurring with this system was not satisfactory. Much more satisfactory resistance readings were obtained with solutions of deuterium oxide at intermediate concentrations in water (5–20% deuterium oxide).

As shown in Fig. 1, the vapor pressure equilibrium process observed under these conditions follows an exponential law, the plot of log ΔR vs. time being linear. It is clear from these data that the concentration of deuterium oxide in the mixture initially can be related

[1]*Issued as N.R.C. No. 7729.*

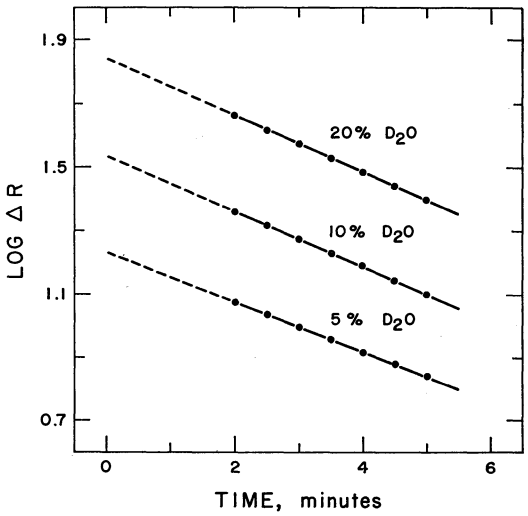

FIG. 1. Thermometric measurement of the vapor pressure equilibration process at 37° C in the system D_2O–H_2O for D_2O concentrations of 5, 10, and 20%; ΔR is a measure of the steady-state temperature difference as a function of resistance.

directly to the logarithm of ΔR at zero time. Hence, measurements of this type should afford a means for estimating the deuterium oxide content of mixtures of unknown composition, at least within the concentration range examined. The ΔR^* values obtained by extrapolation of plots (as in Fig. 1) to zero time were as follows: for 20% deuterium oxide, 68.80 ± 0.28 (average of five runs); for 10% deuterium oxide, 34.12 ± 0.15 (average of five runs); for 5% deuterium oxide, 16.94 ± 0.04 (average of three runs).

As far as we are aware, analyses of deuterium oxide – water mixtures have not been carried out in this way, although a sensitive manometric method based on vapor pressure lowering has been described by Puddington (3). Because of the simplicity and speed with which thermometric measurements may be made, and the small quantity of sample required, a method of this kind might offer specific advantages over some of the analytical procedures now available for heavy water analysis. The sensitivity and range of the measurement undoubtedly could be increased over those pertaining in the present study by suitable modification of the apparatus, most particularly, by use of a recorder in place of manual settings for obtaining ΔR values.

ACKNOWLEDGMENT

The authors express their gratitude to Dr. W. H. Stevens, Atomic Energy of Canada Ltd. for helpful information.

1. A. P. BRADY, H. HUFF, and J. W. MCBAIN. J. Phys. Colloid Chem. **55**, 304 (1951).
2. F. T. MILES and A. W. C. MENZIES. J. Am. Chem. Soc. **58**, 1067 (1936).
3. I. E. PUDDINGTON. Can. J. Res. B, **27**, 1 (1949).
4. A. V. HILL. Proc. Roy. Soc. (London), A, **127**, 9 (1930).
5. E. J. BALDES. J. Sci. Instr. **11**, 223 (1934).

RECEIVED OCTOBER 11, 1963.
PRAIRIE REGIONAL LABORATORY,
NATIONAL RESEARCH COUNCIL,
SASKATOON, SASKATCHEWAN.

**The ΔR values are characteristic for a given thermistor. Hence a different instrument may give substantially different ΔR values than those recorded here.*

Can. J. Chem. Downloaded from www.nrcresearchpress.com by 210.87.254.40 on 09/05/12
For personal use only.

SOME REACTIONS OF ALICYCLIC α-AZIDOKETONES[1]

O. E. EDWARDS AND K. K. PURUSHOTHAMAN[2]

In connection with another problem we examined the preparation and reactions of two alicyclic α-azidoketones. Our initial object was a study of the photochemical decomposition of these compounds, but several factors forced a shift of emphasis to their acid- and base-catalyzed reactions.

The reaction of 2-chlorocyclohexanone and sodium azide in dimethylsulphoxide gave a good yield of yellow oil. This analyzed correctly for the 2-azidoketone and had intense absorption at 2110 cm^{-1} characteristic of an alkyl azide. However, it could not be distilled under reduced pressure without extensive decomposition and polymerization. Irradiation of a hexane solution of 2-azidocyclohexanone in a quartz vessel with ultraviolet light resulted in steady evolution of nitrogen. An oil deposited from the solution. This and the material remaining in the hexane after complete decomposition of the azide had absorption bands characteristic of an α-iminoketone (ν_{max} 3400 and 1670 cm^{-1}). However, the product could only partly be distilled under 15 mm pressure. It seemed that the expected (1) mode of reaction (equation *a*) was taking place, but that the iminoketone

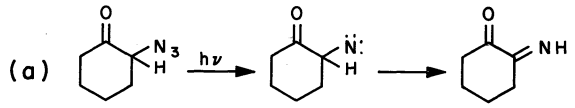

was undergoing rapid polymerization. It appeared probable that acid catalysis would bring about a similar decomposition, as indicated in equation *b*, with the sensitive iminoketone now being rapidly hydrolyzed to the α-diketone. This indeed proved to be a smooth reaction leading in good yield to 1,2-cyclohexanedione. This very convenient

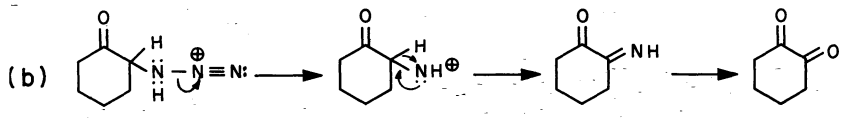

synthesis of the α-diketone is superior to the selenium dioxide oxidation or oximinoketone hydrolysis (2) methods for its preparation. A parallel acid-catalyzed conversion of cycloalkylazides to the corresponding ketones was described some time ago by Boyer and co-workers (3).

Attempts to prepare pure 2-azidocholestanone by the reaction of 2-α-bromocholestan-3-one with lithium azide in methanol or dimethylformamide or with sodium azide in dimethylsulphoxide were unsuccessful. A steady state concentration of the azidoketone was produced, as revealed by the infrared spectrum, but it was continuously being converted to a substance with ν_{max} 1655 cm^{-1}. After 1 hour at 50° in dimethylformamide containing excess lithium azide the bromoketone had been completely converted to the new compound. That this was the α-iminoketone I was shown by its hydrolysis to 2,3-cholestanedione, and by its reduction to a mixture rich in a 2-aminocholestan-3-ol which was characterized as its O,N-diacetate. The derived acetamido alcohol II was oxidized to 2-α-acetamidocholestane-3-one (III) (ν_{max} 1710 cm^{-1}, λ_{max} 279 mμ). Wolff-Kishner reduction of this gave a good yield of cholestane.[3]

[1]*Issued as N.R.C. No. 7701.*

[2]*National Research Council of Canada Postdoctoral Fellow.*

[3]*The elimination of α-substituents in this reaction is well known (4). The olefin which is first produced is often reduced to the hydrocarbon by diimide formed from the hydrazine present (5).*

Can. J. Chem. Downloaded from www.nrcresearchpress.com by 210.87.254.42 on 09/05/12
For personal use only.

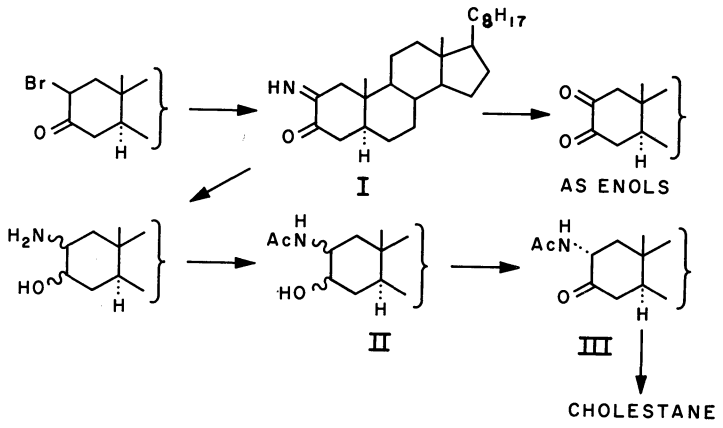

Boyer and Straw observed that thermal decomposition of phenacyl azides requires temperatures around 200° (6). The decomposition of liquid α-azidocyclohexanone began below 100°, but the compound was unchanged after several hours in boiling methanol or in dimethylformamide at 60° with or without added lithium bromide or lithium azide. Hence 2-azidocholestan-3-one is anomalously reactive. Investigation of its instability soon proved that it too was inert in methanol or dimethylformamide near 60°, or in these solvents containing lithium bromide. Clearly then, the observed decomposition during the preparative reaction is a lithium-azide-catalyzed process.

A conformational driving force for the accelerated decomposition of the azidocholestanone seems probable. Spectroscopic evidence (ν_{max}^{CO} 1720 cm^{-1} in chloroform) indicates that the parent bromoketone is 2-α-bromocholestane-3-one, with the bromine equatorial. Since the displacement of the bromine is probably a normal S_N2 reaction the azide should be 2-β-azidocholestane-3-one (IV). Since C-3 is trigonal, and the electrostatic repulsion between the carbonyl and azido groups seems low (2-azidocyclohexanone has an equatorial azido group) it is probable that the azido ketone adopts a ring A conformation closer to the half-boat V than the chair IV in order to help relieve the repulsive interaction of the azido group and the 10-methyl group.[4] This interaction seems the one factor which can

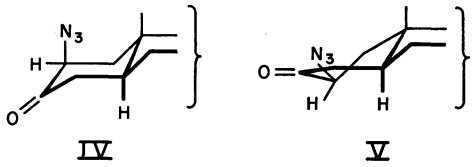

account for the rapid decomposition. We suggest that lithium azide acts as a generalized base aiding abstraction of the 2-hydrogen:

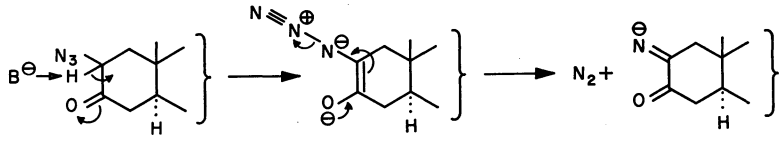

[4]*The azidoketone carbonyl appears as a shoulder on the low-wavelength side of the bromoketone carbonyl band in the infrared spectrum of a mixture of the two compounds. It is hence unlikely that the azidoketone has ring A as a boat with the azido group equatorial.*

Can. J. Chem. Downloaded from www.nrcresearchpress.com by 210.87.254.42 on 09/05/12
For personal use only.

The repulsive interaction between the 10-methyl group and the azide group will be relieved in the enolate anion, thus providing the driving force for enolization by the weak base. The enolate ion must rapidly lose nitrogen to give the anion corresponding to the product.

The above reactions of α-azidoketones may provide valuable alternative routes to steroidal α-diketones (7, 8) and α-amino alcohols (9).

EXPERIMENTAL

2-Azidocyclohexanone

A solution of 2.05 g of sodium azide in 45 ml of dimethylsulphoxide was added to 1.45 g of 2-chlorocyclohexanone. The mixture was stirred at room temperature for 80 minutes. Water containing crushed ice was added, then the product extracted by three 25 ml portions of *n*-pentane. The combined extracts were washed with ice-cold water, dried, and the solvent removed *in vacuo*. The residual yellow oil polymerized if distillation was attempted under water pump pressure. The oil had $\nu_{max}^{CHCl_3}$ 2110 (—N_3) and 1722 cm^{-1} (C=O). Found: N, 29.82. Calc. for $C_6H_9N_3O$: N, 30.20.

A solution of 50 mg of 2-azidocyclohexanone in 20 ml of dimethylformamide was heated at 65°. Aliquots were periodically removed, diluted with water, and extracted with *n*-pentane. The intensity of the azide peak in the infrared spectrum remained unchanged during 1½ hours heating. When the solution was heated above this temperature, however, slow decomposition resulted.

Photolysis of 2-Azidocyclohexanone

The photolysis cell was 1 cm thick and 6.5 cm in diameter with quartz windows equipped with a side reservoir with cooling coil and circulation device. A solution of 750 mg of the azidoketone in 165 ml of cyclohexane was irradiated under nitrogen with a 140 watt Hanovia lamp while the temperature was maintained below 40°. A steady evolution of nitrogen ensued. The azide band at 2110 cm^{-1} had disappeared after 12 hours. The photolysis was interrupted at intervals to remove an oil which collected on the walls of the cell. This oil was soluble in methylene chloride, but the solution deposited polymer on standing. Both the oil and cyclohexane solution had infrared absorption at 3400 and 1670 cm^{-1}.

Acid-Catalyzed Decomposition of 2-Azidocyclohexanone

A mixture of 750 mg of 2-azidocyclohexanone and 15 ml of 10 *N* sulphuric acid was vigorously stirred a s the temperature was raised to 60°. Nitrogen evolution commenced. After 1 hour at 60–65° the oily drops of the azide had completely disappeared. The solution was cooled, saturated with sodium sulphate, and extracted three times with 50 ml portions of ether. The ether extracts were concentrated to 50 ml *in vacuo*, then extracted twice with 15 ml portions of ice-cold 10% potassium hydroxide solution. The aqueous layers were neutralized with cold 6 *N* hydrochloric acid and extracted thoroughly with ether. The dried ether solution was removed at 0° *in vacuo*, leaving 378 mg of 1,2-cyclohexanedione which crystallized from pentane; m.p. 38–40°, $\nu_{max}^{CHCl_3}$ 3500 cm^{-1} (OH), 1675 cm^{-1} (C=O), and 1650 cm^{-1} (C=C) corresponding to the enolic form; λ_{max} 266 mμ, ε 2460 shifted to 308 mμ in alkali. The dione formed a dioxime which melted at 187–188° after recrystallization from acetone. An aqueous solution of the dioxime gave a rose-red precipitate when a nickel sulphate solution was added.

Attempted Preparation of 2-Azidocholestanone

Numerous attempts were made to prepare pure 2-azidocholestanone by the action of alkali azides on 2-bromo(chloro)-cholestane-3-one, varying the solvent and temperature. Aliquots were removed from the reactions at intervals, the ether-extractable products isolated, and the infrared spectra examined. The azidoketone ($\nu_{max}^{CHCl_3}$ 2110 cm^{-1} and 1710 cm^{-1}) soon reached a steady state concentration while a second product steadily grew in concentration ($\nu_{max}^{CHCl_3}$ 1655 cm^{-1}). Of the three solvents used, dimethylformamide, dimethylsulphoxide, and methanol, the highest steady state concentration of azide was reached with the latter solvent, after 1 hour of refluxing. In a typical experiment 300 mg of 2-bromocholestan-3-one in 2 ml of chloroform was added to a solution of 300 mg of lithium azide in 25 ml of dry methanol. After 1 hour of refluxing the solvent was removed *in vacuo*, water added, and the products extracted into ether. After removal of the ether the extracted products were dissolved in benzene and the solution passed through a column of silica gel (20-fold ratio). The readily eluted material contained none of the by-product and had intense azide absorption. However, the product melted over a wide range and analysis for bromine indicated the presence of up to 50% of starting material. Attempts to further purify the azidoketone by chromatography on alumina were unsuccessful, hence this mixture was used to study the reactivity of the azidoketone.

The azide was not decomposed if a solution of 100 mg of the mixture in 10 ml of methanol or in 10 ml of methanol containing 100 mg of lithium bromide was refluxed for 1½ hours. It was also unchanged in a 3:7 mixture of chloroform and dimethylformamide after 2 hours at 50°.

Can. J. Chem. Downloaded from www.nrcresearchpress.com by 210.87.254.42 on 09/05/12
For personal use only.

2-Acetamidocholestan-3-ol Acetate

To a stirred solution of 3.8 g of 2-α-bromocholestan-3-one in 40 ml of dimethylformamide was added 3.8 g of lithium azide. The mixture was maintained at 50° for 1 hour then diluted with methanol and cooled to room temperature. Sodium borohydride (1.5 g) was added in small portions. After standing overnight the reaction mixture was diluted with water and thoroughly extracted with ether. The extracts were concentrated to 100 ml, then shaken with 3 *N* sulphuric acid. A sulphate which precipitated was collected by filtration and washed well with ether. It was then dissolved in 100 ml of hot ethanol, and the solution basified with alcoholic sodium hydroxide. The solvent was removed under reduced pressure, and the residue extracted with chloroform. The organic layer was washed with water and dried over anhydrous sodium sulphate. After removal of the solvent, 20 ml pyridine and 2 ml acetic anhydride were added and the contents left overnight. Pyridine was removed *in vacuo* and the residue taken up in ether. The fraction separated by the usual procedure was crystallized from alcohol to yield 2.6 g of 2-acetamidocholestanol acetate; m.p. 193–195°. $\nu_{max}^{CHCl_3}$ 3500 cm^{-1} (NH), 1722 cm^{-1} (ester), 1665 cm^{-1} (amide). Found: C, 76.74; H, 10.74; N, 2.94%. Calc. for $C_{31}H_{53}O_3N$: C, 76.33; H, 10.95; N, 2.87%.

2-Acetamidocholestan-3-ol

A solution of 2-acetamidocholestanol acetate (2 g) in 40 ml of alcohol was heated on a steam bath and 4 ml of 10% sodium hydroxide solution added to it. The contents were refluxed for 1 hour. The mixture was then concentrated to 25 ml and 20 ml water added. The resulting precipitate was washed with water and recrystallized from ethanol; m.p. 256°. Found: C, 78.16; H, 11.35%. Calc. for $C_{29}H_{51}O_2N$: C, 78.14; H, 11.53%.

2-α-Acetamidocholestan-3-one

One gram of chromic acid was added in small portions to 10 ml of pyridine at 0° C with vigorous shaking. When the formation of the complex was complete 1.5 g of 2-acetamidocholestanol dissolved in 30 ml pyridine was added slowly. The mixture was shaken overnight at room temperature and extracted with 1:1 benzene–hexane mixture. The organic layer was washed with acid and alkali and finally with water. After drying over sodium sulphate the solvent was removed. A chloroform solution of the product was passed through a column of grade III alumina (weight ratio 20:1). The readily eluted material finally crystallized from ether to give 2-α-acetamidocholestane-3-one, m.p. 184–186°, $\nu_{max}^{CHCl_3}$ 3370 cm^{-1}(NH), 1710 cm^{-1} (>C=O), and 1665 (—C(=O)—N<); λ_{max}^{EtOH} 279 mμ, ε 130. Found: C, 78.39; H, 11.09%. Calc. for $C_{29}H_{49}O_2N$: C, 78.5; H, 11.13%.

Wolff-Kishner Reduction

A mixture of 80 mg of 2-acetamidocholestan-3-one, 6 ml triethylene glycol, and 2 ml hydrazine was immersed in a bath at 110°. The temperature was gradually raised to 155–160° and maintained for 1 hour. Two grams of potassium hydroxide was now added and the water condenser replaced with an air condenser. The temperature was raised to 195–205° and kept at that temperature for 5 hours. The mixture was then cooled, diluted with water, and extracted with ether. The ether solution was washed with acid, with water, dried, and distilled. The 60 mg of residue was dissolved in pentane and the solution passed through a column of alumina (grade III). The eluate yielded 42 mg of a solid. Recrystallization from alcohol gave colorless plates, m.p. and mixed m.p. with cholestane 78–81.5°. Found: C, 86.81; H, 13.16. Calc. for $C_{27}H_{48}$: C, 87.02; H, 12.98%.

2,3-Secocholestan-2,3-dioic Acid

Four hundred milligrams of 2-α-bromo-5-α-cholestan-3-one was dissolved in 15 ml dimethyl formamide and 400 mg of lithium azide added. The mixture was heated at 50° for 1 hour, with shaking in nitrogen atmosphere. The contents were evaporated to dryness *in vacuo* and the residue taken up in 15 ml of 80% aqueous dioxane. Five milliliters of 1.5 *N* sulphuric acid was added and the mixture shaken at room temperature for 2 hours. The solution was concentrated to half its volume, diluted with water, extracted with ether. The residue (approx. 300 mg) obtained after the removal of the ether had $\lambda_{max}^{alcohol}$ 272 mμ which was shifted to 320 mμ in alkali (2).

Crude diketone (150 mg) was dissolved in 15 ml alcohol and a mixture of 1 ml hydrogen peroxide (30%) and 1 ml of 10% potassium hydroxide added. The mixture was heated on a steam bath. The same mixture of hydrogen peroxide and alkali was added twice more at 15 minute intervals. After 1 hour, the heating was stopped and the contents left overnight. After diluting with water the solution was extracted with ether to remove non-acidic materials. The clear aqueous layer was then acidified with 3 *N* sulphuric acid and ether-extracted. After washing with water the organic layer was dried over anhydrous sodium sulphate. Removal of solvent and crystallization of the residue from ethyl acetate gave 100 mg of the dicarboxylic acid, m.p. 193–194° (lit. m.p. 195° (2)). Found: C, 74.5; H, 10.29. Calc. for $C_{27}H_{46}O_4$: C, 74.61; H, 10.67%.

1. D. H. R. Barton and L. R. Morgan. J. Chem. Soc. 622 (1962).
2. E. G. Rauh, G. F. Smith, C. V. Banks, and H. Diehl. J. Org. Chem. **10**, 199 (1945).
3. J. H. Boyer, F. C. Canter, J. Hamer, and R. K. Putney. J. Am. Chem. Soc. **78**, 325 (1956).

Can. J. Chem. Downloaded from www.nrcresearchpress.com by 210.87.254.42 on 09/05/12
For personal use only.

4. R. B. TURNER, R. ANLIKER, R. HEBLING, J. MEIER, and H. HEUSSER. Helv. Chim. Acta, **38**, 411 (1955).
5. E. J. COREY, D. J. PAST, and W. L. MOCK. J. Am. Chem. Soc. **83**, 2957 (1961). E. E. VAN TAMELIN and R. J. TIMMONS. J. Am. Chem. Soc. **84**, 1067 (1962).
6. J. H. BOYER and D. STRAW. J. Am. Chem. Soc. **75**, 1642, 2683 (1953).
7. H. MORI, V. S. GANDHI and E. SCHWENK. Chem. Pharm. Bull. (Tokyo), **10**, 842 (1962).
8. C. DJERASSI (*Editor*). Steroidal reactions. Holden-Day Inc., San Francisco. 1963. Chap. 13.
9. M. SVOBODA, M. TICHY, J. TAJKOS, and J. SICHER. Tetrahedron Letters, No. 16, 717 (1962).

RECEIVED OCTOBER 23, 1963.
DIVISION OF PURE CHEMISTRY,
NATIONAL RESEARCH COUNCIL,
OTTAWA, CANADA.

Can. J. Chem. Downloaded from www.nrcresearchpress.com by 210.87.254.42 on 09/05/12
For personal use only.

Canadian Journal of Chemistry

Issued by THE NATIONAL RESEARCH COUNCIL OF CANADA

VOLUME 42 APRIL 1964 NUMBER 4

Can. J. Chem. Downloaded from www.nrcresearchpress.com by 210.87.254.42 on 09/05/12
For personal use only.

REACTIONS OF (i) ALUMINUM TERTIARY BUTOXIDE WITH ACETYL CHLORIDE AND (ii) ALUMINUM CHLORIDE WITH TERTIARY BUTYL ACETATE

R. C. MEHROTRA AND R. A. MISRA

Chemical Laboratories, University of Rajasthan, Jaipur, India

Received October 29, 1963

ABSTRACT

The reactions between aluminum tertiary butoxide and acetyl chloride have been studied. The addition of 1 mole of acetyl chloride to aluminum tertiary butoxide forms monochloride ditertiary butoxide, which, with another mole of acetyl chloride, appears to give the dichloride monotertiary butoxide derivatives. Further, these products appear to react with tertiary butyl acetate formed in the reaction itself, giving acetate derivatives. The above is confirmed by a detailed study of the reactions between aluminum chloride and tertiary butyl acetate, which have been found to result in the acetate derivatives. A plausible mechanism has been suggested.

Considerable work has been done on the reactions of acetyl chloride with the alkoxides of zirconium (1), titanium (2), and aluminum (3). In the cases of normal and secondary alkoxides, the reactions proceed in a straightforward manner yielding chloride alkoxides. For example, the reactions of aluminum isopropoxide with acetyl chloride can be represented by the following equation:

$$Al(OR)_3 + nCH_3COCl \rightarrow Al(OR)_{3-n}Cl_n + nCH_3COOR,$$

(where R = isopropyl radical and n = 1, 2, or 3).

However, for the three metals, their tertiary alkoxides showed a different behavior towards acetyl chloride. The reaction of the tertiary butoxides with acetyl chloride appeared to be quite facile up to the formation of the monochloride derivative, but further replacement appeared to be slow, a conclusion which was based on the determination of Cl:Al ratio in the product. A number of other physical and chemical properties (e.g., volatility (4), molecular complexity (5), reactivity with alcohols (4), and esters (6)) of the tertiary alkoxides in general, appeared to be explained easily on the steric hindrance caused in the molecule by the ramified alkyl groups. The same explanation was, therefore, offered (1, 3) for the comparative slowness of the reactions of the tertiary alkoxides with acetyl chloride. However, maximum steric hindrance should have been presented in the initial stages of the reaction between aluminum tertiary butoxide and acetyl chloride. The replacement of the first tertiary butoxide group by chloride should decrease the steric hindrance and aluminum monochloride ditertiary butoxide should react more readily with acetyl chloride. However, experimental results are just the opposite.

Can. J. Chem. Downloaded from www.nrcresearchpress.com by 210.87.254.42 on 09/05/12
For personal use only.

TABLE I

Reactions of aluminum tertiary butoxide with acetyl chloride

Reaction mixture	Molar ratios	Conditions of the experiment	Nature of the product	Analysis						
				Found				Required		
				% M	% Cl	Cl:M	Alk. eq. in moles	% M	% Cl	Alk. eq. in moles
$Al(OBu^t)_3$ (1.183 g), CH_3COCl (0.38 g), in benzene (8.5 g)	1:1	Room temperature 7 hours	$AlCl_{0.43}(OBu^t)_{2.57}$ (1.0574 g) white powder	12.2	6.9	0.43	0.44	11.75	6.64	0.43
$Al(OBu^t)_3$ (1.859 g), CH_3COCl (0.596 g), in benzene (11.8 g)	1:1	Room temperature overnight	$AlCl(OBu^t)_2$ (1.489 g) white powder	13.6	18.7	1.0	1.04	12.95	17.02	1.0
$Al(OBu^t)_3$ (1.406 g), CH_3COCl (0.896 g), in benzene (5.3 g)	1:2	Room temperature 5 hours	$AlCl_{1.2}(OAc)_{0.3}(OBu^t)_{1.5}$ (1.0214 g) white powder	13.96	22.07	1.2	1.5	13.71	21.64	1.5
$Al(OBu^t)_3$ (1.527 g), CH_3COCl (0.98 g), in benzene (9.0 g)	1:2	Refluxing 4 hours	$AlCl_{0.6}(OAc)_{1.6}(OBu^t)_{0.8}$ (1.22 g) white powder	13.9	10.8	0.6	2.2	13.43	10.6	2.2
$Al(OBu^t)_3$ (1.435 g), CH_3COCl (1.39 g), in benzene (5.8 g)	1:3	Room temperature overnight	$AlCl_{0.7}(OAc)_{1.8}(OBu^t)_{0.5}$ (1.265 g) white powder	13.04	12.4	0.7	2.5	13.8	12.7	2.5
$Al(OBu^t)_3$ (1.65 g), CH_3COCl (2.65 g), in benzene (16.0 g)	1:5	Refluxing ½ hour	$AlCl_{0.5}(OAc)_2(OBu^t)_{0.5}$ (1.247 g) white powder	14.02	9.05	0.49	2.5	13.6	8.92	2.5

Can. J. Chem. Downloaded from www.nrcresearchpress.com by 210.87.254.42 on 09/05/12
For personal use only.

TABLE II

Reactions of aluminum chloride with tertiary butyl acetate

Reaction mixture		Molar ratios	Conditions of the experiment	Nature of the product	Analysis						
					Found				Required		
					% M	% Cl	Cl:M	Alk. eq. in moles	% M	% Cl	Alk. eq. in moles
$AlCl_3$ Bu^tOAc in benzene	(2.52 g), (2.32 g), (16 cc)	1:1	Carried out at 0–5° C and left overnight at room temperature	$AlCl_2(OAc)$ (3.35 g) dark brown sticky solid	*14.53	34.94	1.9	2.9	17.2	45.2	3.0
$AlCl_3$ Bu^tOAc in benzene	(1.706 g), (3.01 g), (12 cc)	1:2	Reaction at 0–5° C kept overnight at room temperature	$AlCl(OAc)_2$ (2.792 g) white powder	13.2	17.6	1.0	2.9	14.9	19.6	3.0
AlCl Bu^tOAc in benzene	(1.144 g), (3.01 g), (12 cc)	1:3	Room temperature overnight	$AlCl(OAc)_2 0.3Bu^tOAc$ (2.02 g) white powder	12.56	15.94	0.98	3.0	12.52	16.4	3.0
$AlCl_3$ Bu^tOAc	(2.240 g), (large excess)	1: large excess	Room temperature overnight	$AlCl(OAc)_2 0.5Bu^tOAc$ (4.09 g) white powder	11.05	15.0	1.0	2.8	11.3	14.88	3.0
$AlCl_3$ Bu^tOAc	(2.469 g), (24.0 g)	1: large excess	Refluxing at 110° C (20 minutes)	$AlCl_{0.42}(OAc)_{2.57}$ (4.2 g) white powder	13.4	7.8	0.43	2.8	13.9	7.8	3.0
$AlCl_3$ Bu^tOAc	(2.7 g), (35.0 g)	1: large excess	Refluxing at 110° C (6 hours)	$Al(OAc)_3$ (3.55 g), white powder	12.95			2.9 OAc 83.7%	13.2		3.0 OAc 86.7%

*The compound is sticky and appears to retain the solvent because of which the analyses are low. The reaction has, therefore, been repeated in *h*-hexane in place of benzene, which has been used as an inert solvent in all the other reactions and the effect of heat on the compound has been studied.

The first clue pointing to an entirely new explanation of the above facts was obtained in the reaction of silicon tetrachloride with tertiary butyl acetate, in which case silicon tetraacetate (7) was obtained in a quantitative yield at the room temperature. It was conjectured that in the present reactions also the aluminum chloride tertiary butoxide initially produced may react with the tertiary butyl acetate formed in the reaction itself, to yield the acetate derivative:

$$Al(OBu^t)_{3-n}Cl_n + xBu^tOOCCH_3 \rightarrow Al(OBu^t)_{3-n}(—OOCCH_3)_xCl_{(n-x)} + xBu^tCl,$$

(where $n = 1, 2,$ or 3
$x \leqslant n$).

The reactions of aluminum tertiary butoxide with acetyl chloride were, therefore, carried out in different molecular proportions, when the results shown in Table I were obtained.

A perusal of the data in Table I clearly indicates that monochloride ditertiary butoxide and dichloride monotertiary butoxide derivatives are formed initially by the reactions:

$$Al(OBu^t)_3 + CH_3COCl \rightarrow AlCl(OBu^t)_2 + Bu^tOOCCH_3,$$

$$AlCl(OBu^t)_2 + CH_3COCl \rightarrow AlCl_2(OBu^t) + Bu^tOOCCH_3.$$

However, the dichloride monotertiary butoxide appears to react with the tertiary butyl acetate produced in the reaction with the replacement of chloride groups by the acetoxy groups.

For testing the correctness of the above assumption, the reactions of aluminum trichloride with tertiary butyl acetate were carried out in different molar ratios, when the results shown in Table II were obtained.

A study of the data in Table II reveals that the reaction between aluminum chloride and tertiary butyl acetate is a straightforward reaction which can be represented by the following equation:

$$AlCl_3 + nBu^tOAc \rightarrow AlCl_{3-n}(OAc)_n + nBu^tCl + \text{heat},$$

(where $n = 1, 2,$ or 3).

The reaction at first is very vigorous and exothermic, and two of the chlorine atoms of aluminum trichloride are replaced with facility by the acyl group at room temperature. Later on the reaction becomes slow and the triacetate of aluminum is obtained only under refluxing conditions:

$$AlCl_3 + 3Bu^tOAc \xrightarrow[110^\circ C]{\text{reflux}} Al(OAc)_3 + 3Bu^tCl.$$

The reactions thus provide alternative routes for the synthesis of aluminum chloride acylates (8) and the triacetate (9), the existence of which was doubted for a long time and which were synthesized for the first time in these laboratories.

Possible Reaction Mechanism

The reaction between aluminum chloride and tertiary butyl acetate could be represented by the following probable mechanism :

Can. J. Chem. Downloaded from www.nrcresearchpress.com by 210.87.254.42 on 09/05/12
For personal use only.

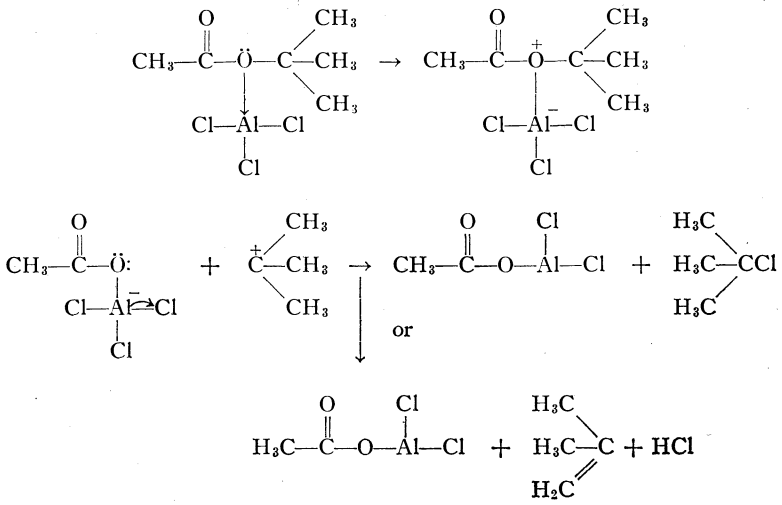

. . . and so on.

The facile manner of the reaction could be understood easily on the stability of tertiary butyl cations. As the chlorine is replaced in aluminum chloride by acetate groups, the electrophilic nature of the aluminum will decrease and can be expected to make the third stage of the reaction rather slow.

The above mechanism is similar to the alkyl fission mechanism suggested by Bunton, Comyns, and Wood (10) for the acid hydrolysis of tertiary butyl acetate:

$$(CH_3)_3COOCCH_3 + HO^{18}H \xrightarrow[HCl]{H_3O} (CH_3)_3CO^{18}H + CH_3COOH$$

In an infrared study of the ester – boron trichloride system, Lappert (11) found that the initial coordination occurs through the acyl oxygen of the ester. The above reaction mechanism will hold equally well in this case also:

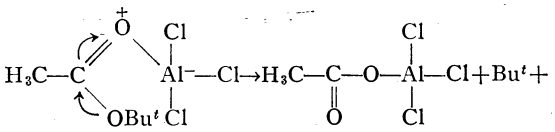

. . . and so on.

However, the reactions of tertiary butyl acetate with the isopropoxides of aluminum (4) and zirconium (6) have been shown to give the corresponding tertiary butoxides and it would be difficult to explain this if the initial coordination were through the acyl oxygen.

EXPERIMENTAL

Apparatus

All-glass apparatus fitted with interchangeable standard joints was employed and adequate precautions were taken to exclude atmospheric moisture. Fractionations were carried out in a column packed with Raschig rings and fitted to a total condensation variable takeoff stillhead.

Materials

Aluminum tertiary butoxide was prepared with aluminum turnings and anhydrous tertiary butyl alcohol (12). It was sublimed (198–200° C at 1.0 mm) and analyzed before use. Found: Al, 10.9. Calc. for $Al(OBu^t)_3$: Al, 10.97%. Acetyl chloride (B.D.H./A.R.) was distilled (51–52° C) before use. Tertiary butyl alcohol was first dried over slaked lime and then on sodium tertiary butoxide and finally distilled (82.5° C). Benzene

Can. J. Chem. Downloaded from www.nrcresearchpress.com by 210.87.254.42 on 09/05/12
For personal use only.

(B.D.H.) was dried by refluxing it over sodium metal for 2 days and distilled. Finally it was dried azeotropically with ethanol. Anhydrous aluminum chloride (sublimed/E. Merck) was resublimed (180° C at 1.5 mm) and analyzed before use. Tertiary butyl acetate was prepared (13) by the action of acetic anhydride on tertiary butanol. After purification and drying over anhydrous potassium carbonate, it was fractionated (96–98° C) twice before use.

Analytical Method

Aluminum and chlorine were estimated as oxinate and silver chloride separately. Acetoxy group was estimated by titrating the weighed sample with $N/10$ caustic soda using phenolphthalein as indicator. It was initially tested by a large number of blank experiments that both aluminum trichloride as well as triacetate require 2.9 equivalents of caustic soda. Further, it was also found that the first drop of sodium hydroxide when added to tertiary butyl acetate and aluminum tertiary butoxide gives immediate color to phenolphthalein. This method of analysis giving the acetate groups is more accurate than elemental analyses.

I. Reaction between Aluminum Tertiary Butoxide and Acetyl Chloride in Benzene

To a solution of aluminum tertiary butoxide in dry benzene was added the calculated amount of acetyl chloride. No heat appeared to be evolved in 1:1 molar reactions and only a slight amount of heat was evolved in the other reactions. After the clear solution was shaken well and allowed to stand at room temperature for a number of hours or after it was refluxed at a bath temperature of nearly 90° C, the volatile fractions were removed at the room temperature under reduced pressure. A white powder was obtained in each case and the analyses of the various products obtained are given in Table I.

II. (a) Reactions of Anhydrous Aluminum Chloride and Tertiary Butyl Acetate in Benzene

The suspension of aluminum chloride in dry benzene was caused to react with tertiary butyl acetate in required amount for definite molar ratio. All the reactions were highly exothermic and were carried out in a cold bath (0–5° C). After the reaction mixture had been shaken and allowed to stand overnight, the volatile fractions were removed and then the product was dried under reduced pressure at room temperature. The final product was a white amorphous solid except in the 1:1 molar reaction, where it was a brownish sticky solid. The results of the analyses are tabulated in Table II.

II. (b) Reaction of Anhydrous Aluminum Chloride with Tertiary Butyl Acetate in Presence of n-Hexane (Molar Ratio 1:1)

In view of the sticky nature of the product in 1:1 molar reaction in benzene, the reaction was repeated in *n*-hexane. A suspension of aluminum chloride (2.92 g) in about 10 cc of *n*-hexane was treated with tertiary butyl acetate (2.56 g) in cold (0–5° C). An exothermic reaction occurred and after about 2 hours the volatile fractions were removed under reduced pressure, leaving a brown, viscous sticky solid. Yield 4.464 g. Found: Al, 14.0; Cl, 37.2; Cl:Al = 2; alkali eq., 2.97 moles. Calc. for $AlCl_2(OAc)$: Al, 17.3; Cl, 45.2%; alkali eq., 3.0 moles.

The above compound (3.60 g) when heated at about 50° C at 1.0 mm for 1 hour gave a brown color sticky solid (3.36 g) which, on analyses, gave: Al, 14.95; Cl, 37.8%; Cl:Al = 1.94; alkali eq., 2.95 moles.

This, on further heating (3.2 g) at 100° C 0.1 mm for 1 hour, gave a brown viscous solid (3.1 g). Found: Al, 15.4; Cl, 38.9%; Cl:Al = 1.91; alkali eq., 2.87 moles.

Further heating of the compound (2.91 g) at 120–130° C at a reduced pressure of 0.1 mm for 2 hours gave a brittle-brown solid (2.84 g). Found: Al, 16.6; Cl, 34.0%; Cl:Al = 1.6; alkali eq., 2.3 moles.

II. (c) Reaction between Aluminum Chloride and Excess of Tertiary Butyl Acetate without any Solvent

To avoid the hardening of the product formed in the reaction, a weighed amount of aluminum chloride was added cautiously, with shaking, to the flask containing tertiary butyl acetate in large excess. The reaction in each case was found vigorous and exothermic. The resulting mixture was shaken well, then kept overnight at room temperature or refluxed at about 110° C. The times of refluxing were varied with the conditions of the particular reaction. In every case, a white solid separated out from the clear solution. The supernatant liquid was decanted off and the product was freed from the volatile fractions under reduced pressure. The analyses of the various products are given in Table II.

REFERENCES

1. D. C. Bradley, F. M. Abdel Halim, R. C. Mehrotra, and W. Wardlaw. J. Chem. Soc. 4609 (1952).
2. D. C. Bradley, D. C. Hancock, and W. Wardlaw. J. Chem. Soc. 2773 (1952).
3. R. C. Mehrotra and R. K. Mehrotra. J. Indian Chem. Soc. **39**, 23 (1962).
4. R. C. Mehrotra. J. Indian Chem. Soc. **30**, 585 (1963).
5. R. C. Mehrotra. J. Indian Chem. Soc. **31**, 85, 704 (1954).
6. R. C. Mehrotra. J. Am. Chem. Soc. **76**, 2266 (1954).
7. R. C. Mehrotra and B. C. Pant. Tetrahedron Letters, **5**, 321 (1963).
8. R. C. Mehrotra and A. K. Rai. J. Indian Chem. Soc. **31**, 1 (1962).

Can. J. Chem. Downloaded from www.nrcresearchpress.com by 210.87.254.42 on 09/05/12
For personal use only.

9. R. C. MEHROTRA. Nature, **172**, 74 (1953). R. C. MEHROTRA and K. C. PANDE. Z. Anorg. Allg. Chem. 291 (1956). R. C. MEHROTRA and K. C. PANDE. J. Inorg. Nucl. Chem. **2**, 60 (1956); **4**, 128 (1957).
10. C. A. BUNTON, A. E. COMYNS, and J. L. WOOD. Research, **4**, 383 (1951).
11. M. F. LAPPERT. J. Chem. Soc. 817 (1961).
12. W. WAYNE and H. ADKINS. Org. Syn. Vol. 21. John Wiley and Sons, Inc. New York. 1941. p. 8.
13. A. I. VOGEL. A text book of practical organic chemistry. Longmans Green and Co., London. 1956. p. 384.

Can. J. Chem. Downloaded from www.nrcresearchpress.com by 210.87.254.42 on 09/05/12
For personal use only.

THE pK_a OF PROTONATED α,β-UNSATURATED CARBOXYLIC ACIDS

T. S. SORENSEN
Department of Chemistry, University of Alberta, Calgary, Alberta
Received October 20, 1963

ABSTRACT

The pK_a of three, protonated α,β-unsaturated carboxylic acids have been determined from their ultraviolet absorption curves by using several of the well-known empirical methods. A detailed study of the absorption curves has been attempted in order to learn more about the "solvent effect" inherent in this spectral method of calculating pK_a values. Methyl substitution at the β-carbon of the acid results in large differences in the calculated pK_a.

The pK_a of protonated *o*- (1) and *p*-substituted (2) benzoic acids and of propionic (3) and acetic (4) acid have been reported. These values range from −6.2* to −8.6 for phthalic acid and *m*-nitrobenzoic acids (the extremes for substituted benzoic acids which have been measured), −6.4 for acetic acid and −7.3 for propionic acid.

The values for acetic and propionic acids are likely to be only approximate since the ultraviolet transition used in the measurement ($n \rightarrow \pi^*$) is weak and in the region of the spectrum where stray light and other effects can cause erroneous absorption. We have measured the complete accessible ultraviolet spectral curves for acrylic, crotonic, and β,β-dimethylacrylic acids in a wide range of sulphuric acid – water mixtures and have used these measurements to calculate the respective pK_a values by several different techniques. In addition, the roughly Gaussian shape of the spectral curves allows us to make an investigation of the "solvent effects" which appear as a serious complication in many pK_a determinations using ultraviolet spectroscopy to determine the concentration of the unprotonated and protonated species.

The structure of the protonated carboxyl group has been discussed by Stewart and Yates (2) and by Palmer and Urch (5) and is considered to have a symmetrical structure, e.g. I for protonated crotonic acid.

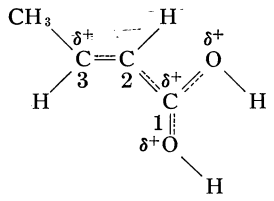

I

A pK_a value is a measure of the stability of the protonated form of a base relative to the unprotonated form, but since there is not likely to be much difference in energy between the unprotonated molecules, differences in pK_a can be attributed to differences in the stability of the protonated forms. It is to be expected that the substitution at carbon 3 of the oxonium ion I will cause some difference in the stability of this ion (tertiary > secondary > primary) but the magnitude is unknown.

Except for a very weak band ($n \rightarrow \pi^*$) which is hardly observable (6), the only accessible ultraviolet absorption in solutions of α,β-unsaturated acids is the intense $\pi \rightarrow \pi^*$

**All literature pK_a values are corrected by using the new H_0 scale in ref. 14.*

Can. J. Chem. Downloaded from www.nrcresearchpress.com by 210.87.254.105 on 09/05/12
For personal use only.

transition. This absorption band is very satisfactory for pK_a measurements except for acrylic acid where the λ_{max} in water is at 1940 Å, only some 100 Å above the cutoff point of the instrument and therefore subject to the usual inaccuracies. It has been reported (7) that Beer's law is not valid for the absorption spectra of certain α,β-unsaturated acids in ethanol solution. We have checked Beer's law for crotonic acid in 50% sulphuric acid and find that it holds well. The reported deviations are likely instrumental since these results were obtained with machines with effective cutoffs at 2100 Å.

We have made recovery and dilution experiments to verify that the spectrum we have recorded is not due to some irreversibly formed decomposition product. Solutions of β,β-dimethylacrylic acid underwent decomposition (decreasing ultraviolet absorption with time) with certain concentrations of sulphuric acid but no difficulty was encountered with crotonic and acrylic acids. We were able to obtain rough kinetics for this decomposition and to extrapolate the spectra to zero time.

RESULTS

The complete spectra for crotonic acid are shown in Fig. 1 plotted in wave numbers.

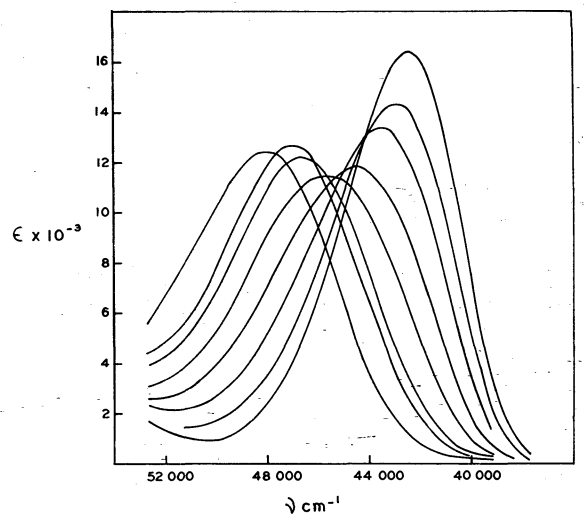

FIG. 1. Ultraviolet spectra of crotonic acid in aqueous sulphuric acid, % w/w sulphuric acid, curves from left to right, 0, 49.2, 58.9, 67.7, 73.2, 77.8, 82.2, 96.2.

The tabulated data for these curves (λ_{max}, ϵ_{max}, and $\Delta\nu$) as well as those for the other two acids are given in the Experimental section. A number of methods can be applied in using these curves to calculate pK_a values. Plots of ϵ_B vs. H_0 and ϵ_{BH^+} vs. H_0 all give sigmoid-shaped curves although the calculated pK_a in each case is not exactly the same. The procedure of Davis and Geissman (8), which has been most widely used, was applied to the absorption curves for each acid and is shown in Fig. 2 for crotonic acid. It is difficult to decide where the midpoint of the sigmoid curve is situated and in these cases Stewart and Granger (1) have shown that a plot of log $(\Delta D_{BH^+}-\Delta D)/(\Delta D-\Delta D_B)$ versus H_0 gives a straight line from which the pK_a can be directly located. We have also used this method to calculate the pK_a values. The remarkable thing about these plots is that they appear to be exact (a straight line is obtained) but the slope of the line is considerably less than unity.

Can. J. Chem. Downloaded from www.nrcresearchpress.com by 210.87.254.105 on 09/05/12
For personal use only.

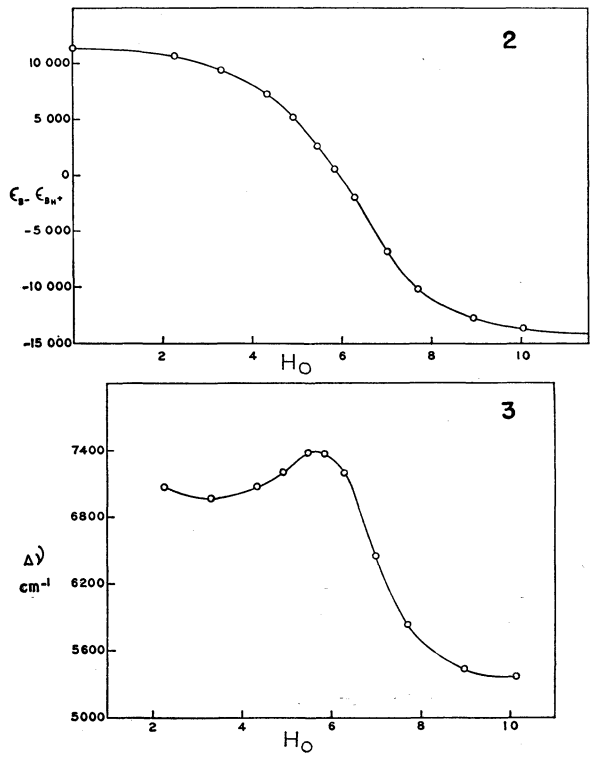

FIG. 2. pK_a calculation using the procedure of Davis and Geissman.

FIG. 3. A plot of the half-width, $\Delta\nu$, for the absorption curves of crotonic acid in aqueous sulphuric acid solutions, against the H_0 of these solutions.

Slopes of less than unity have been found for a number of other carbonyl compounds (9), so-called "non-Hammett bases". Finally the half-widths, $\Delta\nu$, of each curve, over the whole H_0 range, have been plotted against H_0 and, as shown in the following discussion, a rough pK_a can be calculated from this. The shape of this plot for crotonic acid is shown in Fig. 3. The calculated pK_a values, by each method, are collected in Table I along with the observed slopes determined by using the treatment of Stewart and Granger.

DISCUSSION

It is somewhat disturbing that qualitatively there is no real indication of two peaks in any of the complete absorption curves for β,β-dimethylacrylic and crotonic acids as shown in Fig. 1. Similar difficulties have been reported (10) in attempting to measure the pK_a of protonated anisole. The spectral curves of acrylic acid show somewhat better behavior (in that an approximate isobestic point is observed) but unfortunately we cannot measure the complete curves.

Vandenbelt and Henrich (11) have calculated the combined curves resulting from the mixing of two Gaussian curves, varying the separation of the curves and the ratio of the two in the combined curve. If the separation is small definite shoulders or inflection points are not obvious in the combined curve, e.g. if two identically shaped curves have a $\Delta\nu$ of 3 units and if the separation is 2 units, the combined curve also looks roughly Gaussian in shape. The $\Delta\nu$ of the combination curve is increased to 4 units, however, if the two

Can. J. Chem. Downloaded from www.nrcresearchpress.com by 210.87.254.105 on 09/05/12
For personal use only.

TABLE I

pK_a of protonated α,β-unsaturated acids

Method of pK_a determination	Crotonic	Acrylic	β,β-Dimethylacrylic
Davis and Geissman	−6.15	−7.55	−5.4
Stewart and Granger	−6.18	−7.55	−5.35
$\Delta\nu$ versus H_0	−5.8	−7.2*	−4.9
Slope	0.73	0.90	0.67

*Peak width at three-quarters peak height.

separate curves are of equal height. The presence of what appears to be a single peak need not cause any concern therefore except inasmuch as the component curves must be separated by amounts similar to those discussed above.

The curves for these α,β-unsaturated acids in aqueous sulphuric acid, where the H_0 of the solution is equal to the pK_a, must by definition be composed of equal parts of the curve due to the free base and that due to the protonated base. If a curve fitting is made, assuming constant ϵ_{max} and shape for the component curves, it can be shown that the λ_{max} for the absorption curve due to unprotonated acid shifts strongly to the red and that due to the protonated acid (with reference to the peak position at the pK_a point) also shifts, although less than the unprotonated species, to the red. The general theory (12) of solvent effects on $\pi \rightarrow \pi^*$ transitions of this type predicts that a red shift of the absorption curve of unknown magnitude should be observed for the unprotonated molecule but the protonated molecule, being a charged species, is expected to be rather insensitive to solvent polarity.

The red shift of the "free" carbonyl absorption peak has been noted by many workers in this field, beginning with Hammett (13). It has also been noted that the peak for the protonated carbonyl species shifts to the red with increasing acid concentration and also increases in intensity (1). In our spectral curves, the increase in intensity is paralleled by a decrease in $\Delta\nu$, so that the integrated intensity remains nearly constant.

If two identical Gaussian curves overlap strongly the combined curve will have a maximum $\Delta\nu$ when the two contributing curves are present in equal amounts. We have therefore plotted $\Delta\nu$ for the curves of Fig. 1 against H_0 and have calculated a pK_a by: (1) neglecting slight errors due to the different $\Delta\nu$ of the two contributing curves; (2) assuming that the shape of curves for the protonated and unprotonated base do not change with the H_0 of the solution; and (3) that within the 0.1–0.3 H_0 units involved, a plot of log BH^+/B versus H_0 is linear with unit slope so that in the case where ϵ_B is somewhat different from ϵ_{BH^+}, a pK_a can still be calculated. Since the individual curves must by definition be rising and falling very rapidly in the region of the pK_a, the assumptions which have been made do not have much effect on the value of the pK_a which is calculated. The pK_a values calculated in this manner agree fairly well (0.3–0.4 pK_a units lower) with those obtained by the Davis and Geissman method. This method of calculating pK_a values should be applicable to systems where the optical density of the absorption curves are decreasing rapidly with time, providing the time required to make the spectral measurements is fast relative to this decomposition and also that the decomposition products do not absorb themselves.

The calculated pK_a values are in the range reported for other carboxylic acids and a large difference, 1 pK_a unit, is observed between the successive members of this series. This would imply that the double bond is considerably delocalized by resonance with the

Can. J. Chem. Downloaded from www.nrcresearchpress.com by 210.87.254.105 on 09/05/12
For personal use only.

protonated carboxyl group. This difference can be compared with the difference in pK_a between protonated benzoic acid (−7.65) and the *p*-methyl (−7.25) substituted acid.

The decomposition of β,β-dimethylacrylic acid was found to be catalyzed by ultraviolet light. In the absence of light the reaction, as measured by the decrease in ϵ_{max}, was found to be approximately first order and in all cases where there was appreciable reaction, a steady state was reached where no further decomposition occurred. At low H_0 values the rate of decomposition was slow but the position of the equilibrium was almost completely on the side of a non-absorbing species. As the concentration of sulphuric acid increases the rate of decomposition increases but the position of the equilibrium shifts in favor of the α,β-unsaturated acid. This decomposition can be satisfactorily explained as a simple hydration (equation I) since the hydrated species would have virtually no ultraviolet absorption.

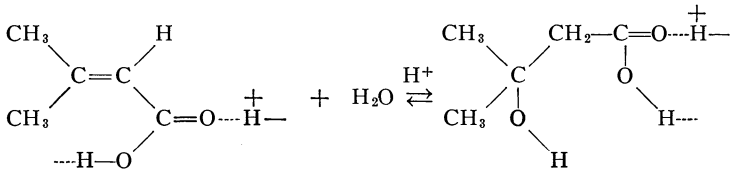

Equation I

EXPERIMENTAL

Ultraviolet measurements were obtained from a Beckman DK-1 spectrophotometer which had been checked for accuracy of intensity and wavelength (down to 2200 Å). The stray light performance of this machine was investigated and this effect can cause errors in the region of the absorption curve near the cutoff point of the machine (1850–1950 Å). No correction has been applied but the curves for acrylic acid are the only ones appreciably affected. The scan speed was 100 Å/minute except where decomposition was occurring when a speed of 500 Å/minute was used. All peak maxima were rerun and an expanded scale was used in order to obtain maximum accuracy. The samples were not thermostated but the temperature did not vary much (22±2° C). The solutions were measured in 0.1 cm "suprasilica" cells, with a solvent blank in the reference cell of the same composition as that in the sample cell. A base-line correction was made where necessary by measuring spectra with only solvent in both cells. The curves for β,β-dimethylacrylic acid have been corrected back to zero time. The optical density of the absorption curve was determined at time intervals measured from the time of preparation of the solution. A rough check was made on curves where substantial decrease in optical density had occurred to make certain that no extraneous absorption was appearing. It was observed that decomposition was more rapid when the sample stayed in the cell compartment with ultraviolet light shining on it than when the sample was kept in the dark. Measurements were continued until a steady state was reached where no further decomposition occurred. The kinetics (as measured by the decrease in optical density in the dark) were approximately first order and the ϵ_{max} of the curves for this acid have been corrected. On fast scan, the time necessary to record most of the absorption (1 minute) is short compared to the decomposition rate. Some rough values for the kinetics of the decomposition are:

% Sulphuric acid	Half-life of decomposition, $T^{1/2}$ (min)	Equilibrium position, % α,β-unsaturated acid
63.76	ca. 90	Small
70.35	ca. 28	38
73.16	ca. 14	55
77.79	ca. 7	83

All curves were measured in duplicate and if the average error for the calculated ϵ_{max} was more than 2%, repeat measurements were made. Tabulated data from the absorption curves are collected in Table II.

Solutions were prepared by weighing out 0.3–0.5 mg of the carboxylic acid on a small glass boat, with a microbalance. This boat was added to the solvent previously made up to mark in a volumetric flask.

Aqueous sulphuric acid solutions were titrated against standard base. The Hammett acidity function H_0 for a given percentage of sulphuric acid was taken from the recent data of Jorgenson and Hartter (14).

Can. J. Chem. Downloaded from www.nrcresearchpress.com by 210.87.254.105 on 09/05/12
For personal use only.

Can. J. Chem. Downloaded from www.nrcresearchpress.com by 210.87.254.105 on 09/05/12
For personal use only.

TABLE II

% sulphuric acid	Crotonic acid			Acrylic acid			β,β-Dimethylacrylic acid		
	ϵ_{max}	λ_{max} Å	$\Delta\nu$ cm^{-1}	ϵ_{max}	λ_{max} Å	$\Delta\nu$ cm^{-1}	ϵ_{max}	λ_{max} Å	$\Delta\nu$ cm^{-1}
0	12,400	2,083	7,290	10,500	1,939	—	12,000	2,203	6,900
38.04	13,100	2,110	7,070	—	—	—	11,700	2,230	6,880
49.21	12,650	2,121	6,960	9,800	1,966	—	11,500	2,255	7,160
58.93	12,200	2,141	7,070	—	—	—	11,700	2,301	7,410
63.76	11,850	2,159	7,260	—	—	—	11,950	2,350	7,430
65.81	—	—	—	—	—	—	12,400	2,367	7,250
67.66	11,500	2,184	7,370	8,900	1,992	—	12,500	2,393	6,980
70.35	11,950	2,221	7,360	—	—	—	13,100	2,420	6,540
73.16	11,750	2,242	7,190	8,800	2,010	—	13,700	2,444	6,160
77.79	13,300	2,292	6,430	8,100	2,038	—	15,100	2,471	5,610
80.36	—	—	—	8,000	2,073	—	—	—	—
82.21	14,250	2,323	5,820	8,250	2,110	—	15,000	2,492	5,440
86.13	—	—	—	8,950	2,142	—	—	—	—
90.25	15,600	2,345	5,420	10,500	2,156	—	16,750	2,508	5,180
96.20	16,300	2,352	5,360	11,000	2,163	—	17,800	2,516	5,050
98.29	—	—	—	—	—	—	17,700	2,518	5,140
100.0	16,150	2,355	5,380	10,500	2,175	—	13,200	2,436	—

The absorption spectra of these carboxylic acids in 100% sulphuric acid are not unusual except in the case of β,β-dimethylacrylic acid where the λ_{max} is at considerably shorter wavelengths than in 98% sulphuric acid. Evidently some other change has occurred in this solvent but we have not investigated this.

Unchanged carboxylic acid can be recovered from its concentrated sulphuric acid solutions. A more quantitative measurement of any decomposition was obtained by dilution experiments. Solutions of the carboxylic acids were prepared and the spectrum measured with 0.1 cm cells. This same solution was diluted 10-fold with ice and water and the spectrum (taken in 1 cm cells) was compared with that of the carboxylic acid in this medium (approximately 10% sulphuric acid). A quantitative recovery was calculated for crotonic acid; for β,β-dimethylacrylic and acrylic acids the recovery was better than 90%.

β,β-Dimethylacrylic and crotonic acids were recrystallized from water, m.p. 69–70° C and 72–73° C respectively. Acrylic acid was redistilled at reduced pressure and kept below 0° C.

REFERENCES

1. R. STEWART and M. R. GRANGER. Can. J. Chem. **39**, 2508 (1961).
2. R. STEWART and K. YATES. J. Am. Chem. Soc. **82**, 4059 (1960).
3. J. T. EDWARD and I. C. WANG. Can. J. Chem. **40**, 966 (1962).
4. A. R. GOLDFARB, A. MELE, and N. GUTSTEIN. J. Am. Chem. Soc. **77**, 6194 (1955).
5. M. H. PALMER and D. S. URCH. J. Chem. Soc. 174 (1963).
6. W. D. CLOSSEN, S. F. BRADY, E. M. KOSOWER, and P. C. HUANG. J. Org. Chem. **28**, 1161 (1963).
7. H. E. UNGNADE and I. ORTEGA. J. Am. Chem. Soc. **73**, 1564 (1951).
8. C. T. DAVIS and T. A. GEISSMAN. J. Am. Chem. Soc. **76**, 3507 (1954).
9. J. T. EDWARD and I. C. WANG. Can. J. Chem. **40**, 966 (1962). A. R. KATRITZKY, A. J. WARING, and K. YATES. Tetrahedron, **19**, 465 (1963).
10. E. M. ARNETT and C. Y. WU. J. Am. Chem. Soc. **82**, 5660 (1960).
11. J. M. VANDENBELT and C. HENRICH. Appl. Spectroscopy, **7**, 173 (1953).
12. N. S. BAYLISS and E. G. MCRAE. J. Phys. Chem. **58**, 1002 (1954).
13. L. A. FLEXSER, L. P. HAMMETT, and A. DINGWALL. J. Am. Chem. Soc. **57**, 2103 (1935).
14. M. J. JORGENSON and D. R. HARTTER. J. Am. Chem. Soc. **85**, 878 (1963).

Can. J. Chem. Downloaded from www.nrcresearchpress.com by 210.87.254.105 on 09/05/12
For personal use only.

POLYCONDENSED ANIONS OF THE TRANSITION METALS

LIGHT SCATTERING AND ULTRACENTRIFUGATION WITH SCHLIEREN AND INTERFERENCE OPTICS OF ALKALINE NIOBIUM(V) SOLUTIONS[1]

WILFRED H. NELSON[2] AND R. STUART TOBIAS
Department of Chemistry, University of Minnesota, Minneapolis

Received October 3, 1963

ABSTRACT

Alkaline aqueous niobium(V) solutions prepared by dissolving the salt $K_{14}Nb_{12}O_{37}\cdot 27H_2O$ were studied by means of light scattering and by equilibrium ultracentrifugation by using both schlieren and interference optics. All three experimental methods indicate that the degree of polymerization of the polycondensed niobate anion is no less than 5 and probably has the value 6. The centrifugation data indicate that only one polycondensed species exists in the solutions. The effective charge of the niobate anion appears to be reduced appreciably by the binding of potassium ions to a value of no greater than −2. The behavior of the solutions is very similar to that observed previously with alkaline tantalum(V) solutions, and it appears very likely that the hexameric anion $[HNb_6O_{19}]^{-7}$ found in niobate crystals also exists in aqueous solutions. The niobate is slightly protonated in comparison to the analogous tantalate. The stability of highly concentrated solutions containing this large polycondensed species is probably the result of the existence of a poly-ion with high symmetry which interacts only weakly with the solvent, water.

INTRODUCTION

Among the best known of the polycondensed inorganic compounds are those formed by the quinquevalent Group V-A and B elements. The polyphosphates in aqueous solution have been very thoroughly studied by modern physicochemical techniques (1). The picture with the V-A elements V, Nb, and Ta is certainly less clear. In the past, there have been many postulates concerning the structure of the polycondensed transition metal compounds based on the structures of the polyphosphates with analogous stoichiometry. With an increase in information on the stereochemistry of these transition metals, it became apparent that most of these analogies were false. Rather than exhibiting regular tetrahedral coordination with respect to oxygen, vanadium(V) occurs in badly distorted structures involving essentially five-coordination while niobium and tantalum seem to exhibit almost regular octahedral coordination.

Recently we completed a study of alkaline aqueous solutions of tantalum(V) prepared by dissolving the compound $K_8Ta_6O_{19}\cdot 16H_2O$ (2). This type of alkali metal tantalate appears to be unique in that it is the only example of a readily soluble tantalum oxy-compound (3). The measurements indicated that $K_8Ta_6O_{19}\cdot 16H_2O$ dissolves in water without appreciable changes in the degree of condensation of the polycondensed anion found in the crystals. X-Ray studies on single crystals of this tantalate have indicated that discrete anions are present which contain six tantalum atoms arranged at octahedral vertices (4). All of the experimental data indicated that the solutions were monodisperse and that the single polyanion had the stoichiometry $[Ta_6O_{19}]^{-8}$ or $[HTa_6O_{19}]^{-7}$.

Although quinquevalent niobium does not form a compound isostructural with $K_8Ta_6O_{19}\cdot 16H_2O$, a single crystal X-ray study of the compound $Na_{14}Nb_{12}O_{37}\cdot 32H_2O$

[1]*This report is based on portions of a doctoral dissertation to be submitted by W. H. Nelson to the Graduate School of the University of Minnesota in partial fulfillment of the requirements for the degree of Doctor of Philosophy. The work has been supported by grants NSF-G14173 and GP-653 from the United States National Science Foundation and by the Graduate School of the University of Minnesota. Presented at the Symposium on Inorganic Polymers, The University of Western Ontario, London, Ontario, September 4–6, 1963.*

[2]*Present address: Department of Chemistry, University of Illinois.*

Can. J. Chem. Downloaded from www.nrcresearchpress.com by 210.87.254.42 on 09/05/12
For personal use only.

has indicated that this structure is also built up out of discrete anions with six niobium atoms arranged at octahedral vertices (5). The potassium niobate which seems to be most easily crystallized from aqueous solution apparently has the stoichiometry $K_{14}Nb_{12}O_{37}\cdot 27H_2O$ (6). In contrast to tantalum, which seems to crystallize in only the aforementioned type of alkali metal salt, niobium gives a series of soluble niobates differing but slightly in the ratio of alkali metal ion to niobium(V) (7). Recently a very thorough preparative study of the system K_2O–Nb_2O_5–H_2O has been carried out (8), and 10 different crystalline phases were identified.

By analogy with the alkaline tantalate solutions, it might be expected that solutions prepared by dissolving $K_{14}Nb_{12}O_{37}\cdot 27H_2O$ would also be monodisperse and contain a hexameric anion. Indeed, this has been suggested to be the case by Jander and Ertel (7) on the basis of measurements of the diffusion coefficient of the niobate species. On the other hand, these same authors had suggested earlier that tantalate solutions contained an anion with five tantalum atoms on the basis of analogous measurements (9). Recent work by Baker and Pope (10) has, however, shown that there is no theoretical or experimental basis for the assumed relation between diffusion coefficient and ionic weight used in the interpretation of Jander and Ertel's data (7, 9).

There is also definite evidence for differing behavior of the transition metals of the second and third long periods. Recent studies on sexavalent molybdenum have shown that the ions $[Mo_7O_{24}]^{-6}$, $[HMo_7O_{24}]^{-5}$, and $[H_2Mo_7O_{24}]^{-4}$ appear to exist in alkaline solutions (11, 12). In the case of tungsten, the anion $[HW_6O_{21}]^{-5}$ appears to be the main polycondensed species together with additionally protonated species with charges down to -2 (13, 14).

Rohmer and Guerchais using salt cryoscopy found a maximum degree of polymerization of 5 for niobate solutions and also concluded that the simple tetrahedral orthoniobate anion NbO_4^{-3} existed in strongly alkaline solutions (15). Although the basic theory of this experimental method has been known for 50 years there are some difficulties attending its use (16). Gridchina estimated the degree of polymerization to be 6 for solutions 2.5×10^{-3} to 2.5×10^{-2} M in niobium and 0.3 M in KOH using a dialysis method (17). Again this experimental method has proved to be erratic in the past, and there is no theoretical basis for the equation used in evaluating the data (18).

Since the studies on the tantalate solutions had indicated that the $[Ta_6O_{19}]^{-8}$ structure was a very stable one, it was decided to examine alkaline niobium solutions to see if there was any evidence for comparable stability of the analogous niobate anion. In the past, many problems have arisen in the study of such solutions, because it is now recognized that the theory used in the interpretation of the experiments was often inadequate. In recent years, there have been many refinements in the theory of multicomponent electrolyte solutions, and the use of sedimentation equilibrium in the ultracentrifuge with schlieren (19) and with interference optics (20) and the application of light scattering (21) for the study of relatively low weight inorganic polyions has been discussed. In order to make a detailed comparison of the experimental methods which all have the same thermodynamic basis, it was decided to undertake a study of the niobate solutions by all three techniques.

EXPERIMENTAL

Synthesis

Reagent grade Nb_2O_5 produced by H. C. Starch, A. G., was fused with KOH in a silver crucible to form the crude niobate. The cold melt was dissolved in a minimum amount of hot water, and the product was freed from the insoluble Ag_2O which resulted from attack on the crucible. Polyethylene vessels were used

Can. J. Chem. Downloaded from www.nrcresearchpress.com by 210.87.254.42 on 09/05/12
For personal use only.

throughout to avoid contamination by silicates. The partially purified product was precipitated by the addition of ethanol. This material was recrystallized several times from dilute KOH; and the crystals were dissolved in water and passed three times through a Millipore ultrafilter with a pore diameter of 4500 Å. Finally, pure crystals were precipitated with ethanol, collected on a glass frit under nitrogen, and dried in a vacuum desiccator. The infrared spectrum showed the final product to be free of ethanol and of carbonate. Niobium was determined by precipitation of the hydrous oxide from an aqueous solution of the salt with HCl. The precipitate was washed with 2% NH_4NO_3, ignited to constant weight at ca. 800° C and weighed as Nb_2O_5. Potassium was determined by precipitating the niobium with sulphuric acid, separating the hydrated Nb_2O_5 by filtration, evaporating the solution, and weighing the residue as K_2SO_4. Differential thermal and gravimetric analyses were run to determine the water of crystallization. The weight loss upon ignition was constant from 450° to 700°. Anal. Calc. for $K_{14}Nb_{12}O_{37}\cdot 27H_2O$: Nb 40.7, K 20.0, H_2O 17.8%. Found: Nb 40.7, K 19.9, H_2O 17.3%. Carbonate-free KOH solutions were prepared by precipitating carbonate with barium hydroxide and passing the solutions through the potassium form of Dowex-50W-X-8 to remove excess barium ions.

Infrared Spectra

The infrared spectrum of the potassium niobate was determined with both mineral oil mulls and KBr discs with a Perkin Elmer 21 spectrometer. The spectrum showed a sharp band at 852 cm^{-1} and broad absorption below 800 cm^{-1} with peaks at 760 and 720 cm^{-1}.

Light Scattering Measurements

The light scattering measurements were carried out as previously described (2, 22) with unpolarized 4358 Å light by using a Brice-Phoenix photometer. All measurements were made with 1 *M* KCl as the supporting electrolyte. Semioctagonal and cylindrical cells were used to determine the dissymmetry of scattering. The solutions were clarified by filtration through 0.10 μ Gelman ultrafilters in a stainless steel system under nitrogen pressure. Each sample was passed through the filter from 5 to 10 times and was discarded if any trend was observed in the turbidities from filtration to filtration. There was no measurable depolarization of the light scattered at 90°.

Sedimentation Equilibrium in the Ultracentrifuge

The experimental procedure was essentially that of Johnson and co-workers (23, 24). The centrifugations were carried out with a Spinco Model E ultracentrifuge using an Analytical "D" rotor. The optical systems standard with the instrument were used. Only one solution in a 12 mm cell was spun at a time. The temperature was controlled to 25±0.1° and the rotor speed to ±15 r.p.m. with accessories available for the centrifuge. All plates were read with a Bausch and Lomb microscope sliding scale comparator. The 5461 Å mercury line isolated with a Wratten 77A filter was used for all measurements. Density measurements were made with a 2 ml pycnometer. The data are summarized in Table I.

Schlieren Measurements

Schlieren patterns were taken at various bar angles between 60° and 85° and were recorded on Eastman Kodak I-N spectroscopic plates. Values of Z, the vertical displacement of the bar image caused by the refractive index gradient in the cell, were tabulated as a function of x, the radius from the center of rotation. Attainment of equilibrium was assured by observing images from day to day and noting the time at which no further change took place. Most of the runs had durations of from 40 to 70 hours. In addition to the centrifugation of the niobate in 1 *M* KCl, a background centrifugation was carried out on 1 *M* KCl. The difference between Z for the solution containing niobate + KCl and the Z for 1 *M* KCl gave Z^* from which the distribution of the polymeric niobate could be calculated.

Interference Optics

Interference optics have the advantage of permitting smaller amounts of solution to be used in the cell so that the distance from the meniscus to the cell bottom is reduced. As a result, equilibrium is much more rapidly attained. In addition, the precision in the determination of the refractive index gradient for a given run is considerably greater so that measurements can be made with more dilute solutions. The Rayleigh interference patterns were recorded on Eastman Kodak II-G spectroscopic plates with high green sensitivity. The plates were read by lining up the fringes, using the air reference fringes, and the distances between "vertical" fringes from the meniscus to the cell bottom were measured. From these measurements, the difference in refractive index between the solution and background compartments at different values of x can be calculated. In some cases, a series of photographs of the fringe pattern was taken throughout the run so that the position of a given fringe could be followed. From these data the absolute values of the refractive index differences at the various x values, n^*, could be obtained in the following way. From the movement of the fringes with time, the point where a given fringe at equilibrium would intersect the "reference fringe," i.e., the position of the fringe before sedimentation, could be noted. At this point the difference between the refractive indices of solution and background compartments is equal to the initial and known difference before sedimentation took place. Since the difference in refractive index between fringes is known, n^* values can be tabulated for the points corresponding to a fringe intersection with the "reference fringe." In most

Can. J. Chem. Downloaded from www.nrcresearchpress.com by 210.87.254.42 on 09/05/12
For personal use only.

TABLE I

Ultracentrifugation of niobium(V) in 1 *M* KCl

Expt. No.	Molarity of component 2 (*M*)	Speed of rotation (r.p.m.)	Optical system	S_e[a] or S	*N* computed for: $Z' = -0.2$	*N* computed for: $Z' = -0.3$
1	0.0444	19,160	*S*,[b] 65°[c]	0.075		
2	0.0444	19,160	S, 65°	0.075	6.0	6.3
					6.0	6.3
3*a*	0.0888	19,160	S, 60°	0.072		
3*b*	0.0888	19,160	S, 65°	0.073	5.8	6.2
3*c*	0.0888	19,160	S, 70°	0.072		
4*a*	0.1776	19,160	S, 65°	0.068		
4*b*	0.1776	19,160	S, 70°	0.072	5.8	6.3
4*c*	0.1776	19,160	S, 75°	0.069		
5*a*	0.2664	19,160	S, 75°	0.067		
5*b*	0.2664	19,160	S, 75°	0.068	5.8	6.4
5*c*	0.2664	19,160	S, 80°	0.068		
6*a*	0.3552	19,160	S, 70°	0.060	5.8	6.7
6*b*	0.3552	19,160	S, 75°	0.058		
1	0.0131	15,183	I	0.0445	5.8	6.0
2	0.0435	17,980	I	0.0600	5.5	5.7
3	0.0643	15,220	I	0.0417	5.4	5.7
4	0.0953	15,220	I	0.0390	5.2	5.4
5	0.1112	12,590	I	0.0280	5.4	5.7
6	0.1114	12,590	I	0.0287	5.4	5.7
7	0.1495	9,330	I	0.0159	5.6	5.9
8	0.1572	12,560	I	0.0284	5.4	5.7
9	0.1697	9,330	I	0.0162	5.7	6.0

[a]Average of the values at different bar angles used in calculations.
[b]S = schlieren and I = interference optics centrifugation.
[c]Bar angle.

cases, the values of n^* were obtained by an integrative procedure which only required values of the difference between the refractive index at the meniscus and at several values of x. The x values corresponded to points of intersection of the curved solution fringes with a reference fringe picked arbitrarily to pass through the meniscus and to intersect a curved fringe. Cell distortions for the interference cell were determined by centrifugations with both compartments filled with water, and fringe deviations from the horizontal were noted as a function of angular velocity. The distortions were found to be very small with our cell, and at speeds under 20,000 r.p.m. they never exceeded 0.1 fringe interval.

Since the solutions were alkaline, Kel-F single-sector and charcoal-filled Epon double-sector centerpieces rather than the usual aluminum-filled centerpieces were used with the usual quartz windows. The difference in refractive index between compartments corresponding to one fringe interval was determined with a capillary-type synthetic boundary cell and found to equal the value predicted from the instrument constants. Solution column thicknesses were determined by measuring the distance between the outer faces of the quartz windows with a micrometer and subtracting the known thicknesses of the quartz windows.

Unfortunately, it was necessary to vary the speed over a wide range as the concentration was varied in order to obtain good interference patterns in all cases.

Ion Exchange Measurements

Initial attempts to bind the anionic niobium(V) species to the hydroxide form of Dowex 2-X-8 were unsuccessful. Apparently the degree of cross-linking was too high to permit diffusion of the large niobate anion into the resin, and when the less highly cross-linked Dowex 2-X-4 was used, the niobate was bound quantitatively. The column was washed with distilled water, and the hydroxide ion in the eluate was titrated with standard acid. The equilibrium solution pH was measured with a Beckman H pH meter.

RESULTS

Light Scattering

Since the refractive index increments for the niobate solute were needed for both the light scattering and centrifugation with interference optics, these were obtained from measurements on solutions with known concentrations of KOH and KCl. The contributions of the latter two compounds to the gross Δn values could be calculated by using

Can. J. Chem. Downloaded from www.nrcresearchpress.com by 210.87.254.42 on 09/05/12
For personal use only.

known refractive index increments of KOH and KCl solutions, and these were subtracted from the gross Δn to give the Δn due to niobate. A plot of the Δn due to the niobate solute versus the niobate concentration is shown in Fig. 1 for the two wavelengths 4358

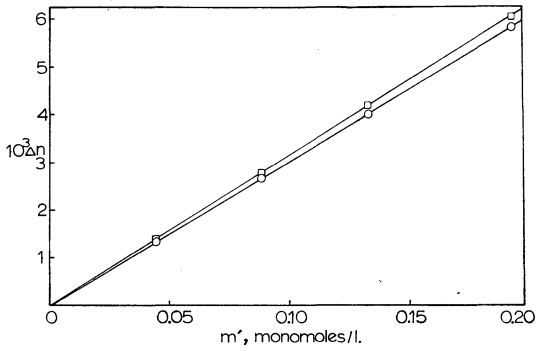

FIG. 1. Refractive index of the niobium(V) solutions as a function of concentration; □ 4358 Å, ○ 5461 Å.

and 5461 Å. The values for dn/dm' for the niobate in solutions 1 M in KCl were 0.0314 and 0.0301 l. monomole^{-1} at 4358 and 5461 Å respectively. The linearity of these plots tends to indicate that there are no condensation reactions leading to larger polycondensed species occurring as the concentration increases.

In order to verify that there were no significant contributions to the 90° scattering from colloidal particles, the angular dependence of the scattering was investigated from $\theta = 45$ to 135°. Typical data are illustrated in Fig. 2, which shows the normalized scattering

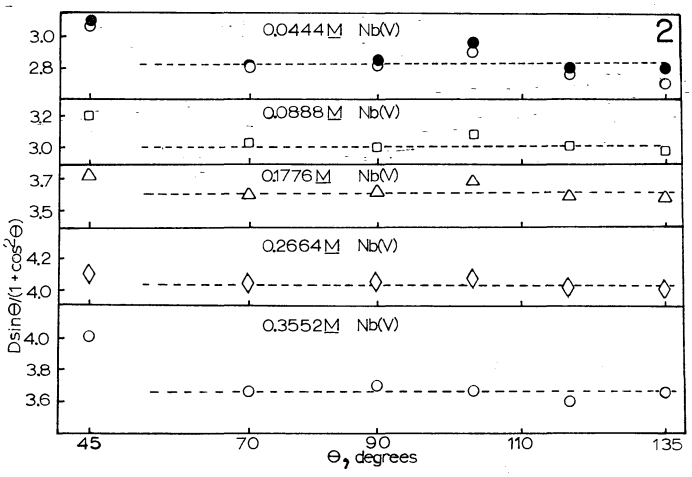

FIG. 2. Angular dependence of the light scattering of the niobate solutions.

envelope obtained by multiplying the observed galvanometer deflections by $\sin\theta/(1+\cos^2\theta)$. The 90° turbidities proved to be essentially the same as those obtained by extrapolation from larger angles.

The experimental turbidity data were used to compute the values of the deviation function (22) given in equation [1] for different values of the charge per monomer unit, Z'.

Can. J. Chem. Downloaded from www.nrcresearchpress.com by 210.87.254.42 on 09/05/12
For personal use only.

$$1/N_{z'} = \frac{\phi H'' \psi'^2 m'}{\tau^*} - \frac{Z'^2 m'}{2(m_3 + m_5)} \qquad [1]$$

Here, $N_{z'}$ is the number of monomer units (niobium atoms) contained in the polyanion, m' is the niobium concentration in monomoles per liter, ψ' is the value of dn/dm' for the monomeric scattering component, H' is a constant, ϕ is the volume fraction of solvent computed for 1 M KCl, and m_3 and m_5 are the concentrations of KCl and KOH respectively. The concentrations of KOH were sufficiently small in all of the solutions to be neglected.

In order to carry out these calculations, it is necessary to define a hypothetical "monomer" unit which contains one niobium atom and which has the proper stoichiometry. Since the compound $K_{14}Nb_{12}O_{37} \cdot 27H_2O$ used in preparing the solutions is obtained by crystallization from aqueous solution, the monomer unit is defined as $[K_{\bar{\nu}}H_{0.17}NbO_{3.17} + (1.17-\bar{\nu})K^+]$ with formula weight $M = 189.55$. In addition, the average value of the charge of the niobate species was determined from the ion exchange measurements coupled with pH measurements of the niobate solutions by using the relation $Z_{av} = ([OH]_{total} - [OH]_{eq})/[Nb]_{total}$. The values $Z_{av} = 0.111$, 0.112, and 0.113 were obtained from three separate determinations, and these are in fairly good agreement with the maximum value assumed above. In the definition of the monomer unit, the electrically neutral unit is written with $\bar{\nu}$ potassium ions to allow for a reduction in the effective average charge on the ion from the maximum value of -1.17. The monomeric *component* is then $K_{(1.17-\bar{\nu})}[K_{\bar{\nu}}H_{0.17}NbO_{3.17}] - (1.17-\bar{\nu})KCl/2$ with a formula weight $M' = M - Z'M_{KCl}/2$; $Z' = (1.17-\bar{\nu})$.

It is necessary to determine both the degree of polymerization, N, and the effective charge per monomer unit, Z', simultaneously from the experimental data (21). This was done graphically, and Fig. 3 shows $1/N_{z'}$ as a function of Z' with concentration as a

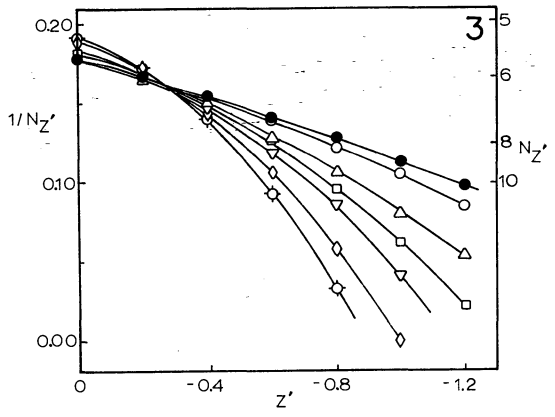

FIG. 3. Light scattering determination of $1/N_z$, as a function of Z' with concentration as parameter; special ○ 0.354 M, ◇ 0.266 M, ▽ 0.177 M, □ 0.133 M, △ 0.0888 M, ○ 00.0444 M, ● 0.0266 M Nb(V).

parameter. From the point of intersection of the curves, the value of N is obtained as ca. 6 and the charge per monomer unit $Z' = -0.3$. The data are very similar to those obtained for tantalate solutions and indicate that the polycondensed niobate species has the approximate formula $[HNb_6O_{19}]^{-7}$ and that the charge is reduced by the binding of potassium ions to ca. -2. It should be noted that the "effective" charge Z' determined

Can. J. Chem. Downloaded from www.nrcresearchpress.com by 210.87.254.42 on 09/05/12
For personal use only.

by light scattering measurements is generally lower than the value obtained, for example, from electrophoresis (25).

Ultracentrifugation

The schlieren data were evaluated in the usual manner (26). The components are defined as in the light scattering analysis, and N and Z' are the same. Once again a simultaneous determination of the degree of polymerization and the effective charge must be made. The experimental data $\ln Z^*/x(x)$ were plotted to determine graphically the value of $\underline{S}_e = d \ln (Z^*/x)/d(x^2)$. In all cases, essentially straight lines were obtained, and this indicates that the system is monodisperse. This is shown in Fig. 4 where the data are

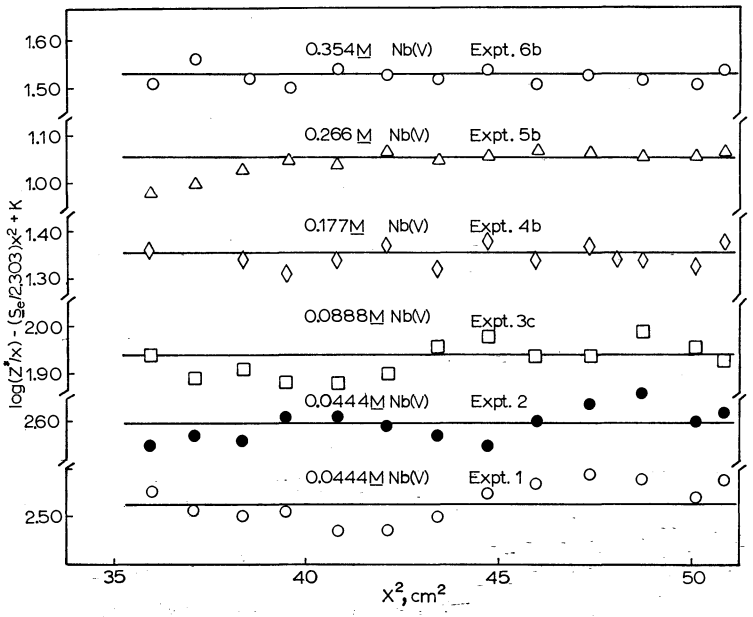

FIG. 4. Test of constancy of S_e for the schlieren ultracentrifugation data.

presented as the deviation functions $(\log Z^*/x) - \underline{S}_e x^2/2.303 + K$. Here K is an arbitrary constant used to normalize the values to ca. 1 to 2.

The degree of polymerization was calculated as a function of charge from equations [2] and [3].

$$d \ln m'/d(x^2) = S = S_e + \frac{\frac{Z'^2 m'}{2A'm_3}(S-\sigma)^2}{1 + \frac{Z'^2 m'\sigma}{2A'm_3}} \qquad [2]$$

$$N_{z'} = \frac{S}{A' - \frac{Z'^2 m'}{2m_3}(S-\sigma)} \qquad [3]$$

Here $A' = M'(1-\bar{\nu}'\rho)\omega^2/2RT$ where ρ is the solution density, ω is the angular velocity, and $\bar{\nu}' = (M\bar{V}_{\text{niobate}} - Z'M_{KCl}\bar{V}_{KCl}/2)/M'$. The apparent molal volume ϕ_{niobate} for the

Can. J. Chem. Downloaded from www.nrcresearchpress.com by 210.87.254.42 on 09/05/12
For personal use only.

niobate was determined to be essentially independent of concentration and had the value 27.5 ml, which was used for the partial molal volume $\bar{V}_{\text{niobate}}$. The value of $\sigma = d \ln m_3/d(x^2)$ was calculated from the relation $\sigma = M_{KCl}(1-\bar{\nu}_{KCl}\rho_{KCl})\omega^2/4RT$. The centrifugation data are tabulated in Table I, and Fig. 5 shows $1/N_{z'}$ as a function of Z' with con-

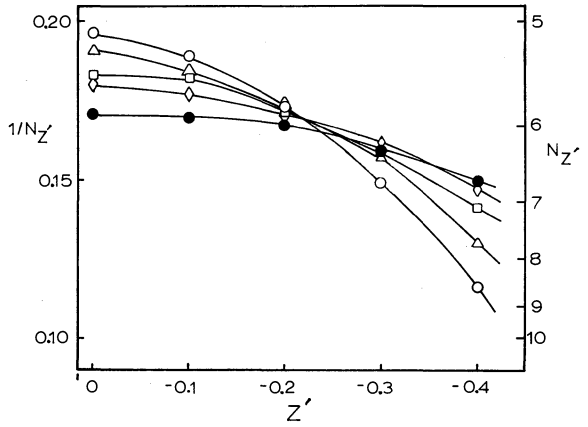

FIG. 5. Schlieren ultracentrifugation determination of $1/N_{z'}$ as a function of Z' with concentration as a parameter; ● 0.0444 M, ◇ 0.0888 M, □ 0.1776 M, △ 0.2664 M, ○ 0.3552 M Nb(V).

centration as the parameter for comparison with the light scattering data in Fig. 3. The results of the two different methods of determination are very similar, and the values $N = 5.8$ and $Z' = -0.2$ are obtained from the centrifugations.

The interference optics data were treated as suggested by Johnson, Scatchard, and Kraus (20). In general, the values of the refractive index differences between the solution and background compartments, n^*, as a function of the radius, x, were calculated by an integration procedure using equation (4) to compute the equilibrium value of n^* at the meniscus, n_α^*.

$$(\psi' m_0' + \psi_3 m_{3(0)} - \psi_3 m_{bg0}(x_\omega^2 - x_\alpha^2) = n_\alpha^*(x_\omega^2 - x_\alpha^2) + \int_\alpha^\omega (n^* - n_\alpha^*) d(x^2) \qquad [4]$$

Since the differences $(n^* - n_\alpha^*)$ were determined from the Rayleigh patterns, the value of n^* at the different points in the cell could then be calculated. Here $m_{3(0)}$ is the initial concentration of component 3, KCl, in the solution compartment and m_{bg0} is the initial concentration in the background compartment. Essentially the same values were obtained by this procedure as by following a fringe throughout the centrifugation. The refractive index data were then used to compute values of $\eta = Z'm'/2m_3$ by solving the quadratic equation [5] derived by Johnson *et al.*

$$(1-\eta^2)(1-\eta_0+\Delta)^2(n^*+\psi_3 m_{bg}^{\pm})^2 = m_{bg}^2(1-\eta_0^2)[2\psi'\eta/Z' + \psi_3]^2 \qquad [5]$$

Here η_0 is the initial value of η, $m_{bg}^{\pm}$ is a corrected background concentration to take into account the unsymmetrical location of the slits in the Spinco optical system, and $\Delta = (m_{bg0} - m_{BX0})/m_{30}$. The distribution of solutes is then obtained from equations [6] and [7].

$$m_3 = \frac{n^* + \psi_3 m_{bg}^{\pm}}{2(\psi'\eta/Z') + \psi_3} \qquad [6]$$

$$m' = 2m_3\eta/Z' \qquad [7]$$

Can. J. Chem. Downloaded from www.nrcresearchpress.com by 210.87.254.42 on 09/05/12
For personal use only.

The data ln m' and ln $(1+\eta)/(1-\eta)$ as functions of x^2 were fitted by a least squares procedure using equal weights to determine the slopes $S = d \ln m'/d(x^2)$ and $d \ln (1+\eta)/(1-\eta)/d(x^2)$. The values of the slope S were quite constant, and the precision of the measurement for a given run was considerably greater than in the case of the schlieren optics. The primary data are presented as the deviation function ln $n^* - \underline{S}(x^2)$ where $\underline{S} = d \ln n^*/d(x^2)$ in Fig. 6. Finally the values of the degree of polymerization as a function

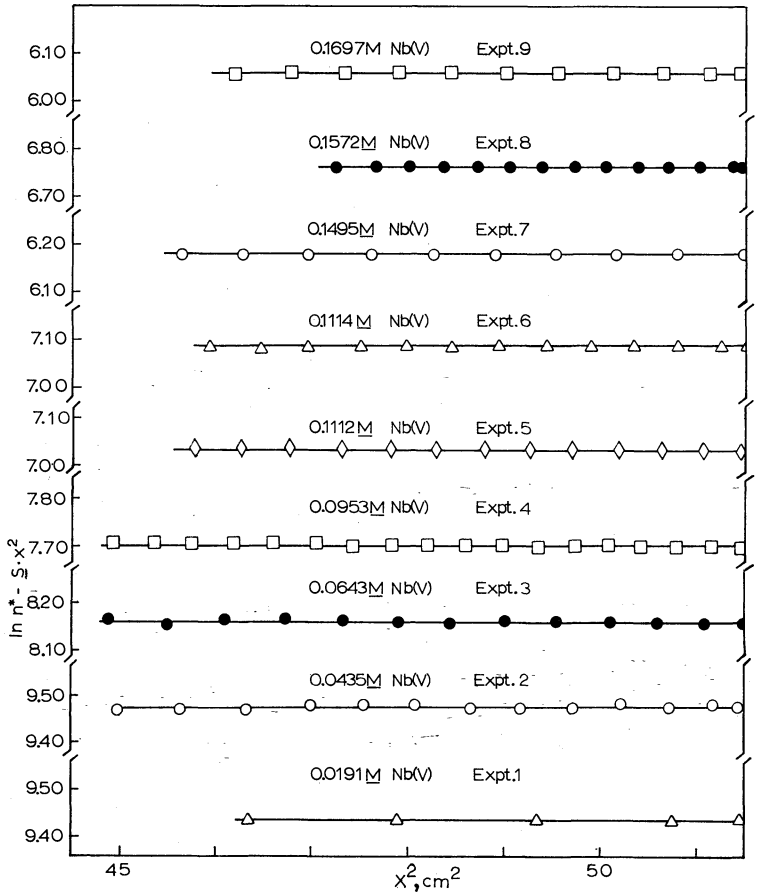

FIG. 6. Test of constancy of S for the interference optics centrifugation data.

of the charge were computed with equation [8].

$$N_{z'} = \frac{S}{A' - \frac{Z'}{2} d \ln [(1+\eta)(1-\eta)]/dx^2} \qquad [8]$$

The entire calculation was programmed in Fortran 60 for the Control Data Corporation 1604 computer at the University of Minnesota.[3] The data are tabulated in Table I and are again displayed in Fig. 7 as $1/N_{z'}$ as a function of Z' with concentration as the parameter for purposes of comparison with the light scattering and schlieren centrifugation

[3]*The complete deck listing, duplicate decks, and a flow sheet for this program ULTRACEN may be obtained by writing R.S.T.*

Can. J. Chem. Downloaded from www.nrcresearchpress.com by 210.87.254.42 on 09/05/12
For personal use only.

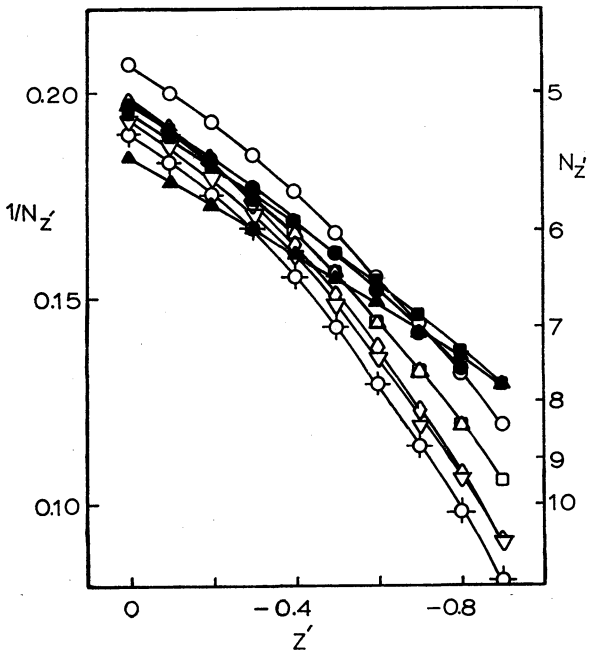

FIG. 7. Interference optics centrifugation determination of $1/N_{z'}$ as a function of Z' with concentration as a parameter; special ○ 0.1697 *M*, ◇ 0.1572 *M*, ▽ 0.1495 *M*, □ 0.1114 *M*, △ 0.1112 *M*, ○ 0.0953 *M*, ● 0.0643 *M*, ■ 0.0435 *M*, ▲ 0.0191 *M*, Nb(V).

data. Although the values of the slope S in the interference optics experiments could be determined much more accurately than the corresponding experimental quantity S_e in the schlieren experiments, the reproducibility of the $1/N_{z'}$ versus Z' curves was only fair. In some cases, the changes in S with concentration were not even in the correct direction. Part of the trouble may have been caused by the large changes in the speeds required in order to obtain good interference patterns as the concentration was changed, causing slightly different amounts of distortion of the cells. Distortions were, however, observed to be very slight. Pronounced experimental difficulties with leakage between the two solutions in the double compartment cell were also encountered initially. Although the curves are similar to those obtained by the other measurements and the degree of polymerization N has a value of ca. 5.4 and 5.8 at $Z' = -0.2$ and -0.3, respectively, it is considerably more difficult to determine the correct value of Z' from these measurements. When using interference optics, the measurements are also very susceptible to errors resulting from slight inaccuracies in the supporting electrolyte concentration in the two compartments. This is especially troublesome when working with dilute polymer solutions and high supporting electrolyte concentrations such as the 1 *M* KCl employed here.

DISCUSSION

The results obtained in these experiments are very similar to those obtained in the light scattering studies on alkaline tantalate solutions (2) which have also recently been confirmed by both schlieren and interference optics centrifugations (27). The agreement among the three experimental methods used here is also good, and in all probability the solute contains six niobium atoms and certainly no fewer than five. The data also indicate

Can. J. Chem. Downloaded from www.nrcresearchpress.com by 210.87.254.42 on 09/05/12
For personal use only.

that there is but one polycondensed anion present in the solutions rather than a series of species with different degrees of polymerization. All things considered, it seems unlikely that such measurements as these can be considered accurate to better than about ±10%.

Although the light scattering measurements are intrinsically simpler from the experimental standpoint, the very large amount of time involved in removing large impurity particles by ultrafiltration makes the centrifugation experiments preferable. The light scattering results provide a valuable confirmation of the centrifugation data. In the derivation of the equations used in the analysis of both the light scattering and sedimentation equilibrium experiments, it is assumed that the polymeric solute is monodisperse, i.e., that a single poly-ion is present. In some of the centrifugations quite large concentration gradients are established, and it is conceivable that this could cause a gradation in the degree of polymerization from one end of the cell to the other with labile species. It is also quite likely that this would be detected from deviations in the linearity of the plots used to determine $\underline{S}_e$ and S. That this was not the case here is clearly shown by the data in Figs. 4 and 6. In addition with the centrifugation calculations, it is necessary to know the formula weight of the monomer unit. In general, the stoichiometry of the solute species will be known from independent measurements on the solute and (or) solution. In the case of the polycondensed species with oxygen bridges, these measurements often do not distinguish between a single oxo group and two hydroxo groups in a complex. With the polycondensed species formed from metals in high oxidation states but which have low net charges, the difference in M' between the oxo and the hydroxo complexes could be appreciable. This in turn affects the value of A' used in calculating the degree of polymerization, although the effect is partially compensated by the changes in the partial specific volume $\bar{v}'$. With light scattering measurements, no comparable assumption need be made. Since structural studies on crystals of the iso- and heteropolyions of the groups V and VI elements have generally indicated that these are built up of octahedra formed from the transition metal and six oxo groups, the dehydrated form of the niobate monomer unit, $(NbO_{3.17}]^{-1.33}$ was assumed as the basic unit. Since both the stoichiometry of the $K_{14}Nb_{12}O_{37}\cdot 27H_2O$ crystals and the value of the average charge per niobium atom determined from the ion-exchange measurements indicated that there was some protonation of the above unit, the anion monomer was taken as $[H_{0.17}NbO_{3.17}]^{-1.17}$.

In comparing the results of the study of the niobate species with the earlier work on tantalum (2), it is apparent that charge effects are slightly less pronounced with the niobate; and the value determined for the "effective" charge is also slightly lower with the niobate. This is qualitatively in accord with the stoichiometry of the crystals obtained from aqueous solution where the tantalate appears to be unprotonated as $[Ta_6O_{19}]^{-8}$ while the niobate is protonated to give $[HNb_6O_{19}]^{-7}$. It is also in accord with the determination of the average charge per niobium in solution from the ion exchange which gave the value 0.112. In general, the effective charge as determined from ultracentrifugation appears to be rather lower than the actual charge on the species as has been found to be the case from the light scattering analysis (25). Thus the species $[Bi_6(OH)_{12}]^{+6}$ has an effective charge of ca. +4 as determined by ultracentrifugation (20) and also by light scattering (22).

It seems very likely that the same structural unit which exists in the niobate and tantalate crystals, i.e., the polycondensed anions with cubic symmetry $[Nb_6O_{19}]^{-8}$ and $[Ta_6O_{19}]^{-8}$ respectively, also persist when these crystals are dissolved in water. The lack of any depolarization of the light scattered at 90° is in accord with the existence of a species with high symmetry. This structure is illustrated in Fig. 8. There certainly do not appear to be any larger condensed species present in the solutions. Large symmetrical

Can. J. Chem. Downloaded from www.nrcresearchpress.com by 210.87.254.42 on 09/05/12
For personal use only.

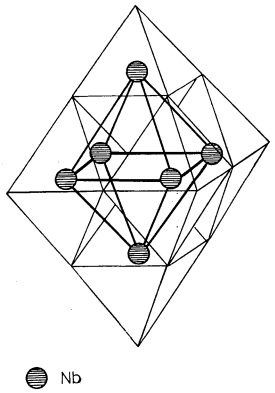

FIG. 8. Structure of the hexaniobate anion.

isopoly-ions such as these appear to behave much like the large heteropoly-ions such as the 12-tungstosilicate anion interacting only weakly with the solvent so that quite concentrated solutions can be obtained. The structural chemistry of niobium and tantalum is very different from that of phosphorus, and there is no evidence for the formation of chains and open ring structures.

The bonding in the hexatantalate anion has been discussed earlier (2), and it seems likely that pi-bonding to the six peripheral oxygens lowers the electron density at these oxygens, making them less susceptible to protonation or to functioning as bridges to give larger polycondensed species. The existence of the band in the infrared spectrum of crystalline $K_{14}Nb_{12}O_{37}\cdot 27H_2O$ at 852 cm^{-1} tends to indicate some metal–oxygen double bond character (27), although the vibration is at a considerably lower frequency than the band at 965 cm^{-1} found in $K_8Ta_6O_{19}\cdot 16H_2O$ or that at 906 cm^{-1} recently assigned to the Nb=O bond in $NbO(NO_3)_3$ (29). Bands attributed to niobium–oxygen double bonds are also found at 922 cm^{-1} in K_3NbOF_6 and at 927 cm^{-1} in $K_2NbOF_5\cdot H_2O$. The highest frequency band in $NbOCl_3$ is at 769 cm^{-1} and is attributed to Nb—O—Nb bridges.

It is interesting that the older semiempirical methods of determining the degrees of polymerization based on diffusion (7), dialysis (17), and salt cryoscopy (15) do appear to give approximately the correct values for the niobate. The latter method has essentially the same thermodynamic basis as the light scattering and equilibrium centrifugation measurements (16). It should also be pointed out that although the light scattering and centrifugation experiments may appear to give N and Z' quite precisely, very much depends on the behavior of the one or two most concentrated solutions. When charge effects are not pronounced, e.g. Figs. 3, 5, and 7, the determination of the intersection point depends largely on the most concentrated solutions, for the curves at concentrations $\leqslant 0.1\ M$ are all very similar. This also removes one of the main advantages of the measurements with interference optics, that of the use of low concentrations of the polymeric solute, since the value of Z' cannot then be easily determined. In some cases it has been necessary to assume values of Z' in order to interpret such measurements (20).

ACKNOWLEDGMENTS

The authors would like to express their appreciation to Professor Rufus Lumry for assistance in making the centrifugation measurements and to Mr. Norman Sweeney of

Can. J. Chem. Downloaded from www.nrcresearchpress.com by 210.87.254.42 on 09/05/12
For personal use only.

Central Research, The Minnesota Mining and Manufacturing Company, St. Paul, who provided the differential thermal and gravimetric analyses.

REFERENCES

1. J. R. VAN WAZER. Phosphorus and its compounds. Vol. I. Interscience, New York–London, 1958.
2. W. H. NELSON and R. S. TOBIAS. Inorg. Chem. **2**, 985 (1963).
3. N. V. SIDGWICK. The chemical elements and their compounds. Oxford, 1950. p. 846.
4. I. LINDQVIST and B. ARONSSON, Arkiv Kemi, **7**, 49 (1954).
5. I. LINDQVIST. Arkiv Kemi, **4**, 247 (1952).
6. F. WINDMAISSER. Osterr. Chemiker-Ztg. **45**, 201 (1942).
7. G. JANDER and D. ERTEL. J. Inorg. Nucl. Chem. **14**, 71, 77, 85 (1960).
8. R. ROHMER and J. E. GUERCHAIS. Bull. Soc. Chim. France, 317, 324 (1961).
9. G. JANDER and D. ERTEL. J. Inorg. Nucl. Chem. **3**, 139 (1956).
10. L. C. W. BAKER and M. T. POPE. J. Am. Chem. Soc. **82**, 4176 (1960).
11. Y. SASAKI, L. G. SILLÉN, and I. LINDQVIST. J. Inorg. Nucl. Chem. **9**, 93 (1959).
12. J. B. GOEHRING and S. Y. TYREE, JR. Proceedings of the Seventh International Conference on Coordination Chemistry, Stockholm, Sweden, 1962. p. 172.
13. Y. SASAKI, Acta Chem. Scand. **15**, 175 (1961).
14. J. A. R. GENGE, J. P. REDFERN, and J. E. SALMON. Proceedings of the Seventh International Conference on Coordination Chemistry, Stockholm, Sweden. 1962. p. 176.
15. R. ROHMER and J. E. GUERCHAIS. Bull. Soc. Chim. France, 334 (1961).
16. R. S. TOBIAS. J. Inorg. Nucl. Chem. **19**, 348 (1961).
17. G. I. GRIDCHINA. Zh. Neorgan. Khim. **8**, 634 (1963).
18. P. SOUCHAY. Bull. Soc. Chim. France, **14**, 914 (1947).
19. J. S. JOHNSON, K. A. KRAUS, and G. SCATCHARD. J. Phys. Chem. **58**, 1034 (1954).
20. J. S. JOHNSON, G. SCATCHARD, and K. A. KRAUS. J. Phys. Chem. **63**, 787 (1959).
21. R. S. TOBIAS and S. Y. TYREE, JR. J. Am. Chem. Soc. **81**, 6385 (1959).
22. R. S. TOBIAS and S. Y. TYREE, JR. J. Am. Chem. Soc. **82**, 3244 (1960).
23. J. S. JOHNSON, K. A. KRAUS, and T. F. YOUNG. J. Am. Chem. Soc. **76**, 1436 (1954).
24. J. S. JOHNSON and K. A. KRAUS. J. Am. Chem. Soc. **81**, 1569 (1959).
25. P. STIGER. J. Phys. Chem. **64**, 242 (1960).
26. J. S. JOHNSON, K. A. KRAUS, and R. W. HOLMBERG. J. Am. Chem. Soc. **78**, 26 (1956).
27. W. H. NELSON and R. S. TOBIAS. Unpublished work.
28. C. G. BARRACLOUGH, J. LEWIS, and R. S. NYHOLM. J. Chem. Soc. 3552 (1959).
29. B. O. FIELD and J. C. HARDY. Proc. Chem. Soc. 11 (1963).
30. J. S. JOHNSON and K. A. KRAUS. J. Am. Chem. Soc. **81**, 1509 (1959).

Can. J. Chem. Downloaded from www.nrcresearchpress.com by 210.87.254.42 on 09/05/12
For personal use only.

N,N-DIACETYLAMINES AS BY-PRODUCTS FROM THE ACETYLATION OF AMINES[1]

R. A. B. BANNARD
Defence Research Chemical Laboratories, Ottawa, Ontario
and
Department of Chemistry, University of Ottawa, Ottawa, Ontario

Received October 3, 1963

ABSTRACT

Acetylation of five alicyclic amines and isopropylamine with a large excess of acetic anhydride for 1 hour under reflux led to formation of appreciable yields (23–35%) of N,N-diacetylamines in addition to the anticipated N-acetylamines, except in the case of *cis*-2-aminocyclohexanol, which gave only the O,N-diacetyl derivative. The N-acetyl derivatives show an acetamido methyl proton resonance in their nuclear magnetic resonance spectra at 8.04–8.09 τ, whereas the N,N-diacetylamines show no absorption in this region but instead a resonance equivalent to six protons at 7.63–7.69 τ due to the N,N-diacetyl group. The infrared spectra of these compounds are consistent with the structures assigned on the basis of their n.m.r. spectra. Splitting of the amide carbonyl band was not generally observed in these compounds although two of the substances exhibited a minor band on the low frequency side of the main band which might be attributed to this cause.

Can. J. Chem. Downloaded from www.nrcresearchpress.com by 210.87.254.40 on 09/05/12
For personal use only.

During the preparation of the acetyl derivatives of a series of 1-alkoxy-2-hydroxy-3-aminocyclohexanes for examination of their nuclear magnetic resonance (n.m.r.) spectra (1), it was found that treatment of 1α-methoxy-2α-hydroxy-3β-acetylaminocyclohexane (I) and 1α-ethoxy-2α-hydroxy-3β-aminocyclohexane (II) with a large excess of acetic anhydride under reflux for 1 hour gave appreciable yields (37–48%) of the O,N,N-triacetyl derivatives I*b* and II*b* in addition to the anticipated O,N-diacetyl compounds

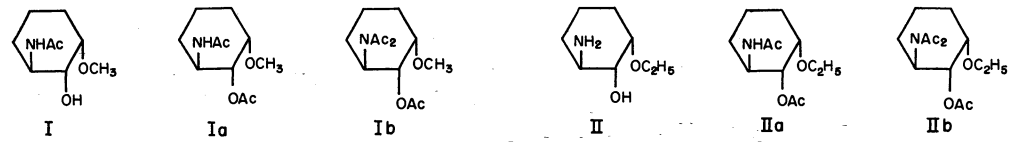

I*a* and II*a*. The formation of N,N-diacylamines during uncatalyzed reaction between aromatic amines and aliphatic acid anhydrides is well known (2) but few examples of diacylation of aliphatic amines under similar conditions have been observed (see, however, ref. 3). This circumstance is somewhat surprising because the formation of diacylamines by the acid-catalyzed acylation of amines (4, 5) and the formation of imides by uncatalyzed (6) and acid-catalyzed (7, 8, 9) acylation of primary amides has been reported, and it does not seem unreasonable to expect the secondary amide resulting from monoacylation of an amine to undergo further acylation to at least some extent. It seemed possible, therefore, that under rather vigorous conditions by which I*b* and II*b* were formed—which were essentially the same as found by Sudborough (2) to produce significant amounts of N,N-diacyl aryl amines—other alicyclic and aliphatic amines would also yield diacetylamines as major by-products.

Accordingly, acetylation of the six amines shown in Chart I was examined under conditions identical with those used earlier (1) with compound II. The results given in Table I* show that with all but one of these compounds, namely, *cis*-2-aminocyclohexanol, such

[1]*Issued as D.R.C.L. Report No. 422.*

**Note: IIIa* = N-*Acetyl derivative of III; IIIb* = N,N-*diacetyl derivative of III, etc. Under these conditions hydroxyl groups were also acetylated.*

conditions lead to formation of 23–35% of the N,N-diacetyl derivative in addition to 76–65% of the normal N-acetyl compound. It is therefore concluded that acetylation of aliphatic and alicyclic as well as aromatic amines in this manner can be expected to yield significant amounts of the N,N-diacetylamines. In each instance, the N,N-diacetyl compound boiled at a lower temperature than the corresponding N-acetyl derivative, as might have been predicted from the lack of an available proton for intermolecular hydrogen bonding in the former.

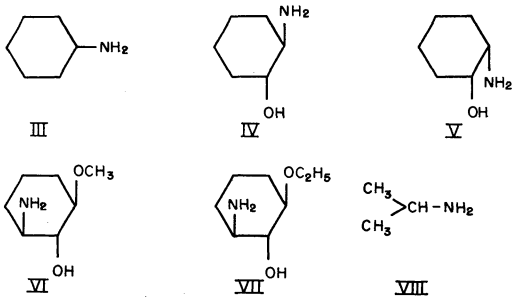

CHART I

In general, the total yield of N-acetylated compounds was 98% or higher† and thus no evidence of nitrile formation was obtained. This result contrasts with the results of Davidson and Skovronek (9), who observed the formation of large quantities of nitrile together with small amounts of imide by interaction of primary amides with acid anhydrides in the absence of acid catalysts. Consequently, the O-acetylation O → N migration mechanism advanced by these workers to explain their product distribution is not necessary to account for the products resulting from the present experiments, which are readily accommodated by the general mechanism for reaction of nucleophiles with anhydrides proposed by Denney and Greenbaum (10).

As in the case of compounds I*b* and II*b* described earlier (1), the structures of the N,N-diacetyl derivatives resulting from acetylation of compounds III to VIII were established from consideration of the n.m.r. and infrared spectra of the products.

In the n.m.r. data, which is summarized in Table II, all the N-acetyl derivatives exhibit a broad doublet at 3.17 to 4.20 τ, which disappears on deuteration by equilibration with deuterium oxide, and which owes its origin to the NH proton coupled with that attached to an adjacent carbon atom. The N,N-diacetyl compounds, on the other hand, show no resonance in this region. The N-acetyl derivatives show an acetamido methyl proton resonance at 8.04 to 8.09 τ, whereas the N,N-diacetyl compounds show no resonance in this region but instead exhibit resonance equivalent to six protons at 7.63 to 7.69 τ, which is assigned to the N,N-diacetyl group.

In the cyclohexane compounds, introduction of the second acetyl group on nitrogen causes the H_2 multiplet to shift to lower field by 0.7–0.9 p.p.m. and H_1 to shift to lower field by ca. 0.2 p.p.m., presumably due to the diamagnetic anisotropy of the newly introduced acetamido carbonyl group. It was reported earlier (1) that acetoxy-methyl protons in the equatorial orientation in cyclohexane derivatives show a resonance at 7.90 to 7.99. Reference to Table II makes it clear, however, that two ranges can be quoted for such

†*The one exception to this statement was provided by the first experiment of the series in which manipulative losses were much greater than in subsequent experiments.*

Can. J. Chem. Downloaded from www.nrcresearchpress.com by 210.87.254.40 on 09/05/12
For personal use only.

Can. J. Chem. Downloaded from www.nrcresearchpress.com by 210.87.254.40 on 09/05/12
For personal use only.

TABLE I

Acetylation of amines

Starting material	N-Acetyl derivative							N,N-Diacetyl derivative							
	% yield	M.p. or b.p. (° C)	Analysis	C	H	N	Ac	% yield	B.p./*p** (° C at mm)	Analysis	C	H	N	Ac	n_D^{25}
III	76.1	105.5–107†	Calc.	68.04	10.71	9.92	30.49	22.6	41 at 0.01	Calc.	65.54	9.35	7.64	46.98	1.4800
			Found	68.00	10.57	10.18				Found	65.50	9.22	7.66		
IV	63.5	117.5–119‡	Calc.	60.28	8.60	7.03	43.21	35.2	79 at 0.01	Calc.	59.73	7.94	5.81	53.50	1.4747
			Found	60.15	8.50	7.16	43.49			Found	59.78	8.16	5.89	53.76	
V	98.0	74 at 0.01	Calc.	60.28	8.60	7.03	43.21			None isolated					
			Found	60.49	8.60	7.03	44.1								
VI	75.5	170–172§	Calc.	57.62	8.35	6.11	37.5	23.5	90 at 0.01	Calc.	57.55	7.80	5.16	46.5	1.4755
			Found	57.85	8.36	6.30				Found	57.75	7.74	5.19	46.1	
I	50.2	138–140§	Calc.	57.62	8.35	6.11	37.5	47.6	75 at 0.01§	Calc.	57.55	7.80	5.16	46.5	1.4726
			Found	57.60	8.37	5.95				Found			5.17	46.45	
VII	74.4	167–169§	Calc.	59.24	8.70	5.76	35.4	24.2	91 at 0.01	Calc.	58.93	8.13	4.91	45.25	1.4707
			Found	59.41	8.83	5.78				Found	59.19	7.94	5.02	45.11	
II	47.6	113.5–115§	Calc.	59.24	8.70	5.76	35.4	37.2	70–72 at 0.01§	Calc.	58.93	8.13	4.91	45.25	1.4756
			Found	59.16	8.78	5.86				Found			4.91	44.93	
VIII	64.8	57 at 0.1‖¶	Calc.	59.37	10.96	13.85	42.6	27.6	73 at 8¶	Calc.	58.72	9.15	9.78	60.2	1.4440
			Found	59.52	11.04	13.87				Found	58.51	9.30	9.63		

*Air bath temperature unless otherwise specified.
†Baeyer (11) reports m.p. 104°.
‡McCasland *et al.* (12) report m.p. 117–119°.
§See Ref. (1).
‖Gertler and Yerington (13) report b.p. 102–104° at 14 and n_D^{25} 1.4291.
¶True boiling point; n_D^{25} 1.4306.

Can. J. Chem. Downloaded from www.nrcresearchpress.com by 210.87.254.40 on 09/05/12
For personal use only.

TABLE II

Chemical shifts and coupling constants in N-acetyl- and N,N-diacetyl-amines

Compound	OCH_3 (1)	OAc (2)	NAc (3)	Chemical shift (τ)				Coupling constant	
				H_1	H_2	H_3	NH	$J_{1,2}$	$J_{2,3}$
III*a*	—	—	8.04	—	—	6.23	3.51	—	—
III*b*	—	—	7.65*	—	—	6.20	—	—	—
IV*a*	—	7.96	8.08	—	5.36	6.10	4.08	—	—
IV*b*	—	8.04	7.69*	—	4.47	6.28	—	—	—
V*a*	—	7.94	8.08	—	5.00	5.98	3.79	—	—
VI*a*	6.62	7.93	8.09	6.79	5.30	6.05	3.91	9.1	9.1
VI*b*	6.65	7.99	7.69*	—	4.40	6.22	—	9.2	9.2
VII*a*	6.37†	7.92	8.08	6.64	5.26	5.99	3.91	8.8	8.8
	8.84								
VII*b*		8.01	7.68*	6.44	4.53	6.44	—	8.9	8.9
	8.88†								
I*a*	6.63	7.90	8.08	6.39	5.29	5.61	4.20	2.3	10.4
I*b*	6.66	7.99	7.66*	6.22	4.51	5.81	—	2.8	10.6
II*a*	6.41†	7.90	8.07	6.25	5.23	5.65	4.11	2.5	10.5
	8.81								
II*b*	6.43†	7.97	7.64*	6.10	4.55	5.76	—	3.0	10.7
	8.84								
VIII*a*	—	—	8.04	—	8.84‡	6.00§	3.17	—	6.4
VIII*b*	—	—	7.63*	—	8.04	5.79§	—	—	6.8

*For NAc_2.
†For OC_2H_5.
‡For doublet of isopropyl group.
§For septet of isopropyl group.

substituents, depending on whether the adjacent carbon atom bears an N-acetyl (7.90–7.96) or an N,N-diacetyl (7.97–8.04) group.

The $J_{1,2}$ and $J_{2,3}$ coupling constants of the N,N-diacetyl compounds were identical within experimental error with those found for the N-acetyl derivatives and the remarks made previously (1) with regard to the magnitude and variation of the coupling constants in relation to the Karplus equation (14) again apply.

Introduction of the second acetyl group into isopropylacetamide causes the resonance of the doublet due to the methyl protons of the isopropyl group to shift to lower field by 0.8 p.p.m. It thus appears that the large shift in the resonance of the multiplet due to a proton on the carbon atom adjacent to that bearing the acetamido group caused by introduction of the second acetyl group on nitrogen, which was observed in the 1,2,3-trisubstituted cyclohexanes, is also characteristic of acyclic amines.

The principal infrared absorption frequencies (exclusive of the C—H stretching region) observed for the N-acetyl- and N,N-diacetyl-amines in 0.05 *M* solution in carbon tetrachloride, together with their assignments (15, 16), are given in Table III. The N-acetyl derivatives show bands at ca. 3400 and 3300 cm^{-1} due to non-bonded and bonded N—H. The latter absorption disappeared in all cases on dilution, indicating that the bonding is of the inter- rather than the intra-molecular type (16, p. 517). The N,N-diacetyl compounds, on the other hand, exhibit no N—H absorption. The amide I absorption at 1680 ± 3 cm^{-1} in the N-acetyl compounds was shifted to 1699 ± 3 cm^{-1} in the N,N-diacetyl compounds in accordance with expectation for introduction of a second electrophilic substituent on the amide nitrogen (18). The amide II absorption at 1501 ± 4 cm^{-1} in the N-acetyl derivatives was absent from the N,N-diacetyl derivatives. All the compounds showed absorption at 1360–1370 cm^{-1} characteristic of the C—H bend in the acetyl methyl group (19). In agreement with this assignment, the intensity of this band increased as the degree of acetylation increased. Those compounds which contained O-acetyl groups showed absorption at 1218–1235 cm^{-1} (20) and at 1010–1049 cm^{-1} (17) due to C—O stretching modes of the acetate group. All these compounds gave a single prominent band at 1218–1235 cm^{-1}, which could be construed as evidence (20) that all the acetoxy groups are in the equatorial orientation, in agreement with the n.m.r. evidence derived from the substituent resonances and coupling constants reported earlier (1). It should be pointed out, however, that these bands are considerably broader than those given by equatorial acetoxy groups in steroids (20) and the appearance of shoulders near the band in several instances possibly detracts from the usefulness of this absorption for assignment of conformation to acetoxy groups in cyclohexane derivatives in the absence of other supporting evidence. The broadening of the band at 1218–1235 cm^{-1} and (or) the appearance of shoulders in some cases could owe its origin to a C–N amide III absorption which is sometimes found in this region (16, p. 220). Some evidence in support of this view was given by compounds III*a*, III*b*, VIII*a*, and VIII*b*, which contain no O-acetyl group yet exhibit medium to weak absorption at 1212–1240 cm^{-1}. Only the examination of a series of similar compounds in which the acetoxy groups have been shown unequivocally to occupy an axial orientation will clarify the usefulness of the acetoxy C—O absorption for assignment of conformation.

Several years ago Abramovitch (21) found that N,N-diacetyl compounds exhibit more than one carbonyl band in chloroform solution when examined at sufficiently slow chart speeds and narrow slit schedules. The effect was more noticeable in ca. 0.25 *M* solution than in ca. 0.05 *M* solution. Examination of the N,N-diacetyl compounds described herein in 0.05 *M* and 0.25 *M* solution in carbon tetrachloride at chart speeds as low as

Can. J. Chem. Downloaded from www.nrcresearchpress.com by 210.87.254.40 on 09/05/12
For personal use only.

Can. J. Chem. Downloaded from www.nrcresearchpress.com by 210.87.254.40 on 09/05/12
For personal use only.

TABLE III

Infrared absorption of N-acetyl- and N,N-Diacetyl-amines

Compound	N—H stretch		Characteristic group frequencies (cm^{-1})						
	Non-bonded	Bonded	Ester carbonyl	Amide carbonyl	Amide II	sym. C—H bend in CH_3 of acetyl*	C—O— stretch in acetate	R—O—R asym.	C—O— stretch No. 2† in acetate
III*a*	3405w	3300w	—	1677s	1498m	1360w	1220m‡	—	—
III*b*	—	—	—	1695s	—	1360m	1212m‡	—	—
IV*a*	3380w	3300w	1723s	1680s	1502m	1365m	1235s	—	1038m
IV*b*	—	—	1739m	1698s	—	1362s	1220s	—	1035m
V*a*	3415w	3320w	1739s	1682s	1497m	1360m	1227s	—	1010m
VI*a*	3380w	3300w	1726s	1682s	1505m	1370m	1233s	1093m	1042m
VI*b*	—	—	1742m	1702s	—	1365s	1218s	1100m	1042m
I*a*	3395w	3320w	1722s	1682s	1504m	1368m	1233s	1100m	1042m
I*b*	—	—	1743m	1700s	—	1363s	1225s	1083m	1048m
VII*a*	3380w	3300w	1725s	1680s	1500m	1370s	1230s	1092m	1040w
VII*b*	—	—	1740m	1701s	—	1365s	1218s	1104w	1040w
II*a*	3410w	3320w	1722s	1683s	1502m	1370m	1233s	1075w	1042m
II*b*	—	—	1742m	1700s	—	1363s	1225s	1076w	1049m
VIII*a*	3400w	3300w	—	1678s	1498m	1365m	1235m‡	—	—
VIII*b*	—	—	—	1696s	—	1365m	1240w‡	—	—

*Nolin and Jones (19).
†Jones and Herling (17).
‡Possibly due to C—N stretch in N-acetyl (amide III (16, p. 220)). s = Strong, m = medium, w = weak.

25 cm^{-1} per minute and a spectral slit width as low as 1.5 cm^{-1} (Perkin–Elmer model 421) did reveal the presence of very low intensity shoulders on the amide carbonyl band in some cases, but in only two compounds was the band resolved. It is therefore concluded that not all diacylamines exhibit multiplicity of amide carbonyl bands as reported earlier (21).

It was noted earlier that *cis*-2-acetamido-1-acetoxycyclohexane (V*a*) is the sole product resulting from the uncatalyzed reaction between *cis*-2-aminocyclohexanol and acetic anhydride. It was at first thought that this behavior might owe its origin to the circumstance that V*a* exists as an equilibrium mixture of conformers V*a*′ and V*a*″, in which the former predominates. If such were the case, the rate of formation of the O,N,N-triacetyl

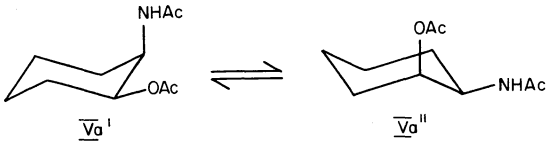

Va′ Va″

derivative could be much slower than in the corresponding trans isomer in which both substituents are equatorial (22). However, extending the period of reflux on interaction of V with acetic anhydride by a factor of three produced no evidence for the presence of an O,N,N-triacetyl derivative by n.m.r. examination of the product and it was concluded that such an explanation is unsatisfactory. A second possible explanation for failure of the N,N-diacetyl compound to form from V*a* is that the proton attached to nitrogen in the latter is firmly held by intramolecular hydrogen bonding to the carbonyl oxygen of the acetoxy group. Although V*a* exhibited both non-bonded and bonded N—H vibrations at 3415 and 3320 cm^{-1} in 0.05 *M* solution in carbon tetrachloride, dilution caused the bonded vibration to disappear, indicating it to be of the inter- rather than the intramolecular type. Alternatively, it is suggested that further acetylation of the amide nitrogen may be prevented in V*a* by intramolecular interaction between the nitrogen atom and the cis ester carbonyl group. Such an interaction would not be expected to occur as readily in the trans derivative and for this reason di-N-acetylation may proceed in this case. No experimental evidence directly supporting this suggestion was obtained in the present study, however, and further work is planned to elaborate the reason for this difference in behavior between cis- and trans-1,2-aminocyclanols toward acetic anhydride.

EXPERIMENTAL[2,3]

trans-2-Aminocyclohexanol (IV)

trans-2-Aminocyclohexanol was prepared as described by Hawkins and Bannard (23).

cis-2-Aminocyclohexanol (V)

trans-2-Acetylaminocyclohexanol (IV*a*) (7.38 g, 0.047 mole) (12, 23) was added portionwise with mechanical stirring over a period of 15 minutes to thionyl chloride (42.4 g, 0.356 mole) at room temperature, contained in a three-necked flask equipped with a "trubore" stirrer and reflux condenser which was protected with a calcium chloride tube. The resultant light red solution was heated with stirring at 52–54° for a further 2½ hour, then poured into anhydrous ether (700 ml). The deep red oil which separated crystallized rapidly on standing at room temperature, changing in color to grayish-white. The ether was decanted, 10% hydrochloric acid (125 ml) was added, and the solution was heated under reflux for 5 hours. The solution was taken to dryness *in vacuo* and residual water was removed by azeotropic distillation with benzene and ethanol. The residue was recrystallized from ethanol, yielding 4.72 g (67.5%) of *cis*-2-aminocyclohexanol hydrochloride as colorless needles, m.p. 189–191°. McCasland *et al.* (12) report m.p. 189–190°. This method

[2]*All melting points and boiling points are uncorrected.*
[3]*Microanalyses by J. G. Helie, Defence Research Chemical Laboratories.*

Can. J. Chem. Downloaded from www.nrcresearchpress.com by 210.87.254.40 on 09/05/12
For personal use only.

of preparation is somewhat more efficient than the similar procedure starting from *trans*-2-benzoylaminocyclohexanol which was reported by Johnson and Schubert (24).

The above hydrochloride was converted to the free base by treatment with one equivalent of sodium hydroxide in ethanol, followed by evaporation to dryness *in vacuo* and extraction with ether. The crystalline material recovered by evaporation of the ether was heated at 60° at 0.001 mm pressure yielding *cis*-2-aminocyclohexanol as a colorless sublimate, m.p. 75.5–77.5°, in 91.4% yield. McCasland *et al.* (12) report m.p. 72°.

1-Alkoxy-2-hydroxy-3-aminocyclohexanes (I, II, VI, VII)

The preparation of these compounds was described previously by Bannard and Hawkins (25).

Acetylation of Amines

The acetylation and isolation procedures were the same for all the compounds examined. The acetylation of *trans*-2-aminocyclohexanol given below is typical.

trans-2-Aminocyclohexanol (3.45 g, 0.03 mole) was added at room temperature to acetic anhydride (79.5 g, 0.78 mole) contained in a round-bottomed flask equipped with a reflux condenser and calcium chloride tube. After the initial exothermic reaction had subsided, the colorless solution was heated under reflux for 1 hour and cooled to room temperature. The excess acetic anhydride was removed by distillation at room temperature at 6 mm pressure, whereupon the residue crystallized. The crystals were collected and washed with anhydrous ether, and the combined filtrate and washings were again evaporated to yield a second crop of crystals. These operations were repeated until no further crystals were obtained from the residual colorless oil. The crops of crystals were combined and recrystallized from anhydrous ether, yielding 3.79 g (63.5%) of *trans*-2-acetylamino-1-acetoxycyclohexane (IV*a*) as colorless platelets, m.p. 117.5–119° (see Table I). The oil fraction was transferred to a four-bulb Späth tube and distilled three times at 0.01 mm pressure at an air bath temperature of 78°, yielding 2.53 g (35.2%) of *trans*-2-diacetylamino-1-acetoxycyclohexane (IV*b*) as a colorless oil, n_D^{25} 1.4747.

The other preparations are summarized in Table I. It should be noted that in some of these the use of air bath temperatures much in excess of that required to barely cause the N,N-diacetyl derivatives to distill also caused the N-acetyl derivatives to sublime, necessitating further distillations to complete the separation. The separation of N-acetyl- and N,N-diacetyl-isopropylamine proved more difficult than that of the derivatives of the alicyclic amines and was accomplished by the use of an 18-inch Stedman column. The boiling points reported for the isopropylamine derivatives are thus true boiling points.

The proton magnetic resonance spectra were measured on a Varian V-4302 spectrometer operating at 60 Mc/second using a Varian V-4351 integrator for baseline stabilization. All solutions were 25% w/v in chloroform and were calibrated with reference to internal tetramethylsilane by the usual sideband technique.

Infrared spectra were measured in carbon tetrachloride (0.05 *M*) using a Perkin–Elmer model 21 double beam recording spectrometer. More dilute solutions (0.01–0.005 *M*) were used to examine hydrogen bonding effects. The 1600–1800 cm^{-1} region of the spectra of the N,N-diacetyl derivatives was re-examined for splitting of the amide carbonyl group using 0.05 *M* (0.1 mm cell) and 0.25 *M* (0.025 mm cell) solutions with both the Perkin–Elmer model 21 and model 421 spectrometers at a chart speed of ca. 25 cm^{-1} minutes.

ACKNOWLEDGMENTS

The author wishes to express his thanks to the Defence Research Board of Canada for granting him leave to participate in this work.

Thanks are also due to Dr. L. D. Hall for recording the n.m.r. spectra, to Mr. R. Lauzon for recording the infrared spectra, and to Professor B. Belleau, Professor F. A. L. Anet, and Dr. R. Norman Jones for the use of laboratory facilities and helpful discussions.

REFERENCES

1. F. A. L. Anet, R. A. B. Bannard, and L. D. Hall. Can. J. Chem. **41**, 2331 (1963).
2. J. J. Sudborough. J. Chem. Soc. **79**, 534 (1901).
3. E. L. Holmes and C. K. Ingold. J. Chem. Soc. **127**, 1800 (1925).
4. P. Dunn, E. A. Parks, and J. B. Polya. Rec. Trav. Chim. **71**, 676 (1952).
5. W. H. Dehn. J. Am. Chem. Soc. **34**, 1399 (1912).
6. W. Hentschel. Ber. **23**, 2394 (1890).
7. J. B. Polya and P. L. Tardrew. J. Chem. Soc. 1081 (1948).
8. J. B. Polya and T. M. Spotswood. Rec. Trav. Chim. **67**, 927 (1948).
9. O. Davidson and H. Skovronek. J. Am. Chem. Soc. **80**, 376 (1958).
10. D. B. Denney and M. A. Greenbaum. J. Am. Chem. Soc. **79**, 3701 (1957).
11. A. Baeyer. Ann. **278**, 104 (1894).
12. G. E. McCasland, R. K. Clark, and H. E. Carter. J. Am. Chem. Soc. **71**, 637 (1949).
13. S. I. Gertler and A. P. Yerington. U.S. Dept. Agr. ARS-33-14 (Nov. 1958), Chem. Abstr. **50**, 7111f (1956).

Can. J. Chem. Downloaded from www.nrcresearchpress.com by 210.87.254.40 on 09/05/12
For personal use only.

14. M. KARPLUS. J. Chem. Phys. **30**, 11 (1959).
15. L. J. BELLAMY. The infrared spectra of complex molecules. John Wiley and Sons Inc., New York. 1958.
16. R. N. JONES and C. SANDORFY. *In* Chemical applications of spectroscopy, technique of organic chemistry. Vol. IX, Chap. IV. *Edited by* A. Weissberger. Interscience Publishers Inc., New York. 1956.
17. R. N. JONES and F. HERLING. J. Am. Chem. Soc. **78**, 1152 (1956).
18. R. E. RICHARDS and H. W. THOMPSON. J. Chem. Soc. 1248 (1947).
19. B. NOLIN and R. N. JONES. Can. J. Chem. **34**, 1392 (1956).
20. R. N. JONES, P. HUMPHRIES, F. HERLING, and K. DOBRINER. J. Am. Chem. Soc. **73**, 3215 (1951).
21. R. A. ABRAMOVITCH. J. Chem. Soc. 1413 (1957).
22. W. G. DAUBEN and K. S. PITZER. *In* Steric effects in organic chemistry. *Edited by* M. S. Newman. John Wiley and Sons Inc., New York. 1956. p. 47.
23. L. R. HAWKINS and R. A. B. BANNARD. Can. J. Chem. **36**, 220 (1958).
24. W. S. JOHNSON and E. N. SCHUBERT. J. Am. Chem. Soc. **72**, 2187 (1950).
25. R. A. B. BANNARD and L. R. HAWKINS. Can. J. Chem. **36**, 1241 (1958).

Can. J. Chem. Downloaded from www.nrcresearchpress.com by 210.87.254.40 on 09/05/12
For personal use only.

THE PHOTOLYSIS OF WATER VAPOR AND REACTIONS OF HYDROXYL RADICALS[1]

A. Y.-M. UNG[2] AND R. A. BACK

Division of Pure Chemistry, National Research Council of Canada, Ottawa, Canada

Received August 17, 1963

ABSTRACT

The photolysis of water vapor at 1849 Å has been investigated as a possible source of hydroxyl radicals for kinetic studies. At temperatures from 23 to 350° C and pressures from 1.3 to 28 mm, H_2 and H_2O_2 were the only detectable products. Experiments with added oxygen indicated that O_2 may have been present as an intermediate at a very low steady-state concentration, although this is not certain. Possible mechanisms are discussed.

At temperatures from 200 to 350° C, carbon monoxide appeared to react quantitatively with the hydroxyl radicals produced in the photolysis of water by the reaction, $OH + CO \xrightarrow{k_{CO}} CO_2 + H$. Rates of this reaction relative to those of the reactions, $OH + H_2 \xrightarrow{k_{H2}} H_2O + H$, and $OH + D_2 \xrightarrow{k_{D2}} HDO + D$, were estimated from the decrement in the yield of CO_2 when H_2 or D_2 was added to the H_2O–CO system, and the following Arrhenius parameters were obtained:

$$E_{H_2} - E_{CO} = 4.0 \pm 0.3 \text{ kcal/mole}, \quad A_{H_2}/A_{CO} = 31 \pm 5,$$

$$E_{D_2} - E_{CO} = 6.4 \pm 0.3 \text{ kcal/mole}, \quad A_{D_2}/A_{CO} = 160 \pm 30,$$

$$E_{D_2} - E_{H_2} = 2.4 \pm 0.6 \text{ kcal/mole}, \quad A_{D_2}/A_{H_2} = 5 \pm 2.$$

At temperatures below 200° C, hydroxyl radicals were not completely converted to CO_2, as the yield of CO_2 increased to a maximum, then decreased again, with increasing pressure of CO. The mechanism of this system is complex, but probably involves secondary reactions of HCO or COOH radicals.

INTRODUCTION

Reactions of hydroxyl radicals in the gas phase at moderate temperatures have not been extensively studied; one reason for this is the lack of a good photochemical source of these radicals. Hydrogen peroxide, an obvious choice, does yield hydroxyl radicals upon photolysis at convenient wavelengths, but rapid reactions of the peroxide with radicals make the system, at moderate temperatures at least, rather complex (1). The photolysis of water vapor offers a possible alternative source of hydroxyl radicals. Its chief virtue lies in the high resistance of the water molecule, with an H—OH bond dissociation energy of 118 kcal, towards radical attack. This must be balanced against the inconvenience of working at wavelengths below about 1860 Å, where water begins to absorb light, and the possible complications of the concomitant production of hydrogen atoms in the photolysis process. A further experimental difficulty in the study of hydroxyl-radical reactions is that simple abstraction of hydrogen produces water, a product not easily measured in small amounts, and obviously impossible to measure if water is used as the radical source. One solution to this problem might be to use as a standard some reaction of hydroxyl that yields an easily measured product. Decrements in this product upon addition of a second reagent could then be used as a measure of the extent of reaction of the second reagent. The reaction, $OH + CO \rightarrow CO_2 + H$, seems particularly promising as such a reference standard (2, 3).

[1]*Issued as N.R.C. No. 7638.*

[2]*National Research Council of Canada Postdoctoral Fellow, 1960–62. Present address: Chemistry Department, McGill University, Montreal, Canada.*

Can. J. Chem. Downloaded from www.nrcresearchpress.com by 210.87.254.42 on 09/05/12
For personal use only.

In the present research, the photolysis of water vapor at 1849 Å was examined as a source of hydroxyl radicals; the use of the reaction of hydroxyl radicals with carbon monoxide as a reference standard was investigated; and, finally, relative rate constants of reactions of hydroxyl radicals with H_2, D_2, and CO were measured by this technique.

EXPERIMENTAL

The photolysis vessel was a quartz cylinder, 10 cm long and 5 cm in diameter, with plane windows of synthetic quartz (Suprasil) at the ends, and was mounted in an air thermostat. The light source was a mercury resonance lamp, similar to that described recently (4), but made from synthetic quartz. A common cylindrical housing enclosed both the lamp and the photolysis vessel, and was kept under a slight positive pressure of dry nitrogen to exclude air from the light path. The end of the housing that contained the lamp was made of brass, and was water-cooled to maintain a constant lamp temperature, while an intermediate section of the cylindrical housing was made of Pyrex to minimize heat transfer from the photolysis vessel.

Both the 2537 and the 1849 Å mercury resonance lines were emitted by the lamp, but all the reagent gases were transparent at 2537 Å. The 1849 Å line lies just within the sharply rising edge of the first absorption continuum of water (5). None of the other reagents (CO, H_2, D_2) absorb light in this region, and product concentrations were always too low to permit appreciable absorption at either 1849 or 2537 Å, so that the photolysis of water at 1849 Å should have been the only primary photolytic process of any importance.

The photolysis vessel was part of a circulatory system comprising the vessel, a glass paddlewheel pump, used to mix and circulate reagents, and two U-traps. One U-trap was mounted in a thermostatic bath which was used to maintain a suitable equilibrium vapor pressure of water in the system. Pressure was measured with a quartz-spiral gauge. The preparation line and reaction vessel were kept free of mercury, with access through suitable guard traps to a conventional gas analysis system.

In the experiments with water vapor alone, non-condensible gases were removed at −196° C by a diffusion-pump – Toepler-pump combination, measured in a gas burette, and analyzed by gas chromatography on an 8-ft, 5A molecular sieve column at 0° C, which gave good separation of H_2, N_2, O_2, and CO. Small amounts of oxygen were added in some experiments; this was done by adding air, so that the amount of oxygen originally added could be deduced from the nitrogen measured in the products. In the experiments in which large pressures of CO were added, CO and H_2 were transferred through a trap at −196° C, by a Toepler pump, into a trap at −220° C which condensed most of the CO. Controlled pumping on this latter trap (by expanding the non-condensed gases three times into a 500-cc volume) removed the hydrogen quantitatively, together with about a thousandfold excess of CO. This was transferred by a Toepler pump and analyzed by gas chromatography. In the same experiments, the trap originally at −196° C was warmed to −78° C and the CO_2 product was distilled off and measured in a gas burette. Mass spectrometric analysis confirmed that this fraction contained only CO_2. When the reaction mixture contained large pressures of H_2 or D_2, the non-condensible gases were pumped away at −196° C, and CO_2 was the only product measured.

Distilled water was used without special purification except for vigorous degassing and several bulb-to-bulb distillations. Blank experiments showed no measurable amounts of N_2, O_2, or CO_2. Carbon monoxide was Matheson C.P. grade from which traces of CO_2 were removed by passage through traps at −196°. This gas contained about 20 p.p.m. of O_2. In some experiments CO was purified by passing it over a potassium–sodium mixture deposited on glass wool, which reduced the oxygen content to less than 2 p.p.m. Hydrogen and deuterium were purified by passage through a hot palladium thimble. The deuterium contained 0.5% hydrogen.

RESULTS

Pure Water Vapor

A number of experiments were performed under a wide variety of conditions of light intensity, reaction time (7.5 to 150 minutes), pressure of water vapor (1.3 to 28 mm), and temperature (23 to 350° C). Hydrogen was the only non-condensible product detected in any of these experiments, although as little as 5×10^{-10} mole of oxygen would have been detectable on the gas chromatograms. Condensible products were not systematically analyzed, but did show a positive reaction to a permanganate test (6) for the hydrogen peroxide which is required by the stoichiometry if oxygen is not a product. Figure 1 shows the dependence of the hydrogen yield on irradiation time at two different light intensities. Table I shows the effect of pressure of water vapor on the hydrogen yield at 23° C with a light intensity corresponding to the lower curve in Fig. 1.

Can. J. Chem. Downloaded from www.nrcresearchpress.com by 210.87.254.42 on 09/05/12
For personal use only.

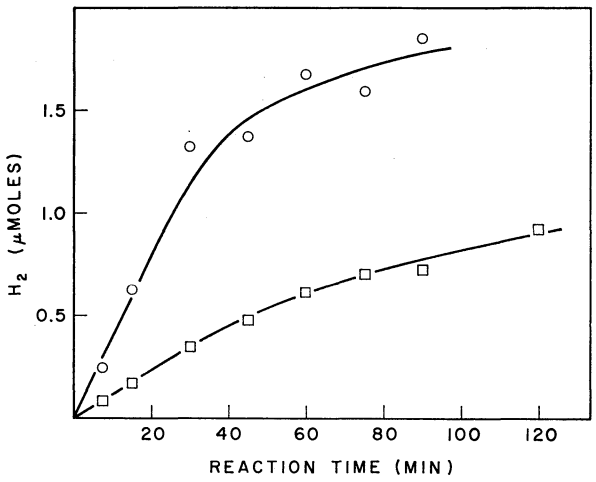

FIG. 1. Yield of hydrogen from the photolysis of water vapor at 25° C at two different intensities.

TABLE I

Effect of pressure in the photolysis of water vapor

Pressure (mm)	Irradiation time (min)	H_2 yield ($\times 10^3$), moles/min
1.3	200	1.12
4.5	75	2.76
19.8	75	9.31

Water Vapor with Added Oxygen

To test the possibility that oxygen was a primary product of the photolysis, but disappeared by rapid secondary reactions, two series of experiments were performed. In the first, shown in Fig. 2, a constant quantity (7.5×10^{-8} moles) of oxygen was added initially,

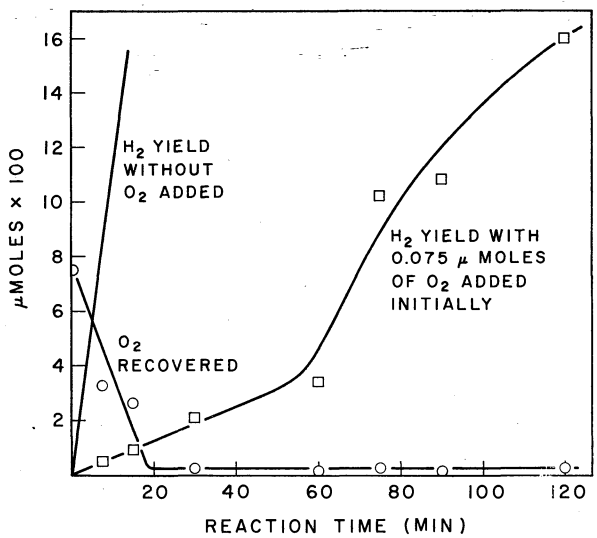

FIG. 2. The effect of 0.075 μmole of oxygen on the photolysis at 23° C and 19.8 mm pressure of water vapor.

Can. J. Chem. Downloaded from www.nrcresearchpress.com by 210.87.254.42 on 09/05/12
For personal use only.

and the hydrogen and oxygen measured after various times of irradiation. In the second series (Fig. 3), various amounts of oxygen were added initially, and hydrogen and oxygen determined after a constant reaction time of 75 minutes. Both series of experiments were performed at a temperature of 23° C and a pressure of water vapor of 19.8 mm.

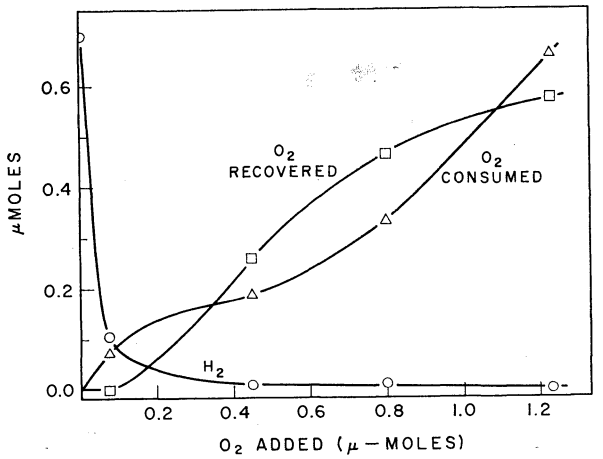

FIG. 3. The effect, at constant reaction time, of various amounts of oxygen on the photolysis at 23° C and 19.8 mm pressure of water vapor.

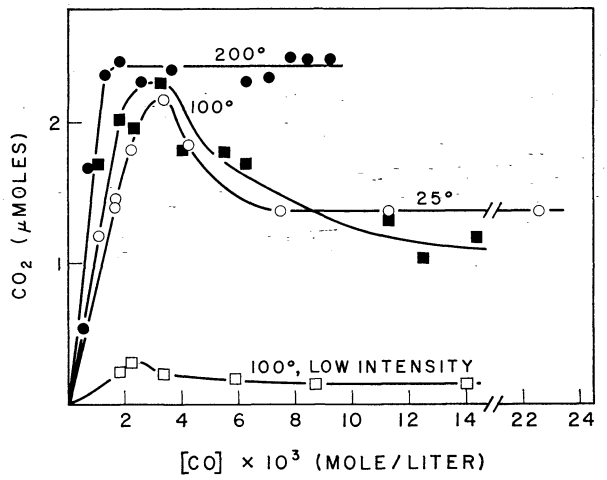

FIG. 4. The yield of CO_2 from the photolysis of water vapor in the presence of CO.

Water Vapor with Added Carbon Monoxide

In Fig. 4, yields of carbon dioxide at constant reaction time are plotted against concentration of carbon monoxide at temperatures of 25, 100, and 200° C. In all experiments at temperatures below 200° C, distinct maxima appear in these curves. At 200° C, and in several similar series of experiments (not shown) at temperatures ranging up to 350° C, the yield of carbon dioxide rose to a constant value, independent of carbon monoxide pressure, with no indication of any falling off from this value.

Can. J. Chem. Downloaded from www.nrcresearchpress.com by 210.87.254.42 on 09/05/12
For personal use only.

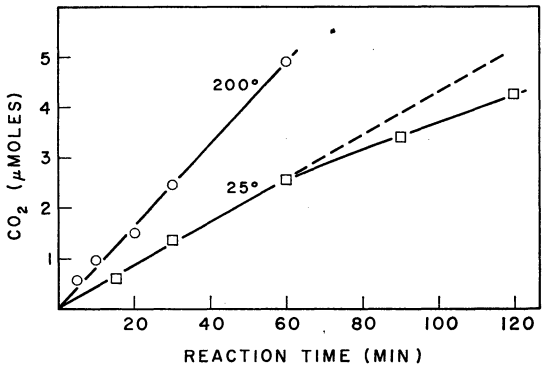

FIG. 5. The dependence on reaction time of the production of CO_2 from the photolysis of water vapor in the presence of about 220 mm of CO.

In Fig. 5, the yield of carbon dioxide at constant high pressure (~220 mm) of carbon monoxide is shown as a function of irradiation time at 25 and 200° C. At both temperatures the carbon dioxide yield was initially linear with time; at 25° C, at longer times, a decrease from the linear rate was observed. These data may be correlated with the curves in Fig. 4.

Hydrogen was a minor product in the experiments with added carbon monoxide. It was not measured systematically, as the analysis was complicated by the presence of hydrogen as a trace impurity in the carbon monoxide, but it was apparent that the yield of hydrogen was very low, less than a few percent of the CO_2.

Water Vapor with Added Carbon Monoxide and Hydrogen

At temperatures of 200° C and above, carbon monoxide appeared to act as a simple scavenger for hydroxyl radicals (Fig. 4), and the constant yield of carbon dioxide at high pressures of carbon monoxide should be a measure of the hydroxyl radicals produced in the photolysis. If, under these conditions, a second reagent such as hydrogen is added, the competition between the two reactions,

$$OH + CO \xrightarrow{k_{CO}} CO_2 + H,$$

$$OH + H_2 \xrightarrow{k_{H_2}} H_2O + H,$$

should lead to a reduced yield of carbon dioxide. The equation,

$$[(CO_2)_0 - CO_2]/CO_2 = (k_{H_2}/k_{CO})([H_2]/[CO]),$$

where $(CO_2)_0$ is the yield of CO_2 in the absence of H_2, should describe this competition. In Fig. 6 are shown typical plots of this equation at several temperatures, and representing a variety of irradiation times and carbon monoxide pressures. Tables II and III summarize the results obtained with the H_2–CO and D_2–CO systems respectively, including values of k_{H_2}/k_{CO} and k_{D_2}/k_{CO} derived from plots similar to those in Fig. 6.

DISCUSSION

The Primary Process in the Photolysis of Water Vapor

There is general agreement that the primary process in the photolysis of water vapor at wavelengths in the first continuum is

$$H_2O + h\nu \rightarrow H + OH \qquad [1]$$

Can. J. Chem. Downloaded from www.nrcresearchpress.com by 210.87.254.42 on 09/05/12
For personal use only.

TABLE II

Reaction of OH with CO and H_2

Temp., ° C	Reaction time (min)	p_{H_2} (mm)	p_{CO} (mm)	p_{H_2}/p_{CO}	$(CO_2)_0$ (μmole)	CO_2 (μmole)	k_{H_2}/k_{CO}
200	30	112	113	0.992	0.524	0.373	
200	30	80	150	0.533	0.524	0.426	
200	60	150	105	1.43	1.048	0.599	0.429
200	30	50	175	0.286	0.524	0.459	
200	60	165	102	1.62	1.048	0.619	
250	30	127	123	1.03	0.569	0.346	
250	60	158	107	1.48	1.138	0.605	0.615
250	30	83	182	0.465	0.569	0.452	
300	30	75	137	0.547	0.569	0.392	
300	30	43	175	0.246	0.569	0.472	0.875
300	30	152	115	1.32	0.569	0.253	
300	30	107	142	0.755	0.569	0.340	
350	28	125	145	0.862	0.925	0.452	1.21

TABLE III

Reaction of OH with CO and D_2

Temp., ° C	Reaction time (min)	p_{D_2} (mm)	p_{CO} (mm)	p_{D_2}/p_{CO}	$(CO_2)_0$ (μmole)	CO_2 (μmole)	k_{D_2}/k_{CO}
200	30	145	110	1.32	1.117	0.957	0.118
200	30	105	142	0.74	1.117	1.038	
300	30	132	130	1.015	2.845	1.875	0.497
300	30	129	116	1.112	1.103	0.718	

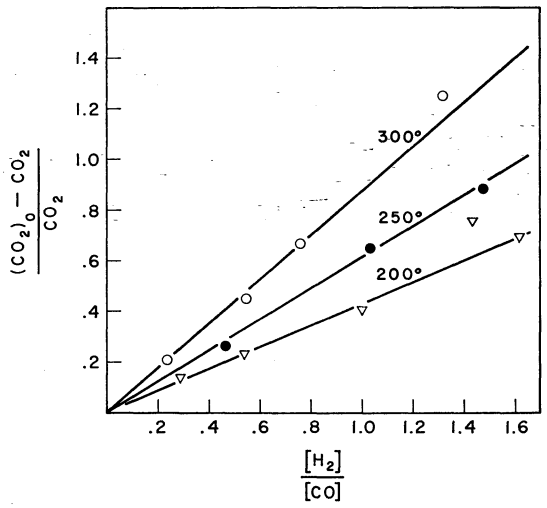

FIG. 6. The competition between the reactions of hydroxyl radicals with CO and H_2.

with both H and OH in their lowest electronic states (7, 8, 9). The present results confirm this conclusion. In particular, the reduction of the hydrogen yield to a negligible value by the addition of small quantities of oxygen (Fig. 3) definitely rules out the primary formation of molecular hydrogen.

Reactions in Pure Water Vapor

The simplest way to account for the absence of oxygen as a product is by the mechanism,

Can. J. Chem. Downloaded from www.nrcresearchpress.com by 210.87.254.42 on 09/05/12
For personal use only.

$$OH + OH + M \rightarrow H_2O_2 + M, \quad [2A]$$

$$OH + H + M \rightarrow H_2O + M, \quad [3A]$$

$$H + H + M \rightarrow H_2 + M, \quad [4]$$

where M is a third body, which has recently been suggested in the flash photolysis of water vapor at total pressures between 100 and 600 mm, in which the disappearance of hydroxyl radicals was observed to be termolecular (9). On the other hand, O_2 might have been formed in the present system, but reduced to an undetectably low steady-state concentration by rapid secondary reactions. The reaction,

$$OH + OH \rightarrow H_2O + O \quad [2B]$$

has been shown to predominate in a fast-flow system at about 1 mm total pressure (10, 11, 12). This is not incompatible with the flash photolysis results (9), as one would expect a gradual transition from reaction [2B] to [2A] as the pressure was increased. The pressures used in the present work lie between those used in the flash photolysis and in the fast-flow experiments, almost overlapping the latter. The abnormally high efficiency of water as a third body (9) may favor reaction [2A], so that a mixture of reactions [2A] and [2B], with [2A] probably predominant, might be expected in the present experiments.

In the low-pressure, fast-flow experiments (10, 11), concentrations of hydroxyl radicals were rather high (1 to 6 microns), and reaction [2B] was thought to be followed exclusively by the fast reaction,

$$O + OH \rightarrow O_2 + H. \quad [5]$$

In the present system, concentrations of hydroxyl were probably orders of magnitude lower, and reactions such as

$$O + O + M \rightarrow O_2 + M, \quad [6]$$

$$O + H + M \rightarrow OH + M, \quad [7]$$

$$O + HO_2 \rightarrow OH + O_2 \quad [8]$$

may also have been important, although reaction [5] should still have predominated.

Oxygen would have disappeared in the reaction,

$$H + O_2 + M \rightarrow HO_2 + M, \quad [9]$$

followed by

$$2HO_2 \rightarrow H_2O_2 + O_2, \quad [10]$$

$$H + HO_2 + M \rightarrow H_2O_2 + M, \quad [11]$$

$$H + HO_2 \rightarrow 2OH, \quad [12A]$$

$$H + HO_2 \rightarrow H_2 + O_2, \quad [12B]$$

$$OH + HO_2 \rightarrow H_2O + O_2, \quad [13]$$

and reaction [8]. If oxygen were formed in the photolysis of water vapor, this reaction sequence must have been fast enough to keep the steady-state concentration of oxygen below 2×10^{-9} moles per liter. It is impossible from the present results to say definitely whether or not oxygen was in fact an intermediate.

The dependence of hydrogen yield on irradiation time (Fig. 1) requires some comment. The fall-off from an initial linear dependence may be attributed to the loss of H, H_2, and H_2O_2 by secondary reactions,

Can. J. Chem. Downloaded from www.nrcresearchpress.com by 210.87.254.42 on 09/05/12
For personal use only.

$$H + H_2O_2 \rightarrow H_2O + OH, \quad [14A]$$

$$H + H_2O_2 \rightarrow H_2 + HO_2, \quad [14B]$$

$$OH + H_2O_2 \rightarrow H_2O + HO_2, \quad [15]$$

$$OH + H_2 \rightarrow H_2O + H. \quad [16]$$

Subsequent reactions of HO_2 radicals [9 to 13] might be expected to yield some oxygen, and it is perhaps significant that even in the experiments with the longest irradiation times, no oxygen was detected. However, reactions [11] and [12A] may well have predominated over [10] and [13], as H was probably much more abundant than HO_2 or OH. Reaction [12B] is an unknown quantity, and it is possible that production of oxygen from reactions of HO_2 was very inefficient. The experiments of Chen and Taylor, using much higher light intensities and conversions, and thus well on in the steady-state region whose approach is evident in Fig. 1, show that, ultimately, oxygen does appear as a major product in the photolysis of water vapor (8).

The dependence of the hydrogen yield on the pressure of water vapor (Table I) suggests that perhaps half the incident light was absorbed at the highest pressures used, which is quite compatible with published estimates of the extinction coefficient of water vapor (5). The observed dependence may be complicated by a dependence of the quantum yield of hydrogen on the absorbed light intensity and on the pressure of water vapor.

The initial quantum yield* of hydrogen in the photolysis of pure water vapor at 25° C was about 0.4. This is somewhat higher than might be expected from either a simple recombination mechanism or one involving oxygen as an intermediate. One possible source of extra hydrogen is the reaction of hydrogen atoms with trace impurities, as is thought to occur in the radiolysis of water vapor (13). The system is highly susceptible to such effects, which can compete effectively with the relatively slow termolecular combination reactions of hydrogen atoms.

Reactions in Water Vapor with Added Oxygen

Figure 2 shows that oxygen does indeed disappear rapidly when it is added to the photolysis system. The yield of hydrogen was initially much reduced by the presence of oxygen, but rose again as the oxygen was consumed. Small but measurable residues of O_2 scattered between about 1 and 3% of that added initially, were found after irradiation times of 30 minutes or longer. These residues may have arisen partly from O_2 remaining in the circulation system, and in several small sidearms attached to it, as the paddlewheel pump was not very efficient at low pressures. They may also have partly arisen from secondary reactions with H_2O_2 (mainly reaction [15] followed by [10]) which would set in earlier in the water–O_2 system than in pure water, and which could generate oxygen and so establish a low steady-state concentration of O_2, although the marked rise in hydrogen production between 50 and 90 minutes suggests that the oxygen concentration in the reaction vessel itself was still decreasing, probably to a very low value, even though the oxygen recovered was approximately constant from 30 minutes onwards. The rate of hydrogen production in Fig. 2 never reached the value found in the absence of oxygen, since by the time the oxygen concentration was sufficiently reduced, the same secondary reactions which led to the decreased hydrogen yield in pure water (Fig. 1) were coming into play.

The initial rate of disappearance of oxygen represented by the straight line drawn in Fig. 2 corresponds to a quantum yield* of 0.14. This gives an upper limit for the rate of

**Assuming a primary quantum yield (for reaction [1]) of unity, and a primary rate of formation of* OH *(and* H*) of* 2.8×10^{-8} *mole/minute as measured by the production of* CO_2 *by reaction with* CO *at 200° C.*

Can. J. Chem. Downloaded from www.nrcresearchpress.com by 210.87.254.42 on 09/05/12
For personal use only.

formation of oxygen in the photolysis of pure water vapor under similar conditions, in order for oxygen not to have accumulated, which is about half the quantum yield of 0.33 expected if all the hydroxyl radicals disappeared by reactions [2B] and [5], which consume 3 OH for each O_2 formed.

Reactions in Water Vapor with Added CO

By adding a sufficiently high pressure of carbon monoxide, it was hoped that hydroxyl radicals could be quantitatively converted to CO_2 by the reaction

$$OH + CO \rightarrow CO_2 + H. \quad [17]$$

Hydrogen atoms from reactions [1] and [17] might be expected to disappear by reactions such as

$$H + CO + M \rightarrow HCO + M, \quad [18]$$

$$H + HCO + M \rightarrow H_2CO + M, \quad [19A]$$

$$H + HCO \rightarrow H_2 + CO, \quad [19B]$$

$$2HCO \rightarrow H_2 + 2CO, \quad [20A]$$

$$2HCO \rightarrow H_2CO + CO, \quad [20B]$$

$$2HCO + M \rightarrow (HCO)_2 + M. \quad [20C]$$

The very low yield of hydrogen observed in this system suggests that reactions [19B] and [20A] were not important. At temperatures below 200° C, complete scavenging of hydroxyl radicals by reaction [17] was not achieved. As the CO pressure was increased, the yield of CO_2 rose to a maximum not far below the limiting value attained at high temperatures, decreased again, and finally became constant at about half its highest value. Two tentative explanations of this behavior may be offered. The first involves the reactions

$$OH + HCO \rightarrow H_2O + CO \quad [21A]$$

and

$$OH + HCO + M \rightarrow HCOOH + M, \quad [21B]$$

which consume hydroxyl radicals in competition with reaction [17]. Although reactions [17] and [18] are both nominally first order in CO pressure, CO can also act as a third body in reaction [18], so that with increasing CO pressure, the rate of formation of HCO, and hence its steady-state concentration, and the rates of reactions [21A] and [21B], will rise more rapidly than the rate of reaction [17]. This can account for a rise through a maximum and a subsequent decrease of the CO_2 yield. As the CO pressure is further increased, reaction [18] will eventually consume all the hydrogen atoms, and become independent of CO pressure. The dependence of reactions [17] and [21B] on further increase in the CO pressure could then lead to a constant yield of CO_2.

A second explanation is rather similar, and involves the COOH radical (14, 15). The formation of this radical again requires a stabilizing collision,

$$CO + OH + M \rightarrow COOH + M. \quad [22]$$

Loss of OH (or CO_2) by subsequent reactions such as

$$OH + COOH \rightarrow H_2O + CO_2, \quad [23]$$

$$2COOH \rightarrow HCOOH + CO_2, \quad [24]$$

and others involving HCO can equally well account for the observed dependence of the CO_2 yield on CO pressure, using arguments roughly analogous to those invoked for the HCO radical.

Can. J. Chem. Downloaded from www.nrcresearchpress.com by 210.87.254.42 on 09/05/12
For personal use only.

A third rather similar mechanism involving HO_2 radicals formed by reaction [9] from the trace of oxygen impurity present in the carbon monoxide was ruled out by experiments with highly purified CO (less than 2 p.p.m. O_2), which showed no change in behavior.

With increasing temperature, both COOH and HCO radicals would tend to dissociate thermally, and the rate of reaction [17] would increase, leading finally to complete scavenging of hydroxyl radicals by CO. It is impossible from the present results to choose clearly between HCO and COOH as the more likely cause of the observed low-temperature behavior.

Loss of OH radicals by reaction with products such as HCOOH or H_2CO might also be invoked, and these probably account for the decrease in CO_2 yield at higher reaction times observed at 25° C (Fig. 5). However, all the data shown in Fig. 4 were obtained at reaction times in the linear portions of the curves in Fig. 5, so that reactions with products were probably unimportant. Partial removal of products such as HCOOH and H_2CO from the circulating reaction gases by solution in the liquid water present in the U-trap may have reduced product concentrations in the reaction vessel and minimized reaction with products.

Reactions in Water Vapor with Added CO, H_2, and D_2

Plots of the type shown in Fig. 6 appeared to give consistent values of relative rate constants over a considerable range of conditions, suggesting that above 200° C, the

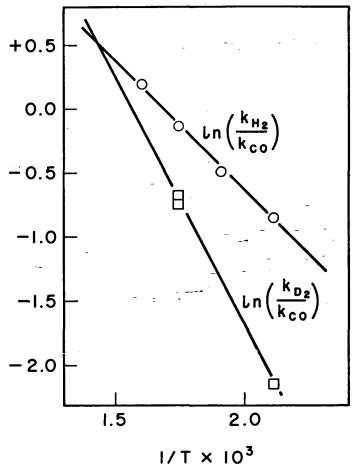

FIG. 7. Arrhenius plot of ratios of rate constants for the reactions of hydroxyl radicals with CO, H_2, and D_2.

simple mechanism suggested was obeyed. In Fig. 7 is shown an Arrhenius plot of the ratios k_{H_2}/k_{CO} and k_{D_2}/k_{CO}, from which the following parameters were derived:

$$E_{H_2} - E_{CO} = 4.0 \pm 0.3 \text{ kcal/mole},$$
$$A_{H_2}/A_{CO} = 31 \pm 5,$$
$$E_{D_2} - E_{CO} = 6.4 \pm 0.3 \text{ kcal/mole},$$
$$A_{D_2}/A_{CO} = 160 \pm 30,$$
$$E_{D_2} - E_{H_2} = 2.4 \pm 0.6 \text{ kcal/mole},$$
$$A_{D_2}/A_{H_2} = 5 \pm 2.$$

Can. J. Chem. Downloaded from www.nrcresearchpress.com by 210.87.254.42 on 09/05/12
For personal use only.

The limits of error suggested are rather arbitrary, and the values for the reaction with deuterium must be regarded as preliminary. The apparatus is presently being modified to permit operation at higher temperatures and thence to obtain more accurate Arrhenius parameters.

Avramenko and Lorentso (3), using a technique of doubtful accuracy, found $E_{CO} = 7$ kcal and $E_{H_2} = 10$. Both these values are supported by the measurements of Fenimore and Jones (16), and are in reasonable accord with our present estimate of $E_{H_2} - E_{CO} = 4$. Del Greco and Kaufman (10), however, have suggested that E_{H_2} must be closer to 6 kcal, which, combined with our data, gives $E_{CO} = 2$; the same value may be derived from $E_{CH_4} = 9$ kcal (17) (for the reaction of OH with CH_4) and $E_{CH_4} - E_{CO} = 7$ measured recently by Hoare (2). Thus E_{CO} would seem to lie somewhere between 7 and 2 kcal. There does seem to be general agreement that A_{CO} is markedly lower than typical values for hydrogen abstraction reactions; our value of $A_{H_2}/A_{CO} = 31$ may be compared with $P_{CH_4}/P_{CO} = 100$ (where P is a collision-theory steric factor) estimated by Hoare (2). Finally, a value of $k_{CO}/k_{H_2} = 15$ measured in aqueous solution at 20° C by Dainton and Hardwick (18) may be compared with a value of about 33 obtained by extrapolation of our present gas-phase data.

The isotope effect observed in the reaction of hydroxyl radicals with H_2 and D_2 in the present work is very close to that found for the parallel reactions of methyl radicals by Majury and Steacie (19), who reported $E_{D_2} - E_{H_2} = 2.5$ kcal and $A_{D_2}/A_{H_2} = 5$. It should be noted again that the present data for the reaction of hydroxyl with deuterium are very tentative.

REFERENCES

1. D. H. Volman. J. Chem. Phys. **17**, 947 (1949).
2. D. E. Hoare. Nature, **194**, 283 (1962).
3. L. E. Avramenko and P. V. Lorentso. Zh. Fiz. Khim. **24**, 207 (1950).
4. R. A. Back and D. van der Auwera. Can. J. Chem. **40**, 2339 (1962).
5. M. Zelikoff and K. Watanabe. J. Opt. Soc. Am. **43**, 753 (1953).
6. I. M. Holthoff and E. B. Sandell. Textbook of quantitative inorganic analysis. Rev. ed. Macmillan, New York. 1943.
7. W. Groth. Z. Electrochem. **45**, 262 (1939).
8. M. C. Chen and H. A. Taylor. J. Chem. Phys. **27**, 857 (1957).
9. G. Black and G. Porter. Proc. Roy. Soc. A, **26**, 185 (1962).
10. F. P. Del Greco and F. Kaufman. Discussions Faraday Soc. **33**, 128 (1962).
11. L. F. Phillips and H. I. Schiff. J. Chem. Phys. **37**, 1233 (1962).
12. M. A. A. Clyne and B. A. Thrush. Trans. Faraday Soc. **57**, 2176 (1961).
13. J. H. Baxendale and G. P. Gilbert. Discussions Faraday Soc. **36** In press. (1963).
14. M. H. Back and A. H. Sehon. Can. J. Chem. **38**, 1261 (1960).
15. A. M. Mearns and R. A. Back. Can. J. Chem. **41**, 1197 (1963).
16. C. P. Fenimore and G. W. Jones. J. Phys. Chem. **62**, 1578 (1958).
17. C. P. Fenimore and G. W. Jones. J. Phys. Chem. **65**, 2200 (1961).
18. F. S. Dainton and T. J. Hardwick. Trans. Faraday Soc. **53**, 333 (1957).
19. T. G. Majury and E. W. R. Steacie. Can. J. Chem. **30**, 800 (1952); Discussions Faraday Soc. **14**, 45 (1953).

Can. J. Chem. Downloaded from www.nrcresearchpress.com by 210.87.254.42 on 09/05/12
For personal use only.

TWO NEW PAPILIONACEOUS ALKALOIDS: ARGYROLOBINE AND (—)-APHYLLIDINE[1]

Y. TSUDA[2] AND LÉO MARION
Division of Pure Chemistry, National Research Council, Ottawa, Canada
Received August 19, 1963

ABSTRACT

Argyrolobium megarhizum Bol. has been found to contain a number of alkaloids, four of which have been well characterized. Two of these were identical with N-methylcytisine and cytisine respectively, while the other two were new. One of these proved to be the levorotatory enantiomorph of aphyllidine, while the other (the major alkaloid), $C_{15}H_{22}O_2N_2$, designated argyrolobine, was shown to be a hydroxyaphyllidine, and its absolute configuration derived by reduction to (−)-sparteine.

Argyrolobium megarhizum Bol. is a small shrub of the family Leguminosae which was collected at Bronkhorstspruit, Transvaal, South Africa.[3] The alcoholic extract of this plant has yielded several alkaloids, four of which have been characterized. Two of these have been found to be identical with N-methylcytisine and cytisine respectively, while the other two are new. N-Methylcytisine was characterized by the formation of its perchlorate, its picrate, and its hexahydro-deoxo derivative. Cytisine was identified as its high-melting picrate.

The first of the two new bases ($C_{15}H_{22}O_2N_2$) was the most abundant alkaloid and we propose to designate it argyrolobine (I). Its infrared spectrum showed it to contain a hydroxyl (3385 cm^{-1}) and a lactam carbonyl (1638 cm^{-1}). In the ultraviolet, a maximum (λ_{max} 239 mμ, ϵ 9400) was suggestive of a C=C—N—CO grouping (cf. aphyllidine, λ_{max} 240 mμ, ϵ 10,300). It formed a normal monohydrochloride, m.p. 170–172°, and a monomethiodide, m.p. 180°, and hence must be a monoacidic base. The n.m.r. spectrum of argyrolobine contained no signals attributable to an N-methyl or a C-methyl group, but contained a signal (δ 6.0) suggesting one olefinic proton.

Mild acetylation of argyrolobine produced a monoacetate, $C_{17}H_{24}O_3N_2$, m.p. 61°. The infrared spectrum of the acetate in chloroform solution showed no hydroxyl absorption, but bands at 1735 and 1225 cm^{-1} attributable to the acetyl group, and at 1650 cm^{-1} due to the lactam carbonyl, while its n.m.r. spectrum contained the signal (δ 2.02) of the acetate protons. The presence of a hydroxyl group in the alkaloid is thus confirmed.

The n.m.r. spectrum of the acetate also contained two signals at fields lower than δ ~4.0, each of which corresponded to one proton. The lower signal (δ 7.21) can be attributed to an olefinic proton situated on the second carbon away from the electron-attracting nitrogen, and since no other olefinic proton signal appeared in the region δ 5.0–7.0, the carbon adjacent to the nitrogen must be fully substituted (CH=C—N—CO). A complex signal centered at δ 4.82 could be attributed to the proton on the carbon bearing the acetoxy group which would indicate that the hydroxyl is secondary.

Although argyrolobine was difficult to hydrogenate in a neutral solvent, it smoothly absorbed 4 moles of hydrogen in hydrochloric acid solution in the presence of Adams' catalyst. The product was an oil, $[\alpha]_D$ −16°, which formed a picrate identified as

[1]*Issued as N.R.C. No. 7779.*
[2]*National Research Council of Canada Postdoctoral Fellow. Present address: School of Pharmacy, Osaka University, Osaka, Japan.*
[3]*We are grateful to Mr. D. H. S. Horn, Pretoria, who had the plant collected and extracted for us.*

Can. J. Chem. Downloaded from www.nrcresearchpress.com by 210.87.254.40 on 09/05/12
For personal use only.

(−)-sparteine dipicrate. The production of (−)-sparteine (II) involved the reduction of the lactam carbonyl, the double bond, and the hydrogenolysis of the hydroxyl; besides proving that argyrolobine possessed the sparteine structure, it showed that the hydroxyl must be present either in a carbinolamine grouping, or in an allylic position to the double bond. That it is the former, and not the latter, is shown by the action of lithium aluminum hydride on the base.

The action of lithium aluminum hydride on argyrolobine, as expected, also reduced the carbonyl and hydrogenolyzed the hydroxyl, giving rise to an unstable oil which in the infrared, in chloroform solution, showed a weak absorption band at 1620 cm^{-1} and in a liquid film showed bands at 1630 and 1650 cm^{-1}. The product, when hydrogenated catalytically, absorbed 1 mole of hydrogen and gave rise to (−)-sparteine, thus confirming the presence of one double bond. The unstable product of the reaction with lithium aluminum hydride, which is a dehydrosparteine, forms a crystalline perchlorate, m.p. 225–228°, showing in the infrared a sharp absorption band at 1677 cm^{-1} characteristic of the grouping $C{=}N^+$, and is therefore an imonium salt, thus confirming the location of the double bond, relative to a nitrogen, already indicated by the n.m.r. spectrum of the alkaloid.

These results suggest that argyrolobine is a hydroxyaphyllidine represented by structure I. Since sodium borohydride converted the perchlorate (m.p. 225–228°) to (−)-sparteine II, although the free base liberated from this salt was inert to lithium aluminum hydride, it follows that this free base arising from the action of lithium aluminum hydride on argyrolobine must be Δ^5-dehydrosparteine III, and its perchlorate $\Delta^{1(6)}$-dehydrosparteinium perchlorate (IV). The identity of the perchlorate was indeed confirmed by direct comparison (melting point of mixture, infrared spectra) with an authentic sample of $\Delta^{1(6)}$-dehydrosparteinium diperchlorate (1).

The hydroxyl group in argyrolobine could not occupy positions C-11, C-15, or C-17 (cf. formula I) for the following reasons: (*a*) argyrolobine could not be oxidized by manganese dioxide to a dilactam, (*b*) argyrolobine hydrochloride is not an imonium salt but a normal salt as shown by its infrared spectrum, and (*c*) argyrolobine is not affected by sodium borohydride.

That the hydroxyl is at C-2 was established by the pyrolysis of acetylargyrolobine (V). On distillation the acetyl-derivative lost the elements of acetic acid, and produced a colorless viscous oil which in the infrared showed absorption bands at 1650 and 1625 cm^{-1}, indicating a lactam carbonyl and unsaturation. The n.m.r. spectrum of the product contained three complex signals (δ 4.73, 5.12, 7.20), each corresponding to one proton, which can be assigned to olefinic protons. The ultraviolet spectrum of the pyro-compound (λ_{max} 252 mμ, ϵ 8300) when compared with that of argyrolobine (λ_{max} 239 mμ, ϵ 9400) reveals that the new double bond, introduced by elimination of acetic acid, has caused a bathochromic shift and, therefore, contributes to the original chromophore. That no skeletal rearrangement took place during pyrolysis was shown by catalytic hydrogenation of the pyro-compound followed by reduction with lithium aluminum hydride, which gave rise to (−)-sparteine. Thus the pyro-compound must be represented by VI or VII depending on whether or not the newly introduced double bond shifted into conjugation with that originally present. The formation of sparteine from VI also eliminates the possibility of structure VIII for argyrolobine since the acetyl derivatives of such a structure could not eliminate acetic acid with formation of a double bond without rearrangement.

Since the absolute configuration of (−)-sparteine is known (2), structure I represents both the structure and absolute configuration of argyrolobine.

Can. J. Chem. Downloaded from www.nrcresearchpress.com by 210.87.254.40 on 09/05/12
For personal use only.

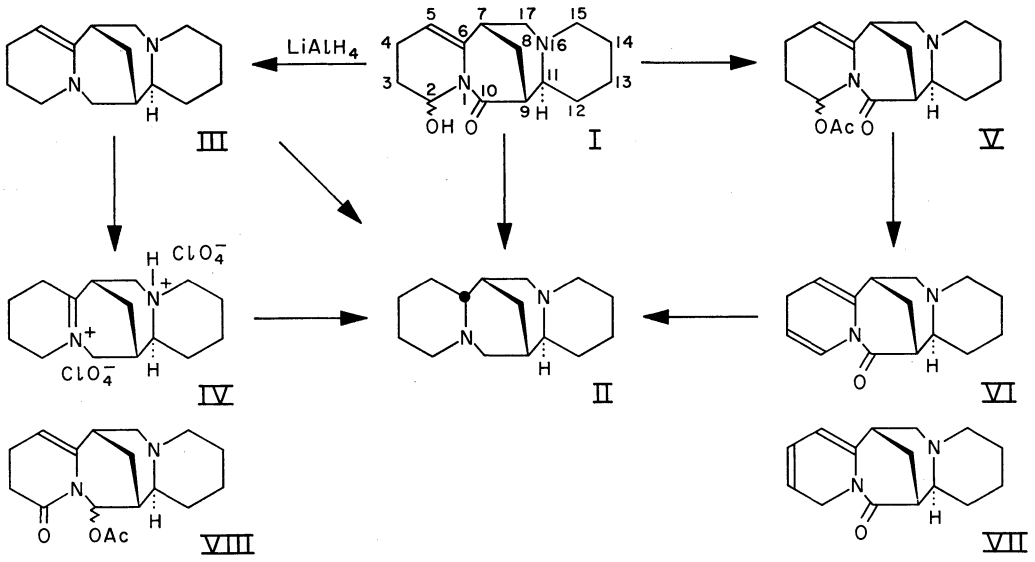

The second new alkaloid was isolated from the mother liquor of the crystallization of argyrolobine by chromatography on alumina and subsequent sublimation. It had the empirical formula $C_{15}H_{22}ON_2$, m.p. 101–106°, $[\alpha]_D$ −9.1° (EtOH). Its ultraviolet spectrum (λ_{max} 240 mμ, ε 12,000) is the same as that of aphyllidine and the infrared spectrum is superimposable on that of the latter. The melting point of the base in admixture with aphyllidine is lowered (63–67°) very appreciably. The alkaloid forms a hydrochloride, m.p. 228–230°, and picrolonate, m.p. 241–243° (decomp.), while the corresponding salts of aphyllidine melt at 235–236° and 235–237° respectively. When hydrogenated catalytically, the base absorbed 3 moles of hydrogen and gave rise to (−)-sparteine, whereas

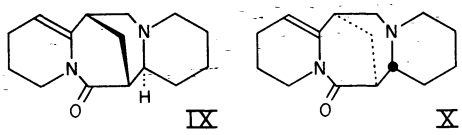

aphyllidine, which is dextrorotatory, was hydrogenated to (+)-sparteine (3). Consequently, the new base is (−)-aphyllidine (IX) and its absolute configuration follows from that of (−)-sparteine (2). It is the enantiomorph of (+)-aphyllidine (X), and its isolation constitutes the first recorded natural occurrence of the levorotatory enantiomorph of this base.

Four more alkaloids were isolated as their salts, but in quantities insufficient to permit proper characterization.

EXPERIMENTAL

Separation of the Alkaloid

The crude, dried methanolic extract (670 g) from *Argyrolobium megarhizum* was stirred with warm 10% hydrochloric acid (2 l.) for 1 hour and filtered. The insoluble material on the filter was washed with water (1 l.) and the combined filtrate and washings extracted repeatedly with ether. The aqueous layer was made basic with sodium hydroxide and extracted with methylene chloride (4×1 l.). The extract was dried over sodium carbonate and evaporated to dryness. The residual brown gum (20.87 g) showed four spots (R_F 0.50, 0.42, 0.32, 0.16) on a paper chromatogram, in which 5% acetic acid – butanol was used as solvent. The

Can. J. Chem. Downloaded from www.nrcresearchpress.com by 210.87.254.40 on 09/05/12
For personal use only.

gum was dissolved in acetone and the solution, when allowed to stand, deposited a crop of crystals, 3.82 g (base A).

The acetone mother liquor was evaporated to dryness and the residue dissolved in 10% hydrochloric acid (500 ml), the solution washed with ether (discarded), neutralized with sodium bicarbonate, and repeatedly extracted with methylene chloride. This extract, on evaporation, left a brown residue (10.32 g) which crystallized on standing (base A and base B). The aqueous solution was made strongly basic with sodium hydroxide and extracted first with ether (yielding a colorless gum, 1.57 g, which crystallized on standing—mainly base A), and then with methylene chloride. This last extract, on evaporation, left a pale brown gum.

All the alkaline aqueous layers, which had been extracted, were combined, acidified with hydrochloric acid, and an aqueous solution of ammonium reineckate was added. The precipitated reineckate was collected by filtration, washed with water, and dried in air (ca. 50 g).

A second lot of the crude extract was worked up differently. The crude extract (100 g) in this case yielded 5 g of basic residue which was dissolved in 10% hydrochloric acid, washed with ether (discarded), made basic with sodium bicarbonate, and extracted with ether. This extract (extract I) yielded a gum, 1.0 g, on evaporation. The aqueous solution was further extracted with methylene chloride which on evaporation left a solid residue (3.4 g—extract II).

Sodium carbonate was added to the aqueous solution, which was extracted with methylene chloride. This extract (III) yielded a gum, 0.07 g. The aqueous solution was finally made strongly basic with sodium hydroxide and thoroughly extracted with methylene chloride (extract IV), which on evaporation left a gummy residue, 0.30 g.

Base A (Argyrolobine)

Base A formed colorless prisms from acetone, m.p. 168–169°. It could be sublimed unchanged at ca. 150° (air bath) and 10^{-3} mm, $[\alpha]_D$ +13.3° (*c*, 1.4 in $CHCl_3$). Found: C, 68.83; H, 8.30; N, 10.45. Calc. for $C_{15}H_{22}O_2N_2$: C, 68.67; H, 8.45; N, 10.68%. Infrared (in Nujol): 3385 (OH), 1638 cm^{-1} (lactam); in chloroform: 3450 (OH), 1620 cm^{-1} (lactam). Ultraviolet: λ_{max} 239 mμ, ϵ 9400. The base was unstable in chloroform solution, which discolored on standing.

Argyrolobine formed a hydrochloride crystallizing from methanol – ethyl acetate as colorless prisms, m.p. 170–172°. Found: C, 60.37; H, 7.63. Calc. for $C_{15}H_{22}O_2N_2.HCl$: C, 60.30; H, 7.76%. Infrared: 3450 (OH), 2360 (broad) (N^+H), 1640 cm^{-1} (lactam). It also gave rise to a methiodide crystallizing from methanol–ether, m.p. 180–183° (decomp.). Found: C, 45.77; H, 5.89. Calc. for $C_{15}H_{22}O_2N_2.CH_3I.H_2O$: C, 45.50; H, 6.44%.

Acetylargyrolobine

Argyrolobine (base A, 0.1 g) was kept overnight at room temperature in a mixture of pyridine (2 ml) and acetic anhydride (1 ml). The reaction mixture was poured into ice water, the solution made basic with potassium carbonate, and extracted with ether. The extract, dried and evaporated, left a colorless oil (0.11 g) which was dissolved in benzene and passed through a column of alumina. The benzene eluate contained the acetylargyrolobine which crystallized from *n*-hexane as colorless prisms, m.p. 61°. Found: C, 66.57; H, 7.70; N, 9.38. Calc. for $C_{17}H_{24}O_3N_2$: C, 67.08; H, 7.95; N, 9.20%. Infrared in chloroform: 1730 (acetyl carbonyl), 1650 cm^{-1} (lactam). The acetate when allowed to stand in the air gradually became discolored.

Hydrogenation of Argyrolobine

Argyrolobine (9.7 mg) was dissolved in 10% hydrochloric acid (6 ml) and hydrogenated at 23° over prereduced Adams' catalyst (35 mg). In the course of 3 hours, 3.4 ml of hydrogen was absorbed (~4.1 mole). The mixture was filtered, the filtrate alkalized with sodium hydroxide, and extracted with methylene chloride. The extract was dried over potassium carbonate and evaporated to dryness. It left a colorless oil which was distilled, b.p. 56–60° (air bath) at 10^{-2} mm, $[\alpha]_D$ −16° (*c*, 1.7 in EtOH). The oil formed a picrate which after recrystallization from methanol, melted at 208–209° either alone or in admixture with (−)-sparteine dipicrate. The infrared absorption spectra of the two were superimposable.

Reduction of Argyrolobine with $LiAlH_4$

Argyrolobine (0.16 g) and lithium aluminum hydride (0.16 g) in dioxane (20 ml) was heated under reflux for 20 hours. The mixture was cooled, a few drops of water added, followed by the addition of methylene chloride. The mixture was filtered, the filtrate dried over potassium carbonate, and evaporated under reduced pressure. There was left a colorless oil, 0.15 g, which could be distilled but with appreciable loss of material by resinification. The product was dissolved in 10% acetic acid and converted to the perchlorate by the addition of sodium perchlorate. The perchlorate thus obtained was recrystallized first from methanol and then from water from which it separated as colorless prisms, m.p. 225–228° (decomp.). Admixture with an authentic sample of $\Delta^{1(6)}$-dehydro(—)sparteinium diperchlorate (m.p. 237–238° (decomp.) (1)) did not depress the melting point. Hence the base itself was Δ^5-dehydrosparteine. Catalytic hydrogenation of this base in ethanol over platinum oxide yielded (−)-sparteine, isolated as its dipicrate.

$\Delta^{1(6)}$-Dehydrosparteinium diperchlorate in methanol was stirred for 30 minutes during which a methanolic solution of sodium borohydride was gradually added. The reaction, worked up as usual, gave an excellent yield of (−)-sparteine, isolated and characterized as its dipicrate. Argyrolobine and its hydrochloride were

Can. J. Chem. Downloaded from www.nrcresearchpress.com by 210.87.254.40 on 09/05/12
For personal use only.

treated in a similar manner with sodium borohydride. In both cases unchanged argyrolobine was recovered in not less than 90% yield.

Pyrolysis of Acetylargyrolobine

Acetylargyrolobine (0.1 g) was distilled *in vacuo* (7×10^{-3} mm). The distillate collected at 130–150° (air bath) was redistilled under the same pressure. Most of the fraction (47 mg) distilled at 130–135° (air bath). The product failed to crystallize. Its infrared spectrum showed no acetate carbonyl absorption but contained bands 1650 and 1625 cm^{-1}. Ultraviolet: λ_{max} 252 mμ, ϵ 8300 (in 95% EtOH).

The pyro-compound (30 mg) dissolved in ethanol (10 ml) was hydrogenated over Adams' catalyst at room temperature for 20 hours. After removal of the catalyst by filtration, the solution was evaporated to dryness *in vacuo* and the residue (which showed an absorption band at 1620 cm^{-1} in the infrared) was heated under reflux in dioxane (5 ml) with excess lithium aluminum hydride for 10 hours. The reaction mixture, worked up as usual, yielded (−)-sparteine, characterized as its dipicrate, m.p. 208–210°, (melting point of mixture with authentic sample and comparison of infrared spectra).

Base B ((−)-Aphyllidine)

The residue obtained from extract I was dissolved in benzene and chromatographed on alumina. Elution with benzene gave a solid which was purified by sublimation at 90–100° (air bath) and 10^{-3} mm. The sublimate was crystallized from ether–hexane from which base B separated as colorless prisms, m.p. 101–106°, $[\alpha]_D$ −9.1° (*c*, 2.2 in EtOH). Ultraviolet: λ_{max} 240 mμ, ϵ 12,000. Found: C, 72.86; H, 8.24; N, 11.01. Calc. for $C_{15}H_{22}ON_2$: C, 73.13; H, 9.00; N, 11.37%. The infrared absorption spectrum was superimposable on that of (+)-aphyllidine.

The base formed a hydrochloride which separated from methanol–acetone–ether as colorless prisms, m.p. 228–230° (decomp.). The reported melting point (3) for (+)-aphyllidine hydrochloride is 235–237°. The base also formed a picrolonate crystallizing from methanol as yellow needles, m.p. 241–243° (decomp.). The literature (4) gives for (+)-aphyllidine picrolonate m.p. 235–236°.

Hydrogenation of (−)-Aphyllidine

(−)-Aphyllidine (base B, 17.1 mg) was hydrogenated over platinum oxide (42 mg) in 10% hydrochloric acid (5 ml) under the same conditions as argyrolobine. The absorption of hydrogen was 5.3 ml (~3.1 moles) in 5 hours. The product of the reaction, a colorless oil, had $[\alpha]_D$ −15°. It was isolated as the dipicrate, m.p. 203–205°. The melting point was unaltered in admixture with (−)-sparteine dipicrate. The identity was also confirmed by comparison of the infrared spectra which were exactly alike.

Base C (N-Methylcytisine)

The residue from extract II consisted of a mixture. Crystallization from acetone removed the argyrolobine present. The mother liquor was evaporated to dryness and the residue dissolved in benzene and chromatographed on alumina. Elution with benzene containing 1% of diethylamine gave first a small quantity of (−)-aphyllidine and then some argyrolobine. Further elution with benzene – methylene chloride (3:1) containing 1% of diethylamine yielded base C as an oil which was distilled at 80–120° (air bath) at 10^{-3} mm.

One-half of the distillate was neutralized with perchloric acid and the salt crystallized from methanol from which it separated as colorless needles, m.p. 274–275° (decomp.). Admixture with N-methylcytisine perchlorate (m.p. 282°) failed to depress the melting point, $[\alpha]_D$ −112° (*c*, 1.7 in H_2O). Found: C, 45.95; H, 5.55; N, 8.50. Calc. for $C_{12}H_{16}ON_2.HClO_4.\frac{1}{2}H_2O$: C, 45.94; H, 5.78; N, 8.93%. The infrared absorption spectrum of the salt was identical with that of N-methylcytisine.

The remaining half of the base in methanol was added to a saturated methanolic solution of picric acid. The precipitated picrate was crystallized several times from methanol and was obtained as yellow needles, m.p. 230–232°, either alone or in admixture with an authentic sample of N-methylcytisine picrate (5). The infrared absorption spectra of both picrates were superimposable.

Hydrogenation of N-Methylcytisine

N-Methylcytisine (base C) perchlorate (14.2 mg) was hydrogenated at 22° in 10% hydrochloric acid (7 ml) over prereduced Adams' catalyst (46 mg). In the course of 5 hours, 5.1 ml of hydrogen was taken up (~4.5 moles). The reaction mixture was filtered, the filtrate alkalized with sodium hydroxide, and repeatedly extracted with methylene chloride. The combined extract was dried over potassium carbonate and evaporated to dryness. It left a residual colorless oil (5 mg) (no lactam carbonyl absorption in the infrared) which was treated with picric acid. The picrate crystallized from methanol as yellow needles, m.p. 225–227° (decomp.). Found: C, 44.45; H, 4.32. Calc. for $C_{12}H_{22}N_2.(C_6H_3O_7N_3)_2$: C, 44.19; H, 4.32%.

Cytisine (Base D)

Extract IV was combined with the uncrystallized fractions from the separation by the first method described. The bases were subjected to fractional distillation at 10^{-2} – 7×10^{-3} mm. The following fractions were collected: I, b.p. ~120–130°; II, b.p. ~150°; III, b.p. ~180°; IV, b.p. ~200°. Fraction III was dissolved in acetone and added to an acetone solution of picric acid. The crystalline picrate was crystallized several times from acetone and then from methanol from which it separated as yellow prisms, wt. 15 mg, m.p. 285°

Can. J. Chem. Downloaded from www.nrcresearchpress.com by 210.87.254.40 on 09/05/12
For personal use only.

(decomp.). The melting point was not altered by admixture with an authentic sample of cytisine picrate. The infrared absorption spectrum of the picrate and that of cytisine picrate were superimposable.

Throughout the fractional distillation, a sublimate came over which crystallized from acetone as colorless needles, m.p. 253–255° (decomp.).

Three other bases were isolated from the distillates as their hydrochlorides or perchlorates. The quantities recovered, however, were insufficient to allow proper characterization.

REFERENCES

1. N. J. LEONARD, P. D. THOMAS, and V. W. GASH. J. Am. Chem. Soc. **77**, 1552 (1955).
2. S. OKUDA, K. TSUDA, and H. KATAOKA. Chem. Ind. 1115 (1961).
3. A. P. OREKHOV. J. Gen. Chem. (USSR), **7**, 2048 (1937); Chem. Abstr. **32**, 572 (1938).
4. A. P. OREKHOV and G. P. MEN'SHIKOV. Ber. **65**, 234 (1932).
5. L. MARION and J. OUELLET. J. Am. Chem. Soc. **70**, 691 (1948).

Can. J. Chem. Downloaded from www.nrcresearchpress.com by 210.87.254.40 on 09/05/12
For personal use only.

HIGH-FREQUENCY TITRATIONS

I. ARGENTIMETRIC DETERMINATION OF HALIDES AND THIOCYANATE IN METHANOL[1]

PETER GREY AND G. C. B. CAVE
Department of Chemistry, McGill University, Montreal, Quebec
Received August 1, 1963

ABSTRACT

A new method is proposed for the determination of milligram amounts of each halide present in a mixture of alkali-metal halides. In some mixtures, thiocyanate also may be determined. A methanol solution of the sample is titrated in a closed-type cell, with a standard solution of silver nitrate in methanol. By using high-frequency titrimetry, and an appropriate concentration of the halide solution, sharp end points were obtained for each halide. Because of solid solutions, the accuracy of the determination of individual halides in mixtures depended on the mole ratios of the halides; the errors found in the titration of various binary, ternary, and quaternary mixtures are reported. For some binary mixtures, the total amount of halide titrated in 120 ml of methanol was varied from 0.5 to 500 micromoles. At the lower concentrations, addition of a small amount of sodium nitrate sharpened the end point. At all concentrations of halide, an excessive amount of indifferent electrolyte essentially eliminated the end points. The alkali-metal halides gave more satisfactory titration graphs than did some other metal halides. The effects of variation in temperature, and of solvent evaporation were noted.

INTRODUCTION

The present work describes the high-frequency argentimetric titration of alkali-metal halides and thiocyanate in their mixtures dissolved in methanol. It was found that such titrations could also be performed in ethanol, in acetonitrile, and in acetone–water mixtures.

Volumetric methods for the halides usually are based on the use of silver nitrate as the titrant. In addition to the use of indicators to detect the end point, potentiometric and amperometric methods may be used (1). The potentiometric titration of halides in aqueous solutions of their mixtures was recently studied by Martin (2), and by Bowers *et al.* (3). The effect of using acetone–water mixtures instead of water in the amperometric determination of halides has been studied (4). Léon (5) determined by potentiometric titration the bromide and the thiocyanate contents of mixtures, in acetone.

High-frequency titrations have also been reported for the determination of chloride alone in aqueous solutions (6) and in other solvents (7), and for the determination of chloride and of sulphate present together in acetone–water solutions (8). Low-frequency conductometric titrations of single halides is practicable, but is not feasible for the individual determination of halides in mixtures, in aqueous solution, or in methanol.

EXPERIMENTAL

Apparatus

The Sargent Model V Oscillometer was used. It is a null-type instrument, with a fixed frequency of 5 megacycles per second. When higher sensitivity was needed, a Sargent cell compensator was coupled in the transmission line ahead of the sample cell. It is a variable inductor, whose reactance can be adjusted to the capacitance reactance due to the walls of the titration cell.

The titration cell was a capacitor in parallel with standard capacitors, to comprise the resonant circuit of the oscillometer's sine-wave oscillator. After each measured addition of titrant, the apparent capacitance

[1]*Presented in part at the Ninth Ottawa Symposium, Canadian Association for Applied Spectroscopy in conjunction with the Analytical Chemistry Division of the Chemical Institute of Canada, September 17–19, 1962.*

of the filled cell was measured by removing standard capacitances from the resonant circuit, until the frequency of the circuit was restored to its original value. This apparent capacitance is a function of the conductance and the dielectric constant of the solution. The principles of high-frequency titrimetry have been described by Reilley and McCurdy (9), and by Sherrick *et al.* (10).

For a titration cell, the closed-type macro cell supplied with the oscillometer was used. Its diameter was 50 mm, and the overall height was 165 mm. It had an outside-fitting ground-glass cap. For the present work, two holes, 9 mm in diameter, were drilled through this cap. A central hole was for the shaft of a polypropylene stirrer. The other hole was for the delivery tip of a buret. The shaft and the delivery tip were each fitted with a sliding washer of silicone rubber having a thin smear of silicone grease, to provide reasonably gas-tight seals at the two holes in the glass cap. A closed-type titration cell has also been used by Hitchcock and Elving, for non-aqueous titrations (11).

The solution for titration was contained in an annulus of 90-ml capacity, which constituted the lower half of the cell. The two outer cylindrical walls of this annulus each had a metal coating, to serve as the plates of the capacitor. Thus, solutions never were in contact with these plates.

A 50-ml buret was used, with its glass stopper lubricated with silicone grease. It had a special delivery tip. This tip was bent sharply at 90 degrees to give a horizontal section of about 8 cm, then sharply at 90 degrees to give a final vertical section of about 11 cm. Part of this 11-cm length projected into the titration cell. The orifice was immersed in the sample solution during stirring.

Burets and pipets were calibrated to deliver methanol.

Reagents

Standard solutions of silver nitrate, 10^{-4} N to 10^{-2} N, were prepared in pure methanol, from reagent-grade silver nitrate previously dried first at 110° C, then for 15 minutes at 255° C. They were standardized by high-frequency titrations, against reagent-grade sodium chloride dried at 550° C. This sodium chloride was the primary standard in the present investigation.

Standard solutions of sodium iodide, sodium bromide, sodium chloride, and potassium thiocyanate in methanol were prepared from dried reagent-grade salts. The iodide and thiocyanate were dried at 120° C, and the bromide at 550° C. The iodide, bromide, and thiocyanate solutions were standardized by high-frequency titrations against a previously standardized solution of silver nitrate.

Standard solutions of sodium nitrate in methanol were prepared from the reagent-grade salt previously dried at 120° C. These solutions were not standardized. Their halide content was found to be negligibly small, in the amounts used.

The methanol was absolute, reagent grade. Its water content was measured in accordance with the method of Willis and Miller (12) by using the infrared peak of water, at 1.950 μ and was found to be 0.03%.

The acetone was reagent grade. It contained about 5% of water, which was not removed.

The Titrimetric Procedure

A dry cell was inserted into the cell holder of the oscillometer. The instrument reading was then adjusted to zero by removing from the circuit a capacitance equal to that of the empty cell. Without removing the cell, the required aliquot of one of the standard solutions of halide in methanol was added by pipet. This aliquot was then diluted to 120±1 ml with methanol. This volume provided for satisfactory stirring, as well as bringing the level of the liquid well above the top of the condenser plates of the cell. The polypropylene stirrer was positioned, with its paddles 5 mm above the top of the condenser plates. The ground-glass cap was then slid down the stirrer shaft, into position. The filled buret was positioned. Finally, the two silicone-rubber washers were positioned at the holes in the cap.

The rate of stirring was not critical. It was adjusted so that the top of the vortex was about 25 mm above the still level of the liquid. The precipitated silver halide was then found not to settle.

After the original solution was stirred, the apparent capacitance due to the solution was measured, and recorded merely as "instrument divisions." A standard solution of silver nitrate in methanol was added in measured increments. After each such addition, the apparent capacitance due to the solution was read. The additions were continued past the end point. Stirring was continuous throughout the titration.

Apparent capacitance (as instrument divisions) was plotted against the volume of titrant added. In general, straight lines could be drawn through the points, and they intersected at the end point. Typical titration graphs are shown in Fig. 2 for the titration of methanol solutions of sodium halides by a standard solution of silver nitrate in methanol.

RESULTS AND DISCUSSION

The Effect of Temperature and Solvent Evaporation

The apparent capacitance due to an electrolyte solution in the titration cell is a function both of the dielectric constant of the solution, and of its conductance. The temperature coefficient of the dielectric constant will be negative, and that of the conductance will be

positive. Therefore, for a solution such as an alkali halide in methanol, the nett temperature coefficient of the apparent capacitance will change sign at some concentration of electrolyte. Measurements on a solution of sodium chloride in methanol confirmed this conclusion. A solution 5.5×10^{-5} M in sodium chloride showed a zero temperature coefficient; at higher concentrations the coefficient was negative.

On titrating stirred methanol solutions of alkali halides in a titration cell similar to the one described above but without the cover, solvent evaporation occurred, with concomitant lowering of the temperature of the solution. This cooling effect is shown in Fig. 1*a*.

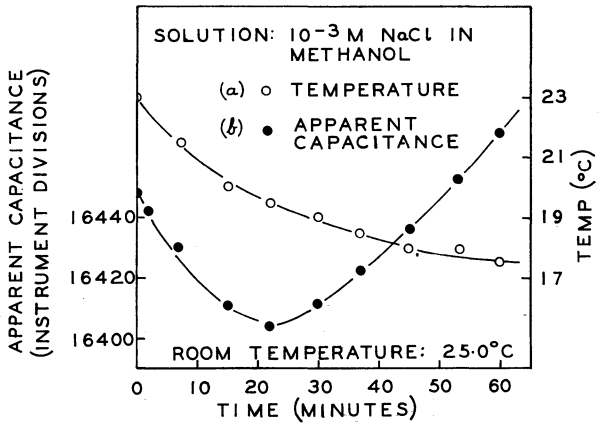

FIG. 1. Changes in temperature and in apparent capacitance due to solvent evaporation from a continuously stirred solution of NaCl in methanol, in an open cell.

The nett change in apparent capacitance due to this solvent evaporation is shown in Fig. 1*b*, as a function of the period of stirring. The curve is the resultant of two opposing effects; both are due to evaporation. The apparent capacitance for this solution has a negative temperature coefficient. The rate of fall of temperature of the solution declined with time. To the left of the minimum, the effect of the negative temperature coefficient predominated over the effect of the increase in concentration due to evaporation. Therefore the apparent capacitance declined. To the right of the minimum the increase in concentration was predominant.

Clearly the slope, and the degree of curvature of the arms of a titration graph will generally be affected by solvent evaporation from an open titration cell. Provided that stirring was continuous and at a reasonably constant rate, the titration graphs were found to be satisfactory for the detection of the end point. However, the slopes of the arms of these graphs varied with the rate of addition of titrant, and with the stirring program. The use of intermittent stirring, with unequal increments of titrant was found to produce anomalous kinks in the titration graphs. For example, when stirring was stopped between increments of titrant, then a change in the size of the increment during a titration produced a change in the slope of the titration graph. This effect was due to a change in the volume of methanol evaporated, per milliliter of titrant added.

Standardization of Solutions

Sodium chloride was the primary standard. The titrimetrically determined normalities of the silver nitrate, sodium iodide, sodium bromide, and potassium thiocyanate solutions were found to be within 1% of the values calculated from the weights of the pure salts

taken to prepare the standard solutions. In general, 1–10 mg of halide were taken for the high-frequency titration.

Titration of Single Halides

Typical titration graphs for single halides in methanol, titrated against silver nitrate in methanol are shown in Fig. 2.

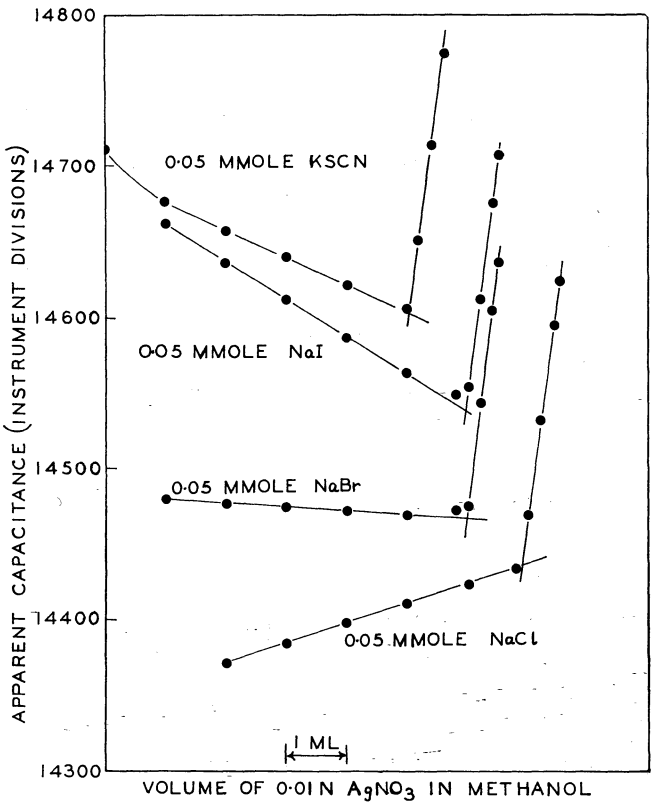

FIG. 2. Typical titration graphs of argentimetric titrations of single halides in methanol.

The slope of the lefthand branch of the graph was found to depend not only on the nature of the halide, but also on its concentration, and the concentration of indifferent electrolyte, such as sodium nitrate, present. These changes in slope will be explained in a subsequent communication.

The precision with which single halides can be titrated by using the proposed high-frequency method was found from replicate titrations; the standard deviations are given in Table I.

Determination of Halides and Thiocyanate in Mixtures

Binary, ternary, and even quaternary mixtures of halides and thiocyanate were satisfactorily titrated, and each component determined. However, the acuteness of the angles at the various end points was found to depend on the concentrations of the halides and thiocyanate present, and on the ionic strength of the methanol solutions. At extreme concentrations, low and high, the end points could not be recognized. The limits within

TABLE I

Precision of high-frequency argentimetric titration of halides present alone in methanol
Initial volume of solution in titration cells: 120 ml
Normality of standard solution of $AgNO_3$ in methanol: 0.01029 *N*

	Chloride (as Cl)	Bromide (as Br)	Iodide (as I)	Thiocyanate (as SCN)
Average found (mg)	1.78	4.08	6.42	2.97
No. samples	3	4	3	3
Std. deviation*	0.012	0.012	0.029	0.020

*Computed for $n-1$ degrees of freedom.

which titrations are feasible can be predicted, and are considered in a subsequent communication.

Typical examples of titrations are shown in Figs. 3 and 4.

Inspection of Fig. 3 shows that for the bromide–chloride mixture, the titration graph has decided curvature at the bromide end point, and practically none at the chloride end point. For a thiocyanate–chloride mixture, curvature was evident at the thiocyanate end point. The degree of curvature at an end point depends on the mixture. Moreover, curvature at the end point occurred when single halides were titrated (see Fig. 2).

In conventional low-frequency conductometric titrations in aqueous solutions, curvature at an end point is usual. This has been attributed to the solubility of the silver halide

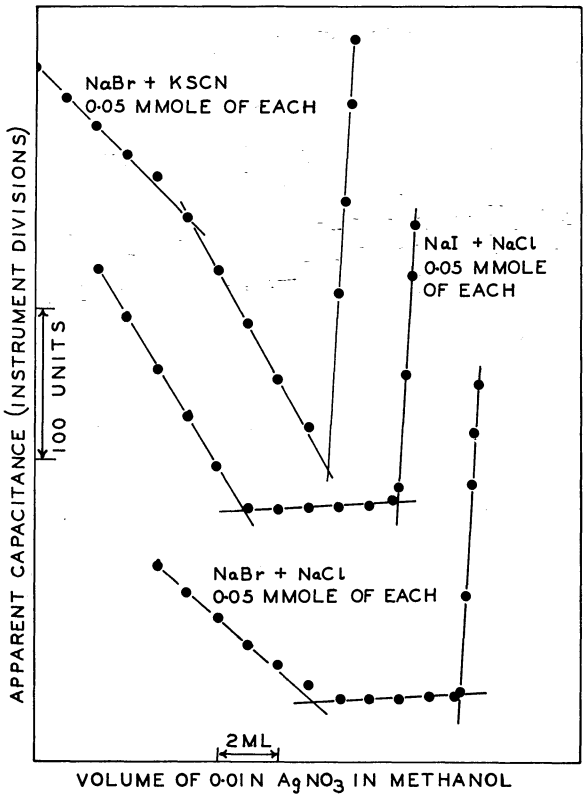

FIG. 3. Typical titration graphs of argentimetric titrations of pairs of halides in methanol.

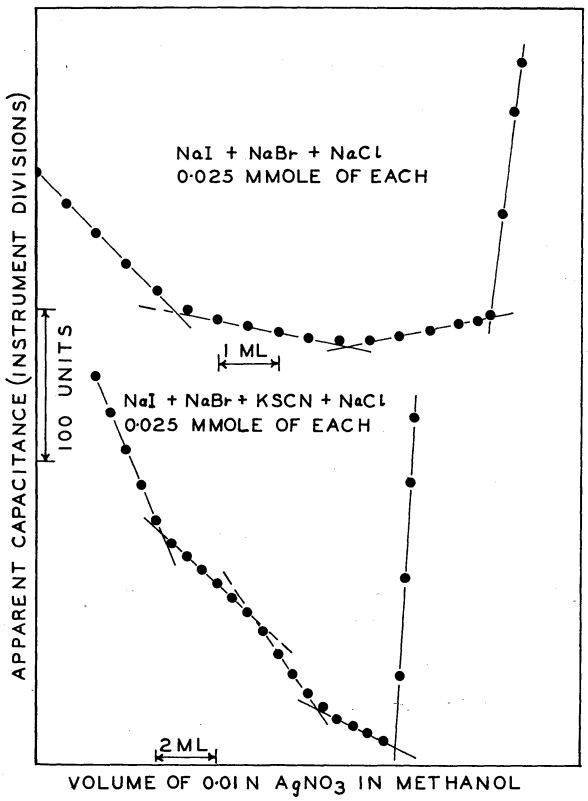

FIG. 4. Typical titration graphs of argentimetric titrations of mixtures of several halides in methanol.

(13), and to the adsorption of ions on the surface of the precipitate (14). In the present high-frequency titrations, the formation of solid solutions would be expected to contribute to curvature at an end point.

Replicate determinations of chloride and bromide in equimolar mixtures were made, in order to find the precision of the analyses as measured by the standard deviation. These results are in Table II. In addition to these replicate titrations, additional single or

TABLE II

Precision of high-frequency argentimetric titrations of sodium chloride and sodium bromide (millimoles) in equimolar mixtures in methanol
Initial volume of solution in titration cell: 120 ml
Normality of standard solution of $AgNO_3$ in methanol: 1.018×10^{-2} *N*

Halide taken (mmole)		Mean halide found (mmole)			Standard deviation	
Br+Cl	Br	Br+Cl	Br	No. samples	Br+Cl	Br
0.1017	0.0506	0.1019	0.0546	6	0.00017	0.0016
0.0509	0.0254	0.0512	0.0285	6	0.00027	0.0015

duplicate titrations were made on assorted mixtures of halides and thiocyanate. The results are in Table III. Attention is drawn to the successful determination of chloride, bromide, iodide, and thiocyanate present together in an equimolar mixture.

In connection with these titrations of mixtures of halides and thiocyanate, as reported in Tables II to IV inclusive, the various solubility-product values are of interest. The pK values of the solubility products of AgCl, AgSCN, AgBr, and AgI in methanol at 25° C have been reported (15) to be, respectively, 13.05, 13.74, 15.24, and 18.22.

The Formation of Solid Solutions of Halides

The novel feature of the present communication is the detection of end points in argentimetric titrations of mixed halides in methanol; the purpose was not the reduction of errors due to the formation of solid solutions. However, several workers (13, 16–19) have studied the formation of solid solutions during the precipitation of halides from aqueous solutions. It was considered of interest to study precipitation from methanol solutions.

Argentimetric high-frequency titrations were carried out in replicate, on mixtures of sodium bromide and sodium chloride present together in various proportions. The results are in Table IV.

In all of the analyses reported in Tables II, III, and IV the end points were observable. However, not all titrations gave equally clear end points. The acuteness of the angle of intersection of two arms of a titration graph, that is, the sharpness of the end point, was found to depend on the total concentration of halide present.

Inspection of Table IV shows that solid solutions were formed in these chloride–bromide systems. The sign of the percentage difference between amount taken and amount found, given in column 6, changes at a point where the ratio of the initial concentration of chloride to that of bromide is less than unity. Flood (17), in considering the precipitation of chloride and bromide in aqueous mixtures, showed that this fact indicates the formation of heterogeneous solid solutions; the percentage differences should go through zero when the halide ratio is unity, if homogenous solid solutions are formed.

The data in Table III, and the relevant solubility products indicate that a thiocyanate–chloride mixture is the other binary mixture for which an argentimetric titration of each component is of limited use.

Range of Titratable Concentrations, and Effect of an Indifferent Electrolyte

When the apparent capacitance due to a solution is plotted against the logarithm of its concentration, a sigmoid curve is obtained. It has relatively flat arms parallel to the concentration axis, at high and low concentrations. Thus, there is a range of concentrations within which the concentration of a solution for titration must be kept, in order to ensure that the instrument will be sufficiently sensitive to changes in concentration to provide a definite break in the titration curve.

Each solute present in a solution contributes, by its conductance or by its dipole moment, to the apparent capacitance. The addition of an indifferent electrolyte, such as sodium nitrate, to a halide solution in methanol therefore increases this apparent capacitance. If too much of an indifferent electrolyte is present in the halide solution, then the response of the oscillometer will be along the upper, flat arm of the above-noted sigmoid curve. As a result, a break will not be evident in the titration graph obtained in the argentimetric titration of the halide. In general, the acuteness of the angle made by the arms of the titration graph will depend on the ionic strength of the solution. This was confirmed, and at about 0.01 M sodium nitrate, there was no break at the end point.

So far in the present report, the amount of alkali halide titrated in 120 ml of methanol has been 5–100 μmoles. However, up to 500 μmoles of sodium chloride and sodium bromide, alone and in their mixtures, were successfully titrated; the upper limit of

TABLE III

High-frequency argentimetric titrations of sodium halides and thiocyanate in mixtures in methanol
Initial volume of solution in titration cell: 120 ml
Normality of standard $AgNO_3$ in methanol: 0.01 *N*

Binary mixtures	Taken (μmoles)	Found (μmoles)	Ternary mixtures	Taken (μmoles)	Found (μmoles)	Quaternary mixture	Taken (μmoles)	Found (μmoles)
I	50.5	50.3	I	50.6	59.6	I	25.2	22.5
I+Cl	102.6	102.0	I+Br	102.0	111.0	I+Br	50.0	53.3
			I+Br+Cl	153.4	154.2	I+Br+SCN	75.6	73.6
I	50.5	49.8				I+Br+SCN+Cl	100.6	100.6
I+Br	102.0	102.8	I	25.2	25.4			
			I+Br	50.0	46.9			
Br	50.4	50.8	I+Br+SCN	75.6	75.0			
Br+SCN	101.0	100.7						
			I	25.2	24.8			
SCN	50.6	36.1	I+SCN	50.8	48.1			
SCN+Cl	100.8	101.1	I+SCN+Cl	75.7	75.6			
SCN	100.5	84.8	Br	24.8	27.8			
SCN+Cl	110.6	109.6	Br+SCN	50.4	50.5			
			Br+SCN+Cl	75.3	75.4			
Cl*	99.4	81.0						
SCN+Cl	109.5	110.6						

*The first end point was attributed in this case to chloride.

TABLE IV

The effect of variation in the mole ratio of chloride and bromide on the accuracy of argentimetric titrations in methanol
Initial volume of solution in titration cell: 120 ml
Normality of standard solution of $AgNO_3$ in methanol: 0.01 *N*

Mole ratio Cl:Br	Chloride taken (micromoles)	Bromide (micromoles) Taken	Found*	Standard deviation	% difference	Chloride + bromide (micromoles) Taken	Found*	Standard deviation	% difference
1:20	4.8	101.5	98.1	0.49	−3.4	106.3	106.3	0.10	0.0
1:10	9.7	101.5	98.8	0.64	−2.6	111.2	111.1	0.25	−0.09
1:3	24.3	76.2	78.3	0.58	2.8	100.5	101.0	0.16	0.5
1:1	51.1	50.6	54.6	1.70	7.9	101.7	101.9	0.17	0.2
3:1	72.8	25.4	27.9	0.41	9.9	98.2	99.3	0.29	1.1
10:1	97.0	10.2	12.1	1.25	19.4	107.2	107.5	0.15	0.28
20:1	97.0	5.1	8.7	0.41	71.2	102.1	102.8	0.23	0.7

*Average of three samples.

titratable concentration was not sought. Amounts down to 0.5 μmole of these two halides were also successfully titrated in their mixtures, provided that 50 μgrams or more of sodium nitrate were also present, and that the Sargent cell compensator was also used, at a setting of about 800 units.

Titration of Halides of Metals other than Alkali Metals

The titration graphs obtained for the alkali-metal halides consisted of linear branches, although in the immediate vicinity of the end points for some mixtures there was curvature. A few titrations were made of anhydrous strontium chloride, anhydrous cupric chloride, and ferric chloride hexahydrate, separately in methanol. Approximately 50 μmoles were titrated with 0.01 *N* silver nitrate in methanol. The titration graphs for strontium chloride and for cupric chloride are shown in Fig. 5; that for ferric chloride was too in-

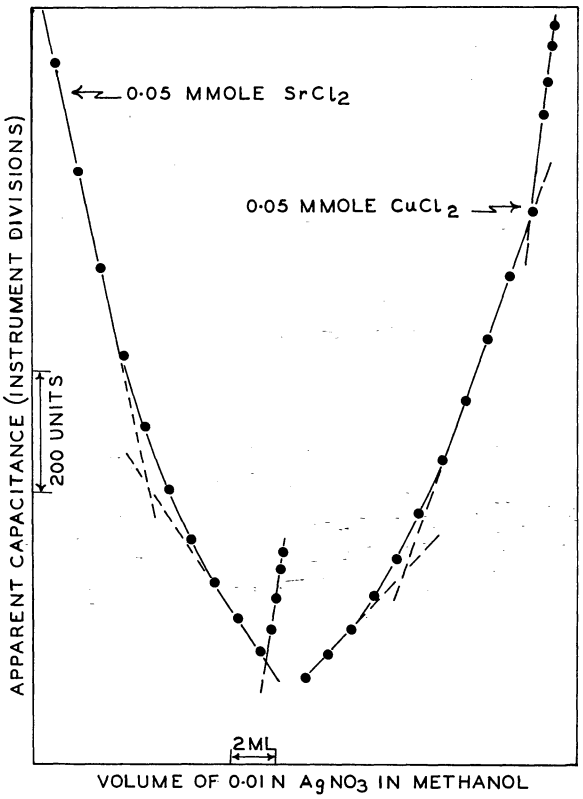

FIG. 5. Titration graphs of the argentimetric titration of strontium chloride and of cupric chloride in methanol.

definite to be useful. The second break in each graph corresponds to the stoichiometric end point. The first break, in the vicinity of which the graphs are curved, corresponds roughly to one-half the stoichiometric end point. However, it would be speculation to suppose that this first break indicates the presence of $CuCl^+$ and of $SrCl^+$.

The illustrated curvature in a titration graph, caused by the presence of a non-alkali metal, could obscure an end point when a mixture of halides is being titrated. Therefore, it may be necessary in analyses of mixtures of halides in which a non-alkali metal is present, to replace that metal by an alkali metal, prior to titration of the halides.

The presence of acid in the methanol solution of halide caused curvature in the branch of the titration graph that preceded the end point; the branch after the end point was linear. Such titration graphs are shown in Fig. 6, for several solutions that contained

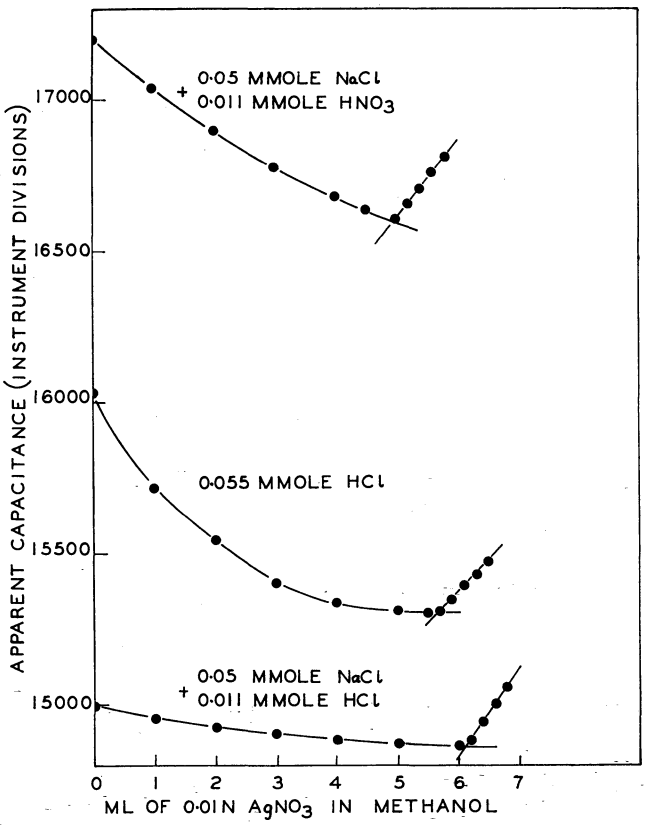

FIG. 6. The effect of acid on the titration graphs in the argentimetric determination of halide in methanol.

hydrochloric acid or nitric acid. As expected, nitric acid produced less curvature than did hydrochloric acid. To permit unequivocal titrations of mixtures of halides, it would seem advisable in general to neutralize almost all of the free acid present, prior to a titration.

ACKNOWLEDGMENTS

We are grateful to Mrs. Nurjahan Begum for obtaining the data in Table IV, to the National Research Council for financial support, and to the Province of Quebec for a scholarship to one of us (P. G.).

REFERENCES

1. G. W. ARMSTRONG, H. H. GILL, and R. F. ROLF. *In* Treatise on analytical chemistry, Part II, Vol. 7. *Edited by* I. M. Kolthoff and P. J. Elving. Interscience Publishers, New York, N.Y. 1961. pp. 363–424.
2. A. J. MARTIN. Anal. Chem. **30**, 233 (1958).
3. R. C. BOWERS, L. HSU, and J. A. GOLDMAN. Anal. Chem. **33**, 190 (1961).
4. H. A. LAITINEN, W. P. JENNINGS, and T. D. PARKS. Anal. Chem. **18**, 355 (1946).
5. C. LÉON. Compt. rend. **233**, 170 (1951).
6. W. J. BLAEDEL and H. V. MALMSTADT. Anal. Chem. **24**, 455 (1952).

7. N. VAN MEURS. J. Electroanal. Chem. **2**, 17 (1961).
8. G. S. BEIN. Anal. Chem. **26**, 909 (1954).
9. C. N. REILLEY and W. H. MCCURDY, JR. Anal. Chem. **25**, 86 (1953).
10. P. H. SHERRICK, G. A. DAWE, R. KARR, and E. F. EWEN. Manual of chemical oscillometry. E. H. Sargent and Company, Chicago, Ill. 1954.
11. E. T. HITCHCOCK and P. J. ELVING. Anal. Chim. Acta, **27**, 501 (1962).
12. H. A. WILLIS and R. G. J. MILLER. Spectrochim. Acta, **14**, 119 (1959).
13. I. M. KOLTHOFF and J. J. LINGANE. J. Am. Chem. Soc. **58**, 1524, 1528 (1936).
14. W. CLARK. J. Chem. Soc. (London), 768 (1926).
15. P. BUCKLEY and H. HARTLEY. Phil. Mag. **8**, 320 (1929).
16. I. M. KOLTHOFF and F. T. EGGERTSON. J. Am. Chem. Soc. **61**, 1036 (1936).
17. H. FLOOD. Z. Anorg. Allgem. Chem. **229**, 76 (1936).
18. H. FLOOD and B. BRUNN. Z. Anorg. Allgem. Chem. **229**, 85 (1936).
19. H. FLOOD and E. SLETTER. Z. Anal. Chem. **115**, 30 (1938).

STUDIES ON THE SOLUBLE INTERMEDIATES IN THE HYDROLYSIS OF DIMETHYLTIN DICHLORIDE

EQUILIBRIUM CONSTANT FITTING WITH A HIGH SPEED DIGITAL COMPUTER[1]

R. STUART TOBIAS AND M. YASUDA[2]

Department of Chemistry, University of Minnesota, Minneapolis

Received October 3, 1963

Can. J. Chem. Downloaded from www.nrcresearchpress.com by 210.87.254.6 on 09/05/12
For personal use only.

ABSTRACT

The hydrolysis of $(CH_3)_2SnCl_2$ has been studied in a medium 0.1 *M* in $(Na^+)Cl^-$ by a potentiometric titration technique. The complexes formed by the hydrolysis reactions together with their formation constants have been determined by analysis of the 394 data sets using a high speed digital computer. The data can be fitted equally well over the range pH 1.5 to 9 by the four formation constants for $(CH_3)_2SnOH^+$ ($\log {}^*\beta_{11} = -3.245\pm0.004$), $[(CH_3)_2SnOH]_2^{+2}$ ($\log {}^*\beta_{22} = -5.00\pm0.02$), $(CH_3)_2Sn(OH)_2$ ($\log {}^*\beta_{21} = -8.516\pm0.004$), and $[(CH_3)_2Sn]_4(OH)_6^{+2}$ ($\log {}^*\beta_{64} = -16.85\pm0.02$) or by the five constants for $(CH_3)_2SnOH^+$ ($\log {}^*\beta_{11} = -3.251\pm0.004$), $[(CH_3)_2SnOH]_2^{+2}$ ($\log {}^*\beta_{22} = -5.05\pm0.02$), $(CH_3)_2Sn(OH)_2$ ($\log {}^*\beta_{21} = -8.535\pm0.005$), $((CH_3)_2Sn)_2(OH)_3^+$ ($\log {}^*\beta_{32} = -9.81\pm0.01$), and $((CH_3)_2Sn)_3(OH)_4^{+2}$ ($\log {}^*\beta_{43} = -11.52\pm0.03$). Thus there is little question about the existence in the solutions of the simple monohydroxo complex and its dimer or of the neutral dihydroxide. Only very low concentrations of species containing more than four tin atoms can exist in aqueous solution. In addition, the data determined previously for the hydrolysis of $(CH_3)_2Sn(ClO_4)_2$ in a medium 3.0 *M* in $(Na^+)ClO_4^-$ have been refined by the least squares procedure. These 762 data sets can also be fitted equally well by the set of constants $\log {}^*\beta_{11} = -3.55\pm0.01$, $\log {}^*\beta_{22} = -4.52\pm0.01$, $\log {}^*\beta_{21} = -9.00\pm0.01$, and $\log {}^*\beta_{64} = -16.14\pm0.03$ or $\log {}^*\beta_{11} = -3.54\pm0.01$, $\log {}^*\beta_{22} = -4.60\pm0.02$, $\log {}^*\beta_{21} = -8.98\pm0.01$, $\log {}^*\beta_{32} = -9.76\pm0.06$, and $\log {}^*\beta_{43} = -10.40\pm0.05$. The tendency of dimethyltin dichloride to form polycondensed species in aqueous solution is slight, and there is no evidence for the formation of large rings or chains. The solid stannoxane which precipitates from chloride solution was studied by infrared and X-ray powder photography and is essentially the same as the compound obtained by reaction of $(CH_3)_2SnO$ and $(CH_3)_2SnCl_2$ in a 1:1 mole ratio in 95% ethanol. This corresponds to a slightly different product than that obtained by a 1:1 reaction of these compounds in benzene which gives $((CH_3)_2SnCl)_2O$. This is in accord with the observation that precipitation occurs only at a pH higher than that at which $((CH_3)_2SnOH)_2^{+2}$ has attained the maximum concentration, and hence precipitation is occasioned by the formation of larger polycondensed species. A comparison of the perchlorate and chloride data also indicates that the tendency to form polycondensed species is reduced by the presence of chloride ion. This is partially an ionic strength effect and partially a result of chloride complexing of the simple aquodimethyltin(IV) ion, and the first chloro-complexing constant was estimated to be 28 l. mole^{-1}.

INTRODUCTION

With the rise in interest in the synthesis of metalloxane polymers, numerous attempts have been made to synthesize tractable polyorganostannoxanes. Although it would appear by analogy with the organodihalosilanes that the dialkyltin dihalides could be used as starting materials in a hydrolytic polycondensation reaction, it was shown quite some time ago by Rochow and Seyferth (1) that this was not the case. The free energy change for the hydrolysis of dimethyltin dichloride is much less negative than for the hydrolysis of dimethyldichlorosilane, the hydrolysis is readily reversible, and large condensation polymers are not formed. It has also been established that dimethyltin dichloride undergoes extensive aquation in solution, and the equilibrium in [1] almost entirely favors the aquodimethyltin cation (2, 3). The value of n is presumed to be 2.

$$(CH_3)_2SnCl_2 + nH_2O = (CH_3)_2Sn(OH_2)_n + 2Cl^- \qquad [1]$$

[1]*This work was supported by the United States National Science Foundation under grant GP-653. Presented at the Symposium on Inorganic Polymers, University of Western Ontario, London, Ontario, September 4–6, 1963.*

[2]*Research Fellow in Chemistry; present address: Department of Chemistry, University of Nagoya, Nagoya, Japan.*

Can. J. Chem. Downloaded from www.nrcresearchpress.com by 210.87.254.6 on 09/05/12
For personal use only.

In the years intervening since these initial experiments, several attempts at other methods of synthesis of the polydialkylstannoxanes have been made. In general, these have been based on the direct reaction of dialkyltin oxides with the dialkyltin dihalides, since Harada showed that these reactions give low molecular weight polycondensation products (4, 5). In addition many attempts have been made to obtain useful materials by the cohydrolysis of organosilicon monomers with organotin monomers. Much of this work has been described in a recent review (6).

A short time ago, a study of the hydrolysis of the aquodimethyltin(IV) cation in a medium 3 *M* in sodium perchlorate was reported (7). It had been previously noted that the dimethyltin(IV) ion behaved, qualitatively, much like the tin(II) ion (8); and it had been shown some time ago that polynuclear hydrolysis products exist in hydrolyzed tin(II) solutions (9). Indeed, it was found that in addition to the simple conjugate base $(CH_3)_2SnOH^+$ appreciable concentrations of a binuclear species $((CH_3)_2Sn(OH))_2^{+2}$ were formed in the hydrolyzed dimethyltin perchlorate solutions. At even higher ratios of base to dimethyltin aquo ion, larger polynuclear complexes appeared to be formed together with the neutral hydroxide $(CH_3)_2Sn(OH)_2$; and the data were fitted in terms of equilibrium constants for the formation of $((CH_3)_2Sn)_2(OH)_3^+$ and $((CH_3)_2Sn)_3(OH)_4^{+2}$. When the total concentration of the dimethyltin was greater than about 5 m*M*, precipitation occurred at an $\bar{n}$ (average number of hydroxo groups bound per dimethyltin group) of ca. 1.4. Systematic deviations of the calculated $\bar{n}(\log [H^+])$ curves from the experimental data indicated that even larger polynuclear complexes were formed at $\bar{n}$ values slightly less than that at which precipitation occurred. In a few cases, the precipitate was filtered off from the solution and dried. This basic dimethyltin(IV) perchlorate burned violently in the open; and because of the potentially explosive nature of the compound, no further studies were made of it. It has been shown that the basic tin(II) nitrate is a rather violent explosive and is more heat- and impact-sensitive than lead azide (10).

Since most of the preparative studies on stannoxanes have been conducted with the halides and especially with the chlorides, it was decided to undertake a thorough study of the species present in solutions of dimethyltin dichloride. In such equilibrium studies, it is necessary to employ a rather high concentration of supporting electrolyte, and the medium 0.1 *M* NaCl was chosen. It was hoped that in comparison to the measurements in 3 *M* $NaClO_4$ the reduction in ionic strength would permit measurements to be made at higher concentrations in the region of extensive hydrolysis without precipitation occurring.

Tin 119 NMR studies on the hydrolysis intermediate with the stoichiometry $((CH_3)_2SnCl)_2O$ have indicated that the tin atoms are found with two different configurations. It was originally suggested that this compound was a tristannoxane (11), but further studies indicated that it was dimeric in benzene, and structures I and II were suggested

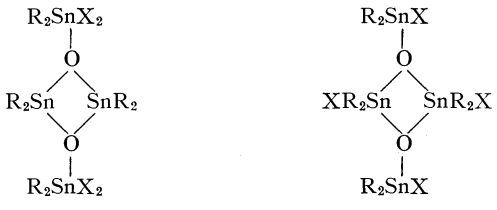

I II

(12). In addition, it has been reported that a single crystal X-ray study of tetramethyl-1, 3-bistrimethylsiloxydistannoxane shows that the tin and oxygen positions are those

suggested in structures I and II (13). Alleston *et al.* (12) also observed that compounds with the stoichiometry $R_4Sn_2X(OH)O$ are formed, and structures III and IV have been suggested for these.

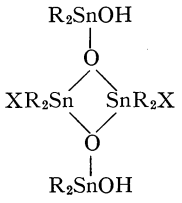

III

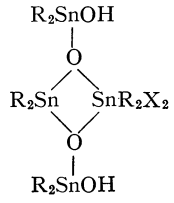

IV

It was hoped that our studies on solutions of dimethyltin dichloride would shed more light on the processes by which these stannoxanes are formed during the hydrolysis. In addition, we have gained access to a Control Data Corporation 1604 computer since our original studies on perchlorate solutions were completed, and this permits us to subject all of our data to a much more rigorous evaluation.

EXPERIMENTAL

Solution Preparation

Solutions of dimethyltin dichloride were prepared by dissolving weighed amounts of $(CH_3)_2SnCl_2$ in distilled water. Hydrochloric acid was standardized against Na_2CO_3 and was added to the stock solution to give a hydrogen ion concentration of ca. 0.2 *M*. The $(CH_3)_2SnCl_2$ was obtained from M and T Chemicals, Inc., New York, and was recrystallized twice from benzene. Anal. Calculated: C 10.94, H 2.75. Found: C 10.94, H 2.82%.

Standard sodium hydrogen carbonate, sodium hydroxide, and sodium chloride solutions were prepared from reagent grade chemicals.

Apparatus and Procedure for Solution Measurements

The hydrogen ion concentration of the solutions was determined with the cell Ag|AgCl|100 m*M* NaCl satd. with AgCl||100 m*M* NaCl||*B* m*M* $[(CH_3)_2Sn]^{+2}$, *H* m*M* H^+, (100−2*B*−*H*) m*M* Na^+, 100 m*M* Cl^-|glass electrode. A Beckman type 40498 glass electrode was used. The glass electrode system was calibrated as a hydrogen ion concentration probe in the range $1.0 \leqslant pH \leqslant 4.0$ by measuring the cell e.m.f. during the titration of hydrochloric acid with sodium hydrogen carbonate and sodium hydroxide solutions. Deviations from ideal behavior are considerably more pronounced in dilute ionic media such as employed here than in the more concentrated media like 3 *M* $NaClO_4$. The potentials are described by the equation $E_g = E' + 59.15 \log [H^+]$. The quantity E' was fitted by least squares to an equation quadratic in $[H^+]$, $E' = E^0 - 0.524 [H^+] + 0.00204 [H^+]^2$; concentrations in m*M*. The apparatus and the general experimental procedure have been described earlier (7).

X-Ray Powder Patterns

All X-ray patterns were taken with a General Electric XRD-3 diffractometer using copper $K\alpha$ radiation.

Infrared Spectra

All infrared spectra were determined with a Perkin Elmer 21 spectrometer equipped with NaCl optics. The split mull technique was employed, using fluorocarbon from 4000 to 1325 cm^{-1} and Nujol from 1325 to 650 cm^{-1}.

Reaction of Dimethyltin Dichloride with Sodium Hydroxide

Ten grams of $(CH_3)_2SnCl_2$ was dissolved in 100 ml of 0.1 *M* NaCl, and NaOH solution was added until the mole ratio of $(CH_3)_2SnCl_2$ to NaOH was 1:1. The white precipitate which formed was filtered by suction, washed with water, and dried over $CaCl_2$. This product was only slightly soluble in benzene or ethanol. Anal. Calculated for $((CH_3)_2SnCl)_2O$: Sn 62.3, C 12.50, H 3.15. Calculated for $((CH_3)_2Sn)_3Cl_2O_2$: Sn 64.9, C 13.10, H 3.31%. Found: C 12.56, H 3.31. The infrared spectrum of the product showed absorption at 2980 and 2900 (C—H str.), 1410 (w. asym. methyl def.), 1197 (s) and 1193 (m) methyl def., at 960, and at 783 (s), 720, and 704 cm^{-1} (CH_3—Sn rock). There was no evidence for an O—H stretch.

Reaction of Dimethyltin Dichloride with Dimethyltin Oxide

A solution was prepared by dissolving 1.1 g of $(CH_3)_2SnCl_2$ in 300 ml of 95% ethanol and adding 0.83 g of $(CH_3)_2SnO$ to give a mole ratio of $(CH_3)_2SnCl_2$ to $(CH_3)_2SnO$ of 1:1. After heating for 3 hours on a hot plate, the unreacted $(CH_3)_2SnO$ was filtered off, the filtrate was evaporated to 100 ml, and the white product

Can. J. Chem. Downloaded from www.nrcresearchpress.com by 210.87.254.6 on 09/05/12
For personal use only.

filtered by suction. This product was only slightly soluble in benzene. Anal. Found: Sn 63.1, C 12.78, H 3.18. The X-ray powder pattern for this compound was identical with that of the compound described above which had been precipitated from aqueous solution and also different from that of either of the starting materials. The infrared spectrum of the product showed absorption at 2980, 2900, 1410 (w), 1196 (s), 1193 (m), 968 (w), 780 (s), 720 (m), and 702 (m) cm^{-1}.

$(CH_3)_2SnCl_2$ and $(CH_3)_2SnO$ were reacted in a 1:1 mole ratio in hot benzene, and the product was separated after filtration and evaporation of a portion of the solvent. This compound was readily soluble in benzene. Anal. Found: Sn 62.3, C 12.68, H 3.14%. The infrared spectrum showed absorption at 2980, 2900, 1407 (w), 1200 (s), 1197 (m), 970 (w), 795 (s), and 725 (m) cm^{-1}.

The above reaction was also carried out in absolute ethanol, the hot solution was filtered after 15 minutes, and the product was obtained by evaporation of a part of the solvent. This product was also very soluble in benzene. The X-ray powder patterns of these last two compounds prepared under anhydrous conditions were identical and somewhat different from that of the first two compounds prepared in the presence of water. Anal. Found: Sn 63.3, C 12.84, H 3.19%. The infrared spectrum showed absorption at 2900, 1405 (w), 1200 (s), 1195 (m), 970 (w), 790 (s), and 725 (m) cm^{-1}.

TREATMENT OF DATA

Hydroxo Complexing

The nomenclature used in the description of the equilibrium constants is that of the Chemical Society Tables (14). The total dimethyltin dichloride concentration was held constant during the determination of the individual $\bar{n}(\log [H^+])_B$ curves. Here $\bar{n}$ is the average number of hydroxo groups bound (or protons transferred) per dimethyltin(IV) group in the solution, and B is the total dimethyltin dichloride concentration. Runs were made with 30.6, 20.4, 10.2, 5.1, and 2.55 mM $(CH_3)_2SnCl_2$. Duplicate runs were made with the three lowest concentrations. In contrast to the studies with the 3 M perchlorate medium (7), no precipitation was observed with $B \leqslant 20$ mM. The data are illustrated in Fig. 1. The general character of the curves is similar to that for the 3 M perchlorate

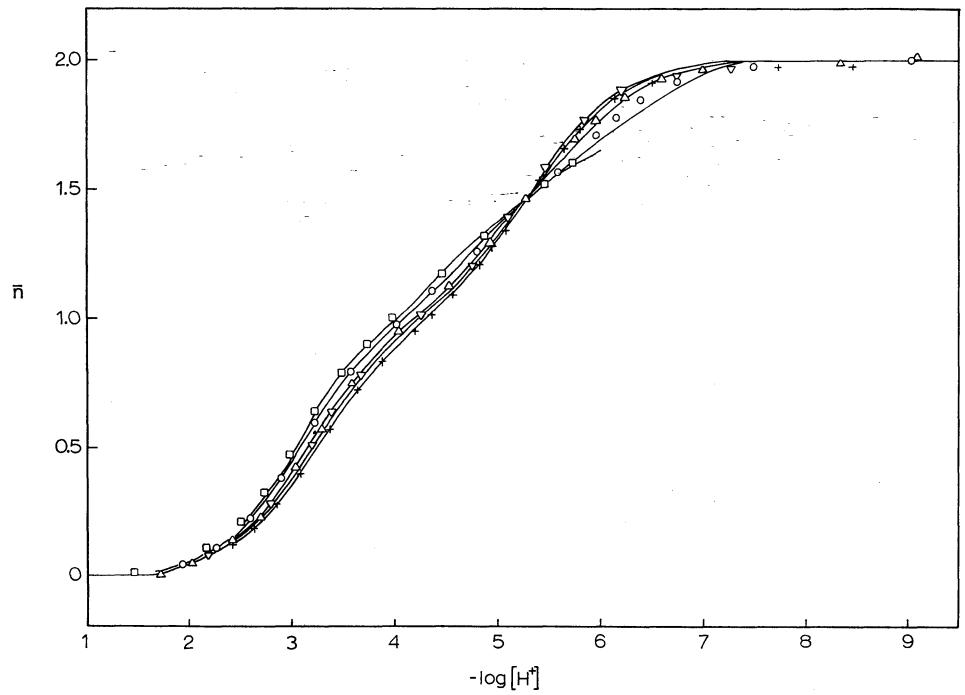

FIG. 1. Average number of protons transferred per dimethyltin(IV), $\bar{n}$, as a function of $-\log [H^+]$. Only about one-fifth of the data items are shown. □ 30.6 mM, ○ 20.4 mM, △ 10.2 mM, ▽ 5.1 mM, × 2.55 mM $(CH_3)_2SnCl_2$. Curves drawn with set of four constants (1, 1), (2, 2), (2, 1), (6, 4) given in Table I.

Can. J. Chem. Downloaded from www.nrcresearchpress.com by 210.87.254.6 on 09/05/12
For personal use only.

medium, although it is immediately obvious that the dependence on the total dimethyltin ion concentration is much reduced. There is thus considerably less tendency to form polycondensed species in the chloride medium. The "isohydric" or crossover point (15) occurs at the same $\bar{n}$ value of 1.43, although the isohydric pH is shifted about 0.3 unit lower. This indicates that essentially the same species, aside from complexing by the medium ions, are formed in both the chloride and perchlorate solutions from pH 1 to 9.

Trial values for the equilibrium constants were obtained by curve fitting procedures. As has been observed for measurements in 3 M $NaClO_4$ (7) and in 0.1 M KNO_3 (16), the data up to $\bar{n} \leqslant 0.8$ could be fitted well in terms of two constants for the formation of $(CH_3)_2SnOH^+$ (1, 1) and the dimer $((CH_3)_2SnOH)_2^{+2}$ (2, 2). Trial values for $^*\beta_{11}$ and $^*\beta_{22}$, the equilibrium constants for reactions 2 and 3, were obtained by fitting the data $\log B(\log [H^+])_{\bar{n}}$ with normalized projection maps (7). The values $\log {}^*\beta_{11} = -3.2$ and $\log {}^*\beta_{22} = -4.9$ were obtained.

$$(CH_3)_2Sn^{+2} + H_2O = (CH_3)_2SnOH^+ + H^+ \quad [2]$$

$$2(CH_3)_2Sn^{+2} + 2H_2O = (CH_3)_2Sn(OH)_2Sn(CH_3)_2^{+2} + 2H^+ \quad [3]$$

At $\bar{n}$ values of from ca. 1 to 2, the predominant species is the uncharged dimethyltin dihydroxide. The trial value for the equilibrium constant $^*\beta_{21}$ for reaction 4 was obtained

$$(CH_3)_2Sn^{+2} + 2H_2O = (CH_3)_2Sn(OH)_2 + 2H^+ \quad [4]$$

from the value of $^*\beta_{11}$ estimated above and the $\bar{n}$ and $[H^+]$ values at the isohydric point according to the relation in [5]. The estimated value of $\log {}^*\beta_{21}$ was -8.6.

$$\bar{n}_{\text{mono}} = \frac{\beta_{11}[H^+]^{-1} + 2\beta_{21}[H^+]^{-2}}{1 + \beta_{11}[H^+]^{-1} + \beta_{21}[H^+]^{-2}} \quad [5]$$

It should be pointed out that since the measurements have been made in media with $NaClO_4$ or with NaCl as the supporting electrolyte, a concentration term such as $[(CH_3)_2SnOH^+]$ actually refers to the sum of the concentrations of several different structural entities, namely, to $\sum_x \sum_y \sum_z [(CH_3)_2SnOH(OH_2)_x(Na^+)_y(ClO_4)_z]^{+(y+1-z)}$ and $\sum_x \sum_y \sum_z [(CH_3)_2SnOH(OH_2)_x(Na^+)_y(Cl^-)_z]^{+(y+1-z)}$, respectively. In the case of measurements with perchlorate media, one generally assumes no appreciable complexing by the medium ions. On the other hand, with a chloride medium a measurable degree of complexing by chloride ions might be expected.

The data at the higher concentrations of the dimethyltin ion indicate that complexes larger than the dimer are formed at $\bar{n}$ values greater than ca. 0.8. In the earlier analysis of the perchlorate data (7), the data in this region were fitted fairly well by the inclusion of equilibrium constants for the formation of two additional species (3, 2) and (4, 3) formed according to equations 6 and 7. There was also some indication that the data

$$2(CH_3)_2Sn^{+2} + 3H_2O = ((CH_3)_2Sn)_2(OH)_3^+ + 3H^+ \quad [6]$$

$$3(CH_3)_2Sn^{+2} + 4H_2O = ((CH_3)_2Sn)_3(OH)_4^{+2} + 4H^+ \quad [7]$$

might also be fitted by adding an equilibrium constant for a (6, 4) complex formed according to equation 8 rather than by adding the constants for the (3, 2) and (4, 3) complexes. Because of the difficulty involved in the calculation of projection maps to try to fit the

$$4(CH_3)_2Sn^{+2} + 6H_2O = ((CH_3)_2Sn)_4(OH)_6^{+2} + 6H^+ \quad [8]$$

data in terms of the set of complexes (1, 1), (2, 2), (2, 1), and (6, 4), it was not feasible earlier to carry out a thorough test of this set of complexes using only a desk calculator.

Can. J. Chem. Downloaded from www.nrcresearchpress.com by 210.87.254.6 on 09/05/12
For personal use only.

The trial values of the constants for the (1, 1), (2, 2), and (2, 1) complexes together with estimated values for the higher constants were used as input to a least squares parameter refinement program for the CDC-1604 computer. Both the 394 chloride and 762 perchlorate data sets were refined. A brief description of some of the Fortran 60 programs used has been given (17). Initially the response surface (MAP Z) or "pit mapping" type of program (18) which adjusts the constants so as to minimize the sum of the squares of the residuals ($\bar{n}_{calcd} - \bar{n}_{exptl}$) was used. Subsequently, it was found that the Gauss method of least squares parameter refinement (19) was much faster, and a program (GAUSS Z) was written to carry out these calculations. This program was similar to the Gauss method program described earlier (17) with the exception that it also minimized the sum of the squares of the residuals in $\bar{n}$ as does MAP Z.[3] The advantage of the higher speed of the Gauss method refinement was quite important with the large numbers of data items involved in these refinements.

It was found that equally good fits to both the chloride and perchlorate data could be obtained with the two sets of complexes ((1, 1), (2, 2), (2, 1), (6, 4)) and ((1, 1), (2, 2), (2, 1), (3, 2), (4, 3)). A survey of the values obtained by the least squares refinement is given in Table I, which gives the constants, their standard errors, σ, and the standard

TABLE I

Survey of the refined values of the equilibrium constants for the dimethyltin(IV) hydrolysis

Medium	0.1 *M* (NaCl)		3 *M* (Na)ClO_4	
log $*\beta_{11}$	−3.251±0.004	−3.245±0.004	−3.54±0.01	−3.55±0.01
log $*\beta_{22}$	−5.05±0.02	−5.00±0.02	−4.60±0.02	−4.52±0.01
log $*\beta_{21}$	−8.535±0.005	−8.516±0.004	−8.98±0.01	−9.00±0.01
log $*\beta_{32}$	−9.81±0.01	—	−9.76±0.06	—
log $*\beta_{43}$	−11.52±0.03	—	−10.40±0.05	—
log $*\beta_{64}$	—	−16.85±0.02	—	−16.14±0.03
log K_d	+1.45	+1.48	+2.48	+2.58
log $*K_{21}$	−5.284	−5.271	−5.44	−5.45
$\sigma_{\bar{n}}$	±0.015	±0.015	±0.035	±0.034

errors to the fit, $\sigma_{\bar{n}}$. Since there were 762 data items in the perchlorate set and 394 in the chloride set, tables of the t test of significance can be entered at an infinite number of degrees of freedom, so the errors at the 95% confidence limit are ±1.960 σ and at the 99% confidence limit are ±2.576 σ (20). Figures 2 and 3 give the least squares residuals ($\bar{n}_{calcd} - \bar{n}_{exptl}$) for the chloride data and the four- and five-parameter fits, respectively.

It is virtually certain that the same hydroxo complexes are formed in both the perchlorate and chloride media, and there is no question about the existence of the (1, 1), (2, 2), and (2, 1) complexes. Without these species, it is impossible to begin to reproduce the experimental data. There is some question about the nature of the larger complexes formed, since only a small fraction of the dimethyltin(IV) is distributed in these species except for a very short pH range before precipitation. As Dunsmore *et al.* (21) have pointed out, it is almost always possible to discern the principal complexes, and in general one tries to reproduce the small systematic deviations caused by additional complexes with the minimum number of additional parameters. Here it is difficult to choose between the fits with the sets of four and five parameters. Neither set reproduces the data ideally about the isohydric point. The variance to the fit is essentially the same with both sets.

[3]*Complete deck listings, duplicate program decks, and flow sheets for both MAP Z and GAUSS Z may be obtained by writing to R.S.T.*

Can. J. Chem. Downloaded from www.nrcresearchpress.com by 210.87.254.6 on 09/05/12
For personal use only.

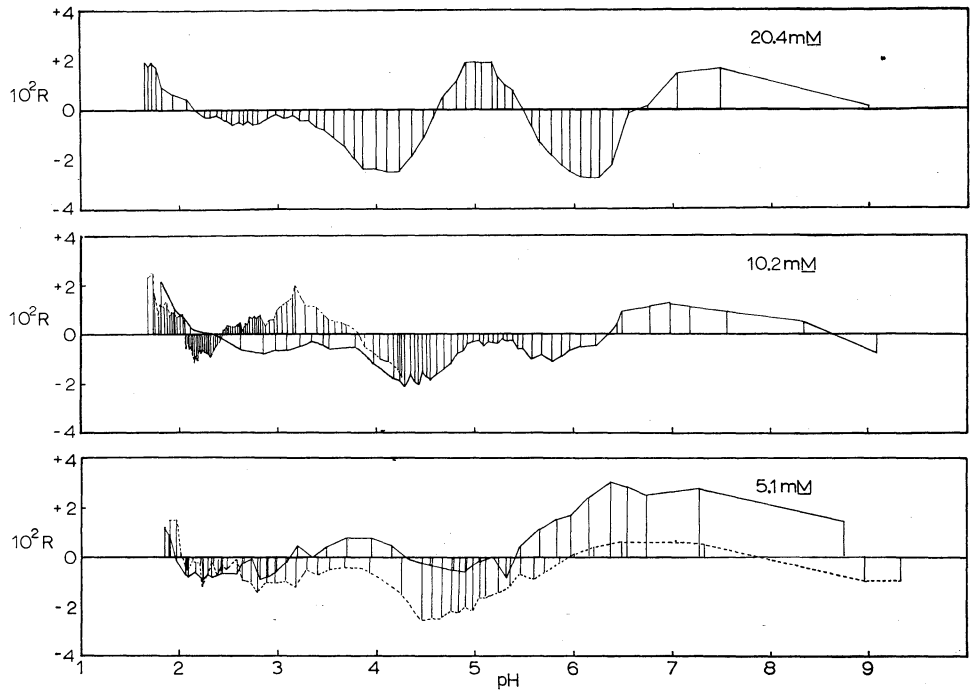

FIG. 2. Least squares residuals, $\bar{n}_{calcd} - \bar{n}_{exptl}$, for the fit with four parameters. Measurements in the 0.1 *M* Cl^- medium.

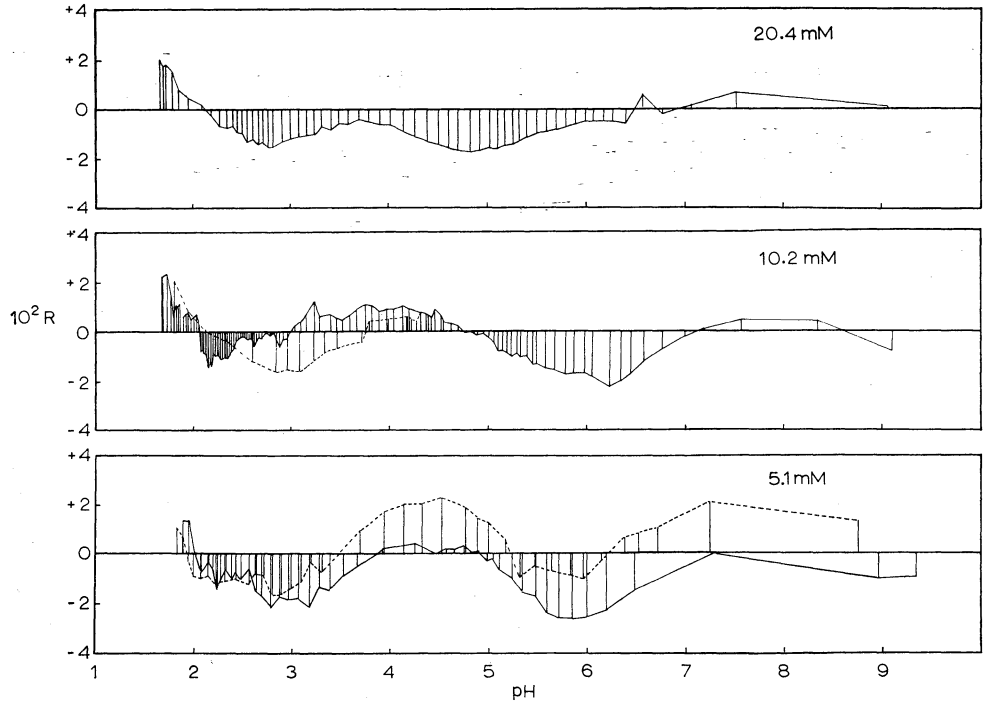

FIG. 3. Least squares residuals, $\bar{n}_{calcd} - \bar{n}_{exptl}$, for the fit with five parameters. Measurements in the 0.1 *M* Cl^- medium.

Can. J. Chem. Downloaded from www.nrcresearchpress.com by 210.87.254.6 on 09/05/12
For personal use only.

The problem is that there is no independent way to determine the correct number of parameters, and there may be several additional complexes present in low concentrations just before the precipitation pH is reached.

Chloro-Complexing of the Aquodimethyltin(IV) Ion

The definite differences observed in the values of the equilibrium constants determined for the two different ionic media can be ascribed to two effects. The first is a result of definite chloro-complexing of the different dimethyltin(IV) species, while the second is a result of changes in activity coefficients due to all other factors. There is no indication in the literature of the magnitude of chloro-complexing of the aquodimethyltin(IV) ion except that it must be rather small. If one considers the difference in the values of log $*\beta_{11}$ in a 0.1 M KNO_3 medium (16, 17) (-3.13 ± 0.02) and in the 0.1 M NaCl medium (3.26 ±0.004) to be caused only by chloro-complexing, an estimate of the degree of complexing can be made. It seems logical to assume that the constant for the first chloro complex of the dipositive ion $(CH_3)_2Sn^{+2}$ should be much larger than for the first chloro complex of the unipositive ion $(CH_3)_2SnOH^+$. If this be true, then the following relation obtains.

$$\log *\beta'_{11} = \log *\beta_{11} - \log \alpha^0 \qquad [9]$$

Here, $*\beta'_{11}$ is the hydrolysis constant for the nitrate medium, $*\beta_{11}$ is for the chloride medium, and α^0 is the fraction of the unhydrolyzed dimethyltin(IV) in a 0.1 M chloride medium which is present as the free aquo ion. This gives an estimate of $\log \alpha^0 = -0.13$, $\alpha^0 = 0.74 = [(CH_3)_2Sn(OH_2)_n^{+2}]/[(CH_3)_2Sn^{+2}]_{total}$. Thus it appears that complexing of the dimethyltin ion by chloride ion is not extensive. With the assumption that chloro-complexing of the unipositive $(CH_3)_2SnOH^+$ is much less than that for the dipositive ion $(CH_3)_2Sn^{+2}$, the first chloro-complexing constant can be estimated to be $\beta_1 = \alpha^0/(1-\alpha^0)$ [Cl] = 28 l. mole^{-1}.

There are indications that the assumption that chloro-complexing of $(CH_3)_2SnOH^+$ is small is valid; for the constant for the dimerization of this complex according to equation [10], K_d, is approximately the same in the 0.1 M chloride medium ($\log K_d = 1.45$ to 1.48)

$$2(CH_3)_2SnOH^+ = (CH_3)_2Sn(OH)_2Sn(CH_3)_2^{+2} \qquad [10]$$

as it is in the 0.1 M nitrate medium ($\log K_d = 1.3$ to 1.6 (17)). Although it is questionable just how much reliance can be placed in the value of the first chloro-complexing constant, it appears to be of the right order of magnitude. For Sn^{+2}, the value for β_1 determined at 25° in a 3 M $NaClO_4$ medium is 15.1 l. mole^{-1} (22); this value should increase with a decrease in the ionic strength; and finally it would be expected that the value for $(CH_3)_2Sn^{+2}$ would be somewhat larger. Efforts made to determine the chloride complexing constants independently were without success. No bands attributable to halide complexing were found in the ultraviolet spectrum of solutions of dimethyltin dihalides with varying concentrations of the sodium halide. In addition, attempts were made to determine these constants by the method of ligand displacement with thio-Michler's ketone as a means of determining the concentration of the dimethyltin cation spectrophotometrically (23), but the solubility of the ketone in water proved to be too low.

Preparative Studies

The X-ray powder patterns for the two compounds prepared by precipitation from the aqueous solution of dimethyltin dichloride with NaOH and by the direct reaction of dimethyltin dichloride with dimethyltin oxide in 95% ethanol were identical and different from either of the starting materials. The analysis of these compounds indicates a slightly

Can. J. Chem. Downloaded from www.nrcresearchpress.com by 210.87.254.6 on 09/05/12
For personal use only.

more hydrolyzed compound than $((CH_3)_2SnCl)_2O$. The patterns for the compounds prepared by direct reaction of the oxide and chloride in benzene or anhydrous ethanol were also identical but slightly different from that of the first compound. The latter compound was quite soluble in benzene, and it is apparently the one studied by Harada (4, 5) and by Alleston *et al.* (11, 12).

There was no evidence from the infrared spectrum that the compound precipitated from aqueous solution contained hydroxo groups after it had been dried over $CaCl_2$. It has, however, been reported that the hydroxo compounds such as $(CH_3)_4Sn_2Cl(OH)O$ dehydrate readily (12). In all cases, the infrared spectra were essentially that given by Brown, Okawara, and Rochow for $(CH_3)_4Sn_2Cl_2O$ (24). This spectrum differs from the oxide mainly in that the band due to the symmetrical methyl deformation at ca. 1200 cm^{-1} is split into two sharp bands in the oxide at 1206 and 1188 cm^{-1} while in the chlorostannoxanes the splitting is much less and the bands are at ca. 1200 and 1196 cm^{-1}.

DISCUSSION

When $(CH_3)_2SnCl_2$ is dissolved to give a dilute solution, almost all of the dimethyltin(IV) in the solution is found in the simple aquo ion. It seems likely that tin is essentially tetrahedrally coordinated in the solution and so the aquo ion is $(CH_3)_2Sn(OH_2)_2^{+2}$. In contrast to the hypothetical silicon analog, this ion is a rather weak aquo acid. If base is added to the solution, most of the aquodimethyltin(IV) is converted to the mono- and then to the neutral di-hydroxo complexes by simple proton transfer reactions. As the concentration of the dimethyltin ion is increased, more of the simple conjugate base $(CH_3)_2Sn(OH)(OH_2)^+$ is converted to the dimer which probably has the structure V. The

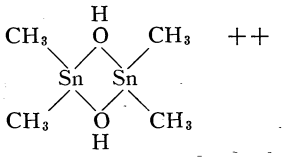

V

basic bridge structure indicated here has been shown to exist in the tetramethyl 1,3-trimethylsiloxydistannoxane (13). If oxygen–tin p_π–d_π bonding were appreciable, such a bridge with ca. 90° Sn—O—Sn angles would not be favored. Since the metal oxygen bonds are not nearly so strong with tin as with silicon, the bridging oxygens are protonated. Thus the stability of the di-μ-hydroxo bridges which satisfy the tetrahedral coordination of tin and hence inhibit the formation of long polycondensed chains is a result of the absence of substantial π bonding. If the hydrolysis is carried to $\bar{n}$ values of 1 and greater by increasing the pH, it should be possible to remove some of the protons on the bridging hydroxo groups. These oxygens could then function as donor atoms replacing water molecules in $(CH_3)_2Sn(OH)(OH_2)^+$ ions. If one proton in I were replaced by the monohydroxo complex, the (4, 3) complex $((CH_3)_2Sn)_3(OH)_4^{+2}$ would be produced while if both protons were replaced the (6, 4) complex $((CH_3)_2Sn)_4(OH)_6^{+2}$ would be produced. The latter complex corresponds to the intermediate described by Alleston *et al.* (12), III and IV. Since the variances to the fits given in Table I for hypotheses including the formation of each of these complexes were the same, there is no clear choice between them; and indeed it is quite possible that both are formed. Finally as the pH approaches 7, the simple monohydroxo complex is converted by a second proton transfer to the dihydroxo complex. Since the complexes are quite labile, this results in the depolymerization of the

Can. J. Chem. Downloaded from www.nrcresearchpress.com by 210.87.254.6 on 09/05/12
For personal use only.

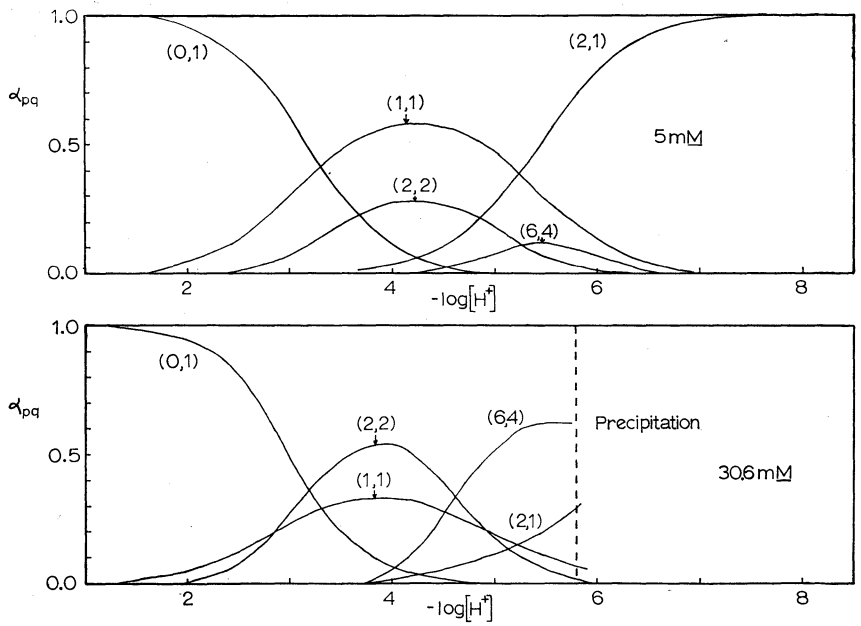

FIG. 4. Distribution of the hydrolysis products in the 0.1 *M* Cl^- medium. Upper curves 5 m*M*, lower curves 30.6 m*M*.

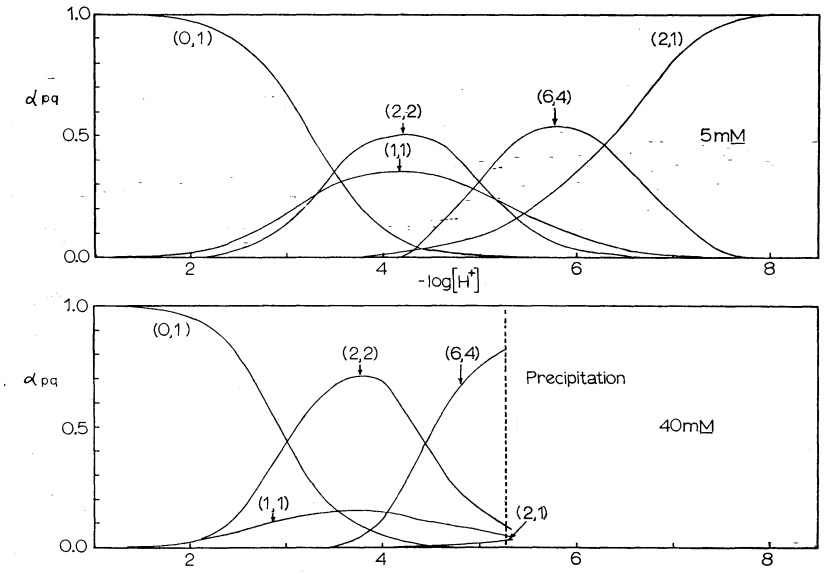

FIG 5. Distribution of the hydrolysis products in the 3.0 *M* ClO_4^- medium. Upper curves 5 m*M*, lower curves 40 m*M*.

larger condensed species; and at pH 9 only the neutral hydroxide exists in the solutions. Figures 4 and 5 illustrate the distribution of hydrolysis products in the 0.1 *M* Cl^- and 3 *M* ClO_4^- media respectively.

The much smaller values for the dimerization constant found for the 0.1 *M* chloride

Can. J. Chem. Downloaded from www.nrcresearchpress.com by 210.87.254.6 on 09/05/12
For personal use only.

and nitrate media compared to the value in 3 M $NaClO_4$ point up the tendency of the concentrated ionic media to stabilize charged polycondensed species.

The white solid which precipitates from the more concentrated solutions is very similar to the compound obtained by reaction of equimolar quantities of $(CH_3)_2SnCl_2$ and $(CH_3)_2SnO$ under anhydrous conditions, although it corresponds to a slightly more hydrolyzed intermediate than $((CH_3)_2SnCl)_2O$. Since no evidence for hydroxo groups was found, additional condensation may occur during the isolation of this product. This would be in accord with the lower solubility found for this product compared to that obtained by reaction in benzene.

The approximate value for the chloro-complexing constant for $(CH_3)_2Sn^{+2}$ was slightly greater than the comparable constant for Sn^{+2} just as it has been observed that the first proton transfer constant for $(CH_3)_2Sn^{+2}$ is slightly greater than the corresponding constant for Sn^{+2} (7). This is to be expected, for the pair of 5*s* electrons should lead to a weakening of the tin ligand bond in tin(II). The fact that these two ions have such similar values can be attributed to the distortions from spherical symmetry which occur with the tin(II) ion (25) which should lead to bonds of comparable strength to those of the dimethyltin(IV) ion.

REFERENCES

1. E. G. Rochow and D. Seyferth. J. Am. Chem. Soc. **75**, 2877 (1953).
2. A. B. Thomas and E. G. Rochow. J. Am. Chem. Soc. **79**, 1843 (1957).
3. K. Gingold, E. G. Rochow, D. Seyferth, A. C. Smith, Jr., and R. West. J. Am. Chem. Soc. **74**, 6306 (1954).
4. T. Harada. J. Sci. Res. Inst. (Tokyo), **35**, 318 (1939).
5. T. Harada. J. Sci. Res. Inst. (Tokyo), **42**, 57, 64 (1947).
6. R. K. Ingham and H. Gilman. Inorganic Polymers. *Edited by* F. G. A. Stone and W. A. G. Graham. Academic Press, New York. 1962. p. 368.
7. R. S. Tobias, I. Ogrins, and B. A. Nevett. Inorg. Chem. **1**, 638 (1962).
8. E. G. Rochow, D. Seyferth, and A. C. Smith, Jr. J. Am. Chem. Soc. **75**, 3099 (1953).
9. R. S. Tobias. Acta Chem. Scand. **12**, 198 (1958).
10. J. D. Donaldson and W. Moser. J. Chem. Soc. 1996 (1961).
11. D. L. Alleston, A. G. Davies, and B. N. Figgis. Angew. Chem. **73**, 683 (1961).
12. D. L. Alleston, A. G. Davies, and B. N. Figgis. Proc. Chem. Soc. 457 (1961).
13. R. Okawara. Proc. Chem. Soc. 383 (1961).
14. J. Bjerrum, G. Schwarzenbach, and L. G. Sillen. Stability constants of metal-ion complexes with solubility products of inorganic substances. Part II, Inorganic ligands. Special Publication No. 7, The Chemical Society, London. 1958. p. xi.
15. F. J. C. Rossotti and H. S. Rossotti. The determination of stability constants. McGraw Hill Book Co., New York. 1961. p. 372.
16. M. Yasuda and R. S. Tobias. Inorg. Chem. **2**, 207 (1963).
17. R. S. Tobias and M. Yasuda. Inorg. Chem. 1307 (1963).
18. L. G. Sillén. Acta Chem. Scand. **16**, 159 (1962).
19. J. C. Sullivan, J. Rydberg, and W. F. Miller. Acta Chem. Scand. **13**, 2023 (1959).
20. R. A. Fisher. Statistical methods for research workers. Hafner Publishing Company, New York. 1954. p. 174.
21. H. S. Dunsmore, S. Hietanen, and L. G. Sillén. Acta Chem. Scand. In press (1964).
22. R. S. Tobias and Z. Z. Hugus. J. Phys. Chem. **65**, 215 (1961).
23. M. Schellenberg and G. Schwarzenbach. Proceedings of the Seventh International Conference on Coordination Chemistry, Stockholm, Sweden. 1962. p. 157.
24. M. P. Brown, R. Okawara, and E. G. Rochow. Spectrochim. Acta, **16**, 595 (1960).
25. L. E. Orgel. J. Chem. Soc. 3815 (1959).

Can. J. Chem. Downloaded from www.nrcresearchpress.com by 210.87.254.6 on 09/05/12
For personal use only.

THE EFFECT OF WATER VAPOR UPON THE DEHYDRATION OF $CaSO_4.2H_2O$

H. G. McAdie
Department of Physical Chemistry, Ontario Research Foundation, Toronto, Ontario
Received August 21, 1963

ABSTRACT

Kinetics of the two-stage dehydration of $CaSO_4.2H_2O$ have been examined under controlled water vapor pressures up to one atmosphere. For both stages water vapor initially accelerated the rate of dehydration and subsequently retarded it. Separate, temperature-dependent water vapor pressures were noted above which each stage could be suppressed.

The hemihydrate was clearly defined either as a change in the rate of weight loss during dehydration or, at higher water vapor pressures, as a fixed composition. The heat of solution of the hemihydrate increased linearly with the partial water vapor pressure present during its formation, but was independent of the formation temperature over the range studied. Activation energy and pre-exponential factor for the dihydrate → hemihydrate process also increased linearly with water vapor pressure. Hemihydrates produced at the extremes of water vapor pressure corresponded to the α- and β-modifications, as defined thermodynamically, and the production of a hemihydrate series with properties varying linearly from one extreme to the other is discussed.

Can. J. Chem. Downloaded from www.nrcresearchpress.com by 210.87.254.40 on 09/05/12
For personal use only.

The dehydration of calcium sulphate dihydrate (gypsum) has been studied for decades by many investigators, few of whom have made provision for controlling the partial water vapor pressure during dehydration. No systematic study of its kinetic influence has been reported, although Weiser and co-workers (1, 2) clearly demonstrated the importance of such isobaric studies to a proper understanding of the system.

Despite earlier controversy (3) the combination of evidence now available (1, 2, 4–8) has established the existence of the hemihydrate as the lower hydrate in the $CaSO_4$–H_2O system. However, the composition in terms of water of hydration can be variable over rather wide limits and has led to speculation that there may exist a zeolitic type of structure rather than that of a true hydrate. Clarification has recently been obtained from nuclear magnetic resonance results (5), showing the hemihydrate to contain definite crystal water as well as a variable quantity of relatively free water "occluded" within the crystal lattice. Two modifications of the hemihydrate are known, differing in thermodynamic properties (4), although being structurally quite similar (9, 10). Speculation that these differences reflect the degree of crystal lattice perfection has recently received support (6).

This paper will describe a systematic study of the influence of water vapor pressure upon the kinetics of the dehydration process and upon the thermodynamic properties of the hemihydrates obtained. Previous studies of these properties involved hemihydrates produced at the extreme conditions, i.e. under essentially anhydrous conditions or in an atmosphere saturated with water vapor, plus some commercial plasters produced under undefined partial water vapor pressures (4, 11). A later paper will discuss the influence of partial water vapor pressure upon such practical properties of the hemihydrate as gauging water requirement.

EXPERIMENTAL

Calcium sulphate dihydrate was precipitated slowly from equal volumes of 0.25 *M* calcium nitrate and sulphuric acid. The precipitate was filtered on sintered glass; washed with water, ethanol, ether; dried at 40° C for 1 hour; sieved; and the 60–80 mesh fraction retained. This material contained the theoretical water of crystallization, 20.93%, and appeared under the microscope to be polycrystalline.

For dehydration, 4-g samples were contained in a 3- to 4-mm annulus between two concentric 100-mesh copper gauze cylinders, 10 cm high and 4 cm o.d. The problem of vapor diffusion within the sample was greatly reduced by this arrangement and by the relatively large particle size of starting material. Using a constant initial weight, the reproducibility of *rate* of weight loss was found to be $\pm 1\%$.

The sample holder was suspended from an ordinary analytical balance by means of an iron–constantan duplex thermocouple wire, the junction being immersed within the powder mass. The dehydration was carried out in a vapor-jacketed cylindrical Pyrex oven in which the appropriate atmosphere was established by passing dry nitrogen directly or through water saturators maintained at the appropriate temperature. Heated lines were used to prevent condensation from the wet nitrogen stream and at flow rates of 50–100 cc min^{-1} the buoyancy correction was negligible.

The hemihydrate produced in each experiment was subsequently analyzed and the heat of solution in 2.0 *N* hydrochloric acid determined in a calorimeter described elsewhere (12). Debye–Scherrer powder patterns were obtained using CuK_α radiation with a nickel filter.

RESULTS

The fractional decomposition, α, was calculated in terms of the maximum possible water loss, so that

$$\alpha = (w_i - w_t)/(w_i - w_f)$$

where w_i = initial sample weight,
w_t = sample weight at any time t,
w_f = sample weight corresponding to complete water loss.

The two stages in the dehydration process:

I. $$CaSO_4.2H_2O\ (s) = CaSO_4.\tfrac{1}{2}H_2O\ (s) + 1\tfrac{1}{2}H_2O\ (v)$$

and

II. $$CaSO_4.\tfrac{1}{2}H_2O\ (s) = CaSO_4\ (s) + \tfrac{1}{2}H_2O\ (v)$$

were indicated in both fractional decomposition and sample temperature plots (Fig. 1), their respective rates being markedly influenced by the partial water vapor pressure (Figs. 2 and 3). Low partial water vapor pressures were found to catalyze both stages (Fig. 3), while further increase in water vapor pressure retarded stage II more rapidly than stage I. Above a definite water vapor pressure, dependent upon the dehydration temperature, no evidence of stage II was detected in the duration of the experiment, a higher water vapor pressure being required for suppression of stage I at the same temperature. Not all dehydration temperatures resulted in the clear-cut suppression of stage II indicated in Fig. 2. In some cases the sample was found to remain at the hemihydrate composition for a considerable period before commencing further loss of water. With increasing water vapor pressure, this induction period in stage II eventually increased to the point where no further reaction was observed. The induction period for stage I was relatively short, even at 1 atm of water vapor.

The calcium sulphate dihydrate used in this work was a polycrystalline material, having generally spherical-shaped particles, whose surface area was unknown except for the general estimate from screen-size data. In attempting to extract meaningful rate constants from the fractional decomposition plots several treatments were applied, including that of Spencer and Topley (13) for the case of rapid nucleation followed by rapid surface growth on spherical particles of known initial radius. The various treatments represented the data over a considerable range, but an equally extensive fit to the experimental points was obtained from the simple linear expression for a zero-order process

$$\alpha = kt.$$

Further, activation energies based on rate constants derived from these two treatments were virtually the same.

Can. J. Chem. Downloaded from www.nrcresearchpress.com by 210.87.254.40 on 09/05/12
For personal use only.

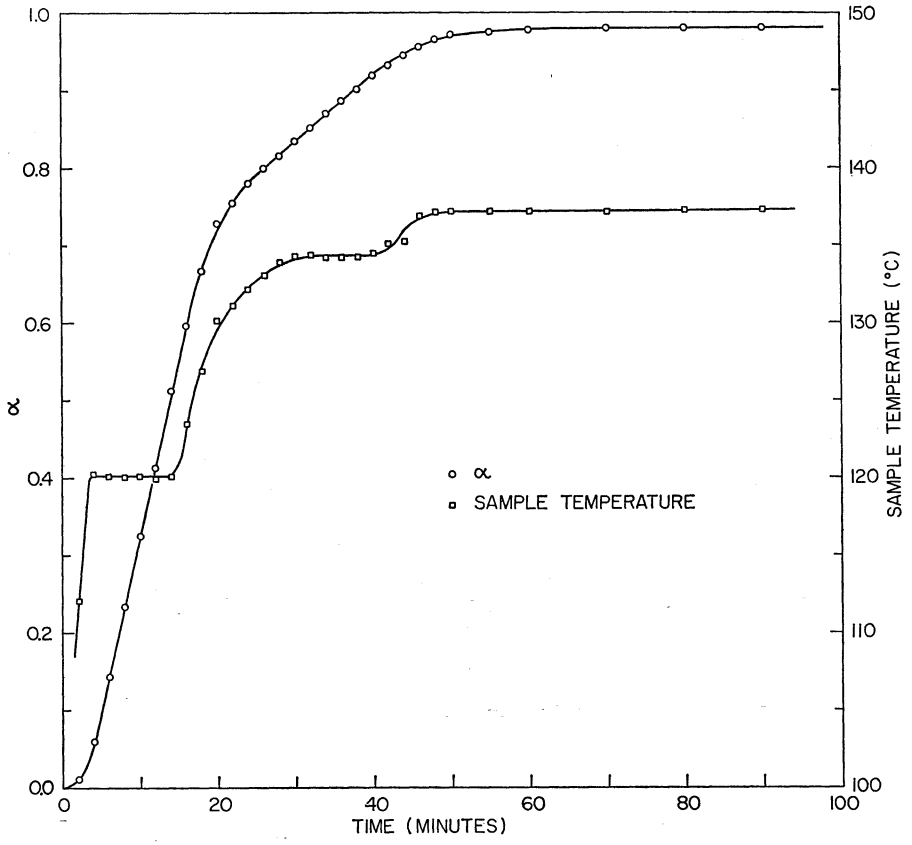

FIG. 1. Experimental fractional decomposition and sample temperature during dehydration at 139° C and 200 mm H_2O.

For simplicity, then, rate constants k_I and k_{II} were assigned for the two stages directly from the linear sections of the fractional decomposition plot, using the approach of Topley and Smith (14). These authors measured all rates at a definite fractional decomposition, and selected as *rate constant* the rate of weight loss at a given stage of decomposition divided by the original weight of the hydrate sample. Such a rate constant is empirical in nature, but has the merit of referring to a definite, although unknown, area of reaction interface and of largely standardizing any impedance effect of the product layer without eliminating it. For stage I, the rate constant and sample temperature were selected at $\alpha = 0.25$ and for stage II at $\alpha = 0.80$. Both these points lie on the respective temperature plateau for the two stages and within the linear regions of the α vs. t plots (Fig. 1), so that further normalization of the curves was unnecessary. The considerable range of dehydration over which the rate is constant indicates the "impedance" effect of the increasing product layer is not of great significance.

The plateau temperatures, T, as recorded by the thermocouple immersed in the sample mass, were considered to be representative of the overall reaction temperature. Care was taken to minimize differences due to packing of the sample and placement of the thermocouple.

The rate constants obtained, reaction temperatures, calculated activation energies, and Arrhenius pre-exponential factors are given in Tables I and II. Also included in Table

Can. J. Chem. Downloaded from www.nrcresearchpress.com by 210.87.254.40 on 09/05/12
For personal use only.

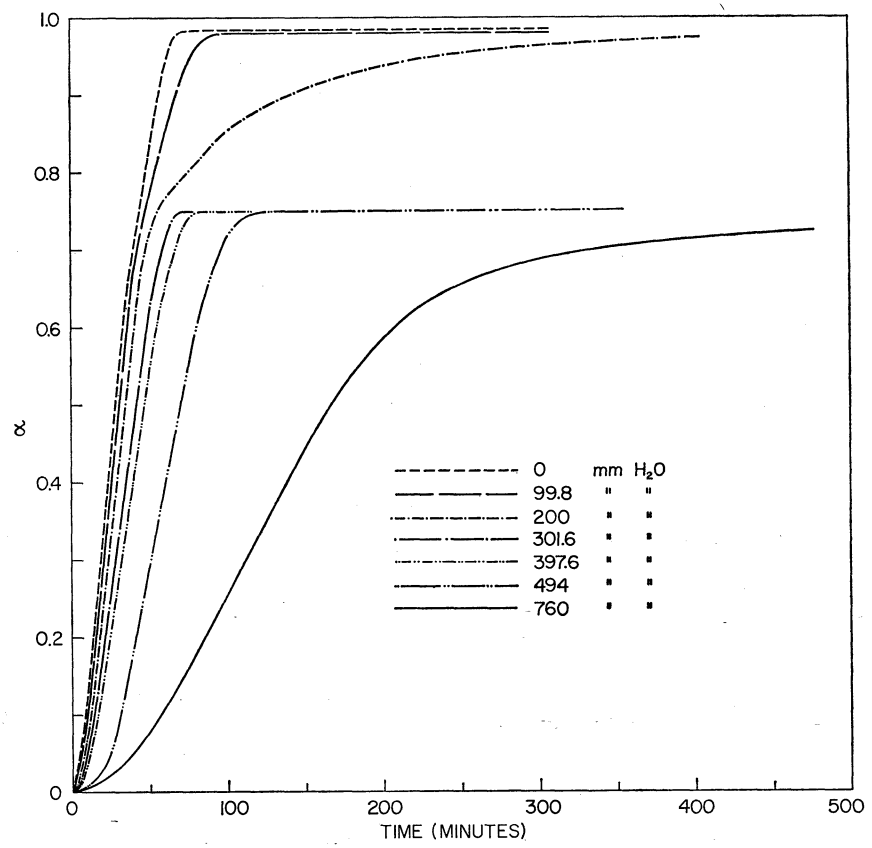

FIG. 2. Variation in fractional decomposition curves with ambient water vapor pressure during dehydration. Jacket temperature 124.3° C.

I are calorimetric heats of solution of the hemihydrates obtained at each partial water vapor pressure. The heat of solution of the hemihydrate was found to be independent of the temperature at which it was produced, over the range 100–140° C, provided the partial water vapor pressure in the system remained constant. In cases where dehydration ultimately resulted in the anhydrous calcium sulphate, a separate dehydration was performed later and the sample removed at a weight loss corresponding to the theoretical hemihydrate composition.

Debye–Scherrer patterns for calcium sulphate dihydrate and for hemihydrates produced under the two extremes of partial water vapor pressure, shown in Fig. 4, illustrate that no gross structural differences were found in the hemihydrates produced over the experimental range of water vapor pressures.

DISCUSSION

The dehydration of calcium sulphate dihydrate has been shown to begin by nucleation on the surface of the crystal at sites other than dislocations (15), followed by growth over the surface until discrete reaction areas overlap, propagation through the individual crystals also occurring along exfoliation planes (16). Representation of a considerable portion of the dehydration by the linear, zero-order relation found in the present work indicates this nucleation–propagation mechanism occurs on a substantially constant

Can. J. Chem. Downloaded from www.nrcresearchpress.com by 210.87.254.40 on 09/05/12
For personal use only.

Can. J. Chem. Downloaded from www.nrcresearchpress.com by 210.87.254.40 on 09/05/12
For personal use only.

TABLE I

Kinetic and thermodynamic parameters for stage I
$CaSO_4.2H_2O$ (s) = $CaSO_4.\frac{1}{2}H_2O$ (s) + $1\frac{1}{2}H_2O$ (v)

Jacket temp. (° C):	100.0		107.4		110.4		117.6		124.3		139.0				
Ambient P_{H_2O} (mm):	k_I	T, ° C	k_I	T, ° C	k_I	T, ° C	k_I	T, ° C	k_I	T, ° C	k_I	T, ° C	E, kcal mole^{-1} H_2O	$\log_{10} A$	ΔH solution kcal mole^{-1} $CaSO_4.\frac{1}{2}H_2O$
0.0	1.618	97.1	2.471	102.3	3.020	103.1	4.302	107.9	5.794	111.9	10.90	119.2	26.1	12.6	1.110
10.0	1.627	97.1	2.261	100.3	3.413	104.3	4.410	108.0	5.916	111.1	10.98	118.3	25.7	12.4	—
20.0	1.411	97.0	2.081	100.2	2.986	104.8	4.461	109.0	5.906	111.2	11.22	118.3	26.5	12.8	1.154
50.0	1.442	97.1	2.200	101.1	2.899	104.2	4.331	108.4	5.895	112.1	10.92	119.1	26.4	12.8	1.098
99.8	1.188	96.9	1.981	99.6	2.834	103.5	4.189	107.3	5.668	111.3	10.34	117.3	27.7	13.5	1.196
200.0	0.835	97.9	1.511	102.0	2.413	105.2	3.729	108.8	5.460	112.2	10.36	119.8	31.6	15.6	1.250
301.6	0.635	98.3	1.071	99.7	2.073	106.7	3.079	110.6	4.728	113.6	9.546	120.3	35.7	17.8	1.322
397.6	0.425	98.7	0.494	99.2	1.563	107.0	2.748	110.4	4.495	114.4	7.107	121.5	42.8	21.8	1.359
494	0.322	98.5	0.358	99.8	1.421	107.1	2.178	110.1	4.152	115.1	5.001	121.4	43.5	22.1	1.412
760	—	—	—	—	0.036	110.2	0.792	116.1	1.548	120.6	2.623	123.6	48.2	24.0	1.564

Can. J. Chem. Downloaded from www.nrcresearchpress.com by 210.87.254.40 on 09/05/12
For personal use only.

TABLE II

Kinetic and thermodynamic parameters for stage II
$CaSO_4.\frac{1}{2}H_2O$ (s) = $CaSO_4$ (s) + $\frac{1}{2}H_2O$ (v)

Jacket temp. (° C):	100.0		107.4		110.4		117.6		124.3		139.0			
Ambient P_{H_2O} (mm):	k_{II}	T, ° C	k_{II}	T, ° C	k_{II}	T, ° C	k_{II}	T, ° C	k_{II}	T, ° C	k_{II}	T, ° C	E kcal mole^{-1} H_2O	$\log_{10} A$
0.0	0.919	99.1	1.238	103.8	1.680	105.5	2.163	111.0	3.077	116.1	6.076	126.3	20.9	9.2
10.0	0.923	98.0	1.367	102.0	1.639	106.9	2.445	110.0	3.258	114.9	6.433	124.9	21.0	9.4
20.0	0.658	98.3	1.003	102.1	1.499	107.2	2.271	112.2	3.122	116.0	6.241	125.2	24.2	11.1
50.0	0.383	99.4	0.999	103.3	1.213	107.1	1.940	112.5	2.458	117.5	5.874	126.1	27.0	12.6
99.8	0.125	99.3	0.261	103.4	0.798	107.5	1.569	114.4	2.141	117.5	4.933	126.7	29.0	13.4
200.0	—	—	—	—	—	—	0.303	115.1	1.307	118.8	3.953	130.0	31.0	16.8
301.6	—	—	—	—	—	—	—	—	—	—	1.837	133.3	—	—
397.6	—	—	—	—	—	—	—	—	—	—	—	—	—	—
494	—	—	—	—	—	—	—	—	—	—	—	—	—	—
760	—	—	—	—	—	—	—	—	—	—	—	—	—	—

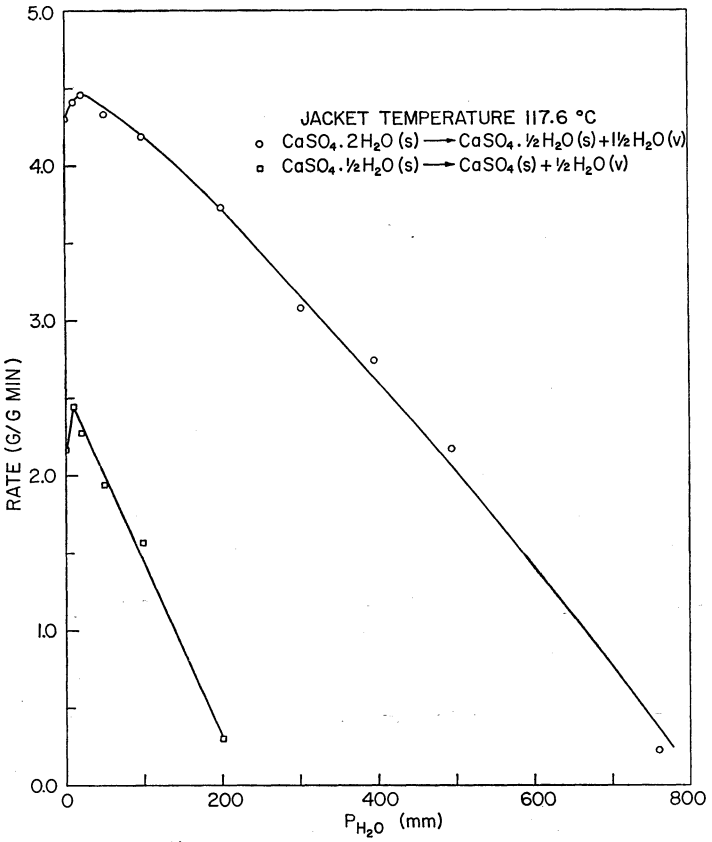

FIG. 3. Variation in dehydration rates with ambient water vapor pressure. Jacket temperature 117.6° C.

reaction interface where the effect of ingesting other potential nuclei may not be of great significance.

The principal effect of increasing partial water vapor pressure is to repress the rate of anhydrous calcium sulphate formation more rapidly than that of hemihydrate formation, as expected (4). Further, it has been shown kinetically that separate, temperature-dependent water vapor pressures exist above which each stage may be effectively suppressed. For example, for the process

$$CaSO_4.2H_2O\ (s) = \alpha\text{-}CaSO_4.\tfrac{1}{2}H_2O\ (s) + 1\tfrac{1}{2}H_2O\ (v),$$

$\Delta F°$ equals 0 at about 106° C (4). No measurable dehydration could be detected at 1 atm H_2O and 107.4° C, although a rate was measurable at 110.4° C under this water vapor pressure. A similar correlation between kinetic and thermodynamic results cannot be made for stage II since, as will be discussed below, the hemihydrate produced at the critical water vapor pressure for suppressing this stage is intermediate in thermodynamic properties between the α- and β-modifications reported (4).

Catalysis of both stages I and II by low water vapor pressures has been observed in other salt hydrate systems (17, 18), the magnitude of the pressures required in this work presumably being due to the less efficient transport of water molecules to and from the reaction site in processes at atmospheric pressure, compared to those carried out in

Can. J. Chem. Downloaded from www.nrcresearchpress.com by 210.87.254.40 on 09/05/12
For personal use only.

Can. J. Chem. Downloaded from www.nrcresearchpress.com by 210.87.254.40 on 09/05/12
For personal use only.

PLATE I

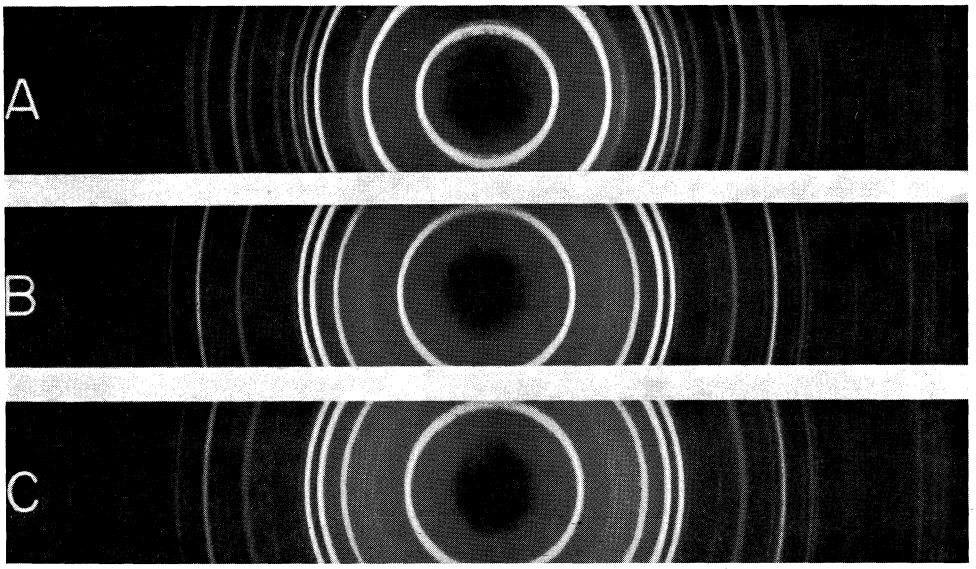

FIG. 4. Debye–Scherrer powder patterns: A, calcium sulphate dihydrate; B, hemihydrate produced under 1 atm water vapor; C, hemihydrate produced under 0 atm water vapor.

vacuum, and to the low surface area of the original materials. The regular decrease in rate with further increase in water vapor pressure may be associated with the increasing competition of the reverse reaction due to an increasing concentration of water molecules in the transition layer (18).

Heat of solution measurements have identified the hemihydrates produced at 0 and 760 mm H_2O to be the β- and α-modifications, as defined thermodynamically (4) and not on the basis of preparation (19). Despite a difference of only 0.5 kcal $mole^{-1}$ in heat of solution, the activation energy for formation of α-hemihydrate is some 20 kcal $mole^{-1}$ greater than that for β-hemihydrate. Heat of solution, activation energy, and pre-exponential factor were found to increase linearly with water vapor pressure (Fig. 5).

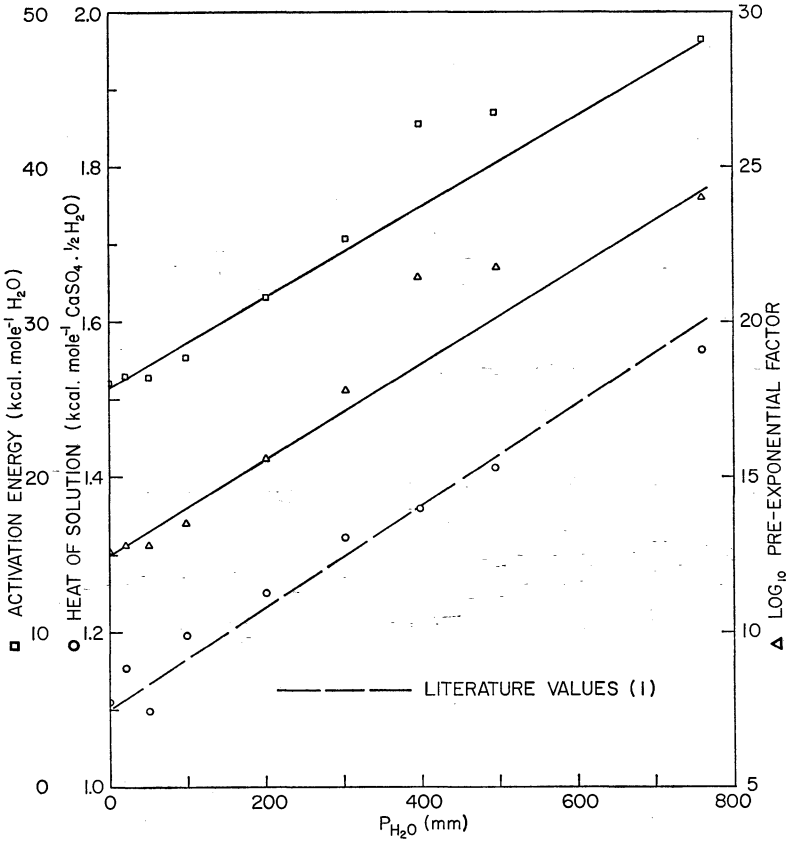

FIG. 5. Variation of kinetic and thermodynamic parameters for production of the hemihydrate with partial water vapor pressure during dehydration.

While a linear relationship between heat of solution and "relative amounts of α- and β-hemihydrate present in a plaster" (4) has been accepted, it has not previously been demonstrated that thermodynamic properties intermediate between these two modifications may be obtained by control of the partial water vapor pressure during dehydration. The possibility of such continuous variation had been suggested (3) on the basis of general considerations.

Some workers feel that differences in the heat of solution of hemihydrates are associated

Can. J. Chem. Downloaded from www.nrcresearchpress.com by 210.87.254.40 on 09/05/12
For personal use only.

with differences in specific surface, similar to the case for magnesium hydroxide (20). It is difficult to accept this viewpoint concerning the hemihydrate. This material exhibits a well-defined range of heats of solution, which would not be expected if these were dependent upon the specific surface which could be induced into the sample. Further, the same heat of solution can be obtained under widely differing methods of preparation. For example, hemihydrates have been produced in this laboratory by crystallization from boiling 50% nitric acid, and by dehydration under 760 mm water vapor pressure, both having the heat of solution reported for α-hemihydrate produced by autoclaving of lump gypsum under pressure followed by grinding (4). Although comparative surface area data are not available, it is difficult to conceive that such different preparative techniques would result in hemihydrates of sufficiently comparable specific surface to yield the same heat of solution. While changes in the rates of other transformations of calcium sulphate (21) may be attributed to differences in specific surface (3), no data are yet available to correlate specific surface with any thermodynamic properties of the hemihydrate. In one case (22) the concept of thermodynamically defined α- and β-modifications was discarded on the basis of heat of solution data outside the reported range (11). However, the lack of adequate description of the samples and calorimetric techniques involved leaves doubt about the purity of the hemihydrates employed.

It appears more reasonable that the range of thermodynamic properties found for hemihydrates reflects the overall order within the hemihydrate lattice, rather than its surface character. On this basis, not only does increasing water vapor pressure influence the kinetics of the dehydration process, it also influences the order with which the hemihydrate lattice is created at the reaction interface. It is significant that the determining factor is the partial pressure of water, not its relative pressure. Since the structure of the hemihydrate lattice (23) is comprised of continuous chains of successive calcium atoms and sulphate tetrahedra, these chains being arranged in bundles so that channels of about 3 Å diameter are formed wherein water molecules can be located, it is possible that at least two lattice features may be influenced by the water vapor pressure at the reaction interface:

(i) the packing of Ca–SO_4 chains with respect to one another, the overall order of these chains being higher in α-hemihydrate producing a higher "stacking order" (6);

(ii) the rotational orientation of a given SO_4 tetrahedron along the Ca–SO_4 chain with respect to succeeding SO_4 tetrahedra, the tetrahedra in the α-hemihydrate being more regularly oriented.

X-Ray evidence obtained in this work again found no gross differences in lattice features accompanying change in heat of solution. Morris (6) has recently demonstrated that any structural differences may be associated with degree of "stacking order" within the crystal, his results being consistent with earlier entropy calculations (4). The possibility of other types of defects in the ionic Ca–SO_4 chains cannot be excluded at the present time.

The continuous variation in thermodynamic properties and kinetic parameters with increasing water vapor pressure further supports the concept that the designations "α" and "β" represent merely the terminals of a hemihydrate series. The α- and β-hemihydrates are not necessarily separate entities which may be present in different proportions in a mixture (although such mixtures may be artificially prepared), but the designation of a hemihydrate as, say, 50% β-modification merely defines its properties as being the average of the two terminals. Because of the continuous variation in properties, depending upon partial water vapor pressure, it is reasonable that the inter- and intra-chain order is determined by conditions prevailing at the reaction interface. If the function of water

Can. J. Chem. Downloaded from www.nrcresearchpress.com by 210.87.254.40 on 09/05/12
For personal use only.

vapor were to promote further change in the lattice following passage of the reaction interface, such a process would presumably also be temperature-dependent and its extent, as determined by heat of solution, would not be constant over a temperature range at a constant water vapor pressure.

The anhydrous calcium sulphates obtained at the lower partial water vapor pressures were not studied extensively, because of difficulties in keeping them completely anhydrous (1, 2). The dehydration times and temperatures involved were such that formation of the insoluble form of anhydrous calcium sulphate was not favored. This was further evident from the fact that the water loss never equalled the theoretical value, although the starting dihydrate was found to contain this amount of water when dehydrated at 450° C. It is known (4) that a small fraction of water is retained by the anhydrous calcium sulphate lattice until its reversion to the insoluble modification at higher temperature, this rearrangement being sufficient to expel residual water.

ACKNOWLEDGMENT

The author wishes to thank Domtar Construction Materials Limited for support of this work and for permission to publish the results obtained.

REFERENCES

1. H. B. WEISER, W. O. MILLIGAN, and W. C. EKHOLM. J. Am. Chem. Soc. **58**, 1261 (1936).
2. H. B. WEISER and W. O. MILLIGAN. J. Am. Chem. Soc. **59**, 1456 (1937).
3. M. J. RIDGE. Rev. Pure Appl. Chem. **10**, 243 (1959).
4. K. K. KELLEY, J. C. SOUTHARD, and C. T. ANDERSON. U.S. Bureau of Mines, Technical Paper No. 625. 1941.
5. T. SAITO. Bull. Chem. Soc. Japan, **34**, 1454 (1961).
6. R. J. MORRIS. Nature, **198**, 1298 (1963).
7. W. E. P. FLECK, M. H. JONES, R. A. KUNTZE, and H. G. McADIE. Can. J. Chem. **38**, 936 (1960).
8. R. A. KUNTZE. Nature, **193**, 772 (1962).
9. W. A. CASPARI. Proc. Roy. Soc. A, **155**, 41 (1936).
10. P. GALLITELLI. Periodico Mineral. **4**, 132 (1933).
11. J. C. SOUTHARD. Ind. Eng. Chem. **32**, 442 (1940).
12. H. G. McADIE. Mater. Res. Std. In press.
13. W. D. SPENCER and B. TOPLEY. J. Chem. Soc. **1929**, 2633.
14. B. TOPLEY and M. L. SMITH. J. Chem. Soc. **1935**, 321.
15. J. E. BRIGHT and M. J. RIDGE. Phil. Mag. **6**, 441 (1961).
16. J. L. AMOROS, J. GALVAN, and P. ALONSO. Bol. Real Soc. Espan. Hist. Nat. G, **59**, 13 (1961).
17. R. W. FORD and G. B. FROST. Can. J. Chem. **34**, 591 (1956).
18. J. A. COOPER and W. E. GARNER. Proc. Roy. Soc. A, **174**, 487 (1940).
19. W. A. DAVIS. J. Soc. Chem. Ind. **26**, 727 (1907).
20. R. FRICKE, R. SCHNABEL, and K. BECK. Z. Elektrochem. **42**, 881 (1936).
21. C. MITSUKI and M. KITA. Nature, **184**, 1481 (1959).
22. E. EIPELTAUER. Zement-Kalk-Gips, **11**, 264 (1958).
23. O. FLÖRKE. Neues Jahrb. Mineral. Abhandl. **84**,(2) 198 (1952).

Can. J. Chem. Downloaded from www.nrcresearchpress.com by 210.87.254.40 on 09/05/12
For personal use only.

AN INFRARED STUDY OF THE ADSORPTION OF AMMONIA ON POROUS VYCOR GLASS

N. W. CANT AND L. H. LITTLE
Department of Chemistry, University of Western Australia, Nedlands, Western Australia
Received October 4, 1963

ABSTRACT

The infrared spectrum of ammonia adsorbed on porous glass at 20° C and 150° C has been studied in the region 1450–4000 cm^{-1}. No absorption band due to the asymmetric bending mode of ammonia was observed but in the NH stretching region, bands occurred at 3280 cm^{-1}, 3320 cm^{-1}, 3365 cm^{-1}, and 3400 cm^{-1}. The bands at 3320 cm^{-1} and 3400 cm^{-1} were easily removed by evacuation and are due to ammonia molecules hydrogen bonded through the nitrogen atom to surface hydroxyl groups. The bands at 3280 cm^{-1} and 3365 cm^{-1} were not removed by evacuation even at 150° C and are due to ammonia molecules held to surface Lewis acid sites by the nitrogen lone-pair electrons. The site for this adsorption is not a surface hydroxyl group. These results are further evidence for the existence of the two adsorption sites proposed by Folman and Yates. Deuteration of the surface OH groups was easily accomplished with D_2O vapor at 300° C and the rate of hydrogen exchange between adsorbed ammonia molecules and surface OD groups was found to be rapid.

INTRODUCTION

The infrared spectrum of ammonia adsorbed on porous Vycor glass has been studied several times, most extensively by Folman and co-workers. They have correlated the infrared spectra (1, 2) with measurements on length changes (1, 3) and dielectric properties (4) of the adsorbent. Their results show that two sites with different kinetics of adsorption exist on evacuated porous glass: one is associated with residual hydroxyl groups and the other is assumed to be surface silicon or oxygen atoms. At room temperature, adsorption occurs principally on the surface OH groups by hydrogen bonding through the nitrogen atom of the ammonia molecule and this produces an initial contraction in the length of the glass. At higher temperatures a relatively larger number are adsorbed on the other sites and the initial contraction is not observed. Folman and Yates (2) were unable to distinguish spectroscopically between ammonia adsorbed on the two different sites although they reported that the characteristic stretching frequencies of ammonia did shift to lower values as the temperature was increased. In the present study it has been possible to resolve adsorption bands in the region 3250–3400 cm^{-1} due to two forms of adsorbed ammonia.

EXPERIMENTAL

In the present work, we used 0.1-mm thick porous glass in a cell with sodium chloride windows. This system has several advantages over that used by Folman wherein a 0.4-mm sample was placed in a silica cell. Measurements could be made of the bands that were due to the surface OH groups and residual water molecules both in the stretching and bending regions of the spectrum. Moreover, studies could be carried out at higher surface coverages and with greater spectral resolution when the thinner sample was employed.

Two types of infrared cells were used. One was similar to that used by Little, Sheppard, and Yates (5). For temperatures above 100° C a silica test tube of diameter 2.4 cm and length 15 cm was used. A ground glass joint at the upper end gave access for the sample and a simple external furnace was used for heating. For use in either cell the sample was supported in a metal holder and after evacuation in the furnace section of the cell it was carefully aligned in the infrared beam. All adsorption and desorption measurements were made without disturbing the alignment. The gasline was a conventional volumetric B.E.T. apparatus. Mercury levels could be read to ±0.005 cm by a cathetometer.

The samples of porous glass had the approximate dimensions 1 cm × 1 cm × 0.01 cm and weighed between 20 and 40 mg. They were cleaned by being heated to 450° C in air and outgassed at the same temperature.

Can. J. Chem. Downloaded from www.nrcresearchpress.com by 210.87.254.42 on 09/05/12
For personal use only.

Deuteration was carried out by exposing evacuated samples to D_2O vapor at 300° C for 3 hours. Ammonia was obtained from cylinders and purified by bulb-to-bulb distillation.

After evacuation of the sample, doses of ammonia were admitted until the 3337 cm^{-1} band of the gas phase ammonia spectrum became appreciably intense (approximately 10 cm pressure). About 10 doses were admitted for each experiment and 30 minutes was allowed for equilibrium to be reached in each case. Desorption was carried out by successive expansions into the evacuated line. Finally the sample was evacuated and the spectrum of any residual ammonia recorded.

Because of small sample weights and large cell volumes it was possible to obtain only approximate isotherms for ammonia adsorbed on the samples during the course of spectral studies. More accurate adsorption–desorption isotherms were determined on a number of small pieces of the glass contained in a cell with a dead space of only 12 ml. This procedure introduced errors in that the exact temperature of the sample in the infrared cell could not be reproduced in the small cell because of the undetermined heating effect of the infrared beam. Comparison of the isotherms obtained in the two cells indicated that the temperature in the beam was possibly 20° C higher. This effect is shown in Fig. 1.

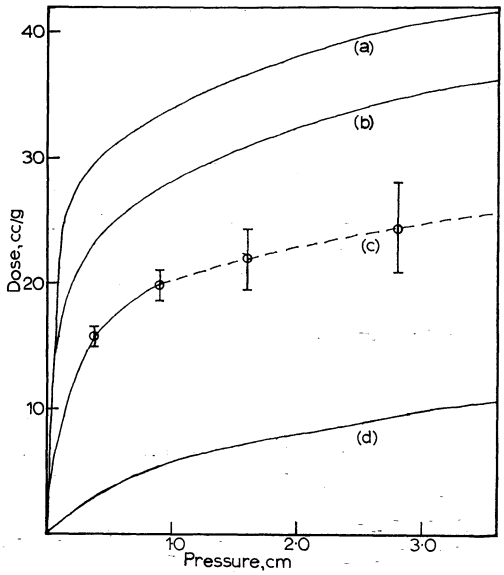

FIG. 1. Isotherms for ammonia adsorbed on porous Vycor glass at different temperatures (*a*) 13° C, (*b*) 20° C, (*c*) sample in infrared beam, (*d*) 150° C. The dotted section is extrapolated and the approximate error shown.

Spectra were recorded with a Perkin–Elmer Model 137G spectrophotometer which has only two scanning speeds, 350 cm^{-1}/minute and 110 cm^{-1}/minute. However, manual checks at particular wavelengths showed that the peak heights of bands were not affected by the finite scanning time at the slower scanning speed and this was used for all measurements. The error in determination of the optical densities is difficult to estimate but is probably less than ±5% for optical densities less than 1.0. Frequencies are accurate to ±5 cm^{-1}. Spectra as directly recorded were on the usual linear transmission scale. For comparison purposes they were replotted on a linear optical density scale at 50 cm^{-1} intervals and more closely for narrow bands.

The integrated molar intensity of the NH stretching modes of ammonia in carbon tetrachloride solution was measured for comparison with that of the surface species. The concentration of ammonia in carbon tetrachloride was determined by titration.

RESULTS

Figure 2 shows the spectra of representative doses of ammonia adsorbed on porous glass at temperatures of 20° C and 150° C and the effect of subsequent evacuation on the bands. The bands at 3665 cm^{-1} and 3730 cm^{-1} are due to surface hydroxyl groups, those from 3250–3400 cm^{-1} to NH stretching vibrations, and the broad band at 3000 cm^{-1} to OH groups hydrogen bonded to ammonia molecules. The optical densities of the NH bands

Can. J. Chem. Downloaded from www.nrcresearchpress.com by 210.87.254.42 on 09/05/12
For personal use only.

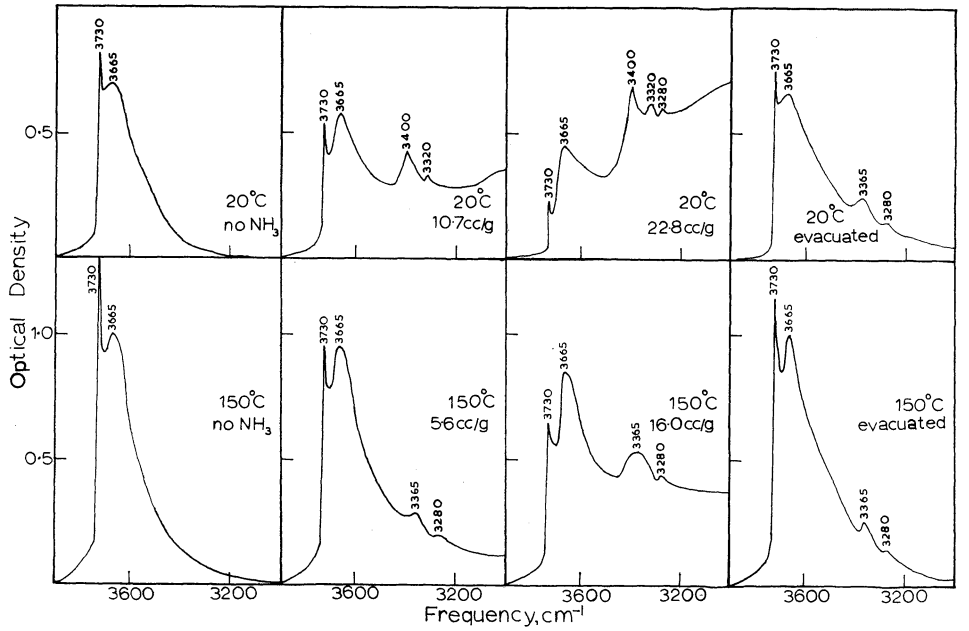

FIG. 2. The infrared spectrum from 4000 cm^{-1} to 3000 cm^{-1} of different amounts of ammonia adsorbed on 0.1-mm porous Vycor glass at 20° C and 150° C.

alone have been replotted in Fig. 3. The bands were graphically resolved from the background absorption. The peak optical densities of the main bands evident in Fig. 2 are plotted in Fig. 4 as a function of the dose of ammonia adsorbed. These doses of ammonia were estimated by measuring the equilibrium gas pressure over the sample in the infrared cell and then referring to the adsorption isotherms of Fig. 1 (*c*) and 1 (*d*) for the temperatures 20° C and 150° C respectively.

To investigate further the nature of the hydrogen bonding, the spectrum of ammonia adsorbed on deuterated porous glass was studied. Figures 5 (*a*) and 5 (*b*) are spectra of the evacuated glass before and after deuteration. The exchange was approximately 85% for both types of hydroxyl groups and may have been limited only by the purity of the D_2O used. After a dose of ammonia had been exposed to the sample for 1 hour, spectrum 5 (*c*) was obtained. Evacuation for 15 minutes at room temperature gave spectrum 5 (*d*).

A continuous absorption covering the region 1450–3000 cm^{-1} is a prominent feature of the spectrum of ammonia-covered Vycor glass. The optical density at any frequency in the region varies linearly with the amount of adsorbed ammonia. No band was observed in this region that could be assigned to the asymmetric NH bending mode of ammonia, which occurs at 1627 cm^{-1} in the gas phase spectrum.

DISCUSSION

Absorption Bands Due to the Evacuated Adsorbent

In the spectral region from 3500 cm^{-1} to 4000 cm^{-1}, two bands can be assigned to the adsorbent: a sharp symmetrical band at 3730 cm^{-1} to free surface hydroxyl groups; and a comparatively broad asymmetrical band with peak at approximately 3665 cm^{-1} to two adjacent hydroxyl groups hydrogen bonded to each other. The optical density of the 3730 cm^{-1} band was found to vary from 0.9 to 2.0 according to the individual sample and the

Can. J. Chem. Downloaded from www.nrcresearchpress.com by 210.87.254.42 on 09/05/12
For personal use only.

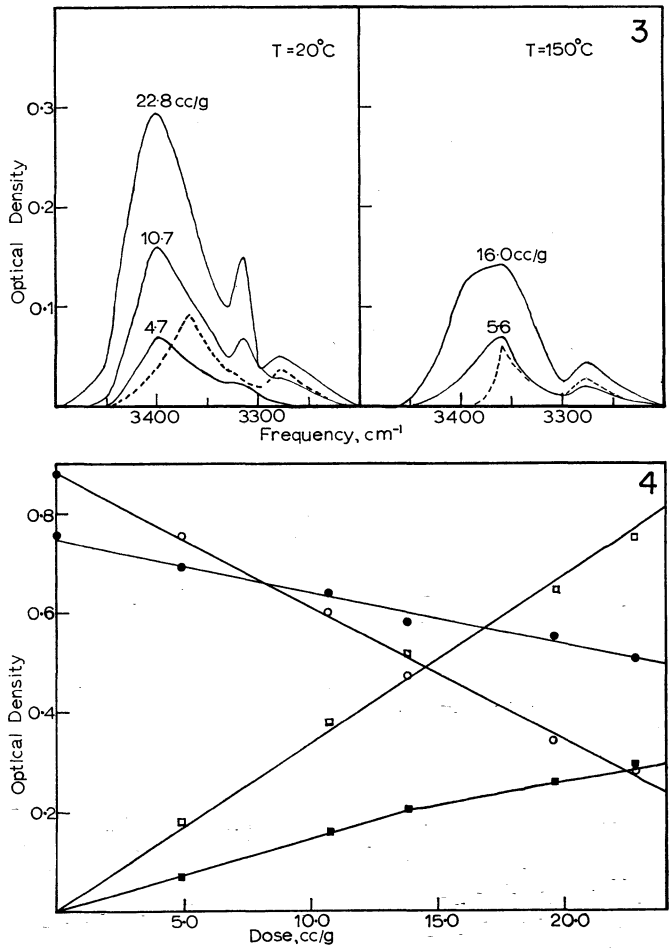

FIG. 3. The detailed structure of the infrared absorption bands of ammonia adsorbed on 0.1-mm porous Vycor glass at 20° C and 150° C. Evacuation after adsorption of the largest dose of ammonia gave the dotted spectra.

FIG. 4. Dependence of the intensities of the main absorption bands from 4000 cm^{-1} to 3000 cm^{-1} on the dose of ammonia adsorbed at 20° C: ○, 3730 cm^{-1}; ●, 3665 cm^{-1}; ■, 3400 cm^{-1}; □, 3000 cm^{-1}.

experimental conditions of evacuation. The final optical density depended more on the temperature than the time of evacuation. On the other hand variations of temperature in the range 400° C to 500° C produced only minor changes in the optical density of the hydrogen-bonded band, which was always between 0.8 and 1.0. These results are in general agreement with those published by Little and Mathieu (6) for the evacuation of similar samples, although intensities and band widths reported here are smaller for the same evacuation temperature. These variations are probably due to different sample preparations. The evacuated samples used here became slightly contaminated with hydrocarbons from the stopcock grease during the 24-hour period of the experiments.

Figures 5 (*a*) and 5 (*b*) show that both types of hydroxyl groups are easily exchanged for deuteroxyl groups. This agrees with the infrared studies of Benesi and Jones (7) on silica gel, although Pimentel *et al.* (8) found the rate of exchange to be much slower. The rate of exchange between adsorbed NH_3 and deuteroxyl groups was also very rapid as

Can. J. Chem. Downloaded from www.nrcresearchpress.com by 210.87.254.42 on 09/05/12
For personal use only.

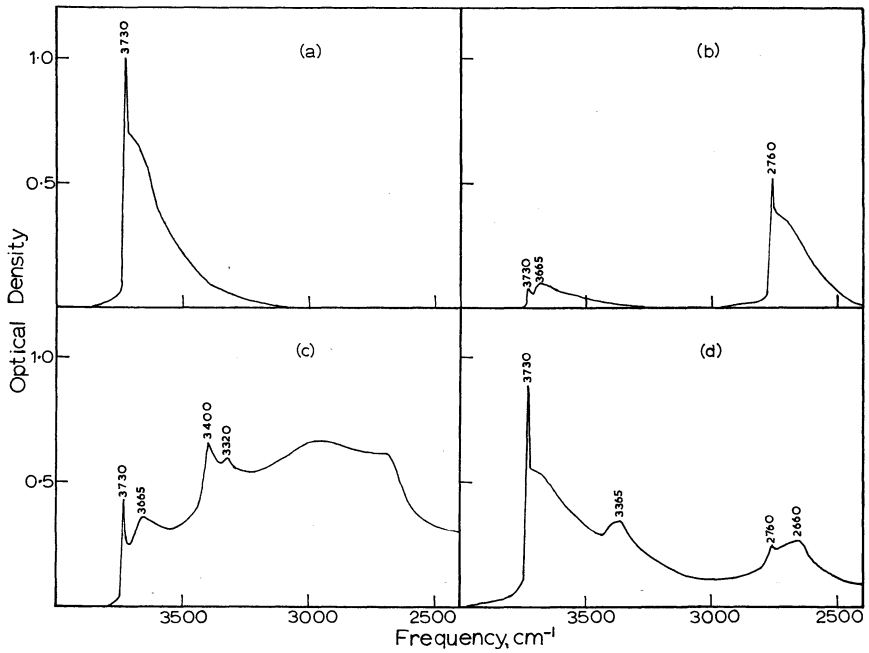

FIG. 5. The infrared spectrum of 0.1-mm porous Vycor glass at 20° C after (*a*) evacuation at 450° C, (*b*) subsequent deuteration at 300° C for 2 hours, (*c*) adsorption of approximately 20 cc/g of ammonia for 1 hour at 20° C on the deuterated sample, (*d*) subsequent evacuation at 20° C.

Figs. 5 (*c*) and 5 (*d*) show. Only weak OD bands were evident after 1 hour at room temperature; subsequent evacuation almost completely restored the original OH band.

When ammonia was adsorbed onto the porous glass the intensity of the free OH band at 3730 cm^{-1} decreased markedly, as is shown in Fig. 4. Those samples, for which the initial optical density of the band was less than 1.0, showed an approximately linear decrease with dosage. More intense bands could not be measured accurately. The slope of the line in Fig. 4 corresponding to the 3730 cm^{-1} band was unaffected by temperatures to 150° C. The optical density of the 3665 cm^{-1} band decreased much more slowly with increasing dosage of ammonia. In fact the observed decrease at this frequency may have been due to the decreased contribution from the free OH band, the wings of which overlap this band. Evacuation for 15 minutes at the temperature of the experiment restored the OH bands to almost the original intensity. These results show that free OH groups are better sites than hydrogen-bonded ones for the adsorption of ammonia and some, at least, of the ammonia is adsorbed on them at temperatures up to 150° C. Sidorov (9) found that the hydrogen-bonded hydroxyl groups on porous glass are better sites for the adsorption of water than free hydroxyl groups. It seems likely that the adsorption of ammonia and water proceeds by different means especially since Folman and Yates (10) found that water causes only expansions in the length of the glass.

Bands Due to Adsorbed Ammonia Molecules

Figure 4 shows that for the most intense NH band (3400 cm^{-1}), a graph of optical density against dosage is approximately linear. The marked flattening of the curve

Can. J. Chem. Downloaded from www.nrcresearchpress.com by 210.87.254.42 on 09/05/12
For personal use only.

reported by Folman and Yates (2) is not evident even though the surface coverage used here is much higher.

It was not possible to measure directly the amount of residual ammonia on a sample after evacuation. However, a comparison of the intensities of bands of residual ammonia on the sample was made after (*a*) adsorption of ammonia at 20° C and evacuation at 20° C and (*b*) adsorption of ammonia at 150° C followed by evacuation at 150° C. It was found that the intensities and frequencies (3280 cm^{-1} and 3365 cm^{-1}) were the same for both experiments. This result is consistent with the existence of a limited number of sites which will strongly adsorb the ammonia responsible for the 3280 cm^{-1} and 3365 cm^{-1} absorption bands (Figs. 2 and 3).

The main features of the observed spectra in the NH stretching region are summarized in Table I.

TABLE I

Frequencies and intensities of infrared bands due to ammonia adsorbed on 0.1 mm porous Vycor glass

Temperature	Dose, cc/g	Absorption bands			
20° C	10	3400 (0.15)*		3320 (0.06)	
	23	3400 (0.3)		3320 (0.15)	3280 (0.05)
After evacuation at 20° C			3365 (0.09)		3280 (0.04)
150° C	7		3365 (0.09)		3280 (0.04)
	16	3400 (0.13)	3365 (0.15)		3280 (0.04)
After evacuation at 150° C			3365 (0.07)		3280 (0.03)

*The values in parentheses are optical densities.

This table shows the existence of two types of ammonia on the porous glass—a comparatively weakly held species which gives absorption peaks at 3320 cm^{-1} and 3400 cm^{-1} and a more strongly held one with peaks at 3280 cm^{-1} and 3365 cm^{-1}. The close similarity between the two pairs of bands, as regards intensity ratios and frequency separations, indicates a mere difference in adsorption site and not a fundamental difference in the structure of the adsorbed species.

For comparison purposes a summary of the infrared absorptions of the NH groups of various molecules in the region 2800 cm^{-1} to 3600 cm^{-1} is presented in Table II.

There is no evidence for the presence of ammonium ions in the spectrum of ammonia adsorbed on porous glass and it can therefore be assumed that the adsorption is not on

TABLE II

Infrared absorption by NH groups of various molecules from 2800 cm^{-1} to 3600 cm^{-1}

Molecule	Phase	NH stretching modes		Overtone and combination bands	Reference
		Asymmetric	Symmetric		
NH_3	Gas	3443 (0)*	3337 (1)		(11, 12)
NH_3	Liquid	3375 (3)	3285 (2)	3220 (1)	(13)
NH_3	Solid	3378 (8)	3223 (1)†	3297 (4)†	(14)
NH_3	Dissolved in CCl_4	3417 (3)	3315 (2)	3230 (1)	(15)
NH_3	Suspended in solid N_2	3440 (3)	3332 (1)	—	(16)
$F_3B{:}NH_3$	Solid	3340 (3)	3230 (1)	—	(17)
Aniline	Dissolved in CCl_4	3470 (2)	3390 (3)	—	(18)
$-NH_2$	Chemisorbed on porous glass	3520 (1)	3445 (2)	—	(19)
				3042 (2)	
NH_4Cl	Solid	3140 (2)		2805 (1)	(19)

*Values in parenthesis give relative optical densities.
†It seems likely that the assignment of these bands has been reversed in reference (14).

Can. J. Chem. Downloaded from www.nrcresearchpress.com by 210.87.254.42 on 09/05/12
For personal use only.

surface Bronsted acid sites, as was the case for some of the ammonia adsorbed on the silica–alumina cracking catalyst used by Mapes and Eischens (20).

The 3320 and 3400 cm^{-1} pair of bands most closely approximates those for ammonia dissolved in carbon tetrachloride and therefore interaction with the surface must be weak (no asymmetric bending vibration was evident in the spectrum of adsorbed ammonia and therefore the first overtone would not be expected to appear in this region of the spectrum). This pair of bands is easily removed by evacuation at room temperature and at the same time the broad hydrogen-bonded absorption at 3000 cm^{-1} disappears, to be replaced by bands identical in the OH stretching region with those of the sample before adsorption of ammonia. In view of this, the most likely assignment of the 3320 and 3400 cm^{-1} bands is to ammonia weakly held by hydrogen bonding to surface hydroxyl groups.

From comparison with the spectrum of the Lewis acid complex $F_3B{:}NH_3$ (Table II), it is suggested that the pair of bands at 3280 cm^{-1} and 3365 cm^{-1} are the stretching frequencies of ammonia bound to Lewis acid sites on the adsorbent by the nitrogen lone-pair electrons. These bands cannot be due to ammonia bound to either type of hydroxyl group since evacuation does not remove them but does remove all evidence of hydrogen bonding between ammonia and OH groups. Since the porous glass contained 3% of B_2O_3 and as it has been shown that the number of sites is limited, it is not impossible that this ammonia is adsorbed on the surface electron-deficient boron atoms themselves. It has been suggested (21) that surface aluminum atoms are active sites for the adsorption of olefinic hydrocarbons on porous Vycor.

Absorption Bands Due to Perturbed OH Groups

The integrated molar intensity of all bands due to adsorbed ammonia in the 3300–3400 cm^{-1} region is 4000 ± 1000 moles^{-1} liter cm^{-2} compared to 900 ± 200 moles^{-1} liter cm^{-2} for ammonia dissolved in carbon tetrachloride. It seems likely, therefore, that all adsorbed ammonia is contributing to the bands in this region and that it is unnecessary to assume that there is any contribution by hydrogen-bonded NH groups to the broad 3000 cm^{-1} band. The band must then be due to perturbed OH groups.

A graph of the optical density of this absorption band against dosage is linear at 20° C (Fig. 4) and also at 150° C. The slopes for the two temperatures are not markedly different, which is not in accord with the findings of Folman and Yates (2). In the present work and also in that of Folman and Yates (2) approximately 4 cc/g of ammonia remained on the glass after evacuation at 150° C and the optical density of the perturbed OH band (3000 cm^{-1}) was then zero.

Roev (22) and Basila (23) have suggested that the type of continuous absorption observed in the 1450–3000 cm^{-1} region arises from a photodesorption process, whereby the incident infrared radiation is responsible for the desorption of weakly held surface species.

A solution of sodium methoxide in methanol shows (24) a similar absorption over the frequency range accessible to study with this system (2050–2300 cm^{-1}). Here it is not possible for photodesorption to occur and it seems likely that a more satisfactory explanation for this phenomenon is forthcoming from the study of Zundel and Schwab (25) on a polystyrene – sulphonic acid – water system. The continuous absorption was shown to originate in the high exchange probability of a proton in such strongly hydrogen-bonded systems.

In the present study it is considered that the less strongly held ammonia (3320 and 3400 cm^{-1} bands) and surface hydroxyl groups are involved in hydrogen bonding. The

Can. J. Chem. Downloaded from www.nrcresearchpress.com by 210.87.254.42 on 09/05/12
For personal use only.

continuous absorption spectrum observed would be consistent with the rapid exchange of the surface hydroxyl proton with the ammonia. This view is supported by the rapid exchange between surface OD groups and adsorbed ammonia.

It is interesting to note that while the spectrum of the surface OH group is considerably perturbed to give the continuous absorption pattern, the spectrum of the adsorbed ammonia resembles that of ammonia in a nonpolar environment (Tables I and II). Perhaps it might have been reasonable to consider that the spectrum of this ammonia would have resembled more closely that of the ammonium ion.

ACKNOWLEDGMENTS

The porous glass used was a gift of Dr. M. E. Nordberg, of the Corning Glass Works, New York. One of us (N. W. C.) gratefully acknowledges the receipt of a Commonwealth Scientific and Industrial Research Organisation Senior Studentship.

REFERENCES

1. M. FOLMAN and D. J. C. YATES. Proc. Roy. Soc. (London), A, **246**, 32 (1958).
2. M. FOLMAN and D. J. C. YATES. J. Phys. Chem. **63**, 183 (1959).
3. M. FOLMAN and D. J. C. YATES. Trans. Faraday Soc. **54**, 429 (1958).
4. D. FIAT, M. FOLMAN, and U. GARBATSKI. Proc. Roy. Soc. (London), A, **260**, 409 (1961).
5. L. H. LITTLE, N. SHEPPARD, and D. J. C. YATES. Proc. Roy. Soc. (London), A, **259**, 242 (1960).
6. L. H. LITTLE and M. V. MATHIEU. Proceedings of the Second International Congress on Catalysis, Paris. 1960. Paper 34. Editions Technip, Paris. 1961.
7. H. A. BENESI and A. C. JONES. J. Phys. Chem. **63**, 179 (1959).
8. G. C. PIMENTEL, C. W. GARLAND, and G. JURA. J. Am. Chem. Soc. **75**, 803 (1953).
9. A. N. SIDOROV. Opt. Spectr. **8**, 424 (1960).
10. M. FOLMAN and D. J. C. YATES. Trans. Faraday Soc. **54**, 1684 (1958).
11. C. CUMING. Can. J. Phys. **33**, 635 (1955).
12. G. HERZBERG. Infrared and Raman spectra. D. Van Nostrand Co. Inc., New York, N.Y. 1945. p. 294.
13. I. V. DEMIDENKOVA and L. D. SHCHERBA. Izv. Akad. Nauk SSSR, Ser. Fiz. **22**, 1122 (1958).
14. F. P. READING and D. F. HORNIG. J. Chem. Phys. **19**, 594 (1951).
15. C. G. CANNON. Spectrochim. Acta, **10**, 425 (1958).
16. G. C. PIMENTEL, M. O. BULANIN, and M. VAN THIEL. J. Chem. Phys. **36**, 500 (1962).
17. A. A. BABUSHKIN, I. V. KOVALEV, and V. M. EMEL'YANOVA. Opt. Spektroskopiya, **4**, 468 (1958).
18. S. CALIFANO and R. MOCCIA. Gazz. Chim. Ital. **87**, 58 (1957).
19. M. FOLMAN. Trans. Faraday Soc. **57**, 2000 (1961).
20. J. E. MAPES and R. P. EISCHENS. J. Phys. Chem. **58**, 1059 (1954).
21. L. H. LITTLE, H. E. KLAUSER, and C. H. AMBERG. Can. J. Chem. **39**, 42 (1961).
22. L. M. ROEV. Dokl. Akad. Nauk SSSR. **133**, 561 (1960).
23. M. R. BASILA. J. Phys. Chem. **66**, 2223 (1962).
24. N. S. BAYLISS, R. L. HEPPOLETTE, L. H. LITTLE, and J. MILLER. J. Am. Chem. Soc. **78**, 1978 (1956).
25. G. ZUNDEL and G. M. SCHWAB. J. Phys. Chem. **67**, 771 (1963).

Can. J. Chem. Downloaded from www.nrcresearchpress.com by 210.87.254.42 on 09/05/12
For personal use only.

Can. J. Chem. Downloaded from www.nrcresearchpress.com by 210.87.254.105 on 09/05/12
For personal use only.

ENERGY LEVELS OF TRIARYLMETHYL CARBONIUM IONS

E. K. NG AND F. C. ADAM
Department of Chemistry, University of Alberta, Calgary, Alberta

Received November 12, 1963

ABSTRACT

The near ultraviolet and visible spectra of the various phenyl-, *p*-biphenyl methyl carbonium ions have been investigated and the polarization of the absorptions relative to the fluorescence band have been determined. An assignment of the transitions is made, using as a basis simple molecular orbital calculations and the expectations based on the structure representation. These are compared to the assignments made in earlier researches. The calculated intensities are found to agree favorably with the observed values.

I. INTRODUCTION

The absorption spectra of various aryl hydrocarbon cations have been investigated with the end in view of comparing the transitions to those found in triaryl methane dyestuffs (1, 2, 3). The characteristics of the electronic state of the latter compounds are relatively well understood, and symmetry assignments have been made to these states by consideration of the properties of the various optical transitions. In this respect, the absorption energies, intensities, and the polarizations, related to a molecular fixed frame, are especially important. Most of the present work concerns the particular sequence of cations resulting from successive substitution of *p*-phenyl groups into the triphenylmethyl carbonium ion. This particular series of compounds has been studied by Chu and Weissman (4). We have essentially duplicated their results with the exception that particular attention has been paid to the polarizations of some of the weaker transitions of the spectrum. These are of critical importance in the final analysis of these systems, and their significance was apparently overlooked by the earlier authors. This has led us to a different assignment, but one which is more in accord with that of crystal violet and analogous dye compounds. Although the importance of these transitions of lesser intensity can be demonstrated by simple Huckel (HMO) calculations, the situation may be more easily visualized from consideration of the interaction between the four low-energy (N-state) species taken as equivalent to the paper structures (5).

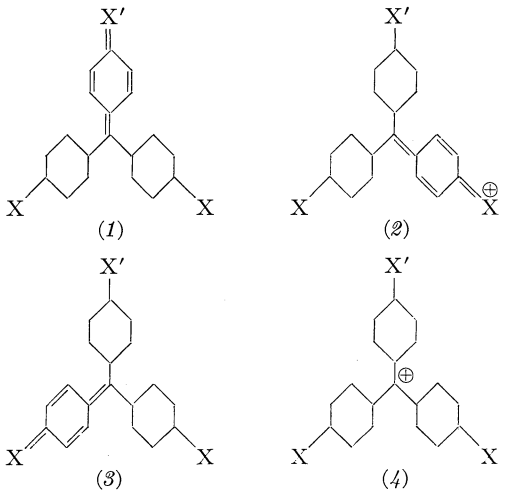

For crystal violet, for instance, X′ = X = —N̈Me$_2$, so that structures (*1*) to (*3*) are related by the threefold axis of rotation. It can be shown by group theoretical arguments that interactions between these structures will give rise to four electronic states that may be described in terms of an arbitrary constant, c, by the following functions:

$$\psi_0 = (c/\sqrt{3})\ (1 + 2 + 3) + (1 - c^2)^{\frac{1}{2}}\ (4),$$
$$\psi_1 = (1/\sqrt{6})\ (2\,1 - 2 - 3),$$
$$\psi_2 = (1/\sqrt{2})\ (2 - 3),$$
$$\psi_3 = [(1-c^2)/3]^{\frac{1}{2}}\ (1 + 2 + 3) - c\ (4),$$

ψ_0 and ψ_3 are of the totally symmetric, A, representation and ψ_1 and ψ_2 are a degenerate pair, of symmetry E. Transitions between states of the representations E and A are allowed and in-plane while those between two states of the symmetric representation are allowed out-of-plane (i.e. parallel to the threefold axis, or "z" direction in the molecular frame). These considerations apply to any molecule with a threefold axis and are independent of twisting of the phenyl group, as long as the distortions are symmetrical. On the other hand, any perturbation which destroys this threefold axis of symmetry by preferential interaction with only one of the rings reduces the original molecular symmetry from D_3 or C_3 to C_2. If this preferential axis of perturbation is defined as the "y" axis, then the originally degenerate wave function will be split into symmetric (A) and antisymmetric (B) state wave functions with respect to this axis. Furthermore, all $A \leftrightarrow A$ intercombinations become allowed in-plane, and y-polarized, while the $A \leftrightarrow B$ combinations are also allowed, but x-polarized. Chemical substitution of one of the dimethylamino groups (i.e. X′ ≠ —N̈Me$_2$) is a perturbation of this sort, and to some reasonable order of approximation such substitution will affect only the energy of structure (*1*). The functions of symmetry B, because of the nodal plane in the axis of the perturbation, will, to the same approximation, be unaffected, experiencing only a relatively small and arbitrary shift in energy. Whether the symmetric states are lowered or raised in energy depends largely on whether the perturbation stabilizes or destabilizes structure (*1*). The situation is as depicted in Fig. 1. Both types of perturbations have been observed in the crystal violet series of dyes (2, 3).

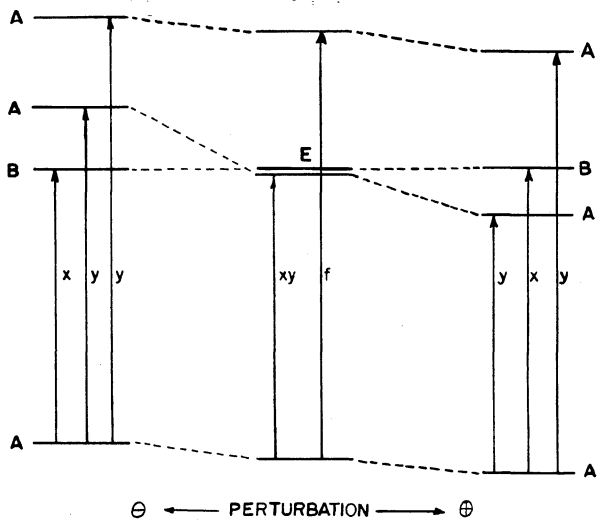

FIG. 1. Effect on energy level scheme of a y-axis perturbation on a trigonal molecule. "Stabilizing" perturbations are designated as positive.

Can. J. Chem. Downloaded from www.nrcresearchpress.com by 210.87.254.105 on 09/05/12
For personal use only.

Can. J. Chem. Downloaded from www.nrcresearchpress.com by 210.87.254.105 on 09/05/12
For personal use only.

Experimentally, a pattern such as this is found; a low-energy intense transition ($\epsilon > 10^4$) being followed at higher energies by a weaker transition ($\epsilon < 10^3$). Considerations of HMO energies yield the same conclusions, with the same type of perturbation leading to the same prediction of the polarization axis for the long wavelength transition. Since the reverse of this particular transition is the only process occurring in fluorescence, it is possible to relate all absorptions to the single emission process. Absorptions are described as "parallel" or "perpendicular" to the fluorescence depending on whether the axis of polarization of the absorption is in the same direction or at right angles to the polarization axis of the emission. The key factor to the analysis is that the weak transition, when allowed in-plane, is always polarized "y", regardless of the particular perturbation affecting the molecule. Accordingly, this absorption is "parallel" with "stabilizing" perturbations, but is otherwise "perpendicular". These conclusions are perfectly general for trigonal molecules and should apply to the hydrocarbon cations, anions, and dye materials alike. In particular, the structure (*1*) for triphenyl methyl carbonium would be a composite of the ortho and para cation structures, each weighted about equally in the

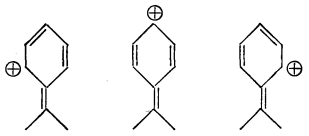

final function. Furthermore, it would be expected that the biphenyl carbonium structures would be stabilized relative to the phenyl, since the composite function contains nine structures. The implication is that for monoxenyl diphenyl methyl carbonium (Mono), the degenerate state will be split and the function ψ_1, of symmetry A, will correspond to a state of lowered energy relative to that with the function of symmetry B, ψ_2. By comparison with Fig. 1, this corresponds to a stabilizing perturbation (to the right) so that the absorptions at increasing energy are polarized y, x, y. The absorptions will be accordingly described as $\|$, $\perp$, $\|$, relative to the fluorescence. On the other hand, dixenyl phenyl methyl (Di) carbonium may be considered as a perturbation of the symmetrical trixenyl carbonium (Tris). In this case, the substitution of biphenyl by phenyl results in destabilization, so that by analogy, the polarizations of the absorptions are in the order x, y, y, which will give $\|$, $\perp$, and $\perp$ absorptions respectively. It can be seen that it is the relative polarization of the third absorption band that is determined by the nature of perturbation. The converse is also true, that the determination of the polarization of this transition allows one to obtain the polarization of all other in-plane transitions.

II. EXPERIMENTAL

The absorption spectra of the mono-, di-, and tri-xenyl derivatives were taken by dissolving the corresponding carbinols in 10% sulphuric acid – 90% acetic acid mixtures at room temperature. These compounds sulphonated at varying rates in pure sulphuric acid but not in acetic – sulphuric acid mixtures. On the other hand, TPM carbonium ion was itself found to be very stable in sulphuric acid but did not result in complete conversion of the carbinol in the above mixture. Accordingly, the spectrum of the TPM ion was obtained in 95% sulphuric acid. The spectrum of each carbinol in acid is similar in essential details to those of the corresponding fluoroborate and perchlorate salts dissolved in various anhydrous solvents. A calibrated Beckman D.U. was used for all intensity measurements, and the transition moment magnitudes determined according to the formula,

$$[q(\text{Å})]^2 = 9.17\times10^{-4}\int \epsilon\, d \log \lambda.$$

Emission spectra and polarization ratios were determined from the carbonium ions dissolved in syrupy phosphoric acid at −130° C. The output of a Hanovia 1000-w mercury–xenon compact arc was passed through a Bausch and Lomb 250-mm monochrometer. The emergent beam was reflected from a stack of

quartz microscope cover slips at Brewster's angle in such a manner as to give a vertically oriented electric plane of polarization. The intensity of the beam was modulated at line frequency, since it is powered by alternating current. The fluorescence was detected at 90° to the propagation direction of the incident light, using a Du Mont K-1292 infrared sensitive photomultiplier tube. This fluorescence was observed through an adjustable Polaroid, which could be oriented to transmit either vertical or horizontal components of the electric vector of the fluorescence. Suitable Corning filters were used to further increase the spectral purity of the fluorescence. The power supply for the photomultiplier tube was a series of batteries, shielded so that pickup of spurious 60-cycle radiation was below the limits of detection as determined by a capacatively coupled Tetronix 805 oscilloscope on its most sensitive range ($\frac{1}{2}$ mv per cm). In this way any emission process of lifetime short enough to follow the modulated exciting light appears as a sinusoidal signal on the oscilloscope, with voltage amplitude proportional to the intensity of the emission. Two voltage readings corresponding to the vertical and horizontal settings of the analyzing Polaroid were taken. The ratio of these values is the polarization ratio "p", its value being between 1 and 3 for parallel processes, but between 1 and 0 for perpendicular absorptions. The results are set out in Table I, with energies quoted in kilokaisers, i.e. $cm^{-1} \times 10^{-3}$.

TABLE I

Spectral characteristics of the xenyl–phenyl carbonium ions

Compd. (carbonium ion)	Energy (kk)	Intensity[‡] (Å)	Polarization	Assignment (upper state)
TPM	23.4, 24.6 } 24.0	1.64	(x, y)	E
	34.5	0.20	(y or z)	A
Mono	19.8	1.62	(y)	A
	24.0	1.13	(x)	B
	29.8	0.38	(y)	A
Di	18.5	1.84	(x)	B
	21.7	1.40	(y)	A
	28.3	0.62	(y)	A
	(36.0)	—	(x)	B
Tris	18.5, 18.5 } 18.5	2.5	(x, y)	E
	26.0	0.58	y or z	A
	37.0	—		
	40.0	—		

III. SYMMETRY ASSIGNMENTS

The transition energies, intensities, and polarizations for each of the ions have been calculated by the HMO method, and the values appear in Table II. Only those transitions of significant intensity in any of the x, y, or z directions, and those transitions predicted to have energies less than 40 kk are included, this last being the excitation energy of the B_{2u} transition of an isolated benzene molecule. No corrections have been made for overlap or non-planar distortions; nor have further improvements such as the ω-technique been employed (6). The value of $\beta = 26.3$ kk has been chosen for each cation except TPM where the value of $\beta = 24.0$ kk has been used. The observed energies are in each case those of the vertical transition, since it is clearly impossible to choose the 0–0 vibronic component in any consistent way for all of the transitions. The agreement between the observed and calculated quantities given in Table II is very good, although the calculated intensities are too large. This difficulty often obtains in HMO calculations and more refined techniques usually lower these values materially. It should be noticed that the second transition of Mono, relative to that of TPM, and the first transition of Di, relative to that of Tris, are predicted to lie at the same energy. This prediction is clearly borne out in the experimental results and is in accordance with observations made on other compounds of this type (7).

Within the framework of the experiments we have conducted, we have been able to

Can. J. Chem. Downloaded from www.nrcresearchpress.com by 210.87.254.105 on 09/05/12
For personal use only.

reproduce all of the results of Chu and Weissman and at the same time experienced most of the difficulties that they mentioned in their paper. In particular, the fluorescence of TPM does not correlate with the absorption, and the fluorescence of Tris is not polarized during excitation of the long wavelength transitions. On the other hand excitation in the weak absorption band is perpendicularly polarized, a factor which would indicate that this transition is polarized in the z direction, as predicted by the group theoretical arguments and by the HMO calculations. Accordingly the transitions to degenerate states are assigned on the basis of intensity and of spectral energy, there being little doubt about the validity of this assumption. Even in the case of TPM this degeneracy has been lifted to some extent by some solvent or interionic interaction, so the observed band has two distinct maxima, and the upper states no longer lie at the same energy.

TABLE II

The spectral characteristics of triarylmethyl carbonium ions as calculated by the HMO method

	Energies				Intensities	
Compound	β	(kk)	Obs.	Symmetry	Calc.	Obs.
TPM	0	0	0	A	—	—
	1.0000	(24)	24.0	E	2.5495	1.64
	1.5060	35.2	34.5	A	0	0.2
Mono	0	0	0	A	—	—
	0.7512	19.8	19.8	A	2.3494	1.62
	1.000	26.3	24.0	B	1.2394	1.13
	1.2232	32.2	29.8	A	0.5266	0.45
	1.5024	39.6	37.0	A	1.0946	—
	1.5590	41.0			0.0913	—
Di	0	0	0	A	—	—
	0.7046	18.5	18.6	B	2.6303	1.84
	0.8106	21.3	21.7	A	1.8664	1.40
	1.1361	29.9	28.3	A	0.8110	0.62
	1.3174	34.6		B	0.2636	—
	1.4092	37.1	36	A B	0.8804	—
	1.5152	39.9		B	1.4216	—
Tri	0	0	0	A	—	—
	0.7046	(18.5)	18.6	E	3.6272	2.5
	0.9270	24.4	26.0	A	0	0.58
	1.3174	34.8	37.0	E	1.7465	—
	1.4093	37.1		E		
	1.6126	40.0	40.0	A	0	—
	1.6316	42.9		E	1.1977	—

It is the question of the assignment of the Mono and the Di derivatives which brings disagreement with the earlier work and which is the main reason for this present research. Chu and Weissman have based their assignment on the assumption that localized excitation of the biphenyl rings was responsible for the absorption in the region of 2800 Å. They noted, first of all, that the net absorption at 2580 Å increased through the carbinol series TPM to Tris in a way proportional to the number of biphenyl rings. They then assumed that the increase in absorption in the 2800 Å region is due to similar process in the cation series. Secondly, the polarization ratio is observed to be larger (2) in the case of Mono than in the case of the Di compound (~1.2). For long axis polarized low-energy absorption in biphenyl, this leads to the assignment of the first excited states of both Mono and Di to the symmetric representation, A. This is at variance with the HMO calculations and the experimental results presented here for the lowest energy transitions. Reconsidering the 2800 Å region there is predicted by the HMO theory to be increasing

Can. J. Chem. Downloaded from www.nrcresearchpress.com by 210.87.254.105 on 09/05/12
For personal use only.

absorption through the series of compounds. In the case of Mono, this is predominantly polarized parallel to the fluorescence. For the Di compound there is substantial overlapping of transitions of both polarizations, but the larger part of the absorption is predicted to be parallel. The polarization ratios would be expected to reflect these facts and Di would have a value reduced from that of Mono which would be expected to have a ratio typical of a solitary parallel transition. Accordingly, the measured polarization ratios have an alternative explanation, and it appears that the present assignment agrees in every detail with the experimental observations as well as with the expectations of the HMO and structure methods. At the same time there are fewer assumptions of a tentative nature.

IV. DISCUSSION

The critical factor in this determination, as in the case of the dye molecules, is that of the relative polarization of the low intensity band in the 300–400 mμ region of the spectrum. Similar transitions are found in the carbanion spectra of the hydrocarbon species. As far as the molecules of trigonal symmetry are concerned, it must be assumed that this transition gains intensity through slight distortions from the perfect symmetry. This might occur through non-totally symmetric vibrations, or through unsymmetrical perturbations in solution. The presence of such distortions and interactions are particularly evident in the case of TPM, where the loss of symmetry has resulted in a splitting of the degeneracy of the first excited states; there appear to be slight variations in this energy difference with the fluoroborate and perchlorate derivatives in various solvents, and the most reasonable explanation appears to be that the perturbations arise from a loose ion pairing. Crystal violet exhibits a similar tendency, and the perchlorate salt in non-polar solvents may exhibit as large a splitting as 2100 cm^{-1}. Nevertheless, the demonstration that these off-axis perturbations exist is not, in itself, sufficient to prove that the forbidden transition has gained sufficient intensity to correlate with the assignment. A considerably more valid test is to be found in some calculation where the assumed transition energy appears explicitly. In the structure representation a calculation of the transition intensities achieves this end in the following way. The first three term values for the molecule may be expressed in the Heisenburg form as a diagonal matrix,

$$\mathbf{E} = \begin{pmatrix} a & & \\ & 0 & \\ & & 0 \\ & & & b \end{pmatrix}$$

wherein a is the ground-state energy relative to the degenerate pair of states whose energy is arbitrarily taken as zero, b then is the energy of the normally inaccessible state, so that $(b-a)$ is the energy of the nominally symmetry forbidden transition. Using standard methods (3), it is possible to compute for the unperturbed molecule both $\mathbf{E}'$ and $\mathbf{S}^{-1}$ from the transformation equation,

$$\mathbf{E}' = \mathbf{S}^{-1}\,\mathbf{E}\,\mathbf{S}.$$

The intensities of the transitions are obtained from the square of the appropriate matrix element in the transition moment matrix, $\mathbf{X}$, resulting from the transformation,

$$\mathbf{X}' = \mathbf{S}\,\mathbf{X}\,\mathbf{S}^{-1},$$

where $\mathbf{X}'$ is, for instance, the dipole moment matrix for the structures in a specified

Can. J. Chem. Downloaded from www.nrcresearchpress.com by 210.87.254.105 on 09/05/12
For personal use only.

direction and $\mathbf{S}^{-1}$ is the same matrix as before. The elements in $\mathbf{X}'$ can be computed from the geometry and charge distribution of the structures. In particular,

$$\mathbf{X}' = \begin{pmatrix} 0 & 2.51 & \\ & & -2.51 \\ & & 0 \end{pmatrix}$$

for TPM, since it was assumed that the matrix is diagonal in the structure representation and that the ortho and para charged species contribute equally to each structure. The origin of the molecular frame is taken at the central carbon atom. Thus the calculated intensities depend upon $\mathbf{S}^{-1}$, which, in turn, depends upon the relative magnitudes of a and b. The magnitude of the forbidden band will always be zero, since $\mathbf{S}^{-1}$ incorporates the requirements of perfect symmetry. On the other hand, the intensities calculated for the intense bands will also reflect a faulty choice of b. The calculation of the transition moment lengths for the degenerate transitions for TPM and for Tris gives, in fact, the values 1.60 Å and 2.30 Å, which compare favorably with the experimentally determined values 1.64 Å and 2.50 Å respectively. By using the b values of transitions further in the ultraviolet, this agreement is lost. It should be noted that with the heterosubstituted dye molecules, the relative contributions of the ortho, para and extracyclic positive charge distributions are impossible to estimate a fortiori, so the required moments had to be determined empirically. This was not necessary in the present cases, a fact which lends credulity to the assumptions leading to formulation of $\mathbf{X}'$ as given above. It can be concluded that the use of structures results in a fairly accurate description of the charge distribution in the first few excited states of these carbonium ions.

Consideration of the matrix elements of $\mathbf{S}^{-1}$ of TPM leads to the conclusion that .043 units of electronic charge are distributed in each of the three phenyl rings. Unfortunately this is not in agreement with the estimates reached through nuclear magnetic resonance studies (8) which indicate that there is nearly twice this charge density on the ortho, meta, and para positions alone. Furthermore it would appear that the meta positions carry more positive charge than do ortho positions. This clearly contradicts the assumptions made above regarding the charge distribution within the rings. Roughly the same results are obtained for the carbanion of TPM (9). Using the suggested charge distribution as a basis for a calculation of the intensities of the optical transitions leads to much too high a value. On the other hand, proton chemical shifts are the resultant of many effects of both electrical and magnetic nature. As mentioned, there is good evidence that ion pairing exists with TPM salts in solution, and such association could in itself lead to considerable magnetic anisotropy. This would still be true if the counter ions undergo rapid exchange, in the time frame of n.m.r. measurements, but slow exchange as far as optical measurements are concerned (about 10^{-7} seconds in the present case). The possibility of rapid exchange may not be detectable by conductometric determinations (10) and could, in fact, account for some of the observed discrepancies. There is not much data available concerning the anisotropies associated with the highly charged central atom in TPM, and atomic contributions from this site might also modify the proton chemical shifts, but at the same time have relatively little effect on the charge distribution in the rings. Accordingly these purely magnetic effects would not necessarily show up in the optical spectra. Further investigations of other systems are under way in an effort to find the source of incongruity between the various measurements.

Can. J. Chem. Downloaded from www.nrcresearchpress.com by 210.87.254.105 on 09/05/12
For personal use only.

ACKNOWLEDGMENTS

Financial aid from the University of Alberta and National Research Council of Canada is very gratefully acknowledged.

REFERENCES

1. W. T. SIMPSON and C. W. LOONEY. J. Am. Chem. Soc. **76**, 6285 (1954).
2. C. W. LOONEY and W. T. SIMPSON. J. Am. Chem. Soc. **76**, 6293 (1954).
3. F. C. ADAM and W. T. SIMPSON. J. Mol. Spec. **3**, 363 (1959).
4. T. L. CHU and S. I. WEISSMAN. J. Chem. Phys. **22**, 21 (1954).
5. W. T. SIMPSON. J. Am. Chem. Soc. **75**, 597 (1953).
6. A. STREITWIESER, JR. J. Am. Chem. Soc. **82**, 4123 (1960).
7. R. GRINTER and S. F. MASON. Proc. Chem. Soc. 386 (1961).
8. T. SCHAEFER and W. G. SCHNEIDER. Can. J. Chem. **41**, 966 (1963).
9. V. R. SANDEL and H. H. FREEDMAN. J. Am. Chem. Soc. **85**, 2328 (1963).
10. K. ZEIGLER and H. WOLLSCHITT. Ann. **479**, 123 (1930).

Can. J. Chem. Downloaded from www.nrcresearchpress.com by 210.87.254.105 on 09/05/12
For personal use only.

THERMOCHEMICAL STUDIES OF SOME ACRYLATE AND METHACRYLATE POLYMERIZATIONS IN EMULSION SYSTEMS

K. G. McCurdy and K. J. Laidler
The Department of Chemistry, University of Ottawa, Ottawa, Canada
Received October 3, 1963

ABSTRACT

With the use of a Tian–Calvet microcalorimeter, the heats of polymerization of a number of monomers have been measured in aqueous emulsion systems: the emulsifying agent was cetyltrimethylammonium bromide, and initiation was by Fenton's reagent ($Fe^{++} + H_2O_2$). The monomers employed were acrylic acid, methyl, ethyl, and butyl acrylates, 2-hydroxyethyl methacrylate, 2-hydroxypropyl methacrylate, methacrylic acid, and methyl, ethyl, butyl, and hexyl methacrylates. The heats of polymerization lie in the range from 13 to 19 kcal per mole, the experimental standard deviations being 40 to 110 cal per mole. A steady increase was observed for acrylic acid and its CH_3, C_2H_5, and C_4H_9 esters, and for methacrylic acid and its CH_3, C_2H_5, C_4H_9, and C_6H_{13} esters. This change is attributed to a steady increase in the proportion of head-to-head, tail-to-tail polymers, leading to a decrease in steric hindrance. Abnormally low heats observed with hydroxyethyl methacrylate and 2-hydroxypropyl methacrylate are attributed to the solvation of the monomer, less solvation being possible in the polymer as a result of shielding.

Can. J. Chem. Downloaded from www.nrcresearchpress.com by 210.87.254.42 on 09/05/12
For personal use only.

INTRODUCTION

During the past few years a considerable amount of attention has been devoted to heats of polymerization, including those of monosubstituted (CH_2=CHX) and 1,1-disubstituted (CH_2=CXY) ethylenes. Estimates of heats ($-\Delta H$) of polymerization on the basis of bond and group energies lead to values close to 20 kcal per mole (1). Heats of polymerization of the monosubstituted ethylenes agree with this value, but the disubstituted ethylenes have heats that are less by 3 to 9 kcal per mole. This difference has been attributed (2, 3) to the energy of repulsion between the neighboring side-units in the polymer formed. The vinyl polymers exist predominantly in the head-to-tail arrangement, and in polymers formed from 1,1-disubstituted monomers there is steric hindrance involving side-groups or neighboring monomer residues. Valuable support for this point of view has been obtained by Baxendale and Madaras (4) in a study of heats of copolymerization.

The work done so far has shown that the heats evolved in the polymerization of the methacrylates (1,1-disubstituted ethylenes, H_2C=C(CH_3)COOR) are significantly lower than with the acrylates (monosubstituted ethylenes, H_2C=CHCOOR). No systematic study of the effect of substituents has, however, been carried out on these compounds. This has been done in the present investigation, the object of which was to learn more about the magnitude of the effects of steric hindrance. The polymerizations were carried out in aqueous emulsions, the emulsifying agent being cetyltrimethylammonium bromide. Initiation was brought about by Fenton's reagent: this produces OH radicals,

$$Fe^{++} + H_2O_2 \rightarrow Fe^{+++} + OH^- + OH,$$

and these initiate polymerization by adding on to double bonds.

EXPERIMENTAL

Calorimetry

The heats of polymerization were measured using a Tian–Calvet microcalorimeter that has been described in previous publications from this laboratory (5, 6); the amplification and integration circuits have been

described in detail by Attree and co-workers (7). The instrument was calibrated electrically by passing a known current through a measured resistance for a definite period of time. As a check the heat of solution of anhydrous lithium sulphate was measured; the value obtained, -6.54 ± 0.10 kcal per mole, is in satisfactory agreement with the value of -6.61 kcal per mole reported in the N.B.S. tables (8). The calories reported in this paper are defined calories, equal to 4.1840 joules.

Materials

The monomers employed in this work were kindly supplied by the Rohm and Haas Company, and had been purified. They were all reported to be over 99% pure except for 2-hydroxyethyl methacrylate and 2-hydroxypropyl methacrylate, which were both 96.5% pure. When received, the monomers contained a few parts per million of inhibitor. Just prior to polymerization of a monomer the inhibitor was removed by distillation under reduced pressure of nitrogen. The middle fraction of the distillate was collected and kept under refrigeration until used.

The emulsifying agent, cetyltrimethylammonium bromide, was an Eastman Kodak product; it was purified by recrystallizing it twice from acetone. The ferrous sulphate and hydrogen peroxide were reagent-grade chemicals. The materials used in the volumetric determination of the monomers were Fisher Certified Reagents.

Reaction Cell Assembly

A special cell was designed for measuring the heats of polymerization, and is shown in Fig. 1. The function

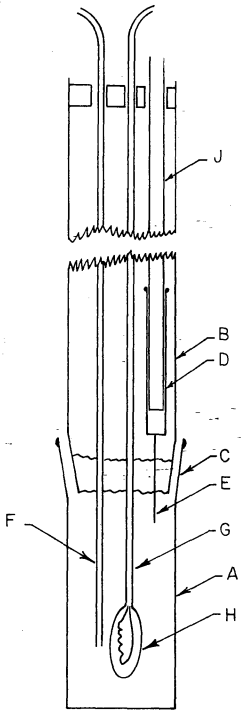

Fig. 1. The reaction cell assembly.

of the apparatus is to add the initiator to the reactants and to bring about gentle stirring. The cell A is constructed completely of glass, and it is connected to the upper part B by means of a 19/38 ground glass joint C. The monomer solution is contained in A, while the initiator is held in a 1-ml syringe, D. The syringe needle E passes through the ground glass joint, as does a small diameter glass tube F and a glass tube G carrying electrical leads; these are sealed in with epoxy resin, and the glass tube ends in a bulb H, which contains a calibrated resistor immersed in oil. This bulb is held submerged in the middle of the liquid in the reaction cell. The tube F is used for stirring, small regular alterations in pressure causing the liquid to oscillate through a short distance in the tube. The plunger of the syringe D was extended by a glass rod J that extended out of the top of the assembly; in this way the initiator solution could be injected into the reaction cell by merely depressing the plunger.

Can. J. Chem. Downloaded from www.nrcresearchpress.com by 210.87.254.42 on 09/05/12
For personal use only.

Experimental Procedure

The general procedure used for measuring heats of polymerization was as follows. The two syringes in the reaction assembly were loaded with the appropriate amount of hydrogen peroxide to give a 10^{-3} M solution after injection into 10 ml of solution in the reaction cell. An oxygen-free solution was prepared containing 1% of emulsifier and 10^{-2} N with respect to sulphuric acid and 10^{-3} M with respect to ferrous sulphate. Part of this solution (10 ml) was placed in one of the reaction cells, to be used as a blank. Monomer was introduced into the remainder of the solution and 10 ml of this placed in the other reaction cell. Both cells were allowed to stand in the calorimeter block long enough for thermal equilibrium to be attained. To initiate the polymerization in the cell containing monomer, the syringe plungers were then depressed. At the same time stirring was begun (and continued through the experiment) and the recording was started. When the reaction had essentially stopped, the heat evolved was estimated, and approximately the same quantity of electrical heat was developed in the reaction cell. At the conclusion of this calibration the exact heat evolved was calculated from the ratio of the two curve heights on the recorder that was connected to the integrator circuit.

Immediately after the completion of the calibration, the amount of monomer in the initial solution and in the final partially polymerized solution was determined by titration. The titration procedure was a modification of that described by Mitchell *et al.* (9). Ten milliliters of bromide solution was placed in each of three stoppered iodine-number flasks and the flasks were cooled in ice water. To one flask was added 5 ml of initial monomer solution and 5 ml of chloroform. Into a second flask was introduced the partially polymerized solution from the reaction cell, which was rinsed twice with 2 ml of water and twice with 2.5 ml of chloroform. The contents of the other reaction cell was introduced in a similar manner to the third flask. Each iodine-number flask was placed on an oscillating shaker immediately after the addition of the solution. The flasks were shaken for 1-hour periods, and then again chilled in the water. A 25-ml portion of a 10% KI solution was then added to each flask, which was then shaken. The solutions were then titrated with sodium thiosulphate solution until the chloroform layer was clear.

The amount of monomer polymerized can readily be shown to be given by

$$\text{no. moles polymerized} = \{N(Na_2S_2O_3)/2000\}\ (V_B - 2V_{mi} + V_{mp})$$

where $N(Na_2S_2O_3)$ is the normality of the thiosulphate solution, V_B is the titer of the blank, V_{mi} is the titer of the initial monomer solution, and V_{mp} is the titer of the partially polymerized solution. Duplicate titrations of monomer solutions were in agreement with each other to within 1%. Titrations on weighed quantities of monomer showed that gravimetric and volumetric determinations agreed to better than 1%.

Special checks were made to confirm that neither the initiation reaction nor the stirring contributed to the heat measured.

RESULTS

A number of measurements, at least five, were made on each monomer. The results obtained with 2-hydroxypropyl methacrylate are shown in Table I. Most of the measurements, including all of those in Table I, were made with a fixed initiator concentration and emulsifier concentration, namely 10^{-3} M initiator and 1.0% emulsifier. A number of measurements were made with different initiator and emulsifier concentrations, the range covered being from 0.5 to 2.0% emulsifier and 0.5×10^{-3} M to 4×10^{-3} M initiator. No effect on the heat was observed.

TABLE I

Heats of polymerization of 2-hydroxypropyl methacrylate

Expt. No.	Initial monomer conc. (mmoles/10 cc)	Final monomer conc. (mmoles/10 cc)	Amount polymerized (mmoles/10 cc)	Polymerization (%)	Heat evolved (cal)	Molar heat of polymerization (kcal/mole)
1	2.310	0.555	1.755	76.0	21.06	12.00
2	2.453	0.839	1.614	65.8	19.53	12.10
3	2.516	0.573	1.943	77.2	23.41	12.05
4	2.060	0.427	1.633	79.3	19.67	12.04
5	2.002	0.410	1.512	75.5	18.42	12.18
6	2.486	0.338	2.148	86.4	26.15	12.18
7	2.424	0.295	2.129	87.7	25.90	12.16
				Mean =	12.10	
				Standard deviation =	0.07	

Can. J. Chem. Downloaded from www.nrcresearchpress.com by 210.87.254.42 on 09/05/12
For personal use only.

Table II summarizes the final results for the various monomers.

TABLE II

Summary of heats of polymerization, $T = 25.0°$ C

Monomer	No. measurements	Molar heat of polymerization (kcal/mole)	Standard deviation (kcal/mole)
Acrylic acid	6	18.40	0.04
Methyl acrylate	5	18.58	0.05
Ethyl acrylate	5	18.79	0.04
n-Butyl acrylate	5	19.07	0.05
2-Hydroxyethyl methacrylate	5	11.94	0.08
2-Hydroxypropyl methacrylate	7	12.10	0.07
Methacrylic acid	6	13.46	0.07
Methyl methacrylate	21	13.57	0.06
Ethyl methacrylate	9	13.78	0.05
n-Butyl methacrylate	12	13.86	0.11
n-Hexyl methacrylate	6	14.00	0.08

DISCUSSION

Comparison with Previous Results

Heats of polymerization have previously been reported for some of the monomers used in the present study. These heats relate to a number of different states of the monomer and polymer, and Dainton and Ivin (10) have suggested a notation, which is summarized in Table III, for these states. Table IV summarizes the results obtained by

TABLE III

Summary of standard states

Notation	State of monomer	State of polymer
gg	Gas	Gas (usually hypothetical)
gc	Gas	Condensed (liquid or amorphous solid)
lc	Liquid	Condensed
ls	Liquid	Solution in monomer
ss	Solution	Solution
sc	Solution	Condensed

TABLE IV

Monomer	Standard states	Molar heat of polymerization (kcal/mole)	Temperature of polymerization	Reference
Acrylic acid	ss	18.5 ± 0.3 (18.40 ± 0.04)	20	12
	ls	16.0 ± 0.2	74.5	23
Methyl acrylate	lc	18.7±0.2	76.8	11
	ss	20.2±1.0 (18.58±0.05)	20	12
n-Butyl acrylate	ls	18.5±0.2	74.5	24
Methacrylic acid	ss	15.8±0.2 (13.45±0.07)	20	12
	ls	10.1±0.2	74.5	23
Methyl methacrylate	lc	13.0±0.2	76.8	13
	lc	13.9±0.3	76.8	18
	ls	13.8±0.2 (13.57±0.06)	26.9	19
	ls	13.3±0.1	74.5	24
	lc	13.4±0.5	130	20, 21
	lc	12.9±1.1	20	12
Ethyl methacrylate	lc	14.4±0.6	120	22
	ls	13.8±0.2 (13.78±0.05)	26.9	19
n-Butyl methacrylate	lc	13.5±0.2	76.8	13
	ls	14.3±0.3 (13.86±0.11)	26.9	19
n-Hexyl methacrylate	ls	14.4±0.3 (14.00±0.08)	26.9	19

Can. J. Chem. Downloaded from www.nrcresearchpress.com by 210.87.254.42 on 09/05/12
For personal use only.

various previous workers, our own values being shown in parentheses. Our values are best compared to the solution–solution values where available; they are measured at a different temperature (25.0° C) from those of previous studies, but the effect will be small.

The agreement between our results and those of other workers is good in some cases (acrylic acid and ethyl methacrylate) but not in others. In the case of methyl acrylate we agree with the lc value of Tong and Kenyon (11), but the ss value of Evans and Tyrrall (12) is considerably higher than ours. Their estimated error of 1 kcal, amounting to 5%, indicates a large degree of uncertainty in their results. Their value for methacrylic acid also differs considerably from ours, again being much higher. In the case of methyl methacrylate our value does not differ greatly from any of the several previous values, especially when the estimated errors are taken into account. The value of Tong and Kenyon (13) may be too low because they assumed complete polymerization.

The results of Joshi (23, 24), for bulk polymerization, were obtained at 74.5° C. They are in fair agreement for methyl methacrylate and *n*-butyl methacrylate, but differ significantly from previous results, and from the results of the present paper, for the two monomeric acids.

Interpretation of Results

Addition of a free radical to a monosubstituted or 1,1-disubstituted ethylene may occur in one of two different ways:

$$R— + H_2C{=}CXY \rightarrow R{-}CH_2{-}CXY—$$

$$R— + XYC{=}CH_2 \rightarrow R{-}CXY{-}CH_2—$$

The former process leads to a head-to-tail (HT) polymer, the latter to a head-to-head, tail-to-tail (HHTT) polymer. The relative rates of the two processes depend on the energies of the corresponding activated complexes, and the following two factors are of primary importance:

(1) In the radical R—CH_2—CXY— the substituents X and Y provide the possibility of resonance structures in which the unpaired electron resides on the radical, and this has the effect of stabilizing the radical. This resonance stabilization will also enter to some extent into the activated complex. No such resonance stabilization is possible in the case of the radical R—CXY—CH_2— or of its corresponding activated complex. This factor therefore favors the formation of HT polymers, and structural studies (14, 15, 16) in fact indicate that these are the most common.

(2) Steric effects, on the other hand, tend to favor the HHTT arrangement, as is shown schematically in Fig. 2. There is more steric interference in the case of an HT polymer than in an HHTT polymer, and this is also true in the case of the activated complexes. A polymer radical in which the odd electron is on the —CH_2— group (I and II in Fig. 2) will therefore prefer to add on to the —CH_2 end (I) rather than the —CXY end (II). Similarly a polymer radical with the odd electron on the CXY group will prefer to add on to the —CXY end of the monomer (IV) rather than to the —CH_2 end (III). As a result, the HHTT polymers tend to be preferred if there is much steric hindrance. In agreement with this, Marvel and Cowan (17) have shown that the monomers

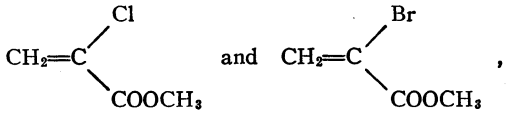

Can. J. Chem. Downloaded from www.nrcresearchpress.com by 210.87.254.42 on 09/05/12
For personal use only.

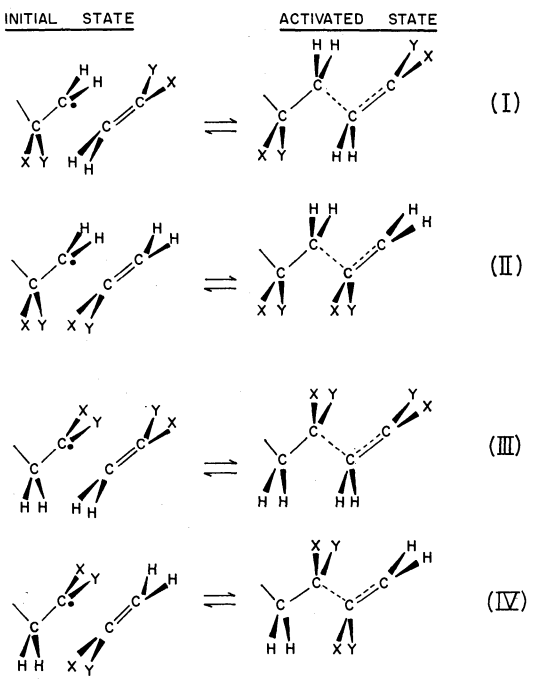

Fig. 2. Initial and activated states in polymerization.

where considerable steric effects are expected, lead predominantly to the HHTT arrangement.

These considerations lead naturally to an interpretation of the apparently paradoxical result that in both the acrylate and methacrylate series the change from methyl to ethyl to *n*-butyl leads to a steady increase in the heat of polymerization. It must be supposed that in these series the increasing steric hindrance leads to an increase in the proportion of HHTT polymer, so that in the products there is actually less hindrance with the more bulky substituents than with the smaller ones.

2-Hydroxyethyl methacrylate and 2-hydroxypropyl methacrylate both exhibit lower heats of polymerization than do the monomers having no hydroxyl groups. The difference seems too large to explain on the basis of changes in the bond strengths, or by steric hindrance, brought about by the hydroxyl groups. The most likely explanation appears to be that in solution the hydroxyl group in the monomer is solvated, but that in the polymer chain the hydroxyl groups are only partially solvated. The heats of solvation of alcohols are in the range from 2.5 to 4 kcal per mole, so that the effects observed could be explained if only part of the solvation shell is removed on polymerization.

It must be emphasized that since all of the effects discussed above are small, the explanations are necessarily tentative. Factors such as heats of emulsification of the monomers, or heats of wetting of the polymers, might also play a part.

ACKNOWLEDGMENT

The work was supported in part by the Defence Research Board under Grant 1028-28. One of us (K. G. McC.) is indebted to the National Research Council for a Scholarship.

Can. J. Chem. Downloaded from www.nrcresearchpress.com by 210.87.254.42 on 09/05/12
For personal use only.

REFERENCES

1. P. J. FLORY. Principles of polymer chemistry. Cornell Univ. Press, Ithaca, New York. 1953. Chap. VI.
2. F. D. ROSSINI. Chem. Rev. **27,** 1 (1940).
3. E. J. PROSEN and F. D. ROSSINI. J. Res. Nat. Bur. Std. **27,** 519 (1941).
4. J. H. BAXENDALE and G. W. MADARAS. J. Polymer Sci. **19,** 171 (1956).
5. H. M. PAPEE, W. J. CANADY, and K. J. LAIDLER. Can. J. Chem. **34,** 1677 (1956).
6. W. J. CANADY, H. M. PAPEE, and K. J. LAIDLER. Trans. Faraday Soc. **54,** 502 (1958).
7. R. W. ATTREE, R. L. CUSHING, J. A. LADD, and J. J. PIERONI. Rev. Sci. Instr. **29,** 491 (1958).
8. U.S. Nat. Bur. Std. Selected values of chemical properties. Ser. I. Washington. 1952.
9. J. MITCHELL, I. M. KOLTHOFF, E. S. PROSKAUER, and A. WEISSBERGER. Organic analyses. Vol. III. Interscience Publishers Inc., N.Y. 1956. p. 240.
10. F. S. DAINTON and K. J. IVIN. Quart. Rev. (London), **12,** 61 (1958).
11. L. K. J. TONG and W. O. KENYON. J. Am. Chem. Soc. **69,** 2245 (1947).
12. A. G. EVANS qnd E. TYRRALL. J. Polymer Sci. **2,** 387 (1947).
13. L. K. J. TONG and W. O. KENYON. J. Am. Chem. Soc. **68,** 1355 (1946).
14. C. S. MARVEL. The chemistry of large molecules. Interscience Publishers, New York. 1943. Chap. VII.
15. G. D. COUMOLOS. Proc. Roy. Soc. (London), A, **182,** 166 (1943).
16. H. W. THOMPSON and P. TORKINGTON. Trans. Faraday Soc. **41,** 254 (1945).
17. C. S. MARVEL and J. C. COWAN. J. Am. Chem. Soc. **61,** 3156 (1939).
18. S. EKEGREN, S. OHRN, K. GRANATH, and P. KINELL. Acta Chem. Scand. **4,** 126 (1950).
19. F. S. DAINTON, K. J. IVIN, and D. A. G. WALMSLEY. Trans. Faraday Soc. **56,** 1784 (1960).
20. S. BYWATER. Trans. Faraday Soc. **51,** 1267 (1955).
21. K. J. IVIN. Trans. Faraday Soc. **51,** 1273 (1955).
22. R. E. COOK and K. J. IVIN. Trans. Faraday Soc. **53,** 1132 (1957).
23. R. M. JOSHI. Makromol. Chem. **55,** 35 (1962).
24. R. M. JOSHI. J. Polymer Sci. **56,** 313 (1962).

Can. J. Chem. Downloaded from www.nrcresearchpress.com by 210.87.254.42 on 09/05/12
For personal use only.

RATES OF POLYMERIZATION OF ACRYLATES AND METHACRYLATES IN EMULSION SYSTEMS

K. G. McCurdy and K. J. Laidler
Department of Chemistry, University of Ottawa, Ottawa, Canada
Received October 3, 1963

ABSTRACT

The microcalorimeter has been used to obtain rates of polymerization of a number of monomers in emulsion systems. The rates with the acrylates are consistently higher than those with the methacrylates, and this is attributed to less steric hindrance. Low rates found with monomers containing a hydroxyl group are explained as due to solvation in the initial state. In both the acrylates and methacrylates the rates go through a maximum as one goes up the series methyl: ethyl: butyl: hexyl. This is discussed in terms of inductive and steric effects.

INTRODUCTION

The preceding paper (1) describes a microcalorimetric study of a number of vinyl polymerizations in emulsion systems. Several investigators (2–6) have described procedures for determining rate constants on the basis of calorimetric measurements, and in particular Baumgartner and Duhaut (7) and Lueck, Beste, and Hall (8) have developed methods that are especially suitable for our technique using the Tian–Calvet microcalorimeter. Lovering and Laidler (9) have recently applied the Baumgartner–Duhaut procedure to the determination of alcohol–isocyanate rate constants. The method of Lueck, Beste, and Hall (8), which is very similar, applies specifically to the differential method, which is the one employed in the present work.

EVALUATION OF THE RATE CONSTANTS

Kinetics of Emulsion Polymerization

The kinetic laws applicable to emulsion polymerization have been worked out in detail, and the present brief account covers only the essential points. Soap solutions such as those used in the present work, in which cetyltrimethylammonium bromide is the emulsifying agent, have been shown by McBain (10) and Harkins (11, 12) to contain micelles consisting of layers of oriented soap molecules. When substances such as the monomers used in the present investigation are added to such a soap solution they are "solubilized", which means that some of the monomer penetrates the micelles. Some of the monomer also remains as suspended droplets in the aqueous phase.

Harkins (13) proposed that in emulsion systems there are two principal loci of polymerization. Initially, when there is not much polymer present, the micelles contain largely monomer, and because the radii of the micelles are much smaller than those of the droplets the micelles present a much larger interfacial area. Most of the polymerization therefore takes place in these micelles. The process is that the free radicals generated by the initiation in the aqueous phase are captured by the micelles, and that monomer is supplied to the growing radicals from the droplets in the surrounding solution. The micelles therefore grow larger and soon consist largely of polymer particles with soap adsorbed on them. After 2 to 3% of the monomer has been converted into polymer the micelles have in fact largely disappeared, and have been replaced by polymer particles. From this point on, therefore, the locus of polymerization is the polymer particles.

Can. J. Chem. Downloaded from www.nrcresearchpress.com by 210.87.254.105 on 09/05/12
For personal use only.

A quantitative formulation of this theory was put forward by Smith and Ewart (14). Applied to the later phase of the process, when polymerization is occurring in the polymer particles, the number of which has become constant, the treatment may be outlined as follows. On the average there are 10^{14} particles per cubic centimeter and in a typical experiment 10^{13} radicals are produced per cubic centimeter per second; if all of these enter the polymer particles a particle will acquire a radical once in about 10 seconds on the average. Once a radical has entered a particle it proceeds to grow by adding monomer units at a rate equal to the rate constant for the propagation process, k_p, multiplied by the monomer concentration [M] in the particles.

If a radical enters a particle that already contains a radical it will at once combine with it, and from this it follows that at any time one-half of the polymer particles will contain one radical and the other half no radical. If N is the total number of polymer particles the rate of polymerization is therefore given by

$$[1] \qquad v_p = \tfrac{1}{2}k_p[\mathrm{M}]N.$$

This relationship has been confirmed (15–19) for a number of systems, and the k_p values derived are in reasonable agreement with those obtained in other ways. Relationships between the number, N, of particles and the concentrations of emulsifier and initiator have been derived by Smith and Ewart (14) and by Medvedev (20), whose model is a little different from that outlined above.

The essential point as far as the present investigation is concerned is that the monomer concentration is sufficiently low (0.2 M) that all of the monomer is solubilized. The monomer concentration in the particles is therefore proportional to the overall monomer concentration.

The experiments were all carried out at an emulsifier concentration of 1% and an initiator concentration of 10^{-3} M; this ensures constancy of the number N of particles. Since this number remains constant throughout a run the kinetics will be first-order.

THE THERMAL METHOD FOR DETERMINING RATE CONSTANTS

The principle of the method used has been described by Lovering and Laidler (9). It is sufficient here to note that the extent of reaction at time t is measured by the area of the e.m.f. vs. time curve up to that point, plus a contribution due to the loss of heat from the cell to the calorimeter block; this is determined by a separate measurement in which electrical heat is supplied to the cell.

In this way the amount reacted can be determined at various times, and the rate constant calculated in the usual way. This was carried out at various times, covering the initial part of the reaction, up to 50% completion. A graphical method was employed for obtaining the first-order rate constants.

RESULTS

Fig. 1 shows a typical plot used for the determination of a rate constant; it relates to experiment 1 (cf. Table I) for methyl methacrylate. Table I gives the rate constants calculated on the basis of a number of completely different experiments, under identical experimental conditions, for the polymerization of methyl methacrylate. The values are seen to be reasonably constant. Table I summarizes also the averaged rate constants, and standard deviations, for all of the polymerizations studied.

DISCUSSION

Comparison with Previous Results

Rate constants previously derived for the polymerizations of the monomers employed in the present work are derived from bulk polymerization studies; they are second-order

Can. J. Chem. Downloaded from www.nrcresearchpress.com by 210.87.254.105 on 09/05/12
For personal use only.

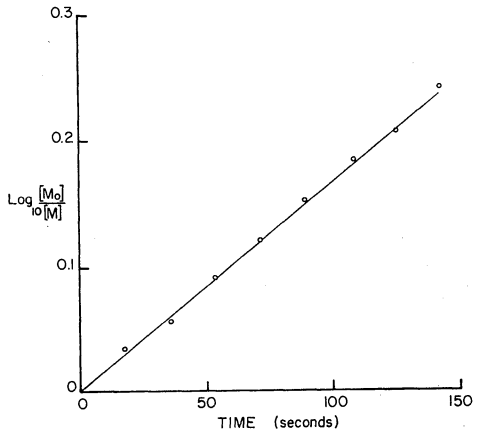

Fig. 1. A typical first-order plot, for the polymerization of methyl methacrylate.

TABLE I

Rate constants for the polymerization of methyl methacrylate and all compounds studied

Polymerization of methyl methacrylate		All polymerizations studied (T = 25° C)	
Expt. No.	Rate constant × 10^3 (sec^{-1})	Monomer	Rate constant × 10^3 (sec^{-1})
1	1.66	Methacrylic acid	2.15 ± 0.19
2	1.70	Methyl methacrylate	1.83 ± 0.28
3	1.68	Ethyl methacrylate	2.84 ± 0.28
4	1.72	*n*-Butyl methacrylate	2.66 ± 0.23
5	1.68	*n*-Hexyl methacrylate	1.35 ± 0.18
6	1.72	Acrylic acid	4.19 ± 0.43
7	1.68	Methyl acrylate	8.83 ± 0.60
8	1.70	Ethyl acrylate	12.64 ± 0.41
9	1.67	*n*-Butyl acrylate	9.62 ± 0.10
10	1.52	Hydroxyethyl methacrylate	1.24 ± 0.19
11	1.60	2-Hydroxypropyl methacrylate	1.97 ± 0.39

rate constants, and relate to those of the present work through N, the concentration of particles. The values agree provided that N is 10^{15} to 10^{16} particles per cc, and this is the value of N obtained in a number of investigations of emulsion polymerization (15–19, 21).

The previous kinetic studies of bulk polymerization are consistent with the results of the present work as far as general trends are concerned. Thus in the methacrylate series previous work shows the maximum in rate constant in going from methyl to butyl. Some previously obtained rate constants are:

methyl methacrylate at 24° C: 310 liter $mole^{-1}$ sec^{-1}, (22)

n-propyl methacrylate at 30° C: 467 liter $mole^{-1}$ sec^{-1}, (23)

n-butyl methacrylate at 30° C: 362 liter $mole^{-1}$ sec^{-1}. (24)

For the acrylates the only previously reported values are:

methyl acrylate at 30° C: 769 liter $mole^{-1}$ sec^{-1}, (25)

n-butyl acrylate at 25° C: 13 liter $mole^{-1}$ sec^{-1}. (26)

Our value (cf. Table I) for methyl acrylate is lower than that for *n*-butyl acrylate. There is evidence, however, that the previously reported value (25) for methyl acrylate is too high on account of autoacceleration (27).

Also, the previous value for *n*-butyl acrylate (26) is lower than that for *n*-butyl methacrylate (24), which is contrary to expectation on steric grounds.

Can. J. Chem. Downloaded from www.nrcresearchpress.com by 210.87.254.105 on 09/05/12
For personal use only.

Interpretation of Results

The propagation rate constants are seen from Table I to be consistently higher for the acrylates than for the corresponding methacrylates. As discussed in the preceding paper (1), with reference to heats of polymerization, there is considerably less steric hindrance to polymerization in the case of the acrylates than in the methacrylates, and this may well explain the difference in rates.

In the acrylate series the rate constants increase from acrylic acid to methyl acrylate to ethyl acrylate, but then decrease on going to butyl acrylate. The behavior in the methacrylate series is similar: the apparent deviation for methacrylic acid and methyl methacrylate is within the experimental error. There is a decrease from ethyl to butyl to hexylmethacrylate. These trends can be explained in terms of inductive effects and steric effects. The increases in rates from methyl to ethyl are attributed to the greater electron-donating power of the ethyl group as compared with methyl. It would appear that the increased electron-donating power facilitates the opening of the double bond, and in this way increases the rate of addition of the monomer to the polymer radical. The steric difference between methyl and ethyl is probably unimportant.

In the series ethyl: butyl: hexyl the inductive effects will be very similar, and the steric effects will now become predominant, leading to a progressive decrease in rate. This steric effect is envisaged as simply arising from the physical size of the monomers; as this size is increased there is more interference between substituent groups, a bulky monomer having greater difficulty in approaching a polymer radical.

Hydroxyethyl methacrylate and 2-hydroxypropyl methacrylate both exhibit low rates of polymerization, and this is to be related to their low heats of polymerization (1). The monomers will be more solvated than the activated complexes, and the free energies of activation will therefore be higher than with the monomers not containing hydroxyl groups.

ACKNOWLEDGMENT

The work was supported in part by the Defence Research Board under Grant 1028-28. One of us (K. G. McC.) is indebted to the National Research Council for a Scholarship.

REFERENCES

1. K. G. McCURDY and K. J. LAIDLER. Can. J. Chem. This issue.
2. H. HARTRIDGE and F. J. W. ROUGHTON. Proc. Roy. Soc. A, **104**, 376 (1923).
3. R. P. BELL and J. C. CLUNIE. Proc. Roy. Soc. (London), **212**, 16 (1952).
4. N. H. RAY. J. Chem. Soc. 4023 (1960).
5. P. A. H. WYATT. J. Chem. Soc. 2299 (1960).
6. W. J. ALBERTY and R. P. BELL. Trans. Faraday Soc. **57**, 1942 (1961).
7. P. BAUMGARTNER and P. DUHAUT. Bull. Soc. Chim. France. 1187 (1960).
8. C. H. LUECK, L. F. BESTE, and H. K. HALL. J. Phys. Chem. **67**, 972 (1963).
9. E. G. LOVERING and K. J. LAIDLER. Can. J. Chem. **40**, 31 (1962).
10. J. W. McBAIN. Advances in colloid chemistry. Vol. I. Interscience Publishers Inc., N.Y. 1942. p. 124.
11. W. D. HARKINS. J. Chem. Phys. **13**, 381 (1945).
12. W. D. HARKINS and R. S. STEARNS. J. Chem. Phys. **14**, 215 (1946).
13. W. D. HARKINS. J. Am. Chem. Soc. **69**, 1428 (1947).
14. W. V. SMITH and R. H. EWART. J. Chem. Phys. **16**, 592 (1948).
15. W. V. SMITH. J. Am. Chem. Soc. **70**, 3695 (1948).
16. W. V. SMITH. J. Am. Chem. Soc. **71**, 4077 (1949).
17. M. MORTON, P. P. SANATIELLO, and H. LANDFIELD. J. Polymer Sci. **8**, 111 (1952).
18. M. MORTON, P. P. SANATIELLO, and H. LANDFIELD. J. Polymer Sci. **8**, 215 (1952).
19. M. MORTON, P. P. SANATIELLO, and H. LANDFIELD. J. Polymer Sci. **8**, 279 (1952).
20. S. S. MEDVEDEV. International symposium on macromolecular chemistry. Pergamon Press, N.Y. 1959. p. 174.
21. J. G. BRODNYAN, J. A. CALA, T. KONEN, and E. L. KELLEY. J. Colloid Sci. **18**, 73 (1963).

Can. J. Chem. Downloaded from www.nrcresearchpress.com by 210.87.254.105 on 09/05/12
For personal use only.

22. M. H. MacKay and H. W. Melville. Trans. Faraday Soc. **45,** 323 (1949).
23. G. M. Burnett, P. Evans, and H. W. Melville. Trans. Faraday Soc. **49,** 1105 (1953).
24. G. M. Burnett, P. Evans, and H. W. Melville. Trans. Faraday Soc. **49,** 1096 (1953).
25. M. S. Matheson, E. E. Auer, E. B. Bevilacque, and E. J. Hart. J. Am. Chem. Soc. **73,** 5395 (1951).
26. H. W. Melville and A. F. Bickel. Trans. Faraday Soc. **45,** 1049 (1949).
27. C. H. Bamford, W. G. Barb, A. D. Jenkins, and P. F. Onyon. The kinetics of vinyl polymerization by radical mechanisms. Butterworth Scientific Publications, London. 1958. p. 82.

Can. J. Chem. Downloaded from www.nrcresearchpress.com by 210.87.254.105 on 09/05/12
For personal use only.

EXTRACELLULAR GLYCOLIPIDS OF RHODOTORULA SPECIES

THE ISOLATION AND SYNTHESIS OF 3-D-HYDROXYPALMITIC AND 3-D-HYDROXYSTEARIC ACIDS[1]

A. P. TULLOCH AND J. F. T. SPENCER
National Research Council of Canada, Prairie Regional Laboratory, Saskatoon, Saskatchewan
Received November 27, 1963

ABSTRACT

Several species of the red yeast *Rhodotorula* produce extracellular glycolipids which consist of a mixture of mannitol and pentitol esters of 3-D-hydroxypalmitic and 3-D-hydroxystearic acids. One molecule of the long chain acid is attached to each polyol molecule and most of the remaining hydroxyl groups including the one on the fatty acid are acetylated.

Can. J. Chem. Downloaded from www.nrcresearchpress.com by 210.87.254.42 on 09/05/12
For personal use only.

The formation of extracellular lipid by *Rhodotorula graminis* was reported by di Menna in 1958 (1). Later Deinema (2, 3) studied extracellular lipid production in *R. graminis* and in two strains of *R. glutinis*. She also investigated the composition of the lipids and found acetic acid, a number of known and unknown long-chain fatty acids, and polyols among the hydrolysis products. In an investigation of the production of extracellular lipids by yeasts which is being carried out in this laboratory (4), three species of *Rhodotorula*, which form such lipids, were isolated.

The composition of the lipids produced by these species and also that produced by *R. glutinis* CBS 4648, originally studied by Deinema, were investigated. The "oily" extracellular material, obtained when the yeasts were grown in shaken culture, was heavier than water and therefore was easily isolated. It was found to be a mixture of polyol esters, which was soluble in both methanol and hexane. However, on one occasion when *R. glutinis* strain 4648 was grown in fermentors the oil produced was only partly soluble in methanol, and could be separated by solvent distribution into polyol esters and triglycerides. The principal fatty acids of the latter were oleic and palmitic acids. It is probably this extracellular triglyceride which gave rise to the ordinary fatty acids found by Deinema (2, 3).

Acid methanolysis of the polyol esters gave free polyols, the methyl esters of hydroxy acids, and methyl acetate. The relative amounts of the first two groups of components corresponded approximately to a ratio of 1 molecule of fatty acid to 1 molecule of polyol. The polyols were analyzed as the acetates by gas liquid chromatography (GLC) and consisted of a mixture of D-mannitol, D-arabitol, and minor amounts of xylitol. The fatty acid ester portion was almost the same for each strain and was a mixture of 3-D-hydroxypalmitic (85%) and 3-D-hydroxystearic (15%) acids. The evidence for this conclusion is described below.

A mixture of palmitic and stearic acids was obtained by reduction of the hydroxy acids with red phosphorus and hydrogen iodide followed by zinc and hydrochloric acid, showing that the fatty acids contained unbranched carbon chains. This finding and the observation that the carbon numbers, on a silicone column, were 17.7 and 19.7, or almost two units greater than the carbon numbers of palmitic and stearic acids, suggested that

[1]*Issued as N.R.C. No. 7801.*

the fatty components were hydroxy acids (5, 6). The methyl esters were partly separated into C_{16} and C_{18} components by countercurrent distribution. The only isolatable product of chromic acid oxidation of the C_{16} ester was myristic acid, which indicated that the hydroxyl group was at position 3.

Further evidence for this was derived from the action of base on the original polyol esters and on the acetoxy ester, obtained by acetylation of the hydroxy ester. Treatment of the polyol ester with sodium methoxide solution, to effect methanolysis, produced an unsaturated C_{16} ester in addition to the hydroxy ester. The acid corresponding to this ester was found to be *trans*-2-hexadecenoic acid. This acid was also obtained by alkaline hydrolysis of the polyol ester or the C_{16} acetoxy ester. Linstead *et al.* (7) have shown that when β-acetoxy esters are treated with bases β-elimination of acetic acid occurs and an α,β-unsaturated acid is produced. The relative amounts of unsaturated and hydroxy acid obtained by alkali treatment of the polyol ester and of methyl 3-acetoxypalmitate were compared by GLC analysis. The relative amount of unsaturated acid yielded by the polyol ester was slightly lower than that yielded by the pure acetoxy ester indicating that in most, but not all, of the polyol ester molecules the 3-hydroxyl group was acetylated. The results showed that the 3-hydroxystearic acid was also mainly acetylated. Therefore in working with a lipid which contains a 3-acetoxy fatty acid grouping hydrolysis must be carried out in an acid medium. The previous workers (2, 3) employed alkaline hydrolysis and consequently obtained confusing results.

Racemic methyl 3-hydroxypalmitate was synthesized and compared with the ester obtained from the glycolipid. The carbon numbers, on the silicone column, were the same and the infrared spectra in carbon tetrachloride solution were indistinguishable. However, the infrared spectra, compared as Nujol mulls, were quite different. The 3-hydroxy esters and acids obtained from the glycolipid were quite strongly laevorotatory in chloroform, but in methanol the specific optical rotation was quite small, which is characteristic of 3-hydroxy fatty acids (8). The negative rotation suggests that the compounds have the D-configuration (9).

To establish the configuration and structure of the acids of the glycolipid 3-D-hydroxypalmitic and 3-D-hydroxystearic acids were synthesized from (+) methyl hydrogen β-acetoxyglutarate by the general method of Serck-Hanssen (8). The products were identical with those obtained from the yeast lipid.

It appears that these two particular 3-hydroxy acids have not been obtained from natural sources previously, but 3-D-hydroxymyristic acid has been isolated from *Escherichia coli* (10), 3-D-hydroxylauric acid from a metabolite of *Isaria cretacea* (11), and 3-D-hydroxycapric acid from a metabolite of *Pseudomonas aeruginosa* (12).

Approximately 3.5 molecules of acetic acid were obtained per molecule of glycolipid but the points of substitution of the acetic acid and fatty acid residues on the polyol were not investigated. The product is probably a complex mixture of isomers. The fatty acids and polyols of the intracellular lipids of three of the four strains were also analyzed. The composition of the polyol fraction is shown in Table I. The two lipids are quite different, the intracellular lipid being mostly triglycerides and the extracellular lipid a mixture of esters of 5 and 6 carbon polyols. Table II shows the composition of the fatty acid fractions. The two lipids obtained from *R. glutinis* strain 4648 closely resemble each other in fatty acid composition and strain 16A8 is also similar. However, the acids from *R. graminis* strain 6CB contain different relative amounts of palmitic and oleic acids. The composition of the cell fat of *R. graminis* di Menna has been reported (13) but differed from that of the strain used here in having a considerably lower oleic acid content.

Can. J. Chem. Downloaded from www.nrcresearchpress.com by 210.87.254.42 on 09/05/12
For personal use only.

TABLE I

Polyols of the intra- and extra-cellular lipids

		Glycerol	Arabitol (mol. %)	Xylitol (mol. %)	Mannitol
R. glutinis strain 4648	Intracellular	86.9	8.2	1.2	3.7
	Extracellular triglycerides	94.5	5.5	—	—
	Extracellular polyol esters	—	49.7	—	50.3
R. glutinis strain 16A8	Intracellular	81.3	4.9	1.1	12.7
	Extracellular	—	24.0	3.5	72.5
R. graminis strain 6CB	Intracellular	97.9	0.8	—	1.3
	Extracellular	—	15.6	7.5	76.9

TABLE II

Fatty acid composition of lipids other than polyol esters

Fatty acids, weight %	*R. glutinis* strain 4648		*R. glutinis* strain 16A8	*R. graminis* strain 6CB
	Extracellular	Intracellular		
Myristic	1.2	1.1	1.5	1.3
Palmitic	31.4	32.7	28.7	21.6
Palmitoleic	1.2	1.1	3.2	1.6
Stearic	8.3	8.7	2.4	2.3
Oleic	43.2	40.0	46.3	61.0
Linoleic	12.3	11.4	10.6	11.3
Linolenic	1.9	2.3	5.2	0.7
Unidentified	0.5	2.7	2.1	0.2
Oil content %	—	71	64	74

EXPERIMENTAL

Melting points were determined using a Leitz hot-stage microscope. Optical rotations were measured at 25° C in a 1 dm tube.

Method of Oil Production

The yeasts were isolated from flowers obtained from several localities in Canada. On the basis of carbon assimilation tests (14) the yeasts were considered to be *R. glutinis* strain 16A8, *R. mucilaginosa* strain S6A1, and *R. graminis* strain 6CB. The last strain resembled *R. graminis* di Menna C.B.S. 2826 but differed from this culture in not assimilating cellobiose, L-arabinose, dulcitol, and salicin (J. F. T. Spencer and H. Phaff, unpublished work). The medium used consisted of glucose (4%), yeast extract (0.2%), potassium dihydrogen phosphate (0.1%), and magnesium sulphate heptahydrate (0.02%). Flasks containing 50 ml of medium were agitated on a Gump shaker having a radius of 1 in. at 230 r.p.m. for a period of 8–10 days. Three liter fermentors were used at 28° C, with an air flow of 1 liter/minute, a stirring speed of 400 r.p.m., and inoculated with 100 ml of 24-hour shaken culture. The yield of extracellular lipid was 1–2 g/liter. The cells and lipid were allowed to settle and the lipid was washed away from the cells with light petroleum, b.p. 60–80° C.

Gas–Liquid Chromatographic Analysis

The hydroxy fatty acid esters were analyzed by means of a silicone on celite column as previously described (5). Methyl 3-hydroxypalmitate and methyl 3-hydroxystearate had carbon numbers of 17.7 and 19.7 respectively. On this column methyl 2-hexadecenoate has a carbon number of 16.5 and is completely separated from methyl palmitate. On the other hand, methyl 9-hexadecenoate has a carbon number which is very slightly lower than that of methyl palmitate.

The separation of all the pentitol and hexitol acetates except for those of glucitol and galactitol was described by Jones and co-workers (15) using a column packing which consisted of a mixture of polyester and non-polar phases. In the present work an 8 ft × 3/16 in. copper column packed with 1:30 butanediol. succinate (16) on 40–60 mesh acid-washed firebrick was used. The oven temperature was 212° C and the

Can. J. Chem. Downloaded from www.nrcresearchpress.com by 210.87.254.42 on 09/05/12
For personal use only.

helium flow rate 60 ml/minute. This column partly separated glucitol and galactitol acetates and the retention times of the acetates relative to arabitol pentaacetate were as follows: ribitol 0.89, arabitol 1.00 (18 minutes), xylitol 1.24, mannitol 2.60, galactitol 2.97, glucitol 3.12. The column used by Jones and co-workers separated the acetates in the same order, except for the last two, and also effected a good separation of allitol, talitol, and iditol acetates from the other three. It is probable that the present column would separate all six hexitol acetates.

To separate and collect larger quantities of arabitol and mannitol acetates and fatty acid esters an 8 ft × 5/16 in. copper column with 1:6 silicone grease on acid-washed celite was used at 240° C, with injector at 290° C, and a flow rate of 60 ml helium/minute.

Composition of the Extracellular Lipids

The lipid had a molecular weight (osmometric in acetone) of 560, a saponification equivalent of 110.5, and gave 0.44 g of volatile acid (calculated as acetic acid) per gram of lipid. The volatile acid was analyzed by gas chromatography as the decyl ester (17) and acids of chain length longer than two carbon atoms were absent. The analyses do not correspond to a definite composition and the lipid is probably quite a complex mixture. It contains approximately 3 to 4 molecules of acetic acid for each lipid molecule.

Acid Methanolysis of the Extracellular Lipid

Lipid (11.56 g) was refluxed for 1 hour with 3% methanolic hydrogen chloride and the acid neutralized with silver carbonate. After filtration the volatile material was removed on a rotary evaporator and collected in a dry-ice trap. This fraction, which contained methyl acetate, was saponified and a portion of the salt obtained treated with S-benzyl thiouronium chloride to give S-benzyl thiouronium acetate with a melting point of 135–138° C, which was not depressed by an authentic sample.

Hydroxy fatty acid esters (5.30 g) were extracted from the residue, obtained after removing the methyl acetate, by stirring with ether. The polyols (3.18 g) remained and when analyzed by paper chromatography (*n*-butanol–ethanol–water 40:11:19 v/v) only pentitols and hexitols were found. When the polyols from *R. glutinis* strain 4648 were examined a portion was acetylated and separated in 35 mg batches by means of the preparative silicone column. D-Mannitol hexaacetate, so obtained, had $[\alpha]_D$ +32.0° (*c*, 1.0, $CHCl_3$) and melting point 120–123° C, after crystallization from ethanol. The mixed melting point with an authentic sample of D-mannitol hexaacetate was 122–124° C. D-Arabitol pentaacetate was crystallized from ethanol–hexane and had $[\alpha]_D$ +36.8° (*c*, 1.5, $CHCl_3$) and melting point 71–73° C. The mixed melting point was not depressed by an authentic sample.

Structure of the Hydroxy Fatty Acids

The composition of the hydroxy fatty acid methyl ester portion, as analyzed by GLC, was almost the same for the lipids from all the strains examined. Palmitic and stearic acids were very minor components (0.3% or less), the approximate composition was 3-hydroxypalmitate (85%), and 3-hydroxystearate (15%).

Mixed esters (10 mg) were refluxed overnight with 47% aqueous hydrogen iodide (5 ml) and red phosphorus (100 mg), the mixture poured into water, and the acids isolated. The saturated acids obtained by refluxing for 5 hours with concentrated hydrochloric acid (1 ml) and zinc dust (100 mg) were identified, by GLC, as palmitic and stearic acids. Hydroxy methyl esters (3 g) were distributed between 85% ethanol and light petroleum b.p. 40–60° C by 125 cycles of a modified E.C. Apparatus Co. fractionater with 100 tubes and 20 ml capacity each phase. Only a partial separation of the C_{16} and C_{18} esters was obtained. Tubes 52–70 contained methyl 3-hydroxypalmitate (1.3 g) and tubes 84–88 contained methyl 3-hydroxystearate (0.075 g). After crystallization from acetone, methyl 3-D-hydroxypalmitate had melting point 48–49° C and $[\alpha]_D$ −13.8° (*c*, 5.6, $CHCl_3$) and −0.3° (*c*, 7.1, MeOH). Calculated for $C_{17}H_{34}O_3$: C, 71.3%; H, 12.0%. Found: C, 71.2%; H, 11.9%. The peaks in the OH and carbonyl regions of the infrared spectra were as follows: 3380 (s), 3300 (s), 1735 (s), 1690 (s), (Nujol mull); 3550 (w), 1727 (s) cm^{-1}, (0.2% in carbon tetrachloride). Saponification of the methyl ester with potassium hydroxide (5% in 90% ethanol) at 60° C for 1 hour yielded 3-D-hydroxypalmitic acid which had melting point 78–79° C, after crystallization from acetone, and $[\alpha]_D$ −12.9° (*c*, 1.3, $CHCl_3$) and +2.1° (*c*, 6.8, MeOH). Calculated for $C_{16}H_{32}O_3$: C, 70.5%; H, 11.8%; neutral equivalent, 272.5. Found: C, 70.8%; H, 11.7%; neutral equivalent, 275.5.

The C_{18} fraction was crystallized from acetone and yielded methyl 3-D-hydroxystearate, m.p. 55.5–56.5° C; $[\alpha]_D$ −15.0° (*c*, 1.9, $CHCl_3$). Calculated for $C_{19}H_{38}O_3$: C, 72.6%; H, 12.2%. Found: C, 72.5%; H, 12.0%. The peaks in the infrared spectrum (Nujol mull) in the OH and carbonyl regions were 3380 (s), 3300 (s), 1735 (s), 1690 (s) cm^{-1}. Saponification yielded 3-D-hydroxystearic acid which had melting point 84–86° C, after crystallization from acetone and $[\alpha]_D$ −12.0° (*c*, 1.2, $CHCl_3$). Calculated for $C_{18}H_{36}O_3$: C, 71.95%; H, 12.1%. Found: C, 71.8%; H, 12.0%.

Chromic Acid Oxidation

Methyl 3-D-hydroxypalmitate (0.12 g) was oxidized overnight with 0.1 *N* chromium trioxide in acetic acid (50 ml); water was added, the excess oxidant reduced with sulphur dioxide and the product (0.1 g) extracted with ether. The product was converted to the methyl ester and purified by gas chromatography using the preparative silicone column at 200° C. Saponification and crystallization from hexane yielded myristic acid with melting point 53–54° C, which was not depressed by admixture with pure myristic acid.

Can. J. Chem. Downloaded from www.nrcresearchpress.com by 210.87.254.42 on 09/05/12
For personal use only.

Synthesis of the Hydroxy Esters

Racemic Methyl 3-Hydroxypalmitate

Methyl 3-oxopalmitate was prepared from myristoyl chloride (18) and hydrogenated over Raney nickel (19) to give methyl 3-hydroxypalmitate, m.p. 41–43° C. Calculated for $C_{17}H_{34}O_3$: C, 71.3%; H, 12.0%. Found: C, 71.4%; H, 11.8%. Infrared maxima in the OH and carbonyl regions were 3390 (m), 3570 (sh), 1730 (s), (Nujol mull); 3550 (w), 1727 (s) cm^{-1}, (0.2% in carbon tetrachloride.)

3-D-Hydroxypalmitic Acid

(+) Methyl hydrogen β-acetoxyglutarate (8) (1 g) and tridecanoic acid (3 g) were electrolyzed in 0.022 *N* sodium methoxide in methanol (30 ml) until the solution was just alkaline. After the solution was acidified with acetic acid, it was filtered from hydrocarbon by-products, part of the methanol was taken off, 3% methanolic hydrogen chloride added, and the mixture refluxed for 3 hours. Water was added and the product extracted with ether. The crude product (1.1 g) was chromatographed on silicic acid (60–200 mesh); elution with light petroleum (b.p. 60–80° C) containing 2% acetone gave a small amount of methyl tridecanoate followed by the desired hydroxy ester (0.45 g). Crystallization from acetone yielded methyl 3-D-hydroxypalmitate, m.p. 49–50° C, which was not depressed when mixed with the natural ester, $[\alpha]_D$ was −14.3° (*c*, 2.5, $CHCl_3$). Calculated for $C_{17}H_{34}O_3$: C, 71.3%; H, 12.0%. Found: C, 71.1%; H, 12.0%. The infrared spectrum (Nujol mull) and the X-ray powder photograph were indistinguishable from those of the natural product. 3-D-Hydroxypalmitic acid was obtained by saponification, and after crystallization from acetone had melting point 77–79° C and $[\alpha]_D$ −13.8° (*c*, 2.4, $CHCl_3$); the melting point was not depressed by admixture with natural acid. Calculated for $C_{16}H_{32}O_3$: C, 70.5%; H, 11.8%. Found: C, 70.5%; H, 12.0%.

3-D-Hydroxystearic Acid

Pentadecanoic acid was prepared by stepwise oxidation of 1-hexadecene in the same way as the preparation of heptadecanoic acid (5). (+) Methyl hydrogen β-acetoxyglutarate (1 g) was electrolyzed with pentadecanoic acid (3 g) and worked up as in the preparation of the C_{16} ester. After silicic acid chromatography methyl 3-D-hydroxystearate (0.47 g) was obtained and crystallized from light petroleum (b.p. 60–80° C). The melting point was 56.5–57.5° C, undepressed by admixture with the natural ester, and $[\alpha]_D$ was −12.9° (*c*, 4.1, $CHCl_3$). The infrared spectrum (Nujol mull) and the X-ray powder photograph were indistinguishable from those of the natural ester. Calculated for $C_{19}H_{38}O_3$: C, 71.6%; H, 12.2%. Found: C, 72.3%; H, 12.2%. Hydrolysis yielded 3-D-hydroxystearic acid which was crystallized from acetone and had melting point 83–85° C, which was not depressed by the natural acid; $[\alpha]_D$ was −12.2° (*c*, 1.4, $CHCl_3$). Calculated for $C_{18}H_{36}O_3$: C, 71.95%; H, 12.1%. Found: C, 71.9%; H, 12.1%.

Reaction of the Lipid and of Methyl 3-Acetoxypalmitate with Alkali

The glycolipid was treated with 0.022 *N* sodium methoxide in methanol both at room temperature and under reflux. The relative amounts of methyl 2-hexadecenoate, methyl 3-hydroxypalmitate, and methyl 3-acetoxypalmitate, found in the product by GLC, varied with the time and temperature of the reaction. Similar results were obtained starting with methyl 3-acetoxypalmitate. The latter was prepared by refluxing synthetic racemic methyl 3-hydroxypalmitate with 20 times its weight of acetic anhydride for 1 hour and removing the excess reagent. The acetate ester was distilled with boiling point 110–115° C (bath) at 0.05 mm. The following conditions were found to give the best yield of 2-hexadecenoic acid. Acetoxy ester (0.3 g) was added to boiling *M*/50 potassium hydroxide in methanol (100 ml) and refluxed for 1 hour, potassium hydroxide (0.5 g) in water (5 ml) was then added and the mixture refluxed for a further 30 minutes. Water was added followed by dilute hydrochloric acid and the acids extracted with ether. The product was extracted with light petroleum (b.p. 40–60° C) leaving insoluble 3-hydroxypalmitic acid (0.065 g). The extract was concentrated to 4 ml and cooled to −10° C and *trans*-2-hexadecenoic acid (0.080 g) was obtained with melting point 47–48° C. Reported melting point is 48.7–49° C (20).

Methyl 3-D-acetoxypalmitate (0.3 g) was prepared from the natural hydroxy acid and treated in the same way. GLC analysis of the methyl esters of the crude product showed that the ratio of 2-hexadecenoic acid to 3-hydroxypalmitic acid was 3.44:1. 2-Hexadecenoic acid (0.052 g) was isolated and the melting point and mixed melting point with the 2-hexadecenoic acid, prepared as above from synthetic racemic acetoxy ester was 46.5–47.5° C. The polyol ester from yeast was also treated with *M*/50 potassium hydroxide as described above and the ratio of 2-hexadecenoic acid to 3-hydroxypalmitic acid was 2.82:1.

The Polyols of the Extra- and Intra-cellular Lipids

The intracellular lipids were extracted from the dried yeast cells by the method used for rust spores (21). The lipids were treated with methanolic hydrogen chloride (3%), the acid neutralized with silver carbonate, the mixture filtered, and the methanol taken off. The fatty esters were extracted with ether and the remaining polyols were acetylated by heating at 100° C with a mixture of acetic anhydride and pyridine (1:1). The excess reagent was removed and the acetates were analyzed by GLC. The results are shown in Table I.

The Fatty Acid Composition of the Lipids Other than Polyol Esters

The methanol-insoluble extracellular lipid produced by *R. glutinis* CBS 4648 when grown in fermentors was separated from polar polyol esters by distribution between 90% methanol and light petroleum (b.p. 40–60° C) in four separatory funnels. Methyl esters were prepared from this lipid as before. The fatty acid

Can. J. Chem. Downloaded from www.nrcresearchpress.com by 210.87.254.42 on 09/05/12
For personal use only.

methyl esters were analyzed on silicone and polyester columns as previously described (21). The methyl esters from the above-mentioned extracellular triglycerides produced by *R. glutinis* CBS 4648 were oxidized with the permanganate–periodate reagent and the oxidation fragments analyzed (22). The results confirmed the assumption that the unsaturated fatty acids had the usual structures, and no evidence for the presence of isomeric acids was found. The esters of the other lipids were also assumed to have the usual structures. The results are summarized in Table II.

ACKNOWLEDGMENTS

The authors thank Mr. L. L. Hoffman and Mr. N. R. Gardner for technical assistance, Mr. M. Mazurek for the microanalyses, and Mr. W. C. Haid for the infrared spectra and the X-ray powder photographs.

REFERENCES

1. M. E. DI MENNA. J. Gen. Microbiol. **18**, 269 (1958).
2. M. H. DEINEMA and C. A. LANDHEER. Biochem. Biophys. Acta, **37**, 178 (1960).
3. M. H. DEINEMA. Thesis, Agricultural University, Wageningen, Netherlands. 1961.
4. P. A. J. GORIN, J. F. T. SPENCER, and A. P. TULLOCH. Can. J. Chem. **39**, 846 (1961).
5. A. P. TULLOCH, J. F. T. SPENCER, and P. A. J. GORIN. Can. J. Chem. **40**, 1326 (1962).
6. A. P. TULLOCH. Paper presented at the 37th Fall Meeting of the American Oil Chemists' Society, Minneapolis, Minnesota. October 1963.
7. R. P. LINSTEAD, L. N. OWEN, and F. R. WEBB. J. Chem. Soc. 1211 (1953).
8. K. SERCK-HANSSEN. Arkiv Kemi, **10**, 135 (1956).
9. J. A. MILLS and W. KLYNE. *In* Progress in stereochemistry. Vol. I. *Edited by* W. Klyne. Butterworths Ltd., London.
10. M. IKAWA, J. B. KOEPFLI, S. G. MUDD, and C. NIEMANN. J. Am. Chem. Soc. **75**, 1035 (1953).
11. L. C. VINING and W. A. TABER. Can. J. Chem. **40**, 1579 (1962).
12. F. G. JARVIS and M. J. JOHNSON. J. Am. Chem. Soc. **71**, 4124 (1949).
13. L. HARTMAN, J. C. HAWKE, F. B. SHORLAND, and M. E. DI MENNA. Arch. Biochem. Biophys. **81**, 346 (1959).
14. L. J. WICKERHAM. U. S. Dept. Agr. Tech. Bull. 1029, 1–56 (1951).
15. S. W. GUNNER, J. K. N. JONES, and M. B. PERRY. Can. J. Chem. **39**, 1892 (1961).
16. B. M. CRAIG and N. L. MURTY. J. Am. Oil Chemists' Soc. **36**, 549 (1959).
17. B. M. CRAIG, A. P. TULLOCH, and N. L. MURTY. J. Am. Oil Chemists' Soc. **40**, 61 (1963).
18. S. STALLBERG-STENHAGEN. Arkiv Kemi, Mineral. Geol. **20A**, No. 19, 1 (1945).
19. M. SKOGH. Acta Chem. Scand. **6**, 809 (1952).
20. R. S. SWEET and F. L. ESTES. J. Org. Chem. **21**, 1426 (1956).
21. A. P. TULLOCH and G. A. LEDINGHAM. Can. J. Microbiol. **8**, 379 (1962).
22. A. P. TULLOCH and B. M. CRAIG. J. Am. Oil Chemists' Soc. In press.

Can. J. Chem. Downloaded from www.nrcresearchpress.com by 210.87.254.42 on 09/05/12
For personal use only.

PREPARATIONS OF DIALKYLAZOXYBENZENES AND THEIR DERIVATIVES[1]

BRIAN T. NEWBOLD AND DANIEL TONG
Department of Chemistry, University of Moncton, Moncton, New Brunswick
Received June 19, 1963

ABSTRACT

The three isomeric symmetrical dimethylazoxybenzenes have been prepared in very good yield by oxidation of the corresponding azobenzenes with peracetic acid. 2,2′- and 4,4′-Diethylazoxybenzenes have been synthesized by oxidation of the azobenzenes and reduction of the ethylnitrobenzenes. The diethylazoxybenzenes were also reduced to the corresponding azo- and hydrazo-benzene derivatives.

INTRODUCTION

Some work on the oxidation of mono- and di-methylazobenzenes has been reported in the chemical literature. For instance, 2- and 4-methylazobenzene have been oxidized by means of peracetic acid (1, 2) and the rates of oxidation of some dimethylazobenzenes with perbenzoic acid have been determined (3). One object of this work was to prepare dimethylazoxybenzenes from the azobenzenes by oxidation with hydrogen peroxide in glacial acetic acid.

Schultz reported in an earlier paper (4) that 2- and 4-nitroethylbenzenes are reduced to the corresponding diethylazobenzenes by zinc dust and sodium hydroxide, and recently Wheeler (5) has studied the polarographic reduction of these nitroethylbenzenes. In the present work, new diethylazoxybenzenes were prepared both from the nitroethylbenzenes by reduction with reducing sugars in alkaline medium, and from the diethylazobenzenes by oxidation with peracetic acid.

DISCUSSION

2,2′-, 3,3′-, and 4,4′-Dimethylazoxybenzenes were prepared in very good yield from the corresponding azobenzenes by oxidation with peracetic acid. Some results are shown in Table I. The 2,2′-dimethylazobenzene proved difficult to oxidize, a great excess of hydro-

TABLE I

Peracetic acid oxidations of dialkylazobenzenes*

Azobenzene, g		H_2O_2, ml	Time, hr	Temp., °C	Azoxybenzene yield, %
2,2′-Dimethyl-	0.510	25	17½	65–75	70
2,2′-Dimethyl-	1.337	25	21	65–77	68
2,2′-Dimethyl-	0.423	30	2	61–66	91
3,3′-Dimethyl-	0.407	25	3	61–65	87
4,4′-Dimethyl-	0.405	15	1	65–70	89
4,4′-Dimethyl-	0.398	15	5	65–66	70
2,2′-Diethyl-	0.307	5	20	65–70	66
2,2′-Diethyl-	0.789	5	24½	80–90	71
2,2′-Diethyl-	1.858	10	½	Reflux	64
2,2′-Diethyl-	0.408	25	4	55–65	40
2,2′-Diethyl-	0.517	10	6½	60–70	84
4,4′-Diethyl-	0.200	5	1½	65–70	52
4,4′-Diethyl-	0.200	5	5 minutes	Reflux	67

*Glacial acetic acid (50 ml) was used in all oxidations.

[1]*Presented at the 46th Annual Conference of the Chemical Institute of Canada, Toronto, Ontario, June 1963.*

Can. J. Chem. Downloaded from www.nrcresearchpress.com by 210.87.254.42 on 09/05/12
For personal use only.

gen peroxide being necessary to obtain the azoxybenzene in over 90% yield. The azo linkage in this case is sterically hindered by the methyl groups and this impedes oxidation. A similar effect was encountered previously with the oxidation of 2,2′-dichloroazobenzene (6, 7). Prolonged oxidation of the dimethylazobenzenes led in each case to decomposition and lower yields of the dimethylazoxybenzenes.

2,2′- and 4,4′-Diethylazoxybenzenes were also prepared from the corresponding azobenzenes by oxidation with hydrogen peroxide in glacial acetic acids and fair yields were achieved. The details are found in Table I. To prepare 2,2′-diethylazoxybenzene in over 60% yield, either an extended period of reaction or elevated temperature was necessary, and this can be attributed to steric hindrance by the bulky ethyl groups.

The diethylazoxybenzenes were synthesized also by reduction of the nitroethylbenzenes with reducing sugars. The sterically hindered 2-nitroethylbenzene was very difficult to reduce as expected. With dextrose, over 80% of the starting material was recovered, whereas when lactose was used more reduction occurred. In both cases, 2,2′-diethylazoxybenzene and 2-ethylaniline were obtained in very low yield. Attempts were also made to reduce 2-nitroethylbenzene with sodium arsenite in alkaline medium but these were not successful. Reductions of 4-nitroethylbenzene with dextrose or lactose gave low yields of 4,4′-diethylazoxybenzene. Some results are given in Table II.

TABLE II

Reductions of nitroethylbenzenes

Nitrobenzene, moles		Reducing agent, moles		NaOH, moles	H_2O, ml	Time, hr	Temp., °C	Products, %		
								Rec. Nitro	Azoxy	Amine
2-Ethyl-	0.17	Dextrose	0.13	0.75	285	1½	60–70	80.4	4.6	Nil
2-Ethyl-	0.17	Dextrose	0.13	1.00	285	2	65	80.4	2.4	5.5
2-Ethyl-	0.17	Lactose	0.13	0.75	285	2	60–70	65.2	1.7	4.1
2-Ethyl-	0.17	Lactose	0.13	0.75	285	1	80–85	56.5	1.5	5.2
2-Ethyl-	0.17	Lactose	0.13	0.75	280	2	55–60	61.0	8.3	5.0
2-Ethyl-	0.17	As_2O_3	0.15	0.75	150*	3	82	95.6	Nil	Nil
4-Ethyl-	0.033	Dextrose	0.025	0.14	57†	1	75	18.2	5.6	Nil
4-Ethyl-	0.033	Lactose	0.025	0.14	57†	1	78	16.0	4.8	Nil

*Methanol (65 ml).
†Methanol (25 ml).

The diethylazoxybenzenes described in this work were synthesized for the first time. The structure of 2,2′-diethylazoxybenzene was established by reduction to 2,2′-diethylhydrazobenzene and oxidation of the latter to the known 2,2′-diethylazobenzene. Confirmation of the structure was also achieved by reduction to 2-ethylaniline with stannous chloride. The structure of 4,4′-diethylazoxybenzene was determined by conversion to the known 4,4′-diethylazobenzene via the new hydrazobenzene.

The compounds 2,2′-diethylazo- and azoxy-benzene are of interest since the bulky ethyl groups should present steric hindrance to coplanarity and this effect can be detected by ultraviolet absorption spectroscopy. Badger and Buttery (8) showed by a model that 2,2′-dimethylazoxybenzene must be non-coplanar and observed a hypsochromic shift of about 20 mμ in the *K*-band (conjugation) of the ultraviolet spectrum on conversion of 2,2′-dimethylazobenzene to the azoxybenzene. Here conjugation is inhibited and the *K*-band should occur at shorter wavelength. Gore and Wheeler (9) have reported that the hypsochromic shift in the above case is 18 mμ. The ultraviolet spectra of 2,2′-diethylazo- and azoxy-benzene are compared in Fig. 1. The introduction of the oxygen atom into

Can. J. Chem. Downloaded from www.nrcresearchpress.com by 210.87.254.42 on 09/05/12
For personal use only.

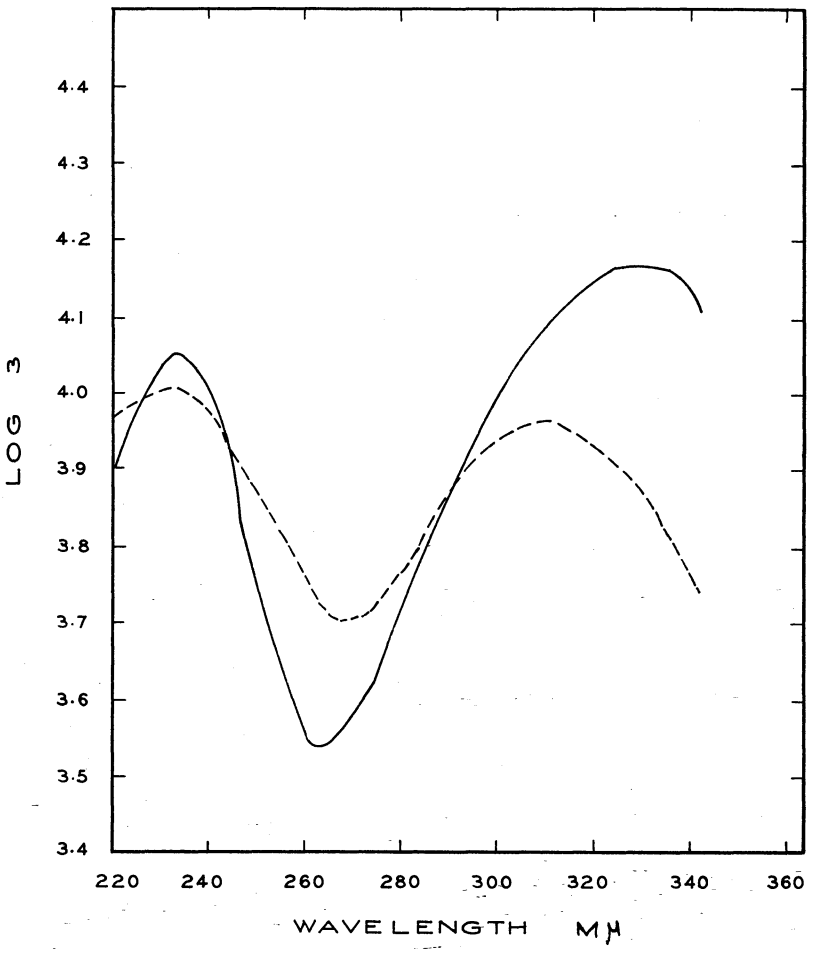

FIG. 1. Absorption spectra of 2,2′-diethylazobenzene (—) and 2,2′-diethylazoxybenzene (– – –).

2,2′-diethylazobenzene caused a hypsochromic shift of 21 mμ in the *K*-band due to inhibited conjugation. Spectral data for the diethylazoxybenzenes and their derivatives are given in Table III.

The ultraviolet spectrum of azobenzene has been shown to possess a *K*-band at 320 mμ (ε17,300) (10). In Table IV, the shifts and changes in intensity of the *K*-bands for dimethyl- and diethyl-azobenzenes are compared. The *K*-bands of the 2,2′-dialkylazobenzenes undergo bathochromic shifts accompanied by decreases in intensity. The results indicate that the more bulky ethyl group leads to increased steric hindrance to coplanarity. If it is assumed that the molecular extinction coefficient of the *K*-band of the 2,2′-disubstituted azobenzenes will be as high as that of the 4,4′-disubstituted derivatives in the absence of steric effects, then the degree of non-coplanarity or total deformation angle can be calculated using the method of Braude and Sondheimer (11). The deformation angle for 2,2′-diethylazobenzene is 33° compared to 23° for 2,2′-dimethylazobenzene as reported by Gore and Wheeler (10). The deformation angle should increase with the effective size of the substituent and such is the case here.

Can. J. Chem. Downloaded from www.nrcresearchpress.com by 210.87.254.42 on 09/05/12
For personal use only.

TABLE III

Absorption spectra of diethylazoxy-, azo-, and hydrazo-benzenes*

Substituent	Bands					
	E		*K*		*R*	
Azoxybenzenes						
2,2′-Diethyl-	234	(10,600)	309	(9,300)	None	
4,4′-Diethyl-	236	(13,500)	334	(20,700)	None	
Azobenzenes						
2,2′-Diethyl-	235	(11,300)	330	(14,800)	460	(560)
4,4′-Diethyl-	236	(13,900)	331	(21,000)	440	(1,000)
Hydrazobenzenes						
2,2′-Diethyl-†	245	(18,500)	287	(3,200)	None	
2,2′-Diethyl-‡	245	(17,700)	289	(5,200)	450	(210)
4,4′-Diethyl-§	248	(21,700)	298	(4,500)	437	(85)
4,4′-Diethyl-‖	244	(9,700)	330	(6,700)	—	—
4,4′-Diethyl-¶	236	(14,800)	330	(19,800)	442	(960)

*Wavelength is recorded in mμ, and the molecular extinction coefficients, ε, values are shown in parentheses.
†Freshly prepared sample kept in vacuum desiccator.
‡Sample kept in air for several weeks. A *K*-band was also present, λ_{max}, 330 mμ (ε, 3200).
§Freshly prepared sample kept under nitrogen.
‖Sample kept for several days in air.
¶Sample kept for 2 weeks in air.

TABLE IV*

Shifts and intensity changes of the *K*-bands of dialkylazo- and azoxy-benzenes

Substituents	Azobenzenes		Azoxybenzenes	
	Shift, mμ	Intensity change	Shift, mμ	Intensity change
2,2′-Dimethyl-	+10	−900	−11	−3400
2,2′-Diethyl-	+10	−2500	−14	−5200
4,4′-Dimethyl-	+10	+2000	+ 7	+3600
4,4′-Diethyl-	+11	+3700	+11	+6200

*The results for the dimethylazo- and azoxy-benzenes are those of Gore and Wheeler (9, 10).

The *K*-band in the ultraviolet spectrum of azoxybenzene has been shown to occur at 323 mμ (ε 14,500) (9). The data in Table IV shows that the *K*-bands of 2,2′-dimethyl- and diethyl-azoxybenzene exhibit hypsochromic shifts together with decreases in intensity. There is, however, more pronounced steric hindrance to coplanarity in the 2,2′-diethyl-azoxybenzene. The deformation angle for the latter compound is 48° compared to 38° for the 2,2′-dimethylazoxybenzene (9). There is greater hindrance in the 2,2′-dialkylazoxy-benzenes than the azobenzenes due to the presence of the oxygen atom of the azoxy group. Moreover, our results show that for both the azoxy- and the azo-benzenes the replacement of the methyl groups by ethyl groups causes an increased distortion of 10° in the molecule. The total deformation angle is also increased by 15° for both 2,2′-di-methyl- and 2,2′-diethyl-azobenzene on passing to the corresponding azoxybenzene, due to the insertion of the coordinated oxygen atom.

Data concerning the *K*-bands of the ultraviolet spectra of the 4,4′-dialkylazo- and azoxy-benzenes is also given in Table IV. The *K*-band of both 4,4′-dimethyl- and diethyl-azobenzene showed a bathochromic shift and increased intensity. If the ethyl groups contribute equally to the polarization of the molecule, the results indicate that each ethyl group causes a bathochromic shift of 5.5 mμ, and an increase in intensity of 1850

Can. J. Chem. Downloaded from www.nrcresearchpress.com by 210.87.254.42 on 09/05/12
For personal use only.

compared to 5 mμ, and 1000 per methyl group. Similar results were obtained with 4,4′-dimethyl- and diethyl-azoxybenzenes, the increases in intensity of the *K*-bands being greater. These results show that for the 4,4′-dialkylazo- and azoxy-benzenes, the electron-releasing inductive effect of the alkyl groups is the important factor rather than the hyperconjugative effect.

The ultraviolet spectra of the diethylhydrazobenzenes possess two bands, a high intensity *E*-band at 245–250 mμ, and a low intensity band at about 285–300 mμ (Table III). Oxidation of the diethylhydrazobenzenes to the azobenzenes causes the latter band to disappear and a high intensity *K*-band to occur in the ultraviolet spectrum. The formation of the azo group is also shown by the appearance of a low intensity *R*-band in visible spectrum.

The diethylhydrazobenzenes showed quite different sensitivities to air oxidation. After it had been standing in air for several weeks the 2,2′-diethylhydrazobenzene turned pink but was only slightly oxidized. Furthermore, it was not completely oxidized to the azobenzene when boiled in alcoholic solution for 10 minutes. In contrast, 4,4′-diethylhydrazobenzene was extremely sensitive to oxidation, turning deep yellow when in contact with air for a few minutes and oxidizing to the azobenzene completely after 2 weeks.

The resistance of 2,2′-diethylhydrazobenzene to air oxidation can be accounted for by steric hindrance, whereas in 4,4′-diethylhydrazobenzene this effect is not operative. Recent results (12) have shown that the sterically hindered 2,2′-diethoxyhydrazobenzene can only be converted to the azobenzene by refluxing with peracetic acid.

EXPERIMENTAL*

Materials

The nitroethylbenzenes used in this work for reductions were commercially available samples.

Reductions of Nitroethylbenzenes

Since essentially the same procedures were used in all reductions carried out using the sugars and sodium arsenite, only one procedure for each method is described.

Reduction of 4-Nitroethylbenzene with Dextrose

4-Nitroethylbenzene 5.0 g (0.033 mole) was dissolved in methanol (25 ml), and sodium hydroxide 5.8 g (0.14 mole) in water (57 ml) was added. Dextrose 4.56 g (0.025 mole) was then added in portions and the mixture stirred vigorously and heated at 75° for 1 hour. The reaction mixture was steam distilled to give a distillate containing a yellow liquid. The distillate was acidified with hydrochloric acid and the yellow liquid separated off, dried, and purified by distillation to give recovered 4-nitroethylbenzene, b.p. 240° at 758 mm (lit. b.p. 245–246° at 760 mm) (13), yield, 18.2%. The acid layer was made alkaline with sodium hydroxide and allowed to stand overnight in the refrigerator, but no 4-ethylaniline separated out. The mixture in the flask after steam distillation contained an oily liquid which was extracted with ether to give a yellow extract. The latter was dried and removal of solvent left a reddish liquid, which was distilled under reduced pressure to give a deep yellow oil, b.p. 244° at 16 mm. When it had been cooled in the refrigerator, the oil solidified to give orange-yellow crystals, m.p. 16–17°. Anal. Calc. for $C_{16}H_{18}N_2O$: C, 75.56%; H, 7.13%; N, 11.01%. Found: C, 76.30%; H, 7.14%; N, 11.28%. The product was 4,4′-diethylazoxybenzene, yield, 5.6%. Infrared spectrum bands at: 3.08, 3.42, 3.50, 3.51, 3.61, 5.98, 6.28, 6.74, 6.90, 7.10, 7.60, 7.69, 7.88, 8.61, 8.98, 9.45, 9.51, 9.85, 10.32, 10.92, 11.82, and 14.78 μ.

In the reduction of 2-nitroethylbenzene, besides the azoxybenzene, some 2-ethylaniline was formed and identified by conversion to the acetyl derivative.

Reduction of 2-Nitroethylbenzene with Sodium Arsenite

2-Nitroethylbenzene 25.9 g (0.17 mole) was dissolved in methanol (65 ml), and sodium hydroxide 30.0 g (0.75 mole) in water (125 ml) was added. Then arsenic trioxide 29.7 g (0.15 mole) as a paste mixed with water (25 ml) was added in portions to the mixture, which had been heated to 60°. The reaction mixture was vigorously stirred throughout and the reaction carried out at 82° for 3 hours. Steam distillation gave recovered 2-nitroethylbenzene, in the acidified distillate, b.p. 223–225° at 756 mm (lit. b.p. 227–228° at 760 mm) (13), yield, 95.6%. No other products were isolated.

**All melting points are uncorrected.*

Can. J. Chem. Downloaded from www.nrcresearchpress.com by 210.87.254.42 on 09/05/12
For personal use only.

Preparations of Dialkylazobenzenes

The dimethylazobenzenes were prepared from the appropriate nitrotoluenes by reductions with zinc dust and sodium hydroxide. Reductions of 2- and 4-nitroethylbenzene by the method described by Schultz (4) gave 2,2′-diethylazobenzene, red needles, m.p. 45–46°. Anal. Calc. for $C_{16}H_{18}N_2$: N, 11.75%. Found: N, 11.66%. (Lit. m.p. 46.5° (4), and 4,4′-diethylazobenzene, orange needles, m.p. 59–60°.) Found: N, 11.47%. (Lit. m.p. 63° (4).)

Peracetic Acid Oxidations of Dialkylazobenzenes

Only one oxidation will be described since essentially the same procedure was employed in all cases.

Oxidation of 2,2′-Diethylazobenzene

2,2′-Diethylazobenzene (1.858 g) was dissolved in glacial acetic acid (50 ml) and 30% hydrogen peroxide (10 ml) added. The red solution was then refluxed for 30 minutes (at which time the color had turned to yellow) and poured into an excess of cold water. The mixture was cooled and extracted with ether to give a yellow extract, which was dried and the solvent removed. The residue, a deep yellow oil, was purified by distillation under reduced pressure, b.p. 168–169° at 2.7 mm. When cooled in the refrigerator, the oil solidified to give orange-yellow crystals, m.p. 12–13°. The product was 2,2′-diethylazoxybenzene, yield, 64.0%. Anal. Calc. for $C_{16}H_{18}N_2O$: C, 75.56%; H, 7.13%; N, 11.01%. Found: C, 75.62%; H, 7.16%; N, 10.91%. Infrared spectrum bands at: 3.35, 3.50, 3.51, 3.58, 6.34, 6.79, 6.90, 7.30, 7.60, 8.08, 8.43, 8.63, 8.75, 8.92, 9.20, 9.46, 9.69, 10.50, 10.80, 10.90, 11.80, 12.58, 12.91, and 14.91 μ.

In the peracetic acid oxidations of the dimethylazobenzenes, the azoxybenzene separated out as a yellow solid when the reaction solution was cooled after dilution and the product was recrystallized from aqueous ethanol.

Reductions of Diethylazoxybenzenes

2,2′-Diethylazoxybenzene

2,2′-Diethylazoxybenzene (1.313 g) was dissolved in a minimum of ethanol and 40% sodium hydroxide solution (4 ml) added, together with an excess of zinc dust. The mixture was refluxed for 1 hour (at which time all color had disappeared), decanted, and poured into an excess of cold water. A yellow product separated out when the mixture was allowed to stand. This product was washed with water and, to decolorize it, was dissolved in ethanol containing a little glacial acetic acid and warmed in the presence of a little zinc dust. The solution was then poured into cold water to precipitate the colorless product, m.p. 106–108°. Repeated recrystallizations from aqueous ethanol gave 2,2′-diethylhydrazobenzene, colorless needles, m.p. 108–108.5°, yield, 62.8%. Anal. Calc. for $C_{16}H_{20}N_2$: C, 79.95%; H, 8.38%; N, 11.66%. Found: C, 80.08%; H, 8.27%; N, 11.55%. Infrared spectrum bands at: 2.80, 3.30, 3.35, 3.40, 3.48, 6.28, 6.64, 6.71, 6.81, 6.92, 7.33, 7.61, 7.75, 8.05, 8.64, 8.95, 9.52, 9.75, 10.43, 10.68, 11.90, 12.64, 12.97, 13.30, and 14.92 μ. This compound slowly oxidizes in air when it has been left standing and takes on a pinkish color. After preparation it must be dried in a vacuum desiccator and stored there.

2,2′-Diethylazoxybenzene (0.5 g) was treated with an excess of stannous chloride dihydrate and concentrated hydrochloric acid for several minutes and the reaction mixture shaken and warmed. The latter was then cooled, diluted with water, and made alkaline. Ether extraction and removal of the solvent gave a dark yellow oil, which was 2-ethylaniline, the infrared spectrum being identical with that of an authentic sample. Acetylation with acetic anhydride also gave 2-ethylacetanilide (from ethanol), m.p. 108–109.5°, alone or with an authentic sample.

4,4′-Diethylazoxybenzene

4,4′-Diethylazoxybenzene (0.352 g) was dissolved in ethanol and 40% sodium hydroxide (1.5 ml) added, together with an excess of zinc dust. The reaction was carried out under a nitrogen atmosphere and the mixture warmed and shaken until all color disappeared. The solution was decanted into an excess of water, the nitrogen atmosphere being maintained throughout. When the solution had been shaken, a colorless product separated out and was collected by very rapid filtration. The substance was 4,4′-diethylhydrazobenzene, which immediately turned pale yellow, m.p. 87–89°, yield, 40.8%. Anal. Calc. for $C_{16}H_{20}N_2$: C, 79.95%; H, 8.38%; N, 11.66%. Found: C, 79.66%; H, 7.64%; N, 11.41%. Infrared spectrum bands at: 2.98, 3.30, 3.35, 3.40, 3.48, 6.20, 6.58, 6.70, 6.88, 7.10, 7.70, 8.02, 8.10, 8.52, 8.70, 9.00, 9.46, 11.78, 12.00, 12.10, 13.87, and 14.45 μ. This reduction, when carried out in air gives a product which turns deep yellow and must be decolorized with glacial acetic acid and zinc dust. 4,4′-Diethylhydrazobenzene oxidizes very rapidly in air and must be stored under a vacuum or nitrogen.

Reductions of Diethylazobenzenes

To 2,2′-diethylazobenzene (0.3 g) in a minimum of ethanol, 40% sodium hydroxide (1 ml) and excess zinc dust were added, and the mixture refluxed for 2 hours. Extraction, using the procedure described for the reduction of 2,2′-diethylazoxybenzene, gave 2,2′-diethylhydrazobenzene, m.p. 107–108°, identity confirmed by infrared spectral analysis.

Reduction of 4,4′-diethylazobenzene with sodium hydroxide and zinc dust using the method employed for the reduction of 4,4′-diethylazoxybenzene gave 4,4′-diethylhydrazobenzene, whose infrared spectrum was identical with that of an authentic sample.

Can. J. Chem. Downloaded from www.nrcresearchpress.com by 210.87.254.42 on 09/05/12
For personal use only.

Oxidations of Diethylhydrazobenzenes

2,2′-Diethylhydrazobenzene

2,2′-Diethylhydrazobenzene (0.15 g) was dissolved in ethanol and the solution boiled in air to the point of crystallization. The product was dissolved in ethanol again and the treatment repeated several times to give a mixture of red and colorless crystals. The red product was 2,2′-diethylazobenzene, m.p. 44–46° alone or with an authentic sample. The colorless product was 2,2′-diethylhydrazobenzene, m.p. 107–108° alone or with an authentic sample.

4,4′-Diethylhydrazobenzene

When 4,4′-diethylhydrazobenzene (0.09 g) was dissolved in ethanol and the solution was boiled for several minutes, an orange color developed. Evaporation produced orange crystals, m.p. 57–58°. Repeated recrystallizations from ethanol gave 4,4′-diethylazobenzene, orange needles, m.p. 60–61° alone or with an authentic sample.

4,4′-Diethylhydrazobenzene (0.05 g) was allowed to stand in air for several days and was oxidized to 4,4′-diethylazobenzene, m.p. 58–60° alone or with an authentic sample.

Spectra

The infrared spectra were recorded on a Perkin–Elmer Infracord model 137B spectrophotometer. The spectra of the diethylazoxybenzenes were obtained from liquid samples and those of the diethylhydrazobenzenes by the potassium bromide pellet technique. The other infrared spectra were recorded by employing Nujol mulls. The visible and ultraviolet spectra were determined on a Beckman model DK-2 ratio-recording spectrophotometer, using absolute ethanol as solvent.

ACKNOWLEDGMENT

The authors wish to express their profound gratitude to the National Research Council of Canada for a grant during the course of this work.

REFERENCES

1. T. Parsons, Jr. and J. C. Bailar, Jr. J. Am. Chem. Soc. **58**, 268 (1936).
2. D. Bigiavi and V. Sabbatteli. Gazz. Chim. Ital. **57**, 557 (1927).
3. G. M. Badger and G. E. Lewis. J. Chem. Soc. 2147 (1953).
4. G. Schultz. Ber. **17**, 473 (1884).
5. O. H. Wheeler. Can. J. Chem. **41**, 192 (1963).
6. P. E. Gagnon and B. T. Newbold. Can. J. Chem. **37**, 366 (1959).
7. B. T. Newbold. J. Org. Chem. **27**, 3919 (1962).
8. G. M. Badger and R. G. Buttery. J. Chem. Soc. 2156 (1953).
9. P. H. Gore and O. H. Wheeler. J. Am. Chem. Soc. **78**, 2160 (1956).
10. P. H. Gore and O. H. Wheeler. J. Org. Chem. **26**, 3295 (1961).
11. E. A. Braude and F. Sondheimer. J. Chem. Soc. 3754 (1955).
12. B. T. Newbold. Unpublished results.
13. I. Heilbron. Dictionary of organic compounds. Oxford University Press. 1953.

Can. J. Chem. Downloaded from www.nrcresearchpress.com by 210.87.254.42 on 09/05/12
For personal use only.

CATALYTIC HYDRODESULPHURIZATION OF THIOPHENE

V. THE HYDROTHIOPHENES. SELECTIVE POISONING AND ACIDITY OF THE CATALYST SURFACE[1, 2]

P. DESIKAN[3] AND C. H. AMBERG

Received August 15, 1963

ABSTRACT

The hydrogenolysis of tetrahydrothiophene over sulphided cobalt molybdate – alumina was shown to proceed in two ways. The main reaction was hydrodecyclization to *n*-butanethiol and conversion of the latter to butenes and butane; the second and less prominent reaction involved dehydrogenation to thiophene, which was also desulphurized. The overall desulphurization activity decreased in the order *n*-butanethiol > tetrahydrothiophene > 2,3-dihydrothiophene > thiophene. A better understanding of the dual catalytic nature of the catalyst resulted from selective poisoning experiments with H_2S, thiophene, methylthiophene, pyridine, and NH_3. The sites responsible for olefin hydrogenation were shown to have strong affinity for thiophenes, H_2S, and pyridine, as well as limited capacity to dehydrogenate thiolane and desulphurize thiophenes. Sites weakly electrophilic in character were also shown to be present on the catalyst surface. These could be poisoned only by ammonia or alkali and have been identified with the bulk of the desulphurization in the hydrogenolysis of thiophenes, hydrothiophenes, and thiol.

Can. J. Chem. Downloaded from www.nrcresearchpress.com by 210.87.254.42 on 09/05/12
For personal use only.

INTRODUCTION

During earlier investigations on thiophene hydrogenolysis (1) saturated derivatives still containing sulphur, such as tetrahydrothiophene and *n*-butanethiol, could not be detected as gas-phase intermediates over a sulphided cobalt molybdate catalyst under the conditions used. It was noted also (2) that in the conversion of thiolane (tetrahydrothiophene) over the catalyst a small amount of thiophene was present among the products in addition to the C_4 hydrocarbons. Essentially the same products had been observed earlier by Girelli, Helm, Thompson, Meyer, and Ball (3), who dehydrogenated thiolane both thermally and over several catalysts. Apparently, the hydrogen produced in the dehydrogenation served to decyclize the thiolane to the hydrocarbons through intermediate formation of *n*-butanethiol.

Previous experiments in this laboratory (1, 4) had also focussed attention on the selective effect of hydrogen sulphide on the desulphurization and hydrogenation activities of sulphided cobalt molybdate. There was enough evidence to suggest two different catalytic functions to be operative, and this included the possibility that one type of site was responsible for both. Sulphided chromia (5, 6) perhaps exemplifies such a case.

On all considerations, it seemed attractive to look into the reaction of thiolane over the catalyst in some detail. Primarily the reaction could be expected to show characteristics relevant to the hydrogenolysis of thiophene itself, the latter having been found among the products. Also, it was felt that a molecule like thiolane with a non-aromatic, saturated ring might react differently on a strong acid site which could polarize one of its carbon atoms, and on a much weaker site to which the lone pair of electrons on the sulphur atom might have affinity.

The hydrogenolysis of thiolene (2,3-dihydrothiophene) and *n*-butanethiol (representing the two routes by which thiolane decomposes thermally (3)) was also studied and the results compared with those for thiophene and thiolane.

[1]*Issued as N.R.C. No. 7755.*
[2]*For Parts I to IV see refs. 1, 5, 6, and 4.*
[3]*N.R.C. Postdoctoral Fellow 1961–63.*

Finally, selective poisoning techniques were employed to accentuate one or more steps involved in the hydrogenolysis reaction.

EXPERIMENTAL

The apparatus was the same as in Part IV of the series (4). The catalysts employed were all cobalt molybdate on alumina, sulphided before use: G_1, G_2, and G_3 were samples of Girdler catalyst G35A previously described (1), which differed merely in that G_1 had been used in earlier experiments and in that G_2 consisted of somewhat larger granules than our normal 32–65 mesh size. G_2 was used only in a few experiments with ammonia. A catalyst designated as HM was made to contain 1.3% Co and 6.1% Mo to equal the commercial sample in composition. In its preparation a batch of highly acidic alumina, made from aluminum isopropoxide by the method of Pines and Haag (7), was impregnated successively with aqueous ammonium molybdate and aqueous cobalt acetate and ignited after each impregnation. The blue powder so obtained was reduced and sulphided as usual at 400°. One-gram catalyst beds were employed throughout.

The thiolane and *n*-butanethiol used (Eastman) were found to be chromatographically pure. A sample of 2,3-dihydrothiophene was prepared by a slight modification of Sosnovsky's procedure (8, 9) and purified by preparative gas chromatography. The hydrocarbons used for reference were all Phillips research grade. Hydrogen from a cylinder was passed through a palladium catalyst and drying column to remove oxygen and water. The pyridine used in poisoning experiments contained a maximum of 20 p.p.m. of ammonia. A portion of this was purified by drying and repeated distillation through a Vigreux column. Research grade ammonia (Matheson) was passed over a drying column and used either as such or in admixture with hydrogen.

Hydrocarbon analysis was carried out using a propylene carbonate column (25 ft copper tube; 30% w/w on 30–48 mesh Chromosorb). Squalane and tricresyl phosphate (6 ft glass U-tubes; 20 and 28.6% w/w respectively on 30–48 mesh Chromosorb) were employed for separating the C_4 hydrocarbons from the sulphur-containing starting materials and intermediates.

RESULTS AND DISCUSSION

The main hydrocarbon products of the desulphurization of thiolane, predictably, were butenes and butane. Thiophene and *n*-butanethiol were found under certain conditions and will be discussed in detail below. Butadiene, which could be expected to be formed from thiophene (1), was probably hydrogenated too fast to be detected.

The distribution of the butene isomers obtained from thiolane over catalyst G_1 at 308° C is presented in Table I and compared with similar distributions from thiophene, butanethiol, and thiolene, as well as with the thermodynamic equilibrium values.

TABLE I

Distribution of *n*-butene isomers over catalyst G_1 at 308° C, using 2-μl pulses of C_4 sulphur compounds
H_2 flow rate: 50 cc/minute

	Thiophene	Thiolene	Thiolane	Butanethiol	Equilibrium calc. from (10)
1-Butene, %	19.5	17.8	17.7	16.0	14.0
trans-2-Butene, %	42.1	44.0	44.0	44.0	53.5
cis-2-Butene, %	38.4	38.2	38.3	40.0	32.5

It is apparent that *trans*-2-butene cannot be the initial mono-olefin formed from any of the four sulphur compounds considered. Both 1-butene and *cis*-2-butene are in excess of thermodynamic equilibrium and it is not possible to decide from the distribution alone which of these two isomers could have formed first. It has been shown in the case of thiophene over chromia catalyst that 1-butene is the initial isomer formed (1) presumably through 1,2-hydrogenation of butadiene. Vernon and Richardson (11) working with MoS_2 catalysts promoted with different amounts of cobalt also reported the initial formation of 1-butene. If, as will be pointed out, *n*-butanethiol is the principal gas phase

Can. J. Chem. Downloaded from www.nrcresearchpress.com by 210.87.254.42 on 09/05/12
For personal use only.

intermediate in thiolane conversion, 1-butene can be expected to be the initial isomer in that case as well.

The amounts of C_4 hydrocarbons formed from 2-μl pulses of thiolane over catalyst G_1 at different temperatures, and the extent of their saturation, are presented in Table II

TABLE II

Hydrocarbon products from the hydrogenolysis of C_4 sulphur compounds over 1.0 g G_1. Propylene carbonate column in series with reactor; H_2 flow: 50 cc/minute

% C_4 = % total C_4/sulphur compound
% sat. = % butane in C_4

Temp., °C	Thiophene		Thiolene		Thiolane		Thiol	
	% C_4	% sat.	% C_4	% sat.	% C_4	% sat.	% C_4	% sat.
270*	41.9	30.6	49.1	23.8	64.3	20.5	94.8	35.9
280	54.3	30.6	—	—	81.1	41.4	98.3	56.1
298	—	—	—	—	91.1	53.3	—	—
308*	57.5	28.9	74.9	33.9	93.9	35.4	100.0	46.2
313	63.9	30.8	—	—	96.4	69.6	100.0	72.1
365	—	—	—	—	100.0	98.0	—	—
372*	88.1	28.2	77.3	45.4	100.0	47.1	100.0	61.2

along with corresponding data for thiophene, thiolene, and butanethiol. In the runs marked with an asterisk, the pulses were injected 7 minutes after a 5-μl thiophene pulse. In the other runs, the catalyst had been flushed for at least 1 hour in H_2 at reaction temperature before introducing the pulse. The predosing with thiophene was carried out to determine whether it could act as a poison. Preliminary experiments had shown that two equal consecutive pulses of thiolane spaced at an interval of about 7 minutes gave approximately the same amount of C_4 product with nearly the same butene to butane ratio. On the other hand, if the thiolane pulse was injected ~7 minutes after an equivalent hydrogen sulphide pulse, some suppression of butane formation (olefin hydrogenation) was evident. This could mean that H_2S formed as a result of reaction is not able to compete successfully with thiolane for adsorption on the hydrogenation sites; if preadsorbed, however, it can suppress the hydrogenation of olefins. Eventual displacement of H_2S by the organosulphur compound is thought to be too slow to have any effect on the conversion of the pulse. Therefore in the experiments with thiophene-predosing (Table II) if there was any poisoning effect, it could be attributed to the thiophene rather than to the H_2S formed from it. If, as will be shown presently, the hydrogenation sites are strong acid sites, thiophene should at any rate adsorb more strongly on them than H_2S.

The table shows the normal effect of temperature on overall activity. Also, the conversion decreases in the order thiol > thiolane > thiolene > thiophene. Furthermore, on a clean catalyst both thiolane and thiol yield a larger amount of butane than does thiophene. Predosing with thiophene indeed suppresses the saturation appreciably except when thiophene is also the reactant. Since the H_2S originating from the thiophene can be assumed to be relatively ineffective (as in the case of thiolane), and the hydrocarbons are only weakly adsorbed (1), these observations clearly show that thiophene is strongly adsorbed on the hydrogenation sites; they also explain why the butane formed from thiophene is always less than that from thiolane. Predosing affects the desulphurization activities only to a slight extent, presumably because thiophene reacts on the

Can. J. Chem. Downloaded from www.nrcresearchpress.com by 210.87.254.42 on 09/05/12
For personal use only.

desulphurization sites. Suppression of hydrogenation activity, which was in remarkably close agreement with the thiophene results, was also observed when 3-methylthiophene was used as a poison (98% reduced to 48% with an 8 minute 20 second interval between poison and reactant pulses).

Earlier experiments in this laboratory (1) implied that the main selective poison for butene hydrogenation in continuous flow desulphurization of thiophene over cobalt molybdate would be the H_2S which is being maintained at high levels of concentration. This view must now be modified to include the organosulphur compounds themselves which are able to compete as hydrogenation poisons.

The gas phase intermediates in thiolane hydrogenolysis were studied in some detail. As already mentioned, thiophene and *n*-butanethiol were found among the products of thiolane conversion. Using the squalane column for analysis it was observed that small amounts of the thiol could be obtained at temperatures below 270° and small amounts of thiophene above 300°. The amount of thiophene formed varied with the history of the catalyst. The older catalyst G_1 gave much less thiophene than did G_3. Assuming that the thiophene formed by dehydrogenation of thiolane reacted further with hydrogen at the same rate at which it would normally react in the absence of thiolane, it was possible to calculate the contribution of the thiophene route in the overall reaction. With 10-μl shots of thiolane at ~400°, the dehydrogenation route accounted for approximately 20% of the reaction over freshly sulphided G_3, 10% over G_1, and 15% over HM. Pyridine, ammonia, and H_2S all poisoned the dehydrogenation reversibly; some irreversible suppression of dehydrogenation activity was noticeable in catalysts that had been extensively used in desulphurization or after repeated poisoning with pyridine or ammonia. The strong (reversible) poisoning by H_2S was evident from continuous flow experiments on G_1 and HM when no thiophene could be detected among the products as a result of the steady H_2S level on the catalyst surface.

Thiophene was also formed in the hydrogenolysis of pulses of dihydrothiophene and the latter is therefore a possible intermediate in thiolane dehydrogenation. In fact, Girelli *et al.* (3) were able to detect dihydrothiophene by mass spectrometric analysis of the products of decomposition of thiolane; no success, however, was achieved in our attempts to detect it in the thiolane hydrogenolysis product. Liquid thiolene readily polymerizes, even under refrigeration, and loss by polymerization on the catalyst surface may well cause the disappearance of unreacted material in the course of hydrogenolysis. Other mechanisms might be operative, such as a relatively faster second dehydrogenation step to thiophene. It is difficult to decide between the two possibilities, considering the very small concentrations involved.

It should be emphasized, however, that in the conversion of thiolane, the maximum contribution of the thiophene route was only 20%, and that the principal intermediate, therefore, is *n*-butanethiol. If the hydrodecyclization step leading from thiolane to thiol had been very much faster than the removal of H_2S from the latter (see the rates for compounds I and IV, Fig. 1) the rates of hydrogenolysis of thiolane and thiol should have been much closer to each other. One may reasonably conclude that the decyclization is also a slow step with a significant contribution to the overall rate.

Earlier experiments with alkali modified specimens of Girdler G35A catalysts had revealed that with sufficient amount of alkali both the hydrogenation and the desulphurization activities for the hydrogenolysis of thiophene could be almost completely poisoned, indicating that practically all the catalytic sites involved in the reaction were acidic. The distinction between desulphurization sites and hydrogenation sites could then be

Can. J. Chem. Downloaded from www.nrcresearchpress.com by 210.87.254.42 on 09/05/12
For personal use only.

one of relative acidities. To define this more clearly, pyridine was used to poison the hydrogenolysis of thiophene as well as of thiolane.

Most of the experiments were carried out with catalyst G_1 and pyridine containing a maximum of 20 p.p.m. ammonia. Later experiments with purified pyridine led us to expect that this impurity had negligible effect at least in reversible poisoning. A quantitative assessment of the effect of pyridine on the various steps of the reactions studied was hampered by two factors: (1) the presence of strong and weak types of adsorption leading to a single chromatographic peak with a sharp front and a diffuse tail and (2) a gradual irreversible modification of the catalyst.

A 5-μl pyridine sample was introduced on freshly sulphided G_1 at 367°, followed at various intervals by several pulses of 2 μl thiophene. Independently, without using an analytical column but employing the same temperature and hydrogen flow rate, we obtained an adsorption–desorption peak for 5 μl pyridine. The shape of the peak did not unequivocally suggest two types of adsorption, and could very well have been taken to signify fast adsorption and slow desorption. The amounts of pyridine which resided on the surface at the various time intervals during the poisoning of the thiophene reaction were calculated and are shown in Table III along with the corresponding poisoning effects.

TABLE III

Poisoning of thiophene desulphurization by pyridine
Catalyst G_1 at 367° C
Sample sizes: 5 μl pyridine, 2 μl thiophene
H_2 flow: 50 cc/minute

Time after pyridine injection, minute	Pyridine on surface, cc (N.T.P.)	C_4 product/ thiophene, %	Butane in C_4 product, %
2.2	1.00	84	24.8
10.0	0.62	81	21.6
22.0	0.31	83	21.9
28.4	0.18	77	21.2
Fresh catalyst	0.00	92	44.0

If the peak had been governed by adsorption on one kind of site, there should have been considerably more poisoning of butane formation at the 1.0-cc pyridine level (close to the maximum) than at the lower levels (representing the tail). The sharp portion of the peak therefore represents a weak adsorption–desorption mechanism on one type of site conceivably associated with the bulk of the desulphurization (Table III, col. 3). On the other hand, the tail is due to strong adsorption of pyridine on, and slow desorption from, sites which mainly catalyze butene hydrogenation (Table III, col. 4) and to a small extent also thiophene desulphurization. This latter fact may well be the origin of the slow recovery of desulphurization (col. 3): recovery should have been faster if desulphurization were to take place exclusively on weakly adsorbing sites. The association of the weakly adsorbing sites with desulphurization was confirmed by thiolane hydrogenolysis experiments using pulses mixed with different amounts of pyridine over catalyst G_1. These runs were spaced at intervals of over 1 hour, although a few thiolane pulses without pyridine were injected in between. The results are shown in Table IV. They distinguish sharply between the strong and immediate suppression of desulphurization and the somewhat weaker one of hydrogenation. Moreover, the persistence of the latter effect shows desorption of pyridine from the hydrogenation sites to be much slower than from the

Can. J. Chem. Downloaded from www.nrcresearchpress.com by 210.87.254.42 on 09/05/12
For personal use only.

TABLE IV

Effect of pyridine on thiolane conversion
Catalyst G_1 at 358° C; H_2 flow: 50 cc/minute

Description of pulse	Total C_4, %	Saturation, %
1 μl thiolane on fresh catalyst	100	90
1 μl thiolane + 2 μl pyridine	31	59
1 μl thiolane 6.8 minutes later	100	47

Can. J. Chem. Downloaded from www.nrcresearchpress.com by 210.87.254.42 on 09/05/12
For personal use only.

desulphurization sites. This is consistent with the hydrogenation sites being the more strongly acidic ones. A slow drift in the saturation values (e.g. 59 to 47%) was consistently noted after the first introduction of poison, but could not be explained. The original value of 90% was restored after about 1 hour.

The irreversible modification of G_1, briefly referred to earlier, became measurable after about 30 μl pyridine had passed over the catalyst. The most significant effect was that the catalyst (G_1) no longer produced thiophene from thiolane within the temperature range studied; the overall desulphurization and olefin hydrogenation activities, however, remained virtually unchanged.

To examine thiolane dehydrogenation further, poisoning experiments were carried out on fresh catalysts G_2 and G_3 using ammonia and purified pyridine, respectively. Successive injections of ammonia mixed with hydrogen on to 1.0 g of catalyst G_2 reduced the thiophene yield at 418° from 4.8% to 1.4% when about 0.4 cc of ammonia had been adsorbed (5 to 8 μl thiolane pulses). Further increase of ammonia increased the yield to 2.3%, probably because some of the more weakly acidic thiophene desulphurization sites were also getting poisoned. The original 4.8% yield could not be restored. Purified pyridine reduced thiophene yields at 402° on G_3 by about one-quarter of the value on fresh catalyst, when the cumulative amount of pyridine injected had reached 45 μl. The contribution of the thiophene route in the thiolane conversion fell from 20% to 15%. The fact that this decrease was less marked than with G_1 (10% to 0% with 30 μl of unpurified pyridine) can be attributed to the longer use of G_1 in desulphurization runs and (or) the higher purity of the second sample of pyridine. It is tempting to speculate on the mechanism by which dehydrogenation becomes irreversibly poisoned. One possibility might be that thiolane is adsorbed on the desulphurization sites and the bulk of the hydrogenation sites through the S-atom. In addition a small number of strong acid sites are capable of polarizing one of the C-atoms of thiolane, i.e. they are able to chemisorb thiolane by a dissociative mechanism, giving adsorbed carbonium and hydride ions. These sites, which are responsible for the limited dehydrogenation reaction, can be progressively and irreversibly neutralized by ammonia or pyridine.

The hydrogenolysis of *n*-butanethiol, which did not undergo any side reaction (e.g. dehydrogenation) in the temperature range under consideration, showed good selectivity in the effect of pyridine on its constituent steps. The results on catalyst G_3 at 247° are presented in Table V and once again indicate that H_2S elimination and butene hydrogenation take place on different sites.

In conclusion, we propose the following functional model of the catalyst surface as meeting all the requirements of the results described. The sulphided cobalt molybdate desulphurizes thiophene and thiolane with the use of only two types of sites, one very strongly acidic and the other having low affinity for electrons. The strong acid sites are

TABLE V

Effect of pyridine on *n*-butanethiol conversion
Catalyst G_3 at 247°; pulse size: 2 μl; H_2 flow: 50 cc/minute

Description of pulse	% Thiol converted to: total C_4	butane
On fresh catalyst	68.9	40
7 minutes after 5 μl pyridine pulse	58.3	18.2
40 minutes after 5 μl pyridine pulse	52.5	18.8

sufficiently electrophilic to interact with olefins and to hydrogenate them (see also ref. 4). Hydrogen sulphide, thiophene, and pyridine can be strongly adsorbed on them. Prior to irreversible modification by poisoning, these sites include a small number capable of dissociatively chemisorbing thiolane and dehydrogenating it. All the strong sites can also catalyze desulphurization to a limited extent when the compound to be desulphurized is sufficiently basic, i.e., when it has sufficiently high electron density at the surface-directed portion of the molecule.

The weaker acid sites can be poisoned irreversibly only by a sufficiently strong base or alkali. These sites can be expected to desulphurize in two ways, either by adding H_2 across a C—S or C=S bond or by removing SH from a C—SH, forming an adsorbed carbonium ion. Thus starting from thiophene, one can obtain butadiene and H_2S either in one concerted action (*a*) or through several surface intermediates (*b*):

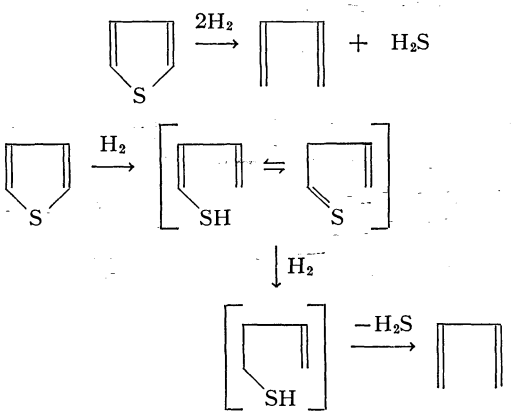

(*a*)

(*b*)

Decyclization of thiolane on the other hand leads to butanethiol, followed by H_2S removal:

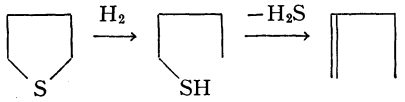

The butadiene or butene if produced on the stronger acid sites will, without leaving the sites, get hydrogenated further. If formed on the weaker sites, they can desorb into the gas phase or migrate to the strong sites for saturation.

The major steps involved in the reaction scheme involving thiophene, the hydrothiophenes, butanethiol, and the C_4 hydrocarbons on the sulphided cobalt molybdate are

Can. J. Chem. Downloaded from www.nrcresearchpress.com by 210.87.254.42 on 09/05/12
For personal use only.

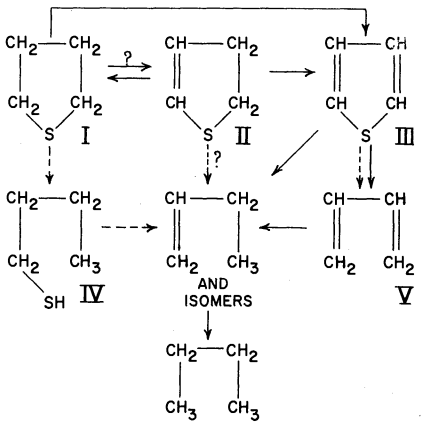

FIG. 1. Reaction scheme and the catalytic sites. ⟶ Strong acid site. ----→ Weaker site. ? = Route not definitely identified.
Approximate rates of conversion to butenes and butane for I to V at 280° C were found to be 24, 18, 16, 35, and 75 micromoles per gram catalyst per second, respectively.

featured in Fig. 1. Approximate rates of conversion to butenes and butane at 280° on a fresh catalyst are also given for the various starting materials and intermediates.

It is easily seen that the surface species involved in H_2S removal from a saturated C_4 mercaptan and the hydrodesulphurization of an olefinic mercaptan (which may be involved in thiophene hydrogenolysis) would be similar. It was therefore of interest to see whether the activation energy for continuous flow hydrogenolysis of thiolane was of the same order as for thiophene. Using low thiolane feed and high H_2 flow and a squalane column for analysis, continuous flow hydrogenolysis of thiolane was carried out over catalyst G_3 (before contacting with pyridine) in the temperature range 200 to 300°; the E value obtained was 23.6 ± 1.5 kcal, close to the value 24.4 ± 1.6 obtained earlier (4) for thiophene.

ACKNOWLEDGMENT

We thank M. Bednas for purifications by preparative gas chromatography.

REFERENCES

1. P. J. OWENS and C. H. AMBERG. Advances in Chemistry, Ser. No. 33, 182 (1961).
2. P. J. OWENS and C. H. AMBERG. Unpublished.
3. A. GIRELLI, R. V. HELM, C. J. THOMPSON, R. A. MEYER, and J. S. BALL. Preprints, Division of Petroleum Chemistry, American Chemical Society, Kansas City. 1954. p. 165.
4. P. DESIKAN and C. H. AMBERG. Can. J. Chem. **41**, 1966 (1963).
5. P. J. OWENS and C. H. AMBERG. Can. J. Chem. **40**, 941 (1962).
6. P. J. OWENS and C. H. AMBERG. Can. J. Chem. **40**, 947 (1962).
7. H. PINES and W. O. HAAG. J. Am. Chem. Soc. **82**, 2471 (1960).
8. G. SOSNOVSKY. Tetrahedron, **18**, 15 (1962).
9. G. SOSNOVSKY. Tetrahedron, **18**, 903 (1962).
10. F. D. ROSSINI. Selected values of physical and thermodynamic properties of hydrocarbons and related substances. Carnegie Press, Pittsburgh. 1953.
11. L. W. VERNON and J. T. RICHARDSON. Abstracts, Division of Colloid and Surface Chemistry, American Chemical Society, Atlantic City. 1962. p. 7 I.

Can. J. Chem. Downloaded from www.nrcresearchpress.com by 210.87.254.42 on 09/05/12
For personal use only.

SECONDARY KINETIC ISOTOPE EFFECTS IN BIMOLECULAR NUCLEOPHILIC SUBSTITUTIONS

I. DEUTERIUM EFFECTS IN THE BUNTE SALT REACTION[1]

K. T. LEFFEK
Department of Chemistry, Dalhousie University, Halifax, Nova Scotia
Received October 30, 1963

ABSTRACT

The secondary deuterium isotope effects have been measured for the reaction between sodium thiosulphate and α-deuterated methyl, ethyl, and *n*-propyl bromide, and also for β- and γ-deuterated *n*-propyl bromide, in aqueous ethanol solvent. The α-deuterium isotopic rate ratios (k_H/k_D) are all greater than unity. These unexpected results are discussed with respect to the suggested use of the α-deuterium isotope effect as a test of mechanism in nucleophilic substitutions.

Can. J. Chem. Downloaded from www.nrcresearchpress.com by 210.87.254.105 on 09/05/12
For personal use only.

There are many examples in the literature of changes in the rates of nucleophilic substitutions when some of the hydrogen atoms of the reactant, which are not directly involved in the reaction, are replaced by deuterium (1–5). However, nearly all of these examples pertain to S_N1-type solvolytic reactions. Of the bimolecular reactions studied, many are solvolyses in water which show regular changes of isotope effect with changes of alkyl group and the site deuterated (6–9); very few isotope effects have been measured in non-solvolytic S_N2 reactions (10, 11). It is not known whether the regularities found in the solvolytic reactions are general for all bimolecular substitutions; hence, the present investigation is part of a program of systematic study of secondary deuterium isotope effects in non-solvolytic bimolecular substitutions.

Since the known isotope effects in this type of substitution are small (11), it is necessary to choose reactions for study which allow the precise determination of their rate constants. The attack of thiosulphate ion on alkyl bromides, in 50% v/v ethanol–water solvent, to yield S-alkyl thiosulphates, known as Bunte salts (12), is one such group of reactions, and may be represented by the equation

[1] $$S_2O_3^{2-} + RBr \rightarrow RS_2O_3^- + Br^-.$$

The unreacted sodium thiosulphate can be estimated quite accurately by titration with standard iodine solution.

Hammett and co-workers (13, 14) made a careful investigation of this reaction in their study of the changes which occur in the enthalpy and entropy of activation with structure of the alkyl group. They used an acetate buffer to avoid decomposition of thiosulphate ion in an acidic medium which could result from solvolysis of the alkyl bromide to give hydrobromic acid and an alcohol (or ether). The rate of acetate ion attack on the alkyl bromide was found to be negligibly slow under the conditions of reaction. For the straight-chain alkyl bromides, the rate of solvolysis was too slow to necessitate correction of the observed rate constants of the thiosulphate reaction.

Subsequently, Bevan and Monk showed that Hammett's rate constants for the reaction of sodium thiosulphate with *n*-propyl bromide in 50% v/v ethanol–water solvent, calculated using stoichiometric molarities of thiosulphate, are not the true rate constants

[1]*Presented at the XIXth International Congress of Pure and Applied Chemistry, London, England, July 10–17, 1963.*

because sodium thiosulphate is incompletely dissociated in this solvent (15). Corrected rate constants measured by Bevan and Monk (16) gave the same activation energy but a higher Arrhenius frequency factor for the above reaction compared to those obtained by Hammett *et al.* However, since Hammett's discussion was based on comparisons between the activation parameters for different alkyl groups, his conclusions are not invalidated by the use of apparent rate constants. In the determination of secondary isotope effects the use of apparent rate constants is equally valid, as the correction factor used by Bevan and Monk is the same for normal and deuterated alkyl bromides and therefore would cancel in the ratio of the rates.

RESULTS AND DISCUSSION

Results of kinetic experiments on the reactions between sodium thiosulphate and methyl, ethyl, and *n*-propyl bromide and their α-deuterated analogues are given in Table I.

TABLE I

Secondary α-deuterium isotope effects for the reactions between alkyl bromides and sodium thiosulphate in 50% v/v ethanol–water at 25.00±0.05° C

Compound	No. runs	$10^4\, k_2 \pm$ Std. dev. (l./mole sec)	$k_H/k_D \pm$Std. dev.
Methyl bromide	5	872±7	
Methyl-d_3 bromide	3	846±6	$1.03_1 \pm 0.01$
Ethyl bromide	9	12.23±0.04	
Ethyl-1,1,d_2 bromide	3	11.45±0.10	$1.06_8 \pm 0.01$
n-Propyl bromide	11	6.03±0.04	
n-Propyl-1,1,d_2 bromide	4	5.61±0.05	$1.07_5 \pm 0.01$

These rate ratios are interesting as they constitute a critical test of the α-deuterium isotope effect as an indicator of mechanism of nucleophilic substitution.

At the time of their discovery α-deuterium isotope effects were recognized as a possible means of distinguishing between the S_N1 and S_N2 mechanisms (17, 18). The first evidence for this was given by Johnson and Lewis (11), who showed that whereas normal isotope effects ($k_H/k_D > 1$) are obtained with S_N1 reactions, inverse effects ($k_H/k_D < 1$) result for S_N2 reactions. Their examples of inverse effects were reactions of methyl-d_3 *p*-bromobenzenesulphonate, the methanol solvolysis ($k_H/k_D = 0.94$) and the non-solvolytic methoxide ion attack ($k_H/k_D = 0.96$).

An elegant demonstration of the correlation between α-deuterium isotope effect and mechanism for solvolytic reactions was given by Hartman and Robertson (19). A plot of secondary deuterium isotope effect, k_H/k_D, for methyl and deuterated methyl compounds solvolyzing in water, against the ratio $k_{2(OH^-)}/k_{1(H_2O)}$, the rate of attack by hydroxide ion to the rate of solvolysis by water, gave a good straight-line relationship. The latter ratio has been used as a diagnostic test of mechanism for many years (20) and it is generally accepted, although some criticism can be levelled against it (21). Thus it was assumed that k_H/k_D for α-deuteration indicated mechanism equally well.

The rate ratios for α-deuterated alkyl bromides for the Bunte salt reaction, listed in Table I, are all greater than unity, the opposite effect to that expected according to the mechanistic test outlined above and also the opposite effect to that obtained for the water solvolyses of these bromides, for which the rate ratios are less than one (6, 7). There is little doubt from the work of Hammett *et al.* (13, 14) that the Bunte salt reaction is a bimolecular nucleophilic substitution. Thus, one of two conclusions must be drawn—

Can. J. Chem. Downloaded from www.nrcresearchpress.com by 210.87.254.105 on 09/05/12
For personal use only.

either that the α-deuterium isotope effect is not a generally reliable indicator of mechanism, or that there is some special peculiarity in the Bunte salt reaction which makes it alone an exception to the rule. There are insufficient data in the literature at the present time to decide between these two possibilities on the basis of experimental evidence, but the lack of any gross peculiarity in the isotope effects observed for β- and γ-deuterated *n*-propyl bromide for the Bunte salt reaction, collated in Table II, and certain theoretical considerations, favor the first of the alternatives.

TABLE II

Secondary β- and γ-deuterium isotope effects for the reaction between *n*-propyl bromide and sodium thiosulphate in 50% v/v ethanol–water at 25.00±0.05° C

Compound	No. runs	$10^4\, k_2 \pm$ Std. dev. (l./mole sec)	$k_H/k_D \pm$Std. dev.
n-Propyl bromide	11	6.03±0.04	
n-Propyl-2,2,d_2 bromide	4	5.91±0.04	$1.02_1 \pm 0.009$
n-Propyl-3,3,3,d_3 bromide	3	6.09±0.01	$0.99_0 \pm 0.006$

Both the β- and γ-deuterium isotope effects for thiosulphate ion attack of *n*-propyl bromide, although very small, are of the same sign as those found for the same compounds solvolyzing in water. Thus the anomaly of the α-effect is not carried through to the rest of the molecule, although there is some change in the γ-effect towards unity.

Calculations made by Wolfberg, Seltzer, and Freund (22) lead them to the conclusion that secondary isotope effects are brought about by force field changes and only in a subsidiary manner by geometrical changes, between the initial and transition states. Thus, the geometry of the transition state will correlate with the secondary isotope effect only insofar as the force field change correlates with the geometrical change during the activation process. A comparison of force constants for sp^2 and sp^3 hybridized carbon–hydrogen bonds tabulated by Robertson and co-workers (7) showed that the direction of the change in force constant, when the molecular geometry is changed, is unpredictable. It may therefore be overly optimistic to expect the α-deuterium isotope effect to change in a systematic manner with the geometry of the transition state, i.e., with the mechanism, for all nucleophilic substitutions, despite the fact that it has been shown to do so in certain cases.

Even if the non-universality of the α-deuterium isotope effect test of mechanism is accepted, the problem remains to explain why the attack of thiosulphate ion on α-deuterated alkyl bromides gives significantly different rate ratios from those obtained for the same compounds solvolytically attacked by water. Pertinent to this problem is the question of the immediate source of these isotope effects. The rate changes may be brought about by a difference in the enthalpies of activation, a difference in the entropies of activation, or by a difference in both, between the normal and deuterated compounds. To separate the free energy of activation difference between two isotopic analogues into its enthalpy and entropy contributions, the rate ratio must be determined at several different temperatures. Meaningful results can be obtained only when the rate difference is quite large and the errors in the rate measurements are small. Unfortunately, the isotope effects observed for both the Bunte salt and the water solvolysis reactions are too small to allow this analysis to be made experimentally. Previous work (23), however, on the temperature

Can. J. Chem. Downloaded from www.nrcresearchpress.com by 210.87.254.105 on 09/05/12
For personal use only.

dependence of the β-deuterium isotope effects in the water solvolysis of isopropyl compounds, in which the effects were shown to be entirely in the entropy of activation, demonstrates that it can no longer be assumed that all secondary deuterium isotope effects are enthalpy of activation effects. Recently a 12% inverse effect observed in the reactions of 2-methyl pyridine with methyl and deuterated methyl iodide, in benzene solvent, has also been found to be entirely an entropy of activation effect (24).

The immediate conclusion which may be drawn from the Bunte salt reaction isotope effects is that the α-deuterium effect test of mechanism is probably not completely reliable and should therefore be used with great care.

EXPERIMENTAL

Materials

The deuterated alkyl bromides, supplied by Merck and Co. Ltd., each had a minimum isotopic purity of 98%. The normal alkyl bromides were reagent grade chemicals and were dried and distilled immediately before the commencement of the kinetic measurements.

Anhydrous sodium thiosulphate was prepared from the hydrous salt using the method described by Vogel (25) and dried to constant weight at 115° C. This was used in the kinetic runs and also as a primary standard for the iodine solutions used in the titrations. Sodium acetate was dried over potassium hydroxide before use.

The solvent was prepared by mixing equal volumes of water and dry ethanol at 25.0° C. Absolute ethanol was dried according to the method of Lund and Bjerrum (26) and distilled. The exact composition of the solvent was established by density measurements: $d_4^{25} = 0.9229$, which corresponds to 44.05% ethanol, by weight.

Kinetic Method

Stock solutions of sodium acetate and sodium thiosulphate were prepared. The calculated volumes of these solutions and of solvent, all at the temperature of the thermostat, were mixed in a volumetric flask. A solution of appropriate concentration of alkyl bromide in the solvent was prepared, brought to thermostat temperature, and added to the reaction mixture. After rapid mixing a 5-ml sample was withdrawn and run into 50 ml of ice-cold water. The time of quenching was taken as the kinetic zero. Subsequent samples were withdrawn at appropriate intervals and each sample was analyzed by titration of the unreacted thiosulphate against a standardized iodine solution, using 1 ml of 1% starch solution as an indicator. Immediately after each 5-ml sample was withdrawn from the reaction flask a sufficient quantity of small glass ampoules was added to restore the air space above the solution to its original volume. By this procedure, steady rate constants were obtained from the integrated rate equation for a second order irreversible reaction.

Initial concentrations of approximately 0.05 *M* sodium thiosulphate and 0.025 *M* alkyl bromide were used for all the runs except those involving methyl bromide, for which the concentrations were reduced to 0.02 *M* and 0.01 *M* respectively. The sodium acetate buffer used for the ethyl and *n*-propyl bromide reactions was 0.020 *M*. Two illustrative runs are shown in Table III.

Each isotope effect was measured by carrying out runs with the protium and deuterium compounds simultaneously, which gave a constant check on the kinetic operations and ensured that any errors due to fluctuations in temperature would affect both compounds equally. The temperature of the thermostat was measured with a mercury-in-glass thermometer which had been compared with a standard thermometer certified by H. J. Elliott Ltd. (E-mil). The observed fluctuations in the bath temperature were less than 0.01° C, but the limit of accuracy of E-mil standardization was ±0.05° C. At least three pairs of runs were carried out with each deuterated compound.

As the second order rate constant for this reaction under the described conditions varies with the initial concentration of thiosulphate, presumably due to a medium effect (13), care was taken to ensure that the initial thiosulphate concentration did not vary from run to run sufficiently to introduce rate differences from this source. The magnitude of the medium effect was determined separately before the isotopic measurements, to be certain that this was feasible.

Since the rate constants did not show any variation from this source or from temperature fluctuations, the final rate ratios were calculated from the mean rate constant of all the runs carried out with each compound. The standard deviation in the rate ratio was computed from that calculated for k_H and k_D separately, according to the treatment by Crumpler and Yoe (27).

ACKNOWLEDGMENT

The author is grateful for financial support of this work by the National Research Council.

Can. J. Chem. Downloaded from www.nrcresearchpress.com by 210.87.254.105 on 09/05/12
For personal use only.

TABLE III

Illustrative kinetic runs for the reactions between alkyl bromides and sodium thiosulphate in 50% v/v ethanol–water at 25.00±0.05° C

Run 13 Initial conc. $Na_2S_2O_3$ = 0.04994 *M* Initial conc. CH_3CD_2Br = 0.02229 *M* Conc. CH_3COONa buffer = 0.020 *M*			Run 55 Initial conc. $Na_2S_2O_3$ = 0.01895 *M* Initial conc. CH_3Br = 0.00845 *M*		
t (minutes)	Iodine titer* (ml)	$10^4 k_2$ (l./mole sec)	*t* (minutes)	Iodine titer† (ml)	$10^4 k_2$ (l./mole sec)
0	9.79	—	0	9.34	—
30	9.36	11.79	2.11	8.59	876.6
60	9.00_5	11.50	4.31	8.00	857.6
120	8.39_5	11.59	6.40	7.56	865.3
180	7.92	11.60	8.63	7.17	866.6
240	7.55	11.52	10.71	6.92	849.6
300	7.22	11.70	13.02	6.62_5	867.2
360	6.98_5	11.54	14.58	6.50	856.9
1740	5.42	—	86.59	5.19	—
1770	5.42	—	95.96	5.17	—
Average k_2 = 11.61×10^{-4} l./mole sec			Average k_2 = 862.8×10^{-4} l./mole sec		

*Volume of 0.02543 *N* I_2 solution equivalent to 4.98_5 ml sample, corrected for burette errors.
†Volume of 0.01010 *N* I_2 solution equivalent to 4.98_5 ml sample, corrected for burette errors.

REFERENCES

1. L. MELANDER. Isotope effects on reaction rates. Ronald Press Co., New York. 1960. Chap. 5.
2. W. H. SAUNDERS. Technique of organic chemistry. Vol. VIII, Pt. I. Interscience Publishers Inc., New York. 1961. Chap. 9.
3. R. E. WESTON, JR. Ann. Rev. of Nucl. Sci. **11**, 439 (1961).
4. A. STREITWIESSER, JR. Ann. N.Y. Acad. Sci. **84**, 576 (1960).
5. V. J. SHINER, JR., H. R. MAHLER, R. H. BAKER, JR., and R. R. HIATT. Ann. N.Y. Acad. Sci. **84**, 583 (1960).
6. J. A. LLEWELLYN, R. E. ROBERTSON, and J. M. W. SCOTT. Can. J. Chem. **38**, 222 (1960).
7. K. T. LEFFEK, J. A. LLEWELLYN, and R. E. ROBERTSON. Can. J. Chem. **38**, 1505 (1960).
8. K. T. LEFFEK, J. A. LLEWELLYN, and R. E. ROBERTSON. J. Am. Chem. Soc. **82**, 6315 (1960).
9. K. T. LEFFEK, J. A. LLEWELLYN, and R. E. ROBERTSON. Can. J. Chem. **38**, 2171 (1960).
10. V. J. SHINER, JR. J. Am. Chem. Soc. **74**, 5285 (1952).
11. R. R. JOHNSON and E. S. LEWIS. Proc. Chem. Soc. 52 (1958).
12. B. MILLIGAN and J. M. SWAN. Rev. Pure Appl. Chem. **12**, 72 (1962).
13. T. I. CROWELL and L. P. HAMMETT. J. Am. Chem. Soc. **70**, 3444 (1948).
14. P. M. DUNBAR and L. P. HAMMETT. J. Am. Chem. Soc. **72**, 109 (1950).
15. J. R. BEVAN and C. B. MONK. J. Chem. Soc. 1392 (1956).
16. J. R. BEVAN and C. B. MONK. J. Chem. Soc. 1396 (1956).
17. A. STREITWIESER, JR. and R. C. FAHEY. Chem. Ind. 1417 (1957).
18. K. MISLOW, S. BORCIC, and C. PRELOG. Helv. Chim. Acta, **40**, 2477 (1957).
19. S. HARTMAN and R. E. ROBERTSON. Can. J. Chem. **38**, 2033 (1960).
20. E. D. HUGHES. J. Chem. Soc. 255 (1935).
21. J. HINE. Physical organic chemistry. McGraw-Hill Book Co. Inc., New York. 1962. p. 131.
22. (*a*) *Quoted in* M. FELD, A. P. STEFANI, and M. SZWARC. J. Am. Chem. Soc. **84**, 4453 (1962). (*b*) M. WOLFSBERG. Private communication.
23. K. T. LEFFEK, R. E. ROBERTSON, and S. E. SUGAMORI. Can. J. Chem. **39**, 1989 (1961).
24. K. T. LEFFEK and J. W. MACLEAN. Unpublished results.
25. A. I. VOGEL. Quantitative inorganic analysis. Longmans, Green and Co., London. 1951. p. 334.
26. A. I. VOGEL. Practical organic chemistry. Longmans, Green and Co., London. 1954. p. 166.
27. T. B. CRUMPLER and J. H. YOE. Chemical computations and errors. Wiley and Sons, Inc., New York. 1940. p. 178.

Can. J. Chem. Downloaded from www.nrcresearchpress.com by 210.87.254.105 on 09/05/12
For personal use only.

PYRIDINE N-OXIDE COMPLEXES OF ZIRCONYL, THORIUM, AND URANYL PERCHLORATES

P. RAMA MURTHY AND C. C. PATEL

Department of Inorganic and Physical Chemistry, Indian Institute of Science, Bangalore, India

Received October 2, 1963

ABSTRACT

Pyridine N-oxide complexes having the composition $ZrO(Py.O)_6(ClO_4)_2$, $Th(Py.O)_8(ClO_4)_4$, and $UO_2(Py.O)_5(ClO_4)_2$ have been prepared. The infrared and electronic absorption spectra show that the bonding between the metal and pyridine N-oxide in the complexes has occurred by donation of the lone pair of *p*-electrons on oxygen to the metal, and that the π-bond character of NO group increases in the complexes as uranyl < thorium < zirconyl. The decrease in the vibrational structure of the UO_2^{2+} spectrum in the visible region indicates strong coordination of pyridine N-oxide to the uranyl group. The decomposition temperatures of zirconyl, thorium, and uranyl complexes are 307, 350, and 319° C respectively.

Recently Quagliano (1) *et al.* have prepared a number of metal complexes of pyridine N-oxide and determined their conductivity and magnetic susceptibilities. The same workers (2, 3) have also investigated the infrared spectra of these complexes. Carlin (4) has also prepared a number of pyridine N-oxide complexes of metal perchlorates and investigated their visible spectra.

The survey of the literature shows that the pyridine N-oxide complexes of IV A group metal perchlorates and of uranyl perchlorate have not been prepared before. The pyridine N-oxide complexes of zirconyl, thorium, and uranyl perchlorates were, therefore, prepared for the first time and some of their properties studied.

EXPERIMENTAL

Materials Employed

Pyridine N-oxide was prepared according to the method of Ochiai (5), purified by repeated vacuum distillations, and finally recrystallized from chloroform.

Zirconyl perchlorate dihydrate and thorium perchlorate tetrahydrate were prepared as reported earlier (6, 7).

Uranyl perchlorate hexahydrate was prepared by digesting uranyl nitrate hexahydrate with the calculated amount of perchloric acid and evaporating the mixture to dryness. Uranyl perchlorate formed was crystallized until free from nitrate ions.

Preparation of the Complexes

To 1 g of zirconyl perchlorate dihydrate in 20 ml of anhydrous ethanol, 2.5 g of pyridine N-oxide in 20 ml of ethanol was added. The solution was allowed to stand for 15 hours in the refrigerator and the crystals obtained were filtered, washed with ethanol, dried over phosphorus pentoxide under vacuum, and analyzed. Zirconium was estimated gravimetrically by precipitating the hydroxide with ammonium hydroxide and weighed as ignited oxide. Perchlorate was estimated by Kurz's method (8) by reducing the perchlorate with sodium nitrite at about 500° C and estimating the chloride formed by Volhard's method. Nitrogen was estimated by Duma's semimicro method. (Zr = 10.32, ClO_4 = 22.38, and N_2 = 9.48%. Calc. for $ZrO(Py.O)_6(ClO_4)_2$: Zr = 10.40, ClO_4 = 22.69, and N_2 = 9.58%.)

Crystals of the thorium complex were obtained immediately by mixing the reactants as above. The crystals were purified, dried as before, and analyzed in the same way as in the above case. (Th = 16.79, ClO_4 = 27.86, and N_2 = 7.99%. Calc. for $Th(Py.O)_8(ClO_4)_4$: Th = 16.68, ClO_4 = 28.45, and N_2 = 8.06%.)

In the case of uranyl complex, it was necessary to evaporate the solution almost to dryness to get the crystals of the complex. The crystals were purified, dried, and analyzed as before. (U = 24.85, ClO_4 = 20.85, and N_2 = 7.40%. Calc. for $UO_2(Py.O)_5(ClO_4)_2$: U = 25.10, ClO_4 = 21.06, and N_2 = 7.42%.)

Properties

Zirconyl and thorium pyridine N-oxide complexes were white while uranyl complex was bright yellow in color. All the complexes were non-hygroscopic, insoluble in non-polar solvents, and soluble in water,

Can. J. Chem. Downloaded from www.nrcresearchpress.com by 210.87.254.5 on 09/05/12
For personal use only.

acetonitrile, and dimethyl formamide. When the complexes were heated, they exploded. To minimize the impact of explosion, the differential thermal analysis of the complexes were carried out by mixing the complexes with alumina in the ratio of 1:10. The DTA for zirconyl, thorium, and uranyl complexes gave a big exothermic peak at 307°, 350°, and 319° C respectively.

Infrared and Electronic Absorption Studies

The infrared spectra of the complexes were taken in Nujol mull with Perkin–Elmer infrared spectrophotometer model 21, equipped with sodium chloride optics. The infrared absorption frequencies of these complexes together with those of pyridine N-oxide (2) are given in Table I.

TABLE I

Infrared frequencies (cm^{-1}) of zirconyl, thorium, and uranyl complexes together with pyridine N-oxide

Py.O in solution (2)	$ZrO(Py.O)_6(ClO_4)_2$	$Th(Py.O)_8(ClO_4)_4$	$UO_2(Py.O)_5(ClO_4)_2$	Assignments
3070 w	3125 w	3096 m	3106 m	CH stretching
1930	2016 w	2010 w	2000 m	$2.\nu_5$
1909	1901 v w	1888 v v w	1883 v w	$\nu_{10b}+\nu_{17a}$
~1780	1832 v v w	1832 v v w	—	$\nu_{10a}+\nu_5$
1760	1792 w b	—	—	$\nu_{10a}+\nu_{17a}$
—	1689 m	1681 m	1686 w	$\nu_{11}+\nu_{10b}$
1610 m	1631 m	1631 m	1637 m	Ring def
	1555 v w			
	1464 s	1460 s	1460 s	
	1427 w			Ring def
1463 s	1414 v w	1408 sh	1414 sh	
	(1332 sh)			
1265 v s	1222 v s	1218 v s	1207 v s	NO str
1188 w	1198 sh	1183 sh	1189 sh	
	1179 sh	1173 w	1175 sh	
1166 s	1136 w	1163 sh	1155 w	C–H in plane def
1068 w	1053 sh	1050 w	1068 sh	
			(1053 sh)	
	1085 v s	1081 v s	1081 v s	ClO_4^-
	1075 sh	1070 sh		
1014 s	1022 sh	1024 sh	1020 w	Ring breathing
965	1009 v w	1004 sh	~999.2 w sh	ν_5
950 v w sh	968.9 w	970.9 sh	961.9 sh	ν_{17a}
887 m	930.9 w	918.5 m b	923.4 w	ν_{10b}
840 s	840 s	836 s	837 s	NO bending
820 v w sh	822 v w sh	823 sh	830 v w sh	ν_{10a}
758 v s	763 v s	768 v s	770 v s	ν_{11}
667 v s	668 v s	668 v s	669 v s	—

NOTE: v = very, s = strong, m = medium, w = weak, b = broad, sh = shoulder.

Electronic absorption spectra of the complexes in pure dry acetonitrile were taken with Hilger Uvispek spectrophotometer, model H 700, using 1 cm matched pair of quartz cells. The spectra are given in Figs. 1 and 2.

DISCUSSION

The three main vibration frequencies of pyridine N-oxide which are likely to be influenced on complex formation with metal ion are NO stretching vibration, NO bending vibration, and C–H out-of-plane vibration frequencies (3).

Shindo (9–11) has assigned the strong band at 1265 cm^{-1} to NO stretching vibration in the spectrum of pyridine N-oxide in carbon disulphide, while in the solid state the band occurs around 1243 cm^{-1}. The NO stretching frequency of the complexes in mull is lowered to below 1225 cm^{-1} (Table I). The decrease in the frequency is attributed to the change in the nature of the NO bond as a result of coordination. With the formation of M ← O bond, there is a decrease in the π-bond character of NO. The NO stretching vibrational frequencies of zirconyl, thorium, and uranyl complexes are at 1222, 1218, and 1207 cm^{-1}

Can. J. Chem. Downloaded from www.nrcresearchpress.com by 210.87.254.5 on 09/05/12
For personal use only.

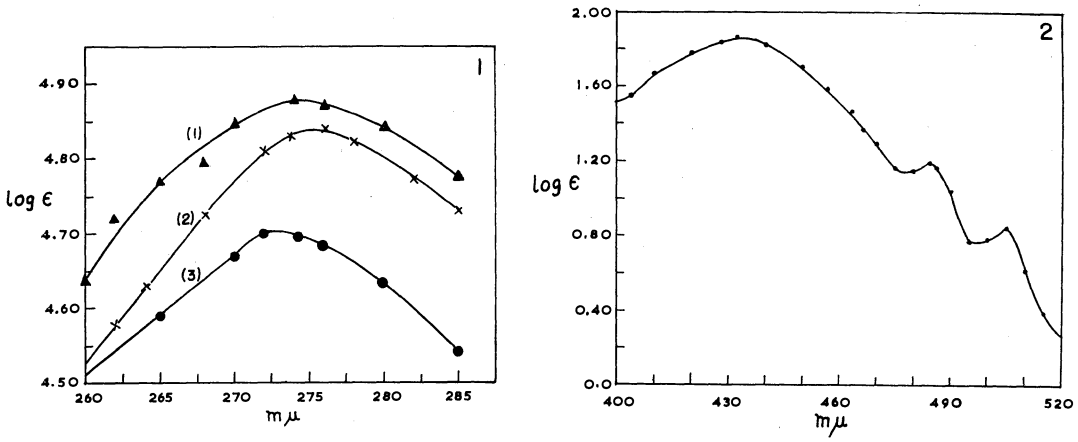

FIG. 1. Ultraviolet absorption spectra of (1) $Th(Py.O)_8(ClO_4)_4$, (2) $ZrO(Py.O)_6(ClO_4)_2$, and (3) $UO_2(Py.O)_5(ClO_4)_2$ in acetonitrile.
FIG. 2. Absorption spectra of uranyl pyridine N-oxide complex in acetonitrile in the visible region.

respectively, showing gradual decrease in the π-bond character of NO and consequent increase in the bond strength between the metal and the oxygen. Using these frequencies, the force constants calculated for the NO group in the complexes are 6.577, 6.531, and 6.398 millidynes per Å respectively. The decreasing order also follows the decreasing order of π-bond character of the NO group in the complexes.

The 840 cm^{-1} band in the spectrum of pyridine N-oxide has been assigned to NO bending vibration (2). Because of the coordination of oxygen atom of NO group to the metal atom, a noticeable shift of NO bending could be expected. However, a very slight shift of this vibration is observed in these complexes. The small shift is due to the two opposing effects. One, similar to that of coordinated water where bending vibration, δOH, is shifted to the higher frequency and the other, lowering in the frequency because of the decrease in π-bond character of the NO bond. If both these effects are practically equal, a very small shift in the frequency would result.

Kakiuti (3) and co-workers have assigned C–H out-of-plane vibrations at 741 (ν_{11}), 935 (ν_{10b}), 993 (ν_5), 846 (ν_{10a}), and 972 cm^{-1} (ν_{17a}) for pyridine N-oxide. In the complexes studied almost all vibrations except (ν_{11}) and (ν_{10b}) appear as weak shoulders, and all are considerably shifted to higher frequencies owing to the decrease in the electron density of the pyridine ring. This observation is in agreement with the findings of Kross (12).

All the remaining bands due to the pyridine ring are very little affected on complex formation and their assignments are made after the work of Kida (2). The in-plane ring vibration band of pyridine N-oxide around 1475 cm^{-1} has merged with the Nujol band. In the uranyl complex, the strong band at 907 cm^{-1} is due to the asymmetric stretching frequency and the 858 cm^{-1} weak band due to the symmetric stretching frequency of uranyl ion (13). The asymmetric vibration band is shifted to the lower frequency. A similar shift was observed by Comyns *et al.* (14) in uranyl acetylacetone complex. Such a shift is possible when the ligand groups are presumed to lie in or nearly in a plane perpendicular to the axial O–U–O direction (16). The force constant K_{eff}, and $r_{U-O(2)}$, $r_{U-O(1)}$ distances calculated for UO_2^{2+} group in the complex are 6.87 millidynes per Å and 1.74 Å and 1.72 Å respectively. The U–O distances are calculated using equations of Jones (15) and McGlynn (16) respectively. The broad strong band at 1085 cm^{-1} in all the three complexes is due to the degenerate stretching vibration of the perchlorate ion.

Can. J. Chem. Downloaded from www.nrcresearchpress.com by 210.87.254.5 on 09/05/12
For personal use only.

The electronic absorption of spectrum of pyridine N-oxide in *n*-heptane gives one intense band at 280 mμ and a weak band at about 320 mμ. The former band is assigned to $\pi \rightarrow \pi^*$ transition, and the latter to the $n \rightarrow \pi^*$ transition by Ito (17) *et al.* On complex formation the weak band at 320 mμ disappears while the band at 280 mμ shifts to lower wavelength around 275 mμ. This shows that the complex formation has taken place by donation of the lone pair of *p*-electrons on oxygen of the NO group to the metal atom, thus supporting the findings by the vibrational spectra. The absorption maximum in zirconyl, thorium, and uranyl complexes occurs at 276, 274, and 272 mμ respectively. This shows that π-electrons in the NO group are held in the following increasing strength: uranyl < thorium < zirconyl complex. This observation is in agreement with the decrease in NO stretching frequency. The intensity of the band around 275 mμ is roughly proportional to the number of pyridine N-oxide ligands attached to the metal atom.

In place of nearly 10 bands due to the free uranyl ion in solution, uranyl pyridine N-oxide complex gave only three weak bands in the visible region at 432 ($\epsilon = 71.88$), 484 ($\epsilon = 15.07$), and 505 mμ ($\epsilon = 6.955$) (Fig. 2). From their position and low intensity, the 432 and 484 mμ bands are the modified form of uranyl bands. The lowest intensity 505 mμ band may also be due to the uranyl ion, although it falls just outside the range of absorption usually observed in the spectrum of uranyl ions in solution. The decrease in the number of bands indicates the strong coordination between pyridine N-oxide and uranyl group.

From the number of pyridine N-oxide molecules in the metal complexes, the coordination number for both zirconium and uranium is seven and that for thorium is eight. In general, compounds with coordination number of seven are rare. However, both zirconium and uranium (18) exhibit coordination number of seven in complex ions $(ZrF_7)^{3-}$ and $(UO_2F_5)^{3-}$. The zirconyl complex with coordination number seven may be represented either as a face-centered octahedron (d^5sp hybridization) having the extra oxygen atom at the center of one face of the octahedron or as a trigonal prism with the extra oxygen at the center of one square face (face-centered trigonal prism with d^4sp^2 hybridization). The uranyl complex with coordination number seven may have pentagonal bipyramidal arrangement. In this case, two separate sets of hybrids are possible: d^2sp^2 to give five planar bonds and $d_{z^2}p_z$ or df to give the axial bonds (18). The arrangement may resemble that of $(UO_2F_5)^{3-}$ complex ion (19). Thorium complex with eight coordination number may have the square-antiprism structure with d^5p^3 hybridization as in the acetylacetonate complexes of Th(IV), U(IV), and Ce(IV) (20).

ACKNOWLEDGMENT

The authors are thankful to Professor M. R. A. Rao for his interest in the work.

REFERENCES

1. J. V. Quagliano, J. Fujita, G. Franz, D. H. Phillips, J. A. Walmsley, and S. Y. Tyree. J. Am. Chem. Soc. **83**, 3770 (1961).
2. S. Kida, J. V. Quagliano, J. A. Walmsley, and S. Y. Tyree. Spectrochim. Acta, **19**, 189 (1963).
3. Y. Kakiuti, S. Kida, and J. V. Quagliano. Spectrochim. Acta, **19**, 201 (1963).
4. L. Carlin. J. Am. Chem. Soc. **83**, 3773 (1961).
5. E. Ochiai. J. Org. Chem. **18**, 534 (1953).
6. P. Rama Murthy and C. C. Patel. Naturwiss. **22**, 693 (1961).
7. P. Rama Murthy and C. C. Patel. J. Inorg. Nucl. Chem. **25**, 310 (1963).
8. E. Kurz, G. Kober, and M. Berl. Anal. Chem. **30**, 1983 (1958).
9. H. Shindo. Pharm. Bull. (Tokyo), **4**, 460 (1960); Kagaku No Ryôiki, Zôkam, **28**, 163 (1958).
10. H. Shindo. Chem. Pharm. Bull. (Tokyo), **6**, 117 (1958).
11. H. Shindo. Chem. Pharm. Bull. (Tokyo), **7**, 791 (1959).
12. R. D. Kross, V. A. Fassel, and M. Margoshes. J. Am. Chem. Soc. **78**, 1332 (1956).

Can. J. Chem. Downloaded from www.nrcresearchpress.com by 210.87.254.5 on 09/05/12
For personal use only.

13. G. K. T. CONN and C. K. WU. Trans. Faraday Soc. **34**, 1483 (1938).
14. A. E. COMYNS, B. M. GATEHOUSE, and E. WAIT. J. Chem. Soc. 4655 (1958).
15. L. H. JONES. Spectrochim. Acta, **15**, 409 (1959).
16. S. P. MCGLYNN, J. K. SMITH, and W. C. NEELY. J. Chem. Phys. **35**, 105 (1961).
17. M. ITO and N. HATA. Bull. Chem. Soc. Japan, **28**, 260 (1955).
18. E. CARTMELL and G. W. A. FOWELS. Valency and molecular structure. 2nd ed. Butterworths, London. 1961. p. 236.
19. W. H. ZACHARIASEN. Acta Cryst. **7**, 183 (1954).
20. D. GRADENIC and B. MATKOVIC. Acta Cryst. **12**, 817 (1959).

Can. J. Chem. Downloaded from www.nrcresearchpress.com by 210.87.254.5 on 09/05/12
For personal use only.

Can. J. Chem. Downloaded from www.nrcresearchpress.com by 210.87.254.40 on 09/05/12
For personal use only.

REACTIONS OF DIETHYLBERYLLIUM AND DIETHYLBERYLLIUM TRIMETHYLAMINE WITH THE METHYLHYDRAZINES

NEIL R. FETTER
Chemistry Division, U. S. Naval Ordnance Laboratory, Corona, California

Received November 7, 1963

ABSTRACT

The reactions of Et_2Be and $Et_2Be{:}NMe_3$ with the methylhydrazines produce the following compounds: $Et_2Be{:}NMe_3$ and H_2NNMeH give $(EtBeMeNNH_2)_n$, Et_2Be and H_2NNMeH give $Be(MeNNH_2)_2$, Et_2Be and H_2NNMe_2 give $Be(HNNMe_2)_2$, Et_2Be and HMeNNMeH give $(EtBeMeNNMeH)_n$, $Et_2Be{:}NMe_3$ and $HMeNNMe_2$ give approximately 50% $Et_2Be{:}HMeNNMe_2$ and 50% $(EtBeMeNNMe_2)_n$, Et_2Be and $HMeNNMe_2$ give primarily $(EtBeMeNNMe_2)_n$, and Et_2Be and Me_2NNMe_2 give $(Et_2Be_2){:}Me_2NNMe_2$.

INTRODUCTION

The first preparation of an organo-beryllium–nitrogen compound was reported by Gilman and Schulze (1), who prepared

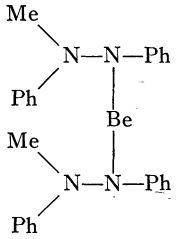

from the reaction of azobenzene and dimethylberyllium. Several years later this area of beryllium chemistry was extensively investigated by Coates and co-workers. They first reported the preparation of $Me_2Be{:}NMe_3$ and an unstable compound $(Me_2Be)_2{:}(NMe_3)_3$ (2). Also reported was the preparation of $(MeBeNMe_2)_3$ from the reaction of dimethyl beryllium and dimethylamine and the preparation of $Me_2Be{:}H_2NMe$, MeBe—NHMe, and $(MeBe—NHMe{:}Be{:}NMe)_y$ from dimethylberyllium and methylamine. Later Coates and Glockling (3) prepared $(i\text{Pr})_2Be{:}NMe_3$, $i\text{PrBeNMe}_2$, $Be(NMe_2)_2$, and $(BeNHMe_2)_n$ from reactions of diisopropylberyllium with trimethylamine and dimethylamine. These authors also prepared $(t\text{-Bu})_2Be{:}NMe_3$ by reaction of $(t\text{-Bu})_2Be{:}Et_2O$ with NMe_3 and $Be(NMe_2)_2$ by reaction of di-*t*-butylberyllium with dimethylamine (4).

Recently Coates and Green (5) have described the preparation and properties of two bipyridyl complexes, Et_2bipyBe and Ph_2bipyBe, and a series of ethylenediamine complexes with dimethylberyllium. A 1:1 adduct is formed between dimethylberyllium and N,N,N′,N′-tetramethylethylenediamine; N,N,N′-trimethylethylenediamine gave the dimer $(Me_2NCH_2CH_2NMe—BeMe)_2$: N,N′-dimethylethylenediamine produced a polymer with the structure

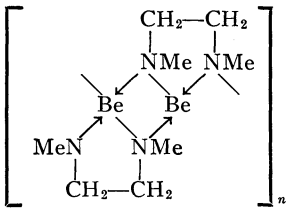

N,N-dimethylethylenediamine gave the dimer $(Me_2NCH_2CH_2NH—BeMe)_2$: and ethylenediamine reacted with dimethylberyllium to give a compound with the empirical formula $(C_2H_4N_2BeH_2)_x$.

The present work was undertaken to observe the behavior of diethylberyllium and its trimethylamine complex with several methylhydrazines. The hydrazines, in their reactions with beryllium alkyls, are chemically similar to the ethylenediamines, but sterically less flexible; hence, complexes involving these amines, which have nitrogen atoms that can be positioned to form the type

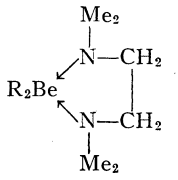

reported by Coates (5), are less likely to be found.

EXPERIMENTAL

Apparatus and Reagents

The compounds described below were prepared on a conventional glass high-vacuum system, which was equipped with a Toepler pump and calibrated volume for measurement of evolved gases. The products were handled in a nitrogen-filled dry box.

The methyl hydrazine (Matheson, Coleman and Bell), 1,1-dimethylhydrazine (Olin Mathieson Corp.), and tetramethylhydrazine (Metalectro Corp.) were vacuum distilled over CaH_2 before use. The 1,2-dimethylhydrazine was isolated from its dihydrochloride (K and K Laboratories) by treatment with liquid ammonia, and the trimethylhydrazine was prepared by the method of Class, Aston, and Oakwood (6). The diethylberyllium was prepared by the method of Gilman and Schulze (7), and the diethylberyllium trimethylamine was prepared by treatment of Et_2Be in heptane with a slight excess of NMe_3. The Et_2Be:NMe_3 was distilled under high vacuum before use. Solvents were reagent grade and were used without further purification except benzene, which was distilled over $LiAlH_4$ before use.

Molecular weight determinations were done cryoscopically in benzene with a Bender-Hobein apparatus, and infrared spectra were taken with NaCl cells on a Beckman IR-5 spectrophotometer. Elemental analyses were performed by the Schwarzkopf Microanalytical Laboratories, Woodside, New York. Nuclear magnetic resonance spectra were made on a Varian Associates Model V-4302 operating at 60 mc. Samples were 10–15% by weight in benzene solutions.

Reaction of Diethylberyllium Trimethylamine with Methylhydrazine

Onto 0.797 g (6.33 mmole) of Et_2Be:NMe_3, dissolved in 20 ml of *n*-octane, at −196° C was transferred 0.455 g (9.90 mmole) of H_2NNMeH. The mixture was allowed to warm to room temperature and stand for 2 hours. The evolved ethane was measured after the condensible substances were passed through a −100° C trap and into a calibrated volume by a Toepler pump. The reaction yielded 228 ml (10.2 mmole) of ethane and 61.5 ml (2.96 mmole) of trimethylamine.

Removal of the solvent via vacuum transfer left a powdery white solid which did not sublime or dissolve in hydrocarbons. Elemental analysis of the crude product gave results which agree with the formula $C_3H_7N_2Be$. Anal. Calc.: C, 43.44; H, 12.12; N, 33.70; Be, 10.84. Found: C, 42.55; H, 12.23; N, 33.05; Be, 10.70.

Methanolysis of 0.0963 g (1.16 mmole) of the crude product yielded 27.4 ml (1.20 mmole) of ethane. The infrared spectrum of the product has a strong N—H band at 3100 cm^{-1} and a weak NH_2 band at 1700 cm^{-1}.

Reaction of Diethylberyllium with Methylhydrazine

The above reaction was repeated with 0.831 g (12.1 mmole) of Et_2Be and 1.308 g (28.4 mmole) of H_2NNMeH. The reaction mixture stood at 25° C for 2 days after having reached room temperature. During this period 408 ml (18.2 mmole) of ethane evolved. After the solvent was removed there remained a powdery white solid which was sufficiently unstable that a sample for the C and H analysis exploded before results could be obtained. The Be and N analyses were in closest agreement with the formula $C_3H_7N_2Be$. Anal. Calc.: N, 33.70; Be, 10.84. Found: N, 36.98; Be, 10.97.

Methanolysis of 0.392 g (4.71 mmole) of the crude product, $C_3H_7N_2Be$, gave only 58.2 ml (2.60 mmole) of ethane. This material had infrared bands at the same wavelengths for N—H and NH_2 as the product obtained from the reaction of Et_2Be:NMe_3 with H_2NNMeH.

Can. J. Chem. Downloaded from www.nrcresearchpress.com by 210.87.254.40 on 09/05/12
For personal use only.

In another experiment, 0.473 g (7.07 mmole) of Et_2Be and 0.794 g (17.2 mmole) of H_2NNMeH were combined in 10 ml of nonane at −196° C. The mixture was warmed to room temperature and heated at 65° C for 14 hours. During this period 258.3 ml (11.5 mmole) of ethane was collected. The solvent and any unreacted H_2NNMeH were removed under vacuum and 0.1547 g (1.84 mmole $EtBeNMeNH_2$) of the powdery white product was treated with methanol, yielding 9.4 ml (0.42 mmole) of ethane. The ethane was 22.8 mole% of that calculated for 0.1547 g of $EtBeNMeNH_2$. The infrared spectrum of the product had an NH band at 3100 cm^{-1} and a weak NH_2 band at 1680 cm^{-1}.

Reaction of Diethylberyllium with 1,1-Dimethylhydrazine

By vacuum transfer, 1.347 g (22.5 mmole) of H_2NNMe_2 was placed on 0.540 g (8.05 mmole) of Et_2Be dissolved in 20 ml of *n*-octane at −196° C. The mixture was allowed to warm to room temperature, stand overnight, and was then heated at 50° C for 1 hour. A total of 341 ml (15.2 mmole) of ethane was recovered. After solvent and excess H_2NNMe_2 were removed under vacuum a light-yellow, gummy material remained. Since the crude product could not be distilled or sublimed, an elemental analysis of this material was obtained and the results agree with the formula $Be(HNNMe_2)_2$. Anal. Calc.: C, 37.70; H, 11.09; N, 44.05; Be, 7.08. Found: C, 37.58; H, 11.70; N, 43.85; Be, 7.03.

Methanolysis of approximately 0.5 g of crude product produced no ethane measured on a mercury manometer. The infrared spectrum of the product had no NH_2 band at 1700 cm^{-1}, but did have an N—H band at 3100 cm^{-1}. The reaction is: $Et_2Be + 2H_2NNMe_2 \rightarrow Be(HNNMe_2)_2 + 2C_2H_6$.

Reaction of Diethylberyllium with Trimethylhydrazine

Under vacuum, 1.248 g (15.5 mmole) of $HMeNNMe_2$ was transferred to a solution at −196° C containing 0.858 g (12.8 mmole) of Et_2Be and 20 ml of *n*-octane. The mixture was allowed to warm to room temperature and stand for 2 hours. During this period, 263 ml (11.8 mmole) of ethane evolved. The solvent was removed under vacuum to a −196° C trap and the clear fluid that remained was vacuum transferred (0.05 mm) at 25° C onto a −196° C cold surface. Approximately 15% of the crude product was collected in this manner and was a clear mobile liquid. The remainder of non-volatile material was a viscous fluid.

Elemental analysis of the volatile liquid gave results which agree with the formula $Et_2Be{:}HMeNNMe_2$. Anal. Calc.: C, 59.52; H, 14.27; N, 19.83; Be, 6.38. Found: C, 59.75; H, 13.95; N, 20.00; Be, 5.91.

There was not sufficient material to do a methanolysis. Elemental analysis of the non-volatile material gave results which agree with the formula $EtBe{-}NMeNMe_2$: Anal. Calc.: C, 54.01; H, 12.69; N, 25.20; Be, 8.10. Found: C, 54.86; H, 11.03; N, 25.30; Be, 8.06.

Methanolysis of 0.2027 g (1.82 mmole) of $EtBe{—}NMeNMe_2$ gave 35.7 ml (1.60 mmole) of ethane.

The above reaction was repeated with a 2:1 ratio of Et_2Be to $HMeNNMe_2$ in an attempt to prepare $Be(NMeNMe_2)_2$. In heptane, 0.585 g (8.73 mmole) of Et_2Be was added to 1.29 g (17.4 mmole) of $HMeNNMe_2$ at −196° C. The mixture was allowed to reach room temperature and was heated at 55° C for 4 hours. During this period 302 ml (13.5 mmole) of ethane was evolved. The solvent and any unreacted $HMeNNMe_2$ were removed at 25° C under vacuum, and the product that remained was a clear, viscous, non-volatile fluid.

Methanol hydrolysis of 0.2146 g of the product produced 33.2 ml (1.48 mmole) of ethane and the results of an elemental analysis suggest only a partial formation of $Be(NMeNMe_2)_2$ had occurred. Anal. Calc. for $Be(NMeNMe_2)_2$: C, 46.41; H, 11.68; N, 36.08; Be, 5.80. Calc. for $EtBe{—}NMeNMe_2$: C, 54.01; H, 12.69; N, 25.20; Be, 8.10. Found: C, 51.08; H, 12.25; N, 29.76; Be, 7.51.

The reactions of Et_2Be with $HMeNNMe_2$ may be summarized by the following equations:

$$(1)\ Et_2Be + HMeNNMe_2 \rightarrow Et_2Be{:}HMeNNMe_2$$

$$(2)\ Et_2Be{:}HMeNNMe_2 \rightarrow EtBe{—}NMeNMe_2 + C_2H_6$$

and presumably, if vigorous enough conditions are used,

$$(3)\ EtBe{—}NMeNMe_2 + HMeNNMe_2 \rightarrow Be(NMeNMe_2)_2 + C_2H_6.$$

Reaction of Diethylberyllium Trimethylamine with Trimethylhydrazine

The reaction of $Et_2Be{:}NMe_3$ with $HMeNNMe_2$ is essentially the same as the reaction with Et_2Be, except that a higher yield of $Et_2Be{:}HMeNNMe_2$ is obtained (approx. 50% by wt. of crude product). The reaction of 0.819 g (6.50 mmole) of $Et_2Be{:}NMe_3$ with 0.596 g (8.05 mmole) of $HMeNNMe_2$ in 15 ml of *n*-octane yielded 151 ml (6.72 mmole) of ethane during warming to 25° C over a period of 1 hour. The crude product that was obtained after solvent removal was vacuum transferred at 25° C onto a −78° C cold surface. Approximately 50% of this crude material transferred as a clear, mobile liquid. Its elemental analysis agreed with the formula $Et_2Be{:}HMeNNMe_2$. Anal. Calc.: C, 59.52; H, 14.27; N, 19.83; Be, 6.38. Found: C, 58.72; H, 13.07; N, 20.07; Be, 6.16.

Methanolysis of 0.0695 g (0.49 mmole) of $Et_2Be{:}HMeNNMe_2$ yielded 15.7 ml (0.70 mmole) of ethane. Elemental analysis of the non-volatile liquid gave results which agreed with the formula $EtBe{—}NMeNMe_2$: Anal. Calc.: C, 54.01; H, 12.69; N, 25.20; Be, 8.10. Found: C, 54.86; H, 11.03; N, 24.40; Be, 8.25.

Reaction of Diethylberyllium with 1,2-Dimethylhydrazine

Under vacuum, 1.384 g (23.1 mmole) of HMeNNMeH was transferred to a solution of 1.584 g (23.7

Can. J. Chem. Downloaded from www.nrcresearchpress.com by 210.87.254.40 on 09/05/12
For personal use only.

mmole) of Et_2Be and 15 ml of *n*-octane at −196° C. The mixture was allowed to warm to room temperature, the solvent was removed, and the crude product was then heated at 75° C for 3 hours. During this period, 620 ml (27.7 mmole) of ethane evolved leaving a non-volatile gummy yellow fluid product. Elemental analysis of this material gave results which agree with the formula EtBe—NMeNMeH. Anal. Calc.: C, 49.44; H, 12.45; N, 28.84; Be, 9.27. Found: C, 49.90; H, 11.66; N, 29.00; Be, 9.03.

Methanolysis of 0.3244 g (3.34 mmole) of EtBe—NMeNMeH yielded 68.7 ml (3.07 mmole) of ethane.* The infrared spectrum of the product had a strong NH band at 3120 cm^{-1}. The reaction is:

$$Et_2Be + HMeNNMeH \rightarrow EtBe—NMeNMeH + C_2H_6.$$

Reaction of Diethylberyllium with Tetramethylhydrazine

Under vacuum, 1.108 g (12.5 mmole) of tetramethylhydrazine was transferred to a solution at −196° C containing 0.748 g (11.1 mmole) of Et_2Be in 20 ml of octane. The reaction mixture was allowed to warm to room temperature and stand overnight. No gas evolution occurred. The solvent was removed under vacuum and the product that remained was a white crystalline solid (m.p. 84–87° C). Elemental analysis of the crude product gave results which agree with the formula $(Et_2Be)_2{:}Me_2NNMe_2$. Anal. Calc.: C, 64.80; H, 14.50; N, 12.60; Be, 8.10. Found: C, 64.46; H, 14.31; N, 12.35; Be, 8.31.

Methanolysis of 0.1980 g (0.893 mmole) of $(Et_2Be)_2{:}Me_2NNMe_2$ produced 87.3 ml (3.90 mmole) of ethane.

DISCUSSION

The reactions of Et_2Be and $Et_2Be{:}NMe_3$ with methylhydrazines follow the same general course observed for Me_3Al–hydrazine reactions (8). The following two general reactions, illustrated by the equations, show (1) the formation of a dative Be:N bond, and (2) the formation of a covalent Be—N bond by elimination of ethane:

$$(1)\ Et_2Be + HMeNNMe_2 \rightarrow Et_2Be{:}HMeNNMe_2$$

$$(2)\ Et_2Be{:}HMeNNMe_2 \rightarrow EtBe—NMeNMe_2 + C_2H_6.$$

The products obtained from these reactions suggest that steric effects may determine the number of ethyl groups which are substituted by a hydrazine. It was found that, at 50° C, 1,1-dimethylhydrazine readily reacts with diethylberyllium to give $Be(HNNMe_2)_2$, but trimethylhydrazine under similar conditions gave a compound which still contained 20.0% by weight of active ethyl (calc.: 26.1% for EtBe—$NMeNMe_2$). Also, 1,2-dimethylhydrazine gave only EtBe—NMeNMeH at 75° C. Even methylhydrazine, which forms $Be(MeNNH_2)_2$ upon reaction with diethylberyllium at 65° C, still does not replace all the active ethyl on Et_2Be. When treated with $Et_2Be{:}NMe_3$ at 25° C, methylhydrazine replaces one ethyl group and the resulting compound may have the formula EtBe—NHNHMe or EtBe—$NMeNH_2$.

From these results, it appears that the presence of a methyl group on a hydrazine nitrogen atom which also has an active hydrogen atom, in some manner limits the substitution of ethyl groups on diethylberyllium to one. It may be that the N-methyl group sufficiently hinders the close approach of another molecule of the same hydrazine that it cannot react with the remaining Be-ethyl. If this effect applies to all of the methylhydrazines, then it is possible to choose one of the two formulas indicated above for the Et_2Be—methylhydrazine monosubstituted reaction product. Since the compound contains an active Be-ethyl, then the Be—N bond must be at the nitrogen atom with the methyl group and the reaction may be written:

$$Et_2Be + H_2NNMeH \rightarrow EtBe—NMeNH_2 + C_2H_6.$$

This formula is supported by the infrared spectrum which exhibits an NH_2 absorption at 1700^{-1}.

**In some methanolyses the amount of ethane is less than the calculated amount. In this case, the polymeric nature of the product may prevent complete reaction, but in other cases no evident explanation is available.*

Can. J. Chem. Downloaded from www.nrcresearchpress.com by 210.87.254.40 on 09/05/12
For personal use only.

The reaction between diethylberyllium and 2 moles of methylhydrazine may yield three products, $H_2NNMe—Be—MeNNH_2$, $MeHNNH—Be—MeNNH_2$, and $H_2NNMe—Be—MeNNH_2$; however, no attempt was made to determine which species were present.

Unlike $Me_3Al{:}Me_2NNMe_2$, which is a 1:1 complex (8), tetramethylhydrazine reacts with 2 molecules of diethylberyllium even though the molar ratio of reactants was 1:1. This reaction is the only one in this series in which two molecules of diethylberyllium were bonded to a hydrazine, although 1,1-dimethylhydrazine and trimethylhydrazine present possibilities for such datively bonded diethylberyllium. The fact that compounds

$$\begin{matrix} BeEt_2 & Et_2Be & BeEt_2 \\ \| & \| & \| \end{matrix}$$

such as $EtBe—NMeNMe_2$ and $Me_2NHN—BeNHNMe_2$ were not isolated may be the result of charge transfer from the nitrogen atom not covalently bonded to a beryllium atom. Such an effect may reduce the basicity of the nitrogen atoms sufficiently to prevent further complexing by diethylberyllium.

The n.m.r. spectrum of $(Et_2Be)_2{:}Me_2NNMe_2$ has a single sharp N—Me proton peak (τ = 8.11 p.p.m.) and a triplet–quartet characteristic of ethyl protons. Since the N—Me protons are identical, the structure of this complex is probably

$$\begin{matrix} & & Et_2Be \\ & & \| \\ Me_2N— & NMe_2, & \text{for the} \\ & \| & \\ & BeEt_2 & \end{matrix}$$

monomeric species.

The molecular weight data shown in Table I indicate that all of the compounds which are soluble in benzene are associated, but not in integral numbers.

TABLE I

Molecular weights of Et_2Be–methylhydrazine complexes

Compound	Molecular weight		Degree of association	Solution molality
	Found	Calc.		
$(Et_2Be)_2{:}Me_2NNMe_2$	315	222.4	1.42	.0271
	337		1.52	.0238
$EtBe—NMeNMe_2$	464	111.2	4.18	0.143
	464	111.2	4.18	0.107
$EtBe—NMeNMeH$*	1468	97.1	15.1	0.142
	772		7.95	0.216

*Poorly soluble in benzene.

The remaining compounds were insoluble in hydrocarbons. All of the products, except $(Et_2Be)_2{:}Me_2NNMe_2$, appeared to be highly associated or polymeric as indicated by molecular weight data, insolubility in hydrocarbons, low volatility, and very high melting temperatures (usually decomposition occurred before melting). Since all compounds but $Be(HNNMe_2)_2$ contained at least one beryllium–ethyl group, the polymers probably involve dative Be:N bonds between molecules as illustrated below using $EtBeNMeNH_2$ as an example:

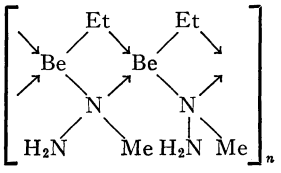

Can. J. Chem. Downloaded from www.nrcresearchpress.com by 210.87.254.40 on 09/05/12
For personal use only.

or, in the case of $(Et_2Be)_2Me_2NNMe_2$, which is also associated, only ethyl bridging may be involved:

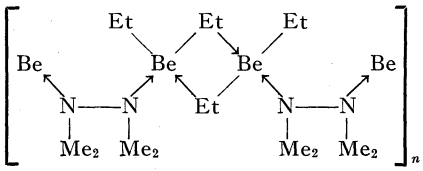

Since the n.m.r. of $(Et_2Be)_2Me_2NNMe_2$ has only one set of ethyl peaks it is assumed that exchange among the Be—ethyl bonds is rapid enough at room temperature to give only an average ethyl proton spectrum and the N—Me protons will be identical in either the monomer or associated molecule.

ACKNOWLEDGMENTS

The author wishes to acknowledge the valuable suggestions of Drs. Peter J. Slota and Charles P. Haber of the U. S. Naval Ordnance Laboratory, Corona, California, and to thank Mr. Donald W. Moore of the U. S. Naval Ordnance Test Station, China Lake, Calif. for the n.m.r. spectra.

This work was supported by funds from the Advanced Research Projects Agency and the U. S. Navy Department, Bureau of Naval Weapons.

REFERENCES

1. H. GILMAN and F. SCHULZE. Rec. Trav. Chim. **48**, 1129 (1929).
2. G. E. COATES, F. GLOCKLING, and N. D. HUCK. J. Chem. Soc. 4496 (1952).
3. G. E. COATES and F. GLOCKLING. J. Chem. Soc. 22 (1954).
4. G. E. COATES and F. GLOCKLING. J. Chem. Soc. 2526 (1954).
5. G. E. COATES and S. I. E. GREEN. J. Chem. Soc. 3340 (1962).
6. J. B. CLASS, J. G. ASTON, and T. S. OAKWOOD. J. Am. Chem. Soc. **75**, 2937 (1953).
7. H. GILMAN and F. SCHULZE. J. Chem. Soc. 2663 (1927).
8. N. R. FETTER and B. BARTOCHA. Can. J. Chem. **39**, 2001 (1961).

Can. J. Chem. Downloaded from www.nrcresearchpress.com by 210.87.254.40 on 09/05/12
For personal use only.

EFFECTS ON THE N.M.R. SPECTRA OF THE STEREOCHEMISTRY OF 3,4-DIARYLADIPIC ESTERS AND 1,2-DIARYLCYCLOPENTANES[1]

D. Y. CURTIN AND S. DAYAGI

Noyes Chemical Laboratory, University of Illinois, Urbana, Illinois

Received September 27, 1963

Can. J. Chem. Downloaded from www.nrcresearchpress.com by 210.87.254.42 on 09/05/12
For personal use only.

ABSTRACT

Examination of the n.m.r. spectra of *cis*- and *trans*-1,2-diphenylcyclopentane and 3,4-diphenylcyclopentanone substituted in the para positions of both rings with methoxyl, methyl, and chloro substituents has shown that the previous explanation (1) of the effect of temperature on the n.m.r. spectra of 1,2-diphenylcyclopentane and 3,4-diphenylcyclopentanone (unsubstituted) was incorrect. The n.m.r. spectra provide no evidence of restriction of rotation of the aromatic rings of these compounds. An alternative explanation is offered.

Comparison of the spectra of the compounds above and those of *meso*- and *dl*-3,4-diphenyladipic esters with the para substituents mentioned leads to the observation that in the *dl*-adipates and the *cis*-cyclopentanes the position of absorption of the protons ortho to the central structure (H_R) is shifted to higher field compared to the corresponding meso or trans isomer by an amount ranging from 0.2 to 0.7 p.p.m. The protons ortho to the substituent X (H_X) are also shifted to higher field but by only about 0.1 p.p.m.

Shifts of the benzylic protons of the *trans*-cyclopentanes and cyclopentanones to higher field amount to 0.3–0.6 p.p.m. in agreement with previous work (1, 34). The corresponding shift of the benzylic protons of the *meso*-adipic esters is only 0.1–0.2 p.p.m. The methylene protons and the methyl ester protons of the *meso*-adipates are also shifted to higher field by about 0.3 and 0.2 p.p.m. respectively.

These shifts seem adequately explained in terms of ring current effects of the benzene rings and lead to the possibility of obtaining detailed information concerning the stereochemistry of such substances. They are of immediate value in making configurational assignments to related compounds.

INTRODUCTION

In the course of an investigation (1) of the steric interaction of cis phenyl groups (relative to trans) in the 1,2-diphenylcyclopentanes I and a number of other related compounds it was observed that the nuclear magnetic resonance spectrum of *cis*-I, either without any solvent or in carbon tetrachloride, at room temperature showed the absorption attributable to the aromatic protons as two incompletely resolved broad sets of absorptions. Similar behavior was shown by *cis*-3,4-diphenylcyclopentanone *cis*-II, but the corresponding trans isomers and either *cis*- or *trans*-1,2-diphenylcyclopropane showed the narrow absorption to be expected by analogy with the aromatic proton spectrum of toluene (2). The aromatic proton spectrum of the *cis*-diphenylcyclopentanes narrowed on heating. Thus, the aromatic proton spectrum of *cis*-I with a bandwidth at half-height of 25 c.p.s. at 60 Mc sec at 25° had a bandwidth at half-height of 5 c.p.s. at 182°. It was proposed that the origin of the broadening in the *cis*-diphenylcyclopentanes *cis*-I and *cis*-II was due to restricted rotation of the phenyl rings with consequent non-equivalence of the "inside" and "outside" hydrogens. The present investigation of derivatives of *cis*- and *trans*-I, substituted in the para position, was undertaken to simplify and to make possible a more rigorous interpretation of the spectra. It has from the outset shown that the proposed explanation of the n.m.r. spectra of compounds such as *cis*-I in terms of restricted rotation of the phenyl rings is erroneous.

[1]*We are indebted to the Na ional Science Foundation (Grant G 14-480) for support of this work.*

Can. J. Chem. Downloaded from www.nrcresearchpress.com by 210.87.254.42 on 09/05/12
For personal use only.

EXPERIMENTAL[2]

Preparation of Materials

The compounds employed in the present investigation were either known compounds or close relatives of compounds which had already been prepared. Their physical properties and the syntheses employed are outlined in Table I. In addition to the para-substituted *cis*-1,2-diphenylcyclopentanes and *cis*-3,4-diphenylcyclopentanones originally sought a number of other compounds whose n.m.r. spectra are relevant to the present discussion are tabulated.

Nuclear Magnetic Resonance Spectral Determinations

Unless otherwise indicated n.m.r. spectra were obtained in deuterochloroform with tetramethylsilane as

TABLE IA

Physical properties of compounds studied

p-Substituent	Stereoisomer	M.p. of acid (° C)	Lit. m.p. (° C)	M.p. or [b.p.] of ester	Lit. value	Reference: Synthesis	Reference: Properties
		Methyl *trans*-cinnamates, X—$C_6H_4CH = CHCOOCH_3$					
CH_3O	—	—	—	89–90	89	3, 7	4
CH_3	—	—	—	57–57.5	57–58	7	6
Cl	—	—	—	75–76	75–76	6, 7	5
		Methyl hydrocinnamates, X—$C_6H_4CH_2CH_2COOCH_3$					
CH_3O	—	—	—	[278]	[278 at 1 atm]	10	9
HO	—	127–8	128–129	[195–197 at 16 mm]	[186–187 at 17 mm]	8, 12	8, 12
CH_3	—	120	120	[120–130 at 12 mm]	[132 at 20 mm]	12	8, 13
Cl	—	122	123	[145 at 8 mm]	*		14
		Dimethyl diaryladipates					
CH_3O	*meso*-IV	252–253	257–258	154–155	154.5–155.5 [165–185 at 0.5 mm]	7, 11	15, 16
	dl-IV	180–182	178–180	66–67 [235–237 at 2 mm]	63.5–64.5, 67 [235–250 at 0.8–1 mm]	7, 11	15, 16
HO	*meso*	326–328 (dec.)	†	215–216	‡	7, 13	—
	dl	224–225	§	147–148°	‖	7	—
CH_3	*meso*-VII	319–322	320	150–151	150	8	8
	dl-VII	200	—	Oil	—	8	—
H	*meso*	277–278	270–273	175–176°	177	7, 11	16
	dl	185–186	185–186	74.5–75.0	73–74	7, 11	16
Cl	*meso*-X	—	—	175	¶	8, 18	—
	dl-X	198–200	199–200	Oil [270 at 8 mm]	**	7, 8, 18	—
NO_2	*meso*	340 (d)	337–338(d)	243–244	234–235	7, 17	17
	dl	265	262–263	134–135	136–137	7, 17	17

*Found for the ester: C, 60.1; H, 5.5; Cl; 17.0. Calc. for $C_{10}H_{11}ClO_2$: C, 59.3; H, 5.5; Cl, 17.5.

†The same hydroxy acid was obtained both from the *meso*-methoxyphenyladipic acid by treatment for 50 minutes with 70 ml of 47 percent hydriodic acid and 10 ml of glacial acetic acid and from the *meso*-nitrophenyl acid by the method of ref. 17.

‡Found for the hydroxy ester: C, 66.5; H, 6.4. Calc. for $C_{20}H_{22}O_6$: C, 67.0; H, 6.2. The diacetyl derivative prepared from the hydroxy ester and acetyl chloride when recrystallized from ethanol had m.p. 175°. Found for $C_{24}H_{26}O_8$: C, 65.3; H, 6.0. Calc. for $C_{24}H_{26}O_8$: C, 65.2; H, 5.9.

§The *dl*-acid was prepared from the *dl*-dimethoxylphenyladipic acid by the hydriodic acid treatment employed for the meso isomer.

‖Found for the *dl*-ester: C, 66.6; H, 5.9. Calc. for $C_{20}H_{22}O_6$: C, 67.0; H, 6.2.

¶The meso ester was purified by recrystallization from methanol. Found: C, 60.6; H, 5.0; Cl, 17.9. Calc. for $C_{20}H_{20}Cl_2O_4$: C, 59.6; H, 5.0; Cl, 17.6.

**Found for the *dl*-ester: C, 59.3; H, 5.1; Cl, 17.5. Calc. for $C_{20}H_{20}Cl_2O_4$: C, 59.6; H, 5.0; Cl. 17.6.

[2]*All melting points are corrected and were determined with a microscope with a Koffler hot stage. Nuclear magnetic resonance spectra, unless otherwise indicated, were obtained by Mr. Dick Johnson and his associates. Microanalyses were provided by Mr. J. Nemeth and his associates.*

TABLE IB

Physical properties of compounds studied

p-Substituent	Stereoisomer	M.p. or [b.p.] (° C)	Lit. value	Reference: Synthesis	Reference: Properties
		3,4-Diarylcyclopentanones and [oximes]			
CH_3O	*cis*-VI	[oxime 124–125]	[oxime 124.5–125]	19	19
	cis-V*	[260–280 at 2–20 mm]			
	trans-V	111	110–111	19	19
	trans-VI	[oxime 127–128]	†		
CH_3	*cis*-VIII	80–82 [220–230 at 20 mm]	‡	19	—
	trans-VIII	102	§	19	—
H	*cis*-II	106	107	20	21
	trans-II	178–179	177	20	21
Cl	*cis*-XI	100	‖	19	—
	trans-XI	125–126	—	19	—
		1,2-Diarylcyclopentanes			
CH_3O	*cis*-III	56–57 [230–235 at 18 mm]	¶	22	23
	trans-III	72–72.5	**	22	—
CH_3COO		124.5	—	††	—
CH_3	*cis*-IX	[200–208 at 10–12 mm]	‡‡	22	—
	trans-IX	45.5	§§	22	—
		Other cyclopentanes			
p-Methoxyphenylcyclopentane		[149 at 22 mm]	[78–79 at 0.35 mm]	24	24
1,2-Bis-(*p*-methoxyphenyl)-cyclopentene		87–88	87.5–89	23	23

*Purified by distillation after recovery from the oxime (which had been chromatographed on alumina and recrystallized from benzene: ligroin 1:2) by hydrolysis with 4 *N* sulphuric acid containing a small amount of formaldehyde.

†Found for the oxime after recrystallization from benzene: ligroin 1:4: C, 73.3; H, 7.1; N, 4.0. Calc. for $C_{19}H_{21}NO_3$: C, 73.3; H, 6.8; N, 4.5.

‡Found for the *cis*-ketone after distillation and recrystallization from methanol: C, 86.4; H, 7.9. Calc. for $C_{19}H_{20}O$: C, 86.3; H, 7.6.

§Found for the *trans*-ketone after recrystallization from methanol: C, 86.4; H, 7.6. Calc. for $C_{19}H_{20}O$: C, 86.3; H, 7.6.

‖Found for the *cis*-ketone after recrystallization from chloroform – petroleum ether: C, 66.9; H, 4.6; Cl, 23.2. Calc. $C_{17}H_{16}Cl_2O$: C, 66.9; H, 4.6; Cl, 23.2.

¶A melting point of 56.5–57.5° has been reported (20) for an isomer of which the stereochemistry was not assigned. Found for the *cis*-cyclopentane after distillation and recrystallization from aqueous ethanol: C, 80.7; H, 8.0. Calc. for $C_{19}H_{22}O_2$: C, 80.8; H, 7.9.

**Found for the *trans*-cyclopentane after crystallization from ligroin: C, 80.0; H, 7.7. Calc. for $C_{19}H_{22}O_2$: C, 80.8; H, 7.9.

††Hydrolysis of *trans*-III by 2 hours of refluxing with 10 ml of acetic acid and 50 ml of 47% hydriodic acid gave a 67% yield of what was presumably the dihydroxyphenyl derivative, m.p. 173°, (recrystallized from carbon tetrachloride). The n.m.r. spectrum was in agreement with this structure. However, even at 100° under vacuum it apparently did not lose solvent imbedded in the crystal because the carbon analysis was 3.4% below that expected. The compound dissolved in dilute sodium hydroxide solution and when the basic solution was treated with acetic anhydride there resulted the diacetyl compound, m.p. 124.5° (recrystallized from ethanol). Found: C, 74.1; H, 6.5. Calc. for $C_{21}H_{22}O_4$: C, 74.5; H, 6.6. Hydrolysis of cis-III in the same way gave what was probably the *cis*-dihydroxy- compound, m.p. 72–73°.

‡‡Found after purification by distillation: C, 90.6; H, 9.0. Calc. for $C_{19}H_{22}$: C, 91.1; H, 8.9.

§§Found after crystallization from aqueous methanol: C, 90.9; H, 8.8. Calc. for $C_{19}H_{22}$: C, 91.1; H, 8.9.

an internal standard with a Varian A-60 spectrometer. As a check on the reliability of the instrument in the aromatic region, the absorption due to a trace of chloroform present in the deuterochloroform when it could be observed was found to be 2.75±0.05 p.p.m. Although the position of absorption of the chloroform proton is notoriously subject to shifts due to the interaction with other species present it appears that the values reported for the aromatic protons are reliable to about ±3 c.p.s. The n.m.r. results reported in τ units (25) are presented in Tables II, III, and IV.

DISCUSSION

Aromatic Proton n.m.r. Spectra

As will be seen from the data in Table IIIA the spectrum of the *cis*-di-*p*-methoxyphenylcyclopentane *cis*-III in deuterochloroform showed a single aromatic proton absorption in sharp contrast to the unsubstituted compound *cis*-I, which showed a broad

Can. J. Chem. Downloaded from www.nrcresearchpress.com by 210.87.254.42 on 09/05/12
For personal use only.

Can. J. Chem. Downloaded from www.nrcresearchpress.com by 210.87.254.42 on 09/05/12
For personal use only.

TABLE II

Positions of the aromatic protons in the n.m.r. spectra of monoaryl compounds, *meso*-diaryladipic esters and *trans*-diarylcyclopentanes

A. *para*-Methoxy compounds

Compound	Chemical shift (τ units)*			
	H_X	H_X(corr.)†	H_R	H_R(corr.)†
Methyl *p*-methoxyhydrocinnamate‡	3.16	3.17	2.86	2.87
p-Methoxyphenylcyclopentane	3.17	3.18	2.85	2.86
Dimethyl *meso*-di-(*p*-methoxyphenyl)-adipate (*meso*-IV)§	3.13	3.16	2.80	2.83
trans-Dimethoxyphenylcyclopentanone (*trans*-V)	3.18	3.19	2.94	2.95
trans-Dimethoxyphenylcyclopentanone oxime (*trans*-VI)	3.22	3.21	2.98	2.97
trans-Dimethoxyphenylcyclopentane (*trans*-III)‖	3.26	3.19	2.98	2.91¶
Range	3.19±0.07	3.18±0.03	2.89±0.09	2.90±0.07
p-Methoxytoluene (27)	3.20		2.95	

B. *para*-Methyl compounds

	$H_X \simeq H_R$	H(corr.)
Methyl *p*-methylhydrocinnamate	2.87	2.88
Dimethyl *meso*-di-(*p*-methylphenyl)-adipate (*meso*-VII)	2.80	2.84
trans-Di-(*p*-methylphenyl)-cyclopentanone (*trans*-VIII)	2.90	2.92
trans-Di-(*p*-methylphenyl)-cyclopentane (*trans*-IX)	2.97	2.85
Range	2.87±0.09	2.88±0.04
p-Methylisopropylbenzene (28)	2.92	

C. *para*-Chloro compounds

	H_X	H_X(corr.)	H_R	H_R(corr.)
Methyl *p*-chlorohydrocinnamate	2.66	2.77	2.76	2.87
Dimethyl *meso*-di-(*p*-chlorophenyl)-adipate (*meso*-X)	2.62	**	2.70	**
trans-Di-(*p*-chlorophenyl)-cyclopentanone (*trans*-XI)††	2.60	**	2.70	**
Range	2.63±0.03		2.73±0.03	
p-Chlorotoluene‡‡	2.73		2.83	

*Although, strictly speaking, the spectra are those of an A_2B_2 type they approximate the spectra to be expected of two independent AB systems superimposed as has been observed in previous studies (29) of *p*-disubstituted benzenes. Accordingly when the AB quartette was observed J and δ were calculated from the equation (30) $(1-3) = (2-4) = \sqrt{[(\delta_B-\delta_A)^2+J^2_{AB}]}$. In all cases where the spectrum was of this type, J, estimated as the separation between peaks 1 and 2 or 3 and 4, was found to be 9±0.5 c.p.s.

Spectra were obtained with 10–25% solutions (generally 20% in deuterochloroform unless otherwise specified. Spectra obtained in acetone agreed well with those in deuterochloroform, in general, and data obtained in acetone will be presented in footnotes to the Tables when they are available.

†The correction was applied by adding or subtracting the error estimated from a comparison of the position of the peak due to chloroform present as an impurity in the deuterochloroform with that of pure chloroform (2, p. 8), τ 2.73. The corrected values appear to have somewhat better internal consistency but the major conclusions are unaffected by the correction.

‡Methyl *p*-hydroxyhydrocinnamate (20% in acetone) had H_X 3.15, H_R 2.85 τ.

§In acetone (7%) dimethyl *meso*-di-(*p*-hydroxyphenyl-adipate had H_X 3.18, H_R 2.82 τ.

‖In acetone (20% solution) *trans*-III had H_X 3.27 and H_R 2.95. The analogous dihydroxyphenyl compound (20% in acetone) had H_X 3.28, H_R 3.00.

¶The spectrum of a neat sample showed H_X 3.71, H_R 2.81.

**No correction was possible since the chloroform peak was obscured by the aromatic absorption.

††The *trans*-ketone was obtained by the ring closure employed for the other *trans*-ketones in very small amount and not purified fully. The spectrum was obtained with a 4.8% solution in deuterochloroform.

‡‡In carbon tetrachloride the values were H_X 2.84, H_R 2.96. Although the positions of H_X and H_R of *p*-chlorotoluene have not been reported in a form which would make possible direct comparison with the present values their difference of 0.113 with H_R at higher field (29) agrees with the values here.

Can. J. Chem. Downloaded from www.nrcresearchpress.com by 210.87.254.42 on 09/05/12
For personal use only.

TABLE III

Positions of the aromatic protons in the n.m.r. spectra *dl*-diaryladipic esters and *cis*-diarylcyclopentanes

A. *para*-Methoxy compounds

Compound	Chemical shift (τ units)*			
	$H_X \simeq H_R$	H(corr.)	$(H_X^{dl} - H_X^{meso})$ or $(H_X^{cis} - H_X^{trans})$	$(H_R^{dl} - H_R^{meso})$ or $(H_R^{cis} - H_R^{trans})$
Dimethyl *dl*-di-(*p*-methoxyphenyl)-adipate (*dl*-IV)†	3.22†	3.25†	+0.09	+0.30
cis-Dimethoxy-phenylcyclopentanone (*cis*-V)‡	3.32	3.31	+0.12	+0.36
cis-Dimethoxyphen-ylcyclopentanone oxime (*cis*-VI)	3.27	3.28	+0.09	+0.33
cis-Dimethoxyphen-ylcyclopentane (*cis*-III)§	3.31	3.28	+0.09	+0.37
Range for the cyclopentane derivatives	3.29 ±0.03	3.29 ±0.02	+0.10 ±0.02	+0.35 ±0.02

B. *para*-Methyl compounds

	H_X	H_X(corr.)	H_R	H_R(corr.)		
Dimethyl di-(*p*-methylphenyl)-adipate (*dl*-VII)	2.92	2.88	3.14	3.10	0.00	+0.22
cis-Di-(*p*-meth-ylphenyl)-cyclo-pentanone (*cis*-VIII)	2.93	2.85	3.21	3.13	+0.01	+0.29
cis-Di-(*p*-methylphenyl)-cyclopentane	3.08	3.02	3.24	3.18		
(*cis*-IX)‖ (Av.)	3.11 (3.10)	3.03 (3.03)	3.27 (3.26)	3.19 (3.19)	+0.06	+0.34
Range for the cyclopentane derivatives	2.97 ±0.4	2.94 ±0.09	3.23 ±0.04	3.16 ±.03	+0.03 ±.03	0.31 ±0.03

C. *para*-Chloro compounds

Methyl *dl*-di-(*p*-chlorophenyl)-adipate (*dl*-X)	2.75	2.79	3.09	3.13	+0.13¶	+0.39¶
cis-Di-(*p*-chlorophenyl)-cyclopentanone (*cis*-XI)	2.88	2.90	3.32	3.34	+0.28¶	+0.62¶

*The *J*'s had values from 8.5 to 9.0 c.p.s. Spectra were obtained with 10–25% solutions in deuterochloroform unless otherwise specified.

†8% solution in deuterochloroform. Dimethyl *dl*-(*p*-hydroxyphenyl)-adipate (15% solution in acetone) had H_A 3.11, H_B 3.25, for the aromatic proton absorption.

‡At −52° there was no noticeable change in the shape of the spectrum (determined by Mr. O. Norton) and $H_X = H_R$ was 3.37 (uncorrected). *cis*-3,4-(Dihydroxyphenyl)-cyclopentanone (20% acetone solution) had $H_X = H_R$ 3.37.

§A 16% solution of *cis*-III in acetone showed H_X and H_R at 3.23 and 3.43. In decalin (20% solution) at room temperature the corresponding values were 3.31 and 3.50. The separation between the peaks was essentially the same (12 c.p.s. between peaks 1 and 3) when the sample was heated to 180° as it was at room temperature (11 c.p.s. between peaks 1 and 3). The corresponding hydroxy compound had the aromatic chemical shifts at 3.33 and 3.45 in deuterochloroform and at 3.26 and 3.36 in acetone (20% solution). It will be noted that there is some possible ambiguity in making assignments of the H_X and H_R absorptions. They have been made here with the assumption that the H_X band is the lower one but without good justification.

‖A 20% solution of *cis*-IX in decalin showed H_X 3.25, H_R 3.37. On heating to 180° the two branches coalesced with $H_X = H_R$ 3.57. On recooling the AB quartette returned with H_X 3.11, H_R 3.27. The values of the chemical shifts in decalin were obtained with no calibration of the instrument in the region of interest and accordingly this result has only qualitative significance.

¶Since no corrected values could be obtained for the *meso-trans*-compounds, the uncorrected values were used throughout.

TABLE IV

Chemical shifts (τ units) of the aliphatic protons*

	Benzilic protons			Methylene protons			Ester protons		
p-Substituent or	meso (trans)	*dl* (cis)	*dl*−meso (cis−trans)	meso (trans)	*dl* (cis)	*dl*−meso (cis−trans)	meso (trans)	*dl* (cis)	*dl*−meso (cis−trans)
				A. Dimethyl diaryladipates					
CH_3O	6.72	6.63	−0.09	7.60	7.37	−0.23	6.60	6.42	−0.20
HO†	—	6.65	—	—	7.29	—	6.56	6.40	−0.16
CH_3	6.75	6.60	−0.15	7.58	7.33	−0.25	6.62	6.42	−0.20
H	6.69	6.51	−0.18	7.58	7.27	−0.31	6.63	6.41	−0.22
Cl	6.63	6.52	−0.11	7.58	7.29	−0.29	6.56	6.40	−0.16
NO‡	—	—	—	—	—	—	(6.59)	(6.40)	(−0.04)
Range	6.69 ±0.06	6.58 ±0.07	−0.14 ±0.05			−0.27 ±0.04			−0.19 ±0.03
				B. Cyclopentanones and oximes					
CH_3O	6.65	6.30	−0.35						
HO†	—	6.24	—						
CH_3	6.59	6.14	−0.45						
H	6.60 (6.52)	6.20 (6.17)	−0.40 (−0.45)§						
Cl	6.55	6.20	−0.35						
CH_3O	6.97	6.42	−0.55						
				C. Cyclopentanes					
CH_3O	7.04	6.67	−0.37						
CH_3	6.94	6.61	−0.33						
H	(7.00)	(6.68)	(−0.32)§						
CH_3COO	6.92	—	—						
Range	6.98 ±0.06	6.65 ±0.04	−0.44 ±0.12						

*Solvent deuterochloroform unless otherwise specified.
†Solvent acetone.
‡Solvent dimethylsulphoxide.
§Data from ref. (1) (solvent, carbon tetrachloride).

complex aromatic proton spectrum (1). (In acetone or decalin the aromatic proton spectrum of *cis*-III has the appearance of an AB spectrum (26) (doubled in this case) with a chemical shift between the A and B protons of 0.10–0.12 p.p.m.) This would seem at the outset not to be in accord with the previous postulation (1) of restricted rotation of the aromatic rings. In a further analysis of the n.m.r. data it is instructive first to consider together the spectra of those *p*-methoxy compounds which have only one phenyl ring and those which might be expected to have the maximum physical separation of the two phenyl rings and, hence, the minimum interaction of one phenyl ring with the other. Such a series, presented in Table IIA, includes, in addition to the compounds containing only one *p*-methoxyphenyl ring, the *meso*-dimethoxyphenyladipic ester (*meso*-IV) and the *trans*-dimethoxyphenylcyclopentane derivatives *trans*-III, *trans*-V, and *trans*-VI. The inclusion of the *meso*-adipic ester *meso*-IV is based on the somewhat intuitive premise to be discussed later that the predominate conformation is that (*meso*-A) with the aryl groups trans to each other, which places the CH_3OCOCH_2— groups trans to each other also. Each of these compounds had an aromatic proton spectrum which approximated the typical AB quartette as does *p*-methoxytoluene (27). The proton ortho to the substituent is designated by H_X; that ortho to the point of attachment of the molecule proper by H_R.

Can. J. Chem. Downloaded from www.nrcresearchpress.com by 210.87.254.42 on 09/05/12
For personal use only.

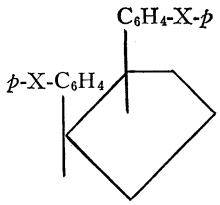

cis-I
cis-III
cis-IX

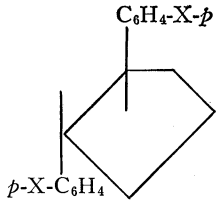

trans-I X = H
trans-III X = CH_3O
trans-IX X = CH_3

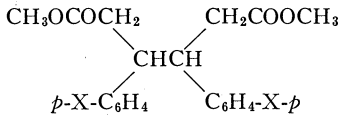

IV X = CH_3O
VII X = CH_3
X X = Cl

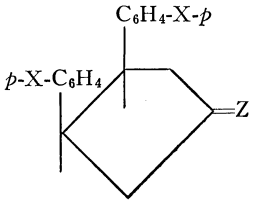

cis-II
cis-V
cis-VI
cis-VIII
cis-XI

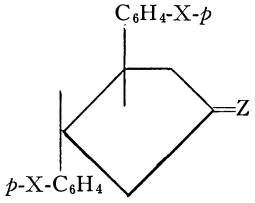

trans-II X = H
trans-V X = CH_3O, Z = O
trans-VI X = CH_3O, Z = NOH
trans-VIII X = CH_3 Z = O
trans-XI X = Cl, Z = O

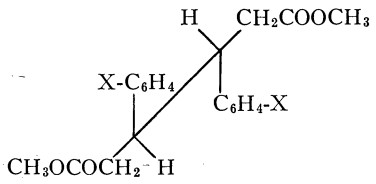

meso-A

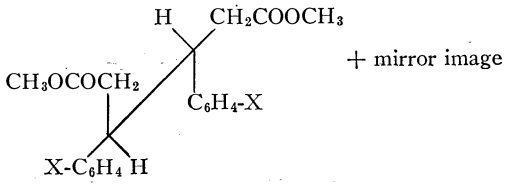

dl-A

The data in Table IIA show the chemical shifts of the aromatic protons to be quite insensitive to changes in the carbon skeleton to which the benzene rings are attached. It can be seen further that the values for the two kinds of protons are scattered around the values of τ 3.20 and 2.95 for H_X and H_R obtained from the Varian Spectra Catalogue (27) for *p*-methoxytoluene. A similar situation exists in the *p*-methyl series (Table IIB) and also with the more limited and less dependable data available for the *p*-chloro series (Table IIC). Thus, the chemical shifts of H_X and H_R for the methyl compounds in Table IIB are sufficiently close to each other to appear as a single aromatic proton absorption close to the position of absorption (28) of *p*-methylisopropylbenzene.

In Table III are summarized the data for the aromatic proton spectra of the *dl*-diaryladipic esters and *cis*-diarylcyclopentane derivatives. The methoxy compounds (Table IIIA), in contrast to the meso–trans series, show, in deuterochloroform a single absorption attributable to both H_X and H_R. The methyl and chloro compounds (Tables IIIB and IIIC) have, as the aromatic proton spectrum, an AB quartette (28). As was the case with the series of Table II, the H_X (or H_R) values of the methoxy compounds (Table IIIA) are quite insensitive to the structural changes involved and this seems to be true also for the methyl compounds (Table IIIB) and chloro compounds (Table IIIC) although the data are rather limited. Most striking is the difference between the position of the H_X (or H_R) proton in the *dl*-cis series and that of the corresponding proton in the meso–trans

Can. J. Chem. Downloaded from www.nrcresearchpress.com by 210.87.254.42 on 09/05/12
For personal use only.

series. There is clearly a structural effect on the positions of the aromatic protons which is stereochemical in origin and which leads to a small shift to higher field (0.03–0.1 p.p.m.) of the H_X protons, in the *dl*–cis series and a somewhat larger shift (0.2–0.7 p.p.m.) again to higher field of the H_R protons. Although there is some indication that this difference is largest with the *p*-chloro compounds and smallest with the *p*-methyl the precision of the data is hardly adequate to justify any such correlation of the shift with the electrical effect of the substituent.

The shift to higher field of the aromatic protons of the compounds in the *dl*-cis series would seem to be primarily the result of the effect of the ring currents of each ring on the magnetic environment of the protons of the other adjacent to it. Such an effect was observed by Waugh and Fessenden (31) in their study of the paracyclophanes and in the series of *cis*-olefins and cyclic compounds (1, 30 p. 119 *ff.*) which led to the present investigation. It is of interest to compare the value of 0.57 p.p.m. for the shift to higher field relative to *p*-xylene of [2,2]paracyclophane (31) with the present data. Although it is not possible to make calculations with more than qualitative significance (32) because of the freedom to rotate of the phenyl rings in the diphenylcyclopentanes, inspection of molecular models makes it appear reasonable both that the shift of the paracyclophane should be comparable to those observed for H_R in the present examples and that shifts of H_R should be considerably larger than those of H_X.

The questions of the complexity and temperature dependence of the shape of the aromatic proton spectrum of the unsubstituted diphenylcyclopentane *cis*-I and the related diphenylcyclopentanone can now be considered. The results obtained with the *p*-substituted compounds just discussed explain readily the complexity of the spectra since the position of absorption of the ortho protons could be expected to be shifted more to higher field than the meta or para by the adjacent ring. Although the spectra of the unsubstituted compounds are too complex to permit assignments of chemical shift values to the ortho, meta, and para protons, the separation previously observed (1) between the centers of the two multiplets (0.2–0.3 p.p.m.) is of the order of magnitude expected from the study of the para-substituted relatives in Tables II and III.

A possibility which might be considered is that although rotation of the aromatic rings in the diphenyl compounds without para substituents is slow (on the n.m.r. time scale) it is accelerated by an electronic effect (which might alter the effective size of the π-electron cloud) of the para substituents. Substituents of the compounds studied include the methoxyl group with σ_{meta} negative, σ_{para} positive; the methyl group with σ_{meta} and σ_{para} both negative; and the chlorine atom with both σ_{meta} and σ_{para} positive. Since in none of these para-substituted compounds has there been complexity in the aromatic proton spectrum beyond that to be expected in molecules with freely rotating phenyl rings, such an explanation appears to be ruled out. As was noted in Table IIIA an attempt to slow the rotation of the *p*-methoxyphenyl rings of *cis*-III by cooling the solution to −52° made no significant change in the spectrum. It is anticipated that at lower temperatures or with appropriate ortho or meta substituents on the phenyl rings their rotation rates may be measured with n.m.r. techniques.

The most probable explanation of the narrowing at 180° (1)[3] of the phenyl proton spectrum in the cis compounds *cis*-I and *cis*-II appears to involve the non-coplanarity of the cyclopentane ring (33). Suppose, for example, that a solution of the *cis*-hydrocarbon *cis*-I contains at room temperature a mixture of molecules in two or more conformations

[3]*The examination of the n.m.r. spectrum of cis*-I *in decalin at room temperature and at 180° has been repeated with complete confirmation of the previous results (1).*

Can. J. Chem. Downloaded from www.nrcresearchpress.com by 210.87.254.42 on 09/05/12
For personal use only.

Can. J. Chem. Downloaded from www.nrcresearchpress.com by 210.87.254.42 on 09/05/12
For personal use only.

of the cyclopentane ring, which differ in the relative positions of the phenyl groups with respect to each other and which are in rapid equilibrium. The effective magnetic field at each H_R is then a weighted average which depends on the field at that proton in each of the conformations and on the equilibrium constant (*s*) describing the degree to which each conformation is populated. If the increase in temperature were to increase the populations of conformations in which the phenyl groups were most separated there would then be a preferential shift to lower field of the resonance position of the H_R protons and a corresponding narrowing of the proton resonance band.[4] This leads to the prediction that there should be a preferential shift to lower field of the H_R protons in the *cis*-1,2-diphenylcyclopentane derivatives. A compound which might be expected to show this effect most dramatically is the *para*-methyl compound *cis*-X, which was studied as a 20% solution in decalin. At room temperature as mentioned in the footnote to Table IIIB the AB quartette had a chemical shift between H_X and H_R of 0.12 p.p.m. At 180° the quartette had a single peak, in agreement with expectation. The *para*-methoxy compound *cis*-III (20% solution) in decalin failed to show a significant change in the shape of the aromatic proton spectrum. As was noted in Table IIIA, this substance, in contrast to its behavior in deuterochloroform, shows an AB quartette with a chemical shift between H_X and H_R of about 0.19 p.p.m. This separation did not change appreciably on heating. It seems clear that a detailed understanding of the temperature dependence of *cis*-diarylcyclopentanes awaits the accumulation of further experimental data. The difference between the spectra of deuterochloroform and acetone or decalin solutions in the cis series indicates that part of the chemical shift differences considered above between the cis–*dl* and trans–meso series is due to solvent interactions which are probably most serious with the deuterochloroform solutions (34).

Absorption of the Benzylic Protons

It was pointed out previously (1, 35) that a few *vic*-diphenylcyclic compounds and the stilbenes had a shift of the benzylic proton 0.32–0.50 p.p.m. to higher field in the trans isomer (in which the benzylic proton is cis to the phenyl ring on the adjacent carbon). In Tables IVB and IVC are presented data showing the benzylic proton absorptions of compounds now available. The value given is the center of the unresolved multiplet. Both the previous generalization relating configuration with benzylic proton absorption and the configurational assignments of the compounds in Tables IVB and IVC are confirmed with the benzylic protons of the trans isomers absorbing 0.44 ± 0.11 p.p.m. higher than the corresponding protons of the cis isomers.

Conformations of the Diphenyl Adipic Esters

It is of interest to compare more fully the n.m.r. spectra of the *meso*- and *dl*-adipic esters. At the outset it might be supposed that the staggered conformation in which the small hydrogen atom lies between the two larger groups on the adjacent carbon atom, as in *meso*- and *dl*-A, is the most populated one in each case. As a beginning then it is instructive to examine the positions of the proton resonances with the assumption that the meso isomers have the conformation *meso*-A, and that the *dl*-isomers have those shown as *dl*-A. On this basis it has already been noted (Table II) that the phenyl proton positions of the *meso*-adipic esters (with a dihedral angle of 180° between the bonds to the phenyl rings) are the same to within the present limits of the experimental measurement as those

[4]*Substantially this explanation was proposed by Dr. F. A. L. Anet, to whom we are indebted, in a letter written in April, 1962, before the results with the para-substituted compounds were available.*

of the *trans*-diarylcyclopentanones and cyclopentanes with a dihedral angle of 120°, neglecting the twisting of the five-membered ring.

The data in Table III might be interpreted as showing that the phenyl proton positions are not shifted quite as much to higher field in the *dl*-adipic esters (dihedral angle 60° as in conformation *dl*-IVA) as they are in the *cis*-cyclopentanes (dihedral angle nearly O°). The precision of these data is not sufficient to permit more than a suggestion that this difference may be real. In any case the trend is reasonable, the greatest shift to higher field occurring with the smallest dihedral angle between the bonds to the phenyl rings. If the postulated conformations *meso*-A and *dl*-A are interpreted literally with the benzylic proton on one carbon atom centered between the bonds to the phenyl and methylene groups on the adjacent carbon atom, then the spacial relationship of the benzylic proton to the two aromatic rings is the same in the two conformations and there should be no shift due to a change in the effect of ring currents on the proton's environment. Data in Table IVA show that this prediction is not verified. The benzylic protons in the meso series are consistently somewhat higher (0.14 ± 0.05 p.p.m.) than the corresponding protons in the *dl*-series.[5] An improved picture would take into account the possibility that the stabilities of conformations *meso*- and *dl*-A can be increased by distorting them slightly so that the proton is not equidistant from the two bonds opposite it, and also the probable existence of an appreciable fraction of the molecules in the other staggered conformations, as well as the non-planarity of the cyclopentane ring. This over-simplified picture is of value, however, in a consideration of the shifts of the methylene protons and ester methyl protons (Table IVA). It is seen that the meso isomers which had the H_R protons at lower field (relative to the *dl*) have both the methylene and methyl protons shifted to higher field. This is readily explained if conformations *meso*-A and *dl*-A are assumed to be the most important conformations, since in *meso*-A the methylene and methyl ester groups are above the face of the opposite benzene ring and therefore subject to a ring-current shift to higher field. In the *dl*-isomer (conformation *dl*-A) the phenyl groups are adjacent.

It seems clear that with more refined data, n.m.r. studies are capable of giving detailed structural information about positions of conformational equilibria in systems such as the diphenyladipic esters. Hyne (36) has reported such studies of the diastereoisomeric ephedrines. In any case the positions in the n.m.r. spectrum of the H_R protons together with the methylene and methyl protons appears to provide a reliable method of assigning configuration to compounds similar to those studied here.

REFERENCES

1. D. Y. Curtin, H. Gruen, Y. G. Hendrickson, and H. E. Knipmeyer. J. Am. Chem. Soc. **83**, 4838. (1961); **84**, 863 (1962).
2. Varian Spectra Catalogue. Varian Associates, Palo Alto, Cal. 1962. Spectrum No. 157.
3. R. K. Callow, J. M. Gulland, and R. D. Haworth. J. Chem. Soc. 1444 (1929).
4. G. R. Ramage and R. Robinson. J. Chem. Soc. 607 (1933).

[5] *Another basis on which to make a comparison is to consider the chemical shift in relation to the approximate dihedral angle between the* C—*phenyl and* C—H *bonds on adjacent carbon atoms. Data for the two series available*

Series	*Dihedral angle) (approximate*	*Chemical shift* X═CH_3O	(τ) CH_3
cis-Cyclopentane	*120°*	*6.67*	*6.61*
dl-Diphenyladipate	*60°*	*6.63*	*6.60*
meso-Diphenyladipate	*60°*	*6.72*	*6.75*
trans-Cyclopentane	*0°*	*7.04*	*6.94*

in deuterochloroform (shown here) suggest that the dl-shifts fall quite close to the cis with the meso-adipates somewhat larger. The differences are too small to permit further analysis.

Can. J. Chem. Downloaded from www.nrcresearchpress.com by 210.87.254.42 on 09/05/12
For personal use only.

5. G. P. Scott. J. Org. Chem. **20**, 736 (1935).
6. K. C. Pandya and R. B. Pandya. Proc. Indian Acad. Sci. **14A**, 112 (1941).
7. T. Posner and G. Schreiber. Ber. **57**, 1127 (1924).
8. G. R. Ramage. J. Chem. Soc. 397 (1938).
9. W. Körner and P. Corbetta. Ber. **7**, 1731 (1874).
10. C. Paal and J. Gerum. Ber. **41**, 2273 (1908).
11. E. Bowden and H. Adkins. J. Am. Chem. Soc. **62**, 2422 (1940).
12. E. Fischer and O. Nouri. Ber. **50**, 611 (1917).
13. T. Koreber. Ber. **23**, 1033 (1890).
14. K. Kindler. Ann. **452**, 111 (1927).
15. C. L. Wilson and K. B. Wilson. Trans. Electrochem. Soc. **84**, 153 (1943).
16. A. L. Wilds and R. E. Sutton. J. Org. Chem. **16**, 1371 (1951).
17. H. E. Fierz-David, L. Blangey, and M. Uhlig. Helv. Chim. Acta, **32**, 1414 (1949).
18. I. Vogel. J. Chem. Soc. 594 (1927).
19. G. P. Mueller and F. C. Bateman. J. Am. Chem. Soc. **74**, 3959 (1952).
20. K. Bernhauer and R. Hoffmann. J. Prakt. Chem. **149**, 319 (1937).
21. H. A. Weildlich. Ber. **71B**, 1601 (1938).
22. H. Burton and C. W. Shoppee. J. Chem. Soc. 570 (1939).
23. G. P. Mueller, J. G. Fleckenstein, and W. H. Tallent. J. Am. Chem. Soc. **73**, 2651 (1951).
24. R. R. Burtner and J. M. Brown. J. Am. Chem. Soc. **75**, 2334 (1953).
25. G. v.D. Tiers. J. Phys. Chem. **62**, 1151 (1958).
26. J. A. Pople, W. G. Schneider, and H. J. Bernstein. High resolution nuclear magnetic resonance. McGraw-Hill Book Co., New York. 1959. p. 119 ff.
27. Varian Spectra Catalogue. Varian Associates, Palo Alto, Cal. 1962. Spectrum No. 205.
28. Varian Spectra Catalogue. Varian Associates, Palo Alto, Cal. 1962. Spectrum No. 268.
29. R. E. Klinck and J. B. Stothers. Can J. Chem. **40**, 2329 (1962). See also R. E. Richards and T. P. Schaefer. Trans. Faraday Soc. **54**, 1280 (1958); P. F. Cox. J. Am. Chem. Soc. **85**, 381 (1963) and references therein cited.
30. L. M. Jackman. Applications of nuclear magnetic resonance spectroscopy in organic chemistry. Pergamon Press, New York. 1959. pp. 89–90. J. J. Drysdale and W. D. Phillips. J. Am. Chem. Soc. **79**, 319 (1957).
31. J. S. Waugh and R. W. Fessenden. J. Am. Chem. Soc. **79**, 846 (1957).
32. C. E. Johnson and F. A. Bovey. J. Chem. Phys. **29**, 1012 (1958).
33. E. L. Eliel. Stereochemistry of carbon compounds. McGraw-Hill Book Co., New York. 1962. p. 248 ff.
34. J. A. Pople, W. G. Schneider, and H. J. Bernstein. High resolution nuclear magnetic resonance. McGraw-Hill Book Co., New York. 1959. p. 428 ff. See also R. Kaiser. Can. J. Chem. **41**, 430 (1963).
35. D. Y. Curtin, H. Gruen, and B. A. Shoulders. Chem. Ind. 1205 (1958).
36. J. B. Hyne. Can. J. Chem. **39**, 2536 (1961).

Can. J. Chem. Downloaded from www.nrcresearchpress.com by 210.87.254.42 on 09/05/12
For personal use only.

STUDIES ON THE URANIUM EXTRACTION EQUILIBRIA, PHOTOLYTIC, AND HYDROLYTIC REACTIONS IN SYSTEMS CONTAINING TRI-*n*-BUTOXYETHYL PHOSPHATE[1]

M. HALPERN,[2] T. KIM, A. S. KERTES, AND N. C. LI
Duquesne University, Pittsburgh, Pennsylvania, and The Hebrew University, Jerusalem, Israel
Received September 23, 1963

Can. J. Chem. Downloaded from www.nrcresearchpress.com by 210.87.254.6 on 09/05/12
For personal use only.

ABSTRACT

The extraction equilibria in the system aqueous hydrochloric acid – uranyl chloride – undiluted tri-*n*-butoxyethyl phosphate, TBEP, were examined as a function of increasing uranyl concentration (0.44 to 4.41 *M*) in the initial aqueous solution, the acid content of the initial aqueous solution being kept constant at 6.76 *M*. The extraction behavior of TBEP is found to be different from that of tributyl phosphate. Evidence has been presented to show that the three ethereal oxygen atoms in the TBEP molecule are, under high organic phase loading conditions, available for participation in complexation. The hydrochloric acid promoted hydrolysis of TBEP and the instability toward light of the TBEP layer containing hydrochloric acid and uranium were also examined.

INTRODUCTION

Numerous papers (1–9) have been presented on the comparison of tri-*n*-butyl phosphate, TBP, with other neutral organophosphorus extractants. In the extraction of uranyl nitrate, the extraction ability of the phosphorus compounds usually increases in the order of phosphate $(RO)_3PO$, phosphonate $(RO)_2RPO$, phosphinate $(RO)R_2PO$, and phosphine oxide R_3PO. The explanation is that the alkoxy oxygen lowers the electron donor properties of the phosphoryl oxygen, which is the only coordination site in the extractants. It was thought, accordingly, that combination of three oxygen atoms (in addition to the three alkoxy oxygens) with the phosphoryl oxygen might lead to an inferior extractant in comparison with TBP. Tri-*n*-butoxyethyl phosphate, $(C_4H_9OC_2H_4O)_3PO$, TBEP, was chosen as the representative of this class of compounds, since it is commercially available in pure state.

A roughly comparable distribution ratio of uranyl nitrate by TBP and TBEP has been observed (1, 7) under otherwise identical conditions. Halpern, Kim, and Li (10) observed a weaker extraction by TBEP in comparison to TBP of micro quantities of zinc, indium, and uranyl chlorides from dilute hydrochloric acid solutions. To compare TBP and TBEP further, we felt that experiments have to be carried out under conditions of high organic loading. The extraction of uranyl chloride from concentrated hydrochloric acid was chosen, since the system for comparison, $HCl–UO_2Cl_2–TBP$, was recently investigated by two of the present authors (11) and others (12, 13).

Although there are no general considerations which make it possible to predict the effect of degree of hydration on the extraction ability of a given organophosphorus compound, Sidall (14) has reported that the order of affinity for water increases in the order of phosphate, phosphonate, phosphinate, and the same order is kept in the extraction ability. Usually the acid or metal salt entering the organic phase will remove one or more ester molecules as a water acceptor. This is certainly true for the nitrate systems, and is

[1]*This investigation was supported in part by the U.S. Atomic Energy Commission through Contract No. At-(30-1)-1922.*
[2]*On leave of absence from the Hebrew University.*

also true for systems containing uranyl chloride (11) and cobalt chloride (12). The unusually high degree of hydration of the HCl·TBEP complex (10), as compared to that of the corresponding HCl·TBP complex (15), places TBEP far ahead of TBP in the order of extraction capacity, which is not in agreement with the previous reasoning on the possible inferior effect of the ethereal oxygens on the extraction ability of TBEP. In order to resolve this question, experiments had to be carried out with high aqueous electrolyte concentration leading to saturation of the extractant and causing, consequently, an appreciable transfer of water to the organic phase. Since the presence of an inert diluent in the organic phase affects the hydration of both the extractant and the extracted solute, we have used undiluted TBEP throughout this study.

An additional emphasis has been placed in this study upon the chemical stability of the TBEP phase. Recently Kertes and Halpern (16, 17) reported on the hydrochloric acid promoted hydrolysis of TBP and the instability of the TBP layer containing both hydrochloric acid and uranyl chloride. They found that, when aqueous hydrochloric acid and TBP were mixed together and the equilibrium phases separated, after a few days the homogenous TBP phase became heterogenous; a second phase was formed. If the organic layer had been separated from the equilibrated aqueous phase containing both HCl and uranyl chloride, after a period of several days a solid appeared. The uranium (VI) initially present was photolytically reduced to uranium (IV) and the TBP hydrolyzed to alkyl phosphates, resulting in a greenish precipitate. In our studies with TBEP, we have observed similar phenomena, and the results of our study on the instability of TBEP are included in this paper.

EXPERIMENTAL

Materials

Samples of pure TBEP and uranyl chloride monohydrate were obtained from the Food Machinery and Chemical Corp., New York and S. W. Shattuck Chemical Co., Denver, Colo., respectively. A determination of the molecular weight by means of a vapor pressure osmometer showed that TBEP is at least 99% pure. The TBEP was washed with 1 *N* HCl, then with 1 *N* sodium hydroxide, and finally with water. In its general physical properties TBEP differs but little from TBP (18). The solubility of water in the phosphorus esters corresponds to the formation of a monohydrate for TBP, and to a TBEP:water mole ratio of 1:1.5. The latter value has been confirmed by equilibrating dry undiluted TBEP with water (10).

Procedure

The initial aqueous solutions were prepared by mixing calculated amounts of stock solutions of hydrochloric acid and uranyl chloride with water to give the desired initial concentrations. Undiluted TBEP was used as extractant throughout the experiments. After equilibration by shaking for 15 minutes and centrifugation, the TBEP phase was immediately diluted with a 1:2 water–ethanol mixture and then analyzed. The uranium content of the equilibrated aqueous phase was determined gravimetrically using 8-hydroxyquinoline. The amount of uranium extracted into the TBEP phase was calculated by difference from the total uranium content. The concentrations of hydrochloric acid in the equilibrium aqueous and TBEP layers were calculated by subtracting twice the uranium concentration values from the chloride values obtained by titrations using the Volhard method.

The conductivity of the equilibrium organic phases having the composition as listed in Table I has been measured by a procedure previously given (10). The water content of the organic layers was found by means of the Karl Fischer reagent using the dead-stop end-point method as determined with a Fisher titrimeter.

In experiments designed to study the degradation of TBEP, the procedure was essentially identical with that previously described (16), except that they were run at 60±0.4° C for periods ranging from 2 to 12 days. The concentrations of the acidic degradation products, H_2DBEP and HMBEP, in the organic phase were determined potentiometrically while the aqueous phase was analyzed for orthophosphoric acid spectrophotometrically (19).

RESULTS AND DISCUSSION

(A) Extraction of Uranyl Chloride

In this set of experiments the hydrochloric acid content of the initial aqueous solution

Can. J. Chem. Downloaded from www.nrcresearchpress.com by 210.87.254.6 on 09/05/12
For personal use only.

TABLE I

The equilibrium distribution of 6.67 *M* HCl and UO_2Cl_2 between aqueous and undiluted TBEP as a function of the uranyl concentration in the initial solution. All concentrations, *M*

$[UO_2Cl_2]$ initial aq. solution	Swelling of the organic phase, ml*	$[HCl]_{aq}$	$[UO_2Cl_2]_{aq}$	$[HCl]_{org}$	$[UO_2Cl_2]_{org}$	$[H_2O]_{org}$
0.44	1.00	6.34	0.02	1.41	0.357	6.55
0.89	1.12	6.60	0.09	1.34	0.667	5.13
1.33	1.20	6.78	0.30	1.30	0.890	5.82
1.78	1.50	6.89	0.57	1.47	1.06	6.55
2.22	1.50	6.93	0.89	1.50	1.23	6.82
2.66	1.80	6.83	1.28	1.76	1.36	7.43
3.11	2.05	6.59	1.64	2.04	1.52	7.32
3.55	2.47	6.69	2.01	2.26	1.69	9.31
4.00	2.85	6.34	2.44	2.57	1.88	10.33
4.44	3.25	5.87	2.93	2.85	2.07	11.46

*Initial organic phase volume 5.0 ml (2.56 *M* TBEP).

was kept constant at 6.67 *M*, and the extraction by undiluted TBEP was examined as a function of increasing uranyl chloride concentration in the initial aqueous solution. The above initial HCl concentration was chosen to approach "saturation" of the extractant, leaving practically none of the extractant unreacted (10). Table I and Figs. 1–4 summarize the results obtained. Figures 1–3 include the results obtained with TBP (11) for comparison with TBEP. Since the volume change measurements were reproducible to ±0.05 ml, we believe that the values in Table I are accurate to ±3%. Figure 1 shows that there is very probably a change in the extraction mechanism at about 1 *M* uranyl chloride in the organic phase (as discussed previously for TBP (11)), coinciding with the intersection of the lines in Fig. 4. The latter corresponds to a TBEP:UO_2Cl_2 ratio of nearly 2. The

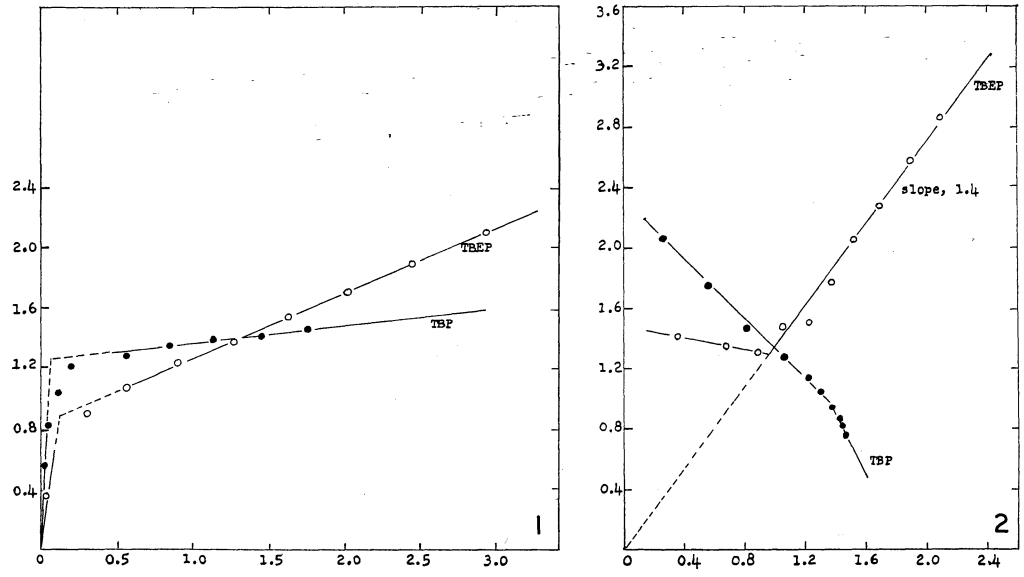

FIG. 1. Molarity of UO_2Cl_2 in the equilibrium organic phase (ordinate) vs. molarity of UO_2Cl_2 in the equilibrium aqueous phase (abscissa).

FIG. 2. Molarity of HCl in the equilibrium organic phase (ordinate) vs. molarity of UO_2Cl_2 in the equilibrium organic phase (abscissa).

Can. J. Chem. Downloaded from www.nrcresearchpress.com by 210.87.254.6 on 09/05/12
For personal use only.

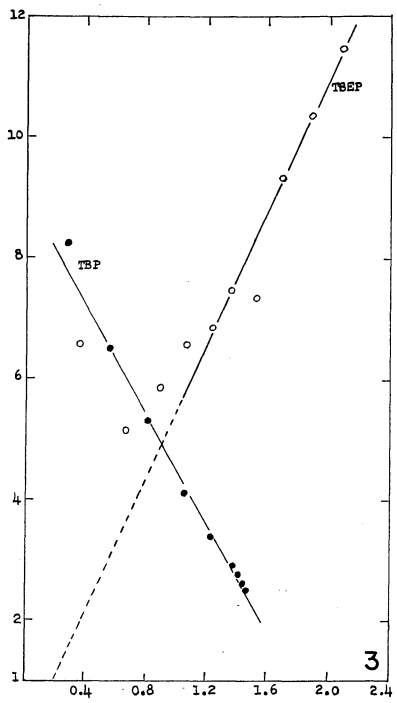

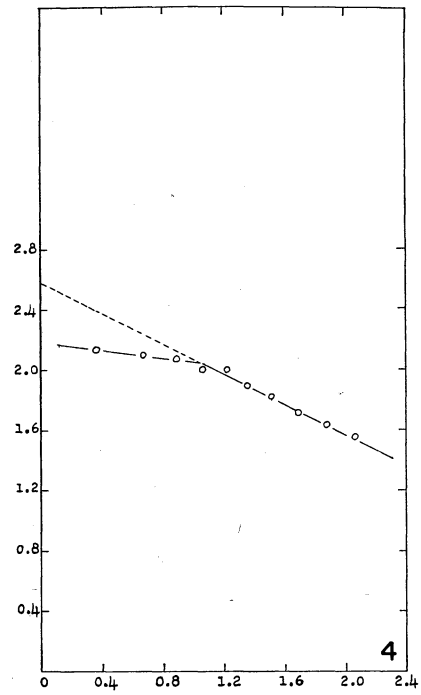

FIG. 3. Molarity of H_2O in the equilibrium organic phase (ordinate) vs. molarity of UO_2Cl_2 in the equil. organic phase (abscissa).

FIG. 4. Molarity of TBEP in the equilibrium organic phase (ordinate) vs. molarity of UO_2Cl_2 in the equilibrium organic phase (abscissa).

slope of the second part of the curve in Fig. 4 seems not to be incidental since by extrapolation to zero uranium content the molarity of undiluted TBEP, 2.56 *M*, is obtained. Figure 2 suggests that the acid content of the TBEP phase decreases up to about 1 *M* UO_2Cl_2 in the organic phase and increases afterwards. The line with a slope of 1.4 has its origin at zero concentrations of the solutes. Up to about 1 *M* UO_2Cl_2 in the organic phase, the concentration of HCl in TBEP is smaller than in TBP, both decreasing with increasing concentration of uranyl chloride. Beyond 1 *M* uranyl chloride, however, a different behavior is noted. The concentration of HCl in TBEP is now greater than that in TBP, and is increasing with increase in uranium concentration, while the concentration of HCl in TBP is still following the same trend. We would like to suggest that, up to the concentration of 1 *M* uranyl chloride, there is only one coordination site in TBEP, namely the phosphoryl oxygen, just as in TBP. At higher concentrations, however, the acid may be coordinated additionally to the ethereal oxygens in TBEP, hence the increase in the TBEP phase over TBP. This is confirmed in the comparison between TBEP and TBP in the extraction of water, as shown in Fig. 3. The same general trends are observed for the extraction of HCl in Fig. 2.

The most striking result for TBEP is that the extraction of uranium, acid, and water shows no indication of levelling off. This is in contrast to the behavior of neutral alkyl phosphates containing no ether linkage, but is in line with that of certain ethers (19). It has been observed that about 5.5 *M* UO_2Cl_2 and 6.67 *M* HCl in the aqueous phase result in complete miscibility with the undiluted TBEP, a phenomenon which has so far

Can. J. Chem. Downloaded from www.nrcresearchpress.com by 210.87.254.6 on 09/05/12
For personal use only.

been observed only for undiluted TBP with pure nitric acid (21) and anhydrous phosphoric acid (22).

When the aqueous HCl concentration is less than 2 *M* (corresponding to organic phase HCl concentration of less than 0.2 *M*), the extraction ability of TBEP for tracer amounts of Zn(II) and In(III) is less than that of TBP (10). In extraction from dilute aqueous solutions there is but one coordination site in TBEP, namely, the phosphoryl oxygen. Because of the presence of three additional oxygen atoms in TBEP, the electron donor strength of the phosphoryl oxygen becomes slightly weaker in TBEP than in TBP, and hence also the extraction ability. In extractions from concentrated aqueous solutions, however, three additional coordination sites (the ethereal oxygens) become available in TBEP. Since TBP still has only one coordination site, its total extraction capacity now becomes lower than that of TBEP.

Additional evidence for the formation of a compound with TBEP:UO_2Cl_2 ratio of 2 and for different extraction mechanisms involved is shown in Fig. 5, representing the resistance curve of the organic phase as a function of its UO_2Cl_2 content. The maximum resistance is observed at about 1 *M* UO_2Cl_2 in the TBEP phase (corresponding according to Fig. 4 to 2 *M* TBEP) and as more uranium goes into the organic phase, together with ever-increasing amounts of acid and water, the conductance of the organic phase increases. This behavior is very different from that of a TBP system under comparable conditions.

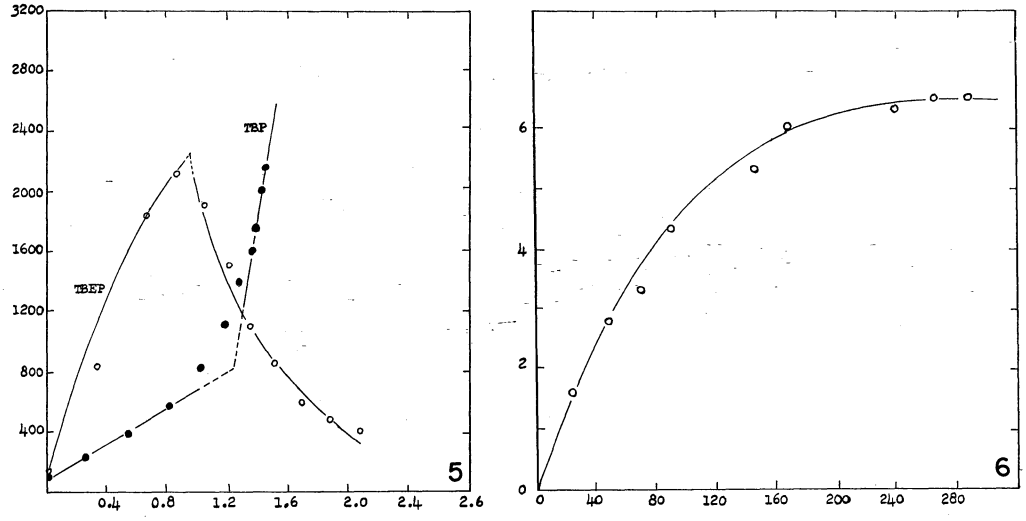

FIG. 5. Resistance in scale reading units of the equilibrium organic phase (ordinate) as a function of its UO_2Cl_2 content in molarity (abscissa).
FIG. 6. Volume decrease in ml at 60° of the equilibrium TBEP phase (ordinate) vs. ageing time in hours (abscissa).

(B) Hydrochloric Acid Promoted Degradation of TBEP

When equal volumes (15 ml) of undiluted TBEP and 12.1 *N* HCl were mixed at 60°, the result was that the organic layer increased in volume to 20.30 ml. Thereafter, as degradation of TBEP proceeded, the volume of the equilibrium organic phase decreased, reaching a constant volume of 14.00 ml after 238 hours at 60°; the liquid ejected from the organic layer was completely miscible with the aqueous layer. This decrease in volume as a function of time is plotted in Fig. 6. A separate experiment in

Can. J. Chem. Downloaded from www.nrcresearchpress.com by 210.87.254.6 on 09/05/12
For personal use only.

which the aqueous phase was discarded after equilibration, while the TBEP phase was left standing in a thermostat at 60° for 205 hours, has shown that the ejected phase is an aqueous HCl solution of 6.13 *M* concentration. Qualitative experiments have shown that the phenomenon of an ejected layer also occurs when TBEP is equilibrated with as dilute a solution as 2 *M* HCl.

In a simple and formal analogy with the dealkylation of TBP (16), the corresponding degradation of TBEP may be represented as

$$\underset{\text{TBEP}}{(C_4H_9OC_2H_4O)_3PO} + HCl_{aq} \xrightarrow{k_1} \underset{\text{HDBEP}}{HO(C_4H_9OC_2H_4O)_2PO} + C_4H_9OC_2H_4Cl,$$

$$\text{HDBEP} + HCl_{aq} \xrightarrow{k_2} \underset{\text{H}_2\text{MBEP}}{(HO)_2(C_4H_9OC_2H_4O)PO} + C_4H_9OC_2H_4Cl,$$

$$H_2MBEP + HCl_{aq} \xrightarrow{k_3} H_3PO_{4aq} + C_4H_9OC_2H_4Cl.$$

The analytically determined values of the concentrations of the decomposition products are shown in Table II. The values of log unreacted TBEP plotted against the ageing

TABLE II

Degradation of TBEP at 60°. All concentrations, *M*

Ageing time, hours	Unreacted $[TBEP]_{org}$	$[H_2MBEP]_{org}$	$[HDBEP]_{org}$	$[H_3PO_4]_{aq}$
51	1.750	0.122	0.685	0.003
97	1.489	0.225	0.834	0.012
143	1.179	0.315	1.043	0.023
191	1.065	0.391	1.065	0.039
263	0.989	0.409	1.127	0.045
315	0.929	0.450	1.133	0.048

time gives a straight line only for the first four values tabulated. Assuming for these four values a first-order reaction, the rate constants represented by the equation $d[TBEP]/dt = k_1[TBEP]$ have been calculated. The four values: 4.6×10^{-3}, 5.4×10^{-3}, 5.6×10^{-3}, and 7.5×10^{-3} hour^{-1} show a trend, demonstrating that the rates of formation of HDBEP, H_2MBEP, and H_3PO_4 are dependent on other variables and that the rate of reaction is much more sensitive to these products than in the case of TBP. This evidence was sufficient to discourage further quantitative study of the degradation process.

This failure is not surprising in view of the presence of ethereal oxygens in TBEP. At higher temperatures the degradation of TBEP is more complicated, since the possibility of electrophilic attack by hydrogen ion on the ethereal oxygen increases, presumably by the higher dissociation of HCl in the organic phase at the higher temperature.

(C) Hydrolytic Degradation of TBEP and the Simultaneous Photolytic Reduction of Uranium (VI)

If TBEP is equilibrated with an aqueous solution of 1–4 *M* uranyl chloride in 7–8 *M* HCl and the loaded organic phase separated and stored in the dark, no transformation occurs. However, if it is left 2 days on open shelves, the organic solution, initially homogenous and yellow in color, develops a greenish tinge, characteristic of uranium (IV), and a greenish precipitate. The solid obtained is apparently non-hygroscopic and does not undergo oxidation at room temperature. The infrared spectrum, using KBr disc, shows strong absorption at 3350 cm^{-1} indicating free OH. Powder diffraction data were not

Can. J. Chem. Downloaded from www.nrcresearchpress.com by 210.87.254.6 on 09/05/12
For personal use only.

definitive in establishing the nature of these compounds. Only diffuse powder lines were obtained characteristic of amorphous type substances.

The results of phosphorus and carbon analysis for the uranium (IV) compound are as follows: P, 8.2%; C, 31.2%. If no degradation occurred in TBEP, the C/P ratio would be 7.0; whereas if degradation to HDBEP and H_2MBEP occurred, the C/P ratios would be 4.6 and 2.3, respectively. The actually observed C/P ratio, 31.2/8.2, is 3.8, so that about two thirds of TBEP is degraded into HDBEP, and one third degraded into H_2MBEP.

ACKNOWLEDGMENTS

The authors wish to thank Drs. B. S. Fraenkel and Lionel Cohen for X-ray, and Dr. Anna Feilchenfeld, of the Hebrew University, for the infrared results.

REFERENCES

1. L. L. Burger. J. Phys. Chem. **62**, 590 (1958).
2. T. H. Siddall, III. J. Am. Chem. Soc. **81**, 4176 (1959); J. Inorg. Nucl. Chem. **13**, 151 (1960); Ind. Eng. Chem. **51**, 41 (1959).
3. T. V. Healy and J. Kennedy. J. Inorg. Nucl. Chem. **10**, 128 (1959).
4. T. V. Healy, J. Kennedy, and G. M. Waind. J. Inorg. Nucl. Chem. **10**, 137 (1959).
5. A. V. Nikolaev, S. M. Shubina, and N. M. Sinitsyn. Radiokhimiya, **2**, 3 (1960).
6. K. A. Petrov, V. B. Shevchenko, V. G. Timoshev, F. L. Maklyaev, A. V. Fokin, A. V. Rodinonov, A. V. El'kine, Z. I. Nagnibeda, and A. A. Volkova. Zh. Neorgan. Khim. **5**, 498 (1960).
7. V. G. Timoshev, K. A. Petrov, A. V. Rodionov, V. V. Salandine, A. A. Volkova, A. V. El'kine, Z. I. Nagnibeda. Radiokhimiya, **2**, 419 (1960).
8. C. A. Blake, Jr., A. T. Gresky, J. N. Schmitt, and R. G. Mansfield. Paper presented at the American Nuclear Society, Chicago. June 1960.
9. K. Oshima. J. Atomic Energy Soc. Japan, **4**, 166 (1962).
10. M. Halpern, T. Kim, and N. C. Li. J. Inorg. Nucl. Chem. **24**, 1251 (1962).
11. A. S. Kertes and M. Halpern. J. Inorg. Nucl. Chem. **16**, 308 (1961).
12. H. Irving and D. N. Edgington. J. Inorg. Nucl. Chem. **10**, 306 (1959).
13. I. V. Gal and A. Ruvarac. Bull. Inst. Nucl. Sci. Belgrade, **8**, 67 (1958). V. M. Vdovenko, A. A. Lipovskii, and S. A. Nikitina. Zh. Neorgan. Khim. **5**, 449 (1960). V. B. Shevchenko, I. G. Slepchenko, V. S. Schmitt, and E. A. Nenarokomov. Zh. Neorgan. Khim. **5**, 526 (1960).
14. T. H. Siddall, III. J. Phys. Chem. **64**, 1340 (1960).
15. A. S. Kertes. J. Inorg. Nucl. Chem. **14**, 104 (1960).
16. A. S. Kertes and M. Halpern. J. Inorg. Nucl. Chem. **20**, 117 (1961).
17. A. S. Kertes and M. Halpern. J. Inorg. Nucl. Chem. **19**, 359 (1961).
18. L. L. Burger and R. M. Wagner. J. Chem. Eng. Data, **3**, 310 (1958).
19. R. A. Koenig and R. Johnson. Ind. Eng. Chem. Anal. Ed. **14**, 155 (1942).
20. D. G. Tuck. J. Chem. Soc. 3202 (1957). V. M. Vdovenko and N. A. Alekseeva. Radiokhimiya, **1**, 450 (1959).
21. T. J. Collopy and J. F. Blum. J. Phys. Chem. **64**, 1324 (1960).
22. C. E. Higgins and W. H. Baldwin. J. Org. Chem. **21**, 1156 (1956); J. Inorg. Nucl. Chem. **24**, 415 (1962).

Can. J. Chem. Downloaded from www.nrcresearchpress.com by 210.87.254.6 on 09/05/12
For personal use only.

THE CHEMISTRY OF ALUMINUM–NITROGEN COMPOUNDS

IV. THE REACTIONS OF Me_3Al AND $H_3Al{:}NMe_3$ WITH SEVERAL TERTIARY POLYAMINES

NEIL R. FETTER AND DONALD W. MOORE[1]

U.S. Naval Ordnance Laboratory, Corona, California

Received August 29, 1963

ABSTRACT

The reactions of Me_3Al with $Me_2N(CH_2)_3NMe_2$, $Me_2NCH_2CH{=}CHCH_2NMe_2$, $(CH_2)_6N_4$, and $(Me_2N)_2C{=}C(NMe_2)_2$ have yielded complexes with two molecules of Me_3Al per amine. The structures of these complexes are rationalized on the basis of a pentacoordinated aluminum atom with a linear N → Al ← N dative bond. The reactions of $H_3Al{:}NMe_3$ with these amines have produced a variety of products in which the amines appear to have undergone rearrangements. The complexes are 1:1 except the $(Me_2N)_2C{=}C(NMe_2)_2$ complex, which has 2 moles of H_3Al per amine.

Can. J. Chem. Downloaded from www.nrcresearchpress.com by 210.87.254.5 on 09/05/12
For personal use only.

INTRODUCTION

In this paper are presented further investigations into the proposal made recently (1) that ditertiary amines will form 2:1 complexes with trimethylaluminum whose nitrogen atoms are separated by more than two methylene groups and 1:1 complexes with one or no intervening methylene groups. In our last communication (1) it was stated that $Me_2NCH_2NMe_2$ formed a 1:1 complex while $Me_2N(CH_2)_2NMe_2$ formed a 2:1 complex. We are now reporting the results obtained from the reactions of Me_3Al with $Me_2N(CH_2)_3NMe_2$ and $Me_2NCH_2CH{=}CHCH_2NMe_2$. The latter amine was chosen not only because it contains four carbon atoms between the N—Me_2 groups, but also because we wished to see whether Me_3Al would react with the double bond. We have also treated $H_3Al{:}NMe_3$ with these amines.

The reactions of Me_3Al and $H_3Al{:}NMe_3$ with two unusual tertiary tetramines, namely, hexamethylenetetramine and *tetrakis*-dimethylaminoethylene, have been studied. The n.m.r. spectra of some of these complexes have revealed new structural possibilities for aluminum–nitrogen dative bonded complexes.

EXPERIMENTAL

Apparatus and Reagents

The experimental apparatus and procedures have been described in earlier publications (2, 3). The $Me_2N(CH_2)_3NMe_2$ and the $Me_2NCH_2CH{=}CHCH_2NMe_2$ were supplied by the Ames Laboratories of Milford, Conn., and were used without further purification. The hexamethylenetetramine was Eastman White Label grade and the $(Me_2N)_2C{=}C(NMe_2)_2$, generously donated by the Chemistry Division of the U.S. Naval Ordnance Test Station, was vacuum fractionated once before use. The trimethylaluminum was obtained from the Ethyl Corp., New York, N.Y., and the triethylaluminum was obtained from Texas Alkyls, Houston, Texas. Both of these materials were vacuum distilled before use. All solvents were reagent and were used without further treatment, except benzene which was distilled over CaH_2 and stored in a dry box.

The n.m.r. spectra were obtained with a Varian Associates Model V-4302 spectrometer operating at 60 Mc. Liquid compounds were diluted 10% with benzene and the solid compounds were dissolved in benzene to 15% by weight. All solutions were sealed under vacuum in 5 mm pyrex tubes. All spectra were taken at 30° C unless otherwise noted.

Cryoscopic molecular weight data were obtained in a Bender-Hobein apparatus employing benzene as a solvent. The samples were prepared in a dry box to eliminate moisture contamination. The elemental analyses were performed by the Schwarzkopf Microanalytical Laboratories of Woodside, N.Y.

All melting points are uncorrected.

[1]*Present address: U.S. Naval Ordnance Test Station, China Lake, California.*

Reaction of Trimethylaluminum with N,N,N′,N′-Tetramethylpropanediamine

By vacuum transfer, 2.79 g (21.4 mmole) of $Me_2N(CH_2)_3NMe_2$ was added to 1.54 g (21.4 mmole) of Me_3Al dissolved in 20 ml of *n*-heptane. The reaction was started at −196° C and completed at 25° C. During the warming period (30 minutes) a white precipitate formed and the solvent was then removed by vacuum transfer. The crude product was sublimed (0.05 mm) at 100° C. Elemental analysis of the sublimate (m.p. 158–168° C) agreed with the formula $C_{13}H_{36}N_2Al_2$. Anal. Calc.: C, 56.89; H, 13.22; N, 10.21; Al, 19.66. Found: C, 55.90; H, 12.90; N, 10.53; Al, 20.69.

Methanol hydrolysis of 0.187 g (0.683 mmole) of the sublimate gave 90.2 ml (4.02 mmole) of methane. Yield of sublimate was approximately 65 mole% based on Me_3Al.

Reaction of Aluminum Hydride Trimethylamine with N,N,N′,N′-Tetramethylpropanediamine

When the amine was used as a solvent, 15 g was condensed on 1.58 g (17.8 mmole) of $H_3Al{:}NMe_3$ at −196° C. The mixture was allowed to warm to room temperature, stand overnight, and was then heated at 80° C for 2 hours. During the heating, the $H_3Al{:}NMe_3$ dissolved in the amine and 243.0 ml (10.5 mmole) of NMe_3 evolved. The mixture was cooled to 25° C, the excess amine was removed via vacuum transfer, and the remaining white solid was sublimed at 80° C under 0.05 mm vacuum. Elemental analysis of the sublimate (m.p. 136–140° C) gave results in fair agreement with the formula $C_7H_{21}N_2Al$. Anal. Calc.: C, 52.14; H, 13.13; N, 17.38; Al, 16.73. Found: C, 51.19; H, 12.49; N, 17.37; Al, 15.55.

Methanol hydrolysis of 0.1224 g (0.760 mmole) of the sublimate gave 58.3 ml (2.60 mmole) of hydrogen. Yield of sublimate was 75 mole% based on $H_3Al{:}NMe_3$.

Reaction of Trimethylaluminum with N,N,N′,N′-Tetramethyl-2-butene-1,4-diamine

By vacuum transfer, 1.28 g (9.05 mmole) of $Me_2NCH_2CH{=}CHCH_2NMe_2$ was placed on a solution of 1.27 g (17.6 mmole) of Me_3Al and 20 ml of *n*-heptane at −196° C. When the components melted during the warming to room temperature, a flocculent precipitate formed. After reaching room temperature, the solvent was removed and the crude product was vacuum sublimed at 85° C (0.05 mm). Elemental analysis of the sublimate (m.p. 141–144° C) gave results which agreed with the formula $C_{14}H_{36}N_2Al_2$. Anal. Calc.: C, 58.71; H, 12.67; N, 9.78; Al, 18.83. Found: C, 58.55; H, 12.52; N, 9.75; Al, 18.49.

Methanol hydrolysis of 0.3327 g (1.14 mmole) of the sublimate gave 138.0 ml (5.93 mmole) of methane. Yield of sublimate was approximately 80 mole% based on Me_3Al.

Reaction of Aluminum Hydride Trimethylamine with N,N,N′,N′-Tetramethyl-2-butene-1,4-diamine

By vacuum transfer, 1.04 g (7.35 mmole) of $Me_2NCH_2CH{=}CHCH_2NMe_2$ was added to an *n*-octane solution at −196° C containing 1.52 g (17.0 mmole) of $H_3Al{:}NMe_3$. The mixture was warmed to room temperature and heated with stirring at 40° C for 2 hours. During this period, 18.1 ml (0.807 mmole) of hydrogen evolved and the trimethylamine was recovered as $H_3Al{:}(NMe_3)_2$. The solvent was removed and the crude product was vacuum sublimed at 105° C (0.05 mm). Elemental analysis of the white crystalline sublimate (m.p. 150–155° C) gave results which give closest agreement with the formula $C_9H_{23}N_2Al$. Anal. Calc.: C, 58.03; H, 12.44; N, 15.04; Al, 14.48. Found: C, 58.13; H, 12.49; N, 13.23; Al, 14.51.

Methanol hydrolysis of 0.2174 g (1.16 mmole) of the sublimate yielded 78.8 ml (3.52 mmole) of hydrogen. Yield of sublimate was approximately 50 mole% based on $Me_2NCH_2CH{=}CHCH_2NMe_2$.

Reaction of Trimethylaluminum with Hexamethylenetetramine

By vacuum transfer, 2.12 g (29.0 mmole) of Me_3Al was added to 20 ml of *n*-octane and 2.00 g (14.3 mmole) of $(CH_2)_6N_4$ at −196° C. The mixture was allowed to warm to room temperature and stand for 2 additional hours. At the end of this period the solvent was removed leaving behind a white solid. This material was vacuum sublimed at 90° C (0.05 mm) and elemental analysis of the resulting sublimate (m.p. 146–148° C) gave results which agreed with the formula $C_{12}H_{30}N_4Al_2$. Anal. Calc.: C, 50.69; H, 10.62; N, 19.69; Al, 18.99; Found: C, 50.74; H, 10.58; N, 19.90; Al, 18.87.

Methanol hydrolysis of 0.1785 g (0.625 mmole) of the sublimate gave 82.2 ml (3.67 mmole) of methane. Yield of sublimate was approximately 65% based on Me_3Al.

The above reaction was repeated employing a 4:1 starting ratio of Me_3Al (21.8 mmole) to $(CH_2)_6N_4$ (5.44 mmole), but the sublimate obtained melted at 225–228° C and its elemental analysis agreed with the formula $C_{11}H_{28}N_3Al_2$. Anal. Calc.: C, 51.54; H, 11.00; N, 16.39; Al, 21.07. Found: C, 51.55; H, 11.36; N, 16.39; Al, 21.54.

Methanol hydrolysis of 0.2417 g (0.945 mmole) of $(Me_3Al)_2{:}(CH_2)_5N_3$ yielded 128.2 ml (5.73 mmole) of methane. Yield was approximately 40% based on $(CH_2)_6N_4$. Both products were soluble in benzene.

Reaction of Aluminum Hydride Trimethylamine with Hexamethylenetetramine

A mixture containing 1.70 g (19.1 mmole) of $H_3Al{:}NMe_3$, 1.34 g (9.95 mmole) of $(CH_2)_6N_4$, 15 ml of nonane, and a stirring bar was stirred for 3 days at 25° C. During this period the granules of $(CH_2)_6N_4$ were reduced to a fine powder, and 119.0 ml (5.31 mmole) of NMe_3 evolved. The solvent and a small amount of $H_3Al{:}(NMe_3)_2$ were removed by vacuum transfer leaving a powdery white material. This material could not be vacuum sublimed up to 120° C and would not melt up to 200° C; at this temperature an aluminum mirror appeared on the melting point tube. Elemental analysis of the crude material gave results which agree

Can. J. Chem. Downloaded from www.nrcresearchpress.com by 210.87.254.5 on 09/05/12
For personal use only.

with the formula $C_6H_{15}N_3Al$. Anal. Calc.: C, 45.90; H, 9.63; N, 26.78; Al, 17.18. Found: C, 46.12; H, 10.26; N, 26.68; Al, 17.29.

Methanol hydrolysis of 0.3407 g (2.17 mmole) of $H_3Al:(CH_2)_6N_3$ yielded 159.2 ml (7.10 mmole) of hydrogen.

Reaction of Trimethylaluminum with Tetrakis-dimethylaminoethylene

By vacuum transfer, 1.91 g (9.60 mmole) of $(Me_2N)_2C{=}C(NMe_2)_2$ was added to 1.35 g (18.8 mmole) of Me_3Al dissolved in 20 ml of heptane at −196° C. The mixture was allowed to warm to room temperature and an immediate precipitation occurred when the components thawed. At room temperature (25°) the solvent was removed under vacuum and the remaining white solid was vacuum sublimed at 60° C (0.05 mm). Elemental analysis of the sublimate (m.p. 141–143° C) gave results which were in fair agreement with the formula $C_{16}H_{42}N_4Al_2$. Anal. Calc.: C, 55.78; H, 12.29; N, 16.27; Al, 15.66. Found: C, 56.75; H, 12.51; N, 16.33; Al, 14.60.

Methanol hydrolysis of 0.6810 g (1.98 mmole) of the sublimate gave 271.0 ml (12.0 mmole) of methane. Yield of sublimate was approximately 75 mole% based on $(Me_2N)_2C{=}C(NMe_2)_2$.

The sublimate was very soluble in benzene, but after standing a few minutes a dense phase separated from solution. The dense phase contained $C_{16}H_{42}N_4Al_2$ and benzene and the light layer contained only benzene. The n.m.r. spectrum of the dense layer is shown in Fig. 1.

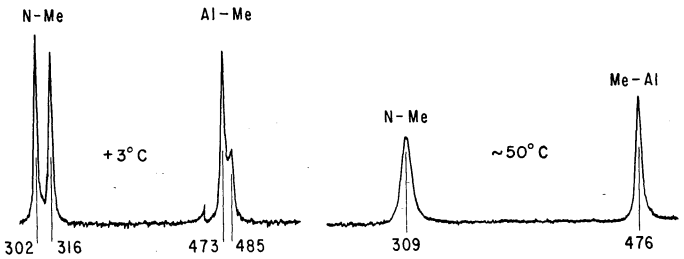

Fig. 1. Nuclear magnetic resonance spectrum of $(Me_3Al)_2{:}(Me_2N)_2C{=}C(NMe_2)_2$.

This compound was found to have another interesting property, namely, exposure of the solid or solutions to even a trace of dry oxygen produced an intense red color. It was also noted that dry solvents such as acetone and methanol developed this color. A benzene solution of 0.597 g (1.73 mmole) of compound was exposed to an atmosphere of dry oxygen for 3 days at 30° C. At the end of this period the material was a viscous red fluid and 58.0 ml (2.59 mmole) of O_2 had been absorbed. Elemental analysis of the oxidized compound gave results which agree most closely with the formula $C_6H_{14}NO_2Al$: Anal. Calc.: C, 45.27; H, 8.86; N, 8.80; O, 20.10; Al, 16.94. Found: C, 42.69; H, 9.35; N, 9.74; O, 20.13; Al, 18.09.

Methanol hydrolysis of 0.0874 g (0.550 mmole) of the oxidized material gave 25.9 ml (1.16 mmole) of methane. The infrared spectrum exhibits a strong absorption at 1690 cm^{-1} and two weaker bands at 912 cm^{-1} and 3420 cm^{-1}. The first of these suggests a $\diagdown\!\!\diagup C{=}O$ absorption and the latter appear to be —OH modes.

The reaction of Me_3Al with $(Me_2N)_2C{=}C(NMe_2)_2$ was repeated with a 4:1 starting ratio of reagents. Using the procedure described above, 1.25 g (6.27 mmole) of $(Me_2N)_2C{=}C(NMe_2)_2$ was mixed with 1.81 g (25.1 mmole) of Me_3Al in heptane. The solvent and any unreacted Me_3Al were removed and the crude product was vacuum sublimed at 95° C.

Elemental analysis of the sublimate (m.p. 58–68° C) gave results which agree most closely with the formula $C_{14}H_{36}N_4Al_2$: Anal. Calc.: C, 53.46; H, 11.54; N, 17.81; Al, 17.15. Found: C, 53.98; H, 11.88; N, 17.70; Al, 17.17.

Methanol hydrolysis of 0.3108 g (0.987 mmole) of the sublimate yielded 108.2 ml (4.85 mmole) of methane. The infrared spectrum exhibits a weak band at 1800 cm^{-1}, indicating the presence of ethylenic bonds.

Reaction of Aluminum Hydride Trimethylamine with Tetrakis-dimethylaminoethylene

This reaction is not as simple as the two described above. Some of the $H_3Al{:}NMe_3$ is consumed by the formation of $H_3Al{:}(NMe_3)_2$ and the elemental analysis of the sublimed product suggests some rearrangement may occur during sublimation.

When 20 ml of *n*-octane was used as the solvent, 3.25 g (16.3 mmole) of $(Me_2N)_2C{=}C(NMe_2)_2$ was transferred to a solution at −196° C containing 1.45 g (16.3 mmole) of $H_3Al{:}NMe_3$. The mixture was allowed to warm to room temperature and it was then heated at 40° C for 3 hours. No hydrogen or trimethylamine evolution was observed; however, considerable $H_3Al{:}(NMe_3)_2$ was present in the solvent removed from the mixture. Also the infrared spectrum of the solvent showed the presence of unreacted $(Me_2N)_2C{=}C(NMe_2)_2$. After removal of the solvent, $H_3Al{:}(NMe_3)_2$, and $(Me_2N)_2C{=}C(NMe_2)_2$, a white powdery material remained which was vacuum sublimed at 75° C. Sublimation at this temperature is slow, but, if the temperature is

Can. J. Chem. Downloaded from www.nrcresearchpress.com by 210.87.254.5 on 09/05/12
For personal use only.

raised, discoloration of the crude product commences. Elemental analysis of the sublimate gave results which most closely fit the formula $C_{15}H_{40}N_4Al$. Anal. Calc.: C, 51.54; H, 12.21; N, 16.97; Al, 16.34. Found: C, 52.97; H, 12.04; N, 18.18; Al, 16.20.

Methanol hydrolysis of 0.2138 g (0.647 mmole $(H_3Al)_2C_{15}H_{34}N_4$) gave 108.0 ml (4.83 mmole) of hydrogen. Exposure to oxygen produced no color change.

RESULTS AND DISCUSSION

As can be seen from the experimental data presented, $Me_2N(CH_2)_3NMe_2$ and $Me_2NCH_2CH{=}CHCH_2NMe_2$ react with Me_3Al, to form the 2 to 1 complexes $Me_3Al{:}Me_2N(CH_2)_3NMe_2{:}AlMe_3$ and $Me_3Al{:}Me_2NCH_2CH{=}CHCH_2NMe_2{:}AlMe_3$. The double bond in the latter complex does not appear to be involved with the trimethylaluminum, because the n.m.r. spectrum shows both the Al—Me and N—Me protons as sharp single peaks and no other unusual proton bands for the amine. (N—Me, τ = 8.07 p.p.m.; Al—Me, τ = 10.46 p.p.m.).

TABLE I

Molecular weights of several Me_3Al – tertiary amine complexes

Compound	Molecular weight		Degree of association	Solution molality
	Found	Calc.		
1. $Me_3Al{:}Me_2NNMe_2$*	164	160.3	1.02	.0675
2. $Me_3Al{:}Me_2NCH_2NMe_2$	246	174.3	1.41	.0491
	232		1.33	.0505
3. $(Me_3Al)_2{:}Me_2N(CH_2)_2NMe_2$	359	260.4	1.38	.0690
	342		1.32	.0840
4. $(Me_3Al)_2{:}Me_2N(CH_2)_3NMe_2$	300	274.4	1.09	.0324
	291		1.06	.0400
5. $(Me_3Al)_2{:}Me_2NCH_2CH{=}CHCH_2NMe_2$	296	286.4	1.03	.0418
	303		1.06	.0500
6. $(Me_3Al)_2{:}(CH_2)_6N_4$	296	284.2	1.05	.0333
	295		1.05	.0306

*Measured in cyclohexane.

The cryoscopic molecular weights of the trimethylaluminum–amine complexes from tetramethylhydrazine to N,N,N′,N′-tetramethyl-2-butene-1,4-diamine, where the intervening carbon atoms range from zero through four, are presented in Table I. It will be noted that with the exception of $Me_3Al{:}Me_2NNMe_2$, which appears to be monomeric, there is a trend toward monomeric character as the number of intervening carbon atoms increases. This pattern of association suggests that $Me_3Al{:}Me_2NCH_2NMe_2$ may be in rapid equilibrium with a species involving a pentacoordinated aluminum atom:

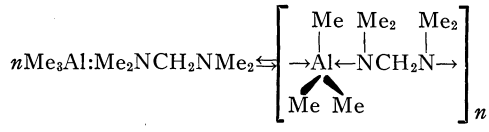

Such a scheme is a better rationalization of both n.m.r. and molecular weight data, than is the cyclic structure

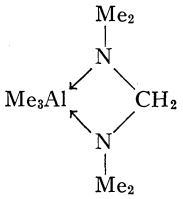

Can. J. Chem. Downloaded from www.nrcresearchpress.com by 210.87.254.5 on 09/05/12
For personal use only.

proposed earlier (1); however, the third complex in Table I must be associated in a different manner because there is a Me_3Al on each amino nitrogen atom. Within experimental error ($\pm 10\%$) the fourth, fifth, and sixth complexes are monomeric.

Although the analytical data are poorer, it appears that H_3Al forms only 1:1 complexes with $Me_2N(CH_2)_3NMe_2$ and $Me_2NCH_2CH{=}CHCH_2NMe_2$. These results fall into the pattern established for $Me_2NCH_2NMe_2$ and $Me_2N(CH_2)_2NMe_2$ complexes of AlH_3. All of these complexes are insoluble in hydrocarbons and it has been difficult to obtain n.m.r. and cryoscopic molecular weight data.

A clue to the possible structure of the polyamine complexes with aluminum hydride and trimethylaluminum has been provided by a recent publication of Heitsch, Nordman, and Parry (4), and by the preliminary data of Palenik (5). The former authors have reported that $H_3Al{:}(NM_3)_2$ in the crystal state is a monomer with a trigonal bipyramidal structure and a linear N—Al—N bond:

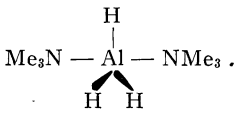

The work of Palenik indicates the complex $H_3Al{:}Me_2N(CH_2)_2NMe_2$ has a similar structure with a unit cell containing eight dimer units:

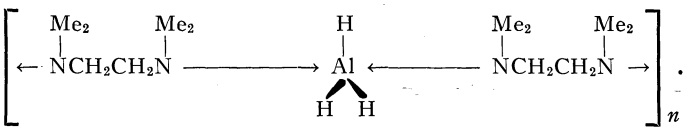

Since all the aluminum hydride – amine complexes are 1:1, the structure proposed for the aluminum hydride – N,N,N,′N′-tetramethylethylenediamine may be assumed to apply to the complexes with $Me_2NCH_2NMe_2$, $Me_2N(CH_2)_3NMe_2$, and $Me_2NCH_2CH{=}CHCH_2NMe_2$.

The trimethylaluminum complexes present a different problem because some are 1:1 and others are 2:1. The linear structure for $Me_3Al{:}Me_2NCH_2NMe_2$ has already been proposed above to rationalize both molecular weight and n.m.r. data. The n.m.r. spectrum of $(Me_3Al)_2{:}(CH_2)_6N_4$ may also be explained by considering hexamethylenetetramine to be similar to $Me_2NCH_2NMe_2$ or by considering it to be a series of $—CH_2NCH_2NCH_2—$ groups. If the Me_3Al molecules, which are datively bonded to the nitrogen atoms, are pentacoordinated and if the bonds are oscillating rapidly among all possible positions, then the n.m.r. spectrum in Fig. 2 and the 2:1 stoichiometry are compatible. The hexamethylenetetramine–trimethylaluminum complex may be illustrated as follows:

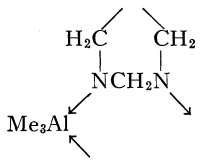

employing one-half of an amine molecule and one Me_3Al molecule. It should be noted that the monomeric molecular weight shown in Table I for this complex does not appear consistent with the bonding scheme proposed above and this discrepancy cannot be readily explained since the n.m.r. sample concentration was approximately 10 times greater than those used for the molecular weight determinations.

Can. J. Chem. Downloaded from www.nrcresearchpress.com by 210.87.254.5 on 09/05/12
For personal use only.

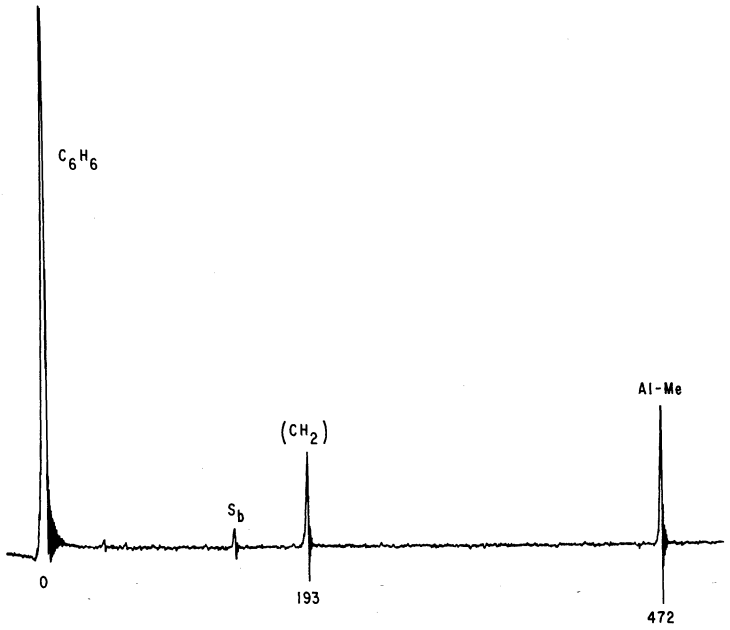

Fig. 2. Nuclear magnetic resonance spectrum of $(Me_3Al)_2{:}(CH_2)_6N_4$.

If *tetrakis*-dimethylaminoethylene is considered to be two $Me_2N—C—NMe_2$ groups connected by a double bond at the center carbon atoms, then the bonding proposed for $Me_3Al{:}Me_2NCH_2NMe_2$ could also apply to this complex. A structure of the type

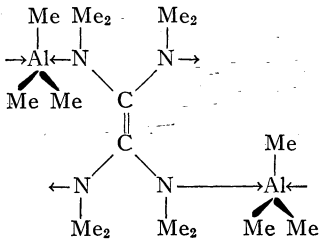

would be consistent with the n.m.r. data at 50° C, for if all Al ← N dative bonds are equivalent, then all Al—Me protons are identical and so are all N—Me protons. The structure of the complex at 5° C may be

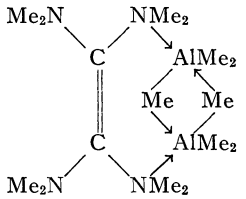

to give the proper number and area ratios to the n.m.r. peaks shown in Fig. 1.

Since n.m.r. is the only technique employed to characterize this complex, it should be noted that other structures are consistent with the observed spectra. An equilibrium

Can. J. Chem. Downloaded from www.nrcresearchpress.com by 210.87.254.5 on 09/05/12
For personal use only.

involving a species recently described by Wiberg and Buchler (6) for the boron trifluoride – *tetrakis*-dimethylaminoethylene complex would also fit the n.m.r. data:

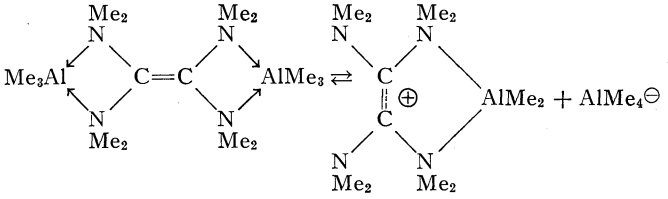

I

and they may also be explained by a structure similar to I in which the system is planar and each $AlMe_3$ molecule is situated above this plane over a pair of nitrogen atoms.

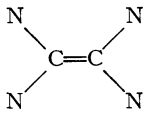

If such a bonding system were "frozen" the protons are in a position such that they may produce the n.m.r. spectrum observed at 5° C. As the Al ← N dative bond system "thaws" and bond rotation is possible, the N—Me protons become identical and so do the Al—Me protons. The selection of the correct structure may be possible from a single crystal X-ray examination.

An anomalous reaction was observed between Me_3Al and $(Me_2N)_2C{=}C(NMe_2)_2$ when the starting ratio of Me_3Al to amine was increased to 4 to 1. Although no methane or ethane was observed, the analysis of the sublimate indicated a formula in which a 2 to 1 complex had formed, but which contained two methyl groups less than that needed for the dative-bonded complex. The structure of such a compound could be

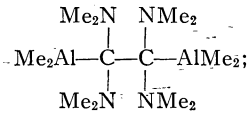

however, structural confirmation must await further study.

Although no n.m.r. spectrum of the aluminum hydride – *tetrakis*-dimethylaminoethylene complex could be made, the elemental analysis indicates a higher carbon content than is required for the simple 2 to 1 complex. Since hydrolysis shows only active hydrogen, the amine appears to have undergone a change which as yet has not been characterized. It should be noted that the aluminum hydride – N,N,N,′N′-tetramethyl-2-butene-1,4-diamine complex also has a high carbon value for the 1 to 1 complex. In this case hydrolysis also showed only active hydrogen. Again, it appears the amine may have undergone rearrangement.

The reaction of $H_3Al{:}NMe_3$ with hexamethylenetetramine appears to have disrupted the amine, because the elemental analysis, for a 1 to 1 complex, agrees best with a formula which is minus one nitrogen atom. The amine also appears to have changed when the starting ratio of Me_3Al to amine is raised to 4 to 1. In this case the analysis of the sublimed product agrees best with a formula which is short one methylene or methyl group and a nitrogen atom. Possible formulas may be $(Me_3Al)_2{:}(CH_2)_5N_3$ or $(Me_3Al){:}(Me_2Al—)(CH_2)_6N_3$.

Can. J. Chem. Downloaded from www.nrcresearchpress.com by 210.87.254.5 on 09/05/12
For personal use only.

This brief study of AlH_3 and Me_3Al amine complexes has posed a few questions which we hope to answer by further investigations. One of these is, why does AlH_3 form only 1 to 1 complexes with amines which are separated by as many as three or four carbon atoms whereas $AlMe_3$ forms 2 to 1 complexes? The linear bonding scheme proposed above would favor 1 to 1 complexing because of the apparent higher stability of the pentacoordinated aluminum atom. However, the fact that $H_3Al{:}NMe_3$ and Me_3Al are employed as starting compounds may have some influence upon the product formed. Repeating this series of reactions with $Me_3Al{:}NMe_3$ may cast some light on this problem. Also, repeating the reactions with bulkier aluminum alkyls may indicate whether steric effects have an influence on stoichiometry.

ACKNOWLEDGMENTS

The authors acknowledge the valuable suggestions made by Dr. Peter J. Slota, Jr. and Dr. Charles P. Haber of the U. S. Naval Ordnance Laboratory, Corona, California; Dr. Frederick E. Brinckman, Jr. of the U. S. Naval Propellant Plant, Indian Head, Maryland; and Dr. Gus Palenik of the U. S. Naval Ordnance Test Station, China Lake, Calif.

This work was supported by funds from the Advanced Research Projects Agency and the U. S. Navy Department, Bureau of Naval Weapons.

REFERENCES

1. N. R. FETTER, B. BARTOCHA, F. E. BRINCKMAN, JR., and D. W. MOORE. Can. J. Chem. **41,** 1359 (1963).
2. N. R. FETTER and B. BARTOCHA. Can. J. Chem. **39,** 2001 (1961).
3. N. R. FETTER and B. BARTOCHA. Can. J. Chem. **40,** 342 (1962).
4. C. W. HEITSCH, C. E. NORDMAN, and R. W. PARRY. Inorg. Chem. **2,** 508 (1963).
5. Private Communication from Gus Palenik, Chemistry Division, U.S. Naval Ordnance Test Station, China Lake, California.
6. N. WIBERG and J. W. BUCHLER. J. Am. Chem. Soc. **85,** 243 (1963).

Can. J. Chem. Downloaded from www.nrcresearchpress.com by 210.87.254.5 on 09/05/12
For personal use only.

THE CONFORMATIONS IN SOLUTION OF *trans*-CYCLOHEXENE DIHALIDES AND *cis*- AND *trans*-1,2-CYCLOHEXANEDIOLS AND DERIVATIVES

R. U. LEMIEUX AND J. W. LOWN[1]

The Department of Chemistry, University of Alberta, Edmonton, Alberta

Received September 20, 1963

ABSTRACT

trans-1,4,4-Trideuteriocyclohexene dichloride, dibromide, and diiodide and the 1,4,4-trideuterio-*cis*- and *trans*-1,2-cyclohexanediols together with their *O*-acetyl, *O*-tosyl, and *O*-isopropylidene derivatives were synthesized. Their nuclear magnetic resonance (NMR) spectral parameters were obtained with a spectrometer operating at 100 Mc.p.s. and employing double irradiation to establish the chemical shifts and the signs of the coupling constants. The interpretation of the data according to expectations based on the Karplus relationship, for dihedral angles and coupling constants, support the conformational equilibria assigned to the *trans*-dichloride and *trans*-dibromide of cyclohexene on the basis of dipole moment measurements (previously published results). The results indicate that *trans*-cyclohexene diiodide exists to about 84% in the diaxial conformation. In the case of the 1,2-cis-disubstituted cyclohexanes, the occurrence of the signal for the 3-hydrogen in trans relation to the 2-hydrogen at lower field than its geminal 3-hydrogen is assigned to the deshielding influence on the 3-hydrogen when in axial orientation by an opposing axial oxygen at the 1-position. Support for this contention was obtained by determination of the chemical shifts of the geminal hydrogens at the 3- and 5-positions of the *cis*- and *trans*-4-*t*-butyl-2,2,6,6-tetradeuterio-1-methylcyclohexanols. The conformational equilibria indicated for the 1,2-diol, 1,2-diacetoxy, and 1,2-ditosyloxy trans derivatives of 1,4,4-trideuteriocyclohexane by NMR parameters obtained from the spectrum of the *O*-isopropylidene derivatives of the *trans*-diol allowed conclusions regarding the non-bonded interaction energies involved. The Karplus relation had to be adjusted to the form, $J_\phi = 14.7 \cos^2\phi - 0.2$ (0°–ϕ–90°) and $J_\phi = 11.2 \cos^2\phi - 0.2$ (90°–ϕ–180°), to accommodate the results. Solvent effects on conformation are noted. Also, the investigation provided further evidence for the opposite signs of the coupling constants for geminal and vicinal hydrogens. A consideration of the chemical shifts observed for a variety of derivatives of cyclohexanol appears to indicate that intramolecular shielding effects are better accounted for on the basis of neighboring atomic groupings than on the basis of individual chemical bonds.

Can. J. Chem. Downloaded from www.nrcresearchpress.com by 210.87.254.42 on 09/05/12
For personal use only.

Attempts have been made previously to study the conformational equilibria of the *trans*-cyclohexene dihalides in benzene solution by the measurement of dipole moments (1) and by observation of the chemical shifts of protons adjacent to the halogen atoms (2). Both of these methods suffer from disadvantages; in the first, it is impossible to estimate the molecular dipole in the diaxial conformation, i.e. of allowing for dipolar contributions from the cyclohexane skeleton (3). The second method requires the assumption that the usual orientational effects on chemical shifts apply (4, 5). This latter assumption, as it transpired, proved to be justified in the case of the *trans*-dihalides but could not have been foreseen and would not have applied to the series of *cis*-1,2-cyclohexane derivatives. Moreover, it would be impossible to study the conformational equilibrium of the diiodide by the dipole method since this compound exists in solution in chemical equilibrium with cyclohexene and iodine. A more attractive approach was to use nuclear magnetic resonance (NMR) spectroscopy to measure appropriate coupling constants. By preparing specifically deuterium-labelled cyclohexene, the NMR spectra of the dihalides could be simplified sufficiently to measure coupling constants which could then be related by the Karplus (6) expression to the corresponding dihedral angles. The actual shape of the molecules could then be examined. It was realized that the theoretical Karplus

[1]*University of Alberta, Postdoctoral Fellow, 1961–62.*

relation, which has been supported by experimental observations (7), has its own limitations (8, 9). However, it was thought to be of interest to show that the two procedures afforded consistent results. This was found to be the case and in addition the NMR coupling constant method gave information on the conformational equilibrium of the diiodide. The method also appeared to provide interesting new insight on ring distortions, conformational equilibria, solvent effects, and orientation effects on chemical shift in the case of the *cis*- and *trans*-1,2-cyclohexanediols and their *O*-acetyl, *O*-tosyl, *O*-*p*-toluenesulphonate, and *O*-isopropylidene derivatives.

1,4,4-Trideuteriocyclohexene was selected as a suitable starting material for the preparation of the corresponding *trans*-dihalides and *cis*- and *trans*-glycols. These afford spectra of the ABX type (10) arising from the protons at the 2,3,3-positions. It turned out that the paramagnetic shift of the substituent at the 2-position on the 2-proton was always sufficient to render the ABX approximation valid. Analysis of the ABX spectra then gave the conformationally averaged coupling constants J_{AX} and J_{BX} from which the dihedral angles could be deduced. Except for the diacetate, the trans compounds gave spectra in good approximation to the AMX type (11).

Cyclohexane-1,4-dione was reduced in tetrahydrofuran with lithium aluminum deuteride, and the resulting 1,4-dideuteriocyclohexane-1,4-diols were dehydrated over alumina (12) to provide 1,4-dideuterio-1,4-epoxycyclohexane, which produced virtually no detectable signal (at 4.6 p.p.m. from internal tetramethylsilane) in the NMR spectrum for hydrogens at the 1- and 4-positions. The maximum hydrogen content at these positions was estimated to be 5%. The epoxide was cleaved in 87% yield to the 1,4-dideuterio-*trans*-4-bromocyclohexanol using hydrogen bromide in diethyl ether at room temperature. Again the NMR spectrum was devoid of signals (at 3.7 and 4.1 p.p.m.) for hydrogens at the 1- and 4-positions. This reaction was found to be much cleaner than that involving the direct action of hydrogen chloride to the epoxide (12). The bromine atom was replaced by deuterium through very rapid deuterolysis in the presence of a palladium-on-charcoal catalyst in methanol containing sodium methoxide. It is noteworthy that no difference in the deuterium content of the product was observed when methanol-*O*-*d* was used as solvent. The resulting 1,4,4-trideuteriocyclohexanol showed no detectable absorption at the position in the NMR spectrum for the 1-hydrogen of cyclohexanol.

Recently, Premuzic and Reeves (13) described the preparation of 1,3,3-trideuteriocyclohexene by the conventional dehydration of 2,2,6,6-tetradeuteriocyclohexanol with orthophosphoric acid, but gave no indication of the extent of deuteration of the product. A similar trial dehydration of our 1,4,4-trideuteriocyclohexanol resulted in complete loss of deuterium by acid-catalyzed exchange, so that this method was abandoned in favor of base-catalyzed cleavage of the tosylate. The *O*-tosyl derivative of the alcohol was treated with potassium hydroxide in dry diethylene glycol to yield 1,4,4-trideuteriocyclohexene (I). Gas–liquid partition chromatography showed the presence of cyclohexene only and integration of the NMR spectrum showed the relative intensities of the ethylenic and methylenic hydrogens to be 1:5.8 (expected for I, 1:6). The spectrum (see Fig. 1) clearly required that the reductions in the intensities of the signals relative to those in cyclohexene be at the 1- and 4-positions. Compound I was converted to the dichloride and the dibromide by halogenations in benzene. The diiodide was prepared by mixing equimolar amounts of I and iodine at about −70°. On warming of the mixture to room temperature, the iodine had dissolved and the resulting mixture was taken up in benzene for the NMR experiment. The *cis*-diol was prepared by osmium tetraoxide oxidation in pyridine (14) and decomposition of the osmiate with sodium bisulphite (15).

Can. J. Chem. Downloaded from www.nrcresearchpress.com by 210.87.254.42 on 09/05/12
For personal use only.

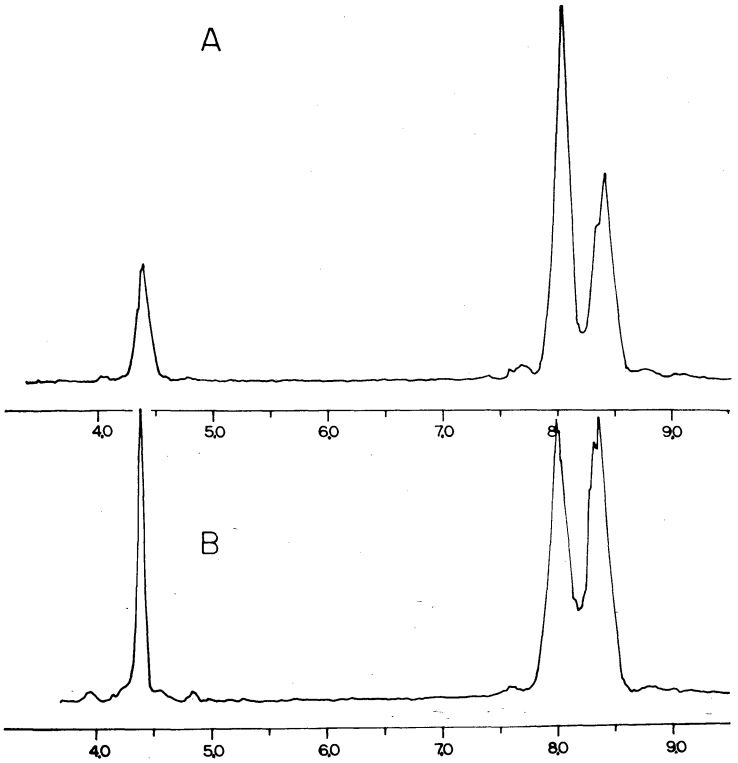

FIG. 1. (A) 1,4,4-Trideuteriocyclohexene. (B) Cyclohexene. Both 5% solutions in CCl_4 at 60 Mc.p.s. with tetramethylsilane (1%) as internal reference. The scale is in τ units.

Performic acid oxidation followed by hydrolysis gave the *trans*-diol (14). Each spectrum showed a clearly resolved triplet or quartet due to the X-proton (which was broadened by neighboring deuterium coupling) but a direct ABX analysis was not possible owing to the overlap of the AB signals by the equivalent protons at the 6-position. The ABX parameters could, however, be determined by the spin decoupling or double resonance method (16–19).

By this means it could be shown that the X-proton was coupled to two and only two other protons at higher field in the methylene envelope, thereby confirming the structures. By measuring the decoupling frequencies, the chemical shifts of the A- and B-protons could be found within two cycles per second. Spin decoupling has been used with considerable success in assigning relative signs of coupling constants in spectra which approximate to first order (16, 17). In view of the theoretical interest in the relative signs of the vicinal and geminal couplings (20–22), it was of interest to determine the relative signs of the coupling constants in these systems. This refinement had added advantages in that it provided an additional consistency check on the measured decoupling frequencies and allowed a rationalization of those experiments (see below) where anomalous double resonance effects occurred owing to a small AB chemical shift as described by Freeman (23). Also the method provided a reasonable estimate of the third coupling constant J_{AB} and so provided all the spectral parameters including the relative signs of the coupling constants. Thus, it was possible to derive better approximations to the true coupling constants and chemical shifts by iterative calculations of theoretical spectra. By using

Can. J. Chem. Downloaded from www.nrcresearchpress.com by 210.87.254.42 on 09/05/12
For personal use only.

the values for the coupling constants and chemical shifts to predict the appearance of the experimentally observable X-part of the ABX spectrum at both 60 and 100 Mc.p.s., an additional check on the accuracy of the derived parameters was obtained.

Valuable qualitative information is obtained directly by this selective decoupling of the individual groups of A and B transitions in that one can tell from the appearance of a decoupled quartet which proton, high field or low field (B or A by definition), gives rise to the larger coupling.

Spin decoupling may be carried out with the integrator of the Varian 100 Mc.p.s. spectrometer (24). The observed frequency difference, Δw, which produces optimum decoupling is not exactly equal to the chemical shift difference of the two spin-decoupled nuclei. Anderson and Freeman (25) have shown that, for two sets of nuclei whose chemical shifts are w_A and w_X, the condition for optimum decoupling is given by the expression,

$$\Delta w = w_A - w_X - (\gamma H_2)^2/2(w_A - w_X),$$

where H_2 is the decoupling radio-frequency field strength and γ is the magnetogyric ratio of the proton. For nuclei with large relative chemical shifts such as are considered here the correction term $(\gamma H_2)^2/2(w_A - w_X)$ is small and $\Delta w \simeq (w_A - w_X)$. An estimate of the magnitude of the correction to be made in the least favorable case gave a value of 0.2 c.p.s., which was considered negligible.

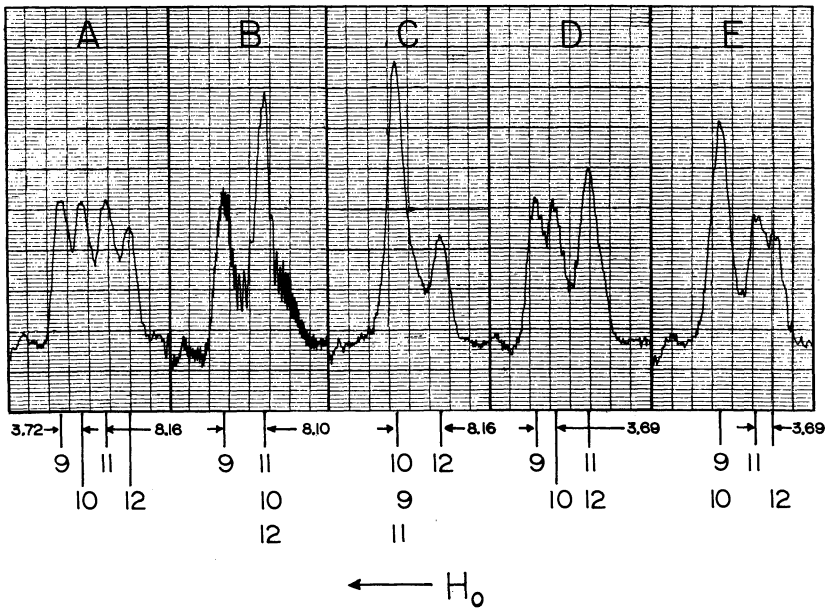

FIG. 2. The signal for the 2-hydrogen (X-part) of *trans*-1,4,4-trideuteriocyclohexene dichloride, taken at 100 Mc.p.s. in benzene at room temperature, showing the effects of double irradiation performed with first lower sideband. (A) Single resonance spectrum. (B) With double irradiation frequency at 239.8 c.p.s. (C) With double irradiation frequency at 223.7 c.p.s. (D) With double irradiation frequency at 179.8 c.p.s. (E) With double irradiation frequency at 160.8 c.p.s.

It was anticipated that the geminal coupling J_{AB} would be large, ca. 12 c.p.s., and experience showed that δ_{AB} was about 50 c.p.s. for the *trans*-dihalides at 100 Mc.p.s. Consequently, the general appearance of the ABX spectra would be three widely separated sets of quartets. For reference purposes, the 12 transitions are numbered with decreasing

Can. J. Chem. Downloaded from www.nrcresearchpress.com by 210.87.254.42 on 09/05/12
For personal use only.

field from 1 to 12. The possibility arises of irradiating the branches of the A- and B-quartets selectively so that four decoupling frequencies are measured. The relative signs of the coupling constants may be deduced from the appearance of the decoupled multiplet (18). The determination of relative signs of coupling constants in this way is illustrated by the appearance of the X-proton quartet of the *trans*-dichloride in Fig. 2. It can be seen from Fig. 2 that when the largest decoupling frequency, which must necessarily correspond to the 1- and 2-transitions, is employed there resulted a collapse of lines 10 and 12. The next lowest decoupling frequency irradiates the 3- and 4-transitions and caused the collapse of lines 9 and 11. This showed that J_{AX} and J_{AB} are of opposite sign and also that J_{BX} is greater than J_{AX}. This result is in accordance with the usual orientational effects on chemical shifts in 6-membered rings (4). A similar experiment carried out by irradiating in the region of the A-nucleus confirmed that J_{AB} and J_{BX} are opposite in sign and that J_{AX} was the smaller constant. It thus followed that, as expected (20–23), the signs of the coupling constants for vicinal hydrogens were opposite to that for the geminal hydrogens.

It follows that the four decoupling frequencies observed will be given by the following expressions:—

Lines irradiated		Decoupling frequency (c.p.s.)	
1 and 2		$\delta_{BX} + \frac{J_{AB}}{2} + \frac{J_{AX}}{2}$	(1)
	B-quartet		
3 and 4		$\delta_{BX} - \frac{J_{AB}}{2} - \frac{J_{AX}}{2}$	(2)
5 and 6		$\delta_{AX} + \frac{J_{AB}}{2} + \frac{J_{BX}}{2}$	(3)
	A-quartet		
7 and 8		$\delta_{AX} - \frac{J_{AB}}{2} - \frac{J_{BX}}{2}$	(4)

where δ_{BX} etc. represent the chemical shifts in c.p.s. Therefore, the difference between expressions 1 and 2 equals $J_{AB}+J_{AX}$; similarly the difference between expressions 3 and 4 equals $J_{AB}+J_{AX}$. It can be shown that the calculated separations of the X-quartet are very insensitive to the magnitude of J_{AB}, therefore an estimate of J_{AB} could be obtained from the differences in decoupling frequencies by subtracting the corresponding spacings of the quartet measured at 100 Mc.p.s.

Thus, two estimates of J_{AB} are obtained from decoupling of the B- and A-protons, respectively. Now by substituting the approximate values of J_{AB}, J_{AX}, and J_{BX} in equations 1 to 4, values could be obtained for the positions of the four branch lines of the unperturbed AB-quartet, the simple AB analysis then furnished the chemical shifts of the A- and B-protons.

It is seen from Tables I and II that the chemical shifts of the A-, B-, and X-protons were usually large. However, for certain compounds, particularly the *trans*-diacetate and the *cis-O*-isopropylidene compounds, δ_{AB} was quite small. Consequently, transitions 3 and 4, and 5 and 6, of the ABX spectrum tended to overlap or at least be so close together that irradiation of transitions 5 and 6, for example, tended to perturb transitions 3 and 4 (26). Thus, no precise decoupling frequencies could be measured in this region of the spectrum. However, clear-cut spin decoupling was achieved at the outer regions, that is, by irradiation of transitions 1 and 2 of the B-proton and transitions 7 and 8 of the A-proton. The values for δ_A and δ_B were then derived by using the value for J_{AB} obtained

Can. J. Chem. Downloaded from www.nrcresearchpress.com by 210.87.254.42 on 09/05/12
For personal use only.

TABLE I

NMR spectral parameters for *trans*-1,4,4-trideuteriocyclohexene dihalides*

Compound	X-spacings, c.p.s.	Chemical shifts, p.p.m. (TMS)			Calc. coupling constants, c.p.s.†		
		δ_A	δ_B	δ_X	J_{AX}	J_{BX}	J_{AB}
1. Dichloride	3.72, 8.16	1.99	1.39	3.70	3.72	8.16	−12
2. Dibromide	3.69, 5.57	2.10	1.50	4.11	3.69	5.57	−11
3. Diiodide	3.36, 3.36	2.00	1.56	4.73	3.36	3.36	−12

*Determined in benzene at 100 Mc.p.s. and room temperature (about 25°).
†The negative sign is based on the evidence recently presented by Anet (28).

TABLE II

NMR spectral parameters for the *cis*- and *trans*-1,4,4-trideuterio-1,2-cyclohexanediols and derivatives*

	Solvent	X-spacings, c.p.s.	Chemical shifts, c.p.s.† (TMS)			Calculated coupling constants			$J_{AX} + J_{BX}$, c.p.s.
		100 Mc.p.s.	δ_A	δ_B	δ_X	J_{AX}	J_{BX}	J_{AB}	
cis-Compounds									
Di-*O*-acetyl	CCl_4	3.62 6.98	180	157	492	7.1	3.6	−11	10.7
Diol	$CHCl_3$	3.79 7.11	177	153	375	7.1	3.8	−11	10.9
Diol	D_2O	4.29 6.50	218	194	421	6.7	4.1	−11	10.8
Di-*O*-tosyl	$CHCl_3$	2.77 7.72	196	154	451	7.8	2.7	−12	10.5
O-Isopropylidene	CCl_4	5.4 5.4	181	154	396	5.4	5.4	−12	10.8
trans-Compounds									
Di-*O*-acetyl	CCl_4	4.20 10.15	141	129	468	3.5	11.0	−11	
Diol	$CHCl_3$	4.55 11.06	192	123	330	4.5	11.0	−11	
Diol	D_2O	4.26 10.91	240	171	384	4.1	10.5	−12	
Di-*O*-tosyl	$CHCl_3$	3.62 7.82	196	148	440	3.6	7.9	−12	
O-Isopropylidene	CCl_4	3.46 10.99	205	137	310	3.5	11.0	−12	

*The parameters are expressed to the nearest significant figure.
†At 100 Mc.p.s.

for the isomers. It was found that the calculated values for J_{AX} and J_{BX} were quite insensitive to the value of J_{AB} in the range 11 to 12 c.p.s.

$$nJ_{aa} + (1-n)J_{ee} = J_{BX} \quad (5)$$

$$nJ_{ae} + (1-n)J_{ea} = J_{AX} \quad (6)$$

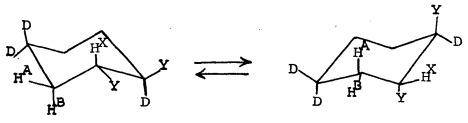

II III

The NMR results obtained for the *trans*-dihalides allow the following conclusions to be drawn. With respect to their relative magnitudes, J_{AX} and J_{BX} represent the weighted averages of the coupling constants for the *cis*- and *trans*-hydrogens, respectively (equations 5 and 6). Judging from structurally closely related compounds wherein the halogens (Y) are axial, only the chair conformations II and III need be considered (27). Bender, Flowers, and Goering (1) have estimated by dipole moment studies that the fraction, n, in the diequatorial form (II) is 0.75 and 0.43 for the dichloride and dibromide, respectively. Substitution of these values for n and the appropriate values for J_{AX} and J_{BX}

Can. J. Chem. Downloaded from www.nrcresearchpress.com by 210.87.254.42 on 09/05/12
For personal use only.

given in Table I into expressions 5 and 6 provides the values $J_{aa} = 10.2$, $J_{ee} = 2.04$, $J_{ae} = 3.74$, and $J_{ea} = 3.66$ c.p.s. These values are in excellent agreement with those to be expected (28) and thus provide confirmation of the significance attached to the dipole moment data. To the extent to which the results from the two methods are in agreement, the assumption that the cyclohexane skeleton makes a negligible contribution to the molecular dipole in the diaxial conformation is justified (1, 3).

Substitution of the above values for J_{aa} and J_{ee} and the value for J_{BX} obtained from the diiodide in equation 5 suggests that this compound exists in benzene at room temperature to an extent of about 84% in the conformation wherein both iodines are in axial orientation. Since the chemical shift for the A- and B-hydrogens (44 c.p.s.) is more than three times greater than J_{AB} the condition is met that the triplet is not degenerate and J_{AX} does equal J_{BX} (29). It is pertinent in this regard that the coupling constant of the 1-hydrogen with the vicinal hydrogens in a number of 2,6-disubstituted cyclohexyl iodides were found (30) to be of the magnitude (necessarily greater than the observed spacings, 9 and 2.5 c.p.s., for hydrogens in trans and gauche relations, respectively) expected on the basis of the present results.

It must be noted that the NMR data taken together with the dipole moment data can only indicate that the hydrogens at the 1- and 2-positions of the *trans*-1,2-dihalogenocyclohexanes are both well staggered with the hydrogens on the vicinal carbon atoms when the halogens are in axial orientation (III). It seems likely that the erection of the halogens into axial orientation to achieve conformation III will cause some distortion of the opposite side of the ring in the direction which will increase the internuclear distance between the halogens and the opposing axial hydrogens. This condition seems likely in view of the results, discussed below, obtained with the di-*O*-tosyl-*cis*-1,2-cyclohexanediol.

TABLE III

Effect of solvent on the conformational equilibria for *trans*-cyclohexene dihalides

Compound	Solvent	Dielectric constant at 20°*	Approx. coupling constants, c.p.s.		n†
			J_{AX}	J_{BX}	
Dichloride	CCl_4	2.24	3.6	6.8	0.58
Dichloride	CH_3CN	37.50	3.7	8.9	0.84
Dibromide	CCl_4	2.24	3.9	4.0	0.24
Dibromide	CS_2	2.64	4.1	4.1	0.25
Dibromide	$CHCl_3$	4.81	4.1	4.2	0.26
Dibromide	$CHBr_3$	4.39	3.7	5.7	0.45
Dibromide	$(CH_3)_2CO$	20.7‡	3.7	6.7	0.57
Dibromide	CH_3CN	37.5	4.1	7.1	0.62

*National Bureau of Standards Circular 514.
†Fraction of conformation II calculated from expression 6, with $J_{aa} = 10.2$ and $J_{ee} = 2.04$ c.p.s.
‡Value at 25° C.

Having established the close correspondence between the results obtained from the dipole moment and NMR studies, it would be predicted that the conformationally averaged spacings would be dependent on the dielectric constant of the solvent. The greater the dielectric constant the greater should be the population of the more polar diequatorial conformation (II). Accordingly, the spacings of the X-quartet for the dichloride and the dibromide dissolved in a number of solvents were determined at

Can. J. Chem. Downloaded from www.nrcresearchpress.com by 210.87.254.42 on 09/05/12
For personal use only.

60 Mc.p.s. (Table III). Since it has been established that the spectra in benzene are close to the AMX type, the spacings can be expected to be approximately equal to J_{AX} and J_{BX}. On this basis, the values for the fraction n of the compounds in the diequatorial conformation II were estimated. It is seen that the quantitative prediction is borne out and illustrates the advantage of the NMR technique for the study of conformational equilibria in highly polar solvents (31).

An inspection of a conformational Barton model allows the conclusion that the dihedral angles defined by the 2-hydrogen of *O*-isopropylidene-*trans*-1,2-cyclohexanediol with the hydrogens at the 3-position are very close to 60° and 180°. Therefore it was concluded from the data in Table III that for this compound $J_{AX} = J_{60°} = 3.5$ c.p.s. and $J_{BX} = J_{180°} = 11.0$ c.p.s. These values are in excellent agreement with those observed by Anet for similar groupings in cyclohexane rings (28). The above value for $J_{60°}$ requires an upward displacement in this region of the original Karplus curve (6) by 1.65 c.p.s. A simple upward displacement of the whole curve would yield $J_{90°} = 1.37$ c.p.s., a value which is not acceptable in view of the evidence that $J_{90°}$ invariably is very small (6, 7, 32).

For the cis compounds listed in Table III, the observed coupling constants must represent the average coupling of the *cis*- and *trans*-3-hydrogens with the 2-hydrogen, respectively, in the two energetically equivalent chair conformations IV and V. Therefore,

$$J_{ae}+J_{ea} = 2J_{BX} \text{ and } J_{aa}+J_{ee} = 2J_{AX}.$$

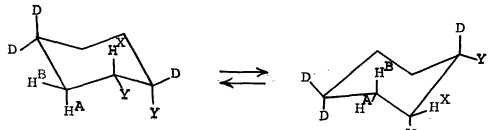

IV V

In view of the near linearity of the Karplus curve in the vicinity of 60°, the sum $J_{ee}+J_{ea}$ should be near constant, and J_{aa}, being only slightly dependent upon dihedral angle in the region 170° to 180°, should have very nearly the same value for all the compounds. Therefore, assuming $J_{ae} = J_{60°} = 3.5$ c.p.s. and $J_{aa} = J_{180°} = 11.0$ c.p.s. it would be expected that for the cis compounds,

$$J_{AX}+J_{BX} = (J_{180°}+3J_{60°})/2 = 10.75 \text{ c.p.s.}$$

It is seen in Table II that the values found for $J_{AX}+J_{BX}$ are in excellent general agreement with this expectation. Evidence has been obtained that the cis compounds exist in solution in the chair forms (33). The slight difference between the shift for unbonded and bonded hydroxyl infrared frequency of 39 cm^{-1} for the *cis*-diol and 32 cm^{-1} for the trans isomer has been ascribed (34) to deformation of the cis compound from the perfect chair. The hydroxyl groups are said to be able to approach each other more readily in the *cis*- than in the *trans*-diol. A similar explanation has been advanced to explain the slightly greater reactivity of the *cis*-diol towards cleavage by lead tetraacetate (35).

Should the cis compounds exist in undistorted chair forms, one would expect $J_{AX} = 7.25$ c.p.s. and $J_{BX} = 3.5$ c.p.s. Indeed, values very close to these were found in the case of the *cis*-diacetate and of the *cis*-diol when dissolved in chloroform. However, the high value for $J_{BX} = 4.1$ c.p.s. and the low value for $J_{AX} = 6.7$ c.p.s. for the *cis*-diol when dissolved in deuterium oxide infer appreciable distortion of the chair for this compound in aqueous solution. The result, as expected, seems best explained on the basis of a dihedral angle of less than 60° for the oxygen atoms. However, it is to be noted that the distortion is

Can. J. Chem. Downloaded from www.nrcresearchpress.com by 210.87.254.42 on 09/05/12
For personal use only.

probably related to the hydration of the hydroxyl groups rather than simple intramolecular hydrogen bonding since the distortion was not present for the compound dissolved in chloroform. Thus, the apparent ring distortion brought on by intramolecular hydrogen bonding when the compound is dissolved at high dilution in carbon tetrachloride (34) must be imposed on the molecule by the state of dilution which has rendered intermolecular hydrogen bonding unfavorable.

The value, 5.4 c.p.s., found for both J_{AX} and J_{BX} in the case of the *cis*-isopropylidene compound requires considerable distortion of the cyclohexane ring (36, 37). Because of unusually strong deuterium broadening of the signal, these coupling constants are not known to better than ± 0.2 c.p.s. Should expressions of the type proposed by Karplus allow an interpretation of these results, in view of the data contained in Table II and the above considerations regarding $J_{90°}$, the following expressions are indicated.

$$J_\phi = 14.7 \cos^2\phi - 0.2 \quad (0° \leq \phi \leq 90°), \tag{7}$$

and

$$J_\phi = 11.2 \cos^2\phi - 0.2 \quad (90° \leq \phi \leq 180°). \tag{8}$$

On this basis, with $\phi_{ae} = \phi_{ea} = 50°$, $\phi_{aa} = 170°$, and $\phi_{ee} = 70°$, the values $J_{AX} = J_{BX} = 5.9$ c.p.s. are obtained. Although these values are in reasonably close agreement with those determined experimentally, a somewhat greater distortion was anticipated on the basis of a conformational model.

The values for J_{AX} and J_{BX} found for the ditosylate appear to require $J_{ee} > J_{60°}$ and $J_{ea} < J_{60°}$. The only distortion apparent from a study of conformational models that can provide such a condition is that wherein the 3-, 4-, and 5-carbons have moved toward coplanarity with the 1-carbon (the position of the axial tosyloxy group). Such a distortion is plausible since it provides a relief of the congestion between the axial tosyloxy group and the opposing axial hydrogens.

The values of J_{BX} ($\simeq J_{aa}$) for the *trans*-diol when dissolved in chloroform and deuterium oxide require the compound to exist almost entirely in the diequatorial orientation in both solvents. This situation could not necessarily be anticipated from the published values for the non-bonded interaction energies involved. The experimentally determined free-energy differences between equatorial and axial hydroxyl groups in aprotic solvents have been estimated (3, p. 236) to be 0.5 (pyridine), 0.4 (carbon disulphide), and 1.0 (carbon tetrachloride) (28) kcal/mole. The differences (so-called A-values) seem greater in protic solvents (3, p. 236); 0.8 (75% aqueous acetic acid), 0.9 (water), 0.96 (isopropanol), 1.25 (deuterium oxide) (28). This change in A-value on change from aprotic to protic solvents has been assigned to solvation phenomena (38, 39). For the purpose of illustrating the present status of our appreciation of the conformation of the *trans*-diol, it is useful to assume average A-values for the hydroxyl group of 0.6 kcal/mole (aprotic solvent) and 1.0 kcal/mole (protic solvent). Only one value has been reported for the non-bonded interaction free energy of hydroxyl groups in gauche relation, namely, 0.35 kcal/mole (40) (we propose the term G-value for this type of non-bonded interaction free energy). On this basis, it was to be anticipated that the conformational equilibrium constant toward the diequatorial conformation (II) at ordinary temperatures for *trans*-1,2-cyclohexanediol should be about 4 for aprotic solvents and about 16 for protic solvents. These constants would require J_{BX} to have values of 9.5 and 10.7 c.p.s., respectively. The value of 9.5 c.p.s. is significantly lower than the experimentally determined value of 11.0 c.p.s. for the *trans*-diol dissolved in chloroform. Clearly, however, because of the possibility of intramolecular hydrogen bonding the G-value for hydroxyl groups can be expected

Can. J. Chem. Downloaded from www.nrcresearchpress.com by 210.87.254.42 on 09/05/12
For personal use only.

to be appreciably dependent on solvent. However, the values found for J_{AX} suggest that such intramolecular bonding effects are negligible at the concentrations required for the NMR experiments. That is, the values of 4.5 and 4.1 c.p.s. observed for J_{AX} reflect a distortion of the cyclohexane ring in the direction which will decrease the dihedral angle defined by the A- and X-hydrogens in the diequatorial conformation (II). This situation can only be achieved by the hydroxyl groups moving somewhat further apart than in the ideal chair form. On the basis of the expressions 7 and 8, only very slight distortions are necessary. Thus, for the *trans*-diol, a dihedral angle of about 58° is indicated for the A- and X-hydrogens when the solvent is either chloroform or water. Our results are best explained using the A-values for the hydroxyl group of 1.25 kcal/mole in deuterium oxide and 1.0 kcal/mole in carbon tetrachloride determined by Anet (28). This conclusion rests on the assumption that the non-bonded interaction energy between two hydroxyl groups in gauche relation (G-value) has the value of 0.35 kcal/mole estimated by Angyal and McHugh (40). The above noted distortions require a repulsion between the hydroxyl groups in the *trans*-diol. It does not seem likely that this repulsion can be substantially less than 0.35 kcal/mole.

A-values of 0.66 kcal/mole (28) and 0.7 kcal/mole (3, p. 236) have been reported for the acetoxy group. The values, $J_{AX} = 3.5$ c.p.s. and $J_{BX} = 10.9$ c.p.s., found for the *trans*-diacetate obviously require the compound to exist essentially only in the diequatorial orientation. Evidently, the G-value for acetoxy groups must be small. Setting this value at 0.35 kcal/mole (the value for the hydroxyl groups) and using an A-value of 0.7 kcal/mole, one would expect the compound to exist to an extent of 85% in the diequatorial orientation, in poor agreement with the NMR data. However, this G-value must be a maximum value in view of the correspondence of J_{AX} with $J_{60°}$. On the other hand, it is difficult to conceive why the A-value for the acetoxy group should be substantially less than for the hydroxyl group. We therefore arbitrarily propose that A- and G-values for the acetoxy groups of 1.0 and 0.2 c.p.s., respectively, are in best agreement with the present data. On this basis, the compound would exist to an extent, 95%, compatible with the NMR data ($J_{BX} = 10.7$ c.p.s.). The low G-value presumably could arise from attractive dipole–dipole interactions between the acetyl groups tending to offset the repulsive non-bonded interactions.

In the case of the *trans*-ditosylate, assuming $J_{aa} = 11.0$ c.p.s. and J_{ee} is in the range 2.6–3.5 c.p.s., since $J_{BX} = 7.9$ c.p.s., it would follow that 59% to 63% of the compound resides in the diequatorial conformation. There thus appears to be a considerably stronger repulsion between tosyloxy groups in *gauche*-orientation than in the case of acetoxy groups. On the basis of the reasonable assumption that the A-value of the tosyloxy group is the same as for the hydroxyl group in aprotic solvents, namely 1.0 kcal/mole, a G-value for the tosyloxy group of 1.8 kcal/mole is indicated. This high value is consistent with the conformational properties of the *trans*-dihalides and provided a basis for explaining the difficulty often experienced in attempts to completely tosylate carbohydrate structures.

It is seen in Table II that the A-protons of the cis compounds are more strongly coupled with the X-proton than are the B-protons. This difference in coupling must arise from the strong coupling to be expected between the 2- and 3-*trans*-hydrogens in conformation IV. Therefore, the A- and X-protons of the cis compounds must be in trans relation as shown in IV and V. The chemical shifts observed for the ring hydrogens of sugars and their derivatives were found to require the assignment of magnetic shielding of an axial hydrogen by an opposing, axially oriented C—O bond (41). On this basis, it

Can. J. Chem. Downloaded from www.nrcresearchpress.com by 210.87.254.42 on 09/05/12
For personal use only.

Can. J. Chem. Downloaded from www.nrcresearchpress.com by 210.87.254.42 on 09/05/12
For personal use only.

could be anticipated that the A-protons of the cis compounds are deshielded relative to the B-protons because of the occurrence of this diaxial arrangement involving the A-protons when in conformation IV. To better assess the magnetic shielding of axial C—O bonds relative to C—CH_3 bonds on opposing axial hydrogens, it was decided to examine the NMR spectra of the *cis*- and *trans*-4-*t*-butyl-2,2,6,6-tetradeuterio-1-methylcyclohexanols. In the case of the *trans*-isomer, wherein the hydroxyl is equatorial, and using carbon tetrachloride as solvent, a rough doublet of intensity 2 centered at 1.7 p.p.m. was assigned to the two equivalent equatorial hydrogens at the 3- and 5-positions. The signals for the geminal axial hydrogens on the basis of intensity measurements appeared to be about 1.0 p.p.m., a position in the field about half-way between the signals for the two kinds of *C*-methyl peaks in the molecule. This chemical shift between the geminal hydrogens at the 3- or 5-positions of about 0.70 p.p.m. is assumed to arise mainly from the diamagnetic anisotropy of the neighboring C—C bonds (42). On the other hand, the spectrum of the *cis*-isomer required both the axial and equatorial hydrogens at the 3- and 5-positions to produce their signal at about the same positions, 1.47 p.p.m. Thus, as expected, the axial hydroxyl has a deshielding effect on the opposing axial hydrogens. The signals for the axial and equatorial hydrogens at the 3- and 5-positions of *trans*-4-*t*-butyl-2,2,6,6-tetradeuteriocyclohexanol under the same conditions were at about 1.0 and 1.8 p.p.m., respectively. A comparison of these chemical shifts with those given above for the 1-*C*-methyl derivative (1.0 and 1.7 p.p.m., respectively) shows the influence of an axial C—CH_3 bond on the chemical shift of an opposing axial hydrogen to be much less than that of a C—OH bond. Since substantially the same results were obtained with pyridine as the solvent, it seems clear that the shielding effects noted are intramolecular in origin.

In conclusion, it is of interest to note that the chemical shifts of the ring hydrogens of cyclohexane and its derivatives appear best rationalized as a first rough approximation (±0.1 p.p.m.) through a consideration of the inductive effects of substituent groups and of the shielding effects from neighboring *groups of atoms* rather than individual chemical bonds. Tau values are used in the following discussion to simplify the presentation. Shielding effects were derived by inspection of the chemical shifts observed in the variety of compounds considered using the chemical shift of the equatorial hydrogens of cyclohexane 8.35 τ (43), as the reference point in the magnetic field. Using Anet's data (28),* the inductive effect of an hydroxyl group on the chemical shift of a hydrogen situated on the same carbon was set at -2.20 τ and on a vicinal carbon at -0.20 τ. Furthermore, the effect on the chemical shift of a hydrogen of projecting between H—C—H, H—C—OH, H—C—CH, and CH—C—OH groupings was estimated to be about 0.0, 0.0, 0.25, and 0.50 τ, respectively. Also, the effect on the chemical shift of an axial hydrogen of being opposed by an axial hydroxyl was set at 0.50 τ. On this basis, it would be anticipated that the equatorial hydrogens at the 2- and 6-positions of the *cis*- and *trans*-4-*t*-butylcyclohexanols and at the 3- and 6-positions of *trans*-1,2-cyclohexanediol would produce their signals at 8.15 τ. The chemical shifts actually observed were 8.23, 8.08, and 8.08 τ, respectively. The 1-hydrogen of *cis*-4-*t*-butylcyclohexanol would be expected to give its signal at 6.15 τ; the observed position was 6.06 τ. The calculations of the chemical shifts for these equatorial hydrogens involved only the inductive effects. However, the shielding effects of neighboring groups influence strongly the chemical shifts of axially oriented hydrogens. Thus, the chemical shifts for the axial hydrogens at the 2- and 6-positions of *trans*-4-*t*-

The authors wish to thank Professor Anet for providing them prior to publication with the chemical shifts of the ring hydrogens of the cis- and trans-4-t-butylcyclohexanols deuterated at the 3-, 4-, and 5-positions.

butylcyclohexanol and at the 3- and 6-positions of *trans*-1,2-cyclohexanediol would both be expected to be at 8.35 + 0.50 + 0.25 − 0.20 = 8.90 τ. The values observed are 8.88 and 8.77 τ, respectively. The position of the 1-hydrogen of *trans*-4-*t*-butylcyclohexanol would be expected at 8.35 + (2×0.25) − 2.20 = 6.65 τ, found 6.62 τ. The signal of the 1- (or 2-) hydrogen of *trans*-1,2-cyclohexanediol would be expected to occur at 8.35 + 0.50 + 0.25 − 2.20 − 0.20 = 6.70 τ, the chemical shift actually observed. In the case of the axial 2- or 6-hydrogens of *cis*-4-*t*-butylcyclohexanol, a chemical shift of 8.35 + (2×0.25) − 0.20 = 8.65 τ is expected. The shift found for this hydrogen was 8.63 τ. A consideration of the chemical shifts for the A-, B-, and X-hydrogens of *cis*-1,2-cyclohexanediol in equal populations of the conformations IV and V gave the following results. The A-hydrogen would be expected to produce its signal at 8.35 + 0.50 + 0.25 − 0.50 − 0.20 = 8.40 τ and at 8.35 − 0.20 = 8.15 τ in conformations IV and V, respectively. Thus, an averaged value of 8.28 τ would be expected which compared well with the observed value of 8.23 τ. In the case of the B-hydrogen, chemical shifts of 8.35 − 0.20 = 8.15 τ and 8.35 + (2×0.25) − 0.20 = 8.65 τ would be expected for conformations IV and V, respectively, with an averaged value of 8.40 τ. The value observed was 8.47 τ. Thus, the relative positions of the A- and B-hydrogens are rationalized. The X-hydrogen would be expected to produce its signal at 8.35 + (2×0.25) − 2.20 − 0.20 = 6.45 τ and 8.35 − 2.20 − 0.20 = 5.95 τ in the IV and V conformations, respectively. The average of these values 6.20 τ, is in good agreement with that observed, 6.25 τ. The agreement could be improved by the introduction of further parameters. However, such refinements would only obscure the main point of the discussion, which is to indicate that reasonably good agreement can be achieved by the addition of shielding effects arising from neighboring groups of atoms. This was not possible when only individual neighboring bonds were considered. The same situation was found to be the case in an attempt to rationalize the chemical shifts observed (4) for the ring hydrogens of isomeric benzene hexachlorides. Reasonable agreement was only obtained when shielding effects were assigned to H—C—Cl, H—C—CH, CH—C—Cl, and axial C—Cl groups in the manner described above for the alcohols.

EXPERIMENTAL

Nuclear Magnetic Resonance Spectra and Double Irradiation Experiments

Solutions, 5–10% (w/v), were prepared in suitable solvents containing 0.5% tetramethylsilane as internal reference. Spectra were first recorded conventionally at 60 Mc.p.s. on a Varian Associates A-60 spectrometer and at 100 Mc.p.s. on a Varian model H.R. 100 spectrometer and line positions calibrated in both cases by the sideband technique using a Hewlett-Packard audiofrequency oscillator model 200AB and electronic counter model 521C. It is possible to operate in the sideband mode by altering the modulation level and altering the audio phase by 90°. Ordinary absorption spectra differing only in sign are then obtained by using the upper or lower 2 kc.p.s. sideband (w_1). Additional field modulation at a variable frequency w_2 c.p.s. can make a portion of the residual rf power available for selective nuclear saturation in the w_1 sideband spectrum. In this way, proton–proton spin decoupling is obtained (24). When operating on the first lower w_1 sideband (which was used throughout these experiments) protons with chemical shifts at higher applied fields (the A- and B-protons) may be decoupled in turn from the X-proton by setting ($w_2 - w_1$) approximately equal to the chemical shifts δ_{AX} or δ_{BX}. Due care was taken to reduce the modulation amplitude so that the observed X-lines were not broadened by saturation. To confirm that successful decoupling had been accomplished, a check was made that the X-quartet or triplet regained its original shape as ($w_2 - w_1$) was increased beyond the optimum decoupling value. Several determinations were made of decoupling frequency for each substance and the results are summarized in Tables IV, V, and VI. In general, as seen from Table II, the agreement between the sums of the X-spacings and the calculated coupling constants ($J_{AX} + J_{BX}$) was as good as the measurement of the spacings (±0.2 c.p.s.). Judging from results with other compounds involving similar chemical shifts, the discrepancy in the case of the *trans*-diol in deuterium oxide must be the result of experimental errors and J_{AX} and J_{BX} likely have values closer to the values reflected by the X-spacings for this compound.

All melting points were determined in capillaries and are uncorrected.

Can. J. Chem. Downloaded from www.nrcresearchpress.com by 210.87.254.42 on 09/05/12
For personal use only.

TABLE IV

Double irradiation experiments on *trans*-1,4,4-trideuteriocyclohexene dihalides* in benzene

Compound	Proton and lines irradiated	Decoupling frequencies,† c.p.s.	Lines collapsed	Appropriate measured spacings,‡ c.p.s.	J_{AB}, c.p.s.	Chemical shifts,§ c.p.s. δ_A	δ_B
Dichloride	B (1 and 2)	239.8	10, 12	3.72	12.38	199	139
	B (3 and 4)	223.7	9, 11				
	A (5 and 6)	179.8	11, 12	8.16	10.84		
	A (7 and 8)	160.8	9, 10				
Dibromide	B (1 and 2)	268.7	10, 12	3.69	11.20	210	150
	B (3 and 4)	253.8	9, 11				
	A (5 and 6)	208.2	11, 12	5.57	11.00		
	A (7 and 8)	191.6	9, 10				
Diiodide	B (1 and 2)	325.3	10, 12	3.36	11.10	200	156
	B (3 and 4)	309.1	9, 11				
	A (5 and 6)	279.4	11, 12	3.36	12.80		
	A (7 and 8)	264.9	9, 10				

*In each case the measurements were made on the signal for the X-proton.
†Average of three to four determinations.
‡These spacings were substituted in either expressions 1 and 2 or 3 and 4 to obtain J_{AB}.
§These shifts are those deduced as described in the text.

trans-1,4,4-Trideuteriocyclohexene

A solution of 26 g of cyclohexane-1,4-dione (L. Lights and Co., purified by sublimation) in 100 ml of purified anhydrous tetrahydrofuran was added dropwise to a rapidly stirred suspension of 5 g of lithium aluminum deuteride (98%) in 100 ml of anhydrous tetrahydrofuran over a period of 1 hour. A considerable quantity of white insoluble complex separated and the mixture became very viscous. After complete addition of the dione the mixture was stirred at room temperature for 12 hours, cooled in ice, and treated cautiously with 20 ml of ice water with rapid stirring, followed by 100 ml of ice-cold 2 *N* sulphuric acid. The organic layer was removed and the aqueous layer saturated with sodium chloride and extracted three times with ether. The combined extract was dried over magnesium sulphate and filtered, and the solvents evaporated. The combined yield of *cis*- and *trans*-1,4-dideuteriocyclohexane-1,4-diols, obtained as a waxy solid from three similar preparations, was 70.5 g, 88%. The mixture of diols was used without further purification.

A mixture of 70 g of reagent aluminum oxide (which had been freshly roasted to drive off absorbed water, and cooled) and 70.5 g of *cis*- and *trans*-cyclohexane-1,4-diols was heated to 240–250° under a Vigreux column for 6 hours and the distillate collected. The organic layer of the distillate was removed and the aqueous layer extracted with ether (3×15 ml). The combined extract was dried over magnesium sulphate, filtered, and fractionated at atmospheric pressure through a spinning-band column. The 1,4-dideuterio-1,4-epoxycyclohexane distilled at 115° at 700 mm (b.p. for hydrogen analogue, 117–118° (12)). The yield was 12.05 g, 20.5%. Gas–liquid chromatographic analysis of the product on a silicone oil column at 80° showed the product to be pure. The NMR spectrum showed no detectable absorption at 4.66 p.p.m. from internal tetramethylsilane at the position expected for the hydrogens at the 1- and 4-positions.

A solution of hydrogen bromide in ether was prepared by passing the dry gas into ice cold anhydrous ether for ½ hour. The concentration of the hydrogen bromide was determined by titration. 1,4-Dideuterio-1,4-epoxycyclohexane (12 g, 0.12 *M*) was dissolved in 250 ml of the anhydrous ether solution of hydrogen bromide (0.18 *M*) and the mixture set aside in the dark at room temperature for 24 hours. The solution was refluxed for ½ hour, the solvent removed *in vacuo* and the residual pink oil purified by chromatography of silicic acid with light petroleum ether (b.p. 60–80°) as eluant. Evaporation of the eluate afforded 1,4-dideuterio-*trans*-4-bromocyclohexanol, 19 g (87%), as a white crystalline solid m.p. 80°. Rothstein (44) has described the preparation of the mixed cis- and trans-compounds.

1,4,4-Trideuteriocyclohexanol

In a typical experiment 2.03 g of 1,4-dideuterio-*trans*-4-bromocyclohexanol was dissolved in a solution of 0.307 g of sodium in 20 ml of anhydrous methanol. The bromide was subjected to rapid deuterolysis over 0.312 g of 5% palladium-on-charcoal with deuterium generated electrolytically from sodium deuteroxide solution. A rapid uptake of gas was observed and when no more deuterium was absorbed the solution was filtered through Celite. The methanol was removed by fractional distillation with a small spinning-band column. The residue was poured into brine and the mixture was extracted several times with ether. The combined extracts from several similar experiments were dried over magnesium sulphate, filtered, and

Can. J. Chem. Downloaded from www.nrcresearchpress.com by 210.87.254.42 on 09/05/12
For personal use only.

Can. J. Chem. Downloaded from www.nrcresearchpress.com by 210.87.254.42 on 09/05/12
For personal use only.

TABLE V

Double irradiation experiments on *cis*-1,2-cyclohexanediols and their derivatives*

Compound	Solvent	Proton and lines irradiated	Decoupling frequencies,† c.p.s.	Lines collapsed	Appropriate measured spacings,‡ c.p.s.	J_{AB}, c.p.s.	Chemical shifts,§ c.p.s. δ_A	Chemical shifts,§ c.p.s. δ_B
Di-*O*-acetyl	CCl_4	B (1 and 2)	346.0	11, 12	6.98	11.2	180	157
		B (3 and 4)	327.8	9, 10				
		A (5 and 6)	318.8	10, 12	3.62	11.4		
		A (7 and 8)	303.8	9, 11				
Diol	$CHCl_3$	B (1 and 2)	231.8	11, 12	7.00	10	177	153
		B (3 and 4)	214.8	9, 10				
		A (5 and 6)	204.6	10, 12	3.80	11.6		
		A (7 and 8)	189.2	9, 11				
Diol	D_2O	B (1 and 2)	237.8	11, 12	6.50	11.5	218	194
		B (3 and 4)	219.8	9, 10				
		A (5 and 6)	209.8	10, 12	4.29	10.7		
		A (7 and 8)	194.8	9, 11				
Di-*O*-tosyl	$CHCl_3$	B (1 and 2)	309.2	11, 12	7.72	12.2	196	154
		B (3 and 4)	288.2	9, 10				
		A (5 and 6)	261.7	10, 12	2.77	12.4		
		A (7 and 8)	246.5	9, 11				
O-Isopropylidene	CCl_4	B (1 and 2)	252	{11, 12}	5.40	11.6	181	154
		B (3 and 4)	234	{ 9, 10}				
		A (5 and 6)	222	{10, 12}	5.40	12.6		
		A (7 and 8)	205	{ 9, 11}				

*In each case the measurements were made on the signal for the X-proton.
†Average of three to four determinations.
‡These spacings were substituted in either expressions 1 and 2 or 3 and 4 to obtain J_{AB}.
§These shifts are those deduced as described in the text.

Can. J. Chem. Downloaded from www.nrcresearchpress.com by 210.87.254.42 on 09/05/12
For personal use only.

TABLE VI

Double irradiation experiments on *trans*-1,2-cyclohexanediols and their derivatives*

Compound	Solvent	Proton and lines irradiated	Decoupling frequencies,† c.p.s.	Lines collapsed	Appropriate measured spacings,‡ c.p.s.	J_{AB}, c.p.s.	Chemical shifts,§ c.p.s. δ_A	Chemical shifts,§ c.p.s. δ_B
Di-*O*-acetyl	CCl_4	B (1 and 2)	345.8	10, 12	4.20	10.8	140	133
		B (3 and 4)	330.8	9, 11				
		A (5 and 6)	335.8	(11, 12)	10.15	9.85		
		A (7 and 8)	315.8	9, 10				
Diol	$CHCl_3$	B (1 and 2)	217.6	10, 12	4.55	11.9	193	123
		B (3 and 4)	201.2	9, 11				
		A (5 and 6)	149.8	11, 12	11.06	10.94		
		A (7 and 8)	127.8	9, 10				
Diol	D_2O	B (1 and 2)	222.2	10, 12	4.26	12.74	241	171
		B (3 and 4)	205.2	9, 11				
		A (5 and 6)	154.2	11, 12	10.91	12.10		
		A (7 and 8)	131.2	9, 10				
Di-*O*-tosyl	$CHCl_3$	B (1 and 2)	300.9	10, 12	3.62	12.88	196	148
		B (3 and 4)	284.4	9, 11				
		A (5 and 6)	252.9	11, 12	7.82	11.88		
		A (7 and 8)	233.2	9, 10				
O-Isopropylidene	CCl_4	B (1 and 2)	181.2	10, 12	3.46	11.54	205	137
		B (3 and 4)	166.2	9, 11				
		A (5 and 6)	116.2	11, 12	10.99	12.31		
		A (7 and 8)	92.9	9, 10				

*In each case the measurements were made on the signal for the X-proton.
†Average of three to four determinations.
‡These spacings were substituted in either expressions 1 and 2 or 3 and 4 to obtain J_{AB}.
§These shifts are those deduced as described in the text.

fractionated to yield 7.32 g (75% yield) of 1,4,4-trideuteriocyclohexanol as a colorless oil. Freshly recrystallized *p*-toluenesulphonyl chloride, 21 g, was added in portions with shaking to a solution of 7.32 g of 1,4,4-trideuteriocyclohexanol in 45 ml of anhydrous pyridine at −2°. The solution was shaken until all the chloride had dissolved, then allowed to warm to room temperature, and set aside for 3 hours. Two milliliters of water was added cautiously with shaking. After several minutes, the mixture was poured into 200 ml of water. On chilling, the precipitated oil crystallized. The product was purified by washing with water, drying, and recrystallizing from (1:2) ether/pentane. The white plates, 16 g (87%), melted at 44–45°, the melting point recorded (45) for cyclohexyl-*p*-toluenesulphonate. The 1,4,4-trideuteriocyclohexyl-*p*-toluenesulphonate, 5 g, was dissolved in a solution of 3 g of potassium hydroxide in 10 ml of redistilled diethylene glycol. The mixture was heated under conditions for distillation at 110° and the distillate was collected in a trap cooled in a mixture of solid carbon dioxide and acetone. The organic layer was removed from the distillate and dried over magnesium sulphate. Gas–liquid chromatographic analysis of the product showed it to be pure. The yield of 1,4,4-trideuteriocyclohexene was 1.3 g, 10%. Integration of the NMR spectrum showed the relative intensities of the ethylenic and methylenic hydrogens to be 1:5.8 (expected for I, 1:6). See Fig. 1.

1,4,4-Trideuteriocyclohexene-trans-1,2-dibromide in Benzene

A 4% (w/v) solution of bromine in cold dry benzene was prepared and a slight molar excess was added with stirring to a solution of 117.6 mg of 1,4,4-trideuteriocyclohexene in 1 ml of dry benzene until a permanent pink color remained. The excess bromine was dispelled with a stream of air, the solution passed down a short column of grade 1 alumina, and the eluate concentrated under a spinning-band column to a small volume. The solution was then made up to 1.0 ml with dry benzene containing 0.5% of tetramethylsilane for the NMR experiment.

1,4,4-Trideuteriocyclohexene-trans-1,2-dichloride in Benzene

A solution of 124.3 mg of 1,4,4-trideuteriocyclohexene in 1 ml of dry benzene was treated dropwise with stirring with a solution of chlorine in cold dry benzene. The course of the reaction was followed by NMR and the reaction was judged to be complete when the olefinic band disappeared. The excess chlorine was dispelled with a stream of air, the solution passed down a short column of grade 1 alumina, and the eluate concentrated under a spinning-band column to a small volume. The solution was then diluted to 1.0 ml with dry benzene containing 0.5% of tetramethylsilane for the NMR experiments.

1,4,4-Trideuteriocyclohexene-trans-1,2-diiodide in Benzene

Finely powdered iodine, 378 mg, in a vial was cooled in an acetone – solid carbon dioxide mixture and treated dropwise with 127 mg of 1,4,4-trideuteriocyclohexene. The iodine reacted immediately and a reddish-brown solution resulted. The mixture was allowed to reach room temperature, then made up to 1.0 ml with dry benzene containing 0.5% of tetramethylsilane. The solution was used immediately for the NMR experiments.

1,4,4-Trideuterio-cis-cyclohexene-1,2-diol

1,4,4-Trideuteriocyclohexene, 0.7 g, and 2 g of osmium tetraoxide in 30 ml of dry pyridine were mixed at 0° with rapid stirring (14). The mixture immediately set to a mass of brown crystals. After 30 minutes, the mixture was treated with a solution of sodium bisulphite in 60 ml of water and 40 ml of pyridine (15) and the mixture stirred until a clear orange solution was obtained. The solution was thoroughly extracted with chloroform and the extract was dried over magnesium sulphate. Evaporation of the filtered extract left a brown gum from which pure 1,4,4-trideuterio-*cis*-cyclohexane-1,2-diol was obtained as a white crystalline solid by sublimation at 70° and 1 mm pressure. The yield was 0.69 g (70%), m.p. 98° (46).

1,4,4-Trideuterio-trans-cyclohexane-1,2-diol

A solution of 1.44 g of 1,4,4-trideuteriocyclohexene in 5 ml of 98% formic acid was warmed to 45° and treated with 30% aqueous hydrogen peroxide (14) with stirring at a rate to maintain an internal temperature of 55–60°. The addition took 75 minutes. The solution was stirred at 60° for 1 hour, then subjected to steam distillation until 90 ml of distillate was collected. Evaporation of the residual aqueous solution *in vacuo* afforded a yellow gum which readily crystallized. The product, 1,4,4-trideuterio-*trans*-cyclohexane-1,2-diol, was dried and purified by sublimation at 70° and 1 mm pressure. The compound was obtained as a white crystalline solid, 1.30 g (65%), m.p. 101° (literature, m.p. 103.5° (46)).

1,4,4-Trideuterio-cis-cyclohexane-1,2-diol Di-p-toluenesulphonate

A solution of 0.10 g of 1,4,4-trideuterio-*cis*-cyclohexane-1,2-diol in 2 ml of dry pyridine at −5° was treated with 0.60 g of freshly recrystallized *p*-toluenesulphonyl chloride in portions with shaking. When all the reagent has been added, the solution was allowed to attain room temperature and was set aside for 3 hours. A few drops of water were added, and after several minutes the solution was poured into 4 volumes of water. The precipitated oil crystallized. The product was washed with water, dried, and purified by recrystallization from ethanol. The yield was 0.25 g (70%), m.p. 127° (literature (47) m.p. of hydrogen analogue 128.5–129.5°).

Can. J. Chem. Downloaded from www.nrcresearchpress.com by 210.87.254.42 on 09/05/12
For personal use only.

1,4,4-Trideuterio-trans-cyclohexane-1,2-diol Di-p-toluenesulphonate

Similar treatment of 0.1 g of the *trans*-deuteriodiol with 0.6 g of *p*-toluenesulphonyl chloride afforded 0.2 g (55%), m.p. 105°, of the di-*p*-toluenesulphonate (literature (47) m.p. of hydrogen analogue 109°).

1,4,4-Trideuterio-cis-cyclohexane-1,2-diol Diacetate

1,4,4-Trideuterio-*cis*-cyclohexane-1,2-diol, 141 mg, was treated with 0.5 ml of acetic anhydride containing a trace of concentrated sulphuric acid as catalyst. The diol dissolved immediately with evolution of heat but the solution soon returned to room temperature and was set aside for an hour. The acid catalyst was neutralized with a little solid calcium carbonate and the filtered solution concentrated to a small volume *in vacuo*. The crude diacetate was purified by elution chromatography on acid-washed alumina using carbon tetrachloride. Evaporation of the eluant afforded diacetate as a colorless oil, 0.2 g (83%), which was characterized by comparison using gas–liquid partition chromatography with an authentic sample.

1,4,4-Trideuterio-trans-cyclohexane-1,2-diol Diacetate

Similar treatment of 0.143 g of the *trans*-trideuteriodiol with 0.5 ml of acetic anhydride and chromatographic purification provided the diacetate as a colorless oil, 0.2 g (82%), which was characterized by gas–liquid partition chromatography.

O-Isopropylidene-1,4,4-trideuterio-cis-cyclohexane-1,2-diol

A solution of 0.201 g of the trideuterio-*cis*-cyclohexane-1,2-diol in 8 ml of dry acetone and 8 ml of pentane containing 20 mg of *p*-toluenesulphonic acid was refluxed for 60 hours in a Dean-Stark apparatus (48). The residual solution was cooled and treated with 10 mg of solid sodium acetate. The filtered solution was concentrated to a small volume *in vacuo*. The residual oil was purified by elution chromatography on acid-washed alumina using carbon tetrachloride. Evaporation of the eluate afforded the isopropylidene derivative as a colorless oil, 0.15 g (56%). The product was shown to be pure by gas–liquid partition chromatography.

trans-O-Isopropylidene-1,4,4-trideuteriocyclohexane-1,2-diol

A solution of 78 mg of the trideuterio-*trans*-cyclohexane-1,2-diol and 9.65 mg of *p*-toluenesulphonic acid in a mixture of 15 ml of 2,2-dimethoxypropane and 5 ml of carbon tetrachloride was heated under reflux for 20 hours. The excess solvents were removed by distillation at atmospheric pressure until the residual volume was about 4 ml. The cooled yellow solution was poured down a silica gel chromatography column covered by a 1-in. section of alumina. The column was developed with carbon tetrachloride and 25-ml fractions of the eluant were collected and concentrated to a small volume by fractionational distillation. The fractions containing the desired product were detected by NMR spectroscopy and combined. The pure product was isolated by preparative gas–liquid partition chromatography on a silicone oil column at 90° and collected in tubes cooled by a mixture of acetone and solid carbon dioxide. The *trans-O*-isopropylidene-1,4,4-trideuteriocyclohexane-1,2-diol, 15 mg (14.5%), produced an NMR spectrum at 100 Mc.p.s. consistent with its structure. Also, it showed the same behavior on gas–liquid partition chromatography as an authentic sample (48).

4-t-Butyl-2,2,6,6-tetradeuteriocyclohexanone

A solution of 2.74 g of 4-*t*-butylcyclohexanone in a mixture of 10 ml of anhydrous dioxane and 7 ml of deuterium oxide containing a trace of sodium was sealed in a Carius tube and heated at 100° for 12 hours. The contents were than rapidly extracted with *n*-pentane. Evaporation of the *n*-pentane gave a yellow oil which was treated for a second time under the above conditions for deuterium exchange. The product was isolated by extraction and purified by sublimation. The yield was 2.05 g of a compound with the expected melting point and deuterium content (NMR analysis).

trans-4-t-Butyl-2,2,6,6-tetradeuteriocyclohexanol

The tetradeuterioketone was reduced with lithium aluminum hydride in ether and the product was isolated in the usual way. The crude product, m.p. 63–65°, was purified by chromatography as described by Winstein and Holness (49).

cis- and trans-4-t-Butyl-2,2,6,6-tetradeuterio-1-methylcyclohexanols

The tetradeuterioketone, 10 g, was reacted with methylmagnesium iodide in ether and the partially crystalline product, isolated in the usual manner, was chromatographed on grade 1 alumina using *n*-pentane – diethyl ether (1:2) for development. Two well-resolved fractions were obtained. The first fraction (cis-isomer) gave a white crystalline material, m.p. 70–71°, after recrystallization from Skellysolve B. The second fraction (*trans*-isomer) melted at 97–98° after recrystallization from ethyl acetate. This latter compound in carbon tetrachloride solution showed absorption in the infrared for intermolecularly hydrogen-bonded hydroxyl which was much more dependent on concentration than was the lower melting, faster moving (chromatogram) former compound. The configurational assignments were made on this basis.

ACKNOWLEDGMENTS

The research was supported in part by a National Research Council of Canada grant-in-aid of research (T172) to R. U. L.

Can. J. Chem. Downloaded from www.nrcresearchpress.com by 210.87.254.42 on 09/05/12
For personal use only.

REFERENCES

1. P. Bender, D. L. Flowers, and H. L. Goering. J. Am. Chem. Soc. **77**, 3463 (1955).
2. L. W. Reeves and K. O. Strømme. Trans. Faraday Soc. **57**, 390 (1961).
3. E. L. Eliel. Stereochemistry of carbon compounds. McGraw Hill Book Co., Inc. 1962. p. 218.
4. R. U. Lemieux, R. K. Kullnig, H. J. Bernstein, and W. G. Schneider. J. Am. Chem. Soc. **80**, 6098 (1958).
5. N. Muller and W. C. Tosch. J. Chem. Phys. **37**, 1167 (1962).
6. M. Karplus. J. Chem. Phys. **30**, 11 (1959); J. Phys. Chem. **64**, 1793 (1960); J. Am. Chem. Soc. **85**, 2871 (1963).
7. F. A. L. Anet. Can. J. Chem. **39**, 789 (1961).
8. R. U. Lemieux, J. D. Stevens, and R. R. Fraser. Can. J. Chem. **40**, 1955 (1962).
9. R. J. Abraham and K. A. McLauchlan. Mol. Phys. **5**, 513 (1962).
10. H. J. Bernstein, J. A. Pople, and W. G. Schneider. Can. J. Chem. **35**, 65 (1957).
11. J. D. Roberts. An introduction to spin–spin splitting in high resolution nuclear magnetic resonance spectra. W. A. Benjamin, Inc., New York. 1961. p. 62.
12. E. A. Fehnel, S. Goodyear, and J. Berkowitz. J. Am. Chem. Soc. **73**, 4978 (1951).
13. E. Premuzic and L. W. Reeves. Can. J. Chem. **40**, 1870 (1962).
14. H. Gunstone. Advances in organic chemistry methods and results. Vol. I. Interscience Publishers. 1960. p. 135.
15. J. S. Baran. J. Org. Chem. **25**, 257 (1960).
16. J. P. Maher and D. F. Evans. Proc. Chem. Soc. 208 (1961).
17. D. W. Turner. J. Chem. Soc. 847 (1962).
18. R. Freeman and D. H. Whiffen. Mol. Phys. **4**, 321 (1961).
19. D. D. Elleman and S. L. Manatt. J. Chem. Phys. **36**, 2346 (1962).
20. R. R. Fraser, R. U. Lemieux, and J. D. Stevens. J. Am. Chem. Soc. **83**, 3901 (1961).
21. F. A. L. Anet. J. Am. Chem. Soc. **84**, 3767 (1962).
22. B. D. Nageswara Rao, J. D. Baldeschweiler, and J. I. Musher. J. Chem. Phys. **37**, 2480 (1962).
23. R. Freeman, K. A. McLauchlan, J. I. Musher, and K. G. R. Pachler. Mol. Phys. **5**, 321 (1962).
24. L. F. Johnson. Varian Associates Technical Bulletin, No. 87-100-082. May 1962.
25. W. A. Anderson and R. Freeman. J. Chem. Phys. **37**, 85 (1962).
26. R. Freeman. Mol. Phys. **4**, 385 (1961).
27. C. Altona, C. Romers, and E. Havinga. Tetrahedron Letters, **10**, 16 (1959).
28. F. A. L. Anet. J. Am. Chem. Soc. **84**, 1053 (1962).
29. K. B. Wiberg and B. J. Nist. Interpretation of N.M.R. Spectra. W. A. Benjamin, Inc., New York. 1962. p. 21.
30. R. U. Lemieux and G. Kavadias. Unpublished results.
31. N. Sheppard and J. J. Turner. Proc. Roy. Soc. London, A, **252**, 506 (1959).
32. J. W. Clark-Lewis and L. M. Jackman. Proc. Chem. Soc. 165 (1961).
33. B. Ottar. Acta Chem. Scand. **1**, 521 (1947).
34. L. P. Kuhn. J. Am. Chem. Soc. **74**, 2492 (1952).
35. R. Criegee, E. Büchner, and W. Walther. Ber. **73**, 571 (1940).
36. S. J. Angyal and C. G. MacDonald. J. Chem. Soc. 686 (1952).
37. R. U. Lemieux, J. D. Stevens, and R. R. Fraser. Can. J. Chem. **40**, 1955 (1962).
38. M. A. Kabayama and D. Patterson. Can. J. Chem. **36**, 563 (1958).
39. E. L. Eliel. J. Chem. Educ. **37**, 126 (1960).
40. S. J. Angyal and D. J. McHugh. Chem. Ind. 1147 (1956).
41. J. D. Stevens and R. U. Lemieux. 45th National Meeting of the Chemical Institute of Canada, Edmonton, Alberta. May 28–30, 1962.
42. A. A. Bothner-By and C. Naar-Colin. J. Am. Chem. Soc. **80**, 1728 (1958). J. I. Musher. J. Chem. Phys. **35**, 1159 (1961).
43. F. R. Jensen, D. S. Noyce, C. H. Sederholm, and A. J. Berlin. J. Am. Chem. Soc. **82**, 1256 (1960).
44. A. Rothstein. Ann. Chim. **14**, 461 (1930).
45. W. Hückel, O. Neunhoeffer, A. Gercke, and E. Frank. Ann. **477**, 99 (1930).
46. S. Winstein and R. E. Buckles. J. Am. Chem. Soc. **64**, 2780 (1942).
47. R. Criegee and H. Stanger. Ber. **69**, 2753 (1936).
48. N. R. Christian, C. J. Gogek, and C. B. Purves. Can. J. Chem. 911 (1951).
49. S. Winstein and N. J. Holness. J. Am. Chem. Soc. **77**, 5562 (1955).

Can. J. Chem. Downloaded from www.nrcresearchpress.com by 210.87.254.42 on 09/05/12
For personal use only.

STATISTICAL PROBABILITIES OF SOME ARRANGEMENTS OF SOLUTE MOLECULES ON SUBSTITUTIONAL SITES IN CUBIC-CLOSE-PACKED CRYSTALS

K. B. HARVEY AND H. F. SHURVELL
Department of Chemistry, University of British Columbia, Vancouver, British Columbia

AND

J. R. HENDERSON
Department of Mathematics, University of British Columbia, Vancouver, British Columbia

Received September 25, 1963

ABSTRACT

Assuming a random distribution of solute molecules on substitutional sites of a cubic-close-packed solvent crystal, the probabilities have been calculated of finding single solute molecules and pairs of solute molecules in various degrees of isolation. The probabilities have been derived as a function of solute concentration and for distances corresponding to the separation of first, second, third, and fourth nearest neighbors.

INTRODUCTION

Following the use of the matrix isolation technique for the trapping and identification of unstable species, a number of investigations have been carried out in this laboratory (1) and others (2, 3) on the effect of the matrix environment on the spectra of the trapped species. The gross features of these spectra can usually be explained in terms of monomeric and polymeric solute molecules (4) but high resolution studies reveal a fine structure which requires a more elaborate explanation. The possibilities of hindered rotation (2) and multiple trapping sites (1, 3) have been put forward as explanations of this fine structure. We have found, however, that even these refinements are unable to account completely for the matrix spectra of water and the halogen acids obtained in this laboratory. In fact, the complexity of these spectra has suggested to us that other than nearest-neighbor solute molecule interactions may be significant; hence the calculations reported here.

Previous calculations on the statistics of isolation in matrices have been reported by Jackson (5) and Behringer (6). In both cases, however, only the probabilities for nearest neighbors were evaluated—our S_1 and D_1.

CALCULATIONS AND RESULTS

In all of the calculations it has been assumed that the solute molecules are randomly distributed throughout the crystal. Following the notation of Behringer the fractional concentration of solute molecules is designated p and the probabilities of finding isolated singlets, doublets, or triplets are denoted by the symbols S, D, and T respectively.

Since the matrices with which we are concerned are all cubic-close-packed at low temperatures, we have considered only this type of lattice. Probabilities for degrees of isolation out to distances corresponding to the fourth nearest neighbor were calculated (Fig. 1); the four different cases being denoted by subscripts. Thus, S_1 represents the probability of finding a solute molecule with no nearest neighbors. S_2 represents the probability of finding a solute molecule with no nearest or second nearest neighbors, and so on.

Can. J. Chem. Downloaded from www.nrcresearchpress.com by 210.87.254.42 on 09/05/12
For personal use only.

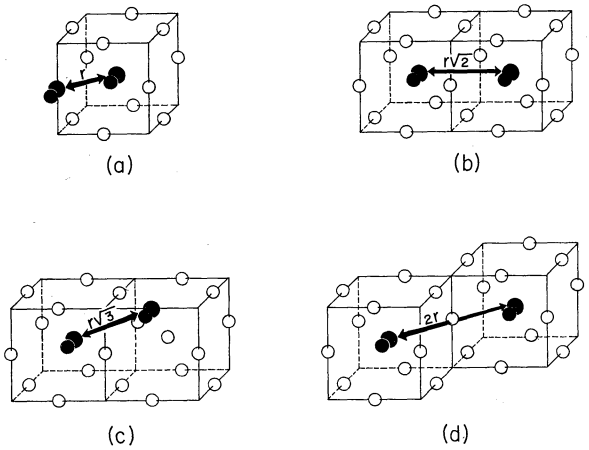

FIG. 1. Structure of a cubic-close-packed lattice showing the first, second, third, and fourth nearest neighbors.

The equations giving the probabilities of finding a single molecule in various degrees of isolation are as follows:

$$S_1 = (1-p)^{12} \qquad S_3 = (1-p)^{42}$$
$$S_2 = (1-p)^{18} \qquad S_4 = (1-p)^{54}$$

Values of S_1, S_2, S_3, and S_4 for matrix ratios between 10:1 and 1000:1 are listed in Table I

TABLE I

Probability of finding isolated single molecules in various degrees of isolation

p	S_1	S_2	S_3	S_4
0.00100	0.9881	0.9822	0.9588	0.9474
0.00125	0.9851	0.9777	0.9488	0.9347
0.00167	0.9801	0.9704	0.9322	0.9137
0.00200	0.9763	0.9646	0.9194	0.8975
0.00250	0.9704	0.9559	0.9002	0.8736
0.00333	0.9608	0.9417	0.8693	0.8352
0.00500	0.9416	0.9137	0.8102	0.7629
0.00667	0.9228	0.8865	0.7550	0.6967
0.01000	0.8864	0.8345	0.6557	0.5812
0.02000	0.7847	0.6951	0.4281	0.3359
0.05000	0.5404	0.3972	0.1160	0.0627
0.10000	0.2824	0.1501	0.0120	0.0034

and plotted in Fig. 2. It should be noted that these equations represent probabilities and not numbers of atoms as in Behringers calculations. They differ by a factor Np, where N is the number of lattice sites in the crystal.

The symbol D_1 denotes the probability of finding a pair of molecules a distance r apart (i.e. in nearest-neighbor positions), with no other molecules in nearest-neighbor positions to either of the pair. D_2 represents the probability of finding a pair of molecules a distance $\sqrt{2}r$ apart (i.e. in second nearest-neighbor positions), with no other molecules in nearest or second-nearest-neighbor positions to either of the pair, and so on.

The equations used in calculating these probabilities are as follows.

$$D_1 = 12p(1-p)^{18} \qquad D_3 = 24p(1-p)^{69}$$
$$D_2 = 6p(1-p)^{30} \qquad D_4 = 12p(1-p)^{90}.$$

Can. J. Chem. Downloaded from www.nrcresearchpress.com by 210.87.254.42 on 09/05/12
For personal use only.

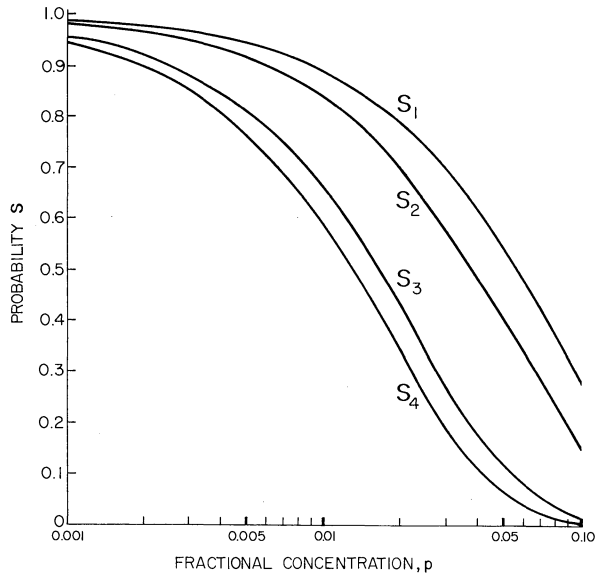

FIG. 2. Probability of finding isolated single molecules as a function of solute concentration, p.

The factors 12, 6, 24, and 12 arise from the number of first, second, third, and fourth nearest neighbors, respectively. These probabilities are listed in Table II and illustrated in Fig. 3.

The systematic classification of triple clusters is a much more difficult problem. It is apparent, however, that the additional factor, p, in the formulae, will reduce the probabilities to a negligibly small value in most cases. Thus, we did not feel a detailed analysis of the problem was worthwhile. On the other hand, when the number of possible arrangements of the triple cluster is large the probability may become of significant magnitude.

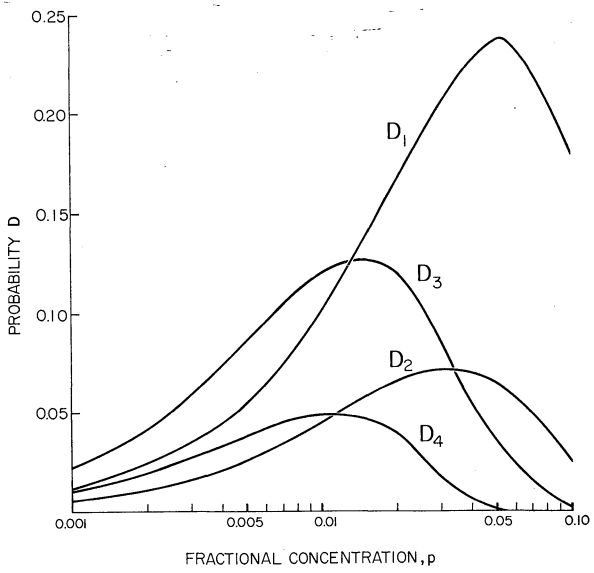

FIG. 3. Probability of finding isolated pairs of molecules as a function of solute concentration, p.

Can. J. Chem. Downloaded from www.nrcresearchpress.com by 210.87.254.42 on 09/05/12
For personal use only.

TABLE II

Probability of finding isolated pairs of molecules in various degrees of isolation and of finding the most probable triple cluster

Isolated pairs					Most probable triple cluster	
p	D_1	D_4	D_3	D_4	p	T_{A1}^3
0.00100	0.0118	0.0058	0.0224	0.0110	0.00100	0.00016
0.00125	0.0147	0.0072	0.0275	0.0134	0.00200	0.00064
0.00167	0.0194	0.0095	0.0357	0.0172	0.00500	0.00365
0.00200	0.0232	0.0113	0.0418	0.0200	0.01000	0.01268
0.00250	0.0287	0.0139	0.0505	0.0239	0.02000	0.03818
0.00333	0.0376	0.0181	0.0635	0.0296	0.05000	0.09988
0.00500	0.0548	0.0258	0.0849	0.0382	0.10000	0.08790
0.00667	0.0710	0.0327	0.1009	0.0438		
0.01000	0.1001	0.0444	0.1200	0.0486		
0.02000	0.1668	0.0655	0.1191	0.0390		
0.05000	0.2383	0.0644	0.0348	0.0059		
0.10000	0.1801	0.0254	0.0017	0.0001		

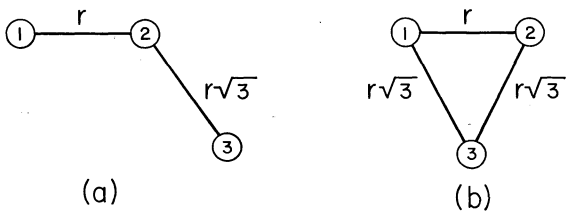

FIG. 4. Open (*a*) and closed (*b*) triple clusters.

A case in point is what we have designated a T_{A1}^3 cluster. The subscript A denotes an open cluster as defined by Behringer (Fig. 4) while the sub- and super-script numerals refer to the two shorter internuclear distances. Thus in a T_{A1}^3 cluster there is a pair of solute molecules in nearest-neighbor positions to each other with a third molecule at a distance of $\sqrt{3}r$ from one of the pair and a distance greater than $\sqrt{3}r$ from the other. None of the three has any molecules in nearest-neighbor positions except as specified above. With 168 possible arrangements, $T_{A1}^3 = 168p^2(1-p)^{28}$, this would appear to be the most probable triple cluster but the probability is still less than 10% (Table II). Behringer's triple cluster, which we would designate a T_{A1}^1, is considerably less probable, although there would appear to be a discrepancy in his calculations. Our calculations indicate a numerical factor of 12 in the formula, i.e. $T_{A1}^1 = 12p^2(1-p)^{23}[5(1-p)+2]$.

DISCUSSION

As expected the S probabilities decrease with increasing p, the falloff being greater the greater the degree of isolation stipulated. The D's, on the other hand, exhibit maxima in the region of $0.01 < p < 0.06$ because the isolation of the pair decreases as p increases. Furthermore, the magnitudes of the maxima are not simply a function of p but depend quite strongly on the number of coordinating positions at the required separation. Thus the probability of finding a D_3 double cluster is considerably higher than that for a D_2 or D_4 when p is less than 0.02. In principle, one could make use of this fact to ascertain the presence of double clusters in the matrix deposits but this conclusion must be accepted with some reservation in the light of practical considerations.

Some diffusion certainly occurs in the matrix during deposition, its extent depending

Can. J. Chem. Downloaded from www.nrcresearchpress.com by 210.87.254.42 on 09/05/12
For personal use only.

on the experimental conditions. In effect, this may be interpreted as a localized increase in the effective value of p. Thus our S probabilities must be considered as maximum values since an increase in p leads to a lower value of S. In the case of the D's the situation is more complicated. Because of the presence of the maxima, the sign of the change in D will depend on both the absolute value of p and the extent of diffusion. For p less than 0.01 a small change in p will lead to an increase in all of the D's calculated. For larger values of p each case must be considered separately. For $p=0.02$, for example, a small amount of diffusion would lead to an increase in D_1 and D_2 but a decrease in D_3 and D_4. The situation would be further obscured by the presence of solute molecules on other than substitutional sites.

The authors are grateful to the National Research Council of Canada and the University of British Columbia for financial support of this work and to the University of British Columbia computing center for assistance with the calculations.

RÉSUMÉ

Pour une distribution faite au hasard des molécules de solute sur les emplacements substitutionals d'une assemblage compacte cubique de molécules solvents, on a calculé les probabilités de trouver une molécule de solute unique ou en paires pour plusieurs degrés d'isolement. Les probabilités ont été derivées comme fonction de la concentration de la solute et pour les séparations des plus proche première, deuxième, troisième et quatrième voisines.

REFERENCES

1. K. B. Harvey and J. F. Ogilvie. Can. J. Chem. **40**, 85 (1962).
2. R. L. Redington and D. E. Milligan. J. Chem. Phys. **37**, 2162 (1962).
3. M. J. Linevsky. J. Chem. Phys. **38**, 658 (1963).
4. M. Van Thiel, E. D. Becker, and G. C. Pimentel. J. Chem. Phys. **27**, 486 (1957).
5. J. L. Jackson. Free radical trapping — theoretical aspects. *In* Formation and trapping of free radicals. *Edited by* A. M. Bass and H. P. Broida. Academic Press, New York. 1960.
6. R. E. Behringer. J. Chem. Phys. **29**, 537 (1958).

Can. J. Chem. Downloaded from www.nrcresearchpress.com by 210.87.254.42 on 09/05/12
For personal use only.

CARBOHYDRATES OF CENTROSEMA SEED. THE CONSTITUTION OF AN ARABINO GALACTAN. I[1]

A. M. UNRAU
Department of Plant Science, University of Manitoba, Winnipeg, Manitoba
Received January 19, 1963

ABSTRACT

Treatment of the water-soluble polysaccharides of *Centrosema plumari* seed with Fehling's solution resulted in the formation of a precipitate in major proportions. The polysaccharide forming a copper complex was composed of D-galactose (92.5%) and L-arabinose (7%). No change was observed in this ratio upon further treatment of the polysaccharide with Fehling's solution. Partial hydrolysis of the arabinogalactan liberated about 80% of the arabinose. Controlled periodate degradation (Smith degradation) indicated a complex branched structure with a preponderance of 1,4-glycosidic linkages. Methylation experiments also indicated a branched structure.

Can. J. Chem. Downloaded from www.nrcresearchpress.com by 210.87.254.6 on 09/05/12
For personal use only.

The isolation and a few characteristics of a galactan present in *Centrosema plumari* seed have been described in an earlier communication (1). Whereas it was previously found that extraction of the crushed seed with hot water yielded an amorphous polysaccharide composed primarily of D-galactose (92%) with lesser amounts of arabinose and mannose, the sample of seed used in this investigation gave a product which contained galactose and arabinose, but no mannose could be detected. It was therefore suspected that two or more related polysaccharides were present in the seed.

The use of complexing agents in the fractionation of polysaccharide mixtures has met with considerable success (2). Probably all galactomannans obtained from leguminous seeds form copper complexes. Neutral copper sulphate solutions, which contain the cation $Cu(OH_2)_4^{++}$ (3), precipitate yeast mannan and the *Lupinus albus* galactan. Alkaline copper sulphate solution, containing the anion $Cu(OH)_4^{--}$ (3), precipitates a greater range of gums and mucilages. It is believed that the same structural characteristics are required in the formation of polysaccharide copper complexes as are necessary for borate complex formation, namely, adjacent cis hydroxyls. In the case of the borate anion, $B(OH)_4^-$, it is believed that cross linkages are formed between two adjacent polymeric chains resulting in a three dimensional network (4, 5). The arabinogalactan with which this communication is concerned showed little or no evidence of forming a borate complex. Treatment of an aqueous solution with Fehling's solution gave a rigid gel. It was found that 80% of the original starting material formed a copper complex. Acid hydrolysis of this polysaccharide showed it to be composed of D-galactose (92.5%) and L-arabinose (7%). Results obtained from partial hydrolysis of the arabinogalactan showed that the greater proportion (80%) of arabinose units were released. This indicated that the arabinose residues were mainly present as nonreducing terminal furanosyl units, a structural feature which has been observed in a fairly large number of polysaccharides containing this pentose (2). A series of internal arabinofuranosyl units could also explain this result although such a structure is less likely.

The further investigation of the structure of the polysaccharide using the Smith degradation (6) largely confirmed the earlier findings (1), although some interior structural systems were found to be much more complex than was at first believed. The absence of

[1]*Contribution No. 74, Department of Plant Science, University of Manitoba.*

ethylene glycol in the mild acid hydrolyzate of the polyalcohol eventually obtained in the reaction sequence showed that few, if any, nonreducing terminal arabinopyranose units were present. The relatively large amount of glycerol (component 1) obtained when considered together with the preferential release of arabinose upon mild acid hydrolysis of the intact polysaccharide further indicated the presence of nonreducing terminal arabinofuranose units. Glycerol would also be formed from terminal as well as 1,6-linked galactopyranose residues and 1,5-linked arabinofuranose units. D-Threitol (component 2) obviously originated from 1,4-linked galactose units. The detection of arabinose (component 3) in the hydrolyzate indicated the presence of periodate-resistant internal arabinose units.

In addition to the above simple degradation compounds, a number of threityl glycosides were obtained which, when hydrolyzed, showed that some galactose and a minor quantity of arabinose units were linked in a manner rendering them immune to periodate cleavage. The simplest galactoside found was 2-O-β-D-galactopyranosyl-D-threitol (component 4), a β-linkage being assigned because of the low specific optical rotation. The structure was deduced from the fact that upon hydrolysis a 1:1 molar ratio of D-galactose and D-threitol was observed. Periodate oxidation of the glycoside followed by borohydride reduction and hydrolysis gave only glycerol (two molar proportions). The amount of formaldehyde released in the periodate oxidation of the glycoside indicated a molecular weight of 300 (7). The compound was readily hydrolyzed by β-D-galactosidase, thus further indicating a β-linkage; and yielded equimolar amounts of galactose and threitol. Methylation of the compound followed by hydrolysis gave crystalline 2,3,4,6-tetra-*O*-methyl-D-galactose. Direct reduction (BH_4) of a portion of the hydrolyzate followed by demethylation with 40% hydrobromic acid gave threitol, characterized as the solid *p*-nitrobenzoate, and galactitol in a 1:1 molar ratio. Treatment of the galactoside with *p*-nitrobenzoyl chloride in the usual fashion gave a powdery derivative which was rather insoluble in organic solvents except pyridine. Elemental analysis gave close to theoretical values for nitrogen.

Component 5 gave upon complete acid hydrolysis galactose, arabinose, and threitol in a 2:1:1 molar ratio. The quantity of formaldehyde released upon periodate oxidation indicated a molecular weight of 430 (7). Reduction of the polyaldehyde with borohydride and complete hydrolysis of the resulting polyalcohol gave galactose, threitol, and glycerol in a 2:3:4 molar ratio. A trace of arabinose was also detected. Part of the glycerol obviously arose from threitol residues. The presence of some galactose in the hydrolyzate indicated that a small number of these units were still linked in a manner rendering them immune to periodate attack. Practically all of the arabinose units were degraded to glycerol indicating that they were present as internal 1,4-linked units.

Paper electrophoretic analysis of component 5 showed the presence of two compounds. Compound 5A, which showed the lower mobility, constituted about 75% of the total. This material gave, upon hydrolysis, galactose and threitol in a 2:1 molar ratio. Periodate oxidation of 5A gave formaldehyde, the amount of which indicated a molecular weight of 440 (7). Borohydride reduction of the polyaldehyde and hydrolysis of the product gave galactose, glycerol, and threitol in a molar ratio of 1:4:1. These results indicated that 5A was composed of two oligosaccharides with the probable partial structures of (*a*) D-Gal*p*(1 → 4)-D-Gal*p*(1 → 2)-D-threitol and, (*b*) D-Gal*p*(1 → 3)-D-Gal*p*(1 → 2)-D-threitol. The specific optical rotation of 5A (−3°) indicated β-glycosidic linkages. Similar experimental procedures applied to 5B showed it to be composed of galactose, arabinose, and threitol (1:1:1 molar ratio). Periodate oxidation released formaldehyde, the amount of which indicated a molecular weight of 420 (7). Borohydride reduction of the polyaldehyde

Can. J. Chem. Downloaded from www.nrcresearchpress.com by 210.87.254.6 on 09/05/12
For personal use only.

followed by hydrolysis gave glycerol and a trace of arabinose. These results indicated that 5B was composed of two oligosaccharides with probable partial structures of (*a*) D-Gal*p*(1 → 4)-L-Arab*p*(1 → 2)-D-threitol and (*b*) D-Gal*p*(1 → 2 or 3)-L-Arab*p*(1 → 2)-D-threitol.

Component 6, which had a specific optical rotation of −4.6°, indicating the predominance of β-glycosidic linkages, gave, upon hydrolysis, galactose, arabinose, and threitol in a 3:1:1 molar ratio. Periodate oxidation gave formaldehyde, the amount of which indicated a molecular weight of 680. Hydrolysis of the reduced (BH_4) product gave galactose, arabinose, threitol, and glycerol in an approximate molar ratio of 2:1:4:4. The threitol arose from galactose residues while the original threityl residues were converted to glycerol by reduction of the aldehyde produced by periodate cleavage between C_3 and C_4. A 1,3-linkage would explain the survival of some galactose residues whereas both 1,3- and 1,2-linked arabinopyranosyl units would account for the survival of such pentose units.

Paper electrophoretic analysis of component 6 showed that it was heterogeneous. A substance with a somewhat greater mobility than the bulk of the material gave, upon complete hydrolysis, galactose and threitol in a molar ratio of 3:1. Periodate oxidation of this oligosaccharide gave formaldehyde, the amount of which indicated a molecular weight of 600. Borohydride reduction of the polyaldehyde and complete hydrolysis of the product gave galactose, threitol, and glycerol in a molar ratio of 1:3:4. The survival of a portion of galactose indicated the presence of two compounds with probable partial structures of (*a*) D-Gal*p*(1 → 4)-D-Gal*p*(1 → 4)-D-Gal*p*(1 → 2)-D-threitol, and (*b*) D-Gal*p*(1 → 4)-D-Gal*p*(1 → 3)-D-Gal*p*(1 → 2)-D-threitol. A few other structures with minor modifications could also fit the experimental results. The specific optical rotation (−6°) indicated β-glycosidic linkages.

Hydrolysis of the slower migrating material gave galactose, arabinose, and threitol in molar ratio of 2:2:1. Periodate oxidation of the material gave formaldehyde, the amount of which indicated a molecular weight of 700. Reduction (KBH_4) of the polyaldehyde and complete hydrolysis of the product gave galactose, arabinose, threitol, and glycerol in a 2:1:4:5 molar ratio. These results indicated considerably more structural complexity than was found for the previously discussed oligosaccharide-type fragments.

The results from experiments with the larger oligosaccharide fractions (components 7 and 8) suggested similar structural features. Component 7, which had a specific rotation of −7.5° indicating a dominance of β-glycosidic linkages, gave, upon complete hydrolysis, galactose, arabinose, and threitol in a 4:2:1 molar ratio. A molecular weight of about 1000 may be deduced from this result. Periodate oxidation gave formaldehyde, the amount of which suggested a molecular weight of about 1550. This result is at variance with that which was deduced from hydrolysis of the oligosaccharide. A possible structural unit to accommodate these observations would be a disubstituted D-threityl glycoside. Since a considerable quantity of formaldehyde was formed upon periodate oxidation of component 7, the greater proportion of oligosaccharide molecules contained the glycosyl-1,2-threitol structure. Borohydride reduction of the polyaldehyde and complete hydrolysis of the polyalcohol gave galactose, arabinose, threitol, and glycerol in a molar ratio of 2:1:2:10. A number of molecular arrangements might be suggested to accommodate these results. The relatively large quantity of glycerol formed by the above reaction sequence considered together with the smaller quantity of formaldehyde evolved suggests that the oligosaccharide originated from a highly branched segment of the original polysaccharide. In these segments must be present multiple-linked galactose units containing 1,3-glycosidic bonds and other combinations such as 1,2,4- and 1,2,3-linkages. To survive two successive

Can. J. Chem. Downloaded from www.nrcresearchpress.com by 210.87.254.6 on 09/05/12
For personal use only.

periodate treatments, the arabinose units must be protected by a series of linkages resisting periodate glycol cleavage. Whereas components 5 and 6 could be further resolved by paper electrophoresis, similar separation was not achieved with component 7.

Component 8, also having a negative specific optical rotation (−7.7°) and being the largest oligosaccharide on the basis of its lowest chromatographic mobility, gave galactose, arabinose, and threitol (5:3:1 molar ratio) upon hydrolysis. Periodate oxidation gave formaldehyde, the quantity of which indicated a molecular weight of approximately 1300. This value is in accord with the molecular weight which can be deduced from the molar proportion of threitol that was released upon hydrolysis. Borohydride reduction of the polyaldehyde and complete hydrolysis of the product gave galactose, arabinose, threitol, and glycerol in a molar ratio of 2:1:4:4. An attempted resolution of fraction 8 by paper electrophoresis was not successful.

The polysaccharide was fully methylated using the Howarth procedure (dimethyl sulphate and strong alkali) followed by extended treatment with Purdie reagents (silver oxide and methyl iodide). Hydrolysis of the alkylated polysaccharide with sulphuric acid (8) gave tetra-, tri-, and di-*O*-methyl sugars. No unmethylated sugar was found and only a trace of mono-*O*-methyl galactose was detected. The color reaction of the tetra-*O*-methyl hexose indicated the presence of tri-*O*-methyl arabinose. The mixture of sugars was resolved into tetra-, tri-, and di-*O*-methyl fractions by cellulose column chromatography (9) using the butanone–water azeotrope solvent (10). The weight of the three fractions indicated a molar ratio of tetra-:tri-:di-*O*-methyl hexose of 3:14:3.

2,3,4,6-Tetra-*O*-methyl-D-galactose and 2,3,5-tri-*O*-methyl-L-arabinose were identified as follows: the mixture was oxidized with bromine, the resulting acids were converted to their lactones, and these separated by vapor phase chromatography. 2,3,4,6-Tetra-*O*-methyl-D-galactono-δ-lactone and 2,3,5-tri-*O*-methyl-L-arabono-lactone both crystallized in the collection tubes. The molar ratio of tetramethyl galactose to trimethyl arabinose was 3:1.

The trimethyl fraction was separated by the following procedure. Treatment of the methyl glycosides with trityl chloride gave a water-insoluble trityl compound which was presumed to be methyl 2,3,4-tri-*O*-methyl-6-*O*-trityl-D-galactoside. Detritylation and hydrolysis gave crystalline 2,3,4-tri-*O*-methyl-D-galactose. The non-tritylated trimethyl galactosides were hydrolyzed and chromatographically resolved into 2,4,6-tri-*O*-methyl-D-galactose, which crystallized spontaneously, and 2,3,6-tri-*O*-methyl-D-galactose, the faster migrating sugar, which did not crystallize. The latter sugar was identified by degradation to 2,3-di-*O*-methyl-L-threose, which was reduced (BH_4) to the corresponding alcohol. Demethylation of the mixture of 2,3-di-*O*-methyl-L-threitol and monomethyl ethylene glycol gave the expected alcohols in a 1:1 molar ratio. Both were transformed to the solid *p*-nitrobenzoates. The molar ratio of 2,4,6-:2,3,6-:2,3,4-trimethyl hexoses was estimated to be 2:10:1. Although a small amount of dimethyl-L-arabinose was expected to be present with the trimethyl galactoses, apparently not enough was present to facilitate detection.

The dimethyl hexose fraction was analyzed in the following manner. Reduction (BH_4) and periodate oxidation gave two reducing sugars which were presumed to be 2,3-di-*O*-methyl-L-threose (arising from 2,3-di-*O*-methyl-D-galactose) and a dimethyl pentose believed to be 2,4-di-*O*-methyl-L-lyxose which would arise from 2,4-di-*O*-methyl-D-galactose. The two sugars were present in a 5:1 molar ratio. Reduction of the dimethyl tetrose and demethylation gave L-threitol, which was transformed to the solid *p*-nitrobenzoate.

Can. J. Chem. Downloaded from www.nrcresearchpress.com by 210.87.254.6 on 09/05/12
For personal use only.

The results from the Smith degradation and those from the methylation experiments are essentially in accord insofar as to show that the polysaccharide investigated has a rather complex structure. Although it was, with possibly one exception, difficult to characterize rigorously the fragments obtained in the Smith degradation, this procedure at least affords a possible opportunity to study in more detail the internal structural units which resist periodate cleavage. With this in mind, it appears that the Smith periodate degradation scheme should be the method of choice when complex or even simple polysaccharides are considered. Small amounts of undegraded sugar present after the more classical periodate degradation of a polysaccharide should not be disregarded since this observation likely has structural significance. The Smith degradation also presents the opportunity to isolate periodate-resistant backbones of certain polysaccharides which then can be studied in further detail. It is believed that the Smith degradation when applied to simple polysaccharides may yield results indicating a somewhat more complex structure.

EXPERIMENTAL

Paper chromatographic separation of compounds was carried out by the descending technique and the following solvent systems: A, butanol – acetic acid – water (12:5:3); B, ethyl acetate – pyridine – water (9:2:2); C, ethyl acetate – acetic acid – water (8:2:2); and D, butanone – water azeotrope (10). Electrophoretic examinations of oligosaccharide components were carried out using either Whatman No. 1 or 3MM paper and sodium borate buffer (0.07 *M*). Compounds were detected with *p*-anisidine trichloroacetate (11), ammoniacal silver nitrate (12) and periodate–permanganate (13) spray reagents. Evaporations were carried out under reduced pressure at 35 to 40° C. Melting points (uncorrected) were determined on a hot-stage apparatus. Optical rotations are equilibrium values unless otherwise stated.

Isolation of Arabinogalactan

Coarsely ground seed (200 g) of *Centrosema plumari* was covered with water and boiled for 1 hour. The slurry was cooled somewhat to facilitate handling and coarse solids removed by pouring the mixture through several layers of cheesecloth. The residue was resuspended twice more in boiling water and filtered as described. To the combined filtrates potassium borohydride (200 mg in 150 ml water) was added and after six hours at room temperature, sodium hydroxide was added to give a final alkali concentration of 7–8% (wt./vol.). The solution was boiled for several hours to decompose protein and then left overnight to allow sedimentation of suspended solids. Insoluble material was removed by centrifugation and the slightly opalescent acidified (acetic acid) supernatant poured with vigorous stirring into three volumes of ethanol. The precipitated polysaccharide was collected and dissolved in hot water. After three re-precipitations of the polysaccharide by addition of aqueous solutions to four volumes of ethanol, a nearly white amorphous product, $[\alpha]_D^{25}$ +11° (*c*, 1.0 in 0.5 *N* NaOH), was obtained in about 40% yield. Hydrolysis (reflux temperature for 7 hours) of a small portion (0.5 g) of the above product with *N* HCl (20 ml) gave a mixture of sugars identified by their characteristic chromatographic mobilities in solvents A, B, and C and reactions with the stated spray reagents. Galactose, arabinose, and xylose were found in a molar ratio, as determined by the phenol – sulphuric acid method (14), of 45:8:1.

Fractionation of Polysaccharide

(a) Passage through ion-exchange resin columns.—A solution (100 ml) of polysaccharide (0.3 g) was slowly passed successively through cation and anion exchange resin columns. The effluent was evaporated to dryness and the residue refluxed in *N* sulphuric acid for 8 hours. Galactose, arabinose, and xylose were identified chromatographically. The molecular proportion of each sugar was found to be unchanged when compared to the original preparation.

(b) Treatment with Fehling's solution.—A preliminary test showed that a precipitate resulted when Fehling's solution was added to a solution of the polysaccharide. To a portion (40 g) of polysaccharide suspended in water (300 ml), Fehling's solution (900 ml) was added, with vigorous stirring. The gel was collected, washed with Fehling's solution, and dissolved in dilute acetic acid. The solution was dialyzed against distilled water and the volume reduced to 300 ml. Fehling's solution (900 ml) was again added and the procedure repeated. After three treatments as described, the polysaccharide was precipitated twice from aqueous solution with ethanol. The product was finally precipitated from an aqueous solution (pH 7.5) in 4 volumes of ethanol containing 8-hydroxyquinoline. The precipitate was thoroughly washed with acetone to remove chelate and excess chelating agent. The polysaccharide in the form of a nearly white powder had $[\alpha]_D^{25}$ +13° (*c*, 1 in water). Complete hydrolysis of a portion (1.5 g) yielded galactose (92.5%) and arabinose (7.0%). The mixture of sugars was resolved on sheets of Whatman 3MM paper using solvent A. D-Galactose was obtained

Can. J. Chem. Downloaded from www.nrcresearchpress.com by 210.87.254.6 on 09/05/12
For personal use only.

crystalline, m.p. and mixed m.p. 165–167° C, $[\alpha]_D^{25}$ +79.5° (*c*, 0.9 in water) and was converted by oxidation with nitric acid to mucic acid, m.p. and mixed m.p. 218–219° C. L-Arabinose was also obtained crystalline, m.p. and mixed m.p. 158–160°, $[\alpha]_D^{25}$ +104° (*c*, 0.4 in water).

Controlled Periodate Degradation of Arabinogalactan (Smith Degradation) (6)

To a quantity (4.45 g) of polysaccharide in water (120 ml) was added 0.5 *M* periodic acid (60 ml) and the solution stored at 5° C in the dark. Periodate uptake was determined periodically by the usual arsenite procedure. After 4 days, 0.82 moles of periodate per hexose unit had been consumed; after 6 days, 1.04 moles of periodate had been consumed per sugar residue with no change noted after 7, 8, and 9 days. Formaldehyde was determined (7) and on the assumption that two molecular proportions of formaldehyde are produced from a galactitol residue linked through C_4, the D.P. was estimated to be 285. Periodate and iodate were removed from the solution by precipitation with $BaCO_3$. To the filtrate containing the polyaldehyde was added KBH_4 (2.7 g) and the solution stored at room temperature for 24 hours. The solution was neutralized with dilute hydrochloric acid and evaporated to dryness. Borate was removed as methyl borate by several additions and evaporations (20° C) of 1% methanolic hydrogen chloride. The residue was dissolved in water, and the acidic solution (pH 2) left at room temperature for 6 hours, after which the solution was deionized using cation and anion exchange resins. Evaporation of the effluent gave a clear, syrupy product which was chromatographed using the three solvent systems and spray reagents mentioned earlier. At least eight components were detected, one of which reacted with *p*-anisidine trichloroacetate whereas the others were nonreducing in that they reacted only with Tollen's reagent. The mobilities (R_g) of the eight major components in solvent B were as shown below. A portion of the mixture was resolved using Whatman 3MM paper sheets and solvent B.

TABLE I

Chromatographic separation of compounds

Component	R_g	Weight (mg)
Glycerol (1)	2.92	465
D-Threitol (2)	1.82	445
L-Arabinose (3)	1.38	24
4	0.75	54
5	0.61	50
6	0.47	65
7	0.30	83
8	0.20	93

Characterization of Components

(a) Glycerol

The oily residue co-chromatographed with a known standard in the three solvent systems. To a portion (100 mg) of the compound in dry pyridine (4 ml) was added *p*-nitrobenzoyl chloride (5% molar excess) and the mixture heated at 70° for 1 hour. Excess aroyl halide was decomposed with water (1 ml) and saturated sodium bicarbonate (50 ml) added to the mixture with vigorous agitation. The precipitate was collected, thoroughly washed with water, and recrystallized from an ethanol:acetone mixture (1:1 v/v). The product, glycerol tri-*p*-nitrobenzoate, had m.p. and mixed m.p. 191–193° C.

(b) D-Threitol

The syrupy residue, $[\alpha]_D^{25}$ +4.5° (*c*, 8 in water), failed to crystallize. Treatment of a portion (100 mg) with 5% molar excess of *p*-nitrobenzoyl chloride in the manner described above gave the solid tetra-*p*-nitrobenzoate, m.p. 219–221° C. Calculated for $C_{32}H_{22}O_{16}N_4$:N, 7.92. Found: N, 7.88, 7.90.

(c) L-Arabinose

The syrup, $[\alpha]_D^{25}$ +103° (*c*, 0.2 in water), crystallized upon addition of a few seed crystals. The product had m.p. and mixed m.p. 158–160° C.

(d) Component 4

This nonreducing substance (54 mg), $[\alpha]_D^{25}$ −2° (approx.) (*c*, 1.8 in water) gave upon hydrolysis of a small portion (12 mg) galactose and threitol. The specific optical rotation changed in the course of hydrolysis from the stated value to approximately 36°. This upward shift constitutes strong evidence for a β-glycosidic linkage. The two constituents were determined using the phenol – sulphuric acid procedure (14) for the sugar and the periodate – chromotropic acid method for the polyol (7, 15). The molar ratio of galactose and threitol was found to be 1:1. The remainder of threityl galactoside (32 mg) was subjected to periodate oxidation (at 5° C) and formaldehyde determined. Approximately 3.4 mg formaldehyde was found from which a molecular weight of 290 was calculated for the compound, theory, 284. Periodate and iodate was precipitated with barium carbonate and the mixture filtered. Potassium borohydride (100 mg) was added to the filtrate and after 24 hours storage at room temperature, the solution was acidified with 2 *N* HCl,

Can. J. Chem. Downloaded from www.nrcresearchpress.com by 210.87.254.6 on 09/05/12
For personal use only.

refluxed, and worked up as described previously. Only glycerol (13 mg characterized as the *p*-nitrobenzoate) was found. The amount of glycerol obtained showed that galactose and threitol were both converted to the polyol. Treatment of a small portion (3.5 mg) of the glycoside in water (10 ml) with β-D-galactosidase (2 mg) gave galactose and threitol (1:1 molar ratio). The reaction was completed in 30 minutes. To a further quantity (5 mg) of this substance in dry pyridine was added *p*-nitrobenzoyl chloride and the reaction mixture handled in the usual fashion. The powdery product, 18 mg, was very sparingly soluble in organic solvents except pyridine and melted at 175–180° C. Calculated for $C_{73}H_{41}O_{40}N_7$: N, 5.92. Found: N, 6.08, 6.01.

A small portion (12 mg) of component 4 was methylated by the Kuhn procedure (16), followed by extended methylation with methyl iodide and silver oxide. The final product, 14 mg, showed no OH absorption in the infrared spectrum. The syrup was hydrolyzed with sulphuric acid (8) and 2,3,4,6-tetra-*O*-methyl galactose identified by paper chromatography. Resolution of a portion of the hydrolyzate by paper chromatography led to recovery of a few crystals of the tetramethyl galactose, m.p. 71–73° C. The remaining portion of the hydrolyzate was reduced (KBH_4) and the reduced residue boiled for 45 minutes with concentrated hydrobromic acid. After removal of the acid by repeated evaporation with methanol, galactitol and threitol were identified chromatographically. The molar ratio of the alcohols was determined by the periodate – chromotropic acid procedure (7, 15) and found to be 1:1 as expected. The experimental results dictate that the identity and structure of the compound must be 2-O-β-D-galactopyranosyl-D-threitol.

(e) Component 5

This substance had $[\alpha]_D^{25}$ −2° (approx.) (*c*, 1.8 in water), and gave, upon complete hydrolysis (N H_2SO_4) of a portion (10 mg), galactose, arabinose, and threitol, in a molar ratio of about 2:1:1. Another aliquot (40 mg) of the material was treated with periodic acid as described above. The molecular weight computed from the quantity (2.79 mg) of formaldehyde evolved was 430. The polyaldehyde was reduced (KBH_4) in the usual manner. The polyalcohol gave upon complete hydrolysis galactose, threitol, and glycerol in a molar ratio of 2:3:4. Paper electrophoresis of component 5 showed two components which will be referred to as 5A and 5B. A quantity (65 mg) of the mixture was resolved by paper electrophoresis. Component 5A constituted about 75% of the total material recovered from the electrophoretograms (75% recovery). Hydrolysis of a portion (7 mg) of 5A gave galactose and threitol in a molar ratio of 2:1. Periodate oxidation of the remaining material (40 mg) gave formaldehyde, the quantity (2.69 mg) of which indicated a molecular weight of 445 for the compound. Reduction (KBH_4) of the polyaldehyde and complete hydrolysis of the product gave galactose, glycerol, and threitol in a molar ratio of 1:4:1. These results indicated that 5A was composed of two oligosaccharides with the probable partial structures of (*a*) D-Gal*p* (1 → 4)-D-Gal*p* (1 → 2)-D-threitol and (*b*) D-gal*p*(1 → 3)-D-Gal*p*(1 → 2)-D-threitol. The oligosaccharide fragments were present in about equal molar proportions. The specific optical rotation (−3°) indicated that the glycosidic linkages were of the β-configuration.

Component 5B was investigated in a manner similar to that used for 5A. Hydrolysis of a portion (5 mg) gave galactose, arabinose, and threitol in a molar ratio of 1:1:1. Periodate oxidation of the remaining material (10 mg) gave formaldehyde, the amount (0.72 mg) of which corresponded to a molecular weight of 417. Reduction of the polyaldehyde (KBH_4) and complete hydrolysis of the product gave glycerol and a trace of arabinose. These results indicated that 5B was composed of two oligosaccharides with the probable partial structures of (*a*) D-Gal*p*(1 → 4)-L-Arab*p*(1 → 2)-D-threitol and (*b*) D-Gal*p*(1 → 2 or 3)-L-Arab*p* (1 → 2)-D-threitol.

(f) Components 6, 7, and 8

These substances were analyzed in the manner described for components 4 and 5. Some of the results are summarized in Table II.

TABLE II

Characteristics, composition, and results from Smith degradation (6) of some oligosaccharide components

Component	$[\alpha]_D^{25}$	Molar ratio of galact:arab: threitol	Molar ratio of galact:arab: threitol:glycerol after IO^-_4 treatment
6	−4.6	3:1:1	2:1:4:4
7	−7.5	4:2:1	2:1:2:10
8	−7.7	5:3:1	2:1:4:4

Paper electrophoresis of component 6 indicated that it was composed of two compounds and possibly three. The resolution of this material was by no means as distinct as for component 5. A portion (approximately 20%) of component 6 showed a somewhat faster electrophoretic mobility under the particular conditions used (350 v, 1–1.5 ma/in. of paper, 36 hours). Hydrolysis of a portion (6.5 mg) of the fast moving fraction gave galactose and threitol in molar ratio of 3:1. Periodate oxidation of the remaining material

Can. J. Chem. Downloaded from www.nrcresearchpress.com by 210.87.254.6 on 09/05/12
For personal use only.

(12 mg) gave formaldehyde, the amount (0.59 mg) of which indicated a molecular weight of 610. Reduction (KBH_4) of the polyaldehyde followed by complete hydrolysis of the polyalcohol gave galactose, threitol, and glycerol in a molar ratio of 1:3:4. The resistance of some galactose to periodate oxidation indicated the presence of at least two compounds with probable partial structures of (*a*) D-Gal*p*(1 → 4)-D-Gal*p*(1 → 4)-D-Gal*p*(1 → 2)-D-threitol and (*b*) D-Gal*p*(1 → 4)-D-Gal*p*(1 → 3)-D-Gal*p*(1 → 2)-D-threitol. The low specific optical rotation (−6°) indicated β-glycosidic linkages.

Hydrolysis of a portion (10 mg) of the slower moving material gave galactose, arabinose, and threitol in a molar ratio of 2:2:1. Periodate oxidation of the substance (60 mg) gave formaldehyde (1.25 mg) the amount of which indicated a molecular weight of 720. Reduction (KBH_4) of the polyaldehyde and complete hydrolysis of the product gave galactose, arabinose, threitol, and glycerol in a molar ratio of 2:1:4:5. These results indicated considerably more structural complexity.

Components 7 and 8 could not be resolved by electrophoresis and were not investigated further than indicated in Table II.

(g) Identification of Constituents of Oligosaccharide Hydrolyzates

The hydrolyzates from the individual oligosaccharides were combined and the constituents (galactose, arabinose, and threitol) separated using solvent C and Whatman 3MM paper. This procedure was adopted because of (*a*) the limited individual quantities involved and (*b*) the qualitative identity, as established by paper chromatography, of the individual oligosaccharide hydrolyzates. D-Galactose, 55 mg, was obtained crystalline after introduction of a few seed crystals and had m.p. and mixed m.p. 165–167° C. The original syrupy product had $[\alpha]_D^{25}$ +79° (*c*, 0.8 in water). Mucic acid, m.p. and mixed m.p. 218–219° C, was obtained upon oxidation of the sugar with nitric acid. L-Arabinose, 20 mg of syrupy material, $[\alpha]_D^{25}$ +101° (*c*, 0.4 in water), did not crystallize. The substance was reduced (KBH_4) to the corresponding alcohol, $[\alpha]_D^{25}$ −12.3° (*c*, 2.4 in water), and the final product, which was freed from borate, was acetylated with acetic anhydride and fused sodium acetate. The pentaacetate was obtained crystalline, m.p. and mixed m.p. 73–75° C.

(h) Identification of Constituents formed in Periodate Degradation of Oligosaccharides

The mixtures from components 5, 6, 7, and 8 were combined and resolved as described in the previous section. D-Galactose was isolated as a syrup (60 mg) which crystallized upon seeding, m.p. and mixed m.p. 165–167° C, $[\alpha]_D^{25}$ +80° (*c*, 0.6 in water). L-Arabinose was obtained as a syrup (30 mg), $[\alpha]_D^{25}$ +101° (*c*, 0.3 in water) and failed to crystallize. Reduction (KBH_4) of the sugar followed by acetylation gave the crystalline L-arabitol pentaacetate, m.p. and mixed m.p. 73–75° C. D-Threitol, obtained as a syrup (100 mg), $[\alpha]_D^{25}$ +4.4° (*c*, 2 in water), gave upon treatment with *p*-nitrobenzoyl chloride the corresponding *p*-nitrobenzoate, m.p. and mixed m.p. 219–220° C. Glycerol (180 mg), isolated as a mobile oil, gave upon treatment with *p*-nitrobenzoyl chloride the crystalline *p*-nitrobenzoate, m.p. and mixed m.p. 192–194° C.

Partial Acid Hydrolysis of Polysaccharide

A quantity (2.0 g) of arabinogalactan was suspended in cold 0.1 *N* HCl (200 ml). No change in viscosity was observed after the suspension had been left several days at room temperature. The solution was placed in a hot water bath (85° C) and after 1.5 hours, the relative viscosity had changed from 2.6 to about 1.2. The solution was cooled to 5° C and examined chromatographically using solvents A, B, and C. Arabinose, galactose, and a series of oligosaccharides were detected with *p*-anisidine trichloroacetate spray reagent. The relative amounts of arabinose, galactose, and oligosaccharide were determined by the phenol – sulphuric acid method (14). Approximately 80% of the arabinose present in the polysaccharide was removed by the above treatment. Increasing the acid concentration and refluxing the solution released the remaining arabinose. The relative quantities of each sugar were in accord with results obtained previously.

Methylation of Polysaccharide

To a sample (2.0 g) of borohydride-reduced polysaccharide in 30% sodium hydroxide (20 ml) was added simultaneously and with vigorous stirring five aliquots of dimethyl sulphate (30 ml) and 30% sodium hydroxide (30 ml). After the third addition, acetone was added to keep the partially methylated polysaccharide in solution. The polysaccharide was recovered from the acidified solution by extraction with chloroform and further methylated over extended time (two 72-hour treatments) with methyl iodide and silver oxide. The final product (2.5 g), a yellow glass, showed no OH^- absorption in the infrared spectrum. The alkylated polysaccharide was dissolved in 72% sulphuric acid (8), and after 45 minutes, the acidic solution diluted to about 2 *N* and boiled for 8 hours. The neutralized ($BaCO_3$) solution was evaporated to a syrup (1.8 g). Paper chromatography of the syrupy residue using butanone–water azeotrope (10) as solvent showed the presence of tetra-, tri-, and di-methyl hexose. The spot for tetramethyl galactose was multicolored, indicating the presence of 2,3,5-tri-*O*-methyl-L-arabinose. The components were separated by cellulose column chromatography (9) using butanone–water azeotrope (10) as irrigant. The weights of the components thus recovered were as follows.

Component		Weight (mg)
No. 1.	Tetramethyl fraction	244
No. 2.	Trimethyl fraction	1023
No. 3.	Dimethyl fraction	211
No. 4.	Monomethyl fraction	7

Can. J. Chem. Downloaded from www.nrcresearchpress.com by 210.87.254.6 on 09/05/12
For personal use only.

Analysis of Components

Component No. 1.—To the syrupy substance dissolved in water (15 ml) was added bromine and lead carbonate. The flask was wrapped in foil and the oxidation allowed to proceed for over 48 hours, after which time the solution was nonreducing. Excess bromine was removed by aeration, the insoluble inorganic lead salts filtered off and the filtrate passed through a cation exchange resin column to generate the free aldonic acids. The effluent was evaporated to a thick syrup which was, in turn, heated (water bath temperature 60° C) under vacuum to facilitate lactone formation. The mixture was resolved by vapor phase chromatography using a column (3 ft long, $\frac{1}{4}$ in. in diameter) packed with silanized chromosorb W coated with Versamid* (7%). With helium flow of 45 ml per minute and column temperature 155° C, the retention time of 2,3,5-tri-*O*-methyl-L-arabono-γ-lactone was 2 minutes. The compound crystallized spontaneously in the collection tube, m.p. 34° C, $[\alpha]_D^{22}$ −46° → −24° (*c*, 1.0 in water). These values are in agreement with those found in the literature (17). The retention time of 2,3,4,6-tetra-*O*-methyl-D-galactono-δ-lactone was 3.5 minutes, and it also crystallized spontaneously in the collection tube, m.p. 84–85° C, $[\alpha]_D^{22}$ +23° (*c*, 1.2 in water). Lit. (18) m.p. 84° C, $[\alpha]_D^{22}$ +22.6° (water). The molar ratio of tetramethyl galactose to trimethylarabinose was estimated using an integrator attachment and found to be 3:1.

Component No. 2.—The syrupy mixture was dissolved in methanol containing 1% hydrogen chloride and the solution refluxed until nonreducing. The solution was neutralized with silver carbonate, filtered, and evaporated. The syrup was dissolved in dry pyridine (10 ml) and trityl chloride added. The mixture was heated on a boiling water bath for 1 hour, cooled, and ice water added. The precipitate that formed was collected and dissolved in methanol (15 ml) containing hydrogen chloride. After the solution was warmed at 60° C for 30 minutes, water (150 ml) and lead carbonate were added. The insoluble material was removed by filtration and the filtrate evaporated. The residue was dissolved in 1 *N* H_2SO_4 and the solution boiled for 8 hours. Neutralization ($PbCO_3$) and evaporation of the solution gave a clear syrup (75 mg) which crystallized spontaneously. After recrystallization from ethyl acetate, the sugar had m.p. 82–84° C, $[\alpha]_D^{22}$ +152° → +117° (*c*, 0.5 in water). These values are in accord with those in the literature (19) for 2,3,4-tri-*O*-methyl-D-galactose.

The non-tritylated glycosides were hydrolyzed to the free sugars by boiling in 1 *N* H_2SO_4 for 8 hours. Paper chromatography indicated two sugars with R_f values similar to those reported (2) for 2,4,6- and 2,3,6-tri-*O*-methyl galactoses. The compounds were separated by cellulose column chromatography. The slower migrating sugar, 150 mg (2,4,6-tri-*O*-methyl galactose) crystallized spontaneously after evaporation of the solvent. After recrystallization from ethyl acetate, the sugar had m.p. 103–106° C, $[\alpha]_D^{22}$ +118 → +90° (*c*, 0.8 in water). These values are in good accord with reported values (20) for 2,4,6-tri-*O*-methyl-D-galactose. The faster migrating sugar, 750 mg, did not crystallize. The syrup had $[\alpha]_D^{22}$ +82° (*c*, 2 in water) indicative of 2,3,6-tri-*O*-methyl-D-galactose. A portion (500 mg) of the sugar was reduced with KBH_4 and the generated alcohol cleaved with periodate. No formaldehyde was evolved. Paper chromatography indicated the presence of a dimethyl tetrose, presumably 2,3-di-*O*-methyl-L-threose. A portion of the reaction mixture was freed from periodate and iodate and KBH_4 added. The reduced alcohols, presumably 2,3-di-*O*-methyl-L-threitol and monomethoxy ethylene glycol, were demethylated with hydrobromic acid to yield ethylene glycol and threitol. These products can only arise from 2,3,6-tri-*O*-methyl-D-galactose by the above reaction sequence. The two alcohols were resolved by paper chromatography using solvent A. Ethylene glycol (42 mg) was converted to the *p*-nitrobenzoate in the usual fashion, m.p. and mixed m.p. 140–142° C. L-Threitol (82 mg) $[\alpha]_D^{22}$ −4.4° (*c*, 4.1 in water) upon treatment with *p*-nitrobenzoyl chloride gave the tetra-*p*-nitrobenzoate, m.p. 220–221° C. Calculated for $C_{32}H_{22}O_{16}N_4$: N, 7.92. Found: N, 7.88, 7.93.

Component No. 3.—A portion (150 mg) of the syrup was dissolved in water and KBH_4 (180 mg) added. The product after removal of borate was oxidized with periodic acid at 5° C. Slightly less than 2 moles of periodate was consumed per mole of dimethyl hexitol. Periodate and iodate was removed by precipitation and the deionized solution evaporated. Paper chromatography of the product indicated the presence of a dimethyl tetrose as the major component with identical R_f value (0.79) as that obtained for 2,3-di-*O*-methyl-L-threose above. A slower-moving dimethyl pentose (R_g 0.5) was evident, presumably 2,4-di-*O*-methyl-L-lyxose. The components were resolved by column chromatography to give 2,3-di-*O*-methyl-L-threose, 65 mg, and 2,4-di-*O*-methyl-L-lyxose, 7 mg. A portion (40 mg) of the tetrose was reduced (KBH_4) and the dimethyl tetritol demethylated with hydrobromic acid. Removal of ionic material from the reaction mixture left L-threitol (22 mg), $[\alpha]_D^{22}$ −4.5° (*c*, 2.2 in water), which was identified chromatographically and as tetra-*p*-nitrobenzoyl-L-threitol, m.p. 219–221° C. The dimethyl pentose was not further investigated.

ACKNOWLEDGMENTS

Financial support from the National Research Council, Ottawa, Canada, is gratefully acknowledged. The author is indebted to Dr. J. C. Moomaw, University of Hawaii, for making available a generous supply of seed.

**Product of F and M Corp.*

Can. J. Chem. Downloaded from www.nrcresearchpress.com by 210.87.254.6 on 09/05/12
For personal use only.

REFERENCES

1. A. M. UNRAU. Chem. Ind. London, 1419 (1960).
2. F. SMITH and R. MONTGOMERY. Chemistry of plant gums and mucilages. Am. Chem. Soc. Monograph No. 141. Reinhold Publ. Co. 1959. pp. 57–65.
3. H. DEUEL and H. NEUKOM. Makromol. Chem. **4**, 97 (1950).
4. H. DEUEL and H. NEUKOM. Makromol. Chem. **3**, 13 (1949).
5. H. DEUEL, H. NEUKOM, and F. WEBER. Nature, **161**, 96 (1949).
6. I. J. GOLDSTEIN, G. W. HAY, B. A. LEWIS, and F. SMITH. Abstr. of papers, 136th Am. Chem. Soc. Meeting, Boston, Mass. April, 1959. p. 3D.
7. A. M. UNRAU and F. SMITH. Chem. Ind. London, 330 (1957).
8. I. CROON, G. HERRSTROM, G. KULL, and B. LINDBERG. Acta Chem. Scand. **14**, 1338 (1960).
9. J. D. GEERDES, B. A. LEWIS, R. MONTGOMERY, and F. SMITH. Anal. Chem. **26**, 264 (1954).
10. L. BOGGS, L. S. CUENDET, I. EHRENTHAL, R. KOCH, and F. SMITH. Nature, **166**, 520 (1950).
11. L. HOUGH, J. K. N. JONES, and W. H. WADMAN. J. Chem. Soc. 1702 (1950).
12. S. M. PARTRIDGE. Nature, **158**, 270 (1946).
13. R. U. LEMIEUX and H. F. BAUER. Anal. Chem. **26**, 920 (1954).
14. N. DUBOIS, J. K. HAMILTON, K. A. GILLES, P. A. REBERS, and F. SMITH. Anal. Chem. **28**, 350 (1956).
15. M. LAMBERT and A. C. NEISH. Can. J. Res. B, **28**, 83 (1950).
16. R. KUHN, I. LOW, and N. TRISHMAN. Ber. **90**, 203 (1957).
17. F. SMITH. J. Chem. Soc. 744 (1939).
18. W. N. HAWORTH, D. A. RUELL, and G. C. WESTGARTH. J. Chem. Soc. **125**, 2468 (1924).
19. D. MCCREATH and F. SMITH. J. Chem. Soc. 387 (1939).
20. A. L. CLINGMAN, J. R. NUNN, and A. M. STEPHEN. J. Chem. Soc. 197 (1957).

Can. J. Chem. Downloaded from www.nrcresearchpress.com by 210.87.254.6 on 09/05/12
For personal use only.

N.M.R. STUDIES OF BRIDGED RING SYSTEMS

II. UNUSUAL MAGNETIC DESHIELDING EFFECT ON THE BRIDGE METHYLENES OF NORBORNADIENE AND BENZONORBORNADIENE

K. TORI, Y. HATA, R. MUNEYUKI, Y. TAKANO, T. TSUJI, AND H. TANIDA
Shionogi Research Laboratory, Shionogi and Co., Ltd., Fukushima-ku, Osaka, Japan

Received October 17, 1963

ABSTRACT

Proton magnetic resonance spectra of some norbornane derivatives having double bonds and (or) a benzene ring in the skeleton were studied. Differences in the chemical shifts between the bridge methylenes of norbornene and benzonorbornene and that of norbornane result from the diamagnetic anisotropy effect of a double bond or a benzene ring being in good agreement with the values calculated theoretically. However, in the norbornadiene derivatives which have two double bonds or one olefinic double bond with a benzene ring in a part of the skeleton, the signals of their bridge methylenes show extraordinarily larger downfield shifts by about 0.8 p.p.m. than those expected from the additive shielding due to each π-electron system. This anomaly is not observed in bicyclo[2.2.2]octane ring series. A large transannular interaction between two π-electron systems in that system would be a major contribution to the above anomaly.

Can. J. Chem. Downloaded from www.nrcresearchpress.com by 210.87.254.105 on 09/05/12
For personal use only.

INTRODUCTION

In the past few years a number of proton magnetic resonance (n.m.r.) spectra of bridged ring systems have been investigated, reporting the relations between the spin coupling constants of ring protons and the stereochemistry (1–10), various types of long-range spin couplings (3, 5, 6, 8–11), the establishment of the configuration of substituents by the evaluation of diamagnetic shielding effects of a double bond or a benzene ring (9, 12–15), and so forth (16–19). However, the substantial features of n.m.r. spectra of bicyclo[2.2.1]heptane derivatives have not received much attention. By the studies of various monohydroxyl derivatives of bicyclo[2.2.1]heptane, Musher (8) has recently reported that (i) a strikingly large difference in the magnetic shielding between an exo and an endo proton was observed, showing larger deshielding on the exo proton, and this difference can not be explained only by the diamagnetic anisotropy of the C—C bonds in the ring; that (ii) the coupling constants between each pair of adjacent protons, $J_{H_x-H_x}$ and $J_{H_n-H_n}$*, are not equal; and that (iii) fairly large long-range spin coupling constants were found. On the basis of these results, he suggested the presence of some π-characters in this ring system. In a previous paper (20), we also suggested the presence of this character on the basis of the increased *s*-character of the C—H bonds, which was reflected in the strikingly large values of carbon–hydrogen spin coupling constants $J_{C^{13}-H}$ obtained from the C^{13}-satellites (21) in the n.m.r. spectra of norbornane (I), norbornene (II), norbornadiene (III), benzonorbornene (IV), benzonorbornadiene (V), and quadricyclene (VI).

This paper deals with the spectra of the compounds of I–VI in comparison with those of bicyclo[2.2.2]octane derivatives, which are bicyclo[2.2.2]octene (VII), bicyclo[2.2.2]-octadiene (VIII), benzobicyclo[2.2.2]octene (IX), benzobicyclo[2.2.2]octadiene (X), and dibenzobicyclo[2.2.2]octadiene (XI). The diamagnetic shielding effects of a double bond (14, 22) or of a benzene ring (23) upon their bridge methylenes and (or) bridge ethylenes are estimated experimentally and are compared with the values theoretically

**Protons* H_{exo}, H_{endo}, H_{anti}, *and* H_{syn} *are abbreviated as* H_x, H_n, H_a, *and* H_s, *respectively.*

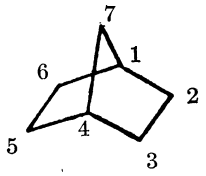

(I)

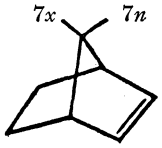

(II)

(III)

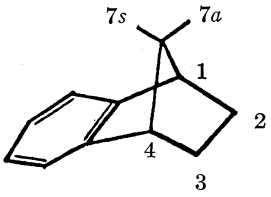

(IV)

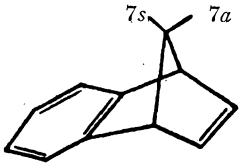

(V)

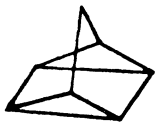

(VI)

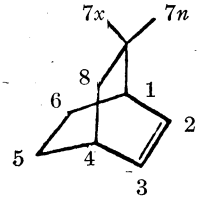

(VII)

(VIII)

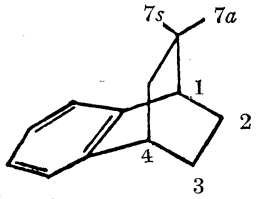

(IX)

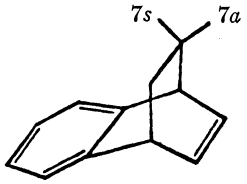

(X)

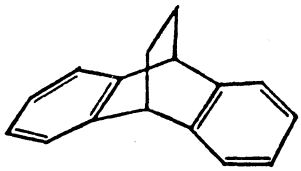

(XI)

calculated (24, 25, 26). Particularly, an unusual deshielding effect on the bridge methylenes of III and V will be discussed.

RESULTS AND DISCUSSION

The chemical shifts of assignable protons in the n.m.r. spectra of bicyclo[2.2.1]heptane derivatives (I–VI) are shown in Table I, in comparison with those of bicyclo[2.2.2]octane derivatives (VII–XI). Figure 1 shows a part of the spectra of II and IV.

Can. J. Chem. Downloaded from www.nrcresearchpress.com by 210.87.254.105 on 09/05/12
For personal use only.

TABLE I

Chemical shifts (τ) of all assignable protons of some bicyclo[2.2.1]heptanes and bicyclo[2.2.2]octanes in deuterochloroform solutions

Compound	Olefinic	Bridgehead	Bridge methylene or ethylene	Reference
Norbornane (I)	—	7.80 7.81*	8.80 8.74*	This work (16)
Norbornene (II)	4.02 4.06*	7.15 7.22*	8.92(n) 8.67(x)	This work (16)
Norbornadiene (III)	3.27 3.35*	6.43 6.53*	8.02 8.05*	This work (16)
Benzonorbornene (IV)	—	6.65	8.52(s) 8.27(a)	This work
Benzonorbornadiene (V)	3.23	6.13	7.80(a) 7.67(s)	This work
Quadricyclene (VI)	—	8.53† 8.59*,†	7.98 8.01*	This work (18)
Bicyclo[2.2.2]octene (VII)	3.75	7.51	~8.73(n) ~8.50(x)	(9)
Bicyclo[2.2.2]octadiene (VIII)	3.73	6.41	8.75	This work (cf. 27)
Benzobicyclo[2.2.2]octene (IX)‡	—	7.04	~8.58(s) ~8.23(a)	(9)
Benzobicyclo[2.2.2]octadiene (X)§	3.52	6.09	~8.57(s) ~8.47(a)	(9)
Dibenzobicyclo[2.2.2]-octadiene (XI)	—	5.71	8.32	This work

*Data on solutions in carbon tetrachloride.
†The strongest peak of the signals of the six cyclopropyl protons.
‡Prepared from X by the catalytic reduction over palladium charcoal.
§Prepared by the procedure of Kitahōnoki and Takano, Tetrahedron Letters, No. 24, 1597 (1963). Also, refer to ref. 13.

In general, the signals of these compounds were easily assignable, except for the chemical shifts of the protons on the bridge methylenes of II and IV, which were assigned according to the following way. The signals of protons on these bridge methylenes generally appear as an AB-type quartet, each of which is further split into a triplet by the bridgehead protons. Additional long-range spin couplings, if they appear, will be small (3, 8, 11). The geminal coupling constant of these bridge methylene protons is believed to be about 8 c.p.s., which is unusually small, by reference to this sort of the coupling constant in V (20). The differences in the chemical shifts between the protons H_x and H_n on the ethylene bridge of II and IV should be much larger than the value observed in I, because of the anisotropy effect of a double bond or a benzene ring. On the basis of the above idea and observed relative integrated areas of signals, we tentatively assigned signals of the bridge methylenes of II and IV, as shown in Fig. 1. The signals of the bridge methylene of V separately appear as an AB-type quartet, each of which is split into a triplet. The detailed assignments of this quartet to the H_{7s} or H_{7a} were achieved on reference to the data of some authentic C_7-derivatives (28). The protons on the bridge ethylenes of VII, IX, and X exhibit the complex signal patterns of an $A_2B_2X_2$ system and the determinations of their exact chemical shifts seemed difficult. However, they closely resemble the AB part of a usual ABX system. Therefore, approximate values of the chemical shifts were obtained according to the treatment of an ABX-type pattern (9). It is of interest to note the presence of a long-range spin coupling

Can. J. Chem. Downloaded from www.nrcresearchpress.com by 210.87.254.105 on 09/05/12
For personal use only.

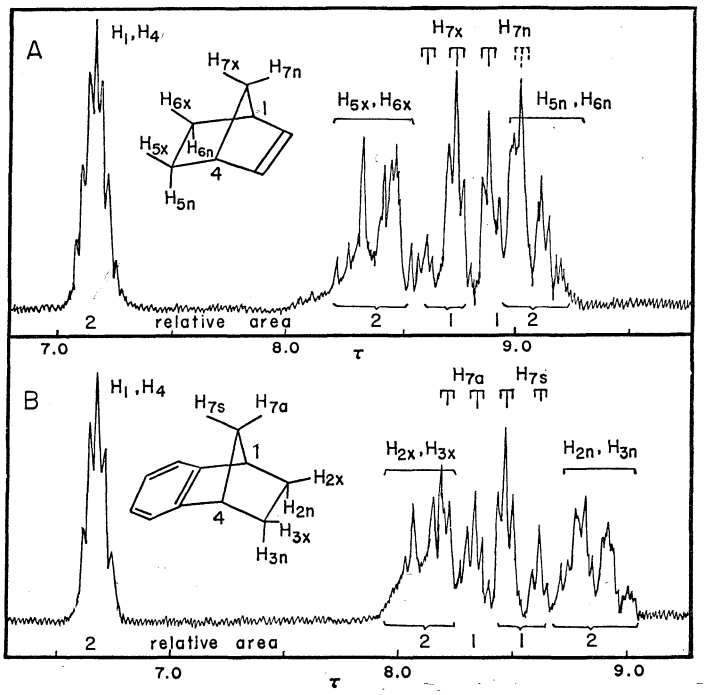

FIG. 1. A: n.m.r. spectrum of norbornene (II); B: n.m.r. spectrum of benzonorbornene (IV). The low field parts of the spectra are not presented.

$J_{7x-2(3)}$ (about 0.3 c.p.s.), being clearly observed on the C^{13}-satellites in the spectrum of III, in addition to the long-range spin couplings, J_{2x-6x} (J_{3x-5x}) and $J_{7n-5x(6x)}$, already observed by several workers (3, 8, 11).*,†

Shielding Effects of a Double Bond upon Bridge Methylenes

Much is now known about the appreciable anisotropy of the diamagnetic shielding effect of a double bond on neighboring protons in the presence of a strong field (22). By this effect, the signal of a proton which lies above the plane of the sp^2-bonds is shifted to upfield, whereas a downfield shift is experienced by the proton which lies in the sp^2-bond plane. Fraser (14) demonstrated these facts in comparison of the signals of the protons H_5 and H_6 on some C_5- or C_6-substituted norbornenes with those of the corresponding norbornanes.

The shift values of the signals of bridge methylenes or ethylenes due to an introduction of a double bond are summarized in Table II.‡ The introduction of a double bond into I induces a downfield shift of the H_{7x} signal by 0.13 p.p.m. and also an upfield shift of the

The coupling constants of the compounds I–VI were reported in the previous paper (20).

†*The long-range spin coupling $J_{7s-2(3)}$ (about 0.8 c.p.s.) is noticed clearly in some 7a-substituted derivatives of V (28).*

‡*It may be somewhat dubious to estimate the effect of a double bond by the difference in proton signal shifts between the saturated and the unsaturated compound because the introduction of a double bond produces a change in the conformation of a ring and consequently in the shielding effects of* C—C *bonds (29) and* C—H *bonds. The* C—H *bond anisotropy has recently been discussed to be not negligible (refer to Discussions of Faraday Soc. 34 (1962)). However, the relative position of a relevant proton on a bridge to the* C—C *bonds, which construct the ring of our compounds, will be almost unchanged with respect to the replacement of a single bond into a double bond. Accordingly, the above treatment will be generally valid.*

Can. J. Chem. Downloaded from www.nrcresearchpress.com by 210.87.254.105 on 09/05/12
For personal use only.

TABLE II

Differences in chemical shifts of the bridge methylenes and ethylenes due to the introduction of a double bond, in p.p.m.

Compound	H_{7exo}	H_{7endo}	$\lvert H_{7exo}-H_{7endo}\rvert$
I → II	−0.13	+0.12	0.25
II → III	−0.90	−0.62	0.28
IV → V	−0.85	−0.47	0.28
Calculated value from eq. [A]*	-0.12_8	$+0.19_2$	0.32_0
VII → VIII	+0.02	+0.25	0.23
IX → X	−0.01	+0.24	0.25
Mean value reported in ref. 9†	−0.07	+0.17	0.24
Calculated value from eq. [A]*	-0.08_8	$+0.18_1$	0.26_9

*See text.
†Derived from the spectral data on eighteen bicyclo[2.2.2]octane derivatives, which were reported in ref. 9.

corresponding H_{7n} signal by 0.12 p.p.m. It is possible to explain quantitatively the difference in these shieldings (in p.p.m.) by using the following formula [A] of Nakagawa *et al.* (25) for the total shielding effect due to two π-electrons of a double bond:

$$\delta(\text{p.p.m.}) = \frac{\Delta\chi}{3}\left(\frac{1-3\cos^2\theta_1}{R_1^3} + \frac{1-3\cos^2\theta_2}{R_2^3}\right) \qquad [A]$$

where R is the distance from a carbon atom **C** of a double bond to an affected proton **H**, θ is the angle formed by the axis of a π-electron (z-axis) and the **C–H** line, as illustrated diagrammatically in Fig. 2, and the constant $\Delta\chi$ was determined empirically as about

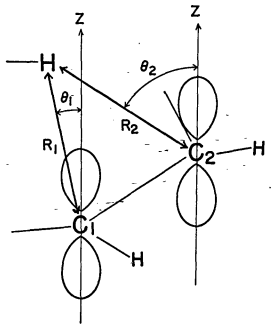

FIG. 2. A diagrammatic illustration of magnetic anisotropy of a double bond.

-10×10^{-30} cm³.* The values calculated from the equation [A] agree well with those observed, as listed in Table II. Molecular geometries were estimated by using the Barton model. The data on bicyclo[2.2.2]octane derivatives are also consistent with the calculated values, as seen from Table II. However, of particular interest is the fact that a further introduction of a double bond into the compounds II and IV already having a double bond or a benzene ring causes an extraordinary downfield shift of the bridge methylene signals, whereas this fact is not experienced in a series of bicyclo[2.2.2]octanes.

**The procedure of Nakagawa et al. (25), which is an application of McConnell's equation (30) and different from the others (14, 24), seemed to us best for obtaining the anisotropic effect of a double bond. A good example is the effects on the protons* $H_{5n}(H_{6n})$ *and* $H_{5x}(H_{6x})$ *in norbornane derivatives, which were obtained to be +0.04 and −0.14 p.p.m. experimentally by Fraser (14), and* $+0.04_7$ *and* -0.22_3 *p.p.m. by the present calculations, respectively.*

Can. J. Chem. Downloaded from www.nrcresearchpress.com by 210.87.254.105 on 09/05/12
For personal use only.

Shielding Effects of a Benzene Ring upon Bridge Methylenes

The shielding effect of a benzene ring on neighboring protons is well known as the ring current effect (23). The effects of a benzene ring are summarized in Table III in the same

TABLE III

Differences in chemical shifts of the bridge methylenes and ethylenes due to the introduction of a benzene ring, in p.p.m.

Compound	H_{7anti}	H_{7syn}	$\lvert H_{7anti}-H_{7syn}\rvert$
I → IV	−0.53	−0.28	0.25
II → V	−1.10	−1.00	0.10
Calculated value from Johnson and Bovey's method*	−0.29	−0.02	0.27
VII → X	−0.26	+0.07	0.33
X → XI	−0.26	+0.09	0.35
Mean value reported in Ref. 9†	−0.30	+0.06	0.36
Calculated value from Johnson and Bovey's method*	−0.23	+0.07	0.30

*See text.
†Derived from the spectral data on eleven bicyclo[2.2.2]octane derivatives, which were reported in ref. 9.

manner as those of a double bond were done. The theoretical shielding effect of a benzene ring can be easily calculated from the molecular geometry according to Johnson and Bovey's method (27). Table III also shows the values obtained from the calculations. Molecular geometries were estimated by using the Barton model. Upon the similar consideration to the case of a double bond, the introduction of a benzene ring into I produces downfield shifts of the H_{7a} and H_{7s} signals by 0.53 and 0.28 p.p.m., respectively. These shifts as well as those of the bicyclo[2.2.2]octane derivatives are comparable to the values obtained from calculations. The analogous interesting fact to the above is found in the case of a condensation of a benzene ring to the C_5- and C_6-positions of II, in which extraordinary downfield shifts appear in the H_{7a} and H_{7s} signals of V. There are not such indications in bicyclo[2.2.2]octane series.

Unusual Deshielding Effects upon Bridge Methylenes of Norbornadienes

If the additivity principle of magnetic shielding effects could be applied to the bicyclo-[2.2.1]heptane series, the bridge methylene signals of III should appear at about 8.8τ and that of V should be at about 8.4τ. However, their signals actually obtained show such a striking large downfield shift as about 0.8 p.p.m. from the expected positions. This fact could not be explained by the change of molecular geometries due to the introduction of two π-electron systems. Recently we proposed the increasing of *s*-character in all the C—H bonds of this ring system (20). Moreover, recent studies of ultraviolet absorption spectroscopy demonstrated a considerably larger transannular interaction between two double bonds of III, and its resonance integral value was estimated to be 0.385 β (SMO) by Wilcox *et al.* (31) and 0.74 eV (SCFMO) by Paldus and Koutecký (32). In contrast, the ultraviolet spectrum of VIII suggests that this kind of interaction is not so large as that of III (33). These findings were also supported by the measurements of the heats of hydrogenation of III and VIII (34).

A clear explanation for these unusual deshielding effects on the bridge methylenes of III and V may be difficult immediately. However, we suppose that this effect can result from a novel type of the magnetic shielding arising from a large transannular interaction between the π-electron systems, besides from the change in the diamagnetic anisotropy

Can. J. Chem. Downloaded from www.nrcresearchpress.com by 210.87.254.105 on 09/05/12
For personal use only.

of C—C bonds of III and V with the "bent" of the bonds due to the more ring strain, as reflected in the increased $J_{C^{13}-H}$ values in the rings (20). The signal of the bridge methylene of VI also appears at a very low field as 7.98τ, as shown in Table I. The latter observation would be due to the change in the diamagnetic anisotropy of C—C bonds, as mentioned above, along with the possible small ring currents of two cyclopropyl rings (35).*

EXPERIMENTAL

All the spectra were observed on 10% (w/v) solutions in deuterochloroform with tetramethylsilane as an internal standard at room temperature, by using a Varian A-60 n.m.r. spectrometer, whose calibration was checked by Tiers and Hotchkiss' method (37). Accuracies of chemical shifts and coupling constants are within $\pm 0.02\ \tau$ and ± 0.03 c.p.s., respectively.

ACKNOWLEDGMENTS

The authors are indebted to Prof. N. Nakagawa, University of Electro-communications, for his helpful discussions on the diamagnetic anisotropy of a double bond, to Prof. C. A. Grob, Universität Basel, for the supply of an authentic sample of bicyclo[2.2.2]octadiene, and to Mr. M. Yamakawa, in this laboratory, for the information about its ultraviolet spectrum. They also acknowledge the encouragement of Drs. K. Takeda, T. Nakagawa, and K. Kitahōnoki in this laboratory.

REFERENCES

1. W. D. Kumler, J. N. Shoolery, and F. V. Brutcher, Jr. J. Am. Chem. Soc. **80**, 2533 (1958).
2. E. J. Corey, M. Ohno, S. W. Chow, and R. A. Scherrer. J. Am. Chem. Soc. **81**, 6305 (1959).
3. F. A. L. Anet. Can. J. Chem. **39**, 789 (1961).
4. M. M. Anderson and P. M. Henry. Chem. Ind. 2053 (1961).
5. J. Meinwald and A. Lewis. J. Am. Chem. Soc. **83**, 2769 (1961).
6. K. B. Wiberg, B. R. Lowry, and B. J. Nist. J. Am. Chem. Soc. **84**, 1594 (1962).
7. K. L. Williamson. J. Am. Chem. Soc. **85**, 516 (1963).
8. J. I. Musher. Mol. Phys. **6**, 94 (1963).
9. K. Tori, Y. Takano, K. Kitahōnoki, and T. Nakagawa. To be published. (*Presented at* The 2nd Symposium on Nuclear Magnetic Resonance (Japan), Tokyo. November, 1962.)
10. J. Meinwald, Y. C. Meinwald, and T. N. Baker, III. J. Am. Chem. Soc. **85**, 2513 (1963).
11. J. Meinwald and Y. C. Meinwald. J. Am. Chem. Soc. **85**, 2514 (1963).
12. R. L. Erskine and S. A. Knight. Chem. Ind. 1160 (1960).
13. H. E. Simmons. J. Am. Chem. Soc. **83**, 1657 (1961).
14. R. R. Fraser. Can. J. Chem. **40**, 78 (1962).
15. W. L. Meyer and R. W. Huffman. Tetrahedron Letters, No. 16, 691 (1962). F. A. L. Anet. Tetrahedron Letters, No. 25, 1219 (1962). W. A. Ayer, C. E. McDonald, and J. B. Stothers. Can. J. Chem. **41**, 1113 (1963).
16. G. V. D. Tiers. Characteristic nuclear magnetic resonance "shielding values" for hydrogen in organic structures. Minnesota Mining and Manufacturing Co., St. Paul, Minn. 1958.
17. P. R. Story. J. Am. Chem. Soc. **82**, 2085 (1960). P. R. Story and M. Saunders. J. Am. Chem. Soc. **84**, 4876 (1962). N. O. Brace. J. Org. Chem. **27**, 3027 (1962).
18. W. G. Dauben and R. L. Cargill. Tetrahedron, **15**, 197 (1961).
19. P. Yates and S. Danishefsky. J. Am. Chem. Soc. **84**, 879 (1962).
20. K. Tori, R. Muneyuki, and H. Tanida. Can. J. Chem. **41**, 3142 (1963).
21. N. Muller and D. E. Pritchard. J. Chem. Phys. **31**, 768, 1417 (1959).
22. L. M. Jackman. Applications of nuclear magnetic resonance in organic chemistry. Pergamon Press, New York. 1961. p. 129.
23. J. A. Pople, W. G. Schneider, and H. J. Bernstein. High-resolution nuclear magnetic resonance. McGraw-Hill Book Co., Inc., New York. 1959. pp. 180, 251.
24. J. A. Pople. J. Chem. Phys. **37**, 53, 60 (1962). J. A. Pople. Discussions Faraday Soc. **34**, 7 (1962).
25. S. Yamaguchi, S. Okuda, and N. Nakagawa. Chem. Pharm. Bull. **11**, 1465 (1963); and private communication.
26. C. E. Johnson, Jr. and F. A. Bovey. J. Chem. Phys. **29**, 1012 (1958).
27. C. A. Grob, H. Kny, and A. Gagneux. Helv. Chim. Acta, **40**, 130 (1957).
28. K. Tori, R. Muneyuki, T. Tsuji, Y. Hata, and H. Tanida. To be published. (*Presented at* The 16th annual meeting of the Chemical Society of Japan, Tokyo. April, 1963.)
29. L. M. Jackman. Applications of nuclear magnetic resonance in organic chemistry. Pergamon Press, New York. 1961. p. 112.
30. H. M. McConnell. J. Chem. Phys. **27**, 226 (1957).

**This ring current may not be fully believed at present (36).*

Can. J. Chem. Downloaded from www.nrcresearchpress.com by 210.87.254.105 on 09/05/12
For personal use only.

31. C. F. WILCOX, JR., S. WINSTEIN, and W. G. MCMILLAN. J. Am. Chem. Soc. **82**, 5450 (1960).
32. P. PALDUS and J. KOUTECKÝ. Collection Czechos. Chem. Commun. **27**, 2139 (1962).
33. M. YAMAKAWA. Private communication.
34. R. B. TURNER, W. R. MEADOR, and R. E. WINKLER. J. Am. Chem. Soc. **79**, 4116 (1957).
35. K. B. WIBERG and B. T. NIST. J. Am. Chem. Soc. **83**, 1226 (1961). J. D. GRAHAM and M. T. ROGERS. J. Am. Chem. Soc. **84**, 2249 (1962).
36. B. P. DAILEY, A. GAWER, and W. C. NEIKAM. Discussions Faraday Soc. **34**, 18 (1962).
37. G. V. D. TIERS and D. R. HOTCHKISS. J. Phys. Chem. **66**, 560 (1962).

Can. J. Chem. Downloaded from www.nrcresearchpress.com by 210.87.254.105 on 09/05/12
For personal use only.

THE KINETICS OF THE CHELATION OF NICKEL (II) AND 1,10-PHENANTHROLINE

P. F. BARRETT AND W. MACF. SMITH
Department of Chemistry, Queen's University, Kingston, Ontario
Received September 17, 1963

ABSTRACT

The kinetics of the formation of the bidentate monocomplex of 1,10-phenanthroline and nickel (II) have been examined spectrophotometrically at ionic strength 0.5 over the range of temperatures 8 to 37° C and over the range of hydrogen ion concentrations 0.01 to 0.30 molar. The kinetic behavior over the range of conditions is consistent with that found at 25° C by Margerum, Bystroff, and Banks. The limiting values for the second-order rate constant for the reaction at high acidities have been assessed and imply associated values of $\Delta H^{\ddagger}$ and $\Delta S^{\ddagger}$ of 9.5 kcal mol^{-1} and −5.3 e.u. respectively.

INTRODUCTION

The reaction between nickel (II) and 1,10-phenanthroline yields a bidentate monocomplex at a rate convenient for kinetic studies both in water and in certain mixed solvents. The kinetics of the reaction involving the formation of the complex was studied in detail by Margerum, Bystroff, and Banks (1) at 25° C. They showed that the second-order rate constant increased with acidity and approached a constant value at higher acidities.

Wilkins and Williams (2) and Ellis, Hogg, and Wilkins (3) estimated the rate of the acid-independent solvolysis of the monocomplex over a range of temperature through measurements on the rate of exchange of ^{63}Ni (II) which, they considered, was directly controlled by the rate of solvolysis.

The work described below assesses kinetic features of the acid-dependent formation of the monocomplex at constant ionic strength and over a range of temperatures and is part of a program to obtain comparable data about the kinetics of the formation of the bidentate complexes of nickel (II) and iron (III) and the effect of solvent composition on the reactions of nickel (II).

EXPERIMENTAL

Materials

Water used in preparing the solutions was triply distilled, the second distillation being from alkaline permanganate. Sodium perchlorate (anhydrous), perchloric acid (70%), and nickel (II) perchlorate were all reagent grade obtained from G. Frederick Smith Chemical Company. The pyridine method outlined by Vogel (4) was used in estimating the nickel content of solutions. Eastman reagent grade 1,10-phenanthroline was used and three different sample lots gave indistinguishable spectra and kinetic properties.

Methods and Apparatus

The reaction was followed spectrophotometrically with light of wavelength 310 mμ. Nickel (II) is essentially transparent at this wavelength for the conditions of this work and the difference in the extinction coefficients of the monocomplex and the monoprotonated phenanthrolium ion is nearly at a maximum. The data discussed below indicate that under the conditions of the kinetic studies over 99.9% of the phenanthroline is in the protonated form and over 98% of the total phenanthroline is complexed at equilibrium. Under these conditions the concentration of complex is proportional to the change in optical density.

All spectrophotometric measurements relating to kinetics and equilibria were made with a Beckman extended range DK-1 spectrophotometer using thermostated quartz cells of path length of 1 cm. The pH was determined with a Radiometer number 4 pH meter on thermostated samples. Standardization for the lower pH's was made with 0.050 molar potassium tetroxalate (5).

In a kinetic run, equal volumes (1.5 ml) of two solutions, one containing nickel (II) perchlorate, the other

Can. J. Chem. Downloaded from www.nrcresearchpress.com by 210.87.254.40 on 09/05/12
For personal use only.

phenanthroline, were mixed in the quartz absorption cell of the spectrophotometer by simultaneous ejection of the solutions from 2-ml syringes fitted with polythene tips directed in a way to ensure mixing. The two solutions were of identical ionic strength and had the same concentrations of perchloric acid. Solutions and pipettes were thermostated prior to the mixing operation. The value of the optical density at equilibrium along with the extinction coefficient of the complex (estimated as indicated below) was used to check the concentration of total phenanthroline using the assumption that substantially all of the phenanthroline was present as the monocomplex.

The Ionization Quotient of Phenanthrolium Ion

The interpretation of the kinetic data required a knowledge of the acid ionization quotient of the monoprotonated phenanthrolium ion. Margerum, Bystroff, and Banks (1) examined the equilibria involving the free and protonated forms. However, quantitative values for the acid ionization quotient of the monoprotonated species covering the range of our experimental conditions were not available and we have carried out measurements relating to the quotient at ionic strength 0.5 and temperatures from 13 to 37°. We have also assessed the extinction coefficient of the monocomplex ($NiPh^{++}$).

If Q_a represents the acid ionization quotient of the monoprotonated species then

$$\log ([Ph]/[HPh^+]) + \log a_{H^+} = \log Q_a\gamma_{H^+} \quad [1]$$

where [Ph] and $[HPh^+]$ represent concentrations of the free and monoprotonated 1,10-phenanthroline and γ_{H^+} is the activity coefficient of hydrogen ions. If the pH, indicated by the meter, were equal to $-\log a_{H^+}$ then $\log Q_a\gamma_{H^+}$ could be estimated. Also the plot of $[Ph]/[HPh^+]$ against the antilog of the pH would be a straight line.

We have estimated by spectrophotometric methods the ratio $[Ph]/[HPh^+]$ for solutions in the range of pH 4.9 to 5.5 and ionic strength 0.5 and find that the plot of $[Ph]/[HPh^+]$ against the antilog of the pH is indeed a straight line over this range. The extinction coefficients for the free base and the monoprotonated species were estimated from absorption measurements in solutions in the pH ranges 7.8 to 8.9 and 1.2 to 2.3. Values of $Q_a\gamma_{H^+}$ estimated from relation 1 are given in Table I. The associated standard deviations are about four percent of the values given. A value of 0.567×10^{-5} for 8° was obtained by extrapolation. These values of $Q_a\gamma_{H^+}$ along with measured pH values and equation [1] were used to estimate the ratio $[HPh^+]/[Ph]$ and $f = [Ph]/([HPh^+] + [Ph])$ for the solutions used in the kinetic experiments. Under all conditions more than 99% of the phenanthroline was in the monoprotonated form. It may be noted that the validity of the procedure depends on the measured estimate of the pH being proportional to $-\log a_{H^+}$ and the value of γ_{H^+} remaining constant.

The extinction coefficient of the $Ni(Ph)^{+2}$ complex at 310 mμ was determined using solutions of pH = 2.0, total phenanthroline concentrations in the range 0.15×10^{-3} to 1.0×10^{-3} molar and Ni (II) in about 10-fold excess. Under these conditions the optical density is proportional to the total concentration of phenanthroline, which indicates essentially complete complexing of this base. The slope of the plot of data obtained at temperature 25° C and ionic strength 0.5 indicated an extinction coefficient of 1338 l. mol^{-1} cm^{-1}. The overall changes in optical density under the conditions of the kinetic runs were consistent with this value and complete complexing of the phenanthroline to ±2%.

TABLE I

The acid ionization quotient of 1,10-phenanthrolium ion: values of $Q_a\gamma_{H^+}$

Temperature, ° C	$Q_a\gamma_{H^+}\times10^5$
13.0	0.613
19.0	0.676
25.0	0.751
31.0	0.888
37.0	1.022
43.0	1.194

Interpretation of the Kinetic Data

For the solutions used in the kinetic runs and at λ 310 mμ the monobidentate complex and the monoprotonated phenanthroline are the only species contributing appreciably to optical density, and the concentration of monocomplex is proportional to the change in optical density which has occurred since zero time. If the reaction is first order in free phenanthroline and first order in Ni (II) ion, which is in large excess, then

$$\text{constant} - \ln (D_\infty - D) = k_f f.M.t \quad [2]$$

where D_∞ and D are the optical densities of the reacting solution at equilibrium and time t, k_f is the second-order constant defined by (d/dt) [complex] $= k_f$ $[Ni^{++}]$ [Ph], f is the fraction of uncomplexed phenanthroline existing as the free base and M is the total concentration of Ni (II).

Can. J. Chem. Downloaded from www.nrcresearchpress.com by 210.87.254.40 on 09/05/12
For personal use only.

A plot of ln $(D - D_\infty)$ against t should yield a straight line with slope $k_f.M.f.$ Data from our runs yield linear plots with the value of k_f depending on acidity and tending to a limit at higher acidities. This was noted by Margerum, Bystroff, and Banks (1), who suggested two mechanisms to account for this behavior.

In their mechanism I, indicated below, a labile intermediate NiPh—$^{++}$ (A) involving a single bond between phenanthroline and nickel ion is formed and this then forms a bidentate complex directly or via a path involving the protonated species NiHPh—$^{+++}$

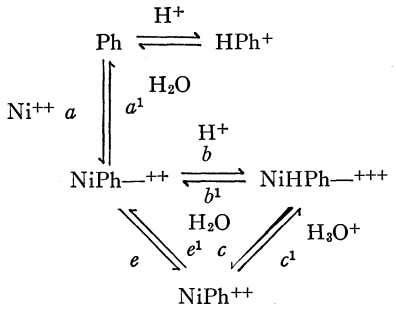

a, a^1, b, etc. represent rate constants.

In their second mechanism the transient species A is formed directly as in mechanism I but in addition phenanthrolium ion (HPh^+) is involved in reaction with nickel to give the singly bonded and protonated intermediate (NiHPh—$^{++}$) which by proton loss yields the species A and this is the sole precursor to the final bidentate complex.

If the back reaction of the final product is neglected it can be shown that both mechanisms imply that at higher acidities the rate of formation of the bidentate complex can be expressed by

$$(d/dt)[\mathrm{NiPh}^{++}] = (m+[\mathrm{H}^+])/(p+n[\mathrm{H}^+])[\mathrm{Ni}^{++}][\mathrm{Ph}]$$

where m, p, and n are related to the rate constants of the various steps. If m is negligible relative to $[H^+]$ the effective rate constant (k_f) becomes $[H^+]/(p+n[H^+])$ and a plot of $1/k_f$ against $1/[H^+]$ would yield a straight line with intercept n. At very low acidities the rate constant is m/p, which on the basis of both mechanisms is equal to $ae/(a^1+e)$. On the basis of mechanism I $1/n$ is equal to a, the rate constant for the first step in the attachment of the ligand. (This corresponds to the condition approached at high acidity where the intermediate A is transformed to bidentate product by the acid-catalyzed path at a rate equal to that of the formation of A.) On the basis of mechanism II, $1/n = e \times K_e^1$ where K_e^1 is the formation constant for A from nickel (II) ion and free phenanthroline. (This corresponds to the condition where the intermediate A is maintained at equilibrium concentration through formation from phenanthrolium ion.)

RESULTS OF THE KINETIC MEASUREMENTS AND DISCUSSION

Measurements of rate were made over the range of temperatures and concentrations of acid shown in Table II. Concentrations of nickel (II) varied from 1×10^{-2} to 4×10^{-2} M and total phenanthroline from 0.6×10^{-4} to 1.3×10^{-4} M. Data from all runs yielded plots of log $(D_\infty - D)$ against time which were good straight lines with no significant dependence of the slope (and rate constants) on the initial concentration of either reactant at a given hydrogen ion concentration. The values of the rate constants (k_f) given in Table II are the means of values from six to eight runs carried out with different concentrations of nickel (II) and phenanthroline.

Plots of $1/k_f$ against $1/[H^+]$ for concentrations of hydrogen ion 0.04 molar and greater are given in Fig. 1 and indicate that data for higher acidities were consistent with a linear relationship. Values of n, p, and m were derived separately from values of the rate constants obtained from smoothed curves of k_f against $[H^+]$ through the experimental points and are given in Table III. The dispersion in the data for highest acidities at the temperatures 8° and 13° was considerable and the values of n, p, and m for these temperatures were obtained by ignoring the data for acid concentrations 0.2 and 0.3 molar.

Included in Fig. 1 are lines drawn in accord with the values of n and p of Table III, p indicating the slope of the plot of $1/k_f$ against $1/[H^+]$ at limiting high acidity. The values

Can. J. Chem. Downloaded from www.nrcresearchpress.com by 210.87.254.40 on 09/05/12
For personal use only.

TABLE II

Rate constants (k_f) for the overall reaction for the formation of the mono complex between nickel (II) and 1,10-phenanthroline. Ionic strength = 0.50

Temperature, ° C	[H⁺] mol l.⁻¹	$k_f \times 10^{-4}$ l. mol⁻¹ sec⁻¹	Temperature, ° C	[H⁺] mol l.⁻¹	$k_f \times 10^{-4}$ l. mol⁻¹ sec⁻¹
8.0	0.30	1.12	25.0	0.30	3.55
	0.20	1.13		0.20	3.37
	0.10	0.96		0.10	2.75
	0.07	0.83		0.08	2.54
	0.04	0.67		0.06	2.16
				0.04	1.79
13.0	0.30	1.66	31.0	0.30	4.76
	0.20	1.88		0.20	4.31
	0.10	1.40		0.10	3.39
	0.07	1.23		0.07	2.99
	0.04	0.94		0.04	2.15
19.0	0.30	2.47	37.0	0.30	6.01
	0.20	2.27		0.20	5.51
	0.10	1.92		0.10	4.45
	0.07	1.64		0.07	3.78
	0.04	1.29		0.04	2.70

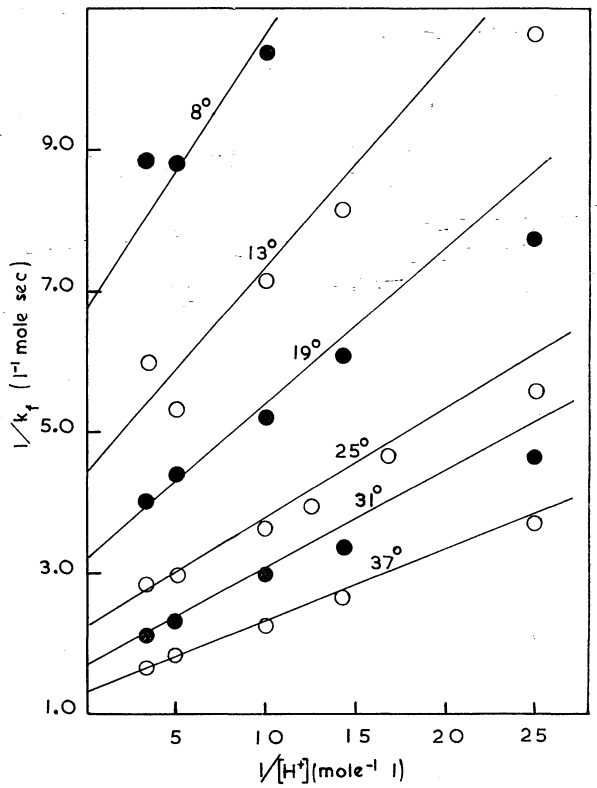

FIG. 1. Plots of $1/k_f$ against $1/[H^+]$ with lines indicating intercepts (n) and limiting slopes (p) for high acidity estimated from the data using the relation $k_f = (m + [H^+])/(p + n[H^+])$.

Can. J. Chem. Downloaded from www.nrcresearchpress.com by 210.87.254.40 on 09/05/12
For personal use only.

TABLE III

Values for the constants n, p, and m in the relation $k = (m + [H^+])/(p + n[H^+])$

Temp. ° C,	$n\times10^5$	$p\times10^6$	$m\times10^3$
8	6.8	3.9	3.9
13	4.5	2.9	4.4
19	3.32	2.16	4.8
25	2.25	1.54	4.2
31	1.67	1.41	6
37	1.34	1.0	3

for the constants n, p, and m are those which best summarize the experimental data but the values for p and more particularly for m have rather wide confidence limits. For example, for 19° C an increase in n of 4% along with an associated decrease in p of 15% and in m of 40% yield values for k_f which fit the smoothed experimental curves to about 3% of the value of k_f.

Our data for 25° C and those of Margerum, Bystroff, and Banks (1) are in fair agreement. Their value for n is 2.62×10^{-5} and ours is 2.25×10^{-5} mol $l.^{-1}$ sec. Their value for p is 2.58×10^{-6}, ours is 1.54×10^{-6} mol^2 $l.^{-2}$ sec. The difference in values for p is probably attributable to the influence of ionic strength on the rate characteristics of the acid dependent path.

Our values for m and p indicate a value of 2.7×10^3 l. mol^{-1} sec^{-1} for the rate constant for the overall acid independent reaction at 25° C. This may be compared with 4.1×10^3 l. mol^{-1} sec^{-1} derived from Ellis, Hogg, and Wilkins (3) value of 6.2×10^{-4} min^{-1} for the rate constant for dissociation and Margerum, Bystroff, and Banks value of 2.5×10^{-9} mole $liter^{-1}$ for the equilibrium constant for the dissociation. In view of the uncertainty associated with the value for equilibrium dissociation constant and our value for m the agreement between the values is satisfactory.

Our values for $1/n$ at various temperatures yield the values 9.5 ± 0.6 kcal mol^{-1} for $\Delta H^{\ddagger}$ and -5.3 ± 2.1 cal mol^{-1} $degree^{-1}$ for $\Delta S^{\ddagger}$. These values apply to the transition state involved in the formation of the unidentate intermediate A if mechanism I applies or to that involved in the formation of final bidentate complex relative to the same initial states of nickel (II) and phenanthroline if mechanism II applies. Although six or seven co-ordinate intermediates are conceivable (6), recent work by Eigen and co-workers (7) suggests that the transition state involving the smaller co-ordination number is more likely. It may be noted that the values of $\Delta H^{\ddagger}$ and $\Delta S^{\ddagger}$ quoted by Basolo and Pearson (8) for the acid-independent solvolysis and based on the data of Ellis, Hogg, and Wilkins (3) apply to the overall reaction and not necessarily to the rate-controlling step.

The work of Eigen and co-workers (7) involving relaxation techniques provides convincing evidence that the reaction between a metal ion and potential ligand involves two types of ion pairs as precursors to the unidentate complex, the immediate precursor being one in which the metal ion and ligand are separated by one molecule of water. This ion pair yields the complex with a first-order rate constant (k_{34}) which, in the case of most bivalent metal ions, is characteristic of the metal ion but nearly independent of the loosely associated ligand of the ion pair. If it is assumed that the concentrations of the two types of ion pairs are small relative to the concentrations of the free reactants then the overall second-order rate constant for complex formation should be $K_e k_{34}$ where K_e is the effective association equilibrium constant for the ion pair from which the complex is

Can. J. Chem. Downloaded from www.nrcresearchpress.com by 210.87.254.40 on 09/05/12
For personal use only.

directly formed. Swift and Connick (9) have used N.M.R. relaxation methods to estimate the rate constant (k_1) for water exchange from the first co-ordination sphere of various cations and find values which are nearly proportional and close in magnitude to the values for k_{34} found by Eigen, e.g. for nickel (II) at 25° C k_1 is 2.7×10^4 seconds^{-1} and k_{34} for nickel (II) and sulphate ion is 1.5×10^4 seconds^{-1}. Both Eigen and Connick have emphasized the implication that the rate of association (anation) is controlled essentially by the rate of water loss from the metal ion and that the rate constant for this process for most bivalent ions is nearly independent of the nature of the neighboring ligand in the ion pair.

If mechanism I of Margerum and co-workers applies to the reaction of nickel (II) and *o*-phenanthroline at high acidity then $1/n$ is the rate constant for the formation of the unidentate intermediate A and is identifiable with $K_e k_{34}$. Eigen's value of 1.5×10^4 sec^{-1} for k_{34} along with a value of 4×10^4 mole^{-1} liter second^{-1} for $1/n$ imply that k_e is approximately 2.7 mole^{-1} liter, a value sufficiently small to lead to a relatively negligible concentration of ion pairs under our range of experimental conditions and consequently to a situation consistent with second-order kinetics. Using Swift and Connick's value for k' in place of Eigen's value for k_{34} leads to the same conclusions. Melson and Wilkins (10) have determined values ranging from 2.5×10^3 to 3.2×10^3 mole^{-1} liter second^{-1} for the overall association rate constant of nickel (II) with three uncharged unidentate ligands which had widely different association equilibrium constants. Davies and Smith (11) found a value of about 4×10^3 mole^{-1} liter second^{-1} for the reaction between nickel (II) and the singly charged thiocyanate ion. The significant excess of our value for $1/n$ (4×10^4) over those obtained by Melson and Wilkins may imply that $1/n$ is not measuring the rate constant for formation of A and that mechanism I does not operate. Melson and Wilkin's finding that the rate constants for association are essentially independent of ligand type, when considered in terms of Eigen's mechanism, implies that the effective association constant (K_e) for ion pair formation is almost independent of the equilibrium constant for complex formation. It follows that if mechanism I operated in a series of reactions involving nickel (II) with various ligands of the same charge, then there should be essential independence of rate constant on ligand type.

Mechanism II implies that at high acidity the concentration of intermediate A is maintained close to that for equilibrium with nickel (II) and phenanthroline via a path involving protonation and deprotonation and $1/n = K_e'k''$ where K_e' is the association constant for the unidentate species A and should be much more dependent on the nature of the ligand than is K_e. k'' is the first-order rate constant for formation of the bidentate complex from the unidentate intermediate A and could conceivably be less than k' (12). If the magnitude of k'' be assumed to be close to that for k', there is implied a value for K_e' which is comparable to K_e and consistent with a second-order rate law.

It appears then that the data for the nickel–phenanthroline reaction are quite consistent with both the data obtained and mechanisms proposed by Eigen and by Connick but taken alone do not permit decision to be made about the detailed nature of the acid-catalyzed mechanism. Our values for $\Delta H^{\ddagger}$ and $\Delta S^{\ddagger}$, while potentially significant, may not be usefully interpreted in the present state of knowledge about solvation in aqueous ionic solutions. It is, however, pertinent to note that a dependence of $1/n$ on K_e' and consequently on the nature of ligand is implied for a series of reactions proceeding by mechanism II and involving nickel (II) and various ligands. Ahmed and Wilkins (13, 14) provide data on the kinetics of the dissociation of complexes of nickel (II) with various aliphatic diamines which suggest a mechanism for association and dissociation similar to that applying to the phenanthroline complex. They find that the rate constant for the dissociation increases

Can. J. Chem. Downloaded from www.nrcresearchpress.com by 210.87.254.40 on 09/05/12
For personal use only.

with acidity and tends to a constant value before increasing again at high acidities. They satisfactorily interpret their results on the basis of a mechanism which is essentially mechanism II. If their values for the dissociation rate constant at intermediate acidities be considered to indicate the limiting value for high acidities, then an estimate of $1/n$ should be obtained by multiplication of this dissociation rate constant and the equilibrium association constant. Values in the range 14×10^4 to 27×10^4 mole^{-1} liter second^{-1} are implied for a temperature of 0.6° C and ionic strength of 2.0. The high magnitude of $1/n$ relative to that anticipated for the rate constant for unidentate ligand formation (3×10^3) seems to support mechanism II while its relative independence on type of ligand suggests mechanism I. However, values for K_e' (for the unidentate intermediate) are not available and it is possible that the range of the values is small. It appears that more extended and accurate data relating to the acid dependence of the association rate constants for nickel (II) with a series of bidentate ligands which could have quite different association equilibrium constants for the unidentate intermediate might help assessment of the acid-catalyzed mechanisms.

ACKNOWLEDGMENTS

The authors thank the National Research Council for financial support of this work and for the award of a Bursary to P. F. B.

REFERENCES

1. D. W. Margerum, R. I. Bystroff, and C. V. Banks. J. Am. Chem. Soc. **78**, 4211 (1956).
2. R. G. Wilkins and M. J. G. Williams. J. Chem. Soc. 4514 (1957).
3. P. Ellis, R. Hogg, and R. G. Wilkins. J. Chem. Soc. 3308 (1959).
4. A. I. Vogel. Quantitative inorganic analysis. 2nd ed. Longmans, Green and Company. 1951. p. 458.
5. R. G. Bates, V. E. Bower, R. G. Miller, and E. R. Smith. J. Res. Nat. Bur. Std. **47**, 433 (1951).
6. F. Basolo and R. G. Pearson. Mechanisms of inorganic reactions. John Wiley and Sons, Inc., New York. 1958. Chap. 3.
7. M. Eigen and K. Tamm. Z. Elektrochem. **66**, 107 (1962).
8. F. Basolo and R. G. Pearson. Advances in inorganic and radiochemistry. Vol. 3. Academic Press, New York. 1961. p. 22.
9. T. J. Swift and R. E. Connick. J. Chem. Phys. **37**, 307 (1962).
10. G. A. Melson and R. G. Wilkins. J. Chem. Soc. 4208 (1962).
11. A. G. Davies and W. MacF. Smith. Proc. Chem. Soc. 380 (1961).
12. D. W. Margerum, D. B. Rorabacher, and J. F. G. Clarke, Jr. Inorg. Chem. **2**, 667 (1963).
13. A. K. Shamsudden Ahmed and R. G. Wilkins. J. Chem. Soc. 3700 (1959).
14. A. K. Shamsudden Ahmed and R. G. Wilkins. J. Chem. Soc. 2895 (1960).

Can. J. Chem. Downloaded from www.nrcresearchpress.com by 210.87.254.40 on 09/05/12
For personal use only.

N.M.R. SPECTRA OF TIN COMPOUNDS

II. Sn^{119} AND H^1 MAGNETIC RESONANCE SPECTRA OF HEXAMETHYLDITIN

H. C. CLARK, J. T. KWON, L. W. REEVES, AND E. J. WELLS
Department of Chemistry, University of British Columbia, Vancouver, British Columbia
Received November 20, 1963

ABSTRACT

The H^1 and Sn^{119} resonances in hexamethylditin have been examined. A coupling constant $J = 4400 \pm 70$ c.p.s. is reported for Sn^{117}—Sn^{119} nuclei directly bonded. Comparison with some other heavy metal couplings is made. Changes in bond type of the Sn—C bond in hexamethylditin from tetrahedrally bonded tin compounds with no Sn—Sn bond is indicated by an anomalously low value for J_{Sn-C-H}.

INTRODUCTION

The proton resonance spectrum of hexamethylditin was first reported by Kaesz (1) but more recently discussed by Brown and Morgan (2). The latter workers have assigned the Sn^{119} and Sn^{117} satellites of hexamethylditin, octamethyltritin, and cyclic and linear polymethyltin compounds. Interpretation of the respective coupling constants from methyl protons to tin followed empirical assignment of *s* character in the tin–carbon bond after suggestions of earlier workers (3, 4). Other coupling constants involving magnetic tin nuclei have recently been reported by the present authors in methyltin derivatives (5). A correlation of coupling constants involving the group IV elements has been published by Reeves and Wells (6).

The purpose of the present work is to investigate the Sn^{119} magnetic resonance spectrum of hexamethylditin and to point out some further features of the H^1 spectrum. The classic work on Sn^{119} spectra in various compounds has been published by Lauterbur and Burke (7).

EXPERIMENTAL

Proton resonance spectra were obtained at 60 Mc using an A60 spectrometer with calibrating side bands. The side bands were produced by a Hewlett Packard 2000CD wide-range audio oscillator and measured with a Hewlett Packard 522B electronic counter. Sn^{119} magnetic resonance spectra were obtained at 15.37 Mc, with a Varian variable-frequency spectrometer model V4210A. Calibration of these spectra was achieved by using modulation side bands on the Li^7 resonance signal in lithium nitrate solution. The procedure for this calibration is as follows. The Sn^{119} resonance was obtained at 15.37 Mc and the field sweep conditions standardized. The sharp Li^7 resonance in dilute $LiNO_3$ solution was then recorded at the same value of H_0. For modulation frequencies much larger than the line width the recorded derivative of absorption signal consists of two absorption mode signals in opposite phase separated by twice the modulation frequency serving to calibrate the spectrum. It was not possible with the experimental conditions available to observe audio side bands on the Sn^{119} resonances. The Sn^{119} spectra appear as derivatives of the absorption spectrum because the main magnetic field was modulated by a 400-c.p.s. variable field.

The compound was prepared in the manner of Clark and Willis (8).

RESULTS AND DISCUSSION

The proton resonance spectrum of hexamethylditin is illustrated in Fig. 1(*a*) with the calibrating audio side bands included at ± 114.9 c.p.s. When the gain of the A60 instrument is increased by 20 times the observation of weak satellite resonances can be investigated as shown in Fig. 1(*b*). The proton resonance spectrum arises in the first approximation from the contribution of 10 molecular types. These are listed with their fractional abundances as follows: (1) $(CH_3)_3SnSn(CH_3)$—no magnetic tin nuclei—0.692;

Can. J. Chem. Downloaded from www.nrcresearchpress.com by 210.87.254.105 on 09/05/12
For personal use only.

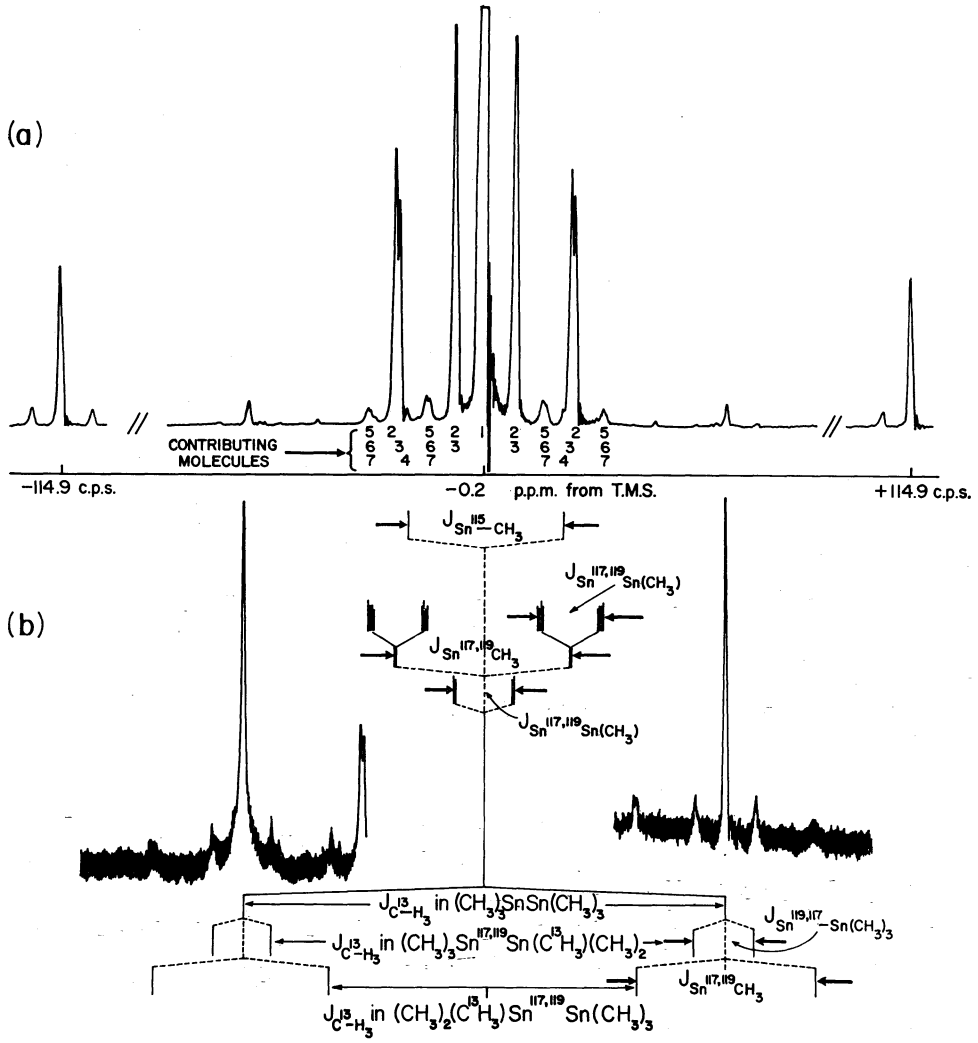

FIG. 1. (*a*) Spectrum of the H^1 resonance in hexamethylditin at low gain (60 Mc). (*b*) Spectrum of the H^1 resonance at 20 × amplitude of (*a*).

(2) $(CH_3)_3Sn^{119}Sn(CH_3)_3$ 0.144; (3) $(CH_3)_3Sn^{117}Sn(CH_3)_3$ 0.128; (4) $(CH_3)_3Sn^{115}Sn(CH_3)_3$ 7×10^{-3}; (5) $(CH_3)_3Sn^{119}Sn^{119}(CH_3)_3$ 7.5×10^{-3}; (6) $(CH_3)_3Sn^{117}Sn^{117}(CH_3)_3$ 5.9×10^{-3}; (7) $(CH_3)_3Sn^{117}Sn^{119}(CH_3)_3$ 0.013; (8) $(CH_3)_3Sn^{119}Sn^{115}(CH_3)_3$ 6×10^{-4}; (9) $(CH_3)_3Sn^{117}Sn^{115}(CH_3)_3$ 6×10^{-4}; (10) $(CH_3)_3Sn^{115}Sn^{115}(CH_3)_3$ 1.2×10^{-6}. Molecules 8, 9, and 10 are in such low abundance as to be unobservable. In Fig. 1 the main central resonance is due to molecules of type 1. The first satellites arise from molecules 2 and 3 and their separation corresponds to an averaged remote coupling, methyl protons to the distant Sn^{117} or Sn^{119}, i.e. $(CH_3)SnSn^{119,117}$. The methyl groups coupling to adjacent Sn^{117} and Sn^{119} are further separated from the central resonance and individually resolved. A resolution of the small abundance of molecules containing an Sn^{115} nucleus is clearly seen just inside the resonances due to adjacently coupled methyl protons (to Sn^{117}, Sn^{119}). The much weaker satellites on each side of these peaks are from the molecules 5, 6, and 7, containing two magnetic

Can. J. Chem. Downloaded from www.nrcresearchpress.com by 210.87.254.105 on 09/05/12
For personal use only.

tin nuclei. The relative intensities of individual peaks of these multiplets are indicated below in Fig. 1(*b*) directly under the peaks in Fig. 1(*a*).

The main C^{13} satellites due to the 1.108% abundant isotope are clearly seen even at the low gain settings in spectrum 1(*a*). Examination of the spectrum in 1(*b*) shows peaks due to C^{13}—H^1 coupling in the molecules 2 and 3 and for both adjacent and remote methyl groups. Each of these weakest C^{13} satellites has an intensity $\sim 10^{-4}$ times that of the main resonance. The coupling constants which uniquely fit the observed spectrum are recorded in Table 1. The estimated error in these values is $\pm 0.25\%$.

TABLE 1

$J_{Sn^{115}-CH_3}$	= 42.9 c.p.s.	$J_{Sn^{119}-Sn-CH_3}$	= 16.3 c.p.s.
$J_{Sn^{117}-CH_3}$	= 47.0	$J_{C^{13}-H_3}$	= 128.9
$J_{Sn^{119}-CH_3}$	= 49.6	$J_{Sn^{117}-Sn^{119}}$	= 4400±70
$J_{Sn^{117}-Sn-CH_3}$	= 15.8	δ_{CH_3}	= −0.2 p.p.m.

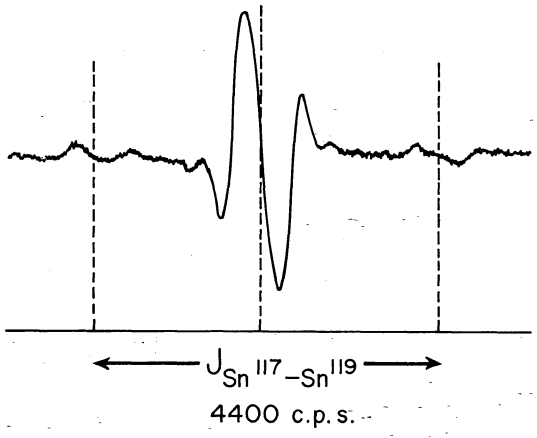

FIG. 2. Sn^{119} spectrum of hexamethylditin showing the coupling to Sn^{117} (15.37 Mc).

The Sn^{119} resonance spectrum is shown in Fig. 2. In order to observe the weak side-band resonances the modulation width exceeded the tin resonance width and the derivative of absorption signals are thus distorted. The weak satellite lines are due to molecules of type 7 in which two dissimilar isotopes Sn^{117}, Sn^{119} occur together. The separation of these two satellite lines is equal to $J_{Sn^{117}-Sn^{119}}$ (4400±70 c.p.s.). Spin-couplings between heavy metal atoms are quite rare in nuclear magnetic resonance and apart from a recent value of the Tl^{203}—Tl^{205} coupling constant of 2560 c.p.s. in the tetramer of thallous ethoxide there seems no other case reported (9). In this tetramer the coupling occurs through an intervening oxygen atom. A large platinum phosphorous coupling of 5700 c.p.s. has been reported in (10) $\{(EtO)_3P\}_2PtCl_2$ and in this case there is no intervening atom between the coupled nuclei. The electronic contribution to these coupling constants can be compared by dividing by the product $\gamma_N\gamma_N'$ where N and N′ are the two nuclear species involved. The result gives for the reduced coupling constants; Tl^{203}—O—Tl^{205} = 248 c.p.s. $\mu^{-1}.I$; Pt^{195}—P^{31} = 2080; Sn^{117}—Sn^{119} = 1062. The Pt^{195}—P^{31} coupling has the largest electronic contribution. We have shown that the coupling constant varies roughly as the square of the atomic numbers of coupled nuclei (6) in a given group of the periodic

Can. J. Chem. Downloaded from www.nrcresearchpress.com by 210.87.254.105 on 09/05/12
For personal use only.

table. The large reduced coupling constants Sn^{117}—Sn^{119} and Pt^{195}—P^{31} are a reflection of the large atomic number of coupled nuclei.

The change in bond type of the Sn—C bond in hexamethylditin is well illustrated by examination of Fig. 3. This is a plot of $J_{C^{13}-H}$ in the methyl group for hexamethylditin,

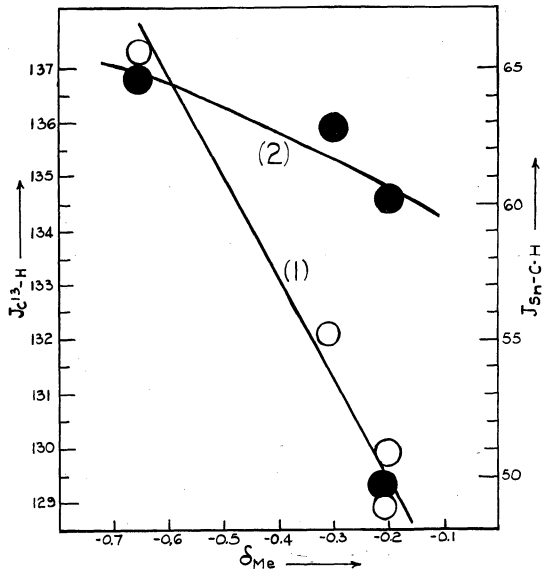

FIG. 3. Coupling constants $J_{Sn^{119}-C-H}$ and $J_{C^{13}-H}$ plotted as a function of δ_{Me} in methyl tin derivatives measured by us.

dimethyltin dihydride, dimethyltetrafluoroethyltin hydride, and dimethylditetrafluoroethyltin (5) against the chemical shift of the methyl protons. The values of $J_{C^{13}-H}$ versus chemical shift fall near a straight line—curve I—in the figure. The coupling constants J_{Sn-C-H} lie near a smooth curve except for the value in hexamethylditin, which is much lower than curve 2 in the figure. The Sn—Sn bond, therefore, considerably influences the Sn—C—H coupling constant and it is tempting to associate this with a reduced *s* character in the Sn—C bond and enhanced *s* character in the Sn—Sn bond.

ACKNOWLEDGMENTS

This work has been supported by the National Research Council of Canada in grants to H. C. Clark and L. W. Reeves.

REFERENCES

1. H. D. KAESZ. Nuclear magnetic resonance spectral data. A.P.I. Research Project 44. Ser. No. 53.
2. T. L. BROWN and G. L. MORGAN. Inorg. Chem. **2**, 736 (1963).
3. VAN DER KELEN. Nature, **193**, 1069 (1962).
4. J. R. HOLMES and H. D. KAESZ. J. Am. Chem. Soc. **83**, 3903 (1961).
5. H. C. CLARK, J. T. KWON, L. W. REEVES, and E. J. WELLS. Can. J. Chem. **41**, 3005 (1963).
6. L. W. REEVES and E. J. WELLS. Can. J. Chem. **41**, 2698 (1963).
7. J. J. BURKE and P. C. LAUTERBUR. J. Am. Chem. Soc. **83**, 326 (1961).
8. H. C. CLARK and C. J. WILLIS. J. Am. Chem. Soc. **82**, 1888 (1960).
9. W. G. SCHNEIDER and A. D. BUCKINGHAM. Discussions Faraday Soc. **34**, 147 (1962).
10. A. PIDCOCK, R. E. RICHARDS, and L. M. VENANZI. Proc. Chem. Soc. 184 (1962).

Can. J. Chem. Downloaded from www.nrcresearchpress.com by 210.87.254.105 on 09/05/12
For personal use only.

Can. J. Chem. Downloaded from www.nrcresearchpress.com by 210.87.254.6 on 09/05/12
For personal use only.

NOTES

THE COVALENT CHARACTER OF ALKALI ALKOXIDES

M. S. BAINS[1]

Alkali metal alkoxides have been little studied (1) as is shown by a general lack of information regarding their structure and properties. Conductance measurements (2) show that dilute solutions of alkoxides of sodium are completely ionized in their parent alcohols. Use of these compounds as synthetic agents (3) in ionizing and polar media (4) appears to confirm the usual belief about their ionic character. Except for certain compounds of lithium, such as alkyls, alkali metals are assumed to form predominantly electrovalent compounds. It is only recently that a study of the crystal structure of lithium methoxide (5) has provided evidence that lithium–oxygen (Li–O) bond in this compound is approaching covalency.

Organic compounds of alkali metals such as alkoxides, amides, and mercaptides are important as catalysts or reagents in the reactions of organic carbonyl or unsaturated compounds (6–9). In view of this, the present work on alkali metal alkoxides was undertaken as a preliminary study of this neglected field by obtaining conditions of sublimation of pure compounds, by determining molecular weights cryoscopically, and by securing nuclear magnetic resonance spectra of the soluble alkali alkoxides.

Lithium *tert*-butoxide, according to present investigation, is found to be the most volatile lithium alkoxide amongst those studied, subliming at 110° C at 0.1 mm; lithium ethoxide is relatively less easily sublimed (155° C at 10^{-4} mm). Lithium isopropoxide sublimes under intermediate conditions, i.e. 170° C at 0.1 mm. It is also observed that, with increasing atomic number of the alkali metal, volatility decreases as, for example, potassium *tert*-butoxide which sublimes at 145° C at 10^{-4} mm. These data show that these compounds might be more covalent than hitherto supposed.

It is also found that pure lithium *tert*-butoxide and lithium iso-propoxide are soluble in benzene and in cyclohexane. Their molecular weights determined in these solvents show that lithium *tert*-butoxide is tetrameric in benzene and hexameric in cyclohexane over a fairly wide range of concentration. Lithium iso-propoxide is found to be undecameric in cyclohexane. The fact that the molecular weight of lithium *tert*-butoxide is lower in benzene suggests that the solvent plays some role in the dissolution of the compound. Cyclohexane has no π-electrons but benzene, by virtue of its sextet of π-electrons, may be expected to share in the covalency of the metal and thus lower its polymerization.

The determination of nuclear magnetic resonance spectra of the two soluble lithium alkoxides reveals their covalent metal–oxygen bond: the diamagnetic shielding of protons due to electrons is less than in the parent alcohol. For instance, the methyl protons in *tert*-butanol have a negative shift of -1.222 p.p.m. with respect to tetramethylsilane, while an even more negative shift is observed in the case of the tert-butoxide for the same protons (-1.527 p.p.m.). This indicates that metal–oxygen bond in lithium alkoxides is more covalent than the hydrogen–oxygen bond in alcohols. This may be explained by the fact that the electrons in the p–π orbitals of oxygen can be accepted by the empty p–π

[1]*National Research Council of Canada Postdoctoral Fellow, 1959–61.*

orbitals of lithium. This effect is probably augmented by the branching alkyl groups of the alkoxides on account of their enhanced +I effect and consequently the metal–oxygen bond is made more covalent by the so-called back-cordination. There is thus a decreased electronic shielding of the protons of the alkyl groups.

It is also possible to suggest as an alternative that steric requirements of the branched alkyl groups cause a weakening in the lattice forces of the crystalline compounds and this in addition to the +I effect may contribute toward the increased volatility of the more branched alkoxides.

EXPERIMENTAL

The desolvated alkoxides were sublimed at as low a temperature as possible and were handled in a dry box or under a continuous stream of dry nitrogen. The molecular weights were determined cryoscopically in both cyclohexane and benzene respectively.

The proton magnetic spectra were run at room temperature through a Varian 4300 B high-resolution spectrometer using frequency of 60 Mc/second. Tetramethylsilane sealed in a fine capillary was used as an external reference. Anhydrous carbon tetrachloride was employed as the solvent and the concentration of tert-butanol and lithium *tert*-butoxide were 11.9 and 3.6% weight/volume respectively.

The details of this work will be published in due course.

ACKNOWLEDGMENTS

The author wishes to thank Professor D. C. Bradley for his interest in this work and Dr. J. B. Stothers for helping to run nuclear magnetic resonance spectra. Thanks are also due to the National Research Council of Canada for the postdoctoral fellowship.

1. D. C. Bradley. Metal alkoxides. Advances in Chemistry Series, No. 23. 1959. pp. 10–36.
2. G. E. M. Jones and O. L. Hughes. J. Chem. Soc. 1197 (1934).
3. A. Kh. Khomenko and A. K. Gorban. Izv. Akad. Nauk SSSR, Otd. Khim. Nauk, 1676 (1959).
4. P. J. Wheatley. Nature, **185**, 681 (1960).
5. P. J. Wheatley. J. Chem. Soc. 4270 (1960).
6. D. W. Young and H. B. Kellog. U.S. Patent No. 2,440,498. (April 27, 1948).
7. P. J. Hanrick, Jr. and C. R. Houser. J. Am. Chem. Soc. **81**, 2096 (1959).
8. A. R. Gantmakhar and Yu. L. Spirin. Russ. Chem. Rev. 299 (1960).
9. A. Zilkha, Ben-Ami Feit, and M. Frankel. Proc. Chem. Soc. 255 (1958); J. Chem. Soc. 928 (1959).

Received May 6, 1963.
Chemistry Department,
Panjab University,
Chandigarh-3, India.

ON THE PORE STRUCTURE OF VYCOR GLASS

D. Basmadjian and K. P. Chu

The narrow pore size distribution believed to be present in porous Vycor glass makes it a suitable material for investigating basic properties of porous solids. Sorption isotherms of various gases on Vycor have been reported by Amberg and McIntosh (1) and Barrer and Barrie (2). The latter have, in addition, made extensive measurements of pure gas permeabilities in the Knudsen flow region. The sorption data have been used to evaluate the main structural parameters of the solid, yielding a B.E.T. area of about 120 m^2/g and a most probable pore radius of 28 Å obtained by application of the Kelvin equation to the desorption branch of the hysteresis loop (1). Using the pore size distribution derived in this manner and assuming a uniform cylindrical pore structure, Amberg and McIntosh

Can. J. Chem. Downloaded from www.nrcresearchpress.com by 210.87.254.6 on 09/05/12
For personal use only.

orbitals of lithium. This effect is probably augmented by the branching alkyl groups of the alkoxides on account of their enhanced +I effect and consequently the metal–oxygen bond is made more covalent by the so-called back-cordination. There is thus a decreased electronic shielding of the protons of the alkyl groups.

It is also possible to suggest as an alternative that steric requirements of the branched alkyl groups cause a weakening in the lattice forces of the crystalline compounds and this in addition to the +I effect may contribute toward the increased volatility of the more branched alkoxides.

EXPERIMENTAL

The desolvated alkoxides were sublimed at as low a temperature as possible and were handled in a dry box or under a continuous stream of dry nitrogen. The molecular weights were determined cryoscopically in both cyclohexane and benzene respectively.

The proton magnetic spectra were run at room temperature through a Varian 4300 B high-resolution spectrometer using frequency of 60 Mc/second. Tetramethylsilane sealed in a fine capillary was used as an external reference. Anhydrous carbon tetrachloride was employed as the solvent and the concentration of tert-butanol and lithium *tert*-butoxide were 11.9 and 3.6% weight/volume respectively.

The details of this work will be published in due course.

ACKNOWLEDGMENTS

The author wishes to thank Professor D. C. Bradley for his interest in this work and Dr. J. B. Stothers for helping to run nuclear magnetic resonance spectra. Thanks are also due to the National Research Council of Canada for the postdoctoral fellowship.

1. D. C. Bradley. Metal alkoxides. Advances in Chemistry Series, No. 23. 1959. pp. 10–36.
2. G. E. M. Jones and O. L. Hughes. J. Chem. Soc. 1197 (1934).
3. A. Kh. Khomenko and A. K. Gorban. Izv. Akad. Nauk SSSR, Otd. Khim. Nauk, 1676 (1959).
4. P. J. Wheatley. Nature, **185**, 681 (1960).
5. P. J. Wheatley. J. Chem. Soc. 4270 (1960).
6. D. W. Young and H. B. Kellog. U.S. Patent No. 2,440,498. (April 27, 1948).
7. P. J. Hanrick, Jr. and C. R. Houser. J. Am. Chem. Soc. **81**, 2096 (1959).
8. A. R. Gantmakhar and Yu. L. Spirin. Russ. Chem. Rev. 299 (1960).
9. A. Zilkha, Ben-Ami Feit, and M. Frankel. Proc. Chem. Soc. 255 (1958); J. Chem. Soc. 928 (1959).

Received May 6, 1963.
Chemistry Department,
Panjab University,
Chandigarh-3, India.

ON THE PORE STRUCTURE OF VYCOR GLASS

D. Basmadjian and K. P. Chu

The narrow pore size distribution believed to be present in porous Vycor glass makes it a suitable material for investigating basic properties of porous solids. Sorption isotherms of various gases on Vycor have been reported by Amberg and McIntosh (1) and Barrer and Barrie (2). The latter have, in addition, made extensive measurements of pure gas permeabilities in the Knudsen flow region. The sorption data have been used to evaluate the main structural parameters of the solid, yielding a B.E.T. area of about 120 m^2/g and a most probable pore radius of 28 Å obtained by application of the Kelvin equation to the desorption branch of the hysteresis loop (1). Using the pore size distribution derived in this manner and assuming a uniform cylindrical pore structure, Amberg and McIntosh

Can. J. Chem. Downloaded from www.nrcresearchpress.com by 210.87.254.105 on 09/05/12
For personal use only.

(1) were then able to calculate a cumulative surface area in good agreement with the B.E.T. value. The cylindrical pore model proposed by these authors is, however, in conflict with the findings of subsequent investigators. de Boer, in a theoretical study (3), showed that the data of Amberg and McIntosh point to the existence of non uniform pores, the most likely shape being a cylindrical pore with globular *enlargements*. Barrer and Barrie (2) found that their measured permeabilities were about five times lower than those calculated on the basis of Knudsen flow through a cylindrical pore of 28 Å radius, even after correction for the percentage of solid in their plugs. Barrer and Gabor (4) attributed this to periodic *constrictions* in the pores, although similar low values could conceivably have resulted from a highly tortuous pore structure or a high percentage of blind pores.

Recent diffusion measurements made by us in the range 0.2–70 atm may serve to throw some fresh light on this discrepancy. A Corning brand Vycor glass (No. 7930, S = 120 m²/g, ϵ = 0.34) was used to measure counterdiffusion of hydrogen and nitrogen at constant pressure and in two directions perpendicular to each other. Details of the apparatus and

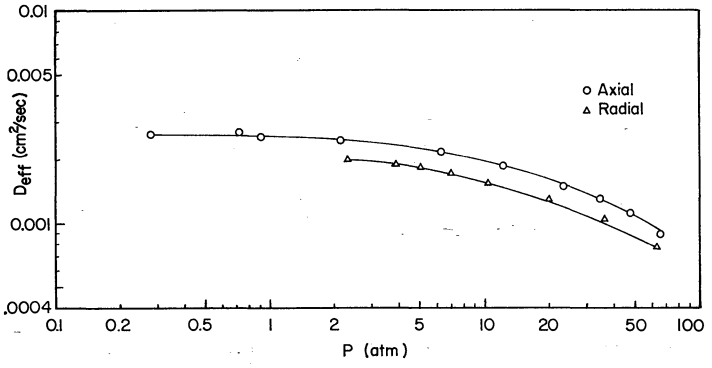

FIG. 1. Effective diffusivity of Vycor glass as a function of pressure.

procedure have been given elsewhere (5) and the results are plotted in Fig. 1. The pertinent equation for calculating effective diffusivities valid for both Knudsen and bulk diffusion as well as the transition zone has been derived by Scott and Dullien (6):

$$[1] \qquad \frac{N_A RTL}{P(y_{A_1}-y_{A_2})} = D_{eff} = \frac{(D_{AB})_{eff}}{(y_{A_1}-y_{A_2})\alpha} \ln \frac{1-\alpha y_{A_2}+(D_{AB}/D_{KA})_{eff}}{1-\alpha y_{A_1}+(D_{AB}/D_{KA})_{eff}}$$

At pressures up to about 5 atm, the data yield constant diffusivities, i.e. the material transport in this region is by Knudsen diffusion, which is independent of the total pressure and directly proportional to the average channel radius R_c. Under these conditions equation [1] reduces to the effective Knudsen diffusivity:

$$[2] \qquad D_{eff} = (D_{KA})_{eff} = \tfrac{2}{3} R_c \cdot v_A \cdot \epsilon \cdot X.$$

The tortuosity factor X accounts for any constrictions of the pore channel below the value R_c, the existence of blind pores, as well as the tortuous path of the pore.

At higher pressures, there is a gradual drop in diffusivity values, indicating a transition to bulk diffusion which is inversely proportional to pressure but independent of channel radius. In the limit, equation [1] reduces to the expression

$$[3] \qquad D_{eff} = (D_{AB})_{eff} = D_{AB} \cdot \epsilon \cdot X.$$

Can. J. Chem. Downloaded from www.nrcresearchpress.com by 210.87.254.105 on 09/05/12
For personal use only.

Substituting measured diffusivities in equations [1] and [2] and eliminating ϵX from equations [1–3], it is possible to evaluate the controlling pore radius R_c independent of any structural considerations and independent also of surface tension and other parameters which are required in the application of the Kelvin equation. The value of R_c obtained in this manner was 28 Å ±2 for both sets of measurements, and is in good agreement with the radius calculated from sorption data (1, 2). The corresponding tortuosities were 0.23 and 0.19. Thus, although Barrer and Barrie's tortuosity factor of 0.18 is essentially confirmed, the reason given by them to explain its small magnitude is not. The latter must instead be attributed to the tortuous pore path and (or) the existence of blind pores.

A possible pore structure which would yield the correct cumulative pore area and volume and be in agreement with the diffusion data as well as de Boer's pore model may be proposed. It would consist of randomly oriented pores with a tortuous path factor of $1/\sqrt{2} = 0.707$ proposed by Wheeler (7) and having globular enlargements part of whose volume would act as blind pores. Calculations have shown that a model of this type would require alternate sections of cylindrical pores ($R_c = 28$ Å, $L = 50$ Å) and spherical cavities ($R_s = 2R_c$). Further refinements of the model are at present not justified, but it may be pointed out that diffusion measurements of the type described may be usefully applied for the independent evaluation of controlling pore radii in similar solids.

NOMENCLATURE

A, B	Components in binary mixture.
D_{eff}	Effective diffusivity of a porous body, defined by equation [1], cm²/second.
$(D_{AB})_{eff}$	Effective diffusivity of a porous body in the bulk diffusion region, defined by equation [3], cm²/second.
$(D_{KA})_{eff}$	Effective diffusivity of a porous body in the Knudsen diffusion region, defined by equation [2], cm²/second.
D_{AB}	Bulk diffusion coefficient in free space, cm²/second.
L	Length of porous disk, cm, or cylindrical pore, Å.
M	Molecular weight.
N_A	Moles of component A diffusing per unit time and area of porous disk, g moles/second cm².
P	Pressure, atm.
R	Gas constant, atm cm³/g mole ° K.
R_c	Radius of cylindrical pore, cm.
R_s	Radius of spherical cavity, cm.
S	Surface area of porous solid, m²/g.
T	Temperature, ° K.
v_A	Average molecular velocity of component A, cm/second.
X	Tortuosity factor, dimensionless.
y_A	Mole fraction of component A, dimensionless.
α	$1+(N_A/N_B) = 1-(M_B/M_A)^{\frac{1}{2}}$.
ϵ	Porosity of material, cc/cc.

Subscripts 1 and 2 refer to the two ends of the porous disk.

Grateful acknowledgment is made for a National Research Council grant in support of this work.

Can. J. Chem. Downloaded from www.nrcresearchpress.com by 210.87.254.105 on 09/05/12
For personal use only.

1. C. H. AMBERG and R. MCINTOSH. Can. J. Chem. **30**, 1012 (1952).
2. R. M. BARRER and J. A. BARRIE. Proc. Roy. Soc. A, **213**, 250 (1952).
3. J. H. DE BOER. *In* Proceedings of the 10th Symposium of the Colston Research Society. Butterworths, London. 1958. p. 68.
4. R. M. BARRER and T. GABOR. Proc. Roy. Soc. A, **251**, 353 (1959).
5. K. P. CHU. M.Sc. Thesis, Department of Chemical Engineering, University of Ottawa, 1963.
6. D. S. SCOTT and F. A. L. DULLIEN. A.I.Ch.E. J. **8**, 113 (1962).
7. A. WHEELER. *In* Advances in catalysis. Vol. III. Academic Press, New York. 1951. p. 250.

RECEIVED SEPTEMBER 26, 1963.
DEPARTMENT OF CHEMICAL ENGINEERING,
UNIVERSITY OF OTTAWA,
OTTAWA, ONTARIO.

Can. J. Chem. Downloaded from www.nrcresearchpress.com by 210.87.254.105 on 09/05/12
For personal use only.

LYCOPODIUM ALKALOIDS. VI. THE NATURE OF ALKALOID L.9

W. A. AYER, A. N. HOGG, AND A. C. SOPER

In 1943 Manske and Marion reported (1) the isolation of a basic substance, m.p. 122°, from *Lycopodium annotinum L.*, which they designated alkaloid L.9. At that time they stated that "alkaloid L.9 is probably a mixture but, owing to its exceptional behaviour, it has been deemed advisable to retain one designation only until more can be ascertained concerning its nature". Through the courtesy of R. H. Manske we have obtained a sample of "alkaloid L.9" and wish at this time to report on its composition.

Thin-layer chromatography (t.l.c.) over alumina revealed the presence of (at least) two components, one having the same R_f value as lycopodine (I), the other having a lower R_f value.

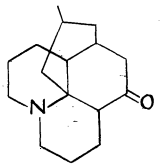

I

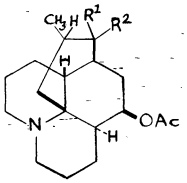

II, $R^1 = H$; $R^2 = OAc$
III, $R^1 = OH$; $R^2 = H$
IV, $R^1 = OAc$; $R^2 = H$

A mixture of lycopodine and "alkaloid L.9" also showed only two spots on t.l.c., suggesting that lycopodine (I) was a component of "alkaloid L.9". Since insufficient material was available for a preparative separation of the components we turned to mass spectrometry as a further aid to identification of the components. The mass spectrum of alkaloid L.9 displayed all the major ions expected for lycopodine (2, 3) and in addition showed weak peaks at m/e 349, 290, 289, and moderately intense peaks at m/e 234 and 174. The infrared spectrum of alkaloid L.9 suggested the presence of O-acetyl groups (1735, 1725, 1250, 1230 cm^{-1}) and thus it seemed reasonable to interpret the extra peaks in the mass spectrum in terms of the following sequence, since it is known (2, 3) that ions of type A and B are readily formed from *Lycopodium* alkaloids:

1. C. H. AMBERG and R. MCINTOSH. Can. J. Chem. **30**, 1012 (1952).
2. R. M. BARRER and J. A. BARRIE. Proc. Roy. Soc. A, **213**, 250 (1952).
3. J. H. DE BOER. *In* Proceedings of the 10th Symposium of the Colston Research Society. Butterworths, London. 1958. p. 68.
4. R. M. BARRER and T. GABOR. Proc. Roy. Soc. A, **251**, 353 (1959).
5. K. P. CHU. M.Sc. Thesis, Department of Chemical Engineering, University of Ottawa, 1963.
6. D. S. SCOTT and F. A. L. DULLIEN. A.I.Ch.E. J. **8**, 113 (1962).
7. A. WHEELER. *In* Advances in catalysis. Vol. III. Academic Press, New York. 1951. p. 250.

RECEIVED SEPTEMBER 26, 1963.
DEPARTMENT OF CHEMICAL ENGINEERING,
UNIVERSITY OF OTTAWA,
OTTAWA, ONTARIO.

Can. J. Chem. Downloaded from www.nrcresearchpress.com by 210.87.254.5 on 09/05/12
For personal use only.

LYCOPODIUM ALKALOIDS. VI. THE NATURE OF ALKALOID L.9

W. A. AYER, A. N. HOGG, AND A. C. SOPER

In 1943 Manske and Marion reported (1) the isolation of a basic substance, m.p. 122°, from *Lycopodium annotinum L.*, which they designated alkaloid L.9. At that time they stated that "alkaloid L.9 is probably a mixture but, owing to its exceptional behaviour, it has been deemed advisable to retain one designation only until more can be ascertained concerning its nature". Through the courtesy of R. H. Manske we have obtained a sample of "alkaloid L.9" and wish at this time to report on its composition.

Thin-layer chromatography (t.l.c.) over alumina revealed the presence of (at least) two components, one having the same R_f value as lycopodine (I), the other having a lower R_f value.

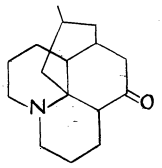

I

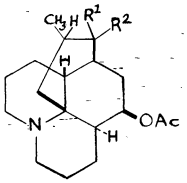

II, $R^1 = H$; $R^2 = OAc$
III, $R^1 = OH$; $R^2 = H$
IV, $R^1 = OAc$; $R^2 = H$

A mixture of lycopodine and "alkaloid L.9" also showed only two spots on t.l.c., suggesting that lycopodine (I) was a component of "alkaloid L.9". Since insufficient material was available for a preparative separation of the components we turned to mass spectrometry as a further aid to identification of the components. The mass spectrum of alkaloid L.9 displayed all the major ions expected for lycopodine (2, 3) and in addition showed weak peaks at m/e 349, 290, 289, and moderately intense peaks at m/e 234 and 174. The infrared spectrum of alkaloid L.9 suggested the presence of O-acetyl groups (1735, 1725, 1250, 1230 cm^{-1}) and thus it seemed reasonable to interpret the extra peaks in the mass spectrum in terms of the following sequence, since it is known (2, 3) that ions of type A and B are readily formed from *Lycopodium* alkaloids:

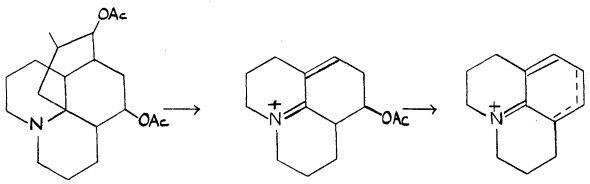

A B

m/e 349 m/e 234 m/e 174

The peaks at m/e 290 and 289 simply represent loss of OAc and HOAc from the molecular ion.

At this point it seemed that the naturally occurring O-acetylfawcettiine (II) (4) might represent the second component of alkaloid L.9. However, when a mixture of II and alkaloid L.9 was subjected to t.l.c. three distinct spots were obtained, O-acetylfawcettiine displaying a lower R_f value than either of the L.9 components. The C-8 epimer of O-acetylfawcettiine, O-acetyllofoline (IV), prepared by acetylation of lofoline (III) (5), was, however, indistinguishable by t.l.c. from the lower R_f component of alkaloid L.9. The mass spectrum of O-acetyllofoline showed the expected peaks (see above), the base peak appearing at m/e 174 (ion B). Crystallization of a 1:1 mixture of lycopodine and O-acetyllofoline from hexane yielded crystals, m.p. 121–122°, identical (mixed melting point, infrared spectrum, t.l.c. behavior) with authentic "alkaloid L.9", which is thus a molecular complex of these two substances. Recrystallization of the complex from either hexane or ether did not alter the melting point. It is interesting to note that the analytical results obtained earlier by Manske and Marion (1) agree well with the composition $C_{16}H_{25}ON \cdot C_{20}H_{31}O_4N$.

The natural occurrence of O-acetyllofoline (IV) has not been reported previously.

EXPERIMENTAL

The mass spectra were determined on a AEI MS2-H mass spectrometer at an ionizing potential of 70 ev and an ionizing current of 100 μa. Samples were introduced through a heated inlet system maintained at 150°. Thin-layer chromatograms were carried out on 0.25 mm layers of alumina G (Research Specialties Co., Richmond, Calif.) on glass plates using chloroform – 0.75% ethanol as the solvent system, and were developed with Dragendorff's reagent (6).

Alkaloid L.9

(*a*) A sample supplied by Dr. R. H. Manske melted at 121–122°. Infrared spectrum: ν_{max}^{nujol} 1735, 1725, 1698, 1250, 1230 cm^{-1}.

(*b*) O-Acetyllofoline (84 mg) and lycopodine (60 mg) were dissolved in a minimum volume of hot hexane. On cooling, colorless crystals (110 mg), m.p. 121–122°, separated. The melting point was not altered by recrystallization from either hexane or anhydrous ether. The material obtained in this way was identical (mixed melting point, infrared spectrum, t.l.c. behavior) with the authentic sample of alkaloid L.9.

O-Acetyllofoline

Lofoline (0.22 g) was dissolved in 1:1 acetic anhydride – pyridine (30 ml) and the solution kept at room temperature for 48 hours, then evaporated at the pump. The oily residue was dissolved in $CHCl_3$ and filtered through alumina (8 g). Evaporation of the solvent left a colorless viscous oil (0.22 g) which showed a single spot on t.l.c. A sample was purified by evaporative distillation under reduced pressure. Calc. for $C_{20}H_{31}O_4N$: molecular weight, 349. Found: molecular weight (mass spec.) 349. Infrared spectrum: $\nu_{max}^{CHCl_3}$ 1720–1730, 1225 cm^{-1}. Nuclear magnetic resonance spectrum (CCl_4): 4.92 τ (1H, triplet, C*H*OAc), 5.25 τ (1H, mult., C*H*OAc), 7.96 and 8.02 τ (6H, two OCOC*H*$_3$), 9.12 τ (3H, doublet, CHC*H*$_3$).

A sample of the base in acetone was converted to the perchlorate by addition of perchloric acid. After recrystallization from acetone–ether the salt melted at 272–273° (dec.). Calc. for $C_{20}H_{31}O_4N.HClO_4$: C, 53.40; H, 7.17; N, 3.11%. Found: C, 53.30; H, 7.06; N, 2.95%. Infrared spectrum: ν_{max}^{nujol} 3040 (—N$^+$H), 1737, 1722, 1235 cm^{-1} (OAc).

Can. J. Chem. Downloaded from www.nrcresearchpress.com by 210.87.254.5 on 09/05/12
For personal use only.

ACKNOWLEDGMENTS

We wish to thank Dr. R. H. Manske for the sample of alkaloid L.9 which enabled us to carry out this work, Dr. P. Kebarle for his help and advice in determining the mass spectra, and the National Research Council for financial support.

1. R. H. F. MANSKE and L. MARION. Can. J. Res. B, **21**, 92 (1943).
2. D. B. MACLEAN. Can. J. Chem. **41**, 2654 (1963).
3. D. A. LAW. Ph.D. Thesis, University of Alberta. 1963.
4. R. H. BURNELL and D. R. TAYLOR. Tetrahedron, **15**, 173 (1961).
5. F. A. L. ANET. Tetrahedron Letters, No. 20, 13 (1960).
6. B. T. CROMWELL. *In* Modern methods of plant analysis. Vol. 4. *Edited by* K. Paech and M. W. Tracey. Springer-Verlag, Berlin. 1955. p. 373.

RECEIVED NOVEMBER 27, 1963.
DEPARTMENT OF CHEMISTRY,
UNIVERSITY OF ALBERTA,
EDMONTON, ALBERTA.

Can. J. Chem. Downloaded from www.nrcresearchpress.com by 210.87.254.5 on 09/05/12
For personal use only.

PROTON MAGNETIC RESONANCE ABSORPTION IN COPPER(II) STEARATE

R. F. GRANT

The magnetic moment of copper in copper(II) acetate is known to decrease as the temperature is lowered (1, 2). This anomalous effect has been explained by assuming that the copper ions are arranged in isolated pairs which interact strongly through exchange forces (3). X-Ray studies, supporting this explanation, have shown that copper(II) acetate monohydrate exists as a binuclear molecule $Cu_2(CH_3CO_2)_4 \cdot 2H_2O$ in which the copper ions are situated close together (4). By analogy, a similar structure has been suggested for copper(II) salts of higher fatty acids (5, 6), although a layer structure allowing a kind of antiferromagnetic interaction between the copper ions has also been proposed (7). This layer structure, which is supposedly characteristic of fatty acid salts (8), infers a cooperative effect between copper ions extending in planes throughout the crystal lattice. In such a structure, the interaction between the copper ions should decrease if the lattice expands with rising temperature and some correlation between motion of the hydrocarbon portion of the molecule and the magnetic moment might be expected. The following investigation of proton magnetic resonance absorption in copper(II) stearate shows no such correlation.

EXPERIMENTAL

The stearic acid used was Eastman Kodak white label grade, purified by repeated crystallization at −20° C in acetone. Copper(II) stearate was prepared by metathesis of potassium stearate in 70% ethanol with an aqueous solution of copper(II) sulphate at 60° C. The soap precipitate was allowed to settle overnight and was then washed repeatedly on a suction filter with distilled water and with aqueous ethanol. The product was dried in an air oven at 100° C and then heated to about 130° C under vacuum to render it more compact. Portions of this soap used in the proton magnetic resonance investigations were reheated under vacuum in sample tubes, dry nitrogen was admitted to the system, and the tubes were sealed off.

Copper(II) stearate has been reported to melt indefinitely to a clear blue liquid at 125° C (9). This was not observed, either for the samples which had been heated under vacuum or for new samples dried in air. On a Fisher–Johns melting block, some sample particles were observed to deform slightly around 120° C,

ACKNOWLEDGMENTS

We wish to thank Dr. R. H. Manske for the sample of alkaloid L.9 which enabled us to carry out this work, Dr. P. Kebarle for his help and advice in determining the mass spectra, and the National Research Council for financial support.

1. R. H. F. MANSKE and L. MARION. Can. J. Res. B, **21**, 92 (1943).
2. D. B. MACLEAN. Can. J. Chem. **41**, 2654 (1963).
3. D. A. LAW. Ph.D. Thesis, University of Alberta. 1963.
4. R. H. BURNELL and D. R. TAYLOR. Tetrahedron, **15**, 173 (1961).
5. F. A. L. ANET. Tetrahedron Letters, No. 20, 13 (1960).
6. B. T. CROMWELL. *In* Modern methods of plant analysis. Vol. 4. *Edited by* K. Paech and M. W. Tracey. Springer-Verlag, Berlin. 1955. p. 373.

RECEIVED NOVEMBER 27, 1963.
DEPARTMENT OF CHEMISTRY,
UNIVERSITY OF ALBERTA,
EDMONTON, ALBERTA.

Can. J. Chem. Downloaded from www.nrcresearchpress.com by 210.87.254.5 on 09/05/12
For personal use only.

PROTON MAGNETIC RESONANCE ABSORPTION IN COPPER(II) STEARATE

R. F. GRANT

The magnetic moment of copper in copper(II) acetate is known to decrease as the temperature is lowered (1, 2). This anomalous effect has been explained by assuming that the copper ions are arranged in isolated pairs which interact strongly through exchange forces (3). X-Ray studies, supporting this explanation, have shown that copper(II) acetate monohydrate exists as a binuclear molecule $Cu_2(CH_3CO_2)_4 \cdot 2H_2O$ in which the copper ions are situated close together (4). By analogy, a similar structure has been suggested for copper(II) salts of higher fatty acids (5, 6), although a layer structure allowing a kind of antiferromagnetic interaction between the copper ions has also been proposed (7). This layer structure, which is supposedly characteristic of fatty acid salts (8), infers a cooperative effect between copper ions extending in planes throughout the crystal lattice. In such a structure, the interaction between the copper ions should decrease if the lattice expands with rising temperature and some correlation between motion of the hydrocarbon portion of the molecule and the magnetic moment might be expected. The following investigation of proton magnetic resonance absorption in copper(II) stearate shows no such correlation.

EXPERIMENTAL

The stearic acid used was Eastman Kodak white label grade, purified by repeated crystallization at −20° C in acetone. Copper(II) stearate was prepared by metathesis of potassium stearate in 70% ethanol with an aqueous solution of copper(II) sulphate at 60° C. The soap precipitate was allowed to settle overnight and was then washed repeatedly on a suction filter with distilled water and with aqueous ethanol. The product was dried in an air oven at 100° C and then heated to about 130° C under vacuum to render it more compact. Portions of this soap used in the proton magnetic resonance investigations were reheated under vacuum in sample tubes, dry nitrogen was admitted to the system, and the tubes were sealed off.

Copper(II) stearate has been reported to melt indefinitely to a clear blue liquid at 125° C (9). This was not observed, either for the samples which had been heated under vacuum or for new samples dried in air. On a Fisher–Johns melting block, some sample particles were observed to deform slightly around 120° C,

but most of the particles became glassy in appearance at 117–122° C and retained their shapes. At 250–252° C the sample particles appeared to melt and flow freely.

The nuclear magnetic resonance spectrometer and associated apparatus have been described previously (10).

Figure 1 shows the variations of the proton magnetic resonance absorption line width of copper(II) stearate as a function of temperature. The line width was taken as the separation, in gauss, of the points of maximum and minumum slope on the resonance line. Also shown in Fig. 1 are the corresponding variations of second moment with temperature. The second moments of the resonance lines were obtained by a graphical method (11) and were corrected for the effects of modulation (12). Between 116 and 120° C, in the vicinity of the reported melting point (9), the line width decreased to a value governed by the depth of modulation which was 0.3 gauss. The narrowed line retained broad wings of comparatively small amplitude, allowing a second moment of 0.9 gauss^2.

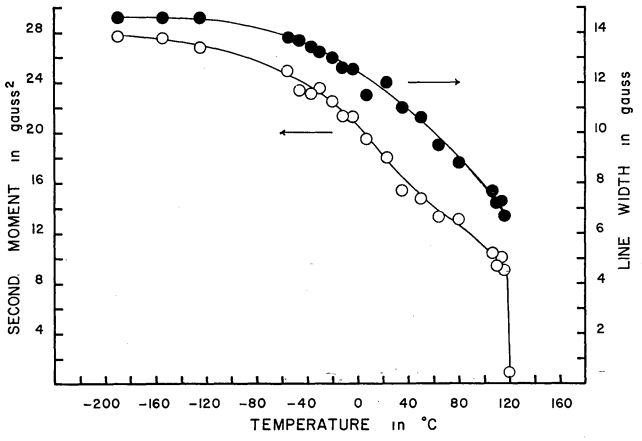

FIG. 1. Line width and second moment of copper(II) stearate as functions of temperature. Filled circles, line width; open circles, second moment.

DISCUSSION

Since details of the copper(II) stearate unit cell are not available, the rigid lattice second moment cannot be directly calculated. However, X-ray studies reporting long and short spacings (13) suggest that the hydrocarbon chain packing in copper(II) stearate may be similar to the chain packing in silver stearate. The crystal structure of silver stearate is well known (14) and a rigid lattice second moment of 28.3 gauss^2 has been calculated for it (15). This value is close to the experimental second moment of 27.7±0.5 gauss^2 obtained for copper(II) stearate at –190° C, and it is assumed that there is little molecular motion at this temperature. The contribution of the paramagnetic copper(II) ions to the second moment was calculated to be less than 0.1 gauss^2. The gradual decrease in the second moment of copper(II) stearate as the temperature is raised between –190° C and 116° C can be interpreted in terms of a torsional oscillation about the longitudinal axis of the hydrocarbon chain portion of the molecule (15). The effect of such motion on the second moment has been calculated for a silver stearate structure (15) and is assumed to be valid for copper(II) stearate. Torsional oscillation amplitudes can therefore be obtained from the copper(II) stearate results by using the second moment versus torsional oscillation curve calculated for silver stearate (15). The temperature dependence of the relative amplitude of torsional oscillation is shown in Fig. 2 along with the magnetic moment results of Martin and Waterman (6). A comparison of the two curves in Fig. 2

Can. J. Chem. Downloaded from www.nrcresearchpress.com by 210.87.254.5 on 09/05/12
For personal use only.

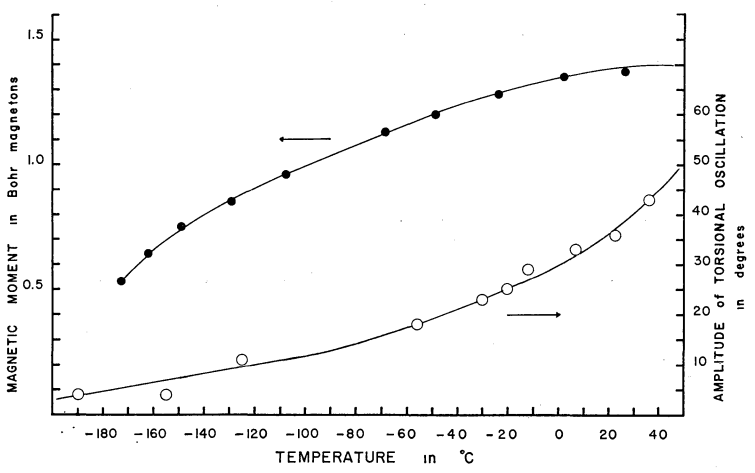

FIG. 2. The copper magnetic moment (6) and amplitude of torsional oscillation of the hydrocarbon chains in copper(II) stearate as functions of temperature. Filled circles, magnetic moment; open circles, torsional oscillation.

suggests that there is little correlation between hydrocarbon chain motion and change in the magnetic moment of the copper ion in copper(II) stearate.

The change in line width and second moment between 116 and 120° C seems to be related to a thermal transition previously reported as the melting point. Since copper(II) stearate does not become a freely flowing liquid until 250° C it is assumed that the melting point reported to occur around 125° C is a mesomorphic transition, perhaps similar in nature to one of the transitions known to occur in alkali metal soaps (15, 16). The second moment of 9.0 gauss^2 at 116° C for copper(II) stearate is slightly larger than the 8.1 gauss^2 predicted for complete rotation of the hydrocarbon chain about the long axis in the silver stearate structure (15). The narrow line at 120° C indicates that the hydrocarbon chain has become free to rotate about many axes, however, the finite second moment implies that the molecules are not free to diffuse through the lattice (17).

1. B. C. GUHA. Proc. Roy. Soc. (London), A, **206**, 353 (1951).
2. B. N. FIGGIS and R. L. MARTIN. J. Chem. Soc. 3837 (1956).
3. B. BLEANEY and K. D. BOWERS. Proc. Roy. Soc. (London), A, **214**, 451 (1952).
4. J. N. VAN NIEKERK and F. R. L. SCHOENING. Acta Cryst. **6**, 227 (1953).
5. R. C. HERRON and R. C. PINK. J. Chem. Soc. 3948 (1956).
6. R. L. MARTIN and H. WATERMAN. J. Chem. Soc. 2545 (1957).
7. A. GILMOUR and R. C. PINK. J. Chem. Soc. 2198 (1953).
8. M. VOLD and G. HATTIANGDI. Ind. Eng. Chem. **41**, 2311 (1949).
9. W. F. WHITMORE and M. LAURO. Ind. Eng. Chem. **22**, 646 (1930).
10. R. F. GRANT and B. A. DUNELL. Can. J. Chem. **38**, 359 (1960).
11. J. G. POWLES. Brit. J. Appl. Phys. **9**, 299 (1958).
12. E. R. ANDREW. Phys. Rev. **91**, 425 (1953).
13. I. SATAKE and R. MATUURA. Kolloid-Z. **116**, 31 (1961).
14. V. VAND, A. AITKEN, and R. K. CAMPBELL. Acta Cryst. **2**, 398 (1949).
15. R. F. GRANT and B. A. DUNELL. Can. J. Chem. **38**, 2395 (1960).
16. G. H. BROWN and W. G. SHAW. Chem. Rev. **57**, 1049 (1957).
17. E. R. ANDREW. Nuclear magnetic resonance. Cambridge University Press. 1956. p. 173.

RECEIVED OCTOBER 25, 1963.
DEPARTMENT OF CHEMISTRY,
CANADIAN SERVICES COLLEGE, ROYAL ROADS,
VICTORIA, BRITISH COLUMBIA.

Can. J. Chem. Downloaded from www.nrcresearchpress.com by 210.87.254.5 on 09/05/12
For personal use only.

THE NUCLEAR MAGNETIC RESONANCE SPECTRA OF THE CARBOLINES

R. A. ABRAMOVITCH AND I. D. SPENSER

Can. J. Chem. Downloaded from www.nrcresearchpress.com by 210.87.254.5 on 09/05/12
For personal use only.

There is no report in the literature on the n.m.r. spectra of the parent fully aromatic carbolines. The spectra of α- (Fig. 1), β- (Fig. 2), and δ-carboline (Fig. 3) have now been measured using a Varian DP-60 instrument. Unfortunately, a sample of the γ-isomer was not available at this time. The spectra had to be determined on dimethyl sulphoxide solutions of the compounds due to their insolubility in the common solvents: the solvent peak was used as internal reference.[1] Solvent corrections have not been applied and a complete analysis of the spectra has not been attempted. A number of features are worth commenting upon, however.

A band (not shown) at 719 c.p.s. towards low field in the spectrum of β-carboline is due to the *ind*-N–H group. The single proton singlet at 555 c.p.s. is undoubtedly due to C_1–H and the doublet centered at 515 c.p.s. ($J_{3,4}$ 6 c.p.s.) to C_3–H. The signals for C_4–H (a pyridine β-proton) overlap with those of the phenyl protons at higher field. The corresponding assignments for δ-carboline appear to be almost as straightforward. The The *ind*-N–H proton gives rise to a line at 704 c.p.s. (not shown). A single-proton doublet ($J_{2,3}$ 4 c.p.s.) centered at 520 c.p.s. may be attributed to C_2–H (pyridine α-proton). At much higher resolution this may be seen to be a quartet ($J_{2,4}$ 1 c.p.s.) as expected. A second single-proton doublet ($J_{3,4}$ 8 c.p.s.), centered at 506 c.p.s., is probably due to C_4–H (pyridine γ-proton). The single-proton doublet (J 8 c.p.s.) at 480 c.p.s. may be due to C_3–H but this seems to be a somewhat low field for a pyridine β-proton absorption (though lines within the range 479–499 c.p.s. have been attributed to pyridine β-protons (1)), and one would have expected the resonance due to this proton to give rise to a quartet. It is more likely that this doublet is due to C_8–H (cf. the lines due to C_8–H in quinoline (2)) and that the lines for C_3–H overlap with those of the phenyl protons. It is of interest to note that, if the above assignments are correct, the signal corresponding to C_1–H in β-carboline is at a much lower field than that for C_3–H in β- and that for C_2–H in δ-carboline, and is certainly at a lower field than is expected for a pyridine α-proton (3). A similar situation is observed in isoquinoline (2). The electron-attracting character of the *ind*-*N* may well also play a role here. An analogous effect appears to exist in δ-carboline, where C_4–H (corresponding to a pyridine γ-proton) absorbs at a lower field than expected.

The interpretation of the α-carboline spectrum is more difficult and only tentative suggestions can be made at this time. The *ind*-N–H absorbs quite unexceptionally at 723 c.p.s. (not shown). Two lines appear at 519 and 511 c.p.s., respectively, each one having an area corresponding to one proton. A single-proton doublet (J 7 c.p.s.) is centered at 496 c.p.s. One of the bands at 519 and 511 c.p.s. is undoubtedly due to C_2–H, and it is then tempting to suggest that these peaks are caused by overlapping doublets due to C_2–H and C_4–H. C_3–H would be expected to give rise to a quartet due to coupling with two non-equivalent protons, so that the doublet at 496 c.p.s. may be due to C_8–H. No firm assignments can be made without further studies.

[1]*The signal of dimethyl sulphoxide is observed at 152.7±0.3 c.p.s. downfield from that of tetramethylsilane when the latter is dissolved in dimethyl sulphoxide.*

Can. J. Chem. Downloaded from www.nrcresearchpress.com by 210.87.254.5 on 09/05/12
For personal use only.

Fig. 1

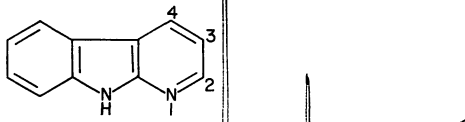

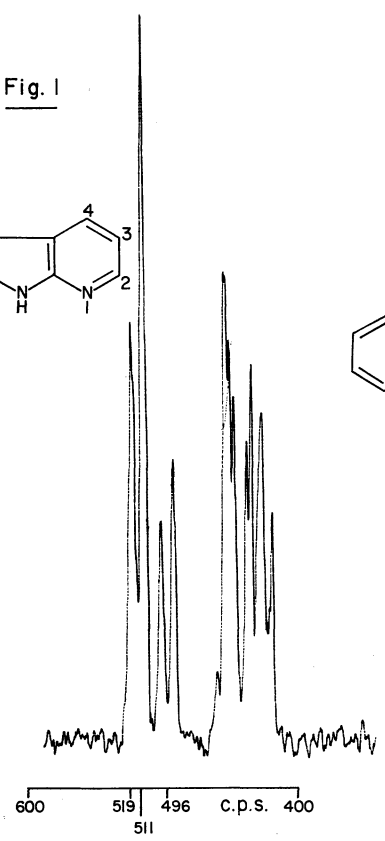

Fig. 2

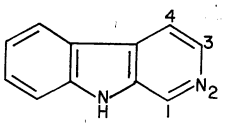

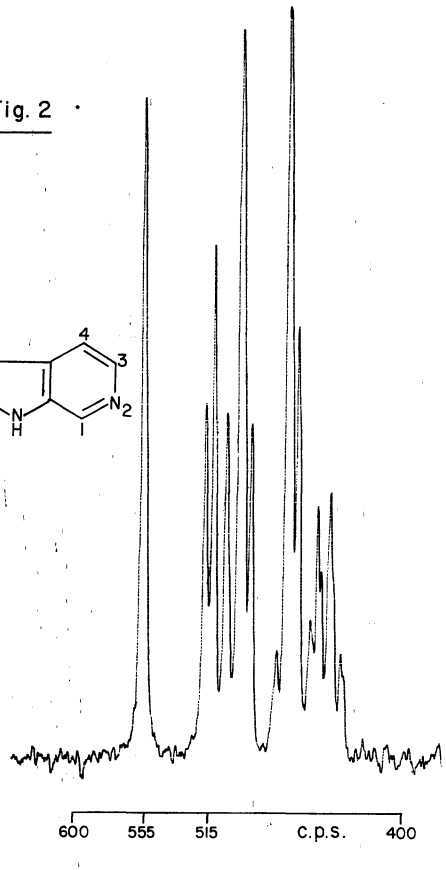

Fig. 3

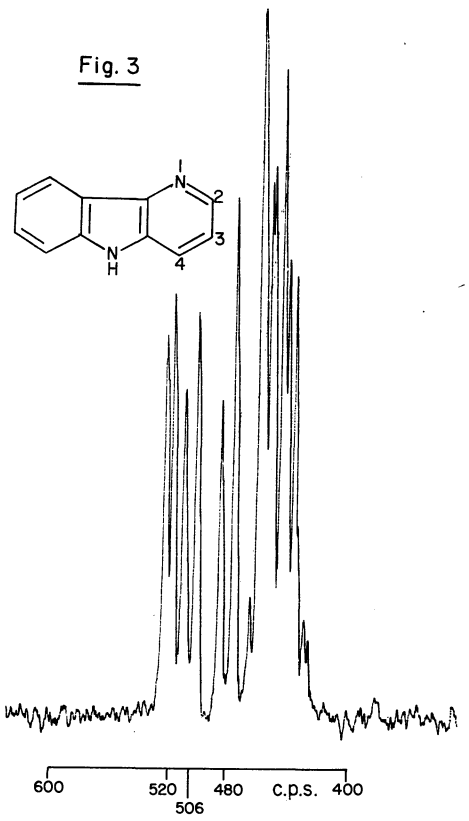

1. E. J. POZIOMEK, D. N. KRAMER, W. A. MOSHER, and H. O. MICHEL. J. Am. Chem. Soc. **83**, 3616 (1961).
2. J. A. POPLE, W. G. SCHNEIDER, and H. J. BERNSTEIN. High resolution nuclear magnetic resonance. McGraw-Hill, Inc., New York. 1959. p. 268.
3. R. A. ABRAMOVITCH, GIAM CHOO-SENG, and A. D. NOTATION. Can. J. Chem. **38**, 761 (1960). L. M. JACKMAN. Application of nuclear magnetic resonance spectroscopy to organic chemistry. Pergamon Press, New York. 1959.

RECEIVED JUNE 27, 1963.
DEPARTMENT OF CHEMISTRY,
UNIVERSITY OF SASKATCHEWAN,
SASKATOON, SASKATCHEWAN,
AND
DEPARTMENT OF CHEMISTRY,
MCMASTER UNIVERSITY,
HAMILTON, ONTARIO.

Can. J. Chem. Downloaded from www.nrcresearchpress.com by 210.87.254.5 on 09/05/12
For personal use only.

REACTION OF BENZALDEHYDE SEMICARBAZONE AND AZINE WITH CARBON MONOXIDE

ALEX ROSENTHAL AND S. MILLWARD

It has been reported previously (1) that benzophenone semicarbazones and benzophenone azine reacted with carbon monoxide in the presence of dicobalt octacarbonyl to yield phthalimidines. The work reported herein deals with an extension of a similar reaction to benzaldehyde semicarbazone and to benzaldehyde azine.

When benzaldehyde semicarbazone was treated with about 4000 p.s.i. of carbon monoxide at 235–245° in the presence of preformed dicobalt octacarbonyl, no cyclization took place but the substrate was converted in 63% yield into benzaldehyde azine. Under similar conditions, except at a lower temperature of 215–220°, the same substrate afforded a 54% yield of the same product. In addition to the azine, about 39% of an insoluble blue organocobalt complex (no catalyst was present after the reaction) and about 6% of bibenzyl were also produced. Presumably, the cyclization reaction did not take place because the catalyst was precipitated out of the reaction mixture. On the other hand, benzaldehyde azine incorporated carbon monoxide at 235–245° to yield 2-(N-benzylcarboxamido)phthalimidine (I), N-benzylphthalimidine (II), and phthalimidine (III) in 5%, 16%, and 13% yields, respectively. In the last experiment some of the catalyst was still present in the reaction mixture. As in the previous experiments, a trace quantity of bibenzyl was produced in addition to about 14% of an organocobalt complex. From the mixture of products which were separated by alumina chromatography, a substance (IV) was also isolated in 12% yield.

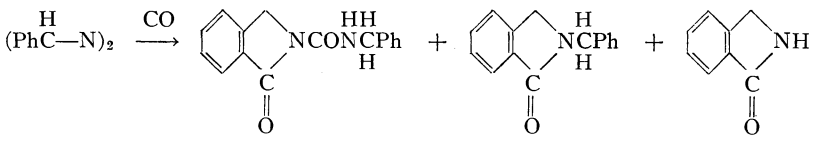

I II III

Structure (I) was deduced on the bases of its elemental analysis and a comparison of its infrared spectrum with that of 3-phenyl-2(N-benzhydrylcarboxamido)phthalimidine (1). Final confirmation of structure (I) was obtained by direct comparison of compound

Presented at the XIXth International Congress of Pure and Applied Chemistry, London, England, July, 1963.

1. E. J. POZIOMEK, D. N. KRAMER, W. A. MOSHER, and H. O. MICHEL. J. Am. Chem. Soc. **83**, 3616 (1961).
2. J. A. POPLE, W. G. SCHNEIDER, and H. J. BERNSTEIN. High resolution nuclear magnetic resonance. McGraw-Hill, Inc., New York. 1959. p. 268.
3. R. A. ABRAMOVITCH, GIAM CHOO-SENG, and A. D. NOTATION. Can. J. Chem. **38**, 761 (1960). L. M. JACKMAN. Application of nuclear magnetic resonance spectroscopy to organic chemistry. Pergamon Press, New York. 1959.

RECEIVED JUNE 27, 1963.
DEPARTMENT OF CHEMISTRY,
UNIVERSITY OF SASKATCHEWAN,
SASKATOON, SASKATCHEWAN,
AND
DEPARTMENT OF CHEMISTRY,
MCMASTER UNIVERSITY,
HAMILTON, ONTARIO.

Can. J. Chem. Downloaded from www.nrcresearchpress.com by 210.87.254.6 on 09/05/12
For personal use only.

REACTION OF BENZALDEHYDE SEMICARBAZONE AND AZINE WITH CARBON MONOXIDE

ALEX ROSENTHAL AND S. MILLWARD

It has been reported previously (1) that benzophenone semicarbazones and benzophenone azine reacted with carbon monoxide in the presence of dicobalt octacarbonyl to yield phthalimidines. The work reported herein deals with an extension of a similar reaction to benzaldehyde semicarbazone and to benzaldehyde azine.

When benzaldehyde semicarbazone was treated with about 4000 p.s.i. of carbon monoxide at 235–245° in the presence of preformed dicobalt octacarbonyl, no cyclization took place but the substrate was converted in 63% yield into benzaldehyde azine. Under similar conditions, except at a lower temperature of 215–220°, the same substrate afforded a 54% yield of the same product. In addition to the azine, about 39% of an insoluble blue organocobalt complex (no catalyst was present after the reaction) and about 6% of bibenzyl were also produced. Presumably, the cyclization reaction did not take place because the catalyst was precipitated out of the reaction mixture. On the other hand, benzaldehyde azine incorporated carbon monoxide at 235–245° to yield 2-(N-benzylcarboxamido)phthalimidine (I), N-benzylphthalimidine (II), and phthalimidine (III) in 5%, 16%, and 13% yields, respectively. In the last experiment some of the catalyst was still present in the reaction mixture. As in the previous experiments, a trace quantity of bibenzyl was produced in addition to about 14% of an organocobalt complex. From the mixture of products which were separated by alumina chromatography, a substance (IV) was also isolated in 12% yield.

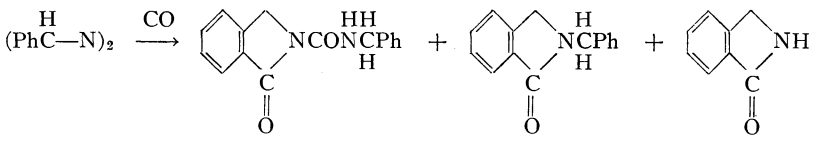

I II III

Structure (I) was deduced on the bases of its elemental analysis and a comparison of its infrared spectrum with that of 3-phenyl-2(N-benzhydrylcarboxamido)phthalimidine (1). Final confirmation of structure (I) was obtained by direct comparison of compound

Presented at the XIXth International Congress of Pure and Applied Chemistry, London, England, July, 1963.

(I) with an authentic sample of 2-(N-benzylcarboxamido)phthalimidine prepared by the condensation, under conditions previously described (2), of benzylisocyanate with phthalimidine.

The structure of compound (II) was established by direct comparison with an authentic sample of N-benzylphthalimidine prepared by the method of Murahashi and co-workers (3). Likewise, compound (III) was directly compared with an authentic sample of phthalimidine (4) and shown to be the same in melting point and infrared spectrum.

Compound (IV) had an empirical formula of $C_9H_8N_2O_2$. When heated with either concentrated sulphuric acid or concentrated sodium hydroxide, carbon dioxide and ammonia, respectively, were evolved. On the bases of elemental, infrared, and proton magnetic resonance analyses, its structure is tentatively suggested to be that represented by structure (IV). Infrared absorptions at 3380 and 3220 cm^{-1} indicated the presence of

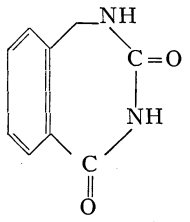

IV

two different monosubstituted amide functions, the one at 3380 cm^{-1} being a non-bonded NH and the one at 3220 cm^{-1}, a bonded NH absorption. The CONHCO group showed a single bonded amide NH absorption in the 3200 cm^{-1} region similar to that of cyclic lactams (5). Absorptions at $\delta = 4.96$ and at about 7.6 in the nuclear magnetic resonance spectrum of compound (IV) were consistent with the presence of a benzylic methylene group and a fused benzene ring in the proposed formulation. As attempts to synthesize compound (IV) by unequivocal methods were without success, further work was abandoned.

EXPERIMENTAL

General Considerations

(*a*) The high-pressure equipment has been described previously (1).

(*b*) In every carbonylation experiment preformed dicobalt octacarbonyl (6) was used, and high purity carbon monoxide (containing 0.01% hydrogen) supplied by the Matheson Co., East Rutherford, N. J., was added to an initial pressure of about 2100 p.s.i. at room temperature.

(*c*) The aluminum oxide (calcined) "Analar" was procured from the British Drug Houses (Canada) Ltd., Toronto 14.

(*d*) All melting points were obtained on a Leitz heating stage and are uncorrected. The infrared analyses were done on a Perkin–Elmer spectrophotometer, Model 21, using a sodium chloride crystal. Microanalyses were done by Dr. A. Bernhardt, Mikroanalytisches Laboratorium, im Max-Planck Institut fur Kohlenforschung, Mülheim (Ruhr), Germany, and by Mrs. Aldridge of this Department. The n.m.r. spectra were obtained on a Varian A-60 instrument using tetramethylsilane as the internal standard (set at $\delta = 0$).

Carbonylation of Benzaldehyde Semicarbazone at 235–245°

To a mixture of 5.90 g of benzaldehyde semicarbazone (0.036 mole) in 45 ml of anhydrous, thiophene-free benzene were added 1.8 g of preformed dicobalt octacarbonyl and 2000 p.s.i. of carbon monoxide. The mixture was heated, with rocking, for 150 minutes at 235–245°. The reaction product consisted of 2.76 g of blue solid (A), and a brown liquid (free of catalyst) which, on evaporation under reduced pressure, yielded 3.50 g of a brown solid (B).

Benzaldehyde Azine (from Solid A)

The solid (A) was extracted with ethyl ether for 48 hours in a Soxhlet apparatus yielding 0.19 g of solid

Can. J. Chem. Downloaded from www.nrcresearchpress.com by 210.87.254.6 on 09/05/12
For personal use only.

residue. Recrystallization of this residue from petroleum ether (b.p. 65–110°) yielded benzaldehyde azine. m.p. 90–92°. The mixed melting point of the latter substance and an authentic sample of benzaldehyde azine (7) was 90–92°. The infrared spectra of the two compounds were identical. Infrared spectrum of benzaldehyde azine (KBr); 3000 (w), 2920 (w), 1619 (m), 1570 (w), 1492 (w), 1446 (m), 1320 (w), 1305 (w), 1288 (w), 1210 (m), 1170 (w), 1070 (w), 1020 (w), 999 (w), 955 (m).

Separation of Substances in Solid B

A 0.87 g sample of solid B was dissolved in a minimum of benzene, and chromatographed on alumina using benzene as a developer. Bibenzyl (0.019 g, 2% yield) was eluted first, followed by benzaldehyde azine (0.569 g, 61% yield). Bibenzyl was compared with an authentic stock sample of bibenzyl and shown to be the same. Further elution of the column with benzene–ethanol (90:10) eluted about 0.03 g of solid which was crystallized from benzene, m.p. 214–215°. The substance was not analyzed because of the lack of material.

Carbonylation of Benzaldehyde Semicarbazone at 215–220°

Similarly, benzaldehyde semicarbazone (10 g) was carbonylated at 215–220° for 3 hours. The reaction product consisted of 5.47 g of blue solid and a brown liquid which afforded, on evaporation, 4.32 g of solid. The products were worked up as described in the 235–245° experiment yielding 6% of bibenzyl, 54% of benzaldehyde azine, and 39% of a blue insoluble complex.

Carbonylation of Benzaldehyde Azine at 235–245°

An amount of 8.20 g of benzaldehyde azine was carbonylated as described in the first experiment for 2.5 hours at 235–245°. The reaction product consisted of 2.28 g of a black solid (C) and a dark green solution which, upon evaporation under reduced pressure, gave 7.15 g of greenish black solid (D). The solid (C) was extracted with chloroform. Evaporation of the chloroform solution yielded a residue which was chromatographed on alumina to yield bibenzyl.

Separation of Substances in Solid (D)

A 2.28 g sample of material (D), dissolved in benzene, was chromatographed on an alumina column (130×60 mm diameter). The following developers were then added consecutively with elutions as indicated:

(1) 1100 ml of benzene eluted 0.372 g of oily material (E);
(2) 1300 ml of benzene yielded no material;
(3) 300 ml of benzene gave 0.449 g (16%) of white solid (II);
(4) 1600 ml of benzene–chloroform (3:1) eluted 0.12 g of solid;
(5) 550 ml of benzene–chloroform (3:1) eluted 0.187 g (6%) of solid;
(6) 1200 ml of benzene–chloroform (1:1) eluted a trace of material;
(7) 600 ml of chloroform eluted a trace of solid;
(8) 1000 ml of benzene–ethanol (4:1) eluted 0.45 g (13%) of solid (III);
(9) 2000 ml of ethanol–water (1:1) afforded 0.37 g (12%) of solid (IV).

Characterization of Fractions

2-(N-Benzylcarboxamido)phthalimidine (I)

Material (E) was rechromatographed on alumina. Petroleum ether (b.p. 30–60°) eluted bibenzyl (0.023 g, 1%). The column was then eluted with 800 ml of benzene – petroleum ether to afford 0.03 g of white solid. Benzene–chloroform (500 ml) removed 0.17 g (5%) of 2-(N-benzylcarboxamido)phthalimidine which was recrystallized from ethyl ether – petroleum ether (b.p. 30–60°), m.p. 127–128°. Infrared spectrum (KBr) of compound (I): 3290 (m), 3030 (w), 2940–2920 (w), 1710 (s), 1675 (m), 1613 (w), 1590 (w), 1533 (s), 1494 (w), 1470 (w), 1442 (m), 1369 (s), 1343 (w), 1324 (m), 1302 (m), 1258 (m), 1237 (w), 1216 (w), 1193 (w), 1155 (m), 1104 (w), 1078 (w), 754 (m), 737 (s), 693 (s).

Synthesis of Authentic 2-(N-Benzylcarboxamido)phthalimidine

Benzyl chloride (15 g) was first treated with silver cyanate (21.6 g) under reflux for about 10 minutes. Distillation of the product under reduced pressure yielded benzylisocyanate. The latter compound (0.07 g) was then condensed with phthalimidine (0.07 g) following the procedure previously described (8) to yield 0.095 g (68%) of a white solid which, after recrystallization from carbon tetrachloride – petroleum ether (b.p. 30–60°) gave white needles, m.p. 126–127°. The mixed melting point with compound (I) was 126–127°. The infrared spectra of the two substances were identical. Anal. Found: C, 72.12; H, 5.13; N, 10.17. Calc. for $C_{16}H_{14}N_2O_2$: C, 72.16; H, 5.30; N, 10.52.

2-Benzylphthalimidine (II)

Compound (II) was repurified by alumina chromatography and then recrystallized from petroleum ether (b.p. 30–60°), m.p. 90–91°. The mixed melting point of compound (II) and an authentic sample of N-benzylphthalimidine, prepared by the method of Murahashi and co-workers (3), was 90–91°. Infrared spectrum of compound (II) (KBr): 3020 (w), 2900 (w), 1667 (s), 1492 (w), 1466 (m), 1450 (m), 1436 (w), 1411 (m), 1354 (m), 1324 (w), 1315 (w), 1298 (w), 1284 (w), 1264 (m), 1219 (w), 1203 (m), 1180 (w), 1140 (w), 1070 (w), 968 (w), 926 (w), 855 (w), 764 (w), 735 (s). Anal. Found: C, 80.61; H, 5.97; N, 6.25. Calc. for $C_{15}H_{13}NO$: C, 80.67; H, 5.87; N, 6.27.

Can. J. Chem. Downloaded from www.nrcresearchpress.com by 210.87.254.6 on 09/05/12
For personal use only.

Phthalimidine (III)

Compound (III) dissolved in benzene–ethanol was treated with Norite, filtered, evaporated to dryness, and then recrystallized from benzene – petroleum ether (b.p. 30–60°), m.p. 154–155°. The mixed melting point of compound (III) with an authentic sample of phthalimidine prepared by the method of Graebe (4) was 154–155°. The infrared spectra of both substances were identical.

Substance (IV)

Substance (IV) was recrystallized from hot benzene, m.p. 255–256° (decomp.). Infrared spectrum (KBr): 3380 (s), 3220 (m), 3030 (w), 2900 (w), 1715 (s), 1664 (s), 1597 (s), 1580 (s), 1555 (m), 1470 (m), 1455 (m), 1391 (m), 1363 (s), 1320 (m), 1300 (m), 1219 (m), 1183 (w), 1154 (m), 1145 (m), 1082 (w), 922 (w), 820 (w), 800 (w), 761 (m), 730 (m), 677 (w). Nuclear magnetic resonance signals (given in δ units); (*a*) spectrum obtained in trifluoracetic anhydride; 4.96 (area = 2H), 7.55, 7.60, 7.79 (area = 4H), 7.90, 8.01 (area = 2H); (*b*) spectrum obtained in dimethylsulphoxide; 4.80 (area = 2H), 7.72 (area = 6H).

Compound (IV), when heated in concentrated sulphuric acid, evolved carbon dioxide, and, when heated with concentrated sodium hydroxide, yielded ammonia. Anal. Found: C, 61.55; H, 4.82; N, 15.78; O, 18.13. Calc. for $C_9H_8N_2O_2$: C, 61.35; H, 4.58; N, 15.91; O, 18.16.

ACKNOWLEDGMENTS

Grateful acknowledgment is hereby made to the National Research Council of Canada and to the Petroleum Research Fund administered by the American Chemical Society for support of this research.

The author (A. R.) expresses his gratitude to University Chemical Laboratory, Cambridge University, for use of its facilities during the writing of this manuscript.

1. A. Rosenthal and S. Millward. Can. J. Chem. **41**, 2504 (1963).
2. P. F. Wiley. J. Am. Chem. Soc. **71**, 1310 (1949).
3. S. Murahashi, S. Horiie, and T. Jo. Bull. Chem. Soc. Japan, **33**, 81 (1959).
4. C. Graebe. Ann. **247**, 288 (1888).
5. L. J. Bellamy. The infrared spectra of complex molecules. 2nd ed. John Wiley and Sons, Inc., New York. 1958.
6. I. Wender, H. W. Sternberg, S. Metlin, and M. Orchin. Inorg. Syn. **5**, 190 (1957).
7. A. Thiele. Ann. **376**, 244 (1910).
8. A Rosenthal and Mary R. S. Weir. Can. J. Chem. **40**, 610 (1962).

Received October 22, 1963.
Department of Chemistry,
University of British Columbia,
Vancouver, British Columbia.

1(7),8-*p*-MENTHADIENE EX PYROLYSIS OF β-PINENE

L. Steinbach, E. T. Theimer, and B. M. Mitzner

The mechanism postulated by Burwell (1) for the pyrolysis of β-pinene I, via a biradical II, predicts the formation of myrcene III, dipentene IV, and 1(7),8-*p*-menthadiene V. Although it is well known (for example, cf. ref. 2) that myrcene and dipentene are products of this pyrolysis, the formation of 1(7),8-*p*-menthadiene has not been reported.

We have found 1(7),8-*p*-menthadiene in an amount of about 5% among the products formed by the vapor-phase pyrolysis of β-pinene. The separation is a difficult one and thus V may easily have been overlooked by previous workers who did not have available refined gas chromatographic equipment.

This confirmation of the presence of 1(7),8-*p*-menthadiene in β-pinene pyrolyzate adds support to the pyrolysis mechanism of Burwell.

Can. J. Chem. Downloaded from www.nrcresearchpress.com by 210.87.254.6 on 09/05/12
For personal use only.

Phthalimidine (III)

Compound (III) dissolved in benzene–ethanol was treated with Norite, filtered, evaporated to dryness, and then recrystallized from benzene – petroleum ether (b.p. 30–60°), m.p. 154–155°. The mixed melting point of compound (III) with an authentic sample of phthalimidine prepared by the method of Graebe (4) was 154–155°. The infrared spectra of both substances were identical.

Substance (IV)

Substance (IV) was recrystallized from hot benzene, m.p. 255–256° (decomp.). Infrared spectrum (KBr): 3380 (s), 3220 (m), 3030 (w), 2900 (w), 1715 (s), 1664 (s), 1597 (s), 1580 (s), 1555 (m), 1470 (m), 1455 (m), 1391 (m), 1363 (s), 1320 (m), 1300 (m), 1219 (m), 1183 (w), 1154 (m), 1145 (m), 1082 (w), 922 (w), 820 (w), 800 (w), 761 (m), 730 (m), 677 (w). Nuclear magnetic resonance signals (given in δ units); (*a*) spectrum obtained in trifluoracetic anhydride; 4.96 (area = 2H), 7.55, 7.60, 7.79 (area = 4H), 7.90, 8.01 (area = 2H); (*b*) spectrum obtained in dimethylsulphoxide; 4.80 (area = 2H), 7.72 (area = 6H).

Compound (IV), when heated in concentrated sulphuric acid, evolved carbon dioxide, and, when heated with concentrated sodium hydroxide, yielded ammonia. Anal. Found: C, 61.55; H, 4.82; N, 15.78; O, 18.13. Calc. for $C_9H_8N_2O_2$: C, 61.35; H, 4.58; N, 15.91; O, 18.16.

ACKNOWLEDGMENTS

Grateful acknowledgment is hereby made to the National Research Council of Canada and to the Petroleum Research Fund administered by the American Chemical Society for support of this research.

The author (A. R.) expresses his gratitude to University Chemical Laboratory, Cambridge University, for use of its facilities during the writing of this manuscript.

1. A. Rosenthal and S. Millward. Can. J. Chem. **41**, 2504 (1963).
2. P. F. Wiley. J. Am. Chem. Soc. **71**, 1310 (1949).
3. S. Murahashi, S. Horiie, and T. Jo. Bull. Chem. Soc. Japan, **33**, 81 (1959).
4. C. Graebe. Ann. **247**, 288 (1888).
5. L. J. Bellamy. The infrared spectra of complex molecules. 2nd ed. John Wiley and Sons, Inc., New York. 1958.
6. I. Wender, H. W. Sternberg, S. Metlin, and M. Orchin. Inorg. Syn. **5**, 190 (1957).
7. A. Thiele. Ann. **376**, 244 (1910).
8. A Rosenthal and Mary R. S. Weir. Can. J. Chem. **40**, 610 (1962).

Received October 22, 1963.
Department of Chemistry,
University of British Columbia,
Vancouver, British Columbia.

1(7),8-*p*-MENTHADIENE EX PYROLYSIS OF β-PINENE

L. Steinbach, E. T. Theimer, and B. M. Mitzner

The mechanism postulated by Burwell (1) for the pyrolysis of β-pinene I, via a biradical II, predicts the formation of myrcene III, dipentene IV, and 1(7),8-*p*-menthadiene V. Although it is well known (for example, cf. ref. 2) that myrcene and dipentene are products of this pyrolysis, the formation of 1(7),8-*p*-menthadiene has not been reported.

We have found 1(7),8-*p*-menthadiene in an amount of about 5% among the products formed by the vapor-phase pyrolysis of β-pinene. The separation is a difficult one and thus V may easily have been overlooked by previous workers who did not have available refined gas chromatographic equipment.

This confirmation of the presence of 1(7),8-*p*-menthadiene in β-pinene pyrolyzate adds support to the pyrolysis mechanism of Burwell.

Can. J. Chem. Downloaded from www.nrcresearchpress.com by 210.87.254.5 on 09/05/12
For personal use only.

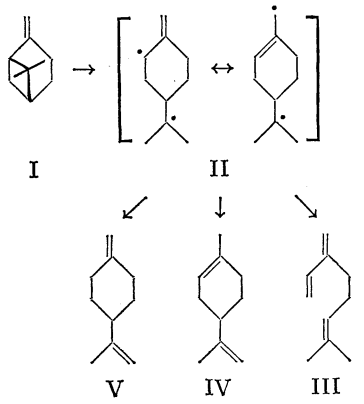

EXPERIMENTAL

Myrcene from the pyrolysis of commercial β-pinene (94%) was used for most of this work. To be absolutely certain that the 1(7),8-*p*-menthadiene was not an impurity in the starting β-pinene, a sample of β-pinene* (99% by gas chromatography) was pyrolyzed under the conditions of Goldblatt and Palkin (2). Here also 5% of 1(7),8-*p*-menthadiene was found in the pyrolyzate. Preparative gas chromatography was carried out using a VPC unit consisting of 10 ft × 1/2 in. O.D. × 7/16 in. I.D. copper tubing packed with 20% Carbowax 20 M on 60–80 mesh silane-treated Celite at a temperature of 120° C and an inlet pressure of 40 p.s.i. helium with a flow rate of 120 ml/minute. The 1(7),8-*p*-menthadiene eluted between myrcene and dipentene. Two passes were required to obtain pure V because of the closeness in elution time to dipentene and myrcene. The relative retention times of 1(7),8-*p*-menthadiene and dipentene are 0.95:1.00. The infrared spectrum of our V was the same as that reported by Webb and Bain (3). It was also the same as that of the 1(7),8-*p*-menthadiene formed (together with dipentene) by the pyrolysis of β-terpinyl acetate VI (4).

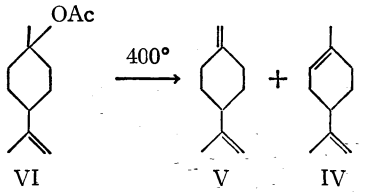

1. R. L. Burwell, Jr. J. Am. Chem. Soc. **73**, 4461 (1951).
2. L. A. Goldblatt and S. Palkin. J. Am. Chem. Soc. **63**, 3517 (1941).
3. R. L. Webb and J. P. Bain. J. Am. Chem. Soc. **75**, 4279 (1953).
4. To be published.

Received November 25, 1963.
Research Laboratories,
International Flavors and Fragrances Inc.,
Union Beach, New Jersey.

**Kindly supplied by Hercules Powder Company.*

INFRARED ABSORPTION OF THE SO_2 CLATHRATE-HYDRATE MOTION OF THE SO_2 MOLECULE

K. B. Harvey, F. R. McCourt, and H. F. Shurvell

Because of their clathrate type of structure, the gas hydrates present an interesting opportunity for the study of intermolecular interactions in the solid state. In many cases the cavities occupied by the molecules of the hydrate-former have a larger free-volume

Can. J. Chem. Downloaded from www.nrcresearchpress.com by 210.87.254.5 on 09/05/12
For personal use only.

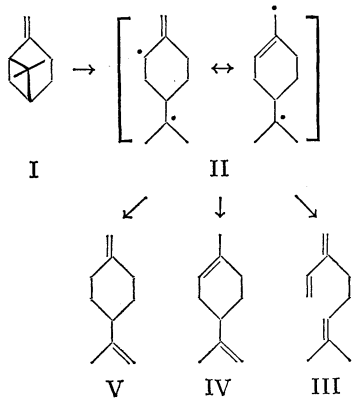

EXPERIMENTAL

Myrcene from the pyrolysis of commercial β-pinene (94%) was used for most of this work. To be absolutely certain that the 1(7),8-*p*-menthadiene was not an impurity in the starting β-pinene, a sample of β-pinene* (99% by gas chromatography) was pyrolyzed under the conditions of Goldblatt and Palkin (2). Here also 5% of 1(7),8-*p*-menthadiene was found in the pyrolyzate. Preparative gas chromatography was carried out using a VPC unit consisting of 10 ft × 1/2 in. O.D. × 7/16 in. I.D. copper tubing packed with 20% Carbowax 20 M on 60–80 mesh silane-treated Celite at a temperature of 120° C and an inlet pressure of 40 p.s.i. helium with a flow rate of 120 ml/minute. The 1(7),8-*p*-menthadiene eluted between myrcene and dipentene. Two passes were required to obtain pure V because of the closeness in elution time to dipentene and myrcene. The relative retention times of 1(7),8-*p*-menthadiene and dipentene are 0.95:1.00. The infrared spectrum of our V was the same as that reported by Webb and Bain (3). It was also the same as that of the 1(7),8-*p*-menthadiene formed (together with dipentene) by the pyrolysis of β-terpinyl acetate VI (4).

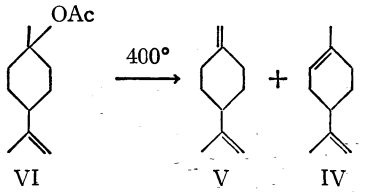

1. R. L. Burwell, Jr. J. Am. Chem. Soc. **73**, 4461 (1951).
2. L. A. Goldblatt and S. Palkin. J. Am. Chem. Soc. **63**, 3517 (1941).
3. R. L. Webb and J. P. Bain. J. Am. Chem. Soc. **75**, 4279 (1953).
4. To be published.

Received November 25, 1963.
Research Laboratories,
International Flavors and Fragrances Inc.,
Union Beach, New Jersey.

**Kindly supplied by Hercules Powder Company.*

INFRARED ABSORPTION OF THE SO_2 CLATHRATE-HYDRATE MOTION OF THE SO_2 MOLECULE

K. B. Harvey, F. R. McCourt, and H. F. Shurvell

Because of their clathrate type of structure, the gas hydrates present an interesting opportunity for the study of intermolecular interactions in the solid state. In many cases the cavities occupied by the molecules of the hydrate-former have a larger free-volume

Can. J. Chem. Downloaded from www.nrcresearchpress.com by 210.87.254.5 on 09/05/12
For personal use only.

than that allowed these molecules in their normal, close-packed crystalline state, so that the gas molecules are permitted a greater than normal freedom of motion. These considerations combined with the results of an X-ray diffraction study led Von Stackelberg (1) to propose freedom of rotation for the SO_2 molecule in the SO_2 hydrate. Pauling (2), on the other hand, found the best agreement with the observed diffraction intensities for Cl_2 hydrate when the Cl_2 molecule was restricted to sterically favorable positions in the non-spherical cavity. The evidence to be presented here indicates that in the case of the SO_2 hydrate, the motion of the SO_2 molecules is similarly limited.

The frequencies of absorption from spectra obtained on a Perkin–Elmer 421 double beam grating spectrometer are listed in Table I. It can be seen that the spectrum of the

TABLE I

Infrared absorption of SO_2 hydrate (frequencies in cm^{-1})

Mode	Hydrate, 78° K	Cubic ice (3), 78° K	SO_2 (4), 78° K	SO_2 (5), gas
$\nu_2(SO_2)$	520 s		520 s	518
$\nu_R(H_2O)$	780 s	812 s		
	1140 m		1140 w	
$\nu_1(SO_2)$				1151
	1155 w		1144 m	
	1340 s		1305 w	
$\nu_3(SO_2)$			1315 m	1362
	1350 w		1322 s	
$\nu_2(H_2O)$	1640 m	1600 m		
$\nu_R + \nu_2(H_2O)$	2220 w	2230 w		
? (H_2O)	2410 w			
$\nu_3(H_2O)$	3230 s	3240 s		
$\nu_1(H_2O)$	3380 m	3380 m		

hydrate is, to a good approximation, simply the combined spectra of solid SO_2 and cubic ice. In the case of the SO_2 absorption the largest shift occurs for the ν_3 peak. This is in the direction of the value for the gas phase and may be attributed to the relative freedom of the SO_2 molecule in the hydrate compared with its environment in solid SO_2.

Of even more interest is the behavior of the absorption due to ν_3 when the temperature is varied. These spectra, shown in Fig. 1, were obtained on a Perkin–Elmer 112G spectrometer with slit widths sufficiently narrow to give a resolution of 1 cm^{-1} or better. The resolution was adequate, therefore, to resolve, at least partially, the J subbranches of a vibration–rotation band of a freely rotating SO_2 molecule (5). No such absorption is observed; however, there are two weak shoulders spaced approximately 10 cm^{-1} above and below the principal absorption peak at 1340 cm^{-1}. This is too large a separation for the energy levels of a free rotator but 10 cm^{-1} is a reasonable value for the first excited state of hindered rotatory or translatory motion. The decrease in intensity of the low frequency component with lowering of the temperature would result from depopulation of the upper level of the hindered rotator in the ground vibrational state.

The spectrum of the H_2O skeletal vibrations exhibits several points of interest. Not unexpectedly, because of the fairly large dipole moment of the SO_2 molecule, there is a substantial downward shift of the librational frequency to 780 cm^{-1}. On the other hand, the peak at 1600 cm^{-1} in cubic ice is shifted upward by some 40 cm^{-1} in the hydrate, confirming its assignment to ν_2 rather than $2\nu_R$ as has been suggested (6). The opposite shifts approximately cancel one another in the combination $\nu_2 + \nu_R$ to give a peak at 2220 cm^{-1}, almost the same frequency as in cubic ice.

Can. J. Chem. Downloaded from www.nrcresearchpress.com by 210.87.254.5 on 09/05/12
For personal use only.

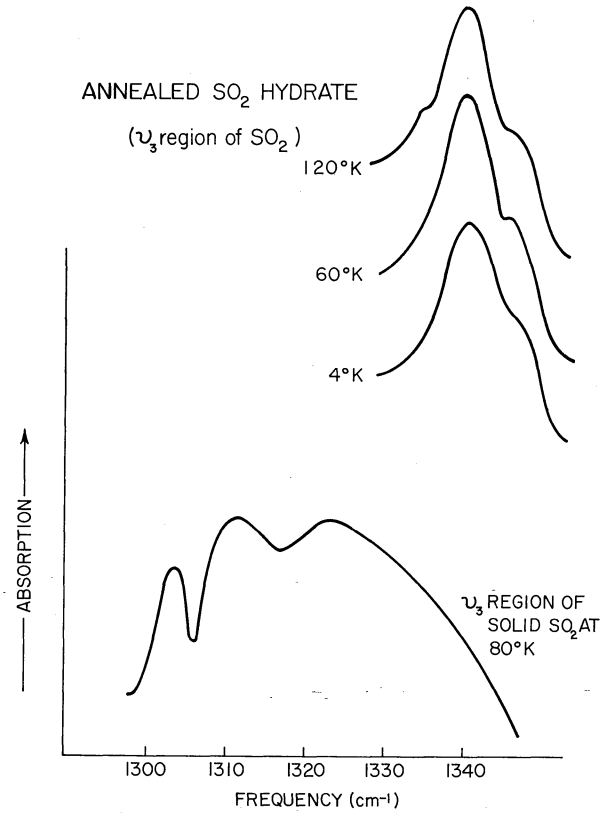

FIG. 1.

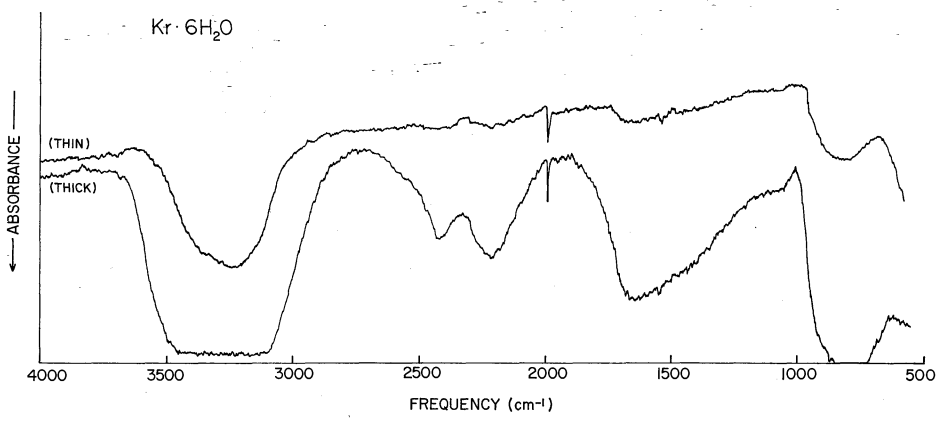

FIG. 2.

Another prominent feature of the H_2O skeletal spectrum is the peak at 2410 cm^{-1}. Absorption at this frequency has also been observed in the spectra of the H_2S and krypton hydrates (Fig. 2) hence it must be associated with the H_2O vibrations. Like the peak at 2220 cm^{-1}, the frequency of peak absorption is approximately the same in all of the

Can. J. Chem. Downloaded from www.nrcresearchpress.com by 210.87.254.5 on 09/05/12
For personal use only.

hydrates we have studied so that neither the 2220 cm^{-1} or 2410 cm^{-1} peaks are overtones of ν_R. There are several possible explanations for the absorption at 2410 cm^{-1} but none are very satisfying and, on the basis of the evidence presented, all are speculative. The two peaks at 2210 cm^{-1} and 2410 cm^{-1} could be assigned as components of $\nu_2 + \nu_R$ of different symmetry arising from correlation field splitting. None of the other vibrations exhibit such a splitting, however, and 200 cm^{-1} seems a rather large difference to explain in this way.

Alternatively, the two peaks in question may arise from combinations of ν_2 with two different librational frequencies ν_R and ν_R'. This implies a value of about 1000 cm^{-1} for the absorption due to ν_R' and no such absorption has been detected. In addition, it has been estimated (7) that the three librational frequencies in ice should not differ from one another by more than 10%. Unless severe distortion of the H_2O molecule occurs in the hydrate, and the spectra do not indicate this, one would expect the librational frequencies to be accidentally degenerate in the gas hydrate also. On the other hand, lack of activity of the fundamental, ν_R', certainly does not exclude activity of the combination $\nu_2 + \nu_R'$.

Obviously, more information is required before a reasonable interpretation can be made. We are hoping to obtain this information from a detailed study of the fundamentals and overtones of both the H_2O and D_2O hydrates.

EXPERIMENTAL

The general technique was to deposit the sample to be investigated on a cesium iodide window at 78° K and anneal it by raising the temperature to approximately 110° K before spectra were recorded. The samples were prepared initially by mixing gaseous SO_2 and H_2O in the correct stoichiometric ratio. This technique does not, however, assure a deposit of the correct stoichiometric ratio since inadequate mixing or fractionation during deposition may lead to a change in composition. To compensate for this the gas phase samples were prepared with an excess of one component when the spectrum of the other component was being observed. This method obviously leaves much to be desired and improved techniques are being devised.

The authors wish to gratefully acknowledge the financial support of the National Research Council of Canada and the University of British Columbia.

1. M. V. Stackelberg and H. R. Muller. Z. Elektrochem. **58**, 25 (1954).
2. L. Pauling and R. E. Marsh. Proc. Nat. Acad. Sci. U.S. **38**, 112 (1952).
3. N. Ockman. Advan. Phys. **7**, 199 (1958).
4. P. A. Giguère and M. Falk. Can. J. Chem. **34**, 1833 (1956).
5. R. D. Shelton, A. H. Nielson, and W. H. Fletcher. J. Chem. Phys. **21**, 2178 (1953).
6. D. F. Hornig, H. F. White, and F. P. Reding. Spectrochim. Acta, **12**, 338 (1958).
7. R. W. Blue. J. Chem. Phys. **22**, 280 (1954).

Received October 3, 1963.
Department of Chemistry,
University of British Columbia,
Vancouver 8, British Columbia.

POLYMER FORMATION IN THE RADIOLYSIS OF BENZENE–CYCLOHEXANE MIXTURES[1]

J. A. Stone, P. J. Dyne, and M. G. Bailey

A polymeric material is formed as a primary product in the radiolysis of benzene–cyclohexane mixtures (1, 2). From a detailed study of the product yields in this system, we had concluded that benzene acts as a nucleus for polymer formation and that, at low

[1]*Issued as A.E.C.L. No. 1906.*

Can. J. Chem. Downloaded from www.nrcresearchpress.com by 210.87.254.5 on 09/05/12
For personal use only.

hydrates we have studied so that neither the 2220 cm^{-1} or 2410 cm^{-1} peaks are overtones of ν_R. There are several possible explanations for the absorption at 2410 cm^{-1} but none are very satisfying and, on the basis of the evidence presented, all are speculative. The two peaks at 2210 cm^{-1} and 2410 cm^{-1} could be assigned as components of $\nu_2 + \nu_R$ of different symmetry arising from correlation field splitting. None of the other vibrations exhibit such a splitting, however, and 200 cm^{-1} seems a rather large difference to explain in this way.

Alternatively, the two peaks in question may arise from combinations of ν_2 with two different librational frequencies ν_R and ν_R'. This implies a value of about 1000 cm^{-1} for the absorption due to ν_R' and no such absorption has been detected. In addition, it has been estimated (7) that the three librational frequencies in ice should not differ from one another by more than 10%. Unless severe distortion of the H_2O molecule occurs in the hydrate, and the spectra do not indicate this, one would expect the librational frequencies to be accidentally degenerate in the gas hydrate also. On the other hand, lack of activity of the fundamental, ν_R', certainly does not exclude activity of the combination $\nu_2 + \nu_R'$.

Obviously, more information is required before a reasonable interpretation can be made. We are hoping to obtain this information from a detailed study of the fundamentals and overtones of both the H_2O and D_2O hydrates.

EXPERIMENTAL

The general technique was to deposit the sample to be investigated on a cesium iodide window at 78° K and anneal it by raising the temperature to approximately 110° K before spectra were recorded. The samples were prepared initially by mixing gaseous SO_2 and H_2O in the correct stoichiometric ratio. This technique does not, however, assure a deposit of the correct stoichiometric ratio since inadequate mixing or fractionation during deposition may lead to a change in composition. To compensate for this the gas phase samples were prepared with an excess of one component when the spectrum of the other component was being observed. This method obviously leaves much to be desired and improved techniques are being devised.

The authors wish to gratefully acknowledge the financial support of the National Research Council of Canada and the University of British Columbia.

1. M. V. Stackelberg and H. R. Muller. Z. Elektrochem. **58**, 25 (1954).
2. L. Pauling and R. E. Marsh. Proc. Nat. Acad. Sci. U.S. **38**, 112 (1952).
3. N. Ockman. Advan. Phys. **7**, 199 (1958).
4. P. A. Giguère and M. Falk. Can. J. Chem. **34**, 1833 (1956).
5. R. D. Shelton, A. H. Nielson, and W. H. Fletcher. J. Chem. Phys. **21**, 2178 (1953).
6. D. F. Hornig, H. F. White, and F. P. Reding. Spectrochim. Acta, **12**, 338 (1958).
7. R. W. Blue. J. Chem. Phys. **22**, 280 (1954).

Received October 3, 1963.
Department of Chemistry,
University of British Columbia,
Vancouver 8, British Columbia.

POLYMER FORMATION IN THE RADIOLYSIS OF BENZENE–CYCLOHEXANE MIXTURES[1]

J. A. Stone, P. J. Dyne, and M. G. Bailey

A polymeric material is formed as a primary product in the radiolysis of benzene–cyclohexane mixtures (1, 2). From a detailed study of the product yields in this system, we had concluded that benzene acts as a nucleus for polymer formation and that, at low

[1]*Issued as A.E.C.L. No. 1906.*

Can. J. Chem. Downloaded from www.nrcresearchpress.com by 210.87.254.5 on 09/05/12
For personal use only.

concentrations of benzene (<3%), the polymer consisted largely of cyclohexyl groups. This note presents further observations on the yield and constitution of the polymer which support these conclusions.

EXPERIMENTAL

Polymer was isolated from 100 ml samples of benzene–cyclohexane mixtures, irradiated to a dose of $\sim 1.6 \times 10^{23}$ ev/liter, by vacuum sublimation. This technique was suggested to us by Dr. J. G. Burr. The irradiated sample was initially frozen in liquid nitrogen; sublimation was carried out at ice temperature under vacuum, the receiver being cooled in liquid nitrogen. When about 95% of the solvent had been removed, the residue was transferred to a smaller weighed flask and the sublimation continued. After it was weighed, the polymer was redissolved in solvent and the unsublimed bicyclohexyl determined by gas liquid chromatography. Molecular weights were determined in benzene solutions with a Mechrolab vapor pressure osmometer. Yields and molecular weights were corrected for residual bicyclohexyl.

The 'benzene' content of the polymer was determined by a radiotracer technique using benzene C-14 obtained from Merck and Company (Canada). A 0.1 mc quantity of benzene-C_{14} was diluted with Phillips Research Grade benzene, treated with bromine to remove 1,3-cyclohexadiene (3), and distilled. The activity in the polymer was measured by scintillation counting of solutions containing the polymer (or an aliquot of the stock solutions), 1 ml of benzene, and 20 ml of liquid scintillator (Nuclear Enterprises WE-293), using a Packard Tri-Carb counting system.

RESULTS

Values of G(monomer → polymer) assuming a monomer molecular weight of 83(C_6H_{11}) are shown in Fig. 1 together with values of G(benzene in the polymer) determined from

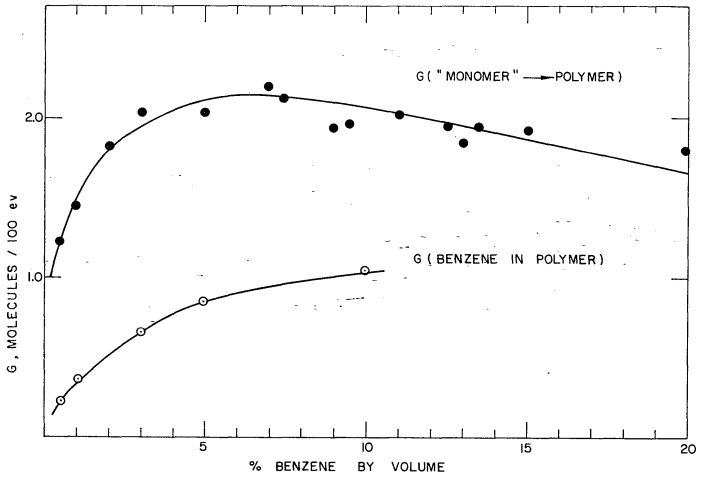

FIG. 1. Yield of polymer formed in the radiolysis of benzene–cyclohexane mixtures and the benzene content of the polymer.

the C-14 assay. The molecular weight of polymer over this concentration range is 335±15 with a trend towards increasing molecular weight at the higher benzene concentrations. Carbon–hydrogen analysis of polymer obtained from 3 and 10% benzene solutions gave compositions of $CH_{1.59}$ and $CH_{1.46}$, respectively. C_{24} hydrocarbons of this composition have molecular weights of 323 and 328. A C_{24} hydrocarbon containing three cyclohexyl residues and one benzene residue would contain 25% benzene; at 1% benzene the aromatic content of the polymer is 21% and it is clear that most of this polymer has this composition. At higher benzene concentrations, the polymer composition averages two cyclohexyl residues to two aromatic residues.

Can. J. Chem. Downloaded from www.nrcresearchpress.com by 210.87.254.5 on 09/05/12
For personal use only.

The molecular weight of the polymer shows a slight dose dependence increasing from 285 at a dose of 2×10^{22} ev/l. to 350 at 3.2×10^{22} ev/l., for solutions containing 1% benzene. While the polymer is, in the main, a C_{24} hydrocarbon it must contain amounts of C_{18} and C_{30} hydrocarbons which vary with dose. It appears that the benzene molecule attaches two and three cyclohexyl groups very readily but that the C_{24} hydrocarbon has a much lower, although not negligible affinity for attachment of a further cyclohexyl group. This variation in the molecular weight of the polymer with dose is similar to that reported by Barker and Hill (4) for the polymer formed in the radiolysis of cyclohexane at high doses. In their system, the polymer is a secondary product formed through cyclohexene, so that G(polymer) is initially very dose dependent. In our system, benzene, the nucleus for polymerization, is always present and G(polymer) varies only slightly with dose.

1. T. GAUMANN. Helv. Chim. Acta **44**, 1337 (1961).
2. J. A. STONE and P. J. DYNE. Radiation Res. **17**, 353 (1962).
3. M. A. TOMAS and R. BILRON. Nucleonics, **21**, (6), 90 (1963).
4. R. BARKER and M. R. H. HILL. Nature, **194**, 277 (1962).

RECEIVED OCTOBER 8, 1963.
ATOMIC ENERGY OF CANADA LIMITED,
CHALK RIVER, ONTARIO.

Can. J. Chem. Downloaded from www.nrcresearchpress.com by 210.87.254.5 on 09/05/12
For personal use only.

6,7-DI-2′-PYRIDYLDODECANE

J. T. EDWARD

Ziegler and Zeiser (1) found that *n*-butyllithium metalated α-picoline to α-picolyllithium, but added to 2-*n*-butylpyridine to give (in undisclosed yield) 2,6-di-*n*-butylpyridine. There was no report of significant metalation in the second reaction. Accordingly an attempt was made to prepare 2-*p*-anisyl-6-*n*-hexylpyridine by the reaction of *p*-anisyllithium with 2-*n*-hexylpyridine. The reaction mixture became red, indicating some metalation of the alkyl group (2) to give 1,2′-pyridyl-1-hexyllithium (I). After reaction of the organolithium compounds, the reaction mixture was stirred under dry air to oxidize dihydropyridine derivatives (3) and then worked up in the usual way (1). A fraction boiling at 155–160° at 0.5 mm was found to be made up of *p*,*p*′dianisyl (known to be produced by the air oxidation of *p*-anisyllithium (4)), a base $C_{22}H_{32}N_2$, and probably the desired 2-*p*-anisyl-6-*n*-hexylpyridine, although the last compound could not be obtained in an analytically pure state.

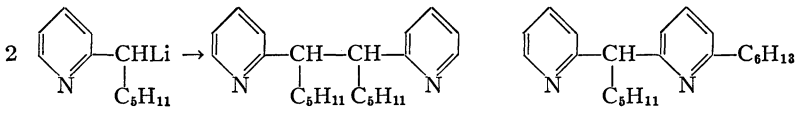

I II III

The base $C_{22}H_{32}N_2$ appeared to be 6,7-di-2′pyridyldodecane (II) produced by air oxidation of the metalation product I (cf. 4). Its ultraviolet absorption (λ_{max}^{EtOH} at 258, 260, 270 mμ; log ϵ_{max} 3.81, 3.86, 3.75) was closely similar to that of 2-alkylpyridines (5) showing that the two pyridine nuclei were linked through an insulating alkyl group,

The molecular weight of the polymer shows a slight dose dependence increasing from 285 at a dose of 2×10^{22} ev/l. to 350 at 3.2×10^{22} ev/l., for solutions containing 1% benzene. While the polymer is, in the main, a C_{24} hydrocarbon it must contain amounts of C_{18} and C_{30} hydrocarbons which vary with dose. It appears that the benzene molecule attaches two and three cyclohexyl groups very readily but that the C_{24} hydrocarbon has a much lower, although not negligible affinity for attachment of a further cyclohexyl group. This variation in the molecular weight of the polymer with dose is similar to that reported by Barker and Hill (4) for the polymer formed in the radiolysis of cyclohexane at high doses. In their system, the polymer is a secondary product formed through cyclohexene, so that G(polymer) is initially very dose dependent. In our system, benzene, the nucleus for polymerization, is always present and G(polymer) varies only slightly with dose.

1. T. GAUMANN. Helv. Chim. Acta **44**, 1337 (1961).
2. J. A. STONE and P. J. DYNE. Radiation Res. **17**, 353 (1962).
3. M. A. TOMAS and R. BILRON. Nucleonics, **21**, (6), 90 (1963).
4. R. BARKER and M. R. H. HILL. Nature, **194**, 277 (1962).

RECEIVED OCTOBER 8, 1963.
ATOMIC ENERGY OF CANADA LIMITED,
CHALK RIVER, ONTARIO.

Can. J. Chem. Downloaded from www.nrcresearchpress.com by 210.87.254.42 on 09/05/12
For personal use only.

6,7-DI-2′-PYRIDYLDODECANE

J. T. EDWARD

Ziegler and Zeiser (1) found that *n*-butyllithium metalated α-picoline to α-picolyllithium, but added to 2-*n*-butylpyridine to give (in undisclosed yield) 2,6-di-*n*-butylpyridine. There was no report of significant metalation in the second reaction. Accordingly an attempt was made to prepare 2-*p*-anisyl-6-*n*-hexylpyridine by the reaction of *p*-anisyllithium with 2-*n*-hexylpyridine. The reaction mixture became red, indicating some metalation of the alkyl group (2) to give 1,2′-pyridyl-1-hexyllithium (I). After reaction of the organolithium compounds, the reaction mixture was stirred under dry air to oxidize dihydropyridine derivatives (3) and then worked up in the usual way (1). A fraction boiling at 155–160° at 0.5 mm was found to be made up of *p*,*p*′dianisyl (known to be produced by the air oxidation of *p*-anisyllithium (4)), a base $C_{22}H_{32}N_2$, and probably the desired 2-*p*-anisyl-6-*n*-hexylpyridine, although the last compound could not be obtained in an analytically pure state.

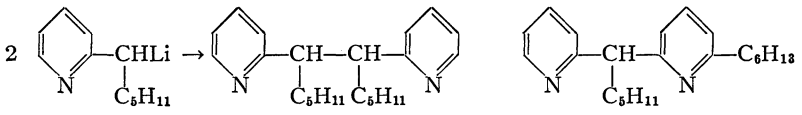

I II III

The base $C_{22}H_{32}N_2$ appeared to be 6,7-di-2′pyridyldodecane (II) produced by air oxidation of the metalation product I (cf. 4). Its ultraviolet absorption (λ_{max}^{EtOH} at 258, 260, 270 mμ; log ϵ_{max} 3.81, 3.86, 3.75) was closely similar to that of 2-alkylpyridines (5) showing that the two pyridine nuclei were linked through an insulating alkyl group,

and not directly together (6). The nuclear magnetic resonance spectrum of the base in carbon tetrachloride (Table I) showed peaks at the positions (7) and having the areas expected for the structure II. It excluded the other possible structure III, formed by addition of I to 2-*n*-hexylpyridine, since such a compound would have only one α-pyridyl proton.

The present work makes it likely that not only methyl groups, but also other alkyl groups at the 2-position of pyridine are metalated by *n*-butyllithium.

TABLE I

Proton magnetic resonance spectrum of 6,7-di-2′-pyridyldodecane

Signal (τ value)	Assignment*	No. protons	
		Theor.	Found†
1.52	6′	2	2.3, 1.8
2.80	4′	2	2.4, 2.3
3.20	3′, 5′	4	3.6, 3.9
6.78	6, 7	2	2.0, 1.9
8.05	5, 8	4	3.9, 4.1
8.80	2, 3, 4, 9, 10, 11	12	17.5
9.17	1, 12	6	

*Ref. 7.
†By cutting out and weighing peaks from trace.

EXPERIMENTAL

2-*n*-Hexylpyridine (81 g) in ether (100 ml) was added in 5 minutes to a stirred solution of *p*-anisyllithium, prepared from *p*-bromoanisole (93.5 g) and lithium (7.0 g) (3). After 50 minutes color test I (8) was only weakly positive, and dry air was passed over the stirred mixture for 18 hours. The mixture, worked up in the usual way, gave several basic fractions boiling below 115° (0.5 mm); these most probably consisted of 2-*n*-hexylpyridine and of 1-(2′-pyridyl)hexan-1-ol (from air oxidation of I), but did not give crystalline picrates or mercurichlorides, and were not investigated further. At 155° to 160° (0.5 mm) a yellow oil (19.5 g) distilled over; at higher temperatures only small amounts of reddish oils were obtained.

The yellow oil dissolved in concentrated hydrochloric acid, leaving a non-basic residue (0.1 g), m.p. 145–155°, which crystallized from ethanol as white flakes, m.p. 172–174°; melting point reported for *p*,*p*′-dianisyl, 172° (9). Calc. for $C_{14}H_{14}O_2$: OMe, 29.0%. Found: OMe, 28.0%. The solid gave a dark blue color with concentrated nitric acid, as reported for *p*,*p*′-dianisyl (9).

Neutralization of the hydrochloric acid solution afforded an oil, which on treatment with picric acid in ethanol gave a gummy solid. Washing with hot ethanol removed a gummy red impurity and left a crystalline solid (25 g, 5% yield), m.p. 145–147°. This was obtained on crystallization from methanol as yellow needles, m.p. 148–150°, analyzing as the *dipicrate* of II. Calc. for $C_{34}H_{38}O_{14}N_8$: C, 52.1; H, 4.9; N, 14.3%. Found: C, 52.4; H, 4.9; N, 14.4, 14.6%.

The free base, recovered from the dipicrate by treatment with sodium hydroxide solution, was redistilled to give a pale yellow oil, b.p. 215–217° (13 mm), d_{25}^{25} 0.9571, n_D^{25} 1.5163. Calc. for $C_{22}H_{32}N_2$: C, 81.5; H, 9.9; N, 8.6%. Mol. wt. 324.5. Found: C, 81.0; H, 10.1; N, 8.4%. Mol. wt. (Rast) 322. R_D calc. from constants of Vogel (10): 101.7. Found: 102.4.

The mother liquors and the red gum removed from the dipicrate were treated with sodium hydroxide to regenerate the free bases, which were taken up in ether and redistilled at reduced pressure. The yellow oil obtained appeared from analysis to be 2-*p*-anisyl-6-*n*-hexylpyridine ($C_{18}H_{23}NO$) contaminated with $C_{22}H_{32}N_2$. Calc. for 63% $C_{18}H_{23}NO$ + 37% $C_{22}H_{32}N_2$: OMe, 7.2; N, 6.13%. Found: OMe, 7.1, 7.4; N, 6.13%. All attempts to form a crystalline derivative (picrate, mercurichloride, hydrochloride, perchlorate, aurichloride, chloroplatinate) were fruitless.

ACKNOWLEDGMENTS

Grateful acknowledgment is made to Professor Henry Gilman, in whose laboratory the reaction was first investigated, for encouragement, Dr. C. Stammer for nuclear magnetic resonance studies, and the National Research Council for financial support.

Can. J. Chem. Downloaded from www.nrcresearchpress.com by 210.87.254.42 on 09/05/12
For personal use only.

1. K. ZIEGLER and H. ZEISER. Ann. **485**, 174 (1931).
2. F. W. BERGSTROM. J. Am. Chem. Soc. **53**, 4065 (1931). H. C. BROWN and W. A. MURPHEY. J. Am. Chem. Soc. **73**, 3308 (1951).
3. H. GILMAN and J. T. EDWARD. Can. J. Chem. **31**, 457 (1953).
4. E. MULLER and T. TOPEL. Ber. **72**, 273 (1939).
5. E. LEETE and L. MARION. Can. J. Chem. **30**, 563 (1952).
6. P. E. FIELDING and R. J. W. LEFEVRE. J. Chem. Soc. 1811 (1951). W. G. FRANKENBURG, A. M. GOTTSCHO, E. W. MAGAUD, and T. C. TSO. J. Am. Chem. Soc. **74**, 4309 (1952).
7. L. M. JACKMAN. Applications of nuclear magnetic resonance spectroscopy in organic chemistry. Pergamon Press, London. 1959. p. 64.
8. H. GILMAN and F. SCHULZE. J. Am. Chem. Soc. **47**, 2002 (1925).
9. A. GILLMEISTER. Ber. **30**, 2843 (1897).
10. A. I. VOGEL. J. Chem. Soc. 1833 (1948).

RECEIVED OCTOBER 16, 1963.
DEPARTMENT OF CHEMISTRY,
MCGILL UNIVERSITY,
MONTREAL, QUEBEC.

Can. J. Chem. Downloaded from www.nrcresearchpress.com by 210.87.254.42 on 09/05/12
For personal use only.

NMR SPECTRA OF O,O-DIALKYLORGANOPHOSPHORUS ESTERS. P^{31} CHEMICAL SHIFTS BY HETERONUCLEAR SPIN DECOUPLING[1]

J. B. STOTHERS AND J. R. ROBINSON

Other studies required the synthesis of a family of organophosphorus esters (I–IV, below) which differ only in the atoms bonded directly to phosphorus:

$(RO)_2P(O)OAr$	$(RO)_2P(S)OAr$	$(RO)_2P(O)SAr$	$(RO)_2P(S)SAr$
I	II	III	IV

where R = CH_3 or C_2H_5 and Ar = C_6Cl_5.

These model compounds, representing the dialkylphosphate (I), phosphorothionate (II), phosphorothiolate (III), and phosphorodithioate (IV) systems, possess a common third ester group; the latter (pentachlorophenyl) was chosen partly to provide solid products, partly to allow a toxicological study of these highly chlorinated aromatic organophosphorus esters. The syntheses and chemical, physical, and toxicological properties will be reported elsewhere.

Because of the four differing chemical environments of the phosphorus nuclei, it seemed of interest to report on the variation in phosphorus chemical shifts. Such information is a useful complement to infrared spectra in confirming the structures of organophosphorus esters, particularly in differentiating P(S)O structures from their P(O)S isomers; many phosphorothionates possess no infrared absorption peak which is assignable to the P(S) group whereas, as shown below, the P^{31} chemical shift in these $(RO)_2P(S)OAr$ materials is quite different from that of the isomeric $(RO)_2P(O)SAr$ compounds. Also, these shift data can be applied generally over a wide range of organophosphorus esters since the values are not altered radically through changes in R and Ar by substitution. Moreover, these closely related model compounds provided a unique opportunity to compare, systematically, two methods of determining phosphorus chemical shifts, the direct P^{31} shift measurement and the indirect heteronuclear spin decoupling technique.

Although the H^1 and P^{31} NMR data for phosphorus esters exactly comparable to those for the present series have not been determined, extensive surveys of P^{31} chemical shift data now available (1–4) allow one to estimate these values for the phosphorus nuclei

[1]*Issued as Part V in the series on nuclear magnetic resonance studies by one of us (J.B.S.) and as Contribution No. 268, Canada Department of Agriculture, Research Institute, London (J.R.R.).*

1. K. ZIEGLER and H. ZEISER. Ann. **485**, 174 (1931).
2. F. W. BERGSTROM. J. Am. Chem. Soc. **53**, 4065 (1931). H. C. BROWN and W. A. MURPHEY. J. Am. Chem. Soc. **73**, 3308 (1951).
3. H. GILMAN and J. T. EDWARD. Can. J. Chem. **31**, 457 (1953).
4. E. MULLER and T. TOPEL. Ber. **72**, 273 (1939).
5. E. LEETE and L. MARION. Can. J. Chem. **30**, 563 (1952).
6. P. E. FIELDING and R. J. W. LEFEVRE. J. Chem. Soc. 1811 (1951). W. G. FRANKENBURG, A. M. GOTTSCHO, E. W. MAGAUD, and T. C. TSO. J. Am. Chem. Soc. **74**, 4309 (1952).
7. L. M. JACKMAN. Applications of nuclear magnetic resonance spectroscopy in organic chemistry. Pergamon Press, London. 1959. p. 64.
8. H. GILMAN and F. SCHULZE. J. Am. Chem. Soc. **47**, 2002 (1925).
9. A. GILLMEISTER. Ber. **30**, 2843 (1897).
10. A. I. VOGEL. J. Chem. Soc. 1833 (1948).

RECEIVED OCTOBER 16, 1963.
DEPARTMENT OF CHEMISTRY,
MCGILL UNIVERSITY,
MONTREAL, QUEBEC.

Can. J. Chem. Downloaded from www.nrcresearchpress.com by 210.87.254.42 on 09/05/12
For personal use only.

NMR SPECTRA OF O,O-DIALKYLORGANOPHOSPHORUS ESTERS. P^{31} CHEMICAL SHIFTS BY HETERONUCLEAR SPIN DECOUPLING[1]

J. B. STOTHERS AND J. R. ROBINSON

Other studies required the synthesis of a family of organophosphorus esters (I–IV, below) which differ only in the atoms bonded directly to phosphorus:

$(RO)_2P(O)OAr$	$(RO)_2P(S)OAr$	$(RO)_2P(O)SAr$	$(RO)_2P(S)SAr$
I	II	III	IV

where R = CH_3 or C_2H_5 and Ar = C_6Cl_5.

These model compounds, representing the dialkylphosphate (I), phosphorothionate (II), phosphorothiolate (III), and phosphorodithioate (IV) systems, possess a common third ester group; the latter (pentachlorophenyl) was chosen partly to provide solid products, partly to allow a toxicological study of these highly chlorinated aromatic organophosphorus esters. The syntheses and chemical, physical, and toxicological properties will be reported elsewhere.

Because of the four differing chemical environments of the phosphorus nuclei, it seemed of interest to report on the variation in phosphorus chemical shifts. Such information is a useful complement to infrared spectra in confirming the structures of organophosphorus esters, particularly in differentiating P(S)O structures from their P(O)S isomers; many phosphorothionates possess no infrared absorption peak which is assignable to the P(S) group whereas, as shown below, the P^{31} chemical shift in these $(RO)_2P(S)OAr$ materials is quite different from that of the isomeric $(RO)_2P(O)SAr$ compounds. Also, these shift data can be applied generally over a wide range of organophosphorus esters since the values are not altered radically through changes in R and Ar by substitution. Moreover, these closely related model compounds provided a unique opportunity to compare, systematically, two methods of determining phosphorus chemical shifts, the direct P^{31} shift measurement and the indirect heteronuclear spin decoupling technique.

Although the H^1 and P^{31} NMR data for phosphorus esters exactly comparable to those for the present series have not been determined, extensive surveys of P^{31} chemical shift data now available (1–4) allow one to estimate these values for the phosphorus nuclei

[1]*Issued as Part V in the series on nuclear magnetic resonance studies by one of us (J.B.S.) and as Contribution No. 268, Canada Department of Agriculture, Research Institute, London (J.R.R.).*

in these compounds. On this basis, one would expect the shifts to occur in the order of increased shielding: $(RO)_2P(S)SAr$, $(RO)_2P(S)OAr$, $(RO)_2P(O)SAr$, $(RO)_2P(O)OAr$. The P^{31} data obtained at 15.1 Mc/sec are listed in Table I and the observed shifts follow

TABLE I

NMR data (35–50% solutions in $CDCl_3$)

Compound	H^1 chemical shifts*		Coupling constants (cycles/sec)			P^{31} chemical shifts†	
	CH_3	CH_2	H–H	P–O–CH	P–O–C–C–H	Direct determ.‡	By decoupling
$(EtO)_3P$	1.24_5	3.85_0	7.1	8.0	0.6	−138.1	−138.1§
$(MeO)_3P$	3.48_5	—	—	10.8	—	−140.5	−140.4
$(MeO)_2P(O)OC_6Cl_5$	3.96_5	—	—	12.0	—	+5.3	+5.6
$(MeO)_2P(O)SC_6Cl_5$	3.91_3	—	—	13.2	—	−21.4	−21.1
$(MeO)_2P(S)OC_6Cl_5$	3.95_6	—	—	14.3	—	−66.1	−65.7
$(MeO)_2P(S)SC_6Cl_5$	3.87_3	—	—	15.6	—	−90.6	−90.6
$(EtO)_2P(O)OC_6Cl_5$	1.41_3	4.36_0	6.9	8.0	1.1	+7.6	+7.3
$(EtO)_2P(O)SC_6Cl_5$	1.37_5	4.28_0	7.1	8.8	0.9	−17.9	−17.0
$(EtO)_2P(S)OC_6Cl_5$	1.40_3	4.33_3	7.1	9.5	1.1	−62.4	−62.1
$(EtO)_2P(S)SC_6Cl_5$	1.36_0	4.27_0	7.0	9.8	0.9	−85.6	−85.2

*P.p.m. from TMS.
†P.p.m. from H_3PO_4 (85%).
‡At 15.1 Mc/sec.
§Assigned value (see text).

the expected trend. The principal disadvantage concerned with the direct determination of these data, however, is the low sensitivity of P^{31} nuclei to NMR experiments, ca. 6.6% of that for H^1 at the same field (5); if larger samples are available this can be overcome to some extent, but at the expense of high resolution results. In addition, a second complete transmitter–receiver unit is required for such measurements (for optimum results at 14.1 kgauss, a 24.3 Mc/sec source). In the present case, only small amounts of material were on hand and the additional radio-frequency unit available operated at 15.1 Mc/sec. These two features restricted the information from the P^{31} spectra to a determination of the chemical shifts only, since the fine structure due to P^{31}–H^1 spin coupling was not clearly resolved for these samples under such conditions.

Spin coupling data, however, are readily obtained from the proton spectra and, furthermore, the P^{31} chemical shifts also may be found by the technique of heteronuclear spin decoupling. The latter involves observation of the proton spectrum at 60 Mc/sec while simultaneously irradiating the P^{31} nucleus at its resonance frequency of 24.3 Mc/sec with a strong radio-frequency field which meets the requirement $\gamma H_2/2\pi \sim J$. The general method has been reviewed (6) and some examples of its application to chemical shift measurements have appeared for N^{14} (7–9) and C^{13} (10–12), but little use of the technique for H^1–P^{31} coupled systems has been reported. For these systems, the method presents a very important advantage to the chemist. Since the size of sample required for proton work is *much* less than that for P^{31} spectra, all of the NMR data could be obtained from a few milligrams of material. The results measured by the spin decoupling method compare well with those measured directly (see table), and the data are readily obtainable in a few minutes.

By its nature, the spin decoupling method for P^{31} chemical shift determinations requires the use of a secondary reference compound, and triethylphosphite was selected since the P^{31} chemical shift has been determined by many workers (2, 3, 4). Using the value −138.1 p.p.m. for $(EtO)_3P$, the rest of the data from the spin decoupling experiments were converted to the more common scale with 85% H_3PO_4 = 0 p.p.m. These results are listed in the table, together with the proton data for the series.

Can. J. Chem. Downloaded from www.nrcresearchpress.com by 210.87.254.42 on 09/05/12
For personal use only.

It can be noted that the methyl protons of the ethyl groups are spin coupled to the phosphorus nuclei with a coupling constant of ca. 1 cycle/sec. The magnitude of this interaction is not greatly affected by the substitution changes at the phosphorus nucleus, although there may be a small decrease for the substitution: $—OC_6Cl_5 \rightarrow SC_6Cl_5$. The stronger P^{31}–H^1 coupling (P–O–C–H), however, is clearly dependent on the substituents on phosphorus. In each case, replacement of an oxygen by sulphur increases the coupling constant, but the increase is larger for the thiono than for the thiolo grouping. This effect of sulphur on the coupling constant has been reported previously (e.g. 2, 13, 14) but the magnitude of the P^{31}–O–C–H^1 coupling constants is significantly larger than those noted in some reviews (1, 2). As indicated above, the P^{31} chemical shifts are close to those "expected" on the basis of previous work (2, 4), and the differences, which are due to the particular substituent groups, are not large enough to change the relative positions of the shifts.

In considering substitution effects upon the P^{31} chemical shift, a comparison of these data with those of Van Wazer *et al.* (4) gives an indication of the changes caused by fully chlorinating the benzene ring. For example, in substituting sulphur for oxygen in the aromatic ester linkage only, $(RO)_2P(O)OAr \rightarrow (RO)_2P(O)SAr$, there is little difference in effect between $Ar = C_6H_5$ and $Ar = C_6Cl_5$ as the replacement effects are −26 p.p.m. (4) and −25.8 p.p.m. (on the average) respectively. However, where sulphur replaces a phosphoryl oxygen only, $(RO)_2P(O)OAr \rightarrow (RO)_2P(S)OAr$, the chlorinated ring has a much greater effect, the corresponding data being −46 p.p.m. for $Ar = C_6H_5$ (4) and −70.5 p.p.m. in the present case. The substituent effects are seen to be approximately additive; for example, when both oxygen atoms are replaced by sulphur, $(RO)_2P(O)OC_6Cl_5 \rightarrow (RO)_2P(S)SC_6Cl_5$, the P^{31} chemical shift is changed by about 94 p.p.m. (average value) while addition of the two separate sulphur replacements gives a 96.3 p.p.m. replacement effect.

EXPERIMENTAL

The H^1 NMR spectra were determined with a Varian DP-60 spectrometer and were calibrated by the usual side-band technique with an audio oscillator whose output was continuously monitored with a Hewlett-Packard 522B frequency counter. The peak positions were determined relative to internal tetramethylsilane (TMS) and the precision is estimated to be within 0.05 p.p.m. for the chemical shifts and 0.05 cycle/sec for the coupling constants. The P^{31} spectra were obtained at 15.1 Mc/sec. Because of the relatively small amounts of material, rapid-passage dispersion mode operation afforded the better result. These peak positions were determined relative to an external 85% H_3PO_4 signal with an estimated accuracy of ±0.5 p.p.m. For both cases, the samples were 35–50% (w/w) solutions in deuterochloroform contained in 5 mm O.D. tubes.

The decoupling experiments were carried out using an NMR Specialties, Inc., Model SD-60 spin decoupler operating at a nominal frequency of 24.3 Mc/sec. Essentially this unit provides a signal whose frequency can be varied continuously. This is achieved by mixing the output of a variable frequency oscillator (VFO), operating close to 5.35 Mc/sec, with the output of a crystal oscillator at 18.95 Mc/sec to produce the required variable frequency near 24.3 Mc/sec. To monitor the output of the decoupler, the VFO output is mixed with that of a 5.30 Mc/sec crystal oscillator (an NMRS Model EC-60 counter adapter) and the difference frequency (in kc/sec) measured using the H-P 522B counter. After locating the desired region of the proton spectrum, for example, the methylene pattern for the ethyl derivatives, the variable 24.3 Mc/sec signal is changed until the approximate decoupling frequency is found. The proton spectrum of the methylene group becomes a simple quartet in the case of the ethyl derivatives, and the spectrum of the methylated compounds collapses to a singlet at the frequency required to decouple the P^{31} nucleus. The decoupler power is then reduced to determine this frequency more accurately, since the higher the power level used, the wider is the frequency range over which decoupling occurs. These operations can be conveniently carried out by following the spectral changes on the oscilloscope of the instrument. The counter reading for maximum decoupling (i.e., complete collapse of the pattern to a quartet) is noted. Similarly, the necessary frequency for each sample is obtained. Since operation in this way does not provide a check on the stability of the fixed oscillator, one can observe the frequency required for the reference sample between each determination, to test for a possible drift of the fixed frequency. The difference between the decoupling frequencies for two compounds provides a measure of the P^{31} chemical shift directly, if the

Can. J. Chem. Downloaded from www.nrcresearchpress.com by 210.87.254.42 on 09/05/12
For personal use only.

shifts of the decoupled protons of the two compounds are identical. Otherwise, a correction for any change in the applied field required to observe the two proton patterns must be included. The frequency measurements are converted to a p.p.m. scale by division by 24.3, after which the correction (if any) may be taken into account. The estimated precision of the present results is ±0.5 p.p.m. Although higher precision could be obtained through the use of a stabilized VFO, e.g. an audio-modulated single side-band oscillator as the source, the large chemical shift differences for P^{31} nuclei do not require that the data be of the highest precision.

As an example of the method, the optimum decoupling frequency for the reference, triethyl phosphite, was found to give a counter reading of 15,585 cycles/sec, while the reading for $(EtO)_2P(S)OC_6Cl_5$ was 17,443 cycles/sec. This difference, 1858 cycles/sec (76.46 p.p.m.), represents the "apparent" chemical shift difference for the two P^{31} nuclei. Since the counter reading monitors only the VFO output relative to another crystal oscillator, the actual direction of change in the decoupler frequency (24.3 Mc/sec) must be established independently. In this case we know that the P^{31} nucleus of the sample absorbs at *higher* field than the reference and so the change in counter reading from reference to sample corresponds to a *lower* decoupling frequency for the sample. The phosphorous nuclei were decoupled at different applied fields and the apparent shift must be corrected for this change, 0.48 p.p.m. (i.e., the chemical shift difference between the proton absorptions used for the two decoupling experiments). In this case, the apparent separation is *larger* than the actual difference since the proton band used for the sample is at *lower* field than that for the reference. The P^{31} chemical shift for this sample is, therefore, 76.0 p.p.m. relative to $(EtO)_3P$ or −62.1 p.p.m. relative to 85% H_3PO_4. The remaining P^{31} shifts were calculated in a similar manner.

ACKNOWLEDGMENTS

We are grateful to the National Research Council for financial assistance.

1. R. A. Y. Jones and A. R. Katritzky. Angew. Chem. **74**, 60 (1962).
2. H. Finegold. Ann. N.Y. Acad. Sci. **70**, 875 (1958).
3. N. Muller, P. C. Lauterbur, and J. Goldenson. J. Am. Chem. Soc. **78**, 3557 (1956).
4. J. R. Van Wazer, C. F. Callis, J. N. Shoolery, and R. C. Jones. J. Am. Chem. Soc. **78**, 5715 (1956).
5. P. C. Lauterbur. NMR spectra of elements other than hydrogen and fluorine in determination of organic structures by physical methods. Vol. 2. *Edited by* F. C. Nachod and W. D. Phillips. Academic Press. 1962. p. 469.
6. J. D. Baldeschwieler and E. W. Randall. Chem. Rev. **63**, 81 (1963).
7. J. A. Glasel, L. M. Jackman, and D. W. Turner. Proc. Chem. Soc. 426 (1961).
8. J. D. Baldeschwieler and E. W. Randall. Proc. Chem. Soc. 303 (1961).
9. J. D. Baldeschwieler. J. Chem. Phys. **36**, 152 (1962).
10. V. Royden. Phys. Rev. **96**, 543 (1954).
11. E. G. Paul and D. M. Grant. J. Am. Chem. Soc. **85**, 1701 (1963).
12. G. V. D. Tiers. J. Phys. Chem. **67**, 1373 (1963).
13. J. B. Stothers and E. Y. Spencer. Can. J. Chem. **39**, 1389 (1961).
14. G. Mavel and G. Martin. J. Chim. Phys. **59**, 762 (1962).

Received November 1, 1963.
Department of Chemistry,
University of Western Ontario,
London, Canada,
and
Canada Department of Agriculture,
Research Institute,
University Sub Post Office,
London, Canada.

Can. J. Chem. Downloaded from www.nrcresearchpress.com by 210.87.254.42 on 09/05/12
For personal use only.

PROTON MAGNETIC RESONANCE AND THE STRUCTURE OF MALEIC HYDRAZIDE

Osamu Ohashi, Mitsuo Mashima,* and Masaji Kubo

There are three possible structures for maleic hydrazide (I). Miller (1) found that the compound exhibits acidic properties with a single pK_a value of 5.65. From this fact and comparison between the ultraviolet spectra of the compound and its derivatives in

*Saga University, Saga, Japan.

shifts of the decoupled protons of the two compounds are identical. Otherwise, a correction for any change in the applied field required to observe the two proton patterns must be included. The frequency measurements are converted to a p.p.m. scale by division by 24.3, after which the correction (if any) may be taken into account. The estimated precision of the present results is ±0.5 p.p.m. Although higher precision could be obtained through the use of a stabilized VFO, e.g. an audio-modulated single side-band oscillator as the source, the large chemical shift differences for P^{31} nuclei do not require that the data be of the highest precision.

As an example of the method, the optimum decoupling frequency for the reference, triethyl phosphite, was found to give a counter reading of 15,585 cycles/sec, while the reading for $(EtO)_2P(S)OC_6Cl_5$ was 17,443 cycles/sec. This difference, 1858 cycles/sec (76.46 p.p.m.), represents the "apparent" chemical shift difference for the two P^{31} nuclei. Since the counter reading monitors only the VFO output relative to another crystal oscillator, the actual direction of change in the decoupler frequency (24.3 Mc/sec) must be established independently. In this case we know that the P^{31} nucleus of the sample absorbs at *higher* field than the reference and so the change in counter reading from reference to sample corresponds to a *lower* decoupling frequency for the sample. The phosphorous nuclei were decoupled at different applied fields and the apparent shift must be corrected for this change, 0.48 p.p.m. (i.e., the chemical shift difference between the proton absorptions used for the two decoupling experiments). In this case, the apparent separation is *larger* than the actual difference since the proton band used for the sample is at *lower* field than that for the reference. The P^{31} chemical shift for this sample is, therefore, 76.0 p.p.m. relative to $(EtO)_3P$ or −62.1 p.p.m. relative to 85% H_3PO_4. The remaining P^{31} shifts were calculated in a similar manner.

ACKNOWLEDGMENTS

We are grateful to the National Research Council for financial assistance.

1. R. A. Y. Jones and A. R. Katritzky. Angew. Chem. **74**, 60 (1962).
2. H. Finegold. Ann. N.Y. Acad. Sci. **70**, 875 (1958).
3. N. Muller, P. C. Lauterbur, and J. Goldenson. J. Am. Chem. Soc. **78**, 3557 (1956).
4. J. R. Van Wazer, C. F. Callis, J. N. Shoolery, and R. C. Jones. J. Am. Chem. Soc. **78**, 5715 (1956).
5. P. C. Lauterbur. NMR spectra of elements other than hydrogen and fluorine in determination of organic structures by physical methods. Vol. 2. *Edited by* F. C. Nachod and W. D. Phillips. Academic Press. 1962. p. 469.
6. J. D. Baldeschwieler and E. W. Randall. Chem. Rev. **63**, 81 (1963).
7. J. A. Glasel, L. M. Jackman, and D. W. Turner. Proc. Chem. Soc. 426 (1961).
8. J. D. Baldeschwieler and E. W. Randall. Proc. Chem. Soc. 303 (1961).
9. J. D. Baldeschwieler. J. Chem. Phys. **36**, 152 (1962).
10. V. Royden. Phys. Rev. **96**, 543 (1954).
11. E. G. Paul and D. M. Grant. J. Am. Chem. Soc. **85**, 1701 (1963).
12. G. V. D. Tiers. J. Phys. Chem. **67**, 1373 (1963).
13. J. B. Stothers and E. Y. Spencer. Can. J. Chem. **39**, 1389 (1961).
14. G. Mavel and G. Martin. J. Chim. Phys. **59**, 762 (1962).

Received November 1, 1963.
Department of Chemistry,
University of Western Ontario,
London, Canada,
and
Canada Department of Agriculture,
Research Institute,
University Sub Post Office,
London, Canada.

Can. J. Chem. Downloaded from www.nrcresearchpress.com by 210.87.254.5 on 09/05/12
For personal use only.

PROTON MAGNETIC RESONANCE AND THE STRUCTURE OF MALEIC HYDRAZIDE

Osamu Ohashi, Mitsuo Mashima,* and Masaji Kubo

There are three possible structures for maleic hydrazide (I). Miller (1) found that the compound exhibits acidic properties with a single pK_a value of 5.65. From this fact and comparison between the ultraviolet spectra of the compound and its derivatives in

*Saga University, Saga, Japan.

solutions at low and high pH's, Miller and White (2) concluded that maleic hydrazide exists as structure IB, i.e., 3-hydroxy-1,6-dihydropyridazin-6-one. One of the present

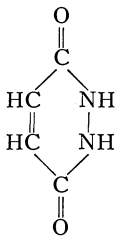
IA

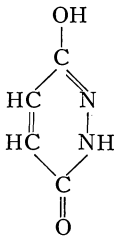
IB

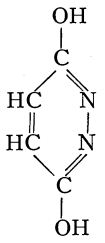
IC

authors (M.M.)(3) observed the infrared absorption of this compound in the rock-salt region. From the presence of absorption bands attributable to CO, NH, and OH groups, it was concluded that the molecules assume form IB in the crystalline state. On the other hand, Gompper and Altreuther (4) interpreted the n.m.r. spectrum of the compound in terms of form IA. However, Katritzky and Waring (5) criticized the interpretation by pointing out that fast exchange can render two or more protons equivalent in a tautomeric compound and therefore the molecules simulate a more symmetric structure. They further suggested that the dangers of misinterpretation can be avoided if proton resonance spectra of potentially tautomeric compounds are compared with those of methylated derivatives (6). Therefore, the present authors undertook to measure the n.m.r. spectra of this compound along with those of maleic methylhydrazide or 1-methyl-3-hydroxy-1,6-dihydropyridazin-6-one (II) for comparison.

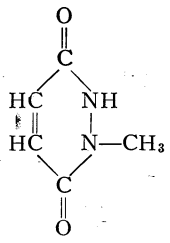
IIA

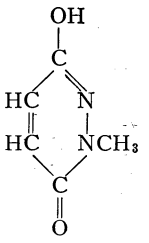
IIB

EXPERIMENTAL

Materials

Maleic anhydride and hydrazine hydrate were heated in ethanol to obtain compound I, which was recrystallized from ethanol, m.p. 263° C (decomp.) (lit. (7) >260° C (decomp.)). Compound II was prepared by a method employed by Eichenberger *et al.* (8), m.p. 209–213° C (lit. (8) 210-211° C).

Apparatus and Experimental Procedure

The proton magnetic resonance spectra were recorded at room temperature with a JNM-3 high-resolution n.m.r. spectrometer from Japan Electron Optics Laboratory Company operating at 60 Mc/sec. Since the compounds under investigation are sparingly soluble in water and other common solvents, dimethylsulphoxide was used as a solvent with tetramethylsilane as an internal standard, the concentration being 11.3 and 8.4% for maleic hydrazide and the methyl derivative, respectively. To obtain definite spectra, it was of crucial importance to keep the samples free from moisture, because dimethylsulphoxide is very hygroscopic.

ASSIGNMENTS

The observed spectra are illustrated in Fig. 1. The spectrum of compound II consists of a sharp intense peak at −3.49 p.p.m., a group of four closely spaced lines centered at −6.99 p.p.m., and a broad absorption at −11.06 p.p.m. The strongest peak is attributable to N—CH_3 protons. The quartet is symmetric about its center with two central

Can. J. Chem. Downloaded from www.nrcresearchpress.com by 210.87.254.5 on 09/05/12
For personal use only.

lines of greater intensity than the outermost lines. The pattern of peak heights and line spacings is characteristic of a two-spin system of nonequivalent protons having J, the spin coupling constant, approximately equal to δ, the internal chemical shift (9). Therefore, the quartet is unequivocally assigned to protons in —CH=CH—. J, equal to the separation between an extreme resonance line and the neighboring line in the quartet, is calculated to be 9.8 c.p.s. The internal chemical shift δ is given by the geometric mean, 0.16_7 p.p.m. or $9._9$ c.p.s., of the frequency separation between the extreme lines and that between the central ones (9). The broad absorption on the low-field side is tentatively attributed to C—OH protons, a final decision being suspended until the detailed discussion is given below.

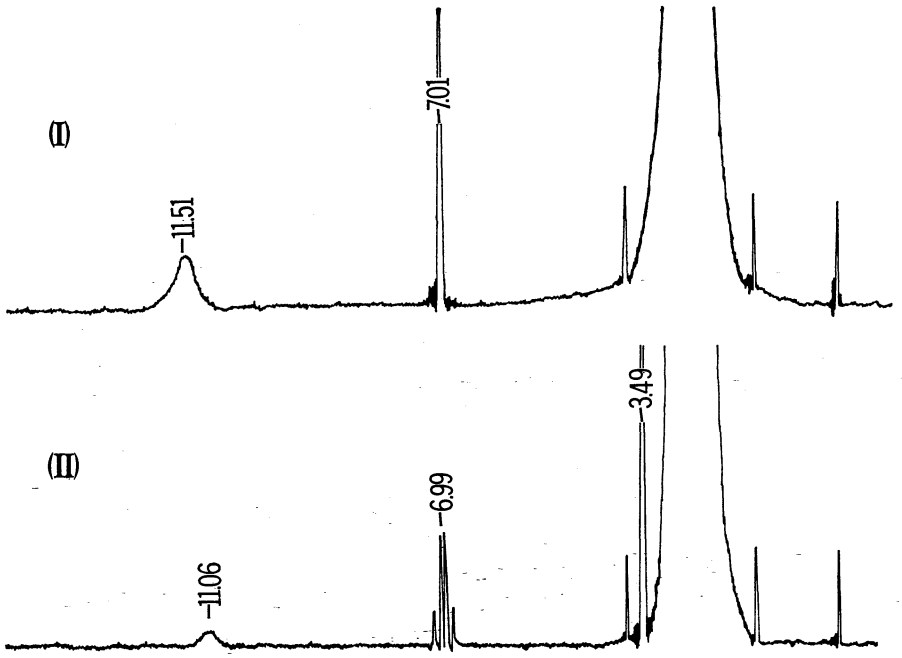

FIG. 1. Proton magnetic spectra of maleic hydrazide (I) and maleic methylhydrazide (II). In each spectrum, the strongest signal is due to dimethylsulphoxide, which was used as solvent. Satellites on either side of this peak are attributable to protons bonded to ^{13}C in solvent molecules. The signal of tetramethylsilane is at the highest field.

The compound I shows only two signals. One of them is a very sharp peak appearing at −7.01 p.p.m., in almost perfect agreement with the center of the aforementioned quartet at −6.99 p.p.m. Accordingly, it is attributable to —CH=CH— protons. The other signal is a broad one at −11.51 p.p.m. and corresponds to the broad absorption of compound II. It became broader and finally disappeared with increasing moisture content. Either the C—OH proton or the N—H proton or both must be responsible for this absorption. The problem is discussed in the succeeding section. The results of assignments are summarized in Table I.

DISCUSSION

The proton signal of $—CH_{(4)}=CH_{(5)}—$ in maleic hydrazide molecules is a singlet indicating that the two hydrogen atoms in a molecule are magnetically equivalent, whereas that of the methyl derivative is a quartet as expected from its chemical formula. In addition, only one line was observed for C—OH and N—H protons in maleic hydrazide. From these two facts, it is concluded that if the structure IB is correct as indicated

Can. J. Chem. Downloaded from www.nrcresearchpress.com by 210.87.254.5 on 09/05/12
For personal use only.

TABLE I

Proton magnetic resonance signals (p.p.m.) of maleic hydrazide (I) and maleic methylhydrazide (II)

Compound	N—CH_3	—CH=CH—	C—OH N—H
I		−7.01	−11.51 (broad)
II	−3.49	−6.79	−11.06 (broad)
		−6.96	
		−7.03	
		−7.19	

by ultraviolet and infrared spectroscopy, prototropic rearrangement takes place leading to keto–enol tautomerism between equivalent structures, IB and IB′, the lifetime of which

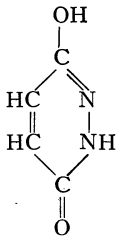

IB

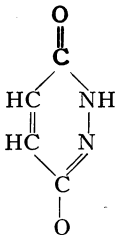

IB′

is much shorter than the relaxation times of proton spin orientations in a magnetic field but is much longer than the lifetime of transitions in infrared vibrations (10). During the relatively longer observation time of n.m.r. measurements, protons bonded to oxygen at a particular time find themselves at another time near nitrogen, and vice versa. The intramolecular rearrangement possibly superposed on the intermolecular exchange of protons as well as the effect of the nuclear quadrupole moment of nitrogen gives rise to the broadening of the observed signal at −11.51 p.p.m. The same explanation can be made for the broad signal of compound II at −11.06 p.p.m. These signals are at a lower field than expected for ordinary non-exchanging N—H or O—H protons. This suggests the presence of intramolecular hydrogen bonds and (or) intermolecular interactions through hydrogen bonding between the N—H or O—H protons of the solute and the > S=O groups of solvent molecules. In summary, the n.m.r. spectra of maleic hydrazide and its methyl derivative are consistent with the results of ultraviolet and infrared spectroscopy and provide experimental support in favor of the conclusions reached by Katritzky and Waring (5).

1. D. M. Miller. Can. J. Chem. **33**, 1806 (1955).
2. D. M. Miller and R. W. White. Can. J. Chem. **34**, 1510 (1956).
3. M. Mashima. J. Chem. Soc. Japan, Pure Chem. Sect. **83**, 981 (1962).
4. R. Gompper and P. Altreuther. Z. Anal. Chem. **170**, 205 (1959).
5. A. R. Katritzky and A. J. Waring. Chem. Ind. London, 695 (1962).
6. R. A. Y. Jones, A. R. Katritzky, and J. M. Lagowski. Chem. Ind. London, 870 (1960).
7. H. Feuer, E. H. White, and J. E. Wyman. J. Am. Chem. Soc. **80**, 3790 (1958).
8. K. Eichenberger, A. Staehelin, and J. Druey. Helv. Chim. Acta, **37**, 837 (1954).
9. P. L. Corio. Chem. Rev. **60**, 363 (1960).
10. W. G. Schneider. *In* Hydrogen bonding. *Edited by* D. Hadži. Pergamon Press, London. 1959. p. 67.

Received November 20, 1963.
Department of Chemistry,
Nagoya University,
Chikusa, Nagoya, Japan.

Can. J. Chem. Downloaded from www.nrcresearchpress.com by 210.87.254.5 on 09/05/12
For personal use only.

CATALYTIC OXIDATION OF LEAD (II) ACETATE BY OZONE[1]

GARSON P. SHULMAN[2]

Can. J. Chem. Downloaded from www.nrcresearchpress.com by 210.87.254.6 on 09/05/12
For personal use only.

Lead tetraacetate is widely used as an oxidizing agent in organic chemistry. Only three methods for its preparation have been reported. A solution of red lead (Pb_3O_4) in acetic acid (preferably with acetic anhydride present to remove water) produces a mixture of lead (II) and lead (IV) acetates (1).

Oxidation of lead (II) acetate by chlorine gives a mixture of lead (II) chloride and lead (IV) acetate (2). These methods have been combined in the generally recommended laboratory procedure for preparation of lead tetraacetate, but because of lead chloride formation, the yield is inherently limited. An alternative preparation involves electrolysis of lead (II) acetate in acetic acid, giving hydrogen and lead (IV) acetate (3). During some experiments involving catalytic decomposition of ozone on metal oxide surfaces, appearance of lead tetraacetate in an acetic acid solution which came into contact with the catalyst suggested the feasibility of oxidizing lead (II) acetate directly with ozone. The initial experiment apparently involved oxidation of the lead (II) oxide followed by solution; a solution of lead (II) acetate (from lead (II) oxide) in acetic acid was not affected by ozone. A number of metal ions known to react with ozone and to form higher valent oxides with oxidation potentials greater than that required for a lead (II) to lead (IV) conversion (4) ($Pb^{++} + 2H_2O \rightarrow PbO_2 + 4H^+ + 2e^-[-1.46\ v]$) were selected and screened as potential catalysts (see Table I). Of these, cobalt appeared to be particularly effective.

Table II summarizes the results of a series of reactions on a small preparative scale. Addition of acetic anhydride to the solution is not necessary to prevent hydrolysis by water formed during the reaction. The rate of hydrolysis of lead tetraacetate in glacial acetic acid must therefore be slow compared to the rate of its preparation. However, failure to add the acetic anhydride markedly affects yield of lead tetraacetate.[3] Cobalt chloride gave a conversion of 11.6% per gram of ozone at 60°, the acetate 8.9% at 60°, and 14.1% at 25°. Changing the anion thus does not affect the catalytic activity greatly, but a marked increase as the temperature is lowered is apparent. The more efficient utilization of ozone at a lower temperature must be due to a decrease in the rate of the catalytic decomposition of ozone to oxygen, resulting in use of a greater share of the absorbed ozone for oxidation. The reaction of equimolar amounts of lead acetate and ozone gives a yield of 72%.

The mechanism of the catalysis is not clear. While it was originally postulated that trivalent cobalt would be capable of oxidizing lead to the tetravalent state, cobalt (III) is not reduced rapidly by lead (II) acetate. The green color of the solution persists for at least 12 hours without noticeable change when the ozonization is interrupted. Because of the inverse effect of temperature, it is most unlikely that oxygen atoms formed from decomposition of ozone are the reactive intermediate. Therefore, direct oxidation of lead

[1]*Presented at the A.C.S. Southwest Regional Meeting, Houston, Texas, December 1963.*
[2]*Present address: The Martin Company, Baltimore 3, Maryland.*
[3]*Hydrolysis of lead tetraacetate gives a brown precipitate (lead dioxide) and would be readily apparent. The water must therefore inhibit the catalytic oxidation.*

acetate by ozone must be catalyzed by cobalt ion (and to a lesser extent, by silver, bismuth, cerium, and manganese ions).

EXPERIMENTAL

Effect of Various Catalysts

Solutions of 0.50 g of yellow lead oxide, 2.5 ml of acetic anhydride, and a small crystal (10±1 mg) of catalyst were dissolved in 100 ml of acetic acid. Ozone was passed through the solution at a rate of about 65 mg/min for 5 minutes, with total unreacted ozone being measured by passing the off-gas stream through a potassium iodide trap, which was then titrated with thiosulphate. The acetic acid solutions were mixed with 8.0 g of potassium iodide, poured into water, filtered, and titrated with thiosulphate. Results are summarized in Table I.

TABLE I

Catalytic oxidation of lead (II) acetate

Catalyst	Temperature, °C	O_3 consumed (meq)	$S_2O_3^=$ required* (meq)
None	25	1.81	0.21
$AgNO_3$	25	0.78	0.59
$Bi(NO_3)_3$	25	1.02	1.6†
$Ce(NO_3)_3$	25	1.05	0.78
$Mn(OAc)_2 \cdot 4H_2O$	25	3.56	2.30
$Mn(OAc)_2 \cdot 4H_2O$	60	6.56	1.31
$Co(OAc)_2 \cdot 4H_2O$	25	2.24	2.04
$Co(OAc)_2 \cdot 4H_2O$	60	3.49	2.58

*Approximate $Pb(OAc)_4$ formed.
†End point difficult to observe.

Preparation of Lead Tetraacetate

A solution of yellow lead oxide, acetic anhydride, and a cobalt salt in 100 ml of acetic acid was treated with a 0.02 c.f.m. stream of ozonized oxygen containing approximately 60 mg/min of ozone. The ozone was produced using a Welsbach Model T-23 Ozonator. Repeated titration of the ozone stream during an 8-hour day showed that variation in ozone concentration was less than the uncertainty in the titration (2%) as long as instrument settings were unchanged. As a precaution, ozone concentration was determined before and after each reaction. Consumption of ozone was determined by connecting the outlet of the reaction vessel (a gas-washing bottle) to a potassium iodide trap periodically and titrating the iodine liberated in 1 minute. A smooth curve of rate of ozone uptake vs. time resulted. Total ozone uptake was determined from the area under the curve. The solid which formed was filtered, washed with benzene, and dried. An additional small crop of crystals was obtained by adding a mixture of benzene and hexane to the acetic acid. Yields were determined from the weight of the precipitate, since the filtrate then contained a negligible amount of lead tetraacetate, as shown by attempted iodimetric titration. Results are summarized in Table II.

TABLE II

Preparation of lead tetraacetate

Temp. (° C)	Wt. of PbO (g)	Wt. of catalyst (g)	Vol. of Ac_2O (ml)	Input O_3 conc. (mg/min)	Reaction time (min)	Wt. of O_3 absorbed (g)	Yield (%)
25	20.6	0	0	57.4	105	0.9	nil
60	5.0	0	5.0	47.5	8	0.2	nil
60	25.0	0.1*	25.0	62.0	75	2.7	24
60	25.0	0.1‡	25.0	53.1	163	4.8	56
25	25.0	1.0*	0	61.6	390	5.9	30
25	25.0	1.0*	25.0	65.0	340	5.4	72†

*$Co(OAc)_2.4H_2O$.
†Melting point 178° C. Reported melting point 175°. Reference 4, p. 592.
‡$CoCl_2$.

I would like to thank Mr. Richard Hughes for competent technical assistance.

Can. J. Chem. Downloaded from www.nrcresearchpress.com by 210.87.254.6 on 09/05/12
For personal use only.

1. A. HUTCHINSON and W. POLLARD. J. Chem. Soc. **63**, 1136 (1893).
2. A. COLSON. Compt. Rend. **136**, 1664 (1903).
3. (*a*) C. SCHALL and W. MELZER. Z. Elektrochem. **28**, 474 (1922).
(*b*) M. YA FIOSHIN and V. A. GUS'KOV. Dokl. Akad. Nauk SSSR, **112**, 303 (1957).
4. C. D. HODGMAN (*Editor*). Handbook of chemistry and physics. 43rd ed. The Chemical Rubber Publishing Co., Cleveland, Ohio. 1961. p. 1744.

RECEIVED NOVEMBER 13, 1963.
RESEARCH LABORATORIES,
ARCHER-DANIELS-MIDLAND COMPANY,
MINNEAPOLIS, MINNESOTA.

Can. J. Chem. Downloaded from www.nrcresearchpress.com by 210.87.254.6 on 09/05/12
For personal use only.

REARRANGEMENT STUDIES WITH ^{14}C. XVIII. 2-PHENYL-2-^{14}C-ETHYL CHLORIDE FROM GAMMA-IRRADIATION OF 2-PHENYL-1-^{14}C-ETHYL CHLORIDE

C. C. LEE AND D. J. KROEGER[1]

The γ-irradiation of propyl halides (1–4) and butyl halides (5, 6) has been shown to result in isomerizations. These isomerizations have been postulated to take place by 1,2-halogen shifts (2, 3) or by 1,2-hydrogen shifts (5, 6). Using ^{14}C as tracer, isotope position rearrangements of the label from the C-1 to the C-2 positions have been observed in the γ-irradiation of 1-^{14}C-ethyl iodide (7), 2-phenyl-1-^{14}C-ethyl iodide (8), 2-phenyl-1-^{14}C-ethyl bromide (9), and 2-*p*-methoxyphenyl-1-^{14}C-ethyl bromide (9). The present communication reports observations on the ^{60}Co γ-induced rearrangement of 2-phenyl-1-^{14}C-ethyl chloride to 2-phenyl-2-^{14}C-ethyl chloride.

The reaction of 2-phenyl-1-^{14}C-ethanol with thionyl chloride in pyridine has been shown to give 2-phenyl-1-^{14}C-ethyl chloride (I) without rearrangement (10). This method of preparation of I was adopted with the modification that the reaction was carried out in benzene as solvent. The modified method led to less tendency for tar formation and high yields of I. Degradation of I so synthesized to benzoic acid showed the presence of 0.09% of the ^{14}C-activity in the C-2 position. In the subsequent studies on γ-induced rearrangements, corrections were made by subtracting this 0.09% of activity present in C-2 before irradiation.

Samples of I were irradiated and analyzed for total decomposition and for rearrangement to 2-phenyl-2-^{14}C-ethyl chloride as described previously for analogous studies with the bromide and iodide (8, 9). The results are shown in Table I. For the range of absorbed doses investigated, the extent of rearrangement increases with increasing dosage. The mean G_r resulting from γ-irradiation of I is 0.21 ± 0.02, which may be contrasted with G_r values of 0.30 ± 0.01 and 0.50 ± 0.05, respectively, for isotope position rearrangements upon γ-irradiation of 2-phenyl-1-^{14}C-ethyl bromide (9) and 2-phenyl-1-^{14}C-ethyl iodide (8).

The extent of decomposition of I also increases with increasing amount of radiation. Since these estimates of decomposition were calculated from small differences between large specific activities, the errors involved may be relatively high (8). If G_d for the first sample (Table I) were neglected, the mean G_d is about 4.5, which may be compared with G_d of about 2 for the irradiation of 2-phenyl-1-^{14}C-ethyl iodide (8).

It has already been pointed out (8) that formation of 2-phenyl-2-^{14}C-ethyl halide from γ-irradiation of 2-phenyl-1-^{14}C-ethyl halide could result neither from a 1,2-halogen shift nor from the addition of hydrogen halide to styrene produced during the irradiation.

[1]*Holder of a National Research Council of Canada Bursary, 1962–1963.*

1. A. HUTCHINSON and W. POLLARD. J. Chem. Soc. **63**, 1136 (1893).
2. A. COLSON. Compt. Rend. **136**, 1664 (1903).
3. (*a*) C. SCHALL and W. MELZER. Z. Elektrochem. **28**, 474 (1922).
(*b*) M. YA FIOSHIN and V. A. GUS'KOV. Dokl. Akad. Nauk SSSR, **112**, 303 (1957).
4. C. D. HODGMAN (*Editor*). Handbook of chemistry and physics. 43rd ed. The Chemical Rubber Publishing Co., Cleveland, Ohio. 1961. p. 1744.

RECEIVED NOVEMBER 13, 1963.
RESEARCH LABORATORIES,
ARCHER-DANIELS-MIDLAND COMPANY,
MINNEAPOLIS, MINNESOTA.

Can. J. Chem. Downloaded from www.nrcresearchpress.com by 210.87.254.6 on 09/05/12
For personal use only.

REARRANGEMENT STUDIES WITH ^{14}C. XVIII. 2-PHENYL-2-^{14}C-ETHYL CHLORIDE FROM GAMMA-IRRADIATION OF 2-PHENYL-1-^{14}C-ETHYL CHLORIDE

C. C. LEE AND D. J. KROEGER[1]

The γ-irradiation of propyl halides (1–4) and butyl halides (5, 6) has been shown to result in isomerizations. These isomerizations have been postulated to take place by 1,2-halogen shifts (2, 3) or by 1,2-hydrogen shifts (5, 6). Using ^{14}C as tracer, isotope position rearrangements of the label from the C-1 to the C-2 positions have been observed in the γ-irradiation of 1-^{14}C-ethyl iodide (7), 2-phenyl-1-^{14}C-ethyl iodide (8), 2-phenyl-1-^{14}C-ethyl bromide (9), and 2-*p*-methoxyphenyl-1-^{14}C-ethyl bromide (9). The present communication reports observations on the ^{60}Co γ-induced rearrangement of 2-phenyl-1-^{14}C-ethyl chloride to 2-phenyl-2-^{14}C-ethyl chloride.

The reaction of 2-phenyl-1-^{14}C-ethanol with thionyl chloride in pyridine has been shown to give 2-phenyl-1-^{14}C-ethyl chloride (I) without rearrangement (10). This method of preparation of I was adopted with the modification that the reaction was carried out in benzene as solvent. The modified method led to less tendency for tar formation and high yields of I. Degradation of I so synthesized to benzoic acid showed the presence of 0.09% of the ^{14}C-activity in the C-2 position. In the subsequent studies on γ-induced rearrangements, corrections were made by subtracting this 0.09% of activity present in C-2 before irradiation.

Samples of I were irradiated and analyzed for total decomposition and for rearrangement to 2-phenyl-2-^{14}C-ethyl chloride as described previously for analogous studies with the bromide and iodide (8, 9). The results are shown in Table I. For the range of absorbed doses investigated, the extent of rearrangement increases with increasing dosage. The mean G_r resulting from γ-irradiation of I is 0.21 ± 0.02, which may be contrasted with G_r values of 0.30 ± 0.01 and 0.50 ± 0.05, respectively, for isotope position rearrangements upon γ-irradiation of 2-phenyl-1-^{14}C-ethyl bromide (9) and 2-phenyl-1-^{14}C-ethyl iodide (8).

The extent of decomposition of I also increases with increasing amount of radiation. Since these estimates of decomposition were calculated from small differences between large specific activities, the errors involved may be relatively high (8). If G_d for the first sample (Table I) were neglected, the mean G_d is about 4.5, which may be compared with G_d of about 2 for the irradiation of 2-phenyl-1-^{14}C-ethyl iodide (8).

It has already been pointed out (8) that formation of 2-phenyl-2-^{14}C-ethyl halide from γ-irradiation of 2-phenyl-1-^{14}C-ethyl halide could result neither from a 1,2-halogen shift nor from the addition of hydrogen halide to styrene produced during the irradiation.

[1]*Holder of a National Research Council of Canada Bursary, 1962–1963.*

TABLE I

Total decomposition and rearrangement to 2-phenyl-2-^{14}C-ethyl chloride from ^{60}Co γ-irradiation of 2-phenyl-1-^{14}C-ethyl chloride

Absorbed dose (megarads)	Compound assayed*	Specific activity† (c.p.m./mmole)	Decomposition		Rearrangement‡	
			%	G_d	%	G_r
0	II	3.07×10^6				
	III	2.82×10^3			0.09	
54.1	II	2.87×10^6	6.5	8.2		
	III	7.89×10^3			0.17	0.22
126	II	2.81×10^6	8.5	4.6		
	III	1.47×10^4			0.39	0.21
181	II	2.67×10^6	13.0	4.9		
	III	2.06×10^4			0.58	0.22
235	II	2.60×10^6	15.3	4.5		
	III	2.36×10^4			0.68	0.20
282	II	2.52×10^6	17.9	4.4		
	III	2.63×10^4			0.77	0.19

*II is $C_6H_5CH_2CH_2COOH$; III is C_6H_5COOH.
†Measured by a liquid scintillation counter.
‡Corrected for the 0.09% of activity in III derived from the unirradiated sample.

These processes could lead to the structurally rearranged 1-phenyl-2-^{14}C-ethyl halide, but not the isotopically rearranged 2-phenyl-2-^{14}C-ethyl halide. The observed rearrangements (Table I) indicated the occurrence of a net 1,2-phenyl shift during radiolysis. If 1,2-shifts take place in the free radicals produced during irradiation, it would be of interest to investigate the effects of added iodine, a free radical scavenger (11), on the extent of γ-induced rearrangements.

Two 5-g samples of I containing 5% (by weight) of iodine were irradiated and then fractionated through a small helix-packed column. About one-half of the material was distilled and the remainder designated as the residue. Both the distillate and the residue from each sample were analyzed for rearrangement and total decomposition. The results are given in Table II. From this table, it can be seen that G_r for the distillate is about one-half as large as G_r for the residue (about 0.18 and 0.36). While the probable errors involved in the calculated G_d may be quite high, a trend is evident in that G_d for the distillate is approximately 0.3 while G_d for the residue is about 7. The small G_d for the distillate suggests that this fraction is relatively pure I while most of the decomposition products remain with the residue. In these experiments, there is a possibility of energy transfer from organic halide to dissolved iodine. No attempt is made in the current work to investigate this problem. If such an energy transfer were to take place, the dose absorbed by I would be lower, and the calculated G values would be higher than those given in Table II. Such a possible change in the absolute magnitudes of the G values, however, should not materially alter the qualitative conclusion that, relatively, G_r and G_d are apparently greater for the residue than for the distillate.

During irradiation of I in the presence of iodine, if 2-phenyl-1-^{14}C-ethyl and 2-phenyl-2-^{14}C-ethyl radicals were produced, both radicals could be scavenged by iodine. If the separation of 2-phenylethyl chloride and 2-phenylethyl iodide were complete, one might then expect no rearrangement in the distillate, which would be pure 2-phenylethyl chloride, and some rearrangement in the residue, which would contain some 2-phenylethyl chloride and all of the 2-phenylethyl iodide. Since the separation of 2-phenylethyl chloride from

Can. J. Chem. Downloaded from www.nrcresearchpress.com by 210.87.254.6 on 09/05/12
For personal use only.

Can. J. Chem. Downloaded from www.nrcresearchpress.com by 210.87.254.6 on 09/05/12
For personal use only.

TABLE II

Total decomposition and rearrangement to 2-phenyl-2-^{14}C-ethyl chloride from ^{60}Co γ-irradiation of 2-phenyl-1-^{14}C-ethyl chloride containing 5% iodine

Absorbed dose (megarads)	Compound assayed*	Distillate					Residue				
		Specific activity† (c.p.m./mmole)	Decomposition		Rearrangement‡		Specific activity† (c.p.m./mmole)	Decomposition		Rearrangement‡	
			%	G_d	%	G_r		%	G_d	%	G_r
0	II	3.65×10^6					3.65×10^6				
	III	3.32×10^3			0.09		3.32×10^3			0.09	
104	II	3.62×10^6	0.8	0.5			3.26×10^6	10.7	7.1		
	III	1.31×10^4			0.27	0.18	2.33×10^4			0.55	0.36
167	II	3.63×10^6	0.5	0.2			3.06×10^6	16.2	6.7		
	III	1.85×10^4			0.42	0.17	3.55×10^4			0.88	0.36

*II is $C_6H_5CH_2CH_2COOH$; III is C_6H_5COOH.
†Measured by a liquid scintillation counter.
‡Corrected for the 0.09% of activity in III derived from unirradiated sample.

2-phenylethyl iodide likely was not quantitative, the observed higher rearrangement in the residue may be regarded as in qualitative agreement with prediction.

The strength of the carbon–halogen bond, as indicated by bond dissociation energies, follows the order chloride > bromide > iodide (12). The G_r value from irradiation of 2-phenyl-1-^{14}C-ethyl chloride is less than that from the bromide, which, in turn, is less than that from the iodide. Such findings suggest that the extent of rearrangement may depend on the strength of the carbon–halogen bond, which could influence the readiness with which the 2-phenylethyl radical is formed during the irradiation. Another factor which may play a role is the relative magnitudes of the favorable energy balance in the dissociative electron attachment process for organic radical formation from radiolysis of organic halides. Feng (12) has estimated the order to be iodide > bromide > chloride, while Geissler and Willard (13) indicated that thermodynamically the process is most favorable for iodide and about the same for bromide and chloride. The observed G_r of about 0.5, 0.3, and 0.2, respectively, for 2-phenylethyl iodide, bromide, and chloride are in the order expected if the rearrangement involved formation of 2-phenylethyl radical by the dissociative electron attachment process.

EXPERIMENTAL

2-Phenyl-1-^{14}C-ethyl Chloride (I)

A solution of 10.1 g (0.082 moles) of 2-phenyl-1-^{14}C-ethanol (10) in 10 ml of benzene was added dropwise with stirring to a solution of 10.7 g (0.090 moles) of thionyl chloride and 2.0 ml of pyridine in 20 ml of benzene. Stirring was continued at room temperature for 1.5 hours and then the mixture was refluxed for 1 hour. The resulting solution was cooled in an ice bath and 20 ml of ice water was introduced. The benzene layer was separated and the aqueous layer was extracted with three 10-ml portions of benzene. The combined extract was washed with 10% sodium carbonate solution and with water and then dried over anhydrous potassium carbonate. After the benzene was removed by distillation, the residue was distilled under reduced pressure, giving 9.8 g (85%) of 2-phenyl-1-^{14}C-ethyl chloride, b.p. 77–78° C at 10 mm (lit. (10) b.p. 85–87° C at 17 mm). The material was diluted with ordinary 2-phenylethyl chloride and redistilled to give a uniform stock for irradiation studies.

Irradiation and Analyses for Decomposition and Rearrangement

The procedures were analogous to those used in previous studies (8, 9). Irradiation of I was continued for periods of up to about 5 months, the dose rates being of the order of 1.9 megarad/day. The irradiated halide was converted to a solid derivative, hydrocinnamic acid, which, in turn, was oxidized to benzoic acid. Based on isotopic dilution, the decrease in specific activity of the hydrocinnamic acid after irradiation measured the extent of decomposition. The ^{14}C-activity of the benzoic acid measured the amount of rearrangement.

ACKNOWLEDGMENT

The financial support given by the National Research Council of Canada is gratefully acknowledged.

1. R. H. Schuler and R. C. Petry. J. Am. Chem. Soc. **78**, 3954 (1956).
2. R. H. Wiley, W. Miller, C. H. Jarboe, Jr., J. R. Harrell, and D. J. Parish. Radiation Res. **13**, 479 (1960).
3. H. L. Benson and J. E. Willard. J. Am. Chem. Soc. **83**, 4672 (1961).
4. R. J. Neddenriep and J. E. Willard. J. Phys. Chem. **65**, 1206 (1961).
5. W. S. Wilcox. Radiation Res. **10**, 112 (1959).
6. E. B. Dismukes and W. S. Wilcox. Radiation Res. **11**, 754 (1959).
7. I. S. Bhardwaj and C. C. Lee. Can. J. Chem. **41**, 2368 (1963).
8. C. C. Lee, D. G. Lee, and I. S. Bhardwaj. Radiation Res. **17**, 536 (1962).
9. D. P. Thornhill and C. C. Lee. Can. J. Chem. **41**, 2482 (1963).
10. C. C. Lee and J. W. T. Spinks. Can. J. Chem. **32**, 1005 (1954).
11. R. H. Schuler. J. Phys. Chem. **62**, 37 (1958).
12. P. Y. Feng. Proc. Second Intern. Conf. Peaceful Uses Atomic Energy, Geneva, 1958, **29**, 166 (1958).
13. P. R. Geissler and J. E. Willard. J. Am. Chem. Soc. **84**, 4627 (1962).

Received November 4, 1963.
Department of Chemistry,
University of Saskatchewan,
Saskatoon, Saskatchewan.

Can. J. Chem. Downloaded from www.nrcresearchpress.com by 210.87.254.6 on 09/05/12
For personal use only.

HIGH-FREQUENCY TITRATIONS. II. ARGENTIMETRIC DETERMINATION OF MICRO AMOUNTS OF HALIDES IN METHANOL

PETER GREY AND G. C. B. CAVE

Can. J. Chem. Downloaded from www.nrcresearchpress.com by 210.87.254.105 on 09/05/12
For personal use only.

INTRODUCTION

In Part I, a new method was proposed for the argentimetric titration of alkali-metal halides present in their mixtures in methanol. The sample volume was 120 ml. Amounts of halide down to about 0.5 micromole (μmole) could be determined.

In the present work, the same method was applied to mixtures of alkali-metal halides in about 6 ml of methanol. Amounts of halides of the order of a few micrograms were successfully determined.

EXPERIMENTAL

Apparatus

The Sargent Model V Oscillometer was used. A Sargent cell compensator was coupled in the transmission line ahead of the sample cell. It is a variable inductor, whose reactance can be adjusted to the capacitance reactance due to the walls of the titration cell.

For the titration vessel, a 10-ml closed-type cell supplied with the oscillometer was used. It was 15 mm in diameter, and 123 mm in height, constructed like the Sargent macrocell used in Part I, but with an annulus 65 mm deep that held only 5 ml of liquid. The outer walls of the annulus were metal plated, to provide a capacitor. In practice, 6 ml of solution were used for a titration. The standard taper 14/10 stopper supplied with the cell was replaced by a cover that consisted of a 25-mm square of silicone rubber, 4 mm thick. A thin smear of silicone grease on the underside of this square provided a reasonably gas-tight seal.

The solution was stirred with a small paddle-type stirrer, made from a flexible Teflon shaft, 3 mm in diameter, with a small polyethylene paddle inserted in a slot at the end. The shaft was rotated in a centrally cut hole in the silicone-rubber cover of the cell. The shaft was coupled to the stirring motor by a flexible cable. A Variac provided for changes in the stirring rate.

The titrant was dispensed into the cell solution from a 5-ml Koch microburet having 0.01-ml graduations. The stopcock had a Teflon plug. The tip supplied was detachable, having a standard No. 5 taper joint which also happened to fit the standard Luer joints of hypodermic needles. This tip was replaced by a lumbar puncture needle of standard gauge 22 G, and 3 in. in length, which had a standard Luer joint. In use, the needle was inserted through the silicone-rubber cover of the titration cell, to a depth such that its orifice was in the solution to be titrated, during stirring.

The microburet and the pipets were calibrated to deliver methanol.

Reagents

The reagents used were those described in Part I. A 0.01 N standard stock solution of silver nitrate was standardized by high-frequency titrimetry against sodium chloride (the primary standard). Standard stock solutions, 0.01 N in sodium chloride, sodium bromide, and sodium iodide in methanol were also prepared; the latter two solutions were standardized against the 0.01 N silver nitrate solution.

From these 0.01 N stock solutions, 10^{-4} N working solutions were prepared by dilution.

The Titrimetric Procedure

An aliquot of the halide solution in methanol was transferred to the titration cell, and the contents diluted to 6 ± 0.2 ml with absolute methanol. In some cases, particularly at very low concentrations of halide, an aliquot of a 5×10^{-4} N solution of sodium nitrate in methanol was added prior to the final dilution to 6 ml. The purpose was to raise the ionic strength of the solution to a point where the sensitivity of the instrument toward changes in concentrations was sufficient. In cases of such additions, titration blanks for halide in the sodium nitrate were always separately run.

The stirrer was then positioned so that the paddle was about 5 mm above the top of the cell electrodes. The tip of the buret needle was placed about 5 mm above the level of the still solution. The silicone-rubber cover was then pressed firmly to the top of the open cell, to form a seal by reason of the applied silicone grease. The rate of stirring was adjusted to cause the outer edge of the solution to rise about 1 cm in the cell.

The Sargent cell compensator was set at 640 dial units. This value gave the maximum instrumental sensitivity, while still keeping the oscillometer readings within the limits of variation of its standard capacitors, for the solutions titrated. Without the cell compensator, breaks were not obtained in the titration graphs for the microgram amounts of halide taken in the present work.

RESULTS AND DISCUSSION

Effect of Temperature

It was shown in Part I of this series that the apparent capacitance due to a solution is temperature dependent. Therefore, a closed-type cell was used in that work and in the present work. The use of only 6 ml of solution instead of the 120 ml used in the macro-titrations of Part I would make the cell solution more susceptible to changes in ambient temperature. Therefore the effect of temperature changes in the 10-ml cell used in the present work was studied. The results are in Table I. The apparent capacitance (as

TABLE I

The effect of temperature on the apparent capacitance due to methanol
Volume of solution: 6 ml
Concentration: Pure methanol for column A; 2×10^{-5} *M* in NaCl for column B
Cell: Closed-type, 10-ml cell
Conditions: Solution was initially at room temperature; stirring was continuous

A			B		
Time (hours)	Room temp. (°C)	Instrument divisions	Time (minutes)	Room temp. (°C)	Instrument divisions
0	23.5	30368	0	23.0	30376
1	23.0	30400	10	23.0	30371
2.25	22.0	30461	30	23.0	30379
4	21.0	30568	50	23.0	30378

instrument divisions) of the closed 10-ml titration cell containing 6 ml of methanol was measured at intervals over a 4-hour period. The decline in room temperature caused a rise in apparent capacitance. Evaporation could not have occurred to cause this change, since at 23° C a 2×10^{-5} *M* solution of sodium chloride in methanol gave no significant change in apparent capacitance over a 50-minute period of continuous stirring.

Titration of microgram amounts gave, in general, rather small changes in the slope of the titration graph, at the end point. Therefore, it is clearly necessary to carry out such titrations at a reasonably constant temperature. This is readily achieved. However, the slopes of the arms of the titration graph also were found to be temperature dependent; the lower the temperature, the more acute the angle of intersection. A change of a few degrees of temperature can produce this effect. The position of the end point was not shifted, in the few titrations performed to observe this effect.

Precision and Accuracy of the Micro Titrations

Replicate determinations on 0.1 μmole amounts of sodium chloride alone in 6 ml of methanol were made, to obtain an estimate of the standard deviation. The results are in Table II. Precision and accuracy are good.

Duplicate determinations were made on several mixtures of sodium bromide and sodium chloride. In addition, replicates ($N = 7$) were run on one such mixture to obtain an estimate of the standard deviation. Results are in Table II, and typical titration graphs are shown in Fig. 1. These results agree with those in Part I, where solid-solution formation was evident.

Lower Limits of Titratable Concentrations

Titrations were performed on various micro amounts of sodium chloride, sodium bromide, and sodium iodide, in 6 ml of methanol. The purpose was to find approximately

Can. J. Chem. Downloaded from www.nrcresearchpress.com by 210.87.254.105 on 09/05/12
For personal use only.

Can. J. Chem. Downloaded from www.nrcresearchpress.com by 210.87.254.105 on 09/05/12
For personal use only.

TABLE II

High-frequency argentimetric titration of micro amounts of halides, alone and in their mixtures, in methanol
Volume of methanol solution: 6 ml
Normality of standard silver nitrate in methanol: 0.001 *N*

Molar ratio Br/Cl	Bromide (μmole)				Chloride (μmole)				Bromide + chloride (μmole)			
	Taken	Found*	Standard deviation	*N*	Taken	Found*	Standard deviation	*N*	Taken	Found*	Standard deviation	*N*
0	Nil				0.1005	0.101	0.0010	6				
1:1	0.1491	0.157	0.0070	7	0.1512				0.3003	0.304	0.011	7
			% diff.								% diff.	
3:1	0.4485	0.443	−1.2	2	0.1511				0.5996	0.578	−3.6	2
2:1	0.2988	0.297	−0.5	2	0.1511				0.4498	0.432	−3.8	2
1:2	0.1491	0.160	7.4	2	0.3046				0.4537	0.438	−3.3	2
1:3	0.1491	0.162	8.7	2	0.4560				0.6051	0.600	−0.8	2

*Average of *N* samples.
NOTE: "% diff." is the percentage difference between the amount taken, and the average of duplicates of the amount found. For the six samples of chloride alone, the methanol solutions were made 1.7×10^{-5} *M* in sodium nitrate; this salt was not added to the chloride–bromide mixtures.

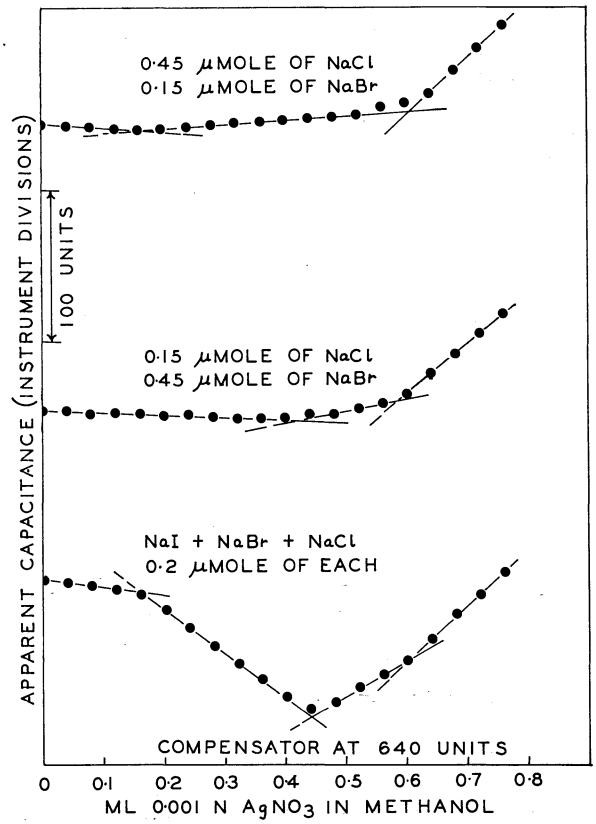

FIG. 1. Typical titration graphs of argentimetric titrations of mixtures of halides in methanol.

the lower limits of concentration, below which the angle of intersection of the arms of the titration graph became very small, and the precision of the titration poor. It is to be noted that these lower limits will be in part defined by the precision required.

In all of the titrations, the methanol was made approximately 2×10^{-5} M in sodium nitrate. This indifferent electrolyte sharpened the end point at the lowest concentrations of halide, but it is not a necessary additive at higher concentrations. The reason for its effectiveness will be given in a subsequent communication.

For the single halides, down to about 6 μg of sodium chloride could be titrated with accuracy and precision. Below that amount, precision became progressively less, although even at 3 μg the two linear arms of the titration graph intersected at about 4–5°, at the end point. At about 10 μg it was possible to dispense with the sodium nitrate. Down to about 10 μg of sodium bromide, and down to about 8–15 μg of sodium iodide were also satisfactorily titrated.

For binary mixtures of these halides, the lower limits were about 50% higher than the corresponding limits for the single halides. It is to be noted that for Table II, the amounts taken were in fact near the lower limits recommended here.

All three halides, present in a favorable ratio, were titrated satisfactorily in their ternary mixture, but the lower limits were about double those for the corresponding single halides. In Fig. 1 is shown a typical titration graph of such a ternary mixture.

Can. J. Chem. Downloaded from www.nrcresearchpress.com by 210.87.254.105 on 09/05/12
For personal use only.

ACKNOWLEDGMENTS

We are grateful to the National Research Council for financial support, and to the Province of Quebec for a scholarship to one of us (P. G).

RECEIVED AUGUST 1, 1963.
DEPARTMENT OF CHEMISTRY,
MCGILL UNIVERSITY,
MONTREAL, QUEBEC.

Can. J. Chem. Downloaded from www.nrcresearchpress.com by 210.87.254.105 on 09/05/12
For personal use only.

3030

Can. J. Chem. Downloaded from www.nrcresearchpress.com by 210.87.254.105 on 09/05/12
For personal use only.

Canadian Journal of Chemistry

Issued by THE NATIONAL RESEARCH COUNCIL OF CANADA

VOLUME 42 MAY 1964 NUMBER 5

THE DECOMPOSITION OF SILYL PEROXIDES[1]

RICHARD R. HIATT[2]

Department of Chemistry, University of Toronto, Toronto, Ontario

Received November 25, 1963

ABSTRACT

The thermal decomposition of *tert*-butyl trimethylsilyl peroxide has been investigated and found to be sensitive to acid and base catalysis and to the nature of the solvent. In heptane and iso-octane the first-order rate constant could be expressed as $1.09\times10^{15}\ e^{-42300/RT}$ and in 1-octene as $3.90\times10^{15}\ e^{-42300/RT}$ (sec^{-1}). The half life at 203° C was about 1 hour. The reaction was faster in aromatic solvents; in chlorobenzene it was complicated by formation of HCl from the solvent.

Products of the reaction were acetone, *tert*-butyl alcohol and hexamethyldisiloxane.

INTRODUCTION

Although the silicon analogues of alkyl peroxides and hydroperoxides have been known for some time (1, 2), and it has been shown that these compounds can initiate free radical polymerizations (1), it has been only recently that careful kinetic studies on their homolytic decomposition have been initiated (3).

The orthodox explanation for the effect of substituents on the stability of the oxygen–oxygen bond concerns the ability of the attached groups to minimize the charge on the opposed dipoles of the two oxygen atoms (4). This argument, advanced to explain rates

$$R\overrightarrow{\ }O-O\overleftarrow{\ }R$$

of decomposition of a large number of substituted benzoyl peroxides, is probably always operative, even though other considerations may be, in some instances, more important (5).

A silicon atom should be particularly effective in delocalizing the electrons on an adjacent oxygen through $d\pi$–$p\pi$ bonding, and should confer stability to a silyl peroxide greater than that of its carbon analogue.* To determine the correctness of this hypothesis, a study of the thermal decomposition of *tert*-butyl trimethylsilyl peroxide (I) was instituted.

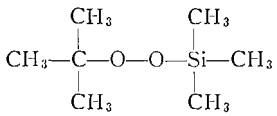

I

[1]*This work received financial assistance from the National Research Council of Canada.*

[2]*Present address: Stanford Research Institute, Menlo Park, California.*

**This has not proved to be the case for bis(trimethylsilyl)peroxide (2) or for triphenylsilyl hydroperoxide (3). But hydroperoxides are notorious for their susceptibility toward induced decomposition, and the seemingly unrealistic activation energy for thermal decomposition, in the former compound, of 6.3 kcal suggests that in neither case was the reaction under consideration the uncomplicated cleavage of the O—O bond.*

Can. J. Chem. Downloaded from www.nrcresearchpress.com by 210.87.254.105 on 09/05/12
For personal use only.

EXPERIMENTAL

tert-Butyl trimethylsilyl peroxide was prepared by the method of Buncel and Davies (1). Distillation at reduced pressure gave material which liberated 96–99% of the theoretical amount of iodine on titrations.

To titrate, the peroxide was added to a solution of 20% acetic acid –80% isopropyl alcohol. Solid sodium iodide was added and the mixture refluxed for 20 minutes, with subsequent titration of the liberated iodine by a standard solution of sodium thiosulphate.

Chlorobenzene, iso-octane, and *n*-heptane were Fisher Reagent Grade materials, used without further purification. Tetralin was freed from peroxides by washing with Fenton's reagent and distilling immediately prior to its use. 1-Octene, 99+% pure, was obtained from Phillips Petroleum Company.

Rates of reaction were measured using solutions 0.04 to 0.2 *M* in peroxide in the appropriate solvent. Solutions were degassed, decanted into ampoules, and sealed off under vacuum. After they were heated for various lengths of time in a constant temperature bath, the ampoules were opened and the contents titrated for remaining peroxide. Depending on the solvent, plots of log peroxide concentration vs. time were linear for 40 to 90% of the reaction.

Products of the decomposition were determined by vapor-phase chromatography, using the F & M Model 500. Columns of isodecylphthalate and on Carbowax 20 M, both on Chromosorb, were equally effective in separating the components.

RESULTS AND DISCUSSION

Like the analogous di-*tert*-butyl peroxide, *tert*-butyl trimethylsilyl peroxide gave clean unimolecular thermal decomposition in a number of solvents (Table I). A fivefold change

TABLE I

Decomposition of *tert*-butyl trimethylsilyl peroxide

Solvent	P_0*	T,° C	$k_1 \times 10^5$ sec^{-1}	ΔE
n-Heptane	0.141	183.5	2.78	
n-Heptane	0.145	192.4	6.64	41.2±0.60
n-Heptane	0.140	203.2	18.8	
n-Heptane	0.0279	203.2	17.8	
Iso-octane	0.141	183.6	2.64	
Iso-octane	0.139	193.1	7.09	
Iso-octane	0.140	203.2	17.9	
1-Octene	0.143	183.4	2.85	
1-Octene	0.162	193.4	7.60	
1-Octene	0.0315	193.9	8.02	42.3±1.0
1-Octene	0.141	203.4	21.0	
1-Octene	0.150	203.4	20.6	
1-Octene	0.0301	203.4	19.6	
Tetralin	0.156	193.9	15.0	
tert-Butylbenzene	0.156	192.8	10.9	
Chlorobenzene	0.140	193.2	27.5†	

*Initial concentration of peroxide in mole/l.
†Initial rate.

in the initial peroxide concentration showed, by its lack of effect on the rate constant, that free radical induced decomposition was not a complicating factor. The peroxide was also found to be unattacked by *tert*-butoxy radicals produced by the decomposition of di-*tert*-butyl peroxalate at 45° C. Similar conditions are found to destroy *tert*-butyl hydroperoxide (6) completely.

The products were those to be expected from subsequent reactions of *tert*-butoxy and trimethylsiloxy radicals. The high temperature necessary for the decomposition and the consequent formation of tars precluded a good material balance. In 1-octene there was considerable attack on the solvent to give low molecular weight polymer.

413732

TABLE II

Products of decomposition (Mole/mole of peroxide; 0.70 g in 30 ml solvent decomposed at 183°)

	In 1-octene	In chlorobenzene
Acetone	0.28	0.32
tert-Butyl alcohol	0.19	—
Hexamethyl disiloxane	0.18	0.21
Undistillable residue	8.22*	0.300*

*Grams.

tert-Butyl trimethylsilyl peroxide is remarkably stable, temperatures of 180–200° C being necessary to give conveniently measurable rates of decomposition. This is 60–70° warmer than is required for di-*tert*-butyl peroxide and is reflected in the activation energy for the reaction of 41 kcal compared with 38 kcal for the carbon analogue (7).

The marked effect of the solvent on the stability of the peroxide is, however, very unlike that of di-*tert*-butyl peroxide, which is relatively indifferent to its environment (8). Since the reaction, which appears to be unimolecular, goes faster in more polar solvents, it might be inferred that it is not homolytic at all but shows a heterolysis similar to those observed for some acyl peroxides (9).

Decomposition in Chlorobenzene

The initial decompositions were done in chlorobenzene, a solvent generally considered inert to free radicals. The difficulties encountered were twofold. The reaction became autocatalytic after about one half life, and the extent of decomposition became increasingly unreproducible as the reaction proceeded. Thus titration after several half lives of two ampoules which had contained identical amounts of peroxide at the beginning of the reaction might show peroxide titers differing by as much as 25%.

In the expectation that adventitious materials on the glass walls of individual ampoules were responsible, several methods of cleaning the glass before use were tried. In ampoules cleaned by steam, by concentrated sulphuric acid, by alcoholic potassium hydroxide, or fitted with quartz liners, the decomposition was faster than in uncleaned pyrex. Packing the ampoules with uncleaned pyrex wool did not enhance the rate appreciably but the onset of unreproducibility was hastened.

It is well known that silicon–oxygen bonds are subject to rapid solvolysis catalyzed by acid or base. The results suggested a reaction of the peroxide with water (formed by condensation of two molecules of trimethylsilanol) catalyzed by the glass walls or by other products of reaction.

$$(CH_3)_3Si{-}O{-}O{-}t\text{-Bu} + H_2O \rightarrow (CH_3)_3SiOH + t\text{-BuOOH}$$

As *tert*-butyl hydroperoxide would be rapidly decomposed at 180° C, the hydrolysis would be rate determining.

Saturation of the chlorobenzene solution with water, prior to reaction, had no effect. Other known products of the decomposition were then tested by adding amounts substantially in excess of those produced by the decomposing peroxide (3% by volume in chlorobenzene). The effect of added *tert*-butyl alcohol was negligible, but both acetone and hexamethyl disiloxane *retarded* the decomposition. Not only was the half life increased by about 20%, but the reaction could be carried to near completion with no evidence of autocatalysis, and duplicate ampoules gave identical titers at all stages. A mixed solvent of 3% 1-octene, 97% chlorobenzene gave similar results.

Can. J. Chem. Downloaded from www.nrcresearchpress.com by 210.87.254.105 on 09/05/12
For personal use only.

TABLE III

Decomposition in mixed solvents*
(97% chlorobenzene + 3% co-solvent†)

Co-solvent	T, ° C	$k_1 \times 10^5$ sec^{-1}
None	191.2	25.7
tert-Butyl alcohol	191.1	26.5
Acetone	191.0	19.2
tert-Butyl hydroperoxide	191.5	19.6
Hexamethyl disiloxane	191.5	17.9
1-Octene	193.1	12.6

*Initial peroxide concentration = 0.14 mole/l.
†By volume.

Clearly the known products of the reaction were not responsible for the autocatalysis, but that the product mixture did contain a powerful catalyst was demonstrated by using this medium as solvent for a new decomposition. This catalyst could be removed by washing the solution with dilute $NaHCO_3$ or its effect could be eliminated by adding 1-octene to the mixture. When the solvent for decomposition was composed of the reaction product solution plus 3% 1-octene, the reaction started out very rapidly but after several minutes slowed to the rate previously observed for a pure chlorobenzene–1-octene mixture.

That the miscreant product might be HCl was suggested by results of Hammond and co-workers (10), who showed that silyl radicals could displace chlorine atoms from chlorobenzene. On treatment with aqueous $AgNO_3$ the product mixture gave a positive test for chloride ion, and titration showed the presence of a minute amount of acid.

The supposition of HCl formation allows a ready explanation of the effect of acetone and of hexamethyl disiloxane, which are much more ready sources of hydrogen atom than is chlorobenzene. Thus trimethyl siloxy radicals would react preferentially with this material suppressing the formation of HCl. 1-Octene is effective not only in this way, but also is capable of reacting with HCl previously formed.

Heterolytic Decomposition

It was suggested (*vide supra*) that the effect of HCl was to catalyze a hydrolysis at the silicon atom. However, peroxides which undergo heterolytic cleavage of the O—O bond are also subject to acid catalysis. From the rate dependence on solvent character it seems likely that there is some contribution from this sort of reaction with *tert*-butyl

$$(CH_3)_3Si—O—O—t\text{-}Bu \rightarrow (CH_3)_3Si—O^- + t\text{-}Bu—O^+$$

trimethylsilyl peroxide. It is not to be expected that t-BuO$^+$ would be formed as such, but that a concerted shift of a methyl group to oxygen would have acetone as the detectable product. That the major product from the decomposition was found to be acetone is not significant, however, since *tert*-butoxy radicals formed at this temperature would be expected to cleave to give acetone also.

While the relative amounts of heterolytic and homolytic decomposition remain in doubt, an upper limit for the rate of homolysis has been established. That this is slower in all the solvents investigated than the similar reaction of di-*tert*-butyl peroxide is significant and leads to a confirmation of the original hypothesis.

REFERENCES

1. E. Buncel and A. G. Davies. Chem. Ind. 1052 (1956).
2. W. Hahn and L. Metzinger. Makromol. Chem. **21**, 113 (1956).
3. R. L. Dannley and G. Jalics. Abstracts of papers presented at the 145th meeting of the American Chemical Society. 1963. p. 75Q.

Can. J. Chem. Downloaded from www.nrcresearchpress.com by 210.87.254.105 on 09/05/12
For personal use only.

4. C. G. SWAIN, W. H. STOCKMAYER, and J. T. CLARKE. J. Am. Chem. Soc. **72**, 5426 (1950).
5. P. D. BARTLETT and R. HIATT. J. Am. Chem. Soc. **80**, 1398 (1958).
6. Unpublished work in these laboratories.
7. F. LOSSING and A. W. TICKNER. J. Chem. Phys. **20**, 907 (1952).
8. C. WALLING. Free radicals in solution. John Wiley and Sons. New York. 1957. p. 470.
9. J. E. LEFFLER. J. Am. Chem. Soc. **72**, 67 (1950).
10. J. CURTICE, H. GILMAN, and G. S. HAMMOND. J. Am. Chem. Soc. **79**, 4754 (1957).

Can. J. Chem. Downloaded from www.nrcresearchpress.com by 210.87.254.105 on 09/05/12
For personal use only.

Can. J. Chem. Downloaded from www.nrcresearchpress.com by 210.87.254.40 on 09/05/12
For personal use only.

THE INFLUENCE OF SUBSTITUENTS ON THE EASE AND DIRECTION OF RING OPENING IN THE $LiAlH_4$–$AlCl_3$ REDUCTIVE CLEAVAGE OF SUBSTITUTED 1,3-DIOXOLANES[1]

B. E. Leggetter and R. K. Brown
Department of Chemistry, University of Alberta, Edmonton, Alberta
Received December 9, 1963

ABSTRACT

The room temperature hydrogenolysis by $LiAlH_4$–$AlCl_3$ of ether solutions of a number of 1,3-dioxolanes has been studied.

Electron donor substituents on the C_2 atom of the ring accelerate while electron acceptor substituents on C_2 retard the reductive ring cleavage. The same effect but to a lesser extent is observed when these substituents are attached to the C_4 or C_5 atom of the ring.

When electron donor substituents are attached to C_4, ring cleavage occurs predominantly at the C_2—O bond remote from the C_4 position. On the other hand, electron-withdrawing groups attached to C_4 give predominantly scission of the C_2—O bond closer to the C_4-substituted position. In contrast to this marked control over the direction of ring cleavage exhibited by substituents on C_4, those on C_2 generally have little or no effect on the direction of ring opening.

A mechanistic interpretation of the results is presented.

INTRODUCTION

The stability of acetals and ketals towards lithium aluminum hydride permits their use as a means of protecting a ketone or aldehyde moiety during hydride reduction of other functional groups in a molecule (1). However, in the presence of acidic reagents such as anhydrous aluminum chloride or boron trifluoride, lithium aluminum hydride reductively cleaves the acetal or ketal to an ether (1–5). Eliel *et al.* (6) have recently examined the $LiAlH_4$–$AlCl_3$ hydrogenolysis of a number of cyclic acetals and ketals (1,3-dioxolanes and 1,3-dioxanes) and obtained a high yield of the corresponding hydroxyethers arising from the cleavage of either the C_2—O_1 or C_2—O_3 bond according to equation (*a*).

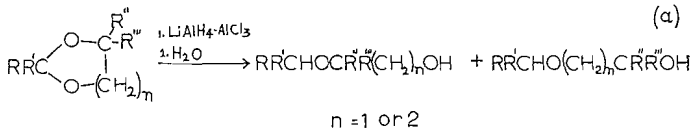

Two mechanisms for this reduction have been suggested (3). One involves hydride attack on the complex formed from the Lewis acid and the acetal, a complex which tends to form the stabilized oxocarbonium ion (equation (*b*)). The other requires prior formation of the α-haloether, which is then readily reduced (equation (*c*)).

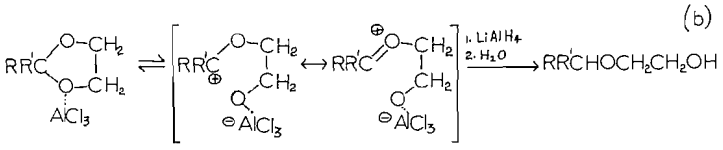

[1]*Taken from the thesis of B. E. Leggetter, submitted to the Graduate School, University of Alberta, Edmonton, Alberta, in partial fulfillment of the requirements for the degree of Doctor of Philosophy.*

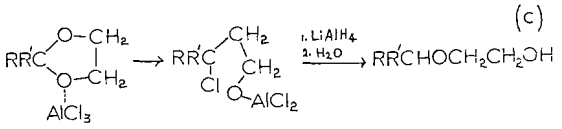

The latter mechanism was preferred for the reductive cleavage of *1,3-oxathiolanes* due to the observation that one of the oxathiolanes could be isomerized by $AlCl_3$ and also reduced by $AlCl_3$–$LiAlH_4$, whereas the same compound could be isomerized by BF_3 but could *not* be reduced by BF_3–$LiAlH_4$ (4, 7). However, since *1,3-dioxolanes* could be reduced by either $AlCl_3$–$LiAlH_4$, or BF_3–$LiAlH_4$, α-haloether formation was not considered necessary in the mechanism of hydrogenolysis of 1,3-dioxolanes (note 18, ref. (7)).

Recent work in this laboratory has shown that BF_3–$LiAlH_4$ *does* hydrogenolyze 1,3-oxathiolanes (8), hence invalidating the main supporting argument for the requirement of α-haloether formation in the reduction of oxathiolanes. The results of the work reported (8) favor the first mechanistic scheme (equation (*b*)) for Lewis acid – $LiAlH_4$ hydrogenolysis of both 1,3-dioxolanes and 1,3-oxathiolanes.

Pertinent to the mechanistic interpretation of acetal hydrogenolysis by $LiAlH_4$ and a Lewis acid is the work recently reported by Bonner and Saville (9), who have shown evidence for α-haloether formation in the reaction of boron trichloride with cyclic acetals of hexitols. But since the experimental conditions* used by Bonner and Saville differed considerably from those employed by Eliel and co-workers (6, 7) or by Leggetter and Brown (8), their results cannot be considered as proof of α-haloether formation in the aluminum chloride – lithium aluminum hydride reductions in *ether* solution.

During part of a program of study of the hydrogenolysis of acetals, interest arose concerning the effect of substituents on the ease and direction of ring opening in C_2- and C_4-substituted dioxolanes and the bearing this might have on the mechanistic interpretation of the hydrogenolysis in ether solution of cyclic acetals and ketals by lithium aluminum hydride in the presence of a Lewis acid. This paper reports some of the results obtained. Since it was discovered quite early in the course of this work that those compounds capable of cis–trans isomerism gave results which depended upon the relative proportion of cis and trans isomers in the mixture, such compounds were omitted from the present study. These will be reported upon in a later publication.

RESULTS AND DISCUSSION

Several 1,3-dioxolanes were prepared by standard methods (see Experimental). The choice of substituents on positions C_2 or C_4 of the dioxolane ring was somewhat limited by the availability of suitable starting materials, but was sufficient to provide a satisfactory range of electron-donating and electron-withdrawing groups. Compounds that were the expected products were synthesized by known routes or prepared originally and characterized.

These acetals and ketals were then dissolved in pure, dry diethyl ether containing an equimolar quantity of lithium aluminum hydride. To this stirred mixture at room temperature was then added slowly an ether solution of an equimolar amount of anhydrous aluminum chloride. The mixture was then allowed to stand, with continuous stirring, for

**Bonner and Saville used methylene chloride as solvent for both the acetals and the BCl_3. They then removed the solvent and excess BCl_3 from the reaction mixture. A solvent such as methylene chloride co-ordinates much less readily with Lewis acids than does diethyl ether, hence even normally stable 1,3-dithiolanes are isomerized by Lewis acids in methylene chloride solution (8). One would expect much more extensive reaction of the boron trichloride with acetals, particularly if the solvent methylene chloride is removed, as found by Bonner and Saville. These conditions might be expected to lead to α-haloether formation more readily than would our conditions.*

Can. J. Chem. Downloaded from www.nrcresearchpress.com by 210.87.254.40 on 09/05/12
For personal use only.

Can. J. Chem. Downloaded from www.nrcresearchpress.com by 210.87.254.40 on 09/05/12
For personal use only.

the requisite time. This was usually 90 minutes except in those cases where the reaction was slow or negligible. In such situations, reactions were allowed to continue for as long as 24 to 48 hours. Analysis by gas–liquid chromatography (g.l.c.) gave information concerning the extent and direction of reductive cleavage of the ring. Identification of products was made by comparison of the products with authentic compounds with respect to retention times, infrared analyses, n.m.r., and the usual boiling points or melting point. The total recovery of products was generally quite high. The products were found to be stable under reaction conditions. The results of these experiments are shown in Table I.

A number of general conclusions can be made from an examination of the data in Table I.

(i) The formyl acetals (experiments 1–6) are hydrogenolyzed with greater difficulty than are the C_2 alkylated or arylated isomers and homologues. For example, when 4,4-dimethyl-1,3-dioxolane (experiment 3) was reduced for a period of 24 hours, 16% of the product was unchanged starting material. On the other hand, the isomer 2,2-dimethyl-1,3-dioxolane, under the same conditions was completely hydrogenolyzed within 90 minutes (experiment 8). Again, no unreacted starting material was found when 2-phenyl-1,3-dioxolane was allowed to react for 60 minutes (experiment 12), whereas 60 hours of reaction yielded a product containing 25% of unreacted 4-phenyl-1,3-dioxolane (experiment 6). The pairs of experiments 4, 21 and 5, 20 further exemplify this point.

Generally a reaction period of 24 to 48 hours left a substantial quantity of the formyl acetal unchanged. The only exception is that of 4-methyl-1,3-dioxolane (experiment 2), which was reduced to the extent of about 90% within 90 minutes. This was checked at least four times to be certain of the results, and is the only case of a formyl acetal that in our experience was largely reduced in so short a period under our conditions.

The slow reaction of formyl acetals has also been observed by Abdun-Nur and Issidorides (5) during their reduction of acetals by a mixture of lithium aluminum hydride and boron trifluoride in ether.

(ii) A greater effect on the rate of reductive cleavage of the dioxolane ring is exerted by substituents on position C_2 than by the same substituents on any other of the ring carbon atoms. Thus 2,2-dimethyl-1,3-dioxolane (experiment 8) was completely hydrogenolyzed within 90 minutes, whereas 4,4-dimethyl-1,3-dioxolane (experiment 3) even after 24 hours of reduction yielded a product containing 16% of unreacted material. Experiments 6 and 12 as well as 4 and 9 further exemplify this observation.

(iii) Electron-donating substituents (methyl, phenyl) accelerate while electron-withdrawing groups (chloromethyl, dichloromethyl) retard or prevent reductive cleavage of acetals or ketals. This effect is much more pronounced when these substituents are on C_2 than on any other carbon atom of the ring. For example, due to the electron-withdrawing effect of the chlorine atom, 2-chloromethyl-1,3-dioxolane (experiment 9), when hydrogenolyzed for 48 hours, gave a product which was 86% unreacted material whereas the electron donor properties of the methyl group caused 2-methyl-1,3-dioxolane (experiment 7) to be completely converted to its reduction product within 60 minutes. That the same phenomenon occurs when such groups are attached to position C_4 rather than C_2 is shown by comparison of experiments 3 and 4. The two methyl groups in 4,4-dimethyl-1,3-dioxolane promote reaction sufficiently so that in 24 hours only 16% of the product is unreacted material. On the other hand, 4-chloromethyl-1,3-dioxolane is nearly three-fourths unchanged even after 48 hours of reduction. In the extreme case of 2,4-bis(chloromethyl)-1,3-dioxolane (experiment 18) practically no reduction occurred in 48 hours.

These observations (i–iii) are consistent with the view that the mechanism of reaction involves first the rapid reversible association of the Lewis acid with the acetal or ketal,

TABLE I

Hydrogenolysis of ether solutions of cyclic acetals and ketals by lithium aluminum hydride in the presence of aluminum chloride ($AlCl_3$:$LiAlH_4$:1,3-dioxolane = 1:1:1)

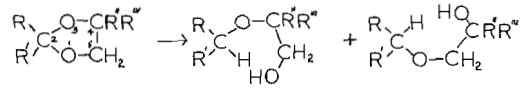

Primary alcohol Secondary or tertiary alcohol

Expt. No.	Compound	Time of reduction	Primary* alcohol, %	Secondary* or tertiary alcohol, %	Recovery† of unreacted material, %	Total‡ recovery, %
1.	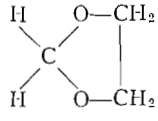	24 hr	only CH_3—O—CH_2—CH_2—OH		40	55§
2.	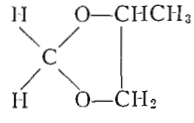	90 min	93	7	8	85
3.	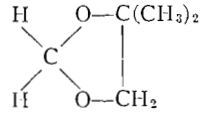	24 hr	92	8	16	67
4.	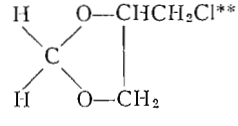	48 hr	10	90	70	93
5.	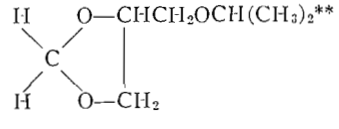	48 hr	24	76	34	93
6.	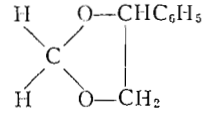	60 hr	73	27	25	83
7.	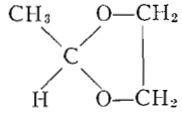	≪60 min	only CH_3—CH_2—O—CH_2—CH_2—OH		0	70
8.	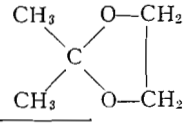	≪90 min	only $(CH_3)_2CHOCH_2CH_2OH$		0	71

Can. J. Chem. Downloaded from www.nrcresearchpress.com by 210.87.254.40 on 09/05/12
For personal use only.

TABLE I—(*Continued*)

Expt. No.	Compound	Time of reduction	Primary* alcohol, %	Secondary* or tertiary alcohol, %	Recovery† of unreacted material, %	Total‡ recovery, %
9.	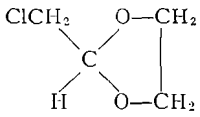	48 hr	only $ClCH_2—CH_2—O—CH_2CH_2—OH$		86	80
10.	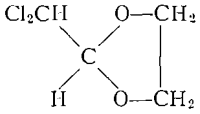	48 hr	(no reduction)		100	85
11.	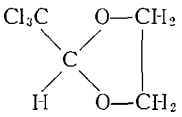	48 hr	only 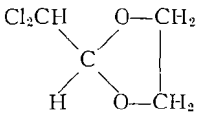		0	76
12.	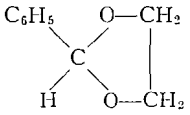	⩽60 min	only $C_6H_5—CH_2—O—CH_2—CH_2—OH$		0	80
13.	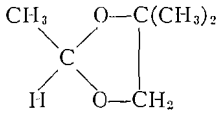	⩽90 min	90	10	0	85
14.	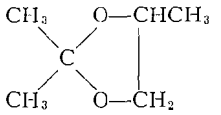	⩽90 min	82	18	0	86
15.	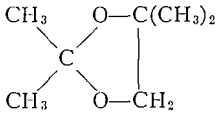	⩽90 min	6	94	0	87
16.	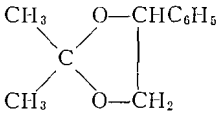	⩽90 min	52	48	0	81
17.	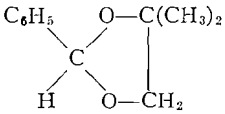	⩽90 min	90	10	3‖	81
18.	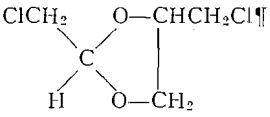	48 hr	very little reduction		~100%	

Can. J. Chem. Downloaded from www.nrcresearchpress.com by 210.87.254.40 on 09/05/12
For personal use only.

TABLE I—(*Concluded*)

Expt. No.	Compound	Time of reduction	Primary* alcohol, %	Secondary* or tertiary alcohol, %	Recovery† of unreacted material, %	Total‡ recovery, %
19.	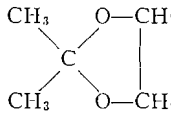	⩽90 min	19	81	0	79
20.	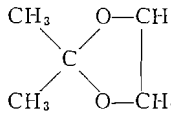	⩽90 min	14	86	0	71
21.	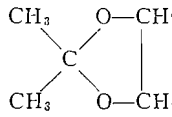	⩽90 min	5	95	0	96

*These figures represent the fraction of the isolated reduction products that is primary or secondary (tertiary) alcohol.
†This represents the fraction of the total recovered material which is unreduced or unchanged.
‡This includes both reduced and unreduced material.
§Considerable loss occurred due to the high water solubility of compounds and to the volatility of the acetal.
‖The small amount of unreduced material (3%) is surprising, since both the phenyl group on C_2 and the *gem*-dimethyl group on C_4 enhance reduction. In experiment 12, the phenyl group on C_2 caused complete and rapid reduction.
¶In 90 minutes there was no sign of reduction. In 48 hours only small amount of reduction occurred. This was not examined thoroughly since isomerization of original acetal occurred and the two acetals are known to reduce at different rates.
**In experiments 4, 5, and 20 the primary alcohol reduction product was assumed to be respectively 3-chloro-2-methoxy-1-propanol, 3-isopropoxy-2-methoxy-1-propanol, and 2,3-diisopropoxy-1-propanol as expected. Due to the unavailability of a different synthetic route for their preparation, these were not made for comparison with the respective products of reductive cleavage. However, the isomers (the secondary or tertiary alcohols) were synthesized by known routes. Because of the invariable dual reduction path of all these dioxolanes, and since only two products were obtained, one of the pair being known, the assumption of the other structure is reasonable.

followed by a slow, rate-controlling cleavage of the ring to form the stabilized oxocarbonium ion which is then rapidly and irreversibly reduced (equation (*b*)). Groups which stabilize the oxocarbonium ion enhance the ring scission and hence the rate of reduction. Substituents R and R′ on C_2, because of their proximity to the incipient carbonium ion, exert a strong stabilizing or destabilizing influence on this ion, more so than do the same substituents on the other two more distant C_4 and C_5 atoms attached to oxygen.

The similarity between the results of the reductive cleavage of acetals and ketals and the rates of acid-catalyzed hydrolysis of substituted acetals (10) is quite striking. Kreevoy and Taft (10), in a study of the influence of substituents on the rates of acid-catalyzed hydrolysis of acetals and ketals of the type $RR'C(OR'')_2$ found that the rates paralleled the inductive order of the substituents R and R′. Electron donors accelerated while electron acceptors retarded the hydrolysis. The results supported their postulated mechanistic path of hydrolysis (equations (*d*) and (*e*)) in which the slow step of oxocarbonium ion formation is rate controlling.

(d)

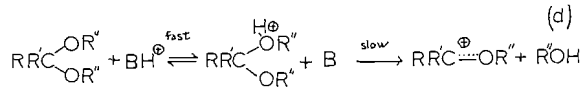

(e)

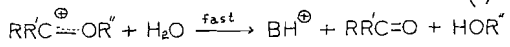

Can. J. Chem. Downloaded from www.nrcresearchpress.com by 210.87.254.40 on 09/05/12
For personal use only.

Can. J. Chem. Downloaded from www.nrcresearchpress.com by 210.87.254.40 on 09/05/12
For personal use only.

We have made no kinetic study of the reductive cleavage of acetals or ketals, but a qualitative estimation of their relative ease of hydrogenolysis has been obtained by subjecting them to a competitive reduction. A mixture of two dioxolanes was treated with a limited amount of reducing agent so as to achieve about 10 to 15% of reduction. If the extent of reduction is limited in this way so that the concentration of the dioxolanes is practically constant, and if we adopt the reasonable assumption that the dioxolane molecule participates in the rate-determining step of the reaction, and also know that the reduction step is irreversible and that under our conditions very little or none of the product is lost by further reaction, then the ratio of the rates of reduction of the two dioxolanes will be directly proportional to the ratio of the amounts of reduction product of these dioxolanes. The total recovery of material was sufficiently good and the ratios sufficiently large to give a clear indication of the relative effects of the substituents on the ease of hydrogenolysis of the acetals or ketals. The results of these experiments are shown in Table II. From an examination of the results in Table II in conjunction with those in

TABLE II

The competitive reduction of 2-substituted -1,3-dioxolanes with lithium aluminum hydride and aluminum chloride*

Expt. No.	Mixtures of dioxolanes	Relative amounts of reduction products (mole %)	Total recovery, %	k_a/k_b
1 (*a*)	2-Phenyl-1,3-dioxolane	2-Benzyloxyethanol (89)	84	8
(*b*)	2,2-Dimethyl-1,3-dioxolane	2-Isopropoxyethanol (11)		
2 (*a*)	2-Phenyl-1,3-dioxolane	2-Benzyloxyethanol (100)	84	$\gg 1$
(*b*)	2-Methyl-1,3-dioxolane	2-Ethoxyethanol (negligible)		
3 (*a*)	2,2-Dimethyl-1,3-dioxolane	2-Isopropoxyethanol†	77	>1
(*b*)	2-Methyl-1,3-dioxolane	2-Ethoxyethanol†		

*In ether solution; reaction time was about 30 minutes for each experiment. The extent of reduction was controlled by limiting the amount of reducing agent to obtain ~15% hydrogenolysis.
†Analysis of reduction products were performed by n.m.r., which indicated a large proportion of 2-isopropoxyethanol. No separation of the reduction products could be obtained by gas–liquid chromatography.

Table I, the groups can be arranged in the following order of their decreasing ability to enhance reductive cleavage of the dioxolane ring when they are attached to the C_2 position of the ring.

$$C_6H_5— > (CH_3)_2— > CH_3— > H— > ClCH_2— > Cl_2CH—$$

This order is in agreement with the stability of the correspondingly substituted carbonium ions.

(iv) A further interesting observation obtained from a study of Table I is that *electron donor or acceptor substituents attached to carbon atoms C_4 or C_5 of the dioxolane ring exert a marked control over the direction of ring cleavage.* The results of the present work show that, by and large, substituents which by electron donation assist in the stabilization of the oxocarbonium ion will favor cleavage of the C_2—O bond remote from the substituted carbon atom, thus yielding a high preponderance of the primary alcohol. Eliel, Badding, and Rerick (6) found similar preferential direction of cleavage of a number of cyclic acetals. On the other hand, electron acceptor groups favor cleavage of the C_2—O bond closest to the C_4-substituted moiety, producing largely the secondary or tertiary alcohol. This is exemplified by 4-methyl-1,3-dioxolane (expt. 2) which, because of the presence of the electron-donating methyl group at C_4, gave 93% of the reduction product as

the primary alcohol, 2-methoxy-1-propanol and only 7% of the secondary alcohol, 1-methoxy-2-propanol (equation (*f*)).

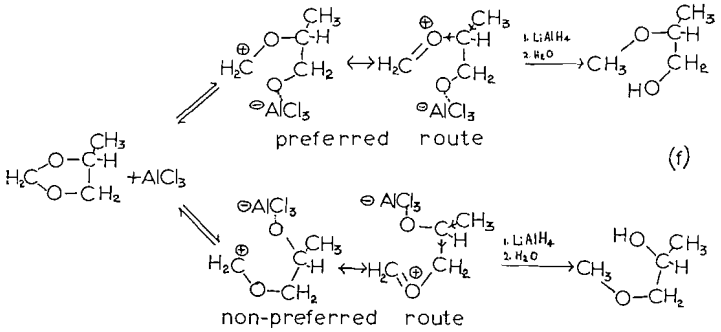

Experiments 13, 14, and 17 also clearly illustrate this point. It is interesting to note that the phenyl group does not appear to exert as much control in this manner as do the alkyl groups (cf. experiments 6 and 16).

The reverse effect due to an electron-withdrawing substituent at C_4 is illustrated by the reduction of 4-chloromethyl-1,3-dioxolane (experiment 4), which, upon reduction, gave a product which consisted of 90% of the secondary alcohol, 1-chloro-3-methoxy-2-propanol, and only 10% of the primary alcohol, 3-chloro-2-methoxy-1-propanol (equation (*g*)).

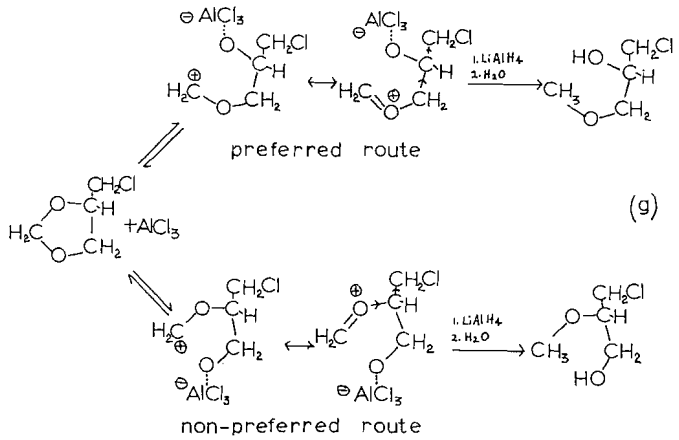

Experiments 5, 19, and 20 supply further illustrations of the effect of electron-withdrawing substituents on the direction of ring cleavage.

These observations are also consistent with the view that the formation of the oxocarbonium ion is the rate-controlling step. In equation (*f*) the preferred path of ring cleavage is that wherein the methyl substituent is closer to the incipient oxocarbonium ion and hence more effective in stabilizing the positive charge on this ion. In equation (*g*) the electron-withdrawing chloromethyl group destabilizes that oxocarbonium ion in which the chloromethyl group is closer to the site of positive charge. Hence the other ion is preferred. However, formation of both ions is retarded as compared with those containing an electron donor substituent at C_4 (equation (*f*)).

The only exception to the general statement of the observation noted in (*iv*) that electron-releasing groups show preferential cleavage of the C_2—O bond remote from the

Can. J. Chem. Downloaded from www.nrcresearchpress.com by 210.87.254.40 on 09/05/12
For personal use only.

substituted C_4 atom is that provided by the compound 2,2,4,4-tetramethyl-1,3-dioxolane (experiment 15). Instead of forming largely the primary alcohol, 2-isopropoxy-2-methyl-1-propanol as expected on the basis of the above observations, there was obtained a greater than 90% yield of the tertiary alcohol, 1-isopropoxy-2-methyl-2-propanol. A similar anomaly has been pointed out by Eliel and co-workers (6), who found that the isobutylene ketal of cyclohexanone gave exclusively the tertiary alcohol (equation (*h*)) in sharp contrast to all their other C_4-substituted dioxolanes.

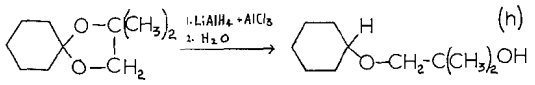

They suggested that this may be the result of either a different mechanism of hydrogenolysis or "a counterplay of polar and steric influences". A report of further investigations in our laboratory concerning this anomalous behavior will be given at a later date.

In contrast to the pronounced effect that C_4 substituents have on the direction of ring opening, those at the position C_2 have little or no effect in this regard. Apart from the peculiar ring cleavage found for 2,2,4,4-tetramethyl-1,3-dioxolane, the ineffectiveness of C_2 substituents is amply demonstrated by the examples found in Table I.

(v) The final observation of interest concerning the data in Table I is that of *the peculiar reduction experienced by 2-trichloromethyl-1,3-dioxolane* (experiment 11). The material recovered from this experiment, rather than being either the reduction product 2-β,β,β-trichloroethoxyethanol or the unchanged starting material, proved to be 2-dichloromethyl-1,3-dioxolane, which is stable to further reduction. Further work showed that the formation of the dichloro compound from the trichloro precursor could be achieved by the use of lithium aluminum hydride *alone*, although it is conceivable that aluminum chloride could in this case have been formed *in situ* during the course of the reaction.

A somewhat analogous result has recently been found by Ruske and Hartmann (11), who studied the action of strong bases such as sodium ethoxide upon the same dioxolane. These workers found that 2-trichloromethyl-1,3-dioxolane, upon treatment with an ethanolic solution of sodium ethoxide, afforded 2-dichloromethyl-2-ethoxy-1,3-dioxolane as indicated in equation (*i*). They postulated the prior elimination of hydrogen chloride from the trichloromethyl compound, followed by addition of the solvent ethanol to the intermediate 2-dichloromethylene-1,3-dioxolane. The elimination of hydrogen chloride in the first portion of the reaction was brought about by attack of base on the strongly acidic C_2 hydrogen atom, followed by departure of a chloride ion.

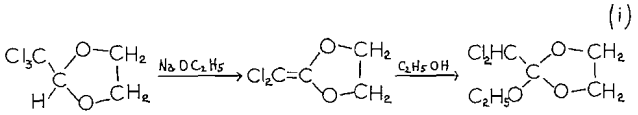

The same line of reasoning may very well hold true for the reaction found in the present instance. The basic character of lithium aluminum hydride could promote elimination of hydrogen chloride from the 2-trichloromethyl-1,3-dioxolane and the intermediate 2-dichloromethylene-1,3-dioxolane could then be reduced by the hydride. The reduction of double bonds upon treatment with lithium aluminum hydride is not without precedent. For instance, allyl alcohol has been reduced to 1-propanol (12) and ω-nitrostyrene to β-phenylethylamine (13).

Can. J. Chem. Downloaded from www.nrcresearchpress.com by 210.87.254.40 on 09/05/12
For personal use only.

The possibility of direct displacement of a chlorine ion of the trichloromethyl group by a hydride ion via an S_N2 substitution seems rather doubtful, since lithium aluminum hydride reduction of chloral hydrate yields β,β,β-trichloroethanol with the trichloromethyl group intact (14).

EXPERIMENTAL

All boiling points and melting points are uncorrected. Except where otherwise stated, g.l.c. analyses were done with a Burrell K-2 Kromo-Tog using a 2-meter column packed with 25% of carbowax 20M on Gas-Chrom P as the solid stationary phase. Helium at a flow-rate of approximately 80 ml per minute was the carrier gas. The column temperature was dependent upon the boiling point of the compounds being analyzed. All compounds were identified by comparison of their g.l.c. retention times and the infrared and n.m.r. spectra with those of authentic samples. Quantitative analyses were made by measuring the integrated areas of the peaks concerned. The areas were compared with those of peaks obtained by use of definite measured amounts of samples.

Infrared spectra were recorded on a Perkin–Elmer Model 221 instrument. Nuclear magnetic resonance spectra were obtained with a Varian Associates A-60 spectrometer.

Preparation or Source of 1,3-Dioxolanes

2-Methyl-1,3-dioxolane was prepared according to the method of Hibbert and Timm (15).

2-Phenyl-1,3-dioxolane was prepared in 57% yield by the method devised by Salmi (16), except that toluene rather than benzene was used as solvent, and a Dean–Stark water separator (17) was employed. B.p. 116° at 20 mm. Lit. b.p. 101° at 10 mm (18).

4,4-Dimethyl-2-phenyl-1,3-dioxolane was prepared from benzaldehyde and 2-methyl-1,2-propanediol in 70% yield by the above modification of the procedure described by Salmi (16). B.p. 85° at 5 mm; η_D^{25}, 1.5015. Calc. for $C_{11}H_{14}O_2$: C, 74.16; H, 7.87. Found: C, 74.26; H, 8.06.

The precursor, *2-methyl-1,2-propanediol*, was prepared as follows: a solution of ethyl α-hydroxyisobutyrate (19) (5.2 g, 0.4 mole) in 100 ml of dry ether was added dropwise to a stirred suspension of lithium aluminum hydride (15.2 g, 0.4 mole) in 500 ml of dry ether. After complete addition of the reagents, the reaction mixture was allowed to stand for 2 hours and then water was cautiously added to decompose any excess hydride and the aluminum complexes. The inorganic solid was then removed by filtration and the filtrate dried over anhydrous magnesium sulphate. Removal of the ether afforded the required product as an oil which was purified by distillation under reduced pressure. Yield, 25.2 g (70%) of material boiling at 55° at 3 mm. Lit. b.p. 79–80° at 12 mm (20).

4-Methyl-1,3-dioxolane.—A mixture of paraformaldehyde (33 g, 1.1 moles), 1,2-propanediol (76 g, 1.0 mole), anhydrous magnesium sulphate (30 g), and concentrated hydrochloric acid (2 ml) was refluxed 5 hours. The reaction mixture was then cooled and filtered free of solid. The filtrate was neutralized with Na_2CO_3, washed, and then dried over anhydrous magnesium sulphate, and finally fractionally distilled to give 55 g (65.5%) of material boiling at 82–83° at 700 mm. Lit. b.p. 88–89° at 755 mm (21).

4-Chloromethyl-1,3-dioxolane was prepared in 82% yield from paraformaldehyde and 3-chloro-1,2-propanediol (Eastman Kodak Co.) according to the preceding experimental conditions. B.p. 76° at 54 mm. Lit. b.p. 126° at 750 mm (22); cf. 146–147° at 745 mm (23).

4-Phenyl-1,3-dioxolane was prepared according to the preceding directions from paraformaldehyde and 1-phenyl-1,2-ethanediol (Eastman Kodak Co.). Yield 75%. B.p. 66° at 1.4 mm. Lit. b.p. 101° at 12 mm (22, 24).

4,4-Dimethyl-1,3-dioxolane was prepared as above in 51.5% yield starting with paraformaldehyde and 2-methyl-1,2-propanediol (see above) but using a reaction time of 20 minutes rather than 5 hours. B.p. 100–102° at 700 mm; η_D^{25}, 1.4004. Calc. for $C_5H_{10}O_2$: C, 58.82; H, 9.80. Found: C, 58.46; H, 10.06.

1,3-Dioxolane was prepared by a modification of the method advocated by Vogel (25). A mixture of 1,2-ethanediol (32 g, 0.5 mole), paraformaldehyde (20 g, 0.67 mole), anhydrous magnesium sulphate (20 g), and 2 ml of concentrated hydrochloric acid was heated at such a rate that the product was taken off through a 4-inch Vigreux column as it was formed. The product was collected, dried over anhydrous sodium carbonate, filtered, and then fractionally distilled giving the required material boiling at 71–73° at 700 mm. Lit. b.p. 75° at 760 mm (26).

2,2-Dimethyl-4-hydroxymethyl-1,3-dioxolane was prepared according to the directions given by Fischer and Pfahler (27). Yield, 80%. B.p. 95° at 24 mm. Lit. b.p. 82.5° at 11 mm (27).

2,2-Dimethyl-4-phenyl-1,3-dioxolane was synthesized in 79% yield by the method of Fischer and Pfahler (27) starting with acetone and 1-phenyl-1,2-ethanediol (Eastman Kodak Co.). B.p. 73° at 2 mm. Lit. b.p. 95–96° at 10 mm (28).

2,2,4-Trimethyl-1,3-dioxolane was prepared by the method of Fischer and Pfahler (27) starting with acetone and 1,2-propanediol (Eastman Kodak Co.). Yield, 33%. B.p. 99° at 700 mm. Lit. b.p. 98–99° at 760 mm (29).

4-Chloromethyl-2,2-dimethyl-1,3-dioxolane was prepared in 78% yield by the procedure of Fischer and

Can. J. Chem. Downloaded from www.nrcresearchpress.com by 210.87.254.40 on 09/05/12
For personal use only.

Can. J. Chem. Downloaded from www.nrcresearchpress.com by 210.87.254.40 on 09/05/12
For personal use only.

Pfahler (27) starting with 3-chloro-1,2-propanediol (Eastman Kodak Co.) and acetone. B.p. 78° at 40 mm. Lit. b.p. 45–50° at 10 mm (30); cf. 157° at 767 mm (27).

2,2-Dimethyl-1,3-dioxolane was prepared in 24% yield from acetone and 1,2-ethanediol using the procedure of Fischer and Pfahler (27). B.p. 89° at 700 mm. Lit. b.p. 92.5° at 760 mm (29).

2,4,4-Trimethyl-1,3-dioxolane was prepared by a modification of the method of Fischer and Pfahler (27). A mixture of paraldehyde (10 ml) and 2-methyl-1,2-propanediol (Eastman Kodak Co.) (8 g), 0.2 g of para-toluene-sulphonic acid, and 8 g of dry magnesium sulphate was kept in a refrigerator overnight, then filtered, and treated according to the procedure cited (27). Yield, 7.4 g (72%). B.p. 97–99° at 720 mm. Lit. b.p. 100.1° at 762 mm (31).

2,2,4,4-Tetramethyl-1,3-dioxolane.—This ketal was prepared by the acetal or ketal exchange reaction using a modification of the procedure described by McElvain and Curry (32).

The precursor, *2,2-dimethoxypropane*, was prepared in 41% yield by the method of Croxall *et al.* (33) starting with isopropyl acetate and methanol. B.p. 79–80° at 700 mm. Lit. b.p. 83° at 760 mm (34).

A mixture of 2,2-dimethoxypropane (7 g, 0.067 mole), 2-methyl-1,2-propanediol (see above) (6 g, 0.067 mole), and 0.05 g of *p*-toluenesulphonic acid was heated in a flask, equipped with a 4-inch Vigreux column, at such a rate that the methanol formed during the reaction slowly distilled over. When the theoretical amount of methanol had been removed, the residual oil was fractionally distilled to give 5.8 g (67%) of material boiling at 106° at 700 mm. Lit. b.p. 109–110° (35).

4-Isopropoxymethyl-1,3-dioxolane was prepared in 42% yield by the acetal exchange method described above, starting with 1-isopropoxy-2,3-propanediol and 1,1-diethoxymethane (Eastman Kodak Co.). B.p. 70° at 20 mm; n_D^{25}, 1.4201. Calc. for $C_7H_{14}O_3$: C, 57.53; H, 9.59. Found: C, 57.30; H, 9.49.

The precursor, *1-isopropoxy-2,3-propanediol*, was synthesized by acid-catalyzed hydrolysis of the corresponding epoxide by a modification of the method advocated by Lucas *et al.* (36). 1,2-Epoxy-3-isopropoxypropane (see above) (25 g, 0.22 mole) was added to a stirred mixture of water (40 ml) and concentrated sulphuric acid (2 ml) at 60°. During the addition, the temperature of the reaction mixture rose to 95° and was kept at this figure for 30 minutes following complete addition of the reagent. Solid sodium carbonate was then added to the cooled solution to neutralize the acid completely, and then the product was extracted with ether. When the ether extract was dried (Na_2CO_3) and the ether removed, an oil was obtained which was distilled under reduced pressure yielding 21.5 g (74%) of material boiling at 94° at 3.5 mm. Lit. b.p. 187–190° (37).

2,2-Dimethyl-4-isopropoxymethyl-1,3-dioxolane was made in 51% yield from 2,2-dimethoxypropane (Eastman Kodak Co. (33)) and 1-isopropoxy-2,3-propanediol (see above). B.p. 68° at 16 mm. Lit. b.p. 56–57° at 10 mm (28). The experimental procedure of McElvain and Curry (32), as modified for the preparation of 2,2,4,4-tetramethyl-1,3-dioxolane, was used for this preparation.

2-Chloromethyl-1,3-dioxolane was prepared in 63% yield from 1-chloro-2,2-dimethoxyethane (Eastman Kodak Co.) and 1,2-ethanediol using the above modification of McElvain and Curry's directions (32). B.p. 154–155° at 700 mm. Lit. b.p. 155–159° at 740 mm (32).

2-Dichloromethyl-1,3-dioxolane was prepared from 1,2-ethanediol and 1,1-dichloro-2,2-diethoxyethane using the above modification of McElvain and Curry's directions (32). B.p. 185° at 700 mm. Lit. b.p. 185–188° (38).

The precursor, *1,1-dichloro-2,2-diethoxyethane*, was made by a modification of the procedure described by Fritsch (39). Chlorine gas was bubbled through ethanol (100 ml) at 25° for 6 hours, after which time the lower layer of the reaction mixture was separated and mixed with 100 ml of ethanol. The resulting solution was treated with sodium carbonate (solid) and then poured into aqueous sodium carbonate solution. The oil that precipitated was taken up in ether and the ether extract then dried over anhydrous sodium carbonate. Removal of the ether afforded an oil which was fractionally distilled under reduced pressure to give 15 g of material boiling at 74–75° at 20 mm. Lit. b.p. 66–71° at 12 mm (40); cf. 178–185° (39).

2-Trichloromethyl-1,3-dioxolane was prepared as described by McElvain and Curry (32).

2,4-Bischloromethyl-1,3-dioxolane was prepared by the modification of McElvain and Curry's acetal exchange method (32), as described above for the preparation of 2,2,4,4-tetramethyl-1,3-dioxolane. From 45 g of chloroacetaldehyde diethylacetal (Eastman Kodak Co.) and 33 g of 3-chloro-1,2-propanediol (Eastman Kodak Co.) there was obtained 46 g (90%) of material boiling at 66° at 2 mm; 58–59° at 1.5 mm. Calc. for $C_5H_8Cl_2O_2$: C, 35.11; H, 4.72; Cl, 41.5. Found: C, 34.88; H, 4.29; Cl, 41.17; n_D^{24}, 1.4761.

Preparation or Source of Reduction Products

2-Ethoxyethanol and *ethylene glycol monomethyl ether* were obtained from Eastman Kodak Co.

2-Benzyloxyethanol was prepared by the procedure of Bennett and Hock (41) with the following modification. After the addition of the benzyl chloride, the mixture was heated at 120° for 2 hours, then cooled, and poured into water. The dried ether extract was then distilled. From benzyl chloride and 1,2-ethanediol there was obtained a 35% yield of the product boiling at 116° at 6 mm. Lit. b.p. 138° at 15 mm (42).

The following compounds were made by a modified version of the method described by Chitwood and Freure (43). After the epoxide had been added to the sodium alkoxide as directed by these authors, the solution was allowed to stand at 25° for 16 hours, then poured into cold water. The organic layer was separated, dried ($MgSO_4$), and distilled.

1-Methoxy-2-propanol.—B.p. 115–116° at 700 mm. Lit. b.p. 118–119° at 765 mm (44).

1-Isopropoxy-2-propanol.—B.p. 68° at 40 mm. Lit. b.p. 137–138° (45).

1-Chloro-3-isopropoxy-2-propanol.—This compound was prepared by a modification of the procedure described by Koelsch for the synthesis of derivatives of 2-propanol (46). 1-Chloro-2,3-epoxypropane (1 mole) (Matheson, Coleman, and Bell, Inc.) was added dropwise to 2-propanol (10 moles) to which three drops of concentrated sulphuric acid had been added. The temperature of the reaction mixture was maintained at 30° during the addition. The mixture stood for 3 hours and was then poured into saturated aqueous sodium carbonate solution. The organic layer was separated, dried (Na_2CO_3), and fractionally distilled. B.p. 80° at 6 mm. Lit. b.p. 87–87.5° at 20 mm (47).

The following compounds were prepared by this modified procedure of Koelsch:

1-Chloro-3-methoxy-2-propanol from 1-chloro-2,3-epoxypropane and methanol. B.p. 77° at 8 mm. Lit. b.p. 95° at 20 mm (46).

1-Isopropoxy-3-methoxy-2-propanol from methanol and 1,2-epoxy-3-isopropoxypropane (Eastman Kodak Co.). Yield, 65%. B.p. 97° at 30 mm. Lit. b.p. 202–203° (48).

1,3-Diisopropoxy-2-propanol from 2-propanol and 1,2-epoxy-3-isopropoxypropane. Yield, 46%. B.p. 101° at 20 mm. Lit. b.p. 74–75° at 2 mm (49).

2-Methoxy-1-propanol was prepared by the reduction of methyl α-methoxypropionate with lithium aluminum hydride according to standard procedure (14). B.p. 125° at 700 mm. Lit. b.p. 130° at 758 mm (44).

The *methyl α-chloropropionate* required to prepare methyl α-methoxypropionate (50) was made by heating under reflux for 3 hours 108.5 g (1 mole) of α-chloropropionic acid (Eastman Kodak Co.) with methanol (400 ml) containing 20 ml of concentrated sulphuric acid. The reaction mixture was cooled and poured into aqueous sodium carbonate and the organic layer removed. The organic layer was washed with sodium carbonate solution, dried (Na_2CO_3), and distilled to give 41 g (33%) of the ester boiling at 127–129° at 700 mm. Lit. b.p. 127–130° (50).

2-Isopropoxy-1,3-propanediol was made by lithium aluminum hydride reduction (14) of the mixed diester of isopropoxymalonic acid. B.p. 93° at 2 mm; η_D^{25}, 1.4430. Calc. for $C_6H_{14}O_3$: C, 53.73; H, 10.45. Found: C, 53.28; H, 10.11.

The mixed diester of isopropoxymalonic acid was prepared as follows: Isopropyl chloroacetate was made in 60% yield from 2-propanol and α-chloroacetic acid using the same procedure described above for the preparation of methyl α-chloropropionate. B.p. 68° at 23 mm. Lit. b.p. 150° (51).

The method of Nieman *et al.* (50) was used to prepare *isopropyl isopropoxyacetate* starting with sodium isopropoxide and isopropyl chloroacetate in 2-propanol. B.p. 65° at 8 mm. Calc. for $C_8H_{16}O_3$: C, 60.00; H, 10.11. Found: C, 60.13; H, 10.25. The isopropyl isopropoxyacetate (55 g, 0.34 mole) was treated with diethyl carbonate in the presence of sodium methoxide, according to the directions of Ames and Bowman (52), to form 30 g of the mixed diester of isopropoxymalonic acid boiling at 89° at 1.5 mm. Confirmation that this was indeed the diester of isopropoxymalonic acid was obtained by shaking a small portion of the diester with concentrated ammonium hydroxide. The diamide separated as a colorless solid. After crystallization from aqueous acetone it melted at 220–221°. Calc. for $C_6N_{12}N_2O_3$: C, 45.00; H, 7.50; N, 17.50. Found: C, 44.86; H, 7.42; N, 17.37.

2-Isopropoxy-1-propanol was prepared by the lithium aluminum hydride reduction (14) of isopropyl α-isopropoxypropionate. B.p. 141–142° at 700 mm. Lit. b.p. 143–144° (43).

The precursor, *isopropyl α-chloropropionate,* was made by the acid-catalyzed esterification of α-chloropropionic acid with 2-propanol using the procedure described for the preparation of methyl α-chloropropionate. Yield, 87%. B.p. 91° at 85 mm; η_D^{25}, 1.4127. Calc. for $C_6H_{11}ClO_2$: C, 47.85; H, 7.36; Cl, 23.57. Found: C, 47.65; H, 7.13; Cl, 23.64.

Using the procedure of Nieman *et al.* (50) *isopropyl α-isopropoxypropionate* was prepared from sodium isopropoxide and isopropyl α-chloropropionate in 2-propanol. B.p. 78° at 23 mm. Calc. for $C_9H_{18}O_3$: C, 62.07; H, 10.34. Found: C, 61.93; H, 10.15.

2-Methoxy-2-methyl-1-propanol was prepared in 82% yield by the reduction of α-methoxy isobutyric acid with lithium aluminum hydride (14). B.p. 137° at 700 mm. Lit. b.p. 141° (53).

The precursor *α-methoxyisobutyric acid* was prepared according to published directions (54) from 2-methyl-1,1,1-trichloro-2-propanol (Eastman Kodak Co.). Yield, 60%. B.p. 84–85° at 7 mm. Lit. b.p. 98–99° at 20 mm (54).

2-Ethoxy-2-methyl-1-propanol was prepared in 56% yield by standard lithium aluminum hydride reduction (14) of α-ethoxyisobutyric acid. B.p. 140° at 700 mm. Lit. b.p. 146–148° (53).

The precursor, *α-ethoxyisobutyric acid,* was prepared by the procedure of Weizmann *et al.* (54) in 36% yield from ethanol and 2-methyl-1,1,1-trichloro-2-propanol. B.p. 85–86° at 7 mm. Lit. b.p. 97° at 19 mm (54).

2-Isopropoxy-2-methyl-1-propanol was prepared in 53% yield by lithium aluminum hydride reduction (14) of α-isopropoxyisobutyric acid (54). B.p. 147–149° at 700 mm. Lit. b.p. 42–46° at 10 mm (55).

2-Benzyloxy-2-methyl-1-propanol was prepared in 78% yield by lithium aluminum hydride reduction (14) of α-benzyloxyisobutyric acid. B.p. 102° at 3.5 mm; η_D^{25}, 1.5088. Calc. for $C_{11}H_{16}O_2$: C, 73.33; H, 8.89. Found: C, 73.58; H, 8.90.

The *α-benzyloxyisobutyric acid* was prepared in 34% yield from benzyl alcohol and 2-methyl-1,1,1-trichloro-2-propanol by the method of Weizmann *et al.* (54) but with the modification that the reaction mixture

Can. J. Chem. Downloaded from www.nrcresearchpress.com by 210.87.254.40 on 09/05/12
For personal use only.

was heated at 100° for 2 hours rather than refluxed for the same length of time. B.p. 139° at 3 mm; η_D^{25}, 1.5048. Calc. for $C_{11}H_{14}O_3$: C, 68.04; H, 7.22. Found: C, 68.36; H, 7.02.

1-Methoxy-2-methyl-2-propanol was prepared by the method mentioned by Palomaa (56). Since no details were given by Palomaa, the procedure employed is described.

Ethyl methoxyacetate was prepared in 59% yield by the acid-catalyzed esterification of methoxyacetic acid (Eastman Kodak Co.) with ethanol. The procedure was the same as that described above for the preparation of methyl α-chloropropionate. B.p. 138–139° at 700 mm. Lit. b.p. 144° at 748 mm (57).

Ethyl methoxyacetate (19.7 g, 0.167 mole) was slowly added to an ethereal solution of methyl magnesium iodide prepared from methyl iodide (52.0 g, 0.37 mole) and magnesium (8.9 g, 0.37 mole) in 200 ml of ether. After the addition of the ester was completed, the reaction mixture was stirred for 3 hours, and then crushed ice was added to decompose the complex. After inorganic salts were removed by filtration, the ethereal solution was dried ($MgSO_4$). Removal of the ether gave an oil which was distilled, yielding 3.7 g (21%) of 1-methoxy-2-methyl-2-propanol. B.p. 112–115° at 700 mm. Lit. b.p. 116.6° (56).

1-Ethoxy-2-methyl-2-propanol was prepared by the method described above to synthesize 1-methoxy-2-methyl-2-propanol. From ethyl ethoxyacetate and methyl iodide there was obtained a 40% yield of the desired alcohol. B.p. 125° at 700 mm. Lit. b.p. 129–130° (53).

Ethyl ethoxyacetate was prepared in 62% yield from ethoxyacetic acid (Eastman Kodak Co.) and ethanol by the method described above for the preparation of methyl α-chloropropionate. B.p. 152–153°. Lit. b.p. 154° (58).

1-Isopropoxy-2-methyl-2-propanol was made in 37% yield from isopropyl isopropoxyacetate (see above) and methyl iodide by the procedure given for the preparation of 1-methoxy-2-methyl-2-propanol. B.p. 75° at 70 mm; η_D^{25}, 1.4055. Calc. for $C_7H_{16}O_2$: C, 63.64; H, 12.12. Found: C, 63.57; H, 12.14.

1-Benzyloxy-2-methyl-2-propanol was made in 46% yield from ethyl benzyloxyacetate and methyl iodide by the method described above for the synthesis of 1-methoxy-2-methyl-2-propanol. B.p. 106° at 6 mm; η_D^{25}, 1.4997. Calc. for $C_{11}H_{16}O_2$: C, 73.33; H, 8.89. Found: C, 73.70; H, 9.12.

Ethyl benzyloxyacetate was prepared in 23% yield from ethyl chloroacetate and sodium benzyloxide in benzyl alcohol by the procedure of Nieman *et al.* (50). B.p. 118–120° at 3 mm. Lit. b.p. 100–102° at 1 mm (59).

2-Methoxy-2-phenylethanol was made by acid-catalyzed methanolysis of 1,2-epoxyethylbenzene (Eastman Kodak Co.), as described by Reeve and Christoffel (60).

2-Isopropoxy-2-phenylethanol was prepared in 54% yield from 1,2-epoxyethylbenzene and 2-propanol using acid catalysis (60). B.p. 94° at 3 mm; η_D^{25}, 1.4982. Calc. for $C_{11}H_{16}O_2$: C, 73.33; H, 8.89. Found: C, 73.51; H, 8.72.

2-Methoxy-1-phenylethanol.—This was prepared by the base-catalyzed reaction between methanol and 1,2-epoxyethylbenzene, as described by Reeve and Christoffel (60). There was obtained 24 g (76%) of material boiling at 108–110° at 6 mm. Lit. b.p. 137–138° at 30 mm (60). This substance was found by g.l.c. to contain a small amount of the isomeric 2-methoxy-2-phenylethanol. This impurity was removed by solution of the product in skellysolve and addition of sodium metal (1.2 g). The precipitated sodium derivative was removed by passing the solution through a column of alumina using skellysolve as eluant. Removal of the solvent from the eluant afforded 2-methoxy-1-phenylethanol which g.l.c. showed to be >99% pure.

2-Isopropoxy-1-phenylethanol was made according to the method of Reeve and Christoffel (60) from 1,2-epoxyethylbenzene and sodium isopropoxide in 2-propanol. Yield, 24%. B.p. 93° at 3 mm; η_D^{25}, 1.4995. Calc. for $C_{11}H_{16}O_2$: C, 73.33; H, 8.89. Found: C, 73.14; H, 8.76.

2-β-Chloroethoxyethanol was prepared by the acid-catalyzed alcoholysis of 1,2-epoxyethane by β-chloroethanol using a modification of the method of epoxide solvolysis described by Lucas *et al.* (61).

1,2-Epoxyethane (8.89 g, 0.2 mole) was slowly added to β-chloroethanol (16 g, 0.2 mole) containing 1 ml of concentrated sulphuric acid. The resulting mixture was allowed to stand at 25° for 48 hours, then poured into a saturated aqueous solution of sodium carbonate. The product was extracted with ether, the ether extract dried (Na_2CO_3), and then freed of solvent. The residual oil upon fractional distillation at reduced pressure gave 2.8 g (11%) of 2-β-chloroethoxyethanol boiling at 70° at 3 mm. Lit. b.p. 180–185° (62).

1-Isopropoxy-2,3-propanediol.—This compound was prepared in 74% yield by the acid-catalyzed hydrolysis of 1,2-epoxy-3-isopropoxypropane (Eastman Kodak Co.) by a modification of the method described by Lucas *et al.* (61).

1,2-Epoxy-3-isopropoxypropane (25 g, 0.22 mole) was added to a stirred mixture of water (40 ml) and concentrated sulphuric acid (2 ml) at 60°. During the addition the temperature of the mixture rose to 95° where it was maintained for 30 minutes after complete addition of reagents. It was then cooled and solid sodium carbonate added to neutralize the acid. The ether extract was dried over anhydrous sodium carbonate. Removal of the ether and distillation of the oil under reduced pressure gave 21.4 g (74%) of material boiling at 94° at 3.5 mm. Lit. b.p. 187–190° (37).

3-Chloro-2-isopropoxy-1-propanol was not made by an independent route but was prepared and characterized as one of the products of the reduction of 4-chloromethyl-2,2-dimethyl-1,3-dioxolane by lithium aluminum hydride in the presence of aluminum chloride. For the details of the procedure see below.

Can. J. Chem. Downloaded from www.nrcresearchpress.com by 210.87.254.40 on 09/05/12
For personal use only.

General Procedure for the Reduction of 1,3-Dioxolanes by Lithium Aluminum Hydride and Aluminum Chloride

A standard reduction procedure was employed throughout the course of this work. This is exemplified by the following description of the reduction of 2,2-dimethyl-4-phenyl-1,3-dioxolane. Anhydrous conditions were observed and maintained where necessary.

A quantity (18.0 g, 0.1 mole) of 2,2-dimethyl-4-phenyl-1,3-dioxolane was added to a stirred suspension of lithium aluminum hydride (3.9 g, 0.1 mole) in 300 ml of diethyl ether. The resulting suspension was stirred whilst a solution of aluminum chloride (13.35 g, 0.1 mole) was added in a dropwise manner. The reaction mixture was stirred for 1 hour after complete addition of the Lewis acid, which usually took about 10 minutes. Cold water was then added cautiously to decompose the aluminum complexes as well as the excess hydride. The inorganic material was removed by filtration and washed with ether. The combined ethereal filtrate and extract was dried ($MgSO_4$) and then freed from the bulk of the ether. The residual oil when analyzed by gas–liquid chromatography was found to be a mixture of 2-isopropoxy-2-phenylethanol (52%) and 2-isopropoxy-1-phenylethanol (48%), each identified by comparison with authentic samples of these compounds. The total product of the reduction distilled over the range 90–92° at 3 mm, yielding 14.7 g (81%) of material.

In many cases the mixture was actually separated by fractional distillation into unreacted dioxolane and the two isomeric hydroxyethers.

The Reduction of 4-Chloromethyl-2,2-dimethyl-1,3-dioxolane with Lithium Aluminum Hydride and Aluminum Chloride and the Resulting Preparation of 3-Chloro-2-isopropoxy-1-propanol

In this case the products of the reduction were separated and characterized due to the fact that one of the reduction products, 3-chloro-2-isopropoxy-1-propanol, was unavailable.

A quantity (40 g, 0.27 mole) of 4-chloromethyl-2,2-dimethyl-1,3-dioxolane was reduced according to the general procedure described above and afforded 36.0 g (86%) of crude reduction product after removal of the ether. G.l.c. analysis of this product showed it to be a mixture of two substances, 1-chloro-3-isopropoxy-2-propanol (95%) and 5% of a second material assumed to be the other possible reduction product, 3-chloro-2-isopropoxy-1-propanol.

These two products were separated by careful fractional distillation with a 12-inch column packed with glass helices. The first fraction (32.0 g) boiled at 114° at 72 mm and was shown to be 1-chloro-3-isopropoxy-2-propanol by comparison of its g.l.c. retention time as well as its n.m.r. and I.R. spectra with those of an authentic sample. The residue (4.0 g) from the fractionation was purified by passing it through a g.l.c. preparative column and collecting the effluent and then finally by distillation under reduced pressure. There was obtained 1.5 g of material boiling at 108° at 35 mm. The n.m.r. spectrum in carbon tetrachloride, with tetramethylsilane as reference, agreed with the structure designated as 3-chloro-2-isopropoxy-1-propanol. n_D^{25}, 1.4430. Calc. for $C_6H_{13}ClO_2$: C, 47.22; H, 8.52; Cl, 23.28. Found: C, 46.87; H, 8.39; Cl, 23.21.

In view of the invariable twofold direction of reduction of dioxolanes found for all previous cases, agreeing with the predicted products, and because of the above evidence, we are convinced that the compound dealt with is actually that designated. Final confirmation of course will have to await the unambiguous synthesis by another route.

Competitive Reduction of 2-Substituted 1,3-Dioxolanes

Equimolar quantities (0.025 mole) of two dioxolanes were dissolved in ether (300 ml) containing 0.05 mole of lithium aluminum hydride. To this stirred solution was added an ether solution of aluminum chloride (0.005 mole) over a period of 3 minutes and the mixture then stirred for 30 minutes. The extent of reduction could be controlled by the amount of Lewis acid added, since no further reduction occurred after the limited amount of aluminum chloride had been added even though there was originally sufficient lithium aluminum hydride to reduce most, if not all, of the dioxolane. Water was then cautiously added and the solution worked up and analyzed by g.l.c. as described in the general procedure.

ACKNOWLEDGMENTS

The authors wish to express their appreciation to the National Research Council of Canada whose financial support made this work possible.

REFERENCES

1. N. G. GAYLORD. Reduction with complex metal hydrides. Interscience Publishers Inc., New York, N.Y. 1956. pp. 673–680.
2. H. M. DOUKAS and T. D. FONTAINE. J. Am. Chem. Soc. **73**, 5917 (1951).
3. E. L. ELIEL and M. N. RERICK. J. Org. Chem. **23**, 1088 (1958).
4. E. L. ELIEL. Record Chem. Progr. Kresge-Hooker Sci. Lib. **23**, 129 (1961).
5. A. R. ABDUN-NUR and C. H. ISSIDORIDES. J. Org. Chem. **27**, 67 (1962).
6. E. L. ELIEL, V. G. BADDING, and M. N. RERICK. J. Am. Chem. Soc. **84**, 2371 (1962).
7. E. L. ELIEL, L. A. PILATO, and V. G. BADDING. J. Am. Chem. Soc. **84**, 2377 (1962).

Can. J. Chem. Downloaded from www.nrcresearchpress.com by 210.87.254.40 on 09/05/12
For personal use only.

8. B. E. LEGGETTER and R. K. BROWN. Can. J. Chem. **41**, 2671 (1963).
9. T. G. BONNER and N. M. SAVILLE. J. Chem. Soc. 2851 (1960).
10. M. M. KREEVOY and R. W. TAFT, JR. J. Am. Chem. Soc. **77**, 5590 (1955).
11. W. RUSKE and I. HARTMANN. J. Prakt. Chem. **18**, 150 (1962).
12. F. A. HOCHSTEIN and W. G. BROWN. J. Am. Chem. Soc. **70**, 3484 (1948).
13. R. F. NYSTROM and W. G. BROWN. J. Am. Chem. Soc. **70**, 3738 (1948).
14. ORGANIC REACTIONS. Vol. VI. J. Wiley and Sons Inc., New York. 1951.
15. H. HIBBERT and J. A. TIMM. J. Am. Chem. Soc. **46**, 1283 (1924).
16. E. J. SALMI. Ber. **71**, 1803 (1938).
17. E. W. DEAN and D. D. STARK. Ind. Eng. Chem. **12**, 486 (1920).
18. M. SULZBACHER, E. BERGMANN, and E. PARISER. J. Am. Chem. Soc. **70**, 2827 (1948).
19. H. HEPWORTH. J. Chem. Soc. 1207 (1919).
20. H. ADKINS and H. R. BILLICA. J. Am. Chem. Soc. **70**, 3118 (1948).
21. H. T. CLARKE. J. Chem. Soc. 1804 (1912).
22. A. VERLEY. Bull. Soc. Chim. France, (3) **21**, 229 (1899).
23. F. F. BLICKE and F. E. ANDERSON. J. Am. Chem. Soc. **74**, 1733 (1952).
24. G. B. TAL'KOVSKII. J. Gen. Chem. USSR, **18**, 68 (1948); Chem. Abstr. **42**, 4973.
25. A. I. VOGEL. J. Chem. Soc. 616 (1948).
26. R. R. LEGAULT and D. C. LEWIS. J. Am. Chem. Soc. **64**, 1354 (1942).
27. E. FISCHER and E. PFAHLER. Ber. **53**, 1606 (1920).
28. F. G. PONOMAREV. Dokl. Akad. Nauk SSSR, **108**, 648 (1956).
29. J. BOESEKEN and P. H. HERMANS. Rec. Trav. Chim. **42**, 1104 (1923).
30. F. G. PONOMAREV, L. G. ESIPOVA, O. G. LAMTEVA, M. F. MIZILINA, and B. SH. FARBEROVA. Tr. Voronezhsk. Gos. Univ. **49**, 9 (1958); Chem. Abstr. **56**, 2435.
31. M. G. VORONKOV and E. S. TITLINOVA. Zh. Obshch. Khim. **24**, 613 (1954).
32. S. M. MCELVAIN and M. J. CURRY. J. Am. Chem. Soc. **70**, 3781 (1948).
33. W. J. CROXALL, F. J. GLAVIS, and H. T. NEHER. J. Am. Chem. Soc. **70**, 2805 (1948).
34. L. CLAISEN. Ber. **31**, 1010 (1898).
35. A. A. PETROV. J. Gen. Chem. USSR, **10**, 981 (1940).
36. H. J. LUCAS, M. T. SCHLATTER, and R. C. JONES. J. Am. Chem. Soc. **63**, 25 (1941).
37. M. S. MALINOVSKI and V. M. VVEDENSKII. Zh. Obshch. Khim. **23**, 219 (1953).
38. M. J. ASTLE, J. A. ZASLOWSKY, and P. G. LAFYATIS. Ind. Eng. Chem. **46**, 787 (1954).
39. P. FRITSCH. Ann. **279**, 300 (1894).
40. A. MAGNANI and S. M. MCELVAIN. J. Am. Chem. Soc. **60**, 2210 (1938).
41. G. M. BENNETT and A. L. HOCK. J. Chem. Soc. 472 (1927).
42. G. M. BENNETT. J. Chem. Soc. 1277 (1925).
43. H. C. CHITWOOD and B. T. FREURE. J. Am. Chem. Soc. **68**, 680 (1946).
44. W. REEVE and A. SADLE. J. Am. Chem. Soc. **72**, 1251 (1950).
45. V. S. ABRAMOV and E. N. NIKOLAEVA. Zh. Obshch. Khim. **20**, 100 (1950).
46. C. F. KOELSCH. J. Am. Chem. Soc. **65**, 2460 (1943).
47. H. FLORES-GALLARDO and C. D. POLLARD. J. Org. Chem. **12**, 831 (1947).
48. M. S. MALINOVSKI and V. M. VVEDENSKII. Ukr. Khim. Zh. **23**, 626 (1957).
49. H. R. HENZE and B. G. ROGERS. J. Am. Chem. Soc. **61**, 433 (1939).
50. C. NIEMAN, A. A. BENSON, and J. F. MEAD. J. Org. Chem. **8**, 397 (1943).
51. T. B. DORRIS, F. J. SOWA, and J. A. NIEUWLAND. J. Am. Chem. Soc. **56**, 2689 (1934).
52. D. E. AMES and R. E. BOWMAN. J. Chem. Soc. 1082 (1951).
53. A. A. PETROV and E. N. PRITULA. J. Appl. Chem. USSR, **28**, 527 (1955).
54. CH. WEIZMANN, M. SULZBACHER, and E. BERGMANN. J. Am. Chem. Soc. **70**, 1153 (1948).
55. K. E. MARPLE, E. C. SHOKAL, and T. W. EVANS. U.S. Patent No. 2,380,185; Chem. Abstr. **39**, 4625 (1945).
56. M. H. PALOMAA. Chem. Zentr. **I**, 1144 (1918).
57. M. H. PALOMAA. Ber. **42**, 1300 (1909).
58. R. C. FUSON and B. H. WOJCIK. Organic syntheses. Coll. Vol. II. John Wiley and Sons Inc., New York. 1943. p. 261.
59. K. M. HAMMOND, N. FISHER, E. N. MORGAN, and E. M. TANNER. J. Chem. Soc. 1062 (1957).
60. W. REEVE and I. CHRISTOFFEL. J. Am. Chem. Soc. **72**, 1480 (1950).
61. H. J. LUCAS, M. T. SCHLATTER, and R. C. JONES. J. Am. Chem. Soc. **63**, 25 (1941).
62. LOURENCO. Ann. Chim. [3], **67**, 290 (1863).

Can. J. Chem. Downloaded from www.nrcresearchpress.com by 210.87.254.40 on 09/05/12
For personal use only.

Can. J. Chem. Downloaded from www.nrcresearchpress.com by 210.87.254.40 on 09/05/12
For personal use only.

ANOMALOUS RING CLEAVAGE DURING LITHIUM ALUMINUM HYDRIDE – ALUMINUM CHLORIDE REDUCTION OF 2,2,4,4-TETRAALKYLATED-1,3-DIOXOLANES[1]

B. E. LEGGETTER AND R. K. BROWN
Department of Chemistry, University of Alberta, Edmonton, Alberta

Received December 6, 1963

ABSTRACT

The anomalous reductive cleavage by $LiAlH_4$–$AlCl_3$ of 2,2,4,4-tetramethyl-1,3-dioxolane in ether solution has been examined. Evidence supports the view that this unexpected direction of ring cleavage is due to steric repression of the formation of the intermediate oxocarbonium ion leading to cleavage of the C_2—O_1 bond of the dioxolane ring.

INTRODUCTION

In a recent publication (1) it was shown that in the reductive ring cleavage of 1,3-dioxolanes with a mixture of lithium aluminum hydride and aluminum chloride in ether solution, substituents on C_4 of the dioxolane ring exerted a marked control over the direction of ring opening. Electron donor substituents attached to C_4 gave predominant cleavage of the C_2—O bond remote from C_4, while electron-attracting groups attached to C_4 resulted in a high proportion of cleavage at the C_2—O bond nearest to the C_4-substituted position. Substituents on C_2 of the 1,3-dioxolane ring system were found to have a negligible effect on the direction of reductive ring cleavage.

This effect was rationalized on the basis of the stabilizing or destabilizing effect that the C_4 substituents exerted on the two possible intermediate oxocarbonium ions, the formation of which was considered to be rate-determining (equation (*a*)). Electron donor substituents (R‴, R^{iv}) would stabilize to a greater extent the oxocarbonium ion shown

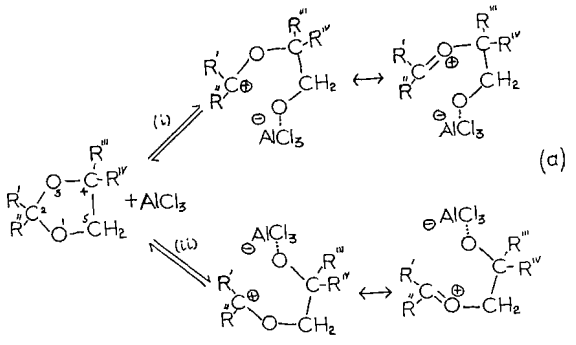

in equation (*a*), route (i), hence this ion would be predominant and reduction would follow largely this route. On the other hand, electron-withdrawing groups (R‴, R^{iv}) would preferentially destabilize the oxocarbonium ion shown in route (i) of equation (*a*), hence the formation of the ion indicated in route (ii) would be predominant and reductive cleavage would follow largely this path. Subsequent reduction to the hydroxy ether was considered to be fast, and found to be irreversible.

[1]*Taken from the thesis of B. E. Leggetter, submitted to the Faculty of Graduate Studies, University of Alberta, Edmonton, Alberta, in partial fulfillment of the requirements for the degree of Doctor of Philosophy.*

Can. J. Chem. Downloaded from www.nrcresearchpress.com by 210.87.254.40 on 09/05/12
For personal use only.

However, the cleavage of one compound encountered in this work (1), that of 2,2,4,4-tetramethyl-1,3-dioxolane, gave 94% of 1-isopropoxy-2-methyl-2-propanol and only 6% of the 2-isopropoxy-2-methyl-1-propanol. This was the reverse of what had been expected considering the results found for all the other cases examined. Its formation could not be rationalized within the framework of the postulated mechanistic pathways. A similar situation has been pointed out by Eliel and co-workers (2), who found that the isobutylene ketal of cyclohexanone gave exclusively the tertiary alcohol (equation (*b*)) in sharp contrast to the results found for all their other C_4-substituted 1,3-dioxolanes. They suggested that this anomaly might be the result of either a different mechanism of hydrogenolysis

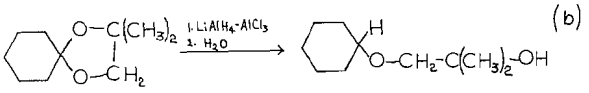

from that occurring for the other examples studied, or a "counterplay of polar and steric influences".

The purpose of this work was to examine this anomalous reductive cleavage in more detail and to provide an explanation for the results obtained.

RESULTS AND DISCUSSION

The reduction of 2,2,4,4-tetramethyl-1,3-dioxolane was repeated as described and the results found to be in agreement with those published (1).

Two explanations may be offered to account for this unexpected direction of ring cleavage. The first is that the steric strain, due to non-bonded repulsion of the four alkyl substituents at C_2 and C_4 positions, outweighs the polar influence normally controlling the direction of the ring opening. This view is supported by the fact that the corresponding 2,4,4-trimethyl-1,3-dioxolane and the 2,2,4-trimethyl-1,3-dioxolane both gave the predicted preferential cleavage at the C_2—O bond (equation (*a*), route (i)) to give the primary alcohols in the proportion of 90% and 82% respectively of the total reduction product (ref. (1), Table I). It thus appears that the fourth group plays a decisive role in the direction of ring opening.

The second explanation of the anomaly is that the oxocarbonium ion formation, necessary for the cleavage at C_2—O_1, is retarded by the steric influence of the substituents on C_2 and C_4, whereas similar steric retardation involving the formation of the alternate oxocarbonium ion does not occur (equation (*c*)).

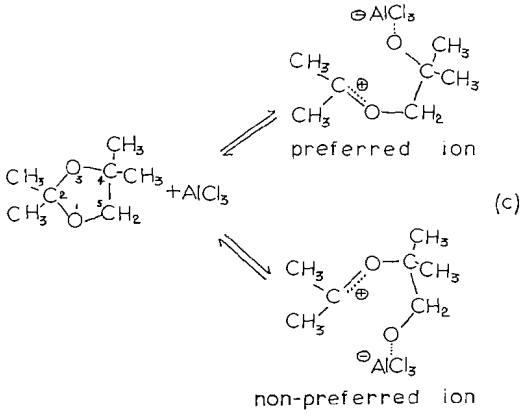

For the cleavage of the C_2—O_1 bond to occur, overlap of the p orbital of the O_3 atom with the developing empty p orbital of the C_2 atom must take place, resulting in the formation of the stabilized oxocarbonium ion. A requirement for effective overlap of these two p orbitals, and hence formation of the "double bond", is a configuration in which the C_2 atom with its two substituents, the oxygen atom with the lone pair in the sp^2 hybrid orbital *and* the C_4 atom are all coplanar as shown below.

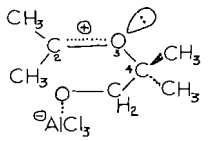

This configuration would result in strong non-bonded interference between one of the two methyl substituents at C_2 and the substituents on the tertiary carbon, C_4. Thus a strain would occur during the formation of the oxocarbonium ion, tending to inhibit its development.

The literature contains a closely analogous case in the explanation offered to account for the anomalous rate of reduction of *t*-butyl phenyl ketone by sodium borohydride compared to the rates of reduction found for the homologous methyl, ethyl, and isopropyl phenyl ketones (3).* It was found that the order of the rates of reduction of the homologues was methyl phenyl ketone > ethyl phenyl ketone > isopropyl phenyl ketone as expected from steric and polar considerations. However, the *t*-butyl phenyl ketone was found to reduce at a rate faster than that of the methyl phenyl ketone. This was rationalized by the postulation that, due to steric repression, there was a much lower contribution of the resonance structure, such as that shown below, for the *t*-butyl compound than for each of the other homologues.

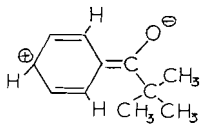

The difference between the two explanations suggested to account for the unexpected ring cleavage found in the present work is that the first requires steric *acceleration* of the cleavage of the C_2—O_3 bond, while the ease of cleavage of the C_2—O_1 bond is unaffected by the substituents on C_2 and C_4, other than by polar influences. On the other hand, the latter explanation requires that the cleavage of the C_2—O_1 bond be *retarded* by steric compression due to the four groups on C_2 and C_4, while the rate of cleavage of the C_2—O_3 bond is not changed other than by polar effects.

One can differentiate between these two routes by a study of the rate of reduction of 2,2,4,4,5,5-hexamethyl-1,3-dioxolane. If the first explanation is correct, then this dioxolane should cleave much more readily than does the 2,2-dimethyl-1,3-dioxolane where no steric strain between C_2 and C_4 substituents occurs. On the other hand, if the latter explanation is correct then the rate of reductive cleavage of the hexa-substituted dioxolane should be greatly retarded.

The ease of reduction has been examined and results show that the reduction of

**The referee has kindly pointed out that the heat of hydrogenation of cis-methyl-t-butylethylene provides a second analogy. This olefin is destabilized through steric strain by about 4.3 kcal/mole relative to the trans isomer. (R. B. Turner, D. E. Nettleton, Jr., and M. Perelman. J. Am. Chem. Soc. 80, 1430 (1958).)*

Can. J. Chem. Downloaded from www.nrcresearchpress.com by 210.87.254.40 on 09/05/12
For personal use only.

2,2,4,4,5,5-hexamethyl-1,3-dioxolane is greatly retarded. After 1 hour of reduction, this compound was practically unchanged, and even after 48 hours of reduction 30% of the original dioxolane was recovered intact. Under identical conditions both 2,2-dimethyl-1,3-dioxolane and 2,2,4,4-tetramethyl-1,3-dioxolane were completely cleaved in less than 90 minutes (1). On the basis of these results, the second explanation is preferred.

EXPERIMENTAL

Analysis of products of the reduction was carried out by gas–liquid chromatography as described in the previous publication (1).

The reduction of the 1,3-dioxolanes were carried out according to the general procedure described by Leggetter and Brown (1).

2,2,4,4,5,5-Hexamethyl-1,3-dioxolane was prepared in 72% yield from 2,2-dimethoxypropane (1) and anhydrous pinacol using the ketal exchange procedure described by McElvain and Curry (4). B.p. 145–146° at 700 mm. Lit. b.p. 147.5–148.5° (5).

ACKNOWLEDGMENTS

The authors wish to thank the National Research Council of Canada for financial assistance throughout the course of this work.

REFERENCES

1. B. E. Leggetter and R. K. Brown. This issue.
2. E. L. Eliel, V. G. Badding, and M. N. Rerick. J. Am. Chem. Soc. **84**, 2371 (1962).
3. H. C. Brown and K. Ichikawa. J. Am. Chem. Soc. **84**, 374 (1962).
4. S. M. McElvain and M. J. Curry. J. Am. Chem. Soc. **70**, 3781 (1948).
5. R. Leutner. Monatsh. **66**, 222 (1935).

Can. J. Chem. Downloaded from www.nrcresearchpress.com by 210.87.254.40 on 09/05/12
For personal use only.

DEUTERIUM–HYDROGEN EXCHANGE BETWEEN WATER AND SILK FIBROIN

JOHN L. MORRISON
Department of Physical Chemistry, Ontario Research Foundation, Toronto, Ontario
Received November 13, 1963

ABSTRACT

A gravimetric method for measuring deuterium–hydrogen exchange between light and heavy waters and macromolecular solids has been applied to the fibrous protein, silk fibroin (*Bombyx mori*). The accessibility of the protein to water vapor can be estimated from the amount of exchange, and it appears to be related to the amorphous regions of the fiber. A comparison of the amount of exchange with the water monolayer content as obtained from the adsorption isotherm and the equilibrium evaporation technique suggests that the water molecules use the polar side chains of the amino acid residues as the sites of primary adsorption.

INTRODUCTION

Isotopic exchange studies are useful in elucidating the secondary and tertiary structures of proteins, celluloses, and other macromolecules. Usually, the isotopic exchange has been followed by indirect methods such as change in composition of the water (1, 2), infrared measurements (3–6), and tritium exchange (7, 8).

Three groups of workers (9–11) have measured the exchange directly by the change in dry weight of the macromolecular solid. All of them used a quartz spring balance, and two of them (9, 11) stated that they made measurements with a sample between 0.1 and 0.2 grams.

In this paper, a simpler gravimetric method of measuring deuterium–hydrogen exchange (12) is applied to a preliminary study of the reaction between light and heavy waters and the protein, silk fibroin (*Bombyx mori*).

EXPERIMENTAL

Materials

The silk fibroin, *B. mori*, was kindly supplied by Belding–Corticelli Limited, Montreal, as Japanese raw silk. It was degummed by the method of Drucker, Hainsworth, and Smith (13). The deuterium oxide was 99.7% pure (Atomic Energy of Canada, Limited).

Apparatus

The same type of glass reaction cell (14, 15) was used for both the exchange measurements and the sorption determinations. It consists of a thin-walled glass bulb, to hold about 5 g fibrous substance, a vacuum stopcock, and an inner ground-glass joint. It was readily removed for weighing. An oil manometer containing Apiezon oil B was used to measure the water vapor pressure. The reaction cell and the light and heavy water reservoirs were immersed in a thermostat at 24.8° C.

The assembly was evacuated by a mercury condensation pump and a rotary oil pump. A trap immersed in a dry ice – methyl cellosolve bath at −86° C was placed between the reaction cell and the mercury pump to avoid the back exchange inherent in the use of drying agents (2) and to prevent mercury from reaching the sample.

Drying Procedures

Fifty hours of continued evacuation at 25° C against a dry ice trap reduced the water content of silk fibroin to about 0.2% compared with the dryness obtained by a further 1 day evacuation at 70° C.

Subsequent evacuation of a 6-g sample of silk fibroin at 70° C for 15 days decreased the weight by about 1 mg. Lang and Mason (16) showed that the evacuation of cellulose at 70° for 24 hours achieved a water content not sensed by isotopic exchange as analyzed by a mass spectrograph.

However, when the silk sample was alternately wetted and dried by a cycle similar to that used in the heavy and light water dosing procedure, a significant weight loss amounting to 0.5 mg per cycle occurred (Fig. 1). The weight loss appeared to be largely independent of dose size or of time of drying at 70°, and only

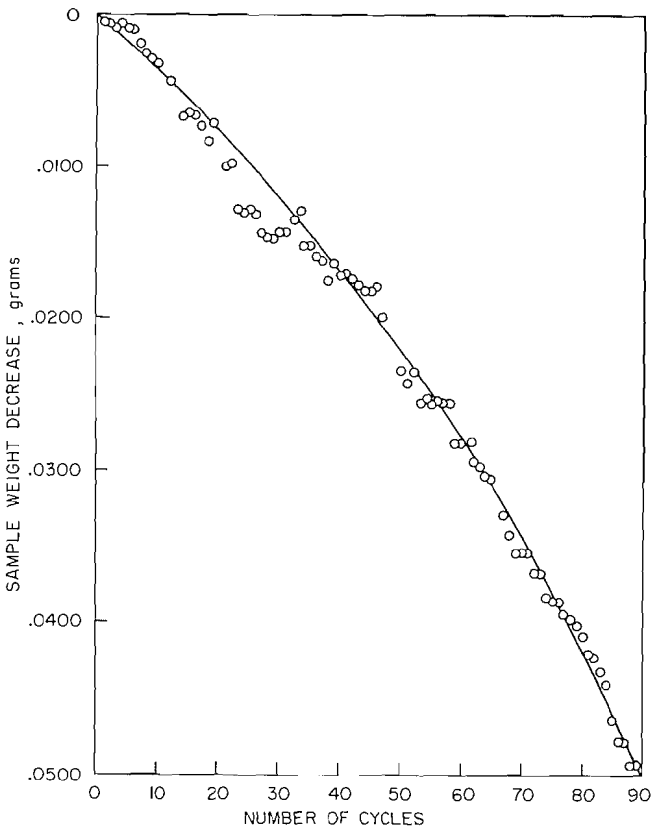

FIG. 1. Cyclic wetting and drying of 6.2 g silk fibroin. Cycles 1–14, 0.05 to 0.44 g H_2O dried 1 day at room temperature and 1 day at 70° C; cycles 15–89, increasing doses from 0.03 to 0.73 g, dried 12 hours at room temperature and 16 hours at 70°.

dependent on the number of wetting and drying cycles. A similar phenomenon has been observed for cellulose by Lang and Mason (8).

In view of an observation that drying at 50° C removed the last amounts of sorbed water as effectively as at 70° C, a number of exchange experiments were dried at the lower temperature. This partially avoided the possibility of thermal decomposition at 70° (17). In all cases, samples undergoing exchange were evacuated at room temperature for 12 to 24 hours before being raised to a higher temperature.

Sorption Characteristics

The adsorption–desorption isotherms of light water and the adsorption isotherm of heavy water on silk fibroin were determined by the same method as was used for cellulose (15). A maximally deuterated sample was used for the heavy water isotherm. Each point was the result of equilibration for at least 24 hours. The isotherms are given in Fig. 2.

From the adsorption isotherms, the B.E.T. monolayer contents (18) on a dry protein basis were found to be 4.47 and 4.98% for H_2O and D_2O, respectively. These values are exactly in their molar ratios.

An independent method for determining monolayer values, recently developed in this laboratory (19), was applied to silk fibroin. The method, an equilibrium evaporation technique, involves experimentally determining the rate of evaporation of water from a wet polymer sample under conditions approaching equilibrium. A completely wetted sample in a cell similar to that used in the other experiments is dried under vacuum through a capillary tube (0.85 mm diameter, 20.5 cm long) for 20 minutes, weighed, left to stand for 12 hours, and again evacuated for 20 minutes. This cycle is repeated until the sample is practically dry. Except for the time of weighing, the sample tube is continually thermostatted at 25.0° C. Figure 3 shows the drying rate below 26% water content. The break at about 5% water content is interpreted as the monolayer value. An even sharper break has been obtained for other polymers by using 24-hour waiting intervals between the evacuation periods.

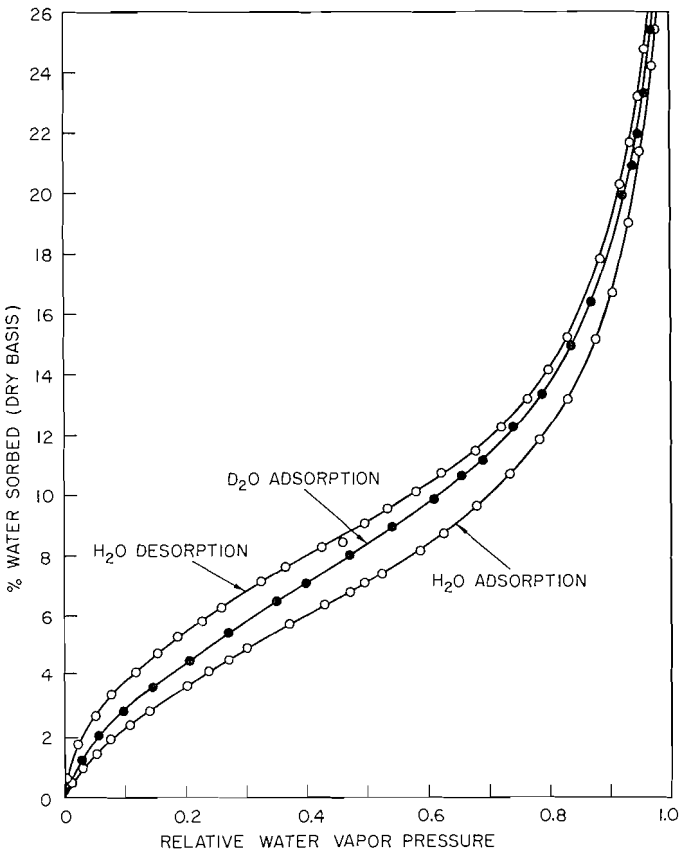

FIG. 2. Sorption isotherms at 24.8° C.

Since the evaporation rate method is a desorption process, it would be better to compare the break at 5% with the B.E.T. monolayer value calculated from the desorption rather than the adsorption branch of the isotherm. The desorption branch value was 5.4%.

Rapid Exchange Experiments

In one experiment 6.20 g silk fibroin were wetted with six doses (8, 9, 4, 9, 6.5, 5.5 g respectively) of heavy water. After 3 to 4 days contact, the sample was evacuated for 12 hours at 25° C and 16 hours at 50° C with each successive dose. By the end of the second cycle, the sample weight was within 6% of the total increase. The final weight increase was 1.04%. Then this sample was used for the heavy water isotherm determination.

Another sample of 5.35 g was similarly treated with five doses (5.7, 6.0, 5.3, 6.0, and 9.0 respectively) of heavy water. After the second cycle, the sample was within 10% of its total increase. The final increase was 1.06%.

This sample was back-exchanged with three doses (14, 13, 12.5 respectively) of light water and finally dried at 50° C when it had recovered exactly its original weight.

Slow Exchange Experiments

The 6.20 g sample was deuterated and protonated by a rate method already applied to insulin (12). Small doses of heavy water (0.142 g) and light water (0.127 g), the latter for the deuterated sample, were admitted to the sample through a capillary tube. After 10.5 minutes, the samples were evacuated for several hours at 24.8° C. The final drying of the first series was carried out at 70° C and of the second at 50° C. When the weight change appoached a maximum, between 15 and 22 doses, much larger doses were admitted to the sample, until the maximum degree of exchange was attained. The results are reported in Figs. 4 and 5.

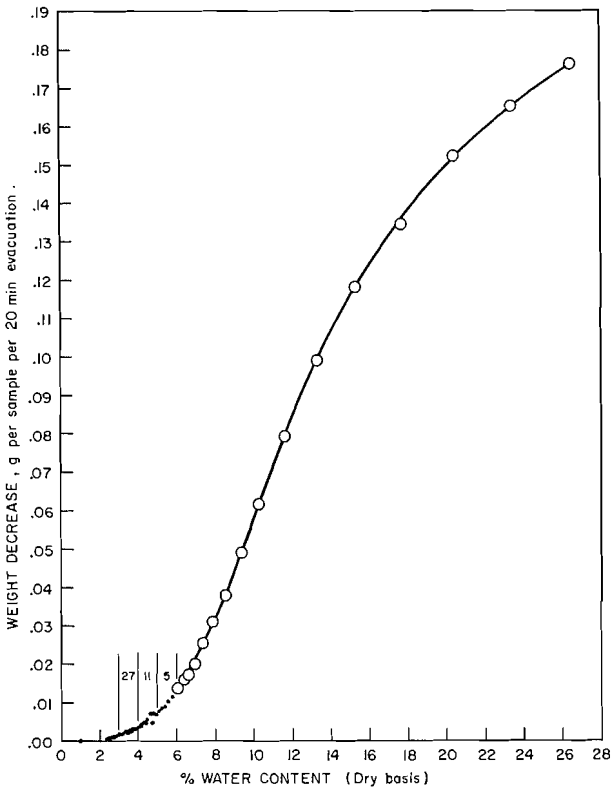

FIG. 3. Weight decreases by a highly wetted sample of silk fibroin (dry wt. = 5.35 g) on evacuation through a capillary tube. Each point represents the *change* in sample weight after 20 minutes evacuation. The numbers 5, 11, and 27 represent the number of 20-minute evacuations between 6 and 5, 5 and 4, and 4 and 3% water contents, respectively.

DISCUSSION

Assuming that the weight decrease in the cyclical wetting and drying (Fig. 1) is a loss in water, one can speculate about its origin. It does not appear to be ordinarily adsorbed water and it is not removed merely by continual heating. This difficultly removable water, which requires for its removal the perturbations of the solid set up by the cyclical wetting and drying process, may be intracrystalline water.

When a correction for the weight loss due to cyclical wetting and drying is applied to the deuteration and protonation curves given in Fig. 4, the two curves come closer together, but they do not coincide. That coincidence does not occur may be due to a number of factors (12). One possible explanation is that the cycling correction has been determined only for light water. Heavy water may have a drying effect arising from the entropy of mixing, that is, it is very hygroscopic. To test this hypothesis, one would carry out wetting and drying experiments with heavy water on a maximally deuterated sample.

The true value of the exchange rate probably lies somewhere between the deuteration and protonation curves of Figs. 4 and 5. In principle it need not be the mean between the two curves because of differences in such properties as zero-point energy.

The maximum value for the exchange, as given by the rapid exchange experiments, corresponds to an increase of 1.05% in the dry weight of the protein. In the slow experiments, with the drying at 50° C, Fig. 5, the mean of the two maxima is 1.0%. For slow

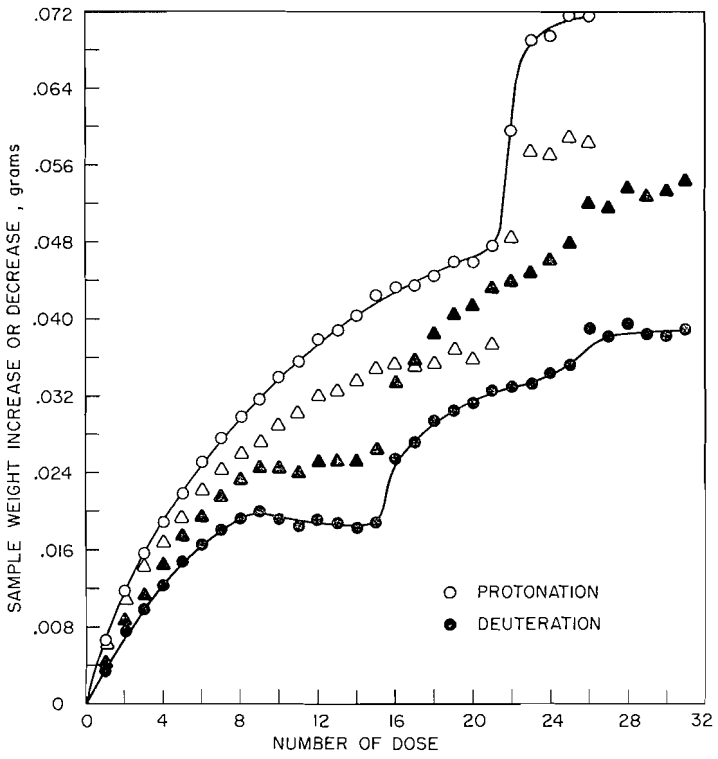

FIG. 4. Deuteration and protonation of 6.20 g silk fibroin by cyclic dosing with each final drying at 70° C. Deuteration: doses 1–12, 0.142 g D_2O for 10.5 minutes, then evacuation; doses 13 and 14, 0.142 g left overnight before evacuation; dose 15, 0.35 g, immediately evacuated; doses 16–23, 0.60 g evacuated after 64½ minutes; dose 24, 0.60 g left overnight; dose 25, 0.88 g left overnight; dose 26, 2.56 g left 2 days; dose 27, 3.04 g left 1 day; doses 28–31, 0.142 g D_2O left overnight. Protonation: doses 1–18, 0.127 g H_2O added for 10.5 minutes, then immediately evacuated; doses 19 and 20, 0.127 g left overnight; dose 21, 1.0 g left 3 days; doses 22–26, 6.5–8.4 g H_2O left several days before evacuation. The symbols ▲, △ are weight changes on deuteration and protonation respectively corrected for the weight losses as shown in Fig. 1.

experiments with the drying at 70°, Fig. 4, the means of the maxima are 0.89% uncorrected, and 0.92% corrected.

Deuterium–hydrogen exchange between water and proteins occurs with hydrogens attached principally to nitrogen and oxygen atoms. These occur on the peptide and other polar groups of the constituent amino acids. In the case of silk fibroin, the total exchangeable hydrogens make up about 1.58% of the weight of the protein. The present results show that 1.05% are exchangeable. The part of the fibroin which is accessible to deuterium–proton exchange is probably the amorphous part, the inaccessible region being the crystalline part (6).

The only experimental work on silk fibroin, *B. mori*, with which to compare the present results is that of Lucas and Smith (20). They separated the fibroin into two fractions by means of chymotrypsin digestion. They suggested that the fraction, CTL (40% of the total protein nitrogen), soluble in the enzyme digest consists of the amorphous region and that the soluble fraction, CTP (60%), is the crystalline region. From their Table II (20), the total exchangeable hydrogen in the soluble fraction is 0.67% of the total fibroin, made up of the hydrogens of 0.499 moles peptide nitrogen and 0.157 moles polar groups per

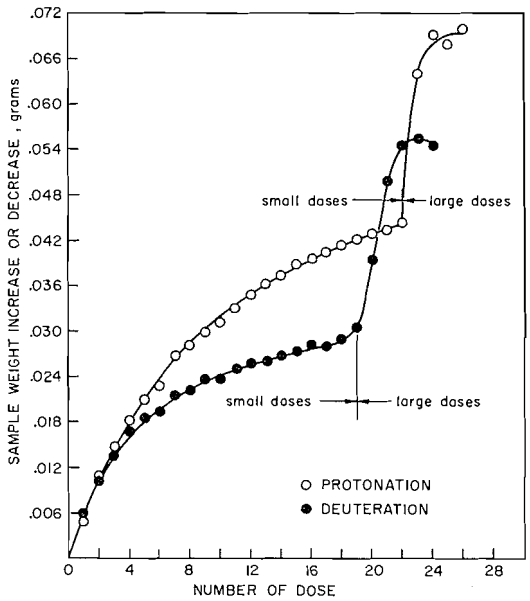

FIG. 5. Deuteration and protonation of 6.20 g silk fibroin by cyclic dosing with each final drying at 50° C. Deuteration: small doses 1–18, same as for 70° experiments; dose 19, same as 1–18 but left 1 day before evacuation; doses 20–24, 0.7, 5.1, 7.0, 6.6, and 9.4 g D_2O, respectively, evacuated after 2 days. Protonation: small doses 1–21, same as for 70° experiments; dose 22, same as dose 19 of deuteration; doses 23–26, 6.2, 6.0, 13.2, and 14.5 g H_2O, evacuated after 2–3 days.

100 g fibroin. On the basis of the present observations it would appear that chymotrypsin dissolves about two-thirds of the amount of fibroin accessible to water exchange. This is not surprising in view of the enormous difference in size between the chymotrypsin and water molecules.

The data of Lucas and Smith (20) can be used in a discussion of the mode of attachment of the water monolayer to the amorphous region. The deuterations and protonations are adsorption processes. The monolayer content on adsorption is 4.5% or 0.25 moles H_2O per 100 g fibroin. There are 1.05 moles exchangeable hydrogen in this amount of fibroin. Consequently water molecules could not be attached directly to all of the exchangeable hydrogens. Pauling (21) suggested that the water molecules are attached to the amino acid residues with polar side groups.

If water is accessible to all of the CTL and part of the CTP fractions of the fibroin, the number of polar side groups is 0.222 moles per 100 g fibroin, made up of 0.157 moles from the CTL and 0.065 from the CTP. The value 0.222 is somewhat less than the 0.25 moles H_2O in the monolayer. Two possible explanations may account for this discrepancy.

The fractional number of polar side groups in the part of the CTP accessible to water is assumed to be the same as that for the whole CTP, namely 0.17. In the case of the CTL, this fraction is 0.315. It is possible that the part of the CTP accessible to water has a greater proportion of polar side groups than the whole CTP.

Another explanation which may not be different from the first one is that there may be more polar side groups on the surfaces of the crystallites than inside them.

Finally, let us consider the fact that small doses of water reach an intermediate maximum in their exchange with silk fibroin. This is particularly clear in the experiments shown in Fig. 4. The levelling off, which is independent of time for the small doses, occurs

at between 0.5 and 0.6% exchange. Two alternative explanations are possible: either the accessibility to the amorphous region is determined by dose size or the amorphous region is completely accessible to any amount of water, and the exchangeable hydrogens exist in different energy levels. There is, of course, the possibility that both effects operate together.

The fact that the equilibrium evaporation rate curve (Fig. 2) can be entered at any point by wetting from the dry state to a moisture content a little higher than the desired entry point strongly suggests that the accessibility is independent of moisture content. It is more probable that the exchangeable hydrogens on each different group have their own equilibrium constant with respect to water.

Of the 1.05% exchangeable hydrogens about 0.23% are attached to polar side groups when the calculations are based on the amino acid contents of the two fractions of fibroin. However, comparison with the monolayer value of 0.25% suggests that the 0.23% may be underestimated. If 0.25 is taken as the percentage of exchangeable hydrogens on polar side groups and if an approximately equal number of peptide hydrogens occurring in the same amino acid residues is added, the total may account for the half more readily exchangeable hydrogens observed during deuteration. This would be consistent with the location of the water monolayer molecules on the polar side groups.

REFERENCES

1. V. J. Frilette, J. Hanle, and H. Mark. J. Am. Chem. Soc. **70**, 1107 (1948).
2. A. Hvidt and K. Linderstrom-Lang. Biochim. Biophys. Acta, **16**, 168 (1955); Compt. Rend. Trav. Lab. Carlsberg, Ser. Chim. **29**, 385 (1955).
3. K. E. Almin. Svensk Papperstid. **55**, 767 (1952).
4. J. Mann and H. J. Marrinan. Trans. Faraday Soc. **52**, 481, 487, 492 (1956).
5. R. D. B. Fraser and T. P. MacRae. J. Chem. Phys. **28**, 1120 (1958).
6. M. Beer, G. B. B. M. Sutherland, K. N. Tanner, and D. L. Woods. Proc. Roy. Soc. Ser. A, **249**, 147 (1959).
7. W. Lobunez and F. Karush. J. Am. Chem. Soc. **81**, 795 (1959).
8. A. R. G. Lang and S. G. Mason. Can. J. Chem. **38**, 373 (1960).
9. W. Hnojewyj and L. H. Reyerson. J. Phys. Chem. **63**, 1653 (1959).
10. T. King and C. Ouellet. Can. J. Res. Ser. B, **14**, 444 (1936).
11. R. W. Burley, C. H. Nicholls, and J. B. Speakman. J. Textile Inst. Trans. **46**, 427 (1955).
12. J. L. Morrison. Biochim. Biophys. Acta, **47**, 606 (1961).
13. B. Drucker, R. Hainsworth, and S. G. Smith. J. Textile Inst. Trans. **44**, 420 (1953).
14. E. O. Wiig and A. J. Juhola. J. Am. Chem. Soc. **71**, 561 (1949).
15. J. L. Morrison and M. A. Dzieciuch. Can. J. Chem. **37**, 1379 (1959).
16. A. R. G. Lang and S. G. Mason. Can. J. Chem. **37**, 1829 (1959).
17. S. G. Smith. Private communication.
18. H. B. Bull. J. Am. Chem. Soc. **66**, 1499 (1944).
19. J. L. Morrison. Nature, **198**, 84 (1963).
20. F. Lucas and S. G. Smith. J. Textile Inst. Trans. **50**, 695 (1959).
21. L. Pauling. J. Am. Chem. Soc. **67**, 555 (1945).

Can. J. Chem. Downloaded from www.nrcresearchpress.com by 210.87.254.6 on 09/05/12
For personal use only.

NEPHELOMETRIC DETERMINATION OF PALLADIUM WITH DI-2-THIENYLKETOXIME

WILLIAM J. HOLLAND AND LEO LEE
Department of Chemistry, University of Windsor, Windsor, Ontario
Received November 25, 1963

ABSTRACT

Di-2-thienylketoxime is used to determine 1 to 4 p.p.m. of palladium nephelometrically. Palladium (II) can be determined in the presence of a 30-fold excess of platinum. A sixfold excess of other platinum metals and gold do not interfere. No interference was found with other common cations or anions with the exception of cyanide.

INTRODUCTION

Of the several methods (1) generally recommended for the determination of microgram quantities of palladium, the most sensitive is that employing *p*-nitrosodiphenylamine as a colorimetric reagent. The reagent 2-thienyl-*trans*-aldoxime has been used for the gravimetric estimation of palladium (2). The nephelometric method described herein constitutes part of the results of an investigation into the use of thienylketoximes as analytical reagents. A previous paper (3) reported the reactions of di-2-thienylketoxime and the structure of the complexes formed with bivalent palladium. Di-2-thienylketoxime reacts with microgram quantities of palladium (II), as the chloride, in acid solution to form a suspension of a complex which could be determined nephelometrically. The method was investigated to determine such factors as optimum concentration of reagent, effect of time of standing, pH, temperature, stabilizing agents, and diverse ions.

EXPERIMENTAL

Reagents

Standard palladium solutions.—Reagent grade palladium (II) chloride was used. This material was analyzed gravimetrically with dimethylglyoxime and was found to contain 60.16% palladium. A palladium (II) stock solution was prepared by dissolving a weighed amount of the reagent in hydrochloric acid and diluting to a given volume. The palladium (II) standard solutions were prepared by appropriate dilution of aliquots of the stock solution with a buffer solution of pH 3.2.

Diverse ions.—Reagent grade chlorides were employed in the preparation of cation solutions and sodium salts were used for the anion solutions.

Stabilizing agent.—A 1% solution of U.S.P. grade gelatin was used.

Di-2-thienylketoxime.—The reagent was synthesized and purified by the method outlined in a previous publication (3). A 0.1% solution in ethanol was employed.

Generator solution.—This solution was prepared by suspending powdered pyrex glass in water. The procedure used in this preparation was that outlined by Fikman (4).

Buffer solution.—pH 3.2. Prepared from potassium acid phthalate and hydrochloric acid solutions.

Instruments.—A Fisher Nefluorophotometer was used for the nephelometric measurements and a Beckman Model G pH meter for the pH determinations.

Procedure

Standard solutions of palladium (II) buffered to pH 3.2 and of various concentrations (0.05 to 0.25 mg per 50 ml final dilution) were prepared by pipetting aliquots of the stock solution (0.1 mg per ml) into 100-ml volumetric flasks and diluting with the buffer. Exactly 25 ml of these solutions were pipetted into 50-ml volumetric flasks. To each flask was added 5 ml of the ketoxime solution and the mixture was allowed to stand for 1 hour. After addition of 5 ml of the gelatin solution and diluting to the mark the mixture was shaken vigorously for 2 minutes. The suspension prepared with the most concentrated of the palladium (II) solutions was transferred to a nephelometric cell and the percentage transmittancy scale set at 100%. The scale readings of the remaining suspensions were measured using the glass suspension as the generator solution. By plotting the scale readings against palladium (II) concentration a straight line was obtained over the range 0.05 to 0.20 mg per 50 ml final solution. The results of this plot are shown in Fig. 1.

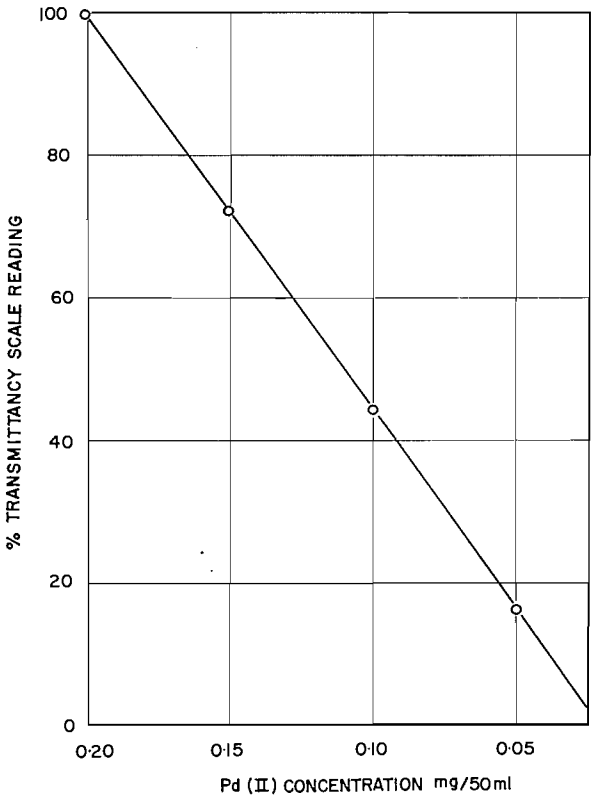

FIG. 1.

Effect of pH.—Constant scale readings were obtained for solutions containing 0.15 mg palladium (II) per 50 ml final dilution between pH 2.8 and 4.2. Solutions of pH less than 1.2 or higher than 4.5 gave very little turbidity. The greatest turbidities were produced between pH 1.5 and 2.5, but these were very sensitive to slight changes in pH. The solutions were adjusted to the desired pH by dropwise addition of 0.1 *N* hydrochloric acid or sodium hydroxide solutions. A diluted glass suspension solution was used as the reference standard.

Effect of time of standing.—The procedure described above was followed with a number of solutions of the same palladium (II) content varying the time allowed after the addition of the reagent and before the addition of the gelatin solution prior to measurement of the turbidity. Constant readings were obtained after 1 hour standing.

Effect of reagent concentration.—Results indicated that a 0.1% solution of the ketoxime was the most suitable concentration. Higher concentrations resulted in precipitation of the reagent with a consequent increase in turbidity. Lower concentrations gave decreasing turbidities.

Effect of ethanol concentration.—The total amount of reagent added to solutions having the same palladium (II) content was maintained constant while the amount of ethanol was varied. Constant readings were obtained when the final dilution contained 5 ml of ethanol per 50 ml. Higher alcohol contents resulted in decreasing turbidity while lesser amounts caused precipitation of the reagent.

Effect of variation of temperature.—Constant readings were obtained in the temperature range 20–25° C. Above 25° the turbidity decreased markedly.

Effect of diverse ions.—Suspensions were prepared for solutions containing the same concentration of palladium (II) to which had been added various amounts of other cations or anions. Readings were taken for the solutions and the results are given in Table I. These results indicate that no serious interference occurs with the ions investigated with the exception of cyanide.

Determination of known samples.—Known palladium (II) solutions were prepared and then concentrations determined using the procedure outlined and the calibration curve of Fig. 1. The results given in Table II show a recovery of at least 95%.

Can. J. Chem. Downloaded from www.nrcresearchpress.com by 210.87.254.6 on 09/05/12
For personal use only.

TABLE I

Effects of diverse ions on the determination of Pd

Palladium (II) concentration, 3 p.p.m.					
Ion	Concentration, p.p.m.	Scale reading	Ion	Concentration, p.p.m.	Scale reading
—	—	70	Cd (II)	40	70.0
Pt (II)	100	70	Cr (III)	40	71.0
Ir (III)	40	70	K (I)	100	70.0
Rh (III)	100	70	Cu (II)	40	70.0
Ru (III)	20	69	HPO_4^{-2}	100	70.5
Au (III)	20	69	OAc^-	40	70.0
Na (I)	100	71	CO_3^{-2}	100	70.5
Co (II)	100	70	CN^-	40	—
Ni (II)	40	70	SO_4^{-2}	100	70.5
Mn (II)	40	71	NO_3^-	100	69.0
Hg (II)	100	70	F^-	100	70.0

TABLE II

Determination of known samples

Pd present, mg/50 ml	Pd found, mg/50 ml	% deviation
0.175	0.180	2.8
0.150	0.145	3.3
0.100	0.095	5.0
0.075	0.079	5.3

Reproducibility.—Ten solutions containing the same amount of palladium (II) were prepared and measured as in the outlined procedure. A comparison of the scale readings showed an average deviation of ±0.6%. The results are given in Table III.

TABLE III

Reproducibility

Palladium (II) concentration, 3 p.p.m.		
Sample	Scale reading	% recovery
1	70.0*	100.0
2	69.0	99.7
3	70.5	100.7
4	70.2	100.3
5	71.0	101.4
6	69.0	98.6
7	69.5	99.3
8	70.5	100.7
9	71.0	101.4
10	69.5	99.3

*Scale reading of 70.0 assumed to represent 100% recovery.

REFERENCES

1. F. H. Beamish and W. A. McBryde. Anal. Chem. Acta, **9**, 349 (1953).
2. S. G. Trandon and S. C. Bhattacharya. Anal. Chem. **32**, 194 (1960).
3. W. J. Holland and L. Lee. Can. J. Chem. **41**, 1657 (1963).
4. B. A. Fikman. Lab. Delo, **4** (2), 53 (1958).

Can. J. Chem. Downloaded from www.nrcresearchpress.com by 210.87.254.6 on 09/05/12
For personal use only.

Can. J. Chem. Downloaded from www.nrcresearchpress.com by 210.87.254.105 on 09/05/12
For personal use only.

PRESSURE EFFECT AND MECHANISM IN THE ACID-CATALYZED HYDRATION OF PROPYLENE AND ISOBUTYLENE[1]

B. T. BALIGA[2] AND E. WHALLEY
Division of Applied Chemistry, National Research Council, Ottawa, Canada

Received October 4, 1963

ABSTRACT

The effect of pressure up to 3 kbar on the rate of the acid-catalyzed hydration of propylene and isobutylene has been measured. The volumes of activation are: for propylene at 100° C $-9.6 \pm \sim 1.0$ cm^3 mole^{-1}, and for isobutylene at 35° C $-11.5 \pm \sim 1.0$ cm^3 mole^{-1}. The effect of temperature in the range 90–120° C on the rate of hydration of propylene at 100 bar was measured. At 100° C the Arrhenius energy is $27.1 \pm \sim 1.0$ kcal mole^{-1} and the entropy of activation is $-5.4 \pm \sim 2.5$ cal deg^{-1} mole^{-1}. Both the volumes and entropies of activation strongly indicate that a molecule of water is present in the transition states, which can therefore be represented as $[\text{olefin}.H^+.H_2O]^{\ddagger}$. There appears to be no strong evidence regarding the molecular structure of the transition states.

1. INTRODUCTION

The acid-catalyzed hydration of olefins in aqueous solution has been studied frequently

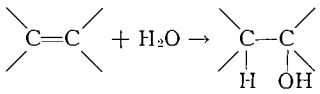

in the past few years, but the mechanism is still not entirely settled. The main direct evidence relating to the mechanism is as follows. The hydration of isobutylene (1, 2, 3) and many other tertiary olefins (4, 5, 6) is specifically acid-catalyzed, and so is catalyzed only by the solvated hydrogen ion. It is first order in hydrogen ion in dilute acid and first order in olefin. The transition states therefore contain one molecule of olefin, one proton, and perhaps one or more molecules of water. When the hydration of 2-methyl-2-butene is carried out (7) under conditions such that the *t*-amyl alcohol formed does not dehydrate appreciably, there is no exchange between the hydrogen of the unreacted olefin and the solvent. A pre-equilibrium proton transfer to form a carbonium ion does not

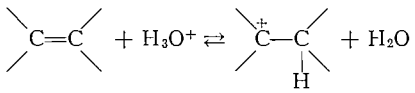

therefore occur since, if it did, then exchange of hydrogen with the solvent would occur. The lack of an acid-catalyzed isomerization of certain olefins under similar conditions (8) is further confirmation of this point.

The foregoing evidence is reasonably direct. The main likely mechanisms that are consistent with it are as follows.

(*a*) A one-step addition of H_3O^+, perhaps via a cyclic transition state

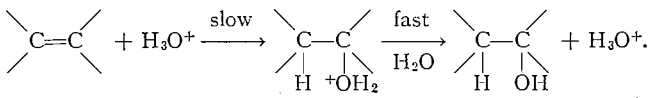

[1]*N.R.C. No. 7841.*
[2]*N.R.C. Postdoctoral Fellow 1962–4.*

(*b*) A slow proton transfer followed by a rapid addition of a molecule of water

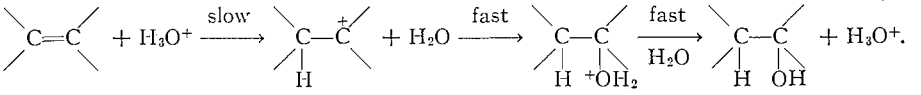

(*c*) A rapid pre-equilibrium protonation of the double bond of the olefin, followed by a slow unimolecular rearrangement to a carbonium ion which then reacts rapidly with water

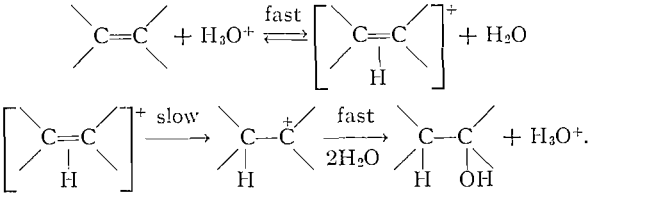

(*d*) A mechanism similar to (*c*) in which the double-bond-protonated olefin reacts slowly with a molecule of water

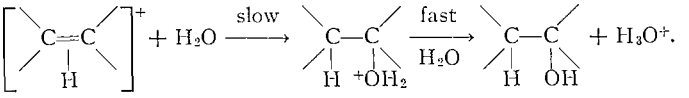

Mechanisms intermediate between these four can, of course, be envisaged. The mechanism could also be more complicated and involve several molecules of water in the transition state (see, for example, ref. 9). More complicated mechanisms will not be discussed here because there is no even moderately sound method at present of distinguishing between one and more than one molecule of water in the transition state.

There are no direct methods at present of distinguishing between mechanisms (*a*)–(*d*), and there is very little indirect evidence of useful weight. Mechanism (*c*) was suggested by Taft and co-workers (10) mainly because the rate of hydration of several olefins, including isobutylene, in concentrated acid is more nearly proportional to Hammett's acidity function h_0 than to the hydrogen-ion concentration. The Zucker-Hammett hypothesis, on which this conclusion was based, is now known to be invalid, and so this evidence has no weight. Other methods of determining the mechanism based on rates in concentrated acids seem to be hardly more soundly based. Kinetic solvent isotope effect studies have been reported on the hydration of some olefins. The ratio of the rates in H_2O and D_2O is close to unity (7) for the hydration of 2-methyl-2-butene and 1-methyl-1-cyclopentene, whereas it is 2.2 (11) for the addition of concentrated sulphuric acid to ethylene and 2.8 for hydration of propylene (12) in 90% aqueous formic acid. Willi (13) has argued that an isotope effect of near unity is consistent with a 4-centered transition state

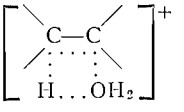

whereas Bunton and Shiner (14) have suggested that an isotope effect of near unity favors either of the following transition states

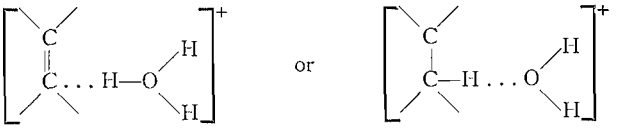

Can. J. Chem. Downloaded from www.nrcresearchpress.com by 210.87.254.105 on 09/05/12
For personal use only.

in which the H—O bond is either only slightly broken or almost completely broken. In short, the solvent deuterium isotope effect can be plausibly explained on the basis of any of the foregoing mechanisms and so does not at present distinguish between them. The dehydration of the *t*-butyl (15) and *t*-amyl alcohols (16) is much slower than the exchange of oxygen between the alcohol and the solvent. However, as it is not known whether oxygen exchange and dehydration go by related or unrelated mechanisms, the relevance of this evidence to the mechanism of dehydration of alcohols and the reverse reaction, the hydration of olefins, is not established. The entropy of activation should provide useful evidence, and indeed it has already been discussed (10) as eliminating mechanism (*b*) and favoring mechanism (*c*). However, as we shall discuss in more detail in Section 4, the analysis that this was based on is incomplete, and the conclusion drawn is probably erroneous.

Volumes of activation of acid-catalyzed reactions have in recent years proved useful for determining whether there is a molecule of water in the transition state (17). In the hope that useful information might be obtained about the acid-catalyzed hydration of propylene and isobutylene, the effect of pressure on the rates has been measured. The effect of temperature on the rate of hydration of propylene was not previously known and has also been measured.

2. EXPERIMENTAL METHODS

Materials

Propylene and isobutylene were Phillips Petroleum Co. research grade, *n*-heptane was Anachemia Chemicals Ltd. pure grade, and other chemicals were reagent grade.

Analysis of Alcohols

The hydrations were followed by estimating the alcohol produced. This was done by Shmulyakovskii's (18) method in which the alcohol is converted to the nitrite, and the nitrite is extracted into *n*-heptane and estimated spectrophotometrically. Five milliliters of the reaction mixture was added to 10 ml of *n*-heptane in a 60-ml separating funnel. Then 2 ml of 1 *N* HCl was added followed by 2 ml of 6% aqueous sodium nitrite. A stop-watch was started when the nitrite was added. The mixture was shaken for 2 minutes, allowed to settle for 2 minutes, and the aqueous layer discarded; 5 ml of 0.5 *N* ammonium carbonate solution was added and the mixture shaken for 1 minute. One minute later the optical density of the heptane layer was measured with a Beckman DU spectrophotometer using 1-cm silica cells. In a separate series of experiments the optical density was verified to be linear in the concentration of alcohol in the original solution in the range of concentration used in the kinetic experiments; the measurements are summarized in Fig. 1. The analysis for ethanol in concentrations that would be obtained by hydrating ethylene in aqueous solution was also tested as it is hoped to study this reaction in the future, and the results are included for convenience in Fig. 1.

Kinetic Measurements

The high-pressure techniques have been described previously (19, 20). Perchloric acid was used as catalyst. Because propylene and isobutylene are only slightly soluble in water, the reaction mixture was prepared by saturating aqueous perchloric acid at 0° C by bubbling the olefin through the solution by means of a sintered glass tube. The solution was taken up in the hypodermic syringe, and the pressure vessel was quickly assembled, put into the thermostat, and pressurized. The thermostat was maintained at 35.000±0.005° C for isobutylene and at 90.00, 100.00, 110.00, and 120.00°±0.015° C for propylene. The fall in temperature of the thermostat when the pressure vessel was put into it was quickly compensated by means of a 1-kw boost heater. To ensure temperature equilibrium, about 15 minutes was allowed for isobutylene and about 30 minutes for propylene before samples were taken. Propylene is much less soluble in water than isobutylene, and it is important to have the solution nearly saturated at 0° C. To reduce the loss of propylene, the syringe, pressure vessel, and mercury were precooled to ~0° C in a refrigerator, and the vessel was pressurized to ~100 bars immediately after assembly.

About six samples were taken during each run. Three samples were taken for the infinity reading after allowing the reaction to go to completion overnight, which was at least 10 half-lives.

To verify that no significant amount of olefin was present at equilibrium, two experiments were done. In the first, 0.5 *M* *t*-butanol in 1 *M* perchloric acid was kept overnight at 70° C and 50 bar. In the second, 0.034 *M* isopropanol in 1 *M* perchloric acid was kept overnight at 110° C and 100 bar. In both experiments there was no change in concentration of the alcohol within the reproducibility (± ~0.3%) of the measurements. There will be an even smaller amount of olefin present at higher pressures because alcohols dehydrate with an increase of volume.

Can. J. Chem. Downloaded from www.nrcresearchpress.com by 210.87.254.105 on 09/05/12
For personal use only.

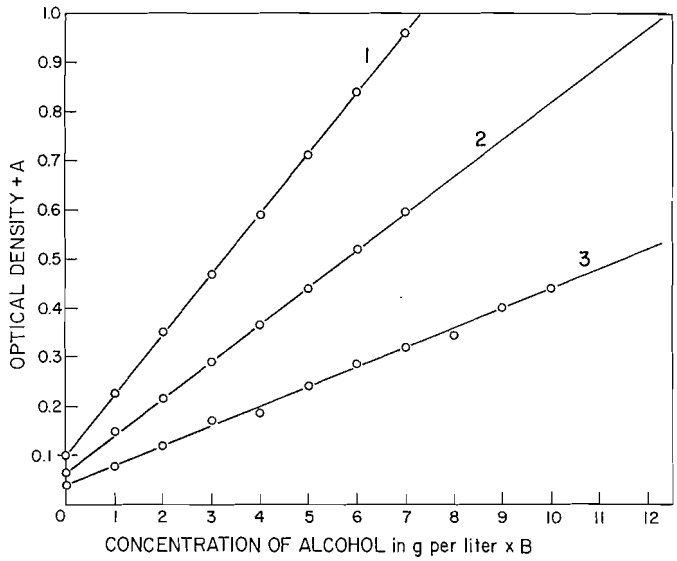

FIG. 1. Optical density of solutions of the alkyl nitrite in *n*-heptane against the original concentration of alcohol. Curve 1: isopropanol at 358 mμ, A = 0.1, B = 0.314. Curve 2: *t*-butanol at 382 mμ, A = 0.05, B = 0.186. Curve 3: ethanol at 357 mμ, A = 0, B = 0.315.

3. RESULTS

All runs were accurately first order in olefin, and the first-order rate constants k_1 were obtained graphically by plotting log $(D_\infty - D_t)$ against time t where D_∞ and D_t are the optical densities of the alkyl nitrite solution when the reaction had gone to completion and after time t respectively. The rate constants are accurate to about 3%. The second-order rate constants k_a were obtained by dividing the first-order constants by the concentration of hydrogen ion at the temperature and pressure of the experiment (21, 22). The results are summarized in Tables I and II.

The kinetics of the hydration of propylene in low concentrations of strong acid in water do not appear to have been studied previously. The measurements described above confirm that it is first order in olefin. It was shown to be first order in perchloric acid at 90° C and 100 bars by doing runs in 0.857 and 1.146 *M* perchloric acid, the results of which are summarized in Table I. The effect of temperature on the rate of hydration of propylene was also measured at temperatures from 90 to 120° C. These reactions were carried out

TABLE I

Rate constants for the acid-catalyzed hydration of propylene in water

Temp., °C	*p*/bar	c_{HClO_4}/M*	$10^6 k_a$/l. mole^{-1} sec^{-1}
90.0	100	0.857	71.1, 72.8
		1.146	74.4
100.00		0.564	182, 177
110.00		0.560	481, 492
120.00		0.278	875, 922
100.00	500	0.576	204, 199
	1000	0.587	226, 232
	2000	0.606	276
	3000	0.623	333

*c_{HClO_4} is the concentration of perchloric acid at the temperature and pressure of the experiment.

Can. J. Chem. Downloaded from www.nrcresearchpress.com by 210.87.254.105 on 09/05/12
For personal use only.

TABLE II

Rate constants for the acid-catalyzed hydration of isobutylene in water at 35° C

p/bar	c_{HClO_4}/M^*	$10^3 k_a$/l. mole^{-1} sec^{-1}
50	0.105	1.29
	0.105	1.25
500	0.107	1.55
	0.104	1.52
1000	0.0544	1.83
	0.0531	1.83
2000	0.0561	2.06
	0.0548	2.08
3000	0.0577	2.66
	0.0549	2.57

*c_{HClO_4} is that at the temperature and pressure of the experiment.

in the pressure vessel, as described above, and a pressure of 100 bars was used to ensure that the propylene did not come out of solution.

For comparison, previous results for $10^3 k_a$/l. mole^{-1} sec^{-1} for the hydration of isobutylene in dilute nitric acid at atmospheric pressure and 35° C are 1.41 (1) and 1.34 (3) compared with our 1.27 (Table II).

The rate constants as a function of pressure are shown in Fig. 2. The volumes of activation $\Delta V^{\ddagger}$ at zero pressure were obtained graphically by plotting mean volumes of activation $\Delta V^{\ddagger}_{mean}$ calculated between adjacent pressures p_1 and p_2 from the formula

$$\log_{10} \frac{k_a(p_2)}{k_a(p_1)} = -\frac{\Delta V^{\ddagger}_{mean}(p_2 - p_1)}{2.303RT}$$

against $(p_1+p_2)/2$, where $k_a(p_1)$ and $k_a(p_2)$ are the rate constants at the adjacent pressures p_1 and p_2, and extrapolating to zero pressure. For isobutylene

$$\Delta V^{\ddagger} = -11.5 \pm \sim 1.0 \text{ cm}^3 \text{ mole}^{-1} \text{ at } 35° \text{ C},$$

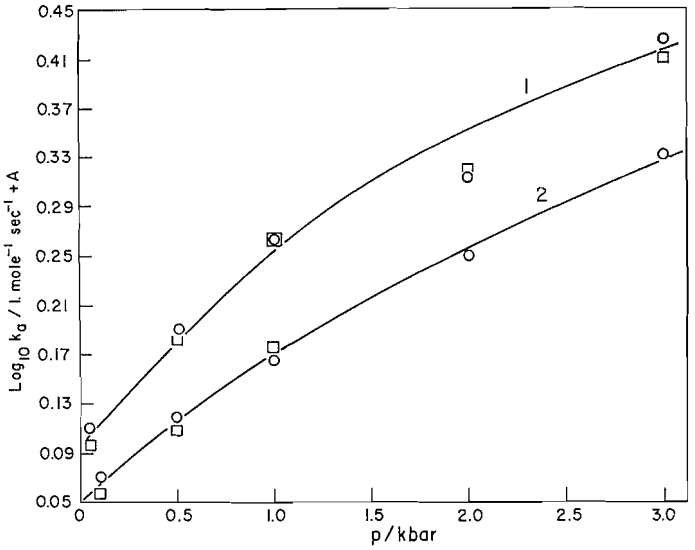

FIG. 2. Effect of pressure on the rate of the acid-catalyzed hydration of propylene and isobutylene catalyzed by aqueous perchloric acid. Curve 1: isobutylene at 35° C, A = 3. Curve 2: propylene at 100° C, A = 3.81.

Can. J. Chem. Downloaded from www.nrcresearchpress.com by 210.87.254.105 on 09/05/12
For personal use only.

and for propylene

$$\Delta V^{\ddagger} = -9.6 \pm \sim 1.0 \text{ cm}^3 \text{ mole}^{-1} \text{ at } 100^\circ \text{ C.}$$

An Arrhenius plot of the second-order constants for the hydration of propylene is given in Fig. 3. There appears to be a curvature, indicating that a change of mechanism may be

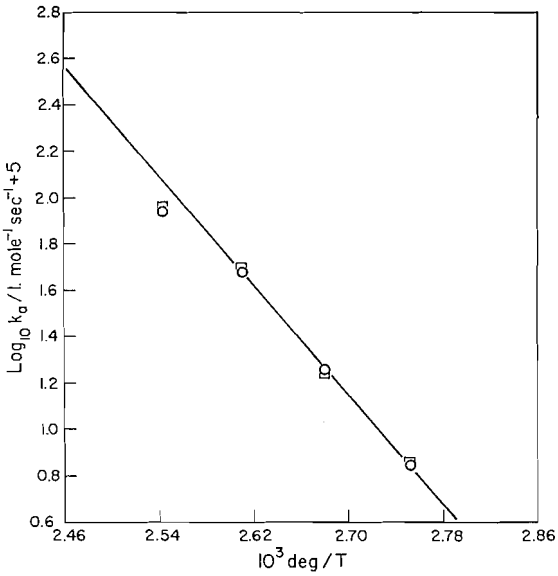

FIG. 3. Effect of temperature on the rate of the acid-catalyzed hydration of propylene at 100 bars.

occurring. However, no great weight should be put on this until the curvature is confirmed. The parameters at 100° C and 100 bars of the Arrhenius equation, obtained graphically from the line drawn in Fig. 3, are

$$E_A = 27.1 \pm \sim 1 \text{ kcal mole}^{-1},$$

$$\log_{10} A/\text{l. mole}^{-1} \text{ sec}^{-1} = 12.1,$$

and the entropy of activation $\Delta S^{\ddagger}$ [$= R \ln(A/\text{l. mole}^{-1})(h/ekT)$] is $-5.4 \pm \sim 2.5$ cal deg^{-1} mole^{-1}. The difference between these values and those for zero pressure or 1 bar will be quite inappreciable.

4. DISCUSSION

The volumes of activation for the acid-catalyzed hydration of propylene and isobutylene are $-9.6 \pm \sim 1.0$ cm^3 mole^{-1} at 100° C and $-11.5 \pm \sim 1.0$ cm^3 mole^{-1} at 35° C respectively. A volume greater than half the volume of a water molecule is therefore lost when the transition state is formed. Information about the mechanism can be extracted from this observation.

The transition states of the slow steps of the mechanisms listed in the Introduction can be divided into two groups according as the transition state is better represented as [olefin.H$^+$]‡ (mechanism (*c*)) or as [olefin.H$^+$.H$_2$O]‡ (mechanisms (*a*), (*b*), and (*d*)). If the formation of the transition state can be represented by

$$\text{olefin} + H_3O^+ \rightarrow [\text{olefin.H}^+]^{\ddagger} + H_2O, \qquad [1]$$

Can. J. Chem. Downloaded from www.nrcresearchpress.com by 210.87.254.105 on 09/05/12
For personal use only.

there is no change in the number of molecules and probably little change in the electrostatic interaction with the solvent when the transition state is formed, and the change in the electrostatic interaction is more likely to be a decrease than an increase due to the larger size of the transition state than of H_3O^+. There is therefore probably little change in volume, or perhaps a slight increase, when the transition state is formed. On the other hand if the formation of the transition state can be represented by the reaction, or sequence of reactions represented by,

$$\text{olefin} + H_3O^+ \rightarrow [\text{olefin}.H^+.H_2O]^{\ddagger}, \qquad [2]$$

a molecule is lost by the conversion of a van der Waals bond into a partial valence bond. On theoretical and empirical grounds (17) this should be accompanied by a loss of volume of very roughly 10 cm^3 $mole^{-1}$. It seems clear therefore that the observed volumes of activation can be readily understood only if a molecule of water is bound into the transition state.

The entropies of activation support this conclusion. The entropy change for reaction [1] is roughly analogous to the entropy changes for the proton transfer reactions

$$R_3N + H_3O^+ \rightarrow R_3NH^+ + H_2O. \qquad [3]$$

The entropy changes for reactions [3] for a variety of substituents R have been collected (23). They are all positive and as high as 15 cal deg^{-1} $mole^{-1}$. While the analogy between reactions [1] and [3] is by no means perfect, it seems likely that the entropy change of reaction [1] is positive. The fact that the entropies of activation of all unimolecular acid-catalyzed (A-1) reactions that have been measured appear to be positive provides further empirical confirmation (17). Reaction [2] can be considered as the sum of reaction [1] and the reaction

$$[\text{olefin}.H^+]^{\ddagger} + H_2O \rightarrow [\text{olefin}.H^+.H_2O]^{\ddagger}.$$

The entropy change of this reaction is undoubtedly negative because of the loss of freedom of the water molecule, unless there is a considerable decrease in the electrostatic interaction with the solvent when the water molecule adds, which seems unlikely. The entropy change of reaction [2] is therefore the sum of a positive and a negative term, and the sign is at present unpredictable. We note, however, that a negative entropy of activation is predicted only if the transition state is $[\text{olefin}.H^+.H_2O]^{\ddagger}$. Empirically, all bimolecular acid-catalyzed (A-2) hydrolyses or hydrations in aqueous solution, in which the transition state can be represented as $[\text{substrate}.H^+.H_2O]^{\ddagger}$, have negative entropies of activation (17), which provides some confirmation for this view.

The entropy of activation for the hydration of propylene is $-5.4 \pm \sim 2.5$ cal deg^{-1} $mole^{-1}$ and of isobutylene is -7.7 cal deg^{-1} $mole^{-1}$ in the range 25–50° C (24). The negative values confirm the conclusion derived from the volumes of activation that the transition states have the composition $[\text{olefin}.H^+.H_2O]^{\ddagger}$, and mechanism (*c*), which has been widely held recently, can be eliminated with good assurance for propylene and isobutylene.

The structure of the transition states, as opposed to their compositions, i.e. whether the mechanisms are best represented as reactions [*a*], [*b*], [*d*], or otherwise, is a subtle question that cannot be answered at present. Several tertiary alcohols have been shown (15, 16) to exchange oxygen with the solvent by acid catalysis faster than they dehydrate. The volume of activation for the acid-catalyzed racemization of *sec*-butanol (25) indicates that the mechanism is best represented as the unimolecular decomposition of the protonated alcohol. It seems likely then that the oxygen exchange in tertiary alcohols occurs by the mechanism

$$ROH_2^+ \rightleftarrows R^+ + H_2O,$$

Can. J. Chem. Downloaded from www.nrcresearchpress.com by 210.87.254.105 on 09/05/12
For personal use only.

and that the carbonium ion reacts with water faster than it is deprotonated to form the olefin. The question whether the dehydration of the alcohol goes by the carbonium ion or by a different mechanism is unanswered by this evidence. Although it is often assumed that both exchange and dehydration go by the carbonium ion (16), there is no strong evidence that this is so.

The results reported in this paper do not, of course, throw any direct light on the mechanism of hydration of other olefins. They do, however, suggest that evidence based on the use of acidity functions should be re-examined. The most useful kinetic parameter for determining whether a molecule of water is bound into the transition state that has hitherto been widely measured is probably the entropy of activation. For many olefins it is negative, but only by a small amount (ref. 6 and this work). This indicates, on the basis of the arguments given above, that a molecule of water is bound into the transition states. However, as the entropies of activation are not far from zero, the evidence is not wholly convincing, and volumes of activation would be worth measuring.

ACKNOWLEDGMENTS

We are greatly indebted to Mr. A. Lavergne for help in maintaining the high-pressure apparatus.

REFERENCES

1. H. J. Lucas and W. F. Eberz. J. Am. Chem. Soc. **56**, 460 (1934).
2. F. G. Ciapetta and M. Kilpatrick. J. Am. Chem. Soc. **70**, 639 (1948).
3. J. B. Levy, R. W. Taft, D. Aaron, and L. P. Hammett. J. Am. Chem. Soc. **73**, 3792 (1951).
4. H. J. Lucas and Y. P. Liu. J. Am. Chem. Soc. **56**, 2138 (1934).
5. R. W. Taft, J. B. Levy, D. Aaron, and L. P. Hammett. J. Am. Chem. Soc. **74**, 4735 (1952).
6. R. W. Taft, E. L. Purlee, P. Riesz, and C. A. DeFazio. J. Am. Chem. Soc. **77**, 1584 (1955).
7. E. L. Purlee and R. W. Taft. J. Am. Chem. Soc. **78**, 5807 (1956).
8. J. B. Levy, R. W. Taft, and L. P. Hammett. J. Am. Chem. Soc. **75**, 1253 (1953).
9. J. Manassen and F. S. Klein. J. Chem. Soc. 4203 (1960).
10. R. W. Taft. J. Am. Chem. Soc. **74**, 5372 (1952).
11. A. E. Shilov, R. D. Sabirova, and V. I. Gorshkov. Dokl. Akad. Nauk SSSR, **119**, 533 (1958).
12. J. S. Coe and V. Gold. J. Chem. Soc. 4571 (1960).
13. A. V. Willi. Z. Naturforsch. **16a**, 838 (1961).
14. C. A. Bunton and V. J. Shiner. J. Am. Chem. Soc. **83**, 3214 (1961).
15. I. Dostrovsky and F. S. Klein. J. Chem. Soc. 791 (1955).
16. R. H. Boyd, R. W. Taft, A. P. Wolf, and D. R. Christman. J. Am. Chem. Soc. **82**, 4729 (1960).
17. E. Whalley. Advances in physical organic chemistry. Vol. 2. Academic Press, London. 1964. p. 93.
18. Ya. E. Shmulyakovskii. Khim. i Tekhnol. Topliv i Masel, 4, No. 12, 46 (1959).
19. A. R. Osborn and E. Whalley. Can. J. Chem. **39**, 1094 (1961).
20. J. Koskikallio and E. Whalley. Trans. Faraday Soc. **55**, 809 (1959).
21. P. W. Bridgman. Proc. Am. Acad. Arts Sci. **48**, 309 (1912); **66**, 185 (1931).
22. W. T. Holser and G. C. Kennedy. Am. J. Sci. **256**, 744 (1958).
23. E. Whalley. Trans. Faraday Soc. **55**, 798 (1959).
24. E. L. Purlee, R. W. Taft, and C. A. DeFazio. J. Am. Chem. Soc. **77**, 837 (1955).
25. R. J. Withey and E. Whalley. Can. J. Chem. **41**, 546 (1963).

Can. J. Chem. Downloaded from www.nrcresearchpress.com by 210.87.254.105 on 09/05/12
For personal use only.

Can. J. Chem. Downloaded from www.nrcresearchpress.com by 210.87.254.40 on 09/05/12
For personal use only.

THE METAL-CATALYZED AUTOXIDATION OF TETRALIN

III. CATALYSIS BY MANGANESE, COPPER, NICKEL, AND IRON[1]

Y. KAMIYA[2] AND K. U. INGOLD

Division of Applied Chemistry, National Research Council, Ottawa, Canada

Received December 20, 1963

ABSTRACT

The catalysis of the autoxidation of tetralin by the decanoates of manganese, copper, nickel, and iron has been examined over a large concentration range at 50° C. With all four metals the oxidation rate approaches a limit at high catalyst concentrations but in each case this limit is smaller than the theoretical maximum rate of oxidation of pure tetralin (Y. Kamiya *et al.* Can. J. Chem. 41, 2020 (1963)). However, upon dilution with an inert solvent, such as chlorobenzene, or with the metal acetates, acetic acid, the theoretical maximum rate is attained. The low limiting rates in pure tetralin are apparently due to the low solubilities of the catalysts and are not due to chain termination by the catalysts.

INTRODUCTION

The previous papers in this series showed that the limiting rate of the cobalt-catalyzed autoxidation of tetralin in acetic acid (1) and of pure tetralin (2) at 50° C was due to the production of a steady-state concentration of hydroperoxide. The experimental limiting rate was in fairly good agreement with the theoretical predictions of Tobolsky (3). This work has now been extended to catalysis by manganese, copper, nickel, and iron since it is of considerable interest to compare and contrast the behavior of several metal oxidation catalysts. The four metals were examined as their decanoates in pure tetralin* and as their acetates in acetic acid. The experimental technique has been described previously (1, 2). All measurements were made at 50° C.

The kinetic scheme describing the production of a steady-state hydroperoxide concentration is given by (1, 4):

$$\mathrm{ROOH} + n\mathrm{M} \xrightarrow{k_1'} \text{radical} \xrightarrow{\mathrm{RH}} \mathrm{R}\cdot, \qquad [1\mathrm{D}]$$

$$\mathrm{R}\cdot + \mathrm{O_2} \xrightarrow{k_2} \mathrm{RO_2}\cdot, \qquad [2\mathrm{D}]$$

$$\mathrm{RO_2}\cdot + \mathrm{RH} \xrightarrow{k_3} \mathrm{ROOH} + \mathrm{R}\cdot, \qquad [3\mathrm{D}]$$

$$\mathrm{RO_2}\cdot + \mathrm{RO_2}\cdot \xrightarrow{k_5} \text{inactive products} + \mathrm{O_2}. \qquad [4\mathrm{D}]$$

When the rate of hydroperoxide decomposition is negligible compared with the rate of formation, the overall rate of oxidation is given by

$$\frac{-d[\mathrm{O_2}]}{dt} = k_3\left(\frac{k_1'}{2k_6}\right)^{1/2}[\mathrm{RH}][\mathrm{ROOH}]^{1/2}[\mathrm{M}]^{n/2}. \qquad [2]$$

As the hydroperoxide concentration increases with time its rate of decomposition will eventually equal its rate of formation. This steady-state concentration is given by

$$[\mathrm{ROOH}]_\infty = \frac{k_3^{\,2}[\mathrm{RH}]^2}{2k_1'k_6[\mathrm{M}]^n}, \qquad [3]$$

[1]*Issued as N.R.C. No. 7842.*

[2]*N.R.C. Postdoctoral Fellow 1962–64.*

**Cobalt decanoate was the most soluble cobalt fatty acid salt examined previously (2).*

and, therefore, the limiting rate of oxidation is given by

$$\left(\frac{-d[O_2]}{dt}\right)_\infty = \frac{k_3^2[RH]^2}{2k_6}. \qquad [4]$$

The limiting rate defined by this equation for pure tetralin at 50° C is 1.0×10^{-3} mole/l. sec (1).

Two papers on the cobalt-catalyzed autoxidation of tetralin that have been published very recently deserve some comment. The first paper by Cerny and Hajek deals with the oxidation in acetic acid (5). These authors conclude, on the basis of very inadequate data, that the Tobolsky theory of limiting rates (3) as outlined by Woodward and Mesrobian (4) is incorrect. They prefer to interpret their results in terms of Denisov's theory (6, 7), which assumes that the radical induced decomposition of hydroperoxide predominates over the metal-catalyzed decomposition. This assumption seems very unlikely to be true at the high catalyst concentrations where limiting rates occur, and, in fact, it leads to the incorrect prediction that $[ROOH]_\infty$ is independent of the catalyst concentration. Since this is obviously incorrect, Denisov introduces two more reactions,

$$RO_2\cdot + M \rightarrow X\cdot + P,$$
$$X\cdot + RH \rightarrow XH + R\cdot,$$

which have the effect of making $[ROOH]_\infty$ inversely proportional to the catalyst concentration at high levels of catalyst. Our own work (1) showed that the radical induced decomposition of hydroperoxide only has an important effect on $[ROOH]_\infty$ at low catalyst concentrations and that the Tobolsky mechanism gives a quantitative explanation of oxidation rates and $[ROOH]_\infty$ values at high catalyst concentrations.

The second paper by Tomiska deals with the oxidation of pure tetralin (8). The initial rate was found to vary with the catalyst concentration but to be independent of the initial peroxide concentration. It was therefore concluded that chain initiation was due to the production of radicals in a reaction between the catalyst and tetralin or between the catalyst and oxygen rather than to a reaction between catalyst and hydroperoxide. However, we have shown (2) that a much more likely explanation of this effect is that chain initiation occurs by the slow decomposition of a rapidly formed cobalt catalyst – hydroperoxide complex. Tomiska showed that the rate at later times in the oxidation depends on the peroxide concentration and is only slightly greater than that of the uncatalyzed oxidation. This provides excellent evidence for catalyst deactivation during the reaction (2).

RESULTS AND DISCUSSION

1. Pure Tetralin

Oxygen Absorption

The effect of manganous, cupric, nickelous, and ferric decanoate on the rate of autoxidation of tetralin at 50° C has been examined in the range of catalyst concentrations from 2×10^{-6} mole/l. to 1.0 mole/l., the exact range depending on the activity of the metal. The maximum rate of oxidation (ρ_m) has been plotted as a function of the metal catalyst concentration in Fig. 1. The data obtained previously for cobalt (2) have been included. All the metals show the same general characteristics. That is, at low concentrations ρ_m is proportional to $[\text{catalyst}]^{1/2}$ as required by equation 2 for catalysis by a monomer of the metal. At high concentrations ρ_m becomes independent of the catalyst concentration. However, certain features of these curves are specific to each metal and therefore each

Can. J. Chem. Downloaded from www.nrcresearchpress.com by 210.87.254.40 on 09/05/12
For personal use only.

metal is separately discussed below. Comparative data on the five metal catalysts have been collected together in Table I.

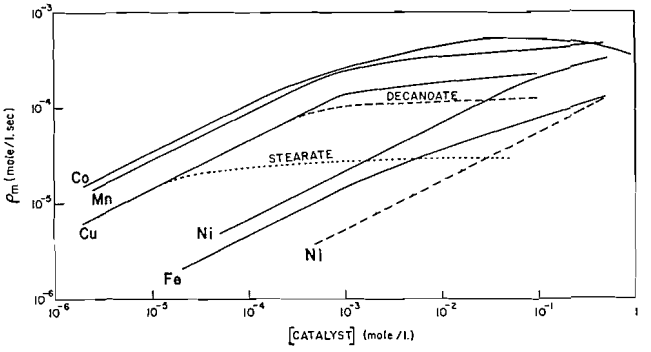

FIG. 1. The maximum rate of oxidation of tetralin as a function of metal decanoate concentration.

Manganese

A typical oxygen absorption curve is shown in Fig. 2 for a manganese decanoate concentration of 5×10^{-3} mole/l. This curve is quite different from those obtained with cobalt (2) and the other metals (see below) in that it shows a very pronounced induction period during which the rate of oxygen absorption is extremely small. The induction period depends on the initial hydroperoxide concentration ($[ROOH]_0$) since it can be readily increased or decreased by removing or adding hydroperoxide without materially affecting the main oxygen absorption curve except at very low manganese concentrations. That is, ρ_m is virtually independent of $[ROOH]_0$ at manganese concentrations above about 5×10^{-5} mole/l.

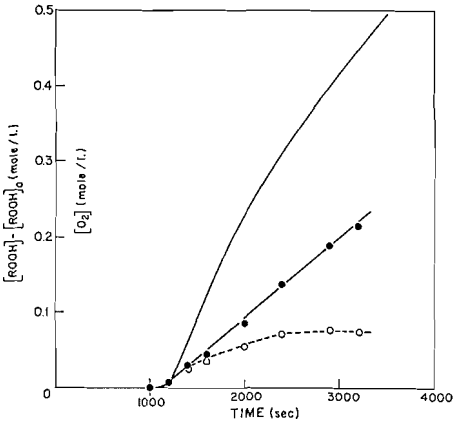

FIG. 2. Oxygen absorption and hydroperoxide formation with 5×10^{-3} mole/l. manganese decanoate. $[ROOH]_0 = 5\times10^{-4}$ mole/l. Measured $[ROOH]-[ROOH]_0$ ●. Calculated $[ROOH]-[ROOH]_0$ ○.

The induction period is roughly proportional to the manganese concentration divided by $[ROOH]_0$. When this ratio is 1.0 or less, the induction period is effectively eliminated, but it rises to about 1000 seconds for a ratio of 10 and to more than 10,000 seconds for a ratio of 100. These results suggest that divalent manganese is a powerful oxidation

Can. J. Chem. Downloaded from www.nrcresearchpress.com by 210.87.254.40 on 09/05/12
For personal use only.

inhibitor that must be almost entirely converted to the trivalent state by reaction with a roughly equivalent amount of hydroperoxide before rapid oxidation can commence, i.e., during rapid oxidation $[Mn^{III}]$ must be $\gg [Mn^{II}]$. Towards the end of the induction period the brownish color of trivalent manganese can often be observed. Once the induction period is over, the maximum rate is reached very rapidly even at high manganese concentrations. The decrease in rate after the maximum generally results from the conversion of the catalyst to a much less active form during oxidation, i.e., the catalyst is deactivated.

The inhibiting property of manganous manganese has been observed previously in autoxidations (7, 9, 10) and can be attributed to chain termination by the catalyst. That is,

$$MnA_2 + RO_2\cdot \rightarrow ROOMnA_2 \qquad [8]$$

or, alternatively,

$$MnA_2 + RO_2\cdot \rightleftarrows ROOMnA_2, \qquad [8']$$

$$ROOMnA_2 + RO_2\cdot \rightarrow \text{inactive products.} \qquad [9]$$

Incidentally, this Mn^{III} chain termination product (and also $ROMnA_2$) may, for steric reasons, be a less active peroxide decomposition catalyst than is the usual form of Mn^{III}, which is produced by reaction of MnA_2 with ROOH, i.e., $HOMnA_2$.

Over a range of manganese concentrations from 1.0×10^{-3} to 4×10^{-1} mole/l., ρ_m rises steadily from 3×10^{-4} to 4.6×10^{-4} mole/l. sec. These rates are rather less than the limiting rate of 5.3×10^{-4} mole/l. sec obtained with cobalt in our earlier work (2) and are considerably less than the theoretical limit of 1.0×10^{-3} mole/l. sec. It was suggested previously that the cobalt ρ_m values should be corrected for three effects: (i) consumption or deactivation of the catalyst (with cobalt this correction was negligible at concentrations above 5×10^{-2} mole/l.); (ii) consumption of the tetralin in those cases where a considerable fraction of the tetralin was oxidized before the maximum rate was reached; (iii) dilution of the tetralin by the catalyst (a rather small correction even at high catalyst concentrations). When these three corrections were applied to the cobalt data a limiting rate of oxidation roughly equal to the theoretical limit was obtained. However, with manganese, the second and third corrections are of little importance and even the first is only 15–20%, compared with 40% for cobalt. The reason for the smaller correction with manganese is that the maximum rate is reached after very little oxygen has been absorbed and, therefore, after comparatively little manganese has been deactivated. The total correction to the measured rate at the highest manganese concentrations is about 20–25%, which is insufficient to raise the rate to its theoretical limiting value. This result does not appear to be due to chain termination by the catalyst. That is, the inclusion of reaction 8 in the normal chain sequence yields the following kinetic expressions:

$$[ROOH]_\infty = \frac{k_3^2[RH]^2 - k_3k_8[RH][Mn]}{2k_1' k_6[Mn]},$$

$$\left(\frac{-d[O_2]}{dt}\right)_\infty = \frac{k_3^2[RH]^2 - k_3k_8[RH][Mn]}{2k_6}.$$

Alternatively, the inclusion of reactions 8′ and 9 yields

$$[ROOH]_\infty = \frac{k_3^2[RH]^2}{2k_1'[Mn](k_6 + K_8' k_9[Mn])},$$

$$\left(\frac{-d[O_2]}{dt}\right)_\infty = \frac{k_3^2[RH]^2}{2k_6 + 2K_8' k_9[Mn]}.$$

Can. J. Chem. Downloaded from www.nrcresearchpress.com by 210.87.254.40 on 09/05/12
For personal use only.

Both expressions predict a smaller limiting rate than that predicted by equation 4 but they also predict that as the manganese concentration is increased the rate will go through a maximum and then immediately decrease.* Since the limiting rate obtained with manganese is drawn out over a very large concentration range (i.e. 1×10^{-3} to 4×10^{-1} mole/l. [Mn]) it seems likely that chain termination by the catalyst is unimportant in determining its magnitude. On the other hand, ρ_m does decrease at manganese concentrations above 0.4 mole/l. (as did ρ_m for cobalt stearate) but not too much significance should probably be attached to rate data obtained in such viscous solutions (2). By and large, it seems probable that the low measured limiting rate is due to the rather low solubility of manganese decanoate in pure tetralin.

The chief evidence in favor of this view is provided by the fact that the measured and theoretical limiting rates become equal upon dilution of the tetralin with an inert solvent. This is shown in Fig. 3 in which ρ_m is plotted against the tetralin concentration at a manganese decanoate concentration of 5×10^{-2} mole/l. The tetralin has been diluted with chlorobenzene, dimethyl phthalate, and α-tetralone. In the last case, the rates have been corrected for the self-oxidation of the α-tetralone at this catalyst concentration (i.e., 6×10^{-5} mole/l. sec). The heavy line represents the theoretical limiting rate. It has a slope of 2.0 (i.e., an order of 2.0 in [RH], see equation 4) and reaches the theoretical rate of 1.0×10^{-3} mole/l. sec in pure tetralin. It can be seen that the experimental rates fall close to this theoretical line in dilute tetralin, i.e., the manganese-catalyzed reaction rate becomes roughly equal to the theoretical limiting rate and has the correct second-order dependence on tetralin concentration required by the Tobolsky theory (3). These dilution experiments provide the best test of this theory since the limiting rate will be reached at lower catalyst concentrations in dilute solution than is required in pure tetralin (2), i.e., the rate becomes less sensitive to catalyst solubilities in dilute tetralin solutions. In addition, the diluent may be a good solvent or dispersing agent for the catalyst, even water being satisfactory in this respect. For example, with 5×10^{-2} mole/l. manganese decanoate, the addition of 10% of water by volume raised the measured rate from 3.7×10^{-4} to 6.0×10^{-4} mole/l. (tetralin) sec. In contrast, organic acids inhibit the reaction. This is probably because they co-ordinate with the metal and are not readily displaced by the hydroperoxide. For example, with 4×10^{-3} mole/l. [Mn] the rate was decreased by a factor of 2.5 on the addition of 0.2 mole/l. of decanoic acid. A similar result was also obtained with copper and nickel under these conditions. On the other hand, decanoic acid increases the rate of the cobalt-catalyzed oxidation (2). In this last case the improved dispersion of the catalyst presumably outweighs any decrease in its activity resulting from association of the catalyst with the acid. Incidentally, the agreement between the measured and theoretical rates at low tetralin concentrations proves that the low limiting rate in pure tetralin is not due to a reaction between the catalyst and hydroperoxide to give non-radical products (rate constant k_1*,

$$\left(\frac{-d[O_2]}{dt}\right)_\infty = \frac{k_3^2[RH]^2}{2k_6}\frac{k_1'}{k_1'+k_1^*} \qquad (2)),$$

nor is it due to a decrease in the propagation rate constant such as might come about if a complex were formed between the chain carrying peroxy radicals and the metal catalyst.

A few experiments were performed with manganese stearate. The change in anion had

*Chain termination by reaction 8 will produce a very sharp decrease in the rate as the catalyst concentration is increased beyond a certain point, the rate reaching zero when $k_3[RH] = k_8[Mn]$ (see, for example, reference 11). Chain termination by reaction 9 will produce a slow and steady decrease in the rate.

Can. J. Chem. Downloaded from www.nrcresearchpress.com by 210.87.254.40 on 09/05/12
For personal use only.

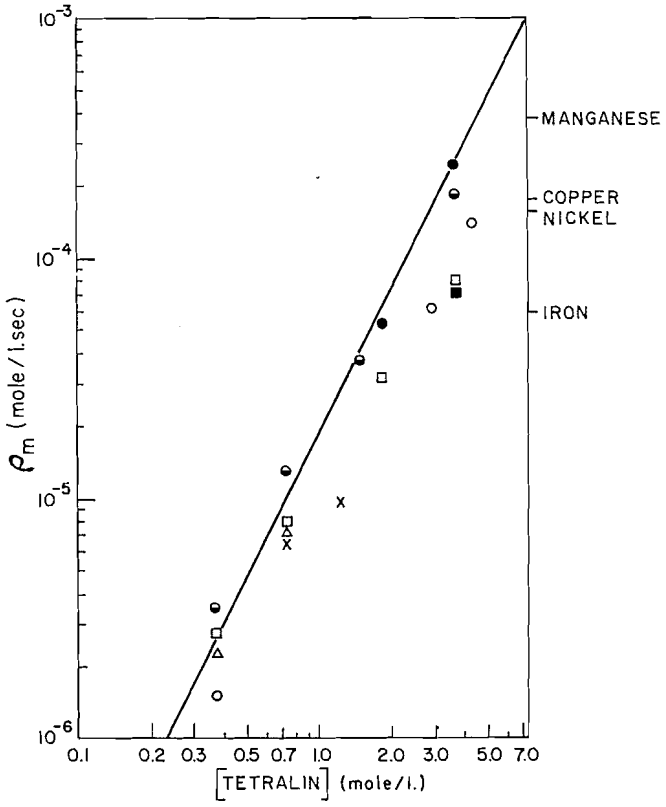

FIG. 3. The maximum rate as a function of tetralin concentration with 5×10^{-2} mole/l. of catalyst. Manganese decanoate diluted with chlorobenzene ○; with dimethyl phthalate ◒; with α-tetralone ●. Copper decanoate diluted with chlorobenzene □; with α-tetralone ■. Nickel decanoate diluted with chlorobenzene △. Ferric decanoate diluted with chlorobenzene ×. The line drawn on the figure represents the theoretical limiting rate.

little effect on the rates at low manganese concentrations but at 10^{-2} mole/l. the measured rate was slightly lower (2.9×10^{-4} mole/l. sec) than that found with the decanoate at this concentration (3.4×10^{-4} mole/l. sec). However, with the stearate the maximum rate was not reached until considerably more oxygen had been absorbed than with the decanoate case. Identical rates were obtained after the two measured rates were corrected for tetralin consumption.

The slow but steady increase in the rate at manganese concentrations above 10^{-3} mole/l. is probably due to catalysis by micelles and by solid, undispersed, catalyst. That is, the catalyst has a small but definite effect on the rate even when it is in an associated form (cf. 2, 9).

As was mentioned previously, manganese catalysts are deactivated during autoxidation. By analogy with cobalt (2), this deactivation probably occurs mainly in the chain-initiating step, the acidic products contributing only slightly to the deactivation. The extent of the deactivation will therefore be dependent on the amount of oxygen absorbed. The amount absorbed when the rate has fallen to half its maximum value ($[O_2]\rho_{m/2}$) has been plotted against the catalyst concentration in Fig. 4. The curve is similar to the one obtained previously with cobalt (2). At manganese concentrations below about 10^{-2}

Can. J. Chem. Downloaded from www.nrcresearchpress.com by 210.87.254.40 on 09/05/12
For personal use only.

mole/l. the straight line is described by the equation,

$$[O_2]\rho_{m/2} = 7.3\,[Mn]^{1/2}\ \text{mole/l.} \qquad [8]$$

This equation gives a measure of the amount of oxygen required to deactivate a given amount of catalyst at a particular concentration (2). The constant in the corresponding equation for cobalt was 12.8 $\text{mole}^{1/2}\text{l.}^{-1/2}$.

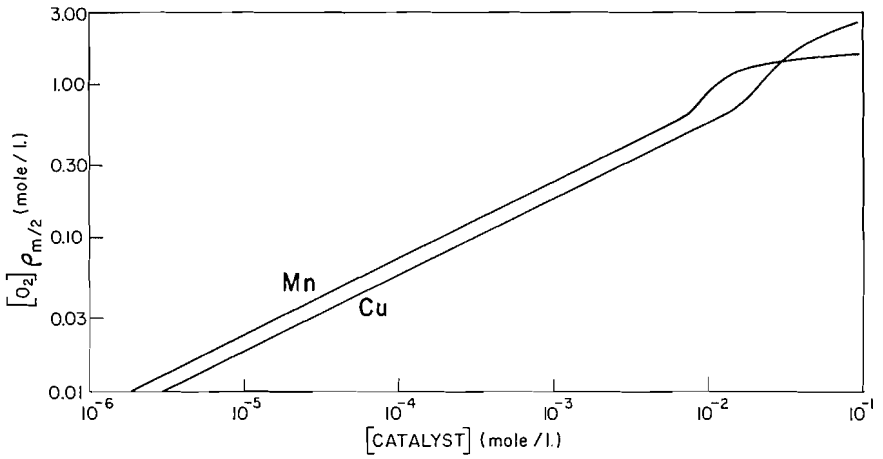

FIG. 4. Amount of oxygen absorbed when the rate reaches half its maximum value as a function of the catalyst concentration.

At manganese concentrations above 7×10^{-3} mole/l., $[O_2]\rho_{m/2}$ shows a sharp increase. This is followed by a levelling off and an approach to a constant value which has been shown to be due to consumption of the tetralin rather than to consumption of the catalyst (2). The theoretical limit of $[O_2]\rho_{m/2}$ is 2.2 mole/l. if it is assumed that each molecule of oxygen oxidizes 1 molecule of tetralin (2). At high catalyst concentrations, it is more probable that 2 molecules of oxygen oxidize 3 molecules of tetralin (1), in which case the limit will be 1.5 mole/l. With cobalt catalysts at concentrations above 2.5×10^{-2} mole/l., $[O_2]\rho_{m/2}$ reached a constant value of about 2.2–2.4 mole/l. This rather high value is probably connected with the fact that a significant fraction of the tetralin is oxidized before the maximum rate is reached (2). Since this does not occur with manganese decanoate it is not surprising to find that $[O_2]\rho_{m/2}$ appears to level off at 1.5–1.6 mole/l.

During autoxidation the deactivated manganese catalyst is precipitated. The precipitate from a 4.5 hour oxidation catalyzed by 10^{-3} mole/l. manganese decanoate contained 33.0% [Mn] by weight, 73% of the manganese being recovered (cf. analysis of a cobalt precipitate under similar conditions (2)). X-Ray examination of the precipitate in a focusing camera using monochromatic CuK_α radiation showed that it was completely amorphous and its infrared spectrum in a nujol mull contained only the broad bands corresponding to hydrogen-bonded hydroxyl groups.

As a result of catalyst deactivation it is quite difficult to obtain meaningful results at low concentrations. For example, the plot of ρ_m against [Mn] tends to show the same too-rapid decrease in rate as the manganese concentration is reduced as was observed previously with cobalt (2), i.e., the apparent order in [Mn] appears to increase as the manganese concentration is reduced. Similarly, in the $[O_2]\rho_{m/2}$ against [Mn] plot, the

Can. J. Chem. Downloaded from www.nrcresearchpress.com by 210.87.254.40 on 09/05/12
For personal use only.

Can. J. Chem. Downloaded from www.nrcresearchpress.com by 210.87.254.40 on 09/05/12
For personal use only.

experimental points show a positive deviation at low manganese concentrations and tend to a limit of about 0.02 mole/l. These deviations from the expected kinetics are more pronounced with manganese than with cobalt, possibly because it is more rapidly deactivated.* Thus, if the induction period is eliminated by the initial addition of hydroperoxide then a significant fraction of the manganese catalyst may be deactivated before any rate measurements are made. Alternatively, if no hydroperoxide is added, the same deactivating process will probably slowly occur during the induction period. In either case, the true manganese concentration will be less than its initial concentration at the point where the first rate measurements are made. However, at manganese concentrations below about 5×10^{-5} mole/l., there is an optimum initial hydroperoxide concentration which minimizes the effects of catalyst deactivation. For example, with 2.5×10^{-6} mole/l. [Mn] the following maximum rates were obtained: 2.6×10^{-6} mole/l. sec ($[ROOH]_0<10^{-5}$ mole/l.); 1.15×10^{-5} ($[ROOH]_0 = 5\times10^{-4}$); 5.8×10^{-6} ($[ROOH]_0 = 10^{-3}$); 4.6×10^{-6} ($[ROOH]_0 = 4\times10^{-3}$); 2.8×10^{-6} ($[ROOH]_0 = 3\times10^{-2}$).† These values can be compared with a rate of 1.4×10^{-5} mole/l. sec, which is obtained by extrapolation of the data in the concentration range from 5×10^{-5} to 1×10^{-3} mole/l. [Mn] where ρ_m is much less sensitive to $[ROOH]_0$ and has the expected dependence on the square root of the manganese concentration. Similarly, at 1×10^{-5} mole/l. [Mn] the extrapolated rate was 2.8×10^{-5} mole/l. sec, which can be compared with measured rates of 1.4×10^{-5} ($[ROOH]_0 = 5\times10^{-4}$ mole/l.); 2.3×10^{-5} ($[ROOH]_0 = 3.5\times10^{-3}$); and 1.7×10^{-5} ($[ROOH]_0 = 7\times10^{-2}$). It is obviously difficult to obtain true maximum rates at low manganese concentrations but, under optimum conditions, the results suggest that ρ_m is proportional to $[Mn]^{1/2}$ in the range from 2.5×10^{-6} to 1.0×10^{-3} mole/l. [Mn]. This implies that chain termination by the catalysts is unimportant at these low concentrations (9). At the optimum initial hydroperoxide concentration, the $[O_2]\rho_{m/2}$ points at low manganese concentrations also fall fairly close to the line obtained by extrapolation from higher concentrations.

The observation that the initial hydroperoxide concentration only increases ρ_m up to a certain limiting value implies that the rate-controlling chain-initiation reaction between manganese and hydroperoxide is not the simple bimolecular process suggested by reaction 1D. Instead, the rate-controlling step must involve the slow decomposition of a rapidly formed complex. By analogy with cobalt (2), this reaction can be written as:

$$ROOH + Mn^{III} \overset{\text{fast}}{\rightleftarrows} [ROOHMn^{III}] \overset{\text{slow}}{\rightarrow} RO_2\cdot + Mn^{II} + H^+. \qquad [1b']$$

By comparing relative rates of oxidation with different catalysts at the same concentration in the region where ρ_m is proportional to $[\text{catalyst}]^{1/2}$ but is independent of [ROOH] we can compare the rates of decomposition of the different catalyst–hydroperoxide complexes. That is, the rate of oxidation will be given by

$$\frac{-d[O_2]}{dt} = k_3\left(\frac{k_1'}{2k_6}\right)^{1/2}[RH][M]^{1/2}$$

where k_1' is the rate constant for decomposition of the ROOH–M complex. Since $(\rho_m)_{Mn}/(\rho_m)_{Co} = 0.83$ for the uncorrected rates, $(k_1')_{Mn}/(k_1')_{Co} = 0.69$. There is only a small error involved in using measured ρ_m values which have not been corrected for catalyst deactivation, etc.

*This would mean that, for a given extent of catalyst deactivation, smaller concentrations of catalyst-solubilizing oxidation products will be formed in the presence of manganese. Differences in measured and in extrapolated rates between cobalt and manganese at high concentrations may be due to this factor rather than to any intrinsic differences in the solubilities of their decanoates.

†In contrast, the rate tends to reach a limiting value as $[ROOH]_0$ is increased with the other metals (including cobalt (2)).

At manganese concentrations above about 2×10^{-2} mole/l. the rate of oxygen absorption frequently goes through two maxima, an effect which becomes more pronounced the higher the manganese concentration. An excellent example of this phenomenon is shown in Fig. 5. After correcting for tetralin consumption the two maximum rates are approximately equal. This suggests that the manganese decanoate in solution at the start of the reaction (solubilized by a large $[ROOH]_0$) is deactivated more rapidly than fresh catalyst can be dissolved into the solution. The rate therefore decreases after the first maximum. Subsequently, the oxidation products solubilize undissolved catalyst so that the concentration of active catalyst in solution rises and the rate goes through the second maximum. This effect was observed previously with cobalt stearate (the first cobalt salt studied (2)) at concentrations above 5×10^{-3} mole/l. provided the stearate was added to the reaction vessel as a solution and the solvent was then removed under vacuum. When the cobalt catalyst was added as a solid the double maxima were not observed. This phenomenon is presumably more noticeable with manganese because it is more rapidly deactivated than cobalt.

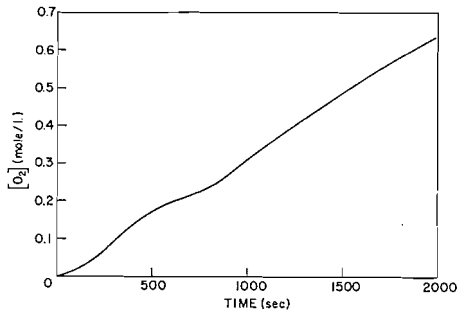

FIG. 5. Oxygen absorption at a manganese decanoate concentration of 0.3 mole/l., $[ROOH]_0 = 0.4$ mole/l.

TABLE I

Comparison of five metal decanoates as catalysts of tetralin autoxidation at 50° C

	Decanoate catalysts				
	Co^{II}	Mn^{II}	Cu^{II}	Ni^{II}	Fe^{III}
Largest measured ρ_m (mole/l. sec $\times 10^4$)	5.3	4.6	2.2	3.1	1.3
Largest corrected ρ_m (mole/l. sec $\times 10^4$)	10	5.7	3.0	4.3	1.8
$(k_1')_M/(k_1')_{Co}$	1.0	0.69	0.18	0.004	0.002
Kk_1' from $(-d[O_2]/dt)_\infty$ and $[ROOH]_\infty$(l./mole sec)	2.9	2.7	0.67	—	—
Kk_1' from direct measurement (l./mole sec)	5.0	3.5	0.33	0.002	—
$k_i/(2k_6)^{1/2}$ (l./mole sec)$^{1/2}$	0.31	0.19	0.14	—	—
$[O_2]\rho_{m/2}/[M]^{1/2}$ (mole/l.)$^{1/2}$	12.8	7.3	5.8	—	2.8

Copper

For initial hydroperoxide concentrations below about 5×10^{-2} mole/l. the maximum rate of oxidation rises steadily from 1.0×10^{-4} to 1.25×10^{-4} mole/l. sec over a range of copper decanoate concentrations from 10^{-3} to 10^{-1} mole/l. (see broken line in Fig. 1). The correction for catalyst deactivation is about 10% at copper concentrations below about 5×10^{-3} mole/l. At higher copper concentrations the correction for tetralin consumption becomes quite significant since appreciable oxidation has to occur before ρ_m is reached (cf. oxidation curves at high cobalt concentrations (2)). This correction amounts to about 40% at 0.1 mole/l. [Cu], giving a corrected ρ_m of about 1.8×10^{-4} mole/l. sec. However,

Can. J. Chem. Downloaded from www.nrcresearchpress.com by 210.87.254.40 on 09/05/12
For personal use only.

this correction is very much smaller if $[ROOH]_0$ is increased to 0.3 mole/l. since the maximum rate now occurs nearly at the beginning of the reaction (see Fig. 6). Further increases in $[ROOH]_0$ only affect ρ_m at copper concentrations above about 10^{-2} mole/l. and even then the effect is quite small. For example, with 0.1 mole/l. [Cu], ρ_m is 1.8×10^{-4} mole/l. sec with 0.3 mole/l. $[ROOH]_0$ and is 2.2×10^{-4} mole/l. sec with 1.0 mole/l. $[ROOH]_0$. Incidentally, the only correction of any significance which has to be applied to these measured rates allows for the dilution of the tetralin by the added hydroperoxide.* The largest measured rates which were actually obtained are shown as the solid line in Fig. 1. They are roughly equal to the corrected rates obtained from the runs with low initial peroxide concentrations. These very large $[ROOH]_0$ values have no effect on ρ_m at low copper concentrations, i.e., ρ_m at 2×10^{-6} mole/l. [Cu] is the same for 0.04 and 0.3 mole/l. $[ROOH]_0$ (cf. cobalt (2)). At high copper concentrations one of the main functions of the added peroxide is probably to solubilize the catalyst. Water also has this effect, 10% by volume increasing the rate with 5×10^{-2} mole/l. [Cu] and 10^{-3} mole/l. $[ROOH]_0$ by about 15%. As with manganese, ρ_m decreases at very high copper concentrations (>0.3 mole/l.). A typical oxygen absorption curve is shown in Fig. 6.

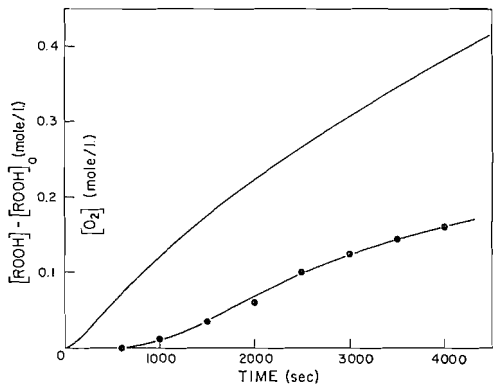

FIG. 6. Oxygen absorption and hydroperoxide formation with 5.0×10^{-3} mole/l. copper decanoate. $[ROOH]_0$ = 0.3 mole/l. Measured $[ROOH] - [ROOH]_0$ ●.

The steady rate obtained with copper stearate at an initial peroxide concentration of 0.04 mole/l. is much smaller than the rate obtained with the decanoate (see dotted line in Fig. 1). This is not unexpected if the rate is determined by the solubility of the catalyst. Increasing the initial peroxide concentration to 0.3 mole/l. at a copper stearate concentration of 10^{-2} mole/l. raised the rate to 1.35×10^{-4} mole/l. sec, which is not much less than the value found with the decanoate under these conditions. The effect of the added peroxide can probably be entirely explained by its solubilizing action on the stearate. However, the possibility that there is a smaller equilibrium constant for the formation of the peroxide–stearate catalyst complex than for the peroxide–decanoate catalyst complex cannot be completely ruled out.

Evidence that the limiting rate is determined by catalyst solubilities was again obtained by experiments in which the tetralin was diluted with an inert solvent. With 5×10^{-2} mole/l. of copper decanoate and 0.3 mole/l. $[ROOH]_0$† the experimental and theoretical rates are in excellent agreement at low tetralin concentrations (see Fig. 3).

**This is also true of the rates obtained with nickel and iron decanoates at high* $[ROOH]_0$.
†*The rate in pure tetralin is marked at this initial peroxide concentration in Fig. 3.*

Can. J. Chem. Downloaded from www.nrcresearchpress.com by 210.87.254.40 on 09/05/12
For personal use only.

Catalyst deactivation again occurs mainly in the initiation reaction (see ref. 12) and therefore the amount of oxygen absorbed when the rate reaches half its maximum value is proportional to the square root of the catalyst concentration (Fig. 4), i.e., $[O_2]\rho_{m/2} = 5.8$ $[Cu]^{1/2}$ mole/l. The experimental ρ_m and $[O_2]\rho_{m/2}$ values at low copper concentrations are much less sensitive to the initial peroxide concentration than are the manganese values and they therefore show a more exact dependence on $[catalyst]^{1/2}$. At concentrations below 0.1 mole/l. the present results show none of the peculiarities which have been observed in some other autoxidation systems and which probably arise from chain termination by the copper catalyst (7, 10, 11, 13).

Nickel

Nickel decanoate appears to be rather more soluble than copper decanoate but it is a much less active catalyst. The ρ_m values depend on $[ROOH]_0$ over the entire concentration range rather than just at high concentrations, which suggests that the added hydroperoxide is not serving solely as a solubilizing agent for the catalyst. This is confirmed by the fact that with 5×10^{-3} mole/l. of nickel decanoate ρ_m is proportional to the square root of the initial peroxide concentration from 0.1 to 1.0 mole/l. $[ROOH]_0$ as required by equation (2) (see Fig. 7). In this $[ROOH]_0$ concentration range ρ_m occurs right at the beginning of the reaction (see Fig. 8). At lower $[ROOH]_0$ concentrations ρ_m is not reached until a significant amount of oxygen has been absorbed (Fig. 9). Therefore, ρ_m can no longer be expected to be proportional to $[ROOH]_0^{1/2}$, particularly in view of the fact that some of the nickel catalyst will have been deactivated by the time ρ_m is reached. At low $[ROOH]_0$, ρ_m actually decreases to a constant value, but the *initial* rates continue to be proportional to $[ROOH]_0^{1/2}$ (see Fig. 7).

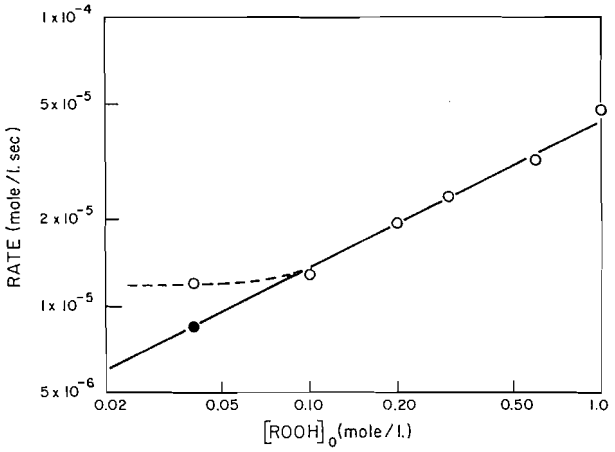

FIG. 7. Measured rates of oxidation with 5×10^{-3} mole/l. nickel decanoate as a function of $[ROOH]_0$. The rates have not been corrected for the diluting effect of the added peroxide. Key: initial rate ● ; maximum rate ○.

The dependence of the rate on $[ROOH]_0^{1/2}$ could arise if the nickel catalyst did not form a complex with the hydroperoxide prior to the formation of free radicals. However, this would make nickel quite different from the other metal catalysts. It therefore seems more reasonable to suppose that the equilibrium constant for the formation of the nickel–peroxide complex is rather smaller than the equilibrium constants for the other metals.

The solid line in Fig. 1 represents ρ_m values obtained with $[ROOH]_0 = 1.0$ mole/l. and

Can. J. Chem. Downloaded from www.nrcresearchpress.com by 210.87.254.40 on 09/05/12
For personal use only.

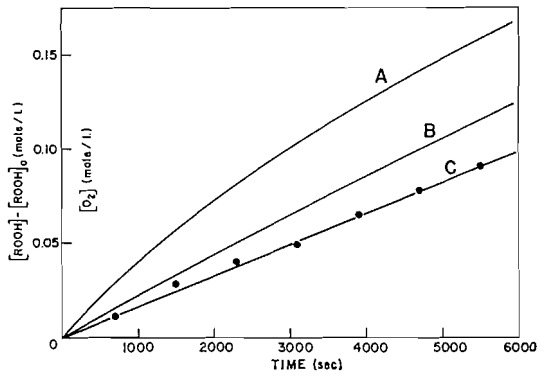

FIG. 8. Oxygen absorption and hydroperoxide formation with 5×10^{-3} mole/l. nickel decanoate. (A) Oxygen absorption with $[ROOH]_0 = 1.0$ mole/l. (B) Oxygen absorption with $[ROOH]_0 = 0.3$ mole/l. (C) Peroxide formation (i.e., $[ROOH] - [ROOH]_0$) with $[ROOH]_0 = 0.3$ mole/l.

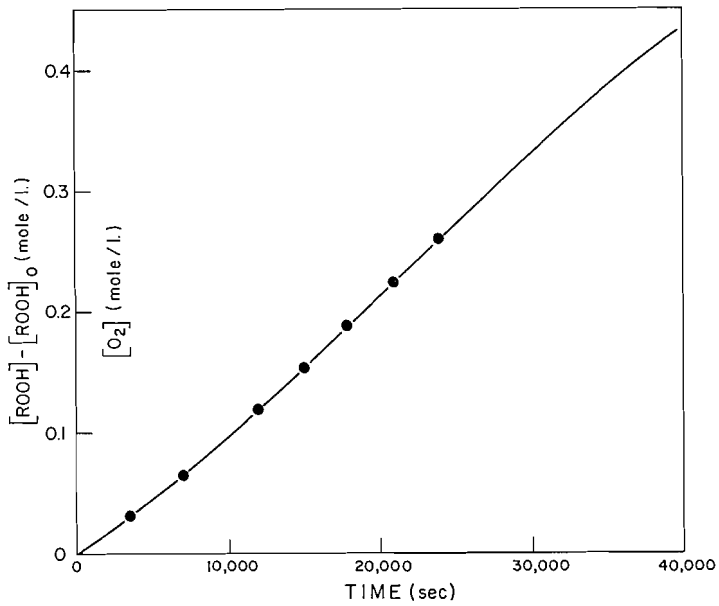

FIG. 9. Oxygen absorption and hydroperoxide formation with 5×10^{-3} mole/l. nickel decanoate. $[ROOH]_0 = 4\times10^{-2}$ mole/l. Measured $[ROOH] - [ROOH]_0$ ●.

the dotted line ρ_m values obtained with $[ROOH]_0 \leqslant 4\times10^{-2}$ mole/l. Since ρ_m depends on $[ROOH]_0^{1/2}$ up to at least 1.0 mole/l. [peroxide] the rate constant for decomposition of the expected nickel-peroxide complex (k_1') cannot be compared with the rate constants for the other metals.

At low initial peroxide concentrations virtually all the absorbed oxygen appears as peroxide (see Fig. 9). This is presumably due to the low rate of chain initiation. That is, since the rate of chain termination is proportional to $[RO_2\cdot]^2$, the chain length will be very long and therefore a large amount of oxygen will be absorbed for every molecule of hydroperoxide decomposed. At the beginning of the reaction the low rate of chain initiation is due to the low peroxide concentration. Later, when the peroxide concentration has

Can. J. Chem. Downloaded from www.nrcresearchpress.com by 210.87.254.40 on 09/05/12
For personal use only.

built up, the rate of chain generation is still small because much of the catalyst will have been deactivated. In general, the amount of peroxide produced will become more nearly equal to the amount of oxygen absorbed as the activity of the catalyst, and hence the rate of radical production, decreases. Such decreases in catalyst activity can include a decrease in $[ROOH]_0$ (cf. peroxide formation in Figs. 8 and 9) as well as a change in the catalyst (cf. peroxide formation in Figs. 6 and 8*).

Dilution with chlorobenzene (0.3 mole/l. $[ROOH]_0$ for diluted tetralin) again suggests that the measured limiting rate is due to the low solubility of nickel decanoate in pure tetralin (see Fig. 3). The relation between $[O_2]\rho_{m/2}$ and the catalyst concentration depends on $[ROOH]_0$ because of the variation in chain length with $[ROOH]_0$. For example, at catalyst concentrations below about 5×10^{-2} mole/l., $[O_2]\rho_{m/2}/[Ni]^{1/2}\approx2.5$ (mole/l.)$^{1/2}$ at $[ROOH]_0 = 0.3$ mole/l. and ≈7.5 (mole/l.)$^{1/2}$ at $[ROOH]_0 = 4\times10^{-2}$ mole/l. Deactivation by acidic products is relatively unimportant (cf. ref. 14).

Iron

Ferric decanoate is a rather inactive catalyst that requires large initial peroxide concentrations to give the true maximum rates even at fairly low catalyst concentrations. For example, with 5×10^{-3} mole/l. $[FeDe_3]\rho_m$ is 2.3×10^{-5}, 2.1×10^{-5}, and 1.0×10^{-5} mole/l. sec at $[ROOH]_0$ values of 1.0, 0.3 (Fig. 10), and 0.1 mole/l., respectively. In the first two cases, although the rate is at its maximum value for only a very short time and for only a small degree of oxygen absorption, the subsequent decrease in the rate is very slow. This suggests that the catalyst may be quite rapidly converted to a slightly less active form that is very resistant to further deactivation. At lower initial peroxide concentrations, ρ_m is not reached until a fair amount of oxygen has been absorbed. The results suggest that the equilibrium constant for the formation of the catalyst–peroxide complex is slightly larger with iron than with nickel but is still much smaller than with the other three metals. The rate constant for decomposition of the complex is smaller with iron than with any of the other metals.

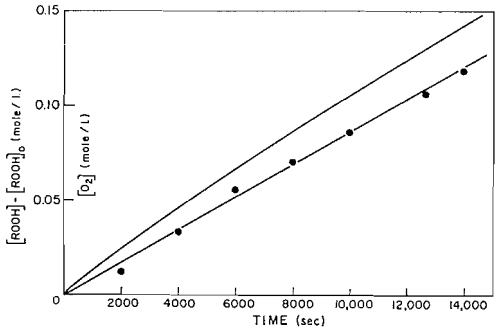

FIG. 10. Oxygen absorption and hydroperoxide formation with 5×10^{-3} mole/l. ferric decanoate. $[ROOH]_0 = 0.3$ mole/l. Measured $[ROOH] - [ROOH]_0$ ●.

At catalyst concentrations above 5×10^{-3} mole/l. ρ_m is noticeably larger with 1.0 mole/l. $[ROOH]_0$ than with 0.3 mole/l. For example, in the latter case ρ_m reaches a constant value of 5.4×10^{-5} mole/l. sec from 0.2 to 0.5 mole/l. $[FeDe_3]$. This limit is probably due both to the low solubility of the catalyst as well as to the fact that 0.3 mole/l. of peroxide will be insufficient to complex all the catalyst, i.e., the chain initiation rate will be dependent

**Similarly, with 5×10^{-3} mole/l. copper decanoate and 4×10^{-2} mole/l. $[ROOH]_0$ after 2500 sec, absorbed $[O_2] = 0.22$ mole/l., and $[ROOH] - [ROOH]_0 = 0.16$ mole/l. (cf. Fig. 9).*

Can. J. Chem. Downloaded from www.nrcresearchpress.com by 210.87.254.40 on 09/05/12
For personal use only.

on the peroxide concentration. Thus, with 1.0 mole/l. $[ROOH]_0$, the rate rises to 1.3×10^{-4} mole/l. sec at 0.5 mole/l. $[FeDe_3]$. The line in Fig. 1 represents ρ_m values obtained with $[ROOH]_0$ equal to 1.0 mole/l. at catalyst concentrations above 5×10^{-3} mole/l. At low catalyst concentrations it represents the values obtained with 0.3 mole/l. $[ROOH]_0$.

Dilution with chlorobenzene (0.3 mole/l. $[ROOH]_0$ for the diluted tetralin) indicates that ρ_m is controlled by catalyst solubility (Fig. 3). With high initial peroxide concentrations the amount of oxygen absorbed at the half maximum rate is given by, $[O_2]\rho_{m/2} = 2.8$ $[Fe]^{1/2}$ mole/l. in the range from 10^{-3} to 10^{-2} mole/l. $[FeDe_3]$. This very rapid deactivation may possibly be due to the production of phenolic inhibitors by the catalytic decomposition of tetralin hydroperoxide (cf. inhibiting action of ferric chloride on the autoxidation of cumene and tetralin (15)).

Hydroperoxide Formation

The formation of tetralin hydroperoxide in the presence of 5×10^{-3} mole/l. catalyst is shown in Figs. 2, 6, 8, 9, and 10. As was mentioned above, the amount of peroxide formed becomes more nearly equal to the amount of oxygen absorbed as the activity of the catalyst decreases. With the exception of copper, the amount of peroxide produced tends to increase steadily during the reaction, there being no steady-state concentration, i.e., no $[ROOH]_\infty$. This was also observed previously with cobalt and was attributed to the low solubility of the catalyst combined with its rapid deactivation (2). The exception, copper, apparently has a steady peroxide concentration equal to $[ROOH]_0$ in the region of the maximum rate at the beginning of the reaction, i.e., $[ROOH]_\infty = [ROOH]_0 = 0.3$ mole/l. Using this value of $[ROOH]_\infty$, the rate constant for chain initiation by copper decanoate in pure tetralin can be calculated from the ratio of equation 4 to equation 3, i.e.,

$$\left(\frac{-d[O_2]}{dt}\right)_\infty \Big/ [ROOH]_\infty = k[Cu]. \qquad [6]$$

Therefore, using the theoretical limiting rate rather than the measured limiting rate, $(k)_{Cu} = (Kk_1')_{Cu} = 0.67$ l./mole sec, where K is the equilibrium constant for the formation of the catalyst–hydroperoxide complex and k_1' is the rate constant for decomposition of this complex.

In our previous work with cobalt it was shown that the measured hydroperoxide concentration could be very roughly corrected to allow for catalyst deactivation by means of the equation relating $[O_2]\rho_{m/2}$ to the square root of the catalyst concentration (i.e. equation 8) and that this corrected peroxide concentration reached a roughly constant value (2). Upon applying the same type of correction to the manganese data, $[ROOH]-[ROOH]_0$ also reaches a steady value (see Fig. 2). However, the actual magnitude of this calculated $[ROOH]_\infty$ depends on the constant in equation 8 and therefore the validity of the results obtained by this method is open to some question. Nevertheless, it is interesting to obtain a rough measure of Kk_1' for manganese by this method for comparison with the directly measured value (see below). From the data in Fig. 2, $[ROOH]_\infty = 0.075$ mole/l., therefore $(Kk_1')_{Mn} = 2.7$ l./mole sec.

It is impossible to estimate $[ROOH]_\infty$ for nickel and iron at 5×10^{-3} mole/l. because they are such inactive catalysts that the kinetic conditions necessary for a constant peroxide concentration cannot exist. That is, with these catalysts at this concentration, $[ROOH]_\infty$ would be greater than its limiting value of 6 or 7 mole/l. for the pure peroxide. No attempt was made to obtain $[ROOH]_\infty$ values at higher catalyst concentrations because the catalysts would probably be only incompletely dissolved.

Can. J. Chem. Downloaded from www.nrcresearchpress.com by 210.87.254.40 on 09/05/12
For personal use only.

Hydroperoxide Decomposition

The rate of the metal–decanoate catalyzed decomposition of tetralin hydroperoxide in chlorobenzene has been measured. Estimation of the rate constant for this reaction is complicated by catalyst deactivation and low catalyst solubilities as well as by a radical induced peroxide decomposition process,

$$\text{radical} + \text{ROOH} \rightarrow \text{radical} + \text{products.} \qquad [i]$$

The rate of hydroperoxide decomposition is given by (2),

$$\frac{-d[\text{ROOH}]}{dt} \Big/ [\text{ROOH}][\text{M}] = Kk_1' + k_t \left(\frac{Kk_1'[\text{ROOH}]}{2k_6'[\text{M}]}\right)^{1/2}$$

and a plot of the lefthand side of this expression against $([\text{ROOH}]/[\text{M}])^{1/2}$ should give a straight line of intercept Kk_1'. A moderately good straight line was obtained with manganese decanoate over the range 1×10^{-4} to 6×10^{-4} mole/l. [Mn] and 1×10^{-2} to 6×10^{-2} mole/l. [ROOH]. The intercept was 3.5 ± 1.0 l./mole sec and the slope was 0.35 l./mole sec. The agreement between this value of Kk_1' and the value obtained indirectly from $[\text{ROOH}]_\infty$ at 5×10^{-3} mole/l. [Mn] provides some support for the assumptions implicit in calculating $[\text{ROOH}]_\infty$ from measured hydroperoxide concentrations. From the intercept and the slope $k_t/(2k_6)^{1/2}$ was calculated to be 0.19 (l./mole sec)$^{1/2}$, which is in moderately good agreement with a value of 0.31 (l./mole sec)$^{1/2}$ obtained in the same way from the cobalt data (2). At manganese concentrations above about 8×10^{-4} mole/l. the half-life for peroxide decomposition becomes virtually constant, which suggests that this concentration represents the limiting solubility of manganese decanoate in chlorobenzene at this temperature, i.e., this catalyst is about equally soluble in tetralin and chlorobenzene.

Copper decanoate is a much less active catalyst for peroxide decomposition than manganese or cobalt and the rate measurements were correspondingly less accurate. Over a range of copper concentrations from 6×10^{-4} to 5×10^{-3} mole/l. and with 1×10^{-2} mole/l. [ROOH], Kk_1' was found to be 0.33 l./mole sec and $k_t/(2k_6)^{1/2}$ was about 0.14 (l./mole sec)$^{1/2}$.

Nickel decanoate is so inactive that it was necessary to work with 5×10^{-2} to 2×10^{-1} mole/l. [Ni], which is probably beyond the limits of solubility of the catalyst in chlorobenzene. However, an approximate first-order dependence of the rate on the nickel concentration was obtained with 1×10^{-2} mole/l. [ROOH]. Neglecting any radical-induced decomposition, $Kk_1' \approx 2\times10^{-3}$ l./mole sec. No rate measurements could be made with ferric decanoate as the solutions were so strongly colored by the catalyst that the peroxide concentration could not be determined by iodometric titration.

2. Tetralin in Acetic Acid Solution

We have shown previously (1) that the kinetics applicable to the cobalt acetate catalyzed oxidation of tetralin in acetic acid are quite different from the kinetics of the cobalt decanoate catalyzed oxidation of pure tetralin and of tetralin in chlorobenzene. However, the limiting oxidation rate in acetic acid is still determined by the Tobolsky mechanism (3), i.e., it is determined by the condition that $d[\text{ROOH}]/dt = 0$ and it is therefore given by equation 4.

No attempt was made to check the overall kinetics in acetic acid for catalysis by manganous, cupric, nickelous, and ferric acetates. This was simply because these metals are all so very much less active than cobalt as catalysts for peroxide decomposition in acetic acid that a thorough kinetic treatment would be extremely tedious at the present

Can. J. Chem. Downloaded from www.nrcresearchpress.com by 210.87.254.40 on 09/05/12
For personal use only.

reaction temperature (50° C). For example, the half-life for the decomposition of 1×10^{-2} mole/l. of tetralin hydroperoxide in a 1:1 by volume acetic acid – benzene solvent mixture is more than 30,000 sec for catalysis by 2×10^{-2} mole/l. of manganese, copper, and nickel acetate.* In contrast, cobalt acetate at 1/10th of this concentration gives a half-life of 710 sec (1).

The variation in ρ_m with catalyst concentration for a 1:1 by volume mixture of tetralin and acetic acid is shown for all five acetates in Fig. 11. The rate only reaches its theoretical limit (which is 2.5×10^{-4} mole/l. sec under these conditions) with cobalt acetate. Manganous manganese is a powerful inhibitor in acetic acid just as it is in pure tetralin. To eliminate a very long induction period at least sufficient peroxide must be added at the start of the reaction to convert all the Mn^{II} to Mn^{III}. The experimental rates for iron, nickel, and copper acetate were also obtained under conditions where $[ROOH]_0 \geqslant$ [catalyst]. The results suggest that in acetic acid the active catalytic species for manganese, iron, and nickel are dimeric just as they are for cobalt (1, 4). The results with copper acetate suggest that although it is a moderately active catalyst it is extremely insoluble under these conditions.

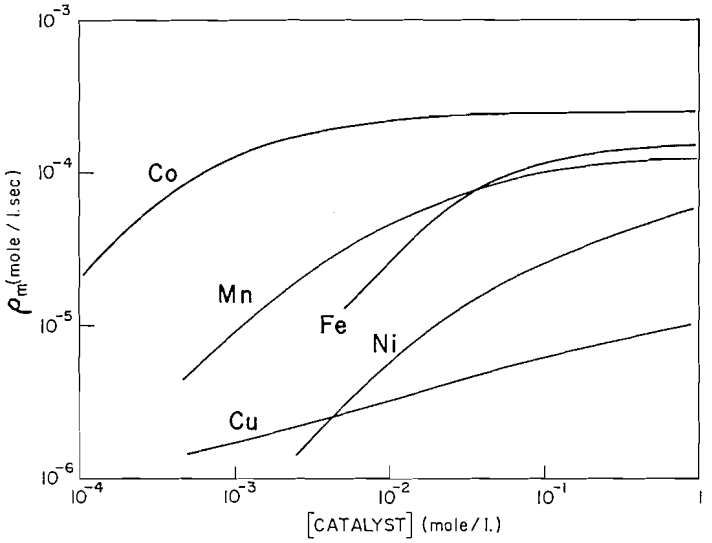

FIG. 11. The maximum rate of oxidation of a 1:1 by volume tetralin: acetic acid mixture as a function of the metal acetate concentration.

The theoretical rate upon dilution of the tetralin to 1.22 mole/l. is 2.8×10^{-5} mole/l. sec. The following rates were obtained with 0.5 mole/l. [catalyst] and 0.5 mole/l. $[ROOH]_0$ at this tetralin concentration. Manganese 2.9×10^{-5}, nickel 1.9×10^{-5}, and copper $\sim3\times10^{-6}$ mole/l. sec. Ferric acetate at 5×10^{-2} gave a rate of 2.8×10^{-5} mole/l. sec. These rates provide convincing evidence that, although manganese, iron, and nickel are less active catalysts than cobalt in acetic acid, they will nevertheless raise the rate to its theoretical limiting value in sufficiently dilute tetralin solutions. The very low rate obtained with copper is most probably due to the low solubility of the cuprous salt.

**Ferric acetate is too highly colored at this concentration for the peroxide to be determined by the usual iodometric procedure.*

Can. J. Chem. Downloaded from www.nrcresearchpress.com by 210.87.254.40 on 09/05/12
For personal use only.

CONCLUSIONS

In pure tetralin the maximum rate of oxidation is proportional to [catalyst]$^{1/2}$ at low metal catalyst concentrations and approaches a limiting value at high concentrations. This limit is controlled by a combination of the catalyst solubility and the condition that $d[\mathrm{ROOH}]/dt = 0$ as was originally proposed by Tobolsky. These two factors become readily apparent upon dilution of the tetralin with an inert solvent. There is no evidence that the magnitude of the limiting rate is in any way controlled by a chain-terminating process involving the catalyst, although such a process may effect the rates at very high catalyst concentrations (> 0.1 mole/l.). The catalysts are all deactivated during the oxidation and the rate of deactivation is proportional to the rate of initiation and, therefore, is also proportional to [catalyst]$^{1/2}$.

Finally, it should be noted that the specific order of catalytic activity of the different metals is obviously a function of the experimental conditions. That is, the curves in Fig. 1 represent rates obtained with large initial peroxide concentrations. If peroxide were not added at the beginning of the reaction, nickel and iron would appear to be much less active and manganese, in a short experiment, would appear to be totally inactive. Similarly, copper appears to be relatively much less active than the other metals in acetic acid solution compared with its activity in pure tetralin.

REFERENCES

1. Y. KAMIYA, S. BEATON, A. LAFORTUNE, and K. U. INGOLD. Can. J. Chem. **41**, 2020 (1963).
2. Y. KAMIYA, S. BEATON, A. LAFORTUNE, and K. U. INGOLD. Can. J. Chem. **41**, 2034 (1963).
3. A. V. TOBOLSKY. India Rubber World, **118**, 363 (1948).
4. A. E. WOODWARD and R. B. MESROBIAN. J. Am. Chem. Soc. **75**, 6189 (1953).
5. O. CERNY and J. HAJEK. Collection Czech. Chem. Commun. **28**, 494 (1963).
6. E. T. DENISOV. Zh. Fiz. Khim. **32**, 1269 (1958).
7. E. T. DENISOV and N. M. EMANUEL. Usp. Khim. **29**, 1409 (1960).
8. J. TOMISKA. Collection Czech. Chem. Commun. **28**, 1177 (1963).
9. A. J. CHALK and A. H. SMITH. Trans. Faraday Soc. **53**, 1214, 1235 (1957).
10. K. U. INGOLD. Lipids and their oxidation. *Edited by* H. W. Schultz and E. A. Day. Avi Publishing Co., Inc., Westport, Conn. 1963. Chap. 5.
11. D. G. KNORRE, L. G. CHUCHUKINA, and N. M. EMANUEL. Zh. Fiz. Khim. **33**, 877 (1959).
12. A. G. KORSUN, V. YA. SHLYAPINTOKH, and N. M. EMANUEL. Izv. Akad. Nauk SSSR, Otd. Khim. Nauk, 788 (1961).
13. P. W. ALLEN. J. Phys. Chem. **65**, 1906 (1961).
14. R. F. VASIL'EV, Z. G. KOZLOVA, L. G. CHUCHUKINA, V. YA. SHLYAPINTOKH, and N. M. EMANUEL. Izv. Akad. Nauk SSSR, Otd. Khim. Nauk, 1337 (1960).
15. G. S. HAMMOND, L. R. MAHONEY, and U. S. NANDI. J. Am. Chem. Soc. **85**, 737 (1963).

Can. J. Chem. Downloaded from www.nrcresearchpress.com by 210.87.254.40 on 09/05/12
For personal use only.

Can. J. Chem. Downloaded from www.nrcresearchpress.com by 210.87.254.40 on 09/05/12
For personal use only.

THE INHIBITED AUTOXIDATION OF STYRENE

PART IV. SOLVENT EFFECTS[1]

J. A. HOWARD AND K. U. INGOLD
Division of Applied Chemistry, National Research Council, Ottawa, Canada

Received November 20, 1963

ABSTRACT

The influence of solvents on the rate of the uninhibited oxidation of styrene can be roughly correlated with the dielectric constants of the solvents. It is suggested that the propagation reaction involves a dipolar transition state and that the magnitude of the solvent effects might be used to identify dipolar transition states in other oxidation reactions. The effect of solvents on the rate of oxidation of styrene inhibited by phenolic antioxidants is attributed to hydrogen bonding interactions between the phenolic hydroxyl group and the solvent. The magnitude of these interactions depends on the acidity of the phenol and on the degree of steric protection afforded the hydroxyl group by ortho-alkyl substituents.

INTRODUCTION

In recent years there has been a growing interest in the effect of the medium upon the rates of radical reactions. To gain a greater understanding of liquid phase oxidations and to continue our study on the inhibition of hydrocarbon autoxidation by phenols (1–4), we have examined the effect of a number of solvents on both the uninhibited and the inhibited autoxidation of styrene.*

The experimental technique has been described in previous papers in this series (1, 2, 3). The oxidation rates are generally reproducible to within $\pm 3\%$. All the work was done at 65° C.

RESULTS AND DISCUSSION

The Uninhibited Oxidation

The theoretical rate of the azo-bis-isobutyronitrile (AIBN) initiated oxidation of styrene is given by

$$P_0 = \rho_0 - (2e-1)k_1[I_2] = k_3[RH]\left(\frac{ek_1[I_2]}{k_5}\right)^{1/2}$$

where ρ_0 is the measured uninhibited rate, e is the efficiency of radical production by the initiator I_2, k_1 is its rate constant for decomposition, and k_3 and k_5 are the propagation and self-termination rate constants (1). RH represents the styrene. Experimentally it was found that $P_0 \propto [I_2]^{0.6}$ over a range of AIBN concentrations from 10^{-4} to 10^{-1} mole/l. (1). However, the data showed some curvature and it was suggested that the high order was due to a first-order chain terminating process occurring concurrently with the

[1]*Issued as N.R.C. No. 7815.*

**In some preliminary experiments on inhibited autoxidations the medium was changed by changing the oxidizable substrate rather than by adding a solvent to a given substrate. However, this proved to be rather unsatisfactory because completely saturated hydrocarbons (which might be expected to behave somewhat differently compared with alkyl aromatics and olefins) are so difficult to oxidize that high temperatures are required even with an initiator and the reactions are then autocatalytic. A second difficulty arises from the fact that the inhibitor may compete very efficiently for peroxy radicals relative to the hydrocarbon so that the inhibited rate is effectively zero. For example, the rate of oxidation of decalin at 100° C, initiated by 0.16 mole/l.[t-butylperbenzoate], is independent of the concentration of 2,6-di-t-butyl-4-methyl phenol over a range from 10^{-3} to 5×10^{-2} mole/l. The residual rate (1.6×10^{-6} mole/l. sec) is due to oxygen absorption by the initiator. Similar problems were encountered with n-decane and with 2,4,4-trimethyl pentane. More satisfactory results were obtained by using styrene as the oxidizable substrate and diluting it with excess inert solvent.*

normal bimolecular termination. The first-order process was considered to involve the reaction of a peroxy radical with a phenolic type inhibitor formed during the oxidation. Recently, it was suggested to us that the high order might be due to a wall effect (5) and it certainly would appear that some chains are terminated on the walls. That is, increasing the volume of styrene from the usual 5 ml to 25 ml increased the rate by 13% and decreasing the volume to 1 ml decreased the rate by 13%. However, the order in AIBN remained 0.6 for both the 1 ml and the 25 ml samples. It therefore seems quite probable that there are two first-order chain-terminating processes occurring during the uninhibited oxidation.

The rate of oxidation of a constant volume of styrene in the solvents listed in Table I is accurately first order in styrene over a concentration range from 0.42 to 1.75 mole/l. Deviations from first-order kinetics at higher styrene concentrations are positive for *n*-decane, CCl_4, *tert*-butylbenzene, etc., and are negative for acetonitrile, nitromethane, nitrobenzene, etc. The reaction is most nearly first order at all concentrations in chlorobenzene (see Table I). Because of the deviations at high styrene concentrations the oxidation rates were compared at 0.42 mole/l. styrene (1.0 ml styrene with 20 ml solvent).* The data in the various solvents are given in Table I at an AIBN concentration of 7×10^{-2} mole/l. The value given for pure styrene is the measured rate for 1.0 ml divided by 21 so that it is directly comparable with the other results. The values for toluene, *p*-xylene, and isopropanol have been corrected to allow for the self-oxidation of these solvents at this initiator concentration. They are probably less accurate than the rates obtained in solvents that resist oxidation. The reaction order with respect to $[I_2]$ was also determined in several solvents over a range of AIBN concentrations from 10^{-3} to 7×10^{-2} mole/l. The measured orders given in Table I are not too significant since with most solvents the curvature in the log (rate) against log $[I_2]$ plots is even greater than in pure styrene. However, these orders do emphasize the fact that specific correlations between the rates in different solvents and any physical properties, etc., of the solvents will depend to some extent on the AIBN concentration at which the rates are compared. As an extreme example, the rate in carbon tetrachloride becomes greater than the rate in *t*-butylbenzene at AIBN concentrations below 2×10^{-2} mole/l.

The rate constant, k_1, for the decomposition of AIBN in several solvents (determined by the rate of nitrogen evolution) is also given in Table I. In agreement with recent work (6, 7) it was found that k_1 is greater in aromatic than in aliphatic solvents.

Some values of ek_1 were determined by the induction period method of Boozer *et al.* (8) using the inhibitor 2,6-di-*t*-butyl-4-methylphenol (BMP) and the equation

$$ek_1 = n[\mathrm{BMP}]/2[I_2]t$$

where t represents the induction period, and the inhibitor stoichiometric factor, n, is assumed to have a value of 2.0. It can be seen from Table I that e appears to vary with the solvent and it is interesting to compare the present results with those reported previously by Hammond, Sen, and Boozer (6). These authors used the same inhibitor but worked with 2 ml of cumene in 4 ml of solvent at 62.5° C. Their values of e were 0.43 (CCl_4), 0.61 (benzene), 0.57 (chlorobenzene), 0.73 (nitrobenzene), and 0.73 (nitromethane). More recently, Hendry (9) has determined ek_1 in several solvents at 60° using BMP together with both cyclohexene and cumene as the substrate. His results indicate a similar variation in e with solvent together with some difference in ek_1 values between the two

*NOTE ADDED IN PROOF. *The effect of solvents on the rate of the AIBN initiated autoxidation of styrene (25% solvent – 75% styrene) at 50° C has been reported by R. Kerber (Z. Elektrochem. 63, 296 (1959)).*

Can. J. Chem. Downloaded from www.nrcresearchpress.com by 210.87.254.40 on 09/05/12
For personal use only.

Can. J. Chem. Downloaded from www.nrcresearchpress.com by 210.87.254.40 on 09/05/12
For personal use only.

TABLE I

Oxidation of 0.42 mole/l. styrene in various solvents at 65° C

Solvent	$\rho_0 \times 10^6$ mole/l. sec AIBN = 7×10^{-2} mole/l.	Order in AIBN	$k_1 \times 10^5$, sec^{-1}	$ek_1 \times 10^5$, sec^{-1}	e	$P_0 \times 10^6$ mole/l. sec	$k_3/k_5^{1/2} \times 10^2$ $l.^{1/2}mole^{-1/2}$ $sec^{-1/2}$
1. None	10.5	0.60	1.9	1.5	0.79*	9.8	2.33
2. *n*-Decane	5.0	0.57	1.2_8	0.9_2	0.72	4.6	1.35
3. Carbon tetrachloride	6.6	0.58	1.3	0.9_4	0.72	6.1	1.79
4. *t*-Butylbenzene	7.4	0.67				6.8	1.66
5. *p*-Xylene	8.6		1.8			8.0	1.95
6. Toluene	8.8	0.67	1.7	1.5	0.88	8.2	2.10
7. Benzene	9.3	0.65	1.6	1.4	0.87	8.7	2.23
8. Propionic Acid	9.6		1.8			9.0	2.20
9. Chlorobenzene	11.1	0.64	1.7_5	1.4	0.80	10.5	2.63
10. Bromobenzene	11.8					11.2	2.73
11. Acetic acid	12.6	0.66	1.8	1.8_5	1.03	12.0	2.93
12. *o*-Dichlorobenzene	13.0	0.61	1.7_5	1.3	0.74	12.4	3.10
13. 2-Propanol	13.1					12.5	3.05
14. *t*-Butanol	13.7		2.0	1.2	0.60	13.0	3.02
15. Ethanol	14.5					13.9	3.39
16. Nitrobenzene	16.5	0.66	2.0	1.6	0.80	15.8	3.67
17. Nitromethane	16.9	0.64	1.6	1.7	1.06	16.3	4.18
18. Acetonitrile	17.5	0.66	1.5	2.0	1.33	17.0	4.59

*Previous value 0.74 (3).

Can. J. Chem. Downloaded from www.nrcresearchpress.com by 210.87.254.40 on 09/05/12
For personal use only.

substrates. In particular, with cyclohexene (but not with cumene) he found that e was about 1.2 in nitromethane (k_1 measured) and about 1.0 in acetonitrile (k_1 not measured). Since e cannot be greater than 1.0 it was suggested that these anomalously high values were due to the catalysis by polar solvents of a reaction between the hydroperoxide formed during the induction period and the phenol or its phenoxy radical. It was, in fact, shown that the addition of hydroperoxide at the start of a run in nitromethane reduced the induction period. However, it does not seem likely that such reactions would be of any importance with styrene since its polyperoxide is much less reactive than most hydroperoxides. This was readily shown to be the case, that is, the induction period of a styrene–nitromethane mixture (1:20 ml) was the same whether the inhibitor was added at the start of the reaction or after the absorption of an amount of oxygen roughly equal to that absorbed at the end of the normal induction period ($\sim$0.01 mole/l.). The apparent variation in e may perhaps be associated with the fact that BMP becomes a relatively less efficient inhibitor in solvents of high polarity, i.e., the styrene competes more favorably with the phenol for peroxy radicals (see following section). As a result, the effective inhibitor concentration will tend to be reduced in these solvents which will lead to a shorter induction period and hence to an apparent increase in e. At all events, there seems no reason to believe that e will vary appreciably with the solvent and an "average" value of 0.75 was therefore used in calculating P_0 and $k_3/k_5^{1/2}$ in all solvents. The rate constant, k_1, was taken to be 1.8×10^{-5} sec^{-1} in those solvents in which it was not measured.* It is clear, that the fairly large solvent effects recorded in Table I must be mainly due to the influence of the solvents on the $k_3/k_5^{1/2}$ ratio. Any correlation that exists between a physical property of the solvents and $k_3/k_5^{1/2}$ should, therefore, apply almost equally well as a correlation with ρ_0. The determination of e and k_1 in each solvent is therefore unnecessary except insofar as it confirms or improves such a correlation.

The importance of solvent effects on free radical abstraction reactions was first demonstrated by Russell for atomic chlorinations (10). It was shown that a π-complex was formed between the chlorine atom and most aromatic solvents with a consequent reduction in the reactivity of the chlorine atom compared with its reactivity in aliphatic solvents or nitrobenzene. The oxidation rates given in Table I cannot be correlated with Russell's chlorination data since they show a completely dissimilar pattern of solvent effects. It must therefore be concluded that peroxy radical – π complexes do not play a very important role in determining $k_3/k_5^{1/2}$ for styrene. A similar conclusion was reached by Hendry as a result of his study of the AIBN-initiated oxidation of cyclohexene and cumene in a number of solvents at 60° C (9). Hendry showed instead that the oxidation rate could be very roughly correlated with the dielectric constant (D) of the solvent by means of the function $(D-1)/(2D+1)$, which describes the bulk effect of solvents on dipole forming reactions.† That is, the rate constant k' for reaction in solution is given by (12),

$$\ln k' = \ln k_0' - \frac{1}{kT}\frac{D-1}{2D+1}\left[\frac{\mu_A^2}{a_A^3}+\frac{\mu_B^2}{a_B^3}-\frac{\mu_M^{\ddagger 2}}{a_M^{\ddagger 3}}\right]+\frac{\phi_A+\phi_B-\phi_M^{\ddagger}}{kT}$$

where k_0' is the specific rate constant in a solvent of unit dielectric constant and μ and a are the dipole moment and radius of the reactants (A and B) and the transition state

Fortunately, the exact values of e and k_1 are relatively unimportant in determining P_0 since the correction factor $(2e-1)k_1[I_2]$ is small in comparison with ρ_0. Moreover, they are also relatively unimportant in determining $k_3/k_5^{1/2}$ since $\sqrt{(ek_1)}$ is comparatively insensitive to changes in e or k_1.

†A similar correlation under very different experimental conditions has been obtained by Zaikov (11) for the oxidation of ethanol and methyl ethyl ketone in benzene.

($M^{\pm}$). ϕ is a correction factor for non-electrostatic forces between the solvent and the reactants and the solvent and the transition state (e.g. dipole–quadrupole forces, van der Waals forces, and other specific solvation effects). Provided the non-electrostatic terms are small enough to be neglected a plot of log k' against $(D-1)/(2D+1)$ should be linear. Deviations from linearity will probably be greatest in solvents of low dielectric constant where the non-electrostatic terms may become relatively important. The data in Table I is presented in terms of this equation in Fig. 1 where $\log_{10}(k_3/k_5^{1/2})$ has been plotted against $(D-1)/(2D+1)$ (the dielectric constant at 25° C having been used to calculate this function). The results show a rather more linear correlation than was obtained by Hendry with cyclohexene but there is still the same sharp increase in rate for the solvents of very high dielectric constant.

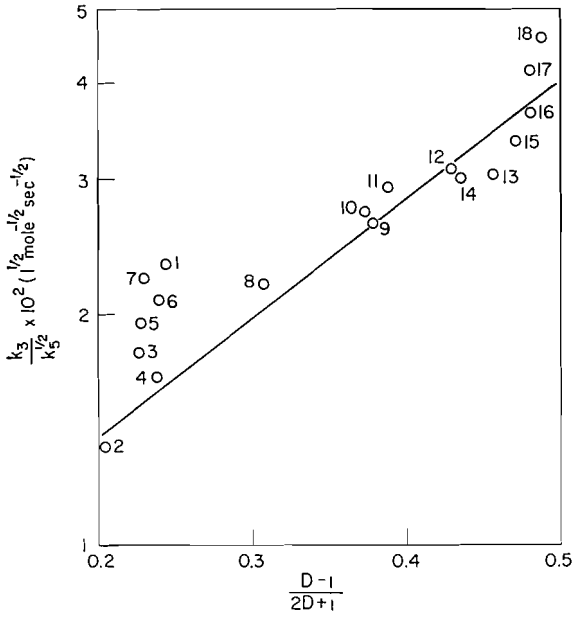

FIG. 1. Plot of $k_3/k_5^{1/2}$ for the uninhibited oxidation of styrene against the dielectric function, $(D-1)/(2D+1)$.

The rates of autoxidation of many organic substrates are extremely sensitive to trace impurities which may be either inhibitors or catalysts. Although considerable care was taken in drying and purifying the solvents used in this work, one can never be absolutely sure that a particular rate is a function of the solvent rather than of some impurity contained in it. A second factor that may produce deviations in Fig. 1 is that the pure solvent itself may become directly involved in the oxidation process, e.g. the decomposition of hydroperoxides to free radicals is accelerated in ketonic solvents (13). As would be expected, the greatest deviations of the experimental rates from the line in Fig. 1 occur in the solvents of low dielectric constant (CCl_4 and the alkyl aromatic solvents). These deviations probably arise from non-electrostatic forces, i.e., from specific solvation effects that can perhaps be attributed to the high polarizability of CCl_4 and of the π electrons of the aromatic ring.

The correlation between $\log_{10}(k_3/k_5^{1/2})$ and $(D-1)/(2D+1)$ is not significantly improved by multiplying this dielectric function by the ratio of the density (d, at 25° C) to

Can. J. Chem. Downloaded from www.nrcresearchpress.com by 210.87.254.40 on 09/05/12
For personal use only.

the molecular weight (M) of the solvent (compare, however, ref. 9), i.e., by plotting $\log_{10}(k_3/k_5^{1/2})$ against $d(D-1)/M(2D+1)$ (see Fig. 2). The factor d/M is introduced on the supposition that the radii of the reactants and of the transition state (the "a" terms in the previous equation) are not independent of the solvent but, instead, depend on its molar volume (14, 15). However, in this plot the aliphatic solvents (with the single exception of *t*-butanol, No. 14) now fall fairly close to one line, and all the aromatic solvents (including even nitrobenzene) fall close to a second steeper line, the two lines having roughly the same intercept on the rate axis. It seems reasonable to ascribe this separation of the aromatic solvents onto a separate line to a specific solvating effect of their π electron clouds.

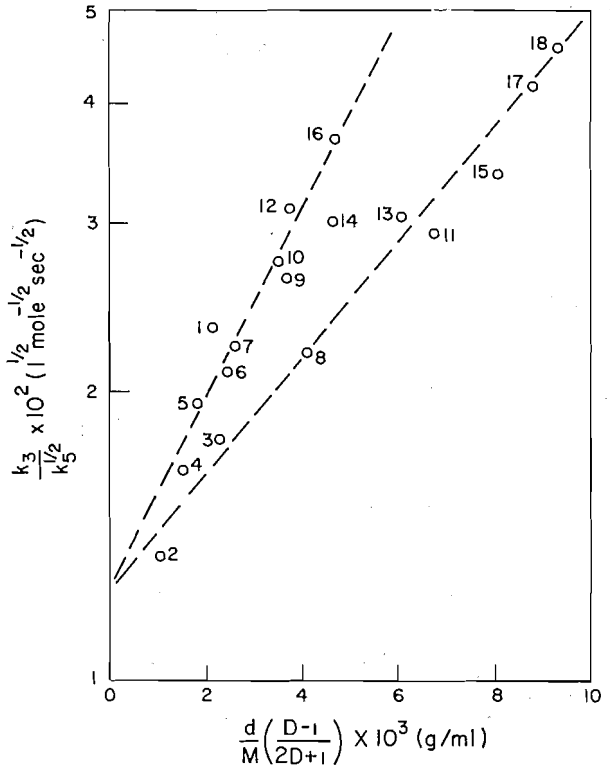

FIG. 2. Plot of $k_3/k_5^{1/2}$ for the uninhibited oxidation of styrene against the dielectric function, $d(D-1)/M(2D+1)$.

The increase of $\log_{10}(k_3/k_5^{1/2})$ with the dielectric function $(D-1)/(2D+1)$ suggests that the dipolar character of the transition state of the propagation reaction is greater than the dipolar character of the reactants,*

i.e., $$\frac{\mu_M^{\ddagger 2}}{a_M^{\ddagger 3}} > \left(\frac{\mu_A^2}{a_A^3}+\frac{\mu_B^2}{a_B^3}\right).$$

**This conclusion is based on the assumption that the increase in the dipolar character of the reactants in the propagation step on going through the transition state of this step outweighs any decrease in the dipolar character of two peroxy radicals which is produced in the transition state of the termination reaction. That is, either effect would cause the overall oxidation rate to increase with increasing solvent dielectric constant, but it is assumed that the former predominates over the latter.*

Can. J. Chem. Downloaded from www.nrcresearchpress.com by 210.87.254.40 on 09/05/12
For personal use only.

In this respect, therefore, the addition of a peroxy radical to styrene is similar to many free-radical hydrogen abstraction reactions from compounds of the type C_6H_5YH (2). It is particularly interesting to note that the rates in the hydroxylic solvents are correlated just about as well as the rates in the aprotic solvents since this is frequently not the case for reactions involving the formation of a dipolar transition state. Instead, hydroxylic solvents generally produce a greatly enhanced reactivity over that which would be expected on the basis of their dielectric constant. This is because the dielectric constant, which is a macroscopic quantity, is not a good measure of solvent-ionizing power. Several empirical methods of estimating solvating power have been suggested, including one based on the rates of solvolysis of *t*-butyl chloride in hydroxylic solvents (Y values (16)), one based on the rates of ionization of *p*-methoxyneophyl *p*-toluenesulphonate in aprotic solvents (log k_{ion} values (17)), another based on the position of the charge-transfer absorption maximum of pyridinium iodides (Z values (18)), and finally, one based on the product distribution in the cyclopentadiene – methyl acrylate addition reaction (Ω values (19)). All four of these measures of solvating power are linearly related to one another and all involve systems in which there is a rather large increase in the dipole on going from the initial state to the transition or final state. The dipoles in these systems must be stabilized by a direct interaction with hydroxylic solvents. Presumably this does not occur in the transition state of the styrene oxidation propagation reaction possibly because the amount of charge and of charge separation is very much less.

Rather convincing evidence that a dipolar transition state is involved in the oxidation of styrene is provided by a comparison of the present results with those reported by R. E. Pincock for the solvent effect on the rate of decomposition of *t*-butylperoxyformate (TBF) catalyzed by pyridine at 90° C (20). The position of attack of the base and the polarity of the transition state for this reaction can be represented by (20):

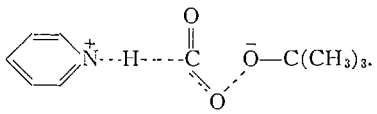

The transition state for this reaction involves a fairly large dipole so the linear relation between the logarithm of the rate constant for the TBF decomposition and log $k_3/k_5^{1/2}$ in the solvents common to both studies* (which unfortunately does not include any hydroxylic solvents) is quite gratifying (see Fig. 3).

In conclusion, we suggest that the relative magnitude of the solvent effects observed in the present work may provide a useful method of identifying dipolar transition states in other reactions.

The Inhibited Oxidation

In the presence of an inhibitor AH which completely suppresses the bimolecular self-termination reaction, the theoretical rate of oxidation is given by,

$$P = \rho - (2e-1)k_1[I_2] = \frac{ek_1k_3[RH][I_2]}{k_6[AH]}$$

where ρ is the measured inhibited rate and k_6 is the rate constant for abstraction of the active hydrogen from AH by a peroxy radical (1). It has been shown previously (3), that at moderately low concentrations of AH, P is exactly proportional to $[I_2]^{1\cdot0}/[AH]^{1\cdot0}$.†

*Point 2, refers to n-decane in our work and to n-heptane in Pincock's work.

†*At very low inhibitor concentrations the apparent order in* [AH] *decreases (even at a fixed* $[I_2]/[AH]$ *ratio) owing to the increasing importance of the self-termination reaction (1).*

Can. J. Chem. Downloaded from www.nrcresearchpress.com by 210.87.254.40 on 09/05/12
For personal use only.

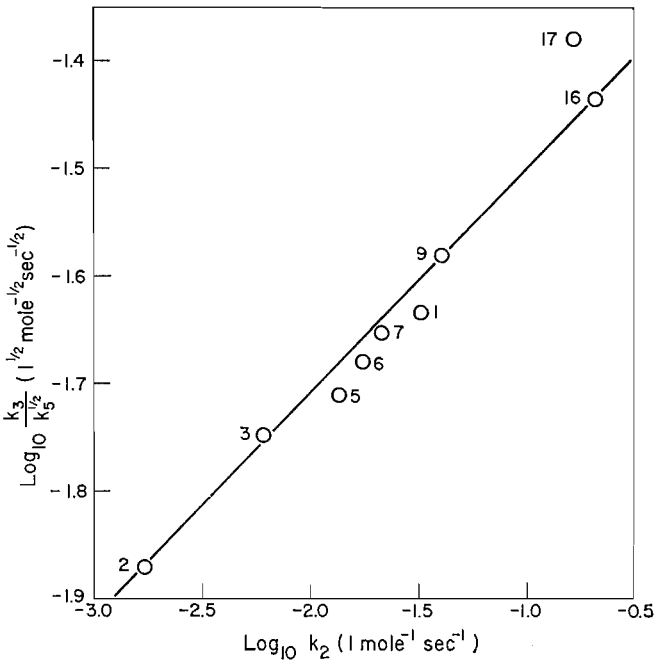

FIG. 3. Plot of $k_3/k_5^{1/2}$ for the uninhibited oxidation of styrene against the rate constant, k_2, for the pyridine-catalyzed decomposition of *t*-butylperoxyformate at 90° C.

This relationship has now been reconfirmed in several solvents at low styrene concentrations with BMP. It has also been confirmed that $P \propto [RH]^{1.0}$ in all the solvents examined at styrene concentrations below about 2.0 mole/l. The order is most nearly unity over the entire styrene concentration range in nitrobenzene (see Table II).

As the inhibitor concentration is raised, the apparent order in [AH] decreases but this is not due to chain transfer nor, in the case of BMP, is it due to intermolecular hydrogen bonding (3). The deviations from first-order kinetics occur at lower AH concentrations as the acidity of the phenolic inhibitor is increased* and as the steric protection afforded the hydroxyl group by ortho-alkyl substituents is decreased. Our initial results on the effect of solvents (particularly CH_3CN) on the rate of the BMP-inhibited oxidation immediately suggested that these kinetic peculiarities were due to complex formation between the phenols and the nitrile groups of the initiator. This is inherently probable in that, at high AH concentrations, $[I_2]$ must also be very large to obtain measurable oxidation rates.

The occurrence of non-hindered phenol–AIBN complexes was readily confirmed by examining the O–H stretching fundamental region in the infrared spectra of such mixtures in CCl_4 at room temperature. For 0.05 *M* phenol – 0.05 *M* AIBN mixtures the percentages of the phenol involved in a complex with AIBN (based on the decrease in the intensity of the free O–H band produced by the AIBN) were 33% for 3-chlorophenol, 20% for phenol, and 16% for 4-methoxyphenol. The difference in the frequencies of the free and bonded O–H band maxima ($\Delta\nu$ cm^{-1}) were 161 cm^{-1}, 138 cm^{-1}, and 137 cm^{-1} respectively, for these three phenols. It is obvious that the strength of the hydrogen bond increases with increasing acidity of the phenol and therefore parallels the kinetic deviations.

**This effect makes the determination of k_6 for phenols containing electron-withdrawing groups doubly difficult since these are also the weakest inhibitors.*

Can. J. Chem. Downloaded from www.nrcresearchpress.com by 210.87.254.40 on 09/05/12
For personal use only.

Replacing the AIBN by 0.05 M acetonitrile (i.e. halving the number of CN groups) reduces the amount of ordinary phenol in hydrogen-bonding complexes to 12%. The hydrogen bond is probably slightly stronger since $\Delta\nu$ is 155 cm^{-1}.

The infrared evidence for complexing between BMP and AIBN is not quite so clear-cut but there seems to be no doubt that it occurs. For example, a 0.05 M BMP – 0.05 M AIBN mixture in CCl_4 shows a very weak band at about 3475 cm^{-1} ($\Delta\nu$ = 175 cm^{-1}) and a second weak band at about 3625 cm^{-1} ($\Delta\nu$ = 25 cm^{-1}) which is not properly resolved and is therefore most easily seen by running the mixture against a 0.05 M BMP solution in the reference beam. These bands can be compared with those at 3627 cm^{-1} (sharp) and 3479 cm^{-1} (broad) reported by Bellamy and Williams for BMP in acetonitrile (21). There appears to be a slight shift of the O–H band maxima to longer wavelengths in the presence of AIBN but the expected small decrease in the intensity of the free O–H band cannot be measured because this band is not properly resolved from the small band at 3625 cm^{-1}. Bands in similar positions were obtained on replacing the AIBN by 0.05 M acetonitrile. With 2,6-di-t-butyl-4-cyanophenol in place of BMP the two hydrogen-bonded bands with AIBN are two or three times as intense and occur at $\Delta\nu$ values of 40 cm^{-1} and 170 cm^{-1}.

These results certainly suggest that the kinetic peculiarities we have noted previously at high phenol concentrations are due to the formation of a complex which causes the inhibitor efficiency to decrease. Further confirmation is provided by the fact that the addition of 0.1% and 1.0% by volume of acetonitrile (i.e., 2×10^{-2} and 2×10^{-1} mole/l., respectively) to a 1.74 M styrene in decane solution raised the BMP-inhibited oxidation rates ([BMP] = 9.8×10^{-5} mole/l., [AIBN] = 4.8×10^{-4} mole/l.) by 13% and 37% respectively, over the rates calculated on a linear basis from the rates in n-decane and in acetonitrile.

The formation of complexes between phenols and AIBN which affected k_6 suggested that these complexes might also affect k_1. The results of nitrogen evolution measurements from 0.2 mole/l. [AIBN] in 5 ml styrene indicated that 0.3 mole/l. [BMP] had no effect on the rate, but that 0.8 mole/l. [phenol] increased the rate by 5–10%. Similar results were obtained in tetralin. The same accelerating effect on k_1 has also been observed by Godsay *et al.* with 4-chlorophenol (22). The magnitude of this effect is such that it can be neglected in calculating k_3/k_6 but it does suggest yet another reason for the non-linear kinetics exhibited by the acidic, unhindered phenols at high concentrations.

For the reasons outlined above, the effect of solvents on the inhibited oxidation of styrene was measured at low styrene concentrations (1.74 mole/l.), low initiator concentrations (4.8×10^{-4} mole/l.), and low inhibitor concentrations (9.8×10^{-5} mole/l.). To obtain measurable rates, these conditions sometimes necessitated the use of rather large samples (up to 100 ml). However, the correction factor $(2e-1)k_1[I_2]$ was always very small. The inhibitors examined were BMP, 2,4,6-trimethylphenol, 2-t-butyl-4-methylphenol, and 4-methylphenol, these representing four general classes of phenolic antioxidants (3). Two members within a class were also examined briefly, 2,6-di-t-butyl-4-cyanophenol (for which the initiator concentration was reduced to 1.0×10^{-4} mole/l.) and 2,6-di-t-butyl-4-methoxyphenol. The values of k_3/k_6 given in Table II have been calculated on the assumption e = 0.75 in all solvents.

The k_3/k_6 values for BMP are shown plotted against $(D-1)/(2D+1)$ in Fig. 4 and against $d(D-1)/M(2D+1)$ in Fig. 5. Although these values show a general increase with D both correlations are rather poor. That is, the alkyl aromatic solvents show large positive deviations in both figures and the solvents of high dielectric constant also show large positive deviations in Fig. 4. In addition, there is considerable random scatter in

Can. J. Chem. Downloaded from www.nrcresearchpress.com by 210.87.254.40 on 09/05/12
For personal use only.

TABLE II

k_3/k_6 as a function of phenol and solvent at 65° C.
Styrene 1.74 mole/l.; AIBN 4.8×10^{-4} mole/l.; phenol 9.8×10^{-5} mole/l.

Solvent	BMP ν_m, cm^{-1}	$k_3/k_6\times10^3$ BMP	2,4,6-Me_3	2Bu^t-4Me	4Me
1. None	3634 (4)	8.47	2.41	4.20*	7.34
2. *n*-Decane	3656†	3.10	0.57	1.23	2.10
3. Carbon tetrachloride	3650 (21)	3.77	0.89	1.38	2.53
5. *p*-Xylene	3639†	5.08			
9. Chlorobenzene	3641†	5.01	1.42	2.30	3.54
10. Bromobenzene	3640 (21)	4.92			
11. Acetic acid		5.42	3.26	4.58	7.58
12. *o*-Dichlorobenzene	3637†	6.55	1.75		
14. *t*-Butanol		6.68	4.50	12.64	19.39
16. Nitrobenzene	3635 (21)	8.18			
17. Nitromethane	3630 (21)	14.77	7.27	9.89	19.0
18. Acetonitrile	3627 (sharp) 3479 (broad) (21)	23.75	14.05	20.8	35.9

*k_6 = 1.6×10^4 l./mole sec as redetermined in this work (cf. (1)).
†Frequency measured for this work.

Fig. 5. The other phenols give generally similar figures except that, in these cases, the k_3/k_6 values in the hydroxylic solvents (Nos. 11 and 14) are greatly enhanced relatively to the other solvents.

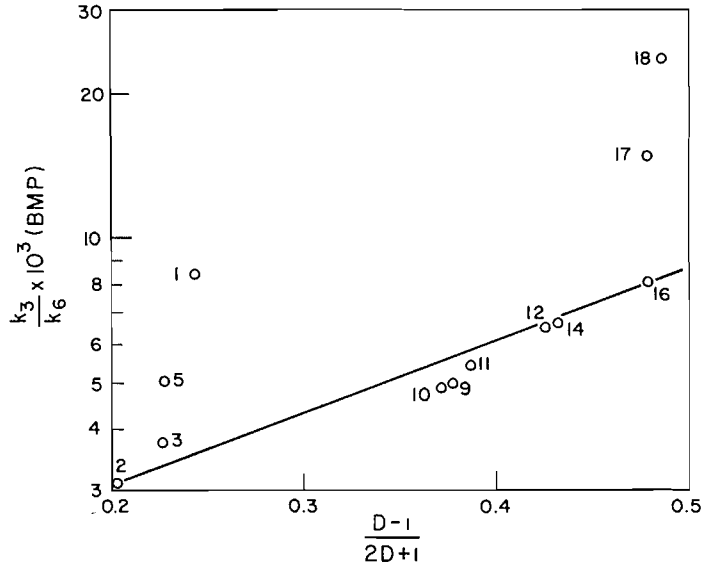

FIG. 4. Plot of k_3/k_6 for the BMP-inhibited oxidation of styrene against the dielectric function, $(D-1)/(2D+1)$.

The failure of the data to correlate with either dielectric function is not too surprising since dipolar transition states are involved in both the propagation reaction (k_3, see above) and in the termination reaction (k_6 (3)). The general increase in k_3/k_6 with D might suggest that the formation of the transition state for the propagation reaction involved the formation of a greater dipole than did the formation of the transition state for the termination

Can. J. Chem. Downloaded from www.nrcresearchpress.com by 210.87.254.40 on 09/05/12
For personal use only.

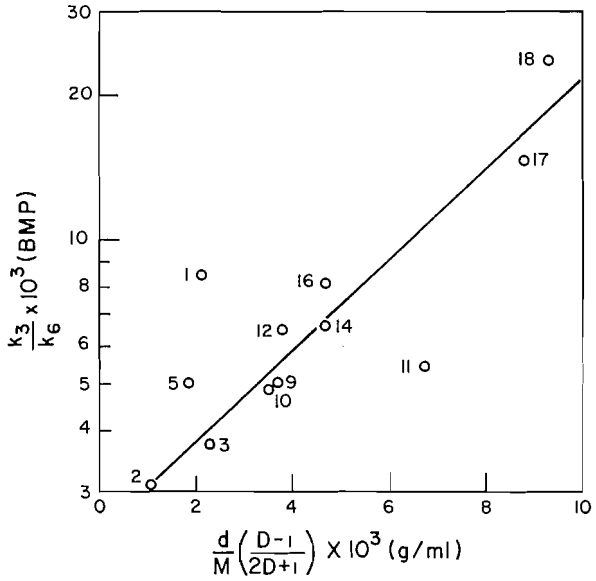

FIG. 5. Plot of k_3/k_6 for the BMP-inhibited oxidation of styrene against the dielectric function, $d(D-1)/M(2D+1)$.

reaction. However, it seems more likely that such purely dielectric effects on the transition state will tend to cancel out in the function k_3/k_6. Changes in this function probably reflect changes in k_6 which arise from hydrogen bonding interactions between the phenolic hydroxyl group and the solvent (cf. hydrogen abstraction from nitrophenols by the 2,4,6-tri-*t*-butyl phenoxy radical (23)). The frequency of the O–H fundamental stretching band (ν_m) in the different solvents gives a very rough relative measure of the strengths of the O–H···solvent interactions. Therefore, a plot of k_3/k_6 against ν_m should show a smooth relation between these two quantities. Since this is indeed the case (see Fig. 6), it strongly suggests that k_3/k_6 is determined by the strength of the hydrogen bond between the phenol and the solvent and that purely dielectric effects are largely cancelled out.

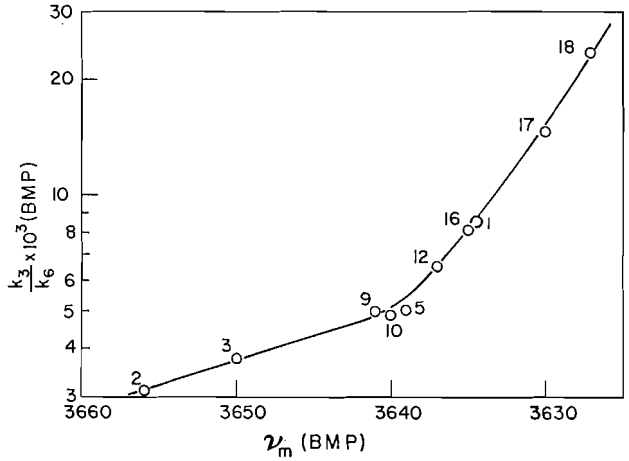

FIG. 6. Plot of k_3/k_6 for the BMP-inhibited oxidation of styrene against the frequency of the fundamental O–H stretching band maxima for BMP in the different solvents.

Can. J. Chem. Downloaded from www.nrcresearchpress.com by 210.87.254.40 on 09/05/12
For personal use only.

Can. J. Chem. Downloaded from www.nrcresearchpress.com by 210.87.254.40 on 09/05/12
For personal use only.

The k_3/k_6 values for the other three phenols have been plotted in Fig. 7 against k_3/k_6 for BMP. With the exception of the two hydroxylic solvents, there is an excellent linear correlation between the different sets of data. The lines in Fig. 7 all have a slope of about 1.5, which implies that 2,4,6-tri-methylphenol, 2-*t*-butyl-4-methylphenol, and 4-methylphenol are more susceptible than BMP to solvent effects, i.e. for a given change in solvent k_6 for any of these three phenols changes more than k_6 for BMP. This result is hardly surprising as these hydroxyl groups are sterically much more poorly protected than is the hydroxyl group in BMP. It is, however, rather surprising that all three are about equally susceptible to solvent effects as one might expect the partially hindered trimethylphenol to be intermediate in behavior between BMP and the other two non-hindered phenols. It seems clear that the relative inhibiting efficiencies of phenolic antioxidants belonging to any of these three general structural classes will be very nearly independent of the solvent or reactant system in which the efficiencies are determined. To judge by the results in *t*-butanol and acetic acid, this generalization may also apply roughly to hydroxylic solvents or reactants (compare, however, k_3/k_6 for trimethylphenol in *t*-butanol relative to the other *t*-butanol and acetic acid results). On the other hand, the efficiency, relative to the other phenols, of the highly hindered antioxidant BMP will show a strong solvent dependence. For example, BMP is a more efficient inhibitor than 4-methylphenol in nitromethane and acetonitrile but is less efficient in all the other non-hydroxylic solvents. It is much more efficient than 4-methylphenol in the two hydroxylic solvents.

The strength of O–H · · · solvent interactions increases as the phenolic hydrogen becomes more acidic (24). Relative inhibiting efficiencies in different solvents must therefore depend not only on the steric protection of the O–H group but also on the extent to which the phenol is substituted on the ring by electron donating or withdrawing groups.

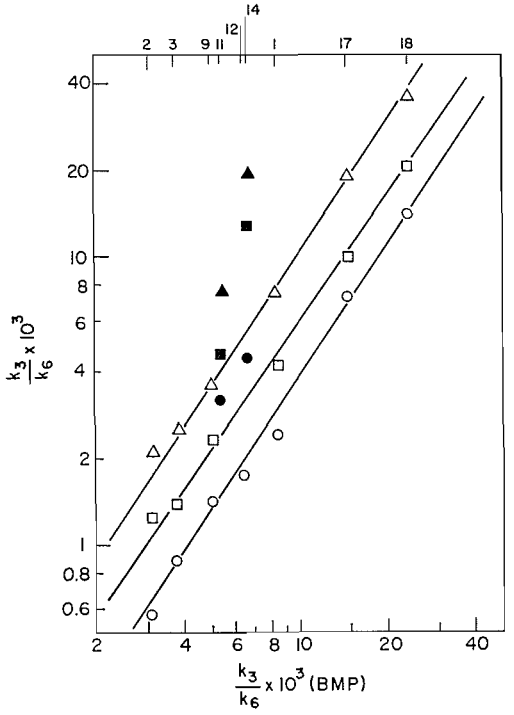

FIG. 7. Plot of k_3/k_6 for 2,4,6-trimethylphenol (○), 2-*t*-butyl-4-methylphenol (□), and 4-methylphenol (△) as a function of k_3/k_6 for BMP. The solid points represent the two hydroxylic solvents.

This effect was demonstrated by measuring the k_3/k_6 values for 2,6-di-*t*-butyl-4-methoxyphenol and 2,6-di-*t*-butyl-4-cyanophenol in *n*-decane (0.6 and 15.6×10^{-3}, respectively) and in acetonitrile (3.7 and 156×10^{-3}, respectively). The slopes of the lines obtained by plotting these values against k_3/k_6 for BMP were 0.95 for the 4-methoxy- and 1.23 for the 4-cyano-phenol. That is, the 4-methoxy derivative is less sensitive and the 4-cyano more sensitive than BMP to solvent effects.

The fact that the relative efficiencies of different classes of phenols are largely solvent independent suggests that since the efficiencies of the meta- and para-substituted phenols of a given class must be correlated in the Hammett equation by means of the σ^+ constants of the substituents in styrene (3), then similar correlations with σ^+ constants must exist in all other solvents.* Moreover, this fact suggests that the ρ factor in the Hammett equation should be nearly independent of the solvent. That is, there is no solvent effect on the type (i.e. σ or σ^+) of substituent constant correlation, nor should there be a significant solvent effect on the sensitivity of the reaction to polar influences (ρ).

In conclusion, the dependence of the relative inhibiting efficiencies of phenolic antioxidants on the solvent probably accounts for much of the conflicting data on relative efficiencies in the literature, i.e., different substrates were employed by different workers. The present work emphasizes that the most efficient inhibitor varies from system to system. The best inhibitor for a given substrate can, therefore, only be found by experimentally testing the more efficient inhibitors of each different structural class under the same conditions as the substrate will eventually be required to withstand in practice.

REFERENCES

1. J. A. Howard and K. U. Ingold. Can. J. Chem. **40**, 1851 (1962).
2. J. A. Howard and K. U. Ingold. Can. J. Chem. **41**, 1744 (1963).
3. J. A. Howard and K. U. Ingold. Can. J. Chem. **41**, 2800 (1963).
4. K. U. Ingold. J. Phys. Chem. **64**, 1636 (1960).
5. F. R. Mayo. Private communication.
6. G. S. Hammond, J. N. Sen, and C. E. Boozer. J. Am. Chem. Soc. **77**, 3244 (1955).
7. G. Henrici-Olivé and S. Olivé. Makromol. Chem. **58**, 188 (1962).
8. C. E. Boozer, G. S. Hammond, C. E. Hamilton, and J. N. Sen. J. Am. Chem. Soc. **77**, 3233 (1955).
9. D. G. Hendry. University Microfilms. Ann Arbor. 1962. Order No. 62-4152.
10. G. A. Russell. J. Am. Chem. Soc. **79**, 2977 (1957); **80**, 4987, 4997, 5002 (1958).
11. G. E. Zaikov. Neftekhimiya, **3**, 381 (1963). G. E. Zaikov and Z. K. Maizus. Dokl. Akad. Nauk SSSR, **150**, 116 (1963).
12. K. J. Laidler and H. Eyring. Ann. N.Y. Acad. Sci. **39**, 303 (1940).
13. E. T. Denisov. Dokl. Akad. Nauk SSSR, **146**, 394 (1963).
14. J. Powling and H. J. Bernstein. J. Am. Chem. Soc. **73**, 1815, 4353 (1951).
15. A. D. E. Pullin. Spectrochim. Acta, **13**, 125 (1958); Proc. Roy. Soc. London, Ser. A, **255**, 39 (1960).
16. E. Grunwald and S. Winstein. J. Am. Chem. Soc. **70**, 846 (1948). S. Winstein, E. Grunwald, and H. W. Jones. J. Am. Chem. Soc. **73**, 2700 (1951). A. H. Fainberg and S. Winstein. J. Am. Chem. Soc. **78**, 2770 (1956); **79**, 1597, 1602, 1608 (1957). S. Winstein, A. H. Fainberg and E. Grunwald. J. Am. Chem. Soc. **79**, 4146 (1957).
17. S. G. Smith, A. H. Fainberg, and S. Winstein. J. Am. Chem. Soc. **83**, 618 (1961).
18. E. M. Kosower. J. Am. Chem. Soc. **80**, 3253, 3261, 3267, (1958). E. M. Kosower, J. A. Skorez, and W. M. Schwartz, Jr. J. Am. Chem. Soc. **82**, 2188 (1960). E. M. Kosower and J. A. Skorez. J. Am. Chem. Soc. **82**, 2195 (1960).
19. J. A. Berson, Z. Hamlet, and W. A. Mueller. J. Am. Chem. Soc. **84**, 297 (1962).
20. R. E. Pincock. Paper 26 presented to the C.I.C. Solvation Symposium held at Calgary, Alberta. August, 1963.
21. L. J. Bellamy and R. L. Williams. Proc. Roy. Soc. London, Ser. A, **254**, 119 (1960).
22. M. P. Godsay, G. A. Harpell, and K. E. Russell. J. Polymer Sci. **57**, 641 (1962).
23. A. L. Buchachenko, M. B. Neiman, O. P. Sukhanova, and Yu. G. Mamedova. Zh. Fiz. Khim. **37**, 221 (1963).
24. K. U. Ingold. Can. J. Chem. **38**, 1092 (1960).

**In some earlier work from this laboratory (4) it was found that the induction periods produced by 2,6-di-t-butyl-4-substituted phenols in a saturated naphthenic hydrocarbon oil at 160° C were correlated by the σ constants of the 4-substituents. The present work shows that this correlation cannot be attributed to the low polarizability of this medium (cf. (2)). However, a variety of factors control the length of an induction period, particularly at 160° C, and the observed correlation may therefore not be directly related to the rate of reaction 6.*

Can. J. Chem. Downloaded from www.nrcresearchpress.com by 210.87.254.40 on 09/05/12
For personal use only.

GAS–LIQUID CHROMATOGRAPHY OF TERPENES

PART X. THE VOLATILE OILS OF THE LEAVES OF SITKA AND ENGELMANN SPRUCE[1]

E. VON RUDLOFF

National Research Council of Canada, Prairie Regional Laboratory, Saskatoon, Saskatchewan

Received December 9, 1963

ABSTRACT

The leaf oils from Sitka and Engelmann spruce were obtained in 0.36 and 0.094% yield respectively. The average percentage composition was determined by gas–liquid chromatography. Sitka spruce leaf oil was found to contain mainly *d*-myrcene (23.5%), *l*-piperitone (23.2%), and *d*-camphor (17.2%). Smaller amounts of 1,8-cineole, *l*-β-phellandrene, *p*-cymene, two aliphatic esters, *d*-bornyl acetate, *d*-borneol, and *d*-terpinen-4-ol were also isolated and several other esters appeared to be present in small amounts. Engelmann spruce leaf oil was found to contain mainly *cis*-hex-3-en-1-ol (18.5%), *d*-camphor (16.0%), *d*-bornyl acetate (8.6%), *d*-linalool (5.8%), and two unidentified compounds. Smaller amounts of myrcene, β-phellandrene, *p*-cymene, piperitone, and several sesquiterpenoids were also recorded. Tricyclene, α-pinene, camphene, β-pinene, 3-carene, limonene, γ-terpinene, and terpinolene were found in small amounts in both oils.

Phylogenetic relationships between the different spruces and other conifers are discussed.

INTRODUCTION

The volatile oils of many different species of eucalyptus (1) and pine wood (2) have been analyzed systematically, and Mirov (2) has discussed the relationship between the chemical composition of these oils and the taxonomic position of the plants. A systematic study of the volatile oils from the leaves of conifers does not appear to have been carried out, although Shaw (3, 4) has analyzed, by fractional distillation, the oils of four Canadian conifers and earlier Lehmann and Lynn (5) investigated those of a number of Washington conifers. In this series, oils from the leaves of several different conifers have been analyzed by gas–liquid chromatography (GLC) and the opinion was advanced (6) that certain of the oxygenated monoterpenes may have considerable taxonomic and phylogenetic value. In part V of this series (7) the analysis of the oils from black spruce (*Picea mariana* (Mill) B.S.P.), white spruce (*P. glauca* (Moench) Voss), and Colorado spruce (*P. pungens* Engelm.) was described. This communication deals with a similar analysis of the oils obtained from the foliage of Sitka spruce (*P. sitchensis* (Bong) Carr) and Engelmann spruce (*P. engelmanni* Parry).

In 1931, Lehmann and Lynn (5) analyzed the oil from Sitka spruce leaves and report the isolation of β-pinene, β-phellandrene, camphor, an α,β-unsaturated ketone and, after saponification, borneol and terpineol. The oil from Engelmann spruce leaves does not appear to have been investigated before.

EXPERIMENTAL

The same experimental procedures as described in the previous paper (6) were followed. Analytical chromatograms were run with 1 to 5 μl aliquots of the oils on 6 ft × ¼ in. O.D. columns having polyethylene glycol (Carbowax 20M, PEG; 15%), neopentyl glycol adipate (NGA; 15%) or polyethylene glycol adipate (PEGA; 15%) polyester, Apiezon N (A-N; 5%) or fluorinated silicone polymer (QF-1; 15%) as liquid phase, and Chromosorb W or Gaschrom P (60–80 mesh) as solid support. Isothermal runs were also carried out on a 10 foot × ¼ inch rapeseed oil (RO; 10%) and a 6 ft ethylene glycol bis-propionitrile (EGPN; 15%)

[1]*Issued as N.R.C. No. 7821.*

column. Preparative runs were carried out on a 20 ft × ⅜ in. O.D. PEG 20M (20%) column using the Aerograph Autoprep model 700 instrument. Infrared spectra (IR) were recorded as films between sodium chloride plates on a Perkin–Elmer model 21 double beam spectrophotometer. Optical rotations were determined as chloroform solutions at room temperature (23 to 27° C) unless otherwise indicated.

Relative retention times (RRT) of monoterpenes were measured relative to limonene and of oxygenated monoterpenes relative to camphor. The values recorded for most of the compounds encountered have been reported previously (6, 7). Those of *cis*-hex-3-en-1-ol (limonene = 1.00) were 0.17, 4.10, 0.41, 1.51, and 5.28 respectively on the A-N, PEG 20M, RO, NGA, and EGPN columns. Those of α-phellandrene were 0.83, 0.82, 0.86, 0.81, and 0.86, and those of β-phellandrene 0.97, 1.06, 1.05, 1.06, and 1.16 respectively. The RRT values (camphor = 1.00) of piperitone on the A-N, PEG 20M, and NGA columns were 2.02, 2.57, and 2.31 respectively.

Isolation of the Oils

Sitka spruce foliage (4.1 kg) from the Prince Rupert district, British Columbia, and water (25 liters) were mascerated in a Waring blendor and the mixture was steam-distilled for 4 to 5 hours. The volatile oil was extracted into a small volume of ether and this solution was washed with aqueous bicarbonate and water. After drying (Na_2SO_4), the ether was evaporated on a steam bath in a flask having a long neck (8). The residue (15.0 g, 0.36%) was a light yellow oil; n_D 1.4735, $[\alpha]_D$ +4.3° (undiluted).

Engelmann spruce (identified by cone morphology) leaves (3.3 kg) from Indian Head, Saskatchewan, were similarly treated to give a yellow oil (3.1 g, 0.094%) with n_D 1.4783 and $[\alpha]_D$ +11.0°.

Temperature-programmed runs (from 65° to 200° C) of each oil (3 μl aliquots) on the PEG 20M columns are shown in Figs. 1 and 2. The average percentage composition, as determined by area measurement (triangulation method) on a variety of analytical columns, is shown in Table I.

Isolation and Identification of Individual Components

Aliquots (50–100 μl) of the oil were injected repeatedly onto the 20-ft PEG column and each individual peak recorded (at 100 ma detector current) was collected in ice-cooled traps. Aliquots (1–2 μl) of each portion thus collected were chromatographed on the analytical columns to determine purity and RRT values. Where sufficient material was collected the IR spectrum, refractive index (at 25° C), and optical rotation was recorded. The following data were obtained for the oil from Sitka spruce leaves:

Peak 2: ester and α-pinene according to the IR spectrum and RRT data (1735–1715 cm^{-1}, no significant absorption at 1250–1200 cm^{-1}); $[\alpha]_D$ +54.8°.

Peak 3: ester and a little camphene (IR 1735–1715 cm^{-1}, RRT); $[\alpha]_D$ +11.6°; n_D 1.4700.

Peak 5: myrcene (IR, RRT) with slight contamination of peak 4 (β-pinene, RRT) and peak 6 (3-carene, RRT); $[\alpha]_D$ +19.3°; n_D 1.4668.

Peak 8: mainly β-phellandrene and 1;8-cineole (IR, RRT) and some contamination with peak 7 (limonene, RRT); $[\alpha]_D$ −18.2°; n_D 1.4661.

Peak 9: γ-terpinene (RRT).

Peak 10: mainly an ester (IR 1735 cm^{-1}) and some terpinolene (RRT); $[\alpha]_D$ +25.6°; n_D 1.4270.

Peak 11: *p*-cymene (RRT, u.v. spectrum).

Peak 12: unsaturated ester and ketone (IR 1732, 1715, weak 1635, and 885 cm^{-1}) (two unknowns, RRT); $[\alpha]_D$ +5.9°; n_D 1.4310.

Peak 18: camphor (IR, RRT); $[\alpha]_D$ +40.5°; m.p. 166–173° C.

Peaks 19 and 20: bornyl acetate and an unsaturated ketone (isopulegone ?) (IR 1735, 1715, 1638, 885 cm^{-1}); $[\alpha]_D$ +7.1°; n_D 1.4901.

Peaks 21 and 22: terpinen-4-ol and an unknown (IR, RRT); $[\alpha]_D$ +48.5°; n_D 1.4910.

Peaks 23 and 24: borneol and an unsaturated ketone (IR 1715, 1675, 1637, 887 cm^{-1}; RRT); $[\alpha]_D$ +69.2°; n_D 1.4890.

Peak 25: piperitone (IR, RRT); $[\alpha]_D$ −15.9°; n_D 1.4823.

Peak 26: C_{15} hydrocarbon (canadene ?) (IR, RRT).

When Sitka spruce oil (0.2 g) was saponified with alcoholic (80%) potassium hydroxide (2 *N*) solution the analytical chromatograms showed a considerable reduction of peaks 10, 12, 29, 32, and some reduction of peaks 2, 3, 19, and 33.

The amount of oil obtained from Engelmann spruce leaves was sufficient only for the isolation of the major constituents.

Peak 4: β-pinene (impure) (IR and RRT).

Peak 5: myrcene (IR and RRT); $[\alpha]_D$ +5°.

Peak 13: *cis*-hex-3-en-1-ol (IR and RRT); n_D 1.4823.

Peak 17: linalool (IR and RRT); $[\alpha]_D$ +10°.

Peak 18: camphor (IR and RRT); $[\alpha]_D$ +35°.

Peak 19: bornyl acetate (IR and RRT); $[\alpha]_D$ +20°.

Saponification removed peak 19 almost entirely.

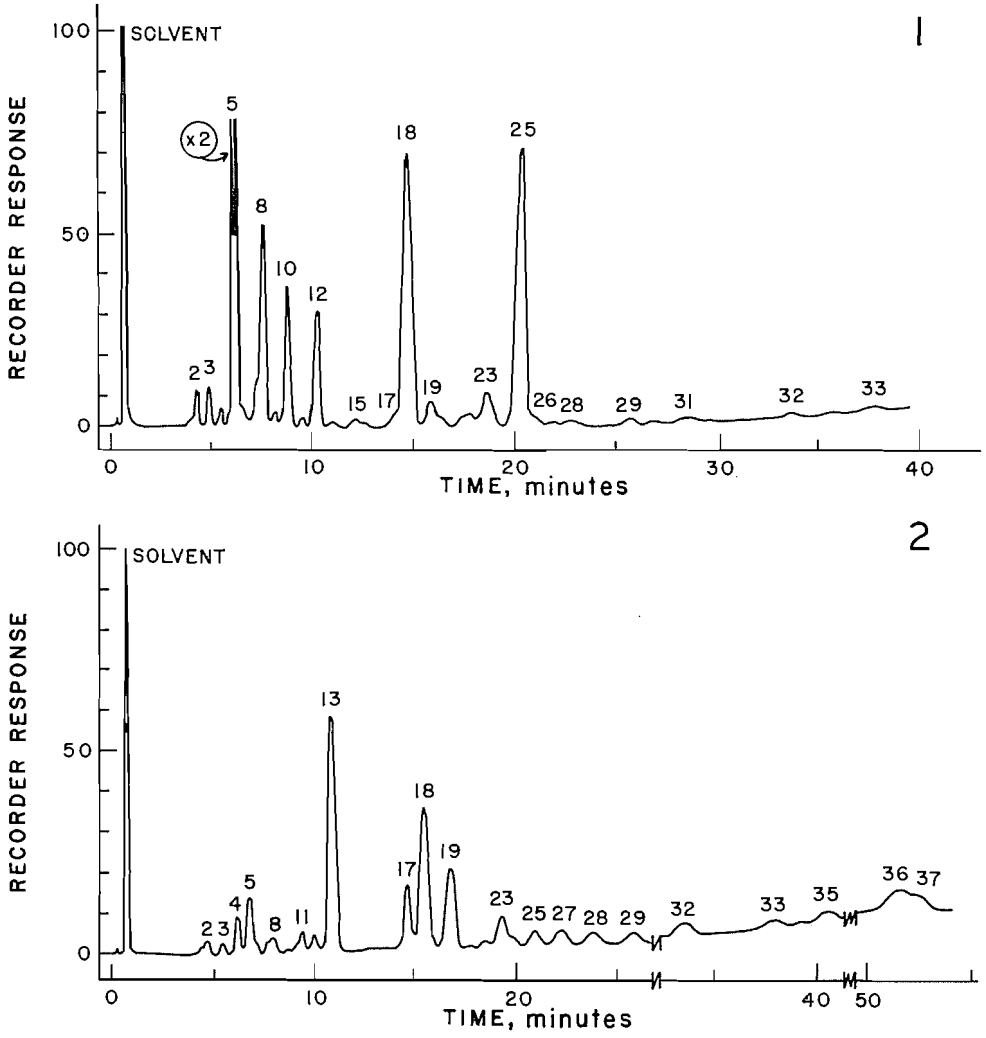

FIG. 1. Temperature-programmed chromatogram of the volatile oil from the leaves of Sitka spruce (see Table I for the peaks which have been identified).

FIG. 2. Temperature-programmed chromatogram of the volatile oil from the leaves of Engelmann spruce (see Table I for the peaks which have been identified).

RESULTS AND DISCUSSION

The oil from Sitka spruce leaves was obtained in comparatively good yield (0.36%), but that from Engelmann spruce leaves was rather poor (0.094%). Both oils were dextrorotatory and the refractive index was in the same range as that of other spruce leaf oils (6). Typical temperature-programmed chromatograms are shown in Figs. 1 and 2, and the average percentage composition of each oil in Table I. Both oils show significant qualitative and quantitative difference with respect to the composition of the oils from the leaves of black, white, and Colorado spruce (6).

The major constituents of Sitka spruce leaf oil were found to be *d*-myrcene, *l*-piperitone, and *d*-camphor. Piperitone appears to be the unidentified ketone (semicarbazone m.p.

TABLE I

Average percentage composition of spruce leaf oils

Peak No.	Compound*	*Picea sitchensis*, %	*P. engelmanni*, %	Peak No.	Compound*	*Picea sitchensis*, %	*P. engelmanni*, %
1	(Tricyclene)	0.2	0.4	20	(Isopulegone?)	0.5	0.4
2	α-Pinene	1.5†	0.8	21	*d*-Terpinen-4-ol	0.6	Trace
3	(Camphene)	1.7†	0.7	22	Unidentified	0.7	1.0
4	(β-Pinene)	0.8	3.1	23*a*	*d*-Borneol	1.1	3.0
5	*d*-Myrcene	23.5	4.3	*b*	Ketone	1.9	1.0
6	(3-Carene)	0.6	Trace	24	(α-Terpinyl acetate)	—	0.6
7	(Limonene)	0.9	0.8	25	*l*-Piperitone	23.2	2.2
8	1;8-Cineole	3.0	—	26	(Canadene?)	0.5	—
	l-β-Phellandrene	4.1	1.5	27	Unidentified	0.2	2.6
9	(γ-Terpinene)	0.5	0.3	28	Unidentified	0.6	2.5
10	Ester (terpinolene)	5.5	1.9	29	(Ester?)	0.8	1.5
11	*p*-Cymene	0.3	1.3	30	Unidentified	0.3	0.2
12	Ester, ketone	5.3	—	31	Unidentified	0.2	0.3
13	*cis*-Hex-3-en-1-ol	0.3	18.5	32	(Ester?)	0.2	2.5
14	Unidentified	0.3	—	33	(Ester?)	0.2	1.3
15	Unidentified	0.6	—	34	Oxygenated sesquiterpenes	—	0.4
16	Unidentified	0.3	—	35		—	2.4
17	*d*-Linalool	0.6	5.8	36		—	9.5
18	*d*-Camphor	17.2	16.0	37		—	4.5
19	*d*-Bornyl acetate	1.8	8.6				

*Compounds in parentheses were identified by relative retention time only.
†Contains an unidentified ester.

231–232° C) isolated by Lehmann and Lynn (5). Read and Smith (9) report that piperitone forms two semicarbazones with melting points 185° and 226° C respectively. The presence of fairly large amounts of 1;8-cineole and β-phellandrene and several non-terpenoid esters (peaks 2, 3, 10, and 12) is also noteworthy. RRT values of peaks 10 and 12 suggest that they are C_8 esters. They were not separated on an Apiezon N column, which suggests that they differ by a double bond. This is substantiated by their infrared spectra. However, neither compound was obtained in pure form, peak 10 being contaminated with terpinolene and peak 12 with a ketone. The retention time on the PEG column of peak 12 is similar to that of citronellal, but this aldehyde did not appear to be present. Lehmann and Lynn also report the isolation of borneol and terpineol from the saponified oil. Free borneol (peak 23*a*) and bornyl acetate (peak 19) were found in small amounts in this study, but α-terpineol (RRT same as peak 23*b*) or α-terpinyle acetate (RRT same as peak 24) were not detected. However, the saponified oil showed a reduction in the relative sizes of peaks 2, 3, 10, 12, 19, 29, 32, and 33 and it is possible that the later peaks are higher esters of α-terpineol. Sesquiterpenes were found only in very small amounts and only canadene, the cadinene isomer (4) found in other spruce leaf oils, was tentatively identified.

The leaf oil from Engelmann spruce was found to contain mainly *cis*-hex-3-en-1-ol (leaf alcohol) and camphor. Monoterpene hydrocarbons were present in relatively small amounts, β-pinene and myrcene being the most prominent members. The typical minor components, including tricyclene and β-phellandrene, were recorded, but 1;8-cineole was not found. Fairly large amounts of linalool and bornyl acetate were isolated and borneol, piperitone, and several unidentified higher boiling constituents were recorded in the 1 to 3 percentage range. Two prominent peaks (Nos. 36 and 37) were recorded in the sesquiterpene alcohol range, but attempts to correlate retention data with those of known compounds (cedrol, eudesmol, cadinols) failed to give conclusive data. Canadene was not recorded.

The presence of piperitone and large amounts of myrcene in the oil from Sitka spruce may have phylogenetic value. In this respect the presence of non-terpenoid esters (e.g. peak 10 and 12) and fairly large amounts of 1;8-cineole and β-phellandrene may also be significant. In Engelmann spruce leaves the formation of large amounts of *cis*-hex-3-en-1-ol, and perhaps also the large number and relatively high amounts of components in the sesquiterpene range, appears to be highly characteristic. *cis*-Hex-3-en-1-ol does not appear to have been isolated from spruce leaf oils before. Engelmann spruce is known to hybridize with white spruce and a distinct western variety of white spruce, *P. glauca* (Moench) Voss var. *albertiana* (S. Brown) Sarg., is recognized (10). Thus the presence of *cis*-hex-3-en-1-ol and major amounts of linalool in the leaf oil from Engelmann spruce may serve as a convenient taxonomic guide. This aspect will be studied further.

On comparing the composition of the oils from the leaves of spruces and other members of the family Pinaceae (11) with those from junipers (6) and cedars (12, 13) (fam. Cupressaceae) a phylogenetic pattern becomes discernible. The latter are characterized by the presence of monoterpenes of the thujane type (thujone, sabinol, sabinene, etc.). Oils from the members of the family Pinaceae contain bornyl acetate, borneol, and frequently camphor. Thus each botanical family has a closely related series of monoterpenes in common. It will be noted, that the oxygenated compounds are all substituted at carbon two of the cyclohexane ring (*p*-menthane nomenclature). Therefore, the finding of large amounts of piperitone, a C_3-substituted terpene, in the leaf oil of Sitka spruce is most remarkable. Its formation would require a separate biogenetic step.

Small amounts of many monoterpene hydrocarbons are found in the volatile oils of

plants from widely different genera. Yet, some of these occur in significant amounts and thus appear to be characteristic for a single family or species. For instance, large amounts of myrcene were found in the Sitka spruce leaf oil. Mirov (2) has shown that α- and β-pinene, as well as the phellandrenes are highly characteristic of pine wood oils. In junipers, sabinene is very prominent and thujene also appears to be a characteristic constituent. An extended study of volatile oils may, therefore, establish further phylogenetic relationships in this group of terpenes. As yet, the data on the sesquiterpenoid constituents are too fragmentary to allow any comparison. The fact that many peaks with different retention characteristics are recorded in this range would indicate that phylogenetic relationships exist. Improvements in the isolation and characterization of these minor constituents are being sought to obtain more conclusive data.

ACKNOWLEDGMENTS

The author wishes to thank Mr. P. J. Salisbury, plant pathologist, Indian Head Forest Nursery, Saskatchewan, for identifying and supplying the Engelmann spruce foliage, Dr. H. Worster, Columbia Cellulose Co., Prince Rupert, B.C., for sending the Sitka spruce leaves, and Mr. M. Granat for technical assistance. Infrared spectra were recorded by Mr. W. C. Haid.

REFERENCES

1. R. T. Baker and H. G. Smith. J. Proc. Roy. Soc. N. S. Wales, **35**, 116 (1901).
2. N. T. Mirov. Ann. Rev. Biochem. **17**, 521 (1948).
3. A. C. Shaw. Pulp Paper Mag. Can. **53**, no. 4, 119 (1952).
4. A. C. Shaw. Can. J. Chem. **31**, 277 (1953).
5. A. J. Lehmann and E. V. Lynn. J. Am. Pharm. Assoc. **20**, 29 (1931).
6. E. von Rudloff. Can. J. Chem. **41**, 2876 (1963).
7. E. von Rudloff. Tappi, **45**, 181 (1962).
8. E. von Rudloff. Can. J. Chem. **39**, 1 (1961).
9. H. G. Read and H. G. Smith. J. Chem. Soc. **121**, 1863 (1922).
10. Canadian Department of Forestry. Native trees of Canada. 6th ed. Queen's Printer, Ottawa. 1956. p. 38.
11. E. Guenther. The essential oils. Vol. VI. D. Van Nostrand Co., Inc., New York. 1952. pp. 216, 224, 244, and 250.
12. E. von Rudloff. Can. J. Chem. **39**, 1200 (1961).
13. E. von Rudloff. Phytochemistry, **1**, 195 (1962).

Can. J. Chem. Downloaded from www.nrcresearchpress.com by 210.87.254.105 on 09/05/12
For personal use only.

COMPLEXES OF PLATINUM (0)

I. COMPLEXES WITH TRIPHENYLPHOSPHINE AND SUBSTITUTED PHENYLACETYLENES

A. D. ALLEN AND C. D. COOK[1]

Department of Chemistry, University of Toronto, Toronto, Ontario

Received December 4, 1963

ABSTRACT

Kinetic and equilibrium measurements have been made on the exchange of one arylacetylene for another of different structure in the compounds bis-triphenylphosphineacetylene-platinum (0). The rate of exchange is proportional to the concentration of the complex but is independent of the reagent. The complexes are stabilized by electron-withdrawing groups in the acetylene ligand. A mechanism for the reactions is proposed in which an intermediate $Pt(Ph_3)_2$ is formed which has a significant stability.

Compounds with the general formula $Pt(PPh_3)_2.ac$, where ac = acetylene or a substituted acetylene, were first prepared in 1957 by Chatt, Rowe, and Williams (1). These authors reported that the compounds are monomeric, that the acetylenic carbons are at least approximately in the same plane as the platinum and phosphorous atoms, and that the stability of the compounds is increased by the presence of alkyl, and even more so by aryl groups attached to the acetylenic carbons. The great stability of the compound formed with di-4-nitrophenylacetylene indicated that electron withdrawing substituents also stabilize the compounds.

We have prepared a series of compounds of this type containing monosubstituted phenylacetylenes and have attempted to determine the effect of the substituent on the properties of the free acetylene and on the stability of the complex formed. The relative stabilities of the various compounds have been determined by carrying out kinetic and equilibrium measurements on the exchange reaction in cyclohexane:

$$Pt(PPh_3)_2.ac + ac' \rightleftarrows Pt(PPh_3)_2.ac' + ac.$$

Use was made of the differences in optical absorption of the different complexes, so that by measuring the change in optical density with time at a selected wavelength the progress of the reaction and the position of equilibrium could be determined. Cyclohexane was chosen as the medium because spectra of solutions of the compounds in it do not change during the time necessary to carry out the experiments, and it is the most inert solvent that will sufficiently dissolve all the compounds.

EXPERIMENTAL

(1) Preparation and Characterization of Substituted Phenylacetylenes

The methods used for the preparations of the substituted phenylacetylenes, their physical properties, and infrared and nuclear magnetic resonance spectra have been reported elsewhere (2, 3).

(2) Preparation of Complexes

The following general method was used to prepare the complexes.* Hydrazine hydrate (100%, 2 ml) was added to a suspension of *cis*-bis(triphenylphosphine)dichloroplatinum (II) (2 g, 0.0025 mole) in 45 ml absolute ethanol. When the suspension was warmed to about 40°, the solid dissolved with slight effervescence. The yellow solution formed was filtered and the appropriate arylacetylene (0.004 mole), dissolved in 5 ml ethanol, was added. Precipitation of the complex generally began after about 30 minutes and was complete

[1]*Present address: Department of Chemistry, University College, London, England.*

**We are indebted to Dr. J. Chatt and Dr. G. A. Rowe, who provided us with details of this general method of preparation used in reference (1).*

when the suspension was left to stand overnight at room temperature. Recrystallization from benzene–methanol or methylene chloride – methanol gave the pure product. The compounds prepared in this way are listed in Table I.

TABLE I

Complex $[Pt(PPh_3)_2.ac]^0$ ac =	M.p. (decomp.)	Analysis Found % C	Found % H	Calc. % C	Calc. % H
$C_6H_5C_2H$	141–148°	64.4	4.4	64.3	4.4
4-NO_2—$C_6H_4C_2H$	117–120°	60.7	3.9	60.8	4.0
3-NO_2—$C_6H_4C_2H$	148–151°	60.8	4.3	60.8	4.0
4-Cl—$C_6H_4C_2H$	124–128°	63.0	4.4	61.7	4.1
2-Cl—$C_6H_4C_2H$	119–124°	62.3	4.2	61.7	4.1
4-Br—$C_6H_4C_2H$	123–129°	58.6	3.9	58.7	3.9
4-F—$C_6H_4C_2H$	117–120°	63.5	4.3	62.9	4.2
2-F—$C_6H_4C_2H$	114–116°	64.0	4.2	62.9	4.2
4-Me—$C_6H_4C_2H$	109–114°	66.6	5.0	64.7	4.6
4-MeO—$C_6H_4C_2H$	136–140°	63.5	4.4	63.5	4.5
2-MeO—$C_6H_4C_2H$	146–150°	63.5	4.5	63.5	4.5
3-MeO—$C_6H_4C_2H$	147–150°	63.5	4.5	63.5	4.5
$C_6H_5C{\equiv}CC_6H_5$	161–169°	66.9	4.8	66.9	4.5

(3) Solvent

Cyclohexane was dried by reflux over lithium aluminum hydride and fractionally distilled. Purity was checked by constancy of boiling point on changing to total reflux.

(4) Kinetic and Equilibrium Measurements

Absorption spectra of cyclohexane solutions of the complexes and the acetylenes were examined in the visible and near ultraviolet region of the spectrum. In the range 300–400 mμ it was usually possible to find a wavelength at which the free acetylenes were essentially transparent and the two complexes involved in a particular reaction to be studied had different extinction coefficients. The common feature of the spectra of these complexes is that they have an intense absorption below about 350 mμ and are more or less transparent at about 400 mμ. The absorption in between these two wavelengths depends on the substituent in the combined acetylene. Most of these systems showed a maximum change in absorbance at about 365 mμ, and many of the reactions were investigated at this wavelength.

Separate solutions of the complex and reagent acetylene in cyclohexane were prepared in a constant temperature (29±0.5°) room. Appropriate volumes of the reagents and solvent were mixed at zero time, and the mixture was rapidly transferred to the spectrophotometer cell. The cell temperature was maintained at 28.8 (±0.1)° by the use of aluminum block cell holder through which constant temperature water was circulated. The spectrophotometer (Bausch and Lomb 505) was set to run at constant wavelength and the recorder was started at zero time. The first reading was usually obtained within 1 minute of mixing. The change in absorbance with time was followed continuously for the first 10–20 minutes, and the final reading was checked after approximately 2 hours. In all cases both the forward and backward reactions were studied and only those which gave close agreement in the final equilibrium position were accepted. Details are given of the readings taken for a typical pair of reactions:

$$Pt(PPh_3)_2.C_6H_5C_2H + C_6H_5C_2C_6H_5 \rightleftarrows Pt(PPh_3)_2.C_6H_5C_2C_6H_5 + C_6H_5C_2H$$

Complex and reagent 1.00×10^{-4} *M* in cyclohexane. Wavelength 365 mμ. Temperature 28.8 (±0.1)°.

Forward reaction:								
Time (minutes)	1	2	3	4	6	8	10	∞
% *T*	70.8	68.8	67.5	66.3	64.3	63.1	62.2	60.5
Backward reaction:								
Time (minutes)	1	2.5	3	4	6	8	10	∞
% *T*	40.7	43.0	43.9	45.0	47.2	49.8	51.1	60.2

It was established that the optical densities are proportional to the concentrations of the two complexes in the solution, so that the equilibrium position can be calculated directly from the optical density at equilibrium. For the above reaction the concentration equilibrium constant, i.e.

$$[Pt(PPh_3)_2.C_6H_5C_2C_6H_5][C_6H_5C_2H]/[Pt(PPh_3)_2.C_6H_5C_2H][C_6H_5C_2C_6H_5],$$

has the value 0.25.

First-order rate coefficients were calculated by two methods: (*a*) from the rate of approach to equilibrium,

Can. J. Chem. Downloaded from www.nrcresearchpress.com by 210.87.254.105 on 09/05/12
For personal use only.

using the equilibrium position to calculate the rate coefficient from the slope of the plot of log [complex] vs. time, and (*b*) from the initial slope of the first-order log plot based on the reaction going to completion. Good agreement was obtained in all cases.

Reactions were carried out in which the concentration of the reagent was varied, and also in which some of the acetylene contained in the complex was used in addition to the reagent acetylene.

DISCUSSION

Tables II, III, IV show the kinetic and equilibrium results obtained for several of these reactions, together with published data on the nuclear magnetic resonance spectra of the free acetylenes.

TABLE II

Reactions of the complex $Pt(Ph_3P)_2.C_6H_5C_2H$ with substituted phenylacetylenes, in cyclohexane at 28.8°. Concentration of complex = 1.00×10^{-4} *M*

Reagent $M \times 10^4$	1	1+1*	2	5	5+5*
Substituent in reagent acetylene	Observed first order rate coefficient $\times 10^4$ sec^{-1}				
4-Nitro	15.5	—	16.1	16.5	15.0
2-Nitro	14.8	—	14.9	15.7	14.6
3-Nitro	14.0	—	—	15.0	—
4-Chloro	15.0	9.2	—	15.8	—
2-Chloro	14.3	8.3	15.0	15.0	—
4-Bromo	14.0	—	—	15.8	—
3-Methoxy	12.2	6.6	12.0	14.0	—
4-Methoxy	12.4	6.5	14.0	14.0	—
2-Methoxy	14.8	—	15.0	—	—

*Indicates addition of phenylacetylene in the stated concentration in addition to the reagent-substituted phenylacetylene.

TABLE III

Reactions of complexes containing substituted phenylacetylenes, $Pt(Ph_3P)_2.X—C_6H_4C_2H$, with phenylacetylene in cyclohexane 28.8°. Concentration of complex = 1.00×10^{-4} *M*

[Reagent] $M \times 10^4$	1	1+1*	2	5	5+1*	10	10+1*
Substituent in complex	Observed first-order rate coefficient $\times 10^4$ sec^{-1}						
4-Nitro	—	—	—	—	—	1.6	0.25
3-Nitro	—	—	—	—	—	1.6	—
4-Chloro	7.1	—	7.3	7.2	4.3	—	—
2-Chloro	9.6	2.8	9.0	9.6	—	—	—
4-Bromo	5.0	—	—	—	—	—	—
3-Methoxy	—	—	13.0	—	—	—	—
Hydrogen	(15)						
4-Methoxy	19.0	14.8	19.0	19.0	—	—	—
2-Methoxy	25.0	13.0	—	—	—	—	—

*Indicates presence of appropriate substituted phenylacetylene in the stated concentration, in addition to the reagent phenylacetylene.

Table II shows the observed first-order rate coefficients for the reaction of the phenylacetylene complex with various substituted phenylacetylenes at several concentrations. It is clear that the rate is insensitive to the nature and concentration of the reagent. In Table III are shown similar first-order rate coefficients for the reaction of various substituted phenylacetylene complexes with phenylacetylene at several concentrations. Again the rate is independent of the concentration of the reagent, but it is apparent that

Can. J. Chem. Downloaded from www.nrcresearchpress.com by 210.87.254.105 on 09/05/12
For personal use only.

TABLE IV

Comparison of equilibrium and rate coefficients with properties of free acetylenes

Substituent in complex	K_c*	$10^4 k_1$ sec^{-1}†	τ, p.p.m.‡
3-Nitro	125	1.6	6.893
4-Nitro	105	1.6	6.793
4-Bromo	10	5.0	7.042
4-Chloro	10	7.2	7.051
2-Chloro	3	9.6	6.806
3-Methoxy	6	13.0	7.113
Hydrogen	1	15	7.125
4-Methoxy	1	19.0	7.213
2-Methoxy	0.5	25.0	6.958

*K_c = $[Pt(Ph_3P)_2X—C_6H_4C_2H][C_6H_5C_2H]/[Pt(Ph_3P)_2C_6H_5C_2H][X—C_6H_4C_2H]$.
†First-order rate coefficient for complex containing substituted phenylacetylene, with phenylacetylene as reagent.
‡From ref. (3).

it depends markedly on the nature of the acetylene in the complex. The simplest interpretation of these results is that the rate-determining step involves the splitting of the complex into the free acetylene and an intermediate $Pt(Ph_3P)_2$, without the direct intervention of the reagent. Thus the rate coefficient is a measure of the ease of rupture of the metal–acetylene bond, and we see that the strongest bond is formed by the acetylene containing the strongly electron-withdrawing nitro group. The only complexes reacting more rapidly than the phenylacetylene complex are those containing the methoxy group in the ortho- or para-position, in which it is weakly electron-releasing.

Table IV shows these rate coefficients together with the equilibrium constants and τ values for the acetylenic hydrogen of the free acetylenes. It will be seen that, with minor variations, the equilibrium constants and rate coefficients follow the same pattern. By both measurements the nitro group strongly stabilizes these complexes. This means that the effect of the substituent is important in the region of the triple bond. Chemical shifts of the acetylenic hydrogen (3) follow the same sequence for substituents in the para- and meta-positions, showing clearly the change in electron density in the region of the hydrogen atom, and thus, presumably, in the triple bond. It is noteworthy that ortho substituents give much lower chemical shifts. The so-called "ortho effect" is well known in aromatic systems, and it is interesting that the ortho-substituted complexes do not show this effect, their stabilities being very similar to those containing analogous para-substituents.

It is clear that the bond between the triple bond and the metal atom has some double bond character, as originally proposed by Chatt *et al.* (1). The ability of the unsaturated system to accept electrons from the *d* orbitals of the metal atom plays an important part in the formation of the bond. An increase in the electron-accepting power of the ligand more than compensates for the decrease in donor properties caused by the presence of an electron-withdrawing substituent.

Also shown in Tables II and III is the effect on the reaction rate of adding to the mixture some of the acetylene which is also contained in the complex, e.g. addition of phenylacetylene to the reaction between the phenylacetylene complex and a substituted phenylacetylene. Two extreme cases are observed: (*a*) addition of a small amount of *p*-nitrophenylacetylene (to give a concentration of only 1/10th of that of the reagent) to the reaction between the *p*-nitrophenylacetylene complex and phenylacetylene produces a

Can. J. Chem. Downloaded from www.nrcresearchpress.com by 210.87.254.105 on 09/05/12
For personal use only.

very marked reduction in the observed first order rate coefficient, from 1.6 to 0.25×10^{-4} sec^{-1}, and (*b*) addition of phenylacetylene to the reverse reaction in a concentration equal to that of the reagent *p*-nitrophenylacetylene produces an insignificant reduction in rate.

These observations are consistent with the formation of a relatively stable intermediate, $Pt(PPh_3)_2$, in the following reaction scheme (4):

$$Pt(Ph_3P)_2.ac \underset{k_{-1}}{\overset{k_1}{\rightleftarrows}} Pt(Ph_3P)_2 + ac,$$

$$Pt(Ph_3P)_2 + ac' \xrightarrow{k_2} Pt(Ph_3P)_2.ac'.$$

If we assume a steady state for the intermediate $Pt(Ph_3P)_2$, the rate expression for the initial forward reaction is:

$$v = k_1[Pt(Ph_3P)_2.ac] \Big/ \left(\frac{k_{-1}[ac]}{k_2[ac']}\right)+1.$$

At the beginning of a reaction in which the reagent ac′ is the only free acetylene present the term $k_{-1}[ac]$ is zero, and a simple first order expression is obtained, $v = k_1[Pt(PPh_3)_2.ac]$. The first-order rate coefficients given in the tables are derived from this expression for the initial part of the reaction. If some free acetylene ac is also added to the reaction mixture, at a concentration equal to ac′, the denominator at the beginning of the reaction becomes $(k_{-1}/k_2)+1$. The effect of this addition upon the observed first order rate coefficient will depend on the relative magnitudes of k_{-1} and k_2. If $Pt(PPh_3)$ is a reactive intermediate its reaction with the acetylene present will depend only on their relative concentrations. The nature of the acetylene will not be important, so that k_{-1} and k_2 will be approximately equal and very large. Their ratio will be close to unity and the denominator in the rate expression will be approximately equal to two. Thus, with a reactive intermediate and with equal concentrations of the two acetylenes, the rates of the forward and backward reactions of the intermediate will be approximately equal and the net forward rate will be about half of that observed in the absence of added ac, irrespective of the nature of ac. Our results show clearly that this is not the case.

If, however, the intermediate $Pt(PPh_3)_2$ is sufficiently stable the rate of its reaction may depend upon the acetylene involved. If, for example, the activation energy for the reaction of this intermediate with *p*-nitrophenylacetylene is substantially less than that for its reaction with phenylacetylene it will react selectively, at a faster rate, with the former reagent. In the reaction scheme above the rate coefficients k_{-1} and k_2 will depend on the acetylene involved, and the observed rate will depend upon the ratio of these coefficients. In the reaction between the *p*-nitrophenylacetylene complex and phenylacetylene, the coefficient k_{-1} appears to be very much greater than k_2, so that addition of small amounts of free *p*-nitrophenylacetylene strongly inhibit the overall rate of the forward reaction. Similarly, for the reverse reaction, addition of relatively large amounts of free phenylacetylene have a very small effect on the overall rate of reaction. With other combinations of acetylenes less extreme results are obtained, as shown in Tables II and III. The results obtained are consistent with the reasonable hypothesis that the activation energy for the reaction of the intermediate with an acetylene is directly related to the stability of the complex formed, i.e. it is lowest for the acetylene which forms the strongest complex.

It follows from this argument that the stability of diphosphine intermediate should be affected by the nature of the phosphine used. Work is in progress to determine the effect of substituted aryl phosphines on the stability of this intermediate.

Can. J. Chem. Downloaded from www.nrcresearchpress.com by 210.87.254.105 on 09/05/12
For personal use only.

ACKNOWLEDGMENTS

The authors thank the National Research Council for financial support, the Shell Oil Company of Canada Limited for a fellowship (to C. D. C.), and Dr. J. Chatt for valuable advice.

REFERENCES

1. J. CHATT, G. A. ROWE, and A. A. WILLIAMS. Proc. Chem. Soc. 208 (1957).
2. A. D. ALLEN and C. D. COOK. Can. J. Chem. **41**, 1084 (1963).
3. C. D. COOK and S. S. DANYLUK. Tetrahedron, **19**, 177 (1963).
4. A. D. ALLEN and C. D. COOK. Can. J. Chem. **41**, 1235 (1963).

Can. J. Chem. Downloaded from www.nrcresearchpress.com by 210.87.254.105 on 09/05/12
For personal use only.

UREA INCLUSION COMPOUNDS OF *n*-ALKYL BROMIDES AND IODIDES

JACK RADELL[1] AND B. W. BRODMAN
Pitman–Dunn Institute for Research, Frankford Arsenal, Philadelphia, Pennsylvania

AND

E. D. BERGMANN
The Hebrew University of Jerusalem, Jerusalem, Israel

Received December 13, 1963

ABSTRACT

The formation and stability of urea inclusion compounds of *n*-alkyl bromides and iodides were established from X-ray powder diffraction data. The stability of both homologous families is greater than would be expected from a consideration of the cross-sectional diameter of the molecules only. The procedure for isolating the complexes has been simplified.

INTRODUCTION

In preparation for studying the effect of radiation on the urea inclusion compounds of *n*-alkyl bromides and iodides it was necessary to demonstrate unequivocally that these compounds form urea inclusion compounds. A second objective was to ascertain the relative stability of these compounds and to determine which compounds were sufficiently stable to make reasonable candidates for a study of radiation effects.

DISCUSSION

It has been previously reported (1) that molecules such as organic acids and ketones are capable of forming urea inclusion compounds for shorter (unbranched) chains than the *n*-alkanes. These molecules which appear to be more effective in their ability to form urea inclusion compounds all contained a polarizable functional group containing pi bonding electrons. In a previous study the effect of fluorine in esters was tested (2). The results indicated that the influence of the fluorine was independent of any inductive effect resulting from the pronounced electronegativity of the halogen atom. In fact, the results could be explained by the larger atomic radius of fluorine (as compared with hydrogen) requiring a slightly greater number of methylene groups in the chain than that required for non-fluorinated esters to form a complex. Since the cross-sectional diameters of the *n*-alkyl bromides and iodides were 4.75 Å (previously reported (1) to form a urea complex) and 4.95 Å (not previously reported to form a complex) respectively, it was anticipated that both would form complexes since the maximum (3) cross section of a urea channel is 6 Å. At the same time it was anticipated that the shortest alkyl iodides and bromides (1) would require a somewhat greater number of methylene groups than the shortest alkane (4.6 Å in cross section) which would form a urea complex. It was surprising, therefore, to find that both the shortest *n*-alkyl bromide and iodide capable of forming a complex were shorter than the shortest *n*-alkane (*n*-octane) which would form a channel complex with urea by the method employed.

Since all the starting materials are liquids, the X-ray powder pattern of the crystalline products obtained after treatment with a urea–methanol solution must be either that of uncomplexed urea (tetragonal) or that of some new product. It is easy to distinguish

[1]*Holder of a U.S. Secretary of the Army Research and Study Fellowship at The Hebrew University of Jerusalem, 1962–1963.*

Can. J. Chem. Downloaded from www.nrcresearchpress.com by 210.87.254.6 on 09/05/12
For personal use only.

between these two since the spacing at 3.98–4.02 Å* is the most intense spacing characteristic of tetragonal (4) (uncomplexed) urea and the spacing at 4.10–4.11 (Table I) or 4.11–4.15 Å (Table II) is the most intense spacing characteristic of the (hexagonal) urea inclusion compound (4). From these spacings which indicate the relative concentration of free urea and the complex, it was concluded that *n*-heptylbromide is the shortest bromoalkane tested which unequivocally gives a complex (Table I). Table I contains all X-ray measurements for the *n*-alkyl bromide urea inclusion compounds. The *n*-heptylbromide complex is appreciably contaminated by free urea as indicated by a relative intensity of 0.19 at 3.98–4.02 Å. The complexes of 1-bromooctane and all higher homologues are free of urea (no interplanar spacing at 3.98–4.02 Å) and retain a maximum intensity for the complex of 1.00 at 4.10–4.11 Å.

The most surprising result was the appreciable formation of a complex by 1-iodopentane (Table II) as indicated by a relative intensity of 0.31 at 4.11–4.15 Å, characteristic of complex formation. The 3.98–4.02 Å spacing, characteristic of free urea, was very strong in the case of 1-iodopentane with a maximum relative intensity of 1.00 which indicated a high concentration of urea contaminating the complex. For 1-iodohexane the value fell to 0.33, and none of the higher homologues above 1-iodohexane showed a spacing at 4.00–4.02 Å (Table II).

The ease of complex formation decreases as the cross-sectional diameter of the molecule in the planar zigzag conformation increases over and above that of a *n*-hydrocarbon (5). This results in the fact that the shortest homologue able to form a complex in a family of compounds which has a high cross section requires a larger number of methylene groups and thus a longer chain to produce enough van der Waals forces for stable inclusion compound formation. For the 1-bromo and 1-iodoalkanes this behavior is reversed. For the cross-sectional diameters we find *n*-RI (5.0 Å) > *n*-RBr (4.8 Å) > *n*-RH (4.6 Å). Consequently, it would be expected that the alkyl iodide would require the longest and the alkane the shortest chain for the complex formation. Instead, the shortest homologue in the three series to form a complex under the same conditions is 1-iodopentane, 1-bromoheptane, and normal octane (4). The shorter chain length requirements for complex formation of the molecules of greater girth can be accounted for by the stabilization resulting from the polarizability of the carbon–halogen bond.

In all cases the most reliable criteria for the relative stability of the complexes was the amount of uncomplexed urea, as determined by the intensity of the strongest urea spacing around 4.00 Å. In the tables it is seen that this spacing decreases in intensity as we proceed to the higher homologues and rapidly disappears.

The formation of urea inclusion compounds of *n*-alkyl bromides was unequivocally identified by the following spacings which occurred in decreasing order of intensity: 4.10–4.11, 3.39–3.40, 2.62, 2.06, and 3.26–3.27 Å. Most of the other spacings are uniformly weak except the one at 3.53–3.57 Å, which is characteristic of both complexed and free urea. The 7.13–7.15 Å spacing which is characteristic of urea complexes is weak and not present in all the complexes (Table I).

Channel complex formation of the *n*-alkyl iodides was identified by the following spacings which occurred in decreasing order of intensity: 4.11–4.15, 3.39–3.40, 2.37–2.38, 2.05–2.06, and 7.13–7.21 Å. Again the spacing at 3.56–3.58 Å cannot be used as it is characteristic of both complexed and free urea (Table II).

To determine whether there is any advantage in washing the filtered crystalline

**The range of 3.98–4.02 Å is used to cover the maximum intensity urea spacing which occurs in Table I and III at 3.98–4.00 Å and Table II at 4.00–4.02 Å and will be used throughout the text.*

Can. J. Chem. Downloaded from www.nrcresearchpress.com by 210.87.254.6 on 09/05/12
For personal use only.

Can. J. Chem. Downloaded from www.nrcresearchpress.com by 210.87.254.6 on 09/05/12
For personal use only.

TABLE I

X-Ray powder diffraction patterns of *n*-RBr–urea inclusion compounds (unwashed)

R	1.94–2.00*	2.06	2.16–2.17	2.62	2.69–2.70	2.82–2.84	3.03–3.05	3.26–3.27	3.39–3.40	3.53–3.57	3.61–3.62	3.86	3.98–4.00	4.10–4.11	7.13–7.15
C_6H_{11}	0.04†	—	0.02	—	—	0.06	0.11	—	—	0.03	0.10	—	1.00	0.06	—
C_7H_{15}	—	0.03	0.03	0.05	—	—	0.05	0.03	0.10	0.42	—	—	0.19	1.00	0.03
C_8H_{17}	0.02	0.04	0.02	0.05	0.03	—	—	0.02	0.15	0.86	—	0.04	—	1.00	0.05
C_9H_{19}	0.03	0.03	0.03	0.05	0.03	—	—	0.03	0.12	0.69	—	0.04	—	1.00	—
$C_{10}H_{21}$	0.03	0.06	0.07	0.05	0.03	—	—	0.03	0.16	0.31	—	0.09	—	1.00	0.03
Urea	0.02	—	—	—	—	0.06	0.24	—	—	0.10	0.02	—	1.00	—	—

*Interplanar spacings in angstroms using CuK_α radiation.
†Relative intensities; 1.00 being the strongest.

TABLE II

X-Ray powder diffraction patterns of *n*-RI–urea inclusion compounds (unwashed)

R	1.98–2.00*	2.05–2.06	2.37–2.38	2.53	2.62	2.83	3.06	3.39–3.40	3.56–3.58	3.63	4.00–4.02	4.11–4.15	7.13–7.21
C_5H_{11}	—	—	—	0.10	—	0.10	0.16	—	0.56	0.14	1.00	0.31	0.07
C_6H_{13}	—	0.05	0.08	—	0.07	—	0.07	0.16	1.00	—	0.33	0.83	0.05
C_7H_{13}	0.03†	0.08	0.05	—	—	—	—	0.08	1.00	—	—	0.20	0.05
C_8H_{17}	0.02	0.04	0.06	—	—	—	—	0.05	1.00	—	—	0.38	—
C_9H_{19}		0.03	0.06	—	—	—	—	0.06	1.00	—	—	0.29	0.03
$C_{10}H_{21}$	—	0.03	0.06	—	0.04	—	—	0.06	1.00	—	—	—	—
Urea	0.02	—	—	0.04	—	0.04	0.24	—	0.10	0.02	1.00	—	—

*Interplanar spacings in angstroms using CuK_α radiation.
†Relative intensities; 1.00 being the strongest.

TABLE III

X-Ray powder diffraction patterns of *n*-RI–urea inclusion compounds (washed)

R	1.98–2.00*	2.05–2.06	2.38–2.42	2.53	2.61–2.62	2.82–2.83	3.05	3.39–3.40	3.56–3.57	3.98–4.00	4.10–4.12	7.13–7.19
C_5H_{11}	—	—	0.06	0.10	0.04	0.06	0.14	0.92	1.00	0.92	0.58	—
C_6H_{13}	—	—	—	—	—	—	0.12	0.24	0.58	0.39	1.00	—
C_7H_{15}	0.04†	0.04	0.09	—	0.04	—	—	0.06	1.00	—	0.50	0.03
C_8H_{17}	0.02	—	0.03	—	—	—	—	0.07	0.88	—	1.00	—
C_9H_{19}	0.02	0.02	0.08	—	—	—	—	0.05	1.00	—	0.37	0.02
$C_{10}H_{21}$	0.04	0.05	0.07	—	0.03	—	—	0.07	1.00	—	0.71	—
Urea	0.02	—	—	0.06	—	0.03	0.02	—	—	1.00	—	—

*Interplanar spacings in angstroms using CuK_α radiation.
†Relative intensities; 1.00 being the strongest.

inclusion compounds with absolute ethanol, the complexes of the *n*-alkyl iodides were prepared in two ways, by simply filtering them (results Table II) or by filtration and washing with ethanol (results in Table III). No advantage could be found by including the washing step since it only reduced the yield of complex. The data in Tables II and III indicate the disappearance or diminution of some of the spacings characteristic of the complex for the washed inclusion compounds. Consequently, the washing step was omitted from the preparation of the 1-bromoalkane complexes.

EXPERIMENTAL

1-Bromo- and iodo-alkanes.—Pure compounds were obtained from the Gallard–Schlesinger Mfg. Corp., Long Island, N.Y.

Urea inclusion compounds.—To 4.5 ml of a urea–methanol solution (0.15 g urea/ml of methanol) in a screw-cap vial was added 30 drops of the alkyl halide. The vial was capped, shaken vigorously for 30 seconds, and allowed to stand for 3–4 hours at 29–30°. Then the compounds were kept at 4° for 24 hours. Crystals that formed were filtered by suction using a rubber sheet to cover the funnel, thereby reducing the possibility of contaminating the complex with free urea resulting from the evaporation of the mother liquor during filtration.

The inclusion compounds of Tables I, II, and III were prepared in the same way except that the inclusion compounds of Table III were washed with 10 ml of absolute ethanol at 4° during the filtration step.

X-ray powder diffraction measurements.—These measurements were made on a North American Phillips Co. X-Ray Diffractometer (Model 5001) which was equipped with a high angle goniometer and a proportional counter. CuK_α radiation was obtained by operating the Cu tube at 35 kv and 15 ma using a nickel filter and passing the radiation through a 1° slit. The goniometer scanning speed was 1°/minute. Samples were mounted on a roughened glass slide using a spatula and enough pressure to make the samples stick to the slide.

Cross-sectional diameters.—These measurements were made on scalar molecular models by a previously described procedure (6).

REFERENCES

1. W. SCHLENK, JR. Ann. **565**, 204 (1949).
2. J. RADELL and J. W. CONNOLLY. J. Am. Chem. Soc. **25**, 1202 (1960).
3. W. SCHLENK, JR. Svensk Kem. Tidskr. **67**, 10 (1955).
4. J. RADELL and J. W. CONNOLLY. *In* W. M. Mueller. Advances in X-ray analysis. Vol. IV. Plenum Press, N.Y. 1961. pp. 140–150.
5. J. RADELL, J. W. CONNOLLY, and L. D. YUHAS. J. Org. Chem. **26**, 2022 (1961).
6. J. RADELL, J. W. CONNOLLY, and W. R. COSGROVE, JR. J. Org. Chem. **26**, 2960 (1961).

Can. J. Chem. Downloaded from www.nrcresearchpress.com by 210.87.254.6 on 09/05/12
For personal use only.

Can. J. Chem. Downloaded from www.nrcresearchpress.com by 210.87.254.105 on 09/05/12
For personal use only.

STUDIES IN THE PYRROLINE SERIES

III. SOME PYRROLINYLPYRROLES AND RELATED COMPOUNDS

R. BONNETT, K. S. CHAN, AND I. A. D. GALE
Chemistry Department, University of British Columbia, Vancouver, British Columbia
and
Chemistry Department, Queen Mary College, London, England

Received November 12, 1963

ABSTRACT

The addition of 5,5-dimethyl-1-pyrroline to pyrrole gives both the 1:1 adduct and the 2:1 adduct. The palladium-catalyzed dehydrogenation of 2,2′-pyrrolidinylpyrrole has been studied at various temperatures. In refluxing toluene the reaction proceeds satisfactorily to the pyrroline level, while in cymene the corresponding bipyrrole is produced. 1,2′-(1′-Pyrrolinyl)-pyrrole has been obtained from the reaction of 2-methoxy-1-pyrroline with pyrrole: on pyrolysis it yields 2,2′-(1′-pyrrolinyl)pyrrole. A similar sequence is observed with 3,4-dimethylpyrrole.

Compounds with two rings of the pyrrole type linked directly at α,α' positions have become of much interest recently with the formulation of vitamin B_{12} and prodigiosin as naturally occurring examples of this class. The most direct routes to such systems appear to be (i) dimerization of suitably substituted pyrroles, e.g. (1, 2):

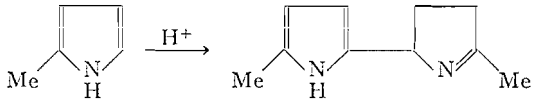

(ii) nucleophilic substitution at position 2 of a suitable 1-pyrroline:

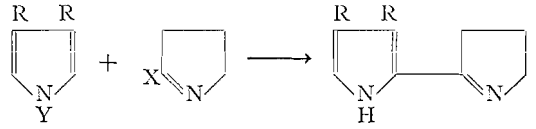

R = Y = H; X = $OPOCl_2.HCl$ (ref. 3)

R = CH_3; Y = MgHal; X = OMe (ref. 2)

and (iii) the addition of a pyrrole to a 1-pyrroline (4):

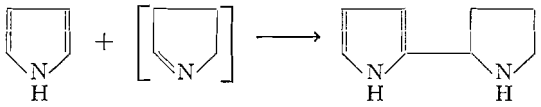

The latter approach now has been investigated further, with particular attention being paid to the dehydrogenation of the resulting 2,2-pyrrolidinylpyrrole under various conditions.

The addition reaction itself was examined at the outset since it appeared likely that the addition of a further pyrroline nucleus to the pyrrolidinylpyrrole might occur. In the case of 1-pyrroline itself the 1:1 adduct is the only isolated product, and this is not surprising in view of the ready trimerization of 1-pyrroline, a process which could effectively limit the concentration of the monomer. 5,5-Dimethyl-1-pyrroline, which does not trimerize so

readily, has now been shown to yield both 1:1 and 2:1 adducts. The former adduct is isolated when the reaction medium contains a considerable excess of pyrrole.

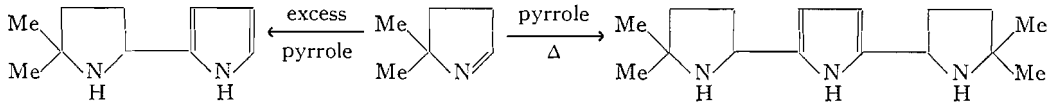

I II

That compound II was in fact the 2:1 adduct was evident from the analysis of the base and that of its dipicrate, and from the equivalent of the base. The assignment of structure II was in accord with the ultraviolet spectrum (λ_{max} 223 mμ; log ϵ 4.04) and the infrared spectrum (two NH bands in dilute solution): 2,5-disubstitution was assigned on the basis of the known relative nucleophilicity of the pyrrole positions ($\alpha > \beta$) and received support from the proton magnetic resonance spectrum, which indicated only one type of aromatic proton (Table I).

TABLE I

Proton magnetic resonance spectra
(τ values, internal T.M.S., A60, $CDCl_3$)

Compound	Pyrrole protons					Pyrroline protons			Other
	1	2	3	4	5	3′	4′	5′	
II	—	—	4.18	4.18	—	—	—	—	5.74 (*tert.* H) 8.82 (Me)
III	−0.33	—	3.54	3.84	3.12	7.12	8.06	6.00*	—
V	—	2.86	3.82	3.82	2.86	7.15	7.98	6.14	—
3,3-Dimethyl-2-phenyl-1-pyrroline	—	—	—	—	—	—	8.07	6.12	8.66† (Me)
3,4-Dimethyl-1,2′-(1′-pyrrolinyl)-pyrrole	—	3.11†	—	—	3.11†	7.17	7.82	6.14	8.00† (Me)

*These values are somewhat lower than those quoted by Rapoport (3). We assign the ~6τ signal to the 5′ protons and the ~7τ signal to the 3′ protons rather than vice versa (cf. (9) and τ values given above for 4′ and 5′ protons in 3,3-dimethyl-2-phenyl-1-pyrroline).
†Singlets. Other values refer to the centers of broad or multiplet signals.

When the dehydrogenation of 2,2′-pyrrolidinylpyrrole was carried out in xylene (5) the major product was a base with a pK_a (aqueous ethanol) of 7.9, and evidently not 2,2′-bipyrrole. Analysis of the base indicated the formula $C_8H_{10}N_2$, which was supported further by the titration results. The ultraviolet spectrum indicated increased conjugation (λ_{max} 279 mμ; log ϵ 4.21) and, moreover, the band experienced a bathochromic shift on acidification of the solution (λ_{max} 318 mμ; log ϵ 4.41). Closely analogous behavior was shown by the Schiff base formed from pyrrole-2-aldehyde and methylamine (6). In ethanol this was found to have a band at 285 mμ (log ϵ 4.20) which shifted to 325 mμ (log ϵ 4.36) in acid solution. The infrared spectrum indicated the presence of the NH group: in addition, a band, which in the infrared of the base was at 1620 cm^{-1}, appeared in the spectrum of the perchlorate at 1655 cm^{-1} (Ar—C=N— → Ar—C=N$^+$H—). These results strongly supported the formulation of the base as 2,2′-(1′-pyrrolinyl)pyrrole III, and this structure was in accord with the proton magnetic resonance spectrum (Table I). After the completion of this work a similar conclusion was reported by Rapoport (3), who isolated 2-(4-aminobutyl)-pyrrole and 2,2′-bipyrrole in addition to the pyrroline. It is of interest that this pyrrylpyrroline (formulated as the Δ^2-tautomer) was reported much earlier (7)

Can. J. Chem. Downloaded from www.nrcresearchpress.com by 210.87.254.105 on 09/05/12
For personal use only.

as the product of the conventional Cloke pyrroline synthesis. This report has recently been shown to be in error; the Cloke synthesis is not of general application to the pyrrylmagnesium halides and the isomer obtained earlier has been characterized as 2-(3-cyanopropyl)pyrrole (8).

Small-scale experiments (evaluated by paper chromatography) were carried out to obtain conditions which would give 2,2′-(1′-pyrrolinyl)pyrrole and the corresponding bipyrrole in satisfactory yields. The results (Table II, Experimental) suggested that the pyrroline oxidation level could be satisfactorily reached in refluxing toluene, while in refluxing cymene the 2,2′-bipyrrole was formed in moderate amount. On a preparative scale the pyrrylpyrroline has been obtained in 54% yield from the reaction in toluene.

The synthesis of 2,2′-(1′-pyrrolinyl)pyrrole has been approached in another way, following the observation that the cyclic iminoether 2-methoxy-1-pyrroline reacted readily with various anilines to give amidines such as IV, which, as would be expected, are strong

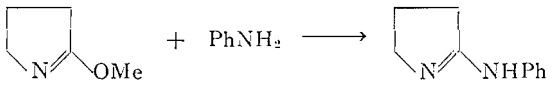

IV

bases (pK_a in aqueous ethanol 9.8 cf. p-$ClC_6H_4NHC(=NH)CH_3$ pK_a 9.5 (10)). It was of interest that pyrrole also reacted with the cyclic iminoether to give a white crystalline substance isomeric with compound III. This compound is assigned the novel structure V, although it is, in fact, a rather weak base (pK_a 5.4). The ultraviolet spectrum of the compound had a maximum at 245 mμ (log ϵ 4.15) which shifted to 252 mμ (log ϵ 4.24) on acidification. This absorption is comparable to that of 1-acetylpyrrole (λ_{max} 238.5 mμ; log ϵ 4.03 (11)), and the shift observed in acid is similar to that recorded for the base for which structure VI has been advanced (2). The infrared spectrum of base V had no prom-

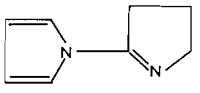

V

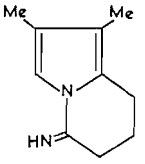

VI

inent absorption in the NH region but did possess a band assignable to the C=N stretching mode at 1650 cm^{-1}. Further support for the proposed structure came from the n.m.r. spectrum (Table I), which had two groups of equally intense signals corresponding to the two types of aromatic protons in V; and from the fact that an analogous compound (n.m.r. spectrum: Table I) could be obtained, though in low yield, from the reaction of 3,4-dimethylpyrrole with 2-methoxy-1-pyrroline. Clearly, although compound V is formally an amidine, the lone pair on the pyrrolic nitrogen has aromatic commitments and cannot be readily involved in the cation VII. On the other hand, the 2,2′-compound (III) gives a

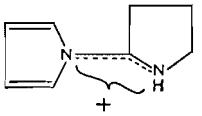

VII

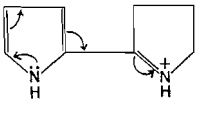

VIII

Can. J. Chem. Downloaded from www.nrcresearchpress.com by 210.87.254.105 on 09/05/12
For personal use only.

cation in which not only has protonation occurred on nitrogen but in which mesomerism may involve the entire π-system (VIII—arrows). Thus the 2,2′-compound is a much stronger base than the 1,2′-compound.

It is striking that the reaction of pyrrole and the cyclic iminoether appears to occur specifically at position 1 under the mild conditions employed; it should be noted (cf. reaction (ii)) that when various pyrrylmagnesium halides are used (2) reaction at carbon (rather than at nitrogen) prevails following the general experience (cf. 12) with magnesium salts of pyrroles. The migration of groups from nitrogen to carbon (especially α-carbon) under thermal stimulus is, however, a well-known reaction in pyrrole chemistry, and it was pertinent to observe whether or not the 1-pyrroline residue could survive such a process. Pyrolysis carried out in a stream of purified nitrogen was attended by much decomposition, but a 12% yield of 2,2′-(1′-pyrrolinyl)pyrrole was isolated, and paper chromatography indicated that 2,2′-bipyrrole was amongst the by-products of this novel pathway to the α,α' direct linkage.

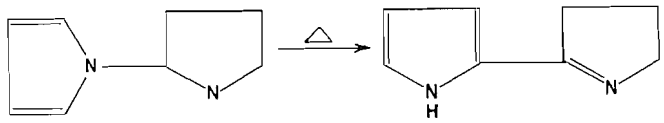

V III

EXPERIMENTAL

The following equipment was used. Melting points: Fisher–Johns heated block. Infrared spectra: Perkin Elmer Infracord or Model 21. Vapor phase chromatography: Aerograph A-90-P. Proton magnetic resonance spectra: Varian A60. The pK_a values refer to the pH recorded at the half-neutralization point at 18° by a Doran pH meter previously standardized with aqueous buffer at pH 9.15. Analyses by Dr. A. Bernhardt, Mulheim.

Reaction of 5,5-Dimethyl-1-pyrroline with Pyrrole

(a) With a large excess of pyrrole.—The pyrroline (0.5 g) and pyrrole (8 g) were kept at 100° for 32 hours in a sealed tube. The pyrrole was removed (rotary evaporator) and the oily residue was sublimed at 95° at 1 mm. The white sublimate (0.27 g, 32%) had m.p. 39° when crystallized from hexane. It gave an orange picrate from ether, which, recrystallized from ethanol, melted at 155°. Found: C, 49.05; H, 5.0; N, 18.0. $C_{16}H_{19}N_5O_7$ requires C, 48.85; H, 4.9; N, 17.8%.

(b) 2,5-Bis-2′-(5′,5′-dimethylpyrrolidinyl)pyrrole (II).—The pyrroline (1 g) and pyrrole (2 g) were heated in a stoppered flask on a steam bath for 24 hours. Readily volatile material was removed on a rotary evaporator and the remaining oil was treated in benzene–hexane with charcoal to give 0.24 g (18%) of colorless prisms, m.p. 127–131°. Recrystallization from the same solvent raised the m.p. to 133°. Found: C, 73.8; H, 10.4; N, 15.8. $C_{16}H_{27}N_3$ requires C, 73.5; H, 10.4; N, 16.1%. $\nu_{max}^{CHCl_3}$ 3430, 3310, 1587, 1475 cm^{-1}. λ_{max}^{EtOH} 223 mμ; log ϵ 4.04. Titration in aqueous ethanol gave an equivalent of 134 (calc. 131). The *picrate*, prepared in moist ether and recrystallized from ethanol, had m.p. 213° (decomp.). Found: C, 46.8; H, 4.7; N, 17.5. $C_{28}H_{33}N_9O_{14}$ requires C, 46.7; H, 4.6; N, 17.5%.

Dehydrogenation of 2,2′-Pyrrolidinylpyrrole

(a) Trial experiments.—2,2′-Pyrrolidinylpyrrole (25 mg (4)) and 5% palladium on charcoal (25 mg) were refluxed in 10 ml of aromatic solvent (Table II) for 4½ hours. The hot solution was filtered (Celite) and the depth of color of the filtrate was observed. The solutions were examined by descending paper chromatography in two systems: (A) Whatman No. 1 with *n*-butanol – acetic acid – water (4:1:5—top phase) over 4½ hours and (B) aluminum oxide paper No. 288 (Schleicher and Schnell, Dassel) with *n*-butanol saturated with water over 15 hours. The spots were developed with iodine vapor. The relative intensities were estimated visually; they give a rough guide to the progress of the reactions as illustrated in Table II.

(b) Preparation of 2,2′-(1′-pyrrolinyl)pyrrole (III).—2,2′-Pyrrolidinyl pyrrole (250 mg) and 5% palladium on charcoal (250 mg) were refluxed in toluene (15 ml) for 4 hours. The hot solution was filtered (Celite) and the pad was washed with ether (45 ml). The filtrate was extracted with two portions of 0.5 *N* HCl (40 ml, 20 ml), and the separated aqueous extract was basified (NaOH) and re-extracted with ether (2×50

Can. J. Chem. Downloaded from www.nrcresearchpress.com by 210.87.254.105 on 09/05/12
For personal use only.

TABLE II

Dehydrogenation of 2,2′-pyrrolidinylpyrrole

Solvent	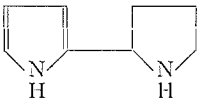	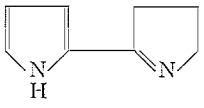	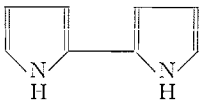	Decomposition*
		Chromatography—R_f values		
System A	0.69	0.69	0.89	—
System B	0.47	0.78	0.78	—
		Dehydrogenation†		
Benzene	XXX	X	—	—
Toluene	—	XXX	X	—
Xylene	—	XX	XX	X
Cymene	—	X	X	XXX

* As judged by depth of color of filtrate.
†Crosses correspond roughly to spot intensities: XXX—major, XX—moderate, X—minor component.

ml). The dried ethereal solution was concentrated to yield (at −10°) 132 mg (54%) of 2,2′-(1′-pyrrolinyl)pyrrole, m.p. 166°. Found: C, 71.1; H, 7.5; N, 20.9. $C_8H_{10}N_2$ requires C, 71.6; H, 7.5; N, 20.9%. $\nu_{max}^{CHCl_3}$ 3450 (sharp, free NH) 3300 (broad, hydrogen-bonded NH), 1620 cm^{-1} (Ar—C═N). In Nujol mull only H-bonded NH absorption was observed. λ_{max}^{EtOH} 279 mμ (log ε 4.21) with inflexion at 240 mμ (log ε 3.61); on acidification the maximum appeared at 318 mμ (log ε 4.41). Potentiometric titration in aqueous ethanol (50% ethanol) gave an apparent pK_a of 7.9 and an equivalent of 138 (calc. 134).

(c) Preparation of 2,2′-bipyrrole.—2,2′-Pyrrolidinylpyrrole (250 mg) and 5% palladium on charcoal (250 mg) were refluxed in *p*-cymene (5 ml), stirred with a slow stream of nitrogen for 3 hours. The cooled mixture was applied to a column (10×1.5 cm) of alumina (activity IV) in petrol and eluted with benzene. The eluate was tested from time to time with the Ehrlich reagent. Those fractions which gave a royal blue color were combined, reduced to a small volume, and diluted with petrol to give 47 mg (19%) of 2,2′-bipyrrole, m.p. 185°. Sublimation (100° at 0.5 mm) raised the m.p. to 187° (lit. 189–190° (3)).

Preparation of 1,2′-(1′-Pyrrolinyl)pyrrole (V)

2-Methoxy-1-pyrroline (2 g (2)) and pyrrole (4 g) were heated together in a sealed tube (40 hours, 100°). The excess pyrrole was removed (rotary evaporator) and the oily residue was sublimed to give 0.93 g (34%) of 1,2′-(1′-pyrrolinyl)pyrrole, m.p. 71°, after two crystallizations from 60–80° petroleum. Found: C, 71.8; H, 7.6; N, 20.8; mol. wt. (Rast) 126. $\nu_{max}^{CHCl_3}$ 1650, 1495, 1378 cm^{-1}. λ_{max}^{EtOH} 245 mμ (log ε 4.15); on acidification 252 mμ (log ε 4.24). Potentiometric titration in aqueous alcohol gave a pK_a value of 5.4 and an equivalent of 135.

Thermal Rearrangement of 1,2′-(1′-Pyrrolinyl)pyrrole

1,2′-(1′-Pyrrolinyl)pyrrole (0.7 g) was distilled in a stream of oxygen-free nitrogen through a column (20×1 cm) of glass beads (2–3 mm diameter, Hopkins and Williams Ltd.) at dull red heat. The crude product (0.46 g) solidified; it was triturated with methanol (0.5 ml) and the liquid withdrawn at the filter stick. The off-white solid remaining was crystallized (charcoal) from ether to give 69 mg of 2,2′-(1′-pyrrolinyl)pyrrole, m.p. and mixed m.p. 166°. A further 12 mg, m.p. 164°, was obtained from the mother liquors (total yield 12%). Paper chromatography (system A) of the mother liquors suggested the presence of 2,2′-bipyrrole (R_f 0.88).

3,4-Dimethyl-1,2′-(1′-pyrrolinyl)pyrrole

3,4-Dimethylpyrrole (1.72 g) and 2-methoxy-1-pyrroline (2 g of a 60% solution in benzene) were heated in a sealed tube (100°, 72 hours). Vapor phase chromatography showed the presence of a new compound (retention volume 620 ml; 5 foot Ucon Polar column at 210°; helium carrier) in addition to starting material. The lower boiling fraction was removed at reduced pressure, and the solid residue was crystallized from petroleum ether (60–80°; charcoal) to give 0.41 g (21%) of 3,4-dimethyl-1,2′-(1′-pyrrolinyl)pyrrole, m.p. 93–94° after two recrystallizations from petroleum. Found: C, 73.9; H, 8.7; N, 17.3. $C_{10}H_{14}N_2$ requires C, 74.0; H, 8.7; N, 17.3%. Electrometric titration in aqueous ethanol gave an equivalent of 152 (calc. 162) and a pK_a of 5.8. ν_{max}^{Nujol} 1650 cm^{-1}, no NH, λ_{max}^{EtOH} 258 mμ (log ε 4.15).

Pyrolysis of this compound as before gave a low yield of 3,4-dimethyl-2,2′-(1′-pyrrolinyl)pyrrole, m.p. 173–177°; after sublimation 178–178.5° (lit. 178–179° (2)).

2-Phenylamino-1-pyrroline (IV)

2-Methoxy-1-pyrroline (0.5 g) and aniline (0.5 g) were heated together in a sealed tube (90°, 5 days).

Can. J. Chem. Downloaded from www.nrcresearchpress.com by 210.87.254.105 on 09/05/12
For personal use only.

Readily volatile material was removed on a rotary evaporator, whereupon the residue solidified. It was crystallized (charcoal) from 60–80° petroleum to give 0.54 g (67%) of 2-phenylamino-1-pyrroline (tautomeric system) m.p. 115° (lit. 114–115°, (13)). Sublimation (95°, 1 mm) and recrystallization raised the melting point to 116–117°. Found: C, 74.9; H, 7.4; N, 17.3. $C_{10}H_{12}N_2$ requires C, 75.0; H, 7.55; N, 17.5%. Titration gave an apparent pK_a of 9.8 and an equivalent of 165 (calc. 160).

ACKNOWLEDGMENTS

Acknowledgment is made to the donors of the Petroleum Research Fund, administered by the American Chemical Society, for their support of this work. Dr. D. E. McGreer and Mr. P. Cook are thanked for the n.m.r. spectra.

REFERENCES

1. C. F. H. Allen, M. R. Gilbert, and D. M. Young. J. Org. Chem. **2**, 227, 235 (1938).
2. H. Booth, A. W. Johnson, and F. Johnson. J. Chem. Soc. 98 (1962).
3. H. Rapoport and N. Castagnoli. J. Am. Chem. Soc. **84**, 2178 (1962).
4. D. W. Fuhlhage and C. A. Vanderwerf. J. Am. Chem. Soc. **80**, 6249 (1958).
5. H. Rapoport and K. G. Holden. J. Am. Chem. Soc. **84**, 635 (1962). H. Rapoport. Private communication.
6. B. Emmert, K. Diehl, and F. Gollwitzer. Ber. **62**, 1733 (1929).
7. L. C. Craig. J. Am. Chem. Soc. **56**, 1144 (1934).
8. A. J. Castro, J. F. Deck, and M. T. Hugo. Abstracts, 139th A.C.S. meeting, St. Louis, Mo. March, 1961.
9. R. Bonnett and D. E. McGreer. Can. J. Chem. **40**, 177 (1962).
10. J. C. Gage. J. Chem. Soc. 221 (1949).
11. R. Andrisano and G. Pappalardo. Gazz. Chim. Ital. **85**, 1430 (1955).
12. A. Treibs and A. Dietl. Ann. **619**, 80 (1959).
13. H. Bredereck and K. Bredereck. Ber. **94**, 2278 (1961).

Can. J. Chem. Downloaded from www.nrcresearchpress.com by 210.87.254.105 on 09/05/12
For personal use only.

Can. J. Chem. Downloaded from www.nrcresearchpress.com by 210.87.254.6 on 09/05/12
For personal use only.

CO-ORDINATION COMPLEXES OF GROUP (IV) HALIDES

PREPARATION AND INFRARED SPECTRA OF THE CO-ORDINATION COMPOUNDS OF TITANIUM TETRACHLORIDE, TITANIUM TETRABROMIDE, ZIRCONIUM TETRACHLORIDE, TIN TETRACHLORIDE, AND BORON TRICHLORIDE WITH ETHYL CYANOACETATE AS LIGAND[1]

SUMER CHAND JAIN AND ROLAND RIVEST
Department of Chemistry, University of Montreal, Montreal, Quebec

Received December 4, 1963

ABSTRACT

Co-ordination compounds between ethyl cyanoacetate and boron trichloride, titanium tetrabromide, and tetrachlorides of titanium, zirconium, and tin have been prepared. The analytical results indicate that under similar experimental conditions, 1:1 addition compounds are obtained in each case. On the basis of infrared spectra it has been postulated that the compounds obtained are six-membered ring chelates, satisfying the most common co-ordination number six for the elements of group IV.

INTRODUCTION

In our previous work (1) on the co-ordination complexes of group (IV) halides with nitriles and dinitriles it has been postulated for some of the compounds that the central element had a co-ordination number five, or a co-ordination number six, where this co-ordination number six was reached through halide bridging. In the complexes with halogen-substituted esters (2) the formation of 1:1 addition complexes was explained on the basis of co-ordination number six for the central titanium atom where both the oxygen atoms of acid and ether groups were involved in co-ordination forming a four-membered-ring chelate. But at the same time the probability of co-ordination number five for titanium where only the carbonyl group was co-ordinated, could not be ruled out. Since titanium compounds having co-ordination number eight have been well established by Nyholm (3) and his co-workers, in the compounds of general formula $TiCl_4.2$ esters titanium can exhibit a co-ordination number six, if only the carbonyl groups act as donors, or it can exhibit a co-ordination number eight if both oxygens of the monoester molecule are involved in co-ordination.

To know more about the possible co-ordination numbers of titanium (IV), it was thought of interest to use a bidentate ligand where it was easy to detect the co-ordination of the two different donor elements and in which one could see what was happening to both donor groups when present on the same molecule. For this purpose ethyl cyanoacetate was chosen where it was possible to differentiate between the co-ordination effects of cyano and carbonyl groups through infrared spectroscopic studies. To investigate the respective influence on the stretching frequencies of the two donor groups when only one of them is involved in co-ordination, boron trichloride was chosen.

EXPERIMENTAL

Material and Manipulations

Boron trichloride obtained from the British Drug Houses Limited (in sealed capsules) was used without further purification. Ethyl cyanoacetate was obtained from Eastman Organic Chemicals through The Fisher Scientific Company and was dried over molecular sieves. The solvent carbon tetrachloride was made anhydrous by appropriate method. The group (IV) halides were purified as mentioned in previous publication (1).

[1]*Presented at the XXXI Congrès de l'Association Canadienne Française pour l'Avancement des Sciences, Québec, November 2, 1963.*

The group (IV) halides and their complexes are extremely sensitive to humidity. Therefore, all manipulations were carried out in a rigorously dried apparatus and handled in an anhydrous chamber, which was continuously flushed with dry nitrogen in a manner described in an earlier paper (4). The experimental methods and the methods of analysis for metal and halogens are essentially the same as described previously (4, 5). Boron was analyzed as boric acid after adding mannitol, and titrating with a standard NaOH solution to a phenolphthalein end point (6).

The spectrophotometric measurements were carried out on a Perkin–Elmer Infrared spectrophotometer, model 21, using sodium chloride prism. Samples were prepared as Nujol mulls.

Preparation of the Complexes

The preparation of these complexes was performed in carbon tetrachloride. In each case except for $SnCl_4$ and BCl_3, insoluble precipitates were obtained which were filtered, washed with the solvent, and dried under vacuum at room temperature. The following proportions of the reactants w/v % were used to obtain the respective compounds.

$TiCl_4.NCCH_2CO_2C_2H_5$.—To 20 ml of 25% solution of the ligand was added 20 ml of 42.25% solution of $TiCl_4$. The analytical and the infrared results of the product so obtained and its sublimate at low pressure were identical.

$2TiCl_4.NCCH_2CO_2C_2H_5$.—To 20 ml of 85% solution of $TiCl_4$ was added 10 ml of 10% solution of the ligand and the reaction allowed to go for 3 days.

$TiBr_4.NCCH_2CO_2C_2H_5$.—To 20 ml of 10% solution of the ligand was added 20 ml of 32.5% solution of $TiBr_4$.

$ZrCl_4.NCCH_2CO_2C_2H_5$.—Twenty milliliters of 15% solution of the ligand and 2 g of $ZrCl_4$ was allowed to react for about 1 week under continuous stirring.

$SnCl_4.NCCH_2CO_2C_2H_5$.—Ten milliliters of 10% solution of the ligand was added to 20 ml of 33.5% solution of $SnCl_4$. In this particular case no product was obtained in the beginning, but when the solution in the reaction flask was evaporated slowly, a white crystalline product separated from the mother liquor.

$BCl_3.NCCH_2CO_2C_2H_5$.—A 25 g capsule of BCl_3 was cooled to 0° C before breaking the seal and was then diluted with 15 ml cold CCl_4 in a reaction flask. To this solution 4 ml ligand was added drop by drop keeping the reaction flask at 0° C. The reaction mixture was then subjected to slow evaporation. The product so obtained and its sublimate at reduced pressure gave the same analytical results of boron and chlorine. The analytical results are included in Table I.

INFRARED SPECTRA AND DISCUSSION

It is well known that the carbonyl stretching frequency is lowered on co-ordination (2, 5). In previous published work it has been shown (2) that the magnitude of the negative shift is largely affected by the number and position of the chlorine atoms on the ester molecules used as ligands. Infrared observations as included in Table II show that the presence of the cyano group seems to have a similar electron pulling effect as the one noticed in the case of chlorine substituted esters, and thus reduces the donor ability of the oxygen of the carbonyl group. A negative bathochrome effect gives an indication that C=O group is involved in co-ordination. On the other hand a positive shift is observed for the C≡N stretching frequency. In our work (1) on the complexes of group IV halides with dinitrile series it was pointed out that on co-ordination the C≡N stretching frequency is increased. Coerver and Curran (7) working with mononitriles and $TiCl_4$, BCl_3, and $SnCl_4$ compounds reported a positive shift of the same order as obtained in the case of ethyl cyanoacetate complexes.

To investigate the relative influence on the stretching frequencies of the two donor groups when only one of them is involved in co-ordination, $BCl_3.NCCH_2COOEt$ was prepared. Though the boron trichloride compound was prepared in large excess of BCl_3 the analytical results confirmed the one to one composition. The infrared spectrum of this compound did not indicate any marked increase in the C≡N frequency while C=O and C′—O stretching frequencies showed marked negative shifts. This is an indication that co-ordination through the carbonyl group has no marked effect on the cyano stretching frequency of the ligand, but does influence the C′—O stretching frequency as shown in the boron trichloride complex.

Another point worth mentioning is that the infrared spectra of 1:1 ethyl cyanoacetate

Can. J. Chem. Downloaded from www.nrcresearchpress.com by 210.87.254.6 on 09/05/12
For personal use only.

Can. J. Chem. Downloaded from www.nrcresearchpress.com by 210.87.254.6 on 09/05/12
For personal use only.

TABLE I

Analytical results

Lewis acid in the compounds	Color	Melting point, °C	Metal %		Halogen %		Nature of adduct
			Theor.	Found	Theor.	Found	
$TiCl_4.E$*	Yellow	150–152	15.81	15.70	46.8	46.20	1:1
$2TiCl_4.E$	Yellow	156–158	19.45	18.96	57.65	55.76	2:1
$TiBr_4.E$	Red	D 200	9.98	9.89	66.66	65.37	1:1
$ZrCl_4.E$	White	D 180	26.35	26.63	40.96	39.90	1:1
$SnCl_4.E$	White	60–62	31.77	29.91	37.95	38.46	1:1
$BCl_3.E$	White	80–82	4.70	4.82	46.20	46.33	1:1

*E = Ethyl cyanoacetate.

TABLE II

Infrared spectra results in Nujol mulls

Name of the compound	Carbonyl stretching frequency (cm^{-1})	Shift $\Delta\nu$ C=O (cm^{-1})	C′—O stretching frequency (cm^{-1})	Shift $\Delta\nu$ C′—O (cm^{-1})	C≡N stretching frequency (cm^{-1})	Shift $\Delta\nu$ C≡N (cm^{-1})
$NCCH_2CO_2C_2H_5$	1750	—	1027	—	2267	—
$TiCl_4.E$*	1665	85	998	29	2318	51
$2TiCl_4.E$	1660	90	1000	27	2315	48
$TiBr_4.E$	1666	84	995	32	2300	33
$ZrCl_4.E$	1668	82	992	35	2305	38
$SnCl_4.E$	1670	80	1002	25	2302	35
$BCl_3.E$	1590	160	1005	22	2770	3

*E = $NCCH_2CO_2C_2H_5$.

complexes are similar to those of the complexes of halogenated esters with $TiCl_4$ in the regions attributed to C=O and C′—O absorption. This leads one to the conclusion that titanium in the compounds of halogenated esters exhibits a co-ordination number five in the 1:1 addition compounds, and a co-ordination number six in the 1:2 addition compounds. These two types of compounds may be assumed to have co-ordination through the carbonyl group only of the monoester molecule. The lowering of the C′—O band in the infrared spectra of these complexes might be due to the mutual interaction of the C=O and C′—O groups. Moreover, a similar lowering of C′—O stretching frequency in boron trichloride complex, where only the carbonyl group is co-ordinating, further supports our interpretation. If the above interpretation was not true then the central metal atom in the ethyl cyanoacetate complexes would have a co-ordination number seven, forming per molecule of complex two chelate rings of six and four atoms. This situation would put an extra strain on the ligand molecule and is to be rejected.

Then, it seems, that in the complexes with the group (IV) halides, where both the cyano and the carbonyl stretching frequencies are changed on co-ordination, six-membered ring chelates are formed. This interpretation is further supported if the melting points of $TiCl_4.NCCH_2COOEt$ (150–152° C) and that of $TiCl_4.CH_3COOEt$ (110–111° C) are compared. In the work with halogenated esters it was shown that with halogen substitution both the carbonyl shifts and the melting points of the compounds fall (2). But in the present case of cyanoacetate compound the carbonyl shift is smaller (85 cm^{-1}) than for the ethyl acetate compound (148 cm^{-1}) but at the same time the melting point is much higher. This would not be the case if co-ordination through C≡N group forming a more strongly co-ordinated and more stable chelated ring was not taking place. On the basis of the above discussion it is quite reasonable to presume that in the cyanoacetate complexes the central elements exhibit a co-ordination number 6, except for the complex with boron trichloride.

From the infrared spectra of all these complexes one can see that in the cases of $TiCl_4$, $TiBr_4$, and $ZrCl_4$ complexes there is not much dissociation as seen from the shifted carbonyl stretching frequencies. But the spectrum of $SnCl_4$ compound clearly shows two carbonyl peaks, one shifted due to co-ordination and the other one in the original region due to dissociation. The low melting point of $SnCl_4$ compound and its solubility in CCl_4 and CH_2Cl_2 in comparison to titanium and zirconium compounds indicate the weakness of tin tetrachloride as a Lewis acid against the tetrahalides of titanium and zirconium mentioned above. The stability of Ti and Zr compounds in question can further be seen by comparing the shifts in C≡N stretching frequency which is maximum in the case of $TiCl_4$ compound and least with $SnCl_4$ compound. The ipsochrome effect of the cyano group in the case of $SnCl_4$ and $ZrCl_4$ compound falls considerably as compared with $TiCl_4$ compound. The reason for this behavior may be attributed to the fact that the 4*d* orbitals of zirconium and tin are more diffused in space than the 3*d* orbitals of titanium and thus lead to weaker bonds.

To investigate the possibility of co-ordination number five of titanium in $TiCl_4$ complexes an experiment, taking very large excess of $TiCl_4$ and adding cyanoester to it in methylene chloride medium, was performed. The analytical results indicate the formation of a 2:1 compound. The infrared spectrum of this 2:1 addition compound clearly shows an increase of the cyano stretching frequency and a decrease of the carbonyl stretching C=O frequency, thereby indicating that out of the two $TiCl_4$ molecules one is involved in co-ordination through the carbonyl group and the other through the cyano group of the same ligand. As shown in Table I and Table II the melting points,

Can. J. Chem. Downloaded from www.nrcresearchpress.com by 210.87.254.6 on 09/05/12
For personal use only.

carbonyl, and cyano stretching frequencies of the 1:1 and 2:1 addition compounds of $TiCl_4$ and ethyl cyanoacetates are quite similar to each other. This observation is in accordance with our previous experience with similar complexes of dinitriles (1) where almost the same ipsochrome effect of the C≡N stretching frequency for both 1:1 and 2:1 complexes was observed. As it was postulated for the 2:1 complexes of dinitriles, the central element can exhibit co-ordination number five or six depending on the absence or presence of chlorine bridging.

ACKNOWLEDGMENT

The authors gratefully acknowledge the continued financial support from the National Research Council of Canada.

SOMMAIRE

Des composés de co-ordination entre le cyanoacétate d'éthyle et le trichlorure de bore, le tétrabromure de titane et les tétrachlorures de titane, de zirconium et d'étain ont été préparés. Les résultats analytiques indiquent que, suivant des conditions expérimentales identiques des composés d'addition un à un sont obtenus. De plus, en se basant sur les spectres infrarouges, on peut proposer que les composés obtenus sont de chélates à six atomes où le nombre de co-ordination 6 des éléments du groupe (IV) est satisfait.

REFERENCES

1. S. C. JAIN and R. RIVEST. Can. J. Chem. **41**, 2130 (1963).
2. S. C. JAIN and R. RIVEST. Can. J. Chem. **40**, 2243 (1962).
3. R. J. H. CLARK, J. LEWIS, and R. S. NYHOLM. J. Chem. Soc. 2460 (1962).
4. J. ARCHAMBAULT and R. RIVEST. Can. J. Chem. **36**, 1331 (1958).
5. E. RIVET, R. AUBIN, and R. RIVEST. Can. J. Chem. **39**, 2343 (1961).
6. A. I. VOGEL. A text book of quantitative inorganic analysis. 3rd ed. Longmans Green and Co., London. 1961. p. 253.
7. H. J. COERVER and C. CURRAN. J. Am. Chem. Soc. **80**, 3522 (1958).

Can. J. Chem. Downloaded from www.nrcresearchpress.com by 210.87.254.6 on 09/05/12
For personal use only.

Can. J. Chem. Downloaded from www.nrcresearchpress.com by 210.87.254.5 on 09/05/12
For personal use only.

PHOTOCONDUCTION AND SEMICONDUCTION IN MONOCRYSTALS OF THE CHARGE-TRANSFER COMPLEX, PERYLENE–FLUORANIL*

H. KOKADO,† K. HASEGAWA,† AND W. G. SCHNEIDER
Division of Pure Chemistry, National Research Council, Ottawa, Canada

Received December 10, 1963

ABSTRACT

Single crystals of the perylene–fluoranil charge-transfer complex were found to be photoconductive throughout the near ultraviolet, visible, and near infrared spectral regions. The temperature dependence of the semiconduction and photoconduction are characterized by apparent activation energies of 0.73 ev and 0.12 ev, respectively. Conductivity parallel to the *c*-crystallographic axis (along which the complex units are stacked in columns) was found to be about threefold greater than that in the perpendicular direction. Attempts to measure carrier mobilities proved unsuccessful. The results suggest extrinsic carrier generation accompanied by pronounced carrier trapping processes.

INTRODUCTION

The electronic behavior of crystalline charge-transfer complexes of aromatic molecules is of particular interest. Because of the enhanced π-electron interaction in complexes of this type the electronic conductivity may be expected to exceed that observed in pure aromatic compounds. Complexes of polycyclic aromatic hydrocarbons with iodine have very high conductivities and small energy gaps (1, 2) together with a pronounced ESR absorption (3). The complexes, however, exhibited negligible photoconductivity. Polycrystalline samples of complexes formed by the anils (chloranil, bromanil, and iodoanil) with aromatic diamines have also been investigated (4, 5). These showed moderate conductivities with apparent activation energies in the range 0.2 to 0.8 ev, and a comparatively very weak ESR absorption (6, 7). Thus in contrast to the iodine complexes, the ground state of these complexes exhibits very little ionic character. A similar behavior was found for complexes of aromatic hydrocarbons with tetracyanoethylene (8). With few exceptions previous experimental measurements have been carried out with compressed powder samples of the complexes. Photoconductivity measurements of charge-transfer complexes have not been reported. The present paper describes an investigation of the semiconduction and photoconduction behavior of single crystals of the charge-transfer complex, perylene–fluoranil (2,3,5,6-tetra-fluoro-*p*-benzoquinone).

EXPERIMENTAL

Monocrystals of the complex, approximately 10×2×2 mm, were grown from a toluene solution of the component compounds. For best results it was found necessary to adjust the relative concentration of the solution to about a 50% excess in fluoranil, the more soluble component. The crystals, which are bluish-black in color, have a prismatic habit with well developed crystal faces. Chemical analysis confirmed a 1:1 stoichiometry for the complex. A crystal structure analysis, carried out by Dr. A. Hanson (9), showed the crystal to be monoclinic with unit cell, $a = 17.3$, $b = 7.49$, $c = 6.97$ Å, and $\beta = 90.4°$ C. The structure is thus very nearly orthorhombic, the crystals tending to be elongated along the *c*-direction. There are four molecules, i.e. two complex units, in the unit cell. In common with other C.T. complexes, the donor (perylene) and acceptor (fluoranil) molecules are alternately stacked in columns which are parallel to the *c*-axis. The perpendicular interplanar spacing between neighboring coparallel donor and acceptor molecules within the column is 3.27 Å.

Electrodes were applied to the crystal specimens by means of silver paste. Conductivity measurements were carried out by means of a four-probe method to be described elsewhere (10). It was established that

*National Research Council No. 7816.
†National Research Council Postdoctoral Fellow, 1961–63.

the presence of air or oxygen had no effect on the dark conductivity or photoconductivity. Accordingly the crystals were mounted in a cell and maintained in an atmosphere of dry air saturated with fluoranil vapor. These conditions were found desirable, since, due to the appreciable volatility of fluoranil, the surface of the crystal tended to deteriorate if the cell was evacuated over extended periods of time.

The spectral dependence of the photocurrent was measured with two silver paste electrodes, one on each end of the elongated crystal, and an area between the two electrodes was illuminated. The light source consisted of an Osram XBO–1001 xenon discharge lamp together with a Beckman DV monochromator. Currents were measured with a Keithley electrometer.

RESULTS AND DISCUSSION

Table I summarizes the results of the semiconductivity and photoconductivity measurements. The results exhibit the anticipated larger (approximately threefold) conductivity

TABLE I

	$\parallel c$-direction	$\perp c$-direction
Dark conductivity (Ω^{-1} cm^{-1})(20° C)	1.5×10^{-14}	5.0×10^{-15}
Semiconduction activation energy (ev)	0.73	0.73
Photoconductivity (Ω^{-1} cm ^{1})* (20° C)	3.0×10^{-12}	—
Photoconduction activation energy (ev)	0.12	—

*Measured with 100-watt tungsten lamp at 1 meter distance.

parallel to the c-axis relative to that in the ab plane. However, the relative magnitudes of the conductivity as well as the semiconduction activation energy are only slightly lower than those usually found in aromatic hydrocarbons (11). This implies that the ground state of the complex has relatively little ionic character. The relatively weak ESR absorption observed in crystals of the complex is consistent with this conclusion.*

The photoconductivity of the complex exhibits a characteristic temperature dependence with an apparent activation energy of 0.12 ev. This may be compared with the corresponding value of 0.17 ev observed in anthracene crystal photoconduction (12). The spectral dependence of the photoconductivity is illustrated in Fig. 1(*a*). Since even the thinnest crystals were virtually opaque to visible light a satisfactory absorption spectrum could not be obtained. Figure 1(*a*) shows the short-wavelength absorption spectrum of the complex measured as a Nujol mull. Under these conditions the charge-transfer band could not be satisfactorily measured. A charge-transfer band centered at 670 mμ was however observed in a toluene solution of the complex. From measurements on sublimed films a low-level absorption throughout the range from 700 to 1300 mμ was indicated. The absorption from 350 to 450 mμ arises mainly from the perylene component of the complex.

The photocurrent response shown in Fig. 1(*a*) has not been corrected for the intensity and dispersion of the light source. It is thus only an indication of spectral activity and not a measure of relative quantum efficiency. Photocurrents were detectable over the entire spectral range measured, 350 to 1500 mμ. The xenon lamp emits a number of strong lines in the near infrared region. Figure 1(*b*) shows for comparison the response of a PbS cell in the region 700 to 1300 mμ when used in place of the crystal complex. Also shown is the region from 350 to 700 mμ recorded by a conventional photocell. It can be seen that the complex exhibits a peak activity between 450 to 500 mμ, and a surprisingly broad activity in the infrared.

Although a true absorption edge or a photoconduction threshold could not be established, it is evidently less than 1 ev. Considering also the measured semiconduction activation energy of 0.73 ev, charge carrier generation would appear extrinsic in nature.

We are greatly indebted to Dr. A. Reddoch for carrying out the ESR measurements.

Can. J. Chem. Downloaded from www.nrcresearchpress.com by 210.87.254.5 on 09/05/12
For personal use only.

Can. J. Chem. Downloaded from www.nrcresearchpress.com by 210.87.254.5 on 09/05/12
For personal use only.

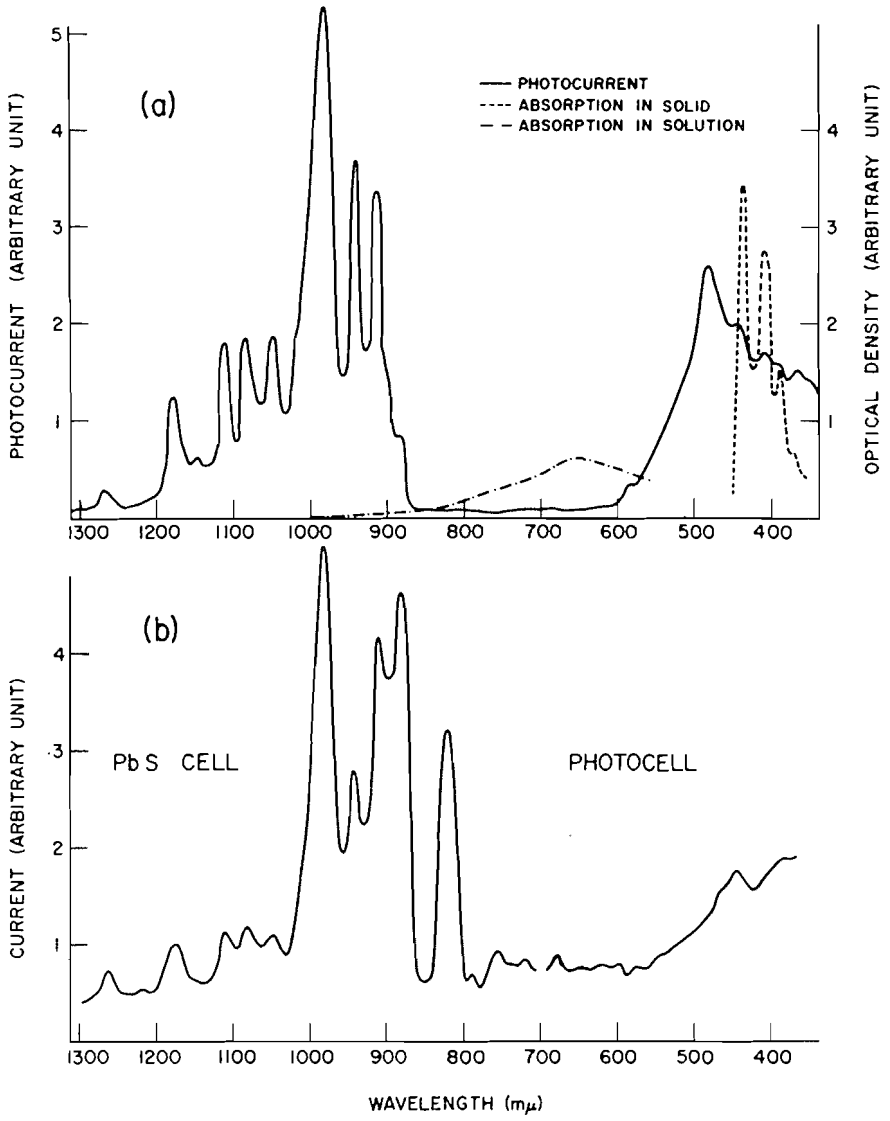

FIG. 1.

There is also evidence of strong carrier trapping effects. For example the photocurrent rise time and decay time are relatively long, particularly in the red and infrared regions, and, as is evident from Fig. 2, they also vary with wavelength. Contributions to the current due to thermal heating of the crystal by the illumination employed in these experiments is negligibly small.*

Attempts were made to determine carrier mobilities by measuring carrier transit times in the crystal of the complex using the microsecond light-flash technique (1, 3). The resulting photocurrent pulse exhibited a fairly rapid exponential decay, indicative of either

*Assuming all the radiant energy incident on the crystal is absorbed, and that no heat is lost, it is estimated the maximum temperature rise of the crystal is approximately 0.2° C per minute. On the other hand, on the basis of the known temperature dependence of the dark current, a temperature rise of 67° C would be required to thermally generate currents of the magnitude of those observed on illumination.

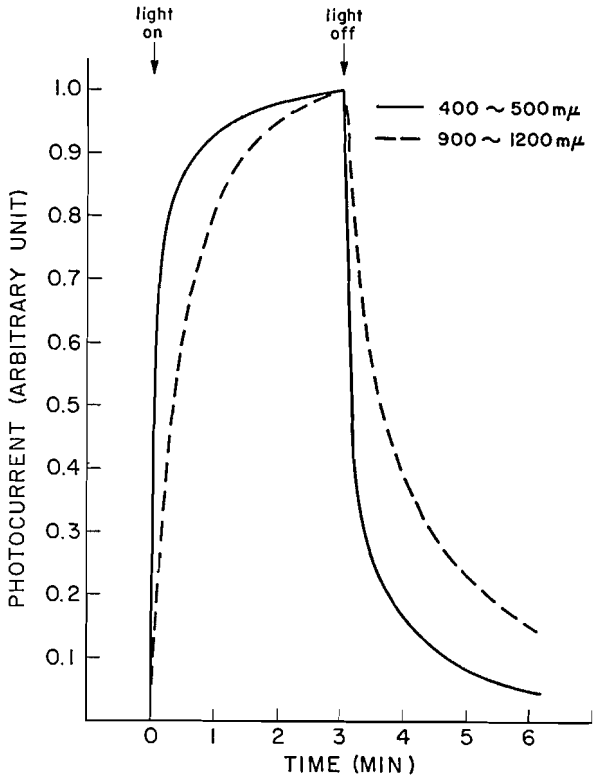

FIG. 2. Rise and decay of photocurrent in perylene–fluoranil monocrystal.

comparatively high mobilities, or of unusually short carrier lifetimes. Attempts to measure carrier transit times along the *c*-axis in crystals 1.0 to 1.5 cm long by the Haynes and Shockley method (14) also proved unsuccessful. This would appear to support the possibility that the carrier lifetime is reduced by trapping effects, although this point requires further investigation.

Preliminary measurements were also carried out on single crystal specimens of the complexes; perylene–chloranil, perylene–TCNQ (tetracyanoquinodimethan), and pyrene–chloranil. All of these crystals are blue-black in color and all proved to be photoconductive on illumination with a tungsten light source. However, in all cases the photoconductivity was somewhat less than that of the perylene–fluoranil complex.

REFERENCES

1. H. AKAMATU, H. INOKUCHI, and Y. MATSUNAGA. Bull. Chem. Soc. Japan, **29**, 213 (1956).
2. J. KOMMANDEUR and F. R. HALL. J. Chem. Phys. **34**, 129 (1961).
3. L. S. SINGER and J. KOMMANDEUR. J. Chem. Phys. **34**, 133 (1961).
4. D. D. ELEY, H. INOKUCHI, and M. R. WILLIS. Discussions Faraday Soc. **28**, 54 (1959).
5. P. L. KRONICK and M. M. LABES. J. Chem. Phys. **35**, 2016 (1961).
6. D. BIJL, H. KAINER, and A. C. ROSE-INNES. J. Chem. Phys. **30**, 765 (1959).
7. R. SEHR, M. M. LABES, M. BOSE, H. UR, and F. WILHELM. Symposium on electrical conductivity in organic solids. Interscience Publishers, N.Y. 1961. p. 309.
8. H. KURODA, M. KOBAYASHI, M. KINOSHITA, and S. TAKEMOTO. J. Chem. Phys. **36**, 457 (1962).
9. A. W. HANSON. In press.
10. K. HASEGAWA. To be published.
11. H. INOKUCHI and H. AKAMATU. Solid state physics. Vol. 12. Academic Press, N.Y. 1961. p. 117.
12. J. KOMMANDEUR, G. J. KORINEK, and W. G. SCHNEIDER. Can. J. Chem. **35**, 998 (1957).
13. R. G. KEPLER. Phys. Rev. **119**, 1226 (1960).
14. J. R. HAYNES and W. SHOCKLEY. Phys. Rev. **81**, 835 (1951).

Can. J. Chem. Downloaded from www.nrcresearchpress.com by 210.87.254.5 on 09/05/12
For personal use only.

THE GLUCOMANNAN OF BLUEBELL SEED (SCYLLA NONSCRIPTA L.)

J. L. THOMPSON[1] AND J. K. N. JONES
Department of Chemistry, Queen's University, Kingston, Ontario
Received November 7, 1963

ABSTRACT

A glucomannan has been isolated from bluebell seeds. It is a linear polymer composed of D-glucopyranose and D-mannopyranose residues in the approximate ratio of 1:1.3. Methylation and periodate oxidation results support this structure. Acetolysis of the polysaccharide led to the isolation of cellobiose, 4-*O*-β-D-mannopyranosyl-D-glucose and 4-*O*-β-D-glucopyranosyl-D-mannose.

INTRODUCTION

It has been shown that seeds and food reserves of some plants of the family Liliaceae contain glucomannans (1). Proof of the presence of glucomannans in plant materials can be of taxonomic value, so that it was of interest to investigate the food reserve of other seeds from this family. Accordingly, the seeds of the English bluebell (*Scylla nonscripta* L.), a member of the Liliaceae, were examined. The powdered alcohol-extracted seeds were found to contain an alkali-soluble polysaccharide which formed an insoluble copper complex and which on hydrolysis yielded D-glucose and D-mannose in the ratio of 1:1.3.

The polysaccharide was obtained as a white powder which on drying rapidly became insoluble in all the common solvents. However, it was found possible to obtain a solution of the polymer in water by dissolving it in aqueous urea solution containing sodium hydroxide.

The methylated polymer on hydrolysis yielded mainly 2,3,6-tri-*O*-methyl-D-glucose and 2,3,6-tri-*O*-methyl-D-mannose which are not readily separated. Very small amounts of a 2,3,4,6-tetra-*O*-methyl hexose (tentatively identified as a D-glucose derivative) and di-*O*-methyl hexose (not identified) were also detected. No attempt was made to isolate the di-*O*-methyl fraction which was very small in amount. The apparent low methoxyl content (42.5%) (see experimental section) of the methylated polysaccharide indicates that it might not have been completely methylated. Experience has shown that end groups are methylated more rapidly than is the main body of the polysaccharide. It is unlikely that the yield of methylated end group is greatly underestimated. The oxidation by periodate of several preparations of polysaccharide was studied. In general it was observed that oxidation proceeded satisfactorily if it was carried out with 0.103 *M* periodate at 2° C or with 0.015 *M* periodate at room temperature. At the end of these experiments the consumption of periodate was approximately 1 mole (±0.05) per mole of hexose. The yield of formic acid corresponded to a chain length of 170–230 units. When the oxidation was made with 0.1 *M* periodate at room temperature overoxidation occurred. The periodate-oxidized polymer yielded no detectable hexose sugar after hydrolysis by acid, indicating the absence of 1,3-linked sugars. Acetolysis of the polymer afforded D-glucose, D-mannose, 4-*O*-β-D-glucopyranosyl-D-glucose (cellobiose), 4-*O*-β-D-mannopyranosyl-D-glucose, and 4-*O*-β-D-glucopyranosyl-D-mannose, all of which were obtained crystalline. 4-*O*-β-D-Mannopyranosyl-D-mannose was tentatively identified on the basis of chromatographic evidence.

The above results, the 2*b* type absorption shown by the polymer in the infrared and

[1]*Present address: Collège Militaire Royal de Saint-Jean, Saint-Jean, Québec.*

Can. J. Chem. Downloaded from www.nrcresearchpress.com by 210.87.254.105 on 09/05/12
For personal use only.

its optical rotation (−24°) indicate that the polysaccharide is linear and is built up in the main of beta 1 → 4-linked D-glucopyranose and D-mannopyranose residues terminated at the non-reducing end by a D-glucopyranose residue and that it is very similar in structure to glucomannans which have been isolated from seeds and bulbs of other members of the family Liliaceae.

EXPERIMENTAL

Paper Chromatography

Paper chromatography was carried out by the descending method, using Whatman No. 1 paper. All paper chromatograms were sprayed with a solution of *p*-anisidine hydrochloride in butanol-1 (2% w/v) and then heated in an oven at about 120° to reveal the positions of the sugars. The solvent systems used for development were: (1) ethyl acetate : acetic acid : formic acid : water (18:3:1:4, v/v); (2) butanol-1:pyridine : water (10:3:3, v/v); (3) benzene:butanol-1:pyridine:water (1:5:3:3, v/v); (4) butanol-1:ethanol:water (3:1:1, v/v); and (5) butanol-1:ethanol:water (4:1:2, v/v).

Concentration of solutions was carried out under reduced pressure unless otherwise stated.

Preparation of Bluebell Polysaccharide

The seeds of the bluebell (*S. nonscripta* L.) were collected near High Wycombe, England, in August 1939. They were powdered in a mill and extracted exhaustively with methanol. The extracts, which contained a crystalline saponin-like material, were discarded. Several preliminary experiments were made in order to obtain the best yield of undegraded polysaccharide from the seeds. The following experimental procedure gave good results.

Preparation of the Polysaccharide (with Exclusion of Air–N_2 Atmosphere)

The dry methanol-extracted seeds (58.1 g) were extracted for 12 hours and then for 10 hours with cold water (750-ml portions) which was decanted and discarded. The seeds were then suspended in hot boiled-out water (1 l.) and homogenized in a Waring Blendor for 5 minutes. The mixture was stirred overnight (N_2 atmosphere) and centrifuged. The water contained only traces of polysaccharide and was discarded. The residue from the hot water extract was stirred overnight with sodium hydroxide (1 *N*, 1 l.) which had been prepared from oxygen-free water. The mixture was centrifuged and the extract was poured into ethanol (2 l.). The precipitate was collected and dissolved in sodium hydroxide (1 *N*, 400 ml). Fehling's solution (75 ml) was added slowly to the solution, which was vigorously stirred. The precipitated copper complex was collected and dispersed in water (400 ml). Dilute cold hydrochloric acid was then added until the complex had dissolved, the solution then had pH 4. The solution was poured into ethanol (1 l.) and the precipitate was collected and washed with ethanol, acetone, and then with ether, and dried over phosphoric oxide. (Yield 5.38 g.)

The residue from the previous extraction was extracted with a solution of urea (50 g) and sodium hydroxide (100 g) in water (1 l.) for 36 hours. The mixture was centrifuged and the clear solution was poured into ethanol (2 l.). The precipitate was extracted with sodium hydroxide (1 *N*, 200 ml) and after 1 hour the suspension was centrifuged. The soluble material (0.73 g) was isolated as the insoluble copper complex and the alkali-insoluble polysaccharide was obtained in 5.9% yield (3.43 g).

The residue from the above extraction was extracted for 3 days with a solution of sodium hydroxide (100 g) and urea (50 g) in water (1 l.). The mixture was centrifuged and the supernatant solution was poured into ethanol (2 l.). The precipitate was collected, washed with ethanol, acetone, and ether, and dried (A). The residual seeds were again extracted with urea and sodium hydroxide solution (as above) but for 4 days. The soluble material isolated as described above was combined with A. Total yield 29.55 g (50.9%). A final extraction of the seeds yielded a further 1.22 g of product. Total yield 40.31 g (69.5%). The major fraction (29.55 g above) was refractionated by dissolving it in water (1500 ml) containing urea (75 g) and sodium hydroxide (150 g). Fehling's solution (75 ml) was added and the precipitated copper complex was collected and converted to the dry polysaccharide (X) by the usual procedure. Yield 13.15 g (44.6%), $[\alpha]_D$, −24°±1° in sodium hydroxide (10%) and urea (5%) solution. A further addition of Fehling's solution yielded a second fraction (Y) (7.58 g, 25.7%) of $[\alpha]_D$ −15°±1° in sodium hydroxide (10%) and urea (5%) solution. Both polysaccharides X and Y showed type 2*b* absorption in the infrared, characteristic of β-linked glycopyranosides (3). Zone electrophoresis in 2 *N* potassium hydroxide solution on glass fiber strips showed one component only to be present in fraction X (4). All the fractions gave mannose and glucose on hydrolysis in a ratio varying from 1.3:1 to 1.0:1. Trace amounts of arabinose or xylose were detectable in some of the fractions.

Methylation of the Polysaccharide

A sample of the polysaccharide (2.1 g) was methylated twice by the Haworth procedure (5). After the first methylation the product separated as a solid, when the reaction mixture was heated to the boiling point. The methylated polymer was isolated by chloroform extraction of the solution after the second methylation.

Can. J. Chem. Downloaded from www.nrcresearchpress.com by 210.87.254.105 on 09/05/12
For personal use only.

This material was then further methylated twice by the Kuhn procedure (6(*a*)). The product (1.2 g) was extracted under reflux with mixtures of hexane and chloroform containing 100%, 95%, 90%, 80%, and 65% (v/v) in turn. The fraction which was soluble in 80% hexane (0.64 g) had $[\alpha]_D$ − 18° (*c*, 4.0 in chloroform) and OMe, 42.5% (mean of three determinations). The infrared spectrum of the sample in potassium bromide was compared with that of a disc of potassium bromide alone. No difference could be detected in the area of OH peak absorption. It was concluded that the low methoxyl values are due in the main to the presence of non-carbohydrate impurities and to the errors in the procedure for the determination of methoxyl. A sample of each of the 95%, 90%, 80%, and 65% hexane-soluble fractions on hydrolysis followed by paper chromatographic examination of the hydrolyzate (solvent 4) showed the apparent presence of one component which moved at the speed and gave the color reactions of a tri-*O*-methyl hexose.

Hydrolysis of the Methylated Glucomannan

The polysaccharide (604 mg, 80% hexane fraction) was dissolved in a mixture of water (12.5 ml) and sulphuric acid (16.7 ml), i.e. in 70% sulphuric acid (w/w) and the mixture was kept at room temperature for 12 hours. The solution was then diluted with water to 300 ml and boiled under reflux for 7 hours. This procedure minimizes demethylation (6(*b*)). The mixture of the syrupy sugars (524 mg) isolated in the usual way was separated on a column of cellulose, using butanol-1 half-saturated with water as irrigant. The effluent was collected portionwise and the sugars isolated in the usual way (7). The *first fraction* (ca. 1 mg) had $[\alpha]_D$ + 20° (*c*, 0.07 in water), moved at the speed of a tetra-*O*-methyl hexose, and on demethylation with boron trichloride (8) gave glucose, detected chromatographically (solvents 2 and 4). The paper chromatogram was run for 4 days to ensure a good separation between the sugars. The tri-*O*-methyl fraction (551 mg) was dissolved in methanolic hydrogen chloride (124 ml, 1% w/v) and the optical rotation of the solution (+ 23.6°) was followed until it became constant at − 5.7° in 20 hours. The hydrogen chloride was neutralized with silver carbonate and the sugars were isolated in the usual way. The syrup was fractionated on Whatman 3MM paper and the tri-*O*-methyl mannose fraction was thus separated from the methyl tri-*O*-methyl glucoside fraction (9).

The *tri-O-methylmannose* (93.9 mg) was characterized as the 1,4-di-*p*-nitrobenzoate of m.p. 187–188° and $[\alpha]_D$ +36°±2° (*c*, 1.0 in chloroform) (9), yield 61.3 mg from 80 mg syrup. De-*O*-methylation of the tri-*O*-methyl fraction with boron trichloride showed the presence (paper chromatography, solvent 4) of mannose only. On the other hand gas–liquid chromatographic analysis (10) of the derived glycosides showed the presence of a trace of the methyl 2,3,6-tri-*O*-methyl-D-glucosides.

The *tri-O-methylglucose fraction* (156 mg) contained none of the mannose isomer since de-*O*-methylation of a sample with boron trichloride yielded glucose only (detected chromatographically). The syrup was converted to the 1,4-di-*O*-*p*-nitrobenzoate in the usual way (9). The product (24 mg) was recrystallized from methanol and then had m.p. 189–190° and $[\alpha]_D$ −31°±2° (*c*, 0.83 in $CHCl_3$), in agreement with the constants recorded in the literature. The *di-O-methyl fraction* was very small indeed (from chromatographic evidence and from the yields of tri-*O*-methyl fraction isolated) and was not examined.

Periodate Oxidation of the Polysaccharide

A sample of the polysaccharide (36.3 mg), which was insoluble in water, was oxidized with periodate (25 ml, 0.015 *M*) in the usual way and the periodate consumption was determined spectrophotometrically (2). After 70 hours 0.9 mole of periodate per $C_6H_{10}O_5$ had been consumed. A second experiment, using a solution of the polysaccharide which had been dialyzed against distilled water, showed the uptake of 0.96 mole of periodate per $C_6H_{10}O_5$ in 137 hours. The determination of formic acid production was unsatisfactory when oxidation was carried out with 0.1 *M* periodate at room temperature. The periodate-oxidized polysaccharide after 70 hours of oxidation (see above) was dialyzed to remove inorganic salts and the residue when tested with Molisch reagent gave a faint positive test for hexoses. However, when the oxidized polysaccharide was hydrolyzed with hot sulphuric acid (0.1 *N*) and the hydrolyzate isolated and examined chromatographically, neither glucose nor mannose could be detected.

Acetolysis of the Polysaccharide

As a result of several experiments the following conditions were chosen for acetolysis of the polysaccharide. The material, polysaccharide X (5.0 g), was treated at 0° with a stirred mixture of ice-cold acetic anhydride (250 ml) and sulphuric acid (50 ml) for 30 minutes. After this time the mixture was allowed to come to room temperature when the polysaccharide slowly dissolved. After 6½ hours the mixture was poured with stirring into ice and water (ca. 1 l.). The derived acetates (9.8 g) were isolated by chloroform extraction in the usual fashion. They were de-*O*-acetylated by the Zemplen procedure (11) and fractionated first on a resin column (12) and then on sheets of Whatmann 3 MM paper, using solvent 4.

The following sugars were isolated and identified.

α-D-*Glucose* (98 mg) was isolated as the crystalline solid of m.p. 140–141° and $[\alpha]_D$ +48° (equilib.) (*c*, 1.14 in water). The infrared spectrum was indistinguishable from that of authentic α-D-glucose.

D-*Mannose* (46 mg) was a syrup from which D-mannose phenylhydrazone of m.p. 195–196° and $[\alpha]_D$ + 21±3° (*c*, 0.3 in pyridine) was prepared. The infrared spectrum of this compound was essentially the same as that of an authentic specimen.

Can. J. Chem. Downloaded from www.nrcresearchpress.com by 210.87.254.105 on 09/05/12
For personal use only.

Cellobiose (32 mg) after recrystallization from ethanol had $[\alpha]_D$ +29°±1° (*c*, 1.0 in water) and m.p. 230–232°. 4-*O*-β-D-Mannopyranosyl-D-glucose was detected (chromatographically, solvent 3) in the mother liquor and also in trace amounts in the infrared spectrum of the crystalline cellobiose fraction (above).

4-O-β-D-Mannopyranosyl-D-glucose (18 mg) had m.p. 170° and $[\alpha]_D$ +14°±1° (const.) (*c*, 1.07 in water) after recrystallization from ethanol. The infrared spectrum of the compound was in good agreement with that prepared from an authentic specimen.

4-O-β-D-Glucopyranosyl-D-mannose behaved as a single component chromatographically. Its rate of movement relative to cellobiose was 1.69 in solvent 3. It crystallized on nucleation with an authentic specimen and then had $[\alpha]_D$ +10° → +8.3° in 5 hours (*c*, 0.6 in water) (13) and m.p. 128–137°. Its infrared spectrum was indistinguishable from that of an authentic specimen.

The mannobiose fraction (16 mg) was chromatographically pure (solvent 3) and had the mobility of 4-*O*-β-D-mannopyranosyl-D-mannose but it could not be induced to crystallize (13).

ACKNOWLEDGMENTS

The authors thank the National Research Council for grant (N.R.C. T.19) and the Ontario Research Foundation for financial assistance. They also wish to thank Dr. M. B. Perry for his interest and advice.

REFERENCES

1. P. Andrews, L. Hough, and J. K. N. Jones. J. Chem. Soc. 181 (1956).
2. G. O. Aspinall and R. J. Ferrier. Chem. Ind. 1216 (1957).
3. W. B. Neely. Advan. Carbohydrate Chem. **12**, 13 (1957).
4. D. R. Briggs, E. F. Garner, and F. Smith. Nature, **178**, 154 (1956).
5. W. N. Haworth. J. Chem. Soc. **107**, 8 (1915).
6. (*a*) R. Kuhn, H. Trischmann, and T. Löw. Angew. Chem. **67**, 32 (1955).
   (*b*) I. Croon, G. Heurrström, G. Kull, and B. Lindberg. Acta Chem. Scand. **14**, 1338 (1960).
7. L. Hough, J. K. N. Jones, and W. H. Wadman. J. Chem. Soc. 2511 (1949).
8. S. Allen, T. G. Bonner, E. J. Bourne, and N. M. Saville. Chem. Ind. 630 (1958).
9. P. A. Rebers and F. Smith. J. Am. Chem. Soc. **76**, 6097 (1954).
10. C. T. Bishop. Methods Biochem. Anal. **10**, 1 (1962).
11. G. Zemplen and E. Pacsu. Ber. **62**, 1613 (1929).
12. J. K. N. Jones and R. A. Wall. Can. J. Chem. **38**, 2285 (1960).
13. J. K. N. Jones and T. J. Painter. J. Chem. Soc. 669 (1957).

Can. J. Chem. Downloaded from www.nrcresearchpress.com by 210.87.254.105 on 09/05/12
For personal use only.

Can. J. Chem. Downloaded from www.nrcresearchpress.com by 210.87.254.6 on 09/05/12
For personal use only.

THE RESPONSE TO 14 MEV NEUTRONS OF SOME CHEMICAL DOSIMETER SYSTEMS*

W. A. Armstrong and W. G. Humphreys
Defence Research Chemical Laboratories, Department of National Defence, Ottawa, Canada
Received October 28, 1963

ABSTRACT

The response to 14 Mev neutrons of 10^{-3} *M* ferrous sulphate – 0.4 *M* H_2SO_4, 10^{-4} *M* ceric sulphate – 0.4 *M* H_2SO_4, 10^{-3} *M* calcium benzoate, and 10^{-4} *M* terephthalic acid – 4×10^{-4} *M* NaOH solutions has been investigated. *G* values as follows:
G(Fe III) = 10.5 ± 0.2, *G*(Ce III) = 3.13 ± 0.06, *G*(salicylic acid) = 0.316 ± 0.006, and *G*(hydroxyterephthalic acid) = 0.474 ± 0.007. These results are compared with those obtained when the same solutions are irradiated with Co^{60} γ-rays. Although the response to 14 Mev neutrons is only about one half the response of Co^{60} γ-radiation, the calcium benzoate and the terephthalic acid systems can measure doses as low as 20 and 2 rads, respectively.

INTRODUCTION

The dosimetric properties of the aqueous calcium benzoate and terephthalic acid systems have been studied in this laboratory for X- and γ-radiations of various energies (1, 2, 3). In this paper the response of these as well as the ferrous sulphate and ceric sulphate systems to 14 Mev neutrons is described and compared with their response to Co^{60} γ-radiation.

EXPERIMENTAL

Materials

Triply distilled water (one distillation from alkaline $KMnO_4$ followed by distillation from dilute H_2SO_4) was used in all solutions and preparations. All chemicals were reagent grade unless otherwise stated. Irradiation vessels were cleaned in an HNO_3–H_2SO_4 mixture (1:3) and washed many times with once-, twice-, and thrice-distilled water. Finally steam from thrice-distilled water was passed through.

The purification of materials and the preparation of solutions used in the 10^{-3} *M* ferrous sulphate – 0.4 *M* H_2SO_4, 10^{-3} *M* calcium benzoate, and the 10^{-4} *M* terephthalic acid – 4×10^{-4} *M* NaOH dosimeter systems has been previously described (4, 2, 3).

The preparation of the 10^{-4} *M* ceric sulphate – 0.4 *M* H_2SO_4 system was similar to that recently reported (5) with one significant change. The dosimeter solution was electrolyzed to oxidize the cerous ions which are always present to some extent in ceric solutions. Solutions so treated could then be used for the measurement of doses as low as 1000 rads. The electrolysis was performed in a simple cell equipped with platinum electrodes and a U-shaped bridge filled with 0.4 *M* H_2SO_4. While being stirred with a glass-encased magnet, the solutions were electrolyzed overnight by means of a $3\frac{1}{2}$-volt dry cell which gave a current of about 0.2 ma through the system. This treatment had no apparent effect on the dosimetric properties of the system since electrolyzed and untreated solutions gave identical results when irradiated with doses of more than 5000 rads. Since the ceric sulphate dosimeter is extremely sensitive to the presence of trace impurities, fresh samples were electrolyzed each day and the cerous ion yield measured for a given Co^{60} γ-ray dose.

Standard 0.5-g sulphur tablets supplied by Atomic Energy of Canada Limited were used in the sulphur activation studies.

Analytical Techniques

The ferric ion yield in irradiated 10^{-3} *M* ferrous sulphate – 0.4 *M* H_2SO_4 solutions was determined by its optical absorption at 224 mμ using a molar extinction coefficient of 4565 at 25° with a temperature coefficient of 0.13% per ° C (6).

The amount of cerous ion formed in irradiated samples of 10^{-4} *M* ceric sulphate – 0.4 *M* H_2SO_4 was determined by comparing its fluorescence intensity with that of a standard cerous sulphate – 0.4 *M* H_2SO_4 solution. The measurements were made with an Aminco–Bowman spectrophotofluorometer using an exciting wavelength of 254 mμ and recording the fluorescence emitted at 350 mμ. Ceric ions reduce the cerous ion fluorescence presumably by absorbing some of the exciting and emitted light. It has been shown that *Q*,

**Issued as D.R.C.L. Report No. 426.*

the ratio of Ce III fluorescence in the absence and presence of Ce IV, may be determined from the equation $\log Q = 3750$ [Ce IV] (5), where the concentration of ceric ion is determined from its absorption at 320 mμ using the value of 5580 for the molar extinction coefficient (7). Hence the formula for calculating the concentration of cerous ion in an irradiated sample is

$$[\text{Ce III}] = [(F - B)/F_S].S.Q,$$

where F is the sample fluorescence, B the blank fluorescence of the unirradiated solution, F_S the fluorescence of the cerous sulphate standard, and S the concentration in g-ions per liter of cerous ion in the cerous sulphate standard.

The fluorometric methods for the determination of salicylic acid in irradiated 10^{-3} M calcium benzoate solutions and hydroxyterephthalic acid in irradiated 10^{-4} M terephthalic acid – 4×10^{-4} M NaOH solutions have been described elsewhere (2, 3).

The specific activity of the activated sulphur pellets was measured by the Radiation Dosimetry Branch of the Biology and Health Physics Division, Atomic Energy of Canada Limited.

Irradiation Techniques

Samples (5.0-ml) were irradiated in Vycor tubes about 10 cm long and having an O.D. of 1.5 cm and an I.D. of 1.3 cm. A small piece of "Saran" was wrapped over the mouth of each tube to keep out dust and to prevent evaporation.

Monoenergetic neutrons (14-Mev) were obtained from a 150 kv Cockroft–Walton accelerator by means of the $H^3(d,n)He^4$ reaction. Four sample tubes were mounted on an aluminum turntable which was bolted to the target assembly flange in such a way that the tubes could be rotated in front of and as close as possible to the target. The turntable was rotated at 60 r.p.m. and the average distance of each sample tube from the target during irradiation was about 4 cm. The average dose rate was approximately 13 rads/minute and total doses of about 2000 rads were usually given. Preliminary experiments showed that each of the four sample tubes received the same dose during an irradiation. Since the γ-ray contamination has been reported as less than 5% of the neutron dose (8), it was considered negligible. A Tullamore BF_3 counter was used to monitor the runs but it was not calibrated.

Co^{60} γ-irradiations were performed at a dose rate of 17 rads/minute with a 500-c source.

RESULTS

Sulphur Activation Studies

Standard sulphur tablets 1.134 cm in diameter, 0.322 cm thick, and weighing 0.509 g were irradiated in the same Vycor tubes as were used for the chemical systems. Each tube was marked with a diamond pencil at the 5.0 ml level and the distance to the bottom of the tube marked off in thirds. Four tablets were placed in each tube, one at the bottom and one at each mark, the intervening spaces being filled with sulphur powder. Two such tubes were irradiated together with two tubes each containing 5.0 ml of ferrous sulphate solution. From the average specific activity of the four tablets in each tube and the half life of P^{32} (14.3 days), the number of P^{32} atoms/mg formed at the time of irradiation was calculated. From the dimensions of the sulphur tablets, the weight of sulphur, as compacted in the tablets, equivalent to the 5.0-ml volume was determined. These calculations are outlined below:

$$\text{specific activity} = -dN/dt = N\lambda$$

where

$$N = \text{no. of } P^{32} \text{ atoms/mg}$$

and

$$\lambda = \text{the disintegration constant} = 0.0485 \text{ days}^{-1},$$

$$N_0 = Ne^{\lambda t},$$

where N_0 = no. P^{32} atoms/mg at the time of irradiation and t is the time when the activity was measured. Since the volume of a sulphur pellet is 0.325 cm^3, the number of pellets equivalent to 5.0 ml is 15.4 and the weight of sulphur is 7.83 g. Thus the total number of P^{32} atoms that would have been formed in a 5.0-ml irradiated volume is $7.83 \times 10^3 N_0$

Can. J. Chem. Downloaded from www.nrcresearchpress.com by 210.87.254.6 on 09/05/12
For personal use only.

and the neutron fluence, the term recommended by the International Commission on Radiological Units and Measurements (9), is

$$[(7.83\times10^{3}\ N_0)/\sigma\cdot S]\ \text{neutrons/cm}^2$$

where σ = the cross section for the reaction $S^{32}(n,p)P^{32}$

$= 0.248\times10^{-24}\ \text{cm}^2$ (10)

S = number of S^{32} atoms in 5.0 ml

$= (7.83/32)\times6.023\times10^{23}\times0.9506$ (95.06% of natural sulphur is S^{32}).

Randolph (11) has calculated that D, the ratio of dose rate to neutron flux density for 14 Mev neutrons interacting with water, is 0.449 Mev/(g-sec-flux). It follows that D', the ratio of dose to fluence, is 7.19×10^{-9} rads/neutrons cm^{-2}. Since about 72.3% of the dose absorbed in water is due to proton recoils (11) and, since the concentrations of elements other than hydrogen and oxygen are very small, it is assumed that the dose absorbed for a given neutron fluence in a sample of $10^{-3}\ M$ ferrous sulphate – 0.4 M H_2SO_4, $10^{-4}\ M$ ceric sulphate – 0.4 M H_2SO_4, $10^{-3}\ M$ calcium benzoate, or $10^{-4}\ M$ terephthalic acid – $4\times10^{-4}\ M$ NaOH is the same as that absorbed by a water sample exposed under similar conditions. The errors involved in this dose determination include an uncertainty of ±5% in the sulphur activation measurements and ±5% in the value of the $S^{32}(n,p)P^{32}$ cross section. Randolph (11) quotes a ±7.5% uncertainty on his value for D but states that the real error should be considerably less. Thus the total error in dose measurements is about ±15%.

In Table I the dose determined by this technique is compared with the yield of ferric

TABLE I

G(Fe III) for 14 Mev neutrons

N_0 (10^6 atom/mg)	Fluence (10^{11} n/cm^2)	Dose (rads)	(Fe III) (10^{-5} moles/l)	G(Fe III) (molecules/100 ev)
1.53	3.44	2480	2.64	10.3
1.49	3.36	2410	2.64	10.6
1.49	3.36	2420	2.63	10.5
1.47	3.30	2380	2.63	10.7

ions in a ferrous sulphate solution which was exposed simultaneously with a sulphur sample. The results give G(Fe III) = 10.5±0.2. It is realized that wall effects introduce an unknown error in the dose determinations. However, a comparison of fluence determinations and ferric ion yields in Vycor tubes of I.D. 0.9 cm with similar measurements in tubes of I.D. 2.3 cm indicate that the error due to proton leakage is small in comparison with other experimental errors.

Chemical Studies

G(Ce III) was determined using G(Fe III) reported above by comparing the concentration of cerous ions formed in $10^{-4}\ M$ ceric sulphate – 0.4 M H_2SO_4 with the concentration of ferric ions formed in $10^{-3}\ M$ ferrous sulphate – 0.4 M H_2SO_4 when two samples of each solution were irradiated together. The results listed in Table II give G(Ce III) = 3.13±0.06. G(salicylic acid) for $10^{-3}\ M$ calcium benzoate and G(hydroxyterephthalic acid) for $10^{-4}\ M$ terephthalic acid – $4\times10^{-4}\ M$ NaOH determined in a similar way were found to be 0.316±0.007 and 0.474±0.007, respectively (Tables III and IV). Considering

Can. J. Chem. Downloaded from www.nrcresearchpress.com by 210.87.254.6 on 09/05/12
For personal use only.

TABLE II

G(Ce III) for 14 Mev neutrons

[Fe III] (10^{-5} moles/l.)	[Ce III] (10^{-5} moles/l.)	G(Ce III) (molecules/100 ev)
3.33	0.987	3.12
3.25	0.978	3.16
2.35	0.714	3.19
2.35	0.672	3.01
4.41	1.33	3.17
4.47	1.34	3.15

TABLE III

G(salicylic acid) for 14 Mev neutrons

[Fe III] (10^{-5} moles/l.)	[Sal] (10^{-7} moles/l.)	G(sal) (molecules/100 ev)
2.21	6.80	0.323
2.21	6.59	0.313
2.25	6.69	0.312
2.21	6.46	0.307
2.20	6.79	0.324
2.20	6.69	0.319

TABLE IV

G(hydroxyterephthalic acid) for 14 Mev neutrons

[Fe III] (10^{-5} moles/l.)	[HTA] (10^{-7} moles/l.)	G(HTA) (molecules/100 ev)
2.18	9.83	0.473
2.14	9.83	0.482
2.26	9.95	0.462
2.16	9.81	0.477

the errors involved in both the sulphur activation and chemical determinations it is felt that G(Fe III) is accurate to about $\pm 17\%$, G(Ce III) to $\pm 25\%$, G(salicylic acid) to $\pm 20\%$, and G(hydroxyterephthalic acid) to $\pm 20\%$.

The results of the Co^{60} γ-irradiation experiments are given in Table V. Each G value is

TABLE V

Comparison of G-values for 14 Mev neutrons and Co^{60} γ-rays

	Co^{60} γ	14 Mev neutrons	% Difference
G(Ce III)	2.63 ± 0.05	3.13 ± 0.06	19.0
G(Sal)	0.654 ± 0.011	0.316 ± 0.006	51.7
G(HTA)	0.988 ± 0.009	0.474 ± 0.007	52.0

the average of 10 results together with the standard deviation. The dose rate was determined with the ferrous sulphate dosimeter assuming G(Fe III) = 15.5 and applying the proper density corrections when the dose rate in calcium benzoate and terephthalic acid solutions was required.

As the response to 14 Mev neutrons of the benzoate and terephthalate systems is about one half as great as to Co^{60} γ-radiation, γ-ray contamination of 5% or less in the neutron

Can. J. Chem. Downloaded from www.nrcresearchpress.com by 210.87.254.6 on 09/05/12
For personal use only.

irradiations (8) might introduce significant errors in the measured G-values for neutrons of these systems. At present there is no way of accurately determining the amount of γ-ray contamination.

DISCUSSION

As a larger fraction of radicals react with each other at higher LET, the yield of ferrous ion oxidation decreases with an increase in LET. The value reported here of $G(\text{Fe III}) = 10.5$ for 14 Mev neutrons falls within the range of values given by Schuler and Allen (12) for deuterons of 8 to 20 Mev (G(Fe III) 9.7 to 11.5) and by Anderson and Hart (13) for protons of 4.8 to 10.6 Mev (G(Fe III) 9.27 to 10.88).

The response of the ceric sulphate system has been shown to be almost independent of LET for helium ions of 11 Mev to 33 Mev and deuterons of 8 Mev to 18 Mev (14) as well as for protons of 11 Mev to 23 Mev (15). Barr and Schuler (14) found G(Ce III) to be 2.33 for Co^{60} γ-radiation and 2.85 for radiations having an LET of about 1.2 ev/Å, the value reported for 14 Mev neutrons (8). More recently Hochanadel *et al.* (15) measured G(Ce III) to be 2.48 for Co^{60} γ-radiation and 2.95 for protons of 11 Mev to 23 Mev. In view of the experimental errors involved our corresponding values of 2.63 and 3.13 are considered to be in good agreement with those of Hochanadel.

The yields of salicylic acid from calcium benzoate solutions and hydroxyterephthalic acid from terephthalic acid solutions are much lower for 14 Mev neutrons than for Co^{60} γ-radiation. This is to be expected if reaction with OH radicals rather than H_2O_2 is the important step in the hydroxylation process since G_{OH} decreases while $G_{H_2O_2}$ increases with increasing LET. It is interesting to note that the radical yield G_{OH} decreases from 2.90 for Co^{60} γ-radiation (16) to 1.45 for 5.4 Mev protons (14), a change comparable to that in G(salicylic acid) and G(hydroxyterephthalic acid) for a similar change in LET.

Although the response of the benzoate and terephthalic acid systems to 14 Mev neutrons is only about one half the response to Co^{60} γ-radiation the extreme sensitivity of the fluorometric analytical technique makes possible the measurement of very low neutron doses. The lower limit of this method is determined by the blank fluorescence of the unirradiated solution. This is equivalent to 10 to 20 rads with the calcium benzoate system and 1 to 2 rads with the terephthalic acid system.

ACKNOWLEDGMENTS

The authors wish to thank Mr. F. G. Strain for constructing the aluminum turntable and for operating the neutron generator. The authors are also grateful to Dr. W. G. Cross, of the Radiation Dosimetry Branch, Biology and Health Physics Division, Atomic Energy of Canada Limited, for measuring the activity of the irradiated sulphur pellets as well as for much helpful advice.

REFERENCES

1. W. A. Armstrong and D. W. Grant. Can. J. Chem. **38**, 845 (1960).
2. W. A. Armstrong, D. W. Grant, R. A. Facey, and W. G. Humphreys. Radiation Res. **9**, 120 (1963).
3. W. A. Armstrong, D. W. Grant, R. A. Facey, and W. G. Humphreys. Can. J. Chem. **41**, 1575 (1963).
4. J. Weiss, A. O. Allen, and H. A. Schwarz. Proc. Intern. Conf. Peaceful Uses of Atomic Energy, Geneva, **14**, 179 (1955).
5. W. A. Armstrong, D. W. Grant, and W. G. Humphreys. Anal. Chem. **35**, 1300 (1963).
6. K. Scharf and R. M. Lee. Radiation Res. **16**, 115 (1962).
7. T. J. Sworski. Radiation Res. **6**, 645 (1957).
8. A. D. Conger, M. L. Randolph, C. W. Sheppard, and H. J. Luippold. Radiation Res. **9**, 525 (1958).
9. Radiation Quantities and Units. Nat. Bur. Std. U.S., Handbook 84 (1962).
10. L. Allen, Jr., W. C. Biggers, R. J. Preswood, and R. K. Smith. Phys. Rev. **107**, 1363 (1957).

Can. J. Chem. Downloaded from www.nrcresearchpress.com by 210.87.254.6 on 09/05/12
For personal use only.

11. M. L. RANDOLPH. Radiation Res. **7**, 47 (1957).
12. R. H. SCHULER and A. O. ALLEN. J. Am. Chem. Soc. **79**, 1565 (1957).
13. A. R. ANDERSON and E. J. HART. Radiation Res. **14**, 689 (1961).
14. N. F. BARR and R. H. SCHULER. J. Phys. Chem. **63**, 808 (1959).
15. G. L. TOCHANNY, Jr., A. TIMMICK, C. J. HOCHANADEL, and C. D. GOODMAN. Radiation Res. **19**, 462 (1963).
16. C. J. HOCHANADEL and S. C. LIND. Ann. Rev. Phys. Chem. **7**, 83 (1956).

Can. J. Chem. Downloaded from www.nrcresearchpress.com by 210.87.254.6 on 09/05/12
For personal use only.

PROTON MAGNETIC RESONANCE ABSORPTION IN HIGH TEMPERATURE PHASES OF ANHYDROUS SODIUM STEARATE

M. R. Barr and B. A. Dunell
Department of Chemistry, University of British Columbia, Vancouver, British Columbia
Received November 18, 1963

ABSTRACT

Nuclear magnetic resonance spectra of anhydrous sodium stearate have been observed between 114° and 320° C. The observed changes in line width and second moment suggest a grouping of the mesomorphic phases into a waxy group in which a lattice structure is preserved for the polar ends of the molecules and a group consisting of the neat and liquid phases in which diffusion takes place freely.

Can. J. Chem. Downloaded from www.nrcresearchpress.com by 210.87.254.40 on 09/05/12
For personal use only.

INTRODUCTION

The extent of motion of the paraffin chains in sodium stearate below 114° C has been investigated previously by nuclear magnetic resonance (1). At 113° C the second moment of 6.7 gauss^2 corresponds to an amount of motion comparable to complete reorientation about the long axis of the hydrocarbon chain or possibly to extensive torsional oscillation of the chain combined with some rocking motion of the long axis itself, the polar ends of the molecules remaining fixed in a rigid layer lattice. The so-called supercurd to subwaxy phase transition is seen in the n.m.r. study as an abrupt decrease in line width and second moment occurring at 114° C. Above this transition the line width recorded by the broad line spectrometer was governed by the depth of modulation used, and the higher temperature transitions between mesomorphic phases observed by other physical methods could not be found using the broad line n.m.r. spectrometer. The work reported here is an extension of the earlier work done in this laboratory to the investigation of the n.m.r. spectrum of higher temperature phases of anhydrous sodium stearate.

EXPERIMENTAL

The sodium stearate sample was the same as the one used in the earlier work (1). Spectra were run on a Varian V-4352 high resolution n.m.r. spectrometer operating at 40 Mc/second. A minimum of six spectra were recorded at each temperature, three sweeps up field and three down, either on a Leeds and Northrup Speedomax recorder or on a photograph of the spectral trace on a Dumont 304-AR oscilloscope. The sweep was calibrated at each temperature by imposing side bands from an audio oscillator on the spectrum. At each temperature the r.f. power level was adjusted to a point below the region of saturation of signal. Temperature control was achieved by passing heated air through dewared leads past the sample tube. The temperature was measured by two thermocouples, one in the air just upstream from the sample and one in the return air stream. Thermocouple readings were controlled to within ±0.5°. Uncertainty in the temperature of the sample is approximately ±1° C near 100° C and ±4° C near 300° C. Demand on machine time precluded the possibility of equilibrating the sample for longer than 2 hours at any particular temperature, except in the special cases of two well-defined transitions at 114° and 246° C, in the vicinity of which 5 hours was allowed for equilibration.

RESULTS

Example spectra for several temperatures are shown in Fig. 1. Width of line between points of maximum and minimum slope is essentially constant at 0.06 to 0.09 gauss between 114° and 246° C. One can see, however, that line shape changes considerably in this range as the wings of the curve become progressively less intense with increasing temperature. The line width at the point of half-maximum intensity $\Delta H_{\frac{1}{2}}$ gives a measure

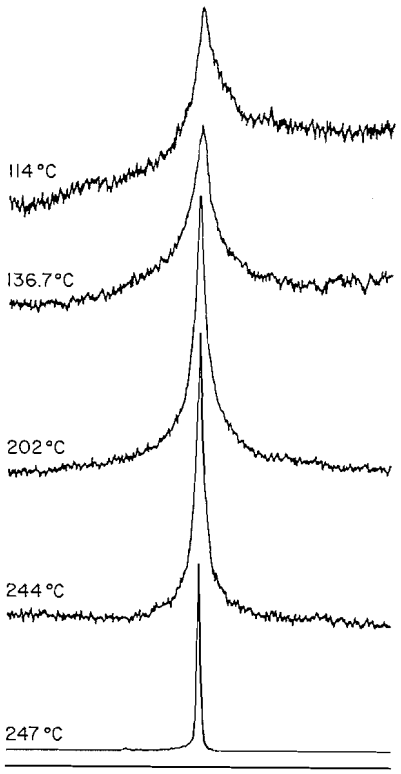

FIG. 1. Absorption spectra of sodium stearate at various temperatures between 110° and 250° C obtained from a high resolution spectrometer.

of this change in line shape and is plotted in Fig. 2 as a function of temperature. Uncertainty as to where to draw the base line because of instability due to noise and drift leads to variation of $\Delta H_{\frac{1}{2}}$ values of some 10% within a group of spectra run in succession at a particular temperature. Each point in Fig. 2 represents the average of such values for at least six spectra. Above 246° C the spectrum is effectively the same as that of water taken in the same field at room temperature.

The second moments which are plotted against temperature in Fig. 3 are also average values for at least six spectra at each temperature. Here, however, individual values are very sensitive to the position of the base line, and may vary by as much as 100% within a group of six spectra run in succession at a particular temperature. Values represented by the open circles are for spectra taken in a preliminary set of runs, and, although they were recorded at a slower sweep rate than the others, they are probably less accurate because the wings of the spectra were cut off by sweeping over an insufficient range of field. The faster sweep rate used in recording the second set of spectra (filled circles) gave a signal whose wings were less affected by noise and base-line drift. A third set of spectra, represented by triangles, shows much smaller second moments above 246° C than the other spectra do. This is thought to be caused by the third set of spectra being run in a more homogeneous field than the earlier spectra. Since we attribute significance only to the change in the second moment at 246° C, the variation from $2(10^{-5})$ to $5(10^{-4})$ gauss^2 above 246° is not important. At both ends of the temperature range 114° to

Can. J. Chem. Downloaded from www.nrcresearchpress.com by 210.87.254.40 on 09/05/12
For personal use only.

Can. J. Chem. Downloaded from www.nrcresearchpress.com by 210.87.254.40 on 09/05/12
For personal use only.

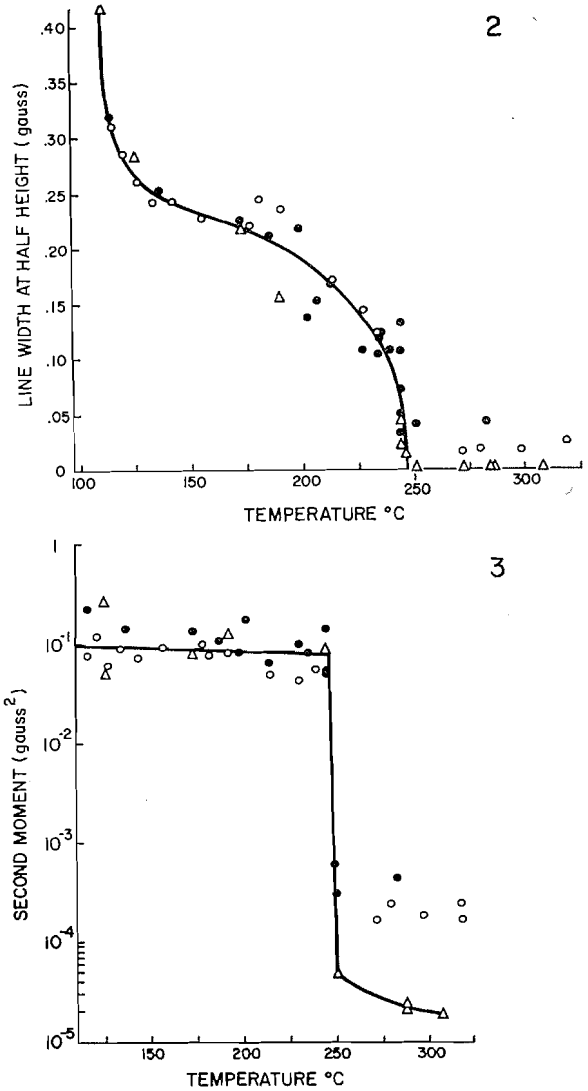

FIG. 2. Line width at half height as a function of temperature.
FIG. 3. Second moment as a function of temperature.

246° C, the observed second moments lie more or less between 0.25 and 0.05 gauss^2, so that there is no evidence of phase transition between these temperatures from second moments.

Above 245° C the second moment falls abruptly to an extremely small value.

DISCUSSION

The appearance at 114±1° C of a line which is narrow enough to observe by the high resolution technique agrees with the previously observed (1) n.m.r. transition at 114° C. From line width and second moment measurements we are led to group together the so-called subwaxy, waxy, superwaxy, and subneat phases (2) as being indistinguishable

one from another by this technique and characterized by very extensive motion of the hydrocarbon chains. The second moments of approximately 0.25 to 0.05 gauss^2 in the temperature range 114° C to 245° C, in which the group of waxy and subneat phases exists, show that the motion is much more extensive than mere rotation about the one long axis of the hydrocarbon chain. The motion is, however, probably restricted throughout this range by the constraining influence of the strongly interacting polar groups and only above 246±3° C where the second moment falls to a value of some 10^{-4} gauss^2 can the motion be said to be that characteristic of a liquid. The "neat" and isotropic liquid phases are not distinguished by this n.m.r. technique, and one might suppose that in the neat phase one is dealing with liquid character in two dimensions, or in which the hydrocarbon chains retain some semblance of parallel array even though rotation and twisting motions are extensive and diffusion takes place freely.

This n.m.r. interpretation supports the X-ray investigation of Skoulios and Luzzati (3), who classified the high temperature phases of sodium stearate into the same groups that we have made. The waxy phases and the subneat phase are understood in their work to form a group possessing a structure which consists of a set of parallel ribbons, indefinite in length, and packed in rectangular array. The polar groups fit end to end in the ribbons and the hydrocarbon chains, in a liquidlike state, fill the rest of the cell. They understand the neat phase to be a lamellar structure with a decidedly liquid character. The X-ray work, however, places the subneat to neat transition at 256° C, an assignment which agrees closely with those from the work of Vold (4) on density, 257° C, Puddington (5) on density, 259° C, Puddington (6) on light transmission, 258° C, and Ravich and Nechitaylo (7) on differential thermal analysis, 256° C. Vold's work on differential thermal analysis (8) gives this transition temperature as 238° C. The abruptness of the n.m.r. transition at 246° C appears to preclude the possibility that this is a non-co-operative transition which could be complete so far as n.m.r. is concerned at an unusually low temperature because of the comparatively low frequencies of molecular motion that are required to change the n.m.r. signal. The reason for the discrepancy between our subneat to neat transition temperature and that obtained from most other investigations is not understood.*

ACKNOWLEDGMENTS

The authors wish to thank the National Research Council for financial assistance by the award of a grant-in-aid for this research.

REFERENCES

1. R. F. Grant and B. A. Dunell. Can. J. Chem. **38**, 2395 (1960).
2. R. D. Vold *et al.* J. Am. Chem. Soc. **63**, 160, 168, 2915 (1941). J. Phys. Chem. **49**, 315 (1945); **52**, 148 (1948).
3. A. E. Skoulios and V. Luzzati. Acta Cryst. **14**, 278 (1961).
4. R. D. Vold, M. Macomber, and M. J. Vold. J. Am. Chem. Soc. **63**, 168 (1941).
5. D. P. Benton, P. G. Howe, R. Farnand, and I. E. Puddington. Can. J. Chem. **33**, 1798 (1955).
6. D. P. Benton, P. G. Howe, and I. E. Puddington. Can. J. Chem. **33**, 1384 (1955).
7. G. B. Ravich and N. A. Nechitaylo. Dokl. Akad. Nauk SSSR, **83**, 117 (1952).
8. R. D. Vold. J. Am. Chem. Soc. **63**, 2915 (1941).

*Note added in proof: *We are indebted to one of the referees for pointing out that Stross and Abrams, J. Am. Chem. Soc. 73, 2825 (1951), reported a phase transition in anhydrous sodium stearate in the range 243°–251° C using differential analysis. This observation gives some support to our assignment of 246° C to the subneat to neat transition.*

Can. J. Chem. Downloaded from www.nrcresearchpress.com by 210.87.254.40 on 09/05/12
For personal use only.

Can. J. Chem. Downloaded from www.nrcresearchpress.com by 210.87.254.42 on 09/05/12
For personal use only.

THE SYNTHESIS AND PROPERTIES OF THE ANHYDROUS HEXACHLOROZIRCONATES OF SODIUM AND POTASSIUM

R. L. Lister and S. N. Flengas
Department of Metallurgical Engineering, University of Toronto, Toronto, Ontario
Received December 30, 1963

ABSTRACT

The hexachlorozirconates of sodium and potassium have been produced in a closed system following the reaction:

$$ZrCl_{4(g)} + 2MCl_{(s)} = M_2ZrCl_{6(s)} \quad [1]$$

where M is Na and K, respectively. The zirconium tetrachloride was reacted at approximately 1 atm. pressure, and at temperatures of the alkali metal chloride between 425° C and 525° C. The densities, melting points, and the corresponding X-ray diffraction patterns for both compounds have been determined.

INTRODUCTION

Because of their high degree of thermal stability, alkali metal hexachlorozirconates offer interesting possibilities as a source of zirconium ions in the recovery of zirconium metal by fused salt electrolysis, especially since zirconium tetrachloride is so reactive.

Morozov *et al.* (1) have prepared sodium and potassium hexachlorozirconate by fusing calculated quantities of the salts in quartz tubes. However, no data on the composition and purity of the compounds thus prepared have been mentioned. Howell *et al.* (2), in their phase diagram study, have shown the compounds Na_2ZrCl_6 and K_2ZrCl_6 should exist, but have not isolated them.

The present investigation deals with the direct synthesis of sodium and potassium hexachlorozirconate by reacting gaseous zirconium tetrachloride with −325 mesh alkali metal chloride, a method similar to that employed in the direct synthesis of the hexachlorotitanates (3).

EXPERIMENTAL

The zirconium tetrachloride used was of commercial grade, Hafnium free, purified further by a triple distillation process. This was carried out by mixing zirconium tetrachloride with finely divided copper filings, preheating the mixture to 160° C to remove any oxychlorides of zirconium present (4), then vacuum distilling at 320° C. The condensed product was then redistilled twice, resulting in a very white zirconium tetrachloride, free of oxychlorides and impurities.

The alkali metal chlorides used were of reagent grade, purified further by vacuum degassing at about 400° C.

The sodium and potassium hexachlorozirconates were produced by the direct reaction,

$$2MCl_{(s)} + ZrCl_{4(g)} = M_2ZrCl_{6(s)}$$

where M is the sodium or potassium, respectively.

An excess of zirconium tetrachloride is placed in a pyrex boat which, in turn, is loaded into the pyrex reaction tube. A weighed amount of between 3 and 7 grams of −325 mesh alkali chloride salt is placed in another pyrex boat and loaded into the cell, as shown in Fig. 1. This step is carried out in a dry box to eliminate any contamination due to hydrolysis. The large end of the cell is then flame sealed and a constriction is made at E to minimize the thermal gradient in the cell. The entire cell is then evacuated through the vacuum outlet at F and simultaneously flamed to remove any traces of moisture in the tube. It is then vacuum sealed at F, and loaded into the furnace. The temperature of the zirconium tetrachloride is regulated to about 330° C, which corresponds to slightly less than 1 atmosphere pressure, while the alkali metal chlorides are heated to 475 ± 50° C.

After a minimum reaction time of 24 hours, the reaction cell is furnace cooled, removed from the furnace, opened at F in a dry box, and the reacted salt weighed to determine the amount of zirconium tetrachloride

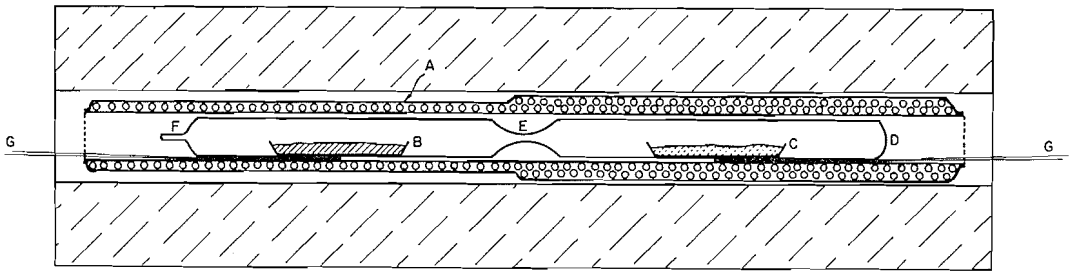

FIG. 1. Reaction apparatus: A, furnace windings; B, Pyrex boat containing purified zirconium tetrachloride; C, Pyrex boat containing alkali metal chloride salt; D, Pyrex reaction tube; E, constriction; F, vacuum-sealed outlet; G, temperature measuring thermocouples.

reacted with the alkali chloride originally placed in the boat. Thus, the exact composition of the reacted product could be easily determined.

RESULTS AND DISCUSSION

In all the preparations, approximately 3 to 7 grams of −325 mesh alkali metal chloride salt was used and the reaction time was at least 24 hours. The reaction temperature was not so critical as it was for the production of the chlorotitanates, but rather any temperature between 425 and 525° C could be readily used. The composition of the reaction products from six typical runs on both the sodium and potassium compounds are given in Table I.

TABLE I

Na_2ZrCl_6 composition				K_2ZrCl_6 composition			
Na	Zr	Cl	Mole ratio, $NaCl/ZrCl_4$	K	Zr	Cl	Mole ratio, $KCl/ZrCl_4$
			Theoretical				
13.14	26.07	60.79	2.000	20.46	23.87	55.67	2.000
			Experimental				
13.13	26.08	60.79	2.000	20.48	23.85	55.67	2.003
13.15	26.06	60.79	2.003	20.44	23.89	55.67	2.000
13.13	26.08	60.79	2.000	20.50	23.89	55.61	1.997
13.16	26.06	60.78	2.003	20.46	23.87	55.67	2.000
13.15	26.05	60.80	2.001	20.47	23.87	55.66	2.001
13.14	26.07	60.79	2.000	20.49	23.85	55.66	2.005
13.16	26.05	60.79	2.003	20.46	23.87	55.67	2.000

Properties of the Hexachlorozirconates

At room temperature, both sodium and potassium hexachlorozirconate are a light grey color, while in the liquid state at about 25° C to 50° C above their melting points, the color observed is a reddish-orange in each case.

The melting points were determined by cooling curve techniques using the pure compounds in sealed quartz vessels. The melting point of Na_2ZrCl_6 was determined to be 646±1° C and that of K_2ZrCl_6 to be 799±2° C, which is in good agreement with those shown by Howell *et al.* (2) and Morozov *et al.* (1) in their respective phase diagram investigations.

With respect to their stability in air, the K_2ZrCl_6 appears to be slightly more stable than the Na_2ZrCl_6. Considering the hydrolyzed product to be $(MCl)_2ZrOCl_2.8H_2O$ (5), approximately 0.5% hydrolysis occurs in the initial hour, 6% in the first day, and 22%

Can. J. Chem. Downloaded from www.nrcresearchpress.com by 210.87.254.42 on 09/05/12
For personal use only.

in the first week for the Na_2ZrCl_6, while 0.3% in the first hour, 4% in the first day, and 22% in the first week for the K_2ZrCl_6. As the hydrolysis occurred, the samples, which in both cases were approximately 6 grams, caked and finally turned to a pale green in color.

X-Ray information was gathered by taking diffractometer measurements on various batches of sodium and potassium hexachlorozirconates. Engel (6) has shown that Rb_2ZrCl_6 and Cs_2ZrCl_6 are of the *Fm3m* space group displaying the hexachloroplatinate structure. In this investigation, the K_2ZrCl_6 has been found to fall in this same group; however, the Na_2ZrCl_6 structure is not of this type and more work is required to solve the space grouping. Due to the hydrolysis of the materials diffractometer measurements were made on different samples, each being used for about 10 minutes only, corresponding to a 2θ value of about 10°.

The lattice parameter of the K_2ZrCl_6 has been determined to be 10.0818 ± 0.003 Å, and the corresponding density was found to be 2.48 g/cc based on four formulae units per cell. The experimental density, found by using reagent grade carbon tetrachloride in a standard density bottle, was 2.44 ± 0.01 g/cc for K_2ZrCl_6 and 2.43 ± 0.01 g/cc for the Na_2ZrCl_6.

Relative peak intensities and interplanar *d* spacings for the K_2ZrCl_6 are found in Table II. Also in Table II is included the 2θ diffraction angles and the relative intensities for the Na_2ZrCl_6.

Some physical properties of the hexachlorozirconates are summarized in Table II.

TABLE II

	A. K_2ZrCl_6		B. Na_2ZrCl_6	
Plane	Observed *d* values	Relative intensities*	2θ	Relative intensities*
(111)	5.8208	100	13.74	30
(200)	5.0420	30	24.59	70
(220)	3.5645	70	31.78	100
(310)			41.39	20
(222)	2.9103	75	43.40	15
(400)	2.5190	100	45.38	60
(313)	2.3123	10	47.02	10
(420)	2.2539	40	48.56	10
(422)	1.9407	20	56.51	10
(511)(333)				
(440)	1.7828	20	75.50	10
(531)	1.7042	10	84.01	10

*Readings of relative intensities of 10 are values which cannot be measured accurately.

TABLE III

Physical properties of the sodium and potassium hexachlorozirconates

	Na_2ZrCl_6	K_2ZrCl_6
Color at room temperature	Light grey	Light grey
Color in liquid state	Reddish-orange	Reddish-orange
Crystal structure		Cubic
Lattice parameter, Å		10.0818 ± 0.003
Space group		*Fm3m*
Density: calculated g/cc		2.48
experimental g/cc	2.43	2.44
Melting point (° C)	646 ± 1	799 ± 2

Can. J. Chem. Downloaded from www.nrcresearchpress.com by 210.87.254.42 on 09/05/12
For personal use only.

ACKNOWLEDGMENT

Acknowledgment is made to the Defence Research Board of Canada for its financial assistance in support of this work.

REFERENCES

1. I. S. Morozov and In'-Chzhu Son. Russ. J. Inorg. Chem. English Transl. 4–11, 1176 (1959).
2. L. J. Howell, R. C. Sommer, and H. H. Kellogg. J. Metals, **209**, 193 (1957).
3. R. L. Lister and S. N. Flengas. Can. J. Chem. **41**, 1548 (1963).
4. T. Sadashige. J. Chem. Soc. Japan, Pure Chem. Sect. **75**, 637 (1954).
5. A. F. Wells. Structural inorganic chemistry. 3rd ed. Oxford University Press. p. 561.
6. G. Engel. Z. Krist. **90**, 341 (1935).

Can. J. Chem. Downloaded from www.nrcresearchpress.com by 210.87.254.42 on 09/05/12
For personal use only.

Can. J. Chem. Downloaded from www.nrcresearchpress.com by 210.87.254.42 on 09/05/12
For personal use only.

THE RELATIVE ACID STRENGTHS OF SUBSTITUTED PICRIC ACIDS[1]

JOHN W. ELDER[2] AND RAYMOND P. MARIELLA[3]
Department of Chemistry, Loyola University, Chicago, Illinois
Received November 26, 1963

ABSTRACT

The relative acidity of substituted picric acids has been determined using special non-aqueous titration techniques. Other organic and inorganic acids, whose acidities in water are well known, were also determined using this non-aqueous method. A correlation of the relative acidities of known acids in water with the relative acidities of these same acids, as measured under the non-aqueous conditions used, was excellent. Using this technique a single relative acidity scale was determined ranging from acids as strong as perchloric to acids as weak as acetic acid.

During recent work with substituted picric acids in reactions with amines and aromatic hydrocarbons (1, 2, 3) it became desirable to know the magnitude of the relative acidities of these acids.

The literature shows that considerable difficulties have been encountered in attempts to evaluate the acid strength of picric acids. The major difficulty is due to the fact that picric acid and its derivatives are too strong for the usual aqueous methods to give good results.

Bates and Schwarzenbach (4) determined the pK_a of picric acid spectrophotometrically in aqueous hydrochloric acid solutions. Because of picric acid's strong acidity, it was not possible to obtain a good value of the absorbance of a solution in which all the picric acid was in the non-ionized form. This difficulty was solved, in part, by selecting several likely values and determining the value that gave the most consistent pK_a values.

Spectrophotometric measurements by Davis *et al.* (5, 6), of methylpicric acid and dimethylpicric acid (7, 8) gave values of 0.81 and 1.38 respectively. Recent work by Davis and Paabo (9) gave the pK_a value of 0.33 for picric acid when measured spectrophotometrically in water containing hydrochloric acid. Attempts to determine the pK_a of picric acid by potentiometric titrations of picric acid and by spectrophotometric measurements of picric acid solutions in the near-saturation range did not yield satisfactory results (9).

The investigation of the acid strength of picric acid in *non-aqueous* solvents has been limited to conductometric measurements. Neale (10) determined the ionization constant of picric acid in acetone and in aqueous acetone solutions, obtaining a value of 10^{-6} in anhydrous acetone.

Goldschmidt (11) determined the dissociation constant of picric acid to be 1.75 times 10^{-4} in absolute methanol. MacInnes (12) using certain refinements in the determination of Λ_0, recalculated Goldschmidt's data to give a value for K of 1.84×10^{-4}.

In the present work several trials were made to find a suitable method to measure the acidities of the various picric acids. The spectral method of Davis *et al.* (5, 6) was applied to the determination of chloropicric acid, where it was found that the spectra of the unionized acid was not readily obtainable, since chloropicric acid was still ionized in 6 N hydrochloric acid. Selection of likely values of the absorbance of the non-ionized species gave values of pK_a ranging from 0.44 to 0.03, but no value gave particularly consistent results.

[1]*Taken in part from the Ph.D. dissertation of J. W. Elder.*
[2]*Present address: Regis College, Willowdale, Ontario.*
[3]*Author to whom inquiries should be directed.*

A method utilizing potentiometric measurements in a non-aqueous system was then adapted, in which the potential of the acetone solution of the acid, half neutralized with tetrabutyl ammonium hydroxide titrant, was taken as characteristic of the acid. The potential of the system was measured with a glass-modified calomel electrode pair. The use of such a non-aqueous potential system follows the methods developed by Heijde (13, 14, 15), Cundiff and Markunas (16, 17), Bruss and Wyld (18), and Fritz and Yamamura (19). The method of measuring the potential of the solution of half-neutralized acid rather than by the usual potentiometric titration method was necessitated by the long interval required before a steady potential value was reached.

The values obtained for the mid-equivalence points are listed in Table I.

TABLE I

Mid-equivalence potentials

	EMF (mv)	ΔEMF (mv)
Perchloric acid	733	243
Trinitrophloroglucinol (1st H)	610	120
Hydrochloric acid	582	92
Chloropicric acid	549	59
Bromopicric acid	542	52
Styphnic acid (1st H)	523	33
Iodopicric acid	509	19
Picric acid	490	—
Methoxypicric acid	467	−23
Ethylpicric acid	457	−33
Methylpicric acid	452	−38
Nitric acid	449	−41
Dimethylpicric acid	380	−110
t-Butylpicric acid	372	−118
Salicylic acid	72	−418
Trinitrophloroglucinol (2nd H)	−66	−556
Styphnic acid (2nd H)	−158	−648
Benzoic acid	−160	−650
Acetic acid	−223	−713

Included in Table I are also some other acids to test the theory. The magnitude of the relative acidities can be seen by comparing the Δ EMF column.

$$(\Delta\ \mathrm{EMF} = \mathrm{EMF}_x - \mathrm{EMF}_{p.a})$$

No value is given for sulphuric acid. Repeated attempts to obtain this value led to erratic results which it is believed are due to the dehydrating action of sulphuric acid on the surface of the electrode, or to the self-condensation of the solvent, caused by the sulphuric acid. The third dissociation of trinitrophloroglucinol could not be measured by our system, since this acidic hydrogen is so very weak.

It is best to consider these values (Table I) as only *relative* values, and no claim is made as to any absolute values. That there is a correlation between our values and those obtained in aqueous systems is seen in Fig. 1.

Figure 1 shows six acids, whose pK_a values are well known from aqueous work, plotted against the EMF values obtained from this work. A good linear relationship can be seen.

Our results agree with the theory that the presence of an increasing bulky group in the meta positions tends to decrease the coplanarity of the nitro groups with benzene ring, thus decreasing the resonance, and hence decreasing the acidity.

Can. J. Chem. Downloaded from www.nrcresearchpress.com by 210.87.254.42 on 09/05/12
For personal use only.

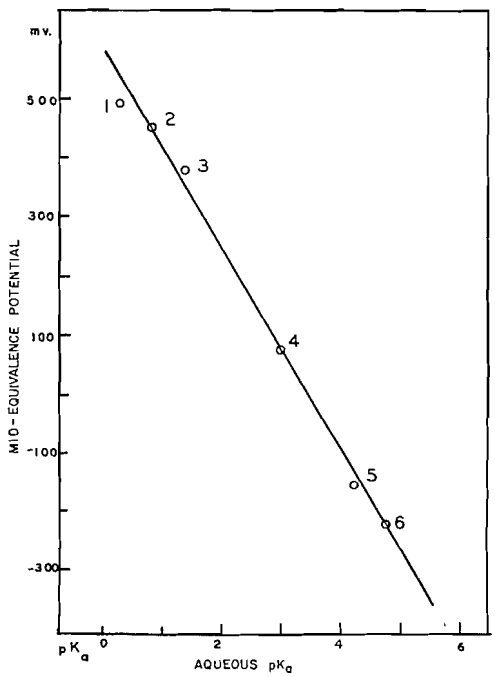

FIG. 1. Mid-equivalence potential vs. aqueous pK_a. 1. Picric acid (4). 2. Methylpicric acid (5, 6). 3. Dimethylpicric acid (5, 6). 4. Salicylic acid (20). 5. Benzoic acid (20). 6. Acetic acid (20).

EXPERIMENTAL

Preparation of Tetrabutylammonium Hydroxide Titrant

Ten grams of tetrabutylammonium iodide (Eastman) and 6 g of purified silver oxide (Eastman) were vigorously agitated for 90 minutes in 25 ml of absolute methanol. The mixture was filtered through a fine sintered glass filter and diluted to 250 ml with absolute methanol, giving a solution about 0.1 *N*. The titrant was standardized against benzoic acid by potentiometric titration.

Potentials were measured with a Beckman Model G pH meter. A Beckman glass electrode (4990-80) and a Beckman fiber-type calomel electrode (1170) were used, the calomel electrode being modified by replacing the aqueous saturated potassium chloride solution with a potassium chloride saturated absolute methanol solution.

The picric acids were prepared (1, 3, 7, 8) and recrystallized at least three times from an appropriate solvent and dried under vacuum in a drying pistol.

Reagent grade acetone was used without purification.

Procedure for Determining the Potential of the Mid-equivalence Points

To 40 ml of acetone solution containing one-third millimole of acid, a volume of titrant was added that would exactly neutralize half of the acid. The solution was stirred and the glass and modified calomel electrodes inserted. Potential readings were taken until the potential became steady (about 20–30 minutes) and this potential was taken as being characteristic of the system. Between determinations the electrodes were removed from the solution, rinsed with acetone, wiped dry with soft tissue, and the glass electrode soaked in distilled water for 10 minutes. After this time the electrodes were again wiped with soft tissue, rinsed with acetone, and introduced into the next solutions (at least two determinations were made on all the acids reported). Duplicate determinations on any one acid usually did not vary by more than 2 mv.

REFERENCES

1. R. P. MARIELLA, M. J. GRUBER, and JOHN W. ELDER. J. Org. Chem. **26**, 3217 (1961).
2. JOHN W. ELDER and R. P. MARIELLA. Can. J. Chem. **41**, 1653 (1963).
3. JOHN W. ELDER and R. P. MARIELLA. Can. J. Chem. To be published (1964).
4. R. G. BATES and G. SCHWARZENBACH. Experientia, **10**, 482 (1954).
5. M. M. DAVIS, M. PAABO, and R. A. ROBINSON. J. Res. Nat. Bur. Std. **64A**, 531 (1960).
6. M. M. DAVIS and M. PAABO. J. Res. Nat. Bur. Std. **64A**, 533 (1960).

Can. J. Chem. Downloaded from www.nrcresearchpress.com by 210.87.254.42 on 09/05/12
For personal use only.

7. C. E. MOORE and R. PECK. J. Org. Chem. **20**, 673 (1955).
8. C. E. MOORE, M. M. LALLY, R. L. ANDERSON, J. L. BRADY, and J. J. MCLAFFERTY. Anal. Chim. Acta, **15**, 1 (1956).
9. M. M. DAVIS and M. PAABO. J. Res. Nat. Bur. Std. **67A**, 241 (1963).
10. S. M. NEALE. Trans. Faraday Soc. **17**, 505 (1922).
11. H. GOLDSCHMIDT. Z. Physik. Chem. **91**, 46 (1916).
12. D. A. MACINNES. The principles of electrochemistry. Dover Publications, New York, N.Y. 1961.
13. H. B. VAN DER HEIJDE and E. A. M. F. DAHMEN. Anal. Chim. Acta, **16**, 378 (1957).
14. H. B. VAN DER HEIJDE. Anal. Chim. Acta, **16**, 392 (1957).
15. H. B. VAN DER HEIJDE. Anal. Chim. Acta, **17**, 512 (1957).
16. R. H. CUNDIFF and P. C. MARKUNAS. Anal. Chem. **28**, 792 (1956).
17. R. H. CUNDIFF and P. C. MARKUNAS. Anal. Chem. **30**, 1450 (1958).
18. D. B. BRUSS and G. E. A. WYLD. Anal. Chem. **29**, 232 (1957).
19. J. S. FRITZ and S. S. YAMAMURA. Anal. Chem. **29**, 1079 (1957).
20. J. F. J. DIPPY. Chem. Rev. **25**, 203 (1939).

Can. J. Chem. Downloaded from www.nrcresearchpress.com by 210.87.254.42 on 09/05/12
For personal use only.

Can. J. Chem. Downloaded from www.nrcresearchpress.com by 210.87.254.6 on 09/05/12
For personal use only.

SYNTHESIS OF MALTOBIOURONIC ACID (4-*O*-[α-D-GLUCOPYRANOSYLURONIC ACID]-D-GLUCOSE)

G. G. S. Dutton and K. N. Slessor
Department of Chemistry, University of British Columbia, Vancouver, British Columbia
Received January 20, 1964

ABSTRACT

Benzyl β-maltobiouronic acid has been isolated from the catalytic oxidation of benzyl β-maltoside. Hydrogenolysis of the benzyl glycoside afforded maltobiouronic acid which was characterized as the methyl ester heptaacetate.

Benzyl hepta-*O*-acetyl-β-maltoside was synthesized from acetobromomaltose (1) and benzyl alcohol by the condensation method described by Helferich and Berger (2). Deacetylation with methanolic ammonia gave the crystalline benzyl β-maltoside (3). Catalytic oxidation (4) as described by Jayme and Demmig (5) in their synthesis of cellobiouronic acid gave a mixture of acidic sugars, which upon esterification with diazomethane and acetylation gave crystalline methyl (benzyl hexa-*O*-acetyl-β-maltosid)uronate. The methyl ester hexaacetate was obtained in 40% yield based on the benzyl β-maltoside consumed.

Saponification was achieved by warming with aqueous barium hydroxide to yield the barium (benzyl β-maltosid)uronate. Hydrogenolysis using palladium on barium sulphate (6), followed by acidification with Amberlite IR 120 (H^+) yielded maltobiouronic acid.

Borohydride reduction of a sample of the acid, followed by acid hydrolysis indicated only glucuronic acid and sorbitol upon paper chromatography. The structure of the synthetic uronic acid is therefore 4-*O*-α-D-glucopyranosyluronic acid-D-glucose.

Esterification of maltobiouronic acid with diazomethane, followed by acetylation with acetic anhydride in pyridine, yielded the crystalline methyl ester heptaacetate.

Future work on enzyme specificity will study the cleavage of this molecule into its constituent monosaccharides. In view of the wide distribution of α-linked glucose residues in the animal and plant kingdom, it is conceivable that maltobiouronic acid may be found in some future study of such polysaccharides.

EXPERIMENTAL

Evaporations were carried out under reduced pressure at a bath temperature of 40–45°. Optical rotations are equilibrium values measured on a Bendix–Ericson ETL-NPL Automatic Polarimeter (Type 143A) at 21±2°. Melting points quoted are uncorrected. Chromatograms were run by the descending technique in ethyl acetate : acetic acid : formic acid : water (18:3:1:4). Sugars were detected on chromatograms by the *p*-anisidine–trichloroacetate spray (7) for reducing sugars and periodate–permanganate spray (8) for non-reducing sugars.

Benzyl Hepta-O-acetyl-β-maltoside

To acetobromomaltose (16.6 g) prepared from maltose (10 g) by the method of Barczai-Martos and Korosy (1) was added freshly distilled benzyl alcohol (32 ml) and mercuric cyanide (6 g). The mixture was heated to 85° on a water bath and stirred vigorously for 45 minutes. The resulting solution was poured with stirring into ethanol (90 ml) and cooled to 5° for 3 hours. The crude product (10.5 g, 61% based on the acetobrom sugar) was collected by suction filtration. Recrystallization from ethanol yielded material melting at 124–125°. Lit. (3), m.p. 125°.

Benzyl β-Maltoside

Deacetylation of benzyl hepta-*O*-acetyl-β-maltoside was accomplished with methanol saturated with ammonia as described by Fischer and Kogl (3). Recrystallization from methanol – ethyl acetate gave the crystalline glycoside, m.p. 148–149°. Lit. (2), m.p. 147–148°.

Platinum Oxidation Catalyst

Modification of a method of Brown (9) facilitated the preparation of an active platinum catalyst. To carbon (10 g, Darco G-60), digested overnight in 6 *N* hydrochloric acid, washed free of chloride with distilled water and dried at 120° for 4 hours, a solution of chloroplatinic acid (5 g) in 50% aqueous ethanol (50 ml)was added. To this mixture, a solution of sodium borohydride (2.5 g) in ethanol (100 ml) was added slowly with stirring. After 5 minutes 6 *N* hydrochloric acid (10 ml) was added and the suspension suction filtered. The precipitate was washed free of chloride with distilled water and dried in vacuum over phosphorus pentoxide. The product (12 g) was pyrophoric and in later experiments drying was not carried out and the product was kept as a moist paste.

Catalytic Oxidation of Benzyl β-Maltoside

To a solution of benzyl β-maltoside (5 g) and sodium bicarbonate (1 g) in distilled water (100 ml) was added platinum catalyst (5 g). The mixture was maintained at 65° and magnetically stirred for 6 hours during which time a stream of oxygen was passed into the solution through a gas dispersion tube. After it had been cooled, the mixture was filtered through Celite, acidified with Amberlite IR 120 (H^+), and passed slowly through a column of Duolite A-4 (OH^-). The Duolite resin was washed with water (500 ml) and the combined eluates evaporated to recover unreacted benzyl β-maltoside (3–4 g). The Duolite resin was eluted with *N* NaOH (15 ml) and washed with water (100 ml), and the combined eluate acidified by passage through Amberlite IR 120 (H^+). The acid mixture obtained was evaporated to a brown sirup (1 g).

Methyl (Benzyl Hepta-O-acetyl-β-maltosid)uronate

To the acid mixture (1.5 g) dissolved in methanol (15 ml) excess diazomethane in ether was added. After 10 minutes the excess diazomethane was decomposed with glacial acetic acid, and the solution evaporated to a sirup. This material was acetylated in pyridine (20 ml) with acetic anhydride (50 ml) overnight. Recovery in the normal way yielded a sirup which crystallized. Recrystallization from ethanol or methanol yielded the methyl ester hexaacetate (0.8 g), m.p. 164–165°, $[\alpha]_D$ 33.8° (*c*, 2.04 in $CHCl_3$). Calculated for $C_{32}H_{46}O_{18}$: C, 53.95; H, 5.62%. Found: C, 53.80; H, 5.71%.

Barium (Benzyl β-maltosid)uronate

To a solution of the methyl ester hexaacetate (415 mg) in methanol (20 ml) a saturated aqueous barium hydroxide solution (40 ml) was added and the solution refluxed on a steam bath for 90 minutes. The solution was neutralized with carbon dioxide and filtered, and the precipitate washed with water (15 ml). The combined filtrates were acidified by passage through Amberlite IR 120 (H^+) and evaporated to a glassy solid. The solid was dissolved in water (2 ml) and neutralized with saturated aqueous barium hydroxide. The precipitate obtained upon the addition of ethanol (30 ml) was centrifuged, washed with ethanol (10 ml), and dried by solvent exchange with ether to give a white powder (300 mg) $[\alpha]_D$ 30° (*c*, 1.53 in H_2O).

Maltobiouronic Acid

A small scale experiment (8.25 mg of barium salt) was conducted in a Warburg type microhydrogenator. Hydrogenolysis was complete after 2 hours with the hydrogen uptake constant at 1.04 moles.

To a solution of the barium salt (202 mg) in water (10 ml) was added palladium oxide on barium sulphate catalyst (270 mg). The mixture was hydrogenolyzed at room temperature in a Paar apparatus at a pressure of 1 atmosphere. After 2 hours the mixture was filtered, the precipitate washed with water (10 ml), and the combined filtrates acidified by passage through Amberlite IR 120 (H^+) and evaporated to a sirup (138 mg). Freeze-drying yielded a product which analyzed as a monohydrate. After it was dried overnight *in vacuo* (0.02 mm) at 80°, the product had lost a weight equivalent to 1.2 moles of water. Upon drying at 100° for 36 hours a further 0.5 moles of water was lost. Drying was discontinued at this stage as the acid began to darken indicating decomposition. Neutralization equivalent: calc. for $C_{12}H_{22}O_{13}$, 374. Found: 367, $[\alpha]_D$ 116° (*c*, 2.52 in H_2O). Calc. for $C_{12}H_{22}O_{13}$ (monohydrate): C, 38.50; H, 5.88%. Found: C, 38.26; H, 5.76%. R_f 0.051, $R_{glucose}$ 0.33, $R_{maltose}$ 0.90 (EtOAc:AcOH:HCOOH:H_2O = 18:3:1:4).

Methyl (Hepta-O-acetyl-β-maltosid)uronate

To maltobiouronic acid (55 mg) in methanol (5 ml) was added excess diazomethane in ether, and after 10 minutes the solution was evaporated to dryness. Acetic anhydride (10 ml) and anhydrous sodium acetate (0.5 g) were added and the mixture heated on a steam bath for 2 hours. The mixture was poured into ice water and extracted into chloroform in the usual manner. Crystals (30 mg) were obtained which upon recrystallization from methanol melted at 197–198°. $[\alpha]_D$ 77° (*c*, 0.54 in $CHCl_3$). Calc. for $C_{27}H_{36}O_{19}$: C, 48.80; H, 5.42%. Found: C, 49.29; H, 5.53%.

Hydrogenolysis of methyl (benzyl hexa-*O*-acetyl-β-maltosid)uronate (145 mg) in glacial acetic acid (5 ml) with Pd/C catalyst (75 mg) for 10 hours at atmospheric pressure gave a material which upon acetylation as described above gave methyl (hepta-*O*-acetyl-β-maltosid)uronate (43 mg). Melting point and mixed melting point 197–198°.

Constitution of Maltobiouronic Acid

To maltobiouronic acid (6 mg) in water (5 ml) sodium borohydride (30 mg) was added. After 17 hours

Can. J. Chem. Downloaded from www.nrcresearchpress.com by 210.87.254.6 on 09/05/12
For personal use only.

at room temperature the solution was neutralized with acetic acid and evaporated to dryness. The sirup was evaporated with 3% HCl in methanol (3×5 ml) and the residue dissolved in water (5 ml), passed through Amberlite IR 120 (H^+), and evaporated to dryness. The resulting material was dissolved in *N* H_2SO_4 (3 ml) and hydrolyzed at 100° in a sealed tube overnight. Neutralization of the hydrolyzate with washed barium carbonate gave a filtrate which upon acidification by passing through Amberlite IR 120 (H^+) indicated only glucuronic acid and sorbitol upon paper chromatography.

ACKNOWLEDGMENTS

We are grateful to the National Research Council for financial support and one of us (K. N. S.) thanks the Council for the award of a studentship. We are also indebted to Mrs. C. Jenkins of this department and Dr. A. Bernhardt, Mulheim (Ruhr), Germany, for analyses.

REFERENCES

1. M. Barczai-Martos and F. Korosy. Nature, **165**, 369 (1950).
2. B. Helferich and A. Berger. Chem. Ber. **90**, 2492 (1957).
3. H. Fischer and F. Kogl. Ann. **436**, 219 (1924).
4. K. Heyns and H. Paulsen. Advan. Carbohydrate Chem. **17**, 169 (1962).
5. G. Jayme and W. Demmig. Chem. Ber. **93**, 356 (1960).
6. R. Kuhn and H. J. Haas. Angew. Chem. **67**, 785 (1955).
7. L. Hough, J. K. N. Jones, and W. H. Wadman. J. Chem. Soc. 1702 (1950).
8. R. U. Lemieux and H. F. Bauer. Anal. Chem. **26**, 920 (1954).
9. H. C. Brown and C. A. Brown. J. Am. Chem. Soc. **84**, 2827 (1962).

Can. J. Chem. Downloaded from www.nrcresearchpress.com by 210.87.254.6 on 09/05/12
For personal use only.

Can. J. Chem. Downloaded from www.nrcresearchpress.com by 210.87.254.5 on 09/05/12
For personal use only.

THE SULPHURIC ACID SOLVENT SYSTEM

PART VI. THE BASICITIES OF COMPOUNDS CONTAINING SULPHUR–OXYGEN BONDS

S. K. Hall and E. A. Robinson
Lash Miller Chemical Laboratories, University of Toronto, Toronto, Ontario

Received December 6, 1963

ABSTRACT

Cryoscopic and conductimetric studies of a variety of compounds containing S—O bonds have shown that dimethyl sulphoxide behaves as a strong base in sulphuric acid whereas dialkyl sulphones behave as weak bases. In contrast diaryl sulphones and aryl sulphonic acids behave as non-electrolytes.

A correlation is established between the basicities of the alkyl sulphones, H_2SO_4, and the HSO_4^- ion, and their sulphur–oxygen stretching frequencies. This relation is used to predict the basicities of other compounds containing S—O bonds. In particular it is shown that the basicity of monomeric sulphur trioxide is similar to that of sulphuric acid, and sulphamide is shown to behave as a strong base in sulphuric acid, which implies protonation on a nitrogen atom rather than on oxygen, since the S—O stretching frequencies indicate only weakly basic behavior for O-protonation.

INTRODUCTION

Previous studies of sulphuric acid solutions of compounds containing sulphur–oxygen bonds have been largely confined to cryoscopic studies (1–6). However, the conductimetric behavior of a few solutes such as SO_2Cl_2 (7), methanesulphonic acid (8), and sulphur dioxide (9), has also been reported.

The earliest studies are due to Hantzsch (1), who studied the cryoscopic behavior of the sodium salts of benzene-, *m*-nitrobenzene-, and *p*-toluene-sulphonic acids. He allowed for solvolysis of the sulphonate anions to their parent acids

$$\text{e.g. } PhSO_3Na + H_2SO_4 = PhSO_3H + Na^+ + HSO_4^-,$$

and concluded that benzene- and *p*-nitrobenzene-sulphonic acids behave as non-electrolytes in sulphuric acid while *p*-toluenesulphonic acid behaves as a weak base. Gillespie (2) carried out similar measurements on solutions of diphenyl sulphone, sodium benzenesulphonate, and sodium *p*-toluenesulphonate in *slightly aqueous* sulphuric acid and concluded that diphenyl sulphone, benzenesulphonic acid, and *p*-toluenesulphonic acid behave as weak bases of the sulphuric acid solvent system ($C_6H_5SO_3H$, $K_b = 0.011$; $CH_3C_6H_4SO_3H$, $K_b + 0.016$).* However, it has been shown more recently that the use of slightly aqueous acid can lead to anomalous freezing point depressions (10, 11), due to salting-in or salting-out of the solute by the electrolyte $H_3O^+.HSO_4^-$, so that these results required re-examination.

In their initial work on the properties of anhydrous sulphuric acid as a non-aqueous solvent Gillespie, Hughes, and Ingold (3) found that SO_2Cl_2 behaves as a non-electrolyte in sulphuric acid. Their results also point to the probable behavior of dimethylsulphate as a non-electrolyte. Later conductivity measurements (7) confirmed the behavior of sulphuryl chloride as a non-electrolyte. Recently (8) the conductimetric behavior of methanesulphonic acid in H_2SO_4 was interpreted in terms of its behavior as either a non-electrolyte or as a *very* weakly ionized base.

Szmant and Brost (4) and Szmant and Lapinski (5) studied solutions of a variety of sulphones, sulphoxides, and sulphides but since they worked with very dilute solutions,

**For $B + H_2SO_4 = BH^+ + HSO_4^-$, $K_b = [BH^+][HSO_4^-]/[B]$.*

and did not correct their results for repression of the solvent self-dissociation, their conclusions, as Gillespie and Passerini have pointed out (6), are invalid.

The latest cryoscopic study of sulphuric acid solutions of some sulphones and sulphoxides is due to Gillespie and Passerini (6), who found that whereas 4-nitrodiphenyl sulphoxide, 4;4′-dinitrodiphenyl sulphoxide, and the corresponding sulphones give stable solutions, diphenyl sulphoxide is unstable in sulphuric acid and the freezing point depressions of its solutions increase with increase in time. This was attributed to protonation of the sulphoxide followed by its rapid sulphonation. Gillespie and Passerini give the following mean cryoscopic ν-factors: 4;4′-dinitrodiphenyl sulphoxide, 2.07; 4-nitrodiphenyl sulphone, 1.34; 4;4′-dinitrodiphenyl sulphoxide, 2.08; and 4;4′-dinitrodiphenyl sulphone, 1.28. Earlier measurements for the solute diphenyl sulphone (2) gave a mean ν-factor of 1.20. The results of these experiments were interpreted in terms of the behavior of aryl sulphoxides as strong bases and of aryl sulphones as weak bases.

One of the present authors has studied the conductimetric behavior of sulphur dioxide in 100% sulphuric acid (9). A slight increase in the electrical conductivity with increasing concentration of SO_2 was observed and was attributed to the behavior of SO_2 as a rather weak base.

In a following paper (12) we shall report the results of cryoscopic, conductimetric, and density measurements on solutions of some other solutes containing S—O bonds (CH_3SO_2F, CH_3SO_2Cl, $C_2H_5SO_2F$, $C_2H_5SO_2Cl$, and $CH_3SO_2.OCH_3$), which were found to behave as non-electrolytes. In this paper we give the results of a study of sulphuric acid solutions of (i) dimethyl sulphoxide, (ii) dimethyl-, diethyl-, di-*n*-propyl-, di-*n*-butyl-, tetramethylene-, diphenyl-, and 4;4′-dinitrodiphenyl-sulphones, (iii) the sodium salts of *p*-toluene-, and 2;4-dinitrobenzene-sulphonic acids, (iv) the monohydrate of *p*-toluene sulphonic acid, and (v) sulphamide.

EXPERIMENTAL

Commercial *dimethyl sulphoxide* (Baker Analysed Reagent) was purified by fractional distillation under reduced pressure (b.p. 55° at 5 mm mercury pressure); *dimethyl sulphone* (Crown Zellerbach Co.) by several recrystallizations from absolute alcohol (m.p. 109°); *n-propyl sulphone* (Eastman Kodak) by fractional crystallization from dry ether (m.p. 29.5°); and *n-butyl sulphone* (Eastman Kodak) by recrystallization from absolute ethanol (m.p. 44°). *Diethyl sulphone* was prepared from the corresponding sulphide by oxidation with ozone in chloroform solution. The product was recrystallized from dry ether (m.p. 73.5°). Pure *tetramethylene sulphone* was obtained by fractional distillation of a commercial product (Eastman Kodak) (b.p. 150° at 15 mm Hg pressure). *Diphenyl sulphone* (Eastman Kodak) was recrystallized from absolute ethanol (m.p. 128°). 4,4′-*Dinitrodiphenyl sulphone* was prepared from the corresponding sulphide by oxidation with an excess of 30% hydrogen peroxide in glacial acetic acid at 100°. It was recrystallized from glacial acetic acid (m.p. 251°).

Sulphuric acid of approximately 100% composition was prepared from analytical grade concentrated sulphuric acid and 30% oleum and the final adjustment to 100% composition carried either cryoscopically or conductimetrically as has been described before. The cells used in the determination of freezing point depressions and electrical conductivities have also been described previously (3, 13).

Cryoscopy

The freezing point depressions were obtained by the Beckmann method using solid stem mercury-in-glass thermometers for temperature measurements. The thermometers were graduated in 1/100° divisions and were calibrated against a platinum resistance thermometer. A supercooling correction, $ks\theta$, was applied to the observed freezing points where k is a constant, s the number of degrees of supercooling, and θ the freezing point depression (3). The affect of the heat capacity of the apparatus on the constant k was allowed for by determining its value experimentally, by comparing the freezing point depressions of solutions of $KHSO_4$ obtained in a particular cryoscope with the very accurate values obtained for this electrolyte by the method of equilibrium cryoscopy (14). An approximately constant amount of supercooling of about 2° was used throughout these experiments. A typical value of k obtained in this way is 0.016, which compares with the value of 0.012, which can be calculated theoretically (3), if the heat capacity of the apparatus is neglected.

Can. J. Chem. Downloaded from www.nrcresearchpress.com by 210.87.254.5 on 09/05/12
For personal use only.

No allowance for the non-ideality of the solutions was possible and cryoscopic ν'-factors were calculated from the equation

$$\nu' = \frac{\theta(1 + 0.002\,\theta)}{6.12\,m} - m_d/m,$$

where θ is the freezing point depression of a solution of molality m, calculated from the freezing point of hypothetical undissociated acid, (10.625°) (15), and m_d is the total concentration of species resulting from unrepressed self-dissociation present in a particular solution. Values of m_d were calculated from the tables given previously (15) via the degrees of ionization deduced from the conductivity measurements. This treatment assumes that the K_b values for sulphones do not change in magnitude in the temperature range 10–25°. This has been shown to be a valid assumption in the case of the weakly basic nitro compounds (17) and is also justified by the present results since the K_b values obtained in this way from cryoscopy at 10° are the same, within experimental error, as those obtained from the conductimetric measurements at 25°.

Conductivity Measurements

Electrical conductivity measurements were carried out at 25 ± 0.003° C. The method of calculating the degrees of ionization, γ, has been described previously (16). Acid–base conductimetric titrations were also carried out for the alkyl sulphones by adding small quantities of sulphone to an approximately 0.1 m solution of $H_2S_2O_7$ in H_2SO_4 and measuring the conductivity after each addition. The specific conductivities were plotted against $n_b/n_a{}^i$, the ratio of moles of added base to the number of moles of $H_2S_2O_7$ initially present, and the position of minimum conductivity, $r = (n_b/n_a{}^i)$ evaluated. The initial concentration of $H_2S_2O_7$ was found from the initial specific conductance. It has been shown previously that r is related to K_b, the ionization constant of the base, according to the equation

$$r = 0.56\,[1 + 0.018/K_b],$$

for an initially 0.1 m solution of $H_2S_2O_7$ (17).

Infrared Spectroscopy

Infrared spectroscopic measurements were carried out on 1–2% solutions of the sulphones in carbon tetrachloride, chloroform, or carbon disulphide, using a Perkin–Elmer 221 double beam spectrometer.

RESULTS

Cryoscopic and conductimetric measurements interpolated at round concentrations from the extensive original experimental data are shown in Table I, which also shows calculated cryoscopic ν-factors and conductimetric γ-values. In the case of those compounds which were found to behave as weak bases the basic ionization calculated from this data is shown in Table II. Figure 1 compares the conductivity curves for the sulphonic acid sodium salts and *p*-toluene sulphonic acid monohydrate with those of solutions of sodium hydrogen sulphate and water, respectively.

Dimethyl sulphoxide.—The observed ν'-factor is slightly greater than two, and the electrical conductivity measurements show that each molecule of solute ionizes to give one HSO_4^- ion, in agreement with complete protonation according to the equation

$$(CH_3)_2SO + H_2SO_4 = (CH_3)_2SOH^+ + HSO_4^-.$$

This result is consistent with those previously reported (6) for 4-nitrodiphenyl sulphoxide and 4;4′-dinitrodiphenyl sulphoxide.

Phenyl sulphones.—Both the cryoscopic and conductimetric measurements are consistent with the behavior of diphenyl sulphone and 4;4′-dinitrodiphenyl sulphone as non-electrolytes in sulphuric acid. These results do not agree with those of Gillespie (2). In the case of diphenyl sulphone the discrepancy is undoubtedly attributable to salting out of the sulphone by the slightly aqueous acid used by Gillespie. This could lead to an anomalously high ν'-factor. In the case of 4;4′-dinitrodiphenyl sulphone the discrepancy is more difficult to explain, since both the experiments of Gillespie and those presented in this paper were carried out in 100% sulphuric acid as solvent. However, our conductivity measurements confirm that both diphenyl sulphone and 4;4′-dinitrodiphenyl sulphone behave as non-electrolytes since the specific conductivities of solutions of both solutes fall below those of pure sulphuric acid.

Can. J. Chem. Downloaded from www.nrcresearchpress.com by 210.87.254.5 on 09/05/12
For personal use only.

TABLE I

Cryoscopic and conductimetric results and calculated ν'- and γ-values

m	F.p. (° C)	θ (° C)	m_d	ν'	$K\times10^3$ (25° C) (ohm^{-1} cm^{-1})	γ
Weak Bases						
1. Dimethyl sulphone						
0.05	10.054	0.571	0.0260	1.34	1.095	0.27
0.10	9.702	0.923	0.0238	1.27	1.187	0.22
0.15	9.348	1.277	0.0220	1.24	1.295	0.22
0.20	8.996	1.629	0.0207	1.22	1.420	0.21
0.25	8.638	1.987	0.0197	1.22	1.547	0.21
0.30	8.279	2.346	0.0190	1.21	1.669	0.20
0.35	7.918	2.707	0.0182	1.21	1.794	0.19
2. Diethyl sulphone						
0.05	10.062	0.563	0.0263	1.31	1.090	0.25
0.10	9.720	0.905	0.0240	1.24	1.177	0.22
0.15	9.372	1.253	9.0222	1.22	1.277	0.20
0.20	9.028	1.597	0.0212	1.20	1.380	0.20
0.25	8.684	1.941	0.0203	1.19	1.483	0.19
0.30	8.342	2.283	0.0195	1.18	1.583	0.18
0.35	7.994	2.631	0.0187	1.18	1.680	0.17
3. Di-*n*-propyl sulphone						
0.05	10.088	0.537	0.0272	1.21	1.069	0.18
0.10	9.770	0.855	0.0254	1.14	1.110	0.15
0.15	9.441	1.184	0.0242	1.13	1.152	0.13
0.20	9.116	1.509	0.0236	1.11	1.194	0.12
0.25	8.796	1.829	0.0230	1.10	1.236	0.11
0.30	8.468	2.157	0.0223	1.10	1.279	0.10
0.35	8.145	2.480	0.0217	1.09	1.310	0.10
4. Di-*n*-butyl sulphone						
0.05	10.106	0.519	0.0278	1.14	1.060	0.14
0.10	9.790	0.835	0.0260	1.10	1.092	0.13
0.15	9.464	1.161	0.0250	1.10	1.125	0.11
0.20	9.140	1.485	0.0242	1.09	1.156	0.10
0.25	8.820	1.805	0.0236	1.08	1.190	0.09
0.30	8.500	2.125	0.0229	1.08	1.220	0.09
0.35	8.176	2.449	00.222	1.08	1.239	0.08
5. Tetramethylene sulphone						
0.05	10.097	0.528	0.0274	1.18	1.063	0.14
0.10	9.780	0.845	0.0257	1.13	1.095	0.14
0.15	9.453	1.172	0.0246	1.11	1.130	0.11
0.20	9.128	1.497	0.0239	1.10	1.160	0.10
0.25	8.808	1.817	0.0233	1.09	1.193	0.09
0.30	8.484	2.141	0.0226	1.09	1.224	0.09
0.35	8.161	2.464	0.0220	1.09	1.253	0.08
Strong Bases						
6. Dimethyl sulphoxide						
0.05	9.864	0.761	0.0208	2.07	1.538	1.0
0.10	9.240	1.385	0.0167	2.10	2.280	
0.15	8.610	2.015	0.0152	2.09	3.020	
0.20	7.985	2.640	0.0141	2.08	3.690	
7. Sulphamide						
0.025	10.174	0.451	0.0266	1.88	1.172	1.0
0.050	9.900	0.725	0.0208	1.95	1.431	
0.075	9.630	0.995	0.0180	1.93	1.724	
0.100	9.357	1.268	0.0167	1.91	2.018	
Non-electrolytes						
8. Diphenyl sulphone						
0.025	10.212	0.413	0.0423	1.01	1.029	
0.050	10.060	0.565	0.0423	1.00	1.011	
0.075	9.904	0.721	0.0423	0.99	1.004	
0.100	9.750	0.875	0.0423	1.01	0.993	
0.125	9.595	1.030	0.0423	1.00	0.981	

Can. J. Chem. Downloaded from www.nrcresearchpress.com by 210.87.254.5 on 09/05/12
For personal use only.

TABLE I (*Concluded*)

m	F.p. (° C)	θ (° C)	m_d	ν'	$K\times10^2$ (25° C) (ohm^{-1} cm^{-1})	γ
9. 4;4′-Dinitrodiphenyl sulphone						
0.025	10.210	0.415	0.0423	1.02	1.038	
0.050	10.058	0.567	0.0423	1.01	1.034	
0.075	9.901	0.724	0.0423	1.00	1.029	
0.100	9.748	0.877	0.0423	1.00	1.024	
0.125	9.592	1.033	0.0423	1.01	1.020	
Salts						
10. Sodium *p*-toluene sulphonate						
0.025	9.993	0.632	0.0266	3.04	1.200	
0.050	9.563	1.062	0.0208	3.05	1.518	
0.075	9.124	1.501	0·0180	3.03	1.850	1.0
0.100	8·685	1.940	0.0167	3.02	2.180	
0.125	8.245	2.380	0.0157	2.98	2.513	
11. Sodium 2;4-dinitrobenzenesulphonate						
0.025	9.998	0.627	0.0266	3.03	1.175	
0.050	9.572	1.053	0.0208	3.03	1.515	
0.075	9.134	1.491	0.0180	3.01	1.865	1.0
0.100	8.700	1.925	0.0167	2.98	2.210	
0.125	8.260	2.365	0.0157	2.96	2.515	
12. *p*-Toluenesulphonic acid monohydrate						
0.050	9.579	1.046	0.0083	(3.25)	1.470	
0.075	9.129	1.496	0.0056	(3.18)	1.772	
0.100	8.684	1.941	0.0042	3.07	2.070	1.0
0.125	8.240	2.385	0.0033	3.07	2.373	
0.150	7.790	2.835	0.0028	3.06	2.675	

TABLE II

Acid–base titrations

Base	$n^i_{H_2S_2O_7}$*	r†	K_b (moles kg^{-1})
Dimethyl sulphone	0.111	1.25	0.0145
Diethyl sulphone	0.108	1.40	0.0120
Di-*n*-propyl sulphone	0.115	2.5	0.0052
Di-*n*-butyl sulphone	0.114	3.1	0.0040
Tetramethylene sulphone	0.135	3.3	0.0036

*Initial molal concentration of $H_2S_2O_7$.
†Position of conductivity minimum.

Alkyl sulphones.—In the case of the alkyl sulphones all of the compounds studied were found to behave as weak electrolytes in sulphuric acid. The basic ionization constants, K_b, were calculated from both the cryoscopic and conductimetric results by the standard methods (5, 16). All the compounds were found to behave as relatively weak bases and their basicities decrease, reasonably, in the series $(CH_3)_2SO_2$, $(C_2H_5)_2SO_2$, $(n\text{-}C_3H_8)_2SO_2$, $(n\text{-}C_4H_{11})_2SO_2$. Tetramethylene sulphone was found to have approximately the same base strength as *n*-propyl sulphone.

To confirm the results of these measurements conductimetric acid–base titrations were carried out where each base was added to an approximately 0.1 *m* solution of the acid $H_2S_2O_7$. The results of these experiments are shown in Fig. 2 and Table II, and give values for the basic ionization constants in good agreement with those from cryoscopy and simple conductimetric studies (Table III).

Sodium salts of sulphonic acids.—Both sodium *p*-toluenesulphonate and sodium 2;4-dinitrobenzenesulphonate gave ν'-factors close to 3.0 and specific conductivities close to

Can. J. Chem. Downloaded from www.nrcresearchpress.com by 210.87.254.5 on 09/05/12
For personal use only.

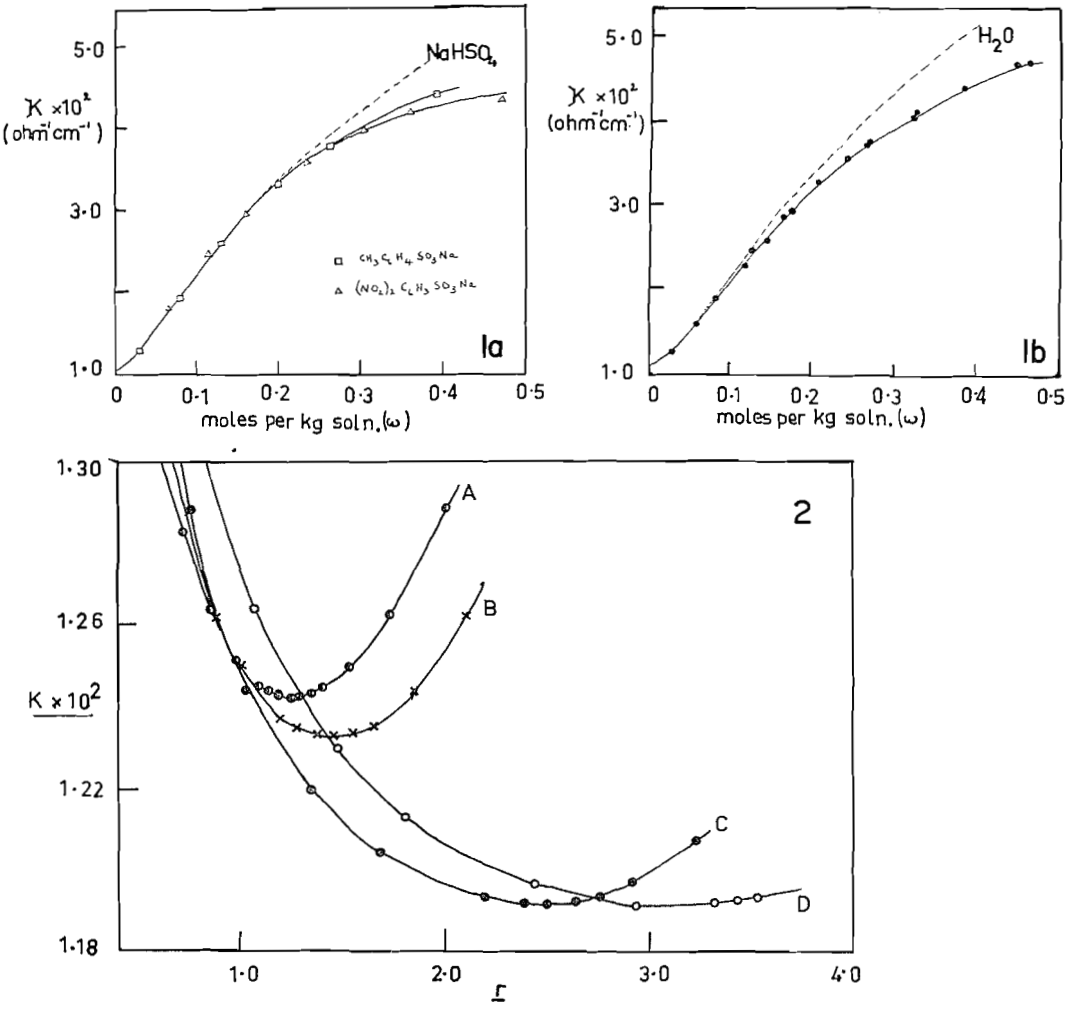

FIG. 1. (*a*) Conductimetric behavior of the salts of *p*-toluene and 2;4-dinitrobenzene sulphonic acids at 25° C.

(*b*) Conductimetric behavior of *p*-toluene sulphonic acid monohydrate at 25° C.

FIG. 2. Conductimetric acid–base titrations at 25° C. A, $(CH_3)_2SO_2$; B, $(C_2H_5)_2SO_2$; C, $(n\text{-}C_3H_7)_2SO_2$; D, $(n\text{-}C_4H_9)_2SO_2$.

those of equimolar solutions of $NaHSO_4$, which is consistent with ionization according to, for example,

$$CH_3C_6H_4SO_3Na + H_2SO_4 = CH_3C_6H_4SO_3H + Na^+ + HSO_4^-.$$

Thus we conclude that these aryl sulphonic acids behave as non-electrolytes in sulphuric acid, which is consistent with the previously reported behavior of methanesulphonic acid (8).

p-Toluenesulphonic acid monohydrate.—It has previously been shown (18) that this compound is best regarded as the salt $H_3O^+.CH_3C_6H_4SO_3^-$. The freezing point depressions and electrical conductivities of its solutions in sulphuric acid are consistent with complete solvolysis of the *p*-toluenesulphonate ion to the parent acid, which then behaves

Can. J. Chem. Downloaded from www.nrcresearchpress.com by 210.87.254.5 on 09/05/12
For personal use only.

TABLE III

Stretching frequencies, K_b values, and pK_{BH^+} values, for some sulphonyl compounds

	ν_{sym} (cm^{-1})	ν_{asym} (cm^{-1})	ν_{SO} (cm^{-1})	K_b (moles kg^{-1}) *	†	‡	§	$-pK_{BH^+}$
$(CH_3)_2SO_2$	1131	1305	1218	0.0150	0.0148	0.0145	0.0150	12.27
$(C_2H_5)_2SO_2$	1133	1311	1222	0.0120	0.0119	0.0123	0.0121	12.37
$(n\text{-}C_3H_7)_2SO_2$	1139	1321	1230	0.0048	0.0051	0.0052	0.0050	12.75
$(n\text{-}C_4H_9)_2SO_2$	1140	1323	1231	0.0041	0.0039	0.0040	0.0040	12.85
$(CH_2)_4SO_2$	1141	1323	1232	0.0036	0.0039	0.0036	0.0036	12.88
H_2SO_4	1195	1365	1280	—	—	—	—	14.88
HSO_4^-	1040	1200	1147	—	—	—	—	9.44

*From cryoscopy.
†From conductivity.
‡From conductimetric titration.
§Mean value.

as a non-electrolyte. The results for the monohydrate are thus consistent with those for the sodium salt.

$$H_3O^+.CH_3.C_6H_4.SO_3^- + H_2SO_4 = H_3O^+ + HSO_4^- + CH_3C_6H_4.SO_3H$$

Sulphamide.—The ν'-factor of 1.9 and the electrical conductivity measurements (γ = 1.0) show that sulphamide probably behaves as a strong base in sulphuric acid.

DISCUSSION

In a following paper (12) we show that alkyl sulphonyl chlorides and fluorides and methylmethanesulphonate behave as non-electrolytes in sulphuric acid and it has been established previously that sulphuryl chloride, dimethyl sulphate, and methanesulphonic acid doubtless also behave as non-electrolytes. In this paper we have found that aryl-sulphonic acids and diaryl sulphones behave as non-electrolytes, dialkyl sulphones as rather weak bases, and dimethyl sulphoxide as a strong base. Previously on the basis of shifts in solvent bands in the infrared spectra Barnard, Fabian, and Koch (19), concluded that sulphoxides form stronger hydrogen bonds than do sulphones. They attributed this result to the greater basicity (polar character), of the S—O bonds in sulphoxides as compared to sulphones, and on the basis of the S—O bond stretching force constants they showed that indeed the S—O bonds in sulphoxides are weaker than those in sulphones. Recently correlations have been obtained between S—O bond lengths, force constants (i.e. stretching frequencies), and bond orders (20). It is thus of interest to attempt to correlate the basicities of compounds containing S—O bonds with the nature of these bonds as shown by, for example, the S—O stretching frequencies.

Tables III and IV show the S—O stretching frequencies of the compounds of interest to this paper. Some of them have been determined in this work while others have been taken from previous papers (18, 25). In the case of compounds containing an SO_2 group use is made of the "Lehmann average rule" (21) to obtain the "equivalent S—O stretching frequency" from the observed symmetric and asymmetric stretches [$\nu_{SO} = (\nu_{sym}+\nu_{asym})/2$]. Immediately it is clear that a decrease in ν_{SO} is paralleled by an increase in basicity.

The H_0 functions for aqueous sulphuric acid solutions have recently been redetermined by Jorgenson and Harrter (22), who found that, near to the composition 100% H_2SO_4, the H_0 function differs by -1.1 log units from the previous scale recommended by Paul and Long (27). It therefore seems reasonable to take H_0 for 100% sulphuric acid equal to -12.2 since Paul and Long give -11.1 for acid of this composition. pK_{BH^+} values

Can. J. Chem. Downloaded from www.nrcresearchpress.com by 210.87.254.5 on 09/05/12
For personal use only.

TABLE IV

pK_{BH^+} and K_b values for some compounds, calculated from their S—O stretching frequencies

	ν_{sym}	ν_{asym}	ν_{SO}	$-pK_{BH^+}$	K_b (moles kg^{-1})
CH_3SO_2F	1204	1400	1302	16.0	3×10^{-6}
CH_3SO_2Cl	1176	1374	1275	14.9	3×10^{-5}
$C_2H_5SO_2F$	1191	1385	1288	15.4	1×10^{-5}
$C_2H_5SO_2Cl$	1170	1368	1269	14·6	7×10^{-5}
$CH_3O\cdot SO_2\cdot CH_3$	1171	1358	1265	14.4	1×10^{-4}
SO_2Cl_2	1182	1414	1298	15.9	3×10^{-6}
$(C_6H_5)_2SO_2$	1161	1326	1244	13.4	1×10^{-3}
$C_6H_5\cdot SO_2\cdot C_6H_4\cdot NO_2$	1163	1341	1252	13.7	4×10^{-4}
$(CH_3O)_2SO_2$	1193	1412	1302	15.9	3×10^{-6}
$C_6H_5SO_3H$	1182	1372	1277	15.1	2×10^{-5}
$CH_3\cdot C_6H_4SO_3H$	1170	1356	1263	14.2	1×10^{-4}
SO_2	1150	1334	1242	13.3	1×10^{-3}
SO_3	1069	1390	1283	15.2	2×10^{-5}
HSO_3F	1230	1445	1338	17.7	6×10^{-8}
HSO_3Cl	1209	1408	1308	16.3	1×10^{-6}
CH_3SO_3H	1174	1354	1264	14.3	1×10^{-4}

for the sulphones can be obtained by combining the expression $K_b = [BH^+][HSO_4^-]/[B]$ with the Hammett acidity function relationship

$$H_0 = pK_{BH^+} - \log [BH^+]/[B]$$

to give

$$H_0 = pK_{BH^+} - \log K_b - \log [HSO_4^-]$$

and since for acid of 100% composition $H_0 = -12.20$ and $[HSO_4^-] = 0.0178\ m$ at 25° C, (23) we obtain

$$pK_{BH^+} = -12.20 + \log K_b + 1.75,$$

or

$$pK_{BH^+} = -10.45 + \log K_b.$$

The pK_{BH^+} values calculated from this equation for the sulphones are shown in Table II. It should be emphasized that the values so obtained are relative to the H_0 function of 100% H_2SO_4, the value of which is based on indicator measurements on amine type bases. It is unlikely that the ratio f_{BH^+}/f_B (the ratio of activity coefficients for charged and uncharged base) will be the same for amines and for compounds containing S—O bonds so that the pK_{BH^+} scale derived here is quite arbitrary.

For the species H_2SO_4 and HSO_4^- the pK_{BH^+} values may be calculated directly from equation [1], since in the case of H_2SO_4 $[BH^+]/[B] = [H_3SO_4^+]/[H_2SO_4] = 0.0139/10.2 = 0.00136$, and for HSO_4^- $[BH^+]/[B] = [H_2SO_4]/[HSO_4^-] = 10.2/0.0178 = 573.3$ (23) (25° C).

pK_{BH^+} values are plotted against ν_{SO} in Fig. 3 and give a linear plot. A similar correlation of pK_{BH^+} with ν_{CO} of carbonyl compounds has been established previously by Stewart and Yates (24), who also found a linear relation. These authors also established a linear correlation between ν_{CO} and the Hammett σ functions of substituted aryl compounds. Recently Marziano, Montaudo, and Passerini (25) obtained similar relationships between ν_{SO} and the Hammett σ functions of substituted aryl sulphones.

Use can now be made of the correlation of pK_{BH^+} values and ν_{SO} to predict the basicities of other compounds containing S—O bonds. ν_{SO} and interpolated pK_{BH^+} and K_b values for a number of compounds are shown in Table IV. Since the ionization of a base with

Can. J. Chem. Downloaded from www.nrcresearchpress.com by 210.87.254.5 on 09/05/12
For personal use only.

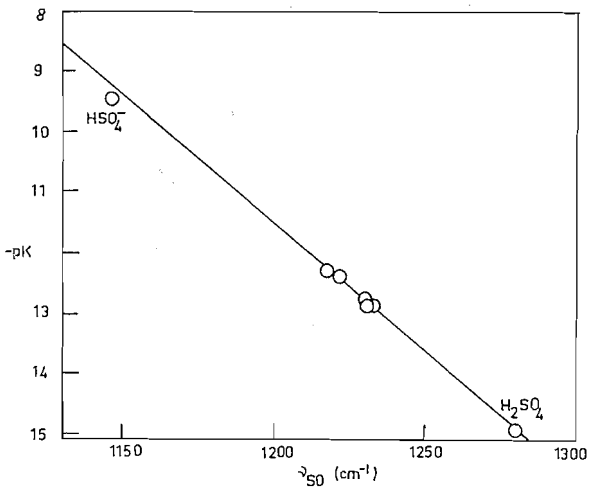

FIG. 3. Correlation of ν_{SO} with pK_{BH^+} values.

a K_b value $<1\times10^{-3}$ would be very difficult to detect experimentally it is quite reasonable that all the compounds less basic than tetramethylene sulphone would appear, from both cryoscopic and conductimetric measurements, to behave as non-electrolytes. Sulphur dioxide and diphenyl sulphone are just on the border line. Cryoscopically a small degree of ionization would be obscured by possible non-ideality effects.

Sulphur trioxide.—For monomeric sulphur trioxide the K_b value of 2×10^{-5} indicates a very weakly basic species, in fact the basicity is very similar to that of H_2SO_4 itself. Since SO_3 occurs only in negligibly small concentration in 95–100% H_2SO_4 it can be concluded that only negligible quantities of HSO_3^+ could be formed in these systems, which rules out the possibility of the participation of HSO_3^+ in sulphonations in these solvents.

Sulphamide.—For protonation on oxygen the S—O stretching frequencies lead us to expect only weakly basic behavior. However, sulphamide is found to behave as a strong base in H_2SO_4 solutions which implies that protonation must occur on a nitrogen atom. This conclusion is in agreement with that from the recent n.m.r. studies of Birchall and Gillespie (26), where N-protonation of sulphamide was found in solvent fluorosulphuric acid.

ACKNOWLEDGMENTS

The National Research Council of Canada and the University of Toronto Advisory Committee on Scientific Research are thanked for generous financial support. Professor R. J. Gillespie of McMaster University is thanked for discussion of the manuscript.

REFERENCES

1. R. HANTZSCH. Z. Physik. Chem. **65**, 41 (1908).
2. R. J. GILLESPIE. J. Chem. Soc. 2542 (1950).
3. R. J. GILLESPIE, E. D. HUGHES, and C. K. INGOLD. J. Chem. Soc. 2473 (1950).
4. H. H. SZMANT and G. A. BROST. J. Am. Chem. Soc. **73**, 4175 (1951).
5. H. H. SZMANT and R. L. LAPINSKI. J. Am. Chem. Soc. **74**, 4395 (1952).
6. R. J. GILLESPIE and R. C. PASSERINI. J. Chem. Soc. 3850 (1956).
7. R. J. GILLESPIE and S. WASIF. J. Chem. Soc. 221 (1953).
8. J. BARR, R. J. GILLESPIE, and E. A. ROBINSON. Can. J. Chem. **39**, 1266 (1961).
9. E. A. ROBINSON. Ph.D. Thesis, University of London, London, England. 1958.
10. R. J. GILLESPIE and E. A. ROBINSON. J. Chem. Soc. 4233 (1957).

Can. J. Chem. Downloaded from www.nrcresearchpress.com by 210.87.254.5 on 09/05/12
For personal use only.

11. J. R. BRAYFORD and P. A. H. WYATT. J. Chem. Soc. 3453 (1955).
12. S. K. HALL and E. A. ROBINSON. Can. J. Chem. To be published.
13. R. J. GILLESPIE, J. V. OUBRIDGE, and C. SOLOMONS. J. Chem. Soc. 1804 (1957).
14. S. J. BASS and R. J. GILLESPIE. J. Chem. Soc. 814 (1960).
15. S. J. BASS, R. J. GILLESPIE, and E. A. ROBINSON. J. Chem. Soc. 821 (1960).
16. R. J. GILLESPIE and C. SOLOMONS. J. Chem. Soc. 1796 (1957).
17. R. H. FLOWERS, R. J. GILLESPIE, and E. A. ROBINSON. Can. J. Chem. **38**, 1363 (1961).
18. E. A. ROBINSON. Can. J. Chem. **39**, 247 (1961).
19. D. BARNARD, J. M. FABIAN, and H. P. KOCH. J. Chem. Soc. 2442 (1949).
20. R. J. GILLESPIE and E. A. ROBINSON. Can. J. Chem. **41**, 2074 (1963).
21. W. J. LEHMANN. J. Mol. Spectry. **7**, 261 (1961).
22. M. J. JORGENSON and R. D. HARRTER. J. Am. Chem. Soc. **85**, 878 (1963).
23. R. J. GILLESPIE, E. A. ROBINSON, and C. SOLOMONS. J. Chem. Soc. 4320 (1960).
24. R. STEWART and K. YATES. J. Am. Chem. Soc. **82**, 4059 (1960).
25. N. MARZIANO, G. MONTAUDO, and R. C. PASSERINI. Gazz. Chim. Ital. **92**, 121 (1962).
26. T. BIRCHALL and R. J. GILLESPIE. Can. J. Chem. **41**, 2642 (1963).
27. M. A. PAUL and F. A. LONG. Chem. Rev. **57**, 1 (1957).

Can. J. Chem. Downloaded from www.nrcresearchpress.com by 210.87.254.5 on 09/05/12
For personal use only.

Can. J. Chem. Downloaded from www.nrcresearchpress.com by 210.87.254.40 on 09/05/12
For personal use only.

PERFLUOROALKYL ARSENICALS

PART IX. SOME REACTIONS OF COMPOUNDS CONTAINING As–As BONDS[1]

W. R. CULLEN AND N. K. HOTA
Department of Chemistry, University of British Columbia, Vancouver, British Columbia

Received August 20, 1963

ABSTRACT

Arsenobenzene reacts with CF_3I to give $C_6H_5As(CF_3)_2$, $C_6H_5As(CF_3)I$, and $C_6H_5AsI_2$. $C_6H_5As(CF_3)I$ and AgCl yield $C_6H_5As(CF_3)Cl$. The compounds $CF_2=CFX$ react with $(CH_3)_2As—As(CH_3)_2$ under mild conditions to give 1:1 adducts $(CH_3)_2As—CF_2CFX—As(CH_3)_2$ (X = CF_3, Br). Some $(CH_3)_2As—CF=CF_2$ is produced when X = Br and is the major product when X = I. When X = F a 1:4 adduct $(CH_3)_2As—(CF_2CF_2)_4—As(CH_3)_2$ is probably formed on ultraviolet irradiation. $(CH_3)_2As—As(CH_3)_2$ reacts with $CF_3C{\equiv}CCF_3$ to give *cis* and *trans* $(CH_3)_2AsC(CF_3){=}C(CF_3)As(CH_3)_2$ and with $\overline{CF{=}CFCF_2CF_2}$ to give $(CH_3)_2AsF$ and $(CH_3)_2As—\overline{CF{=}CFCF_2CF_2}$.

DISCUSSION AND RESULTS

Compounds containing weak bonds such as As–As (1), P–P (1, 2, 3), and Sn–Sn (4, 5) are readily cleaved when treated with perfluoroalkyl iodides, for example,

$$(CH_3)_2As—As(CH_3)_2 + CF_3I \rightarrow (CH_3)_2AsCF_3 + IAs(CH_3)_2.$$

We have now found that the As–As bonds in arsenobenzene, better named hexaphenylcyclohexaarsine (6), undergo a similar reaction when heated with an excess of trifluoroiodomethane at 115°, or at lower temperatures when the reactants are exposed to ultraviolet radiation. The products are phenylbis(trifluoromethyl)arsine, iodophenyltrifluoromethylarsine, and diiodophenylarsine.

$$(C_6H_5As)_6 + CF_3I \rightarrow C_6H_5As(CF_3)_2 + C_6H_5As(CF_3)I + C_6H_5AsI_2$$

Similar products have been isolated from the thermal and photochemical reaction of tetraphenylcyclotetraphosphine with trifluoroiodomethane (2). In an attempt to extend this type of reaction to the preparation of more complex aryltrifluoromethylarsines, *p*-nitroarsenobenzene was heated to 100° with trifluoroiodomethane. After a few hours the reaction tube exploded. This result was reproducible.

Iodophenyltrifluoromethylarsine, a new compound, b.p. 136–137° (35 mm), 158° (65 mm), reacts with silver chloride to give the more volatile chloroarsine, b.p. 118° (65 mm). The iodoarsine does not react with methyl iodide in the presence of mercury to give the expected methylphenyltrifluoromethylarsine (7). However, coupling of the iodoarsine appears to take place to give a white solid diarsine which decomposes in air to benzenearsonic acid.

$$2\ C_6H_5(CF_3)AsI + Hg \rightarrow C_6H_5(CF_3)As—As(CF_3)C_6H_5 + HgI_2$$

Chlorophenyltrifluoromethylarsine reacts with bis(trifluoromethyl)arsine at 100° to give hydrogen chloride, tris(trifluoromethyl)arsine, tetrakis(trifluoromethyl)diarsine, and possibly chlorobis(trifluoromethyl)arsine. A white solid is also produced which decomposes to benzenearsonic acid on exposure to air. The formation of hydrogen chloride and an unstable solid suggests that the main reaction is a coupling one to produce a diarsine.

[1]*For a preliminary publication see W. R. Cullen, D. S. Dawson, N. K. Hota, and G. E. Styan. Chem. Ind. London, 983 (1963).*

Can. J. Chem. Downloaded from www.nrcresearchpress.com by 210.87.254.40 on 09/05/12
For personal use only.

However, analysis of the solid product indicates that it is mainly the symmetrical diarsine $(C_6H_5(CF_3)As)_2$ (Anal. Found: C, 36.6, H, 2.3%. Calc.: C, 37.9, H, 2.3%) rather than the unsymmetrical one $C_6H_5(CF_3)As—As(CF_3)_2$. Either diarsine could decompose to give benzenearsonic acid. The symmetrical diarsine could arise from reactions of the following sort (8).

$$C_6H_5(CF_3)AsCl + HAs(CF_3)_2 \rightarrow C_6H_5(CF_3)As—As(CF_3)_2 + HCl$$

$$- HCl \uparrow \downarrow + HCl$$

$$C_6H_5(CF_3)AsH + ClAs(CF_3)_2$$

$$(CF_3)_2AsH + ClAs(CF_3)_2 \rightleftarrows (CF_3)_2As—As(CF_3)_2 + HCl$$

$$C_6H_5(CF_3)AsH + ClAs(CF_3)C_6H_5 \rightleftarrows C_6H_5(CF_3)As—As(CF_3)C_6H_5 + HCl$$

Such a scheme would also explain the formation of tetrakis(trifluoromethyl)diarsine and chlorobis(trifluoromethyl)arsine. It does not, however, account for the presence of tris(trifluoromethyl)arsine in the reaction products.

There are a few examples known of the addition of olefins and acetylenes to compounds containing M–M bonds (M = P (9, 10), B (11), Sn (12), S (13)), for example

$$(CH_3)_2P—P(CH_3)_2 + C_2F_4 \rightarrow (CH_3)_2P—CF_2CF_2—P(CH_3)_2.$$

Cacodyl (tetramethyldiarsine) has now been found to react similarly with fluorine containing olefins and acetylenes. Thus when the diarsine is treated with excess hexafluoropropene under mild conditions, a 1:1 adduct, 1,2-bis(dimethylarsino)hexafluoropropane, is formed.

$$(CH_3)_2As—As(CH_3)_2 + CF_3CF=CF_2 \rightarrow (CH_3)_2As—CF(CF_3)CF_2—As(CH_3)_2$$

The adduct distills at 116–117° (50 mm) and is hydrolyzed by hot alkali to give 1,2,3,3,3,-pentafluoroprop-1-ene. The olefin is probably produced by HF elimination from the initially formed propane, which would contain two adjacent CHF groups (14).

$$(CH_3)_2As—C(CF_3)F—CF_2—As(CH_3)_2 \xrightarrow{NaOH} (CH_3)_2AsONa + CF_3CFH—CF_2H$$

$$CF_3CFH—CF_2H \longrightarrow CF_3CF=CFH + HF$$

Cacodyl also reacts easily with hexafluorobut-2-yne to give a 1:1 adduct 2,3-bis(dimethylarsino)hexafluorobut-2-ene, b.p. 42° (10^{-3} mm), 99° (17 mm).

$$(CH_3)_2As—As(CH_3)_2 + CF_3C\equiv CCF_3 \rightarrow (CH_3)_2As—C(CF_3)=C(CF_3)—As(CH_3)_2$$

The F^{19} nuclear magnetic resonance spectrum shows only two peaks of approximately equal intensity such as would be shown by an approximately equimolar mixture of the *cis* and *trans* forms of the adduct. The infrared spectrum of the adduct shows only a weak double-bond absorption at 1570 cm^{-1}. Hydrolysis gives a small amount of *trans*-1,1,1,4,4,4,-hexafluorobut-2-ene. The adduct reacts with mercuric chloride to give a complex of indefinite constitution. A similar adduct is obtained from hexamethylditin and hexafluorobut-2-yne on ultraviolet irradiation, although in this case the F^{19} n.m.r. spectrum has only one peak, indicating that only one isomer is formed (15). Grant (2) has found that the iodine catalyzed reaction of tetrakis(trifluoromethyl)diphosphine with acetylene gives a *trans* adduct.

$$(CF_3)_2P—P(CF_3)_2 + HC\equiv CH \rightarrow (CF_3)_2P—CH=CH—P(CF_3)_2$$

In the present investigation we have found that tetrakis(trifluoromethyl)-diphosphine and -diarsine do not react with hexafluorobut-2-yne at 100°. The nature and variety of

these addition reactions and their products makes it difficult to suggest a reaction mechanism without a much more detailed study; however, the *trans* orientation of one product and the 1:1 distribution of isomers in another seems to rule out a general four-center mechanism.

Cacodyl does not react immediately with tetrafluoroethylene at 20°, but, when the two are irradiated with ultraviolet light, reaction does occur. Trimethylarsine is produced in small amounts, but the main reaction product is an involatile, air-stable liquid which analysis indicates to be mainly the 1:4 adduct $(CH_3)_2As—(C_2F_4)_4—As(CH_3)_2$. The F^{19} n.m.r. spectrum supports this result. It shows three broad lines with chemical shifts of the magnitude expected for CF_2 groups in a chain (16). The relative areas of the peaks are 58:30:27, but because of overlap the ratio of the smaller peaks, 30:27, is not very accurate. However, their total relative area of 57 is reliable. These figures strongly indicate that the relative areas are in fact 2:1:1 or 4:2:2, the ratios which would be expected from the compound

$$(CH_3)_2As\cdot\overset{i}{C}F_2\cdot\overset{ii}{C}F_2\cdot(\overset{iii}{C_2F_4})_2\cdot\overset{ii}{C}F_2\cdot\overset{i}{C}F_2\cdot As(CH_3)_2$$

where the fluorines on carbon atoms i, ii, and iii would have different chemical shifts (16). Similar products have been obtained from the iodine-catalyzed reaction of tetrafluoroethylene with dimethyl disulphide (13).

$$(CH_3)_2S_2 + C_2F_4 \rightarrow CH_3S(C_2F_4)_nSCH_3$$

The reaction of cacodyl with hexafluorocyclobutene at 20° yields fluorodimethylarsine and the novel compound 1-dimethylarsinopentafluorocyclobutene, b.p. 125°, in good yield. The n.m.r. spectrum of this compound, which will be reported in detail later, is complex but contains three general regions of fluorine absorption as expected. The infrared spectrum shows a strong double-bond absorption at 1659 cm^{-1}. The method of preparation of the compound and the results described above suggest that the first product of the reaction is a 1:1 adduct which eliminates fluorodimethylarsine to give the cyclobutene derivative.

$$(CH_3)_2As—As(CH_3)_2 + \overline{CF{=}CF_2CF_2}\overline{CF_2} \rightarrow [(CH_3)_2As—\overline{CFCF_2CF_2}\overline{CF}—As(CH_3)_2]$$
$$\downarrow$$
$$FAs(CH_3)_2 + \overline{CF_2CF_2CF{=}C}—As(CH_3)_2$$

A similar reaction sequence has been suggested (17) to account for the formation of 1-alkyl-pentafluorocyclobutenes from the reaction of hexafluorocyclobutene with alkylmagnesium halides. The same cyclobutene derivative can be made by reacting hexafluorocyclobutene with the "Grignard reagent" made from dimethylarsine (18).

$$(CH_3)_2AsMgBr + \overline{CF{=}CFCF_2}\overline{CF_2} \rightarrow (CH_3)_2As—\overline{C{=}CFCF_2}\overline{CF_2} + MgBrF$$

A 1:1 adduct is probably formed when the diarsine reacts with bromotrifluoroethylene under mild conditions, although in this case analysis of the product 1-bromo-1,2-bis(dimethylarsino)trifluoroethane, b.p. 65° (10^{-3} mm), indicated it to be impure. The adduct slowly decomposes at 20° to give dimethyltrifluorovinylarsine and presumably bromodimethylarsine.

$$(CH_3)_2As—As(CH_3)_2 + CF_2{=}CFBr \rightarrow (CH_3)_2As—CF_2CFBr—As(CH_3)_2 \rightarrow$$
$$(CH_3)_2AsCF{=}CF_2 + (CH_3)_2AsBr$$

Both these decomposition products as well as fluorodimethylarsine, the dimer of bromotrifluoroethylene, and other unidentified fractions are also formed in the initial reaction

Can. J. Chem. Downloaded from www.nrcresearchpress.com by 210.87.254.40 on 09/05/12
For personal use only.

to produce the adduct. Addition followed by elimination is probably the source of the dimethylperfluorovinylarsine and the bromodimethylarsine. In a similar way the reaction of bromotrifluoroethylene with tetrakis(trifluoromethyl)-diarsine and -diphosphine at 100° probably gives bis(trifluoromethyl)trifluorovinyl-arsine and -phosphine (19). Dimethyltrifluorovinylarsine is also produced when cacodyl and trifluoroiodoethylene interact at 20°. Iododimethylarsine and an unidentified volatile yellow solid are the other products. A stable adduct $(CH_3)_2As—(CF_2CFI)_n—As(CH_3)_2$ does not seem to be formed in this last reaction; the least volatile reaction products are air sensitive and the analytical data fit cacodyl better than any adduct of cacodyl with the olefin.

Dimethyltrifluoromethylarsine is produced when trifluoroiodomethane reacts with trimethylarsine (20) and with iododimethylarsine in the presence of mercury (1). It has now been found that trimethylarsine slowly interacts with trifluorovinyl bromide and iodide but does not give the expected dimethyltrifluorovinylarsine. This compound can, however, be prepared in low yield from the reaction of trifluorovinyl iodide with iododimethylarsine in the presence of mercury.

$$CF_2{=}CFI + Hg + IAs(CH_3)_2 \rightarrow CF_2{=}CFAs(CH_3)_2 + HgI_2$$

Trifluorovinyl bromide does not react with either iododimethylarsine or diiodomethylarsine in the presence of mercury. Since the vinyl bromide readily reacts with cacodyl yet does not react with iododimethylarsine and mercury, it seems that cacodyl itself is not a reactive intermediate in these coupling reactions. This conclusion is substantiated by the failure of hexafluorobut-2-yne to react with iododimethylarsine in the presence of mercury.

Dimethyltrifluorovinylarsine, b.p. 71°, is a colorless liquid slightly less volatile than trimethylarsine, b.p. 51°, and dimethyltrifluoromethylarsine, b.p. 58°. It is slowly hydrolyzed by hot alkali to trifluoroethylene, a result analogous to the slow hydrolysis of dimethyltrifluoromethylarsine to fluoroform (21). There appears to be a considerable difference in the hydrolytic stability of the easily hydrolyzed tris(trifluoromethyl)arsine and the stable tris(trifluorovinyl)arsine (22).

EXPERIMENTAL

Apparatus and Techniques

Most of the methods used in the present investigation have been described in earlier papers in this series. The F^{19} n.m.r. spectra were obtained using a Varian spectrometer operating at 56.4 Mc/sec. The spectra are reported relative to a trifluoroacetic acid external standard. A dinonylphthalate on firebrick column (12 ft) in an Aerograph instrument was used for vapor phase chromatographic separations. Helium was used as the carrier gas and the temperature of the column is indicated in the text. Starting materials were prepared by methods described in the literature.

Reaction of Arsenobenzene with Trifluoroiodomethane

(*a*) Arsenobenzene (10.0 g) and trifluoroiodomethane (18 g) did not react at 20° (3 days). However, reaction occurred at 115° (1 day) giving a dark-brown liquid product. Trifluoroiodomethane (5.4 g) was recovered, and the remaining contents of the reaction tube were distilled in a nitrogen atmosphere (65 mm) to give phenylbis(trifluoromethyl)arsine (8 g, 42% yield, b.p. 88°) of known infrared spectrum and a pale-yellow liquid shown by analysis to be *iodophenyltrifluoromethylarsine* (6.2 g, 27% yield, b.p. 158°). Anal. Found: C, 23.9; H, 1.54%. Calc. for $C_7H_5AsF_3I$: C, 24.2; H, 1.44%. The residue in the still pot (5.3 g) was largely diiodophenylarsine. The infrared spectrum of iodophenyltrifluoromethylarsine showed the following absorption bands (liquid film): 3055(w), 2230(vw), 1575(vw), 1482(m), 1435(m), 1330(m), 1302(w), 1252(m), 1185(s), 1110(broad vs), 1072(s), 1020(m), 997(m), 735(s), 725(m), 687(s) cm^{-1}.

(*b*) A similar reaction took place when arsenobenzene and trifluoroiodomethane were irradiated with ultraviolet light.

Reactions of Iodophenyltrifluoromethylarsine

(a) With silver chloride.—The arsine (3.4 g) and an excess of freshly prepared, dry silver chloride were shaken at 20° for 2 days. A colorless liquid, *chlorophenyltrifluoromethylarsine*, which was sufficiently volatile

Can. J. Chem. Downloaded from www.nrcresearchpress.com by 210.87.254.40 on 09/05/12
For personal use only.

to be taken into the vacuum system, was quantitatively produced. It distilled at 118° (65 mm) in a nitrogen atmosphere. Anal. Found: C, 33.0; H, 1.76; As, 28.9; Cl, 13.6%. Calc. for $C_7H_5AsClF_3$: C, 32.7; H, 1.93; As, 29.2; Cl, 13.8%. The infrared spectrum was almost identical with that of the iodoarsine.

(b) With iodomethane in the presence of mercury.—The arsine (6.2 g), iodomethane (13.4 g), and mercury (40 g) were shaken for 3 weeks at 20°. Iodomethane (13.3 g) was quantitatively recovered. A white solid in the reaction tube was extracted with benzene to give a solution which slowly deposited crystals of benzenearsonic acid. The acid was identified by means of its X-ray powder photograph.

Reaction of Chlorophenyltrifluoromethylarsine with Bis(trifluoromethyl)arsine

The chloroarsine (0.7 g) and bis(trifluoromethyl)arsine (0.812 g) were left at 100° for 7 days. Trap-to-trap distillation gave hydrogen chloride (0.043 g; mol. wt. 36.6), bis(trifluoromethyl)arsine (0.466 g), chlorophenyltrifluoromethylarsine (0.14 g), and a middle fraction which contained tris(trifluoromethyl)arsine, tetrakis(trifluoromethyl)diarsine, and possibly a trace of chlorobis(trifluoromethyl)arsine, all of known infrared spectra. A cream solid which was left in the reaction tube was highly unstable to air. Anal. Found: C, 36.5; H, 2.33%. The end product of the decomposition was benzenearsonic acid.

Reaction of Cacodyl with Hexafluoropropene

The diarsine (5.3 g) and the propene (16.0 g) were left at 20° for 13 days. A small amount (1.9 g) of a liquid, b.p. 36–38° (10^{-3}) mm, which fumed slightly in air was isolated. The infrared spectrum of this fraction showed the presence of C–F and As–CH_3 groups. All reactants and products were combined and heated to 50° (7 days). Distillation of the less volatile material in a nitrogen atmosphere at 50 mm gave 1.1 g of cacodyl, b.p. 78°; a middle fraction, b.p. 78–114°; and 1.6 g (18% yield) of *1,2-bis(dimethylarsino)-1,1,2,3,3,3-hexafluoropropane*, b.p. 114–116°. The last fraction still fumed in air, so air was bubbled through it until the fuming had ceased. An analytical sample, b.p. 116–117° (50 mm) was obtained from another distillation. Anal. Found: C, 23.2; H, 3.29; As, 41.6; F, 31.8%. Calc. for $C_7H_{12}As_2F_6$: C, 23.3; H, 3.33; As, 41.6; F, 31.7%. The infrared spectrum (liquid film) showed the following bands; 3005(w), 2915(w), 1670(w), 1418(m), 1277(s), 1265(s), 1195(broad, vs), 1142(s), 1158(broad, m), 999(w), 912(broad, m), 850(m), 798(w), 720(w) cm^{-1}. When the adduct (0.291 g) was heated (100°, 24 hours) with 8 ml of 10% aqueous sodium hydroxide, 0.034 g of 1,2,3,3,3-pentafluoroprop-1-ene, of known infrared spectrum (23), was produced.

Reaction of Cacodyl with Hexafluorocyclobutene

Cacodyl (5.0 g) and the butene (17.8 g) were left for 12 days at 20°. Apart from some white deposit on the glass all the contents of the tube were volatile. Trap-to-trap distillation isolated 1.149 g of fluorodimethylarsine, which attacked glass and which stopped in a trap cooled to −64°. Anal. Found: C, 18.2; H, 4.7%; mol. wt. 127; b.p. 66–68° (by distillation in a nitrogen atmosphere at 760 mm). Calc. for C_2H_6AsF: C, 19.4; H, 4.8%; mol. wt. 124; b.p. 75° (24). The most volatile fraction was perfluorocyclobutene (14.6 g), which contained some fluorodimethylarsine. The least volatile fraction (7.0 g) was distilled in a nitrogen atmosphere to give 0.52 g of fluorodimethylarsine, b.p. 70–75°, and 4.9 g (83% yield) of *1-dimethylarsinopentafluorocyclobutene*, b.p. 122–125°. An analytical sample, b.p. 125°, was obtained by redistillation. Anal. Found: C, 29.0; H, 2.41; As, 30.0; F, 38.0%. Calc. for $C_6H_6AsF_5$: C, 29.0; H, 2.42; As, 30.1; F, 38.4%. The infrared spectrum showed the following bands (liquid film): 3010(w), 2920(w), 2360(w), 2349(sh,w), 1695(s), 1424(w), 1397(s), 1374(m), 1275(vs), 1206(m), 1117(vs), 1104(s), 950(vs), 900(w), 865(m), 812(m) cm^{-1}.

Reaction of Cacodyl with Bromotrifluoroethylene

The diarsine (4.0 g) and bromotrifluoroethylene (16.5 g) were left for 7 days at 20°. Qualitative investigation showed that although some reaction had occurred considerable amounts of the diarsine were still present. The reactants were then heated to 50° (5 days). The volatile material was taken into the vacuum system leaving 4.3 g of a pale-yellow liquid in the reaction tube. Trap-to-trap distillation gave 13.5 g of bromotrifluoroethylene, 0.4 g of 1,2-dibromohexafluorocyclobutane (25), and 1.7 g of a mixture which was separated by vapor phase chromatography (v.p.c.) at 135° into fluorodimethylarsine (0.2 g; mol. wt. 121; calc. mol. wt. 124) of known infrared spectrum, bromodimethylarsine (0.4 g) of known retention time and infrared spectrum, and one other volatile fraction. This last fraction was a mixture of dimethyltrifluorovinylarsine and one other unidentified unsaturated compound.

The involatile reaction product distilled at 65° (10^{-3} mm) and analysis of the pale-yellow distillate suggested that it was an impure sample of 2-bromo-1,2-bis(dimethylarsino)-1,1,2-trifluoroethane. Anal. Found: C, 21.0; H, 3.47; As, 40.3; Br, 18.7; F, 16.9%. Calc. for $C_6H_{12}As_2BrF_3$: C, 19.4; H, 3.24; As, 40.4; Br, 21.6; F, 15.4%. The infrared spectrum showed the following bands (liquid film): 2985(m), 2905(m), 2800(w), 2330(w), 1723(m), 1705(m), 1420(m), 1290(m), 1265(m), 1152(m), 1110(m), 1067(s), 1015(m), 985(m), 904(m), 850(s), 825(m), 792(m), 682(m) cm^{-1}. An ethanolic solution of the adduct reacted with an ethanolic solution of mercuric chloride to give a white precipitate which was insoluble in boiling ethanol. An infrared spectrum of the solid showed the presence of C–H and the absence of C–F groups. The adduct slowly decomposed on standing at 20°, since some months after its preparation it was found to be volatile enough to be taken into the vacuum system where trap-to-trap distillation isolated slightly impure dimethyltrifluorovinylarsine.

Can. J. Chem. Downloaded from www.nrcresearchpress.com by 210.87.254.40 on 09/05/12
For personal use only.

Reaction of Cacodyl with Iodotrifluoroethylene

Cacodyl (1.7 g) and the ethylene (10.0 g) were left for 7 days at 20°. Trap-to-trap distillation gave iodotrifluoroethylene (8.9 g), a volatile unidentified yellow solid, iododimethylarsine, and dimethyltrifluorovinylarsine. These fractions could not be separated quantitatively. The trifluorovinylarsine was purified by v.p.c. (90°) to give 0.1 g of product. An involatile air-sensitive material which contained As–CH_3 and some C–F remained in the reaction tube. Anal. Found: C, 24.8; H, 4.9%.

Reaction of Cacodyl with Tetrafluoroethylene

When cacodyl (1.5 g) was exposed to the olefin at a pressure of 30 cm (20°) there was no drop in pressure. The diarsine (1.5 g) and the olefin (2.9 g) were irradiated in a sealed tube with ultraviolet light (24 hours), to give tetrafluoroethylene (0.4 g) and trimethylarsine (0.053 g) of known infrared spectra. The air-stable colorless involatile product (4.3 g) distilled at 10^{-3} mm in the range 110–125°. Elemental analysis of a middle cut, b.p. 120°, showed it to be probably a 1:4 addition product of the diarsine and the olefin, $(CH_3)_2As(CF_2CF_2)_4As(CH_3)_2$. Anal. Found: C, 23.2; H, 1.8; As, 22.7; F, 51.7%. Calc. for $C_{12}H_{12}As_2F_{16}$: C, 23.6; H, 1.97; As, 24.6; F, 49.9%. Two other cuts were taken and these analyzed as follows: C, 23.5; H, 2.4% (110–120°); C, 22.5; H, 1.6% (120–125°). The infrared spectra of the three fractions were very similar. The F^{19} n.m.r. spectrum of the third cut showed peaks at +2450, +2290, and +2240 c/s of relative area 58:30:27.

Reaction of Cacodyl with Hexafluorobut-2-yne

The acetylene (7.5 g) and the diarsine (5.0 g) reacted on warming to 20° to give a reddish-brown solution. The tube was left at 20° for 14 days. Hexafluorobut-2-yne (4.3 g) was the only volatile substance present in the tube. The involatile, air-stable reaction product distilled at 42° (10^{-3} mm) and at 99° (17 mm) and was identified as *2,3-bis(dimethylarsino)-1,1,1,3,3,3-hexafluorobut-2-ene*. Anal. Found: C, 26.0; H, 3.4; As, 40.2; F, 30.9%, mol. wt. 350. Calc. for $C_8H_{12}As_2F_6$: C, 25.8; H, 3.22; As, 40.3; F, 30.6%, mol. wt. 372. The infrared spectrum showed the following bands (liquid film): 2990(w), 2915(w), 1570(w), 1425(m), 1300(w), 1230(vs), 1175(sh,s), 1152(vs), 1135(vs), 897(w), 867(w), 852(w), 652(m) cm^{-1}. The F^{19} n.m.r. spectrum consisted of two peaks of nearly equal intensity at −1368 and −1483 c/s. The adduct (0.283 g) was hydrolyzed with 15% aqueous sodium hydroxide (5 days, 110°) to give a small amount (0.019 g) of *trans*-1,1,1,3,3,3-hexafluorobut-2-ene, of known infrared spectrum. The adduct had partially decomposed to a black solid and unidentified volatile products after 3 days at 150°. When ethanolic solutions of the adduct and mercuric chloride were mixed, a cream precipitate was obtained which was recrystallized from ethanol. Anal. Found: C, 11.5; H, 1.29; As, 12.7; Cl, 14.4; F, 10.7; Hg, 38.1%.

Reaction of Hexafluorobut-2-yne with Tetrakis(trifluoromethyl)-diarsine and -diphosphine

The arsine (1.53 g) and the acetylene (4.9 g) did not react after 7 days at 100° or, in a separate experiment, after 10 days at 150°. The acetylene (4.9 g) and the diarsine (1.50 g) were recovered. Similarly, the acetylene and the diphosphine did not react when heated to 100° for 2 days.

Reaction of Bromotrifluoroethylene with Iodoarsines in the Presence of Mercury

(*a*) Iododimethylarsine (25.7 g), mercury (250 g), and bromotrifluoroethylene (49.0 g) were shaken at 20° for 11 days. The only volatile substance present in the reaction tube was bromotrifluoroethylene (48.7 g).

(*b*) Diiodomethylarsine (18.9 g), mercury (200 g), and bromotrifluoroethylene (49.6 g) did not produce any trifluorovinylarsine after being shaken for 18 days at 20°. The weight of the ethylene recovered was 49.0 g.

Reaction of Iodotrifluoroethylene with Iododimethylarsine in the Presence of Mercury

Iododimethylarsine (24.2 g), mercury (240 g), and iodotrifluoroethylene (66 g) were shaken for 10 days at 20°. Iodotrifluoroethylene (64.4 g) was recovered and *dimethyltrifluorovinylarsine* (1.0 g) was produced. The arsine was identified by its molecular weight of 181 (calc. mol. wt. 186). An analytical sample was obtained by v.p.c. at 55°. Found: C, 26.0; H, 3.31; As, 40.3; F, 30.4%. Calc. for $C_4H_6AsF_3$: C, 25.8; H, 3.26; As, 40.4; F, 30.6%. Infrared spectrum (vapor): 3010(m), 2920(m), 1780(w), 1730(s), 1428(m), 1298(s), 1140(s), 1020(s), 897(m), 852(m), 715(m) cm^{-1}. The boiling point was found to be 71°, the latent heat of vaporization 8180 cal/mole, and Trouton's constant 23.8. When the arsine (0.086 g) was hydrolyzed by 15% aqueous sodium hydroxide (100°, 24 hours) trifluoroethylene (0.0094 g) was produced. Unreacted arsine was also isolated.

Reaction of Iododimethylarsine with Hexafluorobut-2-yne in the Presence of Mercury

Iododimethylarsine (21.0 g) and hexafluorobut-2-yne (30.0 g) did not react on being shaken for 7 days at 20° in the presence of 217 g of mercury. The butyne was recovered quantitatively.

Reaction of Trimethylarsine with Bromotrifluoroethylene and Iodotrifluoroethylene

Trimethylarsine (0.60 g) and bromotrifluoroethylene (6.5 g) were kept at 20° for 1 year. Trap-to-trap distillation of the volatile material recovered 6.4 g of bromotrifluoroethylene and 0.54 g of trimethylarsine. A small amount of unidentified brown solid remained in the reaction tube. The recovered arsine was left with 6.0 g of iodotrifluoroethylene for 14 days. Examination of the volatile contents of the reaction tube showed only the presence of starting materials. A small amount of dark solid remained in the reaction tube.

Can. J. Chem. Downloaded from www.nrcresearchpress.com by 210.87.254.40 on 09/05/12
For personal use only.

ACKNOWLEDGMENTS

The authors wish to acknowledge financial assistance from the National Research Council of Canada. They are also indebted to Dr. L. W. Reeves and Dr. E. J. Wells for assistance in obtaining and interpreting the n.m.r. spectra. Microanalyses were carried out by Dr. Alfred Bernhardt.

REFERENCES

1. W. R. CULLEN. Can. J. Chem. **38**, 439 (1960).
2. M. A. A. BEG and H. C. CLARK. Can. J. Chem. **39**, 564 (1961).
3. M. A. A. BEG and H. C. CLARK. Can. J. Chem. **40**, 283 (1962).
4. H. C. CLARK and C. J. WILLIS. J. Am. Chem. Soc. **82**, 1888 (1960).
5. H. D. KAESZ, J. R. PHILLIPS, and F. G. A. STONE. J. Am. Chem. Soc. **82**, 6228 (1960).
6. K. HEDBERG, E. W. HUGHES, and J. WASER. Acta. Cryst. **14**, 369 (1961).
7. W. R. CULLEN. Can. J. Chem. **38**, 445 (1960).
8. W. R. CULLEN. Can. J. Chem. **41**, 322 (1963).
9. A. B. BURG. J. Am. Chem. Soc. **83**, 2226 (1961).
10. L. R. GRANT. Ph.D. Thesis, University of Southern California, Los Angeles, California. 1961.
11. A. K. HOLLIDAY and A. G. MASSEY. J. Chem. Soc. 43 (1960).
12. M. A. A. BEG and H. C. CLARK. Chem. Ind. London, 140 (1962).
13. W. E. MANFORD. U.S. Patent No. 2,443,003 (1948).
14. R. N. HASZELDINE and B. R. STEELE. J. Chem. Soc. 1199 (1953).
15. W. R. CULLEN and G. E. STYAN. Unpublished results.
16. J. A. POPLE, W. G. SCHNEIDER, and M. I. BERNSTEIN. High resolution nuclear magnetic resonance. McGraw-Hill. New York. 1959.
17. J. D. PARK and R. FONTANELLI. J. Org. Chem. **28**, 258 (1963).
18. W. R. CULLEN and D. S. DAWSON. Unpublished results.
19. W. R. CULLEN and N. K. HOTA. Unpublished results.
20. R. N. HASZELDINE and B. O. WEST. J. Chem. Soc. 3631 (1956).
21. R. N. HASZELDINE and B. O. WEST. J. Chem. Soc. 3880 (1957).
22. H. D. KAESZ, S. L. STAFFORD, and F. G. A. STONE. J. Am. Chem. Soc. **81**, 6336 (1959).
23. CHEMICAL SOCIETY LONDON. Infrared spectrum No. 43.
24. W. R. CULLEN and L. G. WALKER. Can. J. Chem. **38**, 472 (1960).
25. W. R. CULLEN and P. SINGH. Can. J. Chem. **41**, 2397 (1963).

Can. J. Chem. Downloaded from www.nrcresearchpress.com by 210.87.254.40 on 09/05/12
For personal use only.

Can. J. Chem. Downloaded from www.nrcresearchpress.com by 210.87.254.42 on 09/05/12
For personal use only.

REARRANGEMENT STUDIES WITH ^{14}C

XIX. THE REACTION OF 2-PHENYL-1-^{14}C-ETHANOL WITH THIONYL CHLORIDE

C. C. Lee, D. J. Kroeger,[1] and D. P. Thornhill[2]

Department of Chemistry, University of Saskatchewan, Saskatoon, Saskatchewan

Received January 8, 1964

ABSTRACT

The reaction of 2-phenyl-1-^{14}C-ethanol with thionyl chloride in pyridine, dioxane, toluene, or excess thionyl chloride as solvent gave 2-phenylethyl chloride showing, respectively, about 0, 15, 44, and 48% rearrangement of the ^{14}C-label from the C-1 to the C-2 positions. When reactions of 2-phenyl-1-^{14}C-ethanol or 2-*p*-anisyl-1-^{14}C-ethanol with thionyl chloride in dioxane or excess thionyl chloride were carried only to partial completion and the undecomposed chlorosulphites hydrolyzed by aqueous sodium hydroxide, the recovered alcohols showed only 0.1 to 0.5% isotope position rearrangement. This indicated a lack of return from ion-pairs to isotopically rearranged 2-arylethyl chlorosulphite and suggested that the first stage of ionization may involve ion-pairs with structures that will not result in rearrangement on return to covalent bonding, or that the first ion-pair may decompose faster than it can return to reactant. The possibility that rearrangements via rigidly oriented ion-pairs and via the concerted S_Ni' mechanism may represent the two extremes of a graded series is discussed. It is suggested that the relative contributions from the ion-pair and from the S_Ni' mechanisms will depend on the stability of the carbonium ion as well as on the nature of the reaction solvent.

As one approach in studying the ionic nature of reactions between alcohols and thionyl chloride, isotope position rearrangements in the thermal decomposition of 1-^{14}C-2-butyl chlorosulphite and in the reaction between 2-*p*-anisyl-1-^{14}C-ethanol and thionyl chloride, carried out in various solvents, have recently been investigated in this laboratory (1, 2). The results were explained by suggesting the involvement of carbonium ion – chlorosulphite ion-pairs. In 1954, Lee and Spinks (3) reported no isotope position rearrangement in the reaction of 2-phenyl-1-^{14}C-ethanol (I) with thionyl chloride in pyridine, while the reaction of I in excess thionyl chloride without pyridine resulted in extensive rearrangement (48–50%) to 2-phenyl-2-^{14}C-ethyl chloride. Since the use of dioxane or toluene as solvent could apparently affect the course of such reactions (1, 2, 4, 5), the present study extended the work of Lee and Spinks by carrying out the reaction of I with thionyl chloride in dioxane or toluene as solvent. Moreover, the possibility of returns from ion-pairs to covalent bonding was investigated. The reactions of I or 2-*p*-anisyl-1-^{14}C-ethanol (II) with thionyl chloride were interrupted before completion. The unreacted chlorosulphites were hydrolyzed and the recovered alcohols degraded to find whether isotope position rearrangements have or have not taken place.

RESULTS AND DISCUSSION

The reaction of 2-phenyl-1-^{14}C-ethanol (I) with thionyl chloride was carried out in pyridine, excess thionyl chloride, dioxane, or toluene as solvent. In some of these experiments, the dioxane or toluene contained about 1% dissolved hydrogen chloride. The 2-phenyl-*x*-^{14}C-ethyl chloride obtained in each case was converted to hydrocinnamic acid, which, in turn, was oxidized to benzoic acid. The activity in the benzoic acid was taken as a measure of the extent of rearrangement of the ^{14}C-label from the C-1 to the C-2 positions (3). The results are summarized in Table I.

[1]*Holder of a National Research Council of Canada Bursary, 1962–63.*
[2]*Holder of a Commonwealth Scholarship, 1961–63.*

TABLE I

Rearrangements in the reaction between 2-phenyl-1-^{14}C-ethanol and thionyl chloride

Solvent	^{14}C-Activity (c.p.m./mmole)*		% rearrangement
	Hydrocinnamic acid	Benzoic acid	
Pyridine	868,000	116	0.01
Pyridine	897,000	143	0.02
Thionyl chloride	826,000	401,000	48.5
Thionyl chloride	827,000	391,000	47.3
Dioxane	826,000	125,000	15.1
Dioxane	851,000	140,000	16.4
Dioxane	381,000	57,300	15.0
Dioxane	385,000	55,600	14.4
Dioxane + 1.3% HCl	521,000	81,500	15.6
Dioxane + 1.3% HCl	530,000	84,100	15.9
Toluene	888,000	391,000	44.0
Toluene	850,000	343,000	40.3
Toluene	379,000	170,000	44.9
Toluene	385,000	171,000	44.4
Toluene + 1.0% HCl	390,000	180,000	46.2
Toluene + 1.0% HCl	390,000	177,000	45.4

*Measured by a liquid scintillation counter.

The data obtained for the reactions carried out in pyridine or excess thionyl chloride confirmed the earlier findings of Lee and Spinks (3). That essentially no rearrangement was observed for the reaction in pyridine is as expected, an S_N2 process being operative when pyridine is present (3, 6). Reactions effected in dioxane and in toluene gave, respectively, about 15% and 44% rearrangement in the product. The inclusion of hydrogen chloride in the solvents dioxane and toluene was an attempt to ascertain the extent, if any, of involvement of a chain process, such as shown by equation [1],

[1] $$HCl + ROSOCl \rightarrow ClR + SO_2 + HCl,$$

a possibility suggested by Sharman and co-workers (5). The fact that neither the rearrangement nor the yield of 2-phenyl-*x*-^{14}C-ethyl chloride was significantly affected by the hydrogen chloride indicated that under the conditions of the present experiments, the presence of about 1% hydrogen chloride did not materially influence the course of these reactions.

If the rearrangements observed in the reactions of I with thionyl chloride effected in dioxane, toluene, or excess thionyl chloride were to involve carbonium ion – chlorosulphite ion-pairs, it would be of interest to investigate if any returns would occur from ion-pairs to covalent bonding to give rise to 2-phenyl-1-^{14}C-ethyl as well as 2-phenyl-2-^{14}C-ethyl chlorosulphites. Since rearrangements observed in the reaction of 2-*p*-anisyl-1-^{14}C-ethanol (II) with thionyl chloride were best explained in terms involving ion-pairs (2), possible returns in the reactions between thionyl chloride and I as well as II were studied. The alcohols, I or II, were added, with cooling, to excess thionyl chloride or thionyl chloride in dioxane and then allowed to stand at room temperature overnight. The resulting solutions of the corresponding chlorosulphites were refluxed for suitable lengths of time. The undecomposed fraction of chlorosulphite in each experiment was then hydrolyzed with aqueous sodium hydroxide to regenerate the alcohol, which was recovered, with the aid of inactive carrier, as the urethan. From the specific activities of the urethans derived from the original alcohol and from the diluted alcohol recovered after partial reaction, calculations based on isotopic dilution permitted an estimation of the extent of decomposition of the chlorosulphite. Each sample of recovered urethan was in turn

Can. J. Chem. Downloaded from www.nrcresearchpress.com by 210.87.254.42 on 09/05/12
For personal use only.

hydrolyzed back to the alcohol (7) and then oxidized to give benzoic acid or *p*-anisic acid. The ^{14}C-activities in these acids would measure the returns from ion-pairs to isotopically rearranged 2-phenyl-2-^{14}C-ethyl chlorosulphite or 2-*p*-anisyl-2-^{14}C-ethyl chlorosulphite. The results are summarized in Table II.

The possibility that the small amounts of rearrangement recorded in Table II might have arisen from hydrolysis of the reaction products, 2-phenyl-*x*-^{14}C-ethyl chloride or 2-*p*-anisyl-*x*-^{14}C-ethyl chloride, was investigated. The chlorosulphite from non-labeled 2-phenylethanol or 2-*p*-anisylethanol was subjected to partial decomposition. To the resulting material, some 2-phenyl-1-^{14}C-ethyl chloride or 2-*p*-anisyl-1-^{14}C-ethyl chloride was added and then the reaction mixture was treated with aqueous sodium hydroxide as before. The alcohols regenerated from the unreacted chlorosulphites gave urethans containing practically no radioactivity, indicating that the added labeled chlorides were not hydrolyzed under these conditions.

The data in Table II show that the extents of return from ion-pairs to isotopically rearranged 2-arylethyl chlorosulphite are very small, if any. These findings are in sharp contrast to the results obtained in the solvolyses of 2-phenyl-1-^{14}C-ethyl *p*-toluenesulphonate (8, 9) and 2-*p*-anisyl-1-^{14}C-ethyl *p*-toluenesulphonate (7). After partial solvolyses, the recovered sulphonates showed very significant amounts of isotope position rearrangements, indicating returns from nonclassical carbonium ion-*p*-toluenesulphonate ion-pairs to covalent bonding.

It has previously been pointed out (1) that the ionic nature of the thermal decomposition of alkyl chlorosulphites has been supported by studies on kinetics, stereochemistry, solvent effects, and rearrangements. The isotope position rearrangements observed in the present work (Table I) and in the reaction of II with thionyl chloride (2) may also involve carbonium ions. An ionic mechanism would be consistent with the estimated extents of reaction shown in Table II, which clearly indicate a faster decomposition of the chlorosulphite with a *p*-methoxyphenyl substituent than the one with a phenyl substituent. The lack of returns to rearranged 2-arylethyl chlorosulphites (Table II) could be explained by assuming that the first ion-pair formed may have classical structure III, or the first ion-pair may be rigidly oriented (1, 5) with the oxygen and chlorine atoms of the anion

$$ArCH_2{}^{14}CH_2{}^{+} \ldots\ldots\ldots OSOCl^{-}$$

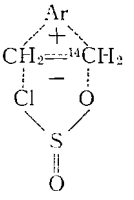

III IV

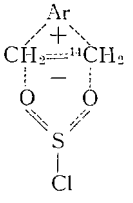

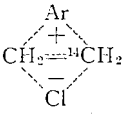

V VI

oriented, respectively, towards C-1 and C-2 as shown in IV. Any return to covalent bonding from III or IV would not result in rearrangement. Another possible rigidly

Can. J. Chem. Downloaded from www.nrcresearchpress.com by 210.87.254.42 on 09/05/12
For personal use only.

Can. J. Chem. Downloaded from www.nrcresearchpress.com by 210.87.254.42 on 09/05/12
For personal use only.

TABLE II

Data from recovered alcohols after partial decomposition of the chlorosulphites from 2-phenyl-1-^{14}C-ethanol (I) and 2-*p*-anisyl-1-^{14}C-ethanol (II)

Reactant	Solvent	Reaction time at reflux temp.* (minutes)	% reacted		^{14}C-Activity (c.p.m./mmole)				% rearrangement	
					Recovered urethan		Oxidation product†			
			Run 1	Run 2	Run 1	Run 2	Run 1	Run 2	Run 1	Run 2
I	$SOCl_2$	90	32	28	1,070,000	1,080,000	1400	1400	0.1	0.1
I	$SOCl_2$	240	70		755,000		3020		0.4	
II	$SOCl_2$	8	56	53	1,520,000	1,550,000	4130	2970	0.3	0.2
II	$SOCl_2$	12	69	61	106,000	118,000	280	250	0.3	0.2
I	Dioxane	60	11		356,000		1490		0.4	
I	Dioxane	240	31		1,070,000		5150		0.5	
II	Dioxane	30	74	72	96,000	101,000	150	110	0.2	0.1

*The chlorosulphite solutions were prepared by adding I or II, with cooling, to $SOCl_2$ in the appropriate solvent and then allowed to stand overnight at room temperature. Decomposition of such solutions without any heating at reflux temperature followed by degradation of the recovered alcohols gave benzoic acid or *p*-anisic acid with less than 0.1% rearrangement.

†Benzoic acid or *p*-anisic acid from oxidation of I or II, respectively.

oriented ion-pair may have structure V. Return from V would lead to isotopically rearranged reactant; but this is excluded by the observed results. It might then be argued that ion-pair IV is also not involved in these reactions. However, Sharman and co-workers (5) have suggested that energetically IV is more favorable than V due to the greater polarizability of chlorine relative to oxygen. The decomposition of 1-^{14}C-allyl chlorosulphite to 3-^{14}C-allyl chloride was attributed by these workers (5) to an ion-pair oriented as in IV to the exclusion of one analogous to V. The anion of the first ion-pair formed in the reactions under study is "complex" and, as suggested by Cram (10), will collapse to a simple ion-pair, with structure VI or its equivalent, which will give rise to products having a maximum of 50% rearrangement. The results in Table II might also be explained by assuming that the first ion-pair could decompose to simple ion-pair VI faster than it could return to reactant (cf. ref. 11).

It is of interest to compare the rearrangement data recorded in Table I with those reported earlier (2) for analogous reactions between II and thionyl chloride. In the reaction of I with thionyl chloride, more rearrangement was noted with toluene than with dioxane as solvent (Table I). This behavior is similar to that observed in the thermal decomposition of 1-^{14}C-2-butyl chlorosulphite (1). On the other hand, in the reaction of II with thionyl chloride, more rearrangement was obtained when the reaction was carried out in dioxane than in toluene (2). For the reaction in dioxane, it was suggested (2) that because of the greater tendency of neighboring *p*-anisyl groups to form bridged ions, the carbonium ion moiety of the ion-pairs may have developed considerable nonclassical structure (such as IV, Ar = *p*-$CH_3OC_6H_4$) before being solvated by dioxane. The net result is a relatively large amount of rearrangement in the product. Since dioxane can apparently exert a specific solvent effect by solvating the carbonium ion as it displaces the chlorosulphite anion (4), the relatively lesser ability of neighboring hydrogen or phenyl to participate and displace dioxane would account for the smaller rearrangements in the products from reactions involving the 1-^{14}C-2-butyl and 2-phenyl-1-^{14}C-ethyl systems. The observed isotope position rearrangements of about 4% (1), 15% (Table I), and 44% (2), respectively, for the decomposition of the chlorosulphites from 1-^{14}C-2-butanol, 2-phenyl-1-^{14}C-ethanol (I), and 2-*p*-anisyl-1-^{14}C-ethanol (II) are in good qualitative agreement with this picture.

The observed rearrangements may also be explained by an S_Ni' mechanism as depicted by VII. In the reaction of II with thionyl chloride (2), the finding that the extents of rearrangement apparently followed the capability of the medium in supporting ionization

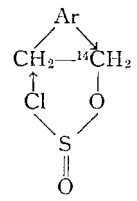

VII

suggested that ion-pairs rather than the largely covalent S_Ni' process may play the dominant role. Pegolotti and Young (12) have suggested for allylic rearrangements that the process via an intimate ion-pair analogous to IV and the S_Ni' mechanism analogous to VII may represent extremes of a graded series or a range of mechanisms. In the decomposition of the chlorosulphites from I or II in various solvents, the contribution from IV

Can. J. Chem. Downloaded from www.nrcresearchpress.com by 210.87.254.42 on 09/05/12
For personal use only.

and VII will depend on both the stability of the carbonium ion and the nature of the solvent. Because of the greater carbonium ion stability, reaction of II with thionyl chloride may involve ionic characteristics even when effected in hydrocarbon solvents. In the present study, the rearrangements observed in the reaction of I with thionyl chloride may arise from intermediate ion-pairs when the chlorosulphite was decomposed in excess thionyl chloride or in dioxane. When the reaction was effected in toluene, the rearrangement was almost as high as that found for reaction in excess thionyl chloride. The contribution from the concerted, highly covalent S_Ni' process may be largely responsible for this fairly extensive amount of rearrangement when the reaction of I with thionyl chloride was carried out in toluene.

EXPERIMENTAL

The preparation of 2-phenyl-1-^{14}C-ethanol (I) and its reaction with thionyl chloride in pyridine were carried out essentially as described by Lee and Spinks (3).

Reaction in Excess Thionyl Chloride

To 30 ml of thionyl chloride, cooled in an ice bath, was added dropwise 3.0 ml of I. The mixture was stirred at room temperature for 3 hours and then refluxed for 24 hours. After cooling, 30 ml of ice-water was introduced and the resulting material was extracted several times with ether. The combined extract was washed successively with water, 10% sodium carbonate solution, and again water, and then dried over anhydrous sodium sulphate. After removal of the ether, the residue was distilled under reduced pressure, giving, for duplicate runs, 1.6 g (46%) and 1.4 g (40%) of 2-phenyl-*x*-^{14}C-ethyl chloride (VIII), b.p. 76–78° C at 10 mm (lit. (3) b.p. 85–87° C at 17 mm).

Reaction in Dioxane

A solution of 3.0 ml of I in 15 ml of dioxane was added dropwise at room temperature to a solution of 5.0 ml of thionyl chloride in 15 ml of dioxane. The resulting solution was stirred at room temperature for 24 hours and then refluxed for 48 hours. After cooling, ice-water was added and the mixture worked up as before. The yields of VIII for four similar runs were 1.2 g (34%), 1.4 g (40%), 1.8 g (51%), and 1.4 g (40%).

For the reaction in dioxane with hydrogen chloride present, gaseous hydrogen chloride was bubbled into dioxane and the increase in weight indicated that 1.3% hydrogen chloride was absorbed. Using this dioxane containing hydrogen chloride as solvent, the reaction was carried out exactly as described above. The yields of product VIII for duplicate runs were 1.3 g (37%) and 1.7 g (48%).

Reaction in Toluene

A solution of 3.0 ml of I in 15 ml of toluene was added dropwise to 5.0 ml of thionyl chloride in 15 ml of toluene, stirred at room temperature for 24 hours and then refluxed for 100 hours. The resulting solution was treated with ice-water and worked up as before to give, for dulpicate runs, 2.0 g (57%) and 1.8 g (51%) of product VIII.

Because of the prolonged refluxing, in order to avoid excessive decrease in volume, twice the amount of toluene (total volume of 60 ml) was used in two further experiments. The yields of chloride VIII obtained in these runs were 1.7 g (48%) and 1.2 g (34%).

For the reaction in toluene containing hydrogen chloride, gaseous hydrogen chloride was bubbled into toluene and the increase in weight indicated the presence of 1.0% hydrogen chloride. When the reaction of 3.0 ml of I with 5.0 ml of thionyl chloride in a total of 60 ml of toluene containing 1.0% hydrogen chloride was effected as described above, the yields of VIII for duplicate runs were 1.2 g (34%) and 1.5 g (42%).

Degradation of 2-Phenyl-x-^{14}C-ethyl Chloride (VIII)

The product, VIII, from each experiment was converted to a solid derivative, hydrocinnamic acid, which, in turn, was oxidized with alkaline potassium permanganate to give benzoic acid. The procedures have been described previously (3).

Partial Decomposition of the Chlorosulphites from 2-Phenyl-1-^{14}C-ethanol (I) and from 2-p-Anisyl-1-^{14}C-ethanol (II) in Dioxane

To a cooled and stirred solution of 3.0 ml of thionyl chloride in 50 ml of dioxane was added dropwise 3.0 g of alcohol I or II. The mixture was stoppered and allowed to stand overnight. The resulting solution, presumably containing the corresponding chlorosulphite of I or II, was refluxed for a suitable length of time (Table II) and then cooled in an ice bath. The undecomposed portion of chlorosulphite was hydrolyzed by the addition with stirring of 8.0 g of sodium hydroxide in 40 ml of water. One gram of inactive 2-phenylethanol or 2-*p*-anisylethanol was then introduced as carrier. The resulting mixture was extracted four times with ether, the combined extract washed with water, and then dried over anhydrous sodium

Can. J. Chem. Downloaded from www.nrcresearchpress.com by 210.87.254.42 on 09/05/12
For personal use only.

sulphate. After removal of the ether, the residue was distilled under reduced pressure to give about 2 g of recovered alcohol.

The recovered, diluted alcohol, I or II, was heated for 5–10 minutes with phenyl isocyanate according to standard procedure to give the corresponding phenylurethans. Each sample of urethan was purified by repeated recrystallization from carbon tetrachloride – petroleum ether. The phenylurethan of I melted at 80° C (lit. (13), m.p. 79–80° C), and that of II melted at 128° C (lit. (7), m.p. 127–128° C).

Each sample of phenylurethan was hydrolyzed by treatment with alcoholic potassium hydroxide as described by Jenny and Winstein (7) and the resulting I or II was oxidized with alkaline potassium permanganate to give benzoic acid or *p*-anisic acid.

Partial Decomposition of the Chlorosulphites from I and from II in Excess Thionyl Chloride

To 50 ml of thionyl chloride, stirred and cooled in an ice bath, was added dropwise 3.0 g of alcohol I or II, and then stoppered and allowed to stand at room temperature overnight. The resulting solution was refluxed for a suitable length of time (Table II). Most of the excess thionyl chloride was removed at room temperature under reduced pressure. When the residual volume was about 3 ml, 40 ml of ether was added, and the solution treated with aqueous sodium hydroxide. One gram of inactive alcohol was introduced as carrier and the resulting mixture worked up in the same manner as described above.

Hydrolysis of Inactive Chlorosulphite in the Presence of Labeled Chloride

To ascertain whether 2-phenyl-1-^{14}C-ethyl chloride or 2-*p*-anisyl-1-^{14}C-ethyl chloride would undergo hydrolysis under the conditions by which unreacted chlorosulphite was hydrolyzed with aqueous sodium hydroxide, the chlorosulphite from inactive 2-phenylethanol or 2-*p*-anisylethanol in dioxane solution was refluxed to effect partial decomposition. Two grams of 2-phenyl-1-^{14}C-ethyl chloride or 2-*p*-anisyl-1-^{14}C-ethyl chloride was introduced into the reaction mixture and then the undecomposed chlorosulphite was hydrolyzed with aqueous sodium hydroxide. The regenerated alcohol, isolated as the phenylurethan as described above, contained practically no radioactivity, thus indicating that the labeled chlorides did not hydrolyze to the respective alcohols under these conditions.

The 2-phenyl-1-^{14}C-ethyl chloride used in this experiment was prepared from the reaction of I with thionyl chloride in pyridine. It is, however, known that reaction of II with thionyl chloride in pyridine gave a chloride product with about 0.5% rearrangement (2). 2-*p*-Anisyl-1-^{14}C-ethyl bromide has been prepared from the reaction of 2-*p*-anisyl-1-^{14}C-ethyl *p*-toluenesulphonate with anhydrous lithium bromide in dry acetone (14). An analogous attempt to obtain the chloride using lithium chloride in acetone failed, presumably because of the low solubility of lithium chloride in acetone. However, 2-*p*-anisyl-1-^{14}C-ethyl chloride without rearrangement was successfully prepared in 48% yield by refluxing for 3 hours a mixture of 19.0 g of 2-*p*-anisyl-1-^{14}C-ethyl *p*-toluenesulphonate and 8.0 g of anhydrous calcium chloride in 200 ml of dry acetone.

ACKNOWLEDGMENT

The financial support given by the National Research Council of Canada is gratefully acknowledged.

REFERENCES

1. C. C. Lee, J. W. Clayton, D. G. Lee, and A. J. Finlayson. Tetrahedron, **18**, 1395 (1962).
2. C. C. Lee, D. Newman, and D. P. Thornhill. Can. J. Chem. **41**, 620 (1963).
3. C. C. Lee and J. W. T. Spinks. Can. J. Chem. **32**, 1005 (1954).
4. C. E. Boozer and E. S. Lewis. J. Am. Chem. Soc. **75**, 3182 (1953).
5. S. H. Sharman, F. F. Caserio, R. F. Nystrom, J. C. Leak, and W. G. Young. J. Am. Chem. Soc. **80**, 5965 (1958).
6. J. Hine. Physical organic chemistry. 2nd ed. McGraw-Hill. 1962. pp. 139–140.
7. E. F. Jenny and S. Winstein. Helv. Chim. Acta, **41**, 807 (1958).
8. C. C. Lee, R. Tkachuk, and G. P. Slater. Tetrahedron, **7**, 206 (1959).
9. J. W. Clayton and C. C. Lee. Can. J. Chem. **39**, 1510 (1961).
10. D. J. Cram. J. Am. Chem. Soc. **75**, 332 (1953).
11. J. L. Kice and R. A. Bartsch. Tetrahedron Letters, No. 25, 1693 (1963).
12. J. A. Pegolotti and W. G. Young. J. Am. Chem. Soc. **83**, 3251 (1961).
13. I. Heilbron and H. J. Bunbury. Dictionary of organic compounds. Vol. 4. Eyre and Spottiswoode London. 1953. p. 125.
14. D. P. Thornhill and C. C. Lee. Can. J. Chem. **41**, 2482 (1963).

Can. J. Chem. Downloaded from www.nrcresearchpress.com by 210.87.254.42 on 09/05/12
For personal use only.

Can. J. Chem. Downloaded from www.nrcresearchpress.com by 210.87.254.42 on 09/05/12
For personal use only.

STUDIES ON THE THERMODYNAMICS AND CONDUCTANCES OF MOLTEN SALTS AND THEIR MIXTURES

PART I. THE DENSITIES AND MOLAR VOLUMES OF LITHIUM CHLORATE AND OF LITHIUM CHLORATE – LITHIUM NITRATE MIXTURES

A. N. Campbell and M. K. Nagarajan
Chemistry Department, University of Manitoba, Winnipeg, Manitoba

Received October 24, 1963

ABSTRACT

The densities at different temperatures of pure molten lithium chlorate and of mixtures of lithium chlorate with lithium nitrate have been determined by a method of high precision. The change of molar volume with temperature has been interpreted in the light of possible structural changes in the melt.

In recent years a number of studies dealing with molten salts have been made. Since there is no adequate theory of the molten state, many of these studies have been quite speculative in nature. We confine ourselves in the present work to the presentation of some precise thermodynamic measurements on a particular binary fused salt system, the $LiClO_3$–$LiNO_3$ system, and results which can be inferred from these measurements. Because of the low melting points involved considerable improvement in experimental accuracy is possible over that obtained in work involving higher melting salt systems.

From a knowledge of the density and molar volume changes with temperature, information on the change in structure of the melt can be obtained. Some approximate relations between the molar volumes and the ionic character of a melt have been given by Drossbach (1).

EXPERIMENTAL

Lithium chlorate was prepared by a method originally suggested by Potilitzin (2) and by Kraus (3), and later modified by Campbell and Griffiths (4). The method involves the mixing of equimolar proportions of barium chlorate and lithium sulphate. The precipitated barium sulphate is filtered off and the clear solution titrated alternately with solutions of lithium nitrate and of barium chlorate until all excess over stoichiometric proportions is removed. The solution is then concentrated by vacuum distillation at about 60°. When the solution has attained a concentration of about 90% lithium chlorate, it is cooled in an ice-bath, when crystals of lithium chlorate separate out. The lithium chlorate crystals are removed by filtration and kept over sulphuric acid for a period of from 2 to 3 weeks. After the salt is sufficiently dry, it is ground to a fine powder in a dry-box. Final drying is then carried out under vacuum, evolved water being trapped in barium oxide. At various stages of this latter process, the melting point and specific conductance were determined, as criteria of dryness. Our final figure for the melting point of anhydrous lithium chlorate was 127.9° C. The specific conductance (electrical) was determined as 0.1148 ± 0.0002 ohm^{-1} cm^{-1} at 131.8°. The lithium nitrate used as addition material was a Fisher Reagent Grade material and it was not further purified except to dry it thoroughly.

The thermostat fluid used was Dow–Corning silicone fluid 550. The temperature was controlled by means of a Thyratron relay and did not vary more than ±0.1° at 130°.

The form of the dilatometers is shown in Fig. 1(*a*). They were made of pyrex glass and had a 1-mm bore capillary, 8 cm long. The capillaries were precision drilled and had a manufacturer's (Corning Glass) reported precision of ±0.002 mm. The slanted sidearm, terminating in a bulb, served as an overflow for the excess melt.

The dilatometers were calibrated with redistilled reagent grade mercury, at four temperatures. The meniscus level of the mercury column was adjusted to coincide with one of the stem marks, by means of a long hypodermic needle. The dilatometer and its contents were then weighed. This procedure was repeated for the remaining two of the three calibration marks. This calibration was carried out at four controlled temperatures. The plots of volume versus temperature, for each calibration mark, were essentially linear. The advantage of this method of calibration is that it does not require any correction for the expansion of the glass.

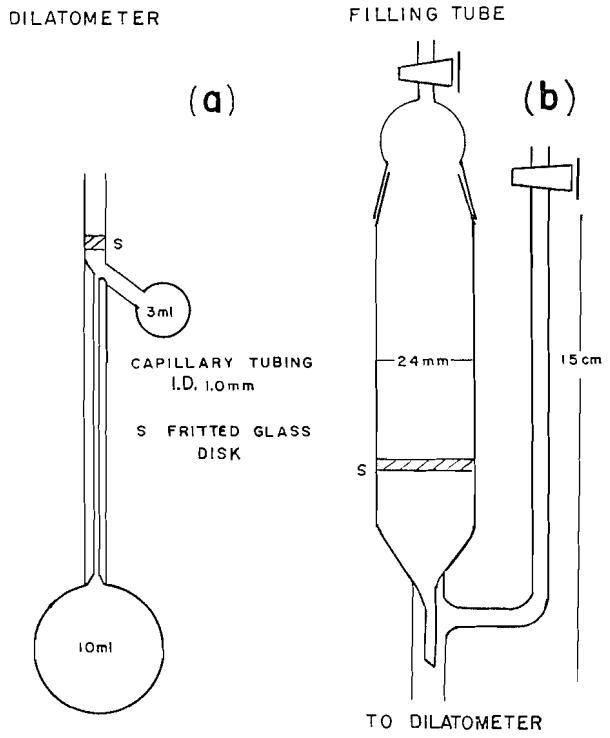

FIG. 1.

Because of the extreme hygroscopicity of lithium chlorate (it is as bad as phosphorus pentoxide) all operations with it have to be conducted in a completely moisture-free atmosphere. The transferring apparatus is shown in Fig. 1(*b*). This apparatus was sealed to the top of the dilatometer, as indicated in the diagram. The top compartment was loaded with anhydrous lithium chlorate, in a nitrogen-filled dry-box. The entire assembly was then evacuated and kept in a thermostat, at about 165°. As the lithium chlorate melted it flowed down and collected gradually in the bulb of the dilatometer, filling it without gas bubbles. When bulb and stem were full, excess lithium chlorate overflowed into the side bulb. In this way it was possible to fill the dilatometer to the desired level without having to add or remove material. The dilatometer was removed from the thermostat and sealed under vacuum at the constriction just above the smaller fritted glass disk. It was then weighed. This disk was very effective and is essential to the accuracy of all measurements with molten salts: it prevents any silt (arising from the decomposition of the thin layer of lithium chlorate during sealing) getting into the capillary bore. When we were dealing with mixtures of lithium chlorate and lithium nitrate, it was necessary to prepare the mixtures in advance and transfer the completely homogeneous melt to the transfer apparatus. All operations were carried out within the dry-box.

The filled dilatometer was now placed in the accurate thermostat. After the attainment of thermal equilibrium, the height of the liquid meniscus with reference to one of the three marks on the stem was determined with a microcathetometer. The distances between the marks were also measured at this temperature. From these data and the calibration graph, the volume of the liquid was obtained by interpolation. The procedure was repeated at intervals of about 2° over the range 130° to 170°. At constant temperature, the heights were reproducible to ±0.01 mm. The weight of the sample was obtained by breaking the dilatometer and weighing the broken pieces. Density measurements were made with pure lithium chlorate and four mixtures containing 0.108, 0.171, 0.227, and 0.292 mole fraction lithium nitrate.

A careful estimate of the overall precision of the method showed that the maximum possible error in the determination of density amounted to ±0.0002 g ml^{-1}.

RESULTS

Table I gives the densities and molar volumes of pure lithium chlorate and of the four mixtures, at different temperatures. When these values are plotted against temperature,

Can. J. Chem. Downloaded from www.nrcresearchpress.com by 210.87.254.42 on 09/05/12
For personal use only.

Can. J. Chem. Downloaded from www.nrcresearchpress.com by 210.87.254.42 on 09/05/12
For personal use only.

TABLE I

Densities and molar volumes

Pure lithium chlorate freezing point: 401.0° K			Lithium chlorate – lithium nitrate, freezing point: 397.6° K, n_2 = mole fraction lithium nitrate = 0.108			Lithium chlorate – lithium nitrate, freezing point: 395.5° K, n_2 = mole fraction lithium nitrate = 0.171		
t, ° C	d(g ml^{-1})	V(ml mole^{-1})	t, ° C	d(g ml^{-1})	V(ml mole^{-1})	t, ° C	d(g ml^{-1})	V(ml mole^{-1})
135.0	2.0854	43.3476	141.2	2.0743	42.8244	138.7	2.0689	42.3016
138.5	2.0825	43.4079	144.1	2.0721	42.8698	141.3	2.0666	42.3486
139.9	2.0812	43.4350	147.3	2.0698	42.9175	143.1	2.0649	42.3835
141.8	2.0798	43.4643	148.5	2.0688	42.9382	145.0	2.0634	42.4143
143.8	2.0783	43.4957	150.1	2.0674	42.9673	147.0	2.0622	42.4390
145.3	2.0770	43.5229	152.3	2.0659	42.9985	148.8	2.0609	42.4658
147.9	2.0750	43.5648	153.8	2.0646	43.0256	150.2	2.0598	42.4885
148.3	2.0741	43.5837	155.8	2.0632	43.0548	151.7	2.0587	42.5112
149.7	2.0728	43.6111	157.9	2.0614	43.0924	153.4	2.0569	42.5484
151.2	2.0713	43.6426	159.3	2.0604	43.1133	155.2	2.0558	42.5711
152.7	2.0699	43.6722	161.0	2.0591	43.1405	157.3	2.0537	42.6147
154.3	2.0685	43.7017	162.7	2.0579	43.1657	158.8	2.0526	42.6375
155.5	2.0673	43.7271				160.2	2.0514	42.6624
157.6	2.0657	43.7610				161.1	2.0506	42.6791
"Best" line: $V = 35.503 + 0.019_2\,T$ Standard deviation = ± 0.0063 ml			"Best" line: $V = 36.130 + 0.016_2\,T$ Standard deviation = ± 0.0021 ml			"Best" line: $V = 35.156 + 0.017_3\,T$ Standard deviation = ± 0.0074 ml		

Lithium chlorate – lithium nitrate, freezing point: 392.9° K, n_2 = mole fraction lithium nitrate = 0.227			Lithium chlorate – lithium nitrate, freezing point: 389.2° K, n_2 = mole fraction lithium nitrate = 0.292		
t, ° C	d(g ml^{-1})	V(ml mole^{-1})	t, ° C	d(g ml^{-1})	V(ml mole^{-1})
139.6	2.0585	41.8759	138.4	2.0514	41.1415
141.7	2.0567	41.9126	139.7	2.0505	41.1595
144.2	2.0551	41.9452	141.0	2.0496	41.1776
145.7	2.0534	41.9799	142.8	2.0484	41.2017
148.2	2.0519	42.0106	144.0	2.0475	41.2198
150.0	2.0505	42.0393	146.2	2.0459	41.2521
151.4	2.0494	42.0619	147.9	2.0447	41.2763
153.5	2.0479	42.0927	149.4	2.0435	41.3005
154.8	2.0467	42.1174	150.8	2.0424	41.3228
156.2	2.0457	42.1380	152.4	2.0412	41.3471
157.8	2.0445	42.1627	154.1	2.0399	41.3734
160.3	2.0424	42.2060	156.0	2.0386	41.3998
161.5	2.0417	42.2205	158.3	2.0368	41.4364
			160.0	2.0356	41.4608
"Best" line: $V = 35.733 + 0.014_9\,T$ Standard deviation = ± 0.0066 ml			"Best" line: $V = 35.031 + 0.014_8\,T$ Standard deviation = ± 0.0020 ml		

admirable straight lines are obtained, both for density and molar volume. The molar volume data were analyzed, by the method of least squares and using a Bendix computer, on the basis of the straight line equation, and this equation is reproduced at the bottom of each section of the table.

Isothermal cuts from the basic molar volume data were made, to show the dependence of molar volume on composition. The interpolations at arbitrarily chosen temperatures (390° K to 450° K at 10° intervals) were carried out on the computor. The values so obtained are given in Table II. The dependence of molar volume on the mole fraction of

TABLE II

Isothermal molar volume as a function of mole fraction of lithium nitrate

	n_2				
T	0.000	0.108	0.171	0.227	0.292
390.0	(42.985)	(42.428)	(41.916)	(41.548)	40.819
400.0	(43.177)	42.590	42.089	41.697	40.968
410.0	43.369	42.751	42.262	41.846	41.116
420.0	43.561	42.913	42.436	41.995	41.264
430.0	43.753	43.074	42.609	42.144	41.413
440.0	43.945	43.236	42.782	42.293	41.561
450.0	44.137	43.397	42.956	42.442	41.710

NOTE: Values in parentheses refer to the hypothetical molar volumes in the supercooled liquid state.

lithium nitrate (n_2) at constant temperature satisfies the quadratic equation:

$$V = A_0 + A_1 n_2 + A_2 n_2^2$$

where A_0, A_1, and A_2 are constants. The data were fitted to a "best" curve by the method of least squares. The values of the constants, at different temperatures, are given in Table III.

TABLE III

Values of constants in the equation for the "Best" curve by the method of least squares ($V = A_0 + A_1 n_2 + A_2 n_2^2$)

Temp. (° K)	A_0	A_1	A_2
390.0	42.983	−3.961	−11.573
400.0	43.172	−4.158	−11.386
410.0	43.363	−4.386	−11.101
420.0	43.553	−4.578	−10.942
430.0	43.744	−4.800	−10.672
440.0	43.934	−5.000	−10.488
450.0	44.124	−5.200	−10.284

The values of the coefficients of thermal expansion, α, were obtained from the equation $V = V_0(1+\alpha t)$; they are given in Table IV.

DISCUSSION

The dependence of the molar volume of molten lithium nitrate on temperature is given by the linear relation:

$$V = (35.503 + 0.0192\ T)\ \text{ml},$$

with an observed deviation of ±0.006 ml. It is generally agreed (5) that salts with non-spherical polyatomic anions, such as nitrates and chlorates, possess a more covalent

Can. J. Chem. Downloaded from www.nrcresearchpress.com by 210.87.254.42 on 09/05/12
For personal use only.

TABLE IV

Coefficient of thermal expansion for mixtures of lithium chlorate and lithium nitrate
$V = V_0(1 + \alpha t)$

n_2	V_0 (ml)	$\alpha \times 10^4$
0.000	40.747	4.71
0.108	40.554	4.00
0.171	39.881	4.34
0.227	39.802	3.74
0.292	39.073	3.79

character than salts with spherical anions (e.g. chlorides, bromides, iodides). Klemm's rule (1) states that, in general, covalent melts possess higher molar volumes than ionic melts, owing to the weaker intermolecular forces in salts of the former type. For the same reason, the coefficient of expansion (α) is also generally higher in covalent melts than in ionic melts. The values of molar volume and of α for molten lithium chlorate suggest that the melt is probably more covalent than ionic in character but such a deduction is only approximate and requires further corroborative evidence.

We discuss the molar volume data for lithium chlorate – lithium nitrate mixtures according to an argument closely related to that developed by Papousek and Kucirek (6). All changes in molar volume of lithium chlorate – lithium nitrate mixtures are discussed relative to an assumed standard or reference state, in this case, 1 mole of pure lithium chlorate at its melting point (401.0° K). This assumption implies that the basic lattice of the reference state predominates over the entire region of temperature and composition involved, in other words, no major change or breakdown of the basic reference state lattice occurs in the region of investigation. The molar volume is considered to be a function of only two variables, viz. temperature and composition, i.e. $V = f(T,n_2)$, where n_2 is the mole fraction of lithium nitrate. The change in molar volume (dV) from the reference state is then defined by the complete differential

$$dV = (\partial V/\partial T)_{n_2}.dT + (\partial V/\partial n_2)_T.dn_2$$

where $(\partial V/\partial T)_{n_2}$ is the rate of change in molar volume with temperature at a fixed composition and $(\partial V/\partial n_2)_T$ is the rate of change of molar volume with composition at constant temperature, and dT and dn_2 are increments of temperature and composition.

The term $(\partial V/\partial T)_{n_2}$ is the thermal expansivity and the term $(\partial V/\partial n_2)_T$ is related to the partial molar volume $\bar{V}_2$ by the equation

$$(\partial V/\partial n_2)_T = \bar{V}_2.[n_T/(1-n_2)],$$

where n_T = total moles in the system. We think it instructive to separate these two quantities and to evaluate their respective effects on ΔV, the change in volume from the standard state, in this case pure molten lithium chlorate at its melting point.

Writing

$$V_T = (\partial V/\partial T)_{n_2}$$

$$V_n = (\partial V/\partial n_2)_T$$

the equation

$$\Delta V = \int_{T_0}^{T} V_T.dT + \int_{n_2=0}^{n_2=n_2} V_n.dn_2$$

Can. J. Chem. Downloaded from www.nrcresearchpress.com by 210.87.254.42 on 09/05/12
For personal use only.

represents total change of volume from the standard state. The values of $V_T = (\partial V/\partial T)_{n_2}$ at different compositions were obtained by differentiation of the equations of "best" lines given in Table I and are tabulated in Table V.

TABLE V

Values of V_n (interpolated) at different compositions for $LiClO_3 - LiNO_3$ mixtures (n_2 = mole fraction lithium nitrate)

n_2	V_n
0.000	0.0192
0.100	0.0168
0.200	0.0155
0.300	0.0145

Differentiation of the quadratic equation representing the change in the isothermal volume with addition of lithium nitrate yields

$$V_n = (\partial V/\partial n_2)_T = A_1 + 2A_2 n_2.$$

From the values of A_1 and A_2 in Table IV, the values of V_n have been calculated at selected fixed temperatures and these are shown in Table VI.

TABLE VI

Values of V_T at different temperatures for $LiClO_3 - LiNO_3$ mixtures (n_2 = mole fraction of lithium nitrate)

T, °K	$n_2 = 0.000$	$n_2 = 0.100$	$n_2 = 0.200$	$n_2 = 0.300$
390.0	−3.961	−6.276	−8.590	−10.905
410.0	−4.386	−6.606	−8.826	−11.047
430.0	−4.800	−6.934	−9.069	−11.203
450.0	−5.200	−7.257	−9.314	−11.370

The individual parts of the equation

$$\Delta V = \int_{T_0}^{T} V_T . dT + \int_{n_2=0}^{n_2=n_2} V_n . dn_2,$$

viz., the part due to temperature change, $\int V_T . dT$, and the part due to composition change, $\int V_n . dn_2$, of the total volume change, from the reference state, have been obtained by evaluating the integrals graphically, within appropriate limits. These parts are collected in Table VII and are shown graphically in Fig. 2, as functions of the composition of the melt. At low temperatures, and high concentrations of lithium nitrate, the change due to change of composition predominates. Thus, though the temperature effect is always positive above the reference temperature, the composition effect, which is presumably connected with interactions in the melt, contributes a large negative value, and the net effect is negative. It is noteworthy that the temperature effect increases considerably with increasing temperature and this may indicate a breakdown in the internal configurations.

Can. J. Chem. Downloaded from www.nrcresearchpress.com by 210.87.254.42 on 09/05/12
For personal use only.

Can. J. Chem. Downloaded from www.nrcresearchpress.com by 210.87.254.42 on 09/05/12
For personal use only.

TABLE VII

Temperature and composition parts of total change in molar volume (n_2 = mole fraction of lithium nitrate)

	$n_2 = 0.000$			$n_2 = 0.100$			$n_2 = 0.200$			$n_2 = 0.300$		
T, ° K	$\int V_T dT$	$\int V_n dn_2$	ΔV	$\int V_T dT$	$\int V_n dn_2$	ΔV	$\int V_T dT$	$\int V_n dn_2$	ΔV	$\int V_T dT$	$\int V_n dn_2$	ΔV
390.0	−0.211	0.000	−0.211	−0.185	−0.512	−0.697	−0.171	−1.255	−1.426	−0.160	−2.230	−2.390
410.0	+0.173	0.000	+0.173	+0.151	−0.550	−0.399	+0.140	−1.322	−1.182	+0.131	−2.316	−2.185
430.0	+0.557	0.000	+0.557	+0.487	−0.587	−0.100	+0.450	−1.388	−0.938	+0.421	−2.403	−1.982
450.0	+0.941	0.000	+0.941	+0.823	−0.623	+0.200	+0.760	−1.452	−0.692	+0.711	−2.487	−1.776

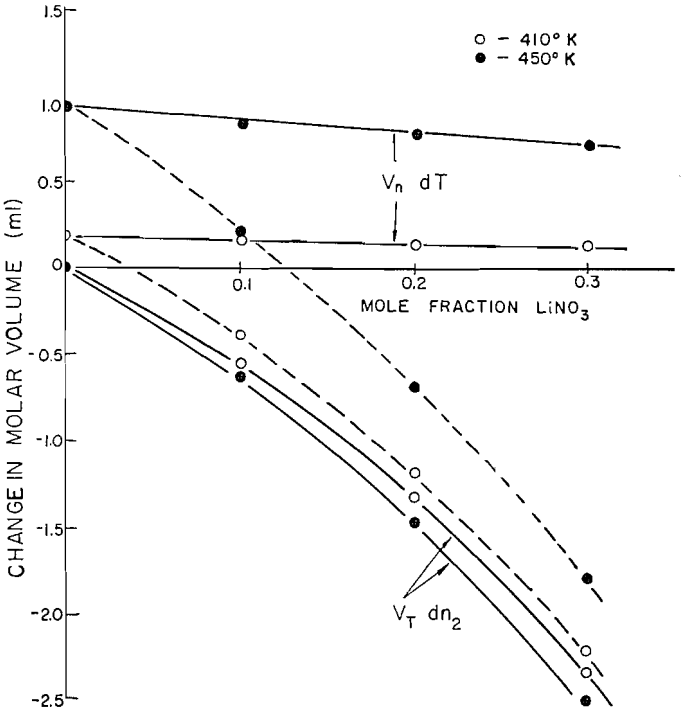

FIG. 2. Structural and geometrical parts of change in volume.

REFERENCES

1. P. DROSSBACH. Elektrochemie geschmolzener Salze. Berlin. 1938.
2. A. POTILITZIN. J. Russ. Phys. Chem. Soc. **16**, 840 (1883).
3. C. A. KRAUS and W. M. BURGESS. J. Am. Chem. Soc. **49**, 1226 (1927).
4. A. N. CAMPBELL and J. E. GRIFFITHS. Can. J. Chem. **34**, 1647 (1956).
5. E. RHODES and A. R. UBBELOHDE. Trans. Faraday Soc. **55**, 1075 (1959).
6. D. PAPOUSEK and J. KUCIREK. J. Phys. Chem. USSR **34**, 168 (1960).

Can. J. Chem. Downloaded from www.nrcresearchpress.com by 210.87.254.42 on 09/05/12
For personal use only.

RELATIVE RATES OF ABSTRACTION OF HYDROGEN FROM PROPANE AND *n*-BUTANE BY ATOMIC HYDROGEN

H. A. KAZMI[1] AND D. J. LE ROY
Department of Chemistry, University of Toronto, Toronto, Ontario
Received October 28, 1963

ABSTRACT

The activation energy for the abstraction of hydrogen from *n*-butane by atomic hydrogen was found to be approximately 1 kcal mole^{-1} smaller than for the analogous reaction with propane. The A factor is smaller by a factor of two. The A factors are discussed in terms of activated complex theory.

The recent determination in this laboratory (1) of the absolute value of the rate constant for the reaction

[1] $$H + C_3H_8 = H_2 + C_3H_7$$

has provided the opportunity for the determination, by relative methods, of the rate constants for other H atom reactions having comparable rates. In the present paper we report the results of experiments in which we determined the rate constant for reaction [2] relative to that for [1].

[2] $$H + n\text{-}C_4H_{10} = H_2 + C_4H_9$$

If H atoms are allowed to react with a mixture of propane and butane, and if the only reactions leading to propane and butane consumption are [1] and [2], and if neither compound is re-formed, then

[i] $$k_1/k_2 = \frac{\log [C_3H_8]_0/[C_3H_8]_t}{\log [C_4H_{10}]_0/[C_4H_{10}]_t}.$$

The experimental conditions used in the present work were similar to those used previously in studying the reaction with propane alone (1). The total concentration of hydrocarbons in the reaction vessel was approximately 10^{14} molecules cm^{-3}, while the H atom concentration was an order of magnitude greater. Since no products other than methane were found under these circumstances, it seems reasonable to assume that the use of [1] is valid.

The consumption of each hydrocarbon was measured relative to the concentration of an inert substance, carbon dioxide. The gases were analyzed by gas chromatography, using helium as the carrier gas and silica gel as the column material. Peak areas were measured with a planimeter, and are subject to an error of about 1%. The differing response factors for the detection of the three gases cancel out, permitting areas to be substituted for concentrations. The areas for the original gas mixture were in the proportion $C_3H_8:C_4H_{10}:CO_2::0.412:0.627:1$.

The results are shown in Fig. 1 in the form of an Arrhenius plot. Least squares treatment of the data yielded the expression

$$k_1/k_2 = (A_1/A_2) \exp - [(E_1 - E_2)/RT] = 2.0 \exp (-1.07 \times 10^3/RT).$$

[1]*Present address: Department of Chemistry, University of Peshawar, Peshawar, Pakistan.*

Can. J. Chem. Downloaded from www.nrcresearchpress.com by 210.87.254.42 on 09/05/12
For personal use only.

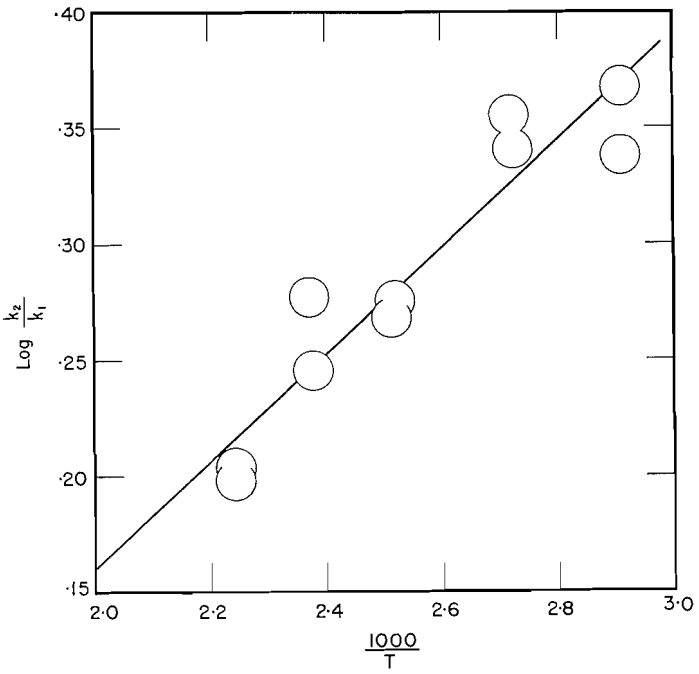

FIG. 1. Arrhenius plot of k_2/k_1.

Thus, utilizing the value $k_1 = 2.2\times10^{-10}$ exp $(-8.2\times10^3/RT)$ cm^3 molecule^{-1} sec^{-1} obtained previously (1), we find

$$k_2 = 1.1\times10^{-10} \exp(-7.1\times10^3/RT) \text{ cm}^3 \text{ molecule}^{-1} \text{ sec}^{-1}$$

$$\text{or } 6.6\times10^{13} \exp(-7.1\times10^3/RT) \text{ cm}^3 \text{ mole}^{-1} \text{ sec}^{-1}.$$

In the previous work, on reaction [1], the experimental evidence indicated that the reaction was predominantly with the secondary hydrogen atoms. It was not possible to draw any conclusion regarding this matter for reaction [2]. For the purpose of the following discussion, however, it will be assumed that only secondary hydrogen atoms are abstracted from *n*-butane.

DISCUSSION

Activated complex theory, in its original form (2), predicts that the A factor for a bimolecular reaction can be written in the form

[ii] $$A = \kappa e^2(kT/h) \exp(\Delta S^{\ddagger}/R),$$

in which $\Delta S^{\ddagger}$ refers to the molar entropy of formation of the activated complex from the reagents in the standard state of 1 mole cm^{-3}.

It has been pointed out a number of times, and most recently and convincingly by Schlag (3), that equation [ii] does not take into consideration the possibility of multiple paths. Account of this may be taken in two ways. One can disregard the external symmetry numbers of the reagents and the activated complex, defining $\Delta S^{\ddagger}$ on the basis that these are all unity, and then multiply the right-hand side of [ii] by n, the number of possible reaction paths; this would introduce a factor of two for reaction [1], four for reaction [2].

Can. J. Chem. Downloaded from www.nrcresearchpress.com by 210.87.254.42 on 09/05/12
For personal use only.

Alternatively, one can retain the actual external symmetry numbers in defining $\Delta S^{\ddagger}$ and multiply the right-hand side of [ii] by $n' = n/s$, where s is the product of the symmetry numbers of the reagents divided by the symmetry number of the complex. This would introduce a factor of unity for reaction [1], two for reaction [2].

In the case of reaction [2] it can be seen that the factor $n' = 2$ is required on *thermodynamic* grounds (if one is to retain the concept that the complex is in equilibrium with the reagents). Both the complex and the secondary butyl radicals formed from it must exist in two distinct forms, which are non-superimposable mirror images, say *d* and *l*. If C_d^* and C_l^* are the equilibrium concentrations of the two complexes then the forward rate of the reaction A + B = X + Y will be equal to $k^*C_d^* + k^*C_l^* = 2k^*K^*[A][B]$, where k^* is the unimolecular rate constant for the decomposition of either complex into products and K^* is the equilibrium constant for the formation of either complex from the reagents. Benson and Nangia (4) have preferred to consider this factor of two as an $R \ln 2$ term in the entropy of formation of the complex, arising from the entropy of mixing of the two forms of the complex.

If we define $\Delta S_{\text{II}}^{\ddagger}$ as the intrinsic internal contribution to the entropy of formation of the complex, omitting the translational and symmetry contributions, as well as that from the coordinate of decomposition, the corrected form of [ii] can be written:

[iii] $$A = \kappa n'(N^5h^4/8\pi^3ekT)^{1/2}\,\mu^{-3/2}(\sigma_a\sigma_b/\sigma^{\ddagger})\exp(\Delta S_{\text{II}}^{\ddagger}/R),$$

in which σ_a and σ_b refer to the two reactants and μ is the reduced molecular weight.

The square root term is only slightly dependent on temperature and it is convenient to calculate its value for 400° K, in the usual range of experimental values. Thus, at 400° K,

[iv] $$A = 2.02\times10^{13}n'\mu^{-3/2}(\sigma_a\sigma_b/\sigma^{\ddagger})\exp(\Delta S_{\text{II}}^{\ddagger}/R),$$

when κ is assumed to be unity.

In many instances the external symmetry numbers are known, or can be estimated with some degree of certainty, and hence the only unknowns are κ, which is usually assumed to be close to unity, and the factor $\exp(\Delta S_{\text{II}}^{\ddagger}/R)$. By making the assumption that the rotational contribution to $\Delta S_{\text{II}}^{\ddagger}$ is separable, and making reasonable assumptions about bond lengths and bond angles in the complex (5), the uncertainty in A can be reduced to that in the vibrational (and possibly electronic) contributions. For reactions in which a = H and b is a hydrocarbon, Bywater and Roberts (6) showed that rotation about the center of gravity contributed +2.3 e.u. to $\Delta S_{\text{II}}^{\ddagger}$ for methane, −0.1 e.u. for ethane, and a negligible amount for higher hydrocarbons. Internal rotations would have to be taken into account in certain instances, but in the case a = H (or even a = D) their contribution to $\Delta S_{\text{II}}^{\ddagger}$ would be quite small, except for possible changes in the symmetry numbers for internal rotations. In a series of reactions involving hydrogen abstraction from a paraffin by atomic hydrogen, one would therefore expect the relative values of the A factors to be determined almost exclusively by the relevant values of κ, n', μ, σ, and the vibrational contribution to $\Delta S_{\text{II}}^{\ddagger}$.

Herzberg's assumption (7) that propane has C_{2v} symmetry has recently been confirmed by Lide (8); it therefore has the symmetry number $\sigma = 2$. Presumably $\sigma^{\ddagger} = 1$. Using the value $A_1 = 1.3\times10^{14}$ cm^3 mole^{-1} sec^{-1} obtained in this laboratory (1), and assuming κ and n' to be equal to unity, we obtain the value $\Delta S_{\text{II}}^{\ddagger} = 6.8$ e.u. for reaction [1].

The complex has three more internal degrees of freedom than propane. One of these has been taken into account in the factor kT/h of equation [ii], namely the C–H_2 stretching vibration. By making the usual assumption that all frequencies except the doubly

Can. J. Chem. Downloaded from www.nrcresearchpress.com by 210.87.254.42 on 09/05/12
For personal use only.

degenerate C–H–H bending and the H–H stretching are the same in the complex as in the propane molecule, it follows that the vibrational contribution to $\Delta S_{11}^{\pm}$ will arise from these new frequencies and the disappearance of one of the C–H frequencies on the secondary carbon of propane.

To affect A by as much as 10% any contribution to $\Delta S_{11}^{\pm}$ would have to be at least as large as 0.19 e.u.; from tables of Einstein functions it can be seen that this would necessitate a fundamental frequency of less than 1100 cm^{-1}. The loss of the C–H frequency will therefore have no effect. If we assume an H–H stretching frequency greater than 1100 cm^{-1} we are left with the doubly degenerate bending frequency as the only important contribution to $\Delta S_{11}^{\pm}$. To contribute 6.8 e.u. at 400° K it would have to have a value of 138 cm^{-1}.

From the result $A_2 = 6.6 \times 10^{13}$ $cm^3\,mole^{-1}\,sec^{-1}$ obtained from the present experiments, we calculate that $\Delta S_{11}^{\pm} = 4.2$ e.u. A statistical analysis of the results shows a probable error of 0.24 e.u. in the difference of 2.6 e.u. between the values of $\Delta S_{11}^{\pm}$ for reactions [1] and [2]. The difference is therefore significant. If, as before, the whole of $\Delta S_{11}^{\pm}$ is attributed to the doubly degenerate C–H–H bending frequency in the complex, then its value here must be 273 cm^{-1}, approximately twice that found for the complex C_3H_9.

The reason for the smaller value of $\Delta S_{11}^{\pm}$ for reaction [2] is not easily explained. However, the discrepancy is not unique to the abstraction of secondary hydrogen by atomic hydrogen. The observed ratio of the A factors, A_4/A_3, for secondary hydrogen abstraction from propane [3] and *n*-butane [4] by atomic chlorine (9) is 1.2_2; the value calculated from [iv], assuming $\Delta S_{11}^{\pm}$ to be the same for each reaction is 1.79, giving a discrepancy factor of 0.63. The effect is even larger for the abstraction of tertiary hydrogen from isobutane [5] and 2,3-dimethylbutane [6] by methyl radicals (10); the observed value of A_6/A_5 is 0.63; the calculated value is 1.8, yielding a discrepancy factor of 0.35. Since the present experiments give a discrepancy factor of 0.25 for A_2/A_1, one might conclude that the effect of adjacent hydrogen atoms on the C–H–X bending frequency is greatest when the abstracting radical X has the smallest mass, although the amount of supporting evidence is very limited.

ACKNOWLEDGMENTS

We are indebted to the National Research Council for continued financial support, and to the Senate of the University of Toronto for the L. V. Redman Fellowship and the Special Open Fellowship awarded to one of us (H. A. K.).

REFERENCES

1. H. A. Kazmi, R. J. Diefendorf, and D. J. Le Roy. Can. J. Chem. **41**, 690 (1963).
2. S. Glasstone, K. J. Laidler, and H. Eyring. The theory of rate processes. McGraw-Hill Book Company, Inc., New York and London. 1941.
3. E. W. Schlag. J. Chem. Phys. **38**, 2480 (1963).
4. S. W. Benson and P. S. Nangia. J. Chem. Phys. **38**, 18 (1963).
5. D. J. Wilson and H. S. Johnston. J. Am. Chem. Soc. **79**, 29 (1957).
6. S. Bywater and R. Roberts. Can. J. Chem. **30**, 773 (1952).
7. G. Herzberg. Infrared and raman spectra of polyatomic molecules. Van Nostrand, New York. 1945.
8. D. R. Lide. J. Chem. Phys. **33**, 1514 (1960).
9. J. H. Knox and R. L. Nelson. Trans. Faraday Soc. **55**, 954 (1959).
10. A. F. Trotman-Dickenson. Gas kinetics. Butterworth Scientific Publications, London. 1955.

Can. J. Chem. Downloaded from www.nrcresearchpress.com by 210.87.254.42 on 09/05/12
For personal use only.

FORMATION CROSS SECTIONS OF VARIOUS RADIONUCLIDES FROM Ni, Fe, Si, Mg, O, AND C FOR PROTONS OF ENERGIES BETWEEN 130 AND 400 MEV[1]

GARIMELLA V. S. RAYUDU
Department of Chemistry, Carnegie Institute of Technology, Pittsburgh 13, Pennsylvania
Received August 14, 1963

ABSTRACT

Formation cross sections of Co^{56}, Mn^{54}, Mn^{52}, Cr^{51}, V^{48}, P^{32}, and Be^{7} from Fe and Ni; of Na^{24}, Na^{22}, and Be^{7} from Si and Mg; and of Be^{7} from C and O have been measured for incident protons of energies between 130 and 400 Mev to assist in the interpretation of data on cosmic-ray-produced nuclides in iron and stone meteorites. Formation cross sections of Mn^{54}, Mn^{52}, Cr^{51}, V^{48}, and P^{32} are found to be a factor of 2 to 3 lower from Ni than from Fe, whereas those of Co^{56} are 20- to 50-fold higher than from Fe. Be^{7} cross sections from C are found to be almost the same as from O, within experimental uncertainties. Cross sections of Na^{24} and Na^{22} from Mg and Si are found to be relatively energy independent, whereas those of P^{32} and Be^{7} from Ni and Fe are found to increase rapidly with increasing energy. Some qualitative conclusions are drawn about the production of cosmogenic activities in meteorites.

INTRODUCTION

This paper describes the variation of formation cross sections of various product radionuclides when meteoritic elements (Ni, Fe, Si, Mg, O, and C) are irradiated by protons of energies between 130 and 400 Mev. In most of the previous studies of cross sections and excitation functions for high energy nuclear reactions, as described by Miller and Hudis (1), the main interest has been on the mechanism of the interactions. Such studies have acquired additional interest in connection with the study of cosmogenic activities in meteorites. Recently, several experiments have been done by Davis (2), Fireman and Zähringer (3), Honda and Lal (4, 5), Rayudu and Shedlovsky (6–12), and Rudstam *et al.* (13, 14) using targets, projectiles, and energies directly applicable to this problem. Ideally, one should have experimental excitation functions for all cosmogenic nuclides for protons of energies from threshold to several billion electron volts and for the important secondary particles (especially neutrons, π-mesons, and photons) of energies up to hundreds of million electron volts. In practice this is impossible, and one must be satisfied with representative data which will permit reasonably accurate interpolations, extrapolations, and theoretical calculations for the more important cases.

It is important to mention that α-particle-induced reaction cross sections in medium-weight elements are comparable to proton reaction cross sections in the 130–400 Mev energy region, as reported by Koterling (15), who bombarded Nb with protons and helium ions. In addition, Davis (2) bombarded Ni and Fe with 880 Mev α-particles, and the measured cross sections of $A^{37,39}$ agreed with proton-induced formation cross sections. Because cosmic rays consist of approximately 90% protons and 8% α-particles, measurements of proton excitation functions of several relatively short-lived radioactive products from meteoritic elements were undertaken.

EXPERIMENTAL PROCEDURE AND RESULTS

The target materials are listed in Table I. Silicon targets were sliced at Westinghouse Research Laboratories; half-inch square targets of the other elements were punched in this laboratory.

[1]*This work was supported by the U.S. Atomic Energy Commission.*

Can. J. Chem. Downloaded from www.nrcresearchpress.com by 210.87.254.6 on 09/05/12
For personal use only.

TABLE I

Target elements	Thickness (mg/cm²)	Chemical form
Ni	45	Metal foil
Fe	40	Metal foil
Si	120	Thin slice
Mg	22	Metal foil
C	75	Polyethylene (85% C)
C + O	75	Delrin (40% C and 53% O)[a]
Al	7	Metal foil (monitor)

[a]A polymer with the composition: —CH_2O— produced by Dupont Co., U.S.A.; supplied by Commercial Plastics Co., Pittsburgh 13, Pa., U.S.A.

Irradiations were carried out in the circulating beam of the Carnegie Institute of Technology Synchrocyclotron with proton energies between 130 and 400 Mev. The irradiation time varied between 8 and 12 minutes. The incident proton energy was varied by placing the target at different radial distances in the circulating beam. The energy spread was estimated to be about 10% at 130 and 208 Mev and 5% at 297 and 396 Mev. Fe, Ni, Mg, and Si targets were irradiated in maximum beam currents (as much as 1 microampere), whereas for the polyethylene and Delrin targets the beam currents were of the order of 0.1 microampere. All the cross sections were measured relative to the cross sections for the $Al^{27}(p,3pn)Na^{24}$ monitor, using 1-mil aluminum foils. The cross section values used in this work are 10, 9.3, 11, and 10.6 mb at 130, 208, 297, and 396 Mev respectively. For detailed discussion of the monitor cross sections see Gray (16) and Treytl (17). Na^{24} activity was measured from the monitor foil, using an end-window proportional counter.

Fe and Ni targets.—Fe and Ni targets were dissolved in aqua regia in the presence of Co, Mn, Cr, V, Ca, P, Na, and Be carriers. Chemical separation was started 2 to 3 days after the irradiation. The chemical separation procedure is summarized in the form of a flow sheet in Fig. 1. Fe was retained in the anion-exchange step, whereas Ni was decanted with the Na and Ca fraction. After the final purification, Co was electroplated. Mn was counted as MnO_2, V as $Pb(VO_3)_2$, Cr as $BaCrO_4$, Be as BeO, and P as $MgNH_4PO_4$. Yields were estimated by weighing finally mounted samples except in the case of V, for which the yield was estimated spectrophotometrically by the peroxide method.

Si, Mg, O, and C targets.—Be^7 from polyethylene and Delrin, and Na^{24}, Na^{22}, and Be^7 from Mg and Si were measured directly using a 2 in. × 2 in. NaI (Tl) scintillation crystal in conjunction with a 512-channel pulse-height analyzer.

The radiation characteristics of the nuclides measured are given in Table II. The measured cross sections are presented in Tables III, IV, and V. The total estimated uncertainties reported for various cross sections in Tables III, IV, and V include the errors and uncertainties involved in counting, chemical yield determination, beam monitoring, and saturation factor. In all cases, duplicate determinations agreed within 5 to 12%. Fifteen percent uncertainty was estimated for cross sections at energies of 208, 297 and 396 Mev. Higher uncertainties, up to 20%, are estimated for results at 130 Mev, because of low beam current. In the case of Be^7 from O, Mg, and Si, 20 to 25% uncertainties were estimated because of the difficulties in processing the data. From Mg and Si containing both Na^{22} and Be^7 activity, the intensity of the 480-kev Be^7 photopeak was estimated from the composite 480- and 511-kev photopeak by subtracting the Na^{22} contribution to the 511-kev photopeak (calculated from its corresponding 1280-kev peak). The multiplication factor used to calculate counts due to the 511-kev peak from the counts of the 1280-kev peak was determined by counting a pure Na^{22} source under similar conditions.

DISCUSSION

The formation cross sections of Co^{56} in Fe are in good agreement with the values of Treytl (17) and Koch (18), who studied $Ni^{64}(p,n)Cu^{64}$. P^{32} cross sections from Fe and Ni are in agreement with Gray's (16) P^{32} cross sections from Co, which are between the present values from Ni and Fe. Be^7 cross sections from C are almost the same, within experimental uncertainties, as from O. This observation is in agreement with Honda and Lal (4), who reported Be^7 cross sections from C and O at 225, 300, and 400 Mev. In Table V, Na^{24} cross sections were calculated from Mg on the basis of total mass and also on the basis of Mg^{25+26}. The latter calculations are justified in the case of Mg because the (p,2p) contribution could be as much as 20 mb according to Morrison (19), who determined the $Si^{30}(p,2p)Al^{29}$ cross sections in this energy region.

Can. J. Chem. Downloaded from www.nrcresearchpress.com by 210.87.254.6 on 09/05/12
For personal use only.

Can. J. Chem. Downloaded from www.nrcresearchpress.com by 210.87.254.6 on 09/05/12
For personal use only.

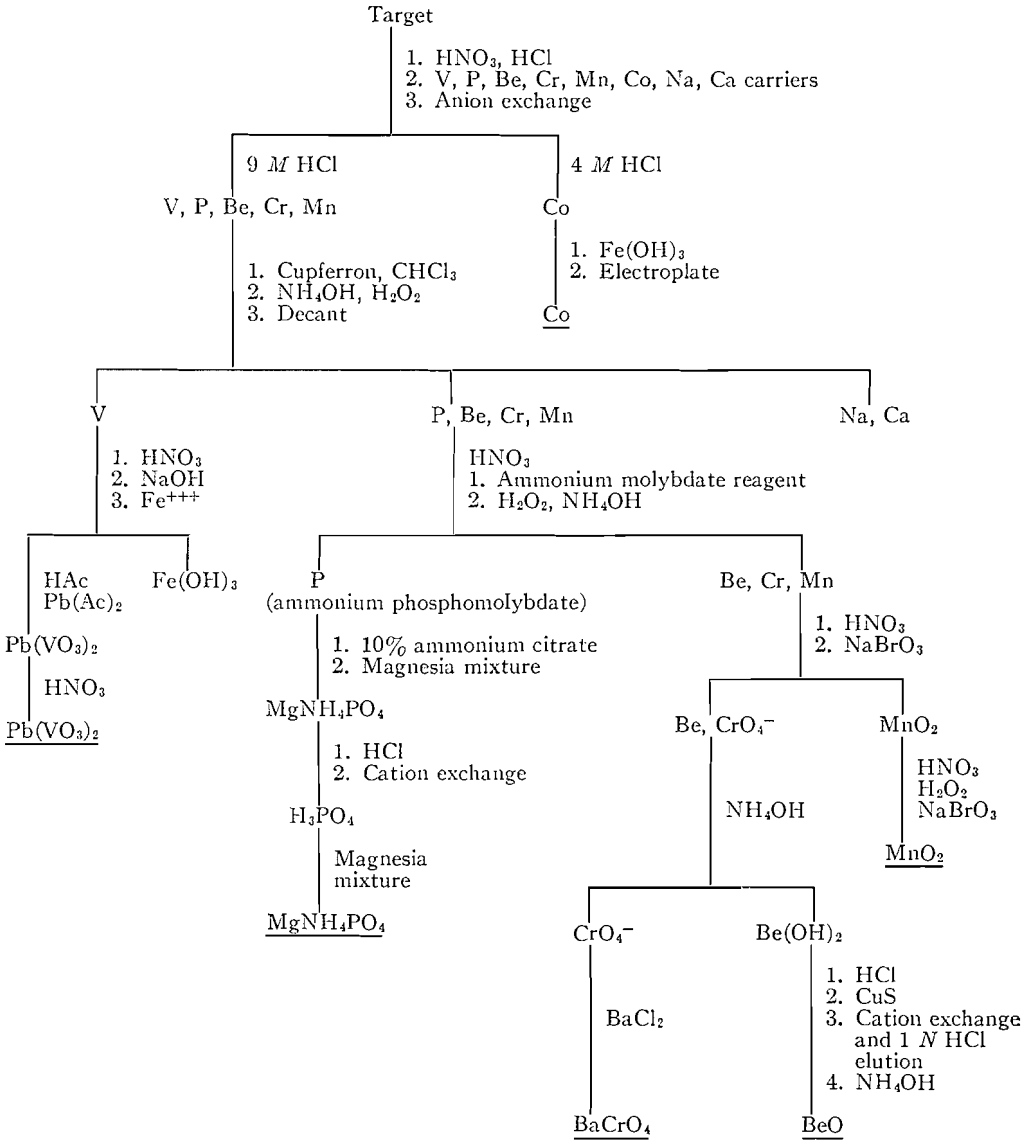

FIG. 1. Flow diagram of the chemical separation scheme for Fe or Ni targets.

From the cross sections reported in this work, some qualitative conclusions may be drawn about the production of cosmogenic activities in iron and stone meteorites.

Iron meteorites.—Production of cobalt activities from Ni is considerably higher than from Fe. High-energy products such as H^3, Be^7, Be^{10}, C^{14}, Na^{22}, Na^{24}, etc., have almost the same cross section from Fe as from Ni, whereas formation cross sections of low-energy products such as Mn^{54}, Mn^{52}, Cr^{51}, V^{48}, and P^{32} from Ni are found to be lower by a factor of 2 to 3 than from Fe. In the case of low-energy products, therefore, corrections are necessary, corresponding to Fe(~93%) and Ni(~7%) contents in meteorites.

TABLE II

Relevant properties of radionuclides measured

Nuclide[a]	Half-life[b]	Radiation measured (Mev)	Branch abundance	Type of cross section
		From Fe and Ni		
Co^{56}	77 day	β^+	0.18	I (independent)
Mn^{54}	310 day	0.850γ	1.00	I
Mn^{52}	5.7 day	β^+	0.33	C (cumulative)
Cr^{51}	27.8 day	0.320γ	0.10	C
V^{48}	16.1 day	β^+	0.56	C
P^{32}	14.3 day	β^-	1.00	I
Be^7	53 day	0.477γ	0.11	C
		From Si, Mg, O, and C		
Na^{24}	15 hour	2.75γ	1.00	I
Na^{22}	2.58 year	1.28γ	1.00	C
Be^7	53 day	0.477γ	0.11	C

[a]Co^{56} and P^{32} were measured using a methane flow-window proportional counter. Mn^{54}, Mn^{52}, Cr^{51}, V^{48}, $Na^{24,22}$, and Be^7 were measured using a 2 in.×2 in. NaI(Tl) scintillation crystal in conjunction with a 512-channel pulse-height analyzer.

TABLE III

Cross sections from iron (mb)

Proton energy (Mev)	Co^{56a}	Mn^{54}	Mn^{52}	Cr^{51}	V^{48b}	P^{32}	Be^7
130	4.25±0.85	38.2±7.6	68.6±10.3	30±6.0	5.87	0.020±0.004	0.175±0.035
208	2.26±0.34	27.7±4.2	49.0±7.4	22±3.00	6.40	0.086±0.013	0.313±0.047
297	1.50±0.22	21.4±3.2	33.7±5.1	25±3.75	8.50	0.320±0.050	0.47 ±0.071
396	0.89±0.13	18.63±2.8	24.2±4.0	25±3.75	9.50	0.61 ±0.092	0.57 ±0.086

[a]Cross sections based on 96.18% of the weight of Fe.
[b]Because up to 80–90% of the Cr^{48} had decayed by the time of separation, the V^{48} cross sections may be considered as lower limits for cumulative cross sections.

TABLE IV

Cross sections from nickel (mb)

Proton energy (Mev)	Co^{56}	Mn^{54}	Mn^{52}	Cr^{51}	V^{48}	P^{32}	Be^7
130	90	10.5±2.0	39.5±6.0	20.0±4.0	3.50	0.0070±0.0014	0.206±0.041
208	59	8.5±1.3	33.5±5.6	19.0±2.8	4.62	0.025 ±0.004	0.380±0.070
297	62	9.8±1.4	38.5±5.9	19.2±2.8	6.50	0.1330±0.020	0.594±0.090
396	45	6.95±1.0	28.0±4.3	18.0±2.7	7.50	0.2720±0.041	0.810±0.122

[a]Since 30% of the 6.4d Ni^{56} had decayed by the time of chemical separation, the cross sections may be considered as upper limits for independent formation.
[b]Since up to 80 to 90% of the Cr^{48} had decayed by the time of separation, the V^{48} cross sections may be considered as lower limits for cumulative cross sections.

Stone meteorites.—It is obvious that Fe contributes to the production of nuclides mainly in the region $15 \leqslant Z \leqslant 26$. It follows that the production of nuclides with low Z(Na^{22}, C^{14}, Be^{10}, H^3, etc.) by low-energy ($\leqslant$ 700 Mev) cosmic-ray protons comes from Si, Mg, and O rather than from Fe. Even at high energies (0.7 Bev–7 Bev), products in the region $1 \leqslant Z \leqslant 15$ are produced mainly from Si, Mg, and O rather than from Fe, because the Fe content is low in stones.

Can. J. Chem. Downloaded from www.nrcresearchpress.com by 210.87.254.6 on 09/05/12
For personal use only.

Can. J. Chem. Downloaded from www.nrcresearchpress.com by 210.87.254.6 on 09/05/12
For personal use only.

TABLE V

Cross sections from Si, Mg, C, and O (mb)

Proton energy (Mev)	From Si			From Mg				From C	From O
	Na^{24}	Na^{22}	Be^{7}	Na^{24a}	Na^{24b}	Na^{22}	Be^{7}	Be^{7}	Be^{7}
130	3.378±.660	10.41±1.06	1.07±.27	28.2±4.2	6.10±.61	28.3±4.20	2.66±.66	8.32±1.66	7.85±1.96
208	3.662±.366	10.28±1.03	0.76±.19	25.2±3.76	5.37±.54	21.6±3.22	2.31±.58	6.8±1.05	4.89±1.22
297	4.740±.474	13.09±1.3	1.69±.34	29.0±4.30	6.18±.62	23.8±3.55	2.48±.62	8.50±1.30	6.54±1.63
396	4.78 ±.478	12.46±1.3	2.02±.40	30.5±4.55	6.48±.65	22.2±3.31	3.25±.88	7.05±1.08	7.47±1.87

[a]Cross sections based on Mg^{25+26} as target weight.
[b]Cross sections based on total weight of magnesium as target weight.

ACKNOWLEDGMENTS

The author acknowledges the encouragement and support offered by Professor T. P. Kohman during the progress of the work. He also thanks Dr. H. F. John of Westinghouse Research Laboratories for supplying the Si targets, the crew of the Synchrocyclotron for their kind cooperation, and Mr. F. Mesojedec for servicing the counters used in this work.

REFERENCES

1. J. M. MILLER and J. HUDIS. Ann. Rev. Nucl. Sci. **9**, 159 (1959).
2. R. DAVIS. Private communication. July, 1963.
3. E. L. FIREMAN and J. ZÄHRINGER. Phys. Rev. **107**, 1695 (1957).
4. M. HONDA and D. LAL. Phys. Rev. **118**, 1618 (1960).
5. M. HONDA. J. Geophys. Res. **67**, 4847 (1962).
6. G. V. S. RAYUDU. Progr. Rept. Nuclear chemistry research at Carnegie Institute of Technology. Subsection II.A.2. 1962–1963.
7. G. V. S. RAYUDU. Progr. Rept. Nuclear chemistry research at Carnegie Institute of Technology. Subsection II.A.3. 1962–1963.
8. G. V. S. RAYUDU. Progr. Rept. Nuclear chemistry research at Carnegie Institute of Technology. Subsection II.A.5. 1962–1963.
9. G. V. S. RAYUDU and J. P. SHEDLOVSKY. Progr. Rept. Nuclear chemistry research at Carnegie Institute of Technology. Subsection II.A.6. 1962–1963.
10. G. V. S. RAYUDU and J. P. SHEDLOVSKY. Progr. Rept. Nuclear chemistry research at Carnegie Institute of Technology. Subsection II.A.7. 1962–1963.
11. J. P. SHEDLOVSKY and G. V. S. RAYUDU. Progr. Rept. Nuclear chemistry research at Carnegie Institute of Technology. Subsection II.A.4. 1962–1963.
12. J. P. SHEDLOVSKY. Progr. Rept. Nuclear chemistry research at Carnegie Institute of Technology. Subsection II.B.10. 1961–1962.
13. G. RUDSTAM. Spallation of medium weight elements. Thesis. University of Uppsala, Uppsala, Sweden. 1956.
14. G. RUDSTAM, P. C. STEVENSON, and R. L. FOLGER. Phys. Rev. **87**, 358 (1952).
15. R. G. KOTERLING. High-energy nuclear reactions of niobium with incident protons and helium ions. Thesis. University of California, Berkeley, California. UCRL-10461. 1962.
16. J. GRAY. Excitation functions and recoil behavior of specific products from the interaction of high energy protons with Al, Co, Ag and Au. Thesis. Carnegie Institute of Technology, Pittsburgh 13, Pa. 1962.
17. W. J. TREYTL. A systematic study of (p,n) reactions in the 100–400 Mev region. Thesis. Carnegie Institute of Technology. Pittsburgh 13, Pa. 1963.
18. R. E. KOCH. A radiochemical study of (p,n) reactions at high energies and some proton-induced reactions in nickel. Thesis. University of Chicago, Chicago, Illinois. 1955.
19. D. L. MORRISON and A. A. CARETTO, JR. Phys. Rev. **127**, 1731 (1962).

Can. J. Chem. Downloaded from www.nrcresearchpress.com by 210.87.254.6 on 09/05/12
For personal use only.

Can. J. Chem. Downloaded from www.nrcresearchpress.com by 210.87.254.105 on 09/05/12
For personal use only.

FIELD DEPENDENCE AND ANOMALOUS TEMPERATURE DEPENDENCE OF TAFEL SLOPES FOR PROCESSES OCCURRING AT HIGH ELECTROSTATIC FIELDS

M. J. DIGNAM
Department of Chemistry, University of Toronto, Toronto, Ontario
Received December 11, 1963

ABSTRACT

A consideration of the probability per unit time for the transport of a charged species over a potential barrier in the presence of a high external electrostatic field shows that the net activation energy for such a process is in general a complex function of the field strength. Both the field dependence and the anomalous temperature dependence of the Tafel slope for the steady-state anodic oxidation of Ta, Nb, and Al are accounted for quantitatively by a simple model according to which the field independent component of the potential energy function for displacement of a mobile charged species is assumed to resemble a Morse function. Accordingly, the steady-state anodic oxidation data for these metals may be represented within experimental error by only three empirical constants, the pre-exponential factor, the activation energy, and the Morse function distance parameter. If, in place of a Morse function, a parabolic or cosine potential energy function is assumed, less satisfactory agreement with the data is obtained. Although there is some doubt concerning the uniqueness of the Morse function in explaining the data, there is no doubt that the present considerations are able to account entirely for the anomalous Tafel slope behavior.

INTRODUCTION

The recent data of Young (1) on the anodic oxidation of tantalum shows an unmistakable field dependence of the Tafel slope $(\partial E/\partial \ln i)$ where E is the field strength in the oxide and i the current density. This dependence was accounted for quantitatively, over a range of temperatures, by an empirical equation of the form:

$$i = i_0 \exp\left[-(Q-\alpha E+\gamma E^2)kT\right] \qquad [1]$$

where Q, α, and γ are all positive constants. At the time equation [1] was first postulated, no theoretical justification for the quadratic term in the field, γE^2, was offered. Young (1) showed that it could not be justified by assuming a range or distribution of parameters associated with an amorphous film. Recently, Young (2) has suggested that the quadratic term may be explained in terms of an increase in the activation energy with increasing condenser pressure. As the condenser pressure is proportional to E^2, this explanation predicts a quadratic term of the correct sign.

Using Young's estimates of the magnitudes of the parameters involved, the predicted value of γ is only about 1/20 of the empirical value.* Admittedly, the estimate of the effect of pressure on the activation energy could be too small by a factor of 20. It is at least equally probable, however, that the influence of the condenser pressure is below the limit of detection. This is certainly the case for the actual estimate given by Young.

The purpose of the present paper is to show that a quadratic term of precisely the correct magnitude arises quite naturally from a more detailed analysis of ion transfer processes at high field strengths. The results obtained for the steady-state anodic oxidation of tantalum, niobium, and aluminum are compared with the theoretical predictions.

**As Young states (2) "a rule of thumb given by Jost is that, with materials such as AgCl, 100 atm are about equivalent to 1° C". Accordingly, $100\partial(Q'/kT)/\partial P \sim -\partial(Q'/kT)/\partial T$ where $Q' = Q + \Delta Q$ is the activation energy at a pressure P (in atm), $\Delta Q = 0$ when $P = 0$, and T is the temperature in °K. We also have P (atm) $= 1.2\times10^5[E\,(V/Å)]^2$ (2) so that since $\Delta Q \ll Q$ and $T \sim 300°$ K, $\Delta Q \sim 4Q[E(V/Å)]^2$ and hence $\gamma \sim 4Q = 8.6$ eÅ^{2}V^{-1} for $Q = 2.185$ ev (1). The empirical value for γ is 167.5 eÅ^{2}V^{-1} (1).*

Can. J. Chem. Downloaded from www.nrcresearchpress.com by 210.87.254.105 on 09/05/12
For personal use only.

THEORY

For generality, we shall not refer to any particular mechanism, but shall concern ourselves solely with the determination of the probability per unit time for a given charged species to cross a potential energy barrier. The results should be applicable to any high-field ionic transport process, whether it be anodic oxidation with metal–oxide interface control as suggested by Cabrera and Mott (3), anodic oxidation with transport of ions through the film rate controlling, or indeed conventional electrode processes such as hydrogen evolution.

The central problem, therefore, is to calculate the probability of an ion transfer process, p, in the presence of a very high field, E. To calculate this we must assume a form for the interaction potential between the ionic species in question and its immediate surroundings. Since we are concerned solely with highfield strengths, only the transfer probability in the direction assisted by the field need be considered. Accordingly, the potential energy function at zero applied field may be represented by $U_1'(\chi)$, where χ is the position variable chosen to increase in the ion transfer direction. It is now reasonable to suppose that the potential energy function in the presence of a field E will be given by:

$$U'(\chi,E) = U_0' + U_1'(\chi) - E\chi q \qquad [2]$$

where q is the absolute magnitude of the charge on the mobile species concerned and U_0' the usual arbitrary constant. In writing this equation, it is assumed that the interaction potential between the charged species and its surroundings is independent of the field (i.e. $\partial U'(\chi)/\partial E = 0$). If all of the bonding involved is purely ionic, this is probably a satisfactory approximation and we could proceed with equation [2] assuming quite properly that q is a constant. If covalent bonding is involved, however, q would in general be a function of both field strength and position. If q varies with field strength, it follows that $U_1'(\chi)$ would also vary with field strength for a given value of χ. In an attempt to generalize equation [2] to cover the cases where bonding has both ionic and covalent character, we shall consider the following equation:

$$U(\mu,E) = U_0 + U_1(\mu) - E\mu \qquad [3]$$

where μ is the product of the charge on the ionic species and its displacement from an arbitrary origin. It is worth noting initially that equations [2] and [3] are fundamentally identical if q is independent of χ and E. Furthermore, they differ only in the specific form of the functions U_1' and U_1 if μ is independent of field strength for fixed χ, provided that μ increases monotonically with χ over the region of interest. The difference between the equations arises, therefore, when μ is a function of E for fixed χ. For this case equation [2] implies that the potential interaction term, $U_1'(\chi)$, depends only on nuclear displacement, χ, which is clearly not valid, whereas equation [3] implies that the potential interaction term, $U_1(\mu)$, depends only on the charge displacement, μ, an assumption difficult to assess. Since an increase in μ for fixed χ (brought about by increasing E) should lead to a reduction in the bonding energy, the correction to equation [2] contained in equation [3] appears to be in the right direction. Whether or not it is of the correct magnitude, however, is not known. In the absence of detailed theoretical calculations, therefore, we must regard $U_1(\mu)$ as, in fact, a function of both E and μ. Fortunately, for realistic values of the current density for high field processes, the field can be varied only over a fairly narrow range (i.e. about $\pm 10\%$ from the mean value for anodic oxidation of the value metals). Therefore, provided $U_1(\mu)$ does not vary too rapidly with E for μ constant,

equation [3] should represent a fairly good approximation to the true behavior for field strengths in this range. We shall proceed on this assumption. The success ultimately achieved on this basis can be regarded either as evidence in support of equation [3], or as evidence that q is constant over the experimental range of field strengths.

For any given functional form for $U_1(\mu)$, it is now a simple matter to determine the net activation energy, $W(E)$, for the transfer process and hence the transfer probability, p, as a function of field. The values of μ corresponding to minima and maxima in $U(\mu,E)$, μ_0 and μ_m respectively, are obtained on solving the equation:

$$\partial U(\mu,E)/\partial\mu = 0. \qquad [4]$$

The net activation energy is then given by

$$W(E) = U(\mu_m,E) - U(\mu_0,E) \qquad [5]$$

and the transfer probability per unit time by

$$p(E) = \nu \exp [-W(E)/kT] \qquad [6]$$

where ν is the usual frequency term.

From equations [3] to [5] we may now derive the form of $W(E)$ for any reasonable representation of the potential energy function $U_1(\mu)$. If $U_1(\mu)$ contains enough disposable constants, agreement between the theoretical and empirical form of $W(E)$ can always be arranged. Such a procedure, however, has little to recommend it. We shall therefore restrict our attention to potential energy functions which involve only two disposable constants and are qualitatively of the correct form. In this way the three empirical constants of equation [1] (Q, α, and γ) will be replaced by only two independent constants, thus providing a fairly stringent test of the theory. Three obvious functions meeting these requirements are the parabolic function, the cosine function, and the Morse function. In the following sections each of these functions is considered in turn; the predictions derived from each are ultimately compared with experimental data.

"Clipped" Parabolic Potential

The simplest function one can choose to represent $U_1(\mu)$, which is qualitatively of the correct form, is the "clipped" parabolic function:

$$U_1(\mu) = \varphi(\mu/\mu^*)^2 \text{ for } \mu^* \geqslant \mu \geqslant 0 \qquad [7]$$

$$= \varphi \text{ for } \mu \geqslant \mu^*.$$

For this representation of $U_1(\mu)$, φ can be thought of as the zero field activation energy and μ^* the zero field charge-activation distance product, or "activation dipole". In view of the foregoing discussion concerning equation [3], these interpretations should not be taken too literally. It is preferable to consider φ and μ^* as extrapolated values, the extrapolation to $E = 0$ being based on experimental data at high fields only.

From equations [3], [4], and [7] we obtain:

$$[\partial U(\mu,E)]/\partial\mu = 0 = (2\varphi\mu/\mu^{*2}) - E \qquad [8]$$

from which $\mu_0 = E\mu^{*2}/2\varphi$. Since $\partial U_1(\mu)/\partial\mu$ has a discontinuity at $\mu = \mu^*$, μ_m cannot be obtained from equation [8], but is clearly given by $\mu_m = \mu^*$. We now have:

$$W(E) = \varphi - E\mu^*[1 - E\mu^*/4\varphi]. \qquad [9]$$

Before discussing this result, $W(E)$ will be calculated for a cosine and a Morse potential energy function.

Can. J. Chem. Downloaded from www.nrcresearchpress.com by 210.87.254.105 on 09/05/12
For personal use only.

Cosine Potential

Assuming the following cosine potential energy function

$$U_1(\mu) = (\varphi/2)[1-\cos \pi\mu/\mu^*] \qquad [10]$$

where both φ and μ^* have the same significance as for the parabolic potential, we can write:

$$[\partial U(\mu,E)]/\partial\mu = 0 = (\pi\varphi/2\mu^*) \sin (\pi\mu/\mu^*)-E$$

or

$$\sin \pi\mu/\mu^* = 2\mu^*E/\pi\varphi. \qquad [11]$$

Solving equation [11] for μ, the values for μ_0 and μ_m are given by the solutions which lie in the intervals $(0, \mu^*/2)$ and $(\mu^*/2, \mu^*)$ respectively. It therefore follows that:

$$U_1(\mu_0) = (\varphi/2)\left\{1-\left[1-\frac{4}{\pi^2}\left(\frac{\mu^*E}{\varphi}\right)^2\right]^{\frac{1}{2}}\right\} \qquad [12]$$

$$U_1(\mu_m) = (\varphi/2)\left\{1+\left[1-\frac{4}{\pi^2}\left(\frac{\mu^*E}{\varphi}\right)^2\right]^{\frac{1}{2}}\right\} \qquad [13]$$

and

$$\mu_0 = \frac{\mu^*}{\pi}\sin^{-1}\frac{2\mu^*E}{\pi\varphi} = \mu^*-\mu_m. \qquad [14]$$

Substituting these values into equations [3] and [5] we obtain

$$W(E) = \varphi\left[1-\frac{4}{\pi^2}\left(\frac{\mu^*E}{\varphi}\right)^2\right]^{\frac{1}{2}}-\mu^*E+\frac{2\mu^*E}{\pi}\sin^{-1}\frac{2\mu^*E}{\pi\varphi}. \qquad [15]$$

Expanding the square root term and the inverse sine function as power series in (μ^*E/φ) gives:

$$W(E) = \varphi-\mu^*E\left[1-\frac{2}{\pi^2}\frac{\mu^*E}{\varphi}-\frac{4}{3\pi^4}\left(\frac{\mu^*E}{\varphi}\right)^3 \cdots\right]$$

or

$$W(E) \simeq \varphi-\mu^*E\left[1-\frac{2}{\pi^2}\frac{\mu^*E}{\varphi}\right] \qquad [16]$$

for

$$\mu^*E/\varphi \lesssim 1.$$

Equation [16] is of the same form as that obtained for the parabolic potential energy function, the coefficient of E^2 being, however, somewhat smaller.

Morse Potential

Proceeding now with the Morse function, we have:

$$U_1(\mu) = \varphi[1-\exp(-\mu/\omega^*)]^2 \qquad [17]$$

where φ has approximately the same significance as for the other two potential functions. There is no very useful physical interpretation of ω^*, it being best regarded simply as a parameter with the same dimensions as μ. Proceeding as before, we have:

$$\frac{\partial v(\mu,E)}{\partial\mu} = 0 = \frac{2\varphi}{\omega^*}\left[1-\exp\left(-\frac{\mu}{\omega^*}\right)\right]\exp\left(-\frac{\mu}{\omega^*}\right)-E$$

or

$$\exp\left(-\frac{\mu}{\omega^*}\right) = \frac{1}{2}\left[1 \pm \left(1-\frac{2\omega^*E}{\varphi}\right)^{\frac{1}{2}}\right]. \qquad [18]$$

Can. J. Chem. Downloaded from www.nrcresearchpress.com by 210.87.254.105 on 09/05/12
For personal use only.

The two roots give values for μ_0 and μ_m which on substitution into equations [3] and [5] lead to the following equation:

$$W(E) = \varphi\left[1-\frac{2\omega^*E}{\varphi}\right]^{\frac{1}{2}}-\omega^*E\ln\left[\frac{1+(1-2\omega^*E/\varphi)^{\frac{1}{2}}}{1-(1-2\omega^*E/\varphi)^{\frac{1}{2}}}\right]. \quad [19]$$

Expanding the square root terms as power series in ω^*E/φ yields:

$$W(E) = [1-z-\tfrac{1}{2}z^2-\tfrac{1}{2}z^3\ldots]+\omega^*E\ln(z/2)$$
$$+\omega^*E\ln[(1+\tfrac{1}{2}z+\tfrac{1}{2}z^2.\ldots)/(1-\tfrac{1}{2}z-\tfrac{1}{4}z^2.\ldots)] \quad [20]$$

where $z = \omega^*E/\varphi$.

Expanding the second logarithm as a power series in z and collecting terms we obtain:

$$W(E) = \varphi-\omega^*E\left[1-\ln\frac{\omega^*E}{2\varphi}-\frac{\omega^*E}{2\varphi}-\left(\frac{\omega^*E}{2\varphi}\right)^2\ldots\right] \quad [21]$$

In order to arrange equation [21] in a form similar to equations [9] and [16] we shall make the following approximations:

$$(\omega^*E/2\varphi)^2 \lll 1$$

and

$$\ln\frac{\omega^*E}{2\varphi} = \ln\omega^*\left[\frac{\bar{E}+E-\bar{E}}{2\varphi}\right] = \ln\frac{\omega^*\bar{E}}{2\varphi}+\ln\left[1+\frac{E-\bar{E}}{\bar{E}}\right]$$
$$\simeq \ln\frac{\omega^*E}{2\varphi}+\frac{E}{\bar{E}}-1 \text{ for } \frac{E-\bar{E}}{\bar{E}} \ll 1$$

where $\bar{E}$ may be regarded as the mean value of the field strength for the set of measurements in question. Equation [21] then becomes

$$W(E) \simeq \varphi-\mu^*E\left[1-\frac{\mu^*E}{C\varphi}\right] \quad [22]$$

where

$$\mu^* = \omega^*\left[2-\ln\frac{\omega^*\bar{E}}{2\varphi}\right] \quad [23]$$

and

$$\frac{1}{C} = \left(\frac{\varphi}{\mu^*\bar{E}}\right)\frac{\omega^*}{\mu^*}+\frac{1}{2}\left(\frac{\omega^*}{\mu^*}\right)^2. \quad [24]$$

For comparison with experiment, it is desirable to obtain a single equation relating the experimental parameters φ, μ^*, C, and $\bar{E}$. Accordingly, from equation [24]:

$$\frac{\omega^*\bar{E}}{\varphi} = \left[1+\frac{2}{C}\left(\frac{\mu^*\bar{E}}{\varphi}\right)^2\right]^{\frac{1}{2}}-1. \quad [25]$$

Substituting this value for ω^* into equation [23] gives

$$y = \left[\left(1+\frac{2y^2}{C}\right)^{\frac{1}{2}}-1\right]\left\{2+\ln 2-\ln\left[\left(1+\frac{2y^2}{C}\right)^{\frac{1}{2}}-1\right]\right\} \quad [26]$$

where

$$y = \mu^*\bar{E}/\varphi.$$

From equation [26] y has been calculated for various values of y^2/C, from which corresponding values of $\mu^*\bar{E}/\varphi$ and C were obtained. The result of these calculations is shown

Can. J. Chem. Downloaded from www.nrcresearchpress.com by 210.87.254.105 on 09/05/12
For personal use only.

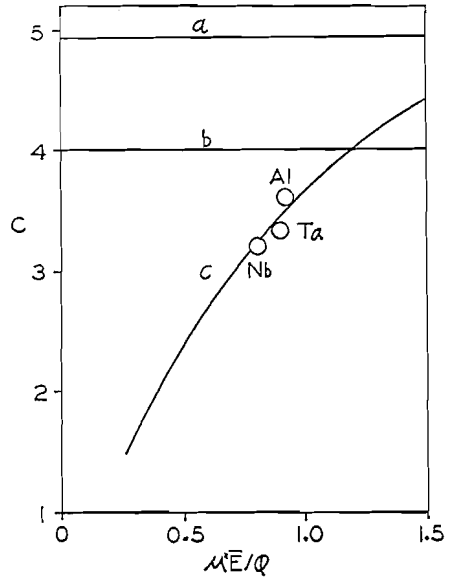

FIG. 1. The quadratic parameter, C, as a function of the mean field strength calculated assuming the potential energy function to be given by: (*a*) a cosine function, (*b*) a clipped parabolic function, (*c*) a Morse function. Experimental points are for the steady-state anodic oxidation of tantalum, niobium, and aluminum. (Both C and $\mu^*\bar{E}/\varphi$ are dimensionless.)

graphically in Fig. 1 along with the corresponding relations obtained for the parabolic and cosine potential energy functions. The points are experimental values, the calculations for which are discussed in a following section.

Summary

We may now summarize the results of the present section. The probability per unit time for a high field strength ion transfer process can be represented by the equation:

$$p(E) \simeq \nu \exp\left\{-\left[\varphi-\mu^*E\left(1-\frac{\mu^*E}{C\varphi}\right)\right]/kT\right\} \qquad [27]$$

where the three parameters φ, μ^*, and C are not independent constants but are related through the form of the potential energy function, as indicated in Fig. 1, making only two of them independent. If we assume for a given electrode process that the overall rate is controlled solely by the high field transfer of one kind of ionic species, then we may write

$$i = i_0 \exp\left\{-\left[\varphi-\mu^*E\left(1-\frac{\mu^*E}{C\varphi}\right)\right]/kT\right\}. \qquad [28]$$

The validity of this assumption in connection with the steady-state anodic oxidation of the valve metals will depend, of course, on the mechanism for the process. It will be valid for the Cabrera–Mott mechanism (3) and for the mechanism proposed recently by the author (4) but will not be strictly valid for the high field Frenkel defect model proposed by Bean, Fisher, and Vermilyea (5).

Equation [28] may also be applied to electrode reactions, such as hydrogen evolution from high overpotential metals, provided, of course, that the mechanism is consistent with the restrictive condition on this equation. For these processes, however, it is more

Can. J. Chem. Downloaded from www.nrcresearchpress.com by 210.87.254.105 on 09/05/12
For personal use only.

convenient to replace μ^*E in equation [28] by $q^*\psi$ where $q^* = \mu^*/\delta$, ψ is the absolute value of the potential drop across the Helmholtz double layer, and δ the width of the Helmholtz layer. The evaluation of ψ from experimental data and the correction for the field dependence of δ are by no means trivial problems. The application of the foregoing to the hydrogen evolution reaction will therefore be treated in a subsequent paper.

COMPARISON OF AVAILABLE EXPERIMENTAL DATA WITH THEORY

The only valve metals for which data of sufficient precision* are available to allow the parameters in equation [28] to be evaluated are Ta (1), Nb (6), Al (7), and Ti (8). Of these four the first three can be fitted to an equation of the form of [28] or [1] with C or γ positive. The behavior of Ti, however, is markedly different from the first three and, although the data may be fitted to an equation of the form of [1], γ is negative. Since the monoxide of titanium displays very large deviations from the stoichiometric composition (9), it is possible that effects arising from gross non-stoichiometry are responsible for the different anodic behavior of Ti.

The evaluations of the parameters for Ta, Nb, and Al are outlined in the following sections.

Tantalum

From analysis of extensive steady-state data for the anodic oxidation of tantalum in 0.1 N aqueous sulphuric acid, Young (1) calculated the following values for the constants in equation [1]:

$$i_0 = 10^{8.24} \text{ amp/cm}^2 \; Q = 2.185 \text{ ev}, \; \alpha = 34.98 \text{ e Å}, \; \gamma = 167.5 \text{ e Å}^2\text{v}^{-1}.$$

Comparing equations [1] and [27], we have

$$\varphi = Q, \; \mu^* = \alpha, \; C = \alpha^2/\gamma Q$$

from which $C = 3.33$. The mean field strength for the set of experiments from which the above parameters were calculated is about 0.056_5 v/Å $= \bar{E}$.

Niobium

For niobium, Young (6) found that the Tafel slope measured over the current density range 10^{-5} to 10^{-3} amp/cm^2 was, within experimental error, independent of temperature between 0° C and 70° C. This result may be expressed mathematically as follows

$$\partial^2 E/\partial(\ln i)\partial(1/T)] \simeq 0 \text{ for } \log i \simeq -4, \; T \simeq 273+35. \qquad [29]$$

Assuming that the current density is given by equation [27], we may solve for E and obtain

$$E = \frac{C\varphi}{2\mu^*}\left[1-\left(1-\frac{4}{C}-4\frac{kT}{C\varphi}\ln\frac{i}{i_0}\right)^{\frac{1}{2}}\right] \qquad [30]$$

from which

$$\frac{\partial E}{\partial(1/T)} = S = -\left[\frac{kT^2}{\mu^*}\ln\left(\frac{i}{i_0}\right)\right]\Big/\left[1-\frac{4}{C}-4\frac{kT}{C\varphi}\ln\left(\frac{i}{i_0}\right)\right]^{\frac{1}{2}}. \qquad [31]$$

Setting $$\partial S/\partial \ln i = 0$$

we obtain $$C = 4+2(kT/\varphi)\ln(i/i_0). \qquad [32]$$

**Data for metals which show a dependence of anodic oxidation parameters on film thickness have been excluded since additional complicating phenomena are clearly involved.*

Can. J. Chem. Downloaded from www.nrcresearchpress.com by 210.87.254.105 on 09/05/12
For personal use only.

The reciprocal Tafel slope, β, will be defined as follows:

$$\beta = \frac{\partial \ln i}{\partial E} = \mu^*\left[1-\frac{2\mu^*E}{C\varphi}\right]/kT. \qquad [33]$$

Solving for C, μ^*, and $(\mu^*E/C\varphi)$ from equations [28], [31], [32], and [33], the following equations can be obtained:

$$C = 4\left[1+\left(\frac{1}{1+TE/S}\right)^2\right]^{-1} \qquad [34]$$

$$\mu^* = (1+TE/S)kT\beta \qquad [35]$$

$$\frac{\mu^*E}{C\varphi} = \frac{1}{2}\left[1+\frac{S}{TE}\right]^{-1}. \qquad [36]$$

Young determined five independent values for the slope of E versus $1/T$, the current density being 10^{-5}, 10^{-4}, and 10^{-3} amp/cm^2. Within experimental error, they were all the same, the mean value being 13.0 v Å^{-1} °K with a standard deviation of 1%. We shall assume that this represents the slope of the tangent, $S = \partial E/\partial(1/T)$, for the median condition (i.e. $T = 308°$ K and $\log i = -4$). Again, Young determined values for $\Delta E/\Delta \log i$ for i changing from 10^{-5} to 10^{-3} amp/cm^2 at eight different temperatures from 0° C to 70° C. They were found to be the same within experimental error, the mean value being represented in the expression $\Delta \ln i/\Delta E = 635$ Å/v with a standard deviation of 3%. Again we shall consider this as the slope of the tangent, $\beta = \partial \ln i/\partial E$, for the median conditions stated above. The median field value corresponding to $\log i = -4$ and $T = 308°$ K is, from Young's data, 0.0428 v/Å. Substituting these results into equations [34] to [36] the following values for the parameters are obtained:

$$C = 3.21,\ \mu^* = 34.0 \text{ e Å},\ \varphi = 1.80 \text{ ev}.$$

Using these values, i_0 can be calculated from equation [27] by setting $i = 10^{-4}$ for $E = 0.0428$ v/Å and $T = 308°$ K, obtaining $i_0 = 10^{7.61}$ amp/cm^2. From these constants, the data may be reproduced within the accuracy of the data.

Aluminum

Recently, measurements of the variation of the steady-state Tafel slope with field strength for the anodic oxidation of aluminum have been made in the author's laboratory (7). From these, the following values were calculated:

$$\mu^* = 23.5 \text{ e Å},\ C\varphi = 7.83 \text{ ev},\ i_0 \exp[-\varphi/kT] = 10^{-28.7}.$$

Unfortunately, at the present time measurements have been made at 25° C only, so that to obtain values for C and φ separately a value for i_0 of $10^{-8.0}$ amp/cm^2 was assumed. Since i_0 for tantalum and niobium differ by only a factor of 4, it is unlikely that i_0 for aluminum would differ from their geometric mean value by as much as a factor of 10. An error of about 3% would be introduced in C and φ by a factor of 10 error in i_0. The values for C and φ calculated in this way are 3.61 and 2.17 ev. The mean field strength for the set of experiments from which these constants were calculated was 0.085_0 v/Å $= \bar{E}$.

Discussion

The calculated values for C for these three systems are plotted against $\mu^*\bar{E}/\varphi$ in Fig. 1. The results are clearly in excellent accord with the theoretical curve calculated assuming

Can. J. Chem. Downloaded from www.nrcresearchpress.com by 210.87.254.105 on 09/05/12
For personal use only.

a Morse function potential energy surface. Accordingly, the Morse function parameter, ω^*, was determined from equation [25], the values for C and $(\mu^*\bar{E}/\varphi)$ used for the calculation being read from curve c of Fig. 1 at a position close to the experimental point in question. A summary of the results is presented in Table I.

TABLE I

Kinetic parameters for the steady-state anodic oxidation of Ta, Nb, and Al

Oxide	i_0 amp/cm²	φ ev	μ^* e Å	C	$\bar{E}$ v/Å	ω^* e Å
Ta_2O_5	$10^{8.21}$	2.18_5	34.9_8	3.33	0.056_5	7.8
Nb_2O_5	$10^{7.64}$	1.80	34.0	3.21	0.042_8	7.7
Al_2O_3	$10^{8.0*}$	2.17	23.5	3.61	0.085_0	5.7

*An assumed value based on the experimental values for Ta_2O_5 and Nb_2O_5.

A more precise calculation of the best value for ω^* would require a computer analysis of the data using equations [6] and [19] (or [21]) directly. Indeed, in view of the results, the proper conduction equation for these systems might well be:

$$i = i_0 \exp\left\{-\left[\varphi - \omega^* E\left(1 - \ln\frac{\omega^* E}{2\varphi} - \frac{\omega^* E}{2\varphi}\right)\right] \Big/ kT\right\} \qquad [37]$$

in accordance with equation [21].

Very accurate data over a wide range of field strengths (which would require obtaining data over a wide temperature range) would be needed for a more stringent test of the suitability of equation [37] and hence of the Morse function. There is no doubt, however, that the Morse function accounts for the quadratic term in the field in the net activation energy with an accuracy which is rather surprising.

It is worth noting that at low field strengths the Morse function cannot represent a satisfactory approximation to the true potential energy function since in the limit as $E \to 0$ the activation charge–distance product will become infinite. However, for the present valve metal systems, only the shape of the Morse function from about 0 to $2\omega^*$ is of any consequence, the shape of the potential energy curve beyond about $2\omega^*$ having no effect on the net activation energy for field strengths which give rise to measurable currents.

The very large values found for both μ^* and ω^* is deserving of some comment. The result is readily explained if the effective field strength assisting the ion transfer process includes an appreciable contribution from the electrostatic polarization of the oxide dielectric medium. A new mechanism based, in part, on this notion has been proposed recently by the author (4).

Preliminary attempts to interpret the anomalous temperature dependence of the Tafel slope for hydrogen evolution from Hg, observed by Bockris and Parsons (10), by assuming a Morse function potential for displacement of the proton from its hydration shell have been successful, the agreement between theory and experiment being comparable to that presented here for the valve metals. This data, along with other data for hydrogen evolution, will be discussed in a future publication.

ACKNOWLEDGMENTS

The author would like to thank Dr. J. P. Valleau and Dr. R. G. Barradas for reading the manuscript and for helpful suggestions.

Can. J. Chem. Downloaded from www.nrcresearchpress.com by 210.87.254.105 on 09/05/12
For personal use only.

REFERENCES

1. L. YOUNG. Proc. Roy. Soc. Ser. A, **258**, 496 (1960).
2. L. YOUNG. J. Electrochem. Soc. **110**, 589 (1963).
3. N. CABRERA and N. F. MOTT. Rept. Progr. Phys. **12**, 163 (1949).
4. M. J. DIGNAM. In preparation. (Presented at Meeting of American Electrochemical Society, Pittsburgh, Penn. April, 1963.)
5. C. P. BEAN, J. C. FISHER, and D. A. VERMILYEA. Phys. Rev. **101**, 551 (1956).
6. L. YOUNG. Trans. Faraday Soc. **52**, 502 (1956).
7. M. J. DIGNAM, D. GOAD, and M. SOLE. In preparation.
8. W. MIZUSHIMA. J. Electrochem. Soc. **108**, 825 (1961).
9. P. EHRLICK. Z. Elektrochem. **45**, 362 (1939).
10. J. O'M. BOCKRIS and R. PARSONS. Trans. Faraday Soc. **45**, 916 (1949).

Can. J. Chem. Downloaded from www.nrcresearchpress.com by 210.87.254.105 on 09/05/12
For personal use only.

VAPOR-PHASE RADIOLYSIS OF CYCLOHEXANE AND MIXTURES OF BENZENE AND CYCLOHEXANE[1]

J. BLACHFORD AND P. J. DYNE
Research Chemistry Branch, Atomic Energy of Canada Ltd., Chalk River, Ontario
Received January 10, 1964

ABSTRACT

The vapor-phase radiolysis of cyclohexane and benzene–cyclohexane mixtures has been studied with isotopic tracer techniques using C_6D_{12} and C_6D_6. Benzene does not quench the molecular detachment of hydrogen, $C_6D_{12} \rightsquigarrow D_2 + C_6D_{10}$, but interacts with the second-order processes giving HD in C_6D_{12}–C_6H_{12} mixtures. This interaction is not H-atom scavenging and an ionic mechanism is preferred. The radiolysis of all these systems is very different from their liquid-phase radiolysis.

The low radiolytic yields in liquid benzene–cyclohexane mixtures are a classic example of 'protection'. The interactions causing these low yields are physical; they do not involve the making or breaking of chemical bonds. This has been shown in two ways: by complete product analysis (1) and by techniques using isotopically labelled hydrocarbons (2). These isotopic techniques have revealed similar interactions in alkane mixtures (3) which are, however, absent in the vapor phase (4). As a result, we expect the vapor-phase radiolysis of benzene–cyclohexane mixtures to show marked differences from the liquid-phase radiolysis.

We have applied our isotopic techniques to the vapor-phase radiolysis. In the liquid, benzene quenches both the first-order process, which gives D_2 by molecular detachment from C_6D_{12}, and the second-order processes which give HD in C_6H_{12}–C_6D_{12} mixtures. In the vapor, however, the D_2 yield is reduced much more slowly than would be expected if H-atom scavenging were occurring and so we favor an ionic mechanism for this interaction. Physical interactions quenching the first-order processes are absent.

EXPERIMENTAL

Fisher 'Spectranalyzed' cyclohexane and benzene and Merck benzene-d_6 and benzene-free cyclohexane-d_{12} were used as received.

To minimize air contamination the sample vessels (volume about 330 ml) were evacuated to 5×10^{-6} mm Hg at 500° C for at least 24 hours before being filled and irradiated. Even so, the gaseous radiolytic products contained about 3% air. The vessels were sealed to a grease- and mercury-free preparation line; the sample (about 2 ml of liquid) was degassed by repeated freezing, pumping, and thawing and was then distilled into the irradiation vessel.

During irradiation in our Co^{60} source, the vessels were kept at a constant temperature (±2° C) in an electric furnace. Using the techniques already described (4), we found the dose rate to be 4.87×10^{15} ev/sec g cyclohexane; the dose in most experiments was 3.61×10^{19} ev/g organic vapor.

After irradiation the sample was frozen in liquid nitrogen; the gaseous products were pumped through two liquid-nitrogen traps and their volume measured with a McLeod gauge. This fraction, which contained mainly hydrogen and methane, was analyzed by mass spectrometry. A second fraction volatile at −112° C, consisting of C_2–C_4 hydrocarbons, was analyzed by gas chromatography on a silica-gel column.

The yields of the liquid products, cyclohexene, bicyclohexyl, and phenylcyclohexane, were determined by gas–liquid chromatography. Cyclohexene was separated on a 12-ft column packed with 20% 1,2,3-tris-(2-cyanoethoxy)propane on acid-washed firebrick. Bicyclohexyl and phenylcyclohexane were separated on a 6-ft column packed with silicone – gum rubber on firebrick.

[1]*Issued as A.E.C.L. No. 1924.*

Can. J. Chem. Downloaded from www.nrcresearchpress.com by 210.87.254.5 on 09/05/12
For personal use only.

Can. J. Chem. Downloaded from www.nrcresearchpress.com by 210.87.254.5 on 09/05/12
For personal use only.

RESULTS

C_6H_{12}–C_6D_{12} Mixtures

A mixture containing 4.77 mole % C_6D_{12} was used in all experiments. In dilute solutions we can define $G_1(D)$ as the number of molecules of D_2 per 100 ev absorbed in the deuterated hydrocarbon. It has previously been shown (2) that in dilute solutions D_2 arises from a first-order reaction in which both D atoms come from the same molecule. Similarly, $g(HD)$ is the number of molecules of HD per 100 ev absorbed in the deuterated hydrocarbon. This quantity is a measure of second-order reactions leading to hydrogen.

The values of G(total hydrogen), $g(HD)$, and $G_1(D)$ as a function of temperature are given in Fig. 1. Over the range 70–250° C the yields are independent of temperature, but the yields of total hydrogen and HD increase rapidly above 250° C. The temperature-independent values are given in Table I together with the values for the liquid-phase radiolysis (2).

TABLE I
Liquid- and vapor-phase yields of the isotopic hydrogens, molecules/100 ev

	Vapor, average values between 100° and 225° C	Liquid (2)
G (total hydrogen)	5.3	5.3_4
$g(HD)$	3.6	3.5_6
G_1 (D)	0.8	0.3_2

TABLE II
Yields in cyclohexane radiolysis, molecules/100 ev

Product	γ-Radiolysis, this work	α-Radiolysis (5)	Liquid (6)
H_2	5.3	8.0	5.5_5
C_6H_{10}	2.2	0.77	3.2_7
$(C_6H_{11})_2$	1.0	0.45	1.9_5
CH_4	0.6	0.13	<0.05
C_2H_6	1.9	0.28	—
C_2H_4	2.8	2.48	—
C_2H_2	—	0.65	—
C_3H_8	2.2	0.95	—
C_3H_6	0.43	0.78	—
iso-C_4H_{10}	0.18	0.04	—
n-C_4H_{10}	0.038		—

Product yields at 125° C are shown in Table II together with the vapor-phase α-radiolysis data of Ramaradhya and Freeman (5) and the liquid-phase data (γ-rays) of Dyne and Stone (6). The temperature dependence of the yields of bicyclohexyl, methane, and cyclohexene are shown in Fig. 2. From 70 to 235° C the yields of the first two products increase but little, while cyclohexene increases by a factor of two. The dose dependence of the hydrogen and cyclohexene yields is shown in Table III.

C_6H_{12}–C_6D_{12}–C_6H_6 Mixtures

The effect of benzene on the radiolytic yields in cyclohexane was examined by adding various amounts of benzene to a mixture of 4.77 mole % C_6D_{12} in C_6H_{12}. The dependence of the normalized yields of H_2, HD, and D_2 on temperature and benzene concentration is shown in Figs. 3*a*, *b*, and *c*. The normalizing factors are temperature-independent yields in Table I.

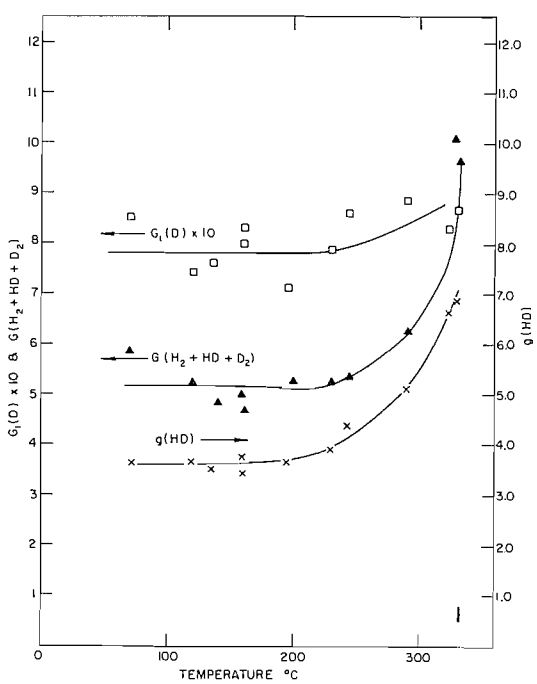

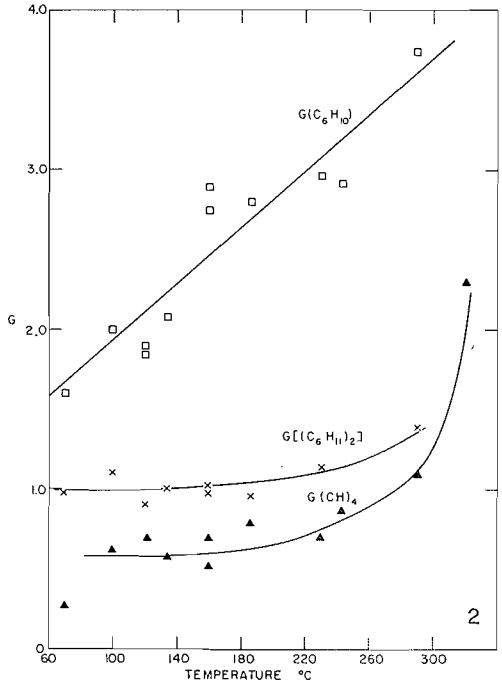

FIG. 1. The temperature variation of the yields of total hydrogen, HD, and D_2 (expressed as $G_1(D)$) in the radiolysis of C_6H_{12} with 4.77 mole % C_6D_{12}.

FIG. 2. The temperature variation in the yields of cyclohexene, bicyclohexyl, and methane in the gas-phase radiolysis of cyclohexane.

TABLE III

Dose dependence on the yields of hydrogen and cyclohexene

Dose, 10^{19} ev/g	Temperature, ° C	$G(H_2)$	$G(C_6H_{10})$
3.51	125	5.44	2.2
7.02	125	4.93	1.7
3.51	235	5.55	3.1
7.02	235	4.73	2.3

We shall compare all yields to those predicted by the mixture law which can be stated as follows (3). If G^0_M is the yield of M derived from a pure material A and X_A is the fraction of energy absorbed by A in a mixture, then the yield in the mixture is $G^0_M X_A$. In its simplest form this means that the yields are linear functions of composition.

No significant deviation from the mixture law is exhibited by $G(D_2)$ at any temperature. Both $G(H_2)$ and $G(HD)$ deviate from the mixture law at low temperatures. At higher temperatures the deviation is reduced and at 235° C the total hydrogen yield obeys the mixture law.

The effect of benzene on the other product yields at 125° C is shown in Fig. 4. Phenylcyclohexane is a significant product at low benzene concentration. As with hydrogen the effect of benzene on these yields is reduced at higher temperatures; the yield of phenylcyclohexane is also reduced.

Can. J. Chem. Downloaded from www.nrcresearchpress.com by 210.87.254.5 on 09/05/12
For personal use only.

Can. J. Chem. Downloaded from www.nrcresearchpress.com by 210.87.254.5 on 09/05/12
For personal use only.

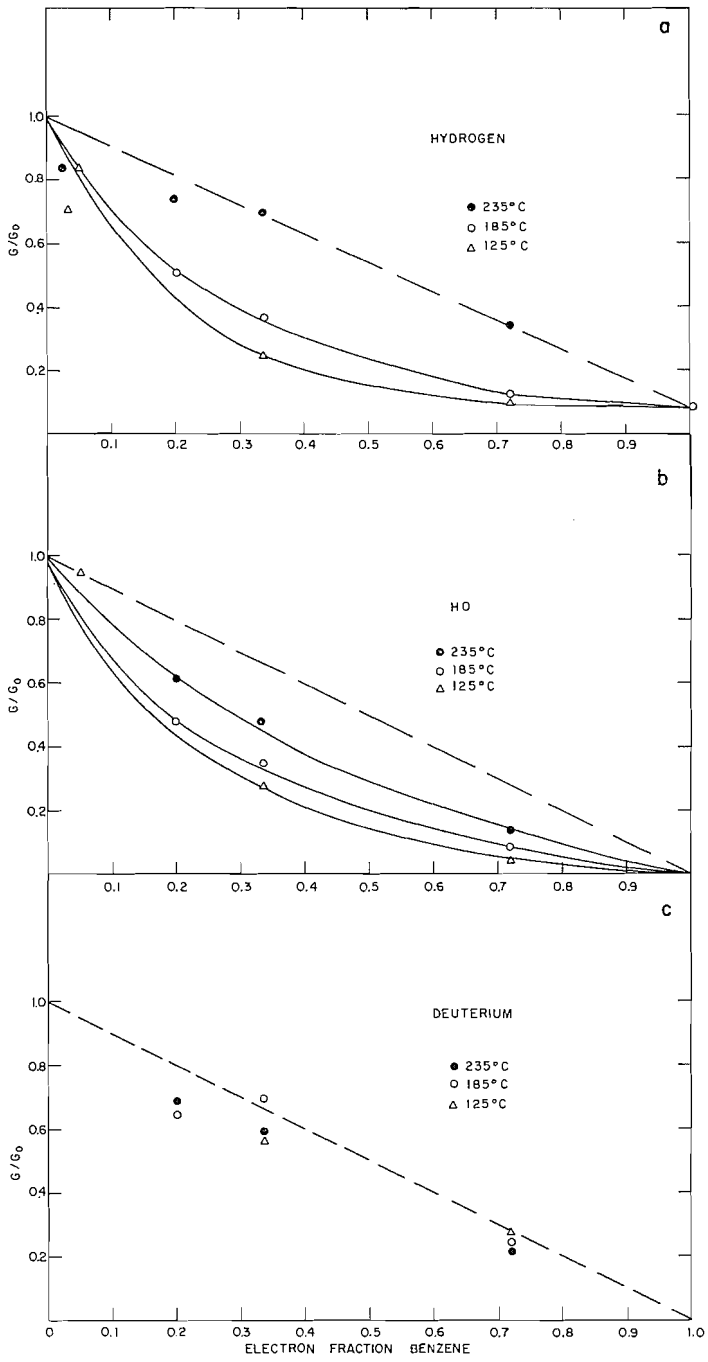

FIG. 3. The normalized yields of total hydrogen (3*a*), HD (3*b*), and D_2 (3*c*) in the radiolysis of mixtures of benzene with cyclohexane containing 4.77 mole % C_6D_{12}. The broken line represents the mixture law. The values of G_0 are, respectively, G (total hydrogen), g(HD), and G(D) as given in Table I.

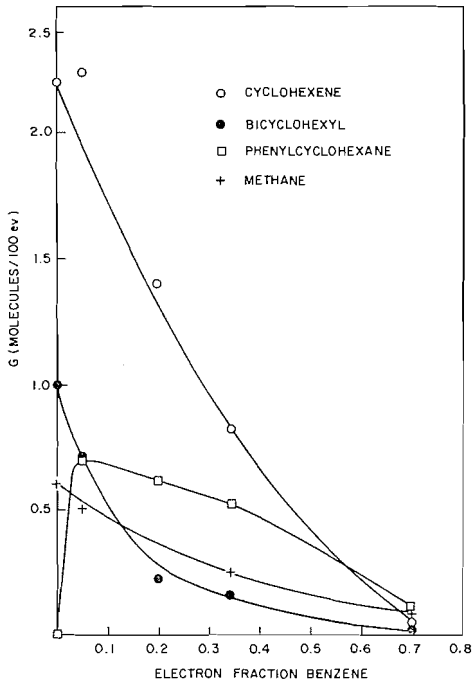

FIG. 4. Yields of cyclohexene, bicyclohexyl, phenylcyclohexane, and methane in benzene–cyclohexane mixtures at 125° C.

C_6H_{12}–C_6D_6 Mixtures

Benzene also takes part in second-order reactions which *produce* hydrogen. This is shown in the HD yields found in mixtures of 5 mole % C_6D_6 (Table IV). The high HD

TABLE IV

Isotopic composition of hydrogen from 5 mole % C_6D_6 in C_6H_{12}

Temperature, ° C	$G(H_2)$	G(HD)	$G(D_2)$	g(HD)
125	3.68	0.147	0.0049	2.92
235	4.52	0.278	0.0050	5.50

yield, comparable with that observed in similar C_6D_{12}–C_6H_{12} mixtures, shows that the efficiency of this reaction is comparable with the corresponding second-order reaction in the C_6H_{12}–C_6D_{12} system.

DISCUSSION

C_6H_{12}–C_6D_{12} Mixtures

We interpret the isotopic yields in terms of two reactions: a first-order molecular detachment and a second-order abstraction. If one writes $C_6H_{12} \equiv C_H$ and $C_6D_{12} \equiv C_D$, these may be written

$$C_H \rightsquigarrow H_2 + \ldots \quad [1]$$

$$C_H \rightsquigarrow X_H + \ldots \quad [2]$$

$$X_H + C_H \rightarrow H_2 + \ldots \quad [3]$$

Can. J. Chem. Downloaded from www.nrcresearchpress.com by 210.87.254.5 on 09/05/12
For personal use only.

where X_H is the reactive intermediate in the bimolecular process. In mixtures of C_H and C_D where $C_H \gg C_D$, D_2 is formed only by the analogue of [1]

$$C_D \rightsquigarrow D_2 + \ldots . \qquad [4]$$

The function $G_1(D)$ is a measure of reaction [4]. HD is formed by the analogues of [3]

$$X_H + C_D \rightarrow HD + \ldots \qquad [5]$$

$$X_D + C_H \rightarrow HD + \ldots . \qquad [6]$$

The function $g(HD)$ is a measure of the sum of reactions [5] and [6].

In the liquid we suppose that the first- and second-order processes have a common precursor, viz.

$$C_D \rightsquigarrow C_D^* \begin{cases} \nearrow D_2 + \text{products} \\ \searrow X_D + \text{products} \end{cases} \qquad [7]$$

since we find that, whatever the environment of the deuterated cyclohexane,

$$g(HD) \simeq A\, G_1(D) + B, \text{ where } A \simeq 4 \text{ and } B \simeq 1.5.$$

The gas-phase values of $g(HD)$ and $G_1(D)$ do not fit this equation. For $G_1(D) = 0.78$, this equation gives $g(HD) \sim 5$ which is significantly greater than the observed value of 3.6. This difference is discussed further in relation to the effect of benzene on $g(HD)$ and $G_1(D)$.

The negligible temperature coefficient of $G_1(D)$ is to be expected if it measures a true 'molecular' process such as reaction [4]. The small temperature dependence of the HD yield deserves comment. If one takes into account the scatter of the data, it appears that between 100 and 200° C $g(HD)$ increases by, at the most, 10%; a 20% increase would have been readily apparent. Part of the HD yield is formed in reaction [5], which is in competition with reaction [3]; this competition is likely to be temperature dependent. The rest of the HD comes from reaction [6], which (in dilute solutions of the deuterated hydrocarbon) is not involved in any competitive reactions. If reaction [6] contributed significantly to the HD yield, then the temperature dependence of reactions [3] and [5] would be masked. Wiberg (7) has estimated that the maximum effect due to the difference between C–H and C–D bond-dissociation energies would lower k_H/k_D ($\equiv k_3/k_5$) by about 25% between 100 and 200° C. If about half the HD yield came through reaction [6], then the observed, very small, temperature coefficient is in accord with Wiberg's estimate.

The sharp increase in the H_2 and HD yields above 250° C is similar to that observed in polyphenyls (8) at higher temperatures, >400° C. At these temperatures a radiation-induced pyrolysis is appearing which leads to further decomposition. As the aromatic hydrocarbons are thermally more stable than the aliphatic hydrocarbons, this induced pyrolysis appears at a higher temperature.

Product yields are tabulated in Table II for comparison with the α-radiolysis data at 108° C of Ramaradhya and Freeman (5). Back, Woodward, and McLauchlin (9) have already pointed out that $G(H_2)$ in the α-radiolysis of hydrocarbons is higher than that obtained in γ-radiolysis. These data show that even larger changes may be observed in the yields of higher molecular weight products.

For cyclohexene this comparison may be complicated by secondary reactions which lower the yield from the true 'initial' value at very low dose. These secondary reactions are

Can. J. Chem. Downloaded from www.nrcresearchpress.com by 210.87.254.5 on 09/05/12
For personal use only.

shown in the increase in the cyclohexene yield between 100 and 220° C. This increased yield is not due to an increase in C–H bond breaking since $G(H_2)$ is temperature independent, nor is it due to an increase in radical disproportionation since bicyclohexyl (which would presumably be formed in the competing combination reaction) does not show a corresponding decrease. The increase in yield must be due to a reaction destroying cyclohexene and forming a polymer, whose efficiency decreases with an increase in temperature. Such a reaction will also cause $G(C_6H_{10})$ to decrease with dose (Table IV). Polymer formation is also shown, indirectly, by the poor hydrogen balance. The yields of hydrogen and molecules containing extra hydrogen relative to cyclohexane exceed the total yield of hydrogen-deficient molecules by about 7 G units. A similar inbalance was reported in Ref. (5).

The high yield of C_2, C_3, and C_4 hydrocarbons in the gas phase as compared with their small yields in the liquid phase has been discussed by Ramaradhya and Freeman (5) and by Kevan and Libby (10). Carbon–carbon bond breakage is strongly inhibited in condensed phases.

C_6H_6–C_6H_{12} Mixtures

From our measurements of $g(HD)$ and $G_1(D)$ in benzene–cyclohexane mixtures, we see that benzene does not interact with the first-order molecular-detachment process

$$C_D \rightsquigarrow C_D^* \rightarrow D_2 + \ldots .$$

The interaction of benzene with the second-order process

$$X_D + C_H \rightarrow HD + \text{products}$$

can be written

$$X_D, X_H + \text{benzene} \rightarrow \text{no hydrogen} \qquad [8]$$

Here we note that X_D and X_H could be any intermediates in the second-order process, and they are not, necessarily, the ones which react in the final steps, reaction [3] and/or [6].

Ramaradhya and Freeman (11) measured the total hydrogen yield in benzene–cyclohexane mixtures. When they used the H-atom scavenging mechanism

$$H + C_6H_{12} \rightarrow H_2 + C_6H_{11} \qquad [9]$$

$$H + C_6H_6 \rightarrow H_2 + C_6H_5 \qquad [10]$$

$$H + C_6H_6 \rightarrow C_6H_7 \rightarrow \text{no hydrogen} \qquad [11]$$

to interpret their results they found that reaction [10] had to have an unreasonably high efficiency (k_{10} was large). Because of this they rejected this mechanism. Our isotopic techniques also show that this analysis is invalid; there is another source of hydrogen—the unquenched molecular detachment. As reaction [10] is, in effect, a source of hydrogen, their kinetic analysis would express any other source of hydrogen as a high value of k_{10}.

In our opinion, an H-atom scavenging mechanism is unlikely because of the unreasonably low value required for k_{11}. If we assume that the contribution of the unquenched molecular-detachment process in C_6D_{12}–C_6H_{12}–C_6H_6 mixtures is equal to $G_1(D)$, 0.78, then from the hydrogen yield at 50% benzene we find $k_9/k_{11} \sim 0.16$. Now, Schiff and Steacie (12) found the collision yield for reaction [9] to be 1.4×10^{-7} and Allen, Melville, and Robb (13) found the collision yield of [11] to be 1.3×10^{-4} so that $k_9/k_{11} \sim 10^{-3}$ at 25° C. As our experiments were carried out at 125° C, the activation-energy difference would have to be ~12 kcal to reconcile these two values. The best estimate for the activation energy of reaction [9] is 8 kcals (12) and for reaction [11] is 4 kcal (14) giving ΔE

Can. J. Chem. Downloaded from www.nrcresearchpress.com by 210.87.254.5 on 09/05/12
For personal use only.

$\sim$ 4 kcal. The observed ratio of k_9/k_{11} is therefore too large for the interaction to be attributed to hydrogen-atom scavenging. Our conclusion agrees with that of Ramaradhya and Freeman although our arguments differ.

As ionic reactions play an important part in the gas-phase radiolysis of hydrocarbons (15), it seems likely that X_D and X_H are ions and we suggest that they may be fragment (C_2–C_3) ions. Futrell (16) has proposed a mechanism for the radiolysis of *n*-hexane in which these fragment ions react rapidly with *n*-hexane in a hydride-ion transfer reaction to give fragment molecules or radicals and a $C_6H_{13}^+$ radical ion. This radical ion decomposes on capturing an electron to give a hydrogen atom and an olefin (or a biradical). A molecule of hydrogen is then formed by H abstraction by this H atom from a *n*-hexane molecule.

According to Borkowski and Ausloos (17), benzene does not take part so readily in hydride transfer reactions with fragment ions but forms addition complexes which decompose by other routes. In their studies benzene reduces the yields of products formed from fragment ions. Molecular elimination processes are unaffected and are, consequently, more prominent. Using Futrell's mechanism this interaction would affect the hydrogen yields in the same way; the molecular elimination would be favored, in agreement with our observations. As fragment ions are not formed in the liquid, benzene must, in this environment, reduce the hydrogen yield by a different mechanism.

The high yield of HD from dilute mixtures of C_6D_6 in C_6H_{12} shows that benzene contributes D atoms to the radiolysis almost as readily as does C_6D_{12}. A high HD yield is also observed in liquid C_6D_6–C_6H_{12} mixtures (18). It is unreasonable to attribute this to the abstraction

$$X_H + C_6D_6 \rightarrow HD + \ldots$$

because this requires the C–D bond in C_6D_6 to be essentially as reactive as the C–D bond in C_6D_{12}, whatever the nature of X_H. It is more reasonable to attribute the yield of HD to the reaction of an intermediate X_D', formed from C_6D_6

$$C_6D_6 \rightsquigarrow X_D' + \ldots, \qquad [12]$$

which can react with cyclohexane to give HD. Neglecting the possibility of energy transfer from cyclohexane to benzene then the yield of this reaction is equal to g(HD)—i.e. 3 molecules/100 ev absorbed in the benzene. This is, of course, much greater than $G(H_2)$ from pure benzene in the liquid or vapor. As the hydrogen yield in pure liquid benzene is much less than G(-benzene), it is not a proper measure of the radiation stability of benzene. While in pure benzene the intermediate X_H' gives a low hydrogen yield, it may react much more efficiently when the benzene is diluted with another hydrocarbon. A high yield of reaction [12] is not improbable and so it is not necessary to have efficient energy transfer from cyclohexane to benzene to give this high yield of HD.

The differences in the interactions in the gas and liquid eliminate any physical interaction with depends only on the electron-stopping power of the molecules. Such a mechanism has been proposed by Lamborn and Swallow (19). From calculations by Inokuti (20) of the excitation cross sections of π-electrons in aromatic molecules, they concluded that the electron-stopping power of benzene was considerably greater than that of cyclohexane. While their measurements of polymer yield in benzene–cyclohexane mixtures were consistent with Inokuti's estimates of the excitation cross sections, our gas-phase measurements are not; we find that one of the decomposition paths, the first-order decomposition is unaffected. The difference in stopping powers predicted by Lamborn and Swallow

Can. J. Chem. Downloaded from www.nrcresearchpress.com by 210.87.254.5 on 09/05/12
For personal use only.

should also be detectable by direct measurement. Recently, however, Rauth and Hutchinson (21) found the electron-stopping power of polystyrene and Formvar (polyvinyl formal, empirical composition $C_5H_8O_2$) to be identical, and no large effect of π-electron excitation was observed.

The differences in mechanism between the liquid- and vapor-phase are the most interesting part of this study. The common intermediate C_D* in reaction [7] is either not formed and the first- and second-order yields are not coupled, or else the lifetime and other properties of C_D* in the vapor differ from those in the liquid, so that (*a*) the HD/D_2 ratio (the branching ratio of [7]) is changed and (*b*) benzene cannot interact with it. While it is possible to devise *ad hoc* reasons for the properties of C_D* being changed, there is still no positive evidence for a common intermediate of the first- and second-order yields (C_D*) in the gas phase.

ACKNOWLEDGMENTS

It is a pleasure to thank Dr. D. R. Smith for his advice on experimental techniques and Dr. J. A. Stone for his candid criticisms of earlier drafts of this paper.

REFERENCES

1. J. A. Stone and P. J. Dyne. Radiation Res. **3**, 353 (1962).
2. P. J. Dyne and W. M. Jenkinson. Can. J. Chem. **39**, 2163 (1961).
3. P. J. Dyne and J. Denhartog. Can. J. Chem. **40**, 1616 (1962).
4. P. J. Dyne, J. Denhartog, and D. R. Smith. Discussions Faraday Soc. In press. (1964).
5. J. M. Ramaradhya and G. R. Freeman. J. Chem. Phys. **34**, 1726 (1961).
6. P. J. Dyne and J. A. Stone. Can. J. Chem. **39**, 2381 (1961).
7. K. B. Wiberg. Chem. Rev. **55**, 713 (1955).
8. A. W. Boyd. J. Nucl. Mater. **9**, 1 (1963).
9. R. A. Back, T. W. Woodward, and K. A. McLauchlan. Can. J. Chem. **40**, 1380 (1962).
10. L. Kevan and W. F. Libby. J. Chem. Phys. **39**, 1288 (1963).
11. J. M. Ramaradhya and G. R. Freeman. Can. J. Chem. **39**, 1769 (1961).
12. H. I. Schiff and E. W. R. Steacie. Can. J. Chem. **29**, 1 (1951).
13. P. E. M. Allen, H. W. Melville, and J. C. Robb. Proc. Roy. Soc. London, A, **218**, 311 (1953).
14. A. F. Trotman Dickenson. Gas kinetics. Butterworths, London. 1955. p. 287.
15. P. J. Dyne, D. R. Smith, and J. A. Stone. Ann. Rev. Phys. Chem. **14**, 313 (1963).
16. J. H. Futrell. J. Am. Chem. Soc. 5921 (1959).
17. R. P. Borkowski and P. Ausloos. J. Chem. Phys. **39**, 818 (1963).
18. P. J. Dyne and W. M. Jenkinson. Can. J. Chem. **40**, 1746 (1962).
19. J. Lamborn and A. J. Swallow. J. Phys. Chem. **65**, 920 (1961).
20. M. Inokuti. Isotopes Radiation Tokyo, **1**, 82 (1958).
21. A. M. Rauth and F. Hutchinson. *In* Biological effects of ionizing radiation at the molecular level. International Atomic Energy Agency, Vienna. 1962. p. 25.

Can. J. Chem. Downloaded from www.nrcresearchpress.com by 210.87.254.5 on 09/05/12
For personal use only.

Can. J. Chem. Downloaded from www.nrcresearchpress.com by 210.87.254.40 on 09/05/12
For personal use only.

THE THEORY OF ULTRASONIC ABSORPTION: RELAXATION OF TWO INTERACTING REACTIONS

J. P. VALLEAU
Department of Chemistry, University of Toronto, Toronto, Ontario
Received October 9, 1963

ABSTRACT

The purpose of this paper is to extend the theory of ultrasonic absorption in fluids to the case of the relaxations of two interacting reactions. The linear theory of the absorption and dispersion of sound waves is developed in terms of a frequency-dependent viscosity coefficient. This coefficient is then evaluated for the familiar case of a single relaxing reaction and for the more complex case of two reactions interacting in an arbitrary way. The absorption and dispersion of the sound waves are related to familiar physical chemical quantities by explicit formulae, and non-ideality has been taken account of by the use of activity coefficients. Some discussion of the results is presented. The intention of this development is to make possible the extraction of physical chemical data from ultrasonic investigations of systems involving interacting equilibria, and such an application has been made in an accompanying paper.

1. INTRODUCTION

The viscosity of fluids leads to an absorption of sound waves, the classical absorption, calculated by Stokes (1) in 1845. To this may be added an absorption due to thermal conductivity (Kirchhoff (2), 1868). The latter measures a deviation from adiabaticity of the sound propagation, and is usually relatively small (except in liquid metals and He II). Subsequent interest has attached to the "relaxation absorption" caused by chemical and physical processes having time constants comparable with the period of the sound waves. From these absorptions it is possible to derive information about the rates and energetics of the processes responsible.

Until recently adequate account was not taken of the interaction between the simultaneous variations of pressure and temperature in the sound wave, an effect certain to be important in the case of chemical processes. This was rectified in 1958 (Davies and Lamb (3), and see Ref. (4), p. 138 ff.), giving a theory adequate for single processes in ideal solutions. More recently (Tamm (5), Eigen and Tamm (6)), activity coefficients have been introduced into the theory.

Work in our laboratory has focussed on ultrasonic absorption in electrolyte solutions, and we have been faced with the need to interpret relaxation processes occurring among simultaneous equilibria. An extension of the theoretical treatment was therefore necessary. A special case of the problem was treated by Eigen and Tamm (6), who considered an association reaction taking place in a number of steps, e.g.

$$A^+ + B^- \rightleftharpoons (AB)' \rightleftharpoons (AB)'' \rightleftharpoons AB,$$

the intermediates presumably being ion pairs separated by varying numbers of solvent layers. The authors solved this case by introducing a set of "normal coordinates", under the assumption that the rates of the various steps are (*a*) all well-separated, and (*b*) decrease from left to right. They believe that such an analysis is required to explain the famous and puzzling results on the sulphates of divalent metals.

In the present paper, we wish to develop the theory of sound absorption for the general case of any two interacting equilibria in non-ideal solutions and having arbitrary rate constants. This will be done only in the usual "linear" approximation.

It is well known that there are several possible starting points for ultrasonic theory, so that absorption may be regarded as due to a frequency-dependent viscosity, or to a heat capacity, or to a compressibility. We have chosen to develop the theory by introducing a "relaxation viscosity". Not only does this approach appear particularly simple, but it keeps ultrasonic theory within the "classical" mold established by Stokes. The classical viscous result appears, in fact, as an incidental product of the general theory. It seemed helpful to include, for completeness, a discussion of the case of a single relaxation process. A detailed example of the use of the results for simultaneous processes can be found in an accompanying paper (7).

2. GENERAL TREATMENT

Consider a fluid through which a plane wave passes in the x-direction. The fluid may be described by a local density ρ_l and a local hydrodynamic velocity u_x in the direction of propagation. The conservations of mass and momentum may be expressed, as usual, by the "continuity equation"

$$d\rho_l/dt+\rho_l(\partial u_x/\partial x) = 0, \qquad [1]$$

and the "equation of motion"

$$(1/\rho_l)(du_x/dt)+\partial p_{xx}/\partial x = 0. \qquad [2]$$

In these equations p_{xx} is the "longitudinal" pressure in the x-direction (more precisely, the x,x-component of the pressure tensor), and d/dt signifies the substantial time derivative: that is, it describes changes in an element of volume moving with the local hydrodynamic velocity.

As is well known, the classical sound absorption (1) is obtained from [1], [2] after inserting the viscous pressure tensor p_{xx}. We wish to modify the argument only by adding to the shear viscosity η and the bulk viscosity κ, a "relaxation viscosity" ξ due to slow dissipative processes. That is

$$p_{xx} = p_0-[(4/3)\eta+\kappa+\xi](\partial u_x/\partial x), \qquad [3]$$

where p_0 is the equilibrium hydrostatic pressure, determined by the instantaneous density and entropy of the fluid. The ξ term, unlike the η and κ terms, need not be in phase with the rate of expansion $\partial u_x/\partial x$, so we set

$$\xi = \xi_1-i\xi_2. \qquad [4]$$

We consider damped plane sine waves of circular frequency ω, when we may set

$$u_x = u_x' \exp\{i(\omega t-kx)\},$$
$$\rho_l = \rho+\rho' \exp\{i(\omega t-kx)\}, \qquad [5]$$

ρ being the density of the fluid. Then

$$k = (\omega/c)-i\alpha, \qquad [6]$$

in which c and α are the velocity and the amplitude absorption coefficient of the sound wave.

When [3] and [5] are inserted in [1] and [2] there results a pair of equations for ρ' and u_x'; these equations are linearized by dropping terms in $\rho'u_x'$. If the equations are to be satisfied for an arbitrary wave amplitude ρ', the determinant of their coefficients must vanish; i.e.

$$\left(\frac{k}{\omega}\right)^2\left\{\left(\frac{\partial p_0}{\partial \rho}\right)_s+\frac{i\omega}{\rho}\left(\frac{4}{3}\eta+\kappa+\xi\right)\right\} = 1. \qquad [7]$$

Can. J. Chem. Downloaded from www.nrcresearchpress.com by 210.87.254.40 on 09/05/12
For personal use only.

The linearization is valid when the absorption per wavelength, $\mu = 2\pi\alpha c/\omega$, is much less than unity; in view of this, and using [4] and [6], [7] may be rewritten

$$\alpha = (\omega^2/2\rho c^3)[(4/3)\eta+\kappa+\xi_1], \qquad [8]$$

$$c^2 = c_0{}^2+(\omega\xi_2/\rho), \qquad [9]$$

where c_0 is the classical sound velocity, $c_0 = \sqrt{(\partial p_0/\partial\rho)_s}$.

The first two terms of [8] give the viscous sound absorption (1). Since the contributions to α are, in the present approximation, additive, we need consider the viscous terms no more. In what follows we shall use α_r to refer to the final term, $\omega^2\xi_1/2\rho c^3$, by which we take account of "relaxation processes" in the fluid.

We now wish to obtain, for such processes, a description of the resulting hydrodynamic parameter ξ. We presume that the processes may be described by a number of "ordering parameters", z, y, etc., which have equilibrium values of $\bar{z}$, $\bar{y}$, etc. that may be regarded as determined by the specific volume and entropy of the fluid. Such ordering parameters might be, for example, the concentrations of certain substances taking part in chemical reactions, or the populations of certain vibrational levels of a particular molecular species. They will differ from their equilibrium values if they are involved in a process which does not proceed rapidly enough to maintain equilibrium during the fluctuations of temperature and pressure occurring in a sound wave. Then $-\xi(\partial u_x/\partial x)$ will describe, in view of [3], the deviation of the pressure due to the deviations $\Delta z = z-\bar{z}$, $\Delta y = y-\bar{y}$ etc., of the ordering parameters. We can write

$$-\xi(\partial u_x/\partial x) \equiv -(\xi/V)(dV/dt) = (\partial p/\partial z)_{s,v,y,\ldots}\Delta z+(\partial p/\partial y)_{s,v,z,\ldots}\Delta y+\ldots$$

or, putting $dV/dt = \dot{V}$,

$$\xi = -V\{(\partial p/\partial z)_{s,v,y,\ldots}(\Delta z/\dot{V})+(\partial p/\partial y)_{s,v,z,\ldots}(\Delta y/\dot{V})+\ldots\}, \qquad [10]$$

where V is the specific volume of the fluid. We make the assumption that the deviations Δz, Δy, etc. depend only on the magnitude and rate of the volume fluctuations $\dot{V}$, not on the geometry of the fluctuations; that is, ξ corresponds to a time-dependent bulk viscosity, not to a shear viscosity.

It only remains to evaluate the ratios $\Delta z/\dot{V}$, $\Delta y/\dot{V}$, etc. To do this we need the rate equations which govern changes in the parameters z, y, etc. Sufficiently close to equilibrium, these equations may always be written as linear relaxation equations:

$$dz/dt = -(\Delta z/\tau_z)-(\Delta y/\tau_z{}^y)-\ldots, \qquad [11]$$

$$dy/dt = -(\Delta z/\tau_y{}^z)-(\Delta y/\tau_y)-\ldots, \text{ etc.},$$

which define the relaxation times τ_z, $\tau_z{}^y$, $\tau_y{}^z$, τ_y, etc. In view of the definitions of Δz, Δy, etc., the relaxation times are those applying to constant entropy and volume ("$\tau_{s,v}$"; compare Ref. (10)). Naturally the above relaxation times are not all independent; there are only as many independent time constants as independent ordering parameters. We shall return to these matters.

The rate equations [11] may be combined with the identities

$$d\bar{z}/dt \equiv (\partial\bar{z}/\partial V)_s\dot{V}, \text{ etc.},$$

to give equations for the time variations of the deviations Δz, Δy, etc. For example

$$d\Delta z/dt \equiv (dz/dt)-(d\bar{z}/dt) = -(\Delta z/\tau_z)-(\Delta y/\tau_z{}^y)-\ldots-(\partial\bar{z}/\partial V)_s\dot{V}. \qquad [12]$$

Can. J. Chem. Downloaded from www.nrcresearchpress.com by 210.87.254.40 on 09/05/12
For personal use only.

These equations, [12], may easily be solved for $\Delta z/\dot{V}$, $\Delta y/\dot{V}$, etc., and hence for ξ [10], α [8], and c [9]. It is sufficient to consider a sinusoidal density fluctuation, $\dot{V} \propto \exp(i\omega t)$. We shall not consider more than two interacting processes in this paper. The case of a single process is first discussed, and forms a useful introduction to the more complex case.

3. SINGLE RELAXING PROCESS

The deviation, Δz, of the single ordering parameter z, will not generally be in phase with the rate of expansion

$$\dot{V} = A \exp(i\omega t), \qquad [13]$$

and must be written

$$\Delta z = (B+iC) \exp(i\omega t). \qquad [14]$$

Equation [12] is then easily solved, and gives (with $\tau_z = \tau$)

$$\frac{\Delta z}{\dot{V}} = \frac{B+iC}{A} = -\left(\frac{\partial \bar{z}}{\partial v}\right)_s \frac{\tau(1-i\omega\tau)}{1+\omega^2\tau^2}. \qquad [15]$$

Thus ξ([4], [10]) takes the predicted form, $\xi_1 - i\xi_2$, and with [8] and [9] we obtain

$$\frac{\alpha_\tau}{\omega^2} = \frac{\xi_1}{2\rho c^3} = \frac{\tau V}{2\rho c^3(1+\omega^2\tau^2)} \left(\frac{\partial p}{\partial z}\right)_{s,v} \left(\frac{\partial \bar{z}}{\partial V}\right)_s, \qquad [16]$$

$$c^2 = c_0^2 + \frac{\omega\xi_2}{\rho} = c_0^2 + \frac{\omega^2\tau V}{\rho(1+\omega^2\tau^2)} \left(\frac{\partial p}{\partial z}\right)_{s,v} \left(\frac{\partial \bar{z}}{\partial V}\right)_s. \qquad [17]$$

In this simple case the absorption and the velocity dispersion are related, since $c \approx c_0$, by

$$c - c_0 \approx c^2\tau\alpha_\tau. \qquad [18]$$

One now wishes to relate the quantities $(\partial p/\partial z)_{s,v}$, $(\partial \bar{z}/\partial V)_s$, and τ more closely to the details of the process described by z. We are most interested in the case of a chemical process. Suppose therefore that z is the concentration of a substance Z taking part in a reaction which may in general be written, using an obvious notation,

$$\nu_z Z + \sum_i \nu_i X_i = 0. \qquad [19]$$

We may define a "stoichiometric quotient"

$$Q = z^{\nu_z} \prod_i x_i^{\nu_i}. \qquad [20]$$

When the system is at equilibrium $z = \bar{z}$, $x_i = \bar{x}_i$, and Q is given by

$$\bar{Q} = K/\bar{F}, \qquad [21]$$

where K is the thermodynamic equilibrium constant and F the quotient of the activity coefficients:

$$F = f_z^{\nu_z} \prod_i f_i^{\nu_i}. \qquad [22]$$

Then (cf. Appendix B)

$$\left(\frac{\partial \bar{z}}{\partial V}\right)_s = \frac{dz}{d\ln Q}\left(\frac{\partial \ln(K/\bar{F})}{\partial V}\right)_s = \frac{\frac{dz}{d\ln Q}\left\{\frac{\Delta H}{RT^2}\left(\frac{\partial T}{\partial V}\right)_s - \frac{\Delta V}{RT}\left(\frac{\partial p}{\partial V}\right)_s\right\}}{1+\frac{dz}{d\ln Q}\left(\frac{\partial \ln F}{\partial z}\right)_{p,T}}, \qquad [23]$$

Can. J. Chem. Downloaded from www.nrcresearchpress.com by 210.87.254.40 on 09/05/12
For personal use only.

where $\Delta H = \nu_z(\partial H/\partial z)_{p,T}$ and $\Delta V = \nu_z(\partial V/\partial z)_{p,T}$ are the enthalpy and volume change in the reaction [20]. It should be noted that we are assuming the activity coefficients to be determined by the temperature, pressure, and concentrations only. That is, we assume they adjust more quickly than the reactions under study; this will, of course, be true for most cases of practical interest (cf. (8)).

To evaluate the reaction quantity $(\partial p/\partial z)_{s,v}$ we first write the total differential

$$dp = (\partial p/\partial s)_{v,z}dS + (\partial p/\partial V)_{s,z}dV + (\partial p/\partial z)_{s,v}dz.$$

Then, considering a process at constant temperature and pressure, we easily find

$$\left(\frac{\partial p}{\partial z}\right)_{s,v} = -\frac{\left(\frac{\partial p}{\partial S}\right)_v \frac{\Delta S}{\nu_z} + \left(\frac{\partial p}{\partial V}\right)_s \frac{\Delta V}{\nu_z}}{1 - \left(\frac{\partial z}{\partial S}\right)_v \frac{\Delta S}{\nu_z} - \left(\frac{\partial z}{\partial V}\right)_s \frac{\Delta V}{\nu_z}}. \qquad [24]$$

This expression [24] repays some further thought. It is apparent that for our present purposes we may discard the second and third terms of the denominator, for they would lead to terms of higher order than are included in the present approximation; these terms would be of the fourth power in ΔH, ΔV, rather than the second. The reason for laboring the matter is that this denominator may be shown (cf. (9)) to be the ratio, $\tau_{s,v}/\tau_{p,t}$, of the relaxation time at fixed entropy and volume to that at fixed pressure and temperature. In what follows the distinction between such relaxation times will be ignored, since this is similarly consistent with the approximation.

Returning to [24], we note that $(\partial p/\partial S)_v \equiv -(\partial T/\partial V)_s$ and, at equilibrium, $\Delta H = T\Delta S$; thus, to the present approximation, we may set

$$\left(\frac{\partial p}{\partial z}\right)_{s,v} = \frac{1}{\nu_z}\left[\frac{\Delta H}{T}\left(\frac{\partial T}{\partial V}\right)_s - \Delta V\left(\frac{\partial p}{\partial V}\right)_s\right] \qquad [25]$$

$$= \frac{\rho^2 C_0^2}{\nu_z}\left[\Delta V - \frac{\Delta H}{C_p}\left(\frac{\partial V}{\partial T}\right)_p\right].$$

In writing the final form of [25] we imply that all extensive quantities and concentrations are expressed per unit mass of the system (so that $V\rho = 1$) and we have recalled that $c_0^2 = (\partial p/\partial \rho)_s$.

With the help of [23] and [25], and recalling that $c \approx c_0$, the absorption coefficient [16] may be written

$$\frac{\alpha_\tau}{\omega^2} = \frac{c - c_0}{\omega^2 c^2 \tau} = \frac{\tau\rho^2 c_0 (dz/d\ln Q)[\Delta V - (\Delta H/C_p)(\partial V/\partial T)_p]^2}{2RT\nu_z(1+\omega^2\tau^2)[1+(dz/d\ln Q)(\partial \ln F/\partial z)_{p,T}]}. \qquad [26]$$

The same result can be recovered from the equations of ref. (6), p. 101, 102.

The value of $(1/\nu_z)(dz/d\ln Q)$ follows from the definition [20] of Q, and is given (dropping unnecessary subscripts) in Appendix B, equation [B8]. In a similar way the relaxation time τ takes the form discussed in the appendix for a more general case. The activity coefficient derivatives $(\partial \ln F/\partial z)_{p,T}$ will generally prove difficult to estimate. Relevant data will not usually be available, and, since rather concentrated solutions are often required in ultrasonic work, theoretical estimates of activity coefficients will usually be unreliable. Sometimes $\bar{Q}$ is known as a function of the ionic strength I, and one might then make the rather gross approximation

$$\left(\frac{\partial \ln F}{\partial z}\right)_{p,T} \approx -\left(\frac{\partial \ln \bar{Q}}{\partial I}\right)_{p,T}\left(\frac{\partial I}{\partial z}\right);$$

Can. J. Chem. Downloaded from www.nrcresearchpress.com by 210.87.254.40 on 09/05/12
For personal use only.

this regards the activity coefficients as depending on concentration through the ionic strength only.

Vibrational relaxation involving a single excited level may be regarded as a special case of the above. If z is the population of the excited state, $Q = z/x$ is given at equilibrium by the Boltzmann factor $K = \exp(-h\nu/kt)$, and we may assume that $F \approx 1$ and $\Delta V \approx 0$. These simplifications lead to the usual result for such a case. Situations involving more than one vibrational level have been discussed by Beyer (10) and others (cf. ref. (4), pp. 90–138); they could be treated as special cases of interacting equilibria, to which subject we now turn.

4. TWO SIMULTANEOUS EQUILIBRIA

Where two ordering parameters y, z are required, it is necessary to solve two equations like [12], to obtain $\Delta y/\dot{V}$ and $\Delta z/\dot{V}$. This is easy but laborious. The results are put into [10] to obtain the "relaxation viscosity", $\xi = \xi_1 - i\xi_2$. Before doing this we indulge in a few preliminary considerations which somewhat simplify the procedure.

It is convenient (and always possible) to choose the concentrations y and z in such a way that each is included in only one of the stoichiometric quotients. That is, we can put (cf. [20], [22])

$$\begin{aligned} Q_y &= y^{\nu_y}\prod_i x_i^{\nu_i(y)}, & F_y &= f_y^{\nu_y}\prod_i f_i^{\nu_i(y)}, \\ Q_z &= z^{\nu_z}\prod_i x_i^{\nu_i(z)}, & F_z &= f_z^{\nu_z}\prod_i f_i^{\nu_i(z)}, \end{aligned} \qquad [27]$$

where $\nu_i(y)$, $\nu_i(z)$ are the stoichiometric numbers for X_i in the y and z reactions respectively. At equilibrium, $\bar{Q}_y\bar{F}_y = K_y$ and $\bar{Q}_z\bar{F}_z = K_z$ as before.

Although it is natural to define the four relaxation times τ_y, τ_y^z, τ_z^y, τ_z of [11], only two times can, of course, be independent. Both τ_y and τ_y^z, for example, depend (under [27]) on the rate constants, k_y, k_{-y} governing the y-reaction, but not on k_z, k_{-z}. In fact we may set

$$\tau_y = \mathscr{Y}\tau_y^z, \quad \tau_z = \mathscr{Z}\tau_z^y. \qquad [28]$$

The ratios $\mathscr{Y}$, $\mathscr{Z}$ prove to be very important; they are given in Appendix A, and it is pointed out that they are purely thermodynamic quantities.

We now solve for ξ, and using the definitions [28] we may write the result:

$$\begin{aligned} \frac{\xi_1}{V} = \frac{2\rho c^3\alpha_\tau}{\omega^2 V} = \Bigg\{ &\frac{\tau_y}{1-\mathscr{Y}\mathscr{Z}}\left(\frac{\partial\bar{y}}{\partial V}\right)_s\left[\left(\frac{\partial p}{\partial y}\right)_{s,v,z} - \mathscr{Z}\left(\frac{\partial p}{\partial z}\right)_{s,v,y}\right] \\ &+\left(\frac{\omega\tau_y}{1-\mathscr{Y}\mathscr{Z}}\right)^2\tau_z\left(\frac{\partial p}{\partial z}\right)_{s,v,y}\left[\left(\frac{\partial\bar{z}}{\partial V}\right)_s + \mathscr{Z}\left(\frac{\partial\bar{y}}{\partial V}\right)_s\right] + \text{similar terms with } y \text{ and} \\ &z \text{ interchanged}\Bigg\} \Big/ \left\{1+\frac{\omega^2[\tau_y^2+2\mathscr{Y}\mathscr{Z}\tau_y\tau_z+\tau_z^2]+\omega^4\tau_y^2\tau_z^2}{(1-\mathscr{Y}\mathscr{Z})^2}\right\} \end{aligned} \qquad [29]$$

$$\begin{aligned} \frac{\omega\xi_2}{V} = \rho^2(c^2-c_0^2) = \left(\frac{\omega}{1-\mathscr{Y}\mathscr{Z}}\right)^2\Bigg\{ &\tau_y\left[\tau_y\left(\frac{\partial\bar{y}}{\partial V}\right)_s\mathscr{Y}\tau_z\left(\frac{\partial\bar{z}}{\partial V}\right)_s\right]\left[\left(\frac{\partial p}{\partial y}\right)_{s,v,z} - \mathscr{Z}\left(\frac{\partial p}{\partial z}\right)_{s,v,z}\right] \\ &+\text{a similar term with } y \text{ and } z \text{ interchanged}\Bigg\} + \frac{\omega^4\tau_y^2\tau_z^2}{(1-\mathscr{Y}\mathscr{Z})^2}\left\{\left(\frac{\partial\bar{y}}{\partial V}\right)_s\left(\frac{\partial p}{\partial y}\right)_{s,v,y}\right. \\ &\left.+\left(\frac{\partial\bar{z}}{\partial V}\right)_s\left(\frac{\partial p}{\partial z}\right)_{s,v,y}\right\} \Big/ \left\{1+\frac{\omega^2[\tau_y^2+2\mathscr{Y}\mathscr{Z}\tau_y\tau_z+\tau_z^2]+\omega^4\tau_y^2\tau_z^2}{(1-\mathscr{Y}\mathscr{Z})^2}\right\}. \end{aligned} \qquad [30]$$

These expressions may be compared to [16], [17] of the former argument. Once again we wish to relate the result more closely to the details of the reactions.

Can. J. Chem. Downloaded from www.nrcresearchpress.com by 210.87.254.40 on 09/05/12
For personal use only.

The reactions quantities $(\partial p/\partial y)_{s,v,z}$ and $(\partial_p/\partial z)_{s,v,y}$ may be found much as before ([24], [25]). To the relevant approximation they may be written

$$\left(\frac{\partial p}{\partial y}\right)_{s,v,z} = \frac{\rho^2 c_0^2}{\nu_y}\left[\Delta V_y - \frac{\Delta H_y}{C_p}\left(\frac{\partial V}{\partial T}\right)_p\right] = \frac{\rho^2 c_0^2}{\nu_y}\delta_y,$$

$$\left(\frac{\partial p}{\partial z}\right)_{s,v,y} = \frac{\rho^2 c_0^2}{\nu_z}\left[\Delta V_z - \frac{\Delta H_z}{C_p}\left(\frac{\partial V}{\partial T}\right)_p\right] = \frac{\rho^2 c_0^2}{\nu_z}\delta_z, \qquad [31]$$

where we have introduced the abbreviations δ_y, δ_z. The equilibrium quantities $(\partial\bar{y}/\partial V)_s$ and $(\partial\bar{z}/\partial V)_s$ are evaluated in Appendix B, where it is shown that

$$\left(\frac{\partial \bar{y}}{\partial V}\right)_s = \frac{\rho^2 c_0^2 (\partial y/\partial \ln Q_y)_z[\delta_y - (\nu_y/\nu_z)\mathscr{Z}\delta_z]}{RT(1-\mathscr{Y}\mathscr{Z})[1+(\partial y/\partial \ln Q_y)_z(\partial \ln F_y/\partial y)_{p,T,z}]}, \qquad [32]$$

$$\left(\frac{\partial \bar{z}}{\partial V}\right)_s = \frac{\rho^2 c_0^2 (\partial z/\partial \ln Q_z)_y[\delta_z - (\nu_z/\nu_y)\mathscr{Y}\delta_y]}{RT(1-\mathscr{Y}\mathscr{Z})[1+(\partial z/\partial \ln Q_z)_y(\partial \ln F_z/\partial z)_{p,T,y}]}.$$

With the help of [31] and [32], and recalling that $c \approx c_0$, we may rewrite α_r [29] and c [30] as follows:

$$\frac{\alpha_\tau}{\omega^2} = \frac{\rho^2 c_0}{2RT}\left\{\frac{\tau_y(\partial y/\partial \ln Q_y)_z[\delta_y - (\nu_y/\nu_z)\mathscr{Z}\delta_z]^2}{(1-\mathscr{Y}\mathscr{Z})^2\nu_y[1+(\partial y/\partial \ln Q_y)_z(\partial \ln F_y/\partial y)_{p,T,z}]}\right.$$

$$+\left(\frac{\omega\tau_y}{1-\mathscr{Y}\mathscr{Z}}\right)^2\frac{\tau_z(\partial z/\partial \ln Q_z)_y[\delta_z]^2}{\nu_z[1+(\partial z/\partial \ln Q_z)_y(\partial \ln F_z/\partial z)_{y,p,T}]} + \text{similar terms with } y \text{ and}$$

$$\left.z \text{ interchanged}\right\} \Big/ \left\{1+\frac{\omega^2[\tau_y^2+2\mathscr{Y}\mathscr{Z}\tau_y\tau_z+\tau_z^2]+\omega^4\tau_y^2\tau_z^2}{(1-\mathscr{Y}\mathscr{Z})^2}\right\}, \qquad [33]$$

$$\frac{c-c_0}{c_0^2} = \frac{\rho^2 c_0}{2RT(1-\mathscr{Y}\mathscr{Z})^3}\left\{\left[\frac{(\partial y/\partial \ln Q_y)_z}{\nu_y[1+(\partial y/\partial \ln Q_y)_z(\partial \ln F_y/\partial y)_{p,T,z}]}\right]\right.$$

$$\times\left[\omega^2\tau_y^2\left[\delta_y - \frac{\nu_y}{\nu_z}\mathscr{Z}\delta_z\right]^2 - \omega^2\tau_y\tau_z\frac{\nu_y}{\nu_z}\mathscr{Z}\left[\delta_y - \frac{\nu_y}{\nu_z}\mathscr{Z}\delta_z\right]\left[\delta_z - \frac{\nu_z}{\nu_y}\mathscr{Y}\delta_y\right]\right.$$

$$\left.\left.+\omega^4\tau_y^2\tau_z^2\delta_y\left[\delta_y - \frac{\nu_y}{\nu_z}\mathscr{Z}\delta_z\right]\right]\right\} + \text{a similar term with } y \text{ and}$$

$$\left.z \text{ interchanged}\right\} \Big/ \left\{1+\frac{\omega^2[\tau_y^2+2\mathscr{Y}\mathscr{Z}\tau_y\tau_z+\tau_z^2]+\omega^4\tau_y^2\tau_z^2}{(1-\mathscr{Y}\mathscr{Z})^2}\right\}. \qquad [34]$$

The absorption and dispersion are not so simply related as for a single relaxation [26]. In the appendices $\mathscr{Y}$, $\mathscr{Z}$, τ_y, τ_z, and the thermodynamic derivatives are related to more familiar quantities. With the help of [A1] and [B8] it can be shown that α_r and $(c-c_0)$ are necessarily positive.

5. DISCUSSION

A detailed example of the use of the results may be found elsewhere (7), but some general illustrative remarks may not be out of place here.

It will be convenient, for the purposes of this discussion, to abbreviate the thermodynamic expressions in [33], putting the equation in the form

$$\frac{\alpha_\tau}{\omega^2} = \frac{\tau_y A_{yz} + \tau_z A_{zy} + (\omega\tau_y/1-\mathscr{Y}\mathscr{Z})^2\tau_z B_z + (\omega\tau_z/1-\mathscr{Y}\mathscr{Z})^2\tau_y B_y}{1+\{\omega^2[\tau_y^2+2\mathscr{Y}\mathscr{Z}\tau_y\tau_z+\tau_z^2]+[\omega^4\tau_y^2\tau_z^2]\}/(1-\mathscr{Y}\mathscr{Z})^2}. \qquad [35]$$

Can. J. Chem. Downloaded from www.nrcresearchpress.com by 210.87.254.40 on 09/05/12
For personal use only.

This general result [33], [35] is most easily surveyed in the special case $\tau_z \ll \tau_y$. There will then be two fairly distinct relaxation regions. These may be seen in Fig. 1, which shows the frequency dependence of the absorption per wavelength, $\mu_v = 2\pi\alpha_r c/\omega$, in such a case; τ_z is here $0.01\tau_y$. This and the subsequent figures refer to the same arbitrary choice of parameters: $\mathscr{Y} = \mathscr{Z} = 0.7$, $\nu_y = \nu_z = 1$, $B_y = B_z$, $\delta_y = \delta_z$. This may be regarded as a case of fairly strong interaction.

We would expect it to be a good approximation, when $\tau_z \ll \tau_y$, to discard the B_y term of [35]. At the same time the denominator will be well approximated, at all frequencies, by $(1+\omega^2\tau_y^2/(1-\mathscr{Y}\mathscr{Z})^2)(1+\omega^2\tau_z^2)$. These approximations lead us to express the absorption as the sum of two single relaxations, in the form

$$\frac{\alpha_r}{\omega^2} \approx \frac{\tau_y A_{yz}+\tau_z(A_{zy}-B_z)}{1+\omega^2\tau_y^2/(1-\mathscr{Y}\mathscr{Z})^2}+\frac{\tau_z B_z}{1+\omega^2\tau_z^2}. \qquad [36]$$

Very often there will be substantial cancellation of A_{zy} with B_z in this expression, so that we might write

$$\frac{\alpha_r}{\omega^2} \approx \frac{\tau_y A_{yz}}{1+\omega^2\tau_y^2/(1-\mathscr{Y}\mathscr{Z})^2}+\frac{\tau_z B_z}{1+\omega^2\tau_z^2}, \qquad [37]$$

which we shall call a "first approximation" to [35]. In the present case (Fig. 1) this is an excellent approximation, while the "second approximation" [36] is scarcely distinguishable from the complete result [33], [35]. They make a sharp contrast with what may be called the "zeroth approximation": i.e. the sum of single relaxations for the y and z processes, with no allowance for interaction. The zeroth approximation is given by

$$\frac{\alpha_r}{\omega^2} \approx \frac{\tau_y B_y}{1+\omega^2\tau_y^2}+\frac{\tau_z B_z}{1+\omega^2\tau_z^2}, \qquad [38]$$

and is shown by broken lines in the figures.

The failure of the zeroth approximation in the region of the low frequency relaxation is very striking. Not only the magnitude of the predicted absorption peak but also its position is grossly incorrect. In fact the characteristic time of the low frequency relaxation is $\tau_y/(1-\mathscr{Y}\mathscr{Z})$ rather than τ_y, as we may see from [36] and [37]; with the present parameters these times differ by a factor of two. This shift is helpful in that it always provides an "extra" separation of the two relaxation regions, but it means that estimates of $\mathscr{Y}$ and $\mathscr{Z}$ must be available if one is to extract precise kinetic data from the observed relaxation frequency (7). The low frequency absorption involves the energetics of both reactions, their interaction being expressed in the term $[\delta_y-(\nu_y/\nu_z)\mathscr{Z}\delta_z]^2$ of A_{yz} (cf. [33] and [35]). The small size of the peak in the present case is due to the near cancellation of δ_y by $\mathscr{Z}\delta_z$ in this squared bracket.

It is worth noting that these shortcomings of [38] persist even in the limit $\tau_z/\tau_y \to 0$, in which case no evidence of a high frequency absorption would be observable. They depend only on the *existence* of a fast interacting process, as expressed in non-zero values of $\mathscr{Y}$ and $\mathscr{Z}$. This fact implies that a certain caution should be used when interpreting the results even where there appears to be a simple single relaxation.

Evidently [38] is of no use in understanding multiple relaxation processes, while [36] and [37] will be satisfactory for most cases of well-separated relaxations. In Fig. 2 we turn to less well-separated relaxations, in this case $\tau_z = 0.1\tau_y$. The B_y term is no longer so very small, so that [36] and [37] will be somewhat low at the higher frequencies. At lower frequencies ($\omega\tau_y < 5$) [36] remains a good approximation: with the present parameters

Can. J. Chem. Downloaded from www.nrcresearchpress.com by 210.87.254.40 on 09/05/12
For personal use only.

it is everywhere within 5%. It can be seen that the first approximation [37] is still a helpful one, but that it is beginning to break down. Where results like these occur experimentally it will be natural to extract chemical parameters from the ultrasonic data by a method of successive approximations, beginning with [37] (cf. (7)). These approximations will be better for cases of weaker interaction. Of course our earlier remarks about the inadequacy of [38] continue to apply.

In Fig. 3 we show the limiting case $\tau_z = \tau_y$. The approximate formulae [36] and [37] have no longer any relevance. The absorption curve is not that of a single relaxation, but slightly broader; rather precise measurements would be needed to display this, however. The high frequency part of the absorption approaches the zeroth approximation, as usual. The noticeable suppression and shift of the peak, as compared to that approximation, may

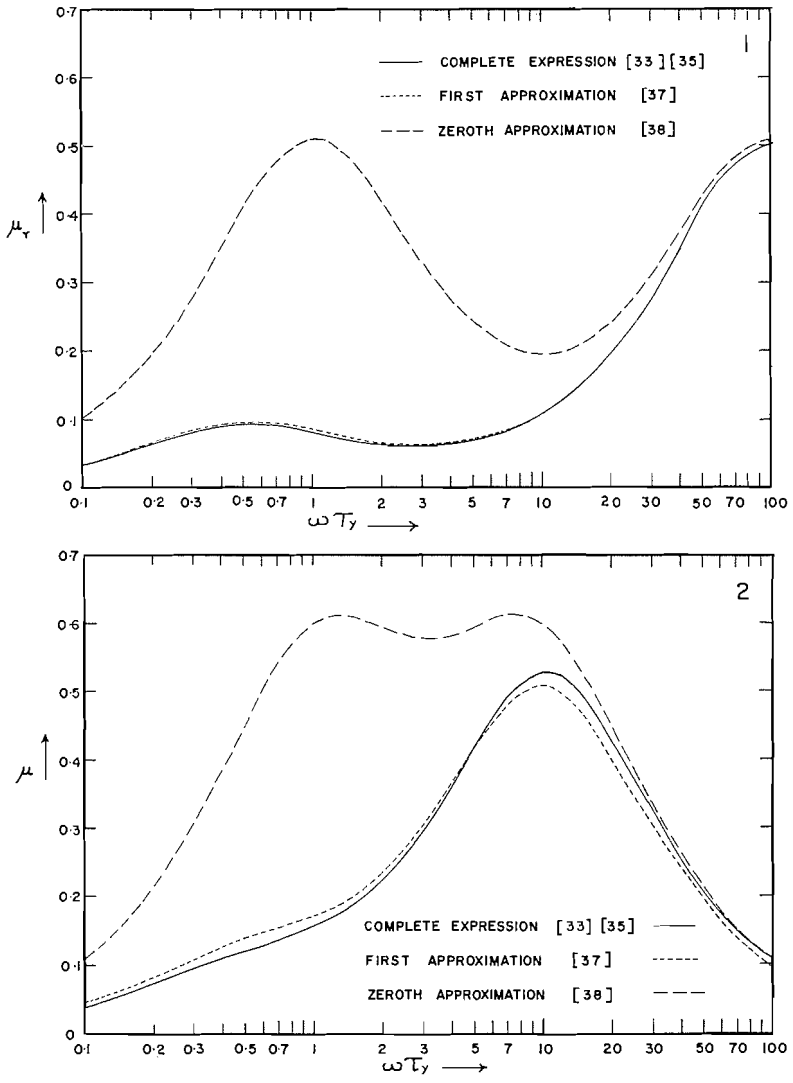

FIG. 1. $\tau_y/\tau_z = 100$.
FIG. 2. $\tau_y/\tau_z = 10$.

Can. J. Chem. Downloaded from www.nrcresearchpress.com by 210.87.254.40 on 09/05/12
For personal use only.

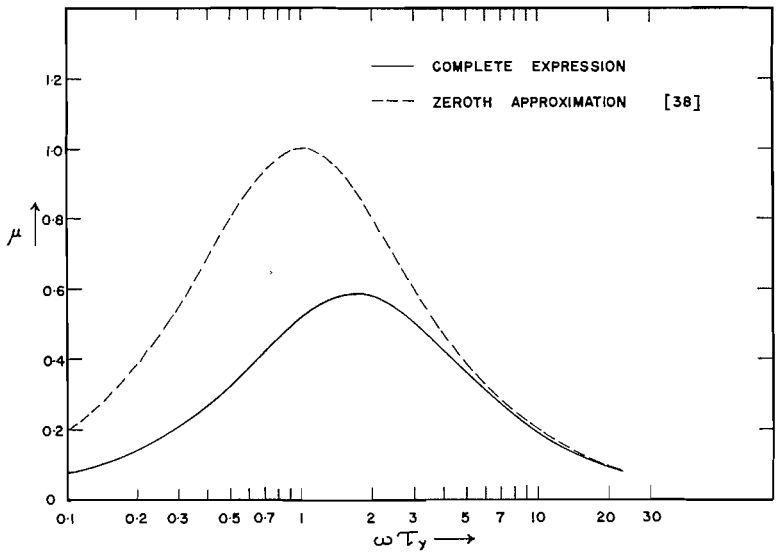

FIG. 3. $\tau_y/\tau_z = 1$.

be attributed to the small size of the low frequency terms A_{yz}, A_{zy}. This was ascribed earlier to the partial cancellation within the brackets $[\delta_y - (\nu_y/\nu_z)\mathscr{Z}\delta_z]$ and $[\delta_z - (\nu_z/\nu_y)\mathscr{Y}\delta_y]$. It should be mentioned that this interaction may have quite the opposite effect. Suppose that we take $\delta_z = -\delta_y$, leaving the other parameters unchanged. Now the terms within the brackets *augment* each other. When they are squared there results a large magnification of the low frequency terms, in contrast to the suppression shown in all the figures here. In the case $\tau_z = \tau_y$ (Fig. 3), for example, it will lead to an absorption peak much bigger than that of the zeroth approximation, and shifted to *lower* frequencies. The qualitative remarks we have made continue to apply, however.

The author appreciates the encouragement of Dr. W. G. Schneider, and the financial support of the National Research Council. He has had helpful discussions with Dr. M. J. Dignam and Mr. S. J. Turner.

APPENDIX A

The Relaxation Times

We consider first the ratios $\mathscr{Y} = \tau_y/\tau_y{}^z$ and $\mathscr{Z} = \tau_z/\tau_z{}^y$, [28]. Close to equilibrium the net rate of a chemical reaction is strictly proportional to the free energy charge, ΔG, of the reaction. This has been demonstrated by Manes, Hofer, and Weller, (11), for example, using purely thermodynamic arguments. It follows that

$$\mathscr{Y} = \frac{(\partial(\Delta G_y)/\partial z)_{y,T,p}}{(\partial(\Delta G_y)/\partial y)_{z,T,p}} = \frac{(\partial \ln Q_y/\partial z)_y + (\partial \ln F_y/\partial z)_{y,T,p}}{(\partial \ln Q_y/\partial y)_z + (\partial \ln F_y/\partial y)_{z,T,p}}, \qquad [A1]$$

$$\mathscr{Z} = \frac{(\partial(\Delta G_z)/\partial y)_{z,T,p}}{(\partial(\Delta G_z)/\partial z)_{y,T,p}} = \frac{(\partial \ln Q_z/\partial y)_z + (\partial \ln F_z/\partial y)_{z,T,p}}{(\partial \ln Q_z/\partial z)_y + (\partial \ln F_z/\partial z)_{y,T,p}}.$$

To take a different point of view, it can easily be shown that unless the ratios $\mathscr{Y}$, $\mathscr{Z}$ take the values shown, the absorption coefficient [33] will not be definitely positive. This would constitute a violation of the second law of thermodynamics, and is therefore a sufficient proof of the relations [A1].

Can. J. Chem. Downloaded from www.nrcresearchpress.com by 210.87.254.40 on 09/05/12
For personal use only.

Can. J. Chem. Downloaded from www.nrcresearchpress.com by 210.87.254.40 on 09/05/12
For personal use only.

The separate relaxation times are, of course, more difficult to manage. It is convenient to denote by N_y and D_y the numerator and denominator of the quotient Q_y [27]. For the rapid reactions studied by ultrasonic methods one may expect the simplest sort of reaction rate law, which may be written, assuming $\nu_y > 0$, in the form

$$dy/dt = -k_{-y}N_y + k_y D_y, \qquad [A2]$$

which defines rate constants k_{-y}, k_y. It is equally convenient, however, to write the somewhat more general rate law

$$dy/dt = P(-k_{-y}N_y^m + k_y D_y^m), \qquad [A3]$$

where m is any power and P an arbitrary positive function of concentration $P(y, z, x_i, \ldots\ldots)$. At equilibrium

$$dy/dt = 0 = \bar{P}(-\bar{k}_{-y}\bar{N}_y^m + \bar{k}_y\bar{D}_y^m). \qquad [A4]$$

Subtracting [A4] from [A3], and retaining only linear deviations from equilibrium, we obtain

$$\begin{aligned} dy/dt &= -\bar{k}_{-y}\bar{N}_y^m\bar{P}\{m\Delta \ln Q_y + \Delta \ln (k_{-y}/k_y)\} \\ &= -\bar{k}_{-y}\bar{N}_y^m\bar{P}\left\{\left[m\left(\frac{\partial \ln Q_y}{\partial y}\right)_z + \left(\frac{\partial \ln (k_{-y}/k_y)}{\partial y}\right)_{z,T,p}\right]\Delta y \right. \\ &\qquad \left. + \left[m\left(\frac{\partial \ln Q_y}{\partial z}\right)_y + \left(\frac{\partial \ln (k_{-y}/k_y)}{\partial z}\right)_{y,T,p}\right]\Delta z\right\}, \end{aligned} \qquad [A5]$$

which gives the relaxation times τ_y, $\tau_y{}^z$ by comparison with [11]. (For $\nu_y < 0$, the sign is, of course, changed in [A5].)

At equilibrium $(\bar{k}_{-y}/\bar{k}_y) = (\bar{F}_y/K_y)^m$; it is rather natural to identify (k_{-y}/k_y) with $(F_y/K_y)^m$ even away from equilibrium, and this assumption has often been made. It is physically very plausible that the two ratios are at least asymptotic at equilibrium. If this is assumed,

$$\begin{aligned} (\tau_y)^{-1} &= m\bar{k}_{-y}\bar{P}\bar{N}_y^m\left[\left(\frac{\partial \ln Q_y}{\partial y}\right)_z + \left(\frac{\partial \ln F_y}{\partial y}\right)_{z,T,p}\right], \\ (\tau_y{}^z)^{-1} &= m\bar{k}_{-y}\bar{P}\bar{N}_y^m\left[\left(\frac{\partial \ln Q_y}{\partial z}\right)_y + \left(\frac{\partial \ln F_y}{\partial z}\right)_{y,T,p}\right]. \end{aligned} \qquad [A6]$$

These expressions [A6] lead immediately to [A1]. It should be emphasized, however, that the relations [A1] are purely thermodynamic and do not depend on any kinetic assumption. Neither do they depend on the form of the rate law, and of course more general rate laws that [A3] are possible (cf. (11)).

APPENDIX B

The Thermodynamic Parameters

We begin by noting that

$$\left(\frac{\partial \bar{y}}{\partial V}\right)_s = \left(\frac{\partial y}{\partial \ln Q_y}\right)_z\left(\frac{\partial \ln (K_y/\bar{F}_y)}{\partial V}\right)_s + \left(\frac{\partial y}{\partial z}\right)_{Q_y}\left(\frac{\partial \bar{z}}{\partial V}\right)_s. \qquad [B1]$$

However, it is easy to show that

$$\left(\frac{\partial \ln (K_y/\bar{F}_y)}{\partial T}\right)_{p,y,z} = \frac{\Delta H_y}{RT^2},$$

$$\left(\frac{\partial \ln (K_y/\bar{F}_y)}{\partial p}\right)_{T,y,z} = -\frac{\Delta V_y}{RT},$$

so that we may write

$$\left(\frac{\partial \ln (K_y/\bar{F}_y)}{\partial V}\right)_s = \frac{\Delta H_y}{RT}\left(\frac{\partial T}{\partial V}\right)_s - \frac{\Delta V_y}{RT}\left(\frac{\partial p}{\partial V}\right)_s - \left(\frac{\partial \ln F_y}{\partial y}\right)_{p,T,z}\left(\frac{\partial \bar{y}}{\partial V}\right)_s - \left(\frac{\partial \ln F_y}{\partial z}\right)_{p,T,y}\left(\frac{\partial \bar{z}}{\partial V}\right)_s. \quad [B2]$$

It follows that

$$\left(\frac{\partial \bar{y}}{\partial V}\right)_s = \left(\frac{\partial y}{\partial \ln Q_y}\right)_z\left[\frac{\Delta H_y}{RT^2}\left(\frac{\partial T}{\partial V}\right)_s - \frac{\Delta V_y}{RT}\left(\frac{\partial p}{\partial V}\right)_s\right] + \left(\frac{\partial \bar{z}}{\partial V}\right)_s\left[\left(\frac{\partial y}{\partial z}\right)_{Q_y} - \left(\frac{\partial y}{\partial \ln Q_y}\right)_z\left(\frac{\partial \ln F_y}{\partial z}\right)_{p,T,y}\right] \Big/ 1 + \left(\frac{\partial y}{\partial \ln Q_y}\right)_z\left(\frac{\partial \ln F_y}{\partial y}\right)_{p,T,z}. \quad [B3]$$

When $(\partial y/\partial z)_{Q_y}$ is evaluated from the total differential (cf. [27])

$$d \ln Q_y = \left(\frac{\partial \ln Q_y}{\partial y}\right)_z dy + \left(\frac{\partial \ln Q_y}{\partial z}\right)_y dz, \quad [B4]$$

and the value [A1] of $\mathscr{Y}$ is noted, the result [B3] may be put (using the abbreviation $\delta_y = \Delta V_y - (\Delta H_y/C_p)(\partial V/\partial T)_p$, [31])

$$\left(\frac{\partial \bar{y}}{\partial V}\right)_s + \mathscr{Y}\left(\frac{\partial \bar{z}}{\partial V}\right)_s = \frac{\rho^2 c_0^2 \delta_y (\partial y/\partial \ln Q_y)_z}{RT[1+(\partial y/\partial \ln Q_y)_z(\partial \ln F_y/\partial y)_{p,T,z}]}. \quad [B5]$$

This equation and the corresponding equation for $(\partial \bar{z}/\partial V)_s + \mathscr{Z}(\partial \bar{y}/\partial V)_s$ may be solved for $(\partial \bar{y}/\partial V)_s$ and $(\partial \bar{z}/\partial V)_s$ separately. The result is

$$\left(\frac{\partial \bar{y}}{\partial V}\right)_s = \frac{\rho^2 c_0^2 [\delta_y - (\nu_y/\nu_z)\mathscr{Z}\delta_z](\partial y/\partial \ln Q_y)_z}{RT(1-\mathscr{Y}\mathscr{Z})[1+(\partial y/\partial \ln Q_y)_z(\partial \ln F_y/\partial y)_{p,T,z}]}. \quad [B6]$$

In writing [B6] use was made of the values [A1] of $\mathscr{Y}$ and $\mathscr{Z}$, and also of the relation

$$\nu_z\left[\left(\frac{\partial \ln Q_y}{\partial z}\right)_y + \left(\frac{\partial \ln F_y}{\partial z}\right)_{p,T,y}\right] = \nu_y\left[\left(\frac{\partial \ln Q_z}{\partial y}\right)_z + \left(\frac{\partial \ln F_z}{\partial y}\right)_{p,T,z}\right], \quad [B7]$$

which may be demonstrated with the help of the Gibbs-Duhem equation. The definitions [27] allow us to write

$$\nu_z\left(\frac{\partial \ln Q_z}{\partial z}\right)_y = \frac{\nu_z^2}{z} + \sum_i \frac{(\nu_i(z))^2}{x_i}, \quad [B8]$$

$$\nu_z\left(\frac{\partial \ln Q_y}{\partial z}\right)_y = \nu_y\left(\frac{\partial \ln Q_z}{\partial y}\right)_z = \sum_i \frac{\nu_i(y)\nu_i(z)}{x_i}. \quad [B9]$$

REFERENCES

1. G. STOKES. Trans. Cambridge Phil. Soc. **8**, 287 (1845).
2. G. KIRCHHOFF. Ann. der Phys. **134**, 177 (1868).
3. R. O. DAVIES and J. LAMB. Quart. Rev. **11**, 134 (1957); Proc. Phys. Soc. **73**, 767 (1959).
4. K. F. HERZFELD and T. A. LITOVITZ. The absorption and dispersion of ultrasonic waves. Academic Press, New York. 1959.
5. K. TAMM. Handbuch der Physik. **XI/1**, 202 (1961).
6. M. EIGEN and K. TAMM. Z. Elektrochem. **66**, 93 (1962).
7. J. P. VALLEAU and S. J. TURNER. Can. J. Chem. This issue.
8. M. EIGEN. Discussions Faraday Soc. **24**, 25 (1957).
9. R. O. DAVIES and J. LAMB. Proc. Phys. Soc. B, **69**, 293 (1956).
10. R. T. BEYER. J. Acoust. Soc. Am. **29**, 243 (1957).
11. M. MANES, L. J. E. HOFER, and S. WELLER. J. Chem. Phys. **18**, 1355 (1950).

Can. J. Chem. Downloaded from www.nrcresearchpress.com by 210.87.254.40 on 09/05/12
For personal use only.

Can. J. Chem. Downloaded from www.nrcresearchpress.com by 210.87.254.6 on 09/05/12
For personal use only.

AN ULTRASONIC STUDY OF SOME OF THE COMPLEXING REACTIONS OF CHLORIDE WITH CADMIUM ION

J. P. VALLEAU AND S. J. TURNER
Department of Chemistry, University of Toronto, Toronto, Ontario

Received October 9, 1963

ABSTRACT

The ultrasonic absorptions of 0.25 *M* aqueous solutions of cadmium ions, containing various amounts of hydrochloric acid, have been measured by a pulse technique between 13 and 143 Mc/second at 16°, 25°, and 35° C. A relaxation occurs in this region, and it has been interpreted in terms of the interacting association reactions

$$CdCl_2 + Cl^- \rightleftharpoons CdCl_3^-$$
$$CdCl_3^- + Cl^- \rightleftharpoons CdCl_4^{2-}$$

An ultrasonic determination of the equilibrium quotient of the second of these reactions has been made, and the association and dissociation rate constants are reported for both reactions. In addition, the volume changes, ΔV, in the two reactions have been estimated, along with the activation energy for the dissociation of $CdCl_3^-$. The analysis breaks down at low ligand concentrations, and this is ascribed to the influence of a third interacting reaction.

1. INTRODUCTION

There has recently been increasing interest (1, 2, 3) in the use of ultrasonic absorption techniques of studying rapid chemical reactions near equilibrium. The magnitude and frequency dependence of the absorptions depend on the free energy, enthalpy, and volume changes in the reactions, as well as on the rate constants. In favorable cases both kinetic and thermodynamic data may therefore be extracted from ultrasonic experiments.

One of the attractions of the ultrasonic method is that when there occurs a series of interacting equilibria (as in complex ion formation), it is in principle possible to obtain kinetic and thermodynamic data for the separate reaction steps (4). In the present paper the chloride complexes of cadmium are studied from this viewpoint, making use of an extension (5) of ultrasonic theory to embrace relaxations involving two simultaneous equilibria.

In the cadmium–chloride system there occur the four association reactions

$$Cd^{2+} + Cl^- \rightleftharpoons CdCl^+, \qquad [1w]$$
$$CdCl^+ + Cl^- \rightleftharpoons CdCl_2, \qquad [1x]$$
$$CdCl_2 + Cl^- \rightleftharpoons CdCl_3^-, \qquad [1y]$$
$$CdCl_3^- + Cl^- \rightleftharpoons CdCl_4^{2-}. \qquad [1z]$$

The existence of higher complexes has occasionally been suggested, but there is no firm evidence of their existence at the solution concentrations in question. There have been several determinations of the first three stoichiometric equilibrium quotients $\bar{Q}_w$, $\bar{Q}_x$, $\bar{Q}_y$ (cf. (6, 7, 8, 9)), of which the most satisfactory appear to be those of Vanderzee and Dawson (7), who measured these quotients, and also the enthalpies (ΔH) of the three reactions as a function of ionic strength. There are also a number of values of $\bar{Q}_z$ in the literature (10, 11, 12, 13), but these differ very widely. A determination of the ultrasonic velocity, and thus of adiabatic compressibility, in cadmium chloride solutions has been made by Subrahmanyan (14) at 750 kc/second.

After describing our experimental measurements, we discuss what physical chemical information is obtainable from the results.

2. EXPERIMENTAL PROCEDURE

(a) Apparatus

The absorption and velocity of ultrasound in the range 13 to 143 Mc/second were determined by a pulse technique similar to that of Pinkerton (15). The sound wave was produced and detected by matched 13 Mc/second quartz crystals, using the circuit shown schematically in Fig. 1. The wave was transmitted into

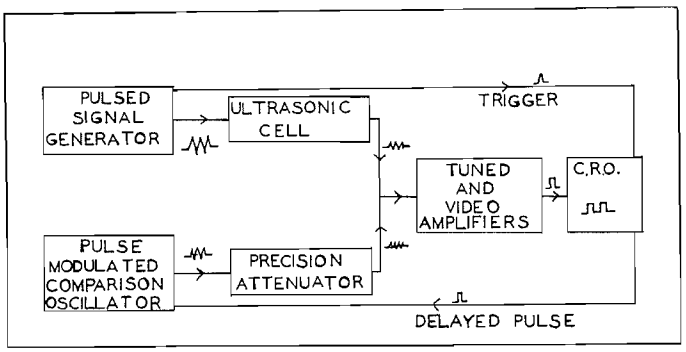

FIG. 1. Schematic circuit diagram of apparatus.

and out of the solution by fused quartz rods, one of which was driven by an accurate lead screw. The changes in ultrasonic attenuation on altering the path length in the solution were compared with electrical attenuation introduced into a comparison circuit by an Airborne Instruments piston attenuator (precision ±0.005 db per db).

The amplitude absorption coefficient α was thus determined for each solution at the five frequencies 13, 39, 65, 91, and 143 Mc/second. The velocity of the sound waves was determined by the interference of reflected pulses at short path lengths.

The precision of the absorption measurements is about 1%, and the estimated error below 3% (cf. (20)). The accuracy of the velocity measurements is estimated to be ±0.5%. Frequency was measured with a calibrated heterodyne frequency meter to within ±0.05%. The cell was thermostatted with a water jacket to within 0.1° C in a given run. The results reported in this paper are for 15.9±0.1° C, 24.7±0.3° C, and 35.1±0.1° C.

(b) Solutions

The solutions discussed in this paper were all 0.25 M in cadmium ion, but contained amounts of hydrochloric acid varying over a wide range (cf. Table I). Hydrochloric acid solutions were prepared by the dilution of Nichols or Baker and Adamson C.P. hydrochloric acid with distilled water, and were subsequently standardized by titrating against mercuric oxide (16). The solutions at 16° and 25° C were prepared by weighing Fisher certified $Cd(NO_3)_2 \cdot 4H_2O$ and adding the required amount of standard hydrochloric acid. The solutions at 35° C were prepared by dissolving weighed amounts of Fisher certified cadmium oxide in standard hydrochloric acid solutions.

The densities of the solutions at 25° C were measured to an accuracy of ±0.3% with hydrometers; the densities at 16° and 35° C were determined to an accuracy of ±0.01% with a specific gravity bottle. Using this data plots were made of density as a function of chloride concentration and from these plots the densities required in the calculations were obtained. Heat capacities and thermal expansion coefficients for the solutions could be estimated from data in the International Critical Tables, since the resulting uncertainties are of no significance.

(c) Determination of the Ultrasonic Parameters

In a single relaxation process the variation of the absorption α with the frequency f determines three constants, A, B, and f_c, according to the relation:

$$\alpha/f^2 = A/[1 + (f/f_c)^2] + B; \qquad [2]$$

f_c is the relaxation frequency. The ultrasonic absorption results on cadmium–chloride solutions were fitted to the expression [2] by the least squares method, using I.B.M. 7090 and 650 computers. The computers were programmed to give A, B, and the standard error $\sqrt{(s/n)}$ for trial values of f_c at 0.2 or 0.5 Mc/second intervals (where s is the sum of the squares of the deviations between the observed and fitted points and n is the number of experimental points).

It was observed that the values of A were quite insensitive to the values of f_c but that this was not so for B. It was of interest to demonstrate that a smooth curve of f_c against chloride ion concentration could be

Can. J. Chem. Downloaded from www.nrcresearchpress.com by 210.87.254.6 on 09/05/12
For personal use only.

TABLE I

Chloride conc. (moles/liter)	f_c (Mc/s)	$A \times 10^{17}$ (sec²/cm)	$B \times 10^{17}$ (sec²/cm)	S.E. $\times 10^{17}$
A. Values of A, B, f_c, and the standard error (S.E.) at 16° C*				
0.301	25.0	29.1	29	0.3
0.500	25.8	63.0	30	0.3
1.038	31.0	146	42	2.8
1.250	35.0	189	46	2.9
1.699	35.0	308	65	6.8
1.901	38.0	346	69	4.3
2.109	38.6	387	71	4.1
2.260	39.0	398	77	6.1
2.349	40.4	414	77	5.4
2.502	41.6	422	78	4.7
2.649	43.6	413	80	7.1
2.775	44.6	400	81	6.1
2.996	46.2	375	80	4.1
3.500	54.0	263	77	3.9
4.000	64.0	161	75	2.2
B. Values of A, B, f_c, and the standard error (S.E.) at 25° C*				
0.306	32.0	11.6	23	1.2
0.436	32.5	36.4	22	0.8
0.562	35.0	37.8	24	1.3
0.874	36.0	99.1	29	0.7
1.260	39.5	164	41	4.2
1.530	41.5	235	47	4.2
1.841	44.5	310	54	3.4
1.890	45.5	321	53	3.5
1.943	45.5	329	54	2.8
1.992	46.0	338	54	4.5
2.043	46.5	345	61	6.0
2.182	47.5	353	63	2.6
2.390	49.0	369	62	4.2
2.618	52.0	357	66	3.8
2.825	53.5	328	75	1.9
3.042	55.5	298	71	4.9
3.272	59.0	264	74	2.1
4.017	94.5	128	44	0.9
C. Values of A, B, f_c, and the standard error (S.E.) at 35° C†				
0.788	39.0	74.4	24	1.2
1.000	40.6	113	31	1.8
1.248	43.8	168	38	2.2
1.552	47.6	234	49	4.6
1.800	49.0	289	55	3.3
2.000	51.6	317	61	5.0
2.201	53.6	330	65	3.9
2.351	55.4	332	68	1.8
2.650	57.9	321	69	4.2
3.000	64.8	274	69	2.8
3.500	81.4	189	61	2.6

*Solutions 0.25 M in cadmium nitrate.
†Solutions made by dissolving cadmium oxide in hydrochloric acid: 0.25 M in cadmium ion.

obtained for values of f_c giving standard errors within the estimated experimental error. These "smoothed" values are given in Table I.* A comparison of the smoothed values with the best least squares values for B and f_c at 35° C is given in Fig. 3. In all cases the experimental results appeared to fit equation [2] very well (cf. Fig. 4), and it is on this basis that the remaining analysis in this paper is carried out.

A, B, and f_c at 25° C are shown in Fig. 2 as a function of hydrochloric acid concentration. It can be seen that both A and B exhibit maxima. Similar curves were obtained at 16° and 35° C. The peak in A is to be expected for a single relaxation process, but the peak in B is explained by the presence of a second, faster, relaxation process in the solution. B contains the classical viscous absorption and the so-called "structural

Only these derived parameters A, B, and f_c are reported here. We shall be glad to supply our absorption data at each frequency to anyone interested.

Can. J. Chem. Downloaded from www.nrcresearchpress.com by 210.87.254.6 on 09/05/12
For personal use only.

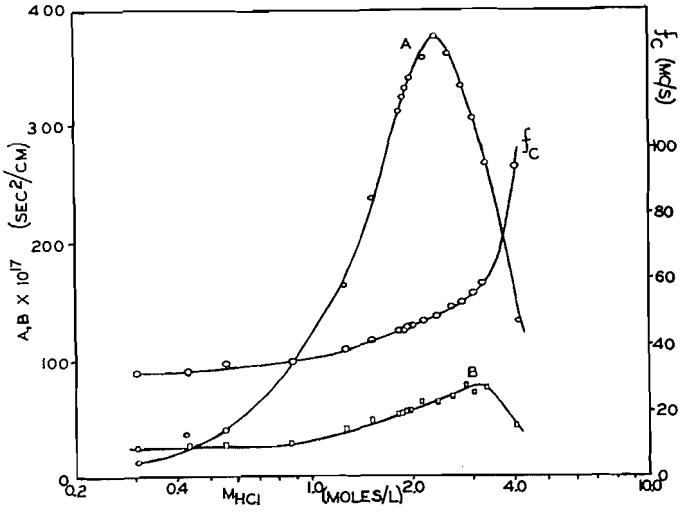

FIG. 2. Variation of A, B, and f_c with concentration of HCl at 25° C (0.25 M in $Cd(NO_3)_2$).

relaxation" of the solvent, plus the absorption of any processes too fast to relax at the frequencies studied. The theory and conclusions which follow are based on the existence of interacting chemical relaxation processes.

3. ANALYSIS OF THE RESULTS

We wish to assign the two peaks, in A and B, to two of the reactions [1]. It is possible to predict roughly the position to be expected for a peak due to a given reaction, and by comparison with such predictions the peaks in A and B have been assigned to reactions [1y] and [1z] respectively. This assignment seems quite unambiguous, for peaks due to [1w] or [1x] would occur at much lower ligand concentrations, below 1 M.

The situation may conveniently be described by the "ordering parameters" $y = [CdCl_2]$ and $z = [CdCl_4^{2-}]$. The general theory of absorption due to such a pair of reactions appears elsewhere (5), and it is shown that the absorption takes the form

$$\frac{\alpha}{\omega^2} = \frac{\alpha_b}{\omega^2} + \frac{\tau_y A_{yz} + \tau_z A_{zy} + (\omega\tau_y/1-\mathscr{Y}\mathscr{Z})^2\tau_z B_z + (\omega\tau_z/1-\mathscr{Y}\mathscr{Z})^2\tau_y B_y}{1+\{\omega^2[\tau_y^2+2\mathscr{Y}\mathscr{Z}\tau_y\tau_z+\tau_z^2]+\omega^4\tau_y^2\tau_z^2\}/(1-\mathscr{Y}\mathscr{Z})^2}, \quad [3]$$

where $\omega = 2\pi f$ and α_b is the absorption due to viscosity and other "background effects". The relaxation times τ_y, τ_z are defined by the rate laws

$$dy/dt = -(\Delta y + \mathscr{Y}\Delta z)/\tau_y, \; dz/dt = -(\Delta z + \mathscr{Z}\Delta y)/\tau_z, \quad [4]$$

where Δy and Δz are the deviations of the concentrations y and z from their equilibrium values. The quantities A_{yz}, A_{zy}, B_y, B_z, $\mathscr{Y}$ and $\mathscr{Z}$ are derived elsewhere (5); for example they may be written, for the above choice of parameters y, z.

$$A_{yz} = \frac{\rho^2 c(-\partial y/\partial \ln Q_y)_z(\delta_y + \mathscr{Z}\delta_z)^2}{2RT(1-\mathscr{Y}\mathscr{Z})^2[1+(\partial y/\partial \ln Q_y)_z(\partial \ln F_y/\partial y)_{p,T,z}]}, \quad [5]$$

$$B_z = \frac{\rho^2 c(\partial z/\partial \ln Q_z)_y \delta_z^2}{2RT[1+(\partial z/\partial \ln Q_z)_y(\partial \ln F_z/\partial z)_{p,T,y}]}, \quad [6]$$

$$\mathscr{Y} = \frac{(\partial y/\partial \ln Q_y)_z[1+(\partial z/\partial \ln Q_y)_y(\partial \ln F_y/\partial z)_{p,T,y}]}{(\partial z/\partial \ln Q_y)_y[1+(\partial y/\partial \ln Q_y)_z(\partial \ln F_y/\partial y)_{p,T,z}]}, \quad [7]$$

Can. J. Chem. Downloaded from www.nrcresearchpress.com by 210.87.254.6 on 09/05/12
For personal use only.

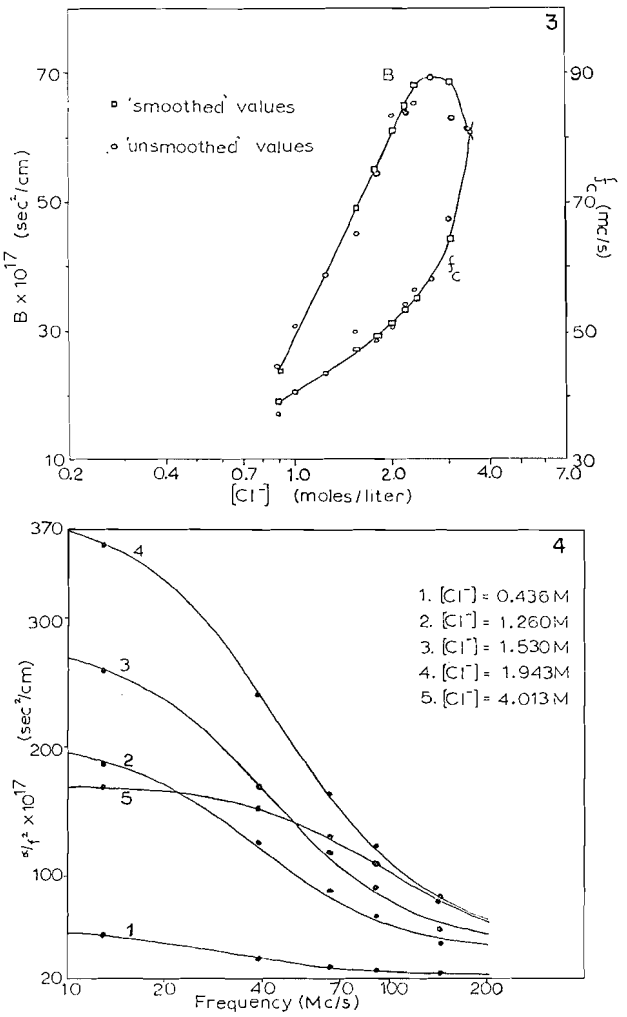

FIG. 3. Comparison of the "smoothed" and "unsmoothed" (best least squares) values for B and f_c at 35° C.

FIG. 4. Some typical fitted relaxation curves at 25° C, with the experimental values.

where

$$\delta_y = \Delta V_y - \left(\frac{\partial V}{\partial T}\right)_p \frac{\Delta H_y}{C_p}, \qquad \delta_z = \Delta V_z - \left(\frac{\partial V}{\partial T}\right)_p \frac{\Delta H_z}{C_p}. \qquad [8]$$

In these equations

ρ and V are the specific gravity and volume of the solution,

c is the sound velocity (cm/second),

C_p is the specific heat of the solution (cal/g deg),

Q_y, Q_z are the stoichiometric quotients for the reactions [1y] and [1z] (liters/mole) (ref. (5), eq. [20]),

F_y, F_z are the corresponding quotients of ionic activity coefficients for the two reactions (ref. (5), eq. [22]), and

ΔV_y, ΔH_y are the volume and enthalpy changes in the y-reaction [1y].

Can. J. Chem. Downloaded from www.nrcresearchpress.com by 210.87.254.6 on 09/05/12
For personal use only.

It is understood that a derivative such as $(\partial z/\partial \ln Q_z)_y$ refers to fixed overall concentrations, and that in calculating the derivative we regard reaction [1y] as frozen (as indicated by the subscript), and need not take into account other reactions, such as [1w] and [1x], which are assumed not to be in interaction with the relaxing processes. In this case we obtain

$$\left(\frac{\partial y}{\partial \ln Q_y}\right)_z = \frac{-[CdCl_3^-]}{1+\bar{Q}_y([CdCl_2]+[Cl^-])}, \qquad [9]$$

$$\left(\frac{\partial z}{\partial \ln Q_z}\right)_y = \frac{[CdCl_4^{2-}]}{1+\bar{Q}_z([CdCl_3^-]+[Cl^-])},$$

$$\left(\frac{\partial y}{\partial \ln Q_z}\right)_z = -\left(\frac{\partial z}{\partial \ln Q_y}\right)_y = \frac{[CdCl_4^{2-}]}{\bar{Q}_z([CdCl_3^-]-[Cl^-])}.$$

Some simplification results from the fact that the observations can be fitted to single relaxation curves. Under this condition we can use the approximation $\omega\tau_z \ll 1$, $\omega\tau_z \ll \omega\tau_y$, when we get the approximate results (5)

$$A \approx \tau_y A_{yz}, \qquad [10]$$

$$B \approx \tau_z B_z + (\alpha_b/f^2),$$

$$1/(2\pi f_c) \equiv \tau_{\text{expt}} \approx \tau_y/(1-\mathscr{Y}\mathscr{Z}).$$

We have attempted to fit our experimental results to the complete expression [3] by a method of successive approximations, beginning with [10].

It will be recalled that the reported values of $\bar{Q}_z$ are widely discrepant. We therefore decided to extract a new value from our data. This is possible because the position and shape of the peak in $[B-(\alpha_b/f^2)] \approx \tau_z B_z$ ([6], [10]) depends primarily on $\bar{Q}_z$. Various trial values of $\bar{Q}_z$ were used, in conjunction with the data of Vanderzee and Dawson (7) on $\bar{Q}_w$, $\bar{Q}_x$ and $\bar{Q}_y$, to calculate, as a function of total halide concentration, a quantity proportional to $\tau z(\partial_z/\partial \ln Q_z)_y$ and thus to $[B-(\alpha_b/f^2)]$. The value of $\bar{Q}_z$ giving the most satisfactory agreement with the B curve was adopted as the best value for this quotient. (In doing this, (α_b/f^2) was given the values 29×10^{-17} (16° C), 21×10^{-17} (25° C), and 16×10^{-17} sec^2 cm^{-1} (35° C) as found in pure water. The absorption of 2.8 M hydrochloric acid solution without cadmium ion was found to be 23×10^{-17} sec^2 cm^{-1} at 25° C, showing that the error in using the above constant values for (α_b/f^2) was well within the estimated accuracy of B.) This should be regarded as an ultrasonic determination of $\bar{Q}_z$ for ionic strengths near three. At 25° C the value $\bar{Q}_z = 0.55$ thus determined agrees fairly well with two of those previously reported (10, 12). In the determination of $\bar{Q}_z$ at 16° and 35° C, it was necessary to know the values of $\bar{Q}_w$, $\bar{Q}_x$, $\bar{Q}_y$ for these temperatures, at various ionic strengths. These quantities were obtained by interpolation of the data of Vanderzee and Dawson (7), by means of plots of $\ln \bar{Q}$ vs. $1/T$ and of $\bar{Q}$ vs. ionic strength.

It should be emphasized that we have chosen only the best *constant* value of $\bar{Q}_z$, and have tacitly ignored, as well, any variation of δ_z or of the rate constants k_z, k_{-z} with concentration. In view of the experimental uncertainty in B, and especially of the imprecise estimate of α_b, it didn't appear justified to attempt more than this. We could, of course, have made our theoretical curve fit the experimental curve exactly by allowing $\bar{Q}_z$, or k_z, or both, to vary with the concentration. The fit based on constant parameters (Fig. 7) appears quite satisfactory, however, and is likely within the uncertainty in our estimate of $\tau_z B_z$ [9]. The very small reported variation of $\bar{Q}$ for $CdBr_3^- + Br^- \rightleftharpoons CdBr_4^{2-}$ (17) is also

Can. J. Chem. Downloaded from www.nrcresearchpress.com by 210.87.254.6 on 09/05/12
For personal use only.

encouraging with respect to our procedure. It appears, from our calculations using other trial values of $\bar{Q}_z$, that the uncertainty in the derived value of $\bar{Q}_z$ is about ± 0.2 liters/mole.

It should be mentioned that in the present analysis we have suppressed all the activity coefficient terms in the theoretical equations, on the following basis: the assumption that the activity coefficients depend on concentration through the ionic strength, I, only (so that $F_y = F_y(T, p, I)$, etc.) allows one to write*

$$(\partial \ln F_y/\partial y)_z = (\partial \ln F_y/\partial z)_y = (\partial \ln F_z/\partial y)_z = 0;$$

this follows from the fact that $(\partial I/\partial y)_z = 0$ (cf. ref. (5), eqs. [B7], [B9]). There is no useful data on F_z, but our constant value of $\bar{Q}_z$ is consistent, on the above assumption, with $(\partial \ln F_z/\partial z)_y = 0$, and we have accepted this value.

The analysis is now carried out as follows. From τ_{expt} we can calculate τ_y [10]. The experimental A values can then be compared with $\tau_y A_{yz}$ [10]; this gives us a trial value of $(\delta_y + \mathscr{Z}\delta_z)^2$ as a function of acid concentration. In order to proceed we need, however, values of δ_y and δ_z separately. There is no rigorous way of carrying out this separation, since both δ_y and δ_z could in principle vary arbitrarily with the concentration. If, on the other hand, δ_y and δ_z are independent of concentration, a plot of $|\delta_y + \mathscr{Z}\delta_z|$ against $\mathscr{Z}$ should be linear; in fact such a plot proves to be very closely linear except at the lowest chloride concentrations (cf. Fig. 5). The linear region extends through the concentration range of

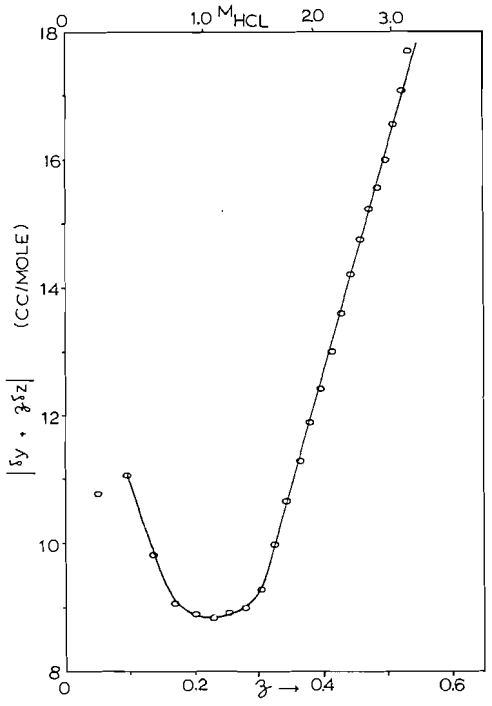

FIG. 5. $|\delta_y + \mathscr{Z}\delta_z|$ vs. $\mathscr{Z}$ at 25° C.

On the other hand, the same assumption allows one to calculate a small finite value for $(\partial \ln F_y/\partial z)_y$ from the reported variation of $\bar{Q}_y$ with ionic strength. Presumably the above assumption is (as one expected) at fault. Fortunately the terms remain so small that they can be neglected, however.

Can. J. Chem. Downloaded from www.nrcresearchpress.com by 210.87.254.6 on 09/05/12
For personal use only.

both the A and the B peaks. The low concentration deviation will require a separate discussion later in the paper. From the linear plot we obtain trial values of δ_y and δ_z (these are of opposite signs and at 25° C their magnitudes are 1.4 and 36 cc/mole, respectively).

Using this value of δ_z, B_z [6] may be calculated. Comparison of this with $(B-\alpha_b/f^2)$ [10] gives a trial value for τ_z at each concentration. The set of trial values of δ_y, δ_z, and τ_z were then used to improve the approximation. With their help the corrections [3] to the first approximation [10] were calculated. These corrections are fortunately small, and allow a second cycle of determinations of δ_y, δ_z, and τ_z. The resulting values of $|\delta_y|$ and $|\delta_z|$ at 25° C are 1.8 and 36 cc/mole. The dissociation rate constant k_{-z} of $CdCl_4^{2-}$ [1z] was determined from τ_z according to the relation

$$\tau_z^{-1} = k_{-z}[1+\bar{Q}_z([CdCl_3^-]+[Cl^-])], \qquad [11]$$

which is equation [A6] of ref. (5) for the rate law

$$dz/dt = (d[CdCl_4^{2-}])/dt = -k_{-z}[CdCl_4^{2-}]+k_z[CdCl_3^-][Cl^-].$$

At 25° C its mean value was found to be 7.6×10^9 sec^{-1}. These values and the values obtained earlier were used to calculate the complete expressions for A and B, and at 25° C these are compared with experiment in Figs. 6 and 7; similar results were obtained at the other temperatures.

No dispersion could be observed in the velocity measurements at different frequencies. In fact the expected dispersion can be calculated from the absorption and was found to be within our experimental accuracy. Also no definite variation with concentration of HCl was found, the individual velocity determinations being scattered about the mean values given in Table II, with a maximum deviation of 0.7%.

TABLE II

Summary of parameters derived for the cadmium–chloride system

Temp. (° C)	ΔV_y (±5) (cc mole^{-1})	ΔV_z (±4) (cc mole^{-1})	$\bar{Q}_z$ (±40%) (l. mole^{-1})	k_z (±50%?) (l. mole^{-1} sec^{-1})	k_{-z} (±50%) (sec^{-1})	Mean velocity (cm sec^{-1})
15.9±0.1	3.8	−38	0.5	5×10^9	10×10^9	1.48×10^5
24.7±0.3	2.8	−35	0.55	4×10^9	8×10^9	1.50×10^5
35.1±0.1	5.8	−42	0.6	6×10^9	10×10^9	1.52×10^5
	Mean = 4.1	−38				

4. DISCUSSION

The discrepancy (Figs. 5 and 6) in our fit of A at low ligand concentrations will be discussed presently. Meanwhile we shall comment only on the more extensive region for which our interpretation appears to be successful.

To carry out our analysis, we were forced to assume the constancy of δ_y and δ_z over a wide range of concentration. Happily this is consistent with our results, and indeed the linearity of $|\delta_y+\mathscr{Z}\delta_z|$ with $\mathscr{Z}$ would be highly fortuitous on any other assumption. The assumed constancy of $\bar{Q}_z$ is perhaps more worrying, although the resulting fit (Fig. 7) is probably within the uncertainty of our estimate of $\tau_z B_z$. There remains however some uncertainty in the constant value chosen—it may be in error by as much as 40%. The calculations have been repeated with the values $\bar{Q}_z = 0.3$ and 0.4, and from these calculations it appears that the uncertainty in $\bar{Q}_z$ leads to uncertainties of about ±3 cc/mole in

Can. J. Chem. Downloaded from www.nrcresearchpress.com by 210.87.254.6 on 09/05/12
For personal use only.

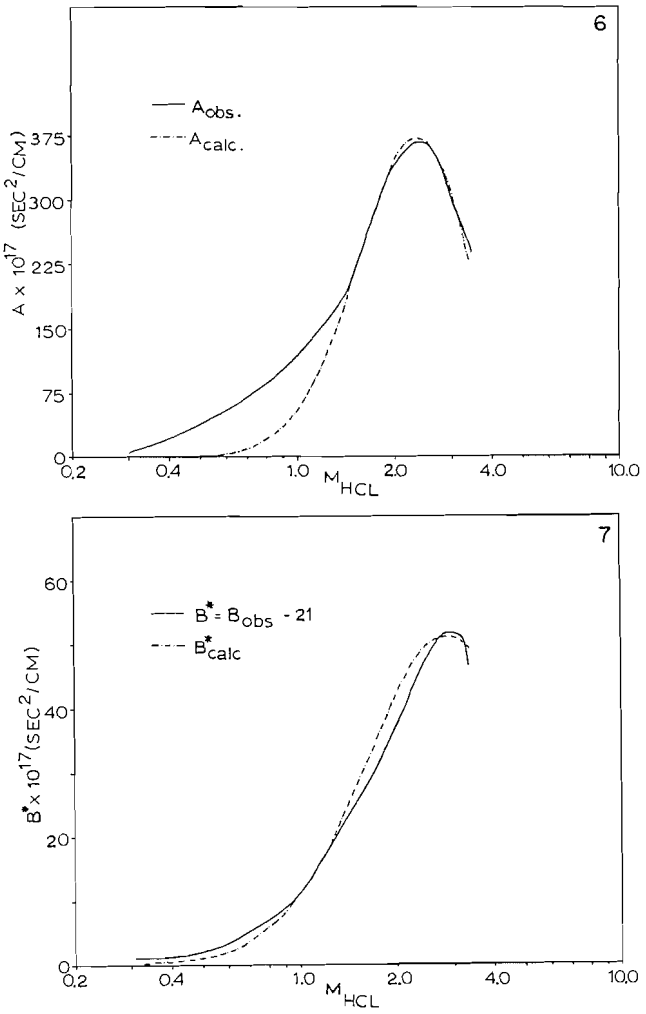

FIG. 6. Comparison of A_{obs} and A_{calc} at 25° C.
FIG. 7. Comparison of $B^* = [B_{obs} - (\alpha_b/f^2)]$ and B^*_{calc} at 25° C.

δ_y and ± 2 cc/mole in δ_z. There will be additional uncertainty in δ_y and δ_z due to errors in τ_y and the remaining $\bar{Q}$'s.

Since A_{yz} is proportional to $(\delta_y + \mathscr{Z}\delta_z)^2$ our plot (Fig. 5) allows us to determine only the magnitudes and the relative sign of δ_y and δ_z. However, one might expect ΔV_z and hence δ_z for the reaction [1z] to be negative, as discussed below. With the help of data from Vanderzee and Dawson (7) and Shchukaryev *et al.* (12) we can calculate the ΔH contributions to δ_y and δ_z [8], and thus extract ΔV for each reaction. Fortunately the ΔH contributions turn out to be small in both cases, and the resulting ΔV values are shown in Table II.

It is perhaps interesting to compare ΔV_z with that predicted by the empirical equations of Couture and Laidler (18). According to these authors the partial molal volume of monatomic anions may be represented by: $4 + 4.9\ r^3 - 14|z|$, where r is the crystallographic radius and z the charge. If we apply this expression to the present more complicated case it leads to:

Can. J. Chem. Downloaded from www.nrcresearchpress.com by 210.87.254.6 on 09/05/12
For personal use only.

$$\Delta V_z = 4.9(r^3_{CdCl_4^{2-}} - r^3_{CdCl_3^-} - r^3_{Cl^-}) - 4.$$

Taking $r_{CdCl_4^{2-}} = r_{CdCl_3^-}$, this gives $\Delta V_z \approx -33$ cc/mole, quite close to our experimental value of -38 cc/mole. If, instead, we attempt to apply to the cadmium complex anions the expressions which the above authors (19) intended for oxyanions, it leads to a numerically smaller, but still negative, value for ΔV_z.

The experimental relaxation time [10] gives us the relaxation time τ_y of reaction [1y]. Since (cf. [11])

$$\tau_y^{-1} = k_{-y}[1+\bar{Q}_y([CdCl_2]+[Cl^-])],$$

we can derive the dissociation rate, k_{-y}, of $CdCl_3^-$, and then the association rate $k_y = \bar{Q}_y k_{-y}$. These rate constants and τ_y are given in Table III. It is interesting that the association rate k_y appears virtually constant, the variation of $\bar{Q}_y$ corresponding almost entirely to that of the dissociation rate; this is contrary to an expectation expressed elsewhere (1).

TABLE III

Derived rate parameters at selected ligand concentrations

	$k_y \times 10^{-8}$ (l. mole^{-1} sec^{-1})			$k_{-y} \times 10^{-8}$ (sec^{-1})			$\tau_y \times 10^9$ (sec)		
[Cl^-]	15.9° C	24.7° C	35.1° C	15.9° C	24.7° C	35.1° C	15.9° C	24.7° C	35.1° C
1.59	0.87	1.1	1.4	1.6	2.0	2.1	3.80	3.07	2.75
1.98	0.96	1.2	1.5	1.5	1.8	1.9	3.54	2.85	2.55
2.34	1.0	1.3	1.5	1.3	1.5	1.6	3.34	2.71	2.40
2.69	1.1	1.3	1.6	1.1	1.2	1.4	3.16	2.61	2.27
3.03	1.1	1.3	1.6	0.92	1.0	1.2	2.96	2.49	2.13
3.35	1.1	1.3	1.7	0.78	0.83	1.0	2.76	2.36	1.91

NOTE: The apparent activation energies for the association and dissociation reactions are 4.5 ± 0.8 kcal/mole and 2.3 ± 0.5 kcal/mole, respectively.

The activation energy for the dissociation reaction [1y] was determined from an Arrhenius plot to be 2.3 ± 0.5 kcal per mole. The linearity of these plots deteriorated at low chloride ion concentrations. This suggests that the relation [10] between τ_y and τ_{expt} may be breaking down at these concentrations. We shall later argue that this is probably due to the presence of a third relaxation process. Combining the above activation energy with the estimated heat of the reaction (7), we find that the activation energy of the association reaction is about 4.5 kcal per mole.

The method of extracting τ_y from the experimental data involves an uncertainty of about 8%. The accuracy of k_y or k_{-y} depends as well on the uncertainty of $\bar{Q}_y$ (7), giving an estimated uncertainty of about 15% in these rate constants. The corresponding figures for τ_z and for the rate constants k_{-z}, k_z are very difficult to estimate, but it appears they may amount to as much as 25% and 50% respectively.

We turn now to discussing the considerable discrepancy between the observed A curve at low concentrations and that predicted by parameters derived at higher concentrations; this discrepancy corresponds to the non-linear region of Fig. 5. The following explanations suggest themselves:

(*a*) a variation of δ_y or δ_z with low concentrations,
(*b*) errors in the $\bar{Q}$'s used in the calculations,
(*c*) a breakdown of the approximation $\tau_y \gg \tau_z$,
(*d*) the presence of a third interacting process.

The first two suggestions require implausibly large changes in the parameters involved,

Can. J. Chem. Downloaded from www.nrcresearchpress.com by 210.87.254.6 on 09/05/12
For personal use only.

however. The implication of (*c*) is that our method of analyzing the results becomes inapplicable at low concentrations. If this were to be important, however, there should appear at least some region in which the relaxation curves were far from those of a single relaxation; nor do the results at higher concentrations suggest that any such calamity is to be expected, a factor of 30 remaining between τ_y and τ_z at [HCl] = 1.5.

We therefore turn to (*d*), the possibility of a third interacting process. Since the deviation occurs at low ligand concentrations, it is natural to suspect that the other complexing reactions [1*x*] or [1*w*], could be responsible, and in fact the deviation goes through a peak at [HCl] = 0.8, very close to the position to be expected for absorption due to reaction [1*x*]. There remains the very surprising fact that the relaxation appears to be single at each concentration. This could only happen if the relaxation time τ_x of the interacting process obeyed one of the following conditions:

(i) $\tau_x \gg \tau_y$, when the *x*-reaction would be frozen and make no contribution to the absorption.

(ii) $\tau_x \ll \tau_y$, when the *x*-reaction could influence the magnitude of A in the same way as we have seen the *z*-reaction to do. Against this, one would expect a peak in the B curve for such a case.

(iii) $\tau_x \approx \tau_y$ when (cf. (5)) it would be very difficult to distinguish the relaxation curve from that of a single relaxation.

The complete analysis of this third case requires a further extension of ultrasonic theory. One can see from the theory for two processes (5) that τ_x and τ_y would not be simply related to f_c in this case, and for that reason we have taken no kinetic data from our results below 1.5 M HCl. An attempt is being made to investigate the matter more thoroughly.

5. CONCLUSION

The experimental results have been interpreted in terms of the two interacting processes [1*y*] and [1*z*]. On this basis we have derived a variety of kinetic and thermodynamic information about these reactions, and this is summarized in Tables II and III.

It appears, however, that these results should be accepted with some caution, inasmuch as the analysis in terms of only two reactions is not satisfactory throughout the range of concentrations studied. It appears that the validity of the present interpretation can only be examined by carrying out a more complete analysis in terms of more than two processes. This is being attempted.

It is felt that the temperature variations in the derived values of the ΔV's, k_z, and k_{-z} are not significant, in view of the uncertainty in the determinations.

The relaxation we have observed is that of the third reaction, [1*y*], in the sense that it is controlled by the rates of this reaction. On the other hand, almost the whole of the magnitude of the absorption is "borrowed" from the fourth reaction [1*z*], due to the large size of ΔV_z compared to ΔV_y. This behavior lends weight to the warning given in a previous paper (5) concerning naive interpretations of apparently single relaxations. In the present case the absorption at [HCl] = 2.3 M, for example, if assigned to a simple relaxation of [1*y*] alone, would have led to the very different value $|\Delta V_y| = 13.5$ cc/mole.

ACKNOWLEDGMENTS

The financial assistance of the National Research Council is gratefully acknowledged and one of us (S. J. T.) wishes to thank the N.R.C. for the award of a bursary.

Can. J. Chem. Downloaded from www.nrcresearchpress.com by 210.87.254.6 on 09/05/12
For personal use only.

REFERENCES

1. M. EIGEN and K. TAMM. Z. Elektrochem. **66**, 93 (1962).
2. J. STUEHR, E. YEAGER, T. SACHS, and F. HOVORKA. J. Chem. Phys. **38**, 587 (1963).
3. M. KRISHNAMURTHI and M. SURYANARAYANA. Acustica, **12**, 33 (1962).
4. M. EIGEN. Discussions Faraday Soc. **24**, 25 (1957).
5. J. P. VALLEAU. Can. J. Chem. This issue.
6. L. ERIKSSON. Acta Chem. Scand. **7**, 1146 (1953).
7. C. E. VANDERZEE and H. J. DAWSON, JR. J. Am. Chem. Soc. **75**, 5659 (1953).
8. I. LEDEN. Z. Phys. Chem. A, **188**, 160 (1941).
9. E. L. KING. J. Am. Chem. Soc. **71**, 319 (1949).
10. A. M. GOLUB. Ukr. Khim. Zh. **19**, 205 (1953).
11. Y. MARCUS. Ph.D. Thesis, The Hebrew University of Jerusalem, Jerusalem, Israel. 1955.
12. S. A. SHCHUKARYEV, L. S. LILICH, and V. A. LATYSHEVA. Uch. Zap. Leningr. Cos. Univ. Ser. Khim. Nauk, **15** (211), 17 (1957).
13. H. L. RILEY and V. GALLAFENT. J. Chem. Soc. 514 (1932).
14. S. V. SUBRAHMANYAN. Trans. Faraday Soc. **56**, 971 (1960).
15. J. M. M. PINKERTON. Proc. Phys. Soc. B, **62**, 286 (1949).
16. I. M. KOLTHOFF and E. B. SANDELL. Textbook of quantitative inorganic analysis. 3rd ed. MacMillan. 1952. p. 525.
17. P. KIVALO and P. EKARI. Suomen Kemistilehti, B, **30**, 116 (1957).
18. A. M. COUTURE and K. J. LAIDLER. Can. J. Chem. **34**, 1209 (1956).
19. A. M. COUTURE and K. J. LAIDLER. Can. J. Chem. **35**, 207 (1957).
20. J. H. ANDREAE, R. BASS, E. L. HEASELL, and J. LAMB. Acustica, **8**, 131 (1958).

Can. J. Chem. Downloaded from www.nrcresearchpress.com by 210.87.254.6 on 09/05/12
For personal use only.

Can. J. Chem. Downloaded from www.nrcresearchpress.com by 210.87.254.5 on 09/05/12
For personal use only.

THE PYROLYSIS OF TRIMETHYLINDIUM

M. G. JACKO[1] AND S. J. W. PRICE
Department of Chemistry, University of Windsor, Windsor, Ontario
Received December 12, 1963

ABSTRACT

The pyrolysis of trimethylindium has been studied in a toluene carrier flow system from 550° K to 781° K using total pressures from 6.0 to 33.5 mm. The progress of the reaction was followed by measuring the amount of methane, ethane, ethylene, propane, and ethylbenzene formed and in a number of cases by direct indium analysis. The decomposition occurs in three steps:

$$In(CH_3)_3 \rightarrow In(CH_3)_2 + CH_3 \quad [1]$$

$$In(CH_3)_2 \rightarrow In(CH_3) + CH_3 \quad [2]$$

$$In(CH_3) \rightarrow In + CH_3 \quad [3]$$

At all temperatures reaction [2] follows rapidly after reaction [1]. Reaction [3] occurs at a measurable rate only at temperatures sufficiently high that reactions [1] and [2] are completed in a very small fraction of the contact time. At lower temperatures the $InCH_3$ produced deposits in the reaction zone as a white film of $(InCH_3)_n$.

Both k_1 and k_3 decline rapidly if the toluene-to-alkyl ratio is decreased below 150. In an unseasoned vessel, the decomposition is markedly dependent on surface conditions. In the unpacked conditioned vessel the reaction is at least 89% homogeneous in the first bond region and 97% homogeneous in the third bond region. Both k_1 and k_3 depend on the total pressure in the system, the dependence of k_1 being very slight. A least squares analysis of the experimental results gives:

$$\log_{10} k_1\ (sec^{-1}) = 15.72 - (47{,}200/2.303RT)$$

$$\log_{10} k_3\ (sec^{-1}) = 10.91 - (38{,}700/2.303RT)$$

at 13.0 mm. E_1 may be directly related to $D[(CH_3)_2In—CH_3]$. A rough calculation based on unimolecular pressure effects indicates that $D[In—CH_3]$ is probably about 2 kcal/mole greater than E_3.

INTRODUCTION

No previous kinetic studies of the thermal decomposition of trimethylindium have been reported.

A study of the reaction of triisobutylindium with 1-decene at 150° C for 100 hours (1) yielded tridecylindium and 83% isobutylene. The tridecylindium broke down further to yield only 64% free indium metal plus 1/2 CH_2=CH—C_8H_{17} and 3/2 CH_3—CH_2—C_8H_{17}. The remaining indium was assumed to be in some polymeric form.

A kinetic study of the thermal decomposition of trimethylgallium has been reported (2). The rate constants obtained were extremely sensitive to the nature of the surface in the reaction zone. After a series of runs, the reaction zone became conditioned and reproducible results were obtained. The experimental results showed $D_1 = 59.5$ kcal/mole and $D_2 = 35.4$ kcal/mole. From a knowledge of the total bond energies, $D_3 = 77.5$ kcal/mole was calculated.

The thermal decomposition of trimethylindium is expected to be similar to that of trimethylgallium and the other neighboring methyl metallic alkyls that have been studied (3, 4, 5). The mean metal–carbon bond dissociation energy in trimethylindium has not been reported. However, from available data on the methyl compounds of groups II*b*, III*b*, IV*b*, and V*b*, a value for trimethylindium of $E = 41 \pm 3$ kcal/mole may be estimated.

[1]*Recipient of a National Research Council of Canada Studentship.*

Can. J. Chem. Downloaded from www.nrcresearchpress.com by 210.87.254.5 on 09/05/12
For personal use only.

EXPERIMENTAL

Materials

(*a*) Trimethylindium was prepared by refluxing indium metal with dimethylmercury in an atmosphere of dry nitrogen using mercuric chloride as catalyst (6). After 8 days the reaction flask was cooled to 0° C (vapor pressure of trimethylindium, 0.2 mm) and the unreacted dimethylmercury (vapor pressure, 17 mm) was distilled off. The crude trimethylindium was transferred to the main alkyl storage system where the remaining dimethylmercury was removed by repeated degassing at 0° C. The final product melted at 89.5° C and gave vapor pressure measurements consistent with literature values (6). It was stored under its own vapor pressure at −190° C.

(*b*) Toluene from sulphonic acid (Eastman Organic, X325) was dried by refluxing over sodium under vacuum and then degassed by bulb-to-bulb distillation.

Apparatus and Procedure

The experiments were carried out in a typical toluene carrier flow system in which the reaction zone was 195 cc. To test for surface effects the reaction vessel was packed with thin-walled quartz tubing of 2 mm O.D. The surface area in the reaction zone was increased by a factor of 10 and its volume reduced to 145 cc. Pressures were measured with a mercury-dioctylphthalate differential manometer designed to give a magnification of 10 to 1.

Trimethylindium was added to the carrier stream by a variable split-stream U-tube pickup system. Before a run, 0.1 to 0.2 gram of the alkyl was distilled from a weighed vessel into the U-tube and the vessel reweighed to determine the exact quantity used. The entire sample in the U-tube was used in the run. The period of alkyl injection was preceded by a 5- to 10-minute flow of toluene to stabilize flow conditions and was followed by a 5- to 10-minute flow of toluene to remove all volatile products from the reaction zone.

An acetone – dry ice trap removed unreacted trimethylindium, toluene, ethylbenzene, dibenzyl, and similar products. The remaining products were transferred by a diffusion pump to a trap at −100° C (acetone–toluene sludge) to remove traces of toluene and hydrocarbons higher than C_4. The remaining gaseous mixture was transferred past a non-return valve to a gas burette with the aid of a Toepler pump. After the gaseous mixture was measured, a sample was taken for chromatographic analysis.

Chromatographic analysis of the gaseous products was carried out using a 2-meter silica-gel column at 80° C with a helium flow rate of approximately 20 cc/min. The contents of the acetone – dry ice trap were analyzed using a 2-meter diisodecylphthalate on diatomaceous earth column at 130° C with a helium flow rate of 38.5 cc/min. This method is sensitive to better than 0.0002 parts ethylbenzene or xylenes in toluene. In the later stages, a Perkin–Elmer Model 800 gas chromatograph equipped with a 150-foot Golay column, 0.02 inch I.D. coated with poly(propylene glycol) was used. This increased the sensitivity of the analyses to better than 0.000002 parts ethylbenzene in toluene.

In 18 selected runs, the contents of the acetone – dry ice trap were analyzed for indium. Approximately 100 cc of concentrated hydrochloric acid (12 *N*) was added and the resultant mixture vigorously stirred and evaporated to 1 to 2 cc. The resulting indium trichloride solution was diluted to about 50 ml with distilled water, buffered with hexamethylenetetramine, and titrated with 0.02 *M* EDTA using xylenol orange as indicator (7). In 7 of these 18 runs, the indium content of the solid in the reaction zone was similarly analyzed.

RESULTS AND DISCUSSION

The experimental results are given in Tables I and II. They may be discussed in terms of the following mechanism:

$$In(CH_3)_3 \rightarrow In(CH_3)_2 + CH_3 \quad [1]$$

$$In(CH_3)_2 \rightarrow In(CH_3) + CH_3 \quad [2]$$

$$In(CH_3) \rightarrow In + CH_3 \quad [3]$$

$$n[In(CH_3)] \rightarrow [In(CH_3)]_n \quad [4]$$

$$CH_3 + C_6H_5{-}CH_3 \rightarrow C_6H_5{-}CH_2 + CH_4 \quad [a]$$

$$2CH_3 \rightarrow C_2H_6 \quad [r]$$

followed by the usual reactions of the benzyl radicals to produce dibenzyl or ethylbenzene. The abstraction reaction [*a*] is a composite reaction proceeding mainly as written but with a small percentage of abstraction from the ring. The ethylene and hydrogen observed in small amounts result from the reactions:

$$CH_3 + C_2H_6 \rightarrow C_2H_5 + CH_4 \quad [5]$$

$$C_2H_5 \rightarrow C_2H_4 + H \quad [6]$$

$$H + C_6H_5{-}CH_3 \rightarrow C_6H_5{-}CH_2 + H_2. \quad [7]$$

Can. J. Chem. Downloaded from www.nrcresearchpress.com by 210.87.254.5 on 09/05/12
For personal use only.

TABLE IA

Temp. (°K)	Contact time (sec)	Total pressure (mm)	Millimoles of:						k_3 (sec^{-1})	$k_a/k_r^{\frac{1}{2}}$ (cc/mole sec)$^{\frac{1}{2}}$
			$In(CH_3)_3$	CH_4	C_2H_6	C_2H_4	C_3H_8	$\phi-C_2H_5$		
781	1.702	13.0	0.670	0.704	0.430	0.0307	0.0228	0.196	1.02	127
779	1.643	13.0	0.644	0.687	0.417	0.0404	0.0336	0.161	1.47	124
773	1.648	13.0	0.742	0.858	0.387	0.0249	0.0286	0.215	0.681	144
768	1.671	13.0	0.645	0.710	0.370	0.0201	0.0298	0.199	0.850	121
768	1.632	13.0	0.656	0.814	0.299	0.0358	0.0228	0.196	0.685	147
757	1.690	13.0	0.884	1.100	0.423	0.0330	0.0284	0.267	0.662	152
752	1.756	13.0	1.050	1.182	0.523	0.0323	0.0277	0.296	0.445	145
744	2.550	6.1	1.112	0.975	0.681	0.0200	0.0260	0.257	0.227	149
744	2.200	8.1	0.591	0.501	0.354	0.0095	0.0150	0.160	0.251	127
744	1.740	13.0	0.569	0.550	0.273	0.0055	0.0075	0.195	0.259	120
744	1.720	13.0	0.908	0.865	0.502	0.0095	0.0185	0.320	0.410	111
744	1.803	13.0	0.635	0.701	0.244	0.0076	0.0076	0.270	0.346	109
744	1.632	17.6	1.092	0.938	0.663	0.0081	0.0081	0.327	0.375	109
744	1.526	25.9	0.512	0.496	0.331	0.0116	0.0116	0.094	0.533	97.0
744	1.452	28.5	0.989	1.074	0.555	0.0560	0.0061	0.322	0.622	81.0
744	1.490	29.4	0.351	0.487	0.108	0.0047	0.0031	0.178	0.557	92.4
744	1.444	31.6	1.062	1.172	0.547	0.0210	0.0110	0.430	0.532	96.0
744	1.448	33.2	0.738	0.833	0.328	0.0203	0.0110	0.278	0.472	91.2
716	1.845	13.0	0.603	0.613	0.221	0.0005	0.0075	0.239	0.1342	130
709	1.980	13.0	0.822	0.820	0.351	0.0039	0.0038	0.251	0.1000	155
708	1.842	13.0	0.921	0.901	0.397	0.0065	0.0065	0.358	0.0924	133
705	1.888	13.0	0.694	0.625	0.305	0.0116	0.0146	0.204	0.0997	117
691	1.865	13.0	1.072	0.945	0.450	0.0198	0.0151	0.291	0.0417	120
687	1.878	13.0	0.931	0.749	0.396	0.0071	0.0071	0.350	0.0385	128
680	1.885	13.0	1.225	0.839	0.606	0.0062	0.0093	0.428	0.0268	105

Can. J. Chem. Downloaded from www.nrcresearchpress.com by 210.87.254.5 on 09/05/12
For personal use only.

TABLE IB

Temp. (°K)	Contact time (sec)	Total pressure (mm)	Millimoles of:						k_1 (sec^{-1})	$k_a/k_2^{\frac{1}{2}}$ (cc/mole sec)$^{\frac{1}{2}}$
			$\ln(CH_3)_3$	CH_4	C_2H_6	C_2H_4	C_3H_8	$\phi-C_2H_5$		
663	1.900	13.0	1.062	0.563	0.498	0.0050	0.0050	0.308	1.162	86.8
656	1.895	13.0	1.088	0.573	0.444	0.0026	0.0052	0.321	0.929	81.7
650	2.055	13.0	0.794	0.438	0.352	0.0030	0.0000	0.250	1.030	58.6
646	1.900	13.0	0.812	0.411	0.267	0.0180	0.0180	0.225	0.682	76.6
638	1.950	13.0	1.038	0.293	0.472	0.0146	0.0146	0.158	0.385	60.2
633	2.090	13.0	1.138	0.376	0.279	0.0021	0.0020	0.213	0.339	61.7
629	2.101	13.0	0.948	0.312	0.161	0.0000	0.0000	0.137	0.290	61.0
629	2.090	13.0	0.665	0.187	0.111	0.0017	0.0016	0.114	0.244	65.0
623	2.005	13.0	2.010	0.348	0.264	0.0018	0.0019	0.158	0.147	61.2
623	1.962	13.0	1.388	0.168	0.103	0.0082	0.0082	0.079	0.103	49.2
618	2.100	13.0	1.262	0.209	0.123	0.0010	0.0005	0.135	0.127	35.5
614	2.050	13.0	1.112	0.269	0.105	0.0010	0.0000	0.076	0.139	47.5
610	2.790	6.2	0.576	0.0476	0.0538	0.0005	0.0003	0.0246	0.0614	57.9
610	2.640	8.5	0.556	0.0600	0.0423	0.0003	0.0003	0.0290	0.0601	56.0
610	1.723	22.3	0.634	0.0665	0.0211	0.0003	0.0003	0.0250	0.0655	39.0
610	1.618	27.6	0.706	0.0784	0.0210	0.0003	0.0003	0.0361	0.0739	34.1
610	1.593	33.5	0.550	0.0611	0.0162	0.0002	0.0002	0.0282	0.0728	34.1
605	2.025	13.0	1.354	0.1400	0.0685	0.0003	0.0007	0.0413	0.0620	40.8
596	1.968	13.0	1.219	0.0477	0.0183	0.0001	0.0002	0.0176	0.0219	32.2
591	2.110	13.0	1.258	0.0585	0.0207	0.0002	0.0081	0.0000	0.0240	26.0
578	2.340	13.0	0.875	0.0148	0.0011	0.0000	0.0004	0.0000	0.0088	35.6
577	2.170	13.0	1.492	0.0313	0.0085	0.0001	0.0007	0.0000	0.0063	25.0
560	2.350	13.0	1.302	0.0077	0.0009	0.0000	0.0000	0.0000	0.0014	20.8
557	2.291	13.0	0.700	0.0066	0.0003	0.0000	0.0000	0.0000	0.0022	35.8
550	2.120	13.0	2.213	0.0098	0.0010	0.0000	0.0000	0.0000	0.0013	18.6

TABLE II

Temp. (°K)	% decomposition		Trap analysis (%)	k_g (sec^{-1})	k_m (sec^{-1})
	Gas	Metal			
First bond region:					
556	1.2		98.0		
594	16.3		83.0		
610	15.0		81.0		
613	11.0		90.1		
613	12.0		87.8		
613	40.0		58.0		
620*	19.7	13.3	85.7	0.219	0.138
623*	57.2	40.7	59.0	0.338	0.209
624*	50.3	36.9	63.7	0.292	0.183
633*	77.8	51.8	48.1	0.606	0.298
637*	64.8	46.5	53.2	0.533	0.320
644*	91.7	73.5	26.5	0.945	0.510
Third bond region:					
684	45.3		1.2		
697	63.1		2.5		
720	72.8		0.9		
726	57.9		3.9		
729*		98.3	1.5		
753	83.3		1.5		

*Runs in an unconditioned vessel.

The values of $k_a/k_r^{1/2}$ given in Tables IA and IB have been calculated using the equation

$$k_a/k_r^{1/2} = \frac{[\text{moles } CH_4]}{[\text{moles } C_2H_6+C_2H_4]^{1/2}} \times \frac{1}{V^{1/2}t^{1/2}[\text{toluene}]}$$

where V = volume of reaction zone, and t = length of run.

If in the decomposition of a compound of the type $M(CH_3)_n$ we have

$$M(CH_3)_n \rightarrow M(CH_3)_{n-y} + yCH_3 \qquad [I]$$

occurring over a temperature range T_1 to T_2 while

$$M(CH_3)_{n-y} \rightarrow M(CH_3)_{n-y-z} + zCH_3 \qquad [II]$$

occurs appreciably only above T_2, we shall have a number of factors which will influence the value of $k_a/k_r^{1/2}$. First, in a flow reaction, the temperature increases as the reaction zone is approached, therefore when the temperature in the reaction zone T_3 is above T_2, reaction [I] will occur partly in the tube leading to the reaction zone and will be complete in some small fraction of this zone. This has a dual effect on $k_a/k_r^{1/2}$:

(i) reaction [I] is occurring at an average temperature above T_2 but below T_3, and

(ii) the volume over which reaction [I] occurs is no longer the total volume of the reaction zone.

The net effect is to hold the apparent observed value of $k_a/k_r^{1/2}$ approximately constant as T increases. Actually, the net effect might be a slight decrease except for the fact that reaction [II] is occurring over the entire reaction zone at T_3. Experimentally, for dimethylzinc,

$$Zn(CH_3)_2 \rightarrow ZnCH_3 + CH_3 \qquad [I]$$
$$ZnCH_3 \rightarrow Zn + CH_3 \qquad [II]$$

the ratio shows a slight decrease above T_2 (4). For trimethylgallium

$$Ga(CH_3)_3 \rightarrow Ga(CH_3)_2 + CH_3 \qquad [I]$$
$$Ga(CH_3)_2 \rightarrow Ga(CH_3) + CH_3 \qquad [II]$$

Can. J. Chem. Downloaded from www.nrcresearchpress.com by 210.87.254.5 on 09/05/12
For personal use only.

the ratio continues to rise slightly (2). In any case, a sharp break in the $k_a/k_r^{1/2}$ curve is observed.

The Arrhenius plot of $k_a/k_r^{1/2}$ for the present work is shown in Fig. 1. In this case, the characteristic break occurs at 67% theoretical yield of methyl radicals indicating that below 670° K reaction [2] follows rapidly after reaction [1], but reaction [3] does not occur to any appreciable extent. Rate constants below this temperature (k_1) have therefore

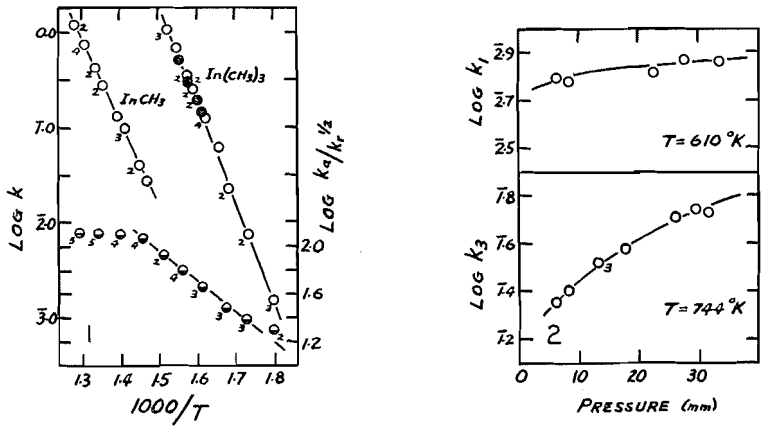

FIG. 1. Arrhenius plots for the pyrolysis of trimethyl- and methyl-indium and the reaction of methyl radicals with toluene. ○ rate constants based on gas analysis; ● rate constants based on metal analysis; ◒ log $k_a/k_r^{1/2}$. Subscripts denote the number of runs averaged to obtain the given point.

FIG. 2. Variation of k_1 and k_3 with pressure. Subscripts denote the number of runs averaged to obtain the given point.

been calculated assuming that two methyl radicals are released for each trimethylindium undergoing reaction. Above 680° K all of the trimethylindium is converted to methylindium plus two methyl radicals in a very small fraction of the contact time. Rate constants in this region (k_3) have therefore been calculated assuming that the fraction of the third bond ruptured is given by:

$$\frac{(\text{moles of methyl radicals}) - (2 \text{ moles trimethylindium})}{\text{moles of trimethylindium}}.$$

Although the break in the Arrhenius curve of $k_a/k_r^{1/2}$ is indicative of the process outlined, independent tests have been made to verify the mechanism.

(i) In 18 runs, the contents of the acetone – dry ice trap located at the outlet of the furnace were analyzed for indium. If reaction [4] is responsible for the removal of $In(CH_3)$, then above 670° K all the indium should be deposited in the reaction zone. Table II shows that over the entire third bond region only traces of indium reach the acetone – dry ice trap. Below this temperature the quantity of indium found in the trap was always in agreement with the proposed mechanism.

(ii) In 7 of the 18 runs listed in Table II a clean pyrex vessel was used. In each of these seven runs the indium content of the reaction zone was analyzed. The values of k_1 calculated assuming moles of indium in the reaction zone equal the moles of trimethylindium decomposed are shown in Fig. 1. The agreement with k_1 values in a seasoned vessel calculated assuming two methyl radicals released for each trimethylindium decomposed is excellent.

Can. J. Chem. Downloaded from www.nrcresearchpress.com by 210.87.254.5 on 09/05/12
For personal use only.

Can. J. Chem. Downloaded from www.nrcresearchpress.com by 210.87.254.5 on 09/05/12
For personal use only.

(iii) The rate constants for the reaction in a clean vessel based on gas analysis lie above the Arrhenius curve. The difference in extent of reaction based on metal analysis is a result of reaction on the unconditioned surface. The most probable surface reactions consistent with the experimental results are the surface decomposition of methylindium to give indium metal plus a methyl radical and the surface decomposition of trimethylindium. The first of these reactions leads to a decrease in the quantity of $(InCH_3)_n$ deposited in the reaction zone. Hence in an experiment in an unconditioned vessel in which 1.0 millimole of methylindium would have been deposited in the reaction zone in a conditioned vessel, addition of bromine vapor to the hot reaction vessel (637° K) while still under vacuum produced only 0.34 millimole of hydrogen bromide and a quantity of polymethylene qualitatively in agreement with the reaction

$$2nBr_2 + (InCH_3)_n \rightarrow nInBr_3 + n(CH_2) + nHBr$$

followed by the polymerization of the methylene radicals in cooler regions of the reaction vessel. The 0.66 millimole of methylindium apparently lost by surface decomposition was in good agreement with the additional methyl radicals detected in the gas analysis (0.58 millimole).

Starting with a clean vessel, both k_1 and k_3 decrease over several runs to a fixed minimum value in what is subsequently called a conditioned vessel. If air is admitted to the reaction vessel between runs, an additional two to three runs are required to recondition the surface of the reaction vessel. The percentage of heterogeneous reaction in the conditioned vessel was estimated by carrying out a series of runs in a packed vessel with a surface-to-volume ratio 12 times that of the unpacked vessel. Because of the large surface area, complete conditioning was probably not obtained, but after a series of runs k_1 was reduced to about 2.2 times its value in the unpacked vessel and k_3 to about 1.3 times its value in the unpacked vessel. Therefore, in the unpacked vessel used in this work, the reaction is at least 89% homogeneous in the first bond region and at least 97% homogeneous in the third bond region.

Both k_1 and k_3 depend on the total pressure in the system, although the dependence of k_1 is very slight (Fig. 2). The slight pressure dependence of k_1 is similar to that observed in the decomposition of trimethylgallium (2). As shown in Fig. 3, the pressure dependence

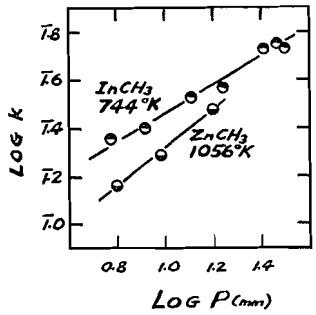

FIG. 3. Comparison of the effect of pressure on the rate of thermal decomposition of $InCH_3$ and $ZnCH_3$.

of the decomposition of methylindium is somewhat less than that of methylzinc (4). This is presumably due to the large temperature difference at which these decompositions occur.

The pressure dependence of $k_a/k_r^{1/2}$ is shown in Fig. 4. The fall-off with increasing

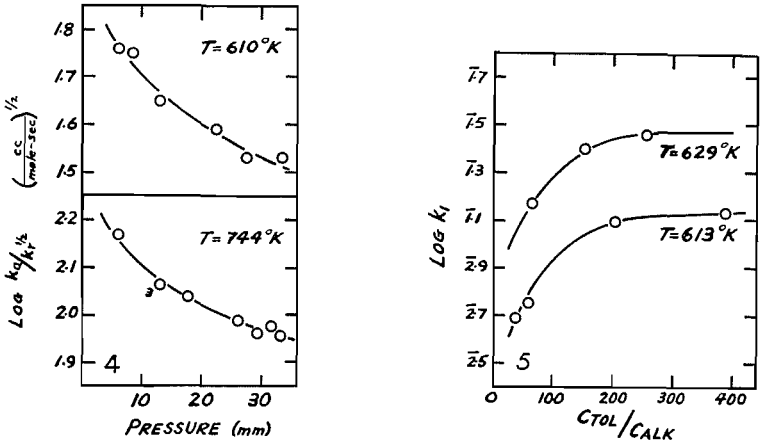

FIG. 4. Variation of $k_a/k_r^{1/2}$ with pressure at 610° K (first bond region) and 744° K (third bond region). Subscripts denote the number of runs averaged to obtain the given point.
FIG. 5. Variation of k_1 with the ratio of moles toluene to moles alkyl using fixed toluene concentrations.

pressure is similar to that previously observed (2–5) and may be attributed to the third body requirements of the methyl radical recombination reaction.

As shown in Fig. 5, the value of k_1 falls sharply when the toluene-to-alkyl ratio is decreased below 150. Values for k_3 are similarly affected. The Arrhenius curves shown in Fig. 1 were therefore plotted using only rate constants obtained in runs where the toluene-to-alkyl ratio was greater than 150. At 13.0 mm, the curves may be represented by:

$$\log_{10} k_1\ (\text{sec}^{-1}) = 15.72 - (47{,}200/2.303RT),$$

$$\log_{10} k_3\ (\text{sec}^{-1}) = 10.91 - (38{,}700/2.303RT).$$

The experimental evidence indicates that the activation energies may be approximately related to the bond strengths, although a rough estimate based on unimolecular pressure effects indicated that D_3 is about 2 kcal/mole greater than E_3. Thus $D[(CH_3)_2In—CH_3]$ equals 47.2 kcal/mole and $D[In—CH_3]$ equals 40.7 kcal/mole. The mean bond energy in trimethylindium is not known. However, comparison of neighboring methyl metallic alkyls indicate that $\bar{E}(In—CH_3)$ in trimethylindium is probably 41 ± 3 kcal/mole. Allowing limits of error of ±1 kcal/mole in D_1 and D_3 would give $D[CH_3In—CH_3]$ equal to 35 ± 5 kcal/mole, a value consistent with the proposed mechanism.

ACKNOWLEDGMENTS

This work has been supported by a grant from the National Research Council of Canada.

REFERENCES

1. J. J. EISCH. J. Am. Chem. Soc. **84**, 3605 (1962).
2. M. G. JACKO and S. J. W. PRICE. Can. J. Chem. **41**, 1560 (1963).
3. S. J. W. PRICE and A. F. TROTMAN-DICKENSON. Trans. Faraday Soc. **54**, 1630 (1958).
4. S. J. W. PRICE and A. F. TROTMAN-DICKENSON. Trans. Faraday Soc. **53**, 1208 (1957).
5. S. J. W. PRICE and A. F. TROTMAN-DICKENSON. Trans. Faraday Soc. **53**, 937 (1957).
6. L. M. DENNIS, R. W. WORK, E. G. ROCKOW, and E. M. CHARMOT. J. Am. Chem. Soc. **56**, 1047 (1934).
7. J. KINNUNEN and B. WENNESTRAND. Chemist-Analyst, **46**, 92 (1957).

Can. J. Chem. Downloaded from www.nrcresearchpress.com by 210.87.254.5 on 09/05/12
For personal use only.

Can. J. Chem. Downloaded from www.nrcresearchpress.com by 210.87.254.42 on 09/05/12
For personal use only.

DISPLACEMENT OF C_4-HYDROCARBON MOLECULES ADSORBED ON PLATINUM[1]

S. AFFROSSMAN[2] AND R. J. CVETANOVIĆ
Division of Applied Chemistry, National Research Council, Ottawa, Canada

Received September 27, 1963

ABSTRACT

A special technique has been used in an attempt to determine the nature and the amount of the C_4-hydrocarbons desorbed by displacement with "poisons" (CO, CS_2) from the "active" sites of a platinum on asbestos hydrogenation catalyst. The "active" area of the catalyst determined in this way is found to decrease with increasing adsorption of the poison molecules, and is approximately related in the expected manner to the observed catalytic activity for butene hydrogenation. The likely nature of the adsorbed hydrocarbon species is discussed.

INTRODUCTION

Considerable progress has been made in recent years in the understanding of the mutually related processes of olefin hydrogenation, isomerization, and isotopic exchange on metallic catalysts (1). At the same time, a choice between the alternative mechanisms cannot be made with certainty and the overall situation in this respect is still far from being free from ambiguities. The present study has been carried out in an attempt to explore an experimental approach which would permit preferential detection of the molecules adsorbed on the "active" catalyst sites. A special technique has been employed using a flow system with gas chromatographic analysis at short intervals. Although it has been possible to carry out only an investigation of preliminary character, the technique appears capable of providing useful information and the results are therefore briefly reported here.

Removal of the molecules adsorbed in the course of the hydrogenation of butene on a platinized asbestos catalyst was attempted by displacement with catalyst poisons. For this purpose, use was made mainly of carbon monoxide and, to a smaller extent, of carbon disulphide. Since it has been shown that CO adsorbs only on metal surfaces and not on carrier (2, 3), the hydrocarbon molecules displaced from the surface by CO should also come only from the metal. As catalyst poisons have an immediate strong effect on the reaction rates, it may be assumed that initially they adsorb preferentially on active sites.

EXPERIMENTAL

Apparatus

The apparatus is shown schematically in Fig. 1. Greaseless stopcocks (Teflon needle valves, Fischer & Porter Co.) were used throughout. The reactor tube was attached to the system by small sections of Tygon tubing. The catalyst was held in place by clean glass wool. The gases coming from the reactor tube were split into two parts, one half going to a flowmeter and the other half to a gas sampling valve connected to a Perkin–Elmer 300 ft squalane capillary column and flame ionization detector. The back-pressure of carrier gas introduced into the system from the chromatography unit on rotating the gas sampling valve was thereby much reduced. The gas sampling valve was operated automatically by an air cylinder and timer, enabling the samples to be injected every minute into the nitrogen stream leading into the capillary column. The olefin used as reactant and the reaction products were all separated chromatographically within 1 minute. CS_2 was added to the system by allowing it to diffuse from the "poison tube" into the gas stream.

[1]*Issued as N.R.C. No. 7829.*
[2]*National Research Council Postdoctoral Fellow, 1961–1963. Present address: The Royal College of Science and Technology, Glasgow, Scotland.*

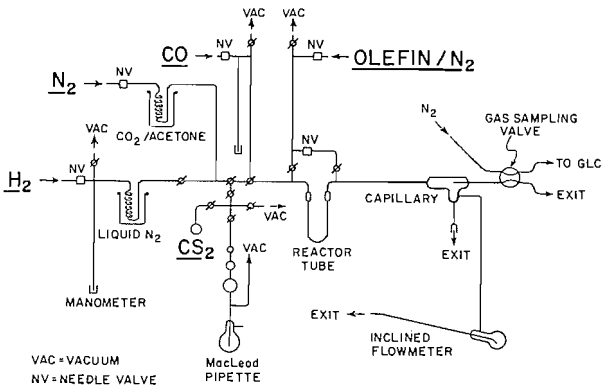

FIG. 1. Schematic diagram of the apparatus.

Materials

The catalyst was 5% Pt on asbestos (Matheson, Coleman & Bell Co.) and its weight was close to 0.03 g. Before each run, air was displaced from the apparatus by a stream of nitrogen. The catalyst was then pretreated with hydrogen for about 20 minutes before olefin was added. The BET surface area of the catalyst was close[3] to 11 m^2/g. Phillips research grade *trans*-butene-2 was used as reactant. A small amount of olefin was introduced into an empty cylinder and the pressure brought to 50 lb/in^2 with prepurified nitrogen. The gases were thoroughly mixed and this diluted olefin was used directly. In the experiments carried out, the partial pressure of olefin was varied from about 0.4 to 5 mm. The partial pressure of hydrogen was approximately 250 mm.

The nitrogen was a prepurified grade (Matheson Co.) and the only further treatment consisted of its passage through an acetone/CO_2 bath. Ultrapure hydrogen (Matheson Co.) was passed through a liquid nitrogen trap, and C.P. grade carbon monoxide (Matheson Co.) was used directly.

Procedure

After pretreating the catalyst with H_2, the olefin was introduced into the gas stream. Analysis of the products gave a measure of the activity of the catalyst as all runs were at one flow rate. Only *trans*-butene-2 and butane were detected when H_2 was present.

To measure the adsorption on the surface, the H_2 stream was first cut off; when no further reaction product was observed, the olefin stream was cut off as well. Only a N_2 stream remained at this stage, and the analysis showed only a decreasing amount of loosely held *trans*-butene-2. CO at a small partial pressure was then added continuously to the system. The following molecules were then observed: *trans*-butene-2, *cis*-butene-2, butane, butene-1. All except butane decreased rapidly in concentration with time. The effects of some alterations of this procedure will be indicated in the following section.

When CS_2 was used as a poison, a barely measurable amount was introduced into the "poison tube". The valve connecting this section to the main gas stream was then opened for a prescribed time: the amount of CS_2 diffusing into the gas stream was proportional to this time (as judged by its effect on the reaction).

It was found that CO was only a temporary poison but that CS_2, once adsorbed, was not easily removed.

RESULTS AND DISCUSSION

Most of the experiments were carried out at room temperature (25±2° C). The reaction was found to be first order in olefin and approximately zero order in H_2. This suggests that the rate-controlling process involves the adsorption of olefin at a low surface coverage on the active surface, as would be reasonable to expect at the very low olefin to hydrogen ratios used.

Table I shows the effect of altering the experimental conditions. Runs 1 and 2 provide evidence that during a reaction, in presence of H_2, the surface is only sparsely covered by olefin. In run 1, on cutting off H_2, adsorption of olefin immediately takes place. In run 2, passage of CO stops the reaction but does not displace any detectable quantity of olefin,

[3]*After outgassing for 17 hours at 0° C: 10.9 m^2/g; after outgassing for 36 hours at 125° C: 11.4 m^2/g. The areas are accurate to ±0.5 m^2/g. The authors are grateful to Mr. D. Kulawic for the surface area determinations.*

Can. J. Chem. Downloaded from www.nrcresearchpress.com by 210.87.254.42 on 09/05/12
For personal use only.

TABLE I

The effect of alterations in the experimental procedure (reaction of *trans*-butene-2 and H_2 in a N_2 carrier over Pt/asbestos at 0° C)

Run	Step 1: cut off	Step 2: cut off	Step 3: poison added	Molecules desorbed or adsorbed
1	H_2	—	—	Adsorption of olefin occurs
2	—	—	CO	None observed
3	H_2	—	CO	Butene-1 desorbed
4	H_2	Olefin	Small[a] CO	Butene-1 (mainly) desorbed
5	H_2	Olefin	Large[b] CO	Butene-1, *trans*-butene-2, *cis*-butene-2, butane, desorbed

[a]Approximately 1 ml (NTP) injected as a pulse.
[b]Approximately 1 ml (NTP) per minute, fed continuously until no further adsorption was detected.

in contrast to runs 3, 4, and 5. These last three runs show that only small amounts of CO are needed to poison the reaction, and that the olefin molecules adsorbed on cutting off H_2 give mainly butene-1 when displaced. Figure 2 shows the manner of desorption of the

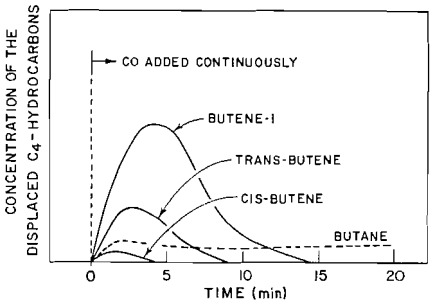

FIG. 2. Displacement of C_4-hydrocarbons from the catalyst by carbon monoxide. (The graph represents a typical example. Ordinate scale is in arbitrary units.)

butenes and butane as a result of displacement by CO (added continuously at a small partial pressure).

When carbon monoxide is added during a reaction, as in run 2 of Table I, it rapidly inhibits the reaction. It would therefore be expected that under conditions of present experiments the hydrocarbon molecules adsorbed on the active sites would be rapidly displaced from the catalyst. As shown in Fig. 2, the butenes desorb in the expected manner, but not the butane. Butane desorbs for a considerable time and when smaller partial pressures of CO are used, the rate of butane desorption decreases while the butenes are unaffected. The mechanism responsible for such behavior of butane is not clear[4] although there are indications that it does not contribute significantly to butene hydrogenation under reaction conditions.[5] For the latter, the butenes desorbed from the surface should

[4]*Perhaps slow displacement of the more strongly adsorbed butyl radicals is involved.*
[5]*When the catalyst is poisoned by injecting a small amount of* CS_2 *or* CO *into the hydrogen stream before the olefin is admitted, trans-butene-2 fed subsequently into the gas stream is not hydrogenated. Nevertheless, when the sequence of steps as in run 5 of Table I is then applied, butane is desorbed from the surface but not butene-1.*

Can. J. Chem. Downloaded from www.nrcresearchpress.com by 210.87.254.42 on 09/05/12
For personal use only.

Can. J. Chem. Downloaded from www.nrcresearchpress.com by 210.87.254.42 on 09/05/12
For personal use only.

provide an appropriate measure of the active surface of the catalyst. Since butene-1 forms the greater part of the butenes desorbed,[6] its amount could be used as an approximate indicator of the number of active sites.

The fact that butene-1, thermodynamically the least stable isomer, forms the major part of the desorbed butenes is of interest. A selective double-bond migration and a stereoselective formation of *cis*-2-butene have been repeatedly observed in recent years in the catalytic isomerization of *n*-butenes (4–10). Selective production of butene-1 is evidently also a part of the process of butene desorption by catalyst poisons under conditions of present experiments. Furthermore, isomerization of butene-2 to butene-1, i.e. double-bond migration, cannot involve in this case a concerted ("hydrogen switch") mechanism (9, 11), involving interaction of chemisorbed hydrogen atoms with the vapor phase or physically adsorbed molecules of butene which do not become chemisorbed at any time during the process.

It is also of interest that when butene-1 was substituted for *trans*-butene-2 as the initial reactant under otherwise identical conditions, the main olefin desorbed by displacement with CO was still butene-1. In terms of the Horiuti–Polanyi mechanism (1, p. 254) this would suggest that the "half-hydrogenated" species is the same in the two cases, perhaps the 2-adsorbed *n*-butane (i.e. the chemisorbed *sec*-butyl radical). If this is true, this species could give either butene-2 or butene-1 on desorption by CO displacement. That it gives predominantly the thermodynamically less stable butene-1 is perhaps due to the steric factors, since a vicinal H atom has to be donated to the surface prior to the re-formation of the double bond.

If there is a correlation between the active area of the catalyst and the amount of butene-1 desorbed by CO displacement, as suggested above, there should also be a proportionality between the latter and the catalyst activity.

The specific reaction rate is given by the equation

$$k = \frac{F}{V.A} \ln \frac{1}{1-Q} \qquad [1]$$

where F is the flow rate, V the reactor volume, A the active area of the catalyst, and Q the fraction of olefin reacted. This can be written in the form

$$\log u = 2 - \frac{k.V.A}{2.3\,F} \qquad [2]$$

where u is the percentage unchanged olefin. In this equation V is unknown but is constant for a given sample of catalyst. Therefore, at a constant flow rate,

$$\log u = 2 - k^*A. \qquad [3]$$

The percentage unchanged olefin, u, is obtained from the gas chromatographic analysis just before the H_2 is cut off. The active area, A, is assumed to be, to a good approximation, proportional to the amount of butene-1 desorbed on displacement with CO.

If the active area of a given sample of the catalyst can be varied by some means, equation [3] predicts linear dependence of $\log u$ on A. This, however, would be strictly true only for a homogeneous catalyst; if the sites are non-uniform and A decreases, for example, as a result of preferential deactivation of the sites of high activity (those on which the hydrogenation proceeds more rapidly) the expected plot would be concave to

[6]*Cis-butene-2 is formed in negligible amounts and trans-butene-2 could conceivably be desorbed also from the catalyst support and the reactor walls, since it is the original reactant.*

the ordinate. If, on the other hand, the sites of lower activity are initially deactivated preferentially, the plot would be convex to the ordinate. It should also be remembered that the effect of poisons on a surface is not necessarily only a pure blocking of sites (12, 13). Furthermore, the reaction conditions under which the activity is measured are not necessarily closely comparable with the conditions in the displacement experiments. The catalytic hydrogenation of olefins is of considerable kinetic complexity and, also, the H_2 content of a catalyst appears to affect its activity (14). In view of these difficulties, and the fact that measurements of this kind are experimentally exacting, only an approximate relation of the kind predicted by equation [3] may be hoped for.

The reaction was found to be slowly self-poisoning, leading to gradual decrease in catalyst activity. Decrease in activity could also be achieved by adding very small amounts of CS_2, and this was the main method used to reduce the active area of a catalyst sample.

Figure 3 shows some of the results obtained on decreasing the active area of the catalyst

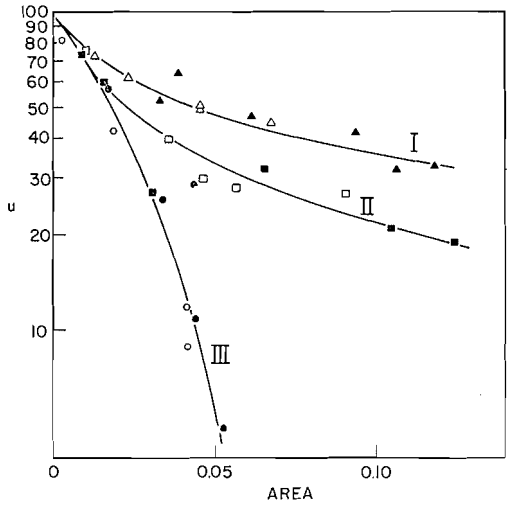

FIG. 3. Plot of equation [3] for three samples (I, II, and III) of the catalyst. (Catalyst weight: 40 mg of 5% Pt on asbestos. The arbitrary unit of the active areas shown on the abscissa corresponds to 1.9×10^{-2} micromoles of butene desorbed. Open and filled symbols indicate two different sets of experiments on the same catalyst samples.)

by poisoning. Qualitatively the trend is as predicted, and a correlation is evident between the activity and the active area measured from the amount of the displaced butene-1. However, there is an appreciable scatter of points and the plots are not linear. Moreover, both convex and concave curvatures are obtained.

In conclusion, it appears that, in spite of the difficulties indicated above, the described technique is capable of providing useful information. More extensive observations with a variety of olefins and, in particular, with simultaneous use of isotopic labelling are likely to enhance further its usefulness. These extensions were not feasible in the course of the preliminary work reported in this communication.

ACKNOWLEDGMENTS

The authors would like to thank Dr. Y. Amenomiya for much helpful discussion and Mr. M. Bednas for assistance in setting up the gas chromatographic part of the apparatus.

Can. J. Chem. Downloaded from www.nrcresearchpress.com by 210.87.254.42 on 09/05/12
For personal use only.

REFERENCES

1. G. C. Bond. Catalysis by metals. Academic Press, London and New York. 1962.
2. H. L. Gruber. Anal. Chem. **34**, 1828 (1962).
3. J. J. F. Scholten and A. Van Montfert. J. Catalysis, **1**, 85 (1962).
4. H. Pines and W. O. Haag. J. Org. Chem. **23**, 328 (1958).
5. W. O. Haag and H. Pines. J. Am. Chem. Soc. **82**, 387, 2488 (1960).
6. P. J. Lucchesi, D. L. Baeder, and J. P. Longwell. J. Am. Chem. Soc. **81**, 3235 (1959).
7. R. J. Cvetanović and N. F. Foster. Discussions Faraday Soc. **28**, 201 (1959).
8. N. F. Foster and R. J. Cvetanović. J. Am. Chem. Soc. **82**, 4274 (1960).
9. D. M. Brouwer. J. Catalysis, **1**, 22 (1962).
10. S. Ogasawara and R. J. Cvetanović. J. Catalysis, **2**, 45 (1963).
11. J. Turkevich and R. K. Smith. J. Chem. Phys. **16**, 466 (1948).
12. C. M. Quinn and M. W. Roberts. Trans. Faraday Soc. **58**, 569 (1962).
13. E. H. Yeneekeyeff and A. V. Krilova. Kinetics and catalysis. (Abstr. *In* J. Catalysis, **1**, 197 (1962)).
14. Z. Csuros and J. Petro. Acta Chim. Acad. Sci. Hung. **30**, 461 (1962).

Can. J. Chem. Downloaded from www.nrcresearchpress.com by 210.87.254.42 on 09/05/12
For personal use only.

Cl^{35} PURE QUADRUPOLE RESONANCE FREQUENCIES IN THE CYCLIC PHOSPHONITRILIC CHLORIDE POLYMERS

M. A. WHITEHEAD
Chemistry Department, McGill University, Montreal, Quebec
Received July 11, 1963

ABSTRACT

Pure nuclear quadrupole resonance frequencies of Cl^{35} in the cyclic phosphonitrilic chloride polymers, $(PNCl_2)_n$ have been observed for $n = 3$, 4, 5, and 6. For both the tetramer and hexamer two different crystal structures were studied. The observed frequencies are discussed assuming that the phosphorus–nitrogen ring system possesses a polyallylic bond structure. Several substituted polymers were examined ($P_3N_3Cl_4\phi_2$, $P_4N_4Cl_7\phi_4$, $P_3N_3(i\text{-}PrNH)_4Cl_2$, $P_3N_3Cl_2\phi_4$) but only diphenyl-tetrachloro trimer, $P_3N_3Cl_4\phi_2$, gave a frequency measurement. The ratio of the Cl^{35} quadrupole frequencies in two compounds is compared with the ratio of the effective orbital electronegativities of the phosphorus atom in the compounds.

INTRODUCTION

The pure nuclear quadrupole (n.q.r.) resonance of Cl^{35} has been observed in the cyclic phosphonitrilic halide polymers $(PNCl_2)_n$, for $n = 3$, 4, 5, and 6. The resonances were detected with a self-quenching super-regenerative oscillator unit, of the type described by Dean (2, 3). Low frequency (30–60 c.p.s.) frequency modulation across the resonance frequency allowed direct oscilloscope display of the signal. The signal was recorded using an on–off antisymmetric square wave of magnetic field over the sample, a phase-sensitive detector, and a narrow band amplifier. The resonance frequencies were measured with a BC 221 frequency meter; they are listed in Table I. The average frequency of the closely spaced lines from a given polymer is listed in Table II, which also lists the frequencies for comparable compounds.

TABLE II

Average Cl^{35} nuclear quadrupole resonance frequencies at 77° K in Mc

Ring compounds		Linear compounds	
Formula	Frequency in Mc/second	Formula	Frequency in Mc/second
$(PNCl_2)_3$	28.4564	SO_2Cl_2	37.7
$a\text{-}(PNCl_2)_4$	28.6483	$SOCl_2$	31.9
$b\text{-}(PNCl_2)_4$	28.6483	$POCl_3$	28.96
$(PNCl_2)_5$	28.15	PCl_3	26.2
$a\text{-}(PNCl_2)_6$	28.42	$COCl_2$	35.7
$b\text{-}(PNCl_2)_6$	27.97	CCl_4	40.6
$(SNCl)_3$	29.8	BCl_3	21.62
$(CNCl)_3$	36.3	$\phi POCl_2$	25.357
$(BNHCl)_3$	19.937		

Van Wazer (4) reports that from atom–atom distances the trimer and tetramer have 0.2 π character in the P—N bond and 0.1 π character in the P—Cl bond, but no such results are available for the higher polymers. Since all the polymers display similar chemical properties (5), it is to be expected that all will have similar amounts of π bonding, and that the frequencies will be in the same region throughout the series, as is the case (Table II). The actual shape of each polymer differs (6, 7), however, and their frequencies differ in detailed structure due to crystal field effects (Table I). The P—N ring is slightly

puckered in the solid state, the exact shape depending on which polymer is examined (8–14). In all the polymers the chlorine atoms are in a plane perpendicular to the P—N ring. When these molecules are packed together in a crystal, models show that several possible crystallographically inequivalent lattice sites are available to the chlorine atoms. These are responsible for the closely spaced lines in the quadrupole resonance (15). Two crystal forms of the tetramer $(PNCl_2)_4$ and hexamer $(PNCl_2)_6$ were examined. These have been differentiated in this work as *a*- and *b*-forms. The *a*-$(PNCl_2)_4$ is obtained from crystallization of the polymer from benzene near room temperature and is metastable. All the P—N bonds are of identical length. The ring is tub shaped. The *b*-$(PNCl_2)_4$ is obtained by crystallization from solvents at 60°, or from the melt. It has the same space group (P_{4_2}/n) as the *a*-form but different unit cell dimensions. In the hexamer both *a*-$(PNCl_2)_6$ and *b*-$(PNCl_2)_6$ are triclinic with different unit cell dimensions (13).

The puckered ring has several possible structures divisible into "tub" and "chair" forms (16); both forms are expected to be possible in the tetramer; the chair form may therefore be responsible for the second crystal structure, since the *a*-form is known to be tub shaped. This is true in $(PN(NMe)_2)_4$ and $(PN(CH_3)_2)_4$, but $(PNF_2)_4$ has a planar ring, due to special considerations.

In the trimer no such variable crystal structures occur (17). The trimer structure has been fully elucidated by X-ray analysis (17). The ring is almost planar and has ring angles of approximately 120°, is orthorhombic, and belongs to the *Pnma* space group.

The two crystal forms of the tetramer give almost identical n.q.r. frequencies at the liquid nitrogen temperature; they distinctly differ at room temperature. At room temperature the *b*-$(PNCl_2)_4$ lines are broad and indistinct, while the *a*-$(PNCl_2)_4$ lines are well separated and sharp.

The change in frequency with temperature of the *a*- and *b*-tetramer shows an interesting phenomenon. Both crystal forms show a frequency increase with temperature decrease. This is quite normal (18, 19). However, the *a*-form has line separations of 0.1314 mc/second at 293° K, and 0.0225 at 77° K, while the *b*-form appears to have a very small separation (if one at all) at 293° K and 0.0207 at 77° K. The *a*-$(PNCl_2)_4$ line separation depends on temperature as predicted by Gutowsky and McCall (20), while the *b*-$(PNCl_2)_4$ shows a dependence similar to that previously found in 2,2,2′,2′-tetrachlorobicyclopropyl, $Cl_2C_3H_3C_3H_3Cl_2$ (21). The *a*-$(PNCl_2)_4$ lines should coalesce at even lower temperatures and the *b*-$(PNCl_2)_4$ should separate further.

Neither crystal form of $(PNCl_2)_4$ displayed four lines similar to those reported by Negita and Satou for the $(PNCl_2)_4$ sample that they examined at room temperature (22). Initially it was assumed that they must have examined *a*-$(PNCl_2)_4$ since the sample displayed distinct lines. However, if the two distinct crystal forms are due to the molecule being in the tub and chair configurations, then the frequency differences between them would be due to molecular inequivalence rather than crystallographic inequivalence of the chlorine atoms. Thus if the two molecular configurations were to occur together, the lines due to both would be observed, and due to molecular dilution of one configuration by the other, the spectrum could have a larger signal-to-noise ratio and a sharper spectrum for each than in the pure molecular form. If, as discussed above, the *b*-lines approach as the temperature is raised, while the *a*-lines diverge, then at room temperature the mixed *a*- and *b*-$(PNCl_2)_4$ would have a pattern very similar to that of Negita and Satou. We have failed to resolve the absolute frequency difference (Fig. 1(*b*)) (22). Our results agree with those of Torizuka (23) both to the number of lines, and absolute frequency at room temperature.

TABLE I

Cl^{35} pure quadrupole resonances at room and liquid nitrogen temperatures

Compound	Frequency (megacycles per second)	Temperature	Approximate signal-to-noise ratio	Method of measurement	Comments*
$(PNCl_2)_3$	27.5391	293° K	2:1		
	27.6201		1:1	Visual	The lines at room temperature were broad. They narrowed but did not increase size at liquid nitrogen temperature
	27.7101		1:1		
	27.8101		2:1		
	28.3158	77° K	1:1		
	28.3275		2:1	Visual	There is a frequency discrepancy with previously reported frequencies. This is still being investigated†
	28.5471		1:1		
	28.6563		2:1		
a-$(PNCl_2)_4$ Crystal A	28.0251	293° K	3:1	Visual, recorder	There was no sign of the additional lines of Negita and Satou† at either temperature
	28.1565		3:1		
	28.6371	77° K	3:1	Visual, recorder	
	28.6596		3:1		
b-$(PNCl_2)_4$ Crystal B	27.9	293° K		Visual, recorder	Distinct single line, broad disturbance, but no multiplicity of lines detected
	28.6380	77° K	2:1	Visual	Rather broad lines but reproducible peak centers
	28.6587		2:1		
$(PNCl_2)_5$	26.8 → 27.4	293° K		Visual, recorder	No lines detectable, only overall disturbance
	27.6876	77° K	3:1		
	27.8415		4:1		
	27.9270		3:1		
	27.9423		2:1		
	28.2220		3:1	Visual	The recorder results were too complicated to interpret. Definitely not piezoelectric effect
	28.2474		3:1		
	28.4400		2:1		
	28.4850		3:1		
	28.7442		1:1		

TABLE I (*concluded*)

Compound	Frequency (megacycles per second)	Temperature	Approximate signal-to-noise ratio	Method of measurement	Comments*
a-$(PNCl_2)_6$ Crystal A	28.4	77° K	2:1	Recorder	Broad and diffuse, and difficult to fix
b-$(PNCl_2)_6$ Crystal B	27.6822 27.7470 27.7938 27.8262 27.8730 27.9216 27.9720 28.0260 28.0395 28.0890 28.3095 28.4157	77° K		Visual	
$P_3N_3Cl_4\phi_2$	27.4 27.8	77° K	3:1 1:1	Recorder Visual	Lines broad and indistinct. Both ϕ on same phosphorus atom
$P_4N_4Cl_4\phi_4$ $P_3N_3(i\text{-}PrNH)_4Cl_2$ $P_3N_3\phi_4Cl_2$	Failed to give any results or disturbance in region 20 → 35 Mc				
$(PNCl_2)_3.HClO_4$	28.3040 28.3296 28.6024 28.6888	77° K	1:1 2:1 1:1 2:1	Visual	Only broad disturbance at 293° K about 27.8 Mc distinct sharp lines at 77° K
$(PNCl_2)_3.HBF_4$	Disturbance at 293° K and very strong at 77° K, but no individual lines detectable visually or by recorder. 28.3 28.5 Mc				
$(CH_3NPCl_3)_2$	No signal 20 → 45 Mc				

* No attempt was made to measure line widths; lines are reported as sharp, broad, or diffuse in accordance with accepted n.q.r. nomenclature. (P. J. Bray, R. G. Barnes, and R. Bersohn. J. Chem. Phys. 25, 813 (1956).)

†H. Negita and S. Satou. J. Chem. Phys. 24, 621 (1956). K. Torizuka. J. Phys. Soc. Japan, 11, 84 (1956).

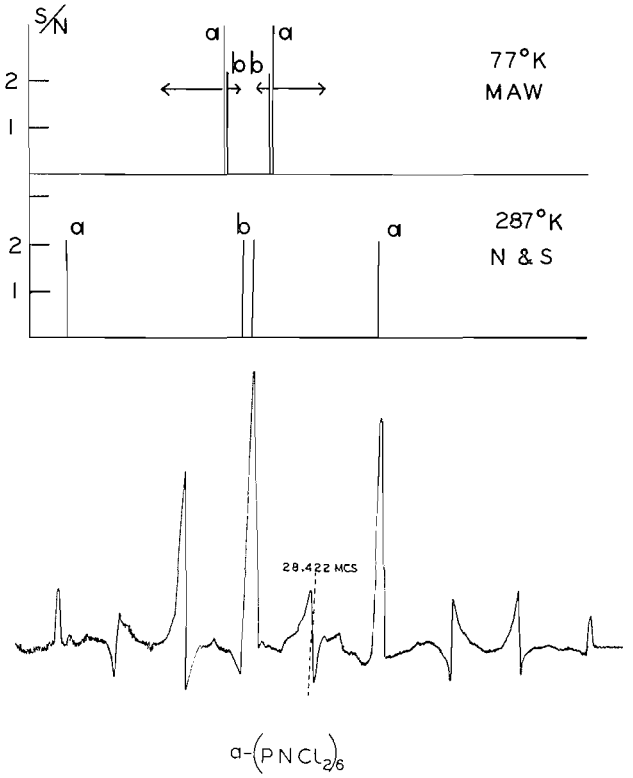

FIG. 1. (*a*) The superimposed spectra of *a*-$(PNCl_2)_4$ and *b*-$(PNCl_2)_4$ at 77° K and the predicted change of frequency with increasing temperature from the results and discussion in this paper. (*b*) The spacing of the four spectral lines in $(PNCl_2)_4$ at 287° K as measured by Negita and Satou, which may be due to their sample being a mixture of the two crystal forms *a*-$(PNCl_2)_4$ and *b*-$(PNCl_2)_4$. (*c*) Recorded nuclear quadrupole spectrum of *a*-$(PNCl_2)_6$, having only one resonance line, using a self-quenching superregenerative oscillator and 50 c/second antisymmetric square wave magnetic modulation. The quench frequency was 50 kc/second. Eight side bands are shown.

In the case of $(PNCl_2)_3$, the signal-to-noise ratio and the number of lines observed agree with the results of Negita and Satou at 293° K, but again an unresolved frequency shift is observed. When the temperature is changed to 77° K, the order of lines (as judged from their signal-to-noise ratio) changes, showing that the various frequencies have different temperature dependences. In the trimer Torizuka (23) reported only two lines which agree with two of the four lines reported in this paper.

While the relative signal-to-noise ratios describe the relative numbers of chlorine atoms in a given crystallographic situation, they do not show whether these chlorine atoms are on the same or different molecules; thus it is impossible to deduce whether there are twice as many molecules in one crystallographic situation as in another, or only twice as many chlorine atoms (15).

Only the diphenyl-tetrachloro-substituted trimer in which the disubstitution occurred on a single phosphorus atom gave a frequency. No frequencies were detected for the tetraphenyl-dichloro tetramer, $\phi_4P_4N_4Cl_4$, the tetra-isopropylamine-dichloro trimer, $P_3N_3(i\text{-}PrNH)_4Cl_2$, or the tetraphenyl-dichloro trimer, $\phi_4P_3N_3Cl_2$, as a result of any of the following effects: (i) the increased crystallographic disorder which results from packing non-symmetrical ring systems together, (ii) the strain occurring in the crystal,

and (iii) the dilution of the chlorine density in the crystal. The broadness and indistinctness of the diphenyl-tetrachloro trimer, $\phi_2P_3N_3Cl_4$, resonance, even at liquid nitrogen temperature, shows that the bulky phenyl groups cause not only a chlorine density dilution (which decreases the signal to noise ratio) but also either, or both, of effects (i) and (ii) (24).

EXPERIMENTAL

The phosphonitrilic chloride polymers were lent by Albright and Wilson Ltd., by arrangement with Dr. Childs, in the pure crystalline state and in sealed tubes of the exact size to fit the resonance coil; the substituted polymers were lent by Dr. R. A. Shaw, of Birkbeck College, London, and made in his Research School by S. K. Ray. They were spectroscopically pure and sealed in appropriate size tubes. Those samples for which resonance frequencies were not detected were recrystallized slowly from the melt in an attempt to obtain strain-free crystals, the work being carried out in a dry box under nitrogen gas, free of oxygen and hydrogen.

The $(PNCl_2)_3.HClO_4$ was made and purified by the procedure of Bode *et al.* (25), and preparation of the $(PNCl_2)_3.HBF_4$ followed the same procedure, replacing the 60% $HClO_4$ by 60% HBF_4 at the appropriate step. The crystals were subsequently filtered and dried under an atmosphere of pure dry nitrogen.

The super-regenerative oscillator (15) has a basic disadvantage when multiple lines are observed in a sample. Both self- and external-quenching produce frequencies on either side of the fundamental carrier, spaced at integral multiples of the quench frequency. Thus any side band of sufficient intensity can excite a quadrupole resonance as the oscillator carrier frequency is scanned. The actual frequency is obtained by re-examining the spectrum at a new quench frequency, when the side band frequencies will change but the fundamental frequency will remain unchanged. In the apparatus used, three side bands were observed on either side of the fundamental, or seven lines per true resonance. Thus for *b*-$(PNCl_2)_6$ a total of up to 84 lines could be seen. Actually 65 were observed at any one time, since side bands due to one true resonance can add to, or subtract from, side and fundamental lines due to another true resonance. Up to 10 different quench settings were needed to analyze the complex spectrum of $(PNCl_2)_5$ and *b*-$(PNCl_2)_6$. It was impossible to use the recording techniques available with either of these spectra. Figure 1(*c*) shows a recorded line from *a*-$(PNCl_2)_6$ which has only a single true resonance. The recording system was used to search for lines, but frequency measurement was made on the visual signals.

DISCUSSION I

The chemical condition of the chlorine atoms in the phosphonitrilic chlorides is quite similar to those in $(SNCl)_3$ trithiazyl chloride, the two frequency averages being alike (26, 27) (Table II). The differences appeared to be easily explained by recent work on orbital electronegativities (28, 29).

In both the phosphorus and sulphur compounds the central atom (P or S) is tetrahedrally(*te*) hybridized:* in the phosphorus compound to form four bonding orbitals, in the sulphur three bonding orbitals, and a lone pair orbital. The χ, orbital electronegativities, are (30):

$$\chi_{te}{}^{P} = 2.79$$

$$\chi_{te}{}^{S} = 3.21$$

for the atoms in the ($te^2tetete$) and (te^2te^2tete) state respectively. The promotion of one electron to the *d* orbital in the phosphorus atom may increase the $\chi_{te}{}^{P}$ slightly, but this will be similar to the change in $\chi_{te}{}^{S}$ when such a promotion occurs. However, in the phosphorus case the fourth bond is joined to chlorine and is not a lone pair orbital, so that the effective orbital electronegativity, $\chi_0{}^{eff}$, presented to a given chlorine, is changed

*The convention used in this paper is:
te = tetrahedral σ orbital,
tr = trigonal σ orbital,
di = digonal σ orbital,
π = pi orbital.
The superscript number designates the number of electrons in the orbital. Thus:
te = singly occupied tetrahedral orbital,
te^2 = doubly occupied tetrahedral orbital, or a lone pair orbital.

from the pure *te* value in both series but by different amounts. The change can be estimated from the empirically and theoretically established relation (30, 31)

$$\chi_o^{eff} = \tfrac{1}{2}(\chi_M^0)+\tfrac{1}{6}(\chi_A^0+\chi_B^0+\chi_C^0) \qquad [1]$$

where χ_M^0 is the orbital electronegativity of the central atom, and χ_A^0 etc. of the atoms joined to it. $(PNCl_2)_3$ and $(SNCl)_3$ only differ in one chlorine ligand as compared to a lone pair. Using the values of χ^0 for chlorine and nitrogen (29) and equation [1] a rough estimate of χ^{eff} for both the phosphorus and sulphur atoms can be made.

The nitrogen atom in the ring (1) is trigonally hybridized with a single p_π electron and a lone pair, *trtrtr*^{2} π; the chlorine can be assumed to be pure unhydridized $s^2p^2p^2p$; the sulphur and phosphorus are respectively *te*^{2}*tetetetd*, and *tetetetetd*. The various electronegativities (Table III) are:

$$\chi_N^{tr} = 4.13, \qquad \chi_{Cl}^{p} = 2.95, \qquad \chi_S^{te^2} = 2.01 \text{ (32)}.$$

TABLE III

Various orbital electronegativities used in the text given in Pauling units*

Atom	Orbital	χ°	Atom	Orbital	χ°
Cl	*s*	5.69	B	*s*	3.26
	p	2.95		*p*	1.26
				di	2.27
N	*s*	6.67		*tr*	1.93
	p	2.27		π	1.44
	di	5.05			
	tr	4.13	P	*s*	4.63
	π	2.47		*p*	1.84
	tr^2	1.58		*di*	3.58
				tr	3.05
C	*s*	4.84		*te*	2.79†
	p	1.75		*te*^{2}	1.59
	di	3.29			
	tr	2.75	S	*s*	5.12
	te	2.48		*p*	2.28
	π	1.68		*di*	3.96
				tr	3.46
H	*s*	2.21		*te*	3.21†
				te^2	2.01†

* J. Hinze and H. H. Jaffe. J. Am. Chem. Soc. 84, 540 (1962).

†These values of χ are calculated for the states *te*^{2}*tetete* (*P*) and *te*^{2}*te*^{2}*tete* (*S*). They are used for the states *tetetetd* and *te*^{2}*tetetd* respectively in the text since no estimation of the change in χ under such a promotion is available.

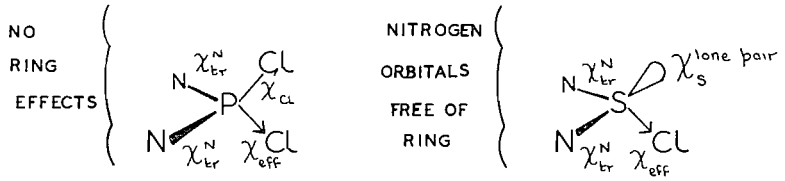

FIG. 2. The central atom is shown bonding either four ligands in the case of the phosphorus atom, or three ligands and a lone pair of electrons in the case of S. The nitrogen atoms are assumed to use pure trigonal hybrids towards the central atom and to be free of any ring influence.

To a first approximation the central atom can be considered as bonding four (P) or three ligands and a lone pair (S), independent of the rest of the ring, Fig. 2. Then using equation [1]

$$\chi_P^{eff} = 3.263, \qquad \chi_S^{eff} = 3.316,$$

giving $$\chi_P^{eff}/\chi_S^{eff} = 0.984,$$

while the n.q.r. frequency ratio is

$$[\nu_{(PNCl_2)_3}/\nu_{(SNCl)_3}] = 0.95.$$

This is quite good agreement when only σ bonds are considered and the ring ignored, but the electronegativity ratio is too high. The inclusion of the lone pairs of the nitrogen in any assessment of χ^{eff} would lower the value of χ^{eff}, to a slightly greater extent in the phosphorus than in the sulphur compound.

The disubstituted trimer, $P_3N_3Cl_4\phi_2$, has a frequency 0.86 Mc lower than the unsubstituted trimer. The pure p orbital electronegativity for chlorine, χ_o^p, is 2.95; if there is s hybridization in the orbital then the orbital electronegativity is given by (33)

$$\chi_{orbital} = s\chi_{orbital}^{s} + (1-s)\chi_{orbital}^{p} \qquad [2]$$

where s is the amount of s hybridization. The $\chi_{orbital}$ will exceed χ_o^p. The orbital electronegativity of the chlorine atoms is in consequence at least 2.95. Their replacement by phenyl groups (ϕ) means that the electronegativity is lowered. The phenyl group can display two electronegativities, the inductive χ^I, and conjugative χ^C. These are respectively (34):

$$\chi_\phi^I = 2.542, \qquad \chi_\phi^C = 1.68.$$

Measurement of the disubstituted trimers containing CH_3, C_2H_5, and $ClCH_2$ groups (as was possible in the $RPOCl_2$ series) would have decided whether the phenyl groups were inductively or conjugatively linked to the ring. This was not possible.

The following discussion allows a decision to be made. The change in frequency from $POCl_3$ to $\phi POCl_2$ is 3.6052 Mc when the phenyl group is conjugatively bonded; displaying $\chi_\phi^C = 1.68$. If it were inductively bonded then $\chi_\phi^I = 2.542$. Assuming the chlorine orbital to be pure p, $\chi_o^p = 2.95$, and thus a change in the electronegativity of 1.27 units changes the frequency by 3.6 Mc; a change of 0.41 units (the phenyl acting inductively) would be expected to cause, approximately, one-third the frequency change, 1.2 Mc. Allowing for the separation of the "phenyl phosphorus" from the phosphorus bonded to the chlorine atoms, a reduction of one-third per bond in the transmission of the effect, similar to that observed in organic ring systems, might be expected (35). Thus the conjugatively linked ϕ would cause a drop of 0.4 Mc per ϕ, or 0.8 Mc for the diphenyl, whereas the inductively linked ϕ would result in a drop of less than 0.3 Mc. It thus appears that the ϕ are conjugatively linked like the ϕ in the $RPOCl_2$ series. The absolute frequencies of the $(PNCl_2)_n$ compounds and the $RPOCl_2$ and R_2POCl series are also similar, suggesting that there is no fundamental difference between the bonding in the various types of compounds (27).

To explain the frequency behavior of the $RPOCl_2$ compounds, the use of the phosphorus d orbitals in d_π–p_π bond formation was stipulated; with the oxygen p_x and p_y orbitals two such bonds are formed, while only two of the remaining d orbitals have the correct symmetry to overlap the p orbitals on the RCl_2 atoms. The orbitals on all three groups can equally overlap the degenerate pair of d orbitals (Fig. 3(a)). The overlap will be less than that in the case of the phosphorus and oxygen orbitals because the RCl_2 atoms lie below the x–y plane containing the phosphorus–oxygen bond and also because the phosphorus–chlorine or phosphorus–R bond is longer than the phosphorus–oxygen bond (36). It was concluded that there would be weak conjugation between the orbitals

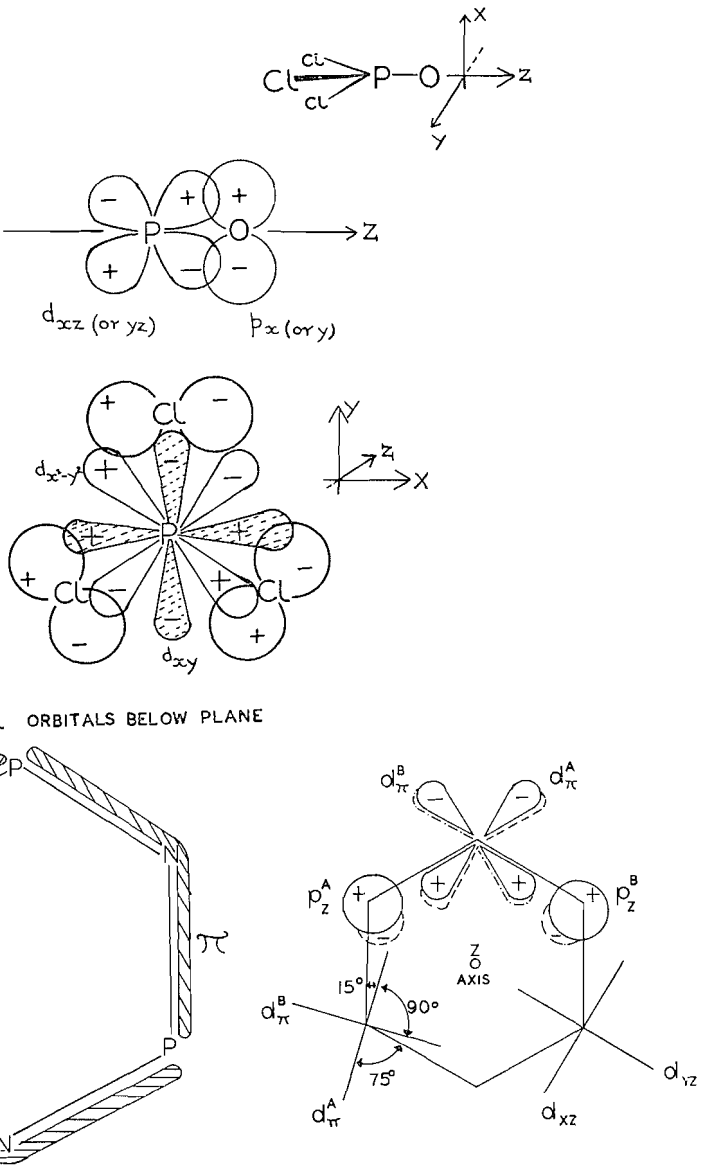

FIG. 3(*a*). The phosphorus oxychloride molecule has C_{3v} symmetry. With the z axis along the PO bond, the oxygen lone pair p orbitals lie in the xy plane. The transformation properties of the five d orbitals of phosphorus and these two p orbitals of oxygen, under both the C_{3v}, molecular, and C_v, bond, symmetry groups, show that the p_x and p_y orbitals can give a multiple π bond with d_{xz} and d_{yz} as shown in (*a*). It is a *triple* bond. The remaining d orbitals of phosphorus are of two symmetry types (i) the d_{z^2} orbital cannot d_π–p_π bond, (ii) the $d_{x^2-y^2}$ and d_{xy} orbitals can overlap with the chlorine orbitals, arbitrarily shown in (*b*). The chlorine orbitals can all equally well overlap, lie below the plane of the d orbitals and are further from the phosphorus than the oxygen atom orbitals.

FIG. 3(*b*). The polyallylic π bond structure of $(PNCl_2)_3$ and $(SNCl_2)_3$ showing the node present in the d_π–p_π system at each phosphorus (sulphur) atom. Any number of PN units may be combined either linearly or in rings and such an allylic structure will fit.

FIG. 3(*c*). The unhybridized d_{xz} and d_{yz} of a phosphorus or sulphur are shown. The hybridized

$$d_\pi^A = (1/\sqrt{2})\,(d_{yz} + d_{xz})$$

and

$$d_\pi^B = (1/\sqrt{2})\,(d_{yz} - d_{xz})$$

are shown and the angle between their lobes and the σ bond framework. The build-up of the allylic π bonds results from the overlap of a phosphorus d_π^A and nitrogen p_z^A which can overlap with the d_π^A of the next phosphorus atom. Since d_π^A and d_π^B are orthogonal orbitals there will be a break in the π orbital, or anode, at each phosphorus.

on the substituents and those on the phosphorus atom, and consequently between themselves, but that there would be no conjugation between the orbitals on the substituents and those forming the phosphorus–oxygen π bond.

In the phosphonitrilic halides it has been shown (1) that the stability of the phosphonitrilic halide ring can be explained by a polyallic structure for the ring. Each phosphorus atom makes use of two d_π orbitals in forming π bonds and these interact with the nitrogen atom p_π orbital to give a system of weakly interacting three-centered π bonds, embracing two phosphorus atoms and a central nitrogen atom (Fig. 3(*b*)).

Craig (16) criticized the formulation of Dewar *et al.* (1) on the grounds that it required the two *d* orbitals d_{xz} and d_{yz} to have identical electronegativities, which they could not, due to their different orientations towards the bonded atoms causing their polarization. However, in his papers (37–40) the effect of the ring nitrogen atoms is the only ligand effect considered. The other bonded ligands, whether halogen, aryl, alkyl, or another electronegative group (41–43) are not considered as affecting the size, or polarization, of the phosphorus *d* orbitals. While it is true that "we may expect, therefore, that d_{xz} will be more polarized than d_{yz} because of its greater overlap with the neighbor nitrogens" (40) it is equally true that we should expect the d_{yz} to be more polarized than the d_{xz} due to its greater overlap with the exocyclic ligand groups. This polarization will depend on the exocyclic group actually attached, or, more exactly, on the electronegativity of the σ orbital by which it is joined to the phosphorus, and these are comparable in electronegativity to the σ orbital of the ring nitrogen (30).

The difference between d_{xz} and d_{yz} orbitals should therefore be considerably less than suggested by Craig's arguments. Further, in the most recent paper (16), he postulates the inclusion of other *d* orbitals, as had been considered earlier by Dewar *et al.* (1). The inclusion of other *d* orbitals permits the non-planarity of the ring. The $d_{\pi a}$, $d_{\pi b}$ formed, have the form

$$d_{\pi a} = 1/\sqrt{(a^2+b^2+c^2+d^2)}\ \{ad_{yz}+bd_{xz}+cd_{xy}+dd_{x^2-y^2}\},$$
$$d_{\pi b} = 1/\sqrt{(a^2+b^2+c^2+d^2)}\ \{ad_{yz}-bd_{xz}-cd_{xy}-dd_{x^2-y^2}\}.$$

The hybridized orbitals do not have to be of precisely the same electronegativity but only similar electronegativities (i.e. energies or sizes), nor do they have to contribute equally to the hybrid. In forming two equal *sp*-hybrids at an angle θ_{ij} (44) where the *s* and *p* orbitals are not of the same χ, the orbitals

$$\phi_1 = s+ap_i$$
$$\phi_2 = s+bp_j$$

are constructed which are orthogonal if $\int \phi_1\phi_2 d\tau = \int (s+ap_i)(s+bp_j)d\tau = 0$ and normalized if

$$\int s^2 d\tau = \int p_i^2 d\tau = 1 \text{ and } \int p_i p_j d\tau = \cos\theta_{ij}.$$

Since any two perpendicular *p* orbitals or an *s* and *p* orbital are orthogonal, $\int sp_i d\tau = \int sp_j d\tau = 0$, so that orthogonality with equal hybrids requires $1+a^2\cos\theta_{ij} = 0$. Similar requirements can be applied to the various *d* orbitals and hybrids can always be constructed which are orthogonal. The polyallylic structure fits the ultraviolet spectra results for the linear and ring molecules, which show no increased conjugation path as the *n* in $(PNCl_2)_n$ increases, but a steady increase in ϵ, which is proportional to *n*.

The d_π orbitals are formed from the d_{yz} and d_{xz}, etc., orbitals by rehydridization. The d_π orbitals, $d_{\pi a}$ and $d_{\pi b}$, are orthogonal and do not conjugate with each other. The remaining orbitals on the phosphorus atom are the d_{xy}, $d_{x^2-y^2}$, and d_z orbitals. The phosphorus

atom is tetrahedrally bonded to the two nitrogen atoms and two chlorine atoms by sp^3 σ bonds, the chlorine atoms being above and below the plane of the ring (17). The $\widehat{ClPCl}$ is 109°. The d_{xy} orbital is therefore of the wrong symmetry to interact with the chlorine atom p_π orbital while both the d_{z^2} and $d_{x^2-y^2}$ orbitals can interact with one lobe of one of the chlorine p_π orbitals.

Thus, as in the $RPOCl_2$ case, there will be weak conjugative bonding between the chlorine atoms via the phosphorus atom, but not between the chlorine atoms and the allylic π bonding of the ring. Therefore the n.q.r. frequency would be expected to be similar in the phosphonitrilic halides and the phosphonyl halides.

The case of the $\phi_2P_3N_3Cl_4$ molecule is interesting. The phenyl groups are, as discussed above, weakly π bonded to the central phosphorus atom, displaying a conjugative rather than inductive electronegativity. This affects both the phosphorus σ and d_π electronegativities which transmit the effect to the next phosphorus atom, which is weakly conjugated to the chlorine atoms. The phenyl groups thus display conjugative electronegativity at the chlorine atoms via a conjugative path containing two nodes.

Similar arguments explain the resemblance between the $SOCl_2$ and $(SNCl)_3$ frequencies, the greater difference being due to the lone pair which has a greater "flexibility", than a bonded pair, to suffer rehybridization.

The perchlorate and borofluoride complexes of the phosphonitrilic chlorides have n.q.r. frequencies so close to those of pure $(PNCl_2)_3$ as to suggest that the $(PNCl_2)_3.HClO_4$ and $(PNCl_2)_3.HBF_4$ do not exist; their frequencies should differ greatly from those of the pure substance. If the bonding of the perchlorate and borofluoride were such as to give a salt, the proton adding to one of the ring nitrogen atoms, then there should be a distinct change in the pattern of the resonance. The four chlorine atoms on the phosphorus atoms adjacent to the protonated nitrogen atom should give higher frequencies, while the other two chlorine atoms should not. The increase of only 0.022 Mc from $(PNCl_2)_3$ to $(PNCl_2)_3.HClO_4$ seems rather small.

DISCUSSION II

It appeared at first as if the use of effective electronegativities could distinguish between π-bonded and non-π-bonded chlorine atoms, since when the ratio of the χ^{eff} was close to the frequency ratio then there would be no π bonding, but when π bonding was present, causing an abnormally low frequency to be measured, there would be a large discrepancy between the frequency and χ^{eff} ratios.

This was a fallacious expectation as the following sequence of results will show; these results confirmed the views expressed previously (21) that "quadrupole data may be correlated by means of χ^{eff} so long as a homologous series or family is maintained. Otherwise both hybridization and ionic character must be considered."

From Table II the following frequency ratios can be determined

$$(\nu_{POCl_3})/(\nu_{PCl_3}) = 1.105,$$

$$[\nu_{(PNCl_2)_3}]/(\nu_{POCl_3}) = 0.982,$$

and $$[\nu_{(PNCl_2)_3}]/(\nu_{PCl_3}) = 1.086,$$

while the χ^{eff} for the ring compound will be that calculated above, and for $POCl_3$ and PCl_3 with $\chi_P{}^{te} = 2.79$, $\chi_P{}^{te^2} = 1.59$, $\chi_O{}^{p} = 3.04$ and pure p chlorine orbitals of $\chi_{Cl}{}^{p} = 2.95$, then equation [1] yields $\chi^{eff}_{POCl_3} = 2.885$ and $\chi^{eff}_{PCl_3} = 2.643$, which give for the ratios

of the frequencies shown above

$$\chi^{eff}_{POCl_3}/\chi^{eff}_{PCl_3} = 1.092, \qquad \chi^{eff}_{(PNCl_2)_3}/\chi^{eff}_{POCl_3} = 1.131,$$

and

$$\chi^{eff}_{(PNCl_2)_3}/\chi^{eff}_{PCl_3} = 1.234.$$

The oxygen orbital is assumed to be pure p, since the inclusion of s character would increase the electronegativity and match the tetrahedral phosphorus orbital less well (45). However, a small amount of s character in either the chlorine or oxygen orbital would still permit a complete match of the frequency and effective electronegativity ratios in the case of $POCl_3$ and PCl_3; the lower $\chi^{eff}_{(PNCl_2)_3}$ resulting from the inclusion of ring effects would match the ratios in the other cases.

Despite the impressive match in the comparison of ν and χ of $POCl_3$ and PCl_3, there is some difficulty with using PCl_3 at all in this work, since it has yet to be established whether there is π bonding present between the chlorine atoms and the central phosphorus and hence between each other. It is possible to assume that the orbitals on the central atom point toward the ligand orbital (orbital following). Two estimates of PCl_3 have been made, with and without this assumption, and with and without π bonding. The various possibilities were:

(i) $\rho = 0.477 \quad \chi_P{}^{hyb} = 2.58 \quad s_P = 0.15$ from bond angles

$$\chi_{Cl}{}^{hyb} = 3.80 \quad s_{Cl} = 0.313$$

bond ionic character = 0.31;

(ii) if P is assumed to be pure "*te*"

$$\chi_P{}^{hyb} = 2.99 \quad s_P = 0.25$$

$$\chi_{Cl}{}^{hyb} = 3.89 \quad s_{Cl} = 0.343$$

bond ionic character = 0.28;

(iii) if π bonds are assumed present and estimated by Pauling's method (44) from bond length changes

$$\pi \text{ character} = 0.10$$

then

$$s_{Cl} = 0.231 \quad \chi_{Cl}{}^{hyb} = 3.64$$

$$i = 0.25.$$

This focusses the difficulties and dangers of correlating theories which ignore the individual nature of each molecule (21).

If the compounds $SOCl_2$ and SO_2Cl_2 are compared (Table II) then

$$(\nu_{SO_2Cl_2})/(\nu_{SOCl_2}) = 1.182$$

The χ^{eff} is estimated by the above method. The χ^{eff} is the effective σ orbital electronegativity displayed by the sulphur to a single chlorine atom which is not π bonded to the oxygen and only weakly π bonded to the sulphur. With $\chi_s{}^{te} = 3.21$, $\chi_s{}^{te^2} = 2.01$, $\chi_o{}^p = 3.04$, and with the chlorine orbital pure p in character (displaying the lowest possible χ) $\chi_{Cl}{}^p = 2.95$ and

$$\chi^{eff}_{SO_2Cl_2}/\chi^{eff}_{SOCl_2} = 1.058.$$

The inclusion of a small and different amount of s hybridization in the chlorine σ orbital

in the two compounds would make the agreement perfect. The comparison of $(SNCl)_3$ with $SOCl_2$ and SO_2Cl_2 gives for the frequency ratio 0.934 and 0.790. The corresponding χ^{eff} ratios are 1.154 and 1.066. These are high due to overassessment of the $\chi^{eff}_{(SNCl)_3}$ when the ring is not considered.

The interesting aspect of this approach is that the bond electronegativities seem to be qualitatively and semiquantitatively related to the n.q.r. frequency changes in all compounds where there is a small amount of conjugation between the chlorine and central atom, but no conjugation between the orbitals on the chlorine atoms and the π bonds of the system.

The compounds CCl_4, $COCl_2$, and $(CNCl)_3$ give nuclear quadrupole frequencies which are distinctly different from the phosphorus and sulphur compounds (27). It has been previously shown (45) that CCl_4 displays 9.7% s character in the chlorine σ orbital and 17.4% ionic character in the carbon–chlorine bond; assuming that the chlorine orbitals in $COCl_2$ are similar to those in CCl_4 with a similar amount of hybridization, then from Table II,

$$(\nu_{COCl_2})/(\nu_{CCl_4}) = 0.879$$

while $\chi^{eff}_{COCl_2}/\chi^{eff}_{CCl_4} = 1.004$ using a pure p orbital

or $= 1.028$ with 9.7% s hybridization.

The χ^{eff} are calculated using equation [1], modified in the case of $COCl_2$ to

$$\chi^{eff} = \tfrac{1}{2}\chi_c{}^{tr} + \tfrac{1}{4}[\chi_o{}^p + \chi_{Cl}{}^p].$$

The oxygen orbital is assumed to be pure p, the chlorine orbital to be pure p and hybridized respectively.

When χ ratio is less than the ν ratio, increased s hybridization in the chlorine σ orbital of $COCl_2$ could match the two ratios. However, s hybridization will increase the mismatch in this case. Any π bonding between the central carbon p orbital and the chlorine atom lone pair p would lower the $COCl_2$ frequency more than would be estimated from the χ^{eff} changes, and recent work supports the view that the chlorine atoms in $COCl_2$ are π bonded to the central carbon atom (36, 46–49).

It might be expected that the $(CNCl)_3$ molecule would resemble $COCl_2$ in its bonding to chlorine. The ratio

$$[\nu_{(CNCl)_3}]/(\nu_{CCl_4}) = 0.894$$

is very similar to the value for $COCl_2$ of 0.879. Treating $(CNCl)_3$ in the same way as the phosphorus and sulphur compounds, with trigonal carbon, the χ^{eff} ratio is 1.203, high due to the ring structure being ignored. If $(CNCl)_3$ is compared with $COCl_2$ then the frequency ratio is 1.017, while the χ^{eff} ratio is 1.171.

Finally in this series of comparisons one can consider $(BNHCl)_3$ and BCl_3 which with trigonal boron give a ν ratio of 0.922 and a χ ratio of 1.247.

CONCLUSION

In the compounds known to have aromatic ring character and π-bonded chlorine atoms, the χ^{eff} ratio differs from the ν ratio by 0.309, $(CNCl)_3$, and 0.325, $(BNHCl)_3$. In the single bonded cases $(PNCl_2)_3$ and $(SNCl)_3$ the differences are only 0.136 and 0.148 (compared to $POCl_3$ and PCl_3 respectively) but 0.22 and 0.27 (compared to $SOCl_2$ and SO_2Cl_2), while in $COCl_2$, now thought to have doubly bonded chlorine atoms and π bonding also

between the carbon and oxygen atoms (48, 49), the discrepancy between χ and ν for $COCl_2$ compared to CCl_4 is 0.149, in the singly bonded region.

The initially hopeful trend seen in comparing the $(SNCl)_3$ and $(PNCl_2)_3$ χ^{eff} ratio with their frequency ratio thus comes to naught. It does not appear possible to interpret structural differences from the comparison of the ratio of the nuclear quadrupole ratios with the ratios of the effective orbital electronegativity of the atom joined to the chlorine atom.

ACKNOWLEDGMENTS

We wish to thank Dr. Childs, of Albright and Wilson, and Dr. R. A. Shaw, of Birkbeck College, London, for the loan of samples, without which this research would never have occurred, and especially Dr. E. A. Lucken for useful views and discussion. The experimental measurements were performed at Queen Mary College, the University of London.

The author is indebted to the referee for very helpful criticism and suggestions.

REFERENCES

1. M. J. S. Dewar, E. A. C. Lucken, and M. A. Whitehead. J. Chem. Soc. 2423 (1960).
2. C. Dean. Thesis, Harvard University, Cambridge, Mass. 1952.
3. M. A. Whitehead. Thesis, University of London, London, England. 1960.
4. J. R. Van Wazer. J. Am. Chem. Soc. **78**, 5709 (1956).
5. N. L. Paddock and H. T. Searle. Advan. Inorg. Chem. Radiochem. **1**, 348 (1959).
6. A. Wilson and D. F. Carrol. Chem. Ind. 158 (1958).
7. A. Liquori, F. Pompa, and A. Ripamonti. Intern. Congr. Pure Appl. Chem. Munich, 1959. A1025.
8. G. J. Bullen. Proc. Chem. Soc. 425 (1960).
9. J. A. A. Ketelaar and T. A. de Vries. Rec. Trav. Chim. **58**, 1081 (1939).
10. H. McD. McGeachin and F. R. Tromans. Chem. Ind. 1131 (1960); J. Chem. Soc. 4777 (1960).
11. F. M. Jaeger and J. Beintema. Proc. Acad. Sci. Amsterdam, **35**, 756 (1932).
12. M. W. Dougill. J. Chem. Soc. 5471 (1961).
13. L. G. Lund, N. L. Paddock, J. E. Proctor, and H. T. Searle. J. Chem. Soc. 2542 (1960).
14. R. Hazekamp, T. Migchelsen, and A. Vos. Acta. Cryst. **15**, 539 (1962).
15. T. P. Das and E. L. Hahn. Nuclear quadrupole spectroscopy. Academic Press, New York. 1958.
16. D. P. Craig and N. L. Paddock. J. Chem. Soc. 4118 (1962).
17. A. Wilson and D. F. Carrol. J. Chem. Soc. 1548 (1960). E. A. Lucken. To be published.
18. J. Vanier. Can. J. Phys. **38**, 1397 (1960).
19. C. Dean and R. V. Pound. J. Chem. Phys. **20**, 195 (1952).
20. H. S. Gutowsky and D. W. McCall. J. Chem. Phys. **32**, 548 (1960).
21. J. Todd, M. A. Whitehead, and K. E. Weber. J. Chem. Phys. **39**, 404 (1963).
22. H. Negita and S. Satou. J. Chem. Phys. **24**, 621 (1956); Bull. Chem. Soc. Japan, **29**, 426 (1956).
23. K. Torizuka. J. Phys. Soc. Japan, **11**, 84 (1956).
24. Y. Koi, A. Tsujimura, and T. Fuke. J. Chem. Phys. **23**, 1346 (1955).
25. H. Bode, K. Bütow, and G. Lienau. Ber. **81**, 547 (1948).
26. H. Negita. Hiroshima Univ. Ser. A, **21**, 261 (1958).
27. H. Negita and Z. Hiraro. Bull. Chem. Soc. Japan, **31**, 660 (1958).
28. J. Hinze and H. H. Jaffé. Can. J. Chem. **41**, 1315 (1963).
29. J. Hinze and H. H. Jaffé. J. Am. Chem. Soc. **84**, 540 (1962).
30. J. Hinze, M. A. Whitehead, and H. H. Jaffé. J. Am. Chem. Soc. **85**, 148 (1963).
31. R. E. Kagarise. J. Am. Chem. Soc. **77**, 1377 (1955).
32. J. Hinze and H. H. Jaffé. To be published.
33. M. A. Whitehead. J. Chem. Phys. **36**, 3006 (1962).
34. E. A. C. Lucken and M. A. Whitehead. J. Chem. Soc. 2459 (1961).
35. R. W. Taft. Steric effects in organic chemistry. *Edited by* M. S. Newman. Wiley, New York. 1956. p. 592.
36. A. F. Wells. Structural inorganic chemistry. 3rd ed. Oxford, Clarendon Press. 1962.
37. D. P. Craig, M. L. Hefferman, R. Mason, and N. L. Paddock. J. Chem. Soc. 1376 (1961).
38. D. P. Craig and N. L. Paddock. Nature, **181**, 1052 (1958).
39. D. P. Craig. J. Chem. Soc. 997 (1959).
40. D. P. Craig. Chem. Soc. London Spec. Publ. **12**, 343 (1958).
41. D. D. Eley and M. R. Willis. J. Chem. Soc. 1534 (1963).
42. S. K. Ray and R. A. Shaw. Chem. Ind. 1173 (1961).
43. R. A. Shaw. Chem. Ind. 52, 53, 54, 412 (1959).
44. C. A. Coulson. Valence. Oxford, Clarendon Press. 1962.
45. M. A. Whitehead and H. H. Jaffé. Theoret. Chim. Acta, **1**, 209 (1963).
46. Interatomic Distances. Chem. Soc. London Spec. Publ. **11** (1958).
47. G. W. Robinson. J. Chem. Phys. **21**, 1741 (1953).
48. R. Livingston. J. Phys. Chem. **57**, 496 (1953).
49. K. M. Sinnott. J. Chem. Phys. **34**, 857 (1961).

Can. J. Chem. Downloaded from www.nrcresearchpress.com by 210.87.254.40 on 09/05/12
For personal use only.

NOTES

SYNTHESES OF ALPHA AMIDE AND PEPTIDE DERIVATIVES OF DL-ASPARTIC ACID

A. ZILKHA AND N. LERMAN

In previous work we have prepared α and β amide and peptide derivatives of aspartic acid starting with N-benzyl-aspartic acid as the anhydride hydrochloride (1) or as the mixed anhydride with chloroformic acid obtained by reaction with phosgene (2, 3, 4). Exclusive preparation of the β derivatives in good yield was obtained starting with maleic anhydride (5). In the previous methods, α amides and peptides were obtained sometimes exclusively, and sometimes in admixture with β derivatives (2, 3, 4). The use of active amines or aminoacid esters led to the formation of α derivatives, while with weak aromatic amines β derivatives were obtained (2, 4, 6). From weak aromatic amines, α derivatives were obtained only on using large excess of amine (6).

In the present work the use of β-benzyl N-benzyl-DL-aspartate (I) as starting material for the exclusive formation of α-aspartyl amides and peptides is described. In this compound the β-carboxyl group is masked with a benzyl group, which can be removed easily by hydrogenolysis. The use of other ester groups such as the methyl group [the corresponding N-benzyl derivative has been prepared (7)] did not seem feasible, as these can be removed only by hydrolysis, and it has already been shown that such hydrolysis leads to the formation of imide derivatives as cyclic intermediates, which afterwards may open to yield either the α or β derivatives (8, 9).

β-Benzyl N-benzyl-DL-aspartate (I) was prepared starting from benzyl maleate as follows:

$$\begin{array}{l} \mathrm{CHCOOCH_2C_6H_5} \\ \| \\ \mathrm{CHCOOH} \end{array} + \mathrm{C_6H_5CH_2NH_2} \rightarrow \begin{array}{l} \mathrm{CH_2COOCH_2C_6H_5} \\ | \\ \mathrm{CHCOOH} \\ | \\ \mathrm{NHCH_2C_6H_5} \end{array}$$

I

One equivalent of benzylamine was used, and it led exclusively to opening of the double bond without attacking the ester group, showing that addition to the double bond is preferable to amidation (7). DL-Aspartic acid was obtained on hydrogenolysis of (I). Reaction of (I) with phosgene in dioxane gave an active intermediate from which α-aspartyl amide and peptide derivatives were obtained on reaction with two equivalents of amine or amino-acid ester in dioxane. The product usually was difficult to crystallize, so that the dioxane solution was evaporated after filtration from the amine hydrochloride that precipitated, and the product was hydrogenolyzed with alcohol in the presence of palladium chloride (30% on carbon). In the case of cyclohexylamine, the intermediate product N^2-benzyl-N-cyclohexyl-α-asparagine β-benzyl ester was isolated. By this method the yields in many cases were much higher than those obtained previously (2, 4).

The α amides and peptides gave positive biuret reactions and purple spots on paper chromatograms as was found previously (2).

Structure of the Active Intermediate (II)

To ascertain the nature of the active intermediate (II), the known determinations (10) of acid chlorides, anhydrides, and amino acids by anhydrous titrations with sodium

methoxide and Triton B (trimethylbenzylammonium hydroxide) were used, as shown in the equations below:

$$RCOCl + NaOCH_3 \rightarrow RCOOCH_3 + NaCl \text{ (no back-titration with } HClO_4)$$

$$RCOCl + 2\,(CH_3)_3NC_7H_7OH \rightarrow RCOON(CH_3)_3C_7H_7 + (CH_3)_3NC_7H_7Cl + H_2O$$

$$\underset{\underset{NH_2}{|}}{RCHCOOH} + NaOCH_3 \rightarrow \underset{\underset{NH_2}{|}}{RCHCOONa} + CH_3OH \xrightarrow[\text{back-titration}]{2HClO_4} \underset{\underset{NH_2.HClO_4}{|}}{RCHCOOH} + NaClO_4$$

It may be noted that while 1 equivalent of sodium methoxide is required for the titration of a chloride or anhydride, 2 equivalents of Triton B are required. However, we found that a solution of carbon dioxide in dioxane required 1 equivalent of Triton B for titration, using thymol blue as indicator, the same as with sodium methoxide.

The intermediate (II) was prepared directly in dioxane solution (excess phosgene expelled) and aliquot portions analyzed. Volhard titration for chlorine showed the presence of approximately 1 equivalent of chlorine. Anhydrous titration with sodium methoxide using thymol blue as indicator required the use of 2 equivalents of reagent, while titration with Triton B required the use of 3 equivalents of reagent (10). Back-titration of the sodium methoxide titrated aliquot with perchloric acid in dioxane required the use of 2 equivalents of reagent, one to titrate the sodium carboxylate formed, and the other the amino group. Addition of *p*-toluidine to the dioxane solution of II led to the generation of 1 mole equivalent of CO_2. Also, the dioxane solution of the intermediate did not titrate directly with perchloric acid in dioxane with thymol blue as indicator, presenting evidence that the amino group was blocked.

All these results are consistent with the formation of an N-chloroformyl derivative (II*a*), but not a mixed anhydride with chloroformic acid (II*b*), which has a free amino group, or a simple anhydride hydrochloride between two molecules of the benzyl ester derivative.

$$\begin{array}{l} CH_2COOCH_2C_6H_5 \\ | \\ CHCOOH \\ | \\ NCOCl \\ | \\ CH_2C_6H_5 \end{array} \qquad \text{(II}a\text{)}$$

$$\begin{array}{l} CH_2COOCH_2C_6H_5 \\ | \\ CHCOOCOCl \\ | \\ NHCH_2C_6H_5 \end{array} \qquad \text{(II}b\text{)}$$

Such an N-chloroformyl derivative was formed in the reaction of phosgene with N-phenyl-β-alanine or N-*p*-tolyl-β-aminobutyric acid (11). It can cyclize (11) on reaction with amines to an N-carboxyanhydride, which decomposes with carbon dioxide evolution on reaction with additional amine.

We tried to obtain more evidence from examination of the infrared spectra of the active intermediate (II). A mixed anhydride structure, such as (II*b*), must have double absorption peaks at about 5.4 μ and 5.6 μ which are not given by the N-chloroformyl structure (II*a*). The dioxane solution was evaporated to dryness *in vacuo* at 30°, and the residue showed a double absorption peak in the infrared at 5.4 μ and 5.65 μ, which is consistent with either a mixed anhydride or an N-carboxyanhydride structure. However, during the evaporation, the compound must have undergone considerable transformation as its chlorine content was reduced by some 50%. The dry compound also evolved fumes of hydrogen chloride on standing. After several fractional crystallizations of the residue from dioxane – petroleum ether or chloroform–ether, the N-carboxyanhydride derivative of (I) was isolated. This was identical with that obtained on addition of an equivalent of

Can. J. Chem. Downloaded from www.nrcresearchpress.com by 210.87.254.40 on 09/05/12
For personal use only.

Can. J. Chem. Downloaded from www.nrcresearchpress.com by 210.87.254.40 on 09/05/12
For personal use only.

TABLE I

α-DL-Aspartyl amides and peptides

N-Alkyl (or aryl)-DL-α-asparagine	M.p.,* °C	Yield, %	R_f	Formula	Carbon, %		Hydrogen, %		Nitrogen, %		Nitrogen, % (Van Slyke)	
					Calc.	Found	Calc.	Found	Calc.	Found	Calc.	Found
Phenyl (6)	252	60	0.79	$C_{10}H_{12}N_2O_3$	57.7	57.6	5.8	5.9	13.4	13.0	6.7	6.5
α-Naphthyl	227	95		$C_{14}H_{14}N_2O_3$					10.8	10.6	5.4	5.2
p-Tolyl (1)	235	60	0.79	$C_{11}H_{14}N_2O_3$	59.5	59.5	6.3	6.2	12.6	12.7	6.3	6.3
Isobutyl	242	80	0.87	$C_8H_{16}N_2O_3$	51.1	51.1	8.5	8.6	14.9	14.5	7.4	7.3
n-Butyl (4)	226	70	0.89	$C_8H_{16}N_2O_3$	51.1	51.1	8.5	8.5	14.9	14.7	7.4	7.4
n-Hexyl (4)	223	65	0.83	$C_{10}H_{20}N_2O_3$	55.5	55.1	9.3	9.3	13.0	13.1	6.5	6.6
Carbethoxymethyl (2)	175	60	0.89	$C_8H_{14}N_2O_5$	44.0	43.7	6.4	6.2	12.8	12.7	6.4	6.5
2-Carbethoxyethyl (3)	188	50	0.93	$C_9H_{16}N_2O_5$	46.5	46.5	6.9	6.9	12.0	12.3	6.0	6.3

*Substances were recrystallized from ethanol or water.

triethylamine to the dioxane solution of the active intermediate, filtration of the precipitated triethylamine hydrochloride, evaporation of the dioxane, and crystallization of the N-carboxyanhydride from chloroform–ether. The N-carboxyanhydride showed absorptions at 5.4 μ and 5.65 μ besides the absorption at 5.8 μ (ester group).

EXPERIMENTAL

Melting points were determined in a Fisher–Johns apparatus, and the ascending method of paper partition chromatography (80% phenol) was used. A procedure for one typical example of each reaction step is given and the remainder are summarized in Table I. Benzyl maleate (12) m.p. 51–52°, was prepared in 92% yield by heating equimolar quantities of maleic anhydride and benzyl alcohol at 125°.

*β-Benzyl N-benzyl-*DL*-aspartate (I).*—Benzyl maleate (51.5 g, 0.25 mole) was dissolved in dry dioxane (400 ml) and cooled. Benzylamine (26.8 g, 0.25 mole) was added in one portion and the reaction mixture was stirred at 125° for 3 hours. The product started to precipitate after a few minutes. It was filtered and washed with acetone, yield 60 g (76%), m.p. 195° on recrystallization from water or better from 50% ethanol. Anal. Calc. for $C_{18}H_{19}NO_4$: C, 69.0; H, 6.1; N, 4.5. Found: C, 68.9; H, 5.9; N, 4.7.

*Reaction of β-Benzyl N-Benzyl-*DL*-aspartate with Phosgene.*—Dry, finely powdered β-benzyl N-benzyl-DL-aspartate (15.7 g, 0.05 mole) was suspended in dry dioxane (400 ml) in a three-necked flask equipped with a gas leading tube, a reflux condenser connected to a calcium chloride tube, and a mechanical stirrer. Dry phosgene was bubbled in with stirring for 90 minutes and the temperature was kept constant at 50°. After 10 minutes the solution cleared. Excess phosgene, but not the solvent, was removed *in vacuo* at 20° (4–5 hours). The solution was used as such for the preparation of the amides and peptides.

*N^3-Benzyl-N-cyclohexyl-α-*DL*-asparagine β-Benzyl Ester.*—To an ice-cold solution of the reactive intermediate (II) prepared from (I) (4.1 g, 0.013 mole) in dioxane (100 ml) was added cyclohexylamine (2.7 g, 0.028 mole). The reaction mixture was shaken in the cold for 30 minutes and left overnight at room temperature. The precipitate consisting of cyclohexylamine hydrochloride was filtered off, and the filtrate evaporated *in vacuo*. On cooling the residue crystallized. It was dissolved in a small volume of ethanol, water was added to incipient cloudiness, and the substance was left to recrystallize; yield 4.85 g. (95%), m.p. 80°. Anal. Calc. for $C_{24}H_{30}N_2O_3$: C, 73.1; H, 7.6; N, 7.1. Found: C, 73.4; H, 7.9; N, 7.1.

*N-Cyclohexyl-*DL*-α-asparagine.*—N^3-Benzyl-N-cyclohexyl-DL-α-asparagine (1 g) was dissolved in ethanol (100 ml) and 0.2 g of 30% palladium chloride on charcoal (2) was added. The hydrogenolysis was carried out in a Parr low-pressure hydrogenation apparatus for 10 hours at 50°. The product precipitated in the ethanol solution and was extracted from the catalyst by boiling water. The aqueous solution was evaporated, and the product which crystallized was washed with ethanol and filtered; yield 0.55 g. (quantitative), m.p. 247° on recrystallization from water, R_f 0.92. Anal. Calc. for $C_{10}H_{18}N_2O_3$: C, 56.1; H, 8.4; N, 13.1; N (Van Slyke), 6.6. Found: C, 56.0; H, 8.5; N, 13.2; N (Van Slyke), 6.6.

*N-Carboxyanhydride of β-Benzyl N-Benzyl-*DL*-aspartate.*—To a solution of the reactive intermediate (III) in dioxane prepared as above from 3.1 g (I), an equivalent amount of dry triethylamine (sufficient to react with the chlorine) was added dropwise in the cold with stirring. The reaction mixture was stirred for 2 hours and the precipitate of triethylamine hydrochloride was filtered. The dioxane filtrate was evaporated to dryness at 40°, and the N-carboxyanhydride crystallized on standing overnight in the cold under petroleum ether, yield 2.8 g (82%). It was recrystallized from chloroform – petroleum ether or chloroform–ether, m.p. 92°. Anal. Calc. for $C_{19}H_{17}NO_5$: C, 67.2; H, 5.0; N, 4.1; mol. wt. 339. Found: C, 66.9; H, 5.2; N, 4.3; mol. wt. 335, determined by anhydrous titration with 0.1 *N* sodium methoxide in dioxane using thymol blue as indicator (13).

1. A. Zilkha and Y. Liwschitz. J. Chem. Soc. 4397 (1957).
2. Y. Liwschitz and A. Zilkha. J. Am. Chem. Soc. **76**, 3698 (1954).
3. Y. Liwschitz and A. Zilkha. J. Chem. Soc. 4394 (1957).
4. Y. Liwschitz, Y. Pfefferman, and Y. Lapidot. J. Am. Chem. Soc. **78**, 3069 (1956).
5. Y. Liwschitz and A. Zilkha. J. Am. Chem. Soc. **77**, 1265 (1955).
6. Y. Liwschitz, E. Nemes, and A. Zilkha. Bull. Res. Council Israel, **4**, 107 (1961).
7. A. Zilkha and M. D. Bachi. J. Org. Chem. **24**, 1096 (1959).
8. A. R. Battersby and J. C. Robinson. J. Chem. Soc. 259 (1955).
9. S. A. Bernhard, A. Berger, J. H. Carter, E. Katchalski, M. Sela, and Y. Shalitin. J. Am. Chem. Soc. **84**, 2421 (1962).
10. A. Patchornik and S. Ehlrich-Rogozinski. Anal. Chem. **31**, 985 (1959).
11. L. Birkofer and R. Modic. Ann. **604**, 56 (1957).
12. D. D. Hicks. U.S. Patent No. 2,934,516 (April, 1960). S. N. Ushakov, A. F. Nikolaeva, A. M. Toroptseva, and M. S. Trizno. Zh. Prikl. Khim. **32**, 667 (1959).
13. A. Berger, M. Sela, and E. Katchalski. Anal. Chem. **25**, 1554 (1954).

Received November 12, 1963.
Department of Organic Chemistry,
The Hebrew University of Jerusalem,
Jerusalem, Israel.

Can. J. Chem. Downloaded from www.nrcresearchpress.com by 210.87.254.40 on 09/05/12
For personal use only.

ISOLATION OF 4,6-O-(1′-CARBOXYETHYLIDENE)-D-GALACTOSE FROM THE EXOCELLULAR POLYSACCHARIDE OF CORYNEBACTERIUM INSIDIOSUM[1]

P. A. J. GORIN AND F. J. T. SPENCER

In a previous publication the polysaccharide formed exocellularly by the alfalfa wilt organism, *Corynebacterium insidiosum*, was shown to yield two oligosaccharides and two unidentified acidic products on partial acid hydrolysis (1). The oligosaccharides were identified as 4-O-β-D-glucopyranosyl-L-fucose and O-β-D-glucopyranosyl-(1 → 4)-[O-D-galactopyranosyl-(1 → 3)]-L-fucose. The two unidentified acidic products consisted of a D-galactose residue (I) substituted by an unknown moiety and a trisaccharide (II) in which the D-galactose unit was also substituted.

C.Et.GAL (I)

C.Et.GALp —(1,3α)→ L-FUC (III)

C.Et.GALp
|
(1,3α)
|
(1,4β) ↓
D-GLp ——→ L-FUC (II)

(C.Et.GAL = 4,6-O-(1′-carboxyethylidene)-D-galactose)

I, II, III. Partial acid hydrolysis products of *Corynebacterium insidiosum* polysaccharide.

Re-examination of the crystalline galactose derivative, derived from I, by nuclear magnetic resonance spectroscopy (n.m.r.) indicated the presence of ethyl and uncoupled C-methyl protons. Since the compound appeared to be $C_{11}H_{20}O_9$ on the basis of carbon and hydrogen analysis and its neutral equivalent, the data were consistent with a carboxyethylidene galactose structure with 1 mole of ethanol of crystallization. The latter was removed by evaporation of an aqueous solution of the ethanolate. Further evidence for the structure was provided by the previous data (1), which showed a gradual consumption of lead tetraacetate by the ethanolate increasing to 1.32 moles after 20 minutes, indicating a 4-linkage (2). Compound I was converted to crystalline 4,6-O-(1′-carboxymethyl-ethylidene)-D-galactitol by treatment with sodium borohydride and then diazomethane. The product consumed 2 moles of sodium periodate with concomitant release of 1 mole of acid. Thus the structural assignment for the galactose derivate (I) was confirmed.

A third acidic component (III) was detected on re-examination of the partial hydrolysis products of the polysaccharide after charcoal and cellulose column chromatography. Its n.m.r. spectrum was indicative of the presence of a carboxyethylidene group. Compound III had a migration rate on paper chromatograms similar to that of glucose and was characterized as 3-O-[4,6-O-(1′-carboxyethylidene)-α-D-galactopyranosyl]-L-fucose as follows. Its hydrolysis products before and after sodium borohydride reduction indicated a fucose-reducing end. The lead tetraacetate oxidation characteristics of the reducing sugar showed it to be substituted in the 3-position. The specific rotation, +50°, of the derived fucitol derivative suggested an α-galactosidic linkage.

The data obtained show that a major structural component of the polysaccharide is O-β-D-glucopyranosyl-(1→4)-[4,6-O-(1′-carboxyethylidene)-α-D-galactopyranosyl-(1→3)]-L-fucose (II). The undegraded polymer consists of D-glucose, D-galactose, and L-fucose in

[1]*Issued as N.R.C. No. 7827.*

Can. J. Chem. Downloaded from www.nrcresearchpress.com by 210.87.254.42 on 09/05/12
For personal use only.

the ratio 1:1:2 and has a neutral equivalent of 912 (1). Since acidic derivatives of sugars other than galactose have not been detected, 80% of the total galactose units must be substituted by a carboxyethylidene group. Also, the structure of II would indicate that the D-glucose units are the site of the periodate consumption (0.60 moles) and acid production (0.28 moles) in the polysaccharide (1). Therefore the D-glucose units are either non-reducing end-units or are glycosidically substituted at C-6.

The occurrence of 4,6-O-(1′-carboxyethylidene) groups in the exocellular polysaccharide of *Xanthomonas campestris* has been reported by Sloneker and Orentas (3). Hydrolysis of the product obtained by treatment of the polymer with sodium periodate and then sodium borohydride yielded 1,3-O-(1′-carboxyethylidene)-D-erythritol. This material appeared to be derived from the 4,6-O-(1′-carboxyethylidene)-D-glucosyl residues. Previous to this Hirase demonstrated the presence of 4,6-O-(1′-carboxyethylidene)-D-galactose linked to 3,6-anhydro-L-galactose in a disaccharide isolated from commercial red seaweed (4). Similar acidic substituents were detected in partial acid hydrolyzates of *C. michiganense* and *C. sepodonicum*. In all these materials the absolute configuration of the carboxyethylidene groups has yet to be determined.

EXPERIMENTAL

Evaporations were carried out under reduced pressure. Specific rotations were measured at 25° C. Acidic sugars were separated on paper chromatograms using ethyl acetate – acetic acid – water (9:2:2 v/v) as solvent. Galactose was identified by paper chromatography using the solvent, butanol–pyridine–water (3:1:1 v/v) and the spray reagent, *p*-anisidine hydrochloride (5). Nuclear magnetic resonance spectra were obtained in D_2O using tetramethylsilane as the external standard.

4,6-O-(1′-Carboxyethylidene)-D-galactose Ethanolate (Ethanolate of I)

The ethanolate was characterized previously as $C_{11}H_{20}O_9$ and had an equilibrium rotation of +49° in water (1). When examined by n.m.r. spectroscopy, the ethanolate gave a signal at 1.65 p.p.m. corresponding to uncoupled C-methyl protons and a triplet at 1.12, 1.23 and 1.35 p.p.m. from the methyl protons of an ethyl group. Re-examination of the product by n.m.r. spectroscopy after the material had been dissolved in water and the solvent then removed gave a spectrum in which there was no evidence of an ethyl group.

Partial Hydrolysis of C. insidiosum Polysaccharide

Crude polysaccharide (50 g) was stirred in *N* sulphuric acid (1 liter) at 70° C for 3 hours. The solution was neutralized ($BaCO_3$), filtered, decationized with Amberlite IR 120, and fractionated on a charcoal column. The monosaccharide components were eluted with water and the acidic components were eluted by increasing the concentration of ethanol in water to 10%. The acidic compounds were designated as I, II, and III, respectively, and had migration rates on paper chromatograms similar to those of arabinose, cellobiose, and glucose. Compounds I, II, and III were fractionated on a cellulose column using ethyl acetate – acetic acid – water (9:2:2 v/v) as solvent. This procedure gave I (0.48 g), corresponding to the previously isolated material (1), and III (0.30 g). Compound II (0.92 g) was obtained when the proportions of the solvent were changed to 3:1:1. Its n.m.r. spectrum contained a signal at 1.54 p.p.m. corresponding to an uncoupled methyl group.

Preparation of 4,6-O-(1′-Carboxymethyl-ethylidene)-D-galactitol

Compound I (0.17 g) was reduced with sodium borohydride (0.20 g) in water (5 ml). After 2 hours excess reagent was destroyed with acetic acid and cations were removed with Amberlite IR 120. The solution was filtered and the filtrate was evaporated to a crust which was repeatedly treated with methanol to remove boric acid as methyl borate, which was then evaporated. The residue was dissolved in methanol and ethereal diazomethane was added until the solution was neutral. The esterified product, when chromatographed in the solvent *n*-butanol–ethanol–water (40:11:19 v/v), was detected with ammoniacal silver nitrate spray reagent (6), and consisted mainly of a substance which had a migration rate similar to that of glycerol. Chromatography on cellulose with benzene–methanol–water (200:50:1 v/v) as solvent yielded the required material. Two recrystallizations of the product from ethyl acetate gave the methyl ester with m.p. 104–105° C and $[\alpha]_D$ −18° (*c*, 0.6, MeOH). Calculated for $C_{10}H_{18}O_8$: C, 45.1%; H, 6.8%; mol. wt., 266. Found: C, 45.3%; H, 6.9%; mol. wt. in ethanol, 260. The ester consumed 2.0 moles of sodium periodate after 30 minutes, 0.92 moles of acid being formed concomitantly. There was no change in the next 30 minutes.

Compound III

Compound III gave galactose and fucose on hydrolysis in *N* H_2SO_4 at 100° C for 3 hours. After reduction with sodium borohydride the product gave galactose and fucitol. Nuclear magnetic resonance spectroscopy

Can. J. Chem. Downloaded from www.nrcresearchpress.com by 210.87.254.42 on 09/05/12
For personal use only.

indicated the presence of uncoupled C-methyl protons at 1.55 p.p.m. similar to the signals found in compounds I and II. Compound III had $[\alpha]_D$ +25° (*c*, 1.0, MeOH) and consumed 0.85, 1.07, 1.14, and 1.26 moles of lead tetraacetate after 2, 5, 10, and 20 minutes, respectively. The derived fucitol derivative had $[\alpha]_D$ +50° (*c*, 1.0, MeOH).

ACKNOWLEDGMENTS

The authors wish to thank Mrs. S. F. Hector and Mr. N. Gardner for technical assistance. Thanks are due to Mr. M. Mazurek and Mr. W. C. Haid for carrying out carbon and hydrogen analyses, n.m.r. determinations, and the molecular weight measurements.

1. P. A. J. Gorin and J. F. T. Spencer. Can. J. Chem. **39**, 2274 (1961).
2. A. J. Charlson and A. S. Perlin. Can. J. Chem. **34**, 1200 (1956).
3. J. H. Sloneker and D. G. Orentas. Can. J. Chem. **40**, 2188 (1962).
4. S. Hirase. Bull. Chem. Soc. Japan **30**, 68, 70, 75 (1957).
5. L. Hough, J. K. N. Jones, and W. H. Wadman. J. Chem. Soc. 1702 (1950).
6. S. M. Partridge. Nature, **158**, 270 (1946).

Received December 9, 1963.
Prairie Regional Laboratory,
National Research Council,
Saskatoon, Saskatchewan.

Can. J. Chem. Downloaded from www.nrcresearchpress.com by 210.87.254.42 on 09/05/12
For personal use only.

REACTION OF PERFLUOROALKYL RADICALS WITH MOLECULAR HYDROGEN[1]

K. O. Kutschke

A certain ambiguity exists in the interpretation of data obtained in studies of reactions of the type $R + H_2 \rightarrow RH + H$ (and analogous reactions with D_2 and HD) in which R is some free radical. The discussion below is developed with those systems in mind in which R is a perfluoroalkyl radical. The ambiguity arises because it has not been possible to specify precisely the fate of the atom formed in the reaction.

In most studies the photolysis of the appropriate perfluoroketone was used as the radical source (R = CF_3, ((1), see also (2)); R = C_2F_5, (3); R = C_3F_7, (4)). Recently an investigation was made of the reaction, with R = C_2F_5 and C_3F_7, in which the radicals were generated by the photolysis of the corresponding aldehyde, RCHO (5). Values of the Arrhenius parameters obtained from the different studies involving the two radical sources are closely similar. However, Pritchard and Foote (5)[2] present evidence which indicates that the atoms disappear predominantly by reaction with aldehyde in their systems. Insofar as this evidence of a unique fate for atoms in the aldehyde systems is valid, the agreement between the results from the aldehyde and ketone systems indicates that the atoms enter only one reaction in the ketone system as well. The basis for this statement is given here; the argument is developed for the reaction $R + H_2$.

The mechanism appropriate to the ketone systems is given below. All combination reactions are written to show their dependence on pressure since the lifetime of the excited state will be considered later. In the mechanism, A represents a molecule of the radical source.

[1]*Issued as N.R.C. No. 7849.*
[2]*I am indebted to Dr. Pritchard for a prepublication copy of this work and for useful correspondence in connection with it.*

indicated the presence of uncoupled C-methyl protons at 1.55 p.p.m. similar to the signals found in compounds I and II. Compound III had $[\alpha]_D$ +25° (*c*, 1.0, MeOH) and consumed 0.85, 1.07, 1.14, and 1.26 moles of lead tetraacetate after 2, 5, 10, and 20 minutes, respectively. The derived fucitol derivative had $[\alpha]_D$ +50° (*c*, 1.0, MeOH).

ACKNOWLEDGMENTS

The authors wish to thank Mrs. S. F. Hector and Mr. N. Gardner for technical assistance. Thanks are due to Mr. M. Mazurek and Mr. W. C. Haid for carrying out carbon and hydrogen analyses, n.m.r. determinations, and the molecular weight measurements.

1. P. A. J. Gorin and J. F. T. Spencer. Can. J. Chem. **39**, 2274 (1961).
2. A. J. Charlson and A. S. Perlin. Can. J. Chem. **34**, 1200 (1956).
3. J. H. Sloneker and D. G. Orentas. Can. J. Chem. **40**, 2188 (1962).
4. S. Hirase. Bull. Chem. Soc. Japan **30**, 68, 70, 75 (1957).
5. L. Hough, J. K. N. Jones, and W. H. Wadman. J. Chem. Soc. 1702 (1950).
6. S. M. Partridge. Nature, **158**, 270 (1946).

Received December 9, 1963.
Prairie Regional Laboratory,
National Research Council,
Saskatoon, Saskatchewan.

Can. J. Chem. Downloaded from www.nrcresearchpress.com by 210.87.254.40 on 09/05/12
For personal use only.

REACTION OF PERFLUOROALKYL RADICALS WITH MOLECULAR HYDROGEN[1]

K. O. Kutschke

A certain ambiguity exists in the interpretation of data obtained in studies of reactions of the type $R + H_2 \rightarrow RH + H$ (and analogous reactions with D_2 and HD) in which R is some free radical. The discussion below is developed with those systems in mind in which R is a perfluoroalkyl radical. The ambiguity arises because it has not been possible to specify precisely the fate of the atom formed in the reaction.

In most studies the photolysis of the appropriate perfluoroketone was used as the radical source (R = CF_3, ((1), see also (2)); R = C_2F_5, (3); R = C_3F_7, (4)). Recently an investigation was made of the reaction, with R = C_2F_5 and C_3F_7, in which the radicals were generated by the photolysis of the corresponding aldehyde, RCHO (5). Values of the Arrhenius parameters obtained from the different studies involving the two radical sources are closely similar. However, Pritchard and Foote (5)[2] present evidence which indicates that the atoms disappear predominantly by reaction with aldehyde in their systems. Insofar as this evidence of a unique fate for atoms in the aldehyde systems is valid, the agreement between the results from the aldehyde and ketone systems indicates that the atoms enter only one reaction in the ketone system as well. The basis for this statement is given here; the argument is developed for the reaction $R + H_2$.

The mechanism appropriate to the ketone systems is given below. All combination reactions are written to show their dependence on pressure since the lifetime of the excited state will be considered later. In the mechanism, A represents a molecule of the radical source.

[1]*Issued as N.R.C. No. 7849.*
[2]*I am indebted to Dr. Pritchard for a prepublication copy of this work and for useful correspondence in connection with it.*

$$R + R \underset{2b}{\overset{2a}{\rightleftharpoons}} R_2^*$$

$$R_2^* + A \xrightarrow{2c} R_2 + A \qquad R + H_2 \xrightarrow{3} RH + H$$

$$R_2^* + H_2 \xrightarrow{2d} R_2 + H_2$$

$$R + H \underset{4b}{\overset{4a}{\rightleftharpoons}} RH^* \qquad H + H \underset{5b}{\overset{5a}{\rightleftharpoons}} H_2^*$$

$$RH^* + A \xrightarrow{4c} RH + A \qquad H_2^* + A \xrightarrow{5c} H_2 + A$$

$$RH^* + H_2 \xrightarrow{4d} RH + H_2 \qquad H_2^* + H_2 \xrightarrow{5d} 2H_2$$

Deactivation by product species has been neglected in view of the low conversions usually employed. Combination on surfaces has also been neglected because the total pressures usually used have been relatively high. Finally, the alternative mechanism for combination (e.g. $H + M \rightleftharpoons HM^* \xrightarrow{H} H_2 + M$) has not been included; the application of such a mechanism leads to intractable algebraic relations.

If the mechanism describes completely the disappearance of R radicals and H atoms, the steady state treatment leads to [i] as the expression for the measured quantity $\rho \equiv R_{RH}/R_2^{\frac{1}{2}}[H_2]$ in which R_X is the rate of formation of the product X.

$$\rho = (k_3/k_{2a}^{\frac{1}{2}}\beta_2^{\frac{1}{2}})(2+2r)/(1+2r) \qquad [i]$$

Here $r = k_{5a}\beta_5[H]/k_{4a}\beta_4[R]$ and $\beta_n = (k_{nc}[A]+k_{nd}[H_2])/(k_{nb}+k_{nc}[A]+k_{nd}[H_2])$, the fraction of excited molecules formed in reaction [na] which suffer deactivation for the conditions used. Usually those conditions are such that the sequence [2] is in its high pressure region so that β_2 is unity and k_{2a} is replaced by k_2. Depending on the magnitude of $2r$ relative to the numerical constants, the correction factor in [i], i.e. $(2+2r)/(1+2r)$, tends to limiting values of two or unity. Usually it has been assumed that one or the other limit is valid over the whole range of temperature.

The correction factor can be independent of temperature if one of the following requirements is met (1). The disappearance of H atoms for all conditions is represented adequately by one of the sequences [4] and [5] (2). The temperature coefficient of r is zero; such a fortuitous cancellation of the temperature coefficient of [H]/[R] with that of $k_{5a}/\beta_5/k_{4a}/\beta_4$ is neglected.

If both sequences [4] and [5] should be included, it is anticipated that the correction factor varies with temperature. Since R_{RH}/R_{R_2} increases with temperature, it is expected that [H]/[R] will show a similar dependence so that the correction factor tends to 2 at low values of temperature (and for low $[H_2]$ and high I_a at a given temperature) and to unity for the opposite conditions. Thus, if both [4] and [5] are included, the temperature coefficient of ρ leads to an activation energy difference which is less than $E_3-\frac{1}{2}E_2$. It is difficult to assess the magnitude of the error in a real system. The maximum effect is obtained if the correction factor changes from 2 to unity over the temperature range studied; if the limits of that range are 300° and 450° K, the error is 1.4 kcal/mole.

When aldehydes are used as the source of free radicals, reaction [6] must be considered as well.

$$R + RCHO \rightarrow RH + RCO \qquad [6]$$

Can. J. Chem. Downloaded from www.nrcresearchpress.com by 210.87.254.40 on 09/05/12
For personal use only.

For this mechanism the correction factor contains a third additive term, $k_6[A]/k_{4a}\beta_4[R]$, in both the numerator and the denominator. If, as Pritchard and Foote suggest (5), [6] is the predominant fate of H atoms for all conditions, the correction factor cancels to unity and the temperature coefficient of ρ yields $E_3-\frac{1}{2}E_2$ unambiguously. Because of the relative smaller amount of R_2 formed in the aldehyde system, the value of $E_3-\frac{1}{2}E_2$ derived is possibly less precise than that obtained from ketone studies. On the other hand the agreement is quite good as shown below.

Reaction:	$C_2F_5 + H_2$		$C_3F_7 + H_2$		$C_3F_7 + D_2$	
System:	Ald. (5)	Ket. (3)	Ald. (5)	Ket. (4)	Ald. (5)	Ket. (4)
$E_3-\frac{1}{2}E_2$, kcal/mole	12.4	11.9	12.1	12.3	14.0	13.8
$A_3/A_2^{\frac{1}{2}}$, $(\text{mole/ml})^{\frac{1}{2}}$ $\text{sec}^{-\frac{1}{2}} \times 10^{-5}$	15.9	5.25	7.2	4.37	9.6	6.01

Values cited for the ketone systems have been calculated with the assumption that the correction factor is 2 and is independent of temperature as was done in the original publications. This agreement in the determinations of $E_3-\frac{1}{2}E_2$, especially for C_3F_7 reactions, is, in itself, indicative that one of the sequences [4] and [5] predominates in the ketone systems.

Unfortunately it is doubtful whether the data are sufficiently precise to permit a reliable decision about which of the limiting values of the correction factor should be used in the ketone systems. A comparison of the apparent values of $A_3/A_2^{\frac{1}{2}}$ from the two systems suggests that the correction factor should be unity, i.e. that sequence [5] predominates over [4] in the ketone systems, but the uncertainties are such as to inspire little confidence in this conclusion. The same conclusion was reached by Ayscough and Polanyi (1) in an experimental test involving the attack of CF_3 on an equilibrium mixture of the isotopes of hydrogen.

On the other hand, Miller and Steacie (4) gave theoretical reasons which suggested that [4] predominates over [5]. A rather more quantitative basis is now available for this argument in view of recent data (6)[3] which permits a calculation of the rate constant for the dissociation of CH_3D^* (formed from $CH_3 + D$); the value at room temperature is of the order $10^9\ \text{sec}^{-1}$. If RH^* in the present systems is assumed to have a similarly long life so that k_{4b} is also of this order, and if k_{4c} is taken near $10^{13}\ (\text{mole/ml})^{-1}\ \text{sec}^{-1}$, i.e. about 10% of the collisions are effective in deactivation, and if H_2 is assumed to have negligible deactivation efficiency, then, for the conditions used, β_4 is close to unity. However, it might be expected that k_{5b} would be closer to $10^{13}\ \text{sec}^{-1}$ so that, with similar rates of deactivation, β_5 is of the order 10^{-4}. Since there is no a priori reason to expect k_{4a} to differ greatly from k_{5a}, the long life of RH^* requires that [H]/[R] approach 10^4 if the $2r$ term in the correction factor of [i] is to compare in magnitude to the numerical constants. Such a large ratio of concentrations is most improbable in these systems. Thus the theoretical argument favors the predominance of [4] while the available experimental evidence suggests that [5] is the more important reaction consuming H atoms.

This disagreement between theoretical expectation and experiment might be resolved if the alternative mechanism for the combination of H atoms were involved. Experimental work to test this possibility has been undertaken.

[3]*I am indebted to Dr. F. W. Lampe for a prepublication copy of this work.*

Can. J. Chem. Downloaded from www.nrcresearchpress.com by 210.87.254.40 on 09/05/12
For personal use only.

1. P. B. AYSCOUGH and J. C. POLANYI. Trans. Faraday Soc. **52**, 960 (1956).
2. G. O. PRITCHARD, H. O. PRITCHARD, H. I. SCHIFF, and A. F. TROTMAN-DICKINSON. Trans. Faraday Soc. **52**, 849 (1956).
3. S. J. W. PRICE and K. O. KUTSCHKE. Can. J. Chem. **38**, 2128 (1960).
4. G. H. MILLER and E. W. R. STEACIE. J. Am. Chem. Soc. **80**, 6486 (1958).
5. G. O. PRITCHARD and J. K. FOOTE. J. Phys. Chem. In press.
6. A. MASCHKE and F. W. LAMPE. J. Phys. Chem. In press. (Mentioned briefly in connection with the presentation of Paper 107, Division of Physical Chemistry, 145th A.C.S. meeting, September, 1963.)

RECEIVED DECEMBER 13, 1963.
DIVISION OF PURE CHEMISTRY,
NATIONAL RESEARCH COUNCIL,
OTTAWA, CANADA.

Can. J. Chem. Downloaded from www.nrcresearchpress.com by 210.87.254.40 on 09/05/12
For personal use only.

AN IMPROVED METHOD FOR DECARBOXYLATING INDOLE-2-CARBOXYLIC ACIDS AND ITS APPLICATION IN THE SYNTHESIS OF 7-AMINO-DL-TRYPTOPHAN

GIOVANNI CASINI* AND LEON GOODMAN†

A projected synthesis of 7-bis(2-chloroethyl)amino-DL-tryptophan in these laboratories required the preparation of large quantities of 7-nitroindole (I). The general procedure of Parmerter *et al.* (1) for the preparation of I was very convenient except for the final step, the decarboxylation of 7-nitroindole-2-carboxylic acid in boiling quinoline. When

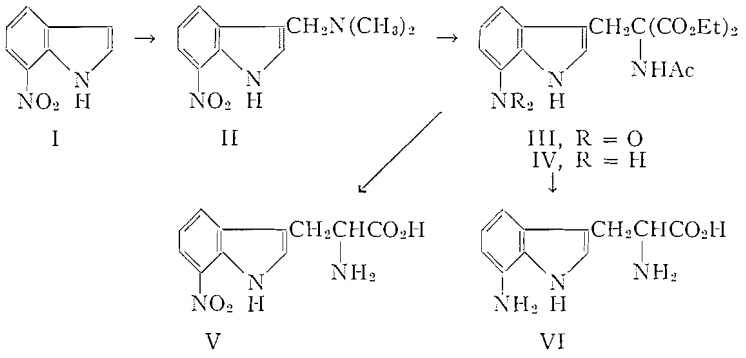

the decarboxylation was effected in refluxing N,N-dimethylacetamide employing as catalyst the copper salt of the acid, prepared by the method of Piers and Brown (2), the yield of I was higher and the isolation was much simpler than in the conventional quinoline procedure. The dimethylacetamide method of decarboxylation should be generally useful in the preparation of substituted indoles.

While this work was in progress, Da Settimo (3) and Hiremath and Siddappa (4) reported the synthesis of 7-nitro-DL-tryptophan (V), utilizing the same intermediates, the gramine (II) and the acetamidomalonate ester (III), that were used to prepare VI. Catalytic reduction of the diester (III) afforded a good yield of the crystalline amino-ester (IV), which was hydrolyzed directly to 7-amino-DL-tryptophan (VI) isolated as

**Holder of a NATO fellowship during 1962. Permanent address: Istituto di Chimica Farmaceutica e Tossicologica, Universita di Roma, Italy.*
†Author to whom reprint requests should be addressed.

1. P. B. AYSCOUGH and J. C. POLANYI. Trans. Faraday Soc. **52**, 960 (1956).
2. G. O. PRITCHARD, H. O. PRITCHARD, H. I. SCHIFF, and A. F. TROTMAN-DICKINSON. Trans. Faraday Soc. **52**, 849 (1956).
3. S. J. W. PRICE and K. O. KUTSCHKE. Can. J. Chem. **38**, 2128 (1960).
4. G. H. MILLER and E. W. R. STEACIE. J. Am. Chem. Soc. **80**, 6486 (1958).
5. G. O. PRITCHARD and J. K. FOOTE. J. Phys. Chem. In press.
6. A. MASCHKE and F. W. LAMPE. J. Phys. Chem. In press. (Mentioned briefly in connection with the presentation of Paper 107, Division of Physical Chemistry, 145th A.C.S. meeting, September, 1963.)

RECEIVED DECEMBER 13, 1963.
DIVISION OF PURE CHEMISTRY,
NATIONAL RESEARCH COUNCIL,
OTTAWA, CANADA.

Can. J. Chem. Downloaded from www.nrcresearchpress.com by 210.87.254.42 on 09/05/12
For personal use only.

AN IMPROVED METHOD FOR DECARBOXYLATING INDOLE-2-CARBOXYLIC ACIDS AND ITS APPLICATION IN THE SYNTHESIS OF 7-AMINO-DL-TRYPTOPHAN

GIOVANNI CASINI* AND LEON GOODMAN†

A projected synthesis of 7-bis(2-chloroethyl)amino-DL-tryptophan in these laboratories required the preparation of large quantities of 7-nitroindole (I). The general procedure of Parmerter *et al.* (1) for the preparation of I was very convenient except for the final step, the decarboxylation of 7-nitroindole-2-carboxylic acid in boiling quinoline. When

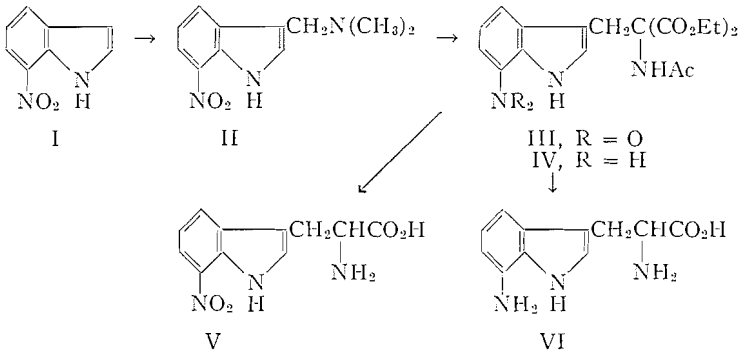

the decarboxylation was effected in refluxing N,N-dimethylacetamide employing as catalyst the copper salt of the acid, prepared by the method of Piers and Brown (2), the yield of I was higher and the isolation was much simpler than in the conventional quinoline procedure. The dimethylacetamide method of decarboxylation should be generally useful in the preparation of substituted indoles.

While this work was in progress, Da Settimo (3) and Hiremath and Siddappa (4) reported the synthesis of 7-nitro-DL-tryptophan (V), utilizing the same intermediates, the gramine (II) and the acetamidomalonate ester (III), that were used to prepare VI. Catalytic reduction of the diester (III) afforded a good yield of the crystalline amino-ester (IV), which was hydrolyzed directly to 7-amino-DL-tryptophan (VI) isolated as

**Holder of a NATO fellowship during 1962. Permanent address: Istituto di Chimica Farmaceutica e Tossicologica, Universita di Roma, Italy.*
†Author to whom reprint requests should be addressed.

the hydrated dihydrochloride. Alternatively, 7-nitro-DL-tryptophan (V) (3) could be hydrogenated catalytically to the free base (VI), which was obtained as a crystalline solid and also converted to the dihydrochloride.

EXPERIMENTAL

7-Nitroindole (I)

A mixture of 4.0 g of 7-nitroindole-2-carboxylic acid (1), recrystallized from ethanol and *completely free* of inorganic salts, 0.4 g of the copper salt of 7-nitroindole-2-carboxylic acid, prepared by the method of Piers and Brown (2), and 20 ml of N,N-dimethylacetamide was refluxed, under nitrogen, until carbon dioxide evolution ceased (about 5 hours), then was poured onto 200 g of cracked ice. The yellow-green precipitate was washed and dried, then crystallized from 60 ml of boiling petroleum ether (60–110°) using Norit A, to afford 2.8 g (89%) of I, m.p. 96–97° (lit. (1) gives m.p. 95–96°).

7-Nitrogramine (II)

7-Nitrogramine (II) was prepared essentially as described by Da Settimo (3) although different physical constants were obtained. Thus, 7.0 g of 7-nitroindole (I) gave 11.2 g of crude II, m.p. 47–59°. Recrystallization of material by dissolving in 1 volume of hot methanol and adding 4 volumes of water gave the hydrate of II, m.p. 55–60°. Anal. Calc. for $C_{11}H_{13}N_3O_2.H_2O$: C, 55.7; H, 6.37; N, 17.7. Found: C, 55.7; H, 6.31; N, 17.9.

Alternatively, recrystallization from boiling toluene with azeotropic removal of any water gave the anhydrous compound, m.p. 91–92° (lit. (3, 4) give m.p. 69–71° and 79–80°, respectively). Anal. Calc. for $C_{11}H_{13}N_3O_2$: C, 60.3; H, 5.98; N, 19.2. Found: C, 60.4; H, 6.16; N, 18.8.

Ethyl α-Acetamido-α-carbethoxy-β-(7-amino-3-indolyl)propionate (IV)

A suspension of 3.0 g of ethyl α-acetamido-α-carbethoxy-β-(7-nitro-3-indolyl)propionate (III), prepared using the same procedure described by Da Settimo (3), 0.3 g of 5% palladium-on-charcoal, and 150 ml of absolute ethanol was treated with hydrogen at 25 p.s.i. and room temperature until the hydrogen uptake ceased (about 2 hours). The solution was filtered rapidly and the filtrate concentrated *in vacuo* to about 30 ml. The solution, after being chilled and scratched, deposited 2.3 g (82%) of crystalline product. The mother liquors were concentrated and treated with water, giving a second crop of crystals which raised the total crude yield to 95%. The analytical sample was recrystallized from ethanol and had m.p. 182–183°; $\lambda_{max\,(\mu)}^{Nujol}$ 2.90, 2.95, 3.10 (NH), 5.73 (ester C=O), 6.02 (amide C=O). Anal. Calc. for $C_{13}H_{23}N_3O_5$: C, 59.8; H, 6.42; N, 11.6. Found: C, 60.1; H, 6.62; N, 11.5.

7-Amino-DL-tryptophan (VI) and the Dihydrochloride

Method A

A stirred mixture of 0.13 g of 7-nitro-DL-tryptophan (3), 0.01 g of platinum oxide, and 50 ml of water was treated with hydrogen at atmospheric pressure until the theoretical amount of gas was absorbed (about 1 hour). The warm (50°) mixture was filtered rapidly and the filtrate was evaporated *in vacuo*, leaving a grey, crystalline powder which was dissolved in 20 ml of hot 60% aqueous ethanol. The solution was cooled, filtered through a thin layer of Norit A, and the filtrate concentrated *in vacuo*, affording 0.07 g (61%) of white crystals. The analytical sample, which slowly decomposed above 250°, was obtained by recrystallization from 3 ml of hot water; $\lambda_{max\,(\mu)}^{Nujol}$ 2.97 (NH), 3.6–4.0 and 4.75 ($NH_3\oplus$), 5.99 (NH_2), 7.04 ($CO_2\ominus$). Its paper chromatographic behavior in the isopropanol – 2 *N* hydrochloric acid system was identical with that of the dihydrochloride (see below). Anal. Calc. for $C_{11}H_{13}N_3O_2$: C, 60.3; H, 6.00; N, 19.2. Found: C, 59.8; H, 6.19; N, 18.9.

The dihydrochloride was obtained from the free base (VI) by dissolving it in a small volume of conc. hydrochloric acid. The chilled solution deposited crystals which were recrystallized from methanol–ether, affording a solid which decomposed slowly above 200°; $\lambda_{max\,(\mu)}^{Nujol}$ 3.08 (NH), 3.7–4.0 ($NH_3\oplus$), 5.69 (carboxyl C=O). The compound was homogeneous on paper chromatography (Whatman No. 1) in isopropyl alcohol – 2 *N* hydrochloric acid (65:35) with R_f 0.51, detected both by ninhydrin spray and ultraviolet examination. Anal. Calc. for $C_{11}H_{15}Cl_2N_3O_2.\frac{1}{4}H_2O$: C, 44.5; H, 5.27; Cl, 23.9; N, 14.2. Found: C, 44.7; H, 5.63; Cl, 24.0; N, 14.0.

Method B

A solution of 0.50 g of the aminoester (IV) in 4.0 ml of conc. hydrochloric acid was heated at reflux under nitrogen for 4 hours, then chilled. A crystalline solid, 0.26 g (65%), was collected and washed with acetone. The product was crystallized three times from methanol and ether, affording the analytical sample, which was identical with dihydrochloride prepared by method A (see above) according to infrared spectral and paper chromatographic comparison.

Can. J. Chem. Downloaded from www.nrcresearchpress.com by 210.87.254.42 on 09/05/12
For personal use only.

ACKNOWLEDGMENTS

This work was carried out under the auspices of the Cancer Chemotherapy National Service Center, National Cancer Institute, National Institutes of Health, Public Health Service, Contract No. SA-43-ph-1892. The opinions expressed in this paper are those of the authors and not necessarily those of the Cancer Chemotherapy National Service Center.

The authors are indebted to Dr. Peter Lim for infrared interpretations and to his staff for paper chromatography. They also wish to thank Mr. O. P. Crews and his staff for the large-scale preparation of certain intermediates.

1. S. M. Parmerter, A. G. Cook, and W. B. Dixon. J. Am. Chem. Soc. **80**, 4621 (1958).
2. E. Piers and R. K. Brown. Can. J. Chem. **40**, 561 (1961).
3. A. Da Settimo. Ann. Chim. Rome, **52**, 17 (1962).
4. S. P. Hiremath and S. Siddappa. J. Karnatak Univ. **6**, 1 (1962); Chem. Abstr. **59**, 8855 (1963).

Received December 12, 1963.
Life Sciences Research,
Stanford Research Institute,
Menlo Park, California.

Can. J. Chem. Downloaded from www.nrcresearchpress.com by 210.87.254.42 on 09/05/12
For personal use only.

THE INITIAL RATE OF DECOMPOSITION OF WATER VAPOR BY AN ELECTRICAL DISCHARGE[1]

S. S. Barton, R. A. Jones, and D. E. Thyne[2]

Gill and Townsend (1), in a mathematical analysis, based on classical kinetic theory, of the motions of free electrons in a high-frequency gas discharge, developed an expression which predicts that the transfer of energy from the field to the gas molecules will have a maximum value when the frequency of the electrical field (ν) is equal to the kinetic theory frequency of elastic gas–molecule collisions (f).

If the density of free electrons remains constant with pressure for a high-frequency discharge in water vapor and if dissociative excitation of water molecules is the main consequence of the electron–molecule collisions while no further destruction of water occurs during subsequent reactions then the rate of decomposition should exhibit a maximum at the pressure where $\nu = f$.

In this work, $\nu < f$, except at very low pressures, and hence the maximum in the rate dependence on pressure may not be observed. However, the rate of decomposition should decrease with increasing pressure.

EXPERIMENTAL

The reaction cell was a 250-ml rectangular volumetric flask upon opposite sides of which were deposited two rectangular (4 × 6 cm) indium electrodes. The distance between the electrodes was approximately 5.7 cm. One electrode was grounded and the other connected to a Tesla coil (standard leak tester). The power

[1]*Based on a paper presented at the 45th Canadian Chemical Conference and Exhibition, Edmonton, Alberta, May 1962.*
[2]*Present address: c/o Department of Chemistry, University of Ottawa, Ottawa, Canada.*

ACKNOWLEDGMENTS

This work was carried out under the auspices of the Cancer Chemotherapy National Service Center, National Cancer Institute, National Institutes of Health, Public Health Service, Contract No. SA-43-ph-1892. The opinions expressed in this paper are those of the authors and not necessarily those of the Cancer Chemotherapy National Service Center.

The authors are indebted to Dr. Peter Lim for infrared interpretations and to his staff for paper chromatography. They also wish to thank Mr. O. P. Crews and his staff for the large-scale preparation of certain intermediates.

1. S. M. Parmerter, A. G. Cook, and W. B. Dixon. J. Am. Chem. Soc. **80**, 4621 (1958).
2. E. Piers and R. K. Brown. Can. J. Chem. **40**, 561 (1961).
3. A. Da Settimo. Ann. Chim. Rome, **52**, 17 (1962).
4. S. P. Hiremath and S. Siddappa. J. Karnatak Univ. **6**, 1 (1962); Chem. Abstr. **59**, 8855 (1963).

Received December 12, 1963.
Life Sciences Research,
Stanford Research Institute,
Menlo Park, California.

THE INITIAL RATE OF DECOMPOSITION OF WATER VAPOR BY AN ELECTRICAL DISCHARGE[1]

S. S. Barton, R. A. Jones, and D. E. Thyne[2]

Gill and Townsend (1), in a mathematical analysis, based on classical kinetic theory, of the motions of free electrons in a high-frequency gas discharge, developed an expression which predicts that the transfer of energy from the field to the gas molecules will have a maximum value when the frequency of the electrical field (ν) is equal to the kinetic theory frequency of elastic gas–molecule collisions (f).

If the density of free electrons remains constant with pressure for a high-frequency discharge in water vapor and if dissociative excitation of water molecules is the main consequence of the electron–molecule collisions while no further destruction of water occurs during subsequent reactions then the rate of decomposition should exhibit a maximum at the pressure where $\nu = f$.

In this work, $\nu < f$, except at very low pressures, and hence the maximum in the rate dependence on pressure may not be observed. However, the rate of decomposition should decrease with increasing pressure.

EXPERIMENTAL

The reaction cell was a 250-ml rectangular volumetric flask upon opposite sides of which were deposited two rectangular (4 × 6 cm) indium electrodes. The distance between the electrodes was approximately 5.7 cm. One electrode was grounded and the other connected to a Tesla coil (standard leak tester). The power

[1]*Based on a paper presented at the 45th Canadian Chemical Conference and Exhibition, Edmonton, Alberta, May 1962.*
[2]*Present address: c/o Department of Chemistry, University of Ottawa, Ottawa, Canada.*

Can. J. Chem. Downloaded from www.nrcresearchpress.com by 210.87.254.105 on 09/05/12
For personal use only.

dissipated in the Tesla coil and the discharge was adjusted by the spark gap control and was measured with a voltmeter and an ammeter in the primary of the Tesla.

The frequency range over which the Tesla coil operated was determined with a General Radio Precision Wavemeter. The range extended from 200 kc to 800 kc with a maximum output at 500 kc.

The pressure rate of decomposition was recorded on a recording potentiometer (chart speed 8 in./minute) suitably connected to record the off-balance of a Consolidated Electrodynamics Corp. Micromanometer.

Water vapor from an outgassed sample of distilled water was allowed to enter the evacuated cell until a suitable pressure had been attained. The cell and the micromanometer were then isolated from the rest of the system and when pressure equilibrium had been reached the Tesla coil was turned on for 10–15 seconds. Initial rates of reaction were obtained from the slope of the initial straight-line portion of the recorded pressure vs. time curve. This straight-line portion extended over about a 0.1- to 0.5-fold pressure increase. When the discharge was allowed to continue for periods of up to 5 minutes, the pressure continued to rise past the 1.5-fold increase expected from the stoichiometry, $2H_2O = 2H_2 + O_2$. Presumably this excess pressure was due to absorbed water which left the surface of the cell as the reaction proceeded.

RESULTS AND DISCUSSION

Experiments were carried out at two levels of power consumption by the Tesla coil and discharge; 5.8 and 9.2 watts respectively. The pressure rates, dp/dt, were found to be proportional to the total power and in Fig. 1, which shows $2\,dp/dt$ vs. p_0 data from

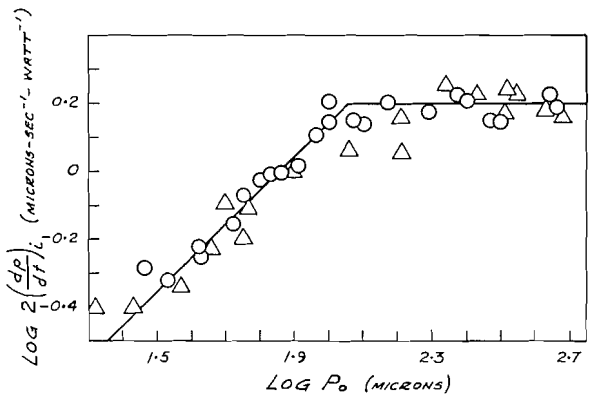

FIG. 1. Log–log plot of p_0 vs. $2\,dp/dt$ per watt data.

both sets of experiments in a log–log plot, the rates are expressed in microns sec^{-1} $watt^{-1}$. The initial pressure rate of reaction increases with increasing initial pressure and the reaction appears to be second order below $p_0 = 100$ microns. Above 100 microns the reaction becomes zero order.

If the Gill–Townsend mechanism is valid for this case and if the assumptions noted above hold then the rate should decrease with increasing pressure from a maximum value at about 2.4 μ, where $f = 4\times10^5$ sec^{-1}. It is not possible from the data to decide whether failure to follow this course can be ascribed to an increase in free-electron density with pressure or to decomposition reactions following the primary dissociation of water.

1. E. W. B. GILL and J. S. TOWNSEND. Phil. Mag. **26**, 290 (1938).

RECEIVED DECEMBER 10, 1963.
DEPARTMENT OF CHEMISTRY,
ROYAL MILITARY COLLEGE OF CANADA,
KINGSTON, ONTARIO.

Can. J. Chem. Downloaded from www.nrcresearchpress.com by 210.87.254.105 on 09/05/12
For personal use only.

AN ESTIMATE OF THE HYDRONIUM ION ACTIVITY IN CONCENTRATED ACIDS

KEITH YATES

Deno and Spink (1) have suggested that H_R' (2) is the simplest acidity function since in equilibria of the type

$$[1] \qquad RH_2^+ \rightleftharpoons RH + H^+ \qquad K_{RH_2^+} = a_{RH} \cdot a_{H^+}/a_{RH_2^+}$$

where RH is a hydrocarbon base, for example a diarylolefin, and RH_2^+ is a carbonium ion, the ratio $f_{RH_2^+}/f_{RH}$ should be nearly invariant with acid concentration. Thus

$$H_R' = pK_{RH_2^+} - \log RH_2^+/RH = -\log a_{H^+} f_{RH}/f_{RH_2^+}$$

should be approximately equal to $-\log a_{H^+}$. The assumption about the invariance of $f_{RH_2^+}/f_{RH}$ is based on the fact that the hydrocarbons and their resulting carbonium ions are of practically the same size, that neither will strongly hydrogen bond to solvent, and that extensive charge delocalization in the large organic cations would be expected to minimize differences in electrostatic effects on $f_{RH_2^+}$ and f_{RH}. There is experimental evidence to support such a view (3) (see also last paper in (2)). However, in equilibrium (1) the conjugate acid RH_2^+ must transfer its proton to at least one water molecule, therefore $K_{RH_2^+}$ should involve some power of the water activity if it is to be considered as an equilibrium constant in any but a purely operational sense. From estimated values of the proton affinity of water (4) and from spectroscopic evidence (5) H_3O^+ can be regarded as a well-defined species in solution. Although other water molecules are undoubtedly fairly firmly held to H_3O^+ (6) the process $H^+ + H_2O \rightarrow H_3O^+$ involves formation of a very strong covalent bond (180–200 kcal mole^{-1}), whereas subsequent waters are attached through hydrogen bonds. Thus to a first approximation the olefin–carbonium ion type of equilibrium can be written in terms of H_3O^+ as a *formal* species,

$$RH_2^+ + H_2O \rightleftharpoons RH + H_3O^+.$$

In this case $K_{RH_2^+} = a_{RH} \cdot a_{H_3O^+}/a_{RH_2^+} \cdot a_{H_2O}$ and $H_R' = -\log a_{H_3O^+} f_{RH}/a_{H_2O} f_{RH_2^+}$. Thus $\log a_{H_3O^+} = -H_R' + \log a_{H_2O} + \log f_{RH_2^+}/f_{RH}$ and if the last term is nearly invariant with acid concentration a function H_R^* can be defined such that $H_R^* = H_R' - \log a_{H_2O} \approx -\log a_{H_3O^+}$. Values of H_R^* have been calculated for sulphuric, perchloric, and nitric acids in the range 0–70% acid and are shown in Table I. If calculations of H_R^* are extended

TABLE I

Calculated values for H_R^* for sulphuric, perchloric, and nitric acids

% acid (w/w)	$-H_R^*(H_2SO_4)$	$\log a_{H^+}/f_{TEA^+}$[a]	$-H_R^*(HClO_4)$	$-H_R^*(HNO_3)$
5	0.05	0.06[b]	0.22	0.46
10	0.68	0.54	1.00	1.24
20	1.80	1.61	2.33	2.49
30	2.97	2.86	3.56	3.58
40	4.30	4.23	5.07	4.65
50	5.69	5.76	6.88	5.69
60	7.34	7.39	9.09	—
70	8.81	9.43	—	—

[a]Taken from Ref. (7).
[b]Calculated from data in Ref. (7).

Can. J. Chem. Downloaded from www.nrcresearchpress.com by 210.87.254.40 on 09/05/12
For personal use only.

beyond 70% sulphuric acid it is interesting to note that H_R* reaches a maximum at almost exactly the equimolar composition of H_2SO_4–H_2O, where the concentration of H_3O^+ must also reach a maximum. This is shown in Fig. 2. The experimentally observed rise in indicator acidity above this region may be attributed to a continued large increase in $f_{H_3O^+}$, but can also be reasonably explained as being due to the drastic reduction in "free" water available and to the involvement of less basic species such as HSO_4^-, H_2SO_4 in the indicator equilibria.

To test the variance of $\log f_{RH_2^+}/f_{RH}$, the functions H_0 and H_R' can be combined to give

$$H_R' - H_0 - \log f_{BH^+}/f_B = \log f_{RH_2^+}/f_{RH}.$$

Experimental values of H_R' and H_0 are available and the recent work of Boyd (7) can be used to estimate $\log f_{BH^+}/f_B$ for the Hammett indicators. Hence estimates of $\log f_{RH_2^+}/f_{RH}$ can be made. Since Boyd's ionic activity coefficients are referred back to TEA^+ as standard ion, the estimated values of $f_{RH_2^+}$ will also be based on this standard. The variation of $\log f_{RH_2^+}/f_{RH}$ with acid concentration is shown in Fig. 1 with $\log f_{BH^+}/f_B$ for comparison.

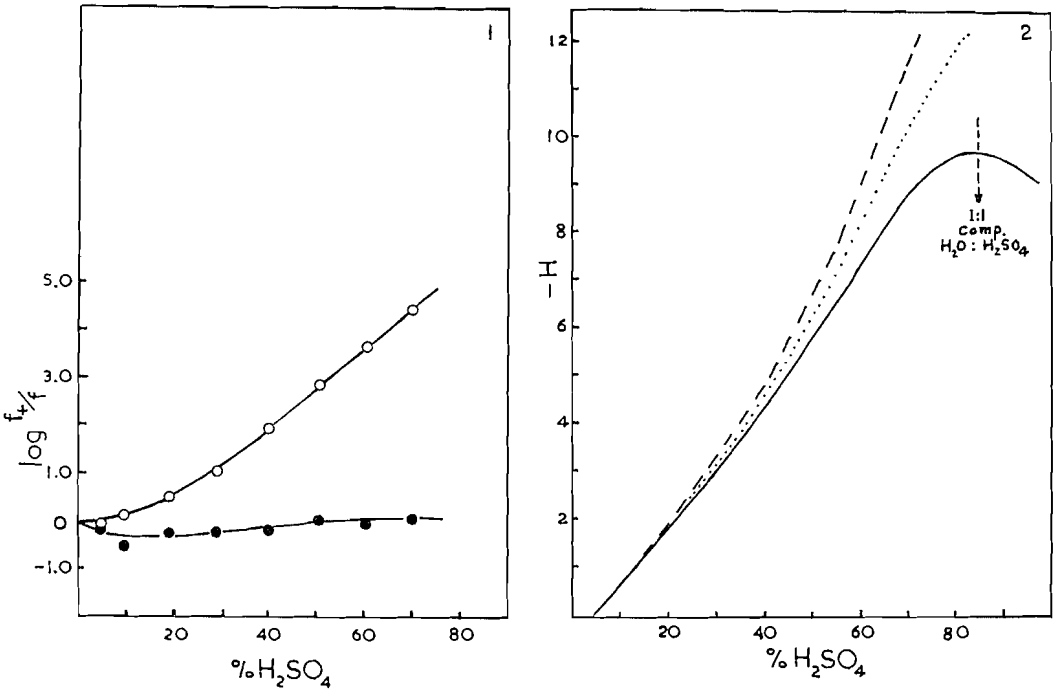

FIG. 1. Variation of activity coefficient ratios with acid concentration. Open circles, $\log f_{BH^+}/f_B$. Solid circles, $\log f_{RH_2^+}/f_{RH}$.

FIG. 2. Variation of hydrocarbon type acidity functions with concentration. – – – H_R, ... H_R', —— H_R*.

It can be seen that $\log f_{RH_2^+}/f_{RH}$ shows little change with concentration compared to the variation of $\log f_{BH^+}/f_B$. This provides support for Deno and Spink's suggestion but does not establish the invariance of $\log f_{RH_2^+}/f_{RH}$ since $f_{RH_2^+}$ is based on the reference f_{TEA^+}, which itself might show considerable variation with acidity. However, Boyd's study (7) of the effect of N-substitution on the activity coefficient of anilinium ion shows that the variation of $\log f_{BH^+}$ decreases with the number of N-alkyl groups. Therefore it seems reasonable that f_{TEA^+} might be expected to show little variation, presumably because of

Can. J. Chem. Downloaded from www.nrcresearchpress.com by 210.87.254.40 on 09/05/12
For personal use only.

the shielding of the cationic charge on nitrogen by four tetrahedrally arranged ethyl groups.

It is therefore proposed that H_R^* can be used as an approximate measure of the hydronium ion activity in concentrated mineral acids. This function can be obtained for any acid for which H_R data and water activities are available, without the difficulties inherent in attempting to evaluate appropriate solute activity coefficients.

It is of interest to compare the H_R^* values in sulphuric acid with Boyd's values of log a_{H^+}/f_{TEA^+} (7) which are also shown in Table I. Some divergence is apparent in the high acidity region but the two sets of values agree within 0.19 log unit up to 60% acid. This agreement is surprising in view of the fact that log a_{H^+}/f_{TEA^+} values were derived without any reference to the water activity and must be at least partly fortuitous. It is possible that a more sophisticated treatment involving variable hydration numbers for all species may provide an explanation of this.

CALCULATIONS

Water activities in sulphuric acid at 25° C have been taken from the recent measurements of Giauque and co-workers (8). Average values of the water activity data at 25° C of Pearce and Nelson (9) and of Robinson and Baker (10) have been used for perchloric acid. Since Giauque (11) has criticized the available data for nitric acid at 25° C on the grounds that it does not obey the Duhem–Margules equation, the water activity data of Potier (12) at 0° C and 20° C have been extrapolated to 25° C. Calculations show that these results are in reasonable accord with the Duhem–Margules relation. Values of H_R and hence H_R' have been taken from Deno and co-workers (13). Estimates of log f_{BH^+}/f_B in 0–70% sulphuric have been made by averaging Boyd's (7) results for anilinium, *p*-chloroanilinium, and *p*-nitroanilinium to obtain log f_{BH^+} (relative to log f_{TEA^+}) and by averaging log f_B values for 2,4-dinitro-, 2,4-dichloro-6-nitro-, and 2,6-dichloro-4-nitro-anilines. These six indicators are typical of those which would be used to set up the H_0 scale in the 0–70% acid range. The equilibrium constant $K_{RH_2^+}$ as defined in this paper is only strictly correct if the activity of water is based on the same concentration scale as the activities of the solute species, namely the molarity scale, which is usually employed for indicator equilibria. However, if the water activity in

$$K_{RH_2^+} = a_{RH} \cdot a_{H_3O^+}/a_{RH_2^+} \cdot a_{H_2O}$$

is based on the mole fraction scale, it can be shown (14) that this expression is related to the true equilibrium constant by the relation

$$K^{true}_{RH_2^+} = 55.5 K_{RH_2^+} \cdot \left(\frac{d + 0.001(18\Sigma c_i - \Sigma c_i w_i)}{(\Sigma c_i) d_0} \right)$$

where d = the density of the solution, d_0 = the density of the pure solvent, c_i = molar concentration of the ith species. The summations are over all species present in solution. The factor of 55.5 enters in so that $a_{H_2O} \rightarrow 1$ in dilute solution on the molarity scale. Thus in dilute solution $K^{true}_{RH_2^+} = K_{RH_2^+}$ and in 70% sulphuric acid, assuming complete ionization of H_2SO_4, the above relation gives $K^{true}_{RH_2^+} = (1.31)\ K_{RH_2^+}$. This corresponds to a variation of 0.12 log units in $pK_{RH_2^+}$ over the range 0–70% sulphuric acid. Hence no serious error is introduced by using mole fraction water activities obtained directly from vapor pressure measurements. This is also illustrated by the fact that H_R' values derived from H_R using mole fraction water activities are directly applicable to olefin-carbonium ion equilibria (2).

Can. J. Chem. Downloaded from www.nrcresearchpress.com by 210.87.254.40 on 09/05/12
For personal use only.

ACKNOWLEDGMENTS

The author gratefully acknowledges financial support from the National Research Council of Canada.

1. N. C. DENO and C. H. SPINK. Personal communication.
2. A. J. KRESGE and Y. CHIANG. Proc. Chem. Soc. 81 (1961). N. C. DENO, P. GROVES, J. JARUSZELSKI, and M. LUGASCH. J. Am. Chem. Soc. **82**, 4719 (1960). N. C. DENO, P. GROVES, and G. SAINES. J. Am. Chem. Soc. **81**, 5790 (1959).
3. N. C. DENO and C. PERIZZOLO. J. Am. Chem. Soc. **79**, 1345 (1957). C. H. SPINK. Ph.D. Thesis, Pennsylvania State University, Penn. 1962.
4. J. SHERMAN. Chem. Rev. **11**, 164 (1932). K. FAJANS. Ber. **21**, 709 (1919). F. HUND. Z. Physik, **32**, 1 (1925).
5. M. FALK and P. A. GIGUÈRE. Can. J. Chem. **35**, 1195 (1957).
6. R. P. BELL. The proton in chemistry. Cornell University Press, Ithaca, N.Y. 1959. Chap. VI.
7. R. H. BOYD. J. Am. Chem. Soc. **85**, 1 (1963).
8. W. F. GIAUQUE, E. W. HORNUNG, J. E. KUNZLER, and T. R. RUBIN. J. Am. Chem. Soc. **82**, 62 (1960).
9. J. N. PEARCE and A. F. NELSON. J. Am. Chem. Soc. **55**, 3075 (1933).
10. R. A. ROBINSON and O. J. BAKER. Trans. Proc. Roy. Soc. New Zealand, **76**, 250 (1946).
11. W. R. FORSYTHE and W. F. GIAUQUE. J. Am. Chem. Soc. **64**, (1942).
12. A. POTIER. Ann. Fac. Sci. Univ. Toulouse, **20**, 1 (1956).
13. N. C. DENO, J. J. JARUSZELSKI, and A. SCHRIESHEIM. J. Am. Chem. Soc. **77**, 3044 (1955). N. C. DENO, H. E. BERKHEIMER, W. L. EVANS, and H. J. PETERSON. J. Am. Chem. Soc. **81**, 2344, 6535 (1959).
14. R. A. ROBINSON and R. H. STOKES. Electrolyte solutions. Butterworths, London. 1959. p. 30.

RECEIVED OCTOBER 22, 1963.
DEPARTMENT OF CHEMISTRY,
UNIVERSITY OF TORONTO,
TORONTO, ONTARIO.

Can. J. Chem. Downloaded from www.nrcresearchpress.com by 210.87.254.40 on 09/05/12
For personal use only.

ACID-CATALYZED REACTIONS OF VINYL COMPOUNDS

PART III. 2,7,9,10-TETRAMETHYLANTHRACENE FROM VINYL ACETATE AND TOLUENE

J. M. PEPPER, MARGARET HOWELL, AND B. P. ROBINSON

In previous communications (1, 2), the nature of the products obtained by the aluminum chloride catalyzed reaction of vinyl acetate and benzene was reported. As part of a subsequent, more detailed study of the mechanism of formation of the principal product, namely 9,10-dimethylanthracene, the similar reaction involving vinyl acetate and toluene was investigated. The isolation of 2,7,9,10-tetramethylanthracene rather than the 2,6,9,10-tetramethyl isomer supported a mechanism of formation of the anthracene derivatives which consisted of the initial synthesis of the 1,1-diarylethane followed by ring closure involving incorporation of a two-carbon fragment. Details of this mechanism will appear in a forthcoming publication. This note describes the synthesis and structure proof of the previously unreported 2,7,9,10-tetramethylanthracene.

Chromic acid oxidation of the purified reaction product gave a substance identical with 2,7-dimethylanthraquinone. An Elbs reaction performed upon 2,4,4′-trimethylbenzophenone, obtained from a Friedel–Crafts reaction of *p*-toluoyl chloride with *m*-xylene, afforded a mixture of 2,7-dimethylanthracene and 3,6-dimethylanthrone either of which, when oxidized with chromic acid, gave authentic 2,7-dimethylanthraquinone.

EXPERIMENTAL

Melting points are uncorrected. Infrared spectra were measured using a Perkin–Elmer Model 21 spectrometer with sodium chloride optics.

ACKNOWLEDGMENTS

The author gratefully acknowledges financial support from the National Research Council of Canada.

1. N. C. DENO and C. H. SPINK. Personal communication.
2. A. J. KRESGE and Y. CHIANG. Proc. Chem. Soc. 81 (1961). N. C. DENO, P. GROVES, J. JARUSZELSKI, and M. LUGASCH. J. Am. Chem. Soc. **82**, 4719 (1960). N. C. DENO, P. GROVES, and G. SAINES. J. Am. Chem. Soc. **81**, 5790 (1959).
3. N. C. DENO and C. PERIZZOLO. J. Am. Chem. Soc. **79**, 1345 (1957). C. H. SPINK. Ph.D. Thesis, Pennsylvania State University, Penn. 1962.
4. J. SHERMAN. Chem. Rev. **11**, 164 (1932). K. FAJANS. Ber. **21**, 709 (1919). F. HUND. Z. Physik, **32**, 1 (1925).
5. M. FALK and P. A. GIGUÈRE. Can. J. Chem. **35**, 1195 (1957).
6. R. P. BELL. The proton in chemistry. Cornell University Press, Ithaca, N.Y. 1959. Chap. VI.
7. R. H. BOYD. J. Am. Chem. Soc. **85**, 1 (1963).
8. W. F. GIAUQUE, E. W. HORNUNG, J. E. KUNZLER, and T. R. RUBIN. J. Am. Chem. Soc. **82**, 62 (1960).
9. J. N. PEARCE and A. F. NELSON. J. Am. Chem. Soc. **55**, 3075 (1933).
10. R. A. ROBINSON and O. J. BAKER. Trans. Proc. Roy. Soc. New Zealand, **76**, 250 (1946).
11. W. R. FORSYTHE and W. F. GIAUQUE. J. Am. Chem. Soc. **64**, (1942).
12. A. POTIER. Ann. Fac. Sci. Univ. Toulouse, **20**, 1 (1956).
13. N. C. DENO, J. J. JARUSZELSKI, and A. SCHRIESHEIM. J. Am. Chem. Soc. **77**, 3044 (1955). N. C. DENO, H. E. BERKHEIMER, W. L. EVANS, and H. J. PETERSON. J. Am. Chem. Soc. **81**, 2344, 6535 (1959).
14. R. A. ROBINSON and R. H. STOKES. Electrolyte solutions. Butterworths, London. 1959. p. 30.

RECEIVED OCTOBER 22, 1963.
DEPARTMENT OF CHEMISTRY,
UNIVERSITY OF TORONTO,
TORONTO, ONTARIO.

Can. J. Chem. Downloaded from www.nrcresearchpress.com by 84.22.46.98 on 09/08/12
For personal use only.

ACID-CATALYZED REACTIONS OF VINYL COMPOUNDS

PART III. 2,7,9,10-TETRAMETHYLANTHRACENE FROM VINYL ACETATE AND TOLUENE

J. M. PEPPER, MARGARET HOWELL, AND B. P. ROBINSON

In previous communications (1, 2), the nature of the products obtained by the aluminum chloride catalyzed reaction of vinyl acetate and benzene was reported. As part of a subsequent, more detailed study of the mechanism of formation of the principal product, namely 9,10-dimethylanthracene, the similar reaction involving vinyl acetate and toluene was investigated. The isolation of 2,7,9,10-tetramethylanthracene rather than the 2,6,9,10-tetramethyl isomer supported a mechanism of formation of the anthracene derivatives which consisted of the initial synthesis of the 1,1-diarylethane followed by ring closure involving incorporation of a two-carbon fragment. Details of this mechanism will appear in a forthcoming publication. This note describes the synthesis and structure proof of the previously unreported 2,7,9,10-tetramethylanthracene.

Chromic acid oxidation of the purified reaction product gave a substance identical with 2,7-dimethylanthraquinone. An Elbs reaction performed upon 2,4,4′-trimethylbenzophenone, obtained from a Friedel–Crafts reaction of *p*-toluoyl chloride with *m*-xylene, afforded a mixture of 2,7-dimethylanthracene and 3,6-dimethylanthrone either of which, when oxidized with chromic acid, gave authentic 2,7-dimethylanthraquinone.

EXPERIMENTAL

Melting points are uncorrected. Infrared spectra were measured using a Perkin–Elmer Model 21 spectrometer with sodium chloride optics.

Reaction of Vinyl Acetate and Toluene

Vinyl acetate (8.6 g, 0.1 mole) was added over a period of 1 hour to a cooled mixture of toluene (92 g, 1.0 mole) and aluminum chloride (40 g, 0.3 mole). The mixture was heated at 80° for 3 hours and the resulting complex decomposed and worked up in the usual manner. The crude product (18.9 g) was distilled and a fraction, boiling at 140–180° at 0.2 mm, was collected. This product solidified slowly and was recrystallized several times from absolute ethanol to yield 2,7,9,10-*tetramethylanthracene*, m.p. 124–125°. (Found: C, 92.74; H, 7.61. $C_{18}H_{18}$ requires C, 92.26; H, 7.74%.) Infrared spectrum (main peaks only): 2900, 1630, 1450, 1345, 910, 805, and 755 cm^{-1}.

Oxidation of 2,7,9,10-Tetramethylanthracene

Chromic acid (1.2 g) was dissolved in the minimum amount of water and this solution added slowly to 2,7,9,10-tetramethylanthracene (0.74 g) dissolved in glacial acetic acid (10 ml). The mixture was heated under reflux for 40 minutes and then poured into water (40 ml). The resulting precipitate was collected, partially purified by boiling in 5% sodium hydroxide solution, and recollected. Recrystallization from absolute ethanol gave 2,7-dimethylanthraquinone as colorless needles (0.55 g), m.p. 165–169°; no melting point depression with an authentic synthetic sample.

Synthesis of 2,7-Dimethylanthraquinone

2,4,4′-Trimethylbenzophenone.—A procedure similar to that reported by Morgan and Coulson (3) was used. A solution of *p*-toluoyl chloride (6.25 g) and *m*-xylene (4.3 g) in petroleum ether (b.p. 37–49°) (10 ml) was added slowly to aluminum chloride (6.3 g). The mixture was heated under reflux for 2 hours before decomposition of the complex. Distillation of the crude product gave 2,4,4′-trimethylbenzophenone (5.15 g, 57%), b.p. 208–210° at 19 mm; reported b.p. 169° at 4 mm (3).

Pyrolysis of 2,4,4′-Trimethylbenzophenone.—By application of the Elbs pyrolysis reaction by the method of Morgan and Coulson (3), two products were obtained: 2,7-dimethylanthracene, m.p. 240–243°, reported m.p. 241° (3), and 3,6-*dimethylanthrone*, m.p. 163–164°. (Found: C, 86.60; H, 6.56. $C_{16}H_{14}O$ requires C, 86.45; H, 6.35%.)

2,7-Dimethylanthraquinone.—Oxidation of either 2,7-dimethylanthracene or 3,6-dimethylanthrone, using chromic acid according to the method of Morgan and Coulson (3), gave 2,7-dimethylanthraquinone, m.p. 171–172°; reported m.p. 170° (4).

ACKNOWLEDGMENT

Grateful acknowledgment is made of the financial assistance provided by Imperial Oil Limited.

1. J. M. Pepper, B. P. Robinson, and G. W. Schwanbeck. Can. J. Chem. **40**, 122 (1962).
2. J. M. Pepper and B. P. Robinson. Can. J. Chem. **41**, 2103 (1963).
3. G. T. Morgan and E. A. Coulson. J. Chem. Soc. 2203 (1929).
4. P. F. Southern and W. A. Waters. J. Chem. Soc. 4340 (1960).

Received December 28, 1963.
Department of Chemistry,
University of Saskatchewan,
Saskatoon, Saskatchewan.

THE EFFECT OF STRUCTURE ON THE THERMAL STABILITY OF HYDROPEROXIDES. II[1]

R. Hiatt[2] and Teunis Visser

In our attempt to discover a hydroperoxide which would give unambiguous evidence for a concerted unimolecular decomposition, we have studied the

$$R_3C{-}O{-}O{-}H \rightarrow R\cdot + R_2C{=}O + \cdot OH$$

thermal decomposition of 2,3,3-trimethyl-2-butyl hydroperoxide. Assisting in a possible

[1]*This research was supported, in part, by a grant from the National Research Council.*
[2]*Present address: Stanford Research Institute, Menlo Park, California.*

Can. J. Chem. Downloaded from www.nrcresearchpress.com by 84.22.46.98 on 09/08/12
For personal use only.

Reaction of Vinyl Acetate and Toluene

Vinyl acetate (8.6 g, 0.1 mole) was added over a period of 1 hour to a cooled mixture of toluene (92 g, 1.0 mole) and aluminum chloride (40 g, 0.3 mole). The mixture was heated at 80° for 3 hours and the resulting complex decomposed and worked up in the usual manner. The crude product (18.9 g) was distilled and a fraction, boiling at 140–180° at 0.2 mm, was collected. This product solidified slowly and was recrystallized several times from absolute ethanol to yield 2,7,9,10-*tetramethylanthracene*, m.p. 124–125°. (Found: C, 92.74; H, 7.61. $C_{18}H_{18}$ requires C, 92.26; H, 7.74%.) Infrared spectrum (main peaks only): 2900, 1630, 1450, 1345, 910, 805, and 755 cm^{-1}.

Oxidation of 2,7,9,10-Tetramethylanthracene

Chromic acid (1.2 g) was dissolved in the minimum amount of water and this solution added slowly to 2,7,9,10-tetramethylanthracene (0.74 g) dissolved in glacial acetic acid (10 ml). The mixture was heated under reflux for 40 minutes and then poured into water (40 ml). The resulting precipitate was collected, partially purified by boiling in 5% sodium hydroxide solution, and recollected. Recrystallization from absolute ethanol gave 2,7-dimethylanthraquinone as colorless needles (0.55 g), m.p. 165–169°; no melting point depression with an authentic synthetic sample.

Synthesis of 2,7-Dimethylanthraquinone

2,4,4′-Trimethylbenzophenone.—A procedure similar to that reported by Morgan and Coulson (3) was used. A solution of *p*-toluoyl chloride (6.25 g) and *m*-xylene (4.3 g) in petroleum ether (b.p. 37–49°) (10 ml) was added slowly to aluminum chloride (6.3 g). The mixture was heated under reflux for 2 hours before decomposition of the complex. Distillation of the crude product gave 2,4,4′-trimethylbenzophenone (5.15 g, 57%), b.p. 208–210° at 19 mm; reported b.p. 169° at 4 mm (3).

Pyrolysis of 2,4,4′-Trimethylbenzophenone.—By application of the Elbs pyrolysis reaction by the method of Morgan and Coulson (3), two products were obtained: 2,7-dimethylanthracene, m.p. 240–243°, reported m.p. 241° (3), and 3,6-*dimethylanthrone*, m.p. 163–164°. (Found: C, 86.60; H, 6.56. $C_{16}H_{14}O$ requires C, 86.45; H, 6.35%.)

2,7-Dimethylanthraquinone.—Oxidation of either 2,7-dimethylanthracene or 3,6-dimethylanthrone, using chromic acid according to the method of Morgan and Coulson (3), gave 2,7-dimethylanthraquinone, m.p. 171–172°; reported m.p. 170° (4).

ACKNOWLEDGMENT

Grateful acknowledgment is made of the financial assistance provided by Imperial Oil Limited.

1. J. M. Pepper, B. P. Robinson, and G. W. Schwanbeck. Can. J. Chem. **40**, 122 (1962).
2. J. M. Pepper and B. P. Robinson. Can. J. Chem. **41**, 2103 (1963).
3. G. T. Morgan and E. A. Coulson. J. Chem. Soc. 2203 (1929).
4. P. F. Southern and W. A. Waters. J. Chem. Soc. 4340 (1960).

Received December 28, 1963.
Department of Chemistry,
University of Saskatchewan,
Saskatoon, Saskatchewan.

THE EFFECT OF STRUCTURE ON THE THERMAL STABILITY OF HYDROPEROXIDES. II[1]

R. Hiatt[2] and Teunis Visser

In our attempt to discover a hydroperoxide which would give unambiguous evidence for a concerted unimolecular decomposition, we have studied the

$$R_3C—O—O—H \rightarrow R\cdot + R_2C{=}O + \cdot OH$$

thermal decomposition of 2,3,3-trimethyl-2-butyl hydroperoxide. Assisting in a possible

[1]*This research was supported, in part, by a grant from the National Research Council.*
[2]*Present address: Stanford Research Institute, Menlo Park, California.*

Can. J. Chem. Downloaded from www.nrcresearchpress.com by 210.87.254.105 on 09/05/12
For personal use only.

concerted mechanism would be not only the formation of a fairly stable free radical but also considerable steric pressure.

Shown in Table I are the rates of decomposition of this hydroperoxide at several

TABLE I

Thermal decomposition in benzene

Rate constants			Products	
T, °C	H_0, mole/l.	$k_1 \times 10^5$, sec^{-1}	Product	Mole %
168.7	0.0121	25.6	Acetone	39
168.7	0.0573	25.4	*t*-Butyl alcohol	6.5
168.7	0.0615	26.3	2,3,3-Trimethyl-	
168.7	0.0622	25.5	2-butanol	55
			Isobutylene	Some
159.1		10.4	*t*-Butylbenzene	4.1
148.6		2.43		
139.6		1.11		
	ΔH^* 39 kcal			
	ΔS^* +13 e.u.			

temperatures and initial concentrations. It was found that at initial concentrations of below 0.1 molar the first-order rate constants were independent of the initial concentration, as shown for the reactions at 168.7° C. The values at the lower temperatures are each averages of four runs with initial concentrations of 0.1 molar or less. It is believed that these represent true rates of unimolecular homolysis, uninfluenced by the complications of induced decomposition. 2,3,3-Trimethyl-2-butyl hydroperoxide is not much different in its rate of decomposition, at temperatures where this is conveniently measurable, from other hydroperoxides (1). We previously pointed out, however, that *t*-butyl hydroperoxide was different from other hydroperoxides in having a considerably higher ΔH^* and ΔS^* for thermal decomposition (2). 2,3,3-Trimethyl-2-butyl hydroperoxide is now found to be anomalous in these respects also. The products, too, show a similarity to those obtained from the decomposition of *t*-butyl hydroperoxide. The large amount of parent alcohol indicates a substantial lifetime for the 2,3,3-trimethyl-2-butoxy radical. To the extent that this radical cleaves, acetone is formed, as well as *t*-butyl radical, which appears as *t*-butyl alcohol and isobutylene. It is apparent that tertiary hydroperoxides at least may be classified in two groups: those which have high activation energies for unimolecular thermal decomposition (39–40 kcal) and give a large amount of the parent alcohol, and those with lower activation energies, which give little or no alcohol (1, 2). If the human time scale were such that the decompositions could be measured at 50° C, large differences in thermal stability would be manifest.

These arguments, which in the case of perester decomposition led to a proposed difference in mechanism of homolysis (3), would seem to make a similar difference for hydroperoxides not unlikely.

EXPERIMENTAL

2,3,3-Trimethyl-2-butyl hydroperoxide was prepared by the method of Criegee (4). The hydroperoxide, recrystallized from pentane (m.p. 109–111° C), gave an iodometric titration of 95%. Alternately it was extracted from the reaction mixture with benzene and not isolated. Rates of decomposition of this material did not differ from those obtained with hydroperoxide that had been crystallized.

The kinetic studies were done in benzene with initial concentrations of hydroperoxide ranging from 0.01 to 0.5 molar. It was found that the presence of air had a profound effect where concentrations were less than 0.05 molar, and all runs were carried out in evacuated sealed tubes.

Products from completely decomposed samples were determined gas chromatographically.

Can. J. Chem. Downloaded from www.nrcresearchpress.com by 210.87.254.105 on 09/05/12
For personal use only.

1. J. R. THOMAS. J. Am. Chem. Soc. **77**, 246 (1955).
2. R. HIATT and W. M. J. STRACHAN. J. Org. Chem. **28**, 1893 (1963).
3. P. D. BARTLETT and R. HIATT. J. Am. Chem. Soc. **80**, 1398 (1958).
4. R. CRIEGEE and H. DIETRICH. Ann. **560**, 136 (1948).

RECEIVED DECEMBER 9, 1963.
DEPARTMENT OF CHEMISTRY,
UNIVERSITY OF TORONTO,
TORONTO, ONTARIO.

Can. J. Chem. Downloaded from www.nrcresearchpress.com by 210.87.254.105 on 09/05/12
For personal use only.

ON THE DIFFERENTIATION OF *endo*- AND *exo*-NORBORNYL DERIVATIVES BY CHEMICAL SHIFTS IN N.M.R. SPECTROSCOPY

EDWARD W. C. WONG* AND C. C. LEE

Recently, Fraser (1) investigated the possibility of correlating the chemical shift of a proton to its *endo*- or *exo*- position in the products of Diels–Alder reactions between cyclic dienes and derivatives of ethylene. Examination of the n.m.r. spectra of a number of bicyclo[2.2.1]hept-2-enes, and the corresponding dihydro compounds, led this author to conclude that the configuration of a proton, or proton-bearing substituent, in this bicyclic system can be ascertained by observing the change in its chemical shift when the double bond is removed by hydrogenation. It was suggested that the effect of the magnetically anisotropic double bond would shift the absorption frequency of the *exo*-proton downfield and that of the *endo*-proton upfield. Thus the change in chemical shift upon hydrogen, $\Delta\tau$, should be positive for an *exo*-proton and negative for an *endo*-proton. To test this hypothesis, we have measured the chemical shifts of the *endo*- and *exo*-protons in three pairs of *endo*- and *exo*-dehydronorbornyl derivatives and in the corresponding norbornyl compounds.

In the *endo*- and *exo*-dehydronorbornyl and norbornyl derivatives examined (I–IV),

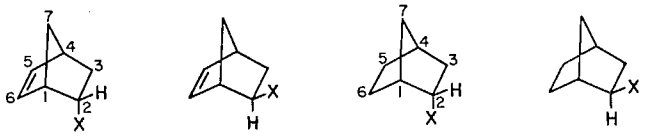

I II III IV

a x = OH
b x = OAc
c x = OBs

the numbering of the carbon skeleton of the dehydro derivatives follows that of the saturated norbornyl derivatives to minimize confusion. The spectra of the brosylates (*p*-bromobenzenesulphonates) are shown in Fig. 1. The mixture of *endo*- and *exo*-dehydronorbornyl brosylates (I*c* and II*c*) was derived from the mixed products of the Diels–Alder reaction between cyclopentadiene and vinyl acetate (2, 3). Partial solvolysis removed all the *exo*-isomer, giving pure *endo*-brosylate I*c* (3). The assignment of the various peaks of Fig. 1A and B is as follows. The intense absorption and its side bands at low field are due

*Holder of a National Research Council of Canada Studentship, 1963–64.

1. J. R. THOMAS. J. Am. Chem. Soc. **77**, 246 (1955).
2. R. HIATT and W. M. J. STRACHAN. J. Org. Chem. **28**, 1893 (1963).
3. P. D. BARTLETT and R. HIATT. J. Am. Chem. Soc. **80**, 1398 (1958).
4. R. CRIEGEE and H. DIETRICH. Ann. **560**, 136 (1948).

RECEIVED DECEMBER 9, 1963.
DEPARTMENT OF CHEMISTRY,
UNIVERSITY OF TORONTO,
TORONTO, ONTARIO.

Can. J. Chem. Downloaded from www.nrcresearchpress.com by 210.87.254.105 on 09/05/12
For personal use only.

ON THE DIFFERENTIATION OF *endo*- AND *exo*-NORBORNYL DERIVATIVES BY CHEMICAL SHIFTS IN N.M.R. SPECTROSCOPY

EDWARD W. C. WONG* AND C. C. LEE

Recently, Fraser (1) investigated the possibility of correlating the chemical shift of a proton to its *endo*- or *exo*- position in the products of Diels–Alder reactions between cyclic dienes and derivatives of ethylene. Examination of the n.m.r. spectra of a number of bicyclo[2.2.1]hept-2-enes, and the corresponding dihydro compounds, led this author to conclude that the configuration of a proton, or proton-bearing substituent, in this bicyclic system can be ascertained by observing the change in its chemical shift when the double bond is removed by hydrogenation. It was suggested that the effect of the magnetically anisotropic double bond would shift the absorption frequency of the *exo*-proton downfield and that of the *endo*-proton upfield. Thus the change in chemical shift upon hydrogen, $\Delta\tau$, should be positive for an *exo*-proton and negative for an *endo*-proton. To test this hypothesis, we have measured the chemical shifts of the *endo*- and *exo*-protons in three pairs of *endo*- and *exo*-dehydronorbornyl derivatives and in the corresponding norbornyl compounds.

In the *endo*- and *exo*-dehydronorbornyl and norbornyl derivatives examined (I–IV),

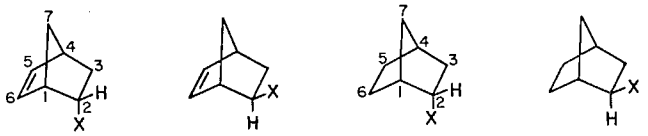

I II III IV

a x = OH
b x = OAc
c x = OBs

the numbering of the carbon skeleton of the dehydro derivatives follows that of the saturated norbornyl derivatives to minimize confusion. The spectra of the brosylates (*p*-bromobenzenesulphonates) are shown in Fig. 1. The mixture of *endo*- and *exo*-dehydronorbornyl brosylates (I*c* and II*c*) was derived from the mixed products of the Diels–Alder reaction between cyclopentadiene and vinyl acetate (2, 3). Partial solvolysis removed all the *exo*-isomer, giving pure *endo*-brosylate I*c* (3). The assignment of the various peaks of Fig. 1A and B is as follows. The intense absorption and its side bands at low field are due

*Holder of a National Research Council of Canada Studentship, 1963–64.

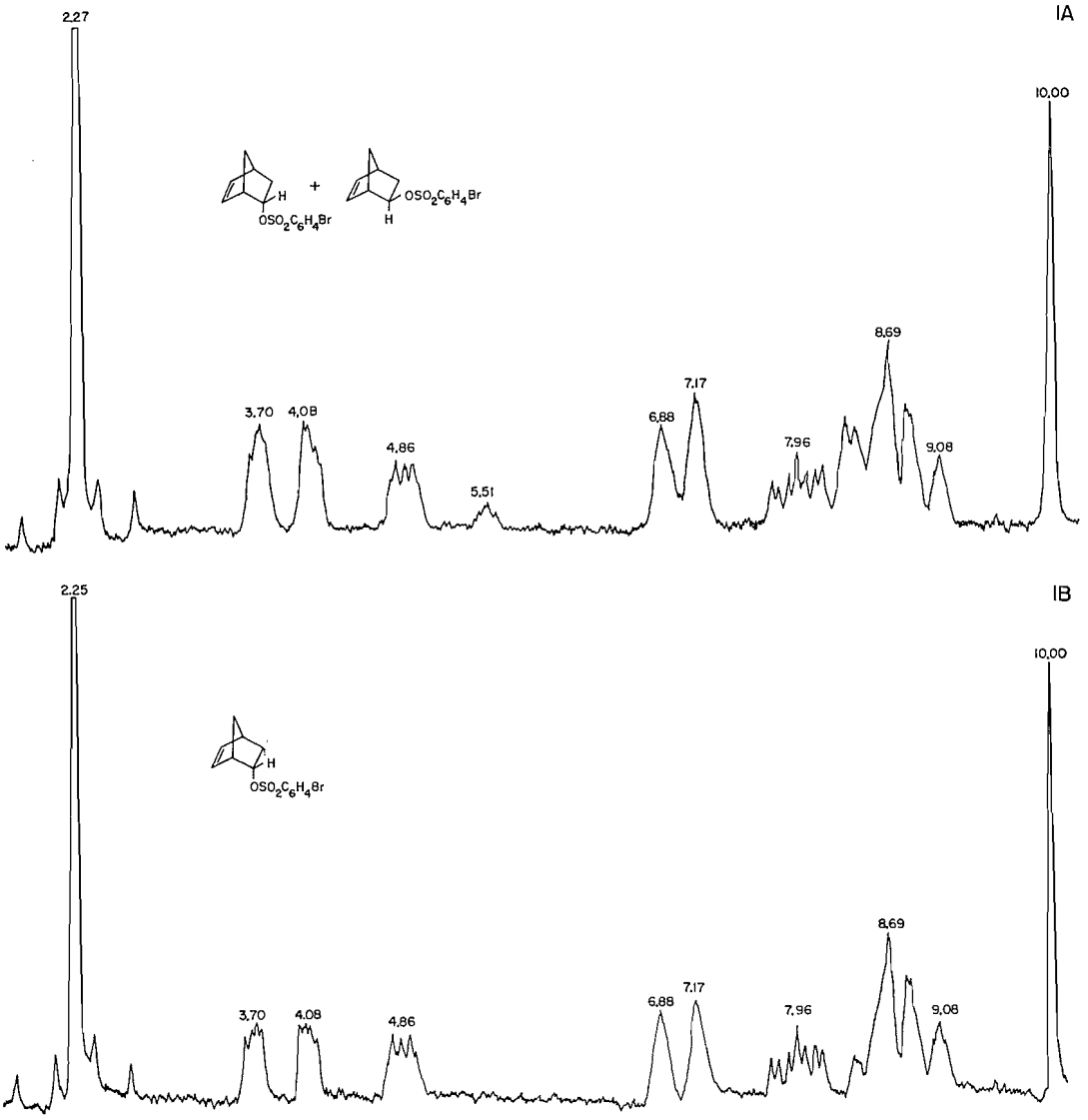

FIG. 1. Nuclear magnetic resonance spectra. A, B, C, and D are, respectively, a mixture of *endo*- and *exo*-dehydronorbornyl, *endo*-dehydronorbornyl, *endo*-norbornyl, and *exo*-norbornyl brosylates.

to the protons of the benzene ring. The multiplets centered at 3.70 and 4.08τ are assigned to the two olefinic protons. The multiplet at 4.86τ is due to the *exo*-proton (of the *endo*-brosylate) at C-2. The absorption of the C-2 *endo*-proton (of the *exo*-brosylate) is centered at 5.51τ. The peaks at 6.88 and 7.17τ are due to the bridgehead protons at C-1 and C-4. Following the reasonings of Fraser (1), the multiplet centered at 7.96τ is assigned to the *exo*-proton at C-3, while the peak at 9.08τ is part of the absorption of the *endo*-proton of C-3. The remaining peaks centered about 8.69τ may be assigned to the two protons of C-7.

As noted by Fraser (1), the saturated compounds show fewer well-resolved peaks. For *endo*-norbornyl brosylate (Fig. 1C), the absorption of the *exo*-proton at C-2 is centered

Can. J. Chem. Downloaded from www.nrcresearchpress.com by 210.87.254.105 on 09/05/12
For personal use only.

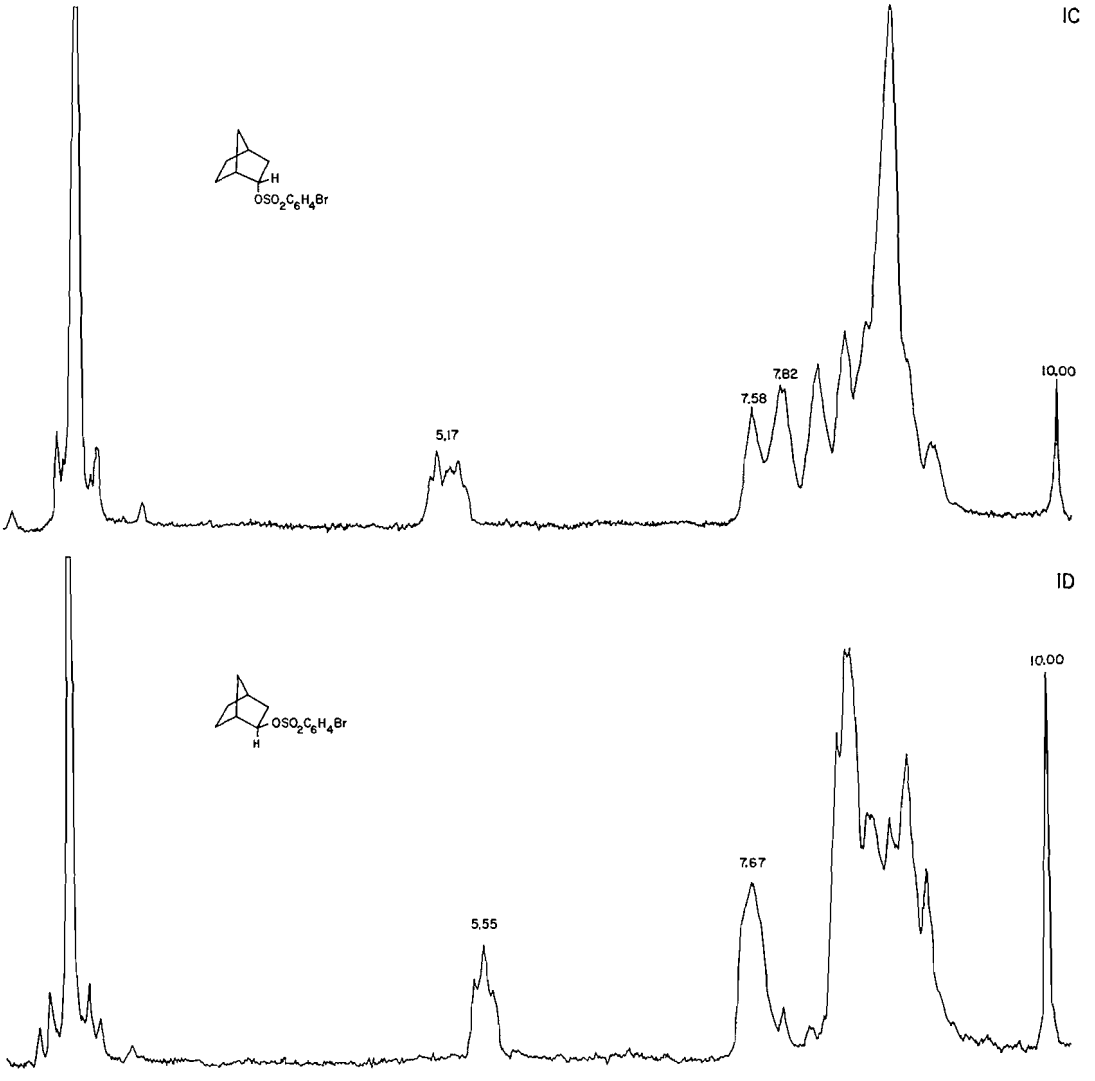

FIG. 1, C and D.

at 5.17τ. The other easily recognized peaks are those at 7.58 and 7.82τ due to the bridgehead protons. With *exo*-norbornyl brosylate (Fig. 2D), τ for the C-2 *endo*-proton is 5.55. Even the bridgehead protons are not resolved in this case.

The τ values for the *exo*- or *endo*-protons at the C-2 position of compounds I to IV were ascertained in a manner similar to that illustrated with the brosylates. These are summarized in Table I. It may also be pointed out that the correctness of the assignments is supported by the fact that the absorption of the C-2 proton of the norborneols disappeared in the spectrum of norborneol-2-*d* (chiefly *endo*) obtained from the reduction of norcamphor with lithium aluminum deuteride.

If the generalization of Fraser (1) regarding the effect of the double bond on chemical shifts of *exo*- and *endo*- protons were valid, the change in τ upon removal of the double

Can. J. Chem. Downloaded from www.nrcresearchpress.com by 210.87.254.105 on 09/05/12
For personal use only.

TABLE I

Chemical shifts of *exo*- and *endo*-protons at the C-2 position of dehydronorbornyl and norbornyl derivatives

	Alcohol		Acetate		Brosylate	
	τ	$\Delta\tau$*	τ	$\Delta\tau$*	τ	$\Delta\tau$*
endo-Dehydronorbornyl	5.54		4.81		4.86	
endo-Norbornyl	5.83	0.29	5.13	0.32	5.17	0.31
exo-Dehydronorbornyl	6.18		5.43		5.51	
exo-Norbornyl	6.34	0.16	5.46	0.03	5.55	0.04

*Change in τ upon removal of double bond.

bond, obtained by subtracting τ of the dehydronorbornyl derivative from that of the corresponding norbornyl derivative, should be positive if the proton at C-2 is *exo* and negative if this proton is *endo*. As can be seen from Table I, all values of $\Delta\tau$ obtained for the present cases are positive, regardless of whether the C-2 proton is *exo* or *endo*. Thus the suggestion that the *exo*- or *endo*-configuration may be established by the sign of $\Delta\tau$ does not hold for the dehydronorbornyl and norbornyl alcohols, acetates, and brosylates.

For the examples examined in the present study, the presence of the double bond shifted the absorption downfield for both *exo*- and *endo*-protons at C-2, although the magnitude of this shift is very small for the *endo*-proton (of the *exo*-epimer). While it is not possible to use $\Delta\tau$ to establish the *exo*- or *endo*-configuration, if both epimers were available, a differentiation can be made by the fact that the *exo*-proton at C-2 absorbs at lower field than the *endo*-proton. The finding that the C-2 *exo*-proton is deshielded relative to the *endo*-proton has also been noted by Musher (4) for a number of bicyclo [2.2.1]heptanols including *endo*- and *exo*-norborneols. Moreover, the absorption of the C-2 *exo*-proton appears to be a quintet, while that of the C-2 *endo*-proton is split into lesser number of peaks. The splitting into a quintet observed for the *exo*-proton of *endo*-2-nitronorbornane and *endo*-2-nitronorbornene (numbering of carbon skeleton as given in I–IV) has been ascribed by Fraser (1) to strong coupling with the *exo*-proton at C-3 and weaker coupling with both the *endo*-proton at C-3 and the bridgehead proton at C-1. More recently, the complexity of the couplings of the *exo*- and *endo*-protons of bicyclo [2.2.1]heptanols has been described by Musher (4). The less extensive splitting shown by the C-2 *endo*-proton may largely be due to its inability to couple with the bridgehead proton at C-1 (5).

It was mentioned earlier that norborneol-2-*d* (chiefly *endo*) showed no absorption for the C-2 proton. It may be of interest to record that after treatment in the presence of sodium and fluorenone in refluxing toluene to give an equilibrated mixture of *exo*- and *endo*-norborneols (2), some C-2 proton absorption reappeared, indicating loss of some deuterium and its replacement by hydrogen. This observation is consistent with the suggestion that such equilibrations may proceed via norcamphor as an intermediate (6).

EXPERIMENTAL

Preparations of compounds I–IV, either as mixtures of epimers or as individual pure compounds, have been described previously (2, 3).

The n.m.r. spectra were taken at 60 Mc on a Varian A-60 spectrometer. Samples were of 15–20% concentration dissolved in carbon tetrachloride containing 1% tetramethylsilane as internal standard.

The reproducibility of the chemical shifts was better than 0.02τ. The relatively high sample concentration of 15–20% was used to provide absorption peaks of good intensity for the C-2 protons. Chemical shifts of the *exo*- or *endo*-protons at C-2 were not affected by variations of sample concentration within the range

Can. J. Chem. Downloaded from www.nrcresearchpress.com by 210.87.254.105 on 09/05/12
For personal use only.

of 5–20%. Chemical shifts of hydroxylic protons are known to be sensitive towards changes in concentration because of association (7). As expected, the absorptions of the hydroxylic protons of the norborneols and dehydronorborneols shifted markedly downfield with increasing concentration. However, the positions of other absorption peaks, corresponding to protons not bonded to oxygen, showed no association effects.

ACKNOWLEDGMENT

The financial support given by the National Research Council of Canada is gratefully acknowledged.

1. R. R. Fraser. Can. J. Chem. **40**, 78 (1962).
2. J. D. Roberts, C. C. Lee, and W. H. Saunders, Jr. J. Am. Chem. Soc. **76**, 4501 (1954).
3. J. D. Roberts, C. C. Lee, and W. H. Saunders, Jr. J. Am. Chem. Soc. **77**, 3034 (1955).
4. J. I. Musher. Mol. Phys. **6**, 93 (1963).
5. J. Meinwald, Y. C. Meinwald, and T. N. Baker, III. J. Am. Chem. Soc. **85**, 2513 (1963).
6. W. F. Wilcox, Jr., M. Sexton, and M. F. Wilcox. J. Org. Chem. **28**, 1079 (1963).
7. L. M. Jackman. Applications of nuclear magnetic resonance spectroscopy in organic chemistry. Pergamon Press, New York. 1959. p. 66.

Received September 12, 1963.
Department of Chemistry,
University of Saskatchewan,
Saskatoon, Saskatchewan.

TRANSFER CELL FOR GAS CHROMATOGRAPHY

M. E. Bednas and D. S. Russell

In the literature there are few transfer cells (1–6) that enable a sample to be transferred from a vacuum manifold to a gas chromatograph in another location. Those designs which utilize two stopcocks are somewhat inconvenient to use and result in some peak broadening.

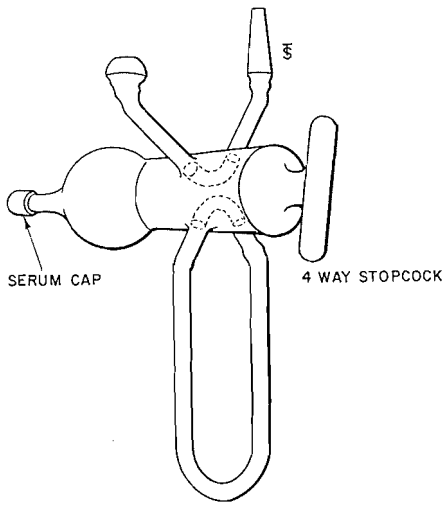

We have constructed a new transfer cell from a single four-way vacuum stopcock (see figure). In 1958, the first model had to be made with a non-vacuum stopcock; it leaked occasionally. Subsequently, Johns Glass Co., Toronto, has made some vacuum stopcocks according to the authors' design and they are now readily available. A serum bottle cap

Can. J. Chem. Downloaded from www.nrcresearchpress.com by 210.87.254.105 on 09/05/12
For personal use only.

of 5–20%. Chemical shifts of hydroxylic protons are known to be sensitive towards changes in concentration because of association (7). As expected, the absorptions of the hydroxylic protons of the norborneols and dehydronorborneols shifted markedly downfield with increasing concentration. However, the positions of other absorption peaks, corresponding to protons not bonded to oxygen, showed no association effects.

ACKNOWLEDGMENT

The financial support given by the National Research Council of Canada is gratefully acknowledged.

1. R. R. Fraser. Can. J. Chem. **40**, 78 (1962).
2. J. D. Roberts, C. C. Lee, and W. H. Saunders, Jr. J. Am. Chem. Soc. **76**, 4501 (1954).
3. J. D. Roberts, C. C. Lee, and W. H. Saunders, Jr. J. Am. Chem. Soc. **77**, 3034 (1955).
4. J. I. Musher. Mol. Phys. **6**, 93 (1963).
5. J. Meinwald, Y. C. Meinwald, and T. N. Baker, III. J. Am. Chem. Soc. **85**, 2513 (1963).
6. W. F. Wilcox, Jr., M. Sexton, and M. F. Wilcox. J. Org. Chem. **28**, 1079 (1963).
7. L. M. Jackman. Applications of nuclear magnetic resonance spectroscopy in organic chemistry. Pergamon Press, New York. 1959. p. 66.

Received September 12, 1963.
Department of Chemistry,
University of Saskatchewan,
Saskatoon, Saskatchewan.

TRANSFER CELL FOR GAS CHROMATOGRAPHY

M. E. Bednas and D. S. Russell

In the literature there are few transfer cells (1–6) that enable a sample to be transferred from a vacuum manifold to a gas chromatograph in another location. Those designs which utilize two stopcocks are somewhat inconvenient to use and result in some peak broadening.

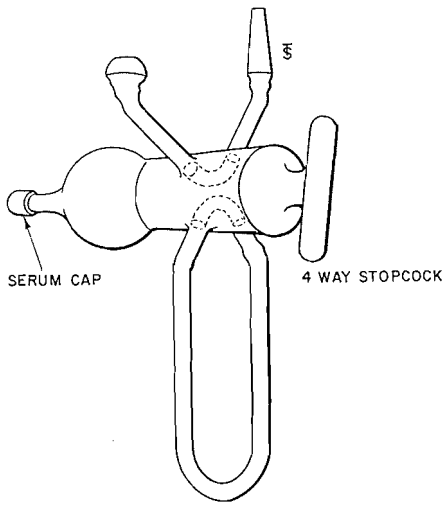

We have constructed a new transfer cell from a single four-way vacuum stopcock (see figure). In 1958, the first model had to be made with a non-vacuum stopcock; it leaked occasionally. Subsequently, Johns Glass Co., Toronto, has made some vacuum stopcocks according to the authors' design and they are now readily available. A serum bottle cap

Can. J. Chem. Downloaded from www.nrcresearchpress.com by 210.87.254.105 on 09/05/12
For personal use only.

is placed on the stopcock so that the barrel of the stopcock may be evacuated with a hypodermic needle cemented to a vacuum line.

Samples may be collected by one of the following methods:

(1) by evacuating the cell and filling it with the sample to some definite pressure.
(2) by evacuating the cell and freezing the whole sample from a vacuum manifold into it.
(3) by blowing or sucking the sample gas through a cold trap (as in the case of air pollutants).

The transfer cell may be used with any gas chromatographic apparatus. It may be connected directly to a four-way or six-way gas sampling valve. In these cases the connecting leads can be flushed with carrier gas first and, when equilibrium is re-established, the stopcock on the transfer cell can be turned to flush in the sample. To use the transfer cell with an instrument equipped with a septum, a hypodermic needle cemented to a 10/30 standard taper joint is fitted to the appropriate end of the cell and an auxiliary carrier gas line to the other end. The leads are flushed out, needle injected through the septum and stopcock turned to flush in the sample.

The authors have constructed cells with 4 to 20 ml capacity and used them under vacuum and up to 30 p.s.i.g. During 5 years of extensive use with these cells, 100% transfer of the sample has been achieved with an overall precision of $\pm 1\%$, including sample introduction, recording, and integration errors.

1. D. S. Russell and M. E. Bednas. Anal. Chem. **29**, 1562 (1957).
2. D. H. Desty and B. H. F. Wyman. Anal. Chem. **29**, 320 (1957).
3. D. N. Glew and D. M. Young. Anal. Chem. **30**, 1890 (1958).
4. D. Harvey and D. E. Chalkley. Fuel, **34**, 191 (1955).
5. A. Kreuchunas. Chemist-Analyst, **49** (3) 82 (1960).
6. R. N. Smith, J. Swinhart, and G. D. Lesnini. Anal. Chem. **30**, 1217 (1958).

Received January 3, 1964.
Division of Applied Chemistry,
National Research Council,
Ottawa, Canada.

SOLVENT EFFECTS ON HYDROCARBON AUTOXIDATIONS[1]

J. A. Howard and K. U. Ingold

We have recently shown that the rate of the α,α'-azo-bis-isobutyronitrile- (AIBN-) initiated autoxidation of 0.42 mole/l. of styrene in oxidation-resistant solvents at 65° C increases with increasing dielectric constant of the solvent (1). The similarity between the effect of solvents on this reaction and their effect on the rate of the pyridine-catalyzed decomposition of *t*-butylperoxyformate at 90° C (2) led us to conclude that a dipolar transition state was probably involved in the addition of a peroxy radical to styrene, i.e., in the propagation reaction. It was suggested that the magnitude of the solvent effects on other oxidation reactions should indicate whether or not their propagation steps also involved dipolar transition states. Four other readily oxidizable hydrocarbons have now been examined in 11 of the solvents used in the previous work with styrene. The same experimental conditions were employed, i.e., 1 ml of reactant to 20 ml of solvent, initiated by 7×10^{-2} mole/l. [AIBN] at 65° C.

[1]*Issued as N.R.C. No. 7865.*

Can. J. Chem. Downloaded from www.nrcresearchpress.com by 210.87.254.105 on 09/05/12
For personal use only.

is placed on the stopcock so that the barrel of the stopcock may be evacuated with a hypodermic needle cemented to a vacuum line.

Samples may be collected by one of the following methods:

(1) by evacuating the cell and filling it with the sample to some definite pressure.
(2) by evacuating the cell and freezing the whole sample from a vacuum manifold into it.
(3) by blowing or sucking the sample gas through a cold trap (as in the case of air pollutants).

The transfer cell may be used with any gas chromatographic apparatus. It may be connected directly to a four-way or six-way gas sampling valve. In these cases the connecting leads can be flushed with carrier gas first and, when equilibrium is re-established, the stopcock on the transfer cell can be turned to flush in the sample. To use the transfer cell with an instrument equipped with a septum, a hypodermic needle cemented to a 10/30 standard taper joint is fitted to the appropriate end of the cell and an auxiliary carrier gas line to the other end. The leads are flushed out, needle injected through the septum and stopcock turned to flush in the sample.

The authors have constructed cells with 4 to 20 ml capacity and used them under vacuum and up to 30 p.s.i.g. During 5 years of extensive use with these cells, 100% transfer of the sample has been achieved with an overall precision of $\pm 1\%$, including sample introduction, recording, and integration errors.

1. D. S. Russell and M. E. Bednas. Anal. Chem. **29**, 1562 (1957).
2. D. H. Desty and B. H. F. Wyman. Anal. Chem. **29**, 320 (1957).
3. D. N. Glew and D. M. Young. Anal. Chem. **30**, 1890 (1958).
4. D. Harvey and D. E. Chalkley. Fuel, **34**, 191 (1955).
5. A. Kreuchunas. Chemist-Analyst, **49** (3) 82 (1960).
6. R. N. Smith, J. Swinhart, and G. D. Lesnini. Anal. Chem. **30**, 1217 (1958).

Received January 3, 1964.
Division of Applied Chemistry,
National Research Council,
Ottawa, Canada.

SOLVENT EFFECTS ON HYDROCARBON AUTOXIDATIONS[1]

J. A. Howard and K. U. Ingold

We have recently shown that the rate of the α,α'-azo-bis-isobutyronitrile- (AIBN-) initiated autoxidation of 0.42 mole/l. of styrene in oxidation-resistant solvents at 65° C increases with increasing dielectric constant of the solvent (1). The similarity between the effect of solvents on this reaction and their effect on the rate of the pyridine-catalyzed decomposition of *t*-butylperoxyformate at 90° C (2) led us to conclude that a dipolar transition state was probably involved in the addition of a peroxy radical to styrene, i.e., in the propagation reaction. It was suggested that the magnitude of the solvent effects on other oxidation reactions should indicate whether or not their propagation steps also involved dipolar transition states. Four other readily oxidizable hydrocarbons have now been examined in 11 of the solvents used in the previous work with styrene. The same experimental conditions were employed, i.e., 1 ml of reactant to 20 ml of solvent, initiated by 7×10^{-2} mole/l. [AIBN] at 65° C.

[1]*Issued as N.R.C. No. 7865.*

Can. J. Chem. Downloaded from www.nrcresearchpress.com by 210.87.254.105 on 09/05/12
For personal use only.

The rate of gas absorption is given by (1),

$$\rho_0 = (2e-1)k_1[\mathrm{AIBN}]+k_3[\mathrm{RH}]\left(\frac{ek_1[\mathrm{AIBN}]}{k_5}\right)^{1/2}$$

where RH represents the hydrocarbon, e is the efficiency of radical production by the initiator, k_1 is its rate constant for decomposition, and k_3 and k_5 are the propagation and self-termination rate constants. In calculating $k_3/k_5^{1/2}$ the same k_1 values were used as previously and e was taken to be 0.75 (1). The data are given in Table I for α-methyl styrene,* tetralin, 4-methyl cyclohexene, and cumene together with the data obtained previously for styrene. The $k_3/k_5^{1/2}$ values for the first three hydrocarbons have been plotted against $k_3/k_5^{1/2}$ for styrene in Fig. 1. The slopes of the best straight lines so

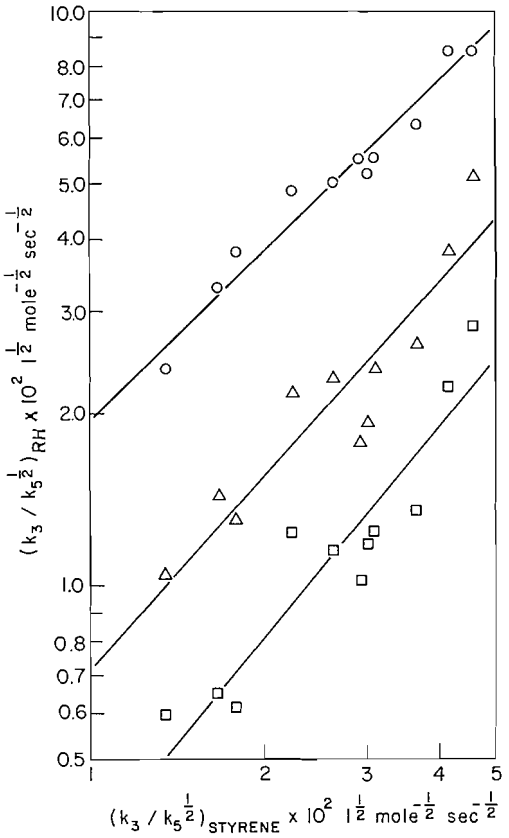

FIG. 1. $k_3/k_5^{1/2}$ for α-methyl styrene ○, 4-methyl cyclohexene △, and tetralin □, plotted against $k_3/k_5^{1/2}$ for styrene at 65° C.

obtained, together with their standard deviations (in $\log_{10}$ units), have been included in Table I.

The very close similarity of the solvent effects on the $k_3/k_5^{1/2}$ values for styrene and α-methyl styrene implies, as we originally suggested (1), that the solvent has a much greater influence on the propagation step (k_3) than on the termination step (k_5). That is,

*The oxygen pressure was kept constant at 740 mm in all the experiments with this hydrocarbon since its oxidation rate shows a slight variation with pressure up to at least 3200 mm (3).

Can. J. Chem. Downloaded from www.nrcresearchpress.com by 210.87.254.105 on 09/05/12
For personal use only.

TABLE I

$k_3/k_5^{1/2} \times 10^3$ l.$^{1/2}$ mole$^{-1/2}$ sec$^{-1/2}$ at 65° C in various solvents

Solvents	Styrene (1)	α-Methyl styrene	Tetralin	4-Methyl cyclohexene	Cumene
n-Decane	13.5	24.0	5.99	10.5	1.56
t-Butylbenzene	16.6	33.1	6.50	14.3	0.84_5
Carbon tetrachloride	17.9	38.1	6.16	13.0	0.76_3
Benzene	22.3	48.8	12.3	21.5	4.38
Chlorobenzene	26.3	50.1	11.5	22.8	3.94
Acetic acid	29.3	55.5	10.2	17.9	3.20
t-Butanol	30.2	52.0	11.8	19.2	1.72
o-Dichlorobenzene	31.0	55.7	12.4	23.7	2.42
Nitrobenzene	36.7	63.2	13.5	26.1	3.43
Nitromethane	41.8	85.1	22.3	38.0	6.97
Acetonitrile	45.9	85.5	28.3	51.4	9.54
Slope $\frac{(k_3/k_5^{1/2})_{RH}}{(k_3/k_5^{1/2})_{styrene}}$		0.97_5	1.21	1.12	1.88
Standard deviation		0.010	0.024	0.023	0.066

the propagation steps must be quite similar for the two hydrocarbons since they will both involve the addition of a peroxy radical to a double bond. In contrast, the reactions involved in chain termination are probably quite different for the *secondary* styrene polyperoxy radicals and for the *tertiary* α-methyl styrene polyperoxy radicals (4). These results therefore provide confirmation that the increase in oxidation rate with increasing solvent dielectric constant results mainly from an interaction of the solvent with the dipolar transition state of the propagation reaction.

The similarity between the solvent effects on styrene and on tetralin and 4-methyl cyclohexene is not quite so close as the similarity between the two styrenes. However, the correlation is close enough to suggest that somewhat similar dipoles are involved in the transition states of both types of propagation reaction i.e., hydrogen abstraction and peroxy radical addition. There appear to be some specific differences in solvent effects for the two types of reaction. For example, $k_3/k_5^{1/2}$ is greater in CCl_4 than in *t*-butylbenzene for addition but is smaller for abstraction. Similarly, $k_3/k_5^{1/2}$ is enhanced in benzene and in acetonitrile for abstraction relative to addition but is depressed in *t*-butanol and in acetic acid.

The data for cumene is much less reliable than for any of the other hydrocarbons because the oxidation rates are so much smaller that the correction for nitrogen evolution from the AIBN (i.e. $(2c-1)k_I$[AIBN]) is a large fraction of the measured rate. Small errors in ρ_0, e, or k_1 will therefore be greatly magnified in the function $k_3/k_5^{1/2}$. This source of error is particularly important in the solvents of low dielectric constant where the rate is very low. For example, the measured rates in *n*-decane, *t*-butylbenzene, and CCl_4 were 8.8, 9.1, and 6.7×10^{-7} mole/l. sec, respectively, but the corrected rates were only 4.4, 2.8, and 2.1×10^{-7} mole/l. sec. Nevertheless, there appears to be a rough general correlation with the styrene data and a rather better correlation with the tetralin and 4-methyl cyclohexene data. A dipolar transition state is therefore probably involved in the propagation reaction with this substrate. This conclusion is supported by the recent correlation of the rate of oxidation of substituted cumenes with the σ^+ constants of the substituents (5).

Hendry (6) has recently measured $k_3/k_5^{1/2}$ at 60° C for 2.0 mole/l. of cyclohexene and for 2.0 mole/l. of cumene in several of the solvents used in this study. In spite of the different temperatures and the fact that oxidation rates tend to be very sensitive to trace

Can. J. Chem. Downloaded from www.nrcresearchpress.com by 210.87.254.105 on 09/05/12
For personal use only.

impurities there is an excellent correlation between his results and our own data on $k_3/k_5^{1/2}$ for styrene at 65° C. That is, the cyclohexene data (eight solvents) give a slope of 0.79 (standard deviation 0.024) and the cumene data (six solvents) give a slope of 0.25 (standard deviation 0.016) when plotted against $k_3/k_5^{1/2}$ for styrene.

In conclusion, the transition state for the propagation step in autoxidation reactions involves some contribution from a dipolar structure whether the peroxy radical abstracts a hydrogen atom or whether it adds to a double bond.

1. J. A. HOWARD and K. U. INGOLD. Can. J. Chem. This issue.
2. R. E. PINCOCK. Paper 26 presented to the CIC Solvation Symposium held at Calgary, Alberta. August, 1963.
3. F. R. MAYO and A. A. MILLER. J. Am. Chem. Soc. **80**, 2480 (1958).
4. P. D. BARTLETT and T. G. TRAYLOR. J. Am. Chem. Soc. **85**, 2407 (1963).
5. G. A. RUSSELL and R. C. WILLIAMSON, JR. Private communication.
6. D. G. HENDRY. Thesis. University Microfilms. Ann Arbor. 1962. Order No. 62-4152.

RECEIVED JANUARY 14, 1964.
DIVISION OF APPLIED CHEMISTRY,
NATIONAL RESEARCH COUNCIL,
OTTAWA, CANADA.

Can. J. Chem. Downloaded from www.nrcresearchpress.com by 210.87.254.105 on 09/05/12
For personal use only.

Can. J. Chem. Downloaded from www.nrcresearchpress.com by 210.87.254.40 on 09/05/12
For personal use only.

Canadian Journal of Chemistry

Issued by THE NATIONAL RESEARCH COUNCIL OF CANADA

VOLUME 42 JUNE 1964 NUMBER 6

THE ELECTRONIC SPECTRA OF SOME ANIONIC POLYMERIZATION SYSTEMS[1]

S. BYWATER, A. F. JOHNSON,[2] AND D. J. WORSFOLD

Applied Chemistry Division, National Research Council, Ottawa, Canada

Received January 16, 1964

ABSTRACT

The ultraviolet absorption spectra of living anionic polymerizing systems have been measured with sytrene, butadiene, and isoprene as the monomers; with lithium, sodium, and potassium as the alkali metals; and with tetrahydrofuran, cyclohexane, and benzene as the solvents. For any monomer the similarity of the spectra obtained with the various metals and solvents leads to the conclusion that the alkali metal – carbon band has the same structure under the various conditions. From other evidence the bond is considered to be ionic in all cases. The diene monomer anions in tetrahydrofuran solution were found to undergo a series of isomerizations, some of them comparable in speed to the consumption of monomer.

Many polymerizations of olefins by anionic reagents occur by the addition of the metal–organic compound to the monomer molecule, M, as the chain initiation step. Chain propagation then proceeds by the addition of further monomer units to the carbon–metal bond at the end of the chain, re-forming the bond at each step.

$$R—M_n—Metal + M \rightarrow R—M_{n+1}—Metal$$

There is disagreement about the relative amount of ionic or covalent character of this bond when different alkali metals are used and when the polarity of the solvent is changed. With lithium in particular (1, 2), it has been suggested that in nonpolar solvents the carbon–lithium bond is largely covalent in character and that with dienes this covalency is the cause of the stereoregulating action found in nonpolar solvents. Addition of polar solvents such as tetrahydrofuran (THF) was supposed to promote ionization of the carbon–lithium bond, the ion-pair reacting to form a more random microstructure.

If the carbon–metal bond is essentially ionic, charge delocalization may be expected to occur with conjugated monomers, and the resultant polymer anions may be expected to show optical absorption in the near ultraviolet region at roughly the same wavelength as observed for the corresponding cations (3). The use of such an absorption band to measure the concentration of active centers in the butyllithium-catalyzed polymerization of styrene in benzene has been described previously (4). The effect of addition of tetrahydrofuran to such a system has been briefly mentioned (5). To learn more about the carbon–metal bond, a more general study of the changes in absorption spectra observed in the polymerization of styrene, butadiene, and isoprene has now been carried out in hydrocarbon solvents, in tetrahydrofuran, and in their mixtures with organo-lithium, -sodium, and -potassium reagents.

[1]*Issued as N.R.C. No. 7853.*

[2]*Present address: University of Sussex, Brighton, Sussex, England.*

Can. J. Chem. Downloaded from www.nrcresearchpress.com by 210.87.254.40 on 09/05/12
For personal use only.

EXPERIMENTAL

The solvents and monomers were purified by standard methods described elsewhere (4, 6). The spectra were measured in the general type of apparatus (7) previously used involving greaseless high-vacuum apparatus to exclude moisture and air. Sodium and potassium films were used to initiate polymerization in THF and in cyclohexane; butyllithium was used to prepare the corresponding lithium compounds.

RESULTS

The absorption bands observed in the anionic polymerization of styrene are shown in Fig. 1. The positions of maximum absorption are given in Table I and show small changes

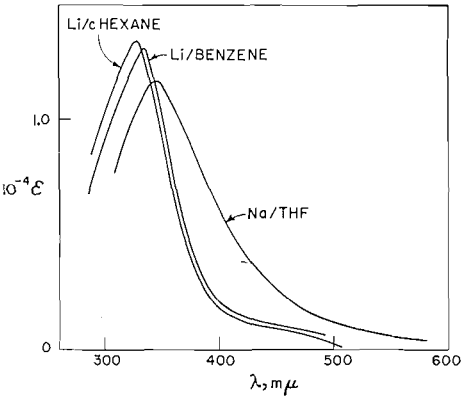

FIG. 1. Absorption spectra of polystyryl anions with different counterions in cyclohexane, benzene, and tetrahydrofuran.

TABLE I

Absorption maxima

Polystyryl anions			
	Counterion	Solvent	λ_{max}, mμ
	K	THF	346
	Na	"	343
	Li	"	338
	"	Benzene	334
	"	Cyclohexane	328

Polydienyl anions				
			λ_{max}, mμ	
Monomer	Counterion	Solvent	Initial	First isomerized
Isoprene	K	THF	318	390
"	Na	"	(300 indistinct)	358
"	Li	"	287	330
"	K	Cyclohexane	(363)	
"	Na	"	297	
"	Li	"	270	
Butadiene	K	THF	312	385
"	Li	"	288	
"	"	Cyclohexane	275	

with alkali metal or with solvent. The absorption is proportional to the initiator concentration, and, since it is known that on complete initiation one polymer molecule is formed

per added initiator molecule, the absorption can be attributed to the reactive end grouping on the polymer chains. The absorption bands are very similar to those observed for benzyl-lithium or -sodium in the appropriate solvent (8, 9).

Similar absorption bands can be observed in the anionic polymerization of isoprene and butadiene; Table I shows the position of the maxima. With isoprene the measurements are complicated by rapid changes which occur in the spectra in tetrahydrofuran solution. After a time comparable to the time taken for the monomer to be consumed, a matter of minutes, the originally formed peaks have declined and other peaks of longer wavelength have appeared. With potassium as initiator, even in cyclohexane, complex spectra are observed. Initiation by metal films is rather slow and with potassium polyisoprene, for instance, the spectrum is already complex when first measured. Only the major band is shown in the table. It is possible that this band is not that of the species causing the polymerization, but is of some already isomerized product.

The effect of small amounts of tetrahydrofuran on the spectrum of polyisoprenyllithium in cyclohexane is a simple broadening of the band. In the presence of 1% tetrahydrofuran, the absorption maximum was still at 270 mμ, but slow isomerization occurred to give an absorption near 320 mμ.

DISCUSSION

Polystyryl–Alkali Metal Compounds

When the metal or solvent is changed, the similarity of the integral extinction coefficient and the positions of maximum absorption is strong evidence that the nature of the absorbing species is the same throughout. It seems likely that the carbon–metal bond is predominantly ionic in character, because in tetrahydrofuran the presence of conducting species has been observed for polystyrylsodium (7). The major part of this compound was shown to exist as ion-pairs in equilibrium with a small concentration of free ions at total concentrations around millimolar. The measured dissociation constant (1.5×10^{-7}) in this solvent is consistent with a simple dissociation process

$$R(M)_n^-Na^+ \rightleftharpoons R(M)_n^- + Na^+$$

rather than the more complex equilibria

$$R(M)_n—Na \rightleftharpoons R(M)_n^-Na^+ \rightleftharpoons R(M)_n^- + Na^+$$

which would also give the same dependence of equivalent conductance on total concentration of organometallic compound. This interpretation is confirmed by the absence in benzene solution of any temperature dependence of the extinction coefficient, which would be observed in the absorption spectrum if significant amounts of covalent form were present in equilibrium.

In tetrahydrofuran, solvation must add significantly to the stability of the ionic species. In hydrocarbon solvents stabilization of the ion-pair form by solvation will be reduced by about 50%, but the loss of solvation energy is apparently replaced by interaction energy between ion-pairs, which are known to be highly associated to dimers in solvents such as cyclohexane and benzene. This association has been demonstrated by kinetic methods (4, 11) and by direct light-scattering measurements on the active and deactivated polymer solutions (12). This phenomenon disappears at relatively low THF concentrations ($\sim$ 25:1 mole:mole calculated on total alkali metal) (5). As the major species changes from the ion-pair dimer to solvated ion-pairs, the ultraviolet absorption broadens without

Can. J. Chem. Downloaded from www.nrcresearchpress.com by 210.87.254.40 on 09/05/12
For personal use only.

changing the position of maximum absorption. At this point insufficient THF is present to materially affect the dielectric constant. The small change in the position of maximum absorption occurs as the bulk dielectric constant of the medium changes.

In nonpolar solvents the absorption spectrum reflects the properties of the ion-pair dimer, whereas the reactive species in polymerization has been shown (4) to be the small amount of free ion-pair present. The absorption in nonpolar solvents can thus give no evidence about the structure of the free ion-pair, which could conceivably differ from that of the associated form.

Polyisoprenyl– and Polybutadienyl – Alkali Metal Compounds

The wavelengths of the absorption maxima of the first peaks formed under the various conditions and assigned to the unisomerized polymer anion vary over a somewhat wider range than do those of the corresponding polystyryl compounds. But if that of the polyisoprenylpotassium in cyclohexane is rejected for reasons given earlier, the shifts are similar to those found in the spectrum of the benzophenone – alkali metal ketyls as the solvent and counterion were changed (13). Warhurst attributed the shifts caused by changing the counterion to perturbations of the energy levels of the anion by the field of the associated cation. This effect will increase as the cation radius decreases. However, it is not clear why the effect should be larger for the polyisoprenyl anion than for the polystyryl anion. McClelland (14) has made an approximate analysis of the cation field effect in the benzophenone compounds. This indicates that in the ground state the counterion is localized near the oxygen atom, but in the excited state the equilibrium position is centered on the aromatic rings. In an optical transition the counterion is therefore not in its equilibrium position after excitation and the transition energy is increased, by an amount which is a function of the cation field. For benzyl type anions a similar shift of effective charge from the side group to the aromatic ring might be expected on excitation, although the spectral shifts found are small.

It seems reasonable to suppose that in tetrahydrofuran the carbon–metal bond is again essentially ionic in nature and that the spectral shifts observed between alkali metals are due to the perturbing effect of the cation. The polymer microstructure in this solvent is predominantly 3:4 and varies little with the metal, suggesting the presence of similar reactive species at the chain ends.

In cyclohexane the polymer microstructure has changed to a predominantly *cis* 1:4 structure when the counterion is lithium and to a more mixed 1:4, 3:4 structure for the other counterions (2). Nevertheless, the spectral evidence suggests little change in the character of the major species present, because the spectral changes with change of alkali metal are very similar to those observed in THF. This similarity suggests that in cyclohexane the bulk of the isoprenyl – alkali metal compounds must have a largely ionic nature, too. Once again stabilization of the ion-pairs is effected through the formation of aggregates. Thus it would seem that there is no connection between the stereoregulating influence of the lithium counterion and the nature of the bond in the bulk of the polymerizing species present. Because of this aggregation, as mentioned before for styrene in hydrocarbon solvents, the spectra do not necessarily reflect the nature of the species active in the polymerization. The active species is probably a free ion-pair form (11), but it does seem likely that it is also ionic. In cyclohexane with 1% THF present, the polymer formed is no longer largely *cis* 1:4 with butyllithium. Although the ion-pairs are largely dissociated in the presence of such an amount of THF (11), the absorption is still at 270 mμ.

Can. J. Chem. Downloaded from www.nrcresearchpress.com by 210.87.254.40 on 09/05/12
For personal use only.

Diene–Carbanion Isomerization in THF

The absorption peaks first formed in tetrahydrofuran soon decay with the formation of peaks at longer wavelengths, and presumably this isomerization gives a more stable carbanion (Fig. 2). This occurs so rapidly for the sodium and potassium compounds, that even the very first spectrum measured one minute after the start of the reaction showed appreciable isomerization (Fig. 3). One isomerization possible with isoprene when 3:4

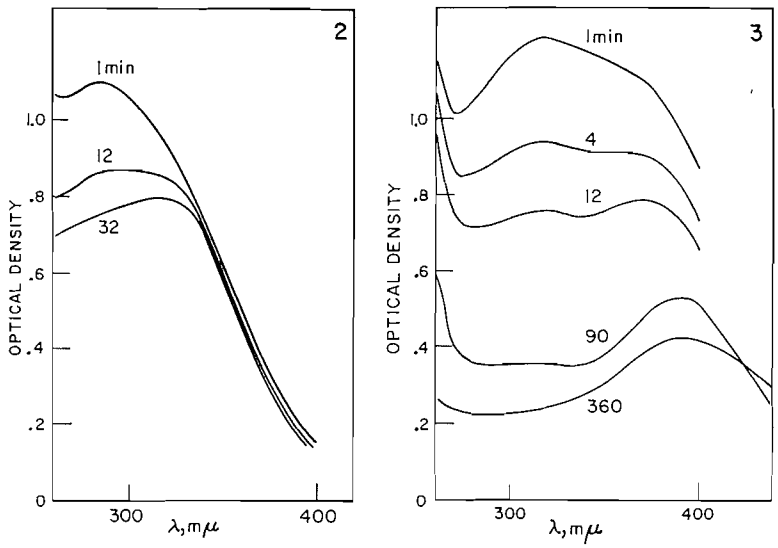

FIG. 2. Changes in spectrum with time after formation of polyisoprenyllithium in tetrahydrofuran.
FIG. 3. Changes in spectrum with time shortly after formation of polyisoprenylpotassium in tetrahydrofuran.

structures are formed is as illustrated and gives a more symmetrical allylic type carbanion.

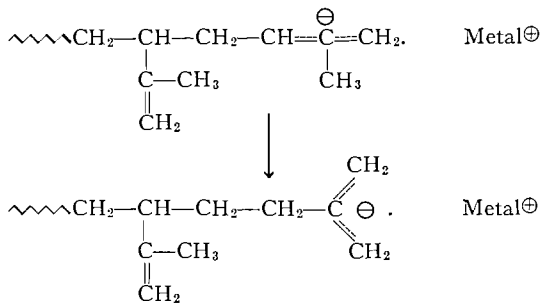

This mechanism is supported by measurements of the positions of the absorption maxima of comparably substituted allyllithiums in tetrahydrofuran solution.

Allylic carbanion	λ_{max}, this work	λ_{max} (10)
Allyllithium	317 mμ	315 mμ
Equilibrium mixture of α- and γ-methylallyllithium		291
β-Methylallyllithium	332	

The absorption maxima of the equilibrium mixture of α- and γ-substituted allyllithium is close to the initially formed, correspondingly substituted carbanion from butadiene and

Can. J. Chem. Downloaded from www.nrcresearchpress.com by 210.87.254.40 on 09/05/12
For personal use only.

butyllithium and is also close to that from isoprene despite the extra methyl group. The β-substituted allyl carbanion absorbs close to the isomerized product from polyisoprenyllithium, the suggested isomerized structure above also having the β-substituent only. No such isomerization is possible in the polybutadienyl carbanion, and indeed it is found that polybutadienyllithium does not isomerize. Polybutadienylpotassium does show an isomerization, however, and this observation casts some doubt on the isomerization mechanism suggested above, but the carbanions from isoprene and butadiene with both sodium and potassium show far more complex behavior than do those with lithium, further isomerizations occurring after the initial rapid one. The initial isomerization may be a distribution of the carbanions among the various sites available, as has been suggested by Morton in alfin catalysis (15). Later isomerizations could well be of the type undergone by the polystyryl anion in ether solutions, with an increase in the stabilization by extra conjugation (16).

The rapid isomerization of polyisoprenyllithium in tetrahydrofuran is reversible in that the addition of another portion of monomer can cause the ion to revert temporarily to the original carbanion. There was little indication that this occurred with sodium or potassium as the counterions. It was found that the first isomerized form would react with styrene to give the polystyryl carbanion. Presumably there is a kinetic balance between the tendency to isomerize and the re-formation of the original ion by reaction of the isomerized form with monomer. The above isomerizations would lead to the presence of extraneous structures in the polymer chains. There is some evidence for abnormal structures in the infrared spectra of the alkali metal initiated polyisoprenes, where considerable deviations from the sum of the spectra of the individual expected (1, 4; 1, 2; 3, 4) structures occur (17).

The occurrence of rapid isomerization must cast some doubt on the usefulness of some of these systems for the production of narrow distribution polymers and block copolymers, unless the conditions are chosen to avoid these isomerizations. Kinetic studies in tetrahydrofuran will also be complicated by this type of rearrangement.

REFERENCES

1. R. S. Stearns and L. E. Forman. J. Polymer Sci. **41**, 381 (1959).
2. A. V. Tobolsky and C. E. Rogers. J. Polymer Sci. **40**, 73 (1959).
3. S. F. Mason. Quart. Rev. London, **15**, 287 (1961).
4. D. J. Worsfold and S. Bywater. Can. J. Chem. **38**, 1891 (1960).
5. D. J. Worsfold and S. Bywater. Can. J. Chem. **40**, 1564 (1962).
6. S. Bywater and D. J. Worsfold. J. Polymer Sci. **58**, 571 (1962).
7. S. Bywater and D. J. Worsfold. J. Chem. Soc. 5234 (1960).
8. R. Waack and M. A. Doran. J. Phys. Chem. **67**, 148 (1963).
9. R. Asami, M. Levy, and M. Szwarc. J. Chem. Soc. 361 (1962).
10. R. Waack and M. A. Doran. J. Am. Chem. Soc. **85**, 1651 (1963).
11. M. Morton, E. E. Bostick, and R. Livigni. Rubber Plastics Age, 397 (1961).
12. A. F. Johnson and D. J. Worsfold. To be published.
13. D. G. Powell and E. Warhurst. Trans. Faraday Soc. **58**, 953 (1962).
14. B. J. McClelland. Trans. Faraday Soc. **57**, 1458 (1961).
15. A. A. Morton. Ind. Eng. Chem. **42**, 1488 (1950).
16. G. Spach, M. Levy, and M. Szwarc. J. Chem. Soc. 355 (1962).
17. J. L. Binder and C. H. Ranshaw. Anal. Chem. **29**, 503 (1957).

Can. J. Chem. Downloaded from www.nrcresearchpress.com by 210.87.254.40 on 09/05/12
For personal use only.

Can. J. Chem. Downloaded from www.nrcresearchpress.com by 210.87.254.5 on 09/05/12
For personal use only.

EXOCELLULAR BACTERIAL POLYSACCHARIDE FROM XANTHOMONAS CAMPESTRIS NRRL B-1459

PART III. STRUCTURE[1]

J. H. Sloneker, Danute G. Orentas, and Allene Jeanes
Northern Regional Research Laboratory,[2] U.S. Department of Agriculture, Peoria, Illinois

Received September 23, 1963

ABSTRACT

Periodate oxidation showed that the *O*-acetyl groups in the polysaccharide sterically affected the rate but not the extent of oxidation of the D-mannose residues, two-thirds of which were glycosidically substituted at C_2 by a D-glucuronic acid residue and one-third of which was linked as a terminal side-chain residue. The D-glucose and D-glucuronic acid residues oxidized by periodate were substituted at C_4, but both were more resistant to oxidation than were the D-mannose residues. One-third of the D-glucose residues and a significant quantity of the D-glucuronic acid residues were inert to vigorous periodate oxidation and may bear side-chain residues. Quantitative recovery of the periodate-stable D-glucose residues as 2-*O*-β-D-glucopyranosyl-D-erythritol, after the oxidized polysaccharide was reduced with sodium borohydride and hydrolyzed with mild acid, revealed that two-thirds of the D-glucose residues were in pairs linked (β, $1 \rightarrow 4$). The pyruvic acid linkage in the polysaccharide was established as a 4,6-*O*-1-carboxyethylidene ketal attached to a terminal D-glucose side-chain residue. The structure of the polysaccharide is discussed in relation to its anomalous viscosity behavior in salt solutions.

In a previous paper the polysaccharide elaborated by *Xanthomonas campestris* NRRL B-1459 was shown to be composed of the sugars D-glucose, D-mannose, and D-glucuronic acid in the ratio 2.8:3.0:2.0 (1). Acetic and pyruvic acid substituents are present in amounts of 4.7% and 3.0–3.5%, respectively. Acetic acid exists as the *O*-acetyl ester, whereas pyruvic acid is attached through a ketal linkage (2). Periodate oxidation of the polysaccharide under various oxidation conditions, followed by reduction with sodium borohydride and examination of the remaining products after acid hydrolysis, has provided further structural information.

RESULTS

Periodate consumption by the polysaccharide depends upon the reaction conditions. At 20° C, the native and deacetylated polysaccharides undergo oxidation at the same rate and to the same extent with either 0.02 *M* periodic acid or sodium metaperiodate. In 140 hours approximately 0.8 mole of periodate was reduced and 0.13 mole of acid produced per sugar residue (Fig. 1). After 140 hours at 4° C, the native polysaccharide had reduced only 0.56 mole of periodate per sugar residue, which is the approximate amount required for complete oxidation of the mannose residues, but the amount of acid produced was the same as that from the oxidation carried out at 20° C. When the periodate concentration was decreased to 0.005 *M* at 4° C, the deacetylated polysaccharide was oxidized at a significantly faster rate than native polysaccharide (Fig. 1), but acid production for both remained at 0.13 mole per sugar residue.

Both the native and deacetylated polysaccharides were oxidized to essentially the same extent by periodate at 20° C as shown by the determination of the residual sugars after borohydride reduction and acid hydrolysis (Table I). All the D-mannose residues

[1]*Presented before the Division of Carbohydrate Chemistry at the 142nd meeting of the American Chemical Society, Atlantic City, New Jersey, September 1962.*
[2]*A laboratory of the Northern Utilization Research and Development Division, Agricultural Research Service.*

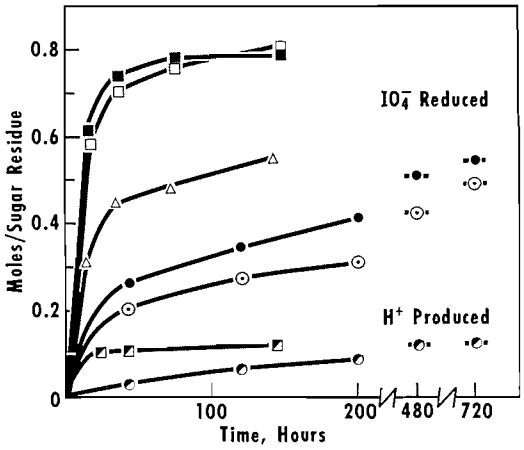

FIG. 1. Periodate oxidation of the native and deacetylated forms of polysaccharide B-1459, 0.02 *M* H_5IO_6 or $NaIO_4$ at 20° C: ■ deacetylated, □ native, ◩ acid-produced from both; 0.02 *M* H_5IO_6 at 4° C: △ native; 0.005 *M* $NaIO_4$ at 4° C: ● deacetylated, ⊙ native, ◐ acid-produced from both.

TABLE I

Periodate oxidation of the native and deacetylated forms of polysaccharide B-1459; measurement of residual components and oxidation fragments after sodium borohydride reduction

	Samples of polysaccharide			
		Oxidized and reduced		
	Unoxidized native T-42	Native MP-3*	Native MP-3†	Deacetylated MP-3†
	Moles/sugar residue			
IO_4^- reduced	—	0.47	0.80	0.79
H^+ produced	—	0.13	0.13	0.13
	Molar proportions			
D-Glucose	2.8	2.24	1.41	1.54
D-Mannose	3.0	0.94	None	None
D-Glucuronic acid	2.0	1.77	0.85	0.83
Erythritol	—	—	1.52	1.45
Pyruvic acid	0.62	0.51	0.62	0.68

Oxidation conditions:
*0.005 *M* $NaIO_4$ at 4° C for 720 hours.
†0.02 *M* H_5IO_6 at 20° C for 140 hours.

and approximately 50% of the D-glucose and D-glucuronic acid residues were oxidized. The quantity of erythritol in the hydrolyzates of both samples was equivalent to the oxidized D-glucose residues. Glycerol, also present in the hydrolyzates, was not measured quantitatively.

When the native polysaccharide was oxidized at 4° C with 0.005 *M* sodium metaperiodate, two-thirds of the D-mannose residues were cleaved, whereas only a small portion of the D-glucose and D-glucuronic acid residues was oxidized. Reduction of this periodate-oxidized product followed by acid hydrolysis yielded a relatively large proportion of glycerol but only traces of erythritol. When this reduced polymeric product

Can. J. Chem. Downloaded from www.nrcresearchpress.com by 210.87.254.5 on 09/05/12
For personal use only.

was acid hydrolyzed under conditions milder than those used for the sugar determination, approximately 7% of the D-glucose was recovered as cellobiose.

Anion-exchange chromatography of the polysaccharide degraded by periodate oxidation, borohydride reduction, and mild acid hydrolysis (3) led to the isolation of 50% of the pyruvic acid as 1,3-*O*-(1-carboxyethylidene)-L-erythritol along with other oxidation products, including L-erythronic acid, 2-*O*-β-D-glucopyranosyl-D-erythritol, and three glucuronic-acid-containing oligosaccharides.

DISCUSSION

Previous reports (4, 5) indicated that uronic-acid-containing compounds have a tendency to "overoxidize" with sodium metaperiodate but not with periodic acid. Therefore, both sodium metaperiodate and periodic acid were employed to study the oxidation behavior of the polysaccharide. As seen in Fig. 1, at 20° C both reagents oxidized the native and deacetylated polysaccharides similarly, and no "overoxidation" was indicated with either reagent under the conditions used (Table I).

A constant quantity of formic acid, 1 equivalent per 8 sugar residues, is produced either under severe oxidation conditions where all three sugars are oxidized or under more mild conditions where only D-mannose residues are oxidized. Presumably the formic acid originates from the oxidation of nonreducing D-mannose end residues. The quantity of formic acid produced is equivalent to one-third of the D-mannose residues in the polysaccharide. Also, one-third of the D-mannose residues is hydrolyzed from the polysaccharide by acid more readily than the other sugar residues (1). Such behavior indicates that these "acid-labile" D-mannose residues are nonreducing end residues that are bound to the polysaccharide chain by a single glycosidic bond. The remaining two-thirds of the D-mannose residues are substituted at C_2 as shown by the isolation of 2-*O*-β-D-glucopyranosyluronic acid-D-mannose (1).

At high concentrations of periodate the native and the deacetylated polysaccharide undergo oxidation at about the same rate, but with low concentrations of periodate the deacetylated polysaccharide is oxidized at a much faster rate. Therefore, the acetyl groups, which are not affected during the oxidation, must sterically hinder oxidation of the D-mannose residues. This conclusion was supported by the observation that removal of the acetyl groups resulted not only in an increased rate of oxidation of the terminal D-mannose residues (increased formic acid production), but also in an increased rate of cleavage of the D-mannose residues linked at C_1 and C_2.

Pyruvic acid appears to be a common substituent in the exocellular polysaccharides produced by members of the genus *Xanthomonas* (6, 7). In the polysaccharide from *X. campestris* the pyruvic acid was not affected by extensive periodate oxidation and was recovered as 1,3-*O*-(1-carboxyethylidene)-L-erythritol after the oxidized polysaccharide had been reduced with sodium borohydride and hydrolyzed with acid under mild conditions (3). Since D-glucose is the sole source of erythritol (Table I) in the polysaccharide, the only structure from which the pyruvic acid ketal can originate directly without rearrangement is a terminal side-chain 4,6-*O*-(1-carboxyethylidene)-D-glucose residue having free hydroxyls at C_2 and C_3. The pyruvic acid content requires approximately one such residue for every 16 sugar residues. This same ketal has been found previously in a pyruvic-acid-containing seaweed agar attached to a D-galactose residue linked at C_1 and C_3 (8).

Both structural and steric factors influence the periodate oxidation of the D-glucose and D-glucuronic acid residues. These two sugar residues were oxidized only slightly under

Can. J. Chem. Downloaded from www.nrcresearchpress.com by 210.87.254.5 on 09/05/12
For personal use only.

the conditions of low temperature and low concentrations of periodate that caused the D-mannose residues to oxidize readily. By increasing the temperature and the concentration of periodate, 50% of the D-glucose and D-glucuronic acid residues were oxidized (Table I). More than 50% of the D-glucose and D-glucuronic acid residues were oxidized when the polysaccharide was subjected to the oxidation conditions used to isolate the pyruvic acid ketal, 1,3-*O*-(1-carboxyethylidene)-L-erythritol. However, even with this extensive oxidation, approximately one-third of the total number of D-glucose residues and a significant portion of the D-glucuronic acid residues were inert. The D-glucose residues were isolated as 2-*O*-β-D-glucopyranosyl-D-erythritol and the D-glucuronic acid residues were recovered in several acidic oligosaccharides after the oxidized polysaccharide was reduced and hydrolyzed with acid under mild conditions (Table II). To be inert

TABLE II

Ion-exchange chromatography of oxidized polysaccharide after reduction and hydrolysis

Fraction	Tube no.	Weight (mg)	Contents after acid hydrolysis*
A	1–10	1180	D-Glucose, glyceraldehyde, glycolaldehyde, glycerol, erythritol, 2-*O*-β-D-glucopyranosyl-D-erythritol, L-erythronolactone
B	100–120	45	D-Glucuronic acid, D-mannose, D-glucose, erythritol
C	129–136	53	L-Erythronic acid
D	145–160	58	D-Glucuronic acid, glyceraldehyde, glycerol, D-glucose
E	260–280	46	D-Glucuronic acid, glyceraldehyde
F	290–320	55	Pyruvic acid, erythritol

*Fraction A was not hydrolyzed.

to periodate oxidation, the glucopyranose residues must have either a glycosidic substituent at C_3 or substituents on at least two of the following positions—C_2, C_3, and C_4. Since the number of inert D-glucose residues is approximately equal to the number of terminal D-mannose side-chain residues, it is believed that the inert D-glucose residues constitute branch points in the polysaccharide and are, therefore, doubly substituted at C_2, C_3, or C_4. Similarly the D-glucuronic acid residues may be inert to periodate oxidation through glycosidic substitution by the side-chain residue, 4,6-*O*-(1-carboxyethylidene)-D-glucose.

The steric factors influencing the oxidation of the "periodate-labile" D-glucose and D-glucuronic acid residues in the polysaccharide are: both the D-glucose and D-glucuronic acid residues are linked in a β-configuration as indicated by the isolation of 2-*O*-β-D-glucopyranosyl-D-erythritol and 2-*O*-β-D-glucopyranosyluronic acid-D-mannose; both are glycosidically substituted at C_4 as shown by the isolation of erythritol and L-erythronic acid, respectively, after periodate oxidation, borohydride reduction, and acid hydrolysis. The *trans*-glycol group at C_2 and C_3 of β-glucosides is much more resistant to periodate oxidation than is that of the α-anomers because an equatorially oriented aglycone on the β-anomer is sufficiently close to the hydroxyl on C_2 to hinder the attack by periodate (9). A bulky equatorial glycoside at C_4 should exert similar steric hindrance on the hydroxyl at C_3. Thus the *trans*-glycol groups at C_2 and C_3 of both the D-glucose and D-glucuronic acid residues should be doubly hindered. The *trans*-glycol group at C_2 and C_3 of the 4,6-*O*-(1-carboxyethylidene)-D-glucose residues would also be doubly hindered if this side-chain residue is β-linked to the polysaccharide backbone, but the steric hindrance will be lessened by the cyclic nature of the carboxyethylidene substituent attached to C_4 and C_6.

In contrast, the D-mannose residues in the polysaccharide should be oxidized by

Can. J. Chem. Downloaded from www.nrcresearchpress.com by 210.87.254.5 on 09/05/12
For personal use only.

periodate more rapidly than the D-glucose or D-glucuronic acid residues. Only a single glycoside substituent at C_2 sterically hinders the periodate oxidation of the *trans*-glycol group at C_3 and C_4 of the D-mannose residues linked at C_1 and C_2. Moreover, this substituent at C_2, although bulky, is in an axial conformation and would have steric effects similar to an aglycone of an α-glucoside (9). The terminal D-mannose side-chain residues have a *cis*, *trans*, triol group at C_2, C_3, and C_4 and should be oxidized rapidly with little hindrance by the substituent at C_1.

A structure consisting of a repeating unit of 16 residues (Fig. 2) is proposed for the

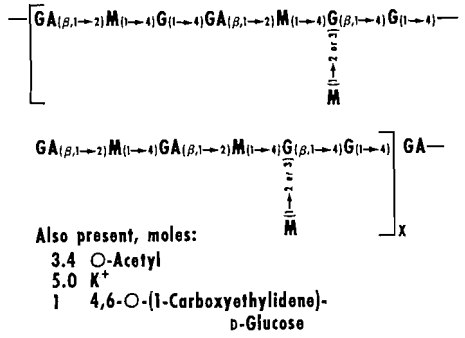

FIG. 2. Block of 16 hexose residues from the polysaccharide elaborated by *Xanthomonas campestris* NRRL B-1459, depicting order of arrangement and linkages: GA, D-glucuronic acid; M, D-mannose; G, D-glucose.

polysaccharide elaborated by *X. campestris* NRRL B-1459 on the basis of the experimental evidence. The linear portion of the polysaccharide consists of D-glucose, D-mannose, and D-glucuronic acid residues. The isolation of 2-*O*-β-D-glucopyranosyluronic acid-D-mannose (1) shows that the D-glucuronic acid residues are linked to C_2 of D-mannose residues. At least part of the D-mannose residues in the polysaccharide backbone are linked glycosidically to D-glucose residues as shown by the isolation of an aldotriouronic acid consisting of all three sugars with a D-glucose residue as the reducing end group (1). The remaining D-mannose residues in the polysaccharide backbone are probably linked to D-glucuronic acid residues, as shown in Fig. 2, although an aldotetraouronic acid containing two 2-*O*-β-D-glucopyranosyluronic acid-D-mannose units was not observed in acid hydrolyzates of the polysaccharide. Quantitative determination of 2-*O*-β-D-glucopyranosyl-D-erythritol indicates that two-thirds of the D-glucose residues are found in pairs linked (β, $1 \rightarrow 4$) to each other. The position of the remaining D-glucose residue in the polysaccharide backbone is not known. It may occur singly as in Fig. 2 or in a sequence of three D-glucose residues.

Six of the glycosidic bonds in the polysaccharide segment (Fig. 2) are known β-linkages. The remainder are presumed to be β also, because the polysaccharide has a low optical rotation [$[\alpha]_D^{25}$ 0°, (*c*, 1.0, water)] and except for the D-mannose side-chain residues is quite resistant to acid hydrolysis.

Studies of molecular models of ($1 \rightarrow 2$) linked sugar residues, such as occur in the main chain of the polysaccharide (Fig. 2), show that the ($1 \rightarrow 2$) linkages do not prevent a linear extension of the polysaccharide chain. However, in the extended molecule, the bulk of a sugar residue linked at C_1 and C_2 projects away from the axis of the main chain to produce a bulge approximately equivalent in size and steric properties to that of a nonreducing side-chain residue. The combined effect of the sugar residues linked

Can. J. Chem. Downloaded from www.nrcresearchpress.com by 210.87.254.5 on 09/05/12
For personal use only.

at C_1 and C_2 and the side-chain residues D-mannose and 4,6-*O*-(1-carboxyethylidene)-D-glucose confer upon the polysaccharide the character of a linear polymer with single unit side-chains, there being seven such apparent protruding groups for every 16 sugar residues (Fig. 2). The relatively frequent occurrence of single side-chain sugar residues and pseudo side-chain effects from $(1 \rightarrow 2)$ linkages does not prevent the polysaccharide from producing excellent water-soluble films with a high degree of flexibility (10). Such behavior is indicative of a polysaccharide which has few, if any, long side branches.

The *O*-acetyl groups are believed to be located on C_6 of the D-mannose residues which are linked at C_1 and C_2. The ratio of the *O*-acetyl groups to these D-mannose residues is 0.85 to 1. Furthermore, the *O*-acetyl groups must be located in a manner that interferes with the periodate oxidation of both forms of the D-mannose residues in the native polysaccharide. The steric hindrance of the D-mannose residues carrying the *O*-acetyl group is in accord with the known steric hindrance produced by bulky groups at C_6 on the periodate oxidation of the *trans* glycol group at C_3 and C_4 of the pyranose ring (9). The manner in which the *O*-acetyl group on the D-mannose residue in the main chain interferes with the oxidation of the D-mannose side-chain residue can be visualized by constructing a molecular model of a D-glucose residue substituted by two D-mannose residues as shown in Fig. 2. The two D-mannose residues are close together and the *O*-acetyl group attached to C_6 of the D-mannose residue in the main chain is in a position to hinder sterically the periodate oxidation of the D-mannose side-chain residue.

Solution viscosities of this anionic polysaccharide are atypically insensitive to the charge-neutralizing effects of electrolytes. Addition of salts to aqueous dispersions of the polysaccharide at concentrations of 0.25% or less resulted in a decrease in viscosity less than that shown by typical polyelectrolytes. For concentrations of polysaccharides greater than 0.25% the solution viscosity is increased markedly by addition of salt (11). Structural and steric factors appear to influence the behavior of the polysaccharide in solutions of electrolyte more than do charge effects. The large number of side-chain residues and $(1 \rightarrow 2)$ linkages restrict the flexibility of the long polysaccharide chains by steric hindrance. The role of side-chains in producing rigidity in polymer chains is well established (12, 13). This structural rigidity limits the loss in viscosity by permitting only a small decrease in the effective solution volume of the polysaccharide even though the coulombic repulsion of the carboxyl groups is reduced by salt (14, 15). The observed increases in viscosity of more concentrated solutions of the polysaccharide, after reduction of ionic repulsion by salt, may be due to an increase in intermolecular association. The rather rigid polysaccharide molecule remains in a more extended state, which favors intermolecular association as well as intermolecular entanglement, to produce a gel-like structure. However, the side-chain groups limit the amount of intermolecular association by steric hindrance (15) and prevent dehydration and precipitation of the polysaccharide from viscous solutions containing high concentrations of salt (16).

EXPERIMENTAL

Materials and Methods

The polysaccharide used for these experiments was an experimental pilot-plant preparation designated MP-3 (17). This material was identical in sugar and *O*-acetyl group content with a laboratory preparation designated T-42, which was used for compositional studies (1, 11). The laboratory preparation, however, contained 20% more pyruvic acid (1). Deacetylated polysaccharide was prepared from MP-3 as previously described (11).

The chromatographic solvents were: (A) ethyl acetate – acetic acid – water (3:1:3) (18); (B) *n*-butyl alcohol – pyridine – water (6:4:3) (19); and (C) *n*-butyl alcohol – ethyl alcohol – water (4:1:5) (20); all v/v. Ammoniacal silver nitrate was used to detect sugars on the developed chromatograms (21). Whatman

Can. J. Chem. Downloaded from www.nrcresearchpress.com by 210.87.254.5 on 09/05/12
For personal use only.

No. 1 paper* was used for quantitative and qualitative chromatography, and Whatman 3MM paper was used to separate and isolate larger quantities of pure sugars. All steps involving reduction of solution volume were carried out on a vacuum rotary evaporator at a bath temperature of 40° C unless otherwise stated.

Periodate Oxidation of Polysaccharide B-1459

For periodate oxidation studies, a portion of a solution containing the required amount of sodium metaperiodate or periodic acid was stirred into a homogeneous dispersion of polysaccharide in water, and the polysaccharide concentration was adjusted to 0.1% by adding a minimum amount of water. A periodate blank was prepared accordingly. Oxidations were carried out in the dark at either 20° C or 4° C. The periodate consumption was measured by the arsenite method (22) and the thiosulphtae method (23). Both methods gave identical values. The acid produced by periodate was measured titrimetrically with 0.01 *N* barium hydroxide (22). The results are shown in Fig. 1.

Sodium Borohydride Reduction of Periodate-oxidized Polysaccharide Samples

After oxidation, excess periodate was reduced with ethylene glycol. The reaction mixture was neutralized to pH 6.7 with solid sodium bicarbonate and dialyzed (Visking tubing) for 6 days against distilled water to remove salts. Toluene was added to each dialysis bag for asepsis. The retentate (24) was removed from the dialysis bag, sodium borohydride (20% by weight of polymer) was stirred in, and the mixture was allowed to react overnight at 25° C. Excess borohydride was destroyed by acidifying the reaction mixture to pH 5.5 with glacial acetic acid. The pH was adjusted to 6.7 with sodium bicarbonate and the solution was dialyzed against distilled water for 6 days. During dialysis the pH of the retentate dropped from 6.7 to between 4.5 and 5.0. Residual borate ions were removed by evaporating the solution to dryness, dispersing the residue in dry methanol, and removing the methanol by vacuum distillation. The oxidized and reduced polysaccharide, after drying over phosphorus pentoxide at room temperature, was a white or light tan powder insoluble in water. Yields of 90 to 95% were obtained.

Quantitative Determination of Residual Sugars and Oxidation Products

Samples of both the native and deacetylated polysaccharides which had been periodate oxidized and borohydride reduced were hydrolyzed in *N* hydrochloric acid for 2.5 hours at 100° C. The free sugars in the hydrolyzates were determined as previously described (1). Erythritol was isolated quantitatively by paper chromatography (solvent C) and determined colorimetrically (25). The results are given in Table I. Glycerol also was observed on the paper chromatograms but was not determined quantitatively.

Isolation of Cellobiose

A 2-g sample of the polysaccharide, which had reduced 0.5 mole of sodium metaperiodate per sugar residue and had been reduced with sodium borohydride, was hydrolyzed with *N* hydrochloric acid for 1 hour at 100° C. The hydrolyzate was neutralized to pH 7 with Dowex 1 (carbonate phase). The resin was filtered off, and the filtrate was concentrated to a small volume. Paper chromatography (solvent B) revealed that the concentrate contained glucose, glycerol, erythritol, and a slow-moving reducing sugar. Preparative paper chromatography (solvent B) and elution of the disaccharide fraction afforded 41 mg of a white amorphous powder after two precipitations from ethanol–water. Acid hydrolysis and chromatography of the disaccharide yielded only glucose. In solvents A and B the disaccharide co-chromatographed with cellobiose. An infrared spectrum of a small portion of the disaccharide, which had been crystallized from an ethanol–water–acetone system, was identical with the spectrum produced by cellobiose.

Mild Acid Hydrolysis and Ion-exchange Chromatography

A 1.5-g sample of the polysaccharide was oxidized with 0.2 *M* sodium metaperiodate, reduced with sodium borohydride, and then was hydrolyzed at room temperature for 24 hours in 150 ml of *N* hydrochloric acid. This material, which had reduced 1.2 moles of sodium metaperiodate per sugar residue, was insoluble in water but dispersed immediately in the acid. The solution was neutralized with silver carbonate, the precipitate was removed by filtration, and excess silver ions were removed as silver sulphide. The solution was concentrated to a small volume, filtered, and neutralized to pH 7 with 0.1 *N* sodium hydroxide. The neutral concentrate was poured onto a 2- × 40-cm ion-exchange column composed of Dowex 1X4, 200–400 mesh (acetate phase). After the concentrate had percolated into the resin, the column was washed with 100 ml of water, and the acidic fractions were separated by gradient elution. An adequate gradient was maintained by passing 5 liters of 3 *N* acetic acid into the mixing flask containing 1500 ml of water. Ten-milliliter fractions were collected at a flow rate of 1 ml per minute.

Pyruvic acid, D-glucuronic acid, and L-erythronic acid were detected qualitatively in the eluate fractions as follows: (A) Pyruvic acid was detected by a method similar to that used to measure the pyruvic acid in the intact polysaccharide (26). Portions of the column eluate (0.5 ml) were transferred to 18- × 150-mm test tubes containing 0.5 ml of 2 *N* hydrochloric acid and were hydrolyzed for 3 hours at 100° C. To the hydrolyzate, 1 ml of 2,4-dinitrophenylhydrazine reagent (2,4-DNP) was added, and the reaction was allowed to proceed for 5 minutes. Ethyl acetate (5 ml) was added, and the pyruvic acid 2,4-DNP was

**Mention of trade names should not be construed as a recommendation or endorsement by the Department over those not mentioned.*

Can. J. Chem. Downloaded from www.nrcresearchpress.com by 210.87.254.5 on 09/05/12
For personal use only.

Can. J. Chem. Downloaded from www.nrcresearchpress.com by 210.87.254.5 on 09/05/12
For personal use only.

extracted from the aqueous layer, which was then discarded. Fifteen milliliters of 10% sodium carbonate was added to the ethyl acetate, and the tube contents were thoroughly mixed. After the two phases separated completely, the absorbance of the carbonate layer was measured at 375 mμ. Aqueous acetic acid produced a slight background color but did not interfere with the assay. (B) The D-glucuronic acid was detected by the use of the carbazole reagent (27). (C) Erythronic acid was detected with fuchsin–sulphite after periodate oxidation (28). A 0.5-ml portion of column eluate was reacted 5 minutes at 23° C with 0.5 ml of periodic acid – B solution. The excess periodate was destroyed by adding excess sulphite solution and then several drops of fuchsin–sulphite solution were added with stirring. Periodate-oxidized erythronic acid produces an immediate pink color of a Schiff's base. Compounds readily oxidized by periodate, such as glycerol and erythritol, react similarly.

On the basis of the qualitative assays, the 10-ml fractions were combined into six different fractions, which were reduced in volume and recovered by lyophilization (Table II).

Components of neutral fraction A.—Glycerol, glycolaldehyde, glyceraldehyde, small quantities of glucose and erythritol, and a significant quantity of a slower moving disaccharide were observed in fraction A when a portion of it was chromatographed in solvents B and C. The remainder of fraction A was dissolved in 5 ml of water to which 5 ml of ethyl alcohol was added. A semicrystalline precipitate formed upon the slow addition of 15 ml of acetone. The precipitate was collected by centrifugation and redissolved in 1 ml of water. Upon paper chromatography in solvents B and C the precipitate appeared to consist primarily of the disaccharide that was observed in the neutral fraction. Preparative paper chromatography in solvent B afforded 114 mg of material which readily crystallized from a water–ethanol–acetone (2:10:30) system. After a second crystallization, the compound had a specific optical rotation of $[\alpha]_D^{25}$ −16 (*c*, 0.94, H_2O); m.p. 185.5–187° C. Glucose and erythritol were produced by acid hydrolysis of the crystalline material. Anal. Calc. for $C_{10}H_{20}O_9$; C, 42.3; H, 7.09. Found: C, 41.9; H, 6.85. These analytical data are in agreement with those reported for 2-*O*-β-D-glucopyranosyl-D-erythritol ($[\alpha]_D^{25}$ −17; m.p. 185–187° C) (29). Upon periodate oxidation, 2-*O*-β-D-glucopyranosyl-D-erythritol reduced 3.13 moles of sodium periodate and produced 0.93 mole of acid and 1.04 moles of formaldehyde; the theoretical values for 2-*O*-β-D-glucopyranosyl-D-erythritol are 3, 1, and 1, respectively.

The yield of 2-*O*-β-D-glucopyranosyl-D-erythritol from the periodate-oxidized, borohydride-reduced polysaccharide was determined on 111 mg of the same polysaccharide product used in the column chromatography experiment. Mild acid hydrolysis was conducted as described above. After neutralization, part of the hydrolyzate was quantitatively chromatographed in solvent C. The area containing 2-*O*-β-D-glucopyranosyl-D-erythritol was eluted and the contents determined by the phenol – sulphuric acid method (30). One mole of 2-*O*-β-D-glucopyranosyl-D-erythritol was produced for every 9.3 sugar units in the polysaccharide.

Components of glucuronic-acid-containing fractions B, D, and E.—These three fractions were subjected to paper chromatography in solvents A and B both before and after acid hydrolysis in *N* hydrochloric acid at 100° C. Each appeared as a single spot before hydrolysis. Paper chromatography in solvent A revealed that the acid hydrolyzates of fractions B, D, and E contained unoxidized D-glucuronic acid (Table II). These fractions appear to be aldobio-, aldotrio-, and aldotetrao-uronic acids in which one of the sugar residues has been oxidized with periodate and reduced with borohydride.

Fraction C, erythronic acid.—Fraction C, a waxy solid, with the chromatographic behavior of erythronic acid, was extracted with hot ethyl acetate to convert the acid to its lactone. Long needlelike crystals (32 mg) formed when the extract was evaporated. After a second crystallization from ethyl acetate, the waxy crystals melted at 100–101° C. The melting point of L-erythronolactone is 103–104° C (31). Pure D-erythronolactone mixed with the crystals depressed the melting point to 85–86° C. Anal. Calc. for $C_4H_6O_4$: C, 40.7; H, 5.12. Found: C, 40.1; H, 5.26. The remainder of the L-erythronolactone was converted to the corresponding crystalline brucine salt, melting point 211° C (reported 212° C (31)). Anal. Calc. for $C_{27}H_{34}N_2O_9$: C, 61.1; H, 6.46; N, 5.28. Found: C, 60.0; H, 6.32; N, 5.27. The lactone of L-erythronic acid also was found in fraction A. It apparently formed during the prolonged acid hydrolysis.

Fraction F, 1,3-O-(1-carboxyethylidene)-L-erythritol.—Fraction F contained 50% of the total pyruvic acid, which had been applied to the column, in a chemically combined state. The lyophilized fraction was dissolved in 2 ml of water and neutralized with saturated barium hydroxide. The barium salt, which precipitated as a soft gel from 70% aqueous ethanol upon addition of acetone, formed an amorphous powder when dried. Acid hydrolysis (*N* hydrochloric acid for 3 hours at 100° C) and quantitative estimation of the products revealed that the compound was composed of pyruvic acid and erythritol in a 1:1 ratio. Anal. Calc. for $(C_7H_{11}O_6)_2Ba$: C, 33.6; H, 4.27; Ba, 26.43. Found: C, 33.1; H, 4.77; Ba, 26.20. Infrared analysis of the barium salt in potassium bromide showed bands at 6.2 and 7.1 μ characteristic of a carboxyl ion and strong bands at 8.5 and 9.4 μ. These strong bands are reported to be characteristic of a six-membered ring structure containing a —C—O—C—O—C-group (32). A nuclear magnetic resonance spectrum shows several hydrogen resonances, CH_3— at 86, —CH—O— and —CH_2—O— at 218 and 226, and —OH at 332 c.p.s. ($(CH_3)_2Si(CH_2)_3SO_3H$ reference). The chemical and spectral evidence indicates that pyruvic acid is bound to erythritol by a ketal linkage. Because the barium salt of the ketal did not react with 0.01 *M* sodium metaperiodate at 4° C, the pyruvic acid must form the six-membered ring

ketal, 1,3-*O*-(1-carboxyethylidene)-L-erythritol. The remainder of the pyruvic acid, like L-erythronolactone, is suspected to be in fraction A as a lactone of 1,3-*O*-(1-carboxyethylidene)-L-erythritol. Evidence for this assumption is indicated by a positive test for pyruvic acid in this fraction.

ACKNOWLEDGMENT

We are gratefully indebted to Mrs. Clara McGrew and Mrs. Bonita Heaton for analytical analyses and to Mr. Curtis Glass for infrared analyses.

REFERENCES

1. J. H. SLONEKER and A. JEANES. Can. J. Chem. **58**, 2066 (1962).
2. J. H. SLONEKER and D. G. ORENTAS. Can. J. Chem. **58**, 2188 (1962).
3. I. J. GOLDSTEIN, G. W. HAY, B. A. LEWIS, and F. SMITH. Abstracts of Papers, 135th Meeting of the American Chemical Society, Boston, Mass. April, 1959. p. 3D.
4. C. F. HUEBNER, S. R. AMES, and E. C. BUBL. J. Am. Chem. Soc. **68**, 1621 (1946).
5. F. SMITH. Private communication.
6. D. G. ORENTAS, J. H. SLONEKER, and A. JEANES. Can. J. Microbiol. **9**, 427 (1963).
7. A. MISAKI, S. KIRKWOOD, J. V. SCALETTI, and F. SMITH. Can. J. Chem. **40**, 2204 (1963).
8. S. HIRASE. Bull. Chem. Soc. Japan, **30**, 68, 70 (1957); Chem. Abstr. **52**, 9479*i* (1958).
9. E. F. GARNER, I. J. GOLDSTEIN, R. MONTGOMERY, and F. SMITH. J. Am. Chem. Soc. **80**, 1206 (1958).
10. P. R. WATSON, A. JEANES, and C. E. RIST. J. Appl. Polymer Sci. **6**, S12 (1962).
11. A. JEANES, J. E. PITTSLEY, and F. R. SENTI. J. Appl. Polymer Sci. **5**, 519 (1961).
12. S. S. WINTER and C. O. BECKMANN. J. Phys. Chem. **60**, 883 (1956).
13. W. BROWN. Arkiv Kemi, **18**(3), 227 (1961).
14. R. M. FUOSS and U. P. STRAUSS. J. Polymer Sci. **3**, 602 (1948).
15. J. JOHNSON, JR., S. KIRKWOOD, A. MISAKI, T. E. NELSON, J. V. SCALETTI, and F. SMITH. Chem. Ind. London, 820 (1963).
16. S. S. WINTER and L. A. PAPAZIAN. J. Phys. Chem. **61**, 1142 (1957).
17. S. P. ROGOVIN, R. F. ANDERSON, and M. C. CADMUS. J. Biochem. Microbiol. Technol. Eng. **3**, 51 (1961).
18. M. A. JERMYN and F. A. ISHERWOOD. Biochem. J. **44**, 402 (1949).
19. E. CHARGAFF, C. LEVINE, and C. GREEN. J. Biol. Chem. **175**, 67 (1948).
20. B. LINDBERG, A. MISIORNY, and C. A. WACHTMEISTER. Acta Chem. Scand. **7**, 591 (1953).
21. S. M. PARTRIDGE. Nature, **158**, 270 (1956).
22. J. C. RANKIN and A. JEANES. J. Am. Chem. Soc. **76**, 4435 (1954).
23. G. HUGHES and T. P. NEVELL. Trans. Faraday Soc. **44**, 941 (1948).
24. E. G. TURNER and J. G. FEINBERG. Nature, **184**, 1139 (1959).
25. M. LAMBERT and A. C. NEISH. Can. J. Research, Ser. B, **28**, 83 (1950).
26. J. H. SLONEKER and D. G. ORENTAS. Nature, **194**, 478 (1962).
27. Z. DISCHE. *In* Methods of biochemical analysis. Vol. II. Interscience Publishers, New York. 1955. p. 342.
28. R. D. HOTCHKISS. Arch. Biochem. Biophys. **16**, 131 (1948).
29. A. J. CHARLSON and A. S. PERLIN. Can. J. Chem. **34**, 1200 (1956).
30. M. DUBOIS, K. A. GILLES, J. K. HAMILTON, P. A. REBERS, and F. SMITH. Anal. Chem. **28**, 350 (1956).
31. O. RUFF. Ber. **34**, 1368 (1901).
32. H. TSCHAMLER and R. LEUTNER. Monatsh. Chem. **83**, 1502 (1952).

Can. J. Chem. Downloaded from www.nrcresearchpress.com by 210.87.254.5 on 09/05/12
For personal use only.

Can. J. Chem. Downloaded from www.nrcresearchpress.com by 210.87.254.40 on 09/05/12
For personal use only.

THE CONFIGURATION AND CONFORMATION OF "DI-D-FRUCTOSE ANHYDRIDE I"

R. U. LEMIEUX AND R. NAGARAJAN*
Department of Chemistry, University of Alberta, Edmonton, Alberta
Received December 17, 1963

ABSTRACT

"Di-D-fructose anhydride I", obtained by acid depolymerization of inulin triacetate, was found to be 1′,2-anhydro-[1-(α-D-fructofuranosyl)-β-D-fructofuranose]. The high resistance to oxidation by periodate found for the α-D-fructofuranoside portion was related to the conformation for the ring wherein the 3′- and 4′-hydroxyl groups are in quasi-axial orientation. This and other conclusions about the conformations of the anhydride were based on a comparison of the 100 Mc.p.s. proton magnetic resonance spectra of the 6,6′-dideoxytetra-*O*-acetyl derivative of the anhydride, sucrose octaacetate, and 1,6-anhydro-α-D-galactofuranose triacetate.

DISCUSSION

When D-fructose reacts with aqueous acid, dimeric D-fructose anhydrides are formed which possess a central 1,4-dioxane ring. Six such di-D-fructose dianhydrides have been described (1). Although both the action of aqueous acid on D-fructose (2) or inulin (3) and the heating of a concentrated aqueous solution of D-fructose (4, 5) lead to mixtures of these anhydrides, the treatment of inulin triacetate in chloroform with fuming nitric acid yields only the hexaacetate of that isomer known as "di-D-fructose anhydride I" (6). The formation of the di-D-fructose anhydrides has been attributed (7, 8) to the stability of the 1,4-dioxane ring.

"Di-D-fructose anhydride I" was first reported almost simultaneously by Jackson and Goergen (3) and by Irvine and Stevenson (6). Methylation followed by hydrolysis to yield 3,4,6-tri-*O*-methyl-D-fructose established the compound to be the 1,2′:1′,2-dianhydride of D-fructose (7). The consumption of 2 moles of periodic acid by the compound provided additional support for this structure (9). The configurations of the anomeric centers in the di-D-fructose anhydrides have not been established.

The α,β-configuration was readily established for "di-D-fructose anhydride I" by application of proton magnetic resonance (NMR) spectroscopy. To achieve better chemical shifts between the various kinds of protons, the spectrum of the hexa-*O*-acetyl derivative (I) of II was determined at 100 Mc.p.s. with chloroform as solvent. Should the compound contain either the α,α- or β,β-configurations, the conformational equilibration would be expected to lead to time-averaging of the resonances for the protons at the corresponding positions in each of the rings. Certainly, the chemical shifts of the protons at the 1- and 1′-positions would be averaged out through rapid conformational change of the dioxane ring (10). This would result in the averaging of the resonances for protons at corresponding positions in the furanoside rings even though these rings should be conformationally rigid. Therefore, the NMR spectra for the 1,2′:1′,2-di-D-fructofuranose anhydride hexaacetates with the α,α- and β,β-configurations should show signals for only five kinds of protons on the sugar residue and three pairs of nonequivalent acetyl groups. However, as seen from the spectrum in Fig. 1, the hexaacetate (1) of "di-D-fructose anhydride I" (II) provided a much more complex spectrum. It is seen, for example, that even the methylenic protons of the dioxane ring are not equivalent. Also, the acetyl group region possessed

**Postdoctoral Fellow, 1961–1963.*

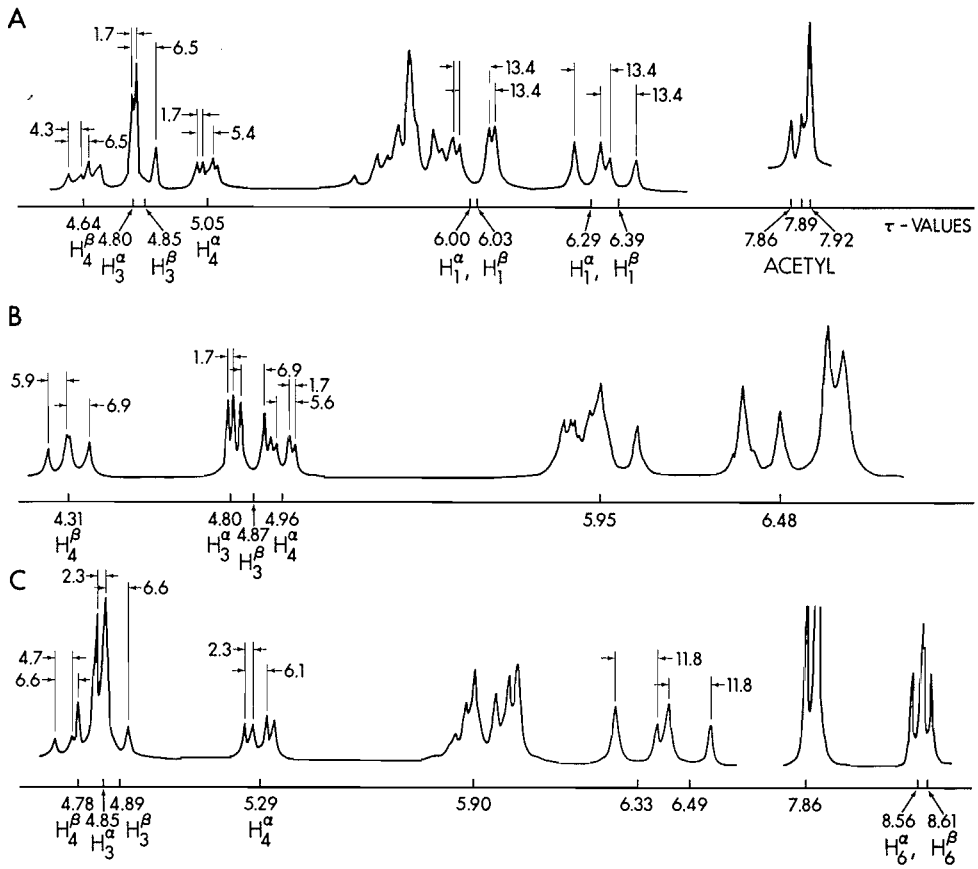

FIG. 1. NMR spectra at 100 Mc.p.s. in chloroform: (A) "di-D-fructose anhydride I" hexaacetate (I); (B) 6,6′-di-*O*-trityl "di-D-fructose anhydride I" tetraacetate (III); and (C) 6,6′-dideoxy-"di-D-fructose anhydride I" tetraacetate (V). The signals for the aromatic and acetyl-group protons are not shown in spectrum B. The spacings are in c.p.s. and the α and β designations refer to the furanoside ring with the corresponding anomeric configuration. The H_1^{α}, H_1^{β} and H_6^{α}, H_6^{β} assignments may in each case be reversed.

three signals of relative intensities 1:1:4. The indication was clear, therefore, that the compound has one of the anomeric centers in the α- and the other in the β-configuration. This conclusion was substantiated by the results obtained in a study of the periodate oxidation of II since, as discussed below, one of the furanoside rings proved to be much more resistant to oxidation than the other. To eliminate the possibility that II was not a 1,2′:1′,2-dianhydride, the compound was fully *O*-methylated and the product hydrolyzed in order that the hydrolyzate could be examined by the modern methods of paper chromatography. In fact, the hydrolyzate contained only one component which gave a color reaction with *p*-anisidine hydrochloride and possessed an R_f value close to that reported for 3,4,6-tri-*O*-methyl-D-fructose.

The formation of the hexaacetate (I) on acid treatment of the triacetate of the 1,2-linked β-D-fructosan (inulin) therefore involved a change in the configuration of the reacting anomeric center. In view of this stereochemical route, the course of the reaction can be depicted as an acid-catalyzed, transglycosidative depolymerization as shown below.

Can. J. Chem. Downloaded from www.nrcresearchpress.com by 210.87.254.40 on 09/05/12
For personal use only.

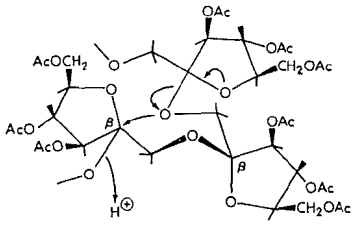

INULIN TRIACETATE

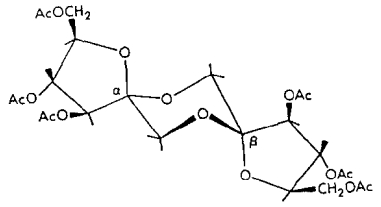

I

Although II consumed 1 mole of periodate at pH 4.05 in 4 hours, 127 hours were required for the consumption of the next 0.86 moles. This slow consumption of periodate by a vicinal glycol group situated on a *simple* five-membered ring appeared without precedent and provided the incentive to determine the conformation of the compound by application of high resolution NMR spectroscopy. Clearly, the high resistance to periodate oxidation exhibited by one of the rings requires a high degree of conformational rigidity. The previous experience with periodate-resistant vicinal glycols indicated a conformation wherein the hydroxyl groups define a dihedral angle greater than 120° (11–13).

McDonald and Jackson (14) subjected II to tritylation followed by acetylation to obtain a crystalline tetra-*O*-acetyl-di-*O*-trityl derivative (III) which was subsequently detritylated to yield a crystalline tetraacetate (IV) of II. The acetyl groups in IV were believed (14) to be at the 3-, 3′-, 4-, and 4′- positions. This conclusion was substantiated in the present investigation by tosylation of IV followed by reaction with sodium iodide to form a tetra-*O*-acetyl-6,6′-dideoxydiiodo derivative of II. Hydrogenolysis of the diiodide gave a crystalline tetra-*O*-acetyl-dideoxy derivative (V) of II. The NMR spectrum of V gave two doublets each of intensity three at 8.56 τ and 8.61 τ with spacings of 6.6 c.p.s. and 6.1 c.p.s., respectively, thus establishing the presence of two *C*-methyl groups each coupled to only one proton (15). It follows, therefore, that compound IV is 3,3′,4,4′-tetra-*O*-acetyl-1′,2-anhydro-[1-(α-D-fructofuranosyl)-β-D-fructofuranose]. As indicated in this name, the prime numbers will be used hereafter to refer to positions in the α-D-fructose residue.

The 100 Mc.p.s. spectra of compounds I, III, IV, and V were examined for information on the conformations of the furanose rings through application of the relationships that appear to exist between the coupling constant and the dihedral angle defined by vicinal protons (16–18). Most of the pertinent NMR data are presented in Fig. 1 and summarized in Table I. The chemical shifts of the protons at the 3-, 4-, and 5- positions in each of the furanose rings are in all cases large as compared to the observed spacings. It can therefore be concluded that the spacings found correspond closely to the coupling constants involved.

Can. J. Chem. Downloaded from www.nrcresearchpress.com by 210.87.254.40 on 09/05/12
For personal use only.

Can. J. Chem. Downloaded from www.nrcresearchpress.com by 210.87.254.40 on 09/05/12
For personal use only.

TABLE I

NMR parameters for a number of derivatives of 1′,2-anhydro-[1-(α-D-fructofuranosyl)-β-D-fructofuranose] (II)

Derivative	Approximate coupling constants (c.p.s.)				Chemical shifts (τ values)					
	H_3,H_4	H_4,H_5	$H_{3'},H_{4'}$	$H_{4'},H_{5'}$	H_3	H_4	H_5	$H_{3'}$	$H_{4'}$	$H_{5'}$
Hexa-*O*-acetyl (I)	6.5	4.3	1.7	5.4	4.85	4.64	—	4.80	5.05	—
Tetra-*O*-acetyl-6,6′-dityril (III)	6.9	5.9	1.7	5.6	4.87	4.31	—	4.80	4.96	—
3,4,3′,4′-Tetra-*O*-acetyl (IV)	6.6	5.2	1.6	5.6	4.82	4.63	—	4.83	5.00	—
Tetra-*O*-acetyl-6,6′-dideoxy (V)	6.6	4.7	2.3	6.1	4.89	4.78	5.9[1]	4.85	5.29	5.9[1]

[1]Established by double irradiation and observation of the collapse of the signals for H_4 and $H_{4'}$.

Can. J. Chem. Downloaded from www.nrcresearchpress.com by 210.87.254.40 on 09/05/12
For personal use only.

The purpose of this research was mainly to gain a better experimental basis for the conformational analysis of furanoside rings (19). The conformation indicated for compound I was suggested by conformational analysis for the following reasons. The two furanoside rings can in theory exist in a number of conformations wherein either one (C_s or envelope conformation) or two (C_2 or twist conformation) of the ring atoms is or are out of the plane of the other ring atoms. In view of the anomeric effect (19) and especially as demonstrated by the conformations of the *trans*-2,5-dichloro- and *trans*-2,3-dibromo-1,4-dioxanes (20), it must be anticipated that the furanoside-ring oxygens will be axially oriented on the dioxane ring of I. Also, in view of the anomeric effect, it can be anticipated that the oxygens of the dioxane will favor quasi-axial orientations on the furanoside rings. Furthermore, it is to be expected that the ring oxygen of a furanoside ring will tend to occupy a central position in that portion of the ring where four of the ring atoms are nearest to coplanarity (19). In other words, it is to be expected that *in general furanoside rings will tend to be puckered in such a manner as to have a carbon meta to the ring oxygen (either the 2- or the 3-carbon for aldofuranosides; either the 3- or 4-carbons for ketofuranosides) furthest out of the mean plane of the ring.* This conclusion is well borne out by the experimental evidence. It is established that the 2-carbon is out of plane in cytidine (21) and the 3-carbon is the atom out of plane in cytidine 3-phosphate (22) and 5′-bromo-5′-deoxythymidine (23). In the case of sucrose (24), it is the 4′-carbon which is out of plane. The 100 Mc.p.s. spectrum for methyl β-D-ribofuranoside was determined in chloroform and showed $J_{1,2} = 0.8$, $J_{2,3} = 4.9$, and $J_{3,4} = 6.3$ c.p.s. These coupling constants are well accommodated by the C_s conformation with the 3-carbon out of the plane of the other ring atoms. These considerations together with the avoidance of the eclipsing of large substituents lead to the conclusion that the conformations for the furanoside rings must be close to those depicted in the conformational formula II. This conformation would account for the periodate oxidation data since the hydroxyls of the two α-glycol groups would define dihedral angles of about 150° and 75° in the α- and β-furanoside rings, respectively.

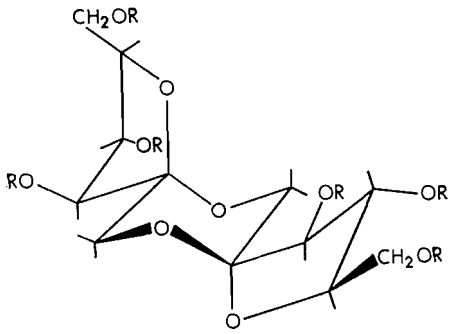

I, R = Ac

II, R = H

The NMR spectral features for compounds I, III, IV, and V are in excellent agreement with this conformation for these compounds. The relevant data are presented in Table I. First of all, it should be noted that the coupling constants for the 3- and 4-protons (average 6.7 c.p.s.) are substantially greater than those for the 3′ and 4′-protons (average 1.8 c.p.s.).

Since the 3- and 4-protons are in *trans*-relationship on a five-membered ring, these hydrogens cannot conceivably define a dihedral angle of less than 60°. Therefore, the large coupling constant, according to the Karplus relationship (16), must arise from hydrogens which define a dihedral angle in the range 150° to 180°. Consequently, the dihedral angle defined by the 3- and 4-hydroxyls in this ring must be in the range 60° to 90° and comprise the glycol group readily susceptible to periodate cleavage. This conclusion was substantiated by treatment of II with 1.1 moles of periodate and reduction of the product with sodium borohydride. Acetylation gave an oil in 93% yield, based on the structure VI for the substance shown in Fig. 2,A. This structure was fully justified by its NMR spectrum. As expected, the coupling constant found for the protons at the 3- and 4-positions of the furanoside ring was small (1.5 c.p.s.). Deacetylation of VI followed by acid hydrolysis liberated fructose, glycerol, and dihydroxyacetone in agreement with the assigned structure.

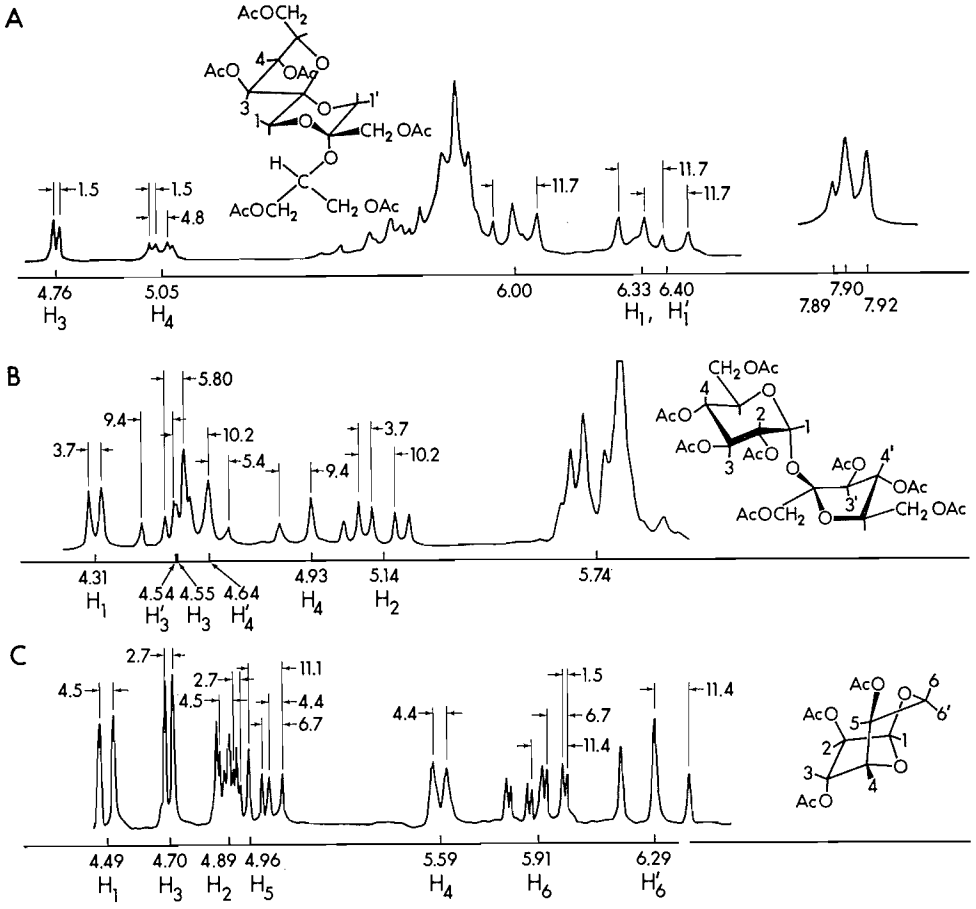

FIG. 2. NMR spectra at 100 Mc.p.s. in chloroform: (A) compound (VI); (B) sucrose octaacetate; and (C) 1,6-anhydro-α-D-galactofuranose triacetate. The signals for the acetyl groups are not shown in spectra B and C. In spectrum A, the H_1, H_1' signals are not specifically assigned.

To fully justify the conformation indicated in formula II for "di-D-fructose anhydride I", it was necessary to gain evidence that the periodate-resistant ring in fact possessed the α-D-configuration. The fact that VI showed a stronger dextrotation (+16°) than I (+0.5°)

Can. J. Chem. Downloaded from www.nrcresearchpress.com by 210.87.254.40 on 09/05/12
For personal use only.

favored this assignment. However, the evidence provided by the NMR spectra of sucrose octaacetate and 1,6-anhydro-α-D-galactofuranose triacetate, reproduced in Fig. 2, provided more definitive evidence. The coupling constant for the 3′- and 4′-protons of the furanose ring in sucrose octaacetate was found to be 5.4–5.8 c.p.s. in agreement with expectations based on the conformation of sucrose (24) and the form for the Karplus expression normally found in carbohydrate structures. The β-D-furanoside ring of sucrose, although less susceptible to periodate oxidation than the α-D-glucopyranoside ring, is readily oxidized. The β-D-furanose ring undergoes lead tetraacetate oxidation extremely readily (25). The coupling constant for the 2- and 3-protons of the 1,6-anhydro-α-D-galactofuranose triacetate is 2.7 c.p.s. (see Fig. 2,C). Since these protons are in *trans*-relationship, this small coupling constant in itself cannot provide information on the dihedral angle defined by the protons. It was possible by double irradiation experiments to definitely locate the resonance for each of the protons in the molecule. The coupling constants found are indicated in Fig. 2,C and are $J_{1,2} = 4.5$, $J_{2,3} = 2.7$, $J_{3,4} \simeq 0$, $J_{4,5} = 4.4$, $J_{5,6} = 6.7$, $J_{5,6'} = 11.4$, and $J_{6,6'} = 11.4$ c.p.s. In addition, the signals for the 4- and 6-protons showed long-range coupling as was observed by Hall and Hough (26) in the spectra for a number of 1,6-anhydroaldopyranose triacetates. Spin-decoupling established that this long-range coupling involves the 2-proton and that $J_{2,4} = 1.1$ and $J_{4,6} = 1.5$ c.p.s. These coupling constants are best rationalized, on the basis of the type of relationship proposed by Karplus, by the conformation for the compound shown in Fig. 2,C wherein the 3-carbon is furthest out of the mean plane of the atoms in the ring. The fact that $J_{2,3}$ is larger than $J_{3,4}$ suggests that the furanose ring is somewhat distorted from the envelope conformation. The main point of interest is that the conformation has the 2- and 3-hydroxyls define a dihedral angle of about 150°, an angle compatible with the resistance to periodate oxidation exhibited by the parent alcohol (11).

In conclusion, "di-D-fructose anhydride I" definitely is 1′,2-anhydro-[1-(α-D-fructofuranosyl)-β-D-fructofuranose] and possesses a conformation close to that presented in structure II. The degree of conformational rigidity displayed by the α-furanoside ring in II is important in relation to the occurrence of furanoside rings in a wide variety of important biological compounds including coenzymes, nucleotides, and antibiotics.

EXPERIMENTAL

The melting points were determined on a Leitz heating stage and are not corrected. The optical rotations were measured at room temperature at the D-line of sodium. The NMR spectra were obtained with a Varian Associates model HR-100 spectrometer at 100 Mc.p.s. and the line positions calibrated by the side-band technique using a Hewlett-Packard audiofrequency oscillator model 200 AB and an electronic counter model 521C. Proton-proton spin decoupling was achieved in the manner previously described (18).

"Di-D-fructose Anhydride I" (II) and Its Hexaacetate (I)

The hexaacetate (I) was prepared according to Irvine and Stevenson (6). The melting point, 137°, optical rotation, +1.08°, and yield were in agreement with those previously reported. The hexaacetate (I), 20 g, was heated for 5 minutes with boiling 0.01 *M* methanolic sodium methoxide. The residue obtained on evaporation of the methanol soon crystallized and was purified by recrystallization from ethanol. The purified product (II) melted at 162–164° with $[\alpha]_D$ +27.6° (*c*, 7.5 in water). The values previously reported (3, 5) are m.p. 164°, $[\alpha]_D^{20}$ +26.9° (*c*, 8.45 in water).

The dianhydride (II) was methylated using dimethyl sulphate and barium hydroxide in dimethyl sulphoxide (27), and the product was separated from a small amount of contaminant by chromatography on a cellulose column using methylethylketone saturated with water as the developing phase (28). The purified product, R_{TG} 1.0, was found to be homogeneous on paper chromatography using *n*-butanol, ethanol, water (5:1:4) (29) and, on hydrolysis at 60° for 1 hour in 1 *N* hydrochloric acid, was converted to only one substance, $R_{TG} = 0.91$. The product of the hydrolysis was also homogeneous when chromatographed on paper using the aqueous methylethylketone (28) as developing phase. *p*-Anisidine hydrochloride was used as spray reagent (30).

Can. J. Chem. Downloaded from www.nrcresearchpress.com by 210.87.254.40 on 09/05/12
For personal use only.

3,4,3′,4′-Tetra-O-acetyl-"di-D-fructose anhydride I" (IV)

3,4,3′,4′-Tetra-*O*-acetyl-6,6′-dityrityl-"di-D-fructose anhydride I" (III) was prepared as described by McDonald and Jackson (14). The compound melted at 192–193° with $[\alpha]_D$ +20.1° (*c*, 8.8 in chloroform) in agreement with the values recorded, m.p. 194°, $[\alpha]_D^{20}$ +21.06 (*c*, 3.73 in chloroform). The NMR spectrum measured in chloroform is reproduced in Fig. 1 (see also Table I). The assignments were made on the basis of the structures of the signals and by comparison with the spectrum obtained for 6,6′-dideoxy-"di-D-fructose anhydride I" tetraacetate (V).

The dityrityl tetraacetate (III), 8.0 g, was hydrogenolyzed at atmospheric pressure in 500 ml of ethanol using 500 mg of 10% palladium on charcoal (purchased from Engelhard Industries Inc.). The compound (III) dissolved in the course of the reaction. When the hydrogen uptake was complete, the catalyst was removed by filtration. On evaporation of the ethanol *in vacuo*, the first crystalline deposit was triphenylmethane, m.p. 93°. After the latter compound was removed, the highly concentrated solution deposited the tetraacetate (IV) in crystalline condition and this product was purified by recrystallization from ethanol. The physical constants, m.p. 187–188°, $[\alpha]_D$ −1.94° (*c*, 20.8 in chloroform), were substantially higher than the values recorded in the literature (14), m.p. 173°, $[\alpha]_D^{20}$ −9.9° (*c*, 3.73 in chloroform).

6,6′-Dideoxy-"di-D-fructose Anhydride I" Tetraacetate (V)

Compound IV, 0.80 g, was dissolved in 15 ml of dry pyridine with 1.55 g of *p*-toluenesulphonyl chloride. After standing for 16 hours at room temperature, the reaction mixture was processed in the usual manner to obtain 1.23 g of a sirupy product. The NMR spectrum of the compound in deuterated chloroform showed signals at 2.43 (quartet), 7.57, and 7.95 τ, the regions characteristic for protons and methyl groups situated on the benzene ring and in acetoxy groups, respectively. The relative intensities of these signals was 4:3:6, respectively, as expected for presence of two tosyl groups in a tetraacetate. The sirup was dissolved in 30 ml of acetone with 11.5 g of sodium iodide and the solution was heated in a sealed tube for 20 hours at 110°. The reaction mixture was added to water and the product isolated by extraction with chloroform followed by evaporation of the chloroform in the usual manner. The yield was 1.02 g of a crystalline product whose NMR spectrum was devoid of signals characteristic for tosyloxy groups. The substance without purification was dissolved in 40 ml of methanol along with 0.45 g of diethylamine. Palladium (10%) on charcoal, 100 mg, was added and the solution was stirred in an atmosphere of hydrogen for 2 hours. After this time, the hydrogen uptake had ceased and the catalyst was removed by filtration. The solvent was removed and the residue was acetylated for 15 hours at room temperature in a mixture of 5 ml of pyridine and 5 ml of acetic anhydride. The product was isolated in the usual manner to provide a sirup which crystallized from ethanol. Purification by recrystallization from ethanol gave 345 mg of compound V, m.p. 169–170°, $[\alpha]_D$ −7.34° (*c*, 23.7 in chloroform). Calc. for $C_{20}H_{28}O_{12}$: C, 52.17; H, 6.13%. Found: C, 52.47, 52.26; H, 5.96, 5.78%.

The NMR spectrum (see Fig. 1) showed two doublets with spacings of 6.57 and 6.06 c.p.s. centered at 8.56 and 8.61 τ, respectively. When the sample was simultaneously irradiated at 5.90 τ, the above-mentioned doublets collapsed to two singlets. The total intensity of the two doublets was one half the intensity of the signal for acetoxy-group protons at 7.86 τ. The irradiation at 5.90 τ also led to the collapse of the two quartets at 4.78 and 5.29 τ. It followed, therefore, that the latter quartets arise from protons at the 4- and 4′- positions, respectively. Irradiation of the quartet at 4.78 τ collapsed the doublet with a spacing of 6.6 c.p.s. at 4.89 τ. Therefore this doublet must arise from the 3-hydrogen. Irradiation of the quartet at 5.29 τ caused a collapse of the doublet with 2.3 c.p.s. spacing at 4.85 τ and this doublet must arise from the 3′-hydrogen. Thus, the spin-decoupling experiments provided the assignment of signals anticipated from first-order analysis of the spectrum.

Periodate Oxidation of "Di-D-fructose Anhydride I" (II)

In a typical experiment, compound II, 151.9 mg (0.468 millimoles), and 289 mg (1.35 millimoles) of sodium metaperiodate were dissolved at zero time in 100 ml of acetate buffer solution at pH 4.05. The periodate consumption was subsequently determined after several intervals of time using the Fleury–Lange arsenite–iodometric method (31). Reaction blanks were determined and 0.391 millimoles of methyl-α-D-glucopyranoside was ozidized under the same conditions in a control experiment. After 3.7, 12.5, 42, and 131 hours at room temperature, compound II consumed per mole 1.03, 1.24, 1.56, and 1.86 moles of periodate, whereas the consumption by the methyl-α-D-glucopyranoside was 1.79, 2.01, 2.06, and 2.09 moles of periodate per mole after the same intervals of reaction time.

The oxidation of "di-D-fructose anhydride I", 0.648 g (2.0 millimoles) in 10 ml of water, with 0.46 g (2.2 millimoles) of sodium metaperiodiate was followed polarimetrically. The specific rotation dropped from +27.6° to a constant value of +5.4° in a period of 2 hours. The resulting solution was reacted with 0.190 g (5 millimoles) of sodium borohydride for 6 hours at room temperature. After this period, the excess of borohydride was destroyed by adding acetic acid and the pH was adjusted to 4.5. The solution was evaporated at 40° *in vacuo* to about 5 ml and then freeze-dried. To the resulting cake, 5 ml of methanol was added, the mixture was heated to the boiling point, and then evaporated to dryness. This procedure was repeated four times. To the dry cake, 10 ml of pyridine and 10 ml of acetic anhydride was added and the reaction mixture was left at room temperature for 15 hours. The usual work-up procedure afforded

Can. J. Chem. Downloaded from www.nrcresearchpress.com by 210.87.254.40 on 09/05/12
For personal use only.

1.08 g (93% yield) of a light sirup, $[\alpha]_D$ +16.2° (*c*, 1.21 in chloroform). The NMR spectrum is reproduced in Fig. 2. The chemical shifts and relative intensities of the various signals clearly required the compound to be essentially pure. The relative intensities of the three sets of signals for the protons in acetoxy groups agreed well with that expected for a hexaacetate (VI), namely 1:3:2. Further evidence of essential purity was provided by deacetylation in 50% aqueous methanol 10% in triethylamine and chromatographic examination. The sirupy product, $[\alpha]_D$ +20.1° (*c*, 6.07 in water), showed only one component in detectable quantity with $R_f = 0.28$ when chromatographed on paper using *n*-butanol, ethanol, water (5:1:4) as developing phase. Hydrolysis of the compound at 95° in 1 *N* sulphuric acid for 15 minutes and chromatographic analysis of the product using pyridine, *n*-butanol, acetic acid, water (4:6:1:3) revealed the formation of fructose, glycerol, and dihydroxyacetone.

ACKNOWLEDGMENTS

This research was made possible by a grant to R. U. L. from the Sugar Research Foundation, Inc., New York as their Project No. 88. The sample of 1,6-anhydro-α-D-galactopyranose triacetate was kindly provided by N. K. Richtmyer. The NMR spectra were determined by Mr. G. Bigam of this department.

1. M. L. WOLFROM, H. W. HILTON, and W. W. BINKLEY. J. Am. Chem. Soc. **74**, 2867 (1952).
2. A. PICTET and J. CHAVAN. Helv. Chim. Acta, **9**, 809 (1926).
3. R. F. JACKSON and S. M. GOERGEN. J. Res. Natl. Bur. Std. **3**, 27 (1929).
4. L. SATTLER and F. W. ZERBAN. Ind. Eng. Chem. **37**, 1133 (1945).
5. M. L. WOLFROM and M. G. BLAIR. J. Am. Chem. Soc. **70**, 2406 (1948).
6. J. C. IRVINE and J. W. STEVENSON. J. Am. Chem. Soc. **51**, 2197 (1929).
7. W. N. HAWORTH and H. R. L. STREIGHT. Helv. Chim. Acta, **15**, 693 (1932).
8. E. J. MCDONALD. Advan. Carbohydrate Chem. **2**, 274 (1946).
9. E. J. MCDONALD and R. F. JACKSON. J. Res. Natl. Bur. Std. **35**, 497 (1945).
10. A. D. COHEN, N. SHEPPARD, and J. J. TURNER. Proc. Chem. Soc. London, 118 (1958).
11. B. H. ALEXANDER, R. J. DIMLER, and C. L. MEHLTRETTER. J. Am. Chem. Soc. **73**, 4658 (1951).
12. S. J. ANGYAL and R. J. YOUNG. J. Am. Chem. Soc. **81**, 5467 (1959).
13. L. F. FIESER and M. FIESER. Steroids. Reinhold Publishing Co., New York, 1959. p. 430.
14. E. J. MCDONALD and R. F. JACKSON. J. Res. Natl. Bur. Std. **24**, 181 (1940).
15. R. U. LEMIEUX and A. G. MCINNES. Can. J. Chem. **40**, 2394 (1962).
16. M. KARPLUS. J. Chem. Phys. **30**, 11 (1959); J. Phys. Chem. **64**, 1793 (1960); J. Am. Chem. Soc. **85**, 2871 (1963).
17. R. J. ABRAHAM, L. D. HALL, L. HOUGH, and K. A. MCLAUCHLAN. J. Chem. Soc. 3699 (1962).
18. R. U. LEMIEUX and J. W. LOWN. Can. J. Chem. **42**, In press.
19. R. U. LEMIEUX. *In* Molecular Rearrangements. Part 2. *Edited by* Paul de Mayo. Interscience Publishers. 1963. pp. 735–743.
20. C. ALTONA, C. ROMERS, and E. HAVINGA. Tetrahedron Letters, No. 10, 16 (1959).
21. S. FURBERG. Acta. Chem. Scand. **4**, 751 (1950).
22. A. ALVER and S. FURBERG. Acta Chem. Scand. **13**, 910 (1959).
23. M. HUBER. Acta Cryst. **10**, 129 (1957).
24. C. A. BEEVERS and W. COCHRAN. Proc. Roy. Soc. London, Ser. A, **190**, 257 (1947).
25. A. K. MITRA and A. S. PERLIN. Can. J. Chem. **37**, 2047 (1959).
26. L. D. HALL and L. HOUGH. Proc. Chem. Soc. London, 382 (1962).
27. R. KUHN and H. TRISCHMANN. Chem. Ber. **96**, 284 (1963).
28. L. A. BOGGS, L. S. CUENDET, I. EHRENTHAL, R. KOCH, and F. SMITH. Nature, **166**, 520 (1950).
29. E. L. HIRST and J. K. N. JONES. Discussions Faraday Soc. **7**, 268 (1949).
30. L. HOUGH, J. K. N. JONES, and W. H. WADMAN. J. Chem. Soc. 1702 (1950).
31. Methods in carbohydrate chemistry. Vol. I. *Edited by* R. L. Whistler and M. L. Wolfrom. Academic Press, N.Y. 1962, p. 437.

Can. J. Chem. Downloaded from www.nrcresearchpress.com by 210.87.254.40 on 09/05/12
For personal use only.

PYRROLE CHEMISTRY

III. FRIEDEL–CRAFTS ISOPROPYLATION OF METHYL 2-PYRROLECARBOXYLATE

HUGH J. ANDERSON AND L. CAMERON HOPKINS
Department of Chemistry, Memorial University of Newfoundland, St. John's, Newfoundland
Received November 14, 1963

ABSTRACT

The reaction between isopropyl chloride and methyl 2-pyrrolecarboxylate catalyzed by aluminum chloride has been investigated. From the reaction mixture 4-isopropyl-, 5-isopropyl-, and 4,5-diisopropyl-2-esters have been isolated and identified. It has been found that while the 4-isopropyl-2-ester rearranged to 5-isopropyl-2-ester under alkylation conditions, neither the latter nor the 4,5-diisopropyl-2-ester underwent any change. Some suggestions as to the course of the reaction are made.

Can. J. Chem. Downloaded from www.nrcresearchpress.com by 210.87.254.6 on 09/05/12
For personal use only.

Interest in the substitution reactions of pyrrole derivatives which possess an electron-withdrawing group in the 2-position (1) has led us to begin an investigation of the Friedel–Crafts isopropylation of such compounds. Often yields in the alkylation of benzene derivatives with only an electron-withdrawing group are too low for preparative value (2), but deactivated furan and thiophene derivatives are still very reactive to electrophilic substitution and several have been alkylated in fair to good yield (3–6) with alkyl halides and aluminum chloride. However, there does not seem to have been any previous study of Friedel–Crafts alkylation using pyrrole or any of its simple derivatives.

The fact that methyl 4-isopropyl-2-pyrrolecarboxylate and the corresponding acid had been prepared and identified previously through ring-closure synthesis (7), while its isomer, methyl 5-isopropyl-2-pyrrolecarboxylate, appeared likely to be fairly easy to synthesize by another path, governed out choice of reactants.

Our starting material methyl 2-pyrrolecarboxylate was produced by the action of methyl chloroformate on pyrrylmagnesium bromide in a modification of the method of Maxim *et al.* (8). In addition to a very small amount of methyl 1-pyrrolecarboxylate (9), two other higher boiling substances were isolated as by-products of the reaction. One of these was methyl 1,2-pyrroledicarboxylate recently reported by Hodge and Rickards (10). The other was identified as methyl 1,3-pyrroledicarboxylate by mild base hydrolysis and partial decarboxylation to the known 3-pyrrolecarboxylic acid (11). The infrared spectrum of this acid was identical with that of an authentic specimen and the mixed melting point was not depressed. The n.m.r. spectrum of the 1,3-diester showed three aromatic type protons as well as two different ester CH_3's. The infrared spectrum showed a peak at 1720 cm^{-1} and another at 1760 cm^{-1}. The peak at higher frequency corresponds to the N-$COOCH_3$ carbonyl which appears at 1765 cm^{-1} in methyl 1-pyrrolecarboxylate.

The action of isopropyl chloride on pyrrylmagnesium bromide produced the known mixture of 2- and 3-isopropylpyrrole (12). Repeated fractionation gave a sample of 2-isopropylpyrrole of greater than 95% purity as determined by gas–liquid partition chromatography. After conversion of this compound to the corresponding Grignard reagent, reaction with methyl chloroformate produced a moderate yield of the desired methyl 5-isopropyl-2-pyrrolecarboxylate. The n.m.r. spectrum was in agreement with the assigned structure.

Can. J. Chem. Downloaded from www.nrcresearchpress.com by 210.87.254.6 on 09/05/12
For personal use only.

Our alkylation reactions were carried out in carbon disulphide using anhydrous aluminum chloride as the catalyst. The products were separated for identification by adsorption chromatography on alumina. Analysis of all reaction mixtures was done by gas–liquid partition chromatography. Standardization against a series of mixtures of known proportions showed that this method gave results accurate to about 2% when peak areas were determined by triangulation. The column used was a commercial Beckman one of Carbowax 4000 Dioleate on firebrick, operating at 220° C, and using helium as carrier gas.

The results of Spaeth and Germain (6) on methyl 2-thienyl ketone led us to expect the predominance of methyl 4-isopropyl-2-pyrrolecarboxylate. This proved to be correct. Column chromatography of early reaction products gave us two compounds as well as some unreacted starting material. One of the products was identified as the known 4-isomer by its melting point, by the n.m.r. spectrum, and by the melting point of the corresponding acid. The other product was shown by n.m.r. and later by elemental analysis to possess two isopropyl groups and to be the 4,5-diisopropyl derivative.

By following the eluate fractions from alumina by gas chromatography it was possible to isolate another major product. This was proved to be the expected methyl 5-isopropyl-2-pyrrolecarboxylate by mixed melting point and comparison of its infrared spectrum with an authentic specimen prepared as described above.

When the 2-isopropylpyrrole used to prepare methyl 5-isopropyl-2-pyrrolecarboxylate contained more than a small amount of 3-isopropylpyrrole then in the gas-chromatographic pattern of the Grignard reaction product two additional peaks were observed. One of these corresponded to the 4-isopropyl-2-ester and the other had the same retention time as an unknown trace peak which appeared in the reaction products from the isopropylation of the ester. The latter would thus appear to be methyl 3-isopropyl-2-pyrrolecarboxylate, the other possible monoisopropylation product. Miyazaki *et al.* (13) found that another Grignard synthesis from 3-isopropylpyrrole gave both 2- and 5-substitution. The amount of 3-substitution in our alkylations was usually of the order of 5% or less. It has not been possible to isolate this substance in a pure state.

Further Friedel–Crafts isopropylation of the now proved 4- and 5-isopropyl-2-esters produced the same diisopropyl-2-ester obtained in the original alkylation. The n.m.r. spectrum was in agreement with methyl 4,5-diisopropyl-2-pyrrole carboxylate. Bromination of the 2-ester has been shown to produce the 4,5-dibromo-2-ester (14). We therefore see no reason to doubt the assignment of the two isopropyl groups to the 4- and 5-positions.

Throughout our experiments no special purification of materials was attempted except for the starting ester which was not used until the gas-chromatographic pattern showed only a single peak. The aluminum chloride was kept in a desiccator but no particular care was used in handling it beyond that which ordinary use demands. Some trial experiments in which a controlled small amount of water was added seemed to have no particularly significant effect on the ratios of products. However, in a series of experiments where extra precautions were used to exclude all atmospheric moisture the extent of reaction was greatly decreased for the same time interval. The alkylation experiments were repeatable and gas–liquid partition chromatography gave consistent results except for some alkylations where the reaction time was quite short. In those experiments where all quantities were carefully measured a high percentage of the ester was accounted for as unreacted starting material or products. Thus there was very little destruction of the heterocyclic ring under these conditions.

Isopropyl chloride and aluminum chloride form a polarized complex in an equilibrium

with the corresponding ion-pair dependent upon the stability of the carbonium ion and the reaction conditions:

$$R\text{-}Cl + AlCl_3 \rightarrow R^{\delta+} \ldots . Cl \ldots . AlCl_3^{\delta-} \leftrightarrows R^+ + AlCl_4^-$$

which is then attacked (15) by the nucleophilic positions of the aromatic system.

Campbell and Spaeth (2) observed that Friedel–Crafts isopropylation of methyl benzoate produced almost exclusively the *meta* isomer, but in low yields. Similar observations on related compounds have been made by these and other authors. Usually the nitration of benzenes with an electron withdrawing group produces from 10 to 30% of the *ortho* plus *para* isomers (16). Other electrophilic substitution studies on such compounds are seldom comparable because of the poor yields. The much smaller proportion of *ortho-para* substitution observed in alkylation of these compounds has been attributed by Campbell and Spaeth to complexing of the carbonyl oxygen by the catalyst which would greatly enhance the electron-withdrawing character of the group. Complexing of carbonyl compounds, including esters, with aluminum chloride and other Lewis acids is well established (17).

Friedel–Crafts isopropylation of methyl 2-furoate and similar compounds was found by Gilman and Calloway (3) to produce only the 5-isomer. However, in the isopropylation of furfural the only product isolated was the 4-isomer (18), in low yield. In contrast, most electrophilic substitution reactions of thiophenes and pyrroles with electron-withdrawing groups in the 2-position have produced mixtures of 4- and 5-isomers (19, 20). Spaeth and Germain (6) observed in the isopropylation of methyl 2-thienyl ketone that more than 90% of the mixture obtained was the 4-isomer, while nitration of this ketone has been reported to produce equal amounts of the 4- and 5-isomers (21).

Although the α-directing influence of the heteroatom may be of some importance, the predominant electronic effect on orientation in our system is expected to be electron withdrawal by the carbomethoxy group, enhanced by complexing with the aluminum chloride, I. This would lead to 4-substitution through deactivation of positions 3- and 5-.

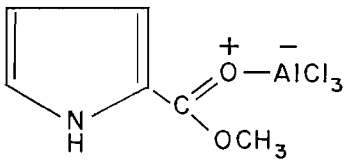

I

In contrast Rinkes (22) found that the reaction of this ester with nitric acid and acetic anhydride produced roughly equal amounts of 4- and 5-substitution.

Our initial observation was that the ratio of 4- to 5-alkyl substitution was roughly 4 or 4.5 to 1. However, it soon became apparent that the ratio varied with time, temperature, and initial concentrations. In addition, the formation of trace amounts of the 3-isopropyl isomer and substantial amounts of the 4,5-diisopropyl-2-ester complicated any explanations of the course of reaction. We also found that the overall reactivity of the pyrrole ring makes up for the strong deactivation of the complexed carbonyl group, and alkylation has preparative value for these products which are readily separated.

Can. J. Chem. Downloaded from www.nrcresearchpress.com by 210.87.254.6 on 09/05/12
For personal use only.

Can. J. Chem. Downloaded from www.nrcresearchpress.com by 210.87.254.6 on 09/05/12
For personal use only.

It was established that when pure methyl 5-isopropyl-2-pyrrolecarboxylate was refluxed for 1 to 2 hours in carbon disulphide with the appropriate quantity of anhydrous aluminum chloride, while a stream of anhydrous hydrogen chloride was admitted, no detectable change occurred. However, when methyl 4-isopropyl-2-pyrrolecarboxylate was subjected to the same conditions there was a rapid rearrangement in which roughly one-half of the 4-isomer was converted to the 5-isomer. At the same time there was a small amount of disproportionation in which nearly equal amounts of starting material and methyl 4,5-diisopropyl-2-pyrrolecarboxylate were formed. Finally it was shown that the diisopropyl-2-ester was also unchanged by the reaction conditions over an 18-hour period, in the presence of starting material.

A series of alkyation experiments was carried out to determine the course of the reaction with time when all other variables were held constant. These results are detailed in Table I. The observed behavior was that roughly equal amounts of 4- and 5-isopropyl-2-ester were formed, along with a rather small amount of diester, until about 1 hour had elapsed. The amounts of both 4-isopropyl- and of 4,5-diisopropyl-2-ester rose more rapidly during the second hour, while the 5-isopropyl-2-ester remained almost unchanged. The reaction was then nearly complete and not a great deal of change took place during the next 16 hours.

Throughout these reactions we have observed the formation of small amounts of yellow solid. In some trials using larger amounts of aluminum chloride a yellow oil separated. Other workers have investigated this type of material (23, 24) and found it to be a complex of aromatic, aluminum chloride and alkyl halide. We observed a more intense color with increased aluminum chloride or isopropyl chloride. Increasing the ester concentration seemed to have little effect.

TABLE I

Product distribution in alkylation experiments

Time (hours)	Conversion (mole %)	Product distribution (mole %)*		
		4-Ipr-2-ester	5-Ipr-2-ester	4,5-Diipr-2-ester
0.25	5.7	4.3	trace	1.4
0.5	15.5	6.9	7.0	1.6
1.0	24.8	11.6	10.1	3.2
1.5	47.3	29.0	10.6	7.7
2.0	53.1	32.4	9.7	11.0
18.0	61.8	34.6	11.6	15.6

*The 3-isopropyl product was ignored in calculations.
Reactants: isopropyl chloride (0.01 mole)
methyl 2-pyrrolecarboxylate (0.01 mole)
aluminum chloride (0.012 mole)
Solvent: carbon disulphide (50 ml)
Temperature: 50° C.

The pattern of our alkylation results is consistent with direct attack taking place primarily at the 4-position leading to the sigma complex II.* This may rearrange intramolecularly by way of a Wagner–Meerwein intermediate III (23, 25). Loss of a proton from these carbonium ions would produce the two monoisopropyl-2-esters. The highly reactive 4-position of the 5-isopropyl-2-ester would then acquire a second isopropyl group to form IV.

Support for this sequence was found in a series of observations in which it is assumed that the 4-position was always the most reactive one to electrophilic attack. Thus alkylation experiments where hydrogen chloride gas was admitted continuously throughout

**The carbonyl groups of II through V undoubtedly remain complexed with aluminum chloride.*

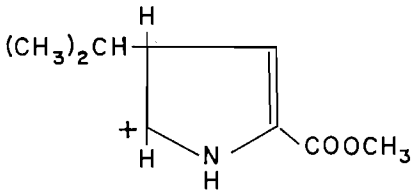

II

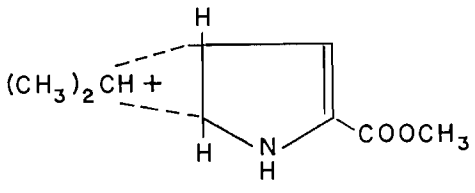

III

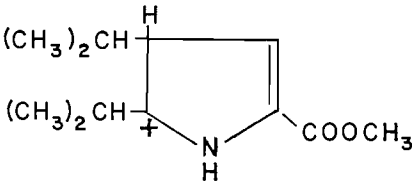

IV

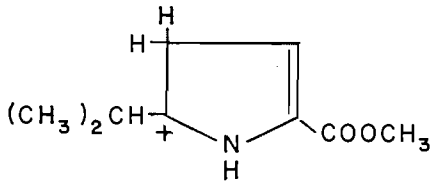

V

led to very low yields, with the 5-isomer predominating. Here protonation of the 4-position exceeded alkylation and such II as was formed rearranged rapidly to the 5-isomer. In rearrangement experiments on the latter and on the diisopropyl-2-ester protonation of the 4-position would produce V and IV respectively, whose rearrangement or disproportionation would be expected to, and did, fail.

On the other hand methyl 4-isopropyl-2-pyrrolecarboxylate protonated to II and would rearrange. Attempts to carry out this rearrangement in the absence of a stream of hydrogen chloride gas produced little of the 5-isomer. The small proton concentration which must have been present was probably supplied by the hydrogen chloride usually associated with commercial grade aluminum chloride. Rearrangement experiments with the 4-isopropyl-2-ester gave, in addition to the 5-isopropyl isomer, equal amounts of methyl 2-pyrrolecarboxylate and 4,5-diisopropyl-2-ester. The fact that we observed no overall loss of isopropyl groups in these rearrangement reactions supports the idea of an intermediate such as III which loses its isopropyl group to a molecule of 5-isopropyl-2-ester in an intermolecular transfer (26). Some loss might have been expected to occur if a free isopropyl cation or its complex with the Lewis acid had formed.

The reactivity of the 4-position is also supported by alkylation experiments using the monoisopropyl-2-esters. Here it was observed that the 5-isomer was converted to 35% of the diisopropyl-2-ester in 15 minutes, while the 4-isopropyl-2-ester gave only 15% after 1 hour. In the latter experiment rearrangement probably preceded alkylation to a large extent. Alkylation experiments using swamping amounts of catalyst gave high yields of product where the 5-isopropyl-2-ester predominated by far and where diisopropylation was negligible.

A small amount of the supposed 3-isopropyl-2-ester was found among the rearrangement products of the 4-isopropyl isomer. While at least some direct attack may occur at the 3- and 5- positions during alkylation, it seems likely that most of the product having isopropyl groups at these positions arises through rearrangement from the kinetically favored 4-position.

Can. J. Chem. Downloaded from www.nrcresearchpress.com by 210.87.254.6 on 09/05/12
For personal use only.

Spaeth and Germain (6) did not examine the diisopropylated product at any time, although they indicated that higher boiling material was present after all alkylations. It may be that the very low percentage of 5-isopropyl-2-thienyl methyl ketone they observed was due to rapid further alkylation. In addition, in rearrangement studies they did not, apparently, use an external source of hydrogen chloride. However, further information is needed to determine whether their thienyl ketone did behave quite differently in Friedel–Crafts isopropylation to our pyrrole ester.

We hope to extend our studies of alkylation to other negatively substituted pyrroles, as well as to investigate the behavior when different Friedel–Crafts catalysts are employed.

EXPERIMENTAL

General

Melting points were determined on a Fisher–Johns apparatus and are uncorrected. Infrared spectra were recorded by a Unicam SP100 Spectrophotometer using the potassium chloride disk technique (2 mg of sample in 200 mg KCl).

Ultraviolet spectra were determined with a Beckman DK-2A recording spectrophotometer; samples were dissolved in ethanol (95%) at a concentration of 10 mg per liter. pK_a's were determined spectrophotometrically as described by Jaffé and Orchin (30).

The nuclear magnetic resonance spectra were determined at 60 Mc/second in carbon tetrachloride or in deuterochloroform. The chemical shifts are in p.p.m. from tetramethylsilane as internal reference.

Analyses of reaction mixtures were carried out by means of gas–liquid partition chromatography using a Beckman GC-2A gas chromatograph, equipped with a 30-in. column (number 70007) packed with Carbowax 4000 dioleate on firebrick and operated at 220° C with helium as the carrier gas (inlet pressure: 20 p.s.i.g.). Analyses were accurate to ±2% as shown by gas-chromatographic examination of a series of known mixtures. Retention times established for pure materials were methyl 2-pyrrolecarboxylate, 3.84 minutes; 5-isopropyl derivative, 4.55 minutes; 4,5-diisopropyl derivative, 5.88 minutes; 4-isopropyl derivative, 7.38 minutes. Another peak at 5.10 minutes is believed to represent the 3-isopropyl derivative.

Elemental analyses were determined by Alfred Bernhardt, Mülheim (Ruhr), Germany.

All Grignard reactions were carried out under an atmosphere of nitrogen.

Methyl 2-Pyrrolecarboxylate

This compound was prepared by an adaptation of the Grignard method of Maxim *et al.* (8) for the ethyl ester. The product was vacuum distilled: b.p. 115–120° at 12 mm; yield 25%. The methyl 2-pyrrolecarboxylate was crystallized from methanol, m.p. 72–73°, literature m.p. 73° (10).

From the forerun was obtained a small amount of methyl 1-pyrrolecarboxylate b.p. 57–59 at 14 mm (n_D^{22} 1.483). Gabel (31) reports b.p. 71–73 at 21 mm (n_D^{20} 1.487).

A higher boiling compound was separated from the 2-ester residue by fractional crystallization from hexane, to give a white crystalline solid, m.p. 142–143.5°. Infrared and n.m.r. spectra showed this compound to be methyl 1,3-pyrroledicarboxylate. Anal. Calc.: C, 52.46; H, 4.95; N, 7.65. Found: C, 52.53; H, 5.06; N, 7.82.

Dimethyl 1,3-pyrroledicarboxylate (0.2 g) was refluxed 2 hours in aqueous methanolic potassium hydroxide. The methanol was distilled and the aqueous solution was washed with ether to remove unreacted ester. Acidification with dilute hydrochloric acid resulted in copious evolution of carbon dioxide. The 3-pyrrolecarboxylic acid was extracted in ether and crystallized from methanol, m.p. 144.5–145.5°. Its infrared spectrum was identical with that of an authentic specimen of 3-pyrrolecarboxylic acid and the mixed melting point was not depressed.

Also isolated was the dimethyl 1,2-pyrroledicarboxylate reported by Hodge and Rickards (10), m.p. 44–45°.* Its infrared spectrum was identical with that of an authentic specimen and the mixed melting point was undepressed.

General Procedure for Alkylations

The reaction vessel was a 100-ml three-neck round bottom flask equipped with stirrer, condenser, and drying tube. The flask was immersed in an oil bath maintained at 50°. Methyl 2-pyrrolecarboxylate, 1.25 g (0.01 mole), and anhydrous aluminum chloride (Fisher Reagent Grade) 1.69 g (0.012 mole) were placed in the reaction vessel with 40 ml of carbon disulphide. Isopropyl chloride, 0.78 g (0.01 mole), in 10 ml of carbon disulphide was added at once and the reaction mixture was stirred for the required period. The reaction was quenched by pouring on ice. The aqueous layer was separated, saturated with sodium chloride, and extracted with ether. The combined organic extract was washed with sodium acetate (saturated aqueous solution) and dried over anhydrous sodium sulphate. The solvent was removed by distillation and the residue analyzed by gas chromatography.

**Dr. Rickards in a personal communication reports m.p. 48–49.5° C.*

Can. J. Chem. Downloaded from www.nrcresearchpress.com by 210.87.254.6 on 09/05/12
For personal use only.

Can. J. Chem. Downloaded from www.nrcresearchpress.com by 210.87.254.6 on 09/05/12
For personal use only.

Isolation of Alkylation Products

The unreacted starting material and its various isopropyl derivatives were separated by adsorption chromatography on alumina (Fisher Reagent Grade) and fractional crystallization from methanol. Methyl 4,5-diisopropyl-2-pyrrolecarboxylate, m.p. 120.5–121°. Calc.: C, 68.87; H, 9.15; N, 6.69. Found: C, 68.77; H, 9.43; N, 6.92. Methyl 4-isopropyl-2-pyrrolecarboxylate, m.p. 89–90° (lit. 90°). Calc.: C, 64.65; H, 7.84; N, 8.38. Found: C, 65.05; H, 7.74; N, 8.50. Methyl 5-isopropyl-2-pyrrolecarboxylate, m.p. 59.5–61°. Calc.: C, 64.65; H, 7.84; N, 8.38. Found: C, 64.67; H, 7.61; N, 8.29. Spectral properties are given in Table II.

2-Isopropylpyrrole

To a refluxing solution of 0.83 mole of pyrrylmagnesium bromide in 400 ml of ether was added an equimolar portion of isopropyl chloride in 50 ml of ether. Refluxing was continued for 18 hours and the reaction mixture cooled and hydrolyzed with 150 ml of a 10% ammonium chloride solution. The aqueous layer was separated and extracted with ether. The combined ether extracts were dried over anhydrous potassium carbonate, the solvent removed by distillation, and the residue vacuum distilled. Redistillation gave a fraction, b.p. 71–73° at 12 mm (n_D^{22} 1.4906), which was better than 95% pure in 2-isopropylpyrrole as determined by gas chromatography, the only other component being 3-isopropylpyrrole. Skell and Bean (12) report b.p. 80° at 25 mm, (n_D^{25} 1.4900) for pure 2-isopropylpyrrole.

Methyl 5-Isopropyl-2-pyrrolecarboxylate

To a cold solution of 0.171 mole of ethylmagnesium bromide in 300 ml of ether was added a solution of 0.171 mole isopropylpyrrole (>95% purity) in 25 ml of ether. The reaction mixture was refluxed for 1 hour and then cooled while methyl chloroformate (0.171 mole) in 25 ml of ether was added dropwise. The reaction mixture was again refluxed for 1 hour then carefully hydrolyzed with 100 ml of 10% ammonium chloride solution. The aqueous layer was separated and extracted with ether. After the combined ether extracts were dried over anhydrous sodium sulphate, the ether was removed by distillation and the product, methyl 5-isopropyl-2-pyrrolecarboxylate, vacuum distilled. Gas-chromatographic analysis showed that the material was homogeneous, the retention time (4.55 minutes) corresponding to that of the alkylation product to which we had tentatively assigned this structure. The 5-isopropyl-2-ester was crystallized from methanol, m.p. 59.5–61°, and was shown to be identical with the alkylation product by mixed melting point and comparison of infrared spectra.

Attempted Disproportionation of Methyl 4,5-Diisopropyl-2-pyrrolecarboxylate

Methyl 4,5-diisopropyl-2-pyrrolecarboxylate (0.001 mole) and methyl 2-pyrrolecarboxylate (0.001 mole) dissolved in 10 ml of carbon disulphide were refluxed for 4 hours in the presence of anhydrous aluminum chloride (0.0024 mole). A continuous stream of dry hydrogen chloride was passed through the reaction mixture. The reaction mixture was worked up in the usual manner and the product analyzed by gas chromatography. No elimination or disproportionation of isopropyl groups was observed.

Rearrangement of Methyl 4-Isopropyl-2-pyrrolecarboxylate

Methyl 4-isopropyl-2-pyrrolecarboxylate (0.001 mole) and aluminum chloride (0.0024 mole) in 10 ml of carbon disulphide were refluxed (50°) for 2 hours in the presence of a continuous stream of dry hydrogen chloride. The reaction mixture was worked up in the usual manner and the products analyzed by gas chromatography:

Product	Mole %
Methyl 4-isopropyl-2-pyrrolecarboxylate	35.2
Methyl 5-isopropyl-2-pyrrolecarboxylate	50.8
Methyl 2-pyrrolecarboxylate	6.9
Methyl 4,5-diisopropyl-2-pyrrolecarboxylate	7.0

Isopropylation of Methyl 5-Isopropyl-2-pyrrolecarboxylate

Methyl 5-isopropyl-2-pyrrolecarboxylate was isopropylated using the general procedure. After a reaction time of 15 minutes at 50° it was found that 35% of the starting material had been diisopropylated giving methyl 4,5-diisopropyl-2-pyrrolecarboxylate.

Isopropylation of Methyl 4-Isopropyl-2-pyrrolecarboxylate

Methyl 4-isopropyl-2-pyrrolecarboxylate was isopropylated using the general procedure. After a reaction time of 1 hour it was found that 15% dialkylation had occurred.

Preparation of acids

The corresponding acids of the alkylation products were prepared by refluxing the esters in 20% aqueous potassium hydroxide solution for 1 to 4 hours. The unreacted ester was extracted in ether and the aqueous layer acidified with dilute hydrochloric acid. The acid derivative was extracted in ether, dried, and

Can. J. Chem. Downloaded from www.nrcresearchpress.com by 210.87.254.6 on 09/05/12
For personal use only.

TABLE II

Spectral properties

Compound	U.V. spectrum		I.R. spectrum		N.M.R. spectrum					
					Aliphatic			Aromatic		
	max (mμ)	log ε	C=O (cm^{-1})	N—H (cm^{-1})	C—CH_3	CH—	O—CH_3	3-	4-	5-
Methyl 2-pyrrolecarboxylate	233.5 265.5	3.72 4.21	1681	3290			3.95	7.04	6.35	7.04
Methyl 4-isopropyl-2-pyrrolecarboxylate	232.5 273.5	3.95 4.20	1698	3297	1.23	2.88	3.88	6.82	—	6.82
Methyl 5-isopropyl-2-pyrrolecarboxylate	233 277.5	3.46 4.31	1690	3300	1.32	2.91	3.82	6.63	5.82	—
Methyl 4,5-diisopropyl-2-pyrrolecarboxylate	236 286	3.72 4.31	1680	3320	1.16 1.32	2.89‡ (2 overlap)	3.78	6.59	—	—
2-Pyrrolecarboxylic acid	222* 258	3.65 4.10	1700	3355						
4-Isopropyl-2-pyrrole-carboxylic acid	237 272.5	3.77 4.15	1695	3368						
5-Isopropyl-2-pyrrole-carboxylic acid	231 277	3.52 4.02	1660	3404						
4,5-Diisopropyl-2-pyrrole-carboxylic acid	235 283.5	3.60 4.23	1680	3296			3.75 (C—) 3.95 (N—)	7.78 (2)	6.58	7.19
Dimethyl 1,3-pyrrole-dicarboxylate	208 233	4.37 4.08	1720† 1760‡	—						

*Ref. 29.
†2-$COOCH_3$.
‡1-$COOCH_3$.

recrystallized from methanol or sublimed under vacuum. Spectral data are recorded in Table II. Melting points and pK_a's as determined spectrophotometrically are as follows:

Acid	M.p.	pK_a
2-Pyrrolecarboxylic acid	210–212°(d)*	4.55†
4-Isopropyl-2-pyrrolecarboxylic acid	182–184°(d)‡	4.77
5-Isopropyl-2-pyrrolecarboxylic acid	133–134°	4.89
4,5-Diisopropyl-2-pyrrolecarboxylic acid	93–94°	4.97

*Ref. 27 gives m.p. 204–205°.
†Ref. 28 gives pK_a 4.38.
‡Ref. 7 gives m.p. 182–184°.

ACKNOWLEDGMENTS

The authors acknowledge with thanks the continued financial support of the National Research Council. They are also indebted to Professors F. A. L. Anet and L. Bauer for determination and interpretation of n.m.r. spectra. Some of the early separations were carried out by Mr. James D. Halliday.

A sample of methyl 1,2-pyrroledicarboxylate was kindly furnished by Dr. R. K. Rickards and one of 3-pyrrolecarboxylic acid by Professor Henry Rapoport.

REFERENCES

1. H. J. Anderson. Can. J. Chem. **37**, 2053 (1959).
2. B. N. Campbell and E. C. Spaeth. J. Am. Chem. Soc. **81**, 5933 (1959).
3. H. Gilman and N. O. Calloway. J. Am. Chem. Soc. **55**, 4197 (1933).
4. T. Reichstein, H. R. Rosenberg, and R. Eberhardt. Helv. Chim. Acta, **18**, 721 (1935).
5. C. D. Hurd and G. L. Oliver. J. Am. Chem. Soc. **76**, 50 (1954).
6. E. C. Spaeth and C. B. Germain. J. Am. Chem. Soc. **77**, 4066 (1955).
7. T. Sugawa, Y. Sanno, and A. Kurita. Chem. Abstr. **50**, 4119 (1956).
8. N. Maxim, I. Zugranescu, and I. Fulga. Chem. Abstr. **32**, 2938 (1938).
9. R. M. Acheson and J. M. Vernon. J. Chem. Soc. 457 (1961).
10. P. Hodge and R. W. Rickards. J. Chem. Soc. 2543 (1963).
11. H. Rapoport and D. Wilson. J. Org. Chem. **26**, 1102 (1961).
12. P. S. Skell and G. P. Bean. J. Am. Chem. Soc. **84**, 4655 (1962).
13. M. Miyazaki, H. Watanabe, C. Mizuno, T. Takano, and A. Morimoto. Chem. Abstr. **50**, 10078 (1956).
14. I. J. Rinkes. Rec. Trav. Chim. **60**, 303 (1941).
15. H. C. Brown and J. Jungk. J. Am. Chem. Soc. **77**, 5584 (1955); **78**, 2182 (1956). H. C. Brown and M. Grayson. J. Am. Chem. Soc. **75**, 6285 (1953).
16. P. B. D. de la Mare and J. H. Ridd. Aromatic substitution. Butterworths, London. 1959. p. 83.
17. M. F. Lappert. J. Chem. Soc. 817 (1961); 522 (1962). B. Mori, J. Gohring, D. Cassimatis, and B. P. Susz. Helv. Chim. Acta, **45**, 77 (1962).
18. H. Gilman, N. O. Calloway, and R. R. Burtner. J. Am. Chem. Soc. **57**, 906 (1935). N. Elming. Acta Chem. Scand. **6**, 605 (1952).
19. H. J. Anderson. Can. J. Chem. **35**, 21 (1957).
20. S. Gronowitz. *In* Advances in heterocyclic chemistry. Vol. I. *Edited by* A. R. Katritsky. Academic Press, New York. 1963. p. 52.
21. I. J. Rinkes. Rec. Trav. Chim. **52**, 538 (1933).
22. I. J. Rinkes. Rec. Trav. Chim. **53**, 1167 (1934).
23. G. Baddeley, G. Holt, and D. Voss. J. Chem. Soc. 100 (1952).
24. G. A. Olah and S. J. Kuhn. J. Am. Chem. Soc. **80**, 6535, 6541 (1958).
25. R. H. Allen. J. Am. Chem. Soc. **82**, 4856 (1960).
26. D. A. McCaulay and A. P. Lien. J. Am. Chem. Soc. **75**, 2411 (1953).
27. O. Sus, K. Moller, R. Dietrich, H. Eberhardt, M. Glos, M. Grundkotter, and H. Bubrich. Chem. Abstr. **50**, 7828 (1956).
28. C. M. McCay and C. L. A. Schmidt. J. Gen. Physiol. **9**, 333 (1926).
29. R. Andrisano, G. Papalardo, and L. Bolognari. Gazz. Chim. Ital. **85**, 1430 (1955).
30. H. H. Jaffé and M. Orchin. Theory and applications of ultraviolet spectroscopy. John Wiley and Sons, Inc., New York. 1962.
31. N. W. Gabel. J. Org. Chem. **27**, 301 (1962).

Can. J. Chem. Downloaded from www.nrcresearchpress.com by 210.87.254.6 on 09/05/12
For personal use only.

Can. J. Chem. Downloaded from www.nrcresearchpress.com by 210.87.254.42 on 09/05/12
For personal use only.

REACTIONS OF ORGANOTIN COMPOUNDS

III. ADDITIONS OF DIMETHYLTIN DIHYDRIDE TO SIMPLE OLEFINS[1]

H. C. CLARK AND J. T. KWON

Department of Chemistry, University of British Columbia, Vancouver, British Columbia

Received January 27, 1964

ABSTRACT

The addition reactions of dimethyltin dihydride with ethylene, butadiene, and *cis*- and *trans*-butene are described. With ethylene and butadiene, the products $(CH_3)_2SnH(R)$ and $(CH_3)_2SnR_2$ are fully characterized, where R = C_2H_5, or $—CH_2CH=CHCH_3$, the latter being the first butenyltin compounds to be reported. The butenes were virtually unreactive towards the dihydride. From a consideration of these and previous results, the possible reaction mechanism is discussed, and the tentative conclusion is reached that the rate-determining factor involves the formation of radicals from the tin dihydride.

INTRODUCTION

In a previous paper (1) we showed that, contrary to earlier reports (2), simple olefins do add to organotin dihydrides, the systems examined involving the addition of some fluoro-olefins to dimethyltin dihydride. Not only was addition shown to occur, but the stepwise character of the addition was also established, so that for the reaction of tetrafluoroethylene to dimethyltin dihydride, both dimethyl(tetrafluoroethyl)tin hydride, $(CH_3)_2SnH(C_2F_4H)$, and dimethylbis(tetrafluoroethyl)tin, $(CH_3)_2Sn(C_2F_4H)_2$, were isolated. It seemed probable that similar addition products should also be formed from hydrocarbon olefins and, moreover, it now seemed worthwhile to re-examine the reaction of butadiene with a dihydride, despite the earlier report (2) that butadiene and hexadiene do not react with aliphatic organotin dihydrides. The extension to other olefins also allows some general statements to be made concerning the mechanism of these additions.

DISCUSSION

That olefins behave towards an organotin dihydride in much the same way as fluoro-olefins is shown by comparing the reactions of tetrafluoroethylene (1) and ethylene. Ethylene apparently reacts somewhat more slowly than tetrafluoroethylene, since the former did not react with dimethyltin dihydride at 50° in the dark during periods up to 180 hours, while tetrafluoroethylene and dimethyltin dihydride undergo 63% reaction at 25° in the dark after 160 hours (1). However, in both cases, the reaction is accelerated by ultraviolet irradiation, so that with ethylene in a 1:1 molar ratio with the dihydride, dimethylethyltin hydride, $(CH_3)_2SnH(C_2H_5)$, and dimethyldiethyltin $(CH_3)_2Sn(C_2H_5)_2$ were obtained in 37% and 31% yields respectively after 24 hours of irradiation at 25°. (In this discussion, experimental yields, calculated on the basis of the tin dihydride, have been rounded to two significant figures.) With a 2:1 molar ratio of ethylene to dimethyltin dihydride, a 69% yield of dimethyldiethyltin was obtained, with only a trace of dimethylethyltin hydride. The most notable difference from the reaction with tetrafluoroethylene is in the much lower stability of $(CH_3)_2SnH(C_2H_5)$ as compared with $(CH_3)_2SnH(C_2F_4H)$. The latter is apparently stable indefinitely at 25° *in vacuo*, but dimethylethyltin hydride decomposes under these conditions at a rate sufficiently rapid to make the determination

[1]*Presented in part at the Symposium on Current Trends in Organometallic Chemistry, Cincinnati, June 12–15, 1963.*

of accurate physical properties difficult. The products of decomposition were dimethyltin dihydride and dimethyldiethyltin, so that apparently a simple disproportionation occurs, similar to that proposed (1) for the decomposition of $(CH_3)_2SnH(C_2F_4H)$ at 160°. There is, however, no obvious reason for this difference in stability between $(CH_3)_2SnH(C_2H_5)$ and $(CH_3)_2SnH(C_2F_4H)$.

Since ethylene reacted readily with the tin dihydride, the reaction of butadiene with dimethyltin dihydride was examined, this being of further interest since a five-membered heterocyclic ring might be formed according to the reaction

$$(CH_3)_2SnH_2 + CH_2{=}CH{-}CH{=}CH_2 \rightarrow (CH_3)_2Sn\begin{array}{l}\diagup CH_2{-}CH_2\\ \diagdown CH_2{-}CH_2\end{array} \quad [1]$$

Reaction occurs more readily than with ethylene, since from 1:1 molar ratio mixture of dimethyltin dihydride and butadiene after 163 hours at 50° in the dark, only 34% of the reactants was recovered. Some decomposition products of the dihydride, notably hydrogen and an involatile white solid, were formed but the main product (34%) was dimethyl(2-butenyl)tin hydride, $(CH_3)_2SnH(CH_2CH{=}CHCH_3)$. This, like the corresponding product with ethylene, decomposed slowly at 25°, but characterization was possible by means of its proton magnetic resonance and infrared spectra, as well as by its conversion by mild chlorination to dimethyl(2-butenyl)tin chloride.

$$(CH_3)_2SnH(CH_2{-}CH{=}CH{-}CH_3) + CCl_4 \rightarrow (CH_3)_2SnCl(CH_2CH{=}CHCH_3) + CHCl_3 \quad [2]$$

The other product of the original reaction, formed in 19% yield, was dimethylbis(2-butenyl)tin, $(CH_3)_2Sn(CH_2CH{=}CHCH_3)_2$; this may form either by addition of butadiene to dimethyl(2-butenyl)tin hydride (equation [3]), or by disproportionation (equation [4]).

$$(CH_3)_2SnH(CH_2CH{=}CHCH_3) + C_4H_6 \rightarrow (CH_3)_2Sn(CH_2CH{=}CHCH_3)_2 \quad [3]$$

$$2(CH_3)_2SnH(CH_2CH{=}CHCH_3) \rightarrow (CH_3)_2SnH_2 + (CH_3)_2Sn(CH_2CH{=}CHCH_3)_2 \quad [4]$$

The reaction represented by equation [4] probably accounts for the spontaneous decomposition of $(CH_3)_2SnH(CH_2CH{=}CHCH_3)$. Ultraviolet radiation alone was not particularly effective in this addition of butadiene, since 92% of the reactants were recovered from a mixture of dimethyltin dihydride and butadiene after irradiation at 25° for 20 hours, although after 112 hours under these conditions, dimethyl(2-butenyl)tin hydride and dimethylbis(2-butenyl)tin were formed in 37% and 30% yields respectively. Reaction at 50° under ultraviolet irradiation for 20 hours, using a 1:1 molar ratio, leads to the consumption of 82% of the reactants and the formation of $(CH_3)_2SnH(CH_2CH{=}CHCH_3)$ and $(CH_3)_2Sn(CH_2CH{=}CHCH_3)_2$ in 6% and 32% yields respectively. Clearly under these conditions, the reaction proceeds so as to give extensive addition across both Sn—H bonds. Similarly, when a mixture of dimethyltin dihydride and butadiene in 1:2 molar ratio was irradiated at 50° for 23 hours, the corresponding yields of $(CH_3)_2SnH(CH_2CH{=}CHCH_3)$ and $(CH_3)_2Sn(CH_2CH{=}CHCH_3)_2$ were 6% and 71% respectively.

These are the first butenyl organotin compounds to be reported, and they are formed by a simple 1:4 addition to the conjugated system of butadiene. The configuration about the C=C bond is of interest, since *cis* and *trans* isomers are possible. The infrared spectra of $(CH_3)_2SnH(CH_2{-}CH{=}CHCH_3)$ and $(CH_3)_2Sn(CH_2CH{=}CHCH_3)_2$ show absorption at 1640 and 1639 cm^{-1} which can be assigned to the C=C stretching vibration, in comparison with the average values (3) of 1673 and 1657 cm^{-1} for $CHR_1{=}CHR_2$ (*trans*) and $CHR_1{=}CHR_2$ (*cis*). The C—H stretching vibrations of —CH=CH— are observed,

Can. J. Chem. Downloaded from www.nrcresearchpress.com by 210.87.254.42 on 09/05/12
For personal use only.

as expected, at 3020 cm^{-1} in both compounds. The out-of-plane =CH deformation vibration is particularly significant, since only *trans* isomers give medium to strong bands at 990–965 cm^{-1}. For $(CH_3)_2SnH(CH_2CH{=}CCH_3)$ and $(CH_3)_2Sn(CH_2CH{=}CHCH_3)$, medium to strong bands are observed at 993 and 961 cm^{-1} and 991 and 960 cm^{-1} respectively. Although the correlation is much less certain, *cis* disubstituted ethylenes appear to show (3) the out-of-plane =CH deformation vibrations in the 675–728 cm^{-1} region. For the compounds being considered, a medium to strong band is observed in each case at approximately 725 cm^{-1}. The infrared evidence is therefore ambiguous, although the correlation of out-of-plane =CH deformation vibrations for *trans* isomers with absorption in the 990–965 cm^{-1} region has been found so reliable, that $(CH_3)_2SnH(CH_2CH{=}CHCH_3)$ and $(CH_3)_2Sn(CH_2CH{=}CHCH_3)_2$ may tentatively be assigned *trans* configurations. The nuclear magnetic resonance spectra are too complex, and hence at present do not allow any distinction between the isomers to be made.

As a final extension, the reactions of dimethyltin dihydride with *cis*- and *trans*-2-butene were examined. Mixtures were heated to 50°, or irradiated with ultraviolet light at 25°, but in all cases, the reactants were recovered virtually quantitatively. That the double bond in the 2,3 position should be inactive towards the tin hydride is consistent with all previous reports (2), which clearly indicate that addition occurs only with terminal olefinic bonds. Moreover, the lack of reactivity of the 2-butenes is also consistent with the observation that the C=C bond of $(CH_3)_2SnH(CH_2CH{=}CHCH_3)$ or $(CH_3)_2Sn(CH_2CH{=}CHCH_3)_2$ is apparently unreactive towards further addition with tin hydride.

It is clear that our earlier (1, 4) reports and this present work describe a general characteristic of organotin dihydrides, namely their ability to add under very mild conditions across terminal C=C bonds in a stepwise fashion. An examination of all these results leads to some general conclusions regarding the mechanism of these additions. The original workers (2) proposed an ionic mechanism, but more recently a radical mechanism has been suggested (5, 6), since it has been found that the addition can be catalyzed by radical sources which decompose at low temperatures, e.g. benzyl hyponitrite. Other workers (7) have investigated the addition of piperylene to trimethyltin hydride, and have suggested that the rate-determining step is the formation of radicals from the olefins. From our own results, the following statements can be made.

1. The addition of simple olefins to organotin dihydrides requires no solvent or catalyst, and in some cases (e.g. $(CH_3)_2SnH_2 + C_2F_4$) occurs at a reasonable rate in the dark at 25°. The addition to a dihydride is stepwise, and the rates of formation of $R_2Sn(R'H)H$ and $R_2Sn(R'H)_2$ seem to be comparable.

2. Ultraviolet irradiation always accelerates the reaction considerably. As the present results show, ethylene and dimethyltin dihydride in 1:1, 8:1, or 10:1 molar ratio were always recovered quantitatively after prolonged periods (up to 180 hours) at 50° in the dark. In a 1:1 molar ratio, after 23 hours at 25° under ultraviolet irradiation, the reaction was approximately 85–90% complete.

3. In the absence of ultraviolet irradiation, for cases where little or no reaction occurred, the percentage recovery of both olefin *and* dihydride was quantitative. However, in the presence of ultraviolet radiation, for cases where reaction was not complete (e.g. $(CH_3)_2SnH_2$ and ethylene), *only* olefin was recovered quantitatively, and involatile, tin-containing residues were formed. Moreover, we have previously shown (1) that ultraviolet irradiation greatly accelerates the decomposition of dimethyltin dihydride.

4. Under the same conditions of temperature and irradiation, an increase in the ratio olefin:tin dihydride from 1:1 to 14:1 has little effect on yields. Thus, for C_2F_4 with

Can. J. Chem. Downloaded from www.nrcresearchpress.com by 210.87.254.42 on 09/05/12
For personal use only.

$(CH_3)_2SnH_2$, in 4:1 and 14:1 molar ratio, the chief product was $(CH_3)_2Sn(C_2F_4H)_2$ in yields of 66% and 70% respectively. For C_2H_4 and $(CH_3)_2SnH_2$ in 2:1 and 8:1 molar ratio, the yields of $(CH_3)_2SnH(C_2H_5)$ and $(CH_3)_2Sn(C_2H_5)_2$ changed from 6 and 69% respectively, to 39 and 22% respectively. That is, the reaction proceeds more slowly when both the molar ratio and actual pressure of olefin are increased.

5. In no instance is there evidence for the formation of products containing $Sn[(C_2X_4)_nH]$ groups where $n > 1$.

All these factors argue convincingly against an ionic mechanism. It is less easy to distinguish between a process involving a four-center transition complex, and a free radical mechanism. However, contrary to previous suggestions (7), our evidence does indicate that the tin dihydride plays a major role and that the formation of radicals from the olefin is probably *not* the rate-determining step. The weight of evidence favors the formation of radicals from the tin dihydride as the determining factor, but detailed kinetic studies are necessary to provide conclusive evidence. It is assumed here that the same mechanism is involved in the addition of olefins to triorganotin monohydrides (5–7) as to diorganotin dihydrides. It must be conceded that there is no direct evidence showing that the same rate-determining step is involved. However, this may well be so since the rates of formation of $R_2Sn(R'H)H$ and $R_2Sn(R'H)_2$ from R_2SnH_2 seem comparable, although detailed kinetic studies are clearly necessary to justify this assumption and to provide conclusive evidence concerning the mechanism.

EXPERIMENTAL

The general experimental techniques have been described previously (1). Infrared spectra were recorded on model 137 sodium chloride and potassium bromide, and model 21 double beam Perkin–Elmer spectrophotometers, while n.m.r. spectra were obtained with Varian A60 and H.R. 60 spectrometers.

Reactions with Ethylene

(*a*) Dimethyltin dihydride (0.956 g, 6.30 mmole) and ethylene (0.384 g, 13.7 mmole) were allowed to react under ultraviolet irradiation for 24 hours at 25°. Vacuum fractionation gave a trace of hydrogen, unreacted ethylene (0.160 g, 5.0 mmole), fractions which condensed at −78° (0.031 g) and −46° (0.059 g, mol. wt. 150–179), and the major product which condensed at −23°. The latter (0.901 g, 69.0%) was dimethyldiethyltin (mol. wt. obs. 208, calc. 208; vapor pressure (25°) 14 mm; b.p. 132±3°, ΔH_v = 8.9 kcal mole^{-1}, lit. values (8) 131–132° and 144–146°. Calc. for $C_6H_{16}Sn$: C, 34.61; H, 7.69. Found: C, 34.64; H, 6.29%. The infrared spectrum of a liquid film showed the following absorption maxima: 2950 (sh), 2920 (s), 2880 (s), 1703 (vw), 1680 (vw), 1470 (m), 1460 (sh), 1428 (m), 1380 (m), 1234 (w), 1197 (m), 1190 (m), 1014 (m), 1000 (sh), 960 (w), 940 (m), 765 (sh), 744 (s), 700 (m), 668 (m), 556 (vw), 519 (s), and 509 (sh) cm^{-1}. The −78° fraction was shown spectroscopically to consist of unreacted dimethyltin dihydride and tetramethyltin. The −46° fraction decomposed at 25°, so that its molecular weight could only be determined approximately. Decomposition was rapid above 30° but the boiling point (extrapolated) was 95±2°, ΔH_v = 7.5 kcal mole^{-1}. The infrared spectrum showed bands at 2960 (s), 2910 (sh), 1837 (vs, Sn—H stretch), 1720 (vw), 1485 (sh), 1474 (w), 1432 (w), 1388 (w), 1205 (w), 1197 (w), 1014 (m), 947 (w), 800 (sh), 763 (s), 713 (m), 675 (sh), 550 (m), 517 (s), and 493 (sh) cm^{-1}. The proton magnetic resonance spectrum indicated one hydrogen attached to tin, this appearing as an unresolved multiplet with δ_{Sn-H} at −4.58 p.p.m. with respect to tetramethylsilane with Sn^{117} and Sn^{119} side bands at −13.60 and −14.20 p.p.m. (9). The ratio of intensities $Sn—H/\Sigma_i H_i$ was 1/10.6. The −46° fraction was therefore *dimethylethyltin hydride*, $(CH_3)_2SnH(C_2H_5)$.

(*b*) When dimethyltin dihydride (1.737 g, 11.5 mmole) and ethylene (0.322 g, 11.5 mmole) were allowed to react under conditions identical with those in (*a*), the products were hydrogen (5%), an involatile residue (0.30 g) containing metallic tin, unreacted ethylene (0.036 g), unreacted tin hidydride (0.136 g, mol. wt. obs. 150, calc. 150), a fraction (0.095 g) which condensed at −64°, dimethylethyltin hydride (0.757 g, 4.28 mmole, 37.1%) as an unstable fraction condensed at −46°, and dimethyldiethyltin (0.733 g, 3.54 mmole, 30.8%). The −64° fraction was shown spectroscopically to be largely $(CH_3)_4Sn$.

(*c*) Dimethyltin dihydride (1.605 g, 10.6 mmole) and ethylene (0.298 g, 10.6 mmole) were heated to 50° in the dark for 180 hours. The reaction mixture separated cleanly into fractions condensing at −125° (1.549 g, mol. wt. obs. 155, calc. for $(CH_3)_2SnH_2$, 150) and at −196° (0.291 g, mol. wt. obs. 28.7, calc. for C_2H_4, 28.0). There were no less volatile fractions and no residue, the total recovery of dihydride and ethylene being 97.3%.

Can. J. Chem. Downloaded from www.nrcresearchpress.com by 210.87.254.42 on 09/05/12
For personal use only.

(*d*) A mixture of the dihydride (0.225 g, 1.49 mmole) and ethylene (0.422 g, 14.9 mmole) was heated at 50° in the dark for 92 hours. Both reactants were recovered quantitatively.

(*e*) Dimethyltin dihydride (0.572 g, 3.79 mmole) and ethylene (0.847 g, 30.3 mmole) were irradiated with ultraviolet light at 25° for 26 hours. The volatile fraction condensed at −23° (0.170 g) was dimethyldiethyltin (mol. wt. obs. 205, calc. 206, 22% yield), and the −46° fraction was dimethylethyltin hydride (0.265 g, 39%, mol. wt. obs. 150, calc. 178), both also identified spectroscopically. Unreacted dihydride (0.127 g, 22%) and ethylene (0.740 g, 87.2%) were also recovered.

Reactions with 1,3-Butadiene

(*a*) Dimethyltin dihydride (2.158 g, 14.3 mmole) and butadiene (0.774 g, 14.3 mmole) were irradiated with ultraviolet light at 25° for 20 hours. The reaction mixture contained no hydrogen, and all products were volatile. The volatile mixture was separated into fractions condensing at −23° (0.227 g, 7.8%, mol. wt. 210), and at −125° (2.692 g, mol. wt. approx. 110). The former fraction was characterized more fully in the later experiments, and the −125° fraction was shown spectroscopically to contain only dihydride and butadiene which could not be separated by fractional condensation. Hence 92% of the unchanged reactants were recovered.

(*b*) A mixture of dimethyltin dihydride (1.995 g, 13.2 mmole) and butadiene (0.697 g, 13.2 mmole) was kept at 50° under ultraviolet irradiation for 20 hours. The products were hydrogen (0.4 mmole), fractions which condensed at −23° (0.154 g, mol. wt. 247, vapor pressure (25°) 5 mm, 5.7%) and −125° (0.496 g) and a mixture of an involatile liquid with metallic tin, and other involatile solids. From this mixture, the involatile liquid (1.20 g, 32.4%) was separated by extraction. The −125° fraction was again an inseparable mixture of unchanged reactants. The −23° fraction decomposed slowly at 30° making characterization difficult, but careful refractionation in this and other experiments gave the same product, mol. wt. 203–210, b.p. (extrap.) approx. 200°, identified as *dimethyl(2-butenyl)tin hydride*, $(CH_3)_2SnH(CH_2CH{=}CHCH_3)$. Its infrared spectrum showed absorption bands at 3020 (sh), 2960 (sh), 2910 (m), 2860 (sh), 1823 (s), (Sn—H stretch), 1655 (sh) and 1640 (w) (C=C stretch), 1455 (w), 1444 (w), 1417 (w), 1398 (w), 1379 (vw), 1363 (w), 1302 (vw), 1254 (vw), 1192 (w), 1159 (w), 1095 (w), 1068 (w), 1037 (w), 993 (m), 961 (m), 906 (w), 762 (s) (CH_3—Sn rocking), 748 (sh), 727 (m), 570 (m), 513 (s), and 464 (w) cm^{-1}. The n.m.r. spectrum consisted of a pair of doublets at −5.36, −5.28, −5.26, and −5.19 p.p.m. assigned to —CH=CH—, an unresolved multiplet at −4.80 p.p.m. assigned to Sn—H (3), maxima at approximately −1.6 p.p.m. due to $—CH_2$ and $C—CH_3$, and a peak at −0.04 p.p.m. due to CH_3—Sn, all with respect to tetramethylsilane as internal standard. The intensities of these peaks, taken in the above order, was 1.8:1.2:5.0:6.0, compared with 2:1:5:6 for $(CH_3)_2SnH(CH_2CH{=}CHCH_3)$. Chlorination of this compound with carbon tetrachloride led to the formation of chloroform in the expected amount, and an increase in weight as expected for the formation of *dimethyl(2-butenyl)tin chloride*, $(CH_3)_2SnCl(CH_2CH{=}CHCH_3)$. The infrared spectrum of this product did *not* show absorption in the 1800–1850 cm^{-1} region, so that Sn—H groups were absent, and its n.m.r. spectrum was similar to that of the parent compound, with the exception that no multiplet at approx. −4.8 p.p.m. was observed.

The involatile liquid was shown to be *dimethylbis(2-butenyl)tin*, $(CH_3)_2Sn(CH_2CH{=}CHCH_3)_2$. Calc. for $C_{10}H_{20}Sn$: C, 46.37; H, 7.79. Obs.: C, 46.71; H, 7.70%. The infrared spectrum showed absorption at 3020 (s), 2955 (sh), 2910 (s), 2860 (sh), 1820 (vw), 1740 (vw), 1708 (vw), 1690 (vw), 1675 (vw), 1655 (w), 1639 (m), 1454 (m), 1442 (m), 1417 (m), 1397 (m), 1379 (m), 1362 (m), 1302 (w), 1254 (w), 1191 (m), 1156 (m), 1092 (m), 1066 (m), 1034 (m), 991 (s), 960 (s), 905 (sh), 902 (m), 788 (sh), 764 (s), 750 (sh), 720 (s), 550 (sh), 526 (s), 510 (m), and 480 (w) cm^{-1}. The n.m.r. spectrum showed a complex triplet at −5.36, −5.27, and −5.18 p.p.m., due to —CH=CH—, a series of peaks in the −0.5 to −2.00 p.p.m. region due to $—CH_2$ and $C—CH_3$ protons, and a large singlet at −0.0 p.p.m. due to CH_3—Sn, all with respect to tetramethylsilane. The areas of these peaks in the above order were in the ratio 2.2:1.7:3.2:5.5, compared with the expected ratio of intensities of 2:2:3:6 for $(CH_3)_2Sn(CH_2CH{=}CHCH_3)_2$.

(*c*) Dimethyltin dihydride (1.982 g, 13.1 mmole) and butadiene (0.707 g, 13.1 mmole) were exposed to ultraviolet radiation for 112 hours at 25°. The reaction mixture was separated into unreacted dihydride and butadiene (0.481 g), dimethyl(2-butenyl)tin hydride (0.994 g, mol. wt. obs. 203, 37%), involatile dimethylbis(2-butenyl)tin (1.005 g, 29.5%), and an involatile white solid (0.20 g).

(*d*) A mixture of dimethyltin dihydride (2.060 g, 13.6 mmole) and butadiene (1.470 g, 27.2 mmole) was irradiated for 23 hours at 50° C. The products were hydrogen (2.5 mmole, 19.0%), unreacted butadiene (0.241 g, 4.30 mmole, mol. wt. obs. 56.2, calc. 54), dimethyl(2-butenyl)tin hydride (0.152 g, 0.75 mmole, 5.5%), dimethylbis(2-butenyl)tin (2.562 g, 9.70 mmole, 70.6%), and a residue (0.50 g) composed largely of metallic tin.

(*e*) Dimethyltin dihydride (2.000 g, 13.2 mmole) and butadiene (0.718 g, 13.2 mmole) were heated at 50° in the dark for 163 hours. The products were identified as hydrogen (2.7 mmole), a mixture of unreacted dihydride and butadiene (0.926 g, 33.8%), dimethyl(2-butenyl)tin hydride (0.924 g, 4.50 mmole, 34.1%, mol. wt. obs. 201), dimethylbis(2-butenyl)tin (0.663 g, 2.56 mmole, 19.4%), and an involatile solid (0.205 g).

Reactions with cis-2-Butene

Four experiments were performed in which dimethyltin dihydride and *cis*-2-butene were allowed to react in either a 1:1 or 1:2 molar ratio under two sets of conditions: (*a*) at 50° in the dark for 23 hours, and (*b*)

Can. J. Chem. Downloaded from www.nrcresearchpress.com by 210.87.254.42 on 09/05/12
For personal use only.

at 25° under ultraviolet irradiation for 22 hours. In all cases, the reactants were recovered virtually quantitatively (96% or higher recovery) as a mixture which condensed at −125°. The infrared spectrum of these mixtures showed only the dihydride and *cis*-2-butene to be present. Also, in each experiment, very small fractions (2–10 mg) were condensed at −23°, and −46°, the quantities being too small to allow characterization.

Reactions with trans-2-Butene

Three experiments were carried out using dimethyltin dihydride and *trans*-2-butene under the following conditions: (*a*) dihydride and the butene in a 1:2 molar ratio at 50° in the dark for 68 hours, (*b*) dihydride and the butene in a 1:1 molar ratio at 50° in the dark for 69 hours, and (*c*) dihydride and the butene in a 1:2 molar ratio at 50° in the dark for 70 hours, followed by exposure to ultraviolet radiation at 25° for 23 hours. In each experiment, virtually all of the volatile products was condensed at −125° and was shown spectroscopically and from molecular weight measurements to be just unreacted dihydride and the original olefin. The total recovery was 96.5% or higher. However, in each case, there were also small fractions separated at −23° and −46°, but in amounts (1–5 mg) too small to allow positive identification.

Reactions with Excess Tetrafluoroethylene

(*a*) Dimethyltin dihydride (0.47 g, 3.16 mmole) and tetrafluoroethylene (1.23 g, 12.3 mmole) were sealed in a Pyrex carius tube (100-ml capacity) to give an initial pressure of approximately 5 atmospheres. After being heated at 50° in the dark for 24 hours, the products were hydrogen (0.2 mmole), unreacted C_2F_4 (0.744g, 7.44 mmole), unreacted dihydride (0.053 g, 0.35 mmole), dimethyltetrafluoroethyltin hydride (0.021 g, 3% yield), dimethylbis(tetrafluoroethyl)tin (0.762 g, 65.5% yield), and involatile, yellow residue (0.17 g) which was apparently polymerized C_2F_4. The characterization of $(CH_3)_2SnH(C_2F_4H)$ and $(CH_3)_2Sn(C_2F_4H)_2$ followed previous work (1).

(*b*) Tetrafluoroethylene (2.47 g, 24.7 mmole) and dimethyltin dihydride (0.284 g, 1.87 mmole), giving an initial pressure of approximately 10 atmospheres, were heated at 50° in the dark for 22 hours; unreacted olefin (2.09 g, 84.5%) and unreacted dihydride (0.083 g, 29%) were recovered. Reaction products were dimethyltetrafluoroethyltin hydride (0.027 g, 5.4% yield), dimethylbis(tetrafluoroethyl)tin (0.457 g, 69.6% yield), a trace of hydrogen, and an involatile residue (0.13 g).

(*c*) After an exposure of 21 hours at 25° to ultraviolet irradiation, dimethyltin dihydride (0.270 g, 1.79 mmole) and tetrafluoroethylene (2.38 g, 23.8 mmole), at an approximately 8 atmosphere initial pressure, gave unreacted C_2F_4 (1.86 g, 78.0%), unreacted dihydride (0.061 g, 23%), dimethylbis(tetrafluoroethyl)tin (0.471 g, mol. wt. obs. 350, calc. 351, 75.0% yield), and involatile white residue (0.26 g).

ACKNOWLEDGMENTS

The financial support of the National Research Council is gratefully acknowledged.

REFERENCES

1. H. C. CLARK, S. G. FURNIVAL, and J. T. KWON. Can. J. Chem. **41**, 2889 (1963).
2. J. G. NOLTES and G. J. M. VAN DER KERK. Functionally substituted organotin compounds. Tin Research Institute, Greenford. 1958.
3. L. J. BELLAMY. The infra-red spectra of complex molecules. Methuen and Co., Ltd., London. 1958. p. 36.
4. C. BARNETSON, H. C. CLARK, and J. T. KWON. Chem. Ind. In press (1964).
5. W. P. NEUMANN, H. NIERMANN, and R. SOMMER. Angew. Chem. **73**, 768 (1961).
6. W. P. NEUMANN, H. NIERMANN, and R. SOMMER. Liebigs Ann. Chem. **659**, 27 (1962).
7. D. J. COOKE, G. NICKLESS, and F. H. POLLARD. Chem. Ind. 1493 (1963).
8. R. K. INGHAM, S. D. ROSENBERG, and H. GILMAN. Chem. Rev. **60**, 460 (1960).
9. H. C. CLARK, J. T. KWON, L. W. REEVES, and E. J. WELLS. Can. J. Chem. **41**, 3005 (1963).

Can. J. Chem. Downloaded from www.nrcresearchpress.com by 210.87.254.42 on 09/05/12
For personal use only.

Can. J. Chem. Downloaded from www.nrcresearchpress.com by 210.87.254.5 on 09/05/12
For personal use only.

REACTION MECHANISM STUDIES

2. REDUCTIVE ELIMINATION OF 1,2-DIHALIDES WITH LITHIUM ALUMINUM HYDRIDE

J. F. KING AND R. G. PEWS
Department of Chemistry, University of Western Ontario, London, Ontario

Received February 5, 1964

ABSTRACT

1,2-Dibromides and bromohydrin *p*-toluenesulphonates of favorable geometry are readily reduced by lithium aluminum hydride in good yield to the corresponding olefin. Small quantities of water are found to have a *temporary accelerating effect* on the reduction. The normal course of the reaction is a trans elimination, but when steric factors inhibit this, then substitution or *cis* elimination reactions may occur. It is shown that the *cis* elimination in the case of *cis*-1,2-dibromocyclohexane cannot involve reduction to the monobromide followed by dehydrobromination to the olefin. The reaction of some other 1,2-dihalides and related compounds with lithium aluminum hydride, and the reaction of a 1,2-dibromide with a number of other complex hydrides are reported.

A general scheme for the mechanism of the olefin-forming elimination reaction is proposed. The limits that this study places on the possible positions of the reductive elimination of 1,2-dibromides with lithium aluminum hydride within this general scheme are discussed.

The elimination reaction leading to the formation of an olefin may be expressed generally by the equation 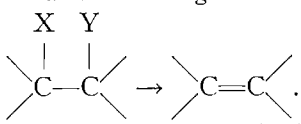 . The conventional description of a reaction as either an oxidation–reduction or metathesis can be usefully applied to classify eliminations as oxidative (e.g. dehydrogenation, in which X, Y = H), reductive (e.g. X, Y = halogen) or metathetical (e.g. X = H, Y = halogen); correspondingly the formal reverse of each of these reactions would be reductive addition (e.g. hydrogenation), oxidative addition (e.g. addition of halogen), and metathetical addition (e.g. addition of hydrogen halide), respectively. Much study has been devoted toward an understanding of the metathetical addition and elimination reactions, but much less work has been carried out on the oxidative and reductive processes. Though some of the most commonly used examples of the latter group are heterogeneous phase reactions whose study is complicated by special problems, a substantial number of oxidative and reductive additions and eliminations take place in solution. Table I lists a number of conditions under which reductive elimination of dibromides has been reported to occur; the great majority of these, in fact, involve a homogeneous system.

Most of the work on the mechanism of homogeneous phase reductive eliminations that had been reported at the beginning of this study had been restricted to the reduction of 1,2-dibromides (and some related species) with alkali iodides.* But the number and variety of other reagents which could effect reductive elimination of 1,2-dibromides (see Table I) suggested the possibility that the mechanism of reaction of some of these reagents might be quite different from that of an alkali iodide. If this were the case it would not be possible to discover all the ramifications of the mechanism of the general reductive elimination reaction were the study to be restricted to the reduction induced by alkali iodides. Accordingly, we decided to investigate the reductive elimination with lithium

**While this work was in progress, an investigation of the reduction of similar compounds with mercaptides was reported (24).*

TABLE I

Reactions reported to result in the reductive elimination of 1,2-dibromides

Reaction conditions	Substrate	Product	Ref.
Sodium in liquid ammonia	*meso*-2,3-Dibromobutane	*cis*-2-Butene (50%) *trans*-2-Butene (50%)	1
Sodium iodide* in acetone	Ethylene dibromide	Ethylene	2
n-Propylmagnesium bromide in ether	*trans*-1,2-Dibromocyclohexane	Cyclohexene (plus cyclohexane)	3
Phenyllithium in ether	*trans*-1,2-Dibromocyclohexane	Cyclohexene (80%)	4
Di-*p*-tolylmercury in toluene	*meso*-Stilbene dibromide	*trans*-Stilbene	5
Trimethyl phosphite in toluene	*trans*-Dibenzoylethylene dibromide	*trans*-Dibenzoylethylene (92%)	6
Potassium cyclohexylphosphide in benzene	Ethylene dibromide	Ethylene (85%)	7
Pyridine at ~ 100°	*meso*-Stilbene dibromide	*trans*-Stilbene	8
Ethanol at 150°	*meso*-Stilbene dibromide	*trans*-Stilbene	9
Aniline at 130°	*meso*-Stilbene dibromide	*trans*-Stilbene	9
Acetic acid	*meso*-Stilbene dibromide	*trans*-Stilbene	10
Phenylhydrazine	*meso*-Stilbene dibromide	*trans*-Stilbene	10
Potassium hydrosulphide in ethanol	*meso*-Stilbene dibromide	*trans*-Stilbene	11
Sodium thiophenoxide in ethanol	*meso*-Stilbene dibromide	*trans*-Stilbene	12
Sodium benzenesulphinate in ethanol	*meso*-Stilbene dibromide	*trans*-Stilbene	12
Water at 170°	2,3-Dibromohexane	2-Hexene	13
Silver oxalate in xylene	*meso*-Stilbene dibromide	*trans*-Stilbene	14
Phenetole at 170°	*meso*-Stilbene dibromide	*trans*-Stilbene (25%)	15
Triphenylphosphine in ether	Methyl 1,2-dibromopropionate	Methyl acrylate (64%)	16
Tri-*n*-butyltin hydride in pentane	1,2-Dibromopropane	Propylene (81%)	17
Chromous chloride in acetone	Stigmasteryl acetate tetrabromide	Stigmasteryl acetate 22,23-dibromide (65%)	18
Ferrous chloride, potassium acetate, and acetic acid in ethanol	Cholesterol dibromide	Cholesterol (72%)	19
Dropping mercury electrode	Ethylene dibromide	Ethylene	20
Zinc* and alcohol	Ethylene dibromide	Ethylene	21
Magnesium in ether	Ethylene dibromide	Ethylene	22
Amorphous arsenic	Ethylene dibromide	Ethylene	23
Lithium aluminum hydride	See Table II		

*An important preparative reaction with numerous variations of conditions; the example quoted is one of the earlier illustrations of its use.

aluminum hydride. From what little was known of this reaction at the beginning of this study, it appeared that this reagent effects reductive elimination of 1,2-dibromides in high yield, but it is otherwise different from alkali iodides in its reactions with organic compounds. Though lithium aluminum hydride is a much-used reagent in organic synthesis, there are serious technical and theoretical problems associated with a study of its mechanism of action. To a considerable extent these have limited the present study. At the same time it is hoped that this work has contributed toward their eventual solution.

Scope of the Reductive Elimination with Complex Metal Hydrides

Previous reports of reduction of 1,2-dihalides with lithium aluminum hydride are listed in Table II. In most of these examples reductive elimination is the only observed course of reaction, though substitution predominates with the following substrates: 1,2-dibromoöctane, ethyl β-chloroethyl ether, and *trans*-1,4-dibromo-2-butene. These anomalies are given further comment in the discussion of the mechanism of the reaction.

Table III summarizes the results of a number of experiments designed to show the range of compounds reducible with lithium aluminum hydride. The rest of this paragraph offers some general conclusions that may be drawn from these data. All of the 1,2-dibromides

Can. J. Chem. Downloaded from www.nrcresearchpress.com by 210.87.254.5 on 09/05/12
For personal use only.

TABLE II

Previous work on reductions of dihalides with lithium aluminum hydride

Substrate	Product	Yield (%)	Reference
meso-Stilbene dibromide	*trans*-Stilbene	98	25
1,2,3,4-Tetrabromobutane	Butadiene	—	25
Styrene dibromide	Styrene	71	25
Ethyl 2,3-dibromo-3-phenylpropionate	Hydrocinnamyl alcohol	59	25
1,2-Dibromoöctane	1-Octene	17	25
	2-Bromoöctane	26	25
2,3-Diiodo-1-propanol	Allyl alcohol	—	25
trans-1,4-Dibromo-2-butene	*trans*-2-Butene	72	25
24,25-Dibromocholest-8-en-3β-ol (zymosterol dibromide)	Cholesta-8,24-dien-3β-ol (zymosterol)	91	26
Ethyl 2,3-dibromo-4,4,4-trifluorobutyrate	4,4,4-Trifluorocrotyl alcohol	50	27
3,4-Dihydro-3,4-dibromohexachloro-1,5-hexadiene	3,4-Dihydrohexachloro-1,3,5-hexatriene	99	28
7,8-Dibromo-1,2,5,6-dibenzocycloöctatriene	1,2,5,6-Dibenzocycloöctatetraene	93	29
Ethyl α,β-dichloroethyl ether	Ethyl β-chloroethyl ether	53	25
Cycloöctatetraene dibromide*	Cycloöctatriene	—	30
	Bicyclo[4.2.0]octa-2,4-diene	—	

*Reaction mixture also contained a small amount of sodium iodide.

listed in Table III gave the corresponding olefin, though in the case of *cis*-1,2-dibromocyclohexane the yield was low. Reductive elimination with formation of *trans*-stilbene took place fairly smoothly with all compounds derived from it including the meso dichloride. The two *trans*-2,3-dichlorocholestanes (I*d* and II*c*), however, both gave a remarkable mixture of products which included only small amounts of the reductive elimination product. It seems likely that the dichlorocholestanes are more representative of 1,2-dichlorides than *meso*-stilbene dichloride; in general, then, formation of the olefin from 1,2-dichlorides probably does not predominate over other possible reactions. A similar result was found with 2-fluorobromides; *trans*-stilbene was formed in good yield from the corresponding fluorobromide, but fluorocyclohexane was the only product obtained from *trans*-1-fluoro-2-bromocyclohexane. As expected, the two diaxial bromohydrin *p*-toluenesulphonates (I*b*) and (I*c*) both gave the corresponding olefin in high yield. Surprisingly, however, the diequatorial isomer II*b* yielded much the same complex mixture of products as that obtained from the dichlorocholestanes, whereas the *cis* isomer IV gave a fairly good yield of the olefin.

The quantity of lithium aluminum hydride consumed by the reduction of 1 mole of *meso*-stilbene dibromide and cholesterol dibromide (V) was estimated by iodometric titration of the unreacted hydride (31) to be 0.47 and 0.42 moles, respectively (see Experimental); this corresponds reasonably well with the equation

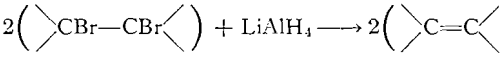

Gas (presumably hydrogen) is evolved in the reaction. The fate of the lithium, aluminum, and bromine atoms after the reduction has not been investigated, though a recent report on the reaction of lithium aluminum hydride with bromine suggests that the inorganic products may be LiBr and $LiAl_2Br_7$ (32).

The reaction of 2β,3α-dibromocholestane (I*a*) with a number of other complex hydrides was briefly investigated. Unreacted starting material was the principal constituent of the product obtained from the following conditions: (*a*) sodium borohydride in methanol at

Can. J. Chem. Downloaded from www.nrcresearchpress.com by 210.87.254.5 on 09/05/12
For personal use only.

Can. J. Chem. Downloaded from www.nrcresearchpress.com by 210.87.254.5 on 09/05/12
For personal use only.

TABLE III

Reaction of lithium aluminum hydride with 1,2-dihalides and halohydrin *p*-toluenesulphonates

Substrate	Solvent	Temp.	Time (hours)	Product	Yield (%)
2β,3α-Dibromocholestane (I*a*) (diaxial)	Tetrahydrofuran	Reflux	1	Cholest-2-ene (III)	90
2α,3β-Dibromocholestane (II*a*) (diequatorial)	Tetrahydrofuran	Reflux	1	Cholest-2-ene (III)	88
trans-1,2-Dibromocyclohexane	Triglyme	25°	1	Cyclohexene	77
		then 100°	1	Cyclohexane	5
cis-1,2-Dibromocyclohexane	Triglyme	25°	1	Cyclohexene	26*
		then 100°	1	Bromocyclohexane	49*
meso-Stilbene dibromide	Tetrahydrofuran	Reflux	1	*trans*-Stilbene	95
dl-Stilbene dibromide	Tetrahydrofuran	(see Table IX)		*trans*-Stilbene *cis*-Stilbene } see Table IX	
meso-2,3-Dibromobutane	Ether	25°	1	*trans*-2-Butene	90
dl-2,3-Dibromobutane	Ether	25°	1	*cis*-2-Butene	86
trans-1-Fluoro-2-bromocyclohexane	Triglyme	25°	1	Fluorocyclohexane	45
		then 100°	1		
erythro-1,2-Diphenyl-2-bromoethyl fluoride	Tetrahydrofuran	25°	0.75	*trans*-Stilbene	86
2β-Bromocholestan-3α-yl *p*-toluenesulphonate (I*b*) (diaxial)	Tetrahydrofuran	Reflux	1	Cholest-2-ene	90
3α-Bromocholestan-2β-yl *p*-toluenesulphonate (I*c*) (diaxial)	Tetrahydrofuran	Reflux	1	Cholest-2-ene	93
2α-Bromocholestan-3β-yl *p*-toluenesulphonate (II*b*) (diequatorial)	Tetrahydrofuran	Reflux	1	Small amounts of: cholest-2-ene, cholestane, cholestan-2β-ol, cholestan-2α-ol, cholestan-3β-ol, cholestan-3α-ol, plus unidentified products	—
2α-Bromocholestan-3α-yl *p*-toluenesulphonate (IV)	Tetrahydrofuran	Reflux	0.5	Cholest-2-ene	75
meso-Stilbene dichloride	Tetrahydrofuran	25°	1	*trans*-Stilbene	75*
2β,3α-Dichlorocholestane (diaxial)	Tetrahydrofuran	Reflux	1	Starting material plus cholest-2-ene, cholestane, cholestan-2β-ol, cholestan-2α-ol, cholestan-3β-ol, cholestan-3α-ol	—
2α,3β-Dichlorocholestane (diequatorial)	Tetrahydrofuran	Reflux	1	Starting material (mainly), plus cholest-2-ene, cholestane, cholestan-2β-ol, cholestan-2α-ol, cholestan-3β-ol, cholestan-3α-ol	—
5α,6β-Dibromocholestan-3β-ol (V)	Tetrahydrofuran	Reflux	2	Cholesterol (VI)	97
erythro-1,2-Diphenyl-2-bromoethyl methyl ether	Tetrahydrofuran	Reflux	5	*trans*-Stilbene	45
2β-Chlorocholestan-3α-yl *p*-toluenesulphonate (I*c*)	Dioxane	Reflux	2	Mainly starting material	—

*Based on reacted starting material.

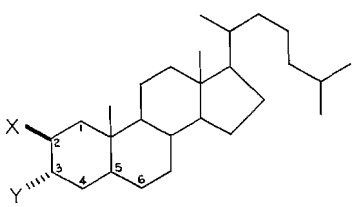

Ia X,Y = Br
Ib X = Br
Y = OSO_2—CH_3
Ic X = OSO_2—CH_3
Y = Br
Id X,Y = Cl
Ie X = Cl
Y = OSO_2—CH_3

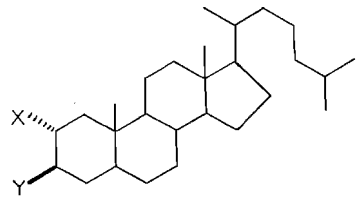

IIa X,Y = Br
IIb X = Br
Y = OSO_2—CH_3
IIc X,Y = Cl

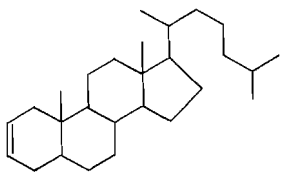

III

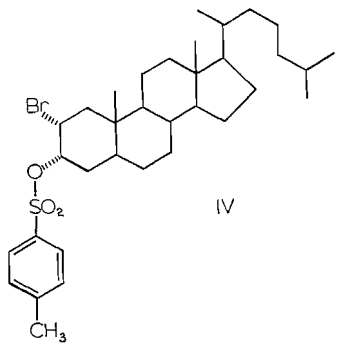

IV

room temperature, (*b*) commercial sodium "trimethoxyborohydride" in diglyme (diethylene glycol dimethyl ether) at room temperature, (*c*) lithium borohydride in ether or tetrahydrofuran under reflux, (*d*) lithium tri-*t*-butoxyaluminohydride in refluxing tetrahydrofuran, (*e*) diborane in diglyme at room temperature. With sodium borohydride in triglyme at 135°, sodium borohydride and aluminum chloride in diglyme at 100°, or lithium tri-*t*-butoxyaluminohydride in triglyme (triethylene glycol dimethyl ether) at 135°, neither starting material nor cholest-2-ene were isolated. Sodium "trimethoxyborohydride" in diglyme at 135° gave cholest-2-ene in 88% yield. Further work on some of these reactions will be described in a subsequent publication. Relevant to these observations is the recent report (17) that tri-*n*-butyltin hydride reduced certain 1,2-dibromides to the corresponding olefin (see Table I).

Rates of Reduction of Dibromides and Bromohydrin p-Toluenesulphonates

To gain further insight into the factors influencing the reductive elimination with lithium aluminum hydride, a study of the approximate rates of reduction of a number of dibromides and bromohydrin *p*-toluenesulphonates (tosylates) was initiated. The reaction was carried out in dry tetrahydrofuran at 0° in an atmosphere of oxygen-free, dry nitrogen under conditions designed to exclude water. Under these conditions the lithium aluminum

Can. J. Chem. Downloaded from www.nrcresearchpress.com by 210.87.254.5 on 09/05/12
For personal use only.

hydride solution, though slightly turbid, was found to maintain the same reducing power (as measured by titration with iodine) over a period of at least 3 months. The rate of the reductive elimination was followed by stopping the reaction with excess water and titrating the bromide ion formed in the reaction. It was found, however, that only the most approximate comparisons of relative rates could be made under these conditions. Individual runs for a certain reaction time using the same lithium aluminum hydride stock solution and the same specimen of the substrate were reasonably reproducible, but the same experiment with similar materials of different origin often gave results incompatible with those obtained previously. In addition, the extent of reaction for different reaction times, even when carried out on the same day with the same materials, did not correspond to any simple rate expression. (These results are discussed in greater detail elsewhere (33).)

Previous investigators (34, 35) had reported that water exhibits a catalytic effect in the lithium aluminum hydride reduction of certain organic halides. It seemed not unreasonable that some of the difficulties described above might be due to traces of water being added with the organic substrate. To test this possibility, a small amount of water was added to the reaction mixture along with the substrate. A notable acceleration was observed, see Table IV, and also Table V experiments No. 1 vs. 9, and 5 vs. 7. However, when the same

TABLE IV

Effect of varying the amount of water added with the substrate in the reduction of *meso*-stilbene dibromide

Time (minutes)	Substrate (mmoles)	Water (mmoles)	$LiAlH_4$ solution* (conc.)	% Reaction of individual experiments	Average % reaction
1.5	0.37	None	0.124 *M*	43, 43, 45	44
1.5	0.37	0.72	0.121 *M*	56, 53, 54	54
1.5	0.37	1.44	0.121 *M*	62, 66, 59, 58	61
1.5	0.37	2.88	0.121 *M*	77, 75, 78	77

*In tetrahydrofuran, 60 ml.

amount of water was added to the lithium aluminum hydride solution and the mixture allowed to stand for 15 minutes *before* adding the dibromide, then the rate of reduction was accelerated only slightly (if at all) over the case in which no water was added: compare experiment 12 (Table V) with 1 and 9, or 8 with 7 and 5. Addition of water, therefore, has a *temporary accelerating effect.* The reproducibility of the above results was checked in two ways: (i) A portion of the first lithium aluminum hydride stock solution (A) was stored under nitrogen for 3 months at room temperature; this solution (B) gave essentially the same results as had been obtained earlier. (ii) A new stock solution (C) was prepared from a fresh lot of lithium aluminum hydride and also gave similar results (see Table V).

It was apparent at this stage that the temporary accelerating effect of water introduces a complication into any attempt to compare the rates of reduction of different organic substrates. In the hope of obtaining a reaction mixture of constant reducing power, water was added gradually and continuously by passing a constant stream of wet nitrogen through the reaction mixture. The results obtained by this procedure using *meso*-2,3-dibromobutane as substrate are recorded in experiments 14–24 (Table V). A plot of log (100 − % reaction) vs. time indicates that under these conditions the reaction is approximately first order in dibromide, indicating that the constant addition of water to a large excess of lithium aluminum hydride produces a reagent of at least roughly constant

Can. J. Chem. Downloaded from www.nrcresearchpress.com by 210.87.254.5 on 09/05/12
For personal use only.

Can. J. Chem. Downloaded from www.nrcresearchpress.com by 210.87.254.5 on 09/05/12
For personal use only.

TABLE V

Effect of added water and its mode of addition to the rate of reduction of *meso*-2,3-dibromobutane*

Expt. No.	Time (minutes)	Amount and mode of addition of H_2O	$LiAlH_4$ concentration†	% Reaction of individual experiments	Average % reaction
1	5	None	0.126 *M* (*C*)	5, 6, 6, 5	5
2	5	None	0.127 *M* (*B*)	5, 7	6
3	10	None	0.126 *M* (*C*)	7, 8, 8	8
4	60	None	0.126 *M* (*C*)	16, 16, 16	16
5	60	None	0.127 *M* (*A*)	15, 13, 16	15
6	60	None	0.127 *M* (*B*)	17, 12, 13	14
7	1.5	1.44 mmoles H_2O with substrate	0.127 *M* (*A*)	22, 23, 25	23
8	1.5	1.44 mmoles H_2O added to reagent; let stand for 15 minutes then substrate added	0.127 *M* (*A*)	6, 4, 5	5
9	2	1.44 mmoles H_2O with substrate	0.126 *M* (*C*)	29, 34, 33	32
10	2	1.44 mmoles H_2O with substrate	0.127 *M* (*B*)	28 (one run only)	(28)
11	2	1.44 mmoles H_2O with substrate	0.127 *M* (*A*)	31 (one run only)	(31)
12	5	1.44 mmoles H_2O added to reagent; let stand for 15 minutes then substrate added	0.126 *M* (*C*)	5, 8, 9	7
13	5	1.44 mmoles H_2O added to reagent; let stand for 15 minutes then substrate added	0.127 *M* (*B*)	13, 7, 9	10
14	3	N_2, saturated at 0° with H_2O, bubbled into reaction mixture at 6.6 cc/second	0.127 *M* (*A*)	14, 15, 14	14
15	5	N_2, saturated at 0° with H_2O, bubbled into reaction mixture at 6.6 cc/second	0.127 *M* (*A*)	22, 23, 25, 24, 23, 21, 23	23
16	5	N_2, saturated at 0° with H_2O, bubbled into reaction mixture at 6.6 cc/second	0.127 *M* (*B*)	20, 29, 21, 20, 22	22
17	5	N_2, saturated at 0° with H_2O, bubbled into reaction mixture at 6.6 cc/second	0.126 *M* (*C*)	19, 25, 23, 23, 21	22
18	7	N_2, saturated at 0° with H_2O, bubbled into reaction mixture at 6.6 cc/second	0.127 *M* (*A*)	32, 34	33
19	7	N_2, saturated at 0° with H_2O, bubbled into reaction mixture at 6.6 cc/second	0.127 *M* (*C*)	31, 29	30
20	10	N_2, saturated at 0° with H_2O, bubbled into reaction mixture at 6.6 cc/second	0.127 *M* (*A*)	42, 41, 43	42
21	10	N_2, saturated at 0° with H_2O, bubbled into reaction mixture at 6.6 cc/second	0.126 *M* (*C*)	46, 44, 43	44
22	15	N_2, saturated at 0° with H_2O, bubbled into reaction mixture at 6.6 cc/second	0.127 *M* (*A*)	58, 54, 58	57
23	15	N_2, saturated at 0° with H_2O, bubbled into reaction mixture at 6.6 cc/second	0.126 *M* (*C*)	58, 57	58
24	30	N_2, saturated at 0° with H_2O, bubbled into reaction mixture at 6.6 cc/second	0.127 *M* (*B*)	94, 96	95

*6.3×10^{-3} *M* in tetrahydrofuran at 0°.

†Letters *A*, *B*, and *C* designate the stock solution of lithium aluminum hydride. Solution *B* was a portion of stock solution *A* that had been allowed to stand under nitrogen for 3 months. Solution *C* was prepared in the same way as *A* from a different lot of lithium aluminum hydride (from the same supplier).

reducing power in which the rate of reaction depends only on the concentration of the substrate. The detailed kinetics of the reduction are, without doubt, considerably more complicated, but the reproducibility of the above results with different stock solutions of lithium aluminum hydride gives confidence that the rates of reduction obtained by this technique would be at least semiquantitatively valid, and hence useful for comparing different organic substrates. It should be noted at this point that the amount of water added was not sufficient to destroy any more than about 10 to 25% of the lithium aluminum hydride, i.e. that the molar ratio of hydride to substrate changed at most from 20 to about 15.

In Table VI are summarized the results of the kinetic experiments which were carried out by passing wet nitrogen (saturated with water vapor at 0°) through solutions of lithium

TABLE VI

Lithium aluminum hydride reductions of 1,2-dibromides and bromohydrin *p*-toluenesulphonates with continuous addition of wet nitrogen at 0°

Substrate	Time (minutes)	% Reaction of individual experiments*	Approximate time for 20% reaction (minutes)	Isolation yield†
meso-Stilbene dibromide	1	75, 82	0.25	95
dl-Stilbene dibromide	1	21, 23	1.0	—
	1.5	28, 30		
meso-2,3-Dibromobutane	5	21, 24	5	90
dl-2,3-Dibromobutane	5	25, 21	5	86
2β,3α-Dibromocholestane (I*a*)	3.5	19	4	87
	3.75	21		
	4.0	23		
	15	70, 56		
2α,3β-Dibromocholestane (II*a*)	15	9, 11	30	85
	20	15		
	30	21, 23		
trans-1,2-Dibromocyclohexane	4	21, 21, 23	4	77
	15	55		
cis-1,2-Dibromocyclohexane	10	27, 29	—	26
	15	36		
2β-Bromocholestan-3α-yl *p*-toluenesulphonate (I*b*) (diaxial)	6	19	6	
	8	27		91
3α-Bromocholestan-2β-yl *p*-toluenesulphonate (I*c*) (diaxial)	5	36, 38	3	85
2α-Bromocholestan-3α-yl *p*-toluenesulphonate (IV)	15	20	15	74

*Concentrations: $LiAlH_4$, 0.128 *M*; substrate, 6.37×10^{-3} *M*; in tetrahydrofuran.
†After titration, the reaction mixture from one run was worked up in the same way that was used for that substrate to obtain the data in Table III. The numbers in the column give the percentage actually isolated of the quantity expected on the basis of the titration.

aluminum hydride and a variety of organic substrates in tetrahydrofuran. From these data it is readily apparent that those compounds reduce most readily in which the dihedral angle formed by the two carbons and the two leaving groups is 180°. In other words the preferred reaction is a trans elimination. Thus *meso*-stilbene dibromide reduces faster than *dl*-stilbene dibromide and the diaxial steroids reduce more readily than their diequatorial (or their cis) isomers. In most instances the rate differences were not very large, and with the 2,3-dibromobutanes there was no apparent rate difference at all. The products from the reduction of the 2,3-dibromobutanes, however, show that the reaction is strictly a trans elimination (see Table III). It is of interest that under the "anhydrous" conditions *meso*-2,3-dibromobutane apparently reduces slightly faster than the racemic isomer.

Can. J. Chem. Downloaded from www.nrcresearchpress.com by 210.87.254.5 on 09/05/12
For personal use only.

Under the "anhydrous" conditions also, 5α,6β-dibromocholestan-3β-ol (V), in which the bromine atoms are diaxial, apparently reduces more than 40 times faster than its di-equatorial isomer (VII).

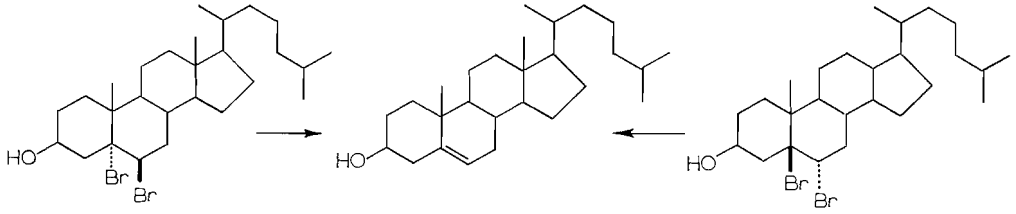

V VI VII

For those compounds in which the dihedral angle of 180° is not readily formed, trans elimination may require extra activation energy, and other reactions, especially cis elimination and substitution, may compete. An example is the reduction of *dl*-stilbene dibromide, which at −10° in tetrahydrofuran gives 5% *cis*-stilbene (the trans elimination product) and 95% *trans*-stilbene (formally, at least, the product of a cis elimination). At higher temperatures a higher proportion of the cis isomer is formed. *cis*-Stilbene is gradually isomerized to *trans*-stilbene under the reaction conditions but the rate is too slow to account for the quantity of *trans*-stilbene produced in these reductions. In addition it was found that 1,2-diphenylethyl bromide yields no *trans*-stilbene under the conditions of the reaction; this clearly demonstrates that this reduction, unlike some cis reductions with sodium iodide (36), cannot be rationalized by a two-step process of initial substitution by one equivalent of the reducing agent followed by a trans elimination. The experiments do not exclude the possibility that under the reaction conditions the *dl*-stilbene dibromide rearranges to the *meso* isomer which is then rapidly reduced; the rearrangement of *dl*-stilbene dibromide above its melting point is well-known (37) but the likelihood of a rapid rearrangement at −10° seems small.

A second compound which undergoes cis elimination is *cis*-1,2-dibromocyclohexane which yields cyclohexane together with a larger amount of the monosubstitution product, bromocyclohexane. *cis*-1,2-Dibromocyclohexane is an apparently stable compound with no tendency to isomerize to the trans isomer; preliminary isomerization followed by trans elimination would seem very unlikely indeed. Again the possibility of substitution followed by metathetical elimination is excluded by the observation that bromocyclohexane yields no cyclohexene under the conditions of the reaction. In the sense that the reaction cannot be reasonably interpreted as involving a preliminary transformation followed by a trans elimination, the formation of cyclohexene from *cis*-1,2-dibromocyclohexane evidently must be regarded as a "true" cis elimination; further mention of this will be made in the discussion of the mechanism.

The reductive elimination of 2α-bromocholestan-3α-yl tosylate (IV), in which the bromine and tosyloxy groups are cis, would also appear to be a true cis elimination for the following reasons. Displacement of the bromine by hydride followed by dehydrohalogenation of the resultant tosylate (cholestan-3α-yl tosylate) is excluded because the latter compound does not give cholest-2-ene (III) under the reaction conditions. The alternative substitution–metathetical elimination pathway, which would require the intermediacy of 2α-bromocholestane, would seem extremely unlikely in view of the lack of olefin obtained from bromocyclohexane.

Referring again to Table VI, another point of interest is the fact that the two diaxial

Can. J. Chem. Downloaded from www.nrcresearchpress.com by 210.87.254.5 on 09/05/12
For personal use only.

bromohydrin tosylates (I*b*) and (I*c*) reduce at about the same rate as the corresponding dibromide (I*a*). In this respect the reduction with lithium aluminum hydride differs from that with sodium iodide. With the latter reagent Cristol *et al.* (36) found that *trans*-2-bromocyclohexyl tosylate reduced about 20 times faster than *trans*-1,2-dibromocyclohexane.

Discussion of Mechanism

It would seem natural, in attempting to determine the mechanism of a reductive elimination reaction, to make use of the concepts which have been developed for the metathetical processes. Extension of the mechanisms of metathetical elimination to reductive

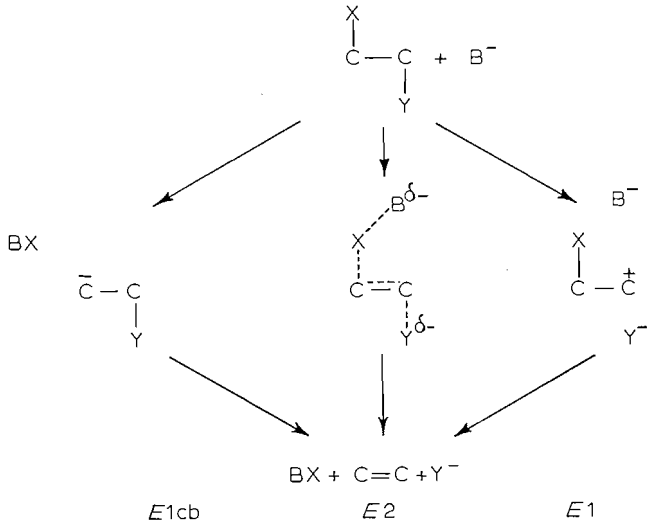

METATHETICAL ELIMINATION MECHANISMS

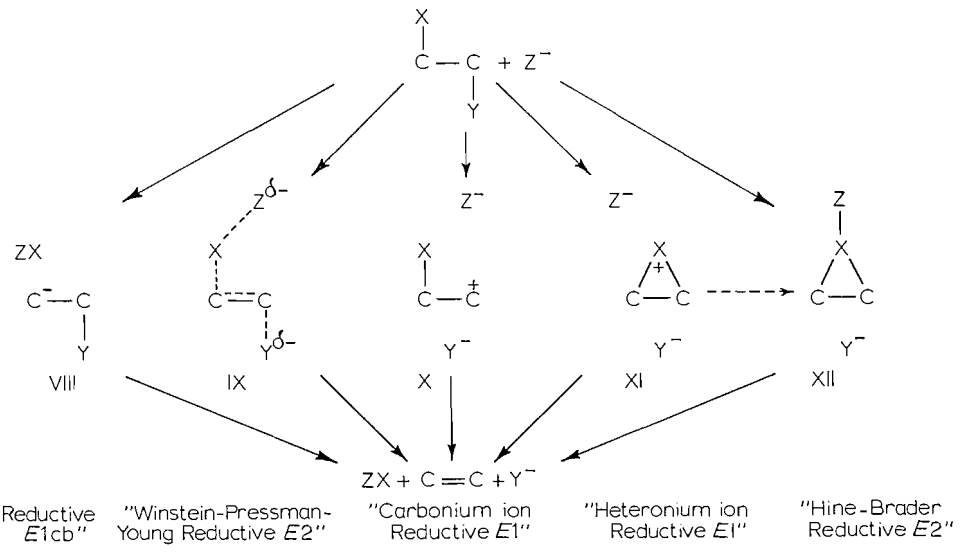

POSSIBLE REDUCTIVE ELIMINATION MECHANISMS

SCHEME 1

Can. J. Chem. Downloaded from www.nrcresearchpress.com by 210.87.254.5 on 09/05/12
For personal use only.

Can. J. Chem. Downloaded from www.nrcresearchpress.com by 210.87.254.5 on 09/05/12
For personal use only.

elimination is in some respects not trivial and some amplification is required at this point. In scheme 1 are set down the three mechanisms, which, together with mechanisms intermediate in character between these extremes, are currently regarded (38, 39) as describing all ionic metathetical eliminations which lead to the formation of olefins. Underneath are extensions which have been or may be made to apply to ionic reductive elimination. The arrangement in scheme 1 is such that between each mechanism and the one adjacent to it, one can easily visualize a continuous range of hybrid or "in between" processes. The five typical mechanisms shown, together with the hybrid mechanisms, constitute a continuous band or spectrum of reaction pathways. This scheme, though discussed here specifically with respect to reductive elimination, is probably general for all eliminations; the somewhat more restricted scheme for metathetical eliminations probably just reflects the inability of hydrogen to form species such as XI and XII, together with the fact that most of the work on metathetical eliminations has been carried out on compounds in which X = H.

At least three of the five reductive elimination mechanisms have been proposed previously. In 1939, Winstein, Pressman, and Young put forward (40) the mechanism involving species IX (scheme 1) to rationalize the observed kinetic and stereochemical data for the reduction of 1,2-dibromides with sodium iodide; since then it has been usual for most authors to discuss the mechanism of other reductive eliminations in terms of this process. Hine and Brader, however, put forward another reductive *E*2 mechanism (proceeding via species XII in scheme 1) for the reaction of dibromides with iodides (41); their chief point in favor of this mechanism is that it allows the halogenation and dehalogenation reactions to proceed via the same species (though, of course, in the reverse sequence). The "reductive *E*1cb" mechanism has been suggested (1) for the reduction of 1,2-dibromides with bivalent metals.* (The designation "reductive *E*1cb" is used in this discussion in order to show the parallel with the metathetical reaction; the literal significance of the term is lost, however, since the intermediate anion (VIII) is not the conjugate base of the starting material.)

To complete this mechanistic scheme it is apparently necessary to postulate mechanisms involving *both* the carbonium and "heteronium" ions, (X) and (XI) respectively, since depending on the nature of the substituent X and on the substitution of the carbon bearing Y, heterolysis of the starting material may lead to either of the extreme species and presumably also to a range of cations of intermediate character. It has recently been reported that an episulphonium salt is reduced to the corresponding olefin with sodium iodide (42). It is attractive to regard this reduction either as representing an example of the second stage of the "heteronium ion *E*1 reaction" (XI → olefin, directly), or alternatively as proceeding first to the Hine–Brader intermediate, as indicated by the dotted arrow, followed by olefin formation (i.e. XI → XII → olefin).

It should be emphasized that the possible reductive elimination mechanisms in scheme 1 are put forward in the hope of creating some order in the study of these transformations. Some of the mechanisms, though plausible, are nonetheless quite speculative. To our knowledge, in no case has *any* of the five mechanisms been established beyond question. It is in the context of this primitive state of the knowledge of these reactions that the following discussion of the lithium aluminum hydride reduction must be viewed.

Of the five mechanisms in scheme 1, two may be readily excluded for the reductive

**These authors do not draw a clear distinction between the "reductive E1cb" and the "Winstein–Pressman–Young reductive E2" mechanisms, but their discussion of the non-stereospecific reduction of the stilbene dibromides and related compounds is, in effect, in terms of the E1cb mechanism.*

elimination with lithium aluminum hydride. Neither the "reductive *E*1cb" mechanism nor the "carbonium ion reductive *E*1" mechanism satisfactorily accounts for the observed predominance of trans elimination and hence cannot be important routes for the reduction. The available data do not allow any definite conclusions to be drawn concerning the other three reductive elimination mechanisms. The "heteronium ion reductive *E*1" and, perhaps more particularly, the "Hine–Brader reductive *E*2" mechanisms might be expected to be strictly trans eliminations,* so that any scheme involving either of these would probably require the postulation of one of the other mechanisms to explain the cis eliminations. On the other hand it has recently been proposed (43, 44) that the metathetical *E*2, reaction takes place most readily when the leaving groups and the carbons to which they are directly attached form a dihedral angle of either 0° or 180°. If the geometrical requirements for the "Winstein–Pressman–Young *E*2" reaction are the same, then it by itself would account for all of the reductive eliminations described in this paper. The fact that the cis elimination is somewhat slower than the trans would be regarded simply as a reflection of the extra energy required for the compound undergoing cis elimination to achieve the totally eclipsed conformation (44). The ability of the "Winstein–Pressman–Young *E*2" mechanism to account for all of the observed elimination products is an attractive feature favoring this possibility, but it cannot be regarded as conclusive evidence.

There does not appear to have been any previous mention of the "heteronium ion reductive *E*1" mechanism,† and lest it be dismissed too lightly it is perhaps worth pointing out that such a mechanism fits readily into the pattern of the reactions of lithium aluminum hydride with organic halides generally. It was early recognized (25) that *substitution* at a saturated carbon with lithium aluminum hydride was a nucleophilic attack on carbon by a hydride ion or its complex equivalent. In addition it has been clearly shown that the displacement in simple secondary bromides and tosylates is predominantly a S_N2 reaction (45). Nonetheless there are a number of cases in which it seems likely that the reaction proceeds via a S_N1 mechanism. Corey and co-workers (46) have observed that the products formed in the reduction of cholesteryl tosylate are not compatible with a S_N2 process but are readily accounted for by assuming that the homoallylic carbonium ion is an intermediate. Other phenomena more readily explained by a S_N1 rather than a S_N2 mechanism are: (i) the high reactivity of triphenylmethyl chloride (25), (ii) the formation of rearranged products from 2-phenyl-3-pentyl tosylate (47), 7-chloronorbornadiene (35, 48), and 1-bromo-7-norbornanone (49) as well as cholesteryl tosylate (46, 50). In addition it may be noted that the tropylium ion is reduced to tropilidene (51), showing that an undoubted carbonium ion can, in fact, be reduced to the hydrocarbon with lithium aluminum hydride.

This expectation rests on two assumptions: (i) that the formation of the intermediates XI and XII involves displacement of Y^- with inversion of configuration, and (ii) that no geometrical isomerization takes place before or during reduction of the intermediate (XI or XII) to the olefin. It is reasonable to expect that these assumptions would be valid in most instances, but it is possible to imagine exceptions, especially with the "heteronium ion E1" reaction; to the extent that such exceptions are plausible in the present instance, then the force of the argument favoring the "Winstein–Pressman–Young E2" mechanism is diminished. The distinction that is being drawn at this point is that there are real *cis eliminations in a reaction which is believed to be analogous to the "Winstein–Pressman–Young E2" reduction, whereas any cis eliminations in the other two eliminations are, at present, hypothetical.*

†NOTE ADDED IN PROOF: *Such a mechanism, as we have belatedly discovered, has, in fact, been proposed by J. W. Cornforth, R. H. Cornforth, and K. K. Mathew (J. Chem. Soc. 112 (1959)). Specifically these authors suggest that a three-membered ring iodonium is an intermediate in the reduction of iodohydrins to olefins by means of a mixture of stannous chloride and phosphorus oxychloride in pyridine. The data in this admirable paper are not sufficient to establish the mechanism rigorously (they would fit equally well with the "Hine–Brader reductive E2" mechanism, for example), and at the moment the proposal would appear to be best described as an attractive and reasonable suggestion.*

Can. J. Chem. Downloaded from www.nrcresearchpress.com by 210.87.254.5 on 09/05/12
For personal use only.

Can. J. Chem. Downloaded from www.nrcresearchpress.com by 210.87.254.5 on 09/05/12
For personal use only.

Ionization of a 1,2-dibromide or bromohydrin tosylate is believed to lead to a bromonium ion (52, 53). Such an ion, in principle, could be attacked by hydride either at carbon or bromine; the former would lead to formation of the monobromide, the latter to the olefin (which reaction is, of course, simply the "heteronium ion *E*1" reduction of scheme 1). Such a direct reduction of a bromonium ion to an olefin is not implausible and finds parallel in the formation of olefins by the reduction of episulphides with lithium aluminum hydride (54) or triethyl phosphite (55), and also the reduction, referred to above, of an episulphonium ion with sodium iodide (42). It is perhaps of interest that the bromonium ion mechanism can account for the formation of 2-bromoöctane (as well as 1-octene) from 1,2-dibromoöctane (see Table II). In this case since one of the carbons of the bromonium ion is primary, attack on that carbon might be expected to be an important reaction path. (Another rationalization of the formation of 2-bromoöctane is mentioned below.)

To sum up this discussion of the three stereospecific mechanisms in scheme 1, it appears that attractive cases may be made for both the "Winstein–Pressman–Young *E*2" and the "heteronium ion *E*1" mechanisms but there is no reason to fault the "Hine–Brader *E*2" mechanism. The possibility either of two or more concurrent mechanisms* or of a hybrid or "in between" mechanism exists but does not warrant discussion until more data are obtained.

Another question raised by this study is the cause of the temporary accelerating effect of water. A priori it is conceivable that reaction of water with lithium aluminum hydride produces a reagent of greater reducing power than lithium aluminum hydride itself. But it has been reported that the lithium alkoxyaluminohydrides in general are weaker reducing agents than lithium aluminum hydride (57); this is in agreement with our finding that lithium tri-*t*-butoxyaluminohydride does not react with $2\beta,3\alpha$-dibromocholestane in refluxing tetrahydrofuran. Eliel and Prosser (34) have called attention to this point in connection with the effect of added water and alcohols in the reduction of chlorohydrins, and have concluded that the accelerating effect in their system may be due to the formation of a more active Lewis acid in the mixture. Such a Lewis acid could accelerate these reactions by adding onto the halide (or tosylate) group to give an easily heterolyzed complex. Such a process would fit in with any of the mechanisms in scheme 1, it would simply mean that the Y groups would be complexed leaving groups rather than the original halide or tosylate functions. A preliminary complexing with a Lewis acid is probably necessary for either the *E*1 or the S_N1 reactions with lithium aluminum hydride (assuming that they exist), since most halides or tosylates do not ionize spontaneously and rapidly in the solvents used for these reactions. Aluminum hydride has been suggested as the active Lewis acid facilitating the formation of an ionic intermediate (58), but the complex of aluminum hydride with tetrahydrofuran is apparently stable under the conditions of our study (59, 60) and therefore is a poor candidate to explain the comparatively short lifetime of the accelerating effect observed in our case. The present data are consistent with the possibility that the accelerating effect of water is due to an hydroxyaluminohydride ($Al(OH)_nH_{4-n}$) which rapidly disproportionates, reacts with solvent, and (or) polymerizes. The inorganic products formed in the reaction do not show any noticeable catalytic activity: a solution of lithium aluminum hydride in which *meso*-stilbene dibromide had been completely reduced showed no greater reactivity than one that had had no stilbene dibromide added to it.

**It has recently been suggested that reduction of ethylene dibromide with sodium iodide in acetone involves* both *the "Winstein–Pressman–Young E2" and the "Hine–Brader E2" mechanisms (56).*

Can. J. Chem. Downloaded from www.nrcresearchpress.com by 210.87.254.5 on 09/05/12
For personal use only.

Among the data in Tables II and III are a number of cases in which direct displacement of halogen by hydride predominates over reductive elimination. These are, in particular, the reactions of (*a*) 1,2-dibromoöctane, in which the displaced bromine is primary, (*b*) *trans*-1,4-dibromo-2-butene, in which the displaced bromine is allylic, and (*c*) ethyl β-chloroethyl ether, in which the displaced chlorine is on the same carbon as the ether oxygen; in each of these cases the relatively fast displacement is easily rationalized in terms of known properties of the S_N2 reaction. The cycloöctatetraene dibromide reduction is readily explained if it is assumed that the reduction proceeds through the monocyclic valence tautomer, in which both bromine atoms are allylic. The formation of bromocyclohexane from *cis*-1,2-dibromocyclohexane presumably reflects the ability of displacement to compete with reductive elimination when steric factors retard the latter reaction.

The reduction of the *trans*-2,3-dichlorocholestanes leads to cholest-2-ene, together with roughly the same amount of what appears to be cholestane, and a smaller amount of a mixture consisting of all four of the 2- and 3-cholestanols in approximately equal proportions. The surprising formation of the cholestanol mixture would appear to result from displacement of chlorine by hydroxide or oxygen bound in some form to aluminum. The most likely source of the oxygen is hydrolyzed reagent though the ratio of mixed cholestanols to other materials in the product is not sensitive to the extent of hydrolysis of the reagent: carrying out the reaction with carefully dried apparatus and solvent gives the same mixture as that obtained in the presence of wet nitrogen. It is not difficult to devise a scheme which accounts for the cholestanols being formed, but it is not particularly obvious why the four isomers should be formed in similar quantities. A similar mixture of cholestanols is also formed in low yield from 2α-bromocholestan-3β-yl tosylate. With this compound the hydroxyl group in the products might conceivably arise by S—O fission of the ester, but the similarity of the composition of the mixture of cholestanols to that obtained from the dichlorocholestanes suggests that they arise by a similar mechanism. Experiments are now being carried out which, it is hoped, will provide evidence as to the origin of the cholestanol mixture.

EXPERIMENTAL

Infrared spectra were obtained using Beckman IR-5 or IR-7 spectrophotometers equipped with sodium chloride optics; all values quoted for the frequencies of infrared maxima were determined with the IR-7 instrument. Melting points, which were determined on a Kofler hot stage, and boiling points are uncorrected. Optical rotations refer to chloroform solutions at room temperature ($c \sim 1.0$). The refractive indices were determined with a thermostatically controlled Bausch and Lomb refractometer. Thin-layer chromatography was carried out using Camag Kieselgel D5 or DF5. Petroleum ether, unless otherwise specified, refers to the fraction of boiling range 35–60°. All glassware used for rate measurements and the distillation of solvents was dried at 200° or more for not less than 2 hours.

The tetrahydrofuran used in this study was Fisher Certified Reagent refluxed for not less than 4 hours with lithium aluminum hydride and then distilled. Triglyme was purified as previously described (61). Dioxane was purified by the method of Vogel (62) and stored under dry nitrogen; it was tested for peroxides before use and if these were found present, it was redistilled from lithium aluminum hydride. The benzene for the iodometric titrations was BDH "Analar" grade refluxed over calcium hydride and distilled. Mallinckrodt "ether anhydrous analytical reagent" was used in reductions without further purification.

2β,3α-Dibromocholestane

Prepared from cholest-2-ene as described by Alt and Barton (63); m.p. 123–124°, $[\alpha]_D$ +76°; reported m.p. 123–124°, $[\alpha]_D$ +76°.

2α,3β-Dibromocholestane

Prepared from 2β,3α-dibromocholestane as described by Alt and Barton (63); m.p. 143–145°, $[\alpha]_D$ −29°; reported m.p. 144–145°, $[\alpha]_D$ −29°.

2β,3α-Dichlorocholestane

Prepared from cholest-2-ene as previously described (63); m.p. 105–108°, $[\alpha]$ +61°; reported m.p. 108–112°, $[\alpha]$ +63°.

2α,3β-Dichlorocholestane
Prepared from cholest-2-ene as previously described (63); m.p. 148–150°, $[\alpha]_D$ −4°; reported m.p. 150–152°, $[\alpha]_D$ −7°.

5α,6β-Dibromocholestan-3β-ol
Prepared as previously described by Fieser (64). Recrystallization from ether – petroleum ether gave a product m.p. 115–117°, $[\alpha]_D$ −45°; reported m.p. 112–114°, $[\alpha]_D$ −44° (65).

5β,6α-Dibromocholestan-3β-ol
The following procedure was found to be more convenient than that of Barton and Miller (65). 5α,6β-Dibromocholestan-3β-ol (3.5 g) was refluxed in spectroscopic grade carbon tetrachloride (100 ml) for 24 hours. About 60 ml of the solvent was removed *in vacuo* and the solution was then diluted rapidly with methanol. The first crop of crystals was unchanged starting material. Further dilution with methanol furnished, after recrystallization from ether–methanol, 5β,6α-dibromocholestan-3β-ol (1.3 g), m.p. 141–143°, $[\alpha]_D$ +45°; reported m.p. 143°, $[\alpha]_D$ +47°.

2β-Chlorocholestan-3α-ol
Prepared from 2α,3α-epoxycholestane as previously described (63); m.p. 118–121°, $[\alpha]_D$ +40°; reported m.p. 118–120°, $[\alpha]_D$ +39°.

2α-Bromocholestan-3α-ol
Prepared by reduction of 2α-bromocholestan-3-one with sodium borohydride as previously described (66); m.p. 116–118°, $[\alpha]_D$ +36°; reported m.p. 117–118°, $[\alpha]_D$ +33°.

2α-Bromocholestan-3α-yl p-Toluenesulphonate
Prepared from the alcohol in the usual way (61); recrystallized four times from acetone, m.p. 237–240°, $[\alpha]_D$ +40°. Calc. for $C_{34}H_{53}O_3SBr$: C, 65.68; H, 8.59; S, 5.16; Br, 12.85%. Found: C, 65.74; H, 8.45; S, 4.97; Br, 13.02%.

2β-Chlorocholestan-3α-yl p-Toluenesulphonate
Prepared from the alcohol in the usual way (61); recrystallized four times from acetone, m.p. 182–183°, $[\alpha]_D$ +46°. Calc. for $C_{34}H_{53}O_3SCl$: C, 70.73; H, 9.25; S, 5.55; Cl, 6.14%. Found: C, 71.20; H, 8.91; S, 5.59; Cl, 5.91%.

2β-Bromocholestan-3α-yl p-Toluenesulphonate
Prepared as previously described (67), m.p. 168–170°, $[\alpha]_D$ +49°; reported m.p. 168–170°, $[\alpha]_D$ +49°.

3α-Bromocholestan-2β-yl p-Toluenesulphonate
Prepared as previously described (61), m.p. 174–177°, $[\alpha]_D$ +49°.

2α-Bromocholestan-3β-yl p-Toluenesulphonate
Prepared as previously described (61), m.p. 135° and around 165°, $[\alpha]_D$ −38.5°.

Derivatives of 1,2-Diphenylethane
meso-Stilbene dibromide: crystallized from toluene, m.p. 237°. *dl*-Stilbene dibromide: m.p. 113–114°. *meso*-Stilbene dichloride: m.p. 191–193°. *dl*-1,2-Diphenylethanol: m.p. 65–67°. *dl*-1,2-Diphenylethyl bromide: prepared by the method of Curtin and Kellom (68): n_D^{20} 1.6015. *erythro*-1,2-Diphenyl-2-bromoethyl fluoride: prepared by Dr. J. Newton (69): m.p. 104–105°. *erythro*-1,2-Diphenyl-2-bromoethyl methyl ether: prepared as described by Bartlett and Tarbell (70): m.p. 117–120°.

Derivatives of Butane
(a) meso-2,3-Dibromobutane.—*trans*-2-Butene (99 mole % minimum, supplied by Phillips Petroleum Company, Special Products Division, Bartlesville, Oklahoma) was bubbled slowly into an ether solution (150 ml) of bromine (16 g) cooled in a dry-ice and carbon tetrachloride bath, until the solution became colorless. The reaction mixture was then poured into water and extracted with ether. The ether extract was washed with dilute sodium sulphite solution, dilute potassium bicarbonate solution, and water, and dried over sodium sulphate. Removal of the solvent and distillation of the residue gave after a small forerun, *meso*-2,3-dibromobutane (8.0 g); b.p. 72–73° (51 mm); n_D^{20} 1.5120; reported b.p. 72.7–72.9° (50 mm), n_D^{20} 1.5116 (71).
(b) dl-2,3-Dibromobutane.—This compound was prepared from *cis*-2-butene (99.97 mole % minimum supplied by Phillips Petroleum Company, Special Products Division, Bartlesville, Oklahoma) by the same procedure as described above for *meso*-2,3-dibromobutane; b.p. 72.5–73.5° (50 mm), n_D^{20} 1.5143; reported b.p. 75.6–75.8° (50 mm), n_D^{20} 1.5147 (71).

Derivatives of Cyclohexane
(*a*) *trans*-1,2-Dibromocyclohexane was prepared by the addition of bromine to cyclohexene in carbon tetrachloride as previously described (72); n_D^{25} 1.5507; reported n_D^{25} 1.5507 (73).

Can. J. Chem. Downloaded from www.nrcresearchpress.com by 210.87.254.5 on 09/05/12
For personal use only.

(*b*) *cis*-1,2-Dibromocyclohexane was prepared by the free radical addition of hydrogen bromide to 1-bromocyclohexene as described by Goering *et al.* (74). Recrystallization from pentane gave the product, m.p. 6–8°; reported m.p. 9–10°.

(*c*) *trans*-1-Bromo-2-fluorocyclohexane was supplied by Mr. F. H. Dean (69), n_D^{20} 1.4820; b.p. 88–90° (84 mm).

Lithium Aluminum Hydride Stock Solutions

Lithium aluminum hydride (Metal Hydrides Inc.) sufficient to give an approximately 0.8 ± 0.2 *M* solution was placed in a Soxhlet extractor and extracted with anhydrous tetrahydrofuran. The stock solution was then attached to the burette assembly as in Fig. 1. The molarity of the stock solution was determined by the addition of excess standardized iodine in anhydrous benzene, followed by back titration with sodium thiosulphate as described by Felkin (31).

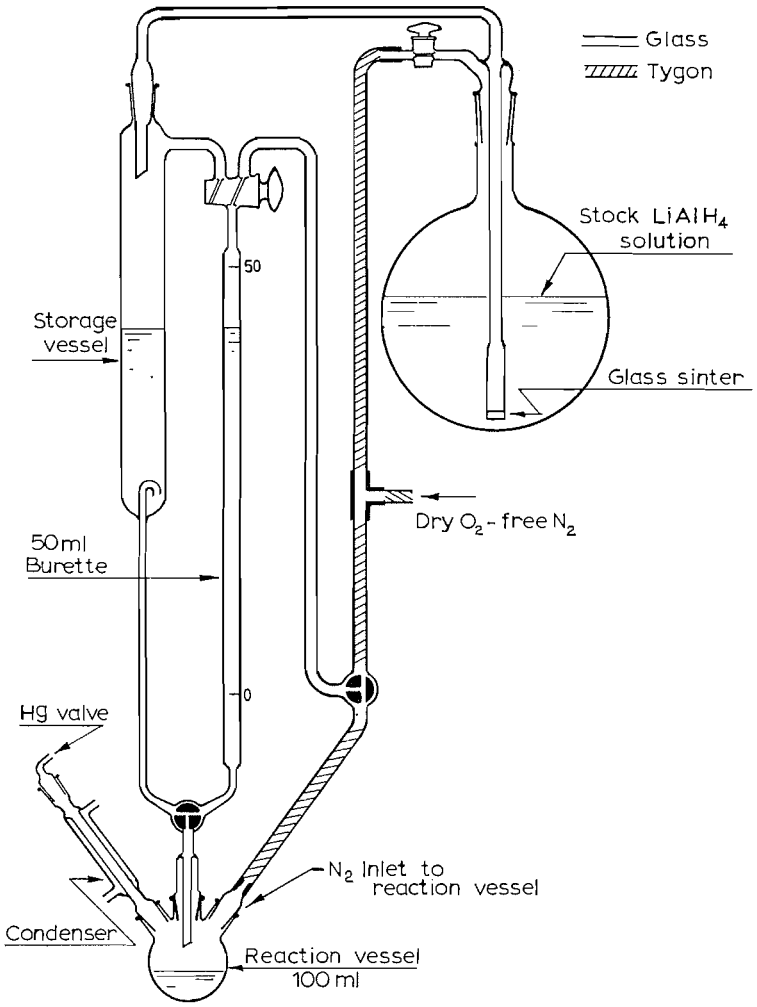

FIG. 1.

Procedure for the Determination of the Stoichiometry

Anhydrous tetrahydrofuran (approx. 150 ml) was distilled under a nitrogen atmosphere into a three-necked flask (300 ml) containing the dibromide (approx. 8 mmoles) and fitted with reflux condenser, magnetic stirrer, and drying tube. The flask was quickly transferred from the distillation assembly to the burette containing the stock solution of lithium aluminum hydride (see Fig. 1), and excess hydride added. After the

Can. J. Chem. Downloaded from www.nrcresearchpress.com by 210.87.254.5 on 09/05/12
For personal use only.

addition of the hydride was complete, the reaction mixture was refluxed for 1 hour in the *meso*-stilbene dibromide experiments and 2 hours in the 5α,6β-dibromocholestan-3β-ol experiments. The active hydride remaining after reduction was titrated with a standardized solution of iodine in benzene (31). Blank experiments with stilbene and cholesterol, respectively, were carried out to determine the amount of hydride lost during the operations. For these experiments both the 5α,6β-dibromocholestan-3β-ol and the cholesterol were recrystallized from ether – petroleum ether and carefully dried. The results are recorded in Table VII.

After the iodine titration, the reaction mixture was poured into water and extracted with ether. The ether extract was washed with dilute sodium sulphite solution, dilute sulphuric acid, and water, dried over sodium sulphate, and the solvent evaporated. The olefin was then recrystallized from ether–ethanol. The yields are summarized in Table VII.

General Procedure for Rate Measurements with Lithium Aluminum Hydride (Tables IV to VI)

(a) The Reaction

The glassware was heated in an oven (minimum temperature 200°) for not less than 4 hours before use. A three-necked, round-bottomed flask (100 ml) equipped with condenser, magnetic stirrer, stopper, and nitrogen inlet tube was quickly assembled and heated with a Bunsen burner flame while dry nitrogen was passed through the apparatus. When the apparatus had cooled to room temperature, the stopper was quickly removed and the substrate (0.366 mmole) and tetrahydrofuran (50 ml) added to the reaction vessel under positive nitrogen pressure. The reactants were cooled in an ice bath to 1±1°. The reaction vessel was quickly transferred from the ice bath to the burette assembly (see Fig. 1) and lithium aluminum hydride (7.32 mmoles) in tetrahydrofuran added. The reduction was stopped by pouring the reaction mixture into water (150 ml). In the kinetic experiments in which water was initially present before the addition of lithium aluminum hydride, the water was mixed with the anhydrous tetrahydrofuran. In all other experiments involving addition of water, nitrogen saturated with water vapor by passage through an ice–water trap was bubbled into the reaction vessel at a constant flow rate. The flow rate (6.6 ml/second) was measured with a burette (50 ml) as a soap bubble flow meter.

(b) Method of Bromide Ion Analysis

The reaction mixture, after being quenched with water, was acidified with glacial acetic acid (approx. 20 ml). The amount of bromide ion was then determined by potentiometric titration with *N*/10 silver nitrate using an Electronic Instruments Ltd. (Surrey, England) Model 23A pH meter, and the following electrode system: silver electrode in contact with the bromide ion solution, with a calomel reference cell in a separate beaker and connected to the titration vessel through an ammonium nitrate bridge. To inhibit gumming of the silver electrode by the organic precipitate, benzene (ca. 50 ml) was added to the titration mixture. Under the titration conditions the organic substrates do not react with silver nitrate. A blank titration of the hydrolyzed reagent showed the presence of a small amount of halide ion (presumably lithium chloride); the quantity of silver nitrate consumed by the hydrolyzed reagent was determined before each run and was subtracted from the titer of that run.

Reaction of Lithium Aluminum Hydride with Water

The following experiments were carried out to measure the amount of lithium aluminum hydride (or active hydride) destroyed by bubbling moist nitrogen into the solution under the conditions described in the above section. In two experiments wet N_2 (saturated at 0°) was bubbled into the mixture at the rate of 6.6 ml/second for an interval and the mixture then titrated immediately with I_2 in benzene. In the other two experiments a quantity of water equal to that calculated to have been added in the wet N_2 experiments was added directly and the mixture allowed to stand for the same length of time as the N_2 had been bubbled in and the mixture then titrated with I_2 in benzene. The results are summarized in Table VIII.

Reaction of Lithium Aluminum Hydride with 1,2-Dihalides and Related Compounds (Table III)

General Procedure

A number of the reactions gave a crystalline product in good yield. In each of these cases, the substrate (ca. 50 mg) was refluxed for 1 hour in 1.0 *M* lithium aluminum hydride (ca. 4 ml). The reaction mixture was poured into water and extracted with ether. The ether extract was washed with dilute sulphuric acid and water, dried with sodium sulphate, and the solvent evaporated. Recrystallization gave a product which was identified by melting point, infrared spectrum, and where useful, optical rotation. The yields are summarized in Table III.

Other reactions are described individually below.

(a) 2α-Bromocholestan-3β-yl p-Toluenesulphonate.—Examination of the reaction product by thin-layer chromatography gave the following results: tile 1 (petroleum ether) indicated only trace amounts of cholestane and cholest-2-ene (identified by authentic samples run on the same tile); tile 2 (petroleum ether – benzene, 1:1) established the absence of starting material; tile 3 (benzene–ether, 3:1) showed the presence of not less than 10 products, four of which appeared to be the 2- and 3-hydroxycholestanes by their R_f values.

(b) 2β,3α-Dichlorocholestane.—In addition to a strong hydroxyl band at 3620 cm^{-1}, only unreacted starting

Can. J. Chem. Downloaded from www.nrcresearchpress.com by 210.87.254.5 on 09/05/12
For personal use only.

Can. J. Chem. Downloaded from www.nrcresearchpress.com by 210.87.254.5 on 09/05/12
For personal use only.

TABLE VII

Stoichiometry experiments

	Dibromide added (mmoles)	$LiAlH_4$ added (mmoles)	$LiAlH_4$ consumed in experiment (mmoles)	$LiAlH_4$ consumed by blank (mmoles)	Net $LiAlH_4$ consumed by reduction (mmoles)	$LiAlH_4$ consumed per mole of dibromide (mmoles)	Yield of olefin (%)
meso-Stilbene dibromide	9.71	12.00	5.67	1.15	4.52	0.47	95
	9.64	11.00	5.69	1.20	4.49	0.47	91
$5\alpha,6\beta$-Dibromocholestan-3β-ol	8.07	11.70	6.05		3.55	0.44	95
	8.10	11.70	5.85	2.50	3.35	0.41	97

TABLE VIII

Reaction of $LiAlH_4$ in water

Time (minutes)	Number of runs	Amount of water (mmoles) added and method of addition	$LiAlH_4$ (mmoles)	I_2 (mmoles) titer	$LiAlH_4$ (mmoles) destroyed
0	1	0	7.32	14.6	(0.0)
15*	3	1.62† in wet N_2	7.32	12.5	1.06
30*	3	3.34† in wet N_2	7.32	10.9	1.86
15‡	2	1.62 added directly	7.32	12.1	1.26
30‡	2	3.34 added directly	7.32	10.4	2.10

*Length of time the wet N_2 was bubbled through the mixture.
†Calculated from the volume of N_2 and the saturated vapor pressure of water at 0°.
‡Time elapsed between water addition and I_2 titration.

material could be identified from the infrared spectrum (IR-7) of the reaction product. Thin-layer chromatography gave the following results: tile 1 (petroleum ether) showed, by comparison of the R_f values of authentic samples, the presence of unreacted starting material, cholestane and cholest-2-ene but none of the diequatorial isomer, 2α,3β-dichlorocholestane; tile 2 (benzene–ether, 3:1) showed, by comparison of the R_f values of authentic samples, the presence of the following alcohols, cholestan-2β-ol, cholestan-2α-ol, cholestan-3β-ol, and cholestan-3α-ol.

(c) 2α,3β-Dichlorocholestane.—The reaction product consisted mainly of unreacted starting material. Examination of the thin-layer chromatograms gave the same results as described for 2β,3α-dichlorocholestane with the exception that the six identifiable products were produced in lesser amounts.

(d) cis-1,2-Dibromocyclohexane.— *cis*-1,2-Dibromocyclohexane (3.5 g), lithium aluminum hydride (1.5 g), and anhydrous triglyme (80 ml) were placed in a three-necked, round-bottomed flask equipped with a nitrogen inlet and a reflux condenser. The condenser was connected to a trap cooled in liquid nitrogen. After wet nitrogen was passed through the reaction mixture at room temperature for 1 hour, the temperature was raised to 100° to distil off the volatile fraction (0.27 g) which was found by vapor-phase chromatography to contain 63% of cyclohexene. The reaction mixture was poured into wet ether to destroy the unreacted lithium aluminum hydride and the ether extract washed with dilute sulphuric acid and water, dried over sodium sulphate, and the solvent evaporated. The residue (1.90 g) was analyzed by vapor-phase chromatography and was found to consist of bromocyclohexane, 51%, and unreacted dibromide 49%. These results are equivalent to the following yields: cyclohexane, 26%, and bromocyclohexane, 49%, based on reacted *cis*-1,2-dibromocyclohexane.

(e) trans-1,2-Dibromocyclohexane.—Following the procedure and method of analysis as outlined for the cis isomer, *trans*-1,2-dibromocyclohexane (28 g) and lithium aluminum hydride (7.5 g) in anhydrous triglyme (100 ml) gave cyclohexane (0.5 g, 5%) and cyclohexene (7.3 g, 77%).

(f) meso-2,3-Dibromobutane.—Following the procedure outlined for *cis*-1,2-dibromocyclohexane, *trans*-2-butene was identified as the principal product of the reduction of *meso*-2,3-dibromobutane by comparison of the infrared spectrum (IR-7) with that of an authentic sample. From the absorption bands in the 2800–3000 cm^{-1} region and at 960 cm^{-1} and the lack of absorption at 975 cm^{-1} it was established that *cis*-2-butene was not produced in appreciable amounts if at all. In a separate experiment, the yield of *trans*-2-butene, isolated as the dibromide, was 90%.

(g) dl-2,3-Dibromobutane.—Following the procedure outlined for *cis*-1,2-dibromocyclohexane, *cis*-2-butene was identified as the principal product of the reduction of *dl*-2,3-dibromobutane by comparison of the infrared spectrum (IR-7) with that of an authentic sample. From the absorption bands in the 2800–3000 cm^{-1} region and at 975 cm^{-1}, and the lack of absorption at 960 cm^{-1}, it was established that *trans*-2-butene was not produced in appreciable amounts if at all. In a separate experiment, the yield of *cis*-2-butene, isolated as the dibromide, was 86%.

(h) 1-Fluoro-2-bromocyclohexane.—Following the procedure outlined in (*d*) 1-fluoro-2-bromocyclohexane (3 g), lithium aluminum hydride (1.5 g), and anhydrous triglyme (100 ml) gave fluorocyclohexane (0.8 g, 45%), identified by comparison of the infrared spectrum with an authentic sample and by retention time upon vapor-phase chromatography.

(i) meso-Stilbene Dichloride.—*meso*-Stilbene dichloride (400 mg) was reacted with lithium aluminum hydride (500 mg) in anhydrous tetrahydrofuran (50 ml) for 1 hour at room temperature. Wet nitrogen (as above) was bubbled gently into the solution during the reaction. Isolation of product as in the general procedure and recrystallization of the crude material from benzene–ethanol gave unreacted *meso*-stilbene dichloride (77 mg). Evaporation of the mother liquors and recrystallization from ethanol gave *trans*-stilbene (200 mg), 75% yield based on reacted dichloride.

(j) erythro-1,2-Diphenyl-2-bromoethyl Methyl Ether.—*erythro*-1,2-Diphenyl-2-bromoethyl methyl ether (300 mg) was refluxed for 5 hours in 1.0 *M* lithium aluminum hydride solution (25 ml). Work-up as in the general procedure and recrystallization from ether–methanol gave *trans*-stilbene (45%). Evaporation of the

Can. J. Chem. Downloaded from www.nrcresearchpress.com by 210.87.254.5 on 09/05/12
For personal use only.

mother liquors yielded an oil (85 mg) which gave a negative Beilstein test and had an infrared spectrum resembling that of the starting material; this material was not further investigated.

(k) erythro-1,2-Diphenyl-2-fluoroethyl Bromide.—*erythro*-1,2-Diphenyl-2-fluoroethyl bromide (300 mg) was reacted with 1.0 *M* lithium aluminum hydride in tetrahydrofuran solution (15 ml) for 45 minutes at room temperature while wet nitrogen was bubbled gently into the solution. Isolation of the product as in the general procedure and recrystallization from ether–methanol gave *trans*-stilbene (166 mg, 86%).

(l) dl-Stilbene Dibromide.—*dl*-Stilbene dibromide (50 mg) or *cis*-stilbene (35 mg) was reacted with 1.0 *M* lithium aluminum hydride (2.0 ml) in tetrahydrofuran as listed in Table IX. The reaction mixture was

TABLE IX

Reaction of $LiAlH_4$ in tetrahydrofuran with *dl*-stilbene dibromide and *cis*-stilbene

Compound	Time (hours)	Temp.	Product (±10%)
dl-Stilbene dibromide	24	−10°	5% *cis*-, 95% *trans*-stilbene
dl-Stilbene dibromide	24	25°	50% *cis*-, 50% *trans*-stilbene
dl-Stilbene dibromide	1	Reflux	65% *cis*-, 35% *trans*-stilbene
dl-Stilbene dibromide	0.5	25°	55% *cis*-, 45% *trans*-stilbene
cis-Stilbene	1	Reflux	70% *cis*-, 30% *trans*-stilbene
cis-Stilbene	24	25°	40% *cis*-, 60% *trans*-stilbene
cis-Stilbene	48	−10°	95% *cis*-, 5% *trans*-stilbene
cis-Stilbene	0.5	25°	95% *cis*-, 5% *trans*-stilbene

poured into water and extracted with ether. The ether extract was washed with dilute sulphuric acid, dilute potassium bicarbonate, water, dried, and the solvent evaporated. The relative amounts of *cis*- and *trans*-stilbene were determined by comparison of the intensities of the infrared absorption bands at 925 cm^{-1} (cis) and 962 cm^{-1} (trans) with those of authentic mixtures. The results are summarized in Table IX.

Reaction of Lithium Aluminum Hydride with Bromocyclohexane

Bromocyclohexane (10 g) and lithium aluminum hydride (5 g) in anhydrous triglyme (75 ml) were reacted under the same conditions as described for *cis*-1,2-dibromocyclohexane. Cyclohexane (0.6 g) was isolated from the liquid nitrogen trap and identified by infrared spectroscopy and vapor-phase chromatography. Cyclohexene was not detected by either method of analysis. The reaction mixture, worked up as previously described, yielded unreacted starting material (5 g).

Reaction of Lithium Aluminum Hydride with Cholestan-3α-yl p-Toluenesulphonate

This compound was reacted with lithium aluminum hydride under identical conditions as described for 2α-bromocholestan-3α-yl *p*-toluenesulphonate. The infrared spectrum of the product indicated little, of any, loss of the tosylate group. Thin-layer chromatography showed the absence of cholest-2-ene and that the reaction product was mostly unreacted starting material.

Reaction of Lithium Aluminum Hydride with dl-1,2-Diphenylethyl Bromide

dl-1,2-Diphenylethyl bromide (600 mg) was added to a solution of lithium aluminum hydride (600 mg) in tetrahydrofuran. The mixture was allowed to stand for 1 hour at room temperature, and then worked up by pouring into water and extracting with ether. The extracts were washed with water, dried with Na_2SO_4, and the solvent evaporated giving dibenzyl (385 mg); m.p. after recrystallization 49–52°. Thin-layer chromatography of the crude product of a second experiment, carried out in the same way, showed the absence of either starting material or any *trans*-stilbene.

ACKNOWLEDGMENTS

We thank the National Research Council of Canada for grants-in-aid and a scholarship, the Research Corporation for a Frederick Gardner Cottrell grant-in-aid, and Dow Chemical of Canada Limited for a scholarship. We are grateful to Professor F. L. M. Pattison, Mr. F. H. Dean, and Dr. J. Newton for generously supplying the fluoro compounds used in this study.

REFERENCES

1. W. M. Schubert, B. S. Rabinovitch, N. R. Larson, and V. A. Sims. J. Am. Chem. Soc. **74**, 4590 (1952).
2. H. Finkelstein. Ber. **43**, 1528 (1910).
3. M. Mousseron and F. Winternitz. Bull. Soc. Chim. France, 604 (1946).
4. G. Wittig and G. Harborth. Ber. **77**, 306 (1944).
5. F. C. Whitmore and E. N. Thurman. J. Am. Chem. Soc. **51**, 1491 (1929).
6. S. Dershowitz and S. Proskauer. J. Org. Chem. **26**, 3595 (1961).

Can. J. Chem. Downloaded from www.nrcresearchpress.com by 210.87.254.5 on 09/05/12
For personal use only.

7. K. Issleib and G. Döll. Chem. Ber. **94**, 2664 (1961).
8. P. Pfeiffer. Ber. **45**, 1810 (1912).
9. H. Limpricht and H. Schwanert. Ann. **145**, 330 (1868).
10. R. von Walther and A. Wetzlich. J. Prakt. Chem. [2] **61**, 169 (1900).
11. K. von Auwers. Ber. **24**, 1776 (1891).
12. R. Otto. J. Prakt. Chem. **53**, 1 (1896).
13. H. Klarfeld. Monatsh. **26**, 83 (1905).
14. C. Forst and T. Zincke. Ann. **182**, 246 (1876).
15. J. F. King and R. G. Pews. Unpublished observations.
16. C. C. Tung and A. J. Speziale. J. Org. Chem. **28**, 1521 (1963).
17. H. G. Kuivila and L. W. Menapace. J. Org. Chem. **28**, 2165 (1963).
18. P. L. Julian, W. Cole, A. Magnani, and E. W. Meyer. J. Am. Chem. Soc. **67**, 1728 (1945).
19. H. Bretschneider and M. Ajtai. Monatsh. **74**, 57 (1941).
20. M. von Stackelberg and W. Stracke. Z. Elektrochem. **53**, 118 (1949).
21. J. H. Gladstone and A. Tribe. Chem. News, **29**, 117 (1874).
22. Tissier and V. Grignard. Compt. Rend. **132**, 835 (1900).
23. V. Auger. Compt. Rend. **145**, 808 (1907).
24. P. Dorn. Dissert. Abstr. **22**, 3396 (1962).
25. L. W. Trevoy and W. G. Brown. J. Am. Chem. Soc. **71**, 1675 (1949).
26. W. J. Adams, V. Petrow, and R. Royer. J. Chem. Soc. 678 (1951).
27. E. T. McBee, O. R. Pierce, and D. D. Smith. J. Am. Chem. Soc. **76**, 3725 (1954).
28. A. Roedig and K. Kiepert. Ann. **593**, 55 (1955).
29. M. P. Cava, R. Pohlke, B. W. Erickson, J. C. Rose, and G. Fraenkel. Tetrahedron, **18**, 1005 (1962).
30. A. C. Cope, A. C. Haven, Jr., F. L. Ramp, and E. R. Trumbull. J. Am. Chem. Soc. **74**, 4867 (1952).
31. H. Felkin. Bull. Soc. Chim. France, 347 (1951).
32. F. Klanberg and H. W. Kohlschütter. Chem. Ber. **94**, 781 (1961).
33. R. G. Pews. Thesis, University of Western Ontario, London, Ont. 1963. pp. 21–26.
34. E. L. Eliel and T. J. Prosser. J. Am. Chem. Soc. **78**, 4045 (1956).
35. P. R. Story. J. Am. Chem. Soc. **83**, 3347 (1961).
36. S. J. Cristol, J. Q. Weber, and M. C. Brindell. J. Am. Chem. Soc. **78**, 598 (1956).
37. J. Wislicenus and F. Seeler. Ber. **28**, 2693 (1895).
38. Sir Christopher Ingold. Proc. Chem. Soc. 265 (1962).
39. J. F. Bunnett. Angew. Chem. Intern. Ed. **1**, 225 (1962).
40. S. Winstein, D. Pressman, and W. G. Young. J. Am. Chem. Soc. **61**, 1645 (1939).
41. J. Hine and W. H. Brader, Jr. J. Am. Chem. Soc. **77**, 361 (1955).
42. D. J. Pettitt and G. K. Helmkamp. J. Org. Chem. **28**, 2932 (1963).
43. C. H. DePuy, R. D. Thurn, and G. F. Morris. J. Am. Chem. Soc. **84**, 1314 (1962).
44. M. M. Kreevoy, J. W. Gilje, L. T. Ditsch, W. Batorewicz, and M. A. Turner. J. Org. Chem. **27**, 726 (1962).
45. G. K. Helmkamp and B. F. Rickborn. J. Org. Chem. **22**, 479 (1957).
46. E. J. Corey, M. G. Howell, A. Boston, R. L. Young, and R. A. Sneen. J. Am. Chem. Soc. **78**, 5036 (1956).
47. D. J. Cram. J. Am. Chem. Soc. **74**, 2152 (1952).
48. S. Winstein, A. H. Lewin, and K. C. Pande. J. Am. Chem. Soc. **85**, 2324 (1963).
49. A. C. Cope, E. S. Graham, and D. J. Marshall. J. Am. Chem. Soc. **76**, 6159 (1954).
50. H. Schmid and P. Karrer. Helv. Chim. Acta, **32**, 1371 (1949).
51. Z. N. Parnes, M. E. Volpin, and D. N. Kursanov. Tetrahedron Letters, No. 21, 20 (1960).
52. S. Winstein, E. Grunwald, and L. L. Ingraham. J. Am. Chem. Soc. **70**, 821 (1948).
53. C. A. Grob and S. Winstein. Helv. Chim. Acta, **35**, 782 (1952).
54. D. A. Lightner and C. Djerassi. Chem. Ind. 1236 (1962).
55. N. P. Neureiter and F. G. Bordwell. J. Am. Chem. Soc. **81**, 578 (1959).
56. J. Mulders and J. Nasielski. Bull. Soc. Chim. Belg. **72**, 322 (1963).
57. H. C. Brown and R. F. McFarlin. J. Am. Chem. Soc. **80**, 5372 (1958).
58. H. C. Brown. *Cited in* D. J. Cram. J. Am. Chem. Soc. **74**, 2152 (1952).
59. E. Wiberg and W. Gösele. Z. Naturforsch. **11b**, 485 (1956).
60. R. Dautel and W. Zeil. Z. Elektrochem. **64**, 1234 (1960).
61. J. F. King, R. G. Pews, and R. A. Simmons. Can. J. Chem. **41**, 2187 (1963).
62. A. I. Vogel. A textbook of practical organic chemistry. 2nd ed. Longmans, Green, and Co., London. 1951. p. 175.
63. G. H. Alt amd D. H. R. Barton. J. Chem. Soc. 4284 (1954).
64. L. F. Fieser. Experiments in organic chemistry. 3rd ed. D. C. Heath and Company, Boston. 1957. p. 68.
65. D. H. R. Barton and E. Miller. J. Am. Chem. Soc. **72**, 1066 (1950).
66. L. F. Fieser and W. Huang. J. Am. Chem. Soc. **75**, 4837 (1953).
67. D. H. R. Barton and J. F. King. J. Chem. Soc. 4398 (1958).
68. D. Y. Curtin and D. B. Kellom. J. Am. Chem. Soc. **75**, 6011 (1953).
69. F. L. M. Pattison, F. H. Dean, and J. Newton. Unpublished observations.
70. P. D. Bartlett and D. S. Tarbell. J. Am. Chem. Soc. **58**, 466 (1936).
71. W. G. Young, R. T. Dillon, and H. J. Lucas. J. Am. Chem. Soc. **51**, 2528 (1929).
72. Organic syntheses. Coll. Vol. 2. *Edited by* A. H. Blatt. John Wiley and Sons, Inc., New York. 1943. p. 171.
73. S. Winstein. J. Am. Chem. Soc. **64**, 2792 (1942).
74. H. L. Goering, P. I. Abell, and B. F. Aycock. J. Am. Chem. Soc. 74, 3588 (1952).

Can. J. Chem. Downloaded from www.nrcresearchpress.com by 210.87.254.5 on 09/05/12
For personal use only.

Can. J. Chem. Downloaded from www.nrcresearchpress.com by 210.87.254.40 on 09/05/12
For personal use only.

ELECTRODE POTENTIALS OF THORIUM TETRACHLORIDE IN ALKALI CHLORIDE MELTS

R. SRINIVASAN* AND S. N. FLENGAS
Department of Metallurgical Engineering, University of Toronto, Toronto, Ontario

Received January 10, 1964

ABSTRACT

The electrode potentials of the system Th, $ThCl_4$ (KCl, NaCl) were measured at various concentrations of thorium chloride, and at temperatures between 670° C and 850° C, using a silver – silver chloride reference electrode. It was shown by a direct gravimetric method that the reaction,

$$Th_{(metal)} + ThCl_{4(melt)} = 2ThCl_{2(in\ melt)},$$

postulated by previous investigators, did not take place.

The activity coefficients, and the other partial molal properties of the solutions of $ThCl_4$ in the equimolar mixture of potassium and sodium chlorides, were calculated as a function of temperature from the e.m.f. measurements.

INTRODUCTION

Measurements of the "apparent standard" potentials of several metal – metal chloride systems in dilute solutions in fused alkali chlorides have been reported in previous investigations (1, 2, 3, 13). Such measurements provide data on activities, help determine the equilibrium constants of chemical reactions in fused salts, and give some of the necessary information for the electrolytic recovery of metals by fused salt electrolysis. An equimolar mixture of potassium and sodium chlorides was used as the solvent melt in all these studies, and a silver – silver chloride electrode developed earlier in this work (1) was used as the reference electrode. In the present investigation, the technique has been applied to the determination of the reversible potentials of thorium tetrachloride, in the temperature range 670° C to 850° C.

The system has also been investigated recently by Yang, Hudson, and Chien (4) in KCl–LiCl melts, in the temperature range 490° C to 550° C, and by Smirnov *et al.* (5, 6, 7) in KCl–NaCl melts. However, the results obtained in these investigations were in complete disagreement. Thus, Smirnov and his associates, from potential–current curves, measured during the electrolysis of $ThCl_4$ in solution in a KCl–NaCl melt, predicted that thorium tetrachloride would be reduced almost quantitatively by thorium metal according to the reaction:

$$Th_{(s)} + ThCl_{4(in\ melt)} = ThCl_{2(in\ melt)}.$$

The redox potential of the Th^{3+}, Th^{4+} system was then measured and the Th, Th^{4+} system was also investigated by using a "non-reacting" Th–Zn alloy. The results of Yang *et al.* (4), however, did not indicate this reduction and, furthermore, Gruen, McBeth, Kooi, and Carnall (8), in an attempt to prepare Th(II) in chloride melts for the purpose of investigating the spectra of the species, did not find any evidence of its existence.

To resolve such conflicting information, it was therefore decided to begin this investigation by the determination of the solubility of thorium metal in a melt containing $ThCl_4$ in solution in the equimolar mixture of potassium and sodium chlorides. It should be noted that the existence of the redox equilibrium postulated by Smirnov *et al.* would make impossible the direct determination of the potentials of the Th, Th^{4+} system.

**Research Fellow, Colombo Plan. 1963–1964.*

Can. J. Chem. Downloaded from www.nrcresearchpress.com by 210.87.254.40 on 09/05/12
For personal use only.

EXPERIMENTAL

Reduction of Thorium Tetrachloride

The method for the determination of the solubilities of thorium metal involved the direct observation of the decrease of weight of a piece of thorium metal, $\frac{1}{2}$ in. long by $\frac{1}{4}$ in. diameter, in contact with a molten solution of thorium tetrachloride, in the equimolar melt of potassium and sodium chlorides. The solution was contained in a platinum crucible and thorium metal was suspended from the end of a calibrated quartz spring balance by means of a platinum wire. The entire system was enclosed in a 2 in. diameter quartz tube under an atmosphere of purified argon, and the contraction of the spring, indicating the loss in weight of thorium metal, was measured by a cathetometer. The apparatus was capable of measuring a minimum loss of weight of 0.1 mg of thorium metal, corresponding to the production of 0.13 mg of thorium dichloride in the melt.

Solutions having compositions between 0.7 and 4.0% by weight of ThCl were investigated at reaction temperatures varying between 730° C and 800° C. The metal samples were immersed in the solutions for about 48 hours, and no loss of weight could be detected during this period of time. Furthermore, the melt remained colorless and there was no evidence of attack on the thorium metal. The reducing power of the melt, after cooling under argon, was also determined by back-titration with a ceric sulphate solution. Again, no trace of the reduced state of divalent thorium chloride could be found. It was therefore concluded that the reduction mechanism postulated by Smirnov *et al.* did not take place to any measurable extent, and that the direct determination of the potential of the Th, Th^{4+} system would be feasible.

Electromotive Force Measurements

The type of cell used for the measurements has been described in detail in previous publications (2, 3). The cell is represented as follows.

$$\begin{array}{c|c|c|c|c|c} \text{Th} & \text{ThCl}_4\ (X_2) & \text{Asbestos} & \text{AgCl}\ (X_1) & \text{Ag} \\ & & \text{fiber} & & \\ (-) & \text{KCl–NaCl (1:1 mole)} & & \text{KCl–NaCl (1:1 mole)} & (+) \end{array}$$

The cell reaction is:

$$Th_{(s)} + 4\,Ag^{+}\ (\text{as AgCl in KCl–NaCl}) = Th^{4+}\ (\text{as } ThCl_4 \text{ in KCl–NaCl}) + 4\,Ag_{(s)}.$$

The Nernst equation for the cell may be written as:

$$E_{cell} = (E^0_{ThCl_4} - E^0_{AgCl}) - \frac{2.303\,RT}{4F}\log\frac{X_2}{X_1^4} - \frac{2.303\,RT}{4F}\log\frac{\gamma_2}{\gamma_1^4} \qquad [1]$$

where $E^0_{ThCl_4}$ and E^0_{AgCl} are the "standard" potentials of thorium tetrachloride and silver chloride, respectively, in their standard states, and the γ's are the corresponding activity coefficients. Equation [1] may be further simplified by substituting the value of unity for the activity coefficient of silver chloride, as found in a previous investigation (2). Equation [1] then becomes:

$$E_{cell} = (E^0_{ThCl_4} - E^0_{AgCl} - \frac{2.303\,RT}{4F}\log\gamma_{ThCl_4}) - \frac{2.303\,RT}{4F}\log\frac{X_2}{X_1^4}. \qquad [2]$$

For dilute solutions obeying Henry's Law, γ_{ThCl_4} becomes constant and the "apparent standard" potential may then be defined as,

$$E^0_{app.} = E^0_{ThCl_4} - E^0_{AgCl} - \frac{2.303\,RT}{4F}\log\gamma_{ThCl_4}. \qquad [3]$$

The final form for equation [1] is:

$$E_{cell} = E^0_{app.} - \frac{2.303\,RT}{4F}\log\frac{X_2}{X_1^4}. \qquad [4]$$

Hence, by plotting E_{cell} against $\log(X_2/X_1^4)$, a straight line should be obtained having a slope of $-2.303\,RT/4F$ and an intercept equal to $E^0_{app.}$. It should be mentioned that the "apparent standard" potential represents the free energy of a hypothetical state of unit mole fraction of solute, having in all respects the properties of the solute in its state at infinite solution.

For the calculation of the activity coefficients of thorium tetrachloride from equation (3), the state of the "pure molten chlorides", at the temperature of the experiments, was chosen as the standard state. Standard potentials for molten silver chloride were obtained from data tabulated by Hamer *et al.* (9). Standard potentials for molten thorium tetrachloride were calculated from the corresponding free energies of formation of the compound. The latter were derived from the available data on the free energies of formation of the solid (10), and the free energies of fusion calculated from the vapor pressure data (11) of solid and liquid thorium tetrachloride, respectively.

In order to account for the entire temperature range of the experiments, i.e. 670° C to 850° C, the free energy equations representing the liquid state were extrapolated to temperatures below the melting point of thorium tetrachloride (765° C). Thus, below 765° C, the standard state is the supercooled liquid. Calculated standard potentials, with respect to the solid and the liquid states, are shown in Fig. 3.

PREPARATION OF MATERIALS

The equimolar mixture of potassium and sodium chlorides was prepared from analytical grade chemicals and dehydrated by heating under vacuum at 500° C for 20 hours.

Anhydrous thorium tetrachloride was prepared by chlorination of thorium oxide. Thorium oxide itself was prepared by calcination of pure thorium nitrate or oxalate. The thorium oxide was mixed with carbon and chlorinated at 800° C. The product was purified by double distillation *in vacuo* and had a purity of 99.3%. The crystalline sublimate was powdered and pelletised in a dry-box to facilitate easy addition to the melt.

The thorium electrode was a rod of reactor-grade thorium metal, cut from a 2 in. ingot supplied by Atomic Energy of Canada Ltd. The dimensions of the electrode were $\frac{1}{4}$ in. square by $2\frac{1}{2}$ in. long. It was threaded onto a copper-coated iron rod which served as the electrode connection. The electrode was cleaned with emery paper and dilute acid. It was then washed well with distilled water and dried with acetone. The cleaned electrode was kept in anhydrous carbon tetrachloride until its use.

The silver electrode was a rod ($\frac{1}{8}$ in) of pure silver connected to a silver wire. The electrolyte for the reference electrode was prepared by intimately mixing weighed amounts of the equimolar mixture of analytical-grade silver chloride with potassium and sodium chlorides, melting the mixture to form a homogeneous solution, and solidifying it, all under argon. The solid was powdered, thoroughly mixed, and kept under dry conditions.

RESULTS

The e.m.f. of Th/Th^{4+} cell was measured as a function of temperature for a given concentration, using the concentrations shown below.

		X_1	X_2
Run *a*	(1)	6.235×10^{-2}	6.468×10^{-3}
	(2)	6.235×10^{-2}	1.417×10^{-2}
Run *b*	(3)	1.05×10^{-2}	1.50×10^{-3}
	(4)	1.05×10^{-2}	5.20×10^{-3}
	(5)	1.05×10^{-2}	7.62×10^{-3}

The results are shown in Fig. 1.

Necessary corrections for the thermoelectric potential, which was measured separately, were made in plotting the results. The material was added in the form of pellets and, after each addition, the potential reached a steady state in about 30 minutes.

From Fig. 1 it is seen that the curves are linear over the temperature range involved, and the cell potentials have a negative temperature coefficient. Potential readings were taken at equilibrium while the temperature was being raised, and were in good agreement with those made while the temperature was decreasing. The duration of a complete heating and cooling cycle was about 24 hours.

Potentials in very dilute solutions of thorium tetrachloride, i.e. below 10^{-4} mole fraction, tended to drift with time as the result of a slow vaporization of thorium tetrachloride from the melt. Furthermore, a slight attack of the silica walls of the container was also observed. Thus, thorium tetrachloride reacted slowly with silica and produced a mirror-like coating, which, on X-ray diffraction analysis, was identified as ThO_2.

Can. J. Chem. Downloaded from www.nrcresearchpress.com by 210.87.254.40 on 09/05/12
For personal use only.

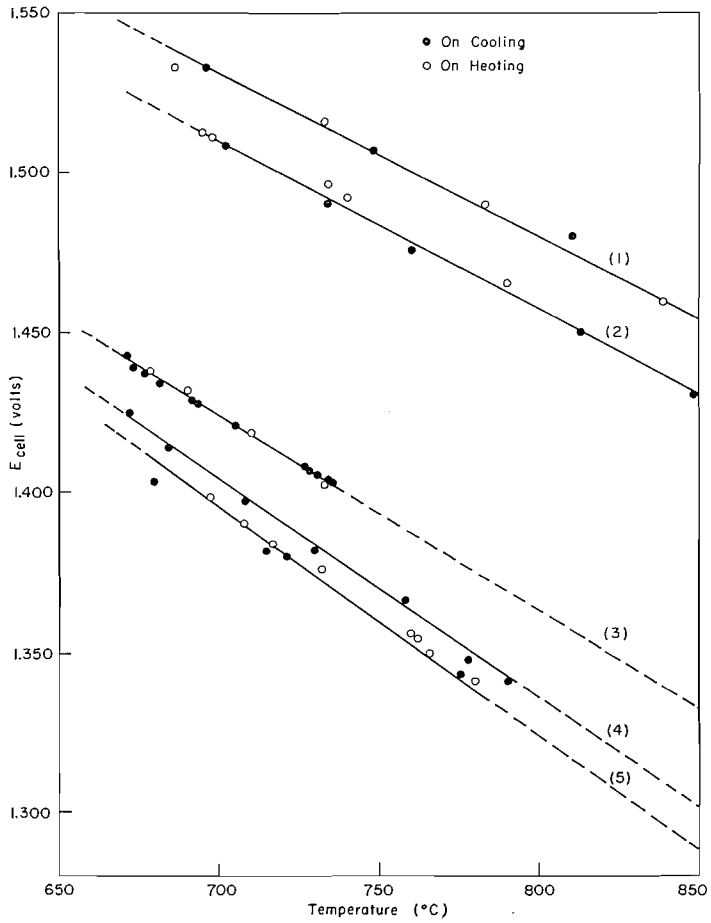

FIG. 1. Electromotive force of the cell Th, $ThCl_4$ (KCl, NaCl) as a function of temperature.

The e.m.f. of the Th/Th^{4+} cell was also measured as a function of $\log X_2/X_1^4$ at various temperatures. The results are shown in Fig. 2. The closed circles are data obtained at selected temperature from the results shown in Fig. 1. The half-closed circles are data representing an independent concentration run at 696° C covering the mole fraction range 4.093×10^{-4} to 2.103×10^{-2} of $ThCl_4$ ($X_1 = 6.235\times10^{-2}$). The slope of the lines in Fig. 2 corresponds fairly well with the theoretical slope for a four-electron electrode reaction calculated by the Nernst equation. For example, at 670° C, the theoretical slope should be 0.047, and the experimental slope is 0.042. At 850° C, the corresponding values are 0.056 and 0.050. The linearity of the curves indicates that the activity coefficient of thorium tetrachloride in dilute solutions is constant, and, at constant temperature, independent of concentration. The "apparent standard potentials" with respect to the silver – silver chloride electrode as the zero potential reference, were obtained by extrapolation of the straight lines to zero $\log (X_2/X_1^4)$ term, and are also shown in Fig. 2. To refer the "apparent standard" potentials to a chlorine electrode, it is only necessary to add to the values shown in Fig. 2 the corresponding standard potential of silver chloride (9).

Can. J. Chem. Downloaded from www.nrcresearchpress.com by 210.87.254.40 on 09/05/12
For personal use only.

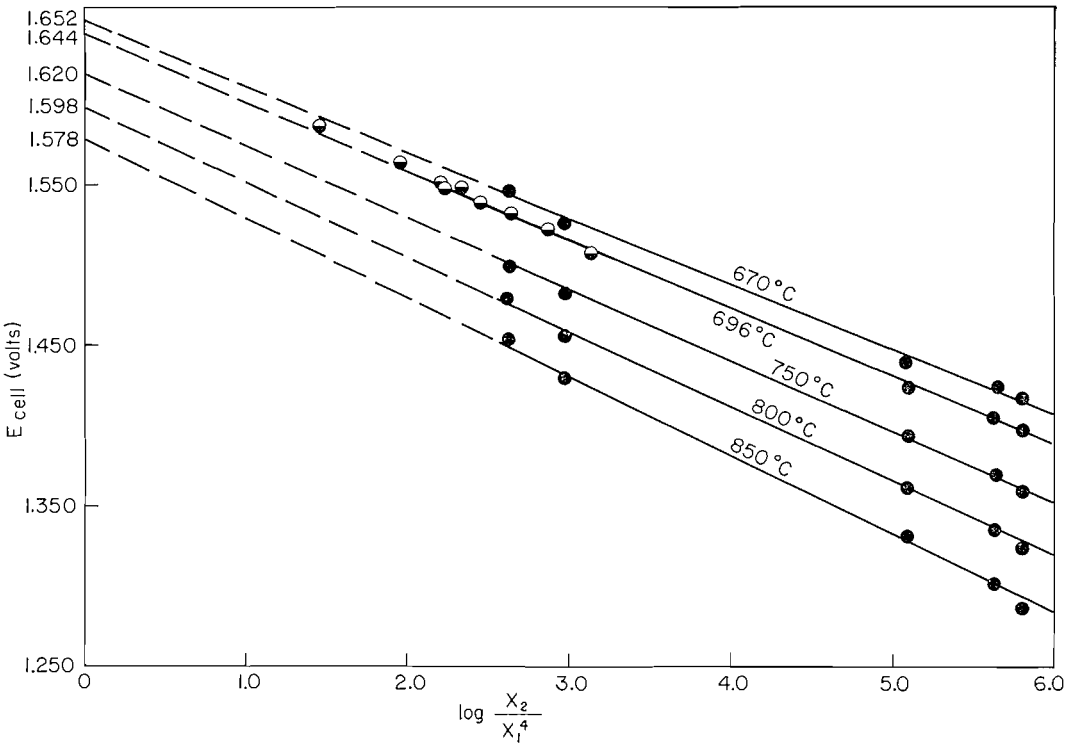

FIG. 2. Electromotive force of the cell Th, $ThCl_4$ (KCl, NaCl) as a function of log X_2/X_1^4 at various temperatures.

The results of these calculations are shown in Fig. 3. The plot is linear and the "apparent standard" potential of thorium tetrachloride, against a chlorine electrode as the zero potential reference, is given by the equation,

$$E^0_{app.} = 3.109 - 6.38\times10^{-4}T \qquad (923° K - 1123° K)$$

where T is in degrees Kelvin.

DISCUSSION

From the data given in Fig. 3, activity coefficients and the other partial molal properties of the solutions of thorium tetrachloride in the KCl–NaCl melt were calculated, and are given in Table I. The "apparent standard" and the standard potentials for thorium tetrachloride, calculated against a chlorine electrode, are also included in this table. The sign of the potentials is given as positive and represents the overall cell potential when one of the electrodes is a chlorine electrode. It will, however, assume a negative sign for the purpose of tabulating the thorium electrode potentials in an e.m.f. series, with respect to a chlorine electrode as the zero potential reference (I.U.P.A.C. convention). It may be noted that potentials calculated from the data of Smirnov and Yushina (7) are about 0.2 volts lower than the values obtained herein.

Within the accuracy of the measurements, the results indicate that the solutions follow Henry's law over a range of concentrations up to $X_{ThCl_4} = 10^{-2}$. Further, the magnitude of the activity coefficients indicates the tendency of thorium tetrachloride to form complex species in the melt. The activity coefficients increase with increasing temperature indicating the dissociation of these complexes at the higher temperatures, as expected.

Can. J. Chem. Downloaded from www.nrcresearchpress.com by 210.87.254.40 on 09/05/12
For personal use only.

Can. J. Chem. Downloaded from www.nrcresearchpress.com by 210.87.254.40 on 09/05/12
For personal use only.

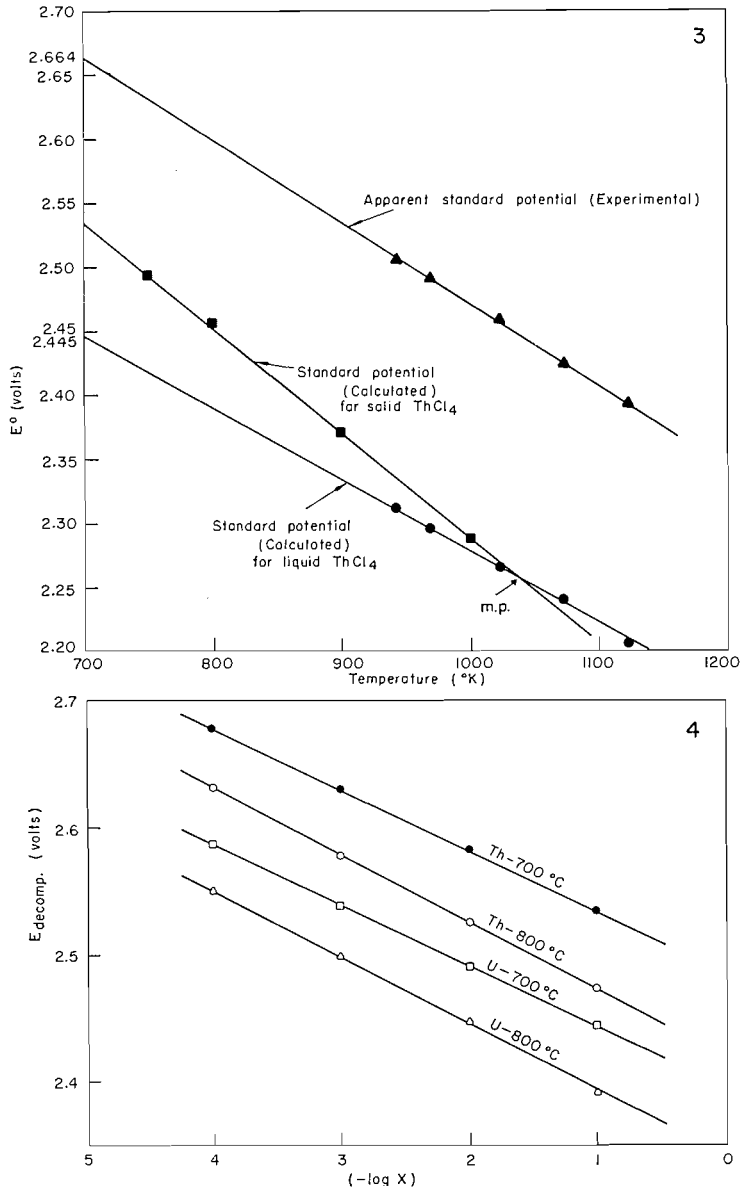

FIG. 3. Apparent standard potentials and standard state potentials of $ThCl_4$, as a function of temperature. All values refer to a chlorine electrode as the zero potential reference electrode.
FIG. 4. Decomposition potentials of UCl_3 and $ThCl_4$ in solution in a KCl–NaCl molten salt solvent, as a function of the mole fraction of the solute.

Activity coefficients of thorium tetrachloride in the KCl–LiCl melt at temperatures between 450° C and 550° C were also calculated by Yang *et al.* (4), and were of the order of 10^{-3}, indicating a weakening of the bonds in the complex species, due to the smaller Li^+ cations in the melt. It should be noted that similar effects were also observed with the complexes of the titanium tetrachloride with alkali metal chlorides. Thus the complex

TABLE I

Partial molal properties of dilute solutions of thorium tetrachloride in 1/1 mole KCl–NaCl

T (°K)	Apparent standard potential (volts)	Standard potential (calculated) (volts)	$\overline{\Delta F^*}$ kcal mole^{-1}	$\overline{\Delta H^*}$ kcal mole^{-1}	$\overline{\Delta S^*}$ e.u.	$\gamma \times 10^3$
943	2.505	2.312	−17.8	+9.6	29.02	0.72
969	2.492	2.296	−18.08	+9.6	28.54	0.81
1023	2.457	2.266	−17.62	+9.6	26.59	1.67
1073	2.424	2.240	−16.97	+9.6	24.74	3.40
1123	2.393	2.207	−17.16	+9.6	23.81	4.46

*Calculated from the well-known relationships

$$\overline{\Delta F} = RT \ln a_{ThCl_4}, \frac{\partial(\overline{\Delta F})}{\partial T} = -\overline{\Delta S}, \text{ and } \overline{\Delta F} = \overline{\Delta H} - T\overline{\Delta S}.$$

K_2TiCl_6 was readily prepared (12), whereas the corresponding lithium complex was found to be unstable.

With respect to the separation of thorium and uranium metals by electrolysis, from a solution containing both species as Th^{4+} and U^{3+} ions dissolved in the equimolar melt of potassium and sodium chlorides, the results obtained herein indicate that such a separation should be difficult.

Figure 4 shows the reversible decomposition potentials of the solutions (13) plotted as a function of concentration, at two temperatures. The corresponding curves are almost parallel in the mole fraction range 10^{-1} to 10^{-4}, with a potential difference of approximately 0.1 volt. Such a difference should not be considered as sufficient in actual practice for the separation and recovery of these two metals by fused-salt electrolysis, and would rather indicate co-deposition.

ACCURACY OF RESULTS

It is difficult to evaluate the limits of accuracy in the potentials measured. It could be said with confidence that the individual potential measurements as shown in Figs. 1 and 2 were stable and reproducible. Potential readings, taken after leaving the cell overnight, coincided within ±1 mv. The slight scattering of the points plotted in Figs. 1 and 2 may be attributed to the difficulties always present in high temperature systems: for example, concentration gradient because of thermal convection, small temperature gradients within the melt, the inevitable presence of some oxygen on the surface of the metal, side reaction in the refractory container, and traces of impurity in the electrolyte. However, it is reasonable to assume that the potential values obtained in this investigation are accurate to within ±2 mv. This variation would result in a change of only 0.4 kcal/mole in the free energy values as listed in Table I.

ACKNOWLEDGMENTS

One of the authors (R. S.) is indebted to the CSIRO, the Government of India, and the Government of Canada for the award of a Colombo Plan Fellowship. The financial aid of the National Research Council of Canada in support of this work is also gratefully acknowledged.

REFERENCES

1. S. N. Flengas and T. R. Ingraham. Can. J. Chem. **35**, 1139 (1957); **35**, 1254 (1957); **36**, 780 (1958); **36**, 1103 (1958); **36**, 1662 (1958).
2. S. N. Flengas and T. R. Ingraham. J. Electrochem. Soc. **106**, 8, 714 (1959).
3. S. N. Flengas. Ann. N.Y. Acad. Sci. **79**, 11, 853 (1959).

Can. J. Chem. Downloaded from www.nrcresearchpress.com by 210.87.254.40 on 09/05/12
For personal use only.

4. L. YANG, R. G. HUDSON, and CHIEN-YEH CHIEN. Physical chemistry of process metallurgy. Part 2. *Edited by* G. R. St. Pierre. Interscience Pub., New York. 1961. pp. 925-942.
5. M. V. SMIRNOV and L. D. YUSHINA. Izv. Akad. Nauk, SSSR, Otd. Khim. Nauk, No. 2, pp. 1285–1293 (1956).
6. M. V. SMIRNOV and L. E. IVANOVSKII. Zh. Fiz. Khim. **31**, 641–647 (1957).
7. M. V. SMIRNOV and L. D. YUSHINA. Izv. Akad. Nauk, SSSR, Otd. Khim. Nauk, No. 2, pp. 251–258 (1959).
8. D. M. GRUEN, R. L. MCBETH, J. KOOI, and W. T. CARNALL. Ann. N.Y. Acad. Sci. **79**, 11, 941 (1959).
9. W. HAMER, M. MALMBERG, and B. RUBIN. J. Electrochem. Soc. **103**, 8 (1956).
10. C. E. WICKS and F. E. BLOCK. Thermodynamic properties of oxides, halides, etc. U.S. Bur. Mines, Bull. 605. 1963.
11. O. KUBASCHEWSKI and E. LL. EVANS. Metallurgical thermochemistry. Pergamon Press. 1958.
12. S. N. FLENGAS. Can. J. Chem. **38**, 813 (1960).
13. S. N. FLENGAS. Can. J. Chem. **39**, 773 (1963).

Can. J. Chem. Downloaded from www.nrcresearchpress.com by 210.87.254.40 on 09/05/12
For personal use only.

Can. J. Chem. Downloaded from www.nrcresearchpress.com by 210.87.254.6 on 09/05/12
For personal use only.

LCAO MO CALCULATIONS ON A SERIES OF NITRILES AND SOME RELATED MOLECULES BY A METHOD OF SELF-CONSISTENT FORMAL CHARGES

J. B. MOFFAT
Department of Chemistry, University of Waterloo, Waterloo, Ontario
Received November 29, 1963

ABSTRACT

A method of self-consistent charges has been applied to an LCAO MO calculation of a series of nitriles and some related molecules. The π-electron bond orders and π-electron densities were calculated for all the molecules considered. The entire calculation was programmed for operation on the IBM 1620 with alterations of the input data for the different molecules. The calculated bond orders yield bond lengths for C—C and C=C bonds in good agreement with experimental data, except when two or more triple bonds are present in the molecule. By the assumption of additivity of the bond orders obtained for the two orthogonal pi-electron systems, bond orders are obtained which yield bond lengths in satisfactory agreement with the experimental results for all CC bonds. For the nitrile bonds the calculated bond orders were fitted to a linear equation with the experimental bond lengths.

INTRODUCTION

It is now well known that the simple LCAO MO method with Huckel approximations yields results for aromatic molecules containing carbon only which are in general in good agreement with experimental data. In the simple LCAO MO method as applied to molecules containing atoms in addition to carbon, data such as electronegativities and effective nuclear charges may be introduced. Such data is usually that obtained for the uncombined atoms. When calculations are then pursued which have the effect of mathematically combining the atoms to form molecules, perturbations of a given atom will occur as a result of the presence of other atoms bonded to it. It is then no longer legitimate to employ the data for the uncombined atoms. In the present work an attempt has been made to allow for such perturbations which will be particularly important where heteroatoms are present in the molecule. In the present calculations the pi-electron density (formal charge) obtained is used to provide "perturbed" values of the Slater nuclear charge and the electronegativity. The calculation is then repeated with these new values included and the pi-electron density again obtained. This process is repeated until a self-consistent pi-electron density is obtained. In the present work, for convenience of programming the calculations, values of the bond orders rather than the pi-electron densities were tested by the computer for self-consistency.

In recent years increased attention has been given to the application of the simple LCAO MO method to heteroatomic molecules. However, as has been pointed out (1), little work has been done on the application of molecular orbital methods to nitriles. Penfold and Lipscomb (2) have carried out some calculations on tetracyanoethylene and 1,1-diamino-2,2-dicyanoethylene in connection with their crystallographic studies. Peacock and Wilkenson have done LCAO MO SCF calculations on benzonitrile (3). As Penfold and Lipscomb point out, reliable estimates of pi-bond orders in nitrile molecules would be most valuable.

Lofthus (4) has considered the values of parameters appropriate for use in molecular orbital calculations on various molecules containing nitrogen and has prepared a bond length:bond order plot for CN bonds. However, the curve for bond order greater than two

is fixed by only one point, namely that obtained by assuming that the bond order for the CN bond in hydrogen cyanide is three.

It therefore seemed worthwhile to attempt to apply the self-consistent method mentioned above to a series of nitrile molecules to determine if bond orders yielding bond lengths in agreement with experimental bond lengths could be obtained. For purposes of comparison, some related molecules have also been considered.

METHOD OF CALCULATION

The method employed here is similar to that suggested by Nagakura (5), and subsequently employed by Brown (6), Orville-Thomas and Jones (7), and Morris and Orville-Thomas (8). However, in the present work, an attempt was made to set up a computer program which could be employed for all "linear" molecules without adjustments, except in the input data.

The program requires the following input data: (1) electronegativities of the atoms, (2) number of atoms in the molecules, (3) experimental bond lengths, (4) value of the overlap integral for the CC bond, (5) effective nuclear charge on the atoms, (6) values of constants in relations for electronegativity and effective nuclear charge. The entire program was set up for operation on an IBM 1620 computer.

The present work considers the π-electron system only and assumes that any interaction with the σ-electron system may be neglected. In the calculation, molecular orbitals are assumed to be capable of representation as a linear combination of atomic orbitals (9)

$$\Psi_r = \sum_i C_{ir}\phi_i \qquad [1]$$

This relation is subsequently introduced into the stationary state form of the Schrodinger equation

$$\hat{H}\Psi = E\Psi$$

and a set of linear equations, one for each molecular orbital, is obtained. For such a set of linear equations, solutions other than those equal to zero are obtained only if the determinant

$$\begin{vmatrix} \alpha_1 - E & \beta_{12} - ES_{12} & \cdots & \beta_{1n} - ES_{1n} \\ \beta_{21} - ES_{21} & \alpha_2 - E & & \vdots \\ \vdots & & \ddots & \vdots \\ \beta_{n1} - ES_{n1} & \cdots & & \alpha_n - E \end{vmatrix} = 0$$

The Coulomb integrals α_i are $(i|H|i)$, the resonance integrals β_{ij} are $(i|H|j)$, and the overlap integrals S_{ij} are $(i|j)$. The polynomial which results from the expansion of the determinant has n real roots. Hence n values of the energy, E, are obtained, each of which may be associated with one of the molecular orbitals. Of course, according to the variational principle the value of the energy which would be obtained by such a calculation is not the "true" eigenvalue as could in principle be obtained from the Schrodinger equation, but rather an upper bound to such an energy. It follows that the wave functions are approximations to the "true" eigenfunctions.

Throughout the present paper, the resonance integrals β_{ij} are taken to be zero, for $j-i > 1$. That is, for atoms which are not nearest neighbors, β_{ij} is assumed to be negligible. On the basis of the exponential decay of the wave functions with distance from the nucleus,

Can. J. Chem. Downloaded from www.nrcresearchpress.com by 210.87.254.6 on 09/05/12
For personal use only.

this seems intuitively correct. In addition the overlap integrals, S_{ij}, where $i \neq j$, are neglected in the so-called secular determinant. This is done so here primarily for mathematical convenience. Although this appears to be a poor approximation at best, it can be shown that this assumption amounts to the introduction of orthogonal atomic orbitals.

For the heteroatoms it is assumed that the Coulomb integral may be written as

$$\alpha_i = \alpha_c + \delta_i \beta_{cc}$$

where β_{cc} is the resonance integral for the CC bond in benzene, α_c is the Coulomb integral for a benzene carbon atom and δ_i is related to the electronegativity of the ith atom. This relation is equivalent to representing the Coulomb integral of the ith atom as a perturbation of that of the carbon atom in benzene with such a change being expressed in units of β_{cc}.

For the purposes of the computer programming, each term in the determinant is divided by β_{cc}. Diagonal terms for a heteroatom then become, by making use of the above substitutions,

$$(\alpha_c - E)/\beta_{cc} + \delta_i$$

or

$$x + \delta_i$$

It is assumed that the Coulomb integral is proportional to the electronegativity (10) so that for a heteroatom such as nitrogen

$$\alpha_i = (\chi_i/\chi_c)\alpha_c.$$

This is equivalent to

$$\begin{aligned} \alpha_i &= \alpha_c + [(\chi_i/\chi_c) - 1]\alpha_c, \\ &= \alpha_c + 4.1\beta_{cc}[(\chi_i/\chi_c) - 1], \end{aligned}$$

where $\alpha_c = 4.1\ \beta_{cc}$ (ref. 11).

Hence

$$\delta_i = 4.1[(\chi_i/\chi_c) - 1].$$

Further it is assumed that the resonance integral is proportional to the overlap integral (12), so that

$$\begin{aligned} \beta_{ij} &= (S_{ij}/S_{cc})\ \beta_{cc}, \\ &= \gamma_{ij}\beta_{cc} \end{aligned}$$

where S_{cc} is the overlap integral for the CC bond in benzene. The off-diagonal terms in the determinant then become γ_{ij}.

The same functional relationships are used for carbon atoms, so that

$$\delta_c' = 4.1[(\chi_c'/\chi_c) - 1]$$

and

$$\beta_{cc}' = (S_{cc}'/S_{cc})\ \beta_{cc}$$

where χ_c is the electronegativity of the uncombined carbon atom and S_{cc} is as defined previously. χ_c' and S_{cc}' are allowed to vary.

The assumptions of the proportionality of the Coulomb integral to the electronegativity, and of the resonance integral to the overlap integral appear to be not unreasonable. The Coulomb integral is related to the density of electrons near the core of the ith atom, which is in turn related to the electronegativity of the ith atom. Both the resonance and overlap integrals are related to the density of electrons near the cores of the ith and jth

Can. J. Chem. Downloaded from www.nrcresearchpress.com by 210.87.254.6 on 09/05/12
For personal use only.

atoms. It should be pointed out that, whereas in the case of the secular determinant the overlap integrals were taken to be zero, for the purposes of determining the resonance integrals, the overlap integrals are now assumed to be non-zero.

The "secular determinant" is now obtained in the reduced form

$$\begin{vmatrix} x_1+\delta_1 & \gamma_{12} & \cdots & \cdots & 0 \\ \gamma_{12} & x_2+\delta_2 & \ddots & & \vdots \\ \vdots & \vdots & \ddots & \ddots & \vdots \\ \vdots & \vdots & & \ddots & \gamma_{n-1,n} \\ 0 & 0 & \cdots & \gamma_{n-1,n} & x_n+\delta_n \end{vmatrix} = 0$$

The computer is programmed to calculate first values of δ_i for each of the carbon, nitrogen, or oxygen atoms in the molecule by employing the initial values of the electronegativity given in the input data. The initial value of δ_c is just 0.

The values of the overlap integrals are calculated from the interatomic distances and the Slater effective nuclear charges (13, 14) by using the equations obtained by Mulliken (15). As has been mentioned, values of the observed interatomic distances and initial values of the Slater charges are contained in the input data. With these values, Mulliken's p and t are calculated within the machine and then are introduced into the appropriate equations for the overlap integrals. A check statement is included to test for the size of t in order that the appropriate relation may be used. These calculated values for the overlap integral are then used with the value of the overlap integral for the CC bond to calculate γ_{ij} values for each of the carbon, nitrogen, and oxygen atoms in the molecule. Of course, the initial value of γ_{cc} is 1.

With these values the secular determinant is transformed to the corresponding polynomial in x. The roots of this equation are obtained by employing the recursion formula of Laguerre as suggested by Pritchard and Sumner (16). The program is set up so that any desired starting value from which the machine may commence to look for roots may be fed into the computer as input data. In practice it was found convenient to insert the value -10.000000. The last two roots are found by solution of the appropriate quadratic equation. The roots are then ordered beginning with the largest negative root first and terminating with the largest positive root.

The eigenvectors are found by the Richardson method (17). If one introduces the value found for the x_1 into the secular determinant and then operates on the resulting determinant with the column matrix composed of the atomic orbital coefficients appropriate to the molecular orbital with that particular value of x, then this product should vanish. Hence if one considers any column matrix or vector as a linear combination of such vectors then on multiplying it by the secular determinant (with x_i introduced), the ith component will be made to vanish. This process may be continued until only one component of the vector remains. This component may then be reintroduced into the start of the process and the calculation continued until repetition of the operation does not alter this component to any assigned degree. The whole operation is then repeated with another value of x_i until all the atomic orbital coefficients have been obtained. In the present programme the initial vector was taken to have all components equal to one. The atomic orbital coefficients so obtained were normalized before further calculations were carried out.

The values of the atomic orbital coefficients so obtained were then employed to calculate mobile π-electron bond orders and π-electron charge densities.

Can. J. Chem. Downloaded from www.nrcresearchpress.com by 210.87.254.6 on 09/05/12
For personal use only.

The π-electron bond order, p_{rs}, for the bond between the r atom and the s atom, is defined as

$$p_{rs} = 2\sum_j C_{jr}C_{js}$$

where the sum is over the j occupied molecular orbitals. The π-electron charge density on the atom r in the ground state is defined as

$$q_r = 2\sum_j C_{jr}C_{jr}.$$

The calculated bond orders were then compared, within the computer, with those calculated in the previous iteration, or in the case of the first iteration with fictitious values (4.5) which were read into the computer at the start of the programme. If the sum of the differences is greater than 0.001, the computer is asked to continue, otherwise it is directed to print the answers, and stop.

In the event that the computer is asked to continue, new values of the Slater function and the electronegativity are determined from the calculated π-electron charges. Slater's rules (13, 14) for obtaining the effective nuclear charge on a given atom are used to relate the Slater nuclear charge to a function of the π-electron density:

$$u_i = u_i' - 0.175\, Q_i$$

where u_i is the value of the Slater function to be used in the next iteration step, u_i' is the appropriate constant for each atom calculated by Slater's method, and Q_i is the π-electron density of the ith atom. This is, of course, equivalent to the assertion that the effective nuclear charge, or the charge on the atom as "seen" by an electron approaching it, will depend on the number of electrons shielding the positively charged nucleus.

Values of the electronegativity adjusted for the π-electron densities are obtained by making use of Pauling's definition of electronegativity. Kurito (18) has obtained a relation from such a definition. This relation is used to obtain an equation,

$$\chi_i = \chi_i' - \tfrac{1}{3}Q_i$$

where χ is the electronegativity on the ith atom adjusted for the π-electron density Q_i, and χ_i' is a constant for the ith atom which contains the value of the "unperturbed electronegativity". Values of u_i' and χ_i' are contained in the input data.

With these adjusted values of the electronegativity and Slater functions, the computer is directed to the start of the program where the entire computation is repeated with these new values. The iterative steps are repeated until the requirements on the bond orders previously mentioned have been satisfied. In practice about 10 iterations were required to achieve the required degree of self-consistency.

RESULTS AND DISCUSSION

Table I shows the experimental bond lengths, the calculated mobile bond orders, and the bond lengths calculated from the latter for the CC and the CN bonds in the various molecules studied. The relationship between the pi-bond order (P_{11}) and bond length (R_{11})

$$R_{11} = 1.511 - 0.173\, P_{11}$$

as found for carbon–carbon bonds by Dewar (19) was assumed to be valid for all CC bonds. The bond lengths for CC bonds were calculated from the bond orders by means of this relation. It should be noted that this relation was derived for sp^2–sp^2 CC bonds. However, throughout this paper it is assumed that the bond lengths are independent of

Can. J. Chem. Downloaded from www.nrcresearchpress.com by 210.87.254.6 on 09/05/12
For personal use only.

TABLE I

Mobile bond orders and calculated bond lengths

Molecule	Bond length, observed	Mobile bond order	Bond length, calculated
C—C bond:			
Vinyl cyanide	1.4256	0.449	1.433
Methyl cyanide	1.458	0.273	1.464
Cyanoacetylene	1.378	0.365	1.448
Vinylacetylene	1.430	0.367	1.447
Cyanogen	1.371	0.312	1.457
Propynal	1.444	0.336	1.453
Malononitrile	1.458	0.284	1.462
Methyl cyanoacetylene	1.454	0.403	1.441
Methyl cyanoacetylene	1.375	0.344	1.451
Propionitrile	1.5479	0.042	1.504
Propionitrile	1.4735	0.297	1.460
Acetylenedinitrile	1.37	0.363	1.44
C=C bond:			
Vinyl cyanide	1.3389	0.881	1.359
Vinylacetylene	1.335	0.927	1.351
C≡C bond:			
Cyanoacetylene	1.2054	0.929	1.177
Vinylacetylene	1.206	0.927	1.178
Propynal	1.2091	0.941	1.175
Methyl cyanoacetylene	1.205	0.859	1.189
Acetylenedinitrile	1.19	0.870	1.187
C≡N bond:			
Vinyl cyanide	1.1637	0.838	1.304
Methyl cyanide	1.1572	0.936	1.283
Cyanoacetylene	1.157	0.892	1.292
Cyanogen	1.127	0.920	1.287
Malononitrile	1.160	0.928	1.285
Methyl isocyanide	1.166	0.753	1.321
Methyl cyanoacetylene	1.157	0.904	1.290
Propionitrile	1.1566	0.919	1.287
Acetylenedinitrile	1.14	0.896	1.292

the σ-electron structure of the molecule. The bond orders shown in Table I are those obtained by considering "in-plane" orbitals only.

As may be seen from Table I, good agreement between the observed and calculated bond lengths of the carbon–carbon 'single' bonds is obtained in all cases where only one triple bond appears in the molecule. However, in those cases where two or more triple bonds appear in the molecule, and where the carbon–carbon 'single' bond separates at least two of these triple bonds, the observed bond length is much smaller than the calculated value. A semiquantitative hypothesis which appears to explain this discrepancy would suggest that in the latter type of molecule there is some delocalization of pi-electrons across the single bond in each of the in-plane and the out-of-plane orbitals. If it be assumed that these two, presumably mutually perpendicular, sets of orbitals are to a first approximation non-interacting one with the other, then the shortening of the bond as a result of the pi-electron delocalization should be additive in the two sets of orthogonal orbitals.

On this basis it should be possible to obtain predicted bond lengths in better agreement with the observed values by a simple addition of the bond orders for the single bond, where such bond orders are obtained from the orthogonal pi-electron systems, and where such a single bond is located between triple bonds. This was done for molecules containing such single bonds in Table I and the results shown in Table IV were obtained. The agreement between observed and calculated bond lengths can be seen to be much improved.

Can. J. Chem. Downloaded from www.nrcresearchpress.com by 210.87.254.6 on 09/05/12
For personal use only.

TABLE II

Calculated values of parameters

Molecule	δ_i	δ_j	γ_{ij}
C—C bond:			
Vinyl cyanide	0.0158	0.647	0.793
Methyl cyanide	−0.0525	0.668	0.756
Cyanoacetylene	0.547	0.669	0.763
Cyanogen	0.669	0.669	0.751
Vinylacetylene	0.0056	0.539	0.811
Propynal	0.544	0.263	0.706
Malononitrile	−0.103	0.669	0.765
Methyl cyanoacetylene	−0.093	0.563	0.790
Methyl cyanoacetylene	0.631	0.672	0.751
Propionitrile	−0.0083	−0.063	0.771
Propionitrile	−0.063	0.673	0.736
Acetylenedinitrile	0.670	0.578	0.769
C=C bond:			
Vinyl cyanide	0.086	0.016	1.057
Vinylacetylene	0.028	0.0056	1.080
C≡C bond:			
Cyanoacetylene	0.586	0.547	1.079
Vinylacetylene	0.539	0.517	1.09
Propynal	0.593	0.543	1.07
Methyl cyanoacetylene	0.563	0.631	1.07
Acetylenedinitrile	0.578	0.578	1.10
C≡N bond:			
Vinyl cyanide	0.647	1.16	0.981
Methyl cyanide	0.668	1.30	0.965
Cyanoacetylene	0.669	1.20	0.984
Cyanogen	0.669	1.24	1.04
Malononitrile	0.670	1.29	0.961
Methyl isocyanide	0.342	1.63	0.941
Methyl cyanoacetylene	0.672	1.23	0.978
Propionitrile	0.674	1.31	0.965
Acetylenedinitrile	0.670	1.21	1.016

To employ the above hypothesis in a consistent manner, the bond orders for the CC 'triple' bonds must also be doubled, since presumably both the in-plane and out-of-plane orbitals will contribute to the contraction of the bond. The bond lengths for the CC 'triple' bonds calculated on the basis of this doubled bond order are also shown in Table IV. An improvement in the agreement between calculated and observed results may again be noted.

For the CN bonds the relation (20) $R_{ij} = 1.478 - 0.208\ P_{ij}$ was initially used for the calculation of bond lengths from bond orders. Examination of the bond lengths calculated for the CN bonds using this equation as found in Table I will indicate a lack of agreement between calculated and experimental values. The bond lengths calculated using this same relation but with doubled bond orders to allow for the in-plane and out-of-plane orbitals are shown for the CN bond in column (1) of Table IV. Although the agreement between calculated and experimental bond lengths has been improved, substantial differences still exist.

It may be argued that changes in the ratio of pi-electron densities of the nitrogen and carbon atoms as one passes from the CN 'double' bond to the CN 'triple' bond may preclude the use of a single relation between bond length and bond order for these two types of bonds. Conveniently, Julg (21) has provided an equation involving the effective charges, Z,

$$R_{ij} = \sqrt{\{3.25/[\tfrac{1}{2}(Z_i+Z_j)]\}}\ (1.52-0.19\ P_{ij})$$

CN bond lengths calculated using this relation are shown in column (2) of Table IV.

Can. J. Chem. Downloaded from www.nrcresearchpress.com by 210.87.254.6 on 09/05/12
For personal use only.

Double bond orders were again employed. The values of Z_C and Z_N for each molecule were calculated from the pi-electron densities given in Table III. It may be seen that in most cases satisfactory agreement between calculated and observed bond lengths is obtained with the Julg relation.

TABLE III

Pi-electron densities

Molecule	Framework	Pi-electron density					
		C_1	C_2	C_3	C_4	N_1	N_2
Vinyl cyanide	$C_1C_2C_3N_1$	0.842	0.970	0.815		1.37	
Methyl cyanide	$C_1C_2N_1$	0.096	0.776			1.13	
Cyanoacetylene	$C_1C_2C_3N_1$	0.928	0.995	0.777		1.30	
Cyanogen	$N_1C_1C_2N_2$	0.774	0.774			1.23	1.23
Vinylacetylene	$C_1C_2C_3C_4$	0.947	0.989	1.01	1.05		
Propynal	$C_1C_2C_3O$	0.915	1.00	0.515			
Malononitrile	$N_1C_1C_2C_3N_2$	0.773	0.189	0.773		1.13	1.13
Methyl isocyanide	$C_1N_1C_2$	0.104	0.372			1.52	
Methyl cyanoacetylene	$C_1C_2C_3C_4N_1$	0.170	0.968	0.844	0.769	1.25	
Propionitrile	$C_1C_2C_3N_1$	0.015	0.116	0.770		1.10	
Acetylenedinitrile	$N_1C_1C_2C_3C_4N_2$	0.772	0.941	0.941	0.772	1.29	1.29

It was thought to be of interest to find the linear relationship between bond order and bond length giving the best fit of the calculated and observed data for the cyano group. Such an equation was found to be

$$R_{ij} = 1.478 - 0.183\ P_{ij}$$

where the constant was assumed to be the same as that employed in the Miller relation. The bond lengths calculated using this fitted relation are given in column (3) of Table IV.

TABLE IV

Revised bond lengths from mobile bond orders

Molecule	Bond length, observed	Bond length, calculated
C—C bond:		
Cyanoacetylene	1.378	1.386
Cyanogen	1.371	1.403
Methyl cyanoacetylene	1.375	1.392
Acetylenedinitrile	1.37	1.385
C≡C bond:		
Cyanoacetylene	1.2054	1.190
Vinylacetylene	1.206	1.190
Propynal	1.2091	1.185
Methyl cyanoacetylene	1.205	1.214
Acetylenedinitrile	1.19	1.210

Molecule	Bond length, observed	Bond length, calculated		
		(1)	(2)	(3)
C≡N bond:				
Vinyl cyanide	1.1637	1.129	1.152	1.171
Methyl cyanide	1.1572	1.089	1.107	1.135
Cyanoacetylene	1.157	1.107	1.139	1.151
Cyanogen	1.127	1.095	1.116	1.141
Malononitrile	1.160	1.092	1.110	1.138
Methyl isocyanide	1.166	1.165	1.174	1.202
Methyl cyanoacetylene	1.157	1.102	1.122	1.147
Propionitrile	1.1566	1.096	1.113	1.142
Acetylenedinitrile	1.14	1.105	1.127	1.150

Can. J. Chem. Downloaded from www.nrcresearchpress.com by 210.87.254.6 on 09/05/12
For personal use only.

Calculated values of the parameters are shown in Table II. The values of δ_N and γ_{CN} are 1.2 ± 0.1 and 1.0 ± 0.05 respectively. It is interesting to note that Fraenkel adopted the values 1.0 and 2.0 respectively for these parameters for the nitriles which he studied. Table V gives a summary of the data on bond lengths and the source of the values which have been used in the present work.

TABLE V

Sources of bond length data

Molecule	Bond C=C	Bond C—C	Bond C≡N	Bond C≡C	Reference
Vinyl cyanide	1.339	1.426	1.164		22
Methyl cyanide		1.4582	1.1572		23
Cyanoacetylene		1.378	1.157	1.205	24
Cyanogen		1.371	1.127		25
Vinylacetylene	1.335	1.430		1.206	26
Propynal		1.444		1.209	27
Malononitrile		1.458	1.160		28
Methyl isocyanide			1.166		29
Methyl cyanoacetylene		1.454 1.375		1.205	30
Propionitrile		1.5479 1.4735	1.1566		31
Acetylenedinitrile		1.37	1.14	1.19	32

The method employed in this work appears to yield reliable values for bond order and pi-electron densities for the compounds considered provided the assumption of additivity of bond order under the conditions described in this work is employed. However, the existence of a systematic variation of bond length of CN 'triple' bonds remains in doubt. Further work is necessary to provide support for any bond order:bond length relationship which is to be applied to the nitrile group.

ACKNOWLEDGMENTS

The generous assistance of the Computation Center of the University of Waterloo is gratefully acknowledged. The author is indebted to the National Research Council of Canada for financial support.

REFERENCES

1. P. H. Rieger and G. K. Fraenkel. J. Chem. Phys. **37**, 2795 (1962).
2. B. R. Penfold and W. N. Lipscomb. Acta Cryst. **14**, 589 (1961).
3. T. E. Peacock and P. T. Wilkinson. Proc. Phys. Soc. **79**, 105 (1962).
4. A. Lofthus. Mol. Phys. **2**, 367 (1959).
5. S. Nagakura. Bull. Chem. Soc. Japan, **25**, 163 (1952).
6. R. D. Brown and M. L. Heffernan. Trans. Faraday Soc. **54**, 757 (1958).
7. W. J. Orville-Thomas and W. J. Jones. Z. Elektrochem. **64**, 714 (1960).
8. F. E. Morris and W. J. Orville-Thomas. J. Mol. Spectry. **6**, 572 (1961).
9. R. Daudel, R. Lefebvre, and C. Moser. Quantum chemistry. Interscience Publishers, Inc., New York. 1959.
10. C. Sandorfy. Bull. Soc. Chim. France, 615 (1949).
11. Y. Kurito and M. Kubo. Bull. Chem. Soc. Japan, **24**, 13 (1951).
12. G. W. Wheland. J. Am. Chem. Soc. **64**, 900 (1942).
13. J. C. Slater. Phys. Rev. **36**, 57 (1930).
14. J. C. Slater. Phys. Rev. **42**, 33 (1932).
15. R. S. Mulliken, C. A. Rieke, D. Orloff, and H. Orloff. J. Chem. Phys. **17**, 1248 (1949).
16. H. O. Pritchard and F. H. Sumner. Proc. Roy. Soc. London, A, **226**, 128 (1955).
17. L. F. Richardson. Phil. Trans. Roy. Soc. London, Ser. A, **242**, 439 (1950).
18. Y. Kurito and M. Kubo. Bull. Chem. Soc. Japan, **24**, 13 (1951).
19. M. J. S. Dewar and H. N. Schmeising. Tetrahedron, **5**, 166 (1959).

Can. J. Chem. Downloaded from www.nrcresearchpress.com by 210.87.254.6 on 09/05/12
For personal use only.

20. R. L. MILLER, P. G. LYKOS, and H. N. SCHMEISING. J. Am. Chem. Soc. **84**, 4623 (1962).
21. A. JULG and P. CARLES. Theoret. Chim. Acta Berlin, **1**, 140 (1963).
22. C. C. COSTAIN and B. P. STOICHEFF. J. Chem. Phys. **30**, 777 (1959).
23. C. C. COSTAIN. J. Chem. Phys. **29**, 864 (1958).
24. B. P. STOICHEFF. Can. J. Phys. **35**, 373 (1957).
25. A. S. PARKER and R. E. HUGHES. Acta Cryst. **16**, 734 (1963).
26. J. SERRE. J. Chim. Phys. **53**, 284 (1956).
27. C. C. COSTAIN and J. R. MORTON. J. Chem. Phys. **31**, 389 (1959).
28. E. HIROTA. J. Mol. Spectry. **7**, 242 (1961).
29. C. C. COSTAIN. J. Chem. Phys. **29**, 864 (1958).
30. L. F. THOMAS, J. S. HEEKS, and J. SHERIDAN. Arch. Sci. Geneva, **10**, 18 (1957).
31. R. G. LERNER and B. P. DAILEY. J. Chem. Phys. **26**, 678 (1957).
32. R. B. HANNAN and R. L. COLLIN. Acta Cryst. **6**, 350 (1953).

Can. J. Chem. Downloaded from www.nrcresearchpress.com by 210.87.254.6 on 09/05/12
For personal use only.

β-KETO ESTERS FROM REACTION OF ETHYL DIAZOACETATE WITH KETONES

W. T. TAI AND E. W. WARNHOFF[1]
Department of Chemistry, University of Western Ontario, London, Ontario
Received January 16, 1964

ABSTRACT

The Lewis acid catalyzed reaction of diazoacetic ester with ketones has been extended. Convenient conditions have been found for the preparation of some pure β-keto esters in fair to good yields by reaction of ethyl diazoacetate with ketones in the presence of boron trifluoride at −40° to −70°. The reaction is apparently general since cyclopentanone, cyclohexanone, and acetophenone gave nearly pure β-keto esters in 44%, 79%, and 38% yields, respectively, based on diazoacetic ester. In the case of acetophenone the phenyl group migrated. Acetone gave 78% of a mixture of β-keto ester and glycidic ester.

Although diazomethane and its alkyl derivatives have served extensively in the homologation of aldehydes and ketones (1), the closely related, but more sluggish, ethyl diazoacetate has been less useful. Several aldehydes bearing electronegative substituents have been reported to yield β-keto esters and (or) glycidic esters with this reagent (2, 3, 4). However, in the few cases studied, ketones and diazoacetic ester in the absence of a Lewis acid catalyst have given enol ethers as the product isolated and no noticeable amount of β-keto ester. Thus, cyclohexanone at 95° in the presence of copper gave 43% of I, and acetone at 93° in the presence of copper gave 23% of II (5). While neither ketone reacted below 120° in the absence of copper, at higher temperatures the same major product was formed as in the copper-catalyzed reactions. Finally, benzosuberone at 120° in the presence of copper gave 50% of III (6). To explain the formation of enol ethers it has been suggested (6) that diazoacetic ester may decompose in the presence of copper or at high temperatures to carbethoxycarbene which could react with the ketone to give the observed product.

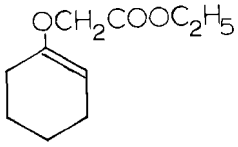

I

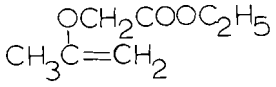

II

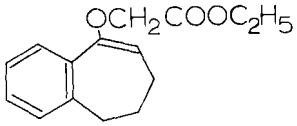

III

Recent work on catalysis of the reactions of ketones with diazoalkanes (7, 8) has revealed means of overcoming the relative inertness of diazoacetic ester and avoiding the formation of enol ethers. While the catalytic action of water and alcohols on the reactions of diazomethane has long been known, it has lately been observed that the catalytic action of boron trifluoride and other Lewis acids is more profound, even altering the course of reaction. Methyl *t*-butyl ketone gave no measurable reaction with diazomethane in methanol at room temperature, but in the presence of boron fluoride etherate at 0° it produced a mixture of homologous ketones and oxide (7). Normally, α,β-unsaturated

[1]*Fellow of the Alfred P. Sloan Foundation.*

ketones and diazomethane give pyrazoline derivatives or else no reaction (1). Δ^4-Cholesten-3-one was found not to react with diazomethane except in the presence of boron trifluoride or fluoboric acid when the homologous ketone was formed (9). Mesityl oxide and benzalacetone with diazomethane each gave a Δ^2-pyrazoline in the absence of a catalyst, but in the presence of the above two catalysts the only products were those of ketone homologation (7, 9). It was also noted that oxide formation was suppressed in the boron trifluoride catalyzed reaction of ketones with diazomethane (7). This result was tentatively ascribed to the decrease in importance of intermediates such as IV with a more nucleophilic alkoxide ion in favor of intermediates such as V with a less nucleophilic

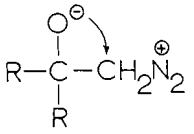

IV

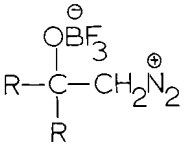

V

complexed oxygen, thus diminishing oxide formation (assumed to occur by nucleophilic displacement of nitrogen) relative to rearrangement. In fact, the two examples of diazoacetic ester and a ketone not giving an enol ether but instead a β-keto ester are the aluminum chloride catalyzed reaction with cycloöctanone which gave the β-keto ester of unspecified purity (8), and the zinc chloride catalyzed reaction with 1,3-cyclohexanedione mono ethylene ketal, which gave 3,3-ethylenedioxy-7-carbethoxycylcoheptanone (21). Since the extension of this reaction could be a convenient synthesis of β-keto esters isotopically labelled on the α-carbon atom which were required for another study, the reaction of ethyl diazoacetate with ketones was examined with cyclopentanone as the model compound.

Several preliminary experiments agreed with previous conclusions. When cyclopentanone and diazoacetic ester were heated in the absence of solvent and catalyst, no nitrogen evolution occurred until 130–150°, and the mixture of products contained no β-keto ester (gas–liquid chromatography and negative ferric chloride test). With refluxing methanol as solvent and catalyst no nitrogen was liberated. On substitution of the higher boiling *n*-amyl alcohol (b.p. 138°) as solvent 86% of the theoretical amount of nitrogen was collected, but the mixture of products contained no β-keto ester (gas–liquid chromatography and a negative ferric chloride test). However, in the presence of boron trifluoride, cyclopentanone and ethyl diazoacetate rapidly evolved nitrogen at room temperature, and the mixture of products gave a positive ferric chloride test. With an excess of cyclopentanone at 0°, a 19% yield of 2-carbethoxycyclohexanone (VI) was separated from other products. There was also considerable (>10%) formation of VII

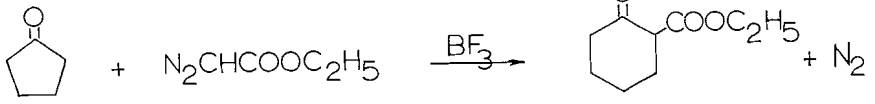

VI

by boron fluoride catalyzed self-condensation of cyclopentanone. This side reaction and others were largely eliminated by lowering the reaction temperature. Subsequent systematic variations of the reaction conditions are summarized in Table I.

TABLE I

Reaction	Moles DAE*	Moles 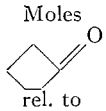 rel. to DAE*	Moles $BF_3.Et_2O$ rel. to DAE*	Solvent	Reaction temp., ° C	Time for DAE addn. (minutes)	% N_2 evolved	Yield VI (%)
1	0.119	1	1	Ether	−2° to 2°	90	53	19
2	0.238	1	1	Petroleum ether	−5° to 2°	82	92	26
3	0.119	3	0.5	None	−5° to 2°	70	100	28
4	0.119	3	3	Ether	−40° to −55°	20	93	44
5	0.119	3	3	Ether	−67° to −70°	25	100	42
6	0.100	5	5	Ether	−67° to −71°	72	96	42
7	0.119	3	3	Ether	−45° to −48°	12	88	43
8	0.119	3	0.1	Ether	−12° to −22°†	31	92	42‡
9	0.150	1	1	Ether	−65° to −40°	35	85	28
10	0.300	3	3	Ether	−65° to −5°	120	51§	43

*DAE = diazoacetic ester.
†The higher temperature was necessary to get a reasonable rate of nitrogen evolution.
‡Contained several impurities.
§Inaccurate since there was a leak in the system.

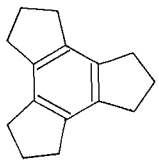

VII

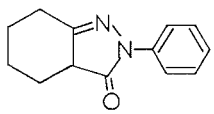

VIII

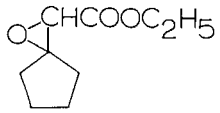

IX

The best results were obtained by the addition of ethyl diazoacetate to a threefold excess of 1:1 ketone:boron trifluoride mixture kept at −40° to −70°. Nitrogen evolution was rapid and almost quantitative.* Distillation of the crude product gave, after removal of excess cyclopentanone, reproducible 42–44% yields of almost pure 2-carbethoxycyclohexanone. There was present a small amount of an impurity which could be removed by fractional distillation. The identity and purity of the product were assured by a violet ferric chloride test, elemental analysis, comparison of the infrared spectrum, and gas–liquid chromatographic behavior with those of an authentic sample, and preparation of the known phenylpyrazolone VIII. The remainder of the diazoacetic ester was transformed into polymeric residue which incorporated cyclopentane groups and was not investigated further. That there was no glycidic ester IX in the once distilled product was demonstrated by comparison with the infrared and n.m.r. spectra of an authentic sample of IX. Nor did the 2-carbethoxycyclohexanone arise by Lewis acid catalyzed rearrangement of initially formed glycidic ester, because authentic IX, when subjected to the reaction conditions, gave a mixture of products containing not more than about 5%, if any, of β-keto ester VI. In addition, the other reaction products from IX would have

*In the absence of a ketone, diazoacetic ester evolved nitrogen only very slowly in the presence of boron trifluoride at −40° to −70°.

appeared in the diazoacetic ester product VI. In contrast to the uncatalyzed diazoacetic ester reactions, there was no evidence of formation of any enol ether analogous to I. Aluminum chloride is a somewhat less effective catalyst. Its substitution for boron trifluoride gave no nitrogen evolution until the reaction temperature was raised to −20°, and the yield of product was only 25%.

The low-temperature boron trifluoride catalyzed reaction is apparently general, since, under the best conditions found for cyclopentanone, other ketones gave fair to good yields of β-keto esters. Cyclohexanone gave 79% of 2-carbethoxycycloheptanone after separation from a small amount of a second product. This β-keto ester was identified from its infrared spectrum, a violet ferric chloride test, and the preparation of the known phenylpyrazolone. In the reaction between acetophenone and diazoacetic ester only the phenyl group migrated to afford in 38% yield ethyl α-phenylacetoacetate. The structure was proved by hydrolysis and decarboxylation to phenylacetone, which could not have

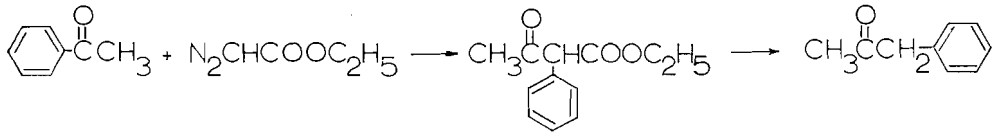

contained more than 2% of propiophenone. From acetone and diazoacetic ester was obtained 78% of a product which was recognized to be a mixture of ethyl α-methylacetoacetate and ethyl β,β-dimethylglycidate in the ratio 5:4 by infrared and n.m.r. spectral comparison of the product with authentic samples. Therefore, boron trifluoride does not always completely suppress oxide formation in this reaction. For those cases where oxide formation is negligible, the yields and convenience are such that the reaction should constitute an acceptable alternative method for preparation of β-keto esters.

EXPERIMENTAL

General

Melting points were taken on a Reichert microscope hot stage unless otherwise stated and are corrected. Infrared spectra were recorded with a Beckman IR-5 spectrophotometer. Only the principal sharply defined peaks are listed. Nuclear magnetic resonance spectra were determined in *carbon tetrachloride* solution on a Varian HR-60 spectrometer and were calibrated by the audio side band technique. Peak positions are given in p.p.m. from the tetramethylsilane peak (=0). The 1-m and 20-cm Nestor and Faust spinning band columns had efficiencies of 9 and 6 theoretical plates, respectively, at total reflux at atmospheric pressure. Petroleum ether refers to the fraction boiling at 60–80°. Microanalyses were by Dr. A. Bernhardt, Mulheim, Germany. Yields of β-keto esters are based on ethyl diazoacetate. For gas–liquid chromatography a Wilkens Aerograph, Model 350 B, was used with ¼ inch O.D. columns of (*a*) 10% Carbowax 20 M, or (*b*) 20–30% Dow Silicone 710, or (*c*) 3% UCON polar, each on 60–80 mesh Johns Manville Firebrick. Gas–liquid chromatography was not very useful with the β-keto esters in the present work. In some cases there were apparently peaks corresponding to keto and enol forms; the relative intensity of the two peaks varied with temperature and flow rate. In other cases decomposition occurred during chromatography. The n.m.r. spectrum was a more reliable criterion of purity.

Reagents

Ethyl diazoacetate was prepared by diazotization of ethyl glycinate according to the directions in Organic Syntheses (10).

Cyclopentanone (B.D.H.), cyclohexanone (B.D.H.), acetophenone, phenylacetone (E.K.C.), and propiophenone (E.K.C.) were redistilled if necessary. In each case the material used gave a single peak on gas–liquid chromatography.

Boron trifluoride etherate (M.C.B.) was redistilled.

Authentic 2-carbethoxycyclohexanone was prepared by the procedure in Organic Syntheses (11).

Ethyl α-methylacetoacetate (Aldrich) was fractionally distilled at reduced pressure.

Ethyl β,β-dimethylglycidate was prepared in 48% yield by condensation of acetone and ethyl chloroacetate according to the procedure of Rutowski and Dajew (19).

Reaction of Cyclopentanone and Ethyl Diazoacetate

(*a*) Cyclopentanone (30 g, 0.35 mole) was cooled to −40° by means of a Dry Ice – acetone bath and 50.7 g (0.35 mole) of redistilled boron trifluoride etherate was added at this temperature with mechanical stirring. Ether (10 ml, reagent grade) was added to prevent the mixture from solidifying. A solution of 13.6 g (0.12 mole) of ethyl diazoacetate in 30 ml of reagent grade ether was added dropwise with stirring over a period of 20 minutes while the temperature was maintained at −40° to −55°. Evolution of nitrogen was instantaneous and 2710 ml (93%) were collected. After addition was complete the cooling bath was removed and the stirring continued for 10 minutes.

The reaction mixture was diluted with ether and washed with saturated aqueous sodium chloride solution until the washings were neutral to litmus paper. The ethereal solution was dried over magnesium sulphate, filtered, and distilled through a 10-cm Claisen head. After removal of ether at atmospheric pressure, distillation gave recovered cyclopentanone, 13.9 g (46%), b.p. 57–62° (50 mm), followed by *2-carbethoxycyclohexanone* (VI), 8.9 g (44% based on diazoacetic ester), b.p. 110-112° (12 mm). The n.m.r. spectrum and gas–liquid chromatography on the UCON column (150 cm, t = 150°, pressure 30 p.s.i.g. He, 3 ml/second) revealed the pressure of ca. 9% of an impurity of retention time 19 minutes whereas VI had a retention time of 12 minutes. This impurity was removed by fractional distillation of the keto ester through a 1-m Nester and Faust spinning band column. The fraction boiling at 83–84° (3.0 mm) (lit. (12): b.p. 106–107° at 11 mm) was pure 2-carbethoxycyclohexanone whose infrared spectrum was identical with that of an authentic sample. R_f 0.70 (silica gel; ethyl acetate:petroleum ether, 50:50). The keto ester gave a deep violet ferric chloride test.

Anal. Calc. for $C_9H_{14}O_3$ (170.20): C, 63.51; H, 8.29. Found: C, 63.43; H, 8.46.

Infrared spectrum: $\nu_{max}^{CCl_4}$ 1745 (ester C=O)(m), 1721 (ketone C=O)(m), 1658 (ester C=O of enol)(s), 1618 (s), 1300 (s), 1261 (s), 1221 (s), 1179 (s), 1085 (s), and 1010 cm^{-1} (m).

The n.m.r. spectrum: δ = 1.27 p.p.m. (3H triplet, J=7 c.p.s., CH_3—[CH_2]); 1.63 p.p.m. (broad peak, ring CH_2); 2.20 p.p.m. (broad peak, CH_2—C=O, CH_2—C=C); 3.27 p.p.m. (broad peak, O=C—CH—C=O); 4.17 p.p.m. (2H quartet, J=7 c.p.s., O—CH_2—[CH_3]); 12.07 p.p.m. (1H singlet, chelated enolic OH).

The β-keto ester was shown to be stable under the reaction conditions by treatment of a 2:1 mixture of cyclopentanone and VI (5.10 g) with boron trifluoride etherate at −60° to −70° for 15 minutes. Work-up and distillation gave back 3.70 g (72%) of VI.

(*b*) From a similar reaction carried out at −2° to 2° there was distilled 19% of 2-carbethoxycyclohexanone followed by a high boiling (130–193° at 0.3 mm) oil that solidified. The solid was recrystallized twice from methanol to give colorless needles of *tris*-cyclopentenobenzene, m.p. 95–96° (lit.(13): m.p. 96–97°), ν_{max}^{melt} 2950 (C—H)(s), 2833 (C—H)(s), 1447 (methylene)(m), and 1425 cm^{-1}(w). The compound did not discolor permanganate solution.

The n.m.r. spectrum: δ = 2.07 p.p.m. (6H multiplet, non-benzylic CH_2); 2.73 p.p.m. (12H multiplet, benzylic CH_2).

(*c*) From a reaction of 13.6 g (0.119 mole) of diazoacetic ester in 200 ml of ether with a mixture of 30 g (0.35 mole) of cyclopentanone and 47.5 g (0.35 mole) of anhydrous aluminum chloride in 50 ml of ether at −20° to −4° there was isolated by distillation 5.15 g (25%) of not quite pure VI.

1-Phenylpyrazolone of Cyclopentanone–Diazoacetic Ester Product

To a solution of 0.85 g (5.9 mmoles) of phenylhydrazine hydrochloride and 1.2 g (14 mmoles) of anhydrous sodium acetate in 10 ml of water was added 1.00 g (5.88 mmoles) of the cyclopentanone – diazoacetic ester product. Sufficient ethanol was added to give a clear solution which was refluxed for 2.5 hours. The cooled solution deposited crystals which were filtered. Concentration of the filtrate gave a second crop from which a brown color was removed by washing with ether. The total yield of crude product, m.p. 172–180°, was 1.03 g (81%). Two recrystallizations from absolute ethanol gave colorless scales of VIII, m.p. 180–181°.

Anal. Calc. for $C_{13}H_{14}ON_2$ (214.26): C, 72.87; H, 6.59. Found: C, 72.79; H, 6.37.

The melting point and appearance of the crystals gradually changed over a period of several weeks to colorless needles, m.p. 163–165° (lit.(12): m.p. 165°) without any change in the infrared spectrum. The melting point of an authentic sample prepared from authentic VI behaved in the same way.

Infrared spectrum: $\nu_{max}^{CHCl_3}$ 1709 (s) (γ-lactam C=O and C=N), 1597 (s), 1379 (s), 1335 (s), 1312 (m), 1152 (m), and 1136 cm^{-1} (m); ν_{max}^{Nujol} 755 (s) and 690 cm^{-1} (s). The last two peaks are from monosubstituted phenyl.

Ethyl β,β-Tetramethyleneglycidate

A literature procedure (14) for cyclohexanone was adapted. A mixture of 16.8 g (0.20 mole) of cyclopentanone and 24.5 g (0.20 mole) of ethyl chloroacetate was cooled to −75° while the powdered sodium ethoxide from 4.6 g (0.20 g-atom) of sodium was added in small portions. After 10 minutes the mixture was allowed to come to room temperature and stand for several hours. The reaction mixture was then heated at 120–140° for 2.5 hours, poured into ice water, and extracted with ether. The combined ether extracts were washed with water, dried, and distilled through a 10-cm Claisen head. After a forerun, the glycidic ester, 8.9 g (26%) distilled as a colorless liquid, b.p. 88–94° at 3 mm. The product was fractionally distilled through a 20-cm Nestor and Faust spinning band column to give 5.97 g of IX, b.p. 92–94° (3.2 mm) (lit. (15): b.p.

90–95° at 3–4 mm). The glycidic ester decomposed during gas–liquid chromatography. Thin-layer chromatography (silica gel; ethyl acetate:petroleum ether, 50:50) gave a main spot, R_f 0.60, and very faint traces of impurities at R_f 0.32, 0.25, and 0.13 which were visible only under ultraviolet light and did not char.

Infrared spectrum: $\nu_{max}^{CCl_4}$ 1761 (s) and 1733 (s) (ester C=O), 1425 (m), 1372 (w), 1339 (w), 1284 (s), 1188 (s), and 1040 cm^{-1} (s). The doublet carbonyl peak probably results from different conformers of IX in solution; it is not caused by an impurity in view of the unambiguous n.m.r. spectrum of the same sample.

The n.m.r. spectrum: δ = 1.28 p.p.m. (3H triplet, J=7 c.p.s., CH_3—[CH_2]); 1.76 p.p.m. (8H apparent singlet, cyclopentane CH_2); 3.37 p.p.m. (1H singlet, O—CH—C=O); 4.17 p.p.m. (2H quartet, J=7 c.p.s. O—CH_2—[CH_3]).

Reaction of Ethyl β,β-Tetramethyleneglycidate with Boron Trifluoride

The glycidic ester IX (4.25 g, 0.025 mole) in 25 ml of reagent grade ether was cooled to −65° and redistilled boron trifluoride etherate (3.55 g, 0.025 mole) was added with stirring (magnetic bar). The temperature was kept at −65° to −55° for 20 minutes and then at −10° for 10 minutes.

The reaction was worked up as for the acetophenone – diazoacetic ester reaction. Evaporation of the ether left 4.2 g of colorless liquid whose infrared spectrum had strong hydroxyl absorption and was quite different from that of the starting material and VI. In particular, the distilled product had none of the strong infrared peaks at 1658, 1618, 1300, 1261, and 1221 cm^{-1} which appear in the spectrum of 2-carbethoxycyclohexanone. Thin-layer chromatography (silica gel; ethyl acetate:petroleum ether, 50:50) gave several spots, R_f 0.61, 0.52, 0.22, 0.10, and 0.03.

Reaction of Cyclohexanone and Ethyl Diazoacetate

A solution of 35.0 g (0.35 mole) of cylcohexanone in 20 ml of reagent grade ether was maintained at a temperature of −45° to −55° while 50.7 g (0.36 mole) of freshly distilled boron trifluoride etherate was added. Then a solution of 13.6 g (0.119 mole) of ethyl diazoacetate in 30 ml of reagent grade ether was added during 22 minutes with the temperature kept at −55° to −40°. The nitrogen evolved amounted to 3010 ml (98%).

The reaction mixture was worked up as for the cyclopentanone reaction. Distillation of the product through a 10-cm Claisen head gave 16.7 g (47%) of recovered cyclohexanone, b.p. 79–81.5° (60 mm), followed by 17.3 g (79%) of *2-carbethoxycycloheptanone*, b.p. 103–109° (3.3 mm) (lit. (16): b.p. 125–126° at 12 mm). Fractional distillation through a 20-cm Nestor and Faust spinning band column gave pure β-keto ester, b.p. 76–79° (1 mm), which produced a violet color with ferric chloride solution.

Anal. Calc. for $C_{10}H_{16}O_3$ (184.23): C, 65.19; H, 8.75. Found: C, 65.11; H, 8.66.

Infrared spectrum: $\nu_{max}^{CCl_4}$ 1748 (ester C=O)(m), 1715 (ketone C=O)(m), 1645 (ester C=O of enol)(s), 1616 (s), 1456 (m), 1404 (m), 1312 (s), 1242 (s), 1217 (s), 1200 (m), 1054 (s), and 975 cm^{-1} (w).

The n.m.r. spectrum: δ = 1.24 (1.29) p.p.m. (3H "doubled" triplet, J=7 c.p.s. for each triplet, CH_3—[CH_2]); 1.70 p.p.m. (broad peak, ring CH_2); 2.46 p.p.m. (broad peak, CH_2—C=O and CH_2—C=C), 3.31–3.53 p.p.m. (broad peak, O=C—CH—C=O); 4.12 (4.19) p.p.m. (2H "doubled" quartet, J=7 c.p.s. for each quartet, O—CH_2—[CH_3]); 12.64 p.p.m. (1H singlet, chelated enolic OH). The "doubling" of the methyl and oxymethylene proton groups is presumably due to slight differences in chemical shift of these groups in the enolic and non-enolic tautomers.

1-Phenylpyrazolone of Cyclohexanone – Diazoacetic Ester Product

The same procedure employed for the cyclopentanone adduct was used to prepare a derivative from 1.00 g (5.43 mmoles) of cyclohexanone–diazoacetic ester product, 0.797 g (5.50 mmoles) of phenylhydrazine hydrochloride, and 0.451 g (5.50 mmoles) of anhydrous sodium acetate in 7 ml of water. The crude product after filtration and drying amounted to 1.105 g (89%), m.p. 200–210°. Three recrystallizations from absolute ethanol gave colorless scales of the pyrazolone, m.p. 210–212° (lit. (17): m.p. 210°).

Infrared spectrum: $\nu_{max}^{CHCl_3}$ 1704 (s) (γ-lactam C=O and C=N), 1645 (m), 1600 (s), 1391 (w), 1340 (m), 1321 (m), and 1116 cm^{-1} (w); ν_{max}^{Nujol} 742 (m) and 690 cm^{-1} (m). The last two peaks are from monosubstituted phenyl.

Reaction of Acetophenone with Ethyl Diazoacetate

A solution of 72 g (0.60 mole) of acetophenone in 700 ml of reagent grade ether was maintained at −60° while 85.2 g (0.60 mole) of redistilled boron trifluoride etherate was added with mechanical stirring. A solution of 22.8 g (0.20 mole) of ethyl diazoacetate in 50 ml of ether was added dropwise at −50° to −30°* during 4 hours. Total nitrogen evolution over a period of 4 hours was 4690 ml (90%).

The reaction mixture was added with vigorous stirring to sodium bicarbonate solution which was then extracted with ether and worked up as for the cyclopentanone reaction. Distillation of the product through a 10-cm Claisen head gave 60.9 g (87%) of recovered acetophenone, b.p. 56–64° (2.8 mm) followed by 15.9 g (38%) of *ethyl α-phenylacetoacetate*, b.p. 120–124° (2.5 mm) (lit. (18): b.p. 145–147° at 11 mm), which gave a violet ferric chloride test. Thin-layer chromatography (silica gel; ethyl acetate:petroleum ether, 85:15) gave a single spot, R_f 0.49. The β-keto ester was fractionally distilled through the 1-m Nestor and Faust spinning band column for analysis and spectra.

**In this reaction evolution of nitrogen was slow at −70° to −50°.*

Anal. Calc. for $C_{12}H_{14}O_3$ (206.23): C, 69.88; H, 6.84. Found: C, 69.78; H, 6.76.

Infrared spectrum: ν_{max}^{film} 1745 (s) (ester C=O), 1721 (s) (ketone C=O), 1642 (s) (ester C=O of enol), 1621 (s), 1401 (w), 1335 (w), 1264 (s), 1225 (s), 1059 (m), 959 (w), 754 (w), 700 (s), and 665 (w).

The n.m.r. spectrum: δ = 1.16 p.p.m. (3H triplet, J=7 c.p.s., CH_3—[CH_2]); 1.80 p.p.m. (3H singlet, CH_3—C(=O)—C=C); 2.12 p.p.m. (3H singlet, CH_3—C=O); 4.14 p.p.m. (2H quartet, J = 7 c.p.s., O—CH_2—[CH_3]); 7.09–7.36 p.p.m. (5H multiplet, aryl H); 13.00 p.p.m. (1H singlet, chelated enolic OH). With better resolution the enolic hydroxyl was a quartet from coupling to the allylic methyl group which was in turn a doublet, $J \sim 0.5$ c.p.s.

Ketonic Cleavage of Acetophenone – Ethyl Diazoacetate Product

The fractionally distilled β-keto ester (6.30 g, 0.030 mole) was heated with 20 ml of 10% aqueous sulphuric acid at 100° for 16 hours at which point the ferric chloride test was negative. The water-insoluble oily layer was extracted with ether. The ethereal solution was washed with dilute sodium bicarbonate solution and with water before being dried over magnesium sulphate. Filtration and distillation of the ether left 3.4 g (83%) of liquid whose infrared spectrum was identical with that of an authentic sample of phenylacetone and quite different from that of authentic propiophenone. Gas–liquid chromatographic comparison (Dow Silicone 710 column, 250 cm, 175°, 50 p.s.i.g., 4.3 ml per second) of the product (retention time 9.6 minutes) with phenylacetone (retention time 9.6 minutes) and propiophenone (retention time 10.8 minutes) also confirmed the identification.

Infrared spectrum (acetophenone + diazoacetic ester product≡phenylacetone): ν_{max}^{film} 1715 (C=O) (s), 1603 (w), 1497 (m), 1456 (m), 1418 (w), 1359 (s), 1230 (m), 1160 (s), 1080 (w), 1033 (w), 730 (s), and 700 cm^{-1} (s) (last two peaks from monosubstituted phenyl).

Infrared spectrum (propiophenone): ν_{max}^{film} 1689 (conjugated C=O) (s), 1600 (m), 1585 (m), 1451 (m), 1416 (w), 1379 (w), 1355 (m), 1222 (s), 1183 (w), 1081 (w), 1016 (m), 1005 (w), 953 (s), 745 (s), and 689 cm^{-1} (s).

The infrared spectrum of a 2% solution (w/w) of propiophenone in phenylacetone gave a definite peak at 953 cm^{-1} from propiophenone. This peak was completely absent from the reaction product. Therefore the phenylacetone from the acetophenone–diazoacetic ester reaction could not have contained as much as 2% of propiophenone.

Reaction of Acetone with Ethyl Diazoacetate

Distilled boron trifluoride etherate (21.3 g, 0.15 mole) was added to 43.5 g (0.75 mole) of reagent grade acetone being stirred (magnetic bar) at −70°. Then 17.1 g (0.15 mole) of ethyl diazoacetate in 75 ml of reagent grade ether was added dropwise at −65° to −60° during 40 minutes. The nitrogen evolved amounted to 3715 ml (93%).

The reaction mixture was added with vigorous stirring to sodium bicarbonate solution and worked up as for the acetophenone reaction. Distillation of the product through a 10-cm Claisen head gave 16.8 g (78%) of colorless liquid, b.p. 73–82° (22 mm). Comparison of the n.m.r. and infrared spectra of the product with those of authentic *ethyl α-methylacetoacetate* and *ethyl β,β-dimethylglycidate* showed the product to be a mixture of these two compounds in the ratio of about 5:4. Fractional distillation of the product through a 1-m Nestor and Faust spinning band column at 22 mm did not separate the mixture.

Repetition of the reaction with a 3:3:1 ratio of acetone:boron trifluoride etherate:diazoacetic ester gave a 63% yield of a mixture of the same two compounds.

Infrared spectrum (ethyl α-methylacetoacetate): $\nu_{max}^{CCl_4}$ 1748 (ester C=O) (s), 1721 (ketone C=O) (s), 1650 (m), 1453 (m), 1245 (s), 1155 (m), 1100 (m), 1078 (w), and 862 cm^{-1} (w).

Infrared spectrum (ethyl β,β-dimethylglycidate): $\nu_{max}^{CCl_4}$ 1757 and 1730 (ester C=O) (s), 1456 (m), 1410 (m), 1381 (m), 1314 (m), 1289 (m), 1255 (w), 1196 (s), 1124 (m), 1112 (m), 1054 (m), and 1037 cm^{-1} (m) (cf. infrared spectrum of ethyl β,β-tetramethyleneglycidate).

The n.m.r. spectrum (ethyl α-methylacetoacetate): δ = 1.25 p.p.m. (3H doublet, J=7 c.p.s., CH_3—C—[H]); 1.26 p.p.m. (3H triplet, J = 7 c.p.s., CH_3–[CH_2]); 2.16 p.p.m. (3H singlet, CH_3—C=O); 3.40 p.p.m. (1H quartet, J = 7 c.p.s.., H—C—(CH_3]); 4.15 p.p.m. (2H quartet, J = 7 c.p.s., O—CH_2—[CH_3]). In addition there were minor peaks from a small amount of the enol tautomer.

The n.m.r. spectrum (ethyl β,β-dimethylglycidate): δ = 1.28 p.p.m. (3H triplet, J = 7 c.p.s., CH_3—[CH_2]); 1.32 p.p.m. and 1.37 p.p.m. (each a 3H singlet, $(CH_3)_2$C(O)—C); 3.14 p.p.m. (1H singlet, C(O)—CH—C=O); 4.17 p.p.m. (2H quartet, J = 7 c.p.s., O(O)—CH_2—[CH_3]).

A 3.00-g sample of the reaction product and a sample of authentic ethyl α-methylacetoacetate were each converted to the pyrazolone by heating with aqueous hydrazine sulphate solution for 11.5 hours. From the authentic sample there was obtained 45% of white prisms of pyrazolone, m.p. 243–263° (cap. uncorr.) (lit. (20): m.p. 268°). From the reaction product the yield was only 35%, m.p. 258–268° (cap. uncorr.).

ACKNOWLEDGMENTS

The financial support of the Alfred P. Sloan Foundation and the National Research Council is gratefully acknowledged. Mr. R. E. Klinck kindly determined most of the n.m.r. spectra.

REFERENCES

1. C. D. GUTSCHE. Org. Reactions, **8**, 364 (1954).
2. F. SCHLOTTERBECK. Ber. **40**, 3000 (1907).
3. F. SCHLOTTERBECK. Ber. **42**, 2565 (1909).
4. E. BUCHNER and T. CURTIUS. Ber. **18**, 2371 (1885). See also W. Dieckmann. Ber. **43**, 1024 (1910), footnote 3.
5. M. S. KHARASCH, T. RUDY, W. NUDENBERG, and G. BÜCHI. J. Org. Chem. **18**, 1030 (1953).
6. C. D. GUTSCHE and M. HILLMAN. J. Am. Chem. Soc. **76**, 2236 (1954).
7. H. O. HOUSE, E. J. GRUBBS, and W. F. GANNON. J. Am. Chem. Soc. **82**, 4099 (1960).
8. E. MÜLLER and M. BAUER. Ann. **654**, 92 (1962).
9. W. S. JOHNSON, M. Neeman, S. P. BIRKELAND, and N. A. FEDORUK. J. Am. Chem. Soc. **84**, 989 (1962).
10. N. E. SEARLE. Org. Syn. **36**, 25 (1956).
11. H. R. SNYDER, L. A. BROOKS, and S. H. SHAPIRO. Org. Syn. Coll. Vol. II, 531 (1943).
12. W. DIECKMANN. Ann. **317**, 94 (1901).
13. O. WALLACH. Ber. **30**, 1094 (1897).
14. W. A. YARNALL and E. S. WALLIS. J. Org. Chem. **4**, 270 (1939).
15. M. S. NEWMAN. J. Am. Chem. Soc. **57**, 734 (1935).
16. P. A. PLATTNER, A. FÜRST, and K. JIRASEK. Helv. Chim. Acta, **29**, 733 (1946).
17. W. DIECKMANN. Ber. **55**, 2486 (1922).
18. W. BECKH. Ber. **31**, 3161 (1898).
19. B. N. RUTOWSKI and N. A. DAJEW. Ber. **64**, 693 (1931).
20. L. WOLFF. Ber. **37**, 2834 (1904).
21. B. EISTERT, F. HAUPTER, and K. SCHANK. Ann. **665**, 55 (1963).

Can. J. Chem. Downloaded from www.nrcresearchpress.com by 210.87.254.105 on 09/05/12
For personal use only.

THE STRUCTURES OF GALACTOSYL-LACTOSE AND GALACTOBIOSYL-LACTOSE PRODUCED FROM LACTOSE BY SPOROBOLOMYCES SINGULARIS[1]

P. A. J. GORIN, J. F. T. SPENCER, AND H. J. PHAFF[2]
National Research Council of Canada, Prairie Regional Laboratory, Saskatoon, Saskatchewan
Received December 12, 1963

ABSTRACT

Sporobolomyces singularis, when grown in a medium containing lactose, utilized the glucose portion as a carbon source and produced by transglycosylation as main products a trisaccharide *O*-β-D-galactopyranosyl-(1 → 4)-*O*-β-D-galactopyranosyl-(1 → 4)-D-glucose (I) and a tetrasaccharide *O*-β-D-galactopyranosyl-(1 → 4)-*O*-β-D-galactopyranosyl-(1 → 4)-*O*-β-D-galactopyranosyl-(1 → 4)-D-glucose (II) (50% combined yield). Oligosaccharides of higher molecular weight were not detected.

INTRODUCTION

Sporobolomyces singularis was isolated by Phaff and do Carmo-Sousa (1) from frass of bark beetles attacking the western hemlock (*Tsuga heterophylla*). This yeast when grown on yeast nitrogen base, a chemically defined medium (Wickerham (2)), utilized lactose but not galactose. It was shown that the galactosyl moiety, instead of occurring free in the medium, was transferred to another lactose molecule to yield a trisaccharide.

Phaff and do Carmo-Sousa showed that a yeast extract – lactose medium at pH 6 supported a more vigorous growth of the yeast, but did not result in any oligosaccharide formation (3). When the pH of the latter medium was adjusted initially to 3.75 the yield of the trisaccharide increased to substantial levels and a tetrasaccharide appeared. The tetrasaccharide is formed preferentially at pH values slightly higher than that optimal for trisaccharide formation.

The oligosaccharides thus formed were fractionated on a charcoal column to give a crystalline trisaccharide and an amorphous tetrasaccharide. The trisaccharide contained galactose and glucose. The latter was shown to be the reducing end-unit by acid hydrolysis before and after sodium borohydride reduction. Partial hydrolysis yielded 4-*O*-β-D-galactopyranosyl-D-galactose (4) and lactose, but in low yield. The *O*-β-D-galactopyranosyl-(1 → 4)-*O*-β-D-galactopyranosyl-(1 → 4)-D-glucose (I) structure indicated by these data was confirmed by conversion to *O*-β-D-galactopyranosyl-(1 → 4)-*O*-β-D-galactopyranosyl-(1 → 2)-D-erythritol (IV) by lead tetraacetate oxidation followed by sodium borohydride reduction (5). This material consumed 4 moles of sodium periodate and released 1 mole of acid.

The tetrasaccharide contained galactose and a glucose reducing end-unit, which was linked in the 4-position as shown by its lead tetraacetate oxidation characteristics (6). The oxidation was carried out on a larger scale and the product reduced with sodium borohydride. The resulting polyol appeared to be *O*-D-galactopyranosyl-(1 → 4)-*O*-D-galactopyranosyl-(1 → 4)-*O*-D-galactopyranosyl-(1 → 2)-D-erythritol since it consumed 5 moles of sodium periodate with concomitant formation of 1 mole of acid. Its specific rotation, which was close to that of galactobiosyl erythritol, suggested β-linkages. The identity of two of the three linkages in the tetrasaccharide was confirmed by prolonged oxidation

Canadian Journal of Chemistry. Volume 42 (1964)

[1]*Issued as N.R.C. No. 7869.*
[2]*Department of Food Science and Technology, University of California, Davis, California.*

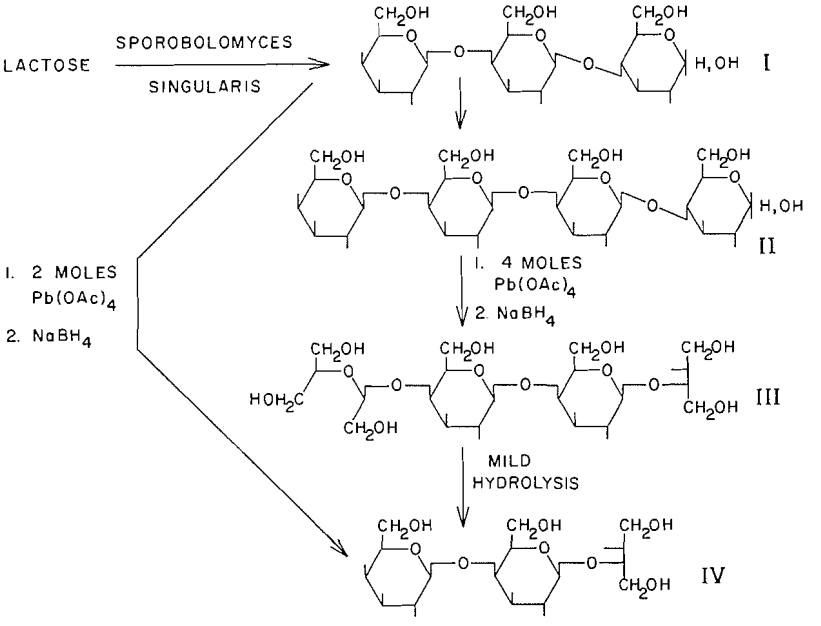

with lead tetraacetate to give a trialdehyde. This was reduced with sodium borohydride to a polyol (III) which was partly hydrolyzed (7) to *O*-β-D-galactopyranosyl-(1 → 4)-*O*-β-D-galactopyranosyl-(1 → 2)-D-erythritol (IV). It was shown that the other linkage in the tetrasaccharide was 1,4 as follows. Oxidation of the galactotriosyl erythritol with periodic acid gave a product which was reduced with sodium borohydride. The polyol was hydrolyzed to erythritol and glycerol, which were compared by gas-phase chromatography as their acetates and shown to be present in equimolar amounts. The tetrasaccharide fraction therefore contained, as a major component, the galactotriosyl glucose structure represented by II.

β-Transglycosyl activity of *Sporobolomyces singularis* under these conditions appears to be quite specific: a galactosyl moiety was transferred to the free 4-hydroxy group of lactose, the predominant sugar in the medium. The trisaccharide thus formed in turn contains a free 4-position which could be substituted with another galactose residue.

The final products have different structures from earlier reactions carried out using β-galactosidases. In general *O*-β-D-galactopyranosyl-(1 → 6)-*O*-β-D-galactopyranosyl-(1 → 4)-D-glucose has been found to be the main product. Pazur and co-workers (8, 9) have isolated this trisaccharide using a yeast lactase preparation. With culture filtrates or cell-free extracts of *P. chrysogenum*, appreciable quantities of this trisaccharide have been prepared by Ballio and Russi (10). When glucose was used as the acceptor, Wallenfels and co-workers (11) have shown with *E. coli* that the 1,6 link is formed in preference to 1,3 and 1,4 links. The only report of preferential synthesis of galactosyl glucoses, other than the 1,6 form has been that of Wallenfels and Fischer (12), who showed that a calf intestine enzyme synthesized 1,3 and 1,4 links rather than the 1,6 link.

The enzyme responsible for the transgalactosylation reaction appears to be associated with the cells. This fact may be responsible for the more quantitative nature of the transgalactosylation reaction in this system than that studied with soluble lactase preparations. Particularly at low pH values, it may be presumed that the galactosyl–enzyme complex,

Can. J. Chem. Downloaded from www.nrcresearchpress.com by 210.87.254.105 on 09/05/12
For personal use only.

formed after one molecule of lactose is cleaved, remains intact until a second molecule of lactose approaches this site. At this stage the galactosyl moiety is transferred to lactose rather than to water. A second galactosyl–enzyme complex could be responsible for transferring an additional galactosyl unit to the trisaccharide, thereby forming a tetrasaccharide.

EXPERIMENTAL

Production of Oligosaccharides

The organism was grown on a medium containing 10% lactose and 0.75% Difco yeast extract. Inoculum was grown in 500 ml Erlenmeyer flasks containing 100 ml medium at 24° C on a Gump shaker (240 r.p.m., 1 inch eccentricity). Cultures 24–28 hours old (100 ml inoculum) were used to inoculate a 5-liter New Brunswick stirred fermentor containing 3 liters of medium at pH 3.75. Initial adjustment of the pH was essential. At pH values above 4, no oligosaccharides were obtained. The incubation temperature was 22° C, air flow rate 1 liter/minute and stirring speed 375 r.p.m. The progress of the fermentation was followed by means of paper chromatography, using ethyl acetate – acetic acid – water (6:2:2 v/v) as solvent and the silver nitrate – alkali dip reagent (13) for detection of the sugars. The process was complete in 3–4 days. The supernatant liquid was recovered by centrifugation and decolorized with activated charcoal (Darco G-60).

Isolation of Oligosaccharides

A portion of the filtered material corresponding to a starting weight of 35 g lactose was fractionated on a column of Darco G-60:Celite 545 (200 g:200 g) (14). This was washed with water, then 5% ethanol which eluted galactose and glucose (trace). Ethanol, 10%, eluted some lactose, then two oligosaccharides moving at a slightly faster rate than lactose on paper chromatograms. Later fractions contained the trisaccharide. Ethanol, 15%, removed the rest of the trisaccharide so that in all 12.0 g were obtained. Increasing the concentration to 20% developed the tetrasaccharide (5.1 g) and later fractions were contaminated with a paper chromatographically slower-moving sugar.

A more quantitative analysis was carried out by cellulose column chromatography. *n*-Butanol, one-half saturated with water, eluted galactose (0.25 g) and a trace of glucose. Acetone–water (4:1 v/v) gave lactose and a disaccharide which ran a little faster (0.64 g), trisaccharide (2.11 g), tetrasaccharide (1.17 g), and a material running slightly slower than the tetrasaccharide (0.21 g).

Characterization of the Trisaccharide (I)

The trisaccharide crystallized from 90% aqueous methanol, yielding a first crop of 5.1 g and a second crop of 2.0 g. Recrystallization from the same solvent gave material with m.p. 228–231° C and $[\alpha]_D$ +68° → +45° (*c*, 1.0, H_2O). Calculated for $C_{18}H_{32}O_{16}$: C, 42.9; H, 6.4. Found: C, 42.6; H, 6.45%.

Hydrolysis at 100° C for 3 hours in *N* sulphuric acid gave galactose and glucose on a paper chromatogram (solvent, butanol–pyridine–water 3:1:1; spray, *p*-anisidine hydrochloride (15)). A portion of the trisaccharide (5 mg) was reduced with sodium borohydride (5 mg) in water (5 cc) for 3 hours. The product on acid hydrolysis gave galactose only on a paper chromatogram with the reducing sugar spray.

The trisaccharide (1.0 g) was partially hydrolyzed in *N* sulphuric acid (5 ml) at 80° C for 45 minutes. The solution was neutralized ($BaCO_3$), filtered, and evaporated. Examination on a paper chromatogram in ethyl acetate – acetic acid – water (9:2:2 v/v) showed the presence of two disaccharides. These were separated on Whatman No. 3 paper sheets in an identical solvent to give lactose (72 mg) (m.p. and mixed m.p. 197–201° C after two recrystallizations from methanol) and faster running 4-*O*-β-D-galactopyranosyl-D-galactose (80 mg). The latter was recrystallized twice from methanol–ethanol to give material (10 mg) which had an X-ray powder diagram identical with an authentic specimen (4).

Lead tetraacetate oxidation showed the reducing end of the trisaccharide to be linked in the 4-position (6), since 0.19, 0.48, and 1.08 moles of oxidant were consumed after 2, 5, and 15 minutes respectively.

The trisaccharide (1.0 g) was oxidized with lead tetraacetate (2 moles) in acetic acid (100 ml), containing water (2 ml). After 1 hour the reaction mixture was treated with oxalic acid (2 moles) in acetic acid. The lead oxalate which formed was filtered off, and residual lead tetraacetate removed by addition of ethylene glycol (0.5 ml). Evaporation yielded a residue which was treated with sodium borohydride (1.0 g) in water (50 ml). After 1 hour excess reagent was destroyed with acetic acid and Amberlite IR120 was added to the solution. Filtration and evaporation gave a material from which boric acid was removed by repeated addition and evaporation of methanol. The resulting polyol mixture was fractionated on a cellulose column using acetone–water (6:1 v/v) as solvent. *O*-β-D-Galactopyranosyl-(1 → 4)-*O*-β-D-galactopyranosyl-(1 → 2)-D-erythritol (0.37 g) was obtained and two recrystallizations from methanol gave material with m.p. 180–183° C and $[\alpha]_D$ +13° (*c*, 1.0, H_2O). Calculated for $C_{16}H_{30}O_{14}$: C, 43.05; H, 6.8. Found: C, 43.1; H, 6.8%. The polyol consumed 3.23, 3.70, 3.97, and 4.26 moles of sodium periodate releasing 0.85, 0.97, 1.07, and 1.19 moles of acid after 1, 3, 5, and 23 hours respectively.

Characterization of the Tetrasaccharide (II)

Using methods identical with those used with the trisaccharide, the tetrasaccharide was shown to contain galactose and a glucose-reducing end. The tetrasaccharide had $[\alpha]_D$ +43° (*c*, 1.2, H_2O) and when oxidized

Can. J. Chem. Downloaded from www.nrcresearchpress.com by 210.87.254.105 on 09/05/12
For personal use only.

with lead tetraacetate it consumed 0.47, 0.86, and 1.59 moles of oxidant after 2, 5, and 15 minutes respectively. The gradual uptake showed that the reducing end was 1,4-linked.

The tetrasaccharide was converted to its corresponding erythritol derivative by lead tetraacetate oxidation followed by sodium borohydride reduction by the method described above. For fractionation of the product on a cellulose column acetone–water (5:1 v/v) eluant was used. The product (0.41 g from 0.80 g starting material) was amorphous and had $[\alpha]_D$ +19° (*c*, 1.0, H_2O). On periodate oxidation it consumed 3.80, 4.40, 4.58, and 5.07 moles of oxidant after 1, 2.5, 4, and 23 hours respectively with concomitant formation of 0.85, 1.06, 1.13, and 1.23 moles of acid. Since these data showed that the two central units of the tetrasaccharide can be linked either 1,2 or 1,4 the following experiment was carried out.

The erythritol derivative (30 mg) was oxidized overnight in water (5 ml) containing periodic acid (100 mg). The reagent was then destroyed with barium carbonate and the solution filtered. The oxidation product was then reduced, with sodium borohydride (100 mg), and the reaction mixture worked up as previously described in this section. The resulting polyol was hydrolyzed by heating for 3 hours at 100° C in *N* sulphuric acid (1 ml). The acid was neutralized ($BaCO_3$) and the solution filtered and evaporated. The product contained erythritol and glycerol, but no hexose. The relative proportion of these polyols was compared by acetylation (hot NaOAc–Ac_2O method) and gas–liquid chromatography (G.L.C.) of the acetates at 150° C on a column of 2% LAC-IR296 on Chromosorb W. In terms of peak areas the glycerol and erythritol acetates were present in the ratio 1.67:1, respectively. When a similar experiment was carried out with galactobiosyl erythritol the polyol mixture on acetylation and G.L.C. examination gave peak areas of 3.63:1 for the glycerol and erythritol acetates. The erythritol:glycerol ratio was 2.2 times that obtained from the galactobiosyl erythritol mixture. This shows the central units of the tetrasaccharide to be 1,4-linked and the structure of the tetrasaccharide to be mainly *O*-D-galactopyranosyl-(1 → 4)-*O*-D-galactopyranosyl-(1 → 4)-*O*-D-galactopyranosyl-D-glucose.

O-β-D-Galactopyranosyl-(1 → 4)-O-β-D-galactopyranosyl-(1 → 2)-D-erythritol (IV) from O-β-D-Galactopyranosyl-(1 → 4)-O-β-D-galactopyranosyl-(1 → 4)-O-β-D-galactopyranosyl-(1 → 4)-D-glucose (II)

The tetrasaccharide (0.90 g) was dissolved in water (5 ml) and treated with lead tetraacetate (3.6 g) in acetic acid (250 ml). After 15 hours ethylene glycol (0.5 ml) was added, followed by oxalic acid (0.9 equivalents) in acetic acid (25 ml). The precipitate which formed was removed by filtration and the filtrate evaporated to dryness. A solution of sodium borohydride (1.0 g) in water (25 ml) was added and the reduction allowed to proceed for 2 hours. Excess reagent was then destroyed with acetic acid and the reduction product (III) was obtained by the method described previously in this section. On a paper chromatogram it ran slightly faster than galactobiosyl erythritol (solvent, acetone–water 4:1 v/v; spray, ammoniacal silver nitrate). Only a small amount of galactotriosyl erythritol was present.

The oxidized tetrasaccharide derivative was hydrolyzed at 60° C overnight in 0.1 *N* hydrochloric acid (25 ml). The solution was then neutralized (Ag_2CO_3), filtered, and the filtrate evaporated to a crust. This was fractionated on a cellulose column using acetone–water (4:1 v/v) as solvent. Galactobiosyl erythritol (0.30 g) was obtained and this was recrystallized twice from aqueous methanol to yield a product with m.p. 186–188° C and $[\alpha]_D$ +17° (*c*, 1.0, H_2O). Calculated for $C_{16}H_{30}O_{14}$: C, 43.05; H, 6.8. Found: C, 42.9; H, 6.8%. The X-ray diffraction patterns of the product and authentic material were identical.

ACKNOWLEDGMENTS

The authors wish to thank Miss E. Barker of the Department of Food Science and Technology, University of California, Davis, and Mr. N. R. Gardner for technical assistance. Thanks are due also to Mr. M. Mazurek for carrying out carbon and hydrogen analyses, and Mr. W. C. Haid for preparing X-ray crystal patterns.

REFERENCES

1. H. J. PHAFF and L. DO CARMO-SOUSA. Antonie Van Leeuwenhoek, J. Microbiol. Serol. **28**, 193 (1962).
2. L. J. WICKERHAM. Taxonomy of yeasts. U.S. Dept. Agr. Tech. Bull. 1029 (1951).
3. H. J. PHAFF and L. DO CARMO-SOUSA. Unpublished work.
4. J. K. GILLHAM, A. S. PERLIN, and T. E. TIMELL. Can. J. Chem. **36**, 1741 (1958).
5. A. J. CHARLSON, P. A. J. GORIN, and A. S. PERLIN. Can. J. Chem. **34**, 1811 (1956).
6. A. J. CHARLSON and A. S. PERLIN. Can. J. Chem. **34**, 1200 (1956).
7. I. J. GOLDSTEIN, G. W. HAY, B. A. LEWIS, and F. SMITH. Abstracts of Papers, 135th Meeting of the American Chemical Society, Boston, Mass. April, 1959. p. 3D.
8. J. H. PAZUR. Science, **117**, 355 (1953).
9. J. H. PAZUR. J. Biol. Chem. **208**, 439 (1954).
10. A. BALLIO and S. RUSSI. Tetrahedron, **9**, 125 (1960).
11. K. WALLENFELS, D. BECK, and J. LEHMANN. Unpublished work. *Cited in* Advan. Carbohydrate Chem. **16**, 255 (1961).
12. K. WALLENFELS and J. FISCHER. Z. Physiol. Chem. **321**, 223 (1960).
13. W. E. TREVELYAN, D. P. PROCTER, and J. S. HARRISON. Nature, **166**, 444 (1950).
14. R. L. WHISTLER and D. F. DURSO. J. Am. Chem. Soc. **72**, 677 (1950).
15. L. HOUGH, J. K. N. JONES, and W. H. WADMAN. J. Chem. Soc. 1702 (1950).

Can. J. Chem. Downloaded from www.nrcresearchpress.com by 210.87.254.105 on 09/05/12
For personal use only.

Can. J. Chem. Downloaded from www.nrcresearchpress.com by 210.87.254.5 on 09/05/12
For personal use only.

MULTISTAGE DEACTIVATION IN THE PHOTOLYSIS OF HEXAFLUOROACETONE[1]

A. N. STRACHAN,[2] R. K. BOYD,[3] AND K. O. KUTSCHKE
Division of Pure Chemistry, National Research Council, Ottawa, Canada

Received December 23, 1963

ABSTRACT

In principle the vibrationally excited molecule in an upper electronic state, formed by absorption in the ultraviolet region of the spectrum, can attain vibrational equilibrium by two mechanisms. In most discussions of this degradation of vibrational energy it has been considered that the data are represented adequately by a single-step deactivation from high to low vibrational levels rather than by a multistep cascade from one group of vibrational levels to the next lower group. The present work suggests new treatments of the experimental data by which it is possible to distinguish between the single- and the multi-step deactivation processes. It is demonstrated that the literature data on the quantum yield for the decomposition of hexafluoroacetone is better interpreted in terms of a multistep deactivation. Some new data are presented which support this conclusion.

Methods to evaluate the efficiencies as deactivating agents of added inert gases are discussed. It is suggested that the deactivation of excited hexafluoroacetone by hydrocarbons might involve chemical rather than, or in addition to, purely physical quenching.

A few measurements were made of the rate of formation of carbon monoxide during the photolysis of hexafluoroacetone in the absence and presence of isobutane. In attempting to interpret these data in terms of the accepted mechanisms, some conclusions were reached concerning the deactivation processes occurring in the photolysis. These conclusions, which are supported by data already in the literature, are of more general interest and are reported here in some detail. The present report is, therefore, largely a reinterpretation of some of the details of the mechanism of the primary process of the photolysis; the few experimental results which give rise to this reconsideration form a relatively minor part of the report. Consequently experimental details are not given although some new results are recorded.

The major conclusion reached is that, contrary to opinions expressed elsewhere (1), there exist several graphical tests which can be used to decide whether deactivation in the upper electronic state reached by absorption involves a single-step process producing electronically excited molecules in low-lying vibrational levels from which dissociation does not occur, or whether a multistep cascade down the vibrational energy levels is involved. Existing data on the photolysis are better interpreted in terms of the cascade process. This conclusion has some bearing on the interpretation of data taken to show the deactivating effect of added gases; this also will be discussed in some detail. In addition a few remarks are offered on the mechanism responsible for the fluorescence observed in this photolysis.

PHOTOLYSIS PRODUCTS

Photoexcitation of hexafluoroacetone in the first absorption band near 3000 Å yields hexafluoroethane and carbon monoxide as photolysis products (2). There is no question that CF_3 radicals are involved (2, 3, 4) and the experiments in the presence of nitric oxide

[1]*Issued as National Research Council No. 7878.*
[2]*Visiting Scientist, Summer, 1961. Permanent address: Department of Applied Chemistry, College of Technology, Loughborough, Leics., England.*
[3]*National Research Council Postdoctoral Fellow 1962–64.*

(4) suggest that no intramolecular formation of C_2F_6 occurs although this latter point has not been definitely established. The relative instability of the trifluoroacetyl radical and the absence of abstractive attack on the ketone molecule permits the use of the quantum yield for the formation of carbon monoxide as a measure of that for decomposition of the molecule.

In earlier work (2, 5) the ratio $R_{C_2F_6}/R_{CO}$ has been taken as unity within experimental error; actually the average values reported are closer to 0.96 and are essentially independent of conditions. An explanation of this observation might be based on the detection (6) of $(CF_3)_3COCF_3$ as a reaction product although the deviation from unity of the ratio of the data in Table I is rather larger than might be expected on the basis of Gordon's rate

TABLE I

C_2F_6/CO ratio in photolysis CF_3COCF_3

Temp., ° C	99.5	105.5	101.5	53.5
$[CF_3COCF_3]$, mm	67	51.5	46.0	46.2
Time, minutes	60	5	3	20
CO, μmole	33.2	3.12	4.61	16.0
C_2F_6, μmole	31.4	3.01	4.45	15.2
C_2F_6/CO	0.94_6	0.96_5	0.96_5	0.95_0
Filter	Pyrex	Pyrex	Quartz	Vycor

constants. That trifluoromethyl radicals are capable of rapid addition to carbonyl bonds is supported by the large decrements in material balance found when hexafluoroacetone was photolyzed in the presence of pivaldehyde or of *t*-butyl formate (7).

The evidence discussed above suggests that for most reaction conditions it is valid to assume that each molecule which decomposes yields one molecule of carbon monoxide so that the quantum yield of dissociation (ϕ) can be taken as R_{CO}/I_a.

DEACTIVATION IN THE PHOTOLYSIS

It has been well established (2, 8) that ϕ is a function of temperature, and of the concentration of ketone and that of other gases which might be present. Mechanisms to explain these effects have been advanced (2, 8). Giacometti, Okabe, and Steacie ((8); referred to as GOS) modified the original mechanism of Ayscough and Steacie ((2); referred to as AS). The modified mechanism is as follows.

$$A + h\nu \rightarrow {}^1A_n \quad [1]$$

$${}^1A_n \rightarrow \text{products} \quad [2]$$

$${}^1A_n + A \rightarrow {}^1A_0 + A \quad [3]$$

$${}^1A_0 \rightarrow A + h\nu^1 \quad [4]$$

$${}^1A_0 \rightarrow {}^3A_0 \quad [5]$$

$${}^3A_0 \rightarrow \text{products} \quad [6]$$

$${}^3A_0 \rightarrow A \quad [7]$$

A represents a molecule of hexafluoroacetone in the ground electronic state, ${}^1A_n$ is a molecule in the *n*th vibrational level of the upper singlet state, ${}^1A_0$ is a molecule in a low-lying, non-dissociating vibrational level of that singlet state, and ${}^3A_0$ is a molecule in a

Can. J. Chem. Downloaded from www.nrcresearchpress.com by 210.87.254.5 on 09/05/12
For personal use only.

low-lying vibrational level of an upper triplet state from which dissociation can occur with an activation energy. This mechanism requires that

$$(1-\phi)^{-1} = (1-\phi_\infty)^{-1} + (1-\phi_\infty)^{-1} k_2/k_3[\mathrm{A}] \qquad [\mathrm{i}]$$

in which $\phi_\infty = k_5k_6/(k_4+k_5)(k_6+k_7)$ and thus represents the quantum yield at infinite concentration of deactivating species.

Plots of the AS data, taken at 3130 Å, and of the GOS data, with 2640 Å excitation, show positive intercepts greater than unity as required by [i]. Evaluation of ϕ_∞ from the intercept of [i] is subject to large uncertainties because of the algebraic form involved. Nevertheless the values obtained are in good agreement with those derived from purely empirical plots of ϕ or ϕ^{-1} vs. $[\mathrm{A}]^{-1}$ in which the algebraic form of the quantities plotted does not lead to a magnification of errors. In those cases where data are available to check the point, the value of the intercept appears to be essentially independent of exciting wavelength at a given temperature.

Equation [i] requires that $(1-\phi)^{-1}$ vs. $[\mathrm{A}]^{-1}$ remain linear while the data show a pronounced upward curvature at low concentrations. Unfortunately, the algebraic form magnifies the experimental errors in the region of greatest curvature since ϕ approaches unity as [A] approaches zero. However, the consistency of the trend at all temperatures and wavelengths suggests that the curvature is not an experimental artifact. Such curvature might be a consequence of multistep deactivation from the nth vibrational level of the upper electronic state, which level is reached by absorption, to the lower vibrational levels from which the emission is thought to occur (8). If k_2/k_3 can be defined for each vibrational level, and if molecules in the zeroth, or highest non-dissociating, vibrational level undergo only reactions [4] and [5] suggested by GOS, then it can be shown that

$$(1-\phi)^{-1} = (1-\phi_\infty)^{-1} + (1-\phi_\infty)^{-1}\{[\textstyle\prod_{i=1}^{n}(1+p_i[\mathrm{A}]^{-1})]-1\} \qquad [\mathrm{ii}]$$

in which $p_i = k_{2,i}/k_{3,i}$. Porter and Connelly (9) give a detailed discussion of the concepts involved. The bracketed portion of [ii] is a power series in $[\mathrm{A}]^{-1}$, of which the first term is $\sum_{i=1}^{n} p_i[\mathrm{A}]^{-1}$, so that [ii] gives a qualitatively correct description of the observations.

Several other tests can be suggested to determine whether or not such multistep deactivation is required by the data. Porter and Connelly (9) use the occurrence of a point of inflection at low values of [A] in a plot of ϕ^{-1} vs. [A] as such a criterion; if $n = 1$, corresponding to a single step deactivation, plots of ϕ^{-1} vs. [A] have a finite initial slope ($\lim_{[\mathrm{A}]\to 0} (d\phi^{-1}/d[\mathrm{A}]) = (1-\phi_\infty)/p_1$), whereas if $n > 1$ the initial slope is zero. While the sensitivity of this test is not great, in the sense that experimental data are required at quite low pressures, the test uses experimental quantities directly. Other tests are proposed below which are more sensitive, in that trends are discernible at higher pressures; however, the algebraic forms involved are such as to amplify the experimental errors.

The characteristics of some plots used in such tests are summarized here.

$$g \equiv (\phi-\phi_\infty)/(1-\phi) = k_2/k_3[\mathrm{A}] \qquad \text{if } n = 1,$$
$$= [\textstyle\prod_{i=1}^{n}(1+p_i[\mathrm{A}]^{-1})]-1 \qquad \text{if } n > 1.$$

Plots of g vs. $[\mathrm{A}]^{-1}$ are predicted to be linear to $g = \infty$ if $n = 1$, but curve upward rapidly as $[\mathrm{A}]^{-1}$ increases ($dg/d[\mathrm{A}]^{-1} \to \infty$) if $n > 1$. Curvature is noted in the AS and GOS data at values of [A] and ϕ which are such that the experimental errors in the data should not introduce too large an error in g. Such plots require a determination of ϕ_∞, which also contributes to the uncertainties, but that particular contribution is minimal in the region

Can. J. Chem. Downloaded from www.nrcresearchpress.com by 210.87.254.5 on 09/05/12
For personal use only.

of greatest curvature. The function g is readily differentiated graphically. Plots of g[A] vs. [A]$^{-1}$ are nearly linear for the AS data; this near linearity cannot be taken to prove that $n = 2$ in this system since the AS data do not extend to sufficiently low pressures.

$$f_1 = (1-\phi)[\mathrm{A}]^{-1} = (1-\phi_\infty)/([\mathrm{A}]+p_1) \qquad \text{for } n = 1$$
$$= (1-\phi_\infty)[\mathrm{A}]^{-1}/\prod_{i=1}^{n}(1+p_i[\mathrm{A}]^{-1}) \qquad \text{for } n > 1.$$

If $n = 1$, plots of f_1 vs. [A] start at $f_1 = (1-\phi_\infty)/p_1$ for [A] = 0 and decrease smoothly to zero as [A] $\rightarrow \infty$; the slope is always negative ($\lim_{[\mathrm{A}]\rightarrow 0} df_1/d[\mathrm{A}] = -(1-\phi_\infty)/p_1^2$) and continuously decreases in magnitude as [A] increases. On the other hand, if $n > 1$, $\lim_{[\mathrm{A}]\rightarrow 0} f_1 = 0$, and the function increases with [A] for small [A], passes through a maximum at a value of [A] such that $\sum_{i=1}^{n} p_i/([\mathrm{A}]+p_i) = 1$, and then decreases to approach $f_1 = 0$ asymptotically as [A] $\rightarrow \infty$. The condition for the maximum in plots of f_1 vs. [A] is such that the concentration at which the maximum appears is larger if n is greater, i.e. if more collisions are required for deactivation to a non-dissociating level of the upper singlet state. An increase in n can be achieved experimentally by doing the photolysis at a higher temperature or at a shorter wavelength. The shift of the maximum to larger concentrations is readily apparent in plots of the AS data (3130 Å; T = 27, 53, 78, and 107° C) and the GOS data (2640 Å; T = 27 and 53° C); such plots are shown in Fig. 1.

The effect of temperature on the position of the maximum probably is the result of two phenomena. (1) Because of the greater population of vibrationally excited molecules in the ground electronic state at higher temperatures and the fact that the photon energy absorbed from a monochromatic beam is independent of temperature, higher vibrational levels of the upper electronic state are reached by absorption. Hence n is larger at higher temperature. This effect will depend exponentially on temperature. (2) Each p_i increases as temperature increases; this increase probably is also exponential. Hence the value of [A] which satisfies the condition for the maximum must be larger at higher temperature. It is not easy to decide unambiguously which of the two effects is the more important or if they are of similar importance.

It might be pointed out that in plots of f_1 vs. [A], $\lim_{[\mathrm{A}]\rightarrow 0} df_1/d[\mathrm{A}] = (1-\phi_\infty)/p_1p_2$ (i.e. > 0) if $n = 2$, whereas if $n > 2$, $\lim_{[\mathrm{A}]\rightarrow 0} df_1/d[\mathrm{A}] = 0$. Therefore there will be a point of inflection if $n > 2$ which is absent if $n = 2$. It is doubtful whether experimental data can be obtained to demonstrate the existence of this point of inflection in an unambiguous way; rather low pressures would be required and such data are suspect because of possible surface effects.

Plots might also be made of f_1 vs. [A]$^{-1}$; a maximum is predicted to occur at a concentration defined by the same condition as that cited above for plots of f_1 vs. [A]. The characteristics of such a plot are that $f_1 = 0$ for [A]$^{-1} = 0$ regardless of the value of n; the initial slope is also independent of n and is equal to $1-\phi_\infty$. f_1 approaches an asymptotic value of $(1-\phi_\infty)/p_1$ for large values of [A]$^{-1}$ if $n = 1$, but passes through a maximum and returns to $f_1 = 0$ at [A]$^{-1} = \infty$ if $n > 1$. The AS data show these broad maxima at 107° and 78° C but the maxima are not distinguishable in the data taken at 53° and 27° C; the plots of the latter data can be interpreted equally well in terms of an approach to an asymptotic value. In plots of any function against [A]$^{-1}$ the data taken at low pressures, which are the least reliable, are emphasized. It might also be noted that values of ϕ_∞ determined from estimates of the initial slopes of f_1 vs. [A]$^{-1}$ are in good agreement with those obtained from plots of ϕ vs. [A]$^{-1}$.

Can. J. Chem. Downloaded from www.nrcresearchpress.com by 210.87.254.5 on 09/05/12
For personal use only.

The function f_1 is the first member of a family of functions defined by $f_m = (1-\phi)[A]^{-m}$. Each such function ($m = 1$, 2, etc.) has the same general shape as that described for f_1 when plotted vs. [A]. In particular, $\lim_{[A]\to 0} f_m = 0$ if $m < n$, $= (1-\phi_\infty)\prod_{i=1}^{n} p_i$ if $m = n$ and $= \infty$ if $m > n$. The predicted values of the initial slopes also depend on the relative values of m and n. A general expression for the slope, which also applies to f_1 if m is set equal to unity in the expression, can be written as $df_m/d[A] = -(1-\phi_\infty)[\prod_{i=1}^{n}([A]+p_i)]^{-1}[A]^{n-1-m}\{m-\sum_{i=1}^{n} p_i/([A]+p_i)\}$. Hence $\lim_{[A]\to 0} df_m/d[A] = 0$ if $n > m+1$, $= +(1-\phi_\infty)/\prod_{i=1}^{m+1} p_i$ if $n = m+1$, $= -(1-\phi_\infty)(\sum_{i=1}^{m} p_i^{-1})/\prod_{i=1}^{m} p_i$ if $n = m$, and $= -\infty$ if m is chosen $> n$. Provided $m > 0$, $\lim_{[A]\to 0} df_m/d[A] = 0$ regardless of the value of n. From the general expression for the slope it is obvious that the maximum is predicted to occur at a value of [A] defined by $\sum_{i=1}^{n} p_i/([A]+p_i) = m$ provided that $m < n$; if $m = n$ the maximum coincides with the intercept at [A] = 0 and if m is chosen $> n$ the function f_m increases without limit as [A] decreases.

Thus a series of plots might be made of f_1, f_2, etc. vs. [A] for a given set of data; for some function there will no longer be any indication of a maximum although one exists in plots of all functions with smaller values of m. The value of m in the function for which the maximum disappears determines a minimum value of n which is compatible with the data in the range of pressures studied. To be of real value, data should be available at quite low pressures and the possibility of surface effects must be kept in mind. The AS and GOS data are not sufficiently extensive to permit a trial of this procedure.

Similar kinds of deductions can be made from plots of the functions f_m vs. $[A]^{-1}$.

Except for the relatively insensitive test involving the detection of a point of inflection in plots of ϕ^{-1} vs. [A], each of the tests suggested above indicates that the AS data and the GOS data are interpreted better in terms of multistep deactivation than by the single-step deactivation proposed originally. It is concluded, therefore, that the multistep deactivation process occurs in this photolysis. Data currently available are insufficiently extensive to permit the determination of the number of vibrational levels involved. Some initial experiments have been done in these laboratories to obtain more extensive data and are shown in Fig. 2. The agreement with the AS data at 78° C is excellent.

Although it provides a sensitive test for the occurrence of multistage deactivation, the function f_1 is subject to large experimental uncertainties. Indeed, the error $\delta f_1/f_1$ introduced into f_1 by an uncertainty $\delta\phi/\phi$ in ϕ is greater than that in ϕ by a factor $\phi/(1-\phi)$; such a factor increases rapidly as ϕ approaches unity. It might be pointed out, however, that ϕ is near 0.7 near the maximum shown in Fig. 2; hence the magnification factor is near 2 which is not unreasonably large. Considerable random scatter is to be expected at lower pressures, of course.

Moreover, it has been brought to our attention (10) that the observable characteristics of plots of f_1 vs. [A], which are ascribed here to the occurrence of multistage deactivation, would also be seen if the quantum yield measurements were systematically too large, i.e., if the quantity measured were $w = (1+\epsilon)\phi$ rather than ϕ, even if the single-stage deactivation process were occurring. With this hypothesis a plot of $(1-w)/[A]$ is predicted to pass through a maximum at $[A] = [A]_c$ such that

$$\epsilon = [A]_c^2(1-w_\infty)/p_1(2[A]_c+p_1). \qquad [iii]$$

Such an artifact type of maximum is not predicted if the measured quantity is systematically less than the true ϕ. It might also be noted that fictitious points of inflection

Can. J. Chem. Downloaded from www.nrcresearchpress.com by 210.87.254.5 on 09/05/12
For personal use only.

Can. J. Chem. Downloaded from www.nrcresearchpress.com by 210.87.254.5 on 09/05/12
For personal use only.

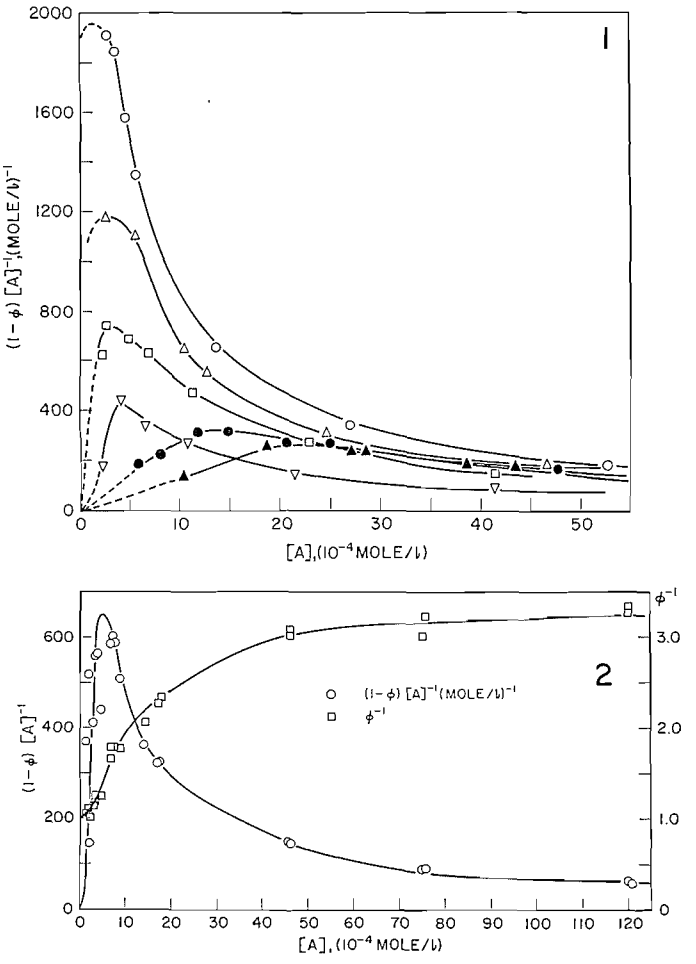

FIG. 1. Plots of $(1-\phi)/[A]$ vs. [A] for GOS and AS data. AS data at 3130 Å are open symbols; GOS data at 2640 Å are filled symbols. Circles, 27°; upright triangles, 53°; squares, 78°; inverted triangles, 107°.
FIG. 2. Plots of $(1-\phi)/[A]$ and ϕ^{-1} vs. [A]. This work, 3130 Å, 78°.

would be drawn in plots of w or w^{-1} vs. [A] if the systematic error in w were not recognized.

Attempts to determine ϵ are frustrated by the necessity of express p_1 in terms of measurable quantities. Four such expressions can be obtained from the initial slopes of plots in which the experimental data are used directly. Thus $p_1 = -(1-w_\infty+\epsilon)/s_1$, $= (1-w_\infty+\epsilon)/(1+\epsilon)^2 s_2$, $= s_3/(1-w_\infty+\epsilon)$ and $= -w_\infty^2 s_4/(1-w_\infty+\epsilon)$ where s_1 to s_4 are the initial slopes of w vs. [A], w^{-1} vs. [A], w vs. $[A]^{-1}$, and w^{-1} vs. $[A]^{-1}$, respectively. If pairs of these four expressions are equated, five quadratic equations in ϵ are obtained; in addition, each expression yields another equation for ϵ after substitution into [iii]. Some of the nine equations have only negative roots and those which yield positive roots lead to values of ϵ which extend from 0.01 to nearly unity. This great scatter arises because of the subjective errors involved in the estimation of an "initial" slope. For various reasons it appears that $s_3 \simeq 5\times10^{-4}$ mole/l. should be the most reliable of all the estimated initial

slopes. This taken together with the more directly observable $w_\infty = 0.27$ (from w vs. $[A]^{-1}$) and $[A]_e \simeq 5\times10^{-4}$ mole/l. (Fig. 2), leads to $\epsilon = 0.20$ after substitution into [iii].

Such a large value of ϵ is not consistent with other aspects of the data nor is it reasonable in view of the precautions taken in obtaining the data in Fig. 2. This is not the place to discuss those precautions; they will be considered in some detail when work now underway is reported.

The conclusion reached in this discussion is one of the first demonstrations of the occurrence of multistep deactivation in the photolysis of polyatomic molecules. Porter and Connelly (9) have discussed the photolysis of ketene and have made extensive calculations based on the theory of unimolecular reactions and the known spectroscopic properties of ketene. It is felt that such detailed considerations of the photolysis of hexafluoroacetone should await the more extensive data now being obtained.

LIGHT EMISSION

Regardless of the detailed mechanism of deactivation, the general GOS mechanism predicts that the function $(Q_\infty - Q)/Q$ (see GOS for the definition of Q; $Q_\infty = k_4/(k_4+k_5)$) should be numerically equal to the function $g = (\phi - \phi_\infty)/(1-\phi)$ for all [A]. Such numerical agreement is very nearly achieved near room temperature between the AS data on the photolysis and the GOS data on the emission; the agreement is increasingly poor as the temperature is raised. Unfortunately the two sets of data were not taken at identical temperatures in the range 25° to 110° C but it is felt that the small temperature differences do not negate the brief comments below.

As shown in Fig. 3 for data taken near 80° C, plots of $(Q_\infty - Q)/Q$ vs. $[A]^{-1}$ show a

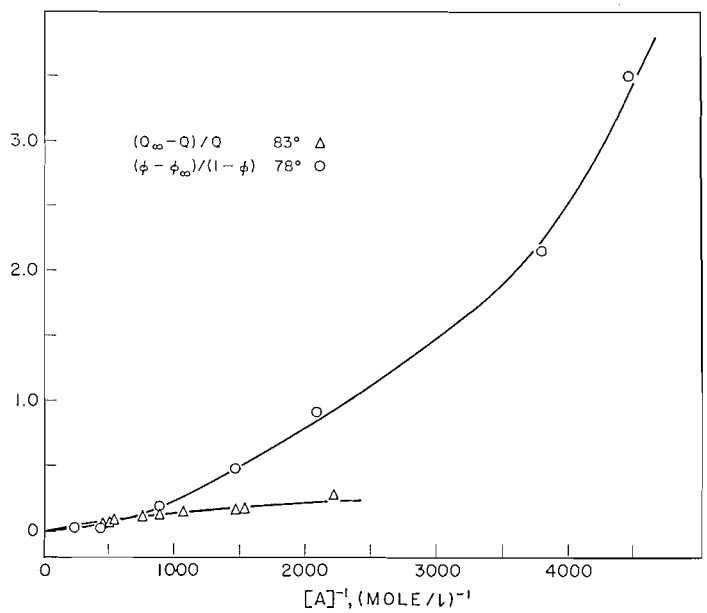

FIG. 3. Plot of $(\phi-\phi_\infty)/(1-\phi)$, AS data, and $(Q_\infty-Q)/Q$ vs. $[A]^{-1}$, GOS data. O, $(\phi-\phi_\infty)/(1-\phi)$ at 78°; Δ, $(Q_\infty-Q)/Q$ at 83°.

rather different dependence on concentration than do plots of g vs. $[A]^{-1}$. It is not our purpose to give a detailed discussion of the light emission in this system. It is, perhaps,

Can. J. Chem. Downloaded from www.nrcresearchpress.com by 210.87.254.5 on 09/05/12
For personal use only.

sufficient to note that further modifications to the mechanism probably will be required to explain these data in detail. On the other hand, estimates of the quantum yield for the emission are rather small values of the order 0.01 (8). Thus, although there might be some ambiguity in the description of the emission, such uncertainties should not affect the conclusions reached in regard to the photodecomposition.

DEACTIVATION BY ADDED GASES

If other species are present which also remove energy from the excited molecule, reaction [8] must be included in the mechanism

$$A_n + M \rightarrow A_{n-1} + M. \qquad [8]$$

The following equation then should be obeyed.

$$\phi = 1 - (1-\phi_\infty)\pi_2\pi_3^{-1}$$

Here $\pi_2 = \prod_{i=1}^{n}(1+q_i[M][A]^{-1})$, $\pi_3 = \prod_{i=1}^{n}(1+p_i[A]^{-1}+q_i[M][A]^{-1})$, p_i has the significance given earlier and $q_i = k_{8,i}/k_{3,i}$. It is possible that the value of k_8/k_3 is independent of the vibrational level involved; this is more likely to be true if M is a polyatomic species. The more exact formulation will be retained for the present.

It is the usual practice to do a series of experiments at constant temperature and incident intensity with a fixed concentration of ketone, $[A]_1$, and various concentrations of the added gas; usually it is found that the absorbed intensity does not vary with [M]. The quantum yield for these conditions at a concentration of ketone $[A]_1$ but with [M] = 0 has been given the symbol ϕ' by AS. When multistep deactivation is included the mechanism requires that $\phi' = 1-(1-\phi_\infty)\pi_1^{-1}$ where $\pi_1 = \prod_{i=1}^{n}(1+p_i[A]_1^{-1})$. Plots of ϕ'/ϕ vs. [M] were made (2), and the relative efficiencies for various gases as deactivating agents were obtained from the slopes of the straight lines drawn through the data. The mechanism outlined here predicts that ϕ'/ϕ rises from unity at [M] = 0 with a finite initial slope given in [iv].

$$S_M^0 \equiv \lim_{[M]\rightarrow 0} d(\phi'/\phi)/d[M] = ((1-\phi')/\phi')\sum_{i=1}^{n} q_i p_i [A]_1^{-2}/(1+p_i[A]_1^{-1}) \qquad [iv]$$

The slope decreases as [M] increases and ϕ'/ϕ is predicted to approach an asymptotic value of ϕ'/ϕ_∞ at large values of [M]. Physical arguments indicate that there should be no point of inflection in such curves for most conditions (see below).

Although the scatter is rather large the AS data fit this general picture. An asymptote calculated from values of ϕ_∞ ($\simeq$0.30 at 78° C) and ϕ' ($\simeq$0.67 at 78° C, $[A]_1$ = 10 mm) derived from the data taken with [M] = 0 is compatible with the plots of ϕ'/ϕ vs. [M]. Some of the data are interpreted better if ϕ_∞ obtained from a plot of ϕ vs. [A] with [M] = 0 differs from that obtained in the limit of large [M], but the data are much too scattered to reach a firm conclusion on this point.

Since plots of ϕ'/ϕ vs. [M] are curves, only the initial slopes are useful for the evaluation of relative efficiencies for deactivation of the various gases. Even these are useful only if the value of q does not depend on the vibrational level, i.e. $q_i = q$ for all $i = 1, 2, \cdots n$, so that q may be removed from within the summation sign in [iv]. Because values are not available for n and the various p_i to permit a calculation of the factor $\sum_{i=1}^{n} p_i/([A]_1+p_i)$ contained in [iv], an absolute value for q cannot be obtained unless use is made of data taken with [M] = 0. One such method for calculating q is outlined below.

When [M] = 0, it can be shown that a plot of ϕ vs. $[A]^{-1}$ is a smooth curve, with no

Can. J. Chem. Downloaded from www.nrcresearchpress.com by 210.87.254.5 on 09/05/12
For personal use only.

point of inflection, which rises from ϕ_∞ at $[A]^{-1} = 0$ to an asymptotic value of unity at $[A]^{-1} = \infty$. The slope of this curve at $[A] = [A]_1$, S_K', may be evaluated graphically or otherwise. Since the general expression for the slope is $d\phi/d[A]^{-1} = (1-\phi)[A]\sum_{i=1}^{n} p_i/([A]+p_i)$, it follows that

$$\sum_{i=1}^{n} p_i/([A]_1+p_i) = S_K'/(1-\phi')[A]_1. \qquad [v]$$

This can be combined with [iv], taking $q_i = q$ for all i, to obtain

$$q = S_M^0\phi'[A]_1^2/S_K'. \qquad [vi]$$

Several other techniques, some possibly more reliable, might be available to evaluate the unknown factors in [iv]; the one outlined was chosen for its relative simplicity.

The AS data have been recalculated using an $S_K' = 1.2\times10^{-4}$ mole/l. obtained graphically, and other data cited above. Values of q obtained are: C_4F_{10}, 0.80; C_3F_8, 0.56; C_2F_6, 0.35; CF_4, 0.33; CO_2, 0.46. The only value of q which differs significantly from those reported by AS is that for C_3F_8 for which AS approximated the curved plot of ϕ'/ϕ vs. [M] by a straight line. The straight lines drawn in AS, Fig. 5, are essentially initial slopes, except that for C_3F_8, since the point at the highest pressure of C_4F_{10}, which indicates the curvature, was omitted from their figure, and the efficiencies of the other gases are so low that the data pertain only to the initial linear portion of the curve. Thus for all the species except C_3F_8 the linear approximation used by AS is close to S_M^0 defined in [iv]. Moreover the AS method of evaluating constants in the photolysis with [M] = 0 yields values which are closely equivalent to S_K'. Thus little difference was expected between values of q calculated by [vi] and those reported by AS.

One further concept should be mentioned. It is difficult to demonstrate mathematically whether or not a point of inflection occurs in plots of ϕ'/ϕ vs. [M]. A qualitative physical argument suggests that its presence or not depends on the value of $[A]_1$ used; the argument is as follows. In a plot of ϕ^{-1} vs. [A] with [M] = 0 at least one point of inflection occurs at some value of [A], say $[A]_p$. At the concentration $[A]_p$ the frequency and efficiency of collisions between excited and ground state molecules presumably are such that deactivation is "taking over" from decomposition as the major mode of disappearance of the "average" vibrationally excited molecule. If $[A]_1$ is chosen to be much greater than $[A]_p$, it seems obvious that deactivation by ketone will continue to keep the system on the "deactivation side" of $[A]_p$ regardless of how inefficient M might be as a deactivating agent. On the other hand, if $[A]_1$ is chosen to be less than $[A]_p$, the same type of argument predicts the existence of a point of inflection in the plots of ϕ'/ϕ vs. [M]. If $[A]_1$ is only slightly less than $[A]_p$ the point of inflection would be difficult to observe if q were large but might be detectable for those M which have a small value of q.

As is demonstrated in Fig. 2, the point of inflection in the plot of ϕ^{-1} vs. [A] for [M] = 0 at 78° C with excitation by 3130 Å occurs at a value of [A] somewhat larger than 5 mm and perhaps as large as the 10 mm which AS used as $[A]_1$. A point of inflection can be identified tentatively in the AS data for C_2F_6, CF_4, and CO_2 for which q is small, but is not discernible in the data involving C_4F_{10} and C_3F_8 for which q is relatively large. Obviously much more data are required before this point can be clarified experimentally.

DEACTIVATION BY HYDROCARBONS

The few data which stimulated the considerations discussed above are recorded in Table II. If these data are treated by the methods outlined in connection with [vi] above, the value of q obtained for isobutane is at least as great as 30 and may be a factor of two

Can. J. Chem. Downloaded from www.nrcresearchpress.com by 210.87.254.5 on 09/05/12
For personal use only.

TABLE II

Effect of isobutane

$[CF_3COCF_3]$ = 46.5 mm; $T = 54 \pm 1°$ C; Vycor filter

[Isobutane] mm	0	4.08	8.53	17.06
Time, minutes	20	10	20	20
CO, μmole	16.0	2.90	5.26	4.58
ϕ'/ϕ*	1.0	2.76	3.04	3.49

*ϕ'/ϕ = ratio of the quantum yields of CO formation in the absence (ϕ') and presence (ϕ) of isobutane.

or three greater. The uncertainty arises in the estimate of $S_M{}^0$, which, because of the steepness of the extrapolated curve, might be grossly in error; the value of 30 was obtained by using a line joining the point at the lowest pressure of isobutane to the origin of the curve. Values of S_K' and ϕ' were taken from the GOS data at 53° C since the exciting wavelength used in that study is more representative, on the basis of energy, of the wavelength used to obtain the data in Table II. If S_K' and ϕ' for 3130 Å excitation were to be used, even larger values would be calculated for the q of isobutane.

This surprisingly large value cannot be considered to be established in view of the paucity of the data available. Nor can it be reconciled readily with concepts of collisional deactivation (physical quenching), which would predict a value near unity. However, similarly large values can be calculated for the efficiency for deactivation by benzene and toluene from the data obtained by Holmes and Kutschke (11). A possible explanation of these large values might be based on the occurrence of a chemical reaction between excited ketone molecules (precise excited state unspecified) and the hydrocarbon. Such chemical quenching is known to exist in several systems (12, 13).

ACKNOWLEDGMENT

Discussions of some of the details involved in this problem with various members of the staff of these laboratories have been of great benefit to the authors. They are particularly grateful for the views expressed by Dr. R. A. Back.

REFERENCES

1. D. J. Wilson, B. Noble, and B. Lee. J. Chem. Phys. **34**, 1392 (1961).
2. P. B. Ayscough and E. W. R. Steacie. Proc. Roy. Soc. London, Ser. A, **234**, 476 (1956).
3. P. B. Ayscough. J. Chem. Phys. **24**, 944 (1956).
4. B. G. Tucker and E. Whittle. Proc. Chem. Soc. 93 (1963).
5. P. B. Ayscough, J. C. Polanyi, and E. W. R. Steacie. Can. J. Chem. **33**, 743 (1955).
6. A. S. Gordon. J. Chem. Phys. **36**, 1330 (1962).
7. A. N. Strachan and K. O. Kutschke. Unpublished work.
8. G. Giacometti, H. Okabe, and E. W. R. Steacie. Proc. Roy. Soc. London, Ser. A, **250**, 287 (1959).
9. G. B. Porter and B. T. Connelly. J. Chem. Phys. **33**, 81 (1960).
10. G. B. Porter. Private communication.
11. J. L. Holmes and K. O. Kutschke. Trans. Faraday Soc. **58**, 333 (1962).
12. I. M. Whittemore and M. Szwarc. J. Phys. Chem. **67**, 2492 (1963).
13. G. B. Porter. J. Chem. Phys. **32**, 1587 (1960).

Can. J. Chem. Downloaded from www.nrcresearchpress.com by 210.87.254.5 on 09/05/12
For personal use only.

Can. J. Chem. Downloaded from www.nrcresearchpress.com by 210.87.254.5 on 09/05/12
For personal use only.

THE BEHAVIOR OF LEAD ELECTRODES IN SULPHURIC ACID SOLUTIONS[1]

K. EKLER
Department of Chemistry, Loyola College, Montreal, Quebec
Received August 1, 1963

ABSTRACT

Lead electrodes were anodically etched in NH_2SO_3H. Immersion potentials, self-passivation potentials, passivation times, PbO_2/O_2 potential, and the potential of the first discharge plateau were determined in H_2SO_4 solutions ranging from 0.5 to 20.0 *N* and were found to be concentration-dependent. Interruption of the anodizing current had no detectable influence on passivation time. Data obtained with the anodizing current turned on fall into three categories; those obtained with (1) short-immersion anodes, (2) anodes which had reached a hydrogen-like potential, and (3) anodes which were self-passivated before the current was switched on. An inflection in the relation between potential and time during charging was investigated. Its length was dependent upon acid concentration and current density, while its potential was $+300 \pm 30$ mv, and seemed to correspond to the self-passivation potential. The lengths of the first and second discharge plateaus increased with the number of coulombs passed and were dependent upon acid concentration, but were identical for electrodes treated by four different methods. The hydrogen-like potential appeared to be due to the presence of $PbO.PbSO_4$. The self-passivation potential seemed to be caused by formation of PbO.

INTRODUCTION

Although there is a voluminous literature on the reactions occurring at Pb electrodes in H_2SO_4 solutions during charge and discharge, there is still considerable uncertainty about the actual mechanism.

From their investigations Gladstone and Tribe (1) concluded that the overall reactions at the two electrodes may be represented by the so-called "double-sulphation" process:

$$Pb + PbO_2 + 2H_2SO_4 \underset{\text{charge}}{\overset{\text{discharge}}{\rightleftharpoons}} 2PbSO_4 + 2H_2O$$

This was subsequently developed in more detail by Müller and Machu (2) and strongly supported by Thirsk and Wynne-Jones (3) as the only mechanism compatible with thermodynamics.

Lander (4) and Burbank (5) found PbO as a product of anodic oxidation in H_2SO_4 in contrast to the observations of Wynne-Jones *et al.* (6), who observed only $PbSO_4$ and PbO_2 as the reaction product. The transformation of $PbSO_4$ to PbO_2 has been assumed by Feitknecht and Gäumann (7) and by Thirsk and Wynne-Jones (3) to involve OH radicals. Two crystallographic modifications of PbO_2 have been noted (8). Feitknecht (9) has also reported PbO as a precursor to the formation of PbO_2 at the anode.

He explained that, during the discharge process, PbO_2 is first reduced to PbO, which is then slowly converted into $PbSO_4$ through the intermediate $PbO.PbSO_4$.

In the present study the conversion of $PbSO_4$ to PbO_2 and the reverse reaction were studied by making potential–time records during charge and open-circuit discharge of the anode.

Since the behavior of the anode during charge and discharge was sensitive to the *immersion time*, i.e. the time during which the anode had been in contact with H_2SO_4

[1]*This paper presented at the Colloquium on Electrochemistry, The Royal Society of Canada, June 1963, Laval University, Quebec.*

before anodization, it was necessary to study also the influence of immersion time on the electrode potential in absence of anodizing current.

EXPERIMENTAL

The measurements were made in a pyrex vessel 10 cm long, 5 cm wide, and 14 cm high, with a $\frac{1}{4}$ inch diameter hole drilled through each end, 6 cm from the top, to allow an electrode to be fastened by a screw and nut which served also to provide electrical contact.

The 2.5 cm × 10.0 cm electrodes were cut from $\frac{1}{4}$ inch rolled Pb sheet (Canada Metal Co., Montreal) of the following analysis: Cd < 0.0001%, Sb = 0.0002%, As < 0.0001%, Ag = 0.0004%, Cu = 0.0004%, Bi = 0.0005%, Fe = 0.0001%, Zn = 0.0001%.

An area of 10.0 cm^2 was measured off on the faces of the anode and cathode and the rest coated with paraffin wax (which had been shown to be chemically inert in H_2SO_4).

The H_2SO_4 used was Reagent Grade (Nicholls Chemical Co., Montreal) with the following analysis: Cl = 0.00002%, NO_3 = 0.00002%, NH_4 = 0.0001%, SO_2 = 0.0002%, As = 0.0000005%, Fe = 0.00002%, heavy metals = 0.00008%, non-volatile = 0.0004%.

The H_2SO_4 electrolyte was saturated with $PbSO_4$ before use. The cell was immersed in a water bath maintained at 25.2 ± 0.1° C. The direct current for the anodization was drawn from a Sorensen regulator (Nobatron 300 B, 150 ma capacity). The galvanostatic method was used for the polarization of the anode. Potential measurements were made with a portable potentiometer (Tinsley, type 3184-D) and a recording oscillograph (Brush RD 232100) in conjunction with a high-gain d-c amplifier (Brush RD 561500). Six chart-speeds were available: the normal speeds 5, 25, and 125 mm/sec and the slow speeds 50, 250, and 1250 mm/hour.

Polarization changes faster than 0.01 second were followed with a cathode-ray oscilloscope (Hewlett-Packard 120 A; P 7 screen) with a sweep-frequency variable from 2 c/sec to 50 kc/sec. Both the oscilloscope and oscillograph could be calibrated by their own internal standards, or against an external circuit consisting of a 1.5 volt battery with voltage divider.

A Luggin-capillary was used to make contact between the electrolyte and the reference electrode. It was filled with H_2SO_4 of the same concentration as that in the reaction vessel.

Electrode potentials were measured relative to the saturated calomel half-cell (Fisher 11-505-10), but are reported here with respect to the N.H.E.

The H_2O used was doubly distilled from KOH.

The anodes were prepared by grinding them on files of various roughness, followed by anodic etching for 32 minutes at a current density of 12.5 amp/dm^2 until the crystal structure of the matrix was exposed. Etching was interrupted every 2 minutes to allow for removal of debris from the electrode, and to dislodge gas bubbles. The electrolyte for etching was 5% aqueous NH_2SO_3H. To obtain satisfactory reproducibility, an anode that had been used once in an experiment had to be reground on the files before it was used in a second experiment. To minimize oxidation of the electrode, after it had been etched, it was washed in three changes of distilled H_2O and transferred, while wet, as rapidly as possible, to the experimental cell.

During the early parts of the study, the electrodes were chemically etched in HNO_3, but reproducibility of the data was very poor. Anodic etching in an electrolyte consisting of 30 g/l. $PbSiF_6$ and 70 g/l. H_2SiF_6 gave good reproducibility, but use of this bath was discontinued in favor of NH_2SO_3H, to rule out any possible influence of adsorbed F^- ion.

Accordingly, most of the electrodes used were etched anodically in the NH_2SO_3H bath, anodically polarized at a current density of 1.0 ma/cm^2 for 7 minutes (for convenience), and discharged on open-circuit, except where specifically stated otherwise.

A typical potential–time record is shown in Fig. 1*a* for an electrode which had been anodically polarized immediately after immersion in H_2SO_4 solution (short immersion).

RESULTS AND DISCUSSION

The potential of the electrode was noted immediately after immersion of the electrode in the H_2SO_4 solution, in the absence of anodizing current. This *immersion potential* ranged from −420 to −240 mv (Fig. 2).

The immersion potential remained constant during a period that ranged from hours to days, depending on the H_2SO_4 concentration, after which it spontaneously assumed a more anodic value of +300 ± 30 mv. The time required to reach this potential decreased with an increase in H_2SO_4 concentration (Fig. 3). After approximately 15 minutes this potential, in turn, slowly became more cathodic, until it reached +20 ± 40 mv, which will be designated the *hydrogen-like potential*. The potential remained constant at this value for

Can. J. Chem. Downloaded from www.nrcresearchpress.com by 210.87.254.5 on 09/05/12
For personal use only.

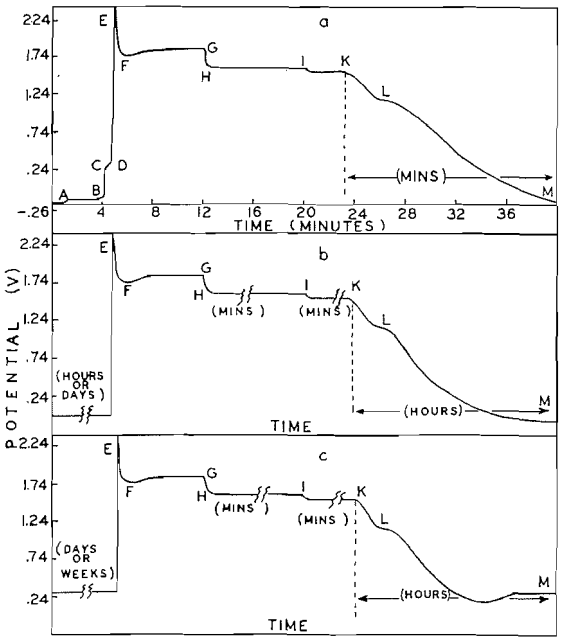

FIG. 1. Typical potential–time recording. A to G: charging; G to M: discharging; A: $Pb/PbSO_4$ potential; F to G: PbO_2/O_2 potential; H to I: $PbSO_4/PbO_2$ potential; L: PbO/PbO_2 potential. Fig. 1*a*: short-immersion electrode; 1*b*: long-immersion electrode (type A); 1*c*: long-immersion electrode (type B).

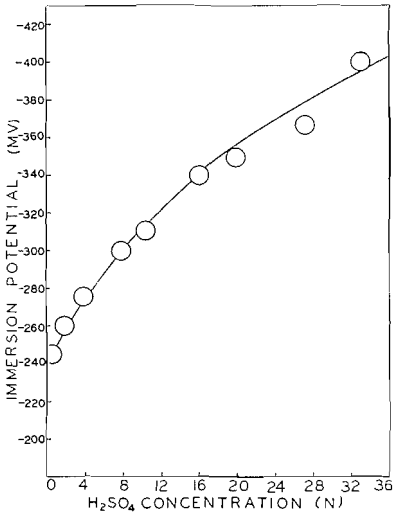

FIG. 2. Immersion potential vs. H_2SO_4 concentration.

about 2 weeks (Fig. 4), after which it changed to the more anodic value of $+300 \pm 30$ mv, hereafter termed the *self-passivation potential.* The change from the immersion potential to the hydrogen-like potential was faster, the higher the concentration of H_2SO_4 into which the electrode was placed.

It appears from the value of $+20 \pm 40$ mv that the hydrogen-like potential might originate from the presence of $PbO.PbSO_4$. Ohse (11) gave a value of +34 mv for the

Can. J. Chem. Downloaded from www.nrcresearchpress.com by 210.87.254.5 on 09/05/12
For personal use only.

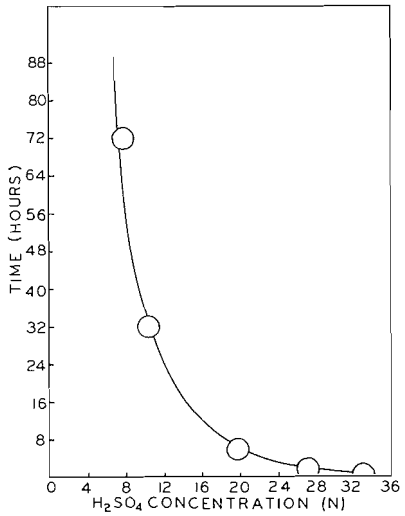

FIG. 3. Time to reach hydrogen-like potential vs. H_2SO_4 concentration.

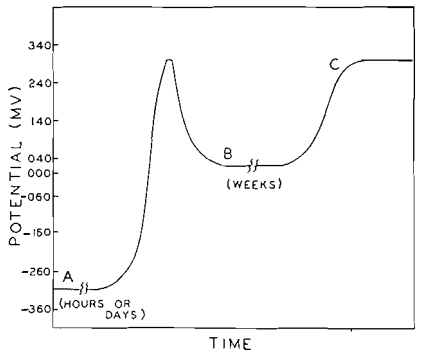

FIG. 4. Change of potential vs. time in absence of anodizing current: A, immersion potential; B, hydrogen-like potential; C, self-passivation potential.

electrode potential of Pb, $PbSO_4/PbO.PbSO_4$ (at pH = 0). He states that: "it is probable that there is $PbO.PbSO_4$ present in the pores of the $PbSO_4$ layer".

The decrease of time required to reach the hydrogen-like potential, with increase in H_2SO_4 concentration, might be attributed to the increased solubility of $PbSO_4$ in more concentrated solutions (12).

The change from the $+300 \pm 30$ mv potential to the hydrogen-like potential could possibly take place by temporary elimination of the impurity centers in concentrated H_2SO_4 solutions, and formation of normal $PbSO_4$, thereby making the potential more cathodic. When sufficient time is allowed, such as on prolonged standing in H_2SO_4, adsorption of O-atoms, which are being formed (Casey and Campney (10)), can then take place to bring the potential to the more anodic self-passivation value. An alternative explanation for the attainment of the self-passivation potential might be the reaction of Pb with H_2O.

With the current turned on data were obtained with anodes which had (i) been immersed

Can. J. Chem. Downloaded from www.nrcresearchpress.com by 210.87.254.5 on 09/05/12
For personal use only.

in the electrolyte for the shortest possible time (*short immersion*), (ii) attained the *hydrogen-like potential*, and (iii) reached the *self-passivation potential* before the current was switched on. When the current was turned on for short-immersion anodes (Fig. 1*a*, A) the potential passed through an "*inflection*" (CD). Interruption of the current had no detectable influence on *passivation time*, i.e. the time to reach the *overshoot* (E).

At constant current density, the passivation time decreased with an increase in H_2SO_4 concentration (Fig. 5). This is probably caused by a decrease in the diffusion coefficient

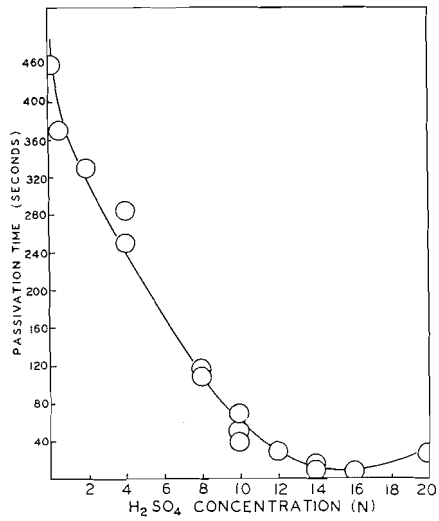

FIG. 5. Passivation time vs. H_2SO_4 concentration.

of $PbSO_4$. A difference in the character of the film may also be involved.

The inflection at CD (Fig. 1*a*) lasted from a fraction of a second to 17 seconds, depending on the current density and H_2SO_4 concentration (Fig. 6). Its potential amounted to $+300 \pm 30$ mv, depending on current density and the concomitant overvoltage, and was essentially identical with the self-passivation potential.

The inflection was absent in H_2SO_4 of less than 0.088 *N*, at which concentration, however, it was just noticeable. It increased in prominence with acid concentration up to 10.5 *N*, beyond which it decreased again. The 10.5 *N* H_2SO_4 gave the optimum inflection for a given current density. The electrochemical reactions which might take place at the inflection are:

(A) $$Pb + H_2O \rightleftarrows PbO_{red} + 2H^+ + 2e$$
$$E = 0.248 - 0.059\ pH$$

(B) $$Pb + H_2O \rightleftarrows PbO_{yellow} + 2H^+ + 2e$$
$$E = 0.253 - 0.059\ pH$$

(C) $$Pb + 2H_2O \rightleftarrows Pb(OH)_2 + 2H^+ + 2e$$
$$E = 0.277 - 0.059\ pH$$

Although present measurements were not sufficiently accurate to permit a decision on the probable occurrence of the above reactions, it might be noted that Burbank (5) reported X-ray identification of both PbO and $Pb(OH)_2$ in the potential range concerned.

Can. J. Chem. Downloaded from www.nrcresearchpress.com by 210.87.254.5 on 09/05/12
For personal use only.

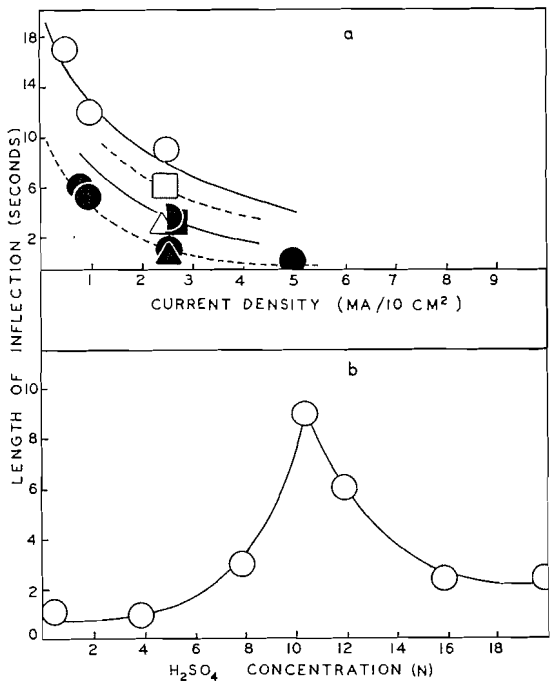

FIG. 6. (*a*) Length of inflection vs. current density:
○ 10.5 *N* H_2SO_4; △ 8.0 *N* H_2SO_4;
● 0.5 *N* H_2SO_4; ▲ 4.0 *N* H_2SO_4;
◗ 20.0 *N* H_2SO_4; □ 12.0 *N* H_2SO_4;
■ 16.0 *N* H_2SO_4.
(*b*) Length of inflection vs. H_2SO_4 concentration: (current density = 2.5 ma/10 cm²).

Since the inflection is a maximum at 10.5 *N* acid, reactions A, B, and C, if they do occur, must have minimum rate for a given current.

When a *short-immersion* electrode was anodized to the inflection and then self-discharged, the potential dropped rapidly to a value that was 40 ± 10 mv more anodic than the immersion potential, the rate depending on acid concentration. When the current was turned on once more, a duplication of the foregoing trace was obtained. When the current was turned off at the inflection, the decay potential was now 80 ± 10 mv more anodic than the immersion potential. The procedure was repeated 3 times and each time the decay potential was more anodic. An interval of 5 minutes was allowed between switching the current off and on, so that concentration effects might dissipate. After the current was switched on for the fourth time no inflection was observable, and the potential rose at once to the overshoot. It may be concluded, perhaps, that more PbO or $Pb(OH)_2$ formed each time the potential was allowed to build up to the inflection, to give a more anodic mixed potential.

Since the potential at the inflection was maintained for a short time only during charging, the total amount of PbO or $Pb(OH)_2$ formed may be calculated to be quite minute.

When a *long-immersion* electrode was anodized, the potential increased at once to the PbO_2/O_2 level without an inflection, which is to be expected, since the electrode potential had already reached the Pb/PbO level before the current was turned on. When the current

Can. J. Chem. Downloaded from www.nrcresearchpress.com by 210.87.254.5 on 09/05/12
For personal use only.

was switched off, with either the short-immersion or long-immersion electrodes anodized for 7 minutes, there was a drop, within 40 seconds, of about 300 mv from the *charging-plateau* (Fig. 1*a*, FG) to a level that might be termed the first *discharge plateau* (Fig. 1*a*, HK). The potentials of the charging- and first discharge-plateaus were concentration dependent (Fig. 7).

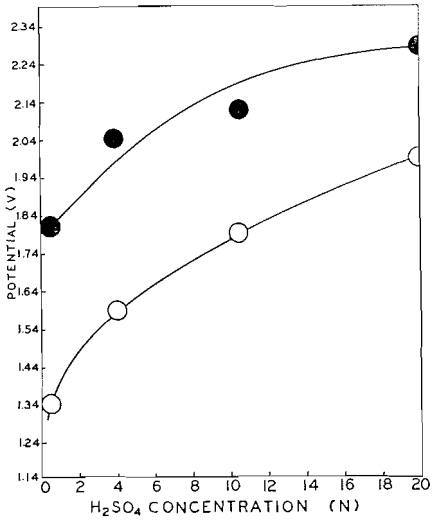

FIG. 7. Potential vs. H_2SO_4 concentration: ● PbO_2/O_2 potential during charging; ○ $PbO_2/PbSO_4$ potential (first plateau).

The duration of the first discharge plateau was concentration dependent with both *short-* and *long-immersion* electrodes, although to markedly different extents (cf. Figs. 8 and 9).

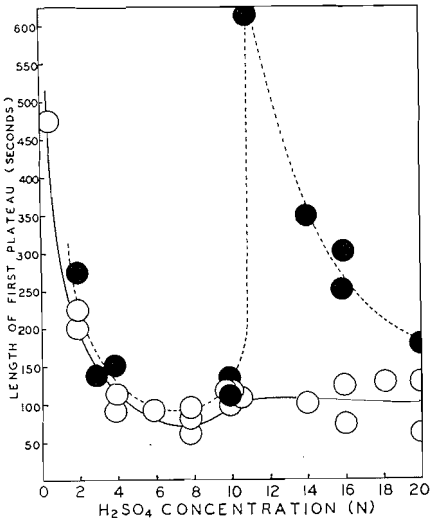

FIG. 8. Length of first plateau vs. H_2SO_4 concentration (short-immersion electrodes): ○ H_2SiF_6 etch; ◍ NH_2SO_3H etch.

Can. J. Chem. Downloaded from www.nrcresearchpress.com by 210.87.254.5 on 09/05/12
For personal use only.

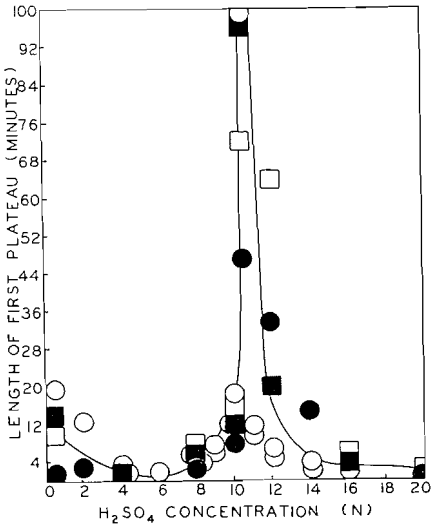

FIG. 9. Length of first plateau vs. H_2SO_4 concentration (long-immersion electrodes): ■ self-passivated in 10.5 *N* H_2SO_4 (NH_2SO_3H etch); ● self-passivated in 16.0 *N* H_2SO_4 (NH_2SO_3H etch); □ filed electrode; ○ self-passivated in own acid (NH_2SO_3H etch).

In accordance with the results of Wynne-Jones *et al.* (13) the length of the first discharge plateau as well as that of the second decay (Fig. 1, KM) increased with the quantity of current passed, i.e. slow formation of PbO_2, in addition to that originating from the initial PbO_2 continued during anodization.

The two sublevels of the first discharge plateau were also observed by Ruetchi and Cahan (8), who associated the higher level with α (orthorhombic) and the lower with β (tetragonal) PbO_2 (Fig. 1*a*, HI and IK).

The behavior of the first discharge plateau for *long-immersion* electrodes was studied with four types of surfaces. The first of these was electrochemically etched, self-passivated in H_2SO_4, and anodized in H_2SO_4 of the same concentration as that used for self-passivation. The maximum plateau-length was observed in 10.5 *N* H_2SO_4 (Fig. 9). The thickness and character of the $PbSO_4$ layer formed might have varied, however, when the electrode was self-passivated in different acid concentrations. Experiments were made, therefore, with a second series of electrodes, self-passivated in 16.0 *N* H_2SO_4 (chosen merely for its relatively short self-passivation time). The electrodes were transferred after self-passivation to another vessel containing the appropriate H_2SO_4 concentration for anodizing. The longest plateau was again obtained in 10.5 *N* H_2SO_4. It was of interest then to check the behavior of a similar series of electrodes, self-passivated in 10.5 *N* H_2SO_4. The results were essentially the same as those obtained with electrodes self-passivated in 16.0 *N* acid. Since there remained the possibility that NH_2SO_3H, used for etching, or an oxidation product thereof, might be adsorbed by the electrodes and form a stabilizing agent, a fourth series of electrodes was prepared by grinding on files without the electrolytic etch. Nevertheless, the first discharge plateaus again showed their peculiar behavior.

It is possible that the length of the first discharge plateau is related to the solubility of $PbSO_4$ and that the slow step in the reaction is the rate of solution of $PbSO_4$ in H_2SO_4. The solubility was determined by Kameyama and Fukomoto (14) over the range 0.5 to 10.5 *N* H_2SO_4 and shows a maximum in 2.0 *N* and a minimum in 10.5 *N*.

Can. J. Chem. Downloaded from www.nrcresearchpress.com by 210.87.254.5 on 09/05/12
For personal use only.

The variation in the length of the first discharge plateau with change in H_2SO_4 concentration raised the question of whether it was caused by a change in the efficiency of PbO_2 formation for a fixed quantity of current or by a variation in the discharge rate. Experiments, in which the anodes were charged in one H_2SO_4 concentration and discharged in another, gave plateaus which reflected the acid concentration used during discharge and thus favor the second answer.

The second decay for *long-immersion* anodes occurred in either of two ways, depending on whether the potential prior to anodization had achieved the hydrogen-like potential $+20 \pm 40$ mv (Fig. 1*b*) or the self-passivation potential $+300 \pm 30$ mv (Fig. 1*c*). If the first condition prevailed, the second decay dipped to -40 ± 30 mv, which was slightly more cathodic than the hydrogen-like potential for the electrode under examination. On continued standing such an electrode gradually assumed the hydrogen-like, and eventually the self-passivation potential.

For the second condition, however, the potential reached a minimum of $+220 \pm 15$ mv, and then gradually regained its self-passivation potential. It would appear that, during the discharge of long-immersion electrodes, a change towards the immersion potential by formation of lower oxides of Pb and (or) $PbSO_4$ from PbO_2 occurs, in opposition to the formation of substances causing the hydrogen-like ($PbO.PbSO_4$) and the self-passivation (PbO or $Pb(OH)_2$) potentials. With short-immersion electrodes the oxidation products apparently were able to revert to $PbSO_4$, whereas this was not possible with the substances formed on long-immersion electrodes and responsible for the hydrogen-like and self-passivation potentials.

To reach the self-passivation potential, an electrode had to stand for an appreciable length of time in acid, giving the H_2SO_4 opportunity to attack the grain-boundaries. It might be that the establishment of the self-passivation potential produces PbO and (or) $Pb(OH)_2$ and that, since PbO is a poor conductor of electricity, it is not all oxidized to PbO_2, even during prolonged anodization, but remains embedded in the intergranular spaces of the surface. Its presence there, in conjunction with $PbSO_4$ formed during discharge, would then give rise to mixed potentials (the hydrogen-like potential). This view would seem to be supported by the observation that anodization experiments of 30 minutes and 2 hours gave results similar to those obtained with only 7 minutes anodization.

Moreover, when *short-immersion* electrodes were electrolytically etched in H_2SiF_6 or in NH_2SO_3H, a plot of the first discharge plateau against H_2SO_4 concentration showed the distinct discontinuity for electrodes treated in NH_2SO_3H (Fig. 8), and microscopic examination showed that NH_2SO_3H attacked the grain-boundaries more strongly than H_2SiF_6.

ACKNOWLEDGMENTS

The present investigation was made with financial assistance from the Defence Research Board of Canada, Grant Number 5480-14, to whom grateful acknowledgment is made.

Thanks are due to Messrs. V. Mimeault, G. Lanthier, R. Cook, J. Devlin, and H. Doherty (student assistants) who helped with the experiments.

The writer would like to express his appreciation to Drs. E. J. Casey and I. Henderson of the Defence Research Chemical Laboratories for several valuable discussions and private communications, Professor C. A. Winkler, Department of Chemistry, McGill University, Montreal, Quebec, for his continued encouragement and advice, and the Canada Metal Company, Ltd., Montreal, Quebec, for their generous gift of high-purity lead sheet.

Can. J. Chem. Downloaded from www.nrcresearchpress.com by 210.87.254.5 on 09/05/12
For personal use only.

REFERENCES

1. J. H. GLADSTONE and A. TRIBE. Nature, **25**, 221 (1882).
2. W. MÜLLER and W. MACHU. Monatsh. Chem. **63**, 347 (1933).
3. H. R. THIRSK and W. F. K. WYNNE-JONES. J. Chim. Phys. **49**, C, 131 (1952).
4. J. J. LANDER. J. Electrochem. Soc. **98**, 213 (1951); **98**, 522 (1951); **103**, 1 (1956).
5. J. BURBANK. J. Electrochem. Soc. **103**, 87 (1956).
6. W. H. BECK, P. JONES, and W. F. K. WYNNE-JONES. Trans. Faraday Soc. **50**, 1249 (1954).
7. W. FEITKNECHT and A. GÄUMANN. J. Chim. Phys. **49**, 135 (1952).
8. J. BURBANK. J. Electrochem. Soc. **104**, 693 (1957). P. RUETCHI and B. D. CAHAN. **104**, 406 (1959). **105**, 396 (1958). P. RUETCHI and R. T. ANGSTADT. **105**, 555 (1958). J. BURBANK. **106**, 369 (1957). P. RUETCHI, R. T. ANGSTADT, and B. D. CAHAN. **106**, 547 (1959).
9. W. FEITKNECHT. Z. Electrochem. **62**, 6/7, 795 (1958).
10. E. J. CASEY and J. CAMPNEY. J. Electrochem. Soc. **102**, 219 (1955).
11. R. W. OHSE. Werkstoffe Korrosion, **11**, 220 (1960).
12. P. DELAHAY, H. POURBAIX, and P. VAN RYSSELBERGHE. J. Electrochem. Soc. **98**, 57 (1951).
13. P. JONES, R. LIND, and W. F. K. WYNNE-JONES. Trans. Faraday Soc. **50**, 972 (1954).
14. N. KAMEYAMA and T. FUKOMOTO. J. Soc. Chem. Ind. Japan, **46**, 1022 (1943).

Can. J. Chem. Downloaded from www.nrcresearchpress.com by 210.87.254.5 on 09/05/12
For personal use only.

Can. J. Chem. Downloaded from www.nrcresearchpress.com by 210.87.254.40 on 09/05/12
For personal use only.

D-MANNOFURANOSE 2,3-CARBONATE. PREFERRED SIZE OF THE SUGAR RING IN SOME FUSED-RING DERIVATIVES[1]

A. S. PERLIN

National Research Council of Canada, Prairie Regional Laboratory, Saskatoon, Saskatchewan

Received December 20, 1963

ABSTRACT

Treatment of 6-*O*-trityl-D-mannose with phosgene gives 6-*O*-trityl-D-mannose 2,3-carbonate (II), which on partial hydrolysis, yields D-mannose 2,3-carbonate (VI). Chemical properties of II and VI agree with the proposition that fusion of the cyclic carbonate group at the 2- and 3-positions of D-mannose converts the latter to a furanose derivative. Nuclear magnetic resonance spectral evidence supports the furanoid assignment and indicates also that in aqueous solution VI does not rearrange significantly to a pyranose form. Substantial disagreement is found between proton-proton coupling observed for VI and corresponding data predicted from the Karplus curve. A similar situation is encountered with a related fused-ring derivative, 2,3-*O*-isopropylidene-L-rhamnose.

5-O-Methyl-D-mannofuranose has been synthesized via methylation of II. 5,6-Di-O-acetyl-α-D-mannofuranosyl bromide 2,3-carbonate (VIII), prepared from VI, permits synthesis of either of the anomeric methyl D-mannofuranosides. On treatment of VIII with methanol in the presence of excess sodium the α-D-glycoside is obtained, whereas in the presence of silver oxide a β-D-anomeric derivative is formed.

D-Mannofuranose 2,3;5,6-dicarbonate is formed by reaction of D-mannose with phosgene in pyridine (1). By analogy with this synthesis, 6-*O*-trityl-D-mannose (I) was treated in similar fashion in attempting to prepare 6-*O*-trityl-D-mannofuranose 2,3-carbonate (II). The reaction product was obtained in crystalline form after chromatography on silicic acid and, in accordance with expectation, it yielded a 5-*O*-methyl ether methyl glycoside (III). Removal of the carbonate group of III with barium methoxide gave 6-*O*-trityl-5-*O*-methyl methyl α-D-mannofuranoside (IV), the furanoside structure of which was clearly shown by a very rapid uptake of lead tetraacetate (2). Location of the ether group in IV was confirmed by acid hydrolysis to give 5-*O*-methyl-D-mannofuranose (V), which was converted to known 5-*O*-methyl-D-*arabino*hexophenylosazone (3).

D-Mannose 2,3-carbonate (VI) was obtained by partial acid hydrolysis of the 6-*O*-trityl ether (II). An α-D-triacetate (VII) of VI was prepared, which, on treatment with hydrogen bromide, afforded di-*O*-acetyl-α-D-mannosyl bromide 2,3-carbonate (VIII). The latter, in methanol containing excess sodium (4), was converted to methyl α-D-mannofuranoside (IX), thus establishing that acetate VII is a furanose derivative of D-mannose 2,3-carbonate. Preparation of IX parallels the conversion of tetra-*O*-acetyl-α-D-mannopyranosyl bromide to methyl α-D-mannopyranoside under the same conditions (4). In both instances, the observed retention of configuration presumably involves an intermediate 1,2-epoxide. When VIII was treated with methanol in the presence of silver oxide, inversion occurred and a β-D-glycoside (X) was obtained; this agrees with the observed behavior of related furanosyl halide 2,3-carbonates (5, 6, 7). Thus, D-mannose 2,3-carbonate is an intermediate suitable for synthesis of either the α- or β-anomer of methyl D-mannofuranoside, and its 6-*O*-trityl ether (II) permits ready synthesis of 5-*O*-methyl-D-mannofuranose (V), which does not appear to have been previously prepared (8).

These syntheses all accord with the original expectation (see (9)) that, in forming a 2,3-carbonate, D-mannopyranose is transformed into a furanose derivative (II and VI).

[1]*Issued as N.R.C. No. 7864.*

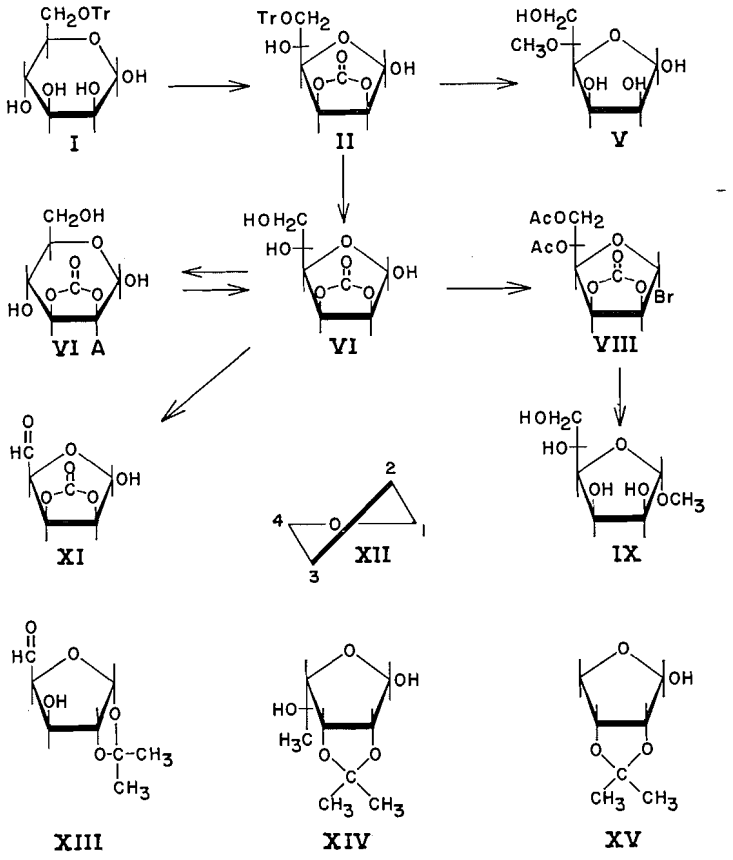

Moreover, D-mannose 2,3-carbonate rapidly consumes a mole of periodate, consistant with degradation of a furanose to a 5-aldo-derivative (XI). Nevertheless, such examples do not entirely eliminate the possibility that in solution the furanose sugar is in equilibrium with a high proportion of the pyranose isomer (e.g. VIA), but reacts preferentially or affords the more stable end-product. Certainly, when the pyranose ring is fixed by glycoside formation a 2,3-carbonate still may be prepared readily (10, 11). If both pyranose and furanose isomers are present in admixture, and if one assumes that they are interconvertible because of free hydroxyl groups at positions -1 and -4 or -5, their equilibrium ratio would depend on the relative stability of the fused-ring structure having two five-membered rings (furanose-carbonate) and the one having a six- and a five-membered ring (pyranose-carbonate).

It appears certain from the n.m.r. spectrum of D-mannose 2,3-carbonate (Fig. 1A) that one particular form of the sugar greatly predominates in aqueous solution.* Thus, the H_1 singlet, H_2 doublet, and H_3 and H_4 quartets are all approximately one proton signals; only the weak signal at 5.3 p.p.m. suggests the presence of a minor constituent. A choice of whether the dominant species is a furanose or pyranose form should be possible by analysis of proton–proton coupling in Fig. 1A, although differences between the two

**The spectrum of the crystalline 6-O-trityl derivative (II) in chloroform solution was more poorly resolved, even after the solution was shaken with deuterium oxide to eliminate OH coupling, but its general characteristics were similar to those of the detritylated derivative (VI).*

Can. J. Chem. Downloaded from www.nrcresearchpress.com by 210.87.254.40 on 09/05/12
For personal use only.

Can. J. Chem. Downloaded from www.nrcresearchpress.com by 210.87.254.40 on 09/05/12
For personal use only.

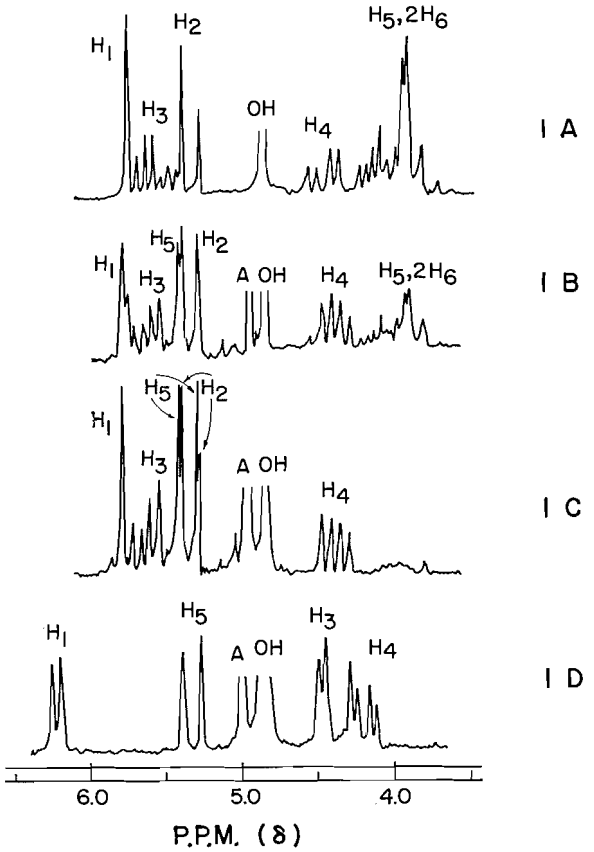

FIG. 1. Nuclear magnetic resonance spectra in deuterium oxide of (A) D-mannose 2,3-carbonate (VI); (B) the solution of VI, five minutes after addition of 0.4 moles of sodium metaperiodate per mole; (C) the product (XI) formed by treating VI with 1 mole of sodium metaperiodate per mole; (D) the product (XII) formed by treating 1,2-*O*-isopropylidene-D-glucofuranose with 1 mole of sodium metaperiodate per mole. Signal A is due to protons of formaldehyde produced.

forms *could* be rather small, depending on the mode of puckering of the furanose ring. This is seen by comparing the observed first-order coupling constants (J) for neighboring protons with corresponding dihedral angles given by the Karplus curve (12, 13).* As

		Dihedral angle		
CH—CH	$J_{H,H}$	α-D-Furanose	Karplus curve value	α-D-Pyranose
1,2	0	95°	90°	85°
2,3	6.5	28°	30°	35°
3,4	3.2	28°	50°, 130°	130°
4,5	9.0	—	180°	180°

shown in the table, the first two dihedral angles are readily approximated in a Barton conformational model (15) of the α-D-furanose isomer (VI) by puckering the ring so that C_2 is above and C_3 below the plane formed by C_4—O—C_1 (XII) ("skew" or cyclopentane

**A modified Karplus equation, derived for use in studies of sugar conformation in deuterium oxide, also gives values close to those listed in the table (14).*

"half chair" form (16, 17)); also there appears to be no restriction to a H_4—H_5 dihedral angle of 180°. In the model of the α-D-pyranose isomer (VIA) approximately the same dihedral angles pertain for the 1,2-, 2,3- and 4,5-proton pairs. Hence the major difference between the two molecules is the angle subtended by H_3 and H_4, although, even in this instance, the parabolic shape of the Karplus curve accommodates the possibility of two widely divergent dihedral values. There is much better agreement on this point between the predicted and found values for the pyranose derivative. A 3,4-dihedral angle larger than 30° appears prohibitive for the furanose isomer, irrespective of the mode of puckering.

If the Karplus curve in its original form is closely applicable to compounds such as D-mannose 2,3-carbonate, it may be inferred that the dominant species in solution is a pyranose form, in marked contrast to the chemical evidence cited above. The value for $J_{3,4}$ of 3.2 c.p.s. requires a gross displacement of the curve, i.e., by almost 3 c.p.s., to accommodate the furanose structure. Nevertheless, discrepancies of this magnitude have been shown for some types of compounds, as influences on proton-proton coupling other than dihedral angle are becoming recognized (18). To test the applicability of the curve in the present instance the spectra of several 2,3-carbonate derivatives were examined (furanoses VII and VIII as well as pyranosides (11)), but these have not yet been adequately interpreted. Pertinent reference data were obtained, however, from the n.m.r. spectrum of the product (XI) formed by periodate scission of VI. The 5,6-diol group of the latter should be readily accessible to the oxidant, whereas a pyranose form (VIA) would have to be converted to a furanose (or an acylcic) form in an equilibrium-displacement reaction; the expected product from either source is the 5-*aldo* derivative (XI). By examination of the spectrum at different stages the course of the oxidation reaction was conveniently followed: on partial oxidation there was a corresponding decrease in the signal intensity for the 5- and 6-protons (e.g. Fig. 1B), but with excess periodate present, cleavage of the diol was complete (Fig. 1C). The production of formaldehyde (signal at 4.95 p.p.m.) from C_6 increased proportionately over these stages, as did the relative intensity of a new doublet (J = 7.2 c.p.s.) overlapping the H_2 doublet. This new signal is attributed to the C_5 aldehydic proton.* Reference to the related 4-*aldo*-pentose (XIII) (Fig. 1D) formed by periodate oxidation of 1,2-*O*-isopropylidene-D-glucofuranose (19) supports the latter assignment by showing that H_5 gives a doublet of resonance frequency 5.35 p.p.m. and that its coupling with H_4 (J = 7.5 c.p.s.) also is clearly analogous to that in XI.† The observed value of 3.2 c.p.s. for $J_{3,4}$ (Fig. 1C) is particularly pertinent here as a guide to possible coupling between H_3 and H_4 in the furanose sugar VI, i.e., in both instances it is equally difficult to correlate the spectra with conformational models and the Karplus curve. Hence, the transformation of D-mannose 2,3-carbonate to XI, which cannot involve retention of a pyranose ring, causes only minute changes in chemical shift and coupling constant for each of the various ring protons. This clear indication of a close conformational similarity between starting material and oxidation product therefore strongly favors the conclusion that D-mannose 2,3-carbonate exists in solution almost entirely as a furanose sugar.‡

By acceptance of a furanose structure for D-mannose 2,3-carbonate, nevertheless the

**The aldehyde group, as well as formaldehyde, must be hydrated, to account for the occurrence of the signal at much higher field than usual for aldehydic protons.*

†Of further note in Fig. 1D are the characteristics of H_3 and H_5. Product XIII has been isolated as a crystalline dimer in which intermolecular bonding renders the 3- and 5-protons non-equivalent (20). Since only one signal is found here for each of these protons, the dimerization process undoubtedly does not take place as the aldehydo compound is generated by oxidation.

‡These data emphasize the difficulty inherent in applying the Karplus equation without a knowledge of the parameters required for the particular system (12, 13, 18).

Can. J. Chem. Downloaded from www.nrcresearchpress.com by 210.87.254.40 on 09/05/12
For personal use only.

n.m.r. spectrum cannot at present be used in turn for deducing the preferred conformation of the compound. The fused-ring system, however, permits relatively few possibilities as compared with a monocyclic compound. The "skew" form of the α-D-anomer depicted in XII has the merit of minimizing interactions between neighboring ring substituents and of a minimal number of *endo*-substituents (21). Also, in this form the cyclic carbonate ring likewise assumes a "skew" conformation which, according to X-ray crystallography, is preferred in ethylene carbonate (22).

There is a close structural analogy between cyclic carbonate and *O*-isopropylidene derivatives. Compounds of the latter class related to D-mannose 2,3-carbonate are 2,3-*O*-isopropylidene-L-rhamnose (XIV) (23, 24) and -D-lyxose (25), both of which have been assigned a furanose structure on chemical grounds. The n.m.r. spectrum of the L-rhamnose derivative (Fig. 2A) is slightly more complex than that of II, and suggests that a proportionately greater mixture of components is present in the solution. This is most evident from the multiplicity of signals for the C-methyl groups: a maximum of only four peaks would have been expected for the latter if a single component were present (two 3-proton singlets for the *O*-isopropylidene group (26; also see Fig. 2B) and a 3-proton doublet for the C_6 methyl group). Nevertheless, a substantial predominance of one component is indicated by major signals attributed to H_1 (singlet), H_2 (doublet), and H_3 (quartet). Of concern, especially to the above discussion, is the fact that values for $J_{1,2}$, $J_{2,3}$, and $J_{3,4}$ derived from these major signals are the same as found with D-mannose 2,3-carbonate. Hence, the current data support the furanose assignment already made, but suggest that a significant proportion of a different species is present in an aqueous solution of XIV.

The only type of fused-ring system possible for 2,3-*O*-isopropylidene-L-erythrose

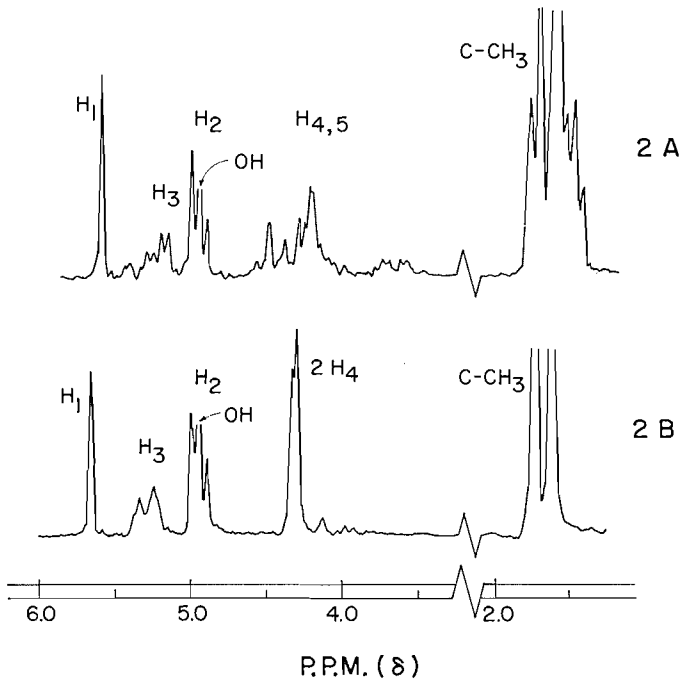

FIG. 2. Nuclear magnetic resonance spectra in deuterium oxide of (A) 2,3-*O*-isopropylidene-L-rhamnose; (B) 2,3-*O*-isopropylidene-L-erythrose.

Can. J. Chem. Downloaded from www.nrcresearchpress.com by 210.87.254.40 on 09/05/12
For personal use only.

(XV; D-isomer) (27) is one that contains two five-membered rings, and the n.m.r. spectrum, (Fig. 2B) as well, indicates that a single isomeric form of this derivative is present in the solution. By contrast, in a solution of D-erythrose itself, only about half of the compound appears to exist as the furanose form (28). Therefore, it may be inferred that the furanose ring is stabilized in XV by fusion of the second five-membered ring.

The strong similarity in general spectral characteristics of VI, XI, XIV, and XV, two of which cannot exist as pyranoses, adds to the chemical evidence in suggesting that this kind of bicyclic structure is more stable when the sugar ring is furanose than when pyranose. On conformational grounds the contrary would appear more reasonable. Thus, by manipulating models of VI and VIA in various ways, the same non-bonded interactions appear possible for both molecules in the region of the ring oxygen, C_1, C_2, and C_3. However, the C_5 group is *cis*-oriented relative to the C_3—O bond in VI and constitutes an unfavorable *endo*-substituent (21), whereas the equatorial C_4 hydroxyl group is *trans* in VIA. Although such interactions are clearly of primary importance in fused-ring systems (21, 29), it is probable that other types of factors also need to be considered when more than one ring size is permitted. The situation is similar for monocyclic sugars, though in a reverse sense: from the evidence available, it appears that most free sugars in solution exist predominantly as pyranose chair forms wherever possible, and various methods of conformational analysis concur in indicating assignment of most favorable chair conformations for the different pyranose sugars. However, the same principles do not necessarily explain why furanose forms should, at most, be minor components of the sugar solutions.

EXPERIMENTAL

Melting points are corrected. Solutions were evaporated *in vacuo* at 40–45° C.

Paper chromatography was carried out using Whatman No. 1 paper and butanol–ethanol–water (40:11:19) as solvent.

Proton magnetic resonance (n.m.r.) spectra were measured with a Varian A-60 spectrometer using tetramethylsilane as external or internal indicator.

6-O-Trityl-D-mannose 2,3-Carbonate (II)

6-*O*-Trityl-D-mannose was prepared according to Helferich and Leete (30): to a solution of D-mannose (10 g) in dry pyridine (60 ml) at 0° C, triphenylchloromethane (17 g) was added, the solution was stored at room temperature for 24 hours, and ice water was then added to turbidity. The suspension was poured with vigorous stirring into ice water containing excess of potassium bicarbonate, and the tacky precipitate was washed well with water.

The crude trityl derivative (10 g) was taken up in chloroform, the solution was passed through anhydrous magnesium sulphate, the chloroform evaporated off, and pyridine (70 ml) added. Phosgene (2.4 g) in toluene (20 ml) (31) was added to the pyridine solution at 0° C over a period of 30 minutes with good stirring, the coolant was removed, and after an additional 30 minutes the suspension was filtered and the filtrate concentrated. Chromatographic purification of the syrupy product (10 g) was carried out using a column of silicic acid (18 cm × 5 cm), the product being applied as a concentrated solution in chloroform and the column then developed with additional chloroform. Fractions of the eluate were concentrated and examined for the presence of a cyclic carbonate derivative by infrared absorption (32). After addition of ether–hexane to selected fractions, crystalline material (2.0 g) was recovered and recrystallized from this mixed solvent; m.p. 106–107° C (with gas evolution), $[\alpha]_D+10°$ (*c*, 1, $CHCl_3$). The product contained ether of crystallization. Calculated for $C_{26}H_{24}O_7 \cdot \frac{1}{2}(CH_3CH_2)_2O$: C, 69.26; H, 6.02; ethoxyl, 9.3. Found: C, 69.50; H, 6.10; ethoxyl, 7.7%. The compound absorbed strongly in the infrared region at 1800 cm^{-1}, characteristic of a cyclic 5-membered carbonate group (32).

6-O-Trityl-5-O-methyl Methyl α-D-Mannofuranoside 2,3-Carbonate (III)

A suspension of 6-*O*-trityl-D-mannose 2,3-carbonate (1.5 g), silver oxide (10 g), and anhydrous calcium sulphate (5 g) in methyl iodide (14 ml) was shaken at room temperature for 1 hour, and then heated under reflux for 24 hours.* The solids were filtered off and washed with chloroform. The filtrate and washings were

**Only product III was obtained when the methylation was carried out with methyl iodide and silver oxide. By using dimethylformamide as solvent for this reaction (33), an additional product was obtained which appeared from its infrared absorption spectrum (32) to contain an acyclic carbonate group.*

Can. J. Chem. Downloaded from www.nrcresearchpress.com by 210.87.254.40 on 09/05/12
For personal use only.

concentrated, and the residue methylated as above. The final product solidified (1.4 g) and, after recrystallization from benzene–ether–hexane, had m.p. 223.5–225° C; $[\alpha]_D$+35° (*c*, 1, $CHCl_3$). Calculated for $C_{28}H_{28}O_7$: C, 70.57; H, 5.92; methoxyl, 13.0. Found: C, 70.68; H, 5.92; methoxyl, 12.9%.

6-O-Trityl-5-O-methyl Methyl α-D-Mannofuranoside (IV)

A suspension of methylation product III (1.0 g) in methanol (50 ml) was heated and sodium methoxide solution (0.1 *N*) was added dropwise until excess of the base was present. The solution was neutralized with carbon dioxide and concentrated fivefold, water was added, the precipitate (0.75 g) was recovered, washed with water, and recrystallized from benzene–ether; m.p. 99–103° C; $[\alpha]_D$+37° (*c*, 2, dioxane) (M_D = +16,650; M_D of methyl α-D-mannofuranoside is +20,500). Calculated for $C_{27}H_{30}O_6$: C, 71.98; H, 6.71; methoxyl, 13.78. Found: C, 71.95; H, 6.74; methoxyl, 13.33%.

To a solution of IV (15 mg) in acetic acid (2 ml) was added lead tetraacetate solution (20 mg in 2 ml of acetic acid). The uptake of oxidant was 1.0 moles/mole, constant value at 2, 5, and 14 minutes reaction time. When oxidized in highly dilute solution as described elsewhere (34), the second-order rate constant found was 30,000 min^{-1} $mole^{-1}$ liter, as compared with a value of 37,800 for methyl α-D-erythrofuranoside (34).

5-O-Methyl-D-mannofuranose (V)

Product IV (0.6 g) in 50 ml of 70% acetic acid (35) was heated on the steam bath for 1 hour, the solution was cooled and concentrated to a volume of 5 ml. Water was added to the concentrate, the precipitated trityl alcohol was filtered off, and the solution was concentrated. Hydrolysis of the glycoside was completed at steam bath temperature with 0.1 *N* sulphuric acid for 1 hour, the solution was neutralized with Dowex-1 resin (bicarbonate form) and concentrated, affording a syrup (0.2 g); $[\alpha]_D$+30° (*c*, 1, H_2O). On paper chromatographic examination, the product was found to consist essentially of one component, travelling at 1.2 times the rate for L-rhamnose or 5-*O*-methyl-D-glucofuranose.

When treated with phenylhydrazine hydrochloride – sodium acetate in water for 1.5 hours on the steam bath, the sugar gave a dark oil which crystallized from ethanol–water; after recrystallization from this ethanol–water and twice from benzene, the yellow crystals had m.p. 131–133° C; the X-ray diffraction pattern was indistinguishable from that of 5-*O*-methyl D-*arabino*hexophenylosazone (m.p. 133–135° C) prepared from 5-*O*-methyl-D-glucofuranose.

D-*Mannose 2,3-Carbonate (VI)*

A solution of 6-*O*-trityl-D-mannose 2,3-carbonate (II) (100 mg) in 70% acetic acid (10 ml) was heated on the steam bath for 1 hour. Several volumes of cold water were added, the suspension was filtered, and the filtrate concentrated; water was again added and extracted material was concentrated to a syrup (35 mg); $[\alpha]_D$ −5° (*c*, 3.5, H_2O). On a paper chromatogram the product travelled at 1.6 times the rate of L-rhamnose.

A larger scale preparation of the carbonate was carried out without isolation of intermediate products: D-mannose (7 g) was tritylated as above, the pyridine solution was shaken thoroughly with excess of solid sodium bicarbonate, and then treated with phosgene as described above. After removal of solvent the final syrupy product was hydrolyzed with hot 70% acetic acid for 1 hour. The hydrolyzate, which was found by paper chromatography to contain VI, free mannose, and unidentified material having a high R_F, was concentrated and extracted with water. The aqueous extract was washed thoroughly with ether, and the water layer then extracted with ethyl acetate in countercurrent fashion in four stages. From those fractions containing chromatographically pure VI, 0.8 g of syrup was obtained. The product crystallized after prolonged storage at 3° C and was recrystallized from ethyl acetate; m.p. 110–112° C. Calculated for $C_7H_{10}O_7$: C, 40.78; H, 4.89. Found: C, 41.06; H, 4.84%. In the infrared region the product absorbed strongly at 1785–1790 cm^{-1} (cyclic carbonate group); the n.m.r. spectrum in deuterium oxide (Fig. 1A) was indistinguishable from that of the product obtained by hydrolysis of crystalline II.

1,5,6-Tri-O-acetyl α-D-Mannofuranose 2,3-Carbonate (VII)

Acetic anhydride (3 ml) and anhydrous sodium acetate (200 mg) were added to D-mannose 2,3-carbonate (200 mg), the suspension was shaken for 1 hour and then heated on the steam bath for 1 hour. Evaporation of the anhydride *in vacuo* at 60° C left a residue which was triturated thoroughly with ice water, dried, and taken up in ethanol from which it crystallized (180 mg). After recrystallization from ethanol the melting point was 110–111° C; $[\alpha]_D$ +40° (*c*, 1.1, $CHCl_3$). Calculated for $C_{13}H_{16}O_{10}$: C, 46.99; H, 4.85. Found: C, 46.94; H, 4.92%. The infrared absorption spectrum showed the presence of a cyclic carbonate group.

5,6-Di-O-acetyl-α-D-mannofuranosyl Bromide 2,3-Carbonate (VIII)

Triacetate VII (60 mg) in ethylene chloride (1 ml) was treated with hydrogen bromide in acetic acid (1 ml; 30%) for 4 hours, the observed rotation of the solution being constant over the period 2–4 hours; calculated for the product, $[\alpha]_D$ +115°. Chloroform (15 ml) was added, the solution was washed successively with ice water, cold sodium bicarbonate solution and ice water, dried, and concentrated. The residue solidified (63 mg), m.p. 117–120° C, and after recrystallization from ether–hexane had m.p. 123–124° C. Calculated for $C_{11}H_{13}O_8Br$: C, 37.41; H, 3.71. Found: C, 37.30; H, 3.99%.

Methyl α-D-Mannofuranoside (IX)

To a solution of bromide VIII (100 mg) in benzene (2 ml) was added methanol (2 ml) containing sodium (8 mg; 1.2 moles per mole of the acyl bromide (4)). After 15 minutes the alkaline solution was heated under

Can. J. Chem. Downloaded from www.nrcresearchpress.com by 210.87.254.40 on 09/05/12
For personal use only.

reflux for 5 minutes, neutralized with carbon dioxide, and concentrated. The residue, in water, was treated with mixed-bed resins and concentrated to a syrup, $[\alpha]_D$ +102° (*c*, 2, H_2O), which was found chromatographically to consist almost entirely of methyl α-D-mannofuranoside. When taken up in 1-propanol (36) and seeded, the product crystallized; m.p. 118–120° C; the X-ray powder diagram was indistinguishable from that of methyl α-D-mannofuranoside.

5,6-Di-O-acetyl Methyl β-D-Mannofuranoside 2,3-Carbonate (X)

A mixture of bromide VIII (80 mg) and silver oxide (600 mg) was taken up in methanol (6 ml), shaken for several hours, filtered, and the solution was concentrated. The residue was taken up in chloroform, filtered, and on concentration a syrup was obtained (60 mg); $[\alpha]_D$ −93° (*c*, 2, $CHCl_3$), its infrared absorption spectrum showed the presence of a cyclic carbonate group and acetyl groups, and its n.m.r. spectrum (in chloroform) showed the presence of an O-methyl group. The non-reducing major product formed by treating the glycoside with sodium methoxide travelled on a paper chromatogram at 0.77 times the rate for methyl α-D-mannofuranoside, and was accompanied by a trace proportion of the latter; it was markedly acid labile, being hydrolyzed to mannose in aqueous solution when shaken with Amberlite IR-120 resin (H^+ form) for 5 hours.

ACKNOWLEDGMENTS

The author expresses his thanks to M. Mazurek and W. Haid, who carried out microanalyses and prepared n.m.r. and infrared absorption spectra. Dr. D. F. Mowery, Jr., very kindly provided a sample of methyl α-D-mannofuranoside.

REFERENCES

1. W. N. Haworth and C. R. Porter. J. Chem. Soc. 649 (1930).
2. R. Criegee. Ann. **495**, 211 (1932).
3. E. E. Percival and E. G. V. Percival. J. Chem. Soc. 1398 (1935).
4. A. S. Perlin. International Symposium on Carbohydrate Chemistry, Birmingham, England. July, 1962. p. 39.
5. W. N. Haworth, C. R. Porter, and A. C. Waine. Rec. Trav. Chim. **57**, 541 (1938).
6. G. M. Tener, R. S. Wright, and H. G. Khorana. J. Am. Chem. Soc. **78**, 506 (1956).
7. G. R. Barker, I. G. Gillam, and J. W. Spoors. Chem. Ind. London, 1312 (1956).
8. G. O. Aspinall. Advan. Carbohydrate Chem. **8**, 217 (1953).
9. L. Hough, J. E. Priddle, and R. S. Theobald. Advan. Carbohydrate Chem. **15**, 91 (1960).
10. L. Hough and J. E. Priddle. Chem. Ind. London, 1600 (1959).
11. P. A. J. Gorin and A. S. Perlin. Can. J. Chem. **39**, 2474 (1961).
12. M. Karplus. J. Chem. Phys. **33**, 316 (1960).
13. F. A. L. Anet. Can. J. Chem. **39**, 789 (1961).
14. R. W. Lenz and J. P. Heeschen. J. Polymer Sci. **51**, 247 (1961).
15. D. H. Barton. Chem. Ind. London, 1136 (1956).
16. J. E. Kilpatrick, K. S. Pitzer, and R. Spitzer. J. Am. Chem. Soc. **69**, 2483 (1947).
17. F. V. Brutcher, Jr., T. Roberts, S. J. Barr, and N. Pearson. J. Am. Chem. Soc. **81**, 4915 (1959).
18. R. U. Lemieux, J. D. Stevens, and R. R. Fraser. Can. J. Chem. **40**, 1955 (1962).
19. K. Iwadare. Bull. Chem. Soc. Japan, **16**, 40 (1941).
20. R. Schaffer and H. S. Isbell. J. Am. Chem. Soc. **79**, 3864 (1957).
21. J. A. Mills. Advan. Carbohydrate Chem. **10**, 1 (1955).
22. C. J. Brown. Acta Cryst. **7**, 92 (1954).
23. K. Freudenberg. Ber. **59**, 836 (1926).
24. P. A. Levene and J. Compton. J. Biol. Chem. **114**, 9 (1936).
25. R. Schaffer. J. Res. Natl. Bur. Std. A, **65**, 507 (1961).
26. R. J. Abraham, K. A. McLauchlan, L. D. Hall, and L. Hough. Chem. Ind. London, 216 (1962).
27. J. N. Baxter and A. S. Perlin. Can. J. Chem. **38**, 2217 (1960).
28. P. A. J. Gorin and K. Horitsu. Private communication.
29. W. G. Dauben and K. S. Pitzer. *In* Steric effects in organic chemistry. *Edited by* M. S. Newman. John Wiley and Sons, Inc., New York. 1956. p. 1.
30. B. Helferich and J. F. Leete. Ber. **62**, 1549 (1929).
31. B. J. Ludwig and E. C. Piech. J. Am. Chem. Soc. **73**, 5779 (1951).
32. L. Hough, J. E. Priddle, R. S. Theobald, G. R. Barker, T. Douglas, and J. W. Spoors. Chem. Ind. London, 148 (1960).
33. R. Kuhn, H. Trischmann, and I. Low. Angew. Chem. **67**, 32 (1955).
34. A. S. Perlin and S. Suzuki. Can. J. Chem. **40**, 1226 (1962).
35. B. Helferich. Advan. Carbohydrate Chem. **3**, 79 (1948).
36. D. F. Mowery, Jr. Methods Carbohydrate Chem. **2**, 330 (1963).

Can. J. Chem. Downloaded from www.nrcresearchpress.com by 210.87.254.40 on 09/05/12
For personal use only.

TRANSFORMATIONS OF ICE VI AND ICE VII AT ATMOSPHERIC PRESSURE*

J. E. Bertie, L. D. Calvert, and E. Whalley
Division of Applied Chemistry, National Research Council, Ottawa, Canada
Received February 7, 1964

ABSTRACT

The irreversible transformations that occur when ices VI and VII are heated at atmospheric pressure from liquid-nitrogen temperature have been examined by simple thermal analysis and by X-ray diffraction. They transform first to cubic ice I (ice Ic) which subsequently transforms to hexagonal ice I (ice Ih). The rates of transformation depend on the temperature. The heat evolved is 16 ± ~2 cal/g for ice VI and 31 ± ~4 cal/g for ice VII.

I. INTRODUCTION

An investigation is being carried out of the properties of the high-pressure ices, and as part of this work the transformations of ices II, III, and V, when they are heated from a metastable state at liquid-nitrogen temperature and atmospheric pressure, have been investigated by simple thermal analysis and by X-ray diffraction (1). The X-ray powder photographs were reported for purposes of identification. In this paper the transformations of ices VI (2(*a*)) and VII (2(*b*)) are described.

II. EXPERIMENTAL METHODS

Ice VI was made using the high-pressure apparatus described earlier (1). Briefly, ice was compressed to ~7 kb at ~253° K in a thick-walled steel cylinder using a hydraulic press, and cooled to 77° K before the pressure was removed. It was removed from the vessel and handled either under liquid nitrogen or in the dry cold gas immediately above the surface of rapidly boiling liquid nitrogen, and was stored under the liquid until required. Ice VII was made (3) in a similar manner using a pressure vessel with one stage of external support (4) at ~253° K and 25 kb. Usually, large cylinders of ice were obtained, and these were washed with liquid nitrogen to remove small fragments, and then ground under liquid nitrogen before use. All of the ice studied in this work was made from H_2O.

When ice II is transformed to ice I on the I–II equilibrium line at 193° K it transforms not directly to the stable form ice Ih, but first to ice Ic (1). It was therefore worth testing whether ice VII transforms directly to ice VI on the equilibrium line. In fact, ice VII transformed at 23 kb and 250° K to ice VI with the same X-ray powder pattern as ice VI made by transformation of ice V at 7 kb and ~250° K.

It is assumed in all this work that the phase recovered at liquid-nitrogen temperature and atmospheric pressure is the same as that formed at high pressure and temperature. This can only be verified by, for example, X-ray diffraction at high pressure, and preparation is being made to do this.

The X-ray powder patterns were photographed as described earlier (1), except that to obtain better resolution a collimator giving a beam size at the specimen of 0.4 mm instead of 0.8 mm was used.

The apparatus and technique used for the thermal analysis has been described in detail elsewhere (1). Basically the temperature of a sample of ice contained in a dewar vessel

Issued as N.R.C. No. 7903.

Can. J. Chem. Downloaded from www.nrcresearchpress.com by 210.87.254.40 on 09/05/12
For personal use only.

of low heat capacity was measured as a function of time as the ice warmed from 77 to 190° K. The calorimeter was then re-cooled to 77° K and the heating curve of the ice I, which had been formed from the ice VI or VII, was measured. No attempt was made to ensure that ice Ih was formed, and the ice I was probably a mixture of ice Ih and ice Ic.

The heating curves were analyzed according to a first-order rate law

$$dT/dt = k(T_\infty - T)/C$$

where T is the temperature at time t, T_∞ is the temperature of the bath surrounding the calorimeter, k is the heating constant, and C is the heat capacity of the calorimeter and contents. T_∞ was 194.6° K.

III. RESULTS

The X-ray powder patterns for ices VI and VII are given in Table I. The values listed

TABLE I

X-ray powder diffraction data for ices VI and VII. Flat-plate camera: specimen to film 6 cm; Zr-filtered Mo radiation, λK_α 0.7107 Å; cutoff ~8 Å; temperature ~90° K

Ice VI		Ice VII	
d/Å	I/I_1	d/Å	I/I_1
4.3	8 h	4.0	2 h
3.6	8 h	3.5	<1 b h
3.4	5 h	3.22	<1 h
3.12	13	2.42	100
2.91	8	2.27	2
2.75	90	2.09	3
2.63	50	1.91	1
2.51	100	1.75	2
2.43	8	1.70	6
2.21	25	1.57	1
2.10	13 b	1.42	3
2.01	20	1.39	9
1.97	20	1.37	<1
1.85	17 b	1.22	2
1.75	1 b	1.20	1
1.64	25 b	1.11	1
1.56	20	1.08	2
1.48	25	0.99	<1
1.44	3		
1.41	12		
1.37	7 b		
1.34	4 b		
1.30	1		
1.26	<1		
1.21	10		
1.14	10		
1.104	2		
1.084	1		
1.050	5		
1.010	4		

NOTE: b Broad line.
h Occurs in region covered by halo due to the silica sample tube.

are averages taken from different samples; a film-shrinkage correction was applied. McFarlan (5) reported obtaining single crystal and powder patterns of ice VI, which he thought was of low symmetry, but he gave no results for comparison. No other measurements have been reported.

Can. J. Chem. Downloaded from www.nrcresearchpress.com by 210.87.254.40 on 09/05/12
For personal use only.

Can. J. Chem. Downloaded from www.nrcresearchpress.com by 210.87.254.40 on 09/05/12
For personal use only.

The heating curve of ice VI is shown as curve 1 of Fig. 1. The transformation begins, at a heating rate of about 1.5 deg/min, at 147° K and is fast at 152° K. A large amount of heat is evolved and the temperature of the thermocouple lags the temperature of the ice by an unknown and uncontrollable amount, and thus the temperatures quoted may be low. Also, the large amount of heat evolved disturbs the pseudo-steady state of the system, causing a temperature peak to occur instead of a monotonic temperature change, and this made it difficult to obtain the temperature change required to calculate the heat evolution in the transition. To obtain this temperature change the heating curve of the ice I that was formed from the ice VI was followed for a long period, and the first-order plot was extrapolated graphically back to the transition temperature. This procedure is not, of course, very precise. It yields a temperature change of 25.4 ± ~0.5° C. From the heating curve of the same sample of ice after it had transformed to ice I, and the heating curve of the empty calorimeter, this temperature change yields a heat evolution of 16 ± ~2 cal/g,* if the heat capacities of ices Ih and Ic are assumed to be the same. From the heating curve of ice VI and the heating curve of the same sample in the form of ice I, the heat capacity of ice VI seems to be greater than that of ice I.

A sample of ice VI was heated in the X-ray camera for 4 minutes successively at the temperatures 106, 113, 127, 137, 146, and 158° K. After each heating it was cooled to ~90° K and the X-ray powder photograph was taken. Between 146° and 158° K the pattern changed from that of ice VI to that of ice Ic. Another sample of ice VI held at 143° K did not change in 10 minutes but had changed to ice Ic in 100 minutes. The rate of transformation is therefore temperature dependent.

The heating curve of ice VII is shown as curve 2 of Fig. 1. Ice VII starts to transform

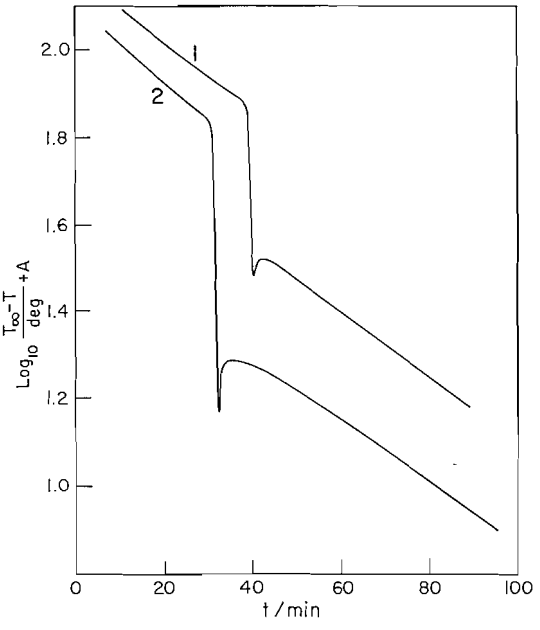

FIG. 1. First-order plot of the heating curves of the high-pressure ices. Curve 1: initially ice VI, A = 0.20. Curve 2: initially ice VII, A = 0.00.

In the previous paper in the series (1) the results for ice V were erroneously reported. The increase in temperature was 15.5 ± ~1° C and the heat evolved 11 ± ~2 cal/g.

at a heating rate of 1.5 deg/min at 123° K, and transforms rapidly at 131° K. The temperature lag between the thermocouple and the ice is likely to be greater for ice VII than for ice VI, because the heat evolved is greater, and the temperatures quoted are likely to be low. Similarly the pseudo-steady state is disturbed by the heat evolution, and the same techniques as outlined above for ice VI were used to find the "steady-state temperature change", which was 48.5 ± ~1° C, and this yielded 31 ± ~4 cal/g for the heat evolved.

A sample of ice VII was heated in the X-ray camera for 4 minutes successively at the temperatures 103, 119, 127, and 138° K. After each heating it was cooled to ~90° K and the X-ray powder photograph was taken. Between 127° and 138° K the pattern changed from that of ice VII to that of Ic with a trace of Ih. Another sample was held at 125° K for 21 hours and cooled to ~90° K and its X-ray powder photograph was taken. About half had transformed to ice Ic. The same sample was then kept at 133° K for 4 hours and cooled to ~90° K, and its X-ray powder photograph again taken. Only a trace of ice VII was left. The rate of transformation of ice VII to ice Ic is therefore temperature dependent. There is no inconsistency in the rates of transformation of ices VI and VII measured by the calorimetric and the X-ray methods. In the calorimetric experiments, the heat of transition autoaccelerates the reaction, and causes the thermocouple temperature to lag the ice temperature, so that the measured transition temperatures are probably low. Whereas in the X-ray experiments, the heat of transition is largely lost to the cooling gas without the ice warming greatly, and the measured temperatures are probably closer to those of the ice, and the transition temperatures are thus more reliable than those obtained in the calorimetric work.

The magnitude of the heat evolved cannot be compared in detail with the thermodynamic properties of the ices because too little is known about the thermodynamic properties. The magnitude is, however, consistent with the appropriate sum of the differences in internal energy on the equilibrium lines (2).

IV. DISCUSSION

For purposes of comparison, the X-ray powder patterns of all the phases of ice we have examined are represented in Fig. 2. As can be seen, they are readily distinguishable one from the other and are detectable in the presence of one another, except for ice Ic in the presence of Ih. The pattern for ice VII has a marked pseudo-cubic appearance and the strong lines can be formally referred to a body-centered cubic cell, $a = 3.45$ Å.

Rough values of the rates and heats of the irreversible transformation of several phases of ice that are metastable at 1 atm have now been obtained, and it is worthwhile to compare them. The data are summarized in Table II. The transformation rates for at least some of the transformations depends on the history of the sample (1), and this is not under perfect control. Nevertheless, the temperatures of transformation for the given heating rate, which is 1–2 deg/min, are probably roughly comparable for all the ices as they were all obtained in roughly the same way. In particular, the ice used was either freshly made or had been stored in liquid nitrogen since it was made.

There appears to be at least a rough relationship between the heat evolved and the temperature of transformation. There is also a rough relationship between these quantities and the infrared and Raman frequencies (3, 7, 8, 9). For example, the larger the O—H stretching frequencies, i.e. the nearer they are to those of the vapor, the lower usually is the transition temperature. Likewise, the dielectric relaxation times (10) correlate roughly with the data in Table II. In particular, ice II, which does not transform until

Can. J. Chem. Downloaded from www.nrcresearchpress.com by 210.87.254.40 on 09/05/12
For personal use only.

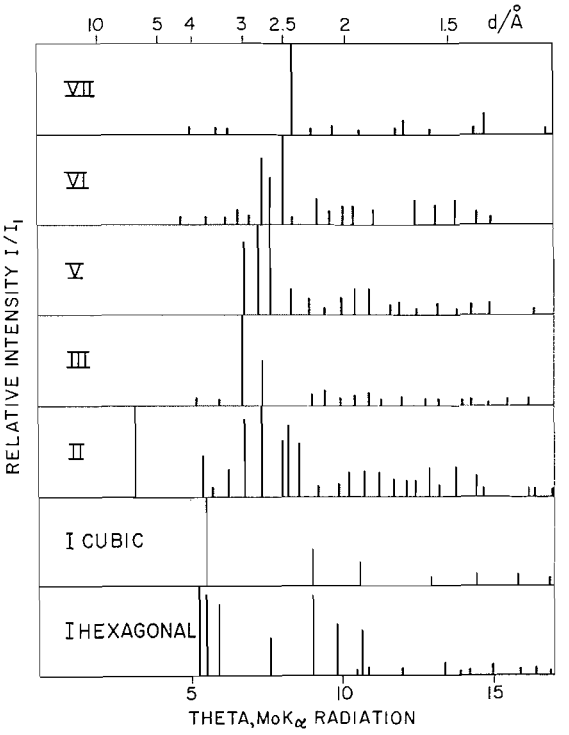

FIG. 2. Summary of the X-ray powder patterns of the various phases of ice at ~90° K.

TABLE II

Comparison of temperatures and heats of irreversible transformation of various phases of ice

Transformation	Temperature*	Heat evolved, cal/g	Reference
VII → Ic	~125°	31	This work
VI → Ic	~150°	16	This work
Iv† → Ic	~150°	12	6
V → Ic	~150°	11‡	1
III → Ic	~150°	4	1
II → Ic	~170°	<0.5	1
Ic → Ih	~200°	Undetected	1

*Temperature of rapid transformation of a freshly made sample, or one that had not previously been heated above 80° K, for a heating rate of about 1–2 deg/min.
†Iv is vitreous ice I.
‡The correct value is given in this paper.

170° K at a heating rate of 1.5 deg/min (1), has no detectable relaxation under any accessible conditions (maximum temperature 243° K) at frequencies as low as 45 c.p.s. and has a low dielectric constant, whereas ices III, V, and VI all relax faster than ice I at the same temperature. There are, however, several exceptions to these correlations, which need not be detailed.

All these processes involve deforming hydrogen bonds, but involve different deformations. It is not surprising that there are rough correlations, nor that there are exceptions.

ACKNOWLEDGMENT

We are indebted to Mr. A. Lavergne for help with the high-pressure equipment, and to Dr. J. Marckmann who made the ices.

Can. J. Chem. Downloaded from www.nrcresearchpress.com by 210.87.254.40 on 09/05/12
For personal use only.

REFERENCES

1. J. E. BERTIE, L. D. CALVERT, and E. WHALLEY. J. Chem. Phys. **38**, 840 (1963).
2. P. W. BRIDGMAN. (*a*) Proc. Am. Acad. Arts Sci. **47**, 441 (1912); (*b*) J. Chem. Phys. **5**, 964 (1937).
3. J. MARCKMANN and E. WHALLEY. To be published.
4. P. W. BRIDGMAN. Proc. Am. Acad. Arts Sci. **72**, 45 (1937).
5. R. L. MCFARLAN. Rev. Sci. Instr. **7**, 82 (1936); J. Chem. Phys. **4**, 60, 253 (1936).
6. R. H. BEAUMONT, H. CHIHARA, and J. A. MORRISON. J. Chem. Phys. **34**, 1456 (1961).
7. J. E. BERTIE and E. WHALLEY. J. Chem. Phys. **40**, 1637 (1964).
8. M. J. TAYLOR and E. WHALLEY. J. Chem. Phys. **40**, 1660 (1964).
9. J. E. BERTIE and E. WHALLEY. J. Chem. Phys. **40**, 1646 (1964).
10. R. K. C. CHAN, G. J. WILSON, D. W. DAVIDSON, and E. WHALLEY. To be published.

Can. J. Chem. Downloaded from www.nrcresearchpress.com by 210.87.254.40 on 09/05/12
For personal use only.

THE DIELECTRIC BEHAVIOR OF THE SYSTEM: ACETIC ACID – CHLOROFORM – WATER AT 25° C

A. N. CAMPBELL AND J. M. T. M. GIESKES[1]
Department of Chemistry, University of Manitoba, Winnipeg, Manitoba
Received January 20, 1964

ABSTRACT

The dielectric constants of mixtures of water and acetic acid, of chloroform and acetic acid, and of water, chloroform, and acetic acid have been determined at 25° C, over a range of concentrations. The apparent molar polarizations, but not the dipole moments, of acetic acid have been calculated and the results interpreted in the light of an assumed structure of the mixtures.

Can. J. Chem. Downloaded from www.nrcresearchpress.com by 210.87.254.40 on 09/05/12
For personal use only.

The work detailed here is a continuing study of the system: acetic acid – chloroform – water. Earlier studies have embraced the isothermal vapor–liquid equilibrium at 25° and the volume changes on mixing (1). A more recent study (2) deals with the isobaric boiling point diagram. The guiding theme of this work is an attempt to find a connection between the very large miscibility gap which exists in this system, and other physical properties of the system. In this connection we thought that the dielectric constants and derived functions might be of interest.

The acetic acid – chloroform – water system stands in sharp contrast to the system acetone–chloroform–benzene, which we have previously investigated (3). In the latter system there is no miscibility gap and a compound is formed by hydrogen bonding between chloroform and acetone. We were able to prove the undoubted existence of this compound by a study of the freezing point curve, but, in addition, we demonstrated it by a study of the dielectric constant, or rather dipole moment, of acetone–chloroform mixtures, when increasing quantities of the inert solvent benzene were added. We have now carried out similar measurements on acetic acid – chloroform mixtures, with increasing additions of the inert, symmetrical carbon tetrachloride. In the case of acetic acid, however, the problem is complicated by the known association of acetic acid. Extrapolation of molar polarization to infinite dilution, in the usual way, becomes meaningless.

Because of the importance of acetic acid and its rather complicated structure, the literature is extensive and need not be gone into in detail. Smyth and Rogers (4) studied the dielectric behavior of acetic acid in benzene and in ethyl ether: Le Fevre and Vine (5) did similar work in the region of low concentration in benzene. More significant is the work of Pohl, Hobbs, and Gross (6), who studied acetic acid in very dilute solutions in benzene and heptane. They found an increase in the polarization of acetic acid at concentrations smaller than 0.004 mole fraction in benzene, and smaller than 0.001 mole fraction in heptane. These results they attribute to a dimer $\rightleftarrows$ monomer equilibrium. The dielectric constant of pure acetic acid increases with rising temperature and this is explained as being due to the favoring, at higher temperatures, of an open-chain polymeric form, rather than the cyclic dimer (7). Results of Raman spectra (8) of solutions of acetic acid in water suggest that an equilibrium exists between ring dimers and open-chain hydrogen bonded complexes with water, thus:

[1]*Holder of C.I.L. Fellowship, 1963–64.*

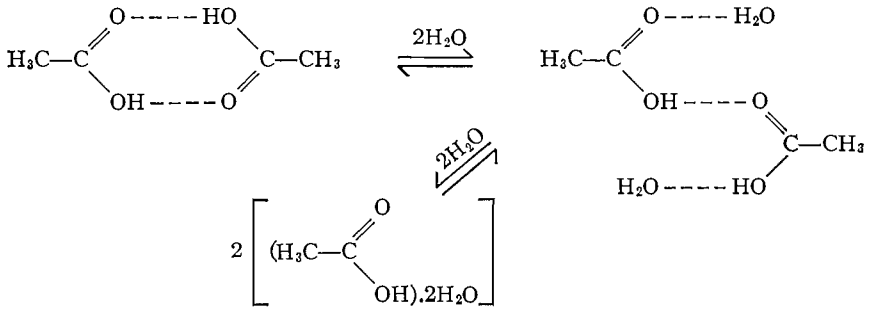

Work on the dielectric constants of acetic acid – water mixtures has been restricted to very dilute solutions (9) and nothing whatever appears to have been done on the dielectric constants of acetic acid – chloroform mixtures.

EXPERIMENTAL

For dielectric constant measurements we used a Sargent Oscillometer Model V and a Sargent Oscillometer Cell Compensator. The oscillometer works at a frequency of 5 megacycles per second. Because of its design, the cell is difficult to immerse in a liquid bath but we found that a well insulated air chamber could be controlled to 25.00 ± 0.05° C; such a temperature fluctuation is well within the accuracy of measurement (0.05%).

Fisher Certified Reagents were used throughout. Water was, therefore, the principal significant impurity, but, because of its high dielectric constant, every trace of it had to be removed. In the case of acetic acid, the freezing point was determined first and this gave a measure of the amount of water present. The calculated amount of acetic anhydride was then added and the mixture refluxed for 12 hours. After distillation, the distillate was submitted to repeated fractional crystallization, until a freezing point of 16.58° C was obtained; this is accepted as the freezing temperature of anhydrous acetic acid. The dielectric constant of this acid was 6.21, against the literature value of 6.18.

Chloroform was treated with concentrated sulphuric acid, washed with water until no acidity was detectable, dried over calcium chloride, and finally distilled from phosphorus pentoxide. The water used had a specific conductance of 5×10^{-6} mhos cm^{-1} at 25° C.

RESULTS

The System: Acetic Acid – Chloroform

1. The Concentrated Region

The accuracy of the measurements of dielectric constant is ±0.01.

TABLE I

Wt. % HAc	$\epsilon_{25°}$	Wt. % HAc	$\epsilon_{25°}$
0.00	4.72	19.06	4.47
1.89	4.68	30.78	4.51
5.41	4.60	43.41	4.68
11.92	4.50	61.46	5.06
15.08	4.48	77.41	5.49
18.30	4.47	100.00	6.21

NOTE: t = 25° C.

2. Solutions in Carbon Tetrachloride

Pure acetic acid.—The apparent polarization of the acetic acid was calculated from the Debye formulae

$$P_{12} = [(\epsilon - 1)/(\epsilon + 2)].[(x_1 M_1 + x_2 M_2)/d_{12}]$$

and

$$P_2 = [(P_{12} - P_1)/x_2] + P_1,$$

Can. J. Chem. Downloaded from www.nrcresearchpress.com by 210.87.254.40 on 09/05/12
For personal use only.

where P_{12} = polarization of the mixture,
P_1 = polarization of carbon tetrachloride,
P_2 = polarization of acetic acid,
x_1, x_2 = mole fractions,
M = formula molecular weight,
d_{12} = density of mixture.

The results are given in Table II.

TABLE II

Wt. % HAc	Mole % HAc	$\epsilon_{25°}$	d_4^{25}	P_{HAc} ml
0.000	0.00	2.228	1.5860	—
0.501	1.27	2.233	1.5812	24.07
0.573	1.45	2.233	1.5804	23.35
1.523	3.81	2.241	1.5716	23.07
1.663	4.15	2.2425	1.5703	23.18
2.786	6.84	2.252	1.5602	23.06
5.137	12.18	2.274	1.5396	23.25
5.350	12.65	2.277	1.5384	23.29
6.135	14.34	2.287	1.5309	23.68
6.930	16.02	2.296	1.5242	23.81
6.960	16.08	2.296	1.5237	23.82
7.084	16.34	2.298	1.5228	23.87
8.705	19.63	2.321	1.5093	24.40
10.22	22.57	2.344	1.4973	24.81
11.25	24.51	2.358	1.4893	24.93

A mixture containing 20.57 mole % $CHCl_3$ and 79.4 mole % HAc in CCl_4.—This is a pseudobinary system, in which the concentration of carbon tetrachloride is variable. To calculate the apparent polarization of the acetic acid, we made use of the Debye formula (as above) but for the polarization of the chloroform we used the value for chloroform at corresponding concentrations in carbon tetrachloride. This value is obtained from a graph of our measurements (not given) of the polarization of chloroform in carbon tetrachloride. Incidentally, this graph, when extrapolated to zero concentration, yields a value for the dipole moment of chloroform of 1.13 D, in good agreement with the literature value (10). The results are tabulated in Table III.

TABLE III

Wt. % HAc	Wt. % CCl_4	$\epsilon_{25°}$	d_4^{25}	P_{HAc}
0.45	99.32	2.2363	—	22.89
1.10	98.33	2.2483	1.5749	23.07
2.15	96.75	2.2680	1.5646	23.17
2.59	96.08	2.2760	1.5604	23.08
4.58	93.06	2.3177	—	23.65
5.54	91.61	2.3425	1.5328	24.30
7.15	89.17	2.3840	—	24.92
8.12	87.69	2.4085	1.5098	25.16

A mixture of 50.04 mole % $CHCl_3$ and 49.46 mole % HAc in CCl_4.—The results are given in Table IV.

A mixture containing 63.39 mole % $CHCl_3$ and 36.61 mole % HAc in CCl_4.—The results are given in Table V.

The System: Acetic Acid – Water

Addition of water to acetic acid causes the electrical conductivity to increase rapidly.

Can. J. Chem. Downloaded from www.nrcresearchpress.com by 210.87.254.40 on 09/05/12
For personal use only.

TABLE IV

Wt. % HAc	Wt. % CCl_4	$\epsilon_{25°}$	d_4^{25}	P_{HAc}
0.166	99.50	2.2362	1.5840	25.08
0.340	98.98	2.2440	1.5819	23.32
0.790	97.64	2.2655	—	23.28
0.825	97.53	2.2671	—	23.18
1.37	95.83	2.2930	1.5697	22.81
2.33	93.04	2.3440	—	23.72
2.41	92.78	2.3477	1.5579	23.45
3.32	90.06	2.3988	1.5478	23.97

TABLE V

Wt. % HAc	Wt. % CCl_4	$\epsilon_{25°}$	d_4^{25}	P_{HAc}
0.340	98.49	2.2535	1.5812	23.37
0.693	96.92	2.2800	1.5764	22.58
0.961	95.73	2.3010	1.5728	22.61
1.41	93.74	2.3385	1.5667	23.14
1.99	91.16	2.3900	—	23.98
2.15	90.45	2.4040	—	24.02

At a concentration of 20% by weight of water, the specific conductance has already risen to 1×10^{-4} mhos cm^{-1}. A conductivity of this magnitude is sufficient to interfere with the determination of dielectric constants, by ordinary methods. Johnson and Cole (11), in their study of formic acid, state that measurements below a frequency of 10^4 cycles and a conductance of 6×10^{-5} mhos cm^{-1} at 25° C, will lead to too large a value of the dielectric constant. In the present study a frequency of 5×10^6 cycles was used, so that, so long as the conductivity did not exceed 10^{-4} mhos, presumably no correction is needed. In this region (up to 20% water), therefore, we continued to use the Sargent Oscillometer. We went to considerable pains to obtain anhydrous formic acid and, having obtained it, we determined the dielectric constant in the Sargent apparatus, and we obtained a value in good agreement with that of Johnson and Cole. We therefore concluded that the Sargent apparatus gives good results up to a conductivity of 6×10^{-5} mhos and we have hopefully assumed that the apparatus continues to function accurately up to a conductivity of 10^{-4} mhos. It is claimed that corrections can be applied when the conductivity exceeds the above figure (12), but we are sceptical of such corrections and therefore we have not entered the region of higher conductivity. For this region of higher conductivity, an entirely different high frequency method is necessary.

Table VI contains data for the specific conductance and the dielectric constants as determined.

The Ternary System: Acetic Acid – Chloroform – Water

For this investigation we made up large amounts of stock solutions of chloroform and acetic acid of known compositions. To each of these stock solutions water was added in known amount, little by little, and the dielectric constant determined. For one set of experiments, in which the water content was allowed to go as high as 16–69% the specific conductances were also determined, to ensure that the allowable limit of conductance had not been exceeded.

DISCUSSION OF RESULTS

System: Acetic Acid – Chloroform

When dielectric constants of mixtures of acetic acid and chloroform are plotted against

Can. J. Chem. Downloaded from www.nrcresearchpress.com by 210.87.254.40 on 09/05/12
For personal use only.

TABLE VI

H_2O wt. %	κ, mhos/cm	$\epsilon_{25°}$
1.795	—	8.76
1.90	—	8.88
2.92	—	10.29
3.46	—	11.06
3.78	—	11.41
5.24	1.99×10^{-6}	—
5.52	—	13.62
5.56	2.39×10^{-6}	13.58
7.27	—	16.06
7.68	—	15.96
8.21	—	16.43
9.06	—	17.48
9.75	1.30×10^{-5}	—
9.77	1.30×10^{-5}	18.43
10.35	—	19.37
13.19	—	24.69
13.37	—	25.10
13.87	3.68×10^{-5}	—
15.29	4.70×10^{-5}	30.10
15.34	—	30.54
15.61	—	31.32
19.14	8.73×10^{-5}	47.44

TABLE VII

Binary mixture 21.0 wt. % HAc 79.0 wt. % $CHCl_3$		Binary mixture 28.2 wt. % HAc 71.8 wt. % $CHCl_3$		Binary mixture 47.1 wt. % HAc 52.9 wt. % $CHCl_3$		Binary mixture 55.7 wt. % HAc 44.3 wt. % $CHCl_3$	
Wt. % H_2O	$\epsilon_{25°}$	Wt. % H_2O	$\epsilon_{25°}$	Wt. % H_2O	$\epsilon_{25°}$	Wt. % H_2O	$\epsilon_{25°}$
0.00	4.47	0.00	4.60	0.00	4.80	0.00	4.95
0.82	5.11	2.53	6.63	2.62	7.52	4.87	10.22
0.89	5.17	3.14	7.04	9.73	14.50	6.99	12.42
1.12	5.32	3.88	7.60	12.16	17.38	8.88	14.60
1.73	5.77					11.21	17.44

Binary mixture 62.5 wt. % HAc 37.5 wt. % $CHCl_3$		Binary mixture 68.1 wt. % HAc 31.9 wt. % $CHCl_3$		Binary mixture 76.5 wt. % HAc 23.5 wt. % $CHCl_3$		
Wt. % H_2O	$\epsilon_{25°}$	Wt. % H_2O	$\epsilon_{25°}$	Wt. % H_2O	κ, mhos/cm	$\epsilon_{25°}$
0.00	5.08	0.00	5.26	0.00	—	5.46
1.53	6.89	2.79	8.67	6.75	—	13.54
2.08	7.54	3.48	9.42	7.58	5.72×10^{-6}	14.35
3.52	9.28	6.61	12.98	13.36	3.09×10^{-5}	23.69
4.54	10.60	9.24	16.30	16.69	5.72×10^{-5}	33.04

weight fraction of acetic acid, a minimum is found to occur at a concentration of about 20% by weight of acetic acid and dielectric value of 4.45, that is, the effective polarization of the mixture is reduced below those of its components. This negative deviation may indicate dipole association of chloroform with acetic acid, or alternatively, that the effect of adding chloroform to acetic acid is to decrease the number of open chain dimers in favor of ring dimers, which have very small dipole moments. The fact, however, that the dielectric constant of acetic acid itself is rather low suggests that the ring dimer form predominates, even in the pure acid.

When the molar polarizations of acetic acid in carbon tetrachloride, evaluated by the

Can. J. Chem. Downloaded from www.nrcresearchpress.com by 210.87.254.40 on 09/05/12
For personal use only.

Debye formula (Table II), are plotted as a function of mole fraction acetic acid, a striking increase in the apparent polarization of acetic acid is apparent, in the region of low concentration. This increase can only be explained on the basis of an increase in the relative amount of monomer, in dilute solution. The polarization of acetic acid in benzene and in heptane behaves in the same way, according to Pohl, Hobbs, and Gross (6): in the latter solvents, however, the effect is observed at a lower concentration. These observations are in agreement with the heats of dimerization as reported by Moelwyn-Hughes (13).

The apparent polarizations of acetic acid – chloroform mixtures, dissolved in carbon tetrachloride, were also obtained by the Debye method. This calculation makes the large assumption that the chloroform retains its molar polarization in the three-component mixture. To offset this assumption to some extent, we have used in our calculations, not the molar polarization of pure chloroform, but that of chloroform in carbon tetrachloride of corresponding concentration. Figures 1, 2, and 3 express the apparent molar polarization

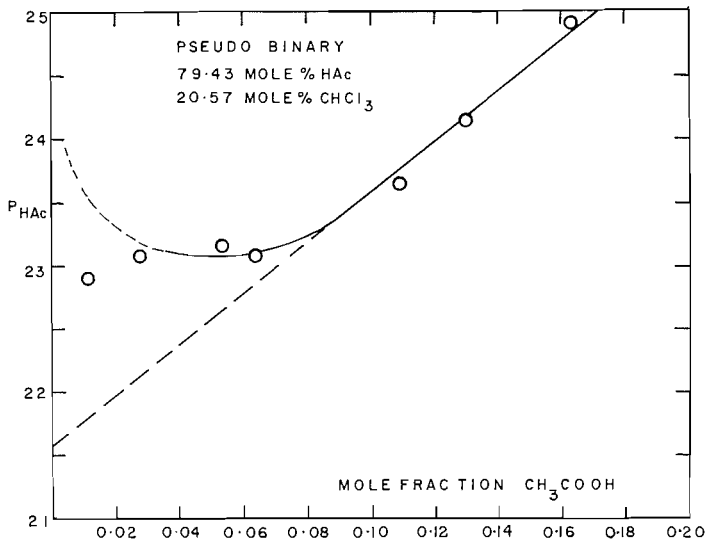

FIG. 1. Apparent polarization of acetic acid in carbon tetrachloride in system 79.43 mole % HAc, 20.57 mole % $CHCl_3$.

of acetic acid in acetic acid – chloroform – carbon tetrachloride mixtures, as a function of mole fraction of acetic acid in the ternary mixture. We have used the concentration of acetic acid as abscissa, rather than that of carbon tetrachloride, for the following reason. For a pseudobinary system of this type, the normal procedure would be to use the concentration of carbon tetrachloride as the obvious axis of reference, but, since the two types of graph (binary and pseudobinary) are very similar in character, it seemed to us that a plot in reference to the concentration of the acid was more instructive. Figures 1, 2, and 3 indicate the same behavior for the molar polarization of acetic acid, as that of acetic acid alone, in carbon tetrachloride. The apparent inaccuracy of the results in the low concentration region is due to the fact that a very slight error in the dielectric constant is very greatly multiplied in the process of calculation. There is no doubt, however, that the upward trend in the low concentration region is real. A striking feature of Figs. 1, 2, and 3 is that in all of them, if the linear portion of the curve is extrapolated to infinite dilution, the extrapolated value is the same, viz. 21.6 $\pm$ 0.1 ml.

Can. J. Chem. Downloaded from www.nrcresearchpress.com by 210.87.254.40 on 09/05/12
For personal use only.

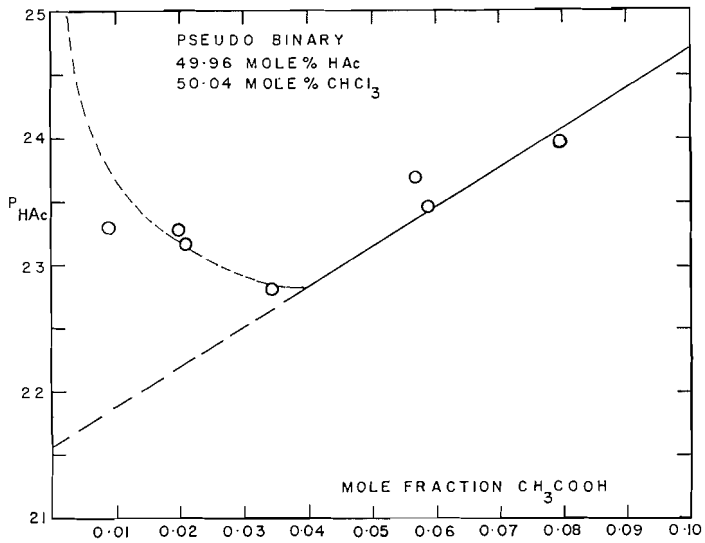

FIG. 2. Apparent polarization of acetic acid in carbon tetrachloride in system 49.96 mole % HAc, 50.04 mole % $CHCl_3$.

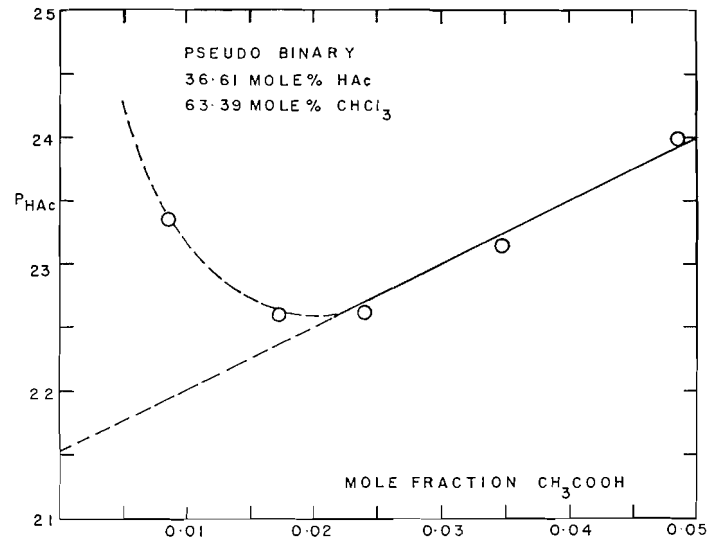

FIG. 3. Apparent polarization of acetic acid in carbon tetrachloride in system 36.61 mole % HAc, 63.39 mole % $CHCl_3$.

From the results of Davies, Jones, Patnaik, and Moelwyn-Hughes (14) on propionic acid in carbon tetrachloride and in chloroform, and also from the study by Brown and Mathieson (15), it appears that the heat of dimerization of acetic acid in carbon tetrachloride is greater than in chloroform and that the monomer concentration is greater in chloroform than in carbon tetrachloride. Similar results and conclusions were arrived at by Barrow and Yerger (16), who think that there is an association, via hydrogen bonding, between an acetic acid monomer and a chloroform molecule, the equilibrium constant being 0.2 at the lower limit.

Can. J. Chem. Downloaded from www.nrcresearchpress.com by 210.87.254.40 on 09/05/12
For personal use only.

It seems to us that our dielectric work confirms the above view. The fact that the increase in polarization is delayed as chloroform is added to acetic acid can be explained on the assumption that the monomer forms a dipole associate with the chloroform. This assumption would also explain the minimum in the dielectric constant of acetic acid – chloroform mixtures. The fact that all extrapolations give the same value, viz. 21.6 ± 0.1 ml, for the polarization of acetic acid, may indicate that, of the two competing equilibria

$$(CH_3COOH)_2 \rightleftharpoons 2CH_3COOH \qquad \text{(i)}$$

and

$$CH_3COOH + CHCl_3 \rightleftharpoons H_3C{-}C(=O\cdots HCCl_3){-}OH \qquad \text{(ii)}$$

the former is still predominant and lies to the side of the dimeric form.

The System: Acetic Acid – Water

Figure 4 shows that up to a concentration of 10% by weight of water, the dielectric

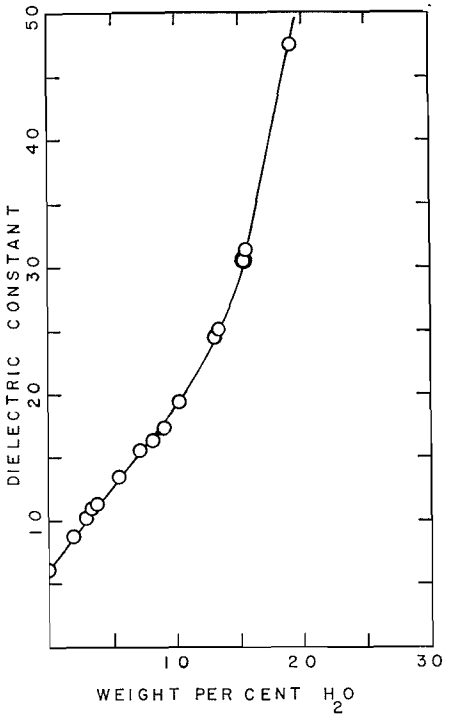

FIG. 4. Dielectric constant in system acetic acid – water at 25°.

constant increases linearly. At higher concentrations of water the slope increases and then becomes linear again. Kozo Nagano (9), who studied the effect of small additions of water, up to 2% by weight, on the dielectric constant of acetic acid, at 30° C, had already noticed the rapid increase in dielectric constant. It has been suggested by S. Fénéant-Eymard (8) as a result of her studies of Raman spectra, that acetic acid, on dilution with

Can. J. Chem. Downloaded from www.nrcresearchpress.com by 210.87.254.40 on 09/05/12
For personal use only.

water, first transforms from ring dimers into chain dimers, followed by hydration with formation of a dihydrated dimeric complex.

The behavior of Fig. 4 suggests that, at first, the ring dimers form open chain dimers, which then, via hydrogen bonding, form a complex with one molecule of water. We suggest this because the change of slope commences in the region of 33 mole % water. We, therefore, suggest a complex of the form

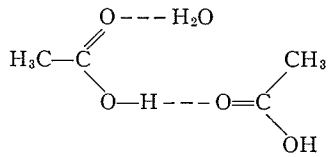

At higher concentrations, the hydroxyl group itself will commence to associate with a water molecule to form the dimeric dihydrate suggested by Fénéant-Eymard (8).

The System: Acetic Acid – Chloroform – Water

In all cases the relation between the dielectric constant and the weight per cent of water is linear. There is a sharp increase in dielectric constant at concentrations greater than 33 mole % of water, similar to the behavior of the system: acetic acid – water. The slopes of the straight lines decrease in the pseudobinary systems with increasing chloroform concentration. Our explanation of this behavior is the same as that offered for acetic acid – water mixtures, but the situation is complicated by the presence of the chloroform. Whereas water has a marked tendency to increase the dielectric constant of acetic acid, chloroform, on the assumption that it associates with the acid monomer to give a less polar complex, will tend to cause a decrease in the dielectric constant. These two competing effects could explain the lesser rate in the increase of the dielectric constant at higher chloroform concentrations.

REFERENCES

1. A. N. Campbell, E. M. Kartzmark, and J. M. T. M. Gieskes. Can. J. Chem. **41**, 407 (1963).
2. A. N. Campbell and J. M. T. M. Gieskes. Can. J. Chem. **42**, 186 (1964).
3. A. N. Campbell, E. M. Kartzmark, and H. Friesen. Can. J. Chem. **39**, 735 (1961).
4. C. P. Smyth and H. E. Rogers. J. Am. Chem. Soc. **52**, 1824 (1930).
5. R. J. W. Le Fevre and H. Vine. J. Chem. Soc. 1795, 1938.
6. H. E. Pohl, M. E. Hobbs, and P. M. Gross. J. Chem. Phys. **9**, 408 (1941).
7. C. P. Smyth. Dielectric behaviour and structure. McGraw-Hill, New York. 1955. J. C. Davis and K. S. Pitzer. J. Phys. Chem. **64**, 886 (1960).
8. S. Fénéant-Eymard. Mem. Serv. Chim. Etat Paris, **37**, 297 (1952). I. Cucurezeanu. Acad. Rep. Populare Romine Studii Cercetari Fiz. **9**, 269 (1958). H. Dunken and P. Fink. Z. Chem. **2**, 117 (1962).
9. K. Nagano. Yakugaku Zasshi, **79**, 1534 (1959).
10. J. W. Williams and I. Kuchma. J. Am. Chem. Soc. **49**, 1676 (1927).
11. J. F. Johnson and R. H. Cole. J. Am. Chem. Soc. **73**, 4536 (1951).
12. P. H. Sherrick, G. A. Dawe, R. Karr, and E. F. Ewen. Manual of chemical oscillometry. Sargent and Co., Chicago. 1954.
13. E. A. Moelwyn-Hughes. Physical chemistry. 2nd ed. Pergamon, New York. 1961. p. 1031.
14. M. Davies, P. Jones, D. Patnaik, and E. A. Moelwyn-Hughes. J. Chem. Soc. 1249 (1951).
15. C. P. Brown and A. R. Mathieson. J. Phys. Chem. **58**, 1057 (1954).
16. G. M. Barrow and E. A. Yerger. J. Am. Chem. Soc. **76**, 5248 (1954).

Can. J. Chem. Downloaded from www.nrcresearchpress.com by 210.87.254.40 on 09/05/12
For personal use only.

Can. J. Chem. Downloaded from www.nrcresearchpress.com by 210.87.254.42 on 09/05/12
For personal use only.

INTRAMOLECULAR DIAZO COUPLING AND MOLECULAR REARRANGEMENT OF *o*-AMINOPHENYLCARBINOLS[1]

ROBERT L. COHEN[2] AND ANTHONY J. SISTI
Department of Chemistry, Adelphi University, Garden City, Long Island, New York
Received November 7, 1963

ABSTRACT

A number of 1-(2-aminophenyl)-1-(substituted aryl)ethanols were deaminated, yielding ketones, formed by a molecular rearrangement and, in some instances, azo ketones formed by intramolecular coupling and cleavage. The sensitivities of these two reactions, one characteristic of the aryl cation and the other of the diazonium group, to relatively small changes in the electrical nature of the migrating group were determined.

The products of decomposition of the aromatic diazonium ion (I) may be classified as resulting from the aryl cation (II) (produced by the irreversible loss of nitrogen from I),

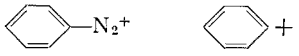

I II

or from the diazonium group functioning as an electrophile. The available data in the literature indicate that the aryl cation (II) is a highly reactive, non-selective moiety (1, 2). Thus, the heterolytic acid-catalyzed decomposition of diazonium salts normally leads to substitution by solvent or other nucleophiles (3, 4), but in certain instances molecular rearrangement (2) and elimination, yielding benzyne intermediate (2, 5, 6), have been observed.

The well-known coupling reaction of aromatic diazonium ions yielding azo compounds illustrates the electrophilic property of the diazonium group. Other reactions indicating this property have been discussed elsewhere (7, 4 (p. 424 ff.)).

Recently, an interesting intramolecular coupling and cleavage of a diazotized amine was reported (8). Namely, when 1-*o*-aminophenyl-1-(2,5-dimethyl-4-methoxyphenyl)-ethanol (III, $R_1 = R_4 = CH_3$, $R_3 = OCH_3$) was treated with nitrous acid, in addition to phenol and the expected rearrangement product (2) (IV), an 18% yield of azo ketone (V)

[1] 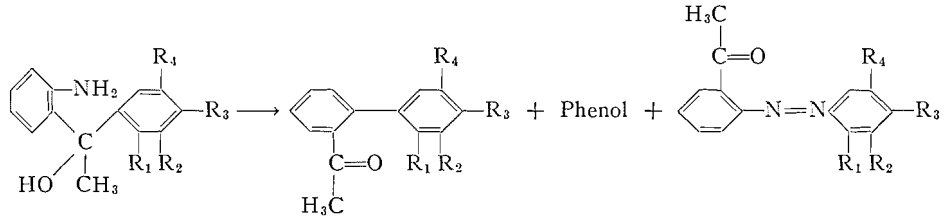

III IV V

was isolated (eq. 1). The intermolecular application of the aforementioned reaction led to an excellent synthesis of aldehydes and ketones (9, 10, 11).

[1]*Taken in part from the Ph.D. thesis of Robert L. Cohen, Adelphi College, 1963; presented at American Chemical Society Meeting, New York, N.Y., September 9–13, 1963.*

[2]*Present address: Jackson Laboratory, Organic Chemicals Department, E.I. du Pont de Nemours and Company, Inc., P.O. Box 525, Wilmington 99, Delaware.*

The present paper deals with a study of the factors (steric and (or) electrical) which promote the novel rearrangement of the anisyl group yielding azo ketone. It is also of interest to note that compounds of type III afford an excellent opportunity to study simultaneously the reactivity and selectivity of the aryl cation (II) and the diazonium group (I) with minor changes in the electrical nature of the migrating group (eq. 1).

RESULTS

The amino alcohols listed in Table I were prepared by treatment of the appropriately substituted *o*-aminobenzophenones with methylmagnesium iodide. The *o*-aminobenzophenones were prepared by conventional Friedel–Crafts acylations. Each compound was diazotized in acidic aqueous dioxane and the resulting diazonium salts were decomposed at room temperature. Three products were isolated: alkali-soluble material presumably phenol, ketones resulting from molecular rearrangement, and azo ketones (when produced) resulting from intramolecular coupling and cleavage. The two ketones were separated chromatographically on an alumina-packed column.

The results of the diazotization of various 1-(2-aminophenyl)-1-(substituted aryl)-ethanols (III), yielding ketone (IV) and azo ketone (V), are given in Table II (eq. 1). No fluorenol resulting from ring closure (2) could be isolated. The ketones (IV and V) were identified by infrared spectra and elemental analysis. Structure determinations were not carried out since ketones (2) and the azo ketone previously isolated (8) from similar reactions were synthesized unequivocally.

DISCUSSION

Inspection of the results presented in Table II reveals that *azo ketone* (V) was produced *only* by those amines which contain alkylated anisole rings (III*f*–III*i*). Significant amounts were produced from the diazotization of amines which bore two alkyl substituents in the anisole nucleus (compare III*e* and III*f* with III*g*–III*i*). The effect of the *ortho*-substituent (R_1) in promoting azo ketone formation cannot be primarily steric in nature (compare III*g* and III*i* with III*j* and III*k*). Specifically it should be noted that the azo coupling of the electrophilic diazonium group is particularly sensitive to the electrical changes in the migrating anisyl group (compare III*g*, III*h*, and III*i* with III*e* and III*f*, and with III*j* and III*k*). A rationalization for the results is best presented by assuming that the transition state for intramolecular azo coupling resembles the intermediate presented in equation 2. Maximum stabilization for the transition state is furnished by the *p*-methoxyl group, however, this substituent is not sufficient to yield a significant amount of coupling product. If the inductive stabilizing effect of the 1-methyl and 2- or 4-methyl groups are added, the rate of intramolecular azo coupling is fast enough to produce reasonable yields of the azo ketone. This interpretation of the results is in complete agreement with previously reported studies (12). The rate of coupling of *p*-nitrobenzenediazonium sulphate with various alkylated anisoles increased in the following order: *m*-methylanisole, 2,3-dimethylanisole, 2,5-dimethylanisole, and 3,5-dimethylanisole (anisole and *o*-methylanisole do not couple at all). Competitive coupling studies of phenols and substituted phenols with *p*-nitrobenzenediazonium sulphate revealed that chlorine and bromine deactivate whether *ortho* or *meta* to the coupling position (coupling occurs *para* to —OCH_3 or —OH group). Thus, the methyl, chloro, and bromo groups, which are sterically similar, whether *ortho* or *meta* to the coupling site exert effects consistent with their respective inductive electrical properties. A rationale for migration is therefore

Can. J. Chem. Downloaded from www.nrcresearchpress.com by 210.87.254.42 on 09/05/12
For personal use only.

Can. J. Chem. Downloaded from www.nrcresearchpress.com by 210.87.254.42 on 09/05/12
For personal use only.

TABLE I

Amino alcohols

	M.p.	Yield,* %	Calc.			Found		
			C	H	N	C	H	N
1-(2-Amino-4,5-dimethylphenyl)-1-(2-chlorophenyl)-ethanol (III*c*)	106–107	71	69.69	6.53	5.08	69.73	6.58	5.05
1-(2-Amino-4,5-dimethylphenyl)-1-(2-bromophenyl)-ethanol (III*d*)	112–112.5	48	60.01	5.66	4.37	60.13	5.60	4.45
1-(2-Aminophenyl)-1-(2-methyl-4-methoxyphenyl)-ethanol (III*f*)	145–147	67	74.68	7.44	5.44	74.55	7.32	5.41
1-(2-Aminophenyl)-1-(2,3-dimethyl-4-methoxyphenyl)-ethanol (III*h*)	178–180	33	75.24	7.80	5.16	75.24	7.67	5.31
1-(2-Aminophenyl)-1-(5-methyl-2-ethyl-4-methoxyphenyl)ethanol (III*i*)	110–112	26	75.76	8.12	4.91	75.73	8.02	4.97
1-(2-Aminophenyl)-1-(2-chloro-5-methyl-4-methoxyphenyl)ethanol (III*j*)	120–122	52	65.86	6.22	4.80	65.85	6.27	4.83
1-(2-Aminophenyl)-1-(2-bromo-5-methyl-4-methoxyphenyl)ethanol (III*k*)	124–126	56	57.15	5.40	4.17	57.33	5.34	4.28
2-Aminophenyldi-(2,5-dimethyl-4-methoxyphenyl)-carbinol† (VI)	161–163	20	76.69	7.47	3.58	76.62	7.37	3.52

*Yields refer to reactions of substituted *o*-aminobenzophenones with methylmagnesium iodide.
†Prepared from methyl anthranilate and the Grignard reagent from 2,5-dimethyl-4-methoxyiodobenzene.

Can. J. Chem. Downloaded from www.nrcresearchpress.com by 210.87.254.42 on 09/05/12
For personal use only.

TABLE II

Yields of ketones, azo ketones, and phenols from diazonium salts

	Amine III							
	R_1	R_2	R_3	R_4	% ketone (IV)*		% azo ketone (V)†	% phenol
(*a*)‖	$-CH_3$	—H	$-CH_3$	—H		10§	0	—
(*b*)‖	—H	—H	—H	—H		3.0§	0	—
(*c*)‡	—Cl	—H	—H	—H	1.34	0.8§§	0	—
(*d*)‡	—Br	—H	—H	—H	1.4	1.4§	0	—
(*e*)‖	—H	—H	$-OCH_3$	—H	—	4.4§	0	—
(*f*)	$-CH_3$	—H	$-OCH_3$	—H	17.2	13.4§	1.7	30
(*g*)‖	$-CH_3$	—H	$-OCH_3$	$-CH_3$	16	(13)	18	22
(*h*)	$-CH_3$	$-CH_3$	$-OCH_3$	—H	18.4	(12)	16.5	17
(*i*)	$-CH_2CH_3$	—H	$-OCH_3$	$-CH_3$	—	(14.2)	15.6	20
(*j*)	—Cl	—H	$-OCH_3$	$-CH_3$	15.0	(11.7)	0	60
(*k*)	—Br	—H	$-OCH_3$	$-CH_3$	15.8	(13.1)	0	40

*Yields in parentheses refer to recrystallized ketone; those without parentheses to chromatographed yield.
†Yields refer to crystallized material.
‡1-(2-Amino-4,5-dimethylphenyl)-1-(substituted aryl)ethanol (VI).
§Yield of 2,4-dinitrophenylhydrazone.
‖The results of these compounds were reported previously (ref. (2)).

envisaged as an intramolecular electrophilic attack by the diazonium group upon the anisyl group (eq. 2).

[2] 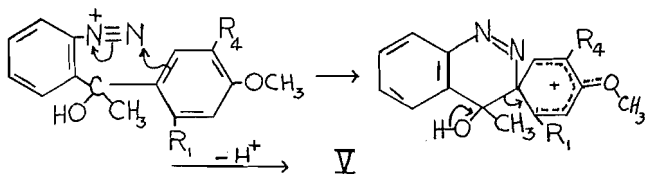

In a previously reported result (2), azo ketone was not isolated when amino alcohol VI was deaminated. Further substantiation of the selectivity and sensitivity of the electro-

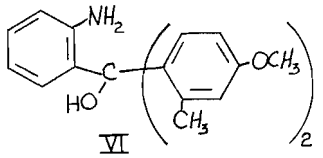

philic diazonium group to relatively minor electrical changes was obtained upon diazotization of the amino alcohol (VII) which resulted in the isolation of a 7% yield of azo ketone (VIII) (eq. 3).*

[3] 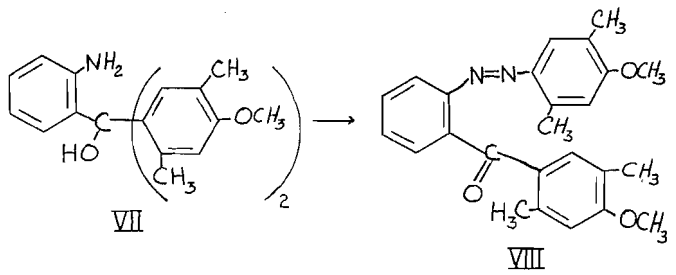

Further inspection of Table II reveals that the yields of ketone (IV), produced by migration of the aryl group to an electron-deficient carbon (2) (aryl cation), were essentially *constant* (III*f*–III*k*). These constant yields are significant since in those cases in which negligible amounts of azo ketone were produced (III*f*, *j*, and *k*), the increased portion of the reaction via aryl cation gave mainly phenol. Thus, the aryl cation is relatively insensitive to these electrical changes in the migrating group. Since it has been demonstrated that the lifetime of the aryl cation is very short (13) these results are not completely unexpected. However, they strongly support the mechanism previously offered for the formation of ketone (2). Thus, the electron-donor group (—OCH_3) in the *para*-position of the migrating group assists rearrangement provided an *ortho*-substituent is present (compare III*c*, *d*, and *e* with III*f*–*k*). This electrical assistance is to be expected in this type of rearrangement. Provided the *p*-methoxyl group is present, the yield of ketone is related to the number of free *ortho*-positions (III*f*–*k*). When the *p*-methoxyl group is absent the effect of an *o*-substituent upon ketone formation appears to be electrical (III*a*–III*d*). The rate of ketone formation, therefore, appears largely determined by the number of free *ortho*-positions, and the ground state electron density, of the migrating

*2,5-Dimethyl-4-methoxy-2'-(2,5-dimethyl-4-methoxyphenyl)benzophenone (27%) and 1,4-dimethyl-3-methoxy-9-(2,5-dimethyl-4-methoxyphenyl)-9-fluorenol (15.3%) were also isolated.

Can. J. Chem. Downloaded from www.nrcresearchpress.com by 210.87.254.42 on 09/05/12
For personal use only.

aryl group. As previously presented (2), the following reaction path is in accord with the data (eq. 4).

[4] 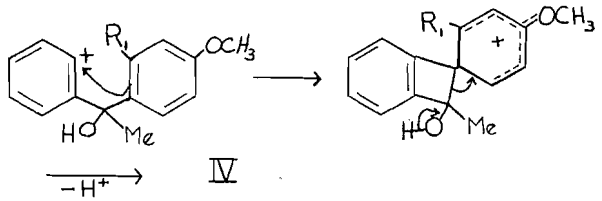

EXPERIMENTAL

Synthesis of o-Aminobenzophenones

The following ketones were synthesized by the method of Kranzlein (14): 2′-chloro-4,5-dimethyl-2-aminobenzophenone, m.p. 121.5–123° (reported (14), 120°); *2′-bromo-4,5-dimethyl-2-aminobenzophenone*, m.p. 111–112.5°; yield, 61%, crystallized from 95% ethanol. Anal. Calc. for $C_{15}H_{14}BrNO$: C, 59.22; H, 4.64; N, 4.61. Found: C, 59.26; H, 4.62; N, 4.53.

2-Amino-4′methoxy-2′-methylbenzophenone

This was prepared according to the procedure of Sternbach *et al.* (15) by treating the Grignard reagent prepared from 4-iodo-3-methylanisole (16) with acetyl anthranil (17); yield, 17%; m.p. 60–61°, crystallized from aqueous ethanol. Anal. Calc. for $C_{15}H_{15}NO_2$: C, 74.66; H, 6.26; N, 5.81. Found: C, 74.53; H, 6.34; N, 5.69.

The following series of substituted benzophenones were prepared according to the procedure of Lothrup (18): 2,3-dimethyl-4-methoxy-2′-aminobenzophenone, m.p. 147–149° (reported (18), 144–145°); *2-ethyl-4-methoxy-5-methyl-2′-aminobenzophenone*, m.p. 116–118°; yield 49%, crystallized from 95% ethanol. Anal. Calc. for $C_{17}H_{19}NO_2$: C, 75.81; H, 7.11; N, 5.20. Found: C, 75.67; H, 7.16; N, 5.33.

2-Chloro-4-methoxy-5-methyl-2′-aminobenzophenone

2-Chloro-4-methoxy-5-methyl-2′-aminobenzophenone, m.p. 124–126°; yield, 29%, crystallized from absolute ethanol. Anal. Calc. for $C_{15}H_{14}ClNO_2$: C, 65.34; H, 5.12; N, 5.08. Found: C, 65.20; H, 5.20; N, 5.15.

2-Bromo-4-methoxy-5-methyl-2′-aminobenzophenone

2-Bromo-4-methoxy-5-methyl-2′-aminobenzophenone, m.p. 139–141°; yield, 22%, crystallized from 95% ethanol. Anal. Calc. for $C_{15}H_{14}BrNO_2$: C, 56.26; H, 4.41; N, 4.37. Found: C, 56.21; H, 4.25; N, 4.52.

The following anisoles were prepared by treating the corresponding phenols with methyl iodide for 5 hours in refluxing alcoholic potassium hydroxide: 2,3-dimethylanisole, b.p. 195–198° at 760 mm (reported (19), 199° at 760 mm), yield, 73%; 5-ethyl-2-methylanisole, b.p. 77–80° at 4.3 mm (reported (20), 96° at 16 mm), yield 81%; 5-chloro-2-methylanisole, b.p. 204–207° at 760 mm (reported (21), 206–208° at 760 mm), yield, 64%; 5-bromo-2-methylanisole, b.p. 75° at 1.4 mm (reported (22), 108° at 15 mm), yield, 83%. 2,3-Dimethylphenol was a commercial product, the other phenols were prepared by the methods described: 5-ethyl-2-methylphenol, b.p. 89° at 2.5 mm (reported (23), 224° at 760 mm); 5-chloro-2-methylphenol, m.p. 70–75° (reported (21), b.p. 225° at 760 mm); 5-bromo-2-methylphenol, m.p. 78–80° (reported (24), 78°).

Synthesis of Amino Alcohols

All of the amino alcohols listed in Table I were prepared from the appropriately substituted *o*-aminobenzophenone and methylmagnesium iodide, except compound VII which was prepared by treating the Grignard reagent of 4-iodo-2,5-dimethylanisole with methyl anthranilate. *4-Iodo-2,5-dimethylanisole* was prepared from 2,5-dimethylanisole by the procedure of Oki and Sato (25), m.p. 46–48°, yield, 60%. Anal. Calc. for $C_9H_{11}OI$: C, 41.25; H, 4.20. Found: C, 41.35; H, 4.36.

In each instance the ethereal solution of the Grignard reagent was cooled in an ice bath during addition of the carbonyl compound. The reactions were completed by refluxing for approximately 24 hours, with the exception of the preparation of VII in which case the reaction mixture was stirred overnight at room temperature. Hydrolysis was effected with aqueous ammonium chloride. All amino alcohols were crystallized from benzene – petroleum ether with the exception of III*h* which was crystallized from 95% ethanol.

Diazotizations

The amino alcohols (5–20 mmoles) were dissolved in a minimum quantity of *p*-dioxane and added to 100–200 ml of 5–10% sulphuric acid solution. The resulting solution or suspension was diazotized with stirring by the dropwise addition of an excess of sodium nitrite dissolved in 10 ml of water. The solution was allowed to stand from ½ hour to 3 hours at 0–10°; it was then permitted to warm to room temperature and stand overnight. The decomposition was completed by warming to 40–50°. The reaction mixture was extracted three times with ether, and the combined ether extracts washed, first with two 100-ml portions of 5% aqueous sodium hydroxide, and then with water, to remove phenolic material, which was not further

Can. J. Chem. Downloaded from www.nrcresearchpress.com by 210.87.254.42 on 09/05/12
For personal use only.

characterized. The neutral ether solution was dried over calcium sulphate, the solvent removed under vacuum, and the residue in each case treated as described below.

Products from IIIc

The residue was dissolved in 15% benzene – petroleum ether and placed on the column. Elution with 45% benzene – petroleum ether yielded 0.063 g (1.34%) of oil, ν 1692 cm^{-1} (chloroform). The ketone was completely converted to its 2,4-dinitrophenylhydrazone. There was obtained 0.062 g of hydrazone, m.p. 235–236°. This was equivalent to 0.036 g (0.8%) of *2-(2-chlorophenyl)-4,5-dimethylacetophenone*. Anal. Calc. for $C_{22}H_{19}ClN_4O_4$: C, 60.21; H, 4.36; N, 12.77. Found: C, 60.10; H, 4.41; N, 12.69. Further elution of the column produced only highly colored oils.

Products from IIId

The residue was dissolved in 20% benzene – petroleum ether, placed on a column, and eluted with 1:1 benzene – petroleum ether. There was obtained 0.066 g (1.4%) of oil, ν 1690 cm^{-1} (chloroform). It was completely converted to its 2,4-dinitrophenylhydrazone, which after purification, yielded 0.104 g of hydrazone, m.p. 231–234° (decomp.). This was equivalent to 0.065 g (1.4%) of *2-(2-bromophenyl)-4,5-dimethylacetophenone*. Anal. Calc. for $C_{22}H_{19}BrN_4O_4$: C, 54.67; H, 3.96; N, 11.59. Found: C, 55.46; H, 4.29; N, 11.98. Further elution of the column produced only highly colored oils.

Products from IIIf

The residue was dissolved in 30% benzene – petroleum ether, placed on a column, and eluted with the same solvent. There was obtained 0.845 g (17%) of light yellow oil, ν 1687 cm^{-1} (chloroform). The oil was completely converted to its 2,4-dinitrophenylhydrazone yielding 1.13 g of hydrazone, m.p. 150–152.5°, equivalent to 0.655 g (13.4%) of *2-(2-methyl-4-methoxyphenyl)acetophenone*. Anal. Calc. for $C_{22}H_{20}N_4O_5$: C, 62.85; H, 4.79; N, 13.33. Found: C, 62.64; H, 4.85; N, 13.20.

Elution of the column with chloroform gave a red oil which crystallized from aqueous ethanol to yield 0.095 g (1.7%) of red needles, m.p. 71–72.5°, ν 1685 cm^{-1} (chloroform). On the basis of previous work (8) it was assigned the structure of *2-acetyl-2'-methyl-4'-methoxyazobenzene*. Anal. Calc. for $C_{16}H_{16}N_2O_2$: C, 71.62; H, 6.01; N, 10.44. Found: C, 71.78; H, 6.19; N, 10.73.

Products from IIIh

The residue was dissolved in 1:1 benzene – petroleum ether, placed on a column, and eluted with petroleum ether. There was obtained 0.862 g (18.4%) of an oil, ν 1685 cm^{-1} (chloroform). The oil was crystallized from benzene – petroleum ether yielding 0.560 g (12%) of *2-(2,3-dimethyl-4-methoxyphenyl)acetophenone*, m.p. 60.5–61.5°. Anal. Calc. for $C_{17}H_{18}O_2$: C, 80.29; H, 7.13. Found: C, 80.17; H, 7.28. The 2,4-dinitrophenylhydrazone melted at 163–165°. Anal. Calc. for $C_{24}H_{22}N_4O_5$: C, 63.58; H, 5.11; N, 12.90. Found: C, 63.39; H, 5.03; N, 13.00.

Elution of the column with 1:1 benzene – petroleum ether gave a red oil which crystallized from ethanol to yield 0.808 g (15.6%) of *2-acetyl-2',3'-dimethyl-4'-methoxyazobenzene*, m.p. 134–135°, ν 1687 cm^{-1} (chloroform). Anal. Calc. for $C_{17}H_{18}N_2O_2$: C, 72.32; H, 6.43; N, 9.92. Found: C, 71.96; H, 6.32; N, 9.80.

Products from IIIi

The residue was dissolved in petroleum ether, absorbed on the column, and eluted with 10% benzene – petroleum ether. There was obtained 0.622 g (14.2%) of *2-(5-methyl-2-ethyl-4-methoxyphenyl)acetophenone*, m.p. 68–70°, ν 1683 cm^{-1} (chloroform), which was crystallized from petroleum ether. Anal. Calc. for $C_{18}H_{20}O_2$: C, 80.56; H, 7.51. Found: C, 80.53; H, 7.59. The 2,4-dinitrophenylhydrazone melted at 170–171.5°. Anal. Calc. for $C_{24}H_{24}N_4O_5$: C, 64.27; H, 5.39; N, 12.50. Found: C, 64.07; H, 5.38; N, 12.38.

Elution of the column with 1:1 benzene – petroleum ether gave a red oil which crystallized in red needles from 80% aqueous ethanol to yield 0.799 g (16.5%) of *2-acetyl-5'-methyl-2'-ethyl-4'-methoxyazobenzene*, m.p. 49–51°, ν 1687 cm^{-1} (chloroform). Anal. Calc. for $C_{18}H_{20}N_2O_2$: C, 72.95; H, 6.80; N, 9.45. Found: C, 73.06; H, 6.69; N, 9.41.

Product from IIIj

The residue was dissolved in 45% benzene – petroleum ether, placed on a column, and eluted with 25% benzene – petroleum ether. There was obtained 0.704 g (15%) of a light yellow oil. The oil was crystallized from ethanol to yield 0.550 g (11.7%) of *2-(2-chloro-5-methyl-4-methoxyphenyl)acetophenone*, m.p. 114–115°, ν 1697 cm^{-1} (chloroform). Anal. Calc. for $C_{16}H_{15}ClO_2$: C, 69.94; H, 5.50. Found: C, 69.92; H, 5.52. The 2,4-dinitrophenylhydrazone melted at 184–186°. Anal. Calc. for $C_{22}H_{19}ClN_4O_4$: C, 58.08; H, 4.21; N, 12.32. Found: C, 57.99; H, 4.15; N, 12.20. Further elution of the column produced only highly colored oils.

Products from IIIk

The residue was dissolved in 30% benzene – petroleum ether, placed on a column, and eluted with 40% benzene – petroleum ether. There was obtained 0.740 g (15.8%) of an oil. The oil was crystallized from benzene – petroleum ether yielding 0.610 g (13.1%) of *2-(2-bromo-5-methyl-4-methoxyphenyl)acetophenone*, m.p. 123–124°, ν 1686 cm^{-1} (chloroform). Anal. Calc. for $C_{16}H_{15}BrO_2$: C, 60.20; H, 4.74. Found: C, 59.98;

Can. J. Chem. Downloaded from www.nrcresearchpress.com by 210.87.254.42 on 09/05/12
For personal use only.

H, 4.72. The 2,4-dinitrophenylhydrazone melted at 195–197°. Anal. Calc. for $C_{22}H_{19}BrN_4O_5$: C, 52.91; H, 3.84; N, 11.22. Found: C, 52.69; H, 3.70; N, 11.18. Further elution of the column produced only highly colored oils.

Products from VII

The residue was dissolved in 1:1 benzene – petroleum ether, placed on the column, and eluted with 2:1 benzene – petroleum ether. There was obtained 0.714 g (38%) of a light yellow oil, ν 1660 cm^{-1} (chloroform). The oil was crystallized from petroleum ether yielding 0.502 g (27%) of *2,5-dimethyl-4-methoxy-2'-(2,5-dimethyl-4-methoxyphenyl)benzophenone*, m.p. 97–99°. Anal. Calc. for $C_{25}H_{26}O_3$: C, 80.18; H, 7.00. Found: C, 79.98; H, 7.07.

Elution of the column with benzene produced a red oil which crystallized from ethanol to give 0.156 g (7.4%) of *2-(2,5-dimethyl-4-methoxybenzoyl)-2',5'-dimethyl-4'-methoxyazobenzene*, m.p. 133–134°, ν 1660 cm^{-1} (chloroform). Anal. Calc. for $C_{25}H_{26}N_2O_3$: C, 74.60, H, 6.51; N, 6.96. Found: C, 74.44; H, 6.58; N, 6.86.

Further elution of the column with 2:1 chloroform–benzene yielded an oil which crystallized from benzene – petroleum ether to give 0.286 g (15.3%) of *1,4-dimethyl-3-methoxy-9-(2,5-dimethyl-4-methoxyphenyl)-9-fluorenol*, m.p. 231–233°, ν 3600 cm^{-1} (chloroform). Anal. Calc. for $C_{25}H_{26}O_3$: C, 80.18; H, 7.00. Found: C, 80.29; H, 7.07.

REFERENCES

1. D. F. DeTar and D. I. Relyea. J. Am. Chem. Soc. **76**, 1680 (1954).
2. R. M. Stiles and A. J. Sisti. J. Org. Chem. **26**, 3639 (1961).
3. H. Zollinger. Azo and diazo chemistry. Interscience Publishers, Inc., New York, N.Y. 1961. p. 138 ff.
4. D. F. DeTar. *In* Organic reactions. Vol. IX. John Wiley and Sons, Inc., New York, N.Y. 1957. p. 409 ff.
5. M. Stiles and R. G. Miller. J. Am. Chem. Soc. **82**, 3802 (1960).
6. R. S. Berry, G. N. Spokes, and M. Stiles. J. Am. Chem. Soc. **84**, 3570 (1962).
7. E. Nolting. Ber. **37**, 2556 (1904).
8. R. M. Stiles and A. J. Sisti. J. Org. Chem. **24**, 268 (1959).
9. R. M. Stiles and A. J. Sisti. J. Org. Chem. **25**, 1691 (1960).
10. A. J. Sisti, J. Burgmaster, and M. Fudim. J. Org. Chem. **27**, 279 (1962).
11. A. J. Sisti, J. Sawinski, and R. Stout. To be published.
12. K. Von Auwers and F. Michaelis. Ber. **47**, 1275 (1914). D. H. Richardson. J. Chem. Soc. 1363 (1937).
13. E. S. Lewis. J. Am. Chem. Soc. **80**, 1371 (1958).
14. P. Kranzlein. Ber. **70B**, 1776 (1937).
15. L. H. Sternbach, R. I. Fryer, W. Metlesics, G. Sachs, and A. Stempel. J. Org. Chem. **27**, 3781 (1962).
16. T. Sato and M. Oki. Bull. Chem. Soc. Japan, **30**, 859 (1957).
17. M. T. Bogert, R. A. Gortner, and C. G. Amend. J. Am. Chem. Soc. **34**, 949 (1912).
18. W. G. Lothrup. J. Am. Chem. Soc. **61**, 2115 (1939).
19. J. Moschner. Ber. **33**, 742 (1900).
20. O. Kruber and A. Lauenstein. Ber. **81**, 221 (1948).
21. M. Kohn and E. Syreia. J. Am. Chem. Soc. **70**, 3950 (1948).
22. J. J. Brown and G. T. Newbold. J. Chem. Soc. 1285 (1953).
23. G. T. Morgan and A. Pettet. J. Chem. Soc. 418 (1934).
24. H. H. Hodgson and F. H. Moore. J. Chem. Soc. 2036 (1926).
25. M. Oki and T. Sato. Bull. Chem. Soc. Japan, **30**, 508 (1957).

Can. J. Chem. Downloaded from www.nrcresearchpress.com by 210.87.254.42 on 09/05/12
For personal use only.

Can. J. Chem. Downloaded from www.nrcresearchpress.com by 210.87.254.105 on 09/05/12
For personal use only.

GAS–SOLID EXCHANGE REACTIONS

ZINC VAPOR AND POLYCRYSTALLINE ZINC SULPHIDE

E. A. SECCO

Chemistry Department, St. Francis Xavier University, Antigonish, Nova Scotia

Received December 19, 1963

ABSTRACT

The exchange kinetics of zinc vapor with polycrystalline zinc sulphide, wurtzite structure, have been studied in a static system in the temperature range 720–960° C.

Plots of $\log_{10}(1-\alpha^*)$, i.e. exchange fraction, versus time reveal two processes. The initial process is a rapid simple exchange, for which the data fit a first-order rate law and which persists to a depth of 15–18 molecular thicknesses. At this depth the second, slower process, which appears to be diffusion-controlled, sets in. Kinetic and structural interpretations of these results along with the existing data on Zn–ZnO exchange are discussed.

INTRODUCTION

Recent results (1, 2) on the exchange reaction between zinc vapor and polycrystalline zinc oxide showed that the exchange rate was controlled by two processes, an initial simple exchange followed by diffusion. The initial rate was not limited to the surface but extended to a depth of 25 molecular thicknesses. On the basis of these data a sequence of rate-controlling steps was postulated, i.e., exchange and interstitial mobility, and interstitial zinc diffusion. That is, the two processes of exchange and zinc mobility via interstices occurred simultaneously, but the exchange rate predominated because it was the slower of the two rates. As the exchange reaction progressed, the "effectively" available interstices became filled, with the result that a second transport mechanism involving a coupled interstitial-lattice type of movement, i.e. interstitial diffusion, became rate-controlling and superseded the exchange rate. The present investigation on the Zn–ZnS system was undertaken to elucidate the rate-controlling steps postulated for ZnO. Zinc sulphide was suitable for this study because it possesses a structure similar to ZnO, i.e. wurtzite, along with interstices available for interstitial mobility of zinc.

EXPERIMENTAL

The polycrystalline ZnS used in this work was from two sources: I, BDH Laboratory Reagent and II, crushed single crystals prepared by sublimation of the vapor (3). In both cases the X-ray diffractograms showed only peaks characteristic of the wurtzite structure. The surface area of sulphide II was found to be 1.2 m^2/g by nitrogen adsorption measurements. The particle radius is calculated to be ca. 6.1×10^{-5} cm. The sulphide samples were dried in an oven at 150° C overnight before use.

The exchange runs were carried out in a static system with the use of quartz vessels (4), and the extent of reaction was determined by the uptake of radiozinc, as previously described (1).

RESULTS

In Figs. 1 and 2 are shown typical $\log_{10}(1-\alpha^*)$ versus time plots at different temperatures for constant Zn pressure (0.11 atm) and constant mole fraction of zinc sulphide (0.50). The features of two distinct rate processes are evident. The logarithms of the rate constants, k_e' and k_e'', obtained from the slopes of the straight lines in Fig. 1(*a*) and 1(*b*),[1] are plotted against the reciprocal of the absolute temperature in Fig. 3, lines *a* and *b*. For the initial exchange process it is found that $k_e' = 3.3\times10^3 \exp(-32.5 \text{ kcal}/RT) \text{ sec}^{-1}$.

[1]*The plot for 780° C is not included, since these data are only slightly different from the data at 800° C, as evidenced by the k_e'' value in Fig. 3, line a.*

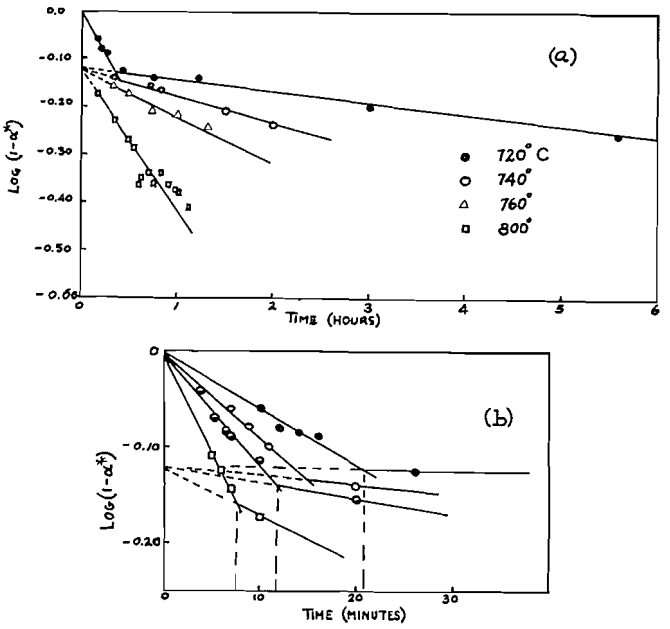

FIG. 1(*a*). Plot of $\log_{10}(1-\alpha^*)$ versus time showing two processes for sulphide I.
(*b*). Plot of $\log_{10}(1-\alpha^*)$ versus time for sulphide I, showing the first process on an expanded scale.

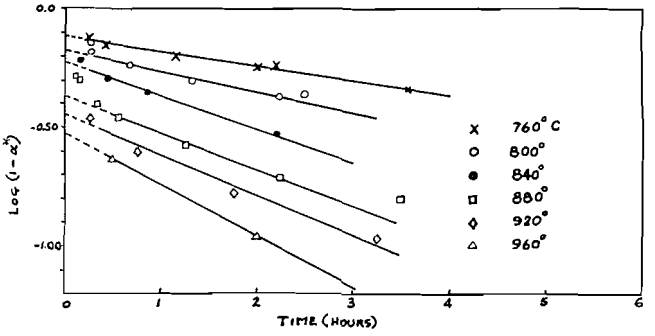

FIG. 2. Plot of $\log_{10}(1-\alpha^*)$ versus time for sulphide II.

The plot of $\log_{10} k_e''$, i.e. the second process, against $1/T$ yields a straight line corresponding to an energy of 61.5 kcal. An interesting fact is the common nonzero intercept of -0.12 corresponding to 25% reaction for the second process of sulphide I.

Figure 2 shows a similar $\log_{10}(1-\alpha^*)$ versus time plot for sulphide II. The slope for the second process at 760° C extrapolates to the same positive intercept value obtained for sulphide I, whereas the slopes above 800° C do not extrapolate to a common intercept. Above 880° C the plots do not show the distinct breaks evident at the lower temperatures.

It is most probable that the second process is a diffusion-controlled (5) transport mechanism whose rate is a function of depth. The particle radius for sulphide I was calculated to be 5.0×10^{-5} cm, using the particle size obtained from gas adsorption measurements of sulphide II, assuming a constant diffusion coefficient, D, at 760° C from the relationship $D = r^2 \times$ slope. The solutions to the diffusion equation for the case of small

Can. J. Chem. Downloaded from www.nrcresearchpress.com by 210.87.254.105 on 09/05/12
For personal use only.

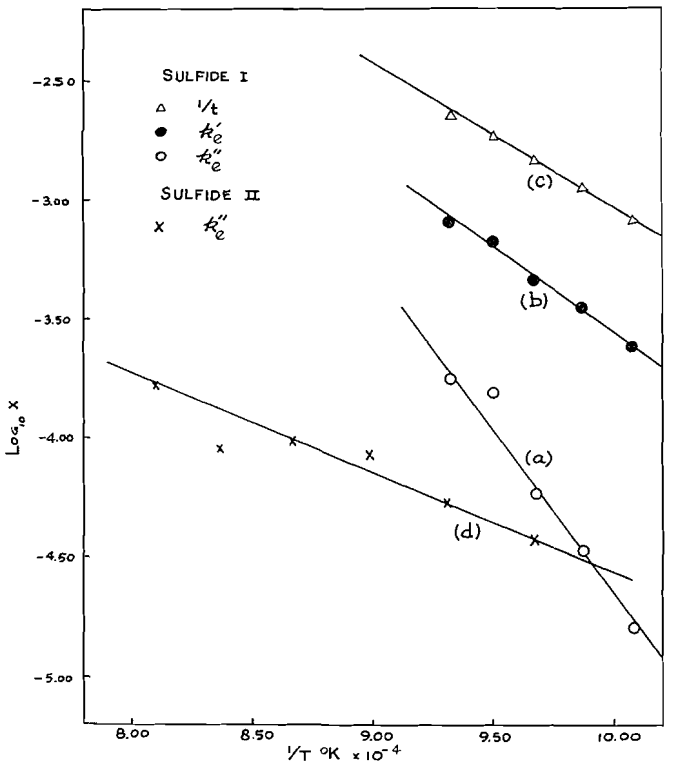

FIG. 3. Plot of $\log_{10} x$ (where $x = k_e'$, k_e'', or $1/t$) versus reciprocal temperature in °K.

spheres (1, 6), to which the polycrystalline sulphide powder approximate sufficiently well,[2] were used to calculate the diffusion coefficient for sulphide I,

$$D = 4.5 \exp (61.5 \text{ kcal}/RT) \text{ cm}^2 \text{ sec}^{-1}.$$

The plot of $\log_{10} k_e''$ versus $1/T$ (from Fig. 2) for sulphide II as given in Fig. 3 yields a straight line, *d*, corresponding to an activation energy of 20 ± 3 kcal. The k_e'' values were obtained from the best slope at a constant time of 2 hours.

DISCUSSION

The sequence of rate-controlling steps postulated for the zinc oxide exchange data may be invoked to explain the experimental results on the zinc sulphide exchange reaction reported here. The two processes of lattice exchange and zinc mobility via interstices occur simultaneously but the exchange process predominates, since it is the slower of the two. The "effectively" available interstices become filled, with the result that a transport mechanism of the interstitial diffusion type supersedes the exchange step. For zinc oxide (1) the activation energy for this latter process was found to be a composite quantity, consisting of an exchange term E_e and an interstitial mobility term, E_i, i.e.

$$E_D = E_e + E_i.$$

From the above data E_i is evaluated as 29.0 kcal, i.e. the activation energy for the direct

[2]*Since the initial and boundary conditions are somewhat ill-defined, use of the standard solutions to the diffusion problem involves some inaccuracy, which would be reflected in the pre-exponential term of the diffusion equation.*

Can. J. Chem. Downloaded from www.nrcresearchpress.com by 210.87.254.105 on 09/05/12
For personal use only.

interstice-to-interstice movement. If the time required for saturation of the sulphide interstices with zinc is taken as the time when interstitial diffusion begins, it is possible to check the value of 29.0 kcal for interstitial mobility. The plot of $\log_{10} 1/t$, i.e. the reciprocal of time (assuming a diffusion mechanism), against $1/T$ (°K) as given in Fig. 3 yields a straight line, c, corresponding to 28.0 ± 2 kcal. Furthermore, the simple relationship of $r^2 = 2Dt$, where r is the particle radius, is used to obtain the diffusion equation,

$$D_i = 10^{-2} \exp(-28 \text{ kcal}/RT) \text{ cm}^2 \text{ sec}^{-1},$$

where D_i is the interstitial mobility.

The diffusion equation for zinc in zinc sulphide differs from that for zinc in zinc oxide only in the pre-exponential factor. If the probability of an interstitial jump per second is given by

$$p_i = \nu_i \exp(-\Delta G_i^*/RT),$$

where ν_i is frequency or the number of attempts per second made by the interstitial zinc to cross the energy barrier ΔG_i^*; and since $\Delta G_i^* = \Delta H_i^* - T\Delta S_i^*$; then

$$p_i = \nu_i \exp(\Delta S_i^*/R - \Delta H_i^*/RT),$$

where ΔS_i^* is the entropy difference between the activated state and an equilibrium interstitial position and ΔH_i^* is the activation energy. The diffusion coefficient, $D_i = 10^{-2} \exp(-28 \text{ kcal}/RT) \text{ cm}^2 \text{ sec}^{-1}$, corresponds to $\Delta H^* = 26$ kcal and $\Delta S^* = -20$ cal deg^{-1} for the parameters of the Eyring diffusion equation,

$$D = (kT/h)\, \lambda^2 \exp -(\Delta H^* - T\Delta S^*)/RT,$$

with the jump distance $\lambda = 3.60$ Å. Therefore, the value of p_i is greater for ZnS than for ZnO by the difference in their entropic factors or, in structural terms, in the radii of their respective interstices.

The changing intercept value in Fig. 2 and the activation energy of 20 kcal obtained from Fig. 3, line b, indicate the appearance of another parameter which reduces the effect of temperature on the second slope. A very likely parameter is that of sintering or aggregation causing an increase in the particle size, which in turn is reflected on the slope, which is an inverse function of particle thickness, i.e. slope $\propto 1/r^2$. Assuming sintering to be the predominant process responsible for the increasing intercept value, we can evaluate the activation energy associated with sintering. The apparent temperature dependence of the diffusion-controlled exchange rate will depend on the extent of sintering that has occurred, but the actual temperature dependence is assumed to remain unchanged. In Fig. 3 the observed straight line, d, corresponding to 20 kcal is an apparent activation energy and represents a net value for the two processes. This interpretation suggests an activation energy of 41 kcal for the sintering process. This problem of sintering in an ambient of zinc vapor and in inert atmospheres is planned to be the subject of a future study.

NOTE ADDED IN PROOF: Sintering studies of zinc sulphide in an ambient of inactive zinc vapor by the radioactive-exchange method are now being carried out in this laboratory. Preliminary results show that the initial rapid exchange process persists after pretreatment in zinc vapor. These results are not concordant with the sequence of rate-controlling steps postulated for the zinc – zinc oxide exchange reaction.

Can. J. Chem. Downloaded from www.nrcresearchpress.com by 210.87.254.105 on 09/05/12
For personal use only.

ACKNOWLEDGMENTS

Grateful acknowledgment is made to the National Research Council of Canada for support of this research.

REFERENCES

1. E. A. SECCO. Fourth International Symposium on Reactivity of Solids, Amsterdam. *Edited by* J. H. de Boer. 1960. pp. 188–194.
2. E. A. SECCO. Can. J. Chem. **39**, 1544 (1961).
3. W. W. PIPER. J. Chem. Phys. **20**, 1343 (1952).
4. E. A. SECCO and W. J. MOORE. J. Chem. Phys. **26**, 942 (1957).
5. K. E. ZIMENS. Arkiv. Kemi Mineral. Geol. A, **20**, No. 18 (1945).
6. J. CRANK. The mathematics of diffusion. Clarendon Press, Oxford. 1956. p. 90.

Can. J. Chem. Downloaded from www.nrcresearchpress.com by 210.87.254.105 on 09/05/12
For personal use only.

Can. J. Chem. Downloaded from www.nrcresearchpress.com by 210.87.254.40 on 09/05/12
For personal use only.

THE INTERACTION OF *o*-DIPHENOLS WITH α-DIKETONES

THE REACTION OF 5,6-DIHYDROXY-*N*-METHYLINDOLE WITH DEHYDROASCORBIC ACID[1,2]

G. L. MATTOK AND R. A. HEACOCK
Psychiatric Research Unit, University Hospital, Saskatoon, Saskatchewan

Received February 3, 1964

ABSTRACT

5,6-Dihydroxy-*N*-methylindole readily reacts with dehydroascorbic acid in aqueous solution at room temperature. The *o*-diphenol system of the indole derivative interacts with the α-diketone function of dehydroascorbic acid to form a 1,4-benzodioxane derivative. This type of reaction appears to be a general one since similar interactions occur between other *o*-diphenols and α-diketones. The mechanism by which the 1,4-benzodioxane derivative is obtained when adrenochrome is reduced with ascorbic acid is discussed.

The reduction of adrenochrome (I) in aqueous solution by ascorbic acid was first described in 1948 by Beauvillain and Sarradin (1), who reported that at least two molecules of ascorbic acid were required to completely reduce 1 molecule of adrenochrome (I). Although these authors did not identify the products of the reaction they did report the spectral characteristics of the reaction mixture, which showed the presence of the typical indole chromophoric system in the ultraviolet region. Beauvillain and Sarradin also noted noted that a different "leuco" derivative was obtained from adrenochrome (I) with sodium bisulphite to that obtained with ascorbic acid. These findings were essentially confirmed 1 year later by Fischer (2); Gero and Parrot reported at about the same time that adrenochrome accelerated the decomposition of ascorbic acid solutions (3).

The products of this reaction (using an excess of ascorbic acid, i.e. five molecular equivalents) have been studied paper chromatographically (4, 5) and it was demonstrated that, along with some dehydroascorbic acid and unchanged ascorbic acid, there were three other products (with R_f values of ca. 0.42, 0.56, and 0.65 respectively when 2% acetic acid in water was used as the developing solvent) present in the reaction mixture. The first of these products was isolated as a crystalline solid and shown to be 5,6-dihydroxy *N*-methylindole (II) (i.e. DHMI)[3] (4). The second product (R_f = 0.56) (III), which could not be extracted from the reaction mixture with ether and which gave a characteristic blue-green color with Ehrlich's reagent, was not identified, although its ultraviolet spectral characteristics suggested that the indole chromophore remained intact (4). Recently it was reported in a preliminary communication that the substance giving the blue-green color with Ehrlich's reagent (R_f = 0.56) (i.e. III) was, in fact, a secondary product derived from the interaction of DHMI and dehydroascorbic acid (6). A consideration on the structure of the product (III) forms the basis of the present paper.

Paper chromatographic examination of samples of an adrenochrome – ascorbic acid reaction mixture, over a period of time, showed that the spot due to DHMI (R_f ca. 0.42) lessened in intensity whilst that due to (III) increased in intensity with increased reaction time (6); the DHMI spot eventually disappeared completely. Therefore, the substance

[1]*This investigation was supported by grants from the Department of National Health and Welfare (Ottawa) and the Government of Saskatchewan (Department of Public Health).*

[2]*Presented in part at the 46th annual conference of the Chemical Institute of Canada, Toronto, Ontario, June 1963.*

[3]*DHMI will be used as an abbreviation for 5,6-dihydroxy-N-methylindole throughout this paper.*

giving the blue-green Ehrlich spot is probably a secondary product resulting from an interaction of DHMI with ascorbic acid or one of its oxidation products. A substance chromatographically identical with (III) was produced by the interaction of DHMI and dehydroascorbic acid, but was not formed from DHMI with ascorbic acid or 2,3-diketogulonic acid (calcium salt), or from an interaction between adrenochrome and dehydroascorbic acid. The product (III) was decomposed (under nitrogen) by 40% aqueous sodium hydroxide and DHMI was regenerated (6).

Evidence which confirmed that (III) was a secondary product, derived from DHMI, was obtained from the reduction of adrenochrome by ascorbic acid in an ether–water system. In this system the DHMI was removed from the aqueous reaction mixture as soon as it was formed and in this case no secondary product was detected in the aqueous phase; only DHMI was found in the ether layer. 5,6-Diacetoxy-*N*-methylindole did not react with dehydroascorbic acid indicating that the *o*-diphenol system of DHMI must have been involved in the interaction. A paper chromatographic study showed that the 1-, 2-, 3-, and 7-positions of the 5,6-dihydroxyindole nucleus were not involved in this interaction, since chromatographically similar products, to that obtained from DHMI and dehydroascorbic acid, were obtained from dehydroascorbic acid and the following *o*-diphenols: (i) 5,6-dihydroxy-7-iodo-*N*-methylindole; (ii) 5,6-dihydroxy-7-iodoindole; (iii) 5,6-dihydroxy-2-methylindole, and (iv) adrenolutin (i.e. 3,5,6-trihydroxy-*N*-methylindole or 5,6-dihydroxy-*N*-methylindoxyl). A further indication that the interaction of DHMI with dehydroascorbic acid involved the α-dicarbonyl function of the dehydroascorbic acid molecule was obtained by treating DHMI with a sreies of α-dicarbonyl compounds (see Table I). All the α-dicarbonyl compounds used were found to react with DHMI.

TABLE I

Paper chromatography of products obtained from the interaction of: (A) several *o*-diphenols with dehydroascorbic acid, and (B) several α-diketones with 5,6-dihydroxy-*N*-methylindole (Solvent: 2% acetic acid – water; chromogenic reagent: Ehrlich's reagent)

	R_f	Color
(A) *o*-Diphenol		
5,6-Dihydroxy-*N*-methylindole	0.57	Blue-green
5,6-Dihydroxy-2-methylindole	0.57	Blue
5,6-Dihydroxy-7-iodo-*N*-methylindole	0.32	Green
5,6-Dihydroxy-7-iodoindole	0.29	Yellow-green
Adrenolutin	0.41*,†,‡	Yellow-green§
Adrenaline	0.56‖,†	Pink¶
(B) α-Diketone		
Dehydroascorbic acid	0.57	Blue-green
5,6-Isopropylidenedehydroascorbic acid**	0.06††	Brown → dark green
2,3-Diketogulonic acid (Ca salt)	0.37	Yellow
Oxalic acid	0.20, 0.33	Pink, yellow‡
Diacetyl	0.61	Purple

*Using paper washed overnight with 2% acetic acid:water.
†Ascending paper development.
‡Self-indicating.
§Color of fluorescence of spot in ultraviolet light.
‖Solvent: methanol (160 ml) – water (40 ml) – quinoline (8 ml).
¶Chromogenic reagent: 3% potassium ferricyanide.
**Formed during the reduction of adrenochrome by 5,6-isopropylideneascorbic acid.
††On formamide-treated paper using ethyl acetate (4 ml) – chloroform (16 ml) – formamide (0.15 ml) as running solvent. Radial development.

The molecular composition of the product (III) was determined by allowing a known amount of dehydroascorbic acid to react with excess DHMI in aqueous solution. After the interaction was completed the unreacted DHMI was extracted and determined

Can. J. Chem. Downloaded from www.nrcresearchpress.com by 210.87.254.40 on 09/05/12
For personal use only.

Can. J. Chem. Downloaded from www.nrcresearchpress.com by 210.87.254.40 on 09/05/12
For personal use only.

spectroscopically. By this procedure it was ascertained that the secondary product (III) was, in fact, derived from one molecule each of DHMI and dehydroascorbic acid.

Attempts to isolate the compound (III) in the solid state, from its aqueous solutions, were not successful as the compound decomposed on concentration of the solutions. However, it was possible to isolate a crystalline diacetate of (III) by acetylating the crude product obtained from either: (i) an adrenochrome – ascorbic acid reaction mixture (after removal of any unreacted DHMI by ether extraction), or (ii) a DHMI–dehydroascorbic acid reaction mixture. The acetylation procedure used was similar to that described by Walsh for the acetylation of adrenaline (7) (i.e. acetic anhydride in aqueous sodium bicarbonate). The fact that the same diacetate was obtained in both the aforementioned cases is further evidence that the compound (III), observed among the reduction products obtained from adrenochrome with ascorbic acid, is derived from the reaction of DHMI with dehydroascorbic acid. The diacetate could be readily converted into a crystalline tetraacetate by acetic anhydride and pyridine in chloroform solution.

Adrenochrome was readily reduced by 5,6-isopropylideneascorbic acid in acrylonitrile solution and gave DHMI and a secondary product analagous to (III). The chromatographic system used to examine the adrenochrome – ascorbic acid reaction mixtures (i.e. 2% acetic acid and Whatman No. 1 paper) was not satisfactory for the isopropylidene derivatives since hydrolysis of the isopropylidene group occurred. However, satisfactory separation of the products was obtained with a formamide – (ethyl acetate – chloroform) (1:4) system.

Although it had not proved possible to isolate the DHMI – dehydroascorbic acid product in the solid state, it was possible to isolate the corresponding compound derived from 5,6-isopropylidineascorbic acid as a white microcrystalline solid. However, this compound decomposed on storage and a completely satisfactory elemental analysis could not be obtained. A crystalline diacetyl derivative of this isopropylidene derivative of (III) was obtained, which, after removal of the isopropylidene group with aqueous acetic acid, gave a diacetate of (III) which was different to the diacetyl derivative obtained by acetylation of (III) by acetic anhydride in aqueous sodium bicarbonate. However, both diacetates, on further acetylation, were converted to the same tetraacetate. Acetylation of (III) by the acetic anhydride – sodium bicarbonate reagent, therefore, occurred at the 5- and 6-positions in the dehydroascorbic acid moiety of the molecule. Compound (III) (i.e. 2,3-*C*,*C*-(1′-methyl-5′,6′-indolodioxy)-L-threohexono-1,4-lactone) is probably formed in the following manner, when adrenochrome (I) is reduced by ascorbic acid. The initially formed "leucoadrenochrome" (i.e. 3,5,6-trihydroxy-*N*-methylindoline (IV)) rapidly loses water giving DHMI (II), which can then react with the dehydroascorbic acid, formed by oxidation of the ascorbic acid. The interaction between DHMI and dehydroascorbic acid occurs between the *o*-diphenol system of DHMI and the 2,3-dicarbonyl system of dehydroascorbic acid with the formation of the substituted 1,4-dioxane ring system in (III).

Although the nature of the reactions involved in the formation of the secondary product during the reduction of adrenochrome by ascorbic acid are clear, the relative positions involved are less certain. It is probably safe to assume that the lactone carbonyl of the dehydroascorbic acid molecule is not involved, but interaction could take place between the 2-carbonyl group and either of the 5- or 6-hydroxyl groups in the DHMI molecule and with similar possibilities existing for the 3-carbonyl group of the dehydroascorbic acid molecule. Structure (III) could, therefore, be written equally well with the indole system

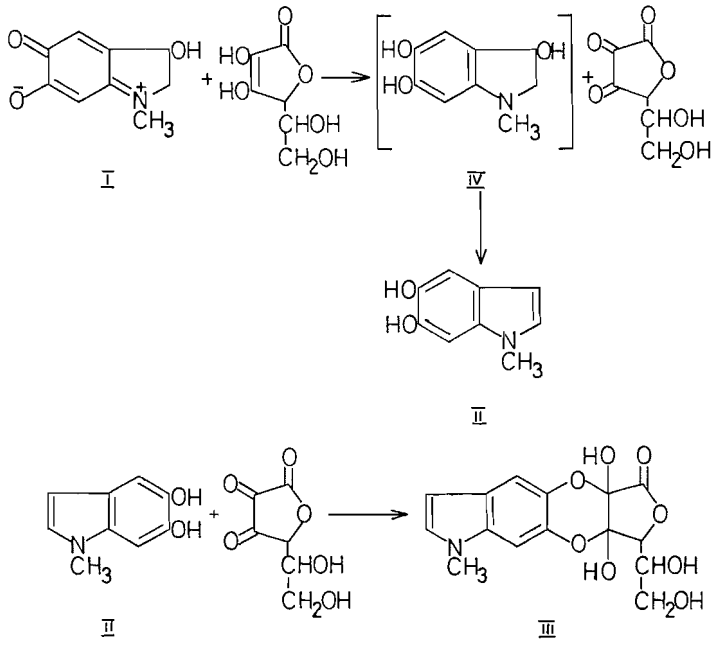

inverted. There was no evidence that mixtures of such products were formed but it was not possible to favor either of these structures.

This type of interaction between an *o*-diphenol and an α-dicarbonyl system seems to be a general one. Paper chromatographically it has been shown that, as well as reacting with dehydroascorbic acid and 5,6-isopropylidenedehydroascorbic acid, DHMI reacts with 2,3-diketogulonic acid, diacetyl, and oxalic acid. Similarly dehydroascorbic acid has been shown to react with the following *o*-diphenols: 5,6-dihydroxy-7-iodo-*N*-methylindole; 5,6-dihydroxy-7-iodoindole; 5,6-dihydroxy-2-methylindole; 5,6-dihydroxy-*N*-methylindoxyl; adrenaline; and catechol. The products of such interactions (as yet unidentified) may have structures similar to (III).

This type of interaction is possibly of physiological significance, particularly in view of the very mild conditions under which it takes place. Ascorbic acid is known to protect catechol derivatives (e.g. adrenaline) against oxidation. This protection arises primarily from the preferential oxidation of the ascorbic acid. However, the formation of interaction products, such as those described above, could provide an additional explanation of the usefulness of ascorbic acid for the protection of catechol derivatives from oxidation. Stabilizations of this type have been reported by Gero (8, 9).

One of the most widely used chemical assay procedures for the catecholamines is the so-called "trihydroxyindole" (or "lutin") method (cf. 10). In this procedure the catecholamines (after extraction from the biological material) are oxidized to the corresponding aminochromes which are then rearranged, usually with a solution of ascorbic acid in strong alkali, to the highly fluorescent "lutins" (i.e. 5,6-dihydroxyindoxyls). The presence of ascorbic acid is necessary to "stabilize" the fluorescent products. The mechanism of this protective action is not clear. The simplest explanation, i.e. that ascorbic acid merely protects the fluorescent products against oxidation by being itself preferentially oxidized is not completely satisfactory. In view of the known instability of ascorbic acid in alkaline

Can. J. Chem. Downloaded from www.nrcresearchpress.com by 210.87.254.40 on 09/05/12
For personal use only.

solution (11) the possibility that the protective action is due, at least in part, to some oxidation or degradation product of ascorbic acid (i.e. dehydroascorbic acid, 2,3-diketogulonic acid, or even oxalic acid) cannot be completely ruled out. Von Euler and Lishajko have, in fact, reported that alkali – ascorbic acid mixtures, of the type usually used in this procedure, spontaneously develop a reddish tint after about 7–10 minutes and this color progressively deepens with time with an accompanying increase in the "blank" fluorescence of this mixture (12), suggesting that the alkaline ascorbic acid reagent is not particularly stable.

The products of the interaction of the "lutins" with the transformation products of ascorbic acid mentioned above, which contain the α-dicarbonyl system, would retain the indoxyl structure, and consequently their intense fluorescence. The product obtained from adrenolutin (5,6-dihydroxy-*N*-methylindoxyl) by interaction with dehydroascorbic acid is still strongly fluorescent and appears to be more stable than adrenolutin. The excitation and emission wavelengths for maximum fluorescence of this interaction product are close to those of adrenolutin itself (excitation, 405 mμ; fluorescence, 535 mμ).

EXPERIMENTAL

All melting points were measured on a Leitz hot-stage instrument. The ultraviolet spectra were measured on a Beckman DK-2 spectrophotometer. The infrared spectra were recorded in chloroform solution on a Perkin–Elmer Model 137 spectrophotometer. Peroxide-free ether (or ether from freshly opened cans, Fisher reagent grade) was used throughout this investigation. The light petroleum used was B.D.H. AnalaR grade (b.p. 60–80°). Unless otherwise stated the paper chromatography was carried out on Whatman No. 1 paper with 2% acetic acid in water as running solvent with descending development. The Ehrlich's reagent used in this investigation was prepared by dissolving *p*-dimethylaminobenzaldehyde (1 g) in a mixture of methanol (75 ml) and conc. hydrochloric acid (25 ml).

A. Preparation of Starting Materials

Adrenochrome (13), 5,6-dihydroxy-*N*-methylindole (14), 5,6-diacetoxy-*N*-methylindole (15), 5,6-dihydroxy-7-iodiondole[4] (15), 5,6-dihydroxy-7-iodo-*N*-methylindole[4] (16), 5,6-dihydroxy-2-methylindole (17), adrenolutin (i.e. 5,6-dihydroxy-*N*-methylindoxyl) (18), and calcium diketogulonate (19) were prepared by the methods described in the literature. 5,6-Isopropylideneascorbic acid was prepared by the method of Vargha (20); colorless needles (m.p. 190.5–192°), Vargha reported a melting point of 220–222°). (Found: C, 50.24; H, 5.85; $C_9H_{12}O_6$ requires C, 50.00; H, 5.60%.) Dehydroascorbic acid was obtained as the methanol complex from the Nutritional Biochemicals Corporation.

B. Reduction of Adrenochrome by Ascorbic Acid

(i) In water

Ascorbic acid (60 mg) was added to a solution of adrenochrome (20 mg) in water (2 ml). Nitrogen was bubbled through the solution and after about 2 hours a sample of the reaction mixture was examined paper chromatographically (see Table I). After spraying the developed chromatogram with Ehrlich's reagent two main products (R_f's: ca. 0.42 and 0.57) and several minor products were detected (cf. 4, 6). The blue Ehrlich-staining substance (R_f 0.42), which had previously been characterized as DHMI (4), was removed by extraction with ether (6 × 1 ml) leaving an aqueous solution of the other major product (R_f 0.57: λ_{max}, 299 mμ) together with ascorbic and dehydroascorbic acids. The absence of DHMI in the aqueous mother liquors was confirmed by paper chromatography. This solution was then treated (under nitrogen) with 40% aqueous sodium hydroxide solution (1 drop), and after 1 minute, acidified with glacial acetic acid. DHMI was then detected in the reaction mixture by paper chromatography and the blue-green Ehrlich-staining substance (III) (R_f 0.57) was no longer present.

Isolation of (III) as its diacetyl derivative.—The product (III) was obtained in aqueous solution, as described above, and acetylated by the method described in section D (*ii*) to give a diacetyl derivative (m.p. 118–119°) identical with that obtained by acetylation, under similar conditions, of the DHMI – dehydroascorbic acid interaction product (III) (see section D (*ii*)).

The diacetate was fully acetylated by the method described in section D (*iii*) to give a tetraacetate (m.p. 108–109°), identical with the fully acetylated derivative of the interaction product (III).

(ii) In an Ether–Water System

Adrenochrome (5 mg) was added to a solution of ascorbic acid (25 mg) in water (1 ml) covered with ether

[4]*These compounds were erroneously referred to as 2-iodo derivatives in the references cited to the preparative procedures (cf. ref. 21).*

Can. J. Chem. Downloaded from www.nrcresearchpress.com by 210.87.254.40 on 09/05/12
For personal use only.

(1 ml), and nitrogen bubbled through the system. After 2 hours, the ether and aqueous layers were separated and each layer was examined paper chromatographically, the ether extract was observed to contain DHMI, and in this case the aqueous phase contained no blue-green Ehrlich-staining substance (i.e. (III)). A control reaction mixture, prepared as above but omitting the ether, showed, on paper chromatographic examination, only a trace of DHMI and a strong blue-green spot due to (III).

C. Reduction of Adrenochrome by 5,6-Isopropylideneascorbic Acid

(i) Paper Chromatographic Examination

Adrenochrome (25 mg) and 5,6-isopropylideneascorbic acid (40 mg) were suspended in acrylonitrile (3 ml), and from time to time the mixture was shaken. The reaction mixture was kept at room temperature and the progress of the reaction was followed by paper chromatographic examination of small samples at various reaction times, using the ethyl acetate – chloroform (1:4) – formamide system (radial development) (15). The initial products were DHMI (R_f 0.48) (cf. 15), giving the usual blue color with Ehrlich's reagent and a compound (R_f 0.06) giving a brown spot with this chromogenic reagent, which quickly became dark green in color. After 24 hours virtually all the DHMI had disappeared from the reaction mixture.

(ii) Isolation of the Product

After 30 hours the reaction mixture was filtered and the filtrate evaporated to dryness at room temperature and under reduced pressure (nitrogen "leak"). The product was extracted from the syrupy residue by ether (5 ml), and obtained as a white crystalline solid (35 mg) by the addition of light petroleum and rapidly filtered in an atmosphere of nitrogen. The product (presumably a 1:1 interaction product of 5,6-isopropylidenedehydroascorbic acid and DHMI) on exposure to air became grey in color and finally turned black. It was not possible to obtain a melting point since the substance became black on heating. It was also impossible to obtain a completely satisfactory analysis. (Found: C, 57.18; H, 6.10; N, 3.58%; and mol. wt. 388. $C_{18}H_{19}NO_8$ requires C, 57.29; H, 5.08; N, 3.71%; and mol. wt. 377.)

(iii) Isolation of the Product as its Diacetyl Derivative

Acetic anhydride (0.15 ml) was added to a solution of the residue (obtained from the reduction of adrenochrome by 5,6-isopropylideneascorbic acid by the method described in section D (*ii*)) in a mixture of dry chloroform (3 ml) and pyridine (0.15 ml). After 20 minutes the reaction mixture was washed with 2 *N* hydrochloric acid (3 × 2 ml); saturated aqueous sodium bicarbonate (3 × 2 ml) and finally water (3 × 2 ml). The dried (Na_2SO_4) chloroform solution was then evaporated to dryness *in vacuo* (nitrogen "leak") at room temperature and the residue obtained was extracted with ether (5 ml); on addition of light petroleum to the ether extract a flocculent white precipitate (137 mg) was obtained. Recrystallization from ether: light petroleum raised the melting point of the diacetyl derivative of the 5,6-isopropylidene derivative of (III) to 135–136°. (Found:[5] C, 57.09; H, 5.19; N, 3.06%; and mol. wt. 471. $C_{22}H_{23}NO_{10}$ requires C, 57.26; H, 5.02; N, 3.04%; and mol. wt. 461.) The product showed the characteristic indole absorption maximum in the ultraviolet region at 284 mμ (in methanol).

(iv) Attempted Preparation of a Second Diacetyl Derivative of (III)

The diacetyl-isopropylidene derivative of (III), prepared by the method described in section C (*iii*) (15 mg), was dissolved in 30% acetic acid – water and the solution maintained at 60° for 1 hour. The reaction mixture was then extracted with chloroform (6 × 1 ml) and the combined, dried (Na_2SO_4), chloroform extracts concentrated, under reduced pressure (nitrogen "leak"), to about 0.2 ml. Ether was added to the concentrated chloroform extract and a white precipitate was then obtained, which decomposed (smelling strongly of acetic acid) on the filter.

A similar concentrate was treated with pyridine (0.3 ml) and acetic anhydride (0.15 ml); after standing for 10 minutes at room temperature, the reaction mixture was diluted with chloroform (1 ml) and washed successively with 2 *N* hydrochloric acid, saturated aqueous sodium bicarbonate, and finally water. The dried (Na_2SO_4) chloroform solution was concentrated to ca. 0.1 ml and light petroleum added. A white microcrystalline precipitate (yield: 0.9 mg; m.p. 109–110°) was obtained, which was identical with the tetraacetate of (III) obtained in Section D (*iii*).

D. Interaction of 5,6-Dihydroxy-N-methylindole with Dehydroascorbic Acid

(i) Paper Chromatographic Examination

DHMI (10 mg) and dehydroascorbic acid (methanol complex; 18 mg) were suspended in water (1 ml) and nitrogen bubbled through the suspension; after 15 minutes dissolution was complete. Chromatographic examination of the reaction mixture showed that the intensity of blue-green Ehrlich staining spot increased with time, with a corresponding decrease in the intensity of the spot due to DHMI. After 1 hour the spot due to DHMI had virtually disappeared.

(ii) Acetylation of (III)

A reaction mixture prepared as described in D (*i*) was allowed to stand at room temperature for 1½ hours, after which time it was extracted with ether (6 × 1 ml) to remove unreacted DHMI. The product (III) was then obtained in aqueous solution and acetylated by a procedure similar to that described by Walsh for the

[5]*Acetyl determinations on the same sample varied with the method used, presumably due to hydrolysis of the lactone ring and generation of catechol derivatives during the assay procedure.*

Can. J. Chem. Downloaded from www.nrcresearchpress.com by 210.87.254.40 on 09/05/12
For personal use only.

acetylation of adrenaline (7). Sodium bicarbonate (200 mg) and acetic anhydride (0.09 ml) were added to the aqueous mother liquors. The reaction mixture was allowed to stand for 20 minutes and then extracted with chloroform (6 × 1 ml). The dried (Na_2SO_4), combined, chloroform extracts were then concentrated on a water bath to about 0.2 ml and on addition of ether a white precipitate was obtained immediately (yield, 5 mg; m.p. 114–117°). After recrystallization from chloroform – light petroleum the product had a melting point of 118–119°. (Found:[6] C, 54.45; H, 4.76; N, 3.54%; and mol. wt. 419. $C_{19}H_{19}NO_{10}$ requires: C, 54.16; H, 4.55; N, 3.32%; and mol. wt. 421.) The infrared spectrum was consistent with that expected for a diacetate of (III), showing the expected carbonyl absorptions at 5.62 μ and 5.71 μ and hydroxyl absorption at ca. 2.85 μ, The ultraviolet spectrum showed a λ_{max} at 286 mμ (in methanol).

(iii) Further Acetylation of the Diacetate of (III)

The diacetate of (III) was obtained in chloroform solution by the procedure described in section D (*ii*). The volume of this solution was reduced to about 1 ml, and pyridine (0.2 ml) and acetic anhydride (0.1 ml) added. After 10 minutes, the reaction mixture was washed successively with 2 *N* hydrochloric acid (2 × 2 ml), aqueous sodium bicarbonate, and finally water. The dried (Na_2SO_4) solution was then evaporated to dryness and the residue extracted with ether (4 ml); addition of light petroleum to the ether extract gave a white precipitate (3 mg). After recrystallization from ether – light petroleum the product had a melting point of 108–109°. (Found:[7] C, 54.48; H, 4.70; N, 2.76%; and mol. wt. 521. $C_{23}H_{23}NO_{12}$ requires: C, 54.65; H, 4.55; N, 2.77%; and mol. wt. 505.) The infrared spectrum was consistent with that expected for a fully acetylated derivative of (III) showing no absorption in the OH stretching region and main carbonyl absorption peaks at 5.52 μ and 5.74 μ with shoulders at 5.60 μ and 5.70 μ; the ultraviolet spectrum showed a typical indole absorption with a λ_{max} of 285 mμ (in methanol). The tetraacetate obtained by this procedure was identical with that obtained by application of a similar acetylation procedure to the adrenochrome – ascorbic acid reduction product (see section B (*i*)).

E. Estimation of the Molecular Composition of the 5,6-Dihydroxy-N-methylindole – Dehydroascorbic Acid Interaction Product

The method used involved a reaction in water between dehydroascorbic acid and an excess (1 to 2 times) of 5,6-dihydroxy-*N*-methylindole (DHMI). The unreacted DHMI was extracted with ether and estimated from its absorbance at 298 mμ in water. Preliminary controls and calibrations that were carried out were as follows: (*i*) the efficiency of extraction of DHMI by ether from its aqueous solution in the presence of dehydroascorbic acid (using the procedure described below, this was found to be better than 95%); (*ii*) a calibration curve for DHMI (the absorbances of several aqueous solutions of DHMI were determined at its λ_{max} (298 mμ); the relation between absorbance and concentration for the solutions of DHMI was linear over the range studied); and (*iii*) the purity of the commercial sample of dehydroascorbic acid. The commercial sample of dehydroascorbic acid (as the methanol complex) available to the authors was analyzed by the 2,4-dinitrophenylhydrazine method described by Roe (22) and found to contain 74% dehydroascorbic acid.

In a typical determination, DHMI (8.5 mg, 5.22×10^{-2} mmoles) and dehydroascorbic acid (4.68 mg, 2.69×10^{-2} mmoles) were dissolved in water (1 ml); nitrogen was bubbled through the suspension and dissolution was complete in 15 minutes. After 2½ hours the solution was extracted with ether (5 × 1 ml); the combined ether extracts were concentrated (under nitrogen) and the residue dissolved in water (100 ml). The absorbance at 298 mμ was measured and the unreacted DHMI estimated from its extinction coefficient (ϵ, 7740 in water) at this wavelength. It was found that 4.40 mg of DHMI had reacted with 4.68 mg of dehydroascorbic acid, corresponding to an interaction product composed of one molecule of DHMI and 1 molecule of dehydroascorbic acid. (For such an interaction the calculated weight of DHMI to react with 4.68 mg of dehydroascorbic acid is 4.38 mg.) Similar determinations were carried out after reaction times of 3 and 3½ hours, and with various amounts of DHMI; in each case the results obtained corresponded to those expected for a 1:1 interaction.

F. Interaction of Other o-Diphenols and α-Diketones

Several other α-diketones were caused to react in aqueous solution with DHMI and, on the other hand, several *o*-diphenols were caused to react with dehydroascorbic acid. The reaction mixtures were prepared as described in Section D (*i*). In one series the dehydroascorbic acid was replaced in turn by: (*a*) calcium 2,3-diketogulonate, (*b*) oxalic acid, (*c*) diacetyl. In the series where the *o*-diphenol was varied, the DHMI, in the reaction mixture prepared according to section C (*i*), was replaced in turn by: (*a*) 5,6-dihydroxy-2-methylindole; (*b*) 5,6-dihydroxy-7-iodo-*N*-methylindole; (*c*) 5,6-dihydroxy-7-iodoindole; (*d*) adrenolutin; (*e*) adrenaline hydrochloride; and (*f*) catechol. The products of these interactions were, except in the case of catechol with dehydroascorbic acid, detected by paper chromatography (see Table I).

When catechol was allowed to react with dehydroascorbic acid no product was detected in the reaction mixture after 3 days reaction. However, when unreacted catechol was completely extracted, from the reaction mixture by ether, and the aqueous mother liquors treated with one drop of 40% aqueous sodium hydroxide, prior to acidification with glacial acetic acid, an ether extractable product (R_f 0.73 in 2% aqueous acetic acid), which gave a blue-black color with the ferric chloride reagent, was obtained. The chromatographic properties

[6]*See footnote 5.*
[7]*See footnote 5.*

Can. J. Chem. Downloaded from www.nrcresearchpress.com by 210.87.254.40 on 09/05/12
For personal use only.

of this product were identical with those of catechol. No interaction between 5,6-diacetoxy-*N*-methylindole and dehydroascorbic acid was detected after a solution containing these two compounds had stood at room temperature for 3 days. *n*-Butanol – acetic acid – water (6:1:2) was used as the chromatographic solvent in this case. (The R_f of 5,6-diacetoxy-*N*-methylindole, in this solvent, was 0.90.)

REFERENCES

1. A. Beauvillain and J. Sarradin. Bull. Soc. Chim. Biol. **30**, 478 (1948).
2. P. Fischer. Bull. Soc. Chim. Belges, **58**, 205 (1949).
3. E. Gero and J. L. Parrot. Compt. Rend. Soc. Biol. **144**, 389 (1950).
4. R. A. Heacock and B. D. Laidlaw. Nature, **182**, 526 (1958).
5. R. A. Heacock and B. D. Laidlaw. Chem. Ind. London, 1510 (1958).
6. G. L. Mattok and R. A. Heacock. Nature, **198**, 993 (1963).
7. L. H. Walsh. J. Am. Chem. Soc. **74**, 4967 (1952).
8. E. Gero. Compt. Rend. **240**, 1941 (1955).
9. E. Gero. Compt. Rend. **240**, 2176 (1955).
10. S. Udenfriend. Fluorescence assay in biology and medicine. Academic Press, Inc., New York. 1962. p. 140.
11. Z. Csuros and J. Petro. Acta Chim. Acad. Sci. Hung. **7**, 199 (1955).
12. U. S. von Euler and F. Lishajko. Acta Physiol. Scand. **51**, 348 (1961).
13. R. A. Heacock, C. Nerenberg, and A. N. Payza. Can. J. Chem. **36**, 853 (1958).
14. G. L. Mattok and R. A. Heacock. Can. J. Chem. **42**, 484 (1964).
15. R. A. Heacock, M. E. Mahon, and B. D. Scott. Can. J. Chem. **39**, 231 (1961).
16. R. A. Heacock and B. D. Scott. Can. J. Chem. **38**, 508 (1960).
17. J. Harley-Mason. J. Chem. Soc. 200 (1953).
18. R. A. Heacock and M. E. Mahon. Can. J. Chem. **36**, 1550 (1958).
19. J. R. Penney and S. S. Zilva. Biochem. J. **39**, 1 (1945).
20. L. von Vargha. Nature, **130**, 847 (1932).
21. R. A. Heacock, O. Hutzinger, B. D. Scott, J. W. Daly, and B. Witkop. J. Am. Chem. Soc. **85**, 1825 (1963).
22. J. H. Roe. Methods Biochem. Analy. **1**, 115 (1954).

Can. J. Chem. Downloaded from www.nrcresearchpress.com by 210.87.254.40 on 09/05/12
For personal use only.

Can. J. Chem. Downloaded from www.nrcresearchpress.com by 210.87.254.42 on 09/05/12
For personal use only.

ALIPHATIC CHEMISTRY OF FLUORENE

PART IX. SOME BIFUNCTIONAL DERIVATIVES

P. M. G. BAVIN[1]

Smith Kline and French Laboratories Ltd., Mundells, Welwyn Garden City, England

Received October 24, 1963

ABSTRACT

Methyl phenanthrene-9-carboxylate, dimethyl phenanthrene-9,10-dicarboxylate, and N,N-dimethyl phenanthrene-9-carboxamide have been prepared directly from fluorene by a novel route. Neighboring group participation by carbomethoxy has been clearly demonstrated in the reactions of some 9,9-disubstituted fluorenes.

This paper describes the preparation and reactions of a number of fluorene derivatives having two functional groups in the 9-position. The ultimate objective has been to provide a synthesis of 4-nitrophenanthrene from 4-nitrofluorene. As a necessary preliminary to experiments with nitrofluorenes, a route has been worked out to phenanthrene derivatives from fluorene without using reducing agents at any stage.

The formation of phenanthrene derivatives from substituted fluorenes is illustrated in Fig. 1. The group R may be hydrogen, alkyl, or aryl and X may be chlorine, bromine,

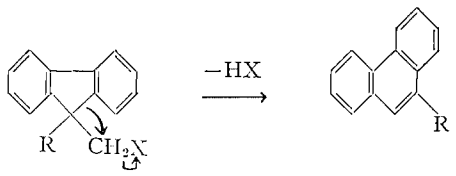

hydroxyl, *p*-toluenesulphonate, or similar leaving group. (For typical references see 1, 2, 3.) Examples where R is a functional group have not been recorded and are rare in the broad field of Wagner–Meerwein rearrangements. Methyl fluorene-9-carboxylate (I*a*) was chosen as starting point for these experiments because it is highly reactive (4, 5) and carboxyl groups are readily eliminated from phenanthrene carboxylic acids (6, 7). Initially, experiments were made with derivatives of the hydroxy-ester (I*b*). These were not successful and are briefly summarized later in this paper. More subtle methods appeared necessary and attention was turned to halo-esters. The bromo- and chloro-esters ((I*c*) and (I*d*) respectively) were prepared in excellent yields from the appropriate dihalomethanes. As expected, bromo-ester (I*c*) failed to react with a further molecule of fluorene ester and was recovered unchanged after it was heated with sodium iodide in methyl ethyl ketone. It was also unchanged after it was heated in 98% formic acid or dimethylformamide or alone at 220°. Like other neopentyl-type halides it reacted rapidly in the presence of silver ions,* for example with silver trifluoracetate in trifluoracetic acid to give diester (I*e*). The diester (I*e*) did not decompose at 220° but solvolyzed smoothly in 98% formic acid, giving methyl phenanthrene-9-carboxylate in 80% yield. Since Pschorr (6) saponified

[1]*Much of the work was carried out at The University, Hull, during the tenure of an I.C.I. Fellowship (1958–60).*

* *For general reviews of electrophilically assisted S_N1 reactions see refs. 8, 9, 10.*

Can. J. Chem. Downloaded from www.nrcresearchpress.com by 210.87.254.42 on 09/05/12
For personal use only.

and decarboxylated the phenanthrene ester, solvolysis of I*e* completes a novel synthesis of phenanthrene from fluorene without employing reducing agents. It also provides a new route to functionally substituted phenanthrenes which should prove valuable in the synthesis of hydrocarbons which show optical isomerism (cf. 11, pp. 472–478; 12). Chlorodiester (I*f*), prepared from methyl dichloroacetate, was converted similarly to dimethyl phenanthrene-9,10-dicarboxylate (62%), whilst N,N-dimethyl phenanthrene-9-carboxamide (53%) was obtained from bromo-amide (II*a*). Reactions of other halo-esters which did not lead to phenanthrene derivatives are discussed below.

In Part I of this series (13) we described some reactions of the chloride (III). It melted with decomposition up to 99° and underwent solvolysis in 98% formic acid, both decompositions giving good yields of 9-methyl-10-phenylphenanthrene. However, reaction with silver acetate in anhydrous acetic acid gave unrearranged acetate. The stabilization of neopentyl carbonium ions by an α-phenyl group has been noted elsewhere (14). The bromo-ester (I*c*) has also given only unrearranged products from reactions with silver salts: trifluoracetate (I*e*) from silver trifluoracetate in trifluoracetic acid; acetate (I*g*) from silver perchlorate in acetic acid; hydroxy-ester (I*b*) in poor and variable yield from silver perchlorate in 'moist' nitromethane. Both the bromides (IV*a*) and (IV*b*) decompose rapidly in the presence of silver salts to give 9-phenyl- and 9-methylphenanthrene respectively. Consequently the formation of unrearranged products from bromo-ester (I*c*) can be confidently attributed to neighboring group participation by the carbomethoxy group. Although it has been concluded (8, p. 120) that neighboring carboxylic ester has no significant effect in solvolytic reactions, an opposite view has been taken regarding silver-catalyzed reactions of certain aliphatic compounds (15) and, more recently, participation has been demonstrated for ester groups in the formation of 3-phenylphthalide (16). The striking neighboring group effect observed with bromo-ester (I*c*) has its origin in the very favorable stereochemistry associated with the rigid 9-disubstituted fluorene.

The contrast between the chemistry of bromo-ester (I*c*) and chloride (III) prompted the preparation of the chloro-ester (I*h*), which appeared to be a suitable intermediate for 9-phenyl-10-phenanthroic acid (13, 17, 18, 19).* Like III, the chloro-ester (I*h*) gave unrearranged diesters, e.g. the trifluoracetate (I*j*), in the presence of silver ion but, in contrast, gave unrearranged formate (I*k*) from solvolysis in formic acid and was recovered unchanged following attempted pyrolysis. The absence of rearrangement accompanying formolysis of (I*h*) can be attributed to additional stabilization by neighboring carbomethoxy. Formolysis of the trifluoracetate (I*j*) resulted in fragmentation to benzaldehyde and fluorene ester probably through a reversed aldol condensation (20) of hydroxy-ester (I*l*), cf. instability of I*b*, facile clearage by base of 9-fluorenyl ketones (13, 21, 22) and fragmentation of *t*-alkoxides (23), the driving force for all of these decompositions being the stability of fluorene anion. Related fragmentations of 9-fluorenylmethanols have been noted (24, 25, 26).

The secondary trifluoroacetate (I*m*), prepared from bromo-ester (I*n*), proved to be remarkably stable. It was recovered largely unchanged after being heated in 98% formic acid for several days or following attempted pyrolysis at 220°. Only slight decomposition occurred at 300–320° and phenanthrene derivatives were not detected by ultraviolet spectroscopy. Since the secondary *p*-toluenesulphonate (V*b*) undergoes formolysis 65 times as fast as the primary ester (V*a*) (27), the inertness of I*m* compared with I*e* is

**The formation of ethyl 9-phenylphenanthrene-10-carboxylate from 9-phenyl-9-bromofluorene and ethyl diazoacetate (19) may proceed by way of an unusual carbenoid insertion between carbon and bromine.*

surprising. As a check on the structure of I*n*, the isomeric bromo-ester (I*p*) was synthesized and non-identity established by comparison of melting points and infrared spectra.

Quinoline has already been used successfully to effect dehydrohalogenation and rearrangement of fluorenylalkyl halides (2), and it has now been shown to react with neopentyl-type halides, giving a good yield of 9-phenylphenanthrene from IV*a* and of 9-methylphenanthrene from IV*b*. The similar reactions of the halo-esters I*c*, I*h*, and I*n* gave only 9-methylene, 9-benzylidene, and 9-ethylidenefluorene, respectively. Previous experience with 9-fluorenylmethanols (1, 2, 3, 13, 21, 28) suggests that the formation of these olefins is anomalous and may proceed by way of the β-lactones (29, but see also 30, 31, 32, 33, 34). Decomposition of α,α-diphenyl-β-propiolactone to α,α-diphenylethylene has already been noted (35). Although the formation of β-lactones (29) and the (transient) α-lactones (9, pp. 117–119) is generally effected by intramolecular attack of carboxylate anion on carbon carrying halogen, examples are known of β-(36) and γ-lactone (37) formation involving explusion from carbomethoxy of methyl cation as methyl bromide. This process is illustrated in Fig. 2 for comparison with the formation of the alkylidene-

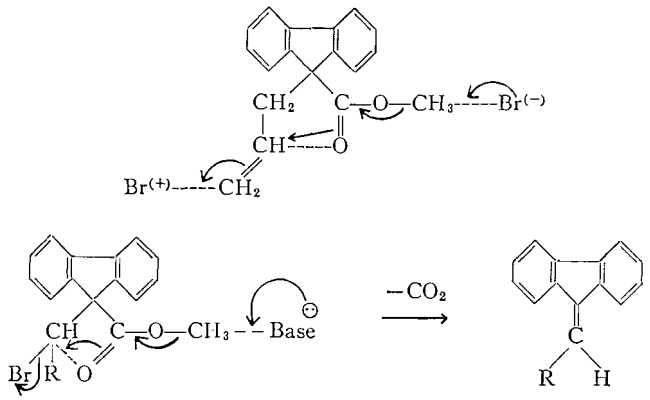

fluorenes (Fig. 3). Few examples have been recorded (38) of the decarboxylation of hindered acids in polyphosphoric acid. Consequently the decomposition in this reagent of hydroxy-ester (I*q*) may also proceed by way of the β-lactone.

The alkylation of N,N-dimethyl fluorene-9-carboxamide (II*b*) was successful only in *t*-butanol, esters being obtained in methanol or ethanol. Alkylation of 9-cyanofluorene (VI*a*) was effected under more general conditions (4), the 9-methyl (VI*b*), bromomethyl (VI*c*), and allyl (VI*d*) derivatives being obtained in satisfactory yields. Only a poor yield

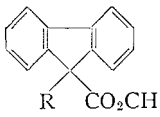

I*a* R =	H	I*j* R =	$C_6H_5CH(O.COCF_3)$
I*b*	$HOCH_2$	I*k*	$C_6H_5CH(O.CHO)$
I*c*	$BrCH_2$	I*l*	$C_6H_5CH(OH)$
I*d*	$ClCH_2$	I*m*	$CH_3CH(O.COCF_3)$
I*e*	$CF_3CO.OCH_2$	I*n*	CH_3CHBr
I*f*	$CH_3O_2C.CHCl$	I*p*	$BrCH_2CH_2$
I*g*	$CH_3CO.OCH_2$	I*q*	$CH_3CH(OH)$
I*h*	C_6H_5CHCl	I*r*	CH_3OCH_2
		I*s*	$CH_3.CO$

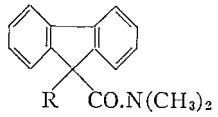

II*a* R =	$BrCH_2$
II*b*	H
II*c*	CH_3
II*d*	HO

Can. J. Chem. Downloaded from www.nrcresearchpress.com by 210.87.254.42 on 09/05/12
For personal use only.

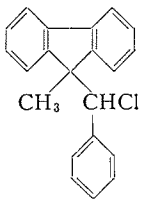

III

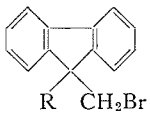

IV*a* R = C_6H_5
IV*b* CH_3

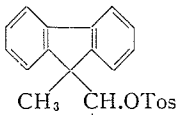

V*a* R = H
V*b* CH_3

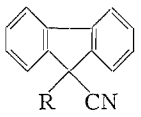

VI*a* R = H
VI*b* CH_3
VI*c* $BrCH_2$
VI*d* CH_2=$CHCH_2$
VI*e* $(CH_3)_3C$

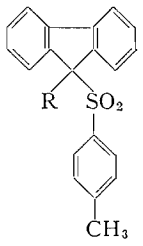

VII*a* R = $BrCH_2$
VII*b* $HOCH_2$

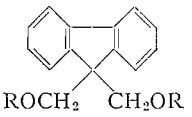

VIII*a* R = H
VIII*b* CF_3CO

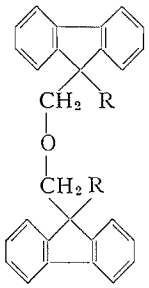

IX*a* R = CO_2CH_3
IX*b* CH_2OH

of the 9-*t*-butyl compound (VII*e*) was obtained and, even under nitrogen, the major product was fluorenone. It was noted that some cyanide ion was liberated during these alkylations. This is interesting because it could have originated from anionic displacement of cyanide ion (39, 40) or, more probably, by autoxidation (41) followed by decomposition of the unstable cyanohydrin (42). The bromosulphone (VII*a*) was prepared by a modification of an earlier general method (43). Attempts to bring about rearrangement of bromonitrile (VI*c*) and bromosulphone (VII*a*) were not successful. A number of other compounds did not rearrange to give phenanthrene derivatives. These included the glycol (VIII*a*) and bistrifluoracetate (VIII*b*); hydroxyester (I*b*) and diester (I*g*); ether (I*r*) and the complex ethers (IX*a*) and (IX*b*) (see Experimental for details).

The infrared spectra of several of the derivatives of fluorene ester described in this paper have proved particularly interesting. In view of a recent publication (44), they will be discussed in detail elsewhere (45).

To provide reference compounds, 9-bromo-10-methylphenanthrene (46) was converted to the nitrile. Alkaline hydrolysis under forcing conditions stopped at the amide.

EXPERIMENTAL

Melting points are uncorrected. Microanalyses are by Weiler and Strauss (Oxford) or Mr. Michael Graham (Smith Kline and French Laboratories Ltd.).

Can. J. Chem. Downloaded from www.nrcresearchpress.com by 210.87.254.42 on 09/05/12
For personal use only.

Methyl fluorene-9-carboxylate was prepared as described earlier (3). 9-Cyanofluorene was prepared from fluorene-9-aldehyde without purifying intermediates (47). 9-Fluorenyl *p*-tolyl sulphone was available from earlier work (43).

N,N-Dimethyl Fluorene-9-carboxamide (IIb)

Fluorene-9-carboxylic acid (3) (20 g) and thionyl chloride (20 ml) were warmed gently until the acid had dissolved. Excess reagent was evaporated under reduced pressure, final traces being removed by codistillation with dry benzene. The residual oil in cold dry benzene (30 ml) was added slowly to a cold solution of dimethylamine (30 g) in dry benzene (200 ml). After half an hour, the mixture was evaporated under reduced pressure and the residue thoroughly washed with hot water. Crystallization of the dried product from toluene gave colorless prisms (11 g), m.p. 256.5–258.0°. Found: C, 81.21; H, 6.53. Calc. for $C_{16}H_{15}NO$: C, 80.98, H, 6.37%.

Derivatives of Methyl Fluorene-9-carboxylate

The following were prepared by alkylating (or acylating) fluorene ester in methanol (4).

*Methyl 9-acetylfluorene-9-carboxylate** (Is) crystallized from acetone–methanol as pale yellow prisms (40–70% for four preparations), m.p. 65–66°. Found: C, 76.91; H, 5.41. Calc. for $C_{17}H_{14}O_3$: C, 76.67; H, 5.30%.

Methyl 9-bromomethylfluorene-9-carboxylate (Ic) separated from methanol as flattened prisms showing extensive twinning (88%), m.p. 112–113°. Found: C, 60.92; H, 4.17. Calc. for $C_{16}H_{13}BrO_2$: C, 60.58; H, 4.13%.

Methyl 9-chloromethylfluorene-9-carboxylate (Id) formed colorless prisms (78%) from methanol, m.p. 96–97°. Found: C, 70.40; H, 4.75. Calc. for $C_{16}H_{13}ClO_2$: C, 70.46; H, 4.80%. Both this and the preceding compound were contaminated when crude with polymeric formaldehyde, easily removed during crystallization.

Methyl 9-methoxymethylfluorene-9-carboxylate (Ir) crystallized from benzene–hexane (1:10) as white prisms (84%), m.p. 129–131°. Found: C, 76.10; H, 6.15. Calc. for $C_{17}H_{16}O_3$: C, 76.10; H, 6.01%.

Methyl 9-α-chlorobenzylfluorene-9-carboxylate (Ih) formed white felted needles (73%) from hexane, m.p. 127.0–127.5°. Found: C, 75.37; H, 4.94; Cl, 10.41. Calc. for $C_{22}H_{17}ClO_2$: C, 75.75; H, 4.91; Cl, 10.17%.

Methyl 9-1'-bromoethylfluorene-9-carboxylate (In) crystallized as colorless irregular prisms from hexane (72%), m.p. 129–130°. Found: C, 61.70; H, 4.48. Calc. for $C_{17}H_{15}BrO_2$: C, 61.64; H, 4.57%.

Methyl 9-2'-bromoethylfluorene-9-carboxylate (Ip) separated from hexane as colorless needles (67%), m.p. 189–190°. Found: C, 61.88; H, 4.72%.

Methyl 9-carbomethoxychloromethylfluorene-9-carboxylate (If) formed irregular prisms (81%) from cyclohexane, m.p. 102–103°. Found: C, 65.48; H, 4.68; Cl, 10.91. Calc. for $C_{18}H_{15}ClO_4$: C, 65.36; H, 4.57; Cl, 10.72%.

α-α'-bis-(9-Carbomethoxy-9-fluorenyl)-dimethyl ether (IXa), prepared by alkylating fluorene ester with α,α-dichlorodimethyl ether, crystallized from isopropyl alcohol as colorless prisms (89%), m.p. 170.5–171.0°. Found: C, 78.17; H, 5.54. Calc. for $C_{32}H_{26}O_5$: C, 78.35; H, 5.34%. The same compound (melting point, mixed melting point, and infrared spectra) was obtained in variable yield (30–60%) when fluorene ester was alkylated with impure chloromethy acetate, and was also isolated (10%) when methyl 9-hydroxymethylfluorene-9-carboxylate (VIIg) was acetylated with acetic anhydride and a trace of sulphuric acid. It was characterized by reduction with ethereal $LiAlH_4$ to IXb.

α,α'-bis-(9-Hydroxymethyl-9-fluorenyl)-dimethyl ether (IXb), which separated from benzene–heptane as fine white needles (91%), m.p. 158–159°, not identical with bis-9,9-hydroxymethylfluorene (VIIIa). Found: C, 82.84, 83.0; H, 6.36, 6.11. Calc. for $C_{30}H_{26}O_3$: C, 82.92; H, 6.03%.

bis-(9,9-Trifluoracetoxymethyl)-fluorene (VIIIb)

Dimethyl fluorene-9,9-dicarboxylate, prepared by acylating fluorene ester with methyl chloroformate, separated from cyclohexane as small colorless prisms (64%), m.p. 166–167° (lit. m.p. 167° (49)). Reduction with ethereal $LiAlH_4$ gave bis-9,9-hydroxymethylfluorene, identical with a sample supplied by Sprinzak (26). Found: C, 79.62; H, 6.24. Calc. for $C_{15}H_{14}O_2$: C, 79.56; H, 6.13%. Esterification of the glycol (3 g) with trifluoracetic anhydride (5 ml) gave *diester* (VIIIb), crystallizing as colorless needles (2.53 g, 45%) from hexane, m.p. 73–74°. Found: C, 54.87; H, 2.95. Calc. for $C_{19}H_{12}F_6O_4$: C, 54.55; H, 2.90%. Brief boiling with 98% formic acid regenerated the glycol, m.p. 146–147° (26), the ultraviolet spectrum of the crude product showing phenanthrene derivatives to be absent. The diester was recovered unchanged after attempted pyrolysis.

9-Hydroxy-9-fluorenylmethanol

Methyl 9-hydroxyfluorene-9-carboxylate was reduced with ethereal $LiAlH_4$, the *diol* crystallizing from benzene–hexane as long white needles (89%), m.p. 108–109°. Found: C, 79.45; H, 5.89. Calc. for $C_{14}H_{12}O_2$: C, 79.21; H, 5.69%. The diol was decomposed by phosphorus pentoxide under boiling xylene without formation of phenanthrene derivatives.

**Infrared measurements have established the keto-ester rather than the ketene–acetal–acylal structure for the corresponding ethyl ester (48).*

Can. J. Chem. Downloaded from www.nrcresearchpress.com by 210.87.254.42 on 09/05/12
For personal use only.

Experiments with Methyl 9-Bromomethylfluorene-9-carboxylate (Ic)

Methyl 9-Acetoxymethylfluorene-9-carboxylate (Ig)

The bromoester (4.2 g) reacted rapidly with silver perchlorate (5 g) in acetic acid (20 ml) which had been previously dried by boiling for 1 hour with 10% of its volume of acetic anhydride. Precipitation of silver salts was completed by the addition of an excess of dilute hydrochloric acid. Filtration and extraction with ether gave crude *diester* which crystallized from hexane as colorless prisms (3.1 g, 79%), m.p. 106–107°. Found: C, 72.72; H, 5.60. Calc. for $C_{18}H_{16}O_4$: C, 72.96; H, 5.44%.

Reduction of the diester with ethereal $LiAlH_4$ gave the glycol (VIII*a*), identical with an authentic specimen (above).

The diester (0.5 g) was heated with polyphosphoric acid for half an hour at 160°. Chromatography of the products (hexane–alumina) gave phenanthrene (0.07 g), identical with an authentic specimen, together with traces of an unidentified substance, m.p. 164–168°.

Methyl 9-Trifluoracetoxymethylfluorene-9-carboxylate (Ie)

The bromoester (2.1 g) reacted rapidly with a warm solution of silver trifluoracetate (50) (2.1 g) in trifluoracetic acid (12 ml)*. The *diester* crystallized from hexane as irregular prisms (1.6 g, 69%), m.p. 72–75°, raised to 81–83° (not sharp) by several further crystallizations. Found: C, 61.66; H, 3.60. Calc. for $C_{18}H_{13}F_3O_4$: C, 61.72; H, 3.74%. The diester was recovered unchanged after attempted pyrolysis at 220°.

Formic acid (5 ml, 98%) and diester (0.5 g) were boiled under reflux for 2 hours. The product separated from methanol as white needles (0.28 g, 82%), m.p. 114–115°, identical with authentic (5, 51) methyl phenanthrene-9-carboxylate.

p-Toluenesulphonic acid monohydrate (30 g) was heated in a thick-walled test tube at 0.01 mm pressure until melting was complete, and was then maintained at 70–90° for 2 hours. To the cooled acid was added bromoester (1 g) and silver *p*-toluenesulphonate (52) (2 g) and the mixture maintained at 35–40° for 2 hours with occasional shaking. Moisture was excluded by maintaining an atmosphere of dry nitrogen. The product was precipitated by pouring into dilute hydrochloric acid, and was extracted into methylene chloride, purified by chromatography (hexane–alumina) and crystallized from methanol. Methyl phenanthrene-9-carboxylate crystallized as white needles (0.4 g), m.p. 113–115°, identical with the previous sample.

Methyl 9-Hydroxymethylfluorene-9-carboxylate (Ib)

The bromoester (1.5 g) reacted rapidly with silver perchlorate (2 g) in nitromethane (20 ml) containing water (0.5 ml). The product formed colorless needles from benzene, m.p. 117–118° (0.7 g, 58%). Found: C, 75.52; H, 5.53. Calc. for $C_{16}H_{14}O_3$: C, 75.57; H, 5.55%. The yield was not reproducible and paraformaldehyde was always obtained.

Attempts to esterify the hydroxy-ester with methanesulphonyl or *p*-toluenesulphonyl chlorides were not successful. The reaction with acetic anhydride and a trace of sulphuric acid gave dimeric ether (IX*a*) (6–10%), isolated by crystallization from hexane, and acetoxy derivative (Ig) (27%), isolated by chromatography (hexane–alumina).

When heated with polyphosphoric acid at 160° or with phosphorus pentoxide under boiling xylene, the hydroxy-ester gave only tars.

The bromo-ester (Ic) was recovered unchanged after attempted pyrolysis at 220°, after it was heated with sodium iodide and boiling methyl ethyl ketone for 1 week, and after attempts at solvolysis in boiling dimethylformamide or 98% formic acid. It decomposed when heated with boiling quinoline for 1 hour, giving 9-methylenefluorene which, after purification by chromatography (hexane–alumina), crystallized from methanol as small colorless prisms (37%), m.p. 42–44°, strongly depressed by 9-methylfluorene (m.p. 45–46°). (Lit. m.p. 53° (53).) Found: C, 93.04; H, 6.58. Calc. for $C_{14}H_{10}$: C, 94.34; H, 5.66%. Calc. for $C_{14}H_{12}$: C, 93.29; H, 6.71%. The identity of the product as slightly impure 9-methylenefluorene was confirmed by its ultraviolet spectrum, which was almost identical with that of 9-ethylidenefluorene (54), and by hydrogenation over palladized charcoal to 9-methylfluorene.

Experiments with Methyl 9-α-Chlorobenzylfluorene-9-carboxylate (Ih)

Methyl 9-α-Formyloxybenzylfluorene-9-carboxylate (Ik)

Colorless prisms (0.9 g, 88%) separated after chloro-ester (Ih) (1 g) and 98% formic acid (10 ml) had been boiled under reflux for 1 hour. One crystallization from hexane gave the analytical sample, m.p. 164–165°. Found: C, 76.90; H, 5.16. Calc. for $C_{23}H_{18}O_4$: C, 77.08; H, 5.06%. Warming the diester with KOH in aqueous methanol gave benzaldyehde (2,4-dinitrophenylhydrazone, m.p. 232–234°) and fluorene-9-carboxylic acid (m.p. 226–228° decomp.).

Methyl 9-α-Trifluoracetoxybenzylfluorene-9-carboxylate (Ij)

The preparation was carried out as described for Ie but with the addition of 10% by volume of trifluoracetic anhydride to the trifluoracetic acid. The *diester* crystallized from hexane as colorless prims (71%), m.p. 128–129° after sintering at 120°. Found: C, 68.34; H, 4.47. Calc. for $C_{24}H_{17}F_3O_4$: C, 67.60; H, 4.02%. The analyses were not improved following further crystallizations.

**In later experiments silver trifluoracetate was replaced by the equivalent of silver oxide, which dissolved readily in trifluoracetic acid containing a slight excess of trifluoracetic anhydride.*

Can. J. Chem. Downloaded from www.nrcresearchpress.com by 210.87.254.42 on 09/05/12
For personal use only.

The trifluoracetate solvolyzed in 98% formic acid with fragmentation (see above) and with formation of small amounts of the formate (I*k*), but, like the chloroester (I*h*), was recovered unchanged after attempted pyrolysis at 220°.

9-Benzylidenefluorene

The chloroester (0.2 g) was decomposed by boiling under reflux for 2 hours with anhydrous quinoline (4 ml). After purification by chromatography (hexane–alumina), the product formed colorless prisms (0.11 g, 75%) from hexane, m.p. 74–76°, identical with an authentic sample (lit. m.p. 76° (55)).

Experiments with Methyl 9-1'-Bromoethylfluorene-9-carboxylate (I*n*)

The bromoester (I*n*) was recovered unchanged after attempted pyrolysis or after attempted solvolysis in formic acid. It was decomposed by boiling quinoline with formation of 9-ethylidenefluorene (61%), identical with an authentic specimen (55), m.p. 103–104°.

Methyl 9-1'-Trifluoracetoxyethylfluorene-9-carboxylate (I*m*)

The *trifluoracetate* (I*m*), prepared in the usual way from bromoester (I*n*), crystallized from hexane as well-defined prisms (74%) m.p. 99.5–101°. Found: C, 62.39; H, 4.32. Calc. for $C_{19}H_{15}F_3O_4$: C, 62.64; H, 4.15%. It was remarkably stable, being recovered unchanged after boiling for 1 week with 98% formic acid or for 12 hours with dimethylformamide, and was not decomposed to phenanthrene derivatives by distillation in a nitrogen atmosphere at atmospheric pressure (300–320°), although some tar formation occurred.

Methyl 9-1'-Hydroxyethylfluorene-9-carboxylate (I*q*)

The ketoester (1 g) was reduced with sodium borohydride (0.5 g) in methanol (15 ml). The *hydroxyester* crystallized as colorless slender needles (0.94 g, 92%) from hexane, m.p. 104–105°. Found: C, 76.21; H, 5.96. Calc. for $C_{17}H_{16}O_3$: C, 76.10; H, 6.01%. Attempts to prepare the methanesulphonate or toluenesulphonate in the usual way (3) failed but esterification with trifluoracetic anhydride gave the trifluoracetate (I*m*). The hydroxyester decomposed when boiled with phosphorus pentoxide under xylene, giving 9-ethylidenefluorene as the only crystalline neutral product.

9-Methyl-10-phenanthryl Nitrile

9-Bromo-10-methylphenanthrene (46) (1.3 g) was boiled under reflux for 3 hours with cuprous cyanide (1.5 g), pyridine (2 drops), and dimethylformamide (20 ml) (56). After it was cooled and diluted with water, the product was extracted into chloroform, purified by chromatography (hexane–alumina), and crystallized from benzene–heptane to give colorless prisms (0.7 g, 68%), m.p. 176.5–177.5°. Found: C, 88.66; H, 5.41. Calc. for $C_{16}H_{11}N$: C, 88.45; H, 5.10%. The infrared spectrum showed a C≡N stretching band at 2230 cm^{-1}.

9-Methylphenanthrene-10-carboxamide

The nitrile (0.4 g) and potassium hydroxide (2 g) were boiled under reflux for 6 hours with diethylene glycol (50 ml) and water (3 ml). The *amide* crystallized from toluene as slender colorless needles (0.15 g), m.p. 181–182°. Found: C, 81.25; H, 5.38; N, 5.67. Calc. for $C_{16}H_{13}NO$: C, 81.67; H, 5.57; N, 5.95%.

Derivatives of 9-Cyanofluorene

9-Methyl-9-cyanofluorene (VI*b*)

9-Cyanofluorene (1 g) was alkylated in the usual way (3, 4) with methyl iodide. After purification by chromatography (hexane–alumina) the product formed colorless well-defined prisms (0.6 g, 56%) from methanol, m.p. 92–93°. Found: C, 87.82; H, 5.53. Calc. for $C_{15}H_{11}N$: C, 87.77; H, 5.40% (C≡N stretching band at 2240 cm^{-1}). Acidification of the mother liquors remaining after isolation of the crude product liberated hydrocyanic acid, detected by its odor.

The following were prepared similarly:

9-Allyl-9-cyanofluorene (VI*d*), crystallizing as rhombohedral plates (69%) from methanol, m.p. 74–76°. Found: C, 88.56; H, 5.88. Calc. for $C_{17}H_{13}N$: C, 88.27; H, 5.67% (C≡N stretching band at 2240 cm^{-1}).

9-t-Butyl-9-cyanofluorene (VI*e*), which formed small colorless needles (8%) from hexane, m.p. 144–145°. Found: C, 87.11; H, 6.65. Calc. for $C_{18}H_{17}N$: C, 87.41; H, 6.93% (C≡N stretching band at 2230 cm^{-1}). Fluorenone, m.p. 69–72° (63%) was isolated by chromatography.

9-Bromomethyl-9-cyanofluorene (VI*c*)

9-Cyanofluorene (3.8 g) dissolved in dry *t*-butyl alcohol (30 ml) containing potassium *t*-butoxide (from 1.2 g potassium) to give a deep green sloution. The color was rapidly discharged following the addition of dibromomethane (8 g). The product separated from isopropyl alcohol as irregular prisms (3.9 g, 68%), m.p. 125–127°, raised to 126–127° by one crystallization from benzene. Found: C, 63.52; H, 3.55; N, 5.19. Calc. for $C_{15}H_{10}BrN$: C, 63.40; H, 3.55; N, 4.93%. Reaction with silver trifluoracetate gave the trifluoracetate (carbonyl stretching band: 1790 cm^{-1}), which decomposed in hot 98% formic acid during 4 hours with formation of the formate (carbonyl stretching band: 1725 cm^{-1}). Comparison of infrared spectra showed that 9-cyanophenanthrene was not formed. The bromo-nitrile decomposed in boiling quinoline to give tars in which 9-cyanophenanthrene was not detected.

Can. J. Chem. Downloaded from www.nrcresearchpress.com by 210.87.254.42 on 09/05/12
For personal use only.

Experiments with N,N-Dimethyl Fluorene-9-carboxamide

N,N-Dimethyl 9-Methylfluorene-9-carboxamide (II*c*)

Prepared by alkylation in *t*-butyl alcohol as described for (VI*c*), the *amide* crystallized as slender colorless needles (83%) from hexane, m.p. 161–162°. Found: C, 81.78; H, 6.94. Calc. for $C_{17}H_{17}NO$: C, 81.24; H, 6.82%. When the methylation was carried out in methanol, only methyl 9-methylfluorene-9-carboxylate was isolated, identical with an authentic specimen (3).

N,N-Dimethyl 9-Hydroxyfluorene-9-carboxamide (II*d*)

The only product isolated from attempts at *t*-butylation in methanol or *t*-butyl alcohol was the *hydroxy-amide* (55%), m.p. 121.5–122.0°. Found: C, 75.69, 75.94; H, 5.99, 6.08. Calc. for $C_{16}H_{15}NO$: C, 75.87; H, 5.97%.

N,N-Dimethyl 9-Bromomethylfluorene-9-carboxamide (II*a*)

The *bromo-amide* was prepared in *t*-butanol and formed very pale yellow prisms (91%) from hexane, m.p. 110–111°. Found: C, 61.66; H, 4.95. Calc. for $C_{17}H_{16}BrNO$: C, 61.83; H, 4.88%.

N,N-Dimethyl Phenanthrene-9-carboxamide

The crude product from the reaction between bromo-amide (II*a*) (1 g) and silver trifluoracetate (1.5 g) in trifluoracetic acid (10 ml) was boiled under reflux for 1 hour with 98% formic acid (8 ml). The phenanthrene amide formed small white needles (0.4 g, 53%) from ethanol, m.p. 185–186°, identical with an authentic specimen, m.p. 185–187° (lit. m.p. 182.5–183.0° (57)).

Preparation of 9-Phenylphenanthrene

9-Phenyl-9-fluorenylmethyl Bromide (IV*a*)

9-Phenylfluorene (17.5 g) was alkylated in ether with dibromomethane (40 g), using phenyllithium as base (58), the red color of the anion disappearing during 5 minutes. The product was obtained as well-defined colorless prisms (14.8 g, 61%) from benzene–hexane, m.p. 142–143°. Found: C, 71.55; H, 4.67; Br, 23.85. Calc. for $C_{20}H_{15}Br$: C, 71.65; H, 4.51; Br, 23.84%.

The bromo compound (1 g) reacted very rapidly with silver perchlorate (1 g) in anhydrous acetic acid (15 ml). 9-Phenylphenanthrene crystallized from ethanol as white needles (0.5 g, 66%), m.p. 103–104° (lit. m.p. 105–106° (17)).

The bromo compound (0.5 g) was boiled under reflux for 1 hour with quinoline (5 ml). Crystallization of the product from ethanol gave 9-phenylphenanthrene (0.28 g, 74%), m.p. 104–105°. The picrate formed orange needles from ethanol, m.p. 116–117° (lit. m.p. 115° (17)).

Preparation of 9-Methylphenanthrene

9-Methyl-9-fluorenylmethyl Bromide (IV*b*)

9-Methylfluorene (6.24 g) (13) was alkylated in the usual way (58) (preceding compound). The product crystallized as colorless prims (4.2 g, 49%) from methanol, m.p. 53–54°. Found: C, 65.89, 66.17; H, 4.65, 4.65. Calc. for $C_{15}H_{13}Br$: C, 65.95; H, 4.80%.

The bromide (IV*b*), (1 g), was warmed with silver perchlorate (1 g) in acetic acid (20 ml). The product crystallized from methanol as colorless prismatic needles (0.54 g, 77%), m.p. 91–92°, identified as 9-methylphenanthrene by comparison with an authentic specimen (3). 9-Methylphenanthrene (70%) was also obtained by decomposition of the bromide in boiling quinoline.

Experiments with 9-Bromomethyl-9-fluorenyl p-Tolyl Sulphone (VII*a*)

9-Bromomethyl-9-fluorenyl p-Tolyl Sulphone (VII*a*)

9-Fluorenyl *p*-tolyl sulphone (1 g) was alkylated with dibromomethane (5 ml) in a mixture of dimethylformamide (15 ml) and methanol (8 ml) containing sodium methoxide (from 0.4 g sodium). The product crystallized from benzene–hexane as small colorless prisms (0.6 g, 48%), m.p. 200–202°, raised to 202–203.5° by a further cyrstallization. Found: C, 60.97; H, 4.68; S, 7.44. Calc. for $C_{21}H_{17}BrO_2S$: C, 61.02; H, 4.15; S, 7.76%. Decomposition of the bromo-sulphone in boiling quinoline did not yield phenanthrene derivatives.

9-Hydroxymethyl-9-fluorenyl p-Tolyl Sulphone (VII*b*)

The bromosulphone reacted rapidly with silver trifluoracetate in trifluoracetic acid, but, even in the presence of trifluoracetic anhydride, the trifluoracetate was not obtained pure. Brief solvolysis of the crude product in 98% formic acid gave the *hydroxy-sulphone* (VII*b*) which, after chromatography (hexane–alumina), crystallized as colorless well-defined prisms (59%) from benzene–hexane, m.p. 158–159°. Found: C, 71.77, 71.89; H, 5.15, 5.39. Calc. for $C_{21}H_{18}O_3S$: C, 71.98; H, 5.18%. The hydroxy-sulphone did not give phenanthrene derivatives when boiled with phosphorus pentoxide and xylene.

REFERENCES

1. W. G. Brown and B. Bluestein. J. Am. Chem. Soc. **62**, 3256 (1940).
2. E. J. Greenhow, D. McNeil, and E. N. White. J. Chem. Soc. 986 (1952).
3. F. A. L. Anet and P. M. G. Bavin. Can. J. Chem. **34**, 991 (1956).
4. P. M. G. Bavin. Anal. Chem. **32**, 554 (1960).

Can. J. Chem. Downloaded from www.nrcresearchpress.com by 210.87.254.42 on 09/05/12
For personal use only.

5. W. WISLICENUS and W. MOCKER. Ber. **46**, 2772 (1913).
6. R. PSCHORR. Ber. **29**, 496 (1896).
7. D. H. HEY and J. M. OSBOND. J. Chem. Soc. 3172 (1949).
8. A. STREITWEISER. Solvolytic displacement reactions. McGraw-Hill Book Co., New York. 1962.
9. J. HINE. Physical organic chemistry. McGraw-Hill Book Co., New York. 1956.
10. C. K. INGOLD. Structure and mechanism in organic chemistry. Cornell University Press, Ithaca, N.Y. 1953.
11. M. S. NEWMAN (*Editor*). Steric effects in organic chemistry. John Wiley and Sons, Inc., New York. 1956.
12. P. M. G. BAVIN. Can. J. Chem. **40**, 1399 (1962).
13. P. M. G. BAVIN. Can. J. Chem. **37**, 2023 (1959).
14. P. SKELL and C. R. HAUSER. J. Am. Chem. Soc. **64**, 2633 (1942).
15. W. VON DOERING and L. K. LEVY. J. Am. Chem. Soc. **77**, 509 (1955).
16. A. SINGH, L. J. ANDREWS, and R. M. KEEFER. J. Am. Chem. Soc. **84**, 1179 (1962).
17. C. F. KOELSCH. J. Am. Chem. Soc. **56**, 480 (1934).
18. CH. WEIZMANN, E. BERGMANN, and T. BERLIN. J. Am. Chem. Soc. **60**, 1331 (1938).
19. I. A. D'YAKANOV and J. V. DOMAREVA. Zh. Obsch. Khim. **29**, 3098 (1959).
20. L. CLAISEN. Ber. **23**, 976 (1890).
21. P. M. G. BAVIN. Can. J. Chem. **38**, 1099 (1960).
22. G. W. H. SCHERF and R. K. BROWN. Can. J. Chem. **39**, 1613 (1961).
23. P. M. G. BAVIN. Can. J. Chem. **38**, 882 (1960).
24. J. G. BURR, JR. J. Am. Chem. Soc. **73**, 823 (1951).
25. H. E. ZAUGG. J. Am. Chem. Soc. **72**, 3001 (1950).
26. E. GHERA and Y. SPRINZAK. J. Am. Chem. Soc. **82**, 4945 (1960).
27. F. A. L. ANET and P. M. G. BAVIN. Unpublished data.
28. M. MATZNER, S. GLAZNER-TARASIEJSKA, and R. H. MARTIN. Bull. Soc. Chim. Belges, **69**, 551 (1960).
29. H. E. ZAUGG. Org. Reactions, **VIII**, 305 (1954).
30. G. PRAUSNITZ. Ber. **17**, 595 (1884).
31. H. JOHANSSON and S. M. HAGMAN. Ber. **55**, 647 (1922).
32. R. B. WOODWARD and R. B. LOFTFIELD. J. Am. Chem. Soc. **63**, 3167 (1941).
33. S. J. CRISTOL and W. P. NORRIS. J. Am. Chem. Soc. **75**, 632, 2645 (1953).
34. E. GROVENSTEIN, JR. and D. E. LEE. J. Am. Chem. Soc. **75**, 2639 (1953).
35. H. E. ZAUGG. J. Am. Chem. Soc. **72**, 2998 (1950).
36. N. J. TOIVONEN. Chem. Zentr. **II**, 39 (1928).
37. R. T. ARNOLD, M. DE MOURA CAMPOS, and K. L. LINDSAY. J. Am. Chem. Soc. **75**, 1044 (1953).
38. F. D. POPP and W. E. MCEWEN. Chem. Rev. **58**, 321 (1958).
39. W. G. KOFRON, W. R. DUNNAVANT, and C. R. HAUSER. J. Org. Chem. **27**, 2737 (1962).
40. TAKEO HIGASHINO. Yakugaku Zasshi, **80**, 1404 (1960); Chem. Abstr. **55**, 5515i (1961).
41. Y. SPRINZAK. J. Am. Chem. Soc. **80**, 5449 (1958).
42. A. LAPWORTH and R. H. F. MANSKE. J. Chem. Soc. 2548 (1928).
43. P. M. G. BAVIN. Can. J. Chem. **38**, 917 (1960).
44. K. BOWDEN, N. B. CHAPMAN, and J. SHORTER. Can. J. Chem. **41**, 2154 (1963).
45. G. HIGGINS and P. M. G. BAVIN. In preparation.
46. R. DE RIDDER and R. A. MARTIN. Bull. Soc. Chim. Belges, **69**, 534 (1960).
47. J. A. KING, R. I. MELTZER, and J. DOCZI. J. Am. Chem. Soc. **77**, 2217 (1955).
48. R. KUHN and U. BREYER. Chem. Ber. **94**, 745 (1961).
49. W. SCHLENCK, H. HILLEMANN, and I. RODLOFF. Ann. **487**, 135 (1931).
50. R. N. HASZELDINE. J. Chem. Soc. 584 (1951).
51. P. M. G. BAVIN and M. J. S. DEWAR. J. Chem. Soc. 164 (1956).
52. N. KORNBLUM, W. J. JONES, and G. J. ANDERSON. J. Am. Chem. Soc. **81**, 4113 (1959).
53. H. WIELAND, F. REINDEL, and J. FERRER. Ber. **55B**, 3313 (1922).
54. E. J. GREENHOW, A. S. HARRIS, and E. N. WHITE. J. Chem. Soc. 3116 (1954).
55. F. ULLMANN and R. VAN WURSTEMBERGER. Ber. **38**, 4105 (1905).
56. L. FRIEDMAN and H. SHECHTER. J. Org. Chem. **26**, 2522 (1961).
57. J. VAN DE KAMP, A. BURGER, and E. MOSETTIG. J. Am. Chem. Soc. **60**, 1321 (1938).
58. P. M. G. BAVIN. Can. J. Chem. **38**, 882 (1960).

Can. J. Chem. Downloaded from www.nrcresearchpress.com by 210.87.254.42 on 09/05/12
For personal use only.

Can. J. Chem. Downloaded from www.nrcresearchpress.com by 210.87.254.6 on 09/05/12
For personal use only.

FISSION FRAGMENT IRRADIATIONS OF HYDROCARBONS

I. YIELD AND ISOTOPIC COMPOSITION OF HYDROGEN FROM MIXTURES OF CYCLOHEXANE AND BENZENE WITH THEIR DEUTERATED ANALOGUES[1]

A. W. Boyd and H. W. J. Connor
Research Chemistry Branch, Atomic Energy of Canada Limited, Chalk River, Ontario

Received January 20, 1964

ABSTRACT

Cyclohexane and benzene and mixtures of each of these with cyclohexane-d_{12} and benzene-d_6 have been irradiated with fission fragments using thin sources of $U_3^{235}O_8$. The hydrogen yield $G(H_2)$ for cyclohexane is 7.73, and is only slightly reduced by the addition of benzene. $G(H_2)$ for benzene is 2.14. The isotopic composition of the hydrogen from the four mixtures indicates that most is formed in bimolecular processes.

To correlate these results with those obtained in gamma radiolysis, a mechanism is proposed based on hydrogen formation by reactions between transient species in both cyclohexane and benzene.

INTRODUCTION

The linear energy transfer (LET) of ionizing radiation is defined as the rate of energy loss per unit length of track. An increase in LET increases the concentration of the primary products along the track and thus favors reactions between these products over their reactions with the substrate. The determination of the effect of LET on product yields may therefore aid in the formulation of a mechanism for the radiolysis of a compound.

LET dependence in the radiolysis of cyclohexane has been investigated by Schuler, Allen, and Dewhurst (1–3), who found the yields of hydrogen and the liquid products to be constant within 10% over the range 0.02–2 eV/Å.

Burns (4) assumed that the hydrogen formed in the radiolysis of cyclohexane is due to reactions [1]–[3]

$$C_6H_{12} \curvearrowright\!\!\!\!\rightarrow C_6H_{11} + H \qquad [1]$$

$$H + C_6H_{12} \rightarrow H_2 + C_6H_{11} \qquad [2]$$

$$H + H \rightarrow H_2 \qquad [3]$$

and calculated that at low LET values reaction [3] is not likely to compete with [2] but at 50–100 eV/Å the hydrogen yield should be lower due to the favoring of [3] over [2].

Gaumann and Schuler (5) and Burns *et al.* (6, 7) have found, in contrast to the behavior of cyclohexane, that in irradiations of benzene the yields of hydrogen and acetylene increase with increasing linear energy transfer.

The yield of hydrogen from benzene using fast electrons (LET ~0.02 eV/Å) is 0.036–0.04 (6) and increases to 0.075 at ca. 3 eV/Å and to 0.57 at ca. 15 eV/Å. Burns (6) has suggested that the increase is due to the favoring of reaction [4] over [5]

$$B^* + B^* \rightarrow H_2 + \text{radicals or stable products} \qquad [4]$$

$$B^* + B \rightarrow B + B \qquad [5]$$

at higher track densities, where B* is an excited molecule.

In this mechanism the intermediate is deactivated by the substrate instead of reacting with it to produce hydrogen as is assumed to occur in the radiolysis of cyclohexane.

[1]*Issued as AECL No. 1943.*
Presented in part at the American Chemical Society Meeting in New York, September 1960.

Fission fragments have an LET of about 400 eV/Å so that they provide a means of testing Burns' calculations of the LET dependence of hydrogen yield in cyclohexane. They also make it possible to determine if there is a further increase in decomposition yields of benzene with LET. We have therefore irradiated cyclohexane, benzene, and mixtures of these with their deuterated analogues with fission fragments. The irradiations of the mixtures were done for comparison with the analogous gamma-ray irradiations of Dyne and Jenkinson (8, 9).

EXPERIMENTAL

The benzene and the cyclohexane were both Fisher Spectrograde and the benzene-d_6 and cyclohexane-d_{12} were obtained from Merck and Co. The isotopic purity, as given by the manufacturer, of the former was 99.5% and of the latter, 99%.

The samples, which were 5–8 ml in volume, were thoroughly outgassed by five cycles of melting, freezing, and evacuating in quartz capsules. The uranium was 93% U^{235} in the form of a thin layer of U_3O_8 on stacked aluminum disks. An irradiation capsule with the aluminum disks is shown in Fig. 1. Chemically polished

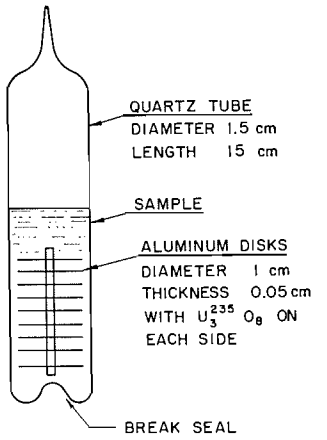

FIG. 1. Fission fragment irradiation capsule.

superpure aluminum was used for these sources and the layer of U_3O_8 was formed using the method of Glover and Burrell (10). The isotopic composition of the uranium, which was obtained from Oak Ridge National Laboratory, measured with a Consolidated Model 21–702B mass spectrometer, was U^{234} 0.984 atom %, U^{235} 93.18 atom %, U^{236} 0.471 atom %, U^{238} 5.37 atom %.

Each source was counted using a windowless proportional alpha counter, and the amount of U^{235} calculated from the alpha activity and the isotopic composition assuming the following half-lives: U^{234} 2.50×10^5 yr, U^{235} 6.985×10^8 yr, U^{236} 2.435×10^7 yr, and U^{238} 4.53×10^9 yr. The alpha counter was calibrated using a standardized Pu^{239} source.

The amount of fission fragment energy deposited in the sample was calculated from the weight of U^{235} and the integrated thermal neutron flux, assuming that half of the total energy of the fission fragments was released in the hydrocarbon. The integrated thermal neutron flux was determined using Johnson and Matthey spectroscopically pure 0.005 in. diameter cobalt wire. The following effective cross sections were used: $\hat{\sigma}$ $Co^{59}(n,\gamma)Co^{60}$ 36.1 b, $\hat{\sigma}$ $U^{235}(n,f)$ 551 b; total energy of fission fragments per fission 165 MeV. The values for these cross sections were taken from Westcott's compilation (11).

The maximum average thickness of the U_3O_8 on the sources was 64 $\mu g\ cm^{-2}$, and, as the range of fission fragments in U_3O_8 is 10 mg cm^{-2}, the loss of energy of the escaping fragments in the sources was negligible (12). The total uncertainty in the energy deposition values due to counting errors and to the uncertainties in the values of cross sections and half-lives is estimated to be less than ±10%.

The quartz capsules were placed in aluminum cans and suspended in an air annulus (the J-rod annulus) in the graphite reflector of the NRX reactor. Irradiation times were 1–2 minutes for the cyclohexane samples. As the yield of hydrogen from benzene is independent of dose (6), the benzene was irradiated for 30–60 minutes in order to obtain more easily measured volumes of gas. The thermal flux was approximately 1×10^{13} n $cm^{-2}\ sec^{-1}$, and the dose rate due to gamma rays and fast neutrons was approximately 30 mW g^{-1}.

Can. J. Chem. Downloaded from www.nrcresearchpress.com by 210.87.254.6 on 09/05/12
For personal use only.

To correct for the decomposition due to reactor radiation, samples without uranium were irradiated at the same time. The total dose in the cyclohexane samples from both fission fragments and reactor radiation was ca. 4×10^{19} eV g^{-1}, with 75% being due to the former. In the benzene samples, the corresponding values were $(1–2)\times10^{20}$ eV g^{-1} and 50%.

The volumes of hydrogen evolved were measured on a conventional gas analysis apparatus. The isotopic composition was determined with a calibrated Consolidated 21-610 mass spectrometer.

Samples of benzene and cyclohexane were given doses of the same order as those above in a Co^{60} source as a check upon the methods of sample preparation and analysis. The hydrogen yields were 5.5 and 0.04 for cyclohexane and benzene, respectively, in good agreement with the accepted values (13, 6).

RESULTS

The data for cyclohexane and the mixtures with C_6D_{12} and C_6D_6 are given in Table I. They have been corrected for the reactor radiation contribution so that the G values are for fission fragments only.

The data from fission fragment irradiations of benzene–benzene-d_6 mixtures and benzene–cyclohexane-d_{12} mixtures are shown in Table II.

TABLE I

Yields and isotopic composition of hydrogen from fission fragment irradiations of C_6H_{12}–C_6D_{12} and C_6H_{12}–C_6D_6 mixtures

Composition (volume %)	G (total hydrogen)	% HD	% D_2	G(HD)	$G(D_2)$	$G(D_2)/F$*
C_6H_{12}	7.73†	—	—	—	—	—
2% C_6D_{12}	8.11	2.63	0.095	0.25	0.0068	0.33
4% C_6D_{12}	8.21	5.14	0.226	0.46	0.018	0.43
6% C_6D_{12}	7.64	7.59	0.376	0.65	0.28	0.44
C_6D_{12}	5.96	5.06	94.94	—	—	—
2% C_6D_6	8.09	1.83	0.044	0.14	0.0035	0.14
6% C_6D_6	7.31	5.05	0.106	0.40	0.0082	0.103
6% C_6D_6	6.97	5.25	0.130	0.40	0.0098	0.125

*F is the mole ratio of the deuterated hydrocarbon to the light hydrocarbon.
†This is the average of five irradiations with an average deviation of 0.15. No significant difference in yields was observed between irradiations of frozen (−60–0°) and liquid (20–30°) cyclohexane.

TABLE II

Yields and isotopic composition of hydrogen from C_6H_6–C_6D_6 and C_6H_6–C_6D_{12} mixtures

Composition (volume %)	G(total hydrogen)	% HD	% D_2	G(HD)	$G(D_2)$	$G(D_2)/F$
C_6H_6	2.14*	—	—	—	—	—
	2.54†					
C_6D_6	1.45	—	—	—	—	—
2.5% C_6D_6–C_6H_6‡		4.15	0.1	0.089	0.002	0.078
2.5% C_6D_6–C_6H_6‡		4.19	0.088	0.090	0.0019	0.074
5% C_6D_6–C_6H_6‡		8.65	0.27	0.175	0.0058	0.114
5% C_6D_6–C_6H_6‡		7.84	0.24	0.168	0.0062	0.12
10% C_6D_6–C_6H_6‡		14.85	0.88	0.318	0.0189	0.17
16% C_6D_6–C_6H_6‡	1.74	23.68	2.01	0.395	0.0335	0.18
2% C_6D_{12}–C_6H_6	2.61	5.83	0.25	0.15	0.0064	0.38
6% C_6D_{12}–C_6H_6	2.37	15.63	1.18	0.37	0.028	0.53

*This is the average of five determinations with an average deviation of 0.12. No significant difference in the yields was observed between frozen and liquid samples. The total dose was approximately 1×10^{20} eV g^{-1}.
†This is the average of four determinations with an average deviation of 0.32. The total dose was approximately 2×10^{22} eV g^{-1}.
‡The total hydrogen yields were assumed to be the same as in pure C_6H_6, i.e. 2.14.

In the calculation of the yields in Tables I and II it is assumed that 50% of the total energy of the fission fragments is deposited in the hydrocarbon. This percentage may if anything be lower so that the yields may be too low. The isotopic composition of acetylene from the fission fragment irradiation of benzene was also obtained. $G(C_2H_2)$ values are

Can. J. Chem. Downloaded from www.nrcresearchpress.com by 210.87.254.6 on 09/05/12
For personal use only.

of the same order as the hydrogen yields. An 8% solution of C_6D_6 in C_6H_6 gave 15.2% C_2HD and 7.3% C_2D_2, and 16% C_6D_6 in C_6H_6 gave 17.4% C_2HD and 15.5% C_2D_2.

DISCUSSION

The salient points shown by comparison of the fission fragment total hydrogen yields with those previously obtained are as follows.

(1) The hydrogen yield in the fission fragment radiolysis of cyclohexane is approximately 40% greater than that obtained in gamma radiolysis.

(2) The hydrogen yield in the fission fragment radiolysis of 6% C_6D_6–C_6H_{12} is 90% or more of the yield in pure cyclohexane, while in gamma radiolysis the addition of 6% C_6D_6 lowers the hydrogen yield by 50%.

(3) The hydrogen yield from benzene increases by a factor of 4 over the LET range 15–400 eV/Å compared to an increase of ~12 over the range 0.02–15 eV/Å.

In the following discussion we shall assume that the yields of the primary products (excited molecules, radicals, or ions) in the irradiation of both cyclohexane and benzene are independent of LET. This assumption is implicit in Burns' (4) discussion of the effect of LET on the hydrogen yield from cyclohexane, and if it is correct then the mechanism represented by reactions [1]–[3] must be wrong. The observed increase in the cyclohexane hydrogen yield with LET suggests that there is competition between a deactivation of the primary species by the substrate and the reaction of two of these species to form hydrogen. Thus the mechanism suggested by Burns (6) to explain the effect of LET in the irradiation of benzene can be used to explain the dependence of $G(H_2)$ values on LET in the irradiation of cyclohexane.

The reaction scheme for cyclohexane can be written as follows.

$$C_6H_{12} \rightsquigarrow C_6H_{12}' \qquad [6]$$

$$C_6H_{12}' + C_6H_{12}' \rightarrow H_2 + P \qquad [7]$$

$$C_6H_{12}' + C_6H_{12} \rightarrow P \qquad [8]$$

$$C_6H_{12}' + C_6H_6 \rightarrow P \qquad [9]$$

With high LET radiation reaction [7] is favored over reactions [8] and [9] so that the hydrogen yield is higher than at low LET values and is unaffected by the addition of benzene.[2]

Analysis of Isotopic Data

Let us consider what evidence can be derived for the above mechanism from the isotopic composition of the hydrogen from the mixtures of cyclohexane and benzene with C_6D_{12} and C_6D_6.

Dyne and Jenkinson (9) have derived equations for the HD and D_2 yields based on the following processes:

(1) a unimolecular decomposition yielding H_2 (or D_2)

(2) the formation of reactive intermediates which produce H_2, HD, or D_2 by abstraction from light or deuterated molecules.

We shall also assume that there is unimolecular decomposition as in reactions [10] and [11].

$$C_H \rightarrow H_2 + P \qquad \text{Yield } G_1(H) \qquad [10]$$

$$C_D \rightarrow D_2 + P \qquad \text{Yield } G_1(D) \qquad [11]$$

[2]*This mechanism is not inconsistent with the invariance of the H_2 yield over the range 0.02–2 eV/Å as the excited species and the spur sizes may be such that fission fragment track densities are needed to reduce reactions [8] and [9].*

Can. J. Chem. Downloaded from www.nrcresearchpress.com by 210.87.254.6 on 09/05/12
For personal use only.

The notation is theirs, with C_H and C_D being the light and the deuterated hydrocarbons, P other products, and $G_1(H)$ and $G_1(D)$ the yields of these reactions. Instead of abstraction we assume the bimolecular process producing hydrogen to be as follows.

$C_H \rightarrow C_H'$	Yield $G_t(H)$	[12]
$C_D \rightarrow C_D'$	Yield $G_t(D)$	[13]
$C_D' + C_H' \rightarrow HD + P$	Rate constant for HD formation, k_1	[14]
$C_D' + C_D' \rightarrow D_2 + P$	Rate constant for D_2 formation, k_2	[15]
$C_H' + C_H' \rightarrow H_2 + P$	Rate constant for H_2 formation, k_3	[16]

In solutions where $C_D \ll C_H$ the yields of D_2 and HD will be given by (i) and (ii).

$$G(D)_2 = FG_1(D) + \frac{F^2G_t(D)}{2}\frac{G_t(D)}{G_t(H)}\frac{k_2}{k_1} \qquad [i]$$

$$G(HD) = FG_t(D) \qquad [ii]$$

For the pure deuterated compound

$$G(D_2) = G_1(D) + \frac{G_t(D)}{2} \qquad [iii]$$

$G_1(D)$ can be obtained by determining the intercept in the plot of $G(D_2)/F$ against F. The yield of the transient species, $G_t(D)$, is given by the initial slope in the plot of $G(HD)$ vs. F, and is designated $g(HD)$ by Dyne and Jenkinson. It is important to note that an independent value of $G_t(D)$ can be obtained from equation (iii) above and is given by $2[G(D_2) - G_1(D)]$.

The values of $G_1(D)$ and $G_t(D)$ calculated from equations (i)–(iii) for all four of the isotopic mixtures used are given in Table III. Dyne and Jenkinson's values for gamma radiolysis are given in parentheses. The values for each of the mixtures in Table III are discussed below.

TABLE III

$G_1(D)$ and $G_t(D)$ values for mixtures of cyclohexane and benzene with their deuterated analogues

Mixture	$G_1(D)$	$G_t(D) = g(HD)$	$G_t(D) = 2[G(D_2)^* - G_1(D)]$
C_6D_{12}–C_6H_{12}	0.3 ± 0.05 (0.32)	12 (3.6)	11.3 (7.4)
C_6D_{12}–C_6H_6	0.3 ± 0.1 (0.06)	9.0 (0.17)	11.3 (8)
C_6D_6–C_6H_{12}	0.1 ± 0.05 (0.01)	5.6 (>2.9)	2.7 (0.006)
C_6D_6–C_6H_6	0.05 ± 0.01 (0.0032)	3.4 (0.027)	2.7 (0.02)

*This is the yield of D_2 from the pure deuterated hydrocarbon.

Cyclohexane-d_{12}/Cyclohexane Mixtures

Insofar as the two $G_t(D)$ values agree with each other our mechanism fits the fission fragment data. The overall increase in yield with LET can, as we have said, be explained by the favoring of reaction [7] over [8]. The disagreement between the $G_t(D)$ values in gamma radiolysis can be explained by an isotope effect in reaction [8] so that C_D' suffers more deactivation proportionally than C_H'. This isotope effect can be written as reaction [17]

$$C_D' + C_H \rightarrow C_D + C_H'. \qquad [17]$$

The $G_1(D)$ values appear to be independent of LET. This does not seem to exclude the possibility that the unimolecular and bimolecular processes have a common precursor.

Can. J. Chem. Downloaded from www.nrcresearchpress.com by 210.87.254.6 on 09/05/12
For personal use only.

Dyne and Jenkinson (14) have suggested the following reactions

$$C_6D_{12} \wwarrow\!\!\!\rightarrow C_6D_{12}^* \quad [18]$$

$$C_6D_{12}^* \rightarrow D_2 + P \quad [19]$$
$$\searrow X_D + P$$

$$X_D + C_6H_{12} \rightarrow HD + P \quad [20]$$

$$C_6D_{12} + C_6H_6 \text{ (or } I_2) \rightarrow P \quad [21]$$

to account for the similar reductions in both $G_1(D)$ and $g(HD)$ on the addition of benzene or iodine in the radiolysis of cyclohexane. Introducing a common precursor into the mechanism we have used, we have

$$C_6D_{12} \wwarrow\!\!\!\rightarrow C_D' \quad [22]$$

$$C_D' \rightarrow D_2 + P \quad [23]$$

$$C_D' + C_H' \rightarrow HD + P \quad [24]$$

$$C_D' + C_6H_{12} \text{ (or } C_6H_6) \rightarrow P \quad [25]$$

In the mechanism of Dyne and Jenkinson an increase in total yield of hydrogen in pure cyclohexane with LET can be explained by assuming that there is some deactivation of the precursor by cyclohexane. This deactivation would be reduced at high LET, but both $G_1(D)$ and $g(HD)$ should then increase, as the branching ratio in reaction [19] and the yield of [20] should not be affected by LET.

The mechanism represented by equations [22]–[25] does not appear to be inconsistent with the increase in $g(HD)$ and the invariance of $G_1(D)$ with increasing LET. At high LET values the substrate concentration in the track will be low; both reactions [23] and [24] will be favored over [25], and [24] will be favored over [23]. Therefore, the certain effects of increasing LET are to increase the yield of [24] and to decrease the yield of [25]. The yield of [23] may increase, decrease, or stay the same.

Cyclohexane-d_{12}/Benzene Mixtures

The values in Table III for these mixtures provide striking evidence of how great the difference can be between fission fragment and gamma radiolysis. In the gamma radiolysis of dilute solutions of C_6D_{12} in benzene $G_1(D)$ is 0.06 and $g(HD)$ only 0.17. In the fission fragment radiolyses of these solutions $G_1(D)$ is 0.3 and $g(HD)$ is 9.0, within 25% of the corresponding values for C_6D_{12} in cyclohexane. That is, the decomposition of C_6D_{12} in fission fragment radiolysis is much the same in 95% benzene as it is in 95% cyclohexane.

The 25% reduction in $g(HD)$ that is observed between C_6D_{12}–C_6H_{12} and C_6D_{12}–C_6H_6 can be explained by assuming that, even with fission fragments, reaction [9] occurs to some extent.

Benzene-d_6/Benzene Mixtures

The increase with LET in the $G_1(D)$ values for these mixtures is not in disagreement with a mechanism involving a common precursor similar to that given in reactions [22] to [25]. An increase in LET favors both reactions [23] and [24] over [25] but, since [24] is second order in the primary species, it should also increase relative to [23].

The difference between the two $G_t(D)$ values indicates that with benzene there is more interaction between the primary species and the substrate. That C_6D_{12}–C_6H_{12} mixtures behave "ideally" with fission fragments and C_6D_6–C_6H_6 mixtures do not is probably due to the greater reactivity of benzene in reactions such as [25].

Can. J. Chem. Downloaded from www.nrcresearchpress.com by 210.87.254.6 on 09/05/12
For personal use only.

Benzene-d_6/Cyclohexane Mixtures

The fission fragment value of g(HD) for these mixtures is twice the value of G_t(D) derived from the D_2 yield in pure C_6D_6. This can be explained by assuming as above that, even with fission fragments, benzene deactivates the primary products. Thus the hydrogen yield from benzene-d_6 is lower in 95% C_6H_6 than it is in 95% C_6H_{12}. The "true" yield of primary products from benzene, i.e. the yield before any deactivation of these products occurs, is, therefore, perhaps around 6 rather than 3.

The results from the gamma radiolysis of C_6D_6–C_6H_{12} mixtures are not consistent with hydrogen formation from the interaction of two primary species. The high value of g(HD) and the low values of G_1(D) in these mixtures and $G(D_2)$ in pure C_6D_6 are most easily explained by abstraction reactions such as [26]

$$X_H + C_6D_6 \rightarrow HD + P \qquad [26]$$

where X_H is an intermediate in the radiolysis of cyclohexane.

Further Comments

The mechanism we have discussed can be extended to explain the effect of HCl on the hydrogen yield in gamma ray irradiations of cyclohexane. If reaction [27] occurs and competes with reaction [8], then as has been found (15) the addition of HCl should increase the hydrogen yield.

$$HCl + C_6H_{12}' \rightarrow H_2 + P \qquad [27]$$

We have obtained a preliminary yield of G(cyclohexene) <1.5 and G(bicyclohexyl) <0.4, but have not identified the other hydrogen-deficient products. These values are supported by Burns and Parry (16) who obtained $G(C_6H_{10}) = 1.9$ and $G(C_6H_{11})_2 = 0.9$ using 1.5 MeV alpha particles. Falconer and Burton (17) found that the ratio of the yields of bicyclohexyl to cyclohexene decreased with increasing LET.

These results show that the reactions leading to the formation of liquid products in cyclohexane are different at high LET, but further speculation as to the mechanism of hydrogen formation should await identification of the other products.

The high C_2D_2 content of the acetylene from fission fragment irradiations of C_6D_6–C_6H_6 mixtures implies that the majority is formed by unimolecular decomposition. The increase in the total acetylene yield with LET is comparable to the increase in the hydrogen yield so that there is an apparent increase in unimolecular or first-order decomposition of 50- to 100-fold. This is much higher than the increase in the unimolecular yield of hydrogen with LET.

Again it is desirable to have the yields of the other products in the fission fragment radiolysis for the interpretation of these results.

ACKNOWLEDGMENTS

The mass analyses of the uranium were done by Dr. M. Lounsbury and Mr. R. W. Jones. It is a pleasure to acknowledge many helpful discussions with Dr. P. J. Dyne, Dr. R. H. Betts, and Dr. J. A. Stone.

REFERENCES

1. R. H. SCHULER and A. O. ALLEN. J. Am. Chem. Soc. **77**, 507 (1955).
2. H. A. DEWHURST and R. H. SCHULER. J. Am. Chem. Soc. **81**, 3210 (1959).
3. R. H. SCHULER. J. Phys. Chem. **63**, 925 (1959).
4. W. G. BURNS. J. Phys. Chem. **65**, 2261 (1961).
5. T. GAUMANN and R. H. SCHULER. J. Phys. Chem. **65**, 703 (1961).
6. W. G. BURNS. Trans. Faraday Soc. **58**, 961 (1962).
7. W. G. BURNS and C. R. V. REED. Trans. Faraday Soc. **59**, 101 (1963).

Can. J. Chem. Downloaded from www.nrcresearchpress.com by 210.87.254.6 on 09/05/12
For personal use only.

8. P. J. DYNE and W. M. JENKINSON. Can. J. Chem. **38**, 539 (1960).
9. P. J. DYNE and W. M. JENKINSON. Can. J. Chem. **40**, 1746 (1962).
10. K. M. GLOVER and P. BURRELL. J. Nucl. Energy, **1**, 214 (1955).
11. C. H. WESTCOTT. AECL Report CRRP-960, Jan. 1962.
12. M. STEINBERG. Nucleonics, **21**, 8, 151 (1963).
13. P. J. DYNE and J. A. STONE. Can. J. Chem. **39**, 2381 (1961).
14. P. J. DYNE and W. M. JENKINSON. Can. J. Chem. **39**, 2163 (1961).
15. P. J. HORNER and A. J. SWALLOW. J. Phys. Chem. **65**, 953 (1961).
16. W. G. BURNS and J. R. PARRY. Nature. In press. 1964.
17. J. W. FALCONER and M. BURTON. J. Phys. Chem. **67**, 1743 (1963).

Can. J. Chem. Downloaded from www.nrcresearchpress.com by 210.87.254.6 on 09/05/12
For personal use only.

Can. J. Chem. Downloaded from www.nrcresearchpress.com by 210.87.254.5 on 09/05/12
For personal use only.

THE MERCURY-PHOTOSENSITIZED DECOMPOSITION OF AMMONIA AND AMMONIA–PROPANE MIXTURES*

S. TAKAMUKU† AND R. A. BACK
Division of Pure Chemistry, National Research Council, Ottawa, Canada
Received January 30, 1964

ABSTRACT

A study of the mercury-photosensitized decomposition of ammonia, both with pure ammonia and with propane added as a scavenger for hydrogen atoms, suggests that the quantum yield of the primary decomposition into H and NH_2 is much less than unity at 33° C and rises with increasing temperature. The interaction of ammonia–propane mixtures with Hg $6(^3P_1)$ atoms cannot be explained in terms of simple competitive quenching; a tentative mechanism involving a long-lived Hg $6(^3P_1)$ – propane complex and Hg $6(^3P_0)$ atoms has been suggested. A temperature dependence in the relative quenching rates of C_3H_8 and C_3D_8 has also been observed.

INTRODUCTION

It was recently observed that the primary quantum yield in the mercury-photosensitized decomposition of methane was much less than unity at 33° C and was temperature dependent, rising with increasing temperature (1). The mercury-photosensitized decomposition of ammonia at room temperature also shows a quantum yield considerably less than unity which in the past has been attributed to efficient back reactions (2). The present experiments were undertaken to determine whether ammonia, like methane, might also show an inefficiency and a temperature dependence in its primary reaction with Hg $6(^3P_1)$ atoms.

EXPERIMENTAL

Apparatus and techniques have been described previously (1). The 200-cc cylindrical reaction vessel was part of a circulation system of about 4 liters volume. The intensity of light absorbed was about 2×10^{-9} einsteins/liter/second. Mercury was at its equilibrium vapor pressure at 0° C, which gave between 40 and 90% absorption of the 2537 resonance line in the reaction vessel. After irradiation, gases non-condensable at −196° C were removed and measured in a gas burette and analyzed for hydrogen content by diffusion through hot palladium. These analyses were confirmed by mass spectrometer and showed that H_2 and N_2 were the only non-condensable products from pure ammonia, while H_2 and CH_4 were the only ones from ammonia–propane mixtures.

Anhydrous ammonia was obtained from Matheson, while propane was Phillips' Research-grade, known to be free of olefins. Both gases were subjected to several bulb-to-bulb distillations. Deuterated ammonia and propane of high purity were obtained from Merck and Co. of Canada.

RESULTS AND DISCUSSION

Experiments with Pure Ammonia

The most thorough study of the mercury-photosensitized decomposition of ammonia was that of McDonald and Gunning (2) in which, with rather high light intensities, the following mechanism was shown to prevail in the initial stages:

$$Hg^* + NH_3 \rightarrow Hg + NH_2 + H \quad [1]$$

$$H + NH_2 \rightleftharpoons NH_3^* \quad [2]$$

$$NH_3^* + M \rightarrow NH_3 + M \quad [3]$$

$$H + H + M \rightarrow H_2 + M \quad [4]$$

$$NH_2 + NH_2 \rightarrow N_2H_4 \quad [5]$$

*Issued as N.R.C. No. 7879.

†*National Research Council of Canada Postdoctoral Fellow, 1961–62. Present address: Osaka University, The Institute of Scientific and Industrial Research, Osaka, Japan.*

As the reaction progressed further, very efficient secondary reactions (of H and NH_2) destroyed hydrazine, producing nitrogen, so that at conversions of about 0.1% and greater, the ratio N_2/H_2 equalled the stoichiometric value of 1/3. As conversion was reduced, this ratio fell towards zero; the lowest value actually attained was 0.017 at 0.005% conversion.

It was hoped in the present experiments, by reducing the light intensity and by maintaining very low conversions, that, first, reactions 2, 3, and 4 could be suppressed, and replaced by the reaction,

$$H + NH_3 \rightarrow H_2 + NH_2, \qquad [6]$$

and, second, that the yield of nitrogen could be reduced effectively to zero. Under these conditions the hydrogen produced would become a direct measure of the extent of the primary process.

These simplifying conditions were not in fact achieved. Table I shows quantum yields of

TABLE I

Quantum yields in the mercury-photosensitized decomposition of ammonia

Temp. (°C)	Ammonia pressure (mm)	H_2	N_2	N_2/H_2
32	303	0.059	0.034	0.58
38	570	0.057*	0.046*	0.81*
38	22	0.059	0.050	0.85
90	320	0.119	0.089	0.75
100	320	0.146	0.102	0.70
108	303	0.167	0.090	0.54
116	303	0.185	0.106	0.57
172	303	0.358	0.178	0.50
198	300	0.518	0.211	0.41
198	293	0.529	0.208	0.39
200	302	0.562	0.242	0.43
205	302	0.527	0.232	0.44
246	302	0.860	0.320	0.37

*Average of seven experiments.

nitrogen and hydrogen (based on comparison with the propane decomposition) and it is seen that there is a marked increase with rising temperature. It is further seen that the yield of nitrogen, far from being zero, was never less than one-third of the hydrogen. Thus although the fraction of ammonia decomposed was about 10 times smaller than in the shortest experiments of McDonald and Gunning, in which nitrogen formation was largely suppressed, secondary reactions with hydrazine had in the present system apparently already led to a steady state in which nitrogen and hydrogen were effectively the only products. This seemingly contradictory behavior is, on closer examination, simply explained. In the earlier experiments, light intensities were about 5000 times higher than in the present ones, and reactions 2, 3, and 4, all second-order in radicals, predominated at low conversions over reactions of H or NH_2 with hydrazine. The much lower intensities used in the present experiments would favor the latter reactions. Reaction 6, if it were fast enough to scavenge all the hydrogen atoms, would suppress their reaction with hydrazine, but reaction of NH_2 with hydrazine would not be prevented, so that efficient destruction of hydrazine occurs in the present system despite the lower conversions.

Yields of nitrogen not only failed to fall below the value of $N_2/H_2 = 1/3$, but were

Can. J. Chem. Downloaded from www.nrcresearchpress.com by 210.87.254.5 on 09/05/12
For personal use only.

actually considerably higher than this maximum stoichiometric limit. There was apparently a loss of hydrogen from the system; this was further investigated by experiments in which a few micromoles of pure hydrogen were irradiated in the reaction vessel. There was a steady loss of hydrogen observed comparable in magnitude to the missing hydrogen in the ammonia decomposition (about 1 micromole/day). Prolonged irradiation of hydrogen progressively reduced this loss to negligible proportions, but when ammonia was again irradiated in the hydrogen-conditioned vessel, loss of hydrogen was almost the same as before. This suggests a surface reaction of hydrogen atoms, perhaps catalyzed by adsorbed ammonia, resulting in permanent loss of hydrogen. The low light intensities used favor such a process.

The rise in quantum yield with rising temperature evident in Table I may arise in part from a temperature-dependent primary process, although it is impossible to separate this effect unequivocally from temperature dependence in the secondary reactions. The product yields in Table I were approximately independent of ammonia pressure, which suggests that most of the hydrogen atoms were disappearing by reaction 6, although the hydrogen deficit indicates that this process was not quantitative. Uncertainties in the mechanisms of the secondary reactions consuming hydrazine also complicate the interpretation of the data.

Experiments with Ammonia–Propane Mixtures

Failure to achieve the simple conditions in which hydrogen was a direct measure of the primary process in the decomposition of pure ammonia suggested the use of propane as an efficient scavenger for hydrogen atoms. In pure propane, under the prevailing conditions of low light intensity and low conversion, the decomposition followed the following simple mechanism (3).

$$RH + Hg^* \rightarrow R + H + Hg \quad [7]$$

$$H + RH \rightarrow R + H_2 \quad [8]$$

$$2R \rightarrow R_2 \text{ or } RH + \text{propylene} \quad [9]$$

Loss of hydrogen atoms by reaction with propylene product was negligible, so that the yield of hydrogen was a measure of reaction 7, which is known to have an efficiency close to unity. If then reaction 1 also has a quantum yield of unity, the addition of ammonia should simply replace reaction 7 by reaction 1, and the hydrogen yield should be unaffected. Any inefficiency in reaction 1, on the other hand, should be reflected in a decrease in the hydrogen production.

In Fig. 1 the hydrogen yields from ammonia–propane mixtures at three different temperatures are plotted against the calculated percentage quenching of Hg $6(^3P_1)$ by ammonia, based on cross sections of 2.94 and 1.30 Å^2 for ammonia and propane respectively (4, 5). Results are also shown for mixtures of ND_3 with C_3H_8 and of NH_3 with C_3D_8, assuming cross sections of 1.09 and 0.09 Å^2 for ND_3 and C_3D_8 respectively (4, 6). The latter mixture takes advantage of the very low quenching cross section of C_3D_8 to attain almost complete (93%) quenching by ammonia. In all these experiments, propane pressure was 150 mm, which should have been enough to scavenge all hydrogen atoms by reaction 8. Corrections were made to allow for measured variations in the absorption of the mercury resonance radiation in the reaction vessel with varying temperature and pressure, which were quite appreciable.

It appears superficially from Fig. 1 that reaction 1 has an efficiency which is much less than unity at 33° C, and which increases with increasing temperature until at 300° C it is about as efficient as reaction 7. It is evident, however, that the interaction between

Can. J. Chem. Downloaded from www.nrcresearchpress.com by 210.87.254.5 on 09/05/12
For personal use only.

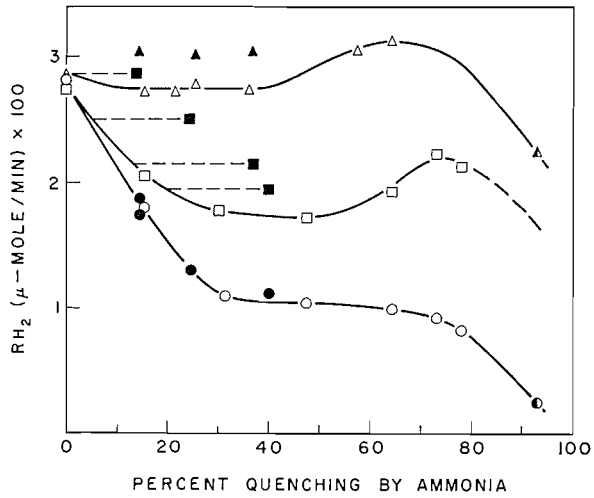

FIG. 1. Hydrogen yield from the mercury-photosensitized decomposition of ammonia–propane mixtures. The abscissae were calculated on the basis of simple competitive quenching. ○, □, △ = NH_3–C_3H_8; ●, ■, ▲ = ND_3–C_3H_8; ◐, ◭ = NH_3–C_3D_8. Circles = 33° C; squares = 200° C; triangles = 300° C.

ammonia and propane is much more complex than a simple competition between reactions 1 and 7. There is a common pattern of behavior at all three temperatures which may be separated into three parts.

(1) The initial effect of added ammonia is much greater than predicted from the quenching cross sections of ammonia and propane. Thus at 33° C the hydrogen yield had fallen by about 50% at a point where quenching by ammonia should have been only 20%. This deviation seems to be far beyond any possible errors in the values of the cross sections. The effect is less pronounced at 200° C and not evident at all at 300° C.

(2) There is an interaction in the region between 40 and 80% quenching by ammonia which leads to an enhancement of the hydrogen yield.

(3) There is a final decrease in hydrogen yield as complete quenching by ammonia was approached.

A simple competition between reactions 1 and 7, it might be noted, would have led to hydrogen yields linearly dependent upon the percentage quenching by ammonia.

The following mechanism can account for the general features of the ammonia–propane system:

$$Hg^* + RH \rightarrow (RH.Hg^*) \quad [10]$$

$$(RH.Hg^*) \rightarrow R + H + Hg \quad [11]$$

$$NH_3 + (RH.Hg^*) \rightarrow RH + NH_3 + Hg \quad [12]$$

$$Hg^* + NH_3 \rightarrow Hg^\circ + NH_3 \quad [13]$$

$$Hg^\circ + RH \rightarrow Hg + R + H \quad [14]$$

$$Hg^\circ + NH_3 \rightarrow Hg + NH_3 \quad [15]$$

$$NH_3 + (Hg^* \text{ or } Hg^\circ) \rightarrow Hg + NH_2 + H \quad [16]$$

where Hg, Hg*, and Hg° represent the ground state, the 6^3P_1 state, and the 6^3P_0 state, respectively. There are several pairs of concurrently competitive reactions in this sequence. At low pressures of ammonia, reaction 12 begins to compete efficiently with reaction 11, reducing the hydrogen yield. As ammonia pressure is further increased, reaction 13 begins to compete with 10, and reaction 14 causes a rise in the hydrogen production. Finally,

Can. J. Chem. Downloaded from www.nrcresearchpress.com by 210.87.254.5 on 09/05/12
For personal use only.

reaction 15 competes more and more efficiently with 14, and the hydrogen yield falls again. Reaction 16 is required to account for the decomposition observed in pure ammonia. The temperature dependence in both ammonia and ammonia–propane mixtures can be explained if reaction 16 and perhaps reactions 11 and 14 increase in rate with rising temperature.

The isotopic composition of the hydrogen produced from the ND_3–C_3H_8 and NH_3–C_3D_8 mixtures (Tables II and III) lends some support to this mechanism. From ND_3–C_3H_8

TABLE II

Isotopic composition of hydrogen produced from ND_3–C_3H_8 mixtures

Temp. (°C)	ND_3 (mm)	C_3H_8 (mm)	Quenching by ND_3 (%)	H_2 (%)	HD (%)	D_2 (%)
33	30	150	14.4	98.8	1.2	0.0
33	30	150	14.4	98.5	1.4	0.1
33	59	150	24.6	98.8	1.2	0.0
33	120	150	40.1	98.4	1.6	0.0
200	120	150	40.1	92.3	7.7	0.0
200	29	150	13.7	98.6	1.4	0.0
200	57	150	24.2	95.5	4.5	0.0
200	105	150	37.0	96.8	3.2	0.0
300	30	150	14.4	96.5	3.5	0.0
300	62	150	25.6	95.9	4.1	0.0
300	105	150	37.0	93.1	6.9	0.0

TABLE III

Isotopic composition of hydrogen produced from NH_3–C_3D_8 mixtures

Temp. (°C)	NH_3 (mm)	C_3D_8 (mm)	Quenching by NH_3 (%)	H_2 (%)	HD (%)	D_2 (%)
33	0	150	0	7.0	42.7	50.2
33	60	150	92.9	11.0	56.2	32.8
300	0	150	0	1.5	9.7	88.8
300	60	150	92.9	3.8	52.2	44.0

mixtures, with calculated percentage quenching by ammonia ranging up to 40%, the decomposition of ND_3 as indicated by production of HD was never more than a few per cent of the total hydrogen, even at 300° C where there was no reduction in the hydrogen yield. This suggests that it was reactions 11 and 14, rather than 16, that were responsible for the increase in hydrogen yield with rising temperature on the left-hand side of Fig. 1. The experiments with NH_3–C_3D_8 mixtures, on the other hand, while complicated by a large yield of HD and H_2 arising from preferential decomposition of hydrogen-containing propane impurity, show that the increased hydrogen yield at 300° C arose largely from enhanced decomposition of NH_3. Thus reaction 16 must finally become important as "complete quenching" by NH_3 is approached. This, combined with the failure of reaction 16 to compete successfully in the ND_3–C_3H_8 experiments implies that Hg^0 rather than Hg^* is the effective reagent in reaction 16.

There are several further conclusions to be drawn from the experiments with ND_3–C_3H_8 and NH_3–C_3D_8 mixtures. One of these is that reactions 12 to 16 have relative rates which approximately parallel the cross sections for quenching of Hg^*. For example, the data

Can. J. Chem. Downloaded from www.nrcresearchpress.com by 210.87.254.5 on 09/05/12
For personal use only.

obtained with ND_3 at 33° C fits perfectly with the NH_3 data when corrected according to their known quenching cross sections. It also appears that C_3D_8 is very ineffective in reaction 14, as it is known to be in quenching Hg*. A further conclusion is that several of the quenching reactions show a marked variation with temperature. At 200° C, ND_3 appears to be much less efficient, relative to NH_3, in reducing the hydrogen yield (Fig. 1), although at 33° their relative efficiencies appeared to follow their quenching cross sections. This seems to imply a temperature dependence in the relative rates of NH_3 and ND_3 in reaction 12. Also notable are the two experiments with C_3D_8 alone (Table III). The yields of H_2 and HD at 33° C are quite compatible with the estimated isotopic purity of the C_3D_8 (> 98%) and the known preferential reaction of protiated propanes both in reaction 7 and to a lesser extent in reaction 8 (6, 7). At 300° C, the percentage yields of H_2 and HD were very much lower, apparently reflecting an increased quenching efficiency of C_3D_8 at the higher temperature. Quenching cross sections for Hg* have usually been measured at a single temperature, and no temperature dependence has been previously reported.

The experiments at 300° C shown in Fig. 1, in which the hydrogen yield in ammonia–propane mixtures apparently rose above that in pure propane, require a brief comment. There is a fairly large correction for incomplete absorption of light made to these data, and while the absorption was measured in each experiment, uncertainties arising in the correction may well account for the discrepancy. However, while the quantum yield of the propane decomposition is usually taken as close to 1.0 actual estimates of the yield (3, 8) lie closer to 0.9, which would make the highest yields in Fig. 1 about unity. A new absolute measurement of the yield of the propane decomposition is obviously desirable.

One final point concerns the fate of the NH_2 radicals in the ammonia–propane system. The complete absence of nitrogen as a product in these experiments suggests either that NH_2 radicals were efficiently removed by reaction with propane,

$$NH_2 + RH \rightarrow NH_3 + R \qquad [17]$$

or that hydrazine, if formed, was not converted to nitrogen by secondary reactions as it was in pure ammonia. There is further evidence that, at least at 300° C, NH_2 radicals reacted quantitatively by reaction 17; the yield of methane, which arose from decomposition of propyl radicals and hence reflects their concentration, was unaffected by the addition of ammonia (9).

The mechanism suggested for the ammonia–propane system is necessarily tentative. Its chief innovation is perhaps reaction 12; some reaction of this sort seems to be required to explain the abnormally high efficiency of ammonia in reducing the hydrogen yield at low temperatures. The existence of a propane–Hg* complex with sufficient lifetime to react with ammonia gains some support from recent evidence that with several alkanes, the initial rate-controlling quenching process, which involves a single C—H bond, is followed by formation of a reaction complex (perhaps cyclic) in which one of several C—H bonds may finally be broken (7, 10). A similar complex capable of deactivation by collision, might be invoked in the mercury-photosensitized decomposition of methane to explain the observed dependence on pressure and temperature (1). It is becoming increasingly evident that quenching of Hg $6(^3P_1)$ atoms by alkanes and probably by other hydrides such as ammonia and water is a fairly complex chemical reaction rather than a simple physical transfer of energy.

REFERENCES

1. R. A. BACK and D. VAN DER AUWERA. Can. J. Chem. **40**, 2339 (1962).
2. C. C. MCDONALD and H. E. GUNNING. J. Chem. Phys. **23**, 532 (1955).

Can. J. Chem. Downloaded from www.nrcresearchpress.com by 210.87.254.5 on 09/05/12
For personal use only.

3. R. A. BACK. Can. J. Chem. **37**, 1834 (1959).
4. M. G. EVANS. J. Chem. Phys. **2**, 445 (1934).
5. B. DE B. DARWENT. J. Chem. Phys. **18**, 1532 (1950).
6. Y. ROUSSEAU and H. E. GUNNING. Can. J. Chem. **41**, 465 (1963).
7. G. N. C. WOODALL and H. E. GUNNING. Bull. Soc. Chim. Belges, **71**, 725 (1962).
8. R. J. CVETANOVIĆ. Progress in reaction kinetics. Vol. II. *Edited by* G. Porter. Pergamon Press. 1963.
9. R. A. BACK and S. TAKAMUKU. J. Am. Chem. Soc. In press. 1964.
10. Y. ROUSSEAU, O. P. STRAUSZ, and H. E. GUNNING, J. Chem. Phys. **39**, 962 (1963).

Can. J. Chem. Downloaded from www.nrcresearchpress.com by 210.87.254.5 on 09/05/12
For personal use only.

Can. J. Chem. Downloaded from www.nrcresearchpress.com by 210.87.254.42 on 09/05/12
For personal use only.

NUCLEAR MAGNETIC RESONANCE STUDIES OF THE PROTONATION OF WEAK BASES IN FLUOROSULPHURIC ACID

IV. PHENOLS AND AROMATIC ETHERS

T. Birchall, A. N. Bourns, R. J. Gillespie, and P. J. Smith
Department of Chemistry, McMaster University, Hamilton, Ontario

Received January 21, 1964

ABSTRACT

The n.m.r. spectra of phenol, anisole, and other phenols and aromatic ethers in solution in fluorosulphuric acid and in 70% perchloric acid show that in every case they protonate on an aromatic carbon. Earlier evidence from ultraviolet spectroscopy that phenol and anisole protonate on oxygen is reinterpreted.

INTRODUCTION

The protonation of methylbenzenes has been studied by a variety of techniques and it has been established that protonation occurs at the most electronegative aromatic carbon atom (1–6). The carbonium ions formed have characteristic absorptions at approximately 350 mμ and 250 mμ. The n.m.r. spectra of these compounds in solution in HF/BF_3 (7) and HSO_3F (8) confirm the spectrophotometric results.

Phloroglucinol and its methyl ethers in solution in concentrated acid have absorption bands at 365 mμ and 250 mμ suggesting that protonation occurs on the ring; this has been confirmed by n.m.r. evidence (9). In the case of anisole in strong acid solution Arnett and Wu (10) concluded that protonation occurs on the oxygen atom because they did not observe any new bands in the absorption spectrum down to 250 mμ. However the n.m.r. spectrum of anisole in HF/BF_3 (7) and HSO_3F (8) solutions at low temperature has been explained on the basis of protonation at the ring position *para* to the methoxy group, in complete contrast to the evidence from the ultraviolet spectra.

This discrepancy is discussed below and further evidence is presented which indicates that in aromatic bases where the ring is activated by an OR group protonation occurs on the most activated ring carbon atom and not on the oxygen atom.

N.M.R. SPECTRA

The chemical shifts of the compounds studied are given in Table I.

TABLE I

Chemical shifts of ethers and phenols in fluorosulphuric acid

Base	Temp., °C	$-\delta$ p.p.m. from ext. T.M.S.						
		CH				OCH_3	CH_2	CH_3
Anisole	25	8.87	8.71	7.74	7.58	4.79	4.46	
Diphenyl ether	−56.5	8.95	8.79	7.77	7.53		4.53	
Phenol	−64	8.82	8.66	7.57	7.42		4.34	
m-Cresol	−67	8.58	8.43	7.41	7.28		4.29	2.76
Phloroglucinol	25*				6.57		4.40	
	−80				6.26		4.07	
2,4,6-Trihydroxybenzoic acid	−55*				6.67		4.71	
	−63				6.70		4.72	

*Solutions in 70% $HClO_4$.

Can. J. Chem. Downloaded from www.nrcresearchpress.com by 210.87.254.42 on 09/05/12
For personal use only.

Anisole

Because of the large difference between the temperatures at which the original ultraviolet and n.m.r. measurements were made we attempted to observe the n.m.r. spectrum of the conjugate acid of anisole at room temperature. This can be done by increasing the acidity of the fluorosulphuric acid solvent by the addition of SbF_5. The n.m.r. spectrum of a solution of anisole in fluorosulphuric acid containing 7.55 mole % SbF_5 was recorded at 25° (Fig. 1); no new peaks appear on cooling the solution to −90°. If protonation occurred at the oxygen atom peaks of relative area 5:3:1 would result with the peak due to the methoxy protons being split into a doublet by the captured proton. However, the relative areas of the peaks A, B, and C were found to be 3.89:3.00:1.90 in good agreement with the relative areas of 4:3:2 expected for ring protonation; these peaks are therefore assigned to the ring protons and the OCH_3 and CH_2 groups respectively. No splitting of the methoxy peak was observed. The simple AB pattern of the signal given by the ring protons indicates that protonation occurs at the position *para* to the OCH_3 group; each component of the lower doublet has a triplet structure ($J \approx 2$ c.p.s.) indicating that it is spin–spin coupled to two protons, i.e. to the CH_2 group. No structure was observed in the CH_2 peak, possibly due to these protons having a shorter relaxation time and as a result broader lines.

Diphenyl Ether

The solution in fluorosulphuric acid when prepared at low temperatures (−85°) is yellow and gives an n.m.r. spectrum which has a peak B at −4.5 p.p.m. from an external tetramethylsilane reference which is characteristic of a CH_2 group (Fig. 2). That protonation occurs on the ring is confirmed by the relative areas of the absorptions A and B which are 9.0:1.93 and not 10:1 as would be the case for protonation on oxygen.

Phenol

A solution of phenol in fluorosulphuric acid at low temperatures gives an n.m.r. spectrum which can only be explained on the basis of protonation at the *para* position. This spectrum is shown in Fig. 3; the relative areas of A:B are 4.0:1.8. If protonation occurred at the oxygen atom the relative areas of the peaks would be 5:2 and the OH_2^+ signal would occur at lower field than the OH resonance of phenol itself. Moreover, the complicated A_2B_2C pattern of the ring protons of phenol is changed on protonation to give a relatively simple quartet pattern which is very similar to that given by the conjugate acid of anisole. The lower doublet is attributed to the ring protons adjacent to the protonated site. Each component of this lower doublet appears to have a triplet structure, as in the case of anisole. This is consistent with spin–spin coupling to the CH_2 protons: again no structure is observed in the CH_2 peak which has a width of approximately 7 c.p.s. No resonance for the OH proton is observed presumably because of rapid exchange with the solvent; this has been found to be the case for acid solutions of other phenols (9).

m-Cresol

The n.m.r. spectrum of *m*-cresol in fluorosulphuric acid is shown in Fig. 4. This spectrum can be accounted for only if protonation occurs at an aromatic carbon atom; the relative areas of the peaks A:B:C are 3.13:1.97:3.0. If protonation had occurred on the oxygen atom the relative areas would be 4:2:3. The spectrum of the ring protons which is an AB pattern overlapping a single peak is very similar to that obtained for the conjugate acid of *m*-xylene (7, 8). For *m*-cresol there are two possible sites for protonation, i.e. *ortho* or *para* to the OH group (I and II).

Can. J. Chem. Downloaded from www.nrcresearchpress.com by 210.87.254.42 on 09/05/12
For personal use only.

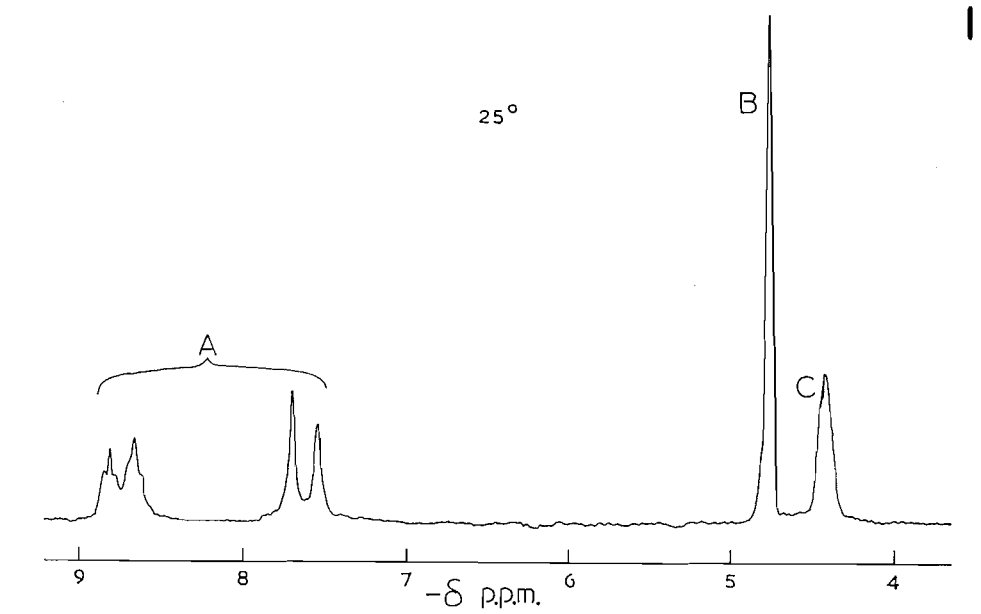

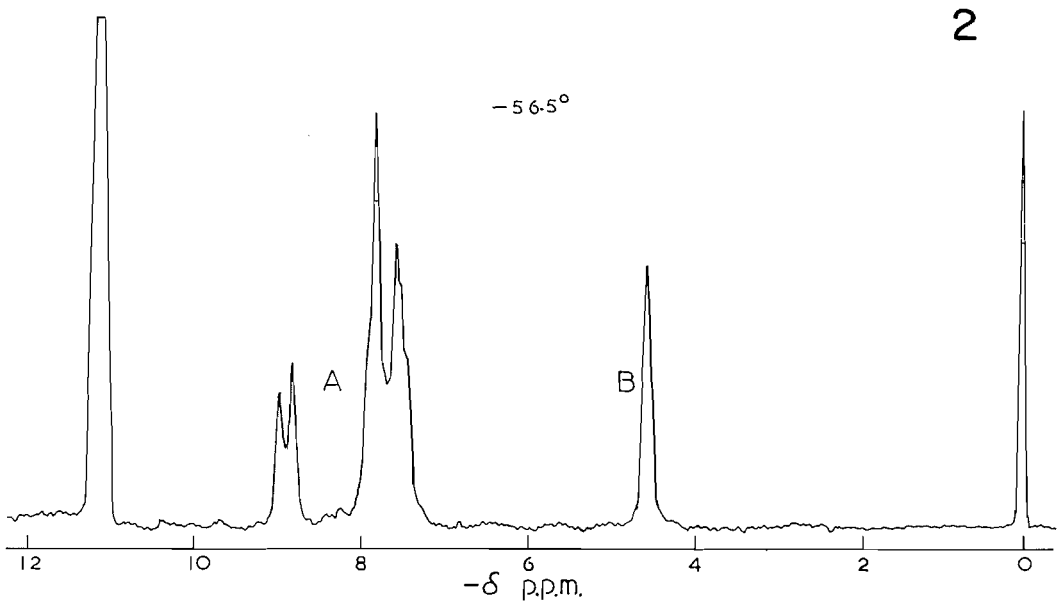

FIG. 1. The n.m.r. spectrum of a solution of anisole in fluorosulphuric acid – antimony pentafluoride.
FIG. 2. The n.m.r. spectrum of a solution of diphenyl ether in fluorosulphuric acid.

Can. J. Chem. Downloaded from www.nrcresearchpress.com by 210.87.254.42 on 09/05/12
For personal use only.

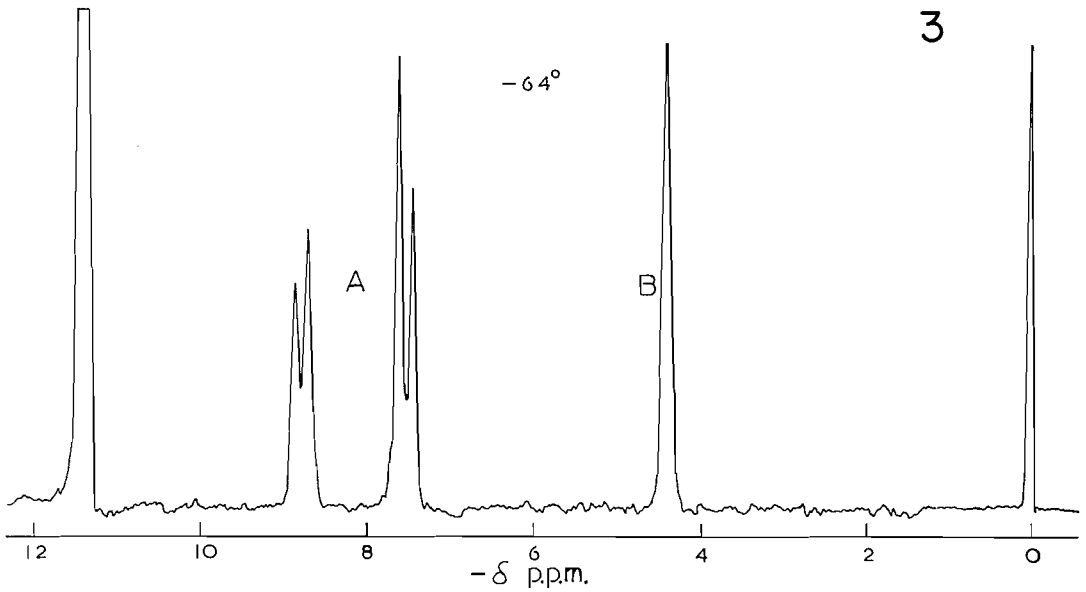

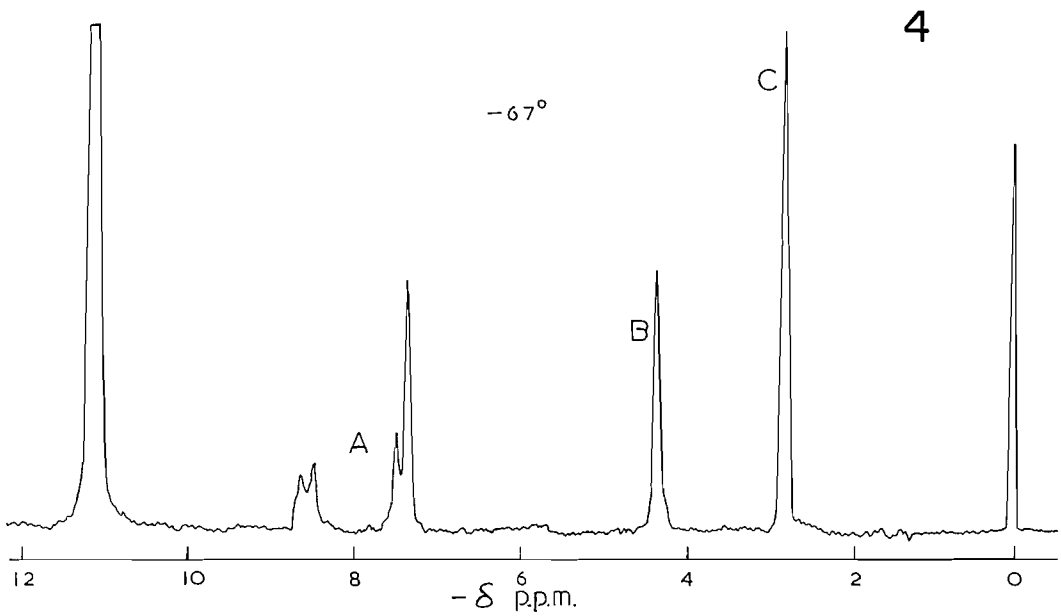

FIG. 3. The n.m.r. spectrum of a solution of phenol in fluorosulphuric acid.
FIG. 4. The n.m.r. spectrum of a solution of *m*-cresol in fluorosulphuric acid.

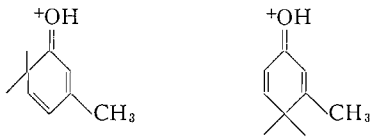

I II

It seems likely that II is the predominant form for reasons discussed below.

Polyhydroxy Compounds

In aqueous 70% perchloric acid phloroglucinol has only two peaks of equal area in its n.m.r. spectrum which have been attributed to the "aromatic" protons and the CH_2 group of the ring protonated base (9). We have obtained essentially the same n.m.r. spectrum in fluorosulphuric acid solution (Table I), although the peaks are much sharper because exchange is slower in the more acidic solvent. No resonance due to the OH proton was observed even on cooling the solution to $-100°$.

We have also examined solutions of 2,4,6-trihydroxybenzoic acid in 70% $HClO_4$ and in HSO_3F. No peaks, other than the solvent, are visible in the n.m.r. spectrum at room temperature but on cooling the 70% $HClO_4$ solution to $-55°$ two broad peaks appear. In the much stronger acid HSO_3F it is possible to slow down the exchange process so that these two peaks become much narrower. At $-63°$ the relative areas of these two peaks are found to be 1.0:1.77. From these relative areas and the chemical shifts of the two peaks they can be attributed to the single ring proton and the CH_2 group respectively showing that the conjugate acid has the structure III.

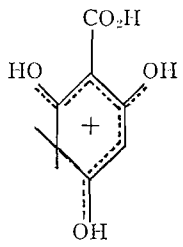

III

Under conditions of very slow exchange the areas should be 1:2. It was not possible to observe peaks due to OH or COOH protons presumably due to rapid exchange of these protons with the solvent.

ULTRAVIOLET SPECTRA

The ultraviolet spectra of these bases were recorded in neutral and strongly acid solution and the positions of the bands are given in Table II. Solutions of diphenylether in HSO_3F at low temperature were found to have a yellow color but we did not have suitable equipment for recording the spectrum at low temperatures; at higher temperatures ($> -10°$) a reaction, probably sulphonation, occurs between the solvent and the ether. Peaks in the 350 mμ region of the spectrum in acid solution were observed only in the cases of phloroglucinol and 2,4,6-trihydroxybenzoic acid. In 70% $HClO_4$ 2,4,6-trihydroxybenzoic acid is incompletely protonated and peaks due to both the free base and the conjugate acid are visible.

Can. J. Chem. Downloaded from www.nrcresearchpress.com by 210.87.254.42 on 09/05/12
For personal use only.

TABLE II

Base	Solvent	λ mμ			
Anisole	H_2SO_4*		240	284	
	Diethylether	220		270	
Phenol	H_2SO_4*		230	270	
	Diethylether	210		273	
m-Cresol	H_2SO_4*		240	270	
	Cyclohexane	220		273	
Phloroglucinol	$HClO_4$†		243		343
	Methanol	230		268	
2,4,6-Trihydroxybenzoic acid	$HClO_4$†	220	260	283	330
	Diethylether		266	305	

*100% H_2SO_4.
†70% $HClO_4$.

DISCUSSION

The conjugate acids of the methylbenzenes are found to give bands at 350 mμ and 250 mμ and protonation is known to occur at the most electronegative carbon atom (1–6), hence the appearance of these bands in the ultraviolet spectrum upon protonation has been taken to indicate ring protonation and the absence of these bands has been assumed to indicate protonation at a site other than the ring carbon atom. In the case of anisole it was assumed, on this basis, that protonation occurs on the ether oxygen (10).

In the cases of phloroglucinol, dimethoxybenzene, and trimethoxybenzene in 70% perchloric acid solution bands at 240 mμ and 350 mμ are present in the ultraviolet spectra. This has been assumed to indicate that protonation occurs on a ring carbon atom and this is confirmed by the n.m.r. evidence (9). We have obtained similar results for phloroglucinol and trihydroxybenzoic acid in both 70% perchloric acid and in fluorosulphuric acid.

However, in the cases where there is only one OR group attached to the aromatic ring the conjugate acid does not have a band in the 350 mμ region of the ultraviolet spectrum but nevertheless the n.m.r. evidence can only be explained on the basis of ring protonation. It is suggested that protonation of ArOR compounds occurs at the position *para* to the OR group, the ion resulting having the quinonoid structure IV; this would result in a localization of the positive charge on the oxygen atom. The ultraviolet spectrum of IV

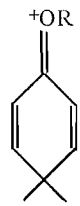

IV

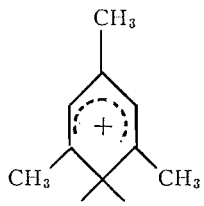

V

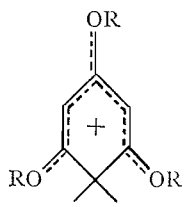

VI

is quite consistent with other quinone systems reported in the literature, e.g., benzoquinone has peaks at 240 mμ, 290 mμ, and a weak band at 480 mμ, but none at 350 mμ (11); 2,4,6-tribromo-4-chloro-2,5-cyclohexadienone has a peak at 275–280 mμ (12); other similar compounds (13, 14) have peaks in the 275–280 mμ region but not in the 350 mμ region. The conjugate acid of *m*-cresol is assumed to have structure II rather than I since its ultraviolet spectrum closely resembles that of phenol and anisole in acid solution.

In contrast, in the case of the conjugate acids of the methylbenzenes, and the polyhydroxybenzenes and their ethers the positive charge is dispersed around the aromatic

Can. J. Chem. Downloaded from www.nrcresearchpress.com by 210.87.254.42 on 09/05/12
For personal use only.

system (V and VI). Thus the bands at 250 mμ and 350 mμ which have been assumed to be characteristic of a protonated aromatic ring may be more satisfactorily regarded as arising from the positively charged conjugated systems present in V and VI. The absence of a band at 350 mμ in the ultraviolet spectrum of the conjugate acid of a base of the ArOR type cannot therefore be taken to indicate protonation on the oxygen atom.

In the case of a solution of diphenylether in fluorosulphuric acid at low temperature, the yellow color suggests the presence of a band at 350 mμ. This presumably arises as a result of some delocalization of the positive charge into the second ring.

EXPERIMENTAL

All of the bases were purified either by recrystallization or distillation and stored under a dry atmosphere. The n.m.r. samples were prepared as previously described (15) and recorded on a Varian H.R. 60 spectrometer equipped with a low temperature probe and integrator. The ultraviolet spectra were recorded on a Bausch and Lomb Spectronic 505 instrument.

ACKNOWLEDGMENT

We thank the Petroleum Research Fund of the American Chemical Society and the Directorate of Chemical Sciences of the United States Air Force Office of Scientific Research for financial support of this work. We also thank the Dow Chemical Company of Canada for the award of a fellowship (to T. B.) and the National Research Council for the award of a studentship (to P. J. S.).

REFERENCES

1. D. A. McCauley and A. P. Lien. J. Am. Chem. Soc. **73**, 2013 (1951).
2. V. Gold and F. L. Tye. J. Chem. Soc. 2172 (1952).
3. C. Reid. J. Am. Chem. Soc. **76**, 3264 (1954).
4. A. A. Verrijn Stuart and E. L. Mackor. J. Chem. Phys. **27**, 826 (1957).
5. G. Dallinga, E. L. Mackor, and A. A. Verrijn Stuart. Mol. Phys. **1**, 123 (1958).
6. M. Kilpatrick and H. H. Hyman. J. Am. Chem. Soc. **80**, 77 (1958).
7. C. MacLean and E. L. Mackor. Discussions Faraday Soc. **34**, 165 (1962).
8. T. Birchall and R. J. Gillespie. Can. J. Chem. **42**, 502 (1964).
9. A. J. Kresge, G. W. Berry, K. R. Charles, and Y. Chiang. J. Am. Chem. Soc. **84**, 4343 (1962).
10. E. M. Arnett and C. Y. Wu. J. Am. Chem. Soc. **82**, 5660 (1960).
11. E. A. Fehnel and M. Cormack. J. Am. Chem. Soc. **70**, 1813 (1948).
12. C. A. R. Elston, A. T. Peters, and F. M. Rowe. J. Chem. Soc. 367 (1948).
13. J. A. Price. J. Am. Chem. Soc. **77**, 5436 (1955).
14. L. G. Cannell. J. Am. Chem. Soc. **79**, 2927 (1957).
15. T. Birchall and R. J. Gillespie. Can. J. Chem. **41**, 148 (1963).

Can. J. Chem. Downloaded from www.nrcresearchpress.com by 210.87.254.42 on 09/05/12
For personal use only.

BASE-CATALYZED DIMERIZATIONS OF ALKYLIDENEMALONONITRILES

MARY R. S. WEIR AND J. B. HYNE
Department of Chemistry, University of Alberta, Calgary, Alberta
Received December 23, 1963

ABSTRACT

The base-catalyzed dimerizations of several alkylidenemalononitriles have been studied, and proton nuclear magnetic resonance (n.m.r.) spectral evidence is presented in support of the suggested cyclic structures of these dimers.

Can. J. Chem. Downloaded from www.nrcresearchpress.com by 210.87.254.42 on 09/05/12
For personal use only.

The preparation of α,β-unsaturated dinitriles of the type $R_2C{=}C(CN)_2$ by base-catalyzed condensation of the corresponding carbonyl compound ($R_2C{=}O$) with malononitrile has been the subject of investigation from the time of Heuck onwards (1–9). In addition to the expected unsaturated dinitrile, however, a second substance, considered to be a dimer of the dinitrile, has been isolated in several instances (5). The formation of this dimeric product has previously led to confusion about the nature of the monomeric product. For example, cyclohexylidenemalononitrile (5) and isopropylidenemalononitrile (4) were originally reported to be crystalline solids and it was later shown (6) that they are, in fact, liquids.

These crystalline products are obtained in varying yields from the base-catalyzed condensations of both aromatic and aliphatic ketones with malononitrile. The structures of some of them have recently been investigated (7, 8, 9). Thus, Anderson, Bell, and Duncan (7) studied the solid products obtained from the base-catalyzed reactions of malononitrile with several carbonyl compounds including acetone, acetophenone, and benzil. They suggested, largely on the basis of infrared spectral analysis, that the structure of the dimer of isopropylidenemalononitrile was linear ($Me_2C{=}C(CN).C(NH_2){=}CH.CMe{=}C(CN)_2$). Williams later investigated some of the reactions of this dimer and concluded that it was cyclic (see Chart A (I*a*)(I*c*)). In a recent communication (9) we have suggested that the dimer of cyclohexylidenemalononitrile is likewise cyclic.

We have now investigated the base-catalyzed dimerizations of other alkylidenemalononitriles in an attempt to determine whether or not the formation of *cyclic* dimers can be considered to be a general reaction of these compounds. The proton n.m.r. spectral evidence which we have obtained leaves little doubt that the dimers are cyclic, but they appear to differ from isopropylidenemalononitrile dimer in the location of the carbon–carbon double bond.

The mechanism for cyclic dimer formation proposed for isopropylidenemalononitrile by Williams (8) can be expanded into the general form shown in Chart A. Compounds I in Chart A represent the reaction sequence for isopropylidenemalononitrile itself. Compounds II, III, and IV represent the three other alkylidenemalononitrile systems studied in this work. Our n.m.r. spectrum of the isopropylidenemalononitrile dimer is included in Fig. 1 for comparison with the spectra of the other dimers.

2-Butylidenemalononitrile Dimer (Chart A, $R = CH_3$; $R' = H$)

The linear form (Chart B, IV (*d*), IV (*e*)) of this dimer analogous to that first suggested for isopropylidenemalononitrile by Anderson, Bell, and Duncan (7) would arise from attack of the primary carbanion on a *nitrile* group of the second molecule rather than on

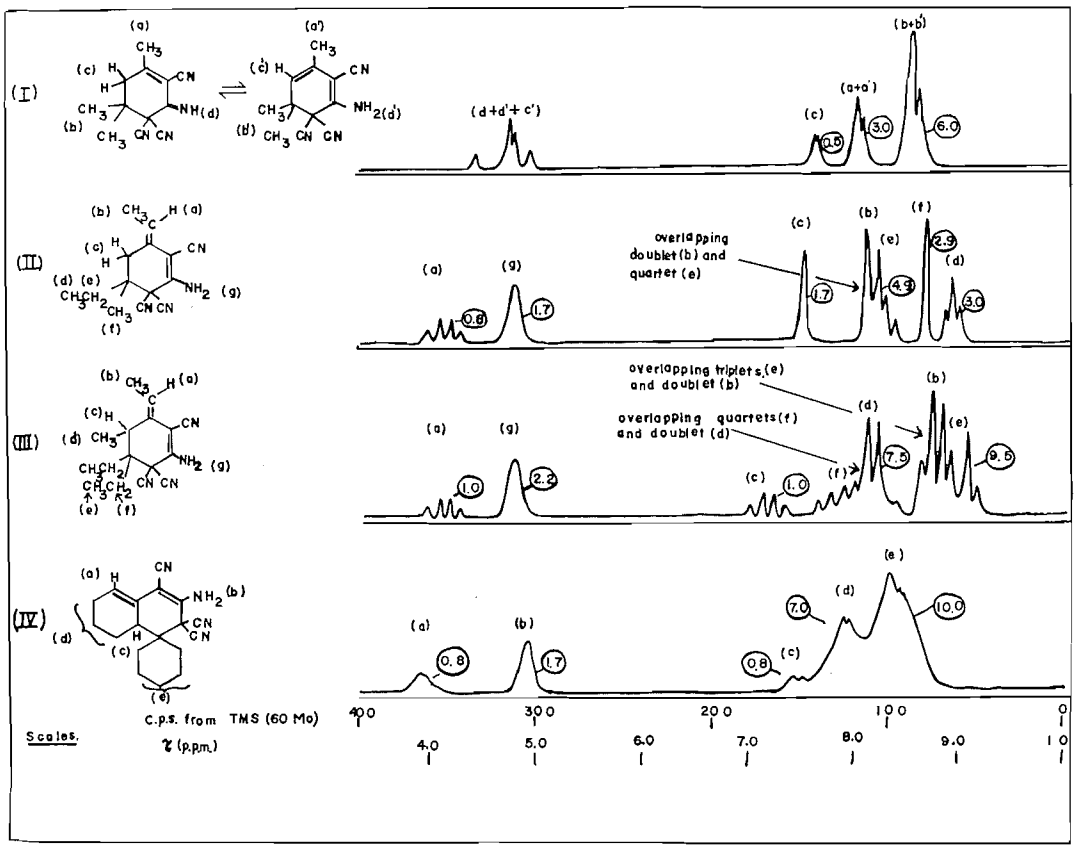

FIG. 1. (i) Assignments as shown by letters, (ii) relative peak areas circled numbers, (iii) spectra all 20% approximately in $CDCl_3$, and (iv) TMS internal standard.

the β-carbon atom. The n.m.r. spectrum (Fig. 1 (II)) of the dimeric product in this case suggests that the material is largely in the amino form II (*b*), the relative areas of the NH_2 absorption at 4.9τ and of the ethylenic hydrogen absorption at 4.1τ being 1.7 and 0.8 respectively. The linear structure can be ruled out since the 8.7τ value for the methyl singlet places it on a saturated carbon. This cannot be accommodated in structures VI (*d*) or VI (*e*). The amino form has been assigned structure II (*b*), with the double bond *exo*cyclic, rather than II (*c*), since the latter would be inconsistent with the 8.1τ doublet and with the 4.2τ quartet, which are due to the splitting in the CH_3—CH= group.

3-Pentylidenemalononitrile Dimer (Chart A, R = R′ = CH_3)

The n.m.r. spectrum (Fig. 1 (III)) of the dimer again suggests that it is largely in the amino form III (*b*) (relative area of NH_2 = 2.2). In the linear form VII (*d*), VII (*e*), only one H_3C—C—H group is present, while the spectrum shows *two* hydrogen quartets, which must arise from this kind of grouping. Hence the linear structure can be ruled out. The presence of these two quartets likewise rules out structure III (*c*).

Cyclohexylidenemalononitrile Dimer (Chart A, R + R′ = —$(CH_2)_5$—)

The proton n.m.r. spectrum has been reported and discussed in a recent communication (9). It is shown for comparison in Fig. 1 (IV).

Can. J. Chem. Downloaded from www.nrcresearchpress.com by 210.87.254.42 on 09/05/12
For personal use only.

CHART A

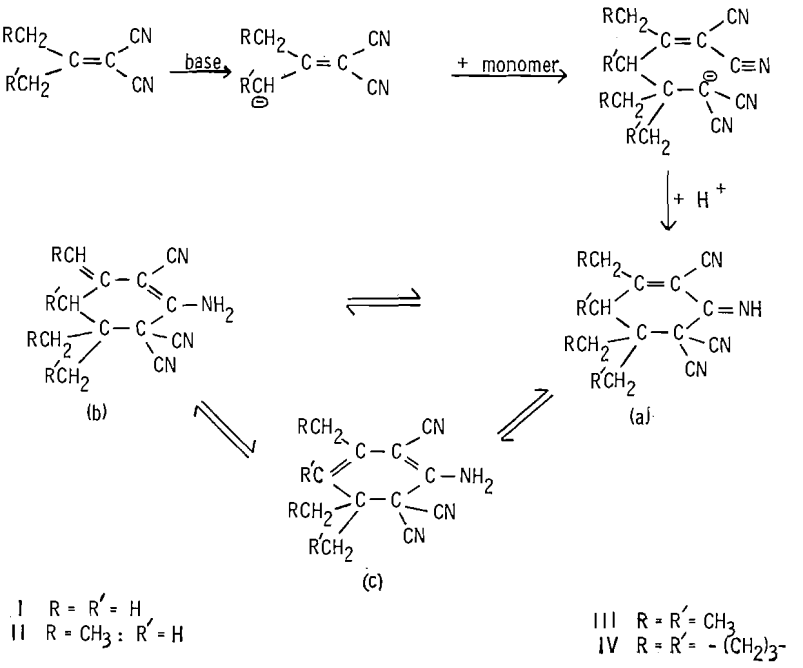

CHART B

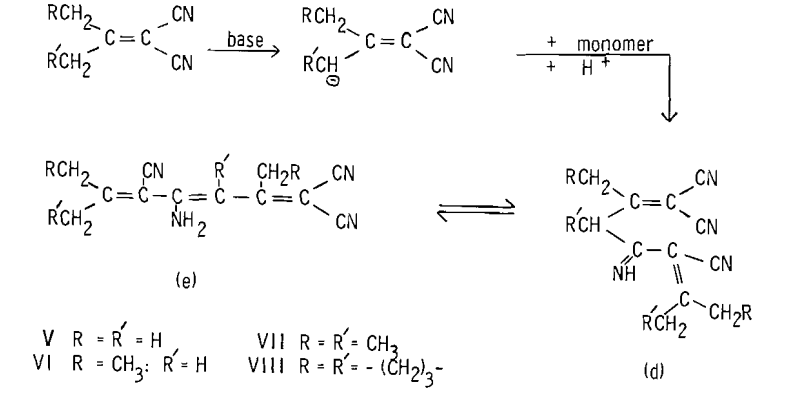

DISCUSSION

The evidence presented in support of the cyclic form of the dimeric products would appear to be conclusive. This implies that attack of the carbanion on the β-carbon of the ene-nitrile is preferred over attack on the cyano group in all the examples considered. The reasons for the observed product distribution among the three tautomeric forms indicated in Chart A remain to be discussed.

This product distribution may be explained in terms of (*a*) the steric repulsion of the

Can. J. Chem. Downloaded from www.nrcresearchpress.com by 210.87.254.42 on 09/05/12
For personal use only.

larger alkyl groups in II and III compared to I, and (*b*) the degree of substitution of the exocyclic double bond in II and III as compared to I.

The *amino* forms of dimers II and III can be written as either II (*b*), III (*b*) with the double bonds exocyclic, or as II (*c*), III (*c*) with the double bonds endocyclic. The n.m.r. evidence suggests that the (*b*) form with exocyclic double bonds is preferred here in contrast to the endocyclic structure I (*c*), favored in the isopropylidene case. It would appear that in II (*b*) and III (*b*) R and R′ have less steric interaction than would be the case in the corresponding (*c*) form. It also suggests that the preferred geometric isomer about the RCH=C(ring) double bond is that with the R group *trans* to the ring segment carrying the R′CH-entity. Steric interaction of this kind would not be important where R = R′ = H, i.e. in isopropylidenemalononitrile dimer.

The second major difference between dimer I and dimers II and III is in the nature of the substituents on the exocyclic double bond. The presence of a methyl substituent here appears to enhance the stability relative to that of an exocyclic methylene group. Thus, as a consequence of both of these factors, the (*b*) forms appear to be favored in the butylidene and pentylidene dimers, in contrast to the endocyclic double bond form (*c*) in isopropylidenemalononitrile dimer.

The apparent absence of *imino* forms II (*a*) and III (*a*) in the dimer products again points to the presence of a driving force favoring relief of steric repulsion between R and R′, possible with an exocyclic double bond as in II (*b*) and III (*b*). The presence of some 40% to 50% of the imino form in isopropylidenemalononitrile dimer (see Fig. 1 and Ref. 8) means that in itself the *imino* form is not significantly less stable than the *amino* form. It appears then that the dominant factors which determine the almost exclusive production of the amino form must be (i) the steric repulsion between R′ and R, and (ii) the added stability conferred by a methyl substituent on the exocyclic double bond.

Similar arguments may be applied to the structure of cyclohexylidenemalononitrile (IV). We previously suggested (9) that the structure of this dimer is the mixture IV (*a*), IV (*c*). However, there is also the possibility of the existence of form IV (*b*), analogous to II (*b*) and III (*b*), where the compounds were essentially 100% in these forms. Recent thermodynamic studies (10) have shown that the four hexahydronaphthalenes shown below have relative stabilities as indicated;

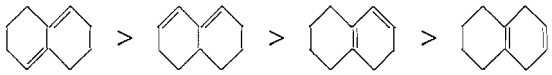

IX X XI XII

These studies might suggest that, in the amino form of cyclohexylidenemalononitrile dimer, IV (*b*) would be thermodynamically favored over IV (*c*). If the 3.9τ peak (Fig. 1 (IV)) were considered to be due to the hydrogen on the exocyclic double bond in IV (*b*) then the relative positions of the peaks in the n.m.r. spectrum of the dimer fit structure IV (*b*), if it is assumed that the material is essentially *all* in the IV (*b*) form. As previously noted (9), however, the broad and overlapping character of the cyclohexane hydrogen bands make accurate area correlations difficult.

Dimerization Mechanism

In the examples considered the ease of dimerization appears to depend on the availability of a base-extractable β-hydrogen in the monomeric ene-nitrile. Thus, the dimers of isopropylidenemalononitrile, 2-butylidenemalononitrile, and cyclohexylidenemalononitrile are produced rapidly (1–2 hours) by the action of base. It is also noteworthy that

Can. J. Chem. Downloaded from www.nrcresearchpress.com by 210.87.254.42 on 09/05/12
For personal use only.

in 2-butylidenemalononitrile the base attacks the methyl group exclusively rather than the ethyl CH_2. This agrees with the observation (11) that unsymmetrical ketones, such as ethyl methyl ketone, undergo enolization-controlled reactions on the ethyl CH_2 group in acid, and on the methyl group in base. On the other hand, the fourth monomer, 3-pentylidenemalononitrile, where the intermediate carbanion will be destabilized by the adjacent CH_3 group, and which is also more sterically hindered, undergoes dimerization much less rapidly. Some investigators (6) have, in fact, reported that they did not obtain any crystalline dimer from this compound. It may be noted in addition that 3-methyl-2-butylidenemalononitrile appears to react sluggishly, and we have as yet obtained only small amounts of the crystalline dimer. Presumably the steric effect of the isopropyl group is coming into play to a significant extent.

Of the base-catalyzed condensations considered here either the monomers or mixtures of the precursor ketones and malononitrile appear to give rise to simple cyclic dimers, except in the case of equimolar mixtures of acetone and malononitrile. In this case there is produced a crystalline solid which analyzes $C_{15}H_{14}N_6$ and which is reported (8) to arise from 1,4-addition of malononitrile to tautomer I (*a*). The production of more complex condensation products of this type from base catalyzed condensations of *arylidene-malononitriles*, such as benzalmalononitrile, appears to be common and will be the subject of a later communication.

EXPERIMENTAL

Preparation of Isopropylidenemalononitrile Dimer (7, 8)

Diethylamine (0.2 ml) was added to a solution of malononitrile (5 g, 0.07 mole) in acetone (19.8 g, 0.34 mole) at room temperature. The reaction mixture became very hot, and, on standing overnight, a solid product formed which was recrystallized from 95% ethanol to give needle crystals; m.p. 170–175° (lit. 171–174°). Anal. Calc. for $C_{12}H_{12}N_4$: C, 67.92; H, 5.67; N, 26.40. Found: C, 67.82; H, 6.08; N, 26.33. Mol. wt. Calc.: 212. Found: 204.

Preparation of 2-Butylidenemalononitrile Dimer

Malononitrile (3.3 g, 0.05 mole) was dissolved in 3.6 g (0.05 mole) of ethyl methyl ketone and 0.2 ml of diethylamine was added to the mixture, which rapidly became very hot. The mixture was left at room temperature overnight, and the solid thus produced was recrystallized from 95% ethanol; m.p. 167–169°. Anal. Calc. for $C_{14}H_{16}N_4$: C, 70.01; H, 6.67; N, 23.30. Found: C, 70.14; H, 6.92; N, 23.35. Mol. wt. Calc.: 240. Found: 255.

Preparation of 3-Pentylidenemalononitrile (6)

Malononitrile (26.4 g, 0.4 mole) and diethyl ketone (38 g, 0.44 mole) were dissolved in 50 ml of benzene, and 3.08 g (0.04 mole) of ammonium acetate plus 4.8 g (0.08 mole) of acetic acid were added to the solution. The mixture was refluxed for 40 minutes under a Dean Stark trap, and 7.8 ml of water was collected. It was then cooled, washed with water several times, and distilled under vacuum. Yield, 48.7 g, (90%); b.p. 150°/19 mm (lit. 122–125°/23 mm); $n_D^{20} = 1.4708$ (lit. $n_D^{25} = 1.4692$).

Preparation of 3-Pentylidenemalononitrile Dimer

Several initial attempts at the dimerization using different bases (piperidine, diethylamine, aqueous ammonia, aniline) resulted in the production of black tars. The following method eventually worked. To 3.4 g (0.025 mole) of 3-pentylidenemalononitrile was added 0.2 ml of diethylamine. The mixture did not become hot, but on standing overnight a glass was formed, which, on addition of 95% ethanol, could be crystallized. Recrystallization from 95% ethanol gave needles; m.p. 165–167°. Anal. Calc. for $C_{16}H_{20}N_4$: C, 71.60; H, 7.46; N, 20.85. Found: C, 71.83; H, 7.60; N, 2.70. Mol. wt. Calc.: 268. Found: 253.

Molecular weights were determined osmometrically.

ACKNOWLEDGMENTS

The research for this paper was supported in part by the Defence Research Board of Canada, Grant No. 2001-01.

Can. J. Chem. Downloaded from www.nrcresearchpress.com by 210.87.254.42 on 09/05/12
For personal use only.

REFERENCES

1. W. HUECK. Ber. **28**, 2251 (1895).
2. G. J. ÖSTLING. Ofersich Finska Vetenskaps Soc. Forhandl, A, **57**, No. 11, 13 (1915).
3. O. DIELS, H. GARTNER, and R. KAACH. Ber. **55**, 3439 (1922).
4. R. SCHENK and H. FINKEN. Ann. **462**, 273 (1928).
5. B. B. CORSON and R. W. STOUGHTON. J. Am. Chem. Soc. **50**, 2825 (1928).
6. A. C. COPE and K. E. HOYLE. J. Am. Chem. Soc. **63**, 733 (1941).
7. D. W. M. ANDERSON, F. BELL, and J. L. DUNCAN. J. Chem. Soc. 4705 (1961).
8. J. K. WILLIAMS. J. Org. Chem. **28**, 1054 (1963).
9. M. R. S. WEIR and J. B. HYNE. Can. J. Chem. **41**, 2905 (1963).
10. R. B. BATES, R. H. CARNIGHAN, and C. E. STAPLES. J. Am. Chem. Soc. **85**, 3030 (1963).
11. E. S. GOULD. Mechanism and structure in organic chemistry. Holt, Rinehart and Winston, Inc. 1959. p. 383.

Can. J. Chem. Downloaded from www.nrcresearchpress.com by 210.87.254.42 on 09/05/12
For personal use only.

Can. J. Chem. Downloaded from www.nrcresearchpress.com by 210.87.254.105 on 09/05/12
For personal use only.

THE ELECTRICAL POLARIZATION OF 1,4-BENZOQUINONE AND RELATED SUBSTANCES

HELMUT HUBER AND GEORGE F WRIGHT
Department of Chemistry, University of Toronto, Toronto, Ontario
Received August 28, 1963

ABSTRACT

A determination of the atom polarization of 1,4-benzoquinone from low-frequency infrared absorptions does not confirm the results of Becker and Charney. Therefore the total polarization of this substance must partly be due to orientation of a dipole. Also tetracyanoethylene and tetracyanoquinodimethane seem to have appreciable dipole moments although they both have abnormally high distortion polarization.

In the gaseous state (1) and in solution (2) the total polarization ($P_T = P_O + P_E + P_A$) of 1,4-benzoquinone has been found to about 37 cc, thus exceeding the electronic polarization (P_E) by about 6 cc. Originally (1) this difference was ascribed to abnormally high atom polarizations, an assignment in lieu of orientation polarization (P_O) which seemingly has been confirmed by observations that microwave absorptions (3, 4) are insufficient to account for a dipole moment and by absence of a negative Kerr effect (5). Most recently, optical dispersion theory (3, 5) has been applied by Becker and Charney (6) to the estimation of atom polarization (P_A) by calculation from absorption spectra of 1,4-benzoquinone in the 1700 to 50 cm^{-1} region. According to these workers the 6 cc difference between total polarization and electronic polarization is accounted largely in terms of this calculation as P_A.

On the other hand, some studies in this laboratory show that the atom polarization of benzoquinone does not exceed a few percent of the electronic polarization (2). Moreover, the total polarizations are both solvent and temperature dependent, and the polarization–temperature plots for several solvents intersect at the value of 37.6 cc, very close to the value obtained (1) from the gaseous state (36 cc) when the latter is extrapolated to lower temperature. Such behavior is presumptive of orientation polarization due to a dipole moment rather than to atom polarization, which ought to be, and has in general been found to be (7), temperature independent.

In view of the conflicting opinions in several laboratories we have elected to repeat with benzoquinone our direct determination of distortion polarization ($P_D = P_E + P_A$). This analysis is effected by capacitance measurements in respect of air on wafers of the solid substance finely ground for random particle orientation and compressed to maximum density. Because of the edge effect common to capacitors of this diameter (about 0.25 in.) a series of different thicknesses is measured and the apparent dielectric constants, if they are linearly related, are extrapolated to zero thickness. The original value for this extrapolation (2) was 30.1 cc. Our new value derived with more precise equipment is 31.4 cc.

This revised value for P_D does not vitiate our conclusion about the polarization of benzoquinone. However, the value of P_A included in it will depend upon the choice of P_E which is subtracted. The value of P_E derived from addition of bond or group polarizabilities at visible frequencies is 26.8 cc but a better evaluation is due to Syrkin *et al.* (8) from their measurements of refractive indices. These measurements led to molecular refraction at several wavelengths: 509 mμ (30.06 cc); 546 mμ (29.7 cc); 579 mμ (29.4 cc); and 644 mμ (29.0 cc). Extrapolation of these volumes to infinite wavelength by Sellmeier's formula led

to their value of 28.4 cc for MR_∞. The difference between this value and that derived by summation of atom (9) or bond (10) polarizabilities was not unreasonably attributed by Syrkin *et al.* to exhaltation.

Within experimental error their MR_∞ represents electronic polarization at radio frequencies. On this basis the difference between our experimental value for P_D and P_E at 10^6 c.p.s. may be assigned as $P_A = 3.0$ cc. This portion, almost 10% of the entire distortion polarization, is larger than is found for many substances but it is much less than is needed to account for 37 cc of total polarization. The alternative is orientation polarization due to a dipole moment.

Also because of the conflicting opinions, we have, like Becker and Charney, examined the spectrum of benzoquinone over the spectral range of 1700 to 50 cm^{-1}. We used the same type of spectrophotometer (PE-301) and altered their procedure only by using dispersions (15 wt. %) in polyethylene wax (7) for measurement of intensities.

Our results are shown in Table I. High accuracy cannot be claimed because there is

TABLE I

Calculation of atom polarization from spectral absorption (900–50 cm^{-1}) by *p*-benzoquinone

Sample No.	Freq., cm^{-1}	Band envelope	Baseline, % *T*	Intensity, cm^2 $mole^{-1}$	Band width cm^{-1}	P_{Aj}
1*	117	Unsym	95	8,199	54	2.37
2	117	Unsym	68–90	11,713	51	3.38
2	411	Unsym	68	8,901	153	0.73
1	117	Sym	95	7,412	52	2.14
2	117	Sym	68	9,043	38	2.61
2	411	Sym	68	1,104	43	0.09
3†	411	Sym	100	1,375	20	0.11
3	882	Sym	97	842	37	0.003

*Sample 1 and 2 in P.E. wax were examined in PE-301.
†Sample 3, 40 g.p.l. in benzene examined in IR-4.

much distortion of the absorption bands on the low-frequency side. In view of this distortion we have calculated our intensities in two ways: integrated area of the entire bands as they were observed (unsymmetric) and also by assuming that the band contour on the low-frequency side ought to be identical with that on the high-frequency side (symmetrical), of course, with limitations imposed by the background of polyethylene wax in the same amount as has been used in the candidate samples.

According to the results of duplicate determinations with different samples we have found that for benzoquinone the absorption which is of principal interest occurs mainly at 117 cm^{-1}. This divergence from the 108 cm^{-1} reported by Charney and Becker (6) cannot be due to differences in the dilution medium because the absorption peak which we obtained from a 12% benzene solution also occurred at 117 cm^{-1}. Moreover the determination in benzene was carried out through the courtesy of the Eastman Kodak company on a duplicate 301 spectrometer. Our calibration was effected in terms of the band at 411 cm^{-1}, which corresponds with the frequency we observed for benzene solutions of benzoquinone in the Beckman IR-4 instrument.

The atom polarizations, P_{Aj} in Table I at each frequency for 1,4-benzoquinone, might be calculated from the equation of Whiffen (I) derived from the Kramers–Kronig relationship.

$$P_A = \frac{Nc}{3\pi^2} \int \frac{\alpha(\nu)d\nu}{\nu^2 C'} \qquad (I)$$

Can. J. Chem. Downloaded from www.nrcresearchpress.com by 210.87.254.105 on 09/05/12
For personal use only.

where α is the extinction coefficient integrated over the bandwidth $d\nu$, N is the Avogadro number, c is the vacuum velocity of light, C' is the concentration in moles per liter, and ν is frequency. Actually P_{A_j} values in Table I have been evaluated from Charney and Becker's form of equation I in which ν is expressed in wave numbers.

$$P_{A_j} = \int \frac{(I_0/I)d\nu}{3\pi^2\nu_j^2 C'(\mathrm{I})} \qquad \text{(II)}$$

and $P_A = \sum P_{A_j}$.

The deviation in P_{A_j} for the important 117 cm^{-1} band in different determinations makes it questionable whether meaningful results are possible with this spectrometer in its present state of development. Nevertheless for purposes of comparison the total of P_A calculated by inclusion of the complete bands (unsymmetrical) and including the high frequency contributions listed by Charney and Becker amounts to 3.5–4.5 cc. By a more realistic inclusion only of a symmetrical envelope of the bands the total P_A is 3.2–3.7 cc. Even the largest of these values (4.5 cc) is much less than the 6.97 cc reported by Charney and Becker.

Actually it is questionable whether equation II is applicable to a calculation of P_A for substances like benzoquinone. Whiffen's application of equation I was justified in the use of 3.1×10^{10} cm sec^{-1}, the vacuum velocity of electromagnetic radiation, because he applied it to gases for which the dielectric constants do not differ markedly from unity. But this approximation is not valid for condensed systems in which the dielectric constant usually exceeds 2. The velocity of radiation in such media has not been measured directly but theoretically (12) it ought to be less than the vacuum velocity by the factor $1/\sqrt{\epsilon}$ (i.e. $1/n$) in the spectral region in which P_A has been evaluated. When the reciprocal root of the dielectric constant of solid benzoquinone, $1/\sqrt{2.845}$, which is 0.5917, is applied to the P_{A_j} values of Table I then 4.5 cc (maximum of unsymmetrical band interpretation) and 3.2 cc (maximum for symmetrical band interpretation) become respectively 2.7 cc and 1.9 cc. But these values for P_A are both less than the magnitude determined as the difference between our measured distortion polarization and the measured electronic polarization by Syrkin *et al.* Contributions from overtones and minor absorptions over the entire spectral range is not expected to augment 1.9–2.7 cc to more than 3 cc.

Therefore our estimation of atom polarization from contributions due to absorption in the infrared region falls easily within the 31.4 cc of distortion polarization measured for the density and dielectric constant of the crystalline solid benzoquinone. Whether or not the estimation from spectra is reliable, it does not provide a contradiction of the value of distortion polarization derived by the wafer method. The estimation from spectra cannot account for the difference between this P_D and the total polarization found in the gas phase or in the solution. There is still no valid interpretation of the difference except as orientation polarization.

One may question our contradiction of Charney and Becker on the basis that our absorption coefficients were inordinately low (i) because of the difference in spectrometers or in their operation or (ii) because we used polyethylene wax suspensions rather than the benzene solution of Charney and Becker, or (iii) that our dispersion of the candidate substance in the wax was non-uniform. On the contrary, it may be seen in Table I that integrated intensity of the band at 411 cm^{-1} when determined by use of the PE-301 by use of polyethylene wax suspensions is much higher than that in benzene solution by IR-4 until it is corrected for asymmetry, after which the results from the two machines and the two media are comparable in magnitude.

Can. J. Chem. Downloaded from www.nrcresearchpress.com by 210.87.254.105 on 09/05/12
For personal use only.

Further evidence that spectral intensities observed with the PE 301 spectrometer tend to be high rather than low is provided by examination of *trans*-2,2,4,4-tetramethylcyclobutane-1,3-diol. The spectral data are recorded in Table II. In contrast to those of benzoquinone these bands are nicely symmetrical. Moreover, the absorption determined in the

TABLE II

Calculation of atom polarization from spectral absorption (900–50 cm^{-1}) of *trans*-2,2,4,4-tetramethyl-1,3-cyclobutanediol, in polyethylene wax

Freq., cm^{-1}	Concentration, %	Baseline, % T	Intensity, $cm^2 mol^{-1}$	Band width, cm^{-1}	P_{Aj}
512*	10	55	5,759	40	0.4
399*	10	70	7,134	28	0.6
317*	10	80	3,508	10	0.4
319	15	80	10,363	55	1.1
276	15	80	9,721	53	1.0
241	15	80	7,513	50	0.8
130	15	80	13,445	45	1.4

*These values were determined with the Beckman IR-4 spectrometer. The PE-301 machine was used for the remainder.

PE-301 spectrometer may be correlated reliably with those from the IR-4 by the overlapping frequency range at 317–319 cm^{-1}, especially since the data from the IR-4 spectroanalysis comprised results from six different samples with not more than 10% deviation among intensities. However, there is a wide discrepancy between the integrated intensities at the overlapping region, indicating that those determined with the PE-301 may be as much as 3 times too high. If P_{A_j} is calculated from the intensities as they were observed then $\sum P_{A_j}$ is 5.3 cc, while P_{A_j} is 2.4 cc if the intensities of bands observed in the PE-301 machine are weighted to conform with the IR-4 results in the ratio 3508/10363 of the 317–319 cm^{-1} absorptions.

Both of these values of P_A are larger than that calculated from the dielectric constant of compressed wafers of the solid substance. Actually the measured value of the distortion polarization is 0.9 cc less than that calculated from bond and atom polarizabilities (32.9 cc versus 40.1 cc). Since it is one of six alcohols for which the difference value, P_A, varies over a range of 2.5 cc (of which the *cis* diol at $P_A = +0.7$ cc is about average) it may be considered to have a minimal atom polarization comprising about 2% of P_D. It may be noted that a reduction of the intensity-corrected $\sum P_{A_j}$ (from the spectral study) by $1/\sqrt{\epsilon}$, i.e., $1/\sqrt{2.157} = 0.68$ provides a value of $P_A = 1.6$ cc, at least within magnitude of value obtained by wafer measurement. This apparent agreement does not increase our confidence in the value derived from spectral absorption.

The spectral studies have not altered the earlier conclusion (2) that part of the polarization of 1,4-benzoquinone is due to orientation due to a dipole in the electric field. However, the nature of this dipole has been obscure. In the hope of gaining an insight we have now examined tetracyanoquinodimethane, TCNQ (13) and its simpler vinylog, tetracyanoethylene, TCNE (14). The choice of TCNQ was made in the expectation that the quinonoid properties would be enhanced by the polar cyano groups, while TCNE was examined to evaluate these cyano groups in non-quinonoid attachment.

In contrast to benzoquinone the distortion polarizations of both substances, shown in Table III, are appreciably higher than would be expected from consideration of the electronic polarization calculated atom (Eisenlohr) or bond (Vogel) polarizabilities. It is of interest that the differences, P_A, are of the same order of magnitude for both of the tetracyano compounds.

Can. J. Chem. Downloaded from www.nrcresearchpress.com by 210.87.254.105 on 09/05/12
For personal use only.

TABLE III
Dielectric constants of solid TCNQ and TCNE

Substance	d_4^{23}	ϵ	P_D, cc	MR_D, cc Eisenlohr	Vogel	Av.	$P_D - P_E$
TCNE	1.323	2.927	37.9	27.6	28.6	28.1	9.8
TCNQ	1.3185	2.976	61.5	51.7	53.0	52.4	9.1

The data showing the total polarizations of TCNQ and TCNE are presented in Table IV.

The dipole moments have been calculated after subtraction of the additive molecular refraction (μ_{MR}) and of the measured distortion polarization (μ_{P_D}) in order to show the hazard of reliance on the additive refraction. Only μ_{P_D} should be considered to be significant. Unfortunately this significance is limited by the low solubility of the substances to a precision of not better than ± 0.03 D.

Within this limitation certain qualitative comparisons may be made. The reality of the TCNE moment is attested by the higher moment of TCNQ which is to be expected from greater charge separation in the latter, even though the difference will be minimized by conjugation resonance. Also notable is the marked enhancement of moment in dioxane versus benzene. This difference (about 30%) is greater than is ordinarily observed and may be considered to be a consequence of the Lewis acid character of TCNE (15) exemplified by charge separation shown as TCNE-R. It may be remarked that the difference is about 3 times that which was observed for benzoquinone in benzene versus dioxane.

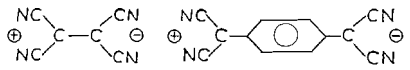

TCNE-R TCNQ-R

Unlike benzoquinone, the apparent moment of which was found (2) to decrease with respect to increasing temperature, the moment of TCNQ (within the precision of the determinations) seems to be invariant with respect to temperature. This invariance may be a consequence of the resonance hybrid exemplified by TCNQ-R or it may be due to a Lewis acid–base complex (16) with dioxane. Unfortunately TCNQ could not be examined in benzene because of inordinately low solubility. Undoubtedly the apparent moment in benzene would have been lower than in dioxane. But lower moments in benzene would not preclude the involvement of this solvent in a Lewis base complex with either TCNE or TCNQ. A better understanding of these apparent moments must await further studies.

Nevertheless the behaviors of TCNE and TCNQ in respect of solvent and temperature are sufficiently different from that of 1,4-benzoquinone that a lateral charge separation such as BP-R is not a reasonable postulation.

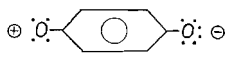

BP-R

On the basis of present evidence the polarization of benzoquinone is best explained in terms of a "bent" molecule. Nor is this unreasonable. The existence of an absorption band at 117 cm^{-1} (reported by Charney and Becker as 108 cm^{-1}) implies a condition at 20–40° C where about half of the molecules are in this state of excitation (17). This band has been designated as due to out-of-plane bending of carbonyl groups (6).

Can. J. Chem. Downloaded from www.nrcresearchpress.com by 210.87.254.105 on 09/05/12
For personal use only.

Can. J. Chem. Downloaded from www.nrcresearchpress.com by 210.87.254.105 on 09/05/12
For personal use only.

TABLE IV

Electrical polarization of TCNQ and TCNE

Substance	Solvent	Temp., °C	$d\epsilon/d\omega$	dv/dw	ϵ_0	ϵ extrap	$\overline{V_0}$	$\overline{V}$ extrap	P_T, cc	μ_{MR}	μ_{PD}
TCNE	Dioxane	40°	1.838	−0.232	2.2196	2.2200	0.98943	0.98955	67.3	1.41	1.15
TCNE	Benzene	40°	0.792	−0.332	2.2409	2.24117	1.16697	1.6701	51.1	1.08	0.82
TCNQ	Dioxane	40°	1.540	−0.158	2.2191	2.2188	0.98942	0.98944	101.5	1.58	1.42
TCNQ	Dioxane	30°	1.694	−0.190	2.2395	2.2392	0.97818	0.98714	103.5	1.59	1.44
TCNQ	Dioxane	20°	1.760	−0.220	2.2603	2.2596	0.96692	0.96698	102.6	1.54	1.40

Charney and Becker, among others (1), have attributed to this oscillation an abnormally high atom polarization for benzoquinone. We have confirmed by our direct measurement of distortion polarization that abnormality does not exist. Indeed it would not be expected to exist if a large percentage of the benzoquinone molecules are already in resonance with the collision field around them since the frequency of this collision field will be higher than that of the electromagnetic field (10^6 c.p.s.) which is imposed on the substance for measurement of dielectric constant. On the other hand, that half of molecules which are excited at temperatures of 20–40° C will in solution be oriented in the field as a consequence of the dipole moment of the excited species.

The evidence against this argument heretofore has seemed to be in the fact that the apparent dipole moment of benzoquinone in benzene, dioxane, or carbon tetrachloride decreases to an extent dependent upon each solvent with increasing temperature. One might expect that if the carbonyl group out-of-plane oscillation were coupled, the amount of BP-2 would increase according to a simple Boltzmann distribution as the temperature was increased.

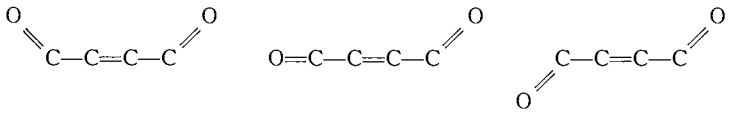

BP-2 BP-1 BP-3

If, on the other hand, the carbonyl oscillators are not coupled but, instead, are independent or mutually are only slightly perturbed, then one may expect an equilibrium among BP-1, 2, and 3. The temperature dependence of such an equilibrium, especially when it involves solvent effects, is not easily predictable. It is not unreasonable to expect that at higher temperatures the reversion of BP-2 and BP-3 to BP-1 would be greater than the rate at which BP-1 reverts to the ground state. If this were the fact the moment of the system would decrease with increasing temperature. Therefore the decreasing moment with increasing temperature does not necessarily contradict the explanation that the apparent moment of 1,4-benzoquinone is due to an excited state of bent molecules in the temperature region 20–40° C.

In view of the expectation that the benzoquinone molecule must partially be nonplanar at 20–40°C, the absence of appreciable Kerr effect (5) might seem to be anomalous. However, Charney's calculations show that a large effect would not be expected. Indeed a small effect has recently been noted (18). Moreover, a consideration of the thermally excited forms that are possible shows that the polarizabilities of BP-2 and BP-3 will be opposite in sign and thus compensatory. Therefore the findings in respect of dipole moment and Kerr effect need not be contradictory.

The discrepancy between the results of moment determination at low radio frequencies versus those at microwave frequencies (3, 4) must also be considered. The difference cannot be explained in terms of solute purity (19), at least in one instance, because the material used by Di Carlo and Smyth (4) and by Meredith *et al.* (2) was prepared in the same laboratory with the same criteria of purity.

Moreover, the discrepancy between microwave and radio frequency valuation extends to a number of other substances (4) such as 2,2,4,4-tetramethylcyclobutanedione for which the radio frequency (5×10^6 c.p.s.) reactance measurements assigns a dipole moment value of 0.7 D (20). On the other hand, the microwave frequency (2.40 and 0.93×10^{10} c.p.s.,

Can. J. Chem. Downloaded from www.nrcresearchpress.com by 210.87.254.105 on 09/05/12
For personal use only.

Can. J. Chem. Downloaded from www.nrcresearchpress.com by 210.87.254.105 on 09/05/12
For personal use only.

1.25 and 3.22 cm) loss measurement does not indicate a moment. Yet a moment would be expected in this diketone if the cyclobutane ring is not planar. Evidence is accumulating that the tetramethylcyclobutane ring deviates by about 20–30° from planarity (summarized in Ref. 20). Also electrical polarization measurements (21) on *cis*- and *trans*-2,2,4,4-tetramethyl-1,3-diisonitriles and -dinitriles give polarizations of such magnitude that they cannot be explained away as atom polarizations. Moreover, the values for the moments of these *cis* diisonitriles and nitriles are best explained on the basis of a bending rather than a bent ring. This dynamic nonplanarity also explains the single proton absorption shown in the n.m.r. spectrum of tetramethylcyclobutanedione as a consequence of the slow reading rate of the latter measurement. The frequencies of the ring oscillations of the diketone, diisonitriles, and dinitriles have not yet been measured, but it may be expected that these cyclobutanes will absorb in the region of the band at 130 cm^{-1} found for 2,2,4,4-tetramethylcyclobutane-1,3-diol (Table II). This band probably is due to the out-of-plane bending of the tetramethylcyclobutane ring.

If a moment by microwave measurement cannot be discerned for tetramethylcyclobutanedione which seems, on the basis of the foregoing evidence, not to be strictly centrosymmetric, then one must seek an explanation for this apparent anomaly. An explanation which will apply equally well to benzoquinone is exemplified by consideration of BP-2 and BP-3 as ephemeral dipoles.

The reactance of all dipoles, even those of short life that are induced at frequencies of 10^{14} and higher c.p.s. will be integrated by the field at 10^6 c.p.s. in media of low viscosity such as are used for solution measurements, by the low-frequency method. Ordinarily the population of such induced dipoles is so small as to be unmeasurable. Only in the unique circumstance where absorption occurs in the thermal region will the population of induced dipoles be large enough to be measurable as in the case with benzoquinone.

By contrast with the same solvents at the higher frequencies of the microwave region the molecules lag behind the field; indeed the relaxation time is the basis for the loss measurement of the determination. But induced dipoles of shorter life than this relaxation time will not be appreciably measurable in the microwave field. This may well be the circumstance during the measurements made (3, 4) with benzoquinone and other substances which absorb strongly in the far infrared regions.

If the dipole moment of benzoquinone is indeed due to excitation in the thermal region it is a question of semantics whether one is justified in designating the geometry of the molecule as non-planar, i.e. as a bent molecule. In its ground state the molecule may be planar. But the circumstances in which the substance is chemically used and characterized places a majority of the molecules in the excited state where it is dipolar. It would seem that as chemistry becomes more sophisticated the necessity for designation of a substance in respect of its environment will increase.

The authors are grateful to the Defence Research Board for financial aid, to Drs. E. Whalley and J. Bertie of the National Research Council for use of their PE-301 spectrometer, and to Drs. Le Roy and Polanyi of this department for helpful discussions.

EXPERIMENTAL

Reagents

Tetracyanoquinodimethane (TCNQ, kindly supplied by Dr. W. R. Hertler, E. I. duPont de Nemours) melted at 288.5°–289.5° and was used as received. Tetracyanoethylene (TCNE) was crystallized from benzene (ca. 16 ml per g) to melt at 199°. Benzoquinone was crystallized repeatedly from ethanol and zone-refined to melt at 113.5°.

Spectral Studies

Both benzene solutions and polyethylene wax wafers were used for studies with the Beckman IR-4 spectrometer and both media were used in the Perkin–Elmer 301 spectrometer. These wafers were prepared according to the method already outlined (1) and reference wafers were made from the same thickness of polyethylene wax in the sample wafer despite the relatively high percentage (2) of candidate substance required for the low frequency spectrometer. The wafers containing benzoquinone were examined in the IR-4 spectrometer during a time interval of 48 hours to show that no appreciable loss by sublimation occurred. The benzene solutions were not used for intensity evaluation.

The PE-301 spectrometer was maintained dry by a positive pressure of gas from a liquid nitrogen container. Samples were examined by use of both globar and mercury arc energy sources with appropriate gratings and reststrahlen filters with scanning rates from 2.75 cm^{-1} per minute (grating No. 29) to 1 cm^{-1} per minute (grating No. 8).

The spectral intensities were obtained by summation of the 1 cm^{-1} increments on the chart and also by weight-integration of the graph paper.

Distortion Polarizations

The improved apparatus described recently (7) was used for measurements with benzoquinone, TCNE, and TCNQ. Density was determined for benzoquinone by air displacement (22) and for the other two substances by flotation. According to the present determination the extrapolated dielectric constant for benzoquinone is 2.842 (Fig. 1) instead of 2.730 while the density at 23° is 1.309 instead of 1.313. The dielectric constant extrapolations for TCNE and TCNQ are as linear as those shown in Fig. 1.

Total Polarizations

The measurements have been made according to earlier descriptions (2) and are recorded as Fig. 2 for TCNE and Fig. 3 for TCNQ.

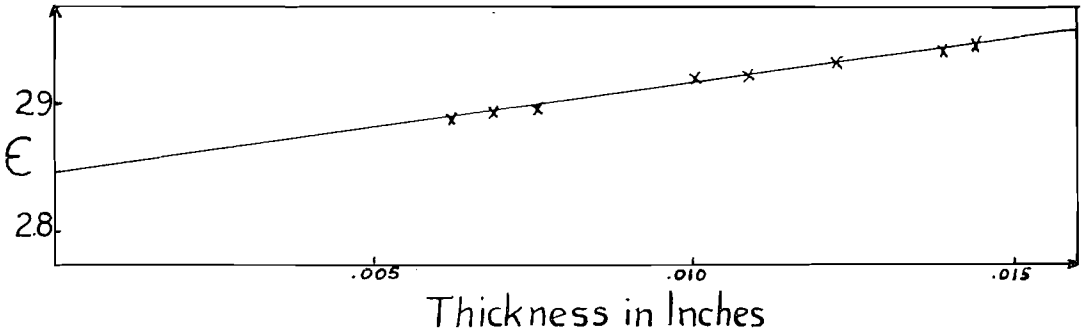

FIG. 1.

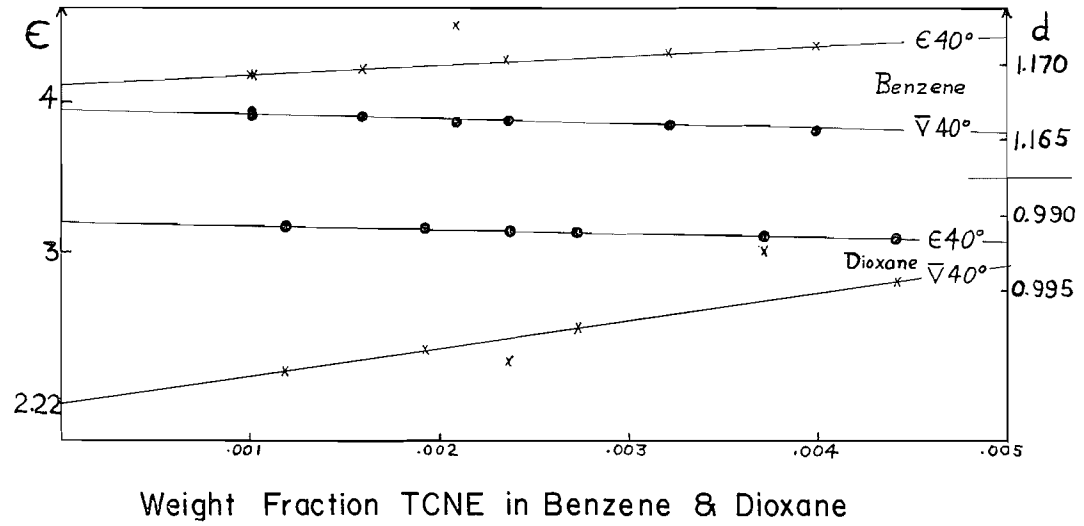

FIG. 2.

Can. J. Chem. Downloaded from www.nrcresearchpress.com by 210.87.254.105 on 09/05/12
For personal use only.

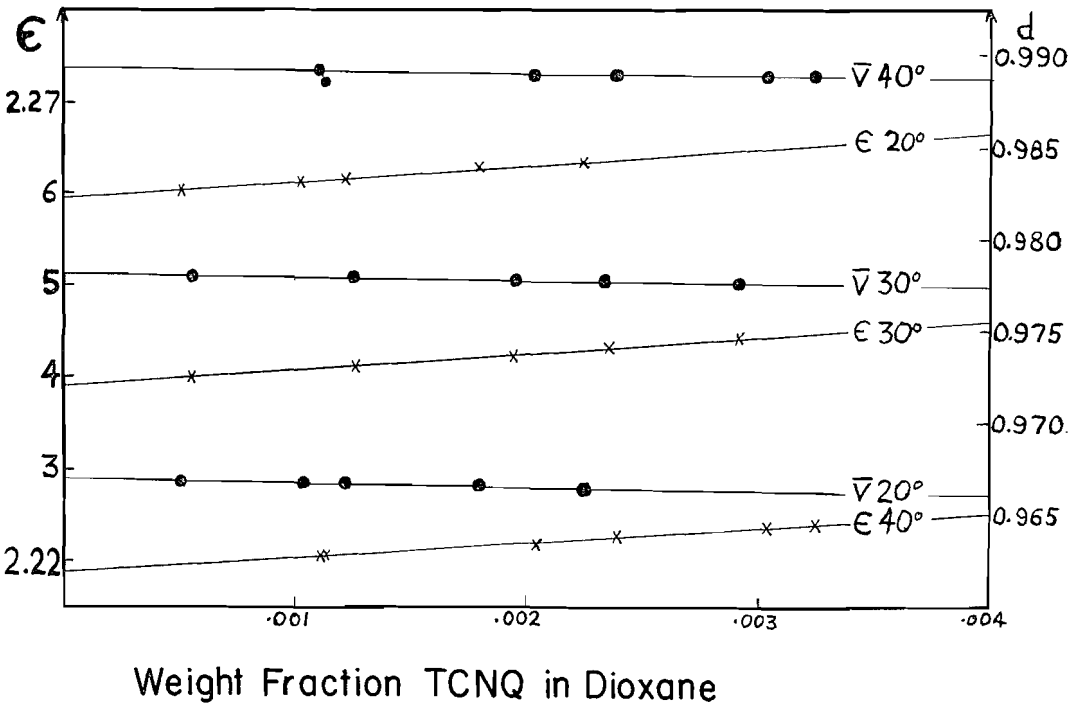

FIG. 3.

REFERENCES

1. E. I. COOP and L. E. SUTTON. J. Chem. Soc. 1269 (1938).
2. C. C. MEREDITH, L. WESTLAND, and G. F. WRIGHT. J. Am. Chem. Soc. **79**, 2385 (1957).
3. R. S. ARMSTRONG, C. G. LEFEVRE, and R. J. W. LEFEVRE. J. Chem. Soc. 371 (1957).
4. E. N. DI CARLO and C. P. SMYTH. J. Am. Chem. Soc. **84**, 1128 (1962).
5. E. CHARNEY. J. Am. Chem. Soc. **83**, 578 (1961).
6. E. CHARNEY and E. D. BECKER. J. Am. Chem. Soc. **83**, 4468 (1961).
7. M. BEDARD, H. HUBER, J. L. MYERS, and G. F WRIGHT. Can. J. Chem. **40**, 2278 (1962).
8. G. G. KIKINA, YA.K. SYRKIN, and E. A. SHOTT-LVOVA. Izv. Acad. Nauk SSSR, Otd. Chim. Nauk, 563 (1954); Chem. Abstr. **48**, 13316 (1954).
9. F. EISENLOHR. Z. Physik. Chem. **75**, 585 (1910); **79**, 129 (1912).
10. A. I. VOGEL. J. Chem. Soc. 134 (1946); 654 (1958).
11. D. H. WHIFFEN. Trans. Faraday Soc. **54**, 327 (1958).
12. R. W. WOOD. Physical optics. Macmillan and Co. 1934. p. 405.
13. D. S. ACKER and W. R. HERTLER. J. Am. Chem. Soc. **84**, 3370 (1962).
14. T. L. CAIRNS *et al.* J. Am. Chem. Soc. **80**, 2775 (1958).
15. R. E. MERRIFIELD and W. D. PHILLIPS. J. Am. Chem. Soc. **80**, 2778 (1958).
16. L. R. MELBY *et al.* J. Am. Chem. Soc. **84**, 3374 (1962).
17. T. L. BROWN. Spectrochim. Acta, **18**, 1071 (1963).
18. R. J. W. LEFEVRE, A. SUNDARAM, and K. M. S. SUNDARAM. J. Chem. Soc. 974 (1963).
19. L. PAOLONI. J. Am. Chem. Soc. **80**, 3879 (1958).
20. P. PODLESCHKA, L. WESTLAND, and G. F WRIGHT. Can. J. Chem. **36**, 574 (1958).
21. F. LAUTENSCHLAGER and G. F WRIGHT. Can. J. Chem. **41**, 863 (1963).
22. M. V. GEORGE and G. F WRIGHT. Can. J. Chem. **36**, 189 (1957).

Can. J. Chem. Downloaded from www.nrcresearchpress.com by 210.87.254.105 on 09/05/12
For personal use only.

Can. J. Chem. Downloaded from www.nrcresearchpress.com by 210.87.254.6 on 09/05/12
For personal use only.

THE ACID HYDROLYSIS OF GLYCOSIDES

I. GENERAL CONDITIONS AND THE EFFECT OF THE NATURE OF THE AGLYCONE

T. E. TIMELL[1]

Department of Chemistry, McGill University, and the Pulp and Paper Research Institute of Canada, Montreal, Quebec

Received December 23, 1963

ABSTRACT

First-order rate coefficients and energies and entropies of activation have been determined for the acid-catalyzed hydrolysis of a number of methyl D-glycopyranosides and disaccharides. The relation between the logarithm of the rate coefficients and values for Hammett's acidity function was linear, although different for different acids. All compounds had entropies of activation indicating a unimolecular reaction mechanism. Glucosides of tertiary alcohols were hydrolyzed very rapidly, triethylmethyl β-D-glucopyranoside, for example, 30,000 times faster than the corresponding methyl compound.

Increase in size of the aglycone caused a slight increase in the rate of hydrolysis of β-D-glucopyranosides, steric hindrance thus being of no significance. Electron-attracting substituents in the aglycone had little or no influence on the rate of hydrolysis, obviously because they would tend to lower the equilibrium concentration of the conjugate acid, while facilitating the subsequent heterolysis, the two opposing effects more or less cancelling out. These results were discussed in connection with recent studies on the acid hydrolysis of various phenyl glycopyranosides and with reference to the postulated occurrence of an activating inductive effect in oligo- and poly-saccharides containing carboxyl or other electronegative groups at C-5. It was concluded that there is little evidence for the existence of any such effect and that, for example, pseudoaldobiouronic acids should be hydrolyzed at the same rate as corresponding neutral disaccharides.

INTRODUCTION

The acid-catalyzed hydrolysis of glycosides has attracted much attention in recent years. The mechanism now accepted was first suggested by Edward (1), experimentally proved by Vernon and co-workers (2–5), and later confirmed by Overend *et al.* (6, 7). For example, with methyl β-D-glucopyranoside (I), it involves a rapid, equilibrium-controlled protonation of the glycosidic oxygen to give the corresponding conjugate acid (II). In the slow, rate-determining step, the acid decomposes in a unimolecular heterolysis with formation of alcohol and a carbonium–oxonium ion (III, IV), which is most likely present in the half-chair conformation (V). Finally, water is rapidly added, giving glucose and hydronium ion.

It was the aim of the present series of investigations to study the effect of functional groups, and especially of carboxyl groups, on the acid hydrolysis of glycosides. Such a study, it was hoped, would provide information about the acid hydrolysis of polysaccharides containing such or similar groups. Because of the paucity of data available, it was decided first to study the hydrolysis of a few common methyl glycosides and disaccharides. This paper is concerned with this aspect and with the influence of the aglycone on the hydrolysis of glycosides. After completion of the experimental part of this study, an investigation by Overend, Rees, and Sequeira (6) on the acid-catalyzed hydrolysis of a number of glycosides has appeared.

RESULTS AND DISCUSSION

Most experiments were carried out with 0.05 *M* sugar solutions in 0.5 *M* aqueous sulphuric acid. The hydrolysis was followed with the aid of a photoelectric polarimeter.

[1]*Present address: Department of Forest Chemistry, State University College of Forestry at Syracuse University, Syracuse 10, New York.*

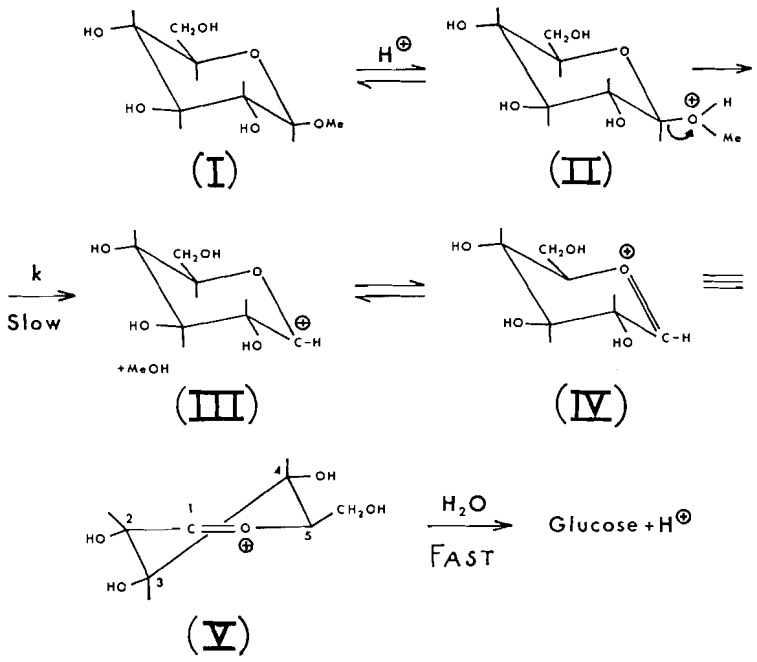

Final rotations usually agreed well with calculated values, although it is known that under the conditions used both disaccharides (6, 8) and 1,6-anhydro-β-D-glucopyranose (9) are formed to a small extent.

Hydrolysis of Some Methyl Glycosides and Disaccharides

The first compounds to be studied were methyl α- and β-D-glucopyranosides, which were hydrolyzed at seven temperatures, ranging from 60 to 120° C. Rate constants with their deviation from the mean and energies and entropies of activation are given in Table I. The Arrhenius plot of log k versus $1/T$ gave a straight line through all experimental points. The ratio of k_β/k_α decreased linearly with increasing temperature, reaching unity at 132° C on extrapolation. The corresponding temperature reported by Moelwyn-Hughes (8) was 116° C. Overend, Rees, and Sequeira (6) found the k_β/k_α ratio to vary very little with temperature.

In Table II a comparison has been made between energies of activation obtained by various investigators for the acid hydrolysis of methyl α- and β-D-glucopyranosides. With the exception of the values of Moelwyn-Hughes (10) and Nakano and Rånby (14), which were based on limited experimental data, the agreement between the various investigators is reasonably good.

A similar comparison between the rate coefficients, presented in Table III, gives a different result. Here, published values have been recalculated to be valid at 60, 70, and 80° C with the aid of the respective energies of activation and then referred to a value of +0.13 for H_0, Hammett's acidity function (15–17), valid for 0.5 M sulphuric acid (18). This treatment is justified because the acid hydrolysis of glycosides (2), and of acetals in general (19), has been shown to be proportional to h_0 rather than to H_3O^+. The agreement between the various investigators is not very good. The values of Easty (13) are conspicuously larger than the others. The fact that he alone used a chemical method (determination

Can. J. Chem. Downloaded from www.nrcresearchpress.com by 210.87.254.6 on 09/05/12
For personal use only.

Can. J. Chem. Downloaded from www.nrcresearchpress.com by 210.87.254.6 on 09/05/12
For personal use only.

TABLE I

Rate coefficients and kinetic parameters for the hydrolysis of methyl α- and β-D-glucopyranosides (0.05 M) in 0.5 M sulphuric acid

	60° C		70° C		80° C		90° C		100° C		110° C		120° C		E, kcal mole^{-1}	$\Delta S^{\ddagger}$ at 60°, cal deg^{-1} mole^{-1}
Compound	k*	D†	k	D	k	D	k	D	k	D	k	D	k	D		
Methyl α-	0.637	2.2	2.85	0.3	12.6	2.0	50.3	3.0	202	0.1	675	1.5	2049	4.4	35.1	+ 16.9
Methyl β-	1.38	2.0	6.25	1.2	24.1	2.1	90.2	1.8	325	2.5	921	3.7	2400	4.0	32.5	+ 10.6

*Rate coefficient $\times 10^{-6}$ sec^{-1}.
†Deviation from mean in percent.

TABLE II

Activation energies for methyl α- and β-D-glucopyranosides

Investigator	Reference	Activation energy, kcal. mole^{-1}	
		Methyl α-	Methyl β-
Moelwyn-Hughes	10	38.2	33.7
Veibel and Frederiksen	11		32.6
Heidt and Purves	12	34.8	33.5
Armour *et al.*	4	33.7	
Easty	13	34.9	
Nakano and Rånby	14	31.0	30.9
Overend, Rees, and Sequeira	6	34.1	34.3
Present		35.1	32.5

TABLE III

First-order rate coefficients for the acid hydrolysis of methyl α-D-glucopyranoside. Recalculated to be valid at an H_0 value of +0.13

Investigator	Reference	Acid	$k \times 10^{-6}$ sec^{-1}		
			60° C	70° C	80° C
Moelwyn-Hughes	10	HCl	0.61		16.2
Bunton *et al.*	2	$HClO_4$		3.77	
Easty	13	H_2SO_4		6.79	
Nakano and Rånby	14	H_2SO_4		3.39	12.9
Overend, Rees, and Sequeira	6	HCl	1.07	4.64	19.9
Present		H_2SO_4	0.64	2.85	12.6

of the methanol formed) for following the hydrolysis might be of relevance in this connection. The rate coefficients of Overend and co-workers (6) are almost twice as large as those obtained in the present study.

It was thought that this could perhaps be attributed to the fact that different acids were used in these two investigations. Rate constants were accordingly determined with four different mineral acids at concentrations ranging from 0.5 to 9 *M*. The results are presented graphically in Fig. 1. The logarithm of the rate coefficients vary linearly with H_0 as required by the Zucker–Hammett hypothesis. The requirement of slope unity, however, is only approximately fulfilled for three of the acids and not at all for phosphoric acid. Instead of coinciding, the plots are displaced with respect to each other, hydrochloric acid giving the highest and phosphoric acid the lowest rate coefficients at concentrations higher than 1 *M*. Data obtained with one of these four acids cannot accordingly be recalculated to be valid for another acid by referring to the same value for H_0, as has often been done in the past.

According to Hammett, a linear relationship in acid-catalyzed reactions between log k and H_0 implies that the rate-determining step involves a unimolecular decomposition of the conjugate acid without participation of water (A-1), while a bimolecular reaction (A-2) involving a molecule of water will lead to proportionality between log k and pH. This hypothesis has lately been critically reviewed by Bunnett (20) with special emphasis on the fact that many of the plots of log k against H_0 have slopes departing from unity. His treatment leads to the conclusion that, for example, methyl α-D-mannopyranoside should be hydrolyzed by the unimolecular mechanism, while methyl α-D-glucopyranoside should be hydrolyzed by an S_N2 mechanism, entailing a nucleophilic attack of water on

Can. J. Chem. Downloaded from www.nrcresearchpress.com by 210.87.254.6 on 09/05/12
For personal use only.

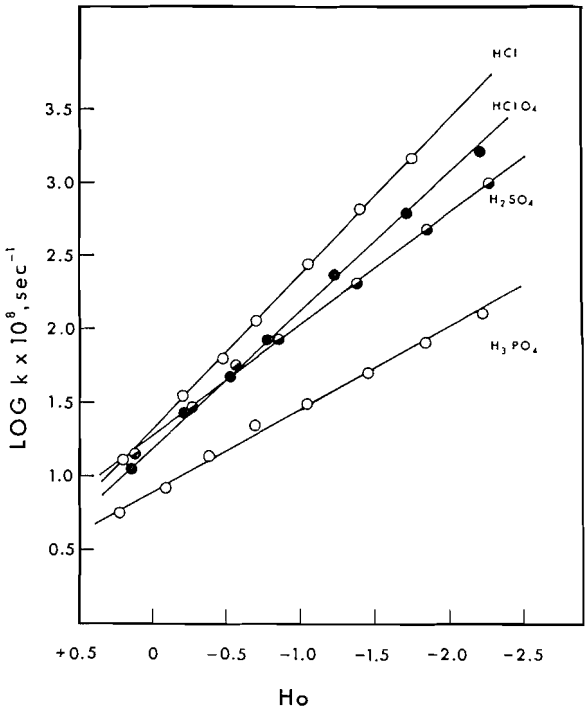

FIG. 1. Variation of log k with H_0 for hydrochloric, perchloric, sulphuric, and phosphoric acids.

the conjugate acid. As pointed out by Bunnett himself, this conclusion is difficult to accept in view of the similarity of the two compounds.

When the rate of hydrolysis of methyl α-D-glucopyranoside was measured at 60° C under exactly the same experimental conditions as those used by Overend, Rees, and Sequeira (6), a k-value of 5.56×10^{-6} sec^{-1} was obtained, compared with a value of 7.08×10^{-6} in the earlier study. A similar difference was found for all compounds studied in both of these investigations. This consistent discrepancy remained unexplained.

Kinetic data for five additional methyl α- and β-D-glycopyranosides are presented in Table IV. When referred to the rate constants valid for a single reference compound, such as methyl α-D-glucopyranoside, the present data agree well with those reported by Riiber and Søorensen (21) and by Overend, Rees, and Sequeira (6). If the reaction involved a

TABLE IV

Rate coefficients and kinetic parameters for the hydrolysis of five methyl glycopyranosides (0.05 M) in 0.5 M sulphuric acid

Compound	$k\times10^{-6}$ sec^{-1}			E	$\Delta S^{\neq}$
	60° C	70° C	80° C		
Methyl α-D-galactopyranoside	3.04	13.6	56.4	34.0	+16.7
Methyl β-D-galactopyranoside	5.87	23.3	94.4	32.0	+12.0
Methyl α-D-mannopyranoside	1.45	6.56	28.9	34.7	+17.3
Methyl α-D-xylopyranoside	3.06	13.9	57.9	33.4	+14.9
Methyl β-D-xylopyranoside	6.56	28.6	121.0	33.9	+17.9

Can. J. Chem. Downloaded from www.nrcresearchpress.com by 210.87.254.6 on 09/05/12
For personal use only.

molecule of water (A-2), the transition state would constitute a more highly ordered structure than the ground state (the conjugate acid). This would involve a decrease in entropy, and $\Delta S^{\ddagger}$ would thus tend to be negative. In a unimolecular type of reaction, on the other hand, the structure in the transition state would be less ordered than in the ground state, and $\Delta S^{\ddagger}$ would be positive. Positive entropies of activation were obtained for all compounds investigated here. A unimolecular (A-1) type of mechanism is thus strongly indicated. Overend and co-workers (6) have previously reached a similar conclusion, basing their arguments both on their own data and on those reported by Heidt and Purves (11, 22). Recently, Withey and Whalley (23) have studied the effect of pressure on the rate of acid hydrolysis of methyl α-D-glucopyranoside. The value for the volume of activation thus obtained shows clearly that the reaction must be unimolecular.

Overend and his co-workers also observed that, with exception of the smallest aglycones, the rate differences between anomeric pairs of glycosides are caused by differences in the entropy rather than in the energy of activation, suggesting that the α-anomers are more highly oriented in the ground state than the β-anomers. Thus, the higher reactivity of the α- as compared to the β-glycosides is due to the greater change in entropy associated with the hydrolysis of the former compounds. An alternative explanation was previously offered by Edward (1), who pointed out that with large-size aglycones, such as a phenyl group, an α- (axial) aglycone would be less stable than the β-(equatorial) aglycone because of steric strain. In the present study, both the energies and entropies of activation are larger for the α- than for the β-anomer in the case of the methyl gluco- and galactopyranosides. The higher rate of hydrolysis of the β-anomer is accordingly in this case associated with its lower energy of activation, the entropy change having an opposite effect. The kinetic parameters observed for the two xylopyranosides are very close to those reported by Overend *et al.* (6). The energies of activation of the two anomers are the same, while $\Delta S^{\ddagger}$ is larger for the more labile β-compound.

Data for eight disaccharides are presented in Table V. For maltose, cellobiose, and gentiobiose the energies of activation are close to those previously reported by Moelwyn-Hughes (10). It is interesting to note that $\Delta S^{\ddagger}$ is larger for maltose (α-anomer) than for cellobiose (β-anomer) in accordance with the results of Overend and co-workers (6).

TABLE V

Rate coefficients and kinetic parameters for the hydrolysis of eight disaccharides (0.05 *M*) in 0.5 *M* sulphuric acid

Compound	$k \times 10^{-6}$ sec^{-1}			E	$\Delta S^{\ddagger}$
	60° C	70° C	80° C		
4-*O*-α-D-Glucopyranosyl-D-glucose (maltose)	5.56	23.6	91.0	32.7	+14.0
4-*O*-β-D-Glucopyranosyl-D-glucose (cellobiose)	2.72	9.63	39.5	31.5	+9.0
6-*O*-β-D-Glucopyranosyl-D-glucose (gentiobiose)	1.29	5.22	21.5	32.9	+11.7
4-*O*-β-D-Glucopyranosyl-D-mannose (glucosyl mannose)		9.40	35.3	32.0	+10.2
4-*O*-β-D-Mannopyranosyl-D-mannose (mannobiose)	4.06	16.8	67.5	32.7	+13.4
4-*O*-β-D-Galactopyranosyl-D-glucose (lactose)	5.45	22.5	78.3	33.0	+14.9
6-*O*-β-D-Galactopyranosyl-D-glucose (melibiose)	4.95	21.2	88.3	33.8	+17.1
4-*O*-β-D-Xylopyranosyl-D-xylose (xylobiose)	19.0	69.8	274	32.7	+16.5

Can. J. Chem. Downloaded from www.nrcresearchpress.com by 210.87.254.6 on 09/05/12
For personal use only.

4-*O*-β-D-Glucopyranosyl-D-mannose is hydrolyzed at the same rate as cellobiose, while mannobiose is almost twice as reactive. Xylobiose is hydrolyzed about three times faster than methyl β-D-glucopyranoside and seven times faster than cellobiose. A β-(1 → 4)-linked xylan has been reported to be hydrolyzed by acid four times faster than cellulose under homogeneous conditions (24).

Effect of the Nature of the Aglycone

The influence of the aglycone on the acid hydrolysis of glycosides has attracted little attention. Nath and Rydon (25) found that acid hydrolysis was facilitated by the presence of electron-repelling and impeded by electron-attracting substituents in the phenyl group of various phenyl β-D-glucopyranosides. The same observation has later been made with phenyl- and *p*-chlorophenyl β-D-gluco-, galacto-, and xylo-pyranosides (26).

The effect of the *size* of the aglycone was studied with nine β-D-glucopyranosides listed in Table VI. It is clear from the data that steric hindrance was of no importance, not even

TABLE VI

Rate coefficients and kinetic parameters for the hydrolysis of nine β-D-glucopyranosides (0.05 *M*) in 0.5 *M* sulphuric acid

	$k \times 10^{-6}$ sec^{-1}				
Compound	60° C	70° C	80° C	E	$\Delta S^{\ddagger}$
Ethyl	1.54	6.72	28.0	33.8	+14.8
Propyl	1.82	7.94	31.2	32.9	+15.1
Isopropyl	2.65	11.3	44.5	33.2	+14.0
n-Butyl	1.62	6.98	27.9	33.6	+14.3
Isobutyl	1.90	8.21	34.4	33.8	+15.2
Neopentyl	2.41	10.6	39.9	36.2	+22.9
Cyclohexyl	3.25	13.9	56.4	33.5	+15.3
Benzyl	1.56	6.75	28.3	33.6	+14.2
Allyl	1.83	8.02	32.8	33.8	+15.1

in the case of the neopentyl β-D-glucopyranoside. [The steric substituent constant, E_s, of the neopentyl group is as high as −1.74 (27).] The absence of steric hindrance is, of course, not unexpected, considering the unimolecular nature of the reaction mechanism. There is a slight and somewhat irregular increase in the rate coefficients with increasing size of the aglycone. This effect is undoubtedly due to the steric strain imposed on the molecule by the bulky aglycones. The higher rate of hydrolysis of isopropyl as compared to propyl β-D-glucopyranoside has been previously reported (28). The values for energy and entropy of activation are remarkedly constant, with exception of the neopentyl glucoside where both are larger than the average.

Three of the compounds investigated were hydrolyzed much more rapidly than the remainder namely *tert*-butyl β-D-glucopyranoside, triethylmethyl β-D-glucopyranoside, and sucrose. Measurements were carried out in both 0.5 *M* and 0.01 *N* sulphuric acid with the first glycoside, while the other two compounds could be studied only in the weaker acid. Experimental and extrapolated rate constants and kinetic parameters are given in Table VII. Sucrose is hydrolyzed by acids 4200 times faster than methyl β-D-glucopyranoside. The data of Heidt and Purves (29) indicate a factor of 3800. The low energy of activation is in agreement with previous results (10, 14). The value for $\Delta S^{\ddagger}$, +2.3 kcal deg^{-1} mole^{-1}, is not unexpected for this fructofuranoside considering that $\Delta S^{\ddagger}$ for ethyl β-D-galactofuranoside is −7.1 cal deg^{-1} mole^{-1} at the same temperature (6). Overend, Rees, and

Can. J. Chem. Downloaded from www.nrcresearchpress.com by 210.87.254.6 on 09/05/12
For personal use only.

Can. J. Chem. Downloaded from www.nrcresearchpress.com by 210.87.254.6 on 09/05/12
For personal use only.

TABLE VII

Rate coefficients and kinetic parameters for the hydrolysis of *t*-butyl and triethylmethyl β-D-glucopyranosides and sucrose (0.05 *M*) in 0.5 *M* and 0.01 *N* sulphuric acid

	30° C		40° C		50° C		60° C		70° C		80° C			
Compound	*k*	*D*	*k*	*D*	*k*	*D*	*k*	*D*	*k*	*D*	*k*	*D*	*E*	$\Delta S^{\ddagger}$
0.5 *M* H_2SO_4														
tert-Butyl	8.44	1.1	42.2	1.1	190	0.8	767*		2916*		10,360*		30.4	+16.9
0.01 *N* H_2SO_4														
tert-Butyl							7.56	1.6	27.7	1.6	94.4	1.0	29.3	+13.0
Triethylmethyl	8.37	1.6	34.9	1.9	125	5.0	422*		1343*		3900*		26.0	+11.0
Sucrose			5.43	2.7	19.6	2.8	58.3	2.9	192*		537*		24.4	+ 2.3

*Value obtained by extrapolation.

Sequeira (6) have suggested that furanosides might be hydrolyzed by an A-2 mechanism, low or negative $\Delta S^{\ddagger}$ values being expected in this case.

Vernon and co-workers (4) have recently shown that the hydrolysis of *tert*-butyl β-D-glucopyranoside involves alkyl–oxygen cleavage, as it does in the acid hydrolysis of esters of tertiary alcohols. The reason is, in both cases, the great stability of this type of alkyl carbonium ion, which is far greater than that of the glycosyl carbonium ion. It is likely that all glycosides of tertiary alcohols hydrolyze by this mechanism. The rate of hydrolysis of the *tert*-butyl glucoside was 550 times higher than that of methyl β-D-glucopyranoside. The triethylmethyl β-D-glucopyranoside was hydrolyzed no less than 30,600 times faster than methyl β-D-glucoside, a truly astonishing rate which actually caused difficulties in the synthesis of this compound. The triethylmethyl carbonium ion is probably more stable than the *tert*-butyl carbonium ion. Part of the difference in stability might, however, reside in the greater release of steric strain on hydrolysis of the triethylmethyl glucoside.

The effect of polar groups in the aglycone was studied with six β-D-glucopyranosides. The kinetic data are given in Table VIII (30). The carboxymethyl β-D-glucopyranoside

TABLE VIII

Rate coefficients and kinetic parameters for the hydrolysis of β-D-glucopyranosides with polar aglucones (0.05 *M*) in 0.5 *M* sulphuric acid

	$k \times 10^{-6}$ sec^{-1}				
Compound	60° C	70° C	80° C	E	$\Delta S^{\ddagger}$
Carboxymethyl	4.11	16.2	61.0	31.4	+9.5
2-Carboxyethyl	1.58	6.40	26.9	33.1	+12.7
2-Hydroxyethyl	1.73	7.56	30.2	33.6	+14.4
2-Methoxyethyl	1.83	8.10	33.2	33.9	+15.4
2-Chloroethyl	2.21	9.67	37.5	32.7	+12.2
3-Hydroxypropyl	1.24	5.45	23.4	34.4	+16.1

was hydrolyzed three times faster than methyl β-D-glucopyranoside, a relatively small increase. The rate coefficients of the other five glucosides show that introduction into the aglycone of an electron-attractive group separated by two or more carbon atoms from the glycosidic oxygen has little or no effect on the rate of hydrolysis of the glycoside. These results are exactly those to be expected in a reaction of the present type. An electron-attracting substituent in the aglycone will decrease the electron density around the glycosidic oxygen, thus lowering the equilibrium concentration of the conjugate acid (II). The transfer of the electron pair to the oxygen in the heterolysis step (II → III), on the other hand, will be facilitated. The two opposing effects will tend to cancel out, and thus the overall rate should be almost unaffected by any polar group in the aglycone. This is a situation very similar to that found in the acid hydrolysis of esters by the A-2 mechanism. Contrary to Richards (31), Capon, Overend, and Sobell (32) have concluded that the rate of hydrolysis of the benzylidene group is approximately the same in methyl 4,6-*O*-benzylidene-α-D-glucopyranoside and in methyl 4,6-*O*-benzylidene-3-deoxy-α-D-glucopyranoside. This seemingly surprising fact is, as pointed out by the investigators, the result of the same two effects, one hindering and the other promoting the removal of the benzylidene group.

In a very strongly acidic solution the conversion of the glycoside to its conjugate acid should be more complete than in a more dilute solution, and an electron-attracting group

Can. J. Chem. Downloaded from www.nrcresearchpress.com by 210.87.254.6 on 09/05/12
For personal use only.

in the aglycone might accordingly increase the rate of hydrolysis of a glycoside under these conditions. The rate coefficients for the hydrolysis of 2-methoxyethyl and methyl β-D-glucopyranosides were 1.83 and 1.38×10^{-6} sec^{-1} at 60° C in 0.5 *M* sulphuric acid and 42.2 and 34.2×10^{-6} sec^{-1} in 5 *M* sulphuric acid, corresponding to a ratio of the rate constants of 1.33 and 1.23, respectively. There was accordingly no increase in the relative rate with increasing acid concentration. It is not known whether the glycosides were still only slightly protonated in the stronger acid, or whether the substituents did not affect the rate.

Hall, Hollingshead, and Rydon (33) have recently reported that the presence of polar groups in the aglycone has no effect on the rate of acid hydrolysis of phenyl α-D-glucopyranosides. As an explanation they suggest that the conjugate acid is protonated on the ring oxygen (34). Its decomposition would then involve the *trans*-elimination of two axial groups and would thus be sterically controlled. Substitution in the aglycone should under these circumstances be of little significance. This, they consider, is a more satisfactory explanation than a coincidentally exact cancellation of two opposing effects. This mechanism cannot be invoked for the equatorially substituted aryl β-D-glucopyranosides (25) or for the present alkyl β-D-glucopyranosides, yet, the influence of the aglycone on the rate of hydrolysis is in both series relatively minor. It should also be noted that the effects are opposite in these two cases. Thus, for example, *p*-chloro and *p*-methoxy substituents in the phenyl group slightly decrease the rate of hydrolysis of the phenyl β-D-glucopyranosides, while the same groups cause a small increase for the alkyl β-D-glucopyranosides. The operation of the same reaction mechanism in all three cases is therefore more likely, the net effect of the polar substituents being a matter of chance and always small.

The present results are of special interest in connection with a recent proposal by Marchessault and Råånby (35–37) concerning the influence of polar groups in general, and carboxyl groups in particular, on the acid hydrolysis of cellulose and other polysaccharides.

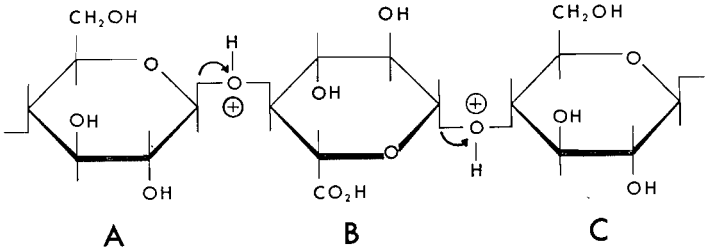

According to these investigators, the linkage (A → B) will be activated by the inductive effect of the carboxyl group, while the linkage (B → C) will be stabilized by the same effect which here will work in the opposite direction.

It is evident from the previous discussions that the concept of the "activating inductive effect" entails an oversimplification of the reaction mechanism involved, only the heterolysis step in the hydrolysis having been considered. The equilibrium concentration of the conjugate acid is certainly not a factor which can be ignored. In the present series, the 2-carboxyethyl β-D-glucopyranoside is an especially good model for unit A → B since both carry a carboxyl group in the aglycone portion, separated by two carbon atoms from the glycosidic oxygen. The 2-chloroethyl β-D-glucopyranoside can also be used as the HO_2CCH_2— and the $ClCH_2$— groups have the same polar substituent constant ($\sigma^* = +1.05$ (27)). The carboxy compound was actually hydrolyzed at the same rate as ethyl β-D-glucopyranoside and the chloroglucoside only slightly faster.

Can. J. Chem. Downloaded from www.nrcresearchpress.com by 210.87.254.6 on 09/05/12
For personal use only.

Summarizing, there is no reason to believe that cellulose or any other polysaccharide should contain "weak links" because of the presence of carboxyl or any other electronegative group at C-5. Similarly, it is to be expected that pseudoaldobiouronic acids should be hydrolyzed at the same rate as the corresponding neutral oligosaccharides. Several acids of this type are presently being synthesized with a view of providing direct experimental evidence on this point (38).

EXPERIMENTAL

All melting points are corrected. Evaporations were carried out *in vacuo* at 50° C. Chromatographic separations were with ethyl acetate – acetic acid – water (9:2:2). The spray reagent was silver nitrate in acetone followed by ethanolic sodium hydroxide.

MATERIALS

Glycopyranosides

Methyl α-D-glucopyranoside, methyl α-D-xylopyranoside, and methyl β-D-xylopyranoside were commercial preparations, recrystallized once from methanol, 2-butanone, and ethanol, respectively. Methyl α- and β-D-galactopyranosides were obtained as a mixture after treatment of D-galactose with methanolic hydrogen chloride as described by Dale and Hudson (39). The anomers were separated by repeated crystallization from ethanol and ethanol – ethyl acetate. Methyl α-D-mannopyranoside was obtained in a yield of 97% by boiling D-mannose under reflux with *N* methanolic hydrogen chloride for 10 hours (40). All other β-D-glucopyranosides were synthesized by condensing acetobromoglucose in the presence of silver carbonate with the respective alcohol according to the method of Königs and Knorr (41), followed by de-*O*-acetylation with methanol in the presence of sodium methoxide according to Zemplén (42). Use of mercuric cyanide (43, 44) rather than silver carbonate always gave lower yields of the β-glucosides. Whenever possible, the condensation was carried out with the alcohol itself as the solvent. The following is a typical example.

Synthesis of Neopentyl β-D-glucopyranoside (45)

Neopentyl alcohol (35 g) was dissolved in anhydrous benzene (250 ml) and shaken in the dark at room temperature for 2 hours with silver carbonate (30 g) and Drierite (30 g). 1-Deoxy-1-bromo-2,3,4,6-tetra-*O*-acetyl-α-D-glucopyranose (acetobromoglucose, m.p. 88–90° C, 20 g) was added, together with a little iodine, and shaking was continued for another 15 hours. After filtration through Celite and washing of the solid residue with benzene, the combined filtrate and washings were evaporated to a colorless sirup. When the latter was dissolved in hot ethanol, crystals formed immediately. After one recrystallization, the neopentyl 2,3,4,6-tetra-*O*-acetyl-β-D-glucopyranoside (10.0 g, 49%) had m.p. 134.5–135.5° C and $[\alpha]_D$ −16.7° (*c*, 2.0 in chloroform). Anal. Calc. for $C_{19}H_{30}O_{10}$: C, 54.4; H, 7.22. Found: C, 54.5; H, 7.71%.

The tetraacetate was dissolved in 0.1 *N* methanolic sodium methoxide (200 ml) and the solution was allowed to stand at room temperature for 15 hours. After addition of some water, treatment with Amberlite IR-120 and IR-45 exchange resins and with Darco G-60 charcoal, filtration, and evaporation, the colorless sirup was dissolved in acetone (15 ml). On addition of benzene (10 ml) crystallization began slowly. The solid, crystalline mass finally formed was washed with acetone–benzene (1:1) and dried *in vacuo*. Yield: 5.0 g, 41%. The neopentyl β-D-glucopyranoside had m.p. 138–139° C and $[\alpha]_D$ −35.3° (*c*, 2.0 in water). Anal. Calc. for $C_{11}H_{22}O_6$: C, 52.8; H, 8.84. Found: C, 52.8; H, 8.80%.

The tetraacetate derivatives of the β-D-glucopyranosides with substituted aglucones were all crystalline, but only two of the glycosides were obtained in a crystalline state. The carboxyethyl β-D-glucopyranoside was prepared in the usual way from acetobromoglucose and methyl hydracrylate. The five sirupy glycosides were purified by preparative paper chromatography on Whatman No. 3 MM filter paper. The carboxymethyl and carboxyethyl compounds gave infrared spectra with the typical carbonyl absorption at 1735 cm^{-1}. Melting points and specific rotations of the glycosides and their tetraacetates (whenever synthesized) are summarized in Tables IX and X.

TABLE IX

Physical data for methyl D-glycopyranosides

Compound	M. p., °C	$[\alpha]_D$*, degrees	Reference
Methyl α-D-glucopyranoside	166–167	+159	51
Methyl β-D-glucopyranoside	112–113	−32.2	41
Methyl α-D-galactopyranoside H_2O	108–110	+175	39, 52
Methyl β-D-galactopyranoside	176–177	±0	39, 53
Methyl α-D-mannopyranoside	193–194	+79.2	54, 55
Methyl α-D-xylopyranoside	90–92	+154	53, 56
Methyl β-D-xylopyranoside	156–157	−66	53, 56

*In water (*c*, 2.0).

Can. J. Chem. Downloaded from www.nrcresearchpress.com by 210.87.254.6 on 09/05/12
For personal use only.

Can. J. Chem. Downloaded from www.nrcresearchpress.com by 210.87.254.6 on 09/05/12
For personal use only.

TABLE X

Physical data for β-D-glucopyranosides

Compound	Tetraacetate			Glucoside		
	M. p., °C	$[\alpha]_D$* degrees	Ref.	M. p., °C	$[\alpha]_D$†, degrees	Ref.
Ethyl	101–103	−20.4	41, 44, 57	93–94.5	−37.3	57, 58
Propyl	96–97	−17.3	44, 57	101–103	−37.9	52, 57, 58
Isopropyl	134–136	−19.3	44, 57, 59	129–130.5	−35.8	57, 60
n-Butyl	61–62	−20.6	44, 61	64–65	−34.1	58, 61
Isobutyl	118–120	−18.2	44, 61	108–110	−39.8	58
Neopentyl	134.5–135.5	−16.7		138–139	−35.3	45
Cyclohexyl	119–120	−22.8	44, 62	133–135	−39.8	62
Benzyl	94–95	−50.0	44, 62	119.5–120.5	−51.4	62
Allyl	85–87	−18.1	44, 63	98–99	−41.9	58, 63, 64
tert-Butyl	143–144.5	−10.6	44, 61	165–166	−19.4	61
Triethylmethyl	92.5–94	− 8.0	61	109–110.5	−13.7	61
Carboxymethyl	77–78‡	−30	62		−35.6	62
				166–167§	−43.2	62
2-Carboxyethyl	89–91‡	−10			−29	
2-Hydroxyethyl	99–100	− 5.7	44, 65, 66		−29.5	65, 66
2-Methoxyethyl	73–76	−14.2	67	118–119	−28.1	67
2-Chloroethyl	116–117	−11.1	44, 68		−28.4	68, 69
3-Hydroxypropyl	94–95	−17	66, 67		−36.1	66, 67

*In chloroform (*c*, 2.0).
†In water (*c*, 2.0).
‡Methyl ester.
§Amide.

Disaccharides

Maltose, cellobiose, lactose, melibiose, and sucrose were commercially available specimens. They were all recrystallized at least twice. Gentiobiose was synthesized according to Reynolds and Evans (46). Glucosyl mannose and mannobiose were obtained by partial acid hydrolysis of a wood glucomannan (47). Xylobiose was formed on enzymatic hydrolysis of a 4-*O*-methylglucuronoxylan (48). Accepted and found values for the melting points and specific rotations of the disaccharides are given in Table XI.

TABLE XI

Physical data for disaccharides

Compound	Melting point, °C		Specific rotation, $[\alpha]_D$*, degrees	
	Reported	Found	Reported	Found
Maltose		120–121	+130.4	+134.9
Cellobiose	225–231	242.5–243	+34.6	+34.1
Gentiobiose	190–195	190–192	+10.5	+9.0
Glucosyl mannose.H_2O	133 to 139	136–137	+5 to +16	+14.3
Mannobiose	193 to 210	208–210	−5 to −9	−8.6
Lactose.H_2O	201–202	203–203.5	+52.6	+52.2
Melibiose.H_2O	184–185	185–186	+142	+139.1
Xylobiose	185–186	185–186	−25.5	−25.6
Sucrose	160 to 186	182–183	+66.5	+66.0

*In water (*c*, 2.0).

Kinetic Measurements

Hydrolyses were carried out in a Townson and Mercer thermostat bath, accurate within ±0.01° C. When open flasks fitted with a reflux condensor were used, the data were exceedingly erratic, probably because of the varying amounts of water that condensed on the side of the flask and in the lower portion of the condensor. Good results were obtained throughout with ampoules, made from Pyrex glass tubing, 9 mm wide and approximately 12 cm long, which were sealed at both ends and completely immersed in the bath.

Polarimetric measurements were made at 405 mμ with a Zeiss precision photoelectric polarimeter, accurate within ±0.005°. The sample to be measured was quickly cooled to 25° C, the ampoule was opened, the sugar solution was transferred to the polarimeter tube, and the rotation was determined. These operations normally required only 2 to 3 minutes. On one occasion, hydrolysis was carried out directly in a jacketed polarimeter tube at 60° C. This technique gave more consistent values, required less material, and involved less manipulations. Unfortunately, however, the design of the polarimeter did not allow the use of temperatures higher than 60° C. Initial rotations were determined immediately after the glycoside solution had been prepared. In most cases the optical rotation to be expected at infinite time was checked by actual measurements. The few discrepancies observed were never large enough to affect the values of the rate constants significantly. As a check, the Shaffer–Hartmann–Somogyi (49, 50) alkaline copper reagent was used in three experiments to follow the hydrolysis. The results are presented in Table XII.

TABLE XII

Comparison between polarimetric and titrimetric determination of rate coefficients

Compound		$k \times 10^{-6}$ sec^{-1}	
		Polarimetric	Titrimetric
Methyl α-D-glucopyranoside	90	50.3	48.0
Carboxymethyl β-D-glucopyranoside	70	16.2	20.1
2-Carboxyethyl β-D-glucopyranoside	70	6.61	6.30

The same stock solution of 0.500 *M* (1.00 *N*) aqueous sulphuric acid was used throughout. Because of their rapid rate of hydrolysis, sucrose, and *t*-butyl- and triethylmethyl-β-D-glucopyranoside were studied in 0.01 *N* sulphuric acid solution. All measurements were carried out with 0.05 *M* solutions of the compounds. The following kinetic data (in min^{-1} and $_{10}$log) were typical.

Deviations from the mean were determined throughout and were usually in the range of 0.5 to 2.0%, with no value exceeding 5%. Data obtained on hydrolysis of methyl α-D-glucopyranoside in hydrochloric, perchloric, sulphuric, and phosphoric acid at 50° C are summarized in Table XIII.

Can. J. Chem. Downloaded from www.nrcresearchpress.com by 210.87.254.6 on 09/05/12
For personal use only.

Methyl α-D-glucopyranoside (0.05 *M*) in 0.5 *M* sulphuric acid at 100° C

Time, min	0	30	45	60	75	90	105
α, degrees	+3.555	2.810	2.540	2.295	2.080	1.920	1.785
$k\times10^4$, min^{-1}	—	52.4	51.5	52.1	53.2	52.9	52.8
Time	120	135	150	165	180	195	210
α	1.685	1.575	1.490	1.430	1.370	1.340	1.295
$k\times10^4$	51.9	52.6	53.3	52.8	53.3	51.8	52.4
Time	225	240	255	270	300	315	∞
α	1.260	1.235	1.215	1.195	1.170	1.150	1.100
$k\times10^4$	52.7	52.5	52.1	52.3	51.5	53.7	—

Mean value of k: 52.5×10^{-4} min^{-1}, 202.0×10^{-6} sec^{-1}
Mean deviation: 0.7%

Triethylmethyl β-D-glucopyranoside (0.05 *M*) in 0.01 *N* sulphuric acid at 30° C

Time	0	270	330	1320	1448	1560	1680
α	−0.425	−0.235	−0.200	+0.320	+0.350	+0.405	+0.455
$k\times10^4$	—	2.14	2.10	2.21	2.13	2.19	2.22
Time	1770	2760	2820	3000	3120	∞	
α	+0.475	+0.730	+0.740	+0.765	+0.775	+1.100	
$k\times10^4$	2.19	2.23	2.22	2.19	2.15	—	

Mean value of k: 2.18×10^{-4} min^{-1}, 8.37×10^{-6} sec^{-1}
Mean deviation: 1.6%

2-Chloroethyl β-D-glucopyranoside (0.05 *M*) in 0.05 *M* sulphuric acid at 70° C

Time	0	255	315	360	420	1380	1448	1502
α	−0.805	−0.545	−0.485	−0.445	−0.405	+0.240	+0.270	+0.300
$k\times10^4$	—	2.50	2.54	2.53	2.44	2.50	2.49	2.51
Time	1575	1695	1740	1800	1860	∞		
α	+0.330	+0.385	+0.415	+0.440	+0.480	+1.100		
$k\times10^4$	2.50	2.51	2.55	2.56	2.62	—		

Mean value of k: 2.52×10^{-4} min^{-1}, 9.67×10^{-6} sec^{-1}
Mean deviation: 1.3%

Melibiose (0.05 *M*) in 0.5 *M* sulphuric acid at 60° C

Time	0	1245	1365	1545	2685	2805	2985
α	+5.750	4.825	4.740	4.650	4.120	4.090	4.010
$k\times10^4$	—	1.29	1.33	1.29	1.27	1.25	1.27
Time	4125	4245	4425	8445	10,005	∞	
α	3.650	3.600	3.565	2.995	2.900	2.760	
$k\times10^4$	1.28	1.29	1.29	1.31	1.33	—	

Mean value of k: 1.29×10^{-4} min^{-1}, 4.95×10^{-6} sec^{-1}
Mean deviation: 1.3%

Calculation of Energies and Entropies of Activation

Energies of activation were obtained from a minimum of three rate constants, usually determined at 60, 70, and 80° C. When log k was plotted against $1/T$, straight lines were obtained throughout.

Entropies of activation were calculated for 60° C from the relationship

$$T\Delta S^{\ddagger} = E - RT - RT \ln (kT/h) + RT \ln (k'/h_0),$$

where R = 1.9871 cal deg^{-1} $mole^{-1}$,
T = 333.16 °K,
k = 1.3805×10^{-16} erg deg^{-1} $molecule^{-1}$,
h = 6.6252×10^{-27} erg sec,
k' = first order rate coefficient, sec^{-1},
h_0 = +0.741 for 0.5 *M* sulphuric acid.

Can. J. Chem. Downloaded from www.nrcresearchpress.com by 210.87.254.6 on 09/05/12
For personal use only.

Can. J. Chem. Downloaded from www.nrcresearchpress.com by 210.87.254.6 on 09/05/12
For personal use only.

TABLE XIII

Rate coefficients for the hydrolysis of methyl α-D-glucopyranoside (0.05 *M*) in various mineral acids

Hydrochloric acid			Perchloric acid		Sulphuric acid		Phosphoric acid		
Molarity	H_0*	$k\times10^{-6}$	H_0	$k\times10^{-6}$	H_0	$k\times10^{-6}$	Molarity	H_0	$k\times10^{-6}$
0.5	+0.20	0.130	+0.16	0.115	+0.13	0.138	2.0	+0.24	0.058
1.0	−0.20	0.353	−0.22	0.280	−0.26	0.300	3.0	−0.08	0.080
1.5	−0.47	0.664	−0.53	0.487	−0.56	0.578	4.0	−0.37	0.150
2.0	−0.69	1.15	−0.78	0.863	−0.84	0.917	5.0	−0.69	0.230
3.0	−1.05	2.82	−1.23	2.37	−1.38	2.11	6.0	−1.04	0.334
4.0	−1.40	6.87	−1.72	5.99	−1.85	4.80	7.0	−1.45	0.514
5.0	−1.76	15.0	−2.23	16.0	−2.28	10.3	8.0	−1.85	0.779
							9.0	−2.22	1.25

*Reference 18.

ACKNOWLEDGMENTS

The author wishes to express his gratitude to Mr. Willem Steyn and Mr. Fred Spencer for technical assistance. This investigation was supported by a United States Public Health Service Research Grant A-4258 (AM 07193 MCHA) from the National Institute of Arthritis and Metabolic Diseases, Public Health Service.

REFERENCES

1. J. T. EDWARD. Chem. Ind. London, 1102 (1955).
2. C. A. BUNTON, T. A. LEWIS, D. R. LLEWELLYN, and C. A. VERNON. J. Chem. Soc. 4419 (1955).
3. A. J. RHIND-TUTT and C. A. VERNON. J. Chem. Soc. 4637 (1960).
4. C. ARMOUR, C. A. BUNTON, S. PATAI, L. H. SELMAN, and C. A. VERNON. J. Chem. Soc. 412 (1961).
5. B. E. C. BANKS, Y. MEINWALD, I. SHEFT, and C. A. VERNON. J. Chem. Soc. 3240 (1961).
6. W. G. OVEREND, C. W. REES, and J. S. SEQUEIRA. J. Chem. Soc. 3429 (1962).
7. C. BAMFORD, B. CAPON, and W. G. OVEREND. J. Chem. Soc. 5138 (1962).
8. E. A. MOELWYN-HUGHES. Trans. Faraday Soc. **24**, 321 (1928).
9. S. PEAT, W. J. WHELAN, T. E. EDWARDS, and O. OWEN. J. Chem. Soc. 586 (1958).
10. E. A. MOELWYN-HUGHES. Trans. Faraday Soc. **24**, 309 (1928); **25**, 81, 503 (1929).
11. S. VEIBEL and E. FREDERIKSEN. Kgl. Danske Videnskab. Selskab, Mat. Fys. Medd. **17**, No. 6 (1940).
12. L. J. HEIDT and C. B. PURVES. J. Am. Chem. Soc. **66**, 1385 (1944).
13. D. B. EASTY. J. Org. Chem. **27**, 2701 (1962).
14. J. NAKANO and B. G. RÅNBY. Svensk Papperstid. **65**, 29 (1962).
15. L. ZUCKER and L. P. HAMMETT. J. Am. Chem. Soc. **82**, 499 (1960).
16. L. P. HAMMETT. Physical organic chemistry. McGraw-Hill Book Co., Inc., New York, N.Y. 1950. pp. 273–277.
17. L. P. HAMMETT. Chem. Rev. **16**, 67 (1935).
18. F. A. LONG and M. A. PAUL. Chem. Rev. **57**, 1, 935 (1957).
19. D. MCINTYRE and F. A. LONG. J. Am. Chem. Soc. **76**, 3240 (1954).
20. J. F. BUNNETT. J. Am. Chem. Soc. **83**, 4916, 4968, 4973, 4978 (1961).
21. C. N. RIIBER and N. A. SØORENSEN. Kgl. Norske Videnskab. Selskabs Skrifter, No. 1 (1938).
22. B. CAPON and W. G. OVEREND. Advan. Carbohydrate Chem. **15**, 11 (1960).
23. R. J. WITHEY and E. WHALLEY. Can. J. Chem. **41**, 1849 (1963).
24. A. A. KONKIN, N. I. KAPLAN, and Z. A. ROGOVIN. Zh. Prikl. Khim. **28**, 693 (1955).
25. R. L. NATH and H. N. RYDON. Biochem. J. **57**, 1 (1954).
26. B. N. STEPANENKO and O. G. SERDYUK. Dokl. Akad. Nauk SSSR, **139**, 1132 (1961); Chem. Abstr. **56**, 1516 (1962).
27. R. W. TAFT, JR. *In* Steric effects in organic chemistry. *Edited by* M. S. Newman. John Wiley and Sons, Inc., New York, N. Y. 1956. pp. 556–675.
28. A. A. KONKIN, V. K. BUYANOVA, L. M. VINOGRADOVA, and Z. A. ROGOVIN. Soobshch. Nauch. Rabot. Chlenov Vsesoyuz. Khim. Obshch. im. Mendeleeva, No. **3**, 1–5 (1953); Chem. Abstr. **53**, 8002 (1959).
29. L. J. HEIDT and C. B. PURVES. J. Am. Chem. Soc. **60**, 1206 (1938).
30. T. E. TIMELL. Chem. Ind. London, 1208 (1963).
31. G. N. RICHARDS. Chem. Ind. London, 228 (1955).
32. B. CAPON, W. G. OVEREND, and M. SOBELL. Tetrahedron, **16**, 106 (1961).
33. A. N. HALL, S. HOLLINGSHEAD, and H. N. RYDON. J. Chem. Soc. 4290 (1961).
34. F. SHAFIZADEH. Advan. Carbohydrate Chem. **13**, 9 (1958).
35. R. H. MARCHESSAULT and B. G. RÅNBY. Svensk Papperstid. **62**, 230 (1959).
36. B. G. RÅNBY and R. H. MARCHESSAULT. J. Polymer Sci. **36**, 561 (1959).
37. B. G. RÅNBY. J. Polymer Sci. **53**, 131 (1961).
38. E. J. SOLTES and T. E. TIMELL. Unpublished results.
39. J. K. DALE and C. S. HUDSON. J. Am. Chem. Soc. **52**, 2534 (1930).
40. E. FISCHER. Ber. **26**, 2400 (1893); **28**, 1145 (1895).
41. W. KÖNIGS and E. KNORR. Ber. **34**, 957 (1901).
42. G. ZEMPLÉN and A. KUNZ. Ber. **56**, 1705 (1923).
43. G. ZEMPLÉN and A. GERECS. Ber. **63**, 2720 (1930).
44. B. LINDBERG. Acta Chem. Scand. **3**, 151 (1949).
45. S. VEIBEL and E. HJORTH. Acta Chem. Scand. **6**, 1353 (1952).
46. D. D. REYNOLDS and W. L. EVANS. J. Am. Chem. Soc. **60**, 2559 (1938).
47. A. JABBAR MIAN and T. E. TIMELL. Svensk Papperstid. **63**, 884 (1960).
48. T. E. TIMELL. Svensk Papperstid. **65**, 435 (1962).
49. P. A. SHAFFER and A. F. HARTMANN. J. Biol. Chem. **45**, 377 (1921).
50. P. A. SHAFFER and M. SOMOGYI. J. Biol. Chem. **100**, 695 (1933).
51. T. S. PATTERSON and T. ROBERTSON. J. Chem. Soc. 300 (1929).
52. E. FISCHER and L. BEENSCH. Ber. **27**, 2480 (1894).
53. E. FISCHER. Ber. **28**, 1145 (1895).
54. E. FISCHER. Ber. **28**, 1429 (1895).
55. J. E. CADOTTE, F. SMITH, and D. SPRIESTERSBACH. J. Am. Chem. Soc. **74**, 1501 (1952).
56. C. S. HUDSON. J. Am. Chem. Soc. **47**, 265 (1925).
57. S. VEIBEL and F. ERIKSEN. Bull. Soc. Chim. France, 5e Sér. **3**, 277 (1936).

Can. J. Chem. Downloaded from www.nrcresearchpress.com by 210.87.254.6 on 09/05/12
For personal use only.

58. E. BOURQUELOT and M. BRIDEL. Compt. Rend. **154**, 1375, 1737 (1912).
59. W. T. HICKINBOTTOM. J. Chem. Soc. 3140 (1928).
60. E. BOURQUELOT and M. BRIDEL. Compt. Rend. **155**, 854 (1912).
61. S. VEIBEL and H. LILLELUND. Bull. Soc. Chim. France, 5e Sér. **5**, 494 (1938).
62. E. FISCHER and B. HELFERICH. Ann. **383**, 68 (1911).
63. E. FISCHER and H. STRAUSS. Ber. **45**, 2474 (1912).
64. E. BOURQUELOT, H. HERISSEY, and M. BRIDEL. Compt. Rend. **156**, 1493 (1913).
65. E. FISCHER and H. FISCHER. Ber. **43**, 2528 (1910).
66. S. KARJALA and K. P. LINK. J. Am. Chem. Soc. **62**, 917 (1940).
67. B. HELFERICH and R. HILTMANN. Ann. **531**, 160 (1937).
68. J. COMPTON. Contrib. Boyce Thompson Inst. **11**, 21 (1940).
69. L. P. MILLER. Contrib. Boyce Thompson Inst. **9**, 425 (1938); **10**, 139 (1939).

Can. J. Chem. Downloaded from www.nrcresearchpress.com by 210.87.254.6 on 09/05/12
For personal use only.

Can. J. Chem. Downloaded from www.nrcresearchpress.com by 210.87.254.6 on 09/05/12
For personal use only.

SYNTHESIS OF ALKYL 2-DEOXY-α-D-GLYCOPYRANOSIDES AND THEIR 2-DEUTERIO DERIVATIVES[1]

R. U. LEMIEUX[2] AND S. LEVINE[3]
Department of Chemistry, University of Ottawa, Ottawa, Ontario
Received December 17, 1963

ABSTRACT

The methyl, cyclohexyl, and *t*-butyl 2-deoxy-2-iodo-α-D-manno- and β-D-glucopyranoside triacetates were formed in near quantitative yield on reaction of equimolar amounts of the corresponding alcohol, iodine, D-glucal triacetate, silver perchlorate, and 2,4,6-trimethylpyridine (collidine) in dry benzene. The proportion of the α-D-*manno* isomer in the product increased in the order, *t*-butyl > cyclohexyl > methyl. Deuterolysis of the iodide in the presence of palladium proceeded with retention of configuration when the iodine was in equatorial orientation (β-D-*gluco*-configuration) but with near complete lack of stereospecificity when axially oriented (α-D-*manno*-configuration).

2-Deoxyglycopyranosides have been prepared by reaction of *O*-acylated 2-deoxyglycopyranosyl halides with alcohols (1, 2), acid-catalyzed addition of alcohols to acylated glycals (3–6), and the acid-catalyzed alcoholysis of 2-deoxysugars (7). Also, the condensation of *O*-acyl-2-deoxy-2-halogenoglycopyranosyl halides with alcohols followed by hydrogenolysis of the 2-deoxy-2-halogenoglycoside has been employed (8–12).

The syntheses involving substituted glycosyl halides are of most general application. Since anomeric halogens are normally in axial orientation and their replacement tends to proceed with inversion of the reacting center, 2-deoxyglycopyranosides with equatorial aglycons are the expected products. This corresponds to the β-configuration for the hexoses. The formation of the α-glycoside on reaction of 2,6-dideoxy-D-ribohexopyranosyl chloride tri-*p*-nitrobenzoate with digitoxigenin (1) is undoubtedly related to the instability of the α-configuration for the chloride in the presence of the axial 3-acyloxy group. The purpose of this research was to achieve a stereochemically controlled synthetic route to the 2-deoxy-α-glycopyranosides which would proceed in high yield.

It has long been recognized that the reaction of an alkene with a halogen in the presence of a source of carboxylate ion leads to the formation of *O*-acylated halohydrin (13, 14). The halogenation of an alkene in an alcohol results in formation of *O*-alkyl halohydrin (15, 16). The yields of these substituted halohydrins are enhanced through depression of the concentrations of halide ion by addition of silver ion (13, 14, 15, 17, 18). It was observed (17) that the reaction of cyclohexene with iodine and silver perchlorate in dry ether gave a product which was hydrolyzed to cyclohexene iodohydrin on the addition of water. This observation is in keeping with the now well-recognized inability of the perchlorate ion to form covalent bonds.

D-Glucal triacetate was converted to 1-*O*-benzoyl-2-deoxy-2-iodo-D-hexose triacetates on treatment with silver benzoate and iodine (19). The product was recently found to comprise an about equimolar mixture of the isomers with the α-*manno*- and β-*gluco*-configurations (20). Evidently, it could be expected that alkyl 2-deoxy-2-iodoglycopyranoside triacetates would form on reaction of an acetylated glycal dissolved in an alcohol with iodine and a silver salt. The preparation of *trans*-2-methoxycyclohexyl iodide in

[1]*Presented by R.U.L. at the International Symposium on Carbohydrate Chemistry sponsored by the Chemical Society and the University of Birmingham (Chemistry and Industry, 1703 (1962)).*
[2]*Present address: Department of Chemistry, University of Alberta, Edmonton, Alberta.*
[3]*Present address: Department of Chemistry, University of Saskatchewan, Regina Campus, Saskatchewan.*

Can. J. Chem. Downloaded from www.nrcresearchpress.com by 210.87.254.6 on 09/05/12
For personal use only.

90% yield on reaction of cyclohexene in methanol with iodine in the presence of silver perchlorate and calcium carbonate at −80° (17) would serve as a precedent. The use of silver perchlorate was found to be an unnecessary precaution in the iodomethoxylation of D-glucal triacetate when a large excess of methanol was used. Thus, the reaction in the presence of silver benzoate gave the methyl 2-deoxy-2-iodo-α-D-manno- and β-D-glucopyranoside triacetates in near quantitative yield. The isomer with the α-D-*manno*-configuration comprised about 55% of the mixture as evidenced by the relative intensities of the signals for the methoxy groups in the proton magnetic resonance (NMR) spectrum. The hydrogenolysis of these glycosides was previously shown (20) to yield the α- and β-methyl glycosides of 2-deoxy-D-glucose.

This approach to the synthesis of 2-deoxyglycopyranosides would likely not find useful application unless the acetylated glycal and the alcohol could be used in equimolar amounts to provide the 2-deoxy-2-halogenoglycoside in high yield. This goal was achieved through the anticipation that both glycosyl perchlorates and the *N*-glycosides of 2,4,6-trimethylpyridine (collidine) would prove to be unstable in the presence of an alcohol. Thus, the addition of iodine to equimolar amounts of D-glucal triacetate, silver perchlorate, collidine, and an alcohol (methanol, cyclohexanol, or *t*-butanol) provided the alkyl 2-deoxy-2-iodo-D-glycopyranoside triacetates as mixtures of α-D-*manno*- and β-D-*gluco*-configurations in near quantitative yields. The content of the isomer with the α-D-*manno*-configuration increased with increasing substitution of the α-carbon of the alcohol (methyl, 55%; cyclohexyl, about 70%; *t*-butyl, 85%). This result is reminiscent of the increased resistance displayed by 1,2-anhydro-α-D-glucopyranose triacetate with alcohols as the bulk of the group about the hydroxyl is increased (21). Thus, it seems likely that the amount of the α-D-*manno*-isomer increased because the formation of the intermediate iodonium ions is reversible and the diequatorial opening of the intermediate 1,2-α-D-*gluco* iodonium ion became less favored than the diaxial opening of the 1,2-β-D-*manno* iodonium ion with increasing size of the alkyl group.

The configurations of the iodoglycosides were established by application of NMR spectroscopy as previously described (12) and by hydrogenolysis to the corresponding α- and β-2-deoxy-D-glucopyranosides. It seemed of interest to investigate the stereochemical route of the reduction of these iodides with deuterium since it could be anticipated that the configurations of the 2-deoxy-2-deuterioglycosides could be readily interpreted from their NMR spectra. Deuterolysis of methyl 2-deoxy-2-iodo-β-D-glucopyranoside in deuterium oxide using palladium on charcoal as catalyst proceeded with apparent complete retention of configuration. The chemical shift and the triplet structure of the signal of intensity one at 1.78 p.p.m. requires the proton to be in axial orientation at the 2-position (see Fig. 1) and coupled with axial hydrogens at the 1- and 3-positions. As expected, the quartet signal (4.62 p.p.m. and spacings of 1.9 and 9.9 c.p.s.) for the anomeric hydrogen of the 2-deoxy-β-glucoside collapsed to a doublet with the larger spacing on introduction of the equatorial deuterium.

Treatment of the methyl 2-deoxy-2-deuterio-β-D-glucopyranoside with methanolic hydrogen chloride provided the α-anomer. The spectrum of this compound is shown in Fig. 2. A comparison of this spectrum with that shown in the same figure for methyl 2-deoxy-α-D-glucopyranoside clearly substantiates the configuration shown. The structure of the signal for the anomeric hydrogen allows the assignment of the larger spacing, 3.9 c.p.s., to the coupling of the anomeric hydrogen (H_1) with the axial hydrogen (H_2) at the 2-position. This result, on the basis of the Karplus relationship (22), indicates that H_1 defines a somewhat smaller dihedral angle with H_2 than with $H_{2'}$. This distortion of

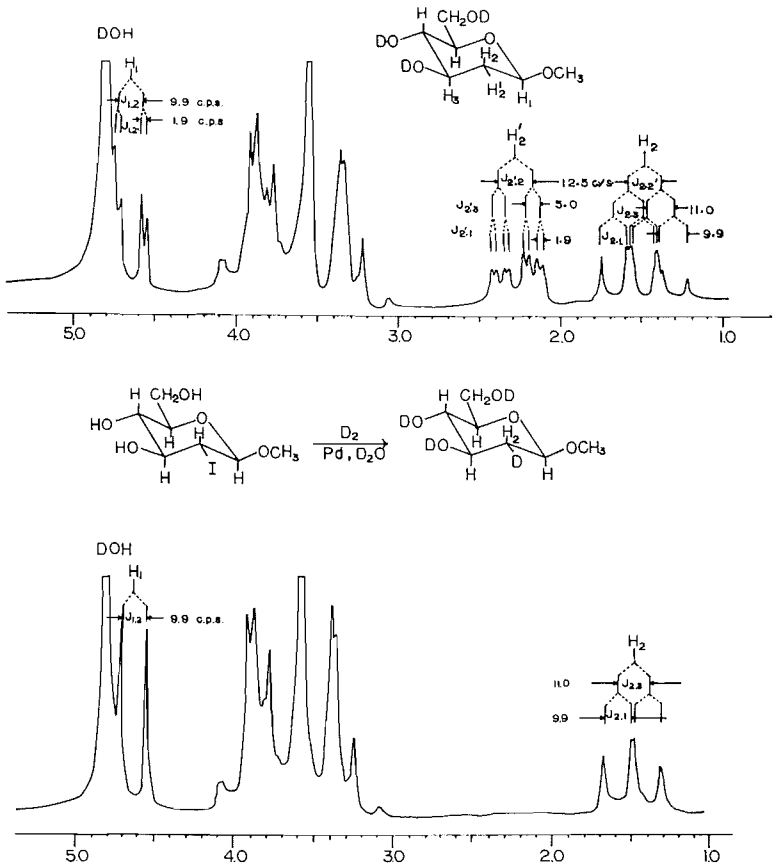

FIG. 1. NMR spectra at 60 Mc.p.s. in deuterium oxide of methyl 2-deoxy-β-D-arabohexopyranoside and methyl 2-deoxy-2-deuterio-β-D-glucopyranoside. The spacings are in c.p.s. and the chemical shifts in p.p.m. from tetramethylsilane used as an external reference.

the pyranose ring would be in the direction expected on the basis that the non-bonded interactions between the axial oxygen and the opposing axial hydrogens do not allow the oxygen to assume an exactly axial orientation. The spacings of 5.0 and 11.4 c.p.s. observed in the signals for the 2′- and 2-hydrogens, respectively, which arise from coupling with the 3-hydrogen, together with the above-mentioned spacings for the anomeric hydrogen obviously require the compound to possess the chair conformation.

The deuterolyses of both the methyl and *t*-butyl 2-deoxy-2-iodo-α-D-mannopyranosides both proceeded with extensive inversion (about 40%) of the reacting center. That the deuterium replaced the iodine is evident from the structures of the signals for hydrogens at the 2-position (see Fig. 3). The relative intensities of these signals provided the relative amounts of the two epimers in the mixture. Since the spacings found in the signals for these hydrogens are virtually the same for both the methyl and the *t*-butyl 2-deoxy-2-deuterio-α-D-glucopyranosides, it is clear that the size of the alkyl group of the aglycon has little if any influence on the conformation of the pyranose ring. The extent of racemization of the 2-position in the deuterolysis of the axially oriented iodine requires the reaction in this case to proceed by way of a configurationally labile intermediate such as a free radical or carbanion.

Can. J. Chem. Downloaded from www.nrcresearchpress.com by 210.87.254.6 on 09/05/12
For personal use only.

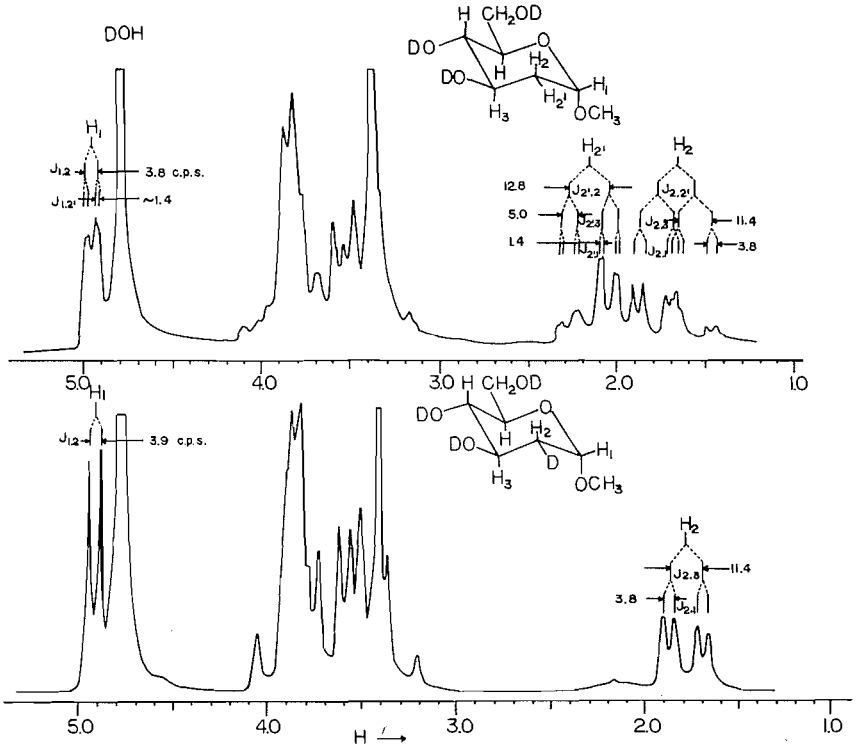

FIG. 2. NMR spectra at 60 Mc.p.s. in deuterium oxide of methyl 2-deoxy-α-D-arabohexopyranoside and methyl 2-deoxy-2-deuterio-α-D-glucopyranoside. The spacings are in c.p.s. and the chemical shifts in p.p.m. from tetramethylsilane used as an external standard.

Incidental to this research, the NMR spectrum of the methyl 2-deoxy-α-D-ribopyranoside was determined both in chloroform and deuterium oxide (see Fig. 4). It is of interest to note that the structures of the signals for the anomeric hydrogen changed from a triplet to a quartet on changing the solvent from chloroform to deuterium oxide. In view of the dependence of the coupling constant for hydrogens on vicinal carbons on the dihedral angles defined by the hydrogens (22), it is clearly apparent that the 1-axial conformation wherein the anomeric hydrogen is *gauche* to both the 2-hydrogens is much more favored in the non-hydroxylic solvent. It seems most probable that this conformation is favored in chloroform since it allows an intramolecular hydrogen bond between the 3-hydroxyl and the methoxyl. In the deuterium oxide solution, hydrogen bonding of the hydroxyl groups with the solvent is favored over intramolecular hydrogen bonding and therefore, the 1-equatorial conformation is preferred since it avoids non-bonded interaction between the 1- and 3-substituents.

EXPERIMENTAL

All melting points were determined on a heating stage and are uncorrected. The proton magnetic resonance spectra were determined in chloroform with a Varian Associates HR-60 spectrometer and the chemical shifts are reported in p.p.m. from tetramethylsilane.

Methyl 2-deoxy-2-iodo-β-D-gluco- and -α-D-mannopyranosides

(*a*) To a stirred suspension of 1.15 g (5 mmoles) of dry silver benzoate in a solution of 1.36 g (5 mmoles) of D-glucal triacetate (23) in 150 ml of dry methanol, 1.27 g (5 mmoles) of iodine were added over a period

Can. J. Chem. Downloaded from www.nrcresearchpress.com by 210.87.254.6 on 09/05/12
For personal use only.

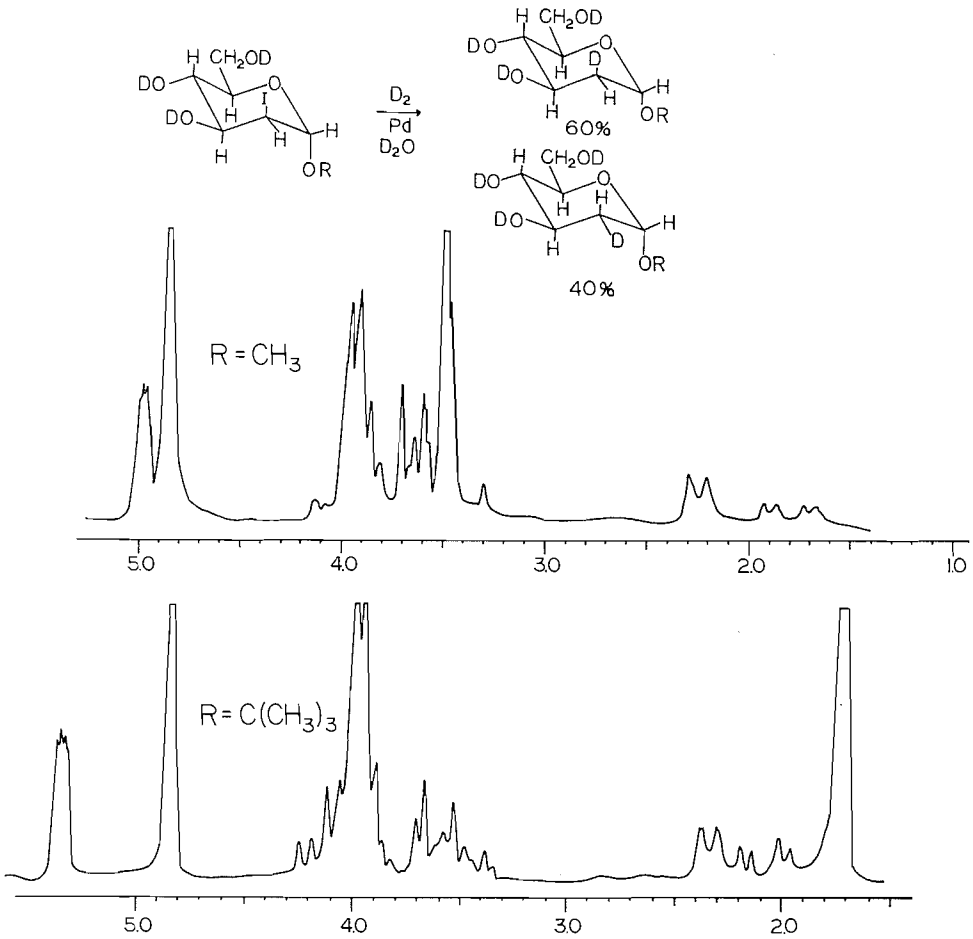

FIG. 3. The NMR spectra at 60 Mc.p.s. in deuterium oxide of the mixtures obtained on deuterolysis of the methyl and *t*-butyl 2-deoxy-2-iodo-α-D-mannopyranosides. The chemical shifts are in p.p.m. from tetramethylsilane used as an external standard. The doublets at 2.25 and 2.33 p.p.m. in the upper and lower spectra, respectively, are assigned to the equatorial 2-protons of the component with the *manno*-configuration. The lower intensity quartets to higher field centered at 1.8 and 2.1 p.p.m., respectively, are assigned to the axial 2-protons of the *gluco*-isomers.

of 5 minutes. Except for the last addition when slight coloration remained, the iodine coloration rapidly disappeared after each addition. After the suspension was stirred at room temperature for 30 minutes, the silver salts were removed by filtration, the filtrate was evaporated to near dryness, and the residue was dissolved in chloroform. The solution was washed with aqueous sodium thiosulphate, then with aqueous bicarbonate, and finally with water before drying. Removal of the chloroform left a viscous oil, 2.01 g (93.5% yield). The NMR spectrum showed two signals for methoxyl-group protons of relative intensities 10:13. The sirup was dissolved in 50 ml of dry methanol saturated with ammonia. After 1 day at room temperature, the solution was evaporated to dryness. The residue was freed of acetamide by chromatography on silicic acid using 5% methanolic chloroform as eluant. The acetamide-free sirup was dissolved in ethyl acetate. On seeding of the solution with methyl 2-deoxy-2-iodo-β-D-glucopyranoside (20), crystals of this material were deposited. The yield (based on the D-glucal triacetate) after one recrystallization from ethyl acetate was 21%. The sirup obtained on evaporation of the mother liquor was seeded with methyl 2-deoxy-2-iodo-α-D-mannopyranoside. After crystallization was complete, the crystals were washed with ethyl acetate and recrystallized from this solvent to provide a 30% yield of the mannoside. The identifications were based on melting points and mixed melting points with authentic samples (20).

(*b*) Anhydrous silver perchlorate, 0.451 g (2.19 mmoles) was added to a solution of 0.590 g (2.19 mmoles)

Can. J. Chem. Downloaded from www.nrcresearchpress.com by 210.87.254.6 on 09/05/12
For personal use only.

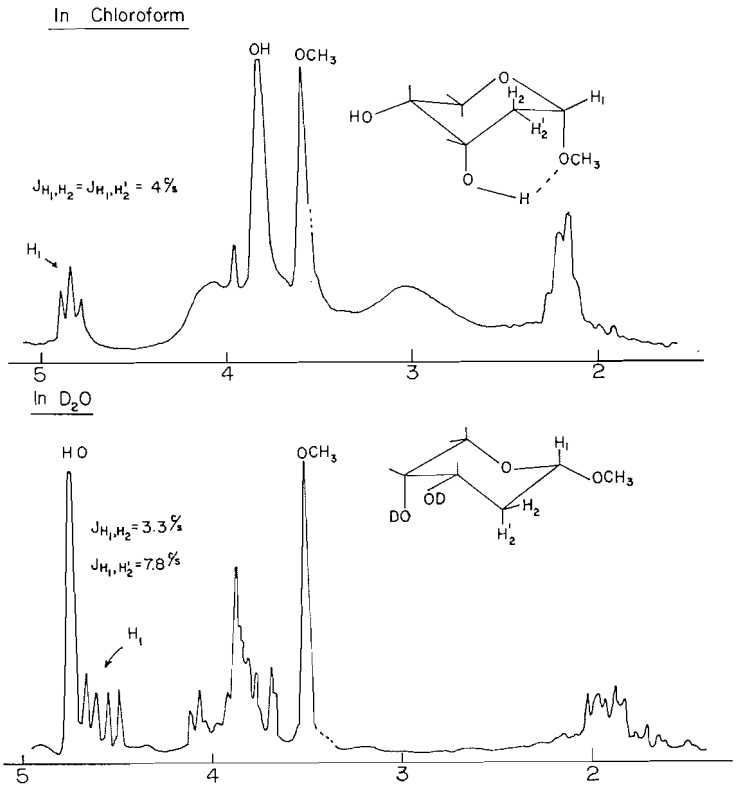

FIG. 4. The effect of solvent on the NMR spectrum at 60 Mc.p.s. of methyl 2-deoxy-α-D-ribopyranoside

of D-glucal triacetate, 0.071 g (2.23 mmoles) of anhydrous methanol, and 0.497 g (2.25 mmoles) of 2,4,6-trimethylpyridine (collidine) in 50 ml of dry benzene. A white precipitate was formed. Iodine, 0.55 g (2.19 mmoles) was added and the mixture was stirred at room temperature for 20 minutes. The reaction product was isolated in a manner similar to that described above. The yield was 0.895 g (95%) of a viscous oil which gave NMR and IR spectra almost identical with those obtained in the reaction described above using methanol as the solvent. The NMR spectrum indicated the product to contain 43% and 57% of the compounds with β-D-*gluco* and α-D-*manno* configurations, respectively. The mixture was deacetylated and the methyl 2-deoxy-2-iodoglycosides were isolated as described in the above preparation in pure condition for positive identification.

Cyclohexyl 2-deoxy-2-iodo-β-D-gluco- and -α-D-mannopyranosides

Reaction of 1.28 g (4.71 mmoles) of D-glucal triacetate, 0.480 g (4.80 mmoles) of dry cyclohexanol, 1.02 g (4.71 mmoles) of silver percholate, 1.20 g (4.71 mmoles) of iodine, and 0.431 (4.77 mmoles) of collidine in 50 ml of dry benzene for 20 minutes, followed by the isolation procedure described above, gave 2.28 g (97% yield). The NMR spectrum of the product required it to be free of D-glucal triacetate. The substance was deacetylated in methanol saturated with ammonia and chromatographed on silicic acid using chloroform as the developing phase. The faster moving of the components was isolated as an amorphous powder, in 50% overall yield, which resisted crystallization. The specific rotation was +68.7° (*c*, 1.9 in methanol). The slower moving component was eluted from the chromatographic column using 5% methanolic chloroform. This compound was obtained in crystalline condition on evaporation of the solvent in 23% overall yield. After purification by recrystallization from benzene, the melting point was 151–152.5° with $[\alpha]_D$ +16.0° (*c*, 2.1 in methanol).

Anal. Calc. for $C_{12}H_{21}O_5I$: C, 38.72; H, 5.69; I, 34.10. Found: C, 38.50; H, 5.83; I, 33.61%.

Cyclohexyl 2-Deoxy-α-D-glucopyranoside

The above-described cyclohexyl 2-deoxy-2-iodo-α-D-mannopyranoside, $[\alpha]_D$ +68.7°, 372 mg, was dissolved in 15 ml of methanol with 138 mg of diethylamine, and 40 mg of 5% palladium on charcoal was added to catalyze a hydrogenolysis. The theoretical amount of hydrogen was consumed within 30 minutes. After

Can. J. Chem. Downloaded from www.nrcresearchpress.com by 210.87.254.6 on 09/05/12
For personal use only.

filtration to remove the catalyst, silver carbonate was added to remove the iodide ion. The silver salts were removed and the filtrate was treated with hydrogen sulphide. Treatment with charcoal, filtration, and evaporation gave viscous oil, 206 mg (84% yield), which completely crystallized on trituration with benzene. Recrystallization from benzene gave white crystals, m.p. 123–124°, $[\alpha]_D$ +129.3° (*c*, 1.1 in methanol).

Anal. Calc. for $C_{12}H_{22}O_5$: C, 58.52; H, 9.00. Found: C, 58.71; H, 8.98%.

Cyclohexyl 2-Deoxy-β-D-glucopyranoside

The above-described cyclohexyl 2-iodo-2-deoxy-β-D-glucopyranoside, $[\alpha]_D$ +16.0°, 185 mg, was hydrogenolyzed and the product, 117 mg (95% yield), was isolated as described for the α-anomer. The crystalline compound melted at 126–127° with $[\alpha]_D$ + 46.3° (*c*, 0.9 in methanol) after recrystallization from benzene.

t-Butyl 2-Deoxy-2-iodo-β-D-glucopyranoside and -α-D-mannopyranosides

A mixture of the triacetates of these two compounds was obtained in 97% yield using the reaction conditions described above for the preparation of the cyclohexyl 2-deoxy-2-iodoglycoside triacetates except that dry *t*-butanol was used instead of the cyclohexanol. The product was deacetylated and chromatographed as reported for the corresponding cyclohexyl glycosides. The band eluted with chloroform provided a 59% yield of a crystalline product which, after one recrystallization from benzene, melted at 146–147° with $[\alpha]_D$ +65.2° (*c*, 2.1 in methanol).

Anal. Calc. for $C_{10}H_{19}O_5I$: C, 34.69; H, 5.53; I, 36.67. Found: C, 34.55; H, 5.30; I, 36.02%.

Elution of the chromatographic column with 5% methanolic chloroform gave a sirup from which a 4% yield of compound, m.p. 153–154°, $[\alpha]_D$ +13.2° (*c*, 0.08 in methanol), was obtained.

Anal. Calc. for $C_{10}H_{19}O_5I$: C, 34.69; H, 5.53; I, 36.67. Found: C, 35.02; H, 5.56; I, 36.20%.

A sample of the reaction mixture was deacetylated and its NMR spectrum in deuterium oxide showed a chemical shift for the *t*-butyl groups of the two components. The relative intensities of the signals required the mixture to comprise 85% of the α-D-mannoside and 15% of the β-D-glucoside.

t-Butyl 2-Deoxy-α-D-glucopyranoside

The above-described *t*-butyl 2-deoxy-2-iodo-α-D-mannopyranoside, $[\alpha]_D$ +65.2°, was hydrogenolyzed under the same conditions as described for the cyclohexyl mannoside except that water was used as solvent. The yield was 84% of a crystalline product which was recrystallized from benzene. On heating, the compound, $[\alpha]_D$ +123.0° (*c*, 0.7 in methanol), first melted at 136–138° then solidified to a crystal form which melted at 144–145°.

Anal. Calc. for $C_{10}H_{20}O_5$: C, 54.53; H, 9.15. Found: C, 54.42; H, 9.01%.

Deuterolysis of the Iodoglycosides

Methyl 2-deoxy-2-iodo-β-D-glucopyranoside and the methyl and *t*-butyl 2-deoxy-2-iodo-α-D-mannopyranosides after exchange of the active hydrogens using deuterium oxide, were treated with deuterium at atmospheric pressure and room temperature in the presence of 5% palladium on charcoal and diethylamine using deuterium oxide as solvent. The product in each case was isolated by first precipitating the iodide ion with silver carbonate as described above in similar preparations. The yields in each case were near quantitative. The NMR spectra of the 2-deoxy-2-deuterioglycosides are reproduced in Figs. 1 and 3. Methyl 2-deoxy-2-deuterio-α-D-glucopyranoside was obtained by allowing a solution of the β-anomer in 5% methanolic hydrogen chloride to achieve constant rotation. The α-glucoside was readily isolated in crystalline condition using the usual isolation procedure. Its NMR spectrum is reproduced in Fig. 2.

ACKNOWLEDGMENTS

The authors thank the Bristol Laboratories Incorporated and the National Research Council of Canada for the financial support of this research through grants to R.U.L. The nuclear magnetic resonance spectra were determined by Mrs. A. Westland and the microanalyses were conducted by Miss E. Busk of these laboratories. The methyl 2-deoxy-α-D-ribopyranoside was prepared by Mr. M. Saeed from a sample of 2-deoxy-D-ribose kindly donated by Hoffmann LaRoche Inc.

REFERENCES

1. W. W. Zorbach and T. A. Payne. J. Am. Chem. Soc. **82**, 4979 (1960).
2. W. W. Zorbach and G. J. Durr, Jr. J. Org. Chem. **27**, 1474 (1962).
3. I. W. Hughes, W. G. Overend, and M. Stacey. J. Chem. Soc. 2846 (1949).
4. W. G. Overend, F. Shafizadeh, and M. Stacey. J. Chem. Soc. 992 (1951).
5. K. Wallenfels and J. Lehmann. Ann. **635**, 166 (1960).
6. R. J. Ferrier, W. G. Overend, and A. E. Ryan. J. Chem. Soc. 3667 (1962).
7. W. G. Overend and M. Stacey. Advan. Carbohydrate Chem. **8**, 45 (1953).
8. E. Fischer, M. Bergmann, and H. Schotte. Ber. **53**, 509 (1920).

Can. J. Chem. Downloaded from www.nrcresearchpress.com by 210.87.254.6 on 09/05/12
For personal use only.

9. J. C. IRVINE and J. W. H. OLDHAM. J. Chem. Soc. **127**, 2729 (1925).
10. F. H. NEWTH and G. O. PHILLIPS. J. Chem. Soc. 2900 (1953).
11. M. AKAGI, S. TEJIMA, and H. NAKAMURA. Yakugaku Zasshi, **82**, 1337 (1962).
12. R. U. LEMIEUX and B. FRASER-REID. Can. J. Chem. **42**, 532 (1964).
13. C. PROVOST. Compt. Rend. **196**, 1129 (1933); **197**, 1661 (1933); **200**, 942 (1935).
14. R. B. WOODWARD and F. V. BRUTCHER, JR. J. Am. Chem. Soc. **80**, 209 (1958).
15. K. MEINEL. Ann. **510**, 129 (1934); **516**, 231 (1935).
16. P. D. BARTLETT and D. S. TARBELL. J. Am. Chem. Soc. **58**, 466 (1936).
17. L. BIRCKENBACH and J. GOUBEAU. Ber. **65**, 395 (1932).
18. L. BIRCKENBACH, J. GOUBEAU, and E. BERNINGER. Ber. **65**, 1339 (1932).
19. J. STANEK and V. SCHWARZ. Collection Czech. Chem. Commun. **20**, 42 (1955).
20. R. U. LEMIEUX and S. LEVINE. Can. J. Chem. **40**, 1926 (1962).
21. R. U. LEMIEUX and G. HUBER. J. Am. Chem. Soc. **78**, 4117 (1956).
22. M. KARPLUS. J. Chem. Phys. **30**, 11 (1959).
23. W. W. PIGMAN and H. S. ISBELL. J. Res. Natl. Bur. Std. **19**, 204 (1937).

Can. J. Chem. Downloaded from www.nrcresearchpress.com by 210.87.254.6 on 09/05/12
For personal use only.

Can. J. Chem. Downloaded from www.nrcresearchpress.com by 210.87.254.5 on 09/05/12
For personal use only.

MOLECULAR SIEVE SORBENTS FROM CLINOPTILOLITE

R. M. Barrer and M. B. Makki
Chemistry Department, Imperial College, London, England
Received February 17, 1964

ABSTRACT

Clinoptilolite has been investigated as a source of porous, largely crystalline, molecular sieve sorbents. By treating the zeolite with mineral acid of different strengths a range of high area sorbents has been produced, in which all the original cations have been replaced by hydronium ions, and in which the aluminum has been progressively removed from the frameworks. The new sorbents and the original clinoptilolite have been characterized by sorption studies, and by X-ray, electron optical, differential thermal analysis, and thermogravimetric methods. The most open molecular sieve sorbents, able to imbibe considerable amounts of larger molecules such as benzene and isopentane, were obtained using 1 *N* and 2 *N* acid, but as acid strength increased further there was a decline in both crystallinity and sorption capacity until with 30 *N* acid an amorphous product resulted.

INTRODUCTION

Clinoptilolite is a silica-rich zeolite related to heulandite (1, 2). It has recently attracted attention because of its ability to scavenge Cs^+ from radioactive effluents (3, 4) and because it is one of several zeolites (including heulandite, laumontite, phillipsite, and erionite) which have been discovered in substantial deposits (5–8). Some natural crystalline zeolites are thus available as potential ion exchangers and molecular sieve sorbents in competition with synthetic crystalline zeolites.

When aluminosilicates are treated with mineral acids there may be exchange of their cations by hydronium ions, and there may be hydrolysis of Al—O—Si bonds. Hydrolysis occurs readily for the most aluminous minerals, and results in complete disintegration to colloidal silica and to aluminum salts. As the silica content increases, colloidal silica is replaced by silica gel (9). It could be anticipated that as the silica content increases still further the gel will retain more and more "memory" of the parent structure, so that highly specific silica-rich sorbents may be obtained. Clinoptilolite is one of the most siliceous aluminosilicates and accordingly sorbents obtained by acid treatment of the zeolite may have molecular sieve properties of special interest. To test this hypothesis we have investigated in various ways the products obtained from clinoptilolite treated with hydrochloric acid solutions.

EXPERIMENTAL MATERIALS AND METHODS

The original clinoptilolite and the products obtained from it were examined by X-ray diffraction, thermogravimetry, d.t.a., and as sorbents. Nitrogen sorption at the temperature of liquid nitrogen was measured in a volumetric sorption unit of standard design, and the sorption of a number of vapors was determined above room temperature using several silica spring balance sorption units. The sorbates were distilled water, 'AnalaR' methanol and ethanol, and benzene and isopentane. The hydrocarbons were supplied as pure chemicals by the National Chemical Laboratory, Teddington. Before sorption studies were made the sorbents were outgassed at 350° C for 15 hours.

CHARACTERIZATION OF THE CLINOPTILOLITE

Clinoptilolite, from Mount Hector, California, was supplied by the courtesy of Dr. L. L. Ames, Jr., of General Electric Company, Richland, Washington. The overall purity was

given as 85–95%, and the zeolite appeared as small hard fragments with conchoidal fracture to which a certain amount of pale green bentonite material was adhering. The main X-ray spacings from our sample are given in Table I, and are compared with the

TABLE I

d-Spacings of sample rich in clinoptilolite

		Values of Mumpton (2)	
d-Spacing	Intensity	*d*-Spacing*	Intensity, I/I_0
8.9	vs	9.00 (8.90)	10 (10)
7.8	w	7.94 (7.94)	4 (2)
6.7	vw	6.77 (6.80)	3 (1)
6.5_5	vw	6.64 (6.63)	2 (1)
5.2_0	vvw	5.24 (5.24)	3 (1)
5.1_0	vw	5.11 (5.09)	1 (1)
4.6_2	vw	4.69 (4.69)	2 (1)
—	—	4.48 (4.45)	2 (2)
4.3_4	vw	4.34 (4.36)	2 (1)
†4.2_0	vw	— —	— —
3.9_3	vs	3.96 (3.97)	10 (2)
3.8_7	w	3.90 (3.89)	8 (3)
—	—	3.73 (3.71)	1 (1)
3.5_3	vw	3.55 (3.56)	2 (1)
3.4_3	vw	3.46 (3.47)	2 (1)
3.4_0	vw	3.42 (3.40)	6 (2)
†3.3_5	vw	— —	— —
3.3_2	vw	— —	— —
3.1_3	w	3.12 (3.12)	3 (1)
3.1_0	vvw	3.07 (3.07)	2 (1)
3.0_5	vvw	3.04 (3.03)	2 (1)
2.9_5	vvw	2.97 (2.97)	5 (4)
—	—	2.87 —	1 —
—	—	2.82 —	3 —
2.7_9	vvw	2.80 (2.80)	1 (1)

*Specimen from Mt. Hector, California. Figures in parentheses are for a heulandite from Prospect Park, New Jersey.
†Lines due to quartz.

corresponding spacings reported by Mumpton (2) for clinoptilolite and heulandite. There is a satisfactory correspondence after several lines due to quartz, which was a further impurity, are subtracted, although the similarity with heulandite is as close as that with clinoptilolite. The clinoptilolite powder pattern was still observed, somewhat weakened, after the zeolite was heated to 750° C for considerable periods. At still higher temperatures an amorphous, glassy phase was formed, although the quartz impurity was detectable up to 1000° C. Evidently clinoptilolite possesses very considerable thermal stability.

A differential thermal analysis curve is shown in Fig. 1. The endothermic reaction in the lower temperature range corresponds to the evolution of zeolitic water. A further endothermic change begins near 600° C and persists over a range of temperature. The loss of zeolitic water is a continuous process as shown by the full thermogravimetric curve of Fig. 2.

Because it was not easy to free the clinoptilolite from quartz and bentonite it was analyzed without further purification. The sample lost 15.2% by weight on ignition, which should primarily be water. The ratio Al_2O_3:SiO_2 was 1:10.8, and sodium was the main cation, with a little potassium and calcium. The latter may have been present as carbonate.

PREPARATION OF SORBENTS FROM CLINOPTILOLITE

Ten-gram samples of clinoptilolite were refluxed with 150 cm^3 of hydrochloric acid solutions for 4 hours at a temperature of a little above 100° C. The acid solutions used in different preparations were 0.25, 0.5, 1, 2, 5,

Can. J. Chem. Downloaded from www.nrcresearchpress.com by 210.87.254.5 on 09/05/12
For personal use only.

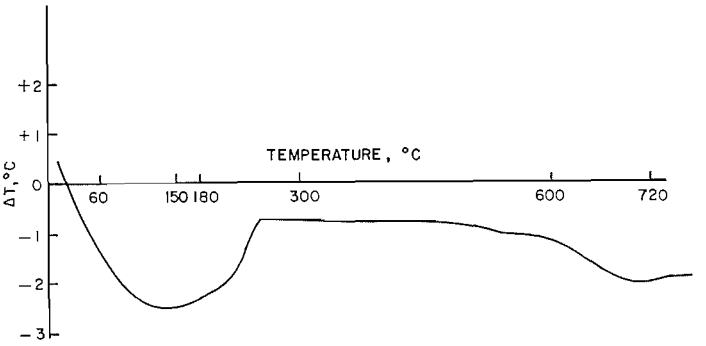

FIG. 1. The differential thermal analysis curve of the original clinoptilolite.

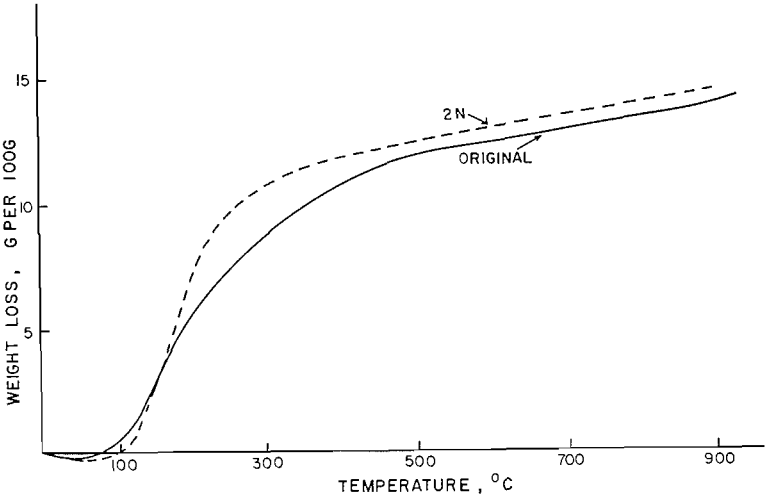

FIG. 2. Thermogravimetric curves of the original clinoptilolite (full line) and of clinoptilolite treated with 2 *N* HCl.

10, 15, and 30 *N*. After treatment the suspended particles were filtered off and washed first with cold and then with hot distilled water, until all traces of entrained acid were removed. The preparations were then air-dried and investigated as follows.

(a) Chemical Analysis

All exchangeable cations were found to be replaced by H_3O^+ by treatment with excess of 0.25 *N* HCl. With increasing acid strength Al and H_3O^+ were removed progressively, and in equal amount, until with the 5 *N* acid a hydroxylated silica free of Al or H_3O^+ remained. Removal of Al and H_3O^+ involves the intracrystalline reaction:

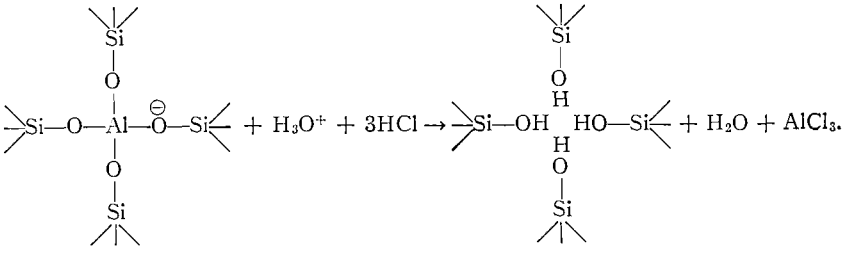

Can. J. Chem. Downloaded from www.nrcresearchpress.com by 210.87.254.5 on 09/05/12
For personal use only.

TABLE II

Compositions of acid-treated clinoptilolites

Treatment of sample	Molar ratio Al_2O_3:SiO_2	Approximate composition of crystalline product
Original	1:10.8	$Na^+[AlSi_{5.4}O_{12.8}]^-4.3_5H_2O$
0.25 *N* HCl	0.95:10.8	$H_3O^+_{0.95}[Al_{0.95}Si_{5.4}O_{12.6}(OH)_{0.2}]^-nH_2O$
0.5 *N* HCl	0.84:10.8	$H_3O^+_{0.84}[Al_{0.84}Si_{5.4}O_{11.96}(OH)_{0.64}]nH_2O$
1 *N* HCl	0.35_5:10.8	$H_3O^+_{0.35_5}[Al_{0.35_5}Si_{5.4}O_{10.02}(OH)_{2.58}]nH_2O$
2 *N* HCl	0.08_1:10.8	$H_3O^+_{0.08}[Al_{0.08_1}Si_{5.4}O_{9.1}(OH)_{3.7}]nH_2O$
5 *N* HCl	0.00 :10.8	$[Si_{5.4}O_{8.8}(OH)_4]nH_2O$

Table II shows the Al and H_3O^+ remaining after each treatment. The compositions in the last column will underestimate the total hydroxyl because partial hydrolysis which does not eliminate Al is not shown by the analysis. The elimination reaction produces nests of four hydroxyls in number equal to the Al removed.

(b) X-ray Diffraction

X-Ray powder photographs were taken with Guinier cameras, using filtered Cu K_α radiation, for all the products, after preparation as described above, and after the prepared samples had been outgassed at 350° C before their examination as sorbents. The results are shown in Fig. 3, in which the left-hand side shows the diffraction patterns before, and the right-hand side the same patterns after, the outgassing. Reading from top to bottom of the figure the samples are: original clinoptilolite and the products respectively obtained with 0.25, 0.5, 1, 2, 5, 10, and 15 *N* acid.

Complete replacement of Na^+ by H_3O^+ has no appreciable influence upon the powder pattern, and the hydrogen-ion exchanged clinoptilolite is quite stable to heating to 350° C. Moreover, one can replace some or all of the aluminum and H_3O^+ with hydroxyl, still leaving crystalline hydroxylated phases which are pseudomorphs of the parent clinoptilolite. This is the situation up to the treatment with 1 *N* HCl, for which there is noted merely some loss of intensity of the clinoptilolite lines. For the products derived by treatment with 2 *N* and higher strength acids, although virtually all Al is removed (Table II), considerable crystallinity still persists even to 15 *N*. The general weakening in intensity of the lines continues, however, and for 30 *N* acid the crystallinity of the original clinoptilolite has practically disappeared. Certain lines in Fig. 3 are unchanged by the acid treatments, but are due to the quartz impurities (Table I).

Heating the products to 350° C produces some further loss in intensity and number of diffraction lines for the products from which Al has been largely or wholly removed, but not for the products from 0.25 *N*, 0.5 *N*, and 1 *N* acid treatments (Fig. 3). Evidently defect-rich crystalline silicas of considerable stability can be prepared from clinoptilolite, in which the defects comprise hydroxyl groups appropriately distributed throughout the structure.

(c) Electron Optical Examination

The photomicrographs taken with a Philips 100 electron microscope showed no great difference among the samples until the product obtained by treatment with 15 *N* acid was reached, although aggregates of plates and laths were found to be progressively dispersed. The amorphous product of the treatment with 30 *N* acid was, however, much more finely divided.

(d) Thermogravimetry

In Fig. 2 we have compared the thermogravimetric curves for the original clinoptilolite and for the product obtained by treatment with 2 *N* hydrochloric acid. The dehydration of the latter sample is more rapid, so that at 300° C the original clinoptilolite had lost 9.5% of water, while the acid-treated product had lost 11%. The heating rate approached 10° C per minute.

BEHAVIOR AS SORBENTS

(a) Nitrogen Isotherms

Sorption isotherms for nitrogen and the vapors were of type II in the Brunauer classification (10). The monolayer equivalent areas were obtained from the isotherms at −195° C for nitrogen by the BET method, taking the area of a nitrogen molecule as 16.2 Å². The results are shown in Fig. 4. A very great increase is seen as the strength of the acid employed to treat the clinoptilolite is increased, until from a value of ~30 m² per g for the original clinoptilolite, the curve passes through a maximum of ~380 m² per g when the acid used is 2 *N*. Thereafter the monolayer equivalent area steadily declines to ~250 m² per g for the sorbent from 15 *N* acid and to ~90 m² per g for the sorbent from 30 *N* acid.

Can. J. Chem. Downloaded from www.nrcresearchpress.com by 210.87.254.5 on 09/05/12
For personal use only.

Can. J. Chem. Downloaded from www.nrcresearchpress.com by 210.87.254.5 on 09/05/12
For personal use only.

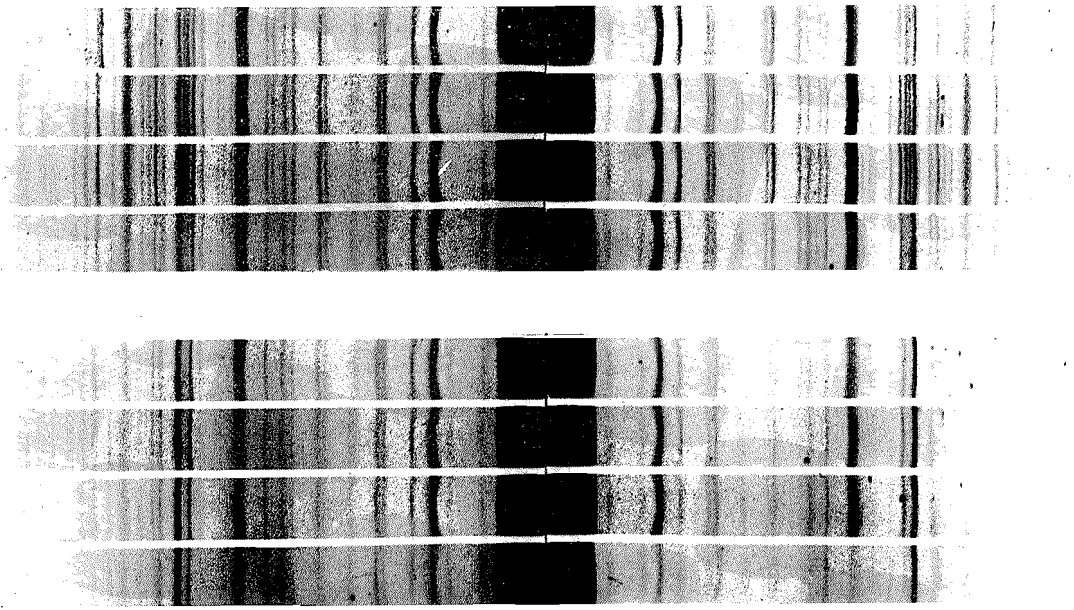

FIG. 3. X-ray powder photographs of the original clinoptilolite and of clinoptilolites treated with acid of varying normality.

1. Original clinoptilolite.
2. Clinoptilolite with 0.25 *N* HCl.
3. Clinoptilolite with 0.5 *N* HCl.
4. Clinoptilolite with 1 *N* HCl.
5. Clinoptilolite with 2 *N* HCl.
6. Clinoptilolite with 5 *N* HCl.
7. Clinoptilolite with 10 *N* HCl.
8. Clinoptilolite with 15 *N* HCl.
9. As 1, outgassed at 350° C for 15 hr.
10. As 2, outgassed at 350° C for 15 hr.
11. As 3, outgassed at 350° C for 15 hr.
12. As 4, outgassed at 350° C for 15 hr.
13. As 5, outgassed at 350° C for 15 hr.
14. As 6, outgassed at 350° C for 15 hr.
15. As 7, outgassed at 350° C for 15 hr.
16. As 8, outgassed at 350° C for 15 hr.

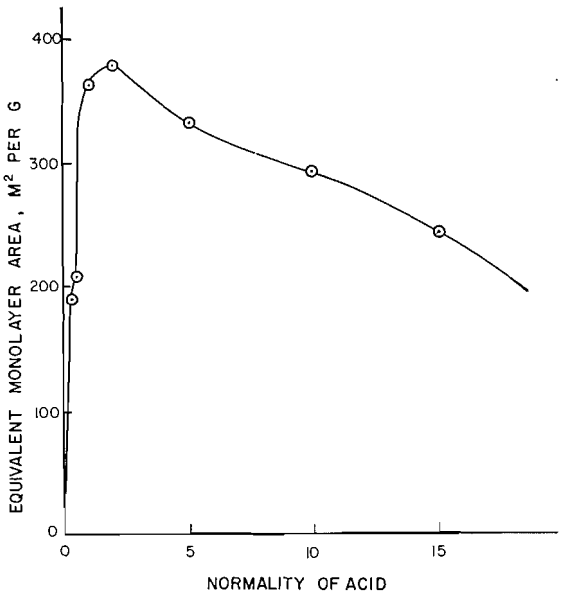

FIG. 4. The equivalent monolayer areas, determined using nitrogen sorption, for the original clinoptilolite and for clinoptilolites treated with HCl of different normalities.

Since the parent clinoptilolite crystals are not permeable to nitrogen, as shown by the area of only 30 m^2 per g, the exchange of Na^+ by H_3O^+, followed by outgassing, has rendered the intracrystalline volume of the crystals much more accessible to this gas. Outgassing at 350° C should remove the zeolitic water and most of the water of hydration of the protons (11), but should not remove significant amounts of hydroxyl water (in kaolin, for example, hydroxyl water is not evolved below about 500° C). The protons, on account of their small size, then offer little obstruction to diffusion of nitrogen into the crystals. The removal of ($Al + H_3O^+$) as shown in Table II improves still more the uptake of nitrogen in the intracrystalline channels, at least as far as the 2 *N* product.

(b) Molecular Sieve Aspects

While the intracrystalline channels of outgassed acid-treated clinoptilolites may be accessible to small molecules such as nitrogen, it by no means follows that they will be available to larger molecules. For this reason we have determined the sorption isotherms of a series of vapors of increasing molecular dimensions (H_2O, CH_3OH, C_2H_5OH, C_6H_6, and iso-C_5H_{12}). Except for water some hysteresis persisted between adsorption and desorption branches down to low relative pressures. The isotherms were measured at 55° C for all vapors save isopentane. In this instance sorption was measured at 30° C. From the adsorption branches at $p/p_0 = 0.5$, assuming that the co-volumes of sorbed molecules equal those of the same molecules in their liquids, one obtained the cm^3 of liquid sorbed per 100 g of outgassed sorbent which are recorded in Table III. For water, the smallest, most polar molecule, the volume sorbed did not vary greatly among all the sorbents. However, as the sorbate molecules became larger the volumes sorbed became progressively smaller both in the original clinoptilolite, and also in the silicas obtained by treatment with the stronger acid solutions. Maximum uptake tends to be observed with sorbents prepared by the action of 0.5, 1, and 2 *N* hydrochloric acids.

Can. J. Chem. Downloaded from www.nrcresearchpress.com by 210.87.254.5 on 09/05/12
For personal use only.

TABLE III

Liquid sorbate (cm^3) per 100 g outgassed clinoptilolite at $p/p_0 = 0.5$

Sorbate \ Sorbent	Original zeolite	0.25 *N*	0.5 *N*	1 *N*	2 *N*	5 *N*	10 *N*	15 *N*
H_2O	13.5	14	14.2	14	11.9	11.6	12.1	11.4
CH_3OH	10.1	15	17.5	15.5	15.9	15.5	13.7	13.9
C_2H_5OH	5.5	17	15.7	17.7	15.5	14.9	13.1	12.7
C_6H_6	2	4.5	5.7	8.7	10.7	8.9	3.7	2.8
iso-C_5H_{12}	0.65	3.5	4.5	6.5	5.4_5	3.8	2.0	1.4

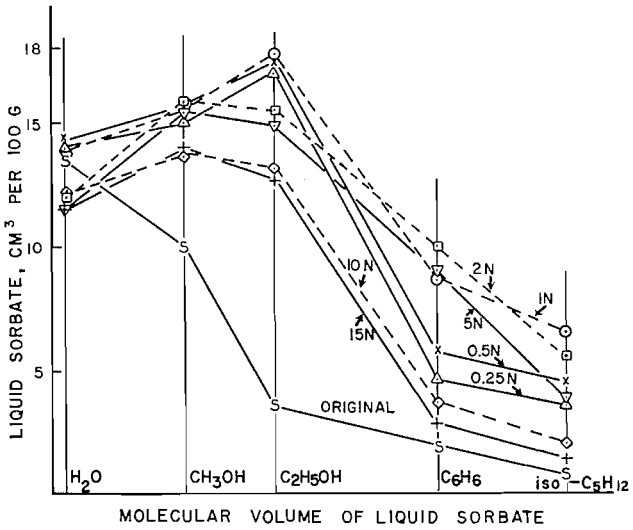

FIG. 5. The relation between sorption at $p/p_0 = 0.5$ of a range of sorbates and the molecular volume of the sorbates, for clinoptilolite and a range of acid treated clinoptilolites.

When the volumes sorbed (as cm^3 of liquid per 100 g of outgassed sorbent at $p/p_0 = 0.5$) are plotted as functions of the molecular volume of the sorbate, the curves of Fig. 5 are obtained. Except in the case of the original clinoptilolite, well-defined maxima appear; in all cases molecular sieve effects are seen which result in substantial reductions in the volumes sorbed for the larger sorbates.

DISCUSSION AND CONCLUSION

To check the reproducibility of the chemical treatment of the clinoptilolite a second treatment of a new sample of the zeolite with 1 *N* acid was given. For the two treatments the amounts of alumina were 3.5% and 3.6% respectively, the monolayer equivalent areas to nitrogen were 370 and 361 m^2 per g respectively, and the sorptions of methanol and ethanol were also almost unchanged. Thus, good control appears to be possible in the formation of sorbents from clinoptilolite. However, color changes, which may be evidence of catalytic activity, were observed in a number of instances. For example, after sorption of ethanol in the sorbent obtained with 15 *N* acid and outgassed at 350° C, the sorbent became blue. The '2 *N*' and '5 *N*' sorbents became black after adsorption of benzene and outgassing at 350° C, while '0.5 *N*' and '1 *N*' sorbents also darkened after occlusion of methanol and outgassing, although here the change of color was less marked. While the character of these reactions is so far unknown, they may in part correspond to deposition of carbon associated with catalytic cracking.

Can. J. Chem. Downloaded from www.nrcresearchpress.com by 210.87.254.5 on 09/05/12
For personal use only.

From Table III about 10 cm³ of liquid benzene are seen to be imbibed per 100 g of H-clinoptilolite obtained by treatment with 1, 2, and 5 *N* acid, while a comparable uptake was observed also in H-mordenite (11). In the best H-clinoptilolite for the purpose, Table III also shows that 6.5 cm³ of liquid isopentane were imbibed, as compared with 7.5 cm³ of liquid neopentane in H-mordenite (11). Evidently the sorption capacity for these size-able hydrocarbon molecules is very similar for H-mordenite and for appropriate H-forms of clinoptilolite.

By condensation polymerization, starting with monosilicic acid, one may prepare extremely fine-pored but amorphous silicas (12). This procedure is the antithesis of that which we have used but has yielded sorbents with much molecular sieve character. Thus in a particular sample the pore volume accessible to small molecules such as nitrogen was 10 cm³ per 100 g, to benzene it was 4 cm³ and to carbon tetrachloride (equal in size to neopentane) only 2 cm³. Thus much of the porosity of this gel is less accessible to larger molecules than are either the crystalline H-clinoptilolites or H-mordenite, and certainly than sodium faujasite (13). The same also can be said of certain carbon sorbents (14). Thus amorphous sorbents can actually overlap substantially in pore accessibility and inaccessibility with some crystalline molecular sieves, although they show a less clear cut-off in accessibility of the pores as the molecular size of the sorbate is increased.

The behavior which we have observed and studied for clinoptilolite should be found with other siliceous zeolites such as mordenite, ferrierite, yugawaralite, or the synthetic lithium zeolite of Barrer and White (15). Although no details are available it is probable that hydrogen-"Zeolon" is produced by acid treatment of sodium-"Zeolon", which is a synthetic mordenite (16). The interesting possibility is thus revealed of multiplying the number of porous molecular sieve sorbents, and the range and type of these, by complete hydrogen ion exchange, and also of subsequently altering the hydrogen ion content in a regulated manner, and hence of modifying the catalytic activity, by removal of various amounts of aluminum from the framework. It is intended to study further, with other zeolites, the preparation and properties of such new molecular sieve materials, using the methods of this paper and other previously developed methods of hydrogen ion exchange of zeolites (17, 18).

One of us (M. B. M.) took part in this work while on sabbatical leave from the University of Aleppo, Syria. We are indebted to Dr. I. S. Kerr of these laboratories for the electron optical investigation.

REFERENCES

1. B. Mason and L. B. Sand. Am. Mineralogist, **45**, 341 (1960).
2. F. A. Mumpton. Am. Mineralogist, **45**, 351 (1960).
3. L. L. Ames, Jr. Am. Mineralogist, **45**, 689 (1960).
4. L. L. Ames, Jr. Am. Mineralogist, **46**, 1120 (1961).
5. D. S. Coombs. Trans. Roy. Soc. New Zealand, **82**, 65 (1954).
6. D. S. Coombs. 4th Triennial Mineral Conference, School of Mines and Metallurgy, University of Otago, New Zealand. September 1959. Paper 162.
7. K. S. Deffeyes. J. Sediment. Petrol. **29**, 602 (1959).
8. K. S. Deffeyes. Am. Mineralogist, **44**, 501 (1959).
9. K. J. Murata. Am. Mineralogist, **28**, 545 (1943).
10. S. Brunauer. The adsorption of gases and vapours. Oxford University Press. 1944. p. 150.
11. R. M. Barrer and D. L. Peterson. Proc. Roy. Soc. In press.
12. D. Dollimore and G. R. Heal. Trans. Faraday Soc. **59**, 2386 (1963).
13. R. M. Barrer. Brit. Chem. Eng. **7**, 267 (1959).
14. J. E. Metcalfe, M. Kawahata, and P. L. Walker, Jr. Fuel, **42**, 233 (1963).
15. R. M. Barrer and E. A. White. J. Chem. Soc. 1267 (1951).
16. A. H. Kerough and L. B. Sand. J. Am. Chem. Soc. **83**, 3536 (1961).
17. R. M. Barrer and D. C. Sammon. J. Chem. Soc. 675 (1956).
18. R. M. Barrer. Nature, **164**, 112 (1949).

Can. J. Chem. Downloaded from www.nrcresearchpress.com by 210.87.254.5 on 09/05/12
For personal use only.

Can. J. Chem. Downloaded from www.nrcresearchpress.com by 210.87.254.6 on 09/05/12
For personal use only.

NOTES

SYNTHESIS OF 4-TRIFLUOROMETHYLPHTHALIC ACID

BERNARD LOEV

During a study of reactions of phthalic acids, it became necessary to prepare 4-trifluoromethylphthalic acid (I). This compound, not previously described, proved to be unexpectedly difficult to prepare; most of the standard methods either failed entirely or gave, at some stage in the reaction sequence, such low yields as to be unsuitable for preparative purposes. In this paper, we describe a convenient synthesis of this compound.

The synthetic scheme is outlined below and proceeds from the commercially available 3-amino-4-chlorobenzotrifluoride.

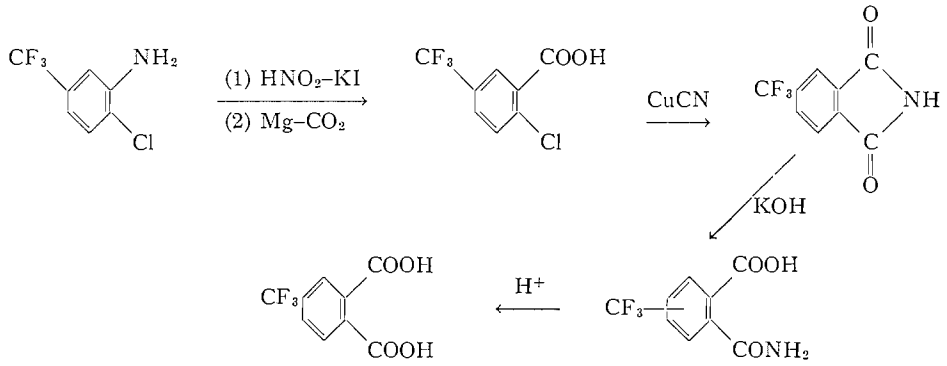

I

Reaction of 2-chloro-5-trifluoromethylbenzoic acid with cuprous cyanide gave 4-trifluoromethylphthalimide (70% yield) rather than the expected 2-cyano-5-trifluoromethylbenzoic acid.

4-Trifluoromethylphthalimide, on being stirred with base, gave the phthalamic acid, which, on being warmed with dilute acid, gave I. The hydrolysis of the imide can be carried out without isolation of the phthalamic acid; in this way, I is obtained in 90% yield.

Another far less satisfactory route to I involved the Diels–Alder reaction. Dehydrogenation of the adduct (II) was accomplished in 30% yield by heating it with sulphur at 230 to 250° C.

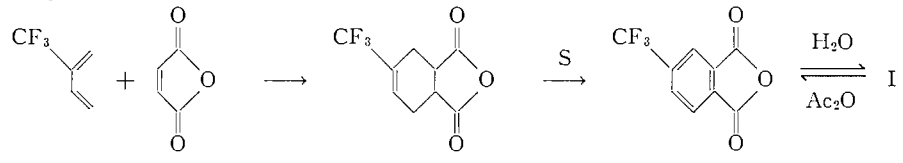

II

Adduct II could not be aromatized using chloranil, bromine, or palladium-on-carbon in refluxing quinoline or dimethylformamide. 4-Trifluoromethylphthalic anhydride, surprisingly, was a very fluid liquid; on being heated with water it was reconverted to the acid (I).

This route to I was not suitable on a preparative scale because of the difficulty of obtaining 2-trifluoromethylbutadiene; this difficulty has been observed by others (1, 2).

Some of the other methods that were investigated, unsuccessfully, for the synthesis of I were via diazotization of 3-nitro-4-aminobenzotrifluoride and 3,4-diaminobenzotrifluoride (in attempts to prepare the corresponding nitriles), via oxidation of 5- or 6-trifluoromethyl isatins,[1] via a Rosenmund–vonBraun reaction on 2-nitro-3-chlorobenzotrifluoride,[2] and via reaction of 4-carboxyphthalic ester and anhydride with sulphur tetrafluoride.

EXPERIMENTAL[3]

3-Iodo-4-chlorobenzotrifluoride

Two 22-liter three-necked round-bottom flasks equipped with an efficient stirrer, addition funnel, and thermometer were charged with 2 liters of concentrated sulphuric acid in 4 liters of water. To this hot solution was added rapidly 616.5 g (3 moles, 95% pure) of 3-amino-4-chlorobenzotrifluoride,[4] after which the solution was slowly cooled to 0–5° C with vigorous stirring. The suspension of the white sulphate salt was then diazotized with a solution of 207 g of sodium nitrite (3 moles) in 840 ml of water. After this addition was completed, there was added 549 g (3.3 moles) of potassium iodide in 815 ml of water over a period of 25 minutes. The brown oily mixture was then heated to 50° C for 1 hour, cooled in an ice water bath, and extracted with three 5 liter portions of ether. The ether extracts were washed with an aqueous solution of sodium thiosulphate, then water, and finally dried over anhydrous magnesium sulphate. The ether solution was filtered and concentrated, and the reddish-colored residue was distilled at 58–60° C (0.5 mm) to give 1620 g (83.5%) of a pink-colored liquid. Anal. Calc. for $C_7H_3ClF_3I$: C, 27.44; H, 0.98. Found: C, 27.37; H, 0.96.

2-Chloro-5-trifluoromethylbenzoic Acid

A 22-liter three-necked round-bottom flask equipped with an efficient stirrer, condenser, gas inlet tube, thermometer, and addition funnel was charged with 150 g (6.25 moles) of magnesium and 2 liters of ether. This solution was kept under a nitrogen atmosphere, as, with vigorous stirring, the solution was heated to reflux, at which time a few drops of ethylene bromide and 1620 g of 3-iodo-4-chlorobenzotrifluoride in 9400 ml of ether was added over a period of 2 hours. The mixture was refluxed and stirred vigorously for another 2 hours, and 1 ml of ethylene bromide was added after each hour. The mixture was cooled to −20° C in a dry ice – acetone bath and 800 g (18.2 moles) of dry carbon dioxide was bubbled into it over a period of 90 minutes. After it was allowed to stand overnight at room temperature, the reaction mixture was hydrolyzed at 0° C with 3 liters of cold 10% hydrochloric acid and was then extracted with three 2-liter portions of ether, and the ethereal solutions extracted with three 2-liter portions of a 10% potassium carbonate solution. The aqueous solution was treated with a small amount of charcoal and the solution filtered. Acidification of the filtrate with concentrated hydrochloric acid gave 663 g (49.5%) of an off-white material which was recrystallized from benzene–petroleum ether, m.p. 91–92° C. Anal. Calc. for $C_8H_4ClF_3O_2$: C, 42.78; H, 1.80. Found: C, 42.91; H, 1.89.

4-Trifluoromethylphthalimide

A mixture of 50 g (0.223 mole) 2-chloro-5-trifluoromethylbenzoic acid, and 30 g (0.335 mole) cuprous cyanide in 80 ml dimethylformamide was heated at reflux, with stirring, for 45 minutes. The resulting dark suspension was cooled slightly, and a solution containing 75 g of ferric chloride and 25 ml of concentrated hydrochloric acid in 125 ml of water was added over a period of 5 minutes. The mixture was then heated at 65° C for 15 minutes, chilled, diluted with 50 ml of ice water, and filtered. The dark brown solid was triturated with 5% sodium bicarbonate and filtered, giving 46.5 g of 4-trifluoromethylphthalimide, m.p. 164–166° C. A small sample recrystallized from benzene melted at 168.5–169.5° C. Anal. Calc. for $C_9H_4F_3NO_2$: C, 50.25; H, 1.87; N, 6.51. Found: C, 50.35; H, 1.85; N, 6.74.

4- (or 5)-Trifluoromethylphthalamic Acid

A suspension of 0.5 g 4-trifluoromethylphthalimide in 2.5 ml of 25% potassium hydroxide was stirred for 4 hours; then sufficient water was added to dissolve all the solid. The solution was cooled and acidified. The resulting waxy white solid was recrystallized from a mixture of isopropanol and hexane, m.p. 154–155° C. Anal. calc. for $C_9H_6F_3NO_3$: C, 46.36; H, 2.59. Found: C, 46.38; H, 2.94.

[1]*The oximino acetanilides could not be cyclized to the isatins as claimed by P. M. Maginnity and C. A. Gaulin. J. Am. Chem. Soc. 73, 3579 (1951).*

[2]*On mixture with potassium cyanide in dimethyl formamide there was no reaction. When sodium cyanide was used the reaction was almost explosively exothermic, but no product could be isolated.*

[3]*All melting points are corrected. Analyses were carried out by Miss Margaret Carroll and her staff of these laboratories.*

[4]*Aldrich Chemical Company.*

Can. J. Chem. Downloaded from www.nrcresearchpress.com by 210.87.254.6 on 09/05/12
For personal use only.

4-Trifluoromethylphthalic Acid

(a) From 4-Trifluoromethylphthalimide

A suspension of 1 g 4-trifluoromethylphthalimide in 5 ml of 25% potassium hydroxide was stirred for 10 hours, then the solution was made strongly acidic with concentrated hydrochloric acid. The solution was heated at reflux for 1 hour, filtered, then chilled, giving 0.9 g of a glistening waxy solid. Recrystallization from water gave the 4-trifluoromethylphthalic acid as a partial hydrate. Anal. calc. for $C_9H_5F_3O_4.3/4\ H_2O$: C, 43.83; H, 2.64. Found: C, 43.84; H, 2.38.

Prolonged drying at 100° C *in vacuo* did not remove the water. The melting point varied with the rate of heating and temperature at which the sample was placed in the melting point bath (phthalic acid shows the same behavior). After recrystallization from benzene, the sample analyzed the anhydrous form, and melted smoothly at melting point 169–170° C. The infrared was identical with that of a sample prepared via the Diels–Alder reaction, described below. Anal. calc. for $C_9H_5F_3O_4$: C, 46.17; H, 2.15. Found: C, 45.76; H, 2.50.

(b) Via Diels–Alder Reaction

A solution of 5 g (0.041 mole) 2-trifluoromethylbutadiene(2) and 4 g (0.041 mole) maleic anhydride in benzene was placed in a sealed bottle and kept at room temperature for 2 hours, then heated at 100° C for 8 hours. The solution was cooled and diluted with hexane. The precipitated 4-trifluoromethyltetrahydrophthalic anhydride was filtered (8 g) and recrystallized from benzene–hexane, m.p. 107–107.5° C (lit. (1) m.p. 107°).

The anhydride (5 g, 0.0228 mole) and 2 g sulphur were heated to 240° C in an oil bath, and maintained at 240–250° C for 3 hours. On cooling, the unreacted sulphur separated. Isopropyl ether was added and the sulphur was filtered off. The filtrate, on evaporation, left 4-trifluoromethylphthalic anhydride as a fluid oil. The oil was boiled with water until it all dissolved (approx. 15 minutes), then the solution was concentrated *in vacuo* leaving 5 g of a viscous oil. This was taken up in a large volume of benzene, then the solution was concentrated to 10 ml and cooled. The product separated as a white solid, m.p. 165–167° C. When a sample of the acid was refluxed with acetic anhydride for 1 hour, then concentrated, it was reconverted to the liquid anhydride.

ACKNOWLEDGMENT

We are indebted to Dr. Dale W. Blackburn and Mr. Gerald E. Jaffe for assistance in preparing some of the intermediates used in this work.

1. A. L. HENNE and P. E. HINKAMP. J. Am. Chem. Soc. **76**, 5147 (1954).
2. P. TARRANT and R. E. TAYLOR. J. Org. Chem. **24**, 1888 (1959).

RECEIVED JANUARY 23, 1964.
SMITH, KLINE & FRENCH LABORATORIES,
PHILADELPHIA, PA.

DIRECT CONVERSION OF AROMATIC NITRILES INTO PHTHALIMIDINES AND UREAS USING DICOBALT OCTACARBONYL*

ALEX ROSENTHAL AND J. GERVAY

This note summarizes the principal results (shown in Table I) of a study on the direct carbonylation of benzonitrile, *m*-tolunitrile, and phenylacetonitrile. In 1959 Murahashi and Horiie (1) reported that benzonitrile was reduced with a 1:1 molar mixture of carbon monoxide and hydrogen in the presence of dicobalt octacarbonyl to yield amines. When the mole ratio of substrate to hydrogen was about 1:1 in the presence of a large excess of carbon monoxide, Rosenthal and Gervay (2) found that a cyclized product, namely, N-benzylphthalimidine, was produced in low yield.

The yield of N-benzylphthalimidine was increased about threefold by the concomitant

**Presented in part before the XIX International Congress of Pure and Applied Chemistry at London, England, July, 1963.*

Can. J. Chem. Downloaded from www.nrcresearchpress.com by 210.87.254.6 on 09/05/12
For personal use only.

4-Trifluoromethylphthalic Acid

(a) From 4-Trifluoromethylphthalimide

A suspension of 1 g 4-trifluoromethylphthalimide in 5 ml of 25% potassium hydroxide was stirred for 10 hours, then the solution was made strongly acidic with concentrated hydrochloric acid. The solution was heated at reflux for 1 hour, filtered, then chilled, giving 0.9 g of a glistening waxy solid. Recrystallization from water gave the 4-trifluoromethylphthalic acid as a partial hydrate. Anal. calc. for $C_9H_5F_3O_4.3/4\ H_2O$: C, 43.83; H, 2.64. Found: C, 43.84; H, 2.38.

Prolonged drying at 100° C *in vacuo* did not remove the water. The melting point varied with the rate of heating and temperature at which the sample was placed in the melting point bath (phthalic acid shows the same behavior). After recrystallization from benzene, the sample analyzed the anhydrous form, and melted smoothly at melting point 169–170° C. The infrared was identical with that of a sample prepared via the Diels–Alder reaction, described below. Anal. calc. for $C_9H_5F_3O_4$: C, 46.17; H, 2.15. Found: C, 45.76; H, 2.50.

(b) Via Diels–Alder Reaction

A solution of 5 g (0.041 mole) 2-trifluoromethylbutadiene(2) and 4 g (0.041 mole) maleic anhydride in benzene was placed in a sealed bottle and kept at room temperature for 2 hours, then heated at 100° C for 8 hours. The solution was cooled and diluted with hexane. The precipitated 4-trifluoromethyltetrahydrophthalic anhydride was filtered (8 g) and recrystallized from benzene–hexane, m.p. 107–107.5° C (lit. (1) m.p. 107°).

The anhydride (5 g, 0.0228 mole) and 2 g sulphur were heated to 240° C in an oil bath, and maintained at 240–250° C for 3 hours. On cooling, the unreacted sulphur separated. Isopropyl ether was added and the sulphur was filtered off. The filtrate, on evaporation, left 4-trifluoromethylphthalic anhydride as a fluid oil. The oil was boiled with water until it all dissolved (approx. 15 minutes), then the solution was concentrated *in vacuo* leaving 5 g of a viscous oil. This was taken up in a large volume of benzene, then the solution was concentrated to 10 ml and cooled. The product separated as a white solid, m.p. 165–167° C. When a sample of the acid was refluxed with acetic anhydride for 1 hour, then concentrated, it was reconverted to the liquid anhydride.

ACKNOWLEDGMENT

We are indebted to Dr. Dale W. Blackburn and Mr. Gerald E. Jaffe for assistance in preparing some of the intermediates used in this work.

1. A. L. HENNE and P. E. HINKAMP. J. Am. Chem. Soc. **76**, 5147 (1954).
2. P. TARRANT and R. E. TAYLOR. J. Org. Chem. **24**, 1888 (1959).

RECEIVED JANUARY 23, 1964.
SMITH, KLINE & FRENCH LABORATORIES,
PHILADELPHIA, PA.

DIRECT CONVERSION OF AROMATIC NITRILES INTO PHTHALIMIDINES AND UREAS USING DICOBALT OCTACARBONYL*

ALEX ROSENTHAL AND J. GERVAY

This note summarizes the principal results (shown in Table I) of a study on the direct carbonylation of benzonitrile, *m*-tolunitrile, and phenylacetonitrile. In 1959 Murahashi and Horiie (1) reported that benzonitrile was reduced with a 1:1 molar mixture of carbon monoxide and hydrogen in the presence of dicobalt octacarbonyl to yield amines. When the mole ratio of substrate to hydrogen was about 1:1 in the presence of a large excess of carbon monoxide, Rosenthal and Gervay (2) found that a cyclized product, namely, N-benzylphthalimidine, was produced in low yield.

The yield of N-benzylphthalimidine was increased about threefold by the concomitant

**Presented in part before the XIX International Congress of Pure and Applied Chemistry at London, England, July, 1963.*

Can. J. Chem. Downloaded from www.nrcresearchpress.com by 210.87.254.6 on 09/05/12
For personal use only.

Can. J. Chem. Downloaded from www.nrcresearchpress.com by 210.87.254.6 on 09/05/12
For personal use only.

TABLE I

Reactions of aromatic nitriles with carbon monoxide and hydrogen

Expt. No.	Substrate	Substr., mole	Catalyst, mole	Solvent, ml	CO, p.s.i.	H_2, mole	Reaction temp., °C	Reaction time, hr	Products	Yield, %
1	Benzonitrile	0.083	0.004	50	2030	—	225	2.5	N-Benzylphthalimidine	0.3
									Benzamide	0.6
2	Benzonitrile	0.093	0.004	50	2040	—	275	6	N-Benzylphthalimidine	3
									Benzamide	2
3	Benzonitrile*	0.029	0.015	25	2220	—	235	8	N-Benzylphthalimidine	8
									Benzamide	4
4	Benzonitrile	0.132	0.018	50	1800	0.12	250	10	N-Benzylphthalimidine	15
									N,N′-Dibenzylurea	8
5	Benzonitrile*	0.026	0.014	22	2320	0.02	235	8	N-Benzylphthalimidine	16
									Benzamide	10
6	Benzonitrile†	0.029	0.015	10	2120	0.035	235	8	N-Benzylphthalimidine	41
									N,N′-Dibenzylurea	16
7	*m*-Tolunitrile	0.052	0.006	50	1900	0.103	240	8.5	N-*m*-Xylylurea‡	10
									N,N′-Di-*m*-xylylurea§	14
									m-Toluamide	12
8	Phenylaceto-nitrile	0.10	0.004	50	2100	—	250	6	Phenylacetamide	3
9	Phenylaceto-nitrile	0.10	0.007	50	1740	0.20	250	8	N-Phenylacetyl-2-phenylethylamine‖	30
									Di-[2-phenylethyl]-amine¶	23
									N,N′-Di-[2-phenylethyl]-urea**	3
									Phenylacetamide	4

*0.006 mole of pyridine was added.
†0.006 mole of pyridine and 0.03 mole of benzylamine were added.
‡M.p. 150°; mixed m.p. with authentic N-*m*-xylylurea 149–150° (6).
§M.p. 137–138°; mixed m.p. with an authentic sample (7) of N,N′-di-*m*-xylylurea 137–138°.
‖M.p. 93–94°; mixed m.p. with an authentic sample (8) was 93–94°.
¶M.p. of HCl was 260–262°.
**M.p. 136–137°; mixed m.p. with an authentic sample (9) was 136–137°.

addition of pyridine to the reactants. Such an enhancement of catalytic activity of cobalt carbonyls by the addition of tertiary amines has been noted previously (3, 4). An even more dramatic increase in yield of cyclized product was achieved by the inclusion of benzylamine with the reactants. The critical dependence of cyclized product on the quantity of hydrogen was clearly shown by the fact that when the mole ratio of hydrogen to substrate was greater than 1:1, then both N-benzylphthalimidine and ureas were simultaneously produced.

The inability of phenylacetonitrile to undergo cyclization with carbon monoxide and hydrogen might be explained by the fact that the nitrile group was not conjugated with the aromatic ring. A similar lack of reactivity of non-conjugated imino groups of Schiff bases towards carbon monoxide has been previously observed (5).

In an attempt to ascertain the probable mechanism of cyclization, benzonitrile was also reacted with mixtures of carbon monoxide, hydrogen, and deuterium, and the structures of the partially deuterated N-benzylphthalimidines determined by proton nuclear magnetic resonance analysis. In two different experiments in which the deuterium content was varied (as shown in the Experimental section) the cyclic methylene group contained less than 50% normal hydrogen and approximately the same amount as that of the exocyclic methylene group. It would therefore appear that the direct transfer of the ortho hydrogen on the aromatic ring to the carbon of the C≡N group cannot be simultaneous with the cyclization process as envisaged by Murahashi and Horiie (5), but rather the catalyst must first extract the ortho hydrogen to yield a cobalt hydrocarbonyl. The latter must then rapidly equilibrate with deuterium to yield a mixture of deuterated and normal hydrogen cobalt carbonyl. Subsequent transfer of hydrogen or deuterium to the carbon would then account for the fact that the cyclic methylene group had less than one normal hydrogen atom. As attempts to isolate the reactive intermediate by chromatographic procedures were unsuccessful, further work on a study of the mechanism was abandoned.

EXPERIMENTAL

General Considerations

These have been described previously (2, 10).

Reaction of Benzonitrile with Carbon Monoxide and Hydrogen

A typical experiment was as follows.

Benzonitrile (3 g) was allowed to react with carbon monoxide (2120 p.s.i. containing 0.04% hydrogen), hydrogen (70 p.s.i., 0.035 mole), benzylamine (3.5 g), and pyridine (0.5 g) in the presence of dicobalt octacarbonyl. Work-up of the product afforded 3.1 g of solid organic material (A) and 2 g of insoluble cobalt containing residue (B).

Alumina chromatography of material (A), using benzene–chloroform (4:1 by volume) as developer, yielded the following:

(1) 0.08 g of unreacted benzonitrile;
(2) 0.08 g of slightly impure N-formyl piperidine (indicated by n.m.r. analysis);
(3) 0.65 g (42%) of N-benzylphthalimidine;
(4) 0.25 g (16%) of N,N′-dibenzylurea.

Each of the fractions was confirmed by direct comparison with authentic samples.

Insoluble Material (B)

Anal. Found: C, 16.09; H, 1.86; N, 8.20. As the chemical analyses of different samples varied considerably, no further work was done on them.

Reaction of Benzonitrile with Carbon Monoxide and Deuterium

Procedure 1

This was similar to that described above except that 50 p.s.i. of deuterium was used instead of hydrogen, and benzylamine was excluded.

Nuclear magnetic resonance of partially deuterated N-benzylphthalimidine showed cyclic methylene group (0.50 H and 1.50 D); exocyclic methylene group (0.40 H and 1.60 D).

Can. J. Chem. Downloaded from www.nrcresearchpress.com by 210.87.254.6 on 09/05/12
For personal use only.

Procedure 2

This was the same as procedure 1 except that 40 p.s.i. of deuterium was used.

Nuclear magnetic resonance of deuterated N-benzylphthalimidine showed cyclic methylene group (0.76 H and 1.24 D); exocyclic methylene group (0.76 H and 1.24 D).

ACKNOWLEDGMENTS

Grateful acknowledgment is made to the National Research Council of Canada and to the Petroleum Research Fund administered by the American Chemical Society for support of this work.

The senior author (A. R.) expresses his gratitude to University Chemical Laboratory, University of Cambridge, for use of their facilities during the writing of this manuscript.

1. S. MURAHASHI and S. HORIIE. Bull. Chem. Soc. Japan, **33**, 78 (1959).
2. A. ROSENTHAL and J. GERVAY. Chem. Ind. London, 1623 (1963).
3. R. H. HASEK and C. W. WAYMAN. U.S. Patent 2,820,059 (1958); Chem. Abstr. **53**, 13040 (1959).
4. R. IWANAGA. Bull. Chem. Soc. Japan, **35**, 865 (1962).
5. S. HORIIE and S. MURAHASHI. Bull. Chem. Soc. Japan, **33**, 247 (1960).
6. R. BRÖMME. Chem. Ber. **21**, 2703 (1888).
7. T. L. DAVIS and K. C. BLANCHARD. J. Am. Chem. Soc. **45**, 1816 (1923).
8. H. DECKER and W. KROPP. Chem. Ber. **42**, 2075 (1909).
9. J. THIELE and R. H. PICKARD. Ann. **309**, 189 (1899).
10. A. ROSENTHAL and M. R. S. WEIR. Can. J. Chem. **40**, 610 (1962).

RECEIVED NOVEMBER 1, 1963.
DEPARTMENT OF CHEMISTRY,
UNIVERSITY OF BRITISH COLUMBIA,
VANCOUVER, BRITISH COLUMBIA.

THE MOLECULAR CONFORMATION OF TRIPHENYLARSINE

M. J. ARONEY, R. J. W. LE FÈVRE, AND J. D. SAXBY

Trotter (1, 2) has recently shown, from an X-ray examination of tri-*p*-tolylarsine and tri-*p*-xylylarsine in the crystal state, that the aromatic rings in each molecule are similarly disposed relatively to the symmetry (C_3) axis. He defines the ring orientations within a molecule by angles of rotation, $\alpha°$, from an ideal model having maximum interaction of the arsenic lone pair and the aromatic π-electrons, the three rotations being in the same sense. For tri-*p*-tolylarsine the mean value of α is given as 36° and for tri-*p*-xylylarsine as 37° (the individual ring rotations for this molecule are reported as 34.6°, 37.0°, and 38.0°).

The conformations thus described agree remarkably well with that found by Aroney, Le Fèvre, and Saxby (3) for triphenylarsine in benzene solution. In our work, electric birefringence and polarity measurements [$_{\infty}(_{m}K_2) = -37.6 \times 10^{-12}$; $\mu = 1.23$ D] were interpreted as indicating a preferred conformation for triphenylarsine in which the angles of rotation (α) of the phenyl groups were 37 ± 3°. It should be noted that ϕ in ref. 3 is the complement of α. Solution of equation (3) in ref. 3 for ϕ required a knowledge of the bond angle C—As—C, which, for these calculations, was assumed to be 96° as quoted by Kuz'min and Kamai (4). If, however, the mean C—As—C angle (102°) newly reported by Trotter (1, 2) is utilized, then α for triphenylarsine as a solute in benzene is calculable as 40 ± 3°.

Can. J. Chem. Downloaded from www.nrcresearchpress.com by 210.87.254.6 on 09/05/12
For personal use only.

Procedure 2

This was the same as procedure 1 except that 40 p.s.i. of deuterium was used.

Nuclear magnetic resonance of deuterated N-benzylphthalimidine showed cyclic methylene group (0.76 H and 1.24 D); exocyclic methylene group (0.76 H and 1.24 D).

ACKNOWLEDGMENTS

Grateful acknowledgment is made to the National Research Council of Canada and to the Petroleum Research Fund administered by the American Chemical Society for support of this work.

The senior author (A. R.) expresses his gratitude to University Chemical Laboratory, University of Cambridge, for use of their facilities during the writing of this manuscript.

1. S. MURAHASHI and S. HORIIE. Bull. Chem. Soc. Japan, **33**, 78 (1959).
2. A. ROSENTHAL and J. GERVAY. Chem. Ind. London, 1623 (1963).
3. R. H. HASEK and C. W. WAYMAN. U.S. Patent 2,820,059 (1958); Chem. Abstr. **53**, 13040 (1959).
4. R. IWANAGA. Bull. Chem. Soc. Japan, **35**, 865 (1962).
5. S. HORIIE and S. MURAHASHI. Bull. Chem. Soc. Japan, **33**, 247 (1960).
6. R. BRÖMME. Chem. Ber. **21**, 2703 (1888).
7. T. L. DAVIS and K. C. BLANCHARD. J. Am. Chem. Soc. **45**, 1816 (1923).
8. H. DECKER and W. KROPP. Chem. Ber. **42**, 2075 (1909).
9. J. THIELE and R. H. PICKARD. Ann. **309**, 189 (1899).
10. A. ROSENTHAL and M. R. S. WEIR. Can. J. Chem. **40**, 610 (1962).

RECEIVED NOVEMBER 1, 1963.
DEPARTMENT OF CHEMISTRY,
UNIVERSITY OF BRITISH COLUMBIA,
VANCOUVER, BRITISH COLUMBIA.

THE MOLECULAR CONFORMATION OF TRIPHENYLARSINE

M. J. ARONEY, R. J. W. LE FÈVRE, AND J. D. SAXBY

Trotter (1, 2) has recently shown, from an X-ray examination of tri-*p*-tolylarsine and tri-*p*-xylylarsine in the crystal state, that the aromatic rings in each molecule are similarly disposed relatively to the symmetry (C_3) axis. He defines the ring orientations within a molecule by angles of rotation, $\alpha°$, from an ideal model having maximum interaction of the arsenic lone pair and the aromatic π-electrons, the three rotations being in the same sense. For tri-*p*-tolylarsine the mean value of α is given as 36° and for tri-*p*-xylylarsine as 37° (the individual ring rotations for this molecule are reported as 34.6°, 37.0°, and 38.0°).

The conformations thus described agree remarkably well with that found by Aroney, Le Fèvre, and Saxby (3) for triphenylarsine in benzene solution. In our work, electric birefringence and polarity measurements [$_{\infty}(_{m}K_2) = -37.6 \times 10^{-12}$; $\mu = 1.23$ D] were interpreted as indicating a preferred conformation for triphenylarsine in which the angles of rotation (α) of the phenyl groups were 37 ± 3°. It should be noted that ϕ in ref. 3 is the complement of α. Solution of equation (3) in ref. 3 for ϕ required a knowledge of the bond angle C—As—C, which, for these calculations, was assumed to be 96° as quoted by Kuz'min and Kamai (4). If, however, the mean C—As—C angle (102°) newly reported by Trotter (1, 2) is utilized, then α for triphenylarsine as a solute in benzene is calculable as 40 ± 3°.

Can. J. Chem. Downloaded from www.nrcresearchpress.com by 210.87.254.6 on 09/05/12
For personal use only.

ACKNOWLEDGMENT

The award of a Commonwealth Research Scholarship to J. D. S. is gratefully acknowledged.

1. J. TROTTER. Can. J. Chem. **41**, 14 (1963).
2. J. TROTTER. Acta Cryst. **16**, 1187 (1963).
3. M. J. ARONEY, R. J. W. LE FÈVRE, and J. D. SAXBY. J. Chem. Soc. 1739 (1963).
4. K. I. KUZ'MIN and G. KAMAI. Dokl. Akad. Nauk SSSR, **73**, 709 (1950).

RECEIVED MARCH 5, 1964.
DEPARTMENT OF CHEMISTRY,
UNIVERSITY OF SYDNEY,
SYDNEY, N.S.W.,
AUSTRALIA.

Can. J. Chem. Downloaded from www.nrcresearchpress.com by 210.87.254.6 on 09/05/12
For personal use only.

BONDING IN THE SULPHITE ION

E. A. ROBINSON

Recently (1), R. J. Gillespie and the author discussed the nature of bonding in compounds containing sulphur–oxygen bonds and obtained a linear correlation between their bond orders and force constants. The general applicability of such a relationship was discussed later (2).

A bond order of 1.13 was calculated for the S–O bonds in the sulphite ion on the basis of incorrect values of the stretching frequencies. Investigations of the Raman spectra of the sulphite ion in aqueous solution (and of solid Na_2SO_3) by Simon and Waldmann (3) led to assignments of the stretching frequencies at 925 cm^{-1} (symmetric stretch) and 966 cm^{-1} (asymmetric stretch). These authors calculate a force constant, k_{SO}, of 5×10^5 dynes cm^{-1} for the S–O bonds in SO_3^{2-} while direct calculation from the stretching frequencies by the simple method we used previously (1), gives $k_{SO} = 5.70 \times 10^5$ dynes cm^{-1} [i.e. $\nu_{SO} = (\nu_{sym} + \nu_{asym})/2 = 953\ cm^{-1}$, and $k_{SO} = 0.6282\ \nu_{SO}^2$].

On the basis of the linear relation between force constant and bond order [$n = 1.11\times 10^{-6}k_{SO} + 0.7$ (1)], $k_{SO} = 5.7\times10^5$ corresponds to a bond order of *1.33*, consistent with the valence bond formulation I, for which the bond length should be 1.54 Å.

It was suggested recently (4) that in sulphur–oxygen compounds a double bond orbital occupies approximately the same amount of space in the valency shell of the sulphur atom as does a lone pair orbital. Thus a bond order of 1.33 for the sulphite ion is consistent with this idea which would predict a structure for SO_3^{2-} similar to that established for the sulphate ion II (1), with a lone pair in place of one of the double bonds.

It was also shown that the bond order of the Cl–O bonds in the chlorate ion is also near to $1\frac{1}{3}$, consistent with structure III, which may be regarded as formed from the perchlorate ion IV by replacing a double bond by a lone pair of electrons. It thus appears likely that the sulphite ion and the chlorate ion, which are isoelectronic, have similar molecular structures.

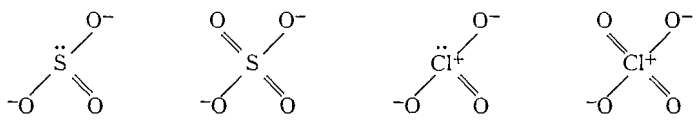

I II III IV

ACKNOWLEDGMENT

The award of a Commonwealth Research Scholarship to J. D. S. is gratefully acknowledged.

1. J. TROTTER. Can. J. Chem. **41**, 14 (1963).
2. J. TROTTER. Acta Cryst. **16**, 1187 (1963).
3. M. J. ARONEY, R. J. W. LE FÈVRE, and J. D. SAXBY. J. Chem. Soc. 1739 (1963).
4. K. I. KUZ'MIN and G. KAMAI. Dokl. Akad. Nauk SSSR, **73**, 709 (1950).

RECEIVED MARCH 5, 1964.
DEPARTMENT OF CHEMISTRY,
UNIVERSITY OF SYDNEY,
SYDNEY, N.S.W.,
AUSTRALIA.

Can. J. Chem. Downloaded from www.nrcresearchpress.com by 210.87.254.5 on 09/05/12
For personal use only.

BONDING IN THE SULPHITE ION

E. A. ROBINSON

Recently (1), R. J. Gillespie and the author discussed the nature of bonding in compounds containing sulphur–oxygen bonds and obtained a linear correlation between their bond orders and force constants. The general applicability of such a relationship was discussed later (2).

A bond order of 1.13 was calculated for the S–O bonds in the sulphite ion on the basis of incorrect values of the stretching frequencies. Investigations of the Raman spectra of the sulphite ion in aqueous solution (and of solid Na_2SO_3) by Simon and Waldmann (3) led to assignments of the stretching frequencies at 925 cm^{-1} (symmetric stretch) and 966 cm^{-1} (asymmetric stretch). These authors calculate a force constant, k_{SO}, of 5×10^5 dynes cm^{-1} for the S–O bonds in SO_3^{2-} while direct calculation from the stretching frequencies by the simple method we used previously (1), gives $k_{SO} = 5.70 \times 10^5$ dynes cm^{-1} [i.e. $\nu_{SO} = (\nu_{sym} + \nu_{asym})/2 = 953\ cm^{-1}$, and $k_{SO} = 0.6282\ \nu_{SO}^2$].

On the basis of the linear relation between force constant and bond order [$n = 1.11\times 10^{-6}k_{SO} + 0.7$ (1)], $k_{SO} = 5.7\times10^5$ corresponds to a bond order of *1.33*, consistent with the valence bond formulation I, for which the bond length should be 1.54 Å.

It was suggested recently (4) that in sulphur–oxygen compounds a double bond orbital occupies approximately the same amount of space in the valency shell of the sulphur atom as does a lone pair orbital. Thus a bond order of 1.33 for the sulphite ion is consistent with this idea which would predict a structure for SO_3^{2-} similar to that established for the sulphate ion II (1), with a lone pair in place of one of the double bonds.

It was also shown that the bond order of the Cl–O bonds in the chlorate ion is also near to $1\frac{1}{3}$, consistent with structure III, which may be regarded as formed from the perchlorate ion IV by replacing a double bond by a lone pair of electrons. It thus appears likely that the sulphite ion and the chlorate ion, which are isoelectronic, have similar molecular structures.

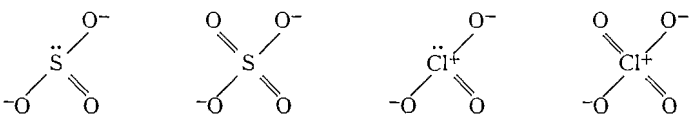

I II III IV

1. R. J. GILLESPIE and E. A. ROBINSON. Can. J. Chem. **41**, 2074 (1963).
2. E. A. ROBINSON and M. W. LISTER. Can. J. Chem. **41**, 2988 (1963).
3. A. SIMON and K. WALDMANN. Z. Physik. Chem. **204**, 235 (1955).
4. E. A. ROBINSON. Can. J. Chem. **41**, 3021 (1963).

RECEIVED FEBRUARY 6, 1964.
DEPARTMENT OF CHEMISTRY,
UNIVERSITY OF TORONTO,
TORONTO 5, ONTARIO.

Can. J. Chem. Downloaded from www.nrcresearchpress.com by 210.87.254.5 on 09/05/12
For personal use only.

THE SYNTHESIS OF ANHYDROUS ZIRCONIUM TRICHLORIDE

B. SWAROOP AND S. N. FLENGAS

INTRODUCTION

Zirconium trichloride was first prepared by Ruff and Wallstein (1) by the reduction of zirconium tetrachloride with aluminum. The product, however, was contaminated with up to 4 weight % aluminum metal, and also contained oxygen. Larsen and Leddy (2) eliminated the aluminum contamination by carrying the reaction at 500° C in sealed pyrex ampoules containing stoichiometric amounts of zirconium tetrachloride, and aluminum or zirconium metal powders as the reductants. To prevent the explosion of the system, because of the vaporization of the excess zirconium tetrachloride during the initial stage of the reaction, the ampoules were placed within a stainless steel pressurized container filled with nitrogen gas. The gas pressure inside the bomb was then regulated to match the internal pressure of zirconium tetrachloride in the system, and pressures as high as 15 atmospheres were found necessary.

Under these conditions, $ZrCl_3$ of a maximum purity of only 85 weight % was obtained, the remainder being $ZrCl_2$ formed by disproportionation. The method was applied only to small quantities of zirconium tetrachloride (about 1 g) because of the obvious difficulty in balancing accurately the pressure in the system during the reaction.

In the present investigation, zirconium trichloride of a purity over 98 weight % was produced by the direct reaction between finely divided zirconium metal and zirconium tetrachloride at atmospheric pressure. The method, although essentially a batch process, could be adopted for preparation of larger quantities of the compound, if required.

EXPERIMENTAL AND RESULTS

Hafnium-free zirconium tetrachloride of commercial grade was further purified by double sublimation in vacuum in the presence of finely divided copper filings. The front and end tailings of the distillate were rejected and the middle portion was stored in sealed containers. Reactor grade zirconium metal containing less than 200 p.p.m. Hf was filed in a dry box filled with nitrogen gas to a particle size of about 80 mesh.

The zirconium trichloride was produced by the direct reaction:

[1] $$3ZrCl_{4\ (gas\ at\ 1\ atm)} + Zr_{(s)} = 4ZrCl_{3\ (s)}.$$

Figure 1 shows the reaction apparatus which was constructed from quartz glass.

The zirconium tetrachloride was placed in the right-hand compartment of the reaction cell, and the finely divided zirconium metal was placed in the left-hand compartment, which was completely lined with either zirconium or platinum foil. The cell was then evacuated and heated under vacuum to about 150° C for 6–8 hours, and then the ends were flame sealed under vacuum. The part of the reaction tube containing the zirconium metal was then heated slowly to about 700° C–750° C, while the compartment containing the zirconium tetrachloride in the system was heated to 330° ± 2° C. At this temperature, the pressure of zirconium tetrachloride vapor in the system was about 1 atm. To prevent the condensation of $ZrCl_4$, the two compartments were separated by a ¼ in. diameter quartz tube which was also heated to about 350° C.

1. R. J. GILLESPIE and E. A. ROBINSON. Can. J. Chem. **41**, 2074 (1963).
2. E. A. ROBINSON and M. W. LISTER. Can. J. Chem. **41**, 2988 (1963).
3. A. SIMON and K. WALDMANN. Z. Physik. Chem. **204**, 235 (1955).
4. E. A. ROBINSON. Can. J. Chem. **41**, 3021 (1963).

RECEIVED FEBRUARY 6, 1964.
DEPARTMENT OF CHEMISTRY,
UNIVERSITY OF TORONTO,
TORONTO 5, ONTARIO.

Can. J. Chem. Downloaded from www.nrcresearchpress.com by 84.22.46.98 on 09/08/12
For personal use only.

THE SYNTHESIS OF ANHYDROUS ZIRCONIUM TRICHLORIDE

B. SWAROOP AND S. N. FLENGAS

INTRODUCTION

Zirconium trichloride was first prepared by Ruff and Wallstein (1) by the reduction of zirconium tetrachloride with aluminum. The product, however, was contaminated with up to 4 weight % aluminum metal, and also contained oxygen. Larsen and Leddy (2) eliminated the aluminum contamination by carrying the reaction at 500° C in sealed pyrex ampoules containing stoichiometric amounts of zirconium tetrachloride, and aluminum or zirconium metal powders as the reductants. To prevent the explosion of the system, because of the vaporization of the excess zirconium tetrachloride during the initial stage of the reaction, the ampoules were placed within a stainless steel pressurized container filled with nitrogen gas. The gas pressure inside the bomb was then regulated to match the internal pressure of zirconium tetrachloride in the system, and pressures as high as 15 atmospheres were found necessary.

Under these conditions, $ZrCl_3$ of a maximum purity of only 85 weight % was obtained, the remainder being $ZrCl_2$ formed by disproportionation. The method was applied only to small quantities of zirconium tetrachloride (about 1 g) because of the obvious difficulty in balancing accurately the pressure in the system during the reaction.

In the present investigation, zirconium trichloride of a purity over 98 weight % was produced by the direct reaction between finely divided zirconium metal and zirconium tetrachloride at atmospheric pressure. The method, although essentially a batch process, could be adopted for preparation of larger quantities of the compound, if required.

EXPERIMENTAL AND RESULTS

Hafnium-free zirconium tetrachloride of commercial grade was further purified by double sublimation in vacuum in the presence of finely divided copper filings. The front and end tailings of the distillate were rejected and the middle portion was stored in sealed containers. Reactor grade zirconium metal containing less than 200 p.p.m. Hf was filed in a dry box filled with nitrogen gas to a particle size of about 80 mesh.

The zirconium trichloride was produced by the direct reaction:

[1] $$3ZrCl_{4\ (gas\ at\ 1\ atm)} + Zr_{(s)} = 4ZrCl_{3\ (s)}.$$

Figure 1 shows the reaction apparatus which was constructed from quartz glass.

The zirconium tetrachloride was placed in the right-hand compartment of the reaction cell, and the finely divided zirconium metal was placed in the left-hand compartment, which was completely lined with either zirconium or platinum foil. The cell was then evacuated and heated under vacuum to about 150° C for 6–8 hours, and then the ends were flame sealed under vacuum. The part of the reaction tube containing the zirconium metal was then heated slowly to about 700° C–750° C, while the compartment containing the zirconium tetrachloride in the system was heated to 330° ± 2° C. At this temperature, the pressure of zirconium tetrachloride vapor in the system was about 1 atm. To prevent the condensation of $ZrCl_4$, the two compartments were separated by a ¼ in. diameter quartz tube which was also heated to about 350° C.

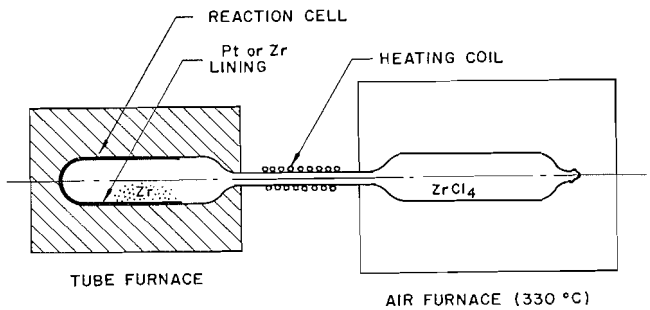

FIG. 1. Reaction apparatus.

It should be noted that all operations involving the handling and transfer of the reactive zirconium halides were done inside a dry box filled with nitrogen gas.

To drive reaction (1) to completion, and to avoid the possible disproportionation of the zirconium trichloride, an excess of zirconium tetrachloride was always present, i.e., 1.5 times the quantity required by the stoichiometry of the reaction. Thus, amounts of approximately 1 g of zirconium powder to about 12 g of zirconium tetrachloride were used in each of the preparations. The reaction time was about 72 hours. After the end of the run, the temperature of the zirconium trichloride compartment was gradually reduced to about 400° C, while that of the zirconium tetrachloride was reduced to about 250° C. When all the unreacted zirconium tetrachloride had been removed from the reaction site, the cell was rapidly cooled down, transferred to the dry box, and opened under an atmosphere of nitrogen gas.

The reaction products were free zirconium trichloride powder, and zirconium trichloride adhering to the surface of the unreacted zirconium metal. To separate the unreacted metal, the product was screened through a 200-mesh screen, and the zirconium trichloride was stored in sealed containers. The screened product was analyzed by three different methods.

(*a*) By the chlorine content determined by Volhard's method (3).

(*b*) By measuring the reducing power of the material with an $N/10$ ceric ammonium sulphate solution. To this purpose, 0.15 to 0.25 g of material was added to the solution containing the ceric salt, which was then back titrated with a $N/10$ sodium oxalate solution.

(*c*) By measuring the volume of hydrogen gas evolved when zirconium trichloride is added to distilled water, following the reaction:

$$[2] \qquad ZrCl_3 + H_2O = ZrOCl_2 + HCl + \tfrac{1}{2}H_2.$$

The results of analysis of the various batches are shown in Table I.

Zirconium trichloride is a blue-black powder which changes to brown when exposed to air. The compound dissolves in water to give a yellow-brown solution, but the color fades away when the solution is allowed to stand.

At high temperatures, both zirconium metal and zirconium tetrachloride react with the silica container in the reaction cell, and without the zirconium or platinum foil linings, all reaction efficiencies become much lower. The overall efficiency of the reaction before screening of the product is about 45%, and attempts to increase this efficiency by increasing the reaction temperature, failed. This is shown in Fig. 2, where the relative total efficiency of the reaction for the same amounts of reactants is plotted against temperature. The reaction time for the runs shown on the graph was always 72 hours. The effect of lining the reaction zone with zirconium and platinum foil is also indicated.

It is evident that the optimum temperature is about 700° C–750° C and that a platinum-lined cell gives only slightly higher efficiencies. The plateau of the efficiency curve in Fig. 2 indicates that the reaction reaches a pseudoequilibrium for that particular particle size of zirconium metal used in the study. It is probable that the reaction is diffusion controlled, and the use of more finely divided metal would increase the overall efficiency, and the purity of the product.

ACKNOWLEDGMENT

The authors are indebted to the Defence Research Board of Canada for its financial assistance in support of this work.

1. O. RUFF and R. WALLSTEIN. Z. Anorg. Allgem. Chem. **128**, 96 (1923).
2. E. N. LARSEN and J. J. LEDDY. J. Am. Chem. Soc. **78**, 5983 (1956).
3. J. R. CALDWELL and H. V. MOYER. Ind. Eng. Chem. **7**, 1, 38 (1935).

Can. J. Chem. Downloaded from www.nrcresearchpress.com by 84.22.46.98 on 09/08/12
For personal use only.

Can. J. Chem. Downloaded from www.nrcresearchpress.com by 84.22.46.98 on 09/08/12
For personal use only.

TABLE I

Analysis of zirconium trichloride

Run No.	Cell lining	Chlorine analysis				Redox titration			Hydrogen evolution		
		Wt. of sample (g)	Wt. % chlorine (theor.)	Wt. % chlorine (expt.)	Wt. % $ZrCl_3$	Wt. of sample	$ZrCl_3$ content (g)	Wt. % $ZrCl_3$	Wt. of sample (g)	Corrected vol. of H_2 at °C in cm^3	g-equivalent weight of $ZrCl_3$ (theor. = 197.8)
1	Zr	—	—	—	—	0.205	0.1150	95.8	0.120	6.19	218
2	Zr	0.1555	53.9	51.6	95.7	—	—	—	—	—	—
3	Zr	0.2115	53.9	51.3	95.0	—	—	—	—	—	—
4	Pt	0.2220	53.9	52.2	97.0	0.1998	0.1952	98.2	0.152	8.50	200
5	Pt	0.1120	53.9	50.8	94.5	—	—	—	—	—	—
6	Pt	0.2260	53.9	53.5	99.2	0.2015	0.1982	98.7	—	—	—
7	Pt	—	—	—	—	—	—	—	0.122	6.94	198

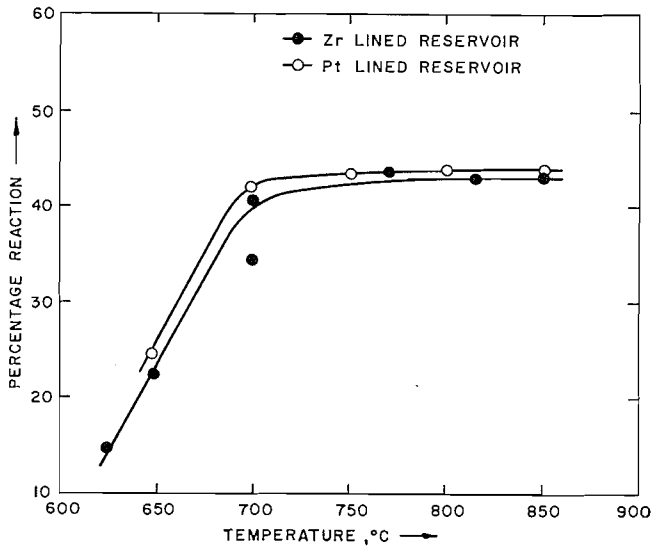

FIG. 2. Reaction efficiencies.

RECEIVED JANUARY 23, 1964.
DEPARTMENT OF METALLURGICAL ENGINEERING,
UNIVERSITY OF TORONTO,
TORONTO, ONTARIO.

CONFORMATIONAL STUDIES OF THE CYCLOHEXANE RING BY NUCLEAR MAGNETIC RESONANCE. VII.* THE REACTION OF 1,4-CYCLOHEXANEDIOL WITH CONCENTRATED HYDROCHLORIC ACID

E. PREMUZIC AND L. W. REEVES

In our investigation of the chemistry of cyclohexane and its derivatives suitable for conformational analysis by n.m.r., we investigated a reported reaction for preparation of 4-chlorocyclohexanol. Owen and Robins (1) and Grewe *et al.* (2) reported a procedure in which a cis and trans mixture of 1,4-cyclohexanediol on treatment with an excess of fuming hydrochloric acid yields 4-chlorocyclohexanol in a good yield (more than 50%). We wish to comment on this reaction.

A mixture of *cis-* and *trans*-1,4-cyclohexanediol (0.98 moles) and concentrated hydrochloric acid (4.1 moles) was sealed in a Carius tube and then heated at 80–90° for 14 hours (1). On cooling of the reaction mixture an oily layer separated. The reaction mixture was then extracted with chloroform, washed with aqueous sodium bicarbonate, and dried over anhydrous sodium sulphate. Chloroform was removed by distillation. Fractional distillation of the residue at 4 mm yielded a colorless oil (75 g), b.p. 80–85°. The oily derivative was then cooled at −10°. A heavy white crystalline precipitate formed, which was collected and recrystallized from ethanol (F_1, m.p. 102–103°). The filtrate was redistilled at 5 mm, yielding 9 g of a colorless oil, b.p. 80–82°, n_D^{16} 1.4964, F_2, and 3 g of

* *VI in preparation.*

Can. J. Chem. Downloaded from www.nrcresearchpress.com by 84.22.46.98 on 09/08/12
For personal use only.

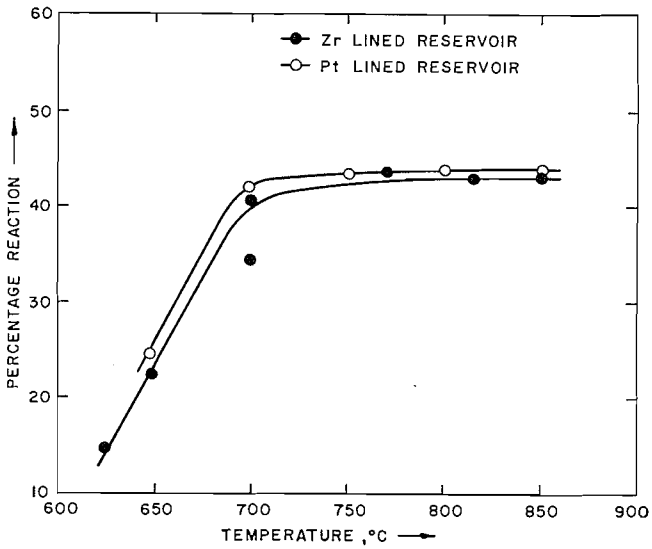

FIG. 2. Reaction efficiencies.

RECEIVED JANUARY 23, 1964.
DEPARTMENT OF METALLURGICAL ENGINEERING,
UNIVERSITY OF TORONTO,
TORONTO, ONTARIO.

Can. J. Chem. Downloaded from www.nrcresearchpress.com by 210.87.254.42 on 09/05/12
For personal use only.

CONFORMATIONAL STUDIES OF THE CYCLOHEXANE RING BY NUCLEAR MAGNETIC RESONANCE. VII.* THE REACTION OF 1,4-CYCLOHEXANEDIOL WITH CONCENTRATED HYDROCHLORIC ACID

E. PREMUZIC AND L. W. REEVES

In our investigation of the chemistry of cyclohexane and its derivatives suitable for conformational analysis by n.m.r., we investigated a reported reaction for preparation of 4-chlorocyclohexanol. Owen and Robins (1) and Grewe *et al.* (2) reported a procedure in which a cis and trans mixture of 1,4-cyclohexanediol on treatment with an excess of fuming hydrochloric acid yields 4-chlorocyclohexanol in a good yield (more than 50%). We wish to comment on this reaction.

A mixture of *cis-* and *trans*-1,4-cyclohexanediol (0.98 moles) and concentrated hydrochloric acid (4.1 moles) was sealed in a Carius tube and then heated at 80–90° for 14 hours (1). On cooling of the reaction mixture an oily layer separated. The reaction mixture was then extracted with chloroform, washed with aqueous sodium bicarbonate, and dried over anhydrous sodium sulphate. Chloroform was removed by distillation. Fractional distillation of the residue at 4 mm yielded a colorless oil (75 g), b.p. 80–85°. The oily derivative was then cooled at −10°. A heavy white crystalline precipitate formed, which was collected and recrystallized from ethanol (F_1, m.p. 102–103°). The filtrate was redistilled at 5 mm, yielding 9 g of a colorless oil, b.p. 80–82°, n_D^{16} 1.4964, F_2, and 3 g of

* *VI in preparation.*

residue, F_3. The residue, on being cooled at $-10°$, yielded a small amount of white crystals identical with those collected in F_1 (mixed m.p. 102–102.8°). The mother liquor, F_4, was kept in cold for further investigation. The n.m.r. spectra of fractions F_1 to F_4 (30% solutions in carbon tetrachloride, with internal tetramethylsilane standard), recorded on a Varian A60 spectrometer, showed the following general pattern: F_1, no hydroxyl peak; F_2, hydroxyl peak present; F_3, crystals, identical spectra with F_1; F_4 showed presence of F_1 and a peak at low field. The F_2 fraction would thus seem to be consistent with the *cis–trans*-4-chlorocyclohexanol obtained by Owen and Robins (1). This fraction was then oxidized with chromic acid to 4-chlorocyclohexanone (b.p. 81–90° at 12 mm). Melting point of the semicarbazone, 178°, is consistent with the result obtained by Grewe *et al.* (2). 4-Chlorocyclohexanone was then adjacently deuterated in the usual manner (5). Nuclear magnetic resonance spectra (30% solution in carbon tetrachloride, tetramethylsilane internal standard, Varian A60 spectrometer) have shown the expected nine lines (6) in the —CHCl— region ($\tau = 5.5$), the coupling constants being $|J| = 4.10 \pm 0.1$ c.p.s. and $|J| = 5.6 \pm 0.1$ c.p.s. (Fig. 1). Unlike 3,3,4,4,5,5-hexadeuterocyclohexanol where the two

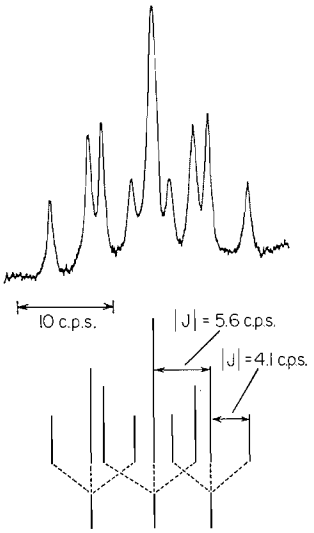

FIG. 1. C-4 proton resonance of 4-chlorocyclohexanone-2,2,6,6-d_4 at 60 Mc.

vicinal coupling constants are 9.77 and 3.93 c.p.s. (6), the ketone shows two almost equal coupling constants. The high-field $(AB)_2$ components of the spectrum were broad and marred by some 1,4-*trans*-dichlorocyclohexane, which was present as impurity. It was not possible to extract reliable chemical shift measurements in the high-field region. The values of these coupling constants in the ketone are indicative of two contributing pseudochair forms in which the carbon atoms of the cyclohexanone ring are much nearer a plane than in cyclohexane. This is reasonable in view of the trigonal carbon at the 1 position. An equally plausible explanation is the assumption that bond angles at the 3, 4, and 5 position are not appreciably distorted and the chlorine atom has ~60% probability of being axial. From the results obtained, it is evident that the reaction suggested by Owen and Robins (1) gives rise to only a small amount of 4-chlorocyclohexanol, viz., only 12% of the total yield.

Can. J. Chem. Downloaded from www.nrcresearchpress.com by 210.87.254.42 on 09/05/12
For personal use only.

Recently, Franzus and Hudson (3), and Russell and co-workers (4) reported an extensive study of 1,3-dibromocyclohexanes and 1,3- and 1,4-dichlorocyclohexanes. Acidic treatment, with either hydrobromic acid or hydrochloric acid of 1,4- (or 1,3-) cyclohexanediols yielded cis–trans mixtures of dihalogen-substituted cyclohexanes.

The bulk of our product (F_1), when isolated and recrystallized from ethanol, melts at 102–103°, in agreement with *trans*-1,4-dichlorocyclohexane prepared by Russell and co-workers by a similar procedure. Proton magnetic resonance spectra show a peak at $\tau = 5.9$ (Russell *et al.* $\tau = 5.82$), due to the methine protons in 1,4-dichlorocyclohexane, the C-1 and C-4 protons being predominantly diaxial. Proton magnetic resonance spectra of F_4 showed presence of *trans*-1,4-dichlorocyclohexane ($\tau = 5.9$) and a peak at $\tau = 5.67$, consistent with the signal due to methine protons of *trans*-1,3-dichlorocyclohexane (4). The reaction between 1,4-cyclohexanediol and hydrochloric acid was then followed up in the manner described below.

A series of Carius tubes each containing 0.98 moles of the diol and 4.1 moles of hydrochloric acid were sealed and heated at 80–90°. At regular intervals one tube was cooled, and the reaction mixture worked up as described at the beginning of the note. The isolated products were then analyzed by n.m.r. (30% carbon tetrachloride solution, int. TMS). In addition to unreacted material, 4-chlorocyclohexanol, 1,4-dichlorocyclohexane, peaks at $\tau = 4.45$ and $\tau = 2.9$ appeared. The $\tau = 4.45$ peak is consistent with formation of 1,4-cyclohexadiene and the $\tau = 2.9$ peak is consistent with formation of aromatic by-products. Presence of 1,3-dichlorocyclohexane in our F_4 fraction can thus be explained as due to the random addition of hydrochloric acid across the double bonds in 1,4-cyclohexadiene.

1. L. N. Owen and P. A. Robins. J. Chem. Soc. 329 (1949).
2. R. Grewe, W. Lorenzen, and L. Vining. Chem. Ber. **87**, 796 (1954).
3. B. Franzus and B. E. Hudson, Jr. J. Org. Chem. **28**, 2238 (1963).
4. J. A. Russell, A. Ito, and R. Konaka. J. Am. Chem. Soc. **85**, 2988 (1963).
5. E. Premuzic and L. W. Reeves. Can. J. Chem. **40**, 1870 (1962).
6. F. A. L. Anet. J. Am. Chem. Soc. **84**, 1053 (1962).

Received February 5, 1964.
Chemistry Department,
University of British Columbia,
Vancouver 8, B.C.

CONDENSATION OF HEXACHLOROCYCLOPENTADIENE WITH DIETHANOLAMINE*

Marwan R. Kamal and John E. Wicklatz

The reactivity of the allylic chlorine atoms in hexachlorocyclopentadiene and the ease of their displacement by nucleophiles had been previously demonstrated by other workers (1, 2). Recently, McBee and co-workers (3) demonstrated this type of reaction with secondary amines.

We wish to report the reaction between the amino alcohol diethanolamine and hexachlorocyclopentadiene. In this reaction the expected product (I) was not isolated. Instead, the spiro compound (II) resulting from the condensation of 1 mole of diethanolamine with hexachlorocyclopentadiene followed by a cyclization step with the elimination of a mole of hydrogen chloride was obtained.

Journal Series Number 354, Central Research Laboratories, General Mills, Inc.

Can. J. Chem. Downloaded from www.nrcresearchpress.com by 210.87.254.42 on 09/05/12
For personal use only.

Recently, Franzus and Hudson (3), and Russell and co-workers (4) reported an extensive study of 1,3-dibromocyclohexanes and 1,3- and 1,4-dichlorocyclohexanes. Acidic treatment, with either hydrobromic acid or hydrochloric acid of 1,4- (or 1,3-) cyclohexanediols yielded cis–trans mixtures of dihalogen-substituted cyclohexanes.

The bulk of our product (F_1), when isolated and recrystallized from ethanol, melts at 102–103°, in agreement with *trans*-1,4-dichlorocyclohexane prepared by Russell and co-workers by a similar procedure. Proton magnetic resonance spectra show a peak at $\tau = 5.9$ (Russell *et al.* $\tau = 5.82$), due to the methine protons in 1,4-dichlorocyclohexane, the C-1 and C-4 protons being predominantly diaxial. Proton magnetic resonance spectra of F_4 showed presence of *trans*-1,4-dichlorocyclohexane ($\tau = 5.9$) and a peak at $\tau = 5.67$, consistent with the signal due to methine protons of *trans*-1,3-dichlorocyclohexane (4). The reaction between 1,4-cyclohexanediol and hydrochloric acid was then followed up in the manner described below.

A series of Carius tubes each containing 0.98 moles of the diol and 4.1 moles of hydrochloric acid were sealed and heated at 80–90°. At regular intervals one tube was cooled, and the reaction mixture worked up as described at the beginning of the note. The isolated products were then analyzed by n.m.r. (30% carbon tetrachloride solution, int. TMS). In addition to unreacted material, 4-chlorocyclohexanol, 1,4-dichlorocyclohexane, peaks at $\tau = 4.45$ and $\tau = 2.9$ appeared. The $\tau = 4.45$ peak is consistent with formation of 1,4-cyclohexadiene and the $\tau = 2.9$ peak is consistent with formation of aromatic by-products. Presence of 1,3-dichlorocyclohexane in our F_4 fraction can thus be explained as due to the random addition of hydrochloric acid across the double bonds in 1,4-cyclohexadiene.

1. L. N. Owen and P. A. Robins. J. Chem. Soc. 329 (1949).
2. R. Grewe, W. Lorenzen, and L. Vining. Chem. Ber. **87**, 796 (1954).
3. B. Franzus and B. E. Hudson, Jr. J. Org. Chem. **28**, 2238 (1963).
4. J. A. Russell, A. Ito, and R. Konaka. J. Am. Chem. Soc. **85**, 2988 (1963).
5. E. Premuzic and L. W. Reeves. Can. J. Chem. **40**, 1870 (1962).
6. F. A. L. Anet. J. Am. Chem. Soc. **84**, 1053 (1962).

Received February 5, 1964.
Chemistry Department,
University of British Columbia,
Vancouver 8, B.C.

CONDENSATION OF HEXACHLOROCYCLOPENTADIENE WITH DIETHANOLAMINE*

Marwan R. Kamal and John E. Wicklatz

The reactivity of the allylic chlorine atoms in hexachlorocyclopentadiene and the ease of their displacement by nucleophiles had been previously demonstrated by other workers (1, 2). Recently, McBee and co-workers (3) demonstrated this type of reaction with secondary amines.

We wish to report the reaction between the amino alcohol diethanolamine and hexachlorocyclopentadiene. In this reaction the expected product (I) was not isolated. Instead, the spiro compound (II) resulting from the condensation of 1 mole of diethanolamine with hexachlorocyclopentadiene followed by a cyclization step with the elimination of a mole of hydrogen chloride was obtained.

Journal Series Number 354, Central Research Laboratories, General Mills, Inc.

Can. J. Chem. Downloaded from www.nrcresearchpress.com by 210.87.254.6 on 09/05/12
For personal use only.

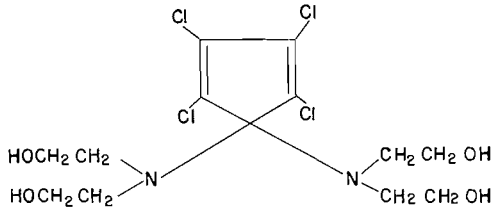

I

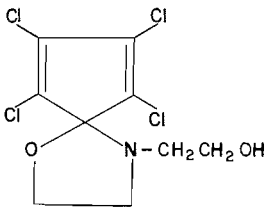

II

The structure of II was elucidated by mass spectrometry, nuclear magnetic resonance, and infrared spectra. The mass spectrum showed a parent peak at 303 (based on Cl^{35} isomer) with characteristic isotope peaks for an ion containing 4 Cl atoms. The n.m.r. spectrum showed a pair of triplets for the ring $—CH_2—N\langle$ and $—CH_2—O$ protons at 3.39 and 4.28 p.p.m. respectively. Another pair of triplets for the open chain $—CH_2—N\langle$ and $—CH_2—O$ protons was seen at 2.67 and 3.57 p.p.m. respectively. A single proton, attributed to —OH, was seen at 1.89 p.p.m. An examination of the n.m.r. spectrum of β-dimethylaminoethanol showed a pair of triplets at 2.38 and 3.50 p.p.m. for the $—CH_2—N\langle$ and $—CH_2—O$ protons respectively.

This cyclization is presumably favored over the further condensation of another diethanolamine molecule which would give the 5,5-bis-(dihydroxyethylamino)-1,2,3,4-tetrachlorocyclopentadiene (I). Steric factors probably contribute to the tendency toward cyclization.

The aminoketal product (II) is easily hydrolyzed in an acid medium to give octachloro-3a,4,7,7a-tetrahydro-4,7-methanoindene-1,8-dione (III). The diketone is undoubtedly the product obtained by the dimerization of the unstable intermediate tetrachlorocyclopentadienone (4).

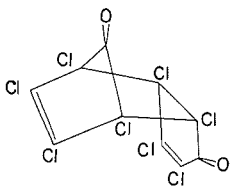

III

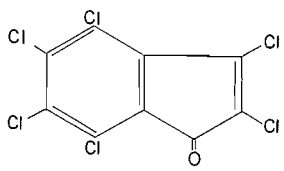

IV

The diketone III was readily converted to hexachloroindone IV by treatment with aqueous acetone (5).

Can. J. Chem. Downloaded from www.nrcresearchpress.com by 210.87.254.6 on 09/05/12
For personal use only.

Can. J. Chem. Downloaded from www.nrcresearchpress.com by 210.87.254.6 on 09/05/12
For personal use only.

EXPERIMENTAL*

1-Oxa-4-hydroxyethylazaspiro[4.4]6,7,8,9-tetrachlorononona-6,9-diene [II]

Potassium hydroxide (22.4 g) was dissolved in 200 ml of isopropanol in a 500-ml, three-necked flask fitted with a stirrer, a thermometer, and a water-cooled condenser. Forty-two grams of diethanolamine and 54.6 g of hexachlorocyclopentadiene were added to the above solution. An immediate exothermic reaction occurred raising the temperature to about 75° C and a solid began to form. The flask was cooled with an ice-water bath to 30° C. The mixture was stirred for 48 hours while the temperature was maintained at 30° C ±5°. The solid which was formed was filtered and identified as potassium chloride. After removing the solvent under reduced pressure, the dark viscous residue was dissolved in benzene and extracted several times with a slightly acidic 20% sodium chloride solution until the aqueous phase was acidic. The organic phase was washed with water and then dried over anhydrous sodium sulphate. The solvent was then removed and pentane added to the residue.† After cooling in an ice bath 48.7 g of solid material was formed. The solid was dissolved in Skelly-B, the solution treated with charcoal, filtered, and the filtrate cooled to give 35.0 g (57%) of white needles II, m.p. 61–63° C. Anal. Calc. for $C_9H_9NO_2Cl_4$: C, 35.45; H, 2.97; N, 4.59; Cl, 46.51. Found: C, 35.76; H, 3.07; N, 4.91; Cl, 46.23.

The infrared spectrum of the product in carbon tetrachloride showed the following peaks between 6.17 and 10.47 μ: 6.17 (s), 6.29 (w-m), 8.28 (s), 8.54 (m), 8.86 (m), 9.32 (s), 9.97 (s), and 10.47 (s) μ.

Acid Hydrolysis of II

A solution of II (18 g) in 240 ml of acetone and 600 ml of concentrated hydrochloric acid was refluxed for 90 minutes. After the solution was cooled to room temperature, the precipitate was filtered. The solid was dried in a vacuum oven to give 11.9 g of III, m.p. 159–161° C dec. Recrystallization from hexane gave 11.7 g (92%) of pure product, m.p. 160–161° C dec.; λ_{max}^{KBr} 5.40 (s), 5.68 (s), 6.27 (s) μ; ϵ mol. = 9100 at 255 mμ in cyclohexane. Anal. Calc. for $C_{10}O_2Cl_8$: Cl, 65.09. Found: Cl, 64.90.

1. J. A. Krynitsky and R. W. Bost. J. Am. Chem. Soc. **69**, 1918 (1947).
2. E. T. McBee, D. L. Crain, R. D. Crain, L. R. Belohlav, and H. P. Braendlin. J. Am. Chem. Soc. **84**, 3557 (1962).
3. E. T. McBee, J. O. Stoffer, and H. P. Braendlin. J. Am. Chem. Soc. **84**, 4540 (1962).
4. J. S. Newcomer and E. T. McBee. J. Am. Chem. Soc. **71**, 946 (1949).
5. P. Eaton, E. Carlson, P. Lombardo, and P. Yates. J. Org. Chem. **25**, 1225 (1960).

Received January 22, 1964.
Central Research Laboratory,
General Mills, Inc.,
Minneapolis, Minnesota.

**All melting points are uncorrected. The mass and n.m.r. spectra were furnished by Dr. L. E. Peterson, General Mills. A 10% concentration of the compound in CCl_4 was used for the n.m.r. and chemical shifts are reported in p.p.m. relative to internal tetramethylsilane. Infrared and ultraviolet spectra were furnished by Mr. Robert Fisher and Miss Delores Bell, General Mills.*

†An attempt to distill the residue prior to the addition of pentane resulted in heavy gas evolution with a great deal of exotherm. Thus, distillation would not be recommended as a purification method.

REARRANGEMENT STUDIES WITH ^{14}C. XX. SOME OBSERVATIONS ON REACTIONS BETWEEN GRIGNARD REAGENT, COBALTOUS BROMIDE, AND 2-PHENYLETHYL BROMIDE

C. C. Lee and D. P. Thornhill*

In a previous paper (1), it was demonstrated that contrary to an earlier report of Smith and Anderson (2), the reaction of 2-phenyl-1-^{14}C-ethyl bromide with magnesium and cobaltous bromide in refluxing ether gave ethylbenzene and styrene with no isotope position rearrangement. Since this reaction has some resemblance to the cobaltous halide catalyzed reaction between a Grignard reagent and an organic halide (designated by Slaugh (3) as the Kharasch reaction), which is believed to involve intermediate free radicals

**Holder of a Commonwealth Scholarship, 1961–63.*

Can. J. Chem. Downloaded from www.nrcresearchpress.com by 210.87.254.105 on 09/05/12
For personal use only.

EXPERIMENTAL*

1-Oxa-4-hydroxyethylazaspiro[4.4]6,7,8,9-tetrachlorononona-6,9-diene [II]

Potassium hydroxide (22.4 g) was dissolved in 200 ml of isopropanol in a 500-ml, three-necked flask fitted with a stirrer, a thermometer, and a water-cooled condenser. Forty-two grams of diethanolamine and 54.6 g of hexachlorocyclopentadiene were added to the above solution. An immediate exothermic reaction occurred raising the temperature to about 75° C and a solid began to form. The flask was cooled with an ice-water bath to 30° C. The mixture was stirred for 48 hours while the temperature was maintained at 30° C ±5°. The solid which was formed was filtered and identified as potassium chloride. After removing the solvent under reduced pressure, the dark viscous residue was dissolved in benzene and extracted several times with a slightly acidic 20% sodium chloride solution until the aqueous phase was acidic. The organic phase was washed with water and then dried over anhydrous sodium sulphate. The solvent was then removed and pentane added to the residue.† After cooling in an ice bath 48.7 g of solid material was formed. The solid was dissolved in Skelly-B, the solution treated with charcoal, filtered, and the filtrate cooled to give 35.0 g (57%) of white needles II, m.p. 61–63° C. Anal. Calc. for $C_9H_9NO_2Cl_4$: C, 35.45; H, 2.97; N, 4.59; Cl, 46.51. Found: C, 35.76; H, 3.07; N, 4.91; Cl, 46.23.

The infrared spectrum of the product in carbon tetrachloride showed the following peaks between 6.17 and 10.47 μ: 6.17 (s), 6.29 (w-m), 8.28 (s), 8.54 (m), 8.86 (m), 9.32 (s), 9.97 (s), and 10.47 (s) μ.

Acid Hydrolysis of II

A solution of II (18 g) in 240 ml of acetone and 600 ml of concentrated hydrochloric acid was refluxed for 90 minutes. After the solution was cooled to room temperature, the precipitate was filtered. The solid was dried in a vacuum oven to give 11.9 g of III, m.p. 159–161° C dec. Recrystallization from hexane gave 11.7 g (92%) of pure product, m.p. 160–161° C dec.; λ_{max}^{KBr} 5.40 (s), 5.68 (s), 6.27 (s) μ; ϵ mol. = 9100 at 255 mμ in cyclohexane. Anal. Calc. for $C_{10}O_2Cl_8$: Cl, 65.09. Found: Cl, 64.90.

1. J. A. Krynitsky and R. W. Bost. J. Am. Chem. Soc. **69**, 1918 (1947).
2. E. T. McBee, D. L. Crain, R. D. Crain, L. R. Belohlav, and H. P. Braendlin. J. Am. Chem. Soc. **84**, 3557 (1962).
3. E. T. McBee, J. O. Stoffer, and H. P. Braendlin. J. Am. Chem. Soc. **84**, 4540 (1962).
4. J. S. Newcomer and E. T. McBee. J. Am. Chem. Soc. **71**, 946 (1949).
5. P. Eaton, E. Carlson, P. Lombardo, and P. Yates. J. Org. Chem. **25**, 1225 (1960).

Received January 22, 1964.
Central Research Laboratory,
General Mills, Inc.,
Minneapolis, Minnesota.

**All melting points are uncorrected. The mass and n.m.r. spectra were furnished by Dr. L. E. Peterson, General Mills. A 10% concentration of the compound in CCl_4 was used for the n.m.r. and chemical shifts are reported in p.p.m. relative to internal tetramethylsilane. Infrared and ultraviolet spectra were furnished by Mr. Robert Fisher and Miss Delores Bell, General Mills.*

†An attempt to distill the residue prior to the addition of pentane resulted in heavy gas evolution with a great deal of exotherm. Thus, distillation would not be recommended as a purification method.

REARRANGEMENT STUDIES WITH ^{14}C. XX. SOME OBSERVATIONS ON REACTIONS BETWEEN GRIGNARD REAGENT, COBALTOUS BROMIDE, AND 2-PHENYLETHYL BROMIDE

C. C. Lee and D. P. Thornhill*

In a previous paper (1), it was demonstrated that contrary to an earlier report of Smith and Anderson (2), the reaction of 2-phenyl-1-^{14}C-ethyl bromide with magnesium and cobaltous bromide in refluxing ether gave ethylbenzene and styrene with no isotope position rearrangement. Since this reaction has some resemblance to the cobaltous halide catalyzed reaction between a Grignard reagent and an organic halide (designated by Slaugh (3) as the Kharasch reaction), which is believed to involve intermediate free radicals

**Holder of a Commonwealth Scholarship, 1961–63.*

(4), Smith and Anderson suggested an adaptation of the Kharasch mechanism, explaining the formation of ethylbenzene and styrene as arising from the 2-phenylethyl radical. It should be noted, however, that considerable differences exist between the experimental conditions of Kharasch and those of Smith and Anderson. In the Kharasch reaction, the organic halide is added to an ether solution of a Grignard reagent, usually phenylmagnesium halide, containing only a catalytic amount of cobaltous salt. The major products are saturated and olefinic hydrocarbons, and biphenyl. Under the conditions of Smith and Anderson (2), the organic halide, magnesium, and an *excess* of cobaltous halide are refluxed together in a relatively large volume of ether. As an attempt to shed some light on possible mechanistic differences between these reactions, interactions between Grignard reagent, cobaltous bromide, and 2-phenylethyl bromide (I) or 2-phenyl-1-^{14}C-ethyl bromide (I-^{14}C), under various experimental conditions, were studied and the results reported in this communication.

The observations from these studies are summarized in Table I. In the experiments where radioactive reactants were used, the mixtures of ethylbenzene (II) and styrene (III) were hydrogenated to II and then oxidized to benzoic acid whose activity measured the extents of ^{14}C-rearrangement (1).

The reaction conditions of expts. 1–3 were analogous to those used by Urry and Kharasch (5) in their study on the cobaltous chloride catalyzed reaction between phenylmagnesium bromide and neophyl chloride, which gave products attributable to rearrangement of the neophyl radical. The 0.5% isotope position rearrangement observed in expts. 1 and 2 (Table I) is real, indicating the occurrence of small amounts of a net 1,2-phenyl shift, possibly involving the 2-phenylethyl radical.

The Kharasch conditions were again used in expts. 4 and 5; but instead of phenylmagnesium bromide, phenylethylmagnesium bromide was employed. The 0.1% rearrangement may be of some significance as it corresponded to observed activities of about three times background for benzoic acid samples weighing about 15 mg. Such amounts of activity likely were beyond the experimental errors. The yields of II and III, as well as their relative compositions, are significantly different from those observed in expts. 1–3.

It is of interest to record that the specific activity of the 2-phenyl-1-^{14}C-ethylmagnesium bromide used in expt. 4 and that of the 2-phenyl-1-^{14}C-ethyl bromide (I-^{14}C) used in expt. 5 were the same, each equalling 5.40×10^5 c.p.m./mmole. The specific activities of the mixed products II and III from expts. 4 and 5 were, respectively, 3.02×10^5 and 2.08×10^5 c.p.m./mmole. If interchange of 2-phenylethyl groups between Grignard reagent and organic halide were complete before decomposition, the specific activities of II and III would be one-half of that of the active starting material. The data obtained suggest that complete interchange was not established before decomposition, as was observed recently by Parker and Noller (6) in their studies with isopropylmagnesium bromide and isopropyl bromide. Apparently, more of II and III were derived from the Grignard reagent than from the organic halide. Possibly, in expts. 4 and 5, two processes may be superimposed on each other. One of these might be a cobaltous bromide catalyzed decomposition of the Grignard reagent itself, which does not give any rearrangement. The other might be a cobaltous bromide catalyzed reaction between Grignard reagent and organic halide (the Kharasch reaction), which is capable of giving a small amount of rearrangement as observed in expts. 1 and 2.

In expts. 6–11, the use of excess cobaltous bromide and larger volumes of ether approximated the conditions of Smith and Anderson. In these trials, the Grignard reagent was first prepared and then the excess cobaltous bromide was introduced. This was followed,

Can. J. Chem. Downloaded from www.nrcresearchpress.com by 210.87.254.105 on 09/05/12
For personal use only.

Can. J. Chem. Downloaded from www.nrcresearchpress.com by 210.87.254.105 on 09/05/12
For personal use only.

TABLE I

Data from reactions between Grignard reagent, cobaltous bromide, and 2-phenylethyl bromide (I) or 2-phenyl-1-^{14}C-ethyl bromide (I-^{14}C)

	Reaction mixture				Products II and III*				
Expt. No.	Grignard reagent	Organic halide	$CoBr_2$	Ether (ml)	Yield† (%)	Composition %II	%III	Yields of other products‡	^{14}C rearrangement in II and III (%)
1	PhMgBr	I-^{14}C	Catalytic	60	25	69	31	62% biphenyl	0.5
2	PhMgBr	I-^{14}C	Catalytic	60	21	72	28	67% biphenyl	0.5
3	PhMgBr	I	Catalytic	60	22	76	24	60% biphenyl	—
4	Ph^{14}CH_2CH_2MgBr	I	Catalytic	60	44	86	14		0.1
5	$PhCH_2CH_2MgBr$	I-^{14}C	Catalytic	60	37	84	16		0.1
6	Ph^{14}CH_2CH_2MgBr	I-^{14}C	Excess	300	68	64	36	92% recovered I-^{14}C	0.0
7	Ph^{14}CH_2CH_2MgBr	I-^{14}C	Excess	300	65	64	36	81% recovered I-^{14}C	0.0
8	$PhCH_2CH_2MgBr$	I	Excess	300	61	62	38	90% recovered I, 68% Co metal	—
9	$PhCH_2CH_2MgBr$	I	Excess	300	65	65	35	85% recovered I, 69% Co metal	—
10	$PhCH_2CH_2MgBr$	None	Excess	250	64	65	35	67% Co metal	—
11	$PhCH_2CH_2MgBr$	None	Excess	250	62	63	37	69% Co metal	—
12	$PhCH_2CH_2MgBr$	None	Catalytic	250	7	62	38	45% hydrocinnamic acid§	—

*II and III are ethylbenzene and styrene, respectively.
†Percentage yields for expts. 1–5 were based on organic halide; those for expts. 6–12 were based on the Grignard reagent.
‡Yields of biphenyl or cobalt metal were based on the Grignard reagent.
§From treatment of reaction mixture with Dry Ice, indicating presence of unreacted Grignard reagent. No hydrocinnamic acid was obtained from Dry Ice treatment of reaction mixtures from expts. 4–11.

in some cases, by the addition of organic halide I or I-^{14}C (expts. 6–9). Most of the added I or I-^{14}C was recovered at the end of the reaction, indicating that the organic halide is not a reactant. The data from expts. 6–11 clearly show that reaction between 2-phenylethylmagnesium bromide and excess cobaltous bromide can take place, the identified products being II and III, with no rearrangement, and cobalt metal (there was no attempt to isolate cobalt metal from expts. 6 and 7). When 2-phenylethylmagnesium bromide in dilute ether solution was treated with only a small amount of cobaltous bromide (expt. 12), a very low yield of II and III was obtained, and the presence of unreacted Grignard reagent was indicated by its carbonation to hydrocinnamic acid.

The results discussed above strongly indicate that reaction of 2-phenylethyl bromide with magnesium and cobaltous bromide under the conditions of Smith and Anderson likely follow a course different from that of the Kharasch reaction. In the presence of excess cobaltous bromide, 2-phenylethylmagnesium bromide may give rise to unstable organocobalt (7), which decomposes to ethylbenzene (II), styrene (III), and cobalt metal. Such a decomposition may not even involve the actual liberation of free radicals (4). If the assumption is made that the 2-phenylethyl radical is an intermediate in all of the reactions investigated, the predominance of II over III in the products, the very small amount of 1,2-phenyl shifts under the Kharasch conditions, and the complete lack of such shifts under the conditions of Smith and Anderson might be rationalized, as discussed previously (1), on the basis of a predominance of hydrogen abstraction and a lack of sufficiently high reaction temperature to overcome the activation energy for the 1,2-shift. The complexity of the Kharasch reaction has been shown by some recent experiments (3, 6). In particular, Parker and Noller (6) have suggested that in the metal halide catalyzed reaction between alkylmagnesium halide and alkyl halide, part of the reaction may be due to decomposition of a molecular complex of Grignard reagent, alkyl halide, and catalyst to give equivalent amounts of saturated and olefinic hydrocarbons while another portion of the reaction proceeds via free radical hydrogen abstraction to give only saturated hydrocarbon. The net result is more alkane than alkene in the overall products. Such possible processes might also be applied in explaining the present results.

EXPERIMENTAL

Experiments 1–3

To a solution of phenylmagnesium bromide, prepared from 9.5 g (0.061 mole) of bromobenzene and 1.7 g of magnesium in 50 ml of ether, 0.4 g (0.0018 mole) of anhydrous cobaltous bromide was introduced. A solution of 10.0 g (0.054 mole) of I or I-^{14}C in 10 ml of ether was then added dropwise. After about one-half of this solution was added, a further introduction of 0.4 g of cobaltous bromide was made before the addition of the remaining solution of I or I-^{14}C was completed. The resulting mixture was heated under reflux for 3 hours. Following decomposition with dilute hydrochloric acid, the monomeric products II and III were isolated and their relative composition measured by vapor phase chromatography as previously described (1).

After removal of II and III, further distillation under reduced pressure gave a second fraction which solidified on cooling. After recrystallization three times from methanol, colorless crystals were obtained which melted alone or on admixture with authentic biphenyl at 69–70° C.

Experiments 4 and 5

The Grignard reagent was prepared from 10.0 g (0.054 mole) of I-^{14}C or I and 1.7 g of magnesium in 50 ml of ether. The solution was treated with catalytic amounts of cobaltous bromide and 10.0 g (0.054 mole) of I or I-^{14}C in 10 ml of ether as in expts. 1–3. Dry Ice was added to the reaction mixture before it was worked up in the usual way (1). No hydrocinnamic acid was obtained from the alkaline extract after the Dry Ice treatment. Following the removal of the mixed products II and III, attempted further distillation of the residue failed to give any 1,4-diphenylbutane.

Experiments 6–9

The Grignard reagent was prepared from 10.0 g (0.054 mole) of I or I-^{14}C and 1.7 g of magnesium in 250 ml of ether. The solution was decanted under nitrogen to remove any excess magnesium. A total of 14.5 g

Can. J. Chem. Downloaded from www.nrcresearchpress.com by 210.87.254.105 on 09/05/12
For personal use only.

(0.066 mole) of anhydrous cobaltous bromide was introduced, either in one batch or portionwise. The mixture turned dark and refluxing occurred without external heating. A solution of 10.0 g of I or I-^{14}C in 50 ml of ether was then added, either rapidly or dropwise. The resulting mixture was heated under reflux for 3 hours, treated with Dry Ice, and worked up to give II and III. Further distillation under reduced pressure gave unreacted I or I-^{14}C, identified by conversion to a solid derivative, hydrocinnamic acid.

In expts. 8 and 9, after removal of unreacted I, the residue was subjected to repeated washing with aqueous acetone followed by centrifugation. When the washing was colorless, the finely divided cobalt metal that remained was dried under vacuum and stored under nitrogen. It showed magnetic and pyrophoric properties. After dissolution in dilute hydrochloric acid, treatment with hydrogen sulphide gave a black precipitate.

Experiments 10–12

The solution of Grignard reagent was prepared from 10.0 g of I and 1.7 g of magnesium in 250 ml of ether. It was decanted from excess magnesium and then treated with 14.5 g or 0.8 g of cobalt bromide. After refluxing of the mixture for 3 hours, Dry Ice was added and the mixture worked up to give II, III, and cobalt metal. When only 0.8 g of cobalt bromide was used (expt. 12), 3.7 g (45%) of hydrocinnamic acid was recovered from the sodium hydroxide extract after the reaction mixture was treated with Dry Ice.

ACKNOWLEDGMENT

The financial support given by the National Research Council of Canada is gratefully acknowledged.

1. D. P. THORNHILL and C. C. LEE. Can. J. Chem. **41**, 2861 (1963).
2. W. B. SMITH and J. D. ANDERSON. J. Am. Chem. Soc. **82**, 656 (1960).
3. L. H. SLAUGH. J. Am. Chem. Soc. **83**, 2734 (1961).
4. M. S. KHARASCH and O. REINMUTH. Grignard reactions of nonmetallic substances. Prentice-Hall, New York. 1954. Chap. 5.
5. W. H. URRY and M. S. KHARASCH. J. Am. Chem. Soc. **66**, 1438 (1944).
6. V. D. PARKER and C. R. NOLLER. Tetrahedron Letters, No. 25, 1737 (1963).
7. D. L. INGLES and J. B. POLYA. J. Chem. Soc. 2280 (1949).

RECEIVED JANUARY 22, 1964.
DEPARTMENT OF CHEMISTRY,
UNIVERSITY OF SASKATCHEWAN,
SASKATOON, SASKATCHEWAN.

SYNTHESIS OF POTENTIAL ANTINEOPLASTIC AGENTS. XII. SOME BIS(2-CHLOROETHYL)AMINES CONTAINING A *p*-FLUOROPHENYL GROUP AND RELATED COMPOUNDS[1,2]

FRANK D. POPP AND DRU W. ALWANI

During the past few years we have prepared a large number of nitrogen mustard Schiff bases of the type I (1, 2, 3). One of the most promising compounds in this series (4) (I, R = H, R′ = CH_3, R″ = *p*-FC_6H_4—) was derived from *p*-fluoroaniline. In a series of compounds of the type II (5) the one derived from *p*-fluoroaniline (II, R = *p*-FC_6H_4—) was ranked the highest of the series in screening against an established Dunning leukemia in Fischer rats (4). In view of these results, it was decided to prepare a number of other bis(2-chloroethyl)amines containing a *p*-fluorophenyl group.

Reaction of the readily available (6) *p*-[N-bis(2-chloroethyl)amino]benzhydrazide with *p*-fluorobenzaldehyde gave the compound III. At the same time a number of other hydrazides related to III were prepared and these are listed in Table I. None of these

[1]*Refer to F. D. Popp and A. Catala. J. Heterocyclic Chem. in press, for part XI of this series.*
[2]*Supported in part by grants from the American Cancer Society (T 177C) and from the National Cancer Institute, U.S.P.H.S. (CA 06606-02).*

Can. J. Chem. Downloaded from www.nrcresearchpress.com by 210.87.254.105 on 09/05/12
For personal use only.

(0.066 mole) of anhydrous cobaltous bromide was introduced, either in one batch or portionwise. The mixture turned dark and refluxing occurred without external heating. A solution of 10.0 g of I or I-^{14}C in 50 ml of ether was then added, either rapidly or dropwise. The resulting mixture was heated under reflux for 3 hours, treated with Dry Ice, and worked up to give II and III. Further distillation under reduced pressure gave unreacted I or I-^{14}C, identified by conversion to a solid derivative, hydrocinnamic acid.

In expts. 8 and 9, after removal of unreacted I, the residue was subjected to repeated washing with aqueous acetone followed by centrifugation. When the washing was colorless, the finely divided cobalt metal that remained was dried under vacuum and stored under nitrogen. It showed magnetic and pyrophoric properties. After dissolution in dilute hydrochloric acid, treatment with hydrogen sulphide gave a black precipitate.

Experiments 10–12

The solution of Grignard reagent was prepared from 10.0 g of I and 1.7 g of magnesium in 250 ml of ether. It was decanted from excess magnesium and then treated with 14.5 g or 0.8 g of cobalt bromide. After refluxing of the mixture for 3 hours, Dry Ice was added and the mixture worked up to give II, III, and cobalt metal. When only 0.8 g of cobalt bromide was used (expt. 12), 3.7 g (45%) of hydrocinnamic acid was recovered from the sodium hydroxide extract after the reaction mixture was treated with Dry Ice.

ACKNOWLEDGMENT

The financial support given by the National Research Council of Canada is gratefully acknowledged.

1. D. P. THORNHILL and C. C. LEE. Can. J. Chem. **41**, 2861 (1963).
2. W. B. SMITH and J. D. ANDERSON. J. Am. Chem. Soc. **82**, 656 (1960).
3. L. H. SLAUGH. J. Am. Chem. Soc. **83**, 2734 (1961).
4. M. S. KHARASCH and O. REINMUTH. Grignard reactions of nonmetallic substances. Prentice-Hall, New York. 1954. Chap. 5.
5. W. H. URRY and M. S. KHARASCH. J. Am. Chem. Soc. **66**, 1438 (1944).
6. V. D. PARKER and C. R. NOLLER. Tetrahedron Letters, No. 25, 1737 (1963).
7. D. L. INGLES and J. B. POLYA. J. Chem. Soc. 2280 (1949).

RECEIVED JANUARY 22, 1964.
DEPARTMENT OF CHEMISTRY,
UNIVERSITY OF SASKATCHEWAN,
SASKATOON, SASKATCHEWAN.

Can. J. Chem. Downloaded from www.nrcresearchpress.com by 210.87.254.105 on 09/05/12
For personal use only.

SYNTHESIS OF POTENTIAL ANTINEOPLASTIC AGENTS. XII. SOME BIS(2-CHLOROETHYL)AMINES CONTAINING A *p*-FLUOROPHENYL GROUP AND RELATED COMPOUNDS[1,2]

FRANK D. POPP AND DRU W. ALWANI

During the past few years we have prepared a large number of nitrogen mustard Schiff bases of the type I (1, 2, 3). One of the most promising compounds in this series (4) (I, R = H, R′ = CH_3, R″ = *p*-FC_6H_4—) was derived from *p*-fluoroaniline. In a series of compounds of the type II (5) the one derived from *p*-fluoroaniline (II, R = *p*-FC_6H_4—) was ranked the highest of the series in screening against an established Dunning leukemia in Fischer rats (4). In view of these results, it was decided to prepare a number of other bis(2-chloroethyl)amines containing a *p*-fluorophenyl group.

Reaction of the readily available (6) *p*-[N-bis(2-chloroethyl)amino]benzhydrazide with *p*-fluorobenzaldehyde gave the compound III. At the same time a number of other hydrazides related to III were prepared and these are listed in Table I. None of these

[1]*Refer to F. D. Popp and A. Catala. J. Heterocyclic Chem. in press, for part XI of this series.*

[2]*Supported in part by grants from the American Cancer Society (T 177C) and from the National Cancer Institute, U.S.P.H.S. (CA 06606-02).*

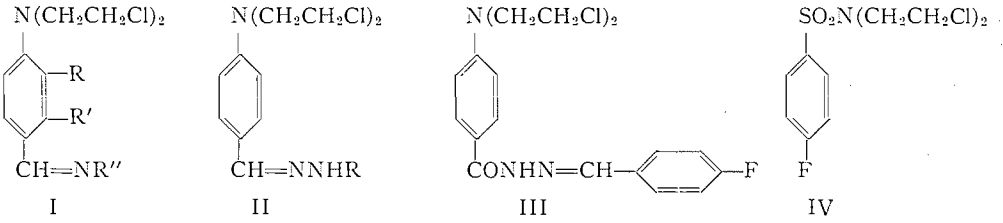

TABLE I

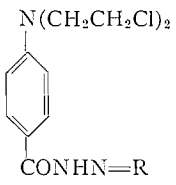

R	M.p.	Yield	Analysis Calc. C	Calc. H	Calc. N	Found C	Found H	Found N
p-FC_6H_4CH=	161–162[a]	87	56.54	4.71	10.99	56.79	4.69	11.15
p-ClC_6H_4CH=	208–209[b,c]	96	54.23	4.55	10.54	54.26	4.76	10.38
	127–128[a]	99	56.14	6.18	12.27	56.18	6.13	12.25
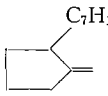	113–114[d,e]	84	62.72	8.01	9.54	63.03	7.86	9.35

[a]Recrystallized from toluene.
[b]Recrystallized from dioxane.
[c]Calc.: Cl, 26.68. Found: Cl, 26.32.
[d]Recrystallized from ether.
[e]Calc.: Cl, 16.10. Found: Cl, 15.91.

compounds exhibited anything but minimal activity against an established Dunning leukemia (4), although III was active ($ED_{50} = 1.7 \times 10^0$, slope = -1.1) when screened against KB line tissue culture.[3]

Reaction of N-bis(2-chloroethyl)amine with *p*-fluorobenzenesulphonyl chloride and with *p*-fluorophenyl isocyanate gave compounds IV and V respectively. These agents were essentially inactive against the Dunning leukemia (4). An additional Schiff base of the type I was prepared from 4-fluoro-2-nitroaniline.

The reaction of *p*-fluorobenzoyl chloride and N-bis(2-chloroethyl)amine gave N-bis-(2-chloroethyl)-4-fluorobenzamide. This compound could be purified only with difficulty and was readily rearranged during purification to the corresponding 2-(2′-chloroethyl-amino)ethyl ester hydrochloride. Before this compound could be submitted for screening or reduced to the corresponding *p*-fluorobenzylamine its preparation was reported by Pettit.[4] In the same publication (7) Pettit speculates that the cycloalkyl amide mustards which we had prepared earlier (8) were actually the rearranged ester hydrochlorides. After publication of that paper (8) we had independently reached the same conclusion although these esters could never be obtained analytically pure. It should be emphasized, however,

[3]*Results supplied by the C.C.N.S.C. of the U.S.P.H.S.*
[4]*We would like to thank Professor Pettit for making this information available to us prior to publication (7). Professor Pettit has also indicated that the p-fluorobenzl bis(2-chloroethyl)amine was not superior to several related compounds in preliminary screening.*

Can. J. Chem. Downloaded from www.nrcresearchpress.com by 210.87.254.105 on 09/05/12
For personal use only.

that no rearrangement was noted when purification was not attempted and that the materials reduced to the cycloalkyl mustards were indeed the unrearranged amides.

In an attempt to overcome the difficulties in the preparation and purification of mustard amides, we tried to react carboxylic acids and N-bis(2-chloroethyl)amine with dicyclohexylcarbodiimide as condensing agent. Such a condensation has been reported (9) in the synthesis of glycine bis(2-chloroethyl)amide. As indicated in the experimental section, our attempts led only to a substituted N-acylurea (VI). This type of compound has been noted by others (10–14) in the attempted preparation of amides.

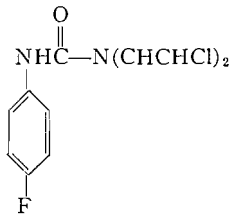

V

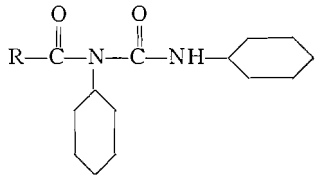

VI

EXPERIMENTAL

1,1-Bis(2-chloroethyl)-3-(p-fluorophenyl)urea.—Reaction of *p*-fluorophenyl isocyanate and N-bis(2-chloroethyl)amine as previously described (15) gave, after recrystallization from carbon tetrachloride, an 82% yield of solid, m.p. 97–99°. Ultraviolet maximum 279–281 mμ and 241 mμ. Infrared (KBr): N–H, 3150–3200 cm^{-1}; C=O, 1625–1630 cm^{-1}. Anal. Calc. for $C_{11}H_{13}Cl_2FN_2O$: C, 47.33; H, 4.69; N, 10.04; Cl, 25.40. Found: C, 47.60; H, 5.12; N, 10.10; Cl, 25.65.

N,N-Bis(2-chloroethyl)-p-fluorobenzenesulphonamide.—A mixture of 0.02 mole of *p*-fluorophenylsulphonyl chloride, 5 ml of pyridine, 60 ml of anhydrous benzene, and the N-bis(2-chloroethyl)amine from 0.022 mole of the hydrochloride was allowed to stand for several days at room temperature and filtered. The filtrate was washed with water, dried, and concentrated to give after recrystallization from methanol a 78% yield of solid, m.p. 70–72°. Anal. Calc. for $C_{10}H_{12}Cl_2FNO_2S$: C, 40.00; H, 4.03; N, 4.67; Cl, 23.62. Found: C, 40.17; H, 4.11; N, 4.47; Cl, 23.30.

N′,N′-Bis(2-chloroethyl)-4-fluoro-2-nitro-2′-methyl-N,4′-methylidynedianiline.—The appropriate amine and aldehyde were refluxed in absolute ethanol for 30 minutes. After cooling of the solution, a solid was collected and recrystallized from benzene to give an 80% yield of solid, m.p. 135–136°. Anal. Calc. for $C_{18}H_{13}N_3Cl_2FO_2$: C, 54.28; H, 4.55; N, 10.55. Found: C, 54.43; H, 4.74; N, 10.46.

Hydrazides of p-[Bis(2-chloroethyl)amine]benzoic acid.—Equimolar quantities of p-[N-bis(2-chloroethyl)-amine]benzhydrazide and the appropriate aldehyde or ketone were refluxed for 30 minutes in absolute ethanol and cooled to give the compounds included in Table I.

Attempted amide formation with dicyclohexylcarbodiimide.—A mixture of 0.02 mole of the appropriate carboxylic acid in a minimum amount of a suitable solvent (benzene, dioxane, or tetrahydrofuran), N-bis(2-chloroethyl)amine, from 0.022 mole of the hydrochloride, in benzene, and 0.03 mole of dicyclohexylcarbodiimide was allowed to stand at room temperature for 24 to 48 hours. The mixture was filtered and the filtrate concentrated *in vacuo* to give a residue which was triturated with a solvent (ether, acetone, or ethanol) and recrystallized to give compounds of the type VI in 30 to 60% yields. When quinaldic acid was used the product was recrystallized from ethyl acetate and had m.p. 132–134°. Anal. Calc. for $C_{23}H_{29}N_3O_2$: C, 72.79; H, 7.70; N, 11.07. Found: C, 72.39; H, 7.72; N, 10.81. When levopimaric acid[5] was used the product was recrystallized from acetone and had m.p. 143–144°. Anal. Calc. for $C_{33}H_{52}N_2O_2$: C, 77.90; H, 10.30; N, 5.51. Found: C, 78.22; H, 10.31; N, 5.41.

1. F. D. Popp. J. Org. Chem. **26**, 1566 (1961).
2. F. D. Popp and W. Kirsch. J. Org. Chem. **26**, 3858 (1961).
3. F. D. Popp. J. Med. Chem. **7**, 210 (1964).
4. L. Rane. University of Miami Medical School. Private communication.
5. F. D. Popp. J. Med. Pharm. Chem. **5**, 627 (1962).
6. R. C. Elderfield and T.-K. Liao. J. Org. Chem. **26**, 4996 (1961).
7. G. R. Pettit, D. S. Blonda, and E. C. Harrington. Can. J. Chem. 41, 2962 (1963).
8. F. D. Popp, S. Roth, and J. Kirby. J. Med. Chem. **6**, 83 (1963).

[5]*We wish to thank the Naval Stores Research Station, Olustee, Fla., for a generous sample of levopimaric acid.*

Can. J. Chem. Downloaded from www.nrcresearchpress.com by 210.87.254.105 on 09/05/12
For personal use only.

9. S. BIEN and O. M. FRIEDMAN. Chem. Ind. 2062 (1962).
10. H. G. KHORANA. Chem. Ind. 1087 (1955).
11. J. C. SHEEHAN, M. GOODMAN, and G. P. HESS. J. Am. Chem. Soc. **78**, 1367 (1956).
12. H. C. KOPPEL, I. L. HONIGBERG, R. H. SPRINGER, and C. C. CHENG. J. Org. Chem. **28**, 1119 (1963).
13. E. M. ACTON and R. M. SILVERSTEIN. J. Org. Chem. **24**, 1487 (1959). H. H. LAU and H. HART. J. Org. Chem. **24**, 280 (1959).
14. K. YAMAKAWA, H. OCHI, and K. ARAKAWA. Chem. Pharm. Bull. **11**, 905 (1963).
15. F. D. POPP and H. SWARZ. J. Org. Chem. **26**, 4764 (1961).

RECEIVED JANUARY 30, 1964.
DEPARTMENT OF CHEMISTRY,
CLARKSON COLLEGE OF TECHNOLOGY,
POTSDAM, NEW YORK, U.S.A.

Can. J. Chem. Downloaded from www.nrcresearchpress.com by 210.87.254.105 on 09/05/12
For personal use only.

Can. J. Chem. Downloaded from www.nrcresearchpress.com by 210.87.254.105 on 09/05/12
For personal use only.

Canadian Journal of Chemistry

Issued by THE NATIONAL RESEARCH COUNCIL OF CANADA

VOLUME 42 JULY 1964 NUMBER 7

COMPOUNDS OF THE TYPE M_5X_2: Pd_5As_2, Ni_5Si_2, AND Ni_5P_2[1]

G. S. SAINI,[2] L. D. CALVERT, AND J. B. TAYLOR

Division of Applied Chemistry, National Research Council, Ottawa, Canada

Received January 13, 1964

ABSTRACT

Space group, lattice parameters, and powder data indicate that Pd_5As_2, Ni_5Si_2, and Ni_5P_2 are structurally related. Single crystal studies have established that Pd_5As_2 exhibits polytypism. Pd_5As_2 has $a = 7.31 \pm 0.01$ Å but c-values of 13.7, 10.34, 27.48, and 96.2 Å were observed on different crystals corresponding to a "single layer" repeat distance of 3.43 Å along the c-axis. The last three cells have trigonal symmetry, space group $P\bar{3}m1$, (D_{3d}^3), $P3m1(C_{3v}^1)$, or $P321(D_3^2)$ and the first cell has hexagonal symmetry, space group $P6_322(D_6^6)$. The Guinier focussing camera pattern of polycrystalline Pd_5As_2 can be indexed on a hexagonal cell with $a = 7.320 \pm 0.002$, $c = 96$ Å. Single crystal and focussing camera studies of Ni_5Si_2 showed it to be of trigonal symmetry with $a = 6.68 \pm 0.02$, $c = 12.28 \pm 0.03$ Å, and space group $P321$, $P3m1$, or $P\bar{3}m1$. A Guinier pattern of Ni_5P_2 can be indexed with hexagonal parameters $a = 13.220 \pm 0.002$ Å, $c = 24.632 \pm 0.002$ Å; a subcell with $a = 6.610$ and $c = 12.316$ Å can be used to index the strong lines. Comparison of the powder data for Pd_5As_2, Ni_5Si_2, and Ni_5P_2 with previously published data for Ni_5As_2 and Mn_5Ge_2 shows that the compounds are structurally related.

INTRODUCTION

Binary transition metal compounds with either pnigogens, chalcogens, silicon, boron, carbon, or germanium having the general formula M_5X_2 have been discussed previously (1). The present work concerns those compounds having hexagonal or trigonal symmetry, i.e. Pd_5As_2 (2), Ni_5Si_2 (3, 4), and Ni_5P_2 (5). Single crystal data have been used to establish the space groups for Pd_5As_2 and Ni_5Si_2 and Guinier patterns have been obtained for Pd_5As_2, Ni_5Si_2, and Ni_5P_2. Comparison of these has established a close structural relationship between them.

EXPERIMENTAL

The preparation techniques were different for the various M_5X_2 phases examined and details are contained under the relevant subheadings. High purity starting materials were used in all cases. Powder patterns were obtained in a Guinier–deWolff focussing camera using As_2O_3 as an internal standard. The intensities were estimated by comparison with a logarithmic interval density scale. Single crystal photographs were taken on a precession camera using zirconium filtered molybdenum radiation.

Pd_5As_2

Polycrystalline specimens were prepared by reacting palladium and arsenic powders in stoichiometric quantities in vacuum-sealed clear fused quartz ampoules. The bead resulting from the initial reaction was crushed and annealed *in vacuo* at 600 °C (2). Single crystal fragments were obtained by breaking up an ingot prepared by slow directional freezing of a melt of composition Pd_5As_2 contained in an evacuated, sealed clear fused quartz ampoule.

Preliminary investigation of the powder patterns showed that their quality was not sufficiently high to enable unambiguous indexing of what appeared to be a low symmetry cell. Accordingly single crystals were

[1]*Issued as N.R.C. No. 7912.*

[2]*Present address: Department of Chemical Engineering Technology, Panjab University, Chandigarh-3, India.*

studied and found to be trigonal or hexagonal with $a = 7.32 \pm 0.02$ Å but having different values for c ranging from 10.34 Å to 96.2 Å. Following the definition given by Strock and Brophy (6), these crystals are polytypes with a "single layer" repeat distance along the c-axis of 3.43 Å. Some crystals proved to be intergrowths of different polytypes and many were apparently of poor quality which could have resulted from the presence of giant polytypes or from imperfect annealing. One crystal gave sharp spots on precession photographs and the reciprocal lattice nets $hk.0$, $hk.1$, $hk.2$, $hk.3$, $hk.4$, $h0.l$, $h1.l$, $h2.l$, were recorded. For the other crystals the indices of the reciprocal lattice nets observed are listed in Table I, where the crystallographic data is summarized. The quantity N represents the multiplicity along the c-axis of the "single layer" repeat distance (3.43 Å).

TABLE I

Polytypes of Pd_5As_2

Multiplicity along c-axis, N	Cell parameters		Nets observed	Symmetry	Space group
	a	c			
3	7.32	10.34	$h0l$	Trigonal	$P\bar{3}m1$ (D_{3d}^3), $P3m1$ (C_{3v}^1) or $P321$ (D_3^1)
4	7.32	13.70	$h0l$	Hexagonal	$P6_322$ (D_6^6)
8	7.32	27.48	See text	Trigonal	$P\bar{3}m1$, etc.
28	7.32	96.2	$h0l$, $hk1$ $h1l$, $hk0$	Trigonal	$P\bar{3}m1$, etc.

A strongly marked subcell with $a = 2.44$ Å and $c = 6.87$ Å is visible in all the precession photographs. The intensities of the reflections corresponding to this subcell were very similar in all the specimens studied.

The crystal with $N = 28$ was re-examined after 2 months and found to have become a mixture of $N = 8$ and $N = 28$. It is assumed that this crystal had annealed at room temperature to form the mixture although it is worthy of record that the crystal had received a total X-ray exposure of 120 hours.

An indexed powder pattern of Pd_5As_2 is listed in Table II. Most of the lines have been indexed on the basis of hexagonal axes $a = 7.320 \pm 0.002$ Å; $c = 27.523 \pm 0.002$ Å. Two weak lines at d values of 4.712 and 4.401 Å were observed in photographs of three separate preparations and required the use of $c = 96$ Å to obtain satisfactory indexing. Two possible explanations are offered. Firstly, the preparations consistently contain a large amount of the polytype with $c = 27.523$ Å and a small amount of the polytype with $c = 96$ Å; secondly, the polytype present is the 96 Å one but the only lines requiring the 96 Å cell are the two weak ones at $d = 4.712$ and 4.401 Å.

Ni_5Si_2

Ni_5Si_2 was prepared by reacting stoichiometric quantities of nickel and silicon powders sealed in an evacuated clear fused quartz ampoule. After the initial reaction, the product was melted and then allowed to solidify slowly from 1300 °C. The ingot thus obtained was broken open and single crystal fragments separated. A portion of the ingot was crushed, screened through a 300-mesh sieve, and sealed under vacuum in a clear fused quartz tube with the minimum of void volume. This sample was annealed at 400 °C for 8 days, quenched, and used directly in the Guinier camera.

One single crystal was selected and the reciprocal lattice nets $hk0$, $hk1$, $hk2$, $h0l$, $h1l$ examined. It was found to be trigonal with diffraction symbol $\bar{3}mP\ldots$ The possible space groups are $P\bar{3}m1$, $P3m1$, and $P321$. The cell parameters from the single crystal photographs are $a = 6.68 \pm 0.02$, $c = 12.28 \pm 0.03$ Å.

The Guinier powder pattern of Ni_5Si_2 is given in Table III and has been indexed on hexagonal axes $a = 6.667 \pm 0.002$, $c = 12.277 \pm 0.002$ Å. Two very weak lines were observed in this pattern but could not be indexed even on a cell $a = 6.68$, $c = 85.94$ Å. These lines were not observed on patterns obtained from other preparations of Ni_5Si_2 but the measured pattern was considerably sharper than the others.

Ni_5P_2

Weighed quantities of nickel and phosphorus powders in stoichiometric proportions were sealed under vacuum in a clear fused quartz ampoule and reacted at 700 °C for 2 days. The product was subsequently crushed, resealed, and annealed at 700 °C for 8 days. This sample was used to obtain a Guinier pattern. Attempts to grow single crystals of this low temperature form of Ni_5P_2 by iodide vapor transport were not successful.

The Guinier pattern of Ni_5P_2 given in Table IV has been completely indexed with hexagonal parameters $a = 13.220 \pm 0.002$ Å, $c = 24.632 \pm 0.002$ Å. The strong lines can be indexed with parameters $a = 6.610$, and $c = 12.316$, and all but three lines at d values of 2.114, 1.7335, and 1.6581 can be indexed on the cell $a = 13.220$, $c = 12.316$.

Can. J. Chem. Downloaded from www.nrcresearchpress.com by 210.87.254.105 on 09/05/12
For personal use only.

Can. J. Chem. Downloaded from www.nrcresearchpress.com by 210.87.254.105 on 09/05/12
For personal use only.

TABLE II

Powder diffraction pattern of Pd_5As_2

Hexagonal parameters $a = 7.320 \pm 0.002$ Å, $c = 27.523 \pm 0.002$ Å, $c/a = 3.760$; $U = 1277.1$ Å^3; $Z = 12$; F.W. = 681.84; $D_x = 10.64$ g cm^{-3}; $D_m = 10.72$ g cm^{-3}. Guinier focussing camera, diameter 11.46 cm; monochromated Cu K_α radiation $\lambda_{\alpha 1} = 1.5405$ Å; temp. 24 °C; internal standard As_2O_3 ($a = 11.075_5$ Å); d values > 1.28 Å; cutoff 35 Å

I/I_1	$\sin^2\theta_{obs}\times10^3$	$\sin^2\theta_{calc}\times10^3$	d_{obs} (Å)	$h\ k\ l$
2.2	26.72		4.712	
2.2	27.28	27.30	4.663	1 0. 4
4.4	30.63		4.401	
5.5	33.62	34.36	4.201	1 0. 5
2.2	38.63	38.41	3.919	0 0. 7
<2.2	43.10	42.98	3.710	1 0. 6
11	71.53	71.59	2.880	2 0. 4
11	72.54	72.51	2.860	1 1. 6
8.6	87.49	87.27	2.604	2 0. 6
13	94.36	94.45	2.508	1 1. 8
		94.84		0 0.11
13	97.56	97.46	2.466	2 0. 7
17	104.24	104.12	2.386	2 1. 1
33	106.64	106.48	2.359	2 1. 2
41	109.33	109.21	2.330	2 0. 8
		109.60		1 0.11
21	116.22	115.88	2.259	2 1. 4
100	122.56	122.67	2.200	1 1.10
		122.54		2 0. 9
		122.94		2 1. 5
80	132.86	132.86	2.113	3 0. 0
		132.46		0 0.13
13	141.68	141.75	2.046	2 1. 7
26	153.25	153.50	1.9676	2 1. 8
		153.62		0 0.14
26	156.87	157.16	1.9447	1 1.12
13	166.63	166.83	1.8869	2 1. 9
4.4	171.68	171.92	1.8590	2 0.12
		171.27		3 0. 7
17	180.30	180.29	1.8140	2 2. 2
17	182.98	183.02	1.8006	3 0. 8
21	195.08	195.05	1.7439	3 1. 2
8.6	204.46	204.45	1.7034	3 1. 4
4.4	220.13	220.13	1.6417	3 1. 6
		220.65		1 1.15
26	255.67	255.53	1.5233	2 2.10
		255.40		3 1. 9
		255.80		4 0. 5
7	281.32	281.26	1.4522	3 2. 1
13	290.17	290.02	1.4299	2 2.12
8.6	300.29	300.08	1.4056	3 2. 5
		299.69		4 0. 9
13	305.10	304.78	1.3945	3 1.12
13	313.52	313.52	1.3756	0 0.20
		313.15		4 1. 2
		313.00		2 0.18
11	319.00	318.89	1.3638	3 2. 7
26	331.23	331.04	1.3383	4 0.11
		330.77		2 2.14
		330.64		3 2. 8
11	344.19	343.97	1.3129	3 2. 9
21	356.83	357.29	1.2894	2 1.18

TABLE III

Powder diffraction pattern of Ni_3Si_2

Trigonal; diffraction symbol $\bar{3}mP\ldots$; $a = 6.667 \pm 0.002$ Å, $c = 12.277 \pm 0.002$ Å, $c/a = 1.841$; $U = 472.6$ Å^3; $Z = 6$; F.W. = 349.72; $D_x = 7.37$ g cm^{-3}. Guinier focussing camera, diameter 11.46 cm; monochromated Cu K_α radiation $\lambda_{\alpha_1} = 1.5405$ Å; temp. 24 °C; internal standard As_2O_3 ($a = 11.075_5$ Å); d values > 1.21 Å; cutoff 35 Å

I/I_1	d_{obs} (Å)	d_{calc} (Å)	$h\ k\ l$
2.8	6.16	6.14	0 0. 2
1.8	5.23	5.23	1 0. 1
2.8	4.21	4.21	1 0. 2
2.2	4.05	4.09	0 0. 3
2.2	3.96		
2.2	3.85		
13	3.337	3.334	1 1. 0
		3.339	1 0. 3
11	3.217	3.217	1 1. 1
7	3.069	3.069	0 0. 4
17	2.931	2.930	1 1. 2
4.4	2.887	2.887	2 0. 0
3.5	2.811	2.810	2 0. 1
8.6	2.712	2.710	1 0. 4
33	2.613	2.612	2 0. 2
33	2.585	2.585	1 1. 3
4.4	2.457	2.456	0 0. 5
17	2.260	2.260	1 0. 5
		2.258	1 1. 4
21	2.184	2.182	2 1. 0
64	2.150	2.149	2 1. 1
64	2.103	2.103	2 0. 4
26	2.057	2.056	2 1. 2
7	2.044	2.046	0 0. 6
100	1.9766	1.9770	1 1. 5
100	1.9244	1.9246	3 0. 0
		1.9256	2 1. 3
26	1.8717	1.8704	2 0. 5
5.5	1.8380	1.8365	3 0. 2
41	1.7780	1.7785	2 1. 4
26	1.7420	1.7439	1 1. 6
		1.7416	3 0. 3
21	1.6693	1.6694	2 0. 6
11	1.6519	1.6516	2 2. 1
21	1.6311	1.6312	2 1. 5
		1.6305	3 0. 4
2.2	1.6087	1.6085	2 2. 2
7	1.5991	1.6016	3 1. 0
26	1.5883	1.5879	3 1. 1
13	1.5427	1.5436	2 2. 3
8.6	1.5332	1.5346	0 0. 8
5.5	1.5151	1.5147	3 0. 5
5.5	1.4911	1.4927	2 1. 6
		1.4912	3 1. 3
7	1.4806	1.4831	1 0. 8
5.5	1.4645	1.4647	2 2. 4
7	1.4418	1.4434	4 0. 0
8.6	1.4315	1.4336	4 0. 1
8.6	1.4190	1.4197	3 1. 4
8.6	1.4036	1.4019	3 0. 6
		1.4051	4 0. 2
41	1.3786	1.3790	2 2. 5
8.6	1.3656	1.3671	2 1. 7
		1.3641	0 0. 9
8.6	1.3532	1.3551	2 0. 8
8.6	1.3424	1.3413	3 1. 5
26	1.3169	1.3170	3 2. 1
11	1.3055	1.3062	4 0. 4

Can. J. Chem. Downloaded from www.nrcresearchpress.com by 210.87.254.105 on 09/05/12
For personal use only.

TABLE III (*Concluded*)

I/I_1	d_{obs} (Å)	d_{calc} (Å)	h k l
26	1.2931	1.2923	2 2. 6
21	1.2606	1.2611	3 1. 6
		1.2602	3 2. 3
		1.2599	4 1. 0
8.6	1.2529	1.2534	4 1. 1
8.6	1.2264	1.2277	0 0.10
33	1.2156	1.2162	3 2. 4

TABLE IV

Powder diffraction pattern of Ni_5P_2

Hexagonal parameters $a = 13.220 \pm 0.002$ Å, $c = 24.632 \pm 0.002$ Å, $c/a = 1.863$; $U = 3728.0$ Å^3; $Z = 24$; F.W. = 355.49; $D_x = 3.80$ g cm^{-3}; Guinier focussing camera, diameter 11.46 cm; monochromated Cu K_α radiation $\lambda_{\alpha_1} = 1.5405$ Å; temp. 24 °C; internal standard As_2O_3 ($a = 11.075_5$ Å); d values > 1.20 Å; cutoff 35 Å

I/I_1	d_{obs} (Å)	d_{calc} (Å)	h k l
1.8	3.314	3.304	2 2. 0
5.5	2.912	2.912	2 2. 4
5.5	2.596	2.596	4 0. 4
17	2.573	2.574	2 2. 6
		2.569	3 2. 2
4.4	2.467	2.469	2 0. 9
		2.464	0 0.10
33	2.160	2.163	4 2. 0
4.4	2.144	2.146	5 0. 4
		2.141	2 1.10
17	2.132	2.134	4 1. 6
		2.131	4 2. 2
		2.128	3 3. 3
5.5	2.114	2.120	1 1.11
21	2.097	2.096	4 0. 8
13	2.073	2.077	5 0. 5
		2.075	3 3. 4
		2.073	3 1. 9
		2.070	3 0.10
7	2.054	2.056	5 1. 0
		2.053	0 0.12
13	2.041	2.041	4 2. 4
2.8	2.017	2.020	1 0.12
13	2.001	2.000	5 0. 6
		1.999	3 2. 8
100	1.9754	1.9778	4 0. 9
		1.9754	2 2.10
26	1.9465	1.9465	3 1.10
100	1.9072	1.9079	6 0. 0
3.5	1.8226	1.8226	6 0. 4
		1.8212	1 1.13
7	1.8030	1.7997	4 3. 4
13	1.7704	1.7704	4 2. 8
3.5	1.7558	1.7640	4 3. 5
		1.7571	5 2. 4
		1.7564	5 0. 9
		1.7539	4 1.10
33	1.7458	1.7458	6 1.10
		1.7440	2 2.12
7	1.7335	1.7360	2 1.13
2.2	1.6698	1.6681	4 0.12
		1.6676	4 1.11
4.4	1.6581	1.6598	4 3. 7

Can. J. Chem. Downloaded from www.nrcresearchpress.com by 210.87.254.105 on 09/05/12
For personal use only.

TABLE IV (*Concluded*)

I/I_1	d_{obs} (Å)	d_{calc} (Å)	$h\ k\ l$
11	1.6374	1.6380	4 4. 2
		1.6353	5 3. 0
			7 0. 0
11	1.6221	1.6221	6 0. 8
		1.6215	5 3. 2
			7 0. 2
2.8	1.5410	1.5396	0 0.16
2.8	1.5331	1.5331	4 4. 6
4.4	1.3963	1.3963	7 2. 1
		1.3955	2 2.16
		1.3952	5 0.14
13	1.3725	1.3732	6 2. 9
		1.3725	4 4.10
		1.3721	4 1.15
13	1.2873	1.2882	1 0.19
		1.2882	3 0.18
		1.2879	7 3. 0
		1.2873	4 4.12
		1.2864	7 3. 1
13	1.2784	1.2790	5 3.12
			7 0.12
		1.2775	5 0.16
13	1.2584	1.2584	5 5. 6
13	1.2483	1.2491	8 2. 0
		1.2475	8 2. 1
13	1.2431	1.2428	8 2. 2
13	1.2322	1.2325	5 1.16
		1.2317	9 0. 5
		1.2317	0 0.20
13	1.2084	1.2081	6 4. 8

DISCUSSION

The similarity between the structure of Ni_5As_2 and the structures of the various polytypes of Pd_5As_2 was established in the first instance by comparing the intensities of single crystal reflections. It was found that the intensities of corresponding reflections, referred to the subcell common to all the crystals, were very closely similar on both zero and upper level nets. Secondly, the similarity of the structures was established by comparing the powder data for Pd_5As_2, Ni_5Si_2, and Ni_5P_2 which have been plotted in Fig. 1 together with previously published data for Ni_5As_2 (1, 7) and Mn_5Ge_2 (8) (designated $Mn_{2.65}Ge$ by Ohoyama). The strong lines common to all the five compounds are shown in their observed positions with relative intensities and indices as indicated. It is apparent that the five structures are closely related.

It should be noted that all the lines in Fig. 1 can be indexed on the smaller cells having $a \approx 6$ Å and $c \approx 12$ Å. The larger cells are necessary in the cases of Pd_5As_2 and Ni_5P_2 to index some of the weak lines in these patterns. In the case of Pd_5As_2, the polytypism has been demonstrated by the single crystal work and the origin of the increase necessary in the c-axis parameter for satisfactory indexing is clear. The occurrence of polytypism implies a layered structure with layer planes at right angles to the c-axis. For Ni_5P_2 it is necessary to double both a and c parameters to index the pattern completely. No possible extension of c alone is satisfactory up to $c = 86$ Å.

In the absence of single crystal data on a number of crystals of Ni_5Si_2 and Ni_5P_2 it is not possible to draw any definite conclusions on the occurrence of polytypism in these compounds.

It is interesting to note that the β and β' phases of Ni_5As_2 reported by Heyding and

Can. J. Chem. Downloaded from www.nrcresearchpress.com by 210.87.254.105 on 09/05/12
For personal use only.

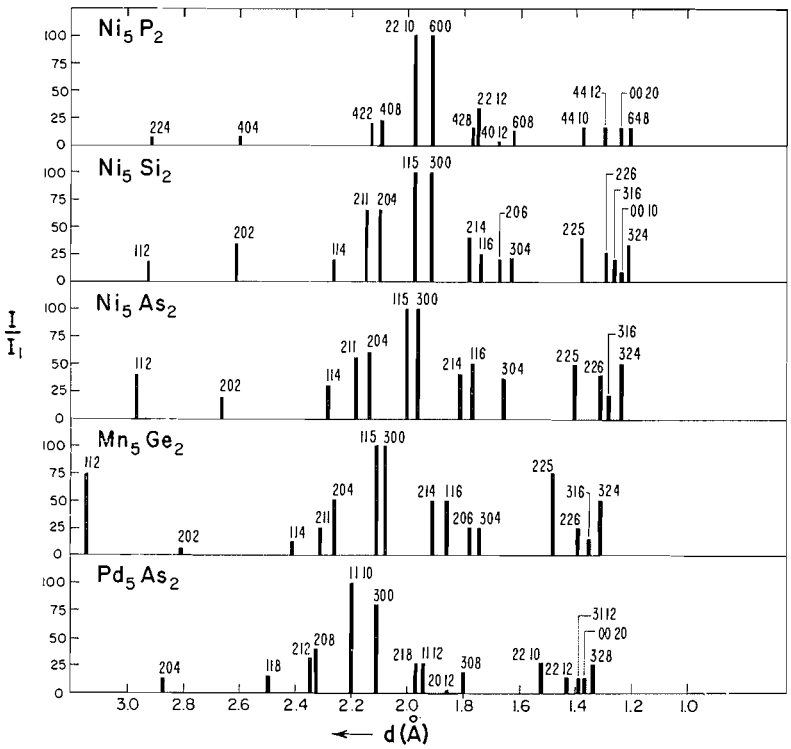

FIG. 1. Comparison of powder patterns of some M_5X_2 compounds.

Calvert (7) have powder patterns which are related in the same way as would be the powder patterns of hexagonal and trigonal polytypes of Pd_5As_2. The trigonal polytypes have reflections *h0l* for all values of *l* whereas the hexagonal polytypes have reflections *h0l* only where *l* is even.

ACKNOWLEDGMENT

The authors are indebted to Mr. G. J. G. Despault, who prepared all the materials used in this investigation.

REFERENCES

1. G. S. SAINI, L. D. CALVERT, and J. B. TAYLOR. Can. J. Chem. **42**, 150 (1964).
2. G. S. SAINI, L. D. CALVERT, and J. B. TAYLOR. Can. J. Chem. In press.
3. G. PILSTRÖM. Acta Chem. Scand. **15**, 893 (1961).
4. A. OSAWA and M. OKAMOTO. Sci. Rept. Tohoku Univ. First Ser. **27**, 331 (1939).
5. S. RUNDQVIST. Arkiv Kemi, **20**, 67 (1962).
6. L. W. STROCK and V. A. BROPHY. Am. Mineralogist, **40**, 94 (1955).
7. R. D. HEYDING and L. D. CALVERT. Can. J. Chem. **35**, 1205 (1957).
8. T. OHOYAMA. J. Phys. Soc. Japan, **16**, 1995 (1961).

Can. J. Chem. Downloaded from www.nrcresearchpress.com by 210.87.254.105 on 09/05/12
For personal use only.

Can. J. Chem. Downloaded from www.nrcresearchpress.com by 210.87.254.42 on 09/05/12
For personal use only.

THE RELATIVE ACCEPTOR POWER OF BORON TRIHALIDES AND BORANE TOWARD TRIMETHYLAMINE BY PROTON N.M.R. MEASUREMENTS[1]

J. M. MILLER[2] AND M. ONYSZCHUK
Inorganic Chemistry Laboratory, McGill University, Montreal, Quebec
Received January 29, 1964

ABSTRACT

Proton n.m.r. spectra of trimethylamine adducts of the boron trihalides and borane have been measured in chloroform solution. Chemical shifts of methyl protons relative to tetramethylsilane decrease in the order: $BBr_3 > BCl_3 > BH_3 > BF_3$, suggesting that this is the order of acceptor activity toward trimethylamine. This is supported by the existence of a linear relationship between methyl proton chemical shifts and the heats of formation, dipole moments, or infrared vibrational shifts of boron trihalide and borane adducts. Splitting of methyl proton resonances into quartets have been observed for $(CH_3)_3N \cdot BCl_3$ and $(CH_3)_3N \cdot BBr_3$ but not for $(CH_3)_3N \cdot BF_3$ and $(CH_3)_3N \cdot BH_3$.

INTRODUCTION

Nuclear magnetic resonance measurements have been used recently to determine relative stabilities of BX_3 (where X = F, H, CH_3, or C_2H_5) addition compounds (1–8). Relative basicities of donor molecules and relative acceptor powers of BX_3 molecules have been inferred from such data. Calorimetric (9, 10), dipole moment (11), infrared (12, 13), and displacement reaction (14) measurements have shown recently that the relative acceptor power of boron trihalides toward a variety of donor molecules is $BBr_3 > BCl_3 > BF_3$. Methyl proton chemical shifts of their trimethylamine adducts should also indicate this order. The measurements reported here were made to examine this possibility.

RESULTS AND DISCUSSION

Chemical shifts of methyl protons in trimethylamine adducts of boron trihalides and borane were found to decrease in the order: $BBr_3 > BCl_3 > BH_3 > BF_3$. The measured values for 1 mole % solutions of the adducts in chloroform were 190.8, 180.2, 159.5, and 157.3 c.p.s., respectively, below the proton resonance of dilute tetramethylsilane ($\delta = 0$ c.p.s.). The corresponding proton chemical shift of trimethylamine in chloroform was 132.2 c.p.s. Line diagrams of the measured spectra are compared in Fig. 1. Chemical shifts were affected to an extent of only 1 or 2 c.p.s. by changes of concentration in the range of 1.0 to 0.2 mole %. The difference between chemical shifts of the BH_3 and BF_3 adducts was only 2.2 c.p.s. in chloroform solution, but this appears to be significant because almost the same effect was obtained for measurements in benzene solution.

The observed order of decrease in chemical shift can be rationalized as follows. If the acceptor power increases progressively from BF_3 to BBr_3, the electron pair of the B–N bond of the trimethylamine complex should be drawn progressively closer to the boron atom. The resulting decrease in electron density at the nitrogen atom should be compensated in part by electron release from the attached methyl groups. This effect, in turn, should result in a decrease in the electron density about the methyl protons and their shielding should be reduced. Consequently, proton resonances should shift to lower field

[1]*This work was supported by a grant from the Defence Research Board of Canada (Grant number 9530-20, Project D46-95-30-20).*
[2]*Holder of an N.R.C. Bursary, 1961–1962, and N.R.C. Studentships, 1962–1964.*

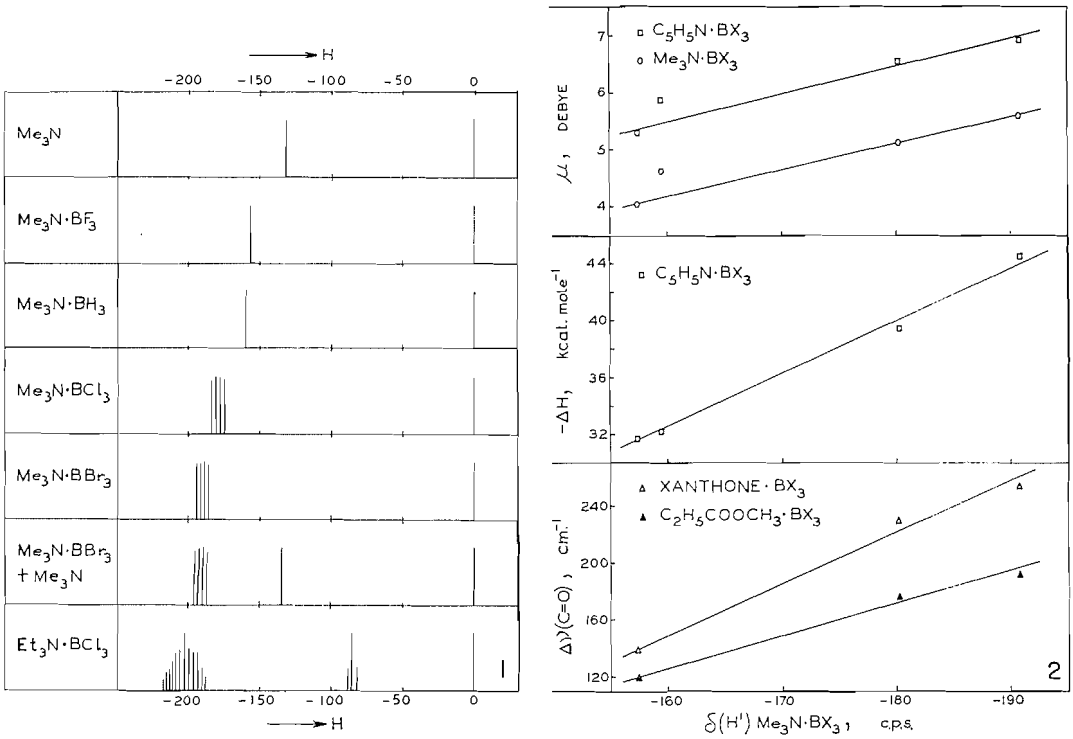

FIG. 1. Methyl proton n.m.r. spectra of $Me_3N \cdot BX_3$ (where X = H, F, Cl, Br) and $Et_3N \cdot BCl_3$.
FIG. 2. Correlations of methyl proton chemical shifts of $Me_3N \cdot BX_3$ with dipole moments, heats of formation, and infrared carbonyl shifts of various BX_3 complexes.

as the electron acceptor power of the boron species increases. Since methyl proton chemical shifts decreased in the order $BBr_3 > BCl_3 > BH_3 > BF_3$, we conclude that this is also the order of acceptor power toward trimethylamine.

The above explanation may not be the only one. Changes in electronegativity and (or) magnetic anisotropy due to substitution of one halogen atom for another might account for the observed order. Several workers (15, 16) have suggested that in some *n*-haloalkanes these effects produce shifts to lower field in the order I > Br > Cl > F for β protons and the opposite order for α protons. However, in the case of isopropyl halides the order in α and β proton chemical shifts is I > Br > Cl > F, whereas the reverse order applies for α protons in *n*-propyl halides. These unusual shifts have yet to be explained satisfactorily. Dr. M. A. Whitehead and his co-workers in this department are now trying to estimate theoretically the relative magnitudes of inductive, magnetic anisotropy, and hyperconjugative effects in $Me_3N \cdot BX_3$ and the isoelectronic Me_3CCX_3 compounds. Their results will be reported at a later date.

Coyle and Stone (5) found that with dichloromethane as solvent and concentrations of adduct of 10%, the methyl proton chemical shifts of $Me_3N \cdot BF_3$ was 0.02 p.p.m. greater than that of $Me_3N \cdot BH_3$. In the case of triethylamine adducts they observed a greater internal shift (measured as the difference between methyl and methylene proton resonances) for $(C_2H_5)_3N \cdot BF_3$ than for $(C_2H_5)_3N \cdot BH_3$; the difference was 0.14 p.p.m. corresponding to 8.4 c.p.s. at 60 Mc. In both cases BF_3 appears to be a slightly stronger acceptor than BH_3. Our chemical shift data agree with recent calorimetric (9, 10) and dipole

Can. J. Chem. Downloaded from www.nrcresearchpress.com by 210.87.254.42 on 09/05/12
For personal use only.

moment (11) measurements which indicate that BH_3 is a slightly stronger acceptor than BF_3.

As shown in Table I and Fig. 2, linear relationships exist between our chemical shift

TABLE I

Physical data for some BX_3 complexes

Property	Complex				Ref.
	BF_3	BH_3	BCl_3	BBr_3	
$-\Delta H$, kcal mole^{-1}, for $C_5H_5N(l) + BX_3(l)$ in $C_6H_5NO_2$ solution	31.7	32.2*	39.5	44.5	9, 10
Dipole moment, debye,					
$Me_3N \cdot BX_3$	4.04	4.62	5.13	5.57	11
$C_5H_5N \cdot BX_3$	5.31	5.86	6.52	6.90	11
Infrared shift, $\Delta\nu$(C=O), cm^{-1}					
$C_2H_5COOCH_3 \cdot BX_3$	119	—	176	191	12
Xanthone$\cdot BX_3$	138	—	229	253	13
Methyl proton chemical shift, δ c.p.s. $Me_3N \cdot BX_3$	157.3	159.5	180.2	190.8	this work

*Corrected for the dimerization energy of BH_3.

data and dipole moments, heats of formation, and infrared shifts of various BX_3 (where X = H, F, Cl, Br) complexes, even though these values refer to different donor molecules. These linear correlations strongly suggest that proton chemical shifts reflect the same fundamental property of the complexes as do dipole moments, heats of formation, and infrared shifts. The property in common is probably the strength of the donor–acceptor bond, which, as suggested by Bax *et al.* (11) increases progressively from BF_3 to BBr_3 adducts because of a corresponding decrease in halogen valence shell electron-pair repulsions in the same order. Calorimetric and displacement results have been explained in terms of dative π-bonding and reorganization energies of boron trihalides (17, 14). This explanation cannot be used to account for dipole moment, infrared, and proton n.m.r. results because these data refer to properties of the complexes themselves and not to the energetics of their formation, as do heats of formation and displacement data. It is clear, nevertheless, that proton n.m.r. shifts, like heats of formation, dipole moments, and infrared shifts, indicate a relative acceptor power order of $BBr_3 > BCl_3 > BH_3 > BF_3$. Although displacement reaction studies showed that BF_3 is a slightly stronger acceptor than B_2H_6, it was evident that by taking the dimerization energy of BH_3 into account, BH_3 should be a stronger acceptor than BF_3. This expectation is confirmed by dipole moment, heat of formation, and our proton n.m.r. measurements.

Methyl proton n.m.r. spectra $Me_3N \cdot BH_3$ and $Me_3N \cdot BF_3$ consisted (Fig. 1) of slightly broadened singlets, whereas $Me_3N \cdot BCl_3$ and $Me_3N \cdot BBr_3$ gave quartets with peaks of almost equal intensity and a splitting constant $J = 2.7$ and 2.8 c.p.s., respectively (Fig. 3). These splittings were independent of concentration in the range 1.0 to 0.2 mole % and were the same in chloroform, *o*-dichlorobenzene, and benzene solutions. Chemical shifts for $Me_3N \cdot BCl_3$ and $Me_3N \cdot BBr_3$ were measured from the center of each quartet. Each peak of the quartet appeared to be a closely spaced doublet with $J \simeq 0.7$ c.p.s. Ohashi *et al.* (6) have also observed a quartet for $Me_3N \cdot BCl_3$ with a splitting constant of 2.6 c.p.s., in excellent agreement with our value. However, they did not detect further splitting of the quartet into doublets. They also reported that the peak at highest field was weaker than the other three. We found this effect depended upon the

Can. J. Chem. Downloaded from www.nrcresearchpress.com by 210.87.254.42 on 09/05/12
For personal use only.

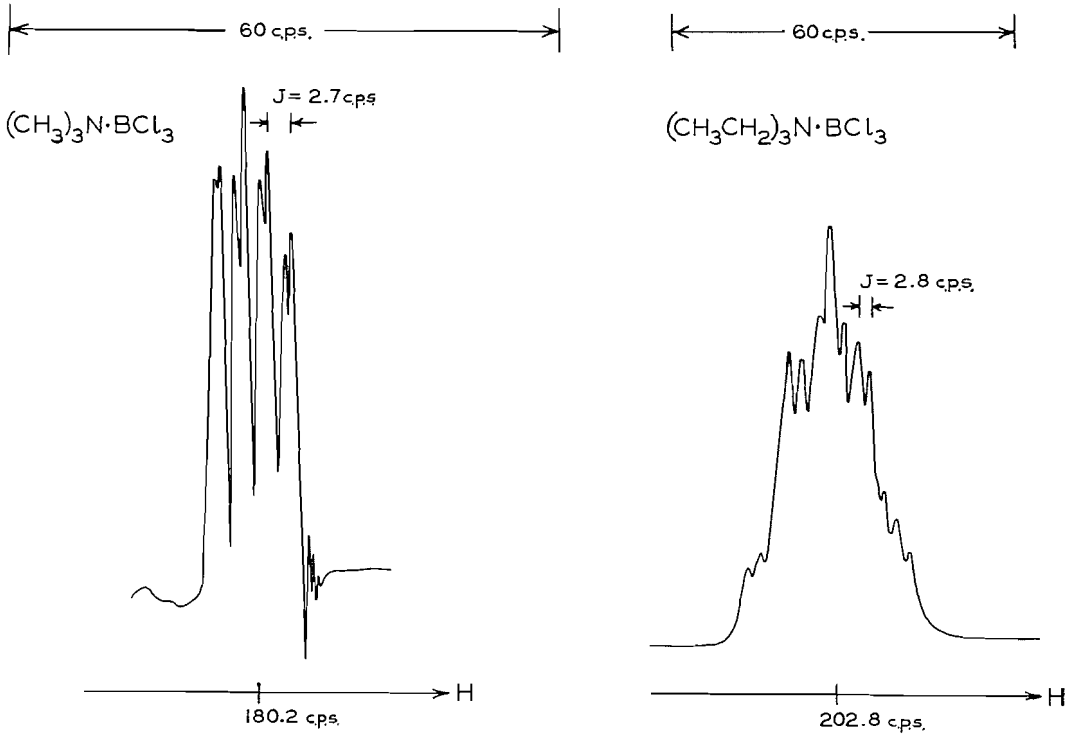

FIG. 3. Splitting of methyl proton resonances of $Me_3N \cdot BCl_3$ and of methylene proton resonances of $Et_3N \cdot BCl_3$.

direction of scan since it appeared at high field when scanned with increasing magnetic field and at low field when scanned in the opposite direction. This effect appears to be due to imperfect adjustment of the spectrometer.

If the main splitting was such as to produce a triplet with peaks of equal intensity, the effect could be ascribed to N^{14} spin–spin splitting, as has been proposed for anhydrous ammonia (18), $(CH_3CH_2)_4N^+I^-$ in D_2O solution (19), $(CH_3CH_2)_4N^+X^-$ (where X is Cl, Br, or OH) in Me_2SO, CH_3CN, and D_2O solution (19), and $(CH_3CH_2)_4N^+Br^-$ in H_2SO_4 solution (20). The same explanation has been suggested by Ohashi *et al.* (6) for the splittings in $Me_3N \cdot BCl_3$, even though they observed a quartet rather than a triplet. We think that N^{14} spin–spin coupling must be ruled out, because we observed quartets rather than triplets for $Me_3N \cdot BCl_3$ and $Me_3N \cdot BBr_3$.

Another possibility is coupling of methyl protons to B^{11} (spin 3/2) which should give a quartet with peaks of equal intensity. This effect should be just as likely to occur in $Me_3N \cdot BH_3$ and $Me_3N \cdot BF_3$ as in $Me_3N \cdot BCl_3$ and $Me_3N \cdot BBr_3$, but splittings were observed for the last two only. Perhaps restricted rotation about the B–N bond is necessary for coupling to be appreciable. Spatial models (of the Courtauld type) reveal that free rotation about the B–N bond is drastically restricted in $Me_3N \cdot BCl_3$ and $Me_3N \cdot BBr_3$ but not in $Me_3N \cdot BF_3$ and $Me_3N \cdot BH_3$. Hindered rotation might affect the electric field in such a way as to promote coupling of methyl protons with B^{11} and thereby give a quartet. An unambiguous test for B^{11} coupling could be made by double irradiation at the B^{11} resonance frequency. This test would be positive if a single methyl proton peak resulted. Unfortunately, we do not have the equipment to make this test. In an attempt

Can. J. Chem. Downloaded from www.nrcresearchpress.com by 210.87.254.42 on 09/05/12
For personal use only.

to examine the possibility of hindered rotation in $Me_3N \cdot BCl_3$, its proton resonance spectrum was measured at temperatures between 25 and 100°. There was no detectable change.

The observed quartets could conceivably be caused by coupling of methyl protons with chlorine and bromine, both of which have nuclear spins of 3/2, in the hindered molecules. However, this is unlikely because these nuclei do not normally produce first-order splitting of proton resonances in organic compounds. Moreover, three halogens should produce splittings more complex than a quartet. Further splitting of each peak of the quartet into a doublet might be due to non-equivalence of the methyl groups arising from a loss of axial symmetry along the B–N bond in the sterically hindered BBr_3 and BCl_3 adducts. Less likely is the possibility that spin coupling to B^{10} (present as 20% of natural boron, spin 3) superimposes new lines on the quartets. Such coupling should produce more complex splitting than the well-defined doublets observed. The same objection should apply to an explanation involving spin coupling of methyl protons to the Cl^{35},Cl^{37} and Br^{79},Br^{81} isotopic pairs (spin 3/2).

We observed that $Me_3N \cdot BBr_3$ and excess Me_3N in chloroform solution gave two separate methyl proton resonances, one for the free amine and the other for the complex. This clearly shows that there is no or only very slow exchange of BBr_3 between Me_3N molecules. The quartet splitting constant and chemical shift was unaffected by the excess Me_3N.

No unusual splitting of ethyl proton resonances in BH_3, BF_3, and BMe_3 complexes of triethylamine were reported by Coyle and Stone (5), and none for $Et_3N \cdot BCl_3$ by Ohashi *et al.* (6). We found that $Et_3N \cdot BCl_3$ in chloroform solution gave a methyl proton triplet centered at 84.3 c.p.s. and a complex band (Fig. 3) centered at 202.8 c.p.s. where methylene resonances are expected. The latter has 12 distinct inflections, but may well have more buried in the complex envelope. A splitting of the expected 1:3:3:1 methylene quartet into 12 peaks is expected if N^{14} spin–spin coupling occurred, and into 16 for B^{11} coupling. We are unable to decide between these possibilities. It is interesting to note that in $Et_4N^+I^-$ the methyl triplet and not the methylene quartet is split, and this has been attributed to N^{14} spin–spin coupling (19). Such coupling does not occur in $Me_3NH^+Br^-$ and $Et_3NH^+Br^-$, the spectra of which in H_2O (19) and chloroform solution show no unusual splitting.

EXPERIMENTAL

Materials

Trimethylamine complexes of BH_3, BF_3, BCl_3, and BBr_3 were prepared and purified as described previously (14). A solution of $Et_3N \cdot BCl_3$ in chloroform was prepared by bubbling BCl_3 (Matheson) into a solution of Et_3N (Eastman) in chloroform. Triethyl and trimethyl ammonium bromides were prepared by bubbling anhydrous HBr (Matheson) into chloroform solutions of the respective amines.

Chloroform (Fisher Spectral Grade) was purified of its ethanol preservative by extracting six times with distilled water and then drying over calcium hydride, followed by fractional distillation. An n.m.r. spectrum of the purified chloroform showed it to be completely free of ethanol. Benzene (Mallinkrodt) was first dried over sodium–lead alloy and then fractionally distilled. Tetramethylsilane (Anderson) was used without further purification.

Apparatus and Methods

Spectra were measured with a Varian HR-60 High Resolution NMR Spectrometer which has a fixed frequency of 60 Mc. Calibration was by means of 60 c.p.s. side bands on the tetramethylsilane peak. Each spectrum was scanned several times in each direction and average values of chemical shifts were taken relative to tetramethylsilane, the internal reference ($\delta = 0$ c.p.s.). Complexes were dissolved in purified chloroform or benzene such that concentrations were approximately 1 mole %.

Can. J. Chem. Downloaded from www.nrcresearchpress.com by 210.87.254.42 on 09/05/12
For personal use only.

ACKNOWLEDGMENTS

We thank Dr. A. Taurins and Dr. C. Stammer for the n.m.r. measurements and for helpful discussions. We are grateful to the Defence Research Board for financial assistance and to the National Research Council for the award of scholarships to one of us (J. M. M.). We are also grateful to a referee for several helpful comments.

REFERENCES

1. P. DIEHL and R. A. OGG. Nature, **180**, 1114 (1957).
2. P. DIEHL and J. GRANACHER. Helv. Phys. Acta, **31**, 43 (1958).
3. T. P. ONAK, H. LANDESMAN, R. E. WILLIAMS, and I. SHAPIRO. J. Phys. Chem. **63**, 1533 (1959).
4. W. D. PHILLIPS, H. C. MILLER, and E. L. MUETTERTIES. J. Am. Chem. Soc. **81**, 4496 (1959).
5. T. D. COYLE and F. G. A. STONE. J. Am. Chem. Soc. **83**, 4138 (1961).
6. O. OHASHI, Y. KURITA, T. TOTANI, H. WATANABE, T. NAKAGAWA, and M. KUBO. Bull. Chem. Soc. Japan, **35**, 1317 (1962).
7. R. A. CRAIG and R. E. RICHARDS. Trans. Faraday Soc. **59**, 1962 (1963).
8. R. R. HOLMES and R. P. CARTER, JR. Inorg. Chem. **2**, 1146 (1963).
9. H. C. BROWN and R. R. HOLMES. J. Am. Chem. Soc. **78**, 2173 (1956).
10. H. C. BROWN and L. DOMASH. J. Am. Chem. Soc. **78**, 5384 (1956).
11. C. M. BAX, A. R. KATRITZKY, and L. E. SUTTON. J. Chem. Soc. 1258 (1958).
12. M. F. LAPPERT. J. Chem. Soc. 542 (1962).
13. D. COOK. Can. J. Chem. **41**, 522 (1963).
14. J. M. MILLER and M. ONYSZCHUK. Can. J. Chem. **41**, 2898 (1963).
15. B. P. DAILEY and J. N. SCHOOLERY. J. Am. Chem. Soc. **77**, 3977 (1955).
16. A. A. BOTHNER-BY and C. NAAR-COLIN. J. Am. Chem. Soc. **80**, 1728 (1958).
17. F. A. COTTON and J. R. LETO. J. Chem. Phys. **30**, 993 (1959).
18. J. A. POPLE, W. G. SCHNEIDER, and H. J. BERNSTEIN. High resolution nuclear magnetic resonance. McGraw-Hill, New York. 1959. p. 101.
19. E. BULLOCK, D. G. TUCK, and E. J. WOODHOUSE. J. Chem. Phys. **38**, 2318 (1963).
20. J. T. EDWARD, A. TAURINS, and C. STAMMER. Private communication.

Can. J. Chem. Downloaded from www.nrcresearchpress.com by 210.87.254.42 on 09/05/12
For personal use only.

Can. J. Chem. Downloaded from www.nrcresearchpress.com by 210.87.254.6 on 09/05/12
For personal use only.

CHEMISTRY OF ETHYL 2-METHYL-4-OXO-Δ^2-PYRROLINE-3-CARBOXYLATE AND RELATED COMPOUNDS

R. S. ATKINSON
Department of Chemistry, University of Nottingham, Nottingham, England

AND

E. BULLOCK
Department of Chemistry, Memorial University, St. John's, Newfoundland

Received February 13, 1964

ABSTRACT

Ethyl 2-methyl-4-oxo-Δ^2-pyrroline-3-carboxylate (I*a*) is oxidized by one-electron oxidizing agents to a colored dimer which has been synthesized by an alternative route. Acetylation of (I*a*) and its N-methyl derivative (I*b*) gives a variety of products some of which show unusual infrared absorptions. The products of dimerization of (I*a*) and (I*b*) in strong acid show nuclear magnetic resonance absorptions at variance with previously claimed structures and alternatives are suggested.

The formation of dimeric compounds from pyrrolic monomers by reaction with one-electron oxidizing agents has been claimed only for certain oxygenated pyrrolic systems (1, 2). (The results of Siedel *et al.* (2) have recently been questioned (3).)

Benary (1) stated that oxidation of (I*a*) (which he formulated as a hydroxypyrrole (cf. ref. 4)) with ferric chloride gave a dimer (II), but had no evidence beyond analysis and the reversible reduction of the product.

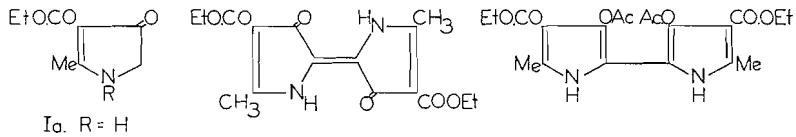

Ia. R = H
b. R = CH_3

II

III

Many one-electron oxidizing agents produce (II) from (I*a*) (see Experimental section) and the reaction appears to be similar to the production of indigo from indoxyl. The product, however, shows few reactions typical of the indigo system and is very sensitive to acid and heat, both of which produce blue-black decomposition products. No crystalline derivatives of (II) have been reported previously, but we have now prepared a crystalline leuco-acetate (III) which, on treatment with base and subsequent neutralization, yields starting material. Dimerization of the iodo-acetate (IV*a*), under modified Ullmann conditions (5), gave (III) and thus proves Benary's formulation of the dimer (II). Infrared spectra of (II) in potassium bromide disks showed slight variations in different samples. The NH region varied considerably in the relative heights of the "bonded" and "unbonded" absorption bands and occasionally the single peak at 1647 cm^{-1} (extended-amide carbonyl) appeared as a close doublet. The rest of the absorptions were reproducible and since there were no variations in electronic spectra, the effect is probably due to polymorphism.

Treatment of (IV*a*) with base and air gave a purple salt which, after neutralization, yielded a compound showing superficial resemblance to (II), although its infrared and

electronic absorption spectra were significantly different. Reductive acetylation yielded (III) and we conclude, therefore, that this product is (or contains) the *cis*-isomer of (II).

Attempts to prepare the iodo-acetate (IV*a*) prompted investigation of the acetylation of (I*a*).

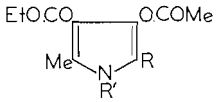

	R	R′
IV*a*.	I	H
b.	H	COMe
c.	H	H
d.	H	Me
e.	I	Me

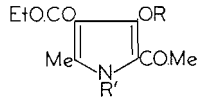

	R	R′
V*a*.	COMe	COMe
b.	COMe	H
c.	H	H
d.	COMe	Me
e.	H	Me

Other workers have assigned structures to some of the acetates described here, but the use of nuclear magnetic resonance spectroscopy (n.m.r.) shows that certain of the earlier formulations were incorrect. In particular, the number of acetate groups present has been difficult to establish by analysis but is obvious from the n. m. r. results. The O,N-diacetate (IV*b*) has previously been reported as an O-acetate (6) and a triacetate (7). The latter formula was based on the infrared absorption around 1700 cm^{-1} which shows four resolvable peaks which might reasonably be attributed to carbonyl groups. In fact, the O-acetate absorption is a doublet, as it is also in (III) and (IV*d*). This double absorption is probably due to the existence of the O-acetate group in two conformations relative to the pyrrole ring (8).

Other unreported acetates which can be prepared from (I*a*) are (IV*c*) and (V*a*). The N-acetates are very readily hydrolyzed and preparation of (IV*a*) from (IV*b*) with iodine and sodium acetate proceeds in one step. Similarly, the authentic triacetate (V*a*) is converted to (V*b*) (9) by treatment with aqueous sodium acetate. The O-monoacetate (IV*c*) undergoes Fries-type rearrangement to (V*c*) (10) either on heating or treatment with aluminum chloride. A similar lability of acetoxy residues has previously been reported for 2-acetoxypyrrole derivatives (11).

To eliminate a possible tautomeric structure for (II) we tried, unsuccessfully, to prepare the di-N-methyl analogue. Benary attempted the synthesis of ethyl 1,2-dimethyl-4-oxo-Δ^2-pyrroline-3-carboxylate (I*b*) by base induced cyclization of (VI), but reported that the only product was a hygroscopic oil.

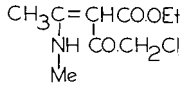

VI

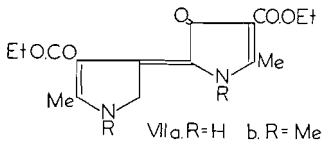

VII *a*. R = H *b*. R = Me

Our results are precisely similar, but we have good evidence that the oil is mainly the desired product. (For example, a group of acetates analogous to those of (I*a*) can be prepared by similar methods.) Attempts to synthesize a dimer analogous to (II) by oxidation were quite unsuccessful and the N-methyl iodoacetate (IV*e*) gave only (IV*d*) under Ullmann conditions.

Acid treatment of (I*a*) gives a crystalline product which has been formulated as a dimer, either (VII*a*) or (VIII*a*) (1, 7). The N-methyl-oxo-pyrroline (I*b*) gives an analogous

Can. J. Chem. Downloaded from www.nrcresearchpress.com by 210.87.254.6 on 09/05/12
For personal use only.

compound and examination of the n. m. r. spectra of the two products suggests that formulas (VII) and (VIII) are incorrect. Thus, apart from two non-equivalent ester groups, ring-methyl groups, and NH (or NMe) absorptions, both compounds show additional absorption equivalent to two protons. Compound (VII) requires that this absorption is either a singlet (intensity two) or an AB quartet, depending on the stereochemistry and rigidity of the ring containing the CH_2 group. Compound (VIII) requires that there be two singlets (intensity one each), one of which (the —OH) would exchange readily with heavy water. Both dimers showed two additional singlets, neither of which exchanged with D_2O, and hence both (VII) and (VIII) are incorrect.

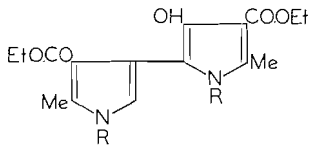

VIII a. R=H b. R=Me

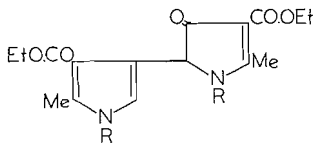

IX a. R=H b. R=Me

Further evidence comes from the fact that neither dimer gives a color with ferric chloride (which makes (VIII) unlikely) and that the ultraviolet absorption, especially of the N-methyl dimer, is extremely similar (in the longer wavelength bands) to the parent oxo-pyrroline (I*b*). The alternative formula (IX) is consistent with all of the observed properties. It is perhaps surprising that the substitution of the pyrryl-residue in the 2-position of ethyl 2-methyl-4-oxo-Δ^2-pyrroline-3-carboxylate does not convert the oxo-pyrroline to the hydroxypyrrole form but we have so far found only the acetyl-substituted compound (V*c*) in which the hydroxypyrrole structure is favored.

EXPERIMENTAL

Ultraviolet and visible spectra were recorded on Perkin–Elmer Model 137 UV and Unicam SP-700 instruments using ethanol solutions. Infrared data were determined on a Unicam SP 100 spectrometer and n. m. r. spectra on A.E.I. RS-2 or Varian A-60 instruments. Melting points (hot stage) are uncorrected.

Oxidation of Ethyl 2-Methyl-4-oxo-Δ^2-pyrroline-3-carboxylate (Ia)

The oxidation was carried out preparatively according to Benary (1). The yield of product is markedly reduced if less than 3 molar equivalents of ferric chloride are used. Using more than 3 moles per mole of pyrrole, the yield is 73%. The same dimer was obtained in varying yield when ferric chloride was replaced by potassium ferricyanide, Fremy's salt, lead tetraacetate, iodine in potassium iodide solution, silver nitrate, or selenium dioxide. A small yield of the sodium salt of the dimer was isolated when air was bubbled through an alkaline solution of (I*a*) for 24 h (precise analogue of indigo preparation).

The dimer gave little indication of similarity to indigo, e.g. direct acetylation gave no isolable product nor did attempts to prepare a dehydroindigo analogue. Oxidation gave no recognizable product. The compound was reversibly reduced by hydrogen over Adams' catalyst and by sodium dithionite.

Diethyl 2,2'-Dimethyl-4,4'-diacetoxydipyrrole-3,3'-dicarboxylate (III)

The oxidation product (0.2 g, see above) was suspended in 50% aqueous ethanol (20 ml) and treated with sodium dithionite (1 g). The reaction mixture remained heterogeneous but on shaking and warming (water bath) the red color of the oxidation product was slowly discharged. The mixture was filtered and the residual solid, after washing once with water, was dissolved in acetic anhydride (10 ml) containing a few drops of pyridine. The mixture was kept for 12 h when the white precipitate was separated and crystallized from chloroform–methanol to colorless needles; m. p. 265–266° (0.201 g, 80%). Calc. for $C_{20}H_{24}O_8N_2$: C, 57.13; H, 5.75; N, 6.66. Found: C, 57.40; H, 5.74; N, 6.60%. Ultraviolet spectrum: λ_{max} 222, 263 mμ; ϵ_{max} 31,200, 15,700 respectively. Infrared absorptions (KBr) at 3373, 1785, 1751, 1700 cm^{-1} (*inter alia*).

Ethyl 1-Acetyl-2-methyl-4-acetoxypyrrole-3-carboxylate (IVb)

This compound was prepared by the procedure reported to give a triacetate (7). The product formed colorless needles (94%); m. p. 123–124° (lit.123°). Calc. for $C_{12}H_{15}O_5N$: C, 56.91; H, 5.97; N, 5.53. Found: C, 56.80; H, 5.88; N, 5.60%. Ultraviolet spectrum: λ_{max} 223, 241 mμ; ϵ_{max} 21 450, 10 540. The infrared

Can. J. Chem. Downloaded from www.nrcresearchpress.com by 210.87.254.6 on 09/05/12
For personal use only.

absorptions included strong bands at 1765, 1744, 1709 cm^{-1} ($CHCl_3$); 1781, 1768, 1745, 1716 cm^{-1} (CCl_4). The n. m. r. spectrum ($CHCl_3$) showed peaks at τ 8.61 (ester CH_3); 7.65, 7.39 ($COCH_3$); 7.11 (—C—CH_3); 5.67 (ester CH_2); 2.99 (pyrrolic CH).

The product gave a red Ehrlich reaction slowly in the cold.

Ethyl 1,5-Diacetyl-2-methyl-4-acetoxypyrrole-3-carboxylate (Va)

The diacetate (IV*b* above, 0.5 g) was suspended in acetic anhydride (10 ml) and treated with 1 drop of 70% perchloric acid. The mixture was stirred in the cold for 10 min and then treated with cold water (30 ml). As the anhydride decomposed a crystalline solid separated. When the anhydride was completely decomposed, the solid was separated and recrystallized from ethanol–water to colorless needles (0.508 g, 87%); m.p. 105–107°. This compound gave no Ehrlich reaction. Calc. for $C_{14}H_{17}O_6N$: C, 56.94; H, 5.80; N, 4.74. Found: C, 56.80; H, 5.76; N, 4.69%. Ultraviolet spectrum: λ_{max} 228, 287 mμ; ϵ_{max} 19 340, 13 550 respectively. The infrared spectrum (CCl_4) showed strong peaks at 1780, 1711, 1654 cm^{-1} whilst n. m. r. absorptions ($CHCl_3$) occurred at τ 8.64 (ester CH_3); 7.59 (2) 7.53 (1) ($COCH_3$); 7.49 (—C—CH_3); 5.73 (ester CH_2).

Ethyl 2-Methyl-4-acetoxy-5-iodopyrrole-3-carboxylate (IVa)

The diacetate (IV*b*; 2.0 g) and potassium acetate (1 g) were dissolved in boiling ethanol (100 ml) and iodine (2 g) in ethanol (70 ml) was added from a dropping funnel over a period of 2 h. The solution was boiled for a further 1 h and the solvent removed. The residual solid was extracted with water to remove salts and then crystallized (charcoal) from aqueous ethanol (2.0 g, 76%) m. p. 140–143.5° (dec.). Calc. for $C_{10}H_{12}O_4NI$: C, 35.62; H, 3.56; N, 4.16; I, 37.69. Found: C, 35.20; H, 3.29; N, 3.82; I, 38.00. Ultraviolet spectrum: λ_{max} 208, 261 mμ; ϵ_{max} 30 410, 5075 respectively. The n. m. r. spectrum ($CHCl_3$) showed peaks at τ 8.93 (ester CH_3); 7.59 ($COCH_3$); 7.46 (C—CH_3); 5.90 (ester CH_2).

Ethyl 2-Methyl-4-acetoxypyrrole-3-carboxylate (IVc)

(i) The O,N-diacetate (IV*b*; 4 g) was heated under reflux with sodium acetate (4 g) in ethanol (60 ml) for 2 h. The solvent was removed and the residual solid was treated with water and ether. The ether extract was dried (sodium sulphate) and the solvent removed. The oily, reddish residue solidified on scratching with a glass rod and was distilled (96°/0.5 mm) to a colorless oil which solidified to a low-melting solid (3.01 g, 90%). The analytical sample was prepared by repeated distillation. Calc. for $C_{10}H_{13}O_4N$: C, 56.86; H, 6.20; N, 6.63. Found: C, 56.70; H, 6.33; N, 7.04%. The n. m. r. spectrum ($CHCl_3$) which showed peaks at τ 8.67 (ester CH_3); 7.80 ($COCH_3$); 7.66 (>C—CH_3); 5.73 (ester CH_2); 3.65, 3.69 (pyrrolic H); 0.55 (broad, NH), confirms the proposed structure. The pyrrolic hydrogen resonance is a doublet, possibly by interaction with the N–H proton; integration confirms that the two absorptions are together equivalent to one proton. The compound gave an intense Ehrlich reaction in the cold.

(ii) Hydrogenation of the iodoacetate (IV*a*) in ethanol over Adams' catalyst gave an oil which had ultraviolet, infrared, and n. m. r. spectra identical with those of the above product.

(iii) Fries rearrangement of IV*c*. Ethyl 2-methyl-4-acetoxypyrrole-3-carboxylate (IV*c*; 0.3 g) was mixed with anhydrous aluminum chloride (0.38 g) and heated at 110° for 20 min. The residue was treated with cold, dilute hydrochloric acid (20 ml) and the mixture extracted with ether. Extraction of the ether with aqueous sodium hydroxide, followed by acidification of the aqueous phase yielded a white solid. After purification by sublimation *in vacuo*, this product was shown to be identical with ethyl 2-methyl-4-hydroxy-5-acetylpyrrole-3-carboxylate (V*e*, (9)) by m. p., mixed m. p., and infrared spectrum. Yield: 69 mg, 23%.

Diethyl 2,2′-Dimethyl-4,4′-diacetoxydipyrrole-3,3′-dicarboxylate (III)

Ethyl 2-methyl-4-acetoxy-5-iodopyrrole-3-carboxylate (IV*a*; 1 g) was dissolved in dimethylformamide (20 ml) and stirred overnight at room temperature with copper powder (1 g). The solvent was removed *in vacuo* and the residue extracted with boiling chloroform from which a white solid was isolated by evaporation. Crystallization from chloroform–methanol gave a product (0.57 g, 92%) identical (m.p., mixed m.p., and infrared spectrum) with the leuco-acetate (III) described above.

Hydrolysis of the iodo-acetate (IV*a*). Ethyl 2-methyl-4-acetoxy-5-iodopyrrole-3-carboxylate (IV*a*; 1.15 g) in methanol (15 ml) was treated with aqueous sodium hydroxide (5 ml, 2.5 *N*). After standing in the cold for 2 h the solution, which had become purple, was neutralized (dilute hydrochloric acid) and the suspended solid (0.19 g) removed. The product showed a superficial resemblance to the normal oxidation product (II) but had rather different infrared and electronic absorption spectra, e.g. ultraviolet and visible spectrum showed bands at 253.5, 309.0, 473.0 mμ compared with 253.5, 300.6, 490.2 mμ for (II). Upon recrystallization from chloroform, the product became identical with (II). Reductive acetylation of this material yielded a substance identical with (III). We were unable to effect any controlled interconversion of the two compounds. The dimerization may proceed as follows: A dimerization sequence based on a similar 'indoleninone' intermediate has been suggested (12).

Ethyl 1,2-Dimethyl-4-oxo-Δ^2-pyrroline-3-carboxylate (Ib)

This compound was prepared, probably in rather impure form, by the method of Benary and Silbermann (1), by the base induced cyclization of ethyl α-chloroacetyl-β-methylaminocrotonate.

Can. J. Chem. Downloaded from www.nrcresearchpress.com by 210.87.254.6 on 09/05/12
For personal use only.

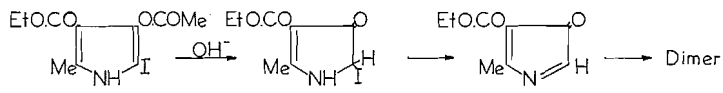

Ethyl 1,2-Dimethyl-4-acetoxypyrrole-3-carboxylate (IVd)

The yellow oil prepared above (15 g) was dissolved in acetic anhydride (20 ml) and treated with potassium acetate (1 g). The mixture was boiled for 1 min and cooled, and the anhydride was decomposed with cold water. The crystalline product (12.7 g, 69%) was separated and recrystallized from ethanol–water to colorless prisms; m. p. 96–97°. Calc. for $C_{11}H_{15}O_4N$: C, 58.65; H, 6.71; N, 6.22. Found: C, 58.90; H, 6.92; N, 6.44%. Infrared spectrum showed carbonyl absorption at 1759, 1698 cm^{-1} ($CHCl_3$) and 1782, 1764, 1709 cm^{-1} (CCl_4). Ultraviolet spectrum: λ_{max} 205.9, 234.0, 258.7; ϵ_{max} 16,750, 8870, 5270 respectively. The n. m. r. absorptions (CCl_4) occurred at τ 8.67 (ester CH_3); 7.80 ($COCH_3$); 7.55 ($\rangle C—CH_3$); 6.49 ($N—CH_3$); 5.77 (ester CH_2); 3.68 (pyrrolic H). The compound gave no color with ferric chloride, but a strong positive Ehrlich reaction in the cold.

Ethyl 1,2-Dimethyl-4-acetoxy-5-acetylpyrrole-3-carboxylate (Vd)

The monoacetate above (IV*d*; 1.0 g) was suspended in acetic anhydride (10 ml) in the cold and treated with 1 drop of 70% perchloric acid solution. After the solution was shaken for 10 min the anhydride was decomposed with water and the white crystalline product separated (0.95 g, 81%). The product was recrystallized from aqueous ethanol to white needles; m. p. 100–100.5°. Calc. for $C_{13}H_{17}O_5N$: C, 58.42; H, 6.42; N, 5.24. Found: C, 58.70; H, 6.28; N, 5.54%. The compound showed n. m. r. absorptions ($CHCl_3$) at τ 8.66 (ester CH_3); 7.67 (2) ($COCH_3$); 7.42 ($—C—CH_3$); 6.09 ($N—CH_3$); 5.68 (ester CH_2). The product gave no reaction with ferric chloride or Ehrlich's reagent.

Ethyl 1,2-Dimethyl-4-hydroxy-5-acetylpyrrole-3-carboxylate (Ve)

Ethyl 1,2-dimethyl-4-acetoxy-5-acetyl-pyrrole-3-carboxylate (V*d*; 0.2 g) was dissolved in cold ethanol (7 ml) and treated with 2.5 *N* sodium hydroxide solution (10 ml). The solution was neutralized after standing at room temperature and the resulting white solid (0.13 g, 85%) was crystallized from aqueous ethanol to colorless needles; m. p. 118–119°. Calc. for $C_{11}H_{15}O_4N$: C, 58.65; H, 6.71; N, 6.22. Found: C, 58.80; H, 6.71; N, 6.13%. The product gave an intense purple ferric chloride test but no color with Ehrlich's reagent.

Ethyl 1,2-Dimethyl-4-oxo-5-(1′,2′-dimethyl-3′-ethoxycarbonyl-pyrrol-4′-yl)-Δ^2-pyrroline-3-carboxylate (IXb)

The above monoacetate (IV*d*; 1 g) was treated with concentrated hydrochloric acid (15 ml) and then the mixture was allowed to evaporate to dryness *in vacuo* over solid sodium hydroxide. The residual oil crystallized on standing and was recrystallized from ethanol to white prisms; m. p. 137–142° (0.55 g, 71%). The product gave an intense purple color with Ehrlich's reagent. The n. m. r. spectrum ($CDCl_3$) peaks were observed at τ 8.91, 8.66 (ester CH_3); 7.55, 7.49 ($—C—CH_3$); 6.79, 6.48 ($N—CH_3$); 5.93, 5.70 (ester CH_2); and 3.54, 2.43 (singlets, unassigned). The spectrum was unchanged after treatment of the solution with D_2O. Calc. for $C_{18}H_{24}O_5N_2$: C, 62.05; H, 6.94; N, 8.04. Found: C, 62.00; H, 7.02; N, 8.38%. Ultraviolet spectrum: λ_{max} 205.4, 245.8, 296.7 mμ (inflection); ϵ_{max} 28 300, 24 550, 4370.

This compound was easily acetylated by acetic anhydride – potassium acetate to a mono-O-acetate which crystallized from aqueous ethanol to small white needles; m. p. 89–92°. Calc. for $C_{20}H_{26}O_6N_2$: C, 61.52; H, 6.71; N, 7.18. Found: C, 61.30; H, 7.03; N, 6.97%.

Ethyl 2-Methyl-4-oxo-5-(2′-methyl-3′-ethoxycarbonylpyrrol-4′-yl)-Δ^2-pyrroline-3-carboxylate (IXa)

Ethyl 2-methyl-4-oxo-Δ^2-pyrroline-3-carboxylate (I*a*; 5 g) in glacial acetic acid (25 ml) was heated under reflux for 15 min. The product was isolated by pouring the mixture on to ice and formed colorless prisms from aqueous acetic acid; m. p. 156–157° (lit. 157.5°). Calc. for $C_{16}H_{20}O_5N_2$: C, 59.99; H, 6.29. Found: C, 60.40; H, 6.26%. The n. m. r. spectrum ($CDCl_3$) showed peaks at τ 8.63 (ester CH_3); 7.54, 7.52 ($\rangle C—CH_3$); 5.69 (ester CH_2); 2.85, 2.81 (unassigned singlets); 1.87 (broad, NH). The ultraviolet spectrum: λ_{max} 203.3, 241.2, 274.2, 311.0 mμ; ϵ_{max} 17,230, 24,220, 6240, 6525 respectively.

A monoacetate was prepared as above and formed colorless needles; m. p. 171–173° (from chloroform – petroleum ether). Calc. for $C_{18}H_{22}O_6N_2$: C, 59.66; H, 6.12; N, 7.73. Found: C, 59.50; H, 6.06; N, 7.80%.

REFERENCES

1. E. Benary and B. Silbermann. Ber. **46**, 1363 (1913).
2. W. Siedel and H. Möller. Z. Physiol. Chem. **259**, 119 (1939).
3. H. von Dobeneck, W. Graf, and W. Ettel. Z. Physiol. Chem. **329**, 168 (1962).
4. R. S. Atkinson and E. Bullock. Can. J. Chem. **41**, 625 (1963).
5. R. Grigg, A. W. Johnson, and J. W. F. Wasley. J. Chem. Soc. 359 (1963).
6. H. Fischer and M. Herrmann. Z. Physiol. Chem. **122**, 1 (1922).

Can. J. Chem. Downloaded from www.nrcresearchpress.com by 210.87.254.6 on 09/05/12
For personal use only.

7. A. TREIBS and A. OHORODNIK. Ann. **611**, 149 (1958).
8. S. J. HOLT, A. E. KELLIE, D. G. O'SULLIVAN, and P. W. SADLER. J. Chem. Soc. 1217 (1958).
9. W. KÜSTER and P. SCHLACK. Z. Physiol. Chem. **121**, 152 (1922).
10. H. FISCHER and E. LOY. Z. Physiol. Chem. **128**, 59 (1923).
11. C. A. GROB and P. ANKLI. Helv. Chim. Acta, **32**, 2023 (1949).
12. A. HASSNER and M. J. HADDADIN. J. Org. Chem. **28**, 224 (1963).

Can. J. Chem. Downloaded from www.nrcresearchpress.com by 210.87.254.6 on 09/05/12
For personal use only.

Can. J. Chem. Downloaded from www.nrcresearchpress.com by 210.87.254.42 on 09/05/12
For personal use only.

N.M.R. STUDIES

PART VI. THE COMPLETE ANALYSIS OF THE PROTON SPECTRA OF TWO ISOMERIC METHYL FLUOROBROMOPROPANOATES WITH THE AID OF HETERONUCLEAR SPIN DECOUPLING[1]

J. B. STOTHERS AND J. D. TALMAN[2]

Department of Chemistry and the Department of Pure and Applied Mathematics, University of Western Ontario, London, Ontario

AND

R. R. FRASER[3]

Department of Chemistry, University of Ottawa, Ottawa, Canada

Received February 17, 1964

ABSTRACT

The 60 Mc/s proton spectra of methyl 2-bromo-3-fluoropropanoate and the 3-bromo-2-fluoro isomer have been analyzed completely with the aid of heteronuclear spin decoupling to illustrate an extension of the double resonance technique to ABCX spin systems. These results provide confirmatory evidence of the magnitude and relative signs of geminal and vicinal proton–proton and proton–fluorine coupling constants.

INTRODUCTION

This paper reports the complete analysis of the proton magnetic resonance spectra of methyl 2-bromo-3-fluoropropanoate and its isomer, methyl 3-bromo-2-fluoropropanoate. These spectra belong to the ABCX classification (1), for which A,B,C = H, X = F. The only previous example of a similar analysis is that of Banwell and Sheppard for vinyl fluoride (2). These authors discussed the general features of analysis of such systems and from its application determined the magnitude and sign of all parameters. In our case, the saturated aliphatic esters are particularly amenable to a simplified analytical approach. We have employed a standard ABC analysis, in conjunction with perturbation theory and heteronuclear spin decoupling, to obtain the complete set of parameters for each ester.

In the three-spin, ABC system, a complete analysis of the spectrum may be carried out if each of the nuclei are slightly shifted from one another. The choice of the best parameters is made by a careful comparison of the theoretical and experimental line positions and intensities. To check the results, this comparison should also be carried out for the spectrum obtained at a lower frequency. From this analysis the relative signs of the coupling constants as well as their magnitudes are obtained. An alternative method for the determination of relative signs, the double irradiation technique, may be employed in one of a number of ways depending on the complexity of the spectrum (3, and references cited therein, 4). The published reports of the use of this method for the study of relative signs for geminal and vicinal couplings have involved the simultaneous irradiation of one or more of the transitions within the spectrum while observing the changes in the rest of the spectrum (3, 4, 5 and references cited therein, 6). These may be termed "homonuclear" double irradiation experiments. If, however, the system is perturbed by the presence of another nucleus having a different magnetogyric ratio, γ, a "heteronuclear" double irradiation experiment can remove this perturbation and allow a complete analysis of the ABC system.

[1]*Part IV, S. Itô, J. B. Stothers, and S. M. Kupchan, Tetrahedron, 20, 913 (1964); Part V, reference 9.*
[2]*Present address: Department of Physics, University of California, Davis, California, U.S.A.*
[3]*Present address: Bristol Laboratories, Syracuse 1, New York, U.S.A.*

A suitable system for this approach is the ABCX, where $\gamma_{A,B,C} \neq \gamma_X$. In the present case for X = F, according to first-order perturbation theory,* the observed spectrum for the three protons will be a composite of two overlapping ABC patterns, one corresponding to each of the fluorine spin states, $\pm 1/2$. While analysis of each of these ABC patterns will yield the required parameters, it is helpful to have a further check on the results. Removal of the perturbation by the X nucleus on the spectrum produces a third ABC spectrum whose analysis must yield the same proton–proton coupling constants as the original systems. This may be accomplished by a "heteronuclear spin decoupling" experiment in which the X nucleus is strongly irradiated at its resonance frequency with a second radio frequency field which is at least strong enough to meet the requirement, $\gamma_X H_2/2\pi \approx \Sigma J_{HF}$, while observing the ABC portion of the spectrum. In this way, the peak positions and intensities in *three* patterns may be compared to provide confirmation of the choice of parameters.

Two examples of the use of this method are presented to illustrate its applicability and limitations. One of these cases has a strongly coupled ABC system, while the second case is one in which the A nucleus is only moderately coupled with the strongly coupled BC nuclei.

EXPERIMENTAL

Samples of methyl 2-bromo-3-fluoropropanoate and methyl 3-bromo-2-fluoropropanoate were kindly provided by Prof. F. L. M. Pattison, in whose laboratories these compounds were prepared in connection with other studies (8).

Carbon tetrachloride solutions of the two compounds were examined using ca. 25% (w/v) concentrations. All 60 Mc/s spectra were determined with a Varian DP-60 spectrometer and line positions measured by the usual audio side-band method. The audio oscillator was continuously monitored with a Hewlett–Packard 522B frequency counter. All measurements are reported as the average obtained from at least 10 separate spectra. The 15.085 Mc/s spectrum was obtained using the same basic instrument equipped with the necessary V4311 r. f. unit and the measurements given are those averaged from 12 spectra.

The heteronuclear spin decoupling experiments were performed with an NMR Specialties Inc. Model SD-60 spin decoupler equipped with modules to provide a strong variable frequency signal near 56.4 Mc/s. To carry out an experiment, the sample was simultaneously irradiated with the two r. f. signals required (60 and 56.4 Mc/s) and the proton spectrum examined by the field sweep method. Initially, the frequency of the 56.4 Mc/s signal was varied until the proton spectrum showed evidence of spin decoupling, i.e., the collapse of multiplets and a general narrowing of the entire pattern. This coarse adjustment was most easily performed with an oscilloscope presentation of the spectrum. Fine adjustments of the frequency were then made using a graphic recorder to locate the optimum setting of the variable frequency oscillator. Throughout these steps, the power of the fluorine oscillator was maximized to ensure complete decoupling. In the case of the α-fluoroisomer in which the components of the ABC system are well separated, it was necessary to readjust the fluorine resonance frequency to obtain complete decoupling of each multiplet. In these experiments, no measurement of the fluorine chemical shifts was done although this determination can be accomplished by the heteronuclear spin decoupling technique as described in Part V of this series (9).

RESULTS

A full description of the rigorous method of analysis for the ABC Spectrum has been given by Castellano and Waugh (10, 11). Following this method, a program for an IBM 650 computer has been written to carry out the computations, differing somewhat from that used previously by one of us (12, 13).

It has been pointed out by Castellano and Waugh that observation of the line positions does not determine the energy levels (E_i) of the system uniquely, but rather that there are 10 possible inequivalent assignments. We have obtained a simple prescription which, once

An elegant example of the use of perturbation theory for a similar purpose has been given by Anet (7).

Can. J. Chem. Downloaded from www.nrcresearchpress.com by 210.87.254.42 on 09/05/12
For personal use only.

one assignment has been obtained, will generate the other nine. We put

$$\begin{aligned} F_1 &= -1/2(E_4 + E_7) \\ F_2 &= 1/2(E_7 - E_4 - 2E_3) \\ F_3 &= 1/2(E_7 - E_4 - 2E_2) \\ F_4 &= 1/2(E_4 - E_7 - 2E_1) \\ F_5 &= 1/2(E_4 - E_7 - 2E_6) \\ F_6 &= 1/2(E_4 - E_7 - 2E_5) \\ F_7 &= 1/2(E_7 - E_4 - 2E_1). \end{aligned}$$

It is simple to verify that $F_2 + F_3 + F_4 = F_2 + F_6 + F_7 = -F_1$ and that appropriate differences $F_i - F_j$ give the same 15 line positions as the $E_i - E_j$. Since the sets $\{E_2, E_3, E_4\}$ and $\{E_5, E_6, E_7\}$ can be permuted arbitrarily, E_4 and E_7 can be chosen in nine different ways, producing in general nine different values of E_1, and hence all the inequivalent assignments.

The quartic equation for the Castellano–Waugh parameter was solved using Ferrari's method rather than an approximation scheme. This is felt to be superior since in some cases the roots were almost degenerate. In predicting the line positions at a different field strength from a determined set of parameters it is necessary to solve a cubic secular equation. This was done using Cardan's method.

The intensities are well known functions of the components of the eigenvectors of H. Since the eigenvalues E_i of H are known, it is a simple matter to compute the eigenvectors; one way is to evaluate the vector cross product of the first two rows of $H - E_i$.

The effect on the molecular parameters of errors in the input parameters E_i is by no means clear. These effects could be determined by introducing unit increments in each of the E_i's separately and determining the resulting changes in each of the molecular parameters. Rather than do this, we considered the increments in the E's produced by unit increments in the molecular parameters. These changes are readily computed using first-order perturbation theory. Since the E's are not all independent but are related by

$$\begin{aligned} E_1 &= -(E_5 + E_6 + E_7) \\ E_8 &= -(E_2 + E_3 + E_4), \end{aligned}$$

the increments in E_3, E_4, E_5, E_6, E_7, E_8 only were computed. This provides a 6×6 matrix whose elements are

$$\frac{\partial E_i}{\partial P_j} \qquad \begin{aligned} i &= 3.8 \\ j &= 1,6. \end{aligned}$$

The inverse of this matrix determines the effect on P_j of a unit change in E_i or the quantity, $\partial P_j/\partial E_i$. If it is assumed that the E's are valid to within an amount ΔE the quantity,

$$\Delta E \sum_{i=3}^{8} \left| \frac{\partial P_j}{\partial E_i} \right|$$

provides an upper bound to the error in P_j. We have assumed for ΔE the value 0.1 c/s. The tolerances indicated on the molecular parameters represent what we believe to be the maximum possible deviations of the results.

The nomenclature used throughout this paper in reference to the analytical method is that given in the original description (10) and is indicated by italics.

Methyl 2-bromo-3-fluoropropanoate.—The 60 Mc/s proton spectrum of methyl 2-bromo-3-fluoropropanoate is shown in Fig. 1(*a*) and it can be seen that 18 of the maximum 30

Can. J. Chem. Downloaded from www.nrcresearchpress.com by 210.87.254.42 on 09/05/12
For personal use only.

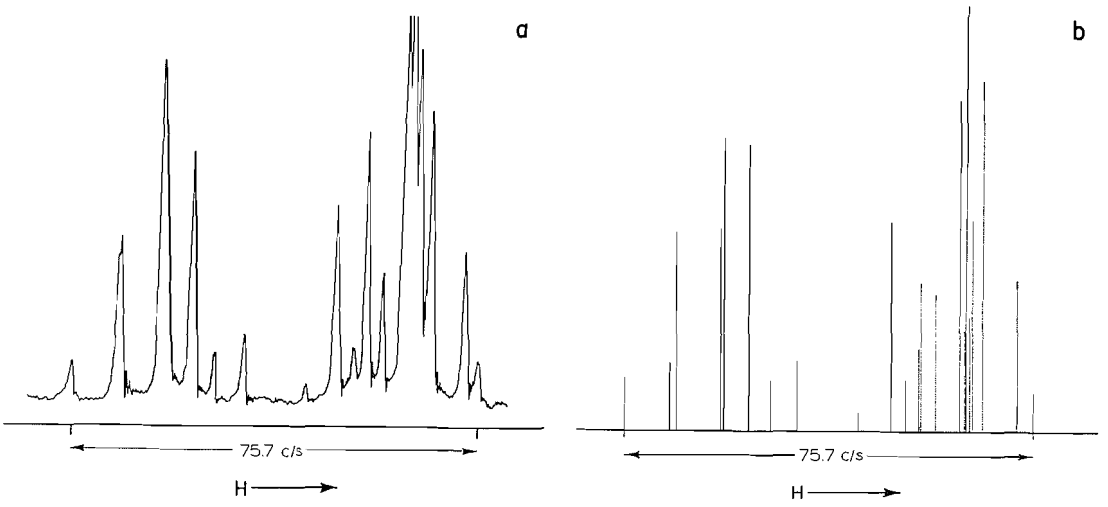

FIG. 1. 60 Mc/s spectra of methyl 2-bromo-3-fluoropropanoate showing the ABC portion only. (*a*) Observed spectrum and (*b*) theoretical spectrum calculated from the averaged parameters given in Table I.

transitions are resolved. By inspection, two "quartets" can be found in the group of seven lines towards lower field. These two multiplets must be a portion of one of the two overlapping ABC systems and would be expected to arise from the methylene protons on the β-carbon atom. The assignment of the third "quartet" for this system, however, is not so readily accomplished even though the required repeated spacings are known from the separations in the low field group. The assignment of the transitions for the remaining, higher field ABC system is still more difficult. The "spin decoupled" spectrum, shown in Fig. 2(*a*)

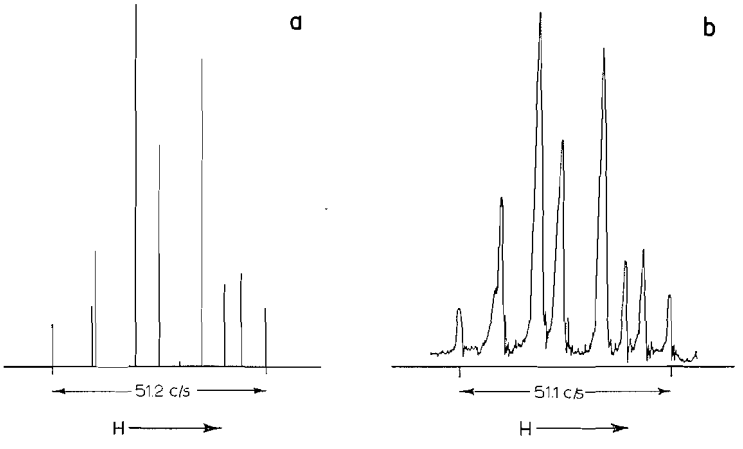

FIG. 2. Decoupled proton spectra of methyl 2-bromo-3-fluoropropanoate showing the ABC portion only. (*a*) Observed spectrum at 60 Mc/s while the fluorine nucleus was being irradiated at its resonance frequency and (*b*) theoretical spectrum calculated from the averaged data in Table I.

however, presents a way around this problem. The nine observable transitions may be assigned in the first-order approximation from the repeated spacings to the three ABC nuclei such that the four lines toward low field form one quartet as do the four lines at

Can. J. Chem. Downloaded from www.nrcresearchpress.com by 210.87.254.42 on 09/05/12
For personal use only.

higher field, while the remaining quartet appears between these overlapping with one line of each of the others. From this assignment, one *grouping* is obtained which yields a possible set of energy levels for the ABC system. Computation of all of the possible arrangements results in a total of three *sets* of eigenvalues, from each of which there arises two sets of chemical shifts, $\nu_0\delta$'s, and coupling constants, J's. A comparison of the calculated intensities for all 15 possible transitions with the experimentally observed spectrum reduces the choice to three of these sets which differ, principally, in the relative signs of the coupling constants. Turning again to the original spectrum, the most probable position for the "missing" highest field quartet belonging to the lower field ABC system can now be found and a choice of suitable transitions made. This yields a set of energy levels for this ABC system from which all possible solutions were computed. A total of six possible solutions resulted, only two of which were found to fit well with the experimental spectrum upon comparing the calculated intensities with those observed. One of these sets of $\nu_0\delta$'s and J's was very close to one of the solutions for the decoupled spectrum. Having identified the C portion of the "low field" ABC, one can now make an assignment of the remaining lines for the other, "high field", ABC system and carry out the sequence of computations as before. This procedure yielded a total of six sets of parameters of which three were in reasonable agreement with the previous results. Only one of these sets, however, compares well with experiment when a comparison of line intensities is done. This set corresponds rather closely to the best results for each of the other two ABC systems. The three best sets of data are collected in Table I together with the averaged parameters. Since the most

TABLE I

Parameters for proton spectra of methyl 2-bromo-3-fluoropropanoate

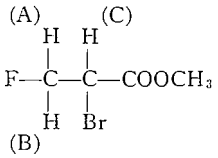

ABC system		Chemical shifts* ($\nu_0\delta$, c/s) A	B	C	Coupling constants (J, c/s) J_{AB}	J_{AC}	J_{BC}
Calculated values	Low field	19.23	6.46	−25.69	−9.45	8.38	5.42
	High field	7.04	−5.53	−1.51	−9.47	8.24	5.93
	Decoupled	13.13	0.47	−13.60	−9.46	8.31	5.65
Averaged values	Low field	19.18	6.52	−25.70			
	High field	7.09	−5.58	−1.51	−9.46	8.31	5.65
	Decoupled	13.13	0.47	−13.60			

*Given in c/s relative to the "center of gravity" of each separate ABC pattern.

precisely determined line positions are those obtained from the original spectrum, the calculated values of the chemical shifts and coupling constants for this spectrum were used for averaging. These averaged figures were then utilized to predict the line positions and intensities of each of the three separate ABC patterns (see Fig. 1(*b*) and 2(*b*)). A comparison of these calculated values with the experimental spectra gave agreement within 0.1 c/s for each line position (see Table II) and within 10% for their intensities.

The proton–fluorine coupling constants were obtained from the calculated chemical shifts after adjustment to a common frequency scale. This is illustrated in Fig. 3. A summary of these and the proton–proton coupling constants is given in Table III.

Can. J. Chem. Downloaded from www.nrcresearchpress.com by 210.87.254.42 on 09/05/12
For personal use only.

Can. J. Chem. Downloaded from www.nrcresearchpress.com by 210.87.254.42 on 09/05/12
For personal use only.

TABLE II

Observed and calculated line positions* for the 60 Mc/s proton spectra of methyl 2-bromo-3-fluoropropanoate (in c/s relative to center of gravity of each pattern)

Normal spectrum					
Low field ABC		High field ABC		Decoupled spectrum	
Calc.	Obs.†	Calc.	Obs.†	Calc.	Obs.†
−42.27	—	−21.59	—	−30.60	—
−33.25	−33.17	−11.76	−11.73	−21.42	−21.35
−27.76	−27.86	−11.58		−16.33	−16.31
−24.89	−24.88	−9.10	−8.99	−12.94	−12.85
−19.40	−19.55	−8.92		−7.95	−7.66
−10.38	—	−2.80	−2.74	−7.43	
−2.23	−2.20	−0.78	−0.82	−2.35	—
+3.26	+3.29	−0.14	−0.02	−0.95	—
+7.12	+7.11	+0.92	+0.91	+1.53	+1.48
+12.28	+12.44	+1.88	+1.95	+6.63	+6.81
+12.61		+9.70	+9.83	+6.83	
+20.64	+20.72	+9.88		+15.21	+15.14
+21.63	+21.60	+11.72	+11.83	+15.81	+15.93
+30.00	+30.00	+11.90		+24.19	+24.10
+52.65	—	+20.68	+20.69	+29.79	+29.73

*Using the averaged data given in Table I.
†In all cases unobserved lines have calculated intensitites which are *less* than 5% of the intensity of the *weakest* line observed.

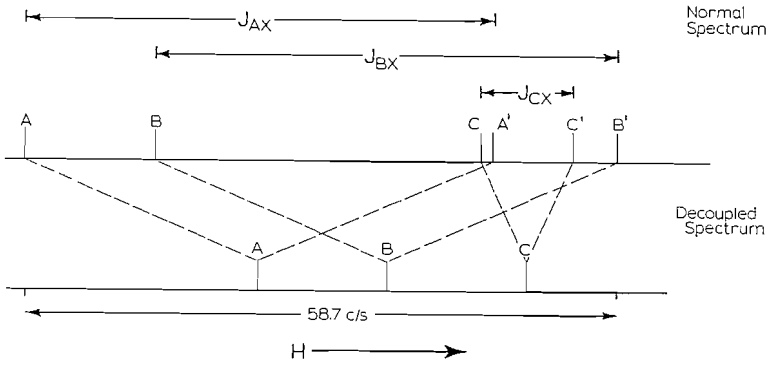

FIG. 3. Schematic chemical shift patterns in the 60 Mc/s spectra of methyl 2-bromo-3-fluoropropanoate showing the "effective" internal shifts in the ABC portion due to the ^{19}F perturbation compared with the decoupled case. The proton–fluorine coupling constants are indicated.

TABLE III

Summary of spin coupling constants for the isomeric methyl fluorobromopropanoates, $XCH_2CHYCOOMe$ (I, X = F, Y = Br; II, X = Br, Y = F)

	Proton–fluorine*		Proton–proton*	
Compound	Geminal	Vicinal	Geminal	Vicinal
I	±46.1±1.4	±9.9±1.4	∓9.5±0.4	±8.3±0.4
				±5.7±0.4
II	±47.4±0.8	±17.9±4.0	∓12.0±0.4	±5.2±0.7
		±26.5±3.8		±3.5±0.7

*Given in c/s.

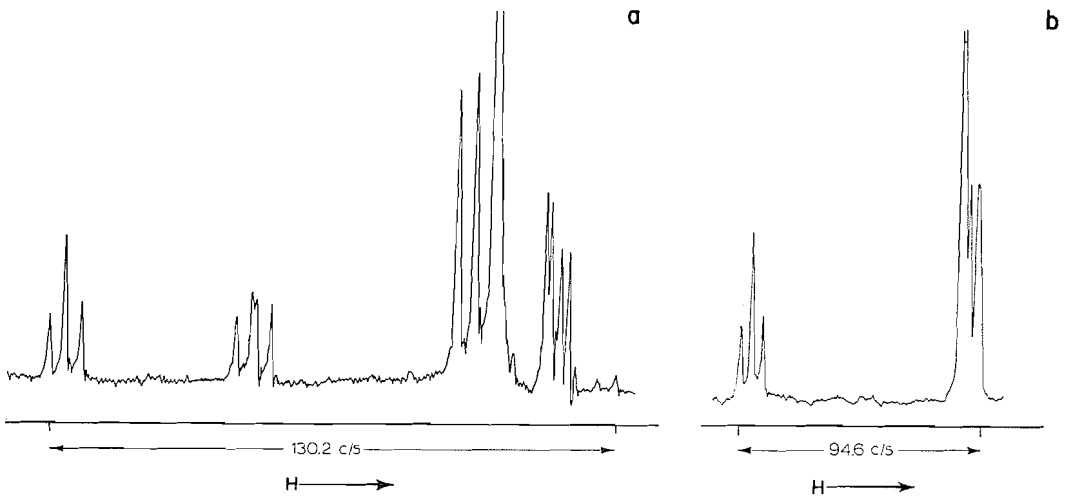

FIG. 4. 60 Mc/s proton spectra of methyl 3-bromo-2-fluoropropanoate. (*a*) Normal spectrum and (*b*) decoupled spectrum obtained by simultaneous irradiation of the fluorine nucleus at its resonance frequency. The strong signal toward higher field in each spectrum is due to the carbomethoxyl protons.

Methyl 3-bromo-2-fluoropropanoate.—The normal 60 Mc/s proton spectrum of methyl 3-bromo-2-fluoropropanoate is shown in Fig. 4(*a*) in which 16 lines are clearly discernible. The two ABC systems within this spectrum are more easily recognized than in the preceding case since one of the protons is shifted to much lower field than the others. Presumably this is the methine proton on the α-carbon. Of the two ABC systems within this spectrum, the one towards higher field is the better starting point for the analysis since more transitions are observed. Using the line positions for the "quartet" at lower field and the seven lines at highest field, an assignment was made from which one of the possible *arrangements* was found. Proceeding as before, all possible *arrangements* were analyzed to compute the physically possible sets of parameters. Four such sets were obtained, two of which gave satisfactory agreement with experiment and the principal difference was the relative sign of the vicinal coupling constant. A similar approach for the low field ABC pattern yielded three sets of parameters for this system. Again, two of these, differing only in the sign of the vicinal coupling constant, gave the most satisfactory agreement with experiment. The "decoupled" spectrum for this compound, shown in Fig. 4(*b*), is an extremely simple pattern having only five observed transitions and is an example of a "deceptively simple" ABX spectrum (14). (The largest peak toward higher field is due to the methoxyl protons.) Thus the data at 60 Mc/s do not allow a decision to be made regarding the relative signs of the coupling constants except by analogy with other similar systems. Furthermore, there are two equally satisfactory chemical shift assignments for the low field ABC pattern. This latter feature has virtually no effect on the proton–proton coupling constants obtained from the analysis but has a significant effect on the proton–fluorine coupling constants. To resolve this problem, the chemical shift data were converted to those expected at 15.1 Mc/s with both possible assignments for the low field ABC shifts included and the theoretical spectra were calculated. A comparison of the experimental 15.1 Mc/s spectrum, shown in Fig. 5(*a*), with those calculated allowed an unequivocal decision between the various possibilities (Table V). The agreement obtained for the best assignment is illustrated by the data in Table IV and schematic spectrum Fig. 5(*b*) for

Can. J. Chem. Downloaded from www.nrcresearchpress.com by 210.87.254.42 on 09/05/12
For personal use only.

Can. J. Chem. Downloaded from www.nrcresearchpress.com by 210.87.254.42 on 09/05/12
For personal use only.

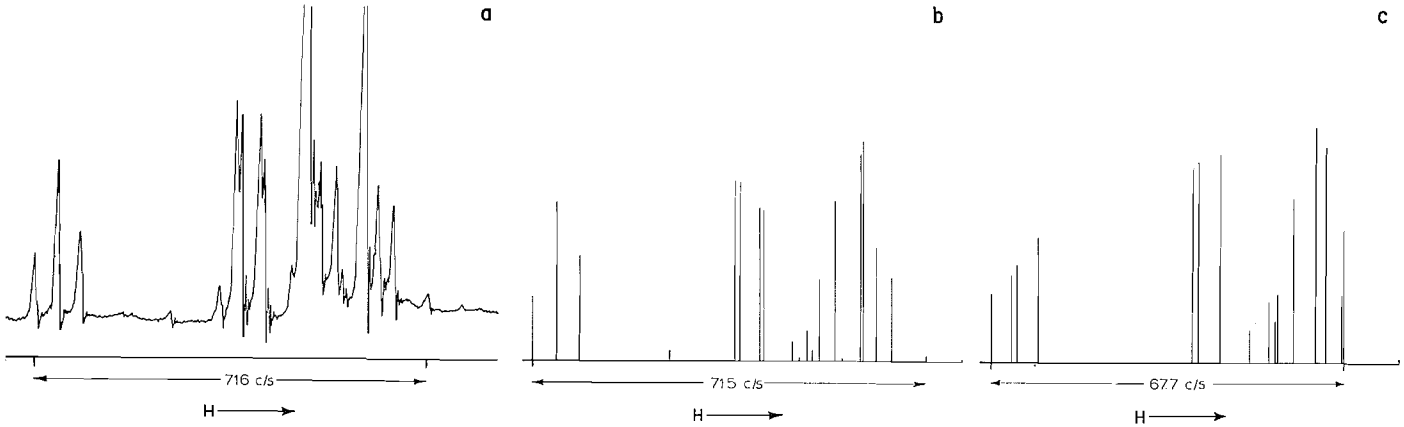

FIG. 5. 15.085 Mc/s proton spectra of methyl 3-bromo-2-fluoropropanoate. (*a*) Observed spectrum (the strong signal near the center of the pattern is due to the three carbomethoxyl protons), (*b*) theoretical spectrum calculated from the data in Table V for the case of opposite sign of the geminal proton–proton coupling constant, and (*c*) theoretical spectrum for the case having the same sign for all J_{H-H} constants.

Can. J. Chem. Downloaded from www.nrcresearchpress.com by 210.87.254.42 on 09/05/12
For personal use only.

TABLE IV

Observed and calculated line positions* for the proton spectra of methyl 3-bromo-2-fluoropropanoate
(in c/s relative to center of gravity of each pattern)

Normal 60 Mc/s spectrum						Normal 15.1 Mc/s proton spectrum			
Low field ABC		High field ABC		Decoupled 60 Mc/s spectrum		Low field ABC		High field ABC	
Calc.	Obs.†	Calc.	Obs.†	Calc.	Obs.†	Calc.	Obs.†	Calc.	Obs.†
79.12	—	63.87	—	70.93	—	35.93	—	20.38	—
71.42	71.40	54.55	54.40	63.01	62.97	27.63	27.41	11.41	11.40
66.96		50.75	50.70	58.86	58.47	23.36	23.23	10.27	—
66.83	67.00	49.71	49.60	58.37		23.33		8.43	‡
62.57	62.60	45.91	45.90	54.22	54.17	19.05	19.06	7.30	7.54
54.67	—	36.58	—	46.30	—	10.77	—	6.06	6.30
−19.24	−19.20	−10.40	‡	−15.02	—	2.76	2.70	3.08	3.32
−23.63	—	−14.20	−14.23	−19.18	—	−1.56	—	−1.40	−1.77
−31.04		−22.39	−22.40	−27.10	−27.23	−9.21	−9.09	−1.67	
−31.54	−31.00	−23.52	−23.50	−27.12		−9.83	−9.97	−4.38	−4.37
−35.63		−26.19	−26.20	−31.27	−31.63	−13.51	−13.31	−5.89	—
−35.79	−35.30	−28.36	−28.40	−31.74		−14.12	−14.11	−7.03	−7.13
−43.33	‡	−35.51	−35.50	−39.19	—	−21.81	−21.93	−13.35	−13.45
−47.79	—	−40.35	−40.30	−43.83	—	−26.07	—	−14.49	—
−133.99	—	−100.46	—	−117.72	—	−46.68	—	−18.70	−18.81

*Using the averaged data for the 60 Mc/s spectra given in Table V and the 15.1 Mc/s data in Table V.
†With the exception of those noted by ‡, unobserved lines have calculated intensities less than 5% of the weakest observed transitions.
‡These transitions are not resolved from the strong carbomethoxyl signal.

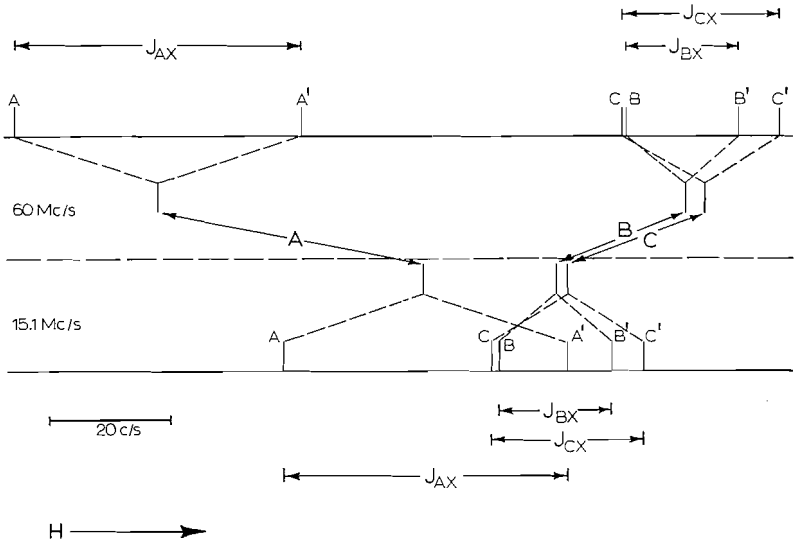

FIG. 6. Schematic chemical shift patterns of the ABC spectra of methyl 3-bromo-2-fluoropropanoate showing the "effective" internal shifts due to the perturbation by ^{19}F compared with the decoupled case at 60 Mc/s (upper portion) and at 15.1 Mc/s (lower part). The proton–fluorine coupling constants are indicated for each.

which the relative sign of the geminal J_{H-H} is opposite to the vicinal. Fig. 5(*c*) shows the spectrum calculated for the case in which these coupling constants have the same sign. The proton–fluorine coupling constants were obtained from the chemical shift data for the two ABC patterns of the normal spectrum as shown in Fig. 6 and are collected in Table III, together with the proton–proton coupling constants.

TABLE V

Parameters for proton spectra of methyl 3-bromo-2-fluoropropanoate

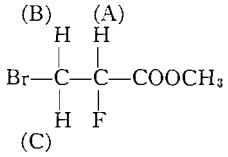

Frequency	ABC system	Chemical shifts* ($\nu_0\delta$) A	B	C	Coupling constants (J, c/s) J_{AB}	J_{AC}	J_{BC}
60 Mc/s							
Calculated	Low field	66.90	−34.50	−32.30	3.66	5.16	−12.10
					2.87	5.64	+11.95
	High field	50.06	−21.84	−28.22	3.31	5.20	−11.96
		50.05	−21.87	−28.18	2.87	5.64	+11.95
	Decoupled	58.47	−28.18	−30.28	3.60	5.20	−12.10
Averaged	Low field	66.90	−34.50	−32.30			
	High field	50.10	−21.80	−28.20	3.45	5.20	−12.00
	Decoupled	58.40	−28.15	−30.25			
15.1 Mc/s							
Calculated	Low field	23.05	−13.41	−9.65	3.45	5.20	−12.00
	High field	6.33	−0.75	−5.59			

*Given in c/s relative to the "center of gravity" of each separate ABC pattern.

Can. J. Chem. Downloaded from www.nrcresearchpress.com by 210.87.254.42 on 09/05/12
For personal use only.

Proton Shifts

The proton chemical shifts relative to internal tetramethylsilane for the two esters were found to be as follows: methyl 2-bromo-3-fluoropropanoate, 3.82 p.p.m. ($COOCH_3$), 4.24 p.p.m. (—CHBr), 4.78 and 4.57 p.p.m. (CH_2F); methyl 3-bromo-2-fluoropropanoate, 3.80 ($COOCH_3$), 5.24 (—CHF), 3.76 and 3.72 p.p.m. (CH_2Br).

DISCUSSION

The question of the relative signs of geminal and vicinal proton–proton spin coupling constants has received much attention recently and the fact that the signs are opposite is well documented (3). For the analogous spin–spin couplings involving proton–fluorine interactions, the constants have been found to have the same sign (5). The present results (see Table III) are in complete agreement with the previous findings and thus confirm the original conclusions. The normal proton spectrum of the α-fluoro isomer (Fig. 4*a*) shows, simply by inspection, the geminal and vicinal proton–fluorine constants to be of the same sign, and while it is not immediately obvious from the spectrum of the β-fluoro isomer, the calculations unequivocally illustrate that this is indeed the case. The agreement between the calculated and observed 60 Mc/s spectra for methyl 2-bromo-3-fluoropropanoate, as shown in the preceding section, confirm the opposite sign relation for the geminal and vicinal proton couplings and the agreement between the calculated and observed 15.1 Mc/s spectra establishes this point for methyl 3-bromo-2-fluoropropanoate. It should be noted that the proton–fluorine coupling constants are given with the same relative sign as the vicinal proton–proton coupling constants, although this was not proved by our analysis. Tiers (15), however, has established that $J_{^{13}C-H}$ and geminal J_{H-F} have the same sign and since $J_{^{13}C-H}$ and geminal J_{H-H} are opposite in sign (16, 17), it follows that geminal J_{H-F} and vicinal J_{H-H} are of like sign.

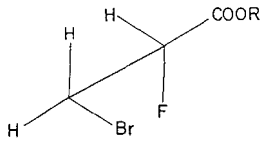

A

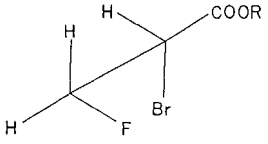

B

The magnitudes of the proton–fluorine coupling constants reported here are within the limits of previously recorded ranges for similar systems (18–22) as are the proton–proton couplings. It is interesting that the electronegativity effect of substituents on the geminal coupling constants is negligible for the proton–fluorine interactions but is appreciable (2.5 c/s) for the proton–proton couplings and is in the expected direction (23) since geminal J_{H-H} = 12.0 c/s for the β-bromo ester and 9.5 c/s for the β-fluoro ester. The factors which affect the magnitude of vicinal J_{H-F} have not been extensively studied. Abraham and Bernstein (24) have concluded from a study of the temperature dependence of the spectrum of CCl_2F—$CHCl_2$ that $J_{trans} \sim 18$ c/s and $J_{gauche} \sim 1$ c/s. In a more recent paper, Fessenden and Waugh (25) report a similar study of $CClF_2$—$CHCl_2$ and were unable to determine with certainty which vicinal coupling constant is the larger. In the present cases, there is a large difference in magnitude for the vicinal J_{H-F} values. There is also an appreciable difference in vicinal J_{H-H} for the two esters. If we assume that the effect of the halogens due to electronegativity and hybridization is the same for both isomers then we can conclude from the Karplus relation (26) that the lower values for

Can. J. Chem. Downloaded from www.nrcresearchpress.com by 210.87.254.42 on 09/05/12
For personal use only.

vicinal J_{H-H} in the α-fluoro isomer reflect a greater proportion of *gauche* interactions than in the β-fluoro isomer. This can only result from a greater contribution of rotamer A to the overall conformational equilibrium of the α-fluoro isomer than the contribution of rotamer B to the equilibrium of the β-fluoro ester. If A contributes more in the α-fluoro case than B for the β-isomer, it follows of necessity that there will be a greater contribution of $J_{trans\ H-F}$ vs. $J_{gauche\ H-F}$ in the α-isomer. Since the observed vicinal J_{H-F} is greater for the α-isomer, our results indicate that $J_{trans} > J_{gauche}$ for vicinal proton–fluorine interactions as concluded by Abraham and Bernstein (24). The above argument is subject to the restrictions recently reiterated by Karplus (27) and requires further work to substantiate it fully. Experiments to shed more light on this problem are in hand.

ACKNOWLEDGMENTS

The authors wish to thank the National Research Council of Canada for financial support of this research. The work of one of us (J. D. T.) was supported in part by a grant from the U.S. Atomic Energy Commission.

REFERENCES

1. J. A. POPLE, H. J. BERNSTEIN, and W. G. SCHNEIDER. High resolution nuclear magnetic resonance. McGraw-Hill Book Co., Inc., New York. 1959.
2. C. N. BANWELL and N. SHEPPARD. Proc. Roy. Soc. London, Ser. A, **263**, 136 (1961).
3. R. FREEMAN and N. S. BHACCA. J. Chem. Phys. **38**, 1088 (1963).
4. J. D. BALDESCHWIELER and E. W. RANDALL. Chem. Rev. **63**, 81 (1963).
5. D. F. EVANS, S. L. MANATT, and D. D. ELLEMAN. J. Am. Chem. Soc. **85**, 238 (1963).
6. R. FREEMAN and W. A. ANDERSON. J. Chem. Phys. **37**, 2053 (1962).
7. F. A. L. ANET. Proc. Chem. Soc. 327 (1959).
8. F. H. DEAN and F. L. M. PATTISON. To be published.
9. J. B. STOTHERS and J. R. ROBINSON. Can. J. Chem. **42**, 967 (1964).
10. S. CASTELLANO and J. S. WAUGH. J. Chem. Phys. **34**, 295 (1961).
11. J. S. WAUGH and S. CASTELLANO. J. Chem. Phys. **35**, 1500 (1961).
12. R. R. FRASER, R. U. LEMIEUX, and J. D. STEVENS. J. Am. Chem. Soc. **83**, 3901 (1961).
13. R. R. FRASER. Can. J. Chem. **40**, 1483 (1962).
14. R. J. ABRAHAM and H. J. BERNSTEIN. Can. J. Chem. **39**, 216 (1961).
15. G. V. D. TIERS. J. Phys. Chem. **67**, 1372 (1963).
16. P. C. LAUTERBUR and R. J. KURLAND. J. Am. Chem. Soc. **84**, 3405 (1962).
17. F. A. L. ANET. J. Am. Chem. Soc. **84**, 3767 (1962).
18. D. D. ELLEMAN, L. C. BROWN, and D. WILLIAMS. J. Mol. Spectry. **7**, 307, 322, 393 (1961).
19. S. L. STAFFORD and J. D. BALDESCHWIELER. J. Am. Chem. Soc. **83**, 4473 (1961).
20. R. L. BUCHANAN, F. H. DEAN, and F. L. M. PATTISON. Can. J. Chem. **40**, 1571 (1962).
21. G. P. VAN DER KELEN and Z. ECKHAUT. J. Mol. Spectry. **10**, 141 (1963).
22. F. H. DEAN and F. L. M. PATTISON. Can. J. Chem. **41**, 1833 (1963).
23. K. L. WILLIAMSON. J. Am. Chem. Soc. **85**, 516 (1963).
24. R. J. ABRAHAM and H. J. BERNSTEIN. Can. J. Chem. **39**, 39 (1961).
25. R. W. FESSENDEN and J. S. WAUGH. J. Chem. Phys. **37**, 1466 (1962).
26. M. KARPLUS. J. Chem. Phys. **30**, 11 (1959).
27. M. KARPLUS. J. Am. Chem. Soc. **85**, 2870 (1963).

Can. J. Chem. Downloaded from www.nrcresearchpress.com by 210.87.254.42 on 09/05/12
For personal use only.

Can. J. Chem. Downloaded from www.nrcresearchpress.com by 210.87.254.5 on 09/05/12
For personal use only.

ON THE ANODIC OVERVOLTAGE IN ALUMINUM ELECTROLYSIS

JOMAR THONSTAD AND EIRIK HOVE
Technical University of Norway, Trondheim, Norway
Received October 2, 1963

ABSTRACT

The overvoltage on the carbon anode in aluminum electrolysis has been measured against a CO_2/C reference electrode placed in the cryolite melt. The behavior of the reference electrode was first investigated against the aluminum cathode. This galvanic cell showed a stable potential of 1.15 V, which was close to the reversible potential for the cell reaction in aluminum electrolysis. Similar measurements were made with CO/C and CO_2,CO/C electrodes. The potential of the CO/C electrode was in fair agreement with the reversible potential for the most probable cell reaction. The potentials obtained with CO_2–CO mixtures were intermediate between those for the pure gases, increasing with increasing CO_2 content. An explanation for the behavior of the CO_2,CO/C electrode is suggested.

The anodic overvoltage depended only to a limited extent on the chemical reactivity of carbon with respect to oxygen. Graphite anodes showed higher overvoltage than all other types of carbon anodes. Catalyzing and inhibiting additives to the carbon had small but significant influences on the overvoltage. Straight Tafel plots were obtained with slopes varying between 0.26 and 0.27. On this basis it is shown that the overvoltage may be due either to slow transport of oxygen ions through the double layer or to slow reaction between chemisorbed oxygen and carbon.

INTRODUCTION

Overvoltage

The decomposition voltage for the aluminum electrolytic cell has been found to be 1.40–1.70 V (1, 2, 3), which is considerably higher than the theoretical values for the two possible overall cell reactions shown below.

$$Al_2O_3 + (3/2)C \rightarrow 2Al + (3/2)CO_2, \qquad E^0_{1000°C} = 1.16 \text{ V (4)} \qquad [1]$$

$$Al_2O_3 + 3C \rightarrow 2Al + 3CO, \qquad E^0_{1000°C} = 1.03 \text{ V (4)} \qquad [2]$$

From measurements with an aluminum cathode Drossbach (5) and Piontelli (6) have shown that the cathodic overvoltage is negligible; hence the observed overvoltage must be confined to the anode.

From experimental evidence (7, 1, 8) it appears that CO_2 is the primary anode product during electrolysis at normal current densities. The anode reaction may tentatively be divided into the following consecutive steps.

Transfer of oxygen-carrying ions through the electric double layer:

$$O^{2-} \text{ (in melt)} \rightarrow O^{2-} \text{ (on surface)} \qquad [3]$$

Discharge and chemisorption: $O^{2-} + C \rightarrow C_xO + 2e$ [4]

Formation of CO_2: $2C_xO \rightarrow CO_2 \text{ (adsorbed)} + C$ [5]

Desorption of CO_2: $CO_2 \text{ (adsorbed)} \rightarrow CO_2 \text{ (g)}$ [6]

The occurrence of chemisorbed oxygen on carbon, usually denoted as C_xO, is also known from the theory of combustion of carbon in air (9, 10).

In measurements with graphite anodes, Welch and Richards (11) found that the anodic overvoltage follows the classical Tafel equation

$$\eta = a + b \log i \qquad (a = 0.52\text{–}0.64,\ b = 0.32\text{–}0.34)$$

and concluded that the overvoltage was caused by slow transport of oxygen-carrying ions through the double layer.

From potential decay measurements on industrial cells, Stern and Holmes (2) concluded that the slow step is a chemical reaction of approximately second order, e.g. reaction [5].

Mashovets and Revazyan (12) have suggested that the overvoltage consists of two components, one "non-inertial" due to slowness of reaction [3] and one "inertial" due to slowness of reaction [5].

Reference Electrodes

Mashovets and Revazyan (13) found that the galvanic element

$$Al/Na_3AlF_6 + Al_2O_3/CO_2/C \qquad [7]$$

gave a stable potential of 1.11 V at 1000° C, which is fairly close to the reversible potential for reaction [1].* Richards (14) has studied the CO_2,CO/C electrode and postulated that the oxygen pressure is determined by the equilibrium

$$CO + (1/2)\ O_2 \leftrightharpoons CO_2, \qquad [8]$$

as originally suggested by Drossbach (5). If p_{O_2} determined from equilibrium [8] is introduced into the formal expression for the cell reaction,

$$Al_2O_3 \rightleftharpoons 2Al + (3/2)O_2, \qquad E_{1000°C} = 2.19 + RT/4F \log p_{O_2}\ (4), \qquad [9]$$

the relation finally becomes

$$E_{1000°C} = 1.30 + 0.126 \log \frac{p_{CO_2}}{p_{CO}}. \qquad [10]$$

This relation is shown by curve I in Fig. 1 where E is plotted against $p_{CO_2}/p_{CO_2}+p_{CO}$.

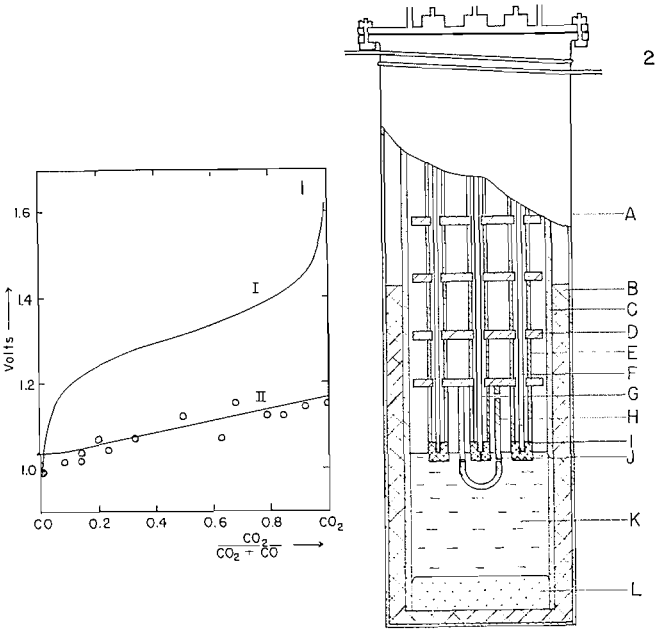

FIG. 1. The dependence of the potential on the ratio CO_2/CO_2+CO. Curve I, following equation [11]; curve II, following equation [16]; O, experimental points.

FIG. 2. Experimental cell.

**There is considerable inconsistency in the thermodynamic data which are used for the calculation of the reversible potentials for reactions [1] and [2]. In recent Russian literature (1) these potentials come out as 1.115 V and 0.98 V respectively at 1000° C, as against 1.16 V and 1.03 V when derived from other sources (4).*

Can. J. Chem. Downloaded from www.nrcresearchpress.com by 210.87.254.5 on 09/05/12
For personal use only.

Richards (14), however, did not get potentials agreeing with equation [10]; the experimental values were much lower (e.g. 1.036 V as compared to 1.40 V for a CO_2/CO ratio of 3), but this was explained as being due to non-reliability of the aluminum cathode.

In the present investigation the CO_2,CO/C reference electrode has been studied. The potentials against the aluminum cathode were measured for the pure gases and for different gas mixtures. The main purpose of the overvoltage measurements has been to study the overvoltage dependence on the chemical reactivity of the carbon anode.

EXPERIMENTAL

The experimental cell for overvoltage measurements is shown in Fig. 2. The crucible consisted of a sintered-alumina tube C (60 mm I.D.) placed in a graphite crucible B, which was protected by an outer crucible A, made of heat-resistant steel. The bottom of the graphite crucible, which also served as the cathode contact, was covered by the aluminum cathode L. The electrolyte K consisted of cryolite saturated with alumina. A Kanthal furnace connected to a temperature controller maintained the temperature of 1000° C.

The reference electrode J (12 mm D), made of AUC grade graphite, was screwed on to a copper tube G and was surrounded by a sintered-alumina crucible H with narrow holes facing each of the anodes I. The anodes, which were accurately machined to the same size (12 mm D), were screwed on to copper rods F protected by sintered-alumina tubes E. Because the baffles, D, resulted in a symmetrical arrangement of the anodes around the reference electrode, possible errors due to a potential drop in the electrolyte would be the same for all anodes, so that the comparison between the measured overvoltage would not be affected.

The potentials were measured with a potentiometer.

REFERENCE ELECTRODE

Results

The reference electrode was tested against the aluminum cathode in separate runs prior to electrolysis. Gas mixtures were prepared in advance in a mercury gasometer.

The cell might be presented schematically as follows:

$$Al/Na_3AlF_6 + Al_2O_3/CO_2,CO/C. \qquad [11]$$

The measured potentials were corrected for the thermoelectrical potential of the cell, which was found to be 5 mV at 1000° C.

With pure CO_2 as the inlet gas, several measurements at 1000° C gave $E = 1.15$ V as the stable potential. This potential could be maintained for hours, the fluctuations not being more than 5–10 mV. When the gas flow was kept above 30 ml/min, the potential was independent of the flow rate.

The temperature dependence of the potential is shown on Fig. 3. The slope of the curve is 6.3×10^{-4} V/°K, which is fairly close to the theoretical value calculated for reaction [1], 5.9×10^{-4} V/°K.

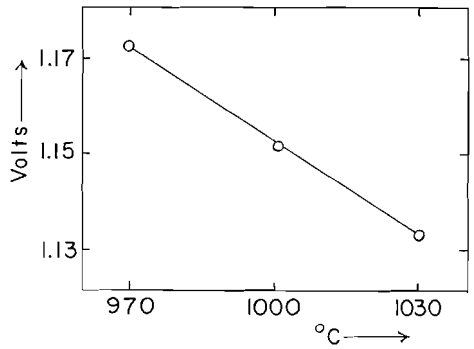

FIG. 3. Temperature dependence of the potential of cell [7].

Can. J. Chem. Downloaded from www.nrcresearchpress.com by 210.87.254.5 on 09/05/12
For personal use only.

With pure CO as inlet gas, the potential values were less stable. The stability of each electrode was usually satisfactory (although not as good as for the CO_2 electrode) but different electrodes gave somewhat different values in the range 0.98 to 1.01 V.

The results obtained with mixtures of CO_2 and CO as inlet gas are plotted as circles on Fig. 1. Although there is considerable scattering of the results, it is evident that the results lie between the values for the pure gases, and that the potential increases with increasing CO_2/CO_2+CO ratio. No curve is drawn to represent the results. Curve II represents calculated potentials from thermodynamic data to be discussed below.

Discussion

The measured potentials for the pure gases agree with the theoretical values for reaction [1] and [2], within the accuracy of these values. It seems therefore reasonable to conclude that the potential-determining overall cell reaction is [1] or [2], depending upon the gas used.

The results for gas mixtures cannot in any way be explained by the theory of Richards (14), as is evident from curve I on Fig. 1. This theory implies that the carbon electrode acts as an inert conductor only, since the oxygen pressure is determined by equation [8]. It seems to be more likely that the oxygen pressure is determined by the following reactions:

$$C + O_2 \leftrightharpoons CO_2 \qquad [12]$$

$$C + (1/2)O_2 \leftrightharpoons CO. \qquad [13]$$

The carbon–oxygen system will not be in equilibrium except at one composition, which at 1000° C is about 99.2% CO, 0.8% CO_2, and 5.4×10^{-17}% O_2 (4).

The following calculation may be suggested: if $p_{CO_2} = x$ and $p_{CO} = 1 - x$, the overall cell reaction with a reversibly acting CO_2,CO/C electrode can be written as:

$$Al_2O_3 + \frac{3}{1+x}C = 2Al + \frac{3x}{1+x}CO_2 + \frac{3(1-x)}{1+x}CO. \qquad [14]$$

The free energy change for this reaction may be expressed in the usual manner from the free energies for reactions [1] and [2], ΔG_1^0 and ΔG_2^0 respectively,

$$\Delta G_x = \frac{2x}{1+x}\Delta G_1^{\,0} + \frac{1-x}{1+x}\Delta G_2^{\,0} + RT \ln \frac{p_{CO_2}^{\,3x/1+x}}{p_{CO}^{\,3(1-x)/1-x}}$$

$(a_{Al_2O_3} = 1, a_{Al} = 1)$

A similar treatment has been suggested by Piontelli (15). By converting the above equation to a Nernst equation, rearranging, and introducing numerical values (4), the final expression becomes:

$$E_x\ (1000°\ C) = 1.03 + \frac{0.26\,x}{1+x} + \frac{0.126}{(1+x)}\,(x \log x + (1-x)\log(1-x)). \qquad [15]$$

This equation is represented by curve II in Fig. 1. It gives a curve which is close to a straight line between E_1^0 and E_2^0.

As an alternative to the treatment above, the anode can be considered as made up of CO_2/C and CO/C half-cells in parallel, the half-cells being located at different spots on the carbon surface. The resulting mixed potential of the electrode towards the aluminum cathode cannot be calculated, but it must evidently lie between the potentials of the pure cells, E_1^0 and E_2^0.

Can. J. Chem. Downloaded from www.nrcresearchpress.com by 210.87.254.5 on 09/05/12
For personal use only.

From the results it appears that the CO_2/C electrode is the best suited reference electrode, because it gives the most stable and reproducible potential. With this electrode the potential against the aluminum cathode is equal to the reversible potential for the overall cell reaction in aluminum electrolysis given by reaction [1].

OVERVOLTAGE MEASUREMENTS

Results

Anodes of different reactivity were obtained by using different kinds of anode materials, by applying different baking temperatures, and by additions of chemicals to the raw materials. The term "reactivity" can here most simply be defined as the tendency to react with oxygen at high temperatures. The reactivity generally decreases with increasing order of the carbon lattice, with graphite as the least reactive material. Addition of various chemicals is known to have substantial influence on the reactivity (17), some acting as catalysts and others as inhibitors.

In this work Fe_2O_3 and Na_2CO_3 were used as catalysts and H_3BO_3 as inhibitor. The additions were made to the raw materials in amounts of 0.4 to 1.3 wt.%. The different types of anodes used are summarized below.

I. Graphite anodes

II. Non-disintegrating anodes
(*a*) With 1.3 wt.% Fe_2O_3
(*b*) With no addition
(*c*) With 1.0 wt.% H_3BO_3

III. Non-disintegrating anodes
(*a*) With 0.6 wt.% Na_2CO_3
(*b*) With no addition
(*c*) With 0.6 wt.% H_3BO_3

IV. Non-disintegrating anodes
(*a*) Baked at 1000° C
(*b*) Baked at 1200° C
(*c*) Baked at 1400° C

V. Industrial type prebaked anodes
(*a*) With 0.4 wt.% Na_2CO_3
(*b*) With no addition
(*c*) With 0.4 wt.% H_3BO_3

All anodes were made by Elektrokemisk A.S. Most of them were of the non-disintegrating type, which earlier had proved not to disintegrate during electrolysis (8). The baking temperature was 1000° C except for type IV.

The current to all four anodes was delivered from the same D.C. source and regulated so that equal currents passed through each anode.

Table I shows a typical set of results on overvoltages obtained with three of the non-disintegrating type anodes, two of which had additions of Fe_2O_3 and H_3BO_3 respectively. In spite of the small differences between the data, there is a distinctive tendency to increasing overvoltage when passing from the most reactive to the least reactive anode. The reproducibility between different runs was not good enough to reveal such differences. However, comparison of the results between a set of anodes of different reactivity in any one experiment indicated clearly this trend.

Corresponding measurements had earlier been carried out in a similar apparatus with non-disintegrating anodes of a different make, type III. These anodes were more porous, and the catalyzing agent was Na_2CO_3 instead of Fe_2O_3. A pure graphite anode was also used. A set of results from these measurements is given in Table II. It is readily seen

Can. J. Chem. Downloaded from www.nrcresearchpress.com by 210.87.254.5 on 09/05/12
For personal use only.

TABLE I

Overvoltages (mV) on carbon anodes with chemical additions

Current density, A/cm²	Anode type		
	II(*a*)	II(*b*)	II(*c*)
0.067	160	162	161
0.10	210	211	212
0.13	219	224	225
0.20	298	300	300
0.26	318	318	319
0.29	334	336	336
0.34	354	354	355
0.44	379	380	381
0.67	433	435	435

that the same tendency of increasing overvoltage with decreasing reactivity is also observed in this case.

With anodes of the same type as those used in industrial cells (type V), the same general trend in the overvoltage was observed, as for the non-disintegrating anodes. The differences were of the same magnitude as in the results shown in Tables I and II, i.e. 1–7 mV.

TABLE II

Overvoltages (mV) on carbon anodes with chemical additions

Current density, A/cm²	Anode type			
	III(*a*)	III(*b*)	III(*c*)	I
0.25	265	265	265	281
0.30	283	284	284	302
0.40	289	290	292	334
0.60	361	363	362	—
0.70	371	373	374	405
0.90	410	412	412	432
1.00	427	429	430	472
1.20	460	463	466	518
1.50	526	528	531	593

The differences between the graphite anodes (type I) and types II, III, and V were approximately 20, 60, and 10 mV respectively, at the highest current density of 1.5 A/cm². This sequence was also confirmed in runs where the types I, II, and V were compared directly, as shown in Table III. Taking the overvoltage as a measure of reactivity provides

TABLE III

Overvoltages (mV) on different types of carbon anodes

Current density, A/cm²	Anode type		
	II(*b*)	V(*b*)	I
0.048	163	168	168
0.086	241	245	247
0.13	289	293	294
0.22	341	344	350
0.38	374	388	400
0.60	411	419	431
1.32	517	529	540

Can. J. Chem. Downloaded from www.nrcresearchpress.com by 210.87.254.5 on 09/05/12
For personal use only.

a reactivity scale, indicating for instance that type II was more reactive than type V. The comparatively great difference with type III was probably due to a larger active surface, because of the higher porosity of this anode material.

Measurements with non-disintegrating anodes baked at different temperatures, type IV, revealed no significant difference in overvoltage.

Discussion

The present results clearly show that the anodic overvoltage in aluminum electrolysis is dependent on the reactivity of the anode material. This dependence is, however, much less pronounced than in combustion of the same materials in oxygen (or CO_2).

In all cases the experimental results gave fairly good Tafel plots. In most measurements the linear relationship between overvoltage and log current density was observed over the entire range investigated (0.04–1.5 A/cm^2), but in a few cases marked inflections in the curves occurred. This phenomenon, which usually indicates that the reaction mechanism has changed, was not further investigated.

Two sets of experimental curves are given in Figs. 4 and 5. In order to keep the curves

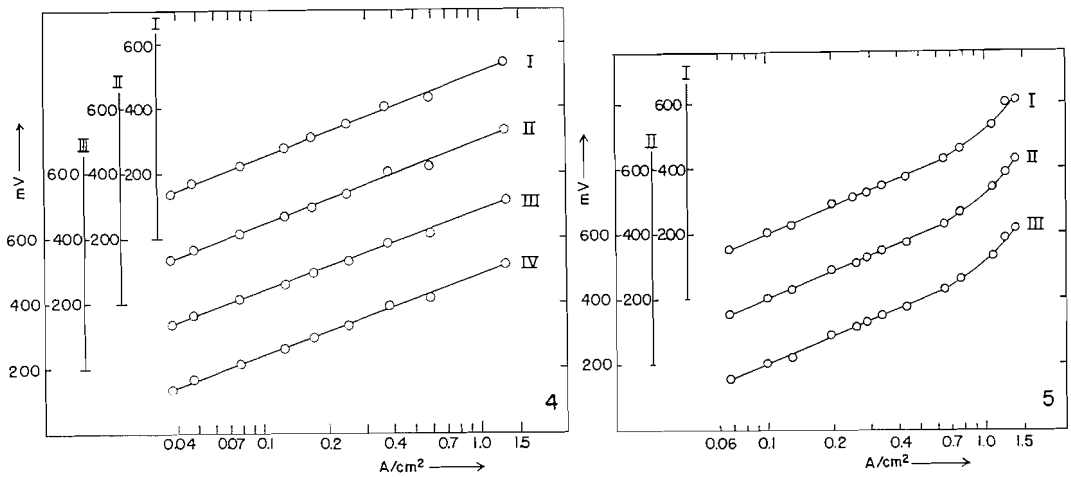

FIG. 4. Tafel plots. Curve I, graphite anode; curve II, industrial type anode; curve III, non-disintegrating anode; curve IV, as above with addition of Fe_2O_3.

FIG. 5. Tafel plots of non-disintegrating anodes. Curve I, with addition of H_3BO_3; curve II, without addition; curve III, with addition of Fe_2O_3.

apart, the ordinate has been displaced successively upwards. Fig. 4 shows the typical case whereas Fig. 5 gives curves which bend at about 0.65 A/cm^2.

The coefficients in Tafel's equation showed fairly constant values. The b value ranged between 0.26 and 0.27 in all runs but two, when it was 0.20. The a value was in the range 0.40–0.52.

Assuming that the overvoltage is caused by slow transport of oxygen-carrying ions through the double layer (reaction [3]), the relationship between overvoltage and current can be expressed by a Tafel equation in the form:

$$\eta = \frac{-RT}{\beta z F} \ln i_0 + \frac{RT}{\beta z F} \ln i \qquad [16]$$

where β is the symmetry factor, z the number of electrons and i_0 the "exchange current".

Can. J. Chem. Downloaded from www.nrcresearchpress.com by 210.87.254.5 on 09/05/12
For personal use only.

Introducing the experimental value, $b = 0.26$–0.27, βz can be calculated as $\beta z = 0.97$–0.94. Assuming that the energy barrier through the double layer is symmetrical, i.e. $\beta = 1/2$, gives $z \simeq 2$, as expected for a reaction involving discharge of divalent oxygen ions.

If, on the other hand, the overvoltage is entirely due to slow formation of CO_2 from chemisorbed oxygen (e.g. reaction [5]), the overvoltage can be described as reaction overvoltage according to the general treatment introduced by Vetter (16). Under certain conditions the reaction overvoltage can be represented by a Tafel equation in the form:

$$\eta = \frac{-RT}{Fpn/\nu} \ln i_r + \frac{RT}{Fpn/\nu} \ln i \qquad [17]$$

where p is the order of reaction for the rate-determining chemical reaction and n/ν is the number of electrons required in the overall cell reaction for the formation of one activated complex. The term i_r is the "reaction limiting current" for the cell reaction going in the reverse direction, when $c \rightarrow 0$ at the interface.

In this case pn/ν would equal 0.97–0.94. The fraction n/ν cannot be less than two if one oxygen atom is involved, and the value of p must then be approximately one-half.

In an investigation of the kinetics of oxidation of graphite in oxygen at 800° C, Blyholder and Eyring (18) found that the order of reaction with respect to oxygen was zero when the reaction occurred only on the surface, and one-half when it also occurred in the pores in the graphite. A zero order of reaction with respect to oxygen indicates that the slow step is the breaking of the C–C bonds in the carbon network. In that case the present experimental results could also be interpreted in terms of the reaction overvoltage theory, providing that the anode reaction also takes place in the pores of the anode. Antipin and Dudyrev (19) observed that the linear dimensions of an anode increased by about 3% when the current density exceeded 0.1 A/cm^2. This expansion may indicate that oxygen becomes internally chemisorbed into the carbon material, so that the reaction could also take place within the pores of the anode.

From the treatment above it can be concluded that slow formation of CO_2 from the chemisorbed oxygen cannot be ruled out as the cause for the overvoltage. The experimental results show that the chemical reactivity of the carbon has a certain influence on the overvoltage. The overvoltage, therefore, can hardly be ascribed entirely to slow transport of oxygen ions through the double layer. It appears that the overvoltage is caused both by slow transport of oxygen ions through the double layer and by slow reaction on the carbon, although our experimental results do not allow the elucidation of the reaction mechanism in detail.

ACKNOWLEDGMENTS

The anodes used in this work were made by Elektrokemisk A/S, Research Department, Kristiansand S, Norway. The authors also wish to thank Prof. Rosenqvist, The Technical University of Norway, for helpful discussions and Prof. Flengas, University of Toronto, for critically reading the manuscript.

REFERENCES

1. A. I. Beljajev, M. B. Rapoport, and L. A. Firsanova. Metallurgie des aluminium. VEB Verlag Technik, Berlin. 1956.
2. H. Stern and G. T. Holmes. J. Electrochem. Soc. **105**, 478 (1958).
3. S. I. Rempel and L. P. Khodak. J. Appl. Chem. USSR, **26**, 857 (1953).
4. O. Kubaschewski and E. L. Evans. Metallurgical thermochemistry. Pergamon Press, London. 1958.
5. F. Drossbach. Z. Elektrochem. **42**, 65 (1936).

Can. J. Chem. Downloaded from www.nrcresearchpress.com by 210.87.254.5 on 09/05/12
For personal use only.

6. R. PIONTELLI. Atti simposio elettroliso sali fusi e produzione metalli speciali. Milan, Italy. 1960.
7. T. G. PEARSON and J. WADDINGTON. Discussions Faraday Soc. **1**, 307 (1947).
8. J. THONSTAD. To be published.
9. A. R. UBBELOHDE and F. A. LEWIS. Graphite and its crystal compounds. Clarendon Press, Oxford. 1960.
10. E. A. GULBRANSEN and K. F. ANDREW. Ind. Eng. Chem. **44**, 1039 (1952).
11. B. J. WELCH and N. E. RICHARDS. AIME International Symposium on the Extractive Metallurgy of Aluminium, New York, New York. 1962.
12. V. P. MASHOVETS and A. A. REVAZYAN. Soviet Electrochem. **II**, 185 (1961).
13. V. P. MASHOVETS and A. A. REVAZYAN. J. Appl. Chem. USSR, **30**, 1069 (1957).
14. N. E. RICHARDS. Southeastern Regional Meeting of the American Chemical Society. 1960.
15. R. PIONTELLI. Ann. N.Y. Acad. Sci. **79**, 1025 (1960).
16. K. J. VETTER. Elektrochemische kinetik. Springer Verlag, Berlin. 1961.
17. G. WRANGLEN. Jernkontorets Ann. **142**, 613 (1958).
18. G. BLYHOLDER and H. EYRING. J. Phys. Chem. **61**, 682 (1957).
19. L. N. ANTIPIN and V. K. DUDYREV. Zh. Fiz. Khim. **31**, 2031 (1957).

Can. J. Chem. Downloaded from www.nrcresearchpress.com by 210.87.254.5 on 09/05/12
For personal use only.

Can. J. Chem. Downloaded from www.nrcresearchpress.com by 210.87.254.105 on 09/05/12
For personal use only.

PLATINUM(II) COMPLEXES: INFRARED SPECTRA IN THE 300–800 CM^{-1} REGION

A. D. ALLEN AND T. THEOPHANIDES[1]
Department of Chemistry, University of Toronto, Toronto, Ontario
Received February 6, 1964

ABSTRACT

Bands have been assigned to stretching frequencies of bonds between platinum and chlorine, nitrogen and oxygen which are observed in the far infrared region. The positions of these bands have been related to the structures of several complexes. Improved procedures are given for the preparation of complexes of the type $K[PtCl_3L]$ and *trans*-$PtCl_2L(am)$, where L is an unsaturated organic ligand and am is an aromatic amine.

As part of a study of the trans effect of unsaturated organic ligands in chloro-complexes of bivalent platinum, the infrared spectra of a series of such compounds have been examined in the 300-800 cm^{-1} region. Variations in the stretching frequencies, ν Pt–Cl, have been investigated and assignments made for the platinum – aromatic nitrogen stretching modes, ν Pt–N. From the spectrum of bis(acetylacetono) platinum(II) stretching frequencies ν Pt–O have been determined.

RESULTS AND DISCUSSION

(a) Chloro-complexes

In Table I are given details of the spectra of salts of the general form $K^+[PtCl_3L]^-$,

TABLE I

Complex	Cl–Pt–Cl, ν cm^{-1}	*trans*-Pt–Cl, ν cm^{-1}	Other bands, ν cm^{-1}
$K[C_3H_6PtCl_3]$†	330 vs	306 s	393 m, 535 vs
$K[C_2H_4PtCl_3]$	340 vs, 331 sh	306 vs	373 m, 403 ms, 492 s
K[olPtCl$_3$]	330 s, 335 sh	305 w	—
K[acPtCl$_3$]	326 vs	312 s	438 m, 486 m, 557 m, 600 s
K[ac*PtCl$_3$]	325 vs, 335 ms	314 s	474 m, 543 s, 618 s
$(MeC_2(OH)C\equiv)_2$	—	—	370 m, 535 s

ol = Allyl alcohol, ac = $(Me_2C(OH)C\equiv)_2$, ac* = $(Me_2C(OMe)C\equiv)_2$.
† = Taken from ref. (2).

where L is an unsaturated organic ligand. Since the complex ion is essentially square planar, with the platinum atom at the center, we expect to find two platinum–chlorine stretching frequencies: (*a*) the asymmetric stretching vibration of the linear Cl–Pt–Cl unit (the symmetric vibration being inactive in the infrared); and (*b*) the stretching frequency of the platinum–chlorine group trans to the ligand L. This latter frequency should be lower than the first because of the weakening of the bond by the high trans effect of the unsaturated ligand (1) as reported by Adams and Chatt (2) for the propene platinous chloride ion. We find that the stretching frequency of the trans chlorine (306–314 cm^{-1}) is some 20 cm^{-1} lower than that of the Cl–Pt–Cl unit (325–340 cm^{-1}), which is in accordance with expectations.

For the allyl alcohol complex the band at 305 cm^{-1} is rather weak and may be affected

[1]*Present address: Howard University, Washington, D.C.*

by any traces of water present, but if this is accepted there is a clear distinction between the *trans*-Pt–Cl stretching frequencies for the olefin and acetylene type complexes which indicates a greater bond weakening, and hence stronger trans effect, for the olefinic ligands.

When salts of the above type are treated with one equivalent of a base such as pyridine a non-ionic product with the formula $[PtCl_2Lpy]^0$ is obtained (3, 4). The *trans* structure of this compound, which would be expected from the fact that the chlorine *trans* to the organic ligand is much more easily displaced than the other two, is shown by its far infrared spectrum. Details of the spectra of this type of compound are given in Table II.

TABLE II

Compound	ν Pt–Cl, cm^{-1}	ν Pt–N, cm^{-1}	Other bands, cm^{-1}
$[Ptpy_4]^{++}Cl_2 3H_2O$	—	474 m	793 m, 781 m, 735 s, 658 m, 302 m, 294 m
trans-$Ptpy_2Cl_2$	343 vs	480 m	778 m, 735 ms, 705 m
cis-$Ptpy_2Cl_2$	344 s, 330 ms	467 m, 454 m	776 m, 738 ms, 706 ms
$Pt_2py_2Cl_4$	349 s, 308 m	454 m	766 m, 736 ms, 688 ms
trans-acPtCl$_2$py	340 vs	474 m	690 m, 597 m, 549 ms, 532 ms, 438 w
trans-acPtCl$_2$(2,pic)	339 vs	477 m	602 m, 549 m, 532 ms, 440 m
trans-acPtCl$_2$(2,6-lu)	337 vs	450 m	645 m, 602 m, 549 m, 535 m, 411 w
trans-olPtCl$_2$(2,6-lu)	344 vs	463 w	855 w, 783 s, 606 s, 511 s, 413 w, 370 m

A single band at about 340 cm^{-1} is observed corresponding to the asymmetric vibration of the linear Cl–Pt–Cl unit, the band at about 310 cm^{-1}, due to the *trans* chlorine, having disappeared. These spectra also show a new band at about 470 cm^{-1}. We assign this band to the stretching mode of the platinum–pyridine bond on the basis of a comparison with the spectra of other compounds containing this bond, also shown in Table II. The ion $[Ptpy_4]^{++}$ has one band at 474 cm^{-1}, and the compound *trans*-$Ptpy_2Cl_2$ has a similar band at 480 cm^{-1}, corresponding to the asymmetric stretching vibration of the linear N–Pt–N unit, as well as the expected band at 343 cm^{-1} for the linear Cl–Pt–Cl unit. In the spectrum of the *cis* isomer of this compound each of these is split into two bands, since both the symmetric and asymmetric stretching modes of the angular *cis* $PtCl_2$ unit and *cis* $Ptpy_2$ unit are active in the infrared. The spectra of these two isomers form the basis of an excellent and simple method of distinguishing between *cis* and *trans* isomers, and for the detection of one in the presence of the other.

From these spectra it has been possible to determine the structure of the material which is formed when a solution of the complex *trans*-$PtCl_2$ac.py in dry benzene is allowed to stand at room temperature. After about 48 hours reddish-brown crystals begin to form, which are insoluble in common organic solvents. The spectrum of this material in the sodium chloride region contains typical pyridine frequencies only, showing that the acetylene has been displaced from the complex. The far infrared spectrum (Table II) shows bands at 308, 349, and 454 cm^{-1}. From these data, and from analyses for carbon, hydrogen, and chlorine, the following bridged structure is proposed:

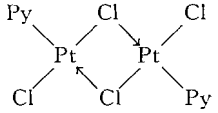

Can. J. Chem. Downloaded from www.nrcresearchpress.com by 210.87.254.105 on 09/05/12
For personal use only.

The band at 454 cm^{-1} is the metal–pyridine stretching frequency, and the band at 349 cm^{-1} is the terminal platinum–chlorine frequency. The band at 308 cm^{-1} is similar to that observed by Adams (5) for the bridging chlorines in platinous chloride (312 cm^{-1}), and is assigned to that vibration. Two similar bands have also been observed (12) for the bridged complexes $[Cr_2Cl_9]^{3-}$ and $[V_2Cl_9]^{3-}$. The trans configuration of the two pyridines is suggested from the fact that only one band is observed for the two bridging chlorines, indicating that they are identical. If the pyridines were in the cis configuration the bridging chlorines would differ from each other and two bands would be expected. This particular compound has not been reported previously. Chatt and Venanzi (13) prepared a series of bridged compounds of bivalent platinum containing aromatic amines from the decomposition (2 months) of *trans*-ethyleneaminedichloroplatinum compounds. The use of the acetylene diol in place of ethylene greatly speeds up the preparation of these compounds since the starting material is easier to prepare and its decomposition in an inert solvent takes place more rapidly.

(b) Bis(acetylacetono) platinum(II)

The far infrared spectrum of bis(acetylacetono) platinum(II) is very similar to that reported by Nakamoto (6) for the analogous palladium(II) compound, who assigns a band at 464 cm^{-1} for the symmetric palladium–oxygen stretching frequency and gives a calculated value of 317 cm^{-1} for the asymmetric metal–oxygen stretching mode. We find (14) a band at 319 cm^{-1}, corresponding to the latter vibration in the platinum complex, and one at 478 cm^{-1} for the symmetric stretching mode. A correlation between this vibration and the stability constant (log K_1K_2) of the acetylacetonate complexes of several bivalent transition metals has been suggested (6). The stability constant of the platinum complex has not been reported, but by extrapolation from these other complexes, based on a stretching frequency for this vibration of 478 cm^{-1}, we obtain an estimated value for the logarithm of the stability constant of between 40 and 45 for this compound. This very high value is consistent with the well-known stability of complexes of bivalent platinum.

EXPERIMENTAL

The ligand 2,5-dimethyl-3-hexyne-2,5-diol was used as supplied by Air Reduction Chemical and Carbide Co. The dimethyl ether of this diol was prepared from it as described in ref. (4).

Potassium Trichloro(ethylene) Platinum(II) Monohydrate (Zeise Salt)

Prepared as described by Chatt and Duncanson (7), decomp. 175–180° (lit. (7)) decomp. about 165°.

Potassium Trichloro(2,5-dimethyl-3-hexyne-2,5-diol) Platinum(II)

In the procedure described by Bukhovets (4, 8) a concentrated aqueous solution of potassium chloroplatinite containing a twofold excess of the diol is allowed to stand at room temperature until the color changes from red to an orange-yellow. This takes from 1 to 2 weeks. It was found that by heating the solution on a water bath the change in color takes place in 2–3 minutes, but that further heating results in rapid decomposition. By cooling the solution in ice as soon as the change in color was observed this decomposition was prevented and the time taken for this step was reduced from several days to a few minutes. The filtered solution was evaporated at 30–40° at reduced pressure, and the procedure of Bukhovets was followed from this point. The yellow product was recrystallized from ether–acetone and dried *in vacuo* at room temperature, decomp. 140–145° (lit. (4, 8) decomp. 140–145°). Calc. for $C_8H_{14}O_2Cl_3PtK$: C, 19.9; H, 2.95. Found: C, 20.1; H, 3.05.

Potassium Trichloro-(2,5-dimethyl-2,5-dimethoxy-3-hexyne) Platinum(II)

Prepared as described by Bukhovets (4, 8). Recrystallization of the dark yellow product from ether–acetone gave yellow crystals, decomp. 154–156° (lit. (4) decomp. 140–145°). Calc. for $C_{10}H_{18}O_2Cl_3PtK$: C, 23.5; H, 3.55. Found: C, 23.3; H, 3.55.

Compounds of the type *trans*-$PtCl_2L(am)$, where am = pyridine, etc., were first prepared by the method of Gel'man, Bukhovets, and Meilakh (3, 4). A more convenient method was later used, as follows. To a concentrated solution of the potassium salt K $[PtCl_3L]$ in dry acetone was added a slight excess of the base

Can. J. Chem. Downloaded from www.nrcresearchpress.com by 210.87.254.105 on 09/05/12
For personal use only.

(pyridine, etc.). A precipitate of potassium chloride formed immediately, and was removed by filtration. The filtrate was evaporated at room temperature, giving yellow crystals, which were thoroughly washed with cold water to remove traces of pyridine and potassium chloride, and dried *in vacuo* at room temperature. Further purification was not necessary, but recrystallization gave well-formed crystals. The following four compounds were prepared in this way:

trans-Dichloro-(2,5-dimethyl-3-hexyne-2,5-diol) (pyridine) platinum(II).—Bright yellow crystals, recrystallized from carbon tetrachloride or ether, m.p. 110–112° (decomp.) (lit. (3) m.p. 97° and (4) 114–116°). Calc. for $C_{13}H_{19}O_2NCl_2Pt$: C, 32.05; H, 3.95. Found: C, 31.8; H, 4.2.

trans-Dichloro-(2,5-dimethyl-3-hexyne-2,5-diol) (2-picoline) platinum(II).—Yellow crystals, recrystallized from ether or acetone, m.p. 127° (decomp.). Calc. for $C_{14}H_{21}O_2NCl_2Pt$: C, 33.55; H, 4.2. Found: C, 33.8; H, 4.1.

trans-Dichloro-(2,5-dimethyl-3-hexyne-2,5-diol) (2,6-lutidine) platinum(II).—This very stable compound has been stored in air for 1 year without detectable decomposition. Fine yellow prisms, recrystallized from benzene, m.p. 154°. Calc. for $C_{15}H_{23}O_2NCl_2Pt$: C, 34.95; H, 4.5. Found: C, 34.75; H, 4.7.

trans-Dichloro-(1-propen-2-ol) (2,6-lutidine) platinum(II).—Yellow crystals, recrystallized from carbon tetrachloride or ether, m.p. 102°. Calc. for $C_{10}H_{15}OCl_2NPt$: C, 27.85; H, 3.5. Found: C, 28.0; H, 3.65.

Tetrachloro-dipyridino-diplatinum(II)

The compound to which this formula is assigned was formed when a solution (3%) of the compound *trans*-dichloro-(2,5-dimethyl-3-hexyne-2,5-diol) (pyridine) platinum(II) in dry benzene was allowed to stand at room temperature. After 2 days reddish-brown crystals began to form. These are insoluble in common organic solvents except acetone (slightly soluble) and pyridine (soluble with reaction), m.p. 170° (decomp.). Calc. for $C_{10}H_{10}N_2Cl_4Pt_2$: C, 17.45; H, 1.45; Cl, 20.55. Found: C, 18.65; H, 1.55; Cl, 19.9.

The Compounds cis- and trans-Dichloro-dipyridino-platinum(II) and Tetrapyridino-platinum(II) Dichloride

These compounds were prepared as described by Kaufmann (9).

Bis(acetylacetono) Platinum(II)

Prepared as described by Werner (10). Recrystallization from benzene gave long yellow needles which begin to darken at 200° and turn black at about 240°. Calc. for $C_{10}H_{14}O_4Pt$: C, 30.5; H, 3.6. Found: C, 30.5; H, 3.45.

Infrared Spectra

The spectra were recorded with a Beckman IR-4 spectrometer, equipped with cesium bromide optics. The samples were prepared in polyethylene films (11). The instrument was calibrated against water vapor.

Microanalyses were done by Alfred Bernhardt, Mulheim.

We are indebted to Miss Mary Wright for assistance with some of the experimental work and to the National Research Council for financial support.

REFERENCES

1. J. Chatt and I. Leden. J. Chem. Soc. 2936 (1955).
2. D. M. Adams and J. Chatt. J. Chem. Soc. 2821 (1962).
3. A. D. Gel'man, S. V. Bukhovets, and E. Meilakh. Compt. Rend. Acad. Sci. URSS, **46**, 105 (1945).
4. J. Chatt, R. G. Guy, L. A. Duncanson, and D. T. Thompson. J. Chem. Soc. 5170 (1963).
5. D. M. Adams. Proc. Chem. Soc. 335 (1961).
6. K. Nakamoto. Infrared spectra of inorganic and coordination compounds. J. Wiley, New York. 1963. p. 217. K. Nakamoto. J. Chem. Phys. **32**, 588 (1960). K. Nakamoto, P. J. McCarthy, and A. E. Martell. J. Am. Chem. Soc. **83**, 1066, 1272 (1961).
7. J. Chatt and L. A. Duncanson. J. Chem. Soc. 2939 (1953).
8. S. V. Bukhovets. Izv. Sektora Platiny i Drug. Blagorodn. Metal. Inst. Obshch. Neorgan. Khim. Akad. Nauk. SSSR, **29**, 55 (1955).
9. G. B. Kauffmann. Inorg. Syn. Vol. VII. pp. 249–252. 1963.
10. A. Werner. Ber. **34**, 2584 (1901).
11. M. Bedard, H. Huber, J. L. Myers, and G. F Wright. Can. J. Chem. **40**, 2278 (1962).
12. D. M. Adams, J. Chatt, J. M. Davidson, and J. Garrett. J. Chem. Soc. 2189 (1963).
13. J. Chatt and L. M. Venanzi. J. Chem. Soc. 2787 (1955).
14. T. Theophanides. Ph.D. Thesis, University of Toronto, Toronto, Ont. 1963.

Can. J. Chem. Downloaded from www.nrcresearchpress.com by 210.87.254.105 on 09/05/12
For personal use only.

Can. J. Chem. Downloaded from www.nrcresearchpress.com by 210.87.254.42 on 09/05/12
For personal use only.

COMPLEXES OF STANNIC CHLORIDE WITH AROMATIC HYDROCARBONS AND OXYGEN-CONTAINING DONORS IN SOLUTION

J. J. Myher and K. E. Russell
Department of Chemistry, Queen's University, Kingston, Ontario
Received February 6, 1964

ABSTRACT

Complex formation between stannic chloride and various alkylbenzenes has been investigated by means of optical measurements. It is found that weak 1:1 complexes are formed in methylene chloride solution at 25 °C. The absorption at 355 mμ can be used to determine the concentration of free stannic chloride in benzene to which oxygen-containing donors have been added. The results are interpreted in terms of 1:1 and 1:2 complex formation between stannic chloride and donor. For the stronger donors such as tetrahydrofuran and acetone, the main complexes formed with excess of stannic chloride must contain equimolar amounts of stannic chloride and donor, and it is probable that they involve tin with a coordination number of five. Ethyl esters of chloroacids are very much weaker donors than ethyl esters of unsubstituted acids. The heat of reaction for the addition of a donor molecule to the 1:1 complex is usually close to the heat of reaction for the addition of the first donor molecule to stannic chloride. The decrease in entropy in each case is approximately 30 e.u./mole.

Extensive studies have been made of complexes between stannic chloride and both oxygen- and nitrogen-containing Lewis bases. In general stannic chloride forms 1:2 complexes with monofunctional donors such as simple aldehydes, ketones, ethers, and esters (1, 2, 3). In some studies, evidence has been obtained for 1:1 complexes; for example, molecular weight studies of complexes of stannic chloride and esters (4), ketones and ethers (2) were interpreted in terms of the dissociation of 1:2 complexes into 1:1 complexes and donor. More recently Kubota and Brown (5) have proved that 1:1 complexes between stannic chloride and aromatic nitriles persist in dilute solution and have determined equilibrium constants for their dissociation into the component donor and acceptor molecules. Laane and Brown (6) have extended this work to include diisobutyl ketone, 9-fluorenone, and ethyl pivulate. Brune and Zeil (7) have shown that both 1:1 and 1:2 complexes between stannic chloride and ethers, alcohols, and nitriles exist in the pure state and in concentrated solution. Satchell and Wardell (8) have interpreted absorption data of solutions of nitroanilines and stannic chloride in *o*-dichlorobenzene on the assumption that 1:1 complexes are formed.

There appears to be little quantitative information concerning the factors which govern the formation of 1:1 and 1:2 complexes between stannic chloride and simple oxygen-containing donors in solution. In principle equilibrium constants may be obtained by studying the infrared spectra of mixtures of stannic chloride and oxygen-containing donor in an inert solvent. The concentration of free donor can be estimated from the intensity of an appropriate infrared absorption band because complexing normally shifts the position of this band. In practice there is some difficulty with overlapping bands when aromatic nitriles are used as donors (5) and with some exceptions (6) the same difficulties are encountered with oxygen-containing donors. An alternative approach is suggested by Satchell's work (9) with toluene solutions of stannic chloride. Satchell confirmed Comyns, Howald, and Willard's observation (10) that such solutions absorb in the near ultraviolet and showed that the absorbance at 380 mμ was proportional to the concentration

of stannic chloride. The addition of acetic acid to a toluene solution of stannic chloride caused a reduction in the absorbance at 380 mμ; the concentration of free stannic chloride was determined from the measured absorbance. Satchell interpreted his results in terms of $SnCl_4 \cdot 3CH_3COOH$ and higher complexes but his conclusions are open to question because he neglected to consider the effects of hydrogen bonding and of dissociation.

Application of the method to other systems appeared attractive because ultraviolet measurements of fairly high precision can be readily made using solutions at controlled temperatures. If the only significant absorbance is due to the complex between stannic chloride and aromatic hydrocarbon, the free stannic chloride concentration can be readily estimated to $\pm 0.0005\ M$ and reasonably accurate estimates of equilibrium constants for the formation of 1:1 complexes between stannic chloride and many donors can be made. In this paper it is shown that weak 1:1 complexes are formed between stannic chloride and each of the aromatic hydrocarbons benzene, toluene, mesitylene, and hexamethylbenzene. Equilibria in dilute solution between stannic chloride and certain ethers and esters and the corresponding 1:1 and 1:2 complexes were studied using benzene as solvent and indicator. Calorimetric data were obtained for four donors and these were interpreted using the equilibrium constants estimated in the ultraviolet studies.

EXPERIMENTAL

Materials

Benzene and methylene chloride were dried over calcium chloride, degassed on the vacuum line and stirred with powdered Drierite for several hours. Mesitylene was treated with concentrated sulphuric acid, washed with sodium carbonate solution and water, and dried over calcium chloride; after standing over calcium hydride it was distilled *in vacuo*. Toluene and the oxygen-containing bases were dried and distilled into ampoules. Stannic chloride was degassed on the vacuum line, distilled three times, and stored at −78.5 °C.

Procedure

Complexes between stannic chloride and benzene, toluene, and mesitylene were investigated using 0.172 *M* solutions of stannic chloride and of hydrocarbon in methylene chloride. Spectra of mixtures containing y ml stannic chloride solution and $5 - y$ ml hydrocarbon solution were taken over the range 300–360 mμ using a Beckman DK1 recording spectrophotometer with cells of 1 cm path length. Complex formation between stannic chloride and hexamethylbenzene was studied using a series of solutions which contained one of the components at constant concentration and the other component at various concentrations; the spectra were recorded over the 300–420 mμ range. The effect of varying the temperature from 15 °C to 40 °C was examined with solutions of stannic chloride in benzene, and of hexamethylbenzene and stannic chloride in methylene chloride, contained in sealed corex cells.

Complex formation between stannic chloride and oxygen-containing donors was investigated with benzene as solvent. The reaction vessel consisted of a corex cell of 1 cm path length sealed to a 50-ml reservoir; ground joints at the top of the vessel provided entry for a small glass stirrer and a microburette. Twenty-five milliliters of an approximately 0.08 *M* solution of stannic chloride in benzene was placed in the cell and the absorbance at 355 mμ measured by means of a DK1 spectrophotometer when temperature equilibrium was reached. A small amount of base was added from the burette, the solution was vigorously stirred and the absorbance was recorded until a steady value was attained. The process was repeated for further additions of base, the maximum amount added generally being in the range of 0.5 ml to 1 ml. Separate experiments involving methylene chloride as solvent established that complexes of stannic chloride and these oxygen-containing donors do not absorb significantly at 355 mμ.

Heats of reaction were obtained by measuring the temperature rise on successive addition of small volumes of donor to 25 ml of stannic chloride solution in benzene. The simple calorimeter consisted of a Dewar flask, micromagnetic stirrer, and Beckmann thermometer. The heat capacity of the assembly was determined from electrical measurements.

Infrared spectra were recorded at room temperature using a Perkin–Elmer Model 21 spectrometer. The solutions were prepared by adding various amounts of ethyl formate, acetate, or propionate to an approximately 0.1 *M* solution of stannic chloride in benzene. The sealed cells were of 0.1 mm path length. Infrared spectra of benzene solutions of the pure esters were obtained under similar conditions.

Can. J. Chem. Downloaded from www.nrcresearchpress.com by 210.87.254.42 on 09/05/12
For personal use only.

RESULTS AND DISCUSSION

Complexes between Stannic Chloride and Aromatic Hydrocarbons

Mixtures of stannic chloride and benzene, toluene, mesitylene, or hexamethylbenzene in methylene chloride solution absorb significantly in the 320 to 360 mμ range, whereas solutions of the individual components show negligible absorption. Continuous variation plots for the absorbance of solutions of stannic chloride and mesitylene in methylene chloride at 25 °C are given in Fig. 1. At both 320 mμ and 340 mμ the absorbance passes

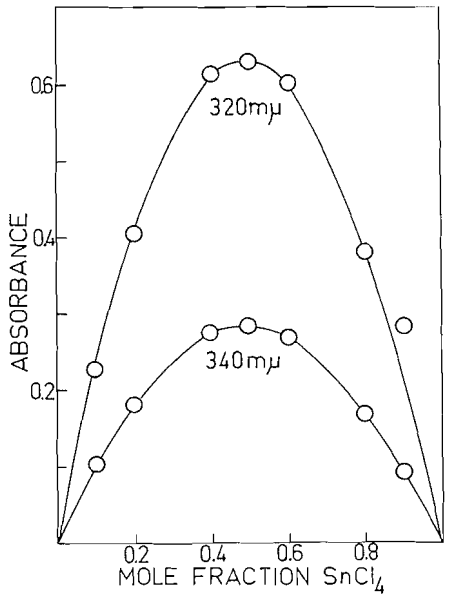

FIG. 1. Absorbance of solutions of stannic chloride and mesitylene in methylene chloride at 25 °C. Mole fraction of stannic chloride refers to the stannic chloride – mesitylene mixture, neglecting the solvent.

through a maximum when the mole fraction of stannic chloride is 0.5 indicating that a 1:1 complex is formed between stannic chloride and mesitylene. The curves are symmetrical, suggesting that only one complex with absorption in this region is formed and the rounded nature of the maximum shows that the complex is largely dissociated. Similar results are obtained with benzene and toluene. With hexamethylbenzene the absorbance in the range 320–410 mμ was found to be proportional to the stannic chloride concentration when the hexamethylbenzene concentration was constant and proportional to the hexamethylbenzene concentration for values up to 0.258 *M* when the stannic chloride concentration was constant (0.0178 *M*).

These observations are explained if a 1:1 complex is formed between stannic chloride and the aromatic hydrocarbon.

$$SnCl_4 + ArH \rightleftharpoons SnCl_4 \cdot ArH$$

In dilute methylene chloride solution the equilibrium is displaced well to the left, the results for hexamethylbenzene in particular indicating that the proportion of complexed stannic chloride is extremely small. Enthalpies of formation were estimated to be approximately −0.2 kcal/mole for the stannic chloride – hexamethylbenzene complex in methylene chloride solution, and 1.2 kcal/mole for the stannic chloride – benzene complex in benzene solution.

Can. J. Chem. Downloaded from www.nrcresearchpress.com by 210.87.254.42 on 09/05/12
For personal use only.

Earlier work in this field includes that of Tsubomura (11), who showed that a benzene solution of stannic chloride absorbs in the 330–360 mμ region. Ulich, Hertel, and Nespital (2) interpreted molar polarization data of such solutions in terms of complex formation between stannic chloride and benzene. Elliott, Evans, and Owen (12) have shown that a comparable 1:1 complex is formed between titanium chloride and benzene.

Complexes between Stannic Chloride and Ethers

The absorbance of benzene solutions of stannic chloride in the 355 mμ region is directly proportional to the concentration of stannic chloride. On the addition of a Lewis base such as tetrahydrofuran (THF), the optical density falls to a new value which is a measure of the concentration of free stannic chloride in the solution. Complexes of stannic chloride and tetrahydrofuran do not absorb in this region. Values of free stannic chloride concentration [$SnCl_4$] obtained at 25 °C are plotted against concentration of added tetrahydrofuran [THF] in Fig. 2. The dotted lines represent the hypothetical results for

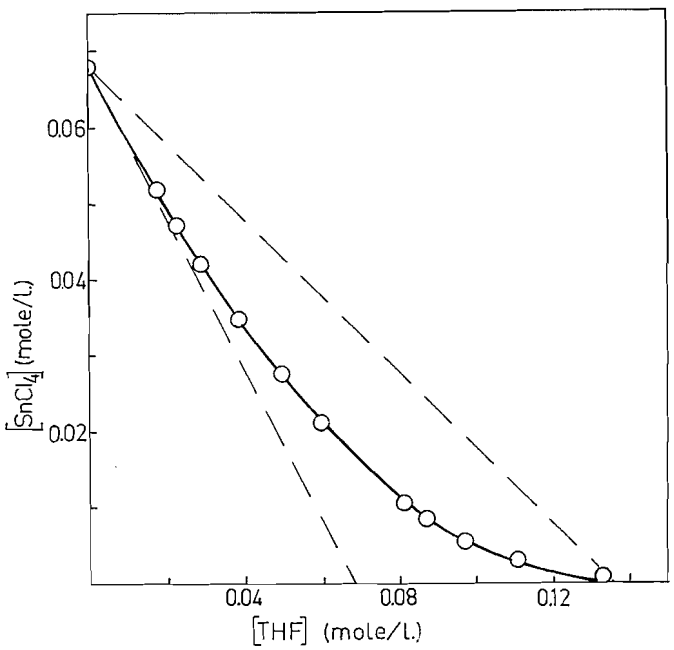

FIG. 2. Effect of added tetrahydrofuran on free stannic chloride concentration in benzene solution at 25 °C.

undissociated $SnCl_4 \cdot THF$ and $SnCl_4 \cdot 2THF$ in solution. The stannic chloride concentration decreases more rapidly with added tetrahydrofuran than is possible for even an undissociated 1:2 complex, and a lower complex must be present. The experimental results could be explained in terms of the complex $2SnCl_4 \cdot 2THF$ or a complex between $SnCl_4 \cdot THF$ and the solvent but the simplest possibility is $SnCl_4 \cdot THF$ in which tin shows a coordination number of five. It is reasonable to assume that the following equilibria are involved

[1] $$SnCl_4 + THF \rightleftharpoons SnCl_4 \cdot THF$$

[2] $$SnCl_4 \cdot THF + THF \rightleftharpoons SnCl_4 \cdot 2THF$$

Can. J. Chem. Downloaded from www.nrcresearchpress.com by 210.87.254.42 on 09/05/12
For personal use only.

Can. J. Chem. Downloaded from www.nrcresearchpress.com by 210.87.254.42 on 09/05/12
For personal use only.

The high degree of complexing precludes accurate estimates of the individual values of K_1 and K_2, the equilibrium constants for reactions [1] and [2], but the ratio K_1/K_2 is found to be equal to four if it is assumed that effectively all the tetrahydrofuran is present as $SnCl_4 \cdot THF$ and $SnCl_4 \cdot 2THF$ in the solution. Infrared spectra of solutions indicate that this assumption is reasonable for molar ratios of tetrahydrofuran to stannic chloride up to 1.4:1. The solid curve in Fig. 2 is calculated on the assumption that K_1/K_2 equals 4. Within experimental error the ratio K_1/K_2 is independent of temperature in the range 17 °C to 44 °C and the values of ΔH for reactions [1] and [2] must be approximately the same. In their thermometric studies of the reaction between tetrahydrofuran and stannic chloride in solution, Cioffi and Zenchelsky (13) showed that the heat evolved is proportional to the tetrahydrofuran added up to a molar ratio of tetrahydrofuran to stannic chloride of almost 2:1 and concluded that the only complex formed is $SnCl_4 \cdot 2THF$. Their experimental results can equally well be explained by the formation of 1:1 and 1:2 complexes and approximately equal values of ΔH for reactions [1] and [2]. The thermometric studies lead to a rough estimate of $K_1 K_2$ of 6×10^7 l^2 mole^{-2} but a rough estimate from the present ultraviolet studies is 2.25×10^6 l^2 mole^{-2} and this value has been used to obtain the approximate values of K_1 and K_2 given in Table I.

TABLE I

Equilibrium constants for the formation of complexes between stannic chloride and oxygen-containing donors at 25 °C

Donor	K_1 (l/mole)	K_2 (l/mole)
Ethyl formate	19	17
Ethyl acetate	61	6
Ethyl propionate	21	5
Ethyl chloroformate	0.13	—
Ethyl chloroacetate	1.1	0.1
Ethyl dichloroacetate	0.45	—
Diethyl carbonate	10.5	3
Tetrahydrofuran	3000	750
Dimethyltetrahydrofuran	50	200
Diethyl ether	3.5	15
Acetone	80	25

Most of the donors studied in this work are very much weaker than tetrahydrofuran and the observed stannic chloride concentration can be used to make estimates of the individual values of K_1 and K_2. The results for 2,5-dimethyltetrahydrofuran and diethyl ether are given in Table I. The estimated error in K_1 when its value is between 2 and 100 l mole^{-1} varies between 6 and 20%, a relatively high error being possible for 2,5-dimethyltetrahydrofuran because solutions of this ether and stannic chloride in methylene chloride show weak absorption.

The order of donor ability is tetrahydrofuran > 2,5-dimethyltetrahydrofuran > diethyl ether. Cioffi and Zenchelsky explain the lower base strength of 2,5-dimethyltetrahydrofuran compared with the unsubstituted compound in terms of steric effects. The weak basicity of diethyl ether compared with cyclic ethers has been observed in other systems e.g. boron trifluoride forms a far stronger 1:1 complex with tetrahydrofuran than with diethyl ether (14).

Complexes between Stannic Chloride and Esters

Table I records values of K_1 and K_2 at 25 °C for equilibria involving a number of ethyl

esters of monobasic acids. The experimental data have been interpreted on the assumption that only 1:1 and 1:2 complexes are formed. It is possible that the 1:1 complexes of stannic chloride and ester are solvated by benzene but the weakness of the complexes between stannic chloride and benzene suggests that such solvation is not significant. Analysis of the experimental data for ethyl formate, acetate, and propionate shows that the 1:1 complexes cannot be significantly dimerized.

The influence of inductive effects on the base strengths of esters is shown by chlorine substitution. The value of K_1 for the reaction between stannic chloride and ethyl chloroacetate is only about one-fiftieth of the equilibrium constant for the corresponding reaction involving ethyl acetate, and an even greater reduction in K_1 is observed in changing the donor from ethyl formate to ethyl chloroformate. The increase in K_1 when ethyl acetate replaces ethyl formate as donor may be ascribed to the inductive effect of the methyl group but the observation that K_1 is only slightly greater for ethyl propionate than for ethyl formate suggests that steric effects may also be involved. The value of K_1 for diethyl carbonate is derived on the assumption that only 1:1 and 1:2 complexes are formed; the weakening in base strength relative to ethyl formate is at least partly due to the inductive effect of the ethoxy group.

Some values of K_2, the equilibrium constant for the addition of a second molecule of ester to the 1:1 complex, are given in Table I. They are of relatively low accuracy but they show that K_2 for a given ester is generally smaller than K_1. Values of K_2 for esters of chloroacids are too small to be measured by the ultraviolet method, a result which is not surprising in view of the susceptibility of K_1 to chlorine substitution.

Infrared studies were confined to benzene solutions of stannic chloride and ethyl formate, acetate, or propionate. In such solutions two new bands appear in the 1620–1700 cm^{-1} range, one of strong intensity 85–105 cm^{-1} below the carbonyl stretching frequency of the pure ester and the other of weak intensity 40–45 cm^{-1} below the carbonyl stretching frequency of the pure ester. The variation of intensity of the strong band with amount of added ester suggests that it is made up of absorptions due to both the 1:1 and 1:2 complexes; the weak absorption probably originates from the 1:2 complex. The reductions in frequency are probably due to complex formation involving the carbonyl oxygen (15).

Absorbance measurements give the concentration of free ester in solution leading to independent estimates of K_1 and K_2. The measurements were made at 20 ± 1 °C and were complicated by the overlapping weak absorption band tentatively ascribed to the 1:2 complex. The values of K_1 and K_2, corrected to 25 °C, agree with those obtained from ultraviolet studies within the estimated experimental error of ±20% for K_1 and ±40% for K_2.

Calorimetric Data

Heats of reaction were measured for the donors ethyl formate, ethyl acetate, acetone, and tetrahydrofuran. Experimentally the heat evolved for a given amount of added donor is obtained and this is corrected for the heat of dilution of added base. The concentrations of 1:1 and 1:2 complexes present in solution are calculated from the spectrophotometric data and the heat of reaction per mole of complexed donor is thus obtained. The heats of reaction per mole of complexed ethyl formate and acetone were −10.9 kcal/mole and −11.0 kcal/mole respectively. The results for various amounts of added donor varied over a range of ±0.1 kcal/mole, which is well within the estimated experimental error of ±0.4 kcal/mole. Since the heat of reaction does not depend on whether primarily 1:1 or 1:2 complexes are being formed, the values of ΔH must be the same within experimental

Can. J. Chem. Downloaded from www.nrcresearchpress.com by 210.87.254.42 on 09/05/12
For personal use only.

Can. J. Chem. Downloaded from www.nrcresearchpress.com by 210.87.254.42 on 09/05/12
For personal use only.

TABLE II

Thermodynamic data for 1:1 and 1:2 complexes of stannic chloride in benzene solution at 25 °C

Donor	K_1 (l/mole)	$-\Delta H_1$ (kcal/mole)	$-\Delta G_1$ (kcal/mole)	$-\Delta S_1$* (e.u./mole)	K_2 (l/mole)	$-\Delta H_2$ (kcal/mole)	$-\Delta G_2$ (kcal/mole)	$-\Delta S_2$* (e.u./mole)
Ethyl formate	19	10.9±.4	1.74±.04	30.7±1.5	17	10.9±.4	1.7±.2	30.9±2.0
Ethyl acetate	61	10.5±.4	2.44±.04	27.0±1.5	6	10.5±.4	1.1±.2	31.6±2.0
Tetrahydrofuran	3000	14.1±.4	4.75±.3	31.4±2.3	750	14.1±.4	3.9±.3	34.2±2.4
Acetone	80	11.0±.4	2.60±.04	28.2±1.5	25	11.0±.4	1.9±.2	30.5±2.0

*Units of l/mole have been used for K_1 and K_2 in the calculation of ΔS_1 and ΔS_2.

error. The heat of reaction [1] for tetrahydrofuran was estimated to be -14.1 kcal/mole and the lack of temperature dependence of K_1/K_2 indicates that the heat of reaction [2] is also -14.1 kcal/mole. Cioffi and Zenchelsky estimated the sum of the two heats of reaction to be -27.5 ± 0.6 kcal/mole. For ethyl acetate the heat of reaction per mole of complexed donor varied from -10.1 kcal/mole to -10.9 kcal/mole over the range of additions. This variation may not be significant because it is still within the estimated experimental error and the heats of reactions [1] and [2] may both be -10.5 kcal/mole. It is possible, however, that for ethyl acetate the heat of reaction [2] is greater than the heat of reaction [1] or that the estimate of K_2 for this donor is low.

Table II summarizes the calorimetric data for reactions [1] and [2] and records the free energy and entropy changes for these reactions in benzene solution at 25 °C. The entropy decreases by approximately 30 e.u./mole in each of the two association reactions. Cioffi and Zenchelsky concluded that the entropy change in the formation of the 1:2 complex from uncomplexed stannic chloride and cyclic ethers is about -60 e.u./mole (13). Laane and Brown (6) observed an entropy decrease of -31.6 e.u./mole for the formation of the 1:1 complex between stannic chloride and diisobutyl ketone but the values for ethyl pivulate and 9-fluorenone were considerably smaller.

ACKNOWLEDGMENTS

The authors are grateful to the National Research Council for a grant and a bursary.

REFERENCES

1. P. Pfeiffer. Ann. Chem. **376**, 285 (1911).
2. H. Ulich, E. Hertel, and W. Nespital. Z. Physik. Chem. B, **17**, 21 (1932).
3. P. Pfeiffer and O. Halperin. Z. Anorg. Allgem. Chem. **87**, 235 (1914).
4. W. Hieber. Ann. Chem. **439**, 97 (1924).
5. T. L. Brown and M. Kubota. J. Am. Chem. Soc. **83**, 331 (1961).
6. J. Laane and T. L. Brown. Inorg. Chem. **3**, 148 (1964).
7. H. A. Brune and W. Zeil. Z. Physik. Chem. **32**, 384 (1962).
8. D. P. N. Satchell and J. C. Wardell. Proc. Chem. Soc. 86 (1963).
9. D. P. N. Satchell. J. Chem. Soc. 4388 (1960).
10. A. E. Comyns, R. A. Howald, and J. E. Willard. J. Am. Chem. Soc. **78**, 3989 (1956).
11. H. Tsubomura. Bull. Chem. Soc. Japan, **27**, 1 (1954).
12. B. Elliott, A. G. Evans, and E. D. Owen. J. Chem. Soc. 689 (1962).
13. F. J. Cioffi and S. T. Zenchelsky. J. Phys. Chem. **67**, 357 (1963).
14. D. E. McLaughlin, M. Tamres, and S. Searles. J. Am. Chem. Soc. **82**, 5621 (1960).
15. M. F. Lappert. J. Chem. Soc. 542 (1962).

Can. J. Chem. Downloaded from www.nrcresearchpress.com by 210.87.254.42 on 09/05/12
For personal use only.

C^{13} CHEMICAL SHIFTS IN ORGANIC CARBONYL GROUPS

J. B. STOTHERS
Department of Chemistry, University of Western Ontario, London, Ontario

AND

P. C. LAUTERBUR
Department of Chemistry, State University of New York at Stony Brook, Stony Brook, Long Island, New York

Received February 4, 1964

ABSTRACT

The results of a study of the resonance position of the carbonyl carbon nucleus in an extensive series of carbonyl derivatives are reported. A discussion of the major factors affecting the position of these carbon resonances is presented and some of the potential applications of these data to chemical problems are indicated.

INTRODUCTION

Earlier reports (1–6) of some preliminary studies of the C^{13} chemical shifts for the carbonyl carbon in a variety of organic compounds have clearly indicated that C^{13} nuclear magnetic resonance (n.m.r.) spectroscopy will prove to have valuable applications to chemical problems. An analogy between the C^{13} carbonyl carbon resonance position and the carbonyl infrared stretching frequency has already been noted (2, 4) since the C^{13} resonances are strong and appear in a relatively uncluttered region of the C^{13} spectrum. The fact that there is no obvious correlation between the C^{13} chemical shifts and the stretching frequencies of the various types of carbonyl group shows that the n.m.r. technique offers a method for studying these groupings which is dependent, at least in part, on different factors. The purpose of this paper is to present the results of a general survey of carbonyl compounds.

Our survey included an examination of more than 150 compounds selected to cover the commonly encountered functional groups such as aldehydes, ketones, carboxylic acids, esters, amides, anhydrides, and acid chlorides as well as a few bifunctional compounds. Examples were drawn from the aliphatic, alicyclic, and aromatic series. A number of general features were found which apply to each class of carbonyl compound, such as the effects of alkyl substitution, of conjugation, and of hydrogen-bonding (either intra- or inter-molecular).

EXPERIMENTAL

N.M.R. Spectra

The spectra were obtained using material containing C^{13} in natural abundance and were measured at either 8.50, 15.085, or 25.143 Mc/s using Varian spectrometers. Some samples were observed at each frequency to check the precision of the measurements. An external reference was used in most cases and was either CS_2 or CH_3I (the latter enriched to 58% C^{13}) contained in a small tube inserted in the larger (15 mm) sample tube. The resonance in CS_2 was taken as the origin of the chemical shift scale. No corrections for bulk magnetic susceptibility were made and the data are judged to be accurate to within ± 0.5 p.p.m. A detailed description of the experimental procedure has been given (7).

Samples

Most of the materials used in this study are commercially available and were purified by standard methods when the C^{13} or H^1 and infrared spectra showed gross amounts of impurities. Most of the members of the series of cyclic ketones (cyclodecanone to cycloheptadeconanone) were kindly supplied by Dr. J. Coops. Whenever possible, the C^{13} spectra were obtained using the neat liquids; otherwise, saturated solutions in

Can. J. Chem. Downloaded from www.nrcresearchpress.com by 210.87.254.5 on 09/05/12
For personal use only.

appropriate solvents (noted in the text) were employed. Although this was done to realize the maximum signal: noise ratio, some preliminary studies of solvent effects for this class of compound were also carried out using 25% solutions.

RESULTS AND DISCUSSION

General

As noted previously (4), the resonances of carbonyl carbons occur over a total range of approximately 70 p.p.m. at the low-field end of the C^{13} spectral region. Some olefinic carbons (4, 5, 8) absorb within the upper portion of this region, as do oximes (4), carbon disulphide, and the central carbon of the allenic structure, $\diagup C{=}C{=}C \diagdown$ (8); otherwise, there is no interference with the C^{13} resonances of other classes of compounds for which data are presently available. As discussed later, it seems likely that a distinction between carbonyl peaks and those due to other carbons may be made on the basis of preferential solvent effects. Certainly, in the case of unknown structures, infrared spectroscopy allows one to determine whether or not a carbonyl group is present. Knowing this, one may be able to obtain further information concerning the environment of the carbonyl grouping from the C^{13} spectrum.

The carbonyl group in aliphatic ketones and aldehydes absorbs in the low-field region of the carbonyl range, -25 to -5 p.p.m. Although the regions are not well separated, no ambiguity arises between these two types because the aldehyde structure gives rise to a widely spaced doublet (J = 165–185 c/s) due to spin-coupling with the directly bonded formyl proton. The resonances of conjugated ketones and aldehydes are shifted to higher field than those in the saturated compounds and, for the most part, appear in the range, -5 to $+5$ p.p.m. Carboxylic acid peaks appear at still higher fields, 10 to 20 p.p.m., while the corresponding esters give rise to carbonyl peaks in the range, 20–30 p.p.m. A few acid anhydride resonances have been found in the upper portion of this ester region, 27–30 p.p.m. and the few amides studied absorb slightly higher, 30–35 p.p.m. Within the group of compounds included in this survey, the resonances of alkyl carbonates and acetylenic esters have been found at the highest field, i.e., 36–40 p.p.m. These general regions for the various carbonyl compounds are shown in Fig. 1 and the various classes are discussed in

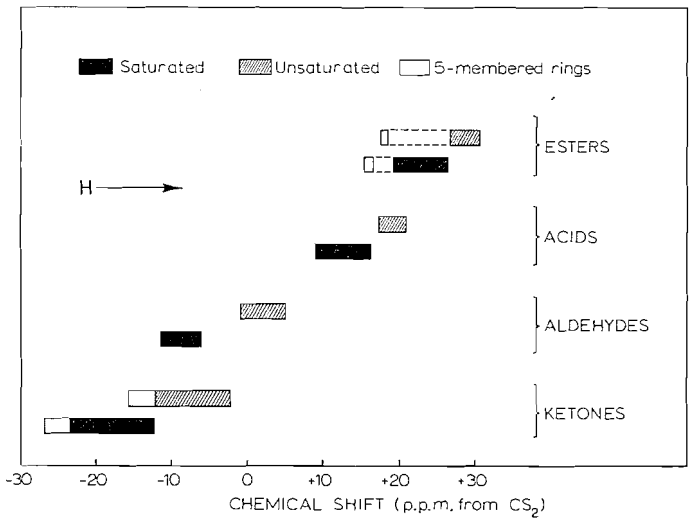

FIG. 1. Ranges of carbonyl carbon chemical shifts in various classes of compounds.

Can. J. Chem. Downloaded from www.nrcresearchpress.com by 210.87.254.5 on 09/05/12
For personal use only.

more detail in the following sections. For reference, it may be noted that the peaks for CO_2 and CO have been found at 68.6 and 11.5 p.p.m. respectively (9).

Aldehydes and Ketones

As mentioned above, the carbonyl carbons of these compounds absorb in approximately the same region of the C^{13} spectrum, but are easily distinguishable. For similar structural types, the ketone appears at the lower field by 5–8 p.p.m. The observed shift to lower field upon alkyl substitution for hydrogen, i.e. $-\overset{\overset{O}{\|}}{C}-H \rightarrow -\overset{\overset{O}{\|}}{C}R$, has been observed for carbon resonances in many different types of structure (1, 5, 7, 8, 10), although the reasons for this trend are not yet fully understood. It has been suggested (10, 11) that the major factor involved is a contribution from the diamagnetic anisotropy of the alkyl group. The difficulty with this explanation is that comparable shifts for protons are not observed although a change in screening due to the anisotropic nature of a substituent grouping should affect both C^{13} and H^1 nuclei equally, except for geometrical factors. To compare the effects of alkyl substitution on carbonyl shifts in some simple aldehydes and ketones, some typical data are collected in Table I. A comparison of the shifts for aldehydes with the corresponding methyl ketones shows that the effect of replacement of hydrogen by a methyl group of ca. −5 p.p.m. is somewhat less than that observed in other systems for a similar substitution. For example, in aliphatic cases, the change, $R\overset{*}{C}H_3 \rightarrow R\overset{*}{C}H_2-Me$, deshields the carbon nucleus marked by an asterisk by ca. −9 p.p.m. (5, 8, 10, 11), while methyl substitution at olefinic and aromatic carbons causes shifts of ca. −10 p.p.m. (8) and ca. −9 p.p.m. (4, 6, 7, 12, 13), respectively. It seems reasonable to suggest that the C—CH_3 bond in methyl ketones is more strongly polarized than that in these other systems resulting in a relatively higher electron density at the carbonyl carbon nucleus. If so, the net

TABLE I

C^{13} chemical shifts of the carbonyl group in ketones and aldehydes (p.p.m. from CS_2)

Substituent, R	Type of compound		
	RCHO	$RCOCH_3$	RCOR
CH_3—	−6.8	−12.3	−12.3
C_2H_5—	−9.0	−13.5	−16.5
n-C_4H_9	—	−14.3	−15.8
n-C_6H_{13}—	−9.0	−14.0	—
n-C_7H_{15}—	−8.5	−13.9	—
$(CH_3)_2CHCH_2$—	—	−13.5	−23.0
$(CH_3)_3CCH_2$—	—	−13.6	—
$(CH_3)_2CH$—	−11.2	−17.4	−22.8
$(CH_3)_3C$—	—	−18.2	−23.0
C_6H_{11}*	−9.0	−15.7	—
CH_2=CH—	0.4	−4.4	—
CH_3CH=CH—	1.4	−3.7	—
CH_3CH=$C(CH_3)$—	0.0	−5.2	—
$(CH_3)_2C$=CH—	—	−3.4	−4.9
ϕ—CH=CH—	1.0	−4.0	—
C_6H_5	1.8	−3.2	−2.4
2-Naphthyl	0.3	−3.0	—
1-Naphthyl	0.3	−6.7	—
9-Anthranyl	0.3	−14.5	—

*Cyclohexyl.

Can. J. Chem. Downloaded from www.nrcresearchpress.com by 210.87.254.5 on 09/05/12
For personal use only.

result would be to offset, at least partially, the deshielding effect of the methyl grouping. Alkyl substitution at the α-position produces a small shift to low field (ca. 2 p.p.m.), but the effects of multiple substitution are not strictly additive. The effects of more distant substituents on alkyl groups are usually small. It may be noted that increased branching at the α-carbon reduces the number of hyperconjugative resonance structures which can contribute to the ground state and it is conceivable that these could be an important factor contributing to the observed chemical shifts since conjugative interactions have marked shielding effects on carbonyl carbon nuclei (see below). The trend to lower field with a decrease in the number of possibilities for hyperconjugation is consistent with this rationalization.

A marked variation in the chemical shift of the carbonyl carbon is found for the series of cycloalkanones, cyclobutanone to cycloheptadecanone. The resonance positions of the carbonyl carbon for this series are presented in Fig. 2 and some typical data are given in

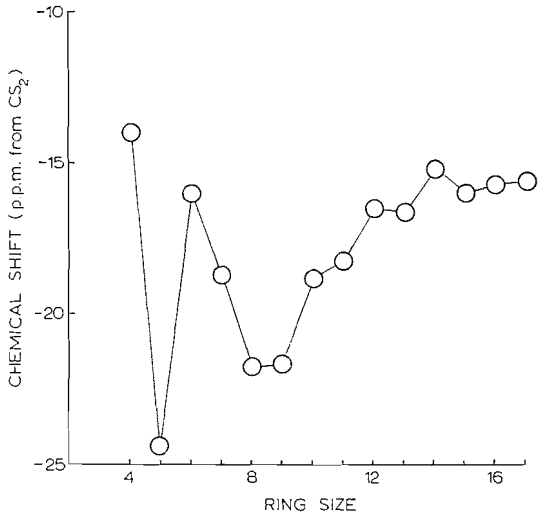

FIG. 2. Variation of carbonyl carbon chemical shifts of cyclanones with ring size.

Table II. Cyclopentanone exhibits the lowest field carbonyl shift of any so far examined (−24.4 p.p.m.). Curiously, the four-membered ring ketone, cyclobutanone, absorbs at approximately the same field as the six- and seven-membered ring ketones and it would appear, therefore, that the low-field position for cyclopentanone is not simply related to ring strain. Other evidence to support this conclusion is provided by the observation that the carbonyl carbons in more highly strained five-membered ring systems, thujone and camphor, are not appreciably different from the parent ketone. (The slightly lower field position for camphor is possibly due, in part, to hydrogen-bonding of the carbonyl group with the chloroform solvent.) Furthermore, the carbonyl resonances of cyclooctanone and cyclononanone appear at significantly lower field (ca. −21.7 p.p.m.) than that of the 6-, 7-, or 10-membered ring ketones, while it is generally assumed that ring strain is comparable in the 8- to 10-membered rings and significantly greater in these than in the five-membered cyclic cases (14). This peculiar effect on the five-membered ring carbonyl carbon is not restricted to the simple ketones but is also found for the corresponding lactone and lactam structures (see Table II) and constitutes one of the more puzzling

Can. J. Chem. Downloaded from www.nrcresearchpress.com by 210.87.254.5 on 09/05/12
For personal use only.

TABLE II

C^{13} carbonyl chemical shifts for some cyclic compounds (p.p.m. from CS_2)

Ring size	Saturated ketones*		Unsaturated ketones		Lactones	
4	Cyclobutanone	−14.1			Propiolactone	22.5
5	Cyclopentanone	−24.4	2-Cyclopentenone	−15.3	γ-Butyrolactone	15.5
	Thujone	−24.9†	1-Indanone	−11.7*	Crotonolactone	17.5
	Camphor	−26.3‡				
6	Cyclohexanone	−16.1	2-Cyclohexenone	−4.3		
			1-Tetralone	−3.0		
7	Cycloheptanone	−18.8				
8	Cyclooctanone	−21.8				
9	Cyclononanone	−21.7				
10	Cyclodecanone	−18.9				
11	Cycloundecanone	−18.3				
12	Cyclododecanone	−16.6				
13	Cyclotridecanone	−16.7				
14	Cyclotetradecanone	−15.3				
15	Cyclopentadecanone	−16.1				
16	Cyclohexadecanone	−15.8				
17	Cycloheptadecanone	−15.7				

*These shifts measured in CS_2 solution except as noted.
†Neat liquid.
‡Saturated solution in $CHCl_3$ (see text).

aspects of C^{13} chemical shifts observed to date, especially when it is compared with the shifts in the corresponding hydrocarbons (15).

The carbonyl resonance position for the large ring ketones, C_{12}–C_{17}, are comparable to those found for the acyclic ketones. This observation is in agreement with many other comparisons of large ring compounds with the corresponding aliphatic derivatives (14), except for the carbon chemical shifts in the cycloalkanes, which have a maximum at C_{12} (15). The trends in the carbonyl shifts of the medium ring cycloalkanones (C_8–C_{11}), however, indicate that a number of factors must contribute to the observed results only one of which is ring strain in the normal sense (i.e., an effect closely associated with changes in normal bond angles). One possible opposing effect could be associated with changes in the electronic structure of the C=O bond as ring size is varied. Further work is clearly required to resolve this difficulty.

Another important factor contributing to the carbonyl chemical shift is conjugation. Comparison of a conjugated system with an analogous saturated derivative shows that in the former the carbonyl peak appears at significantly higher field by ca. 10 p.p.m. (see Tables I and II). This shielding effect is comparable for α,β-unsaturated and aromatic systems, indicating that the electron density about the conjugated carbonyl carbon nucleus may be substantially greater than that about a saturated carbonyl carbon nucleus. If this is so, the electron-withdrawing effect of the carbonyl grouping on the carbonyl-methyl bond in methyl ketones will be reduced in a conjugated system relative to the saturated analogue, and a reduced polarization of this bond would increase the electron density at the methyl carbon nucleus. Evidence to support this view is provided by the observation that acetyl methyl carbons absorb at approximately 4 p.p.m. higher field in conjugated systems than in the corresponding saturated compounds, 168 p.p.m. vs. 164 p.p.m. (5, 6). Studies of proton spectra also indicate a greater electron density at the conjugated carbonyl carbon (16). Finally, it is well-known that conjugated carbonyl compounds are less reactive with the usual carbonyl reagents than are the saturated analogues, presumably because of the greater electron density at the carbonyl carbon in the former cases. In any event, the contribution due to the diamagnetic anisotropy of the aromatic ring cannot be

Can. J. Chem. Downloaded from www.nrcresearchpress.com by 210.87.254.5 on 09/05/12
For personal use only.

important since the observed shifts are in the opposite direction to and much larger than that calculated using the usual ring-current model (17).

To examine the effect of polar substituents on the carbonyl chemical shift, a series of substituted benzaldehydes and acetophenones was examined. These data appear in the first two columns of Table III. It is clear that there is no correlation observed between the

TABLE III

Carbonyl chemical shifts of some aromatic carbonyl compounds (p.p.m. from CS_2)

X	X—C_6H_4—CHO	X—C_6H_4—$COCH_3$	X—C_6H_4—$COOCH_3$
H	1.8	−3.2	27.0
o-NO_2	5.0*	−5.6	28.4
m-NO_2	4.0*	—	—
p-NO_2	—	−3.3*	27.6*
o-CH_3	0.9	−6.5	26.5
m-CH_3	1.4	−2.7	27.2
p-CH_3	1.9	−3.2	27.5
o-OCH_3	5.3	−5.0	26.9
m-OCH_3	—	−3.3	—
p-OCH_3	2.6	−2.9*	27.2*
p-$N(CH_3)_2$	3.1	−2.6*	—
2,6-diCH_3	—	−12.9	23.6
2,4,6-triCH_3	1.9	−13.4	24.2
2,4,6-tri-isoPr	—	−15.1	—

*Sat'd. soln. in $CHCl_3$.

chemical shift and the Hammett parameters for the meta- and para-substituted examples. In fact, the total change in shift between the *p*-$N(Me)_2$ and the *p*-NO_2 acetophenone derivatives is only 0.7 p.p.m. although σ_p changes from −0.83 to +0.77 (18) for these substituents. This change may be compared to the chemical shift difference of 27.5 p.p.m. found for F^{19} in the corresponding *p*-substituted fluorobenzenes (19) and to the difference of less than 1 p.p.m. in the methyl C^{13} resonances of the corresponding toluenes (1). The results for the carbonyl shifts are in direct contrast to the findings from the F^{19} and H^1 nuclear magnetic resonance spectra of aromatic compounds for which the shieldings have been shown to be closely related to the separated σ-constants of Taft (20, 21, 22). There is, however, an important difference between the carbonyl compounds and the fluorobenzenes in that the two types of nuclei examined are not in comparable positions in the resonance system. For the carbonyl compounds, if one considers the resonance forms I and II for electron-releasing and electron-withdrawing substituents, respectively, it seems reasonable that the contribution of these forms would not alter the electron density at the carbonyl

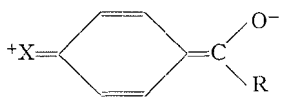

I

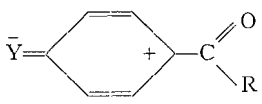

II

carbon appreciably relative to the changes at the terminal nuclei and thus may not affect the carbonyl carbon shielding appreciably. In the fluorobenzenes, however, reasonable resonance forms with a charge on the terminal fluorine may be written, and the effect of substituents on the fluorine shielding should be much more pronounced. Support for this interpretation is provided by an examination of a few *p*-substituted styrenes for which it is found that the β-carbon resonance position shows a dependence on the polar characteristics

Can. J. Chem. Downloaded from www.nrcresearchpress.com by 210.87.254.5 on 09/05/12
For personal use only.

of the substituent while the α-carbon does not (23). In addition, fairly good correlations between the C^{13} chemical shift of the para-carbon of the aromatic ring and the σ_p parameter of the substituent in mono-substituted benzenes (13, 24) have been found whereas a similar correlation is not observed for the meta-carbon shifts vs. σ_m.

More significant changes in the carbonyl shifts of the aromatic derivatives are found for the ortho-substituted acetophenones, particularly in those cases in which the substituent is large and (or) there is 2,6-disubstitution. In these examples, the shift to lower field is explicable in terms of steric inhibition of resonance. If the conjugated interaction of the aromatic nucleus with the carbonyl group is diminished, it follows from the results discussed previously that the carbonyl peak would appear towards lower field relative to an electronically similar, but unhindered, derivative. Furthermore, the acetyl methyl absorption also appears at lower field (6*a*) in the hindered acetophenones. Both of these changes are consistent with the occurrence of steric inhibition of resonance. It has been shown that the C^{13} carbonyl shieldings may be correlated with the angle of twist between the planes of the carbonyl bond and the aromatic ring (6*b*).

Completely analogous trends are found in the polycyclic ketones. Such compounds as 2-acetylnaphthalene and 3-acetylphenanthrene exhibit carbonyl peaks at -3.0 p.p.m., while 1-acetylnaphthalene and 9-acetylphenanthrene give rise to carbonyl peaks at -6.7 and -7.5 p.p.m., respectively, and 9-acetylanthracene shows a carbonyl band at -14.5 p.p.m. It appears, therefore, that the acetyl group in the last three examples is hindered from obtaining co-planarity with the aromatic system by interference with the peri-hydrogens. Further support for these conclusions regarding steric inhibition of resonance is given by a detailed examination of the aromatic ring carbon shifts (6*a*) and a full discussion of the use of C^{13} techniques for the study of steric hindrance in aromatic ketones is in preparation. Studies of similar steric effects in a variety of aromatic compounds have been reported (12).

For acyclic and alicyclic α,β-unsaturated carbonyl compounds, there are two conformations or configurations, respectively, which allow full conjugation between the unsaturated bonds. These are the S-*cis* and S-*trans* forms. The present results indicate that the carbonyl chemical shift is comparable for either of these provided the system is planar. For example, one can compare methyl vinyl ketone, 3-penten-2-one, and mesityl oxide in Table I, since it is generally agreed that the first two exist predominantly in an S-*trans* conformation (25) while mesityl oxide is S-*cis* (26). Further alkyl substitution tends to displace the carbonyl peak to lower field, indicating that such systems are no longer planar. In other words, the situation appears to be analogous to that in hindered aromatic systems. Supporting evidence is provided by the changes in the chemical shifts of the olefinic carbons in these compounds since these also appear to reflect the effect of any factor which hinders the system from attaining a planar conformation (5). A study of these C^{13} spectral changes clearly offers some advantage over the more conventional techniques such as Raman, infrared, and ultraviolet spectroscopies, which do not allow such a clear distinction between a planar S-*cis* form and a non-planar system. A full discussion of this aspect of C^{13} n.m.r. spectroscopy is in preparation.

The effects of a number of polar substituents on the carbonyl chemical shift in aliphatic systems can be seen from the data in Table IV. For comparative purposes, the effects of alkyl substitution are included. In the second column, the chemical shifts for the keto-carbonyl group in some diketones and keto-esters are given. If the second carbonyl group is separated from the first by two or more methylene groups, the shifts are unchanged from the normal saturated values, but the carbonyl shifts are affected in the α-diketo and

Can. J. Chem. Downloaded from www.nrcresearchpress.com by 210.87.254.5 on 09/05/12
For personal use only.

TABLE IV

Effects of substituents on the C^{13} carbonyl absorption for some aliphatic methyl ketones, $R\overset{O}{\overset{\|}{C}}CH_3$ (p.p.m. from CS_2)

R		R	
H	−6.8	$-CH_2CH_2COCH_3$	−14.0
$-CH_3$	−12.3	$-CH_2COCH_3$	−8.9 (keto); 1.9 (enol)
$-CH_2CH_3$	−13.5	$-COCH_3$	−4.9
$-CH_2Cl$	−7.0	$-CH_2CH_2COOEt$	−14.3 (keto); COOEt, 19.8
$-CHCH_3$ (OH)	−19.3	$-CH_2COOEt$	−7.2 (keto); COOEt, 26.0
$-CH_2C(CH_3)_2$ (OH)	−16.9	$-COOEt$	0.8 (keto); COOEt, 32.1

β-diketo examples. In the latter cases, of course, keto–enol tautomeric equilibria are involved and the chemical shift changes are readily rationalized. For example, acetyl acetone shows, in the neat liquid, an enol content of 76–80% (27) and the signals in the C^{13} spectrum (Fig. 3) are readily assigned to the two types of "carbonyl" carbon from the observed intensities. The weaker signal at −8.9 may be assigned to the keto form (A)

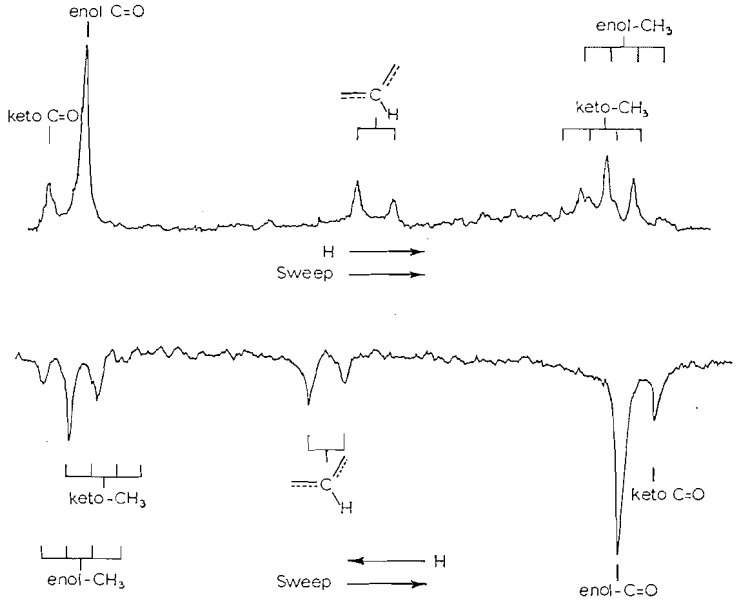

FIG. 3. The 15.085 Mc/s carbon-13 n.m.r. spectra of acetylacetone.

while the more intense peak at 1.9 p.p.m. (ca. 4 times as intense as the lower field signal) must be due to the enol form (B and C or D). The fact that only a single strong band which can be attributed to carbon bearing oxygen is observed indicates that either proton transfer between the two oxygens is rapid (B ⇌ C) or the proton is equidistant from each oxygen

Can. J. Chem. Downloaded from www.nrcresearchpress.com by 210.87.254.5 on 09/05/12
For personal use only.

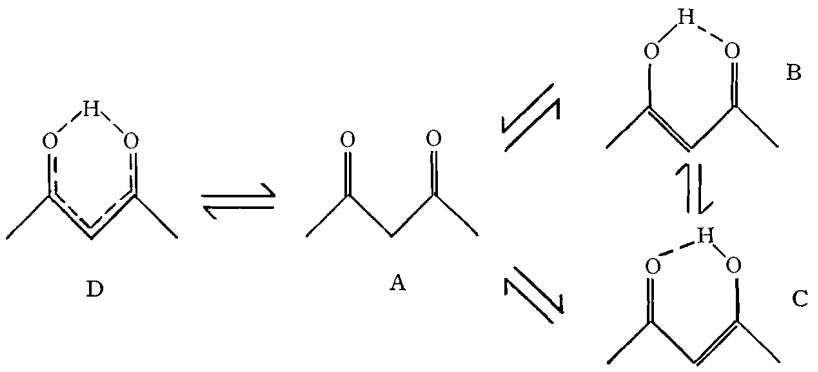

atom (D). The present evidence does not allow one to decide between these two alternatives. Presumably the observed peak position is an average for the chemical shift of a carbon nucleus in the two different environments, i.e., hydrogen-bonded carbonyl carbon and olefinic carbon bearing hydroxyl, of which the former would be expected to appear at the lower field. A number of proton n.m.r. studies of acetylacetone bearing on this phenomenon have appeared (28). Owing to the relatively low sensitivity of the C^{13} method using natural abundance material, coupled with the low enol content for the pure liquid (27), only the keto form is observed in the spectrum of ethyl acetoacetate with the carbonyl peak at −7.2 p.p.m. Thus, it appears that both the acetyl and carboethoxyl groups tend to shield a β-carbonyl carbon. This shielding effect is found to be greater for the α-diketo compounds. A possible interpretation of these results is that the electron withdrawing

$$\overset{+}{\text{C}}{=}\overset{-}{\text{O}}$$

substituents reduce the polarization of the C=O bond such that the electron density is increased at the carbonyl carbon and the nucleus is more screened. Variations in the stretching frequencies of carbonyl bonds have been accounted for in an analogous fashion, by assuming that a reduction in the polarization of the bond by electron-withdrawing groups tends to increase the force constant and, hence, the stretching frequency. Up-field shifts are found also for the α-chlorinated ketones, presumably for the same reason and, in addition, the observed shifts to higher field are approximately additive for each additional halogen atom. The feature of additivity of substituent effects on C^{13} chemical shifts has already been noted for a number of systems (4–8, 12). Further examples of the effects of chlorine substitution are discussed later.

For the case of hydroxyl substituents close to the carbonyl group, the observed shifts are in the opposite direction to those discussed above, i.e. toward lower field. Hydrogen-bonding possibilities, of course, arise for these cases and this effect would tend to increase the polarization of the carbonyl carbon–oxygen bond and thus decrease the screening at the carbon nucleus. Two aliphatic examples are included in Table IV and three examples are given in Table VI for aromatic cases. It is clear that the C^{13} chemical shift provides yet another means for studying hydrogen-bonding effects. One particular area of investigation, namely, solvent effects, is mentioned later in this paper.

Carboxylic Acids and Their Derivatives

Free carboxylic groups exhibit the carboxyl carbon resonance peak at somewhat higher field than aldehydes and ketones, i.e., 9 to 20 p.p.m., with the exception of formic acid at 27.0 p.p.m. Some data are presented in Table V. A comparison of this shift with that for

Can. J. Chem. Downloaded from www.nrcresearchpress.com by 210.87.254.5 on 09/05/12
For personal use only.

TABLE V

Carbonyl chemical shifts of some carboxylic acid derivatives (p.p.m. from CS_2)

R	RCOOH	$RCOOCH_3(C_2H_5)$	CH_3COOR	$(RCO)_2O$	RCOCl	$RCONR_2'$
H	27.0	(33.0)	15.6	—	—	27.9 (R′=H) 30.4 (R′=CH_3)
CH_3	15.6	23.0	23.0	27.6	23.8	—
Et	—	—	22.9	23.0	—	—
n-Pr	12.6	—	22.3	—	—	—
i-Pr	8.9	—	25.7	—	—	—
n-C_4H_9	—	—	25.0	—	—	—
iso-C_4H_9	—	—	22.9	—	—	—
sec-C_4H_9	—	—	19.4	—	—	—
C_5H_{11}—	13.0	20.7 (21.0)				
—(C_2H_4)—*	—	(22.9)	—	—	—	—
—(C_4H_8)—†	—	(20.1)	—	—	19.9	—
CH_2=CH—	20.5	29.2	26.0	—	—	—
CH_2=C(CH$_3$)—	—	26.3	24.8	—	—	—
—(CH=CH)—	—	(28.9)cis (30.4)trans	—	—	—	—
C_6H_5—	20.2	26.7 (28.8)	—	—	25.0	—

*Succinic acid derivatives.
†Adipic acid derivatives.

TABLE VI

Some substituent effects on carbonyl chemical shifts (p.p.m. from CS_2)

R	R—C(=O)—H	R—C(=O)—CH_3	R—C(=O)—R	R—C(=O)—OH	R—C(=O)—Cl	C_6H_5—C(=O)—R
H	—	−5.0	—	27.0	—	+1.8
H_3C	−6.8	−12.3	−12.3	15.6	23.8	−3.2
$ClCH_2$—	—	−7.0	−1.2	19.0*	24.0	+2.8
Cl_2CH—		—	—	23.1*	27.5	7.5
Cl_3C—	+17.5	—	+19.0	25.7*	30.2	12.7
HO—	27.0	+15.6	—	—	—	—
H_2N—	27.9	—	—	—	—	—
$(CH_3)_2N$—	30.4	—	—	—	—	—
o-HO—C_6H_4—	−3.5	−10.9	—	22.5‡	—	—
p-HO—C_6H_4	—	−4.6†	—	—	—	—
o-MeO—C_6H_4—	+5.3	−5.0	—	26.9‡	—	—

*Chloroform solution.
†Dioxane solution.
‡Methyl esters.

acetic acid, 15.6 p.p.m., shows the usual deshielding effect caused by replacement of hydrogen by a methyl group. Again, an increase in the chain length of the substituent alkyl group decreases the shielding slightly while branching at the α-carbon produces a more pronounced shift. It appears that conjugation tends to shield the carboxyl carbon, although the effect is not so large as that observed for simple carbonyl compounds. The position of the carboxyl carbon to higher field than a ketonic carbonyl carbon could be ascribed to the resonance stabilization of the carboxyl due to the additional oxygen atom. This interpretation is consistent with the foregoing while the substituent effects are comparable, at least directionally, to those discussed above. A diminution in the conjugative shielding effect is quite reasonable in view of the resonance stabilization within the carboxyl group itself.

The carboxyl carbon in a variety of carboxylic esters appears at higher field than the

Can. J. Chem. Downloaded from www.nrcresearchpress.com by 210.87.254.5 on 09/05/12
For personal use only.

free acid, in the range 20 to 40 p.p.m. Since the available data for carboxylic acids, are, of necessity, obtained using either neat liquids or concentrated solutions, the observed shift for the free acid is that of the dimeric form rather than the monomeric, and the carbonyl oxygen will be strongly hydrogen-bonded. Hydrogen bonding at carbonyl groups serves to deshield the carbonyl carbon substantially and, thus, it is reasonable to suggest that this is a principal factor giving rise to the chemical shift difference between the carboxyl carbon of the free acid and its corresponding ester. It can be noted that, in general, methyl substitution of the type, $\diagdown\!\!\!\!\diagdown\!\!\!\!\diagdown\!\!\!\!

those in esters, whereas the resonance of the amide grouping appears at slightly higher field. These observations are consistent with the foregoing discussion since, presumably, the nitrogen atom in the amide structure is better able to donate electrons to the carbonyl group as shown, for example, by the lower reactivity of amides relative to esters. It is well known that the C—N bond has considerable "double-bond" character in amides due to contributions from forms such as $R_2—\overset{+}{N}=C(—O^-)—R'$, and the observed C^{13} chemical shifts reflect this effect relative to esters, etc.

To summarize, as well as to allow an intercomparison of the data, the effects of various substituents on "carbonyl" resonances are shown in Table VI. The key feature of this comparison is the remarkable consistency of the effects of various substituents on the different carbonyl groups, a clear indication that the observed variations are due to differences in degree rather than kind. For example, the effect of α-chlorine substitution for the various ketones is reasonably constant at ca. $+4.5 \pm 1$ p.p.m. per chlorine atom, and is found to be slightly less for the acid chlorides and somewhat larger for the aldehydes. It would appear that the electron-withdrawing power of the halogen offsets the same effect due to the carbonyl oxygen such that the electron density at the carbonyl carbon is substantially increased with an increasing number of substituents. The substitution of chlorine at the meta- or para-position of an aromatic ketone does not show the same shielding effect. For example, *p*-chloroacetophenone and *m*-chloroacetophenone absorb at -3.0 and -2.6 p.p.m. respectively, while the carbonyl carbon in acetophenone appears at -3.2 p.p.m. Some of this difference may be due to the diamagnetic anisotropy of the C—Cl bond, and some to a smaller inductive effect in the aromatic ketones, but it is not yet possible to factor the observed effect into its various components. The magnitude of the effect, (3–6 p.p.m. per chlorine atom), seems to be larger than one would expect due to bond anisotropy alone, for reasons mentioned previously.

Miscellaneous Carbonyl Derivatives

A few representative compounds of two other series were examined in the course of this study, namely, alkyl carbonates and metal carbonyls. The alkyl carbonates appear in the high-field region of the carbonyl range, 36–39 p.p.m., which, on the basis of the foregoing, could be attributed to the electron-releasing alkyl oxygen atoms directly bonded to the carbonyl analogous to the effect found for the esters. The two metal carbonyls were found to absorb in the ketone region. Iron pentacarbonyl at -15.6 p.p.m. and nickel tetracarbonyl at 1.2 p.p.m. Contrary to an earlier report (29) on the C^{13} spectra of these two materials, we submit that there is a significant difference between these two chemical shifts, although a better understanding of this difference must await a detailed study of these derivatives. Such an investigation is in progress (30). Since 1958, iron pentacarbonyl has been examined by a number of workers (29, 31, 32) using C^{13} n.m.r. techniques to attempt to establish the structure. No definite conclusions can be drawn as yet since only a single sharp peak is observed. A detailed discussion of this problem has been presented (29).

Hydrogen Bonding Effects

One of the more striking changes in the chemical shift of a carbonyl grouping occurs for hydrogen-bonded structures. In each case, the carbonyl carbon appears at lower field relative to an analogous but non-hydrogen-bonded carbonyl grouping. The effect is clearly illustrated by the data in Table VI for ortho-hydroxy aromatic derivatives. These

Can. J. Chem. Downloaded from www.nrcresearchpress.com by 210.87.254.5 on 09/05/12
For personal use only.

results would suggest that marked solvent shifts should be apparent in hydroxylic solvents relative to non-polar solvents and an examination of acetophenone clearly bears out this prediction. The pertinent data are given in Table VII, for a series of 25% (w/w) solutions

TABLE VII

Solvent effects on C^{13} chemical shifts of acetophenone (25% solutions; p.p.m. from CS_2)

Carbon nuclei	Solvent					
	Nil	CCl_4	C_6H_6	$C_4H_8O_2$	$CHCl_3$	MeOH
CH_3	167.9	167.4	167.4	167.8	166.4	167.5
C_1	56.7	55.4	56.4	55.8	55.4	55.9
$C_{2,3,5,6}$	65.8	64.6	—	65.1	64.4	64.2
C_4	61.2	60.4	61.2	61.5	59.3	59.7
C=O	−3.2	−2.1	−2.9	−3.1	−4.5	−6.3

of acetophenone in a series of solvents. The largest change is noted for the carbonyl shifts in methanol while the down-field shift is also apparent in chloroform. In comparison, the other carbon atoms do not exhibit comparable changes, although there is an indication that the aromatic nuclei are slightly deshielded by hydrogen-bonding. In α,β-unsaturated aliphatic systems, the solvent shifts in methanol (relative to either neat liquid of CCl_4 solution) are comparable for the carbonyl carbons and, in addition, there is a significant shift of the β-olefinic carbon to lower field by ca. 2 p.p.m. (5). One benefit to be derived from these observations is an aid for the assignment of olefinic carbons for those compounds in which the α- and β-nuclei are similarly substituted. Other possible studies of hydrogen-bonding using C^{13} n.m.r. spectroscopy are also indicated, such as in structural studies and detailed solvent effect investigations.

CONCLUSIONS

In general, the C^{13} chemical shifts of organic carbonyl carbon nuclei may be rationalized in terms of the shielding effect of the local electrons about these nuclei. Contributions by neighboring nuclei, as well as the effects of neighboring anisotropic groups, appear to be of secondary importance. A number of potential avenues for investigation which should be rewarding are suggested by this general survey such as (*a*) applications to structural elucidations, (*b*) a new approach to studying steric inhibition of resonance, (*c*) solute–solvent associations, and (*d*) the use of C^{13} techniques for tracer studies. The results of more detailed studies of some of these will be published in the near future.

ACKNOWLEDGMENTS

The financial assistance of the National Research Council of Canada, the Ontario Research Foundation, and the Petroleum Research Fund is gratefully acknowledged, as is the support of some of the work by the Multiple Fellowship on Silicones supported by the Dow Corning Corporation at the Mellon Institute, Pittsburgh 13, Pa. We thank Mr. K. S. Dhami for obtaining some of the data reported herein and acknowledge the generosity of Dr. J. Coops for providing samples of several cycloalkanones.

REFERENCES

1. P. C. LAUTERBUR. Ann. N.Y. Acad. Sci. **70**, 841 (1958).
2. P. C. LAUTERBUR. Abstr. 138th Meeting Am. Chem. Soc. New York, N.Y. 1960. p. 22B.
3. R. E. KLINCK and J. B. STOTHERS. 44th Conf. Chem. Inst. Canada, Montreal, Que. August, 1961.
4. P. C. LAUTERBUR. *In* Determination of organic structures by physical methods. Chap. 7. *Edited by* F. C. Nachod and W. D. Phillips. Academic Press. 1962.

Can. J. Chem. Downloaded from www.nrcresearchpress.com by 210.87.254.5 on 09/05/12
For personal use only.

5. D. H. MARR and J. B. STOTHERS. Abstr. 14th Conf. Anal. Chem. Appl. Spectry. Pittsburgh, Pa. 1963. p. 53.
6. (*a*) K. S. DHAMI and J. B. STOTHERS. 46th Conf. Chem. Inst. Canada, Toronto, Ont. June, 1963. (*b*) K. S. DHAMI and J. B. STOTHERS. Tetrahedron Letters, No. 12, 631 (1964).
7. P. C. LAUTERBUR. J. Am. Chem. Soc. **83**, 1838, 1846 (1961).
8. R. A. FRIEDEL and H. L. RETCOFSKY. J. Am. Chem. Soc. **85**, 1300 (1963).
9. R. ETTINGER, P. BLUME, A. PATTERSON, and P. C. LAUTERBUR. J. Chem. Phys. **33**, 1597 (1960).
10. H. SPIESECKE and W. G. SCHNEIDER. J. Chem. Phys. **35**, 722 (1961).
11. E. G. PAUL and D. M. GRANT. Abstr. 14th Conf. Anal. Chem. Appl. Spectry. Pittsburgh, Pa. 1963. p. 52. J. Am. Chem. Soc. **85**, 1701 (1963).
12. P. C. LAUTERBUR. J. Chem. Phys. **38**, 1406, 1415, 1432 (1963).
13. H. SPIESECKE and W. G. SCHNEIDER. J. Chem. Phys. **35**, 731 (1961).
14. J. SICHER. *In* Progress in stereochemistry. Vol. 3, Chap. 6. Butterworths, London. 1962. E. L. Eliel. Stereochemistry of carbon compounds. Chap. 7. McGraw-Hill, New York. 1962.
15. J. J. BURKE and P. C. LAUTERBUR. To be published.
16. R. E. KLINCK and J. B. STOTHERS. Can. J. Chem. **40**, 1071 (1962).
17. C. E. JOHNSON and F. A. BOVEY. J. Chem. Phys. **29**, 1012 (1958).
18. D. H. MCDANIEL and H. C. BROWN. J. Org. Chem. **23**, 420 (1958).
19. H. S. GUTOWSKY, D. A. MCCALL, B. R. MCGARVEY, and L. H. MEYER. J. Am. Chem. Soc. **74**, 4809 (1952).
20. R. W. TAFT, S. EHRENSON, I. C. LEWIS, and R. E. GLICK. J. Am. Chem. Soc. **81**, 5352 (1959).
21. R. W. TAFT. J. Phys. Chem. **64**, 1805 (1960).
22. R. R. FRASER. Can. J. Chem. **38**, 2226 (1960).
23. K. S. DHAMI and J. B. STOTHERS. Unpublished observations.
24. P. C. LAUTERBUR. Tetrahedron Letters, No. 8, 274 (1961).
25. K. NOACK and R. N. JONES. Can. J. Chem. **39**, 2225 (1961).
26. (*a*) J. B. BENTLEY, R. B. EVERHARD, R. J. B. MARSDEN, and L. E. SUTTON. J. Chem. Soc. 2957 (1949). (*b*) E. S. WAIGHT and R. L. ERSKINE. *In* Steric effects in conjugated systems. Chap. 7. *Edited by* G. W. Gray. Butterworths, London. 1958. p. 73.
27. E. E. ROYALS. Advanced organic chemistry. Prentice-Hall Inc., Englewood Cliffs, N.J. 1956. p. 737.
28. W. G. SCHNEIDER and L. W. REEVES. Ann. N.Y. Acad. Sci. **70**, 858 (1958).
29. R. BRAMLEY, B. N. FIGGIS, and R. J. NYHOLM. Trans. Faraday Soc. **58**, 1893 (1962).
30. P. C. LAUTERBUR and R. B. KING. Unpublished observations.
31. F. A. COTTON, A. DANTI, J. S. WAUGH, and R. W. FESSENDEN. J. Chem. Phys. **29**, 1427 (1958).
32. W. G. SCHNEIDER. Personal communication. R. A. Friedel and H. L. Retcofsky. Personal communication.

Can. J. Chem. Downloaded from www.nrcresearchpress.com by 210.87.254.5 on 09/05/12
For personal use only.

Can. J. Chem. Downloaded from www.nrcresearchpress.com by 210.87.254.6 on 09/05/12
For personal use only.

THE RADIATION CHEMISTRY OF SQUALENE

JEANNE DANON[1] AND MORTON A. GOLUB
Stanford Research Institute, Menlo Park, California
Received February 10, 1964

ABSTRACT

Squalene was irradiated with Co^{60} γ-rays at room temperature and with 1-MeV electrons at $-30°$ C. The main radiation-induced effects, and their *G*-values for the room temperature irradiations, were loss of unsaturation (4.6), crosslinking (1.35), *trans* → *cis* isomerization (0.83), and evolution of hydrogen (0.58). The *G*-values for the first three processes in the low temperature runs were 3.8, 0.82, and 0.83, respectively. The large drop in unsaturation is attributed in part to the formation of crosslinks involving double bonds, but principally to cyclization. The loss of double bonds occurs only in the immediate vicinity of the crosslinks and not at random throughout the irradiated squalene. This result has important implications for the radiolysis of diene polymers. Squalene in 10% benzene solution isomerizes with a much higher yield (apparent *G*-value of 2.6 *trans* double bonds converted initially per 100 eV absorbed by *both* solute and solvent) than that of the pure olefin, indicating very efficient energy transfer from excited benzene molecules to the squalene double bonds. The isomerization in the solution case was accompanied by a loss of double bonds in squalene (*G*-value of 0.98) due to phenylation as well as to the other indicated saturation reactions.

INTRODUCTION

Although there has been considerable interest in recent years in the radiation chemistry of polyisoprene (the pertinent literature will be summarized in reference 1), resulting, in fact, in much controversy regarding the loss of unsaturation in this polymer, very little work has been carried out on the irradiation of low or medium molecular weight prototypes of polyisoprene. This is somewhat surprising in view of the success achieved with appropriate model compounds in understanding the mechanisms of such reactions as vulcanization, crosslinking, and oxidation of natural rubber (2). Thus, while it might be difficult or impossible to characterize adequately the microstructural changes produced in the irradiation of a high polymer, because of intrinsic experimental difficulties with the polymer, the task of resolving some still unsettled questions might be greatly aided by a corresponding study of a small molecule model. From this point of view, we were interested in following up our work on the radiation-induced effects in polyisoprene (1) with a detailed examination of squalene. This compound, which is a hexaisoprene in which the internal double bonds are all of the *trans* configuration, constitutes a medium molecular weight counterpart of balata, but it can presumably serve also as a model for *cis* polyisoprene.

Apparently only two papers have been published to date in which the effects of ionizing radiation on squalene were mentioned. Turner (3), in one of them, has noted that squalene when irradiated *in vacuo* to a dose of 242 Mrad experienced about a 10% loss of double bonds, while Dale (4), in the other paper, reported lack of success in crosslinking squalene with radiation. In the present work, we have focussed attention on the principal radiation-induced reactions common to both squalene and polyisoprene, viz., hydrogen evolution, crosslinking, loss of unsaturation, and *trans* → *cis* isomerization. The aim has thus been to throw additional light on the overall radiation effects in polyisoprene and also to add, if possible, to our knowledge of radiation chemistry generally.

Further interest in a study of the irradiation of squalene derives from the fact that,

[1]*NATO Fellow, 1962–63, from Laboratoire de Chimie Physique, Faculté des Sciences, Orsay (S. et O.), France.*

like polyisoprene, it can be readily cyclized by a conventional carbonium ion mechanism (5, 6). Thus, to the extent that some radiation-induced reactions, such as polymerization of isobutylene (7) and various other monomers, have been found to proceed through an ionic mechanism which may well involve carbonium ions (8), the possibility existed that an ionic cyclization could be induced in squalene on exposure to ionizing radiation. Such a reaction, if realized, would serve as still another example in the increasing evidence for ion–molecule processes in the radiation chemistry of hydrocarbons in the condensed phase.

EXPERIMENTAL

The squalene (Eastman Kodak Co.) was chromatographed through a silica gel column and vacuum distilled prior to use. Portions of the pure squalene were sealed in ampoules *in vacuo* after three or four freeze-thaw outgassing cycles, and irradiated for various periods of time at room temperature using a 1500-curie Co^{60} γ-ray source, and at $-30°$ C using 1-MeV electrons from a G. E. resonant transformer. These samples were exposed to radiation intensities of about 0.3 and 200 Mrad/h, respectively. In addition, benzene solutions of squalene were γ-irradiated in ampoules or special n.m.r. tubes either in air or *in vacuo*.

The gases evolved in certain γ-irradiation runs were measured by compressing the volatile products into a known volume with a Toepler pump and then reading the pressure. They were subsequently analyzed with a mass spectrometer.

For purposes of characterization, some of the γ-irradiated squalenes were vacuum distilled, yielding a fraction which came over almost entirely at 180° C at a pressure of 10^{-5} mm Hg (fraction 1), and a residue which remained in the molecular still (fraction 2). Since the initial squalene gave no such residue on vacuum distillation, fraction 2 evidently comprised all of the crosslinked products present in the irradiated squalene. The relative amounts and molecular weights of fractions 1 and 2 as well as the viscosity of fraction 1 obtained from each irradiated sample were determined. Owing to the small amount of material used in the electron irradiations, it was not practical to carry out either vacuum distillation or viscosity measurements on the products in these runs, but their molecular weights were measured.

The number-average molecular weights of irradiated and unirradiated squalene samples were measured in benzene by means of a Mechrolab vapor pressure osmometer. The accuracy of this instrument in the molecular weight range considered here is claimed to be ±2–3%. However, variations in excess of this amount were found for the initial squalene (measured mol. wt.: 410 ± 38) which were believed to arise from systematic errors involved in the operation of the instrument. To minimize such errors for the irradiated samples, the molecular weight of the unirradiated material (M_0) was generally determined each time the molecular weight of an irradiated squalene (M) was measured. The ratio M_0/M was then essentially free from abnormal variations and could be employed reliably for calculating the degree of crosslinking in the irradiated squalene. The absolute viscosities of the γ-irradiated samples were measured by comparing their flow times in a Cannon–Fenske viscometer at 30° C to that of pure benzene.

To analyze the reaction products for microstructural changes, both infrared and n.m.r. spectra were obtained for irradiated and unirradiated samples of pure squalene as well as for the squalene recovered from some of the benzene solution irradiations. For added convenience, n.m.r. spectra were also run directly on the irradiated n.m.r. tubes containing benzene solutions of squalene.

The infrared spectra of the irradiated squalenes and the various fractions 1 were determined in duplicate in an optical cell of suitable path length, using a Perkin–Elmer Model 221 spectrophotometer. The reliability of the infrared results was verified by comparing the optical density of the 12 μ band (due to the C—H out-of-plane deformation of the *cis* and *trans* —$C(CH_3)$=CH— units) obtained in the given cell with that obtained in another cell of different path length: for each squalene sample examined, the ratio of optical density to path length in one cell was practically the same as in the other. The infrared spectra were examined for changes in the 12 μ band as well as changes in the 6 μ band (C=C stretching vibration of the double bonds) and the 8.7 μ band (C—CH_3 vibration of the *trans* —$C(CH_3)$=CH— unit). Since the fractions 2 were too viscous to be run in the cell, they were placed between salt plates and measurements made of the change in optical density of the 12 μ band relative to that of the 7.25 μ band (due to CH_3 groups) as an internal standard. These measurements were found to be quite satisfactory for the purposes intended, although less precise than the absolute measurements made in the cell. The infrared spectra of the irradiated squalenes, except for evidence of reduction of unsaturation, were only slightly different from that of the initial material. Consequently, there was no need to present them here (9).

The n.m.r. spectra were obtained at room temperature with a Varian HR-60 spectrometer operated at both normal and slow magnetic field sweep rates. The irradiated and unirradiated samples of pure squalene were run as 50% solutions by weight in benzene using tetramethylsilane as internal standard. The spectra obtained for an irradiated sample, before and after fractionation, are shown in Figs. 1 and 2. As can be seen, fraction 2 gives a more poorly resolved spectrum than either the prefractionated sample or fraction 1, a situation which must be related to the higher viscosity of fraction 2. In the case of benzene solutions of squalene (~10% concentration), the n.m.r. spectra were run directly on the irradiated solutions without

Can. J. Chem. Downloaded from www.nrcresearchpress.com by 210.87.254.6 on 09/05/12
For personal use only.

Can. J. Chem. Downloaded from www.nrcresearchpress.com by 210.87.254.6 on 09/05/12
For personal use only.

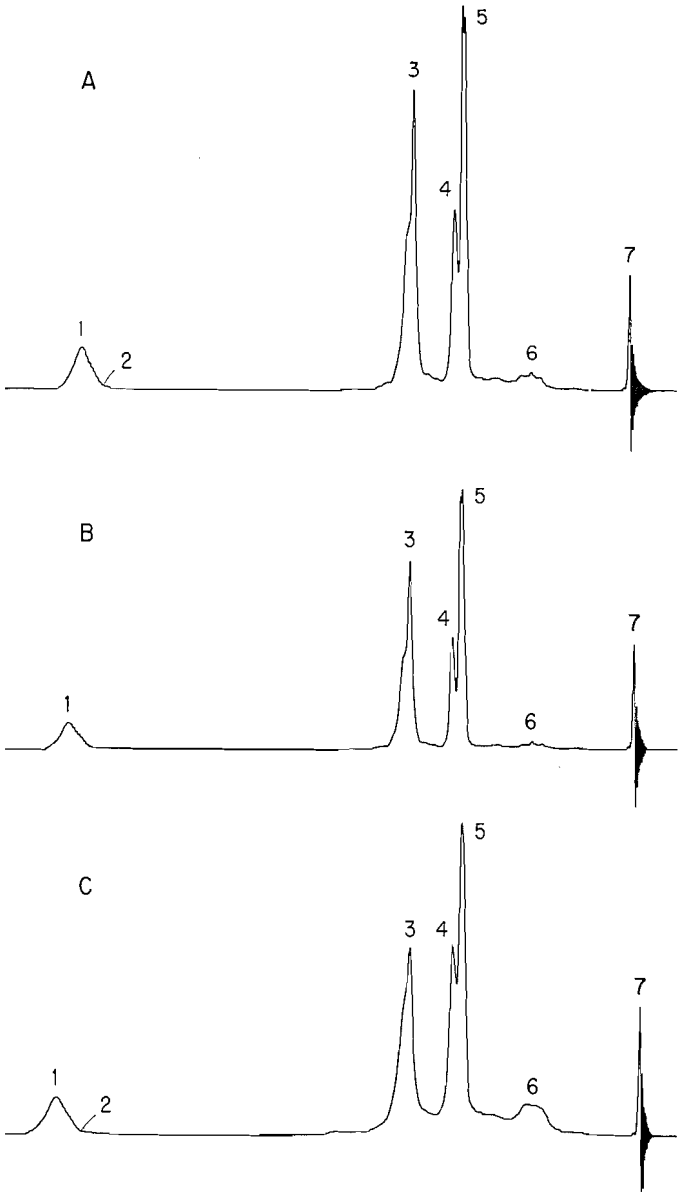

FIG. 1. N.m.r. spectra obtained at normal magnetic field sweep rate of pure squalene γ-irradiated to a dose of 195.5 Mrad: A, before fractionation; B, fraction 1; C, fraction 2. Peak 1, —CH═, 4.85 τ; peak 2, —C(═CH_2)— (?), 5.1 τ; peak 3, —CH_2—C═, 7.95 τ; peak 4, *cis* —C(CH_3)═, 8.34 τ; peak 5, *trans* —C(CH_3)═, 8.43 τ; peak 6, CH_3—C—, 9.0–9.2 τ; peak 7, tetramethylsilane, 10.0 τ.

using tetramethylsilane; since these spectra were very similar to those of Figs. 1 and 2, there was no need to present them here. The normal magnetic sweep spectra (~2 c.p.s./s) were used for the quantitative determination of the olefinic proton content—both planimetrically and by electronic integration—as well as for the qualitative examination for over-all microstructural changes in squalene. The slow sweep spectra (~0.5 c.p.s./s) were employed to give the best possible resolution of the *cis* and *trans* methyl proton

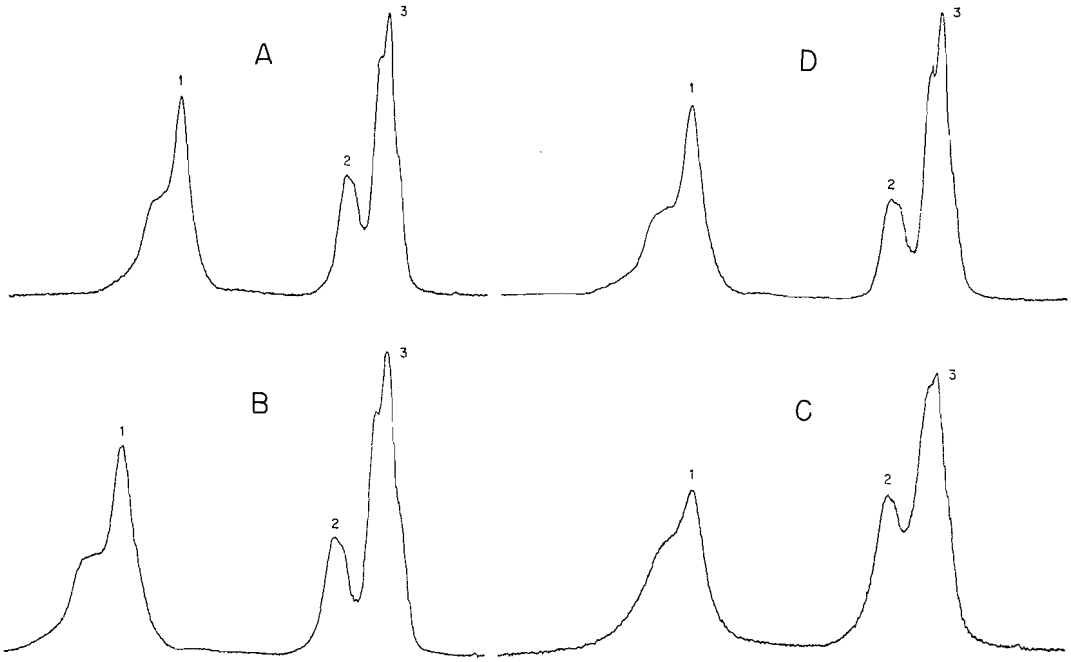

FIG. 2. N.m.r. spectra obtained at slow magnetic field sweep rate of pure squalene γ-irradiated to a dose of 195.5 Mrad: A, same sample as in Fig. 1, before fractionation; B, corresponding fraction 1; C, fraction 2. For comparison, D represents the spectrum of the unirradiated squalene. Peak 1, $-CH_2-\overset{|}{C}=$; peak 2, *cis* $-C(CH_3)=$; peak 3, *trans* $-C(CH_3)=$.

resonance peaks at 8.34 and 8.43 τ (10),[2] following the technique described by Chen (11) for polyisoprenes. The slow sweep spectra were thus used in conjunction with the normal sweep spectra to determine the extent of *trans* → *cis* isomerization of the internal double bonds in irradiated squalene. Two samples of distilled squalene were employed, A and B, which had 94.1 and 97.0% of the theoretical unsaturation, respectively (i.e., 11.25 and 11.65% olefinic proton content compared to the theoretical 12%). Corresponding to the indicated deficiency of double bonds in these samples, the n.m.r. spectra showed some "saturated" methyl protons at around 9.0–9.2 τ. Also, the internal double bonds in A and B were not completely *trans* initially; in fact, sample A, which was used the most, has 1.6% *cis* content.[3]

RESULTS

Gas Evolution

For doses up to 300 Mrad, the evolution of hydrogen, methane, and low molecular weight hydrocarbons in the γ-irradiation of pure squalene at room temperature was linear with dose. The 100 eV yields of these products were found to be $G(H_2) = 0.58$, $G(CH_4) = 0.015$, and G(lower hydrocarbons) = 0.015. These yields are substantiated by the work of Pestaner (12), who obtained $G(H_2) = 0.58$ and $G(CH_4) = 0.02$ for squalene irradiated to a dose of 0.5 Mrad. It is interesting to note that the ratio of hydrogen to methane from squalene (from 29 to 38) is roughly comparable to that from squalane [$G(H_2)/G(CH_4) = 3.4/0.12$ or $\sim$28] (13), which is fully saturated squalene. Moreover, the hydrogen yield

[2]*From an n.m.r. standpoint, two of the methyls on the terminal double bonds are cis and two are trans, the remaining four internal methyls being trans. This accounts for the fact that the initial squalene shows both cis-CH_3 and trans-CH_3 peaks in the ratio of about 25:75.*

[3]*The cis content was calculated from the cis-CH_3 proton values, taking into account the loss of unsaturation which is assumed to be statistically distributed over all six double bonds in squalene.*

Can. J. Chem. Downloaded from www.nrcresearchpress.com by 210.87.254.6 on 09/05/12
For personal use only.

from squalene is somewhat higher than the average value obtained recently in the γ-irradiation of several high molecular weight polyisoprenes [$G(H_2) = 0.48$][4] (14).

Crosslinking

Representative data on the molecular weight and viscosity changes produced in squalene on irradiation *in vacuo* with γ-rays at room temperature and with 1-MeV electrons at $-30°$ C are presented in Table I. From the slopes of the linear plots of M_0/M versus

TABLE I

Radiation-induced crosslinking in pure squalene

Irradiated material before fractionation				Fraction 1			Fraction 2		
Dose, Mrad	M	M_0/M	η, cP	Wt. fraction $1-x$	M_1	η, cP	Wt. fraction x	M_2 Measd.	M_2 Calc.*
				γ-Rays at room temperature					
49.7	398	0.972†	12.5	0.970	413	11.7	0.030		935
52.2	429	0.946‡	13.3						
102.5	416	0.930†	14.9	0.878	412	11.3	0.122	1101	976
150.5	491	0.912§	15.9	0.851	495	11.6	0.149		1000
195	462	0.864‖	19.7	0.788	419	11.4	0.212	998	1140
197	463	0.886‡	17.5						
275	490	0.837‡	23.2	0.733	476		0.267	1594	1050
				Electrons at -30 °C					
53	407	0.976‖							
94	413	0.963‖							
105	410	0.970‖							
171	425	0.936‖							
184	425	0.936‖							
195	419	0.949‖							

*Calculated from equation [2*b*] in the text, through M_0/M_2, and assuming $M_0 = 410$.
†Unirradiated squalene, before fractionation: $M_0 = 387$; $\eta_0 = 11.3$; corresponding fraction 1: $M_1 = 448$; $\eta_1 = 11.1$.
‡$M_0 = 410$.
§$M_0 = 448$.
‖$M_0 = 398$.

dose for the prefractionated irradiated samples, shown in Fig. 3, the G-values for crosslinking were calculated, using the relation (15)

$$[1] \qquad 1/M_0 - 1/M = kD$$

where M_0 and M are the molecular weights before and after irradiation to dose D, and k is the number of crosslinks/g-unit dose. The use of this relation implies that the scissions which could occur in the irradiated squalene have been neglected. According to the findings on polyisoprene where the scission/crosslink ratio is very low (16) crosslinking can indeed be considered to have the greater effect by far on the molecular weight of squalene. $G(X)$ was thus found to be 1.35 and 0.82 for the room temperature and low temperature irradiations, respectively. These values are to be compared with the most probable $G(X)$ value for polyisoprene, viz, 0.9 (17). The fact that $G(X)$ for liquid squalene (room temperature runs) is higher than that for solid squalene (low temperature runs) or for polyisoprene is probably due to the greater mobility of the molecules in the liquid squalene case which is conducive to a higher frequency of crosslinking. As also shown in Fig. 3, the viscosity η of the prefractionated γ-irradiated squalenes is linear with dose up

[4]*This value is supported by Pestaner's work (12) and, moreover, satisfies, better than the value of 0.64 reported earlier by Turner (3), an empirical linear relation which appears to hold between $G(H_2)$ of different isoprenic compounds,* H—(CH_2—$C(CH_3)$=CH—CH_2)$_n$—H, *and the reciprocal of the number n of isoprenic units in these compounds.*

Can. J. Chem. Downloaded from www.nrcresearchpress.com by 210.87.254.6 on 09/05/12
For personal use only.

to ~150–200 Mrad, but becomes more than linear at higher doses. This situation is similar to that found with polymeric systems (15).

The data of Table I indicate that neither the molecular weight nor the viscosity of the various fractions 1 obtained from γ-irradiated squalene or from the unirradiated squalene is significantly different from the corresponding value for the unirradiated compound prior to fractionation. The variations in M_1 and η, although relatively large, are still within limits of experimental error. It would appear, therefore, that each fraction 1 must represent essentially unchanged squalene. This indication will be considered again in connection with infrared and n.m.r. data presented below.

The weight fraction of the crosslinked products (fraction 2 in each γ-irradiation run) when plotted against the dose gave a straight line. From the slope of this line, the G-value for production of crosslinked products was calculated to be 2.45 molecules of crosslinked squalene/100 eV absorbed. In view of the fact that $G(X) = 1.35$ for these runs, it would appear that on the average there is one crosslink per 1.81 squalene molecules. Evidently, the crosslinked products must have a complex structure consisting of dimers, trimers, and possibly even tetramers.[5]

An alternative approach to the structure of the crosslinked product involves a consideration of the molecular weights of the various fractions 2. Since the molecular weight determination of this series was unsatisfactory, it was necessary to get around this difficulty, as follows: For each irradiated sample, the relation

$$[2a] \qquad 1/M = (1 - x)/M_1 + x/M_2$$

is found to hold between the number average molecular weights of the irradiated squalenes before fractionation (M) and those of the corresponding fractions 1 and 2 (M_1 and M_2, respectively), where $(1 - x)$ and x represent the relative amounts of these fractions. Because of the difficulties encountered in measuring the molecular weights, as indicated earlier, it is desirable to use expression ($2a$) in the form

$$[2b] \qquad M_0/M = (1 - x)M_0/M_1 + xM_0/M_2.$$

Substituting the experimental values for M_0/M and x in equation ($2b$) and assuming $M_0/M_1 = 1$, we can calculate values for M_0/M_2, and hence M_2. The calculated values for M_2, given in the last column of Table I, compare satisfactorily with the experimental values in at least two cases and agree qualitatively with the previous observation that there was one crosslink/1.8 squalene molecules in the crosslinked products.[5] A slight upward trend in molecular weights with dose may be seen which, notwithstanding the absence of a corresponding upward curvature in the plot of the weight fractions of the crosslinked products versus dose, might indicate that the latter can undergo slow additional crosslinking on further irradiation. The effect of this additional crosslinking on the molecular weights of the crosslinked products can be eliminated by extrapolation to zero dose. An extrapolated molecular weight of 920 was found indicating that the complex structure of the crosslinked products is not entirely due to additional crosslinking.

Decrease in Original Unsaturation

By means of infrared and n.m.r. analysis of the irradiated unfractionated samples of pure squalene, we have observed a significant drop in the original unsaturation

[5]*This is based on the view that the crosslinked products (molecular weights in the range 935 to 1140, having one crosslink/1.8 squalene molecules) presumably are made up of dimers (mol. wt., 820; one crosslink/2.0 squalene molecules), trimers (mol. wt., 1230; one crosslink/1.5 squalene molecules), and possibly tetramers (mol. wt., 1640; one crosslink/1.33 squalene molecules).*

Can. J. Chem. Downloaded from www.nrcresearchpress.com by 210.87.254.6 on 09/05/12
For personal use only.

(—C(CH_3)=CH—, indicated by the 12, 6, and 8.7 μ bands and the 4.85 τ peak in the respective spectra) and production of some vinylene units (—CH=CH—, indicated by a very weak band at around 10.3 μ) and some vinylidene units (—C(=CH_2)—, indicated by a band at 11.3 μ and possibly also by a very minor peak at around 5.1 τ). Since the vinylene and vinylidene double bonds are of slight or negligible importance, as in polyisoprene (1), we will confine our attention here to the consumption of the original double bonds in pure squalene, as followed by changes in the 12, 6, and 8.7 μ infrared bands and the 4.85 τ n.m.r. peak.

Representative data for the decrease in the 12 μ band in pure squalene irradiated with γ-rays and electrons *in vacuo* are given in Table II. When these results for the irradiated

TABLE II

Radiation induced decrease of unsaturation in pure squalene based on infrared

Dose, Mrad	Irradiated material* before fractionation O.D.$_{12\,\mu}$	Fraction 1		Fraction 2	
		Wt. fraction $1-x$	O.D.$_{12\,\mu}$	Wt. fraction x	O.D.$_{12\,\mu}$/O.D.$_{7.25\,\mu}$
		γ-Rays at room temperature			
0	0.651		0.658		
49.7	0.642	0.970	0.652	0.030	0.325
102.5	0.630	0.878	0.657	0.122	0.370
150.5	0.628	0.851	0.655	0.149	0.316
195.5	0.617	0.788	0.654	0.212	0.433
275.0					0.36
			Av. 0.655 ± 0.003		Av. 0.37† ± 0.06
		Electrons at −30° C			
59	0.649				
94	0.633				
115	0.639				
184	0.630				

*Squalene sample A.
†Corresponding value for unirradiated sample is 0.47. The average loss of double bonds is then (1 − 0.37/0.47)100 = 21%, while the loss of unsaturation, based on the additivity, would be about 30%.

squalene before fractionation were plotted against dose, straight lines with negative slopes were obtained indicating that an important radiation-induced reaction in squalene is a zero-order consumption of double bonds. Straight lines with comparable slopes were obtained for the 8.7 and 6 μ bands. This last result as well as the fact that only very slight changes are observed in the range of wavelengths examined by Cunneen and co-workers (18) for squalene isomerized with sulphur dioxide suggests that if *trans* → *cis* isomerization occurs here, it is not very important. In fact, as we shall soon see, n.m.r. spectra indicated unambiguously that such a reaction does take place but only to a very small extent (1.4% increase in *cis* content after a dose of 200 Mrad). Under these conditions, it was justifiable to take an average value of the rate of decrease of the 12, 6, and 8.7 μ bands for the purpose of obtaining G-values for the loss of double bonds, G(-d.b.). Accordingly, the average decrease in unsaturation after a dose of 200 Mrad was found from infrared to be 7.0 and 5.5% for the room temperature and low-temperature irradiations, respectively; these data correspond to G(-d.b.) values of 4.6 and 3.7. Comparable G-values for the radiation-induced decrease in unsaturation in pure squalene can be obtained from the n.m.r. data given in Table III. Thus, from the slopes of the straight

Can. J. Chem. Downloaded from www.nrcresearchpress.com by 210.87.254.6 on 09/05/12
For personal use only.

Can. J. Chem. Downloaded from www.nrcresearchpress.com by 210.87.254.6 on 09/05/12
For personal use only.

TABLE III

Radiation induced changes in squalene based on n.m.r.

Sample	Irradiated material before fractionation				Fraction 1				Fraction 2			
	Dose, Mrad	% unsatn.*	% *cis*-CH_3	% *cis*†	Wt. fraction $1-x$	% unsatn.*	% *cis*-CH_3	% *cis*†	Wt. fraction x	% unsatn.*	% *cis*-CH_3	% *cis*†
					γ-Rays at room temperature							
Squalene A	0	94.1	25.8	1.6								
	49.7	91.9	26.1	2.2		93.8	25.3					
	102.5	89.5	27.4	4.7								
	150.5	88.7	28.3	6.6								
	195.5	87.5	29.4	8.9	0.788	93.8	26.5	3.0	0.212	78.8‡	32.6	15.1
Squalene B	0	97.0										
	52.2	96.4										
	73.8	93.7										
	106.0	92.2										
	197.0	91.2										
	275.0	88.3	31.5	12.9	0.733	97.0	27.2	4.4	0.267	86.7§	33.6	17.0
10% squalene in C_6H_6	29.0	92.0	30.0	9.8								
	65.3	89.0	34.3	18.5								
	100.3	87.5	36.8	23.6								
	153.3	82.5	40.0	30.0								
	210.6	79.5	42.6	35.0								
					Electrons at −30 °C							
Squalene A	50	92.7	26.1	2.2								
	94	91.2	26.5	3.0								
	115	90.9	26.8	3.6								
	184	89.7	27.8	5.6								

*Calculated from the olefinic proton content which, for a sample having 100% theoretical unsaturation, is 12%.
†Calculated from % *cis*-CH_3.
‡Based on additivity, unsaturation is 63.5.
§Based on additivity, unsaturation is 64.9.

line plots of n.m.r. unsaturation versus dose, G(-d.b.) for the irradiated squalene before fractionation was found to be 4.6 for the room temperature irradiations and 3.9 for the low temperature runs. Although the two samples of irradiated squalene, A and B, had different initial unsaturations, they gave linear unsaturation-dose plots with identical slopes, so that the zero-order reduction in unsaturation in these two samples proceeded at the same rate. The average G(-d.b.) value, from both infrared and n.m.r. data, can then be taken to be 4.6 and 3.8 for the room-temperature and low-temperature irradiations, respectively, indicating a small temperature effect. This corresponds to an activation energy of 0.53 kcal/mole.

It should be noted that the loss of original double bonds reported here for squalene irradiated at room temperature (7% at 200 Mrad) agrees qualitatively with that observed by Turner (~10% at 242 Mrad) (3). Moreover, our corresponding G(-d.b.) for squalene, 4.6, is of the same order of magnitude as that obtained recently for polyisoprene, 5.3 (1).

By comparing the infrared and n.m.r. data for the various fractions 1 with the corresponding data for the starting material (see Tables II and III), and taking into account the molecular weight and viscosity measurements discussed above (see Table I), it is evident that fraction 1 in each run is practically unchanged squalene, except for some *trans–cis* isomerization.

It follows from this last result that the radiation-induced decrease in unsaturation in squalene is localized only in the fractions 2, i.e., in the crosslinked products. At this point, it must be noted that the infrared and n.m.r. data obtained on these fractions were not very consistent with those obtained on the irradiated, prefractionated material and on fractions 1. The desired additivity breaks down,* presumably because of a lack of precision in the infrared analysis of fractions 2 and also because of complications arising in the n.m.r. spectra of samples containing crosslinked products (irradiated, prefractionated squalenes and fractions 2). The major source of difficulty in the n.m.r. case is that the olefinic proton region involves a new peak at around 5.1 τ (perhaps due to vinylidene units, —C(=CH_2)—, but possibly due instead to some other new structure) which broadens the regular 4.85 τ peak (due to —CH= protons), making the integration of these proton areas unreliable. This complication undoubtedly exists to some extent in the case of the irradiated, unfractionated samples, but is probably minor since the infrared and n.m.r. data are in reasonable agreement. This complication is quite serious, however, in the case of the crosslinked fractions 2 in which the production of vinylidene and other perturbing structures appears to be concentrated. At any rate, since the decrease in unsaturation is observed only in the crosslinked products, a simple consideration of the G-values for decrease in unsaturation (4.6) and crosslinking (1.35) in the room temperature irradiation of squalene enables us to find that some 3.4 double bonds are lost per crosslink. This result is difficult to understand on the basis of any known mechanism of crosslinking, and we are led therefore to suggest that some cyclization occurs along with crosslinking.

It may be noted that squalene in a 10% solution in benzene shows a somewhat more rapid linear decrease in unsaturation with dose than in the pure state (Table III), with a G(-d.b.) value of 0.98 double bonds consumed per 100 eV absorbed by both solute and solvent. This is equivalent to 9.8 double bonds/100 eV absorbed directly by the solute, calculated as though there is no energy transfer between excited benzene and squalene molecules. The loss of double bonds in the solution case is no doubt due in part to phenylation as well as to the same processes giving rise to decreased unsaturation in the pure

**See footnotes in Tables II and III for an idea on the discrepancies observed.*

Can. J. Chem. Downloaded from www.nrcresearchpress.com by 210.87.254.6 on 09/05/12
For personal use only.

squalene. Consequently, it is impossible to determine the extent to which the latter processes may have been enhanced in the solution case by benzene sensitization.

Isomerization

Nuclear magnetic resonance data on the radiation-induced *trans–cis* isomerization of squalene in the pure state and in benzene solution are assembled in Table III, and the essential results plotted in Fig. 4. It is immediately obvious that benzene has a profound effect on accelerating the squalene isomerization which approaches an equilibrium in which the *cis* content of the internal double bonds is around 45–50%. Unfortunately, there is no all-*cis* squalene available for studying the approach to equilibrium from the *cis* side. However, extensive γ-irradiation of high molecular weight *cis* or *trans* polyisoprene in benzene resulted in a common structure having a *cis* content ($\sim$50%) (1) which is similar to the above equilibrium value for squalene. Evidently, a parallelism exists between squalene and its high molecular weight counterpart, balata, insofar as radiation-induced isomerization in benzene is concerned. Since the isomerization of pure squalene, like that of solid polyisoprene (1), proceeds very slowly, it was not practicable to examine the equilibrium *cis/trans* ratio in that case; however, it is probably not significantly different from that in the squalene solution case.

In determining the percentage *cis*-1,4 content in the irradiated pure squalene by means of n.m.r. spectra, we encountered the same difficulty as with the unsaturation data, i.e., there is a lack of additivity of the measured *cis* contents of fractions 1 and 2 and prefractionated material. This problem arises in part because, as mentioned above, fractions 2 give spectra which are poorly resolved in the *cis* and *trans* methyl proton region. Much more serious, however, is the fact that the loss of unsaturation in the crosslinked fraction 2 and in the irradiated, prefractionated squalene, involving the reaction

[3] $$-CH_2-C(CH_3)=CH-CH_2- \longrightarrow -CH_2-\underset{|}{C}(CH_3)-\underset{|}{CH}-CH_2-$$

gives rise to "saturated" methylene groups which appear at higher field than the corresponding "unsaturated" methylene groups. The protons of the former groups, along with new tertiary protons, show up fortuitously in the same range of τ values as the "unsaturated" *cis* and *trans* methyl protons, thus perturbing the n.m.r. spectrum in the range of interest, viz., 8.0–9.2 τ (see Figs. 1 and 2). Although mechanistically, there is no reason for the rate of isomerization to differ in one fraction from that in another, the perturbation is such that the *cis* methyl peak, and hence *cis*-1,4 content, is apparently larger in the irradiated, prefractionated squalenes and in the fractions 2 than it is in the fractions 1. The latter, by virtue of not being crosslinked or showing any loss of unsaturation, give n.m.r. spectra which are free of perturbations from saturated methylene or tertiary protons and consequently indicate the actual *trans–cis* isomerization. The *cis* content – dose curves for the irradiated, prefractionated squalenes are curved upwards, as shown in Fig. 4, inasmuch as the perturbation is greater the higher the radiation dose and therefore the more crosslinked the squalene. Moreover, the curve for the room temperature γ-irradiation lies towards higher values of *cis* content than the low-temperature curve, due to the higher yield of crosslinks and hence greater perturbation difficulty in the former case. These curves are seen to originate at the same point on the ordinate, corresponding to the initial *cis* content, and their common tangent P passes through the points of fractions 1. It follows that the tangent line P defines the actual *trans–cis* isomerization of pure squalene and that this process depends neither on the physical state

Can. J. Chem. Downloaded from www.nrcresearchpress.com by 210.87.254.6 on 09/05/12
For personal use only.

Can. J. Chem. Downloaded from www.nrcresearchpress.com by 210.87.254.6 on 09/05/12
For personal use only.

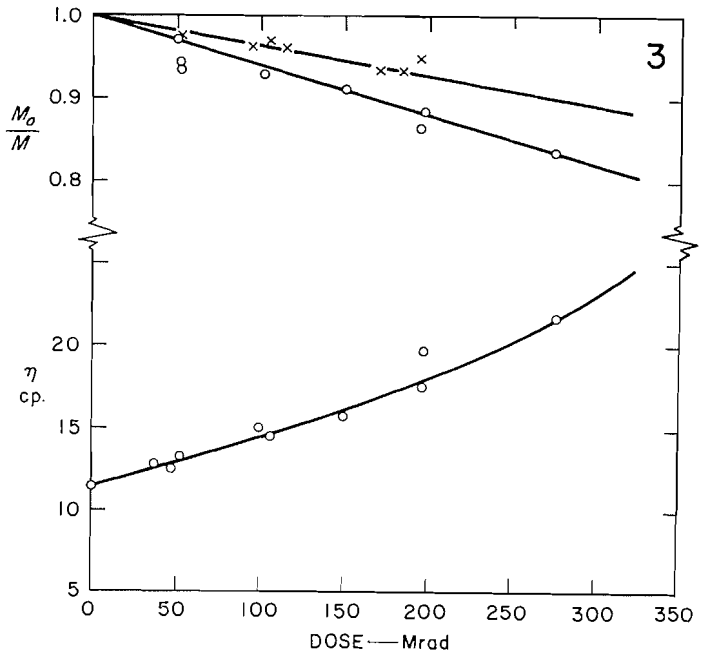

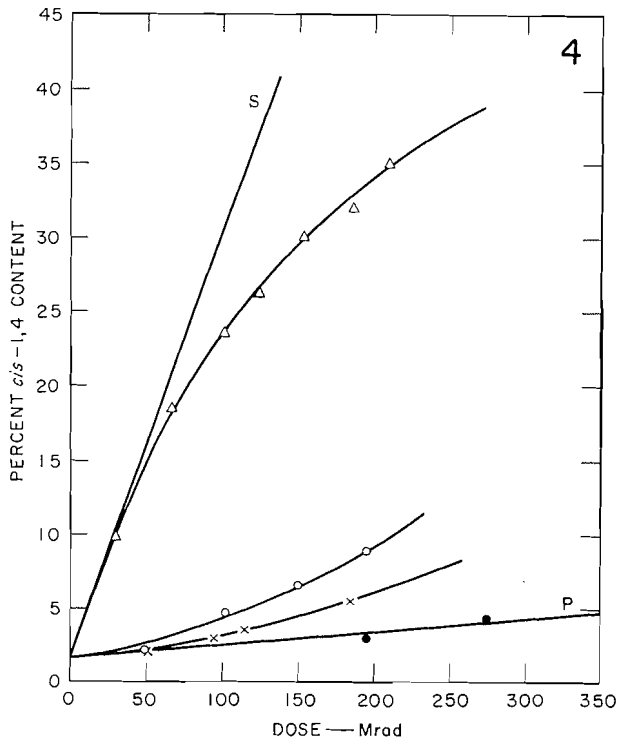

FIG. 3. The effect of dose on the molecular weight and viscosity of prefractionated γ-irradiated (○) and electron-irradiated (×) squalene.

FIG. 4. Radiation-induced *trans–cis* isomerization of squalene: pure squalene irradiated with γ-rays at room temperature (○) and with electrons at −30° C (×) but unfractionated; data on corresponding fraction 1, ●; squalene in benzene irradiated with γ-rays, △.

of squalene (liquid or solid) nor on the temperature. This latter aspect is in keeping with the observed temperature independence of the polybutadiene isomerization (19).

The upward curvature found in the plots for the pure squalene runs is clearly absent in the plot for the squalene solution runs. Here the perturbation effect is perhaps not any smaller than in the pure state but it is certainly obscured by the marked tendency for the plot to curve downward due to the relatively rapid approach towards equilibrium. The tangent line S can be considered to define *only* the upper limit of the initial rate of isomerization of squalene in a 10% benzene solution. The true value for this solution isomerization could thus be much lower than this, although still significantly higher than that in the pure liquid.

It is worth mentioning that, in contrast to the situation with the irradiated pure squalene, the infrared spectra of several samples of squalene recovered from solution irradiations provided qualitative confirmation of partial *trans–cis* isomerization. The infrared changes observed, which were subtle and unsuitable for quantitative purposes, were of the same form but not as extensive as those published for sulphur-dioxide-isomerized squalene (18).

As shown in Table III, the *cis* content in fraction 1 after a dose of 200 Mrad, for example, has increased from 1.6 to 3.0% of the internal double bonds in squalene, whereas in the solution case the *cis* content went from 1.6 to 23.6% for only one-half this dose. From the slopes of the lines S and P, the *G*-values for the *trans–cis* isomerization of squalene in benzene solution and in the pure liquid state were found to be $G_s(t\rightarrow c) \leq 2.6$ and $G_p(t\rightarrow c) = 0.83$, respectively. These energy yields represent the number of *trans* internal double bonds isomerized (initially) to *cis* configuration per 100 eV absorbed by both squalene and solvent, in the solution case, and by squalene alone, in the pure state. By way of comparison, it should be noted that the *G*-values for the *trans–cis* isomerization of balata in a 1% solution in benzene and in the pure solid state were found to be 0.97 and ~10, respectively (1). Evidently, there is a marked difference in ease of isomerization of squalene and balata in the pure state, although their solution isomerizations proceed at rates which have the same order of magnitude. Thus, the effective energy yields, $G_s'(t\rightarrow c)$, for squalene and balata in solution would be around 26 and 97, respectively, when calculated in terms of the energy absorbed directly by the solute, as though there were no energy transfer between solvent and solute.

DISCUSSION

Loss of Unsaturation and Crosslinking

As seen from the results presented above and summarized in Table IV, pure squalene and polyisoprene show considerable similarity in their response to ionizing radiation, quantitatively as well as qualitatively. Thus, for example, the most prominent microstructural change common to both materials is a fairly large consumption of double bonds, with *G*(-d.b.) values of 4.6 and 5.3 for the room temperature irradiations of squalene and polyisoprene, respectively. A somewhat lower *G*-value (3.8) was obtained for squalene in the case of irradiation at −30° C. These various values compare favorably with those calculated for the same compounds from the data of Turner (3) and Hayden (20).

Significantly, it was found in the present study that the loss of unsaturation occurs only in the immediate vicinity of the crosslinks (i.e., it is confined to the crosslinked fraction 2 and is not found in fraction 1), and does not occur randomly throughout the irradiated squalene, in contrast to *trans–cis* isomerization. This interesting result, derived from the

Can. J. Chem. Downloaded from www.nrcresearchpress.com by 210.87.254.6 on 09/05/12
For personal use only.

TABLE IV

G-Values for various structural changes in irradiated isoprenic compounds

Sample	Irradiation temperature	G(-d.b.)	G(X)	$G(H_2)$	$G_p(t \rightarrow c)$	$G_s(t \rightarrow c)$
Squalene	Room	4.6; 5.2*	1.35	0.58	0.83†	$\leqslant 2.9$
	−30° C	3.8	0.82			
cis-Polyisoprene	Room	5.3;‡ 3.2§	0.9‖	0.64;¶ 0.48;** 0.49††	~10‡‡	0.97‡‡

*Calculated from the work of Turner (3).
†As seen in the results, the isomerization is temperature independent.
‡Ref. 1.
§Calculated from the work of Hayden (20).
‖Ref. 16.
¶Ref. 3.
**Ref. 14.
††Ref. 12.
‡‡Data for *trans* polyisoprene (balata) from Ref. 1.

model compound approach pursued here and one which could not have been obtained from a study carried out solely on the high polymer, has important implications for the radiation chemistry of diene polymers. For one thing, it tends to rule out the addition of radiolytically produced hydrogen onto the double bonds of squalene (or polyisoprene) as a significant cause for the loss of unsaturation in the isoprenic compound. Otherwise, this loss would not be limited to the crosslinked products, since there is no reason for the addition of hydrogen to the double bonds to be anything but random. A further argument against this reaction making an important contribution to the loss of unsaturation is that it implies a high transient formation of hydrogen which, on the basis of the mechanisms considered below, would lead to a much higher *G*-value for crosslinking, or production of conjugated diene structures (21), than is actually obtained. It follows, therefore, that hydrogenation of double bonds must play a negligible role in the overall radiation chemistry of squalene or polyisoprene.

In the case of polyisoprene, Turner (3, 16, 17), has shown quite definitely from work with free radical scavengers that both crosslinking and hydrogen evolution involve non-radical as well as radical processes. Thus, he found that free radical scavengers can suppress the C—C crosslinks by about 40% and reduce the hydrogen yield by about 10%. These results afford a rough estimate of the relative contributions of non-radical (NR) and radical (R) processes to crosslinking and hydrogen evolution:

$$G(X)_{NR} = 0.54 \qquad G(H_2)_{NR} = 0.43$$
$$G(X)_{R} = \underline{0.36} \qquad G(H_2)_{R} = \underline{0.05}$$
$$G(X) = 0.90 \qquad G(H_2) = 0.48$$

where we make use of Turner's $G(X)$ value (16, 17) and our own $G(H_2)$ value (14). The non-radical processes, which evidently make a major contribution here, can be represented by the "molecular" reaction

[4] $$2\,RH \longrightarrow R{-}R + H_2$$

suggested by Turner for the radiolysis of polyisoprene (RH), since $G(X)_{NR} \simeq G(H_2)_{NR}$.

The radical processes, on the other hand, can be represented by either mechanism A or mechanism B, although the former appears to be by far the more important of the two, since $G(X)_R \gg G(H_2)_R$.

Can. J. Chem. Downloaded from www.nrcresearchpress.com by 210.87.254.6 on 09/05/12
For personal use only.

Mechanism A

[5] $RH \rightsquigarrow R\cdot + H\cdot$

[6] $H\cdot + RH \longrightarrow RH_2\cdot$

[7] $RH_2\cdot + R\cdot \longrightarrow R_2H_2$

Mechanism B

[5] $RH \rightsquigarrow R\cdot + H\cdot$

[8] $H\cdot + RH \longrightarrow R\cdot + H_2$

[9] $R\cdot + R\cdot \longrightarrow R{-}R$

Consequently, the addition of a hydrogen atom onto a double bond involved in mechanism A (reaction 6) is found to occur much more readily than the abstraction of an α-methylenic hydrogen atom involved in mechanism B (reaction 8). Although this finding is in line with the general view regarding such reactions (22), it is nevertheless somewhat surprising for polyisoprene considering the high concentration of α-methylenic hydrogen atoms present in this macromolecule.*

Mutual combination is perhaps not the only fate of the allylic radicals ($R\cdot$) and the alkyl radicals ($RH_2\cdot$), and two other possibilities need to be considered, viz., disproportionation and addition of these radicals onto double bonds. In the case of the allylic radicals, if they undergo disproportionation a conjugated diene or triene structure would be formed, but such a reaction was shown to be of minor importance (21). Moreover, the two possibilities were ruled out by Moore and Watson (23) on the premise that in their study of the crosslinking of rubber with di-*tert*-butyl peroxide there was no detectable change in efficiency of crosslinking with variation in temperature. Accordingly, we can say quite definitely that the fate of the allylic radicals, apart from the trivial one of recombination with hydrogen atoms, is combination with an alkyl or another radical to form a crosslink.

In the case of the alkyl radicals, their disproportionation at room temperature cannot be very important since it would lead to new types of unsaturation, such as $-CH{=}CH_2$ units, but these are not formed to any appreciable extent. However, the addition of alkyl radicals to polyisoprene double bonds, resulting in further crosslinking

[10] $RH_2\cdot + RH \longrightarrow R_2H_3\cdot$

or their abstraction of α-methylenic hydrogen atoms present in the rubber molecule

[11] $RH_2\cdot + RH \longrightarrow RH_3 + R\cdot$

is not unlikely. Since the crosslinked products, even at very low doses, consist not only of dimers but of higher molecular weight material as well, it would appear that reaction 10 must occur to a certain extent. In fact, we may be dealing here with an allylic type polymerization in which the chain length is very small owing to a competition between reactions 10 and 11 (propagation and allylic termination, respectively). Such a "degradative chain transfer" is known with olefins containing allylic hydrogens (24). Whether or not reactions 10 and 11 take place, mechanism A involves the consumption of one double bond per crosslink formed, without evolution of hydrogen. From this, it may be deduced that the G-value for loss of double bonds involved in crosslinking is $G(\text{-d.b.})_X = G(X)_R - G(H_2)_R = 0.31$, where formation of hydrogen by

[12] $H + H \longrightarrow H_2$

accounts for the $G(H_2)_R = 0.05$.

*See ref. 3, p. 38.

Can. J. Chem. Downloaded from www.nrcresearchpress.com by 210.87.254.6 on 09/05/12
For personal use only.

It is clear that crosslinking is responsible for only a small part of the consumption of double bonds. The major part, $G(\text{-d.b.})_C = G(\text{-d.b.}) - G(\text{-d.b.})_X$ or $5.3 - 0.31 \simeq 5$, is presumably due to cyclization, since the other obvious source of loss of double bonds, hydrogenation, has already been shown to be unimportant.

Since the radiation chemical data for squalene and polyisoprene are evidently very similar (Table IV), the arguments presented for polyisoprene may be considered to apply directly to the case of squalene, and for this reason it appeared necessary to develop them in some detail.

Cyclization

It is now of interest to examine the possible mechanisms for cyclization which must account for the large drop in unsaturation not related to crosslinking, $G(\text{-d.b.})_C \sim 5$. Conceivably, the cyclization takes place through a radical mechanism involving the intramolecular addition of an alkyl radical onto a double bond

[13] 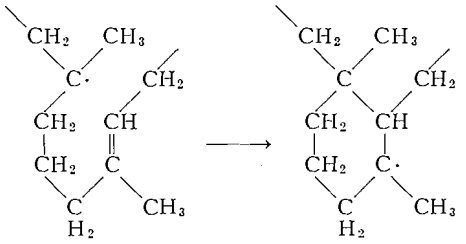

This intramolecular reaction cannot be ignored since the corresponding intermolecular addition of $RH_2\cdot$ radicals onto double bonds (reaction 10) has not been ruled out either. On the other hand, polyisoprene and isoprenoid structures have been known for a long time to undergo facile cyclization by a conventional carbonium ion mechanism

[14] 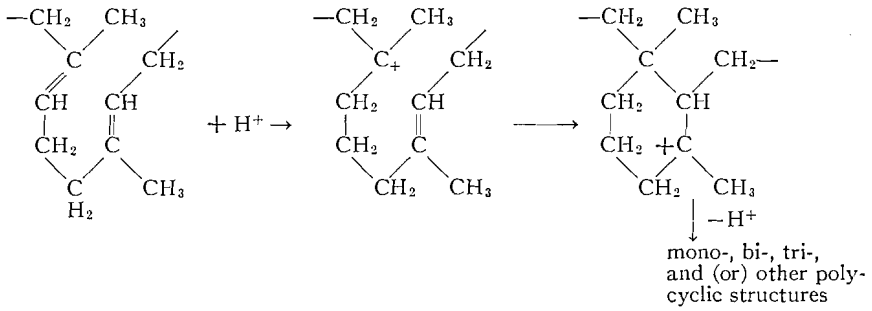

although there has been considerable controversy about whether the product from polyisoprene consists of monocyclic or polycyclic structures (25). Without entering into this controversy, we should note that squalene, when similarly cyclized, gives rise to tetracyclosqualene

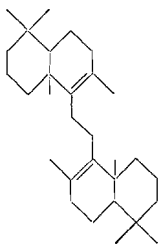

Can. J. Chem. Downloaded from www.nrcresearchpress.com by 210.87.254.6 on 09/05/12
For personal use only.

having a structure consisting of two bicyclic groups connected by two methylene groups (5). In any case, the cyclization reaction can be regarded as a chain process in which a proton, once released in the system, can lead to the consumption of many double bonds without producing crosslinks, hydrogen evolution, or other by-products. If the initially produced molecule ion from irradiated squalene can be converted into an appropriate carbonium ion, analogous to what has been suggested (8) for isobutylene and various other monomers known to undergo a radiation-induced ionic polymerization, it is quite possible that squalene can be cyclized by an ionic mechanism when exposed to ionizing radiation. In that event, the chain nature of the reaction could then be responsible for translating a very low rate of initiation (G_i of the order of 0.2, for example, in the case of isobutylene (7*b*)) into the observed rather high G-value for the cyclization ($\sim$5). If such a cyclization mechanism does operate, the analogous intermolecular reaction

[15] $$\begin{matrix} & -CH_2-\overset{+}{C}(CH_3)-CH_2-CH_2- & \longrightarrow & -CH_2-C(CH_3)-CH_2-CH_2- \\ -CH_2-C(CH_3)=CH-CH_2- & & & -CH_2-\overset{+}{C}(CH_3)-\underset{|}{CH}-CH_2- \end{matrix}$$

is likewise possible: it could, along with reaction 10, account for the higher molecular weight products found in the fractions 2. At any rate, the occurrence of reactions 14 and 15 (carbonium ion mechanism) or reactions 10 and 13 (free radical mechanism) could explain the observation that the cyclization is associated with the crosslinking reaction, i.e., the loss of unsaturation is observed only in the crosslinked products.

Another possible cyclization, involving allylic radicals, is one suggested by Moore and Watson (23)

[16] $$-CH_2-C(CH_3)=CH-CH_2-CH_2-C(CH_3)=CH-\dot{C}H- \longrightarrow$$
$$-CH_2-\dot{C}(CH_3)-CH-CH_2-CH_2-C(CH_3)=CH-CH-$$

to account for the loss of unsaturation observed in the crosslinked products obtained from the rubber-like compounds, dihydromyrcene and digeranyl, when these are reacted with di-*tert*-butyl peroxide. This suggestion does not appear valid, however, due to the small reactivity of allylic radicals and also to the fact that these same authors were led, on other grounds, to dismiss the corresponding *inter*molecular reaction (23). We consider that the loss of unsaturation in their experimental work remains without a satisfactory explanation.

Finally, it should be noted that the slight effect of temperature on G(-d.b.) argues against the free radical reactions 10 and 13 making an important contribution to the radiation chemistry of squalene and polyisoprene. But it would be unjustified to rule out such reactions entirely just as it would be to postulate exclusively a carbonium ion mechanism for cyclization. A study of the radiation-induced loss of unsaturation in the presence of free radical scavengers should help to elucidate this interesting question.

Isomerization

The similarity in the radiation chemistry of squalene and polyisoprene discussed in the foregoing sections clearly extends to the phenomenon of geometric isomerization about their isoprenic double bonds. However, these compounds show notable differences in their relative ease of isomerization in solution and in the pure state. Thus, the G-value for the *trans–cis* isomerization of squalene in the pure liquid (G_p(t$\rightarrow$c) = 0.83) is considerably smaller than that of balata (*trans* polyisoprene) in the solid state ($\sim$10), whereas the

Can. J. Chem. Downloaded from www.nrcresearchpress.com by 210.87.254.6 on 09/05/12
For personal use only.

corresponding effective energy yields for the solution isomerizations ($G_s'(t\rightarrow c)$ of 26 and 97, respectively) are not fundamentally different.

The G_s' value for squalene in benzene is some 30 times the G-value for the pure compound (G_p), while in the case of balata the G_s' value is about 10 times the corresponding G_p value. A similar situation was described several years ago for the radiation isomerization of polybutadiene (26) where the effective yield in a 1% benzene solution is about eight times the yield in the pure polymer. The mechanisms advanced to explain the radiation-induced "unsensitized" isomerization of polybutadiene in solution and in the pure polymer appear to be directly applicable to that of squalene (or polyisoprene). Accordingly, the isomerization of squalene in the pure state can be considered to involve the excitation of the π-electrons of the isoprenic double bonds to an antibonding state where free rotation and hence geometric interconversion can occur. This excitation, resulting from collisions of energetic electrons with the squalene molecules, may take place directly at the double bonds or be produced there indirectly through intramolecular energy transfer out of adjacent methylene groups, or from neutralization of ionized species somewhere in the molecule. In the solution case, however, the important agency for promoting the isomerization can be assumed to be intermolecular energy transfer from excited or ionized benzene molecules to squalene double bonds. A similar explanation has been advanced recently for the radiation-induced isomerization of *cis* and *trans* butene-2 in benzene (27).

Two aspects of the squalene isomerization results deserve additional comment. Firstly, since there is no reason to expect the efficiency of intermolecular energy transfer from benzene to squalene to differ significantly from energy transfer from benzene to polyisoprene, we have to seek an explanation for the fact that the ratio of G_s' to G_p for squalene is around 30 while it is only around 10 for polyisoprene (and about 8 for polybutadiene). Although there is some uncertainty regarding the exact $G_s(t\rightarrow c)$ value for squalene, as noted earlier, it is quite unlikely that its true value would be low enough (say, about 1.0) to bring the G_s'/G_p ratio down from 30 to 10. In view of the work of Cundall and Griffiths (27) on *cis* and *trans* butene-2, a reasonable explanation for the difference between G_s'/G_p ratios for squalene and balata is that the particular values obtained for $G_s(t\rightarrow c)$ depend somewhat on the concentration of the isomerizing compound. In fact, our $G_s(t\rightarrow c)$ for squalene corresponds to a 10% benzene solution while the corresponding value for polyisoprene refers to a 1% solution.

Secondly, we are unable to explain the much lower isomerizability of pure squalene compared to that of pure polyisoprene, even if we allow for the fact that in the former compound only the four internal double bonds can isomerize. Apparently, squalene is less efficient than polyisoprene in using the available excitational energy for isomerization purposes. In this connection, it may be noted that preliminary work on pure *cis* 4-methylpentene-2 indicates that this compound isomerizes either not at all or at most very slightly (28). At first glance, it would seem that the efficiency of isomerization of the pure olefinic compound, in contrast to that of the material in benzene, depends on the size of the molecule, decreasing regularly from the macromolecule down to the very short molecule. Such a point of view appears consistent with the model depicted by Lorquet, ElKomoss, and Magee (29) in which electronic excitation localized in one of the double bonds of a polymer can migrate along the chain to induce the isomerization of several of them. However, both Kaufman (30) and Cundall (31) have recently observed rather high G-values for the isomerization of *cis* butene-2 in the pure state ($G_p\sim4.0$ and 14, respectively), so that the size of the isomerizing molecule per se is not sufficient to account for

Can. J. Chem. Downloaded from www.nrcresearchpress.com by 210.87.254.6 on 09/05/12
For personal use only.

the low isomerizability of pure squalene compared to pure polyisoprene. Further work on this question seems worth while and we plan to extend this research to include dihydromyrcene which, having a diisoprene structure, is intermediate in molecular weight between squalene and pentene-2 or butene-2.

ACKNOWLEDGMENTS

This research was supported in part by Aeronautical Systems Division, U.S.A.F., and in part by Stanford Research Institute. We wish to express our appreciation to W. R. Anderson, Jr., for providing the n.m.r. spectra, to D. E. LeGoullon for the infrared spectra, to L. F. Nye who monitored the irradiations, and to other staff members for various analyses. We wish also to thank Professor P. J. Flory and Dr. A. H. Samuel for helpful discussions.

REFERENCES

1. M. A. GOLUB and J. DANON. To be published.
2. L. BATEMAN and C. G. MOORE. *In* Organic sulfur compounds. Vol. 1. *Edited by* N. Kharasch. Pergamon Press, New York. 1961. L. BATEMAN. Quart. Rev. London, **8**, 147 (1954). E. H. FARMER and C. G. MOORE. J. Chem. Soc. 142 (1951).
3. D. T. TURNER. Polymer, **1**, 27 (1960).
4. J. DALE. Tidsskr. Kjemi, Bergvesen Met. **15**, 162 (1955); Chem. Abstr. **50**, 10048a (1956).
5. B. L. VAN DUUREN and F. L. SCHMITT. J. Org. Chem. **25**, 1761 (1960).
6. M. A. GOLUB and J. HELLER. Can. J. Chem. **41**, 937 (1963); Tetrahedron Letters, 2137 (1963).
7. (*a*) W. H. T. DAVISON, S. H. PINNER, and R. WORRALL. Chem. Ind. 1247 (1957). (*b*) A. CHARLESBY, S. H. PINNER, and R. WORRALL. Proc. Roy. Soc. London, Ser. A, **259**, 386 (1960). (*c*) E. COLLINSON, F. S. DAINTON, and M. A. GILLIS. J. Phys. Chem. **63**, 909 (1959).
8. T. F. WILLIAMS. Trans. Faraday Soc. **57**, 755 (1961). Quart. Rev. London, **17**, 101 (1963).
9. O. ISLER *et al.* Helv. Chim. Acta, **39**, 897 (1956).
10. R. B. BATES and D. M. GALE. J. Am. Chem. Soc. **82**, 5749 (1960).
11. H. Y. CHEN. Anal. Chem. **34**, 1793 (1962).
12. J. PESTANER. Private communication.
13. H. YAMAZAKI and S. SHIDA. J. Chem. Phys. **32**, 950 (1960).
14. M. A. GOLUB. Unpublished results.
15. A. CHARLESBY. Atomic radiation and polymers. Pergamon Press, London. 1959. Chaps. 9, 15.
16. D. T. TURNER. J. Polymer Sci. **B1**, 93 (1963).
17. D. T. TURNER. J. Polymer Sci. **B1**, 97 (1963).
18. J. I. CUNNEEN, G. M. C. HIGGINS, and W. F. WATSON. J. Polymer Sci. **40**, 1 (1959).
19. M. A. GOLUB. J. Phys. Chem. **66**, 1202 (1962).
20. P. HAYDEN. Intern. J. Appl. Radiation Isotopes, **8**, 65 (1960).
21. M. B. EVANS, G. M. C. HIGGINS, and D. T. TURNER. J. Appl. Polymer Sci. **2**, 340 (1959).
22. H. W. MELVILLE and J. C. ROBB. Discussions Faraday Soc. **14**, 55 (1953).
23. C. G. MOORE and W. F. WATSON. J. Polymer Sci. **19**, 237 (1956).
24. C. WALLING. Free radicals in solution. John Wiley and Sons, Inc., New York, N.Y. 1957. p. 175.
25. N. GRASSIE. Chemistry of high polymer degradation processes. Butterworth Scientific Publications, London. 1956. pp. 315–319.
26. M. A. GOLUB. J. Am. Chem. Soc. **82**, 5093 (1960).
27. R. B. CUNDALL and P. A. GRIFFITHS. J. Am. Chem. Soc. **85**, 1211 (1963); Discussions Faraday Soc. In press.
28. M. A. GOLUB. To be published.
29. J. C. LORQUET, S. G. ELKOMOSS, and J. L. MAGEE. J. Chem. Phys. **37**, 1991 (1962).
30. P. C. KAUFMAN. J. Phys. Chem. **67**, 1671 (1963).
31. R. B. CUNDALL. Private communication.

Can. J. Chem. Downloaded from www.nrcresearchpress.com by 210.87.254.6 on 09/05/12
For personal use only.

Can. J. Chem. Downloaded from www.nrcresearchpress.com by 210.87.254.105 on 09/05/12
For personal use only.

FOMECIN A AND B, PHENOLIC ALDEHYDES FROM THE BASIDIOMYCETE FOMES JUNIPERINUS

T. C. McMorris and Marjorie Anchel
The New York Botanical Garden, Bronx Park, Bronx 58, New York
Received February 11, 1964

ABSTRACT

Fomecin A and B obtained previously from the basidiomycete *Fomes juniperinus* Schrenk have been characterized as 6-hydroxymethyl-2,3,4-trihydroxy benzaldehyde and 2,3,4-trihydroxy *o*-phthalaldehyde, respectively.

An investigation of antibacterial substances produced by higher fungi resulted in the isolation some time ago of a crystalline antibiotic from culture liquids of *Fomes juniperinus* Schrenk (1, 2). This compound, which was named Fomecin A, has now been identified as 6-hydroxymethyl-2,3,4-trihydroxy benzaldehyde (I*a*).

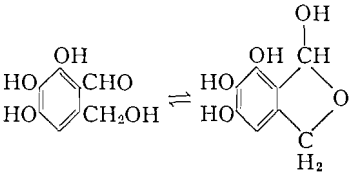

I*a* I*b*

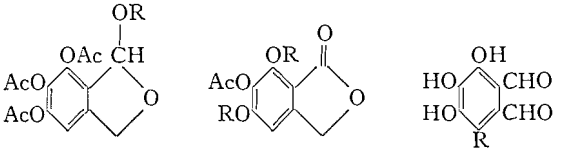

II*a*, R = Ac
b, R = Me

III*a*, R = Ac
b, R = Me

IV*a*, R = H
b, R = Me

Fomecin A, $C_8H_8O_5$, was weakly acidic and gave a blue-black color with ferric chloride solution. It formed a red 2,4-dinitrophenylhydrazone, gave an orange condensation product with aniline, and it rapidly reduced ammoniacal silver nitrate in the cold, thus indicating the presence of an aldehyde function. In agreement, the n.m.r. spectrum showed a singlet at $-0.1\ \tau$.

Treatment of Fomecin A with acetic anhydride and pyridine gave a tetraacetate (II*a*) whose spectral properties indicated it to be a phenolic acetate having no aldehyde group. This reaction is readily explained if there is a hydroxymethyl *ortho* to the aldehyde so that acetylation can proceed through the tautomeric form (*Ib*).

When a methanolic solution of the tetraacetate was refluxed for a short time, solvolysis occurred giving the product (II*b*). The n.m.r. spectrum now showed a singlet at 6.65 (methoxyl) instead of one at 7.97 (acetate) and the unsymmetrical doublet at 2.65 due to the proton on the carbon bearing two oxygen functions had moved upfield to 3.77.

Treatment of (II*a*) with chromium trioxide in aqueous acetic acid gave a crystalline product shown to be 4,5,6-triacetoxy phthalide (III*a*). Thus, on deacetylation and then

methylation it gave a trimethoxy phthalide isomeric with authentic 3,4,5-trimethoxy phthalide. On oxidation, both isomers gave the same trimethoxyphthalic acid. The formation of phthalide (III*a*) establishes the orientation of substituents on the aromatic ring of (I*a*).

In later isolations of Fomecin A a second, less polar, substance called Fomecin B could also be obtained, though in much lower yield. This yellow crystalline compound, $C_8H_6O_5$, also gave a blue-black color with ferric chloride and reduced ammoniacal silver nitrate in the cold. The n.m.r. spectrum revealed the presence of six protons: sharp singlets at −0.8 and 0.05 due to two aldehyde protons, a singlet at 2.92 due to an aromatic proton and broad signals at about −2.66 and 0.4 due to one and to two hydroxyl protons, respectively, which disappeared on addition of deuterium oxide.

Peaks at 1685 and 1630 cm^{-1} in the infrared spectrum are assigned to free and chelated aldehyde groups.

The ultraviolet spectrum (λ_{max} 263, 336 mμ; ϵ 26 400 and 9200) is similar to that of Flavipin (IV*b*), (λ_{max} 261, 264, and 330 mμ; ϵ 23 500, 22 400, and 8700) a metabolite of *Aspergillus flavipes* (3).

The structure (IV*a*) for Fomecin B was confirmed by oxidation of its methylation product to 3,4,5-trimethoxy phthalic acid.

The Fomecins possess the same carbon skeleton as, for example, the well-known metabolite 6-methyl salicylic acid, which is known to be biosynthesized from acetate (4), and they are probably formed in a similar way. Their structures recall those of similarly related pairs of metabolites, dihydrogladiolic and gladiolic acids (5, 6), and cyclopolic and cyclopaldic acids (7).

EXPERIMENTAL

Melting points were taken on a Köfler block. Microanalyses were carried out by Dr. F. Pascher, Bonn, and n.m.r. spectra determined by Dr. D. P. Hollis, Varian Associates, California. Infrared and ultraviolet spectra were determined with Perkin–Elmer Model 21 and Carey Model 11 spectrophotometers, respectively. Petroleum ether refers to the fraction b.p. 66–75°.

The isolation and antibacterial properties of Fomecin A are described elsewhere (1). The final stage of the isolation was a countercurrent distribution between ethyl acetate and water. Fomecin A moved with the aqueous phase while the less polar Fomecin B remained in the ethyl acetate phase in the early funnels.

Fomecin A crystallized from ethanol–water as pale buff-colored spicules which did not melt but charred gradually above 160°. Found: C, 52.28; H, 4.49; O, 43.47; mol. wt. (Rast), 189; equiv., 173. Calc. for $C_8H_8O_5$: C, 52.18; H, 4.38; O, 43.44; mol. wt., 184. λ_{max} (EtOH) 241, 304 mμ (ϵ 10 800 and 15 300). ν_{max} (KBr) 3480, 3150 (broad), 1635, 1615 (shoulder), 1603, and 1510 cm^{-1}. τ (deuterated dimethyl sulphoxide) −0.1 (singlet, —CHO); 3.47 (singlet, aromatic H); 5.32 (singlet, —CH_2—O). The integral curve showed that the hydroxyl protons gave broad resonances overlapping the entire spectrum.

Fomecin B crystallized from ethyl acetate as yellow needles which darkened on heating and melted at about 230°. Found: C, 53.03; H, 3.79; O, 43.31. Calc. for $C_8H_6O_5$: C, 52.75; H, 3.32; O, 43.93. λ_{max} (EtOH) 263, 336 mμ (ϵ 26 400 and 9200). ν_{max} (KBr) 3450 (shoulder), 3100 (broad), 1685, 1630, 1603, and 1510 cm^{-1}. τ ($CDCl_3$) −0.8, 0.05 (singlets, 2 CHO); 2.92 (singlet, aromatic H); −2.66 and 0.4 (broad peaks, 1 and 2 OH, respectively).

Fomecin A Derivatives

(a) 2,4-Dinitrophenylhydrazone.—Addition of a hot solution of 2,4-dinitrophenylhydrazine (300 mg) in acetic acid (6 ml) to a solution of Fomecin A (200 mg) in ethanol (3 ml) gave quickly a red precipitate. It was recrystallized from ethyl acetate and it decomposed without melting. Found: C, 45.55; H, 3.68; N, 14.82. Calc. for $C_{14}H_{12}O_8N_4$: C, 46.16; H, 3.32; N, 15.38.

(b) Anil.—Aniline (0.5 ml) was added to a hot solution of Fomecin A (184 mg) in ethanol (2 ml). When it had been cooled orange crystals separated. It was recrystallized from ethanol and it decomposed without melting. Found: C, 64.60; H, 5.32; N, 5.29. Calc. for $C_{14}H_{13}O_4N$: C, 64.86; H, 5.06; N, 5.40.

(c) Acetate (IIa).—Fomecin A (200 mg) was treated with pyridine (5 ml) and acetic anhydride (2.5 ml) overnight. The solvents were removed *in vacuo* at room temperature, xylene added, and then removed similarly. Addition of ether to the residue caused crystallization. After recrystallization from ethyl acetate – petroleum ether it had m.p. 135°. Found: C, 54.53; H, 4.68; O, 40.98; Ac, 48.60. Calc. for $C_{16}H_{16}O_9$: C,

Can. J. Chem. Downloaded from www.nrcresearchpress.com by 210.87.254.105 on 09/05/12
For personal use only.

54.55; H, 4.58; O, 40.87; 4 Ac, 48.87. λ_{max} (EtOH) 264, 270 (inf.) mμ (ϵ 830, 800). ν_{max} (Nujol) 1785–1755 cm^{-1}. τ ($CDCl_3$) 2.6 (unsymmetrical doublet, J 1.5 c.p.s.; —O—CH—O); 2.9 (somewhat broad singlet, aromatic H); 4.82 (AB spectrum, δ AB .22 p.p.m. J AB 12 c.p.s., —CH_2—O—. The signals of this methylene were broad and ragged indicating coupling to both the O—CH—O and aromatic proton; 7.77, 7.75, and 7.97 (2, 1, and 1 Ac, respectively).

Methanolysis of Tetraacetate

A solution of the tetraacetate (200 mg) in methanol (10 ml) was refluxed for 1 hour, then the solvent removed. The residue crystallized and on recrystallization from ethyl acetate – petroleum ether had m.p. 121–123°. Found: C, 56.08; H, 5.03; O, 39.14; OMe, 9.57; Ac, 39.57. Calc. for $C_{15}H_{16}O_8$: C, 55.55; H, 4.97; O, 39.47; 1 (OMe), 9.56; 3 Ac, 39.8. λ_{max} (EtOH) 263, 270 mμ (ϵ 740, 720). ν_{max} (Nujol) 1785–1765 cm^{-1}. τ ($CDCl_3$) 2.95 (somewhat broad singlet, aromatic H); 3.77 (unsymmetrical doublet, J = 1.5 c.p.s., —O—CH—O—); 4.87 (broad peak, —CH_2—O—. Here the satellite peaks of the AB spectrum were barely visible above the noise); 6.65 (OMe); 7.7 (3 Ac).

Oxidation of Tetraacetate

A solution of chromium trioxide (200 mg) in acetic acid (4 ml) and water (2 ml) was added to one of the tetraacetate (1 g) in acetic acid (12 ml) and water (6 ml). The resulting solution was kept overnight, then the solvents removed *in vacuo*, ethyl acetate added to the dark green residue, and the mixture boiled and filtered. When the filtrate had been concentrated, crystalline material (III) was obtained (prisms, 300 mg) which after recrystallization from ethyl acetate had m.p. 168–170°. Found: C, 54.89; H, 3.93; O, 40.28; Ac, 44.12; mol. wt. (Rast), 309. Calc. for $C_{14}H_{12}O_8$: C, 54.55; H, 3.92; O, 41.53; 3 Ac, 41.85; mol. wt. 308. λ_{max} (EtOH) 236, 277 (inf.), 283 mμ (ϵ 10, 400; 2300; 2500). ν_{max} (Nujol) 1785–1765, 1630, 1615 cm^{-1}. τ ($CDCl_3$) 2.72 (singlet, aromatic H); 4.72 (singlet, —CH_2—O—); 7.6 (Ac); 7.67 (2 Ac).

Hydrolysis and Methylation of Phthalide (III)

The phthalide (110 mg) dissolved in pyridine (4 ml) and water (2 ml) was kept overnight, then the solvents removed *in vacuo* below 30° leaving a residue which crystallized on adding ethanol. Since it tended to color in air it was dissolved in methanol and treated with ethereal diazomethane. There was vigorous effervescence and after 1 hour the excess diazomethane was destroyed and a crystalline product isolated which, after recrystallization from ethyl acetate, had m.p. 181–183°. Found: C, 57.21; H, 4.88; O, 37.78; OMe, 24.66; Ac, 17.01; mol. wt. (Rast), 238. Calc. for $C_{12}H_{12}O_6$: C, 57.14; H, 4.80; O, 38.06; 2 (OMe), 24.59; 1 Ac, 17.06; mol. wt. 252. The values indicate that two acetyl groups were removed in the hydrolysis. They must be the ones *ortho* and *para* to the lactone carbonyl, and the methylated product therefore has the structure (11*b*).

This compound (200 mg) dissolved in methanol (10 ml) was kept overnight with 0.1 *N* NaOH (5 ml). Next morning the solution was made just acid to litmus with dilute HCl then evaporated to dryness *in vacuo*. The residue was suspended in methanol and ethereal diazomethane added. After 1 hour excess diazomethane was destroyed, the methanol removed, water added, and the solution extracted with chloroform. This extract yielded an oil which quickly crystallized as rosettes of needles and after recrystallization from ethyl acetate – petroleum ether they had m.p. 136–137°. A sample was sublimed at 115°, 0.05 mm Hg for analysis. Found: C, 59.55; H, 5.62; O, 35.18; OMe, 41.16; mol. wt. (Rast), 238. Calc. for $C_{11}H_{12}O_5$: C, 58.92; H, 5.40; O, 35.68; 3 (OMe), 41.5; mol. wt. 224.2. λ_{max} (EtOH) 257, 288 mμ (ϵ 13 300; 2800). ν_{max} (KBr) 1755, 1605 cm^{-1}. τ ($CDCl_3$) 3.2 (singlet, aromatic H); 4.75 (singlet, —CH_2—O—) 5.8, 5.98, 6.07 (3 OMe).

3,4,5-Trimethoxy Phthalide

This compound prepared from 3,4,5-trimethoxy benzoic acid (8) had m.p. 135° and gave a depression of mixed melting point with the trimethoxy phthalide from Fomecin A. The infrared spectra of the two compounds were different. However, when both compounds were oxidized by treating the alkaline solutions (5% KOH) with dilute $KMnO_4$ (3%) at 60–65° for 1 hour, the same product, i.e., 3,4,5-trimethoxy phthalic acid was obtained, m.p. and mixed m.p. 174–176°. The infrared spectra were identical.

The phthalide from Fomecin A is, therefore, 4,5,6-trimethoxy phthalide, which is reported to have m.p. 136.5–137 (9).

Methylation and Oxidation of Fomecin B

The compound (100 mg), dry acetone (10 ml), K_2CO_3 (400 mg), and methyl sulphate (0.3 ml) were refluxed under N_2 for 2 hours. The mixture was filtered and the acetone removed from the filtrate leaving an oil. This was taken up in hot KOH solution (5%) and oxidized with dilute $KMnO_4$ as above. The crystalline product was identical (m.p. and infrared spectrum) with 3,4,5-trimethoxy phthalic acid.

ACKNOWLEDGMENT

This work was supported by a grant (E-226) from the National Institute of Allergy and Infectious Diseases, National Institutes of Health.

Can. J. Chem. Downloaded from www.nrcresearchpress.com by 210.87.254.105 on 09/05/12
For personal use only.

REFERENCES

1. M. ANCHEL, A. HERVEY, and W. J. ROBBINS. Proc. Natl. Acad. Sci. **38**, 655 (1952).
2. M. ANCHEL. *In* Essays in biochemistry. *Edited by* Samuel Graff. John Wiley and Sons, Inc., New York, N.Y. 1956. p. 2.
3. H. RAISTRICK and P. RUDMAN. Biochem. J. **63**, 395 (1956).
4. R. BENTLEY. *In* Ann. Rev. Biochem. **31**, 590, 1962. R. W. RICKARDS. *In* Chemistry of natural phenolic compounds. *Edited by* W. D. Ollis. Pergamon Press, 1961. p. 6.
5. H. RAISTRICK and D. J. ROSS. Biochem. J. **50**, 635 (1952).
6. J. F. GROVE. Biochem. J. **50**, 648 (1952).
7. J. H. BIRKINSHAW, H. RAISTRICK, D. J. ROSS, and C. E. STICKINGS. Biochem. J. **50**, 610 (1952).
8. F. E. KING and T. J. KING. J. Chem. Soc. 726 (1942).
9. J. A. MCRAE, R. B. VAN ORDER, F. H. GRIFFITHS, and T. E. HABGOOD. Can. J. Chem. **29**, 487 (1951).

Can. J. Chem. Downloaded from www.nrcresearchpress.com by 210.87.254.105 on 09/05/12
For personal use only.

Can. J. Chem. Downloaded from www.nrcresearchpress.com by 210.87.254.105 on 09/05/12
For personal use only.

SYNTHESIS OF SOME ALKYLATED ADENINES AS POTENTIAL ANTIMETABOLITES

C. J. ABSHIRE* AND L. BERLINGUET
Département de Biochimie, Faculté de Médecine, Université Laval, Québec, Québec
Received January 27, 1964

ABSTRACT

Several substituted adenines and (or) their salts have been prepared by condensing adenine in dimethylformamide with the following halides: benzyl chloride, *p*-methylbenzyl chloride, *n*-propyl bromide, (3-chloropropyl) benzene, α-bromo-γ-butyrolactone, allyl bromide, and cinnamyl chloride. The reaction may be carried out in large quantities and the salts were isolated in high yields.

Characterization of these compounds indicated that they are pure 3-substituted adenines with the possible exception of the allyl and the *n*-propyl derivatives, which may contain little, if any, of the 7- or 9-isomers.

It is well known that derivatives of adenine, such as 6-mercaptopurine, have interesting antimetabolic activities. This paper reports the synthesis of N-alkylated purines to evaluate their biological activities.

Within the recent past, various workers have succeeded in alkylating purines on the basic nitrogens of the heterocyclic rings (1, 2, 3). Some of these compounds have also been isolated as natural products (4–12). Most of the laboratory alkylation studies of purine derivatives have, to date, been achieved in basic media. Recently, however, workers have reported that the alkylation of purines occurs in dimethylformamide or dimethylacetamide without the addition of a basic reagent (1, 2). However, there still exists confusion concerning the site of alkylation. In a recent paper, Pal (13) states that "no correlation between alkylation sites and theoretically predicted relative basicities of the ring nitrogen atoms of adenine was observed." Recently, however, it has been proved by several authors that of all the common purines, adenine is the only one which is alkylated in position 3 (1), in neutral medium.

We have prepared several of these substituted adenines by reacting adenine with excess of an alkyl halide in dimethylformamide. Various halides were chosen, to include a variety of reactivity ranging from highly reactive, such as allyl bromide, to weakly reactive, such as *n*-propyl bromide (see Table I). In all cases, the yields were very good and the compounds could be isolated in fairly large quantities. We have isolated all of our compounds directly from the reaction mixture as the corresponding ammonium salts; these were obtained by removal of most of the solvent and trituration of the residue with acetone. Thus 3-benzyl adenine hydrochloride, 3-(*p*-methylbenzyl) adenine hydrochloride, 3-cinnamyl adenine hydrochloride, 3-(3′-phenyl-*n*-propyl) adenine hydrochloride, 3-(γ-butyrolactonyl-α) adenine hydrobromide, allyl adenine hydrobromide, and *n*-propyl adenine hydrobromide were isolated and characterized. In four cases, we isolated the free bases by neutralizing the salts with sodium hydroxide solution. Leonard and Fujii (2) recently reported the isolation of the free bases 3-benzyl adenine and 3-allyl adenine. The 3-benzyl adenine had also been synthesized previously by Denayer (14).

All of the analyses (C, H, N, halogen, titration) agree with the theoretical values, thereby suggesting purity of the compounds. However, because of the numerous possibilities that alkylation can take place at positions 1, 3, 7, or 9, we cannot disregard the

*Medical Research Council Fellow.

Can. J. Chem. Downloaded from www.nrcresearchpress.com by 210.87.254.105 on 09/05/12
For personal use only.

TABLE I

Preparation of 3-substituted adenine salts

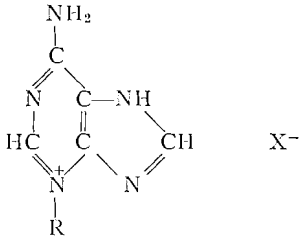

R	Adenine (g)	Halide (ml)	DMF (ml)	Reflux time (h)	Yield (g)	Yield (%)	M.p. (°C)
I 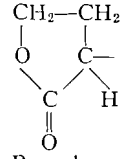	5.0	α-Bromo-γ-butyrolactone (60)	215	1/4	9.5	86	>300
II Benzyl	2.0	Benzyl chloride (17)	100	1/4	2.7	70	261–267
III *p*-Methylbenzyl	1.5	*p*-Methylbenzyl chloride (10)	70	1/4	1.5	49	277–282
IV *n*-Propyl*	20.0	*n*-Propyl bromide (250)	1000	3	20.0	52	252–253
V 3′-Phenyl-*n*-propyl	20.0	(3-Chloropropyl) benzene (100)	1000	3	22.0	45	269–273
VI Allyl*	40.0	Allyl bromide (340)	2000	1/4	50.0	66	196–197
VII Cinnamyl	22.0	Cinnamyl chloride (100)	1000	1/4	21.0	45	237–244

*Isomers present, therefore not all 3-substitution.

presence of two or several isomers. From the evidence accumulated by several authors (1, 2, 3, 13, 14, 15), we have assigned the alkylated chain on the 3-position of the adenine nucleus. The benzyl adenine which we have obtained has a melting point of 284–287 °C compared to 278–280 °C for 3-benzyl adenine reported by Leonard and Fujii (2). We were able to note a slight difference between the ultraviolet data for the free bases and their respective hydrohalides—in general, the free bases absorbed at a slightly lower wavelength than their corresponding hydrohalides. The pK_a' values of cinnamyl adenine and (3′-phenyl-*n*-propyl) adenine were 5.13 and 5.23 respectively, indicating that in both cases, the substitution on the adenine nucleus is in position 3 (3, 15). The allyl adenine and *n*-propyl adenine likewise showed pK_a' values of 5.43 and 5.45 respectively.

From the recent literature (1, 2, 3, 13, 14, 15) and our own work, it would seem that all of our compounds are 3-substituted adenines. To verify the presence or absence of isomers, all the compounds were analyzed by paper chromatography and electrophoresis in different buffers. This last method has proved to be very useful in observing the isomers which have different pK_a' values (see Fig. 1). All of the compounds as isolated showed

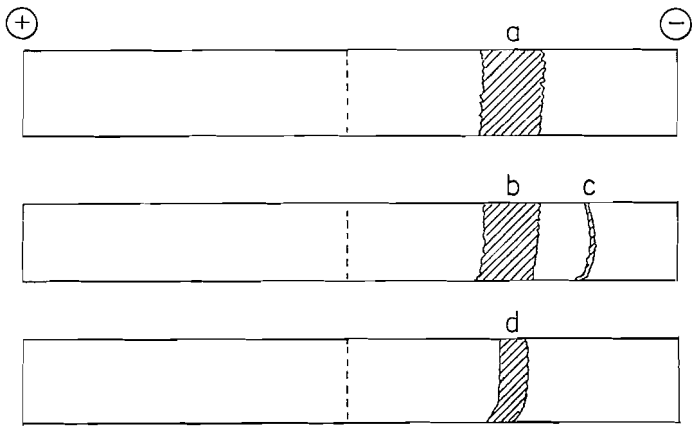

FIG. 1. Electrophoretic migration of adenine and alkylated adenines in buffer pH 1.9, 2 h at 10 mA. The spots are located by means of an ultraviolet lamp: (*a*) pure adenine, (*b*) 3-allyl adenine hydrobromide, (*c*) an uncharacterized allyl adenine isomer, and (*d*) 3-benzyl adenine hydrochloride.

one spotting except the following two: allyl adenine hydrobromide and *n*-propyl adenine hydrobromide. These two compounds showed two spots with both paper chromatography and electrophoresis. Since the elemental analyses and the titration data agreed for purity, the second spot which is somewhat weaker in intensity is obviously due to the presence of a position isomer. No attempts were made to identify the second isomers in question. For both the allyl and the *n*-propyl compounds, the ultraviolet data (λ_{max} = 277 mμ for both) and the pK_a' data (5.43 and 5.45 respectively) point to the fact that these compounds are both primarily 3-substituted.

Before realizing that we were dealing with a mixture of isomers, we prepared derivatives of the allyl compound. Treatment of this compound in acetic acid solution with bromine furnished the perbromide of (2,3-dibromopropyl) adenine hydrobromide (VIII). On heating, the bromine in the perbromide bonding was eliminated and (2,3-dibromopropyl) adenine hydrobromide (IX) resulted. Neutralization with aqueous sodium hydroxide yielded the free base (X). In all of these compounds the ultraviolet absorption peak remained virtually unchanged, indicating that the purine nucleus was not disrupted.

Can. J. Chem. Downloaded from www.nrcresearchpress.com by 210.87.254.105 on 09/05/12
For personal use only.

Elemental analyses and titration data also all agreed. As with the starting material, paper chromatography and electrophoresis showed the presence of a major compound and a minor one (obviously a position isomer).

It is logical that allyl adenine hydrobromide should add bromide on the exocyclic olefinic bond and thus compounds IX and X are easily understood. Evidence for the existence of the heat labile perbromide (VIII) lies in the fact that the compound separates from solution as beautiful orange-colored crystals for which analyses of nitrogen and bromine agreed; the ultraviolet absorption spectra are also similar to that of IX, X, and the starting material. The heat lability of two bromine atoms further suggests that this is really a perbromide. It has similar properties with the perbromide of 2 (or 8)-bromoadenine first reported by Bruhns and Kossel (16).

We are presently doing extensive biological investigation of all the pure compounds.

EXPERIMENTAL

The carbon and hydrogen analyses were done by C. Daessle, Micro Analyses, Montreal. The nitrogen analyses were performed in our laboratory by the Kjeldahl procedure. The acid titrations were done by merely dissolving the compound in water and titrating with 0.1 *M* aqueous sodium hydroxide using phenolphthalein as indicator. The ultraviolet spectra were obtained in ethyl alcohol solution using a Cary Model 15 spectrophotometer. The melting points were determined on a Fisher–Johns melting point apparatus and were not corrected. All paper chromatograms were developed with the organic layer formed from a mixture of 1-butanol, water, and glacial acetic acid (75:20:5). Development was performed by the ascending method in a chamber saturated with solvent vapor. Comparison of samples were made on the same sheet and not by R_f values. Spots were detected by means of ultraviolet absorbance.

All electrophoreses were carried out using a Spinco Duostat apparatus and employing 10 mA for a period of 2 h. Two buffers were used, one at pH 1.9 (98–100% formic acid, glacial acetic acid, and water, 1:4:28) and one at pH 8 (0.667 *M* Na_2HPO_4 – 0.05 *M* borate – KCl – NaOH, 9:10). The pK_a' data for 3-cinnamyl adenine and 3-(3′-phenyl-*n*-propyl) adenine was obtained in dimethyl formamide (DMF), water solution (1:1). In the case of the allyl and *n*-propyl compounds, the salts were dissolved in water, titrated to neutralization with aqueous sodium hydroxide, and, since the free base did not precipitate, the solution was then used as such for pK_a' investigation.

Condensation of Adenine with Alkyl Halides

The halogen compound was added to a stirred solution of adenine in dimethyl formamide solvent at the reflux temperature. The resulting solution was refluxed for some time, then the solvent was removed by vacuum and gentle heat. Trituration of the residue with acetone yielded the ammonium salt in high purity. Table I gives the results obtained with seven different alkyl halides.

The products were analyzed for C, H, N, and either HCl or HBr. Ultraviolet spectral analysis was carried out on each compound; a 1% solution employing ethyl alcohol as solvent was used. Table II contains this data. Paper chromatography and electrophoresis were carried out on all compounds (salts and bases); only in the cases of the allyl and propyl compounds were two spots present. The pK_a' values of four of the compounds were determined as previously mentioned. The free bases 3-benzyladenine, 3-(*p*-methylbenzyl) adenine, 3-(3′-phenyl-*n*-propyl) adenine, and 3-cinnamyl adenine were obtained on neutralization in water of the acid salts. Table III lists the data obtained.

Reaction of Allyl Adenine Hydrobromide with Bromine

Two grams of allyl adenine hydrobromide were dissolved in 80 ml of boiling glacial acetic acid. After the solution was cooled to room temperature, bromine in glacial acetic acid was added. At first, the bromine was decolorized; the bromine solution was added until a slight excess was present. The total resultant solution was about 100 ml. Slight cooling caused precipitation. A 2.7 g yield of orange-colored crystals (perbromide of N-(2′,3′-dibromopropyl) adenine hydrobromide) (VIII) was obtained. These crystals began to change color from orange to white at about 130° and the white crystals subsequently melted with decomposition at 200–207°. Anal. Calc. for $C_8H_{10}N_5Br_3$: N, 12.15; Br, 69.28. Found: N, 12.40; Br, 68.68. The ultraviolet spectrum of this compound in ethyl alcohol showed a λ_{max} at 278 mμ with an ϵ of 19 100.

The above perbromide (800 mg) was dissolved in 25 ml of hot glacial acetic acid. This was heated and distilled. The distillate passed over at 118°; it was reddish in color and probably consisted of bromine and acetic acid. The residue in the distillation flask gradually decolorized from red to colorless. The distillation was stopped when the distillate was completely colorless (about 10 ml remained in the residue). This residue was cooled whereupon a white precipitate formed. This was filtered, washed with ether, and dried. A 550 mg yield of a product melting at 200–208° was obtained (N-(2′,3′-dibromopropyl) adenine hydrobromide) (IX).

Can. J. Chem. Downloaded from www.nrcresearchpress.com by 210.87.254.105 on 09/05/12
For personal use only.

Can. J. Chem. Downloaded from www.nrcresearchpress.com by 210.87.254.105 on 09/05/12
For personal use only.

TABLE II

Analyses of 3-substituted adenine salts

Product	% C		% H		% N		Acid titration (equivalent NaOH)	Ultraviolet	
	Calc.	Found	Calc.	Found	Calc.	Found		λ_{max} (mμ)	$10^{-4}\epsilon$
I	35.98	35.78	3.36	3.58	23.33	23.12	1.99	261	2.26
II	55.07	54.80	4.62	4.62	26.76	26.63	1.01	278	1.74
III	56.62	56.86	5.12	5.36	25.40	25.22	1.00	278	1.97
IV	37.22	36.88	5.04	4.69	27.13	26.86	1.00	277	1.33
V	58.02	58.26	5.55	5.78	24.17	23.79	1.00	277	1.64
VI	37.51	37.73	3.94	3.97	27.35	26.68	0.95	277	1.64
VII	58.43	58.38	4.90	4.98	24.34	24.15	1.00	256	2.21
								276	2.24

TABLE III

3-Substituted adenine free bases

Product	Yield (%)	M.p. (°C)	% N		Ultraviolet		pK_a'
			Calc.	Found	λ_{max} (mμ)	$10^{-4}\epsilon$	
3-Benzyl adenine*	59	284–287	31.09	30.84	274	1.25	—
3-(*p*-Methylbenzyl) adenine	61	284–286	29.27	29.00	273	1.35	—
3-(3′-Phenyl-*n*-propyl) adenine	88	248–253	27.13	26.84	275	1.22	5.23
3-Cinnamyl adenine	57	260–263	27.87	27.67	256	2.48	5.13
					276 shoulder		

*This compound has already been reported by: Leonard and Fujii (2) m.p. 278–280°, Denayer (14) m.p. 278–279°.

Anal. Calc. for $C_8H_{10}N_5Br_3$: N, 16.84; Found: N, 16.64. Titrations: 1 equivalent of NaOH needed for neutralization. The ultraviolet spectrum of this compound in ethyl alcohol also showed a λ_{max} at 277 mμ with an ϵ of 16 700. On neutralization of the above compound with aqueous sodium hydroxide, a white precipitate formed (N-(2′,3′-dibromopropyl) adenine) (X). This was obtained in 50% yield and had a melting point of >300°. Anal. Calc. for $C_8H_9N_5Br_2$: C, 28.67; H, 2.71; N, 20.91; Br, 49.79. Found: C, 28.85; H, 2.50; N, 20.73; Br, 49.36. The ultraviolet spectrum again had a λ_{max} of 280 mμ and an ϵ value of 12 500.

ACKNOWLEDGMENTS

The authors wish to thank the Medical Research Council of Canada for a grant (MBT-831).

REFERENCES

1. J. W. JONES and R. K. ROBINS. J. Am. Chem. Soc. **84**, 1914 (1962).
2. N. J. LEONARD and T. FUJII. J. Am. Chem. Soc. **85**, 3719 (1963).
3. N. J. LEONARD and J. A. DEYRUP. J. Am. Chem. Soc. **84**, 2148 (1962).
4. B. WEISSMAN, P. A. BROMBERG, and A. B. GUTMAN. J. Biol. Chem. **224**, 407 (1957).
5. M. ADLER, B. WEISSMAN, and A. B. GUTMAN. J. Biol. Chem. **230**, 435 (1958).
6. J. D. SMITH and D. B. DUNN. Biochem. J. **72**, 294 (1959).
7. J. D. DUNN and D. B. SMITH. Biochem. J. **68**, 627 (1958).
8. J. W. LITTLEFIELD and D. B. DUNN. Biochem. J. **70**, 642 (1958).
9. D. ACKERMANN and P. H. LIST. Z. Physiol. Chem. **309**, 286 (1957).
10. D. ACKERMANN and P. H. LIST. Z. Physiol. Chem. **318**, 281 (1960).
11. D. B. DUNN. Biochim. Biophys. Acta, **46**, 198 (1961).
12. D. ACKERMAN and P. H. LIST. Naturwissenschaften, **48**, 74 (1961).
13. B. C. PAL. Biochemistry, **1**, 558 (1962).
14. R. DENAYER. Bull. Soc. Chim. France, 1358 (1962).
15. R. DENAYER, A. CAVE, and R. GOUTAREL. Compt. Rend. **253**, 2994 (1961).
16. G. BRUHNS and A. KOSSEL. Z. Physiol. Chem. **16**, 5 (1891).

Can. J. Chem. Downloaded from www.nrcresearchpress.com by 210.87.254.105 on 09/05/12
For personal use only.

Can. J. Chem. Downloaded from www.nrcresearchpress.com by 210.87.254.105 on 09/05/12
For personal use only.

REACTIONS OF PHENYL-SUBSTITUTED HETEROCYCLIC COMPOUNDS

V. NITRATIONS OF 1,3- AND 1,5-DIPHENYLPYRAZOLES[1]

BRIAN M. LYNCH AND YUK-YUNG HUNG[2]
Department of Chemistry, St. Francis Xavier University, Antigonish, Nova Scotia
Received February 17, 1964

ABSTRACT

Dinitration of 1,3- or 1,5-diphenylpyrazole in sulphuric acid yields the corresponding di(*p*-nitrophenyl) compounds, while nitric acid – acetic anhydride yields the 4-nitro-1-*p*-nitrophenyl compounds.

Mononitration at the 4-position occurs when the diphenylpyrazoles and several other 1-phenylpyrazoles are nitrated at 0° by nitric acid – acetic anhydride.

Possible explanations of the dependence of orientation on the nature of the nitrating agent are discussed.

Nuclear magnetic resonance (n.m.r.) spectroscopy was used in demonstrating the structures of many of the nitration products, and a general discussion of the n.m.r. spectra of substituted 1-phenylpyrazoles is given.

INTRODUCTION

In nitrations of aromatic compounds, the stages of successive substitution are usually well defined, since a nitro group is strongly deactivating towards further substitution (1). However, the 1-phenylpyrazole derivatives (IA–IC) are readily *dinitrated* to the 4-nitro-1-*p*-nitrophenyl compounds (IIIA–IIIC), under conditions similar to those employed for *mononitration* of 1-phenylpyrazole (2, 3). In an earlier paper (4), we suggested that 1-phenylpyrazoles (I) will undergo nitration in nitric acid – sulphuric acid as their conjugate acids (II), so that the para-position of the 1-phenyl group is the site of initial nitration. The resulting 1-*p*-nitrophenylpyrazoles (IV) will be far less basic than the parent species (I), and will undergo further nitration as the free bases, in which the 4-position is attacked. Dinitration is thus to be expected, since the various conjugate acids (II) and the 1-*p*-nitrophenylpyrazoles (IV) should be of approximately equal reactivity towards nitronium ion. The generalized conversion I → III is thus to be expected for all 1-phenylpyrazoles with readily accessible 1-para- and 4-positions.

Some assignments of structure to the dinitration products of 1,3- and 1,5-diphenylpyrazoles (ID and IE) conflict with this prediction, although it might be argued that a 3- or 5-phenyl group would shield the 4-position from attack; von Auwers and Mauss (5) suggested that dinitration of 1,3-diphenylpyrazole yielded 1,3-di(*p*-nitrophenyl)pyrazole (VA), while we assigned (4) the dinitro-1,5-diphenylpyrazole, m.p. 185°, obtained by nitric acid – sulphuric acid treatment of 1,5-diphenylpyrazole, as 1,5-di(*p*-nitrophenyl)-pyrazole (VB). In view of these apparent exceptions to the generality of the conversions I → III, we have reexamined the nitrations of 1,3- and 1,5-diphenylpyrazoles in detail. In addition, we have noted several further examples of initial 4-nitration of substituted 1-phenylpyrazoles by nitric acid – acetic anhydride (as predicted in an earlier paper (4)).

The proton nuclear magnetic resonance (n.m.r.) spectra of the various nitration products furnished particularly simple demonstrations of structure, supplementing or replacing classical degradations, syntheses, and conversions into known compounds.

[1]*This work was supported by a grant from the National Research Council. For paper IV, see Can. J. Chem. 41, 2380 (1963).*

[2]*Graduate Research Assistant: holder of a summer scholarship from the Atlantic Provinces Inter-University Committee on the Sciences, July–August 1963.*

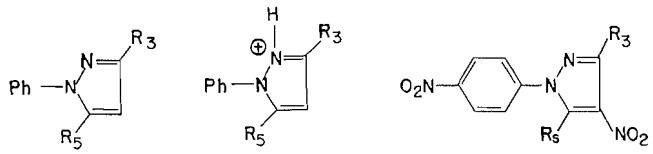

I II III

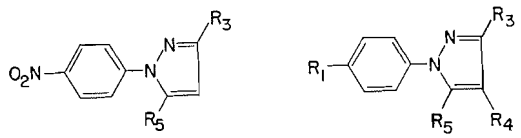

IV V

IA, IIA, IIIA, IVA: $R_3 = R_5 = H$
IB, IIB, IIIB, IVB: $R_3 = CH_3$, $R_5 = H$
IC, IIC, IIIC, IVC: $R_3 = H$, $R_5 = CH_3$
ID, IIID: $R_3 = Ph$, $R_5 = H$
IE, IIIE: $R_3 = H$, $R_5 = Ph$
VA: $R_1 = NO_2$, $R_3 = p\text{-}C_6H_4NO_2$, $R_4 = R_5 = H$
VB: $R_1 = NO_2$, $R_3 = R_4 = H$, $R_5 = p\text{-}C_6H_4NO_2$
VC: $R_1 = R_5 = H$, $R_4 = NO_2$, $R_3 = Ph$
VD: $R_1 = R_3 = H$, $R_4 = NO_2$, $R_5 = Ph$

RESULTS

(a) 1,3-Diphenylpyrazole

Nitration by nitric acid – acetic anhydride at 0° yielded 1,3-diphenyl-4-nitropyrazole (VC), m.p. 123°, together with 1-*p*-nitrophenyl-3-phenylpyrazole and 4-nitro-1-*p*-nitrophenyl-3-phenylpyrazole (IIID), m.p. 238–240°: the dinitro compound (IIID) was the sole product of similar nitration at 20°. Nitration by mixed nitrating acids at 0° yielded 1,3-di(*p*-nitrophenyl)pyrazole (VA), m.p. 228–230°, also obtained by similar nitration of 1-*p*-nitrophenyl-3-phenylpyrazole (cf. von Auwers and Mauss (5)).

The structural assignments were confirmed as follows. The mononitro compound of m.p. 123° has structure VC since its n.m.r. spectrum in dimethyl sulphoxide shows a signal at τ 0.20 integrating for a single proton, and a 10-proton envelope between τ 2.0 and 2.5. The low-field signal is typical of a 5-proton adjacent to a 4-nitro group in a 1-phenylpyrazole derivative (see Discussion section for examples). The assignment of structure VC is subject to little doubt in any case, since other likely nitration products are already known (1-*p*-nitrophenyl-3-phenylpyrazole, m.p. 169° (5), and 3-*p*-nitrophenyl-1-phenylpyrazole, m.p. 137° (6)). Structure VA for the dinitro compound of m.p. 228–230° also follows from its n.m.r. spectrum (measured in dimethyl sulphoxide at 50°), which shows two doublets (*J*, ca. 1 c/s) centered at τ 2.80 and 1.17 assigned to the 4- and 5-protons of the pyrazole ring, and a signal at τ 1.68 corresponding to the 8 (apparently equivalent) protons of the 1- and 3-*p*-nitrophenyl groups (see Discussion section for interpretations of the signal positions). The dinitro compound of m.p. 238–240° has structure IIID since it is obtained by nitration of VC by mixed acids and by nitric acid – acetic anhydride nitration of 1-*p*-nitrophenyl-3-phenylpyrazole, and it differs from the dinitro compound (VA).

Can. J. Chem. Downloaded from www.nrcresearchpress.com by 210.87.254.105 on 09/05/12
For personal use only.

(b) 1,5-Diphenylpyrazole

Our present results confirm previous assignments (4) of structure to the various nitration products of 1,5-diphenylpyrazole, i.e.: 1,5-diphenylpyrazole — (HNO_3/Ac_2O)→VD, m.p. 150°, 1,5-diphenylpyrazole — (HNO_3/H_2SO_4)→VB, m.p. 185°, and confirm that 4-nitro-1-*p*-nitrophenyl-5-phenylpyrazole (IIIE), m.p. 147°, is the product of nitric acid – acetic anhydride nitration of 1-*p*-nitrophenyl-5-phenylpyrazole.

Structure VD for the mononitro-1,5-diphenylpyrazole of m.p. 150° was proved by converting it into 1,4,5-triphenylpyrazole via reduction, diazotization, and Gomberg arylation of benzene (cf. (4)). Furthermore, its n.m.r. spectrum in acetone was consistent with structure VD, in that a single proton signal assignable to the 3-proton, and two five-proton signals at τ 2.56 and 2.63, assignable to the 1- and 5-phenyl groups, are observed. The position of the signal assigned to the 3-proton (at τ 2.77) indicates the presence of some remarkable shielding effect (see Discussion section).

Structure VB for the dinitro-1,5-diphenylpyrazole of m.p. 185° is established, since it is formed by mixed-acid nitration of 1-*p*-nitrophenyl-5-phenylpyrazole, and it yields *p*-nitrobenzoic acid on prolonged oxidation by neutral potassium permanganate. Further confirmation is provided by its n.m.r. spectrum in acetone, which shows two doublets (J, ca. 1 c/s) centered at τ 2.10 and 3.13 assigned to the 3- and 4-protons of the pyrazole ring, together with an A_2B_2 pattern centered at τ 2.05 arising from the two *p*-nitrophenyl groups (which are apparently equivalent: see Discussion section). Similarly, structure IIIE for the dinitro-1,5-diphenylpyrazole of m.p. 147° follows from its n.m.r. spectrum in acetone, which shows a five-proton signal at τ 2.50 due to the 5-phenyl group, an A_2B_2 pattern centered at τ 2.08 arising from the four protons of the 1-*p*-nitrophenyl group, and a single proton signal at τ 1.50 from the 3-proton.

(c) Further Examples of 4-Nitration by Nitric Acid – Acetic Anhydride

Smooth 4-mononitration of the following compounds was effected by nitric acid in acetic anhydride at 0°: 1-*p*-bromo-, 1-*p*-chloro-, 1-*o*-methoxy-, and 1-*p*-phenyl-phenylpyrazoles, and 3-methyl-1-phenylpyrazole. The structures of the first three nitration products were established by comparison with samples synthesized by cyclizing the appropriate arylhydrazine with sodium nitromalonaldehyde hydrate; the structure of 1-*p*-phenylphenyl-4-nitropyrazole (1-*p*-biphenylyl-4-nitropyrazole), m.p. 200° (in previous experiments (4), a polymorphic form, m.p. 170°, having ultraviolet and infrared spectra identical with our present product, was obtained) was proved by synthesis via 1-*p*-aminophenyl-4-nitropyrazole using diazotization and Gomberg arylation (cf. (4)), while our nitro-3-methyl-1-phenylpyrazole had m.p. 110°, identical with that recorded for 3-methyl-4-nitro-1-phenylpyrazole by Finar and Hurlock (3), and its n.m.r. spectrum (see Discussion section) was consistent with the assigned structure.

DISCUSSION

(a) Dependence of Orientation upon the Nitrating Agents

In the dinitrations of both 1,3,- and 1,5-diphenylpyrazoles, the orientations are seen to be reagent-dependent, in the sense that nitration at the para-positions of the N- and C-phenyl groups is favored in sulphuric acid, while 4-nitration is favored when nitric acid – acetic anhydride is used. These results could be rationalized in terms of our previous suggestions (4) if the conjugate acids of the diphenylpyrazoles, and also of the 1-*p*-nitrophenyl-3- and -5-phenylpyrazoles, are the entities undergoing nitration in the strongly acidic solvent, but such a postulate does not appear reasonable. In particular, the

Can. J. Chem. Downloaded from www.nrcresearchpress.com by 210.87.254.105 on 09/05/12
For personal use only.

1-*p*-nitrophenyl compounds would surely exist in measurable proportions as the free bases.

Our present results thus require an interpretation other than deactivation of the pyrazole ring through protonation, with resultant substitution by default in the phenyl rings, to account for the lack of substitution in the pyrazole ring. It is tempting to propose that the adjacent 3- or 5-phenyl group hinders the approach of nitronium ion, but such a suggestion replaces one difficulty by another, since the same factors would operate in the nitric acid – acetic anhydride nitrations, where 4-nitration is favored. However, if a specific interaction occurs between the pyrazole ring and the nitrating agent which is effecting substitution in the nitric acid – acetic anhydride system, such that attack in the pyrazole ring is favored over other sites, then the observed reagent-dependence can be explained.

Since Bordwell and Garbisch (7) have put forward convincing evidence that protonated acetyl nitrate (VI) is the effective species in nitrations by the nitric acid – acetic anhydride reagent, we suggest that the specific interaction suggested above takes the form of an addition of the nucleophilic N_2 of a pyrazole to the electron-deficient carbon of VI, yielding an intermediate (VII). The series of electron shifts shown would then lead to preferred 4-nitration.

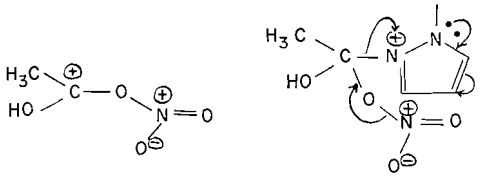

Although an interpretation along these lines seems to be required to account satisfactorily for the results with the diphenylpyrazoles, the selective 4-nitrations of the simpler species noted in part (*c*) of the Results section, and some previous examples (4), may be accounted for in terms of our previous suggestion, i.e., in a simple 1-phenylpyrazole, where the 1-*para*- or 4-positions are the only probable sites of substitution, 4-substitution is favored for attack on the neutral molecule (4). Supporting evidence for this contention is furnished by the results of Friedel–Crafts nitration of 1-phenylpyrazole using nitronium tetrafluoroborate in tetramethylene sulphone, cf. Olah *et al.* (8(*a*), where 4-nitro-1-phenylpyrazole is the only detectable substitution product (8(*b*)).

Intermediates corresponding to VII account neatly for other selective nitrations effected by the nitric acid – acetic anhydride reagent: thus VIII would lead readily to the observed ortho nitration of acetanilide, and IX to the similar nitration of anisole.

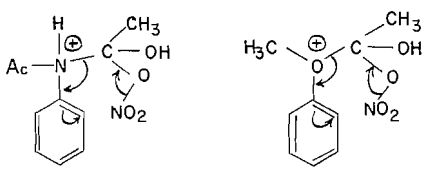

Since previously suggested reaction pathways (9, 10) for these ortho nitrations do not take Bordwell and Garbisch's results into consideration, and the postulated intermediates are consistent with all previous evidence, we are currently engaged in a study (11) seeking to establish VIII as the general intermediate for the selective ortho nitrations of substituted acetanilides.

Can. J. Chem. Downloaded from www.nrcresearchpress.com by 210.87.254.105 on 09/05/12
For personal use only.

Can. J. Chem. Downloaded from www.nrcresearchpress.com by 210.87.254.105 on 09/05/12
For personal use only.

(b) Nuclear Magnetic Resonance Spectra

In addition to their value in facilitating and confirming assignments of structure, the n.m.r. spectra of 1-phenylpyrazole derivatives are of interest in their own right: little previous attention has been focussed either on the chemical shifts of ring protons in pyrazoles, or on the effects of heteroaromatic substituents on the chemical shifts of benzenoid protons. Many of the compounds examined by n.m.r. spectroscopy were 1-parasubstituted-phenyl pyrazoles, in which the presence of a readily recognizable A_2B_2 pattern due to the four protons of the substituted phenyl group facilitated identification of the signals from the pyrazole ring protons. Analyses of these A_2B_2 patterns so as to resolve the individual chemical shifts expected for the A and B protons in the absence of spin–spin coupling gave the results in Table I. The analyses employed the simplified approach adopted by Richards and Schaefer (12), in which it is assumed that $J'_{AB} = 0$ and $J_{AA} = J_{BB}$. It is evident from Table I that 1-pyrazolyl substituents usually have a marked deshielding influence on the protons of a parasubstituted-phenyl group. The deshielding is accounted for readily in terms of the effect of the ring current in the pyrazole ring on the adjacent protons of the 1-phenyl group (13). Although the qualitative effects of various substituents in the 1-phenyl group follow the order expected from the chemical shifts of ortho and meta protons in monosubstituted benzenes (14), no constant chemical-shift parameters could be assigned to the 1-pyrazolyl substituent, since the apparent deshielding contribution varies with the nature of the other substituent, and with the solvent. Fortunately, acetone and dimethyl sulphoxide (the most effective solvents for the compounds studied) appear to be closely comparable in their effects on the chemical shifts of the phenyl-group protons (see No. 1 in Table I).

With the 1-*p*-nitrophenyl-5-phenylpyrazole derivatives (Nos. 7–9 in Table I), where coplanarity of the 1-*p*-nitrophenyl and pyrazole rings is highly unlikely, marked changes from the A_2B_2 pattern typical of other 1-*p*-nitrophenylpyrazoles (e.g., Nos. 1, 3, 4–6) are found. The A–B chemical shift separation (δ_{A-B}), and the extracted A and B chemical shifts, are altered in the direction expected for a decreased deshielding contribution accompanying the increased angle between the planes of the 1-*p*-nitrophenyl and pyrazole rings (13). In No. 9, the 1- and 5-*p*-nitrophenyl groups must be magnetically equivalent, since only one A_2B_2 pattern, closely similar to those for Nos. 7 and 8, was resolved. A corresponding situation was observed with 1,3-di(*p*-nitrophenyl)-pyrazole, although in this instance the center of the system is at τ 1.68 (with $J_{AB} \gg \delta_{A-B}$), indicating that the three rings are coplanar in this compound. Further indications that the 5-phenyl groups in Nos. 7 and 8 are not coplanar with the pyrazole ring are provided by the appearance of discrete signals at τ 2.47 and 2.50, rather than the band envelopes between τ 2.0–2.6 observed for No. 4 and for 1,3-diphenyl-4-nitropyrazole (see Results section). Such differences are to be expected if the ortho protons of the 5-phenyl groups are shielded by comparison with the values characteristic of coplanar C-phenyl and pyrazole rings, and such differences are also noted with 1,5-diphenyl-4-nitropyrazole (see Results section).

The chemical shifts assigned to the pyrazole ring protons in a series of substituted pyrazoles are listed in Table II. In general the τ values fall in the order $4 > 3 > 5$, which is to be expected since (*a*) the 5-proton should be deshielded most effectively by the ring current of the adjacent 1-phenyl group, and (*b*) the 4-carbon should have a higher electron density than the 3-carbon (which will be influenced electrostatically by the adjacent pyridine-type nitrogen). The assignments are based upon the τ values noted for suitably substituted compounds (Nos. 3 and 6, 10 and 11), and upon the observed multiplicities

Can. J. Chem. Downloaded from www.nrcresearchpress.com by 210.87.254.105 on 09/05/12
For personal use only.

TABLE I

Analyses of A_2B_2 patterns in n.m.r. spectra of parasubstituted 1-phenylpyrazoles

No.	Substituents in *p*-A.C_6H_4.B		Solvent	Center of A_2B_2 system	J_{AB} (c/s)	Chemical shifts (τ scale) for protons ortho to:	
	A	B		(τ scale)		A	B
1	NO_2	1-Pyrazolyl	Dioxane	1.83	10.9	1.66	2.00
			Acetone	1.77	10.1	1.66	1.88
			Dimethyl sulphoxide	1.77	10.4	1.66	1.88
2	1-Pyrazolyl	Cl	CCl_4	2.47	9.2_5	2.34	2.60
			Dimethyl sulphoxide	2.25	9.4_5	2.08	2.42
3	NO_2	1-(4-Nitropyrazolyl)	"	1.75	9.0_5	1.67	1.83
4	"	1-(3-Phenylpyrazolyl)	"	1.70	9.2	1.62	1.78
5	"	1-(4-Bromopyrazolyl)	"	1.75	9.2_5	1.62	1.88
6	"	1-(3-Methyl-4-nitro-pyrazolyl)	"	1.75	10.0	1.67	1.83
7	"	1-(5-Phenylpyrazolyl)	Acetone	2.13	8.1	1.77	2.47
8	"	1-(4-Nitro-5-phenyl-pyrazolyl)	"	2.08	8.4	1.76	2.41
9	"	1-(5-(*p*-Nitrophenyl) pyrazolyl)	"	2.05	11.7	1.74	2.36
10	1-(4-Nitropyrazolyl)	NH_2	"	2.80	12.5	2.41	3.19
11	1-(3-Methyl-4-nitro-pyrazolyl)	NH_2	"	2.83	10.5	2.44	3.22
12	1-(4-Nitropyrazolyl)	Br	Dimethyl sulphoxide	2.18	8.4_5	2.08	2.28

Can. J. Chem. Downloaded from www.nrcresearchpress.com by 210.87.254.105 on 09/05/12
For personal use only.

TABLE II

Chemical shifts of ring protons in pyrazoles

Compound (or No. from Table 1)	Solvent	Chemical shifts (τ scale) for: 3-	4-	5-proton	Other signals (τ scale)
1	Dioxane	2.22	3.45	1.68	
	Acetone	2.22	3.42	1.50	
	Dimethyl sulphoxide	2.13	3.35	1.30	
2	CCl_4	3.03	3.61	2.37	
	Dimethyl sulphoxide	2.13	3.39	1.50	
3	"	1.43	—	0.22	
4	"	—	2.80	1.22	Multiplet from 3-phenyl group at τ 2.00–2.60
5	"	2.00	—	1.00	
6	"	—	—	0.30	3-Methyl group at τ 7.47 (measured in pyridine)
7	Acetone	2.20	3.37	—	5-Phenyl group at τ 2.47
8	"	1.50	—	—	5-Phenyl group at τ 2.50
9	"	2.10	3.13	—	
10	"	1.75	—	1.05	
11	"	—	—	1.17	3-Methyl group at τ 7.37 (measured in $CHCl_3$)
12	Dimethyl sulphoxide	1.50	—	0.38	
3-Methyl-4-nitro-1-phenylpyrazole	Chloroform	—	—	1.40	1-Phenyl group at τ 2.67–2.84, 3-methyl group at τ 7.40
1-Methyl-4-nitropyrazole	Acetone	1.96	—	1.47	1-Methyl group at τ 6.00
p-Di(1-pyrazolyl)benzene	Chloroform	2.05	3.50	1.90	Benzene ring protons at τ 2.20
1-*p*-Bromophenylpyrazole	Dimethyl sulphoxide	2.18	3.42	1.49	A_2B_2 pattern from *p*-bromophenyl group centered at τ 2.22
4-Bromo-1-phenylpyrazole	CCl_4	2.68	—	2.22	1-Phenyl group at τ 2.50–2.83
4-Bromo-1-*p*-bromophenylpyrazole	Dimethyl sulphoxide	2.07	—	1.15	*p*-Bromophenyl group protons (all virtually equivalent) at τ 2.20

of signals for the compounds with three adjacent protons (Nos. 1, 2, *p*-di(1-pyrazolyl)-benzene, 1-*p*-bromophenylpyrazole): the 4-protons gave triplets, and the 3- and 5-protons doublets, as expected from simple first-order theory if spin–spin coupling is restricted to adjacent protons. Similarly, doublet signals were observed for compounds with two adjacent protons (Nos. 4, 7, 9, and 1,3-di(*p*-nitrophenyl)pyrazole). The apparent coupling constants between adjacent protons were ca. 1 c/s, and there was no evidence of coupling between non-adjacent protons (the signals from the pyrazole ring protons in Nos. 3, 5, 10, 12, 1-methyl-4-nitropyrazole, 4-bromo-1-phenylpyrazole and 4-bromo-1-*p*-bromophenylpyrazole were singlets). The influence of 4-substituents on the chemical shifts of the 3- and 5-protons qualitatively parallels their influence in monosubstituted benzenes, with one exception.

This exception is 1,5-diphenyl-4-nitropyrazole, where the 3-proton signal falls at τ 2.77 (with most 4-nitro-substituted pyrazoles, the 3-proton signal falls in the range τ 1.4–2.0). The three adjacent groups (the 1- and 5-phenyls, and the 4-nitro group) somehow lead to considerable shielding of the 3-proton. One rationalization of this extraordinary effect is that all three substituents are oriented perpendicularly to the pyrazole ring plane. Circulation of the π-electrons in the nitro group could then produce positive shielding above and below the plane containing the nitro group. Bullock (15) has noted the possibility of such an effect with nitrodurenes and nitromesitylenes, and we find that the n.m.r. spectrum of 3-nitro-*o*-xylene (as the pure liquid), a typical AB_2 system (13, p. 93; 16) may be resolved to give τ 2.67 for the A proton (adjacent to the nitro group) and τ 2.90 for the B protons, while the two methyl groups give a singlet at τ 7.79, thus lending support to the possibility of positive shielding of protons or methyl groups ortho to a nitro group which is in a plane perpendicular to that of an attached aromatic ring.

EXPERIMENTAL

Analyses are by the Schwarzkopf Microanalytical Laboratory, Woodside, N.Y., U.S.A. Melting points were observed using a Fisher–Johns apparatus and are uncorrected. Infrared spectra were recorded using a Beckman IR-8 spectrophotometer: samples were examined as suspensions in potassium chloride disks. Ultraviolet spectra refer to solutions in 95% ethanol, and were recorded using Beckman DK-2 or DK-2A ratio-recording spectrophotometers. Nuclear magnetic resonance spectra were obtained using a Varian A-60 n.m.r. spectrometer. Signal positions are expressed on the τ scale in parts per million from tetramethylsilane, present as an internal reference, and refer to saturated solutions.

Starting and Reference Materials

1-Phenylpyrazole, 1-*p*-biphenylylpyrazole, 4-bromo-1-*p*-bromophenylpyrazole, 4-bromo-1-*p*-nitrophenylpyrazole, 4-bromo-1-phenylpyrazole, 1-*p*-bromophenylpyrazole, 1-*o*-methoxyphenylpyrazole, and 1,5-diphenylpyrazole and its various nitro- and dinitro-derivatives had the properties described previously (4). 1-*p*-Chlorophenylpyrazole, m.p. 51°, 1-methylpyrazole, b.p. 126–127°, and *p*-di(1-pyrazolyl)benzene, m.p. 180° (anal. calc. for $C_{12}H_{10}N_4$: C, 68.55; H, 4.79; N, 26.65; found: C, 68.76; H, 4.83; N, 26.51%) (ultraviolet absorption: λ_{max} 283 mμ, log ϵ 4.37), were prepared by cyclizing the appropriate substituted hydrazine and 1,1,3,3-tetraethoxypropane (4). The 3-methyl-1-phenylpyrazole was purchased from the Aldrich Chemical Co., Inc., Milwaukee, Wisconsin, U.S.A. Authentic samples of 1-*p*-bromophenyl-, 1-*p*-chlorophenyl-, and 1-*o*-methoxyphenyl-4-nitropyrazoles (for melting points, see Table III), and of 1-methyl-4-nitropyrazole, m.p. 88–89° (anal. calc. for $C_4H_5N_3O_2$: C, 37.80; H, 3.96; N, 33.06; found: C, 37.79; H, 4.19; N, 33.11%), were prepared by cyclization using the appropriate substituted hydrazine and sodium nitromalonaldehyde hydrate. 1,3-Diphenylpyrazole, m.p. 85°, and 1-*p*-nitrophenyl-3-phenylpyrazole, m.p. 169° (ultraviolet absorption: λ_{max} 261.5, 337 mμ, log ϵ 4.16, 4.24), were prepared from the appropriate arylhydrazine and hydroxymethyleneacetophenone (5). 4-Nitro-1-*p*-nitrophenylpyrazole, m.p. 146° (ultraviolet absorption: λ_{max} 213.5, 305 mμ, log ϵ 4.22, 4.36), and 3-methyl-4-nitro-1-*p*-nitrophenylpyrazole, m.p. 208–209° (ultraviolet absorption: λ_{max} 216, 312.5 mμ, log ϵ 4.03, 4.30), were prepared by mixed acid nitrations of the parent 1-phenylpyrazoles (2, 3), and 1-*p*-aminophenyl-4-nitropyrazole, m.p. 190° (ultraviolet absorption: λ_{max} 262.5 mμ, log ϵ 4.14), and 1-*p*-aminophenyl-3-methyl-4-nitropyrazole, m.p. 169° (ultraviolet absorption: λ_{max} 261.5 mμ, log ϵ 4.18), were prepared from the corresponding dinitro compounds by partial reduction using ammonium sulphide solution (cf. Finar and Hurlock (3)).

Can. J. Chem. Downloaded from www.nrcresearchpress.com by 210.87.254.105 on 09/05/12
For personal use only.

Nitrations

(a) By Mixed Nitric – Sulphuric Acids

1,3-Diphenylpyrazole (2 g) was dissolved in the minimum volume of sulphuric acid (*d* 1.84), cooled to 0°, and a mixture of nitric acid (4 ml, *d* 1.42) and sulphuric acid (5 ml, *d* 1.84) was added at 0°, and the mixture was kept at 0° overnight, and then poured onto ice. The resulting precipitate was collected and purified by chromatography on alumina and repeated crystallization from methanol, finally yielding 1,3-di(*p*-nitrophenyl)pyrazole (0.7 g, 25%), m.p. 228–230° (anal. calc. for $C_{15}H_{10}N_4O_4$: C, 58.06; H, 3.25; N, 18.06; found: C, 57.85; H, 3.75; N, 18.02%) (ultraviolet absorption: λ_{max} 340 mμ, log ε 4.34; infrared absorption in the 650–1800 cm^{-1} region (cm^{-1}, intensity): 680w, 697w, 746s, 851s, 952m, 1045m, 1105m, 1269w, 1307sh(s), 1333s, 1513s, 1590s). This compound was also obtained in 87% yield by similar nitration of 1-*p*-nitrophenyl-3-phenylpyrazole. Similar nitration of 1,3-diphenyl-4-nitropyrazole yielded 1 g (43%) of 4-nitro-1-*p*-nitrophenyl-3-phenylpyrazole, m.p. 238–240°, after 1 h at 0°. The product was identical (m.p., mixed m.p., superimposable infrared spectra) with that obtained by nitric acid – acetic anhydride nitration of 1,3-diphenylpyrazole or of 1-*p*-nitrophenyl-3-phenylpyrazole (cf. section (*b*) below, and Table III).

(b) By Nitric Acid – Acetic Anhydride

The general procedure used was that adopted in our previous paper (4): A solution of nitric acid (*d* 1.52) in acetic anhydride, prepared at 15–20°, was cooled to 0° and added to the 1-phenylpyrazole derivative (dissolved in the minimum volume of acetic anhydride) over 30 min. The reaction mixture was poured onto ice and the precipitate was collected. Chromatography on alumina, followed by crystallization from methanol or ethanol, yielded the new products listed in Table III. The 4-nitro-1-*p*-nitrophenyl-3-phenylpyrazole (the final entry in Table III) was obtained by nitration of 1,3-diphenylpyrazole at 20°, and showed the following infrared absorption bands in the 650–1800 cm^{-1} region (cm^{-1}, intensity): 680w, 705w, 741s, 826w, 852s, 922w, 952m, 1099m, 1233m, 1307sh(s), 1335s, 1517s, 1590s. This dinitro compound, therefore, differs from 1,3-di(*p*-nitrophenyl)pyrazole (cf. above). 4-Nitro-1-*p*-nitrophenyl-3-phenylpyrazole was also obtained in 40% yield by similar nitration of 1-*p*-nitrophenyl-3-phenylpyrazole at 20°.

Proofs of Structure via Gomberg Reactions

(a) Conversion of 1,5-Diphenyl-4-nitropyrazole into 1,4,5-Triphenylpyrazole

1,5-Diphenyl-4-nitropyrazole (2.3 g) was reduced using tin and hydrochloric acid, and the crude amine thus obtained was diazotized in 10 *N* hydrochloric acid at 0°, and was stirred with benzene for 3 h after basification with sodium hydroxide at 0°. The benzene layer was separated and chromatographed on alumina: evaporation of the eluate followed by crystallization from ethanol yielded 1,4,5-triphenylpyrazole (0.2 g), m.p. 208–211°, undepressed on admixture with an authentic sample, and with infrared absorption identical with that of an authentic sample, showing the following bands in the 650–1800 cm^{-1} region: 654w, 662w, 694s, 718w, 761s, 767s, 773s, 856w, 920w, 952s, 1379s, 1429w, 1439w, 1493s, 1587s.

(b) Synthesis of 1-p-Biphenylyl-4-nitropyrazole

1-*p*-Aminophenyl-4-nitropyrazole (2 g) was diazotized and the basified diazonium salt solution was used to arylate benzene as in (*a*) above. Chromatography on alumina and crystallization from ethanol yielded 1-*p*-biphenylyl-4-nitropyrazole (0.7 g), m.p. 200°, having ultraviolet and infrared absorption identical with the polymorphic form, m.p. 170°, reported previously (4).

Oxidative Degradation of 1,5-Di(p-nitrophenyl)pyrazole

1,5-Di(*p*-nitrophenyl)pyrazole (0.5 g) was heated under reflux with an excess of alkaline potassium permanganate until no further reduction of permanganate occurred (ca. 100 h). Precipitated manganese dioxide was removed using sulphur dioxide, and the reaction mixture was acidified and extracted with hot benzene, re-extracted with sodium hydrogen carbonate, and re-acidified, giving *p*-nitrobenzoic acid (0.1 g), m.p. 237–240°, having infrared absorption identical with that of an authentic sample.

ACKNOWLEDGMENTS

We thank the National Research Council for grants in support of our work, and one of us (Y. H.) gratefully acknowledges the award of a summer scholarship from the Atlantic Provinces Inter-University Committee on the Sciences. The nuclear magnetic resonance and ultraviolet spectroscopic measurements were made during tenure of this scholarship, at the Atlantic Regional Laboratory, National Research Council, Halifax, and we thank Dr. A. G. McInnes for his courtesy in providing facilities for these measurements.

We also thank Dr. H. O. House (Massachusetts Institute of Technology) for a sample of 1,4,5-triphenylpyrazole, Dr. B. T. Newbold (University of Moncton) for a sample of 3-nitro-*o*-xylene, and Dr. H. S. Chang and Mr. M. A. Khan, who furnished several reference samples.

Can. J. Chem. Downloaded from www.nrcresearchpress.com by 210.87.254.105 on 09/05/12
For personal use only.

Can. J. Chem. Downloaded from www.nrcresearchpress.com by 210.87.254.105 on 09/05/12
For personal use only.

TABLE III

4-Nitro-derivatives of substituted 1-phenylpyrazoles

R_1	R_2	R_3	R_5	M.p. (obs.)	M.p. (lit.)	Lit. ref. or analysis	Yield of recrystallized product from 2 g substrate (%)	Ultraviolet absorption	
								λ_{max} (mμ)	log ϵ
H	H	H	Ph	150°	150°	*a*	43	245, 280	4.24, 3.85
H	H	Ph	H	123	—	*b*	25[c]	256, 300sh	4.24, 3.95
H	H	CH_3	H	110	110	*d*	60	300	3.95
H	OCH_3	H	H	89	85–87	*e*	65	—	—
Cl	H	H	H	171	—	*f*	60	—	—
Br	H	H	H	154	—	*g*	60	238, 297	4.13, 4.08
Ph	H	H	H	200	170	*a*	42	265, 315	4.06, 4.08
NO_2	H	H	Ph	147	147	*a*	26	285	4.29
NO_2	H	Ph	H	238–240	—	*h*	80	—	—

[a]M. A. Khan, B. M. Lynch, and Y. Hung. Can. J. Chem. 41, 1540 (1963).
[b]Anal. Calc. for $C_{15}H_{11}N_3O_2$: C, 67.92; H, 4.18. Found: C, 68.18; H, 4.33%.
[c]1-*p*-Nitropheuyl-3-phenylpyrazole (25%) and 4-nitro-1-*p*-nitrophenyl-3-phenylpyrazole (25%) were also isolated.
[d]I. L. Finar and R. J. Hurlock. J. Chem. Soc. 3259 (1958).
[e]C. Alberti and C. Tironi. Farmaco Pavia Ed. Sci. 17, 443 (1962).
[f]Anal. Calc. for $C_9H_6ClN_3O_2$: C, 48.34; H, 2.71. Found: C, 48.67; H, 2.77%.
[g]Anal. Calc. for $C_9H_6BrN_3O_2$: C, 40.31; H, 2.24. Found: C, 40.42; H, 2.43%.
[h]Anal. Calc. for $C_{16}H_{10}N_4O_4$: C, 58.06; H, 3.25; N, 18.06. Found: C, 58.06; H, 3.34; N, 17.52%.

REFERENCES

1. C. K. INGOLD. Structure and mechanism in organic chemistry. Cornell, New York. 1953. p. 248.
2. I. L. FINAR and R. J. HURLOCK. J. Chem. Soc. 3024 (1957).
3. I. L. FINAR and R. J. HURLOCK. J. Chem. Soc. 3259 (1958).
4. M. A. KHAN, B. M. LYNCH, and Y. HUNG. Can. J. Chem. **41**, 1540 (1963).
5. K. VON AUWERS and H. MAUSS. Ann. **452**, 182 (1927).
6. N. K. KOCHETKOV, E. D. KHOMUTOVA, O. B. MIKHALOVA, and A. N. NESMEYANOV. Izv. Akad. Nauk SSSR Otd. Khim. Nauk. 1181 (1957).
7. F. G. BORDWELL and E. W. GARBISCH. J. Am. Chem. Soc. **82**, 3588 (1960).
8. (*a*) G. A. OLAH, S. J. KUHN, and S. H. FLOOD. J. Am. Chem. Soc. **83**, 4571 (1961).
   (*b*) B. M. LYNCH and J. A. MACPHEE. Unpublished experiments.
9. P. B. D. DE LA MARE and J. H. RIDD. Aromatic substitution: nitration and halogenation. Butterworths, London. 1959. p. 76.
10. R. O. C. NORMAN and G. K. RADDA. J. Chem. Soc. 3030 (1961).
11. B. M. LYNCH and Y. HUNG. Unpublished experiments.
12. R. E. RICHARDS and T. P. SCHAEFER. Trans. Faraday Soc. **54**, 1280 (1958).
13. L. M. JACKMAN. Nuclear magnetic resonance spectroscopy in organic chemistry. Pergamon, London. 1959. p. 126.
14. H. SPIESEKE and W. G. SCHNEIDER. J. Chem. Phys. **35**, 731 (1961).
15. E. BULLOCK. Can. J. Chem. **41**, 711 (1963).
16. R. E. RICHARDS and T. SCHAEFER. Mol. Phys. **1**, 331 (1958).

Can. J. Chem. Downloaded from www.nrcresearchpress.com by 210.87.254.105 on 09/05/12
For personal use only.

Can. J. Chem. Downloaded from www.nrcresearchpress.com by 210.87.254.42 on 09/05/12
For personal use only.

STUDIES ON THE THERMODYNAMICS AND CONDUCTANCES OF MOLTEN SALTS AND THEIR MIXTURES

PART II. THE VISCOSITIES, HEATS OF FUSION, AND HEAT CAPACITIES OF LITHIUM CHLORATE AND LITHIUM CHLORATE – LITHIUM NITRATE MIXTURES

A. N. Campbell and M. K. Nagarajan
Department of Chemistry, University of Manitoba, Winnipeg, Manitoba
Received February 6, 1964

ABSTRACT

The viscosities at different temperatures of pure molten lithium chlorate and of mixtures of lithium chlorate with lithium nitrate have been determined with high precision. The heats of fusion, and the molar heat capacities of both solid and liquid lithium chlorate, and of mixtures of lithium chlorate and lithium nitrate have also been determined. The heat of the transition $\alpha\ LiClO_3 \rightleftharpoons \beta\ LiClO_3$ has been obtained as the difference between the heats of solution in water of the two forms. The enthalpy, free energy, and entropy of mixing have been derived.

There is no simple theory which describes quantitatively the relationship between viscosity and composition of molten salt mixtures. Harrap and Heymann (1) determined the viscosity of a number of salt mixtures. They found that the viscosity isotherm was either "ideal", i.e. in conformity with the mixture rule, or exhibited a negative deviation from ideality. In some cases, their results suggested the formation of a complex between the two constituents of the mixture.

The only previous study of molten lithium chlorate is that of Klotschko and Grigorew (2): their value for the viscosity of molten anhydrous lithium chlorate (66.2 cP at 128 °C) is almost twice that found by us. No previous work has been done on the viscosities of mixtures of molten lithium chlorate with other salts.

Since the temperature range of the present investigation was sufficiently low, the conventional Ostwald viscometer, as modified by Campbell, Debus, and Kartzmark (3), was used. A small fritted glass disk was attached to the sidearm used for filling, to prevent any silt or suspended impurities entering the viscometer. The essential feature of the Campbell–Debus instrument is that it can be used at temperatures at which the vapor pressure is greater than 1 atmosphere (up to 20 atmospheres, if precautions are taken to thicken the glass appropriately), or when, as here, the system is extremely hygroscopic. Refilling is brought about simply by rotating the instrument through 180°, without the necessity of opening the viscometer. Our viscometers were calibrated with water in the range of 110° to 160 °C. In each case the water was frozen, evacuated, and remelted four times, to remove dissolved gases before final sealing off. A simple mechanical device, comprising a geared drive and a long handle, made it possible to rotate the viscometer without removing it from the hot thermostat. The nature and accuracy of the thermostat were mentioned in a previous communication (4). Time of flow was measured to $\pm$ 0.1 second, by means of an electrical stop clock. Flow times were measured in the region 100° to 160°. Using the known densities and viscosities of water, a calibration factor $C = \eta/\rho t$ was calculated (t = time). This calibration factor varies consistently with temperature: it was, therefore, plotted against temperature, so that C could be read off for any experimental temperature.

The viscometer was filled by exactly the same technique as was described for the

filling of the dilatometers (4). Here again, the fritted glass disk was of vital importance for removing any silt produced during the sealing operation. With molten salts, the reproducibility of the flow times was ± 5 s on a total time of about 10 000 s. The flow times were measured at different temperatures, for mixtures containing, respectively, the following mole fractions of lithium nitrate: 0.000, 0.030, 0.082, 0.131, 0.206, and 0.260. The appropriate density values were obtained by interpolation from the density data, given in a previous publication (4).

A careful estimate of the various sources of error indicates the error of our experimental work to be not more than $\pm 0.1\%$, but the viscosities of the water used as calibration standard are only known, in this temperature range, with an accuracy of $\pm 1\%$. At lower temperatures, the temperature fluctuation of the thermostat, though only amounting to $\pm 0.1°$, caused an observable change in the viscosity values, since the temperature coefficient of viscosity is large at low temperatures: the deviation due to this effect, however, is well within the accuracy of the determination.

The need for accurate values of the heats of fusion to interpret the results of crysoscopic measurements has been stressed by Janz and Goodkin (5). Since some solid salts undergo allotropic transformation below their melting points, it is necessary to know these heats of transition, to compare their entropies of fusion with those of other salts. The structural changes in the melt, in the immediate neighborhood of the melting point, can be better understood if the heat capacity of the melt is known. The entropy change in the melt from some standard state (e.g. the melting point) is evaluated from the equation

$$\Delta S = \int_{T_s}^{T} C_p \, (\mathrm{d}T/T)$$

where T_s is the temperature of the standard state. This entropy change will be considerable if the melt is associated, as is lithium chlorate. It is possible to make a theoretical calculation of ΔS, on the basis of an assumed structural model for the melt, if certain other data are available, and the comparison of this value of ΔS with the experimental value provides a test of the plausibility of the model.

Calorimetric data on mixtures of molten salts provide an understanding of the interactions in the melt. The heats of mixing (ΔH^m), of a large number of anion mixtures have been shown (6) to satisfy the equation

$$\Delta H^m/n_2 = \Delta H^t(t) + an_1$$

where n_1, n_2 are the mole fractions of the two components, $\Delta H^t(t)$ is the hypothetical heat of fusion of the higher melting component at the temperature of the mixture, and "a" is a constant, designated an "interaction parameter". Kleppa and Meschel (6) suggest that it may be possible to explain their results for the alkali halide – nitrate systems by taking into account, in addition to the electrostatic and van der Waals forces, the short range, anion–anion repulsive potential. They do not give any explicit equation for the interaction parameter "a".

The free energy of mixing can be obtained from the equation $\Delta F^m = \overline{\Delta F}_1 - \overline{\Delta F}_0 = \overline{\Delta H}_1 - \overline{\Delta H}_0 - T(\overline{\Delta S}_1 - \overline{\Delta S}_0) = RT \ln a$, where $\overline{\Delta F}_1$, $\overline{\Delta H}_1$, and $\overline{\Delta S}_1$, refer to the mixture and $\overline{\Delta F}^0$, $\overline{\Delta H}_0$, and $\overline{\Delta S}_0$ to one of its components in the pure state. The deviation of ΔF^m or ΔH^m from ideal behavior is generally related to some type of interionic action, which, in the extreme case, may amount to the formation of definite complexes. Unless, however, corroborative evidence is obtainable from other types of measurement, it is difficult to decide about complex formation in molten salt mixtures, from activity data alone.

Can. J. Chem. Downloaded from www.nrcresearchpress.com by 210.87.254.42 on 09/05/12
For personal use only.

Can. J. Chem. Downloaded from www.nrcresearchpress.com by 210.87.254.42 on 09/05/12
For personal use only.

No calorimetric data of any kind have been reported, either for lithium chlorate or its mixtures. The solid state transition from α lithium chlorate to β lithium chlorate was first reported by Kraus and Burgess (7) and later confirmed by Campbell and Griffiths (8). Campbell, Kartzmark, and Nagarajan (9) obtained a value of 99.1° for the transition temperature, in close agreement with the results of other workers. No determination of the heat of transition had previously been made.

A considerable amount of thermal work has been done on lithium nitrate (10). The heat of fusion of lithium nitrate has been reported as 6060 cal per mole. The molar heat capacity of solid lithium nitrate is 26.68 cal $mole^{-1}$ $degree^{-1}$ at 210° and that of liquid lithium nitrate 26.89 cal $mole^{-1}$ $degree^{-1}$ at 280 °C. No work has been done on the temperature dependence of the heat capacity of lithium nitrate.

Heats of fusion of salts are generally measured by the method of mixtures. A calorimetric assembly is described by Goodkin, Solomons, and Janz (11) for the determination of heats of fusion of inorganic compounds and for this they claim an accuracy of $\pm 2\%$. Our arrangement is quite similar to this, but we introduced a number of modifications to increase the accuracy.

An electric furnace of large heat capacity was kept at constant temperature, by means of the photoelectric control described by Campbell and Kartzmark (21). The furnace was mounted in a vertical position immediately above the calorimeter. The furnace had a swing door, which cut off the heated air space. Within the air space, the heated specimen, contained in a sealed glass container, was suspended by a thread. By swinging aside the door and applying a lighted match to the thread, the sample was precipitated into the calorimeter in a fraction of a second. An examination with a thermocouple probe showed that a band of uniform temperature, 5 inches long, existed in the furnace and within this band the sample was suspended. In the region 90 °C to 180 °C, the temperature was constant within $\pm 0.2°$.

The vacuum-jacketed calorimeter was entirely of glass and was placed in a heavily insulated box. The wooden box was mounted on wheels running on rails. Not until the last moment, that is when we were about to discharge the sample from the furnace, was the calorimeter run under the furnace. The water equivalent of the calorimeter was determined in the usual way from the electrical input necessary to produce an observed rise of temperature. Current was measured from the drop in potential across a standard resistance (about 1 ohm) in series with the calorimeter coil. The heat energy developed is, therefore, given by $E_1E_2t/4.186\,R_s$, where E_1 is the potential across the heating coil, E_2 that across the standard resistance, and R_s the value of the standard resistance. The source of energy was a 6-volt storage battery. The heat energy could be measured to ± 0.1 cal.

A 10-junction copper–constantan thermocouple was inserted in the calorimeter, the cold junctions being kept in a thermostat at 28.0 $\pm$ 0.01 °C. The junctions of the thermocouple were connected to a Varian recorder, which had a voltage span of 3 millivolts. This gave a potential difference of 0.073 °C per division of chart paper and, since it was possible visually to divide the chart paper division into 10 parts, there was an actual sensitivity of measurement of ± 0.007 °C. The calorimeter was stirred with a magnetic stirrer.

Actual temperature measurements were not made. The calculation reduced, after correction for radiation, to the comparison of two heights on the chart paper, one due to the calorimetric experiment and one to a known input of electrical energy. As a check on the accuracy of the apparatus, we determined the specific heat of pure copper, between

Can. J. Chem. Downloaded from www.nrcresearchpress.com by 210.87.254.42 on 09/05/12
For personal use only.

room temperature and 160.0 °C and between room temperature and 198.8 °C. The values we obtained were 0.0959 cal g^{-1} and 0.0967 cal g^{-1}, as against literature values of 0.0953 and 0.0962, respectively.

Anhydrous lithium chlorate and lithium chlorate – lithium nitrate mixtures were loaded into pyrex glass tubes, 20 mm diameter and 5 cm long, using the technique described in Part I of this series (4). Because of the numerous sources of error in calorimetric measurements it is difficult to estimate the accuracy of the final measurement. The only guide, under the circumstances, is the variation from linearity, when molar heat capacity is plotted against temperature. On this basis, the probable error in the molar heat capacities of the solid salts appears to be about $\pm 1\%$ at higher temperatures and closer to $\pm 2\%$ at lower temperatures. The heat capacities of liquid salts and the heats of fusion will have a higher accuracy than this, since larger quantities of heat are involved.

For the heats of solution (in water) the samples were sealed in bulbs which had very thin bottoms and which could therefore be readily broken by the impact of a glass rod. Since the aim of these experiments was to determine the heat of the transition $\alpha \rightleftharpoons \beta$ of the two forms of lithium chlorate it was necessary to prepare both forms in a state of purity. The low temperature α form obtains inevitably in any preparation which has been kept at room temperature for a sufficient length of time. The β form was obtained by heating anhydrous lithium chlorate in a Vycor tube in the controlled furnace at the temperature of 110 °C (transition temperature = 99.1 °C) for 2 weeks. The tube was then dropped into liquid nitrogen, whereby the β form was preserved in the metastable form. We estimate the error of measurement in the determinations of heat of solution to be ± 5 cal on a total of about 400 cal or $\pm 1.5\%$.

RESULTS

The viscosity temperature data have been fitted to the equation

$$\eta = \eta_0 \, e^{(E_{vis}/RT)}$$

by the method of least squares on a computer. Table I gives the numerical values of this equation for pure lithium chlorate and for various values of n_2 = mole fraction of lithium nitrate. The actual experimental data are to be found in the Ph.D thesis of M. K. Nagarajan, University of Manitoba, 1963.

TABLE I

Viscosities of lithium chlorate and lithium chlorate – lithium nitrate mixture in the form of equation $\eta = \eta_0 \, e^{(E_{vis}/RT)}$

n_2 = mole fraction lithium nitrate	Equation	St. dev., P
0	$\eta = 1.979 \times 10^{-5} \, e^{7813/RT}$	±0.005
0.030	$\eta = 1.814 \times 10^{-5} \, e^{8002/RT}$	±0.003
0.082	$\eta = 1.202 \times 10^{-5} \, e^{8481/RT}$	±0.002
0.131	$\eta = 1.446 \times 10^{-5} \, e^{8401/RT}$	±0.003
0.206	$\eta = 1.848 \times 10^{-5} \, e^{8254/RT}$	±0.008
0.260	$\eta = 1.621 \times 10^{-5} \, e^{8399/RT}$	±0.006

Table II contains the values of η_0 and E_{vis} for different mixtures, as obtained from the "best" equation.

The variation of viscosity with composition at constant temperature is shown in Fig. 1. The interpolations at arbitrarily chosen temperatures were carried out by means of the computer, employing the equations of "best" fit. The data so obtained were analyzed

TABLE II

Activation energies for viscous flow

$\eta = \eta_0 e^{E_{vis}/RT}$

n_2	$\eta_0 \times 10^5$	E_{vis}, cal
0.000	1.979	7813
0.030	1.814	8002
0.082	1.202	8481
0.131	1.446	8401
0.206	1.848	8254
0.260	1.621	8399

TABLE III

Values of B_0, B_1, and B_2 in the equation $\eta = B_0 + B_1n_2 + B_2n_2^2$

T, °K	B_0	B_1	B_2	St. dev., P
390.0	0.479	2.676	−5.341	±0.014
400.0	0.372	1.958	−3.828	±0.009
410.0	0.292	1.451	−2.775	±0.006
420.0	0.233	1.088	−2.033	±0.003
430.0	0.187	0.825	−1.503	±0.002
440.0	0.152	0.632	−1.119	±0.001
450.0	0.124	0.489	−0.840	±0.001

by the method of least squares and were found to fit the equation $\eta = B_0 + B_1n_2 + B_2n_2^2$, satisfactorily. The values of B_0, B_1, and B_2 are tabulated in Table III.

Since the calculation of all our results involved a knowledge of the specific heat of Pyrex glass 7740, it was necessary to know this with accuracy. According to the Corning Glass Works (Pyrex Catalogue), this specific heat is 0.20 cal g^{-1}. This value, however, did not seem to satisfy completely all our calculations, and we found it advisable to redetermine the specific heat of Pyrex glass 7740 with the following results:

TABLE IV

Specific heat of Pyrex glass No. 7740

Temperature, °C	Specific heat, cal deg^{-1} g^{-1}
97.5	0.163
126.4	0.166
153.0	0.169
173.1	0.171

Apparently, the value 0.20 must refer to a temperature higher than those at which we have worked.

Table V contains the molar heat capacities of solid and of liquid forms, and the heats and entropies of fusion of pure lithium chlorate and of mixtures of lithium chlorate with lithium nitrate. The specific heats are assumed to be constant over the range of temperature investigated, viz. 156.5 °C to 127.8 °C for the liquid form and 127.8 °C to room temperature (say, 20 °C) for the solid form. It is also assumed that the specific heats of the α and β forms are the same, an allowable assumption, in view of the small heat of transition.

The heat of mixing of n_1 mole fraction of lithium chlorate and n_2 mole fraction of lithium nitrate was calculated as the difference between the observed and calculated

Can. J. Chem. Downloaded from www.nrcresearchpress.com by 210.87.254.42 on 09/05/12
For personal use only.

TABLE V

Calorimetric data on lithium chlorate – lithium nitrate system (n_2 = mole fraction of lithium nitrate)

n_2	Molar heat capacity (C_p), cal deg^{-1} mole^{-1}		Freezing pt. (T_f), °K	ΔH_f, cal mole^{-1}	ΔS_f, cal deg^{-1} mole^{-1}
	Solid	Liquid			
0.000	24.51±0.21	29.20±0.13	401.0	2470±12	6.16
0.050	24.66±0.22	29.17±0.13	399.5	2811±13	7.04
0.105	24.81±0.23	29.11±0.17	397.8	3198±16	8.04
0.146	24.93±0.23	29.06±0.12	396.4	3490±15	8.80
0.196	25.03±0.20	28.98±0.13	394.3	3842±17	9.74
0.255	25.14±0.26	28.84±0.19	391.1	4248±17	10.86

values of heat contents at 401.0 °K (melting point of lithium chlorate), i.e. $\Delta H^m = \Delta H_{obs} - \Delta H_{calc}$. The observed heat content was defined as

$$\Delta H_{obs} = \Delta H_{f(mix)} + \int_{T_f}^{401.0} C_{p(l)} dT$$

where $\Delta H_{f(mix)}$, T_f, and C_p refer to the heat of fusion, freezing temperature, and molar heat capacity in the liquid state of the mixture. The calculated heat content was obtained from the equation:

$$\Delta H_{(calc)} = n_1 \Delta H_{(f)1} + n_2 \Delta H_{(f)2}$$

where $\Delta H_{(f)1}$ and $\Delta H_{(f)2}$ are the molar heats of fusion of lithium chlorate and of lithium nitrate at 401.0 °K. $\Delta H_{(f)2}$ was in turn obtained from the Kirchhof equation

$$\Delta H_{(f)2} = \Delta H_{f(p)} + \int_{T_p}^{401.0} \Delta C_p \, dT$$

where $\Delta H_{(f)p}$ is the heat of fusion of lithium nitrate at its melting point T_p and ΔC_p is the difference between the molar heat capacities of solid and liquid lithium nitrate, i.e. $\Delta C_p = C_{p\ solid} - C_{p\ liquid}$. It is assumed that C_p of lithium nitrate does not alter with temperature. The isothermal heats of mixing, correct to ±2%, are given in Table VI.

TABLE VI

Heats of mixing in lithium chlorate – lithium nitrate system at 401.0 °K (n_2 = mole fraction of lithium nitrate)

n_2	Heat content (calc.) ΔH_{calc}, cal mole^{-1}	ΔH_f of sample, cal mole^{-1}	$\int_{T_f}^{401.0} C_{p(l)}\,dT$, cal mole^{-1}	Heat content (obs.) ΔH_{obs}, cal mole^{-1}	ΔH^m, cal mole^{-1}	$\Delta H^m/n_2$ cal mole^{-1}
0.050	2648	2811	43.8	2855	+207	+4150
0.105	2843	3198	93.2	3291	+448	+4264
0.146	2989	3490	133.7	3624	+635	+4351
0.196	3167	3842	194.2	4036	+869	+4432
0.255	3377	4248	285.5	4533	+1156	+4534

NOTE: $\Delta H_{f(1)} = 2470$ cal mole^{-1}; $\Delta H_{f(2)} = 6060 + \int_{401.0}^{528.1} \Delta C_{p(2)} dT$; $\Delta C_{p(2)} = -0.276$ cal deg^{-1} mole^{-1}.

The heat of the transition $\alpha\,LiClO_3 \rightleftharpoons \beta\,LiClO_3$ was obtained as the difference between the heats of solution of α and β forms, at corresponding concentrations. The heat of solution was calculated in the usual way, viz. values of $(\sum \Delta H_1 / \sum x_1)$ were plotted against

Can. J. Chem. Downloaded from www.nrcresearchpress.com by 210.87.254.42 on 09/05/12
For personal use only.

TABLE VII

Heats of solution of α and β lithium chlorate

	No. moles sample added to 1 liter of solution (x_i)	Heat change during each addition (ΔH_i), cal	Total concn. (Σx_i), mole liter^{-1}	Total heat change per mole (ΔH_{soln}), cal mole^{-1}
α-Form	0.238	+88.1	0.238	+369.6
	0.289	+102.1	0.527	+362.1
	0.268	+91.5	0.795	+354.9
β-Form	0.195	−49.4	0.195	−253.2
	0.117	−28.2	0.312	−248.8
	0.198	−46.2	0.510	−242.8
	0.223	−48.5	0.733	−235.1

NOTE: $\Delta H_{soln}(\alpha)$ extrapolated to infinite dilution = +375.7.
$\Delta H_{soln}(\beta)$ extrapolated to infinite dilution = −258.7.
Heat of transition α $LiClO_3 \rightleftarrows \beta$ $LiClO_3$ = +634.4 cal mole^{-1}.
Entropy of transition = ΔS_{trans} = 1.70 cal deg^{-1} mole^{-1}.

$\sum x_1$ where ΔH_1 and x_1 are the heat change and the molarity at the end of each addition. Three or four additions were made. Table VII reproduces the data.

The equation

$$\ln a = \frac{\Delta H_f}{R}\left(\frac{1}{T} - \frac{1}{T_p}\right) + \frac{\Delta C_p}{R}\left(\ln \frac{T_f}{T} - \frac{T_f - T}{T}\right)$$

was used to calculate the activity of lithium chlorate in mixtures. The values of T and T_f were those of Campbell, Kartzmark, and Nagarajan (9): ΔH_f and ΔC_p were obtained in this investigation. The free energy of mixing results from $\Delta F^m = RT \ln a$. Activities and free energies of mixing are given in Table VIII. The entropy of mixing, ΔS^m was

TABLE VIII

Free energies of mixing in lithium chlorate – lithium nitrate system (n_1 = mole fraction of lithium chlorate)

n_1	T_f (°K)	Activity of lithium chlorate, a	$\Delta F^m = RT_f \ln a$, cal mole^{-1}
1.000	401.0	1.000	—
0.950	399.5	0.988	−9.3
0.854	396.4	0.964	−28.6
0.725	390.2	0.919	−65.8
0.640	384.1	0.875	−102.4
0.585	379.5	0.841	−130.2
0.536	373.9	0.803	−160.9

obtained from these free energies of mixing and the heats of mixing given in Table VI. Table IX contrasts the values of the free energy, enthalpy, and entropy of mixing (at different concentrations of lithium nitrate) at 401.0 °K. The ideal entropies of mixing were also calculated and are shown in the last column of Table IX.

DISCUSSION

We find the viscosity of pure molten lithium chlorate in the temperature range 128° to 170° is represented by the relation

$$\eta = 1.979 \times 10^{-5}\, e^{7813/RT}$$

Can. J. Chem. Downloaded from www.nrcresearchpress.com by 210.87.254.42 on 09/05/12
For personal use only.

TABLE IX

Free energy, enthalpy, and entropy of mixing in lithium chlorate – lithium nitrate system at 401.0 °K (n_1 = mole fraction of lithium chlorate)

n_1	ΔF^m, cal mole^{-1}	ΔH^m, cal mole^{-1}	$T\Delta S^m$, cal mole^{-1}	ΔS^m, cal deg^{-1} mole^{-1}	ΔS^m (ideal), cal deg^{-1} mole^{-1}
1.000	0.000	0.000	0.000	0.000	0.000
0.950	−9.3	+207.5	+216.8	+0.541	+0.102
0.895	−20.8	+447.7	+468.5	+1.168	+0.221
0.854	−28.6	+635.3	+663.9	+1.656	+0.314
0.804	−40.9	+868.7	+909.6	+2.268	+0.433
0.745	−58.9	+1156.2	+1215.0	+3.030	+0.585

NOTE: ΔF^M values obtained by interpolation.

Klotschko and Grigorew (2) reported the values of the viscosity of molten lithium chlorate as 66.2 and 52.2 cp at 128° and 136° respectively. The values consistently obtained by us at these temperatures are 38.3 and 29.8 cP, respectively.

The activation energy of viscous flow is 7.8 kcal, a value similar to those reported in the literature for a number of salts, in fact, the E_{vis} of lithium chlorate is closer to those of ionic melts (NaCl, KCl, etc.) than to those of associated melts, such as the alkali nitrates. It may be that a greater configurational change is involved in the viscous flow of molten lithium chlorate than in other associated melts. The activation energy for electrical conductance has been found by Dr. D. F. Williams of this laboratory, to be 6.13 kcal. Hence the ratio E_{vis}/E_Ω has a value of 1.27, and this is in good agreement with the values reported for associated melts, although this ratio is also affected by the relative sizes of anions and cations.

The presence of nitrate ion in the rather compact lithium chlorate lattice leads to an increase in viscosity and this suggests the possible formation of larger and more unsymmetrical clusters. In all other systems of molten salts hitherto studied, a decrease of viscosity only (negative deviation from ideality) has been noticed (1) and hence the positive deviation exhibited by the lithium chlorate – lithium nitrate system becomes interesting. Even at higher temperatures, the observed viscosity is higher than the ideal value calculated from the relation,

$$\eta_{calc} = n_1\eta_1 + n_2\eta_2$$

where η_1 and η_2 are the viscosities of pure lithium chlorate and of pure lithium nitrate (extrapolated for supercooled melt). Thus, at 440 °C, η_{obs} is 0.237 poise, whereas $n_1\eta_1 + n_2\eta_2$ is 0.154 P, for a mixture containing 0.2 mole fraction lithium nitrate.

We have no direct evidence about the nature of the interaction between nitrate ion and chlorate lattice. A suggested mechansim might be as follows:

1. The activation energy of viscous flow has increased.
2. The unit of viscous flow has become more complex.
3. The number of vacant sites or holes available for the migration of the particles has decreased.

It is possible that some kind of rearrangement takes place on addition of nitrate ion to the chlorate lattice, in such a way as to reduce the volume. Such a reduction in volume would result from the formation of more compact structures, due to the presence of the nitrate ion in the chlorate lattice. The abnormally high viscosity of molten lithium chlorate may be due to the existence of clusters, and the increase in viscosity on the addition of lithium nitrate could result from the bridging of two or more clusters by the nitrate ion.

Can. J. Chem. Downloaded from www.nrcresearchpress.com by 210.87.254.42 on 09/05/12
For personal use only.

Can. J. Chem. Downloaded from www.nrcresearchpress.com by 210.87.254.42 on 09/05/12
For personal use only.

These clusters, which are low energy preferred configurations moving as one unit during the process of transport, need not necessarily contain covalent bonds between the lithium and chlorate ions. The chlorate ion is pyramidal in shape with Cl—O distance of approximately 2.3 Å. Owing to its shape and large size, the chlorate units might give rise to close-packed anionic groupings, with Li^+ ions, ($r = 0.6$ Å) occupying the interspaces. During the process of transport, the chlorate sublattice and Li^+ ions may move as one unit, due to some kind of a co-operative (presumably rotational) effect, thus constituting, in effect, a cluster: thus, the size of the cluster will be partly determined by the co-ordination number and the non-availability of free space for rotation. Increase of temperature will allow more free space for rotation and hence give rise to a decrease in either the size or the number of clusters. The presence of unsymmetrical nitrate ion (flattened disk shape, with a height of 2.2 Å) could augment this co-operative effect, which is essentially a steric effect, yielding apparently bigger clusters.

The value of the entropy of fusion for lithium chlorate, 6.16 cal deg^{-1} $mole^{-1}$, is higher than that of most salts which give rise to an ionic melt, and falls within the general region of salts which are predominantly associated. The entropy of the transition at 99.1 °C, 1.70 cal deg^{-1} $mole^{-1}$, must be added to the entropy of fusion, when discussing the latter. The total entropy change is therefore 7.86 cal deg^{-1} $mole^{-1}$. The abnormally low melting point of lithium chlorate is probably due to entropy contributions from sources other than positional changes. It is possible that particularly low energy configurations occur in molten lithium chlorate which contribute an additional term (ΔS_{assoc}) to the total entropy of fusion. The molar heat capacity of molten lithium chlorate, 29.20 cal deg^{-1} $mole^{-1}$ is similar to those of molten alkali nitrates. It is generally agreed that association of some sort occurs in molten alkali nitrates. It therefore seems probably that similar association occurs in molten lithium chlorate.

The entropy of fusion of lithium chlorate – lithium nitrate mixtures increases sharply with increasing concentration of lithium nitrate (from 6.16 e. u. at $n_2 = 0$, to 10.86 at $n_2 = 0.255$). Although the entropy of fusion of lithium nitrate is itself very high (10.86 e. u.), the increase in entropy of fusion of lithium chlorate when lithium nitrate is added is much greater than that calculated from the mixture rule. For instance, at $n_2 = 0.255$, ΔS_f, calculated from $\Delta S_f = n_1\Delta S_{f(1)} + n_2\Delta S_{f(2)} = 7.51$ e. u., whereas the experimental value is 10.86 e. u. This sharp increase in entropy of fusion may result from some kind of interaction between nitrate ion and chlorate lattice. The change in the molar heat capacity of lithium chlorate – lithium nitrate mixtures also supports this view. If the ideal values of C_p are calculated from the mixture rule, it is found that the observed values exhibit positive deviation from ideality, in both the solid and the liquid states, the deviation being more pronounced in the liquid than in the solid state. The difference here, however, is small (<1%), not much greater than the experimental error, and so no attempt has been made to interpret these differences on a quantitative basis, as was done for molar volume (4). Nevertheless, the fact that the deviation is positive indicates that the nitrate ion (or the chlorate lattice) does not exist in the melt as such but is part of the structural unit resulting from a possible interaction of nitrate ion with chlorate lattice. The formation of a more complex cluster than that present in pure molten lithium chlorate, perhaps by a process of bridging by the nitrate ion, could account for the positive deviation of C_p from ideality, as well as the sharp increase in entropy of fusion.

The heat of mixing in the molten lithium chlorate – lithium nitrate system at 401.0 °K (the melting point of lithium chlorate) is positive and increases with increasing addition of lithium nitrate. This is in agreement with the findings of Kleppa and Meschel (6) that in all the anion mixtures studied by them, the heat of mixing was positive. They find it

useful to plot $\Delta H^m/n_2$ against n_2, the mole fraction of the addendum. They found that their thermal data on a number of systems satisfied the relation:

$$\Delta H^m/n_2 = \Delta H_{f(t)} + a(1 - n_2).$$

Where the "interaction parameter", a, is a constant. The limiting value of a at $n_2 = 0$, represents, according to Kleppa and Meschel, the partial molal enthalpy associated with the transfer of 1 mole of the second component from the pure crystalline state into admixture with the "pure" liquid state of the first component at the temperature of the mixture. They consider this value to be formally composed of two terms: (a) the enthalpy change, $\Delta H_{f(t)}$ of fusion of the second component, at the temperature of the mixture, and (b) the enthalpy change associated with the solution of this supercooled liquid in the pure liquid first component. Hence the value of $\Delta H^m/n_2 = \Delta H_{f(t)} + a$ at $n_2 = 0$, must be the sum of the above two quantities. The factor "a" thus represents the effect of any possible interaction between the two components.

The values of $\Delta H^m/n_2$ listed in Table VI are plotted against n_2 in Fig. 2. The data were

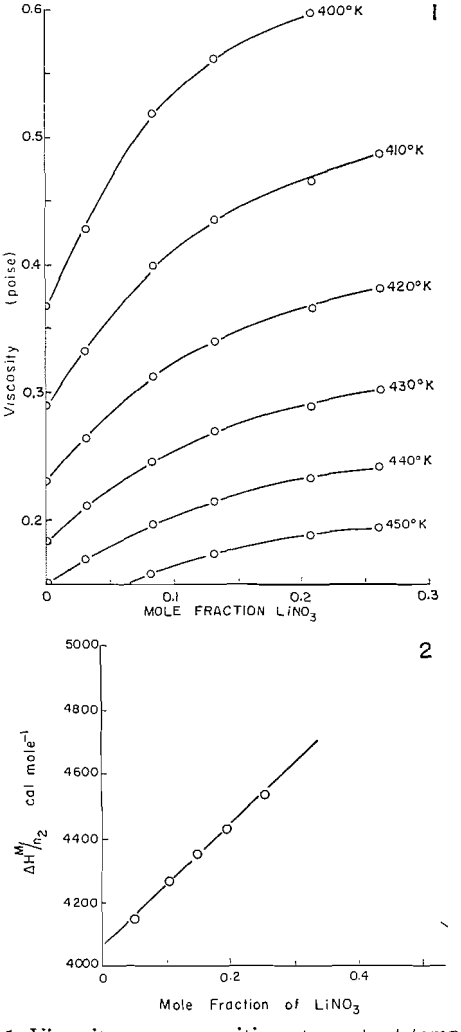

FIG. 1. Viscosity vs. composition at constant temperature.
FIG. 2. Plot of $\Delta H^m/n_2$ vs. n_2.

Can. J. Chem. Downloaded from www.nrcresearchpress.com by 210.87.254.42 on 09/05/12
For personal use only.

found (by least squares technique) to satisfy the linear relation

$$\Delta H^m/n_2 = (4.060 + 1.93\, n_2) \text{ kcal.}$$

Therefore,
$$\Delta H_{f(t)} + a = 4.060 \text{ kcal},$$
$$a = -1.93 \text{ kcal},$$
and
$$\Delta H_{f(t)} = 5.990 \text{ kcal}.$$

The value of $\Delta H_{f(t)}$ is given by the expression:

$$\Delta H_{f(t)} = \Delta H_{f(m.p.)} + \int_{401.0}^{T_p} \Delta C_p dT$$

where $\Delta H_{f(m.p.)}$ is the heat of fusion of pure lithium nitrate at its melting point, T_p, and $\Delta C_p = C_p$ (solid) $- C_p$ (liquid), for lithium nitrate. Using the value of 6060 cal mol^{-1} for $\Delta H_{f(m.p.)}$ the value of ΔC_p (assume to be constant in the temperature region 401.0 °C to T_p) results as -0.55 cal deg^{-1} mole^{-1}. The value of ΔC_p calculated from the data in the literature is -0.22 cal deg^{-1} mole^{-1}.

For the system under study, the interaction parameter, a, is negative and large; Kleppa and Meschal (6) found that the value of "a" is a small positive number (0.2 to 0.4) for the alkali nitrate system studied by them, but that it has decided negative values for the systems $AgNO_3$—AgCl and $AgNO_3$—AgBr ($-$ 1.13 kcal and $-$ 2.17 kcal respectively). They explain the small positive values of "a" as being due to the anion–anion (i.e. second nearest neighbor) core repulsion, in addition to coulombic and van der Waals forces. On the other hand, they explain the decidedly negative values obtaining in the silver salts systems as "evidence for a certain degree of chemical interaction in the mixture". A similar explanation may be offered for the large negative interaction parameter ($a = -1.93$ kcal) for lithium chlorate – lithium nitrate mixtures. Since "a" is a measure of the enthalpy change associated with the solution of undercooled lithium nitrate in molten lithium chlorate at 401.0 °K, a negative value of "a" indicates a negative enthalpy change for the possible interaction of nitrate ion with chlorate lattice.

Although the free energy of mixing given in Table VIII is only approximate and subject to a number of assumptions, it gives additional support to the arguments presented above. The fact that the free energy of mixing is negative shows that the interaction between nitrate ion and chlorate lattice is a spontaneous process. The data of Table VIII show that, in spite of a very large positive enthalpy of mixing ΔH^m, the mixing process is spontaneous (ΔF^m is negative) since $T\Delta S^m$ is also large. Since the entropy of mixing plays such an important role in this system there must be pronounced structural effects. The large positive deviation of ΔS^m from ideality suggests that more stable, low energy configurations result on the addition of nitrate ion to chlorate lattice.

REFERENCES

1. B. S. Harrap and E. Heymann. Trans. Faraday Soc. **51**, 259 (1955).
2. M. A. Klotschko and I. C. Grigorew. Akad. Wiss. USSR, Nacht. Abt. Physik-Chem. Anal. **21**, 288 (1950). (English transl.).
3. A. N. Campbell, G. H. Debus, and E. M. Kartzmark. Can. J. Chem. **33**, 1508 (1955).
4. A. N. Campbell and M. K. Nagarajan. Can. J. Chem. **42**, 1137 (1964).
5. G. J. Janz and J. Goodkin. J. Phys. Chem. **63**, 1975 (1959).
6. O. J. Kleppa and S. V. Meschel. J. Phys. Chem. **67**, 668 (1963).
7. C. A. Kraus and W. M. Burgess. J. Am. Chem. Soc. **49**, 1226 (1927).
8. A. N. Campbell and J. E. Griffiths. Can. J. Chem. **34**, 1647 (1956).
9. A. N. Campbell, E. M. Kartzmark, and M. K. Nagarajan. Can. J. Chem. **40**, 1258 (1962).
10. K. K. Kelley. U.S. Bur. Mines Bull. 371 (1934).
11. J. Goodkin, C. Solomons, and G. J. Janz. Rev. Sci. Instr. **29**, 105 (1958).
12. A. N. Campbell and R. Kartzmark. Can. J. Chem. **34**, 1428 (1956).

Can. J. Chem. Downloaded from www.nrcresearchpress.com by 210.87.254.42 on 09/05/12
For personal use only.

Can. J. Chem. Downloaded from www.nrcresearchpress.com by 210.87.254.105 on 09/05/12
For personal use only.

AROMATIC SUBSTITUTION

PART VII.[1] COMPETITIVE REACTIONS OF PYRIDINE, 3-PICOLINE, AND 3-ETHYLPYRIDINE WITH PHENYLLITHIUM. ACTIVATION OF A NUCLEOPHILIC AROMATIC SUBSTITUTION BY ALKYL GROUPS

R. A. Abramovitch and Choo-Seng Giam[2]
Department of Chemistry, University of Saskatchewan, Saskatoon, Saskatchewan

Received February 2, 1964

ABSTRACT

The relative reactivities of pyridine, 3-picoline, and 3-ethylpyridine towards phenyllithium have been measured under various conditions by a competitive technique and have been found to be in the order: 3-picoline > pyridine > 3-ethylpyridine. A 3-methyl or ethyl substituent *activates* the 2-position relative to that in pyridine itself, while C_6 is deactivated as expected. A possible explanation is put forward for these observations and for the somewhat low yields that are obtained in such reactions. A method is described whereby arylation of pyridines with aryllithium compounds may be effected in high yields.

The predominant formation of 2-phenyl-3-methylpyridine in the reaction of phenyllithium with 3-picoline (1) has been shown to be the result of kinetic control of the addition step in this addition–elimination reaction rather than of thermodynamic control, since this step is irreversible to all intents and purposes (2). Possible explanations of the observed high ortho/para (with respect to the 3-alkyl group) ratio in this and related reactions have been discussed (1) and it clearly was important to establish whether this was due to a selective deactivation of the para position (C_6) with respect to the ortho position, or to some specific *activation* of the ortho position by the 3-substituent, which did not affect the 6-position. Reinheimer and Bunnett have reported cases of activation of an ortho position by a methyl group in certain nucleophilic aromatic substitutions, which they attributed to London dispersion forces between the polarizable approaching nucleophile and the methyl substituent (3).

Serious difficulties were encountered in attempts to study the kinetics of the reaction of phenyllithium with pyridine and with 3-picoline (4). It was, therefore, necessary to turn to competitive experiments in which an excess of equimolar amounts of pyridine and 3-picoline were allowed to react with a small amount of phenyllithium (from bromobenzene and lithium) under various conditions. The results so obtained paralleled those from the preliminary rough kinetic studies (4).

Three methods were used to work up the reactions. In the first (method A), the ether solvent was replaced by dry toluene and the temperature raised to ca. 110° to eliminate lithium hydride from the intermediate addition products. In method B, the ethereal suspension was boiled under reflux, cooled, and oxygen bubbled through to oxidize the intermediates. In method C, the mixtures in ether were stirred at room temperature for varying lengths of time before being oxidized with oxygen. An excess (1.5- to 10-fold, but generally 3-fold) of each pyridine was used and the products were analyzed by gas chromatography after the minimum amount of handling in the work-up. Though the combined yields of 2-phenylpyridine and 2-phenyl-3- and 2-phenyl-5-picoline varied according to the reaction method used, the 2,3-:2,5-isomer ratio remained virtually unchanged (ca. 95:5) within the limits of the experimental error. Table I summarizes a few of the results

[1]*Part VI. R. A. Abramovitch, F. Helmer, and J. G. Saha. Chem. Ind. London, 659 (1964).*
[2]*Present address: Imperial Oil Ltd., Sarnia, Ontario.*

thus obtained. The isomer ratios are correct to $\pm 2\%$ at the outside in most cases. The results of all the experiments described in this paper are the averages of a number of runs.

A number of features are apparent from a consideration of the results in Table I. The yields of products are on the low side and this leads one to worry about whether the isomer ratios and total rate ratios are meaningful or the intermediate σ-complexes are going to by-products at rates which differ according to the structure of the σ-complex. The relative constancy of the ratio of 2,3- to 2,5-phenylpicolines suggested that the isomeric σ-complexes from 3-picoline were not being removed at different rates.

The most striking feature of the results, however, was that it appeared as though, using method C and short reaction times, more phenylpicolines than 2-phenylpyridine were being formed, i.e., 3-picoline was reacting faster than pyridine with a nucleophilic reagent! It also appeared that, with increasing reaction time, the amount of 2-phenylpyridine formed increased with respect to that of the combined phenylpicolines. The following possible explanation had to be considered first, which would have had the merit of avoiding the assumption that 3-picoline was more susceptible to nucleophilic substitution than was pyridine and would account for the change in product ratios with time:

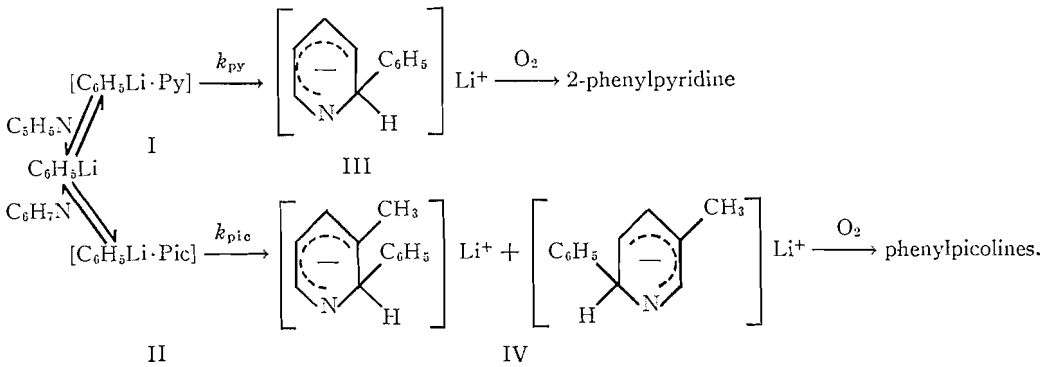

It seems most probable that each base rapidly forms a complex through the nitrogen atom with the organometallic compound.* Since the pyridines are present in excess they would compete for the phenyllithium available and, in view of the slightly greater basicity of 3-picoline over pyridine, one would expect somewhat more of complex (II) to be formed than of (I). These would then react irreversibly (2) to give the intermediate addition products (III) and (IV). Initially, therefore, one might expect more (IV) to be formed than (III). If, however, the 3-alkyl substituent deactivates the nucleus towards electrophilic attack by virtue of its (+I, +M) effect, i.e., $k_{py} > k_{pic}$, the amount of (III) would grow at a faster rate than that of (IV) and lead to the observed results.

To test this possibility an equimolar mixture of pyridine and 3-picoline was treated with *an excess of phenyllithium* to ensure that complexes (I) and (II) would be formed in about equal amounts. If, then, $k_{py} > k_{pic}$, more 2-phenylpyridine than 2-phenylpicolines should be formed from the outset. The results of such experiments are collected in Table II. A number of interesting conclusions may be drawn from the results. It is clear that initially more phenylpicolines are formed than 2-phenylpyridine, confirming that $k_{pic} > k_{py}$. Also, the yields of products obtained under these conditions are quite high (10 min

*This may either undergo intramolecular substitution, or the complex may be attacked by uncomplexed phenyllithium, or uncomplexed pyridine may be substituted by phenyllithium in equilibrium with the complex. Complexing should facilitate nucleophilic attack.

Can. J. Chem. Downloaded from www.nrcresearchpress.com by 210.87.254.105 on 09/05/12
For personal use only.

Can. J. Chem. Downloaded from www.nrcresearchpress.com by 210.87.254.105 on 09/05/12
For personal use only.

TABLE I

Reaction of "ordinary" phenyllithium with an excess of an equimolar mixture of pyridine and 3-picoline

Expt. No.	Moles of:			Relative amounts of:			Combined yields (%)	Method of work-up and time[b]	Ratio of 2-phenyl-pyridine to phenyl-picolines
	pyridine	3-picoline	phenyllithium[a]	2-phenyl-pyridine	2-phenyl-3-picoline	2-phenyl-5-picoline			
1	0.030	0.030	0.010	55	42	3	52	A (6.5 h)	55:45
2	0.030	0.030	0.010	55 (±1)	41	4	33±7	B (1 h)	55:45
3	0.030	0.030	0.0032	44	53	3	29±1	C (1 h)	44:56
4	0.010	0.010	0.0077	40	57	3	16	C (2 min)	40:60
5	0.010	0.010	0.0077	40	57	3	21	C (10 min)	40:60
6	0.010	0.010	0.0077	43	54	3	28	C (55 min)	43:57
7	0.010	0.010	0.0077	45	52	3	28	C (3 h)	45:55
8	0.010	0.010	0.0077	44	53	3	38	C (25 h)	44:56

[a]Determined by titration with acid just prior to use.
[b]In the cases of methods B and C, the time is that between the moment the addition of phenyllithium is complete and that when oxygen is passed through the mixture.

TABLE II

Reaction of mixtures of equimolar amounts of pyridine and 3-picoline with an excess of phenyllithium at 24°[a]

Reaction time (min)	% yield of 2-phenylpyridine	% yield of phenylpicolines[b]	Ratio of phenylpicolines to 2-phenylpyridine
4	36.3	44.0	55:45
6	76.0	76.9	50.5:49.5
10	81.0	79.0	49.5:50.5
21	85.5	78.4	48:52
62	74.5	64.2	46.5:53.5

[a][Pyridine] = [3-picoline] = 0.0015 mole, added within 2 min to phenyllithium (0.02 mole).
[b]Ratio of 2,3- to 2,5-isomers = 95:5. Yields are based on pyridine and 3-picoline, respectively.

and 21 min runs), the highest that have been reported for such reactions. *This now provides a convenient method of obtaining high yields in reactions of organolithium compounds with pyridine derivatives*, i.e., using an excess of the lithium derivative at room temperature and a limited reaction time. The fact that even when the phenylpicolines are formed in 79% yield the ratio of the 2,3- to the 2,5-isomer is still 95:5 confirms that there is no, or almost no, *selective* removal of the isomeric dihydropicolyllithium intermediates to form by-products, but that both isomers undergo side reactions at virtually the same rate (2). From the last column of Table II, it is seen that, whereas more phenylpicolines than phenylpyridine are formed initially, the latter predominates after a reaction time of over 10 minutes. That this is not due to the hypothetical situation discussed above is seen from a brief consideration of the actual yields of products formed at various intervals of time. The phenylpicolines attain a maximum yield of about 80%, after which the actual yield *starts to fall*, while that of 2-phenylpyridine is still increasing and only starts to fall some minutes later. This shows that while intermediates (IV) are being formed more rapidly than is (III) they go to by-products, probably by polymerization, at a faster rate than does (III) (the intermediate dihydropyridine is a *cis*-butadiene-like system and, in the presence of a Ziegler-type catalyst, might be expected to polymerize readily). This explains the apparent increase with time in the amount of 2-phenylpyridine formed relative to the phenylpicolines. It also suggests that the relative reactivities of 3-picoline and pyridine (ratios of phenylpicolines to 2-phenylpyridine (Table I)) are, if anything, on the low side and may be taken as a rough, but conservative, estimate of the total rate ratio ${}^{CH_3}_{H}K$ (see also discussion below). Confirmation that 3-picoline was more readily substituted than pyridine in this reaction was obtained by analysis of the above reaction mixtures (Table II) for unreacted pyridine and 3-picoline. This gave a molar ratio of pyridine:3-picoline consumed of 47:53. From the known concentrations of starting amines and the concentrations of recovered unchanged amines and assuming that equation

$$\frac{\log[\text{picoline}]-\log[\text{recovered picoline}]}{\log[\text{pyridine}]-\log[\text{recovered pyridine}]}=\frac{k_{\text{pic}}}{k_{\text{py}}}={}^{CH_3}_{H}K$$

holds (5), a value of ${}^{CH_3}_{H}K = 1.3$ could be calculated.

It should now be possible to calculate partial rate factors for attack at C_2 and C_6 in 3-picoline, taking the rate of reaction at C_2 in pyridine as a standard. In the light of the above discussion, these partial rate factors should, if anything, be on the low side. As no attack appears to take place at C_4 in the examples studied so far, one can write ${}^{H}K = 2{}^{H}k_2$, where ${}^{H}k_2$ is the rate constant for the reaction at C_2 in pyridine, and ${}^{CH_3}K = {}^{CH_3}k_2 + {}^{CH_3}k_6$

Can. J. Chem. Downloaded from www.nrcresearchpress.com by 210.87.254.105 on 09/05/12
For personal use only.

where $^{CH_3}k_2$ and $^{CH_3}k_6$ are the rate constants for attack at C_2 and C_6 of 3-picoline, respectively. Then $^{CH_3}_{H}K = {}^{CH_3}K/{}^{H}K = (^{CH_3}k_2 + {}^{CH_3}k_6)/2{}^{H}k_2$, i.e., $2^{CH_3}_{H}K = {}^{CH_3}F_2 + {}^{CH_3}F_6$. If the 2-substituted isomer in the phenylpicoline mixture forms a fraction (α_2) of the mixture then $^{CH_3}F_2 = (\alpha_2)(2^{CH_3}_{H}K)$ and $^{CH_3}F_6 = (\alpha_6)(2^{CH_3}_{H}K)$. Partial rate factors calculated in this way for the reactions listed in Table I are given in Table III.

TABLE III

Partial rate factors determined from competitive reactions of "ordinary" phenyllithium with an excess of an equimolar mixture of pyridine and 3-picoline

Expt. No.	1	2	4	5	6	7	8
$^{CH_3}F_2$	1.5	1.5	2.9	2.9	2.5	2.3	2.4
$^{CH_3}F_6$	0.11	0.13	0.15	0.15	0.13	0.12	0.13

In all cases, C_6 in 3-picoline was deactivated about sevenfold compared with the same position in pyridine, a result consistent with the known electrical effect of an alkyl group in nucleophilic aromatic substitution reactions. Also, C_2 in 3-picoline was *activated*—albeit to apparently varying extents according to the reaction conditions—compared with C_2 in pyridine. At the lower temperature used in method C it appears that the selectivity of the attacking species for C_2 is greater than at the higher temperatures.

The solutions of "ordinary" phenyllithium used above contain one equivalent of lithium bromide. Since pyridine and 3-picoline form complexes with lithium bromide [volumetric analyses of the 3-picoline:lithium bromide complex indicate that it is a 2:1 complex (pyridine also forms a 2:1 complex with lithium chloride (6))], it was possible that in the above competitive reactions lithium bromide might have formed a complex with the slightly more basic 3-picoline present in excess. To equalize the influence, if any, of the lithium bromide upon the reactivities of the pyridine nuclei, the above competitive reactions were repeated, this time adding the "ordinary" phenyllithium solutions to solutions of the pyridines containing an excess of anhydrous lithium bromide. The results of these experiments are collected in Table IV. There is a small but probably significant increase in $^{CH_3}F_2$ in all of these reactions, but the overall yields were low compared with those obtained in those reactions in which lithium bromide was not present in excess.

TABLE IV

Reaction of "ordinary" phenyllithium[a] with an excess of an equimolar mixture of pyridine and 3-picoline[b] containing an excess of lithium bromide[c]

Expt. No.	Method of work-up	Combined yields (%) of phenylated pyridines	Ratio of 2,3- to 2,5-phenylpicoline	Partial rate factors	
				$^{CH_3}F_2$	$^{CH_3}F_6$
9	A	42	96:4	3.7	0.16
10	C (30 min)	6.4	94:6	3.8	0.24
11	C (60 min)	13.3	94:6	3.8	0.24

[a][Phenyllithium] = 0.005 mole.
[b][Pyridine] = [3-picoline] = 0.015 mole.
[c][Lithium bromide] = 0.061 mole.

This increase in the selectivity of the phenylating agent might be due to complexing of lithium bromide etherate with phenyllithium (7):

$$C_6H_5Li.LiBr.2(C_2H_5)_2O \rightleftarrows C_6H_5Li + LiBr.2(C_2H_5)_2O.$$

Can. J. Chem. Downloaded from www.nrcresearchpress.com by 210.87.254.105 on 09/05/12
For personal use only.

The presence of an excess of lithium bromide would shift the equilibrium towards the complex which might be less reactive but more selective. It has already been reported (2) that less heat is evolved in the reactions of phenyllithium with pyridines in the presence of an excess of lithium bromide and this would tend to support the above suggestion. Since, however, little is known concerning the structure of phenyllithium (it has been reported to be dimeric in ether solution (8)—contrast with ethyllithium which may be tetrameric or hexameric (9)) further speculation about the reactivity of the complex would be fruitless.

To eliminate the possible influence of lithium bromide similar reactions were carried out using halide-free phenyllithium and the results of these experiments are given in Table V.

TABLE V

Reaction of halide-free phenyllithium[a] with an excess of an equimolar mixture of pyridine and 3-picoline[b]

Expt. No.	Method of work-up	Combined yields (%) of phenylated pyridines	Ratio of 2,3- to 2,5-phenylpicoline	Partial rate factors	
				CH_3F_2	CH_3F_6
12	A	22	96:4	2.6	0.11
13	B (1 min)	6	96:4	2.7	0.11
14	B (30 min)	10	95:5	2.4	0.12
15	B (60 min)	39	96:4	2.5	0.10
16	C (6 min)	33	96:4	2.9	0.09
17	C (60 min)	36	96:4	2.5	0.11

[a][Phenyllithium] = 0.003 mole.
[b][Pyridine] = [3-picoline] = 0.01 mole.

The results indicate once again that the 2-position in 3-picoline is activated relative to that in pyridine in these reactions and that the 6-position is deactivated by the 3-methyl group. It is interesting to note the relative constancies of the partial rate factors when the three different methods of work-up are used. Unfortunately, yields are not very reproducible in those reactions in which halide-free phenyllithium is used.

Similar competitive experiments were carried out using mixtures of pyridine and 3-ethylpyridine under the three sets of conditions and using "ordinary" phenyllithium (Table VI), phenyllithium in the presence of an excess of lithium bromide (Table VII), and halide-free phenyllithium (Table VIII).

TABLE VI

Reaction of "ordinary" phenyllithium[a] with an excess of an equimolar mixture of pyridine and 3-ethylpyridine[b]

Expt. No.	Method of work-up	Combined yields (%) of phenylated pyridines	Ratio of 2,3- to 2,5-phenyl-ethylpyridine	Partial rate factors	
				Et_2F_2	Et_2F_6
18	A	41	91:9	1.5	0.15
19	A	50	91:9	1.5	0.15
20	B (60 min)	37	91:9	1.5	0.15
21	C (60 min)	27	91:9	1.4	0.14

[a][Phenyllithium] = 0.0075 mole.
[b][Pyridine] = [3-ethylpyridine] = 0.01 mole.

The results summarized in Tables VI–VIII indicate again that the 3-ethyl-substituent activates C_2 towards attack by phenyllithium compared with C_2 in pyridine itself. The activation seems to be slightly less in this case than with a 3-methyl-substituent, particularly when halide-free phenyllithium is used. On the other hand, C_6 in 3-ethylpyridine

Can. J. Chem. Downloaded from www.nrcresearchpress.com by 210.87.254.105 on 09/05/12
For personal use only.

TABLE VII

Reaction of "ordinary" phenyllithium[a] with an excess of an equimolar mixture of pyridine and 3-ethylpyridine[b] containing an excess of lithium bromide[c]

Expt. No.	Method of work-up	Combined yields (%) of phenylated pyridines	Ratio of 2,3- to 2,5-phenyl-ethylpyridine	Partial rate factors	
				$^{Et}F_2$	$^{Et}F_6$
22	A	16	91:9	3.9*	0.30
23	B (30 min)	16	90:10	2.0	0.22

*Not accurately reproducible.
[a][Phenyllithium] = 0.005 mole.
[b][Pyridine] = [3-ethylpyridine] = 0.015 mole.
[c][Lithium bromide] = 0.061 mole.

TABLE VIII

Reaction of halide-free phenyllithium[a] with an excess of an equimolar mixture of pyridine and 3-ethylpyridine[b]

Expt. No.	Method of work-up	Combined yields (%) of phenylated pyridines	Ratio of 2,3- to 2,5-phenyl-ethylpyridine	Partial rate factors	
				$^{Et}F_2$	$^{Et}F_6$
24	A	19	90:10	1.6	0.18
25	B (30 min)	13	91:9	1.5	0.15
26	B (60 min)	32	89:11	1.2	0.15

[a][Phenyllithium] = 0.0033 mole.
[b][Pyridine] = [3-ethylpyridine] = 0.01 mole.

would appear to be very slightly less deactivated than in 3-picoline; the difference is so small, however, that it may well be insignificant. Again it should be emphasized that these values of the partial rate factors would, if anything, be on the low side due to the greater ease of polymerization of the 3-ethylphenyldihydropyridine salt compared with the 2-phenyl-1,2-dihydropyridine salt. That a 3-methyl-substituent activates C_2 more than does a 3-ethyl one was confirmed by adding phenyllithium to an excess of an equimolar mixture of 3-picoline and 3-ethylpyridine. The four alkylated phenylpyridines so formed could be resolved by gas chromatography and thus analyzed simultaneously. The results obtained in these experiments are collected in Table IX.

TABLE IX

Reaction of phenyllithium with an excess of an equimolar mixture of 3-picoline and 3-ethylpyridine

Expt. No.	Method of work-up	Ratio of phenylpicolines to ethylphenylpyridines[c]	Combined yield (%) of phenylated pyridines	$^{CH_3}_{Et}K$
27[a]	A	66:34	36.5	1.9
28[a]	B (30 min)	63:37	4.7	1.7
29[b]	C (60 min)	64:36	13.7	1.8

[a]Halide-free phenyllithium (0.005 mole) used. [3-Picoline] = [3-ethylpyridine] = 0.015 mole.
[b]"Ordinary" phenyllithium (0.0032 mole) used. [3-Picoline] = [3-ethylpyridine] = 0.03 mole.
[c]The 2,3-:2,5-ratios for both sets of isomers were the same as in the non-competitive experiments.

Though it is conceivable that these figures may incorporate a reflection of a slightly greater tendency for the intermediate from 3-ethylpyridine to undergo polymerization than that from 3-picoline, this should only be a small effect. The main conclusion drawn from the results is that 3-picoline is more reactive towards phenyllithium than is 3-ethylpyridine. If anything, 3-ethylpyridine should be slightly more basic than 3-picoline, so

Can. J. Chem. Downloaded from www.nrcresearchpress.com by 210.87.254.105 on 09/05/12
For personal use only.

that complexing of the organometallic compound at nitrogen cannot be the factor which determines the apparent relative reactivities.

The reproducibility of competitive results appeared to depend to a small extent on the batch of phenyllithium reagent used. To compare more accurately the reactivities of pyridine, 3-picoline, and 3-ethylpyridine competitive reactions were carried out on the pairs: pyridine/3-picoline, pyridine/3-ethylpyridine, 3-picoline/3-ethylpyridine, under identical conditions, using phenyllithium from the same batch of stock reagent. Table X contains a summary of the results obtained.

TABLE X

Relative reactivities of pyridine, 3-picoline, and 3-ethylpyridine towards phenyllithium[a]

	Pyridine and 3-picoline	Pyridine and 3-ethylpyridine	3-Picoline and 3-ethylpyridine
Combined yields (%) of phenylated derivatives	29	27	14
Total rate ratios	${}^{CH_3}_{H}K = 1.30$	${}^{Et}_{H}K = 0.79$	${}^{CH_3}_{Et}K = 1.80$
Partial rate factors	${}^{CH_3}F_2 = 2.4$	${}^{Et}F_2 = 1.4$	—
	${}^{CH_3}F_6 = 0.13$	${}^{Et}F_6 = 0.13$	—

[a]Phenyllithium (0.0032 mole) added to the pairs of pyridines (0.03 mole of each) at 24°. Oxygen was passed into the mixtures after they had been stirred at that temperature for 1 h.

In addition to the factors already discussed which may lead to an underestimation of the magnitude of K it should be pointed out that this value, which in all the above and previous examples listed was equated with the product ratio, differs slightly from the more accurate value calculated (10) using the equation

$$\frac{k_Y}{k_X} = \log\left(1 - \frac{Z_0}{Y_0}\cdot\frac{R}{1+R}\right) \Big/ \log\left(1 - \frac{Z_0}{X_0}\cdot\frac{1}{1+R}\right)$$

where X_0, Y_0, and Z_0 are the initial amounts of the two pyridines and phenyllithium, respectively, and R is the product ratio (assuming the reactions are bimolecular and irreversible). The difference, however, is very small, e.g., the value calculated using this equation from the data from expt. 27 (Table IX) is 2.05 compared with the product ratio of 1.91; ${}^{CH_3}_{H}K$ calculated from the data in Table X is 1.31, while the product ratio is 1.30. For this reason, the product ratios were taken as the values of K throughout this paper, the difference between these and the values calculated from the Ingold and Shaw equation probably being smaller than the experimental error.

The overall reactivities of the three pyridines studied here towards phenyllithium are in the order 3-picoline > pyridine > 3-ethylpyridine, but both in the case of 3-picoline and 3-ethylpyridine F_2 is greater than unity. The values of the total rate ratios are adequately self-consistent as is indicated by the fact that the value of ${}^{CH_3}_{H}K$, calculated from the relation ${}^{CH_3}_{H}K = {}^{CH_3}_{H}K \cdot {}^{Et}_{H}K$, and from the results in Table X is ${}^{CH_3}_{H}K$ (calc.) = 1.40, in reasonably good agreement with ${}^{CH_3}_{H}K$ (expt.) = 1.30.

Of the possible proposals put forward (1) to explain the preferential formation of the 2,3-isomer in these reactions, only those can be retained which would account for the specific *activation* of C_2 by the alkyl substituent, though it is conceivable and likely that a combination of factors are involved which favor the formation of more 2,3- than 2,5-isomer, but only one of which causes the observed activation. Steric acceleration, resulting from a relief of steric compression of the C_2 proton (by the 3-alkyl substituent and a group complexed at nitrogen) as the phenyl anion attacks almost perpendicularly to the plane

Can. J. Chem. Downloaded from www.nrcresearchpress.com by 210.87.254.105 on 09/05/12
For personal use only.

Can. J. Chem. Downloaded from www.nrcresearchpress.com by 210.87.254.105 on 09/05/12
For personal use only.

of the ring, is ruled out by the fact that ${}^{CH_3}F_2 > {}^{Et}F_2$. The opposite would have resulted from steric acceleration. An attractive interaction, of the nature of London dispersion forces (3), was next considered. As an ethyl substituent is expected to be somewhat more polarizable than a methyl, it would have again been expected that activation by the former would have been the greater of the two, which was not the case. Steric hindrance might play a role here in decreasing the magnitude of ${}^{Et}F_2$. Preliminary studies on the relative reactivities of 2-bromopyridine, 2-bromo-3-methylpyridine, and 2-bromo-5-methylpyridine towards methoxide ion in methanol indicate that these are in the order 2-bromo- > 2-bromo-3-methyl- > 2-bromo-5-methyl- (11), and experiments are now under way using the more polarizable thiophenoxide ion. As has already been pointed out in previous parts of this series, coordination of the organolithium compound at the ring nitrogen is not necessary to explain the observed orientation in other similar cases, though it may be of importance here.

In the reaction of phenyllithium with 3-amino- and 3-methoxy-pyridine the exclusive formation of the 2-phenyl derivative was attributed to complexing between a lone-pair of electrons on the 3-substituent and the phenyllithium (12). It is suggested that a loose complex, e.g., V (in which a monomeric phenyllithium has been assumed for simplicity until further information is available concerning its structure), might be formed between the organolithium reagent and the methyl group of 3-picoline (the ring-nitrogen atom is probably also complexed with lithium bromide or with another molecule of phenyllithium). The attacking molecule would be favorably oriented for attack at C_2 and the energy of activation for the substitution would be sufficiently reduced to overcome the usual deactivation by the methyl group in nucleophilic aromatic substitutions, thus leading to

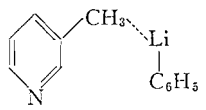

V

the observed activation. The lithium could be weakly bound to the methyl group by an electron-deficient-type bond. The presence of four-centered electron-deficient bonds have been postulated to explain the structures of tetrameric and hexameric ethyllithium both in solution and in the gas phase (9) and that of tetrameric *t*-butyllithium in solution (13). [See, however, 14 in which butyllithium in ether is believed to exist as a solvated dimer.] The existence of electron-deficient bonding is well established in polymeric alkyl beryllium (15) and dimeric aluminum trialkyls (16). The degree of polymerization in the last two systems is decreased by alkyl substitution at the alpha carbon atom and this has been discussed in terms of steric hindrance (17, 18) and of the decreased electronegative character of the branched alkyl groups (19). In either case, a slight decrease in the stability of the electron-deficient bond would be expected on going from 3-picoline to the more branched 3-ethylpyridine and would explain the observed reactivity sequence. It might then be predicted that a 3-isopropyl group would give rise to an even smaller value of F_2, probably less than unity, while with 3-*t*-butylpyridine, in which steric hindrance leads to attack mainly at C_6, ${}^{t\text{-Bu}}F_2$ should be appreciably smaller than ${}^{t\text{-Bu}}F_6$.

EXPERIMENTAL

Starting Pyridines

Commercial 2° pyridine (Reilly Tar and Chemical Co.) was dried (KOH) and fractionally distilled through a Podbielniak Mini-Cal Spinning Band Column, the fraction, b.p. 110–112° at 720 mm, being used. Commercial synthetic 3-picoline was similarly treated: the fraction, b.p. 138–140° at 720 mm, was used.

3-Ethylpyridine, b.p. 165–166° at 720 mm, was obtained in 80–87% yield by the reduction of 3-acetylpyridine with hydrazine hydrate and potassium hydroxide according to the procedure of Fand and Lutomski (20).

"Ordinary" Phenyllithium

This was prepared as usual and its concentration determined before every run by titration with 0.1 *N* hydrochloric acid using methyl orange as indicator.

Halide-free Phenyllithium

This was prepared as described in part V (2) and analyzed similarly.

The preparation of ethereal solutions of anhydrous lithium bromide has been described (2). The concentration of bromide was determined by Volhard titration.

Quantitative Analyses

The products formed in the phenylation reactions were resolved by gas chromatography and the compounds corresponding to the individual peaks identified (i) by comparing the retention times with those of authentic specimens, and (ii) by collecting each compound and comparing its infrared spectrum with that of an authentic phenylpyridine.

Calibration curves were then obtained by plotting areas under peaks vs. known concentration using standard solutions of the individual pyridines and under the conditions used in the quantitative analyses of the mixtures: linear plots were obtained in all cases. The accuracy of the method was checked by the analysis of a number of standard synthetic mixtures. The concentrations of the phenylated pyridines formed during the competitive runs could then be read directly from the calibration curves, provided the conditions established for the chromatographic analysis of each mixture of compounds were kept constant. These conditions are summarized below:

Mixtures of phenylpyridine and phenylpicolines.—A 20 ft × ¼ in. (i.d.) copper tube packed with silicone SE-30 (3%) on glass beads (60–80 mesh); column temperature 153°; injector temperature 230°; carrier gas (helium) inlet pressure 30 p.s.i. Under these conditions the retention times of 2-phenylpyridine, 2-phenyl-3-picoline and 2-phenyl-5-picoline were 13 min 36 s, 16 min 15 s, and 21 min 45 s, respectively.

Mixtures of phenylpyridine and phenylethylpyridines.—A 5 ft × ¼ in. (i.d.) copper tube packed with "Apiezon N" (25%) on Gaschrom P (60–80 mesh); column temperature 220°; injector temperature 245°; helium inlet pressure 30 p.s.i. The retention times of 2-phenylpyridine, 3-ethyl-2-phenylpyridine, and 5-ethyl-2-phenylpyridine were 10 min, 12 min 22 s, and 23 min, respectively.

Mixtures of phenylpicolines and phenylethylpyridines.—A 20 ft × ¼ in. (i.d.) copper tube packed with silicone SE-30 (3%) on glass beads (60–80 mesh); column temperature 170°; injector temperature 235°; helium inlet pressure 30 p.s.i. Under these conditions, the retention times of 2-phenyl-3-picoline, 2-phenyl-5-picoline, 3-ethyl-2-phenylpyridine, and 5-ethyl-2-phenylpyridine were 3 min 9 s, 4 min 9 s, 3 min 45 s, and 5 min 5 s, respectively.

Competitive Reactions

The procedure used will be illustrated by one example of each of methods A, B, and C.

Reaction of "Ordinary" Phenyllithium with an Excess of an Equimolar Mixture of Pyridine and 3-Picoline

Method A.—A solution of pyridine (2.37 g, 0.03 mole) and 3-picoline (2.79 g, 0.03 mole) in anhydrous ether (25 ml) was treated dropwise under a dry oxygen-free nitrogen atmosphere with an ethereal solution of phenyllithium (8.2 ml ≡ 0.01 mole, prepared from bromobenzene and lithium), vigorous stirring being maintained throughout the reaction. The rate of addition was such that the mixture boiled gently under reflux. At the end of the addition the ether was distilled off and simultaneously replaced with dry toluene. The toluene suspension was then boiled under reflux for 6.5 h, cooled, treated carefully with water, and made strongly alkaline with potassium hydroxide; the toluene layer separated and the aqueous layer was extracted with several portions of ether. The combined organic layers were extracted with concentrated hydrochloric acid, the acid extract was made strongly alkaline with potassium hydroxide, and extracted repeatedly with ether. The dried (KOH) ether-extracts were concentrated and analyzed by gas chromatography.

Method B.—The addition of a phenyllithium solution (8.2 ml ≡ 0.01 mole) to a mixture of pyridine (2.37 g, 0.03 mole) and 3-picoline (2.79 g, 0.03 mole) was carried out as in method A. At the end of the addition, the reaction mixture was boiled gently under reflux for a given time (see tables), cooled, and dry oxygen gas bubbled through the mixture until a white suspension had formed. Water was added and the mixture worked up as above.

Method C.—The procedure was essentially the same as that described under method B except that the temperature of the reaction mixture was never allowed to rise above 24° during the addition or after.

The same procedures were used in the runs in which halide-free phenyllithium was used. The concentrations of the phenyllithium solutions were determined by acid titration before every run and the required volume of the solution measured out with a burette, all the transfers being carried out under oxygen-free dry nitrogen.

Can. J. Chem. Downloaded from www.nrcresearchpress.com by 210.87.254.105 on 09/05/12
For personal use only.

When the reactions were carried out in the presence of an excess of anhydrous lithium bromide the procedures were identical with those described above, except that a solution of two molar equivalents of anhydrous lithium bromide in dry ether per mole of pyridine used was added to the solution of the pyridines before the phenyllithium solution was introduced. No appreciable evolution of heat was noted when the phenyllithium solution was added.

ACKNOWLEDGMENTS

This work was carried out during the tenure (by C.-S. G.) of a National Research Council Studentship, and was supported financially by a grant from the National Research Council. The authors thank Dr. K. J. McCallum for reading the manuscript and for helpful comments.

REFERENCES

1. R. A. ABRAMOVITCH and C.-S. GIAM. Can. J. Chem. **40**, 213 (1962).
2. R. A. ABRAMOVITCH and C.-S. GIAM. Can. J. Chem. **41**, 3127 (1963).
3. J. D. REINHEIMER and J. F. BUNNETT. J. Am. Chem. Soc. **81**, 315 (1959). J. F. BUNNETT and J. D. REINHEIMER. J. Am. Chem. Soc. **84**, 3284 (1962).
4. C.-S. GIAM. Ph.D. Thesis, University of Saskatchewan, Saskatoon, Sask. 1962.
5. G. A. RUSSELL. *In* A. Weissberger (*Editor*). Technique of organic chemistry. Vol. VIII, Part I. Investigation of rates and mechanisms of reactions. Part I. 2nd ed. Interscience Publishers, New York. 1961. p. 358.
6. ST. VON LASZCZYNSKI. Ber. **27**, 2285 (1894).
7. T. V. TALALAEVA and K. A. KOCHESHKOV. Dokl. Akad. Nauk. SSSR, **104**, 260 (1955); Chem. Abstr. **50**, 5446*a* (1956).
8. G. WITTIG. Angew. Chem. **62A**, 231 (1950).
9. T. L. BROWN, D. W. DICKERHOOF, and D. A. BAFUS. J. Am. Chem. Soc. **84**, 1371 (1962).
10. C. K. INGOLD and F. R. SHAW. J. Chem. Soc. 2918 (1927).
11. R. A. ABRAMOVITCH and F. HELMER. Unpublished results.
12. R. A. ABRAMOVITCH and A. D. NOTATION. Can. J. Chem. **38**, 1445 (1960).
13. M. WEINER, G. VOGEL, and R. WEST. Inorg. Chem. **1**, 654 (1962).
14. Z. K. CHEEMA, G. W. GIBSON, and J. F. EASTHAM. J. Am. Chem. Soc. **85**, 3517 (1963).
15. A. I. SNOW and R. E. RUNDLE. Acta Cryst. **4**, 348 (1951).
16. E. G. ROCHOW, D. T. HURD, and R. N. LEWIS. The chemistry of organometallic compounds. John Wiley and Sons, Inc., New York. 1957. p. 133.
17. P. H. LEWIS and R. E. RUNDLE. J. Chem. Phys. **21**, 986 (1953).
18. K. S. PITZER and H. S. GUTOWSKY. J. Am. Chem. Soc. **68**, 2204 (1946).
19. G. E. COATES and F. GLOCKING. J. Chem. Soc. 22 (1954).
20. T. I. FAND and C. F. LUTOMSKI. J. Am. Chem. Soc. **71**, 2931 (1949).

Can. J. Chem. Downloaded from www.nrcresearchpress.com by 210.87.254.105 on 09/05/12
For personal use only.

Can. J. Chem. Downloaded from www.nrcresearchpress.com by 210.87.254.42 on 09/05/12
For personal use only.

THE KINETICS OF THE REACTION OF ATOMIC HYDROGEN WITH METHANE

J. W. S. JAMIESON AND G. R. BROWN
Department of Chemistry, St. John's College, University of Manitoba, Winnipeg, Manitoba
Received July 29, 1963

ABSTRACT

Reinvestigation of the reaction of hydrogen atoms, produced by electric discharge, with methane in a fast flow system has given an activation energy of 7.4 ± 1.1 kcal/mole and a steric factor of about 10^{-3} for the primary reaction, $H + CH_4 \rightarrow H_2 + CH_3$.

INTRODUCTION

Earlier studies of the reaction of atomic hydrogen with methane were reviewed by Steacie (1), who concluded that the reliable early investigations led to a mean activation energy of about 12.5 kcal/mole, with the usual assumption of the time that the steric factor was about 0.1. More recently, however, Berlie and Le Roy (2, 3) published very much lower values of both P and E, obtained by production and measurement of the recombination of hydrogen atoms on filaments with and without methane. Steacie (1) also discussed the investigations of the reverse reaction, $CH_3 + H_2 \rightarrow CH_4 + H$, and concluded that the activation energy is 10.0 ± 0.5 kcal/mole. From the known dissociation energy of the H_3C—H bond in methane and from the heat of dissociation of hydrogen, the heat of reaction has been found to be 2.2 ± 1 kcal/mole.

Both the high and low values for the activation energy of the forward reaction are inconsistent with the apparently accurate activation energy of the reverse reaction and the heat of reaction. Thus further study seemed to be warranted and reinvestigation of the reaction of hydrogen atoms, produced by electric discharge, with methane in a fast-flow system became feasible recently as a result of a new method by Demchuk and Gesser (4) for quantitatively trapping methane in such a system.

EXPERIMENTAL

Materials

Reagents were obtained from the following sources:
hydrogen from the Linde Gases Division, Union Carbide Canada Limited,
methane (99% minimum purity) from Matheson Company Inc., East Rutherford, N.J., U.S.A.,
silica gel (28–200 mesh) from the Fisher Scientific Co. Ltd.

Apparatus and Methods

The apparatus was a fast-flow system of the conventional Wood–Bonhöffer type, containing two stopcocks of 15 mm bore and no tubing of smaller inside diameter than 16.6 mm between the reaction vessel and the Welch Duo-seal pump, 1402B, two-stage (vented exhaust), 0.1 micron, 140 liters/min. Hydrogen gas flowed into both ends of the discharge tube, across the aluminum electrodes of which was a potential drop of about 1100 V a-c. at 300 mA, provided by two Hammond 717 × 60 transformers with the primaries in parallel and the secondaries in series.

A mixture of atomic and molecular hydrogen flowed from the discharge tube down through a tube 12 cm long and 23 mm inside diameter to a 500-cc reaction vessel, into the center of which methane flowed. Products condensable at liquid nitrogen temperature were removed by a large trap immediately below the reaction vessel, while a second large trap surrounded by liquid nitrogen and having the inner wall of its outer tube coated with silicone grease and a layer of silica gel (previously degassed at 170 °C) adsorbed methane quantitatively from the gas stream. This gas was removed readily from the silica gel by reheating at 170 °C (4). It is, of course, possible that desorption of methane was complete at a much lower temperature. The flow of methane at room temperature was measured by the pressure drop in a manometer connected to a calibrated volume while the methane recovered from the second trap was allowed to expand into another

known volume of about the same size, where its pressure was measured in a manometer, again at ambient temperature. Products of the reaction were measured in a gas burette and analyzed by gas chromatography using helium as carrier gas, a Gow-Mac thermal conductivity cell Model 9193, TE-II, a Leeds and Northrup Speedomax Type G, Model "S", one second recorder, and a 4-ft molecular sieve 5A column or an 8-ft Beckman No. 17329 di-*n*-butyl maleate column.

RESULTS AND DISCUSSION

The methane used was analyzed by gas chromatography, using both the molecular sieve column and the di-*n*-butyl maleate column. No evidence of impurity was found. Under our fast-flow conditions no hydrogen was collected in either trap. In the high temperature experiments analysis by gas chromatography showed that ethane was the only product collected in the first trap, where it was trapped quantitatively. The quantity of ethane was measured in a gas burette. The methane collected in the second trap was shown by gas chromatography to be free of contamination by other gases. In several blank experiments with the hydrogen discharge off it was shown that the recovery of methane from the second trap was quantitative over the entire range of methane flow rates used in our experiments.

The results of experiments at various temperatures and methane flow rates are given in Table I. In Fig. 1 the amounts of methane reacted per second at various temperatures

TABLE I

Experimental data for the reaction of atomic hydrogen with methane

Expt. No.	T, °C	Atomic hydrogen	Methane flowed	Methane recovered	Methane reacted	Ethane produced
		All flow rates in μmoles/s				
1	227	5.2	5.23	4.67	0.56	
2	218	5.2	6.21	5.57	0.64	
3	212	5.2	12.45	11.56	0.89	
4	213	5.2	16.78	15.67	1.11	
5	317	5.0	3.56	2.92	0.64	
6	315	5.0	10.45	9.44	1.01	
7	314	5.0	13.74	12.31	1.43	
8	318	5.0	16.66	15.28	1.38	
9	519	4.4	4.40	3.29	1.11	0.55
10	483	4.5	9.91	7.50	2.41	
11	530	4.4	11.57	8.85	2.72	
12	513	4.4	11.81	9.06	2.75	
13	492	4.5	13.80	10.54	3.26	1.63
14	516	4.4	19.97	15.57	4.40	2.20
15	528	4.4	20.55	16.19	4.36	
16	514	4.4	24.25	19.87	4.38	2.19

are plotted against the methane flow rate and the amounts of ethane produced per second at the high temperature are also shown. In all experiments the flow rate of molecular hydrogen was 88.2 micromoles/s, which gave a pressure in the reaction system of 1.10 mm.

The atomic hydrogen flow rate was estimated at several temperatures from the reaction of ethylenimine (5) and other cyclic imines (6) with atomic hydrogen in the same system. Thus it was found that the hydrogen atom flow rate decreased approximately linearly with increasing temperature, according to the expression:

$$\text{H-atom flow rate in micromoles/s} = 5.84 - 0.0028\ T\ ^\circ\text{C}.$$

With the use of this relation the applicable hydrogen atom flow rate has been calculated for the temperature of each experiment, as shown in Table I.

Can. J. Chem. Downloaded from www.nrcresearchpress.com by 210.87.254.42 on 09/05/12
For personal use only.

Can. J. Chem. Downloaded from www.nrcresearchpress.com by 210.87.254.42 on 09/05/12
For personal use only.

For the purpose of calculating specific reaction rates it is customary to make the assumption that the reaction is bimolecular and thus second order. Vance and Bauman (7) have derived theoretical equations from which specific reaction rates may be calculated for the case of a stationary state in a streaming, diffusing, and reacting gas mixture. Unfortunately their apparatus was substantially different from the usual Wood–Bonhöffer flow system, particularly since their hydrogen atoms were introduced into the center of the reaction vessel and were carried into the vessel by the other reacting gas, which was assumed to be in great excess so that its concentration could be taken as constant throughout the reaction zone. The treatment of Vance and Bauman does not appear to be applicable to the present experiments and thus the specific reaction rates have been calculated from the usual second-order rate expressions for conditions of both streamline and turbulent flow.

For streamline flow the integrated form of the rate expression is

$$k_s = V/[Nt^2(A - B)] \ln [B(A - X)/A(B - X)] \text{ cm}^3 \text{ molecule}^{-1} \text{ s}^{-1}$$

where k_s is the second-order rate constant for streamline flow,
V is the volume of the reaction vessel in cm^3,
N is Avogadro's number,
t is the reaction time,
A is the flow rate of atomic hydrogen in moles/s,
B is the flow rate of methane in moles/s, and
X is the number of moles of methane reacted/s.

The reaction time, assumed to be the time spent by the reactants in the reaction vessel, may be expressed as:

$$t = n/r$$

where n is the number of moles of gas in the reaction vessel, calculated from the ideal gas law, and r is the total flow rate in moles/s.

For experiments 1 and 9 in which the methane flow rates were virtually equal to the estimated flow rates of atomic hydrogen, the simpler rate expression

$$k_s = V/NAt^2[X/(A - X)] \text{ cm}^3 \text{ molecule}^{-1} \text{ s}^{-1}$$

was used.

Rate constants for conditions of turbulent flow have been calculated without integrating the rate equation by assuming that the reactant concentrations were uniform throughout the reaction zone, using the expression:

$$k_t = XV/[Nt^2(A - X)(B - X)] \text{ cm}^3 \text{ molecule}^{-1} \text{ s}^{-1}$$

where k_t is the second-order rate constant for turbulent flow.

The second-order rate constants and other data for the kinetic calculations are given in Table II. An Arrhenius plot of the data for streamline flow is shown in Fig. 2, for which the line of best fit, calculated by the method of least squares, and also plotted, is

$$-\log k_s = (1.4640 \times 10^3)/T + 12.39.$$

The standard deviations of the slope and intercept of the line may be calculated by statistical analysis (8) of the data. Thus the variance is

$$\sigma^2 = \sum d_i^2/n = 0.01291$$

TABLE II
Data for kinetic calculations

Expt. No.	$10^3/T$, °K	Second-order rate constants, cm^3 molecule^{-1} s^{-1}		$-\log k_s$	$-\log k_t$
		Streamline	Turbulent		
1	2.00	5.63×10^{-16}	6.33×10^{-16}	15.25	15.20
2	2.04	6.02×10^{-16}	6.05×10^{-16}	15.22	15.22
3	2.06	4.16×10^{-16}	4.80×10^{-16}	15.38	15.32
4	2.06	4.33×10^{-16}	5.04×10^{-16}	15.36	15.30
5	1.69	1.33×10^{-15}	1.65×10^{-15}	14.88	14.78
6	1.70	9.07×10^{-16}	1.06×10^{-15}	15.04	14.98
7	1.70	1.04×10^{-15}	1.31×10^{-15}	14.98	14.88
8	1.69	8.74×10^{-16}	1.07×10^{-15}	15.06	14.97
9	1.26	4.58×10^{-15}	6.15×10^{-15}	14.34	14.21
10	1.32	5.58×10^{-15}	9.43×10^{-15}	14.25	14.03
11	1.25	6.89×10^{-15}	1.30×10^{-14}	14.16	13.89
12	1.27	6.62×10^{-15}	1.26×10^{-14}	14.18	13.90
13	1.31	7.43×10^{-15}	1.68×10^{-14}	14.13	13.78

where the d_i are the deviations in Y (or $-\log k_s$) from the least squares line, and n is the number of experimental points.

The standard deviation, σ, then is 0.1136. For convenience a quantity Δ is defined as

$$\Delta = n\sum X_i^2 - (\sum X_i)^2$$

where the X_i are the values of $1000/T$. Therefore

$$\Delta = 16.89.$$

The variance of the slope may then be expressed as

$$\sigma_m^2 = n\sigma^2/\Delta = \sum d_i^2/\Delta = 0.009935$$

and the standard deviation of the slope, $\sigma_m = 0.09967$. The slope, then, may be reported as

$$m = 1.4640 \pm 0.1.$$

Similarly, the variance of the intercept is

$$\sigma_b^2 = (\sigma^2\sum X_i^2)/\Delta = 0.02779$$

and the standard deviation of the intercept, $\sigma_b = 0.1667$, so that the intercept may be written

$$b = 12.39 \pm 0.17.$$

Thus the data of the Arrhenius plot indicate that for streamline flow the activation energy is 6.7 ± 0.5 kcal/mole and the frequency factor is about 4×10^{-13} cm^3/molecule s. Similar calculations for turbulent flow give an activation energy of 8.0 ± 0.6 kcal/mole and a frequency factor of about 1.7×10^{-12} cm^3/molecule s. Since the flow pattern in a Wood–Bonhöffer system has not yet been established it seems desirable to use the mean values: 7.4 ± 1.1 kcal/mole for the activation energy and a frequency factor of about 1×10^{-12} cm^3/molecule s. These values would apply to the primary reaction

[1] $$H + CH_4 \rightarrow H_2 + CH_3$$

provided that the methyl radicals so produced did not regenerate methane either by

Can. J. Chem. Downloaded from www.nrcresearchpress.com by 210.87.254.42 on 09/05/12
For personal use only.

combination with excess hydrogen atoms or by participation in the reverse reaction with molecular hydrogen.

If, however, either the reverse reaction or the $H + CH_3$ combination occurred to even a slight extent the measured rate of consumption of methane by atomic hydrogen would be less than the true value. Thus the measured rate of reaction [1] should tentatively be regarded as minimal and the calculated activation energy should be taken as the upper limit of the true value.

The amounts of methane reacted and ethane produced in experiments at temperatures near 500 °C do, however, provide further evidence that regeneration of methane by either of the two reactions mentioned is negligible. In such experiments, the ethane recovered was found to be one-half the methane reacted. This relation alone might only represent the attainment of a steady state involving several reactions, but at very high methane flow rates not only was the amount of methane reacted per second equal to the estimated hydrogen atom flow rate of 4.4 micromoles/s but the maximum amount of ethane produced was 2.2 micromoles/s, which could only have been formed by combination of 4.4 micromoles/s of methyl radicals, produced by reaction [1]. Thus it appears that, at least under these conditions, all the available hydrogen atoms are consumed by methane, so that none are left to combine with methyl radicals, and the only subsequent reaction is the combination of methyl radicals

$$[2] \qquad 2CH_3 \rightarrow C_2H_6$$

which probably occurs readily in the first cold trap.

In experiments at the high temperature there was no evidence that any of the ethane produced by reaction [2] reacted with hydrogen atoms, since at this temperature there was a material balance between hydrogen atoms and methane reacted, methyl radicals thus formed, and ethane produced by their combination. Furthermore, compounds such as propane, *n*-butane, and higher hydrocarbons, which might have been formed by reactions of ethyl radicals, were not found among the products.

Evidently the reaction

$$CH_3 + H_2 \rightarrow CH_4 + H$$

did not occur at the high temperature and since it has a positive temperature coefficient it would not be expected to occur at the lower temperatures. Therefore the calculated activation energy and frequency factor seem to be applicable to the primary abstraction reaction.

The frequency factor A can be expressed as

$$A = PZ/n_An_B = PZ'$$

where P is the steric or probability factor,

n_A and n_B are the concentrations of the reactants in molecules/cm^3,

Z is the number of molecules colliding/cm^3 s, and

Z' is Z/n_An_B in cm^3/molecule s.

Calculation of Z' at the mean temperature of 389 °C, using 2.1 Å as the collision diameter of the hydrogen atom (9) and 3.75 Å as the collision diameter of methane (10), gives the value 2.06×10^{-9} cm^3/molecule s. Division of the mean frequency factor, 1×10^{-12} cm^3/molecule s, by Z' gives a mean steric factor P of 4.86×10^{-4} for reaction [1].

The present activation energy and steric factor are in substantial agreement with the

Can. J. Chem. Downloaded from www.nrcresearchpress.com by 210.87.254.42 on 09/05/12
For personal use only.

preliminary results of Le Roy (2). The steric factor is within the range predicted by Eyring (11) and the activation energy agrees reasonably well with the activation energy of the reverse reaction and the heat of reaction.

It should, however, be noted that, in a sense, all the kinetic results cited for the reaction of atomic hydrogen with methane are consistent since errors in P and E compensate one another. Thus a plot of the logarithm of the steric factor against the activation energy should be linear. As shown in Fig. 3, this is the case when the present results are plotted

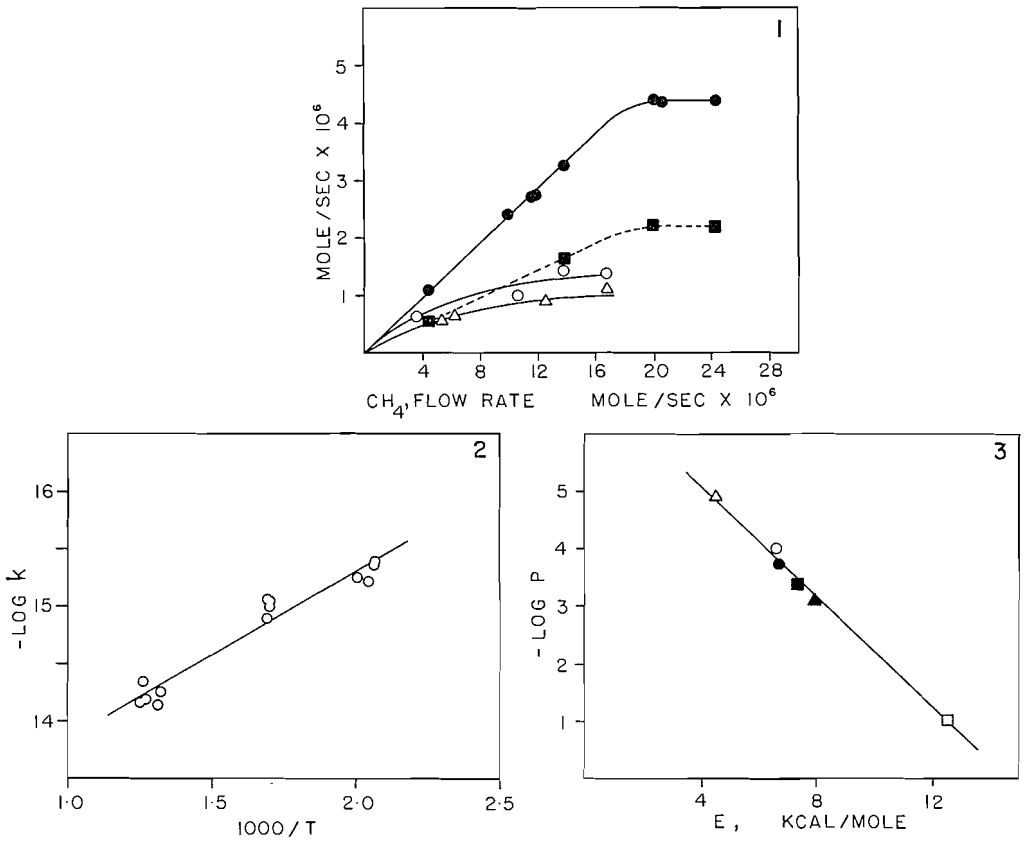

FIG. 1. Methane reacted at 218 °C (△), 316 °C (○), and 512 °C (●); ethane produced at 512 °C. (■).
FIG. 2. Arrhenius plot (streamline flow assumed) for the reaction of atomic hydrogen with methane.
FIG. 3. Logarithm of steric factor vs. activation energy for various studies of the reaction of atomic hydrogen with methane. Early investigations (□), preliminary results of Le Roy (○), Berlie and Le Roy (△), present results, streamline flow (●), present results, turbulent flow (▲), average present results (■).

together with the mean values for the early investigations (1), the preliminary results of Le Roy (2), and the more recent results of Berlie and Le Roy (3).

The results of a recent study (12) of the reaction

$$D + CH_4 \rightarrow HD + CH_3$$

appear to be inconsistent with the various results for reaction [1]. While the activation energy of 7.8 ± 0.6 kcal/mole seems to have the right magnitude, the steric factor, $P = 0.025$ ($-\log P = 1.60$) is too high to fit the line of Fig. 3. These values, however, were

Can. J. Chem. Downloaded from www.nrcresearchpress.com by 210.87.254.42 on 09/05/12
For personal use only.

obtained by the method of competing reactions and thus depend not only on correct values of P and E for the reaction

$$D + D_2CO \rightarrow D_2 + DCO$$

but also on the absence of other reactions which form either D_2 or HD.

ACKNOWLEDGMENT

Financial assistance from the National Research Council is gratefully acknowledged.

REFERENCES

1. E. W. R. STEACIE. Atomic and free radical reactions. American Chemical Society Monograph 125. Reinhold, New York. 1954.
2. D. J. LE ROY. Discussions Faraday Soc. **14**, 120 (1953).
3. M. R. BERLIE and D. J. LE ROY. Can. J. Chem. **32**, 650 (1954).
4. N. DEMCHUK and H. GESSER. Can. J. Chem. **41**, 1645 (1963).
5. J. W. S. JAMIESON and C. A. WINKLER. J. Phys. Chem. **60**, 1542 (1956).
6. J. W. S. JAMIESON, G. R. BROWN, and W. HANCOCK. In preparation.
7. J. E. VANCE and W. C. BAUMAN. J. Chem. Phys. **6**, 811 (1938).
8. H. D. YOUNG. Statistical treatment of experimental data. McGraw-Hill, New York. 1962.
9. W. R. TROST and E. W. R. STEACIE. J. Chem. Phys. **16**, 361 (1948).
10. H. BLADES and C. A. WINKLER. Can. J. Chem. **29**, 1022 (1951).
11. S. GLASSTONE, K. J. LAIDLER, and H. EYRING. The theory of rate processes. McGraw-Hill, New York. 1941.
12. R. KLEIN, J. R. MCNESBY, M. D. SCHEER, and L. J. SCHOEN. J. Chem. Phys. **30**, 58 (1959).

Can. J. Chem. Downloaded from www.nrcresearchpress.com by 210.87.254.42 on 09/05/12
For personal use only.

A GROUP ORBITAL STUDY OF LITHIUM HYDRIDE[1]

I. G. CSIZMADIA,[2] B. T. SUTCLIFFE,[3] AND M. P. BARNETT[2]

Cooperative Computing Laboratory and Solid State and Molecular Theory Group, Department of Physics, Massachusetts Institute of Technology, Cambridge, Massachusetts

Received November 14, 1963

ABSTRACT

A quantum mechanical treatment of lithium hydride in the group orbital approximation is presented. Some excited states and an improved ground state are obtained by means of configuration interaction within a single group.

The total energy obtained for the ground state at several interatomic distances (R = 2.0–8.0 a.u.) omitting and including configuration interaction and for the first excited singlet state compare very well with the values reported by Karo in a comparable simple molecular orbital calculation.

The chemical significance of the group orbital method is discussed. The results of the present calculations are related to some chemical reaction mechanisms and to some spectroscopic phenomena.

1. INTRODUCTION

The molecular orbital treatment of molecular systems allows chemical insight to be used in the choice of the analytical forms for the one-electron wave functions. The most accurate calculations that can be performed with a given set of basis functions in the molecular orbital approximation entails a complete configuration interaction treatment that includes all the electronic states which can be formed from those functions and which satisfy the space and spin symmetry requirements. This can lead to vast computations for relatively small numbers of one-electron basis functions. The "chemical integrity" of the "chemically recognizable" parts of the molecule becomes blurred in this full configuration interaction treatment. McWeeny (1) recently described an approximation that can be used, within the molecular orbital approach, to preserve the conceptual integrity of chemically recognizable molecular fragments such as a π electron cloud, a σ bond, or an atomic core. He calls these fragments "groups", and the approximation, which is defined formally in Section 2, is called the group function approximation. It extends some earlier work of Parr *et al.* (2–4). It allows a "mixing of states" within the individual groups, but requires less computation than the most general molecular orbital configuration interaction calculation which uses the same set of basis functions.

In the treatment of lithium hydride that is reported here, the core electrons on the lithium atom are treated as one group, and the electrons of the lithium hydrogen bond are treated as another group. Variational parameters are included in only the latter group, so that the calculation can be considered as just a conventional molecular orbital treatment in which the lithium 1s orbitals are not varied. A one-determinant, and a multi-determinant calculation have been performed, in a way that allows the results to be compared with those of Karo and Olson (5, 6), who varied all the parameters including those of the lithium core. The agreement is very good. The group function formalism of (1) is followed for convenience, and as an example on which corresponding treatments of larger systems can be modelled.

[1]*Supported by the Army, the Navy, and the Air Force of the United States, and the National Science Foundation.*

[2]*Present address: University of London Computer Unit, London W.C.1, England.*

[3]*Present address: Department of Chemistry, New York University, Washington Square, New York.*

Can. J. Chem. Downloaded from www.nrcresearchpress.com by 210.87.254.5 on 09/05/12
For personal use only.

Can. J. Chem. Downloaded from www.nrcresearchpress.com by 210.87.254.5 on 09/05/12
For personal use only.

The group function approach has been applied to the ground states of some small molecules, which include H_2O (7), NH_3 (8), and NH_2 (9). The present paper applies the group function approach to the ground and excited states of the LiH molecule for a range of internuclear distances. The study was undertaken for several reasons. Lithium hydride is of inherent interest as the smallest neutral heteronuclear molecule. As such it will continue to provide the object of study by theoretical and experimental techniques that are developed to probe molecular structure and behavior with greater detail and precision. Past spectroscopic studies of LiH provide experimental material for several states (10–13). The present calculations have yielded results that may be compared with this material and also some results for states that have not yet been studied experimentally. Experimental corroboration of these latter results would be interesting. Lithium hydride has been studied extensively in different theoretical approximations, so that reference material exists for comparison with the results of a group function treatment, that can give insight into the relative merits of the group function and the other theoretical approaches (14–24). Lithium hydride forms crystals that may provide an interesting subject for subsequent theoretical study. The electronic structure of lithium hydride may also provide a model for the qualitative discussion of certain reactions of organo lithium compounds.

The one electron wave functions that we use are linear combinations of numerical Hartree–Fock functions that were used previously by Karo and Olson in a molecular orbital treatment of the ground state of lithium hydride (5). This has made it possible to use the integrals over basis functions that were computed by Karo and Olson, and hence to obtain a clear comparison of the group function and direct molecular orbital approaches in this instance.

The calculations were performed on an IBM 709 computer, and the programs were coded in FORTRAN. The cathode ray attachment to the computer was used to plot the charge distributions.

The mathematical formulation of our studies is summarized in Section 2. The results are discussed in quantum chemical terms in Section 3. The reaction mechanistic and spectroscopic implications are discussed in Sections 4 and 5. Further details of the mathematical formulation and the computational procedures are provided in a laboratory report that is organized as a set of Appendices to the present paper (25).

2. MATHEMATICAL FORMULATION

In the group function approximation, the electronic wave function for a molecule, molecular fragment or assembly of molecules, and (or) molecular fragments, is approximated by a function Ψ_K that is of the form [1].

$$[1] \qquad \Psi_K(1,2,\ldots,N_t) = \mathscr{A}[\Phi_{R_1,r_1}(1,\ldots,N_1)\Phi_{R_2,r_2}(N_1+1,\ldots,N_2)\ldots \ldots\Phi_{R_t,r_t}(N_{t-1}+1,\ldots,N_t)].$$

Here $\mathscr{A}$ is the normalizing antisymmetry operator (26), and the Φ's are the "group wave functions," which describe the "chemically recognizable" portions of the molecule. Each group function is labelled by two subscripts. The first subscript specifies the group, and conventionally is a capital letter. The second subscript specifies the electronic state of the group, and conventionally is a lower case letter. Equation [1] refers to a system in which there are N_t electrons and t groups. The integers 1 to N_t refer to the space and spin coordinates of the individual electrons. N_t denotes the number of electrons in the groups R_1 to R_t inclusive.

The group wave functions satisfy the orthonormality condition

$$[2] \qquad \int \ldots \ldots \int \Phi^*_{R,r'}(1, \ldots, N)\Phi_{R,r}(1, \ldots, N)d\tau_1 \ldots d\tau_N = \delta_{rr'}.$$

Equation [2] refers to a group R, in states r and r', which contains N electrons. Integration over the space and spin coordinates of the ith electron is denoted by $\int \ldots dv_i$ and $\int \ldots d\omega_i$ respectively and $d\tau_i = dv_i d\omega_i$.

The group wave functions are orthogonalized in the "strong" sense discussed in reference (1). This orthogonality condition refers to the integral [3].

$$[3] \qquad \int\int \Phi^*_{R,r}(i_1, i_2, \ldots, i_N)\Phi_{R',r'}(i'_1, i'_2, \ldots i'_{N'})d\tau_i = 0.$$

In this integral R and R' label two groups that contain N and N' electrons respectively. The groups may or may not be the same. The integrand contains the wave functions for these groups in states r and r' respectively. In the arguments of the wave functions, i_1 to i_N stand for the labels of some N electrons of the molecule, and i'_1 to $i'_{N'}$ stand for the labels of some N' electrons of the molecule. One or more of these labels may be common to the two sets of argument. The integration is over the space and spin of an electron with such a common label, which we denote by i:

$$[4] \qquad i = i_p = i'_{p'} \text{ for some } p, p', 1 \leqslant p \leqslant N, 1 \leqslant p' \leqslant N'.$$

Then the integral [3] is zero, for strong orthogonality, if

$$[5] \qquad R \neq R'.$$

The meaning and effects of this condition have been discussed by Löwdin (27).

As mentioned in the Introduction, we have studied the lithium hydride molecule theoretically, in the group function approximation [1], by considering the electrons of the lithium core as one group, and the electrons of the lithium–hydrogen bond as a second group. We call these groups A and B respectively. We use the letters a and b to designate their states in the early stages of the treatment, extending this notation when necessary. The symbols Φ_{Aa} and Φ_{Bb} are used for the group wave functions of the two groups, with an elaboration of the latter symbol when necessary.

The total wave function Ψ_K thus can be written as

$$[6] \qquad \Psi_K(1, 2, 3, 4) = \mathscr{A}[\Phi_{Aa}(1, 2)\Phi_{Bb}(3, 4)].$$

The integers 1, 2, 3, 4 are used as electron labels.

It is reasonable to assume that the lithium core electrons are affected to only a small extent by the bonding. A wave function that provides an adequate description of the core electrons in the isolated lithium atom therefore is used for Φ_{Aa}. Formally,

$$[7] \qquad \Phi_{Aa}(1, 2) = \phi_A(1)\phi_A(2)\theta_{0,0}(1, 2).$$

The function ϕ_A is the $1s$ one-electron orbital of the lithium atom. It is called a group orbital as it is a one-electron orbital that forms part of a group wave function. $\theta_{0,0}$ is the spin function

$$[8] \qquad \theta_{0,0}(1, 2) = \frac{1}{\sqrt{2}}[\alpha(1)\beta(2) - \beta(1)\alpha(2)].$$

Can. J. Chem. Downloaded from www.nrcresearchpress.com by 210.87.254.5 on 09/05/12
For personal use only.

The lithium–hydrogen bond is described by a group wave function that has the same general structure as the core function

$$\Phi_{Bb}(3, 4) = \phi_B(3)\phi_B(4)\theta_{0,0}(3, 4). \quad [9]$$

The function ϕ_B is also called a group orbital. It is a linear combination of $2s$ and $2p_z$ orbitals on the lithium atom and a $1s$ orbital on the hydrogen atom. These are denoted by χ_{2s}, χ_{2p_z}, and χ_h, respectively, to indicate their chemical nature. They are orthogonal to the lithium $1s$ orbital χ_{1s} and to each other. The z axis on the lithium atom points towards the hydrogen atom.

$$\phi_B = c_1\chi_{2s} + c_2\chi_{2p_z} + c_3\chi_h. \quad [10]$$

The $c_\nu(\nu = 1 \text{ to } 3)$ are variational parameters that are chosen to minimize the total energy of the molecule.

The orbitals χ_{2s}, χ_{2p_z}, and χ_h are linear combinations of the orbitals η_{1s}, η_{2s}, η_{2p_z}, and η_h, which are defined by equations [11*a–c*]. In these equations, the P's are the numerical Hartree–Fock functions obtained by Fock and Petrashen for the lithium atom (28). The letter i is used here as an electron label. The distances of the electron from the lithium and hydrogen atoms are denoted by r_i and r'_i respectively. The polar angle of the electron, measured from the lithium atom as origin and the lithium hydrogen bond as polar axis is denoted by θ_i.

$$\eta_{1s}(i) = (1/4\pi)^{1/2}P_{1s}(r_i) \quad [11a]$$

$$\eta_{2s}(i) = (1/4\pi)^{1/2}P_{2s}(r_i) \quad [11b]$$

$$\eta_{2p_z}(i) = (1/4\pi)^{1/2}P_{2p_z}(r_i)\cos\theta_i \quad [11c]$$

$$\eta_h(i) = (1/\pi)^{1/2}e^{-r'_i} \quad [11d]$$

The relationship between the χ's and the η's can be summarized in matrix form as follows. Replace the chemical subscripts $1s$, $2s$, $2p_z$, and h by the integer labels 1, 2, 3, and 4 respectively. Let $\boldsymbol{\chi}$ be the column vector whose successive components are χ_1, χ_2, χ_3, χ_4. Let $\boldsymbol{\eta}$ be the column vector whose successive components are η_1, η_2, η_3, η_4. Then

$$\boldsymbol{\chi} = \mathbf{Z}\boldsymbol{\eta} \quad [12]$$

$$\mathbf{Z} = \mathbf{V}\mathbf{S}_\zeta^{-1/2} \quad [13]$$

where

$$\mathbf{S}_\zeta = \mathbf{V}'\mathbf{S}\mathbf{V} \quad [14]$$

and

$$\mathbf{V} = \begin{Vmatrix} 1 & 0 & 0 & S_{14}/[1-(S_{14})^2]^{1/2} \\ 0 & 1 & 0 & 0 \\ 0 & 0 & 1 & 0 \\ 0 & 0 & 0 & S_{14}/[1-(S_{14})^2]^{1/2} \end{Vmatrix} \quad [15]$$

and $\mathbf{S}$ is the overlap matrix for the η's, that is

$$S_{ij} = \int \eta_i(1)\ \eta_j(1)\ d\nu_1. \quad [16]$$

The subscripts i and j here refer to orbitals, and the integer 1 is used as the electron label. The matrix $\mathbf{S}_\zeta$ is just the overlap matrix for the orbitals formed from the η's by Schmidt

Can. J. Chem. Downloaded from www.nrcresearchpress.com by 210.87.254.5 on 09/05/12
For personal use only.

orthogonalization. The orbitals χ_2, χ_3, χ_4 must be orthogonal to χ_1 to satisfy the strong orthogonality condition that is discussed in Section 2 by reference to the integral [3]. The orbitals χ_2, χ_3, χ_4 are made orthogonal to each other for computational convenience. This orthogonalization procedure leaves the lithium $1s$ orbital unchanged. It is consistent with the assumption that the core electrons are affected very little by binding. Moreover, a recent calculation of a similar nature to this (7) suggests that, unless such an orthogonalization procedure is adopted, negative binding energies may result.

Karo and Olson (5, 6) used linear combinations of the orbitals η_1 to η_4 in a molecular orbital treatment that varied the coefficients of all four orbitals. Our calculations required less effort, as the form of wave function that we used allowed the variation of just two of the coefficients in the orbital ϕ_B, the third coefficient depending on the other two as a consequence of the normalization condition [2]. In our calculation, the orbitals of the lithium core electrons were not varied. Our results agree closely with those of Karo and Olson, where a comparison can be made. This encourages further use of the group function method.

We determined the coefficients c_1, c_2, c_3 in the orbital ϕ_B in two ways. The first involved a direct variation of parameters. The c_ν were varied until a set of values was found which minimized the energy. This method made it possible to plot contours of the energy surface as a function of the coefficients c_ν. The second method involved a modified self-consistent field (SCF) procedure. The solution of the SCF problem consists of three eigenvectors that are denoted by $\{c_{\nu 1}\}$, $\{c_{\nu 2}\}$, and $\{c_{\nu 3}\}$, and that correspond respectively to the eigenvalues ϵ_1, ϵ_2, ϵ_3, which are labelled so that $\epsilon_1 < \epsilon_2 < \epsilon_3$. These three eigenvectors define three group orbitals, when they are substituted in equation [10]. If the notation

$$\phi_{Bi} = c_{1i}\chi_{2s} + c_{2i}\chi_{2p_z} + c_{3i}\chi_h \qquad [17]$$

is used, then ϕ_{B1} should be identical with the ϕ_B orbital that is obtained by the direct variation of parameters. This is found to be the case.

The three orbitals ϕ_{B1}, ϕ_{B2}, ϕ_{B3} were used in a configuration interaction calculation to construct an improved ground state and a number of excited singlet and triplet states.

The detailed formulation of the computing procedure made extensive use of the concepts and notation of density matrices. The relevant formulae and some related technical matters are reviewed in Appendix 1. Further details of the direct variation of parameters, self-consistent field, and configuration interaction procedures are given in Appendices 2 to 4. The computations are described briefly in Appendix 5. As mentioned in the Introduction these appendices are available as a laboratory report (25). The results and their chemical implications are discussed in the Sections 3 to 5 that follow.

3. COMPUTATIONAL RESULTS

Figures 1A, 1B, and 1C illustrate the relationship between the individual atomic orbitals (η_i), the orthogonalized orbitals (χ_i), and the group orbitals (ϕ_i) respectively. The inflections that are due to the orthogonalization, and which can be seen in Fig. 1B, resemble those which were observed by McWeeny and Ohno, in their study of the water molecule (7). The elements of the orthogonalization matrix $\mathbf{Z}$, which is defined in equation [13], are given for a range of internuclear distances in Table AV of the appendices (25). Figure 1C shows the ϕ_A group orbital, which represents the lithium $1s$ core, and the ϕ_B group orbital, which represents the lithium–hydrogen bond.

The results of the variation of parameters calculation are shown in Table I. This

Can. J. Chem. Downloaded from www.nrcresearchpress.com by 210.87.254.5 on 09/05/12
For personal use only.

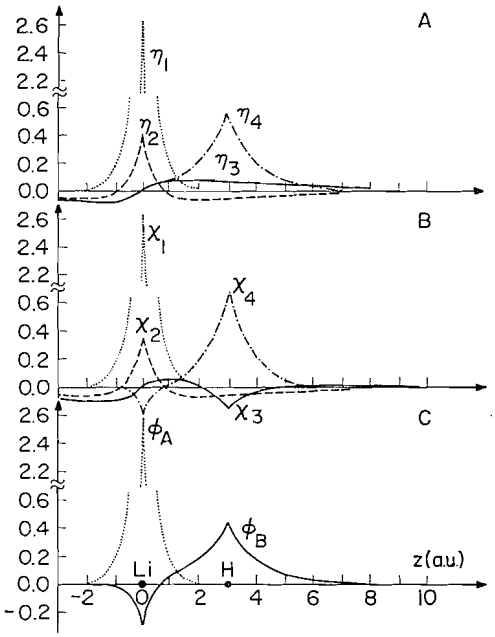

FIG. 1. LiH basis orbital values vs. distance z, for R = 3.0. a.u. (1A) Original basis set. (1B) Orthonormal basis set. (1C) Group orbital basis set.

TABLE I

Coefficients of bond orbital ϕ_{B1} and total energies of lithium hydride molecule in group orbital approximation

		Interatomic distances, R (a.u.)			
		2.0	3.0	5.0	8.0
Orbital coefficients					
c_1	VP	−0.445271	−0.483887	−0.496855	−0.519082
	SCF	−0.445131	−0.488254	−0.496468	−0.516710
c_2	VP	0.347684	0.381893	0.395629	0.303570
	SCF	0.347908	0.376246	0.396198	0.315421
c_3	VP	0.825134	0.787408	0.772407	0.798999
	SCF	0.825118	0.787431	0.772364	0.795940
Energy of group A, $H^4(aa)$		−8.236160	−7.903060	−7.636420	−7.486470
Reproducibility of iteration	VP	$<1.2\ 10^{-7}$	$<1.2\ 10^{-7}$	$<1.2\ 10^{-7}$	$<7.0\ 10^{-5}$
	SCF	$<3.0\ 10^{-8}$	$<3.0\ 10^{-8}$	$<3.0\ 10^{-8}$	$<3.9\ 10^{-3}$
GO total energy	VP	−7.889587	−7.975782	−7.929680	−7.838193
	SCF	−7.889587	−7.975799	−7.929680	−7.838300
Reported (14) MO-SCF total energy		−7.889788	−7.975811	−7.929709	−7.939216

compares the coefficients (c_1, c_2, c_3) defined in equation [10], with the elements (c_{11}, c_{21}, c_{31}) of the lowest eigenvector found in the self-consistent field calculation (see equation [17]). Results are given for a few internuclear distances in Table I. The corresponding results for a greater range of internuclear distances are given in Table AI of the appendices (25). The agreement between the variation of parameter and the self-consistent field calculations is very good. Table AV of the appendices lists the elements of all three eigenvectors that are computed by the self-consistent field procedure, for a range of internuclear distances.

Can. J. Chem. Downloaded from www.nrcresearchpress.com by 210.87.254.5 on 09/05/12
For personal use only.

The coefficients of the χ's that we find in the group orbitals cannot be compared directly with the coefficients that were found by Karo in his molecular orbital calculation (6), as he varied linear combinations of all four basis orbitals, whereas we kept two electrons in the unchanged lithium 1*s* orbitals throughout, in accordance with the group function approximation. The energy that is computed by the two methods may be compared, however, and this comparison shows that the group orbital approach gives results that are very close to those obtained by the comparable molecular calculations of Karo.

The accuracy with which the results can be made self-consistent is shown by the entries in the rows of Tables I and AI that are marked "Reproducibility of iteration". The difference between the energies computed in the last two iterations of the matrix diagonalization is given in this row for each of the internuclear distances at which the calculation was performed. The diagonalization subroutine automatically ended its computation when the results began to oscillate. It can be seen that the accuracy which could be obtained deteriorated with increasing internuclear distance. The dependence of the energy function on the variational parameters is shown graphically in Fig. 2. The energy value becomes extremely shallow at large internuclear distances so that locating the minimum becomes difficult.

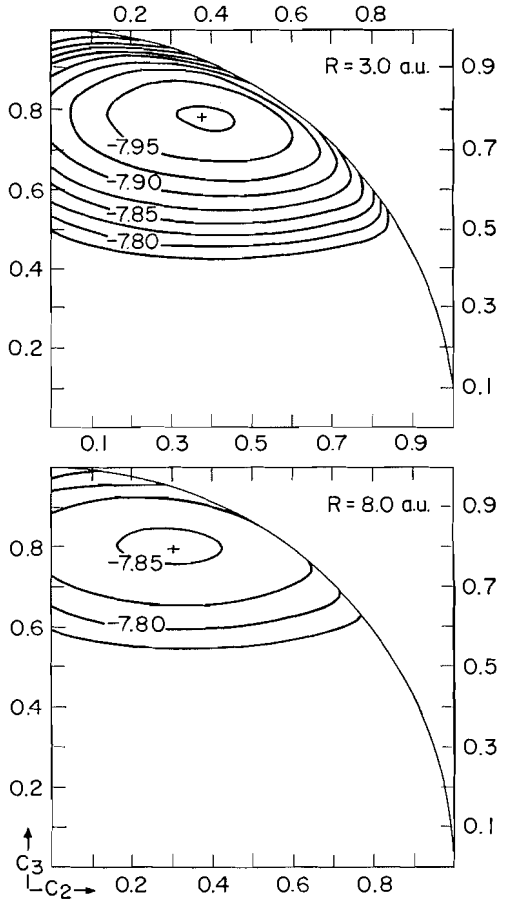

FIG. 2. Contour map of total energy of LiH vs. coefficients c_2 and c_3, for fixed R.

Can. J. Chem. Downloaded from www.nrcresearchpress.com by 210.87.254.5 on 09/05/12
For personal use only.

Figure 3 shows that the generalized product wave function [6] tends to the representation of separated Li^+ and H^- ions at infinite internuclear distance, as does the single determinant wave function of Karo and Olson. To construct a wave function that represents interacting neutral Li and H atoms at large separations, it is necessary to mix the solutions of the self-consistent field calculation (or, equivalently, products of the original χ's) in a configuration interaction treatment. This can still be considered to fall within the group function approximation, in that the orbitals of the bond electrons are mixed independently of the orbitals of the core electrons. In fact, the orbitals of the bond electrons only were mixed, as it seemed that this was most necessary on physical grounds. The configuration interaction treatment seems necessary for reasonable agreement with spectroscopic data.

TABLE II

Comparison of total energies of lithium hydride molecule in group orbital configuration interaction and molecular orbital configuration interaction approximations

		Interatomic distances, R (a.u.)			
		2.0	3.0	5.0	8.0
GOCI					
Singlet	S_0	−7.903083	−7.992182	−7.963833	−7.936200
	S_1	−7.779068	−7.877317	−7.896310	−7.876424
	S_2	−7.493222	−7.560819	−7.642118	−7.706534
Triplet	T_1	−7.833114	−7.917980	−7.931423	−7.918220
	T_2	−7.577554	−7.665784	−7.782805	−7.888330
MOCI					
Singlet	S_0	−7.903237	−7.992175	−7.963838	−7.985161
	S_1	−7.779564	−7.877298	−7.896284	−7.876438

Table II lists the energy values and Table AIII lists the coefficients that are found in this configuration interaction calculation. The results are given in these tables for a few internuclear distances, for the ground state and for the first and second excited singlet and triplet states. The last two rows of Table II contain the results obtained by Karo for the ground state and for the first excited singlet state. These are taken from Tables VI and VI*a* of reference (6). Tables AI and AII of the appendices (25) have the same format as Tables I and II, and contain the results for a larger set of internuclear distances. These results are plotted in Figs. 3 and 4, as graphs of energy versus internuclear distance.

The results of our configuration interaction calculation for the first excited singlet and triplet states suggest that energy minima occur at about 4.6 and 4.2 atomic units respectively. An experimental value of 4.906 atomic units (2.596 A) has been reported for the first excited singlet.

The second excited singlet and triplet states show no minima within the range of internuclear distances which we considered, which is 2 to 8 atomic units. The curves do show definite inflexions, however, which may be attributed to rather weak binding in these dissociating states.

The energy versus internuclear distance curves that we obtain resemble those which were found by Fraga and Ransil (20). The hump that we found in the lowest triplet state, at about 7 atomic units, was unexpected. It was thought at first that it was a numerical artefact due to the difficulty of making the results self-consistent at large internuclear distances. The height of the maximum above the asymptotic value of the energy curve in its neighborhood is about 0.02 atomic units. This is substantially greater than the

Can. J. Chem. Downloaded from www.nrcresearchpress.com by 210.87.254.5 on 09/05/12
For personal use only.

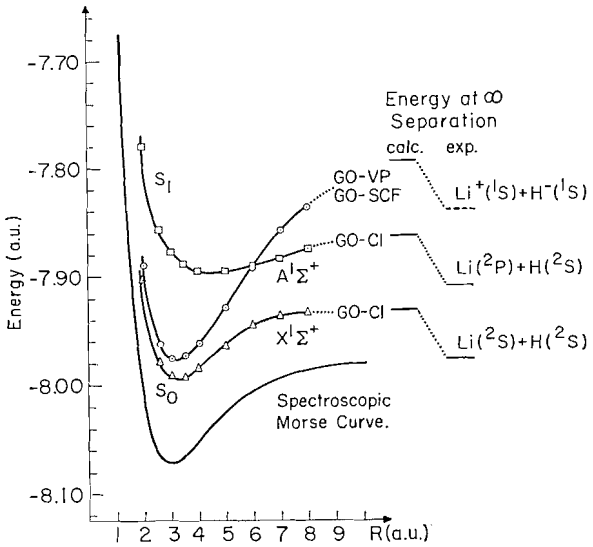

FIG. 3. Total energy vs. internuclear distance for LiH from GO-VP, GO-SCF, and the two lowest singlet GO-CI calculations. (The experimental Morse curve is also shown.)

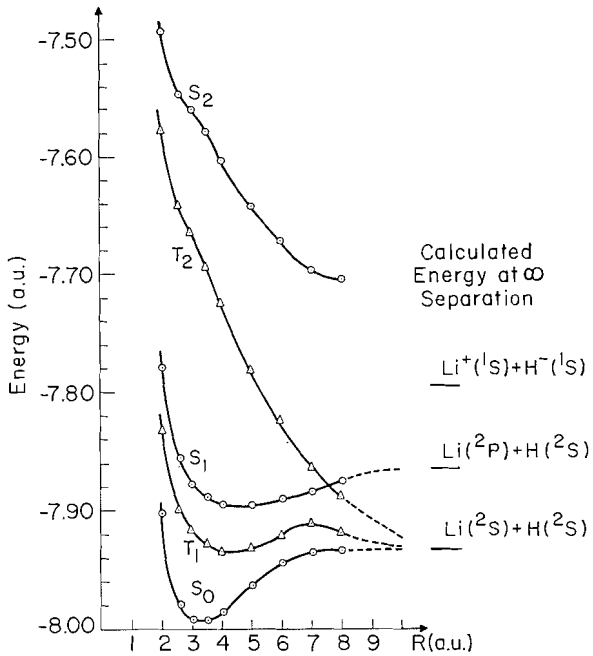

FIG. 4. Total energy vs. internuclear distance for LiH from the singlet and triplet GO-CI calculations.

"reproducibility of iteration", which is less than 0.00004 atomic units at the relevant internuclear distance. We conclude therefore that the hump is significant. Similar humps have been found by other workers in theoretical studies of homonuclear diatomic molecules (29, 30). Examples include H_2 in the $^1\Pi$ state (31), He_2 in the $^3\Sigma$ state (32), and O_2

Can. J. Chem. Downloaded from www.nrcresearchpress.com by 210.87.254.5 on 09/05/12
For personal use only.

in the $^3\Pi$ state (33). Spectroscopic observations of predissociation of the BH species provide experimental evidence for such a hump in the energy curve of this molecule in the $^1\Pi$ state (34). The phenomenon has not yet been explained, however, in terms of any simple physical model.

Figure 4 shows that according to our calculations, the lowest singlet excited state dissociates to an unexcited hydrogen atom and an excited lithium atom in the ^2P state. The lowest excited triplet state of the molecule, however, dissociates, like the ground state, to the unexcited atoms. The energies of the ground state and of the first excited triplet state thus approach asymptotically.

The group orbital approach allows the one-electron densities for the individual groups to be calculated separately. The total electron density of the molecule is the sum of the group densities [28]. Figure 5 is a plot of the electron density distribution along the lithium–

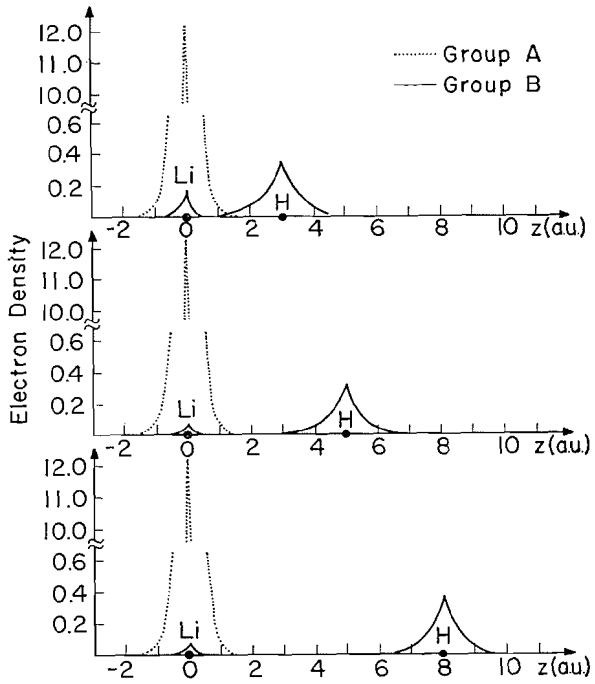

FIG. 5. Group orbital electron densities along the molecular axis (z) of LiH at R = 3.0, 5.0, and 8.0 a.u.

hydrogen bond, as calculated in the self-consistent field group function approximation. Figure 6 contains contour plots of the electron density, in a plane containing the bond, at two internuclear distances. These plots emphasize the group function approximation that we have used, in that the group of core electrons is not changed between the two figures. The density contours of the group of bond electrons in Fig. 6 correspond to the orbital ϕ_{B1}, which is assumed to be doubly filled. Figure 7 shows contour plots of electron density for hypothetical states of the molecule in which the orbitals ϕ_{B2} and ϕ_{B3} are doubly occupied. These states correspond to the states which Karo and Olson label 3σ and 4σ. The geometry of the ϕ_{B2} and ϕ_{B3} antibonding orbitals may have a stereochemical significance, which is discussed in the section that follows.

Can. J. Chem. Downloaded from www.nrcresearchpress.com by 210.87.254.5 on 09/05/12
For personal use only.

Can. J. Chem. Downloaded from www.nrcresearchpress.com by 210.87.254.5 on 09/05/12
For personal use only.

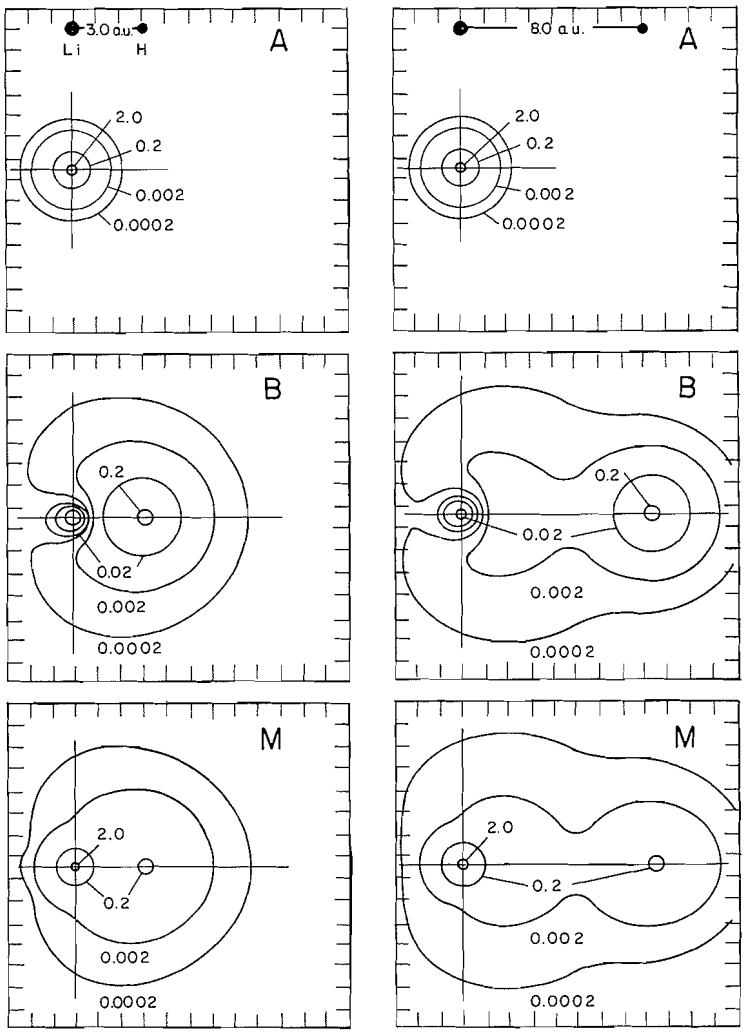

FIG. 6. Group orbital density contours of LiH at $R = 3.0$ and 8.0 a.u. (A) Group A, (B) group B, (M) total electron density.

Electron densities of the group B electrons in the various excited states in the configuration interaction were also found from equations [67] and [68] of Appendix 4 (25). Figure 8 contains plots of density along the Li–H axis for the three lowest singlet states at an internuclear distance of 3 atomic units. Figures 9 and 10 contain contour plots of electron density at several interatomic distances for the ground and several excited states.

These contour plots show that in the first excited states (S_1 and T_1) charge is decreased on both centers and built up in the region behind the lithium atom. In the second excited states (S_2 and T_2) charge is transferred from the lithium to the hydrogen atom. The arrangement of the valence electrons in the excited states may be summarized by simple formulae that depict electrons by arrows whose directions distinguish spin.

[18]

Li↓↑H	↓Li↑H	↑Li↑H	Li↑H↓	Li↑H↑
S_0	S_1	T_1	S_2	T_2

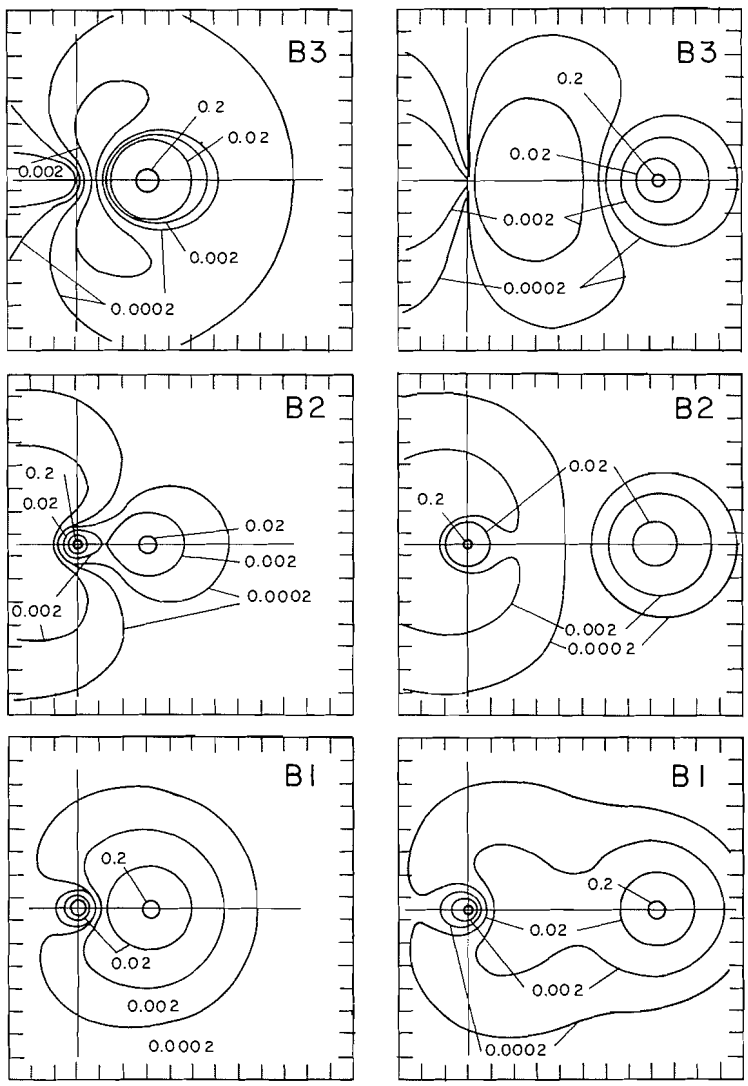

FIG. 7. Group B electron density contours for $B1$, $B2$, and $B3$ of LiH assuming each orbital doubly occupied, at $R = 3.0$ and 8.0 a.u.

Figure 10 contrasts the asymptotic behavior that is predicted by the self-consistent field and configuration interaction calculations. The former leads to ionic dissociation (as does the single determinant molecular orbital wave function) while the latter leads to neutral atom (free radical) dissociation. The fact that self-consistent field wave function goes over into the separated ion wave function at infinite internuclear distance is in a sense accidental. A generalized product function [6] of this form need not represent any particular state of the separated fragments at infinite separation. Nevertheless, advantage may be taken of this accident and the contours ($B1$) shown in Fig. 10 may be taken as representing the behavior of the molecule dissociating into Li^+ and H^- ions.

Contour plots of electron density for several further internuclear distances are given in the Appendix (Figs. A1 to A8). These illustrate the above discussion in greater detail.

Can. J. Chem. Downloaded from www.nrcresearchpress.com by 210.87.254.5 on 09/05/12
For personal use only.

Can. J. Chem. Downloaded from www.nrcresearchpress.com by 210.87.254.5 on 09/05/12
For personal use only.

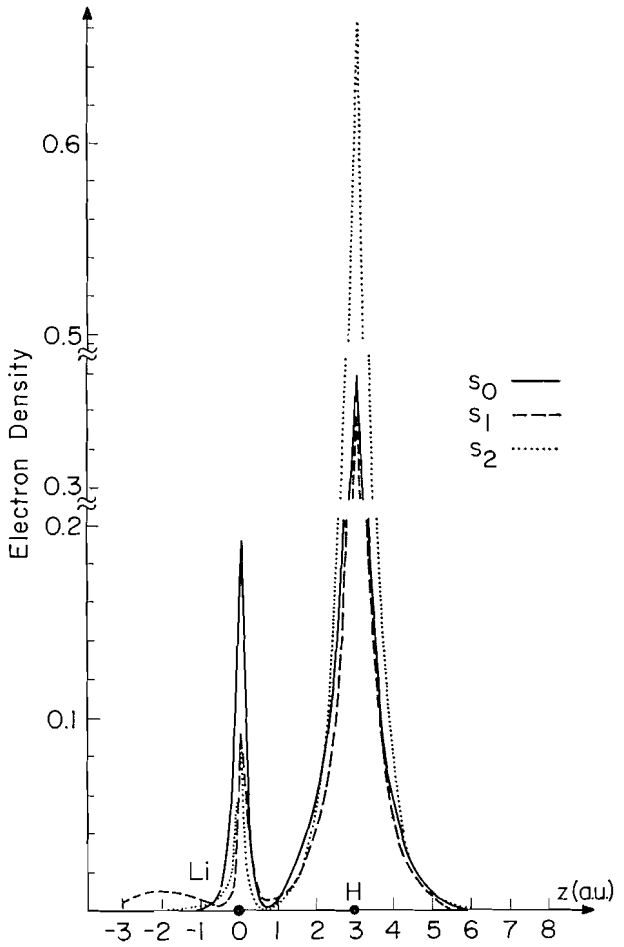

FIG. 8. Valence electron (group B) density along the molecular axis (z) of LiH at $R = 3.0$ a.u. for the three lowest singlet states.

4. A MODEL FOR SOME CHEMICAL REACTIONS

The results that were described in the preceding section may be used to provide a tentative explanation of certain aspects of the chemical behavior of lithium hydride. This explanation is developed, within the framework of the transition state concept, that in every chemical reaction there exists at least one transition state (activated complex) whose electronic structure determines the nature of the reaction products, and the rate with which these products are formed. It is generally assumed that one reactant donates an electron pair to the other reactant to form the transition state in a reaction which proceeds by an ionic mechanism. This is often expressed by the statement that a nucleophilic reagent (Lewis base) attacks the more positive site of a substrate, and an electrophilic reagent (Lewis acid) attacks the more negative site.

[19]

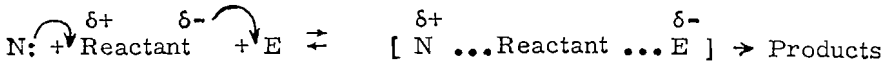

Can. J. Chem. Downloaded from www.nrcresearchpress.com by 210.87.254.5 on 09/05/12
For personal use only.

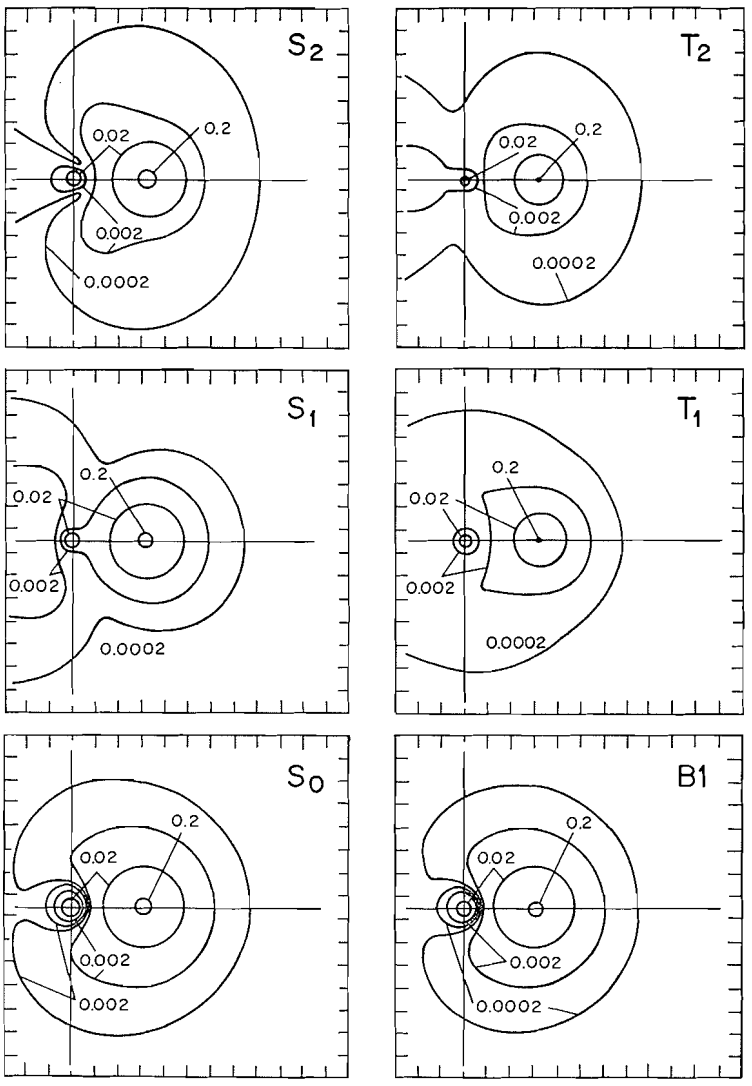

FIG. 9. Group B electron density contours for singlet (S_0, S_1, S_2) and triplet (T_1, T_2) states of LiH, at R = 3.0 a.u. The contour map of $B1$ is shown for comparison.

It is reasonable to assume further that the formation of a transition state in an ionic reaction resembles the formation of a coordination complex with the nucleophilic reagent playing the part of a ligand (35).

We now assume that the center with a net positive charge which is attacked by a nucleophilic agent must also have an unfilled orbital that is energetically accessible to the electron pair of the attacking agent. It would follow that the stereochemical arrangement of such unfilled orbitals affects the structure of the transition state and hence the course of the reaction. When several unfilled orbitals are available at the site of the attack, the orbital of lower energy presumably is occupied in the transition state. The assumptions of this paragraph have meaning within the simple orbital model of chemical structure, and the idea that a pair of electrons forms a chemical bond is implicit. These assumptions now are applied to the reactions of lithium hydride.

Can. J. Chem. Downloaded from www.nrcresearchpress.com by 210.87.254.5 on 09/05/12
For personal use only.

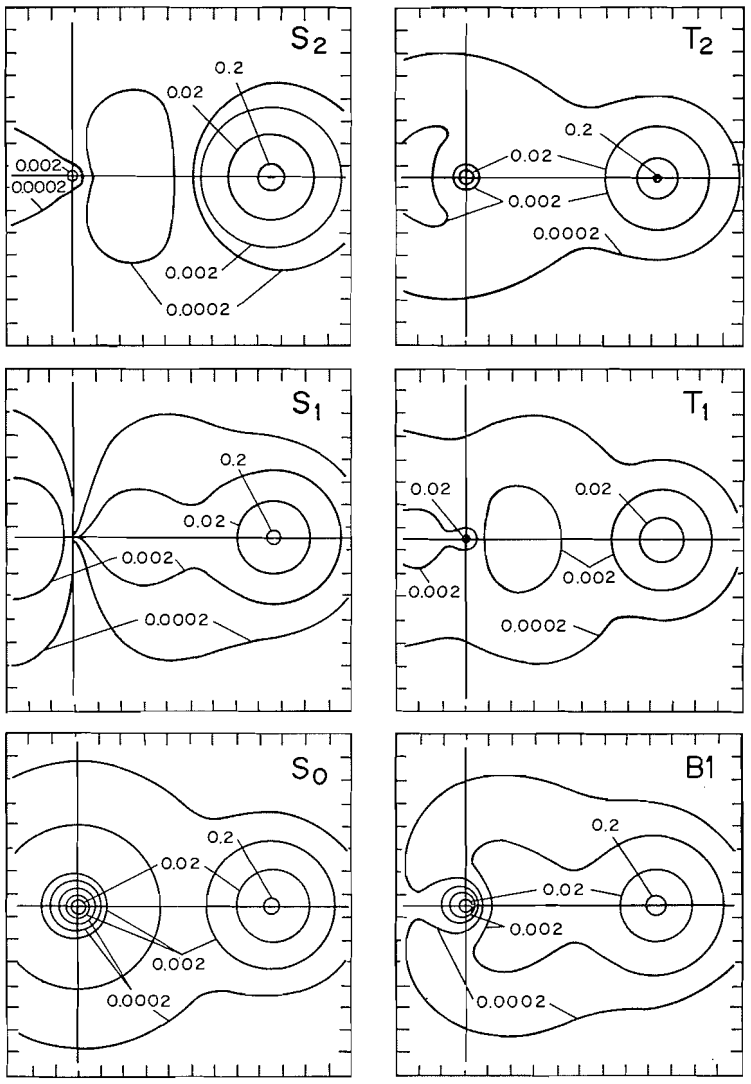

FIG. 10. Group B electron density contours for singlet (S_0, S_1, S_2) and triplet (T_1, T_2) states of LiH, at $R = 8.0$ a.u. The contour map of $B1$ is shown for comparison.

When a molecule of lithium hydride reacts, its atoms separate, and, in accordance with the calculated potential energy curve and electron density maps, it may be assumed that the molecule polarizes $Li^{\delta+} \ldots H^{\delta-}$ in ionic reactions. A nucleophilic reagent therefore should attack the lithium atom, and an electrophilic reagent should attack the hydrogen atom. In accordance with the assumptions of the preceding paragraph, the formation of a linear transition state between LiH and a nucleophilic reagent requires an unfilled orbital on the Li atom whose axis is collinear with the LiH bond.

[20]

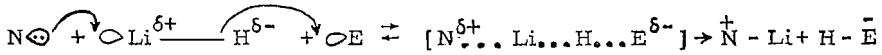

In the bond-breaking step of this proposed mechanism, the valence electrons shift towards the hydrogen atom, where they participate in the formation of a bond with the electrophilic reagent. The valence electrons are described by the orbital ϕ_{B1} in our calculation, and the behavior of the electron density contours plotted for ϕ_{B1} at different internuclear distances probably gives a good representation of the distortion of the valence electron cloud during electrophilic substitution. The antibonding orbital ϕ_{B2} would be assumed to act as an electron acceptor in our scheme, as its geometry favors attack by the nucleophilic agent from the side that is opposite to the hydrogen atom. The orbital ϕ_{B3} is energetically less favorable than ϕ_{B2}, and it points in the opposite direction. We conclude that the orbitals ϕ_{B1} and ϕ_{B2} are of importance in reactions of LiH. Qualitatively, it may be said that as the internuclear distance increases, the region of maximum density of ϕ_{B1} moves away from the Li atom, while the region of maximum density of ϕ_{B2} moves into the region surrounding the Li atom (Fig. 11). Two specific chemical reactions will

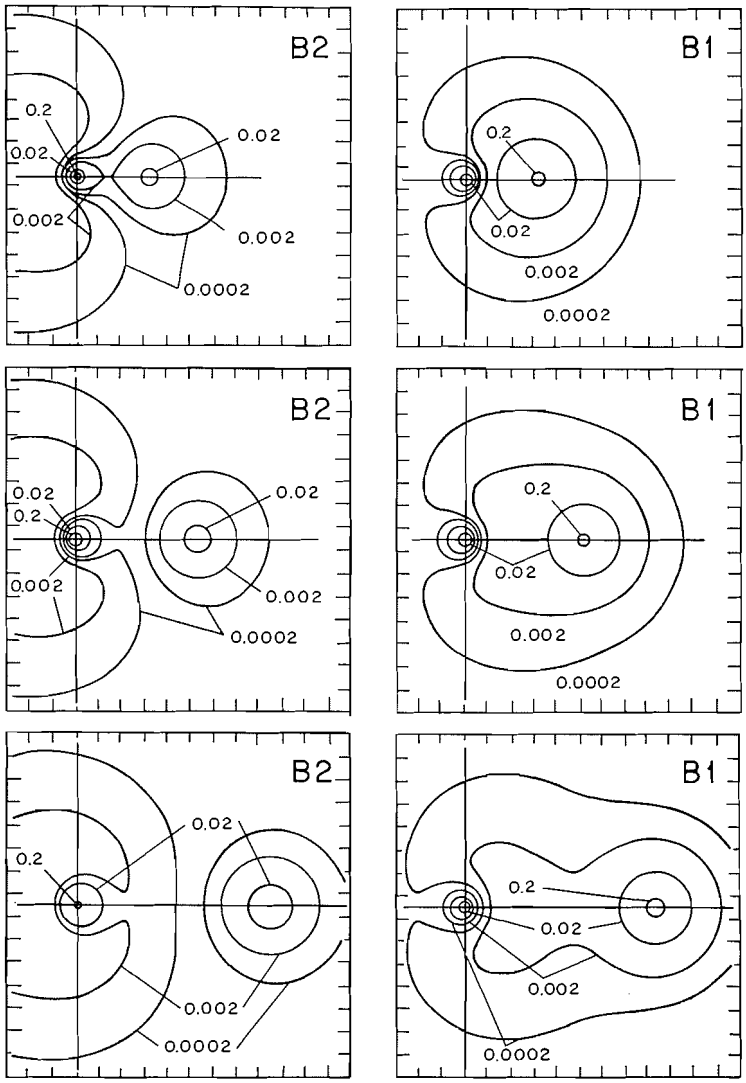

FIG. 11. Group B electron density contours for $B1$ and $B2$ of LiH at R = 3.0, 5.0, and 8.0 a.u.

Can. J. Chem. Downloaded from www.nrcresearchpress.com by 210.87.254.5 on 09/05/12
For personal use only.

now be considered which, it is suggested, proceed by ionic mechanism [20] and in which the ϕ_{B2} orbital acts as an electron acceptor.

The first reaction is the solvolysis of LiH. Molecular hydrogen is formed in this reaction, and not nascent hydrogen. This suggests that molecular hydrogen is formed directly in the decomposition of the activated complex, as would be the case if the reaction proceeded by the following ionic mechanism.

[21]

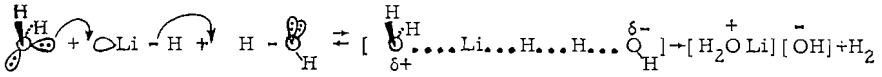

The second reaction is the formation of lithium borohydride from lithium hydride and diborane. Diborane is known to dissociate to BH_3 (36). This would act as an electrophilic reagent. The lithium hydride diborane reaction requires an ether-type solvent (37). It seems reasonable then to assume that the solvent's participation in the reaction involves its lone pair of electrons.

[22]

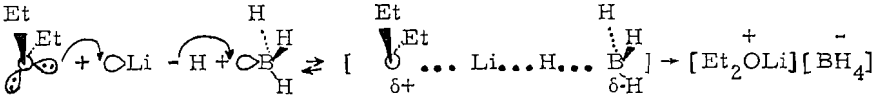

Although this hypothesis is stereochemically plausible, no final conclusion can be drawn as yet from the present calculation since it is not known whether the lowest σ^* or the empty p_x and p_y orbitals of Li are energetically better for electron acceptance. Knowledge of this fact is necessary in the approximation we are using because it is assumed (see above) that of the several unfilled orbitals, the one of lowest energy will be occupied. The utilization of the empty p_x and p_y orbitals in the formation of the transition state would lead to a "bent" or "cyclic" activated complex as opposed to the linear complex presented above [20], [21], [22]. Which orbitals are in fact involved, can only be determined from a separate calculation of the possible transition states in which all three $2p$ orbitals ($2p_x$, $2p_y$, $2p_z$) of Li as well as the reagents are included.

It has, however, been suggested recently, as a result of kinetic measurements (38), that the transition state in butyl lithium – alkyl halide reactions is linear. This suggestion may perhaps be taken as support for a linear transition state in lithium hydride reactions.

5. SPECTROSCOPIC CONSIDERATIONS

The first excited singlet Σ state of lithium hydride is well known (10). We have not found reports of any observations of a triplet state, however. Our calculations predict only one stable triplet Σ state (see Fig. 3). Transition to this state from the ground state, of course, is spin forbidden. Furthermore this state cannot be reached by a radiationless transition from the S_1 state (which could be produced by irradiation), since the curves for S_1 and T_1 do not cross.

If the triplet state T_1 could be generated, however, it might be possible to confirm existence of the potential "hump", by observing rotational predissociation. This is so called "type III" predissociation (34). Although the triplet state cannot be excited directly, two indirect ways may be suggested.

The first involves a perturbation of the LiH molecule by an appropriately selected

Can. J. Chem. Downloaded from www.nrcresearchpress.com by 210.87.254.5 on 09/05/12
For personal use only.

species of unpaired spin, to cause the requisite forbidden transition. The singlet → triplet transition of benzene that occurs in the presence of O_2 and NO molecules is a phenomenon of this type. Theoretical explanations of this process have been given by several authors (39, 40, 41).

The second possible way of exciting LiH to the triplet involves photosensitization. An intermolecular triplet → triplet energy transfer could produce the required $\sigma \rightarrow \sigma^*$ triplet LiH state as shown in Fig. 12. It has been shown that this type of process is responsible

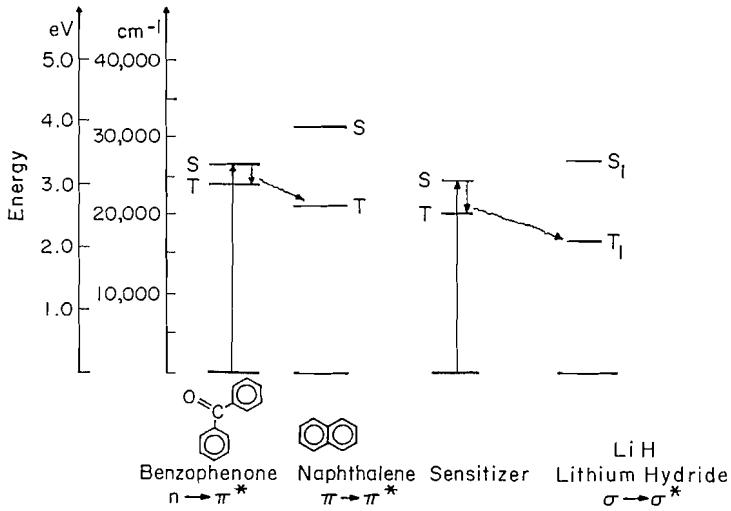

FIG. 12. Photosensitization by means of triplet → triplet energy transfer.

for the production of the $\pi \rightarrow \pi^*$ triplet in naphthalene with the aid of benzophenone (42, 43, 44). An appropriate photosensitizer for LiH would need suitable energy levels, a triplet state with a long enough lifetime for interaction, and should not react chemically with LiH in either its ground or excited states.

If the required triplet state can be obtained by the photosensitization method in an inert matrix at a low temperature (4.2 °K or 77 °K) the possibility of observing e.s.r. signals from both the photosensitizer and the lithium hydride can be considered. The signal from the photosensitizer should decrease as the signal from the lithium hydride increases.

In practice, however, it would be impossible to observe either signal if the lifetimes of the triplet states were too short. Furthermore Weissman suggests that triplet signals from small molecules cannot be observed because of magnetic dipolar coupling between the unpaired electrons (45). Even if the lifetimes of the triplets in the predissociation process were not too short, the signal from the lithium hydride might therefore be unobservable. Observation of a decaying signal from the photosensitizer, however, could still provide evidence for the occurrence of the triplet → triplet energy transfer.

ACKNOWLEDGMENTS

This work forms part of a program of research that is supported by the Army, the Navy, and the Air Force of the United States, and the National Science Foundation. One of us (I.G.C.) would like to thank the National Research Council of Canada for the

Can. J. Chem. Downloaded from www.nrcresearchpress.com by 210.87.254.5 on 09/05/12
For personal use only.

award of a NATO Science Fellowship. One of us (B.T.S.) would like to thank the Fullbright Commission for the award of a Fullbright Travel Scholarship. We should like to thank Professor J. C. Slater for his encouragement and advice, and Drs. J. P. Dahl, M. C. Harrison, J. W. Moskowitz, and R. M. Pitzer for their comments and criticisms.

REFERENCES

1. R. McWEENY. Rev. Mod. Phys. **32**, 335 (1960).
2. R. G. PARR, F. O. ELLISON, and P. G. LYKOS. J. Chem. Phys. **24**, 1106 (1956).
3. P. G. LYKOS and R. G. PARR. J. Chem. Phys. **24**, 1106 (1956).
4. J. M. PARKS and R. G. PARR. J. Chem. Phys. **28**, 335 (1958).
5. A. M. KARO and A. R. OLSON. J. Chem. Phys. **30**, 1232 (1959).
6. A. M. KARO. J. Chem. Phys. **30**, 1241 (1959).
7. R. McWEENY and K. A. OHNO. Proc. Roy. Soc. A, **255**, 367 (1960).
8. A. TSUCHIDA and K. A. OHNO. J. Chem. Phys. **39**, 600 (1963).
9. R. McWEENY and B. T. SUTCLIFFE. Mol. Phys. In press.
10. F. A. CRAWFORD and T. JORGENSEN, JR. Phys. Rev. **49**, 745 (1936).
11. R. VALASCO. Can. J. Phys. **35**, 1204 (1957).
12. T. C. JAMES, W. G. NORRIS, and W. KLEMPERER. J. Chem. Phys. **32**, 728 (1960).
13. L. WHARTON, L. P. GOLD, and W. KLEMPERER. J. Chem. Phys. **37**, 2149 (1962).
14. R. S. MULLIKEN. Phys. Rev. **50**, 1028 (1936).
15. S. BRATOZ and G. BESSIS. J. Chem. Phys. **56**, 1042 (1959).
16. R. J. FALLON, J. T. VANDERSLICE, and E. A. MASON. J. Chem. Phys. **32**, 1453 (1960).
17. A. M. KARO. J. Chem. Phys. **32**, 907 (1960).
18. R. MOCCIA. Gazz. Chim. Ital. **90**, 955, 968 (1960).
19. B. J. RANSIL. Rev. Mod. Phys. **32**, 239 (1960).
20. S. FRAGA and B. J. RANSIL. J. Chem. Phys. **35**, 669 (1961).
21. F. A. MATSEN and J. C. BROWNE. J. Phys. Chem. **66**, 2332 (1962).
22. R. M. STEVENS, R. M. PITZER, and W. N. LIPSCOMB. J. Chem. Phys. **38**, 555 (1963).
23. S. L. KAHALAS and R. K. NESBET. J. Chem. Phys. **39**, 529 (1963).
24. J. C. SLATER. Quantum theory of molecules and solids. Vol. 1. McGraw-Hill Book Co., Inc. 1963. p. 136.
25. I. G. CSIZMADIA, B. T. SUTCLIFFE, and M. P. BARNETT. A group orbital study of LiH—supplementary material. Technical Note No. 32, Cooperative Computing Laboratory, MIT (December 30, 1963).
26. W. MOFFITT. Proc. Roy. Soc. London, A, **210**, 245 (1951).
27. P. O. LÖWDIN. J. Chem. Phys. **35**, 79 (1961).
28. V. FOCK and M. J. PETRASHEN. Phys. Zh. Sovjetunion, **8**, 547 (1935).
29. J. O. HIRSCHFELDER, C. F. CURTISS, and R. B. BIRD. Molecular theory of gases and liquids. John Wiley and Sons Inc., New York. 1954. pp. 990, 1100.
30. G. HERZBERG. Molecular spectra and molecular structure I. Diatomic molecules. 2nd ed. 1950. pp. 296, 380.
31. G. W. KING and J. H. VAN VLECK. Phys. Rev. **55**, 1165 (1939).
32. R. BUCKINGHAM and A. DALGARNO. Proc. Roy. Soc. A, **213**, 327 (1952).
33. A. MECKLER. J. Chem. Phys. **21**, 1750 (1953).
34. G. HERZBERG and L. G. MUNDIE. J. Chem. Phys. **8**, 263 (1940).
35. F. BASOLO and R. G. PEARSON. Mechanism of inorganic reactions. John Wiley and Sons Inc., New York. 1958. p. 34.
36. W. N. LIPSCOMB. Recent studies of boron hydrides. *In* Advances in inorganic chemistry and radiochemistry. Vol. 1. *Edited by* H. J. Emeleus and A. G. Sharpe. Academic Press, N.Y. 1959. p. 148.
37. N. G. GAYLORD. Reduction with complex metal hydrides. Interscience Publishers Inc., N.Y. 1956. p. 20.
38. J. F. EASTMAN and G. W. GIBSON. J. Am. Chem. Soc. **85**, 2171 (1963).
39. H. TSUBOMURA and R. S. MULLIKEN. J. Am. Chem. Soc. **82**, 5966 (1960).
40. G. J. HOIJTINK. Mol. Phys. **3**, 67 (1960).
41. J. N. MURRELL. Mol. Phys. **3**, 319 (1960).
42. A. TERENIN and V. ERMALOV. Trans. Faraday Soc. **52**, 1042 (1956).
43. G. PORTER and F. WILKINSON. Trans. Faraday Soc. **57**, 1686 (1961).
44. J. B. FARMER, C. L. GARDNER, and C. A. McDOWELL. J. Chem. Phys. **34**, 1058 (1961).
45. S. I. WEISSMAN. J. Chem. Phys. **29**, 1189 (1958).

Can. J. Chem. Downloaded from www.nrcresearchpress.com by 210.87.254.5 on 09/05/12
For personal use only.

Can. J. Chem. Downloaded from www.nrcresearchpress.com by 210.87.254.105 on 09/05/12
For personal use only.

NEW REARRANGEMENTS OF THE CARYOPHYLLENE SKELETON: THE DINITROPHENYLHYDRAZONES FROM CARYOPHYLLENE OXIDE

E. W. WARNHOFF[1]
Department of Chemistry, University of Western Ontario, London, Ontario
Received January 27, 1964

ABSTRACT

Caryophyllene oxide (I) and dihydrocaryophyllene oxide (II) have been found to give 2,4-dinitrophenylhydrazones. Structures IV, V, and VII are assigned to three of these compounds on the basis of nuclear magnetic resonance data, other spectral and chemical data, and mechanistic considerations. Structure VII is the product of a new cyclization–rearrangement of the caryophyllene system. The dinitrophenylhydrazone previously obtained from isocaryophyllene oxide-*a* (III) is probably identical with VII. Three other new derivatives of caryophyllene are described, one of which (VI) is an intermediate in the conversion of I to VII.

The chemistry of caryophyllene is a rich source of interesting reactions which is not yet exhausted. Among these reactions is the cyclization–rearrangement which occurs when the caryophyllene oxides are treated with aqueous acid (1). The product isolated is a C-9 epimer of the glycol X, but in addition there are carbonyl compounds formed. In the case of caryophyllene oxide (I), the crude hydration product exhibits infrared absorption at 1730 cm^{-1}. In the case of isocaryophyllene oxide, it has been reported (2) that isocaryophyllene oxide-*a* (III) reacts with 2,4-dinitrophenylhydrazine under unspecified conditions to give a derivative, $C_{21}H_{28}O_4N_4$, m.p. 185°. The carbonyl compounds probably result from rearrangement of the oxide ring, and any rearrangement might also have involved the exocyclic methylene group or a transannular reaction. These possibilities prompted the present investigation of the carbonyl compounds formed during the acid-catalyzed hydration of caryophyllene oxide (I) and dihydrocaryophyllene oxide (II).

The carbonyl compounds are most readily isolated by precipitation as the 2,4-dinitrophenylhydrazones. A mixture of the same derivatives was obtained by addition of 2,4-dinitrophenylhydrazine solution to previously acid-treated I, or, more conveniently, by addition of acidic 2,4-dinitrophenylhydrazine solution directly to I. When caryophyllene oxide was treated with a sulphuric acid solution of 2,4-dinitrophenylhydrazine, an orange precipitate formed in low yield (15%). This proved to be a mixture of three derivatives which was partially separated by thick-layer chromatography into a slower-moving component, m.p. 171°, and a faster-moving component. The faster-moving band was resolved by crystallization into two compounds, m.p. 186° and m.p. 191°. All three derivatives had the molecular formula $C_{21}H_{28}O_4N_4$ (I + 2,4-DNPine-H_2O), and each was revealed to be a true dinitrophenylhydrazone by its infrared and ultraviolet spectra (see Experimental), but these physical constants did not allow a distinction between aldehyde and ketone derivatives (3, 12).

However, the n.m.r. spectrum (Fig. 1*a*) of the 171° compound had a 1-H singlet at 7.39 p.p.m. (tetramethylsilane = 0) from the unsplit proton of an aldehyde dinitrophenylhydrazone —CH=N— system with no α-hydrogen (4). In addition the C-methyl region contained a new 3-H singlet at 1.14 p.p.m. corresponding to a methyl group on

[1]*Fellow of the Alfred P. Sloan Foundation.*

a quaternary carbon atom. The 7 c.p.s. displacement of these methyl protons to lower field relative to the *gem*-dimethyl group at 1.01 p.p.m. can be accounted for by proximity to the —CH=N—dinitrophenyl group.[2] The two olefinic protons at 4.50 and 4.71 p.p.m. showed the exocyclic methylene group to remain undisturbed. A mechanistically reasonable formula consistent with these facts and involving the least structural change is IV, formed by rearrangement of the oxide ring (I → IV) to an 8-membered carbocycle.

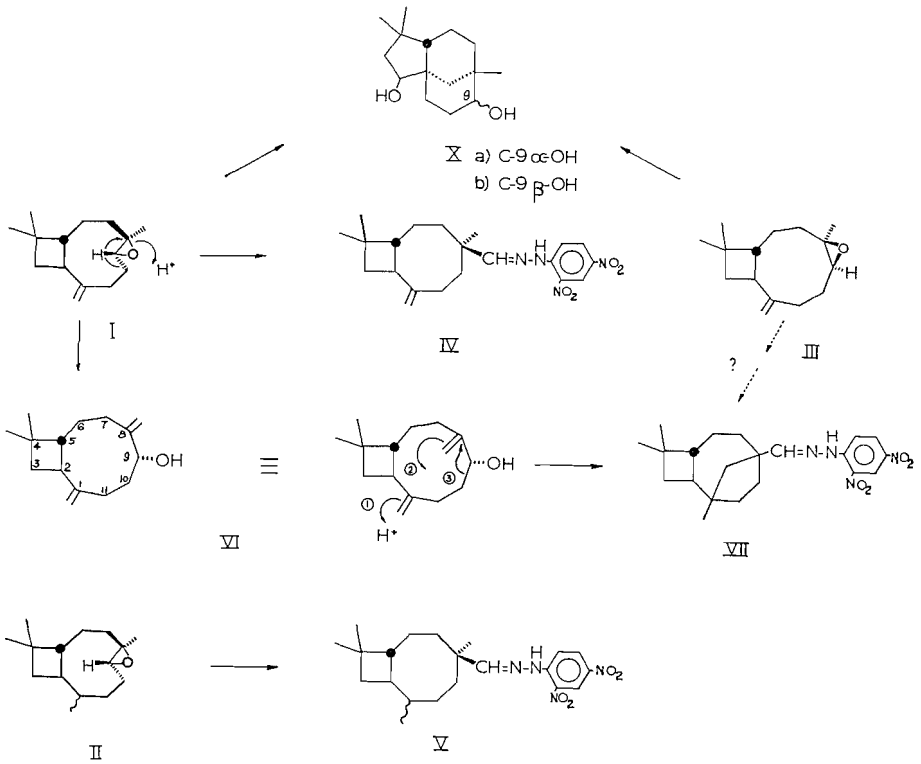

Confirmation for the rearranged structure was sought from dihydrocaryophyllene oxide (II), which should react in the same manner with dinitrophenylhydrazine solution. Only a single derivative, $C_{21}H_{30}O_4N_4$, m.p. 187.5°, was obtained from II in a yield (6%) about equal to that of the 171° compound from I. Again, both the infrared and ultraviolet spectra corresponded to those of a ketone or aldehyde dinitrophenylhydrazone. The n.m.r. spectrum (Fig. 1*b*) of the 187.5° compound also had a 1-H singlet at 7.36 p.p.m. from the unsplit proton of a quaternary aldehyde dinitrophenylhydrazone —CH=N— function. A quaternary methyl substituent adjacent to the —CH=N— dinitrophenyl function gave a 3-H singlet at 1.10 p.p.m., whereas the *gem*-dimethyl group was still present at 0.96 and 0.99 p.p.m. A doublet from the CH_3—CH of the fourth methyl group was centered at 0.82 p.p.m. with an apparent coupling of 6.5 c.p.s., and this doublet was also present in the spectrum of dihydrocaryophyllene oxide (Table I). In the infrared region the only notable difference between the 171° and the 187.5° compounds was the presence of a peak at 890 cm^{-1} (C=CH_2) in the spectrum of the 171° derivative but not of the 187.5° compound. Therefore, the 187.5° dinitrophenylhydrazone has the structure V analogous to that proposed for the derivative IV from

[2]*Proximity to the double bond is excluded by the derivative from II. See below.*

Can. J. Chem. Downloaded from www.nrcresearchpress.com by 210.87.254.105 on 09/05/12
For personal use only.

Can. J. Chem. Downloaded from www.nrcresearchpress.com by 210.87.254.105 on 09/05/12
For personal use only.

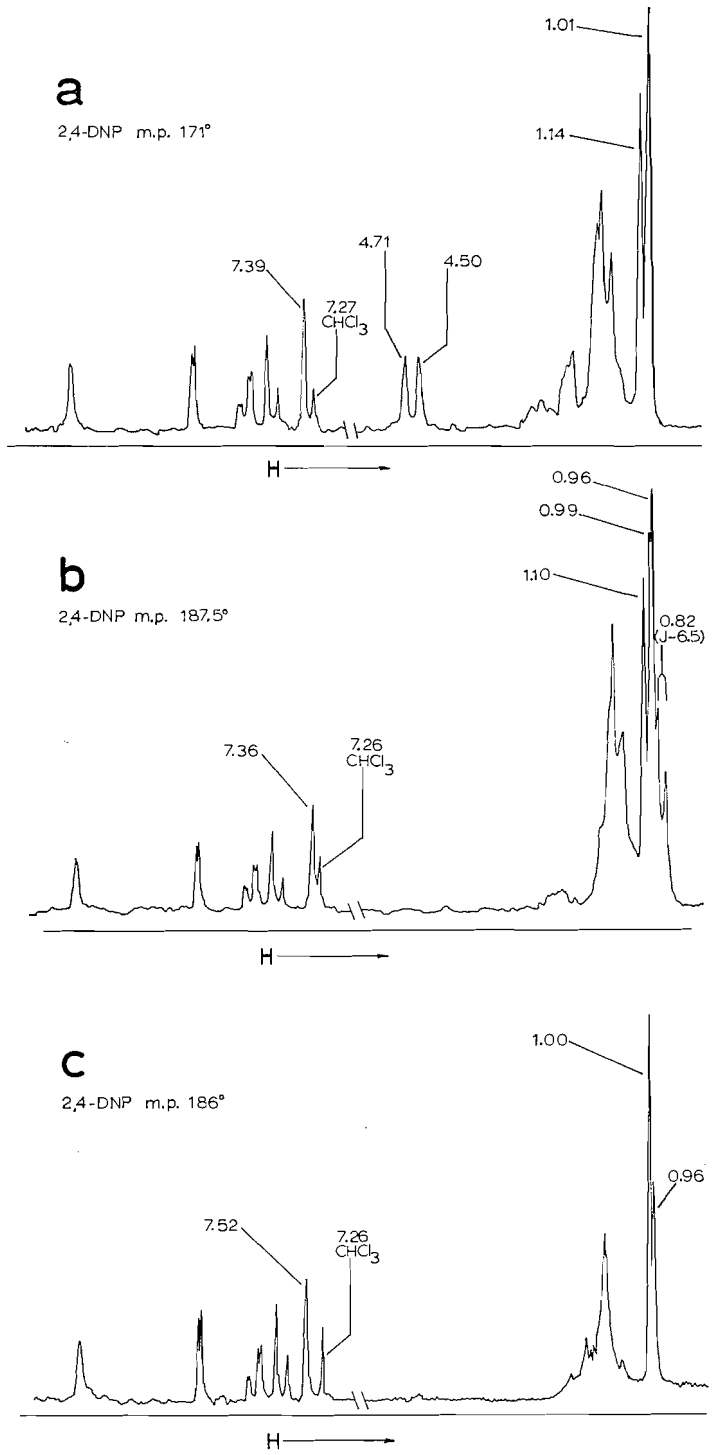

FIG. 1. Nuclear magnetic resonance spectra of 2,4-dinitrophenylhydrazones from caryophyllene oxide and dihydrocaryophyllene oxide.

Can. J. Chem. Downloaded from www.nrcresearchpress.com by 210.87.254.105 on 09/05/12
For personal use only.

TABLE I

Nuclear magnetic resonance absorption of caryophyllene derivatives*

Compound		C_4-*gem*-dimethyl	Exocyclic $=CH_2$	C_8 methyl	C_1 methyl	—CH=N— of DNP	Allylic CH_2	Allylic C—H	O—C_9—H	Other
Caryophyllene oxide	I	0.98(6H,s)	4.87(1H,s) 4.97(1H,s)	1.19 (3H,s)	—	—	ca.1.85–2.34 (m)	ca.2.34–2.65 (m)	2.65–3.02 (1H,m)	—
Dihydrocaryophyllene oxide	II	0.93(6H,s)	—	1.27 (3H,s)	0.84(J ~ 6–7) (3H,d)	—	—	—	2.75–3.02 (1H,m)	—
Dinitrophenylhydrazone m.p. 171°	IV	1.01(6H,s)	4.50(1H,s) 4.71(1H,s)	1.14 (3H,s)	—	7.39 (1H,s)	ca.2.10–2.43 (m)	ca.2.43–3.02 (m)	—	—
Dinitrophenylhydrazone m.p. 187.5°	V	0.96, 0.99 (6H,2-s)	—	1.10 (3H,s)	0.82(J ~ 6.5) (3H,d)	7.36 (1H,s)	—	—	—	—
Dinitrophenylhydrazone m.p. 186°	VII	1.00(6H,s)	—	—	0.96(3H,s)	7.52 (1H,s)	—	—	—	—
Dinitrophenylhydrazone m.p. 191°		1.02(6H,s)	—	1.20 (3H,s)	—	7.45 (1H,s)	?	?	—	1.56(3H,s) 1.73(3H,s) CH_3—C=
Keto allylic alcohol	XV	1.01(6H,s)	4.92(1H,s) 5.00(1H,s)	—	—	—	Indistinguishable from O=C—CH_2 and O=C—CH		4.00–4.24 (1H,m)	2.70(s) OH
Unsaturated diketone	XVI	0.97(6H,s)	5.70(2H,s)	—	—	—	"	"	—	—
Dienol	VI	0.99(6H,s)	4.78(2H,s) 4.95(1H,s) 5.04(1H,s)	—	—	—	ca.1.85–2.4 (m)	ca.2.4–2.7 (m)	4.08 (J ~ 4, 8) (1H,d of d)	2.08(s) OH

*Chemical shifts are given in p.p.m. from tetramethylsilane (=0) for deuterochloroform solutions. The number of protons in the peak(s) and the apparent multiplicity are given in parentheses; s = singlet, d = doublet, d of d = doublet of doublets, m = multiplet.

caryophyllene oxide. The stereochemistry of IV and V follows from the expected inversion during oxide rearrangement.

The 186° dinitrophenylhydrazone from caryophyllene oxide (I) appeared more interesting in that the exocyclic methylene group was missing. Both the peak at 890 cm^{-1} in the infrared spectrum and those at 4.50 and 4.71 p.p.m. in the n.m.r. spectrum were absent. This compound was also derived from an aldehyde with no α-hydrogen since a 1-H singlet at 7.52 p.p.m. was present in the n.m.r. spectrum (Fig. 1*c*). However, the absence of a 1.10–1.14 p.p.m. peak revealed that there was no quaternary methyl substituent on the α-carbon atom of the aldehyde. Instead, close to the *gem*-dimethyl group at 1.00 p.p.m. was a third quaternary methyl group at 0.96 p.p.m. not deshielded by any functional group. Furthermore, in the 2.00–3.10 p.p.m. region there was no absorption from allylic methylene or methine protons such as is present in n.m.r. spectra of unsaturated caryophyllene derivatives (see Table I). With no vinyl or allylic hydrogen present, the 186° compound is necessarily the dinitrophenylhydrazone of a completely saturated cyclization product. The simplest formulation for this derivative is VII arising by the sequence I → VI → VII,[3] which represents a new cyclization–rearrangement of the caryophyllene skeleton. The cyclization itself is not new; this type has been proposed (5) for the reaction of caryophyllene – maleic anhydride adduct with electrophilic reagents, e.g. VIII → IX, and proved (6) for the reaction of caryophyllene keto oxide with hydrogen chloride, XI → XII.

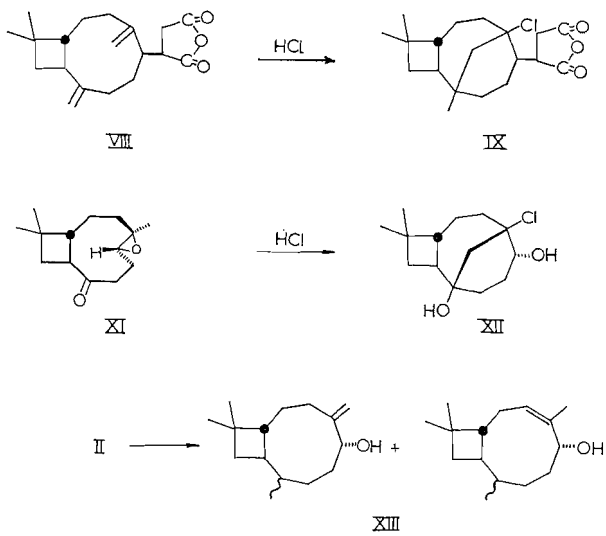

VIII IX XI XII XIII

This interpretation was tested by determining whether VI could be an intermediate, since it has already been demonstrated (7) that the oxide ring of II can be opened to a mixture of allylic alcohols XIII. The allylic alcohol VI was prepared in 80% yield by mild opening of the oxide ring of caryophyllene oxide (I) on passage through a column of alumina. Although the product gave a single spot on thin-layer chromatography, and its infrared spectrum had hydroxyl absorption, increased methylene absorption (C=CH_2, 890 cm^{-1}) relative to I, and no carbonyl absorption, still the n.m.r. spectrum in the olefinic hydrogen region indicated the presence of an impurity. In particular, a small

[3]*More complex changes involving transannular hydride shifts, multiple rearrangements, etc. are regarded as less likely (see below).*

Can. J. Chem. Downloaded from www.nrcresearchpress.com by 210.87.254.105 on 09/05/12
For personal use only.

amount of XIV or the hydroxyl epimer of VI might be difficult to detect. Therefore, a sample of VI was synthesized by a different route.

The oxide ring of caryophyllene keto oxide, XI (8), was opened on alumina to give as the major product the keto allylic alcohol XV, which crystallized. Its structure is substantiated by its infrared spectrum with hydroxyl (3600 and 3440 cm^{-1}), carbonyl (1692 cm^{-1}), and asymmetric disubstituted ethylene (896 cm^{-1}) absorption, and by its n.m.r. spectrum (Table I) with peaks corresponding to two olefinic protons and one H—C—O group. As further structural evidence manganese dioxide oxidation of XV produced the crystalline cisoid conjugated ketone XVI, λ_{max} 227 mμ (ϵ 6150), whose n.m.r. spectrum (Table I) still had two olefinic hydrogens. The Wittig reaction of XV with the ylide from methyltriphenylphosphonium iodide gave VI[4], which, although not crystalline, gave a single spot on thin-layer chromatography with the same R_f value as VI prepared by opening the oxide ring of I. The n.m.r. spectrum (Table I) of VI from the Wittig reaction corresponded with that expected. It had a total of four olefinic protons, one proton (doublet of doublets) on carbon bearing oxygen, and only two methyl groups.

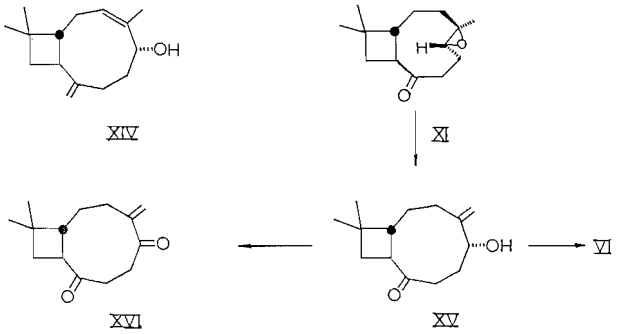

When VI, prepared by either method, was treated with 2,4-dinitrophenylhydrazine under the same conditions used for I and II, orange crystals precipitated in 33–44% yield. These were proved to be the 186° dinitrophenylhydrazone from I by mixture melting point and by comparison of infrared and n.m.r. spectra, optical rotations, and thin-layer chromatographic behavior. No trace of IV could be detected by thin-layer chromatography of the crude precipitate. Nor could any IV or 191° derivative be detected in the n.m.r. spectrum of the crude precipitate, although these would have been readily apparent at 1.14, 1.20, 1.56, and 1.73 p.p.m. if present. The fact that the 186° compound can be obtained from VI, and in much better yield than from I, provides strong support for the proposed structure VII and the reaction sequence leading to it.

Another structure derivable by a more complex transformation of VI, but which also fits the interpretable features of the n.m.r. spectrum (Fig. 1*c*), is XVII formed as outlined below.[5] This possibility was tested by determination of the extent of deuterium incorporation when the cyclization–rearrangement was carried out in deuterium oxide and ethanol-*O*-d_1 solution. The VII formed was found to contain an average of 0.88 atom of deuterium per molecule. Since the 0.96 p.p.m. methyl peak in the n.m.r. spectrum of the deuterated derivative decreased from three to approximately two protons, there

[4]*It has been demonstrated that the 'trans' fusion of the 4- and 9-membered rings with adjacent ketone function is the more stable. Furthermore, in Wittig reactions on ketones of type XV the ring fusion is not altered (9).*

[5]*This possibility was suggested by Professor P. de Mayo.*

Can. J. Chem. Downloaded from www.nrcresearchpress.com by 210.87.254.105 on 09/05/12
For personal use only.

was only one deuterium atom in the deuterated molecules and it was located in the newly formed methyl group.* The formation of XVII would require the introduction of *two* C-deuterium atoms per molecule, and hence this formula is excluded.

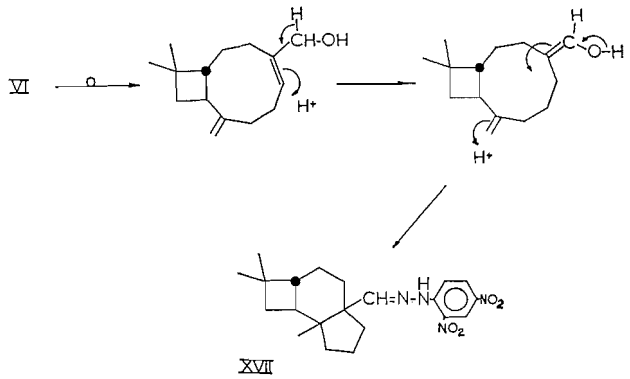

XVII

Consideration of the proposed reaction paths leading to IV and VII suggests that isocaryophyllene oxide-*a* (III), the *cis* epoxide with the same configuration at C_8 as I, could give the same dinitrophenylhydrazones as caryophyllene oxide. In agreement the melting point (185°) of the one derivative reported (2) from III matched the melting point (186°) of VII, and the two compounds may well be identical.

In VII the stereochemistry of the methylene bridge with respect to the C-5 hydrogen is unknown; according to Stuart–Briegleb models, cyclization is possible either above or below the 9-membered ring. Since only one cyclized product was obtained, probably the methylene bridge is *cis* to the C-5 hydrogen as has been found by X-ray crystallography for XII (6). The models also raise an interesting question. The cyclization as depicted in VI cannot be completely concerted without the third "electronic movement" occurring *cis* to the second. On the other hand, a non-concerted cyclization would lead to the bridgehead (S = 8) carbonium ion XVIII of the same [4.3.1] type as that from caryolan-1-ol (β-caryophyllene alcohol). Models indicate that this particular bridgehead ion would not be very strained. There is as yet no evidence whether the cyclization-rearrangement is concerted or not.

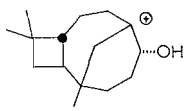

XVIII

Since the dienol VI does not give IV, this derivative and also V must be formed directly from the corresponding oxide by rearrangement, in the case of IV by a reaction competitive with the I → VI → VII path. The 1,2-glycol from hydration of I would not be an intermediate in this rearrangement since the backside of the oxide ring is completely shielded.

The third dinitrophenylhydrazone, m.p. 191°, obtained from I results from more extensive rearrangement of the caryophyllene framework. It is also the derivative of an aldehyde with no α-hydrogen and has *five* methyl groups; the structure is as yet unknown. However, the compound is not formed from the dienol VI.

*NOTE ADDED IN PROOF: *Professor K. Biemann has very kindly determined the mass spectra of both the deuterated and undeuterated VII. No molecules containing two deuterium atoms could be detected.*

Can. J. Chem. Downloaded from www.nrcresearchpress.com by 210.87.254.105 on 09/05/12
For personal use only.

Can. J. Chem. Downloaded from www.nrcresearchpress.com by 210.87.254.105 on 09/05/12
For personal use only.

It was demonstrated that the reactions leading from I to the carbonyl compounds *accompany* the acid-catalyzed cyclization to the glycol X*a*. The filtrate from a preparation of X*a* contained no unreacted I, and yet the addition of dinitrophenylhydrazine gave IV, VII, and the 191° derivative. Furthermore, from the filtrate of the reaction of I with acidic dinitrophenylhydrazine solution at room temperature there was isolated the glycol X*a*. This glycol did not give a precipitate with acidic dinitrophenylhydrazine solution. The dienol VI is not a precursor of glycol X*a* since treatment of VI under conditions yielding 20% of the easily crystallized X*a* from I gave no diol X*a*. More convincingly, the hydration of caryophyllene oxide in acetone-d_6 – deuterium oxide solution with phosphoric acid-d_3 gave glycol X*a* which contained no deuterium. Therefore, at no stage during the hydration of I to X*a* is a proton from solvent incorporated onto carbon; hence X*a* is probably formed directly from I.

The apparent absence of carbonyl products from transannular reactions such as those observed with cycloöctene oxides (10, 11), can probably be ascribed to the peculiarities of the caryophyllene structure. Not only will hydride abstraction from C-2 and C-5 be opposed by the fused cyclobutane ring, but the carbonium ion formed by breaking the oxide ring at the preferred tertiary carbon atom may stabilize itself by proton loss from the C-8 methyl group, or by reaction with the double bond at C-1.

EXPERIMENTAL

General

Melting points were taken on a Reichert microscope hot stage and are corrected. Optical rotations were observed on chloroform solutions in a 1-dm tube with a Schmidt–Haensch polarimeter. Ultraviolet spectra were taken on a Bausch and Lomb Spectronic 505 instrument. Infrared spectra were recorded with a Beckman IR-5 spectrophotometer. Nuclear magnetic resonance spectra were determined in deuteriochloroform solution (10–20% w/v concentration) on a Varian HR-60 or A-60 spectrometer and were calibrated by the audio side band technique. Integrations were by the cut-and-weigh method. Silica gel with calcium sulphate binder was used for thin-layer chromatography. Petroleum ether refers to the fraction boiling at 60–80°. Microanalyses were by Dr. A. Bernhardt, Mulheim, Germany. Combustion deuterium analyses by the falling drop method were by Josef Nemeth, Urbana, Illinois.

Caryophyllene Oxide (I)

Caryophyllene isolated by fractional distillation from clove oil terpene fraction was epoxidized with monoperphthalic acid (2). The crude oxide was recrystallized from methanol to constant m.p. 63.5–64° and constant $[\alpha]_D^{20}$ −79° (*c*, 2.32)(lit. (8): m.p. 63–64°, $[\alpha]_D^{20}$ −68°). It gave a single spot on thin-layer chromatography in ethyl acetate:petroleum ether (15:85).

Dihydrocaryophyllene Oxide (II)

A solution of 2.640 g (12.0 mmoles) of caryophyllene oxide in 30 ml of reagent grade ethyl acetate was hydrogenated over 300 mg of 5% palladium-on-carbon catalyst (Matheson, Coleman and Bell) at atmospheric pressure and room temperature. One equivalent of hydrogen was absorbed in 1 hour. After filtration and evaporation of solvent the oily residue [2.622 g, $[\alpha]_D^{21}$ −81° (*c*, 2.24)] was recrystallized four times from methanol to give 738 mg (29%) of pure dihydrocaryophyllene oxide, m.p. 66.5–68°, $[\alpha]_D^{24}$ −67° (*c*, 2.00) [lit. (8): m.p. 67°, $[\alpha]_D$ −55° (ethanol)]. The pure II gave a single spot on thin-layer chromatography in ethyl acetate:petroleum ether (15:85).

Reaction of Caryophyllene Oxide (I) with 2,4-Dinitrophenylhydrazine Reagent

To a solution of 413 mg (1.88 mmoles) of pure caryophyllene oxide in 1 ml of 95% ethanol was added the reagent prepared from 380 mg (1.92 mmoles) of 2,4-dinitrophenylhydrazine, 0.3 ml of concentrated sulphuric acid, 0.1 ml of water, and 2 ml of 95% ethanol. An exothermic reaction occurred and a voluminous orange precipitate appeared in 10–15 seconds. After 30 minutes the precipitate was separated by centrifugation, washed with ethanol–water and water–pyridine, and dried to yield 116 mg (15%) of orange powder, m.p. 136–160°. Thin-layer chromatography in ethyl acetate:petroleum ether (10:90) gave two spots, R_f 0.30 and R_f 0.36, in about equal amounts. Two other reactions in which the amount of I was varied and the amount of dinitrophenylhydrazine decreased gave no significant change in yield (11–14%).

The combined crude derivative from the reactions was first chromatographed on a thick plate (20 g silica gel per 20×20 cm plate) in benzene to separate the mixture of the main components from traces of slower-moving impurities. The main yellow band (163 mg) was then chromatographed on thick plates (30 mg per

plate) in ethyl acetate : petroleum ether (10:90). Careful manual separation of bands and extraction gave 82 mg of the faster-moving material and 64 mg of the slower-moving derivative.

Three recrystallizations of the slower-moving component (R_f 0.30) from chloroform – 95% ethanol gave matted golden needles of IV, m.p. 170–171°, $[\alpha]_D^{24}$ −14.7° (*c*, 1.77), $\lambda_{max}^{CHCl_3}$ 362 mμ (ε 22,600), $\nu_{max}^{CHCl_3}$ 3300 cm^{-1} (NH), 890 cm^{-1} (C=CH$_2$).[6] Thin-layer chromatography in ethyl acetate : petroleum ether (10:90) showed the IV to be free of VII.

Anal. Calc. for $C_{21}H_{28}O_4N_4$ (400.47): C, 62.98; H, 7.05; N, 13.99. Found: C, 62.84; H, 7.04; N, 14.13.

Five recrystallizations of the faster-moving component (R_f 0.36) from chloroform – 95% ethanol gave matted golden needles of VII, m.p. 184–186°, capillary m.p. 186–188°, $[\alpha]_D^{25}$ +27.5° (*c*, 1.78), $\lambda_{max}^{CHCl_3}$ 369 mμ (ε 20,300), $\nu_{max}^{CHCl_3}$ 3300 cm^{-1} (NH).[6] A mixture of IV and VII melted with depression at 151–173°.

Anal. Calc. for $C_{21}H_{28}O_4N_4$ (400.47): C, 62.98; H, 7.05. Found: C, 63.15; H, 6.91.

From the mother liquors of recrystallization of the upper thick-layer band could be crystallized a third dinitrophenylhydrazone. However, it was more easily obtained from the mother liquors of the original dinitrophenylhydrazone precipitation. These mother liquors were diluted with water and extracted with chloroform. The chloroform solution was washed with water and dilute sodium bicarbonate solution. Evaporation of the chloroform left an oily residue which was extracted with petroleum ether and then with benzene. Evaporation of the benzene solution left 24 mg of dinitrophenylhydrazone. Three recrystallizations from chloroform – 95% ethanol gave matted yellow needles, m.p. 189.5–191°, $\lambda_{max}^{CHCl_3}$ 363 mμ (ε 20 800). On admixture with VII (m.p. 184–186°) the melting point was depressed to 159–186°.

Anal. Calc. for $C_{21}H_{28}O_4N_4$ (400.47): C, 62.98; H, 7.05; N, 13.99. Found: C, 62.81; H, 7.24; N, 14.12.

Reaction of Dihydrocaryophyllene Oxide (II) with 2,4-Dinitrophenylhydrazine Reagent

To a solution of 70 mg (0.315 mmole) of II in 0.8 ml of 95% ethanol was added at room temperature a solution of 63 mg (0.315 mmole) of 2,4-dinitrophenylhydrazine in 1.2 ml of 95% ethanol containing 8 drops of concentrated sulphuric acid and 4 drops of water. The copious orange precipitate which formed after 10 seconds was separated by centrifugation, washed with ethanol–water and water–pyridine and dried to give 7.0 mg (5.5%) of golden powder, m.p. 182–186.5°. Larger-scale reactions (180–230 mg of II) in which the amount of 2,4-dinitrophenylhydrazine was decreased gave no significant change in yield. Three recrystallizations from chloroform – 95% ethanol gave matted golden needles of V, m.p. 186.5–187.5°, $[\alpha]_D^{24}$ +8.5° (*c*, 1.52), $\lambda_{max}^{CHCl_3}$ 363 mμ (ε 22,300), $\nu_{max}^{CHCl_3}$ 3300 cm^{-1} (NH).[6] A mixture of V and VII melted at 159–185°. Thin-layer chromatography in ethyl acetate : petroleum ether (10:90) gave a single spot, R_f 0.36.

Anal. Calc. for $C_{21}H_{30}O_4N_4$ (402.48): C, 62.66; H, 7.51; N, 13.92. Found: C, 62.62; H, 7.51; N, 14.04.

Caryophyllene Keto Oxide (XI)

Caryophyllene oxide was oxidized with permanganate according to Treibs (8) and the product XI purified by chromatography on activity II *basic* Woelm alumina, m.p. 61.5–63°, $[\alpha]_D^{22}$ −148° (*c*, 1.95) (lit. (8): m.p. 61–62°, $[\alpha]_D^{20}$ −124° [methanol]), $\nu_{max}^{CS_2}$ 1695 cm^{-1} (C=O).

Keto Allylic Alcohol XV

A solution of 25 mg of pure caryophyllene keto oxide (XI) in benzene was added to a column of 0.9 g of activity I *neutral* Woelm alumina packed in benzene. Elution with 8 ml of benzene gave 6 mg of recovered XI; further elution with 10 ml of ether gave 17 mg (89%) of keto allylic alcohol XV. Thin-layer chromatography in ethyl acetate : cyclohexane (50:50) showed that XV and recovered XI were the only products of the reaction. Larger-scale reactions gave the same results. Three recrystallizations from chloroform – petroleum ether gave long thin needles of XV, m.p. 110–111°, $[\alpha]_D^{27}$ −46° (*c*, 2.14), $[\alpha]_D^{21}$ −49° (*c*, 2.01), ϵ_{220} 615 (end absorption only), $\nu_{max}^{CHCl_3}$ 3600 and 3440 cm^{-1} (OH), 3030 cm^{-1} (C=CH), 1692 cm^{-1} (C=O), 1640 cm^{-1} (C=C), 916 cm^{-1} (C=CH$_2$).

Anal. Calc. for $C_{14}H_{22}O_2$ (222.32): C, 75.63; H, 9.97. Found: C, 75.43; H, 9.79.

Unsaturated Diketone XVI

A solution of 1.000 g of pure XV in 30 ml of chloroform was stirred (magnetic stirring bar) with 7.0 g of active manganese dioxide (13) for 16 hours. Filtration and evaporation of chloroform left 922 mg of product, which was recrystallized twice from petroleum ether. The recrystallized material (605 mg) was then chromatographed on 5 g of activity II neutral Woelm alumina to remove some unoxidized XV. Elution with petroleum ether gave 470 mg of XVI, which was recrystallized twice from petroleum ether affording colorless prisms, m.p. 48–50°, $[\alpha]_D^{22}$ −14.7° (*c*, 3.06), $\lambda_{max}^{95\%\ EtOH}$ 227 mμ (ε 6150), $\nu_{max}^{CS_2}$ 1703 cm^{-1} (C=O), 1680 cm^{-1} (conjugated C=O), 1622 cm^{-1} (C=C), 925 or 935 cm^{-1} (C=CH$_2$). The compound slowly decomposed to an oil on standing for several weeks.

Anal. Calc. for $C_{14}H_{20}O_2$ (220.30): C, 76.32; H, 9.15. Found: C, 76.47; H, 9.33.

Dienol VI

(a) From the keto allylic alcohol XV.—To a suspension of 6.29 g (15.6 mmoles) of methyl triphenylphosphonium iodide in 50 ml of tetrahydrofuran (freshly distilled from sodium) was added 22 ml (15.6

[6]*Each of the 2,4-dinitrophenylhydrazones IV, V, and VII also had infrared peaks at 1620, 1590, 1510, 1463, 1425, 1333, 1311, 1140, 927, and 846 cm^{-1}, most of which have been found to be characteristic of this derivative (12).*

Can. J. Chem. Downloaded from www.nrcresearchpress.com by 210.87.254.105 on 09/05/12
For personal use only.

Can. J. Chem. Downloaded from www.nrcresearchpress.com by 210.87.254.105 on 09/05/12
For personal use only.

mmoles) of an ethereal solution of phenyllithium. The mixture was refluxed for 5 hours. Then 1.100 g (4.95 mmoles) of XV was added and the reaction mixture refluxed for 19 hours. Dilution of the reaction mixture with ether and extraction with water and dilute sodium bicarbonate solution left a clear-brown organic layer. Steam distillation of this solution left 3.29 g of viscous brown syrup which was chromatographed on 40 g of Woelm neutral alumina, activity I. Fractions eluted with solvents from pure benzene to ether : benzene (25:75) contained dienol VI along with other impurities. These fractions, 991 mg, were chromatographed on thick fluorescent silica-gel plates (20 g silica gel per 20×20 cm plate) and the dienol fraction extracted to give 131 mg (0.60 mmole, 12%) of pure dienol VI as a viscous colorless liquid, $[\alpha]_D^{24}$ +20.8° (*c*, 2.11), $\nu_{max}^{CS_2}$ 3600 and 3370 cm^{-1} (OH), 3060 cm^{-1} (vinyl H), 1640 cm^{-1} (C=C), and 903 cm^{-1} (C=CH_2). The dienol gave a single spot, R_f 0.25, on thin-layer chromatography in ethyl acetate : petroleum ether (30:70).

Anal. Calc. for $C_{15}H_{24}O_2$ (236.34): C, 81.76; H, 10.98. Found: C, 81.91; H, 10.94.

(b) From caryophyllene oxide (I).—To a column of 30 g of activity I *neutral* Woelm alumina packed in petroleum ether was added a solution of 2.000 g of pure I in petroleum ether. Elution with petroleum ether gave 676 mg of recovered I. Further elution with benzene–ether mixtures removed 212 mg of mixed minor products, and pure ether eluted 1.081 g (80%) of liquid dienol VI, $[\alpha]_D^{23}$ −15° (*c*, 2.87), $\nu_{max}^{CS_2}$ 3600 and 3370 cm^{-1} (OH), 3060 cm^{-1} (vinyl H), 1640 cm^{-1} (C=C) and 903 cm^{-1} (C=CH_2). This material gave a single spot, R_f 0.25, on thin-layer chromatography in ethyl acetate : petroleum ether (30:70). However, the dienol was not pure since its optical rotation differed from that of the Wittig reaction product, and its n.m.r. spectrum contained a small additional peak in the olefinic hydrogen region at 4.86 p.p.m., possibly from the hydroxyl epimer of VI.

Reaction of Dienol VI with 2,4-Dinitrophenylhydrazine Solution

(a) With VI from the Wittig reaction.—A solution of 106 mg (0.48 mmole) of pure VI in 1.5 ml of 95% ethanol was treated with the reagent prepared from 96 mg (0.48 mmole) of 2,4-dinitrophenylhydrazine, 10 drops of concentrated sulphuric acid, 4 drops of water, and 1 ml of 95% ethanol. The mixture became cloudy after a minute and crystals precipitated. After several hours the precipitate was separated by centrifugation, washed with ethanol–water and water–pyridine, and dried. There was obtained 67 mg (35%) of orange powder, m.p. 150–173°. Thin-layer chromatography (ethyl acetate : petroleum ether, 10:90) and the n.m.r. spectrum of the crude derivative revealed no trace of IV or the 191° derivative. Four recrystallizations of the crude derivative from chloroform – 95% ethanol gave 24 mg of orange needles of VII, m.p. 184–186°, $[\alpha]_D^{24}$ +27.8° (*c*, 1.94), $\nu_{max}^{CHCl_3}$ 3300 cm^{-1} (NH).[6] On admixture with VII from I the melting point was undepressed, m.p. 181–185°.

Anal. Calc. for $C_{21}H_{28}O_4N_4$ (400.47): C, 62.98; H, 7.05; N, 13.99. Found: C, 63.07; H, 6.98; N, 14.07.

(b) With VI from β-caryophyllene oxide (I).—To a solution of 181 mg (0.82 mmole) of the impure VI in 2 ml of 95% ethanol was added the reagent prepared from 163 mg (0.82 mmole) of 2,4-dinitrophenylhydrazine, 0.5 ml of concentrated sulphuric acid, a few drops of water, and 2 ml of 95% ethanol. There was an immediate precipitation. After several hours the reaction was worked up as in (*a*) above to give 108 mg (33%) of orange powder, m.p. 138–163°. Successive recrystallizations from chloroform – 95% ethanol gave either metallic orange flakes or orange needles, eventually yielding 34 mg of VII, m.p. 184–186°, identical with VII from (*a*) above and from I.[7] Thin-layer chromatography (ethyl acetate : petroleum ether, 10:90) of the recrystallized derivative gave a single spot, R_f 0.36. In another reaction 154 mg of VI gave 124 mg (44%) of crude dinitrophenylhydrazone.

Reaction of Dienol VI with 2,4-Dinitrophenylhydrazine in Deuterated Solvent

Dienol VI (200 mg, 0.91 mmole) was dissolved in 4 ml of ethanol-*O*-d_1 (~99% D) containing 0.25 ml of deuterium oxide (>99.5% D). To this solution was added a solution of 180 mg (0.91 mmole) of 2,4-dinitrophenylhydrazine (NH not previously exchanged for D) in a mixture of 2.0 ml of syrupy phosphoric acid-d_3 (prepared by dissolving phosphorus pentoxide in 99.5% deuterium oxide) and 5 ml of ethanol-*O*-d_1 (99%). The reaction mixture was heated to boiling for a few seconds and then allowed to stand at room temperature for 3 days. The precipitate was centrifuged, washed with ethanol–water and water–pyridine, and dried. The crude product was chomatographed on a thick plate (20 g of silica gel on a 20×20-cm plate) in benzene. The uppermost band was extracted with chloroform to yield 53 mg of orange solid. Recrystallization from chloroform – 95% ethanol gave 34 mg of orange needles, m.p. 182–186°. The n.m.r. spectrum of this material differed from VII only in having a less intense and broadened peak at 0.96 p.p.m. (ca. 2 protons). Integration gave only 8 protons in the methyl groups as compared with 9 protons in the spectrum of VII. The area ratio of the 1.01:0.96 peaks in the non-deuterated derivative was 2:1; in the deuterated derivative 3:1.

Anal. Calc. for $C_{21}H_{27}DO_4N_4$: D, 3.57 atom %. Found: D, 3.18 atom %.

Acid Isomerization of Caryophyllene Oxide (I)

(*a*) Caryophyllene oxide (112 mg) in 1 ml of 95% ethanol was treated with a solution of 3 drops of water and 6 drops of concentrated sulphuric acid in 0.5 ml of ethanol. The reaction mixture was warmed for a minute in

[7]*If the impurity in VI made by opening the oxide ring of I is the hydroxyl epimer of VI, this would also be expected to produce VII in a yield comparable to that from VI.*

a 70° water bath and then allowed to stand at room temperature for 30 minutes. Dilution with water and ether extraction gave 105 mg (93%) of colorless viscous liquid, $\nu_{max}^{CS_2}$ 1730 cm^{-1}. Thin-layer chromatography in ethyl acetate : petroleum ether (10:90) showed the absence of any I.

Addition of an acidic solution of 2,4-dinitrophenylhydrazine to 75 mg (0.34 mmole) of the acid isomerization product in 2 ml of 95% ethanol produced 5.5 mg (4%) of yellow precipitate. Thin-layer chromatography of this derivative in ethyl acetate : petroleum ether (15:85) gave two spots, R_f 0.51 and 0.58, corresponding to authentic IV and VII spotted on the same plate.

(*b*) Following the procedure of Aebi, Barton, and Lindsey (1), a solution of 240 mg of I in 1 ml of reagent grade acetone containing 0.25 ml of water and 0.05 ml of sulphuric acid (1:1, v/v) was refluxed for 2 hours. Dilution with water and extraction with ether gave 246 mg (98%) of colorless viscous oil. Two recrystallizations of a 204-mg sample from chloroform – petroleum ether gave 54 mg (20%) of colorless needles of X*a*, m.p. 150.5–151° (lit. (1): m.p. 152–153°). The glycol X*a* gave no precipitate on treatment with acidic 2,4-dinitrophenylhydrazine solution even at 80°.

The mother liquors from crystallization of X*a* were treated with acidic 2,4-dinitrophenylhydrazine solution whereupon a red oil separated. Thick-layer chromatography of this in benzene gave 32 mg of dinitrophenylhydrazone in the uppermost band. The n.m.r. spectrum of this material had sharp peaks at the positions of the unsplit methyl groups of IV, VII, and the 191° derivative. Thin-layer chromatography (ethyl acetate : petroleum ether, 10:90) gave two spots which had the same R_f as IV and VII plus the 191° derivative.

(*c*) A 150-mg sample (0.68 mmole) of I was treated at room temperature with sulphuric acid–2,4-dinitrophenylhydrazine solution as described earlier. Centrifugation yielded 18.5 mg (7%) of crude dinitrophenylhydrazone mixture. The supernatant mother liquor was diluted with water and extracted with chloroform. Evaporation of the chloroform left a residue which was extracted with petroleum ether. On standing this petroleum ether extract deposited 5.5 mg (2%) of glycol X*a*, m.p. 151.5–152°, after two recrystallizations from chloroform – petroleum ether. The melting point was undepressed on admixture with authentic X*a* prepared in (*b*) above.

Acid Isomerization of Caryophyllene Oxide (I) in Deuterated Solvent

A solution of 600 mg (2.72 mmoles) of I in a mixture of 2.4 ml of acetone-d_6 (>99.5% D), 0.3 ml of deuterium oxide (>99.6% D), and 0.10 ml of phosphoric acid-d_3 : deuterium oxide (3:1) was refluxed for 2.5 hours. The reaction mixture was diluted with water and extracted with ether. The ether extracts were washed with water, sodium bicarbonate solution, and saturated sodium chloride solution and dried. Evaporation of the ether left 580 mg of colorless residue. Recrystallization from chloroform – petroleum ether gave 274 mg (42%) of colorless matted needles of X*a*. A second recrystallization from the same solvent raised the melting point to 150.5–151°. The n.m.r. spectra of this material and the glycol X*a* prepared in protic solvent were compared at 100 mg/0.35 ml concentration in *pyridine* solution for greater solubility. The spectra were identical, and the relative intensities of the unsplit methyl peaks at 1.15 and 1.10 p.p.m. to the unsplit methyl peak at 0.90 was 1.93:1 (protic solvent) and 1.99:1 (deuterated solvent).

Anal. Calc. for $C_{15}H_{25}DO_2$: D, 3.85 atom %. Found: D, 0.00 atom %.

Reaction of Dienol VI with Sulphuric Acid

Dienol VI (200 mg) previously shown by thin-layer chromatography to contain no glycol X*a* was dissolved in 1 ml of reagent grade acetone containing 0.25 ml of water and 0.05 ml of sulphuric acid (1:1, v/v). The solution was refluxed for 2 hours. Dilution with water and extraction with ether gave 222 mg (100%) of colorless viscous oil. The product did not crystallize on trituration with petroleum ether and seeding with X*a*. Thin-layer chromatography in ethyl acetate : petroleum ether (67:33) gave three spots, one of which corresponded closely to authentic glycol X*a*, R_f 0.15. However, the colors developed by this spot on sulphuric acid charring were different from those of X*a*. Also, the infrared spectrum of the acid isomerization product (separated by thick-layer chromatography) corresponding closely in R_f to X*a* was quite different from that of X*a*.

ACKNOWLEDGMENTS

The financial support of the Alfred P. Sloan Foundation and the National Research Council is gratefully acknowledged. Mr. R. E. Klinck kindly determined most of the n.m.r. spectra.

REFERENCES

1. A. Aebi, D. H. R. Barton, and A. S. Lindsey. J. Chem. Soc. 3124 (1953).
2. G. R. Ramage and R. Whitehead. J. Chem. Soc. 4336 (1954).
3. E. A. Braude and E. R. H. Jones. J. Chem. Soc. 498 (1945).
4. (*a*) D. Y. Curtin, J. A. Gourse, W. H. Richardson, and K. L. Rinehart. J. Org. Chem. **24**, 93 (1959). (*b*) J. B. Stothers. *In* Elucidation of structures by physical and chemical methods. Part I. Interscience-Wiley, New York, N.Y. 1963. p. 208.

Can. J. Chem. Downloaded from www.nrcresearchpress.com by 210.87.254.105 on 09/05/12
For personal use only.

5. A. NICKON. J. Am. Chem. Soc. **77**, 1190 (1955).
6. (*a*) J. M. GREENWOOD, I. H. QURRESHI, and J. K. SUTHERLAND. Proc. Chem. Soc. 372 (1963). (*b*) D. ROGERS and M.-UL-HAQUE. Proc. Chem. Soc. 371 (1963).
7. F. SORM, L. DOLEJŠ, and J. PLÍVA. Collection Czech. Chem. Commun. **15**, 186 (1950).
8. W. TREIBS. Ber. **80**, 56 (1947).
9. E. J. COREY, R. B. MITRA, and H. UDA. J. Am. Chem. Soc. **85**, 362 (1963).
10. V. PRELOG and J. G. TRAYNHAM. *In* Molecular rearrangements. Part I. Interscience-Wiley, New York, N.Y. 1963. p. 593.
11. A. C. COPE and J. K. HECHT. J. Am. Chem. Soc. **84**, 4872 (1962).
12. L. A. JONES, J. C. HOLMES, and R. B. SELIGMAN. Anal. Chem. **28**, 191 (1956).
13. J. ATTENBURROW, A. F. B. CAMERON, J. H. CHAPMAN, R. M. EVANS, B. A. HEMS, A. B. A. JANSEN, and T. WALKER. J. Chem. Soc. 1094 (1952).

Can. J. Chem. Downloaded from www.nrcresearchpress.com by 210.87.254.105 on 09/05/12
For personal use only.

RELATIVE RATES OF BASE-CATALYZED EXCHANGE OF ALPHA- AND GAMMA-HYDROGEN IN AN α,β-UNSATURATED KETONE

J. WARKENTIN AND L. K. M. LAM
Department of Chemistry, McMaster University, Hamilton, Ontario
Received January 24, 1964

ABSTRACT

Relative rates of base-catalyzed exchange of vinylic and allylic hydrogen, in an α,β-unsaturated ketone, have been determined. In refluxing heavy water, with OD^- catalyst, vinyl hydrogen was exchanged about 170 times as rapidly as allyl hydrogen. In CD_3OD containing CD_3O^- the two rates were equal or nearly equal at ambient temperature. Factors which may contribute to the observed difference between the relative rates are discussed and results of simple molecular orbital calculations are presented.

We have studied base-catalyzed, hydrogen–deuterium exchange in 6,6-dimethyl-2-cyclohexene-1-one I. Three reactions which might be expected between base and I are (*a*) abstraction of γ-hydrogen to form dienolate II, (*b*) addition to carbonyl carbon, and (*c*) addition at the β-carbon to form III.

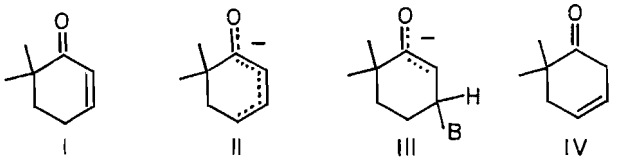

In hydroxylic solvents, II would be converted to enol, to I, and to ketone IV by protonation at oxygen, at C_4 and at C_2, respectively. In basic medium IV would rapidly be isomerized to I. Similarly, III might be destroyed by protonation at oxygen or at C_2 forming products which would not accumulate, but which would readily revert to I. In basic, deuterated, hydroxylic solvent one would therefore expect that I would become labelled at C_2 and at C_4. Reaction (*b*), above, is not of interest in connection with hydrogen–deuterium exchange.

There is evidence that protonation of II should be faster at C_2 than at C_4.* Deconjugation of α,β-unsaturated steroidal ketones can be accomplished in excellent yield by protonation of the corresponding anions with aqueous acetic acid. For example, yields of 17α-methyl-Δ^5-androstene-17β-ol-3-one VII, from 17α-methyltestosterone V, were as high as 95% (1). Alkylation of anions of α,β-unsaturated ketones has also been shown to

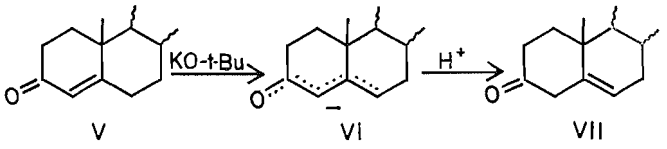

give predominantly the corresponding α-alkyl-α,β-unsaturated ketones and the α,α-dialkyl-β,γ-unsaturated products (2*a* and *b* and references cited therein). Of the two

**We are not concerned here with the rate of protonation at oxygen. That reaction is probably the fastest of all those that destroy II.*

anionic carbons in an ion such as VI, the α-carbon is clearly much more reactive than the γ-carbon, at least in the reactions cited above.

It is readily seen, however, that the rate of exchange of α-hydrogen in our system should not exceed the rate of exchange of γ-hydrogen if both processes involve enolization in the first step. This follows from the fact that α-deuterated IV, in isomerizing to I in deuterated solvent, must pick up deuterium at C_4. Such isomerization could involve loss of either hydrogen or deuterium from C_2 with an associated isotope effect k_H/k_D. From the equations below, for exchange by an enolization mechanism, it is seen that there is only one route leading to exchange at C_2 whereas there are three paths for exchange at C_4.

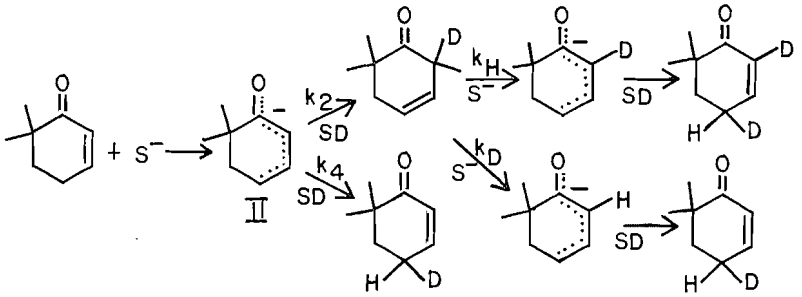

If we designate the rate of labelling at C_2 by dC_2/dt and that of labelling at C_4 by dC_4/dt, then the *initial* rates of exchange are

$$dC_2/dt = [k_2k_H/(k_H + k_D)][SD][II]$$

and

$$dC_4/dt = (k_2 + k_4)[SD][II].$$

Division gives the ratio of initial rates

$$dC_4/dC_2 = [(k_H + k_D)/k_H][1 + (k_4/k_2)].$$

We can set the limits $2 > (k_H + k_D)/k_H > 1$, since k_D will be smaller than k_H. For $k_4 = k_2$, we would then expect $4 > dC_4/dC_2 > 2$, if all exchange occurred via an enolization mechanism. On the other hand, if $k_4 \ll k_2$, then $2 > dC_4/dC_2 > 1$, and if $k_4 \gg k_2$ the rate ratio would be large.

EXPERIMENTAL

General

Rates of exchange were followed by n.m.r. spectrometry with a Varian HR-60 instrument. Exchange with heavy water was followed by periodic withdrawal of samples of ketone from the upper layer of the heterogeneous system. These samples were dissolved in $CDCl_3$ for recording of the n.m.r. spectra (60 Mc). The signals from nonexchangeable groups, such as the methyl groups at C_6 or the C_5 methylene group were used to determine the area per proton. The C_2 proton signal was a doublet at $\tau = 4.03$ while the C_3 proton signal was a sextet centered at $\tau = 3.06$, relative to internal tetramethyl silane. Proton signals centered at $\tau = 8.15$ (triplet) and $\tau = 7.59$ (multiplet) were assigned to the C_5 and the C_4 methylene groups, respectively. Four integrations per sample were averaged to calculate deuterium content.

Exchange with CD_3OD–CD_3O^- was carried out in an n.m.r. tube. Successive integrals of the spectral signals were recorded as rapidly as possible after addition of ketone to the tube.

The number of gram atoms of deuterium per mole incorporated in a given position of the ketone was calculated from the integrated area of the proton signal for that position. Such numbers were plotted against time and initial rates were estimated from the slopes of tangents drawn to the curves at the zero time.

Synthesis of 6,6-Dimethyl-2-Cyclohexene-1-one

6,6-Dimethyl-2-cyclohexene-1-one was synthesized according to a method described in the literature (3). The crude ketone was purified by preparative gas–liquid chromatography (g.l.c.) using a 20 ft × $\frac{3}{8}$ in.

column packed with 30% SE30 on Chromosorb P in the Aerograph A-700 instrument. The ultraviolet spectrum had $\lambda_{max} = 227$ and the semicarbazone of the hydrogenation product had m.p. 196–198° (3).

Exchange in D_2O

The ketone (10.0 g, 0.087 mole) was refluxed with 15 ml of heavy water (atom % D over 50) containing one pellet of NaOH. Samples of ketone were withdrawn at the intervals shown in Fig. 1.

Exchange in CD_3OD

Deuteromethanol (99 atom % D) was obtained from Merck Sharp and Dohme of Canada. To a sliver of freshly cut sodium in an n.m.r. tube was added 0.35 ml of the alcohol. When the sodium had dissolved, the tube was chilled with dry ice and about 40 mg of 6,6-dimethylcyclohexenone was added from a small syringe. The tube was sealed while cold and it was then warmed rapidly to room temperature. Integration of the n.m.r. signals was begun about 4 minutes after introduction of the ketone. The base strength was found to be 1.8×10^{-4} *M* by titration of the mixture at the end of the kinetic run.

RESULTS AND DISCUSSION

The results indicate that the relative rates of exchange depend on the base and on the medium employed. When exchange was catalyzed by OD^- in D_2O, γ-hydrogen was exchanged about 0.0059 times as rapidly as α-hydrogen (Fig. 1).

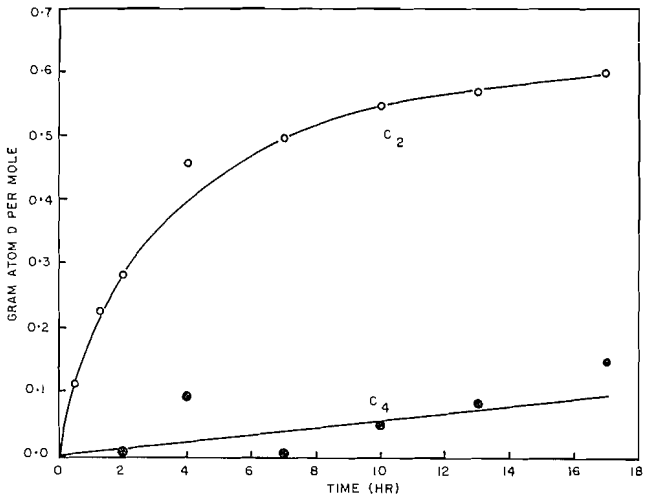

FIG. 1. Rates of exchange, catalyzed by OD^- in D_2O.

Due to the rapidity of exchange in the medium CD_3OD–CD_3O^-, rate data were not obtained in the region below 50% reaction. As our kinetic expression applies to the ratio of initial rates only, it was necessary to estimate that ratio from the experimentally available portion of the rate curves. The fact that these curves lie close together and appear to be nearly parallel allowed us to extrapolate them smoothly to the origin. Although absolute values of initial rates, obtained in this way, would depend critically on the manner of extrapolation, relative values should be more reliable if both curves are extrapolated in the same manner, The ratio of rates dC_4/dC_2, in methanolic medium, was estimated to lie between 1 and 1.7 (Fig. 2).

One way of accounting for the small ratio, dC_4/dC_2, in aqueous medium is to postulate an addition–elimination mechanism as depicted below. Analogy for the reaction is found in the well-known Michael additions of carbanions to α,β-unsaturated ketones. The

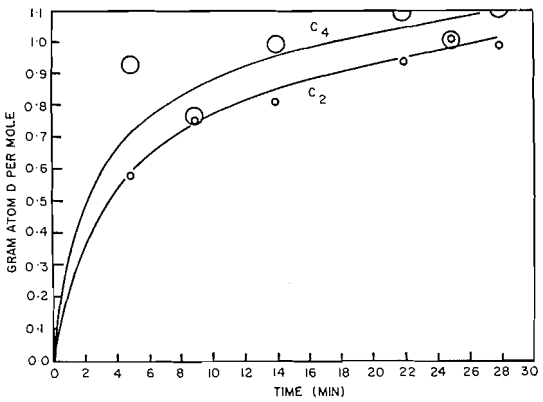

FIG. 2. Rates of exchange, catalyzed by CD_3O^- in CD_3OD.

addition–elimination mechanism has been advanced to account for exchange of α-hydrogen in nonenolizable α,β-unsaturated ketones (4).*

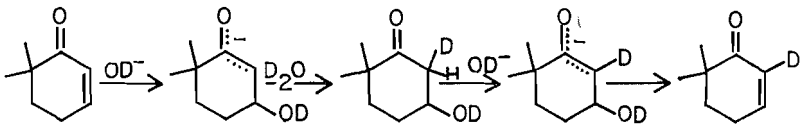

The radically different behavior in the methoxide–methanol system cannot be explained satisfactorily at this time. Factors which may contribute are (*a*) steric hindrance to β-addition and (*b*) different relative nucleophilicities, toward hydrogen and toward unsaturated carbon, of hydroxide and methoxide.

Models of I and III show that steric hindrance to axial-like approach of a base toward the β-carbon of I is not severe for small ions like the ones in question. However, it should be emphasized that exchange with D_2O–OD^- was carried out at about 100°, while that with methoxide occurred at about 20°. Thus any difference between the entropies of activation for β-addition of the two bases to I would exert an effect, on the relative rates of the two addition processes, which would be magnified by the temperature difference. This suggestion is subject to experimental test and we are studying the temperature dependence of the relative rates of exchange at C_2 and C_4.

Nucleophilic reactivity has recently been reviewed (6). The reactivities of nucleophiles toward hydrogen correlate well with their basicities (6), with some exceptions (7, 8, 9).† However, the basicities of hydroxide and methoxide are probably not greatly different (9, p. 45) and the difference is solvent dependent. The relative nucleophilicities of hydroxide and methoxide in Michael-type additions do not appear to be recorded in the literature. Therefore it does not seem possible at this time to predict the magnitude or even the direction of the effect, on rates of exchange, of a difference between the relative nucleophilicities of hydroxide and methoxide toward γ-hydrogen and β-carbon of I.

If the action of methoxide on I, for whatever reason, is primarily the abstraction of

**It has been pointed out by a referee that intramolecular, base-catalyzed isomerization (5) of IV-αd_1 to I-αd_1 may contribute to the enhanced rate of α-exchange relative to that of γ-exchange. Such a process, however, must be unimportant in the aqueous exchange since the isotope effect, k_H/k_D, that would be required to accommodate the data in terms of such a mechanism alone, is too large by more than an order of magnitude.*

†Notable exceptions are some bimolecular eliminations in which thioalcoholate and thiophenolate anions surpass alcoholate and phenolate ions, respectively, as catalysts (7, 8). The effectiveness of carboxylate ions in catalyzing bromination of ketones is also not reliably correlated with their basicities (9).

γ-hydrogen, then the observed rate ratio, $1.7 \geqslant dC_4/dC_2 \geqslant 1$, (see above for predicted ranges of values) requires that the dienolate anion be protonated more rapidly at C_2 than at C_4. Such a rate difference must be responsible for the isomerization of V to VII and finds further analogy in the alkylation reactions of such ions (*vide supra*). Kinetic, rather than thermodynamic, control of the protonation step can be rationalized in terms of a transition state resembling the dienolate anion (10), with the latter having a nonuniform distribution of charge.

We have carried out Hückel molecular orbital calculations (11, 12) to estimate the charge distribution in the anion. In the simplest calculation, with an uncharged system such as the dienol or a dienol ether as the model, we used $\alpha_O = \alpha_C + 2\beta$ for the Coulomb integral of oxygen and $\beta_{CO} = \beta_{CC}$. The following charge densities were obtained.

O	C_1	C_2	C_3	C_4
−0.872	+0.125	−0.155	+0.015	−0.116

An improved calculation for the anion recognizes that oxygen probably bears more of the charge than any of the carbons and that its electronegativity is decreased more as a consequence. Calculation using $\alpha_O = \alpha_C + 1.5\beta$ and $\beta_{CO} = 0.8\beta_{CC}$ gave the charge densities below.

O	C_1	C_2	C_3	C_4
−0.892	+0.107	−0.114	−0.045	−0.057

These qualitative results, for the relative charge densities at C_2 and C_4, support the rationale for the relative reactivities at C_2 and C_4 of the anion of an α,β-unsaturated ketone.

Current work is directed toward testing for the origin of the difference in relative rates of exchange reported here and toward investigation of exchange rates in other systems.

ACKNOWLEDGMENTS

We are indebted to the National Research Council for financial support of this work. Mr. Oswald Tee carried out the second molecular orbital calculation.

REFERENCES

1. H. J. RINGOLD and S. K. MALHOTRA. Tetrahedron Letters, 669 (1962).
2. (*a*) J. M. CONIA. Bull. Soc. Chim. 943 (1954). (*b*) H. J. RINGOLD and S. K. MALHOTRA. J. Am. Chem. Soc. **84**, 3402 (1962).
3. J. COLONGE, J. DREUX, and M. THIERS. Compt. Rend. **243**, 1425 (1956).
4. B. W. ROCKETT, T. M. HARRIS, and C. R. HAUSER. J. Am. Chem. Soc. **85**, 3491 (1963).
5. D. J. CRAM and R. T. UYEDA. J. Am. Chem. Soc. **84**, 4358 (1962).
6. J. F. BUNNETT. Ann. Rev. Phys. Chem. **14**, 271 (1963).
7. P. B. D. DE LA MARE and C. A. VERNON. J. Chem. Soc. 41 (1956).
8. J. F. BUNNETT, G. T. DAVIS, and H. TANIDA. J. Am. Chem. Soc. **84**, 1606 (1962).
9. R. P. BELL. The proton in chemistry. Cornell University Press, Ithaca, New York. 1959. Chap. 6.
10. G. S. HAMMOND. J. Am. Chem. Soc. **77**, 334 (1955).
11. J. D. ROBERTS. Molecular orbital calculations. W. A. Benjamin, Inc., New York, N.Y. 1962.
12. A. STREITWIESER, JR. Molecular orbital theory for organic chemists. John Wiley and Sons, Inc., New York, N.Y. 1961.

Can. J. Chem. Downloaded from www.nrcresearchpress.com by 210.87.254.6 on 09/05/12
For personal use only.

STRONGLY BASIC SYSTEMS

III. THE H_- FUNCTION FOR VARIOUS SOLVENT SYSTEMS[1]

ROSS STEWART AND J. P. O'DONNELL[2]

Department of Chemistry, University of British Columbia, Vancouver, British Columbia

Received January 13, 1964

ABSTRACT

The Hammett acidity function concept has been used to determine simultaneously the pK_a values of 24 substituted anilines and diphenylamines and the H_- values of various solvent systems. The following solvent systems were examined (the most basic H_- value obtained for each is shown in parentheses): water containing benzyltrimethylammonium hydroxide (16.20); pyridine–water containing tetramethylammonium hydroxide (18.91); sulpholane–water containing tetramethylammonium hydroxide (19.18); dimethyl sulphoxide – water containing tetramethylammonium hydroxide (18.61); water containing lithium hydroxide (14.31).

In addition to these results adjustments have been made to previously published scales for hydrazine–water (15.08) and ethylenediamine–water (15.48).

INTRODUCTION

During the past few decades there has been intense interest in the chemistry of strongly acid systems. Studies of the equilibrium protonation of weak bases and of acid catalysis continue to contribute to our knowledge and to a widening of our understanding of the concept of acidity. There is a continuous acidity scale that runs from pure water to pure sulphuric acid and beyond and covers a range in which the acidity varies by a factor of about 10^{20}. Until very recently only a few attempts had been made to extend the region of measurable acidities to strongly basic systems.

Pioneer measurements of the strength of very weak acids using an equilibrium approach were made by Conant and Wheland (3) and McEwen (4). They used ether solutions of carbanions, produced by reaction with metallic potassium, to determine the relative strength of weak acids through the equilibrium

$$HA_1 + A_2^- \rightleftarrows A_1^- + HA_2.$$

They deduced the position of equilibrium by colorimetric methods and so were able to determine acidity constants. They used methanol as a standard, assigning it a value of 16. It should be noted here that apparent acid strengths and even the order of acidity of acids can be different in solvents of low dielectric.

Stearns and Wheland (5) measured the strengths of some very weak acids by measuring the small amount of ionization that is detectable in aqueous or alcoholic alkali and assuming that this is the beginning of an ideal ionization curve. This method is unreliable with certain compounds such as *p*-nitrobenzyl cyanide.

Schwartzenbach and Sulzberger (6) tackled the problem of determining the basicity of concentrated alkalies. They found that the extreme insolubility of indicators prevented a normal spectrophotometric approach. They then added solvents, which contained indicators, to the various aqueous hydroxide solutions and determined the fraction ionized in the solvent layer. The drawbacks of this method have been discussed by Edward and Wang (7), who used thioacetamide as indicator in order to overcome salting-out problems.

[1]*A preliminary account of part of this material has appeared elsewhere (ref. 1); a joint paper dealing with a rate–equilibrium correlation and making use of some of the results reported herein has also appeared elsewhere (ref. 2). These papers can be considered Parts I and II of the series.*

Taken in part from the Ph.D. thesis of J. P. O'Donnell, University of British Columbia, 1962.

[2]*Present address: Imperial Oil Co. Ltd., Sarnia, Ontario.*

In 1952 Deno (8) made the first attempt to construct the H_- function in a mixed solvent system, using water containing various concentrations of hydrazine up to 65% hydrazine in water. The H_- scale for this system reached 16.0 for 65% hydrazine. Deno's pK_a values are also found in Table I. A priori, hydrazine seems to be the best choice of

TABLE I

Summary of previously determined pK_a values

System	Ethylene diamine/ water	Ethanol-amine/ water	Hydra-zine/ water	*t*-Amyl alcohol	Hydra-zine/ water	Sulpho-lane/ water	Etha-nol/ water
Reference	(28, 11)	(12)	(13)	(14)	(8)	(17)	(5)
2,4,6-Trinitroaniline	12.25	—	—	—	—	—	—
3,6-Dinitrocarbazole	13.05	13.05	—	—	13.07	—	—
4-Nitrobenzyl cyanide	13.45	13.45	13.45	—	13.43	13.43	13.4
6-Bromo-2,4-dinitroaniline	—	—	—	—	—	13.71	—
3-Nitrocarbazole	15.10	15.10	15.01	—	14.16	—	—
4,4′-Dinitrodiphenylamine	14.97	14.97	14.90	—	14.48	—	—
2,4,6-Trinitrotoluene	14.45	—	14.50	—	—	—	—
2,4-Dinitrodiphenylamine	14.65	14.65	—	—	—	—	17.71
2,4-Dinitroaniline	15.80	—	—	—	—	15.34	18.46
4-Nitrodiphenylamine	>19	16.95	—	17	15.43	15.76	20.6
4,4′-Dinitrodiphenylmethane	—	—	—	—	15.90	15.82	—
4,4′,4″-Trinitrotriphenylmethane	—	—	—	—	—	—	17.44
4-Chloro-2-nitroaniline	—	—	—	—	—	17.21	—
2-Nitroaniline	>19	>18.75	—	19.40	—	—	—
3-Nitroaniline	>19.4	—	—	—	—	—	—
4-Nitroaniline	>19	—	—	18.95	—	18.47	—
2-Nitrodiphenylamine	>19	18.85	—	18.80	—	—	—

solvent for this type of work from the standpoint of its physical properties: low acidity, high dielectric, suitable optical clarity, freezing point, boiling point, and viscosity. It is, however, difficult to find indicators for this system. Hydrazine reacts rapidly with many nitro compounds which are useful indicators in other systems; with some anions very large shifts in the wavelength of light absorption are observed. For example, Shatenshtein (9) has observed a wavelength shift of 120 mμ for the metanitrophenolate anion between 0.005 N sodium hydroxide and anhydrous hydrazine, with lesser but still troublesome shifts for other anions. In general, Shatenshtein found the comparable shifts in liquid ammonia to be much less and concluded that the shifts in hydrazine were probably due to the formation of molecular compounds. In all, it will be difficult to improve Deno's original choice of indicators for the hydrazine system. Some of the indicators studied by Deno, however, were not fully ionized since, as will be subsequently seen, there is a levelling of the H_- function for hydrazine near 65% composition.

Schaal and co-workers entered this field in 1955, using solutions of ethylene diamine in water as the basic system (10), and since then have published many papers (11–16) covering the systems ethanolamine in water, hydrazine in water, and tertiary amyl alcohol containing its sodium salt. They provided pK_a values for many weak acids, many of which are listed in Table I. Schaal and his co-workers obtained limiting values of 15.35 for anhydrous ethanolamine, 18.2 for ethylenediamine, and 19.4 for the tertiary amyl alcohol solutions.

Langford and Burwell (17) recently investigated sulpholane–water mixtures containing phenyltrimethylammonium hydroxide. They obtained an H_- value near 20 for a solution 95 mole % in sulpholane, 5 mole % in water, and 0.013 molar in phenyltrimethylammonium hydroxide. Sulpholane appears to be a good solvent in which to study a wide

Can. J. Chem. Downloaded from www.nrcresearchpress.com by 210.87.254.6 on 09/05/12
For personal use only.

range of acidities since, as they point out, a 0.01 M solution of sulphuric acid in sulpholane is a much stronger acid than the same concentration of sulphuric acid in water. Similarly, sulpholane containing 5% water is a million times more basic than pure water when both contain 0.01 M hydroxyl ion. Langford and Burwell suggest that most of the difference is due to the increased activity coefficient of the hydroxyl ion.

The pK_a values determined by all these investigators are summarized in Table I. A critical comparison of these values shows that our knowledge of the pK_a values of weak acids is indeed in a state of confusion. Paul and Long (18), in comparing the values reported by Schaal and Deno state "this large discrepancy casts considerable doubt on the assumption that these H_- scales are independent of the indicator used and makes it imperative that this be tested by studies with other indicators."

Kinetic methods have frequently been used to compare acidities (19–23) and this technique has been augmented by the use of deuterium isotope exchange experiments. Shatenshtein (9, 19) concludes that there is usually a direct connection between the point of equilibrium in protolytic reactions and its rate of attainment and that the rate of hydrogen exchange may serve as one method of determining the strengths of very weak acids. He and his colleagues have published extensively in this field, using hydrogen exchange reactions in liquid ammonia. Streitwieser *et al.* (21) have used lithium cyclohexylamide – cyclohexylamine systems to measure deuterium exchange and so determine hydrocarbon acidities. Hofmann, Muller, and Schriesheim (22) have used tritiated dimethyl sulphoxide to measure the acidities of several aromatic hydrocarbons; Dessy, Okuzumi, and Chen (23) have determined relative acidities for a series of weak acids using dimethylformamide as solvent, triethylamine as catalyst, and deuterium oxide as deuterium source. Hart and Crocker (24), using α-deuterioethylbenzene as a deuterium source, measured the rate of deuterium transfer to other related hydrocarbons in the presence of potassium and concluded that cumene was 13 times more acidic than 2,2-dimethyl-3-phenylbutane.

An examination of Table I shows that existing measurements of the acidity constants of very weak acids have led to many differing results. The agreement for 4-nitrobenzyl cyanide will be shown in a subsequent paper to be only apparent. The prime purpose of this work, therefore, was to discover whether consistent values for these weak acids could be found and in so doing determine the H_- function for as many systems as possible.

It was decided to use indicators as closely allied in molecular structure as possible. The substituted anilines and diphenylamines provided a series of compounds of varying acidity well suited to our purpose. A parallel study was therefore initiated on the relation between structure and acidity in these compounds and this is reported in a subsequent publication. Because of the conflicts in values reported by other investigators it was necessary to reexamine their systems in order to pinpoint sources of disagreement.

The term acidity function and the symbol H_- are used to designate the equilibria studied in this work. The well-known Hammett acidity function, H_0, refers to the ability of a solvent to protonate a neutral base.

$$B + H^+ \rightleftharpoons BH^+$$

Hammett (25) pointed out that a different function, H_-, might govern the protonation of an anionic base, and this has proved to be the case in acid solution (26, 27).

$$A^- + H^+ \rightleftharpoons HA$$

In strongly basic systems the ionization of the aniline and related indicators would normally be written as follows.

Can. J. Chem. Downloaded from www.nrcresearchpress.com by 210.87.254.6 on 09/05/12
For personal use only.

$$ArNH_2 \rightleftharpoons H^+ + ArNH^-$$

$$\text{or } ArNH_2 + OH^- \rightleftharpoons H_2O + ArNH^-$$

One can conveniently express these equilibria in terms of the H_- function, however, and this has been done by us and by most other workers in the field. (See Experimental section.)

RESULTS

Establishment of the H_- Function and Acidity Constants

The experimental data on the compounds used as indicators is summarized in Table II.

TABLE II

Spectral data for indicators[a]

Substituent	Neutral molecule λ_{max}	Neutral molecule ϵ_{max}	Anion λ_{max}	Anion ϵ_{max}	Preparation method
Substituted diphenylamines					
2,4,6,2′,4′,6′-Hexanitro	390	16 000	425	23 000	Ref. (41)
2,4,6,2′,4′-Pentanitro	378[b]	18 900[b]	480	25 600	(42)
2,4,6,4′-Tetranitro	377[c]	17 500[c]	465	23 800	(42)
2,4,6,3′-Tetranitro	337[c]	20 700[c]	441[d]	26 000[d]	(42)
2,4,6-Trinitro	372	13 100	450	19 000	(43)
2,4,2′,4′-Tetranitro	413	21 200	510	29 000	(41)
2,4,6-Trinitro-4′-amino	420[e]	11 800[e]	470[e]	19 300	(44)
2,4,4′-Trinitro	385[d]	21 900[d]	520[d]	27 400[d]	(45)
2,4,3′-Trinitro	360[e]	17 850[e]	450[e]	18 700[e]	(46)
2,4-Dinitro	362[d]	16 800[d]	495	16 000	(41)
4,4′-Dinitro	416[d]	35 400[d]	580	37 000	
2,4-Dinitro-4′-amino	375[e]	18 300[e]	495[e]	18 300[e]	
4-Nitro	400[d]	19 550[d]	508[d]	34 600[d]	(47)
2-Nitro	435[e]	6 360[e]	545[e]	9 170[e]	(47)
Substituted anilines					
2,4,6-Trinitro	328[e]	11 000[e]	412	23 400	
	417[e]	6 000[e]			
6-Bromo-2,4-dinitro	350	12 000	395[e]	23 200[e]	
			527[e]	12 700[e]	
2,4-Dinitro	336[f]	14 900[f]	388[d]	21 100[d]	
			535[d]	15 300[d]	
2,6-Dichloro-4-nitro	368[d]	13 700[d]	467[d]	38 800[d]	
2,5-Dichloro-4-nitro	368[d]	11 800[d]	458[d]	37 200[d]	
4-Chloro-2-nitro	417[f]	3 450[f]	516[e]	6 900[e]	
2-Nitro	410[d]	4 490[d]	515[d]	8 400[d]	
4-Nitro	378[d]	16 900[d]	467[e]	32 300[e]	
3-Nitrocarbazole	279[f]	24 600[f]	488[f]	19 000[f]	(28)
	305[f]	41 300[f]			
	364[f]	10 500[f]			

[a]Solvent is water unless otherwise noted.
[b]In ethanol.
[c]In benzene.
[d]In pyridine or aqueous pyridine.
[e]In sulpholane or aqueous sulpholane.
[f]In methanol.

It shows the wavelength of maximal absorption and the extinction coefficient at that wavelength for each compound for both the molecular and anionic species in various solvents.

The pK_a value of 2,4,6-trinitroaniline was determined in aqueous buffers and sodium hydroxide to be 12.20, in good agreement with the work of Schaal (28), who reported 12.25. This indicator was then used to determine the H_- value for several different mixtures of pyridine in water containing 0.011 molar benzyltrimethylammonium hydroxide. It was then possible to determine in the same solutions the fraction ionized for

Can. J. Chem. Downloaded from www.nrcresearchpress.com by 210.87.254.6 on 09/05/12
For personal use only.

2,4,4′-trinitrodiphenylamine. A best fit straight line was then drawn through these measured points to determine the pK_a difference from 2,4,6-trinitroaniline. This procedure could be applied repeatedly for successive indicators. Thus, 2,4,6-trinitroaniline is the compound analogous to 4-nitroaniline which was used in building the H_0 scale in acid solutions (18, 25).

Now pK_a values were assigned to the indicators. These individual pK_a values were then used to calculate the H_- value for each solution in which the position of its ionization equilibrium was measurable. This procedure resulted in several measured H_- values for each solution. These values were averaged, and the results are summarized in Table III.

The H_- values for the various concentrations of pyridine in water were now considered known, and Fig. 1 was produced by plotting the original values of log $[A^-]/[AH]$ against

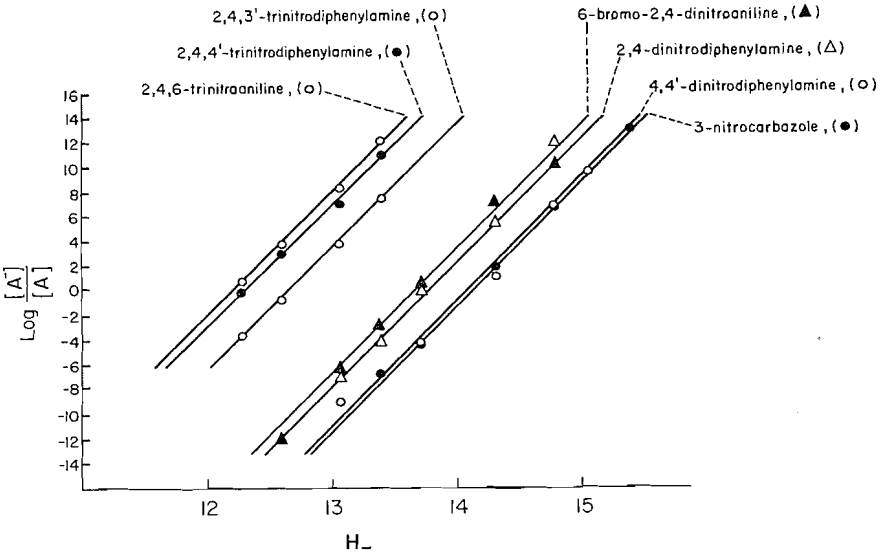

FIG. 1. The ionization of several indicator amines as a function of the basicity of the solution.

H_-. H_- appears to be an acceptable function for the system since the plots are parallel straight lines of unit slope, although it should be pointed out that these indicators are closely similar in molecular structure.

For this system it was not found possible to make determinations above 60 mole % pyridine. Near this point the indicator plots are found to be no longer parallel, and immiscibility problems arise.

Presumably, the irregularities in the ionization plots are chiefly due to decreasing dielectric constant. If it is assumed that change in dielectric is linear with mole fraction in a mixture of the two liquids, the dielectric of 60 mole % pyridine in water will be less than 40. The effects observed in this work seem greater than the expected effect of dielectric on $\log f_{A^-}/f_{AH}$, and it is possible that some effects due to ion pairing or molecular association are present. Hummelstedt and Hume (29) have concluded there is no hope for successful pK_a measurements in solvents such as benzene where association phenomena are very pronounced.

Operations were carried out in the same way for aqueous sulpholane as for aqueous pyridine systems, using the same indicators. The higher dielectric of sulpholane allowed continuance of the measurements from 100% water to 95 mole % sulpholane. The

Can. J. Chem. Downloaded from www.nrcresearchpress.com by 210.87.254.6 on 09/05/12
For personal use only.

Can. J. Chem. Downloaded from www.nrcresearchpress.com by 210.87.254.6 on 09/05/12
For personal use only.

TABLE III

H_- valves for various solvent systems[a]

(*a*) Aqueous solutions of benzyltrimethylammonium hydroxide																				
Molarity of hydroxide	0.01	0.02	0.05	0.29	0.48	0.81	1.19	1.76	2.00	2.38										
H_-	11.98	12.39	12.71	13.29	13.76	14.16	14.55	14.85	15.19	16.20										
(*b*) Aqueous pyridine containing 0.011 molar tetramethylammonium hydroxide																				
Mole % pyridine	1.0	5.3	10.2	14.3	20.0	29.7	40.1	49.4	59.7											
H_-	12.27	12.62	13.03	13.43	13.75	14.35	14.78	15.06	15.35											
(*c*) Aqueous sulpholane containing 0.011 molar tetramethylammonium hydroxide																				
Mole % sulpholane	1.79	3.99	10.12	16.85	20.22	30.1	40.3	50.3	60.7	64.3	68.6	70.7	74.9	77.0	83.9	87.2	89.4	90.9	92.0	93.4
H_-	12.39	12.56	12.63	12.90	13.24	13.73	14.25	14.88	15.60	15.92	16.19	16.52	16.79	17.13	17.51	17.94	18.05	18.28	18.53	19.18
(*d*) Aqueous pyridine (50 mole % of each) containing benzyltrimethylammonium hydroxide																				
Molarity of hydroxide	0.01	0.05	0.10	0.24	0.48	0.96	2.12													
H_-	15.67	16.50	16.75	17.09	17.96	18.10	18.91													
(*e*) Aqueous pyridine (30 mole % pyridine) containing benzyltrimethylammonium hydroxide																				
Molarity of hydroxide	0.03	0.15	0.29	0.83	1.19	1.62	2.19	2.38												
H_-	14.06	14.88	15.66	15.88	16.65	17.52	17.65	16.50												
(*f*) Aqueous lithium hydroxide																				
Molarity of hydroxide	1.0	2.0	3.0	4.0	5.0															
H_-	13.43	13.53	13.93	14.04	14.31															
(*g*) Aqueous dimethyl sulphoxide containing 0.011 molar tetramethylammonium hydroxide																				
Mole % dimethylsulphoxide	5.0	10.0	20.0	30.0	40.0	50.0	60.0	70.0												
H_-	12.17	12.94	14.28	15.29	16.45	17.26	17.85	18.61												
(*h*) Aqueous ethylene diamine[b]																				
Mole % ethylene diamine	9.2	11.4	12.0	13.8	14.4	16.9	17.2	19.7	21.0	23.0	25.2	26.9	31.0							
H_-	12.76	13.40	13.29	13.75	13.62	13.99	14.04	14.38	14.65	14.74	15.19	14.99	15.48							
(*i*) Aqueous hydrazine[c]																				
Mole % hydrazine	23.2	27.4	31.5	36.0	40.7	45.8	51.1	95.0[d]												
H_-	13.06	13.29	13.70	14.02	14.34	14.77	15.08	16												

[a]The systems in (*a*), (*b*), and (*c*) were used to obtain the indicator pK_a values (see Experimental section).
[b]Calculated from data of Schaal (11, 28) using pK values reported herein.
[c]Calculated from data of Schaal and Favier (13) using pK values reported herein (Table IV).
[d]No ionization of 4-chloro-2-nitroaniline (pK_a = 17.22) is detectable in 95% hydrazine.

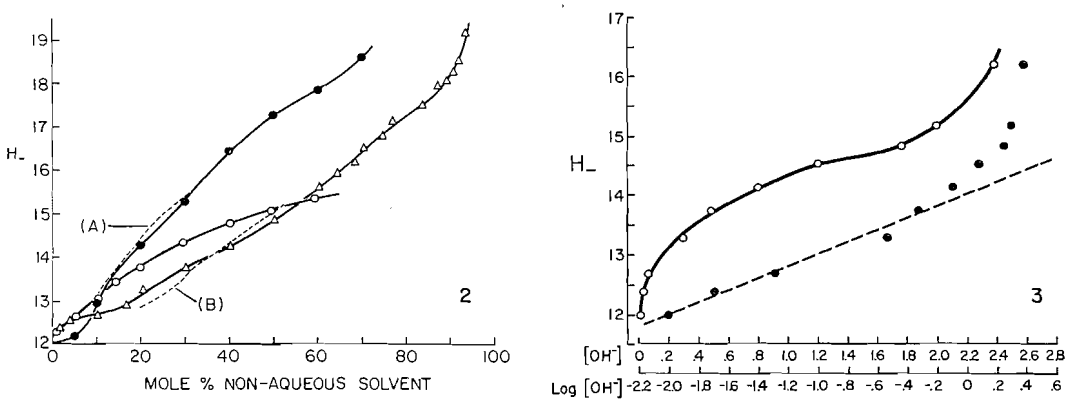

FIG. 2. Variation of basicity with solvent composition in the following systems all containing 0.011 molar tetramethylammonium hydroxide: aqueous dimethyl sulphoxide (●), aqueous sulpholane (△), and aqueous pyridine (○). The broken lines are the calculated values of the basicity of aqueous ethylene diamine (A) and aqueous hydrazine (B) solutions containing no added base, using the data of Schaal *et al.* (11, 13, 28).

FIG. 3. The variation of H_- for aqueous benzyltrimethylammonium hydroxide with the hydroxyl ion molarity (○), and with the logarithm of the hydroxyl ion molarity (●).

quaternary base was added in aqueous solution to bring the base concentration to 0.011 molar. The results are summarized in Table III and Fig. 2.

The entire operation was repeated using solutions of benzyltrimethylammonium hydroxide in water. This quaternary base has high water solubility and may be prepared in 2.38 molar solution. Figure 3 and Table III show the results obtained in this system.

Table IV shows a complete summary of the pK_a values determined in the present work and shows the average values obtained in these basic systems. It may be noted that better agreement is actually found between determinations in different solvents than the variations in log $[A^-]/[AH]$ for an individual indicator would lead one to expect.

Use of Acidity Constants to Establish H_- for Other Solvent Systems

Once an established list of acidity constants, such as Table IV, is available, it can be used to measure H_- values in other solvent systems. An investigation was carried out on the effect of increasing the base concentration in water–pyridine mixtures. Benzyltrimethylammonium hydroxide is available as a 2.19 molar solution in anhydrous pyridine. Thus, by mixing these two solutions in calculated proportions with pyridine or water, one can obtain any desired proportion of pyridine–water containing up to 2.0 molar base. Measurements in each solution were carried out with several indicators. The results are included in Table III. The indicators were also used in this manner to establish the H_- function for dimethyl sulphoxide – water mixtures containing 0.011 molar tetramethylammonium hydroxide. The extinction coefficients of maximal absorption were determined in solutions as close as possible in composition to those in which the measurements were carried out.

The indicators employed in this work possess marginal solubilities in aqueous lithium hydroxide. Measurements were made up to 5 molar (saturated) lithium hydroxide by use of 10 cm cells. Even with this path length optical densities were very low, and the results are accordingly not of high accuracy but are believed to represent at least roughly the H_- function in these systems.

Measurements were even more difficult in aqueous sodium and potassium hydroxides. For 1 molar sodium hydroxide the results agree with those for lithium hydroxide, within

Can. J. Chem. Downloaded from www.nrcresearchpress.com by 210.87.254.6 on 09/05/12
For personal use only.

TABLE IV

Summary of pK_a values determined in this work

Indicator	Average value	Aqueous buffer	Pyridine/ water	BTMA[a]/ water	Sulpholane/ water
2,4,6,2′,4′,6′-Hexanitro-diphenylamine	2.63	2.63	—	—	—
2,6-Dichloro-4-nitrophenol	3.48	3.48	—	—	—
2,4,6,2′,4′-Pentanitro-diphenylamine	6.72	6.72	—	—	—
2,4,6,4′-Tetranitro-diphenylamine	8.88	8.88	—	—	—
2,4,6,3′-Tetranitro-diphenylamine	9.15	9.15	—	—	—
2,4,6-Trinitro-diphenylamine	10.38	10.38	—	—	—
2,4,2′,4′-Tetranitro-diphenylamine	10.82	10.82	—	—	—
2,4,6-Trinitro-4′-amino-diphenylamine	10.82	10.82	—	—	—
2,4,6-Trinitroaniline	12.20	12.20	—	—	—
2,4,4′-Trinitro-diphenylamine	12.35	12.31	12.33	12.44	12.31
2,4,3′-Trinitro-diphenylamine	12.65	—	12.65	12.68	12.62
6-Bromo-2,4-dinitro-aniline	13.63	—	13.66	—	13.60
2,4-Dinitrodiphenylamine	13.84	—	13.83	13.85	13.83
4,4′-Dinitrodiphenylamine	14.08	—	14.09	14.15	14.00
3-Nitrocarbazole	14.10	—	14.16	—	14.03
2,4-Dinitro-4′-amino diphenylamine	14.64	—	—	—	14.64
2,4-Dinitroaniline	15.00	—	—	14.97	15.02
2,6-Dichloro-4-nitroaniline	15.55	—	—	—	15.55
4-Nitrodiphenylamine	15.90	—	—	—	15.90
4-Nitro-2,5-dichloroaniline	16.05	—	—	—	16.05
4-Chloro-2-nitroaniline	17.22	—	—	—	17.22
2-Nitrodiphenylamine	17.57	—	—	—	17.57
2-Nitroaniline	17.88	—	—	—	17.88
4-Nitroaniline	18.37	—	—	—	18.37

[a]Benzyltrimethylammonium hydroxide (aqueous).

TABLE V

Correlation of pK_a values from this work with those recalculated from the work of other investigators

Indicator	Schaal *et al.*		Langford and Burwell		This work
	Original	Adjusted	Original	Adjusted	
2,4,6-Trinitroaniline	12.25	—	—	—	12.20
2,4,4′-Trinitrodiphenylamine	—	—	—	—	12.35
2,4,3′-Trinitrodiphenylamine	—	—	—	—	12.65
6-Bromo-2,4-dinitroaniline	—	—	13.71	13.63[a]	13.63
2,4-Dinitrodiphenylamine	14.65	13.84[a]	—	—	13.84
3-Nitrocarbazole	15.10	14.24[b]	—	—	14.10
4,4′-Dinitrodiphenylamine	14.97	14.13[b]	—	—	14.08
2,4-Dinitro-4′-aminodiphenylamine	—	—	—	—	14.64
2,4-Dinitroaniline	15.80	14.78[b]	15.34	15.26[d]	15.00
2,6-Dichloro-4-nitroaniline	—	—	—	—	15.55
4-Nitrodiphenylamine	16.95	15.93[c]	15.76	15.68[d]	15.90
2,5-Dichloro-4-nitroaniline	—	—	—	—	16.05
4-Chloro-2-nitroaniline	—	—	17.21	17.13[d]	17.22
2-Nitrodiphenylamine	18.85	17.83[c]	—	—	17.57
2-Nitroaniline	19.40	18.38[c]	—	—	17.88
4-Nitroaniline	18.95	17.93[c]	18.47	18.39[d]	18.37

[a]Assigned starting point.
[b]From replot of original data.
[c]Adjusted by 1.02 which is the adjustment found for 2,4-dinitroaniline.
[d]Adjusted by 0.08 log units.

Can. J. Chem. Downloaded from www.nrcresearchpress.com by 210.87.254.6 on 09/05/12
For personal use only.

the experimental error, but attempts to make measurements in more concentrated solutions with these indicators had to be abandoned. (See, however, refs. 6 and 7.)

DISCUSSION

How can we be sure we are actually dealing with a proton removal process producing an anion? At present no cryoscopic work has been done in any of the solvents, so no direct statement of the number of particles present is possible. Partly for these reasons an examination of several compounds which could not lose a proton under the reaction conditions was undertaken. These were *N*,*N*-dimethylpicramide, 1,3,5-trinitrobenzene, the picrate anion, and nitrobenzene. Each of these showed a spectral change when dissolved in a solution of sufficiently high basicity. However, all of them reacted at a finite rate, and for all of them the reverse reaction was also slow when the basicity of the solution was reduced.

This then became one of our main criteria: we accepted as simple proton removal only those reactions which were apparently instantaneous and which reversed instantaneously. All compounds whose pK_a value we have reported obey this criterion. 3,5-Dinitroaniline, for example, reacted slowly in our most basic solutions to produce a stable species, and the reverse reaction was also slow. Because of these observations it was decided that a pK_a determination would not be meaningful.

Difficulties of a similar nature were encountered for 4-nitrophenylhydrazine, 2,4-dinitrophenylhydrazine, and 2,4,6-trinitrophenylhydrazine.

Correlation of Results with Those of Other Investigators

It will be shown in a subsequent publication that the indicator 4-nitrobenzyl cyanide is an unsatisfactory compound on which to build an acidity scale. We have reevaluated the pK_a quantities in Table I by choosing new starting points for the scales of Schaal *et al.* and Langford and Burwell. Accordingly, the value of 13.63 for 6-bromo-2,4-dinitroaniline, as determined in this work, was used as a starting point for Langford and Burwell's work instead of the slightly different value of 13.71, obtained by comparison with 4-nitrobenzyl cyanide (17). The pK_a differences determined by them were then used to build up Table V. (It can be seen that the alteration in pK_a value is very small for every case except 2,4-dinitroaniline.)

Schaal's data for ethylenediamine were replotted after assigning the value of 13.84 instead of 14.65 to 2,4-dinitrodiphenylamine (11, 28).

An examination of Table V shows that disagreements in pK_a determinations are largely removed by these procedures. Also included in Table V are values obtained by Schaal *et al.* in ethanolamine (12) and tertiary amyl alcohol (14). These were determined by an extrapolation procedure since full ionization was not attained. It is satisfying that these values are in at least rough agreement. These values have all been adjusted by 1.02 pK units since we have adjusted 2,4-dinitroaniline by that amount. Hydrazine–water systems were treated in the same way (13).

Interpretation of Solution Basicity

The enhanced basicity of the solutions studied in this work appears to be due chiefly to an enhancement of the hydroxyl ion activity, as suggested by Langford and Burwell (17).[3] The following equilibrium,

$$ArNH_2 + OH^- \rightleftharpoons ArNH^- + H_2O,$$

shifts to the right as water is replaced by a polar aprotic solvent, not merely because of

[3]*See also refs. 30–32.*

Can. J. Chem. Downloaded from www.nrcresearchpress.com by 210.87.254.6 on 09/05/12
For personal use only.

a mass action effect but principally because of the altered activities of the ions involved. As water is replaced by the second solvent, the activity of both OH^- and $ArNH^-$ will rise, since water is very effective at stabilizing anions by hydrogen bonding. The hydroxyl ion is probably coordinated to three water molecules (32–35); three such arrangements are shown below.

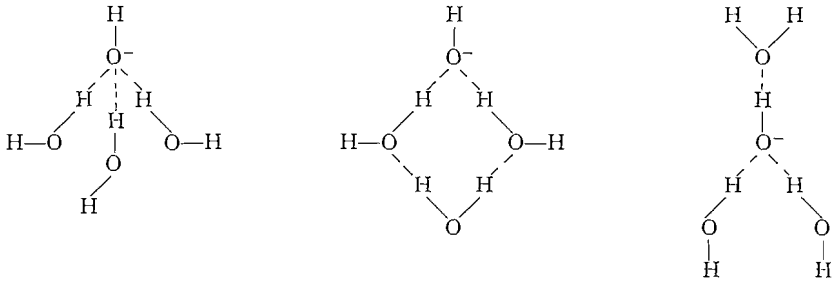

(The third structure above is similar to that of $H_9O_4^+$ (35, 36) less two protons. However, as Yagil and Anbar point out, the OH^- proton is unlikely to form a strong hydrogen bond to water (32)). The larger anion, $ArNH^-$, with extensive internal charge delocalization, is less sensitive to solvation changes and the equilibrium, above, shifts to the right. (In the case of the pyridine, sulpholane, and dimethyl sulphoxide systems it was necessary to add a strong base, but for aqueous hydrazine and ethylenediamine the hydroxyl ion is present because of the intrinsic basicity of the solvent molecules themselves.) It has recently been shown that the rates of nucleophilic displacements and other base-catalyzed reactions are sharply increased by addition of polar aprotic solvents, and similar explanations have been offered (30).

The above ideas explain satisfactorily the general effect of polar aprotic solvents on solution basicity, but they do not account for the individual variations that exist in the effects of the various added solvents (Fig. 2). Specific interactions probably occur between the molecules of added solvent and molecules of water on the one hand and the cations and anions on the other. Ion pairing is probably important only in the solutions that are rich in pyridine (or ethylenediamine), since all the other solvents have reasonably high dielectrics.

The purely aqueous system, containing benzyltrimethylammonium hydroxide (Fig. 3), also shows exalted basicity at high concentrations of the base. The broken line is simply a linear H_- versus log [OH^-] plot and represents the H_- value expected if the various ion activities remained unity. Beyond about 2 molar base the solution basicity rises dramatically, and this rise presumably reflects a decrease in the number of available water molecules for the solvation spheres of the ions.

EXPERIMENTAL

Preparation of Solvent Systems

Sulpholane (tetramethylene sulphone) was purchased from the Shell Development Company and distilled over sodium hydroxide according to the procedure of Langford (17). This solvent, b.p. 112° at 1 mm, was optically clear above 250 mμ. Dimethylsulphoxide was Baker reagent grade and was distilled over sodium hydroxide pellets before use. Fischer reagent grade pyridine was distilled over barium oxide to remove water, and had b.p. 115° at 760 mm. Eastman White Label 95% hydrazine was used without further purification. The percentage hydrazine was determined by the iodine titration procedure given by Audreith and Ogg (36). Eastman 98% ethylenediamine was distilled over sodium to remove water. This solvent does not remain optically clear during storage even if protected from sunlight, moisture, and oxygen. Anhydrous methanol was prepared by distillation over magnesium.

Potassium acid phthalate buffers covering the pH range from 2.2 to 6.2 (37) and potassium dihydrogen phosphate buffers covering the range from 5.8 to 8.0 were prepared. For the range 8.45 to 12.77 glycine

Can. J. Chem. Downloaded from www.nrcresearchpress.com by 210.87.254.6 on 09/05/12
For personal use only.

buffers were used. These buffers were diluted so that the ionic strength was not greater than 0.1. Sodium hydroxide, 0.1 *N*, prepared from commercial standard sodium hydroxide, was used as a 12.88 pH standard. All pH measurements were made using a Beckman model G pH meter, equipped with a calomel reference electrode and a standard glass electrode. The Beckman E_2 "blue" electrode was used for all measurements above pH 11. Benzyltrimethylammonium hydroxide (40% in water) was used as purchased from British Drug Houses. Tetramethylammonium hydroxide (10% in water), tetra-*n*-propylammonium hydroxide (10% in water), and phenyltrimethylammonium hydroxide (20% in methanol) were Eastman White Label. Benzyltrimethylammonium hydroxide (40% in pyridine) was prepared according to the method of Sprinzak (38) from a methanol solution of benzyltrimethylammonium hydroxide, which was purchased from Columbia Organic Chemicals.

The solvent systems were prepared in the following way. Aqueous benzyltrimethylammonium hydroxide (40%) was diluted with freshly distilled water to obtain a series of 10 solutions containing various concentrations of the base. These were then titrated with standard sulphuric acid to a phenolphthalein end point. A series of similar solutions were then prepared by mixing the 10 solutions with varying amounts of pyridine to obtain a set whose pyridine to water mole ratio was 50:50 and a second set in which the pyridine to water mole ratio was 30:70. To keep the base concentration as high as possible, a 40% benzyltrimethylammonium hydroxide solution in pyridine was prepared. The pyridine to water ratio was calculated from a knowledge of the amounts of pyridine and water added, and the final base concentration was determined by titration. Pyridine–water mixtures were prepared by weighing calculated amounts of the components, as were the sulpholane–water mixtures and the dimethyl sulphoxide – water mixtures.

Solutions of lithium and sodium hydroxides were prepared by dissolving a weighed amount of the hydroxide in the calculated amount of water and filtering to remove carbonate. Weighed aliquots of these solutions were then titrated to determine the concentration of hydroxide. The potassium hydroxide solutions were already clear and no carbonate removal step was carried out.

Preparation of Indicators

References to syntheses of indicators are listed in Table II. All other compounds were available commercially.

N-t-butylpicramide had not been prepared previously and was obtained by refluxing 0.02 moles of tertiary butylamine with 0.01 moles of picryl chloride for 1 hour in ethanol. The product, after several recrystallizations from ethanol, was orange needles, m.p. 94–95°. Anal. Calc. for $C_{10}H_{12}N_4O_6$: C, 42.56; H, 4.22; N, 19.31. Found: C, 42.26; H, 4.16; N, 19.71.

Measurement of Spectra

A sample of each indicator was weighed and dissolved in acetone to make a 10^{-3} molar stock solution. Aliquots were pipetted from this solution directly into a 1 cm quartz cell equipped with a ground stopper. The acetone was then evaporated at an aspirator, and 2 ml amounts of the solvent under examination were added by means of a volumetric syringe. This technique was easily adaptable to an oxygen-free method. The cell was sealed with a silicone-rubber stopper of the type used in vapor phase chromatography. The cell was then flushed with dry nitrogen by an inlet and outlet pair of syringe needles. The solvent under consideration could then be added through the silicone stopper. This stopper proved satisfactorily leakproof even after several puncturings by small-gauge needles. Provided the solutions used are degassed previously, this technique prevents oxygen from seriously affecting the equilibria.

It was found that the bases employed reacted reasonably rapidly with sulpholane to produce a species which showed appreciable light absorption below 400 mμ. This reaction was accompanied by a drop in the basicity of the solutions. Because of this change, stock solutions of sulpholane containing the base could not be kept, and the following procedure was adopted. The indicator sample was first dissolved in a solution of known sulpholane–water concentration and the base added in water solution (20 microliters) immediately before taking the spectral measurements. The solvent composition was corrected for the added water. For consistency, this same procedure was adopted for pyridine–water systems and dimethyl sulphoxide – water systems. Also, it was not considered advisable to keep the highly basic solutions for any length of time. Calculation, based on known densities of the mixtures, then provided the final mole % values as reported.

For these systems it was possible to record the molecular spectrum and the anion spectrum in solutions of nearly identical composition. For other systems (buffers, benzyltrimethylammonium hydroxide in water, or hydrazine) the unionized spectrum was recorded in at least two solutions above the point where ionization appeared to be complete. These solutions were shown to be of higher basicity by their effect on a weaker acid. In this way it was possible to be certain that all compounds were fully ionized and to obtain extinction coefficients for both the molecular and anionic form in solutions of reasonably similar composition. All solvents were tested for optical clarity in the regions used, and a solvent blank of the same concentration as that containing the indicator was used.

The spectrum of the indicators employed varied little over the solvent composition range necessary to fully ionize the molecule. This was checked by making measurements at two different positions on the anion spectrum. A good check of this point is the agreement of the ionization equilibria of one indicator with the next. If an indicator shows serious anomalies, the difference in the quantity log $[A^-]/[AH]$ between it and the next indicator will not be constant.

Can. J. Chem. Downloaded from www.nrcresearchpress.com by 210.87.254.6 on 09/05/12
For personal use only.

From one solvent system to another, however, certain significant differences were found for both extinction coefficients and wavelength maxima. (Table II does not include spectral data for all the solvent systems studied; these details may be found in the Ph.D. thesis of J. P. O'D., University of British Columbia, 1962.)

Visible and ultraviolet absorption spectra of the indicators were measured with a Cary Model 14 recording spectrophotometer to locate the wavelengths of maximal absorption of both the molecular and anionic forms. The actual optical density measurements were carried out at two or more wavelengths, using a Beckmann DU spectrophotometer whose cell compartment was maintained at 25° by means of thermospacers. All spectral changes were checked for reversibility.

Treatment of Data

The calculation of H_- and pK_a is carried out using the equation

$$H_- = pK_a + \log [A^-]/[AH].$$

In this work the good agreement of one indicator with another—parallel straight lines of virtually unit slope were obtained in all cases—has been taken as an indication that no serious media effects were encountered.

In aqueous solution calculations in this work were based on the theoretical-curve method because most of the indicators used in the pH range showed considerable absorption by the molecule at the wavelength of maximal absorption for the ion.

This method states that

$$\log [A^-]/[AH] = \log \alpha/(1-\alpha) = \log (\Delta D - \Delta D_u)/\Delta D_i - \Delta D)$$

where the symbols have the following significance.

α is the fraction ionized.

D_u is the difference between the optical density at the wavelength of maximal absorption for the anion and the optical density at the wavelength of maximal absorption of the molecule, when measurements are made in a solution where the amount of ionization is effectively zero.

D_i is the same difference measured in a solution where ionization is effectively complete.

D is this same difference measured in some intermediate test solution.

For many of the indicators in the mixed-solvent systems used in this work, the absorption of the molecule at the anion wavelength was negligible, or very small. In these cases the method described by Schaal (28) was used. In this procedure all measurements are made at the anion wavelength, and the fraction ionized is

$$\alpha = (D - D_{mol})/(D_{ion} - D_{mol})$$

where the symbols have the following significance.

D_{mol} is the optical density of the molecular form measured at the anion wavelength.

D_{ion} is the maximum optical density measurable at this same wavelength when the species is fully in the ionic form.

D is the optical density at this same wavelength measured in some intermediate test solution.

The first of these two methods may be expected to correct somewhat for medium effects on spectra, provided the medium effect on the molecule spectrum is in the same direction as on the anion spectrum.

The second method was favored in this work because of the time-dependent absorption in the blank and the resulting possibility of error in balancing. This error is negligible above 400 mμ, and all anions employed absorbed above this wavelength. Thus, with the second method all measurements could be made in an undisturbed region. Again, provided the Hammett postulate was closely followed, that is, that different solutions gave the same pK_a difference between two indicators, it was felt that medium effects could not be serious.

Probable Error

It is difficult to estimate a precise experimental error, but where simple spectra and good plots are obtained it is estimated to be about 0.05 units. In setting up a scale this error may be cumulative. Considerable effort was expended to measure each pK_a difference in many different solutions and to obtain closely spaced indicators, so that many measurements could be made of H_- for each test solution used. No observations have been used to determine H_- values where $\log [A^-]/[AH]$ was greater than 1.0 or less than -1.0 since the observational experimental error begins to increase rapidly outside this range.

The biggest single problem in obtaining high accuracy was insufficient solubility of the molecular form of the indicator. Particular attention was paid to this problem in aqueous solutions and in the most dilute of the mixed-solvent systems. This problem forced work at lower optical densities than was desired. Whenever work was carried out near the solubility limit, careful checks were made to ensure that complete solution had occurred, so that observational error was as small as possible. For the pH region it was found that several solutions of different but known pH gave the same calculated pK_a value.

No attempt was made to apply a thermodynamic correction. Such corrections are generally less than 0.1 log units and are probably much less than this in the present work, since the ionic strengths of the buffer solutions used were limited to 0.1 (39, 40).

Can. J. Chem. Downloaded from www.nrcresearchpress.com by 210.87.254.6 on 09/05/12
For personal use only.

Some error is probably introduced by solvent effects on spectra, but this error is believed to be small because of the good ΔpK_a agreements among the closely spaced indicators. The solubility problem became serious for solutions of benzyltrimethylammonium hydroxide in water but, fortunately, sufficient solubility to make reasonably accurate measurements was retained. In lithium hydroxide, even though 10 cm cells were employed, only small optical densities could be obtained and the results must be considered of marginal accuracy.

ACKNOWLEDGMENTS

A special award by the Research Corporation is gratefully acknowledged.

REFERENCES

1. R. STEWART and J. P. O'DONNELL. J. Am. Chem. Soc. **84**, 493 (1962).
2. R. STEWART, J. P. O'DONNELL, D. J. CRAM, and B. RICKBORN. Tetrahedron, **18**, 917 (1962).
3. J. B. CONANT and G. W. WHELAND. J. Am. Chem. Soc. **54**, 1212 (1932).
4. W. K. MCEWEN. J. Am. Chem. Soc. **58**, 1124 (1936).
5. R. S. STEARNS and G. W. WHELAND. J. Am. Chem. Soc. **69**, 2025 (1947).
6. G. SCHWARZENBACH and R. SULZBERGER. Helv. Chim. Acta, **27**, 348 (1944).
7. J. T. EDWARD and I. C. WANG. Can. J. Chem. **40**, 399 (1962).
8. N. C. DENO. J. Am. Chem. Soc. **74**, 2039 (1952).
9. A. I. SHATENSHTEIN and Y. M. VARSHAVSKII. Russ. J. Phys. Chem. **22**, 475 (1948). A. I. SHATENSHTEIN. *In* Advances in physical organic chemistry. *Edited by* V. Gold. Academic Press, London. 1963. p. 156.
10. R. SCHAAL. J. Chim. Phys. **52**, 784 (1955).
11. R. SCHAAL. J. Chim. Phys. **52**, 796 (1955).
12. F. MASURE and R. SCHAAL. Bull. Soc. Chim. France, 1138 (1956). F. MASURE, R. SCHAAL, and P. SOUCHAY. Bull. Soc. Chim. France, 1143 (1956). C. JAQUINOT-VERMESSE and R. SCHAAL. Compt. Rend. **254**, 3679 (1962).
13. R. SCHAAL and P. FAVIER. Bull. Soc. Chim. France, 2011 (1959). P. FAVIER and R. SCHAAL. Compt. Rend. **249**, 1231 (1959).
14. C. JACQUINOT-VERMESSE, R. SCHAAL, and P. SOUCHAY. Bull. Soc. Chim. France, 141 (1960).
15. C. JACQUINOT-VERMESSE, R. SCHAAL, and P. RUMPF. Bull. Soc. Chim. France, 2030 (1960).
16. R. SCHAAL and C. GADET. Compt. Rend. **251**, 2171 (1960); Bull. Soc. Chim. France, 2154 (1961).
17. C. H. LANGFORD and R. L. BURWELL, JR. J. Am. Chem. Soc. **82**, 1503 (1960). C. H. LANGFORD. Ph.D. thesis, Northwestern University, 1960.
18. M. A. PAUL and F. A. LONG. Chem. Rev. **57**, 1 (1957).
19. A. I. SHATENSHTEIN. Usp. Khim. **28**, 3 (1959). *Transl. by* C. Reid. Transl. No. 56, Directorate of Scientific Intelligence, Defence Research Board of Canada.
20. J. A. GAUTHIER. Bull. Soc. Chim. France, 1263 (1960).
21. A. STREITWIESER, JR., D. E. VAN SICKLE, and W. C. LANGWORTHY. J. Am. Chem. Soc. **84**, 244 (1962). A. STREITWIESER, JR., and D. E. VAN SICKLE. J. Am. Chem. Soc. **84**, 249, 254 (1963). A. STREITWIESER, JR., W. C. LANGWORTHY, and D. E. VAN SICKLE. J. Am. Chem. Soc. **84**, 251 (1962).
22. J. E. HOFMANN, R. J. MULLER, and A. SCHRIESCHEIM. J. Am. Chem. Soc. **85**, 3000, 3002 (1963).
23. R. E. DESSY, Y. OKUZUMI, and A. CHEN. J. Am. Chem. Soc. **84**, 2902 (1962).
24. H. HART and R. E. CROCKER. J. Am. Chem. Soc. **82**, 418 (1960).
25. L. P. HAMMETT. Physical organic chemistry. McGraw-Hill Book Co., Inc., New York. 1940. Chap. 9.
26. R. H. BOYD. J. Am. Chem. Soc. **83**, 4288 (1961); J. Phys. Chem. **67**, 737 (1963).
27. J. N. PHILLIPS. Austr. J. Chem. **14**, 183 (1961).
28. R. SCHAAL. J. Chim. Phys. **52**, 784 (1955).
29. L. E. I. HUMMELSTEDT and D. N. HUME. J. Am. Chem. Soc. **83**, 1564 (1961).
30. A. J. PARKER. Quart. Rev. London, **16**, 163 (1962).
31. R. G. PEARSON. J. Am. Chem. Soc. **85**, 3533 (1963).
32. G. YAGIL and M. ANBAR. J. Am. Chem. Soc. **85**, 2376, 2380 (1963).
33. T. ACKERMANN. Discussions Faraday Soc. **24**, 180 (1957).
34. W. J. HAMER (*Editor*). The structure of electrolyte solutions. John Wiley and Sons, Inc., New York. 1959.
35. R. P. BELL. The proton in chemistry. Cornell University Press, Ithaca, N.Y. 1959. p. 83.
36. L. F. AUDREITH and B. A. OGG. The chemistry of hydrazine. John Wiley and Sons, Inc., New York. 1951.
38. Y. SPROGEL. Quantitative Inorganic Analysis. Longmans Green and Co., London. 1951.
37. A. I. VINZAK. J. Am. Chem. Soc. **80**, 5449 (1958).
39. R. A. ROBINSON. The structure of electrolytic solutions. *Edited by* W. J. Hamer. John Wiley and Sons, Inc., New York. 1959.
40. V. GOLD. pH measurements, their theory and practice. Methuen and Co., London. 1956.
41. E. J. HOFFMAN and P. A. Dame. J. Am. Chem. Soc. **41**, 1013 (1919).
42. C. F. VAN DUIN and B. C. R. VAN LENNEP. Rec. Trav. Chim. **38**, 358 (1919).
43. F. ULLMANN and G. NADAI. Ber. **41**, 1870 (1908).
44. G. T. MORGAN and F. M. G. MICKLETHEWAIT. J. Chem. Soc. **88**, 608 (1908).
45. H. WIELAND and H. LECHER. Ann. **392**, 156 (1912).
46. E. J. VAN DER KAM. Rec. Trav. Chim. **45**, 722 (1926).
47. I. GOLDBERG. Ber. **40**, 4541 (1907).

Can. J. Chem. Downloaded from www.nrcresearchpress.com by 210.87.254.6 on 09/05/12
For personal use only.

Can. J. Chem. Downloaded from www.nrcresearchpress.com by 210.87.254.105 on 09/05/12
For personal use only.

STRONGLY BASIC SYSTEMS

IV. SUBSTITUENT EFFECTS ON THE ACIDITY OF AROMATIC AMINES

ROSS STEWART AND J. P. O'DONNELL
Department of Chemistry, University of British Columbia, Vancouver, British Columbia

Received January 13, 1964

ABSTRACT

The effect of ring substituents on the acidity of anilines and diphenylamines is examined. In general the effects are similar to those found in the analogous ionization of phenols. The acidities of diphenylamines having two or three nitro groups in one ring and variable substituents in the other ring can be correlated by the Hammett relation.

A good correlation is found between the acidities and basicities of aromatic amines, although basicity is more sensitive to the presence of ring substituents than is acidity. The relation of these results to the general question of first and second dissociation constants of dibasic acids is considered.

In Part III of this series (1) the acidity constants of a great many aromatic amines were reported, together with the H_- functions for several strongly basic solvent systems. The validity of any acidity scale for mixed solvents depends, in turn, on the validity of the general Hammett stepwise method of determining H_- and indicator pK values, a method which involves a considerable extrapolation from the standard state of pure water. Any structure–reactivity or rate–equilibrium correlations that can be tested are important, then, as independent checks of the validity of the scale. A rate–equilibrium correlation was reported previously (2). In this paper we should like to report some structure–acidity correlations that have emerged from this work. These are interesting in their own right, but in addition they strengthen our confidence in the validity of the scale and of the indicator acidities previously reported.

RESULTS AND DISCUSSION

Electron-withdrawing groups in the aromatic rings of the amines increase the acidity of the amino hydrogens and displace the following equilibria to the right.

$$ArNH_2 + OH^- \rightleftharpoons ArNH^- + H_2O$$

$$Ar_2NH + OH^- \rightleftharpoons Ar_2N^- + H_2O$$

If the general Hammett sigma–rho treatment is applied to the ionization of diphenylamines, it is found that the best correlation exists when σ^0 substituent constants (3, 4) are used. Figure 1 shows the correlation obtained for the three series A, B, and C, where Z is a meta or para substituent in all cases. (There is not enough data available to examine the anilines in this way, since all but one of these contain ortho substituents, which frequently produce anomolous effects. Similarly, since only two points are available for series C, below, no decision can be reached about the kind of sigma function being obeyed.)

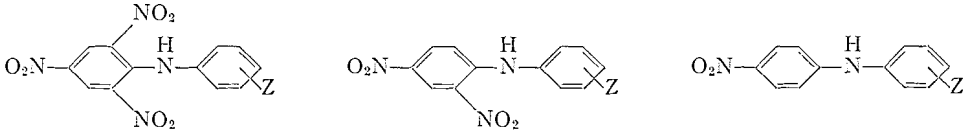

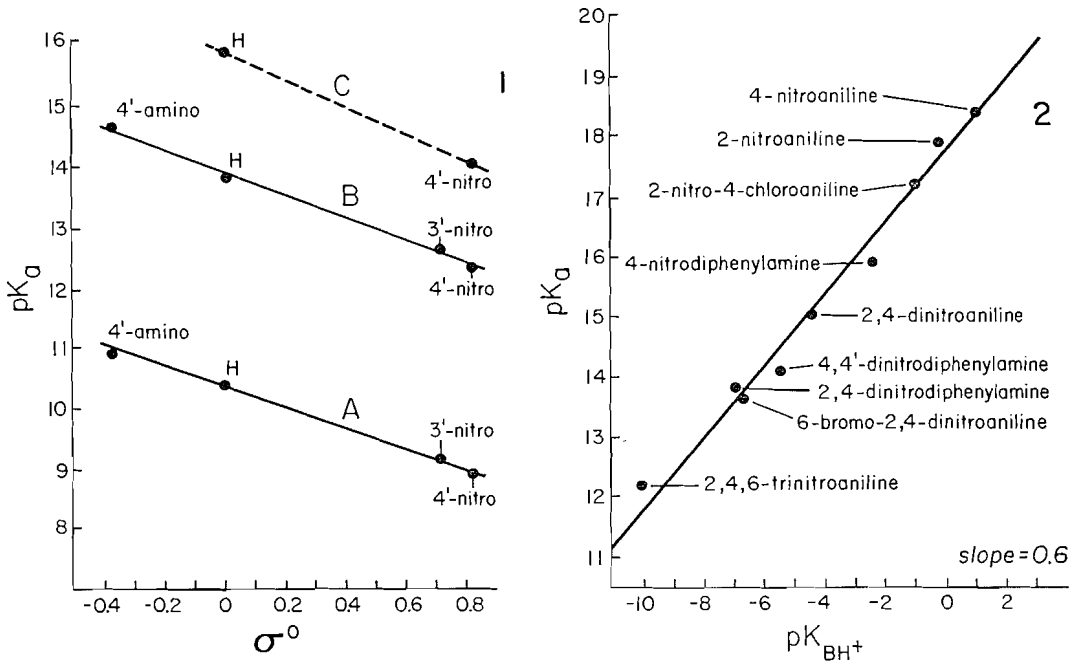

FIG. 1. Effect of an additional substituent on the acidities of nitrodiphenylamines: series A is 2,4,6-trinitrodiphenylamine, series B is 2,4-dinitrodiphenylamine, and series C is 4-nitrodiphenylamine.
FIG. 2. Acidities of aromatic amines (ordinate) plotted against their basicities (abscissa).

The substituent constants, σ^0, normally correlate reactivities for reactions in which conjugation between the substituent and the reactive center is absent (3, 4), whereas σ^- is used for reactions in which there is direct conjugation and σ for systems that possess the limited amount of conjugation present in benzoic acids (5, 6). It seems surprising, at first, that σ^0 constants give the best fit, since ortho and para nitro groups should interact strongly with the central $\rangle$NH and $\rangle$N$^-$ groups. It should be pointed out here that the present correlations are based on four substituents only, and the better agreement with σ^0 may be fortuitous. Nevertheless, it is worth speculating briefly on other possible causes of the less satisfactory correlation that exists for σ and σ^-. This correlation may result from a low degree of conjugation between the amino group and the substituent, simply because of the high degree of conjugation between the amino group and the ring, which is highly nitrated. Thus, for series A the ring with the Z-substituent may be oriented in such a way that much of its contribution to charge delocalization is sacrificed in order that the trinitro ring can interact powerfully with the central nitrogen. Only two points are available for series C, but it is probably significant that the apparent ρ is higher for this series suggesting that the substituent Z exerts a larger effect than in series A or B. (The next series, based on diphenylamine, undoubtedly has a much higher ρ, since work in progress shows that diphenylamine, itself, has a pK near 21.9 (7).)

The effect of substituents on the acidity of substituted anilines and diphenylamines resembles that found with phenols (6). The rho values for diphenylamine and phenol acidities are not strictly comparable, since, as we have seen, the former seem to correlate best with σ^0 values and the latter with σ^- values. Nevertheless, the effects of substituents are similar in the two series.

Can. J. Chem. Downloaded from www.nrcresearchpress.com by 210.87.254.105 on 09/05/12
For personal use only.

There are not enough compounds available to determine ρ for the acidity of anilines, but Table I shows that the effects of substituents on aniline and phenol acidities are also similar.

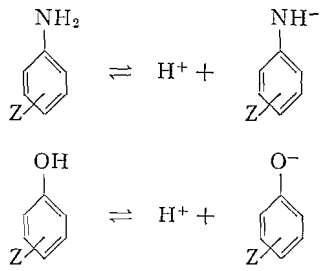

TABLE I

Comparison of the acidities of anilines and phenols

Substituent	pK_a Aniline	pK_a Phenol	ΔpK_a
2-Nitro-	17.88	7.08	10.80
4-Nitro-	18.37	7.15	11.22
2,4-Dinitro-	15.00	4.07	10.93
2-Nitro-4-chloro-	17.22	6.36	10.86
2,6-Dichloro-4-nitro-	15.55	3.48	12.17
2,4,6-Trinitro-	12.20	0.3	11.9

The extraordinary acidity of 2,4,6,2′,4′,6′-hexanitrodiphenylamine, which has a pK_a of 2.63 (1), suggests that both rings contribute strongly to the delocalization of charge (see, however, ref. 8). Charge delocalization may occur if the ion has the planes of its two aryl rings at right angles, so that maximum overlap occurs between the π-orbitals of each ring and two p-orbitals on nitrogen. This structure would require the central nitrogen to be sp hybridized, but the gain in resonance energy may be enough to make sp hybridization the most satisfactory arrangement. (An X-ray diffraction study of the potassium salt of 2,4,6,2′,4′,6′-hexanitrodiphenylamine was kindly undertaken by Dr. J. Trotter of this department, but the diffraction pattern was such that no decision could be reached with regard to the ion's geometry (9).)

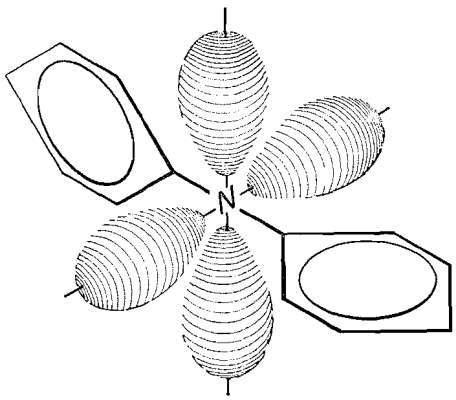

Can. J. Chem. Downloaded from www.nrcresearchpress.com by 210.87.254.105 on 09/05/12
For personal use only.

TABLE II

ΔpK for various nitro-substituted diphenylamines, showing the effect of nitro groups entering "other" ring

Amine	Position			
	3	4	2,4	2,4,6
4-Nitrodiphenylamine	—	1.82	3.59	7.02
2,4-Dinitrodiphenylamine	1.21	1.50	3.01	7.11
2,4,6-Trinitrodiphenylamine	1.23	1.50	3.66	7.75

The addition of an ortho nitro group to 2,4,2′,4′-tetranitrodiphenylamine and to 2,4,6,2′,4′-pentanitrodiphenylamine also produces very large acidity increases; an important contributing factor in all these cases may be the relief of steric strain as the trigonal nitrogen of the amine is converted to the digonal nitrogen of the anion.

Fairly regular increases in acidity result from the introduction of nitro groups into diphenylamine. These effects are shown in Table II.

It is of interest to compare the effect of substituents on the acidity and basicity of diphenylamines. In Fig. 2 the pK_a and pK_{BH^+} values are plotted against one another, and a surprisingly regular effect is observed; surprising because many of the substituents are in the ortho position, and greater irregularities, caused by specific interactions such as the following (10), might have been expected (5, 6, 11, 12).

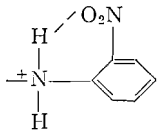

Strong H-bond

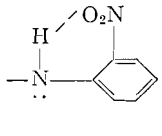

Weak H-bond

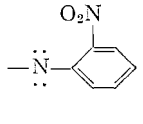

No H-bond

The slope of the line in Fig. 2 is approximately 0.7, meaning that substituents have a larger effect on the amines' basicity than on their acidity.

The matter of amine acidity and basicity is in essence the question of primary and secondary dissociation of a dibasic acid, $ArNH_3^+$ (or $Ar_2NH_2^+$), and it is of interest to see how the information gained in the present work fits into our general knowledge about these processes (13–15).

$$ArNH_3^+ \overset{K_1}{\rightleftharpoons} H^+ + ArNH_2$$

$$ArNH_2 \overset{K_2}{\rightleftharpoons} H^+ + ArNH^-$$

Much of the available information on dissociation of dibasic acids of various charge types is shown in Fig. 3. The filled circles (and the straight line) refer to dibasic acids with a gem diol grouping, that is to HO—Z—OH, where the atom Z may bear other groups and where the charge on the dibasic acid may be +1, 0, or −1. (Sulphuric, which is sometimes included in correlations of this type, has been omitted here because of doubt about the value of its primary dissociation constant.)

It is clear that, in contrast to the HO—Z—OH case, dissociation of dibasic acids of the type H_2Z (open circles) depends very strongly on the nature of the atom Z. This is not unexpected, since for H_2Z the atom Z must bear the charge that is being increased or

Can. J. Chem. Downloaded from www.nrcresearchpress.com by 210.87.254.105 on 09/05/12
For personal use only.

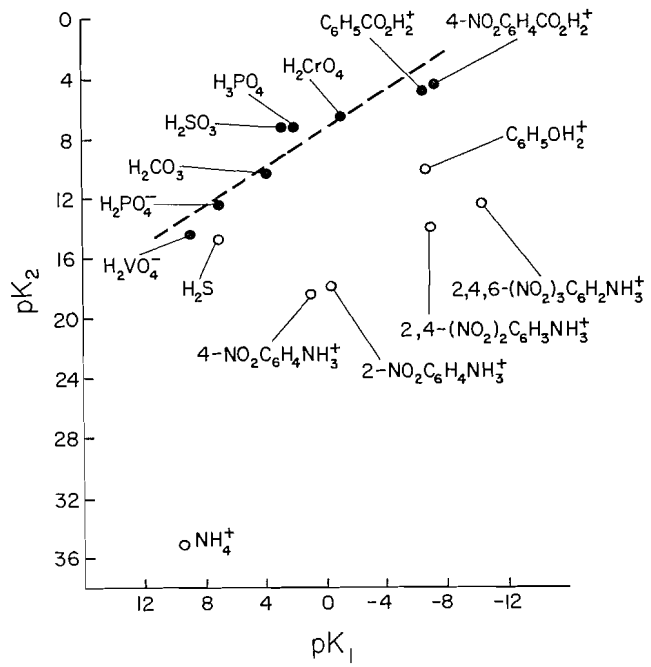

FIG. 3. pK_2 plotted against pK_1 for a variety of dibasic acids: ●, acid of general structure HOZOH; ○, acid of general structure H_2Z.

decreased as a result of the dissociation. (Of all the compounds studied herein only the nitroanilines are included in Fig. 2 for purposes of illustration.)

ACKNOWLEDGMENTS

A special award by the Research Corporation is gratefully acknowledged.

REFERENCES

1. R. STEWART and J. P. O'DONNELL. Can. J. Chem. **42**, 1681 (1964).
2. R. STEWART, J. P. O'DONNELL, D. J. CRAM, and B. RICKBORN. Tetrahedron, **18**, 917 (1962).
3. R. W. TAFT, JR. J. Phys. Chem. **64**, 1805 (1960).
4. R. W. TAFT, Jr., S. EHRENSON, J. C. LEWIS, and R. E. GLICK. J. Am. Chem. Soc. **81**, 5352 (1959).
5. L. P. HAMMETT. Physical organic chemistry. McGraw-Hill Book Co., Inc., New York. 1940. Chap. **7**.
6. H. H. JAFFÉ. Chem. Rev. **53**, 191 (1953).
7. D. DOLMAN and R. STEWART. Unpublished results.
8. S. KERTES and J. M. E. GOLDSCHMIDT. J. Chem. Soc. 401 (1956). W. D. TREADWELL and H. HEPENSTRICK. Helv. Chim. Acta, **32**, 1903 (1949).
9. J. Trotter. Can. J. Chem. **40**, 1218 (1962).
10. P. J. KRUEGER. Can. J. Chem. **41**, 363 (1963). A. N. HAMBLY and B. V. O'GRADY. Chem. Ind. London, 459 (1962).
11. D. H. MCDANIEL and H. C. BROWN. J. Am. Chem. Soc. **77**, 3756 (1955).
12. R. STEWART and M. R. GRANGER. Can. J. Chem. **39**, 2508 (1961).
13. J. E. RICCI. J. Am. Chem. Soc. **70**, 109 (1948).
14. R. J. GILLESPIE. J. Chem. Soc. 2537 (1950).
15. L. PAULING. Nature of the chemical bond. 3rd ed. Cornell University Press, Ithaca, N.Y. 1960. p. 324.

Can. J. Chem. Downloaded from www.nrcresearchpress.com by 210.87.254.105 on 09/05/12
For personal use only.

ANTINEOPLASTIC AGENTS

XI. N-BIS(2-BROMOETHYL)AMINES[1-3]

GEORGE R. PETTIT, MAURICE R. CHAMBERLAND, DAVID S. BLONDA, AND MARTYN A. VICKERS

Department of Chemistry, University of Maine, Orono, Maine

Received February 17, 1964

ABSTRACT

A novel halogen exchange reaction was found to accompany condensation of an acyl chloride with N-bis(2-bromoethyl)amine. Reaction between an acyl bromide and N-bis(2-bromoethyl)-amine, however, gave the expected N-bis(2-bromoethyl)amide. A number of N-alkyl-N-bis(2-bromoethyl)amines were prepared by lithium aluminum hydride reduction of the corresponding N-bis(2-bromoethyl)amides. The overall transformation from N-bis(2-bromoethyl)amine presents a convenient route to certain bromo nitrogen mustards. An efficient synthesis of N-bis(2-iodoethyl)amine hydroiodide is also described.

Can. J. Chem. Downloaded from www.nrcresearchpress.com by 210.87.254.105 on 09/05/12
For personal use only.

The earliest example of a bromo nitrogen mustard[4] appears to have been N-bis(2-bromoethyl)amine hydrobromide, described by Gabriel and Eschenback (2) in 1897. The bromo mustard was obtained by treating 2,2′-iminodiethylphenyl ether with hydrobromic acid. More recent methods ((3); see ref. 1 for an early example) involve modifications of the reaction between hydrobromic acid and 2,2′-iminodiethanol. The small number (4) of known N-substituted-N-bis(2-bromoethyl)amines have generally been prepared from the corresponding diol employing either hydrobromic acid (5), phosphorus tribromide (6), or thionyl bromide (7). A few procedures of more limited scope have also been recorded (3(*c*), 3(*d*), 5(*b*), 8).

Reaction of N-bis(2-bromoethyl)amine with an acyl chloride followed by reduction of the corresponding amide, employing a complex metal hydride reagent, would in principle provide a useful route to bromo nitrogen mustards. Analogous procedures have been developed in these laboratories for obtaining N-alkyl-N-bis(2-fluoroethyl)[1]- and N-alkyl-N-bis(2-chloroethyl)-amines (9). The present study was undertaken in order to explore this potentially useful and relatively mild route to N-alkyl-N-bis(2-bromoethyl)amines and to extend our knowledge of N-bis(2-bromoethyl)amines as potential cancerocidal agents.[5]

Syntheses of N-bis(2-bromoethyl)-derivatives of 3,5-dimethoxy-, 3,4-methylenedioxy-, and 3,4,5-trimethoxy-benzylamines were considered of particular interest as the corresponding chloro nitrogen mustards proved of interest in the Dunning leukemia test-system (9). Preparation of these bromo nitrogen mustards would also allow comparison of biological properties with several of the corresponding fluoro,[1] chloro (9), and iodo[1] (9(*a*)) derivatives. Initially, conversion of 2,2′-iminodiethanol (I*a*) to amine II*a* hydrobromide by the hydrobromic acid method was improved and during this work it was noted that certain acid:alcohol molar ratios lead instead to morpholine (III*a*).[6] Although

[1]*Refer to G. R. Pettit and R. L. Smith, Can. J. Chem. 42, 572 (1964), for the preceding contribution.*

[2]*Abstracted in part from the Master of Science thesis submitted by M. R. Chamberland to the Graduate School, University of Maine, October, 1963.*

[3]*This investigation was aided by Grants Number T-79C and T-79D from the American Cancer Society.*

[4]*The first synthesis of N-bis(2-chloroethyl)amine was reported by V. Prelog and colleagues (1).*

[5]*In preliminary biological studies (refer to footnote 1), N-bis(2-bromoethyl)amine hydrobromide was found to completely inhibit growth of Walker 256 in random-bred albino rats.*

[6]*Morpholine has also been obtained by heating 2,2′-iminodiethanol hydrochloride at 200° (see reference 10).*

Can. J. Chem. Downloaded from www.nrcresearchpress.com by 210.87.254.105 on 09/05/12
For personal use only.

TABLE I

$R—(CH_2)_n\overset{\oplus}{N}H(CH_2CH_2Br)_2Br\ominus$

R	n	M.p.[a] °C	Formula	Carbon		Hydrogen		Bromine		Nitrogen	
				Calc.	Found	Calc.	Found	Calc.	Found	Calc.	Found
4-Methylphenyl	1	162–163	$C_{12}H_{18}Br_3N$	34.64	34.69	4.36	4.53	57.63	57.62	3.37	3.25
4-Methoxyphenoxy	2	146–147	$C_{13}H_{20}Br_3NO_2$	33.79	33.99	4.36	4.52	51.89	51.83	3.03	2.96
3,5-Dimethylphenyl	1	162–163	$C_{13}H_{20}Br_3N$	36.30	36.48	4.69	4.84	55.50	55.62	3.26	3.08
3,5-Dimethoxyphenyl	1	161–163	$C_{13}H_{20}Br_3NO_2$	33.79	33.84	4.36	4.67	51.89	52.07	3.03	3.13
3,4-Methylenedioxyphenyl	1	164–165	$C_{12}H_{16}Br_3NO_2$	33.52	33.16	3.75	3.74	55.75	56.28	3.26	3.35
3,4,5-Trimethoxyphenyl	1	174–176	$C_{14}H_{22}Br_3NO_3$	34.17	34.04	4.51	4.71	48.72	48.80	2.85	3.12

[a]Melting point of the analytical sample which crystallized from methanol – ethyl ether.

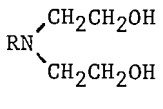

I a, R = H
b, R = $C(CH_3)_3$

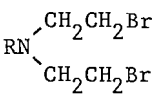

II a, R = H
b, R = CH_3

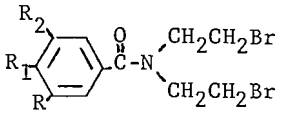

IV a, R-R_1 = OCH_2O, R_2 = H
b, R = R_1 = R_2 = H

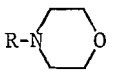

III a, R = H
b, R = $C(CH_3)_3$

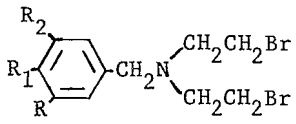

V a, R-R_1 = OCH_2O, R_2 = H
b, R = R_1 = R_2 = H

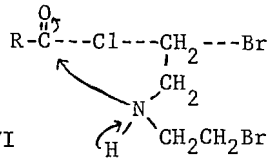

VI

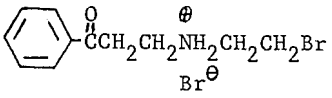

VII

substitution of hydriodic acid for hydrobromic acid, in the procedure used to obtain bromo nitrogen mustard II*a*, afforded an efficient synthesis of N-bis(2-iodoethyl)amine hydriodide (cf. 11), the modified procedure may be limited in scope since analogous reaction between hydrobromic acid and N-*t*-butyl diol I*b* led to morpholine III*b*.

Transformation of N-bis(2-bromoethyl)amine to, e.g., a substance believed to be 3,4-methylenedioxybenzamide, IV*a* and subsequent aluminum chloride – lithium aluminum hydride reduction of the amide gave an unexpected result. Elemental analytical results obtained for the hydrochloride derivative of the product were in poor agreement with theoretical values for benzylamine (V*a*). Repeating the sequence (II*a* → V) with several other benzoyl chlorides was similarly unrewarding. In each case, the bromine content was lower and the chlorine component higher than calculated. Under these circumstances partial exchange of bromine for chlorine present during the reduction step seemed plausible.[7] Introduction of chlorine during isolation of the tertiary amine (V*a*) with hydrogen chloride, or during preparation of the amide precursor, was considered less likely. When the synthesis was repeated employing 3,4,5-trimethoxybenzoyl chloride and an aluminum bromide – lithium aluminum hydride reagent for amide reduction, the problem was rapidly defined. One half of the crude reduction product was converted to a hydrochloride salt, while the second half was isolated as the hydrobromide salt. Microanalyses indicated that chlorine (7.92%) was present in the hydrobromide derivative. A corresponding increase of chlorine in the hydrochloride salt was also apparent. The results of these experiments clearly demonstrated that interchange of chlorine for bromine had occurred during formation of the amide precursor: a novel reaction. In one series of experiments employing 3,4-methylenedioxybenzoyl chloride and aluminum chloride –

[7]*For example, recently a halogen exchange reaction between aluminum chloride and n-propyl bromide has been observed (reference 12).*

Can. J. Chem. Downloaded from www.nrcresearchpress.com by 210.87.254.105 on 09/05/12
For personal use only.

lithium aluminum hydride for reduction of the amide intermediate, nearly one equivalent of chlorine was introduced. The product's elemental composition was consistent with a N-2-bromethyl-N-2′-chloroethyl-3,4-methylenedioxybenzylamine structure. However, the exact course or scope of this interesting halogen-exchange reaction was not pursued further in the present investigation.

Recently, Satchell (13) has predicted the possibility of acylating halogen in alkyl halides (i.e., $RX + R'COY \rightarrow R'COX + RY$) and suggested that "rather powerful acylating agents should be necessary". We have no knowledge of an experimentally verified example of this reaction other than the possibly related transformations noted here. Since attack by an acyl chloride on the bromine–carbon unit of N-bis(2-bromoethyl)-amine occurs under mild conditions, the new reaction may proceed via a transition state such as VI. Under similar conditions, halogen exchange was not noted when N-methyl-N-bis(2-bromoethyl)amine (II*b*) was treated with benzoyl chloride, and this observation lends support to the general reaction pathway suggested by intermediate VI. A more definitive explanation of the reaction will require further study.

As soon as displacement of bromine by the acyl chloride was substantiated, the reaction sequence was restudied employing an acyl bromide. For this purpose benzoyl bromide was prepared from benzoic acid, employing phosphorous tribromide, and the acid bromide was easily converted to N-bis(2-bromoethyl)benzamide (IV*b*). The oily, water-sensitive amide was readily characterized by rearrangement (9), in the presence of aqueous ethanol, to crystalline ester VII.[8] Reduction of amide IV*b* employing lithium aluminum hydride alone or combined with aluminum chloride or aluminum bromide afforded bromo nitrogen mustard V*b*. In each case, the amine was isolated as the crystalline hydrobromide derivative. From these experiments it was ascertained that addition of an aluminum halide was unnecessary.

With exception of amine V*b*, the N-bis(2-bromoethyl)amines summarized in Table I were prepared as follows. The carboxylic acid was treated with oxalyl bromide and the resulting acyl bromide was allowed to react with two equivalents of N-bis(2-bromoethyl)-amine in benzene solution. After removing precipitated amine II*a* hydrobromide, the amide was reduced using an ethereal solution of lithium aluminum hydride. The nitrogen mustard was isolated as the hydrobromide salt.

All of the benzylamines described in Table I were selected for preparation on the basis of interesting biological responses displayed by the corresponding chloro nitrogen mustards (9). For example, preliminary biological studies[9] have shown N-bis(2-chloroethyl)-3,5-dimethylbenzylamine hydrochloride[10] to be capable of markedly inhibiting growth of Walker 256 (subcutaneous) in random-bred albino rats and slowing development of Dunning leukemia (solid) in Fisher 344 rats. Useful results (ca. 98% inhibition) were obtained with the Walker system at a dose of 25 mg/kg (in saline solution given intraperitoneally) beginning on the first day of tumor transplant and continued each of 5 days (tumor growth measured on the tenth day). The same dose regimen was employed in the Dunning experiments. In this case a dose level of 10 mg/kg (in carboxymethylcellulose by the intraperitoneal route) resulted in life extension from 16 days (controls) to 30 days (test).

[8]*A reaction between benzoyl chloride and N-bis(2-bromoethyl)amine, under Schotten–Baumann conditions, was reported (reference 14) in 1934 to yield N-bis(2-bromoethyl)benzamide hydrobromide. The amide salt should now be reassigned the 2-(2′-bromoethylamino)ethyl benzoate hydrobromide (VII) structure.*

[9]*The biological evaluations are being performed under auspices of the Cancer Chemotherapy National Service Center, National Institutes of Health, U. S. Public Health Service.*

[10]*Corresponds to seventh from the top entry in Table I, reference 9(a).*

Can. J. Chem. Downloaded from www.nrcresearchpress.com by 210.87.254.105 on 09/05/12
For personal use only.

Can. J. Chem. Downloaded from www.nrcresearchpress.com by 210.87.254.105 on 09/05/12
For personal use only.

EXPERIMENTAL

Dry benzene was prepared as follows: the solvent was heated at reflux over sodium for 2 h, distilled and then stored over sodium. Glass apparatus used for preparation and subsequent reduction of the moisture-sensitive benzamides was dried at 120°. Ethyl ether (Fisher, A.R. grade) used in the reduction procedures was distilled from lithium aluminum hydride directly into the reaction flask. Solvent extracts were dried over magnesium sulphate.

Melting points are uncorrected and were observed using open Kimble glass capillaries in a silicone oil bath. Elemental microanalyses were performed in the laboratories of Dr. A. Bernhardt, Max Planck Institute, Mülheim, Germany, and Drs. Weiler and Strauss, Oxford, England. Dr. R. A. Hill of these laboratories recorded the infrared data. The infrared spectrum of each pure substance was consistent with the assigned structure.

N-Bis(2-Bromoethyl)amine (IIa) Hydrobromide

The following procedure is a modification of one reported by Bobranski and colleagues (3(*c*)). Commercial 2,2′-iminodiethanol (210 g) was added slowly with cooling to 48% hydrobromic acid (950 ml) contained in a 2-l flask equipped with a 50-cm Vigreaux column. Water was then removed by azeotropic distillation until the distillate temperature rose to approximately 125°. A total of 500 ml of distillate was collected during the 7.5-h heating period. Removal (*in vacuo*, steam bath) of the remaining hydrobromic acid yielded an orange oily residue which crystallized upon cooling. Recrystallizing the crude product from ethanol – ethyl ether gave colorless needles; yield, 322 g (52%), m.p. 199–201°. The reported (3(*c*)) melting point is 199–200°.

Morpholine (IIIa) Hydrobromide

The preceding experiment was repeated employing a reduced volume (670 ml) of 48% hydrobromic acid. In this case, the reaction mixture was heated during 12 h while collecting 590 ml of distillate. The remaining reaction mixture was diluted with methanol, treated with Norit-A, filtered and cooled. The colorless crystals which separated weighed 165 g (49%) and melted at 203–206°. Diluting the mother liquor with ethyl ether led to a second crop weighing 131 g (39%) and melting at 200–201°. Both products were identical[11] with an authentic sample.

N-Bis(2-iodoethyl)amine Hydriodide

A mixture of 2,2′-iminodiethanol (25.0 g) and 47% hydriodic acid (350 ml) was allowed to react as illustrated for preparation of N-bis(2-bromoethyl)amine hydrobromide. After collecting 200 ml of distillate during an 8-h period, the reaction mixture was cooled. The crystalline hydriodide which quickly separated as long colorless needles was collected and washed with ethyl ether; yield, 106 g (97%), m.p. 173–176°. Five recrystallizations from 95% ethanol gave rectangular crystals melting at 183–184°. Calc. for $C_4H_{10}I_3N$: C, 10.61; H, 2.23; I, 84.07; N, 3.09. Found: C, 10.89; H, 2.41; I, 84.00; N, 2.65%.

Upon exposure to light, the iodo nitrogen mustard hydriodide rapidly became light-yellow and subsequently changed to a purple color reminiscent of iodine.

N-t-Butyl-morpholine (IIIb) Hydrobromide

Reaction between N-*t*-butyl-N-bis(2-hydroxyethyl)amine (10.0 g, from Rohm and Haas Co.) and 48% hydrobromic acid (200 ml) was allowed to proceed as described for preparation of N-bis(2-bromoethyl)amine hydrobromide. Recrystallizing the crude hydrobromide from methanol – ethyl ether led to 10.5 g (76%) of colorless crystals decomposing at 253°. Two recrystallizations from the same solvent provided an analytical sample, d.p. 265°. Calc. for $C_8H_{18}BrNO$: C, 42.86; H, 8.09; Br, 35.65; N, 6.25. Found: C, 42.81; H, 8.01; Br, 35.65; N, 6.13%.

Reaction Between N-bis(2-bromoethyl)amine and 3,4,5-Trimethoxybenzoyl Chloride

In a typical experiment, N-bis(2-bromoethyl)amine hydrobromide (78.0 g) in cold water (100 ml) was treated with a cold solution of 20% sodium hydroxide (100 ml). The oily amine[12] which separated was rapidly added to benzene and the remaining aqueous solution was extracted with benzene (2 × 100 ml).

The amine solution was stirred and treated with 3,4,5-trimethoxybenzoyl chlodide (23.1 g, reference 9(*b*)) in dry benzene (100 ml). Addition of the acid chloride was performed over 0.5 h. After a 2-h period at reflux the mixture was cooled and filtered (22.5 g of hydrohalide salt was collected). Concentrating the filtrate *in vacuo* yielded 37.3 g of an oily amide. Several attempts to crystallize the amide were unsuccessful; therefore, the crude substance was used in the following reduction reaction.

A 6.5-g (0.015 mole) sample of the amide in dry benzene (100 ml) was added over a 0.5-h period to a mixture of lithium aluminum hydride (0.35 g, 0.01 mole) and aluminum bromide (4.0 g, 0.015 mole) in

[11]*Identity was established by mixture melting point determination and infrared spectral comparison (potassium bromide).*

[12]*In another experiment, approximately 1 ml of the oily amine was isolated and added to a glass container exposed to the atmosphere. After ca. 1 min a vigorous exothermic reaction ensued. Almost immediately the amine was converted to a black residue and gaseous products.*

diethyl ether (150 ml). Stirring at room temperature was continued for 2 h. Water was then cautiously added dropwise until solid and clear liquid phases were obtained. Following filtration, one-half of the dry filtrate was treated with ethereal hydrogen chloride. The hydrochloride derivative separated as a colorless granular solid; yield, 1.9 g, m.p. 168–172°. Three recrystallizations from methanol – ethyl ether yielded colorless needles melting at 172–173°. Calc. for $C_{14}H_{22}Br_2ClNO_3$: Br, 35.71; Cl, 7.92. Found: Br, 23.13; Cl, 14.92%.

The second half of the amine filtrate was treated with ethereal hydrogen bromide. The resulting hydrobromide derivative weighed 2.3 g and melted at 165–168°. Following three recrystallizations from methanol – ethyl ether, colorless needles melting at 170–173° were obtained. Calc. for $C_{14}H_{22}Br_3NO_3$: Br, 48.72; Cl, 0.00. Found: Br, 36.49; Cl, 7.09%.

Reaction Between N-bis(2-bromoethyl)amine and 3,4-Methylenedioxybenzoyl Chloride

Reaction between piperonyl chloride (16.0 g, reference 9(*b*)) and the amine corresponding to 62.4 g of N-bis(2-bromoethyl)amine hydrobromide was performed as described in the preceding experiment. The resulting amide weighed 30.5 g. A 10.3-g specimen of the amide was reduced employing an aluminum chloride (3.6 g) – lithium aluminum hydride (1.0 g) procedure as illustrated (9(*a*)) in a prior study. The crude product was isolated as a hydrochloride derivative which weighed 5.2 g and melted at 158–161°. Five recrystallizations from methanol – ethyl ether led to a sample of colorless needles melting at 162.5–164°. Calc. for $C_{12}H_{26}BrCl_2NO_2$: C, 40.38; H, 4.52; Br, 22.38; N, 3.92. Found: C, 40.36; H, 4.23; Br, 21.90 to 23.80; N, 3.83%.

N-Methyl-N-bis(2-bromoethyl)amine (IIb) Hydrobromide

A solution composed of 37% formaldehyde (5 ml), 98% formic acid (2 ml) and N-bis(2-bromoethyl)amine hydrobromide (7.5 g) was heated at reflux for 2 h. The mixture was concentrated *in vacuo* to a colorless oil. After removing residual water by azeotropic distillation with benzene, the product crystallized; yield, 8.8 g (65%), m.p. 145–148°. Three recrystallizations from methanol – ethyl ether gave pure needles melting at 147–148°. Calc. for $C_5H_{12}Br_3N$: C, 18.43; H, 3.71; Br, 73.56; N, 4.30. Found: C, 18.65; H, 3.62; Br, 73.68; N, 3.90%.

Applying a similar procedure, Bobranski (3(*c*)) also obtained a hydrobromide melting at 147° but confirming elemental analytical data were not reported.

Treatment of N-Methyl-N-bis(2-bromoethyl)amine (IIb) with Benzoyl Chloride

A sample of amine II*b* hydrobromide (1.0 g) in water (50 ml) was treated with 20 ml of 6 *N* sodium hydroxide solution. The liberated amine was extracted with benzene (2 × 50 ml) and the combined extract was dried. A solution of benzoyl chloride (0.4 g) in benzene (50 ml) was added to the amine solution during 0.25 h. No apparent reaction occurred during a subsequent 2-h period at reflux. Treating the reaction mixture with ethereal hydrogen bromide led to 0.83 g (83%) of colorless solid, m.p. 141–143°. Three recrystallizations from methanol – ethyl ether afforded a specimen of N-methyl-N-bis(2-bromoethyl)amine (II*b*) hydrobromide melting at 145–147°. Calc. for $C_5H_{12}Br_3N$: Br, 73.56; Cl, 0.00. Found: Br, 73.80; Cl, 0.22%.

N-Bis(2-bromoethyl)benzamide (IVb)

The free amine (see above) corresponding to 63.0 g of N-bis(2-bromoethyl)amine hydrobromide in 300 ml of dry benzene was treated dropwise (0.5 h) with a benzene (100 ml) solution of benzoyl bromide (15.8 g, b.p. 218°) prepared (15) from benzoic acid and phosphorous tribromide. Before collecting regenerated amine II*a* hydrobromide (26.1 g, 97%), stirring was continued 2 h at room temperature. Removal of solvent *in vacuo* led to the colorless oily amide (28.3 g). The amide exhibited the following infrared absorption bands: ν_{max}^{neat} 3100, 1670, 1490–1420 (broad), 1295, and 1125 cm^{-1} but several attempts to crystallize this substance were unsuccessful. Consequently, the oily amide was employed without further purification in subsequent experiments.

2-(2′-Bromoethylamino)ethyl Benzoate Hydrobromide (VII)

A solution of N-bis(2-bromoethyl)benzamide (IV*b*, 2.8 g) in 90% ethyl alcohol (50 ml) was heated (steam bath) 2 h. Following concentration *in vacuo* to ca. 5 ml, dilution with ether, and cooling, the ester hydrobromide (VII) was obtained as colorless needles; yield, 2.6 g (93%), m.p. 133–135°. Three recrystallizations from the same solvent afforded an analytical sample melting at 137–139°; ν_{max}^{KBr} 2975, 2900, 2800, 2700, 1720, 1548, 1450, 1125, and 710 cm^{-1}. Calc. for $C_{11}H_{15}Br_2NO_2$: C, 37.42; H, 4.28; Br, 45.27; N, 3.97. Found: C, 37.54; H, 4.43; Br, 45.39; N, 3.87%.

The substance reported by Peacock and Dutta (14) to be N-bis(2-bromoethyl)benzamide hydrochloride, m.p. 135°, most probably corresponds to hydrobromide VII.

N-Bis(2-bromoethyl)benzylamine (Vb) Hydrobromide

Procedure A

A solution of N-bis(2-bromoethyl)benzamide (IV*b*, 6.7 g, 0.02 mole) in benzene (75 ml) was added over a 0.5-h period to a suspension of lithium aluminum hydride (0.8 g, 0.02 mole) in diethyl ether (100 ml). Before eliminating excess lithium aluminum hydride by careful addition of water (until a clear liquid phase

Can. J. Chem. Downloaded from www.nrcresearchpress.com by 210.87.254.105 on 09/05/12
For personal use only.

appeared), stirring was continued 1.5 h at room temperature. The solution was filtered, dried, and treated with hydrogen bromide. Amine V*b* hydrobromide was obtained as colorless crystals; yield, 5.9 g (64%), m.p. 175–178°. Three recrystallizations from methanol – ethyl ether afforded an analytical sample as colorless needles melting at 190–192.5°; ν_{max}^{KBr} 2850, 2500, 1450, 1425, 1370, 1242, 1005, 950, 930, 758, and 700 cm^{-1}. Calc. for $C_{11}H_{16}Br_3N$: C, 32.86; H, 4.01; Br, 59.64. Found: C, 33.13; H, 3.96; Br, 60.17%.

Cerkovnikov (5(*b*)) has reported a melting point of 187–188° for benzylamine V*b* hydrobromide.

Procedure B

The reduction reaction described in Procedure A was repeated with the following modification: Aluminum chloride (2.8 g, 0.02 mole) in ethyl ether (100 ml) was employed as reported earlier (9(*a*)). The crude amine hydrobromide weighed 3.0 g (37%) and melted at 179–183°. The analytical sample, m.p. 190–192°, was obtained as colorless needles following three recrystallizations from methanol – ethyl ether. Found for $C_{11}H_{16}Br_3N$: C, 33.05; H, 3.93; Br, 60.07%.

Procedure C

The preceding experiment (Procedure B) was repeated using aluminum bromide (5.6 g, 0.02 mole) in place of aluminum chloride. The crude hydrobromide derivative of amine V*b* weighed 1.5 g (19%) and melted at 174–178° Recrystallization (3 times) from methanol – ethyl ether raised the melting point to 189–191°. Found for $C_{11}H_{16}Br_3N$: C, 33.17; H, 4.07; Br, 60.02; N, 3.38 (calc. N, 3.49%).

The specimens of N-bis(2-bromoethyl)benzylamine (V*b*) hydrobromide prepared by Procedures A–C were identical.[11]

General Procedure for Preparation of the N-Bis(2-bromoethyl)amines Summarized in Table I

The amine hydrobromides, summarized in Table I, were prepared in good overall yields as illustrated below for synthesis of N-bis(2-bromoethyl)-3,4-methylenedioxybenzylamine (V*a*) hydrobromide. The acid bromide precursors were prepared (16) from the corresponding carboxylic acids and oxalyl bromide. Neither acyl bromides nor their amide derivatives required extensive purification and both were employed soon after formation.

N-Bis(2-bromoethyl)-3,4-methylenedioxybenzylamine (Va) Hydrobromide

A mixture of oxalyl bromide (6 g), prepared (17) from oxalyl chloride and hydrogen bromide, and piperonylic acid (2.5 g) was heated at reflux for 2 h. Removal of excess oxalyl bromide *in vacuo* yielded 3,4-methylenedioxybenzoyl bromide as a pale-yellow solid.

A solution of the acyl bromide in benzene (50 ml) was added dropwise (0.5 h) to a benzene (150 ml) solution of N-bis(2-bromoethyl)amine corresponding to 12.6 g of the bromo nitrogen mustard hydrobromide. Before collecting the regenerated nitrogen mustard hydrobromide which separated, the reaction mixture was stirred at room temperature for 2 h. The benzene filtrate was added over a 0.5-h period to a suspension of lithium aluminum hydride (0.57 g) in diethyl ether (150 ml). Stirring was continued for 2 h at room temperature and then excess lithium aluminum hydride was destroyed by cautious dropwise addition of water until distinct solid and clear liquid phases appeared. The solution was then successively filtered, dried, and dihited with ethereal hydrogen bromide. The colorless crystalline hydrobromide weighed 5.5 g (84%) and melted at 159–160°. Three recrystallizations from methanol – ethyl ether led to an analytical sample in the form of needles (see Table I): ν_{max}^{KBr} 2980, 2625, 2575, 1505, 1488, 1448 (shoulder at 1430), 1385, 1265–1245 (broad), 1105, 1045, 945, and 930 cm^{-1}.

REFERENCES

1. V. Prelog, G. Drîza, and V. Hanousek. Collection Czech. Chem. Commun. **3**, 578 (1931).
2. S. Gabriel and G. Eschenback. Ber. **30**, 810 (1897).
3. (*a*) F. Mann. J. Chem. Soc. 461 (1934). (*b*) Fr. Patent No. 800,369, July 3, 1936; Chem. Abstr. **30**, 8241 (1936). (*c*) B. Bobranski, T. Jakobiec, and D. Prelicz. Acta Polon. Pharm. **12**, 195 (1955); Chem. Abstr. **50**, 11, 938 (1956). (*d*) A. Aronski. Polska Akad. Nauk Zeszyty Probl. Nauki Polskiej. **9**, 137 (1956); Chem. Abstr. **53**, 6, 122 (1959).
4. R. P. Bratzel, R. B. Ross, T. H. Goodridge, W. T. Huntress, M. T. Flather, and D. E. Johnson. Cancer Chemotherapy Rep. **26**, 1 (1963).
5. (*a*) V. Prelog and V. Stepan. Collection Czech. Chem. Commun. **7**, 93 (1935). W. S. Gump and E. J. Nikawitz. U.S. Patent No. 2,504,977 (April 25, 1950); Chem. Abstr. **44**, 6880 (1951). (*b*) E. Cerkovnikov and P. Stern. Arkiv Kemi, **18**, 12 (1946); Chem. Abstr. **42**, 1938 (1948). (*c*) A. E. Kretov and G. V. Tikhonova. Zh. Obshch. Kimh. **28**, 2808 (1958); Chem. Abstr. **53**, 9115 (1959).
6. J. L. Everett and W. C. J. Ross. J. Chem. Soc. 1972 (1949). W. C. J. Ross. J. Chem. Soc. 183 (1949). J. F. Allen and N. B. Chapman. J. Chem. Soc. 1482 (1960). N. B. Chapman and D. J. Triggle. J. Chem. Soc. 4835 (1963).
7. E. Wilson and M. Tishler. J. Am. Chem. Soc. **73**, 3635 (1951).
8. M. H. Benn, L. N. Owen, and A. M. Creighton. J. Chem. Soc. 2800 (1958). R. Sato. Tohoku Igaku Zassi. **60**, 866 (1959). K. Sawatari. Chem. Pharm. Bull. Toyko, **10**, 390 (1962).
9. (*a*) G. R. Pettit, D. S. Blonda, and E. Harrington. Can. J. Chem. **41**, 2962 (1963). (*b*) G. R. Pettit, M. F. Baumann, and K. N. Rangammal. J. Med. Pharm. Chem. **5**, 800 (1962).
10. B. L. Hampton and C. B. Pollard. J. Am. Chem. Soc. **58**, 2338 (1936).
11. O. M. Friedmann and A. M. Seligman. J. Am. Chem. Soc. **76**, 658 (1954).

Can. J. Chem. Downloaded from www.nrcresearchpress.com by 210.87.254.105 on 09/05/12
For personal use only.

12. P. J. TROTTER. J. Org. Chem. **28**, 2093 (1963).
13. D. P. N. SATCHELL. Quart. Rev. London, **17**, 160 (1963).
14. D. H. PEACOCK and U. C. DUTTA. J. Chem. Soc. 1303 (1934).
15. L. CLAISEN. Ber. **14**, 2473 (1881).
16. R. ADAMS and L. H. ULICH. J. Am. Chem. Soc. **42**, 599 (1920).
17. H. STAUNDINGER and E. ANTHES. Ber. **46**, 1427 (1913). N. O. V. SONNTAG. Chem. Rev. **52**, 237 (1953).

Can. J. Chem. Downloaded from www.nrcresearchpress.com by 210.87.254.105 on 09/05/12
For personal use only.

Can. J. Chem. Downloaded from www.nrcresearchpress.com by 210.87.254.105 on 09/05/12
For personal use only.

THE ACTIVATION PROCESS IN SOLVOLYSIS[1,2]

R. E. ROBERTSON
Division of Pure Chemistry, National Research Council, Ottawa, Canada

Received December 6, 1963

ABSTRACT

The structural nature of water is a major factor in determining the solvent isotope effect and the apparent heat capacity of activation for solvolysis. The consequences of this assumption are examined for the S_N2 mechanism in terms of solvation changes at the transition state and the probable make-up of the activation energy.

Our studies of solvolysis (1) have forced us to question certain widely held hypotheses concerning the solvation of the transition state. Most of the current working hypotheses relating to this problem may be traced to the papers in which Hughes and Ingold (2, 3) discussed the solvation differences between the S_N1–S_N2 mechanisms and a series of related papers (4, 5)* in which Polanyi and his students attempted to analyze the components of the activation energy in such reactions. Briefly the latter treated E_{act} (for S_N1) reactions as the residual, Q, determined by the equation

$$[1] \qquad Q = D + I - E - S^+ - S^-$$

where D = heat of dissociation of C—Hal bond, E = electron affinity of Hal atom, I = ionization potential of R, S^+ = heat of solvation of R^+, S^- = heat of solvation of Hal ion. Robertson, Heppolette, and Scott carried out similar calculations for the S_N2 hydrolysis of the methyl halides and showed that the residual, Q, corresponded to the derived experimental activation energy, provided charge development, α, is about 0.8 e (8). While the cumulation of uncertainties in the terms of eq. 1 vitiated the practical value of such a calculation, the principle seemed to be generally accepted.

Since these reactions are exothermic, it will be obvious that there must always be some particular value of α which satisfies this type of calculation, hence apparent agreement cannot be persuasive. If such a calculation approximated reality, it would seem a reasonable corollary to expect evidence of solvation differences characteristic of the product ions. Such anticipated differences are not observed.

For this and other reasons, we have concluded that for the solvolysis of primary and secondary halides and sulphonates in water, exothermic solvation† of the developing anions is only beginning at the transition state. This unfamiliar concept is the logical consequence of the Laughton–Robertson hypothesis for the kinetic solvent isotope effect (9, 10, 11) and the related interpretation of the large negative heat capacity changes which characterize the ionogenic reactions studied (1). The experimental background is outlined in the following section.

DISCUSSION OF EXPERIMENTAL BACKGROUND

Although the kinetic solvent isotope effect (k_{D_2O}/k_{H_2O}) is not a sharp tool for exploring fine differences in solvent reorganization associated with hydrolysis, we have found

[1]*Presented in part at the International Symposium on Solvation, Calgary, Alberta, August 1963.*
[2]*Issued as National Research Council No. 7910.*
**See also Franklin (6) and Streitwieser (7).*
†*Where ion–water interaction exceeds water–water interaction.*

Can. J. Chem. Downloaded from www.nrcresearchpress.com by 210.87.254.105 on 09/05/12
For personal use only.

unmistakable indications of groupings of effects related to the structure of the solute. Thus Laughton and Robertson have shown that the k_{D_2O}/k_{H_2O} ratio for simple primary and secondary sulphonates was 0.92 ± 0.03, the difference between a methanesulphonate and a toluenesulphonate being about 0.02. The ratio for the corresponding halides was 0.80 ± 0.05. The systematic difference between the sulphonates and the halides was attributed to interaction of the sulphonic oxygens with the initial state solvation shell—a conclusion supported by the recent calorimetric studies of Arnett (12). Laughton and Robertson concluded that the major factor determining such solvent isotope effects was the difference in the structural stability of the respective initial state solvation shells compared to the smaller differences in the disrupted state. This assumption and the recognition that part of the activation energy is the work required to break down the initial state solvation shell are the major premises which distinguish the present treatment. Because the assumption of an initial state solvation shell appears to create a semantic stumbling block for some, it is desirable to emphasize that this assumption in no way excludes the existence of a dynamic equilibrium between the solvent shell and the bulk solvent. Our kinetic measurements give only an indication of the time independent difference between the initial and transition states. For convenience we treat this difference as static.

The assumption that the initial state solvation shell has some degree of structural stability follows from our knowledge of the nature of aqueous solutions of weakly polar molecules. Evidence for enhanced initial state water–water interaction due to the presence of the weakly polar solute is drawn from the similarity between the solvation parameters for dissolved gases and the formation of gas hydrates (13); from the negative ΔH and ΔS for solvation but the large positive ΔC_p which characterizes gas–liquid equilibria (14); from the steeper temperature dependence of the k_{D_2O}/k_{H_2O} ratio for the hydrolysis of isopropyl bromide compared to that for the relative fluidity (15); and from the larger partial molar volume of MeBr in such solutions in spite of the existence of empty holes in water structure (16, 17). The reduced temperature dependence for the k_{D_2O}/k_{H_2O} ratio for the sulphonates compared to the halides, as well as the value of the ratio itself, are consistent with the enhanced solute–solvent interaction of the former in the initial state. Limited data indicate that sulphates and phosphates would give values of k_{D_2O}/k_{H_2O} similar to those for sulphonates (10).

The above interpretation has been challenged by Swain and Thornton (17), who would attribute this solvent isotope effect largely to differences in the degree of solvent–ion interaction in the transition state, i.e. a hypothesis consistent with the traditional views concerning solvation of the transition state to which reference has been made above. In principle this is possible but it is snagged by at least one important experimental fact: i.e. the fluorides show similar k_{D_2O}/k_{H_2O} ratios to the remaining halides (Table I), whereas

TABLE I

Comparison of kinetic and ionic coefficients

Halide	k_{D_2O}/k_{H_2O}*	$\gamma_{H_2O}/\gamma_{D_2O}$†
F^-	0.82	1.20
Cl^-	0.77	−0.51
Br^-	0.80	−0.59
I^-	0.81	−0.68

*Typical values for k_{D_2O}/k_{H_2O} (9).
†Ratio of activity coefficients $\Delta F_s = F_s(H_2O) - F_s(D_2O) = R \ln \gamma_{H_2O}/\gamma_{D_2O}$, Table V, ref. 18 based on calorimetric investigation of Lange and Martin (20).

the arguments of Swain and Bader (18) and of Swain and Thornton would lead to a value of $k_{D_2O}/k_{H_2O} > 1$. Another more obvious weakness in the latter analysis is the neglect of the evidence for difference in structural stability between D_2O and H_2O in the absence of a solute. The significance of this omission is made apparent by the fact that when the initial state structure is broken down by the addition of a miscible solvent, the solvent isotope effect is greatly reduced (19).

The heat capacity of activation ($\Delta C_p^{\neq}$) is inherently a more sensitive probe of solvation changes than the solvent isotope effect in that it reflects not only the degree of reorganization but also is more sensitive to the number of molecules involved. In spite of this, there is the same grouping of sulphonates and halide values (Table II) (for the primary and

TABLE II

A comparison of $\Delta C_p^{\neq}$ values for solvolysis involving displacement from primary and secondary carbon centers

	Ions				
Alkyl group	Chloride	Bromide	Iodide	Benzene-sulphonate	Methane-sulphonate
Methyl	52.0*	46.5*	56.6*	33.4†	37.6†
Isopropyl	38.5†	56.4†	59.0†	34.0‡	34.5‡

*Ref. 22.
†Ref. 8.
‡These values supersede those given in ref. 8.

secondary sulphonates -35 ± 5 cal/mol deg. and for the halides -55 ± 8 cal/mol deg.) already noted in the k_{D_2O}/k_{H_2O} ratios. The narrow range of values for $\Delta C_p^{\neq}$ found for the primary and secondary halides or sulphonates suggests that approximately the same number of water molecules are involved in the reorganization accompanying activation and that these have approximately the same initial and transition state relationships. The differences in $\Delta C_p^{\neq}$ for displacement of the same ion from primary and secondary centers apparent in Table II are not significant. There is no apparent correlation with expected differences in the degree of nucleophilic interaction. This may indicate that such interaction is small, or more likely that it appears to have a small effect on $\Delta C_p^{\neq}$. Certainly the introduction of a hydrogen bonding group close to the seat of reaction will show a much larger effect, presumably due to a modification in the initial state solvation shell (21). Similar evidence is seen in the large reduction in $\Delta C_p^{\neq}$ for those systems where sufficient miscible solvent is added to break down the initial state solvation shell (22). The counterpart with respect to the k_{D_2O}/k_{H_2O} value has already been noted (19).

These well-established characteristics for solvolytic reactions of primary and secondary halides and sulphonates in water support the conclusion that a significant component of the activation energy for the hydrolysis in water of alkyl halides and similar compounds is the work, $F_s^{\neq}$, required to break down the initial state solvation shell. The differences in $\Delta F_s^{\neq}$ between H_2O and D_2O already noted for the bulk solvents (23, 24) provide a natural basis for the observed rate difference in the two solvents and for the temperature dependence of this ratio. The second derivative of $\Delta F_s^{\neq}$ with respect to temperature can account for an important part of $\Delta C_p^{\neq}$. It is comparable in sign but larger in magnitude than the temperature dependence of the activation energy for such physical processes as viscosity (24), or time of dielectric relaxation (25), physical processes which necessarily involve the breakdown of water structure. Recent calorimetric studies by Arnett (26) support this interpretation. The familiar changes which are found in $\Delta H^{\neq}$ and $\Delta S^{\neq}$ for

Can. J. Chem. Downloaded from www.nrcresearchpress.com by 210.87.254.105 on 09/05/12
For personal use only.

solvolysis in a series of alcohol–water, and similar mixtures at the high-water end of the series, 26–29 may be regarded as another demonstration of changes in the work to organize the initial state solvation shell $\Delta F_s^{\neq}$. This reduction in $\Delta F_s^{\neq}$, as reflected in $\Delta C_p^{\neq}$ in ethanol–water solutions, lends further support to our hypothesis. It should be noted, however, that $\Delta F_s^{\neq}$ forms but part of the total observed free energy change on activation.

Charge Development at the Transition State

Neither the kinetic solvent isotope effect nor the heat capacity of activation provides a measure of the degree of charge development at the transition state, though each of these phenomena is related to the effect which such charge development has on the initial state solvation shell. The common basis for these diverse effects may be summarized in the composite equation

$$[2]\quad \left\{\text{Water–water interaction}\right\} \begin{matrix} > \\ = \\ < \end{matrix} \left\{\text{water–solute interaction}\right\} \begin{matrix} (a)\ \text{initial state} \\ (b)\ \text{transition state} \\ (c)\ \text{final state} \end{matrix}$$

This statement implies that in the activation process for solvolysis by an S_N2 mechanism, at some point along the reaction co-ordinate the inequality (*a*), characteristic of the initial state, disappears (*b*), then reverses (*c*). As a working hypothesis we have arbitrarily chosen the point of equality as the transition state. Up to the degree of charge development sufficient to satisfy this condition (*b*), work must be supplied to activate the solute and to break down the initial state solvation shell. Charge development beyond this level leads to the familiar complementary making and breaking of bonds without requiring any further increase in free energy but with increasing charge separation to the limiting value.

The Activation Energy in Solvolysis

Equation 2 implies that the activation energy is not a small residual from differences between large heats of ionization and heats of solvation reflecting a position of balance at some 80–100% charge development with a corresponding degree of solvation of both primary ions (8). Rather, E_{act} may be expressed as the sum of terms formally indicated by the following equation.

$$[3]\quad E_{act} = \begin{matrix}\text{Energy to achieve charge} \\ \text{separation to satisfy the} \\ \text{condition of eq. 2}\end{matrix} + \begin{matrix}\text{Energy to break down} \\ \text{the initial state} \\ \text{solvation shell}\end{matrix}$$

Critical charge development for the displacement of a particular anion, X^-, may be achieved by a number of paths depending on the structure of the solute R—X. Where thermal activation is sufficient to achieve critical charge development, S_N1 characteristics are observed. For the solutes under consideration here some degree of nucleophilic interaction is required to achieve this condition.

The first term on the RHS of eq. 3 is complex and probably involves in some measure those factors summarized by Caldin (30) for bimolecular reactions in solution. Some degree of cancellation is necessarily involved in such interaction, but until exothermic solvation is established between the developing anion and the solvent, such interaction will not predicate reaction.

The second term is normally neglected. The evidence of k_{D_2O}/k_{H_2O} and $\Delta C_p^{\neq}$ according to our interpretation, and that arising from the recent work of Arnett (26), shows that for solvolysis in water $\Delta H_s^{\neq}$ is a significant component in $\Delta H^{\neq}$. It is probably largest for reactions in water and tends to assume a constant value in mixed solvents where solvent structure in the initial state is of less importance.

Can. J. Chem. Downloaded from www.nrcresearchpress.com by 210.87.254.105 on 09/05/12
For personal use only.

REFERENCES

1. R. E. ROBERTSON. Suomen Kemistilehti, A, **33**, 63 (1960).
2. E. D. HUGHES. Trans. Faraday Soc. **37**, 603 (1941).
3. SIR CHRISTOPHER INGOLD. Structure and mechanism in organic chemistry. Cornell University Press, Ithaca. 1953. Chap. VII.
4. M. POLANYI and R. OGG. Trans. Faraday Soc. **31**, 604 (1935).
5. A. G. EVANS. The reactions of organic halides in solution. Manchester Press, Manchester. 1946.
6. J. L. FRANKLIN. Trans. Faraday Soc. **48**, 443 (1952).
7. A. STREITWIESER, JR. Chem. Rev. **56**, 571 (1956).
8. R. E. ROBERTSON, R. L. HEPPOLETTE, and J. M. W. SCOTT. Can. J. Chem. **37**, 803 (1959).
9. P. M. LAUGHTON and R. E. ROBERTSON. Can. J. Chem. **34**, 1714 (1956).
10. R. E. ROBERTSON and P. M. LAUGHTON. Can. J. Chem. **35**, 1319 (1957).
11. P. M. LAUGHTON and R. E. ROBERTSON. Can. J. Chem. **37**, 1491 (1959).
12. E. McC. ARNETT. Private communication.
13. D. D. ELEY. Trans. Faraday Soc. **35**, 128 (1939).
14. H. S. FRANK and M. EVANS. J. Chem. Phys. **13**, 507 (1945).
15. R. L. HEPPOLETTE and R. E. ROBERTSON. J. Am. Chem. Soc. **83**, 1834 (1961).
16. D. N. GLEW. J. Phys. Chem. **66**, 605 (1962).
17. C. G. SWAIN and E. THORNTON. J. Am. Chem. Soc. **84**, 822 (1962).
18. C. G. SWAIN and R. F. W. BADER. Tetrahedron, **10**, 182 (1960).
19. W. G. CRAIG, L. HAKKA, P. M. LAUGHTON, and R. E. ROBERTSON. Can. J. Chem. **41**, 2118 (1963).
20. E. LANGE and W. MARTIN. Z. Physik. Chem. A, **180**, 233 (1937).
21. M. J. B. BLANDAMER and R. E. ROBERTSON. Unpublished results.
22. G. KOHNSTAM. Discussions Chem. Soc. **16**, 179 (1962).
23. R. F. HARDAY and R. L. COTTINGTON. J. Res. Natl. Bur. Std. **42**, 573 (1949).
24. C. H. COLLIE, J. B. HASTED, and D. M. RITSON. Proc. Phys. Soc. **60**, 145 (1948).
25. B. E. CONWAY. Can. J. Chem. **37**, 613 (1959).
26. E. McC. ARNETT, P. McC. DUGGLEBY, and J. J. BURKE. J. Am. Chem. Soc. **85**, 1350 (1963).
27. S. WINSTEIN and A. H. FAINBERG. J. Am. Chem. Soc. **79**, 5937 (1957).
28. J. B. HYNE. J. Am. Chem. Soc. **82**, 5129 (1960).
29. E. TOMMILA, M. TIILIKAINEN, and A. VOIPOI. Ann. Acad. Sci. Fennicae, A, **II**, No. 65 (1955).
30. E. F. CALDIN. J. Chem. Soc. 3345 (1959).

Can. J. Chem. Downloaded from www.nrcresearchpress.com by 210.87.254.105 on 09/05/12
For personal use only.

ULTRASONIC ABSORPTION IN CRITICAL BINARY LIQUID SYSTEMS. II

PEETER KRUUS
Department of Chemistry, University of Toronto, Toronto, Ontario
Received February 26, 1964

ABSTRACT

The results of ultrasonic absorption measurements for the systems perfluoromethylcyclohexane – carbon tetrachloride and triethylamine–water are presented. A pulse reflection method was used for the measurements. Intermolecular correlation lengths were calculated from the absorption data for these and two other systems. They are in reasonable agreement with lengths calculated from light scattering data. The absorption results also substantiate the suggestion that, in the critical solution region, the system may already be in two phases. However, these are not present in the form of two distinctly separated phases, but as regions in a type of emulsion.

INTRODUCTION

From the results of ultrasonic absorption measurements in the critical solution region, it is possible to calculate values of an intermolecular correlation length l (1) by using the theory of Fixman (2). Values of l can also be calculated from experimental light-scattering and heat-capacity results.

As both light-scattering (3) and heat-capacity (4) data are available for the system perfluoromethylcyclohexane – carbon tetrachloride, ultrasonic absorption measurements were carried out for this system. An attempt was also made to test the frequency dependence of Fixman's theory by comparing the theory with measurements for the system triethylamine–water.

In addition, some unexpected features in the composition and temperature dependence of the absorption in the system perfluoromethylcyclohexane – carbon tetrachloride were found; these can be explained using the physical picture of the critical solution region suggested by Hildebrand *et al.* (5).

EXPERIMENTAL

Apparatus

The apparatus and the measuring techniques were the same as those described previously (6).

Velocity measurements were made in addition to absorption measurements in some cases. A delayed trigger signal from the pulsed oscillator was sent into the oscilloscope, and the setting of the delay dial was varied to make the delayed trigger signal coincide with the start of the signal of the reflected ultrasonic pulses. The delay dial was calibrated with the velocity of ultrasound at 10 mc in water at 1497 ms^{-1} as reference.

Materials

Perfluoromethylcyclohexane – Carbon Tetrachloride

The perfluoromethylcyclohexane (C_7F_{14}), density 1.789 and purity estimated to be 98.4% from a gas chromatography trace, was obtained from the Imperial Smelting Co. The value of the pressure absorption coefficient divided by the square of the frequency, α/f^2, is $584 \cdot 10^{-17}$ $cm^{-1}s^2$ at 20 mc, 28 °C and $502 \cdot 10^{-17}$ at 60 mc, 20 °C. It is evident from the rather large decrease of α/f^2 with an increase in frequency that C_7F_{14} relaxes in this frequency region. It should be noted that the velocity of ultrasound in C_7F_{14} is the lowest to be found, about 580 ms^{-1}.

Merck analytical grade carbon tetrachloride was used as the other component. It has an α/f^2 of $553 \cdot 10^{-17}$ at 20 mc, 28 °C, compared to $546 \cdot 10^{-17}$ at 107 mc, 25 °C, from ref. 7.

Figure 1 shows a phase diagram (Zimm (3)) for the system. The experimental critical solution temperature is 28.0$_5$ °C compared with 28.3 °C (3) and 26.2 °C (4).

Triethylamine–Water

The second system, triethylamine–water, is an example of a system with a lower critical solution temperature. Ion-exchanged water and Merck "Lab" grade triethylamine were the components of this system.

Can. J. Chem. Downloaded from www.nrcresearchpress.com by 210.87.254.6 on 09/05/12
For personal use only.

The absorption data is as follows: (*a*) Water: $\alpha/f^2 = 24.5 \cdot 10^{-17}$ at 60 mc, 25 °C, compared with $21.2 \cdot 10^{-17}$ at 192 mc, 25 °C (7). Measurements at lower frequencies (8) are in better agreement, but are less precise. (*b*) Triethylamine: $576 \cdot 10^{-17}$ at 17 mc, 18 °C, compared with $410 \cdot 10^{-17}$ at 23 mc, 20 °C (9). When data from ref. 9 is extrapolated to 17 mc, 18 °C, the value of α/f^2 is about $580 \cdot 10^{-17}$.

Values of the critical solution temperature for this system are reported from 12.4 to 19.9 °C (10); the experimental critical solution temperature for the system investigated is 17.8 °C. A phase diagram (10) is shown in Fig. 4.

Results

The results of the measurements are shown in Figs. 1–5. When the precision of the absorption measurements is outside the range given by the size of the symbol indicating points on the graph, the possible range of values is shown by a vertical line, and the most probable value by the symbol.

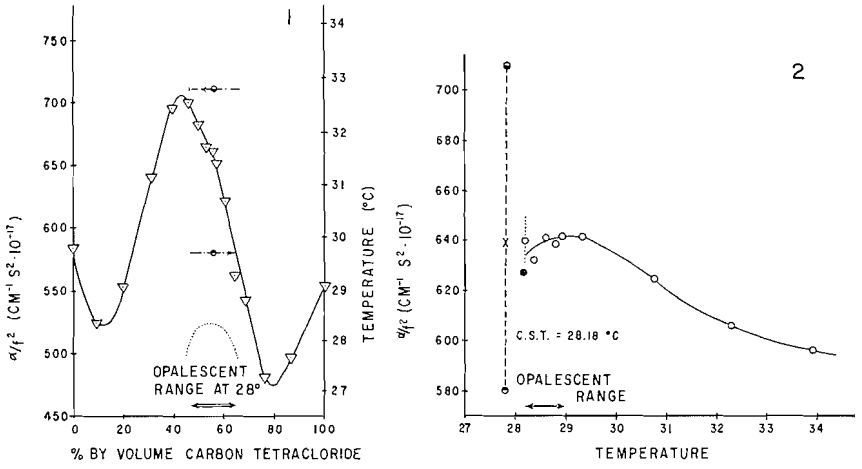

FIG. 1. Phase diagram and absorption in the system perfluoromethylcyclohexane–carbon tetrachloride: ▽ 19.6_7 mc, 28.3_9 °C; ◓ upper phase, 19.6_7 cm, 27.2_9 °C; ◒ lower phase; . . . phase diagram (Zimm (3)).

FIG. 2. Absorption in the system perfluoromethylcyclohexane – carbon tetrachloride: ○ 56.0% carbon tetrachloride, 19.6_7 mc; ● system below critical solution temperature, shaken between readings to prevent separation; ◓ upper phase; ◒ lower phase; × linearly interpolated value using phase–volume fraction data of Zimm (3).

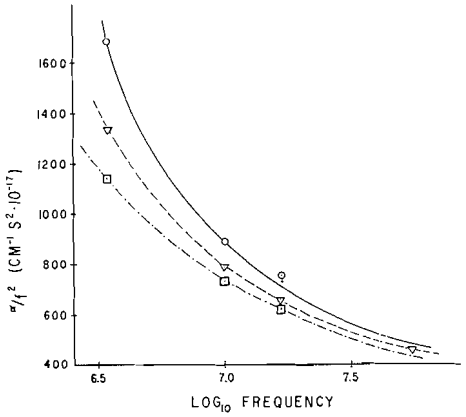

FIG. 3. Absorption in the system perfluoromethylcyclohexane – carbon tetrachloride: ○ 56% carbon tetrachloride, 28.3_7 °C; ▽ 56% carbon tetrachloride, 30.8_6 °C; □ 56% carbon tetrachloride, 33.9_3 °C.

DISCUSSION

The Critical Solution Region

Investigations of light-scattering (3, 11) and heat capacity (4) indicate that these quantities show an abnormally large increase as the critical solution point is approached.

Can. J. Chem. Downloaded from www.nrcresearchpress.com by 210.87.254.6 on 09/05/12
For personal use only.

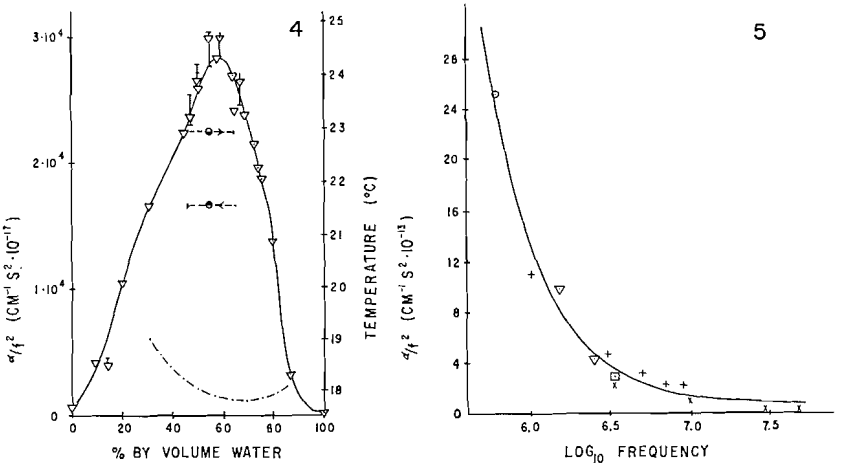

Fig. 4. Phase diagram and absorption in the system water–triethylamine: ▽ 17.0_6 °C, 3.37_7 mc; ◓ upper phase, 18.1_1 °C, 3.37_7 mc; ◒ lower phase; —·— phase diagram (Krichevski, Khasanova, and Linshits (10)).

Fig. 5. Absorption in the system water–triethylamine: ⊙ 17.1 °C, 47.2% water (Chynoweth and Schneider (15)); ▽ 17.1 °C, 69% water (Shimakawa (17)); + 17.1 °C, 59% water (Alfrey and Schneider (16)); × 17.1 °C, 47.2 or 69% water; ⊡ 17.1 °C, 55% water; ----- curve fitted from eq. 2.

When a centrifugal force is applied to a system (5), the critical solution temperature is changed because of hydrostatic and sedimentation effects. The critical solution temperature is here defined as the temperature at which the system first separates into two distinct phases.

The experimental results seem to indicate that the following physical picture of the critical solution region is reasonable.

In the extremely opalescent region, which occurs in some systems just before phase separation takes place, the system is in a form similar to an emulsion (5). It is made up of regions which contain the components in different proportions and are, thus, separated by composition gradients. As the critical solution temperature is approached, the regions become larger and the composition gradients steeper. Separation of the system into two distinct phases is caused by the action of gravity upon the regions of different density when Brownian motion can no longer keep these dispersed.

Related to this composition variation, there are probably also fluctuations (12) which occur inside the regions themselves. Near the critical solution point, these fluctuations can become very large. It is these fluctuations which correspond to the ordinary type of critical fluctuations in a one-component system near the critical point, and which give rise to the high ultrasonic absorption in the critical solution region.

This picture gives a reasonable explanation for all the experimentally observed phenomena. As the critical solution temperature is approached, light-scattering increases because of the critical fluctuations (11, 13), and also because of reflection from the composition gradients between the regions of different composition (5) close to the critical temperature. The heat capacity increases because of entropy changes associated with the inhomogeneities. Since the effective gravitational force is changed in a centrifugal field, it is to be expected that the observed critical solution temperature is also dependent on the centrifugal force.

Can. J. Chem. Downloaded from www.nrcresearchpress.com by 210.87.254.6 on 09/05/12
For personal use only.

Can. J. Chem. Downloaded from www.nrcresearchpress.com by 210.87.254.6 on 09/05/12
For personal use only.

Qualitative Discussion

Composition Dependence

Figure 1 shows the absorption at temperatures just above and just below the critical solution temperature. In the range of composition where the system is visibly opalescent at the higher temperature, the absorption varies about linearly with composition. When a line is drawn between the absorption–composition points at the lower temperature, the result is a good approximation to the absorption at the higher temperature.

This suggests that at the higher temperature, the system is already in two phases. But the phases are present in the form of regions which are too small and too similar in composition to fall into two completely separated phases. Instead, they remain in a dispersed form because of Brownian motion and absorb separately according to the proportion of the phase present in the total system. The ultrasonic absorption hence arises from effects present inside the phases themselves.

The absorption in the system triethylamine–water (Fig. 4) is much greater than in any of the systems which have an upper critical solution temperature. When a system has a lower critical solution temperature, it consequently has a large negative excess entropy. The large negative excess entropy in such a critical binary system is thought to arise from the large critical fluctuations (13). Thus it seems reasonable that the ultrasonic absorption is, at least to a large degree, dependent upon the critical fluctuations, as postulated by Fixman (2).

Because of the high absorption, the measurements are less precise in this second system. This, together with the lack of observed opalescence, makes it impossible to draw any conclusions regarding the physical structure of the system.

Temperature Dependence

Figure 2 shows that in the visibly opalescent temperature range, the absorption decreases slightly as the critical solution temperature is approached. The value just before phase separation is close to the value obtained in an unstable system in which a meniscus is forming. It is also approximately the same as the value obtained by interpolating coefficients of the two separated phases at a temperature slightly below the critical solution temperature. This supports the previous suggestion that in the visibly opalescent region, the system already is in two phases in the form of an emulsion.

Frequency Dependence

The experimental points in Figs. 3 and 5 were fitted with the use of least-squares computer programs. Two theoretical expressions were used: (i) the absorption equation due to a single relaxation frequency,

$$[1] \qquad \frac{\alpha}{f^2} = \frac{A}{1 + f^2/f_c^2} + B;$$

and (ii) the equation obtained from Fixman's theory,

$$[2] \qquad \frac{\alpha}{f^2} = Cf^{-5/4} + B.$$

The fitting was carried out by adjusting the frequency-independent parameters A, B, and f_c in [1] and C and B in [2] to get the lowest value of the relative root-mean-square deviation σ.

The results are shown in Table I and the resulting theoretical curve using equation 2 for triethylamine–water is shown in Fig. 5. It is seen that even though equation 2 has

TABLE I

	Equation 1				Equation 2			B (estimated from graph)
Case	$A \cdot 10^{14}$	$B \cdot 10^{17}$	f_c(mc)	σ	$C \cdot 10^{14}$	$B \cdot 10^{17}$	σ	B
1*	1.4	460	7.1	0.08	3.1	520	0.07	430.10^{-17}
2†	0.85	470	6.4	0.05	6.1	500	0.09	$430 \cdot 10^{-17}$
3‡		No reasonable fit			125.	7600	2.2	$50 \cdot 10^{-17}$

*Case 1: 56% by volume CCl_4 with C_7F_{14}; T = 28.3$_7$ °C.
†Case 2: 56% by volume CCl_4 with C_7F_{14}; T = 33.9$_3$ °C.
‡Case 3: 47 to 69% by volume water with triethylamine; data from (15, 16, 17) included; T = 17.1 °C.

one adjustable parameter less than equation 1, the values of σ obtained using it are of the same order of magnitude as for equation 1. The frequency dependence of the absorption is thus given reasonably well in this frequency range by Fixman's theory.

Quantitative Relationships

Values of an intermolecular energy distance parameter l (1) can be calculated from the temperature dependence of the absorption. The contribution to the absorption, B, due to all effects other than that discussed, is estimated and subtracted from the experimental curve, and the theoretical curve (2) is then fitted to the adjusted experimental curve in two points, giving values for l and C. The parameter C contains too many unknown quantities for a meaningful analysis.

The results of calculations for four systems are given. Values of B for the calculations are taken from Table I and from ref. 6. Since the dependence of B on temperature and frequency is unknown, but small in comparison to the total absorption in these systems, no allowance is made for any such variation of B.

(1) *n*-Heptane–nitrobenzene (6): l = 6 to 7 Å for a range of B-values $270 \cdot 10^{-17}$ to $40 \cdot 10^{-17}$ at 20 mc.

(2) Aniline–cyclohexane (14): l = 7 to 10 Å for a range of B-values $80 \cdot 10^{-17}$ to $180 \cdot 10^{-17}$ at two frequencies, 9 and 27 mc. The value from light-scattering experiments (11) is 12.7 Å.

(3) Perfluoromethylcyclohexane – carbon tetrachloride: l = 6.6 to 14.6 Å for B = $200 \cdot 10^{-17}$ to $520 \cdot 10^{-17}$. The critical solution temperature used in the calculations was 1.5 °C higher than the observed critical solution temperature, as in this 1.5 deg range, the system is probably already in two phases microscopically. The value of l obtained from light-scattering data (3) is 14.7 Å (13), and from heat-capacity data (4), 4.9 Å (13).

(4) Triethylamine–water (15, 16, 17): $l = 2.0 \pm 0.3$ Å for systems at frequencies 0.6 to 9 mc and at varying compositions. The values of l in this system are lower, indicating an interaction range which is shorter than in the other systems.

CONCLUSIONS

The results indicate that near the critical solution temperature, a system may exist as a type of emulsion which already contains two phases in the form of regions of different compositions.

The theory of Fixman postulates that the absorption arises from the interaction of critical fluctuations present in the system with the local temperature changes in the system caused by the passage of the ultrasonic wave. This theory is in reasonable agreement with experimental results, and gives calculated values of l of the same magnitude as those from light-scattering.

Can. J. Chem. Downloaded from www.nrcresearchpress.com by 210.87.254.6 on 09/05/12
For personal use only.

Measurements in a lower frequency range and in a greater number of systems would be helpful in finding out whether Fixman's theory and the physical picture of the critical solution region are more generally valid.

ACKNOWLEDGMENTS

This work was performed in the laboratory of Professor T. A. Bak at the H. C. Ørsted Institute, University of Copenhagen, Denmark, as part of the requirements for the lic. techn. degree from the Technical University of Denmark. The author is indebted to Professor T. A. Bak for his interest and help.

The Ontario Research Foundation gave financial support for this research through a scholarship to the author.

REFERENCES

1. P. DEBYE. J. Chem. Phys. **31**, 680 (1959).
2. M. FIXMAN. J. Chem. Phys. **36**, 1961 (1962).
3. B. H. ZIMM. J. Phys. Colloid Chem. **54**, 1306 (1950).
4. H. SCHMIDT, G. JURA, and J. H. HILDEBRAND. J. Phys. Chem. **63**, 297 (1959).
5. J. H. HILDEBRAND, B. J. ADLER, J. W. BEAMS, and H. M. DIXON. J. Phys. Chem. **58**, 577 (1954).
6. P. KRUUS and T. A. BAK. Acta Chem. Scand. To be published.
7. E. L. HEASELL and J. LAMB. Proc. Phys. Soc. B, **69**, 869 (1956).
8. L. BERGMANN. Der Ultraschall. S. HIRZEL. 1954. p. 464.
9. E. L. HEASELL and J. LAMB. Proc. Roy. Soc. Ser. A, **237**, 233 (1956).
10. J. TIMMERMANS. The physico-chemical constants of binary systems in concentrated solutions. Vol. IV. Interscience. 1959. p. 77.
11. P. DEBYE, B. CHU, and H. KAUFMAN. J. Chem. Phys. **36**, 3378 (1962).
12. O. K. RICE. J. Phys. Colloid Chem. **54**, 1293 (1950).
13. M. FIXMAN. J. Chem. Phys. **36**, 1957 (1962).
14. M. CEVOLANI and S. PETRALIA. Nuovo Cimento, Ser. X, **2**, 495 (1955).
15. A. G. CHYNOWETH and W. G. SCHNEIDER. J. Chem. Phys. **19**, 1566 (1951).
16. G. F. ALFREY and W. G. SCHNEIDER. Discussions Faraday Soc. **15**, 218 (1953).
17. S. SHIMAKAWA. J. Phys. Soc. Japan, **16**, 113 (1961).

Can. J. Chem. Downloaded from www.nrcresearchpress.com by 210.87.254.6 on 09/05/12
For personal use only.

Can. J. Chem. Downloaded from www.nrcresearchpress.com by 210.87.254.5 on 09/05/12
For personal use only.

METHYLATION OF METALATED INDENE AND METHYLINDENE[1]

A. Bosch and R. K. Brown
Department of Chemistry, University of Alberta, Edmonton, Alberta
Received February 12, 1964

ABSTRACT

The reaction of metallic lithium and potassium with indene and fluorene in refluxing 1,2-dimethoxyethane (DME) yields reduction products of indene and fluorene, 1-metalated indene, and 9-metalated fluorene, and as well is accompanied by the production of some hydrogen gas due to the acidic methylene group. The amount of hydrogen is small for fluorene but quite substantial for indene.

Metalation of indene, 1-methylindene, and 3-methylindene in refluxing DME, followed by methylation of these metalated indenes at 0°, gave a mixture consisting of starting material, the corresponding indan, monomethylindene, dimethylindene, and in some cases trimethylindene. Two competing reaction mechanisms resulting in the formation of the metalated indenes are suggested and possible routes for the formation of the di- and tri-methylindenes are examined.

INTRODUCTION

The weakly acidic nature of the methylene group of indene (1) has permitted the preparation of the 1-metalated derivative by use of a variety of basic reagents (2–8). The alkali metal salts of such pseudo acids can also be prepared by direct reaction of the metal with the hydrocarbon in tetrahydrofuran (9) as well as indirectly via metal–aromatic hydrocarbon adducts prepared in ethereal solvents (10–13).

A recent study of the alkylation of the alkali metal salt of fluorene has shown that the proportion of mono- to di-alkylation depends upon both the metal and the solvent employed (14–16). In this work one of the products obtained during the reaction of fluorene with the alkali metals was hydrogen gas. However, it has recently been stated that the reaction of alkali metals with such compounds as fluorene (13) and triphenylmethane (17) produces no hydrogen, but proceeds by initial metal–hydrocarbon adduct formation followed by proton exchange between this adduct and more of the hydrocarbon.

The purpose of this paper is to present results of an investigation of the metalation of indene and alkylation of the resulting salt, and as well of an examination of the question of hydrogen formation during reaction of alkali metals with both fluorene and indene.

RESULTS AND DISCUSSION

A. Hydrogen Evolution vs. Birch Reduction in the Reaction of Lithium or Potassium Metal with Indene or Fluorene

The results of experiments concerning hydrogen formation are shown in Table I.

The blank runs, containing only metal and solvent, produced a volume of gas, due nearly completely to the expansion and displacement of air, equal to 195–200 ml when potassium was used. This gas contained 1–2% of hydrogen as determined by mass spectrometry. When lithium was substituted for potassium, 210 ml of gas was obtained which contained only traces of hydrogen. Gas "evolution" was usually complete within 2 to 3 hours for potassium and 4 to 5 hours for lithium and no further increase in volume of collected material was found in the several runs made where blanks were refluxed for half a day.

[1]*Taken from the thesis of A. Bosch to be submitted to the Faculty of Graduate Studies, University of Alberta, Edmonton, Alberta, in partial fulfillment of the requirements for the degree of Doctor of Philosophy.*

Can. J. Chem. Downloaded from www.nrcresearchpress.com by 210.87.254.5 on 09/05/12
For personal use only.

TABLE I

Production of hydrogen during the reaction of indene or fluorene with lithium or potassium metal in refluxing dimethoxyethane (DME)*
(0.1 mole of hydrocarbon + 0.1 gram-atom of metal in 100 ml of DME)

Expt. No.	Hydrocarbon	Metal used	Amount of metal consumed, %	Time of reflux for complete gas evolution, h	Volume of gas collected, ml	Amount of H_2 in collected gas, %
1	Nil	K	Very little	2–4	200	1–2
2	Nil	K	Very little		195	1–2
3	Nil	Li	Very little		210	Trace
4	Nil	Li	Very little		210	Trace
5	Indene	K	85	3–4	700	At least 50
6	Indene	K	88		725	(No analysis)
7	Indene	Li	80		900	At least 60
8	Indene	Li	77		800	(No analysis)
9	Fluorene	K	Nearly all	3–4	350	35
10	Fluorene	K	Nearly all		390	(No analysis)
11	Fluorene	Li	80	22	220	2
12	Fluorene	Li	85–90	17	215	10
13	Fluorene	Li	(Not estimated)	4 (Incomplete reaction)	200	11

*Generally the reflux was carried out until gas evolution ceased. In some cases reflux time was extended further even though more evolution of gas failed to take place.

A mixture of *indene* and potassium in DME gave 700–725 ml of gas, over 50% of which was hydrogen (presumably 500 ml), while indene and lithium evolved 800–900 ml, over 60% of which was hydrogen (presumably 600–700 ml). Gas evolution ceased in both cases after 3–4 hours. When a mixture of *fluorene* and potassium in DME was refluxed, 350–390 ml of gas was collected (an increase of 150–190 ml above the blank value), at least 35% of which was hydrogen. However, the reaction between lithium and fluorene gave a total volume of gas, 200–220 ml, which mass spectrometry showed to contain about 10% of hydrogen, although in one case out of the three cited only 2% of the collected gas was hydrogen.

Fluorene thus does react with *potassium* to give substantial amounts of hydrogen—but not in the amount equal to that expected if the only reaction between fluorene and the metal were one of hydrogen evolution according to equation *a*.

(a) 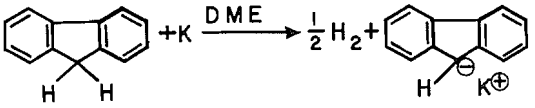

Roughly 11–14% of that theoretically required by equation (*a*) was actually produced. On the other hand, the reaction of *lithium* with fluorene definitely gave hydrogen, but only in small amounts—about 1.5% of that theoretically required by equation *a*. The detection of hydrogen evolution in the present case, but none in the work reported by Eisch and Kaska (13) can be accounted for by the different conditions employed. The latter authors used a larger volume of solvent (400 ml of tetrahydrofuran containing 0.1 mole of fluorene) and room temperature conditions, while the present work employed 100 ml of solvent (DME) containing the same amount of fluorene, and reflux temperature. The latter conditions would promote elimination of small amounts of dissolved hydrogen.*

It is quite evident that a second reaction, consuming the bulk of the metal, has occurred—nearly completely (98–99%) in the case of lithium and fluorene, but to a somewhat lesser extent (85%) with potassium and fluorene. Undoubtedly this occurs by way of reaction *b*, as pointed out by Eisch and Kaska (13), leading to a Birch-type reduction (18) of a portion of the fluorene,

(b) 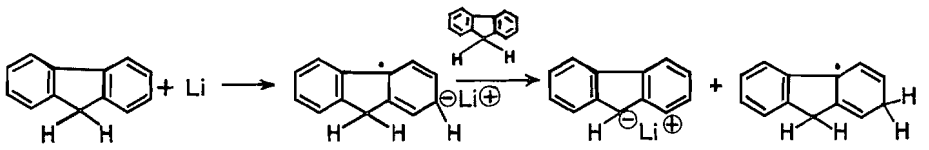

since evidence for the occurrence of such reduction products of fluorene has been presented (13).

The reaction of *indene* with either potassium or lithium metal in DME gave much more hydrogen gas. If the blanks are taken into consideration, the amount of hydrogen evolved when potassium metal reacted with indene was about 40% of the theoretical amount, while reaction with lithium gave about 50% of that required by equation *a*. In these two cases as well, the metal was consumed by the route expressed by equation *a*

**O. F. Beumel, Jr. and R. F. Harris, J. Org. Chem. 28, 2775 (1963) have shown that in the reaction of lithium metal with ethylenediamine in benzene, a competition occurs between (a) direct reaction of the lithium with the diamine to produce hydrogen gas and the lithium amide (b) addition of the metal to the benzene followed by Birch-type reduction of the benzene and lithium amide formation without hydrogen evolution. Hydrogen evolution according to process (a) is less important at lower temperatures, but above 85° a vigorous reaction occurs with evolution of considerable hydrogen.*

Can. J. Chem. Downloaded from www.nrcresearchpress.com by 210.87.254.5 on 09/05/12
For personal use only.

and also by one such as shown in equation *b*. This is supported by the isolation of indan as one of the products of the reaction, to the extent of 15–17% of the product when potassium was used, but only 8–10% with lithium metal* (Table II).

B. Methylation of Indenyllithium and Indenylpotassium

The following observations are made from the methylation data recorded in Table II.

(*i*) The amount of metal consumed appears to be nearly the same regardless of the duration of the reflux period during the metalation, within the limits shown. Whenever equivalent amounts of lithium and indene were employed, 80–90% of the metal reacted, whether the mixture was refluxed 5 or 22 hours, while with potassium 85–90% of the metal was consumed within the limits of 2 to 16 hours. However, in the case of potassium, when a 2:1 molar ratio of metal to indene was used, more than one equivalent amount of metal disappeared and this only when the reflux period was extended to 20 hours. In no case where excess lithium was employed was more than one equivalent of metal consumed even though the reflux time was extended to 72 hours (Table VI).

(*ii*) The amount of indan formed is nearly reproducibly the same regardless of the time of reflux of metal with indene or the use of a twofold excess of metal. The reaction with lithium gave 8–10% of indan while that of potassium yielded 15–17% of the product as indan.

These two observations (*i*) and (*ii*), coupled with the fact that the reaction of both lithium and potassium with indene produced substantial amounts of hydrogen (Table I), strongly support the concept of a competition between two different reactions of the metal with indene. One involves the reaction of indene as an "acid", producing hydrogen (equation *c*) and the other involves the formation of the metal adduct which then metalates more indene with simultaneous formation of reduced indene (equation *d*) via a Birch-type reduction (18).

Equation *c* predicts that equimolar amounts of indene and metal react to produce 0.5

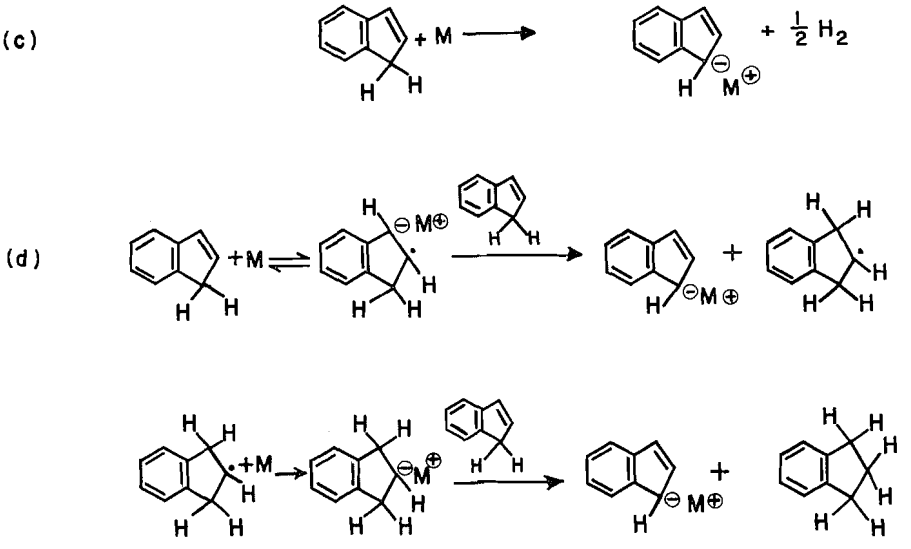

**The source of the lithium metal, as well as particle size, is apparently important. Larger pieces of BDH lithium metal (98%), after 24 hours of heating in refluxing DME, were consumed to the extent of 50%, and gave 23% of the product as indan. Tiny pieces of Fisher Scientific lithium were 90% consumed in 20 hours, but yielded only 9% of the product as indan. In this work only Fisher Scientific lithium was used throughout.*

Can. J. Chem. Downloaded from www.nrcresearchpress.com by 210.87.254.5 on 09/05/12
For personal use only.

Can. J. Chem. Downloaded from www.nrcresearchpress.com by 210.87.254.5 on 09/05/12
For personal use only.

TABLE II

Preparation and methylation of 1-indenyllithium and 1-indenylpotassium in dimethoxyethane*

Metal used	Metal to indene ratio	Time of metalation, h	Amt. of metal consumed, %	Reaction products, mole % of total product								
				Indan	Indene	1-Methyl-indene	3-Methyl-indene	1,1-Dimethyl-indene	1,3-Dimethyl-indene	1,1,3-Trimethyl-indene	Unknown products, %	Total recovery, %
Li†	1	5	~90	9	7	20	51	2	11	0	0	
Li	1	5	~85	8	9	53	19	1	10	0	0	
Li	1	5	~80	8	9	43	27	2	10	0	1	
Li	1	22	~80	10	10	41	26	2	10	0	1	
Li‡	1	18½	~87	9	10	51	23	~0.5	6	0	Trace	
				8	8	42	19	~0.5	5	0	Trace	83
K†	1	2	~85	17	12	0	53	2	14	0	2	
K	1	16½	~90	15	8	0	59	3	13	Trace	2	
K	1	15	~90	15	8	0	60	2	12	1	2	
K	2	3	~45	16	7	0	59	3	12	2	1	
K	2	20	55–60	16	2	0	54	5	14	8	1	
K‡	1	3	~83	15	8	0	64	2	10	0	1	
				15	8	0	58	2	9	0	1	93

*0.1 mole of indene was dissolved in 100 ml of dimethoxyethane and refluxed with the appropriate amount of metal. Methylations were performed at 0–5°.
†Methylations were done at room temperature in these two cases.
‡In these two cases a material balance was made to estimate total recovery, using *t*-butylbenzene as an internal standard. The upper line of figures represents the percentages of each substance based on the total amount of isolated product. The lower line is the percentage of each substance based upon the indene used originally.

mole of hydrogen. Equation (*d*) predicts that 1 mole of indene will react with $\frac{2}{3}$ of a gram atomic weight of metal yielding $\frac{1}{3}$ of a mole of indan and $\frac{2}{3}$ of a mole of the metalated indene. Since the amount of metal consumed actually lies between $\frac{2}{3}$ and 1.0 of a gram atomic weight, and hydrogen as well as indan is produced, both reactions *c* and *d* are required. Furthermore, from the reaction of lithium with indene there has been isolated a small amount of the compound 2,2′-biindanyl, identified by comparison of its n.m.r., i.r., mass spectrum, and melting point (and mixed melting point) with those of an authentic specimen prepared from α,α'-dibromo-*o*-xylene and diethylmalonate (19). The formation of 2,2′-biindanyl is feasible from the indanyl free radical, an intermediate suggested in equation (*d*).

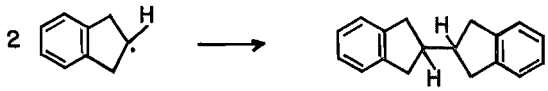

Attempts to isolate this biindanyl from the reaction involving potassium were fruitless. The failure to obtain biindanyl in this instance might be due to the greater electropositive nature of the potassium metal, resulting in *reduction* of the indanyl-free radical before it could dimerize. There was in all cases some unreacted metal left which could do this. The larger amount of indan found in the metalation with potassium (15–17%) than from the metalation with lithium (8–10%) can be rationalized in terms of the greater reducing capability of potassium metal.

(*iii*) The amount of recovered starting material, indene, is nearly constant, regardless of the length of time for metalation, when equivalent amounts of indene and metal are used. No significant change in the amount of recoverable indene occurred when a 2:1 ratio of metal to indene was heated in refluxing DME for a relatively short time (up to 3 hours with potassium metal and 20 hours with lithium metal—Table VI). But extended time of reflux resulted in lowered recovery of starting material (2% rather than 8% recovery of indene when a 2:1 ratio of *potassium* to indene was heated for 20 hours in refluxing DME; 6% rather than 9% of indene recovered when a 2:1 ratio of *lithium* to indene was heated in refluxing DME for 72 hours—Table VI). The decreased indene did not show up as a corresponding increase in the amount of indan, but might have appeared, via further methylation by some route as an increase in the quantity of dimethyl- or trimethyl-indene. A larger amount of the polyalkylated indene did in fact occur under these conditions.

(*iv*) The total amount of monomethylindene (both 1-methylindene and 3-methylindene) is nearly constant regardless of the length of time of metalation. This is to be expected from a reaction involving two competing pathways, *c* and *d*, which would then lead to the formation of a definite amount of metalated indene. For lithium, the total varied between 67% and 74% of the product. At 0 °C, methylation of 1-indenyllithium gave both 1-methylindene and 3-methylindene in the approximate ratio of 2:1, but methylation at room temperature reversed this since the ratio of 1-methylindene to 3-methylindene was now 2:5.

For potassium metal, the total amount of monomethylindene was 59–60% of the product except when the ratio of potassium metal to indene during metalation was 2:1, and then only for reflux periods considerably greater than 15 hours. In this case, 54% of the product was monomethylindene (Table II). The accompanying increase in di- and tri-methylated indene could readily account for this. A 2-hour metalation period yielded less (53%) of the monomethylindene, but also more recoverable indene. This result is

Can. J. Chem. Downloaded from www.nrcresearchpress.com by 210.87.254.5 on 09/05/12
For personal use only.

quite likely due to incomplete metalation in this time. It is significant that all of the monomethylindene obtained is the 3-isomer, whether the methylation was carried out at 0° or at room temperature.

The Isomerization of 1-Methylindene

The isolation of both 1-methylindene and 3-methylindene from the methylation of 1-indenyllithium, but only 3-methylindene from the methylation of 1-indenylpotassium is no doubt due to the isomerization of the initially formed 1-methylindene in the presence of basic reagents (equation *e*).

(e) 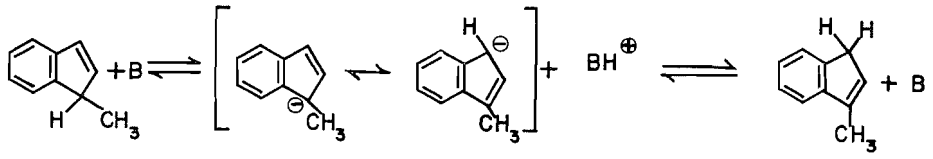

In the presence of the strong base, 1-indenylpotassium, this conversion was rapid (~10 sec) and the equilibrium (equation *e*) appeared to be completely on the side of 3-methylindene. Increase in temperature accelerated this conversion as shown by the greater proportion of 3-methylindene obtained in the methylation of 1-indenyllithium at room temperature than at 0 °C.

1. Thermal Isomerization of 1-Methylindene

The isomerization can be accomplished by heat alone. When 1-methylindene was refluxed in DME (83°/700 mm) for 24 hours, no change to 3-methylindene was perceived. But when 1-methylindene itself was heated to reflux (~184°/700 mm) and aliquots, withdrawn periodically, were analyzed by gas–liquid chromatography the material was converted 94% to 3-methylindene in 80 minutes as shown in Table III.

TABLE III

Isomerization of refluxing 1-methylindene to 3-methylindene (initial reflux temperature, ~184°/700 mm)

Reflux time, min	Product analysis, %	
	1-Methylindene	3-Methylindene
0	99	1
10	93	7
20	79	21
30	62	38
40	47	53
50	27	73
60	22	78
70	13	87
80	6	94
120	4	96
180	4	96

The data do not fit any simple kinetic order, no doubt because of the polymerization which accompanied isomerization at this temperature, as well as change of reflux temperature as the isomerization progressed. After 80 minutes much of the material has polymerized as shown by the viscous material clinging to the walls of the flask. Indenes are known to polymerize readily when exposed to light and heat (20).

The thermal isomerization appears to involve an equilibrium, since no change in the

Can. J. Chem. Downloaded from www.nrcresearchpress.com by 210.87.254.5 on 09/05/12
For personal use only.

4:96 ratio of 1-methylindene to 3-methylindene occurred during the period of reflux between 120 and 180 minutes. The same proportion of these two isomers was obtained when 3-methylindene was refluxed for 7 hours (Table IV).

TABLE IV

Isomerization of refluxing 3-methylindene to 1-methylindene
(initial reflux temperature, ~200°/700 mm)

Expt.	Reflux time, hours	Product analysis, %	
		1-Methylindene	3-Methylindene
1	0.5	2	98
	1.0	3	97
	2.0	4	96
	3.0	4	96
	4.0	4.5	95.5
2	3.0	3	97
	5.0	4	96
	6.0	4	96
	7.0	4	96

The exact position of the equilibrium is not certain since it is not known what the relative rates of polymerization are for 1-methylindene and 3-methylindene. The isomerization, however, occurs much more rapidly than does the polymerization.

2. Base-catalyzed Isomerization of 1-Methylindene

As expected, the base-catalyzed isomerization of 1-methylindene proceeded much more rapidly than did the thermal isomerization, and the rate of this transformation depended upon the strength of the base. The results of several qualitative tests are shown in Table V, and indicate that the effectiveness of the bases used were, in order of decreasing catalytic power, 1-indenylpotassium > methanolic NaOH > 1-indenyllithium > pyridine.

The base-catalyzed isomerization of 1-methylindene eventually yielded only 3-methylindene since only 3-methylindene was obtained from the reaction of 1-indenylpotassium

TABLE V

Isomerization of 1-methylindene in the presence of base
(each run was made with 0.3 ml of 1-methylindene in 1 ml of DME and the base added)

Expt. No.	Base	Time of reaction and conditions	Color, observations	Conversion to 3-methylindene, %
1	Solid K* (about 2 mm cubed)	Shaken 5 sec at room temp.	Slight yellow	1–2
2	Solid K* (about 2 mm cubed)	Shaken 10 sec at room temp.	Dark red	95
3	Solid Li* (about 2 mm cubed)	Shaken 5 min at room temp.	Slight yellow	1–2
4	Solid Li* (about 2 mm cubed)	Boiled 3–4 min volume of solution reduced by ¼	Orange	9
5	2 Drops† methanolic NaOH	Shaken at room temp. for −5 sec	Immediate orange which darkened on standing at room temp.	20
		−15 sec		32
		−120 sec		89
6	4 Drops pyridine	Heated 15 min under reflux	Yellow	8

*Very little of the Li or K was consumed.
†Made from three pellets of NaOH in 10 ml of methanol.

Can. J. Chem. Downloaded from www.nrcresearchpress.com by 210.87.254.5 on 09/05/12
For personal use only.

with methyl iodide. Further support for this view was obtained from the treatment of a solution of *3-methylindene* in DME with methanolic sodium hydroxide. Addition of the base gave an instantaneous yellow color, due to the indenyl carbanion, which became darker when the mixture was shaken for 2 minutes. No conversion of the 3-methylindene to 1-methylindene was detectable by gas–liquid chromatography. Further shaking of the mixture for an additional 15 or 30 minutes failed to alter the result (cf. expt. No. 5, Table V).

The difference between the base-catalyzed and the thermal isomerization may be that in the former case we are dealing with the two contributing structures below, wherein the right-hand form is practically completely predominant. The thermal isomerization,

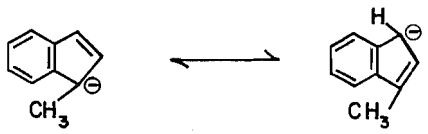

on the other hand, involves the relative stabilities of the neutral molecules, 1-methylindene and 3-methylindene, in which the 3-methylindene, containing the more highly alkylated olefinic bond, is the more stable (21, 22).

No isomerization whatsoever occurred when a solution of 1-methylindene (1.5 g) in 5 ml of DME containing 3 ml of 6 *N* HCl was refluxed for 1.5 hours.

(*v*) Dimethylindene (both 1,1- and 1,3-dimethylindene) was produced in both cases when the metalated indene, obtained from the reaction of equivalent quantities of metal and indene, was treated as usual with a 50% excess of methyl iodide. Under the conditions used, somewhat more dimethylindene was obtained from 1-indenylpotassium (12–16%) than from 1-indenyllithium (11–13%).

About 15–25% of the dimethylindene was the 1,1-dimethyl isomer. This rose to 33% when the metalated indene was prepared by heating an excess of potassium with indene for 20 hours. But, generally, long or short periods of reflux during metalation with an equivalent quantity of metal and indene did not change this proportion (15–25%) much. Further, from the results in Table II, no clear indication exists of the effect of temperature during methylation on the proportion of 1,1-dimethylindene to 1,3-dimethylindene.

Possible Routes Leading to Dimethylindenes

1. Via metal exchange according to equation *f*.
2. Via reaction of residual metal adduct with monomethylated indene (equation *g*).
3. The presence of some unremoved, unreacted metal which, via reactions similar to those in equation *c* and *d* could convert 1-methylindene into the metalated 1-methylindene. The presence of unreacted potassium metal, during methylation of fluorene, has been shown to produce a greater proportion of the dimethylated fluorene (16).
4. Prolonged heating of the metal in refluxing solvent (DME) might produce basic materials which could cause further alkylation of 1-methylindene. Evidence for reaction of alkali metal with a solvent such as dioxane (23) or aryl ethers (24) has already been reported.

The recovery of substantial amounts of indene, but failure to find the expected methylindan (e.g. 2-methylindan) supports the metal exchange process according to equation *f*. But since less indene was recovered than that expected by equation *f* (the ratio of indene to dimethylindene actually found varied between 7/13 and 10/12), formation of

Can. J. Chem. Downloaded from www.nrcresearchpress.com by 210.87.254.5 on 09/05/12
For personal use only.

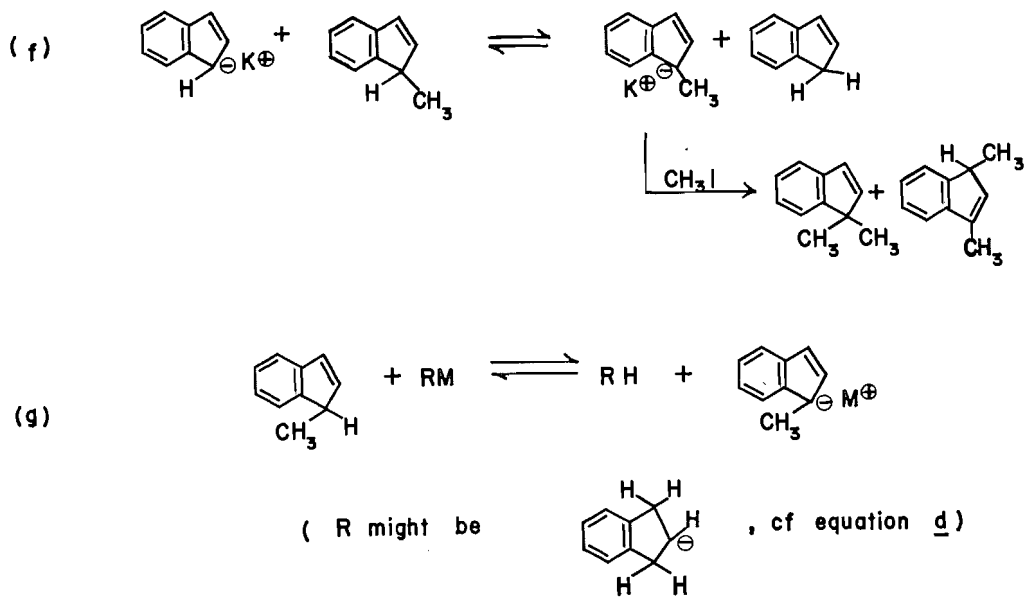

some of the dimethylindene must have taken place by some additional route—for example because of the presence of unreacted metal, or basic decomposition products resulting from metal attack on the solvent DME. We have found that when *potassium* metal was heated in refluxing DME for several hours, a basic material was obtained. This material in the DME, freed from unreacted metal as much as possible, followed by treatment with both indene and methyl iodide simultaneously, gave a product consisting of 3–4% indan, 62% of recovered indene, 4% of 1-methylindene, and 31% of 3-methylindene. The source of the indan is obviously from some unreacted metal present (cf. equation *d*). The amount of methylindene was more, by about one half, than could be obtained from the amount of unreacted metal present (as calculated from the amount of indan found using the data in Table II to obtain an expected ratio of indan to mono- and di-methylindene). When lithium metal was treated similarly, no basic material was obtained and no alkylation of indene was detected.

It is our view that the dimethylindenes are obtained primarily by route 1 above, but assisted by route 3 and, possibly, in the case of the more reactive metal, potassium, by route 4.

Alkylation of the Product Obtained from Metalation of Indene with Two Equivalents of Metal

When metalation was accomplished using a molar ratio of metal to indene of 2:1, alkylation produced the results shown in Table VI. Conclusions drawn from this information can be summarized briefly as follows.

1. When metalation was carried out for short periods (3 hours for potassium, 5–20 hours for lithium) results were nearly identical with those obtained by the use of equivalent amounts of metal and indene (cf. Table II).

2. With potassium, as the time of metalation was increased, the amount of recoverable indene, as well as the newly formed monomethylindene decreased, while the quantity of dialkylated and trialkylated indene increased. The quantity of metal consumed was larger for the longer metalation period.

Can. J. Chem. Downloaded from www.nrcresearchpress.com by 210.87.254.5 on 09/05/12
For personal use only.

Can. J. Chem. Downloaded from www.nrcresearchpress.com by 210.87.254.5 on 09/05/12
For personal use only.

TABLE VI

Results of the methylation* of 1-indenyllithium and 1-indenylpotassium prepared by treatment of indene with two equivalents of the metal

Metal used	Time of metalation, h	Amount of metal consumed, %	Reaction products, mole % of total product								
					Monomethylation		Dimethylation		Trimethylation		
			Indan	Indene	1-Methyl-indene	3-Methyl-indene	1,1-Dimethyl-indene	1,3-Dimethyl-indene	1,1,3-Trimethyl-indene	Unknown products	Total recovery, %
Li	5	~40	9	9	47	26	1	8	0	0	
†	19	~40	10	9	57	18	Trace	6	0	Trace	
			8	7	47	15	Trace	5	0	Trace	82
	20	35–40	10	8	46	26	1	9	0	0	
	72	45–50	10	6	34	36	2	12	0	0	
K	3	~45	16	7	0	59	3	12	2	1	
	3	~48	15	6	0	65	2	11	1	0	
	20	~60	16	2	0	54	5	14	8	1	
	20	~65	17	Trace	0	51	5	18	9	0	
	46	~80	19	0	0	40	8	19	13	1	
†	63	~75	20	0	0	36	7	21	15	1	
			16	0	0	24	5	15	9	1	70
	92	~80	17	0	0	37	7	21	18	0	

*Methylation was done at 0 °C.

†In these two cases a material balance was made to estimate total recovery, using *t*-butylbenzene as an internal standard. The upper line of figures represents the percentages of each substance based on the total amount of isolated product. The lower line is the percentage of each product based upon the indene originally used.

3. With lithium, increase in metalating time gave results about the same as those obtained for shorter metalating periods except that more of the 1-methylindene was isomerized to 3-methylindene.

Metalation and Alkylation of 3-Methylindene

Metalations and alkylations were carried out according to the procedures used for indene itself. The results are compiled in Table VII. Similar reactions were done using 1-methylindene and these results are given in Table VIII. Comparison of the information shown in these tables with those for the analogous reactions involving indene (Table II) lead to the following conclusions.

1. As for the reactions of metal with *indene*, long or short reflux time during metalation produced results which were nearly identical with each other, except that for potassium metal, somewhat more trialkylated indene was formed when the longer reflux time for metalation was used.

2. Total recovery from the metalation and alkylations of the 1-methylindene was 95% for the potassium, and 98% for the lithium. These are substantially higher than those obtained for the analogous reaction using indene.

3. A substantial proportion of the product was the reduced form, 1-methylindan. This was greater (22–27%) than the proportion of indan found from reactions involving indene (Table II).

4. For lithium, the total amount of monoalkylation of methylindene (~70% of product) was about the same as the proportion of monoalkylation of indene while the dialkylation of methylindene to produce 1,1,3-trimethylindene was much less (about 2 to 4% of the product), than that found for indene (about 9–10%). The amount of 1,1,3-trimethylindene from the dialkylation reaction is the *same* as the amount of recovered monomethylindene, suggesting that dialkylation occurs via the metal exchange route shown by equation *f*.

5. With potassium, the amount of monoalkylation (to dimethylindene) is about 30% of the product whereas similar monoalkylation of indene gave about 60% of the product as the monomethylindene. However, the 1,1,3-trimethylindene (from dialkylation) occurred to the extent of 24–29% while recovered unalkylated monomethylindene was found to the extent of 16–18% of the product, indicating that other routes as well as that of metal exchange, brought about dialkylation.

6. Results of the reactions with 1-methylindene (Table VIII) and 3-methylindene (Table VII) are nearly identical. The only significant differences are the slightly higher amounts of metal consumed by the reaction with 1-methylindene, and the recovery of only 3-methylindene rather than the original 1-methylindene as "starting material" (Table VIII).

EXPERIMENTAL

Solvents and Chemicals

1,2-Dimethoxyethane, commercially available, was distilled twice from potassium metal before use. Analysis by gas–liquid chromatography showed it to be free from contaminants.

Potassium metal (BDH reagent) and *lithium metal* (Fischer Scientific Co.) were freed from encrusting oxide or nitride while under Skellysolve B or paraffin oil.

Indene (Eastman Kodak Co.), practical grade, was treated with Drierite, then distilled twice at atmospheric pressure. Analysis by gas–liquid chromatography showed it to be free from impurities and water.

Fluorene (Eastman Kodak Co., 98%) was crystallized six times from 95% ethyl alcohol and then heated for 4 hours at 65° under vacuum in an Abderhalden drier to remove solvent. It was then dried under the same conditions but in the presence of phosphorus pentoxide. The product was stored in a desiccator over phosphorus pentoxide.

Indan (practical grade) was obtained commercially from Matheson Chemical Co.

Can. J. Chem. Downloaded from www.nrcresearchpress.com by 210.87.254.5 on 09/05/12
For personal use only.

Can. J. Chem. Downloaded from www.nrcresearchpress.com by 210.87.254.5 on 09/05/12
For personal use only.

TABLE VII

Metalation and subsequent methylation of 3-methylindene in DME*

Metal used	Metalation time, h	Metal consumed, %	Reaction products, mole % of total product: 1-Methylindan	3-Methylindene	Monomethylation: 1,1-Dimethylindene	Monomethylation: 1,3-Dimethylindene	Dimethylation: 1,1,3-Trimethylindene	Unknown products, %
Li	17	73–75	23	4	11	58	4	0
	45	~72	23	3	11	59	4	0
K	5	~76	27	18	8	23	24	0
	16	~85	26	16	8	22	28	0

*For the metalation step, equimolar amounts (0.1 mole) of metal and methylindene were heated in refluxing DME (100 ml). Methylation was carried out by adding excess methyl iodide to the above solution, first cooled to 0°.

TABLE VIII

Metalation and subsequent methylation of 1-methylindene in DME*

Metal used	Metalation time, h	Metal consumed, %	Reaction products, mole % of total product: 1-Methylindan	1-Methylindene	3-Methylindene	Monomethylation: 1,1-Dimethylindene	Monomethylation: 1,3-Dimethylindene	Dimethylation: 1,1,3-Trimethylindene	Unknown products, %	Total recovery, %
Li	16	~82	22	0	3	11	61	3	0	
	46	~92	24	0	2	11	61	2	0	
†			27	0	2	10	57	2	0	98
K	16	~87	24	0	17	9	21	29	0	
	5	~84	23	0	18	9	23	27	0	
†			27	0	16	8	21	23	0	95

*In the metalation step, equimolar amounts (0.1 mole) of metal and methylindene were heated in refluxing DME (100 ml). Methylation was carried out by adding excess methyl iodide to the above solution, first cooled to 0°.

†These figures represent a material balance using *t*-butylbenzene as an internal standard. The percentage yields are based upon the original amount of methylindene used. The line of figures immediately above are for the same run and represent the yield of each product as a percentage of the total product.

Can. J. Chem. Downloaded from www.nrcresearchpress.com by 210.87.254.5 on 09/05/12
For personal use only.

Gas–Liquid Chromatography (G.L.C.)

A Burrell Model K-2 Kromo-Tog was used for all g.l.c. analyses, utilizing the following 2.5 m columns.

Silicone rubber, 25% by weight on Gas-Chrom P (60–80 mesh). This column separated the following *groups* of compounds from each other but failed to separate the individuals of each group where mixtures are indicated: (*a*) indan and indene, (*b*) 1-methylindene; 1,1-dimethylindene and 1-methylindan, (*c*) 3-methylindene, (*d*), 1,3-dimethylindene and 1,1,3-trimethylindene.

neo-Pentylglycol succinate, 25% by weight on Gas-Chrom P (60–80 mesh). This column separated the following groups from each other but not the individual members of each group: (*a*) indan, (*b*) 1,1-dimethylindene and 1-methylindan, (*c*) indene and 1-methylindene, (*d*) 1,1,3-trimethylindene, (*e*) 3-methylindene and 1,3-dimethylindene.

Apiezon L, 25% by weight on Gas-Chrom P (60–80 mesh). This column separated the following groups from each other but not the individuals contained in each group: (*a*) indan and indene, (*b*) 1,1-dimethylindene, (*c*) 1-methylindene and 1-methylindan, (*d*) 1,1,3-trimethylindene and 3-methylindene, (*e*) 1,3-dimethylindene.

For complete separation of the products of metalation and alkylation it was necessary to change from one column to another. Apiezon L did give better separation than the other two columns, but the peaks were broad and in some cases did not return to the base line satisfactorily, hence quantitative analysis with the integrator attached was not sufficiently satisfactory with this column. The other two columns gave well-resolved, sharp peaks.

Helium, at a flow rate of about 100 ml/min, was the carrier gas. Column temperatures varied with the different packings, but were adjusted to give maximum separation of the products (120–175°). Products were identified by comparison of their retention times with those of authentic samples, as well as by their isolation via the Kromo-Tog and subsequent analysis by n.m.r. and i.r. spectral determinations. These spectra were obtained with a Varian A 60 spectrometer and a Perkin–Elmer Model 421 spectrophotometer respectively.

The paper areas of the various product peaks were measured by an integrator. Analysis of carefully weighed authentic mixtures of the reaction products showed that these paper areas could be used as a direct measure of molar compositions of the reaction mixtures. The addition of a carefully weighed amount of *t*-butylbenzene as an internal standard allowed the calculation of the weights of each individual product and hence determination of the absolute per cent recovery.

General Procedure for the Formation and Collection of Hydrogen Gas

A 250-ml, round-bottom, 3-neck flask equipped with a magnetic stirrer was heated with a bunsen flame to remove adhering moisture. After it was allowed to cool (calcium chloride tube), it was equipped with a short water-condenser and a gas collecting apparatus. To the flask was added 100 ml of DME, 0.10 gram-atom of metal (if the metal was lithium it was cut up into small pieces) and 0.10 mole of the hydrocarbon in the order specified. But in the case of fluorene, 0.10 mole of the hydrocarbon was first dissolved in 100 ml of solvent and the metal added last. The reaction mixture was refluxed till no more gas was evolved (from 2 to 22 hours, see Table I). All gases were collected by the downward displacement of water. Small samples of this gas were taken and analyzed for molecular hydrogen content by mass spectrometry with a Metropolitan Vickers instrument, Model MS-2H, AEI, Manchester. Blanks were run under identical conditions except that the hydrocarbon was not added to the reaction flask.

General Procedure for the Metalation and Methylation of the Indenes

To a dried, 3-neck 250-ml round-bottom flask, equipped with a magnetic stirrer and a reflux condenser, were added 100 ml of DME and 0.10 (or 0.20) gram-atom of metal (Li was cut into small pieces). The redistilled indene (11.6 g, 0.10 mole) was added at once to the mixture, protected by an atmosphere of purified, dry nitrogen. The mixture was refluxed for a specific length of time (see Tables II, VI–VIII), then cooled in an ice-water bath. Any unreacted metal was removed mechanically as completely as possible and weighed. To the cold residual solution, now at 0–5°, was added dropwise over a period of 30–45 minutes, an excess (approximately 1.5 equivalents) of methyl iodide. After the addition was completed, the reaction mixture was stirred for 30 minutes at room temperature, then decomposed with excess dilute aqueous hydrochloric acid. The mixture was then extracted twice with ether (total volume ~400 ml), the ether extract dried ($MgSO_4$), filtered, and freed from solvent. The remaining dark oil was then analyzed by gas–liquid chromatography.

Preparation of Methylated Indenes and Indan

(All melting points are uncorrected.)

3-Methylindene was prepared in 60–75% yield by the method of Parham *et al.* (25), starting with commercially available 1-indanone (Eastman Kodak Co.). The product was a colorless liquid boiling at 56°/2.0 mm; η_D^{23}, 1.5621. Lit. b.p., 76–78°/11 mm; η_D^{25}, 1.5587 (25). The n.m.r. spectrum of this compound is shown in Fig. 1(*a*).

1-Methylindene was synthesized from 3-methyl-1-indanol in 40% yield according to the scheme given by Yarboro, Karr, and Estep (26). Since experimental details were lacking, the procedure is described below.

By a Friedel and Crafts reaction, benzene, crotonic acid, and 3 equivalents of anhydrous aluminum chloride gave 3-methyl-1-indanone (27). B.p., 103°/3.9 mm. Lit. b.p., 132–137°/15 mm (27). Reduction of this ketone with 40–50% excess of lithium aluminum hydride in ether according to general procedure (28) afforded 3-methyl-1-indanol, m.p., 70–72°. Lit. m.p., 71–72° (28).

In the absence of solvent, the alcohol was stirred and heated with 25% of its weight of solid oxalic acid, either in the anhydrous or the dihydrate form, at reflux temperature for 15–20 minutes. After cooling, the substituted indene was extracted from the solidified acid with Skellysolve B. The hydrocarbon layer was dried and fractionally distilled giving a 40% yield of 1-methylindene as a colorless liquid boiling at 54°/3.5 mm; η_D^{25}, 1.5540. Lit. b.p., 55–56°/3.75 mm (or 186°/735 mm); η_D^{20}, 1.5565 (26).

The n.m.r. spectrum of this compound, shown in Fig. 1(*b*), corroborates the structure designated.*

1,3-Dimethylindene was prepared from the 3-methyl-1-indanone, mentioned above, by the method suggested in the literature (29) with the following modifications. After the usual ammonium chloride – water work-up, the ether layer was dried and distilled at reduced pressure yielding both 1,3-dimethyl-1-indanol, m.p., 67–69°; lit. m.p. 72° (29) and 1,3-dimethylindene (colorless oil) b.p., 68°/3 mm; η_D^{21}, 1.5486. Lit. b.p., 66°/3 mm; η_D^{20}, 1.5477 (26).

The n.m.r. spectrum of 1,3-dimethylindene is shown in Fig. 1(*c*).

1,1-Dimethylindene has not been reported in the literature to our knowledge. Its preparation is described below and is similar to the preparation of 1-methylindene. By a Friedel and Crafts reaction a mixture of

**The C_1 proton of 1-methylindene (neat) gives a signal at τ = 6.78 (quartet, J = 8 c.p.s.) while the C_1 proton of indene (neat) shows a signal at τ = 6.98 (triplet, J = 2.0 c.p.s.). This is in agreement with the results found for fluorene and 9-methylfluorene (G. W. H. Scherf and R. K. Brown, Can. J. Chem. 38, 1388 (1961) showing a greater deshielding effect upon the C_1 proton in 1-methylindene and suggesting that it is more "acidic" than is the C_1 proton of indene.*

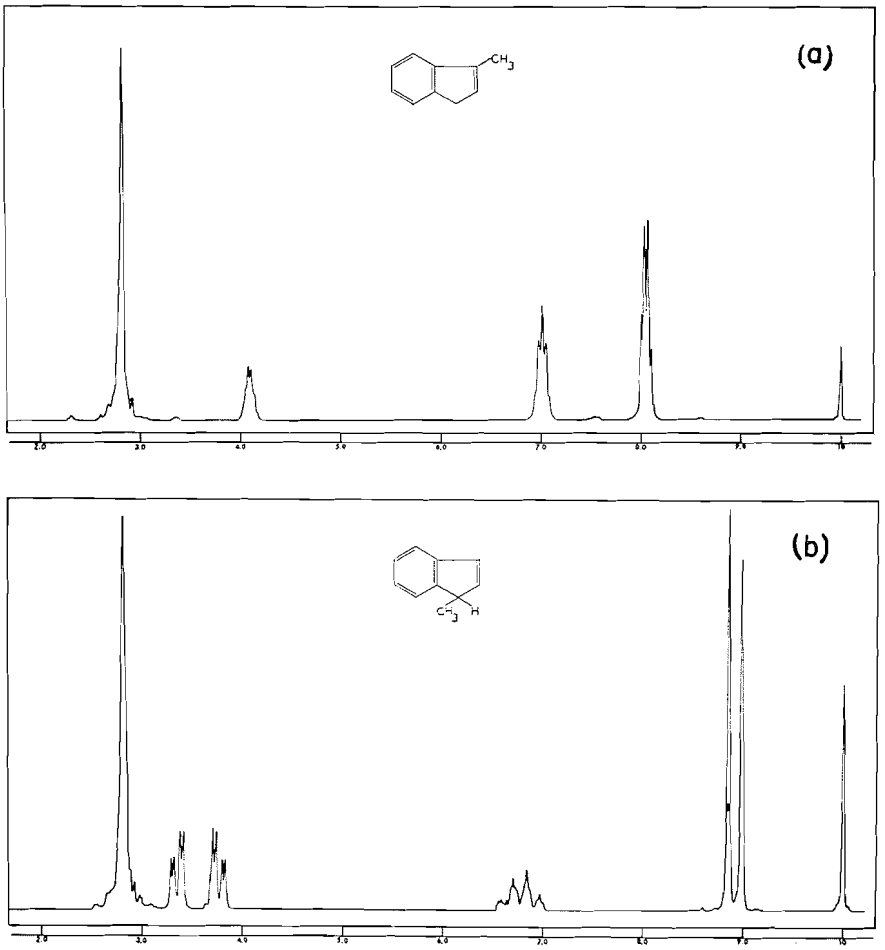

Can. J. Chem. Downloaded from www.nrcresearchpress.com by 210.87.254.5 on 09/05/12
For personal use only.

Can. J. Chem. Downloaded from www.nrcresearchpress.com by 210.87.254.5 on 09/05/12
For personal use only.

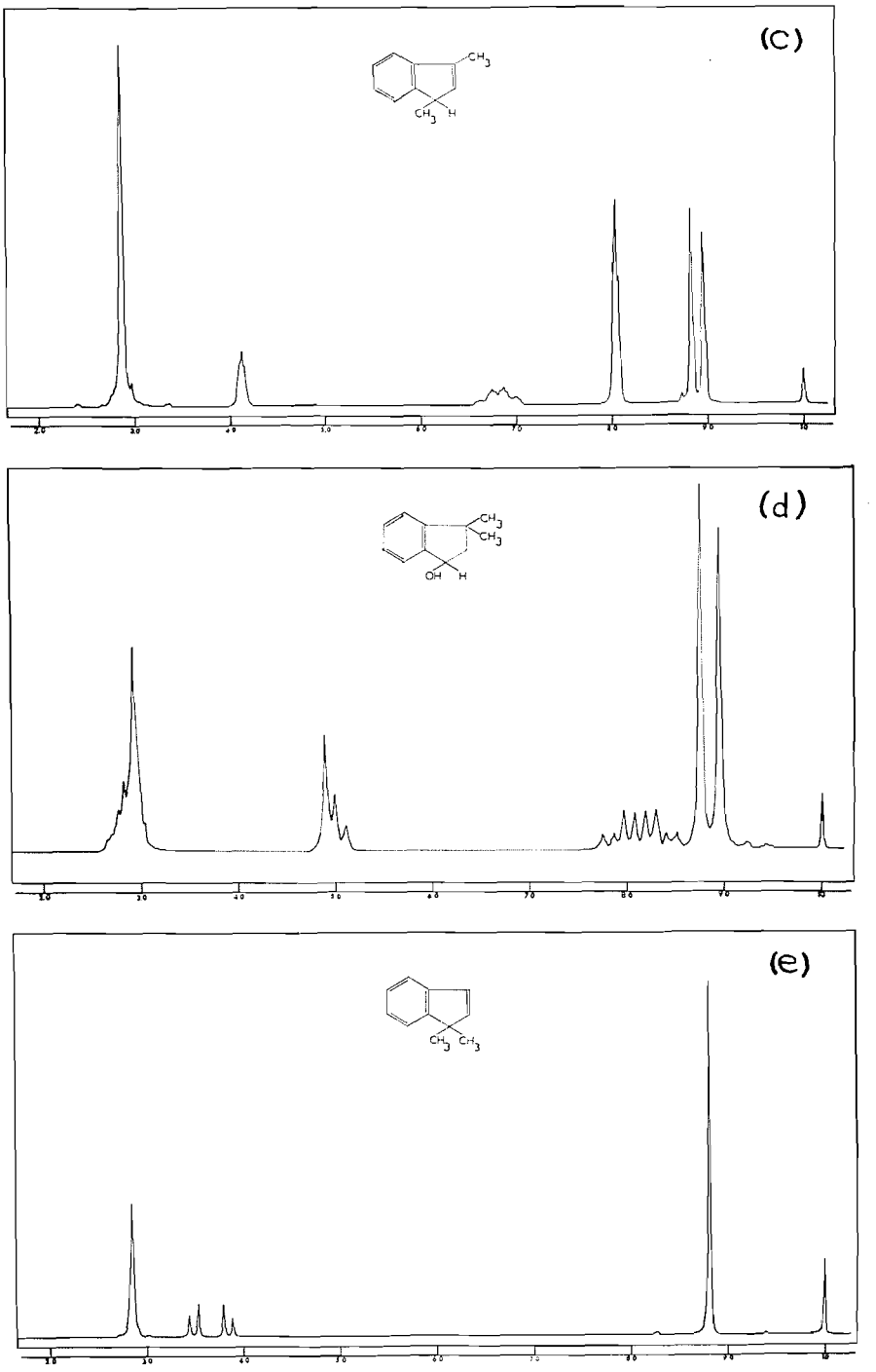

FIG. 1. Nuclear magnetic resonance spectra of indene derivatives (referred to tetramethylsilane, $\tau = 10.00$). All spectra were obtained on the pure liquids, neat, except in the case of 3,3-dimethyl-1-indanol which was diluted with an equal volume of carbon tetrachloride to reduce the viscosity of the hydrocarbon; (*a*) 3-methylindene, (*b*) 1-methylindene, (*c*) 1,3-dimethylindene, (*d*) 3,3-dimethyl-1-indanol, (*e*) 1,1-dimethylindene.

benzene, 3-methyl crotonic acid (Aldrich Chemical Co.) and 3 equivalents of aluminum chloride gave 3,3-dimethyl-1-indanone in 82% yield. B.p. 107°/4.7 mm. Lit. b.p. 130–132°/18 mm (30). Reduction of the ketone with lithium aluminum hydride according to the usual procedure (28) afforded 3,3-dimethyl-1-indanol in 80% yield as a colorless, viscous oil boiling at 107°/4.2 mm; η_D^{24}, 1.5340. Anal. Calc. for $C_{11}H_{14}O$: C, 81.44; H, 8.70. Found: C, 81.75; H, 8.66. The n.m.r. spectrum, shown in Fig. 1(*d*), is consistent with the formulation of this compound as 3,3-dimethyl-1-indanol.

A mixture of 3,3-dimethyl-1-indanol (25 g) and 10 g of solid oxalic acid dihydrate was heated to reflux for 1 hour. The cooled reaction mixture was extracted with Skellysolve B to remove the oil from the solidified oxalic acid. The dried extract ($MgSO_4$) was fractionally distilled and afforded 11 g (yield, 50%) of a colorless oil boiling at 57°/4.8 mm; η_D^{23}, 1.5379. Anal. Calc. for $C_{11}H_{12}$: C, 91.61; H, 8.39. Found: C, 91.47; H, 8.20. The n.m.r. spectrum of the 1,1-dimethylindene is shown in Fig. 1(*e*) and agrees with the structure assigned.

1,1,3-Trimethylindene was prepared quite readily from 3,3-dimethyl-1-indanone (see above) according to published procedure (31). It was a colorless oil boiling at 68°/3.6 mm; η_D^{24}, 1.5348. Lit. b.p., 52–61°/0.5 mm; η_D^{25}, 1.5353 (31).

1-Methylindan was obtained as a colorless oil by the reduction of 3-methylindene in methyl alcohol using a platinum oxide catalyst and hydrogen at an initial pressure of 50 p.s.i. The procedure was similar to directions already published (29) for the reduction of 1,3-dimethylindene. Yield, 81%. B.p. 98°/43 mm; η_D^{24}, 1.5266. Lit. b.p., 189.5/739 mm; η_D^{25}, 1.5241 (32).

2,2′-Biindanyl was prepared according to published directions (19, 33) from α,α'-dibromo-*o*-xylene and diethylmalonate. After three crystallizations from 95% ethyl alcohol, the final product (needles) melted at 168–170°. Lit. m.p., 165–166° (19). Its n.m.r. spectrum showed a peak at $\tau = 2.86$, and a broad, poorly resolved multiplet centered at $\tau = 7.18$. The areas were in the ratio of 4:5. Mass spectral and infrared data were also in complete agreement with the structure.

The above compound was shown to be identical in all respects (n.m.r. and i.r. spectra, melting point, and mixed melting point) with the solid obtained from the metalation of indene with lithium.

ACKNOWLEDGMENT

The authors thank the National Research Council of Canada for their financial support during this work. One of us (A. Bosch) gratefully acknowledges the receipt of a scholarship from the Cities Services Research and Development Company which enabled him to continue his work. We also thank R. Swindlehurst and Mrs. G. Conway for the infrared and n.m.r. spectral determinations of compounds prepared, and R. Taylor for the mass spectrometer analyses.

REFERENCES

1. W. Marckwald. Ber. **28**, 1501 (1895).
2. W. Marckwald. Ber. **33**, 1504 (1900).
3. R. Weissgerber. Ber. **42**, 569 (1909).
4. K. Ziegler and O. Schäfer. Ann. **479**, 150 (1930).
5. O. Blum-Bergmann. Ann. **484**, 26 (1930).
6. V. Grignard and C. Courtot. Compt. Rend. **152**, 272 (1911).
7. Th. Zerewitinoff. Ber. **45**, 2384 (1912).
8. C. Courtot. Ann. Chim. [9], **4**, 76 (1915).
9. H. Gilman and R. D. Gorsich. J. Org. Chem. **23**, 550 (1958).
10. W. Schlenk and E. Bergmann. Ann. **463**, 83 (1928).
11. N. D. Scott, J. F. Walker, and V. L. Hansley. J. Am. Chem. Soc. **58**, 2442 (1936).
12. H. Normant and B. Angelo. Bull. Soc. Chim. France, 354 (1960).
13. J. J. Eisch and W. C. Kaska. J. Org. Chem. **27**, 3745 (1962).
14. G. W. H. Scherf and R. K. Brown. Can. J. Chem. **38**, 697 (1960).
15. G. W. H. Scherf and R. K. Brown. Can. J. Chem. **38**, 2450 (1960).
16. G. W. H. Scherf and R. K. Brown. Can. J. Chem. **39**, 799 (1961).
17. H. O. House and V. Kramar. J. Org. Chem. **27**, 4146 (1962).
18. A. J. Birch and H. Smith. Quart. Rev. **12**, 17 (1958).
19. F. Fichter and H. Stenzl. Helv. Chim. Acta, **22**, 425 (1939).
20. Elsevier's Encyclopaedia of Organic Chemistry. Vol. 12 A, Series III. 1948. pp. 101–102.
21. R. T. Morrison and R. N. Boyd. Organic chemistry. Allyn and Bacon, Inc. 1960. p. 122.
22. L. Bateman and J. I. Cunneen. J. Chem. Soc. 2283 (1951).
23. E. Grovenstein, Jr., E. P. Blanchard, Jr., D. A. Gordon, and R. W. Stevenson. J. Am. Chem. Soc. **81**, 4842 (1959).
24. D. H. Eargle, Jr. J. Org. Chem. **28**, 1703 (1963).
25. W. E. Parham, H. E. Reiff, and P. Swartzentruber. J. Am. Chem. Soc. **78**, 1440 (1956).
26. T. L. Yarboro, C. Karr, Jr., and P. A. Estep. J. Chem. Eng. Data, **6**, 420 (1961).
27. C. F. Koelsch, H. Hochmann, and C. D. LeClaire. J. Am. Chem. Soc. **65**, 59 (1943).

Can. J. Chem. Downloaded from www.nrcresearchpress.com by 210.87.254.5 on 09/05/12
For personal use only.

28. J. A. BARLTROP, R. M. ACHESON, P. G. PHILPOTT, K. E. MACPHEE, and J. S. HUNT. J. Chem. Soc. 2936 (1956).
29. P. A. PLATTNER, A. FÜRST, and K. JIRASEK. Helv. Chim. Acta, **30**, 1325, 1326 (1947).
30. BUU-HOI and R. ROYER. Bull. Soc. Chim. France, 812 (1947).
31. R. A. BARNES and B. D. BEITCHMAN. J. Am. Chem. Soc. **76**, 5430 (1954).
32. J. ENTEL, C. H. RUOF, and H. C. HOWARD. Anal. Chem. **25**, 1303 (1953).
33. W. H. PERKIN, JR. and G. RÉVAY. J. Chem. Soc. **65**, 232 (1894).

Can. J. Chem. Downloaded from www.nrcresearchpress.com by 210.87.254.5 on 09/05/12
For personal use only.

Can. J. Chem. Downloaded from www.nrcresearchpress.com by 210.87.254.40 on 09/05/12
For personal use only.

CLEAVAGE OF XANTHENE ETHERS

A NEW ROUTE TO 9-SUBSTITUTED XANTHENES

N. LATIF, I. FATHY, AND N. MISHRIKY
National Chemical Research Centre, Dokki, Cairo, United Arab Republic

Received January 3, 1964

ABSTRACT

9,9-(Tetrachloro-*o*-phenylenedioxy) xanthene (II*a*) and its thio-analogue (II*b*) are cleaved by hydrazines to give the corresponding hydrazones of xanthone and thiaxanthone, respectively, together with tetrachlorocatechol. The unsaturated nitriles (V*a*), (V*b*), and (V*c*) are produced similarly by the action of malononitrile and cyanoacetic ester. Dixanthenyl ether itself reacts in a similar manner with active hydrogen compounds to give the corresponding 9-xanthyl derivatives. (II*b*) is prepared by the action of 9-diazothiaxanthene on tetrachloro-*o*-benzoquinone and is readily cleaved by lithium aluminum hydride to give thiaxanthene and tetrachlorocatechol. The reaction mechanisms are discussed.

9-Substituted xanthenes have found wide application in biology and industry, and special attention has been directed recently to the study of the chemistry of this group of compounds. It has been shown, in this laboratory, that xanthene ethers of the type (I) have unusual chemical reactivity unrelated to that of previously reported analogous compounds. For example, it is known that ethers are ordinarily not reactive enough as substrate to be hydrolyzed easily; however, it has been found (1) that 9,9-(tetrachloro-*o*-phenylenedioxy) xanthene (II*a*), in contrast to other analogous methylenedioxy derivatives such as (III), is easily cleaved by dilute mineral acids under very mild conditions to give xanthone. Also, it has been reported (2) that xanthene ethers of the type (I) exceptionally undergo reductive cleavage by lithium aluminum hydride yielding xanthene. The unusual reactivity of (I) has been rationalized by assuming that a carbonium ion is first formed as an intermediate and is stabilized by resonance with the unshared electron pair on the oxygen of the xanthylene residue.

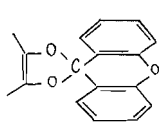

(I)

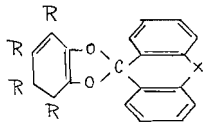

(II*a*): R = Cl, X = O.
(II*b*): R = Cl, X = S.
(II*c*): R = Br, X = S.

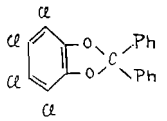

(III)

In the present investigation, it is found that the thiaxanthene analogues have similar reactivity. Thus, when (II*b*) is allowed to react with lithium aluminum hydride in boiling ether, thiaxanthene and tetrachlorocatechol are produced (3). It is assumed that cleavage proceeds by the initial attack of a positive ion such as Li^+ or AlH_2^+ on the oxygen of the dioxole ring followed by the heterolytic fission of the C—O bond to give a resonance stabilized carbonium ion (cf. IV) which readily picks up a hydride ion yielding finally xanthene. A similar mechanism has been previously proposed for the cleavage of the analogous cyclic ether (II*a*) (2). (II*a*) is prepared in good yield by the reaction of 9-diazothiaxanthene with tetrachloro-*o*-benzoquinone. The bromo-analogue (II*c*) is similarly obtained from tetrabromo-*o*-benzoquinone.

This remarkable reactivity of xanthene and thiaxanthene ethers stimulated us to extend our investigations and study their reactivity towards active hydrogen compounds. It is found (3, 4, 5) that when (II*a*) or (II*b*) is allowed to react with phenylhydrazine or benzoylhydrazine in boiling ethanol, the corresponding hydrazones of xanthone and thiaxanthone, respectively, are obtained together with tetrachlorocatechol. However, with hydrazine hydrate, the corresponding hydrazones and ketazines are produced.

It is found also that malononitrile reacts readily with (II*a*) and (II*b*) under similar conditions to give the highly colored unsaturated dinitriles (V*a*) and (V*b*), respectively, in excellent yields, together with tetrachlorocatechol. However, a higher reaction temperature has been found necessary to cleave the cyclic ether by cyanoacetic ester. For example, (V*c*) is only produced when the higher boiling *n*-butyl alcohol is used as a solvent. (V*a*), (V*b*), and (V*c*) have been previously obtained by condensing malononitrile or ethyl cyanoacetate with the corresponding thione in presence of yellow mercuric oxide (6).

Two possible suggestions might be proposed to explain the production of the xanthylene and thiaxanthylene derivatives by the action of active hydrogen compounds on xanthenic ethers. For example, in the case of the reaction of malononitrile with (II*a*), it is assumed

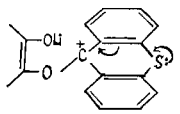

(IV)

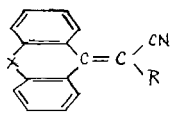

(V*a*): R = CN, X = O.
(V*b*): R = CN, X = S.
(V*c*): R = $OCOC_2H_5$, X = S.

that an intermediate (VI) is first formed which cleaves to give directly Δ^9,α-xanthenemalononitrile by a β-elimination process as shown in Scheme A. The other alternative which immediately suggests itself is that (VI) might react further with another molecule of malononitrile to give a second intermediate (VII) which decomposes under reaction conditions yielding the product as shown in Scheme B. However, the first possibility seems to be more feasible. In this connection, it is worth mentioning that the yield of (V*a*) is found to be the same whether using one or two moles of malononitrile in this reaction.

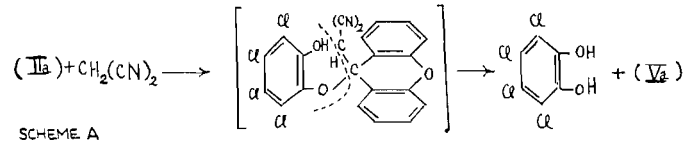

SCHEME A

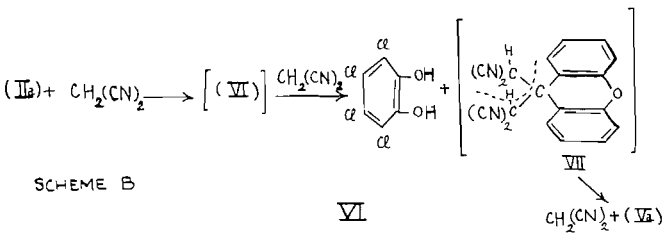

SCHEME B

The production of the corresponding ketazines in the reaction between (II*a*) or (II*b*) with hydrazine hydrate might be explained by assuming that part of the hydrazone first formed reacts further with the cyclic ether to give the azine. This view is supported by the fact that xanthone hydrazone is found to react readily with (II*a*) under the same conditions to give xanthone azine in excellent yield.

Can. J. Chem. Downloaded from www.nrcresearchpress.com by 210.87.254.40 on 09/05/12
For personal use only.

In an attempt to generalize this reaction, the reactivity of dixanthenyl ether itself has been investigated. It is found (4, 5) that the ether reacts readily with active hydrogen compounds to give the corresponding 9-xanthyl derivatives which have been previously obtained by the acid-catalyzed reaction of these compounds with xanthydrol. For example, (VIII*a*), (VIII*b*), and (VIII*c*) are produced, in good yield, by the action of benzoylhydrazine, ethyl cyanoacetate, and malononitrile, respectively, on dixanthenyl ether in boiling ethanol.

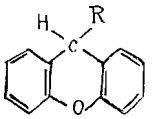

(VIII*a*): R = $HN.HNCOC_6H_5$
(VIII*b*): R = $CH.CN.COOC_2H_5$
(VIII*c*): R = $CH(CN)_2$

Cleavage of xanthene ethers by active hydrogen compounds provides a new method for the direct synthesis of 9-substituted xanthenes which enhances the value of xanthene ethers as synthetic intermediates.

EXPERIMENTAL

Reaction of 9,9-(tetrachloro-o-phenylenedioxy) xanthene (IIa) with hydrazine hydrate.—The xanthene ether (1) (1 g) and hydrazine hydrate (98–100%, 1 ml) in absolute alcohol (25 ml) were refluxed together for 5 hours. The solution was filtered while hot, and the orange crystals obtained (0.01 g) were shown to be xanthone azine (m.p. and mixed m.p. 295 °C). The filtrate was concentrated and left to cool. The yellow solid formed was filtered off and recrystallized from methanol to give xanthone hydrazone (0.1 g) m.p. 126 °C (undepressed when admixed with an authentic sample). The main ethanolic mother liquor was poured onto ice-cold water and acidified with hydrochloric acid. The precipitate formed was filtered off, dried, and refluxed with acetic anhydride (10 ml) for 30 minutes. The solution was left to cool, poured onto ice, and the separated solid was filtered off and washed with water. This was dried and crystallized from methanol to give the diacetate of tetrachlorocatechol, m.p. 184° (undepressed when admixed with an authentic sample prepared as described by Zincke and Kuster (7)).

Reaction of (IIa) with phenylhydrazine.—The cyclic ether (1 g) and phenylhydrazine (1 g) in absolute ethanol (20 ml) were refluxed together for 3 hours. The solution was filtered while hot, concentrated, and left to cool. The solid formed was filtered off and recrystallized from ethanol to give golden yellow crystals, m.p. 152 °C (0.5 g), which proved to be xanthone phenylhydrazone (m.p. and mixed m.p.). Tetrachlorocatechol was produced in the reaction and identified as before.

Reaction of (IIa) with benzoylhydrazine.—The reaction was carried out as above using half a gram of the ether and one-fifth of a gram of the hydrazine. The solution was cooled and the yellow solid formed was crystallized from benzene to give xanthone benzoylhydrazone as yellow crystals, m.p. 150 °C. Calc. for $C_{20}H_{14}O_2N_2$: C, 76.43; H, 4.46; N, 8.91. Found: C, 77.00; H, 4.65; N, 8.66%.

Reaction of (IIa) with xanthone hydrazone.—A suspension of (II*a*) (1 g) and the hydrazone (1 g) in absolute alcohol (20 ml) were refluxed together for 5 hours and the mixture was left to cool. The solid formed was crystallized from xylene to give xanthone azine (0.56 g) as orange yellow crystals, m.p. 295 °C (undepressed when admixed with an authentic sample).

Reaction of malononitrile with (IIa).—Malononitrile (0.3 g) was added to a suspension of (II*a*) (1 g) in absolute alcohol (20 ml) and the reaction mixture was refluxed for 4 hours. During this period the cyclic ether went gradually into solution and a yellow crystalline solid was formed. This was filtered off and recrystallized from benzene to give Δ^9,α-xanthenemalononitrile (V*a*) as green yellow crystals (0.35 g), m.p. 244–245 °C (undepressed when admixed with a sample prepared by condensing 9,9-dichloroxanthene with malononitrile (6)). Tetrachlorocatechol was identified in the ethanolic mother liquor as before. When the reaction was carried out using equimolecular amounts of the reactants, almost the same yield of (V*a*) was obtained.

Preparation of 9,9-(tetrachloro-o-phenylenedioxy) thiaxanthene (IIb).—Tetrachloro-*o*-benzoquinone (0.8 g) was added portionwise, at room temperature (25 °C), to a solution of 9-diazothiaxanthene (8) (1 g) in dry ether (20 ml). A vigorous reaction with evolution of gas took place after each addition and the red color of the quinone disappeared. When all the quinone had been added, the product formed was filtered off, washed with acetone, and recrystallized from the same solvent to give (II*b*) as colorless crystals, m.p. 221 °C (undepressed when admixed with an authentic sample prepared by the reaction of 9,9,dichlorothiaxanthene

Can. J. Chem. Downloaded from www.nrcresearchpress.com by 210.87.254.40 on 09/05/12
For personal use only.

Can. J. Chem. Downloaded from www.nrcresearchpress.com by 210.87.254.40 on 09/05/12
For personal use only.

with tetrachlorocatechol (9)). Both products have identical infrared spectra. Calc. for $C_{19}H_8O_2SCl_4$: C, 51.58; H, 1.81; S, 7.24; Cl, 32.12. Found: C, 51.75; H, 1.99; S, 7.16; Cl, 31.59%.

Preparation of 9,9-(tetrabromo-o-phenylenedioxy) thiaxanthene (IIc).—The reaction was carried out as in the case of the chloro-analogue when (II*c*) was obtained as colorless crystals, m.p. 245 °C (undepressed when admixed with an authentic sample prepared by the reaction of tetrabromo-*o*-benzoquinone with thiaxanthone hydrazone (9)).

Reaction of (IIb) with lithium aluminum hydride.—One gram of (II*b*) was added in small portions to a suspension of lithium aluminum hydride (1 g) in dry ether (40 ml). When all the cyclic ether had been added, the reaction mixture was refluxed for 6 hours on the water bath, and left to cool. It was decomposed with alcohol then with dilute hydrochloric acid, and extracted several times with ether. The combined ethereal extracts were dried over anhydrous sodium sulphate, and the ether was then driven off. The solid left was dissolved in the least amount of boiling methanol and the solution was filtered while hot and left to cool. The separated colorless crystals were shown to be thiaxanthene (m.p. and mixed m.p.). The alcoholic mother liquor was poured onto ice-cold water and acidified with a few drops of hydrochloric acid. The precipitate formed was shown to be tetrachlorocatechol as before.

Reaction of hydrazine hydrate with (IIb).—Hydrazine hydrate (99–100%—0.5 ml) and (II*b*) (0.5 g) in absolute alcohol (20 ml) were refluxed together for 3 hours. The reaction mixture was filtered while hot, and the solid obtained (0.002 g) was shown to be thiaxanthone azine (m.p. and mixed m.p.). The filtrate was concentrated and cooled. The pale yellow solid formed (0.16 g) was filtered off, crystallized from ethanol, and shown to be thiaxanthone hydrazone (m.p. and mixed m.p.). Tetrachlorocatechol was identified in the main alcoholic mother liquor as before.

Reaction of phenylhydrazine with (IIb).—The reaction was carried out as above using half a gram of phenylhydrazine and half a gram of (II*b*). The solution was filtered while hot, concentrated, and left to cool. The crystalline solid formed (0.31 g) was filtered off, and recrystallized from methanol to give thiaxanthone phenylhydrazone as yellow crystals, m.p. 150–151 °C. It gives an olive green color with deep green fluorescence with concentrated sulphuric acid. Calc. for $C_{19}H_{14}SN_2$: C, 75.49; H, 4.63; S, 10.59; N, 9.27. Found: C, 75.27; H, 4.83; S, 10.55; N, 9.25%. Tetrachlorocatechol was produced in the reaction and identified as above.

Reaction of benzoylhydrazine with (IIb).—The reaction was carried out as above. The solution was filtered while hot and evaporated to dryness under reduced pressure, and a few milliliters of methanol was added to the oily residue. The light yellow solid formed (0.24 g) was filtered off and crystallized from methanol to give thiaxanthone benzoylhydrazone as straw yellow crystals, m.p. 177 °C. Calc. for $C_{20}H_{13}OSN_2$: S, 9.72; N, 8.51. Found: S, 10.41; N, 8.36%. Tetrachlorocatechol was identified in the alcoholic mother liquor as above.

Reaction of malononitrile with (IIb).—Malononitrile (0.5 g) and the cyclic ether (II*b*) (0.5 g) in absolute alcohol (30 ml) were refluxed together for 6 hours. The orange yellow crystalline solid formed during the reaction was filtered off, washed with acetone, and crystallized from benzene to give Δ^9,α-thiaxantheneomalononitrile (V*b*) (0.2 g) as orange yellow crystals, m.p. 300–301 °C (undepressed when admixed with an authentic sample prepared by the reaction of 9,9-dichlorothiaxanthene with malononitrile (6)). Tetrachlorocatechol was produced in the reaction and identified as above.

Reaction of ethyl cyanoacetate with (IIb).—A mixture of (II*b*) (1 g) and ethyl cyanoacetate (1 ml) in *n*-butyl alcohol (20 ml) was refluxed for 6 hours. The solution was filtered while hot, evaporated to dryness under reduced pressure, and a few milliliters of methanol was added to the oily residue. The yellow crystalline solid formed (0.35 g) was filtered off, washed with methanol, and crystallized from the same solvent to give Δ^9,α-thiaxantheneacetic acid, α-cyanoethyl ester (V*c*) as yellow crystals, m.p. 129–130 °C (undepressed when admixed with an authentic sample prepared by the reaction of 9,9-dichlorothiaxanthene with ethyl cyanoacetate (6)). Tetrachlorocatechol was identified in the main methanolic mother liquor as before.

Reaction of malononitrile with dixanthenyl ether.—To a suspension of dixanthenyl ether (1.8 g) in absolute alcohol (25 ml), malononitrile (0.6 g) was added, and the reaction mixture was refluxed for 4 hours. During this period the ether went gradually into solution and a crystalline solid was formed. This was filtered off, and the filtrate was concentrated, and left to cool. The solid separated was filtered off, and crystallized from ethanol to give 9-xanthyl malononitrile (VIII*c*) (1.1 g) as colorless crystals, m.p. 186–188 °C (undepressed when admixed with an authentic sample prepared by the reaction of xanthydrol with malononitrile (10)).

Reaction of ethyl cyanoacetate with dixanthenyl ether.—Ethyl cyanoacetate (2.5 g) and dixanthenyl ether (3.7 g) in absolute alcohol (25 ml) were refluxed together for 6 hours. The solution was filtered while hot, and evaporated to dryness. The oily residue obtained was extracted several times with cold petroleum ether (b.p. 40–60°). The solid obtained (1.4 g) was filtered off, washed with methanol, and crystallized from ethanol to give (VIII*b*) (11) as colorless crystals, m.p. 125–127 °C. Calc. for $C_{18}H_{15}O_3N$: C, 73.72; H, 5.11; N, 4.77. Found: C, 74.04; H, 4.97; N, 4.22%.

Reaction of benzoylhydrazine with dixanthenyl ether.—The reaction was carried out as above using 0.8 g of benzoylhydrazine and 1.8 g of the ether. The solution was filtered off, concentrated, and left to cool. The solid separated was filtered off, and crystallized from ethanol to give (VIII*a*) (12) as colorless crystals, m.p. 176–178 °C (yield 1.7 g). Calc. for $C_{20}H_{16}O_2N_2$: C, 75.94; H, 5.10; N, 8.86. Found: C, 75.52; H, 5.37; N, 8.98%.

REFERENCES

1. N. LATIF and I. FATHY. Can. J. Chem. **37**, 863 (1959).
2. N. LATIF and N. MISHRIKY. J. Org. Chem. **27**, 846 (1962).
3. I. FATHY. Ph.D. Thesis, A'in Shams University, Cairo, 1963.
4. N. MISHRIKY. M.Sc. Thesis, A'in Shams University, Cairo, 1962.
5. N. LATIF, I. FATHY, and N. MISHRIKY. Abstracts of Papers, XIXth International Congress of Pure and Applied Chemistry, London, England. July, 1963. p. 244.
6. M. M. HAFEZ, N. LATIF, and I. F. ZEID. J. Org. Chem. **26**, 3988 (1961).
7. T. ZINKE and F. KUSTER. Ber. **21**, 2729 (1888).
8. A. SCHÖNBERG and T. STOLPP. Ber. **63**, 3102 (1930).
9. N. LATIF, I. FATHY, N. MISHRIKY, and A. ATALLAH. J. Org. Chem. **25**, 1618 (1960).
10. E. SAWICIKI and V. OLIVERIO. J. Org. Chem. **21**, 183 (1956).
11. R. FOSSE and A. ROBYN. Compt. Rend. **143**, 240; Beilesteins Handbuch Der Organischen Chemie. Vol. XVIII. p. 342.
12. A. DOUCET. Compt. Rend. **177**, 1120 (1923); Chem. Abstr. **18**, 688 (1924).

Can. J. Chem. Downloaded from www.nrcresearchpress.com by 210.87.254.40 on 09/05/12
For personal use only.

REACTION OF 2-METHYL-2-NITRO-1,3-PROPANEDIOL WITH ALKALI[1]

A. M. UNRAU
Department of Plant Science, University of Manitoba, Winnipeg 19, Manitoba
Received November 25, 1963

ABSTRACT

Hydrolysis of 2-methyl-2-nitro-1,3-propanediol with strong alkali (20% NaOH) resulted primarily, as expected, in a reverse aldol decomposition, although a small but significant quantity of free nitrite ion was detected. Hydrolysis with alkaline borate (pH 10) gave high yields of nitrite ion. Possible mechanisms to explain these results are presented. The major product formed in the borate hydrolysis was identified as 2-C-methyl glycerol (2-methyl-1,2,3-propanetriol). A number of minor products were also detected by vapor-phase chromatography.

DISCUSSION

Mechanisms have been advanced by Haas and Riley (1) and Lippincott (2) for the alkaline hydrolytic removal of the nitro group from primary nitroalkanes and it appears likely the suggested mechanisms were operative in the removal by alkali of the nitro group from β-nitropropionic acid (3). It has been reported (3) that 20 to 25% of the nitro group was removed from this naturally occurring nitro acid to give nitrite ion, when an alkaline borate buffer was used. It was found that the addition of formaldehyde greatly facilitated the removal of the nitro group from β-nitropropionic acid (3, 4) and primary aliphatic nitro compounds (4) and possible mechanisms leading to the greater ease of nitro group elimination have been suggested (4). It is known that 2 moles of formaldehyde may be condensed in an aldol fashion with 1 mole of a primary aliphatic nitro compound, thus removing both acidic α-hydrogens. In the mechanisms proposed by Haas and Riley (1) and Lippincott (2), the presence of α-hydrogens is required. If the α-hydrogens are replaced by hydroxymethyl groups, another mechanism would have to be operative.

An approach which might produce further information regarding the mode of removal of the nitro group would involve suitable model compounds. It was believed that 2-methyl-2-nitro-1,3-propanediol, a crystalline compound commercially available, would serve as a fairly adequate model at this stage. This compound, the nuclear magnetic resonance (n.m.r.) characteristics of which have recently been reported (5), is very soluble in water, methanol, and ethanol; less soluble in acetone; and only sparingly soluble in less polar solvents. The infrared and ultraviolet spectral characteristics of this type of nitro diol have been investigated (6) in some detail. Whereas it was found that 1,3-propanediol has bonded hydroxyl (hydroxyl bands at 2.83 μ in dichloromethane at a number of different concentrations), this feature was reported to be absent for mononitro diols. It has been suggested (6) that the close proximity of the hydroxyl groups and the nitro group might favor an interaction between these groups. Depending on the relative stability of such an interacting system, the ease whereby these nitro diols might be decomposed by alkali could be influenced. It is reasonable that weak alkali would not appreciably disrupt this hydroxyl – nitro group interacting system. Under these conditions, the tertiary, electron-deficient carbon atom might be more easily approached by a nucleophile. A planar intermediate or transition state could lead to a Walden inversion which, however, would not be observable in the optically inactive compound used.

[1]*Contribution No. 83.*

Can. J. Chem. Downloaded from www.nrcresearchpress.com by 210.87.254.42 on 09/05/12
For personal use only.

Can. J. Chem. Downloaded from www.nrcresearchpress.com by 210.87.254.42 on 09/05/12
For personal use only.

The ultraviolet spectra of the nitro diol in methanol with varying concentrations of sodium hydroxide and sodium borate indicated different interactions for these two conditions. A solution of the nitro compound in methanol alone had a well-defined absorption band at 276–278 mμ. Addition of water to the solution caused no appreciable change in the position of the absorption band, although the maximum became progressively less well defined. In water alone, the band at 276–278 mμ appeared as a shoulder. Similar observations have been made (6) for a similar nitro compound, namely 2-hydroxymethyl-2-nitro-1,3-propanediol. This was verified further in this laboratory when the above nitro triol was dissolved in methanol, in methanol containing water, and in water alone. Addition of sodium hydroxide to the methanol solution of the nitro diol caused a marked shift in the absorption band. At low concentrations of this alkali (0.01 to 0.1% w/v), a well-defined band was observed at 296–297 mμ. With increasing base strength (0.08 to 2.0%) this band became obscured with a shoulder evident about 288–290 mμ. In contrast, addition of similar concentrations of sodium borate gave rise to an absorption band at 274–275 mμ at lower concentrations while at higher borate concentrations, a shoulder was observed at 273–274 mμ. These rather different spectra indicated that the nitro group in the nitro diol interacted in a rather different manner under the described conditions (see Fig. 1).

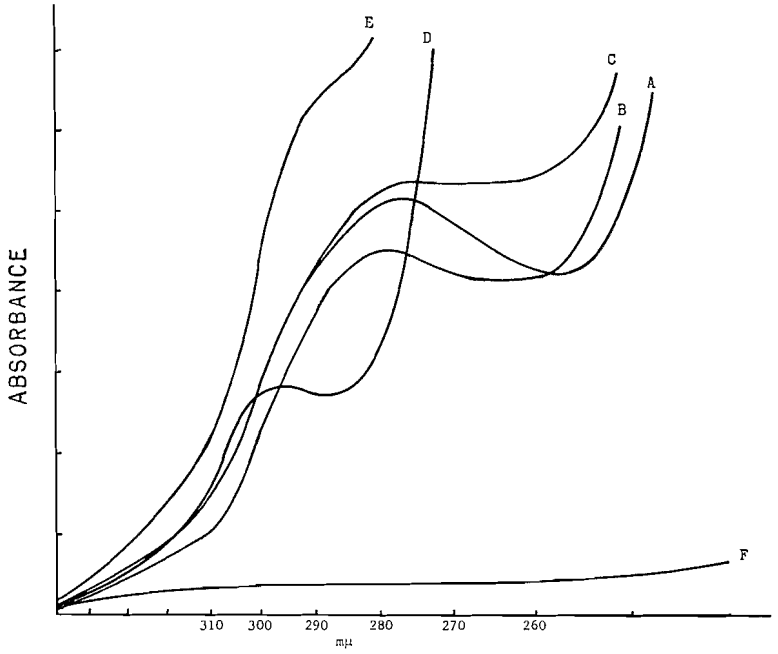

FIG. 1. Ultraviolet absorption spectra of 2-methyl-2-nitro-1,3-propanediol in various solvents. A, in MeOH, B, in water, C, in water and borate (0.02%), D, in MeOH and NaOH (0.01%), E, in MeOH and NaOH (0.08%), F, MeOH – borate blank.

Alkaline hydrolysis (20% NaOH – 15 lb pressure) of the nitro diol resulted in a 5 to 7% release of nitrite ion. A considerable amount of dark-brown, water insoluble polymeric material was formed. It was presumed that the tar consisted of a mixture of formaldehyde and nitroethylene polymers, since nitroethylene and formaldehyde would be formed in the reverse aldol decomposition of the parent compound. The release of a small amount

of nitrite could possibly come about by a direct substitution of the nitro group by hydroxyl or an attack on the tertiary carbon by the neighboring potential oxygenate anion to form an intermediate epoxide. In the experiments involving weak alkali solutions consisting of sodium bicarbonate and dilute sodium hydroxide, considerably less tar was formed and as much as 35% free nitrite was formed. Under these conditions it would be less likely that the neighboring hydroxyl groups would be ionized.

Treatment of the nitro compound with sodium borate buffer resulted in minimal tar formation while nitrite ion release was found to be as high as 90%. It was apparent that under these conditions the reverse aldol decomposition was of minor consequence and the nitro group was rather efficiently eliminated by some other mechanism. As indicated above, the ultraviolet spectrum under these conditions suggests a different interaction. It is known that borate will form charged complexes with *cis* 1,2-diols or form an intermolecular complex with polyhydroxylated compounds (7, 8, 9). Involvement of the nitro group and a hydroxyl with borate could facilitate removal of the nitro group by hydroxylation (nucleophilic attack) of the electron-deficient β-carbon and finally lead to the formation of 2-C-methyl glycerol (2-methyl-1,2,3-propanetriol). An alternative reaction route might involve intermolecular borate complexing of both hydroxyl groups with no direct participation of the nitro group. The nitro group could then be displaced in the same manner as suggested above, namely, nucleophilic displacement by hydroxide.

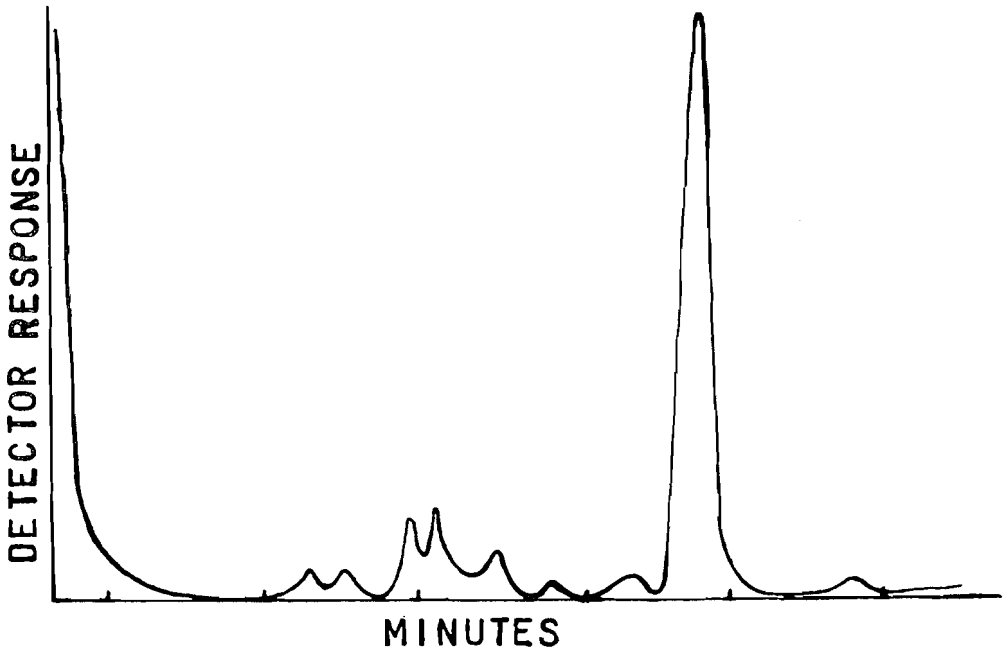

FIG. 2. Gas chromatography of product from alkaline borate hydrolysate. Column temperature programmed from 90 to 190 °C at 10°/min; helium flow 90 ml/min.

The product, a pale-yellow oil, obtained from the alkaline borate hydrolyzate exhibited no absorption bands generally ascribed to the nitro group in its infrared spectrum. Analysis of the product by gas chromatography gave (see Fig. 2) a complex spectrum in which at least eight minor components were evident together with one major peak. The major component, emerging as a sharp, symmetrical peak with a retention time of 8 min

Can. J. Chem. Downloaded from www.nrcresearchpress.com by 210.87.254.42 on 09/05/12
For personal use only.

at a programming rate of 10 °C per min (starting temp. 90 °C), was collected and identified as 2-C-methyl glycerol (2-methyl-1,2,3-propanetriol).

EXPERIMENTAL

Evaporations were carried out under reduced pressure at bath temperatures of 35 °C to 45 °C. Melting points of derivatives were determined on a hot stage apparatus and are uncorrected. The descending technique was used in paper chromatography and solvent systems employed were: (A) ethyl acetate – acetic acid – water (8:2:2) and (B) ethyl acetate – pyridine – water (8:3:2). Ammoniacal silver nitrate solution (10) was used as a spray reagent for detection of polyols. Ultraviolet spectra were obtained with a Perkin–Elmer 4000A spectrophotometer in matched silica cells.

Hydrolysis of Nitro Compound with NaOH and $NaHCO_3$

The nitro compound, 2-methyl-2-nitro-1,3-propanediol, was hydrolyzed with a series of concentrations of sodium hydroxide and sodium bicarbonate. The solutions were boiled at atmospheric pressure for 10 h. In another series of experiments the reactions were carried out in an autoclave under pressure (15 lb/sq. in.) for 2 h. At the end of each run, suitable aliquots (2–5 ml) of the brownish liquid were withdrawn and nitrite determined colorimetrically using sulphanilic acid and naphthylamine reagents (11). The results are summarized in Table I.

TABLE I

Nitrite ion produced in hydrolysis of nitro compound with NaOH and $NaHCO_3$ solutions

Conc. of NaOH (%)	% NO_2^- released	
	Reflux	Autoclave
1	13.5	17.0
5	8.9	10.5
10	7.5	8.8
15	7.1	8.5
20	7.0	8.5
30	7.0	8.4
Conc. of $NaHCO_3$		
0.5	25	35
2	21	30

Hydrolysis of Nitro Compound with Sodium Borate

Analytical runs as described in the previous section were done using 0.7 *M* sodium borate as the alkaline hydrolytic agent (4). Refluxing gave 70 to 75% nitrite while autoclaving gave 80 to 90% nitrite.

Characterization of Hydrolysis Products

A quantity (3 g) of nitro compound in borate buffer (250 ml) was refluxed for 13 h. The small amount of water-insoluble tar was removed and the brownish solution evaporated. Borate was removed by several additions and evaporations of methanolic hydrogen chloride. The reaction product was separated from the inorganic residue by exhaustive extraction with acetone. The extract was evaporated, the thick, brownish liquid taken up in water, and treated with decolorizing charcoal. The filtrate was evaporated leaving a thick, straw-colored liquid (2.2 g). Paper chromatography of the product gave extensive streaking in both solvent systems with at least two darkly staining areas with R_f values of 0.60 and 0.62 in solvents A and B, respectively. The parent compound had an R_f of 0.85 and 0.91 in solvents A and B, respectively.

(a) Vapor-phase chromatography

The product was separated by gas chromatography in the following manner. A 3.5-ft. column (0.25 in. diameter) was packed with silanized Chromosorb W* containing 10% Versamid† as liquid phase. The helium flow was adjusted to 90 ml per min. Figure 1 shows a typical run with the column temperature programmed at 10° per min from a starting temperature of 90° to a temperature of 190°, then held isothermally at the latter temperature until the end of the run. In the separation of the major component, aliquots of 30 μl were injected.

(b) Identification and characterization of 2-C-methyl glycerol as the main component

To a quantity (150 mg) of the substance was added 0.1 *M* sodium periodate (50 ml) and water (50 ml) and the solution stored in the dark at 3 °C. Formaldehyde production (12) and periodate uptake were

**Purchased from Wilkens Instrument and Research Inc.*
†Purchased from F. and M. Corporation.

Can. J. Chem. Downloaded from www.nrcresearchpress.com by 210.87.254.42 on 09/05/12
For personal use only.

determined periodically. After 30 min, 84 mg formaldehyde had been liberated with little or no increase observed thereafter. Periodate consumption became constant (2.80 mmoles) after the above time interval at 2 moles per mole of 2-methyl 1,2,3-propanetriol. Formaldehyde evolved was further characterized as the dimedone derivative which after recrystallization from dilute ethanol had m.p. and mixed m.p. 188–189 °C. Another portion (130 mg) of the compound was treated with bromine after periodate oxidation and the products oxidized with mercuric oxide. Carbon dioxide evolved was trapped in barium hydroxide solution and barium carbonate weighed. From 130 mg of starting material, two proportions of carbon dioxide (484 mg barium carbonate) were obtained. The acidified reaction mixture was extracted with ether and the solution dried with magnesium sulphate. Evaporation of the ether left a small amount of liquid which had a strong odor of acetic acid. The acid was neutralized with dilute alkali and a small quantity (20 mg) of the salt degraded by the Schmidt (13) procedure. The first step yielded 46 mg barium carbonate or one-half of the original carbon, while permanganate oxidation of the remaining amine gave the other half of original carbon (44 mg barium carbonate). The remaining salt (85 mg) was treated with thionyl chloride and the acyl halide reacted with suitable aroyl amines. The *p*-toluide had m.p. and mixed m.p. 145–146 °C and the anilide had m.p. and mixed m.p. 113–114 °C. These constants agree with those of the respective derivatives of acetic acid.

To a quantity (200 mg) of the component in pyridine (5 ml) was added a 10% theoretical excess of *p*-nitrobenzoyl chloride. A solid isolated in the usual fashion had, after recrystallization from acetone, m.p. 170–171 °C. Anal. Calc. for $C_{25}H_{19}O_{12}N_3$: N, 7.6. Found: N, 7.57 and 7.58%. A portion (150 mg) of compound in hot ethanol (100 ml) was saponified (NaOH), alcohol was evaporated, and the solution acidified (HCl). The precipitated *p*-nitrobenzoic acid was washed, dried, and weighed (135 mg). The results showed that the parent alcohol was in fact a trihydric alcohol, namely 2-C-methyl glycerol.

ACKNOWLEDGMENT

Financial support from the National Research Council of Canada is gratefully acknowledged. The helpful discussions with Dr. W. E. Noland, University of Minnesota, are also gratefully acknowledged.

REFERENCES

1. H. B. Haas and E. F. Riley. Chem. Rev. **32**, 373 (1943).
2. S. B. Lippincott. J. Am. Chem. Soc. **62**, 2604 (1940).
3. H. Matsumoto, A. M. Unrau, J. W. Hylin, and B. Temple. Anal. Chem. **33**, 1442 (1961).
4. A. M. Unrau. Can. J. Chem. **40**, 811 (1962).
5. F. Hruska, T. Schaefer, and C. A. Reilly. Can. J. Chem. **42**, 697 (1964).
6. H. E. Ungnade and L. W. Kissinger. Tetrahedron, **19**, 121 (1963).
7. H. Deuel and H. Neukom. Advan. Chem. Ser. 11, 51 (1954). Makromol. Chem. **3**, 13 (1959).
8. A. B. Foster and M. Stacey. J. Appl. Chem. **3**, 19 (1953).
9. D. R. Briggs, E. F. Garner, and F. Smith. Nature, **178**, 154 (1956).
10. S. M. Partridge. Nature, **158**, 270 (1946).
11. A. O. A. C. Methods of analysis. 8th ed. 1955. p. 127.
12. M. Lambert and A. C. Neish. Can. J. Res. Ser. B, **28**, 83 (1950).
13. S. Aronoff. Techniques of radiobiochemistry. The Iowa State College Press, Ames, Iowa. 1956.

Can. J. Chem. Downloaded from www.nrcresearchpress.com by 210.87.254.42 on 09/05/12
For personal use only.

Can. J. Chem. Downloaded from www.nrcresearchpress.com by 210.87.254.6 on 09/05/12
For personal use only.

NOTES

THE STRUCTURE OF FERROCENYL RUTHENOCENYL KETONE

G. J. Small and J. Trotter

Since previous studies have suggested that the cyclopentadienyl rings are staggered in derivatives of ferrocene and eclipsed in ruthenocene derivatives (1), we have investigated the structure of ferrocenyl ruthenocenyl ketone (I) where both entities are contained within the same molecule.

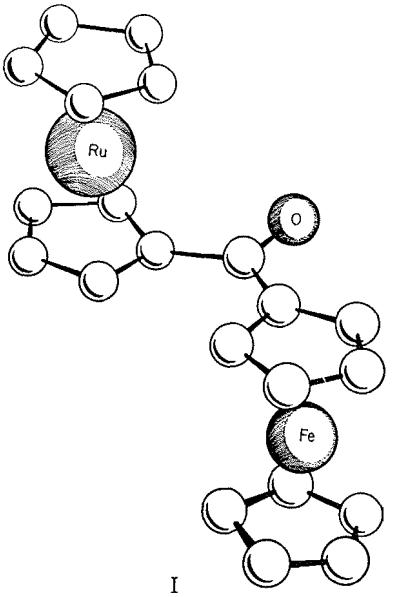

I

Crystals of ferrocenyl ruthenocenyl ketone are orange-red needles elongated along b.

Crystal Data ($\lambda_{Cu\,K_\alpha}$ = 1.5418 Å)

$C_{21}H_{18}OFeRu$, M = 444; m.p. = 216 °C.

Monoclinic, a = 13.29 ± 0.02, b = 6.12 ± 0.01, c = 10.51 ± 0.02 Å, β = 111°17′.

V = 797 Å^3.

D_m (flotation in aqueous $AgNO_3$) = 1.86 g cm^{-3}.

Z = 2.

D_x = 1.85 g cm^{-3}.

$F(000)$ = 444.

Absorption coefficient for Cu K_α X-rays, μ = 160 cm^{-1}.

Absent spectra: $h0l$ when h is odd. In addition hkl weak when $(h + k)$ is odd. Space group is Pa, $P2/a$, or $P2_1/a$.

Intensity data for $h0l$ reflections were recorded on Weissenberg films and estimated visually; no absorption corrections were applied. The heavy atom positions were determined from the Patterson projection assuming space group Pa, and a Fourier series was

summed with phases based on these positions. The resulting electron-density map could best be interpreted as having molecules situated on diad axes of space group $P2/a$, the apparent twofold molecular symmetry being achieved by a disordered arrangement of molecules. The x- and z-coordinates of all the atoms were derived and are listed in Table I; structure factors were calculated with these parameters, with the scattering factors of

TABLE I

Positional parameters (fractional)

Atom	x	z
$\frac{1}{2}$(Ru + Fe)	0.4067	0.2525
C(1)	0.262	0.130
C(2)	0.293	0.251
C(3)	0.296	0.343
C(4)	0.267	0.286
C(5)	0.247	0.145
C(6)	0.520	0.151
C(7)	0.558	0.254
C(8)	0.580	0.382
C(9)	0.556	0.363
C(10)	0.518	0.217
C(11)	$\frac{1}{4}$	0
O	$\frac{1}{4}$	0

the *International Tables* (2) and $B = 3.0$ Å^2 for Fe and Ru and 4.0 Å^2 for the other atoms, and R was 0.14 for 151 observed reflections (a table of measured and calculated structure factors is available from the authors (1)). An electron-density projection along b is shown in Fig. 1. Since hkl reflections are weak when $(h + k)$ is odd, y of $\frac{1}{2}$(Fe + Ru) is about $\frac{1}{4}$.

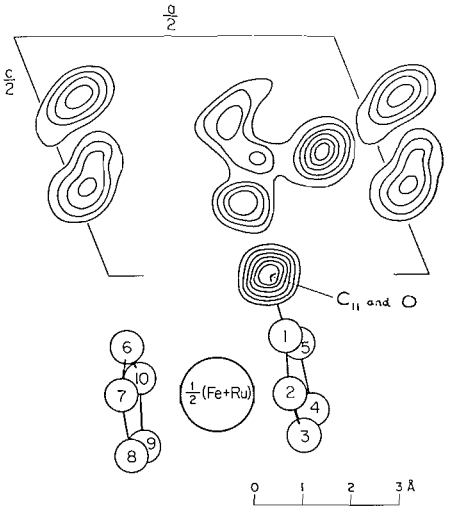

FIG. 1. Electron-density projection along b; contours at intervals of 2 eÅ^{-2}, starting at 4 eÅ^{-2}, except at the heavy atom, where contours are at intervals of 10 eA^{-2}.

Since no superlattice reflections or diffuse scattering are apparent on the films the two molecular orientations, related by a twofold axis, are distributed at random throughout the crystal. The electron-density projection (Fig. 1) indicates that both parts of the molecule have the rings similarly oriented (otherwise the density would be much more

Can. J. Chem. Downloaded from www.nrcresearchpress.com by 210.87.254.6 on 09/05/12
For personal use only.

smeared out), the configuration being about midway between eclipsed and staggered, as in biferrocenyl (3). As a result of the disorder, the further refinement required to establish the structure and configuration more precisely is not profitable; we hope to obtain more accurate information from a study of diferrocenyl ketone. The fact that the rings bonded to the iron atom do have the same disposition as those bonded to the ruthenium suggests that the configuration is influenced to a great extent by intermolecular interactions. The central rings are not quite coplanar, each being rotated a few degrees out of the $C_1C_1'C_{11}O$ plane. No accurate molecular dimensions are available from this study, but all the intra- and inter-molecular distances appear to be normal.

ACKNOWLEDGMENTS

The authors are indebted to the National Council of Canada for financial support, to Dr. M. D. Rausch for the crystal sample, to Dr. F. R. Ahmed for kindly making available his I.B.M. 1620 programs, and to the staff of the U.B.C. Computing Centre for assistance.

1. J. TROTTER. Acta Cryst. **16**, 571 (1963).
2. INTERNATIONAL TABLES FOR X-RAY CRYSTALLOGRAPHY. Vol. III. Kynoch Press, Birmingham. 1962.
3. A. C. MACDONALD and J. TROTTER. Acta Cryst. In press.

RECEIVED MARCH 2, 1964.
DEPARTMENT OF CHEMISTRY,
UNIVERSITY OF BRITISH COLUMBIA,
VANCOUVER 8, BRITISH COLUMBIA.

HYDROGENOLYSIS OF CARBOHYDRATES. X. HYDROGENOLYSIS OF (±)-EPI-INOSOSE-2[1,2]

P. A. J. GORIN

Posternak has shown that catalytic hydrogenation of scyllo-inosose using a platinum catalyst in 5% aqueous sulphuric acid results in the formation of scyllo-quercitol (1). More recently Post and Anderson found that hydrogenation of (+)-vibo-inosose (I) under similar conditions yields (+)-vibo-quercitol (II) and 1,3/2,4-cyclohexanetetrol (III), that is, the tetrol is formed from the inosose by reductive removal of the keto and its adjacent hydroxyl group. This reaction is general among substituted inososes having an axial hydroxyl vicinal to the keto group (2).

In the present work it was observed that by-products were formed during the preparation of (±)-epi-quercitol (VI) from (±)-epi-inosose-2 (V) (purified via its phenylhydrazone (3)). Fractionation of the product on a cellulose column gave tetrol and triol fractions as well as (±)-epi-quercitol. The former consisted mainly of (±)-1,2,3/4-cyclohexanetetrol (VII), which was identified, subsequent to measurement of its periodate characteristics, by comparison with an authentic specimen (4). Oxidation of the triol fraction with sodium periodate resulted in consumption of 2.0 moles of oxidant with concomitant production of 0.9 moles of acid. After crystallization the triol had a melting point corresponding to 1,3/2-cyclohexanetriol (5) (VIII) and differing from those of the 1,2,3- (6) and 1,2/3-isomers (5). Although an authentic specimen was not available the identification was

[1]*Carried out, in part, through the courtesy of Prof. S. J. Angyal, University of New South Wales, Sydney, Australia.*
[2]*Issued as N.R.C. No. 7953.*

Can. J. Chem. Downloaded from www.nrcresearchpress.com by 210.87.254.6 on 09/05/12
For personal use only.

smeared out), the configuration being about midway between eclipsed and staggered, as in biferrocenyl (3). As a result of the disorder, the further refinement required to establish the structure and configuration more precisely is not profitable; we hope to obtain more accurate information from a study of diferrocenyl ketone. The fact that the rings bonded to the iron atom do have the same disposition as those bonded to the ruthenium suggests that the configuration is influenced to a great extent by intermolecular interactions. The central rings are not quite coplanar, each being rotated a few degrees out of the $C_1C_1'C_{11}O$ plane. No accurate molecular dimensions are available from this study, but all the intra- and inter-molecular distances appear to be normal.

ACKNOWLEDGMENTS

The authors are indebted to the National Council of Canada for financial support, to Dr. M. D. Rausch for the crystal sample, to Dr. F. R. Ahmed for kindly making available his I.B.M. 1620 programs, and to the staff of the U.B.C. Computing Centre for assistance.

1. J. TROTTER. Acta Cryst. **16**, 571 (1963).
2. INTERNATIONAL TABLES FOR X-RAY CRYSTALLOGRAPHY. Vol. III. Kynoch Press, Birmingham. 1962.
3. A. C. MACDONALD and J. TROTTER. Acta Cryst. In press.

RECEIVED MARCH 2, 1964.
DEPARTMENT OF CHEMISTRY,
UNIVERSITY OF BRITISH COLUMBIA,
VANCOUVER 8, BRITISH COLUMBIA.

HYDROGENOLYSIS OF CARBOHYDRATES. X. HYDROGENOLYSIS OF (±)-EPI-INOSOSE-2[1,2]

P. A. J. GORIN

Posternak has shown that catalytic hydrogenation of scyllo-inosose using a platinum catalyst in 5% aqueous sulphuric acid results in the formation of scyllo-quercitol (1). More recently Post and Anderson found that hydrogenation of (+)-vibo-inosose (I) under similar conditions yields (+)-vibo-quercitol (II) and 1,3/2,4-cyclohexanetetrol (III), that is, the tetrol is formed from the inosose by reductive removal of the keto and its adjacent hydroxyl group. This reaction is general among substituted inososes having an axial hydroxyl vicinal to the keto group (2).

In the present work it was observed that by-products were formed during the preparation of (±)-epi-quercitol (VI) from (±)-epi-inosose-2 (V) (purified via its phenylhydrazone (3)). Fractionation of the product on a cellulose column gave tetrol and triol fractions as well as (±)-epi-quercitol. The former consisted mainly of (±)-1,2,3/4-cyclohexanetetrol (VII), which was identified, subsequent to measurement of its periodate characteristics, by comparison with an authentic specimen (4). Oxidation of the triol fraction with sodium periodate resulted in consumption of 2.0 moles of oxidant with concomitant production of 0.9 moles of acid. After crystallization the triol had a melting point corresponding to 1,3/2-cyclohexanetriol (5) (VIII) and differing from those of the 1,2,3- (6) and 1,2/3-isomers (5). Although an authentic specimen was not available the identification was

[1]*Carried out, in part, through the courtesy of Prof. S. J. Angyal, University of New South Wales, Sydney, Australia.*
[2]*Issued as N.R.C. No. 7953.*

Can. J. Chem. Downloaded from www.nrcresearchpress.com by 210.87.254.5 on 09/05/12
For personal use only.

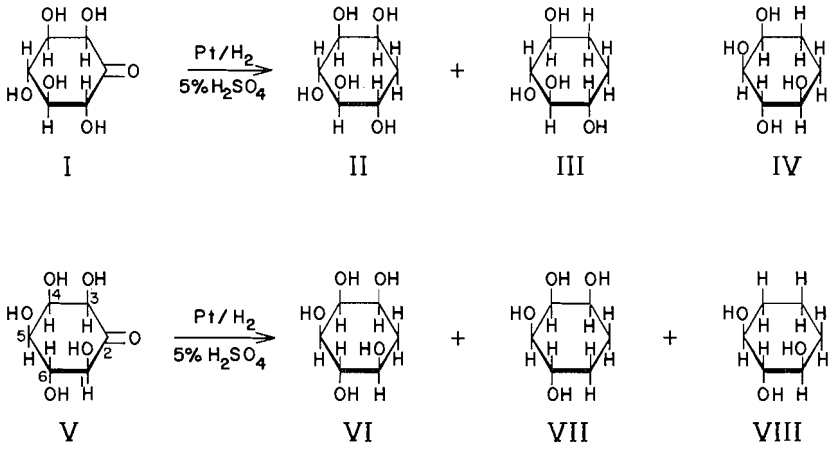

confirmed by examination of the nuclear magnetic resonance (n.m.r.) spectrum of the derived triacetate. It gave one acetoxy-proton signal in the n.m.r. at 2.0 p.p.m., thus indicating three equatorial acetoxy groups. In polyacetoxycyclohexanes which do not interconvert readily from one chair form to the other, equatorial acetoxy protons give signals at 2.0–2.1 p.p.m. Axial acetoxy protons produce signals at slightly lower field. This relation of chemical shift to conformation has been demonstrated with myo-, levo- (7), epi-, and neo-inositol hexaacetates (8) and the acetates of stereoisomeric quinic acid and quinicol derivatives (9).

The mixture, formed by hydrogenolysis of (±)-epi-inosose-2, was acetylated and examined by gas phase chromatography. On a molar basis the composition of the acetate mixture was as follows: (±)-epi-inositol (7%), (±)-epi-quercitol (53%), (±)-1,2,3/4-cyclohexanetetrol (21%), 1,3/2-cyclohexanetriol (9%). Smaller amounts of an unidentified tetrol acetate (5%) and two triol acetates (1% each) were detected. The (±)-1,2,4/3-cyclohexanetetrol tetraacetate was shown to be absent from the mixture.

In the light of the results obtained by Posternak (1) and Post and Anderson (2) it was not anticipated that hydrogenation of (±)-epi-inosose-2 would give appreciable amounts of tetrols and triols. Reductive elimination of the equatorial hydroxyl at C-1 and the keto group takes place, to yield (±)-1,2,3/4-cyclohexanetetrol (VII). A similar elimination at C-3 to form (±)-1,2,4/3-cyclohexanetetrol (IV) does not occur. Instead it appears that the platinum–cyclitol intermediate involving C-2 and C-3 is further hydrogenolyzed at C-4 to give 1,3/2-cyclohexanetriol. In this case the C-4 substituents have a reactivity comparable to those containing an axial hydroxyl group vicinal to a keto group in inososes.

EXPERIMENTAL

The (±)-epi-inosose-2 was prepared by the method of Posternak (10). A crude sample had C, 39.30; H, 5.84. Calc. for $C_6H_{10}O_6$: C, 40.45; H, 5.66%. After purification via its phenylhydrazone and two recrystallizations from water a sample had C, 39.92; H, 5.79%. Examination of the phenylhydrazone and semicarbazone (3) reaction mixtures on a paper chromatogram (solvent: *n*-butanol–ethanol–water 40:11:19 v/v; spray: ammoniacal silver nitrate) did not indicate the presence of any disubstituted derivatives. Melting points are corrected to the nearest degree.

Hydrogenation of (±)-*epi-Inosose-2*

The (±)-epi-inosose-2 (2.0 g) was suspended in 5% sulphuric acid (50 ml) and shaken overnight with platinic oxide (0.20 g) in the presence of hydrogen. The solution was filtered, neutralized with barium carbonate, filtered, and evaporated. The product gave on a paper chromatogram (solvent and spray as above)

Can. J. Chem. Downloaded from www.nrcresearchpress.com by 210.87.254.5 on 09/05/12
For personal use only.

a main spot corresponding to epi-quercitol, and two others running at a faster rate. A trace of epi-inositol was present also.

The product was acetylated and examined by gas phase chromatography using 2% LAC IR296 on Chromosorb W as column packing (11). The gas–liquid chromatograph unit was of conventional design using thermal conductivity cells for detection. At 200 °C a satisfactory separation of epi-inositol, epi-quercitol, and tetrol acetates was obtained and at 160 °C the triol, tetrol, and epi-quercitol acetates gave suitable signals.

The responses of the machine were calibrated using authentic cyclitol acetates. On a molar basis the product consisted of the acetates of (±)-epi-inosose (7%), (±)-epi-quercitol (53%), (±)-1,2,3/4-cyclohexanetetrol (21%), 1,3/2-cyclohexanetriol (9%). An unidentified tetrol acetate (5%), with a slightly higher retention time than the main tetrol acetate, and two triol acetates (1% each), which had higher and lower retention times than the main triol acetate, respectively, were also detected.

The acetate of (±)-1,2,4/3-cyclohexanetetrol (4) was shown to have a lower retention time than the (±)-1,2,3/4-isomer (4).

Isolation of Hydrogenolysis Products

The above hydrogenolysis product was fractionated on a cellulose column using *n*-butanol one-half saturated with water as eluant. The following materials were isolated:

(i) *Triol*—140 mg was isolated and oxidation of this material with aqueous sodium periodate resulted in the consumption of 1.97 moles of oxidant in one day with concomitant production of 0.94 moles of acid.

One crystallization from ethyl acetate yielded 104 mg of material and a further recrystallization from the same solvent gave 1,3/2-cyclohexanetriol with m.p. 107–108 °C. Calc. for $C_6H_{12}O_3$: C, 54.5; H, 9.15. Found: C, 54.6; H, 9.4%. McRae *et al.* (5) report m.p. 107.7–108.2 °C for the 1,3/2-isomer, whereas the 1,2,3-isomer has m.p. 145 °C (6) and the 1,2/3-isomer m.p. 125 °C (5). After 5 h the triol consumed 1.97 moles of sodium periodate releasing 1.05 moles of acid.

The triacetate, obtained by the hot sodium acetate – acetic acid anhydride method, was recrystallized twice from hexane to give a product with m.p. 128–129 °C. Calc. for $C_{12}H_{18}O_6$: C, 55.8; H, 7.0. Found: C, 55.6; H, 7.0%. In the n.m.r., using chloroform as solvent, it gave one signal for acetoxy protons at 2.00 p.p.m. (tetramethyl silane standard).

(ii) *Tetrol*—324 mg was isolated from the column and this was recrystallized from ethanol. The product (0.23 g) was recrystallized and had m.p. 158–159 °C. Calc. for $C_6H_{12}O_4$: C, 48.6; H, 8.2. Found: C, 48.75; H, 8.2%. After 5 and 24 h the tetrol consumed 3.0 moles of sodium periodate, yielding 2.0 moles of acid. The tetrol gave an X-ray diffraction pattern identical with (±)-1,2,3/4-cyclohexanetetrol (4). The derived tetraacetate was recrystallized twice from ether–hexane and had m.p. 113–114 °C. Calc. for $C_{14}H_{20}O_8$: C, 53.3; H, 6.4. Found: C, 53.0; H, 6.45%.

(iii) (±)-*epi-Quercitol*—The majority of the product was represented by epi-quercitol (1.05 g) with m.p. 187–190 °C after two recrystallizations from aqueous ethanol. Calc. for $C_6H_{12}O_5$: C, 43.9; H, 7.4. Found: C, 43.9; H, 7.35%.

ACKNOWLEDGMENTS

The author thanks Prof. T. Posternak for the gift of (±)-1,2,3/4- and (±)-1,2,4/3-cyclohexanetetrols. Thanks are also due to Dr. E. Challen of the University of New South Wales and Mr. M. Mazurek for carrying out carbon and hydrogen analyses, and Mr. W. C. Haid for an n.m.r. determination.

1. T. Posternak. Helv. Chim. Acta, **24**, 1045 (1941).
2. G. G. Post and L. Anderson. J. Am. Chem. Soc. **84**, 471 (1962).
3. T. Posternak. Biochem. Prep. **2**, 57 (1952).
4. T. Posternak and H. Friedli. Helv. Chim. Acta, **36**, 251 (1953).
5. J. A. McRae, R. Y. Moir, J. W. Haynes, and C. G. Ripley. J. Org. Chem. **17**, 1621 (1952).
6. G. W. K. Cavill and D. H. Solomon. J. Chem. Soc. 4426 (1955).
7. R. U. Lemieux, R. K. Kullnig, H. J. Bernstein, and W. G. Schneider. J. Am. Chem. Soc. **79**, 1005 (1959).
8. P. A. J. Gorin. Unpublished work.
9. P. A. J. Gorin. Can. J. Chem. **41**, 2417 (1963).
10. T. Posternak. Helv. Chim. Acta, **19**, 1333 (1936).
11. S. J. Angyal and Z. S. Krzeminski. J. Chem. Soc. 3251 (1962).

Received November 8, 1964.
Prairie Regional Laboratory,
National Research Council,
Saskatoon, Saskatchewan.

Can. J. Chem. Downloaded from www.nrcresearchpress.com by 210.87.254.5 on 09/05/12
For personal use only.

Can. J. Chem. Downloaded from www.nrcresearchpress.com by 210.87.254.42 on 09/05/12
For personal use only.

POLYSACCHARIDES FROM THE SEEDS OF THE HUACRA PONA PALM (IRIARTEA VENTRICOSA)[1]

W. SOWA[2] AND J. K. N. JONES

Many plants produce seeds containing polysaccharides with a high proportion of D-mannose residues. In some cases D-glucose or D-galactose is joined to the main chain of D-mannose units (1). Early studies of ivory nut, the seed of the ivory nut palm (*Phytelephas macrocarpa*), established that mannose was the main carbohydrate component (2). Later work showed that at least two mannans (A and B) were present (3) and that both polymers were linear chains of D-mannopyranose units with β-1 $\rightarrow$ 4 linkages (4). More recently the mannans have been reinvestigated by Aspinall and coworkers (5). Mannan A, $[\alpha]_D$ $-46°$ (*c* 0.7 in *N* sodium hydroxide), was composed of D-mannose (97.6%), D-galactose (1.8%), and D-glucose (0.8%). From methylation studies it was deduced that two types of molecules were present, both comprising an average of 10 to 13 residues, one terminated at the non-reducing end by a D-mannopyranose residue and the other by a D-galactopyranose residue. The majority of the D-mannopyranose units were linked through C1 and C4 with some 1 $\rightarrow$ 6 linkages. A small amount of di-*O*-methyl mannose was found. Mannan B, $[\alpha]_D$ $-26°$ (*c* 0.8 in anhydrous formic acid) was chemically similar to mannan A but of greater molecular size (38 to 40 residues). Partial acetolysis (6) of the polymers yielded a homologous series of mannose oligosaccharides with β-1 $\rightarrow$ 4 linkages. Small amounts of 4-*O*-α-D-mannopyranosyl-D-mannose and β-1 $\rightarrow$ 4 linked oligosaccharides containing mannose and glucose were also found.

The present work describes preliminary results of an investigation of the seeds of the huacra pona tree (*Iriartea ventricosa*), a palm which grows in tropical South America. The fruit of this tree yields a jelly which is used locally as a base in medicinal preparations (7). The seeds are dark brown, about half an inch in diameter, and somewhat cone-shaped. They are extremely hard and in this respect resemble the seeds of the ivory nut palm.

Following the procedure of Aspinall *et al.* (5) for ivory nuts, the seeds were extracted first with 7% and then with 14% potassium hydroxide solutions to obtain polysaccharides. Fraction I, $[\alpha]_D$ $-42°$ (*c* 1.0 in 5 *N* sodium hydroxide), and fraction II, $[\alpha]_D$ $-30°$ (*c* 1.0 in 5 *N* sodium hydroxide), amounted to 15% and 9% of the seeds respectively. Further extraction of the seed residues with 21% potassium hydroxide, then with 14% potassium hydroxide plus 3% boric acid (8) and finally with 14% sodium hydroxide yielded an additional 17.5% of polysaccharide. Most of this (fraction V, 16%) was extracted by the sodium hydroxide solution. Paper chromatographic examination of the hydrolysates of the first four fractions indicated the presence of mannose accompanied by small amounts of galactose, glucose, uronic acid, and a trace of pentose. Fraction V appeared to be a neutral polymer of mannose and glucose. All fractions, especially fraction V, were very unreactive and difficult to hydrolyze.

Fractions I and II moved as discrete spots at slightly different rates when examined by glass paper electrophoresis in a borate buffer (9), suggesting that they were similar in structure but perhaps different in molecular size. The conditions employed for the formation of oligosaccharides from fractions I and II by acid hydrolysis were similar to those used for the formation of oligosaccharides from ivory nut mannan. The change in optical

[1]*Abstracted from the M.Sc. thesis of W.S. (1958 Queen's University).*
[2]*Present address: Ontario Research Foundation, Toronto 5, Ontario.*

Can. J. Chem. Downloaded from www.nrcresearchpress.com by 210.87.254.42 on 09/05/12
For personal use only.

rotation of the solutions during hydrolysis was also of the same order. Fraction I contained 6% of uronic acid anhydride. On periodate oxidation the polysaccharide consumed approximately 1 mole of periodate per mole of hexose and yielded traces of formic acid. Chromatographic examination of the hydrolysate of the oxidized polymer indicated that a small amount (1–2%) of the hexose residues had not been oxidized.

Fraction II was only partially acetylated with pyridine as catalyst and dimethyl formamide as swelling agent (10). Acetylation was effected with trifluoroacetic anhydride as catalyst (11). Attempted methylation of the acetylated product was unsuccessful even after eight treatments by the Haworth procedure (12). On graded hydrolysis of fraction II several oligosaccharides were obtained. These were separated by chromatography on a column of charcoal–Celite (13) and on paper. The major oligosaccharide was identified as 4-*O*-β-D-mannopyranosyl-α-D-mannopyranose. A small amount of an unidentified syrupy disaccharide, containing galactose and mannose, was also isolated. A trisaccharide, according to data obtained from partial hydrolysis and periodate oxidation, appeared to be a mannosyl-mannobiose containing $1 \rightarrow 6$ and $1 \rightarrow 4$ linkages.

The above results suggest that the polysaccharide reserve of the seeds of the huacra pona palm is a β-$1 \rightarrow 4$ linked mannan containing small amounts of D-galactose. The polymer may also contain some $1 \rightarrow 6$ linkages. The significance of the uronic acid portion is unknown but it may be part of an associated polymer, the presence of which may also explain the detection of traces of pentose residues. The polysaccharide fractions occurring in seeds of the huacra palm are thus structurally similar to those in seeds of the ivory nut palm.

EXPERIMENTAL

Paper chromatography was performed by the descending method on Whatman No. 1 paper using the following solvent systems (v/v): (A) ethyl acetate, acetic acid, formic acid, water (18:3:1:4); (B) ethyl acetate, acetic acid, water (9:2:2); (C) butan-1-ol, pyridine, water (10:3:3); (D) butan-1-ol, ethanol, water (3:1:1). Sugars were detected with the *p*-anisidine hydrochloride spray (14), the silver nitrate spray (15) or with a 0.1 *M* solution of 2-aminobiphenyl hydrogen oxalate in acetone (16).

Glass paper electrophoresis was carried out in borate buffer at pH 10.0 (9). Polysaccharides were applied in a 10% solution of sodium hydroxide and detected by spraying the glass paper with a solution of α-naphthol in methanol (3% w/v) followed by concentrated sulphuric acid.

Solutions were concentrated under reduced pressure at a water bath temperature of 40° or less. Optical rotations were determined in water at 20° ± 2° unless otherwise stated.

Isolation of Polysaccharide Fractions

Finely divided seeds (50 g) of huacra pona (*Iriartea ventricosa*) were extracted in a Soxhlet apparatus with benzene for 14 h and then with methanol for 14 h. The residue (32.5 g, 65%) was delignified by the sodium chlorite – acetate acid technique (17). The delignified material (27 g, 54%) was shaken at room temperature with successive solutions (200 g) of alkali of increasing concentration. Each polysaccharide fraction was isolated by pouring the extract into an equal volume of ethanol acidified with acetic acid. The results are shown in Table I.

TABLE I

Polysaccharide fractions obtained by alkaline extraction of seeds

Fraction	$[\alpha]_D$ (*c* 1.0 in 5 *N* NaOH)	Extraction solution	Yield (g)	Yield (% of seeds)
I	−42°	7% KOH	7.5	15
II	−30°	14% KOH	4.5	9
III	−36°	21% KOH	0.3	0.5
IV	−34°	14% KOH + 3% H_3BO_3	0.6	1
V	—	14% NaOH	7.7	16

Fractions I and II were examined for homogeneity by glass paper electrophoresis. Both fractions travelled as single spots with fraction I moving at a slightly greater rate than fraction II.

Hydrolysis of Fractions

Fraction I (1.00 g) was heated with formic acid (50 ml, 90%) in a boiling water bath. The hydrolysis was followed chromatographically and by the change in optical rotation, which was as follows: $[\alpha]_D$ −18° (10 min); −10° (30 min); −1° (1 h); +9° (2 h); +18° (3 h); +21° (8 h), constant value. The concentration of oligosaccharides was a maximum after 3 h hydrolysis. Disaccharides were still present in small amounts after 10 h. Traces of galactose, glucose, pentose, and uronic acids were also present. A colorimetric method employing carbazole (18) showed that fraction I contained 5.8% uronic acid. Fraction II on hydrolysis showed a similar change in optical rotation and in the chromatographic pattern of oligosaccharides. Hydrolysis of small samples of fractions III and IV with 2 *N* sulphuric acid in sealed tubes at 100°, followed by chromatographic examination, showed the presence of the same monosaccharides as in fractions I and II. Fraction V was difficult to hydrolyze with formic acid, 5 *N* sulphuric acid or trifluoroacetic acid at 100°. It was partially dissolved in 72% sulphuric acid and after 5 h the mixture was diluted to 5% sulphuric acid. After the diluted mixture was heated at 100° for 12 h, half the polysaccharide was recovered unhydrolyzed. The sugars in solution were examined chromatographically in solvents (A), (C), and (D) and consisted of glucose and mannose in the approximate ratio 1:1.

Mannan A, obtained by extracting ivory nut shavings with 5% sodium hydroxide solution (3), was hydrolyzed under the same conditions as fraction I. The following change in optical rotation was observed: $[\alpha]_D$ −28° (3 min); −13° (33 min); 0° (50 min); +12° (2.25 h); +15° (3.5 h); +18° (6.5 h); +19° (9.75 h). Paper chromatographic examination showed that the maximum yield of oligosaccharides was obtained after hydrolysis for 50 min.

Oxidation of Fraction I by Sodium Periodate

Samples (100 mg) were suspended in potassium chloride solution (5 ml, 3% w/v) and water (10 ml) was added followed by sodium periodate solution (5 ml, 0.3 *M*). Samples and blanks were shaken at 5° and removed at intervals for the determination of periodate consumption and formic acid yield (19). Found: moles of periodate consumed and formic acid produced per hexose unit ($C_6H_{10}O_5$): 0.66, 0.04 (6 h); 0.68, 0.05 (16 h); 0.81, 0.06 (74 h); 0.97, 0.07 (150 h). A sample of polysaccharide (100 mg) was oxidized for 150 h and excess periodate was then destroyed by the addition of ethylene glycol. The solution was neutralized (barium carbonate) and filtered and sodium borohydride (50 mg) was added. After 18 h the solution was acidified (acetic acid) and evaporated to dryness. The residue was boiled with methanolic hydrogen chloride (100 ml, 1.5%) for 30 min and then evaporated to a syrup. The residue was hydrolyzed for 18 h with *N* sulphuric acid (30 ml) at 100°, cooled, neutralized (barium carbonate), and filtered. The filtrate was concentrated and examined chromatographically in solvents A, B, and C. Erythritol and traces of glycerol, glucose, and mannose were present. The yield of monosaccharides by visual comparison with standards was 1–2%.

Acetylation and Attempted Methylation of Fraction I

Method I (10)

The polysaccharide (0.25 g) was swollen in dimethyl formamide (6 ml) at 20° for 16 h and at 50° for 1 h. Pyridine (10 ml) was then added dropwise at 45° during 1.5 h, followed by acetic anhydride (8 ml). After 1 h at 50° and 14.5 h at 20°, the product was isolated. It contained 7.3% acetyl and the method of acetylation was, therefore, unsatisfactory.

Method II (11)

The polysaccharide (4.00 g) was shaken in acetic acid (75 ml) at 20° for 24 h. Trifluoroacetic anhydride (100 ml) was then added and the mixture was heated at 50° for 2 h. After a further 20 h at 20°, the clear yellow solution was evaporated to 50 ml and poured into sodium bicarbonate solution (500 ml, 2% w/v). The precipitate was collected by filtration, washed well with water, and dried. The product (5.77 g) had $[\alpha]_D$ −18° (*c* 1.0 in acetone) and −34° (*c* 1.0 in chloroform). The acetyl content was 42.9%.

The acetate (5.67 g) was dissolved in acetone–dioxane mixture (150 ml; 2:1 ratio) and methylated with sodium hydroxide (30%) and dimethyl sulphate in the usual way (12). The product (2.4 g) was very difficult to methylate and even after eight treatments was only partially methylated.

Hydrolysis of Fraction II

Fraction II (3.50 g) was hydrolyzed by heating it with formic acid (175 ml, 90%) in a boiling water bath for 1.25 h. The solution was filtered from a small amount of unhydrolyzed material and then evaporated to a syrup (3.61 g). A solution of the syrup in water was placed on top of a column of charcoal–Celite (3 × 30 cm) and fractionated by the method of Whistler and Durso (13). The following 3 major fractions were obtained:

Fraction A

The first fraction (1.70 g), obtained by eluting the column with water, consisted mainly of D-mannose together with traces of a disaccharide, galactose, and xylose.

Fraction B

The second fraction (0.30 g), also obtained by eluting the column with water, was the disaccharide observed

Can. J. Chem. Downloaded from www.nrcresearchpress.com by 210.87.254.42 on 09/05/12
For personal use only.

in fraction A. It was chromatographically indistinguishable from an authentic specimen of 4-*O*-β-D-mannopyranosyl-α-D-mannopyranose. It crystallized from ethanol–water and had m.p. 194–195° and $[\alpha]_D$ −4° → −9° in 1.75 h (*c* 3.3). The X-ray diffraction patterns of the crystals and of the authentic specimen were identical.

Fraction C

Fraction C (0.68 g), $[\alpha]_D$ −14° (*c* 6.7), was a mixture of oligosaccharides, mainly 4-*O*-β-D-mannopyranosyl-D-mannose, which was eluted from the column with water containing from 2% to 50% ethanol (v/v). Paper chromatography of this fraction in solvent (D) yielded two additional oligosaccharides. One was a disaccharide (0.045 g) with $[\alpha]_D$ +11° (*c* 2.2). In solvents A, C, and D it had $R_{galactose}$ 0.38, 0.23, and 0.43, respectively. On partial hydrolysis of the disaccharide with 0.5 *N* sulphuric acid at 100° for 4 h, galactose, mannose, and starting material were observed chromatographically. It was not identified.

The other oligosaccharide (0.14 g) in fraction C had $[\alpha]_D$ −12° (*c* 1.2) and $R_{galactose}$ 0.11 in solvent A. On partial hydrolysis with 0.5 *N* sulphuric acid at 100° for 4 h it yielded D-mannose and a disaccharide which was indistinguishable from 4-*O*-β-D-mannopyranosyl-D-mannose by chromatography in solvents B, C, and D. The degree of polymerization was 3 by the method of Peat, Whelan, and Roberts (20). The trisaccharide (4.0 mg) was oxidized with sodium periodate solution and the yield of formaldehyde was determined using chromotropic acid (21). Found: moles of formaldehyde per mole of trisaccharide: 0.86 (1 h); 0.96 (3 h); 1.33 (5 h); 1.33 (18 h). In a parallel experiment the trisaccharide (4.0 mg) first was reduced in water with sodium borohydride (12 mg) for 1 h. After acidification with *N* sulphuric acid (0.4 ml), the product was oxidized with sodium periodate solution and the yield of formaldehyde was determined. Found: moles formaldehyde per mole of reduced trisaccharide: 1.11 (1 h), 1.47 (3 h), 1.76 (5 h), 1.95 (18 h). The consumption of periodate during oxidation of the trisaccharide was determined spectrophotometrically by the method of Aspinall and Ferrier (22). Found: moles periodate per mole of trisaccharide: 5.0 (2 h); 5.1 (3 h); 5.3 (4 h); 6.7 (6 h); 7.0 (30 h).

ACKNOWLEDGMENTS

The authors thank the National Research Council (N.R.C. T-19) and the Ontario Research Foundation for financial assistance. They thank Baron Walter Frass von Wolfenegg, Director of Colonization for the Oriente, Peru, for the gift of huacra pona seeds (7).

1. F. SMITH and R. MONTGOMERY. The chemistry of plant gums and mucilages. Reinhold Publishin Corporation, New York. 1959. p. 324.
2. R. REISS. Ber. **22**, 609 (1889). E. FISCHER and J. HIRSCHBERGER. Ber. **22**, 1155 (1889).
3. K. HESS and M. LÜDTKE. Ann. **456**, 201 (1927).
4. J. PATTERSON. J. Chem. Soc. **123**, 1139 (1923). F. KLAGES. Ann. **509**, 159 (1934); **512**, 185 (1934).
5. G. O. ASPINALL, E. L. HIRST, E. G. V. PERCIVAL, and I. R. WILLIAMSON. J. Chem. Soc. 3184 (1953).
6. G. O. ASPINALL, R. B. RASHBROOK, and (in part) G. KESSLER. J. Chem. Soc. 215 (1958).
7. L. CLARK. The rivers ran east. Funk and Wagnalls, New York. 1961.
8. J. K. N. JONES, L. E. WISE, and J. JAPPE. Tappi, **39**, 139 (1956).
9. E. J. BOURNE, A. B. FOSTER, and P. M. GRANT. J. Chem. Soc. 4311 (1956).
10. J. F. CARSON and W. D. MACLAY. J. Am. Chem. Soc. **68**, 1015 (1946).
11. E. J. BOURNE, M. STACEY, J. C. TATLOW, and J. M. TEDDER. J. Chem. Soc. 2976 (1949).
12. W. N. HAWORTH and E. G. V. PERCIVAL. J. Chem. Soc. 2277 (1932).
13. R. L. WHISTLER and D. F. DURSO. J. Am. Chem. Soc. **72**, 677 (1950).
14. L. HOUGH, J. K. N. JONES, and W. H. WADMAN. J. Chem. Soc. 1702 (1950).
15. W. E. TREVELYAN, D. P. PROCTER, and J. S. HARRISON. Nature, **166**, 444 (1950).
16. H. T. GORDON, W. THORNBURG, and L. N. WERUM. Anal. Chem. **28**, 849 (1956).
17. L. E. WISE, M. MURPHY, and A. A. D'ADDIECO. Paper Trade J. **122(2)**, 35 (1946).
18. Z. DISCHE. J. Biol. Chem. **183**, 489 (1950). E. A. MCCOMB and R. M. MCCREADY. Anal. Chem. **24**, 1630 (1952).
19. L. MALAPRADE. Compt. Rend. **186**, 382 (1928). A. L. POTTER and W. Z. HASSID. J. Am. Chem. Soc. **70**, 3490 (1948). S. K. CHANDA, E. L. HIRST, J. K. N. JONES, and E. G. V. PERCIVAL. J. Chem. Soc. 1289 (1950).
20. S. PEAT, W. J. WHELAN, and P. J. P. ROBERTS. J. Chem. Soc. 2258 (1956).
21. J. F. O'DEA and R. A. GIBBONS. Biochem. J. **55**, 580 (1953).
22. G. O. ASPINALL and R. J. FERRIER. Chem. Ind. 1216 (1957).

RECEIVED FEBRUARY 14, 1964.
DEPARTMENT OF CHEMISTRY,
QUEEN'S UNIVERSITY,
KINGSTON, ONTARIO.

Can. J. Chem. Downloaded from www.nrcresearchpress.com by 210.87.254.42 on 09/05/12
For personal use only.

ALUMINUM HYDRIDE DERIVATIVES FROM THE REACTIONS OF LITHIUM ALUMINUM HYDRIDE WITH TRIMETHYLAMINE AND DIMETHYLAMINE

FRANCES M. PETERS

Can. J. Chem. Downloaded from www.nrcresearchpress.com by 210.87.254.6 on 09/05/12
For personal use only.

INTRODUCTION

During the preparation of methyl and ethyl aluminum hydride complexes (1), a reaction between lithium aluminum hydride and trimethylamine was observed that yielded aluminum hydride bis-trimethylamine. The treatment of dimethyl or diethyl aluminum chloride with lithium aluminum hydride and trimethylamine in ethyl ether yielded the alkyl aluminum dihydride trimethylamine complexes (1). The route of the reaction, shown here, was determined by combining an excess of lithium aluminum hydride with

$$LiAlH_4 + R_2AlCl \xrightarrow{Et_2O} R_2AlH + [LiAlH_3Cl] \searrow AlH_3 + LiCl$$

$$R_2AlH + AlH_3 \rightarrow 2RAlH_2 \xrightarrow{Me_3N} 2RAlH_2 \cdot NMe_3$$

trimethylaluminum in ether. When trimethylamine was added to the $LiAlH_4$–Me_3Al reaction mixture to produce the stable amine adduct of the methylaluminum hydride product, a substantial amount of aluminum hydride bis-trimethylamine was formed in addition to $Me_2AlH \cdot NMe_3$. Treatment of lithium aluminum hydride with trimethylamine in ether solution afforded $AlH_3(NMe_3)_2$, confirming the suspicion that the source of the $AlH_3(NMe_3)_2$ in the $LiAlH_4$–Me_3Al reaction was the direct reaction of the amine with lithium aluminum hydride.

The isolation of aluminum hydride bis-trimethylamine is inconsistent with the results of Wiberg and co-workers (2), who report that the reaction of lithium aluminum hydride with trimethylamine yields only $LiAlH_4(NMe_3)_x$ where x is 1, 2, or 3. Only the monoamine adduct is reported to be stable at room temperature.

An attempt was made to resolve the inconsistency by a study of the reaction of lithium aluminum hydride with trimethylamine. The study revealed a complex reaction yielding, in addition to aluminum hydride bis-trimethylamine, ether-insoluble solids whose compositions are dependent upon the stoichiometric ratios of the reactants. The study was extended to include the reaction of lithium aluminum hydride with Me_2NH where, with equimolar stoichiometry, dimethylamino aluminum hydride is produced in moderate yield, a result unpredictable from the literature in this area.

EXPERIMENTAL

Starting Materials

Lithium aluminum hydride was obtained from Metal Hydrides, Inc. Trimethylamine and dimethylamine were supplied by the Matheson Company, Inc., and the ethyl ether was provided by Mallinckrodt Chemical Works.

Reactions of Lithium Aluminum Hydride and Trimethylamine

The general procedure may be illustrated by one example: An ether solution of 0.16 mole of trimethylamine was added by drops to the stirred ether solution of $LiAlH_4$ (0.16 mole) in a round-bottom flask. A precipitate began to form immediately. The reaction mixture was stirred for a day, after which time it was filtered in a drybox.[1] The ether was removed from the filtrate and the remaining solid sublimed at 25 °C and 10^{-3} mm

[1]*Model He-43/He-73, D. L. Herring Co., Inc., Sherman Oaks, California.*

Hg onto a cold finger maintained at −78 °C. Five grams (0.034 mole) $AlH_3(NMe_3)_2$ was isolated. The compound melts at 92–94 °C (uncorrected). Anal. Calc. for $C_6H_{21}AlN_2$: C, 48.6; H, 14.3; N, 18.9; Al, 18.2. Found: C, 48.3; H, 14.0; N, 18.9; Al, 18.1. The molar ratio of lithium to aluminum in the sublimation residue was 1 to 1. A sample of the dry sublimation residue was pyrolyzed in a closed system at 120–150 °C for 7 h. A large quantity of hydrogen was evolved and a negligible amount of condensable gas.

An elemental analysis of a sample of the dried reaction residue indicated that the lithium to aluminum molar ratio was 2.5 to 1. Hydrolysis of a sample of the solid with methanol showed a hydridic hydrogen ('H') to aluminum ratio of 4.5 to 1. A strong, broad band in the Al—H frequency range (1600–1900 cm^{-1}) was observed in the infrared spectrum[2] of the reaction residue in Nujol. Pyrolysis of a sample of the reaction residue 3 h at 95–120 °C yielded hydrogen and a condensable gas identified as diethyl ether by its infrared spectrum. No amine was found nor was $AlH_3(NMe_3)_2$ or $AlH_3 \cdot NMe_3$ formed.

Experiments representing a variety of stoichiometries ranging from a large molar excess of Me_3N to a large excess of $LiAlH_4$ were conducted, and the results are summarized in Table I.[3]

Reactions of Lithium Aluminum Hydride and Dimethylamine

1. A solution of 0.24 mole of Me_2NH in ethyl ether was added by drops to a stirred ether solution of 0.24 mole $LiAlH_4$ at room temperature. As each drop of amine solution made contact with the hydride solution, hydrogen was evolved and solid precipitated. There was no noticeable heating of the reaction mixture. The solid was very bulky, and the reaction mixture could be stirred only with difficulty. The reaction mixture remained at room temperature for a day after the amine had been added. No additional hydrogen was formed during this period. The reaction mixture was filtered and the ether removed from the filtrate under vacuum. When the ether-soluble residue was heated in vacuum at 75 °C, 3.4 g of solid (m.p. 75 °C) sublimed and an air-sensitive residue remained. A mixed melting point of the sublimate with an authentic sample of AlH_2NMe_2 showed no depression. Anal. Calc. for C_2H_8NAl: C, 32.9; H, 11.0; N, 19.2; Al, 36.9. Found: C, 32.8; H, 10.8; N, 19.3; Al, 36.6.

2. A reaction of dimethylamine (0.16 mole) and $LiAlH_4$ (0.08 mole) was conducted in ether solution in a manner similar to that used in the previous experiment. Only a few crystals sublimed from the ether-soluble residue at 100 °C and 10^{-3} mm Hg. No sublimate formed when the reaction residue was heated at 100 °C for several hours.

3. The reaction of 0.15 mole Me_2NH and 0.05 mole $LiAlH_4$ in ether solution yielded no sublimable products.

DISCUSSION

Reaction of Lithium Aluminum Hydride and Trimethylamine

The addition of up to 4 moles of trimethylamine to an ether solution of 1 mole of lithium aluminum hydride gives precipitates rich in lithium and aluminum hydride bis-trimethylamine that is sublimed from the ether solution. A non-subliming residue whose lithium to aluminum molar ratio decreases as increasing amounts of trimethylamine are used remains in the sublimation apparatus following the isolation of aluminum hydride bis-trimethylamine. As more than 4 moles of amine to 1 of lithium aluminum hydride are used, the yield of $AlH_3(NMe_3)_2$ approaches zero, the amount of ether-soluble non-volatile material decreases, and the quantity of precipitate increases correspondingly. When 10 moles of amine are used nearly all of the lithium aluminum hydride appears in the non-volatile precipitate containing lithium and aluminum in an approximate 1 to 1 molar ratio, hydrogen, and loosely bound trimethylamine. This precipitate may be the same material that Wiberg, Nöth, and Usón observed in their reaction of a large excess of trimethylamine with lithium aluminum hydride in ether (2). However, their product, reported to be $LiAlH_4 \cdot NMe_3$, was stable in vacuum at 180 °C, whereas the solid obtained here evolves a large non-stoichiometric amount of trimethylamine and a small amount of ether at room temperature (10^{-3} mm Hg), leaving a hydrolytically active substance free of amine.

The solids that are precipitated in the course of the reaction increase in aluminum

[2]*A Model IR-5 Beckman double-beam infrared spectrometer with sodium chloride optics was used to record spectra.*

[3]*Elemental analyses were conducted by Schwarzkopf Microanalytical Laboratory, Woodside, New York.*

Can. J. Chem. Downloaded from www.nrcresearchpress.com by 210.87.254.6 on 09/05/12
For personal use only.

Can. J. Chem. Downloaded from www.nrcresearchpress.com by 210.87.254.6 on 09/05/12
For personal use only.

TABLE I

Reactions of lithium aluminum hydride and trimethylamine

	Mole ratio $Me_3N/LiAlH_4$	Yield $AlH_3(NMe_3)_2$	Analytical results, in mole ratios: Reaction residue Li	Reaction residue Al	Reaction residue N	Reaction residue 'H'	Sublimation residue Li	Sublimation residue Al	Sublimation residue N	Comments
I	1/5 (0.03/0.15)	Not isolated	2.8	1.0	0					
II	1/2 (0.05/0.09)	0.011 mole (44% based on Me_3N)								
III	1/1 (0.16)	0.034 mole (42% based on Me_3N)	2.5	1.0 1.0*	0	 4.5*	1.0	1.0	0	Pyrolysis of the reaction residue at 120° yielded Et_2O and H_2
IV*a*	1/1 (0.13)	Not isolated	2.5	1.0	0					The reaction residue (*a*) was isolated and 0.39 mole Me_3N was added to the filtrate (*a*) for further reaction; pyrolysis of reaction residue (*a*) at 80–150° yielded Et_2O and H_2. Pyrolysis of reaction residue (*b*) at 120–150° yielded Me_3N and H_2
IV*b*	4/1 (Filtrate from IV*a* and 0.39 mole Me_3N)	Trace	1.7	1.0	0.07†					
V	2/1 (0.17/0.08)	0.016 mole (20% based on $LiAlH_4$)	2.7	1.0	0					
VI	3/1 (0.25/0.08)	0.008 mole (10% based on $LiAlH_4$)	2.4	1.0	0					
VII	4/1 (0.34/0.08)	0.005 mole (6% based on $LiAlH_4$)	2.2	1.0	0†					
VIII	5/1 (0.55/0.11)	Trace	1.6	1.0 1.0*	0.04†	 3.2*	1.0	1.6	0.6	
IX	10/1 (0.5/0.05)	Trace	1.0	1.2	0.3†		Only a trace of material remained			
X	10/1 (1.0/0.10)	None		1.0‡	1.5‡	4.7‡				The reaction residue evolved Me_3N at $25°/10^{-3}$ mm. No additional Me_3N was observed in the hydrolyzate

*Hydridic hydrogen 'H' was determined by hydrolysis with methanol. Al was determined as Al_2O_3.
†These nitrogen values are probably low because of amine evolution from the samples prior to analysis. See footnote 3.
‡The mole ratio of nitrogen was determined from HCl–NaOH titration of the Me_3N that evolved at $25°/10^{-3}$ mm prior to hydrolysis of the sample. Hydridic hydrogen was determined with methanol. Al was determined with EDTA and $ZnSO_4$, using Eriochrome black T as indicator.

content as the quantity of trimethylamine used increases. Thus the $AlH_3(NMe_3)_2$ or a species yielding $AlH_3(NMe_3)_2$ present in solution must be able to react with additional amine and dissolved lithium aluminum hydride to give additional solid of different composition than that first deposited (see Table I). (However, aluminum hydride bis-trimethylamine does not react with an ether solution of trimethylamine, nor with an ether solution of lithium aluminum hydride.) Experiment IV illustrates this phenomenon. The reaction mixture was initially equimolar in amine and $LiAlH_4$, a condition known from previous experiments to yield $AlH_3(NMe_3)_2$ from the ether solution (for example, experiment III). The precipitate (IV*a*) had the composition previously found in precipitates from other 1 to 1 reactions, namely 2.5 to 1 lithium to aluminum. The filtrate (IV*a*) was treated with an additional 3 moles of amine. The reaction yielded precipitate (IV*b*) of molar composition 1.7 to 1 lithium to aluminum. The only source of the additional aluminum found in the precipitate is an aluminum-containing species other than $LiAlH_4$ in the ether solution, formed from the earlier encounter of $LiAlH_4$ and Me_3N (IV*a*). As expected, the filtrate from reaction IV*b* contained only a trace of aluminum hydride bis-trimethylamine.

Reaction of Lithium Aluminum Hydride and Dimethylamine

Lithium aluminum hydride reactions with ammonia and primary and secondary amines have been characterized by the elimination of stoichiometric quantities of hydrogen and the formation of amides of undetermined composition (3, 4, 5). If a tetrahydrofuran solution of $LiAlH_4$ is treated with dimethylamine until hydrogen evolution ceases, a precipitate is formed and $LiAl(NMe_2)_4$ solvated with tetrahydrofuran may be isolated from solution (6). The work in this laboratory has demonstrated that the equimolar reaction of lithium aluminum hydride and dimethylamine in ethyl ether solution yields hydrogen, a precipitate, and dimethylamino aluminum hydride. When 2 or 3 moles of amine are used for each mole of $LiAlH_4$, no sublimable products are formed. Amides may be formed in all three reactions. Perhaps in the case of the equimolar reaction of Me_2NH and $LiAlH_4$ the source of AlH_2NMe_2 is the disproportionation of an unstable lithium aluminum amide. The more highly substituted amides formed in the other reactions may be stable to 100 °C or more. Recently Longi, Mazzanti, and Bernardini (7) found that in the reactions of large excesses of Et_2NH and Ph_2NH with $LiAlH_4$, the non-volatile products $LiAl(Et_2N)_3H$ and $LiAl(Ph_2N)_3H$ were formed, the anilide being stable to 140 °C.

ACKNOWLEDGMENT

This work was supported by the Advanced Research Projects Agency through the Navy Department, Bureau of Naval Weapons.

1. F. M. Peters, B. Bartocha, and A. J. Bilbo. Can. J. Chem. **41**, 1051 (1963).
2. E. Wiberg, H. Nöth, and R. Usón. Z. Naturforsch. **11b**, 487 (1956).
3. A. E. Finholt, A. C. Bond, Jr., and H. I. Schlesinger. J. Am. Chem. Soc. **69**, 1199 (1947).
4. F. A. Hochstein. J. Am. Chem. Soc. **71**, 305 (1949).
5. T. Higuchi, T. J. Concha, and R. Kuramoto. Anal. Chem. **24**, 685 (1952).
6. J. K. Ruff. J. Am. Chem. Soc. **83**, 2835 (1961).
7. P. Longi, G. Mazzanti, and F. Bernardini. Gazz. Chim. Ital. **90**, 180 (1960).

Received January 27, 1964.
Chemistry Division, Code 443,
U.S. Naval Ordnance Laboratory,
Corona, California.

Can. J. Chem. Downloaded from www.nrcresearchpress.com by 210.87.254.6 on 09/05/12
For personal use only.

THE REACTION OF SULPHUR TETRAFLUORIDE WITH SOME NITROGEN COMPOUNDS*

B. Marinier and Jean L. Boivin

The reactivity of sulphur tetrafluoride has been studied with compounds rich in nitrogen, such as urea, cyanamide, guanidine, dicyandiamide, melamine, and tetrazoles, and in each case trifluoromethyliminosulphur difluoride was a reaction product.

EXPERIMENTAL

Materials

Sulphur tetrafluoride was obtained from DuPont and was used without further purification. It contained about 5% thionyl fluoride. All other compounds were used as received but had a purity better than 99%.

General Procedure

The reactions with sulphur tetrafluoride were carried out in chrome–vanadium steel pressure vessels of 300-ml capacity. Solid reactants were placed in the bomb, the head was screwed into place, and the air was removed with a vacuum pump. Heat was applied to remove the last traces of water. The bomb was cooled in a dry ice – acetone bath and a known weight of SF_4 was condensed into it. A manometer was attached to the vessel to monitor the variations of pressure with temperature.

After the pressure vessel was heated for the desired period of time, it was cooled, the gases condensed at −196 °C, and weighed. The gases were expanded at 25 °C and analyzed by gas–liquid chromatography and mass spectrometry. The proportion of trifluoromethyliminosulphur difluoride was calculated from the peak areas of the gases present and the yield was reported in Table I for one carbon, whatever the number

TABLE I

Reaction of SF_4 with some nitrogen compounds

Expt. No.	Starting material (mole)	SF_4 (mole)	Temp. (°C)	Starting time (h)	Products (% yield)
			150	6	
1	Urea (0.05)	0.18	200*	2	CF_3NSF_2 (6)
			250	6	
2	Urea (0.05)†	0.24	150	2	CF_3NSF_2 (4)
			350	2	
3	Cyanamide (0.1)	0.22	150	18	CF_3NSF_2 (21)
4	Cyanamide (0.05)	0.2	150	60	CF_3NSF_2 (18)
5	Guanidine hydrofluoride (0.07)	0.15	150	10	CF_3NSF_2 (trace)
6	Guanidine hydrofluoride (0.05)†	0.2	150	48	CF_3NSF_2 (6) Nitrogen
7	Dicyandiamide (0.05)	0.29	150	20	CF_3NSF_2 (25)
8	Melamine (0.05)	0.25	300	48	CF_3NSF_2 (7) Cyanuric fluoride (35)
			150	20	
			200	2	
			250	2	
9	5-Amino-1H-tetrazole monohydrate (0.03)	0.21	300‡	2	CF_3NSF_2 (14)
			350	12	CF_4 (41)
			400	6	Nitrogen

*No reaction up to 200 °C.
†Water (0.05 ml) was added to form a catalytic amount of HF.
‡No reaction up to 300 °C.

of carbon atoms in the starting material. The yield of cyanuric fluoride was found by weighing the liquid obtained.

After each experiment, the bomb contained a solid residue of sulphur, iron salts, and ammonium fluoride.

Analytical Methods

The gas–liquid chromatography was performed with a Perkin–Elmer gas chromatograph Model 154 using a 9-ft long by $\frac{1}{4}$ in. diameter spiral copper column packed with standard Perkin–Elmer Chromosorb A

*Issued as CARDE Tech Memo 725/62 under Project No. D46-10-28-34.

Can. J. Chem. Downloaded from www.nrcresearchpress.com by 210.87.254.6 on 09/05/12
For personal use only.

(containing diisodecyl phthalate as liquid stationary phase), then by a 20-ft long by ¼ in. diameter spiral copper column packed with 33% by weight of grade No. 10 Kel-F polymer oil (3M Co.), supported by 35- to 80-mesh Firebrick C-22 (Johns Manville Co.).

The effluent gases were identified on a Bendix time-of-flight mass spectrometer, model 12-101, which was coupled with the gas chromatograph. The mass spectrum of CF_3NSF_2 was identical with that published (1), and CF_4 showed peaks at *m/e* 69 (CF_3^+), 50 (CF_2^+), and 31 (CF^+), as in the spectrum published by the American Petroleum Institute (serial No. 401).

Cyanuric fluoride obtained by the reaction of melamine with SF_4 (experiment No. 8) was identified by different methods. Its boiling point (74 °C) was the same as that reported (2). Its infrared spectrum, as a liquid film, was identical with that published (3).

The mass spectrum of cyanuric fluoride showed strong peaks in decreasing order of intensity at *m/e* 135 ($C_3N_3F_3$, "parent" ion), 31 (CF^+), 90 ($C_2N_2F_2^+$), 45 (CNF^+), 71 ($C_2N_2F^+$), and 116 ($C_3N_3F_2^+$). Much less abundant ions had mass/charge ratios of 76 ($C_2NF_2^+$), 26 (CN^+), 52 ($C_2N_2^+$), 12 (C^+), 50 (CF_2^+), and 38 (C_2N^+). Upon reducing the ionizing voltage of the mass spectrometer, the peaks due to the smaller charged fragments disappeared very rapidly, except the "parent" ion which disappeared at 9 V only.

1. W. C. Smith, C. W. Tullock, R. D. Smith, and V. A. Engelhardt. J. Am. Chem. Soc. **82**, 551 (1960).
2. A. F. Maxwell, J. S. Fry, and L. A. Bigelow. J. Am. Chem. Soc. **80**, 548 (1958).
3. D. W. Grisley, Jr., W. W. Gluesenkamp, and S. A. Heininger. J. Org. Chem. **23**, 1802 (1958).

Received January 6, 1964.
Chemistry Section,
Canadian Armament and Development Establishment,
Defence Research Board,
Department of National Defence,
Quebec, Quebec.

Can. J. Chem. Downloaded from www.nrcresearchpress.com by 210.87.254.6 on 09/05/12
For personal use only.

THE ALKALOIDS OF ASPIDOSPERMA OBLONGUM A.D.C.

K. H. Palmer

The stem bark of *Aspidosperma oblongum* A.D.C., a tree growing in British Guiana, has been found to contain 0.8–1.0% of alkaloids. From the heptane and methanol extracts of the powdered bark, two crystalline and one amorphous base have been obtained. Thin-layer chromatography (t.l.c.) of alkaloid I, obtained from the heptane extract, was found to be identical in all respects with aspidocarpine (1), which was initially extracted from *Aspidosperma album* root bark. Alkaloid II was obtained by column-partition chromatography (of the total alkaloidal fraction) of the bases obtained from the methanol extract and was shown to be yohimbine. Yohimbine styphnate was found to be an easily prepared and stable derivative. It is of a somewhat unusual composition consisting of two moles of yohimbine and one mole of styphnic acid. Alkaloid III, obtained in extremely low yield as an amorphous powder, had all the physical and chemical characteristics of pseudoyohimbine (2). Four other minor bases, as shown by t.l.c., were not further investigated due to lack of primary plant material.

EXPERIMENTAL

Ultraviolet spectra were determined in 95% ethanol, using a Unicam SP700 spectrophotometer; the infrared spectra were obtained using a Perkin–Elmer DB21 instrument. Melting points are corrected. Thin-layer chromatography employed a 0.25 mm layer of Silicagel G (Merck) on glass plates, using the supersaturated chamber technique of Stahl (3). The solvent was chloroform–hexane–diethylamine (10:20:3) (4). The alkaloids were detected with a modified Dragendorff reagent for alkaloids or a 5% w/v ceric sulphate in 10% sulphuric acid spray.

(containing diisodecyl phthalate as liquid stationary phase), then by a 20-ft long by ¼ in. diameter spiral copper column packed with 33% by weight of grade No. 10 Kel-F polymer oil (3M Co.), supported by 35- to 80-mesh Firebrick C-22 (Johns Manville Co.).

The effluent gases were identified on a Bendix time-of-flight mass spectrometer, model 12-101, which was coupled with the gas chromatograph. The mass spectrum of CF_3NSF_2 was identical with that published (1), and CF_4 showed peaks at *m/e* 69 (CF_3^+), 50 (CF_2^+), and 31 (CF^+), as in the spectrum published by the American Petroleum Institute (serial No. 401).

Cyanuric fluoride obtained by the reaction of melamine with SF_4 (experiment No. 8) was identified by different methods. Its boiling point (74 °C) was the same as that reported (2). Its infrared spectrum, as a liquid film, was identical with that published (3).

The mass spectrum of cyanuric fluoride showed strong peaks in decreasing order of intensity at *m/e* 135 ($C_3N_3F_3$, "parent" ion), 31 (CF^+), 90 ($C_2N_2F_2^+$), 45 (CNF^+), 71 ($C_2N_2F^+$), and 116 ($C_3N_3F_2^+$). Much less abundant ions had mass/charge ratios of 76 ($C_2NF_2^+$), 26 (CN^+), 52 ($C_2N_2^+$), 12 (C^+), 50 (CF_2^+), and 38 (C_2N^+). Upon reducing the ionizing voltage of the mass spectrometer, the peaks due to the smaller charged fragments disappeared very rapidly, except the "parent" ion which disappeared at 9 V only.

1. W. C. Smith, C. W. Tullock, R. D. Smith, and V. A. Engelhardt. J. Am. Chem. Soc. **82**, 551 (1960).
2. A. F. Maxwell, J. S. Fry, and L. A. Bigelow. J. Am. Chem. Soc. **80**, 548 (1958).
3. D. W. Grisley, Jr., W. W. Gluesenkamp, and S. A. Heininger. J. Org. Chem. **23**, 1802 (1958).

Received January 6, 1964.
Chemistry Section,
Canadian Armament and Development Establishment,
Defence Research Board,
Department of National Defence,
Quebec, Quebec.

Can. J. Chem. Downloaded from www.nrcresearchpress.com by 210.87.254.40 on 09/05/12
For personal use only.

THE ALKALOIDS OF ASPIDOSPERMA OBLONGUM A.D.C.

K. H. Palmer

The stem bark of *Aspidosperma oblongum* A.D.C., a tree growing in British Guiana, has been found to contain 0.8–1.0% of alkaloids. From the heptane and methanol extracts of the powdered bark, two crystalline and one amorphous base have been obtained. Thin-layer chromatography (t.l.c.) of alkaloid I, obtained from the heptane extract, was found to be identical in all respects with aspidocarpine (1), which was initially extracted from *Aspidosperma album* root bark. Alkaloid II was obtained by column-partition chromatography (of the total alkaloidal fraction) of the bases obtained from the methanol extract and was shown to be yohimbine. Yohimbine styphnate was found to be an easily prepared and stable derivative. It is of a somewhat unusual composition consisting of two moles of yohimbine and one mole of styphnic acid. Alkaloid III, obtained in extremely low yield as an amorphous powder, had all the physical and chemical characteristics of pseudo-yohimbine (2). Four other minor bases, as shown by t.l.c., were not further investigated due to lack of primary plant material.

EXPERIMENTAL

Ultraviolet spectra were determined in 95% ethanol, using a Unicam SP700 spectrophotometer; the infrared spectra were obtained using a Perkin–Elmer DB21 instrument. Melting points are corrected. Thin-layer chromatography employed a 0.25 mm layer of Silicagel G (Merck) on glass plates, using the super-saturated chamber technique of Stahl (3). The solvent was chloroform–hexane–diethylamine (10:20:3) (4). The alkaloids were detected with a modified Dragendorff reagent for alkaloids or a 5% w/v ceric sulphate in 10% sulphuric acid spray.

The Extraction Aspidosperma oblongum

Finely powdered stem bark (200 g) was continuously extracted in a soxhlet apparatus, first by heptane, then by methanol. Upon concentration of the heptane extract, a light-brown, semicrystalline material (0.14 g) was precipitated. Crystallization of this material from methanol gave (0.065 g) colorless, crystalline prisms, m.p. 166–168°, of alkaloid I. Thin-layer chromatography of the crystals showed one component (R_f 0.46), whereas the mother liquors showed, in addition, a further base (R_f 0.26) alkaloid II. Alkaloid I was vacuum sublimed (0.05 mm/140°) to give colorless prisms, m.p. 168.5–169.5°, $[\alpha]_D^{26}$ +141° (c = 1.0, $CHCl_3$). Found: C, 71.32; H, 8.19; N, 7.54; O, 12.89; OCH_3, 8.30. Calc. for $C_{22}H_{30}O_3N_2$: C, 71.32; H, 8.16; N, 7.56; O, 12.96; 1 OCH_3, 8.38. The sublimed sample was identical in all respects (mixed melting point, ultraviolet, infrared, nuclear magnetic resonance) with an authentic sample of aspidocarpine.

The dark-brown viscous mass (20 g), left after the concentration of the methanol extract *in vacuo*, was dissolved in the minimal volume of boiling glacial acetic acid (30 ml) and the resultant dark-brown syrup was poured into ice-cold water (300 ml). The precipitated dark-brown non-alkaloidal resin was filtered off leaving an amber-brown mother liquid. To this was added strong solution of ammonia to give the pH 9.0 and the resultant solution exhaustively extracted with chloroform. The chloroform extract after evaporation gave a brown viscous alkaloidal residue (0.8 g). This material was fractionated on a 50 g/50 ml Kieselguhr/phosphate buffer (pH 5.8) partition column, first with ether and then chloroform as eluting solvents. The column was then stripped of basic material with ammoniacal chloroform. Both the ether and chloroform eluates were collected in constant volume fractions (10 ml), the progress of the elution was followed by both titrametric and t.l.c. techniques.

The major component of the ether eluate (fraction Nos. 9–21) consisted of a single component, alkaloid II (R_f 0.26). Three other compounds were detected in later fractions (24–40, 43–60, 65–82); these were present in extremely small quantities and were not further investigated. Fractions 4–7 consisted of mainly aspidocarpine and after they were processed gave a further amount of t.l.c. pure aspidocarpine (0.04 g). The chloroform eluate yielded only traces of basic material which was mainly alkaloid II.

Eluate Fractions 9–21

Concentration of these eluate fractions gave a crop of long, colorless needles (0.3 g) m.p. 236–237° of alkaloid II. Further concentration of the mother liquors gave more crystals, m.p. 234–235° of alkaloid II. When the mother liquor evaporated to a very small volume (15 ml), an off-white amorphous powder (0.06 g) m.p. 264–267° (alkaloid III) was deposited. The pale-yellow glass obtained by complete evaporation of the final mother liquors failed to crystallize from the usual solvents and consisted of alkaloid II (R_f 0.26) with traces of probably I (R_f 0.46).

Alkaloid II

Recrystallization of crop m.p. 236–237° from aqueous methanol gave colorless needles of the same melting point identical in all respects (infrared, ultraviolet, nuclear magnetic resonance, and mixed melting point) with yohimbine. The styphnates of alkaloid II and yohimbine were prepared and found to be identical. The styphnate, in contrast to the picrate, easily crystallized in yellow plates, m.p. 204° (dec.), from aqueous ethanol. Found: C, 60.22; H, 5.9; N, 10.2. Calc. for $C_{42}H_{52}O_6N_4$, $C_6H_3O_8N_3$: C, 60.43; H, 5.77; N, 10.2.

Alkaloid III

Recrystallization of the amorphous powder from methanol gave microplates (0.045 g) m.p. 265–266°. Found: C, 71.06; H, 7.40; N, 7.83; mol. wt. (titrametric) 348. Calc. for $C_{21}H_{26}O_3N_2$: C, 71.16; H, 7.39; N, 7.90; mol. wt. 354. Max. 2255 Å (4.49), 2805 Å (3.80), infrared (Nujol mull). Max. 3502 cm^{-1} (NH indole), 3333 cm^{-1} (OH bonded), 1746 cm^{-1} (carbonyl) 1605 and 1589 cm^{-1} (aromatic ring); $[\alpha]_D^{23}$ +29 (pyridine, c = 0.5). Pseudoyohimbine (2, 5) $C_{21}H_{26}O_3N_2$, m.p. 265–266°, $[\alpha]_D^{19}$ +27° (pyridine c = 1). Max. 2250 Å (4.53), 2900 Å (3.79). The infrared spectra appeared to be identical in all respects (5).

ACKNOWLEDGMENTS

I wish to express my thanks to Dr. Léo Marion for the sample of aspidocarpine.

1. S. McLean, K. Palmer, and L. Marion. Can. J. Chem. **38**, 1547 (1960).
2. M. M. Janot, A. Lehir, and G. Goutarel. Ann. Pharm. Franc. **11**, 546 (1953).
3. E. Stahl. Arch. Pharm. **292**, 411 (1959).
4 C. Ferrari, S. McLean, L. Marion, and K. Palmer. Can. J. Chem. **41**, 1531 (1963).
5. Physical data of indole and dihydroindole alkaloids. Vol. 1. Eli Lilly and Company, Indianapolis. 1960.

Received March 16, 1964.
Faculty of Pharmacy,
University of Alberta,
Edmonton, Alberta.

Can. J. Chem. Downloaded from www.nrcresearchpress.com by 210.87.254.40 on 09/05/12
For personal use only.

AN ELECTRON IMPACT STUDY OF METHYLMERCAPTOBENZYL CHLORIDES

F. MEYER AND A. G. HARRISON*

A recent study (1) has shown that the appearance potentials of the $CH_3OC_7H_6^+$ ion from the isomeric meta- and para-methoxybenzyl chlorides differ by 1.15 eV, the meta isomer having the higher appearance potential. This difference is in reasonable agreement with the difference of 0.99 eV predicted for formation of the respective substituted benzyl ions and indicates that rearrangement to the symmetrical tropylium structure (2) does not occur at the appearance potential threshold. This conclusion is supported by the observation of large differences in the mass spectra of the isomeric methoxybenzyl chlorides. Similar differences have also been observed recently (3) in the spectra of the isomeric methoxybenzyl bromides.

We now report a similar study of the related compounds, meta- and para-methylmercaptobenzyl chloride. Partial mass spectra are given in Table I for these two compounds, where the spectra of the methoxybenzyl chlorides (1) are also presented for comparison. The largest peak in the mass spectra of the methylmercaptobenzyl chlorides occurs at $m/e = 137$ corresponding to the $CH_3SC_7H_6^+$ ion formed by loss of Cl. The appearance potential of $m/e = 137$ was found to be 11.20 ± 0.1 eV from the meta isomer and 10.45 ± 0.1 eV from the para isomer. From the correlation (4) of the ionization potentials of substituted benzyl radicals with the σ^+ value for the substituent, we estimate $I(m\text{-}CH_3SC_6H_4CH_2) = 7.97$ eV and $I(p\text{-}CH_3SC_6H_4CH_2) = 7.06$ eV using σ^+ (M-CH_3S) $= +0.158$ and σ^+ (p-CH_3S) $= 0.604$ (5). Since the bond dissociation energies of substituted benzyl derivatives are independent of the nature or position of the substituent (6) the difference of 0.91 eV in the ionization potentials is a measure of the difference expected in the appearance potentials if the benzyl structure for the $CH_3SC_7H_6^+$ ion is retained without migration of the substituent. The experimentally measured difference of 0.75 ± 0.2 eV is in good agreement with the predicted difference and strongly indicates retention of the benzyl configuration at the appearance potential threshold. If rearrangement to the symmetrical tropylium structure had occurred, the orientation of the substituents would have been lost and identical appearance potentials would have been expected. Such a behavior has been found when the ring substituent is CH_3, F, or OH (1).

TABLE I

Partial mass spectra of methylmercaptobenzyl chlorides and methoxybenzyl chlorides

	Methylmercaptobenzyl chlorides (X = S)			Methoxybenzyl chlorides (X = O)		
Formula	m/e	meta	para	m/e	meta	para
$CH_3XC_6H_4CH_2Cl^+$	172	91.6	33.7	156	32.0	13.0
$CH_3XC_7H_6^+$	137	100.0	100.0	121	100.0	100.0
$C_7H_7^+$	91	25.3	8.3	91	31.9	9.3
$C_5H_5^+$	65	8.7	3.1	65	7.9	3.3

*Alfred P. Sloan Research Fellow.

Can. J. Chem. Downloaded from www.nrcresearchpress.com by 210.87.254.6 on 09/05/12
For personal use only.

The spectra of the methylmercaptobenzyl chlorides and the methoxybenzyl chlorides are quite similar and both show the differences expected on the basis of different structures and energy contents for the $CH_2XC_7H_6^+$ ions from the meta- and para-isomers. The $CH_3XC_7H_6^+$ ion from the meta isomer has a much higher energy content than the ion from the para isomer; thus for the meta isomer the abundance relative to the parent ion or the fragmentation product, $C_7H_7^+$ ($m/e = 91$), is greatly reduced compared to the para isomer. Not only is more energy required for formation of the $CH_3XC_7H_6^+$ ion from the meta isomer but also the energy barrier for further decomposition to the $C_7H_7^+$ ion is smaller. The main decomposition path for the $CH_3XC_7H_6^+$ ion appears to be by reaction [1] for both the methoxy- and methyl-mercapto compounds. The $C_7H_7^+$ ion presumably has the tropylium structure.

$$[1] \qquad CH_3XC_7H_6^+ \rightarrow C_7H_7^+ + CH_2X$$

A metastable transition is observed for this decomposition in the case of the methoxy compounds (1); however, for the methylmercapto compounds the metastable transition expected at $m/e = 60.4$ could not be identified with certainty because of a doubly charged ion at $m/e = 60.5$.

The above observations strongly support the conclusion that the methylmercaptobenzyl chlorides behave in a similar manner to the methoxybenzyl chlorides on electron impact and that, in both cases, the ion formed by loss of Cl retains the benzyl configuration.

EXPERIMENTAL

The mass spectra and appearance potentials were measured with an A.E.I. MS-2 mass spectrometer which has been described previously (1). Appearance potentials were determined in the usual manner (7) using xenon to calibrate the voltage scale.

The *p*-methylmercaptobenzyl chloride was prepared from thioanisole and chloromethylmethyl ether by the method of Buu-Hoi (8). The *m*-methylmercaptobenzyl chloride was prepared by reduction of *m*-methylmercaptobenzoic acid with $LiAlH_4$ and treatment of the resulting alcohol with PCl_3 (9). The *m*-methylmercaptobenzoic acid was prepared by the method of Smiles and Stewart (10). The chlorides were purified by fractional distillation.

ACKNOWLEDGMENTS

The authors are indebted to the National Research Council of Canada and to the Alfred P. Sloan Foundation for support of this work.

1. J. M. S. Tait, T. W. Shannon, and A. G. Harrison. J. Am. Chem. Soc. **84**, 4 (1962).
2. S. Meyerson and H. M. Grubb. Mass spectra of alkyl benzenes. *In* Mass spectrometry of organic ions. Academic Press, N.Y. 1963.
3. Z. Pelah, J. M. Wilson, M. Ohashi, H. Budzikiewicz, and C. Djerrasi. Tetrahedron, **19**, 2233 (1963).
4. A. G. Harrison, P. Kebarle, and F. P. Lossing. J. Am. Chem. Soc. **83**, 777 (1961).
5. H. C. Brown and Y. Okamoto. J. Am. Chem. Soc. **80**, 4979 (1958).
6. T. L. Cottrell. The strengths of chemical bonds. 2nd ed. Butterworths, London. 1958.
7. A. G. Harrison and T. W. Shannon. Can. J. Chem. **40**, 1730 (1962).
8. N. G. Buu-Hoi and N. G. Huan. J. Org. Chem. **17**, 350 (1952).
9. R. Pschorr. Ann. **391**, 44 (1912).
10. S. Smiles and J. Stewart. J. Chem. Soc. 1792 (1921).

Received February 24, 1964.
Department of Chemistry,
University of Toronto,
Toronto 5, Ontario.

Can. J. Chem. Downloaded from www.nrcresearchpress.com by 210.87.254.6 on 09/05/12
For personal use only.

METHOXYCARBOSTYRILS

GEORGE R. PETTIT AND ALEXANDER B. NEILL[1]

Can. J. Chem. Downloaded from www.nrcresearchpress.com by 210.87.254.40 on 09/05/12
For personal use only.

The central nervous sytem activity occasionally displayed by carbostyrils (1) led us to prepare several methoxy-substituted 2-hydroxyquinolines (cf. I) and a number of 2-quinolyl esters (Table I) for pharmacological evaluation. In general, the quinoline derivatives were based on structural features[2] of the hypotensive and sedative *Rauwolfia* alkaloids reserpine and resinnamine (2). Certain other 2-quinolyl esters (Table I), ethers, and 2-chloroquinolines were synthesized for comparison purposes.

Initially, it was considered necessary to prepare 6-methoxy-(I*a*), 7-methoxy-(**I*b*)**, and 6,7-dimethoxy-carbostyril (I*c*). Of these, only 7-methoxycarbostyril was previously undescribed and synthesis was accomplished by the following reaction scheme (II → I).[3]

Chromyl chloride oxidation of 2-nitro-4-methoxytoluene (5) gave 2-nitro-4-methoxybenzaldehyde (II) as described by Boon (6). Condensation of benzaldehyde II with malonic acid led to 2-nitro-4-methoxycinnamic acid (III). Ferrous sulphate reduction of nitrobenzene III afforded 2-amino-4-methoxycinnamic acid (IV), which cyclized to 7-methoxycarbostyril (I*b*) in hot 2-propanol – hydrochloric acid solution. Phosphorus oxychloride readily converted carbostyril I*b* to 2-chloro-7-methoxyquinoline (I*d*).

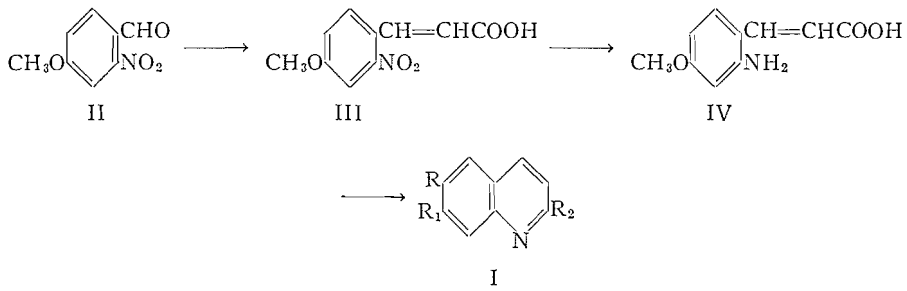

II III IV

I

I*a*. R = OCH_3, R_1 = H, R_2 = OH
b. R = H, R_1 = OCH_3, R_2 = OH
c. R = R_1 = OCH_3, R_2 = OH
d. R = H, R_1 = OCH_3, R_2 = Cl
e. R = R_1 = OCH_3, R_2 = Cl
f. R = R_2 = R_2 = OCH_3
g. R = R_1 = OCH_3, R_2 = $OCH_2(CH_2)_2CH_3$
h. R = R_1 = OCH_3, R_2 = $OCH_2CH_2N(CH_3)_2$
i. R = R_1 = R_2 = OH

Preparation of 2-chloroquinoline I*d* illustrates the general reaction sequence employed for synthesis of 6,7-dimethoxycarbostyril (7) from 6-nitroveratraldehyde and subsequent conversion to 2-chloro-6,7-dimethoxyquinoline (I*e*). Dimethylformamide was found a superior solvent for effecting facile transformation of chloroquinoline I*e* to 2,6,7-trimethoxyquinoline (I*f*) with sodium methoxide. With methanol, Diglyme, or xylene as

[1]*Eaton Laboratories.*
[2]*A number of recent investigations, directed toward preparation of useful ataractic agents, have been inspired by various aspects of the reserpine molecule: see for example, reference 3.*
[3]*Three years after the present investigation was completed, Sidhu (ref. 4) and colleagues reported a similar route to 7-methoxycarbostyril.*

solvent, extended reaction periods were necessary.[4] The butyl (I*g*) and dimethylaminoethyl (I*h*) ethers of dimethoxycarbostyril I*c* were prepared in an analogous manner. In addition, 2,6,7-trihydroxyquinoline (I*i*) was obtained by treating carbostyril I*c* with 48% hydrobromic acid.

The 2-quinolyl esters (Table I) were prepared by warming the respective carbostyril and acyl chloride in pyridine. The infrared spectrum of each ester revealed a single strong band in the 5.78–5.82 μ region, compatible with O-alkylation. Evidence in favor of N-alkylation was not demonstrated.[5]

EXPERIMENTAL[6]

6-Methoxycarbostyril (Ia)

A solution of 6-methoxyquinoline-N-oxide (37.0 g, ref. 11) in 300 ml of acetic anhydride was heated at reflux for 5 h before removal of excess solvent *in vacuo*. The dark residue was warmed (steam bath) for 1 h with 200 ml of 2 *N* sodium hydroxide. After cooling, the product was collected and washed with dilute hydrochloric acid and water. The grayish-brown colored crystals weighed 12.6 g (33%) and melted at 208–216°. Recrystallization from ethanol (Darco) afforded colorless crystals of 6-methoxycarbostyril melting at 220–221°. The product was shown to be identical with an authentic sample (12) by mixture melting point determination and infrared spectral comparison.

2-Nitro-4-methoxycinnamic Acid (III)

To a solution of malonic acid (224 g) in 750 ml of pyridine were added piperidine (20 ml) and 2-nitro-4-methoxybenzaldehyde (127 g, ref. 5 and 6). After a 3-hr period of heating (steam bath), evolution of carbon dioxide appeared to be complete and the solution was poured into 3.2 l of 10% hydrochloric acid. The tan-colored crystalline product weighed 120 g (77%) and melted at 245–247° (with sintering from 190°). Recrystallization from ethanol (Darco) gave pale yellow needles, m.p. 246–248°. A melting point of 240° has been reported (4) for this substance. Anal. Calc. for $C_{10}H_9NO_5$: C, 53.81; H, 4.06; N, 6.28. Found: C, 53.90; H, 3.97; N, 6.56.

7-Methoxycarbostyril (Ib)

A solution of 2-nitro-4-methoxycinnamic acid (120 g) in 1.3 l of 28% aqueous ammonia was added, with stirring, to a warm solution of ferrous sulphate heptahydrate (1.3 kg) in 2 l of water. After the mixture was heated to 80° for 10 min, it was allowed to cool and was filtered through Celite. The filtrate was acidified to pH 6.5 with glacial acetic acid to furnish 44 g (43%) of light brown crystalline product (IV), m.p. 238–242° (dec.). A solution of the amino acid (44 g) in 500 ml of isopropyl alcohol containing concentrated hydrochloric acid (200 ml) was heated at steam bath temperature for 15 min, cooled, and filtered. The greyish-brown crystalline product was dissolved in 2 *N* sodium hydroxide (500 ml) and precipitated with 2 *N* hydrochloric acid. The tan-colored microcrystals weighed 18.3 g (45%) and melted at 198–200° (with sintering from 170°). Recrystallization from ethylene chloride gave colorless needles, m.p. 204–205.5°. An elemental analysis for nitrogen and a melting point of 199° has been reported (4) for carbostyril I*b*. Anal. Calc. for $C_{10}H_9NO_2$: C, 68.56; H, 5.18; H, 8.00. Found: C, 68.30; H, 4.91; N, 7.96.

2-Chloro-7-methoxyquinoline (Id)

A solution of 7-methoxycarbostyril (1.9 g) in 20 ml of phosphorus oxychloride was heated at reflux 3 h. The remaining phosphorus oxychloride was removed *in vacuo*. After addition of ice and aqueous ammonia, the basic mixture was extracted with chloroform. Removal of solvent from the dry (sodium sulphate) extract afforded 1.2 g (59%) of crystalline product; m.p. 96–97°, following recrystallization from benzene

[4]*The unexpected resistance displayed by chlorodeoxydihydroflindersine (ref. 8) (i) to nucleophilic attack by methoxide in methanol or xylene may be cited as another example: cf. also ref. 9.*

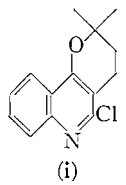

(i)

[5]*An imide structure, arising from N-alkylation, would be expected to exhibit a second band due to carbonyl absorption in the 5.85–6.00 μ region (ref. 10).*

[6]*Unless otherwise indicated, melting points were determined with a Fisher–Johns apparatus and are uncorrected. Elemental analyses were provided by the microanalytical laboratory of Eaton Laboratories. Infrared spectra were measured in chloroform solution using a Perkin–Elmer model 21 infrared spectrophotometer.*

Can. J. Chem. Downloaded from www.nrcresearchpress.com by 210.87.254.40 on 09/05/12
For personal use only.

Can. J. Chem. Downloaded from www.nrcresearchpress.com by 210.87.254.40 on 09/05/12
For personal use only.

TABLE I

2-Quinolyl esters

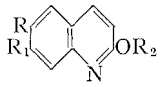

R	R_1	R_2	Yield,[a] %	Solvent[b]	M.p.,[c] °C	Formula	Calculated, %			Found, %		
							C	H	N	C	H	N
H	H	Nicotinyl	29	1	111–112	$C_{15}H_{10}N_2O_2$	71.99	4.03	11.20	72.14	3.94	11.22
H	H	3,4,5-Trimethoxybenzoyl	65	2	129.5–130.5	$C_{19}H_{17}NO_5$	67.25	5.05	4.13	67.00	4.65	4.09
OCH_3	H	3,4,5-Trimethoxybenzoyl	35	1	177–178.5	$C_{20}H_{19}NO_6$	65.03	5.19	3.79	65.20	4.88	3.66
OCH_3	H	3,4,5-Trimethoxycinnamoyl	32	2	120–121	$C_{22}H_{21}NO_6$	66.82	5.35	3.54	66.80	5.42	3.43
OCH_3	OCH_3	Benzoyl	50	2	133–134	$C_{18}H_{15}NO_4$	69.89	4.89	4.53	69.90	4.82	4.40
OCH_3	OCH_3	Nicotinyl	31	2	153–154	$C_{17}H_{14}N_2O_4$	65.80	4.55	9.03	66.00	4.60	8.88
OCH_3	OCH_3	3,4,5-Trimethoxybenzoyl	60	1	221–223	$C_{21}H_{21}NO_7$	63.15	5.30	3.51	63.10	5.01	3.31
CH_3	OCH_3	3,4,5-Trimethoxycinnamoyl	38	1	166–167.5	$C_{23}H_{23}NO_7$	64.93	5.45	3.29	65.10	5.25	3.10

[a]Yield based on a pure specimen.
[b]The ester was recrystallized from benzene (1), or benzene – petroleum ether (2).
[c]Melting point of the analytical sample.

(Darco)–hexane. The analytical sample crystallized as colorless needles from benzene–hexane, m.p. 97–98°. Anal. Calc. for $C_{10}H_8ClNO$: C, 62.02; H, 4.16; Cl, 18.31. Found: C, 62.20; H, 4.14; Cl, 18.05.

2-Chloro-6,7-dimethoxyquinoline (Ie)

A suspension of 6,7-dimethoxycarbostyril (100 g, ref. 7) in 300 ml of refluxing phosphorus oxychloride was stirred 3 h. Excess phosphorus oxychloride was removed *in vacuo* before the residue was cautiously added to an ice – aqueous ammonia mixture. The gray-colored crystalline product was collected and washed with water; yield 104.5 g (96%), m.p. 118–120°. Recrystallization from benzene (Darco) – petroleum ether gave colorless needles melting at 122–124°. Anal. Calc. for $C_{11}H_{10}ClNO_2$: C, 59.07; H, 4.51; Cl, 15.85. Found: C, 59.40; H, 4.50; Cl, 15.82.

2,6,7-Trimethoxyquinoline (If)

To a solution of 2-chloro-6,7-dimethoxyquinoline (I*e*, 5 g) in 100 ml of dimethylformamide was added 6.2 g of sodium methoxide. Before pouring the hot reaction mixture into 1 l of water, the resulting suspension was stirred and heated at reflux for 15 min. Collecting the colorless needles afforded 4.1 g (84%) of product melting at 116–117°. After further recrystallization from petroleum ether, the melting point remained at 116–117°. Anal. Calc. for $C_{12}H_{13}NO_3$: C, 65.74; H, 5.98; N, 6.39. Found: C, 65.75; H, 5.60; N, 6.24.

A fair yield (68%) in Diglyme was obtained after 24 h at reflux, while 48 h in refluxing xylene was needed to obtain a comparable yield (77%). The reaction in refluxing methanol, at periods up to 24 h, gave only crude starting material and was not further investigated. When a methanol solution of 6,7-dimethoxycarbostyril was treated with ethereal diazomethane and allowed to stand at room temperature for 24 h, only starting material was recovered.

2-Butoxy-6,7-dimethoxyquinoline (Ig)

Dimethylformamide (150 ml) and 20 g of 2-chloro-6,7-dimethoxyquinoline (I*e*) were added to solid sodium butoxide, prepared by adding sodium (12.4 g) to 200 ml of refluxing *n*-butyl alcohol (excess alcohol was removed *in vacuo*). Before the mixture was poured into 1.5 l of water, heating was maintained at 110–120° for 15 min. Heating the mixture to reflux caused excessive foaming. The crystalline product weighed 22.9 g and melted at 74–78° (with sintering from 65°). Distillation through a Claisen flask afforded 17.5 g (75%) of viscous oil, b.p. 175–179° (0.02 mm), which crystallized from benzene–petroleum ether as colorless crystals melting at 83–85°. An analytical sample, m.p. 85–86°, was crystallized from the same solvent. Anal. Calc. for $C_{15}H_{19}NO_3$: C, 68.74; H, 7.33; N, 5.36. Found: C, 68.74; H, 6.98; N, 5.08.

2-(2′-Dimethylamino)ethoxy-6,7-dimethoxyquinoline (Ih)

Sodium (12.4 g) was added in small portions to 150 ml of refluxing dimethylaminoethyl alcohol. Excess solvent was removed *in vacuo* and to the crystalline residue was added dimethylformamide (200 ml) and 20 g of 2-chloro-6,7-dimethoxyquinoline (I*e*). Before the mixture was poured into 2 l of cold water, stirring and heating at reflux was continued for 15 min. The aqueous solution was saturated with sodium chloride and extracted with chloroform. Removal of solvent from the dry (sodium sulphate) organic extract left a dark brown mobile oil. A portion of the oily residue (1.7 g) in benzene–hexane (1:1) was chromatographed on 50 g of activated alumina (Merck "Suitable for Chromatography"). Elution with 750 ml of the same solvent gave 0.42 g of colorless crystals. Further elution with 1 l of benzene afforded 0.28 g. After recrystallization from benzene – petroleum ether, the two crystalline fractions melted, respectively, at 108–110° and 112-114°. An analytical sample crystallized as colorless platelets from benzene – petroleum ether, m.p. 113–114°. Anal. Calc. for $C_{15}H_{20}N_2O_3$: C, 65.19; H, 7.30; N, 10.14. Found: C, 65.65; H, 7.23; N, 10.05.

The remaining reaction product was distilled through a Claisen flask. The main fraction boiled at 184-186° (0.01 mm) and separated from benzene – petroleum ether as colorless crystals (8.8 g), m.p. 100–107°. Several additional recrystallizations from benzene – petroleum ether raised the melting point to 109–111°. A mixture melting point determination with the chromatographed product showed no depression. The total yield of crystalline material amounted to 9.5 g (38%).

6,7-Dihydroxycarbostyril (Ii)

A stirred suspension of 6,7-dimethoxycarbostyril (I*c*, 30 g, ref. 7) in 600 ml of 48% hydrobromic acid was heated at reflux 24 h. The dark-colored solution was cooled and the brown needles (27.6 g) collected, washed with water, and recrystallized from glacial acetic acid (Darco). The straw-colored crystalline salt weighed 19.5 g and melted at 268–270° (with sintering from 260°). Precipitation from 450 ml of 2 *N* sodium hydroxide solution, with 2 *N* hydrochloric acid, gave 13 g of tan-colored *6,7-dihydroxycarbostyril*, m.p. 330–334° (dec.) with sintering from 315° .The yield was increased to 17.5 g (68%) by diluting the hydrobromic acid filtrate with ca. 100 ml of water and converting the second crop of hydrobromide to 6,7-dihydroxycarbostyil as previously described. An analytical sample was obtained as colorless crystals from glacial acetic acid, m.p. 338–340° (dec.) with darkening from 315°.[7] Anal. Calc. for $C_9H_7NO_3$: C, 61.01; H, 3.98; N, 7.91. Found: C, 60.90; H, 3.90; N, 7.82.

2-Quinolyl Esters (Table I)

Details for the preparation of 2-quinolyl-3′,4′,5′-trimethoxybenzoate will illustrate the general procedure

[7]*Capillary tube melting point.*

Can. J. Chem. Downloaded from www.nrcresearchpress.com by 210.87.254.40 on 09/05/12
For personal use only.

(13). To a warm solution of carbostyril (263 g) in 1.2 l of pyridine was added 418 g of 3,4,5-trimethoxybenzoyl chloride (14). Before pouring the solution into 13 l of water, heating was maintained at steam bath temperature for 1 h. The crude product was collected, dissolved in 2 l of chloroform, and washed successively with five 300 ml portions of 2 *N* sodium hydroxide and then with water. After removal of solvent from the dry organic extract, the residue was recrystallized (Table I).

Nicotinyl chloride was prepared as described by Clark-Lewis and Thompson (15). The following method was employed for preparation of *3,4,5-trimethoxycinnamoyl chloride*. Oxalyl chloride (35 ml) was added to 3,4,5-trimethoxycinnamic acid (39 g) and, after the initial reaction had subsided, the mixture was heated at reflux 1 h. Removal of excess oxalyl chloride *in vacuo* left a dark-colored crystalline residue which recrystallized from benzene – petroleum ether as yellow-colored crystals; yield 37 g (88%), m.p. 88–90°.

1. W. F. von Oettingen. The Therapeutic Agents of the Quinoline Group. American Chemical Society Monograph Series, No. 64. Chemical Catalog Co., Inc., New York, N.Y. 1933. p. 47.
2. E. Tucker. Agnew. Chem. **75**, 524 (1963). J. A. Schneider. *In* Rauwolfia: Botany, Pharmacognosy, Chemistry and Pharmacology. Little, Brown and Company, Boston, Mass. 1957.
3. I. Jirkovsky and M. Protiva. Collection Czech. Chem. Commun. **28**, 2582 (1963). V. M. Solov'ev, A. P. Arendaruk, and A. D. Skoldinov. Zh. Obsch. Khim. **31**, 2405 (1961). T. Kralt, W. J. Asma, and H. D. Moed. Rec. Trav. Chim. **80**, 431 (1961). T. Kralt, W. J. Asma, H. H. Haeck, and H. D. Moed. Rec. Trav. Chim. **80**, 313 (1961). K. Macek and S. Vaněček. Collection Czech. Chem. Commun. **26**, 2705 (1961). R. A. Lucas, D. F. Dickel, R. L. Dziemian, M. J. Ceglowski, B. L. Hensle, H. B. MacPhillamy. J. Am. Chem. Soc. **82**, 5688 (1960). G. P. Schiemenz and H. Engelhard. Chem. Ber. **92**, 857 (1959). R. A. Lucas, M. E. Kuehne, M. J. Ceglowski, R. L. Dziemian, and H. B. MacPhillamy. J. Am. Chem. Soc. **81**, 1928 (1959). R. Ratouis and G. Combes. Bull. soc. chim. France, 576 (1959). B. V. Rama Sastry and A. Lasslo. J. Org. Chem. **23**, 1577 (1958).
4. G. S. Sidhu, G. Thyagarajan, and S. Ansari. Ann. **627**, 218 (1959).
5. I. Keimatsu and E. Yamaguchi. Yakugaku Zasshi, **57**, 274 (1937).
6. W. R. Boon. J. Chem. Soc. S230 (1949).
7. J. F. Kefford. J. Chem. Soc. 1209 (1940).
8. R. F. C. Brown, J. J. Hobbs, G. K. Hughes, and E. Ritchie. Australian J. Chem. **7**, 348 (1954).
9. M. P. Cava and N. K. Bhattacharyya. J. Org. Chem. **23**, 1287 (1958).
10. R. A. Abramovitch. J. Chem. Soc. **1413** (1957).
11. A. M. van Arendonk. U. S. Patent No. 2,416,658 (1947).
12. F. Montanari and L. Pentimalli. Gazz. Chim. Ital. **83**, 273 (1953).
13. C. J. Cavallito and T. H. Haskell. J. Am. Chem. Soc. **66**, 1166 (1944).
14. F. Benington and R. D. Morin. J. Am. Chem. Soc. **73**, 1353 (1951).
15. J. W. Clark-Lewis and M. J. Thompson. J. Chem. Soc. **442** (1957).

Received March 23, 1964.
Department of Chemistry,
University of Maine,
Orono, Maine,
and
Eaton Laboratories Division,
The Norwich Pharmacal Co.,
Norwich, New York.

SYNTHESIS OF TRYPTOPHAN-CARBOXYL-^{14}C[1]

G. P. Slater

Tryptophan labelled in the carboxyl group with carbon 14 was required for studies on the biosynthesis of a fungal metabolite, but was not commercially available. The synthesis was achieved from indole-3-aldehyde and hydantoin-4-^{14}C* using a modification of the procedure described by Bond (1) for the corresponding ^{13}C-labelled compound.

In the modified method, the indolylidenehydantoin (I) was reduced by the action of Raney nickel alloy in dilute sodium hydroxide solution, instead of using Raney nickel catalyst in sodium hydroxide (2). The reduction product, indolylmethylhydantoin (II),

[1]*Issued as N.R.C. No. 7952.*
**Merck, Sharp & Dohme of Canada Ltd., Montreal.*

Can. J. Chem. Downloaded from www.nrcresearchpress.com by 210.87.254.40 on 09/05/12
For personal use only.

(13). To a warm solution of carbostyril (263 g) in 1.2 l of pyridine was added 418 g of 3,4,5-trimethoxybenzoyl chloride (14). Before pouring the solution into 13 l of water, heating was maintained at steam bath temperature for 1 h. The crude product was collected, dissolved in 2 l of chloroform, and washed successively with five 300 ml portions of 2 *N* sodium hydroxide and then with water. After removal of solvent from the dry organic extract, the residue was recrystallized (Table I).

Nicotinyl chloride was prepared as described by Clark-Lewis and Thompson (15). The following method was employed for preparation of *3,4,5-trimethoxycinnamoyl chloride*. Oxalyl chloride (35 ml) was added to 3,4,5-trimethoxycinnamic acid (39 g) and, after the initial reaction had subsided, the mixture was heated at reflux 1 h. Removal of excess oxalyl chloride *in vacuo* left a dark-colored crystalline residue which recrystallized from benzene – petroleum ether as yellow-colored crystals; yield 37 g (88%), m.p. 88–90°.

1. W. F. von Oettingen. The Therapeutic Agents of the Quinoline Group. American Chemical Society Monograph Series, No. 64. Chemical Catalog Co., Inc., New York, N.Y. 1933. p. 47.
2. E. Tucker. Agnew. Chem. **75**, 524 (1963). J. A. Schneider. *In* Rauwolfia: Botany, Pharmacognosy, Chemistry and Pharmacology. Little, Brown and Company, Boston, Mass. 1957.
3. I. Jirkovsky and M. Protiva. Collection Czech. Chem. Commun. **28**, 2582 (1963). V. M. Solov'ev, A. P. Arendaruk, and A. D. Skoldinov. Zh. Obsch. Khim. **31**, 2405 (1961). T. Kralt, W. J. Asma, and H. D. Moed. Rec. Trav. Chim. **80**, 431 (1961). T. Kralt, W. J. Asma, H. H. Haeck, and H. D. Moed. Rec. Trav. Chim. **80**, 313 (1961). K. Macek and S. Vaněček. Collection Czech. Chem. Commun. **26**, 2705 (1961). R. A. Lucas, D. F. Dickel, R. L. Dziemian, M. J. Ceglowski, B. L. Hensle, H. B. MacPhillamy. J. Am. Chem. Soc. **82**, 5688 (1960). G. P. Schiemenz and H. Engelhard. Chem. Ber. **92**, 857 (1959). R. A. Lucas, M. E. Kuehne, M. J. Ceglowski, R. L. Dziemian, and H. B. MacPhillamy. J. Am. Chem. Soc. **81**, 1928 (1959). R. Ratouis and G. Combes. Bull. soc. chim. France, 576 (1959). B. V. Rama Sastry and A. Lasslo. J. Org. Chem. **23**, 1577 (1958).
4. G. S. Sidhu, G. Thyagarajan, and S. Ansari. Ann. **627**, 218 (1959).
5. I. Keimatsu and E. Yamaguchi. Yakugaku Zasshi, **57**, 274 (1937).
6. W. R. Boon. J. Chem. Soc. S230 (1949).
7. J. F. Kefford. J. Chem. Soc. 1209 (1940).
8. R. F. C. Brown, J. J. Hobbs, G. K. Hughes, and E. Ritchie. Australian J. Chem. **7**, 348 (1954).
9. M. P. Cava and N. K. Bhattacharyya. J. Org. Chem. **23**, 1287 (1958).
10. R. A. Abramovitch. J. Chem. Soc. **1413** (1957).
11. A. M. van Arendonk. U. S. Patent No. 2,416,658 (1947).
12. F. Montanari and L. Pentimalli. Gazz. Chim. Ital. **83**, 273 (1953).
13. C. J. Cavallito and T. H. Haskell. J. Am. Chem. Soc. **66**, 1166 (1944).
14. F. Benington and R. D. Morin. J. Am. Chem. Soc. **73**, 1353 (1951).
15. J. W. Clark-Lewis and M. J. Thompson. J. Chem. Soc. **442** (1957).

Received March 23, 1964.
Department of Chemistry,
University of Maine,
Orono, Maine,
and
Eaton Laboratories Division,
The Norwich Pharmacal Co.,
Norwich, New York.

SYNTHESIS OF TRYPTOPHAN-CARBOXYL-^{14}C[1]

G. P. Slater

Tryptophan labelled in the carboxyl group with carbon 14 was required for studies on the biosynthesis of a fungal metabolite, but was not commercially available. The synthesis was achieved from indole-3-aldehyde and hydantoin-4-^{14}C* using a modification of the procedure described by Bond (1) for the corresponding ^{13}C-labelled compound.

In the modified method, the indolylidenehydantoin (I) was reduced by the action of Raney nickel alloy in dilute sodium hydroxide solution, instead of using Raney nickel catalyst in sodium hydroxide (2). The reduction product, indolylmethylhydantoin (II),

[1]*Issued as N.R.C. No. 7952.*
**Merck, Sharp & Dohme of Canada Ltd., Montreal.*

Can. J. Chem. Downloaded from www.nrcresearchpress.com by 210.87.254.40 on 09/05/12
For personal use only.

was not isolated, but its aqueous solution was hydrolyzed with barium hydroxide (2) and the tryptophan isolated by ion-exchange chromatography. This procedure constitutes a facile synthesis of tryptophan and gives a better yield (73%) than that reported by Bond (1) [59% based on hydantoin].

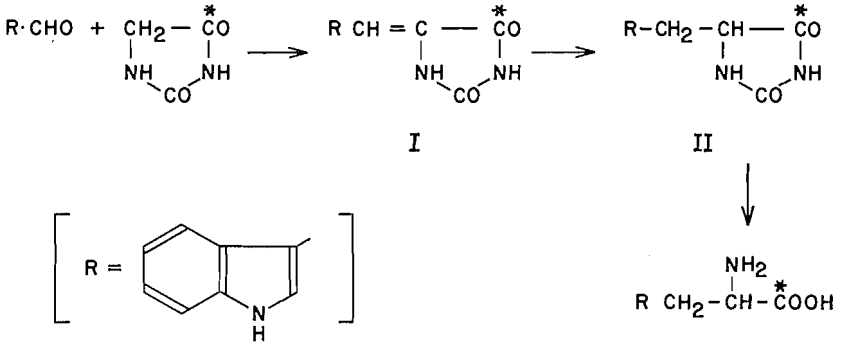

EXPERIMENTAL

Indolylidenehydantoin (I)

Hydantoin-4-^{14}C (45.5 mg, approximately 0.5 mC) and carrier (54.5 mg, total 1 mmole) was mixed with indole-3-aldehyde (160 mg, 1.1 mmole) in a 5-ml round-bottom flask. Piperidine (0.5 ml) was added, the flask fitted with a 6-in. air condenser, and immersed in an oil bath at 150–155 °C (1) until a yellow solid had formed (7 min). The product was suspended in water, the mixture acidified with acetic acid, filtered, and washed to give indolylidenehydantoin (208 mg, 92%).

DL-*Tryptophan-carboxyl-*^{14}*C*

The crude indolylidenehydantoin (208 mg, 0.92 mmole) was dissolved in water (50 ml), containing sodium hydroxide* (800 mg, approximately 20 mmole) in a 250 ml beaker, and stirred at 50–55 °C while Raney nickel alloy (1 g) was added, in portions, until the solution became colorless (6 min). After a further 10 min the mixture was filtered and the pH of the filtrate adjusted to 7.2 with 4 *N* hydrochloric acid to precipitate aluminum hydroxide (3). The mixture was centrifuged and the precipitate washed with water until the washings showed no ultraviolet absorption at 278–386 mμ. Barium hydroxide octahydrate (5.81 g, 18.4 mmole) was added to the combined washings and the mixture boiled for 48 h. The hot mixture was saturated with carbon dioxide (2) and filtered immediately. The filtrate was cooled to room temperature, made alkaline with 5 *N* ammonia, and passed through a Dowex 1 resin (X8, 200–400 mesh, 120 × 28 mm) in the hydroxyl form. The resin was washed with distilled water until the effluent was neutral to litmus and the tryptophan was eluted with 1 *N* acetic acid.† The latter solution was passed through a Dowex 50W resin (X4, 200–400 mesh, 120 × 28 mm) in the hydrogen-ion form, and the column washed as before. The tryptophan was eluted with 1 *N* ammonia and the eluate concentrated under reduced pressure at 50 °C until the product commenced to separate. Dilution of the mixture with ethanol and cooling in ice gave DL-tryptophan-carboxyl-^{14}C (127 mg, 0.386 mC), dec. 255–260 °C. The residue (30 mg) from the mother liquor was dissolved in 1 *N* sodium hydroxide (2 ml), the pH adjusted to 7 with 1 *N* acetic acid, and the solution absorbed on a Dowex 1 resin (220 × 22 mm) in the acetate form. Elution of the column with water and 0.05 *N* acetic acid gave a further quantity of tryptophan (22 mg, total yield 149 mg, 0.73 mmole), dec. 250–255 °C.

The two fractions gave infrared spectra (KBr) identical with that of an authentic sample of DL-tryptophan. Paper chromatography [*n*-butanol – acetic acid – water, 12:3:5] (4) of the product gave a single spot, corresponding to DL-tryptophan, and scanning of the chromatogram showed that the radioactivity was located in the spot of tryptophan only.

Decarboxylation of the product by the method of Van Slyke (5), using pH 4.7 buffer, gave barium carbonate (98% of theory) containing 96% of the radioactivity.

ACKNOWLEDGMENTS

The author wishes to thank Dr. J. C. MacDonald for the decarboxylation of the tryptophan, and Mr. M. Mazurek and Mr. J. Dyck for the radioisotope determinations.

**Barium hydroxide can also be used, but the reaction time is longer (40 min) and more alloy (3 g) is required.*

†The chromatography was followed by ultraviolet spectroscopy to ensure that no tryptophan was lost in the washings or by incomplete elution.

Can. J. Chem. Downloaded from www.nrcresearchpress.com by 210.87.254.40 on 09/05/12
For personal use only.

1. H. W. BOND. J. Biol. Chem. **175**, 531 (1948).
2. J. ELKS, D. F. ELLIOTT, and B. A. HEMS. J. Chem. Soc. 629 (1944).
3. A. I. VOGEL. A text-book of quantitative inorganic analysis. 2nd ed. Longmans, Green, London. 1951. p. 410.
4. I. SMITH. Chromatographic and electrophoretic techniques. 2nd ed. Heineman, London. 1960. p. 83.
5. D. D. VAN SLYKE, D. A. MACFAYDEN, and P. HAMILTON. J. Biol. Chem. **141**, 671 (1941).

RECEIVED MARCH 6, 1964.
NATIONAL RESEARCH COUNCIL,
PRAIRIE REGIONAL LABORATORY,
SASKATOON, SASKATCHEWAN.

Can. J. Chem. Downloaded from www.nrcresearchpress.com by 210.87.254.40 on 09/05/12
For personal use only.

Can. J. Chem. Downloaded from www.nrcresearchpress.com by 210.87.254.105 on 09/05/12
For personal use only.

Canadian Journal of Chemistry

Issued by THE NATIONAL RESEARCH COUNCIL OF CANADA

VOLUME 42 AUGUST 1964 NUMBER 8

REARRANGEMENT STUDIES WITH ^{14}C

XXI. SIDE CHAIN REARRANGEMENT AND FRAGMENTATION FOLLOWING FRIEDEL–CRAFTS ALKYLATION OF BENZENE WITH β-^{14}C-ETHYL IODIDE

C. C. LEE, M. C. HAMBLIN, AND J. F. UTHE

Department of Chemistry, University of Saskatchewan, Saskatoon, Saskatchewan

Received March 2, 1964

ABSTRACT

The aluminum chloride catalyzed reaction between β-^{14}C-ethyl iodide and benzene in 1,2,4-trichlorobenzene as solvent was studied under different conditions of temperature and reaction time. Yields of ethylbenzene were estimated by isotopic dilution. Up to 20% rearranged product, α-^{14}C-ethylbenzene, was found. The trend indicated that yield of ethylbenzene was lower and side chain rearrangement greater when the reaction mixture was heated at higher temperature for longer time. The rearrangement apparently occurred after the initial formation of β-^{14}C-ethylbenzene. After a reaction time of 5 min at 154 °C, only 0.1–0.3% unreacted and unrearranged β-^{14}C-ethyl iodide was recovered while the ethylbenzene obtained from the reaction showed about 2% rearrangement. When β-^{14}C-ethylbenzene was heated with aluminum chloride in 1,2,4-trichlorobenzene for 2 or 24 h, rearrangement to α-^{14}C-ethylbenzene was observed. In some experiments, a fragmentation product, toluene, was isolated. Its specific activity suggested that 1 mole of active ethylbenzene gave 2 moles of toluene only one of which was active. The mechanistic implications of these findings are discussed.

INTRODUCTION

The Friedel–Crafts reaction of β-^{14}C-ethyl chloride (1) or β-^{14}C-ethyl iodide (2) with excess benzene gave β-^{14}C-ethylbenzene with no isotope position rearrangement in the side chain. This observation is consistent with the proposed mechanism of Brown and co-workers (3) that Friedel–Crafts alkylations may be analogous to other substitutions on saturated carbon, with primary alkyl halides reacting by a direct displacement process. Since the Friedel–Crafts catalyst can, by itself, induce rearrangements in alkyl halides, it has been suggested (4, 5) that rearranged products could have arisen from reactions with alkylating agents that have undergone rearrangement prior to the alkylation step. Treatment of β-^{14}C-ethyl chloride or β-^{14}C-ethyl iodide with aluminum chloride (1, 2), or of β-^{14}C-ethyl bromide with aluminum bromide (6), has been shown to cause extensive rearrangement of the ^{14}C-label. However, consideration of reaction rates indicated that no rearrangement of the ethylating agent could take place prior to alkylation when the Friedel–Crafts reaction was effected in excess benzene (2). In the present work, the aluminum chloride catalyzed alkylation of benzene with β-^{14}C-ethyl iodide was carried out in 1,2,4-trichlorobenzene under various conditions. It might then be ascertained if the use of an inert solvent would decrease the alkylation rate sufficiently to allow the aluminum chloride induced rearrangement of the β-^{14}C-ethyl iodide to take place, so that isotopically rearranged ethylbenzene would result. Significant extents of rearrangement were observed only in reactions effected at relatively high temperatures. Experiments were then carried out to show that these rearrangements occurred subsequent to the

formation of ethylbenzene. In addition, a fragmentation product, toluene, was isolated in certain cases and its ^{14}C-contents determined.

RESULTS AND DISCUSSION

The molar ratio of the reactants was 1.0:3.0:3.2 for $AlCl_3$:C_6H_6:C_2H_5I. The solvent, 1,2,4-trichlorobenzene, has previously been used by Brown and co-workers (3). The reaction mixture was heated at different temperatures for various lengths of time. A known amount of ordinary ethylbenzene was then added as carrier, and the crude product was isolated by distillation. Pure ethylbenzene was finally separated by preparative vapor-phase chromatography (v.p.c.). The ethylbenzene recovered was oxidized to benzoic acid, whose activity, relative to that of ethylbenzene, measured the extent of rearrangement of the ^{14}C-label from the β- to the α-positions in the ethyl side chain. The results are summarized in Table I.

In most of the experiments, the specific activity of the original β-^{14}C-ethyl iodide was also determined. Since the amount of added ethylbenzene carrier and the specific activity of the diluted product were known, the yields of ethylbenzene for various runs were estimated by isotope dilution calculations. The basis of these calculations is as follows.

For every experiment, the theoretical yield of ethylbenzene was 3.18 g and the amount of carrier added was 1.73 g (2.0 ml).

Let x = g of ethylbenzene formed; if no carrier had been used, the specific activity of the ethylbenzene would have been the same as that of the β-^{14}C-ethyl iodide.

(Specific activity of $C_2H_5I)x$ = (observed specific activity of $C_6H_5C_2H_5)(1.73 + x)$. Solving for x, % yield = $(x/3.18) \times 100$. The yields calculated in this way are also included in Table I.

The data in Table I show that both yield of ethylbenzene and ^{14}C-rearrangement in the side chain are dependent on reaction temperature and reaction time. Under the relatively milder conditions of lower temperature and shorter reaction time, reproducibilities in yields and extents of rearrangement were fair. When the reaction mixtures were heated at higher temperatures for 24 h, results with much greater deviations were obtained. The general trend indicated by the data of Table I is that higher temperature and longer reaction time could cause greater amounts of rearrangement and lower yields of ethylbenzene. These observations strongly suggest the occurrence of processes which destroyed part of the ethylbenzene subsequent to its formation, and gave rise to side chain rearrangements in the ethylbenzene that remained.

To show more definitely that rearrangement did occur after ethylbenzene formation, first of all it was demonstrated that rearrangement did not arise prior to alkylation. In expt. 7 and 8 (Table I), which involved heating the reaction mixture at 154 °C for 5 min, besides the usual inactive ethylbenzene carrier, 2.0 ml of inactive ethyl iodide carrier was also added. The ethyl iodide fraction obtained by distillation would then contain unreacted β-^{14}C-ethyl iodide. This fraction was used for a Friedel–Crafts alkylation of an excess of benzene to give ethylbenzene, a process which does not cause appreciable rearrangement (2). From the activities of the ethylbenzene so obtained, calculations based on isotope dilution showed that only 0.1% and 0.3% of unreacted β-^{14}C-ethyl iodide were recovered in expt. 7 and 8. Moreover, oxidation of the ethylbenzene derived from the recovered ethyl iodide gave inactive benzoic acid, indicating no rearrangement of the β-^{14}C-ethyl iodide during the course of expt. 7 and 8. Thus the possibility of slowing down the alkylation by inert solvent to allow β-^{14}C-ethyl iodide to rearrange before alkylation was not realized.

Can. J. Chem. Downloaded from www.nrcresearchpress.com by 210.87.254.105 on 09/05/12
For personal use only.

Can. J. Chem. Downloaded from www.nrcresearchpress.com by 210.87.254.105 on 09/05/12
For personal use only.

TABLE I

Yields of ethylbenzene and rearrangements to α-^{14}C-ethylbenzene from aluminum chloride catalyzed reaction of benzene with β-^{14}C-ethyl iodide

Expt.	Reaction temp. (°C)*	Reaction time (h)	Specific activities (c.p.m./mmole)			Yield of $C_6H_5C_2H_5$(%)‖	Rearrangement (%)
			C_2H_5I†	$C_6H_5C_2H_5$‡	C_6H_5COOH§		
1	80	24	251 000	121 000	1 010	51	0.8
2	110	2	—	231 000	2 080	—	0.9
3	110	2	—	226 000	2 820	—	1.2
4	110	24	570 000	212 000	5 770	32	2.7
5	110	24	570 000	217 000	4 210	33	1.9
6	154	1/12	—	725 000	14 900	—	2.1
7	154	1/12	925 000	389 000	7 270	40	1.9
8	154	1/12	925 000	396 000	7 390	41	1.9
9	154	2	—	218 000	8 060	—	3.7
10	154	2	612 000	206 000	10 200	28	4.9
11	154	24	—	173 000	20 900	—	12.0
12	154	24	—	138 000	11 700	—	8.5
13	154	24	612 000	80 200	14 100	8	17.6
14	154	24	570 000	172 000	11 300	24	6.6
15	190	2	295 000	114 000	5 290	34	4.6
16	190	2	438 000	126 000	17 700	22	14.0
17	190	2	438 000	120 000	13 400	21	11.2
18	190	24	438 000	87 800	13 700	14	15.6
19	190	24	438 000	71 500	14 500	11	20.2
20	208	2	—	173 000	6 210	—	3.9
21	208	2	612 000	283 000	11 000	47	3.6
22	208	24	295 000	29 300	6 000	6	20.5
23	208	24	295 000	50 300	8 120	11	16.1

*Temperatures of 80, 110, 154, 190, and 208 °C were maintained by the vapor of refluxing benzene, toluene, bromobenzene, benzonitrile, and 1,2,4-trichlorobenzene, respectively.
†Original reactant before dilution.
‡Diluted with carrier.
§From diluted ethylbenzene.
‖Estimated by isotope dilution calculations.

When the Friedel–Crafts alkylation was carried out at 154° for 2 or 24 h with ordinary ethyl iodide, but with some β-^{14}C-ethylbenzene added at the beginning of each trial, the ethylbenzene finally recovered gave, on oxidation, radioactive benzoic acid, indicating rearrangement of the added active ethylbenzene. Moreover, when β-^{14}C-ethylbenzene in trichlorobenzene containing aluminum chloride was heated at 154 °C for 2 or 24 h, the ethylbenzene re-isolated with the aid of carrier also showed side chain ^{14}C-rearrangement. The results are summarized in Table II. The extents of rearrangement obtained in these

TABLE II

Data from heating β-^{14}C-ethylbenzene at 154 °C in alkylation reaction mixture or in 1,2,4-trichlorobenzene containing aluminum chloride

Expt.	Reaction time (h)	Specific activities (c.p.m./mmole) Initial $C_6H_5C_2H_5$	Recovered $C_6H_5C_2H_5$	C_6H_5COOH*	$C_6H_5C_2H_5$ recovery (%)†	Rearrangement (%)
24	2	481 000	74 400	1 880	—	2.5
25	2	481 000	251 000	8 550	36	3.4
26	24	481 000	51 900	5 350	—	10.3
27	24	481 000	124 000	13 300	23	10.7

*From recovered ethylbenzene.
†Estimated by isotope dilution calculations. In expt. 24 and 26, β-^{14}C-ethylbenzene was heated while an inactive alkylation was carried out. Besides the inactive ethylbenzene carrier added, an unknown amount of inactive ethylbenzene derived from the alkylation reaction was also present; hence no isotope dilution calculations could be made.

trials are of about the same magnitude as those observed in the corresponding experiments 9–10 and 11–14 (Table I). These findings, therefore, support the conclusion that the side chain ^{14}C-rearrangement recorded in Table I arose after the initial formation of unrearranged alkylation product, β-^{14}C-ethylbenzene.

In the course of the v.p.c. separation of ethylbenzene from various experiments, peaks corresponding to benzene and toluene were observed (no attempt was made to identify or separate diethylbenzenes). Probably, benzene resulted from dealkylation and toluene from fragmentation. In some of the experiments with a reaction time of 24 h, sufficient amounts of toluene were present to allow its collection and determination of its specific activity. The results are shown in Table III. As expected, the yield of this fragmentation product was higher when the reaction mixture was heated at higher temperature. It may be of interest to note that under the most drastic conditions employed (expt. 22 and 23), the yields of toluene were comparable to the yields of surviving ethylbenzene.

In these experiments, the toluene was obtained without the addition of any carrier. When the specific activity of the toluene is compared with that of the corresponding ethylbenzene before any dilution of the latter by inactive carrier, the specific activity ratio is about 0.5 in all cases. This is an interesting observation, as it suggests that each mole of active ethylbenzene gave rise to 2 moles of toluene, one of which is active and the other is not. Such a situation would result if the toluene arose from 1,2-diphenyl-1-^{14}C-ethane, which could be derived from either β-^{14}C-ethylbenzene or α-^{14}C-ethylbenzene. In their studies on dealkylation and fragmentation of alkylbenzenes, Roberts, Baylis, and Fonken (7) reported the isolation of *meso*-2,3-diphenylbutane as a minor product after treatment of *sec*-butylbenzene with water-promoted aluminum chloride. A mechanism for fragmentation involving diphenylalkane as intermediate was suggested (7). Such a mechanism applied to ethylbenzene would involve 1,2-diphenylethane as intermediate, which is consistent with the observed specific activity ratio for toluene to ethylbenzene of

Can. J. Chem. Downloaded from www.nrcresearchpress.com by 210.87.254.105 on 09/05/12
For personal use only.

Can. J. Chem. Downloaded from www.nrcresearchpress.com by 210.87.254.105 on 09/05/12
For personal use only.

TABLE III

Fragmentation of β-^{14}C-ethylbenzene to toluene from experiments with reaction time of 24 h

Expt.	Reaction temp. (°C)	Specific activities (c.p.m./mmole)		Specific activity ratio ($C_6H_5CH_3/C_6H_5C_2H_5$)	Yield of $C_6H_5CH_3$		Yield of $C_6H_5C_2H_5$ (%)‡
		Undiluted $C_6H_5C_2H_5$*	$C_6H_5CH_3$		(mg)	(%)†	
14	154	570 000	311 000	0.55	109	4.0	24
27	154	481 000	261 000	0.54	71	2.7	—
18	190	438 000	227 000	0.52	142	5.2	14
19	190	438 000	231 000	0.53	165	6.0	11
22	208	295 000	148 000	0.50	156	5.7	6
23	208	295 000	151 000	0.51	241	8.7	11

*In expt. 27, β-^{14}C-ethylbenzene was added as such; in the other experiments, the specific activity of the undiluted $C_6H_5C_2H_5$ was assumed to be equal to the specific activity of the C_2H_5I initially used (see Table I).

†For expt. 27, based on the β-^{14}C-ethylbenzene added; for the other experiments, based on the limiting reactant, benzene, in the Friedel–Crafts reaction mixture.

‡From Table I, also based on the benzene in the Friedel–Crafts reaction mixture.

about 0.5. The activity data of Table III may, therefore, be regarded as evidence in support of the fragmentation mechanism of Roberts, Baylis, and Fonken.

The disproportionation of ethylbenzene under conditions less severe than those used in the present experiments has been extensively investigated. The pertinent literature has been summarized in a recent paper by Ünseren and Wolf (8). The possibility of side chain rearrangements proceeding through π-complexes has been discussed by Roberts and co-workers (9, 10). It is noteworthy that in the present work, more rearrangement as well as more fragmentation were observed under conditions of higher temperature and longer reaction time. Both of these processes could result from the same intermediate. 1,2-Diphenyl-1-^{14}C-ethane might revert to equal amounts of α-^{14}C-ethylbenzene and β-^{14}C-ethylbenzene, giving rise to the side chain rearrangements observed in the surviving ethylbenzene (Tables I and II). The 1,2-diphenylethane could arise either directly from ethylbenzene or via 1,1-diphenylethane, an intermediate postulated by Streitwieser and Reif (11) for ethylbenzene disproportionation. Isotopically rearranged ethylbenzene via 1,2-diphenylethane would also be consistent with the conclusions of Ünseren and Wolf (8) and of Streitwieser and Reif (11) that disproportionation of ethylbenzene involves considerable extents of intermolecular *trans*-alkylation.

EXPERIMENTAL

The β-^{14}C-ethyl iodide was obtained from New England Nuclear Corp. The β-^{14}C-ethylbenzene was prepared by a Friedel–Crafts reaction between β-^{14}C-ethyl iodide and an excess of benzene, the product showing less than 0.3% ^{14}C rearrangement in the side chain (2). Degradation of ethylbenzene from various experiments to benzoic acid was effected by oxidation with alkaline potassium permanganate (12).

Friedel–Crafts Reactions (Expt. 1–23, Tables I and III)

All reactions were carried out in a pyrex vessel fitted with mechanical stirrer, reflux condenser, and Drierite tube. The vessel was enclosed in a pyrex jacket which was also fitted with a reflux condenser and connected to a pot of boiling liquid. The vapor from the refluxing liquid heated the reaction mixture and maintained a constant temperature.

A mixture of 2.34 g (30 mmoles) of anhydrous benzene, 1.33 g (10 mmoles) of sublimed, anhydrous aluminum chloride, and 50 ml of redistilled 1,2,4-trichlorobenzene was placed in the reaction vessel and brought to the desired temperature. A solution of 5.0 g (32 mmoles) of β-^{14}C-ethyl iodide in a small amount of 1,2,4-trichlorobenzene was then added through the top of the reflux condenser. Heating was continued for the desired length of time and then the reaction stopped by the addition of 50 ml of ice water. Two ml (1.73 g) of inactive ethylbenzene was introduced as carrier. The organic layer was separated and washed successively with 50-ml portions of 5% hydrochloric acid, 2% sodium hydroxide solution containing 5 g of sodium thiosulphate, and water. The washings were extracted with ether and the extract combined with the original organic layer. After the solution was dried over anhydrous magnesium sulphate, it was fractionated. The major portion of the product distilled at 130–135 °C, but the fraction boiling over the range 100–160 °C was collected. Recoveries were of the order of 2–3 g. Final purification was effected by passage through a preparative column packed with Apiezon L on firebrick in a Beckman GC-2A gas chromatograph. Ethylbenzene was recovered in all experiments, while in some cases, toluene, in addition to ethylbenzene, was also collected. The identities of these products were confirmed by n.m.r. spectroscopy. The spectra of the recovered ethylbenzene and toluene were the same as those of corresponding authentic samples. The typical triplet–quartet splitting was shown by the ethyl protons of ethylbenzene and a singlet was observed for the methyl protons of toluene. The τ-values also agree with those given by Tiers (13) for ethylbenzene and toluene.

In expt. 7 and 8, which involved stopping the reaction after heating at 154 °C for 5 min, 2.0 ml of inactive ethyl iodide, in addition to the inactive ethylbenzene carrier, were also added before the mixture was worked up as described above. Two fractions were collected, one contained the ethylbenzene and the other, boiling over the range of 40–80 °C, contained unreacted β-^{14}C-ethyl iodide diluted by carrier. The ethyl iodide fraction was used for a Friedel–Crafts reaction with excess benzene. The ethylbenzene obtained was purified by v.p.c. Its activity measured the amount of unreacted β-^{14}C-ethyl iodide recovered and its oxidation to inactive benzoic acid indicated no rearrangement in the unreacted β-^{14}C-ethyl iodide.

Treatment of β-^{14}C-Ethylbenzene with Aluminum Chloride (Expt. 24-27, Tables II and III)

Two procedures were used. In expt. 24 and 26, a mixture of 1.70 g (22 mmoles) of anhydrous benzene, 1.33 g (10 mmoles) of sublimed, anhydrous aluminum chloride, and 50 ml of redistilled 1,2,4-trichlorobenzene was heated to 154 °C. Inactive ethyl iodide (3.64 g, 23 mmoles) and β-^{14}C-ethylbenzene (0.86 g,

Can. J. Chem. Downloaded from www.nrcresearchpress.com by 210.87.254.105 on 09/05/12
For personal use only.

8 mmoles) were introduced and the reaction mixture heated for 2 or 24 h. The reaction was stopped by addition of ice water. After the introduction of 1.0 ml of inactive ethylbenzene as carrier, the resulting material was worked up as in the Friedel–Crafts reactions to give pure ethylbenzene.

In expt. 25 and 27, 1.33 g (10 mmoles) of sublimed, anhydrous aluminum chloride and 50 ml of 1,2,4-trichlorobenzene were heated to 154 °C and then 2.60 g (24 mmoles) of β-^{14}C-ethylbenzene was introduced. Heating was continued for 2 or 24 h. Ice water was added followed by 1.0 ml of inactive ethylbenzene as carrier. The resulting material was worked up the usual way to give pure ethylbenzene. In expt. 27, which involved 24 h of heating, both ethylbenzene and toluene were recovered in the final purification by v.p.c.

Radioactivity Determination

All activities were measured by a liquid scintillation counter. Active ethyl iodide, ethylbenzene, toluene, and benzoic acid were counted in toluene solution containing PPO and POPOP. Sample concentrations were about 15 mg/20 ml. Ethyl iodide showed appreciable quenching and correction factors were determined by use of a known amount of ^{14}C-toluene as internal standard.

ACKNOWLEDGMENTS

Financial support from the National Research Council of Canada and from the President's Fund awarded by President J. W. T. Spinks of this university are gratefully acknowledged.

REFERENCES

1. R. M. Roberts, G. A. Ropp, and O. K. Neville. J. Am. Chem. Soc. **77**, 1764 (1955).
2. C. C. Lee, M. C. Hamblin, and N. James. Can. J. Chem. **36**, 1597 (1958).
3. H. Jungh, C. R. Smoot, and H. C. Brown. J. Am. Chem. Soc. **78**, 2185 (1956).
4. C. C. Lee, A. G. Forman, and A. Rosenthal. Can. J. Chem. **35**, 220 (1957).
5. C. R. Smoot and H. C. Brown. J. Am. Chem. Soc. **78**, 6249 (1956).
6. F. L. J. Sixma and H. Hendricks. Recueil Trav. Chim. **75**, 169 (1956).
7. R. M. Roberts, E. K. Baylis, and G. J. Fonken. J. Am. Chem. Soc. **85**, 3454 (1963).
8. E. Unseren and A. P. Wolf. J. Org. Chem. **27**, 1509 (1962).
9. R. M. Roberts, S. G. Brandenberger, and S. G. Panayides. J. Am. Chem. Soc. **80**, 2507 (1958).
10. R. M. Roberts and Y. W. Han. J. Am. Chem. Soc. **85**, 1168 (1963).
11. A. Streitwieser, Jr. and L. Reif. J. Am. Chem. Soc. **82**, 5003 (1960).
12. D. P. Thornhill and C. C. Lee. Can. J. Chem. **41**, 2861 (1963).
13. G. V. D. Tiers. Table of characteristic n.m.r. shielding values. Minnesota Mining and Manufacturing Co., St. Paul, Minn. March, 1958.

Can. J. Chem. Downloaded from www.nrcresearchpress.com by 210.87.254.105 on 09/05/12
For personal use only.

Can. J. Chem. Downloaded from www.nrcresearchpress.com by 210.87.254.40 on 09/05/12
For personal use only.

STUDIES ON THE THERMODYNAMICS AND CONDUCTANCES OF MOLTEN SALTS AND THEIR MIXTURES

PART III. DENSITIES, MOLAR VOLUMES, VISCOSITIES, AND SURFACE TENSIONS OF MOLTEN LITHIUM CHLORATE, WITH SMALL ADDITIONS OF WATER, AND OTHER SUBSTANCES

A. N. Campbell and D. F. Williams
Chemistry Department, University of Manitoba, Winnipeg, Manitoba

Received March 10, 1964

ABSTRACT

The density (2.088 g cc^{-1}) at 131.8 °C and viscosity (0.35 P at 131.8 °C) and their temperature dependence, of molten lithium chlorate, have been determined. Similar results have been obtained for lithium chlorate melts containing small quantities of water. The surface tension and its temperature dependence have been determined for lithium chlorate and for several lithium chlorate – water and lithium chlorate – lithium nitrate mixtures. From these measurements the surface heat has been calculated.

The results for pure lithium chlorate indicate that the melt is complex, this complexity probably caused by association of some kind. This is especially evident just above the melting point, since there the temperature change in properties is greatest.

Addition of water to the lithium chlorate melt causes the melt properties, especially the viscosity, to alter considerably. These changes are in part caused by a breakdown of the structural entities in the melt.

In this paper we report our experimental data on the density, viscosity, and surface tension of lithium chlorate (a single-salt melt). As well we report some results for mixtures in which a second component (water or lithium nitrate) was added to lithium chlorate, to assess the sensitivity of these physical properties to the addition of polar molecular species, as well as inorganic salts, as foreign species. It is allowable to discuss these effects in terms of structure, although such a discussion cannot be considered as proving any hypothetical structure.

EXPERIMENTAL

The theoretical implications and the experimental methods used in determining density and viscosity have been described in Parts I and II of this series (1, 2). It should be mentioned, however, that since water was added in these experiments, it was essential that the lithium chlorate be originally completely anhydrous. Accordingly, the residual water, if any, in our preparation was determined by gas chromatography. A precision Chromofrac VP-7 unit was calibrated for water detection by injection of samples of 0.01 ml ethyl alcohol containing known amounts of water. The lower limit of detection was found to be 1 part water in 500 parts alcohol by volume. The dried, powdered lithium chlorate was weighed, mixed with dry sand, and heated strongly. Under the catalytic action of the sand, the lithium chlorate decomposed rapidly, evolving oxygen together with any moisture it contained. The gases were trapped in a liquid nitrogen trap. A test of the residue showed that decomposition was complete. The trapped gases were allowed to warm up slowly to 0 °C and a measured quantity of ethyl alcohol then added. This solution was allowed to warm up to room temperature and a portion passed through the chromatograph. The result showed that the lithium chlorate contained less than 0.006% water by weight. The specific conductivity at 131.8 °C of a sample of this lithium chlorate was found to be $0.1150 \pm 0.0002\ \Omega^{-1}$ and, for all subsequent preparations, this conductance was used as the criterion of the absence of moisture in the specimen. The conductivity water used had a specific conductance of $1.5 \times 10^{-7}\ \Omega^{-1}$.

The method of capillary rise was used for the determination of surface tension. The apparatus is shown in Fig. 1. The inner tube was a precision-bore capillary tube, internal diameter 0.5 ± 0.001 mm. An extension 5 cm wide at the foot of the outer tube made possible a satisfactory reading of the level of the lower meniscus, always a matter of uncertainty in the capillary rise method. The capillary rise was measured by means of a micro-cathetometer, which could be read to 0.01 mm.

The cell was loaded in a dry box with a weighed amount of lithium chlorate, sufficient in amount to cover, when molten, the maximum area of the bottom extension. Weighed amounts of additional substances were

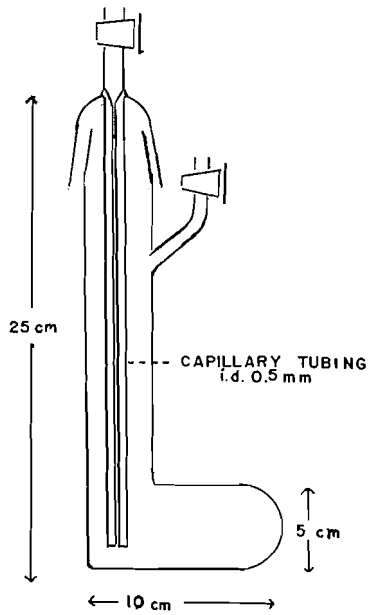

FIG. 1. Surface tension apparatus.

added when necessary. After transference of the apparatus to the thermostat and attainment of temperature equilibrium, the liquid was caused to rise and fall in the capillary by suitably altering the external pressure through the vacuum cocks. After each rise and fall, the capillary rise was measured. To test the apparatus, the surface tension of conductance water was determined in it, at 25 °C, and found to be reproducible to ± 0.5 dyn cm^{-1}.

RESULTS

Density and Molar Volume

The density of pure molten lithium chlorate was determined at temperatures ranging between ca. 130° to 150°, as well as those of mixtures containing 0.046, 0.130, and 0.223 mole fraction water. There is a maximum possible error of 8.0×10^{-4} g cc^{-1} in these measurements. The results are shown in Table I.

The density in each case was found to be linear with respect to temperature, the coefficient of expansion decreasing with increasing water content. The molar volumes, together with the coefficients of expansion, calculated from the relation $V_t = V_0(1 + \alpha t)$ are shown in Table II.

Equations of forms which have been shown experimentally to represent the density–temperature relationship for fused salts have been calculated by a least squares fit of the experimental results of Table I, using a computer. These equations are given in Table III.

Viscosity

The viscosities of pure molten lithium chlorate, and of mixtures containing 0.079, 0.197, and 0.251 mole fraction water, were determined at temperatures between 130° and 180°. The results are given in Table IV.

Both for pure lithium chlorate and the three mixtures with water, a linear relation exists between $\log \eta$ and $1/T$. The activation energies of viscous flow were obtained from these graphs, as $\Delta E_{vis} = 4.576 \times$ slope. The values of the constants are given in Table V. The Arrhenius equations used to represent the viscosity–temperature relations were determined by least squares fit, and they are also included in Table V.

Can. J. Chem. Downloaded from www.nrcresearchpress.com by 210.87.254.40 on 09/05/12
For personal use only.

Can. J. Chem. Downloaded from www.nrcresearchpress.com by 210.87.254.40 on 09/05/12
For personal use only.

TABLE I

Density and molar volume of pure lithium chlorate and lithium chlorate – water mixtures

	t (°C)	Density (g cc^{-1})	Molar volume (cc mole^{-1})
Pure lithium chlorate	133.1	2.0858	43.34
	135.7	2.0838	43.38
	138.7	2.0818	43.42
	140.2	2.0809	43.44
	142.2	2.0794	43.47
	143.7	2.0783	43.49
	146.7	2.0763	43.54
	149.0	2.0742	43.58
	150.5	2.0730	43.60
	152.8	2.0709	43.65
	153.4	2.0700	43.67
Lithium chlorate – water mixture			
Mole fraction water 0.046	130.3	2.0706	42.05
	131.0	2.0696	42.07
	132.0	2.0689	42.08
	132.4	2.0689	42.08
	135.6	2.0664	42.13
	137.1	2.0649	42.16
	139.8	2.0631	
	144.2	2.0595	42.27
	145.6	2.0583	42.30
	147.5	2.0568	42.33
Mole fraction water 0.130	128.8	2.0300	39.89
	130.4	2.0287	39.91
	135.3	2.0251	40.00
	137.5	2.0237	40.02
	141.8	2.0204	40.08
	142.6	2.0188	40.11
	145.0	2.0178	40.14
	145.8	2.0172	40.15
	147.0	2.0162	40.17
	149.6	2.0145	40.20
Mole fraction water 0.223	131.0	1.9722	37.76
	133.0	1.9708	37.78
	135.6	1.9688	37.82
	139.8	1.9657	37.88
	142.2	1.9638	37.92
	145.7	1.9618	37.96
	146.2	1.9614	37.97
	147.0	1.9606	37.98
	148.1	1.9598	38.00
	150.6	1.9580	38.03

TABLE II

Molar volume and coefficient of expansion of lithium chlorate – water mixtures

Mole fraction water	Molar volume at 130 °C (cc)	Coefficient of expansion (deg^{-1})
0.000	43.26	4.12×10^{-4}
0.046	42.04	4.09×10^{-4}
0.130	39.91	3.87×10^{-4}
0.223	37.75	3.77×10^{-4}

TABLE III

Analytical representation of density–temperature relation for lithium chlorate – water mixtures

Mole fraction water	Coefficients in eq. $\rho = \rho_0 \exp(-\alpha T)$		Coefficients in eq. $\rho = a - bt$	
	ρ_0	α	a	b
0.000	2.463	4.12×10^{-4}	2.188	7.672×10^{-4}
0.046	2.437	4.09×10^{-4}	2.172	7.798×10^{-4}
0.130	2.368	3.87×10^{-4}	2.125	7.429×10^{-4}
0.223	2.296	3.77×10^{-4}	2.068	7.304×10^{-4}

TABLE IV

Viscosity

Pure lithium chlorate		Lithium chlorate – water mixture					
		Mole fraction water 0.079		Mole fraction water 0.197		Mole fraction water 0.251	
t (°C)	η(P)	t (°C)	η(P)	t (°C)	η(P)	t (°C)	η(P)
131.8	0.334	130.5	0.241	130.5	0.185	131.0	0.144
133.3	0.320	136.5	0.214	136.0	0.167	134.5	0.132
135.0	0.305	143.7	0.180	142.0	0.147	140.7	0.118
137.5	0.296	150.0	0.160	145.5	0.138	146.8	0.104
138.7	0.277	157.6	0.139	151.5	0.123	154.5	0.090
142.7	0.249	160.0	0.129	159.0	0.107	160.0	0.083
144.7	0.235	162.0	0.128	162.0	0.101	168.2	0.073
148.4	0.218	164.8	0.120	166.0	0.094		
152.4	0.199						
156.3	0.194						
158.6	0.177						
162.1	0.168						
166.9	0.155						

TABLE V

Analytical representation of viscosity

Mole fraction water	Arrhenius eq. $\eta = A_0 \exp(C/RT)$		Activation energy of viscous flow (kcal mole^{-1})
	A_0	C	
0.000	1.979	7813	7.8
0.079	3.314	7124	7.1
0.197	4.144	6740	6.7
0.251	4.573	6452	6.4

Surface Tension

The surface tensions of pure molten lithium chlorate and of mixtures of lithium chlorate with water and with lithium nitrate are given in Table VI. The surface heat of lithium chlorate at different temperatures, calculated from the equation $H^s = \gamma - T(d\gamma/dT)$ (14, 15) was constant at 118 erg/cm^2 in the region 130 to 170 °C. The analytical representations of the temperature dependence of the surface tension of pure lithium chlorate and of the mixtures were obtained from a least squares fit of the results of Table VI. The constants of the equation are shown in Table VII.

Can. J. Chem. Downloaded from www.nrcresearchpress.com by 210.87.254.40 on 09/05/12
For personal use only.

TABLE VI

Surface tension of lithium chlorate, lithium chlorate – water mixtures, and lithium chlorate – lithium nitrate mixtures

	t (°C)	Density (g cc^{-1})	Surface tension (dyn cm^{-1})
Lithium chlorate	132.1	2.0878	87.41
	138.2	2.0828	87.30
	142.6	2.0794	86.91
	150.6	2.0729	86.26
	155.2	2.0691	86.02
	162.0	2.0635	85.43
Lithium chlorate – water mixtures			
Mole fraction water 0.038	133.2	2.0715	86.20
	139.4	2.0666	85.52
	145.7	2.0617	85.10
	146.3	2.0614	83.93
	153.7	2.0552	84.10
	160.1	2.0502	84.07
	164.8	2.0463	83.49
Mole fraction water 0.090	132.3	2.0488	85.97
	139.7	2.0433	84.42
	147.0	2.0378	83.11
	153.3	2.0326	82.66
	156.0	2.0306	82.69
	161.6	2.0262	81.87
Mole fraction water 0.155	137.0	2.0103	83.79
	142.6	2.0062	82.79
	147.7	2.0015	82.49
	152.5	1.9990	81.79
	158.7	1.9944	81.50
	168.0	1.9876	79.39
Mole fraction water 0.236	132.5	1.9617	83.44
	141.7	1.9552	82.57
	144.0	1.9536	82.87
	149.0	1.9500	80.99
	154.4	1.9465	80.90
	155.3	1.9456	80.42
	159.0	1.9431	80.14
Lithium chlorate – lithium nitrate			
Mole fraction lithium nitrate 0.032	132.0	2.0866	88.92
	136.5	2.0828	88.55
	140.0	2.0799	88.60
	145.8	2.0750	87.92
	151.7	2.0700	87.78
	156.1	2.0664	87.69
	161.4	2.0619	87.60
Mole fraction lithium nitrate 0.075	132.0	2.0836	90.00
	138.2	2.0790	89.51
	143.6	2.0747	89.41
	149.0	2.0705	89.02
	156.0	2.0650	88.75
	161.7	2.0606	88.21
Mole fraction lithium nitrate 0.172	133.0	2.0726	91.86
	139.7	2.0672	91.50
	147.5	2.0615	91.34
	156.0	2.0548	90.70
	161.6	2.0506	90.66
Mole fraction lithium nitrate 0.213	130.5	2.0692	92.60
	138.2	2.0632	92.27
	145.6	2.0575	91.64
	153.4	2.0513	91.11
	159.4	2.0467	90.97
	166.7	2.0410	90.44

Can. J. Chem. Downloaded from www.nrcresearchpress.com by 210.87.254.40 on 09/05/12
For personal use only.

TABLE VII

Analytical representation of the surface tension variation with temperature for lithium chlorate, lithium chlorate – water, and lithium chlorate – lithium nitrate mixtures

Additive	Mole fraction additive	Eq. of general type $\gamma = a - bt$	
		a	b
Pure salt	0.000	96.7	6.3×10^{-2}
Water	0.038	96.2	7.7×10^{-2}
Water	0.090	103.2	13.3×10^{-2}
Water	0.155	101.6	13.0×10^{-2}
Water	0.236	101.7	13.6×10^{-2}
Lithium nitrate	0.032	94.9	4.6×10^{-2}
Lithium nitrate	0.075	97.4	5.6×10^{-2}
Lithium nitrate	0.172	97.7	4.4×10^{-2}
Lithium nitrate	0.213	100.5	6.0×10^{-2}

The surface tension of an equimolar mixture of lithium chlorate and water was determined at 132.4 °C and found to be 78.4 dyn cm^{-1}, using a density calculated from the mixture rule and the densities of the pure components at the temperature of determination. The surface tension of this mixture can be calculated from an ideal surface tension relationship proposed by Guggenheim (3).

$$\gamma = \tilde{\gamma} - \frac{kT}{a} \log \cosh \frac{\Delta \delta a}{2kT}$$

where $\tilde{\gamma} = \frac{1}{2}(\gamma_A + \gamma_B)$, $\Delta = \gamma_A - \gamma_B$ and a = area per molecule. Using this relation, the ideal surface tension of the mixture is found to be 69.8 dyn cm^{-1}.* It is obvious that the above relation gives the surface tension of the mixture as being equal to the arithmetic mean surface tension of the two liquids, minus a correction factor. This correction factor will not be very large, unless (*a*) the difference between the surface tensions of the two liquids is very great, (*b*) the temperature is very low on the Kelvin scale, or (*c*) there is a great difference between the surface areas per molecule. In the present case, (*a*) is not large and (*b*) not small, so that the value of the factor is determined by δa, the difference between the surface areas per molecule. This difference is obtained as follows: If we take the densities, at 132.4 °C, of lithium chlorate and of water as 2.0863 and 0.9331, respectively, the molar volumes are 43.33 ml and 19.31 ml, respectively. If these volumes are corrected for the free space in closest packing, they result as 32.06 and 14.29, respectively, but it makes very little difference to the end result whether this is done or not. When we divide by the Avogadro number, the molecular volumes are 5.317×10^{-23} and 2.370×10^{-23} cm^3, respectively. If we assume the molecules to be spherical, the radii are 2.330×10^{-8} and 1.785×10^{-8} cm, respectively. The hemispherical surfaces of such molecules are 3.412×10^{-15} and 2.002×10^{-15} cm^2, respectively. Hence $\delta a = 1.410 \times 10^{-15}$ cm^2. The surface tension of lithium chlorate at 132.4 °C is 87.41 dyn/cm and that of water, by a slight extrapolation from the figure for 130 °C, is 52.36 dyn/cm. Hence $\Delta = 35.05$. With the insertion of these values, together with the value of the Boltzmann constant, the value of the correction factor is 0.11. If the correction in molar volume for the free volume is not made, the correction factor is 0.15. Hence the calculated value of the surface tension of an equimolecular mixture is found to be 69.8, while the experimental value is 78.4.

**For an ideal liquid pair, this relation simplifies to* $\gamma = \tilde{\gamma} - \Delta\,(\delta a/8kT)$.

Can. J. Chem. Downloaded from www.nrcresearchpress.com by 210.87.254.40 on 09/05/12
For personal use only.

Can. J. Chem. Downloaded from www.nrcresearchpress.com by 210.87.254.40 on 09/05/12
For personal use only.

DISCUSSION OF RESULTS

The density of lithium chlorate at 131.8 °C, 2.0880 g cc^{-1}, agrees with the earlier result of Campbell, Kartzmark, and Patterson (4). The value of Klotschko and Grigorjew (5), (1.998 at 128°) is low, probably because of the presence of water in this highly hygroscopic salt. The relation between the density and temperature of molten lithium chlorate can be expressed by either of the following equations

$$\rho = 2.463 \exp(-4.12 \times 10^{-4})T \quad \text{or} \quad \rho = 2.188 - 7.672 \times 10^{-4}t.$$

The general trend of increasing density in the series, chloride–nitrate–chlorate, which is observed with sodium and potassium salts, applies also to the comparable lithium salts. The density of lithium chlorate – water mixtures decreases with increasing water content. The density–temperature variation of these mixtures is represented by equations of the same form as those applicable to pure lithium chlorate. The deviation from the ideal linear relation between molar volume and mole fraction (6, 7, 8) is negligible for the mixtures studied (Fig. 2). Since large deviations have been found for systems in which complex

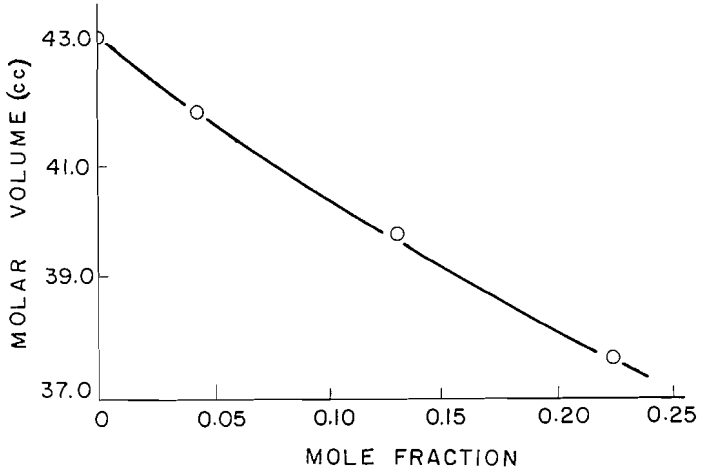

FIG. 2. Molar volume at 130 °C vs. mole fraction water.

formation occurs (9, 10, 11), it appears that there is little immediate association between the water and the lithium chlorate. The decrease in the coefficient of expansion α with increase in water content may be due in part to an increase in the overall ionic character of the melt. A graph of the coefficient of expansion against mole fraction of water (Fig. 3) shows this effect graphically. The viscosity of pure molten lithium chlorate can be represented in its temperature variation by

$$\eta = 1.979 \times 10^{-5} \exp(7813/RT).$$

The value of the viscosity at 131.8 °C, viz. 33.0 cP, is slightly larger than that obtained by Campbell, Kartzmark, and Patterson (4), perhaps because of the improved technique we are now using. On the other hand, Klotschko and Grigorjew (5) report a value of 52.5 cP, almost twice the value obtained by us. There is little doubt that the value of Klotschko and Grigorjew is inaccurate. We suggest as the most probable cause of this discrepancy

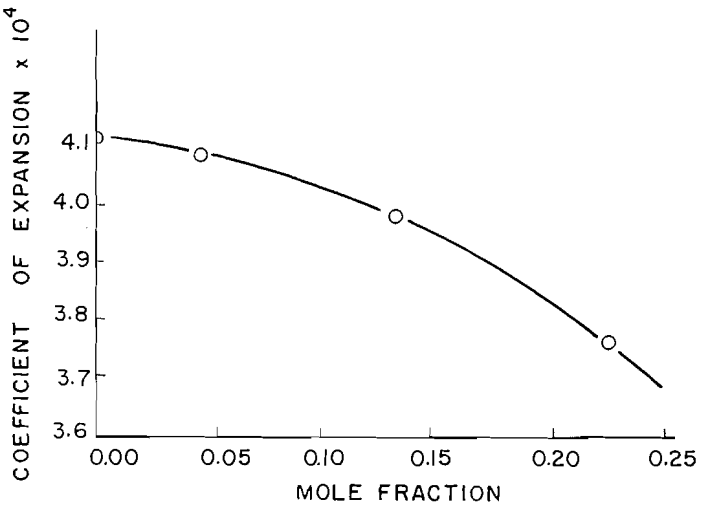

FIG. 3. Coefficient of expansion vs. mole fraction water.

the fact that the Russian workers took no precautions to exclude from their viscometer any decomposition products, formed in the sealing of the apparatus. We have obviated this difficulty by including in the viscometer itself a sintered glass disc, so that the fluid can be filtered as often as desired after sealing (2). If this is not done, the flow times are most erratic, because the capillary of the instrument is more or less choked with insoluble decomposition products.

The viscosity of molten lithium chlorate is much larger than that of simple ionic salts at corresponding temperatures (i.e. taking the melting point of the salt, on the Kelvin scale, as the basis of comparison): e.g. the viscosity of silver nitrate is 2.3 cP at 450 °C against 15 cP for lithium chlorate at 168 °C. Zinc chloride exhibits the very high viscosity of 350 cP at 400 °C, but this is interpreted on the basis of a model in which fragments of the original double layers of crystalline $ZnCl_2$, together with $ZnCl_6^{-4}$ ions, are the predominant species. A marked decrease with temperature of the activation energy for viscous flow is observed for such viscous melts but this is not observed for lithium chlorate, the activation energy being almost constant at 7.8 kcal $mole^{-1}$ between 130 and 170 °C. This is within the range of activation energy of viscous flow for most ionic melts, viz. 3–10 kcal $mole^{-1}$.

Yaffe and van Artsdalen (8) consider that the heat of activation for viscous flow is dependent on two opposing factors. As a melt expands with rising temperature, the total coulombic forces among the constituent ions tend to decrease and hence the activation energy for mass migration also decreases. Opposing this effect and because of the increase in the number of holes in the melt, the average number of nearest neighbors to a given ion may decrease, and hence increase the attractive force per nearest neighbor, with consequent increasing activation energy. In melts in which there is a large disparity in ionic size, such as lithium chlorate, the latter effect should predominate. In fact, however, little change is observed in the activation energy of lithium chlorate: this may be due to the association in the melt breaking down as the temperature rises. If this is so, fewer bonds will be broken in mass transfer at higher temperatures, and this may compensate for the increase in ion-neighbor attractive forces caused by a decrease in coordination number.

Can. J. Chem. Downloaded from www.nrcresearchpress.com by 210.87.254.40 on 09/05/12
For personal use only.

The addition of water to a lithium chlorate melt causes a considerable decrease in the viscosity of the melt. At temperatures slightly above the melting point, the decrease following the initial addition of water is greater than that caused by subsequent additions: at higher temperatures this large difference is not so marked.

Over the temperature range investigated, the viscosity isotherm for each mixture shows a negative deviation from linear dependence on molar composition. Harrap and Heymann (12) have found that this negative deviation is exhibited by all molten salts, regardless of type.

The viscosity–temperature relationship for lithium chlorate – water mixtures is represented by the Arrhenius equations of Table V. The activation energy of viscous flow becomes considerably smaller as the water content increases. The decrease of activation energy is not a linear function of the mole fraction of water. The initial rate of change decreases as water content increases and this indicates that the average size of the mass unit of viscous flow becomes smaller as water is added.

At temperatures slightly above the melting point, and at which, therefore, associated groups may be present in the melt, the effect of water addition on viscosity is pronounced, probably because of the immediate break-up of these groups. At higher temperatures, where associated groups do not exist or exist only to a lesser extent, water additions lower the viscosity to a lesser extent. The changes of activation energy may be interpreted in the same way.

The surface tension of lithium chlorate is typical of group I salts of polyatomic anions. If association occurs within a melt, the associated groups will probably affect the surface energy of the melt considerably, and, if these "associates" lower the surface energy, they will be preferentially adsorbed at the surface. The surface tensions of all group I nitrates are observed to be about the same. The surface tension of lithium chlorate at its melting point, 88.6 dyn cm^{-1}, is much the same as that of potassium chlorate at its melting point, 81.0 dyn cm^{-1} (13). If it is true that the anion determines the surface energy of the group I chlorates, as the nitrate ion does that of the group I nitrates, then it is possible that in these melts the anions pack in contact, with the cations in crevices where their effect on surface tension is slight.

The surface heat, $H^s = \gamma - T(d\gamma/dT)$ is not temperature dependent: it is thought to provide a measure of the covalent character of the melt (14). For nonpolar liquids the surface heat varies between 40 and 65 erg cm^{-2}. Salts which are essentially ionic have the highest values, e.g. sodium chloride 216.7, whereas molten salts which consist largely of covalent molecules have lower values, approaching those of non-polar liquids, e.g. magnesium chloride 76.7. The surface heat of lithium chlorate is 118 erg cm^{-2}, intermediate between the values for ionic melts and those of covalent melts, and indicates that at least some covalent character exists in the lithium chlorate melt.

The temperature coefficient of molecular surface energy is found to be 0.468. Although the calculation has little meaning, since lithium chlorate decomposes at temperatures not much above the melting point, we have used this coefficient to find a hypothetical critical temperature (L $\rightleftarrows$ V) for lithium chlorate, assuming, of course, that the so-called "Law" of Eotvos is applicable, viz. that molecular surface energy is a straight line function of temperature up to the critical temperature. The figure obtained is 2430 °C.

The surface tension of pure lithium chlorate and also those of the mixtures with water and with lithium nitrate decrease linearly with temperature. At any fixed temperature, the lithium chlorate – lithium nitrate mixtures have surface tensions greater than that of pure lithium chlorate, while the mixtures with water have surface tensions lower than

Can. J. Chem. Downloaded from www.nrcresearchpress.com by 210.87.254.40 on 09/05/12
For personal use only.

that of lithium chlorate. This, however, is an almost necessary consequence of the fact that the surface tension of water at, say, 130 °C is lower than that of lithium chlorate while that of lithium nitrate (extrapolated for the supercooled state) is higher (126.0 dyn).

The relation between the isothermal surface tension and mole fraction of either lithium nitrate or water is not linear. Initial additions up to 0.05 mole fraction affect the surface tension of the melt to a greater extent than subsequent additions, both for lithium nitrate and water.

The temperature coefficient of surface tension changes considerably as the water content of the mixture increases. The temperature coefficient of water is much higher than that of molten salts and this accounts for the increase of the temperature coefficient of surface tension when water is added to molten lithium chlorate. On the other hand, the temperature coefficient of lithium nitrate is almost the same as that of lithium chlorate and this accounts for the observed fact that the addition of lithium nitrate hardly affects the temperature coefficient of lithium chlorate.

The surface tension of an ideal equimolecular mixture of lithium chlorate and water (calculated by Guggenheim's relation (3) 69.8 dyn cm^{-1}) is quite different from the experimental value (78.4). Hence the melt is not ideal with respect to surface tension behavior, at higher concentrations of water.

REFERENCES

1. A. N. CAMPBELL and M. K. NAGARAJAN. Can. J. Chem. **42**, 1137 (1964).
2. A. N. CAMPBELL and M. K. NAGARAJAN. Can. J. Chem. **42**, 1616 (1964).
3. E. A. GUGGENHEIM. Trans. Faraday Soc. **41**, 150 (1945).
4. A. N. CAMPBELL, E. M. KARTZMARK, and W. G. PATTERSON. Can. J. Chem. **36**, 1004 (1958).
5. M. A. KLOTSCHKO and J. C. GRIGORJEW. Akad. Wiss. USSR Nacht. Abt. Physik. Chem. Anal., **21**, 288 (1950).
6. H. BLOOM and E. HEYMANN. Proc. Roy. Soc. London, Ser. A., **188**, 392 (1946).
7. N. K. BOARDMAN, F. H. DORMAN, and E. HEYMANN. J. Phys. Chem. **53**, 375 (1949).
8. I. S. YAFFE and E. R. VAN ARTSDALEN. J. Phys. Chem. **60**, 1125 (1956).
9. H. BLOOM, I. W. KNAGGS, J. J. MOLLOY, and D. WELCH. Trans. Faraday Soc. **49**, 1458 (1953).
10. E. W. DEWING. J. Am. Chem. Soc. **77**, 2639 (1955).
11. K. A. SENSE, M. J. SNYDER, and J. W. CLEGG. J. Phys. Chem. **58**, 223 (1954).
12. B. S. HARRAP and E. HEYMANN. Trans. Faraday Soc. **51**, 259 (1955).
13. J. D. FRAME, E. RHODES, and A. R. UBBELOHDE. Trans. Faraday Soc. **55**, 2042 (1959).
14. H. BLOOM, F. G. DAVIES, and D. W. JAMES. Trans. Faraday Soc. **56**, 1179 (1960).
15. G. J. JANZ and M. R. LORENZ. J. Electrochem. Soc. **108**, 11 (1961).

Can. J. Chem. Downloaded from www.nrcresearchpress.com by 210.87.254.40 on 09/05/12
For personal use only.

Can. J. Chem. Downloaded from www.nrcresearchpress.com by 210.87.254.40 on 09/05/12
For personal use only.

THE ELECTROLYSIS OF ω-BROMOCARBOXYLIC ACIDS

II. PREPARATION OF LONG-CHAIN ω-BROMOCARBOXYLIC ESTERS BY MIXED COUPLING REACTIONS[1]

R. G. Woolford, W. Arbic, and Ann Rosser
Department of Chemistry, University of Waterloo, Waterloo, Ontario

Received January 20, 1964

ABSTRACT

An attempt to synthesize long-chain ω-bromocarboxylic esters from the mixed electrolyses of ω-bromocarboxylic acids and half-esters is described. Methyl 15-bromopentadecanoate was successfully prepared in this way in 37% yield, but other reactions producing methyl 16-bromohexadecanoate (by two different routes) and methyl 14-bromotetradecanoate gave low yields (6–18%) and difficulties in purification of products. The product analysis of these electrolyses (symmetrical and unsymmetrical coupling products, methyl esters of starting materials) is given. It is concluded that this method is more likely to be of specific rather than general use.

The use of halogenated carboxylic acids for Kolbe electrolysis reactions has received little study (1). Most of the successful reactions have involved ω-chloro- and ω-bromocarboxylic acids (2–4). Under appropriate conditions the ω-chloro- and ω-bromo-acids with chains of six or more carbon atoms couple normally to produce ω,ω′-dihalides in good (usually 60–70%) yield. The preparation of 1,28-dibromooctacosane by electrolysis of 15-bromopentadecanoic acid is an example (see Experimental section). This dibromide has not been made previously by the Kolbe reaction.

The number of reported mixed electrolyses involving halogenated acids to produce long-chain esters and halides is small. Pattison *et al.* (3) produced 13-fluorotridecyl chloride in 24% yield from the electrolysis of 10-fluorodecanoic acid and 5-chlorovaleric acid. A series of esters have been produced by mixed coupling reactions of ω-fluoroacids (3, 5, 6). However, fluorine is not a typical halogen. The only mixed electrolysis of an ω-bromoacid is the preparation of 1-bromo-2,4-dimethyldocosane from 3,5-dimethyl-6-bromohexanoic acid and stearic acid but no experimental details are given (7).

ω-Bromo-acids and esters are useful as intermediates in multi-step syntheses (e.g. the bromodocosane just mentioned), but their preparation often involves long, tedious routes and low overall yields. Thus a study of the mixed electrolysis of some ω-bromoacids and half-esters seemed appropriate as a possible method offering a one-step route to the longer chain ω-bromoesters. A promising initial reaction seemed to be a mixed electrolysis of 11-bromoundecanoic acid (I; $n = 10$) and methyl hydrogen adipate (II; $m = 4$), both of which are commercially available as fairly inexpensive compounds.

$$\underset{\text{I}}{Br(CH_2)_nCOOH} + \underset{\text{II}}{HOOC(CH_2)_mCOOCH_3} \xrightarrow[\text{d-c. current}]{CH_3OH\ \text{solvent}}$$

$$\underset{\text{III}}{Br(CH_2)_{n+m}COOCH_3} + \underset{\text{IV}}{Br(CH_2)_{2n}Br} + \underset{\text{V}}{CH_3OOC(CH_2)_{2m}COOCH_3}$$

$$+ \underset{\text{VI}}{Br(CH_2)_nCOOCH_3} + \underset{\text{VII}}{CH_3OOC(CH_2)_mCOOCH_3}$$

This reaction produced the primary reaction products III ($n + m = 14$), IV ($n = 10$), and V ($m = 4$) and, in addition, the products VI ($n = 10$) and VII ($m = 4$), methyl

[1]*For Part I, see reference 4.*

esters of the starting materials, resulted from attack of the carboxylate radicals on the solvent. Control reactions showed a negligible tendency to form esters under the reaction conditions if no current were passed. The desired long-chain ω-bromoester, methyl 15-bromopentadecanoate (III; $n + m = 14$) was easily separated from the other products by distillation. The yield of 37% (Table I) is good, considering the number of products possible and bearing in mind that there are few recorded examples in which mixed coupling products are produced in significantly better yields. Moreover, the reaction represents a simpler and more effective means of obtaining this bromoester than hitherto reported (8).

It was previously shown (4) that experimental conditions have to be carefully controlled in reactions of long-chain ω-bromoacids to avoid the almost complete esterification of starting material. Further work indicates that the most critical factor is the temperature of reaction. At temperatures above ca. 54° the yield of coupled product is lowered considerably. Other factors normally considered critical, such as current density, concentration, and solvent, do not affect this yield nearly so much. Therefore, in the present experiments, the temperature was kept between 45 and 54°, while maintaining as high a current density as possible.

The success of this mixed coupling reaction led to its extension to other ω-bromoacids and half-esters. A number of possible combinations were ruled out because of anticipated difficulties in separating products, especially the long-chain bromoester, by distillation. Three reactions were tried: 8-bromooctanoic acid (I; $n = 7$) and methyl hydrogen sebacate (II; $m = 8$) to give methyl 16-bromohexadecanoate (III; $n + m = 15$); 6-bromohexanoic acid (I; $n = 5$) and methyl hydrogen sebacate (II; $m = 8$) to give methyl 14-bromotetradecanoate (III; $n + m = 13$); and 12-bromododecanoic acid (I; $n = 11$) and methyl hydrogen adipate (II; $m = 4$) to give also methyl 16-bromohexadecanoate. In these cases the products IV and V were usually obtained in greater yield, and separation of the products was much more difficult than in the previous reaction producing methyl 15-bromopentadecanoate. A summary of product yields is given in Table I.

TABLE I

Mixed coupling reactions of ω-bromocarboxylic acids

Reagents		Product yield (%)				
I	II	III	IV	V	VI	VII
$n = 10$	$m = 4$	37	39	39	11	5
$n = 11$	$m = 4$	6	21	51	34	1
$n = 5$	$m = 8$	18	23	1	51	50
$n = 7$	$m = 8$	7	24	6	32	30

It must be concluded that, while specific reactions of ω-bromoacids and half-esters may produce a successful mixed coupling, e.g. the preparation of methyl 15-bromopentadecanoate (and thus 15-bromopentadecanoic acid), the method is not likely to be a good general one for the preparation of pure long-chain ω-bromoesters in reasonable yield.

EXPERIMENTAL

General

Melting points, which were corrected, were recorded on a Leitz hot-stage microscope. Boiling points were uncorrected. Analyses were performed by Schwarzkopf Microanalytical Laboratory, Woodside, New York.

A previous article (4) describes the commercial sources or the preparations of ω-bromoacids, methyl hydrogen adipate, and authentic reference samples used in the present work. The electrolytic cell was also fully described, as well as the general method of working up the reaction products into neutral and acidic

Can. J. Chem. Downloaded from www.nrcresearchpress.com by 210.87.254.40 on 09/05/12
For personal use only.

fractions. Methyl hydrogen sebacate was prepared by half-esterification of sebacic acid. Following standard procedure in mixed electrolyses, the half-ester was usually in 1–2 molar excess, so as to improve chances for optimum yield of mixed coupling product. Percentage yields for the mixed electrolyses are recorded in Table I and are based on moles of bromoacid or half-ester reacting (in each case, on whichever was the limiting reagent).

Gas chromatographs used were a Beckman GC-2A and an F and M model 720 with TC3 fraction collector; columns were 6–8 ft Carbowax 20, diethylene glycol succinate, and silicone rubber on Chromosorb-W or its equivalent. Infrared spectra were obtained with a Beckman model IR-5.

Mixed Electrolysis of 11-Bromoundecanoic Acid and Methyl Hydrogen Adipate

11-Bromoundecanoic acid (50 g, 0.19 mole), methyl hydrogen adipate (100 g, 0.63 mole), and sodium (0.9 g, 0.04 g-atom) were dissolved in 95% methanol (130 ml). A current of 1.5–1.7 A was passed for 42 hours (3 × theoretical) at a temperature of 45–50°. A negligible amount of unreacted acid was isolated.

Distillation of the neutral fraction through a short Vigreux column yielded the following fractions: (i) b.p. 80–100° (0.6 mm), 13.8 g; (ii) b.p. 108–111° (0.6 mm), n_D^{25} 1.4346, 28.0 g; (iii) 125–130° (0.6 mm), n_D^{25} 1.4630, 6.0 g; (iv) 130–168° (0.6 mm), 29.5 g; and an undistilled residue of 15.8 g.

Fraction (i) was shown, by gas chromatography, to contain dimethyl adipate, 5.7 g. Fractions (ii) and (iii) were shown by gas chromatography and infrared spectrum analysis to be dimethyl sebacate and methyl 11-bromoundecanoate respectively; Trent *et al.* (9) give b.p. 175° (20 mm), n_D^{25} 1.4342 for dimethyl sebacate, and methyl 11-bromoundecanoate has b.p. 112–116° (0.3 mm), n_D^{25} 1.4630 (4). Fraction (iv) was methyl 15-bromopentadecanoate and was redistilled to yield a white solid, 23.4 g, of b.p. 142–147° (0.25 mm), m.p. 36.5–38.5°. Recrystallization from methanol yielded a solid with m.p. 38.5–39.5°. Anal. Calc. for $C_{16}H_{31}BrO_2$: C, 57.32; H, 9.32; Br, 23.84. Found: C, 57.41; H, 9.32; Br, 23.60. The infrared spectrum was consistent with the structure assumed. The original residue from distillation plus a 3.1 g residue from redistillation of fraction (iv) was recrystallized from methanol to yield 1,20-dibromoeicosane (16.3 g) of m.p. 66.5–68°; Korsching (2) reports m.p. 67.4–68°. A mixed melting point with an authentic sample showed no depression.

Mixed Electrolysis of 12-Bromododecanoic Acid and Methyl Hydrogen Adipate

12-Bromododecanoic acid (23.6 g, 0.085 mole), methyl hydrogen adipate (40.6 g, 0.25 mole), and sodium (0.040 g., 0.017 g-atom) were dissolved in methanol (100 ml) and electrolyzed at 2.0 A for 21 hours (4 × theoretical) at 50–54°. The neutral extract was 46.9 g, and unreacted acids were 5.7 g (1.8 g bromoacid and 6.3 g half-ester, by gas chromatography).

Distillation of the neutral extract and redistillation of each fraction gave the following: (i) b.p. 110–113° (13 mm), n_D^{25} 1.4264, 1.1 g; (ii) b.p. 108–110° (0.6 mm), n_D^{25} 1.4346, 14.1 g; (iii) b.p. 130–135° (0.6 mm), n_D^{25} 1.4625, 7.5 g; (iv) b.p. 152–157° (0.6 mm), m.p. 24–26°, 1.5 g; (v) undistilled residue, 5.4 g.

Gas chromatography and infrared spectrum analysis showed fraction (i) to be dimethyl adipate, fraction (ii) to be dimethyl sebacate, and fraction (iii) to be methyl 12-bromododecanoate; Hunsdiecker and Hunsdiecker (8) give b.p. 130° (0.5 mm). Fraction (iv) was methyl 16-bromohexadecanoate. Seven recrystallizations from methanol gave a white solid of m.p. 28–29° which could not be raised further; Hunsdiecker and Hunsdiecker (8) give m.p. 31°. For fraction (iv) Anal. Calc. for $C_{17}H_{33}BrO_2$: C, 58.46; H, 9.52; Br, 22.88. Found: C, 58.31; H, 9.43; Br, 22.90. Fraction (v) was recrystallized from petroleum ether (30–60°) and methanol to give a white solid (3.6 g) of m.p. 69–70°, undepressed on admixture with authentic 1,22-dibromodocosane.

Mixed Electrolysis of 8-Bromooctanoic Acid and Methyl Hydrogen Sebacate

8-Bromooctanoic acid (40.0 g, 0.18 mole), methyl hydrogen sebacate (78.0 g, 0.36 mole), and sodium (0.21 g, 0.009 g-atom) were dissolved in methanol (150 ml) and electrolyzed at 1.0–1.5 A for 40 hours (3 × theoretical) at 40–50°. At the end of this time the reaction mixture was thick with a solid white precipitate and the temperature could no longer be held below 50°. Gas chromatography showed the recovered acids to be 13.0 g 8-bromooctanoic acid and 25.0 g methyl hydrogen sebacate.

The neutral extract of 44.2 g was distilled and the main fractions redistilled. The following fractions were collected: (i) b.p. 88–90° (0.7 mm), n_D^{25} 1.4605, 8.7 g; (ii) 105–110° (0.6 mm), n_D^{25} 1.4348, 16.7 g; (iii) b.p. 155–160° (0.4 mm), m.p. 24–26°, 2.8 g; (iv) b.p. 165–172° (0.2 mm), m.p. 45–47°, 5.2 g; (v) residue in distilling flask, 2.3 g.

Fraction (i) was shown by gas chromatography and infrared spectrum analysis to be methyl 8-bromooctanoate; Cavanna and Ställberg-Stenhagen (10) give b.p. 91° (0.8 mm). Fraction (ii), identified in the same way, was dimethyl sebacate. Recrystallization of fraction (iii) from methanol gave a white solid of m.p. 28–29°, undepressed on admixture with authentic methyl 16-bromohexadecanoate. Recrystallization of fraction (iv) from petroleum ether (30–60°) gave a solid of m.p. 47.5–48.0°, undepressed on mixing with authentic 1,14-dibromotetradecane. The residue, fraction (v), on recrystallization from low-boiling petroleum ether gave a white solid of m.p. 59–60°, undepressed on admixture with authentic dimethyl 1,16-hexadecanedicarboxylate.

Can. J. Chem. Downloaded from www.nrcresearchpress.com by 210.87.254.40 on 09/05/12
For personal use only.

Mixed Electrolysis of 6-Bromohexanoic Acid and Methyl Hydrogen Sebacate

6-Bromohexanoic acid (25.0 g, 0.13 mole), methyl hydrogen sebacate (83.0 g, 0.39 mole), and sodium (0.6 g, 0.025 g-atom) were dissolved in 150 ml of 1:1 methanol–water. Electrolysis was carried out at 1.5–3.5 A for 28 hours (3 × theoretical) at 45–54°. Products were a neutral extract of 65.5 g and unreacted acids 6-bromohexanoic acid, 1.8 g, and methyl hydrogen sebacate, 6.3 g.

The neutral extract was fractionated and the fractions redistilled to yield: (i) b.p. 66–69° (0.3 mm), n_D^{25} 1.4625, 12.9 g; (ii) 95–102° (0.3 mm), 43.4 g; (iii) 145–150° (0.6 mm), 6.9 g; (iv) undistilled residue, 0.7 g.

Fraction (i) was shown by gas chromatography and infrared spectrum analysis to be methyl 6-bromohexanoate; Skinner, Johnston, and Fisher (11) give b.p. 72° (1 mm), n_D^{22} 1.4635. Fraction (ii) was shown by gas chromatography to be a mixture of 1,10-dibromodecane (4.1 g) and dimethyl sebacate (39.3 g). Fraction (ii) could not be separated further by distillation, but fractionation by gas chromatography yielded small samples of the two compounds; these had the expected infrared spectrum and the correct physical constants: n_D^{25} 1.4265 for dimethyl sebacate, and n_D^{28} 1.4914, m.p. 25–26° for 1,10-dibromodecane (melting point undepressed on admixture with an authentic sample). Fraction (iii) was identified by gas chromatography and infrared spectrum analysis to be methyl 14-bromotetradecanoate; Hunsdiecker and Hunsdiecker (8) give b.p. 164° (0.8 mm), m.p. 22°. Careful recrystallization from methanol gave m.p. 23–23.5°. Fraction (iv), on recrystallization from petroleum ether (30–60°), gave 0.6 g of a white solid of m.p. 59–60°, undepressed on admixture with authentic dimethyl 1,16-hexadecanedicarboxylate.

15-Bromopentadecanoic Acid

Methyl 15-bromopentadecanoate (6.0 g, 0.016 mole) was dissolved in 150 ml of 4 *N* hydrogen bromide in glacial acetic acid and heated under reflux for 24 hours. 5.3 g (95%) of 15-bromopentadecanoic acid of m.p. 65–66° (from low-boiling petroleum ether) was isolated; Hunsdiecker and Hunsdiecker (8) report m.p. 66°. Because of the low solubility of this ester in aqueous systems, attempts to use 48% hydrobromic acid in glacial acetic acid gave less than 0.5% hydrolysis in the same time period.

1,28-Dibromooctacosane

15-Bromopentadecanoic acid (2.00 g, 0.0006 mole) in methanol (50 ml) was electrolyzed at 0.8 A for 10 hours at 45–50°. There was 0.24 g of unreacted acid. The neutral fraction was recrystallized from methanol to yield 0.70 g (51%) of 1,28-dibromooctacosane of m.p. 78–79°. Anal. Calc. for $C_{28}H_{56}Br_2$: C, 60.84; H, 10.23; Br, 28.93. Found: C, 60.54; H, 10.21; Br, 28.62. Gas chromatography of the recrystallization residue indicated 0.38 g, 21%, of the ester methyl 15-bromopentadecanoate.

ACKNOWLEDGMENTS

The authors are indebted to the National Research Council of Canada for financial support.

REFERENCES

1. B. C. L. Weedon. Advan. Org. Chem. **1**, 1 (1960).
2. H. Korsching. Chem. Ber. **86**, 943 (1953).
3. F. L. M. Pattison, J. B. Stothers, and R. G. Woolford. J. Am. Chem. Soc. **78**, 2255 (1956).
4. R. G. Woolford. Can. J. Chem. **40**, 1846 (1962).
5. F. L. M. Pattison and R. G. Woolford. J. Am. Chem. Soc. **79**, 2306 (1957).
6. F. L. M. Pattison and R. G. Woolford. J. Am. Chem. Soc. **79**, 2308 (1957).
7. C. Collin-Asselineau, J. Asselineau, S. Ställberg-Stenhagen, and E. Stenhagen. Acta. Chem. Scand. **10**, 1035 (1956).
8. H. Hunsdiecker and C. Hunsdiecker. Chem. Ber. B, **75**, 291 (1942).
9. F. M. Trent, F. D. Miller, and G. H. Brown. J. Chem. Eng. Data, **5**, 110 (1960).
10. R. Cavanna and S. Ställberg-Stenhagen. Atti Accad. Naz. Lincei, Mem., Classe Sci. Fis., Mat. Nat., Sez. II, **3**, No. 2, 31 (1950).
11. W. A. Skinner, J. D. Johnston, and M. Fisher. J. Am. Chem. Soc. **79**, 5790 (1957).

Can. J. Chem. Downloaded from www.nrcresearchpress.com by 210.87.254.40 on 09/05/12
For personal use only.

Can. J. Chem. Downloaded from www.nrcresearchpress.com by 210.87.254.6 on 09/05/12
For personal use only.

CHEMICAL REACTIONS IN ELECTRICAL DISCHARGES*

I. THE SPECTRUM OF THE METHANE–OXYGEN SYSTEM AT LOW PRESSURE IN THE POSITIVE COLUMN OF A D-C. GLOW DISCHARGE

PIERRE A. BOIS D'ENGHIEN† AND JACQUES M. DECKERS
Department of Chemistry, University of Toronto, Toronto, Ontario

Received March 13, 1964

ABSTRACT

A technique is described which permits the study of changes in the spectra emitted by fast flowing reacting gas mixtures in the plasma of the positive column of a weak d-c. glow discharge. In certain cases a quantitative relationship is shown to exist between the concentration of a species and the intensity of emission of its spectrum. In particular such a correlation exists between the emission intensity of CO and its concentration. Use of this fact is then made to follow the rate of formation of carbon monoxide in methane–oxygen mixtures flowing through a discharge. The mechanism of formation of the various emitters either by means of a chemical reaction or by electron impact on molecules or radicals is discussed. It is concluded that to account for the rate of formation of CO, at least in the early stages of the presence of the gases in the discharge, before the steady state concentrations of atoms, radicals, and molecules have been approached, most of the energy of the electrons is used in breaking chemical bonds. The electric field values needed to impart the necessary amount of energy to the electrons are of the same magnitude as those measured in this laboratory ($\sim$60 V cm^{-1}).

PART 1. INTRODUCTION

This paper describes a method by which it is possible to obtain quantitative information on the rates of reactions occurring in the positive column of a glow discharge. It is by now well established that in the positive column the number of positive and negative charges are approximately equal and form a partially ionized quasi-neutral plasma (1). The chemical reactions occurring under these conditions are indicative of the physical conditions prevailing in this plasma, supplementing or confirming knowledge gained from other types of investigations.

By means of discharges it is possible to induce reactions in a wide variety of gases or gas mixtures over a wide range of pressures and compositions. Because of the flow of electrons and ions and the presence of an electric field, the gas is maintained in a steady state of non-equilibrium. The degree of this non-equilibrium can be changed to a certain extent by varying the overall current through the discharge. By changing the physical parameters of the discharge one can assess the relative importance of changes due to reactive or inelastic collisions, transport phenomena, and relaxation processes. Compared with other non-equilibrium systems, such as flames, in which the enthalpy of the chemical reaction is the only source causing departure from equilibrium, the discharge in gases is clearly a more flexible and versatile method of investigation.

In this laboratory a program has been initiated designed to study the kinetics and mechanisms of reactions in discharges, and assess the influence of these reactions upon the physical parameters of the discharge. After a short description of the apparatus, the spectra emitted by methane, oxygen, and mixtures of these gases, while flowing through a d-c. glow discharge, will be described and discussed.

In this paper we shall restrict ourselves to the description of the influence of a number of parameters, both physical and chemical, upon the emission spectrum of the methane–oxygen system. Our purpose is to illustrate the type of problems which can be solved by

*Supported by grants from the U.S. Air Force Office of Scientific Research, the National Research Council of Canada, and the University of Toronto.

†Present address: Department of Chemistry, Université de Louvain, 96 Rue de Namur, Louvain, Belgium.

using this technique; we reserve detailed kinetic studies of a number of applications outlined in this paper for a later publication.

In particular, the influence of the current, the composition of the gas mixture, and the time spent by the gases in the discharge on the emitted spectrum is discussed. The emission intensity of carbon monoxide has been correlated with its absolute concentration. The overall rate of reaction can hence be measured. We have also been able to show that, during the first few milliseconds that the gases spend in the discharge, most of the energy gained by the electrons under the influence of the electric field is used in breaking chemical bonds. We also discuss the likelihood of a number of reaction mechanisms which could explain some of the observed changes in the spectrum.

Although ion–molecule reactions often are very fast we have assumed that they do not contribute appreciably to the observed overall changes in composition. Electron and ion concentrations, which are equal in the positive column, vary from 10^{10} to 10^{13} ions cm^{-3} (1). In view of the weak currents in the discharge ($<10^{-2}$ A) we can assume that the ion concentrations in our discharge were near the lower limit which makes the above assumption reasonable.

We have limited our observations to the positive column of the discharge because it is known that in this region the electrical field and the density of ions and electrons are the same at all points of the column. Hence the value of the electrical parameters remains constant while the gases proceed downstream through the discharge.

We have also assumed that self-absorption or blockaded radiation could not introduce any significant error in our measurement.

PART 2. EXPERIMENTAL

The gas, or gas mixture, metered by calibrated rotameters, enters a Pyrex observation tube, 80 cm long and 0.7 cm wide through the positive electrode (Fig. 1). The visible and near ultraviolet spectrum emitted

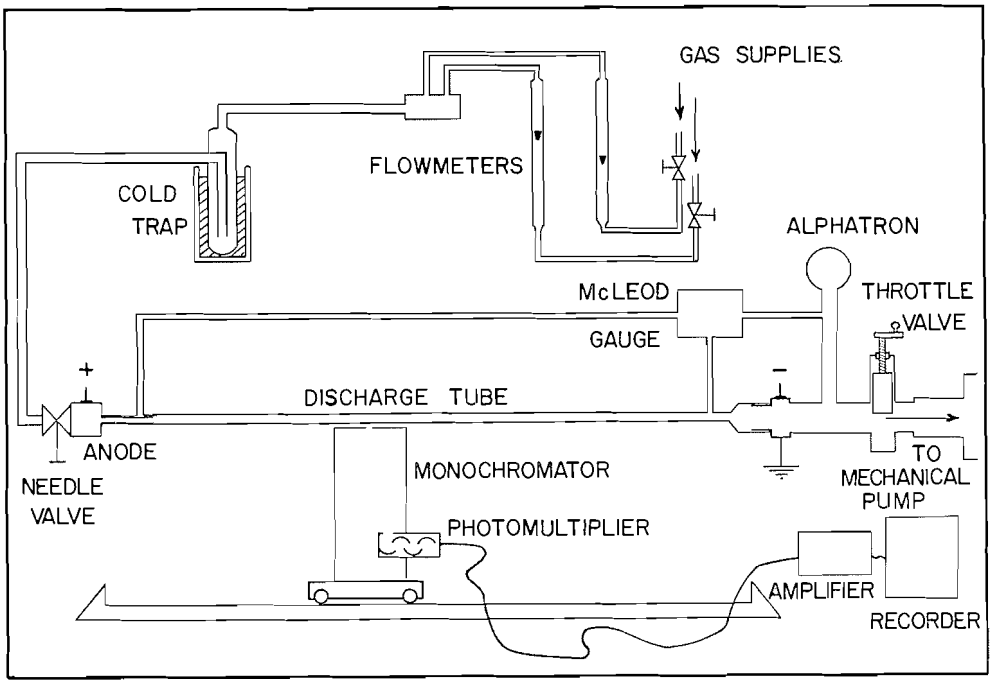

FIG. 1. Schematics of the apparatus.

Can. J. Chem. Downloaded from www.nrcresearchpress.com by 210.87.254.6 on 09/05/12
For personal use only.

by the fast flowing ($\sim$50 m s^{-1}) gas mixture has been analyzed and its intensity measured for various emitters at various distances from the entrance point in the positive column of the discharge.

The gases (methane: Matheson C.P. grade; oxygen: British Oxygen of Canada Ltd.) were passed through dry-ice – acetone cooled traps and used without further purification. After they had passed through the discharge tube the gases were pumped out by means of an N.R.C. model S 30 rotary mechanical pump. Between the pump and the downstream end of the discharge tube a throttling valve allowed us to alter the velocity and the pressure in the discharge tube.

The d-c. glow discharge was sustained by means of an N.J.E. regulated power supply model S 328 (1000 to 10 000 V; 0 to 10×10^{-3} A). A chain of resistors in series with the discharge tube permitted us to adjust the resistance of the overall circuit and limit the current through the discharge tube. The spectrum was analyzed by means of a Jarrell–Ash model 82 000 grating monochromator. At the exit a 1P28 R.C.A. photomultiplier tube measured the light intensity. The monochromator was mounted vertically underneath the discharge tube with its slit parallel to the tube. It was placed on a small carriage rolling on two rails precisely parallel to the tube. This arrangement made it possible to record the spectrum at various positions in the discharge. The output of the photomultiplier tube was fed into a Keithley Model 414 micromicroammeter.

The pressure, both upstream and downstream of the discharge tube could be measured by means of a MacLeod gauge. An alphatron vacuum gauge, mounted downstream of the discharge tube, indicated any changes in pressure during a single run. The pressure gradient along the discharge tube was also measured by constructing a discharge tube similar to the one used for optical observations except for a number of side tubes at which the pressure could be taken.

PART 3. RESULTS

(a) General Remarks

The salient features of the emission spectrum consisted of the 4300 Å and 3900 Å bands of CH, the third positive, 5 B, Angstrom and Herzberg bands of CO, the 3064 Å band system of OH, the C_2 Swann bands, and the atomic lines of hydrogen and oxygen. Since nitrogen was always present as an impurity its second positive band system was always emitted as well. The presence and intensity of the various bands mentioned above were determined by the experimental conditions.

At no time did the intensity of the Swann bands of C_2 exceed the background scatter by more than a factor of three, so that we have not investigated in detail the emission due to this radical.

In addition to the features mentioned above we sometimes noticed a weak continuum in the blue region of the spectrum. A similar continuum appears much more strongly when hydrogen–oxygen mixtures flow through the discharge tube. In pure hydrogen a similar continuum has also been observed (1). It is possible that the origin of this continuum is, at least in part, of the same origin as the blue continuum observed in the emission from hydrogen–oxygen flames, which has been described by Padley (2) and ascribed by him to the radiative association of a hydrogen atom and an OH radical.

In the 3400–3100 Å region some further weak emission bands have been observed, which do not seem to belong to the OH band system. The wavelength of the maximum of emission intensity does correlate with a number of *absorption* maxima reported for ozone, which as far as we know have not yet been observed in emission. However, in view of the poor resolution of the monochromator under our working conditions (see next paragraph) we feel that further work is needed before a definite identification of these bands can be made.

Because of the weakness of the light source we had to use large slit widths on the monochromator which resulted in poor resolution. Hence, we have systematically measured the intensity of emission at the maximum peak height. At no time have we attempted to use integrated line or band intensities. It is probable that various experimental circumstances might affect the rotational populations and that a small error could enter into our measurements in this way. Furthermore, we have attempted to correct the intensities measured at different wavelengths for the variation in sensitivity of the photomultiplier

Can. J. Chem. Downloaded from www.nrcresearchpress.com by 210.87.254.6 on 09/05/12
For personal use only.

tube with wavelength, because we are only interested in relative intensities at one wavelength.

We shall now review in turn the ways in which the time spent by the gases in the discharge tube (as determined by the distance from the entrance electrode), the current through the discharge, and the composition of the gas mixture influence the spectrum.

Unless otherwise indicated, the pressures reported are those at the entrance point of the gas in the discharge.

(b) Variation in the Intensity of Emission over the Length of the Positive Column of the Discharge

Since the gases enter the tube through the electrode and flow through the discharge at a known speed, the various positions downstream of the electrode correspond to the time spent by the gases in the discharge. Hence, the intensity of emission of various bands has been measured at various distances S from the point at which the gases enter the discharge for a wide range of composition of methane–oxygen mixtures. The spectra of the two pure gases have also been investigated as well as those of mixtures containing small known amounts of carbon monoxide.

In pure oxygen the intensity of the atomic oxygen lines shows a linear increase along the length of the positive column as seen in Fig. 2 where the intensity of the 4368.3 Å oxygen line has been plotted as a function of S for three different values of the discharge current. The variation of intensity of the CH emission in pure methane is quite different; as seen in Fig. 3 the intensity is very intense even for small values of S and increases only slightly for larger values. In Fig. 3 the emission intensity of the H_β line and of the 3371.3 Å band of the nitrogen impurity (second positive band system) is also plotted against S.

The behavior of a methane–oxygen mixture is illustrated in Fig. 4. The emission from CO increases in smooth, almost linear, fashion, while the emission of CH and H_β is similar to that in methane alone. The emission of OH increases sharply (but not as fast as the CH emission) at low values of S and more slowly afterwards. For other compositions of methane and oxygen, the behavior is similar. The nearly linear increase of the CO emission has been verified for the Angstrom, the Herzberg, and the triplet bands. We have also added small amounts of carbon monoxide to oxygen, methane, and mixtures of these gases. In Fig. 5 this CO emission from methane or oxygen is shown and that from mixtures in Fig. 6.

(c) Influence of the Current upon the Emission Intensity

The influence of the current upon the emission intensity of the various radicals at fixed distances S has been investigated for the gas mixtures mentioned above.

In Fig. 7 the intensity of emission of the 4368.3 Å oxygen line is plotted as a function of the current for various values of S. In Fig. 8 similar data are given for a discharge through methane, and Fig. 9 shows the linear relationship between the current and the intensity of emission in the case of methane–oxygen mixtures. However, when small amounts of carbon monoxide were added to the above gases and gas mixtures, the variation of the CO emission as a function of the current was not linear (Fig. 10).

(d) Influence of the Composition upon the Emission Intensity

In Fig. 11 the influence of the composition is illustrated; in this graph the intensities of emission of various radicals are plotted against the mole fraction X of methane. One sees that the intensity of the atomic oxygen line becomes negligible at $X = 0.67$; OH and CO emission is at a maximum for $X = 0.55$; the intensity of the H_β line, however, increases very quickly as soon as small amounts of methane are added to a discharge

Can. J. Chem. Downloaded from www.nrcresearchpress.com by 210.87.254.6 on 09/05/12
For personal use only.

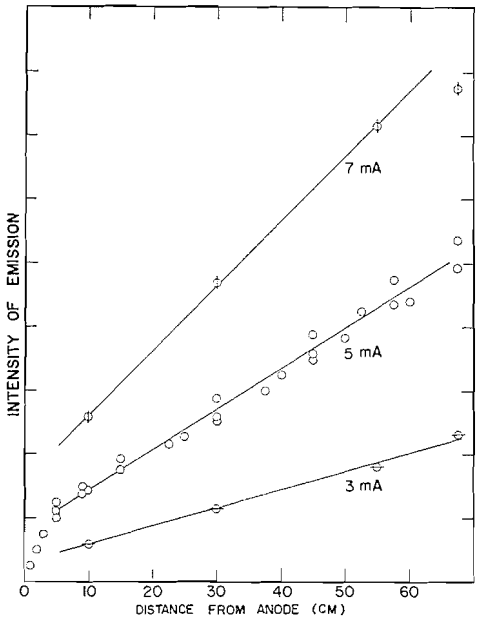

FIG. 2. Emission intensity of the 4368.3 Å atomic oxygen line as a function of S in cm in pure oxygen for three different values of the current through the discharge. Pressure at $S = 0$ cm: 1 torr.

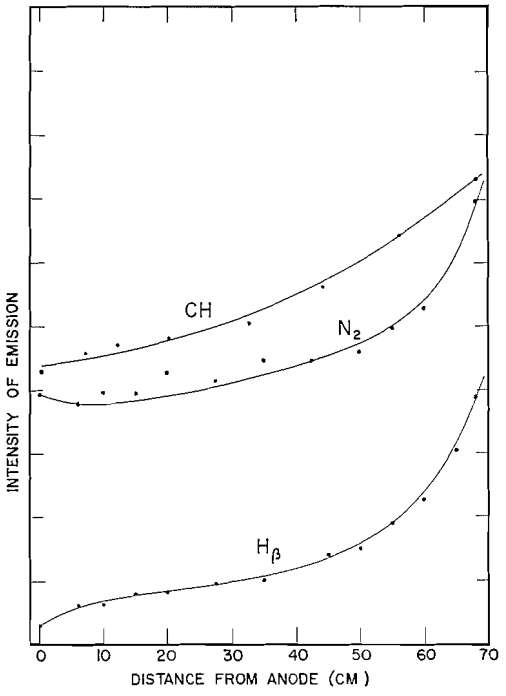

FIG. 3. Emission intensity of the CH 4314.2 band, the N_2 3371.3 Å band (2nd positive system) and of the H_β line as function of S in pure methane. Pressure at $S = 0$ cm: 1 torr.

Can. J. Chem. Downloaded from www.nrcresearchpress.com by 210.87.254.6 on 09/05/12
For personal use only.

Can. J. Chem. Downloaded from www.nrcresearchpress.com by 210.87.254.6 on 09/05/12
For personal use only.

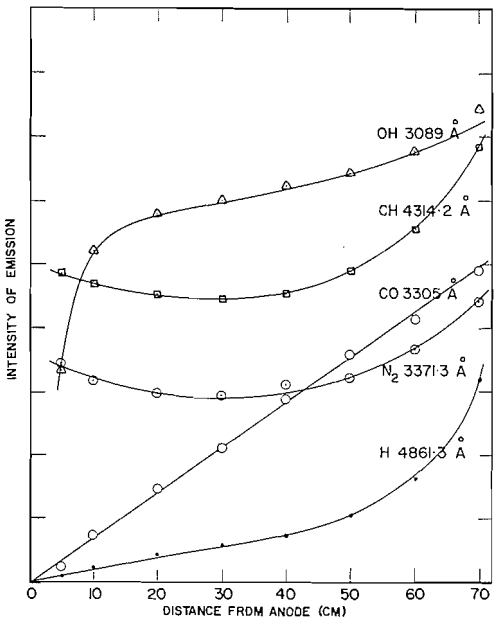

FIG. 4. Emission intensity of the various bands and lines as indicated as a function of S in a mixture containing 33% methane and 67% oxygen (Stoichiometric $\rightarrow CO_2 + H_2O$). Pressure at $S = 0$ cm: 1 torr.

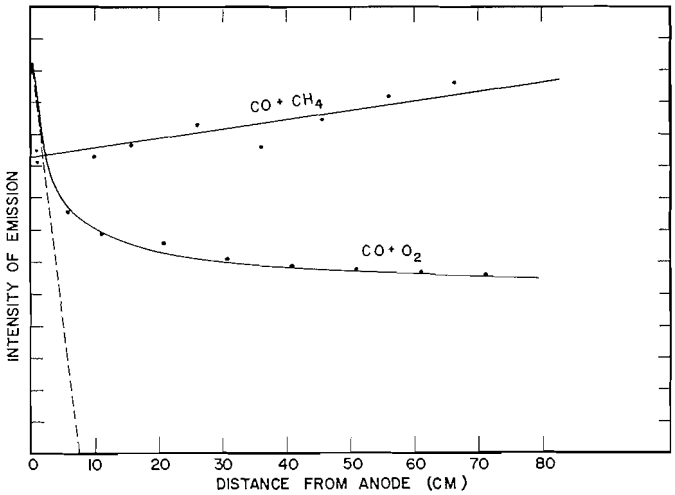

FIG. 5. Emission intensity of the CO 3134.4 Å band in a mixture of 0.58% carbon monoxide and 99.42% methane (upper curve) and in a mixture of 0.55% carbon monoxide and 99.45% oxygen as a function of S. Pressure at $S = 0$: 1 torr.

Can. J. Chem. Downloaded from www.nrcresearchpress.com by 210.87.254.6 on 09/05/12
For personal use only.

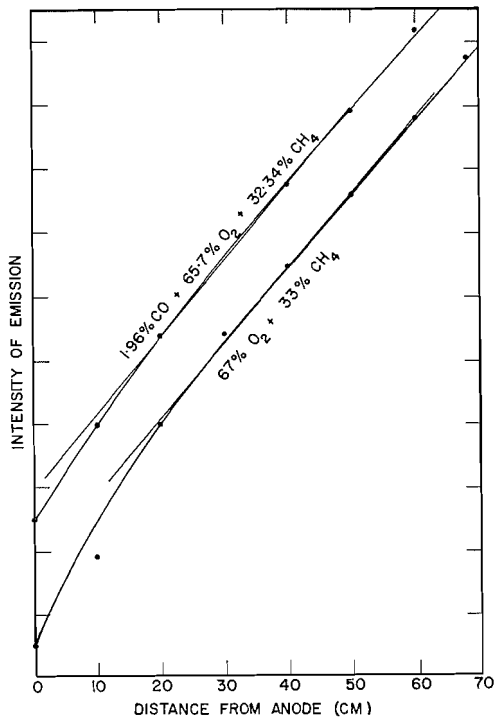

FIG. 6. Emission intensity of the CO 3134.4 Å band in a mixture of 33% methane and 67% oxygen (lower curve) and in a methane–oxygen mixture containing the same methane to oxygen mole ratio and, in addition, 1.96% carbon monoxide (upper curve) as function of S. Pressure at $S = 0$: 1 torr.

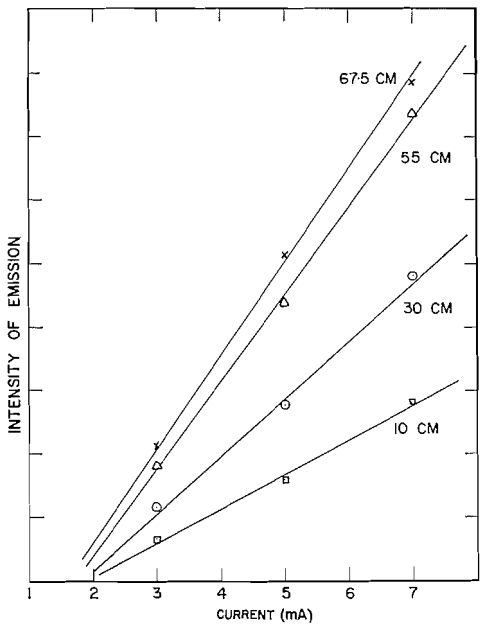

FIG. 7. Intensity of emission of the 4368.3 Å atomic oxygen line in pure oxygen as a function of the current through the discharge for four different values of S. Pressure at $S = 0$ cm: 1 torr.

Can. J. Chem. Downloaded from www.nrcresearchpress.com by 210.87.254.6 on 09/05/12
For personal use only.

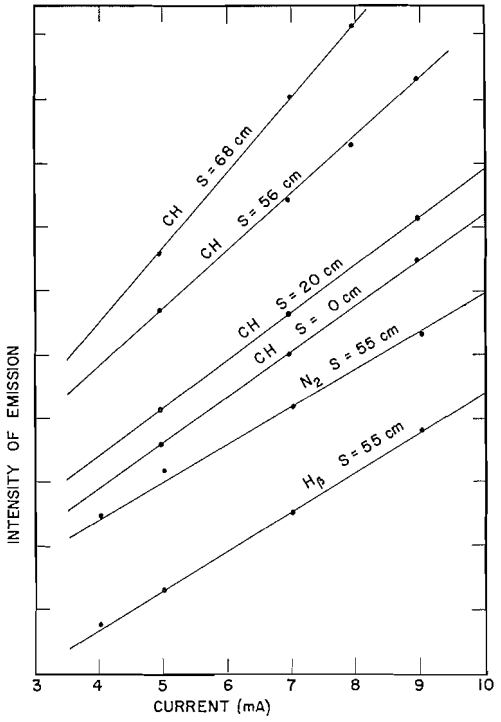

FIG. 8. Intensity of emission of the CH 4314.2 Å band in pure methane as a function of the current through the discharge for four different values of S. The emission of the N_2 3371.3 Å band and of the H_β line is also shown. Pressure at $S = 0$ cm: 1 torr.

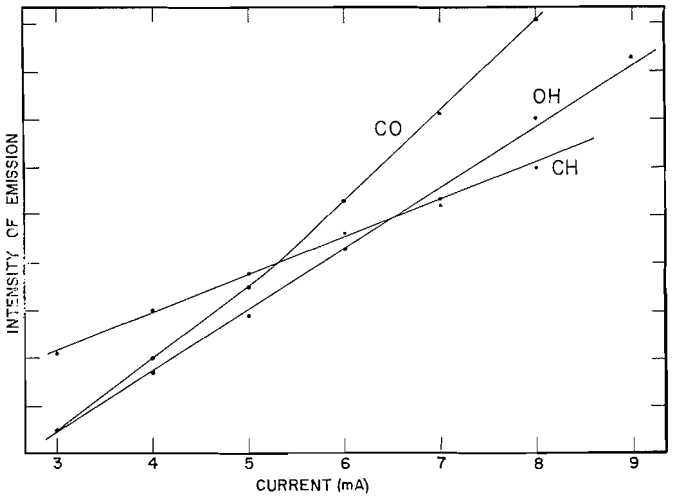

FIG. 9. Intensity of emission of the CH 4314.2 Å band, the CO 3134.4 Å band, and the OH 3089 Å band in a 33% methane 67% oxygen mixture at $S = 40$ cm as a function of the current through the discharge. Pressure at $S = 0$: 1 torr.

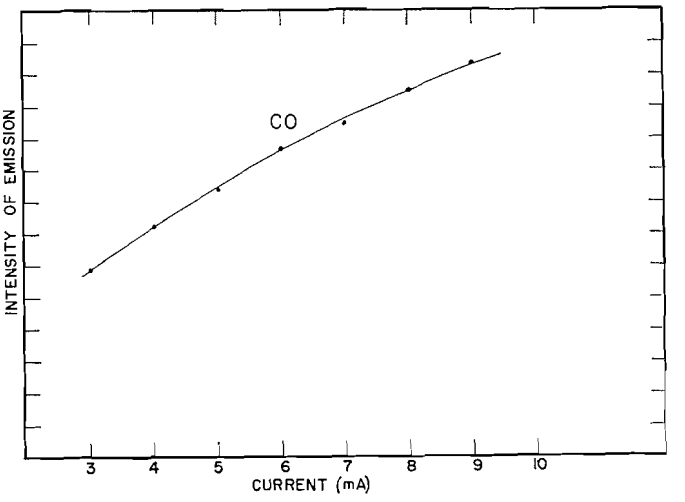

FIG. 10. Intensity of emission of the CO 3134.4 Å band in a mixture of 0.55% carbon monoxide and 99.45% oxygen as a function of the current through the discharge at $S = 40$ cm. Pressure at $S = 0$: 1 torr.

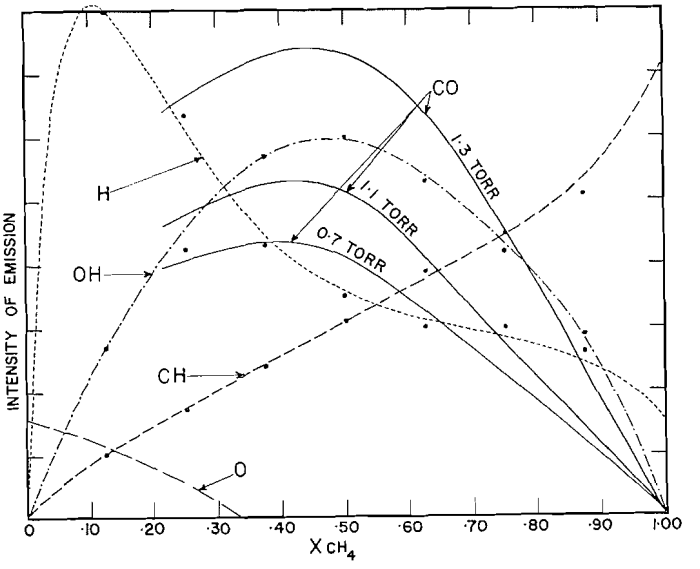

FIG. 11. Influence of the methane–oxygen ratio upon the emission intensity. The intensity of the OH 3089 Å, CH 4314.2 Å bands, and of the H_β and O 4368.3 Å lines is shown for 0.7 torr. The emission of the CO 3134.4 Å is shown at the three indicated pressures.

through pure oxygen and for large concentrations of oxygen, a maximum intensity is reached near $X = 0.88$. The CH emission increases smoothly as the methane concentration increases.

Small, increasing amounts of carbon monoxide were also added to discharges in methane and oxygen (Fig. 12(A) and 12(B)) and the intensity of emission of the CO bands was recorded. We can see that within the range of concentration explored the relation between the percentage of CO added in the mixture and the CO emission is linear. Finally, a

Can. J. Chem. Downloaded from www.nrcresearchpress.com by 210.87.254.6 on 09/05/12
For personal use only.

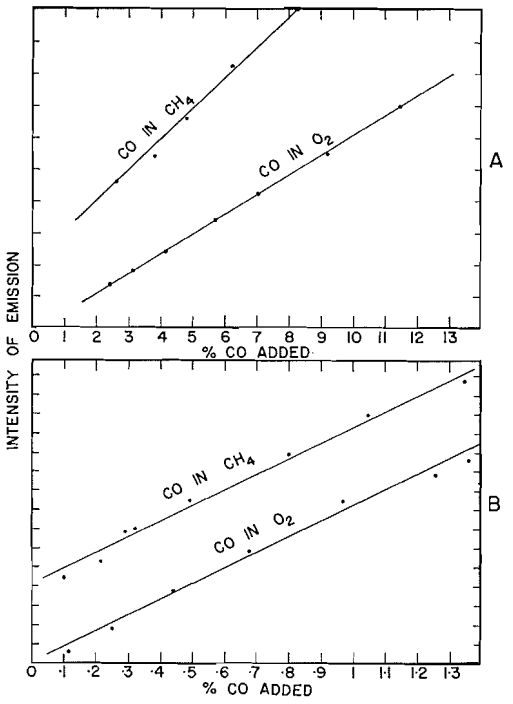

FIG. 12. Influence of the % CO added to methane or oxygen on the intensity of emission of the CO 3134.4 Å band. $S = 40$ cm. Pressure at $S = 0$: 1 torr.

constant amount of carbon monoxide was also added to methane–oxygen mixtures in which the mole fraction of methane varied from 0 to 1 and the intensity of the CO emission was measured. In Fig. 13 the intensity of emission due to the added CO alone (this is the total intensity of CO emission less the emission coming from the CO produced by the reaction) is plotted as a function of the mole fraction; this quantity is equal to the difference separating the two curves shown in Fig. 6. One notices the highly non-linear character of this curve.

(e) Pressure Gradient and Flow Velocity in the Discharge Tube

The total gas flow for all experiments reported in this paper was 150 ml min^{-1} N.T.P. At a pressure of 1 torr this corresponds to an average flow velocity of 50 m sec^{-1}. At that pressure a molecule travels 1 cm along the discharge tube in approximately 2×10^{-4} sec.

Because of the existence of a pressure gradient along the discharge tube, the flow velocity increases with S. This pressure gradient is illustrated in Fig. 14. The ordinate corresponds to the pressure at the entrance point of the gases in the discharge. *Within the limits* that the pressure, flow, or current through the discharge were varied in the experiments reported in this paper, this curve was found to be independent of the absolute value of these parameters. This curve also represents the relative amounts of time spent by a molecule in different sections of the discharge tube. It might also be useful to mention that a molecule, at 1 torr, assuming a collision diameter of 2 Å, suffers approximately 300 collisions during the time it takes to move 1 cm downstream. We have assumed the translational temperature of the gases to remain near 300 °K in the discharge. This last assumption warrants comment because the temperature of a gas in a discharge is not

Can. J. Chem. Downloaded from www.nrcresearchpress.com by 210.87.254.6 on 09/05/12
For personal use only.

Can. J. Chem. Downloaded from www.nrcresearchpress.com by 210.87.254.6 on 09/05/12
For personal use only.

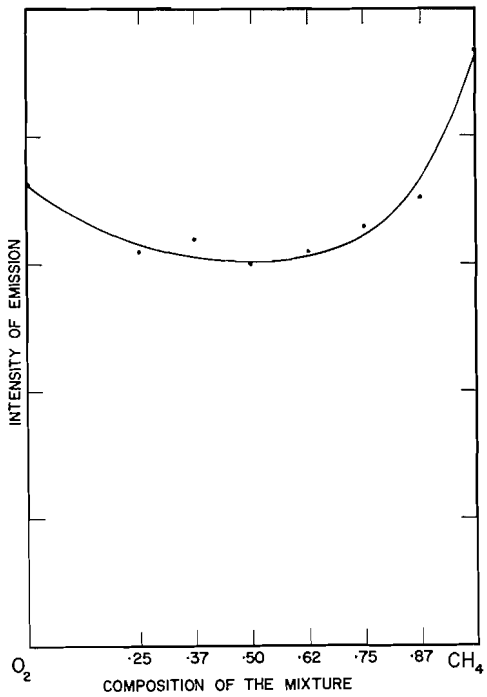

FIG. 13. Intensity of emission of the *added* carbon monoxide as a function of the methane–oxygen ratio at $S = 40$ cm, $p = 1$ torr. The value in ordinate corresponds to the difference separating the two curves in Fig. 6. Amount of CO added 2% (approx.).

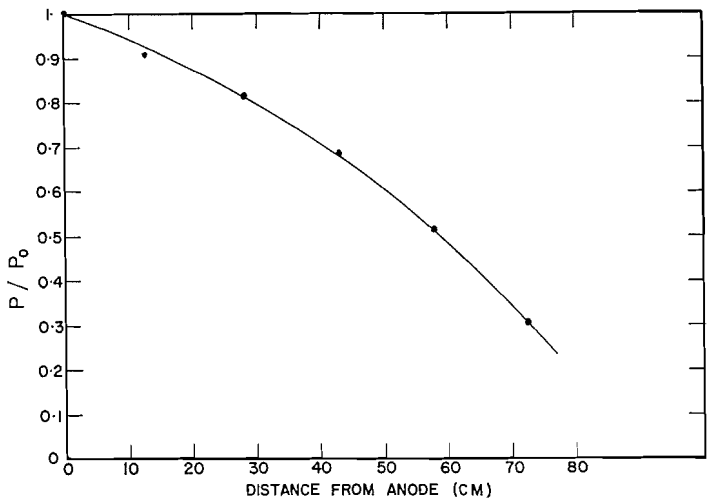

FIG. 14. Reduced pressure drop as a function of S for all experiments reported in this work.

necessarily in equilibrium with the walls. Because of the fast flow and the short residence time of the gases in the discharge it is felt that no appreciable heating of the gas can occur. Electron molecule collisions are very inefficient in transferring translational energy. Heating can hence only result from the succession of two inelastic collisions, the first

between an accelerated electron and a molecule or radical, followed by an inelastic collision of the second kind between two molecules or radicals. This last process competes with the possibility of loss of energy by emission of a photon. The linear increase in the emission of some radicals, further discussed in Part 4, is a further indication that this assumption is a reasonable one.

As was pointed out by the referee* of this paper, the effects of molecular diffusion should be negligible because of the high velocity of the flow.

PART 4. DISCUSSION OF THE RESULTS

A. Characteristics of the Emission

When we compare the emission of the species which have been studied in some detail we notice that we can separate them into two groups, each having a number of features in common. The emission intensity of CO, H, and O was nil at the entrance point of the gases in the discharge and increased monotonically as the gases proceeded further downstream in the observation tube. On the contrary the emission of CH and OH was substantial as soon as the gases entered the discharge tube and increased only very slightly further downstream (more for OH than for CH).

In the reaction zone of a flame a large emission of OH and CH has been observed (3). The origin of this emission is chemiluminescent, the radicals being produced in an excited state by a reactive collision. Vaerman, Nenquin, and Van Tiggelen (4) have indicated the conditions under which one can relate the emission intensity to the concentration of *excited* radicals. No appreciable emission of any of the emitters in the first group has been observed in a flame front.

As can be inferred from Fig. 12 at one point in the discharge tube, the emission due to CO is proportional to the amount of carbon monoxide added to methane or oxygen (up to 12%). This is also the case for methane–oxygen mixtures, provided the emission due to the CO formed in the discharge has been subtracted from the total CO emission (Fig. 6). From a number of similar graphs it was concluded that the emission of CO in mixtures is also proportional to the local carbon monoxide concentration, but the proportionality coefficient is a function of the position in the discharge tube at which the spectrum is recorded and of the methane–oxygen ratio (Figs. 6 and 13).

In this laboratory, Yealland (5) measured the concentration of oxygen atoms in the gases streaming out of a discharge through oxygen as a function of the length of the discharge. He found that this concentration increased linearly with the length of the positive column. We conclude that the emission intensity of the atomic oxygen lines is proportional to the atomic oxygen concentration.

We shall also assume that the emission intensity of the Balmer series of atomic hydrogen is proportional to the atomic hydrogen concentration, because its emission characteristics are rather similar to those of carbon monoxide and of atomic oxygen. For the radicals in group I (CO, H, O) the emission intensity is, we believe, proportional to the *total* concentration, while for the group II radicals (CH, OH) this is not necessarily so.

B. The Pressure Gradient, the Emission, and the Number of Collisions in the Discharge Tube

In most of the experiments the pressure in the discharge tube at the entrance point was 1 torr and the gas flow 150 cc min^{-1} N.T.P. Under these conditions the stream velocity of the gas was about 5×10^3 cm s^{-1}. Because of a pressure drop of about 70% (Fig. 14) the velocity of the gas downstream increased to about 1.5×10^4 cm s^{-1}. The time

*We thank the referee for raising this point.

Can. J. Chem. Downloaded from www.nrcresearchpress.com by 210.87.254.6 on 09/05/12
For personal use only.

spent, on the average, by a molecule in 1 cm of discharge decreased from 2×10^{-4} s to 6.7×10^{-5} s. As a result, the number of collisions suffered by one molecule as it travelled 1 cm depended on the position and under the above conditions this number decreased from about 300 collisions cm^{-1} upstream to about 30 downstream (assuming an average collisional diameter of 2 Å).

For a current of 6 milliamperes there were 3.75×10^{16} electrons s^{-1} crossing a section perpendicular to the axis of the tubes; this number was independent of the pressure; to arrive at this number we assumed that the fraction of the current transported by ions was negligible because of the large difference in velocity between electrons and ions. The number of molecules flowing through a section of the discharge tube, in unit time, was also independent of the value of S throughout the tube because the decrease in density was offset by a corresponding increase in the velocity of the gas stream. Excluding metastable states, the lifetime of an electronically excited radical ($\sim 10^{-8}$ or less) was small compared to the time spent by a molecule in a segment of the tube whose length was comparable to that of the spectrograph slit (1 cm). The intensity of emission at various distances from the entrance point was therefore representative of the number of molecules being excited in that segment.

C. The Production of Excited Species

(a) Oxygen Atoms

The production of excited oxygen atoms could conceivably take place in a single collision:

[1] $$O_2 + e^-(>15.8 \text{ eV}) \rightarrow O + O^* + e^-$$

[2] $$O^* \rightarrow O + h\nu.$$

Emission from the ^5P, ^3P, ^5S, ^5D levels was observed. The intensity of all lines originating from these levels followed closely the behavior of the 4368.3 Å line. If reactions of type [1] were responsible for the observed emission to an appreciable extent, the rates of the production of these various states should increase or decrease proportionately under all experimental circumstances and increase linearly as the gases proceed through the tube. That these two conditions would be fulfilled at the same time is highly improbable; we would have to assume linear changes in the electric properties of the positive column which are contrary to all other observations. The disappearance of the emission of atomic oxygen upon addition of methane (Fig. 11) cannot be explained without assuming unreasonably large collision cross sections, if mechanism [1] is responsible for the production of O*.

It is much more probable that the observed emission is due to the excitation by electrons of oxygen atoms produced in previous collisions.

[3] $$O_2 + e^- (>5.1 \text{ eV}) \rightarrow O + O + e^-$$

[4] $$O + e^- (>12 \text{ eV}) \rightarrow O^* + e^-.$$

If reaction [4] is the only reaction producing excited atoms to any appreciable extent, the emission resulting from such collisions would indeed be proportional to the *total* oxygen atom concentration.

If deactivation of excited atoms by other molecules occurs according to:

[5] $$O^* + M \rightarrow O + M + \text{kinetic energy},$$

Can. J. Chem. Downloaded from www.nrcresearchpress.com by 210.87.254.6 on 09/05/12
For personal use only.

this reaction will be first order with respect to the excited oxygen atoms.

Kaufman and Kelso (6) have suggested that the dissociative collision [3] proceeds via a $^3\Sigma_u^-$ oxygen molecule:

[6] $$O_2 + e^- (>7 \text{ eV}) \rightarrow O_2 (^3\Sigma_u^-) + e^-$$
$$O_2 (^3\Sigma_u^-) \rightarrow O (^3P) + O (^1D).$$

Such a mechanism would produce a ^1D metastable oxygen atom for every ground state atom. The existence of metastable oxygen atoms in the discharge is probable (7, 8) but it seems improbable that they are present in large concentration. It thus seems that as a result of electron impact, a substantial amount of dissociation occurs either from the ground state molecule or via one of the numerous excited states which dissociate into two ^3P oxygen atoms.

Chanin, Phelps, and Biondi (9) have measured the rate coefficient for the reaction

[7] $$O_2 + e^- (>3.5 \text{ eV}) \rightarrow O + O^-.$$

Kaufman and Kelso (6) have calculated that this reaction might account for the small dissociation that they measure in very pure oxygen; in the presence of small amount of impurities (they find N_2, H_2, and H_2O to be very effective) the production rate of oxygen atoms by this process alone is too small to account for the observed dissociation. In their papers these authors also suggest a number of other possible schemes for the production of atoms involving catalytic activity of impurities.

(b) Production of CH Radicals

The intensity of emission of CH in pure methane was fairly uniform throughout the discharge tube. CH emission was observed right at the entrance point of the gases in the discharge even at low pressures ($\sim 4 \times 10^{-2}$ torr). At such pressures a molecule, during the time it drifts 1 cm, suffers only a few collisions (<10) with other molecules. Thus the excited CH radicals must be produced, at least in part, from the methane molecule by electron impact. It is not possible at this stage to decide whether the removal of three hydrogen atoms occurs under the impact of a single electron or, as seems more probable, by successive impacts, as indicated in diagram [8].

[8] $$CH_4 \xrightarrow[e^-]{} CH_3 \xrightarrow[e^-]{} CH_2 \xrightarrow[e^-]{} CH$$
with e^- arrows from CH_3 to CH and from CH_4 to CH.

[9] $$CH + e^- \rightarrow CH^* + e^-$$

[10] $$CH^* \rightarrow CH + h\nu.$$

Excited CH radicals can be produced either directly from methane, or from one of the intermediates or by electron impact with CH radicals in the ground state, via mechanism [9].

At higher pressures some of the hydrogen could be removed from the methane or the radicals CH_3 and CH_2 by reactive collision with H, O, or other radicals which combine with hydrogen.

[11] $$CH_m + M \rightarrow CH_{m-1} + MH.$$

Can. J. Chem. Downloaded from www.nrcresearchpress.com by 210.87.254.6 on 09/05/12
For personal use only.

CH can also be produced by disproportionation of two CH_2.

[11*a*] $$CH_2 + CH_2 \rightarrow CH + CH_3.$$

The reaction $C_2 + OH \rightarrow CO + CH^*$, which has been postulated as being responsible for the CH emission in flames, cannot account for the observed emission because:

(i) at the origin OH concentration is very small,

(ii) emission of C_2 is exceedingly weak and its concentration is too small.

In the case where pure methane flows through the discharge tube the slightly larger rate of increase of the CH emission with S as compared to that in methane–oxygen mixtures is due to the fact that when oxygen is present the CH is consumed by other reactions. It is also possible that some of the CH radicals, produced by reactions of type [11] are formed in excited states.

The fact that the CH emission increases approximately linearly with the concentration of CH_4 is an indication that a substantial amount of the CH might be produced in an excited state.

(c) The Excitation of CO

It can be inferred that no appreciable amount of CO is formed in an excited state, in much the same way that production of excited oxygen atoms in a single collision was excluded. The emission intensity of CO increases linearly with S, and parallel behavior of the emission from the $b_1\Sigma$, $B_1\Sigma$, and $C_1\Sigma$ states has been observed. It is therefore very probable that nearly all the observed emission arises from

[12] $$CO + e^- \rightarrow CO^* + e^-$$

the endothermicity of the process varying from 10.4 to 11.3 eV. Excitation of CO via [12] would make the CO intensity proportional to the total CO concentration.

In the presence of oxygen atoms some CO might be oxidized to CO_2. This possibility is discussed in more detail in the next paragraph. The emission of CO is not directly related to the mole fraction of CO in the discharge. We measure in fact an emission proportional to the sum of the mole fractions of CO and CO_2.

D. Reactions in the Discharge

(a) The Disappearance of CO

In Fig. 5 we notice that the CO emission drops near the origin, both in oxygen and in methane. We ascribe this drop in emission intensity to oxidation or reduction of CO in the discharge. We will discuss first the interaction of carbon monoxide with oxygen.

No reaction occurs at room temperature between CO and O_2 in their ground states. It is highly improbable that electronically excited non-metastable states of CO or O_2, formed under electron impact, are responsible for the formation of CO_2 from CO, because the probability of a collision occurring during the lifetime of an excited CO or O_2 molecule is too small. Although it is known (10, 11) that sizeable concentrations of the metastable $^1\Delta_g$ O_2 are formed in the discharge, this state lies only about 1 eV above the ground state and consequently the reaction

[13] $$CO + O_2^* (^1\Delta) \rightarrow CO_2 + O$$

would still be more than 1.2 eV endothermic. The only reasonable alternative leading to further oxidation of CO would be the reaction

[14] $$CO + O \rightarrow CO_2^*$$

Can. J. Chem. Downloaded from www.nrcresearchpress.com by 210.87.254.6 on 09/05/12
For personal use only.

This reaction has been studied by Mahan and Solo (12), who obtained a rate constant of 10^{10} exp $(-400/RT)$. The possibility that the CO_2* may dissociate is mentioned and discussed. If the decrease in CO emission is due to reaction [14] the value of Mahan and Solo's rate constant is too small. Even the value obtained by Avramenko and Kolesnikova (13), which is about 10 times larger, would be too small.

It is also possible that the initial decrease in the CO emission is due to a rapid removal of CO in the discharge. If this is the explanation of the initial decrease in CO emission in oxygen CO would be broken down under electron impact. The steady state CO emission reached downstream is then the result of the balancing of the breakdown reaction and the further reaction between a carbon atom and an oxygen molecule, regenerating CO.

(b) The Formation of CO

In Part 3(*c*) we assumed the temperature of the gas in the discharge to remain approximately at room temperature; reactions which normally occur in slow combustion or in flames do not occur in this work to any appreciable extent if they have appreciable activation energies.

Fok and Nalbandyan (14) have shown that for large flows at temperatures below 100 °C the only product from reaction between CH_3 and O_2 is a peroxide:

[15] $$CH_3 + O_2 \rightarrow CH_3OO.$$

Only above 100 °C are aldehydes formed as well. Hence the oxidation of a CH_3 radical formed under electron impact according to [8] or [11] will not produce a CO molecule. Similarly a CH_2 radical will probably disproportionate [11*a*] rather than undergo further oxidation. The only reactions which can produce CO are then

[16] $$CH + O_2 \rightarrow CO + OH$$

or

[17] $$CH + O \rightarrow CO + H$$

Most reactions involving H, OH, or CH_3 have activation energies which are large enough to make their occurrence unlikely under our conditions. These activation energies have been summarized by Semenov (15).

In a 50% methane 50% oxygen mixture under the usual conditions, after 5×10^{-3} s (40 cm) 12% CO has been formed. This means that during the time the gas moves 1 cm 4.1×10^{13} molecules have been formed. Since each CO comes from a previously formed CH radical this means that at least 4.1×10^{13} CH radicals were formed in this period of time. As mentioned earlier the only way that CH is produced from CH_4 is either under electron impact (8), or through a reaction of the type

[17*a*] $$CH_m + O \rightarrow CH_{m-1} + OH,$$

which involves an oxygen atom previously formed under electron impact by mechanism [3]. The endothermicity of a CH being produced via mechanism [8] is 12.5 eV while via mechanism [17*a*] it is only 7.7 eV; it only takes 2.55 eV to produce one oxygen atom.

If we assume that the current through the discharge is solely due to the flow of electrons and that the number of additional electrons being produced by ionizing collisions is small, the flux of electrons through a section of the discharge during the time the gas moves 1 cm is 7.5×10^{12} electrons; 4.1×10^{13} CH radicals have thus to be produced during that time. If f is the average number of C—H bonds broken during one electron impact, $(3/f)$ reactive collisions result in a CH being produced from a CH_4. If no reactions of type

Can. J. Chem. Downloaded from www.nrcresearchpress.com by 210.87.254.6 on 09/05/12
For personal use only.

[17*a*] were taking place, each electron must suffer on the average $5.5 \times 3/f$ collisions per centimeter displacement along the axis of the discharge to account for the above calculated rate of formation of CH radicals. In order that the electrons acquire enough energy to produce the calculated number of CH radicals via mechanism [8] the minimum field value has to be 69 V cm^{-1}. If CH were formed completely via mechanism [17*a*], on the other hand, the field value would be decreased to about 38 V cm^{-1}. The experimental values found by Rundle and Miller (16) in this laboratory were intermediate between these values ($\sim$60 V cm^{-1}).

Taking the previous discussion into account, the linear increase of emission with S of the CO emission intensity can be expressed as

$$(dI_{CO}/ds) = (k'd(CO)/ds) = k(i)$$

where I_{CO} is the emission intensity, (CO) the CO concentration, and ds an element of length along the axis of the discharge tube. The proportionality constant k is a function of the current i.

In view of the large pressure gradient in the discharge we have to assume that the rate-controlling step in the production of CO molecules is of zero overall order in the pressure. The right-hand term in the above expression is hence independent of the concentrations of the reagents. This is consistent with the facts reported earlier that the primary step leading to the formation of CO must be the breaking of three C—H bonds by electron impact or by a process such as [17*a*]. Because of the large mass difference electrons do not lose kinetic energy to any significant extent in an elastic collision; they only lose energy in inelastic or reactive collisions. If N_t is the total number of collisions suffered by an electron during the time it moves 1 cm, N_r the number of inelastic and reactive collisions suffered during this time by the electron, and g the average number of collisions it takes an electron before it suffers an inelastic or reactive collision, once it has acquired the minimum amount of energy necessary to excite or break a bond, provided $N_t \geqslant N_r g$, the rate of production of excited species, atoms, or radicals should be pressure independent. This explains the apparent zero order of the above rate law. Since the excitation processes leading to the production of excited CO or O atoms are similar processes, they too should be of zero order in the pressure.

Reactions [16], [17], and [17*a*] must be very fast reactions, occurring within a very few collisions in order to account for the observed rate of formation of the CO, so that the production of the radicals CH or O under electron impact should be rate determining, and thus the overall production of CO be pressure independent, as observed.

If [16] and [17] are fast reactions the concentration of CH should not vary appreciably along the discharge tube; the pressure gradient in the tube will decrease the overall number of collisions taking place per unit length of the discharge tube and result in an increase in the CH concentration. This might explain the slight increase in CH emission seen in Fig. 4.

It might be worthwhile to mention also that ds can be converted into a time dependency when the pressure gradient is known.

It is evident from the above discussion that any process involving accelerated electrons will also have an apparent zero pressure dependency, as long as the condition $N_t \geqslant N_r g$ is met. As was pointed out in Part 4(*a*), the emission of CO, O, or H was found to be proportional to the concentration of that species (to be more precise to the mole fraction of the component). Due to the existence of the pressure gradient in the discharge tube the total number of molecules at various points in the discharge tube varies. Strictly

Can. J. Chem. Downloaded from www.nrcresearchpress.com by 210.87.254.6 on 09/05/12
For personal use only.

speaking the emission intensity is thus not proportional to the absolute concentration but, as long as $N_t \geqslant N_r g$, only to the mole fraction of the emitter in the gas.

The linear increase in the production of CO in methane–oxygen mixture is further evidence that the rate-controlling step in the CO production involves the breakdown of a molecule or radical under electron impact and that under our operating conditions the relation $N_t \geqslant N_r g$ holds.

Ions having comparable masses to the molecules will dissipate their kinetic energy in a few collisions and it is unlikely that a significant amount of energy would be gained by them under the influence of the electric field.

One molecule suffers approximately 300 collisions during the time the gas moves 1 cm (at 1 torr). Schmoluchowsky's formula

$$Z = 3\pi d^2/4\lambda^2$$

gives the average number of collisions suffered by a molecule as it diffuses a distance d with a mean free path of λ.

Assuming an average mean free path of 10^{-2} cm at 1 torr and $d = 0.35 \times 2$ cm as the average distance a radical will diffuse before hitting the wall a molecule suffers about 600 collisions. Hence if appreciable losses or recombinations on the wall are excluded the reactions [16] and [17] should occur within 600 collisions or less.

The relative importance of reactions [16] and [17] will vary with the composition of the gas mixture which flows through the discharge. In oxygen-rich mixtures a significant amount of atomic oxygen is present so that the formation of CO via reaction [17] might become significant.

(c) Other Reactions Involving H, OH, or O Atoms

It has been proposed in the previous sections that the emission of atomic oxygen is due to the collisions of electrons with oxygen atoms (4). When increasing amounts of methane were added to the gas mixture, the emission of atomic oxygen diminished steadily until for 33% methane no emission could be observed. This value is only approximately known because of the weakness of oxygen atom emission and partial overlapping of the N_2 second positive system.

The disappearance of free oxygen atoms might be due to a variety of reasons. If CH is formed from methane it might be that too few electrons are left with enough energy to dissociate an oxygen molecule. Alternately, the oxygen atoms produced may be consumed in further very fast chemical reactions. Recently, Young and Sharpless (17) indicated that the rates of some trimolecular processes might be significant in flow experiments at pressures of 1 torr. However, under our conditions, we doubt that their contribution could be significant.

Reactions likely to occur are:

[18] $\mathrm{CH} + \mathrm{O} \rightarrow \mathrm{CO} + \mathrm{H},$

[19] $\mathrm{OH} + \mathrm{O} \rightarrow \mathrm{O_2} + \mathrm{H},$

[20] $\mathrm{H_2} + \mathrm{O} \rightarrow \mathrm{OH} + \mathrm{H}.$

It is doubtful whether other reactions involving OH take place. Similarly H atoms will not propagate chain reactions at low temperatures because of their relatively large activation energy (15). Reactions [18], [19], and [20] each produce H atoms and together they account for the large H atom emission observed for small amounts of methane in oxygen. We are now attempting to measure the rate of some of the reactions which have been suggested.

Can. J. Chem. Downloaded from www.nrcresearchpress.com by 210.87.254.6 on 09/05/12
For personal use only.

CONCLUSIONS

In this work we have described a technique which permits the study of changes in the spectra emitted by fast flowing, reacting gas mixtures in the positive column of a d-c. glow discharge. We have shown that it is possible in certain cases to obtain a quantitative relation between the emitted intensity and the concentration of the emitting species. To account for the observed reaction rate, we have to postulate a high rate of production of atoms or radicals under electron impact. The electric field values needed to impart the necessary amount of energy to the electrons are of the same magnitude as those measured in this work ($\sim$60 V cm^{-1}). We have thus shown that, at least in the early stages of a discharge, before the steady state of concentrations of atoms, radicals, and molecules has been approached, most of the energy of the electrons is used in breaking chemical bonds.

ACKNOWLEDGMENTS

It is a real pleasure to acknowledge support in the form of grants from the United States Air Force through the Office of Scientific Research (Propulsion Research Division), from the National Research Council of Canada and from the University of Toronto.

Dr. J. F. Vrebosch designed the apparatus and Messrs. J. J. Ryan, R. F. Ferguson, and J. Noolandi were helpful in obtaining part of the data. One of us (P. B d'E.) is indebted to Professor A. Van Tiggelen of the University of Louvain for allowing a year's leave of absence to carry out this work at the University of Toronto.

REFERENCES

1. G. Francis. Handbuch der Physik. Band XXII, Gasentladungen II. Springer Verlag, Berlin. 1956. p. 53.
2. P. J. Padley. Trans. Faraday Soc. **56**, 449 (1960).
3. A. G. Gaydon and H. G. Wolfhard. Flames, their structure radiation and temperature. Chapman and Hall, London. 1960.
4. J. Vaerman, G. Nenquin, and A. Van Tiggelen. Bull. Soc. Chim. Belg. **65**, 435 (1956).
5. R. M. Yealland. Unpublished results.
6. F. Kaufman and J. R. Kelso. Eighth intern. symposium on combustion. The Williams and Wilkins Co., Baltimore. 1962. p. 230.
7. W. D. McGrath and R. G. W. Norrish. Nature, **182**, 235 (1958).
8. F. Kaufman. Progress in reaction kinetics. Vol. 1. *Edited by* G. Porter. Pergamon Press, New York. 1961.
9. L. M. Chanin, A. V. Phelps, and M. A. Biondi. Phys. Rev. Letters, **2**, 344 (1959).
10. S. N. Foner and R. L. Hudson. J. Chem. Phys. **25**, 601 (1956).
11. J. T. Herron and H. I. Schiff. Can. J. Chem. **36**, 1159 (1958).
12. B. H. Mahan and R. B. Solo. J. Chem. Phys. **37**, 2669 (1962).
13. L. Avramenko and R. Kolesnikova. Bull. Acad. Sci. SSSR, **9**, 1506 (1956).
14. N. V. Fok and A. B. Nalbandyan. Dokl. Akad. Nauk SSSR, **86**, 589 (1952); **89**, 125 (1953).
15. N. N. Semenov. Some problems in chemical kinetics and reactivity. *Translation* Boudart. Princeton University Press. 1958.
16. H. W. Rundle and B. H. Miller. Unpublished results.
17. R. A. Young and R. L. Sharpless. J. Chem. Phys. **39**, 1071 (1963).

Can. J. Chem. Downloaded from www.nrcresearchpress.com by 210.87.254.6 on 09/05/12
For personal use only.

Can. J. Chem. Downloaded from www.nrcresearchpress.com by 210.87.254.6 on 09/05/12
For personal use only.

THE REACTION OF UNSATURATED CARBOHYDRATES WITH CARBON MONOXIDE AND HYDROGEN

II. STRUCTURE AND STEREOCHEMISTRY OF THE ANHYDRODEOXYHEXITOLS FROM 3,4-DI-*O*-ACETYL-D-XYLAL

ALEX ROSENTHAL AND DEREK ABSON
Department of Chemistry, University of British Columbia, Vancouver, British Columbia

Received January 20, 1964

ABSTRACT

3,4-Di-*O*-acetyl-D-xylal reacted with carbon monoxide and hydrogen in the presence of dicobalt octacarbonyl to yield 1,5-anhydro-4-deoxy-D-*arabino*-hexitol (I) and 1,5-anhydro-4-deoxy-L-*xylo*-hexitol (II). The stereochemistry at C-5 of the hexitols was elucidated by correlation with the triol ether (VI) obtained by sodium borohydride reduction of the periodate oxidation product of 1,4-anhydro-5-deoxy-D-*arabino*-hexitol (VII). Reaction of 3,4-di-*O*-acetyl-D-xylal with carbon monoxide and deuterium afforded 1,5-anhydro-4-deoxy-D-*arabino*-hexitol-4,6,6-H_3^2 (VIII) and 1,5-anhydro-4-deoxy-L-*xylo*-hexitol-4,6,6-H_3^2 (IX). Examination of the nuclear magnetic resonance (n.m.r.) spectra of the normal and deuterated anhydrodeoxyhexitols confirmed the structural assignments and showed that *cis*-addition to the double bond takes place to give (IX).

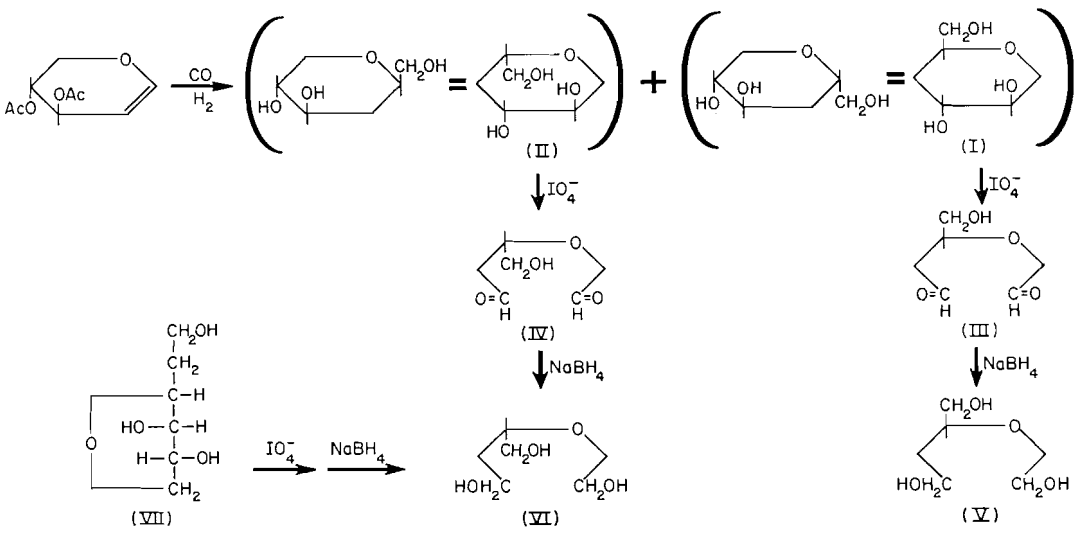

It has been reported previously (1, 2) that 3,4,6-tri-*O*-acetyl-D-galactal reacted with carbon monoxide and hydrogen under oxo conditions (3) to yield an anhydrodeoxyheptitol of unknown stereochemistry. It has now been found that pentals react similarly to yield anhydrodeoxyhexitols in which a hydroxymethyl group has been added to C-1 of the pental. The present paper in the series deals with the oxo reaction of 3,4-di-*O*-acetyl-D-xylal and offers conclusive proof by chemical means of the stereochemistry of the hexitols obtained. In addition, the mechanism of the addition of carbon monoxide and hydrogen to the glycal has been determined by the use of tracer studies.

The 3,4-di-*O*-acetyl-D-xylal, prepared by a modification of the procedure of Helferich and co-workers (4), was reacted with a mixture of carbon monoxide and hydrogen at a

pressure of about 4000 p.s.i. and at a temperature of about 130° in the presence of preformed dicobalt octacarbonyl as catalyst to yield a mixture of products. This was freed from catalyst by filtration through Florisil. After the solvent was removed, the mixture was deacetylated with sodium methoxide in methanol to yield the anhydrodeoxyhexitols (I) and (II). These were subsequently separated by paper chromatography.

The stereochemistry of C-5 of each of the hexitols (I) and (II) was resolved in the following way. Periodate oxidation of these hexitols yielded the dialdehydes (III) and (IV). Sodium borohydride reduction of these dialdehydes afforded the enantiomorphic triol ethers (V) and (VI), having similar infrared spectra and equal but opposite optical rotations. In addition, (V) and (VI) were converted into crystalline *p*-nitrobenzoates having similar infrared spectra and melting points. In connection with the problem of determining the structures of the *p*-nitrobenzoates of the triol ethers, it was noted that Gorin had previously reported (5) the preparation of a *p*-nitrobenzoate of a triol ether which appeared to have the same structure as that of the *p*-nitrobenzoate of either (V) or (VI). Direct comparison (m.p., mixed m.p., and infrared spectra) revealed that the tris-*p*-nitrobenzoate of Gorin's compound (III) was identical with the tris-*p*-nitrobenzoate of compound (V).

The configuration of C-3 of the triol ether (VI) was then correlated with that of C-4 of 1,4-anhydro-5-deoxy-D-*arabino*-hexitol (VII). The latter new compound was prepared by sodium borohydride reduction of the known 3,6-anhydro-2-deoxy-D-*lyxo*-hexose (6). Periodate oxidation of (VII) followed by sodium borohydride reduction of the dialdehyde yielded a triol ether having an optical rotation and infrared spectrum respectively similar to those of the triol ether (VI). Further confirmation of the identity of the two triol ethers was obtained by comparing the crystalline *p*-nitrobenzoates of each (same m.p., mixed m.p., and infrared spectra). Thus, the configuration of C-5 of the hexitol (II) is identical with that of C-4 of 1,4-anhydro-5-deoxy-D-*arabino*-hexitol, and compounds (I) and (II) are 1,5-anhydro-4-deoxy-D-*arabino*-hexitol and 1,5-anhydro-4-deoxy-L-*xylo*-hexitol, respectively.

In conjunction with the study of the structure of each of the hexitols (I) and (II) by classical chemical methods, a parallel investigation of their structures by use of proton n.m.r. has also been carried out. The interpretation of the n.m.r. spectra of (I) and (II) (shown in Fig. 1(A) and (B)) was greatly aided by the excellent n.m.r. analyses of the structures of chalcose (4,6-dideoxy-3-*O*-methyl-D-*xylo*-hexose) and of its methyl glycoside (7), and by comparison of the spectra of (I) and (II) with those of their deuterated analogues prepared by reacting 3,4-di-*O*-acetyl-D-xylal with carbon monoxide and deuterium. The n.m.r. spectra of the deuterated analogues (VIII) and (IX) are shown in Fig. 1(C) and 1(D). Based on the fact that the equatorial C-4 hydrogen of the methylene group of chalcose absorbed at around $\delta = 2.05$ and the axial C-4 hydrogen at around $\delta = 1.0$ to 1.58 (7), the signal at $\delta = 2.0$ in Fig. 1(D) might be attributed to the single equatorial hydrogen on C-4 of the deuterated compound (IX). In Fig. 1(B) both the equatorial and the axial C-4 hydrogen signals at $\delta = 2.0$ and 1.5, respectively, are clearly distinguishable. To account for the wide signal of the axial C-4 hydrogen (about 34 c.p.s.), it is suggested that the hydrogens on C-5 and on C-3 are axial. The three coupling constants of the axial C-4 hydrogen would therefore be $J_{4a,3a}$ $J_{4a,5a}$, and $J_{4a,4e}$ since it would be coupled with the two neighboring hydrogens on C-3 and C-5 and to the equatorial hydrogen on C-4. The fact that the axial C-4 hydrogen of chalcose (7), which gave a series of peaks having a width of 34.5 c.p.s., is also coupled to axial hydrogens on C-5 and on C-3 supports the above postulation. The splitting of the equatorial hydrogen signal around $\delta = 2.0$ clearly

Can. J. Chem. Downloaded from www.nrcresearchpress.com by 210.87.254.6 on 09/05/12
For personal use only.

Can. J. Chem. Downloaded from www.nrcresearchpress.com by 210.87.254.6 on 09/05/12
For personal use only.

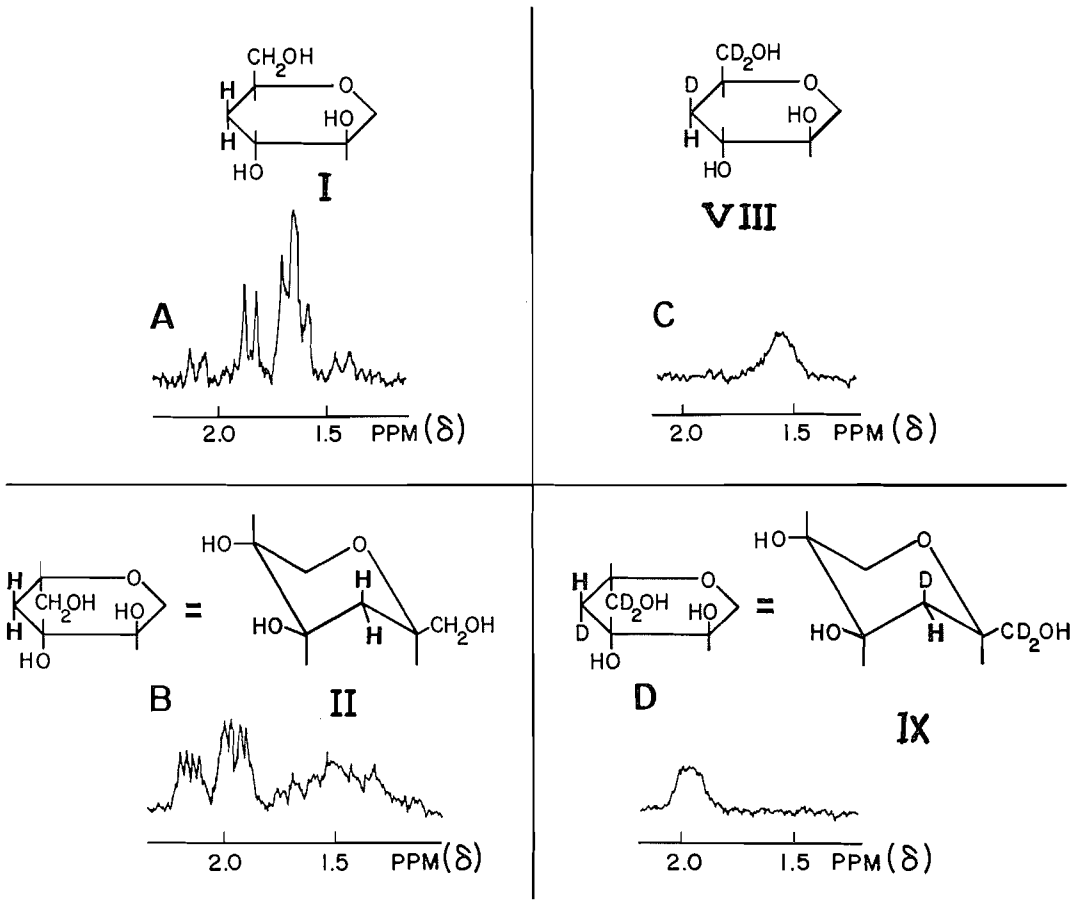

FIG. 1. Proton n.m.r. spectra in D_2O solution at 60 mc with chemical shifts given in p.p.m. from tetramethylsilane as zero: (A) 1,5-anhydro-4-deoxy-D-*arabino*-hexitol; (B) 1,5-anhydro-4-deoxy-L-*xylo*-hexitol; (C) 1,5-anhydro-4-deoxy-D-*arabino*-hexitol-4,6,6-H_3^2; (D) 1,5-anhydro-4-deoxy-L-xylo-hexitol-4,6,6-H_3^2. (Only signals of protons attached to C-4 are shown.)

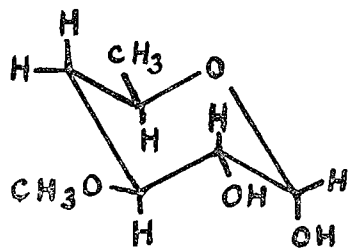

shows the large spin coupling to the geminal hydrogen ($J_{4a,4e}$ approximately 12.5 c.p.s.), and further small splittings by coupling to the adjacent axial hydrogens on C-3 and C-5. Therefore, the hydroxymethyl group in (II) must be in an equatorial position. It is apparent that analysis of the n.m.r. spectra 1B and 1D reveals the stereochemistry of

the hexitol (II) and of the deuterated analogue (IX). An important part of the evidence for axial deuterium in (IX) is the narrowness (~9 c.p.s.) of the signal at 2.0 p.p.m. (had the proton in (IX) been axial, the signal would have been wider (~20 c.p.s.) as well as being at higher field). It is also noteworthy that the deuterated analogue (IX) must have been formed by a *cis*-addition of the hydroxymethyl group and of the deuterium to the 1,2-unsaturated bond of 3,4-di-*O*-acetyl-D-xylal.

The n.m.r. spectra of the normal and deuterated hexitols (I) and (VIII) (Fig. 1(A) and 1(C)) do not reveal the stereochemistry of C-5 because of overlapping of the C-4 axial and equatorial hydrogen signals.

EXPERIMENTAL

General Considerations

The solvent used for paper chromatographic separations was water-saturated 1-butanol containing 5% ethanol and 1% concentrated ammonium hydroxide. The hexitols were detected with ammoniacal silver nitrate (8) or with sodium metaperiodate – Schiff's reagent (9).

The oxo product, first freed from catalyst, was also separated into slightly impure fractions by chromatography on neutral alumina using benzene–methanol (98:2/v:v) as developer. Analysis of the product–mixture was readily carried out using thin layer chromatography on alumina with benzene:methanol (96:4) as developer.

The Florisil was obtained from the Floridin Company, Tallahassee, Florida, United States.

The oxo product was dried by azeotroping with anhydrous benzene followed by methanol, and then deacetylated (10) with 0.1 *N* sodium methoxide in methanol (or in a 1:1 mixture of anhydrous chloroform – methanol) at about 5° for 1 day. Sodium ions were removed by stirring (or elution through a column) with Amberlite IR-120 (H^+) resin. Solutions were evaporated under reduced pressure.

The n.m.r. spectra were obtained in a Varian A-60 instrument using tetramethylsilane as the external standard (set at $\delta = 0$). The infrared analyses were done on a Perkin–Elmer spectrophotometer, Model 21, using a sodium chloride crystal. Microanalyses were done by Mrs. Aldridge of this department and by Dr. A. Bernhardt, Mikroanalytisches Laboratorium im Max-Planck-Institut für Kohlenforschung, Mülheim (Ruhr), West Germany.

Preparation of 3,4-Di-O-acetyl-D-xylal

The 3,4-di-*O*-acetyl-D-xylal was prepared according to a modification of the procedure of Helferich and co-workers (4). During the addition of the tri-*O*-acetyl-α-D-xylosyl bromide to the zinc – acetic acid mixture, the reactants were kept at −5 to −10° for 3 h. Prior to filtration, Celite was added to coagulate the zinc and hasten filtration. Pieces of solid carbon dioxide were added during the filtration process to keep the reaction mixture at −10°. It was imperative that the crude 3,4-di-*O*-acetyl-D-xylal be distilled immediately under reduced pressure to prevent undue decomposition of the product; yield about 60%. All operations in the preparation of 3,4-di-*O*-acetyl-D-xylal were carried out in the same day.

Reaction of 3,4-Di-O-acetyl-D-xylal with Carbon Monoxide and Hydrogen to Yield 1,5-Anhydro-4-deoxy-D-arabino-hexitol (I) and 1,5-Anhydro-4-deoxy-L-xylo-hexitol (II)

To a mixture of 3,4-di-*O*-acetyl-D-xylal (5.6 g) in dry, purified benzene (25 ml) contained in a 300-ml shaker bomb was added preformed dicobalt octacarbonyl (1–2 g). After flushing the bomb with carbon monoxide, carbon monoxide (500 p.s.i.) and hydrogen (2500 p.s.i.) were added and the reactants heated with rocking at 125–130° for about 2 h. The reactants were then added to a column of Florisil (8 × 8 cm diam.) and after the solvent had passed through the dicobalt octacarbonyl was eluted with 30–60° petroleum ether. The product was then eluted with benzene–ethanol (10:1/v:v). Evaporation of the eluent under reduced pressure yielded 6.0 g of sirup. The product contained the anhydrohexitols and traces of sugars. When the same substrate was reacted under similar conditions except at a temperature of about 115° for 0.5 h, the product consisted of 50% unreacted 3,4-di-*O*-acetyl-D-xylal, about 20% of sugars, and about 30% of the same anhydrohexitols as obtained in the 130° experiment.

The oxo product was then deacetylated with sodium methoxide in methanol (10). Fractionation of the deacetylated product was carried out by preparative paper chromatography or by cellulose column chromatography; ratio of fraction (I) and (II) was about 1:1. When the deacetylated product contained appreciable quantities of sugars, better separation of the hexitols was obtained if the mixture was first treated with sodium borohydride in water to reduce the sugars.

Characterization of Fraction (I)

Fraction (I) (1,5-anhydro-4-deoxy-D-*arabino*-hexitol) was crystallized from methanol – isopropyl ether; m.p. 102°; $[\alpha]_D^{20}$ −13° (*c*, 6.3 in water); $R_F = 0.47$. Calc. for $C_6H_{12}O_4$: C, 48.64; H, 8.16. Found: C, 48.35; H, 8.10.

Can. J. Chem. Downloaded from www.nrcresearchpress.com by 210.87.254.6 on 09/05/12
For personal use only.

Preparation of 1,5-Anhydro-4-deoxy-2,3,6-tri-O-p-nitrobenzoyl-D-arabino-hexitol

1,5-Anhydro-4-deoxy-D-*arabino*-hexitol was converted into a tris-*p*-nitrobenzoate according to the procedure used by Gorin (5); m.p. 215°; $[\alpha]_D^{20}$ −50° (*c*, 1.0 in chloroform). Calc. for $C_{27}H_{21}O_{13}N_3$: C, 54.60; H, 3.60. Found: C, 54.56; H, 3.86.

Characterization of Fraction (II)

Fraction (II) (1,5-anhydro-4-deoxy-L-*xylo*-hexitol) could not be crystallized; $[\alpha]_D^{20}$ −44° (*c*, 6.4 in water); R_F = 0.41. Calc. for $C_6H_{12}O_4$: C, 48.64; H, 8.16. Found: C, 48.36; H, 8.39.

Preparation of 2,3,6-Tri-O-acetyl-1,5-anhydro-4-deoxy-L-xylo-hexitol

The 1,5-anhydro-4-deoxy-L-*xylo*-hexitol (70 mg) was acetylated with acetic anhydride – pyridine to yield 109 mg of 2,3,6-tri-*O*-acetyl-1,5-anhydro-4-deoxy-L-*xylo*-hexitol. Recrystallization of the crude acetate from ether – petroleum ether (30–60°) afforded the pure acetate; m.p. 80–81°; $[\alpha]_D^{22}$ −41° (*c*, 0.8 in chloroform). Calc. for $C_{12}H_{18}O_7$: C, 52.55; H, 6.62. Found: C, 52.82; H, 6.58.

Structure and Stereochemistry of Hexitols (I) and (II)

Compound (I) was oxidized with 0.1 *M* periodic acid to yield the dialdehyde (III), which was reduced with sodium borohydride in water, according to the procedure of Gorin (5), to the triol ether (V); $[\alpha]_D^{23}$ −19° (*c*, 2.0 in water). The triol ether was *p*-nitrobenzoylated to afford a tris-*p*-nitrobenzoate, m.p. 102–103°; $[\alpha]_D^{22}$ −28° (*c*, 1.1 in chloroform). Calc. for $C_{27}H_{23}O_{13}N_3$: C, 54.30; H, 3.99. Found: C, 54.57; H, 3.95. The infrared spectra of the tris-*p*-nitrobenzoate of the triol ether (V) and of the tris-*p*-nitrobenzoate of the triol ether obtained from 1,4-anhydro-5-deoxy-D-*arabino*-hexitol (described in the following part of the experimental) were identical.

In a similar way to that described above, compound (II) was oxidized with periodic acid and the dialdehyde (IV) then reduced with sodium borohydride to yield the triol ether (VI) as a sirup; $[\alpha]_D^{25}$ +17° (*c*, 1.7 in water). The triol ether (VI) was then *p*-nitrobenzoylated; m.p. 102–103°; $[\alpha]_D^{24}$ +26° (*c*, 1.4 in chloroform). Calc. for $C_{27}H_{23}O_{13}N_3$: C, 54.30; H, 3.99. Found: C, 54.63; H, 4.09. The mixed m.p. of this *p*-nitrobenzoate and the *p*-nitrobenzoate obtained from 1,4-anhydro-5-deoxy-D-*arabino*-hexitol was 100–102°. The infrared spectra of the two nitrobenzoates were similar.

Synthesis of 1,4-Anhydro-5-deoxy-D-arabino-hexitol (VII)

An amount of 95 mg of "3,6-anhydro-2-deoxy-D-galactose" (6) was reduced with sodium borohydride (50 mg) in water (1 ml) for 1 h. The product, 1,4-anhydro-5-deoxy-D-*arabino*-hexitol (86 mg) was a colorless oil; $[\alpha]_D^{25}$ +21° (*c*, 1.7 in ethanol).

Preparation of 1,4-Anhydro-5-deoxy-2,3,6-tri-O-p-nitrobenzoyl-D-arabino-hexitol

1,4-Anhydro-5-deoxy-D-*arabino*-hexitol was reacted with *p*-nitrobenzoyl chloride in the usual way to yield 1,4-anhydro-5-deoxy-2,3,6-tri-*O*-*p*-nitrobenzoyl-D-*arabino*-hexitol, m.p. 159–160°; $[\alpha]_D^{22}$ −96° (*c*, 0.7 in chloroform). Calc. for $C_{27}H_{21}O_{13}N_3$: C, 54.46; H, 3.56. Found: C, 54.61; H, 3.86.

Conversion of 1,4-Anhydro-5-deoxy-D-arabino-hexitol into 2-Deoxy-3-O-(2-hydroxyethyl)-L-glycero-tetritol (VI)

1,4-Anhydro-4-deoxy-D-*arabino*-hexitol (55 mg) was oxidized with 0.1 *M* periodic acid and the product then reduced with sodium borohydride; yield: 51 mg; $[\alpha]_D^{24}$ +17° (*c*, 2.0 in water). The infrared spectrum of this product was similar to those of the triol ethers (V) and (VI).

A 30-mg portion of the triol ether obtained from 1,4-anhydro-5-deoxy-D-*arabino*-hexitol was *p*-nitrobenzoylated in the usual way; m.p. 101–102°; $[\alpha]_D^{24}$ +27° (*c*, 1.1 in chloroform). Calc. for $C_{27}H_{23}O_{13}N_3$: C, 54.30; H, 3.99. Found: C, 54.61; H, 4.00.

Reaction of 3,4-Di-O-acetyl-D-xylal with Carbon Monoxide and Deuterium to Yield 1,5-Anhydro-4-deoxy-D-arabino-hexitol-4,6,6-H_3^2(cis) (VIII) and 1,5-Anhydro-4-deoxy-L-xylo-hexitol-4,6,6-H_3^2 (cis) (IX)

The 3,4-di-*O*-acetyl-D-xylal was reacted with carbon monoxide and deuterium at 130° under similar conditions to those described in the first experiment to yield the above-mentioned deuterated hexitols (VIII) and (IX). The stereochemistry of the deuterium atoms was determined by proton n.m.r. analysis (see Discussion).

ACKNOWLEDGMENTS

The authors gratefully acknowledge the financial assistance of the National Cancer Institute of Canada, the National Research Council, and the University of British Columbia Research Grant. One of us (D. A.) gratefully acknowledges the Standard Oil Fellowship and the University of British Columbia Research Fellowship.

The authors wish to thank Dr. P. A. J. Gorin for furnishing a sample of the tris-*p*-nitrobenzoate of his triol ether (III).

One of us (A. R.) spent the academic year 1963–64 as a guest of the University Chemical

Can. J. Chem. Downloaded from www.nrcresearchpress.com by 210.87.254.6 on 09/05/12
For personal use only.

Laboratory, Cambridge University, in the laboratories of Professor Lord Todd, where this manuscript was written, and wishes to thank the members of the Department of Chemistry for their hospitality.

REFERENCES

1. A. ROSENTHAL and D. READ. Can. J. Chem. **35**, 788 (1957).
2. A. ROSENTHAL and D. READ. Methods in carbohydrate chemistry. Vol. II. *Edited by* R. L. Whistler and M. L. Wolfrom. Academic Press, New York, N.Y. 1963. p. 457.
3. I. WENDER, H. W. STERNBERG, and M. ORCHIN. Catalysis. Vol. 5. *Edited by* P. H. Emmett. Reinhold Publishing Corp., New York, N.Y. 1957.
4. B. HELFERICH, E. N. MULCAHY, and H. ZIEGLER. Ber. **87**, 233 (1954).
5. P. A. J. GORIN. Can. J. Chem. **38**, 641 (1960).
6. A. B. FOSTER, W. G. OVEREND, M. STACEY, and G. VAUGHAN. J. Chem. Soc. 3367 (1954).
7. P. W. K. WOO, H. W. DION, and L. F. JOHNSON. J. Am. Chem. Soc. **84**, 1066 (1962).
8. S. M. PARTRIDGE. Nature, **158**, 270 (1946).
9. J. BADDILEY, J. G. BUCHANAN, R. E. HANDSCHUMACHER, and J. F. PRESCOTT. J. Chem. Soc. 2818 (1956).
10. G. ZEMPLÉN, A. GERECS, and I. HADÁCSY. Ber. **69**, 1827 (1936).

Can. J. Chem. Downloaded from www.nrcresearchpress.com by 210.87.254.6 on 09/05/12
For personal use only.

Can. J. Chem. Downloaded from www.nrcresearchpress.com by 210.87.254.105 on 09/05/12
For personal use only.

DIAMAGNETIC SUSCEPTIBILITIES OF SOME COMPOUNDS CONTAINING OXYGEN LINKED TO NITROGEN OR PHOSPHORUS

M. W. Lister and R. Marson
Department of Chemistry, University of Toronto, Toronto, Ontario
Received February 7, 1964

ABSTRACT

The diamagnetic susceptibilities of a number of compounds containing oxygen linked to nitrogen or phosphorus have been measured. The results are interpreted in terms of the apparent contribution of the oxygen atoms to the susceptibility in these and other series of compounds, and are compared with other evidence on the nature of the bonds to oxygen. The results support the usual formula of an amine oxide as $R_3N \rightarrow O$, but phosphine oxides behave as would be expected for $R_3P = O$. Phosphorus oxyhalides have molar susceptibilities about 4.6 (in units of -10^{-6} e.m.u.) larger than the corresponding trihalides, a difference close to that for singly bound oxygen in ethers or alcohols. Each oxygen contributes 4.4 in trialkyl phosphites, as might be expected for $P(OR)_3$; but the value in dialkyl phosphites is 4.9 per oxygen, thereby showing behavior similar to that of carboxylic esters. The extra oxygen in trialkyl phosphates as compared with trialkyl phosphites contributes 9.4, a surprisingly large amount.

It has been known since the time of Pascal's extensive work on diamagnetic susceptibilities (1) that the molar susceptibilities of diamagnetic compounds are approximately additive in terms of the atoms they contain, and of certain structural features such as double bonds. Organic compounds of oxygen, in particular, require different values to be assigned to the contribution of an oxygen atom in a ketone, or an ether, or an ester, etc. The object of the present work was to examine the susceptibilities of compounds containing oxygen linked to phosphorus or nitrogen, and to see whether they followed the same pattern as in compounds with oxygen linked to carbon. The interpretation in some cases requires a decision as to whether a given bond is predominantly single or double, and this has been made in the usual way from other properties of the bond, such as its length.

EXPERIMENTAL

Apparatus

The susceptibility measurements were made on a Goüy balance (2). The apparatus was calibrated by oxygen-free benzene, which was assumed to have a susceptibility of -0.7081×10^{-6} e.m.u./g, or -0.6187×10^{-6} e.m.u./ml, as reported by Eggleston, Evans, and Richards (3). The apparent change in weight of the benzene sample in the magnetic field was about 15 mg, and this was measured on a Sartorius microbalance sensitive to 2–3 μg. It was found that the magnetic force for a given magnet current on any particular sample was reproducible to within 0.25%. Since the determination of the molar susceptibilities involves a comparison of the magnetic forces on the sample and on benzene, and since five or six readings of the magnetic forces were always made, it seems reasonable to claim an accuracy in the result of $\pm 0.5\%$.

In order to convert volume susceptibilities to molar susceptibilities, it is necessary to know the density of the substance. Where no reliable value was available in the literature, it was measured in a 10-ml or 25-ml pyknometer, with special precaution against evaporation of volatile liquids. The reproducibility was 0.01% for a non-volatile liquid, but with volatile compounds it was 0.05 to 0.1%.

With solid samples the apparent density was measured directly in the tube used for the magnetic measurements, from the weight and length of the sample. The solid samples were always distilled into the tube, melted, and then allowed to cool. This therefore allows for any shrinkage away from the walls on freezing.

Chemicals

The samples used were prepared as follows. Where a middle fraction of a commercial sample is mentioned, this was always about 20 ml from an initial volume of at least 250 ml. In every case the susceptibility tube was filled by vacuum distillation, and nitrogen was then admitted up to atmospheric pressure.

Triethylamine oxide was prepared by oxidizing triethylamine with 3% hydrogen peroxide for 2 days (4).

The solution was evaporated under reduced pressure to leave an oily residue, which was dried over sodium sulphate and distilled *in vacuo*. It stood in a vacuum desiccator over phosphorus pentoxide for several weeks, and was then redistilled at reduced pressure.

Attempts to prepare trimethylamine oxide in a sufficiently pure state were unsuccessful. Decomposition occurred on melting, and recrystallization from various solvents led to persistent contamination by the solvents. Its instability on melting also prevented filling the susceptibility tube with the molten compound, which gives a uniform column of sample.

Triethylamine from the Eastman Chemical Company was dried over potassium carbonate, and distilled in nitrogen to give a middle fraction boiling at 89.2 °C.

Tripropylamine from the Pennsalt Chemical Company was treated in the same way. The middle fraction boiled at 156 °C.

Tripropylphosphine oxide was prepared by a modification of Pickard and Kenyon's method (5) from phosphorus oxychloride and propyl magnesium bromide in ether. Six hours of refluxing were necessary to give a reasonably complete reaction. After removal of the ether and addition of alkali, the product was distilled off at atmospheric pressure. It was then redistilled *in vacuo*, and dried in a vacuum desiccator. Repeated redistillation under vacuum eventually gave a middle fraction with a constant melting point of 45 °C. Pickard and Kenyon (5) give 38 °C. The compound is very deliquescent.

Trioctylphosphine oxide from Distillation Products Industries Ltd. was fractionally distilled under vacuum to give a sample melting at 57 °C. The melting point was not changed by redistillation.

Phosphorus trichloride from the Eastman Kodak Company was fractionated under reduced pressure, and a middle sample was used which boiled at 76 °C in agreement with earlier measurements (6).

Phosphorus oxychloride from the British Drug Houses Ltd. was fractionally distilled in nitrogen to give a product with a constant b.p. of 106 °C, and m.p. of 1.0 °C. Reference 7 gives m.p. 1.17 °C, b.p. 105.3 to 107.2 °C.

Dialkyl and trialkyl phosphites from the Victor Chemical Company were dried over calcium chloride, and fractionally distilled at low pressures in a slow stream of nitrogen. On redistillation, the middle 10% of the original samples were taken for the susceptibility measurements. The boiling points were checked against the values summarized by Kosolopoff (8) and Van Wazer (9).

Trialkyl phosphates from the Electric Reduction Company were dried briefly over calcium chloride, and redistilled. The boiling points were checked against the values summarized in ref. 8, p. 258; or ref. 9, p. 582.

Phosphorus tribromide was distilled to give a middle fraction boiling at 173 °C in agreement with earlier values (7).

Phosphorus oxybromide was prepared as described in Inorganic Syntheses (10). It was purified by partial crystallization from a melt to give a colorless product melting at 52 °C (ref. 7 gives 51.3 °C).

EXPERIMENTAL RESULTS

The densities were either measured or obtained from the literature. The values used are collected in Table I. The values for tripropylphosphine oxide, trioctylphosphine oxide, and phosphorus oxybromide are effective, and not true, densities, obtained from the length of a known weight of material in the susceptibility tube. The density of solid phosphorus oxybromide had been previously reported (7) as 3.25 g/ml. This is probably too high, as the apparent density was 3.025 g/ml at 25 °C, and the solid showed very little sign of shrinking from the walls of the tube. A density close to 3.025 g/ml is also more consistent with the molar volumes of other phosphorus halides and oxyhalides.

Table I also gives the molar susceptibilities, obtained by multiplying the directly measured volume susceptibilities by the molar volumes. In this table, and in the subsequent discussion, the molar susceptibilities are given in units of -10^{-6} e.m.u.

DISCUSSION OF RESULTS

Earlier measurements have been made on some of the compounds reported above, but these were remeasured either because earlier values disagreed with each other, or as a check on various members of a homologous series. In particular, Francois and Horrau (13) obtained 81.4 for triethylamine, as compared with 83.3 in the present work. Early results (11) gave 66 for phosphorus trichloride, and 68.9 for the oxychloride; more recently Nevgi obtained 61.8 for the oxychloride (14).

Other relevant results in the literature are: phosphorus triethyl, 90.0 (15); triethyl

Can. J. Chem. Downloaded from www.nrcresearchpress.com by 210.87.254.105 on 09/05/12
For personal use only.

TABLE I

Compound	Density, g/ml at 25 °C	Molar susceptibility
$(C_2H_5)_3N$	0.7235*	83.3
$(C_3H_7)_3N$	0.7523*	116.4
$(C_2H_5)_3NO$	0.858	88.4
PCl_3	1.566†	63.1
$POCl_3$	1.668*	67.8
PBr_3	2.880†	89.3
$POBr_3$	3.025‡	93.9
$(C_2H_5)_2HPO_3$	1.068§	81.7
$(C_4H_9)_2HPO_3$	0.986	125.7
$(C_8H_{17})_2HPO_3$	0.922	223.8
$(CH_3)_3PO_3$	1.043	68.3
$(i\text{-}C_3H_7)_3PO_3$	0.908	138.5
$(C_4H_9)_3PO_3$	0.922	170.8
$(CH_3)_3PO_4$	1.2052	77.9
$(C_3H_7)_3PO_4$	1.0023	146.5
$(C_4H_9)_3PO_4$	0.9727	180.7
$(C_3H_7)_3PO$	0.903‡	125.0
$(C_8H_{17})_3PO$	0.9103‡	302.7

These are all normal alkyl groups, unless otherwise noted.
*Reference 7.
†Reference 11.
‡Effective density of a solid.
§Reference 8.
‖Reference 12.

phosphine oxide, 91.6 (15); triethyl phosphate, 115.3 (16); triethyl phosphite, 104.6 (15); and monoethyl phosphate, 68.9 (15).

In comparing members of a homologous series, it is necessary to estimate the contribution of a CH_2 group. Pacault (1) suggests 11.86 for this, and Angus and Hill (17) suggest 11.69. Other workers have used slightly different values, and it is in fact probable that this quantity is somewhat variable. Where possible, this question will be avoided by comparing compounds with the same number of carbon atoms; in other cases a value of 11.7 can be taken as an average.

The contribution of oxygen atoms linked to carbon has been measured in a wide variety of organic compounds. The average of a number of results (1, 17–22) can be summarized as follows: oxygen in alcohols 4.9; ethers 5.1; aldehydes -0.7; ketones -1.2; carboxylic acids 8.2 (two oxygen atoms); and carboxylic esters 7.4 (two oxygen atoms). These results mean that the difference between an ester, RCOOR′, and a ketone, RR′CO, is 8.5; while between an acid, RCOOH, and an aldehyde, RCHO, the difference is 8.9. These values can serve as a basis for comparison with the contributions of oxygen linked to nitrogen or phosphorus.

In interpreting the susceptibility results, we must first consider what evidence is available about the order of the bonds to oxygen. If we first consider triethylamine oxide, the usual view that nitrogen cannot have more than eight valency electrons suggests the formula $(C_2H_5)_3N \rightarrow O$, with singly bound oxygen. This is supported by the length of the N—O bond in trimethylamine oxide, which is about 1.40 Å (23, 24), and by the force constant of the bond which is in the range 3.8 to 4.8×10^5 dyn/cm (25). The susceptibilities of triethylamine and triethylamine oxide differ by 5.1, a value equal to that for singly bonded oxygen in ethers. Consequently the magnetic results support the formula above. The difference between triethylamine and tripropylamine (11.03 per CH_2) is a little low, but the results are consistent with Francois and Horrau's (13) value of 221.7 for trihexylamine.

Can. J. Chem. Downloaded from www.nrcresearchpress.com by 210.87.254.105 on 09/05/12
For personal use only.

Can. J. Chem. Downloaded from www.nrcresearchpress.com by 210.87.254.105 on 09/05/12
For personal use only.

The behavior of phosphine oxides is different, presumably because phosphorus can expand its valency shell at least as far as 12 electrons. The vibration frequency assigned to P—O stretching in trimethylphosphine oxide is 1176 cm^{-1} (26), which would correspond to a force constant of 8.6×10^5 dyn/cm. Robinson (27) has related P—O force constants to bond order in a variety of compounds, and assigns a P—O bond order of 1.76 to this compound. The susceptibilities of phosphine oxides indicate a low contribution by the oxygen. If we allow 11.7 per CH_2, and compare the susceptibilities of triethyl, tripropyl, and trioctyl phosphine oxides with that of triethyl phosphine, the average contribution by the oxygen is 1.2. This is between the values for oxygen in alcohols and ethers (5.0) on the one hand, and aldehydes and ketones (−1.0) on the other, being somewhat closer to the latter. This result is therefore consistent with Robinson's estimate of the bond order.

The phosphorus oxyhalides have stretching force constants of 10.35×10^5 in $POCl_3$, and 9.89×10^5 in $POBr_3$ (27), to which Robinson assigns bond orders of 1.95 and 1.92 respectively. The bond lengths are 1.45 Å in $POCl_3$ (28), and 1.41 Å in $POBr_3$ (29), though the experimental errors are too large to attribute any significance to the apparently shorter bond in $POBr_3$. These distances are much shorter than a single bond, which might be expected to be about 1.71 Å (30). However the susceptibility measurements show a large contribution by oxygen: the difference $\chi(POCl_3) - \chi(PCl_3)$ is 4.7, and $\chi(POBr_3) - \chi(PBr_3)$ is 4.6. This is roughly the contribution of singly bound oxygen, but it is probably better to compare these results with the large contribution of oxygen in oxyacids, and to suggest that in both the electrons are somewhat delocalized by resonance with such structures as

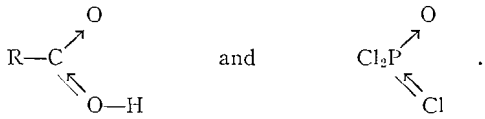

This is supported by the phosphorus halogen distances (see ref. (30), p. 642), which are shorter in $POCl_3$ (1.995 Å) than in either PCl_3 (2.043 Å) or PCl_5 (2.04 and 2.19 Å), and are shorter in $POBr_3$ (2.06 Å) than in either PBr_3 (2.18 Å) or PBr_4^+ (2.13 Å). Against this may be set the fact that the susceptibilities of benzoyl chloride (75.8) and benzyl chloride (82.0) indicate a contribution of −0.4 by the oxygen in benzoyl chloride (if hydrogen has its usual value of 2.9), yet analogous resonance should be possible in compounds of formula RCOCl.

Similarly if we subtract the value for triethyl phosphine from the phosphite and phosphate esters, and allow 11.7 for each extra CH_2, we get the following values for the average contributions of the oxygen atoms: three oxygens in R_2HPO_3, 14.7; three oxygens in $P(OR)_3$, 13.3; four oxygens in R_3PO_4, 22.7. Each oxygen in the trialkyl phosphites contributes 4.4, which is nearly the value for an oxygen in an ether. The bonding of oxygen in trialkyl phosphites and ethers is similar, except for the possibility that the phosphorus can enlarge its valency shell by partial double bonding to the oxygen; if this occurs, it must have only a small effect on the susceptibility.

The usual formula given to dialkyl phosphites is $(RO)_2PH{=}O$, but the contribution of each oxygen is large, being 4.9 on the average. The force constant of the P=O bond in these compounds is about 9.9×10^5 dyn/cm (26, 27), indicating nearly a double bond. Hence their magnetic behavior is like that of the carboxylic esters, whose oxygen contribution is also fairly large (3.7 per oxygen); and their structures are, of course, similar.

The difference $\chi(R_3PO_4) - \chi(R_3PO_3)$ averages 9.4, and is surprisingly large. Here again

the infrared frequency of vibration of the P—O bond is quite high, being about 1275 cm^{-1} (26), corresponding to a force constant (27) of about 10.1×10^5 dyn/cm. This is a much greater susceptibility difference than that for the extra oxygen in going from an ether to a carboxylic ester, which is a somewhat comparable change, since it involves introduction of a doubly bound oxygen. In this latter case the average susceptibility of the extra oxygen is only 2.3. Hence the large increase in the phosphates is not paralleled in compounds with oxygen bound only to carbon. At present no really satisfactory explanation can be offered for this difference.

REFERENCES

1. A. Pacault. Rev. Sci. **86**, 38 (1948).
2. L. G. Goüy. Compt. Rend. **109**, 935 (1889).
3. B. C. Eggleston, D. F. Evans, and R. E. Richards. J. Chem. Soc. 941 (1954).
4. W. R. Dunstan and E. Goulding. J. Chem. Soc. **75**, 1005 (1889).
5. R. H. Pickard and J. Kenyon. J. Chem. Soc. **89**, 262 (1906).
6. N. V. Sidgwick. Chemical elements and their compounds. Oxford University Press. 1950. p. 752.
7. Selected values of properties of chemical compounds. *Edited by* F. D. Rossini. Carnegie Institute. 1959.
8. G. M. Kosolapoff. Organo-phosphorus compounds. J. Wiley and Sons, Inc. 1950. p. 202.
9. J. R. Van Wazer. Phosphorus and its compounds. Vol. 1. Interscience Publishers Inc. 1958. p. 376.
10. Inorganic syntheses. *Edited by* W. C. Fernelius. Vol. II. McGraw-Hill. 1946. p. 151.
11. International critical tables. *Edited by* E. W. Washburn. Vol. I. McGraw-Hill. 1926.
12. D. P. Evans. J. Chem. Soc. 1310 (1930).
13. H. Francois and J. Horrau. Compt. Rend. **240**, 1225 (1955).
14. M. B. Nevgi. J. Univ. Bombay, **7**, pt. 3, 82 (1938).
15. P. Pascal. Compt. Rend. **173**, 144, 712 (1921).
16. D. Voigt. Ann. Chim. **4**, 393 (1949).
17. W. R. Angus and W. H. Hill. Trans. Faraday Soc. **39**, 185 (1943). W. R. Angus, G. I. W. Llewelyn, and G. Stott. Trans. Faraday Soc. **55**, 887 (1959).
18. C. Barter, R. G. Meisenheimer, and D. P. Stevenson. J. Phys. Chem. **64**, 1312 (1960).
19. J. Broersma. J. Chem. Phys. **17**, 873 (1949).
20. P. Pascal. Compt. Rend. **233**, 1078 (1951).
21. W. R. Angus, G. I. W. Llewelyn, and G. Stott. Trans. Faraday Soc. **51**, 241 (1955).
22. J. Farquharson and S. Sastri. Trans. Faraday Soc. **33**, 1472 (1937).
23. M. W. Lister and L. E. Sutton. Trans. Faraday Soc. **35**, 495 (1939).
24. P. W. Allen and L. E. Sutton. Acta Cryst. **3**, 46 (1950).
25. P. A. Giguere and D. Chin. Can. J. Chem. **39**, 1214 (1961).
26. J. V. Bell, J. Heisler, H. Tannenbaum, and J. Goldenson. J. Am. Chem. Soc. **76**, 5185 (1954).
27. E. A. Robinson. Can. J. Chem. **41**, 3021 (1963).
28. (*a*) Q. Williams, J. Sheridan, and W. Gordy. J. Chem. Phys. **20**, 164 (1952).
    (*b*) G. R. Badgley and R. L. Livingston. J. Am. Chem. Soc. **76**, 261 (1954).
29. J. H. Secrist and L. O. Brockway. J. Am. Chem. Soc. **66**, 1941 (1944).
30. A. F. Wells. Structural inorganic chemistry. 3rd ed. Oxford University Press. 1962. p. 57.

Can. J. Chem. Downloaded from www.nrcresearchpress.com by 210.87.254.105 on 09/05/12
For personal use only.

A MODEL FOR THE HYDROGEN BOND AND PROTON TRANSFER REACTIONS

R. F. W. BADER*

Burke Chemical Laboratories, Department of Chemistry, McMaster University, Hamilton, Ontario

Received March 3, 1964

ABSTRACT

A simple extension of Platt's model for determining the force constants in diatomic hydrides is used to investigate the properties of transition states for proton transfer reactions. The model is first tested by comparing the predicted and observed changes in bond lengths and stretching and bending frequencies for O—H···O systems. The quantities predicted for the transition state are the geometry and the perpendicular bending frequencies. The implications of the results with regard to the interpretation of hydrogen–deuterium kinetic isotope effects are discussed. In particular, the variations in both the isotope effect and the geometry of the transition state with changing acid or base strength are considered in detail.

I. INTRODUCTION

In 1950 Platt (1) proposed a simple but successful method for determining the force constants of diatomic hydrides. It is the purpose of the present work to show that a simple extension of Platt's theory provides useful insights into the nature of the hydrogen bond and into the properties of transition states for the transfer of a proton. Platt's method is essentially an application of the Hellmann–Feynman theorem with simplifying assumptions regarding the form and rigidity of the electron density distribution. In the molecule HX the proton is assumed to be imbedded in a spherical electron density distribution of the united atom with nuclear charge $Z_X + 1$ (or in the density of the corresponding ion, X^-). The equilibrium bond length is therefore equal to the radius of a sphere which contains Z_X electrons, for at this position the force on the proton is zero. In addition, if the assumption of the rigidity of the united atom (or negative ion) charge distribution is postulated to hold when the proton undergoes small displacements from its equilibrium position, then by Poisson's equation the force constant is given by

$$k = 4\pi\rho(\mathrm{H})$$

where $\rho(\mathrm{H})$ is the total electron density at the position of the proton. Longuet-Higgins and Brown (2) have successfully applied the same method to binary hydrides. An explanation for the success of the method in the face of the severe assumption regarding the rigidity of the charge density during a vibration has recently been given by Salem (3) (along with an excellent account of the theoretical interpretation of force constants from a number of approaches). Salem's discussion of the method will be referred to during the development of the model for the hydrogen bond.

II. THE MODEL

The proton is considered initially to be imbedded in the charge density of the ion A^- to give the acid species A—H. This initial condition of electrostatic equilibrium is perturbed by the approach of a base molecule B with its accompanying charge density. The final hydrogen-bonded species is A—H···B, which will be characterized by the new equilibrium distances r_a, r_b (and $R = r_a + r_b$) as shown in Fig. 1.

**Alfred P. Sloan Research Fellow.*

Can. J. Chem. Downloaded from www.nrcresearchpress.com by 210.87.254.5 on 09/05/12
For personal use only.

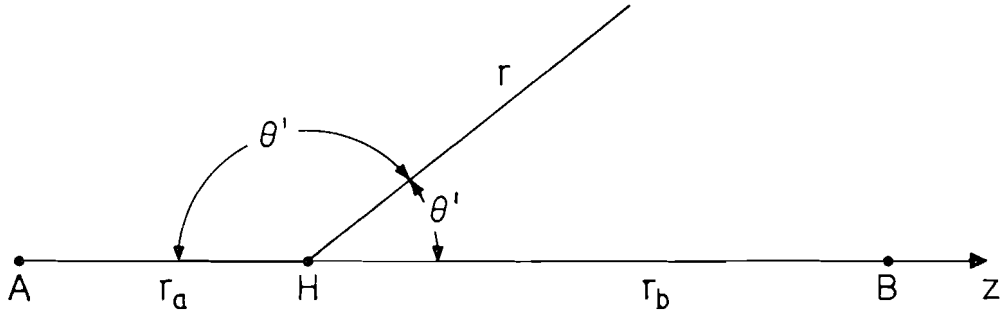

FIG. 1. The coordinate system. The A—B distance is denoted by R in the text.

The atoms A and B may be bonded to atoms other than the proton and the theory will also cover those cases in which the charge densities on A and B are not spherically symmetric.

The potential V of the proton is such that the force exerted on the proton in the z-direction is given by

$$[1] \qquad F_z = -\frac{\partial V}{\partial z_H} = \frac{Z_A}{r_a^2} - \int \frac{\cos\theta'}{r^2}\rho_A d\tau - \frac{Z_B}{r_b^2} + \int \frac{\cos\theta}{r^2}\rho_B d\tau$$
$$= F_{zA} + F_{zB}$$

where ρ_A and ρ_B are the charge densities centered on the acid and base species A and B. Equation [1] assumes that the total charge density is simply

$$\rho = \rho_A + \rho_B.$$

The total charge density correct to the second order in S, the overlap integral for orbitals on A and B is (4)

$$\rho = \rho_A + \rho_B - 2\sum_{i,j}\{2S_{ij}\phi_{iA}\phi_{jB} - S_{ij}^2(\phi_{iA}^2 + \phi_{jB}^2)\}$$

where ϕ_{iA} and ϕ_{jB} are atomic orbitals centered on A and B respectively. The overlap integral for values of R of interest here is 0.02 or less and thus the error in ρ at the position of the proton is less than 0.2%. In addition, applying Mulliken's approximation to the cross term reduces it to

$$S_{ij}\phi_{iA}\phi_{jB} \sim \tfrac{1}{2}S_{ij}^2(\phi_{iA}^2 + \phi_{jB}^2).$$

Thus the bracketed terms in ρ will make no contributions to the electric field and field gradient integrals *evaluated at the proton* when Mulliken's approximation is employed.* The small difference that actually exists between the contribution of $\phi_{iA}\phi_{jB}$ and $(\phi_{iA}^2 + \phi_{jB}^2)$ to these integrals will be multiplied by approximately S_{ij}^2, a very small number.

For a spherical charge distribution

$$\int \frac{\cos\theta}{r^2}\rho_A d\tau = \frac{Q_A}{r_a^2}$$

where Q_A is the total electronic charge contained in a sphere of radius r_a. Thus in this case

**The electric field and field gradient integrals together with the value of ρ at the proton are the only quantities required in the subsequent analysis.*

Can. J. Chem. Downloaded from www.nrcresearchpress.com by 210.87.254.5 on 09/05/12
For personal use only.

the force F_z reduces to

$$[2] \qquad F_z = \frac{1}{r_a^2}(Z_A - Q_A) - \frac{1}{r_b^2}(Z_B - Q_B).$$

Initially, for the isolated acid molecule A—H, $Z_A = Q_A$ (or the two corresponding terms in equation [1] are equal) and there is no net force on the proton. However, when r_b is finite, the density on the base exerts a resultant positive force on the proton. The original value of r_a must increase to the hydrogen-bonded value until the forces exerted on the proton by A and B are again balanced. Thus the formation of a stable hydrogen bond should always result in a lengthening of r_a over the free acid value, as is indeed observed.

A second differentiation of V with respect to z_H will yield the force constant for the linear displacement of the proton. This can be identified with the force constant for the asymmetric motion of the three-atom system A—H$\cdots$B with A and B held fixed. Consider the case of the spherical distributions first and assume further that the charge densities are rigid.

$$[3] \qquad k_\parallel = \frac{\partial^2 V}{\partial z_H^2} = \frac{2}{r_a^3}(Z_A - Q_A) + \frac{2}{r_b^3}(Z_B - Q_B) + 4\pi(\rho_A(H) + \rho_B(H))$$

where $\rho_A(H)$ and $\rho_B(H)$ are the electron densities at the position of the proton due to A and B. (The $4\pi\rho(H)$ terms are a necessary consequence of Poisson's equation. See equation [4] below.)

Initially, for the free acid A—H, $Z_A = Q_A$ at equilibrium and $k_\parallel = 4\pi\rho_A(H)$. In the presence of the base, as explained above, $Q > Z$ for both acid and base at the hydrogen-bonded equilibrium position for the proton. Thus the final perturbed value for $k_\parallel$ is given by the difference between the positive quantity $4\pi(\rho_A(H) + \rho_B(H))$ and the negative field gradients (the first two terms on the R.H.S. of equation [3]). For values of R encountered in hydrogen bonding the overall value of $4\pi(\rho_A(H) + \rho_B(H))$ is less than the initial value of $4\pi\rho_A(H)$ since the increase in r_a on hydrogen bonding leads to a decrease in $\rho_A(H)$ and $\rho_B(H)$ is not large enough to counteract it.* Furthermore, the creation of the negative field gradients at the proton also leads to an overall decrease in $k_\parallel$. The model therefore predicts a decrease in the A—H stretching frequency $\nu_\parallel$ on hydrogen bond formation. This is in fact one of the most striking characteristics of hydrogen bond formation. From Poisson's equation we have

$$\frac{\partial^2 V}{\partial z^2} + \frac{\partial^2 V}{\partial y^2} + \frac{\partial^2 V}{\partial x^2} = 4\pi\rho(H)$$

or

$$[4] \qquad k_\parallel + 2k_\perp = 4\pi(\rho_A(H) + \rho_B(H))$$

where $k_\perp$ is the force constant for the displacement of the proton perpendicular to the bond. For spherical (or axially symmetric) distributions on A and B the two perpendicular frequencies will form a degenerate pair with identical force constants. For the above case $2k_\perp$ is in fact just the negative of the parallel field gradient at the proton.

$$2k_\perp = -\frac{2}{r_a^3}(Z_A - Q_A) - \frac{2}{r_b^3}(Z_B - Q_B)$$

**The electron density falls off exponentially from both centers. Thus, $|d\rho_A/dr_A| > |d\rho_B/dr_B|$ since $r_A < r_B$ and the final value of $\rho(H)$ will therefore, be less than $\rho_A(H)$ initial.*

Can. J. Chem. Downloaded from www.nrcresearchpress.com by 210.87.254.5 on 09/05/12
For personal use only.

Initially, for $Z_A = Q_A$, $k_\perp$ will be zero, but the hydrogen bond formation leads to negative values for the parallel field gradient at the proton and thus to positive values for the perpendicular frequencies. The magnitude of these frequencies will increase as the field gradient becomes more negative and this in turn occurs with increasingly stronger hydrogen bonds. Thus the model predicts the appearance of (or increase in, if A—H was initially polyatomic) the perpendicular bending frequencies and the increase in these frequencies at the direct expense of the parallel frequency (see equation [4]) as the strength of the hydrogen bond increases. This is again in direct accord with observation.

For non-spherical charge distributions, differentiation of equation [1] without assuming the charge clouds to be rigid gives

$$k_\parallel = \frac{2Z_A}{r_a^3} + \frac{2Z_B}{r_b^3} - \int\left(\frac{3\cos^2\theta - 1}{r^3}\right)(\rho_A + \rho_B)\,d\tau + 4/3\pi(\rho_A(H) + \rho_B(H)) - \int\left(\frac{\cos\theta}{r^2}\right)\left(\frac{\partial}{\partial z_H}[\rho_A + \rho_B]\right)d\tau \quad [5]$$

as first shown by Salem (3) for the case of a diatomic molecule. For the correct density distribution ρ, this is an exact equation and follows directly from the Hellmann–Feynman theorem (3). Salem has pointed out that the success of Platt's model is in the fortuitous cancellation of the last term in [5], which arises from the change in the density due to the motion of the proton, with the amount by which the total electron density at the proton is underestimated in the united atom (or negative ion) model. That is, $4\pi\rho(H)$ is underestimated in Platt's model and the last term in [5] is discarded. The result is close to the truth due to the approximate cancellation of these two effects for motions of a hydrogen atom. Thus equation [5] reduces to

$$k_\parallel = \frac{2Z_A}{r_a^3} + \frac{2Z_B}{r_b^3} - \int\left(\frac{3\cos^2\theta - 1}{r^3}\right)(\rho_A + \rho_B)d\tau + 4/3\pi(\rho_A(H) + \rho_B(H)) \quad [6]$$

which in turn reduces to [3] when ρ_A and ρ_B are spherical charge distributions. The discussion of equation [6] for ρ_A and ρ_B of arbitrary symmetry parallels that of equation [3]. Equation [4], of course, holds true for non-symmetrical charge distributions as well.

It can be seen that this simple model embodies all of the important changes which occur on hydrogen bond formation. The close proximity of the base creates an imbalance in the forces operating on the proton with the net result that the original bond length r_a must *increase* to the hydrogen-bonded value. Accompanying this is a decrease in the local electron density in the vicinity of the proton and thus a *decrease* in the frequency of the original A—H stretching mode, one of the most characteristic features of hydrogen bond formation. In addition the parallel field gradient at the proton becomes more negative, leading to an increase in the perpendicular frequencies of vibration, another characteristic feature of hydrogen bond formation.

An even closer approach of the base from its position in the hydrogen-bonded system can result in the transfer of the proton. Thus the same model may be employed for an investigation into the properties of transition states for the transfer of a proton. The model for the transition state is thus a perturbed hydrogen bond, with the special requirement that the force constant $k_\parallel$ go to zero.

We wish to determine, with the aid of this model, what effects changes in the electron densities of the acid and base species have on the properties of a transition state. For this

Can. J. Chem. Downloaded from www.nrcresearchpress.com by 210.87.254.5 on 09/05/12
For personal use only.

reason we retain the electron density ρ as the one flexible parameter. There are more detailed treatments of the hydrogen bond itself, for example, that of Reid (5), but this is accomplished at the expense of employing empirical potential functions with adjustable parameters which can be related to the electronic situation only in terms of "ionic" and "covalent" character. The present model is an attempt to obtain direct relationships between assumed electron densities and the properties of the hydrogen bond and proton transition states.

We shall proceed by first testing the ability of the model to predict the changes in r_a, $\nu_\parallel$, and $\nu_\perp$ brought about by hydrogen bond formation. Since there is a great deal of experimental data regarding O—H···O bonds we consider such a system. Using the same models for the A and B species developed for the hydrogen-bonded systems we then predict values of r_a, $\nu_\perp$, *and* R for transition states involving the transfer of a proton between two oxygen atoms.

III. APPLICATION TO HYDROGEN-BONDED SYSTEMS

Pimentel and Sederholm (6) have shown that an approximate linear relation holds between $\Delta\nu_\parallel$, the shift in the A—H stretching frequency, and R the overall length of the hydrogen bond for O—H····O bonds in crystals. In a crystalline hydrate, the crystal structure is primarily determined by the large forces operative between the ions and the relative sizes of the ions. The net result of these primary effects is the placing of an O—H bond at some distance from an adjacent $\diagup\!\!\diagdown$O atom and thus hydrogen bonds are formed at a number of different R values for different crystals. This situation provides a good opportunity to test the theory, as a single acid and a single base model may be chosen and the calculation carried out at a number of different values of R.

The electron density distribution for the acid species is that of O^- and this is taken to be spherically symmetrical. The fact that the ion is one electron short of a truly spherical density distribution does not change the calculated values by any large amount. The effective nuclear charge for $2s$ and $2p$ orbitals of an O^- ion by Slater's rules is 2.10. This gives a value of $\nu_\parallel = 3840$ cm^{-1} for the free A—H species at the equilibrium bond length for water. The observed value of ν_3 for a free water molecule is 3760 cm^{-1}. It is not necessary to consider the two inner shell electrons in these calculations as

$$\int \frac{\cos\theta}{r^2}\rho(1s_A{}^2)\,d\tau \text{ and } \int\left(\frac{3\cos^2\theta - 1}{r^3}\right)\rho(1s_A{}^2)\,d\tau$$

both reduce simply to $2(1/r_a{}^2)$ and $2(2/r_a{}^3)$ respectively. Thus the inner shell electrons effectively screen two units of the nuclear charge. This follows because the $1s$ electrons are so tightly bound to the nucleus that their entire charge density lies well within the sphere defined by r_a or r_b.* The model for the base must be more sophisticated as a neutral base species with a spherical charge density will not exert an attractive force on a positive charge at any distance. Instead, a density distribution corresponding to some valence state of an oxygen atom is employed. When engaged in hydrogen bonding, the most effective valence state density distribution for an oxygen atom is that corresponding to sp^3 hybridization with two orbitals (the lone pairs) fully occupied and two orbitals (the bonds to the hydrogens) singly occupied. In addition, further polarization of the total

**There is no need to make the 2s orbital orthogonal to the 1s orbital. The required integrals for the force and field gradient change only in the third place due to this nonorthogonality. This again is due to the fact that the 1s electron density is vanishingly small at the proton.*

Can. J. Chem. Downloaded from www.nrcresearchpress.com by 210.87.254.5 on 09/05/12
For personal use only.

charge density may occur through the unequal sharing of the density in the bonding orbitals. This can be taken into account in this simple valence state model by assigning occupation numbers greater than unity to the two bonding orbitals. The final electron density expression for the oxygen atom then becomes

$$\rho_B = \left(1 + \frac{1}{2}n\right)s^2 + \left(5/3 + \frac{1}{6}n\right)p_\sigma{}^2 + 4/3(1 + n)p_\pi{}^2 + \frac{1}{\sqrt{3}}(2 - n)sp_\sigma$$

where the p_σ orbital is directed at the proton and n may vary from 1 to 2. The effective nuclear charge for the neutral oxygen atom by Slater's rules is 2.275. For the case $n = 2$, corresponding to the species $O^=$, ρ_B reduces to a spherical charge distribution with eight electrons. The transfer of charge to the oxygen atom for any value of n is simply $2(n - 1)$. The value of n must be greater than unity to balance the forces exerted on the proton by the A species for the values of R encountered in hydrogen bonding. This is physically reasonable. For a given value of R, r_a and r_b are varied until the force on the proton is zero. The results of the calculations for a range of R values are shown in Fig. 2. All

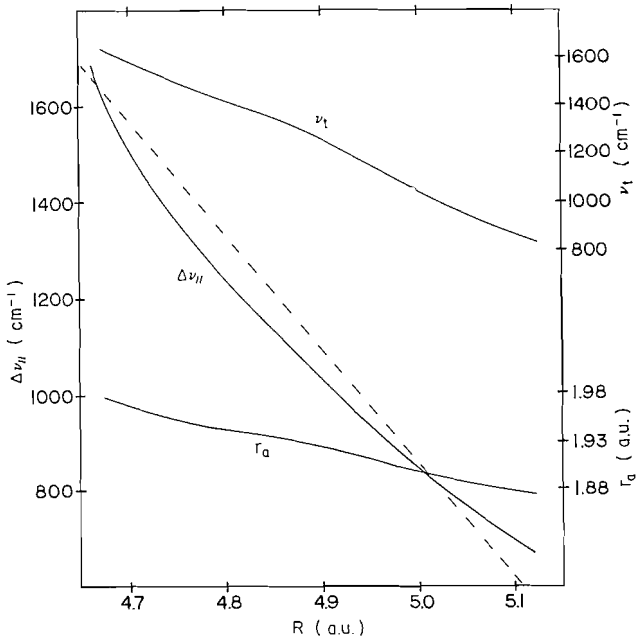

FIG. 2. The calculated values of $\Delta\nu_{\parallel}$, ν_t, and r_a for a hydrogen bonded O—H····O system. The dotted curve is the "experimental" curve of ref. 6. For ice, $\nu_t \sim 850$ cm^{-1} ($R = 5.22$ a.u.) and for carboxylic acids, $\nu_t \sim 950$ cm^{-1} ($R = 5.16$ a.u.).

three graphs were obtained by using just one point on the $\Delta\nu_{\parallel}$ vs. R plot to fix the value of n at 1.27. The predictions of $\Delta\nu_{\parallel}$ are in good agreement with experiment. The calculated curve always lies within ± 100 cm^{-1} of the straight line relation, which is the actual spread of the experimental results. The curve of r_a versus R lies within the observed limits of the "average" experimental curve (7). The present model does not distinguish between the two perpendicular force constants. The sum of these two constants is simply $4\pi\rho(H) - k_{\parallel}$. In hydrogen-bonded systems where A—H is polyatomic the two values of $\nu_{\perp}$ are not necessarily the same. Originally A—H has an in-plane bending mode ν_b and an

Can. J. Chem. Downloaded from www.nrcresearchpress.com by 210.87.254.5 on 09/05/12
For personal use only.

out-of-plane bending mode ν_t. On hydrogen bonding ν_b increases only slightly ($\sim$50 cm^{-1}) but ν_t may undergo remarkable increases and approach ν_b in value. The value of ν_b in hydrogen-bonded systems where water is the acid species is in the range of 1650 cm^{-1} or a k_b of 0.1030 a.u. (7). We can predict a value of ν_t by subtracting this value for k_b from $4\pi\rho(\mathrm{H}) - k_\parallel$, the remainder being k_t. Thus we are testing the prediction that the sum of the force constants for ν_b and ν_t should add up to $4\pi\rho(\mathrm{H}) - k_\parallel$. There is a scarcity of data for ν_t but two experimental observations at values of R just outside the range of Fig. 2 are given in the figure caption. They are for the cubic ice structure and hydrogen-bonded carboxylic acids (7). The values of ν_t (or the total $4\pi\rho(\mathrm{H}) - k_\parallel$) are thus quite reasonable at large values of R. The predicted values of ν_t for shorter R values are seen to approach ν_b. Thus as the hydrogen bond is shortened the model predicts that ν_b and ν_t approach one another in value. In fact as R is further decreased, $k_\parallel$ should become quite small corresponding to a relatively flat-bottomed potential well (as previously suggested by Reid (5)) and the $\nu_\perp$ modes could conceivably surpass $\nu_\parallel$ in value. The same model could be applied to the case where the proton has been transferred and r_a is then greater than r_b, i.e., the system has shifted to the second minimum of a double-well potential.

While the model does not purport to yield the exact values of the electron density at the proton (it is purposely underestimated), it does lead to the conclusion that this density should decrease on hydrogen bond formation. This prediction is in accord with the observation that the proton resonance signal of the hydrogen in the hydrogen bond is shifted to lower magnetic fields relative to its position in the unassociated molecule (8). While, as Pople (9) has pointed out, this decrease in magnetic shielding constant does not necessarily imply a decrease in the electron density at the proton, the present model could account for the observations.

IV. APPLICATION TO TRANSITION STATES OF PROTON TRANSFER REACTIONS

We assume that the potential energy surface in the immediate vicinity of the transition state has zero curvature, i.e., that $k_\parallel$ must equal zero (10, 11). Since F_H and $k_\parallel$ must both be zero at the transition state, equations [1] and [6] will allow one to predict values of both r_a and R. In general, for given density distributions ρ_A and ρ_B there will be only one value of r_a and one value of R which will cause equations [1] and [6] to equal zero simultaneously. For a transition state molecule, equation [4] reduces to

$$[7] \qquad 2k_\perp = 4\pi\rho(\mathrm{H}).$$

This equation, which relates the total electron density at the proton to the restoring force constants for its perpendicular motions, is of great importance in the discussion of isotope effects.

The variation of the force on the proton with r for a given density distribution on either the acid or the base species is shown in Fig. 3. The force initially increases from zero with increasing r because more negative charge is contained in the region between the proton and the nucleus of A or B. Eventually, however, the increase in r becomes overriding and the force decreases. The value of r at which the force is a maximum decreases, and the force itself increases as the total amount of charge is increased, as polarization of the charge density is increased, or as the effective nuclear charge for the orbitals is increased. A discussion of the forces exerted by the electron density distributions obtained from s, p_σ, p_π, and d orbitals may be found in ref. 12. Briefly, these forces decrease in the order $p_\sigma > s > p_\pi$. Thus in Fig. 2 the lower force curve represents a density distribution which may contain a smaller amount of absolute charge or is less polarized than the density

Can. J. Chem. Downloaded from www.nrcresearchpress.com by 210.87.254.5 on 09/05/12
For personal use only.

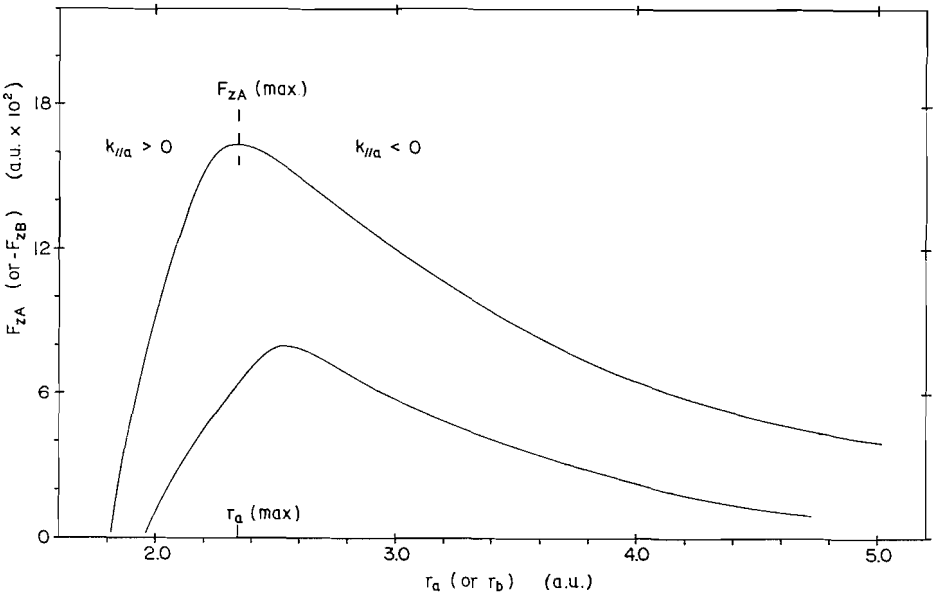

FIG. 3. The variation of F_{zA} or F_{zB} with r_a or r_b. r_a (max.) is the value of r_a at which F_{zA} is a maximum.

given by the upper curve. When we refer to the relative strengths of the acid and base we do so with reference to the respective force curves generated by ρ_A and ρ_B. The species which exerts the greater force on the proton for any value of r will be the stronger of the two, both considered as bases, or the weaker of the two, both considered as acids. We thus have a definite relation between acid or base strength and the electron density distribution.

The terms in equations [3] or [6] for $k_\parallel$ may be regrouped to yield

$$k_\parallel = k_{\parallel a} + k_{\parallel b}$$

where

$$k_{\parallel a} = \frac{2Z_A}{r_a^3} + (4/3)\pi\rho_A(H) - \int\left(\frac{3\cos^2\theta - 1}{r^3}\right)\rho_A d\tau$$

and a corresponding equation for $k_{\parallel b}$. If $k_\parallel$ is to equal zero, either $k_{\parallel a} = -k_{\parallel b}$ or $k_{\parallel a} = k_{\parallel b} = 0$. Since $k_{\parallel a}$ is the gradient of the force F_{zA}, $k_{\parallel a}$ will equal zero only when F_{zA} is a maximum. The same is true for $k_{\parallel b}$. For values of $F_{zA} < F_{zA}$ (max.), $k_{\parallel a}$ is positive, and for values of $F_{zA} > F_{zA}$ (max.), $k_{\parallel a}$ is negative, as illustrated in Fig. 3. Therefore, when ρ_A and ρ_B are identical the transition state will be symmetrical and will occur at a value of $r_a = r_b = r$(max.). Consider next the case where $\rho_A > \rho_B$, i.e., considering both A and B as bases, A is the stronger of the two. Since either $k_{\parallel a}$ or $k_{\parallel b}$ must now be negative in order that their sum equal zero, either $r_a > r_a$(max.) or $r_b > r_b$(max.). In this case both F_z and $k_\parallel$ can be made equal to zero only when $r_a > r_a$(max.) and $r_b < r_b$(max.). Only by having $r_a > r_a$(max.) can $|k_{\parallel a}|$ be reduced to equal $k_{\parallel b}$ with the forces equal and opposite at the same time. In the region $r_a < r_a$(max.) the slope of the F_{zA} curve is too great for values of $F_{zA} = -F_{zB}$. Thus if the density of the acid is held fixed, the original A—H bond must be progressively more broken in the transition state as the strength of the attacking base is decreased. By the same arguments, when $\rho_B > \rho_A$, i.e., the attacking base is a stronger base than is the A^- species, the transition state will occur when

Can. J. Chem. Downloaded from www.nrcresearchpress.com by 210.87.254.5 on 09/05/12
For personal use only.

$r_b > r_b(\text{max.})$ and $r_a < r_a(\text{max.})$. Chemists speak of bonds being more or less than "half broken" in the transition state. We can give a quantitative interpretation to this statement which conveys the same intuitive feeling in terms of $r(\text{max.})$. The distance $r(\text{max.})$ determines the point at which the contribution of either the acid or base to the total force constant changes sign. For $r < r(\text{max.})$ a further increase in r results in an increased force tending to pull the proton back. For $r > r(\text{max.})$ a further increase in r leads to a further decrease in the force tending to bind the proton. Thus when the attacking base is the stronger of the two, the transition state occurs when the original A—H bond is less than "half broken" and the proton is still bound by a positive restoring force constant to the A^- species. When the attacking base is the weaker of the two, then the original A—H bond is more than "half broken" and the new bond is more than "half formed"; i.e., the proton is now bound by a positive restoring force constant to the base rather than to the acid. The other possibility, that of considering a constant density on the base and varying the strength of the A—H species is obtained by simply considering the reverse of the above reactions, i.e.,

$$BH + A^- \rightarrow B^- + A\text{—}H$$

as the transition state species will be identical.

Numerical examples for various acids and bases are given in Tables I and II. The data

TABLE I*

Transition state data for O—H + $O^{\delta-}$

δ	r_a	r_b	R	$4\pi\rho_A(H)$	$4\pi\rho_B(H)$	$\nu_\perp$
1.0	2.32	2.32	4.64	0.1206	0.1206	1790
0.9	2.80	2.21	5.01	0.0233	0.1710	1600
0.8	3.10	2.25	5.35	0.0081	0.1468	1440

*All bond lengths are given in a.u. (1 a.u. = 0.52917 Å) and $\nu_\perp$ is in cm^{-1}. The sum of the van der Waals' radii of two oxygen atoms is 5.29 a.u. and the average O—H bond length is 1.82 a.u.

TABLE II

Transition state data for O—H + $O^{\delta-}$ (polarized)

δ	r_a	r_b	R	$4\pi\rho_A(H)$	$4\pi\rho_B(H)$	$\nu_\perp$
1.0	2.16	2.79	4.95	0.2068	0.0277	1762
0.54	2.22	2.24	4.46	0.1680	0.1217	1960
0.50	2.57	2.05	4.62	0.0515	0.2438	1980
0.44	2.80	2.05	4.85	0.0233	0.2438	1870
0.36	3.00	2.07	5.05	0.0116	0.2260	1780

in Table I are for the simplest type of model, a spherical charge density on both the acid and base species. The model for the acid is that used in the hydrogen bond calculations and the same density is employed for the base with a varying amount of negative charge. When $\delta = 1$, $\rho_A \equiv \rho_B$ and the transition state is the symmetrical one with $r = r(\text{max.})$. The original bond is half broken and the new bond is half formed. As the base strength is decreased r_a increases, r_b is decreased, and R increases. Thus the weaker the base in a series such as this, the "looser" the transition state becomes. This is also reflected in the decrease in $4\pi\rho(H)$ and decreasing values of $\nu_\perp$.

In Table II the acid model is retained but the base density is polarized. The first entry is for a model of the oxygen in the hydroxide ion where we have attempted to take into

Can. J. Chem. Downloaded from www.nrcresearchpress.com by 210.87.254.5 on 09/05/12
For personal use only.

account the fact that the electron density has some preferential p_σ character in the direction of the O—H···O bond. This makes this base stronger than the base with the spherical density even though the total charge is the same on each. The remaining entries are for the base model employed previously in the hydrogen bond calculations with varying amounts of charge. This base is also polarized, i.e., not spherically symmetrical. The model for the hydroxide ion gives a stronger base than the original base A^- species. This is a result of the enhanced force of the base due to the polarization of its charge density. A further decrease in δ results in a weaker attacking base, to values of $r_a > r_a(\text{max.})$ and to values of $r_b < r_b(\text{max.})$. The values of R at first decrease and then increase. The strongest base is able to balance the force and field gradient at large values of R. As the base is weakened R must decrease to achieve a balance and when $\rho_B \sim \rho_A$, R will be a minimum. Further decrease in the base strength necessitates a greater increase in r_a (past $r_a(\text{max.})$) to achieve a balance for both force and field gradient. The variation in the total density at the proton reflects the variation in R, being larger when R is small, and decreasing when R increases. Thus $\nu_\perp$ at first increases, and subsequently decreases. The strength of binding of the proton is proportional to the total electron density at the proton and the separate densities $4\pi\rho_A(H)$ and $4\pi\rho_B(H)$ are included in the tables to illustrate the relative strengths of binding of the acid and base species.

In all of the above examples we have assumed that the density distribution in the acid species remained fixed, regardless of the strength of the base (or vice versa for the reverse reaction). This would correspond roughly to the removal of a proton from an O—H bond which is not conjugated with the rest of the molecule. Because of this fact the proton in all of the transition states so far discussed is relatively tightly bonded (either to the acid or to the base species) as evidenced by the values of $\nu_\perp$ and $4\pi\rho(H)$. There are many chemical reactions in which more than "one bond" is changing at a time and the various changes are coupled together by a facile exchange of electron density from one reacting center to another. There are also many conjugated systems whose reactions show a strong dependence on the possibility of charge density being transferred to or from the reacting center. Thus it is of interest to consider models for transition states in which the density on A (or B) may be increased or decreased quite markedly from what it was initially. As pointed out above, if ρ_A is considered constant, the original A—H bond must be progressively lengthened to attain the transition state as the strength of the base is decreased. The accompanying increase in the energy of activation can be considered as due to the increasing amount of work necessary to stretch r_a to the required value. From this result one can argue that the energy of activation will be minimized if ρ_A (or ρ_B) can be adjusted, by means of electron withdrawal or release, so that ρ_A approaches ρ_B in value. This will result in transition states in which $r_a \sim r_b$. In Table III data are given for symmetrical transition states calculated for the spherical O^- model with varying values for δ.

We now find a wide variation in the binding of the proton in the transition state as

TABLE III

Data for symmetrical transition states with varying total charge

δ	r	R	$4\pi\rho(H)$	$\nu_\perp$
1.0	2.32	4.64	0.2411	1790
0.5	2.58	5.16	0.0925	1100
0.4	2.67	5.34	0.0668	940
0.3	2.78	5.56	0.0449	770

Can. J. Chem. Downloaded from www.nrcresearchpress.com by 210.87.254.5 on 09/05/12
For personal use only.

reflected in the decreasing values of $4\pi\rho(H)$ and $\nu_\perp$. Only in a symmetrical or close to symmetrical transition state can the forces and field gradients be balanced for a loosely bound proton at values of R which are not unreasonably large. Thus if ρ_A is fixed and much greater than ρ_B, the transition state occurs only when r_A has increased to such a large value that R is unreasonable (many times larger than twice the van der Waals' radii). In other words the energy of activation for the removal of a proton from a weak acid by a weak base is so large the reaction does not occur.

V. CONSEQUENCES IN THE INTERPRETATION OF H—D ISOTOPE EFFECTS

Most discussions of hydrogen–deuterium kinetic isotope effects are carried out in terms of a linear model for the transition state in which the bending frequencies are ignored. Examples are the papers of Westheimer (13) and Bigeleisen (14). Bell (15) has given a model for a proton transfer transition state in which a bare proton is placed between two negative charges. This would correspond to the present equation [3] with both ρ_A and ρ_B contracted to the A and B nuclei respectively giving $(Z_A - Q_A) = (Z_B - Q_B) = -1$ and $4\pi\rho(H) = 0$. Then from equation [4] one finds that $2k_\perp = -k_\parallel$. Considering the potential surface at the transition state to have a small negative curvature ($k_\parallel$ is negative) Bell's model necessarily leads to small values for $k_\perp$ and $\nu_\perp$. Bell then demonstrates that the contribution to the isotope effect from $\nu_\perp$ when small in value effectively cancels the contribution from the tunnelling effect. A bare proton is a very idealized model and is bound to underestimate the value of $\nu_\perp$ as ρ_A and ρ_B must always be of finite extent in space and thus $4\pi\rho(H) \neq 0$. Even the present model underestimates $4\pi\rho(H)$ as mentioned in Section II, but hopefully this underestimation is compensated by the neglect of the term which describes the change in density as the proton vibrates. That Bell's model must seriously underestimate $\nu_\perp$ is most easily seen when it is realized that it would predict negative force constants and thus imaginary frequencies for the bending motions in hydrogen-bonded systems for which $k_\parallel$ is positive. In actual fact, as noted in Section III, experimentally it is found that $\nu_b \sim 1600$ cm^{-1} and $\nu_t \sim 800$ cm^{-1}.

The "symmetric" stretching mode (i.e., the other linear motion of the three atom system A—H—B, which in the symmetrical case involves only motions of A and B), plays a dominant role in the above-mentioned discussions (13, 14, 15). The importance of this motion in determining the pre-exponential factor in isotope effect calculations is very well treated in all three expositions. This factor involves only the ratios of the hydrogen and deuterium frequencies, and thus is not dependent upon their absolute magnitudes. The present model cannot predict the second linear frequency (call it ν_s) as A and B are held rigid. It would be possible to add an empirical potential term to our potential expression dependent only upon R and thus obtain a more complete description of the three-atom system. This destroys the simplicity of the model and adds another adjustable parameter which detracts from the predictions that can be made with the present model. Furthermore, we wish to restrict our attention to the exponential term* and all experimental evidence points to the fact that ν_s is invariably small in value and thus relatively not as important as $\nu_\perp$ in determining the total difference in zero-point energies. In all cases where ν_s has been observed for hydrogen-bonded species involving oxygen it has appeared in the region of 250 cm^{-1} or less (7), while $\nu_\perp$ (i.e., ν_t and ν_b) is of the order of 800 cm^{-1} and often higher. Even in the $(HFH)^-$ ion, the shortest hydrogen bond known,

**Westheimer (13) has argued that the pre-exponential factor is always close to unity regardless of the symmetry of the transition state and thus the isotope effect is determined largely by zero-point energy differences as determined here.*

Can. J. Chem. Downloaded from www.nrcresearchpress.com by 210.87.254.5 on 09/05/12
For personal use only.

the value of ν_s is only 600 cm^{-1} as compared to a $\nu_\perp = 1200$ cm^{-1}. In addition, the contribution from $\nu_\perp$ must be doubled since it is degenerate.

Referring first to Tables I and II, it is evident that for all the unsymmetrical transition states $\nu_\perp$ and hence the isotopic shifts in $\nu_\perp$ are quite large in the transition state. The isotope effects for these reactions should thus be quite small or inverse, i.e., less than the "normal" effect of ~10. Westheimer's (13) approach also leads one to expect small isotope effects for unsymmetrical transition states but for a different reason. His argument is that ν_s in the unsymmetrical case will have a significant zero-point energy difference and it is this difference which makes the large contribution in the transition state. This is difficult to reconcile with all known values of ν_s, which would lead one to expect only small zero-point energy differences for this motion. The present model thus ascribes the small isotope effects associated with unsymmetrical transition states as due to the large values of $\nu_\perp$. As pointed out earlier when $r_A \gtrless r_B$ the proton is necessarily relatively tightly bound and hence $\nu_\perp$ must be appreciable in value.

Consider next the results of Table III and symmetrical transition states. Since $\nu_\perp$ can now vary from very large values (~2000 cm^{-1}) to very small values (~700 cm^{-1}), a whole range of isotope effects from very small or inverse to large are possible, *all for a symmetrical transition state.* This is at direct variance with the previous theories which predict only large isotope effects for symmetrical transition states as ν_s in these cases does not involve any motion of the hydrogen atom. Hence it does not contribute to the zero-point energy difference. The present model predicts that for a reaction in which charge density can be readily delocalized, it is possible for the proton to be "tightly or loosely" bonded (large or small values of ρ(H) and $\nu_\perp$) in a symmetrical transition state. There is no a priori reason for not believing this to be possible.

It is an accepted consequence of the previous theories that in a system in which the acid or base strength can be varied over a wide range, one would expect the accompanying isotope effects to pass through a maximum, corresponding to the symmetrical transition state. This has never been observed. As argued earlier, when the electron density is subject to a facile increase or decrease in the transition state, the geometry could always be close to the symmetrical case. A series of such symmetrical transition states will yield isotope effects which simply decrease as the base is made stronger and the proton is increasingly more tightly bound in the transition state. Results of this nature have been observed, an example being the decomposition of substituted β-keto acids (16). In this case as substituents were changed so as to increase the basicity of the keto oxygen, the isotope effect underwent a regular decrease. In this and other systems where this regular decrease in the isotope effect has been observed, a mechanism is available for the adjustment of the electron density on the A and B species such that a symmetrical transition state could result.

A different variation in isotope effect with base strength can be observed in a system with a more or less rigid electron density in the original A—H bond. Consider the results in Table II. The frequency $\nu_\perp$ at first increases and R decreases with increasing base strength. Thus there should be an initial decrease in the isotope effect. After the symmetrical case, which has close to the *minimum* isotope effect, decreasing the strength of the base leads to a further increase in the isotope effect as $\nu_\perp$ again decreases in value. Here then is a prediction in direct contradiction to the previous ones (13, 14). A variation in base strength in a system with an A—H bond which cannot readily delocalize a developing negative charge should yield a set of isotope effects which pass through a minimum, rather than a maximum.

Can. J. Chem. Downloaded from www.nrcresearchpress.com by 210.87.254.5 on 09/05/12
For personal use only.

The predictions of the present model are obtained by considering $\nu_\perp$ and ignoring ν_s, which in a sense is the other possible extreme to the previous models. We have, however, presented both experimental and theoretical results which would seem to indicate that $\nu_\perp$ can be an order or orders of magnitude larger than ν_s. The truth without a doubt involves consideration of both. It is hoped, however, that this model has at least indicated that $\nu_\perp$ can be of crucial importance to an understanding of isotope effects for proton transfer reactions. Other workers (11, 17) have discussed the importance of $\nu_\perp$ for hydrogen atom abstraction reactions. The present model is restricted to proton transfer reactions for only in this case are Platt's basic assumptions valid.

Analytical expressions for the force integrals have been previously reported (18). The method of Pitzer *et al.* (19) was used to derive expressions for the field gradient integrals. All the integrals were calculated on an IBM 650.

ACKNOWLEDGMENT

The author is grateful to Professor A. N. Bourns for helpful discussions concerning the application of the present results to the interpretation of kinetic isotope effects.

REFERENCES

1. J. R. PLATT. J. Chem. Phys. **18**, 932 (1950).
2. H. C. LONGUET-HIGGINS and D. A. BROWN. J. Inorg. Nucl. Chem. **1**, 60 (1955).
3. L. SALEM. J. Chem. Phys. **38**, 1227 (1963).
4. L. SALEM. Proc. Roy. Soc., Ser. A, **264**, 379 (1961).
5. C. REID. J. Chem. Phys. **30**, 182 (1959).
6. G. C. PIMENTEL and C. H. SEDERHOLM. J. Chem. Phys. **24**, 639 (1956).
7. G. C. PIMENTEL and A. L. MCCLELLAN. The hydrogen bond. W. H. Freeman and Co., San Francisco. 1960.
8. W. G. SCHNEIDER. Hydrogen bonding. *Edited by* D. Hadzi. Pergamon Press, London. 1959.
9. J. A. POPLE. Hydrogen bonding. *Edited by* D. Hadzi. Pergamon Press, London. 1959.
10. D. HERSCHBACH, H. S. JOHNSTON, K. S. PITZER, and R. E. POWELL. J. Chem. Phys. **25**, 736 (1956).
11. D. J. WILSON and H. S. JOHNSTON. J. Am. Chem. Soc. **79**, 29 (1957).
12. R. F. W. BADER and G. A. JONES. Can. J. Chem. **41**, 2251 (1963).
13. F. H. WESTHEIMER. Chem. Rev. **61**, 265 (1961).
14. J. BIGELEISEN. Papers presented at the I.A.E.A. Symposium, Vienna, Austria. 1963. Paper SM-50/24.
15. R. P. BELL. Trans. Faraday Soc. **57**, 961 (1961).
16. C. G. SWAIN, R. F. W. BADER, R. M. ESTEVE, JR., and R. N. GRIFFIN. J. Am. Chem. Soc. **83**, 1945 (1961).
17. K. S. PITZER. J. Am. Chem. Soc. **79**, 1804 (1957).
18. R. F. W. BADER. Can. J. Chem. **40**, 2140 (1962).
19. R. M. PITZER, C. W. KERN, and W. N. LIPSCOMB. J. Chem. Phys. **37**, 267 (1962).

Can. J. Chem. Downloaded from www.nrcresearchpress.com by 210.87.254.5 on 09/05/12
For personal use only.

Can. J. Chem. Downloaded from www.nrcresearchpress.com by 210.87.254.5 on 09/05/12
For personal use only.

EFFECT OF PRESSURE ON THE ACID-CATALYZED ENOLIZATION OF ACETONE AND ACETOPHENONE IN VARIOUS ETHANOL–WATER SOLVENTS. ORIGIN OF THE ENTHALPY–ENTROPY COMPENSATION EFFECT[1]

B. T. BALIGA[2] AND E. WHALLEY
Division of Applied Chemistry, National Research Council, Ottawa, Canada

Received March 17, 1964

ABSTRACT

The effect of pressure, temperature, and solvent composition on the rate of the acid-catalyzed enolization of acetone and acetophenone, and the solvent deuterium isotope effect for the enolization of acetophenone, have been measured by following the iodination. The solvent deuterium isotope effect (k^{D_2O}/k^{H_2O}) for the enolization of acetophenone in 16.2% w/w ethanol–water is $2.50\pm\sim0.05$, which undoubtedly proves that there is a pre-equilibrium proton transfer. The effect of solvent in the range water to 33.4% w/w ethanol in water on the rate of enolization of both acetone and acetophenone is small at atmospheric pressure, but is about four times larger at 3 kbar. This cannot be explained on simple electrostatic grounds, and indicates that any simple electrostatic explanation of the solvent effect at atmospheric pressure is invalid. The volumes of activation for the enolizations are strongly dependent on the solvent, that for acetone varying from $-2.1\pm\sim0.5$ to $-6.9\pm\sim0.7$ cm^3 mole^{-1} between solvents water and 33.4% w/w ethanol in water.

An examination has been made of the enthalpy–entropy compensation effect. It is shown that in general if the rate or equilibrium constant of a reaction does not change with changing conditions (such as solvent, substituents, etc.) then either the quantities of activation at constant pressure, $\Delta H_p^{\ddagger}$ and $\Delta S_p^{\ddagger}$, or the corresponding quantities at constant volume, $\Delta U_v^{\ddagger}$ and $\Delta S_v^{\ddagger}$, must vary in a compensating manner, and the existence of an energy–entropy compensation effect is inevitable. For the enolization of acetone and acetophenone in ethanol–water mixtures, $\Delta U_v^{\ddagger}$ and $\Delta S_v^{\ddagger}$ vary only slightly with solvent, whereas $\Delta H_p^{\ddagger}$ and $\Delta S_p^{\ddagger}$ vary in a compensating manner. The main causes of the compensation effect in the constant-pressure parameters are, in a sense, the change with changing solvent of the thermal expansion of the solvent and of the volume of activation of the reaction. On the other hand, both the constant-pressure and the constant-volume parameters vary with substituent from acetone to acetophenone, and the constant-volume parameters vary the more.

1. INTRODUCTION

The acid-catalyzed enolization of ketones is a well-studied reaction (1). It can be conveniently followed by the halogenation (2–5) and the deuterium exchange (6) of the ketones, and by their racemization (7) if they have an asymmetric α-carbon atom. The rates of all these processes are usually identical, and when followed by halogenation they are of zero order in halogen, the zero-order rate constant being itself of first order in both ketone and catalyst. The mechanism of enolization when catalyzed by strong acids is accepted on good grounds to be (see ref. 1 for discussions)

$$R{-}\overset{\displaystyle O}{\overset{\|}{C}}{-}CH_3 + H_3O^+ \underset{}{\overset{\text{fast}}{\rightleftharpoons}} R{-}\overset{\displaystyle \overset{+}{O}H}{\overset{|}{C}}{=}CH_2 + H_2O$$

$$R{-}\overset{\displaystyle \overset{+}{O}H}{\overset{|}{C}}{=}CH_2 + H_2O \xrightarrow{\text{slow}} R{-}\overset{\displaystyle OH}{\overset{|}{C}}{=}CH_2 + H_3O^+.$$

Halogenation then occurs by rapid addition to the enol. The incorporation of a molecule of water in the transition state is not kinetically proved. There is, however, little doubt

[1]*N.R.C. No. 7959.*
[2]*N.R.C. Postdoctoral Fellow 1962–64.*

that it occurs, on the grounds that analogy with the observed base catalysis (1) suggests that water is itself acting as a base. In addition, the entropy of activation, which is usually about -15 cal deg^{-1} mole^{-1} (8), strongly suggests (9–11) that a water molecule is incorporated into the transition state.

Few measurements have been made of the volumes of activation of proton abstraction reactions, and for purposes of comparison with other reactions the volume of activation of the acid-catalyzed enolization of acetone and acetophenone would be interesting. In addition, there are several other points of interest. In the first place, few systematic measurements have been made of the effect of solvent on volumes of activation, and the iodination of ketones is a suitable example of a particular class of reaction that would be worth studying. In the second place, the rate of the reaction is little affected by solvent. It is shown in Section 2 of this paper that for such a reaction, the enthalpy and entropy of activation at constant pressure, or the energy and entropy of activation at constant volume, or both, must vary with solvent so as to compensate one another in the free-energy (energy–enthalpy compensation effect). It is of interest to determine whether only one set of parameters has an appreciable compensation effect or whether both have.

We have therefore measured the effect of temperature and pressure on the rates of the acid-catalyzed iodination of acetone and acetophenone in several ethanol–water mixtures. There was no firm evidence that the iodination of acetophenone goes by a pre-equilibrium proton transfer. The solvent deuterium isotope effect on the rate has therefore been measured to verify it.

2. THE ENTHALPY–ENTROPY COMPENSATION EFFECT

It is frequently found that the enthalpy and entropy changes, ΔH and ΔS, of a reaction, either of its rate or its equilibrium, change with changing conditions in the same direction, so that the changes can be said to compensate one another partially in the free energy ΔG $(= \Delta H - T\Delta S)$. The changing conditions can be a change of solvent for a given reaction, a change of substituents in a series of compounds undergoing a similar reaction, and so on. This compensation has frequently been called the enthalpy–entropy compensation effect. The existence of this effect is frequently considered surprising. The purpose of the following discussion is to show that it is in fact inevitable for many reactions and other processes except in special circumstances.

We first emphasize that processes can be considered to occur at constant pressure or at constant volume (or of course with neither pressure nor volume constant, but these conditions are less interesting). The most useful free energy for constant-pressure processes is the Gibbs free energy, and we have, using the subscript p to indicate the constant-pressure condition

$$\Delta G_p = \Delta H_p - T\Delta S_p. \qquad [1]$$

The most useful free energy for constant-volume processes is the Helmholtz free energy A, and we have

$$\Delta A_v = \Delta U_v - T\Delta S_v \qquad [2]$$

where U is the intrinsic energy, and the subscript v indicates constant-volume conditions. If the rate or equilibrium constant of a reaction is a function of temperature and pressure and not of the extent of reaction then

$$\Delta G_p = \Delta A_v. \qquad [3]$$

Can. J. Chem. Downloaded from www.nrcresearchpress.com by 210.87.254.5 on 09/05/12
For personal use only.

This condition holds in dilute solution. Both the constant-pressure and the constant-volume parameters are equally fundamental thermodynamic parameters, and there is much to be said for the point of view that the constant-volume parameters are simpler than the constant-pressure parameters.

The relation between the quantities of activation at constant pressure and at constant volume can be derived by applying the operational equation

$$\left(\frac{\partial}{\partial T}\right)_v = \left(\frac{\partial}{\partial T}\right)_p + \frac{\alpha}{\kappa}\left(\frac{\partial}{\partial p}\right)_T, \qquad [4]$$

where α is the isopiestic thermal expansivity of the system and κ its isothermal compressibility. This equation can be applied to any quantity that is a function of the temperature and pressure only. It can be applied to ΔG_p $(= \Delta A_v)$ to give

$$\left(\frac{\partial \Delta A_v}{\partial T}\right)_v = \left(\frac{\partial \Delta G_p}{\partial T}\right)_p + \frac{\alpha}{\kappa}\left(\frac{\partial \Delta G_p}{\partial p}\right)_T, \qquad [5]$$

from which

$$T\Delta S_v = T\Delta S_p - T\alpha\Delta V/\kappa, \qquad [6]$$

and hence,

$$\Delta U_v = \Delta H_p - T\alpha\Delta V/\kappa. \qquad [7]$$

We consider first a reaction for which ΔG_p and ΔA_v do not change with the changing conditions. There is no energy–entropy compensation effect in the constant-volume parameters ΔU_v and ΔS_v if both are also independent of the changing conditions. There is then, however, an enthalpy–entropy compensation effect in ΔH_p and ΔS_p, unless the quantity $T\alpha\Delta V/\kappa$ does not vary with changing conditions. Conversely, if there is no enthalpy–entropy compensation effect in the constant-pressure parameters, there is one in the constant-volume parameters unless $T\alpha\Delta V/\kappa$ does not vary with changing conditions. If the changing conditions are changing solvent, α, ΔV, and κ will, in general, all vary and consequently $\alpha\Delta V/\kappa$ will, in general, vary. If the changing conditions are changing substituents in a homologous series, ΔV will, in general, vary. It follows therefore that if ΔG_p and ΔA_v do not vary or vary only slightly, then either the constant-pressure or the constant-volume parameters will usually tend to vary in a compensating manner because of the variation in $T\alpha\Delta V/\kappa$. There may of course be other factors that tend to make the activation parameters vary, and they may dominate the variation in $T\alpha\Delta V/\kappa$.

If ΔG_p or ΔA_v vary strongly there need not necessarily be an enthalpy–entropy or energy–entropy compensation effect unless the variation in $T\alpha\Delta V/\kappa$ is very strong and of the right sign.

In the rest of this section we shall discuss the inevitability of compensation for the particular case of varying temperature and varying pressure. If the changing conditions are merely changing temperature for the same reaction in the same solvent, the changes of the activation parameters necessarily compensate one another. For example

$$\left(\frac{\partial \Delta H_p}{\partial T}\right)_p = T\left(\frac{\partial \Delta S_p}{\partial T}\right)_p = \Delta C_p \qquad [8]$$

and

$$\left(\frac{\partial \Delta U_v}{\partial T}\right)_v = T\left(\frac{\partial \Delta S_v}{\partial T}\right)_v = \Delta C_v. \qquad [9]$$

Can. J. Chem. Downloaded from www.nrcresearchpress.com by 210.87.254.5 on 09/05/12
For personal use only.

Since ΔC_p and ΔC_v are related by the equation (21)

$$[10] \qquad \Delta C_p - \Delta C_v = \frac{T\alpha\Delta V}{\kappa}\left\{\left(\frac{\partial}{\partial T}\ln\frac{\alpha\Delta V^2}{\kappa^2}\right)_p + \frac{\alpha}{\kappa}\left(\frac{\partial}{\partial p}\ln\frac{\Delta V}{\kappa}\right)_T\right\},$$

then either ΔC_p or ΔC_v must differ from zero unless the quantity on the right-hand side of eq. 10 is zero. Consequently, either $\partial\Delta H_p/\partial T$ and $T\partial\Delta S_p/\partial T$, or $\partial\Delta U_v/\partial T$ and $T\partial\Delta S_v/\partial T$, or both, have the same sign, and so there is an energy–entropy compensation effect in at least one of the sets of activation parameters, except in the event that both ΔC_p and ΔC_v are zero.

The volume change of the reaction can be divided into an enthalpy and an entropy part as follows,

$$[11] \qquad \begin{aligned}\Delta V &= \partial\Delta G_p/\partial p,\\ &= (\partial\Delta H_p/\partial p) - T\,(\partial\Delta S_p/\partial p).\end{aligned}$$

Since for the processes we are considering

$$\Delta G_p = \Delta A_v,$$

we can also write

$$[12] \qquad \begin{aligned}\Delta V &= \partial\Delta A_v/\partial p,\\ &= (\partial\Delta U_v/\partial p) - T\,(\partial\Delta S_v/\partial p).\end{aligned}$$

The relation between $\partial\Delta U_v/\partial p$ and $\partial\Delta H_p/\partial T$ is from eq. 7

$$[13] \qquad \frac{\partial\Delta U_v}{\partial p} = \frac{\partial\Delta H_p}{\partial p} - T\frac{\partial}{\partial p}\left(\frac{\alpha\Delta V}{\kappa}\right),$$

and the relation between $\partial\Delta S_v/\partial p$ and $\partial\Delta S_p/\partial p$ is

$$[14] \qquad \frac{\partial\Delta S_v}{\partial p} = \frac{\partial\Delta S_p}{\partial p} - \frac{\partial}{\partial p}\left(\frac{\alpha\Delta V}{\kappa}\right).$$

It follows from these considerations that a zero value of ΔV will necessitate a compensation effect either in $\partial\Delta H_p/\partial p$ and $T\partial\Delta S_p/\partial p$, or in $\partial\Delta U_v/\partial p$ and $T\partial\Delta S_v/\partial p$, or of course in both, unless the quantity $\partial\,(\alpha\Delta V/\kappa)/\partial p$ is zero. There may, of course, be other factors that tend to induce compensation.

The existence of compensation in the variation of the Arrhenius energy and the pre-exponential factor with pressure was first observed experimentally many years ago (12).

3. EXPERIMENTAL

Materials

Mallinckrodt A.R. acetone and Fisher Certified Reagent acetophenone were used directly. Absolute ethanol was used in preparing ethanol–water solvents. D_2O (99.6%) was obtained from Atomic Energy of Canada, Ltd. Ethanol-d_1 was prepared in this laboratory according to the method of Burr (13); it was shown by infrared spectroscopy to be at least 95% deuterated in the hydroxyl group. All other chemicals were of reagent grade.

Kinetics at Atmospheric Pressure

Stock standard aqueous solutions of acetone (0.5 *M*), iodine (0.01 *M*), and perchloric acid (1 *M*) were prepared. A stock solution of acetophenone (0.5 *M*) was made in absolute ethanol. The reaction solution was made in a 100 ml volumetric flask by pipetting to 50 ml of water, standard solutions of perchloric acid (5 ml), ketone (10 ml), and iodine (10 ml). For experiments in water the solution was made up to 100 ml with water. For experiments in ethanol–water solvents, either 20 or 40 ml of ethanol was added before making up the volume to 100 ml with water to give respectively 16.2 and 33.4% w/w ethanol in water. After thorough mixing, the flask was immersed in a water thermostat whose temperature was controlled to ±0.005 °C and was measured by a platinum resistance thermometer. The temperature was maintained

Can. J. Chem. Downloaded from www.nrcresearchpress.com by 210.87.254.5 on 09/05/12
For personal use only.

at 25, 35, and 45 °C for acetone and at 30, 40, and 50 °C for acetophenone. At successive intervals, 10 ml of the reaction solution was removed and titrated with aqueous sodium thiosulphate (0.002 *N*) using starch as indicator. To ensure temperature equilibrium, at least 20 min was allowed before the first sample was removed. About six points were taken and the reaction was followed nearly to completion. Blank experiments without ketone established that iodine did not react with the medium. The absence of iodine at the end of the reaction showed that the reaction went to completion.

For experiments with acetophenone in solvent 16.2% w/w ethanol-d_1 in D_2O, the reaction solution was made in a 25-ml volumetric flask. The acetophenone and perchloric acid (~0.2 g 70.0% w/w $HClO_4$) were weighed directly into the flask, which contained 5 ml of ethanol-d_1, and the flask was nearly filled with D_2O. Three milliliters of a stock iodine solution (~0.008 *M*) in D_2O was added and the solution was made up to 25 ml with D_2O. The proportion of deuterium in this solvent was at least 99%. Five milliliters of the reacting solution was periodically titrated with thiosulphate (0.001 *N*). Four points were taken and the reaction was followed nearly to completion.

In the foregoing experiments, the initial concentration of acetone and the concentration of perchloric acid were about 0.05 *M* at 25 °C and 0.025 *M* at the higher temperatures. The initial concentration of acetophenone and the concentration of perchloric acid were about 0.05 *M* at 30 and 40 °C and 0.03 *M* at 50 °C. The initial concentration of iodine was ~0.001 *M* throughout.

Kinetics at High Pressures

The high-pressure technique was similar to that used previously (14) except for the following modification. Since iodine reacted appreciably with the sampling valve (E of Fig. 1 of ref. 14) a batch method was used to follow the reaction. The reaction vessel was a 2-oz polyethylene bottle provided with a tight-fitting leak-proof cap. The part of the pressure apparatus beyond the junction block F (see Fig. 1 of ref. 14) was eliminated.

The reaction solution was made as in the experiments at atmospheric pressure, a stopwatch being started (stopwatch reading *a*, which is zero) when the iodine solution was added. The polyethylene bottle was filled almost completely with the reaction solution immediately after the solution was mixed, and was placed inside the pressure vessel. The pressure vessel was filled with oil, assembled, immersed in the thermostat, and quickly brought up to pressure. When the desired pressure as read on the Bourdon gauge was reached, the time was noted on the stopwatch (stopwatch reading *b*). After one-half hour (stopwatch reading *c*), the pressure was released and the bottle was removed. The outside oil was wiped off and 10 ml of the solution were pipetted out and titrated (stopwatch reading *d*) with thiosulphate (0.002 *N*). This titer reading was taken as that for zero time. Other samples were put into the bottle and left for different times, i.e., the time interval between *b* and *c* was either 1, 1.5, or 2 h. Four points were taken for each run. The time intervals between *a* and *b* and between *c* and *d* were kept exactly the same for all four samples. In a typical experiment at a pressure of 3 kbar, the time interval between *a* and *b* was 8 min and that between *c* and *d* was 7 min. A blank experiment at 3 kbar without addition of the ketone showed that iodine did not react with the medium. The absence of iodine after a sufficient time at 3 kbar showed that the reaction went to completion. The initial concentration of ketone and the concentration of acid were about 0.05 *M* except for the runs at 3 kbar in 33.4% w/w ethanol in water, for which concentrations of about 0.025 *M* were used.

In all the kinetic experiments the initial concentrations of ketone and acid were kept nearly equal in order to suppress the effect of autocatalysis on the rate of iodination. Further, the molar ratios of ketone to iodine were high enough to exclude the possibility of any di-iodination.

4. RESULTS

All kinetic runs were accurately zero order in iodine, and the zero-order rate constants at atmospheric pressure were obtained by least-squares analysis using a digital computer. The reason for this was that the effect of solvent on the enthalpy and entropy of activation was required, and rate constants of maximum accuracy were required to determine this. The rate constants at higher pressures were obtained by the usual graphical method. The second-order rate constants k_a were obtained by dividing the zero-order constants by the product of the concentrations of ketone and perchloric acid. For kinetic runs in water, the rate constants were corrected for compression of the solution (15) which was assumed without significant error to be that of water. Similar corrections for compression could not be applied to rate constants in ethanol–water solvents since compression of these solutions has not been extensively measured. The rate constants in these solvents were therefore only corrected for the thermal expansion of the solvent at atmospheric pressure. The rate constants at atmospheric pressure are given in Table I, and those at higher pressures in Table II. Our mean value for $10^6 k_a$/l mole^{-1} s^{-1} for acetone (see

Can. J. Chem. Downloaded from www.nrcresearchpress.com by 210.87.254.5 on 09/05/12
For personal use only.

TABLE I

Rate constants for the acid-catalyzed enolization of acetone and acetophenone followed by iodination at atmospheric pressure

Ketone	Solvent	Temp. (°C)	$10^6 k_a$/l mole^{-1} s^{-1}*
Acetone	Water	25.00	28.2, 27.4, 27.5, 27.3
		35.00	84.0, 85.1, 85.7, 84.9
		45.00	243, 244, 242, 243
	16.2% w/w ethanol in water	25.00	31.1, 31.6, 31.4, 31.4
		35.00	94.8, 95.0, 93.5, 95.1
		45.00	266, 273, 262, 266
	33.4% w/w ethanol in water	25.00	33.9, 34.3, 34.4, 34.8
		35.00	100, 101, 103, 101
		45.00	276, 278, 282, 281
Acetophenone	16.2% w/w ethanol in water	30.00	21.5, 21.1, 21.3, 21.7
		40.00	66.6, 66.4, 66.8, 67.2
		50.00	198, 200, 198, 197
	33.4% w/w ethanol in water	30.00	23.7, 23.0, 23.1, 23.8
		40.00	71.4, 71.7, 71.2, 72.0
		50.00	211, 205, 209, 208
	16.2% w/w ethanol-d_1 in D_2O	30.00	54.0, 53.1

*The rate constants are corrected for thermal expansion of the solvent.

TABLE II

Rate constants for the acid-catalyzed enolization of acetone at 25.00 °C and of acetophenone at 30.00 °C followed by iodination at different pressures

Ketone	p/bar	Solvent	$10^6 k$/l mole^{-1} s^{-1}*
Acetone	500	Water	27.8
		16.2% w/w ethanol in water	35.2
		33.4% w/w ethanol in water	39.9
	1000	Water	30.7
		16.2% w/w ethanol in water	37.8
		33.4% w/w ethanoli n water	46.3
	2000	Water	32.9
		16.2% w/w ethanol in water	44.0
		33.4% w/w ethanol in water	58.3
	3000	Water	36.4
		16.2% w/w ethanol in water	51.5
		33.4% w/w ethanol in water	76.5
Acetophenone	500	16.2% w/w ethanol in water	23.8
		33.4% w/w ethanol in water	29.3, 29.1
	1000	16.2% w/w ethanol in water	28.2
		33.4% w/w ethanol in water	33.0
	2000	16.2% w/w ethanol in water	33.8
		33.4% w/w ethanol in water	41.7
	3000	16.2% w/w ethanol in water	36.3
		33.4% w/w ethanol in water	52.2

*k is k_a for solvent water, and $k_a\rho(p)/\rho$ (1 bar), where $\rho(p)$ and ρ(1 bar) are the densities of the solvent at pressure p and 1 bar respectively, for solvents ethanol–water.

Table I) at atmospheric pressure in water is 27.6, which is in good agreement with the literature values; a collection of these can be found elsewhere (16).

The main quantities to be derived from the rate constants that are of interest in this work are the effect of solvent on the enthalpies and entropies of activation at constant pressure, and on the volumes of activation. If k_1 and k_2 represent rate constants at the same temperature in two different solvents, and $\Delta H_p^{\ddagger}$ and $\Delta S_p^{\ddagger}$ represent the enthalpy and entropy of activation in the same solvents, then

[15] $$\ln k_2/k_1 = \Delta\Delta H_p^{\ddagger}/RT - \Delta\Delta S_p^{\ddagger}/R$$

Can. J. Chem. Downloaded from www.nrcresearchpress.com by 210.87.254.5 on 09/05/12
For personal use only.

where

[16] $$\Delta\Delta H_p^{\neq} = \Delta H_{p_1}^{\neq} - \Delta H_{p_2}^{\neq},$$

and

[17] $$\Delta\Delta S_p^{\neq} = \Delta S_{p_1}^{\neq} - \Delta S_{p_2}^{\neq}.$$

Plots of log k_2/k_1 against $1/T$ yield $\Delta\Delta H_p^{\neq}$ and $\Delta\Delta S_p^{\neq}$. These are shown in Fig. 1, and the

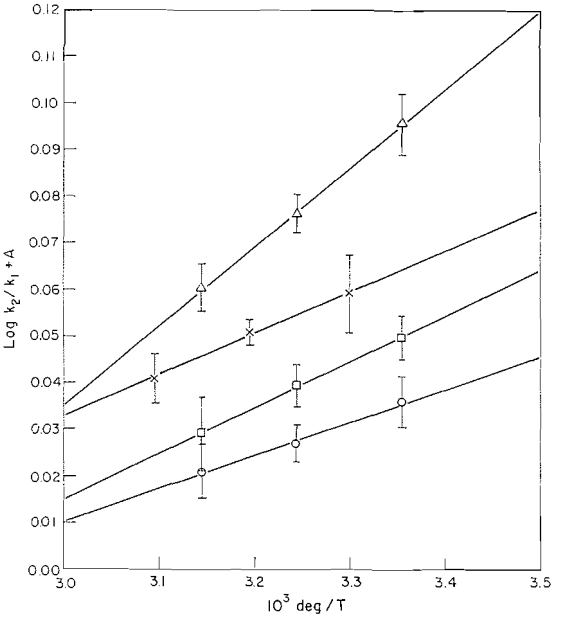

FIG. 1. $\text{Log}_{10}\, k_2/k_1$ against $1/T$ for the acid-catalyzed enolization (iodination) of acetone and acetophenone. Points △, □, and ○ refer to acetone, and × refers to acetophenone. △ ($A = 0$); 33.4% w/w ethanol in water : water. □ ($A = 0.01$), × ($A = 0.02$); 33.4% w/w ethanol in water : 16.2% w/w ethanol in water. ○ ($A = -0.02$); 16.2% w/w ethanol in water : water.

quantities $\Delta\Delta H_p^{\neq}$ and $\Delta\Delta S_p^{\neq}$ are listed in Table IV together with approximate estimates of their standard errors. The values were verified by plotting (plots not shown) $T \log k_2/k_1$ against T. The Arrhenius parameters themselves for the enolization of acetone in water in the range 25–45° obtained by the usual graphical method, are

$$E_A = 20.5 \pm \sim 0.2 \text{ kcal mole}^{-1},$$

$$\log_{10} A/\text{l mole}^{-1}\,\text{s}^{-1} = 10.5 \pm \sim 0.1.$$

These are in excellent agreement with the literature values 20.6 kcal mole^{-1} and 10.6 respectively (17). The Arrhenius parameters for the enolization of acetophenone in 16.2% w/w ethanol in water in the range 30–50 °C are

$$E_A = 21.5 \pm \sim 0.2 \text{ kcal mole}^{-1},$$

$$\log_{10} A/\text{l mole}^{-1}\,\text{s}^{-1} = 10.9 \pm \sim 0.1.$$

Plots of the logarithms of the rate constants against pressure are shown in Figs. 2 and 3. The volumes of activation were obtained by extrapolating plots of log $k(p_2)/k(p_1)$

Can. J. Chem. Downloaded from www.nrcresearchpress.com by 210.87.254.5 on 09/05/12
For personal use only.

Can. J. Chem. Downloaded from www.nrcresearchpress.com by 210.87.254.5 on 09/05/12
For personal use only.

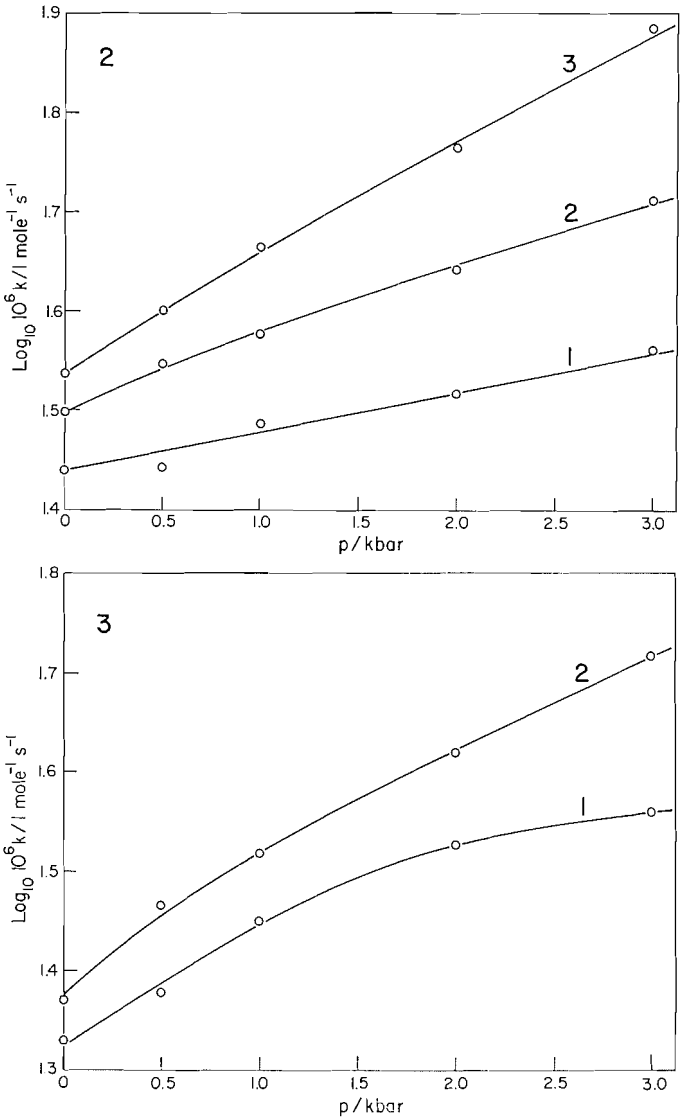

FIG. 2. Effect of pressure on the rate of enolization of acetone at 25.00 °C. Curve 1: in water. Curve 2: in 16.2% w/w ethanol in water. Curve 3: in 33.4% w/w ethanol in water.

FIG. 3. Effect of pressure on the rate of enolization of acetophenone at 30.00 °C. Curve 1: in 16.2% w/w ethanol in water. Curve 2: in 33.4% w/w ethanol in water.

against $\frac{1}{2}(p_2 + p_1)$ to zero pressure, where p_1 and p_2 are adjacent pressures at which the rate constants were measured. The differences in the volumes of activation in two solvents were verified by plotting log k_1/k_2, where k_1 and k_2 are the rate constants in two solvents at the same temperature and pressure, against p. For ethanol–water solvents the compression of the reaction mixture was allowed for by subtracting κRT from the value of $-RT\partial \ln k/\partial p$ at zero pressure (for a similar correction see ref. 18) where κ is the compressibility of the solvent at zero pressure. Using the compressibilities of ethanol–water mixtures as interpolated from Moesveld's data (19), i.e., 39.5×10^{-6} and 44.5×10^{-6}

bar^{-1} respectively, the value of κRT in 16.2% w/w ethanol in water is 1.0 cm^3 mole^{-1}, and in 33.4% w/w ethanol in water is 1.1 cm^3 mole^{-1}. The volumes of activation are given in Table III.

TABLE III

Volumes of activation for the acid-catalyzed enolization of acetone and of acetophenone

Ketone	Solvent	Temp. (°C)	$\Delta V^{\neq}$/cm^3 mole^{-1}
Acetone	Water	25.00	$-2.1\pm\sim0.5$
	16.2% w/w ethanol in water		$-4.2\pm\sim0.7$
	33.4% w/w ethanol in water		$-6.9\pm\sim0.7$
Acetophenone	16.2% w/w ethanol in water	30.00	$-6.0\pm\sim0.7$
	33.4% w/w ethanol in water		$-8.6\pm\sim1.0$

The effect of solvent on the rate constant at various pressures is shown in Fig. 4. The

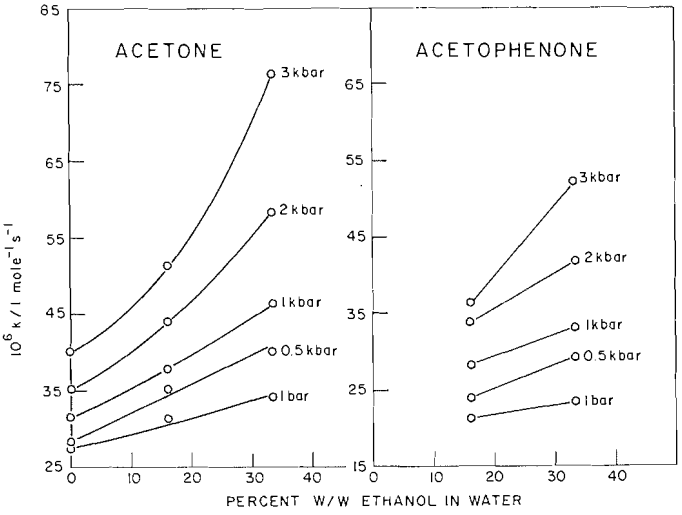

FIG. 4. Effect of solvent on the rate of enolization of acetone at 25.00 °C and of acetophenone at 30.00 °C at different pressures. The definition of k is given in the footnote of Table II.

rate constants for acetone in water at various pressures shown in this plot are uncorrected for compression of the solution, so that a true comparison with the rate constants in ethanol–water solvents, which are also uncorrected for compression, can be made. Because acetophenone is almost insoluble in water, it was not possible to study its iodination kinetics in water under comparable conditions to those used for acetone. The curves for acetophenone in Fig. 4 were therefore drawn as straight, although by comparison with the curves for acetone, they are probably not accurately straight.

5. DISCUSSION

1. Solvent Deuterium Isotope Effect for the Enolization of Acetophenone

The solvent deuterium isotope effect for the enolization of acetophenone k^{D_2O}/k^{H_2O} in 16.2% w/w ethanol in water is $2.50\pm\sim0.05$. This undoubtedly proves that there is a pre-equilibrium proton transfer to the ketone preceding the rate-determining step. The value is similar to the value 2.1 reported (6) for acetone.

Can. J. Chem. Downloaded from www.nrcresearchpress.com by 210.87.254.5 on 09/05/12
For personal use only.

2. Effect of Solvent on the Rate of Enolization

The effect of solvent on the rate of enolization is quite small at atmospheric pressure. Between 0 and 16.2% w/w ethanol in water the rate for acetone increases by about 10%, and between 16.2 and 33.4% w/w ethanol in water the rate for both acetone and acetophenone increases also by about 10%. Solvent effects of a similar magnitude were previously observed for the iodination of acetone in ethanol–water (20) and for the bromination of acetone and acetophenone in acetic acid – water (8) at atmospheric pressure. The slight increase in the rate is in the direction expected if it were due mainly to the electrostatic interaction between the reactants and the solvent, and the electrostatic charge were dispersed over a larger volume in the transition state than in the initial state without a significant increase in the dipole and higher moments (21). However, the change of rate is so small that any small electrostatic effects of this kind could easily be swamped by changes of more specific interactions between the reactants and the solvent. The results cannot therefore be taken as indicating the direction of the change of the polarity when the transition state is formed.

Furthermore, the effect of solvent on the rate (see Fig. 4) is about four times larger at 3 kbar than at 1 bar. The effect of solvent on the compression is much too small to account for this effect. It appears from Figs. 2 and 3 that if the rate constant as a function of pressure could be extrapolated smoothly into the region of negative pressures, then the solvent effect would change sign at about −1 kbar, and at pressures below this, increasing the concentration of organic solvent in the mixture would cause the reaction rate to decrease. The pressure at which the effect of solvent on the rate changes sign has actually been observed for the acid-catalyzed hydrolysis of methyl acetate (Withey, Poulton, Whalley, unpublished work), and more detailed comments will be made when this work is published. It is, nevertheless, clear that caution should be used when one is attempting to interpret small effects of solvent on the rate constant.

The large effect of pressure on the solvent effect for both the enolization of ketones and the hydrolysis of methyl acetate cannot be explained on simple electrostatic grounds, and indicates that any explanation of the solvent effect at 1 bar on simple electrostatic grounds is invalid. Rather, the small solvent effect at 1 bar is almost certainly due to two or more larger effects that in large part cancel one another. The relatively large effect of pressure on the solvent effect is probably due to a smaller relative effect of pressure on one or more of these component solvent effects.

The effect of pressure on the solvent effect and the effect of solvent on the volume of activation are, of course, different ways of describing the same thing. Because

$$\frac{\partial}{\partial x}\left(\frac{\partial \ln k}{\partial p}\right)_T = \frac{\partial}{\partial p}\left(\frac{\partial \ln k}{\partial x}\right)_T$$

where x is the concentration of one component of the solvent mixture, then

$$\frac{\partial}{\partial p}\left(\frac{\partial \ln k}{\partial x}\right) = -\frac{1}{RT}\frac{\partial \Delta V^{\neq}}{\partial x}.$$

The discussion of the effect of solvent on the volume of activation in Section 5.4 is therefore relevant also to this section.

3. Volumes of Activation in Water

The volume of activation for the enolization of acetone in water is $-2.1 \pm \sim 0.5$ cm^3 mole^{-1}. The volume of activation for the enolization of acetophenone is not known in

Can. J. Chem. Downloaded from www.nrcresearchpress.com by 210.87.254.5 on 09/05/12
For personal use only.

water, but it is 1.8 cm^3 $mole^{-1}$ more negative than that of acetone in both 16.2 and 33.4% w/w ethanol in water. It is likely therefore that the volume of activation for acetophenone in water is about -3.9 cm^3 $mole^{-1}$.

Because the ketones are only slightly protonated under the experimental conditions, the volumes of activation are the difference in partial volume between the transition state and the initial ketone and hydronium ion. The volumes of activation for acid-catalyzed reactions of the kind

$$R + H_3O^+ \overset{\text{fast}}{\rightleftharpoons} RH^+ + H_2O,$$

$$RH^+ + H_2O \overset{\text{slow}}{\longrightarrow} \text{products},$$

where a new H_2O—C bond is formed in the slow step are usually about -8 to -12 cm^3 $mole^{-1}$ (21), and similar values are usually found for reactions of the kind (21)

$$R_1O^- + R_2X \rightarrow R_1OR_2 + X^-.$$

It is therefore at first sight a little surprising to find -2.1 cm^3 $mole^{-1}$ for the enolization of acetone. There are probably two reasons for the high volume of activation.

For approximate purposes a volume of activation can be divided into two parts (21), $\Delta V_r^{\neq}$ which is the change of volume due directly to the changing interaction of the reacting molecules with one another, and $\Delta V_s^{\neq}$, which is the change of volume due directly to the changing interaction of the reacting molecules with the solvent. For bimolecular reactions such as we are discussing $\Delta V_r^{\neq}$ is approximately the contraction (or expansion) of the interatomic distance when a partial valence bond is formed (or broken) multiplied by the cross-sectional area perpendicular to the bond. Both the contraction and the cross-sectional area are probably smaller when a water molecule substitutes at a hydrogen atom than when it substitutes at a carbon atom. Consequently, $\Delta V_r^{\neq}$ for the acid-catalyzed enolization of ketone is probably less negative than that for bimolecular (A-2) acid-catalyzed hydrolyses.

If for approximate purposes we represent part of the interaction between an ion and its solvent by that between a charged spherically symmetrical ion and a continuous dielectric, then $\Delta V_s^{\neq}$ can be represented in part as the difference between reactants and transition state of the quantity (22),

$$[18] \qquad \tfrac{1}{2}N\frac{z^2e^2}{a}\left\{\frac{\partial\epsilon^{-1}}{\partial p} + \left(1 - \frac{1}{\epsilon}\right)\frac{\partial \ln a}{\partial p}\right\}$$

where N is Avogadro's number, z is the number of electronic charges e on the ion, a is the radius of the cavity containing the ion, and ϵ is the dielectric constant. The transition state for the enolization of acetone can be represented by

$$CH_3—\overset{\overset{OH^{\delta+}}{\|}}{C}=CH_2\cdots H\cdots OH_2^{(1-\delta)+},$$

and that for a typical A-2 reaction such as the acid-catalyzed hydrolysis of diethyl ether can be represented as

$$CH_3—CH_2\cdots\overset{\overset{(1-\delta)+}{OH_2}}{\overset{|}{O}}H^{\delta+}—CH_2—CH_3.$$

The positive charge is clearly more widely dispersed in the ketone transition state than

Can. J. Chem. Downloaded from www.nrcresearchpress.com by 210.87.254.5 on 09/05/12
For personal use only.

in the ether transition state, and consequently the effective radius of the charge can be considered to be greater. In both transition states the effective radius is, of course, greater than in the initial hydronium ion. $\Delta V_s^{\ddagger}$ for both reactions will therefore be positve and will be more positive for the ketone reaction than for the ether reaction. The increase of volume is composed of an increase of the volume of both the reactants and the solvent due to the decrease of the interaction between them (22).

We see therefore that both $\Delta V_r^{\ddagger}$ and $\Delta V_s^{\ddagger}$ are probably algebraically larger for the ketone enolization than for the ether hydrolysis, and so the volume of activation is probably algebraically larger, in agreement with observation. It is clear that where there is a possibility of a large dispersion of charge, caution may be required in using volumes of activation to help determine mechanisms (21).

The fact that the volumes of activation for acetone and acetophenone are not greatly different and that of acetophenone is more negative than that of acetone suggests that there is little dispersion of charge into the benzene ring of acetophenone. The relatively small effect of para substituents on the rate of enolization of substituted acetophenones (8) agrees well with this view.

4. Effect of Solvent on Volume of Activation

The effect of solvent on the volume of activation (Table III) for both acetone and acetophenone is rather large, the volume of activation for acetone in 33.4% w/w ethanol–water being over three times the value for water. The volumes of activation for the acid-catalyzed hydrolysis of methyl acetate (Withey, Poulton, and Whalley, unpublished work) changes by about the same amount in solvent acetone–water as does that for acetone in ethanol–water of similar concentration, although the relative change for methyl acetate is smaller due to its volume of activation in water being four times bigger than that for acetone (23).

The effect of solvent on a volume of activation is almost by definition an effect on $\Delta V_s^{\ddagger}$ if the mechanism does not change. We have seen in Section 5.3 that $\Delta V_s^{\ddagger}$ is probably positive, and so to explain the observed decrease in $\Delta V^{\ddagger}$ with increasing proportion of organic solvent in terms of the ion-dielectric theory represented by equation 18 requires that $\partial\epsilon^{-1}/\partial p$ should increase in the range of solvent water to 33.4% w/w ethanol–water. This is not a priori unlikely, in spite of the fact that $\partial\epsilon^{-1}/\partial p$ for ethanol is much smaller than that for water (24) because the initial effect of adding ethanol to water is to cause the compressibility to decrease (19). A little more information can be obtained from theory. The dielectric constant of a mixture of polar substances can be represented approximately by the expression (25)

$$[19] \qquad \frac{(\epsilon - 1)(2\epsilon + 1)}{9\epsilon} V = \sum_i \frac{(\epsilon_i - 1)(2\epsilon_i + 1)}{9\epsilon_i} x_i V_i$$

where ϵ and ϵ_i are the dielectric constants of the mixture and of pure component i, V and V_i are the molar volumes of the solution and of component i, and x_i is the mole fraction of component i. For ethanol–water mixtures at room temperature the dielectric constants are much greater than unity, and equation [19] can be simplified approximately to

$$[20] \qquad \epsilon V = \sum_i \epsilon_i V_i x_i,$$

which can also be written

$$[21] \qquad \epsilon = \sum_i \epsilon_i \varphi_i$$

Can. J. Chem. Downloaded from www.nrcresearchpress.com by 210.87.254.5 on 09/05/12
For personal use only.

where φ_i is the volume fraction of component i,

[22] $$\varphi_i = V_i x_i / V.$$

By differentiating equation [21] with respect to pressure and introducing the isothermal compressibility κ_i and the pressure coefficient ζ_i of the dielectric constant

$$\zeta_i = \partial \ln \epsilon_i / \partial p,$$

we find

[23] $$\frac{\partial \epsilon^{-1}}{\partial p} = -\epsilon^{-2} \sum \epsilon_i \varphi_i (\zeta_i - \kappa_i + \kappa).$$

The values of $\partial \epsilon^{-1}/\partial p$ for various ethanol–water mixtures calculated according to equation [23] are as follows.

Solvent	$10^6(\partial \epsilon^{-1}/\partial p)$/bar^{-1}
Water	−0.74
16.2% w/w ethanol in water	−0.74
33.4% w/w ethanol in water	−0.91
Ethanol	−3.58

It seems likely therefore that $\partial \epsilon^{-1}/\partial p$ changes little between water and 33.4% w/w ethanol in water, and perhaps slightly decreases. The effect of solvent on $\Delta V_s^{\neq}$ cannot therefore be explained on the basis of ion-dielectric theory if equation [23] is moderately accurate. It is possibile that part of the decrease in $\Delta V_s^{\neq}$ with increasing proportion of organic solvent is due to there being greater unmixing of water and ethanol around the H_3O^+ ion than around the transition state; since water and ethanol have a larger volume when unmixed than when mixed, greater unmixing around the H_3O^+ ion than around the transition state would tend to make $\Delta V_s^{\neq}$ smaller in water–ethanol mixtures than in water. This could, in principle, be treated in terms of the dielectric theory, but it is not worthwhile. There are also other interactions between the reactant and the solvent about which little is known quantitatively, and they are probably playing their part.

5. Quantities of Activation at Constant Pressure and at Constant Volume: Variation with Solvent

The free-energy of activation ($\Delta G_p^{\neq}$ or $\Delta A_v^{\neq}$) for the enolization of acetone and acetophenone in ethanol–water mixtures changes little with solvent. The volumes of activation for the reactions are not zero, and change considerably with changing solvent. It follows, according to the arguments given in section 2, that there should be compensation either in $\Delta H_p^{\neq}$ and $T\Delta S_p^{\neq}$ or in $\Delta U_v^{\neq}$ and $T\Delta S_v^{\neq}$. The differences, $\Delta\Delta H_p^{\neq}$ and $T\Delta\Delta S_p^{\neq}$, in $\Delta H_p^{\neq}$ and $T\Delta S_p^{\neq}$ between solvents are listed in Table IV together with the changes in $T\alpha\Delta V^{\neq}/\kappa$ and in $\Delta U_v^{\neq}$ and $T\Delta S_v^{\neq}$. It is clear that the intrinsic energy and entropy of activation at constant volume change much less with changing solvent than do the enthalpy and entropy of activation at constant pressure. There is therefore a significant energy–entropy compensation in the constant-pressure parameters of activation but not in the constant-volume parameters. There have been several suggestions in the past that quantities of activation at constant volume should be more easily understood than quantities of activation at constant pressure (see ref. 21 for references). There has, however, been no previous reliable test of this suggestion. A test was made 25 years ago using the homogeneous dimerization of cyclopentadiene (26) but doubts have recently been cast (27) on the reliability of the experimental results used (28).

Can. J. Chem. Downloaded from www.nrcresearchpress.com by 210.87.254.5 on 09/05/12
For personal use only.

Can. J. Chem. Downloaded from www.nrcresearchpress.com by 210.87.254.5 on 09/05/12
For personal use only.

TABLE IV

Changes with solvent of the activation parameters for the acid-catalyzed enolization of acetone and acetophenone. The temperature range was 25–45 °C for acetone and 30–50 °C for acetophenone. Temperature-dependent parameters were evaluated at 25 °C for acetone and at 30 °C for acetophenone

Ketone	Solvent	$\Delta\Delta G_p^{\ddagger}$ (= $\Delta\Delta A_v^{\ddagger}$)* cal mole^{-1} ±∼5	$\Delta\Delta H_p^{\ddagger}$ cal mole^{-1} ±∼120	$T\Delta\Delta S_p^{\ddagger}$ cal mole^{-1} ±∼120	$T\Delta(\alpha\Delta V^{\ddagger}/\kappa)$† cal mole^{-1} ±∼100	$\Delta\Delta U_v^{\ddagger}$ cal mole^{-1} ±∼150	$T\Delta\Delta S_v^{\ddagger}$ cal mole^{-1} ±∼150
Acetone	16.2% w/w ethanol in water	76	325	250	216	109	34
	33.4% w/w ethanol in water	130	775	645	572	203	73
Acetophenone	33.4% w/w ethanol in water	54	405	350	373	32	−23

*Solvent 1 (eqs. 15–17) for acetone is water and for acetophenone is 16.2% w/w ethanol in water. Solvent 2 is listed in column 2 of this table. The quantities $\Delta\Delta G_p^{\ddagger}$ were evaluated from the equation $\Delta\Delta G_p^{\ddagger} = RT \ln k_2/k_1$ where T refers to the temperature at which $\Delta V^{\ddagger}$ has been measured. The quantities $\Delta\Delta H_p^{\ddagger}$ and $T\Delta\Delta S_p^{\ddagger}$ were obtained from plots shown in Fig. 1.

†The thermal expansion ($10^6\,\alpha$/deg^{-1}) for water is 248 (25 °C), for 16.2% w/w ethanol in water is 396 at 25 °C, and 441 at 30 °C, and for 33.4% w/w ethanol in water is 594 at 25 °C, and 613 at 30 °C. These were obtained by plotting log (density) against temperature and evaluating the slopes at the temperatures desired. The densities were taken from the literature (31). The compressibilities ($10^6\,\kappa$/bar^{-1}) of these solvents from Moesveld's data (19) are 43.9, 39.5, and 44.5 respectively at 25 °C, and the same values were assumed for 30 °C. T is the temperature at which $\Delta V^{\ddagger}$ has been measured.

TABLE V

Changes with substituent of the activation parameters for the acid-catalyzed enolization of acetone and acetophenone at 30 °C
($\Delta\Delta$ = $\Delta_{\text{acetophenone}} - \Delta_{\text{acetone}}$)

Solvent	$\Delta\Delta G_p^{\ddagger}$ (= $\Delta\Delta A_v^{\ddagger}$) cal mole^{-1} ±∼5	$\Delta\Delta H_p^{\ddagger}$ cal mole^{-1} ±∼120	$T\Delta\Delta S_p^{\ddagger}$ cal mole^{-1} ±∼120	$T\alpha\Delta V/\kappa$ cal mole^{-1} ±∼100	$\Delta\Delta U_v^{\ddagger}$ cal mole^{-1} ±∼150	$T\Delta\Delta S_v^{\ddagger}$ cal mole^{-1} ±∼150
16.2% w/w ethanol in water	563	1365	803	−146	1511	949
33.4% w/w ethanol in water	557	1510	953	−170	1680	1123

Many attempts have been made in the past to explain the observed enthalpy–entropy compensation effect in a variety of systems (29, 30 and references quoted there). For the system investigated here, the fact that there is little energy–entropy compensation in the constant-volume parameters seems to require no special explanation. The explanation of the enthalpy–entropy compensation in the constant-pressure parameters requires an explanation of the variation of $\alpha\Delta V^{\neq}/\kappa$ with solvent, because of the relationship in equations [6] and [7]. For the enolization of acetone in water and in 33.4% w/w ethanol in water, α changes from 248×10^{-6} to 594×10^{-6} deg^{-1} (Table IV, footnote), $\Delta V^{\neq}$ changes from -2.1 to -6.9 cm^3 mole^{-1} (Table III), and κ changes from 43.9×10^{-6} to 44.5×10^{-6} bar^{-1}. The changes of these quantities between water and 16.2% w/w ethanol in water for the enolization of acetone, and between 16.2% w/w and 33.4% w/w ethanol in water for the enolization of acetophenone (see Tables III and IV) are similar to these changes. The change in $\alpha\Delta V^{\neq}/\kappa$ is therefore due about equally to changes in the thermal expansivity and in the volume of activation and hardly at all to changes in the compressibility. The causes of the change of the volume of activation with solvent are discussed in Section 5.4. The change of the thermal expansitivity with solvent is undoubtedly due largely to the small thermal expansivity of water due to its peculiar structure. The thermal expansivitity of pure water is of course zero near 4 °C, and then the quantities of activation at constant pressure and at constant volume are equal.

6. Quantities of Activation at Constant Pressure and at Constant Volume: Variation with Substituent

Since the intrinsic energy and entropy of activation at constant volume change little with changing solvent (Section 5.5) although the enthalpy and entropy of activation at constant pressure change appreciably, it is worth investigating the change of the two sets of activation parameters with changing substituent. The differences in the activation parameters at constant pressure were obtained from plots analogous to those in Fig. 1. For this purpose, rate constants for acetone at 30 °C were interpolated from Arrhenius plots. The results for both 16.2% w/w and 33.4% w/w ethanol in water are summarized in Table V. There is compensation in both the constant-pressure and the constant-volume parameters, and the compensation in the constant-volume parameters is the greater. There is little doubt that attempts to explain the compensation quantitatively should be based on the constant-volume parameters.

6. CONCLUSIONS

The most important conclusions derived from the experiments reported in this paper are as follows:

1. The effect of solvent on the rate of a reaction may be greatly influenced by pressure, and care is required in interpreting solvent effects, particularly small solvent effects, at atmospheric pressure. It is wise to study the effect of both temperature and pressure on the solvent effect.

2. Reactions whose rates change only slightly with changing conditions (such as substituents, solvent, etc.) inevitably will have an energy–entropy compensation effect in either the enthalpy and entropy of activation at constant pressure or in the energy and entropy of activation at constant volume, or, of course, in both sets of parameters. There is no significant compensation in the variation with solvent of the constant-volume parameters for the enolization of acetone and of acetophenone in ethanol–water mixtures; the compensation in the constant-pressure parameters can be ascribed about

Can. J. Chem. Downloaded from www.nrcresearchpress.com by 210.87.254.5 on 09/05/12
For personal use only.

equally to changes in the thermal expansion and in the volume of activation with changing solvent. There is more compensation in the variation with substituent of the constant-volume parameters for the enolization of acetone and acetophenone than in the constant-pressure parameters. Attempts to explain the compensation in quantitative terms should doubtless be based on the constant-volume parameters if these differ significantly from the constant-pressure parameters.

ACKNOWLEDGMENTS

We are grateful to Mr. R. Ironside for the infrared analysis and to Mr. A. Lavergne for help with the high-pressure apparatus.

REFERENCES

1. R. P. BELL. The proton in chemistry. Cornell University Press, Ithaca, New York. 1959. C. K. INGOLD. Structure and mechanism in organic chemistry. Cornell University Press, Ithaca, New York. 1953.
2. A. LAPWORTH. J. Chem. Soc. 30 (1904).
3. H. M. DAWSON *et al.* J. Chem. Soc. 2282 (1926); 2844 (1928); 1884 (1929).
4. L. ZUCKER and L. P. HAMMETT. J. Am. Chem. Soc. **61**, 2791 (1939).
5. P. D. BARTLETT and J. R. VINCENT. J. Am. Chem. Soc. **55**, 4992 (1933).
6. O. REITZ. Z. Physik. Chem. A, **179**, 119 (1937).
7. P. D. BARTLETT and C. H. STAUFFER. J. Am. Chem. Soc. **57**, 2580 (1935).
8. T. G. BONNER, D. P. EVANS, and H. B. WATSON. J. Chem. Soc. 1353 (1939).
9. E. WHALLEY. Trans. Faraday Soc. **55**, 798 (1959).
10. R. W. TAFT. J. Am. Chem. Soc. **74**, 5372 (1952).
11. F. A. LONG, J. G. PRITCHARD, and F. E. STAFFORD. J. Am. Chem. Soc. **79**, 2362 (1957).
12. S.-L. P'ENG, R. H. SAPIRO, and D. M. NEWITT. J. Chem. Soc. 784 (1938).
13. J. G. BURR. J. Phys. Chem. **61**, 1477 (1957).
14. J. KOSKIKALLIO and E. WHALLEY. Trans. Faraday Soc. **55**, 809 (1959).
15. P. W. BRIDGMAN. Proc. Am. Acad. Arts Sci. **48**, 309 (1912).
16. R. P. BELL and K. YATES. J. Chem. Soc. 1927 (1962).
17. E. A. MOELWYN-HUGHES. Kinetics of reactions in solution. Oxford University Press. 1947. p. 44.
18. J. KOSKIKALLIO, D. POULI, and E. WHALLEY. Can. J. Chem. **37**, 1360 (1959).
19. A. L. TH. MOESVELD. Z. Physik. Chem. **105**, 450 (1923).
20. D. P. N. SATCHELL. J. Chem. Soc. 2878 (1957).
21. E. WHALLEY. Advances in physical organic chemistry. Vol. 2. *Edited by* V. Gold. Academic Press, London. 1964. p. 93.
22. E. WHALLEY. J. Chem. Phys. **38**, 1400 (1963).
23. A. R. OSBORN and E. WHALLEY. Can. J. Chem. **39**, 1094 (1961).
24. B. B. OWEN and S. R. BRINKLEY. Phys. Rev. **64**, 32 (1943).
25. G. OSTER. J. Am. Chem. Soc. **68**, 2036 (1946).
26. D. M. NEWITT and A. WASSERMAN. J. Chem. Soc. 735 (1940).
27. C. WALLING and H. J. SCHUGAR. J. Am. Chem. Soc. **85**, 607 (1963).
28. B. RAISTRICK, R. H. SAPIRO, and D. M. NEWITT. J. Chem. Soc. 1761 (1939).
29. J. F. BUNNETT. Technique of organic chemistry. Vol. VIII. Part I. *Edited by* A. Weissberger. Interscience, New York. 1961. Chap. VI.
30. J. E. LEFFLER and E. GRUNWALD. Rates and equilibria of organic reactions. John Wiley and Sons, Inc., New York, 1963.
1. INTERNATIONAL CRITICAL TABLES. Vol. 3. McGraw-Hill Book Company, Inc., New York. 1928.

Can. J. Chem. Downloaded from www.nrcresearchpress.com by 210.87.254.5 on 09/05/12
For personal use only.

Can. J. Chem. Downloaded from www.nrcresearchpress.com by 210.87.254.40 on 09/05/12
For personal use only.

KINETICS AND MECHANISMS OF THE THERMAL DECOMPOSITION OF ACETALDEHYDE

I. THE UNINHIBITED REACTION

M. Eusuf and K. J. Laidler
Department of Chemistry, University of Ottawa, Ottawa, Canada

Received March 5, 1964

ABSTRACT

The kinetics of the uninhibited decomposition of acetaldehyde have been reexamined. The initial rates of the decomposition of pure acetaldehyde show strict three-halves-order dependence at temperatures from 480 to 525 °C, and the activation energy is 47.6 kcal per mole. Foreign gases, which decrease the rate of reaction, cause a significant increase in order. The rate of ethane formation is second order in acetaldehyde, and Trenwith has found the hydrogen formation to be second order in acetaldehyde. The results are shown to be consistent only with a mechanism involving second-order initiation and the third-order reaction $2CH_3 + M \rightarrow C_2H_6 + M$ as the terminating step. The rate of the initiation process is increased only to a small extent by the addition of inert foreign gases; it is suggested that the initial process may be $CH_3CHO + CH_3CHO \rightarrow CH_3CHOH + CH_3CO$, with a subsequent breakdown of CH_3CHOH into $CH_3CHO + H$. The mechanism is shown to account for the overall kinetic behavior and for the formation of the minor products.

INTRODUCTION

Steacie (1) commented that "the acetaldehyde decomposition is remarkable for the lack of agreement of both mechanism and experimental fact, and for the complications involved." The Rice-Herzfeld mechanism (2), involving first-order initiation and second-order termination ($CH_3 + CH_3$), is a straightforward example of a mechanism leading to three-halves-order kinetics and has commonly been regarded as giving a correct interpretation of the acetaldehyde decomposition. On the other hand, Bril, Goldfinger, Letort, Mattys, and Niclause (3, 4) have proposed an alternative explanation, based largely on the results of experiments in which foreign gases were added to the reaction system; their conclusion was that the termination step, the combination of methyl radicals, is in its third-order region and that the initiation reaction is hardly affected by inert gases. The work of Laidler and Wojciechowski (5) on the ethane decomposition also led to the conclusion that, under the usual conditions of pyrolysis experiments, the methyl-radical combination reaction is third order. A difficulty still remains, however, since a third-order termination reaction requires a second-order initiation reaction in order for the overall order to be three-halves; this, however, appears to be inconsistent with the conclusion that the initiation reaction is hardly influenced by the addition of several foreign gases. The fact that initiation is second order has received support from a recent investigation by Trenwith (6), who found that the rate of hydrogen production (which should be a good measure of the rate of initiation) is second order in acetaldehyde.

Further doubt about the mechanism has arisen as a result of Quinn's work (7) on the kinetics of methane production in the ethane decomposition. This appeared at first sight to require that the dissociation of ethane into $2CH_3$ is first order and the methyl radical combination, therefore, second order, which is inconsistent with conclusions from the acetaldehyde work. Quinn's results are not, however, compelling, since there is a possibility, as suggested by Danby, Spall, Stubbs, and Hinshelwood (8), that the predominant source of methane is the reaction

$$C_2H_6 \rightarrow CH_4 + CH_2.$$

This might occur as a first-order process and be much more important than the second-order dissociation of ethane into methyl radicals. This suggestion was put forward to explain the fact that the methane production is only very slightly inhibited by nitric oxide.

In view of these various difficulties it was decided to reinvestigate the reaction, both uninhibited and inhibited by nitric oxide (see Part II). Since a very large amount of reliable experimental work has been done on this problem, it was not thought necessary, in the present investigation of the uninhibited reaction, to carry out a great deal of additional experimental work. The work has, in fact, been confined to checking the overall order, to studying the kinetics of formation of the minor product ethane, and to obtaining some specific quantitative information about the effect of added foreign gases; in particular, the effect of foreign gases (CO_2, CH_4, N_2, CO, and C_2H_6) on the order of the reaction has been carefully studied. On the basis of these results a mechanism is proposed for the overall reaction.

EXPERIMENTAL

It has been well established by previous work (8–13) that the only major products of the acetaldehyde decomposition are CH_4 and CO and that a pressure increase of 1 mm corresponds to the decomposition of 1 mm of acetaldehyde within the experimental error of 2%. The pressure technique has therefore been used entirely in the present investigation. A quartz Bourdon gauge was used, and its arm was attached to the armature of a Statham pressure transducer which was under some strain. The output from the transducer was recorded on a Philips pen-and-ink recorder, and initial rates were obtained by measuring the initial slopes of the records. The apparatus was calibrated from time to time and was found to be very stable; the displacement on the recorder varied exactly linearly with the pressure difference. The maximum sensitivity of the particular arrangement used was 0.5 inch displacement per mm Hg. All of the runs were, however, done at 1/10 or 1/20 of the maximum sensitivity, in order to give higher stability. Higher sensitivities could readily be obtained by modifications of the Bourdon gauge and in other ways, but only at the expense of a decrease in stability.

The procedure in carrying out a run was to maintain the outside pressure at a value that was slightly less than the initial pressure of the decomposing gas; as the reaction proceeded the differential pressure increased and could be followed on the recorder.

The reaction vessel was a pyrex cylinder 21 cm long and 4 cm in diameter, with a dead space of about 1% of the total volume. It was confined in a furnace consisting of a copper block, the temperature of which was controlled to within 0.2 °C by means of a thermocouple-activated controller. The temperature was measured using a thermocouple and a Minimite potentiometer.

Analysis of the minor product ethane was carried out using gas-phase chromatography. After a certain residence time in the furnace the reaction was stopped by allowing the gas to expand. Acetaldehyde was removed from the expanded gas by a dry ice – acetone mixture, and ethane was condensed in a small evacuated bulb surrounded by liquid nitrogen. With helium as carrier gas the ethane was passed through the chromatographic-analysis unit containing a 2 meter column packed with silica gel and maintained at 30 °C; the gas-chromatographic results were calibrated against known samples taken from the reaction vessel.

The acetaldehyde used was an Eastman product. It was purified by several bulb-to-bulb distillations at temperatures from 0 to −70 °C, special care being taken to free the compound completely from oxygen. The foreign gases used were Matheson Research Grade chemicals and were purified by several distillations.

RESULTS

The results were initially not very reproducible, but after several runs had been carried out in the same vessel a high degree of reproducibility was achieved.

The decomposition was studied from 480 to 525 °C and over the pressure range of 30 to 579 mm Hg. Figure 1 shows a double-logarithmic plot of rate against pressure and shows that the reaction is accurately of three-halves-order over the whole range of temperature and pressure; this agrees with the work of Boyer, Niclause, and Letort (14); Freeman, Danby, and Hinshelwood (15); and Imai, Yoshida, and Toyama (16). Figure 2 shows an Arrhenius plot, and from it the following rate expression is derived:

$$k = 1.16 \times 10^{13}\, e^{-47600/RT}\ cc^{1/2}\ mole^{-1/2}\ s^{-1}.$$

Can. J. Chem. Downloaded from www.nrcresearchpress.com by 210.87.254.40 on 09/05/12
For personal use only.

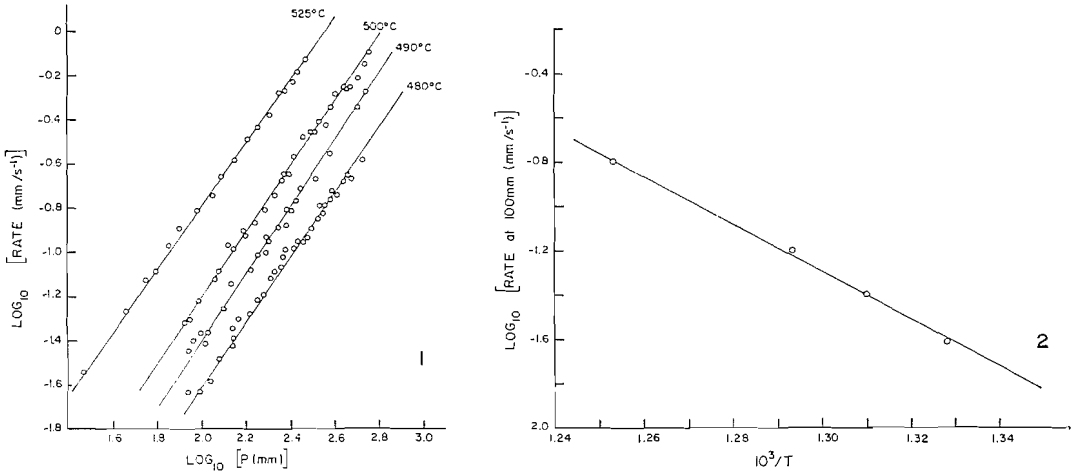

FIG. 1. Plots of log rate against log pressure for the uninhibited reaction.
FIG. 2. Arrhenius plot for the uninhibited reaction.

The activation energy agrees satisfactorily with the value of 48.0 kcal per mole obtained by Boyer, Niclause, and Letort (14) and of 47.7 kcal per mole at high pressure obtained by Fletcher and Hinshelwood (9).

Added foreign gases were found to bring about a decrease in the rate of the reaction, over the entire pressure range investigated, and to increase the order significantly. Figure 3 shows the effect of adding 100 mm of various foreign gases at 525 °C. The order of the

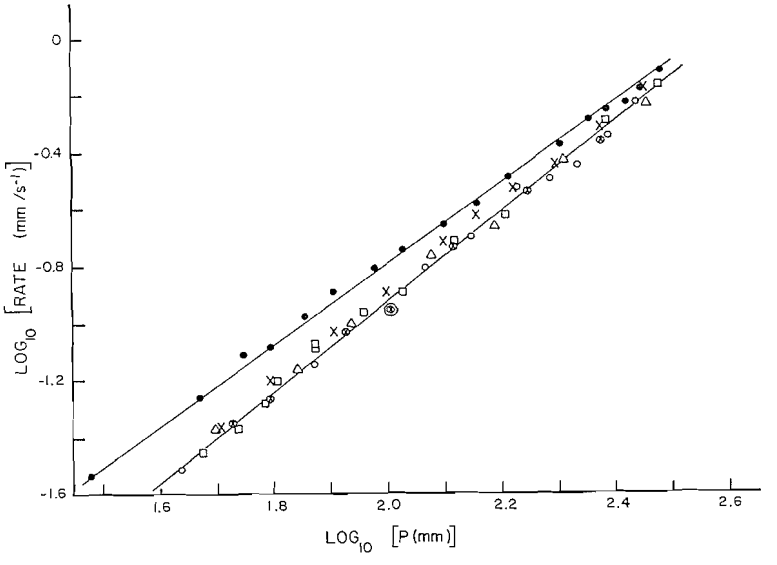

FIG. 3. Plots of log rate against log pressure showing the effects of 100 mm of added foreign gases at 525 °C. The black circles denote rates with no added foreign gases. Rates with added CO_2 are shown as ○, those with CH_4 as □, those with N_2 as △, those with CO as ⊗, and those with C_2H_6 as ×.

reaction has been increased from 1.5 to about 1.6. The figure further shows that essentially the same effect is brought about by adding the same pressure of carbon dioxide, methane, nitrogen, carbon monoxide, and ethane.

Can. J. Chem. Downloaded from www.nrcresearchpress.com by 210.87.254.40 on 09/05/12
For personal use only.

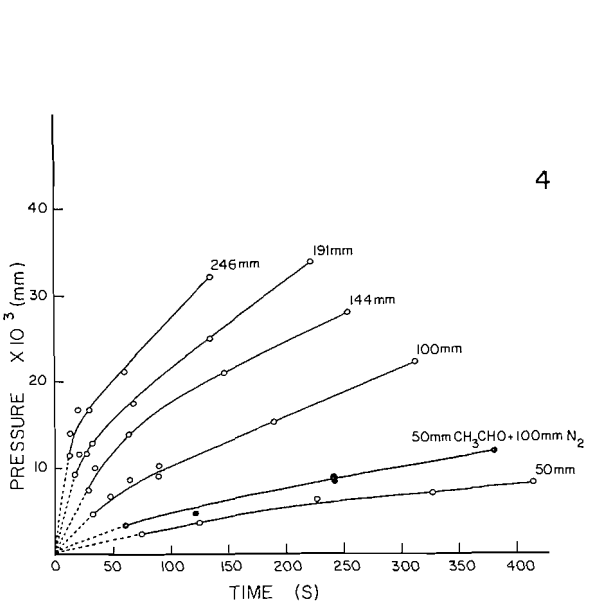

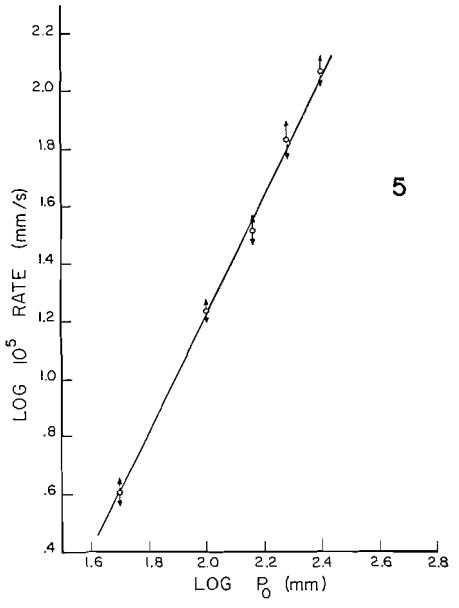

FIG. 4. Plots of the amount of ethane formed as a function of time with different initial pressures of acetaldehyde at 525 °C.

FIG. 5. Plots of log initial rate of formation of ethane against log initial pressure of acetaldehyde at 525 °C.

Figure 4 shows a plot of the amount of ethane formed as a function of time; the estimates of initial slopes have a probable error of 10%. In Fig. 5 the logarithms of the initial slopes, with the probable errors shown, are plotted against the logarithms of the initial acetaldehyde pressure; the slope is close to 2. Figure 4 also shows that the rate of ethane formation is increased by the addition of nitrogen.

DISCUSSION

The Reaction Mechanism

The principal difficulty that exists with regard to the mechanism of the acetaldehyde pyrolysis may be formulated as follows. If one uses the terminology introduced by Laidler, Sagert, and Wojciechowski (17) the possible mechanisms leading to 3/2-order kinetics are ${}^1\beta\beta_{3/2}$, ${}^2\beta\mu_{3/2}$, and ${}^2\beta\beta M_{3/2}$. The first of these, ${}^1\beta\beta_{3/2}$, is the original Rice-Herzfeld scheme; it can be rejected as predicting no inert-gas effect, and because it seems clear that the β radicals, being methyl radicals, must combine by third-order processes (5, 18). The second possibility must be rejected as predicting acceleration by inert gases. The third possibility in its simplest form leads to little or no inert-gas effect; it will now be shown, however, that a modification of the ${}^2\beta\beta M_{3/2}$ mechanism can be made to explain the results in a quantitative fashion.

What is needed is a mechanism that involves third-order termination—and in this way explains the inhibition by inert gases—and an initiation reaction that, as found in particular by Bril, Goldfinger, Letort, Mattys, and Niclause (3, 4), is only slightly affected by inert gas. The initiation reaction must, however, be in its second-order region, and acceleration by inert gas is normally to be expected. Since a variety of inert gases (CO_2, CO, CH_4, N_2, and C_2H_6) give the same effect, it would seem unreasonable to postulate that the gases involved are abnormally ineffective in transferring energy on collision to

Can. J. Chem. Downloaded from www.nrcresearchpress.com by 210.87.254.40 on 09/05/12
For personal use only.

an acetaldehyde molecule. If, however, one postulates that an acetaldehyde molecule plays a very specific role in bringing about the decomposition of another acetaldehyde molecule, the difficulty disappears. The suggestion that is here made is that the initial step in the acetaldehyde decomposition occurs predominantly by the reverse of the "complex" mechanism for radical-combination reactions that has been proposed by Rabinowitch (19) and emphasized by Porter (20) on the basis of experimental results; this mechanism has recently been considered theoretically by Eusuf and Laidler (21). Specifically, it is suggested that the acetaldehyde initiation occurs as the hydrogen-atom transfer reaction

[1′] $$2CH_3CHO \rightarrow CH_3CO + CH_3CHOH$$

followed by

[2] $$CH_3CHOH \rightarrow CH_3CHO + H.$$

The overall process is the split of CH_3CHO into $CH_3CO + H$; the CH_3CHOH radical may also abstract a hydrogen atom from an acetaldehyde molecule or combine with the most abundant radical CH_3. The consequences of these reactions will be considered in a later section. The initiation reaction is second order but is unaffected by inert gases, since one of the acetaldehyde molecules plays a specific role in bringing about dissociation of the other.

The contribution of the proposed initiation reaction by hydrogen transfer may be compared with that of the corresponding splitting reaction

[1] $$2CH_3CHO \rightarrow CH_3 + CHO + CH_3CHO$$

in the following way. According to Benson (22) reaction [1] is more endothermic by about 27 kcal per mole than reaction [1′], and the entropy changes of reactions [1] and [1′] are 28.5 cal $mole^{-1}$ deg^{-1} and 4.5 cal $mole^{-1}$ deg^{-1} respectively (for the standard state of 1 mole per litre). The ratio of equilibrium constants of the two reactions is then calculated to be, at 800 °K,

$$K_1'/K_1 = k_1' \, k_{-1}/k_1 \, k_{-1}' = 1.4 \times 10^5 \text{ ml mole}^{-1}.$$

The value of k_{-1}' may be predicted to a reasonable approximation by simple collision theory and is estimated at 1×10^{14} cc $mole^{-1}$ s^{-1} at 800 °K. The rate of combination of CH_3 and CHO radicals to form CH_3CHO is smaller than that of two CH_3 radicals by a factor of at least 10 (22). The third-order rate constant for the combination of methyl radicals has been estimated at 3.5×10^{18} cc^2 $mole^{-2}$ s^{-1} at 800 °K (23). The maximum value of k_{-1} at 800 °K is, therefore, 3.5×10^{17} cc^2 $mole^{-2}$ s^{-1}. From this it follows that

$$k_1'/k_1 = 40.$$

Even if one allows an uncertainty of 4 kcal per mole in the value of ΔH, and of one power of 10 in the value of k_{-1}', the contribution of reaction [1′] is at least one third of that of reaction [1] at 800 °K and more at lower temperatures. The fact that foreign gases have only a small effect on the initiation reaction indicates that reaction [1′] is probably much more important than reaction [1]. However, both types of initiation will be included in the present scheme of reactions for the sake of completeness.

The reaction mechanism to which these considerations lead is

[1] $$2CH_3CHO \rightarrow CH_3 + CHO + CH_3CHO$$

[1*a*] $$CH_3CHO + X \rightarrow CH_3 + CHO + X$$

Can. J. Chem. Downloaded from www.nrcresearchpress.com by 210.87.254.40 on 09/05/12
For personal use only.

[1′] $2CH_3CHO \rightarrow CH_3CHOH + CH_3CO$

[2] $CH_3CHOH \rightarrow CH_3CHO + H$

[2a] $CHO + X \rightarrow CO + H + X$

[3] $H + CH_3CHO \rightarrow H_2 + CH_3CO$

[4] $CH_3CO + X \rightarrow CH_3 + CO + X$

[5] $CH_3 + CH_3CHO \rightarrow CH_4 + CH_3CO$

[6] $2CH_3 + CH_3CHO \rightarrow C_2H_6 + CH_3CHO$

[6a] $2CH_3 + X \rightarrow C_2H_6 + X$

Application of the steady-state treatment to this scheme leads to the following expressions for the radical concentrations:

[i] $$[CH_3] = \left\{\frac{k_1[CH_3CHO]^2 + k_1'[CH_3CHO]^2 + k_{1a}[CH_3CHO][X]}{k_6[CH_3CHO] + k_{6a}[X]}\right\}^{1/2}$$

[ii] $$[CH_3CO] \simeq \frac{k_5}{k_4}\frac{[CH_3CHO]}{[X]}\left\{\frac{k_1[CH_3CHO]^2 + k_1'[CH_3CHO]^2 + k_{1a}[CH_3CHO][X]}{k_6[CH_3CHO] + k_{6a}[X]}\right\}^{1/2}$$

[iii] $$[CH_3CHOH] = (k_1'/k_2)[CH_3CHO]^2$$

[iv] $$[H] = (k_1/k_3)[CH_3CHO] + (k_1'/k_3)[CH_3CHO] + (k_{1a}/k_3)[X]$$

[v] $$[CHO] = (k_1/k_{2a})[CH_3CHO]^2/[X] + (k_{1a}/k_{2a})[CH_3CHO].$$

The rate of disappearance of acetaldehyde is given by

[vi] $$v = k_5\left\{\frac{(k_1 + k_1')[CH_3CHO] + k_{1a}[X]}{k_6[CH_3CHO] + k_{6a}[X]}\right\}^{1/2}[CH_3CHO]^{3/2}.$$

The rate of disappearance of pure acetaldehyde is therefore

[vii] $$v = k_5\{(k_1 + k_1')/k_6\}^{1/2}[CH_3CHO]^{3/2}.$$

This rate equation is in agreement with the experimental order of three halves for the decomposition of pure acetaldehyde.

Influence of Foreign Gases

Foreign gases such as CO_2, CH_4, CO, N_2, and C_2H_6 inhibit the decomposition of acetaldehyde and increase the order of reaction. The general rate equation [vi] accounts for the observed increase in order as the inert-gas concentration is increased, provided that k_{1a} is small and k_{6a} large.

On the basis of the observed inert-gas effect it is now possible to arrive at a conclusion as to the importance of reaction [1a] as the initiation reaction, in comparison with reactions [1] and [1′], and the importance of reaction [6a] as the termination reaction, in comparison with reaction [6]. With the use of equations [vi] and [vii], the ratio of rates in the presence (v_X) and absence (v_0) of inert gas X can be written as

[viii] $$\frac{v_X}{v_0} = \left\{\frac{[CH_3CHO] + \frac{k_{1a}}{k_1 + k_1'}[X]}{[CH_3CHO] + \frac{k_{6a}}{k_6}[X]}\right\}^{1/2} = \left\{\frac{[CH_3CHO] + r_1[X]}{[CH_3CHO] + r_t[X]}\right\}^{1/2}.$$

Can. J. Chem. Downloaded from www.nrcresearchpress.com by 210.87.254.40 on 09/05/12
For personal use only.

An equation similar to [viii] has been employed by Bril *et al.* (3, 4). The values of r_1 and r_t thus obtained from Fig. 3 are as follows:

$$r_1 = 0.19$$

$$r_t = 1.02.$$

However, these results are highly sensitive to the slopes of the lines in Fig. 3; the r_1 value might, for example, be as high as 0.3. The above results show that reaction [1*a*] plays a smaller part than [1] and [1′] in the initiation reaction and that the efficiencies of CO_2, CH_4, N_2, CO, and C_2H_6 and CH_3CHO in bringing about recombination of methyl radicals are approximately the same. The values of r_1 and r_t are slightly higher than those obtained by Bril *et al.* (3, 4). Traces of oxygen may have a significant effect on the values of r_1 and r_t.

Formation of Ethane

The results given in Figs. 4 and 5 show that the rate of formation of ethane is proportional to the square of the acetaldehyde concentration. Reaction [6] is the only reaction that might be expected to produce ethane. According to the proposed mechanism the rate of formation of ethane from pure acetaldehyde is

[ix] $$v_{C_2H_6} = k_6[CH_3]^2\,[CH_3CHO]$$

[x] $$= (k_1 + k_1')\,[CH_3CHO]^2$$

in agreement with the experimental result. It is obvious that the square in this rate expression will only arise if the initiation reaction is second order. The experimental result that the rate of ethane formation is second order in acetaldehyde is therefore strong evidence that the initiation process is second order and strong evidence for the mechanism proposed.

Formation of Hydrogen

Equally strong evidence is provided by Trenwith's result (6) that the hydrogen production is second order in acetaldehyde. According to the mechanism

[xi] $$v_{H_2} = k_3\,[H]\,[CH_3CHO]$$

[xii] $$= (k_1 + k_1')\,[CH_3CHO]^2,$$

second-order behavior is again only predicted if the initiation reaction is second order.

Trenwith (6) has also found that the hydrogen production shows an induction period of a minute or so, the actual value varying with the temperature and surface area of the reaction vessel but being independent of the acetaldehyde pressure. Trenwith explains this in terms of the initiation reaction

$$CH_3CHO \rightarrow CH_3 + CHO \qquad \text{(second order)}$$

followed by

$$CHO \rightarrow H + CO \qquad \text{(on the surface)}$$

and

$$H + CH_3CHO \rightarrow H_2 + CH_3CO.$$

To explain an induction period of the order of a minute it is necessary to postulate that the half-life of the intermediate CHO is of the order of a minute. The difficulty, however, in assuming that the dissociation of CHO occurs primarily on the surface with such a

Can. J. Chem. Downloaded from www.nrcresearchpress.com by 210.87.254.40 on 09/05/12
For personal use only.

half-life is that the homogeneous decomposition of CHO almost certainly occurs much more rapidly; studies of the photolysis of aldehydes indicate for this reaction an activation energy of about 14 kcal per mole, which would correspond to a half-life of a very small fraction of a second.

A more plausible interpretation of Trenwith's results on the induction period would seem to be provided in terms of the initiation reaction

$$CH_3CHO + CH_3CHO \rightarrow CH_3CO + CH_3CHOH$$

followed by

$$CH_3CHOH \rightarrow CH_3CHO + H,$$

the latter reaction occurring primarily on the surface. The intermediate CH_3CHOH, which probably has the structure

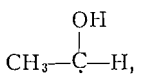

may well have a stability of over 40 kcal so that its dissociation in the gas phase may be slow; there is therefore no difficulty in assuming that it mainly decomposes on the surface. Trenwith's results on the variation of induction period with temperature indicate a frequency factor of $10^{5.3}$ s^{-1} and an activation energy of 26.3 kcal; the very low frequency factor is understandable if it is a surface reaction.

Trenwith (6) reported that the frequency factor for the production of hydrogen, and therefore for the initiation reaction, is $\sim 10^{20}$ cc $mole^{-1}$ s^{-1}. The overall frequency factor was found in the present investigation to be 1.16×10^{13} $cc^{1/2}$ $mole^{-1/2}$ s^{-1}, and this is equal to $A_5(A_1/A_6)^{1/2}$, where the A's are the frequency factors for the elementary processes. A value of $\sim 10^{12}$ cc $mole^{-1}$ s^{-1} has been given for A_5 by Brinton and Volman (24), and A_6 has been estimated (23) as 3.5×10^{18} cc^2 $mole^{-2}$ s^{-1}. These values lead to an estimate of $\sim 5 \times 10^{20}$ for A_1, in reasonable agreement with Trenwith's value.

Formation of Acetone

In a private communication Trenwith (25) has informed us of his results on the formation of acetone, the rate of which is greater than the rate of formation of ethane. At first sight it might be thought that acetone would be formed by the reaction

$$CH_3 + CH_3CO \rightarrow CH_3COCH_3$$

and that this termination reaction is more important than the methyl radical recombination. There are, however, two serious objections to this:

(1) This reaction is a termination reaction of the $\beta\mu$ type, and to obtain three-halves order kinetics the initiation reaction must be second order. This type of mechanism cannot, however, explain the fact that foreign gases reduce the rate of reaction.

(2) If $CH_3 + CH_3CO$ is an important termination reaction in the thermal decomposition of acetaldehyde, it should be so a fortiori in the photochemical decomposition where the temperatures are lower and the radical concentrations, especially of CH_3CO, may be higher. Calvert and Gruver (26) (cf. also Steacie, ref. 1), however, find that acetone formation is unimportant in the photochemical decomposition of acetaldehyde.

This difference between the thermal and photochemical results suggests that the acetone formation is controlled by some process that is temperature dependent. The most plausible reaction would seem to be

Can. J. Chem. Downloaded from www.nrcresearchpress.com by 210.87.254.40 on 09/05/12
For personal use only.

[7] $$CH_3 + CH_3CHO \rightarrow CH_3-\underset{\displaystyle CH_3}{\overset{\displaystyle \dot{O}}{\overset{|}{\underset{|}{C}}}}-H \rightarrow CH_3COCH_3 + H.$$

Several other reactions of this type, involving initial addition of a radical to a double bond, have been proposed (27–29). The hydrogen atoms produced will come to equilibrium with acetaldehyde molecules

[8] $$H + CH_3CHO \rightleftarrows CH_3CHOH,$$

and, owing to the slowness of the dissociation of the radical CH_3CHOH, there will be an induction period for the production of hydrogen molecules.

The point of view that has been arrived at is, therefore, that hydrogen production is due to the two reactions [2] and [7], with the equilibrium [8] leading to an induction period. The maximum rate of hydrogen production by reaction [7] will be roughly equal to the rate of production of acetone. Since hydrogen is also produced as a result of reaction [2], the maximum rate of its production will be somewhat greater than that of acetone, which is what Trenwith (25) found.

Formation of Other Minor Products

Other minor products which have been found in the acetaldehyde pyrolysis are propylene and water (11) and ethylene (15, 25). These products are readily explained as arising through the intermediate CH_3CHOH, as follows:

$$CH_3CHOH + CH_3CHO \rightarrow CH_3CH_2OH + CH_3CO$$
$$CH_3CH_2OH \rightarrow C_2H_4 + H_2O$$
$$CH_3CH_2OH \rightarrow CH_3CHO + H_2$$
$$CH_3CHOH + CH_3 \rightarrow (CH_3)_2CHOH$$
$$(CH_3)_2CHOH \rightarrow CH_3CH{=}CH_2 + H_2O$$
$$(CH_3)_2CHOH \rightarrow CH_3COCH_3 + H_2$$

ACKNOWLEDGMENTS

The authors are indebted to Drs. Margaret H. Back and B. W. Wojciechowski for valuable help and suggestions, and to Dr. P. J. Thomas for a helpful discussion. They also thank Dr. A. B. Trenwith for discussions and for sending them information about his recent unpublished work. One of us (M. E.) is grateful to the Canadian Commonwealth Scholarship and Fellowship Committee for the award of a scholarship. The work was supported in part by the National Research Council and in part by the Petroleum Research Fund.

REFERENCES

1. E. W. R. Steacie. Atomic and free radical reactions. Reinhold Publ. Corp., New York. 1954.
2. F. O. Rice and K. F. Herzfeld. J. Am. Chem. Soc. **56**, 284 (1934).
3. K. Bril, P. Goldfinger, M. Letort, H. Mattys, and M. Niclause. Nature, **166**, 405 (1950).
4. K. Bril, P. Goldfinger, M. Letort, H. Mattys, and M. Niclause. Bull. Soc. Chim. Belg. **59**, 263 (1950).
5. K. J. Laidler and B. W. Wojciechowski. Proc. Roy. Soc. London, Ser. A, **260**, 91 (1961).
6. A. B. Trenwith. J. Chem. Soc. 4426 (1963).
7. C. P. Quinn. Proc. Roy. Soc. London, Ser. A, 275, 190 (1963).
8. C. N. Hinshelwood and W. K. Hutchison. Proc. Roy. Soc. London, Ser. A, **111**, 380 (1926).
9. C. J. M. Fletcher and C. N. Hinshelwood. Proc. Roy. Soc. London, Ser. A, **141**, 41 (1933).
10. C. A. Winkler and C. N. Hinshelwood. Proc. Roy. Soc. London, Ser. A, **149**, 355 (1935).
11. R. V. Sedden and M. W. Travers. Proc. Roy. Soc. London, Ser. A, **156**, 324 (1936).
12. E. Leifer and H. C. Urey. J. Am. Chem. Soc. **64**, 994 (1942).

Can. J. Chem. Downloaded from www.nrcresearchpress.com by 210.87.254.40 on 09/05/12
For personal use only.

13. N. IMAI and O. TOYAMA. Bull. Chem. Soc. Japan, **33**, 1408 (1960).
14. A. BOYER, M. NICLAUSE, and M. LETORT. J. Chim. Phys. **49**, 337, 345 (1952).
15. G. R. FREEMAN, C. J. DANBY, and C. N. HINSHELWOOD. Proc. Roy. Soc. London, Ser. A, **245**, 456 (1958).
16. N. IMAI, Y. YOSHIDA, and O. TOYAMA. Bull. Chem. Soc. Japan, **35**, 752 (1962).
17. K. J. LAIDLER, N. H. SAGERT, and B. W. WOJCIECHOWSKI. Proc. Roy. Soc. London, Ser. A, **270**, 242 (1962).
18. E. K. GILL and K. J. LAIDLER. Proc. Roy. Soc. London, Ser. A, **250**, 121 (1959).
19. E. RABINOWITCH. Trans. Faraday Soc. **33**, 283 (1937).
20. G. PORTER. Discussions Faraday Soc. **33**, 198 (1962).
21. M. EUSUF and K. J. LAIDLER. Trans. Faraday Soc. **59**, 2750 (1963).
22. S. W. BENSON. The foundations of chemical kinetics. McGraw-Hill Book Co., Inc. 1960. pp. 383, 385.
23. D. J. MCKENNEY and K. J. LAIDLER. Can. J. Chem. **41**, 1984 (1963).
24. R. K. BRINTON and D. H. VOLMAN. J. Chem. Phys. **20**, 1053 (1952).
25. A. B. TRENWITH. Private communication.
26. J. G. CALVERT and J. T. GRUVER. J. Am. Chem. Soc. **80**, 1313 (1958).
27. F. E. BLACET and W. E. BELL. Discussions Faraday Soc. **14**, 70 (1953).
28. J. N. PITTS, R. S. TOLLBERG, and T. W. MARTIN. J. Am. Chem. Soc. **76**, 2843 (1954).
29. J. A. KERR and A. F. TROTMAN-DICKENSON. J. Chem. Soc. 3377 (1957).

Can. J. Chem. Downloaded from www.nrcresearchpress.com by 210.87.254.40 on 09/05/12
For personal use only.

Can. J. Chem. Downloaded from www.nrcresearchpress.com by 210.87.254.40 on 09/05/12
For personal use only.

KINETICS AND MECHANISMS OF THE THERMAL DECOMPOSITION OF ACETALDEHYDE

II. THE REACTION IN THE PRESENCE OF NITRIC OXIDE

M. EUSUF AND K. J. LAIDLER
Department of Chemistry, University of Ottawa, Ottawa, Canada

Received March 5, 1964

ABSTRACT

The decomposition of acetaldehyde has been reinvestigated in the presence of various amounts of nitric oxide, over a range of temperatures (495 to 525 °C) and acetaldehyde pressures (36 to 340 mm Hg). At higher acetaldehyde pressures there is no inhibition, the rate steadily increasing with increasing nitric oxide concentration; at low acetaldehyde concentrations increasing amounts of nitric oxide first give inhibition and then give catalysis. The degree of inhibition increases with decrease in temperature. As the nitric oxide concentration is increased, the order rises above 3/2 and then falls to 3/2 again. At higher nitric oxide concentrations the rate varies with $[CH_3CHO]^{3/2}[NO]^{1/2}$. All of the facts are explained by a mechanism according to which initiation occurs by

$$CH_3CHO + NO \rightarrow CH_3CO + HNO$$

together with the processes occurring in the absence of nitric oxide (cf. Part I). Termination is considered to involve the reaction occurring in the case of no inhibition ($CH_3 + CH_3 + X \rightarrow C_2H_6 + X$) together with

$$CH_3 + CH_3NO \rightarrow C_2H_6 + NO$$

and

$$2\ CH_3NO \rightarrow C_2H_6 + 2\ NO.$$

Application of the mechanism to the results is discussed in detail.

INTRODUCTION

The influence of nitric oxide on the kinetics of the thermal decomposition of acetaldehyde has been the subject of a considerable number of investigations (1–5). The reaction has usually been discussed on the assumption that it occurs by a combination of molecular and free-radical mechanisms, the sole function of the nitric oxide being to remove radicals. Wojciechowski and Laidler (6, 7) have recently proposed that when organic decompositions are inhibited by nitric oxide an important role is played by a reaction in which the nitric oxide molecule abstracts a hydrogen atom from the substrate molecule; in addition, they have proposed that chain termination may occur by reaction between radicals and species such as HNO and CH_3NO. These proposals have been successful in leading to a quantitative interpretation of a number of organic decompositions (8–12). The acetaldehyde behavior is a good deal more complicated than the cases previously investigated, and its study therefore provides a valuable test of the validity of the proposed mechanisms. The present paper describes the results of an experimental reinvestigation of the reaction and presents a free-radical mechanism, based on the ideas previously put forward in this laboratory, that appears to be consistent with the results.

EXPERIMENTAL

The apparatus and procedures were the same as described in Part I (13). the nitric oxide used was Matheson Research Grade and was purified by the method of Hughes (14); the distillate collected was completely colorless. Acetaldehyde and nitric oxide were mixed in a spherical flask in appropriate proportions, and complete mixing was ensured by producing a temperature gradient and allowing the gases to stand together for at least 30 minutes.

Can. J. Chem. Downloaded from www.nrcresearchpress.com by 210.87.254.40 on 09/05/12
For personal use only.

RESULTS

Figures 1, 2, and 3 show the effects of nitric oxide on the rate under various conditions. Figure 1 shows that at a relatively low acetaldehyde pressure (52 mm) there is inhibition followed by catalysis; the degree of inhibition decreases with increasing temperatures, there being very little inhibition at 525 °C. The degree of inhibition with acetaldehyde is always very much less than that with the hydrocarbons. Figure 2 shows how the inhibition

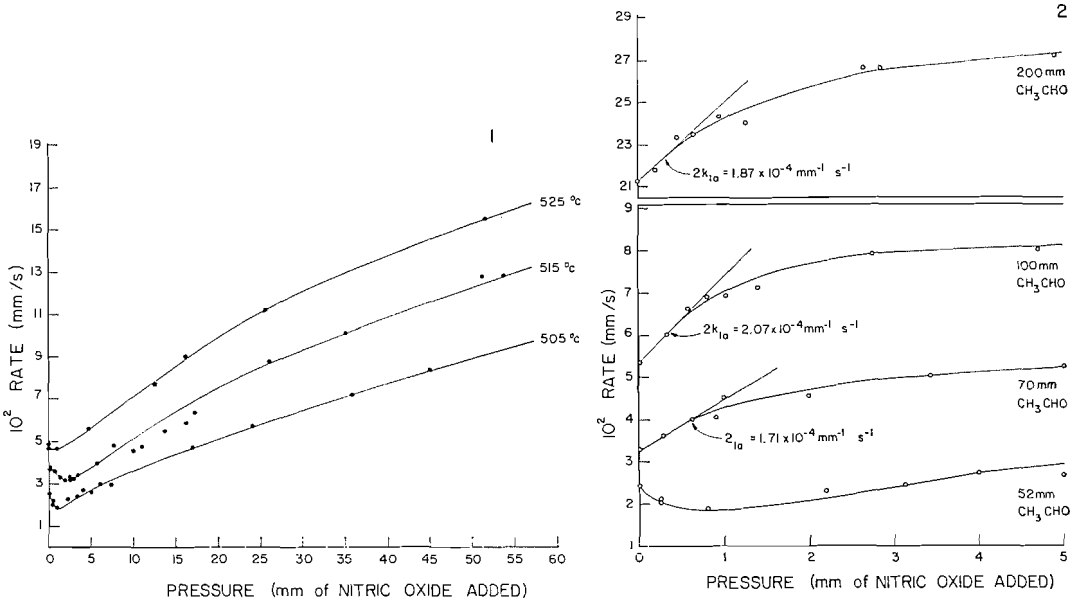

FIG. 1. Effect of temperature on the inhibition by nitric oxide. (Pressure of acetaldehyde = 52 mm).
FIG. 2. Plots of rates against the pressures of nitric oxide added at various acetaldehyde pressures at 505 °C.

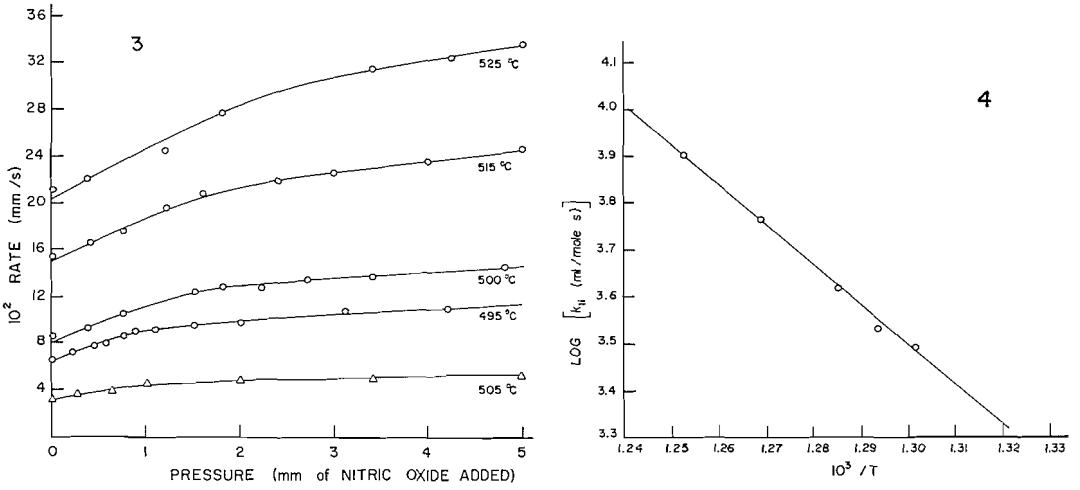

FIG. 3. Plots of rates against the pressures of nitric oxide at different temperatures. ○, 152 mm acetaldehyde; △, 70 mm acetaldehyde.
FIG. 4. Arrhenius plot, the rate constants being those obtained by dividing the initial slopes (Fig. 3) by twice the acetaldehyde concentrations.

curves vary with the acetaldehyde concentration, there being no inhibition at the higher pressures. It will be seen later that at higher acetaldehyde pressures and lower nitric oxide pressures the rate is equal to

$$[i] \qquad v = 2k_{1a}[CH_3CHO][NO] + k'[CH_3CHO]^n$$

where $3/2 < n < 2$ and k_{1a} is the rate constant for the reaction $CH_3CHO + NO \rightarrow CH_3CO + HNO$. From the initial slopes of the curves in Fig. 2, values of k_{1a} have been calculated and are approximately constant.

Figure 3 shows plots of rate against nitric oxide concentration at two acetaldehyde pressures (70 and 152 mm) and at various temperatures. From the k_{1a} values calculated from the initial slopes the Arrhenius plot shown in Fig. 4 has been obtained; the activation energy is 38.9 kcal per mole, and the rate constant can be represented by

$$k_{1a} = 3.46 \times 10^{14}\, e^{-38900/RT} \text{ cc mole}^{-1}\text{ s}^{-1}.$$

The results indicate that the order of the reaction with respect to acetaldehyde is 3/2 when the ratio $[NO]/[CH_3CHO]$ is high, but is greater than 3/2 when the ratio is low. This effect is shown in Fig. 5: the order is 3/2 over the entire range of acetaldehyde pressures when the pressure of nitric oxide is 50 mm, but the order is approximately 1.8 at higher acetaldehyde pressures when the nitric oxide pressure is 5 mm. Figure 6 confirms the 3/2 order at the higher nitric oxide pressure and at four temperatures. The results of Freeman, Danby, and Hinshelwood (4) are added for comparison and are seen to be in excellent agreement.

At higher acetaldehyde pressures the rate varies not only with $[CH_3CHO]^{3/2}$ but with $[NO]^{1/2}$; this result, which was reported by Freeman, Danby, and Hinshelwood (4), is

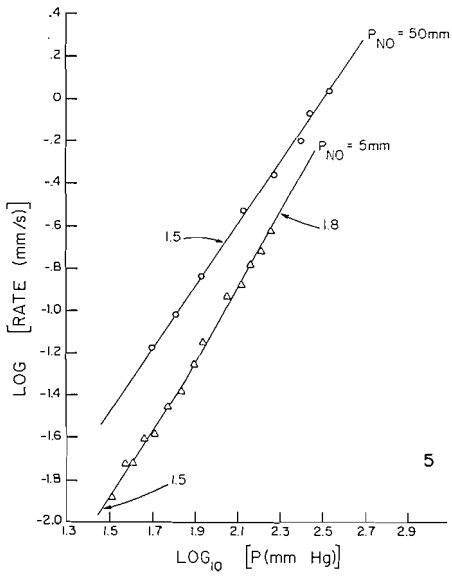

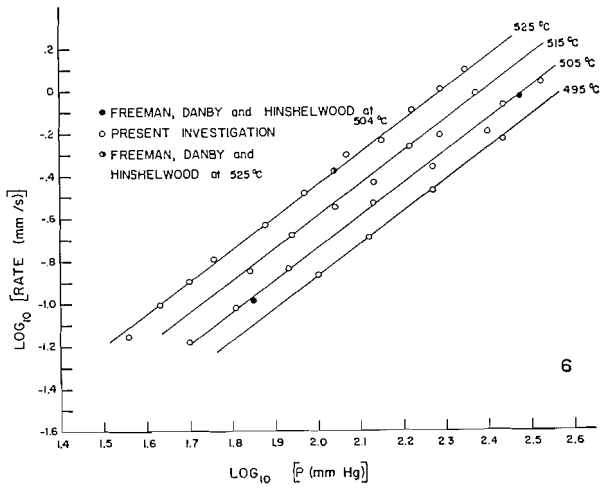

FIG. 5. Plots of log rate against log pressure of acetaldehyde at 505 °C, showing the effects of nitric oxide on the order with respect to acetaldehyde. ○, 50 mm nitric oxide; △, 5 mm nitric oxide.

FIG. 6. Plots of log rate against log pressure of acetaldehyde at different temperatures with 50 mm nitric oxide added.

Can. J. Chem. Downloaded from www.nrcresearchpress.com by 210.87.254.40 on 09/05/12
For personal use only.

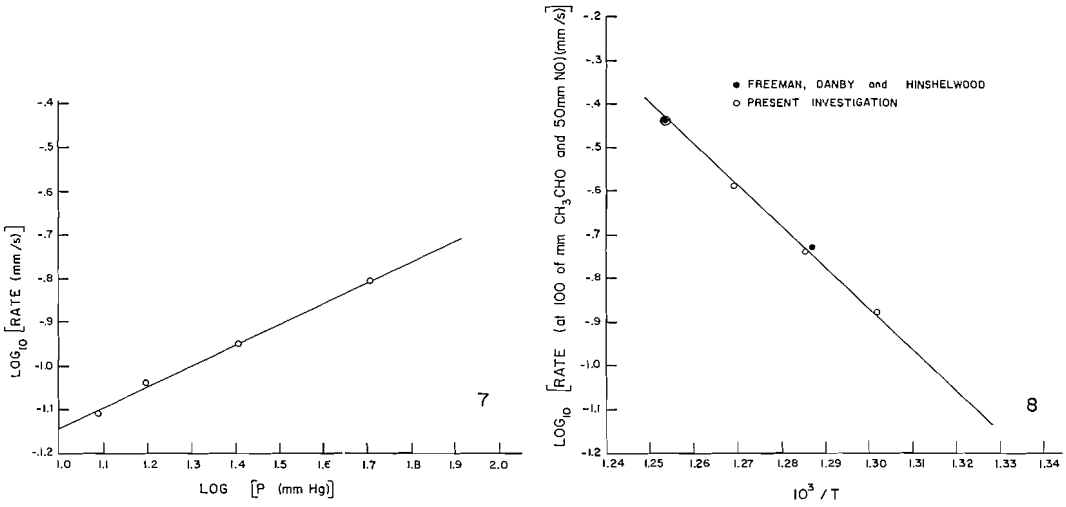

FIG. 7. Plot of log rate against log pressure of nitric oxide added to 52 mm acetaldehyde at 525 °C.
FIG. 8. Arrhenius plot in the region of 3/2 order with respect to acetaldehyde and 1/2 order with respect to nitric oxide.

illustrated by Fig. 7. Figure 8 shows an Arrhenius plot for this region, in which the rate varies with $[CH_3CHO]^{3/2}$ $[NO]^{1/2}$, and leads to the rate constant

$$k = 2.2 \times 10^{15}\, e^{-43500/RT} \text{ cc mole}^{-1}\, s^{-1}.$$

The main results for orders of reaction are summarized in Fig. 9.

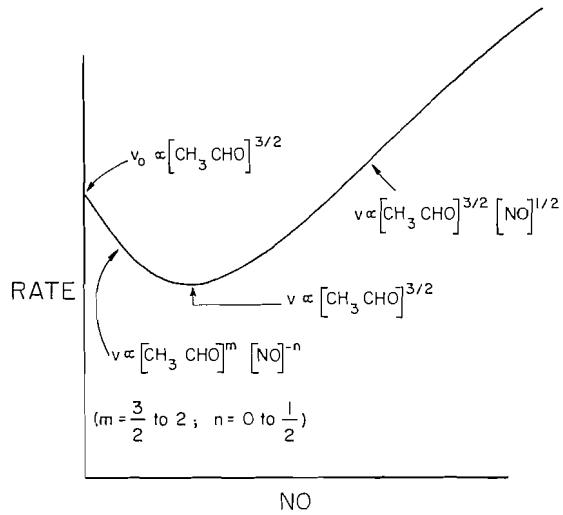

FIG. 9. Schematic diagram showing the reaction orders at various concentrations of nitric oxide.

DISCUSSION

The Reaction Mechanism

In treating the decompositions of hydrocarbons and of ether it has proved expedient to consider, as a separate problem, the situation at maximal inhibition; under these conditions the nitric-oxide-induced initiation reaction can be shown to be much more

Can. J. Chem. Downloaded from www.nrcresearchpress.com by 210.87.254.40 on 09/05/12
For personal use only.

important than the other initiation processes. In the acetaldehyde decomposition, however, there is no flat region when velocity is plotted against nitric oxide concentration. The situation is therefore more complicated, in that one must take into account the initiation processes that occur in the absence of nitric oxide (cf. Part I) together with the reaction

$$NO + CH_3CHO \rightarrow CH_3CO + HNO.$$

In the same way one must include the termination process for the uninhibited reaction (cf. Part I), together with the termination reactions that become important after nitric oxide is added:

$$CH_3 + CH_3NO \rightarrow C_2H_6 + NO$$
$$CH_3NO + CH_3NO \rightarrow C_2H_6 + 2NO.$$

The last reaction has been omitted in previous schemes, but must be included here on account of the higher CH_3NO concentrations resulting from the somewhat lower temperatures employed.

The complete scheme may be written as

[1] $2CH_3CHO \rightarrow CH_3 + CHO + CH_3CHO$

[1′] $2CH_3CHO \rightarrow CH_3CHOH + CH_3CO$

[1i] $CH_3CHO + NO \rightarrow HNO + CH_3CO$

[2a] $X + CHO \rightarrow CO + H + X$

[2] $CH_3CHOH \rightarrow CH_3CHO + H$

[2i] $X + HNO \rightarrow H + NO + X$

[3] $H + CH_3CHO \rightarrow H_2 + CH_3CO$

[4] $CH_3CO + X \rightarrow CH_3 + CO + X$

[5] $CH_3 + CH_3CHO \rightarrow CH_4 + CH_3CO$

[5i] $CH_3NO + CH_3CHO \rightarrow CH_4 + CH_3CO + NO$

$$CH_3 + NO + X \underset{[-9]}{\overset{[9]}{\rightleftharpoons}} CH_3NO + X \underset{[-10]}{\overset{[10]}{\rightleftharpoons}} CH_2{=}NOH + X \xrightarrow{[11]} HCN + H_2O \text{ etc.}$$

[6a] $2CH_3 + X \rightarrow C_2H_6 + X$

[6i] $CH_3 + CH_3NO \rightarrow C_2H_6 + NO$

[6i′] $CH_3NO + CH_3NO \rightarrow C_2H_6 + 2NO.$

The numbering is consistent with the mechanism of Part I. X represents a third body, which may be acetaldehyde itself.

Application of the steady-state treatment, with the usual approximations, leads to the following expressions for the concentrations of CH_3CO, CH_3, and CH_3NO and for the rate of decomposition.

[ii] $$[CH_3CO] = \left(\frac{(k_1 + 2k_1')[CH_3CHO] + 2k_{1i}[NO] + k_5[CH_3] + k_{5i}[CH_3NO]}{k_4}\right)\frac{[CH_3CHO]}{[X]}$$

[iii] $$[CH_3] = \left(\frac{(k_1 + k_1')[CH_3CHO] + k_{1i}[NO]}{k_{6a}[X] + k_{6i}K_9[NO] + k_{6i}'K_9^2[NO]^2}\right)^{1/2}[CH_3CHO]^{1/2}$$

[iv] $$[CH_3NO] = K_9[CH_3][NO] \qquad (K_9 = k_9/k_{-9})$$

[v] $$v = 2(k_1 + k_1')[CH_3CHO]^2 + 2k_{1i}[CH_3CHO][NO] + k_5[CH_3][CH_3CHO] + k_{5i}[CH_3NO][CH_3CHO]$$

Can. J. Chem. Downloaded from www.nrcresearchpress.com by 210.87.254.40 on 09/05/12
For personal use only.

$$[\text{vi}] \qquad = 2k_{1\text{i}}[CH_3CHO][NO] + k_5\left(\frac{k_1 + k_1'}{k_6}\right)^{1/2} \frac{\left(1 + \frac{k_{5\text{i}}}{k_5}K_9[NO]\right)\left([CH_3CHO] + \frac{k_{1\text{i}}}{(k_1 + k_1')}[NO]\right)^{1/2}}{\left([CH_3CHO] + \frac{k_{6\text{i}}}{k_6}K_9[NO] + \frac{k_{6\text{i}}'}{k_6}K_9^2[NO]^2\right)^{1/2}}[CH_3CHO]^{3/2}$$

A number of important special cases of this rate equation are as follows.

(1) If [NO] is zero the equation reduces to

$$v = k_5\left(\frac{k_1 + k_1'}{k_6}\right)^{1/2}[CH_3CHO]^{3/2}.$$

This is merely a check that in the absence of nitric oxide the equation reduces to equation [vii] of Part I.

(2) It can be shown by conventional methods that the second term in equation [vi] passes through a minimum only if

$$[CH_3CHO] < \frac{\frac{k_{6\text{i}}}{k_6}K_9 - \frac{k_{1\text{i}}}{(k_1 + k_1')}}{2\frac{k_{5\text{i}}}{k_5}}.$$

This explains why there is inhibition only at low concentrations of acetaldehyde; at higher concentrations the rate increases steadily with increasing nitric oxide concentration.

(3) If [NO] is sufficiently small that

$$\frac{k_{5\text{i}}}{k_5}K_9[NO] \ll 1, \qquad \frac{k_{6\text{i}}'}{k_6}K_9^2[NO]^2 \ll \frac{k_{6\text{i}}}{k_6}K_9[NO],$$

and

$$\frac{k_{1\text{i}}}{(k_1 + k_1')}[NO] \ll [CH_3CHO],$$

the rate equation reduces to

$$[\text{vii}] \qquad v = 2k_{1\text{i}}[CH_3CHO][NO] + k_5\left(\frac{k_1 + k_1'}{k_6}\right)^{1/2}\frac{[CH_3CHO]^2}{\left([CH_3CHO] + \frac{k_{6\text{i}}}{k_6}K_9[NO]\right)^{1/2}}$$

of which the first term is usually smaller than the second. Three sub-cases are of particular interest.

(*a*) If $[CH_3CHO]$ is also sufficiently small, there will be inhibition by nitric oxide, and the order with respect to acetaldehyde will be between 3/2 and 2. This is exactly the behavior observed. In the limit of very low acetaldehyde concentrations the order will be 2, and the rate will vary with $1/[NO]^{1/2}$.

(*b*) If $[CH_3CHO]$ is not small, the term $(k_{6\text{i}}/k_6)K_9[NO]$ in equation [vii] will be negligible, and there will be no appreciable inhibition. Instead there will be acceleration at all concentrations of nitric oxide, owing to the increase in the term $2k_{1\text{i}}[CH_3CHO][NO]$. It was on this basis that the value of $k_{1\text{i}}$, and that of the corresponding activation energy E, is calculated.

Can. J. Chem. Downloaded from www.nrcresearchpress.com by 210.87.254.40 on 09/05/12
For personal use only.

(*c*) If [CH_3CHO] is small but [NO] is not particularly small, the dominant terms in equation [vi] are

$$\frac{k_{5i}}{k_5}K_9[NO], \qquad \frac{k_{1i}}{k_1 + k_1'}[NO], \qquad \text{and} \qquad \frac{k_{6i}'}{k_6}K_9^2[NO]^2.$$

Under these circumstances the rate equation reduces to

[viii] $$v = 2k_{1i}[CH_3CHO][NO] + k_{5i}\left(\frac{k_{1i}}{k_{6i}'}\right)^{1/2}[CH_3CHO]^{3/2}[NO]^{1/2}.$$

If [NO] is not too high, the second term is dominant, and the orders with respect to acetaldehyde and nitric oxide will therefore be 3/2 and 1/2 respectively, in agreement with experiment.

The Elementary Reactions

Some of the postulated elementary reactions may now be considered in more detail; those occurring in the uninhibited reaction were dealt with in Part I, and only the reactions involving nitric oxide are discussed here. The experimental results show that under certain conditions the reaction is 1/2 order in nitric oxide, and this fact is a very strong indication that nitric oxide is involved in the initiation of a chain reaction. On this basis one can exclude, as an important reaction, the process

$$CH_3CHO + NO \rightarrow CH_4 + CO + NO$$

postulated by Freeman, Danby, and Hinshelwood (4). Freeman *et al.* also suggested the reaction

$$CH_3CHO + NO \rightarrow NO + 2R + \text{product}$$

but this would have a higher activation energy than the experimental value of 38.9 kcal. Reaction [1i], on the other hand, is endothermic by 36.4 kcal (on the basis of $D(HNO)$ = 48.6 kcal and $D(CH_3CO—H)$ = 85 kcal per mole); the activation energy is entirely consistent with this and provides good support for the proposed reaction. Initiation might alternatively occur as

$$CH_3CHO + NO \rightarrow CH_3NO + CHO$$

but there is nothing to support this suggestion.

Reaction [5i], the abstraction of a hydrogen atom by CH_3NO, is an important reaction in the present scheme, since it explains why the degree of inhibition of the acetaldehyde decomposition is much smaller than with hydrocarbon decompositions, in which the analogous reaction has a higher activation energy and therefore occurs more slowly. A reaction analogous to [5i] has been postulated by Szabó and Márta (15, 16) as playing a role in the propionaldehyde decomposition. Ree, Yang, and Eyring (17) have also considered reactions of the same type and have described the action of nitric oxide as a "saloon effect"; the nitric oxide molecule is playing the role of a "chaperon" but acts as a negative catalyst by making the radical less reactive. Ree *et al.* have suggested a method for estimating the activation energies for reactions such as [5i]. For this reaction their method leads to a value of 26 kcal per mole, to be compared with 39.5 in the case of abstraction from a hydrocarbon molecule.

The disappearance of CH_3NO by reactions [10] and [11] has been suggested by Mitchell and Hinshelwood (18). Reaction [11] has been demonstrated by Taylor and Bender (19), and the occurrence of reaction [10] is suggested by the work of Gowenlock and Trotman (20), Batt and Gowenlock (21), and Lüttke (22). Some evidence for reaction [−10] is obtained from the work of Taylor and Bender (19), who found that ethane is formed in the decomposition of formaldoxime $CH_2{=}NOH$.

Can. J. Chem. Downloaded from www.nrcresearchpress.com by 210.87.254.40 on 09/05/12
For personal use only.

Reaction [6i] was suggested by Freeman, Danby, and Hinshelwood (4) in the acetaldehyde decomposition induced by nitric oxide, and McKenney, Wojciechowski, and Laidler (11) postulate it in the dimethyl ether decomposition. Hoare (23) has also found evidence for reaction between nitrosomethane and methyl radicals in the photolysis of acetone at 200 °C. At this lower temperature he found that an average of between 2 and 3 methyl radicals were used up per nitric oxide molecule. Reaction [6i′] was first postulated by Taylor and Vesselowsky (24) in the decomposition of nitromethane, and Szabó and Márta (15, 16) have postulated the analogous reaction involving C_2H_5NO in the propionaldehyde decomposition. An attempt to detect the chain-ending products in the absence and presence of nitric oxide has been made by Freeman, Danby, and Hinshelwood (4), who found that the ratio C_2H_6/CH_4 is increased by the addition of nitric oxide. That nitric oxide reduces markedly the concentration of CH_3 radicals is now beyond question. The increase of ethane production in the presence of nitric oxide must, therefore, be attributed to the occurrence of reactions [6i] and [6i′]. In other words, nitric oxide acts as a 'chaperon' in the combination of methyl radicals. This is an example of the radical–molecule complex mechanism which has recently been considered theoretically by Eusuf and Laidler (25). Porter, Szabó, and Townsend (26) have shown that reactions analogous to [6i] and [6i′] occur in the combination of iodine atoms.

An estimate of the activation energy for reaction [6i′] can be made on the basis of the experimental activation energy of 43.5 kcal for the reaction in which the rate varies with $[CH_3CHO]^{3/2}[NO]^{1/2}$. This activation energy is seen from equation [viii] to be $E_{5i} + \frac{1}{2}(E_{1i} - E_{6i}')$. E_{1i} has been seen to be 38.9 kcal, and E_{5i} was estimated above to be 26 kcal. These figures lead to a value of 3.9 kcal per mole for E_{6i}', which seems reasonable.

ACKNOWLEDGMENTS

One of us (M. E.) is grateful to the Canadian Commonwealth Scholarship and Fellowship Committee for the award of a scholarship. The work was supported in part by the National Research Council of Canada and in part by the Petroleum Research Fund.

REFERENCES

1. L. A. K. Staveley and C. N. Hinshelwood. Nature, **137**, 29 (1936).
2. L. A. K. Staveley and C. N. Hinshelwood. J. Chem. Soc. 812 (1936).
3. J. R. E. Smith and C. N. Hinshelwood. Proc. Roy. Soc. London, Ser. A, **180**, 237 (1942).
4. G. R. Freeman, C. J. Danby, and C. N. Hinshelwood. Proc. Roy. Soc. London, Ser. A, **245**, 456 (1958).
5. F. O. Rice and R. E. Varnerin. J. Am. Chem. Soc. **76**, 2629 (1954).
6. B. W. Wojciechowski and K. J. Laidler. Can. J. Chem. **38**, 1027 (1960).
7. B. W. Wojciechowski and K. J. Laidler. Trans. Faraday Soc. **59**, 369 (1963).
8. K. J. Laidler and B. W. Wojciechowski. Proc. Roy. Soc. London, Ser. A, **260**, 103 (1961).
9. K. J. Laidler, N. H. Sagert, and B. W. Wojciechowski. Proc. Roy. Soc. London, Ser. A, **270**, 254 (1962).
10. N. H. Sagert and K. J. Laidler. Can. J. Chem. **41**, 848 (1963).
11. D. J. McKenney, B. W. Wojciechowski, and K. J. Laidler. Can. J. Chem. **41**, 1993 (1963).
12. K. J. Laidler and D. J. McKenney. Proc. Roy. Soc. In press. 1964.
13. M. Eusuf and K. J. Laidler. Can. J. Chem. In press. 1964.
14. E. E. Hughes. J. Chem. Phys. **35**, 1531 (1961).
15. Z. G. Szabó and F. Márta. J. Am. Chem. Soc. **83**, 768 (1961).
16. Z. G. Szabó and F. Márta. Acta Chim. Acad. Sci. Hung. **32**, 81 (1962).
17. T. Ree, H. Yang, and H. Eyring. Trans. Faraday Soc. **58**, 2375 (1962).
18. J. W. Mitchell and C. N. Hinshelwood. Proc. Roy. Soc. London, Ser. A, **159**, 32 (1937).
19. H. A. Taylor and H. Bender. J. Chem. Phys. **9**, 761 (1941).
20. B. G. Gowenlock and J. Trotman. J. Chem. Soc. 4190 (1955).
21. L. Batt and B. G. Gowenlock. Trans. Faraday Soc. **56**, 682 (1960).
22. W. Lüttke. Z. Elektrochem. **61**, 302 (1957).
23. D. E. Hoare. Can. J. Chem. **40**, 2012 (1962).
24. H. A. Taylor and V. V. Vesselowsky. J. Phys. Chem. **39**, 1095 (1935).
25. M. Eusuf and K. J. Laidler. Trans. Faraday Soc. **59**, 2750 (1963).
26. G. Porter, Z. G. Szabó, and M. G. Townsend. Proc. Roy. Soc. London, Ser. A, **270**, 493 (1962).

Can. J. Chem. Downloaded from www.nrcresearchpress.com by 210.87.254.40 on 09/05/12
For personal use only.

Can. J. Chem. Downloaded from www.nrcresearchpress.com by 210.87.254.6 on 09/05/12
For personal use only.

RADIOLYSIS OF CYCLOHEXANONE

I. PURE LIQUID

AJIT SINGH AND GORDON R. FREEMAN
Department of Chemistry, University of Alberta, Edmonton, Alberta

Received January 31, 1964

ABSTRACT

The G values of the major products of the gamma-radiolysis of liquid cyclohexanone are: hydrogen (0.76), carbon monoxide (0.45), 1-pentene (0.22), 5-hexenal (0.85), cyclohexenone (0.4), cyclohexanol (0.5), "dimer" (1.15), and polymer (1.8 cyclohexanone units). A large number of minor products were also measured.

The amount of ring cleavage that occurs in cyclohexanone is much greater than that which occurs in the radiolysis of cyclohexane. The increase has been attributed to the influence of the carbonyl group on the course of the reaction. Ring cleavage occurs preferentially at the C—C bonds to the carbonyl group.

Much of the radiolytic reaction appears to occur from energy states higher than those of importance in the photolytic studies.

INTRODUCTION

One aim of this investigation was to determine whether the presence of a carbonyl group in a molecule would cause bond cleavage to occur preferentially adjacent to it in a radiation chemical primary reaction. The net amount of ring cleavage that occurs during the radiolysis of liquid cyclohexane is small (1, 2). In cyclohexanone, the activating effect of the carbonyl group should appear as ring cleavage. Moreover, it does not seem likely that ring cleavage would occur in secondary chemical reactions.

The radiolysis of various ketones has been the subject of limited investigations (3–12). Acetone has been studied in some detail (3–9) but, except for a cursory study of cyclopentanone (10), cyclic ketones have been neglected. Some ketones have also been used as solutes in the study of the radiolyses of hydrocarbons, alcohols, and water (13–16).

EXPERIMENTAL

Materials

Cyclohexanone (Eastman Kodak White Label and Allied Chemical) was distilled through an 18 in. fractionating column filled with glass helices. The middle 50% of the distillate was collected and redistilled several times. Multiple distillations reduced the amount of impurities that was initially present, but led simultaneously to the formation of a small amount of an unidentified impurity (U.I.). The purified ketone used in most of the experiments contained less than 0.02% total impurities with each of U.I., cyclohexanol, and cyclohexenone being less than 0.01%. The purity was measured by gas chromatography using Ucon, Carbowax, silicone grease, and Apiezon L columns.

Singly distilled ketone (impurities $<0.04\%$) was used for the 10 ml samples that were irradiated for the measurement of the polymer yield. The distilled ketone was kept in a desiccator until used.

The 2,2′-diketodicyclohexyl (DKDC) was prepared by the reaction of di-*tert*-butyl peroxide with cyclohexanone (17). Gas chromatographic analysis of the reaction mixture indicated the formation of several other dimeric products besides DKDC. Infrared spectral analyses of these dimers showed that they were closely related to DKDC. The reaction mixture was distilled twice under vacuum and the fraction used (b.p. 123°/1–2 mm) contained $\sim$83% DKDC.

The following is a list of the gas chromatographic materials used, with the suppliers given in brackets. Kromat FB, Kromat CE, high activity charcoal, and medium activity silica gel (Burrell Corp.); Carborundum 60SGM (Carborundum Co.); Carbowax 1540 and Ucon LB-1800X (Carbide and Carbon Chemicals Co.); silicone grease (Dow Corning); silicone rubber (Wilkins Instrument and Research Inc.); di-*n*-decyl phthalate (Eastman Kodak); Apiezon L grease (Metropolitan-Vickers Electrical Co.).

Preparation of Samples

Most cells were filled by distillation under vacuum of thoroughly degassed cyclohexanone; others were

filled with a pipette and then degassed under vacuum. Gaseous product yields were the same for both methods.

The density of cyclohexanone at various temperatures was calculated from data in the International Critical Tables.

Irradiation of Samples

The samples were irradiated with ^{60}Co γ-rays. Dose rates were determined with the Fricke dosimeter, using $G(Fe^{3+}) = 15.5$, $\epsilon(Fe^{3+}) = 2225$ at 25 °C and 304 mμ, and the electron densities of the Fricke dosimeter and cyclohexanone. The sample temperature during irradiation was 24 ± 3 °C.

Analyses

Gaseous products were separated by successive distillations through two traps at −196° and then at −70°. Each fraction was collected and measured in a combination Toepler pump – McLeod gauge and then analyzed by gas chromatography. The remaining liquid was analyzed for C_6 products only. Samples that were used only for the analysis of liquid products were opened just before use and were corked and kept in a desiccator between injections of aliquots onto the gas chromatograph. The samples that were irradiated for the estimation of polymeric products, other than dimers, were broken open and most of the contents removed by vacuum distillation at room temperature. When the cyclohexanone seemed to have been removed, the cell was weighed. The soluble contents of the cell were removed by rinsing it with three aliquots of about 1 ml each of Spectrograde chloroform. The chloroform solution so obtained was analyzed by gas chromatography for its monomer and dimer content. The cell was dried and weighed again. The weight of polymer was deduced from the loss of weight of the cell, after correction for the presence of monomer and dimer.

The chloroform soluble polymer was sent to Germany for molecular weight determinations and for C, H, and O analyses.*

Some of the cells were analyzed for insoluble polymer by combustion.*

The identification of most of the products was based on their gas chromatographic retention times, together with information from their infrared and mass spectral analyses. A modified procedure (18) for the reaction of formaldehyde with Eegrive's reagent (19) was used to test for the presence of that aldehyde. A modified (18) arsenious oxide method (20) was used for the estimation of peroxides.

Authentic samples of the identified products were used for calibrations, as far as possible. Calibration factors from 5-hexen-2-one were used for 5-hexenal. Factors from 2-cyclohexenone and DKDC were used for cyclohexenone and dimers, respectively.

Identification of Products

The details of identification of only the less commonly available compounds will be reported here.

5-Hexenal

An authentic sample of 5-hexenal could not be obtained commercially, so this compound was identified as one of the radiolysis products as follows: The retention times of the radiolysis product on various gas chromatographic columns were compared with those of related compounds under the same conditions (18). Infrared analysis of the product, collected after separation on Ucon, di-*n*-decyl phthalate, and Carbowax columns, indicated the presence of $CH_2{=}CH$ (bands at 3070–3080 cm^{-1} and 905 cm^{-1}), C=C (band at 1638 cm^{-1}), aldehydic C—H (2710 cm^{-1} and 2810 cm^{-1}), and C=O (1714 cm^{-1}). If the product was an α,β-unsaturated aldehyde the C=O vibrations should have been in the region 1680–1705 cm^{-1}, and if it had contained a ketonic group in a four or five membered ring the C=O vibrations should have been in the region 1740–1775 cm^{-1}. Thus, the infrared spectrum of the product is consistent with its identification as 5-hexenal.

The product was collected from the Ucon column for mass spectral analysis. A blank from the column was collected for 240 s, whereas the 5-hexenal product peak was collected for 112 s. The blank was assumed to be uniform during the two collections. The mass spectrum of the 5-hexenal, suitably corrected for the blank, is given in Table I. The values for the corresponding ions in the cyclohexanone mass spectrum are listed for comparison. The values of the abundances of the various ions are given relative to the most abundant ion in a given spectrum as 100. Ions that have abundance values less than 3 in 5-hexenal have been omitted. The present mass spectrum of 5-hexenal agrees well with the one obtained by Srinivasan (21). Values of ions from water (m/e = 17 and 18), air (m/e = 28, 32, and 44), and carbon tetrachloride (m/e = 35, 37, 47, 49, 82–86, and 117–123) have been omitted. Carbon tetrachloride contamination of the 5-hexenal was a result of the collection procedure.

Unidentified Impurity (U.I.)

The unidentified impurity gave a doublet peak on the Ucon column. Its infrared spectrum indicated the presence of C=C (1638 cm^{-1}) and a C=O in a C_5 ring (1740 cm^{-1}). Such a product has not been reported in the pyrolysis of cyclohexanone (22).

Cyclohexenone

Cyclohexenone was separated from cyclohexanone on the Ucon and Carbowax columns. Its infrared

F. Pascher and E. Pascher, Mikroanalytisches Laboratorium, Bonn, Buschstrasse 54, Germany.

Can. J. Chem. Downloaded from www.nrcresearchpress.com by 210.87.254.6 on 09/05/12
For personal use only.

TABLE I

Mass spectra of 5-hexenal and cyclohexanone

m/e	5-Hexenal	Cyclohexanone	*m/e*	5-Hexenal	Cyclohexanone
14	5.4	0.9	55	53.7	*100.0*
15	3.4	2.2	56	17.6	11.8
16	3.4	0.0	57	19.5	1.5
26	6.0	3.7	58	5.6	0.1
27	46.6	19.1	67	6.8	1.3
29	52.1	6.7	69	20.9	37.5
38	6.3	2.4	70	12.0	21.2
39	79.1	19.8	71	3.2	1.8
40	12.5	6.1	73	6.1	0.0
41	97.4	29.4	79	5.8	0.7
42	49.0	73.4	80	41.4	4.1
43	63.9	11.2	81	3.5	0.4
45	13.4	0.0	91	8.5	0.0
50	3.4	1.4	92	6.1	0.0
51	5.2	1.8	97	3.9	4.0
53	12.9	2.8	98	11.1	38.6
54	*100.0*	7.5			

spectrum showed the presence of C=C—C=O (1686 cm^{-1}) and CH=CH (3015, 1305, and 665 cm^{-1}) (23), thus indicating the presence of 2-cyclohexenone. However, the presence of 3-cyclohexenone cannot be ruled out on the basis of this work.

C_{12} Products

Analysis of radiolyzed cyclohexanone on the silicone grease column gave five peaks (two of which were doublets) in the region of DKDC. The retention time of the largest peak agreed with that of DKDC and the four smaller peaks were considered to be due to similar compounds.

Quantitative Results

Fragmentation Products

The yield of hydrogen seems to decrease slightly whereas that of carbon monoxide appears to increase slightly with increasing dose (Fig. 1). The initial yields, i.e., the G values extrapolated to zero dose, are $G_i(H_2) = 0.76 \pm 0.03$ and $G_i(CO) = 0.45 \pm 0.03$.

The yields of other fragmentation products were also measured and their yields were independent of dose, within experimental error. The results are summarized in Tables II and III.

TABLE II

Initial yields of major products

Product	G_i[a]
Hydrogen	0.76 ± 0.03
Carbon monoxide	0.45 ± 0.03
1-Pentene	0.22 ± 0.04
5-Hexenal	0.85 ± 0.15
Cyclohexenone	0.4 ± 0.2
Cyclohexanol	0.5 ± 0.3
Total dimer[b]	1.2 ± 0.4
Polymer	1.8 ± 0.3[c]

[a]The possible error, in each case, is estimated visually from appropriate plots.

[b]The value, $G_i \approx 1.2$, was obtained from the average of the G values for total dimer obtained from two columns (silicone grease and Apiezon L).

[c]This value is obtained by linear extrapolation to zero dose from the values obtained in the region 1.8–9.2 (10^{20} eV/ml), and the linear extrapolation might not be valid (see Fig. 4).

C_6 Products

The yields of 5-hexenal and cyclohexenone decrease with increasing dose (Fig. 2). The initial yield of 5-hexenal is 0.85 ± 0.15. The accuracy of the cyclohexenone measurements was not as good as the precision shown in Fig. 2A. Cyclohexenone was measured on the tail of the cyclohexanone peak, and the calibration

Can. J. Chem. Downloaded from www.nrcresearchpress.com by 210.87.254.6 on 09/05/12
For personal use only.

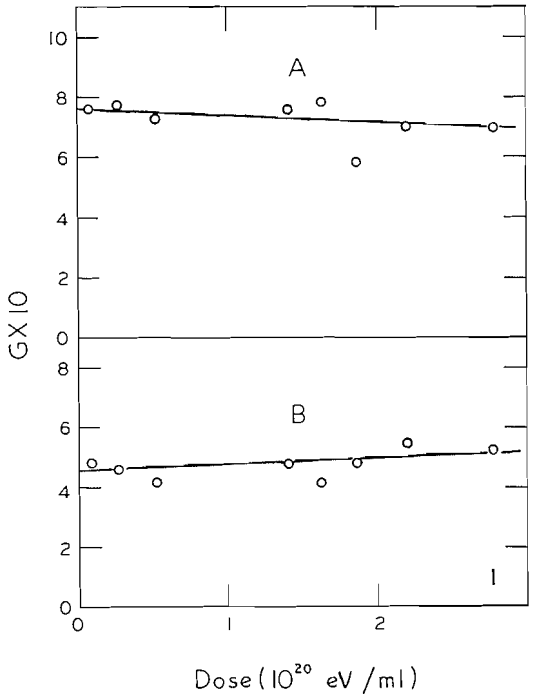

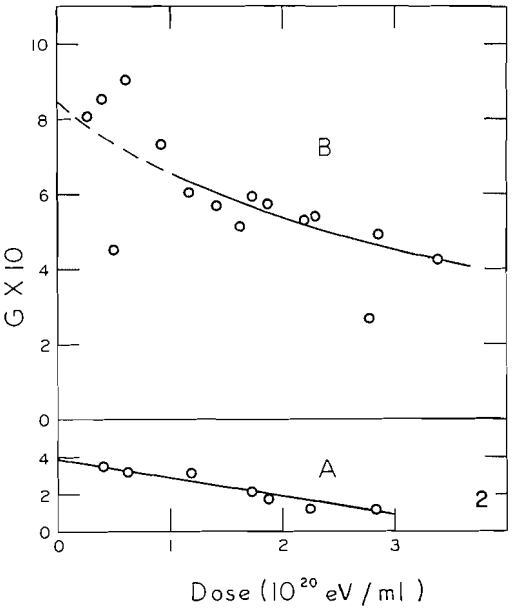

FIG. 1. Hydrogen and carbon monoxide yields: (A) hydrogen, (B) carbon monoxide.
FIG. 2. Yields of cyclohexenone and 5-hexenal: (A) cyclohexenone, (B) 5-hexenal.

TABLE III

Yields of minor products at[a] 2.5×10^{20} eV/ml

Product	G^b
Methane	<0.005
Ethane	0.005±0.002
Ethylene	0.12±0.03[c]
Acetylene	0.003±0.001
Propane	0.002±0.001
Cyclopropane	0.013±0.003[c]
Propylene	0.026±0.004[c]
Methyl acetylene	~0.002
Allene	~0.001
n-Butane	~0.0008
1-Butene	0.002±0.001
Butadiene	~0.001
n-Pentane	0.023±0.004[c]
Cyclopentane	0.04±0.01
2-Pentene	~0.004
Peroxides	≤0.3[d]
Polymer ($CHCl_3$ insoluble)	~0.1[e]

[a]Unless otherwise stated.
[b]The possible error is estimated visually from the appropriate figures.
[c]Extrapolated value for zero dose, G_i.
[d]On the basis of analysis of two samples, one each at 2×10^{20} eV/ml and 5×10^{20} eV/ml.
[e]Average of four samples in the range 1.8–9.2 (10^{20} eV/ml).

factors, determined at various times, were only constant to within about 50%. Therefore, G_i(cyclohexenone) = 0.4±0.2.

Difficulty was also experienced in separating cyclohexanol from a large excess of cyclohexanone. Thus, the results obtained for cyclohexanol are not too satisfactory (Fig. 3). It appears that G_i(cyclohexanol) = 0.5±0.3.

Can. J. Chem. Downloaded from www.nrcresearchpress.com by 210.87.254.6 on 09/05/12
For personal use only.

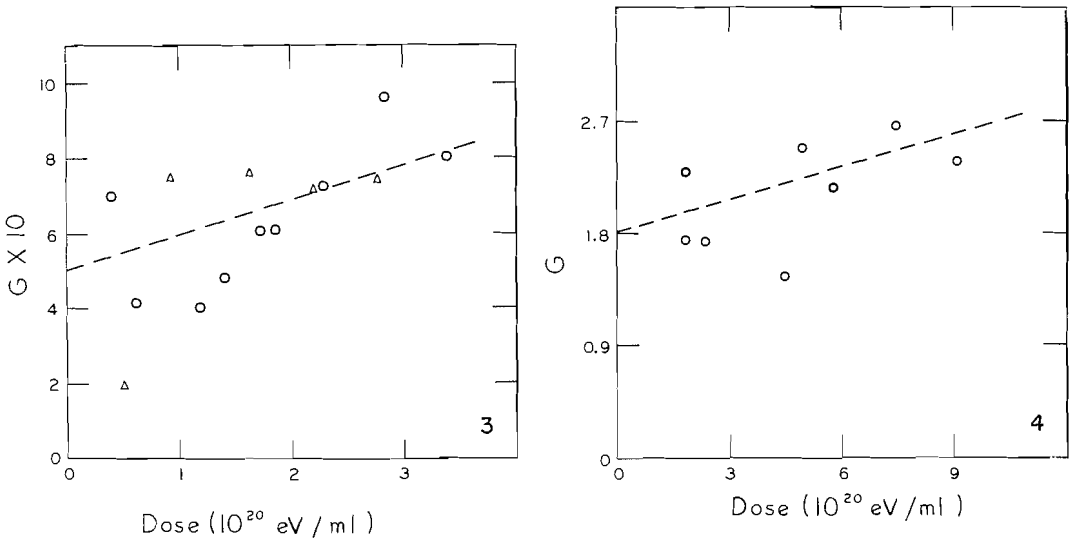

FIG. 3. Cyclohexanol: O average of values from the Ucon and the Carbowax columns; △ values from the Ucon column.
FIG. 4. Yield of polymer.

C_{12} Products

The C_{12} products were analyzed on Apiezon L and on silicone grease columns. At least five different C_{12} compounds were formed but only DKDC was available for standard calibrations. For this reason, it is estimated that the value of G_i(total dimer) = 1.2 might be in error by as much as 0.4 units (Table II). The yield had decreased to G(total dimer) = 0.8 at a dose of 3.4×10^{20} eV/ml. About 50% of the total dimer was DKDC.

Polymer

The yield of the chloroform soluble polymer, in units of cyclohexanone molecules consumed to form polymer, is shown as a function of dose in Fig. 4. The polymer yield probably increases with increasing dose and G_i(polymer) appears to be about 1.8.

For one sample (dose = 5×10^{20} eV/ml), the volatile contents of the cell were removed in the usual way and the cell was sealed while still under vacuum. The cell was then sent to Germany for microanalysis of its remaining contents.* The average composition of the samples referred to in Fig. 4 was polymer:dimer:monomer::70:19:11, and it was assumed that the sample sent for analysis had the same composition. The results of the microanalysis of the polymer, corrected for dimer and monomer content, are shown in Table IV. The values for cyclohexanone are given for comparison. The C, H, and O values are quite similar to

TABLE IV
Microanalysis of polymer

Determination	1	2
C (%)	74.0	73.4
H (%)	9.3	10.3
O (%)[a]	16.7	16.3
Mol. wt.	330	98

[1]Results for the polymer, corrected for the presence of monomer and dimer. All values are averages of two determinations.
[2]Values required for cyclohexanone.
[a]By difference.

those of cyclohexanone, with slight increases in carbon and oxygen and a decrease in hydrogen content. The molecular weight of the polymer (330) lies between those of a trimer (294) and a tetramer (392) of cyclohexanone.

**F. Pascher and E. Pascher, Mikroanalytisches Laboratorium, Bonn, Buschstrasse 54, Germany.*

Can. J. Chem. Downloaded from www.nrcresearchpress.com by 210.87.254.6 on 09/05/12
For personal use only.

The yield of polymer that was insoluble in chloroform was determined for four irradiated samples and two blanks. The blanks were cells that had been filled and put through the usual polymer analysis procedure, but had not been irradiated. The average value of G(insoluble polymer) was about 0.1 cyclohexanone units for the irradiated samples.

DISCUSSION

The initial yields of the major products of the radiolysis of cyclohexanone are listed in Table II. Yields of the minor products are given in Table III. In general, the variations of the yields with dose may be attributed to secondary reactions.

Ring Opening

Extent of Ring Opening

An estimate of the amount of ring opening that occurs during the radiolysis of cyclohexanone is given by

$$[1] \qquad G(\text{ring opening}) \approx G_1(\text{CO} + \text{5-hexenal}) = 1.3.$$

The actual amount of ring opening might be greater than this, depending upon the identity of the dimeric and polymeric products and the mechanism of formation of 5-hexenal (e.g., if 5-hexenal were formed by intramolecular disproportionation of pentamethylene acyl diradicals, $\dot{C}H_2(CH_2)_4\dot{C}O$, then since some of the diradicals would likely regenerate cyclohexanone by intramolecular combination, the observed yield of 5-hexenal would give too low an estimate of the amount of primary ring opening).

An estimate of the amount of initial C—H bond breakage is given by

$$[2] \qquad G(\text{initial C—H breakage}) \approx G_1(H_2 + \text{c-}C_6H_{11}OH) = 1.3.$$

The actual amount of initial C—H bond breakage might be much greater, depending on the identity of the dimeric and polymeric products and on the mechanism of formation of the various products.

The value of the ratio of the amount of ring opening to the amount of initial C—H breakage is given by the ratio of expressions [1] and [2]. Therefore,

$$[3] \qquad (\text{ring opening/initial C—H breakage}) \approx 1.0.$$

In the radiolysis of cyclohexane (1),

$$[4] \quad G(\text{ring opening}) \approx G_1(\text{1-hexene} + \text{methylcyclopentane} + \text{cyclohexylhexene-1}) = 0.77.$$

The actual amount of ring opening may be somewhat greater, depending on the mechanism of formation of 1-hexene, methylcyclopentane, and cyclohexylhexene-1.

An estimate of the amount of initial C—H bond breakage is given by $G_1(H_2)$, which is equal to 5.6 (2). Therefore,

$$(\text{ring opening/initial C—H breakage}) \approx 0.14.$$

TABLE V

Comparison of radiolytic data

Liquid radiolyzed	1	2	3
Cyclohexane	0.77	5.4	0.14
Methylcyclohexane	0.77	4.8	0.16
n-Hexane	1.8	5.3	0.34
Cyclohexanone	1.3	1.3	1.0

[1]Ring opening; except for *n*-hexane where it refers to chain cleavage; G units.
[2]Primary C—H bond breakage; G units.
[3]Ratio, 1/2.

Can. J. Chem. Downloaded from www.nrcresearchpress.com by 210.87.254.6 on 09/05/12
For personal use only.

Similar ratios can also be calculated, on the basis of available results, for methylcyclohexane (24) and for *n*-hexane (25, 26); the data for the four compounds are summarized in Table V. Despite large uncertainties in these values, there are significant differences. In column 3 it is seen that the closed rings of cyclohexane and methylcyclohexane are more stable than the open chain of *n*-hexane, probably due in part to the inability of the free radical ends formed on ring cleavage to escape one another by diffusion, with consequent high probability of reformation of the ring. The cyclohexanone ring, however, is *less* stable than the open chain of *n*-hexane, illustrating the powerful effect of the carbonyl group on the primary radiation chemical reaction.

Site of Ring Opening

The formation of carbon monoxide and 5-hexenal implies cleavage of C—C bonds adjacent to the carbonyl group. Products corresponding to ring opening in other positions were not observed. This behavior, common to both the radiolysis and photolysis of ketones (27), could be attributed to a localization of energy in the carbonyl group, or might simply represent rupture of the weakest bond in the molecule (28). It is impossible at present to distinguish between these two causes in either system. However, the localization of radiolytic activation in specific parts of molecules, before chemical reaction occurs, has been suggested before (29) and it seems probable that it is occurring in the cyclohexanone system.

Comparison of Radiolysis and Photolysis of Cyclohexanone

It is of interest to compare the distribution of reaction products in the radiolytic and photolytic systems to see if any information can be obtained about the relative levels of excitation of the species that undergo reaction.

Carbon monoxide is a major product of both liquid and vapor phase photolyses of cyclohexanone (30–34). The present work shows that it is also a major product of the radiolysis of liquid cyclohexanone. Ethylene, propylene, 1-pentene, and cyclopentane are formed in the radiolysis of the ketone. They were found to be important products of the vapor phase photolysis but seem not to have been looked for in the liquid phase photolysis (34).

Srinivasan found that 5-hexenal is a product of the vapor and liquid phase photolyses of cyclohexanone (34). He also showed that the rate of 5-hexenal formation was 3.7 times greater than that of carbon monoxide in the vapor phase and was about 11 times greater in the liquid phase. The radiolytic yield of 5-hexenal from liquid cyclohexanone is only about twice the radiolytic yield of carbon monoxide.

Polymer formation in the vapor phase photolysis has been reported (32, 33) and Blacet and Miller suggested that the polymer formation increases at lower wavelengths (33). Polymer is a major product of the radiolysis of the ketone.

Hydrogen, cyclohexanol, cyclohexenone, and "dimer" are major products of the radiolysis, but their formation has not been reported in the photolytic studies. It is not certain whether they were looked for. It may be pointed out that the C—H bond dissociation energies in the ketone are likely to be ~90–95 kcal/mole (D(iso-C_3H_7—H) = 94 kcal/mole (28*a*)), so the energy of the light quantum is not sufficient to break a C—H bond where light of wavelength greater than ~300–310 mμ has been used. In the photolysis of cyclopentanone at 313 mμ, hydrogen was reported not to be a product (10). Photolytic formation of cyclohexanol from cyclohexanone has been suggested (35) but it is not certain whether it has been observed as a product.

A large number of minor products are formed in the radiolysis of the ketone, e.g.,

Can. J. Chem. Downloaded from www.nrcresearchpress.com by 210.87.254.6 on 09/05/12
For personal use only.

acetylene, propane, cyclopropane, etc., which have not been reported in the photolytic studies.

It may be concluded that the energy states involved in the radiolytic formation of hydrogen are higher than the energy states involved in most of the photolysis studies. The other products of radiolysis that have not been reported in the photolysis studies may also result from higher energy states. The difference in the relative yields of 5-hexenal and carbon monoxide in the photolysis and radiolysis of liquid cyclohexanone is also indicative of higher states in the radiolysis. However, it is difficult to say whether these states differ mainly in their electronic levels or in their vibrational levels.

ACKNOWLEDGMENTS

The authors are grateful to Dr. R. Srinivasan for sending mass spectral data of 5-hexenal. They also thank Dr. S. Usiskin and the Government of Alberta Cancer Clinic for use of the ^{60}Co therapy unit.

Financial support for this work was received from the National Research Council. Part of the results in this paper were reported at the Annual Conference of the Chemical Institute of Canada, Toronto, June, 1963. The yields of some of the products have been revised slightly from those in the earlier report.

REFERENCES

1. G. R. Freeman. J. Chem. Phys. **33**, 71 (1960).
2. S. K. Ho and G. R. Freeman. J. Phys. Chem. In press.
3. J. C. McLennan and W. L. Patrick. Can. J. Res. **5**, 470 (1931); Chem. Abstr. **26**, 656 (1932).
4. P. Ausloos and J. F. Paulson. J. Am. Chem. Soc. **80**, 5117 (1958).
5. P. J. Ausloos. J. Am. Chem. Soc. **83**, 1056 (1961).
6. L. J. Stief and P. Ausloos. J. Phys. Chem. **65**, 1560 (1961).
7. R. Barker. Nature, **192**, 62 (1961).
8. P. Drienovsky. Collection Czech. Chem. Commun. **27**, 1450, 1614, 1624 (1962); Chem. Abstr. **57**, 9381 (1962).
9. R. Barker. Trans. Faraday Soc. **59**, 375 (1963).
10. M. Katayama, J. C. Whitmer, and C. N. Trumbore. J. Am. Chem. Soc. **84**, 4025 (1962).
11. J. N. Pitts, Jr. and A. D. Osborne. J. Am. Chem. Soc. **83**, 3011 (1961).
12. D. J. Coyle. J. Phys. Chem. **67**, 1800 (1963).
13. W. F. Serat and J. F. Mead. Rad. Res. **11**, 370 (1959).
14. J. D. Strong and J. G. Burr. J. Am. Chem. Soc. **81**, 775 (1959).
15. J. G. Burr and J. D. Strong. J. Phys. Chem. **63**, 873 (1959).
16. T. J. Hardwick. J. Phys. Chem. **66**, 117 (1962).
17. C. G. Moore. J. Chem. Soc. 236 (1951).
18. Ajit Singh. Ph.D. Thesis, University of Alberta, Edmonton, Alta. 1963.
19. J. F. Walker. Formaldehyde. Reinhold Publishing Corp., New York. 1944.
20. S. Siggia. Quantitative organic analysis via functional groups. John Wiley and Sons, Inc., New York. 1949.
21. R. Srinivasan. Private communication (1961).
22. E. Ibuki. J. Chem. Soc. Japan, Pure Chem. Sect. **71**, 96 (1950); Chem. Abstr. **45**, 7025 (1951).
23. A. D. Cross. An introduction to practical infra-red spectroscopy. Butterworth's Scientific Publications, London. 1960.
24. G. R. Freeman. J. Chem. Phys. **36**, 1534 (1962).
25. H. A. Dewhurst. J. Phys. Chem. **62**, 15 (1958).
26. T. J. Hardwick. Can. J. Chem. **64**, 1623 (1960).
27. E. W. R. Steacie. Atomic and free radical reactions. 2nd ed. Reinhold Publishing Corp., New York. 1954.
28. (*a*) T. L. Cottrell. The strengths of chemical bonds. Butterworth's Scientific Publications, London. 1958.
    (*b*) C. Walling. Free radicals in solution. John Wiley and Sons, Inc., New York. 1957.
29. (*a*) R. R. Hentz and M. Burton. J. Am. Chem. Soc. **73**, 532 (1951).
    (*b*) E. Collinson, F. S. Dainton, and D. C. Walker. Trans. Faraday Soc. **57**, 1732 (1961).
30. O. D. Saltmarsh and R. G. W. Norrish. J. Chem. Soc. 455 (1935).
31. C. H. Bamford and R. G. W. Norrish. J. Chem. Soc. 1521 (1938).
32. S. W. Benson and G. B. Kistiakowsky. J. Am. Chem. Soc. **64**, 80 (1942).
33. F. E. Blacet and H. Miller. J. Am. Chem. Soc. **79**, 4327 (1957).
34. R. Srinivasan. J. Am. Chem. Soc. **81**, 2601 (1959).
35. P. de Mayo. *In* Advances in organic chemistry; methods and results. Vol. II. *Edited by* R. A. Raphael, E. C. Taylor, and H. Wynberg. Interscience Publishers, Inc., New York. 1960.

Can. J. Chem. Downloaded from www.nrcresearchpress.com by 210.87.254.6 on 09/05/12
For personal use only.

Can. J. Chem. Downloaded from www.nrcresearchpress.com by 210.87.254.42 on 09/05/12
For personal use only.

RADIOLYSIS OF CYCLOHEXANONE

II. EFFECT OF SOLUTES ON PRODUCTS INVOLVING C—H BOND RUPTURE

AJIT SINGH AND GORDON R. FREEMAN
Department of Chemistry, University of Alberta, Edmonton, Alberta
Received January 31, 1964

ABSTRACT

Some of the products whose formation, during the radiolysis of cyclohexanone, involves the rupture of C—H bonds are hydrogen, cyclohexanol, 2,2′-diketodicyclohexyl, and probably other "dimers" of cyclohexanone.

Benzene appears to inhibit the formation of hydrogen mainly by an activation transfer process. The influence of 2,3-dimethyl-1,3-butadiene (DMB) on the hydrogen yield is more complex and probably involves more than one inhibition reaction.

Less than one mole percent of DMB or of oxygen inhibits the formation of cyclohexanol and of dimers to below their limits of detection on the analytical system ($G < 0.2$). This is probably due to the scavenging of free radicals (G(scavengeable radicals) = 4). Benzene is much less efficient than DMB or oxygen in inhibiting the formation of cyclohexanol and of dimers of cyclohexanone.

INTRODUCTION

The radiolysis of liquid cyclohexanone in binary solutions has been studied in an attempt to elucidate the mechanisms of the formation of some of the products (1). Mechanisms that involve C—H but not C—C bond rupture are considered here.

Benzene has been widely used as an inhibitor in radiolytic studies, (e.g., refs. 2–4). Patrick and Burton studied the radiolysis of propionaldehyde in the presence of benzene (4) and concluded that benzene does not protect propionaldehyde but sensitizes its decomposition. This was attributed to energy transfer from benzene to a low-lying excited state of propionaldehyde.

The photoionization potentials of benzene, propionaldehyde, and cyclohexanone are 9.25, 9.98, and 9.14 eV, respectively (5) and they show absorption maxima in the near ultraviolet at about 260, 285±15, and 290 mμ, respectively (6). It was therefore considered interesting to see whether benzene would protect or sensitize the radiolytic decomposition of cyclohexanone.

It appeared that 2,3-dimethyl-1,3-butadiene (DMB) might be a good radical scavenger (7) and this led to an investigation of its effect on the radiolysis of cyclohexanone.

Oxygen was primarily used to briefly compare its scavenging action with that of DMB.

EXPERIMENTAL

Most of the experimental techniques were described earlier (1). Certain modifications of the techniques were required for this work and these will be described here.

Materials

Phillips Research Grade benzene was distilled and stored under vacuum. Gas chromatographic analysis, using Ucon, Carbowax, silicone grease, and Apiezon L columns, did not reveal detectable amounts of impurities in the benzene. DMB was obtained from Chemical Procurement Labs., K & K Laboratories, and Matheson, Coleman, and Bell. It was distilled under vacuum from a flask at −25 °C into a reservoir at −196 °C. This procedure eliminated high boiling impurities and less than 0.5% of other impurities remained. The distilled DMB was carefully degassed and stored under vacuum.

Preparation and Irradiation of Samples

The amounts of benzene and DMB were measured as liquid in a calibrated tube or as vapor in a calibrated bulb. DMB was distilled from the cooled reservoir (−25 °C) to the measuring tube. For the samples with

added oxygen, a measured amount of cyclohexanone was distilled into the cell and was kept frozen with Dry Ice. Dry oxygen was let into the cell, its pressure recorded, and the cell sealed off. The various solutions were irradiated to a dose of 5.92 ± 0.12 (10^{-4} eV/e$^-$,) which is about 1.9×10^{20} eV/ml. Thus the cyclohexanone in all mixtures received the same dose. The yields of several products were measured as a function of the electron fraction, ϵ_s, of the solute.

Calibrations of Cyclohexanol

The resolution of the cyclohexanol peak from the cyclohexanone peak, on both the Ucon and the Carbowax columns, was not very good and it varied with the amount of the ketone injected. It was therefore necessary to determine a calibration curve for cyclohexanol for each different solution of cyclohexanone and inhibitor used.

RESULTS

If the radiolysis products of a component X in a binary solution are unaffected by the presence of the other component Y, and vice versa, then the expected G value, G_{ex}, for a product P from the solution should be given approximately by the expression:

$$[1] \qquad G_{ex}(P) = G_x^0(P)\ \epsilon_x + G_y^0(P)\ \epsilon_y$$

where G_x^0 (P) and G_y^0 (P) refer to the yields of P from pure X and pure Y, respectively, and ϵ_x and ϵ_y refer to the electron fractions of X and Y in the solution radiolyzed. The values of G_{ex} in the figures are represented by linear dashed lines. Most of the end points are averages of more than one determination.

Hydrogen

The decrease of the hydrogen yield in the low solute concentration region ($\epsilon_s \leq 0.1$) is more pronounced in the DMB solutions (Fig. 1A) than in the benzene solutions (Fig. 1B). However, the decrease is greater than that expected on the basis of equation 1 in both cases. $G(H_2) = 0.038$ for pure benzene and $G(H_2) = 0.19$ for DMB. Hydrogen was not measured for the oxygen solutions.

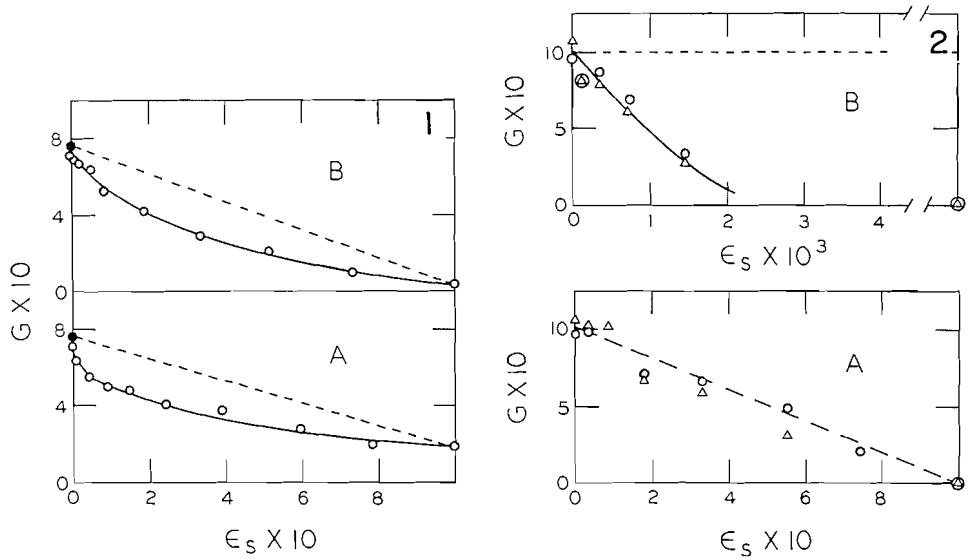

FIG. 1. Hydrogen: ϵ_s = electron fraction of solute; dose = 5.92 ± 0.12 (10^{-4} eV/e$^-$); dashed lines refer to G_{ex}. (A) 2,3-Dimethyl-1,3-butadiene solutions: ○ H_2; ● G_i (H_2). (B) Benzene solutions: ○ H_2; ● G_i (H_2).

FIG. 2. Cyclohexanol: ϵ_s = electron fraction of the solute; dose = 5.92 ± 0.12 (10^{-4} eV/e$^-$); dashed lines refer to G_{ex}. (A) Benzene solutions: ○ cyclohexanol, Ucon column; △ cyclohexanol, Carbowax column. (B) 2,3-Dimethyl-1,3-butadiene solutions: ○ cyclohexanol, Ucon column; △ cyclohexanol, Carbowax column.

Can. J. Chem. Downloaded from www.nrcresearchpress.com by 210.87.254.42 on 09/05/12
For personal use only.

Cyclohexanol

The cyclohexanol yield seemed to decrease about linearly with increasing electron fraction of benzene (Fig. 2). However, in sharp contrast to this, in the DMB solutions the cyclohexanol yield decreased so rapidly that it was not visible as a product in samples containing greater than about 2×10^{-3} electron fraction of the diene. The cyclohexanol yield could not be determined in the oxygen solutions, because of uncertainty in the blank value.

Cyclohexenone

The radiolytic yield of cyclohexenone from pure cyclohexanone is small at this high dose ($G \approx 0.2$ at 1.9×10^{20} eV/ml (1)). It was not seen as a product in any of the solutions ($G < 0.2$).

Cyclohexanone "Dimers"

The G value of total cyclohexanone dimers decreases gradually with increasing benzene concentration, almost all the values being lower than G_{ex} (Fig. 3A). The yields of 2,2′-

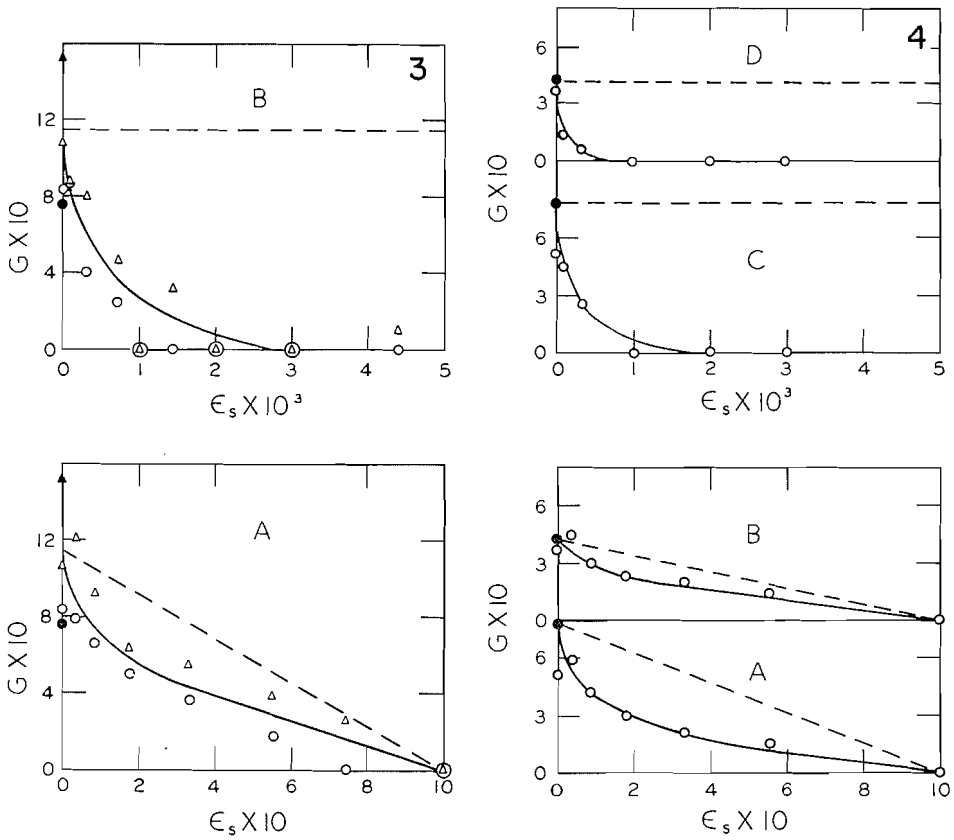

FIG. 3. Total dimers of cyclohexanone from solutions: ϵ_s = electron fraction of the solute; dose = 5.92 ± 0.12 (10^{-4} eV/e$^-$); dashed lines refer to G_{ex}; the filled points refer to values of G_i. (A) Benzene solutions: ○ Apiezon L column; △ silicone grease column. (B) 2,3-Dimethyl-1,3-butadiene solutions: ○ Apiezon L column; △ silicone grease column.

FIG. 4. Yield of individual dimers of cyclohexanone. ϵ_s = electron fraction of the solute; dose = 5.92 ± 0.12 (10^{-4} eV/e$^-$); dashed lines refer to G_{ex}; the filled points refer to values of G_i. (A) 2,2′-Diketodicyclohexyl, benzene solutions; (B) dimer D-1, benzene solutions; (C) 2,2′-diketodicyclohexyl, DMB solutions; (D) dimer D-1, DMB solutions.

Can. J. Chem. Downloaded from www.nrcresearchpress.com by 210.87.254.42 on 09/05/12
For personal use only.

diketodicyclohexyl (DKDC) and of dimer D-1, as obtained by analysis on the silicone grease column, are shown in Fig. 4A and B. They follow a pattern similar to that of the total dimer.

In the DMB solutions, the yields of cyclohexanone dimers decrease very rapidly with increasing electron fraction of the diene (Figs. 3 and 4). The yield had decreased to below the detection limit of about 0.2 G units at $\epsilon_s = 2 \times 10^{-3}$. The three samples with electron fractions of DMB equal to 1×10^{-3}, 2×10^{-3}, and 3×10^{-3} were large samples (20 ml) prepared mainly for polymer analysis and received a lower dose rate (2.3×10^{18} eV/ml h) than did the other samples (5.2×10^{18} eV/ml h) referred to in Figs. 3 and 4. Cyclohexanone dimer formation was inhibited to below the detection limit ($G < 0.2$) in both oxygen solutions.

Additional Products

DMB Solutions

Analysis of radiolyzed pure DMB on Apiezon L and silicone grease columns showed one big peak and three very small peaks after the DMB peak. The big peak, by comparison of its retention time with that of *n*-dodecane, was tentatively identified as the "dimer" of DMB.

The yield of the dimer of DMB increases very rapidly with increasing diene concentration at low concentrations, then remains constant for $\epsilon_s > 0.1$ (Fig. 5B). The G value is greater than G_{ex} throughout.

In the solutions with $\epsilon_s > 0.02$, several new products were formed (4 new peaks on the Apiezon L column and 6 new peaks on the silicone grease column). The new product

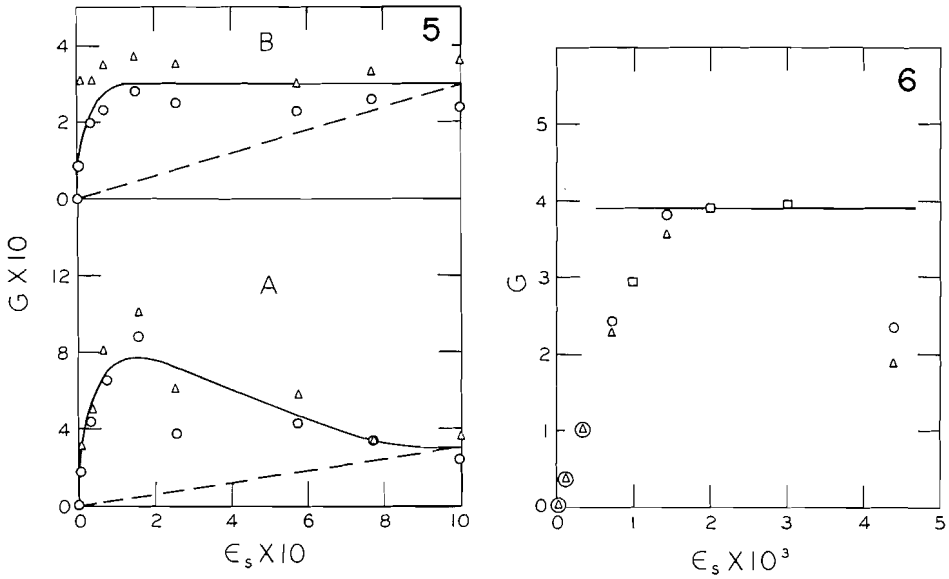

FIG. 5. Dimers that include 2,3-dimethyl-1,3-butadiene units: ϵ_s = electron fraction of the solute; dose = 5.92±0.12 (10^{-4} eV/e$^-$); dashed lines refer to G_{ex}. ○ Apiezon L column; △ silicone grease column. (A) Total C_{12} minus the dimers of cyclohexanone; (B) dimer of DMB.

FIG. 6. G(consumption) of DMB: ϵ_s = electron fraction of DMB; $G = G$(consumption) of DMB; dose = 5.92±0.12 (10^{-4} eV/e$^-$). Dose rate ≈ 5.2×10^{18} eV/ml h); △ silicone grease column; ○ Apiezon L column. Dose rate ≈ 2.3×10^{18} eV/ml h; □ Apiezon L column. NOTE: The values from the sample with $\epsilon_s = 4.4 \times 10^{-3}$ are less trustworthy since they are based on the measurement of a small difference between two large quantities (DMB remaining = 84%).

Can. J. Chem. Downloaded from www.nrcresearchpress.com by 210.87.254.42 on 09/05/12
For personal use only.

peaks appeared between the dimer peak of DMB and the dimer peaks of pure cyclohexanone, on both columns. It is likely that these peaks correspond to "mixed" dimers formed from the diene and the ketone. The combined yield of the mixed dimers plus the dimer of DMB is shown in Fig. 5A. The calibration curves of DKDC were used for calculation of the yields in Fig. 5. Thus the absolute G values in this figure might be wrong by as much as a factor of two, but the shapes of the curves are probably correct.

It is interesting to note that the new C_{12} products were absent in the region of $\epsilon_s = 3 \times 10^{-3}$, where the formation of cyclohexanol and the cyclohexanone dimers was completely inhibited. At these low concentrations of DMB, its rate of destruction was measureable (Table I and Fig. 6). The value of G(consumption) of DMB in the maximally

TABLE I

Percentage of DMB remaining after irradiation: dose = 5.92±0.12 (10^{-4} eV/e$^-$)

Size of sample (ml)	Electron fraction of DMB	Dose rate (10^{18} eV/ml h)	% DMB remaining
2	9.8×10^{-5}	5.2	0
2	3.2×10^{-4}	5.2	0
2	7.2×10^{-4}	5.2	2
20	1.0×10^{-3}	2.3	24
2	1.4×10^{-3}	5.2	32
20	2.0×10^{-3}	2.3	47
20	3.0×10^{-3}	2.3	64
2	4.4×10^{-3}	5.2	86

inhibited system was about 4. Since no gas chromatographic peaks corresponding to new products were observed in this concentration region, the amounts of polymer formed and DMB consumed were measured for a series of 20 ml samples (Table II, see also Table I and Fig. 6). It appears from Table II that the polymer contains an approximately 1:1

TABLE II

DMB consumed and polymer formed: dose = 5.92±0.02 (10^{-4} eV/e$^-$)

Electron fraction of DMB	Weight of polymer (mg)	G(consumption) of DMB[a]	G(consumption) of cyclohexanone to form polymer[b]	Total G(polymer)[c]
0.0	13.0	0.0	2.2	2.2
1.0×10^{-3}	38.6	3.0	4.2	7.2
2.0×10^{-3}	38.6	3.9	3.3	7.2
3.0×10^{-3}	40.0	4.0	3.5	7.5

[a]Based on gas chromatographic measurement.
[b]Calculated from the weight of the polymer with the assumption that all the DMB that reacted formed polymer.
[c]Sum of values in columns 3 and 4.

mole ratio of DMB:cyclohexanone. The average molecular weight of the polymer from two samples with $\epsilon_s = 2.0 \times 10^{-3}$ (dose = 5.9×10^{-4} eV/e$^-$) was 400±30.*

Oxygen Solutions

Peroxides were formed in good yield (Table III), but their identity was not determined.

When the irradiated solution was analyzed on the Apiezon L column, a large product peak was obtained after the cyclohexanone peak. By comparison of the product retention time with those of quinone and hydroquinone, it was tentatively identified as a hydroxycyclohexanone or a cyclohexanedione or a mixture of both. The G values for the product

Samples sent for analysis to F. Pascher, Mikroanalytisches Laboratorium, Bonn, Buschstrasse 54, Germany.

Can. J. Chem. Downloaded from www.nrcresearchpress.com by 210.87.254.42 on 09/05/12
For personal use only.

TABLE III

Products from oxygen solutions:
dose = 5.92±0.12 (10^{-4} eV/e$^-$)

Pressure of O_2 in the sample[a] (mm)	Electron fraction[b] of O_2	G(peroxides)
0	0	$\leqslant 0.3$
71	2.5×10^{-5}	2.5±0.2
412	14.6×10^{-5}	3.5±0.2

[a]Cyclohexanone, 2 ml; oxygen, ~10 ml.
[b]To calculate the electron fraction of dissolved oxygen, its solubility has been assumed to be 0.2 ml per ml of the ketone on the basis of the values for the solubility of oxygen in some oxygenated organic compounds (International Critical Tables).

were estimated to be ~0.8 and ~1.2 from samples with oxygen pressures of 71 and 412 mm, respectively, assuming a calibration factor equal to that of cyclohexanone. There were also three minor products, one of which had the same retention time as caproic acid ($G \approx 0.1$, when calibration factor is assumed equal to that of cyclohexanone).

DISCUSSION

Hydrogen

Benzene and DMB decrease the radiolytic yield of hydrogen from cyclohexanone (Fig. 1). The decrease in hydrogen yield might be due to protection of the ketone by an activation transfer mechanism, which reduces the amount of initial decomposition of the ketone itself, or it might be due to a scavenging mechanism that involves precursors of hydrogen (e.g. H atoms), or it might be a combination of the two. In the following discussion the 'activation transfer-type' and the 'scavenging-type' mechanisms are considered separately.

Several different mechanisms might yield the same type of rate equation. It was therefore decided to classify the mechanisms according to the type of rate equation they obeyed. In an activation transfer-type mechanism, the reaction between the solute and an activated species is in competition with a first order decomposition reaction of the activated species which results in the product under consideration. In a scavenger-type mechanism, the reaction between the solute and an activated species is in competition with a second order reaction of the activated species which results in the product under consideration.

It is assumed in the following treatments that the yield of hydrogen from the direct radiolysis of the solute is proportional to the electron fraction of the solute in the sample.

Mechanism 1 (Activation Transfer-Type)

(1) $C_6H_{10}O \xrightarrow{I_1} C_6H_{10}O^*$
(2) $C_6H_{10}O^* \rightarrow H_2 + P_1$
(3) $C_6H_{10}O^* + S \rightarrow C_6H_{10}O + S^*$
(4) $S^* \rightarrow H_2 + P_2$
(5) $\rightarrow S$

where S refers to the solute. Reactions 2 and 4 could each involve more than one molecule and both could involve more steps than one. Products P_1 and P_2 may each refer to more than one entity.

Can. J. Chem. Downloaded from www.nrcresearchpress.com by 210.87.254.42 on 09/05/12
For personal use only.

The rate of formation of $C_6H_{10}O^*$ is represented by I_1, which is assumed to be proportional to the electron fraction of cyclohexanone, ϵ_c, in the samples.

$$G(C_6H_{10}O^*) = AI_1 \quad [2]$$

where A is a proportionality constant that includes the irradiation dose rate.

The following expression is obtained by the usual steady state treatment of mechanism 1.

$$(1 + u\,[S])\,\rho_1 = 1 + v\,[S] \quad [3]$$

where

$$u = k_3k_4/k_2\,(k_4 + k_5), \quad [4]$$

$$v = k_3/k_2, \quad [5]$$

and

$$\rho_1 = \frac{I_1}{d[H_2]/dt} = \frac{G_{ex}(H_2)_c}{G_{obs}(H_2) - G_s^0(H_2)\epsilon_s}. \quad [6]$$

An equation of the same form as equation 3 can also be obtained from a mechanism that involves charge transfer (8).

The value of ρ_1 can be obtained from experimental data. The production of hydrogen by direct radiolysis of the solute has been excluded from the mechanism, so the "expected" yield of hydrogen is given by

$$G_{ex}\,(H_2)_c = G_c^0\,(H_2)\;\epsilon_c = 0.71\;\epsilon_c \quad [7]$$

at the dose used.* Similarly, $d[H_2]/dt$ excludes the hydrogen produced by direct radiolysis of the solute.

If the value of u were known, the left hand side of equation 3 could be plotted against [S] and a straight line with an intercept of unity would be obtained, if mechanism 1 were applicable. In the present case, various arbitrary values of u (0 to 5) were assumed and several plots of equation 3 were made to see if a straight line with an intercept of unity could be obtained.

(i) Benzene Solutions

For the results from the benzene solutions, the best straight line plot was obtained with $u = 0$ (Fig. 7). A plot with $u = 0.5$ is also shown in Fig. 7 for comparison. The slope of the line with $u = 0$ gives $v = 0.2$ l/mole. The value $u = 0$ means that benzene does not produce an appreciable amount of hydrogen subsequent to protection of cyclohexanone by activation transfer. Many previous workers (e.g. ref. 2) have made the assumption that benzene does not produce hydrogen subsequent to energy absorption from another component in the system, and this is equivalent to the $u = 0$ obtained here.

It is reasonable to expect that either of the reactions 6 and 7

$$A^* + B \rightarrow A + B^* \quad (6)$$

$$A + B^* \rightarrow A^* + B \quad (7)$$

**When the yield of hydrogen from pure cyclohexanone at zero dose, $G_i(H_2) = 0.76$, was used instead of the yield at the dose used in these experiments, the kinetic plots did not give intercepts of unity, even when a straight line was obtained. The use of $G_c^0(H_2) = 0.71$ in equation 7 involves the assumption that the secondary products of radiolysis have a similar effect on the yield of hydrogen in the pure ketone and in the solutions.*

Can. J. Chem. Downloaded from www.nrcresearchpress.com by 210.87.254.42 on 09/05/12
For personal use only.

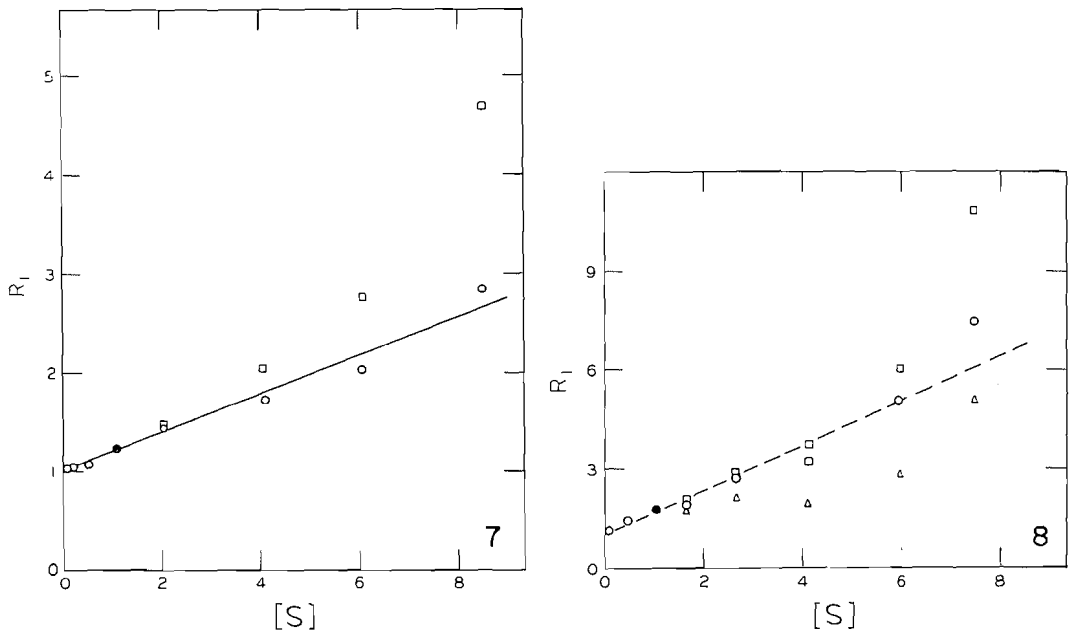

FIG. 7. Kinetic plot for activation transfer-type mechanism: [S] = benzene concentration (M); $R_1 = (1 + u[S])\rho_1$; ○ $u = 0$; □ $u = 0.5$. The curve for $u = 0.5$ has been normalized to that for $u = 0$, using the point ● (i.e. the values of R_1 for the squares have been altered to R_1', where $R_1' = 0.65(R_1 - 1) + 1$). This facilitates the comparison of the linearity of the two curves. Squares are not shown for [S] < 1.1 M because they differed negligibly from the circles in this region.

FIG. 8. Kinetic plot for activation transfer-type mechanism: [S] = DMB concentration (M); $R_1 = (1 + u[S])\rho_1$; △ $u = 0$; ○ $u = 0.3$; □ $u = 1.0$. The curves for $u = 0$ and $u = 1.0$ have been normalized to that for $u = 0.3$, using the point ● (i.e. the values of R_1 have been altered to R_1', where $R_1' = f(R_1 - 1) + 1$; for the triangles and squares $f = 1.3$ and 0.65, respectively). This facilitates the comparison of the linearity of the plots. Triangles and squares are not shown for [S] < 1.1, because they differ negligibly from the circles in this region.

might occur, depending on the relative heights of the energy levels involved (2, 9). The energies of the lowest excited states and the ionization potentials of cyclohexanone and benzene are shown in Table IV.

TABLE IV

Energies of lowest excited states and ionization potentials*

Compound	Triplet	Singlet	Ionization potentials
Cyclohexanone	2.8†	4.27 (6)	9.14 (5)
Benzene	3.58 (11)	4.76 (6, 11)	9.25 (5)
DMB	~2.6 (15)	5.4 (6)	~8.7 (13)

*The energies are expressed in eV and the numbers in parentheses are the references.
†Estimated by comparison with the states of cyclopentanone (6, 11).

Charge transfer from the ground state cyclohexanone ion to a benzene molecule is improbable because the process is endothermic.

States in the vicinity of 4.1 eV (300 mμ) do not contribute significantly to the production of hydrogen (see ref. 1), probably because nearly all of the absorbed energy would have to become localized as vibrational energy in one or two C—H bonds. Such a great degree of vibrational energy localization in the molecule is improbable. Thus, if excited states

Can. J. Chem. Downloaded from www.nrcresearchpress.com by 210.87.254.42 on 09/05/12
For personal use only.

Can. J. Chem. Downloaded from www.nrcresearchpress.com by 210.87.254.42 on 09/05/12
For personal use only.

of the cyclohexanone molecule are involved in the radiolytic production of hydrogen, they must be higher than the lowest singlet and they might well be higher than the lowest states of benzene. Energy transfer from such excited states to benzene, with consequent reduction of the hydrogen yield, would then be possible.

This type of argument is also applicable to the previously studied radiolysis of propionaldehyde (4). Patrick and Burton considered that the inhibition of hydrogen formation was due to the scavenging of hydrogen atoms by benzene (4). Hydrogen has been shown to be a minor product of the photolysis of propionaldehyde even at 238 mμ, or 5.20 eV ($\Phi(CO) \simeq 1$, $\Phi(H_2) \simeq 0.1$, ref. 12). The lowest excited singlet state of propionaldehyde is at about 4.35 eV and its triplet would be still lower in energy (6, 10). Thus, in the radiolysis of propionaldehyde, hydrogen formation must have been due to species with much more energy than that possessed by the lowest excited singlet and triplet states. Inhibition of hydrogen formation by energy transfer to benzene might therefore be possible.

(ii) DMB Solutions

Since the lowest excited states of the ketone are probably not involved in hydrogen production, activation transfer, whether as charge or as excitation energy, must be considered as one possible means of inhibition of hydrogen formation (see Table IV).

A satisfactory straight line could not be obtained with the results from the DMB solutions (Fig. 8) and it appears that this simple mechanism does not apply. It is evident from Fig. 1 that the effect of DMB in the low concentration region ($\epsilon_s < 0.05$) is much greater than the effect of benzene in the same region. At higher concentrations, both solutes appear to have similar effects.

Two processes involving the diene are evident at $\epsilon_s > 1 \times 10^{-2}$, with a maximum at $\epsilon_s \simeq 0.1$. These involve a sharp increase in the yield of the dimer of DMB (Fig. 5B) and a sharp increase of yield of the mixed dimers of cyclohexanone and DMB (Fig. 5A minus Fig. 5B). Both of these effects might result from reactions which contribute to the inhibition of hydrogen formation. An activation transfer-type process is probably involved in the formation of one or both of the types of dimers (containing two and one DMB units, respectively) because the shapes of both of the curves together (Fig. 5) cannot be explained by a simple radical scavenging mechanism. In any case, the scavenging of large ketone radicals is not responsible for the formation of these products because they were not formed at very low diene concentrations ($\epsilon_s \simeq 3 \times 10^{-3}$) where the inhibition of cyclohexanol and the dimers of cyclohexanone was virtually complete. Reactions such as

$$DMB^* + DMB \rightarrow (DMB)_2$$

and

$$C_6H_{10}O^* + DMB \rightarrow C_{12}H_{20}O$$

might be involved (15).

Mechanism 2 (Scavenging-Type)

(8)	$C_6H_{10}O \xrightarrow{I_2} C_6H_{10}O^*$
(9)	$C_6H_{10}O^* \rightarrow H + \cdot C_6H_9O$
(10)	$H + C_6H_{10}O \rightarrow H_2 + \cdot C_6H_9O$
(11)	$\rightarrow (C_6H_{11}O)\cdot$
(12)	$H + S \rightarrow H_2 + R\cdot$
(13)	$\rightarrow HS\cdot$

where R· represents the radical obtained by abstracting a hydrogen atom from S and I_2 has a meaning similar to that of I_1 in mechanism 1.

Steady state treatment of mechanism II yields

$$(1 + y[S]/[C_6H_{10}O])\,\rho_2 = 1 + z\,[S]/[C_6H_{10}O] \quad [8]$$

where

$$y = k_{12}/k_{10} \quad [9]$$

$$\rho_2 = (k_{10}/(k_{10} + k_{11}))/(I_2/(d[H_2]/dt) \quad [10]$$

and

$$z = (k_{12} + k_{13})/(k_{10} + k_{11}). \quad [11]$$

It may be pointed out here that equations of the same form as equation 8 can be obtained from other mechanisms than mechanism 2. Two such mechanisms involve "scavenging" of positive charges and of electrons (8).

Experimentally, ρ_2 is the same as ρ_1,

$$\rho_2 = \frac{0.71\,\epsilon_c}{G_{obs}(H_2) - G_s^0(H_2)\epsilon_s} \quad [12]$$

Various arbitrary values were assumed for y (0 to 5) and the left hand side of equation [8] was plotted against ($[S]/[C_6H_{10}O]$) in an attempt to obtain a straight line with an intercept of unity.

(i) Benzene Solutions

The kinetics plots were not as sensitive to variation in y as might be desired. The best straight line was obtained with $y = 1$ and yielded $z = 3$ (Fig. 9). Plots with $y = 0$ and $y = 2$ are shown for comparison.

For mechanism 2, the values $y = 1$ and $z = 3$ mean that (*a*) the overall rate constant for the reaction of hydrogen atoms with benzene was about three times greater than the corresponding rate constant for the reaction of hydrogen atoms with cyclohexanone; (*b*) the rate constants for hydrogen abstraction by an H atom from benzene, k_{12}, and from cyclohexanone, k_{10}, had the same value.

Since the bond dissociation energies of the C—H bonds in cyclohexanone are likely <95 kcal/mole,* whereas the C—H dissociation energy in benzene is 102 kcal/mole (16), k_{12} would not be expected to be equal to k_{10}. Thus, mechanism 2 seems to be inapplicable in the present case.

The observed values of y and z also make the charge scavenging mechanisms seem improbable (8).

(ii) DMB Solutions

A satisfactory plot could not be obtained (Fig. 10).

To summarize, the role of benzene in reducing the yield of hydrogen appears to involve interference with precursors of hydrogen other than hydrogen atoms. An activation transfer-type mechanism appears to provide a better explanation of the results than does a scavenging-type mechanism. The role of DMB in reducing the hydrogen yield appears to be more complex and probably involves more than one process. Neither the presence nor the absence of hydrogen atoms in the system has been established.

**The C—H bonds on the carbons β and γ to the carbonyl group probably have dissociation energies similar to D(iso-C_3H_7—H) = 94 kcal/mole. The C—H bonds on the carbons α to the carbonyl group are probably weaker than this, due to the formation of a radical that possesses resonance stabilization energy.*

Can. J. Chem. Downloaded from www.nrcresearchpress.com by 210.87.254.42 on 09/05/12
For personal use only.

Can. J. Chem. Downloaded from www.nrcresearchpress.com by 210.87.254.42 on 09/05/12
For personal use only.

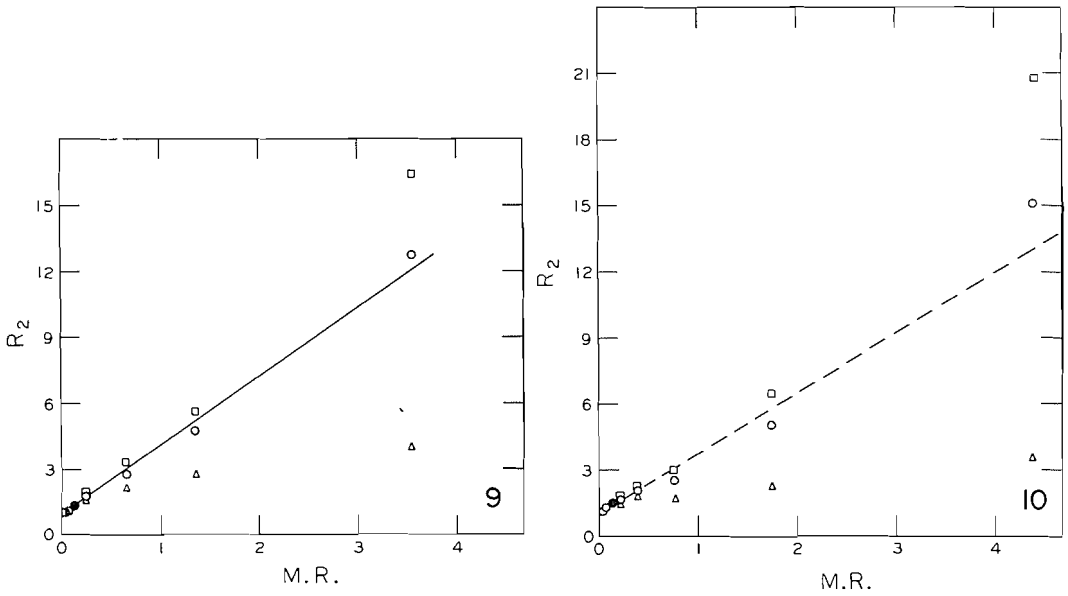

FIG. 9. Kinetic plot for scavenging-type mechanism: $R_2 = (1 + y\,[S]/[C_6H_{10}O])\,\rho_2$; [S] = benzene concentration (M); M.R. = $[S]/[C_6H_{10}O]$; △ $y = 0$; ○ $y = 1$; □ $y = 2$. The points for $y = 0$ and $y = 2$ have been normalized to the curve for $y = 1$, using the point ● (i.e. the values of R_2 have been altered to R_2', where $R_2' = f(R_2 - 1) + 1$; for the triangles and squares $f = 1.13$ and 0.90, respectively). This facilitates the comparison of the linearity of the plots. Triangles and squares are not shown for M.R. < 0.13 because they differ negligibly from the circles in this region.

FIG. 10. Kinetic plot for scavenging-type mechanism: $R_2 = (1 + y\,[S]/[C_6H_{10}O])\,\rho_2$; [S] = DMB concentration (M); M.R. = $[S]/[C_6H_{10}O]$. △ $y = 0$; ○ $y = 1$; □ $y = 2$. The points for $y = 0$ and $y = 2$ have been normalized to the curve for $y = 1$, using the point ● (i.e. the values of R_2 have been altered to $R_2' = f(R_2 - 1) + 1$; for the triangles and squares $f = 1.13$ and 0.90, respectively). This facilitates the comparison of the linearity of the plots. Triangles and squares are not shown for M.R. < 0.13 because they differ negligibly from the circles in this region.

Cyclohexanol

Very small amounts of DMB inhibit the formation of cyclohexanol, whereas benzene has little or no effect. This is consistent with a free radical mechanism for the formation of the alcohol because DMB is a very good radical scavenger and benzene is a very poor one (7, 17).

The cyclohexanol is probably formed by abstraction and disproportionation reactions of the $(C_6H_{11}O)\cdot$ radical. This radical can be formed in several different ways (8) and its most probable structure is I. Structures II and III are also possible, but they are probably

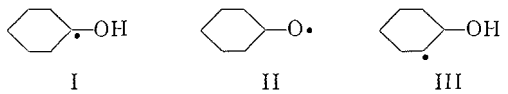

I II III

formed to much smaller extents than is I (8).

C_{12} Products

The C_{12} products are probably formed by the combination of radicals. Half of the dimer yield is accounted for by DKDC (on the silicone grease column; G(total dimer) = 1.53, G(DKDC) = 0.79) which suggests that radical IV is produced in good yield in the system.

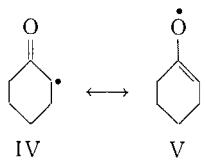

IV V

(14) $2\,\mathrm{IV} \rightarrow \mathrm{DKDC}.$

The reaction

(15) $2\,\mathrm{V} \rightarrow$ 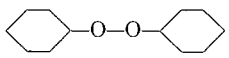

does not occur to a great extent because the yield of peroxides is low ($G \leqslant 0.3$).

Other $\cdot C_6H_9O$ radicals and $(C_6H_{11}O)\cdot$ radicals probably also contribute to C_{12} formation.

Very small amounts of DMB or of oxygen inhibit the formation of cyclohexanone dimers. This can be attributed to the radical scavenging properties of the two additives (7, 18).

The effect of benzene on the radiolytic formation of cyclohexanone dimers (Fig. 3A) is in sharp contrast to the effect of DMB (Fig. 3B). Benzene is a poor radical scavenger and its inhibiting effect might be due to an activation transfer process, although an inefficient radical scavenging action cannot be ruled out.

Further Comments on the Role of Very Low Concentrations of DMB in the Radiolysis of Cyclohexanone

In the low concentration region ($\epsilon_s < 3 \times 10^{-3}$), DMB inhibits the formation of cyclohexanol and the dimers (Figs. 2 and 3). It was suggested in the preceding discussion that the diene was acting as a radical scavenger in these instances. The attack of a free radical on the diene would give an allylic radical (VI).

$$\mathrm{R} + \mathrm{CH_2{=}C(CH_3){-}{-}C(CH_3){=}CH_2} \rightarrow \mathrm{R{-}CH_2{-}C(CH_3)\cdots C(CH_3)\cdots CH_2}$$

VI

The main fate of radical VI is to combine with another free radical to form a product larger than C_{12}. DMB is not consumed in a chain reaction (Fig. 6), so radical VI does not initiate a chain. Nor does radical VI abstract hydrogen or disproportionate to an appreciable extent to form mono-oxo-C_{12} compounds because such products were not observed in solutions with $\epsilon_s \approx 2 \times 10^{-3}$ where the yields of cyclohexanone dimers and cyclohexanol had been reduced to zero.

At DMB concentrations $>1.5 \times 10^{-3}$, radical VI would be the dominant radical in the system, so the main radical reaction product would be the dimer of VI. The formation of polymer with a 1:1 ratio of DMB units to cyclohexanone units in it is consistent with this conclusion. The measured molecular weight (400 ± 30) and iodine number (138 ± 22) of the polymer are in quite good agreement with the molecular weight (360) and iodine number (141) of the dimer of VI.

The Value of G(Scavengeable Radicals)

According to the preceding discussion, the value of G(scavengeable radicals) should equal the value of G(consumption) of DMB in the maximally inhibited reaction. Thus, G(radicals) = 4 (Fig. 6).

The average value of G(peroxides) from the two oxygen containing samples is about 3 (Table III). Since a peroxide may represent either one or two molecules of ketone, a

Can. J. Chem. Downloaded from www.nrcresearchpress.com by 210.87.254.42 on 09/05/12
For personal use only.

value of G(radicals) $\geqslant 3$ may be estimated from this measurement. The yield of dioxocyclohexanes was estimated to be $G \simeq 1$. Thus the value of G(radicals) from the oxygen containing samples would be $\gtrsim 4$.

Thus it appears that G(scavengeable radicals) $\simeq 4$.

An upper limit of the value of G(scavengeable radicals) in pure cyclohexanone can be calculated from the decrease in yields of the various products by low concentrations of DMB and is about 6 ± 3. The uncertainty in this value is due to uncertainties about the mechanisms of formation of the products, to lack of precision in the measurements of the initial product yields, and to the detection limits of the products in the analyses of the solutions.

The overlap of the measured and calculated values of G(scavengeable radicals) is not impressive but is consistent with the proposed free radical mechanisms.

ACKNOWLEDGMENTS

The authors would like to express their appreciation to the National Research Council for financial assistance of this work.

REFERENCES

1. A. SINGH and G. R. FREEMAN. Can. J. Chem. **42**, 1869 (1964).
2. P. MANION and M. BURTON. J. Phys. Chem. **56**, 560 (1952).
3. A. J. SWALLOW. Radiation chemistry of organic compounds. Pergamon Press, Oxford. 1960.
4. W. N. PATRICK and M. BURTON. J. Phys. Chem. **58**, 424 (1954).
5. K. WATANABE, T. NAKAYAMA, and J. MOTTL. J. Quant. Spectr. Radiative Transfer, **2**, 369 (1962).
6. C. N. R. RAO. Ultra-violet and visible spectroscopy; chemical applications. Butterworths, London. 1961.
7. A. RAJBENBACH and M. SZWARC. Proc. Roy. Soc. Ser. A, **251**, 394 (1959).
8. A. SINGH. Ph.D. Thesis, University of Alberta, Edmonton, Alta. 1963.
9. H. SPONER. Radiation Res. Suppl. **1**, 558 (1959).
10. C. REID. Excited states in chemistry and biology. Butterworths Scientific Publications, London. 1957.
11. S. R. LAPAGLIA and B. C. ROQUITTE. J. Phys. Chem. **66**, 1739 (1962).
12. F. E. BLACET and J. N. PITTS, JR. J. Am. Chem. Soc. **74**, 3382 (1952).
13. W. C. PRICE, R. BRALSFORD, P. V. HARRIS, and R. G. RIDLEY. Spectrochim. Acta, **14**, 45 (1959).
14. G. S. HAMMOND, N. J. TURRO, and P. A. LEERMAKERS. J. Phys. Chem. **66**, 1144 (1962).
15. P. DE MAYO. *In* Advances in organic chemistry, methods and results. Vol. II. *Edited by* R. A. Raphael, E. C. Taylor, and H. Wynberg. Interscience Publishers, Inc., New York. 1960.
16. T. L. COTTRELL. The strengths of chemical bonds. Butterworths Scientific Publications, London. 1958.
17. M. LEVY and M. SZWARC. J. Chem. Phys. **22**, 1961 (1954).
18. R. H. SCHULER. J. Phys. Chem. **62**, 37 (1958).

Can. J. Chem. Downloaded from www.nrcresearchpress.com by 210.87.254.42 on 09/05/12
For personal use only.

Can. J. Chem. Downloaded from www.nrcresearchpress.com by 210.87.254.6 on 09/05/12
For personal use only.

GAS–LIQUID CHROMATOGRAPHY OF TERPENES

PART XI. THE VOLATILE OIL OF THE LEAVES OF JUNIPERUS SCOPULORUM SARG.[1,2]

E. VON RUDLOFF AND F. M. COUCHMAN[3]

National Research Council of Canada, Prairie Regional Laboratory, Saskatoon, Saskatchewan

Received March 16, 1964

ABSTRACT

The neutral leaf oil of Rocky Mountain juniper was analyzed by gas–liquid chromatography. *d*-Sabinene was found to be the major constituent (45.7%) and smaller amounts of *d*-limonene (11.4%), *d*-α-pinene (4.2%), γ-terpinene (1.15%), *p*-cymene (1.4%), *l*-linalool (1.2%), *d*-terpinen-4-ol (2.9%), citronellol (0.2%), *l*-β-elemene (0.2–0.3%), three isomeric cadinenes (2.7%), *l*-elemol (6.0%), and safrole (1.85%) were isolated. α-Thujene, camphene, car-3-ene, myrcene, α-terpinene, terpinolene, thujone, isothujone, methyl citronellate, sabinyl acetate, sabinol, geraniol, α- and δ-cadin*ol*, and *trans*-isoeugenol were tentatively identified. An unidentified acetate (II) (4.7%) was isolated from the oxygenated sesquiterpene fraction and another appears to be present in trace amounts.

The composition of the oils from the leaves of four local ornamental plants was found to differ significantly from that of the wild juniper.

Rocky Mountain juniper (*Juniperus scopulorum* Sarg.) is a small bushy tree found mainly in the mountainous areas of Alberta and British Columbia. Except for ornamental purposes this juniper has not any commercial use. The literature is devoid of any reference as to the chemical composition of the foliage or wood. In part IX of this series the analysis of the volatile oil of the leaves of the savin juniper (*J. sabina* L.) was described (1). This communication deals with a similar analysis of the leaf oil of the Rocky Mountain juniper.

In previous work (2) it was noted that prefractionation by fractional distillation may result in considerable isomerization of some terpenes. Prefractionation by low resolution preparative gas–liquid chromatography (g.l.c.) was employed without apparent rearrangement or decomposition (1, 2), but the yield of low boiling monoterpenes was far from satisfactory. In addition, direct preparative g.l.c. of the total oil does not permit collection of many of the minor constituents. Kugler and Kovats (3) report similar findings and have developed group displacement chromatography on modified silica gel to overcome these difficulties. In the present study silicic acid was similarly pretreated with polyethylene glycol to deactivate catalytic sites. On this adsorbent the oil was prefractionated into hydrocarbons and oxygenated components by elution chromatography without apparent rearrangement, dehydration, or polymerization of the more labile components. These fractions were then further subdivided into mono- and sesqui-terpene fractions by preparative g.l.c. on short columns. These four groups were fractionated further into single components by preparative g.l.c. All major and most minor constituents could thus be isolated and characterized, and several of the trace components were tentatively identified by their relative retention times (r.r.t.). The percentage composition (Table I) was determined by measurement of the area under the peaks obtained in linear temperature-programmed runs (Fig. 1). The components identified by r.r.t. only are shown in parentheses. Kugler and Kovats (3) report an analytical error of 3%. However, Janak (4) has shown that the error may be considerably higher on peaks of small area. In our previous studies the errors recorded appeared to be within the range reported by Janak, except that in isothermal runs the

[1]*Part X, Can. J. Chem. 42, 1057 (1964).*
[2]*Issued as N.R.C. No. 8003.*
[3]*National Research Council of Canada Postdoctoral Fellow 1963–64.*

TABLE I

Percentage composition of the volatile leaf oil of Rocky Mountain juniper

Peak No.	Compound	R.R.T.*	%† A	%† B	Peak No.	Compound	R.R.T.*	%† A	%† B
1	Unidentified	—	0.15	Trace	23	Unidentified	—	0.3	0.8
2*a*	(α-Thujene)	0.29	1.5	4.8	24	Unidentified	—	0.6	0.6
2*b*	*d*-α-Pinene	0.29	4.2		25*a*	Safrole	0.45	1.85	4.3
3	(Camphene)	0.42	0.15	Trace	25*b*	(Geraniol)	—	Trace	
4	*d*-Sabinene	0.62	45.7	35.2	26	Unidentified	0.51	0.3	0.1
5	(Car-3-ene)	0.73	0.7	0.5	27	Unidentified	—	0.1	0.1
6	(Myrcene)	0.82	1.4	0.95	28	Unidentified	—	0.1	0.3
7	(α-Terpinene)	0.94	0.7	0.8	29	Unidentified	0.64	0.7	3.85
8	*d*-Limonene	1.00	11.4	3.6	30	Unidentified	—	0.15	
9	γ-Terpinene	1.40	1.15	2.1	31	Unidentified	—	0.45	0.65
10	*p*-Cymene	1.63	1.4	0.95	32	Unidentified	0.76	0.85	0.3
11	(Terpinolene)	1.79	0.3	0.8	33	*l*-Elemol	0.84	6.0	14.4
12	(Thujone)	0.64	0.3	Trace	34	(Acetate I)	0.95	0.45	0.5
13	(Isothujone)	0.68	0.5	0.5	35	Unidentified	—	0.15	1.3
14	*l*-Linalool	1.02	1.2	3.2	36	(α-Cadinol or γ-eudesmol)	1.18	0.6	1.6
15	(Methyl citronellate)	1.20	0.3	0.5	37	Unidentified	—	0.3	0.5
16*a*	*d*-Terpinen-4-ol	1.40	2.9	6.4	38	(δ-Cadinol)	1.25	2.7	3.0
16*b*	*l*-Elemene	1.42	0.3		39	(*trans*-Isoeugenol)	1.40	0.15	Trace
17	Unidentified	1.60	0.15	0.5	40	Unidentified	—	0.15	—
18	(Sabinyl acetate)	1.90	0.15	0.1	41	Acetate II	—	4.7	5.1
19*a*	Unidentified C_{15}	—	0.7	0.5	42	Unidentified	—	1.15	—
19*b*	(Sabinol)	2.20							
20	Cadinene I	2.46	0.3	0.2					
21	Unidentified	—	0.45	Trace					
22*a*	Cadinene II	3.30	2.4	0.65					
22*b*	Citronellol	2.95	0.2						

*Relative retention times on a 6 ft × ¼ in. PEG 20M column: (*a*) monoterpene hydrocarbons (limonene = 1.00) at 65 °C; (*b*) oxygenated monoterpenes and sesquiterpene hydrocarbons (camphor = 1.00) at 120 °C; (*c*) oxygenated sesquiterpenes (cedrol = 1.00) at 180 °C.

†(A) From a tree from the Forest Nursery, Indian Head, Saskatchewan; (B) From a tree from the Invermere district, B.C.

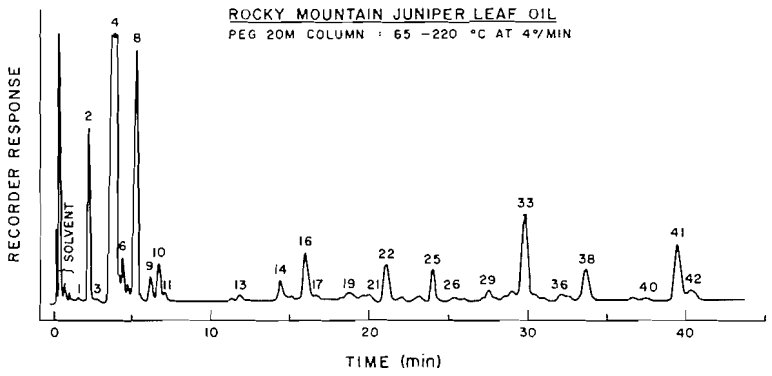

FIG. 1. Gas chromatogram of the volatile oil of Rocky Mountain juniper leaves (6 ft × 3/16 in. o.d. polyethylene glycol 20M column, temperature programmed from 65 to 220 °C at 4° per minute).

values for compounds of high r.r.t. were invariably low. This difficulty was largely overcome by employing temperature programming (1). In the present study an instrument which permitted linear programming was available for the analytical runs and the errors encountered in duplicate runs, or on different columns, were lower than those reported by Janak, but it is unlikely that trace components were recorded with an error of less than 10 to 20%.

Can. J. Chem. Downloaded from www.nrcresearchpress.com by 210.87.254.6 on 09/05/12
For personal use only.

Can. J. Chem. Downloaded from www.nrcresearchpress.com by 210.87.254.6 on 09/05/12
For personal use only.

Comparison of the composition of the leaf oils from Rocky Mountain and savin junipers shows that both contain *d*-sabinene as a major component and the same monoterpene hydrocarbons, although the limonene content (11.4%) of the former was markedly higher. Common to both oils are also thujone, isothujone, methyl citronellate, terpinen-4-ol, citronellol, geraniol, the cadinene isomers, elemol, and perhaps cadinols. These similarities suggest a close phylogenetic relationship between the two juniper species, but the presence of large amounts of sabinyl acetate and some sabinol in the oil of savin may be a significant difference. Also noteworthy are the relatively high amounts of *l*-elemol, safrole, and the unidentified acetate II (peak 41) in the oil from Rocky Mountain juniper leaves. The latter also contained some *l*-linalool (1.2%) which was not isolated from the oil of savin (the trace component 16 did, however, have the same r.r.t. value).

Since the foliage of the Rocky Mountain juniper was obtained from a prairie location (Indian Head, Saskatchewan), it was possible that the composition of the oil was not typical for this species. Therefore, a small amount of the foliage of Rocky Mountain juniper from the Invermere district, B.C., was steam-distilled and the oil analyzed by linear temperature-programmed g.l.c. No significant qualitative differences were recorded (see Table I, last column) and it is thus probable that the composition of the oil is not markedly influenced by environmental factors. The somewhat lower relative amounts of monoterpenes, especially sabinene and limonene, and correspondingly larger amounts of linalool, terpinen-4-ol and elemene, safrole, component 29 or 30, and elemol are the only noteworthy quantitative differences.

A few garden-variety (ornamental) Rocky Mountain junipers were available locally and small amounts of leaf oils were obtained from four plants. The percentage composition was determined by temperature-programmed g.l.c. and the major components are listed in Table II. Peaks were directly compared with those from the charts of the oils discussed

TABLE II

Percentage composition of the leaf oils of local garden variety Rocky Mountain junipers

		Plant*			
Peak	Compound	C	D	E	F
2	α-Pinene and α-thujene	2.6	2.2	3.1	2.1
4	Sabinene	15.6	6.1	22.5	28.3
8	Limonene	0.5	4.4	0.2	0.6
—	Unidentified	—	—	0.8	Trace
9	γ-Terpinene	1.5	0.4	1.1	0.6
11	Terpinolene	0.3	Trace	0.4	0.3
—	Unidentified	—	—	1.4	0.4
13	Isothujone	2.8	1.6	2.0	0.8
14	Linalool	4.2	3.9	14.1	3.3
15	Methyl citronellate	0.5	Trace	0.5	0.6
16	Terpinen-4-ol	4.4	1.7	4.2	1.6
19	Unidentified	1.5	0.6	0.8	1.0
22	Cadinenes	1.0	0.3	0.6	0.6
—	Unidentified	—	—	2.2	0.4
25	Safrole	0.3	7.0	0.1	0.1
26	Unidentified	0.8	Trace	0.5	0.8
28	Unidentified	1.5	0.3	1.0	0.3
30	Unidentified	0.8	18.6	Trace	0.3
31	Unidentified	9.1	11.0	11.2	3.3
32	Unidentified	1.8	0.9	0.5	3.2
33	Elemol	8.0	4.8	10.6	21.6
38	(δ-Cadinol)	1.8	4.1	1.7	0.7
—	Unidentified	1.8	1.1	0.7	0.8
41	(Acetate II)	28.6	24.1	11.2	20.0
42	Unidentified	1.8	1.5	0.3	0.5

*3–4 years old (commercial seedlings).

above, and some very marked quantitative differences were noticed. Thus, the oil from all four local plants had a lower content of the major monoterpene hydrocarbons, most noticeable being the low content of sabinene in plant D and the virtual absence of limonene in the other three. The content of oxygenated monoterpenes also differed somewhat; e.g. the content of linalool in the oil from plant E was 14.1% as compared with 1–3% in that of the wild trees. No significant differences were found in the sesquiterpene hydrocarbon range, but safrole was found only in trace amounts in plants C, E, and F. The markedly higher content of the components in the oxygenated sesquiterpene range is also noteworthy.

Most noticeable is the fact that the oil from plant F contained over 20% elemol and all four oils had a surprisingly high content of component 41 (acetate II). It is possible that the latter has chemotaxonomic significance, and attempts to isolate sufficient amounts for complete characterization are now being made. The large amounts of component 31 in the oils from plants C, D, and E, and of component 30 in that from plant D, are also noteworthy. Since all leaves were harvested during winter, seasonal variations cannot account for the differences recorded. One possibility is that the differences are due to age, the local plants all being relatively young (3–4 years old). Alternatively, the garden varieties may differ genetically from the wild plants. It follows that for the determination of the taxonomically representative composition of conifer leaf oils, the leaves of mature, wild species should be used.

EXPERIMENTAL

The g.l.c. techniques used have been described previously (1, 2). In addition, a F&M model 500 (F&M Scientific Corp.) chromatograph was used for analytical runs using linear temperature programming. Optical rotations were measured at 25 ± 2 °C of either undiluted material or chloroform solutions (1 to 5%). Infrared spectra were recorded with a Perkin–Elmer model 21 double beam spectrophotometer as films between sodium chloride plates. Individual components were identified by comparison of their infrared spectra and relative retention times (r.r.t.).

Materials

The foliage of Rocky Mountain juniper was obtained from the Indian Head Forest Nursery, Saskatchewan (Plant A). Woody branches and berries were removed and the residual leaves (3.90 kg) were steam-distilled for 3–4 h. The distillate was taken up in ether, washed with bicarbonate solution and water, dried over anhydrous sodium sulphate, and the ether then evaporated at 70–80 °C. The residual oil (58.9 g, 1.51%) had n_D 1.4790; $[\alpha]_D$ +40.3°. Acidification of the bicarbonate solution gave only trace amounts of ether-soluble acids. The foliage (5–10 g) from mature Rocky Mountain juniper from the Invermere district, B.C. (Plant B), and from local garden variety plants (3–4 years old, plants C–F) was steam-distilled and the volatile oil (50–100 mg) was isolated as above. Reference compounds were those obtained previously (1, 2). The liquid phases used in g.l.c. columns were commercial products.

Analytical Chromatograms

Temperature-programmed (linear) chromatograms were obtained with 2–3 μl aliquots of oil using 6 ft × 3/16 in. o.d. polyethylene glycol (PEG 20M) or Apiezon N (A–N) columns (Fig. 1). The percentage composition was determined by measurement of the area under each peak (triangulation method) and the average values from two runs on the PEG 20M column are shown in Table I. The values for those components which were unresolved on this column (e.g. α-thujene and α-pinene) were obtained from runs on other columns.

The r.r.t. values and purity of isolated components were determined on PEG 20M, A–N, polyethylene glycol adipate polyester (APEG), rapeseed oil (RO), and ethylene glycol bis-(propionitrile) (EGPN) columns under the conditions (isothermal) described previously (1, 2). The r.r.t. values of monoterpenes were measured relative to limonene, oxygenated monoterpenes and sesquiterpenes relative to camphor, and oxygenated sesquiterpenes relative to cedrol (see Table I).

Prefractionation

Silicic acid was impregnated with polyethylene glycol (carbowax 20M) as described by Kugler and Kovats (3). Aliquots (1.0 g) of oil of savin (1), oil tansy (2), Rocky Mountain juniper leaf oil, and a synthetic mixture of α-pinene, limonene, *p*-cymene, linalool, citronellol, nerol, fenchyl alcohol, and carvone were dissolved in a little hexane and transferred to the top of a column containing the deactivated silicic acid (20–25 g). Elution with hexane (300 ml) gave a mixture of hydrocarbons which showed no oxygenated terpenes on

Can. J. Chem. Downloaded from www.nrcresearchpress.com by 210.87.254.6 on 09/05/12
For personal use only.

g.l.c. analysis. The column was then eluted with methanol (300 ml) and the material eluted showed on g.l.c. analysis less than 2% hydrocarbons and all the oxygenated terpenes previously recorded in the mixtures. Equally good results were obtained when only 10 g modified silicic acid were used, but with 5 g the separation was much poorer.

To test whether any dehydration could be detected, similar runs were carried out with linalool (0.45 g) and *l*-elemol (0.08) alone. In each case, no hydrocarbon peak was recorded and the parent alcohol was recovered unchanged. However, the recovery of elemol was only 85% and it is thus possible that some polymerization does take place.

Rocky Mountain juniper leaf oil (10.63 g) was chromatographed as above on deactivated silicic acid (100 g) to give a hydrocarbon fraction (6.42 g) and the oxygenated terpenes (4.22 g). Aliquots (500 μl) of the hydrocarbon mixture were injected onto a 3 ft × 3/8 in. o.d. SE-30 silicone polymer (25% on Chromosorb W, 40–60 mesh) column, which was programmed (non-linear) from 80 to 150 °C in 20 min. The monoterpenes were eluted within 11 min and collected as a single fraction in an ice-cooled collection flask (5 ml). The sesquiterpenes were collected similarly as a second, unresolved fraction. In the same manner aliquots (100 μl) of the oxygenated terpenes were fractionated into mono- and sesqui-terpenes by use of a 3 ft × 3/8 in. o.d. A–N (20% on Gaschrom P, 60–80 mesh) column, programmed from 100 to 220 °C in 30 min.

Monoterpene Hydrocarbons

Preparative g.l.c. of the monoterpene hydrocarbon fraction (repeated injections of 200 μl aliquots) on a 20 ft × 3/8 in. PEG 20M column programmed from 80 to 160 °C in 50 min resulted in the isolation of components 2, 4, 8, 9, and 10. Component 2 was found to be a mixture of α-pinene and tentatively identified α-thujene (r.r.t. = 0.35 and 0.29 on the A–N and EGPN columns). Component 4, the major constituent of the oil, corresponded in all respects to sabinene; n_D 1.4666; $[\alpha]_D$ +108.0° (*c*, 2.0). The g.l.c. analysis did not reveal the presence of any β-pinene, but up to 2 or 3% of this terpene would not be detectable in sabinene (1). The r.r.t. values and spectral properties showed component 8 to be *d*-limonene; n_D 1.4686; $[\alpha]_D$ +104.6° (*c*, 1.8); component 9: γ-terpinene; n_D 1.4732; and component 10: *p*-cymene. Component 1 could not be isolated and components 3, 5, 6, 7, and 11 were obtained only impure and in small amounts. The r.r.t. values showed the latter to correspond to camphene, car-3-ene, myrcene, α-terpinene, and terpinolene respectively. The infrared spectra of the impure fractions were compatible with these assignments.

Oxygenated Monoterpenes

Aliquots (100 μl) of the mixture of oxygenated monoterpenes were chromatographed on a 6 ft × 3/8 in. PEG 20M column (100 to 210 °C in 35 min). Components 14, 16*a*, and 25*a* were isolated almost pure and were found to correspond to *l*-linalool (n_D 1.4610; $[\alpha]_D$ −12.5°), *d*-terpinen-4-ol (n_D 1.4733; $[\alpha]_D$ +19.7°) and safrole (n_D 1.5214) respectively. Analytical g.l.c. on the A–N column showed that safrole (component 25*a*) could be contaminated by a small amount of geraniol. Component 22*b* was obtained impure (n_D 1.4738; $[\alpha]_D$ +30°). It had the typical smell of citronellol and r.r.t. as well as the infrared spectrum were compatible with this assignment. Components 12, 13, 15, 18, and 19*b* could only be identified tentatively by r.r.t. on the analytical PEG 20M, APEG, A–N, and RO columns (see Table I).

Sesquiterpene Hydrocarbons

Preparative g.l.c. on the 20 ft × 3/8 in. o.d. PEG 20M column (30 μl aliquots, 150 to 205 °C in 50 min) gave components 16*b*, 19*a*, 20, and 22*a* in a fairly pure state. Component 16*b* corresponded to β-elemene, n_D 1.4992, $[\alpha]_D$ −6.0°. Since column chromatography of β-elemol had not given any hydrocarbons (see above), β-elemene is considered to be a genuine component of the oil. Component 19*a* was an unidentified hydrocarbon, n_D 1.5035, $[\alpha]_D$ −8.0°, having r.r.t. values similar to β-caryophyllene, but its infrared spectrum differed somewhat from that of authentic β-caryophyllene (unresolved absorption band at 1377 cm^{-1}; additional bands of medium intensity at 1125, 1050, and 910 cm^{-1}). Component 20 corresponded to the cadinene isomer of low r.r.t. value isolated previously from the oil of savin (1), and found in spruce leaf oils (5, 6); n_D 1.5048; $[\alpha]_D$ −58.4°. Component 22*a* corresponded to cadinene, n_D 1.5057, $[\alpha]_D$ +113.0°, and analytical g.l.c. showed it to be a mixture of γ- and δ-cadinene.

Oxygenated Sesquiterpenes

Aliquots (20 μl) of the last fraction were chromatographed on the 6 ft PEG 20M column (160 to 220 °C in 30 min) and components 33, 36, 38, and 41 could be isolated in a fairly pure state. Component 33 corresponded to *l*-elemol; n_D 1.4993; $[\alpha]_D$ −6.9°. Component 36, n_D 1.5096, $[\alpha]_D$ −13.6°, had the r.r.t. of α-cadinol and γ-eudesmol, but since these two alcohols cannot be distinguished (from one another) by their infrared spectra (7), the identification is uncertain. Component 41 had n_D 1.5000 and $[\alpha]_D$ +147.2° and its infrared spectrum suggested it to be an alcohol containing an acetate group (strong bands at 1730–1720 and 1245 cm^{-1}). When a methanolic solution of this component and sodium methoxide was left overnight the compound appeared to be unchanged. A mixed fraction corresponding to components 33 and 34 was also isolated. As expected, the infrared spectrum showed elemol to be present, but in addition bands at 1735 and 1260–1245 cm^{-1} were recorded. This suggests that component 34 may be another acetate. Component 38 had the retention characteristics and infrared spectrum of δ-cadinol, but seeding with an authentic specimen (m.p. 139–140 °C) failed to induce crystallization.

Can. J. Chem. Downloaded from www.nrcresearchpress.com by 210.87.254.6 on 09/05/12
For personal use only.

ACKNOWLEDGMENTS

We wish to thank Mr. P. J. Salisbury, Plant Pathologist, Forest Nursery, Indian Head, Saskatchewan, for supplying the juniper foliage, Mr. M. Granat for technical assistance, and W. C. Haid for recording the infrared spectra.

REFERENCES

1. E. VON RUDLOFF. Can. J. Chem. **41**, 2876 (1963).
2. E. VON RUDLOFF. Can. J. Chem. **41**, 1737 (1963).
3. E. KUGLER and E. S. KOVATS. Helv. Chim. Acta, **46**, 1480 (1963).
4. J. JANAK. J. Chromatog. **3**, 308 (1960).
5. E. VON RUDLOFF. Tappi, **45**, 181 (1962).
6. E. VON RUDLOFF. Can. J. Chem. **42**, 1057 (1964).
7. E. VON RUDLOFF and G. V. NAIR. Can. J. Chem. **42**, 421 (1964).

Can. J. Chem. Downloaded from www.nrcresearchpress.com by 210.87.254.6 on 09/05/12
For personal use only.

Can. J. Chem. Downloaded from www.nrcresearchpress.com by 210.87.254.6 on 09/05/12
For personal use only.

MECHANISM OF THE BIMOLECULAR NUCLEOPHILIC DISPLACEMENT REACTION ON α-HALOCARBONYL COMPOUNDS

A. Joseph Sisti and Seymour Lowell[1]
Chemistry Department, Adelphi University, Garden City, New York
Received January 9, 1964

ABSTRACT

Two mechanisms have previously been postulated for the high reactivity of α-halocarbonyl compounds in the nucleophilic displacement reaction. Kinetic data for α-halocarbonyl compounds and various nucleophiles (cyanate, acetate, azide, and thiocyanate) in anhydrous methanol are presented. The new data, in conjunction with previously reported results, are in better agreement with the concept of neighboring group overlap than with that of Pearson's electrostatic facilitation between the nucleophile and the α-carbonyl group.

The enhanced reactivity exhibited by α-haloketones in the bimolecular nucleophilic displacement reaction is well known. To a lesser extent, related compounds, α-halonitriles, amides, and esters, manifest similar reactivity. Various interpretations have been offered for the unusual reactivity of these compounds. On the basis of previous evidence (1, 2) many of these interpretations are no longer seriously considered. Two mechanisms are, however, consistent with the data available. Pearson and co-workers (1) postulate that the enhancement results from the proximity of the positively charged carbonyl-carbon atom which electrostatically facilitates the approach of the nucleophile along its normal path to the adjacent carbon atom. They also mention that the enhancement should be larger for the more polarizable nucleophile, since it can be more easily facilitated electrostatically to the reaction site. The mechanism suggested by Dewar (3) and Winstein (see footnote 16 in ref. 4) is based upon neighboring group orbital overlap with the adjoining electron-deficient carbon atom. Thus, the transition state with α-haloketones

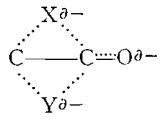

I

is envisaged as including partial bonding of the reagent with the *p*-orbital of the carbonyl-carbon (I). Bartlett and Trachtenberg (2) pointed out that for the latter mechanism to obtain certain stereochemical requirements must be fulfilled. Thus, kinetic measurements (iodide in acetone) were conducted on two model phenacyl systems (II and III). Compound II, which is structurally incapable of attaining the prescribed geometry in the transition

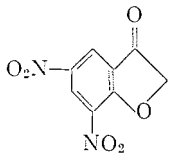

II

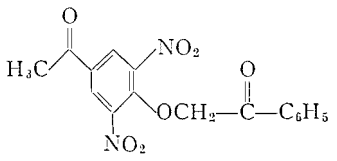

III

[1]*Taken largely from the Ph.D. thesis of S. Lowell, Adelphi University, June 1963.*

state, reacted 9000 times slower than compound III at 0°. These results tend to substantiate the mechanism of Dewar and Winstein. However, the lack of typical phenacyl reactivity in compound II is also consistent with the electrostatic mechanism of Pearson (1), since the electrostatically most favored path, by way of the positive end of the carbonyl dipole, is structurally prohibited (2). The previously reported relative rate ratios, presented in Table I, also do not allow a clear differentiation between the two mechanisms. However,

TABLE I

Relative rates of displacement on α-halocarbonyl compounds

Reaction	Relative rates			
	C_3H_7X	XCH_2CO_2Et	$C_6H_5COCH_2X$	CH_3COCH_2X
R—Br + pyridine[a] in methanol at 35°	1	85	450	—
R—Br + thiourea[a] in methanol at 35°	1	640	10 700	—
R—Cl + KI[b] in acetone at 50°	1	1 600	97 000	33 000
R—Cl + $S_2O_3^{=}$[c] in water at 25°	1	220	1 600	1 400

[a]R. G. Pearson, S. H. Langer, F. V. Williams, and W. G. McGuire. J. Am. Chem. Soc. 74, 5130 (1952).
[b]J. B. Conant, W. R. Kirner, and R. E. Hussey. J. Am. Chem. Soc. 47, 488 (1925).
[c]A. Slater. J. Chem. Soc. 85, 1286 (1904); 87, 481 (1905); A. Slater and D. F. Twiss. J. Chem. Soc. 95, 93 (1909).

it has been pointed out by Bartlett (2) that pyridine which possesses no charge to be acted upon electrostatically, but which does possess an electron pair for neighboring group orbital overlap, is subject to the activating influence of the carbonyl-carbon.

A recently postulated (5) implication of the neighboring group orbital overlap mechanism is the importance of the relative sizes of the electronic orbitals. The rate-enhancing effect seems to be more pronounced when the entering and leaving groups are not first row elements (1) and hence the larger orbitals should be capable of more effective neighboring group overlap.

According to Pearson, α-halocarbonyl and related compounds exhibit rate-enhancement, relative to *n*-propyl halide, because of charge (electrostatics) on the nucleophile. The Winstein–Dewar mechanism manifests enhancement because of neighboring group overlap, and that the magnitude of the enhancement should vary with the orbital size of the entering and leaving reagents. A kinetic study is presented in which three charged nucleophiles with relatively small bonding orbitals and one charged nucleophile with a relatively large bonding orbital were reacted with a series of α-halocarbonyl compounds in an attempt to differentiate between the two mechanisms.

EXPERIMENTAL*

Reagents

All organic chlorides used were commercial products. They were redistilled or recrystallized repeatedly (3–5 times) before use. The chlorides employed were: *n*-propyl chloride (washed with concentrated sulphuric acid before distillation), phenacyl chloride, benzyl chloride, ethyl chloroacetate, and α-chloroacetone. Methanol and ethanol were distilled from magnesium methoxide and ethoxide, respectively. Silver nitrate solutions were prepared from Baker and Adamson analytical reagent grade after drying. Sodium azide (Eastman) was purified by repeated crystallizations from water, then washed with acetone, and dried to constant weight. Sodium ethoxide solution, prepared by treating anhydrous ethanol with sodium, was standardized by titration in water with potassium acid phthalate to the phenolphthalein end point. Solutions of sodium acetate (Baker, reagent grade), potassium cyanate (Baker, reagent grade), potassium thiocyanate (Baker, reagent grade), potassium iodate (Matheson), and sodium thiosulphate (Eastman) were prepared after drying to constant weight.

**All melting points and boiling points were uncorrected. All organic compounds were used within 24 h after purification.*

Can. J. Chem. Downloaded from www.nrcresearchpress.com by 210.87.254.6 on 09/05/12
For personal use only.

General Procedure

In all kinetic studies the solutions were prepared so that the initial concentrations of reactants were in a volume of 25 ml at room temperature. The required volumes of freshly prepared reactants were added from calibrated burettes directly into 100 ml volumetric flasks. The reaction was quenched by the addition of the contents of each flask to a separatory funnel containing an organic solvent (50 ml) and water (100 ml). The layers were separated and analysis was made for the water soluble product or water soluble reactant. Each rate constant given involved a minimum of six flasks and a maximum of ten, each removed at varying time intervals.

Sodium Acetate

The rate constants for sodium acetate and the four organic chlorides in anhydrous methanol were determined as above. Ether was used for quenching the reaction. The method of Fajans (6) was employed for the determination of chloride produced.* At each temperature (45.1° and 55°) equal initial concentrations of each reactant were used: acetate and *n*-propyl chloride 0.400 *M*, acetate and phenacyl chloride 0.222 *M* and 0.142 *M*, acetate and ethyl chloroacetate 0.250 *M*, and acetate and α-chloroacetone 0.250 *M*. An additional kinetic study at 45.1° was conducted in which each flask contained unequal and different concentrations of reactants: organic chlorides 0.100 *M*–0.500 *M*, acetate 0.100 *M*–0.400 *M*. Good results were obtained (from usual second order rate equations), indicating overall second order kinetics and first order in each reactant.

Sodium Azide

All kinetic data were obtained at 30° and 40° in methanol except for phenacyl chloride which was studied at 45.1° and 55.0°. The analytical method described by Swain (7) was used. Kinetic studies were made at the two above temperatures in which unequal and different concentrations of each reactant were employed: organic chlorides 0.020 *M*–0.140 *M*; azide 0.030 *M*–0.160 *M*. The results revealed good overall second order kinetics, first order in each reactant.

Potassium Thiocyanate

All kinetic data were obtained at 30° in anhydrous methanol. The method of Crowell (8) was employed for kinetic measurements. Unequal and different concentrations of each reactant in each flask were used: organic chlorides 0.040 *M*–0.140 *M*; thiocyanate 0.060 *M*–0.160 *M*. Satisfactory results were obtained indicating overall second order kinetics and first order in each component.

Potassium Cyanate

The reaction was quenched with 50 ml of ether and 100 ml of water. The layers were separated and the water solution was acidified to pH 2–3 and boiled 15 min to hydrolyze the cyanate to carbon dioxide and ammonia. The solution was then made basic and boiled for 15 min to expel ammonia. The pH was adjusted to 6.5–7.0 and then the method of Fajans (6) was employed to determine chloride ion concentration. Measured amounts of cyanate in water, and measured amounts of cyanate in presence of measured amounts of chloride in water solution were subjected to the above procedure. The first revealed no cyanate present and the second gave values of chloride ion to within 3% error. All kinetic determinations were conducted at 30° in absolute methanol. Kinetic runs employed *n*-propyl chloride 0.200 *M*–0.800 *M*; cyanate 0.400 *M*–0.096 *M*; all others, cyanate 0.050 *M*–0.100 *M*; and α-chloroacetone, phenacyl chloride, and ethyl chloroacetate 0.050 *M*–0.100 *M*. Overall second order kinetics, first order in each component, were obtained.

Kinetic results were taken over one to four half-lives and are presented in Table II.

Product Analysis

Adequate product studies have been previously conducted and indicate the reaction with α-haloketones and the nucleophiles employed to be nucleophilic substitution reactions. Phenacyl chloride: with potassium acetate yields phenacyl acetate, m.40° (9); with potassium thiocyanate yields phenacyl thiocyanate, m.74° (10); with sodium azide yields phenacyl azide, m.17° (11). Adequate studies were also performed with α-chloroacetone which with sodium azide yields α-azidoacetone (12) and with potassium thiocyanate yields α-thiocyanoacetone (13). All the above reactions were conducted in ethanolic or methanolic solutions. No product studies were undertaken with potassium cyanate.

RESULTS AND DISCUSSIONS

Table II presents the specific reaction rate constants for all reactions. The kinetic order for each reaction studied was overall second order and additional studies indicated each reaction was first order in each component (see experimental). Table II shows the

**The value of the rate constant for benzyl chloride and sodium ethoxide in absolute ethanol at 25° (each reactant 0.300 M) was 3.71 × 10^{-5} l $mole^{-1}$ s^{-1}. The value was obtained by the method of Fajans for chloride determination. The value agrees with that reported, E. D. Hughes, C. W. Bevan, and C. K. Ingold, Nature, 171, 301 (1953), to within 1%.*

Can. J. Chem. Downloaded from www.nrcresearchpress.com by 210.87.254.6 on 09/05/12
For personal use only.

TABLE II

Second order rate constants[a] in methanol

Reaction	Temperature (°C)	R			
		n-C_3H_7—	$C_6H_5COCH_2$—	CH_3COCH_2—	—CH_2CO_2Et
$RCl + CH_3CO_2^-$	55.0	1.46×10^{-7}	3.50×10^{-5}	2.75×10^{-5}	3.90×10^{-6}
	45.1	5.86×10^{-8}	1.38×10^{-5}	1.13×10^{-5}	1.61×10^{-6}
	30.0[b]	1.32×10^{-8}	3.02×10^{-6}	2.61×10^{-6}	3.66×10^{-7}
$RCl + N_3^-$	30.0	5.76×10^{-7}	3.82×10^{-4}[c]	1.21×10^{-4}	1.95×10^{-5}
	40.0	2.29×10^{-6}	6.51×10^{-4}[d]	2.42×10^{-4}	4.38×10^{-5}
			1.57×10^{-4}[b]		
$RCl + NCO^-$	30.0	1.92×10^{-7}	3.44×10^{-5}	2.99×10^{-5}	1.45×10^{-5}
$RCl + NCS^-$	30.0	3.59×10^{-7}	2.76×10^{-4}	1.44×10^{-4}	2.99×10^{-5}

[a]All constants in l mole^{-1} s^{-1}.
[b]Not experimental values, calculated from constants at 45.1° and 55.0° in usual manner.
[c]Rate constant determined at 45.1°.
[d]Rate constant determined at 55.0°.

TABLE III

Relative rates of displacement on α-halocarbonyl compounds at 30.0° in methanol

Compound	Acetate	Azide	Cyanate	Thiocyanate
n-Propyl chloride	1.0	1.0	1.0	1.0
Ethyl chloroacetate	28	33	75	83
α-Chloroacetone	198	210	156	401
Phenacyl chloride	228	276	179	770

relative rates for all the organic substrates employed with each of the four nucleophiles.

The results in Tables I and III may be interpreted as evidence against the Pearson mechanism. The amount of rate-enhancement (relative to n-propyl halide) with the nucleophiles, cyanate, azide, acetate, and pyridine, charged and uncharged, is less than the enhancement of the larger charged and uncharged nucleophiles. It is of interest to note, in particular, the relative rate ratios of azide and cyanate ions. Azide and cyanate, in addition to their charge, possess relatively high polarizabilities (14) and yet their response to the electrostatic activating influence of the α-carbonyl group is comparatively small and essentially the same as the less polarizable nucleophiles, acetate ion and uncharged pyridine. It appears that all the results presented (Table I, III, and the work of Bartlett) are more consistent with the Winstein–Dewar interpretation than the Pearson concept; namely, the enhancement with all nucleophiles is due to additional bonding (covalent) in the transition state with the electron deficient carbonyl-carbon (I). It should be pointed out that one cannot say that the total energy of the additional bonding in the transition state is void of any contribution due to electrostatic interaction. The differences in the relative rate ratios are also tentatively related to the variance in the orbital size of the nucleophiles, i.e., the larger bonding orbital results in more effective neighboring group overlap and a larger relative rate ratio.

In conclusion, the lack of reactivity of certain compounds related to the α-halocarbonyl compounds, namely α-halonitro and α-halosulphonyl compounds, is worthy of comment. Nitrochloromethane and chloromethyl phenyl sulphone have been found unreactive with iodide in acetone (1, 15). Pearson (1) states that the access to the backside of the α-carbon atom, in the region of the positive end of the dipole, in sulphones and nitro compounds is blocked by the negatively charged oxygen atoms. Evidence for the steric rather than the electrical retarding effect of the nitro and sulphonyl groups was supplied by Bordwell (15)

Can. J. Chem. Downloaded from www.nrcresearchpress.com by 210.87.254.6 on 09/05/12
For personal use only.

who found that 1-*p*-toluenesulphonyl-3-chloro-1-propene, IV, and 1-cyano-3-chloro-1-propene, V, reacted, with iodide in acetone at 0°, 1100 and 1400 times faster than *n*-butyl

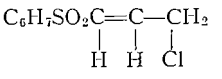

IV

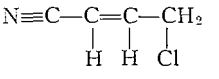

V

chloride. However, the lack of reactivity of nitrochloromethane is also consistent with the Dewar–Winstein concept. Inclusion of the contributing structure, VI, in the transition state may be destabilizing since two negative charges are brought closer together. Similar

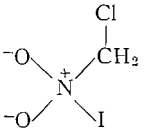

VI

considerations may be offered for the α-halosulphones. Compounds of type IV and V may also have their reactivity accounted for by the Dewar–Winstein concept by inclusion of the stabilizing contributing structure, VII, in the transition state. Since the group,

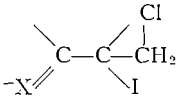

VII

C═C—X, (X = —NO_2, RSO_2—, —CN), possesses similar electrical properties as the carbonyl group, the postulate appears reasonable.

REFERENCES

1. R. G. Pearson, S. H. Langer, F. V. Williams, and W. J. McGuire. J. Am. Chem. Soc. **74**, 5130 (1952).
2. P. D. Bartlett and E. N. Trachtenberg. J. Am. Chem. Soc. **80**, 5808 (1958).
3. M. J. S. Dewar. The electronic theory of organic chemistry. Clarendon Press, Oxford. 1949. p. 73.
4. S. Winstein, E. Grunwald, and H. W. Jones. J. Am. Chem. Soc. **73**, 2700 (1951).
5. A. Streitwieser, Jr. Solvolytic displacement reactions. McGraw-Hill Book Company, Inc. 1962. p. 28.
6. H. F. Walton. Principles and methods of chemical analysis. Prentice Hall, Inc., New York, New York. 1955. p. 356.
7. C. G. Swain and C. B. Scott. J. Am. Chem. Soc. **75**, 146 (1953).
8. T. I. Crowell. J. Am. Chem. Soc. **75**, 6046 (1953).
9. J. Reid. J. Am. Chem. Soc. **41**, 75 (1919).
10. A. Dykerhoff. Ber. **10**, 119 (1877).
11. J. H. Boyer and D. Straw. J. Am. Chem. Soc. **75**, 1642 (1953).
12. J. H. Boyer and J. Hamer. J. Am. Chem. Soc. **77**, 951 (1955).
13. J. Tscherniac. J. Chem. Soc. **115**, 1071 (1919).
14. R. G. Pearson. J. Am. Chem. Soc. **84**, 16 (1962).
15. B. F. Bordwell and G. D. Cooper. J. Am. Chem. Soc. **73**, 5184 (1951).

Can. J. Chem. Downloaded from www.nrcresearchpress.com by 210.87.254.6 on 09/05/12
For personal use only.

THE SYNTHESIS OF SOME DERIVATIVES OF 3,4-METHYLENEDIOXYBENZENE

PRITAM SINGH AND LOUIS BERLINGUET
Department of Biochemistry, Faculty of Medicine, Laval University, Quebec, Quebec
Received July 17, 1963

ABSTRACT

A few derivatives of 3,4-methylenedioxy-α-nitromethylbenzyl alcohol (I) have been prepared. Chlorination with hydrochloric acid and potassium chlorate gave 6-chloro-3,4-methylenedioxy-α-nitromethylbenzyl alcohol (II) which on refluxing with acetic anhydride and sodium acetate gave 6-chloro-3,4-methylenedioxy-ω-nitrostyrene (III). Attempted reduction of (I) with ammonium formate resulted in dehydration to give 3,4-methylenedioxy-ω-nitrostyrene (IV). Reduction of (I) with hydrazine hydrate gave an isobenzaldoxime (VI).

β-(3,4-Methylenedioxyphenyl) serine (VII) was prepared by the condensation of piperonal with glycine. α,β-Dibromo-β-(3,4-methylenedioxyphenyl) propionic acid could not be aminated by a dilute aqueous solution of ethylamine. Decarboxylation and elimination of HBr took place to give ω-bromo-3,4-methylenedioxystyrene (VIII).

INTRODUCTION

The methylenedioxy group is present in many alkaloids with important physiological properties like piperine, narcotine, hydrastine, berberine, etc. Piperonal and its derivatives have been extensively studied biologically. Thus piperonal acts as a vasodilator (1) and thiosemicarbazones of piperonal have been found to inhibit the growth of BCG tuberculus bacteria in vitro (2). It was thought interesting to synthesize some derivatives of 3,4-methylenedioxybenzene with a lateral chain containing amino alcohol groupings for biological evaluation.

RESULTS

It is a well-known fact that halogen substitution, especially chlorination, often enhances the biological activity in a given series of compounds. 3,4-Methylenedioxy-α-nitromethylbenzyl alcohol (I), prepared from piperonal and nitromethane according to the method of Heacock *et al.* (3), was chlorinated with concentrated hydrochloric acid and potassium chlorate. Monochlorination in the 6-position took place and the structure of 6-chloro-3,4-methylenedioxy-α-nitromethylbenzyl alcohol (II) was confirmed by alkaline oxidation of II with potassium permanganate to give 6-chloropiperonylic acid. On refluxing with acetic anhydride and freshly fused sodium acetate, (II) underwent dehydration and 6-chloro-3,4-methylenedioxy-ω-nitrostyrene (III) was obtained.

Heacock, Hutzinger, and Nerenberg recently prepared 3,4-methylenedioxy-α-aminoethylbenzyl alcohol in satisfactory yield by the catalytic hydrogenation of (I) (4). Several different methods of reduction were tried to reduce the nitro group while avoiding the α–β dehydration. When ammonium formate was used as a reducing agent to reduce (I), such a dehydration happened to give 3,4-methylenedioxy-ω-nitrostyrene (IV).

Since this dehydration has been shown to be easily brought about by mineral acids, it was thought formic acid was responsible for it. However, a mixture of 85% formic acid and ethanol (1:4 v/v) did not react with (I). We then tried alkaline reduction with hydrazine hydrate which has been used with some success in the reduction of a nitro group into an amino group (5). But (I), on treatment with hydrazine hydrate, gave with excellent yield a compound to which we have assigned the structure of an isobenzaldoxime (VI).

Can. J. Chem. Downloaded from www.nrcresearchpress.com by 210.87.254.105 on 09/05/12
For personal use only.

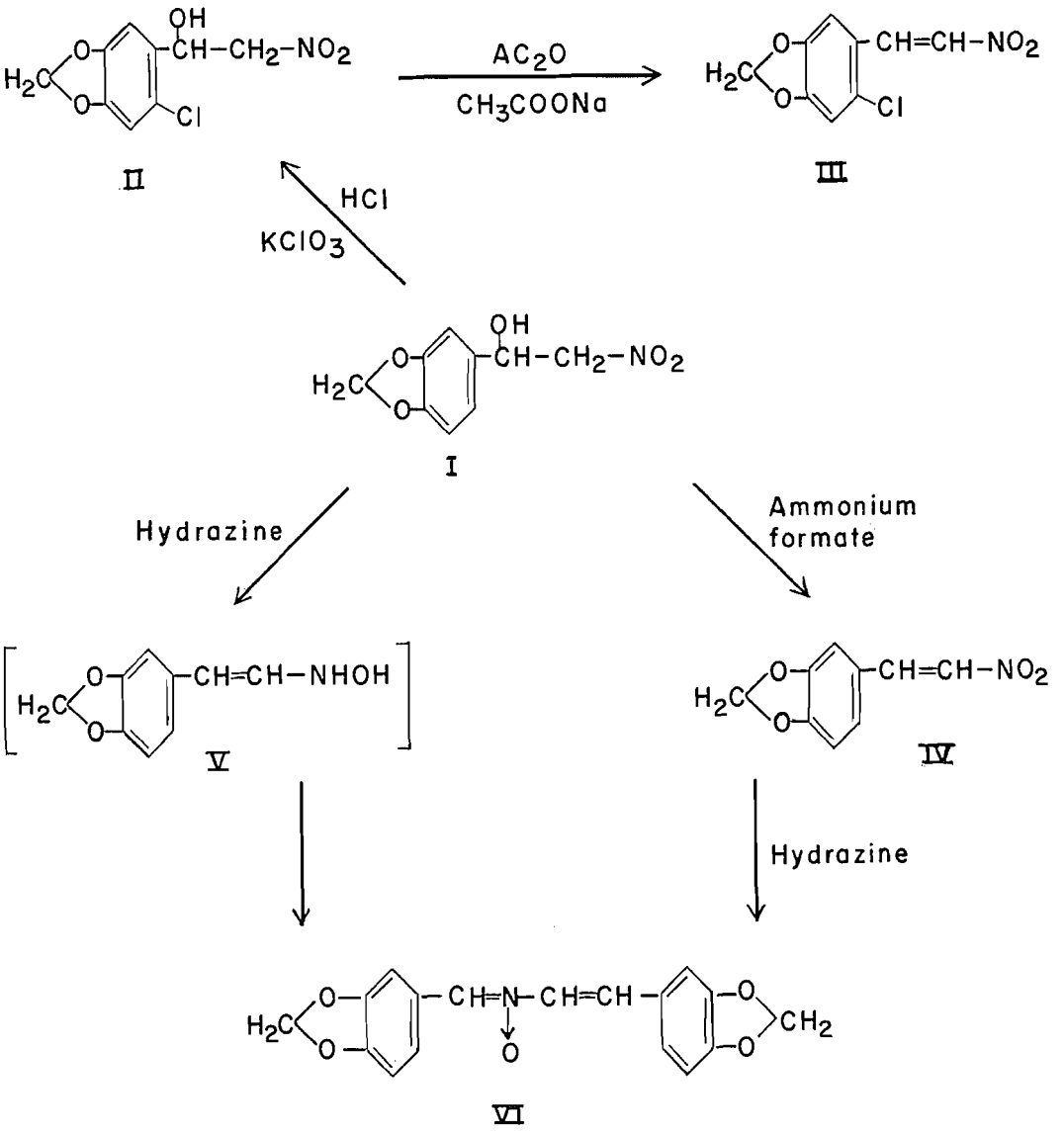

In the above reaction, the formation of the intermediate ω-hydroxylamino-3,4-methylenedioxystyrene (V) by dehydration and reduction was suggested, because the same isobenzaldoxime (VI) could also be prepared by reduction of 3,4-methylenedioxy-ω-nitrostyrene (IV) with hydrazine hydrate. Heacock *et al.* (4) prepared N-(β-hydroxy-β-(3,4-methylenedioxyphenyl)-ethyl)-3′,4′-methylenedioxyisobenzaldoxime from (I) by catalytic hydrogenation with only two moles of hydrogen. The unstable nature of the intermediate hydroxylamino derivative in alkaline medium and the formation of the corresponding isobenzaldoxime has also been shown by Allais (6). It would thus appear that the ultimate product of this alkaline reduction in our case is N-β-(3,4-methylenedioxyphenylvinyl)-3′,4′-methylenedioxyisobenzaldoxime (VI).

Can. J. Chem. Downloaded from www.nrcresearchpress.com by 210.87.254.105 on 09/05/12
For personal use only.

In view of preparing another compound containing the 3,4-methylenedioxphenyl grouping, piperonal was condensed with glycine in presence of alcoholic sodium hydroxide solution (7). A mixture of compounds was obtained from which β-(3,4-methylenedioxyphenyl) serine (VII) could be isolated in 15–20% yield. Drying at 100° for 24 hours at 2 mm pressure was necessary to obtain a pure, dry sample having a melting point of 171–175 ° dec. Kanao and Schinozuka (8) have given a melting point of 200–201° for (VII), while Mahajani and Ray (9) gave a melting point of 125–127°, also for (VII). Probably they were dealing with different isomers. Our compound when chromatographed on paper gave only one spot. It also gave a positive test for α-amino-β-hydroxy amino acids (10).

Efforts to substitute an amino group for a bromine atom in α,β-dibromo-β-(3,4-methylenedioxyphenyl) propionic acid by means of 1% ethylamine gave ω-bromo-3,4-methylenedioxystyrene (VIII). This compound could also be prepared by replacing 1% ethylamine with 0.5 *M* sodium hydroxide in the above reaction. Trumbull and his coworkers (11) have discussed the mechanism of a similar decarboxylative elimination to give ω-bromostyrene. By replacement of 1% ethylamine or sodium hydroxide with dicyclohexylamine or potassium phthalamide, the same type of elimination seemed to take place, since only dicyclohexylamine hydrobromide and phthalimide could be isolated from the reaction mixtures.

EXPERIMENTAL

Infrared spectra were recorded with a Beckman IR-4 spectrophotometer using KBr pellets containing 0.5% by weight of sample. The reported spectra are all calibrated. Ultraviolet spectra were recorded with a Beckman DB spectrophotometer. Analyses were made by Micro-Tech Laboratories, Skokie, Illinois. Melting points are not corrected.

3,4-Methylenedioxy-α-nitromethylbenzyl Alcohol (I)

This was prepared by the method of Heacock *et al.* (3): λ_{max}^{EtOH}, 285 mμ; E_{max}, 8440. Inflection at 235 mμ. V_{max} in cm^{-1}: 3250–3125 (m) (O—H stretching frequency, intermolecular hydrogen bonds); 1565 (s) (C—NO_2 asymm.); 1555 (s), 1510 (s), 1450 (s), 1385 (s), (C—NO_2 asymm.); 1340 (m), 1245 (m).

6-Chloro-3,4-Methylenedioxy-α-nitromethylbenzyl Alcohol (II)

Concentrated HCl (2.5 ml) was added to a solution of 3,4-methylenedioxy-α-nitromethylbenzyl alcohol (1 g in 10 ml ethanol) at room temperature (25°). To prevent a rise in temperature and a possible dehydration, the mixture was cooled. A solution of sodium chlorate (1 g) in water (2.5 ml) was then added and the mixture left undisturbed overnight. Next morning 0.75 g of (II) were obtained (yield varies from 50–70%). Two crystallizations from CCl_4 gave the analytical sample: m.p. 120°; λ_{max}^{EtOH}: 265, 244 mμ; E_{max}: 8575 and 8600 respectively. V_{max} in cm^{-1}: 3250–3125 (m) (O—H); 1565 (s) (C—NO_2 asymm.); 1555 (s), 1490 (m), 1420 (m), 1385 (m) (C—NO_2 asymm.); 1285 (m), 1250 (s), 715 (w) (C—Cl). Anal. Calc. for $C_9H_8ClNO_5$ (245.5): C, 44.08; H, 3.26; N, 5.71. Found: C, 43.81; H, 3.03; N, 5.65.

Alkaline Oxidation of 6-Chloro-3,4-Methylenedioxy-α-nitromethylbenzyl Alcohol (II) to Give 6-Chloropiperonylic Acid

A suspension of 6-chloro-3,4-methylenedioxy-α-nitromethylbenzyl alcohol (0.5 g) in water (10 ml) and aqueous sodium hydroxide (2 *N*, 1.5 ml) was oxidized with 50 ml of a 3% aqueous solution of potassium permanganate at reflux temperature for 5 h. After filtration, the reaction mixture was acidified with dilute sulphuric acid and the white solid that precipitated was crystallized from aqueous ethanol. Colorless needles of 6-chloropiperonylic acid, m.p. 198°, were obtained (m.p. lit. 200°) (12). Anal. Calc. for $C_8H_5ClO_4$ (200.5): C, 47.88; H, 2.49; Cl, 17.45. Found: C, 47.63; H, 2.30; Cl, 17.70. This compound showed no depression in melting point when mixed with an authentic sample of 6-chloropiperonylic acid prepared by the method of Orr *et al.* (12). Infrared spectra of the two samples were also identical.

6-Chloro-3,4-Methylenedioxy-ω-nitrostyrene (III)

A mixture of 6-chloro-3,4-methylenedioxy-α-nitromethylbenzyl alcohol (II) (1 g; 0.004 mole) and freshly fused sodium acetate (1 g), was refluxed with 10 ml of acetic anhydride for ½ h. The reaction mixture was cooled and poured over ice. The yellow solid obtained was filtered and washed free of acidity with water. Recrystallization of the crude product from alcohol gave 6-chloro-3,4-methylenedioxy-ω-nitrostyrene (0.8 g; 72%) in yellow needles (m.p. 156°). λ_{max}^{EtOH}: 368, 316, 264 mμ; E_{max}: 18 368, 11 500, 16 359 respectively. Inflection at 252 mμ. V_{max} in cm^{-1}: 1620 (m), 1510 (m), 1490 (sh), 1425 (w), 1375 (w), 1330 (m),

Can. J. Chem. Downloaded from www.nrcresearchpress.com by 210.87.254.105 on 09/05/12
For personal use only.

1290 (m), 700 (w) (C—Cl). Anal. Calc. for $C_9H_6ClNO_4$ (227.5): C, 47.47; H, 2.64; N, 6.15. Found: C, 47.22; H, 2.53; N, 5.88.

The same compound (III) can also be prepared by treating 1 g of (II) with a mixture of acetic anhydride (10 ml), and pyridine (three drops) overnight at room temperature with a yield of 81%.

3,4-Methylenedioxy-ω-nitrostyrene (IV)

Compound (I) (1 g; 0.005 mole) and ammonium formate (1 g; 0.016 mole) were dissolved in 20 ml of ethanol (95%) and the mixture refluxed for 30 min. The solution was then evaporated to dryness *in vacuo*, washed with water, and dried. Recrystallization of the residue from benzene gave 3,4-methylene-ω-nitrostyrene (0.5 g; 55%) in yellow needles (m.p. 162°), m.p. lit. 159° (13). λ_{max}^{EtOH}: 364, 260 mμ; E_{max}: 16 600, 13 124 respectively. Inflection at 310 and 245 mμ. V_{max} in cm^{-1}: 1640 (m), 1500 (s), 1460 (s), 1370 (m), 1340 (m), 1270 (s), 1250 (s). Anal. Calc. for $C_9H_7NO_4$ (193): C, 55.96; H, 3.62; N, 7.25. Found: C, 56.63; H, 3.65; N, 7.18.

The treatment of 3,4-methylenedioxy-α-nitromethylbenzyl alcohol (I) (1 g; 0.005 mole) with 2.5 ml of formic acid (85%), 10 ml ethanol, at reflux temperature for 1½ h gave no 3,4-methylenedioxy-ω-nitrostyrene (IV). The yield of unreacted material (I) was 0.8 g (80%). But the 3,4-methylenedioxy-ω-nitrostyrene (IV) could be prepared by adding 1 g (0.005 mole) of (I) to a mixture of 4 ml of acetic anhydride and a few drops of pyridine and stirring them at room temperature overnight. The yield of (IV) was 60%. The two samples of 3,4-methylenedioxy-ω-nitrostyrene (IV) obtained by treatment of (I) either with ammonium formate or with acetic anhydride plus pyridine gave identical melting points, ultraviolet spectra, and showed no depression in mixed melting point determination.

N-β(3,4-Methylenedioxyphenylvinyl)-3′,4′-methylenedioxyisobenzaldoxime (VI)

To 5 g (0.025 mole) of 3,4-methylenedioxy-α-nitromethylbenzyl alcohol (I) were added 50 ml of ethanol and 7 ml of 85% hydrazine hydrate. The mixture was refluxed for 45 min and then evaporated to dryness in vacuum. Three crystallizations of the residue from benzene gave the analytical sample. Yield 2.8 g (89%), m.p. 205°. λ_{max}^{EtOH}: 344, 235; E_{max}: 29 545 and 22 703 respectively. Inflection at 292 mμ. V_{max} in cm^{-1}: 1635 (m) conjugated (C=N); 1610 (m) (C=C stretching vibration); 1510 (s), 1495 (sh), 1460 (s), 1360 (w), 1310 (w), 1265 (s), 1195 (w). Anal. Calc. for $C_{17}H_{13}NO_5$: C, 65.59; H, 4.18; N, 4.50; mol. wt. 311. Found: C, 65.11; H, 4.11; N, 4.39; mol. wt. (Rast) 303.

This compound (VI) could also be prepared from 3,4-methylenedioxy-ω-nitrostyrene (IV) in an identical manner. The two samples of (VI) obtained from these two different starting materials, (I) and (IV), gave superimposable infrared and ultraviolet spectra and showed no depression in melting point on mixed melting point determination.

β-(3,4-Methylenedioxyphenyl) Serine (VII)

Piperonal (16.2 g; 0.108 mole) and glycine (4 g; 0.053 mole) were mixed in 20 ml of ethanol. To this mixture was added a solution of 3.2 g (0.08 mole) of sodium hydroxide in 40 ml of water. The mixture was stirred at room temperature (29°) for 48 h, and then neutralized with dilute HCl. After filtration, the white solid that separated was recrystallized from dioxane. A crystalline compound (m.p. 181°) was obtained and was not further identified. (Found: C, 67.83; H, 4.69; N, 3.48%.) When the mother liquor from the above filtration was concentrated by vacuum evaporation and cooled, 2.4 g of a solid separated. This on repeated recrystallizations from hot water gave the pure β-(3,4-methylenedioxyphenyl) serine (VII) (m.p. 171–175° dec., yield varies from 15–20%). Drying *in vacuo* at 2 mm during 24 h at 100° was found to be necessary to completely dry the compound. No attempt was made to isolate the isomers. Sörensen titration of 0.1 g of (VII) gave a neutralization equivalent of 238 (theory, 225). On paper chromatography using Whatman paper No. 1 and the solvent systems pyridine–water (80:20) or phenol–water (81:19), only one spot in each case after spraying with ninhydrin was obtained. R_f values were respectively 0.51 and 0.76. The same spots also gave a positive test for α-amino-β-hydroxy compound when treated with periodic acid and Nessler's reagent (10). $\lambda_{max}^{H_2O}$: 285, 235 mμ. E_{max}: 4100, 4500 respectively. V_{max} in cm^{-1}: 3525 (m), 3200 (s), 3075 (s), 2900 (s), 2025 (w), 1660 (s) (NH_3^+ deformation frequency); 1610 (s) (ionic carboxyl); 1510 (s) (NH_3^+ deformation frequency); 1445 (s), 1400 (s), 1350 (s), 1320 (m). Anal. Calc. for $C_{10}H_{11}NO_5$ (225): C, 53.33; H, 4.90; N, 6.22. Found: C, 53.11; H, 5.21; N, 5.98.

ω-Bromo-3,4-Methylenedioxystyrene (VIII)

α,β-Dibromo-β-(3,4-methylenedioxyphenyl) propionic acid (5 g; 0.014 mole) prepared according to the method of Feuerstein (14) was added slowly in small portions into 280 ml of 1% aqueous solution of ethylamine, cooled to 0 °C. The reaction mixture was stirred at 0 °C for 2 h and then filtered to obtain 1.8 g (56% yield) of ω-bromo-3,4-methylenedioxystyrene, melting at 57–58° (m.p. lit. 59°) (14). This compound could be purified further by crystallization from *n*-hexane. λ_{max}^{EtOH}: 308, 276 mμ; E_{max}: 14 755, 18 160 respectively. V_{max} in cm^{-1}: 1610 (s), 1600 (s), 1510 (s), 1490 (s), 1480 (s), 1440 (s). Anal. Calc. for $C_9H_7BrO_2$ (227): Br, 35.24. Found: 35.11.

The compound (VIII) could also be prepared by substituting 250 ml of 0.5 *M* sodium hydroxide solution for aqueous 1% ethylamine in the above reaction. The reaction was carried out at 55° for 1 h. On acidification with dilute HCl, an oil was obtained which, when crystallized from *n*-hexane, gave crystals melting at 58°.

Can. J. Chem. Downloaded from www.nrcresearchpress.com by 210.87.254.105 on 09/05/12
For personal use only.

The yield of ω-bromo-3,4-methylenedioxystyrene was 40%. A mixed melting point with the compound prepared by reaction with 1% aqueous ethylamine showed no depression, and infrared spectra of the two samples were superimposable.

ACKNOWLEDGMENT

This project was financially supported by the Medical Research Council of Canada, to which we are indebted.

REFERENCES

1. C. WINGARD, P. HITCHCOCK, and R. S. TEAGUE. Arch. Intern. Pharmacodyn. **102**, 65 (1955).
2. Y. OAKI. Japan. J. Bacteriol. **9**, 433 (1954).
3. R. A. HEACOCK, O. HUTZINGER, and C. NERENBERG. Can. J. Chem. **39**, 1143 (1961).
4. R. A. HEACOCK, O. HUTZINGER, and C. NERENBERG. Can. J. Chem. **40**, 133 (1962).
5. J. SINGH, P. SINGH, J. L. BOIVIN, and P. E. GAGNON. Can. J. Chem. **40**, 133 (1962).
6. M. A. ALLAIS. Bull. Soc. Chim. France, 536 (1949).
7. E. ERLENMEYER and E. FRÜSTÜCK. Ann. **284**, 36 (1895).
8. S. KANAO and K. SHINOZUKA. J. Pharm. Soc. Japan, **67**, 218 (1947).
9. P. B. MAHAJANI and J. N. RAY. Current Sci. India, **22**, 146 (1953).
10. L. BERLINGUET. Can. J. Chem. **33**, 1119 (1955).
11. E. R. TRUMBULL, R. T. FINN, K. M. IBNE-RASA, and C. K. SAUERS. J. Org. Chem. **27**, 2339 (1962).
12. A. M. B. ORR, R. ROBINSON, and M. M. WILLIAMS. J. Chem. Soc. **111**, 948 (1917).
13. H. BURTON, J. A. DUFFIELD, and P. F. G. PRAILL. J. Chem. Soc. 1062 (1950).
14. W. FEUERSTEIN and M. HEIMANN. Ber. **34**, 1470 (1901).

Can. J. Chem. Downloaded from www.nrcresearchpress.com by 210.87.254.105 on 09/05/12
For personal use only.

Can. J. Chem. Downloaded from www.nrcresearchpress.com by 210.87.254.40 on 09/05/12
For personal use only.

EFFECTS OF CHLORINE AND BROMINE ON THE RADIOLYSIS OF GASEOUS HCl

R. A. LEE,* R. S. DAVIDOW, AND D. A. ARMSTRONG
Department of Chemistry, University of Alberta, Calgary, Alberta
Received March 31, 1964

ABSTRACT

Using an ionization chamber method, it has been shown that the energy required to create an ion pair in gaseous HCl, W_{HCl}, is 24.4 ± 0.6 eV. The hydrogen yield, $G(H_2)_{HCl\ gas\ at\ 23\ °C} = 8.0 \pm 0.3$, was independent of HCl pressure in the range 19 to 119 cm of Hg. The effects of added bromine demonstrate that at least two species are involved in hydrogen formation, and there are strong indications that one of these is an electron. A second species, designated as H^{II} and formed with a yield $G_{H^{II}} = 2.5$, is not readily scavenged by bromine. The use of chlorine as a scavenger also provides evidence for the presence of more than one hydrogen-forming species. The data of an earlier study of the α-particle radiolysis have been corrected for back reactions of the chlorine which accumulated in the system. The corrected results are in reasonable agreement with those of this study.

INTRODUCTION

The α-particle radiolysis of gaseous HCl was studied in 1932 by Vandame (1). He observed a decrease in the decomposition yield at higher doses and attributed it to back reactions involving hydrogen and chlorine. In view of his observations it was clear that any further study of this system would have to take into account the possible effects of these products on the kinetics of the decomposition. In this study we have investigated the hydrogen yield produced in the ^{60}Co γ-radiolysis of gaseous HCl in the presence of chlorine at concentrations in the range 0–6 mole percent. For reasons which will become apparent later, the effects of bromine over the same concentration range have also been examined. As pointed out in an earlier publication (2), the data also provide evidence for more than one hydrogen-forming species in irradiated gaseous HCl.

EXPERIMENTAL

Apparatus and Chemicals

The vacuum lines employed for the preparation of hydrogen halide samples and the measurement of the hydrogen yields were as previously described (3). The irradiation cells were filled to the desired pressure with hydrogen halide, which had been purified by preirradiation and distillation. Matheson research grade Argon was used without further purification.

The pyrex irradiation cells were usually about 300 ml in volume. Those in which ionization currents were to be measured were of the design shown in Fig. 1. The 2.5-mm thick cylindrical wall, C, was coated internally with colloidal graphite to form the collecting electrode. The central high voltage electrode, A, which consisted of a 7-mm O.D. pyrex tube, and the guard ring, B, were coated in a similar manner. After the coatings had been applied through the tube, D, its end was sealed to form a thimble trap for condensing the hydrogen halide in a liquid nitrogen bath. Tungsten wires passing through the glass walls provided contact between the graphite coatings and the shielded electrical leads A^1, B^1, and C^1. Gases were admitted to the irradiation cell via a stopcock attached to a 30-cm extension of tube E. This stopcock was shielded during irradiations. For some experiments, in which the effects of certain variables were being examined, uncoated cylindrical or spherical cells were employed. All cells were baked out at about 300 °C under vacuum prior to use.

In all but a few experiments, which will be mentioned specifically later, the irradiation source was a 200 curie ^{60}Co unit purchased from Atomic Energy of Canada Ltd. The source was lowered into a concrete cave to a point about 15 cm from the center of the irradiation cells. These were held vertically in an aluminum canister.

Two high voltage supplies of standard design were used in measuring the ionization currents. One covered

**Holder of an N.R.C. Studentship, September 1962 – August 1963; present address: c/o Trinity College, Melbourne St., Port of Spain, Trinidad.*

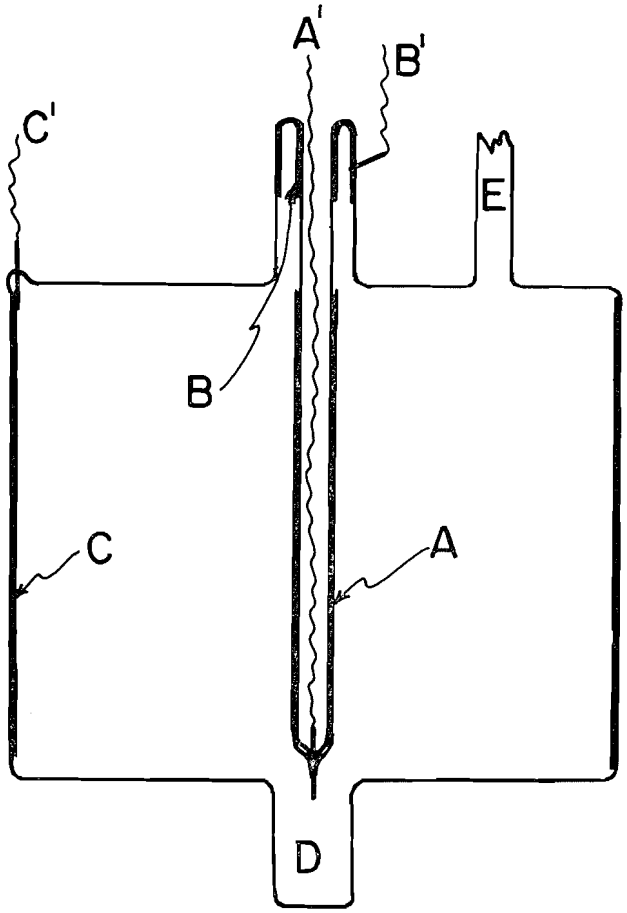

FIG. 1. Irradiation cell for determination W_{HCl} and $G(H_2)_{HCl\ (gas)}$. Double lines represent graphite coatings. Volume of cell = 230 ml; diameter = 7.0 cm.

the range 0–500 V and the second 0–2000 V. One or other of these was connected to the inner electrode, A, and provision was made for reversing the polarity. The ionization currents from the collecting electrode to ground varied between 10^{-8} and 10^{-6} A, and were measured with a Keithley model 621 electrometer. The guard ring, B, was connected directly to ground. All electrical connections to the irradiation cells were passed through a small aperture in the wall of the irradiation cave.

Dosimetry

The simplest and most direct method of dosimetry for gaseous systems is by the measurement of saturation ionization currents. These can be converted to absorbed energy once the value of W, the energy required to create an ion-pair in the gas, is known. Experimental values of W for the hydrogen halides are not available, but reliable measurements of W (see ref. 4) have been obtained for most of the inert gases. Since any given hydrogen halide has the same total number of electrons as the inert gas adjacent to the particular halogen in the periodic table, their electron stopping powers will not differ appreciably and their Compton scattering cross sections will be the same. Thus the energies absorbed by a hydrogen halide and the isoelectronic inert gas at equal pressures in cells subjected to the same flux of ^{60}Co γ-radiation will be very similar. Corrections for the small difference in the stopping powers of the two molecules may be made by means of the Bethe equation.

A somewhat similar approach was employed earlier by Zubler, Hamill, and Williams (5) in their study of the X-radiolysis of HBr and HBr – inert gas mixtures. The use of ^{60}Co γ-rays in the present study represents a distinct advantage, since energy is absorbed almost entirely from secondary electrons arising in γ-ray interactions with the cell walls.

Can. J. Chem. Downloaded from www.nrcresearchpress.com by 210.87.254.40 on 09/05/12
For personal use only.

Can. J. Chem. Downloaded from www.nrcresearchpress.com by 210.87.254.40 on 09/05/12
For personal use only.

RESULTS AND DISCUSSION

Measurement of W_{HCl} and $G(H_2)_{HCl\ gas}$

As shown in Fig. 2 satisfactory ionization current plateaus were obtained with air, HCl, and argon. Figure 3 shows that the relation between the saturation ionization currents and the pressures of the irradiated gases were linear for all three gases over the

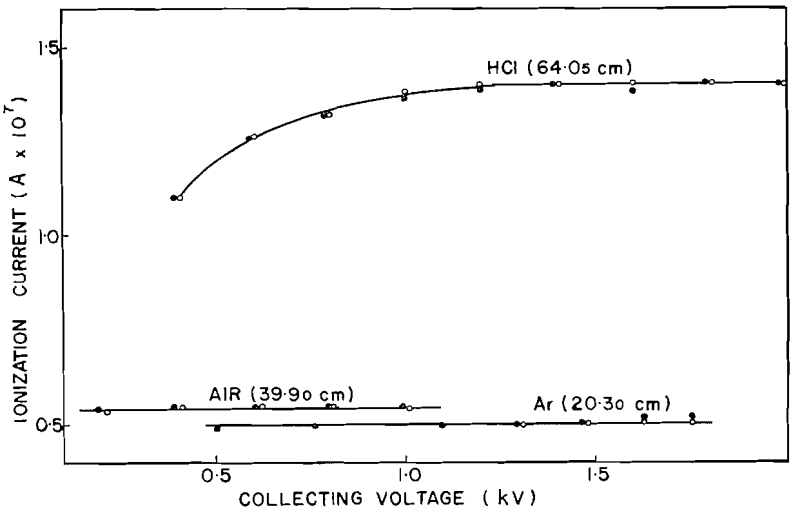

FIG. 2. Typical ionization current – voltage relationships: Open symbols—center electrode negative. Filled symbols—center electrode positive. Where points coincide exactly they have been placed adjacent to each other in the horizontal plane.

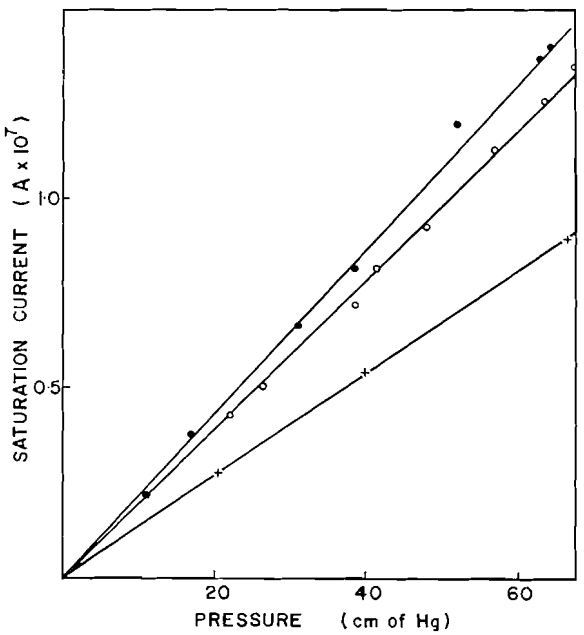

FIG. 3. Saturation ionization currents as a function of pressure. ● HCl; ○ Ar; + air.

range of pressures employed. The slopes of the best lines through the plots in Fig. 3 were $J_{Ar} = 2.0_0$, $J_{HCl} = 2.2_4$, and $J_{air} = 1.3_5 \times 10^{-9}$ A per cm pressure.

Can. J. Chem. Downloaded from www.nrcresearchpress.com by 210.87.254.40 on 09/05/12
For personal use only.

The energy absorbed per cm pressure per second in pure HCl must be equal to the left hand side of the expression:

$$[i] \qquad (W_{HCl} \times J_{HCl})/e = (W_{Ar} \times J_{Ar}\rho_{Ar}^{HCl})/e$$

where e is the electronic charge. If the energy absorption is assumed to be proportional to the stopping powers of the gases and ρ_{Ar}^{HCl} is taken as the ratio of the stopping powers for HCl and Argon, then the remainder of expression [i] follows. As a check on this J_{Ar}/J_{air} was evaluated using an expression analogous to [i] to relate the energy absorption in air and argon. The stopping power ratio ρ_{air}^{Ar} was calculated by means of the equation of Bethe (ref. 6, p. 98, equation 40) with mean excitation potentials of 174* and 85 eV for argon (7) and air (8) respectively. The value of ρ_{air}^{Ar} varied from 1.16, at 1 MeV to 1.11 at 0.05 MeV. The value chosen, 1.13, corresponded to a weighed mean electron energy of about 0.15 MeV (cf. the weighed mean energy in ref. 9) and, together with $W_{air} = 33.7$ and $W_{Ar} = 26.2$ eV (4), gave a ratio for $J_{Ar}/J_{air} = 1.46$. This is in good agreement with the experimental ratio of 1.48. A similar calculation with ρ_{air}^{Ar} based on the ratio of Compton scattering cross sections would predict $J_{Ar}/J_{air} = 1.61$.

The stopping power ratio ρ_{Ar}^{HCl} was evaluated in the same way as ρ_{air}^{Ar} with the mean excitation potentials of hydrogen and chlorine taken as 13.5 and 169 eV (7) respectively. Over the energy range 1.0 to 0.05 MeV the variation is comparatively small (1.02_1 to 1.03_2). It is rather unlikely that the ratio $\rho_{Ar}^{HCl} = 1.0_{28}$, employed in the subsequent calculation of W_{HCl}, can be in error by more than $\pm 1\%$. Substitution of this figure, the above value of W_{Ar}, and the experimental ratio J_{HCl}/J_{Ar} into expression [i] gave $W_{HCl} = 24.4 \pm 0.6$ eV. Hence G (positive ions) must be 100/24.4 (= 4.1), and G_c should be essentially the same.

From the right hand side of expression [i] it can be shown that the dose rate for HCl in cells of the type shown in Fig. 1 was $2.0_3 \times 10^{13}$ eV per minute per cm pressure. Using this factor, the experimental hydrogen yields in moles per minute per cm pressure may be converted to $G(H_2)$ values. The results of four individual determinations have been presented in Table I. The mean value of $G(H_2)_{HCl\ gas\ at\ 23\ °C}$ is 8.0 ± 0.3, and $(M/N)_{-HCl}$

TABLE I

P_{HCl} (cm)	Dose (eV)	Dose (Ion pairs)	H_2 or Cl_2 yield (Molecules)	H_2 or Cl_2 yield (Mole %)	$(M/N)_{-HCl}$ Apparent	$(M/N)_{-HCl}$ Corrected	$G(H_2)$
Data of this study:							
61.49	1.76×10^{18}		1.37×10^{17}			3.80	7.8
61.65	1.26×10^{18}		1.00×10^{17}			3.76	7.7
64.05	1.46×10^{18}		1.22×10^{17}			4.05	8.3
64.05	1.66×10^{18}		1.40×10^{17}			4.00	8.2
				Mean values		3.9±0.1	8.0±0.3
Data of Vandame (Ref. 1):							
32.48	$7.9_2\times10^{19}$	3.12×10^{18}	5.20×10^{18}	0.30	3.3	4.3	8.6
32.48	12.1×10^{19}	4.81×10^{18}	7.75×10^{18}	0.44	3.2	4.6	9.1
70.50	21.4×10^{19}	8.49×10^{18}	13.3×10^{18}	0.36	3.1	4.3	8.5
70.50	38.5×10^{19}	15.21×10^{18}	18.9×10^{18}	0.51	2.5	3.7	7.3
70.50	46.3×10^{19}	18.38×10^{18}	22.7×10^{18}	0.60	2.4	3.9	7.8
				Mean values		4.1±0.2	8.2±0.5

**Calculated from the relationship $I = 9.7 \times Z$. The factor 9.7 is smaller than the experimental value of 10.6 found by Brolley and Ribe (see ref. 8). However, 9.7 is more in keeping with the theoretical analysis made by Brandt (7).*

is 3.9 ± 0.1. It should be emphasized that in separate experiments $G(H_2)$ was found to be independent of absorbed dose over the range $6 \times 10^{17} - 1.7 \times 10^{18}$ eV. Hence, in this range any dose dependence must lie within our experimental error. The reason for the significant differences between our mean value of $(M/N)_{-HCl}$ and Vandame's apparent values will be discussed later.

The effect of HCl pressure on the hydrogen yields was investigated in uncoated pyrex cells of similar volume to those shown in Fig. 1. In Fig. 4 the rate of hydrogen formation

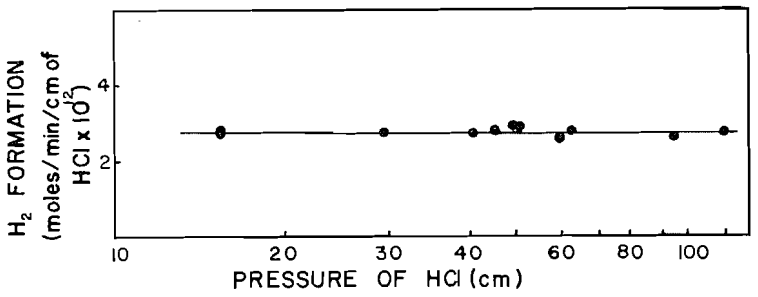

FIG. 4. Effect of pressure on the hydrogen yield from gaseous HCl at 23 °C. Note: dose rate ∝ pressure.

per cm pressure of HCl has been plotted as a function of HCl pressure. Since the dose rate was directly proportional to HCl pressure, the constancy in the rate of formation of hydrogen indicates that $G(H_2)$ is independent of pressure over the range 19 to 119 cm. In view of this, HCl was used as its own dosimeter in all subsequent experiments.

The Effects of Scavengers

The effect of chlorine on the hydrogen yields from gaseous HCl is shown in curve A of Fig. 5. The closed triangles and circles depict results obtained in spherical bulbs of volume 228 and 3690 ml respectively. In both cases HCl pressures were in the range 50–60 cm, varying slightly from one experiment to the next. It can be seen that in this HCl pressure range the effect of chlorine is, within experimental error, independent of bulb size, and hence of surface to volume ratio.

Assuming, as for the liquid phase radiolysis (10), that HCl and chlorine compete for a reactive species, H^1, in accordance with the equations:

[1] $$H^1 + HCl \rightarrow H_2 + \text{products}$$

[2] $$H^1 + Cl_2 \rightarrow \text{products other than } H_2$$

one may carry out the usual kinetic analysis, plotting $1/\Delta G(H_2)$ as a function of $(HCl)/(Cl_2)$. This leads to $G_{H^1} = 6.7$ and $k_{H^1 + HCl}/k_{H^1 + Cl_2} = 3.9 \times 10^{-3}$. In view of the fact that G_{H^1} is less than $G(H_2)$ it is necessary to postulate the existence of a second species, H^{11}. The apparent yield of this is $G_{H^{11}} = 1.3$.

On the basis of the above parameters it may be shown that at any particular chlorine concentration $G(H_2)$ is given by the empirical expression:

[ii] $$G(H_2) = 1.3 + 6.7\left(1 + \frac{(Cl_2)}{3.9 \times 10^{-3}(HCl)}\right)^{-1}.$$

Curve A in Fig. 5 was calculated by means of [ii], and the agreement with the experimental points is quite satisfactory. It is obvious from this curve that the accumulation

Can. J. Chem. Downloaded from www.nrcresearchpress.com by 210.87.254.40 on 09/05/12
For personal use only.

Can. J. Chem. Downloaded from www.nrcresearchpress.com by 210.87.254.40 on 09/05/12
For personal use only.

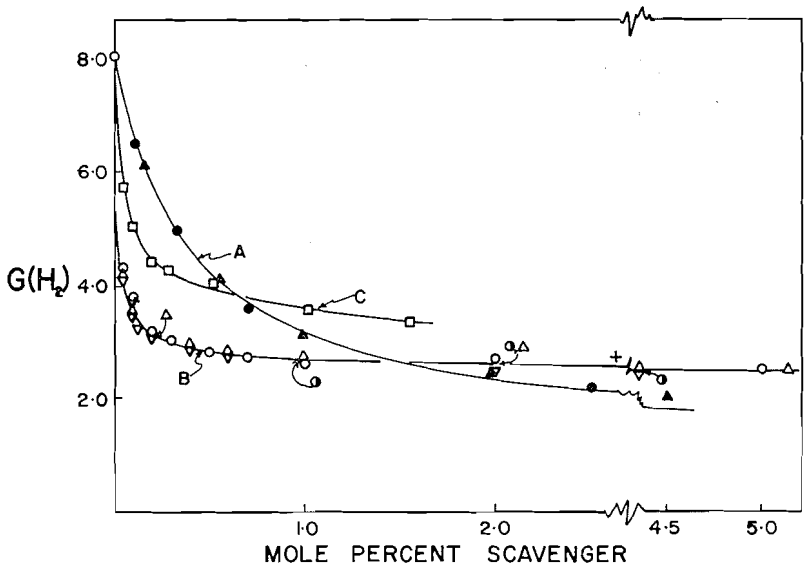

FIG. 5. Effects of Cl_2 and Br_2 on the hydrogen yield.

	Scavenger	Dose rate, I (eV/min/ml)	P_{HCl} (cm of Hg)	Cell type	Square of mean radius (cm^2)	IPr^2
●	Cl_2	3×10^{12}	55	Sphere	81	1.3×10^{16}
▲	Cl_2	5×10^{12}	55	Sphere	11	3.0×10^{15}
○	Br_2	10×10^{12}	115	Sphere	11	1.3×10^{16}
△	Br_2	4×10^{12}	91	Sphere	81	3.0×10^{16}
▽	Br_2	1×10^{12}	19	Sphere	81	1.5×10^{15}
◑	Br_2	5×10^{12}	60	Cylinder coated with graphite	11	3.3×10^{15}
+	Br_2	300×10^{12}	50	Cylinder	11	1.7×10^{17}
□	Br_2	1×10^{12}	16	Sphere	81	1.3×10^{15}

NOTE: The quantity IPr^2 given in the right hand column for each set of conditions is an approximate index of the relative probability of reactive species undergoing homogeneous combination as opposed to diffusion to the cell wall.

of chlorine during the course of an irradiolysis of pure HCl would cause a depletion in the apparent radiolytic yield as Vandame postulated. In the present study the concentration of hydrogen or chlorine (the yields of the two must obviously be equivalent) seldom rose above 0.01 mole percent in any given experiment, and this depletion could not have been significant. However, in Vandame's work percentages of chlorine as large as 0.6 occurred. Corrections to his results may now be applied on the basis of the data of curve A. At any given chlorine concentration the rate of hydrogen formation will be:

[iii] $$\frac{d(H_2)}{dt} = R \times G(H_2)\left\{\alpha \times \left(1 + \frac{k_{H^1+Cl_2}(Cl_2)}{k_{H^1+HCl}(HCl)}\right)^{-1} + (1-\alpha)\right\}$$

where $G(H_2)$ is the "true" initial total hydrogen yield, α represents the proportion of hydrogen formed by H^1 ($\alpha = 6.7_0/8.0_1 = 0.83_2$), and R is the dose rate in eV per unit volume per unit time. Assuming that the values of $k_{H^1+HCl}/k_{H^1+Cl_2}$ and α for the α-particle radiolysis are the same as those above, we may substitute them in expression [iii] and integrate between zero and the time t, at which the yield of hydrogen or chlorine

was measured. This leads to expression (iv), where D $(= Rt)$ is the total accumulated dose per unit volume at time t:

$$[\text{iv}] \qquad G(H_2) = \frac{1}{D}\left[\frac{(Cl_2)}{0.167} - 0.268\ (HCl)\log_{10}\left\{1 + 42.8\frac{(Cl_2)}{(HCl)}\right\}\right].$$

Values of $G(H_2)$ calculated by means of this expression from the data of Table II in Vandame's paper have been included in Table I above. In these calculations it was necessary to replace the figure used by Vandame for the number of ion pairs formed per α-particle by the energy per α-particle (5.48 MeV). No other alterations to his data were made, and the volume of all of his irradiation cells was taken, as he stated, to be 150 ml. An expression analogous to [iv] may be developed for correcting his ion pair yields. Both the corrected and the apparent yields are given in Table I. From this it can be seen that the corrected ion pair yields show a much smaller dose dependence than did the uncorrected ones. Also the corrected ion pair yields and the $G(H_2)$ values are equal to or slightly larger than those obtained in this study. Thus it seems that the discrepancy noted earlier was largely due to a lack of correction for the back reaction involving chlorine.

Experiments analogous to those above (3) have shown that in liquid HCl at -79 °C G_{H^I} is much smaller and $G_{H^{II}}$ much larger ($G_{H^I\ (HCl\ liquid\ at\ -79\ °C)} = 2.4$; $G_{H^{II}\ (HCl\ liquid\ at\ -79\ °C)} = 4.3$). Also $k_{H^I + HCl}/k_{H^I + Cl_2}$ was smaller in liquid HCl ($= 1.7 \times 10^{-3}$). The combination of these three features made it possible to observe the scavenging of H^{II} at high chlorine concentrations, and $k_{H^{II} + HCl}/k_{H^{II} + Cl_2}$ in liquid HCl was shown to be 0.10. This value was sufficiently small to warrant a correction to the apparent values of G_{H^I} and $G_{H^{II}}$ for the scavenging of H^{II} (the values given above are the corrected ones). Obviously Cl_2 may also scavenge H^{II} in gaseous HCl. However, with $G_{H^I} > G_{H^{II}}$ and $k_{H^I + HCl}/k_{H^I + Cl_2}$ larger than in the liquid phase (and hence closer to $k_{H^{II} + HCl}/k_{H^{II} + Cl_2}$) it is not possible to evaluate $k_{H^{II} + HCl}/k_{H^{II} + Cl_2}$ with any reasonable degree of accuracy. Corrections to the apparent values of G_{H^I} and $G_{H^{II}}$* cannot, therefore, be made and they must be treated as upper and lower limits respectively. This does not affect the validity of expression [iv], which is an empirical relationship (cf. the agreement of curve A in Fig. 5 with the experimental points).

To obtain further information about the relative proportions of H^I and H^{II} in gaseous HCl, the effect of bromine under a variety of different conditions was also investigated. As shown in Fig. 5, curve B, the results were similar to those reported earlier by Armstrong and Lee (2), which are in fact included. With small additions of bromine there was a very sharp drop in $G(H_2)$ to a limiting "plateau yield," which decreased only slightly as the bromine concentration was increased beyond 1 mole percent. The position of this plateau was within experimental error independent of HCl pressure, radiation cell volume, and dose rate.† It was also unaffected by coating the irradiation cells with colloidal graphite. It is of considerable interest to be able to decide whether or not this plateau is due to contributions from heterogeneous processes. As a first approximation the rate at which reactive intermediates diffuse to the walls should be inversely proportional to the pressure of HCl (P_{HCl}) and the square of the radius of the irradiation cell (r^2). On the other hand the rate at which they undergo homogeneous combination should be proportional to dose rate (I). The values of IPr^2 have been given for the various points in Fig.

If $k_{H^{II} + HCl}/k_{H^{II} + Cl_2}$ has the same value in gaseous HCl as in liquid HCl, then about 30% of H^{II} would be scavenged at 5 mole percent Cl_2. The errors in G_{H^I} and $G_{H^{II}}$ may therefore be quite large.

†*We are indebted to Dr. J. Stone of the Research Chemistry Branch of Atomic Energy of Canada for the two irradiations at the highest dose rate.*

Can. J. Chem. Downloaded from www.nrcresearchpress.com by 210.87.254.40 on 09/05/12
For personal use only.

Can. J. Chem. Downloaded from www.nrcresearchpress.com by 210.87.254.40 on 09/05/12
For personal use only.

5. It can be seen that the position of the plateau was unaffected by considerable variations in the value of this function. In view of these observations it is extremely unlikely that heterogeneous processes are involved under the conditions of this study. Hence we attribute the hydrogen produced in the bromine concentration range corresponding to the plateau to homogeneous reactions of the species designated above as H^{II}. From the relatively small decreases in hydrogen yield occurring at bromine concentrations in excess of 1 mole percent it may be concluded that (as in liquid HCl (10)) bromine does not compete efficiently for the species H^{II}. The yields of H^{I} and H^{II} measured with bromine are therefore probably closer to the true primary yields than those obtained above with chlorine.

Turning to the region of lower concentrations and assuming (as for chlorine) that bromine competes with HCl for a reactive species, H^{I}, the same kinetic analysis gives $G_{H^{I}} = 5.5$, $G_{H^{II}} = 2.5$, and $k_{H^{I}+HCl}/k_{H^{I}+Br_2} = 2.3 \times 10^{-4}$. Similar effects of bromine in liquid HCl at -79 °C (10) have been attributed to a competition for thermal hydrogen atoms, k_{H+HCl}/k_{H+Br_2} being equal to 8×10^{-4}. In view of the higher temperature and since $E_{H+HCl} > E_{H+Br_2}$* (10), the gas phase ratio should be larger if the same species is involved. In fact it is smaller. Thus it seems that H^{I} in gaseous HCl may not be the same as the species observed in liquid HCl. To confirm this we have made use of the fact that the rate constant ratio k_{H+HBr}/k_{H+Br_2} at 25 °C is known from conventional studies to be $0.1_2 \pm 0.0_2$ (11). The effects of bromine on the hydrogen yields from a gaseous sample of HCl containing 5 mole percent HBr are shown in Fig. 5, curve C. Assuming that HCl and HBr both compete with bromine for H^{I}, one may derive the expression:

$$[v] \qquad \frac{1}{\Delta G(H_2)} = \frac{1}{G_{H^{I}}}\left\{1 + \frac{k_{H^{I}+HCl}(HCl) + k_{H^{I}+HBr}(HBr)}{k_{H^{I}+Br_2}(Br_2)}\right\}$$

and $k_{H^{I}+HBr}/k_{H^{I}+Br_2}$ may be found from the slope of the usual plot on substituting $(k_{H^{I}+HCl})/k_{H^{I}+Br_2})$ from above, the concentrations of HCl and HBr, and $1/G_{H^{I}}$ from the intercept. In this way $k_{H^{I}+HBr}/k_{H^{I}+Br_2}$ was shown to be 5×10^{-3}. It is thus clear that thermal hydrogen atoms cannot be the only species with which bromine reacts in gaseous HCl. The above rate constant ratios should therefore be regarded as "complex" rate constant ratios.

At this point the ionic and free radical reactions, which are responsible for the effects observed, will be considered briefly. As in liquid HCl (see ref. 3 for a more detailed discussion of the following processes) one would expect the formation of HCl^+ ions, viz.:

$$[3] \qquad HCl \rightarrow HCl^+ + e$$

to be the main ionization process. Within a few collisions these ions should undergo reaction [4]:

$$[4] \qquad HCl^+ + HCl \rightarrow H_2Cl^+ + Cl.$$

During the course of their thermalization electrons in the appropriate energy ranges may cause electronic excitation (required energy $\simeq 7$ eV):

$$[5] \qquad e + HCl \rightarrow HCl^* + e$$

$$[5a] \qquad HCl^* \rightarrow H^* + Cl,$$

*E = *activation energy.*

or undergo resonance capture (0.7 − 1.8 eV):

[6] $$e + HCl \rightarrow H + Cl^-.$$

Hence, the major ionic species taking part in neutralization reactions would be:

$$e,\ Cl^-,\ \text{and}\ H_2Cl^+,$$

and ion combinations such as the following would be expected to occur:

[7] $$H_2Cl^+ + e \rightarrow H + HCl$$

[8*a*] $$H_2Cl^+ + Cl^- \rightarrow 2HCl$$

[8*b*] $$\rightarrow H_2 + 2Cl$$

[8*c*] $$\rightarrow H + Cl + HCl.$$

In pure HCl the hydrogen atoms formed in [6], [7], and [8*c*] would give rise to molecular hydrogen through reaction [9]:

[9] $$H + HCl \rightarrow H_2 + Cl.$$

Scavenging of these hydrogen atoms by bromine and chlorine could account in part for the depletion of the hydrogen yield over the concentration range 0–2 mole percent of scavenger. However, as shown above, bromine must react with some sepcies in addition to hydrogen atoms. In view of the rapidity of reaction [4], charge exchange between HCl^+ and Br_2 is unlikely. Also reactions between this halogen and H_2Cl^+ are improbable on energetic grounds. It seems, therefore, that bromine must be scavenging electrons. Strong support for this comes from the fact that its cross section for electron capture in reaction [10] increases from zero for electrons of energy in excess of 1.3 eV to a maximum value

[10] $$e + Br_2 \rightarrow Br^- + Br$$

for electrons of zero energy (12). Its behavior is thus analogous to that of iodine, and the actual magnitude of its capture cross section should also be similar ($\sigma_{e + I_2} \simeq 10^{-16}$ cm^2 (13)). In contrast to bromine and iodine, the electron energy range for resonance capture by chlorine is much higher (1.6 − 3.2 eV (12)). It is not, therefore, likely to be a good electron scavenger (cf. (14)), and its much lower efficiency for suppressing the hydrogen yield from gaseous HCl can be explained on this basis.

At an HCl pressure of 60 cm in our ionization chamber, the saturation ionization current was approximately 10^{-7} A. This corresponds to a rate of formation of ions of 2.8×10^9 ions.ml^{-1}.s^{-1}. Taking 10^{-6} ml.ions^{-1}.s^{-1} as a reasonable order of magnitude for the coefficient of ion recombination (see ref. 15), the steady state ion concentration was estimated to be about 5×10^7 ions.ml^{-1}. From this figure and the above cross section it can be shown that the ratio of electron–ion combination to electron capture by bromine at 1 mole % concentration would be of the order of 10^{-4}. It is thus quite clear that bromine may compete with positive ions for electrons under the conditions of our study. It may also be in competition with reaction [6] and with a modified form of it, [6*a*], viz.:

[6*a*] $$e_{(HCl)} \rightarrow H + Cl^-_{(HCl)}$$

which occurs within an electron–HCl molecule cluster. Mass spectrometric studies (16) in other systems containing polar molecules and measurements of ionic mobilities in HCl

Can. J. Chem. Downloaded from www.nrcresearchpress.com by 210.87.254.40 on 09/05/12
For personal use only.

Can. J. Chem. Downloaded from www.nrcresearchpress.com by 210.87.254.40 on 09/05/12
For personal use only.

and HCl–air mixtures (17) indicate that such clustering will be important under the conditions of temperature and HCl pressure existing in this study. Reactions such as [6*a*] cannot, therefore, be overlooked, and as previously (3, 10) pointed out the capture of thermal electrons is more probable when more than one HCl molecule is involved. Bromine would probably compete for clustered electrons in accordance with the equation:

[10*a*] $$e_{(HCl)} + Br_2 \rightarrow Br + Br^-_{(HCl)}.$$

An additional effect of the clustering of both negative and positive ions would be to reduce the exothermicity of the ion recombination reactions. Thus the excess kinetic energies of the atoms formed in reactions [7], [8*b*], and [8*c*], all of which would be highly exothermic with unclustered ions, should be much less under the conditions of the present study.

The hydrogen produced in the presence of bromine at concentrations in excess of 1 mole percent obviously cannot result from electron–ion combinations. If the species H^{II} is identified as a hot hydrogen atom formed in the reaction sequence [5]–[5*a*], the discrepancies between the values of G_{H^I} and $G_{H^{II}}$ determined with chlorine and bromine would have to be attributed (cf. above) to the fact that chlorine is not sufficiently discriminating in its reactivity toward H^I and H^{II} to indicate their true yields. Also there are reasons for believing that the proportion of hot hydrogen atoms, which undergo thermalization before reacting, may be greater in the gas phase than in the liquid phase (18). Thus, if 3.9 dissociative excitations occurred per 100 eV in gaseous HCl and 1.4 of the resulting hot atoms were thermalized before reacting, one could account for $G_{H^{II}} = 2.5$ and also for the fact that $G_{H^I} - G_e = 1.4$.* In liquid HCl where virtually all hot hydrogen atoms may react before being thermalized, $G_{H^{II}}$ has a value of 4.3.

The only reasonable alternative to the above would be that H^{II} is a composite species consisting of negative halide ions (Cl^- or Br^-, the latter coming from reaction [10] or [10*a*]) and H_2Cl^+ ions. The number of these combining as in [8*b*] to form hydrogen molecules directly might depend on whether Cl^- or Br^- were involved. In this way an alternative explanation can be provided for H^{II} and for the discrepancies between the values of $G_{H^{II}}$ and G_{H^I} determined with chlorine and bromine.

However, since liquid HCl undergoes autoprotolysis (cf. (3)), one would expect [8*a*] to predominate in the liquid phase. Thus it is not easy to explain the larger value of $G_{H^{II}}$ in the liquid phase on the basis of reaction [8*b*].

SUMMARY AND CONCLUSIONS

1. The value of $G(H_2)$ for the γ- (or fast electron) radiolysis of gaseous HCl at 23 °C and over the pressure range 19–119 cm of Hg is 8.0 ± 0.3. The value for α-particle radiolysis is the same or slightly larger.

2. The energy, W_{HCl}, required to create an ion pair in HCl is 24.4 ± 0.6 eV, and hence $G_{HCl^+} \simeq G_e \simeq 4.1$. To explain the fact that $G(H_2)$ is almost twice this, it is necessary to postulate sequences of ionic reactions which give rise to two hydrogen atoms (or molecules) per ion pair (for example: [3]–[4]–[6 or 6*a*]–[8*b* or 8*c*]; or concurrent reaction sequences involving initially both ionization and dissociative excitation (for example: [3]–[4]–[6 or 6*a*]–[8*a*] and [5]–[5*a*]).

3. The effects of bromine on the hydrogen yield show that more than one mode of

**It should be pointed out that, since W = 24.4 eV and the ionization potential of* HCl *is only 12.9 eV (19), there is energy available for at least as many as five excitations per 100 eV. The only alternative explanation for the difference between G_{H^I} and G_e would be the formation of 1.4 thermal hydrogen atoms in a reaction such as [8c].*

hydrogen formation is operative. One of these seems to involve hydrogen atoms formed from electron precursors, and, in contrast to its behavior in liquid HCl, bromine scavenges these electrons with high efficiency. The fact that it does not scavenge them efficiently in liquid HCl must be attributed to their much shorter lifetime in the liquid phase (10).

4. As indicated by the effects of bromine the total yield of thermal hydrogen atoms and hydrogen atoms formed from electron precursors is $G_{H^1} = 5.5$. This is much larger than the yield of the corresponding species in liquid HCl at −79 °C. In contrast the yield of the species H^{11} in gaseous HCl ($G_{H^{11}} = 2.5$) is much smaller than in liquid HCl.

5. The effects of chlorine also provide evidence for more than one mode of hydrogen formation. However, chlorine appears to react much less rapidly with electrons than bromine, and its effect may be almost entirely due to the scavenging of hydrogen atoms.

ACKNOWLEDGMENTS

The authors acknowledge the financial assistance of the National Research Council of Canada. They also express appreciation to Dr. T. Melling and Mr. D. Reece of the Calgary Cancer Clinic, who kindly cooperated in the use of their facilities, and to Dr. R. A. Back of the National Research Council for assistance in the design of the irradiation cells. The use of the 12 000 curie γ-cell at the A.E.C.L. Chalk River Laboratories is also acknowledged.

REFERENCES

1. J. VANDAME. Bull. Soc. Chem. Belges, **41**, 597 (1932).
2. R. A. LEE and D. A. ARMSTRONG. Nature, **200**, 552 (1963).
3. D. A. ARMSTRONG. Can. J. Chem. **40**, 1385 (1962).
4. G. W. WHYTE. Rad. Res. **18**, 265 (1963).
5. E. G. ZUBLER, W. H. HAMILL, and R. R. WILLIAMS. J. Chem. Phys. **23**, 1263 (1955).
6. G. H. HINE and G. L. BROWNELL. Radiation dosimetry. Academic Press Inc., New York. 1956.
7. W. BRANDT. Phys. Rev. **104**, 691 (1956).
8. U.S. DEPT. COM. Natl. Bur. Std. Handbook No. 79. 1961.
9. J. WEISS and W. BERNSTEIN. Phys. Rev. **98**, 1828 (1955).
10. R. C. RUMFELDT and D. A. ARMSTRONG. J. Phys. Chem. **68**, 761 (1964).
11. M. BODENSTEIN and G. JUNG. Z. Physik. Chem. **57**, 168 (1906).
12. D. C. FROST and C. A. MCDOWELL. Can. J. Chem. **38**, 407 (1960).
13. M. A. BIONDI and R. E. FOX. Phys. Rev. **109**, 2012 (1958).
14. J. L. MAGEE and MILTON BURTON. J. Am. Chem. Soc. **73**, 523 (1951).
15. L. B. LOEB. Basic processes of gaseous electronics. University of California Press, Berkeley and Los Angeles. 1961.
16. (*a*) P. F. KNEWSTUBB and A. W. TICKNER. J. Chem. Phys. **38**, 465 (1963).
    (*b*) P. KEBARLE and E. W. GODBOLE. J. Chem. Phys. **39**, 1130 (1963).
17. L. B. LOEB. Proc. Natl. Acad. Sci. **12**, 35 (1926).
18. J. L. MAGEE and W. H. HAMILL. J. Chem. Phys. **31**, 1380 (1959).
19. W. C. PRICE. Proc. Roy. Soc., Ser. A, **167**, 216 (1938).

Can. J. Chem. Downloaded from www.nrcresearchpress.com by 210.87.254.40 on 09/05/12
For personal use only.

Can. J. Chem. Downloaded from www.nrcresearchpress.com by 210.87.254.6 on 09/05/12
For personal use only.

A SPECTROPHOTOMETRIC REEXAMINATION OF THE SPECTRA AND STABILITIES OF THE IRON (III) – TIRON COMPLEXES

W. A. E. McBryde
Department of Chemistry, University of Waterloo, Waterloo, Ontario
Received January 7, 1964

ABSTRACT

Variations in the spectra of the aqueous solutions of the iron (III) – sodium catechol disulphonate (Tiron) complexes may be interpreted in relation to pH of the solutions to show which complexes are present at any chosen pH. With this knowledge it is possible in this system to evaluate equilibrium constants for the formation of each complex in turn. Combining these with separately determined acidity constants for Tiron, the stability constants of the complexes may be calculated. These have been determined for background solutions of potassium nitrate or sodium perchlorate each at three different concentrations, and for three different ratios of reagent to metal. Averages of a number of determinations made under these conditions are given in Table III of the paper. The constant K_1 in perchlorate media shows an unmistakable dependence suggestive of the existence of a protonated species at low pH as well as the simple complex ML. However, there is some ambiguity in the interpretation of the results so that the exact nature of the protonated complex cannot be decided.

INTRODUCTION

In a previous communication (1) the spectrophotometric method introduced by Vareille (2) for determining the successive formation constants of a series of metallic complexes was discussed in some detail. In particular it was shown that the method can only be applied provided the formation constants sought are widely enough separated to give, under appropriate conditions, solutions containing all of the metal exclusively as *one* or *two* species (including the uncomplexed metal). Furthermore, the most suitable complexes for study by this method are those which, as the ligand concentration is changed, will each in turn at some point comprise the *only* metallic species in solution.

The present paper reports a reexamination of the reaction between iron (III) and sodium catechol disulphonate (Tiron) by the Vareille method. This particular reaction was chosen for further study for several reasons. For instance, it was considered desirable to measure "conditional" equilibrium constants at several ionic strengths, since our own observations (3) as well as those of others (4) suggest that even at constant pH and ratio of ligand to metal, different hues of color, indicating different proportions of the colored complex species, are formed according to the ionic strength of the solution. Furthermore, it was hoped to bring additional evidence to bear on the claimed existence of a protonated metallic complex, MHL (5). Finally, it was of interest to try to define conditions under which the metal in solution could be completely converted to the single species ML, for the following reason. It has been noted previously that the red *tris*-complex, ML_3, is produced in alkaline solution irrespective of whether the solution is prepared from an iron (II) or an iron (III) salt; evidently the much greater stability of the iron (III) complex compared to that of iron (II) results in a marked lowering of the reduction potential so that the iron (II) complex is rapidly oxidized by the air (6) or, at high enough pH, by the solvent (3). Similar oxidation was not observed in media suitable for formation of the 1:1 complex. If conditions could be found in which the latter could be produced in stoichiometric amounts, an analytical procedure might be possible in which iron (III) could be determined in the presence of iron (II) in acidic solution, while in the same solution made alkaline total iron could be determined.

Can. J. Chem. Downloaded from www.nrcresearchpress.com by 210.87.254.6 on 09/05/12
For personal use only.

PRINCIPLE OF THE METHOD

In applying Vareille's method for this work certain extensions of the original procedure were introduced. From the optical density of any solution containing metal and ligand, an extinction coefficient based on the total molarity of the metal may be calculated. Calling this ϵ_M, it is evident that

$$\epsilon_M = \epsilon_0 \alpha_0 + \epsilon_1 \alpha_1 + \epsilon_2 \alpha_2 + \epsilon_3 \alpha_3 \quad [1]$$

for a system of three complexes. The symbol α gives the fraction of the metal in the designated species, and the subscripts 0----3 refer respectively to M, ML, ML_2, and ML_3.

From spectra of solutions having a fixed molarity of iron (III) and Tiron and adjusted to various values of pH, values of ϵ_M were obtained, and plotted against pH. The information to be gained from such a plot may be seen by inspection of Fig. 1; two of the wavelengths for which data are portrayed (534 mμ, 670 mμ) are those at which isobestic points occur. The basis of Vareille's method is that one may infer from the horizontal regions in this plot, plus a knowledge of the identity of the complexes found at various regions of pH (1), the following information:

above pH 6.3, $\alpha_3 = 1$; between pH 4.4 and 6.3, $\alpha_2 + \alpha_3 = 1$; at pH 4.3, $\alpha_2 = 1$; between pH 2.8 and 4.2, $\alpha_1 + \alpha_2 = 1$; at pH 2.7, $\alpha_1 = 1$; below pH 2.6, $\alpha_0 + \alpha_1 = 1$.

It is thus possible to obtain at pH 2.7, 4.3, and 6.3 respectively the values of ϵ_1, ϵ_2, and ϵ_3 at any chosen wavelength. It is to be understood that the values and ranges of pH quoted refer only to the experimental conditions under which the data of Fig. 1 were obtained.

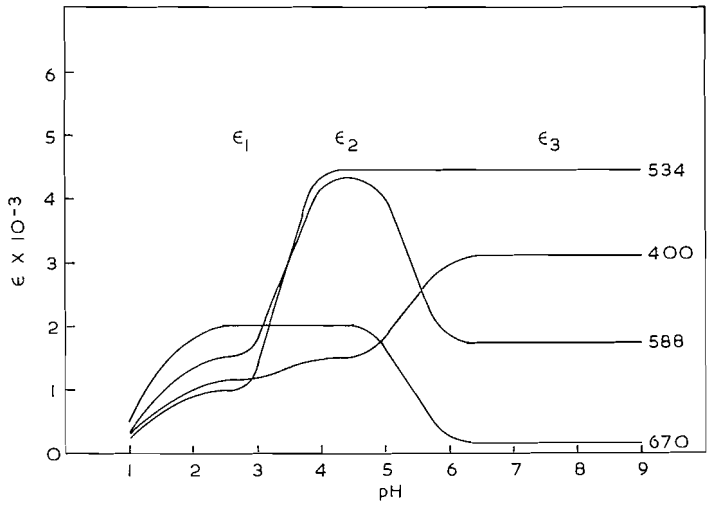

FIG. 1. Variation of molar extinction coefficient for iron (III) – Tiron solutions as a function of pH and at indicated wavelengths. $[M]_T \sim 2 \times 10^{-4}$ M; $[L]_T \sim 2 \times 10^{-3}$ M; 0.5 M KNO_3 background.

Given these characteristics, the composition of mixtures of pairs of metallic species can be deduced from values of ϵ_M. The value of $\epsilon_0 \sim 0$ in the range of wavelengths investigated. Equilibrium constants, $\mathcal{K}_n$, were then calculated for the reactions

$$ML_{n-1} + H_2L = ML_n + 2H \qquad (n = 1, 2, 3)$$

by the expression

$$[2] \qquad \mathcal{K}_n = a_n \, H^2/[H_2L]$$

in which

$$[3] \qquad a_n = (\epsilon_{n-1} - \epsilon_M)/(\epsilon_M - \epsilon_n) = [ML_n]/[ML_{n-1}]$$

$$[4] \qquad H = \text{antilog } (-pH)$$

$$[5] \qquad [H_2L] = ([H_2L]_T - \bar{n}[M]_T)\,(1 + K_{a_1}/H)^{-1}$$

$$[6] \qquad \bar{n} = (n - 1) + a_n/(a_n + 1) = (n - 1) + \alpha_n$$

In these $\bar{n}$ gives the degree of complex formation as defined by Bjerrum. In this system of complexes it has been shown above that at certain values of pH, $\alpha_n = 1$ (for $n = 1$, 2, or 3). Below each such pH is a region where $\alpha_n + \alpha_{n-1} = 1$. In these regions

$$\begin{aligned} \bar{n} &= (n - 1)\alpha_{n-1} + n\alpha_n \\ &= (n - 1)(\alpha_{n-1} + \alpha_n) + \alpha_n \\ &= (n - 1) + \alpha_n. \end{aligned}$$

By substituting from equation [3] in $\alpha_n/(\alpha_n + 1)$ one obtains $[ML_n]/([ML_n] + [ML_{n-1}])$ which is α_n. This is the source of equation [6].

Tiron is represented by H_2L; this stands for the catechol part of the molecule, the sulphonate groups being ionized and assumed inactive in complex formation. By measuring the pH and optical density of any solution in which $(\alpha_n + \alpha_{n-1}) = 1$ an appropriate value of $\mathcal{K}_n$ could be calculated. For calculation of $\mathcal{K}_1$,it is understood that the quantity a_1 gives the ratio [ML]/[M]; however, the quantity [M] includes free ferric ion as well as any products of its hydrolysis. To calculate from a_1 by equation [2] we have divided the expression on the right-hand side by the fraction of the unbound iron (III) actually in the ionic state. Appropriate values of this fraction were taken from calculations [7] based on Hedstrom's hydrolysis constants (8); Fig. 2 shows values of this fraction as a function of pH for concentrations of iron (III) below 10^{-3} molar.

A separate value for the equilibrium constant was obtained from each measurement of

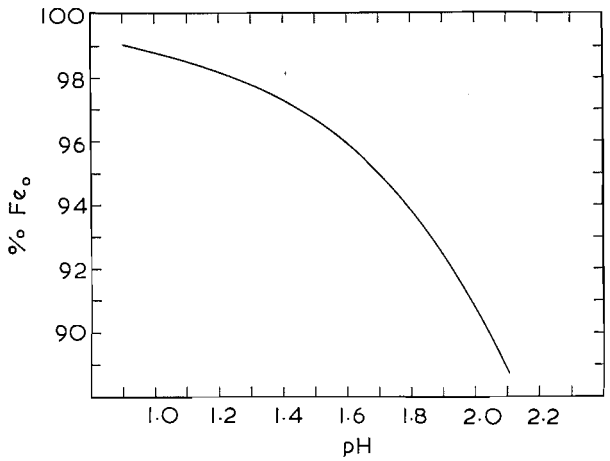

FIG. 2. Percentage of unhydrolyzed iron (III) in solutions $> 10^{-3}$ *M*.

Can. J. Chem. Downloaded from www.nrcresearchpress.com by 210.87.254.6 on 09/05/12
For personal use only.

optical density subject to the restriction that a_n fell between 0.1 and 10. Furthermore, there was no restriction upon the wavelength at which such measurements were made, so that several estimates of $\mathscr{K}_n$ could be obtained from one solution. In the method suggested by Vareille, measurements were made only at wavelengths at which isobestic points occurred, and a single estimate of $\mathscr{K}_n$ made by locating from a graph such as Fig. 1 the pH at which $a_n = 1$ ($n = 2$ or 3).

The acid dissociation constants of Tiron were determined by following the pH during titration of weighed portions with standard alkali. Empirical relationships between pH as detected by a glass electrode and stoichiometric concentrations of free hydrogen or hydroxide ion were first obtained by adding known amounts of acid or alkali to neutral aqueous solutions. It was then assumed that any pH value could be converted to a value of [OH] or [H] in a solution of ionic strength the same as that taken for calibration. The degree of hydrogen bound to Tiron, $\bar{n}_H$ (the average number of hydrogen ions per molecule of Tiron) was given by one or other of the following equations.
In acidic solution

$$\bar{n}_H = ([H]_T - [H])/[H_2L]_T. \quad [7]$$

(This refers to hydrogen bound to the sulphonate groups.)

In neutral or alkaline solution

$$\bar{n}_H = 2 - ([B]_T - [OH])/[H_2L]_T. \quad [8]$$

(This refers to the degree of protonation of L.)

In neutral solution [OH] is negligibly small compared to the other terms. For

$$H_2L = HL + H, \quad pK_{a_1} = pH - \log\{[B]_T/([H_2L]_T - [B]_T)\}. \quad [9]$$

For

$$HL = L + H, \quad pK_{a_2} = pH + \log [\bar{n}_H/(1 - \bar{n}_H)]. \quad [10]$$

The formation constants of the various complexes are given by the relationship

$$K_n = \frac{\mathscr{K}_n}{K_{a_1} K_{a_2}}. \quad [11]$$

It should be noted that the formation constants derived in this way are defined by concentrations of the participating species. They were determined in solutions to which had been added an indifferent electrolyte in sufficient quantity to maintain a known and constant ionic strength. Sets of formation constants were measured at each of these ionic strengths and with two different background electrolytes. These are therefore "conditional" constants applicable, strictly speaking, only in the medium for which they were determined. The acidity constants defined by equations [9] and [10], and the reaction constants defined by equation [2] all contain the quantity H, which is operationally defined, and is neither a concentration nor an activity. These constants, sometimes called Brönsted constants, serve here as means of determining the formation constants.

The foregoing procedure is an extension of that proposed by Vareille in two respects. In his work plots such as Fig. 1 were given and applied only at the wavelengths at which isobestic points were found. Clearly once the spectra of the individual complexes have been identified, there need be no restriction on the wavelength chosen for observation, and indeed one may select wavelengths at which the values of ϵ_n and ϵ_{n-1} in equation [3] differ

Can. J. Chem. Downloaded from www.nrcresearchpress.com by 210.87.254.6 on 09/05/12
For personal use only.

most widely. Secondly, Vareille confined his evaluation of $\mathscr{K}_2$ and $\mathscr{K}_3$ to the case where a_2 or $a_3 = 1$. What has been done here is to use each corresponding pair of measurements of ϵ_M and pH to find an independent value of $\mathscr{K}$.

RESULTS AND DISCUSSION

From the variation of optical density with pH it was possible, as outlined above, to elicit the absorption spectra of the three individual complexes. These are displayed for solutions in 0.5 *M* potassium nitrate in Fig. 3. Somewhat surprisingly the absorption

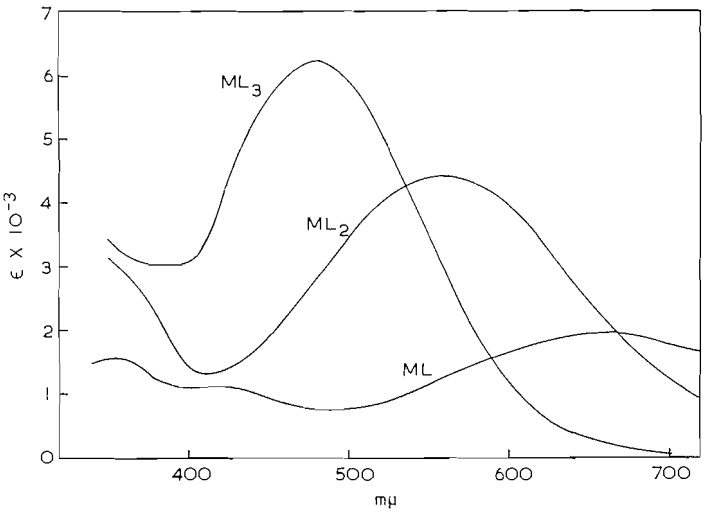

FIG. 3. Absorption spectra of the three iron (III) – Tiron complexes: 0.5 *M* KNO_3 background.

spectra, and hence the wavelength of isobestic points, proved to be slightly different in the different background solutions used. The values of λ_{max} and ϵ_{max} differed between nitrate and perchlorate, and between background solutions of different molarity. The range of values observed was as follows:

FeL:	λ_{max}	670–676 mμ,	ϵ_{max}	1840–1960
FeL_2:		560–562		4550–4600
FeL_3:		478–482		6150–6240

The cause of this variation is not known, but, from the fact that the shift in λ_{max} is appreciable for the complex ML_3, one may presumably rule out the formation of mixed complexes. A more probable explanation, which more applies the higher the degree of complex formation, is that interactions of the complexes occur with cations of the background solution. Such interactions have been postulated by Dyrssen (9), and have been thought to account for shifts in the spectra of the 1:1 ferric–Tiron complex in magnesium perchlorate solutions as compared with sodium perchlorate (3).

At the outset of this work it had been planned to use potassium nitrate as the indifferent electrolyte with which to regulate the ionic strength of the medium. In the more acidic solutions required to measure $\mathscr{K}_1$, however, it became apparent that some change in the Tiron—possibly oxidation by acidified nitrate—was taking place as evidenced by absorption at 400 mμ, and ultimately by a yellow color in the solution. Since the extent of this

Can. J. Chem. Downloaded from www.nrcresearchpress.com by 210.87.254.6 on 09/05/12
For personal use only.

reaction could not readily be determined, and since it introduced an uncertainty in evaluating $[H_2L]$ (equation [5]), a shift was made to a perchlorate medium in which no evidence of this deterioration of the Tiron was observed.

TABLE I

Acidity constants for Tiron (nitrate or perchlorate background)

Background	pK_{a_1}	pK_{a_2}
0.1 *M*	7.65 – 7.69	12.47 – 12.55
0.5 *M*	7.36 – 7.43	12.09 – 12.11
1.0 *M*	7.17	11.74 – 11.81

In Table I are shown values of the acidity constants for Tiron as measured in the two media. The difference between the results with the two background salts was not considered significant. These may also be compared with the values obtained by Schwarzenbach in 0.1 *M* potassium chloride ($pK_{a_1} = 7.66$; $pK_{a_2} = 12.6$). The variation of pK_a is roughly linear with the square root of ionic strength. Extrapolation to zero ionic strength permits the following crude estimates of the thermodynamic dissociation constants: $pK_{a_1} = 7.9$; $pK_{a_2} = 12.9$.

TABLE II

Selected values of molar extinction coefficients for complexes

Nitrate background				Perchlorate background			
λ	ϵ_1	ϵ_2	ϵ_3	λ	ϵ_1	ϵ_2	ϵ_3
400	1130	1480	3090	430		1420	4380
534	980	4440	4440	480			5870
588	1530	4300	1710	500	740	3730	5570
670	1990	1990	150	550	1120	4400	
				600	1620	3730	

Table II lists the values of the molar extinction coefficients selected for evaluation of a in equation [3]. Two of the wavelengths chosen for measurements with nitrate solutions were those at which isobestic points occurred; for the perchlorate solutions wavelengths were taken at which a marked difference in ϵ for adjacent complexes was found.

Table III summarizes all the results for stability constants found at each of three ionic strengths and for three ratios of reagent to metal. The number shown for K_n is an average of six to ten measurements (varying in pH) at each of three wavelengths, except for a few cases with nitrate solutions where only two wavelengths were used. Along with each result is given the average deviation within the set, and these give some indication of the precision of which the method is capable. The variations in K measured at different wavelengths was much greater than the variations among a set made at one wavelength. This fact revealed that the weakest feature in the method is the selection of appropriate ϵ_n values for the individual complexes. Values of K_2 and K_3 showed no dependence on pH; the same could not be said of K_1, and this is the cause of the rather high average deviations for this quantity when measured in perchlorate solutions. The variation of $\mathcal{K}_1$ with pH was made the object of further study, and this was largely confined to perchlorate solutions because of the uncertainty referred to previously in the fate of Tiron in the nitrate solutions at low pH.

Can. J. Chem. Downloaded from www.nrcresearchpress.com by 210.87.254.6 on 09/05/12
For personal use only.

TABLE III

Summary of stability constants for iron (III) – Tiron

Ratio $[L]_T/[M]_T$		20:1	10:1	5:1
Nitrate background				
K_3	1.0 *M*		3.56±0.95	
$\times 10^{-11}$	0.5 *M*	3.77±0.61	4.12±0.69	3.62±0.49
	0.1 *M*		0.59±0.09	
K_2	1.0 *M*		0.50±0.04	
$\times 10^{-15}$	0.5 *M*	1.49±0.11	1.38±0.17	0.98±0.12
	0.1 *M*		1.24±0.25	
K_1	1.0 *M*		0.64±0.11	
$\times 10^{-19}$	0.5 *M*	4.32±0.78	2.10±0.65	3.47±0.48
	0.1 *M*		23.7±5.0	
Perchlorate background				
K_3	1.0 *M*		1.96±0.75	
$\times 10^{-11}$	0.5 *M*	1.95±0.31	2.04±0.28	1.42±0.31
	0.1 *M*		0.124±0.023	
K_2	1.0 *M*		1.28±0.32	
$\times 10^{-15}$	0.5 *M*	1.28±0.21	0.98±0.14	1.24±0.20
	0.1 *M*		0.84±0.19	
K_1	1.0 *M*		1.34±0.54	
$\times 10^{-19}$	0.5 *M*	5.06±1.68	5.46±1.72	5.84±2.92
	0.1 *M*		25.0±10.2	

It was found that $\mathscr{K}_1$ was larger the higher the acidity of the solutions. The spread in values lay approximately within the range pH 1 to 2. Many additional solutions were prepared having pH within this range and various ratios of reagent to metal; the optical densities of each solution were measured at three wavelengths. Some of the results are displayed in Fig. 4; the points shown are the averages for each solution of results at three wavelengths. There can be no doubt that the quantity $aH^2/[H_2L]$ shows some dependence on H; similar trends were found at each level of ionic strength of sodium perchlorate. Schwarzenbach (5) has also observed a variation in the apparent K_1 for this system at low pH, and accounted for this by postulating the formation of a protonated species MHL.

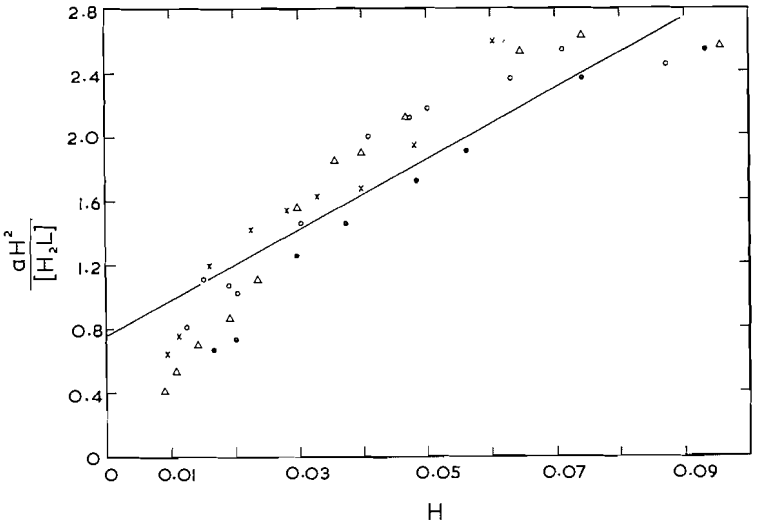

FIG. 4. Variation of apparent $\mathscr{K}_1$ ($= aH^2/[H_2L]$) with H: 0.5 *M* $NaClO_4$ background; $[M]_T \sim 2 \times 10^{-4}$; and ligand to metal ratios: × = 5:1; ○ = 10:1; △ = 10:2; ● = 20:1.

Can. J. Chem. Downloaded from www.nrcresearchpress.com by 210.87.254.6 on 09/05/12
For personal use only.

Can. J. Chem. Downloaded from www.nrcresearchpress.com by 210.87.254.6 on 09/05/12
For personal use only.

The experimental techniques used do not permit any decision to be made concerning the site of this protonation. In Schwarzenbach's discussion of this reaction protonation is assumed to take place on a sulphonate group of the Tiron; this assumption is open to question. Tiron solutions can be titrated with strong acid, and no evidence found from pH measurements of any hydrogen ion being taken up by the molecule down to pH 1. The formula of the complex ML is, presumably,

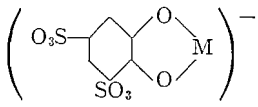

bearing a net charge one unit less negative than the anion of Tiron itself. If we assume that the sulphonate groups in Tiron show no affinity for protons down to pH 1, it seems unlikely that they would show increased tendency to accept protons in the complex. Yet Schwarzenbach's results and ours indicate that interaction of the ML complex with protons occurs above pH 1.

Another possible site for proton exchange in this complex is the hydration shell of the metallic ion which will only partially have been displaced as a result of coordination of one Tiron molecule. There is, however, no variation of $\mathscr{K}_1$ with H in the case of ferric sulphosalicylate or ferric salicylate in the same region of pH and in the same medium (10). These complexes are otherwise fairly similar to the Tiron complexes, and one would expect hydrolysis of the latter to be parallelled by hydrolysis of the former.

It was found that no change in absorption spectrum, in the sense of shifts of absorption maxima or the appearance or disappearance of absorption peaks, occurred in the visible or adjacent ultraviolet region throughout the range of pH in which the protonation appeared to be taking place. If we assume that a protonated species does exist, there seem from the observed spectra to be only two possible conclusions: either it has the same molar extinction coefficient as the unprotonated species, or it has an extinction coefficient undistinguishable from the uncomplexed metal. Making the former assumption, and calling K_H the acidity constant of the protonated species, it can be shown that

$$a\mathrm{H}^2/[\mathrm{H_2L}] = \mathscr{K}_1 + (\mathscr{K}_1\mathrm{H}/K_\mathrm{H}).$$

With reference to Fig. 4, a correlation line through the experimental points should have $\mathscr{K}_1$ as intercept and $\mathscr{K}_1/K_H$ as slope. Correlation lines were found by a least squares calculation with the following results:

Molarity $NaClO_4$	No. of solutions	$\mathscr{K}_1$	K_H	pK_H	Average deviation
0.1	35	0.46	0.018	1.8	0.165
0.5	135	0.75	0.034	1.5	0.36
1.0	51	0.39	0.015	1.8	0.15

The average deviation refers to values of $a\mathrm{H}^2/[\mathrm{H_2L}]$ above and below the line. The value of pK_H for 0.1 M $NaClO_4$ may be compared with Schwarzenbach's value of 1.80 in 0.1 M KCl. It is regrettable that, in spite of a very large number of determinations in 0.5 M $NaClO_4$, the average deviation was as high as shown; this fact creates some doubts about the higher value of $\mathscr{K}_1$ (and hence of K_H) in this medium. The position of the regression line in Fig. 4 is considerably influenced by the values of $a\mathrm{H}^2/[\mathrm{H_2L}]$ at higher H; if the values above H = 0.07 are not included, a regression line much closer to the other two is obtained.

In the event that the protonated species is non-absorbing in the spectral region examined, the quantity a ($= \epsilon_M/(\epsilon_1 - \epsilon_M)$) gives the ratio [ML]/([M] + [MHL]) instead of ([ML] + [MHL])/[M]. This leads to a different relationship involving K_H, namely,

$$[H_2L]/aH^2 = 1/\mathscr{K}_1 + ([H_2L]/K_HH).$$

Provided that there is a sufficient excess of Tiron present $[H_2L] \sim [H_2L]_T$, and is constant for a series of solutions. In this case a plot of the quantity on the left-hand side of the equation against 1/H should also be linear with intercept $1/\mathscr{K}_1$, and have a slope from which K_H can be obtained. Figure 5 shows the data for 0.1 M $NaClO_4$ as background electrolyte,

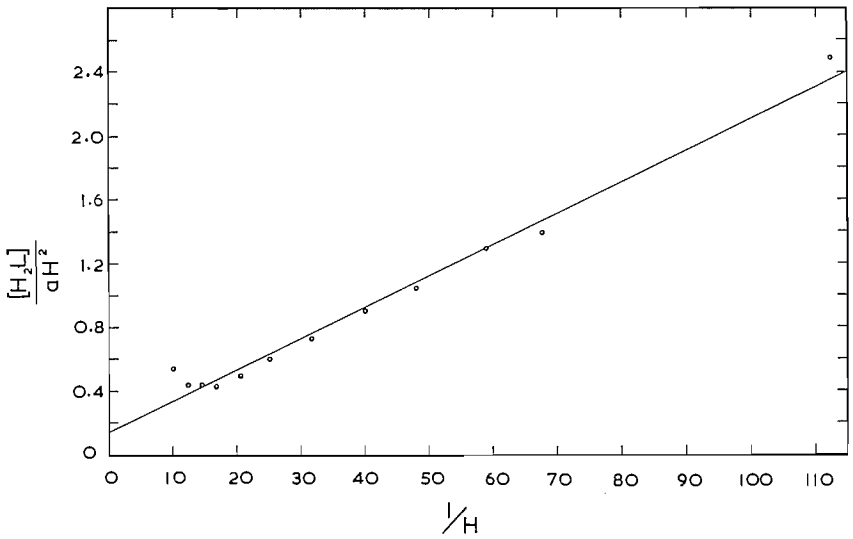

FIG. 5. Variation of apparent $1/\mathscr{K}_1$ ($= [H_2L]/aH^2$) with 1/H: 0.1 M $NaClO_4$ background; $[M]_T \sim 2 \times 10^{-4}$; $[L]_T \sim 2 \times 10^{-3}$.

and it is seen that such a representation also may apply to them. A summary of results for regression lines calculated by least squares, and the resulting values for K_H are given below.

Medium $NaClO_4$	$[L]_T/[M]_T$	No. cases	$\mathscr{K}_1$	K_H	pK_H	Average deviation
0.1 M	10:1	12	6.8	0.09	1.0	0.062
0.5 M	5:1	11	6.2	0.065	1.2	0.05
	10:1	12	4.0	0.15	0.8	0.05
	20:1	9	7.7	0.16	0.8	0.05
1.0 M	10:1	15	5.7	0.10	1.0	0.031

These results do not at all rule out the possibility that the protonated complex is non-absorbing at the wavelengths examined. Moreover, if one takes the data of Willi and Schwarzenbach (5, p. 534) and plots the reciprocal of their $K[H]^2$ (equivalent to our $aH^2/[H_2L]$) against the reciprocal of [H] (equivalent to our H) one gets a reasonably linear relationship, from which we infer that a non-absorbing protonated complex is not ruled out by their measurements. Owing to the fact that their data are taken off a Job curve it is not practical for us to try to evaluate $[H_2L]$, or hence K_H, from this plot.

Can. J. Chem. Downloaded from www.nrcresearchpress.com by 210.87.254.6 on 09/05/12
For personal use only.

The results given above leave little doubt concerning the existence of a protonated complex species below pH 2, in agreement with Willi and Schwarzenbach. It is not possible to deduce from the results where the proton may be attached in this species, nor whether the complex is absorbing or non-absorbing in the region 400–700 mμ. If it does absorb light, its extinction coefficient must be identical with the non-protonated species. If it does not, one may speculate whether the formation of the protonated species involves opening of the chelate ring as a result of addition of a proton at one of the phenolic groups. There is a lack of evidence for the equivalent reaction in nitrate solutions owing to observable deterioration of the Tiron in acidified nitrate solutions. These considerations make it difficult to select a value for $\mathcal{K}_1$ and hence of K_1 for the *mono-* complex in perchlorate solutions. In the absence of further evidence the results for the first stability constant given in Table III are averages of the values obtained without regard to their hydrogen-ion dependence. A few preliminary measurements were made with pyrocatechol as the ligand following the same procedures as with Tiron. The spectra of the resulting solutions showed rather rapid changes with time, and it appeared that the method described in this paper would require some modification before it could successfully be applied to catechol complexes.

Finally, a word should be added about the reaction of ferrous and ferric solutions with Tiron. Below pH 3 a freshly prepared ferrous iron solution gave very little or no color with Tiron. But when solutions containing both ferrous and ferric iron were treated under the same conditions the color developed was roughly equivalent to the total iron present. The induced oxidation of the ferrous iron in the presence of the ferric–Tiron solutions thus rules out the possible discrimination between the two oxidation states for analytical purposes.

EXPERIMENTAL

The Tiron was purchased as the colorimetric reagent sold by British Drug Houses, Ltd. or the G. F. Smith Chemical Co. Each lot was assayed for purity by titration of a weighed portion with standard alkali to the end-point for neutralization of the first phenolic hydrogen as determined with a pH meter. All lots used proved to be 99% or greater in purity if the assumption were made that Tiron was the only acidic substance in the sample. The molarity of solutions of this reagent was calculated with proper regard to the indicated purity.

All other chemicals used were of reagent grade and not further purified. Stock solutions of ferric nitrate in dilute nitric acid or of ferric perchlorate in dilute perchloric acid were standardized gravimetrically by precipitation of the hydrous oxide. A concentrated sodium perchlorate solution, which by dilution could provide selected background ionic strengths, was standardized by passing measured volumes through a column of ion-exchange resin in the hydrogen form, with subsequent titration of the acid set free in the effluent (11).

All pH measurements were made with glass electrodes previously standardized and checked with two or more buffer solutions prepared according to N.B.S. specifications from reagent grade chemicals. Solutions of iron plus Tiron were adjusted in acidity by the addition of small amounts of acid or alkali by means of hypodermic needles; no buffers were used in any of these solutions.

Preliminary spectral measurements on solutions of complexes were made with a Bausch and Lomb Model 505 spectrophotometer. All optical densities required for calculation of ϵ_M were measured in a Beckman Model DU spectrophotometer in 1-cm matched cells. The cell compartment in the latter was fitted out with thermospacers through which water maintained at 25 °C was circulated. The temperature of the solutions was not otherwise controlled, but the prevailing temperature in the laboratory remained quite steady in the range 22 to 25 °C.

ACKNOWLEDGMENTS

This investigation was supported by a grant from the National Research Council of Canada, for which the author records his appreciation. His thanks also go to Miss Jeanne Wittig and Miss Janet Rohr for technical assistance.

Can. J. Chem. Downloaded from www.nrcresearchpress.com by 210.87.254.6 on 09/05/12
For personal use only.

REFERENCES

1. W. A. E. McBRYDE and G. F. ATKINSON. Can. J. Chem. **39**, 510 (1961).
2. L. VAREILLE. Bull. Soc. Chim. France, 870 (1955).
3. G. F. ATKINSON. M.A. and Ph.D. Theses, University of Toronto, Toronto, Ont. 1954, 1959.
4. A. E. HARVEY and D. L. MANNING. J. Am. Chem. Soc. **72**, 4488 (1950).
5. A. WILLI and G. SCHWARZENBACH. Helv. Chem. Acta, **34**, 528 (1951).
6. J. DOLEZAL and J. ADAM. Chem. Listy, **47**, 1467 (1953); Collection Czech. Chem. Commun. **19**, 905 (1954).
7. G. F. ATKINSON and W. A. E. McBRYDE. J. Chem. Educ. **38**, 127 (1961).
8. B. A. O. HEDSTROM. Arkiv Kemi, **6**, 1 (1953).
9. D. DYRSSEN. Private communication. See also J. J. Lothe. Proc. Conf. Co-ordination Chemistry. The Chemical Society, London. 1959.
10. W. A. E. McBRYDE and J. A. PAGE. Unpublished results.
11. O. SAMUELSON. Ion exchange separations in analytical chemistry. 2nd ed. J. Wiley and Sons, New York. 1963. p. 234.

Can. J. Chem. Downloaded from www.nrcresearchpress.com by 210.87.254.6 on 09/05/12
For personal use only.

Can. J. Chem. Downloaded from www.nrcresearchpress.com by 210.87.254.6 on 09/05/12
For personal use only.

RÉACTION DU SULFURE DE BORE AVEC QUELQUES GROUPES CARBONYLES

S. JERUMANIS ET J. M. LALANCETTE
Faculté des Sciences, Université de Sherbrooke, Sherbrooke, Québec

Reçu le 15 janvier 1964

ABSTRACT

The reactions of boron sulphide with some types of carbonyls have been studied. The reaction of boron sulphide with aromatic aldehydes and aliphatic aldehydes which have been deprived of active hydrogen in the α position gives a good yield of the corresponding trithioaldehydes. This reaction is examined for four aldehydes, namely, benzaldehyde, 3-methylbenzaldehyde, 3-nitrobenzaldehyde, and 2,2′-dimethylpropionaldehyde. Through this study the authors have brought out a method which enables either the α-trithiobenzaldehyde, m.p. 166–167 °C, or the β-trithiobenzaldehyde, m.p. 225–226 °C, to be obtained selectively. The reaction of 3-methylbenzaldehyde with boron sulphide yields only one β stereoisomer, but nitrobenzaldehyde remains completely inert. The aldehydes having one active hydrogen in the α position undergo a dehydrogenation at the same time as the oxygen is being replaced by one atom of sulphur. 2,2′-Dimethylthiopropanal exists in a trimeric state at normal temperatures and becomes monomeric at higher temperatures, whereas the trithiobenzaldehydes do not depolymerize. Methyl benzoate reacts with boron sulphide to give tetraphenyldioxadiene. The structure of this extremely inert substance has been established mainly by physical means: infrared, ultraviolet, and n.m.r. spectra. The reaction of benzophenone and acetophenone with boron sulphide has been investigated. The former has been found inert to the action of the sulphide, and the latter reacts quite readily to give 2,4-diphenylthiophene. The structure of this thiophene is established by desulphuration over nickel. The role of boron sulphide as dehydrogenating and deoxygenating agent is discussed, and a laboratory preparation of boron sulphide is described.

INTRODUCTION

La chimie du sulfure de bore n'a pas connu d'apports notables depuis les travaux de Moissan (1, 2) relatifs à la préparation et à la structure de ce composé.

Au cours d'une investigation systématique de l'interaction du sulfure de bore avec divers types de molécules organiques, nous avons voulu étudier le comportement du groupe carbonyle en présence de ce sulfure. Des tests préliminaires ont indiqué qu'un groupe carbonyle rattaché à une chaîne purement aliphatique donne avec le sulfure de bore une réaction relativement complexe, accompagnée à la fois de déshydrogénation indiquée par un dégagement de H_2S et de substitution du soufre à l'oxygène du groupe C=O démontrée par la disparition de la bande carbonyle chez le spectre infrarouge du produit de la réaction. Nous avons voulu aborder le problème par l'étude de carbonyles portés par des molécules à caractère aromatique, afin de prévenir si possible la déshydrogénation et d'observer uniquement la réaction carbonyle – sulfure de bore.

Réactions de quelques groupes carbonyles cétoniques

La première cétone étudiée, la benzophénone, s'est montrée tout à fait inerte vis-à-vis de ce sulfure. L'acétophénone, par contre, réagit énergiquement avec ce sulfure. La réaction est spontanée, s'accompagne d'un dégagement de H_2S et est complétée par un reflux. Au terme du reflux, la totalité du sulfure a réagi et s'est transformée en anhydride borique. De la fraction organique, il a été possible d'isoler un solide blanc, p.f. 121–122 °C, le diphényl-2,4 thiophène. Traitée par le nickel de Raney saturé d'hydrogène (3), cette molécule subit une désulfurisation accompagnée de dégagement de H_2S. Au terme de la réaction, on retrouve un hydrocarbure qu'on a identifié comme étant le diphényl-1,3 butane. La substance de dégradation présente les mêmes spectres dans l'infrarouge (4) et l'ultraviolet qu'un échantillon de diphényl-1,3 butane synthétique préparé à partir de

l'acétophénone et du phényl-2 éthanol-1. Les mesures par résonances magnétiques nucléaires confirment également l'identité du produit de dégradation au produit de synthèse.

Comme cette méthode de désulfurisation a souvent été employée sans que l'on note de réarrangements (5, 6), on peut donc conclure que le diphényl-1,3 butane est représentatif du squelette moléculaire de la substance p.f. 121–122 °C. Les eaux mères de la cristallisation du diphényl-1,3 thiophène à l'évaporation, laissaient un résidu résineux de couleur pourpre, répondant à la description donnée par Champaigne (7) pour la thioacétophénone. Cette substance polymérique dont le spectre infrarouge est dépourvu de bandes carbonyles donne un test positif pour le soufre.

Réaction du benzoate de méthyle

Nous avons constaté que certains esters réagissent avec le sulfure de bore, la réaction procédant selon le mode déjà indiqué, à savoir par une déshydrogénation et désoxygénation simultanées. Cette réactivité ayant été établie par des tests préliminaires, nous avons voulu préciser le comportement du benzoate de méthyle vis-à-vis de ce sulfure. Nous avons noté qu'à la température de reflux de l'ester, soit vers 200 °C, la réaction s'amorce subitement avec un dégagement assez abondant de H_2S. Après un contact prolongé, la masse réactionnelle est filtrée, et on note que le sulfure de bore s'est transformé en anhydride borique. La fraction liquide libère un solide blanc, qu'on a démontré être le tétraphényl-dioxadiène, I. La structure de cette substance, d'une grande stabilité, a pu être établie par

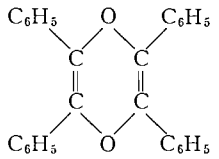

I

des mesures physiques, la dégradation chimique s'avérant inefficace.

Le spectre de résonance magnétique nucléaire révèle l'absence complète de protons aliphatiques dans la molécule, résultat en accord avec le spectre ultraviolet indiquant un système fortement conjugué (ϵ de 23 800 à 237 mμ) et les analyses élémentaires qui montrent une teneur assez faible en hydrogène (5.16%). Le spectre infrarouge présente les bandes propres à des C—H aromatiques dans les régions de 3060 cm^{-1} et 1500 cm^{-1}, et les bandes dans la région de 1050 cm^{-1} suggèrent un groupe éther sur la molécule. L'oxygène positivement indiqué par l'analyse élémentaire de I ne peut être qu'un oxygène de type éther, la possibilité d'un alcool ou d'un carbonyle étant définitivement éliminée par l'absence de bandes caractéristiques dans le spectre infrarouge, et la possibilité de peroxyde ou d'époxyde devant être rejetée par suite de l'inertie de I vis-à-vis l'hydrure de lithium et d'aluminium.

Le spectre de résonance magnétique nucléaire indique la présence de protons aromatiques (δ vers 7.0 p.p.m.). Cependant, au lieu du singlet normalement attendu pour les protons aromatiques portés par le noyau benzénique, on retrouve un triplet (δ = 6.9 p.p.m.) représentant 40% du total des protons et un singlet (δ = 7.1 p.p.m.) représentant 60% des protons. Le triplet à 6.9 p.p.m. ne peut indiquer des protons oléfiniques par suite de son intensité (40%). En effet, un tel pourcentage de ce type d'hydrogène apparaît inconciliable avec les analyses élémentaires et la grande inertie de la substance vis-à-vis les agents d'oxydation. Le dédoublement des bandes, qui ne peuvent être dues qu'à des protons

Can. J. Chem. Downloaded from www.nrcresearchpress.com by 210.87.254.6 on 09/05/12
For personal use only.

aromatiques, pourrait possiblement s'expliquer par un couplage entre les hydrogènes portés par les différents groupes benzéniques.

Réaction de quelques aldéhydes dépourvus d'hydrogène en α

Ayant constaté que les aldéhydes portant en position α un hydrogène actif subissent une déshydrogénation en même temps que la substitution de l'oxygène par un atome de soufre, nous avons choisi des aldéhydes dépourvus d'hydrogène actif tel que les aldéhydes benzoïques, méthyl-4 benzoïque, nitro-3 benzoïque et diméthyl-2,2 propionique. Tous ces aldéhydes simples tant aliphatique qu'aromatiques donnent une réaction exothermique avec le sulfure de bore conduisant à l'anhydride borique et au trithioaldéhyde correspondant. Cependant, le nitro-3 benzaldéhyde ne donne pas de réaction avec le sulfure de bore, sous les conditions expérimentales usuelles.

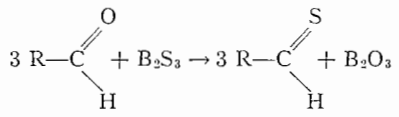

Les thioaldéhydes formés ont une grande tendance à se polymériser. En général, les trois molécules d'un monothioaldéhyde se condensent pour donner le trithioaldéhyde cyclique, composé alternativement de trois atomes de carbone et de trois atomes de soufre.

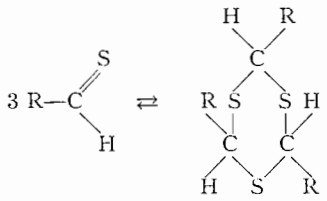

La trimérisation est fortement accélérée par la présence d'un catalyseur tel que l'acide chlorhydrique ou l'iode élémentaire (8). Dans le cas de l'aldéhyde diméthyl-2,2 thiopropionique, la forme trimérique peut être mise en équilibre avec le monomère par le chauffage. En effet, cet aldéhyde existe sous une forme de trimère à la température normale et devient monomérique à la température élévée. Cette transformation a été vérifiée par la détermination cryoscopique du poids moléculaire de ce thioaldéhyde dans le benzène et dans le camphre. Le poids moléculaire trouvé à 175 °C est bien près de celui du monomère (calculé pour le monomère: 102.2; trouvé: 112), mais il se rapproche beaucoup du trimère si on travaille dans le benzène à basse température (calculé pour trimère: 306.6; trouvé: 285). La forme trimérique des thioaldéhydes aromatiques n'admet pas l'équilibre avec la forme monomérique, la température de décomposition étant plus basse que la température de mise en équilibre.

Etant donné que chaque carbone de trithiobenzaldéhyde porte un atome d'hydrogène et un phényle, cette molécule existe sous deux formes stéréoisomériques α ou β, selon la position relative des trois phényles (9). La forme dite α (*cis*) de l'aldéhyde trithiobenzoïque est moins stable et par chauffage dans le chloroforme, dans le sulfure de carbone, ou dans le benzène se transforme, en présence d'un catalyseur (I_2), en isomère β (*trans*) plus stable. La transformation à l'état de solution est lente et incomplète, mais à l'état fondu la transformation est accompagnée d'une forte décomposition (10).

Can. J. Chem. Downloaded from www.nrcresearchpress.com by 210.87.254.6 on 09/05/12
For personal use only.

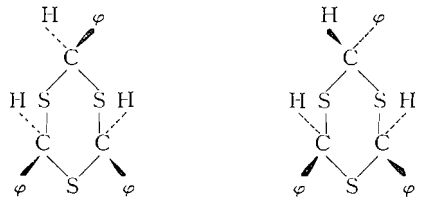

Forme α (*cis*) Forme β (*trans*)

Cependant, on a trouvé que les trithiobenzaldéhydes substitués ne présente qu'un seul stéréomère β (10).

Préparation des isomères α et β de l'aldéhyde trithiobenzoïque

Parmi les auteurs qui ont étudié la question des trithioaldéhydes, certains se sont intéressés à la transformation de l'isomère α en isomère β (8, 9, 10) ou à la réversibilité de ce phénomène et d'autres ont essayé la préparation sélective des deux stéréoisomères (10). Jusqu'ici, la recristallisation répétée du mélange qui se forme à partir du H_2S et de l'aldéhyde dans l'alcool éthylique saturé par l'acide chlorhydrique était le seul moyen pour obtenir l'isomère α de l'aldéhyde trithiobenzoïque. Mais par cette méthode, le rendement en isomère α est faible. En étudiant ce problème de la synthèse stéréoisomérique, nous avons constaté que la formation d'un ou de l'autre isomère de l'aldéhyde trithiobenzoïque peut être déterminée par la nature de l'énergie d'activation apportée au milieu réactionnel.

L'aldéhyde β-trithiobenzoïque

Ce thioaldéhyde se forme presque à l'état pur si la réaction du sulfure de bore avec l'aldéhyde benzoïque est activée par la chaleur. A cause de l'insolubilité du sulfure de bore dans le benzène, qui sert comme solvent, la réaction se passe en milieu hétérogène et par conséquent nécessite un long contact de deux réactifs pour être complète. L'ébullition dans le benzène du produit brut en présence des quelques cristaux d'iode ou de l'acide chlorhydrique assure l'absence complète d'isomère α dans le produit final.

L'aldéhyde α-trithiobenzoïque

La formation d'isomère α nécessite une source d'énergie plus riche. Dans ce but nous avons employé la lumière ultraviolette. Cette façon de procéder paraît une excellente méthode pour la préparation de l'aldéhyde α-trithiobenzoïque. Après la première recristallisation dans le benzène, la substance est déjà pure, comme l'indique son point de fusion.

Préparation du sulfure de bore

Parmi les différentes méthodes qui s'offrent pour la préparation du sulfure de bore: réaction d'échange de l'anhydride borique avec le sulfure d'aluminium (11), réaction du H_2S sur le bore élémentaire (12), et l'action du soufre sur le bore (1), cette dernière méthode a été trouvée la plus pratique, à l'échelle du laboratoire. Cette synthèse ne va pas sans certaines difficultés, car l'union directe des éléments ne débute que vers 650 °C et la réaction tend à s'emballer, par suite de son caractère exothermique. De plus, à ces températures, le sulfure de bore s'avère extrêmement corrosif, attaquant le verre du type "pyrex" ou "Vycor". Ces difficultés expérimentales (réaction explosive, corrosion) sont contrôlées en travaillant en présence d'un excès de soufre, que l'on peut ensuite enlever du produit réactionnel par des lavages au sulfure de carbone. Il nous a été ainsi possible de préparer le sulfure avec des rendements de l'ordre de 65–75%, le composé indiquant 85 à 90% de B_2S_3. Comme l'impureté principale dans le sulfure est constituée de bore élémentaire

Can. J. Chem. Downloaded from www.nrcresearchpress.com by 210.87.254.6 on 09/05/12
For personal use only.

(10–12%) très inerte vis-à-vis les réactifs organiques, nous avons utilisé ce matériel tel quel sans qu'il ait été nécessaire de recourir à une purification plus poussée par sublimation.

Conclusions

L'action du sulfure de bore sur un groupe carbonyle est donc double. Elle implique une désoxygénation et parallèlement une déshydrogénation. Thermodynamiquement, la désoxygénation peut s'expliquer par la grande différence dans la chaleur de formation du sulfure de bore, −57.0 kcal/mole (13), et de l'anhydride borique, −302.0 kcal/mole (13). Cette différence rend compte de la stabilisation apportée au système par l'interchange d'un soufre pour un oxygène sur l'atome de bore.

L'utilisation du sulfure de bore comme agent de sulfuration des molécules organiques constitue une alternative intéressante à la méthode de Pall (14, 15) faisant appel au tri ou penta-sulfure de phosphore comme source de soufre.

Avec les carbonyles aldéhydiques dépourvus d'hydrogènes en α, la réaction s'arrête à un interchange de l'oxygène pour un soufre sur le fragment organique. Le mécanisme suivant lequel cet échange s'opère pourrait possiblement procéder par voie radicalaire, du fait de l'influence de l'irradiation ultraviolette sur l'orientation de la réaction. La forme α, rapportée par Baumann (9) comme correspondant à une structure *cis*, est produite par irradiation ultraviolette alors que la forme β (*trans*) résulte de l'action de B_2S_3 sur le benzaldéhyde en absence de cette source énergétique, et ce fait semble confirmer les conformations assignées par cet auteur à ces deux molécules. Car la forme *cis* (α) correspond à des interactions beaucoup plus importantes que la forme *trans* (β) (modèle Peterson). L'inertie du *p*-nitrobenzaldéhyde peut se comprendre en fonction d'une désactivation du carbonyle par le groupe nitré en position para ou peut résulter d'une action inhibitrice de ce dernier groupement dans l'alternative d'un mécanisme radicalaire. L'état actuel de la question ne permet pas d'opter pour l'une ou l'autre de ces possibilités.

Dans le cas des carbonyles ayant plusieurs hydrogènes portés en α, la substitution de l'oxygène au soufre sur le bore s'accompagne de modifications profondes des réactifs organiques et conduit à des composés fortement déshydrogénés. Bien qu'il soit difficile d'en préciser le mécanisme, un tel type de réaction présente un intérêt certain car il permet d'accéder à des structures nouvelles et difficiles à obtenir par d'autres voies, tel le tétraphényldioxadiène.

PARTIE EXPERIMENTALE*

1. Réaction du sulfure de bore avec des carbonyles cétoniques

1.1 Réaction du sulfure de bore en présence d'acétophénone

A une suspension de 32 g (0.27 mole) de sulfure de bore dans 100 ml de benzène anhydre, on ajoute 110 g (0.92 mole) d'acétophenone "Reagent". La réaction est spontanée à la température de la pièce et très exothermique, en absence de diluant. Suit un reflux de 48 heures, en milieu benzénique, accompagnée de dégagement de H_2S. Au terme de ce contact, le mélange réactionnel est filtré à chaud. Le résidu solide à la filtration qui ne renferme pas de sulfure de bore est constitué d'anhydride borique. Il demeure infondu à 360 °C, et le traitement par un peu d'eau bouillante (3 heures) le transforme en acide borique, p.f. 179–181 °C. Le filtrat, après concentration sous vide, est cristallisé dans l'éther. On retrouve ainsi, après traitement au charbon actif, 12.0 g (25% de la théorie en fonction de l'acétophénone utilisée) de plaquettes minces blanches, p.f. 121–122 °C. Calculé pour $C_{16}H_{12}S$: C, 81.34; H, 5.12; S, 13.54. Trouvé: C, 81.61; H, 5.02; S, 13.40. Spectre infrarouge (10% dans CCl_4, 0.1 mm): épaulement à 3100 cm^{-1}, bandes à 3068 cm^{-1} (moyenne), 3040 cm^{-1} (moyenne), 1599 cm^{-1} (moyenne-forte), 1486 cm^{-1} (moyenne-forte), 1449 cm^{-1} (moyenne), 1363 cm^{-1} (faible), 902 cm^{-1} (faible), 881 cm^{-1} (moyenne), 838 cm^{-1} (moyenne). Spectre ultraviolet (solution

**Les points de fusion ont été déterminés en tubes capillaires et ne sont pas corrigés. Les spectres infrarouges ont été mesurés à l'aide d'un spectromètre "Perkin-Elmer", modèle 125. Les spectres ultraviolets ont été déterminés à l'aide d'un spectromètre "Perkin-Elmer", modèle 4000. Les mesures de résonance magnétiquen ucléaire ont été effectuées à l'aide d'un appareil "Varian", modèle A-60. Les analyses élémentaires sont de C. Daessle, Montréal.*

Can. J. Chem. Downloaded from www.nrcresearchpress.com by 210.87.254.6 on 09/05/12
For personal use only.

4.36×10^{-5} *M* dans l'éthanol absolu à 25 °C): ϵ de 21 440 à 256 mμ; ϵ de 10 000 à 302 mμ. Spectre de résonance magnétique nucléaire: aucune absorption dans la région des protons aliphatiques; bandes multiples entre 7.17 et 7.70 p.p.m., ce qui indique des protons oléfiniques et aromatiques.

1.2 Désulfurisation du diphényl-2,4 thiophène

Une solution de 7.0 g (0.029 mole) du composé p.f. 121–122 °C dans 150 ml d'alcool absolu est traitée par 30 g de nickel de Raney saturé d'hydrogène. La solution est refluée pendant 21 heures. Le reflux s'accompagne d'un dégagement de H_2S. Le catalyseur est filtré, et le filtrat, après concentration sous vide, est doublé de volume par addition d'eau et extrait par l'éther. La solution éthérée est séchée sur chlorure de calcium et concentrée sous Widmer. Le résidu, après distillation pèse 5.0 g, soit 82% de la quantité théorique. Après redistillation sur sodium un échantillon analytique présente les constantes suivantes: éb. 145 °C/18 mm Hg; n_D^{21} 1.5535. Décrit pour le diphenyl-1,3 butane: éb. 150 °C/22 mm; n_D^{20} 1.5535. Spectre infrarouge (solution 10% dans CCl_4 cellule 0.1 mm): bandes à 3105 cm^{-1} (faible), 3083 cm^{-1} (moyenne), 3063 cm^{-1} (forte), 3028 cm^{-1} (forte), 2959 cm^{-1} (forte), 2923 cm^{-1} (forte), 2861 cm^{-1} (moyenne), 2858 cm^{-1} (moyenne). Spectre de r.m.n.: protons aliphatiques à 1.3 p.p.m. (CH_3), à 2.0 p.p.m. (CH_2), à 2.5 p.p.m. (CH), et à 7.1 p.p.m. (protons aromatiques).

1.2.1 Préparation du diphényl-1,3 butane

On prépare le chloro-1 phényl-2 éthane par l'action de 50 g (0.42 mole) de chlorure de thionyle sur 50 g (0.41 mole) de phenyl-2 éthanol-1, à reflux. Par distillation on retrouve 33 g (0.24 mole) du dérivé halogéné cherché; éb. 80 °C/10 mm; décrit, 86 °C/12 mm. Ce dérivé halogéné dans l'éther 33 g (0.24 mole) est ajouté à une suspension de 5.6 g (0.23 mole) de magnésium dans l'éther. Après la mise en solution du métal, une solution éthérée contenant 30 g (0.25 mole) d'acétophénone est ajoutée au magnésium. Les opérations habituelles conduisent au diphényl-1,3 butanol-3, 50 g (0.22 mole) qui est immédiatement déshydraté par l'acide phosphorique 85%, à 170 °C.

Le produit de la déshydratation, après chromatographie sur alumine (alumine Woehm, activité 1, élution par éther de pétrole, éb. 30–40 °C) est hydrogéné en présence de nickel de Raney, à la pression atmosphérique. Le produit saturé, (41 g, 0.19 mole) est chromatographié sur alumine Woehm (activité 1, élution par l'éther de pétrole, éb. 30–40 °C) et redistillé deux fois sur sodium; éb. 149 °C/20 mm, n_D^{21} 1.5535. Spectre infrarouge (solution 10% dans CCl_4, cellule 0.1 mm): bandes à 3105 cm^{-1} (faible), 3083 cm^{-1} (moyenne), 3063 cm^{-1} (forte), 3028 cm^{-1} (forte), 2959 cm^{-1} (forte), 2923 cm^{-1} (forte), 2861 cm^{-1} (moyenne), 2858 cm^{-1} (moyenne). Spectre de résonance magnétique nucléaire: protons aliphatiques à 1.3 p.p.m. (CH_3), à 2.0 p.p.m. (CH_2), à 2.5 p.p.m. (CH), et à 7.1 p.p.m. (protons aromatiques).

1.3 Réaction du sulfure de bore avec la benzophénone

Une solution de 14 g (0.77 mole) de benzophénone dans 125 ml de benzène anhydre est refluée pendant 43 heures en présence de 8.5 g (0.073 mole) de sulfure de bore. La solution se colore en bleu au cours du reflux. La masse réactionelle est filtrée. La fraction solide semble être en quasi totalité du sulfure de bore non réagi (réaction violente de ce résidu avec l'eau). La fraction liquide est distillée sous vide à la température de la pièce pour éliminer le benzène, et le résidu est fractionné sous vide. On retrouve une seule fraction, éb. 160–165 °C/13 mm, p.f. 43–45 °C, représentant 94% du poids de substance mis en expérience. Décrit pour la benzophénone: éb. 172 °C/19 mm, p.f. 45–48 °C. Les spectres infrarouges d'un échantillon authentique de benzophénone et de cette fraction sont identiques.

2. Réaction du sulfure de bore avec un carbonyle ester

2.1 Réaction du sulfure de bore en présence de benzoate de méthyle

On chauffe à reflux (200 °C), pendant 28 heures, en atmosphère inerte, une suspension de sulfure de bore finement pulvérisé (21.0 g, 0.18 mole) dans 75 g (0.55 mole) de benzoate de méthyle redistillé. Après un contact de quelques minutes à la température de reflux, la réaction s'amorce brusquement et s'accompagne d'un abondant dégagement de H_2S. Cette évolution gazeuse se maintient, en diminuant, tout au long de la réaction. Après ce contact, la masse réactionelle est filtrée à chaud, et la fraction solide est lavée par 20 ml de benzoate de méthyle bouillant. Cette fraction solide ne renferme plus de sulfure de bore mais s'avère être de l'anhydride borique. Le filtrat est concentrée sous vide, et le résidu, repris par de l'éthanol, est cristallisé dans ce solvant après traitement au charbon actif. On retrouve ainsi 11.3 g (0.029 mole, 30% de la théorie, en fonction du benzoate de méthyle utilisé) de fines aiguilles blanches, p.f. 184–185 °C. Spectre infrarouge (solution à 10% dans le tétrachlorure de carbone, cellules 0.1 mm, KBr): bandes à 3078 cm^{-1} (faible), 3059 cm^{-1} (moyenne), 3022 cm^{-1} (faible), 1598 cm^{-1} (moyenne), 1574 cm^{-1} (très faible), 1493 cm^{-1} (moyenne), 1476 cm^{-1} (moyenne), 1441 cm^{-1} (moyenne), 1069 cm^{-1} (faible), 1025 cm^{-1} (faible), 912 cm^{-1} (très faible), 905 cm^{-1} (très faible). Spectre ultraviolet (éthanol absolu): ϵ de 23 800 à 237 mμ. Spectre de résonance magnétique nucléaire (solution à 10% dans le tétrachlorure de carbone, référence tétraméthylsilane): absence de protons aliphatiques; triplet à $\delta = 6.9$ p.p.m. (40% du total des protons) et singlet à $\delta = 7.1$ p.p.m. (60% du total des protons). Calculé pour $C_{28}H_{20}O_2$: C, 86.57; H, 5.19; O, 8.24. Trouvé: C, 87.08; H, 5.16; O, 8.31. Poids moléculaire (méthode de Rast): calculé 388.4; trouvé 427.

2.2 Dégradation de la substance p.f. 184–185 °C

Cette substance semble extrêmement résistante aux agents de réduction. Ainsi, le diborane, sous les conditions expérimentales usuelles (16) est sans effet sur le composé que l'on récupère quantitativement au

Can. J. Chem. Downloaded from www.nrcresearchpress.com by 210.87.254.6 on 09/05/12
For personal use only.

terme de la réaction (p.f. du produit brut traité par le diborane, 182–183 °C). De même, l'hydrure de lithium et d'aluminium n'affecte pas le produit que l'on retrouve intact après un reflux de 8 heures, dans l'éther éthylique en présence de $LiAlH_4$. L'oxydation également ne va pas sans difficulté. L'acide nitrique 20% bouillant (reflux de 24 heures) n'attaque pas la molécule, de même que le peroxyde d'hydrogène 30% (reflux de 2 heures). Le permanganate de potassium en milieu alcalin et le bichromate de sodium en milieu acide sont également sans effet. L'inertie de la substance vis-à-vis ces réactifs d'oxydation peut s'expliquer, en partie, par sa grande insolubilité en milieu aqueux. L'oxydation par CrO_3 en milieu acétique a donné, avec difficulté, de faibles rendements (3–5%) en acide benzoïque.

L'action de l'acide iodhydrique ou de l'iodure d'acétyle (17) visant à effectuer l'ouverture d'un éther sur la substance I n'a pas conduit à des espèces purifiables par les techniques usuelles.

3. Préparation des trithioaldéhydes

3.1 β-Trithiobenzaldéhyde

Dans un ballon de 1/2 litre on introduit 23.7 g (0.2 mole) de sulfure de bore et 100 ml de benzène anhydre séché sur la colonne d'oxyde d'aluminium. Le sulfure de bore est maintenu en suspension par une agitation magnétique, et une solution de 29 g (0.27 mole) d'aldéhyde benzoïque dans 100 ml du benzène anhydre est ajoutée goutte à goutte. Pour éviter l'oxidation de l'aldéhyde benzoïque par l'oxygène de l'air et la décomposition du sulfure de bore par l'humidité, le milieu réactionnel est maintenu sous l'atmosphère de l'azote sec. Au cours de l'addition d'aldéhyde, le ballon se réchauffe sensiblement et le benzène se colore légèrement rouge-brun. Quand toute la quantité de réactif est introduite, le mélange est agité et chauffé à reflux du benzène pendant 20 heures.

Le mélange réactionnel est alors filtré à chaud sur l'amiante et refroidi. Les cristaux formés dans le filtrat sont séparés par la filtration et bouillis dans le benzène, en présence de quelques miligrammes d'iode, pendant deux heures pour s'assurer que l'isomère α de l'aldéhyde trithiobenzoïque est transformé complètement en isomère β. Après refroidissement les cristaux sont filtrés et recristallisés dans le benzène. Une nouvelle filtration à froid donne l'aldéhyde β-trithiobenzoïque pur. Cette substance se présente sous forme d'aiguilles blanches très stables et sans odeur. P.f. 225–226 °C. Rdt. 85–90%. Calculé pour $(C_6H_5CHS)_3$: C, 68.81; H, 4.95%; S, 26.24. Trouvé: C, 69.03; H, 5.01; S, 26.10.

3.2 α-Trithiobenzaldéhyde

12 g (0.10 mole) de sulfure de bore est mis en suspension, par une agitation magnétique, dans 100 ml du benzène anhydre. La quantité stoechiométrique de l'aldéhyde benzoïque, préalablement dissout dans 50 ml du benzène anhydre, est ajouté goutte à goutte. Le ballon contenant le mélange réactionel est éclairé par une lampe U.V. (3660 Å) et la solution benzénique portée à ébullition. Après 20 heures environ la réaction est terminée. Le mélange est filtré à chaud sur l'amiante, et le produit formé par refroidissement du filtrat est séparé par une nouvelle filtration. Recristallisé dans le benzène, l'aldéhyde α-trithiobenzoïque précipite sous forme d'aiguilles blanches. P.f. 166–167 °C. Rdt. 90%. Calculé pour $(C_6H_5CHS)_3$: C, 68.81; H, 4.95; S, 26.24. Trouvé: C, 68.92; H, 4.97; S, 26.18.

3.3 Méthyl-3 trithiobenzaldéhyde

En utilisant la même technique que pour la synthèse de l'aldéhyde β-trithiobenzoïque (excepté la transformation catalytique), 12 g (0.10 mole) l'aldéhyde méthyl-3 benzoïque est transformé en trithioaldéhyde correspondant. P.f. 208–210 °C. Rdt. 80–85%. Calculé pour $(CH_3C_6H_4CHS)_3$: S, 23.51. Trouvé: S, 23.72.

3.4 Nitro-4 trithiobenzaldéhyde

15.1 g (0.1 mole) de nitro-4 benzaldéhyde est mis en contact pendant 24 heures avec le sulfure de bore dans les mêmes conditions que l'aldéhyde méthyl-3 benzoïque. Puis le mélange est filtré à chaud et le filtrat refroidi. La précipitation n'apparaît pas. On chasse le benzène sous pression réduite, à température peu élevée. Après évaporation à sec, l'huile jaune restante cristallise; p.f. 50 °C. Le produit est ensuite dissout dans le benzène, décoloré au noir animal, et récupéré par évaporation du solvant; p.f. 52–53 °C. D'après le point de fusion, le produit obtenu est donc l'aldéhyde nitro-4 benzoïque (p.f. 53 °C) inchangé, dont ont retrouve 95% de la quantité mise en expérience.

3.5 L'aldéhyde diméthyl-2,2 trithiopropionique

A une suspension de 7.2 g (0.06 mole) de sulfure de bore dans 30 ml de benzène anhydre, on ajoute sous bonne agitation une solution de 10.0 g (0.16 mole) de l'aldéhyde diméthyl-2,2 propionique dans 20 ml du même solvant. On opère en atmosphère d'azote sec. La réaction s'accompagne d'un léger échauffement de la solution benzénique et dégage une très faible quantité d'acide sulfhydrique. Ce gaz est déterminé sous forme de sulfure de plomb en barbottant le courant d'azote à la sortie de l'appareil dans une solution à 10% d'acétate de plomb.

Après addition de l'aldéhyde suit un léger reflux pendant 18 heures. Le sulfure de plomb ainsi formé pèse 1.42 g. (0.006 mole) après filtration et séchage à poids constant à 100 °C. Le mélange réactionnel est alors filtré et le filtrat concentré par évaporation sous vide. On retrouve ainsi 9.6 g d'une huile rouge foncé qui cristallise lentement. Le solide était extrait par de l'éther de pétrole éb. 30–40 °C et cette solution éthérée passée sur une colonne à chromatographie (50 g d'alumine Woehm neutre, activité 1). L'éther de pétrole élue 8.9 g d'un solide rougeâtre que l'on recristallise dans le même solvant. On trouve ainsi 6.1 g (0.06 mole)

Can. J. Chem. Downloaded from www.nrcresearchpress.com by 210.87.254.6 on 09/05/12
For personal use only.

de fines aiguilles blanches, p.f. 110-112 °C, qui s'avèrent être l'aldéhyde diméthyl-2,2 trithiopropionique. Poids moléculaire par méthode de Rast à 175 °C, 112; par cryoscopie dans le benzène à 10 °C, 285. Calculé pour $C_5H_{10}S$: PM = 102.20; C, 58.76; H, 9.86; S, 31.38. Trouvé: C, 58.56; H, 9.77; S, 31.20.

4. Préparation du sulfure de bore

Une portion d'environ 40 g d'un mélange bien homogène de bore élémentaire 98% (1 mole) finement pulvérisé et de soufre pulvérisé (1.5 mole) est introduite dans une éprouvette en verre épais, 25 mm × 200 mm. L'éprouvette, maintenue inclinée à 45° est purgée par un lent courant d'azote et bouchée par un tampon de laine de verre. Le mélange est alors fondu et chauffé également jusqu'à inflammation de la masse réactionnelle. Le chauffage est ajusté de façon à maintenir la masse au rouge, pendant quelques minutes. Après refroidissement, l'éprouvette est brisée pour libérer le culot de sulfure de bore brut, qui est pulvérisé à l'aide d'un pulvérisateur "Waring Blendor" à l'abri de l'humidité. Suivent trois lavages par le sulfure de carbone anhydre, afin d'enlever le soufre contaminant le sulfure. On obtient ainsi une fine poudre noire extrêmement hygroscopique, qui représente 65–75% de la théorie, le principal facteur d'abaissement du rendement étant la sublimation du sulfure, au cours de sa formation à haute température. Le titre en sulfure de bore du produit de la réaction est déterminé par hydrolyse au moyen de l'eau et détermination du H_2S sous forme de sulfure de plomb, à partir d'une solution à 10% d'acétate de plomb. Au cours d'une expérience typique, un échantillon de 1.00 g de sulfure donne 5.20 g de sulfure de plomb, soit un titre de 85%. L'impureté principale du sulfure est constituée de bore élémentaire (10–12%) isolé en hydrolysant un échantillon de 1.00 g de sulfure par large excès d'eau bouillante. Le résidu à la filtration de cette solution pèse de 0.100 à 0.120 g suivant les échantillons et est identique au bore élémentaire utilisé pour la préparation du sulfure.

REMERCIEMENTS

Les auteurs remercient le "Defence Research Board of Canada" (J. M. L., octroi No. 9530-30) et le Conseil National de Recherches du Canada (S. J.) de leur assistance financière, ainsi que le professeur J. C. Richer, de l'Université de Montréal, qui a bien voulu effectuer les mesures de résonance magnétique nucléaire.

BIBLIOGRAPHIE

1. H. Moissan. Compt. Rend. **115**, 206 (1892).
2. H. Moissan. Ann. Chim. Phys. **6**, 312 (1895).
3. R. Mozingo, D. E. Wolf, S. A. Harris et K. Folkers. J. Am. Chem. Soc. **65**, 1013 (1943).
4. K. T. Serijan, I. A. Goodman et W. J. Yankauskas. Natl. Advisory Comm. Aeron., Tech. Note No. 2557 (1951).
5. J. M. Billy, H. Favre et J. M. Lalancette. Can. J. Chem. **39**, 835 (1961).
6. F. Challenger et B. Rudner. J. Am. Chem. Soc. **73**, 5157 (1951).
7. E. Champaigne. J. Am. Chem. Soc. **66**, 684 (1944).
8. E. Baumann et E. Fromm. Ber. **22**, 2600 (1889).
9. E. Baumann. Ber. **24**, 1419 (1891).
10. M. J. Suyver. Rec. Trav. Chim. **24**, 377 (1905).
11. E. Tiede et M. Thimann. Ber. **59**, 1703 (1926).
12. B. Gauthier. Compt. Rend. **129**, 596 (1899).
13. W. M. Latimer. The oxidation states of the elements. Prentice-Hall. 1952. p. 276.
14. C. Paal. Ber. **18**, 2251 (1885).
15. C. Paal. Ber. **19**, 551 (1886).
16. H. C. Brown et B. C. Subba Rao. J. Am. Chem. Soc. **81**, 6428 (1959).
17. E. L. Gustus et P. G. Stevens. J. Am. Chem. Soc. **55**, 378 (1933).

Can. J. Chem. Downloaded from www.nrcresearchpress.com by 210.87.254.6 on 09/05/12
For personal use only.

Can. J. Chem. Downloaded from www.nrcresearchpress.com by 210.87.254.42 on 09/05/12
For personal use only.

AZOXYCOMPOUNDS

I. THE PHOTOLYSIS OF AZOXYMETHANE[1]

B. G. GOWENLOCK[2]
Division of Pure Chemistry, National Research Council, Ottawa, Canada

Received March 31, 1964

ABSTRACT

A study of the photolysis of azoxymethane has been made. The reaction products include nitrogen, nitrous oxide, methane, and ethane. The ratio N_2:N_2O is independent of temperature and two primary photolytic processes are postulated to account for this fact. On the assumption that methane arises from the reaction $CH_3 + CH_3N_2OCH_3 \rightarrow CH_4 + CH_2N_2OCH_3$, the activation energy of this reaction is 6 ± 2 kcal/mole. Other reactions that take place during the photolysis are discussed.

INTRODUCTION

Azoxymethane and other azoxyalkanes were prepared by Langley, Lythgoe, and Rayner in 1952 (1). A survey of the literature indicates that little attention has been directed to these compounds, the bulk of the published work relating to aromatic azoxyalkanes. By analogy with azoalkanes, it is expected that the primary photolytic (2) and pyrolytic (3) processes will produce two radicals and nitrous oxide. Thus for azoxymethane we expect the reaction [1] to occur.

[1] $$CH_3{-}\underset{\underset{O}{\downarrow}}{N}{=}N{-}CH_3 \xrightarrow{h\nu} CH_3 + N_2O + CH_3.$$

EXPERIMENTAL

Materials

Azoxymethane was prepared by Dr. L. C. Leitch and Mr. N. Kraut by the literature method (1). It was a colorless, mobile liquid with a vapor pressure of about 20 mm at 20 °C. A sample was vaporized and its ultraviolet spectrum determined with a Cary recording spectrophotometer. This spectrum was similar to that given for an ethanol solution (1) and the wavelength of maximum absorption was 212–213 mμ (217 mμ in ethanol (1)). Reference samples of other materials for mass spectrometry and gas chromatography were provided by Dr. F. P. Lossing.

Apparatus

A conventional photolysis apparatus was used. The light source was a Hanovia S-500 medium pressure mercury arc operated on a regulated supply. It was used without filter or lens in order to allow sufficient products to be accumulated in a run of one hour's duration. The beam of light from the lamp passed through two copper tubes, which connected the lamp to the reaction vessel (5 cm diameter and 15 cm length). A piece of thick cardboard could be inserted between the two tubes in order to shut off the arc from the reaction vessel. The reaction vessel could be heated electrically and was mounted in a hot box. The reaction system was isolated from the reactant reservoir gas analysis apparatus and main vacuum line by greaseless mercury cut-offs. Pressures of reactants were measured by means of a spiral gauge, mounted within the hot box, and used as a null instrument in conjunction with a mercury U-tube manometer.

Procedure and Analysis

Thoroughly degassed azoxymethane was admitted to the reaction vessel and the pressure measured. The light beam was allowed to enter the reaction vessel and the run allowed to proceed for 1 h. The products of the run were trapped out at liquid nitrogen temperatures and the remaining noncondensable gases transferred to a combined Toepler/gas burette. After the quantity of the gas was measured, the sample was transferred to a mass spectrometer sampling tube. On occasion a portion was also transferred to a

[1]*Issued as N.R.C. No. 7984.*
[2]*Visiting Scientist, N.R.C., 1963. Permanent address: Department of Chemistry, University of Birmingham, Birmingham, England.*

crusher tube for gas chromatographic analysis using a zeolite column. Further fractions were taken into the Toepler/gas burette, measured, and analyzed. The temperatures and analytical techniques employed were: −160° (mass spectrometry), −131°, −78°, and room temperature (gas–liquid chromatography). All gas–liquid chromatographic analyses were carried out on a Perkin–Elmer fractometer, using a 1 m column of Carbowax 1500 on powdered teflon, helium carrier gas, 50 °C, flow rate 150 cc/min.

RESULTS AND DISCUSSION

The most volatile reaction products were nitrogen, nitrous oxide, methane, and ethane. It was shown by both mass spectrometry and gas chromatography that hydrogen, oxygen, and nitric oxide were absent from the reaction products. The azoxymethane concentration was not varied significantly; the temperature was varied from 27° to 121°, and the ratio N_2:N_2O remained constant at 0.20 ± 0.02 (8 runs). This constancy suggests that the nitrogen is produced by a primary process and the simplest reaction that can be written to account for this is:

[2] $$CH_3{-}\underset{\underset{O}{\downarrow}}{N}{=}N{-}CH_3 \xrightarrow{h\nu} CH_3 + N_2 + OCH_3.$$

Reaction [2] is presumed to take place simultaneously with reaction [1]. Further support for the occurrence of nitrogen elimination from azoxymethane is given by pyrolyzing azoxymethane on a heated quartz surface ($\simeq$ 600 °C) in the inlet of a mass spectrometer, where the primary decomposition process [3] takes place,

[3] $$CH_3{-}\underset{\underset{O}{\downarrow}}{N}{=}N{-}CH_3 \rightarrow CH_3OCH_3 + N_2,$$

and any production of methyl radicals is consequent upon decomposition of the dimethyl ether. (The author is indebted to Dr. F. P. Lossing for this observation.) In addition, pyrolysis of a sample of azoxymethane at about 340 °C for 3.5 h produced nitrogen and nitrous oxide in the ratio 0.92, again indicating the importance of nitrogen production. These observations were contrary to our initial expectation and further investigation is underway. We are unaware of any evidence in the literature for thermal or photolytic production of nitrogen from azoxy compounds, and note that the reaction [2] is more favorable thermochemically than reaction [1] by about 50 kcal/mole (4).

Methane and ethane are prominent reaction products and it is likely that these will be produced from reactions [4] and [5] respectively.

[4] $$CH_3 + CH_3{-}\underset{\underset{O}{\downarrow}}{N}{=}N{-}CH_3 \rightarrow CH_4 + CH_2{-}\underset{\underset{O}{\downarrow}}{N}{=}N{-}CH_3 \text{ (or } CH_3{-}\underset{\underset{O}{\downarrow}}{N}{=}N{-}CH_2\text{)}.$$

[5] $$CH_3 + CH_3 \rightarrow C_2H_6.$$

Consequently, preliminary values have been obtained for the kinetic parameters of reaction [4], $E_4 = 6\pm2$ kcal/mole, $P_4 \simeq 10^{-2}$. It is to be emphasized that these are only preliminary values; it is hoped to obtain a greater number of points over a wider range of experimental conditions. These values compare favorably with those obtained (2) for the comparable reaction [6], $E_6 = 7.6\pm0.2$ kcal/mole, $P_6 \simeq 10^{-3}$.

[6] $$CH_3 + CH_3N{=}NCH_3 \rightarrow CH_4 + CH_2N{=}NCH_3.$$

The ratio $(\frac{1}{2}CH_4 + C_2H_6)/N_2O$ was less than unity and decreased smoothly from about 0.74 at 27° to 0.39 at 121°. Admittedly, this approach to the product balance ignores the contribution of reaction [2], but it makes possible a comparison with the

Can. J. Chem. Downloaded from www.nrcresearchpress.com by 210.87.254.42 on 09/05/12
For personal use only.

azomethane results (2) where the corresponding ratio fell from 0.85 at room temperature to 0.28 at 128°. It was therefore expected that methyl radicals would add to azoxymethane in similar fashion to the azomethane reactions, i.e., [7] and [8] and (or) [9] and [10].

[7] $$CH_3 + CH_3{-}\underset{\underset{O}{\downarrow}}{N}{=}N{-}CH_3 \rightarrow CH_3{-}\underset{\underset{CH_3O}{|}}{N}{-}N{-}CH_3.$$

[8] $$CH_3 + CH_3{-}\underset{\underset{CH_3O}{|}}{N}{-}N{-}CH_3 \rightarrow CH_3{-}\underset{\underset{CH_3O}{|}}{N}{-}N{-}(CH_3)_2.$$

[9] $$CH_3 + CH_3{-}\underset{\underset{O}{\downarrow}}{N}{=}N{-}CH_3 \rightarrow CH_3{-}\underset{\underset{O}{|}}{N}{-}N{-}(CH_3)_2.$$

[10] $$CH_3 + CH_3{-}\underset{\underset{O}{|}}{N}{-}N{-}(CH_3)_2 \rightarrow CH_3{-}\underset{\underset{CH_3O}{|}}{N}{-}N{-}(CH_3)_2.$$

Mass spectrometric investigations of the fractions resolved from g.l.c. analysis of the less volatile reaction products gave no peaks above 80 implying the absence of trimethyl methoxyhydrazine. It is possible that trimethylhydroxylamine (cracking pattern due to Bromberger and Phillips (5)) is formed, and also an azocompound $CH_3{-}N{=}N{-}OCH_3$. Discussion of routes to such products is postponed pending further more detailed investigation of the photolysis, and of reaction products from reaction of methyl radicals with azoxymethane. Methyl alcohol and trace quantities of dimethyl ether were identified from g.l.c. analysis.

A referee has suggested that nitrogen elimination could proceed by reaction [11],

[11] $$CH_3{-}\underset{\underset{O}{\downarrow}}{N}{=}N{-}CH_3 \xrightarrow{h\nu} O + CH_3{-}N{=}N{-}CH_3,$$

followed by photolysis of the azomethane to give nitrogen and hydrocarbon products. This possibility cannot be eliminated completely, but there is some evidence to suggest that it is unlikely. At least some tetramethylhydrazine would be expected as a reaction product, and the absence of peaks above 80 in the mass spectrum of the less volatile products is difficult to reconcile with the presence of azomethane implied by reaction [11]. Reaction [2] is more favorable than reaction [11] by about 70 kcal/mole. If reaction [11] does occur then the absence of oxygen and nitric oxide in the reaction products can be regarded as evidence for the absence of reactions [12] and [13] (because of unfavorable energy requirements, E_{12} and E_{13} being of the order 20 kcal/mole (6)),

[12] $$O + N_2O \rightarrow 2NO$$

[13] $$O + N_2O \rightarrow N_2 + O_2,$$

and the absence of oxygen atom recombination reactions. Photolysis of azoxymethane – nitric oxide mixtures and analysis for nitrogen dioxide reaction product may answer this problem, provided that there is no methyl radical catalyzed disproportionation of the nitric oxide under these reaction conditions. Further evidence against reaction [11] is to be found in the methyl alcohol reaction product of which the methoxy radical is the obvious precursor.

ACKNOWLEDGMENTS

The author is indebted to the National Research Council for the award of the post of visiting scientist during the tenure of which this work was carried out. He wishes to

Can. J. Chem. Downloaded from www.nrcresearchpress.com by 210.87.254.42 on 09/05/12
For personal use only.

thank Mr. R. J. Pilon for mass spectrometric analyses, and Drs. R. A. Back, K. O. Kutschke, and F. P. Lossing for many helpful discussions.

REFERENCES

1. B. W. Langley, B. Lythgoe, and L. S. Rayner. J. Chem. Soc. 4191 (1952).
2. M. H. Jones and E. W. R. Steacie. J. Chem. Phys. **21**, 1018 (1953).
3. B. G. Gowenlock, P. Pritchard Jones, and D. R. Snelling. Can. J. Chem. **41**, 1911 (1963).
4. P. Gray and J. C. J. Thynne. Nature, **191**, 1357 (1961).
5. B. Bromberger and L. Phillips. J. Chem. Soc. 5302 (1961).
6. F. Kaufman. Progress in reaction kinetics. Vol. 1. Pergamon Press, Oxford. 1961. p. 1.

Can. J. Chem. Downloaded from www.nrcresearchpress.com by 210.87.254.42 on 09/05/12
For personal use only.

Can. J. Chem. Downloaded from www.nrcresearchpress.com by 210.87.254.40 on 09/05/12
For personal use only.

FURTHER EVIDENCE FOR THE DIENONE-IMINE INTERMEDIATE IN THE FISCHER INDOLE SYNTHESIS

AN UNCATALYZED FISCHER REACTION UNDER MILD CONDITIONS[1]

F. P. ROBINSON[2] AND R. K. BROWN
Department of Chemistry, University of Alberta, Edmonton, Alberta

Received March 9, 1964

ABSTRACT

Evidence has been presented for the transient formation of a dienone-imine intermediate in the Fischer indole synthesis analogous to the dienone intermediate found in the Claisen rearrangement. The isolation of methylamine hydrochloride, 8-chloro-1,2,3,4-tetrahydrocarbazole, and 5-amino-6-chloro-9-methyl-1,2,3,4-tetrahydrocarbazole from the room temperature, uncatalyzed condensation between cyclohexanone and N′-methyl-2,6-dichlorophenylhydrazine under enamine synthesis conditions can be rationalized only on the assumption of the occurrence of a dienone-imine intermediate. An example of a facile, uncatalyzed Fischer cyclization at room temperature has been described.

INTRODUCTION

Carlin and Fisher (1) have pointed out the close analogy between the mechanism of the Claisen rearrangement (2, 3) and the Robinson mechanism (4) for the Fischer indole synthesis.* A discussion of the Fischer indole synthesis with particular reference to the mechanistic aspect has appeared recently (5). Although the dienone intermediate (I, R = CH_3) has been isolated as the Diels–Alder adduct (6) and has actually been prepared and shown to be a true intermediate in the Claisen rearrangement (7, 8), isolation of the analogous dienone-imine (II, R = CH_3) from the Fischer reaction has not yet been achieved.

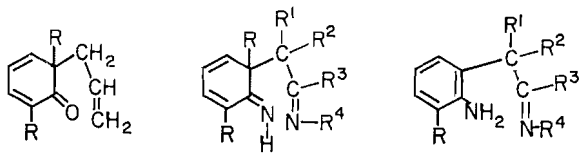

I II III

There are, however, several instances in which a compound of structure III (R = H) has actually been obtained from the Fischer cyclization. Such a compound (III) could quite logically arise from a dienone-imine precursor (II, R = R^4 = H) in which aromatization occurred very rapidly and unavoidably by a tautomeric shift of the hydrogen atom. The isolation of the sparingly soluble hydrochloride of the compound α-amino-β-(*o*-aminophenyl)-γ-butyrolactone (IV) from the cyclization of α-keto-γ-butyrolactone phenylhydrazone (9, 10) and of 3-acetylamino-2-(*o*-aminophenyl)-butene-2 (V) from the treatment of 2-(N,N′-diacetyl-β-phenylhydrazino)-butene-2 (VIII) with hot aqueous potassium hydroxide (11) are specific cases which illustrate this point.

[1]*Taken from the thesis of F. P. Robinson submitted to the Faculty of Graduate Studies of the University of Alberta in partial fulfillment of the requirements for the degree of Doctor of Philosophy.*
[2]*Present address: Department of Chemistry, University of Victoria, Victoria, B.C.*
**A. A. Arbuzov and Y. P. Kitaev, J. Gen. Chem. U.S.S.R. 27, 2388 (1957), have stated that both the Claisen rearrangement and the Fischer indole synthesis are specific cases of the general intramolecular rearrangement in a polarized 1,6-conjugated system.*

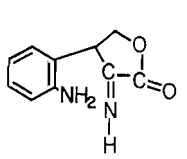

IV

V

There have been reported, also, a number of products obtained from the reaction of phenylhydrazones under Fischer cyclizing conditions which are readily explained only on the basis of a dienone-imine intermediate (II). Examples of these are the isolation of 5,7-dihaloindoles resulting from the halogen migration and interchange during the reaction of 2,6-dihalophenylhydrazones in the presence of zinc halides (1, 12, 13), and of both 2-phenyl-3*a*, 5-dimethyl-3*a*,4,7,7*a*-tetrahydro[3H]pseudoindolone-4 (VI) and the methyl migration product 4,7-dimethyl-3-phenylindole (VII) from the reaction of acetophenone 2,6-dimethylphenylhydrazone in the presence of zinc chloride (14) (equation *a*).

(a)

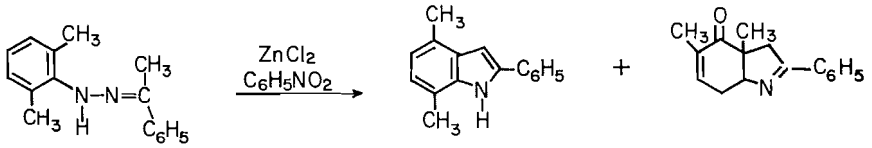

VII VI

An attempt was made by Carlin *et al.* (15) to trap the dienone-imine "intermediate" in the zinc chloride catalyzed reaction of ethyl pyruvate 2,6-dimethylphenylhydrazone as the Diels–Alder adduct with maleic anhydride as had been done by Conroy and Firestone for the Claisen rearrangement of allyl 2,6-dimethylphenyl ether (6). However, no product was obtained indicative of such an adduct, a result considered to be due to the much more rapid conversion of the dienone-imine intermediate into the indole (15). To our knowledge, no other attempt to secure the dienone-imine intermediate has been reported.

This paper describes the isolation from the Fischer indole synthesis of certain products, the formation of which can be rationalized only on the basis of a dienone-imine intermediate.

RESULTS AND DISCUSSION

The isolation from the acid-catalyzed reaction between methyl ethyl ketone phenylhydrazone and acetic anhydride (11) of 2-(N,N′-diacetyl-β-phenylhydrazino)-butene-2, (VIII), which is the diacetylated enamine considered to be the first stage of the Robinson mechanism for the Fischer indole synthesis (4), has suggested the preparation of enamines as starting materials for indole formation. Since such an enamine is one step along in the accepted scheme for Fischer indole synthesis, subsequent conversion of this enamine to an indole might be relatively easily accomplished. Suvorov (11) has shown that acid catalysis is not necessary, although probably helpful, for the second stage of the Fischer indole synthesis; that of conversion of the enamine (VIII) to (IX), the compound analogous to the product of ortho benzidine rearrangement. He found that (IX) was

Can. J. Chem. Downloaded from www.nrcresearchpress.com by 210.87.254.40 on 09/05/12
For personal use only.

Can. J. Chem. Downloaded from www.nrcresearchpress.com by 210.87.254.40 on 09/05/12
For personal use only.

(b) 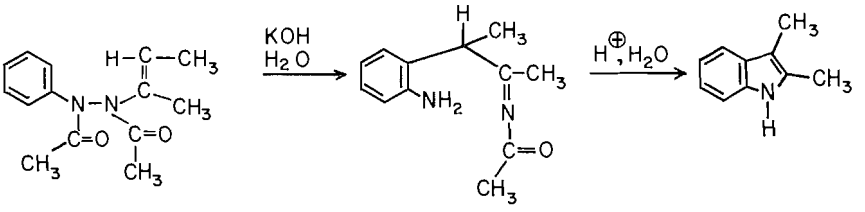

VIII IX

obtained by heating the intermediate diacetyl compound (VIII) in refluxing aqueous sodium hydroxide (equation *b*). Thus, if a suitable enamine were prepared, it might be readily converted to the indole merely by exposure to moderate heat. If, in addition, the 2 and 6 positions of the phenyl group are blocked by substituents which would prevent rapid aromatization (II → III, R = H), it might thus be possible to form, and either retain or trap, the dienone-imine under mild conditions (equation *c*). For the present

(c) 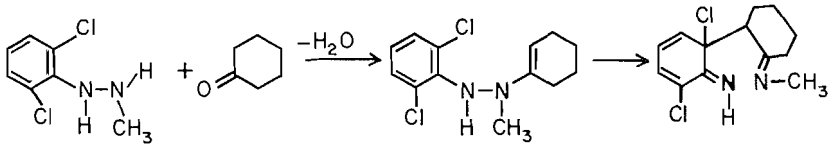

X XI

work, the 2,6-dichlorophenylhydrazine rather than the 2,6-dimethylphenylhydrazine was chosen in view of the latter's well-known instability in air (14). To ensure enamine formation, this hydrazine was converted to the N′-methyl derivative (X).

Formylation of 2,6-dichlorophenylhydrazine (1) with formamide in acetic acid (16) rather than with 50% formic acid (17) gave a good yield of N′-formyl-2,6-dichlorophenylhydrazine which, even with excess methyl sulphate, gave only the monomethyl derivative, N′-formyl-N′-methyl-2,6-dichlorophenylhydrazine (XII). Elemental analysis and a nuclear magnetic resonance spectrum agreed with this structure. Additional proof that the methyl group was on the nitrogen atom remote from the phenyl substituent was obtained by reduction of the formylated hydrazine with Raney nickel and hydrazine (18) to 2,6-dichloroaniline (equation *d*).

(d) 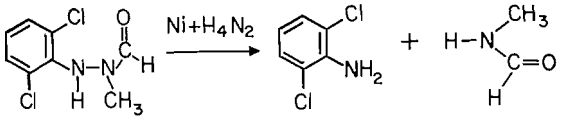

XII

When N′-methyl-2,6-dichlorophenylhydrazine was condensed with cyclohexanone under conditions advocated for enamine preparation (19), using a Dean–Stark apparatus (20) to collect the water removed azeotropically by boiling benzene, a precipitate of methylamine hydrochloride appeared. From the residual dark oil obtained after removal

Can. J. Chem. Downloaded from www.nrcresearchpress.com by 210.87.254.40 on 09/05/12
For personal use only.

of the hydrochloride and the benzene, no pure compound could be isolated. However, the formation of methylamine hydrochloride indicated that a reaction had occurred, in all likelihood forming an indole, since the β-nitrogen atom in hydrazones is eliminated as ammonia during the Fischer cyclization to indoles (21, 32). When the enamine formation was repeated, but this time, to avoid decomposition of products, with the reaction temperature maintained at about 20° by removal of the benzene and water under vacuum with a rotary evaporator, methylamine hydrochloride was again obtained (~15% yield). The residual yellow oil, left after removal of the precipitate and the solvent, when passed through a column of neutral alumina with Skellysolve B as eluant, afforded a 14% yield of a compound which proved to be identical in all respects with an authentic sample of 8-chloro-1,2,3,4-tetrahydrocarbazole (12). Further elution with a 1:1 mixture of Skellysolve B and benzene gave a compound whose elemental analysis and n.m.r. spectrum agreed with the structure 5-amino-6-chloro-9-methyl-1,2,3,4-tetrahydrocarbazole (XVI).

An authentic sample of this compound was prepared from the mixture obtained by Plant and Rosser's (22) cyclization of cyclohexanone 4-chloro-3-nitrophenylhydrazone. Of the two possible products of this reaction, 6-chloro-5-nitro-1,2,3,4-tetrahydrocarbazole and 6-chloro-7-nitro-1,2,3,4-tetrahydrocarbazole (equation *e*), one was later identified (23) as the 6-chloro-5-nitro-1,2,3,4-tetrahydrocarbazole (XIII) by its reduction with tin

(e)

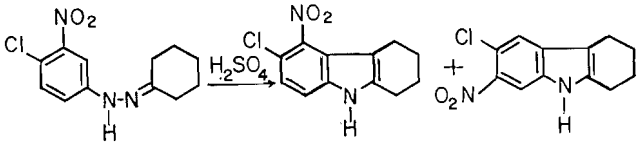

XIII XIV

and hydrochloric acid to the known 5-amino-1,2,3,4,4*a*,9*a*-hexahydrocarbazole. The other isomer, (XIV), must then be the 6-chloro-7-nitrotetrahydrocarbazole.

Compound (XIII) was first converted to the N-methyl derivative (XV) and then reduced with Raney nickel and hydrazine (24) to 5-amino-6-chloro-9-methyl-1,2,3,4-tetrahydrocarbazole (XVI) (equation *f*).

(f)

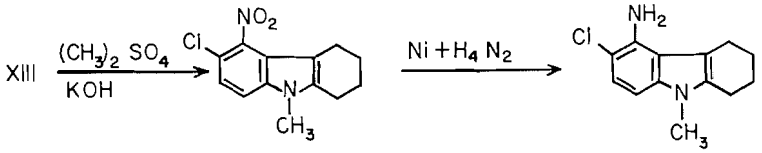

XV XVI

The overall reaction between cyclohexanone and N′-methyl-2,6-dichlorophenylhydrazine can be represented by equation *g*. No enamine corresponding to structure (XI) was obtained.

In our opinion the isolation of both (XVI) and (XVII) is further evidence in favor of the dienone-imine intermediate. Such an intermediate readily explains the formation of (XVI) as shown by the following scheme (equation *h*).

Can. J. Chem. Downloaded from www.nrcresearchpress.com by 210.87.254.40 on 09/05/12
For personal use only.

(g)

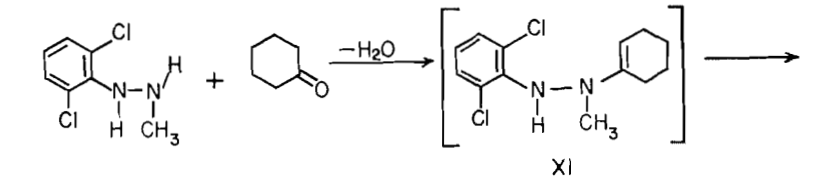

XI

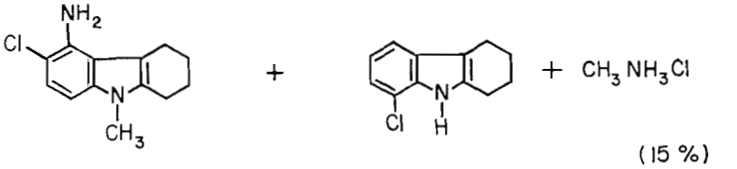

XVI (21 %) XVII (14 %) (15 %)

(h)

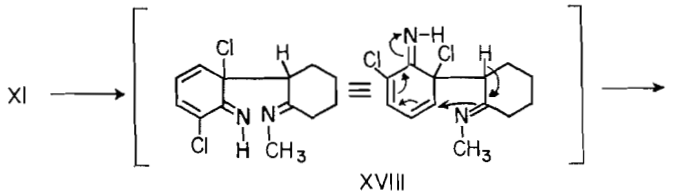

XVIII

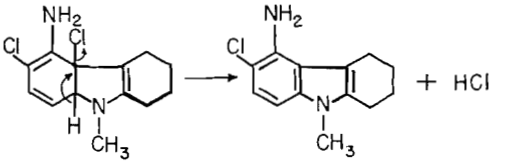

XVI

The mechanism of the formation of compound (XVI) is analogous to that proposed (14) for the formation of 2-phenyl-3*a*,5-dimethyl-3*a*,4,7,7*a*-tetrahydro[3H]pseudoindolone (VI) from the zinc chloride catalyzed cyclization of acetophenone 2,6-dimethylphenylhydrazone.

The formation of the product (XVII) can also be explained on the basis of the dienone-imine intermediate (XVIII) if one postulates that a readily oxidizable substance in the reaction mixture permits the reductive removal of the allylic halogen atom in the dienone-imine intermediate via the scheme shown in equation *i*. That the presence of oxidizable

(i)

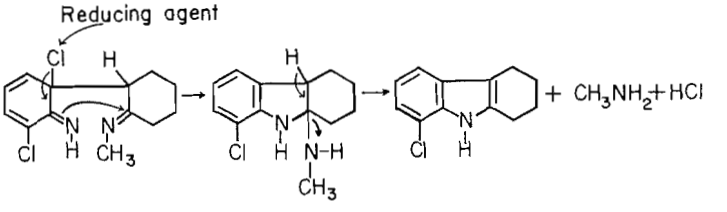

substances does promote the reductive removal of halogen, most likely at the reactive dienone-imine stage, has been supported by the isolation of much 2-allyl-6-chlorophenol during the thermal rearrangement of allyl 2,6-dichlorophenyl ether, particularly in a solvent (e.g. decalin) which is readily oxidizable (25). The isolation of 7-chloroindoles from the stannous chloride catalyzed cyclization of 2,6-dichlorophenylhydrazones (12) can be considered as another example of this reductive removal of allylic halogen at the dienone-imine stage.

The failure as yet to obtain the desired enamine (XI) might be due to the presence of the N′-methyl group which could facilitate cleavage of the N—N bond with subsequent formation of the dienone-imine (XVIII) which then rapidly decomposes. It is known that α-N-methylphenylhydrazones are very readily converted to 1-methylindoles (26, 27).

To our knowledge, this is the first example of a room temperature, non-catalyzed Fischer indole synthesis. The mild conditions required and the much cleaner reaction obtained might now permit isolation of products which under the usual more stringent conditions end up as tars. The surprising ease of the conversion of the enamine (XI) to the dienone-imine and then to indole products supports Suvorov's suggestion that this step need not be acid-catalyzed (11). It might now be possible to obtain, under these modified conditions, an intermediate analogous to compound II (R = CH_3).

We are continuing work on these interesting aspects of the reaction.

EXPERIMENTAL

Preparation of Phenylhydrazines

N′-Formyl-2,6-dichlorophenylhydrazine

Formylation of 2,6-dichlorophenylhydrazine was carried out by the following modification of the method described by Baker *et al.* (16). The use of 50% formic acid (17) proved to be less satisfactory in our experiments.

To a solution of 33.6 g (0.19 mole) of 2,6-dichlorophenylhydrazine (1) in 150 ml of glacial acetic acid was added 7.6 ml (0.19 mole) of formamide in a dropwise fashion. The resulting solution was stirred at room temperature for 1 h during which time the solution thickened because of the formation of a colorless precipitate. The thick slurry was then diluted with 150 ml of water and the solid collected. Crystallization from ethanol gave 29.6 g (76%) of pure product melting at 160–161°. Calc. for $C_7H_6N_2Cl_2O$: C, 40.99; H, 2.95; N, 13.66; Cl, 34.58. Found: C, 41.09; H, 3.10; N, 13.84; Cl, 34.72.

N′-Methyl-N′-formyl-2,6-dichlorophenylhydrazine

Methylation was accomplished by the following modification of a published procedure (17).

To a solution of 41 g (0.20 mole) of N′-formyl-2,6-dichlorophenylhydrazine in 200 ml of dimethylsulphoxide both 21.4 ml (0.22 mole) of dimethylsulphate and a solution of 8.8 g (0.22 mole) of sodium hydroxide in 20 ml of water were added simultaneously and dropwise. The reaction mixture was stirred for 2 h and then diluted with 150 ml of water. The oil which separated solidified on cooling. This oily solid was collected and crystallized from Skellysolve B, yielding 27.6 g (63%) of N′-formyl-N′-methyl-2,6-dichlorophenylhydrazine, m.p. 73–75°. Calc. for $C_8H_8N_2Cl_2O$: C, 43.86, H, 3.68, N, 12.79; Cl, 32.37. Found: C, 43.57; H, 3.64; N, 12.17; Cl, 32.54. That the methyl group was attached to the N′-nitrogen atom was shown by Raney nickel – hydrazine reduction (18) of the compound and isolation of the known 2,6-dichloroaniline. The other product, N-methylformanide was not isolated. The n.m.r. spectrum of N′-formyl-N′-methyl-2,6-dichlorophenylhydrazine showed a sharp signal for the methyl group at 7.1 τ and also agreed with the structure assigned.

N-Methyl-2,6-dichlorophenylhydrazine Hydrochloride

The following procedure is a modification of that described by Neber *et al.* (17).

A solution of 43.8 g (0.20 mole) of N′-formyl-N′-methyl-2,6-dichlorophenylhydrazine, 80 ml of concentrated hydrochloric acid, and 60 ml of ethanol was refluxed for 6 h. The solution was cooled, and poured into ice water whereupon an oil separated. An ether extract of this oil was dried ($MgSO_4$) and after removal of the drying agent was treated with anhydrous hydrogen chloride gas until precipitation of the hydrochloride of N′-methyl-2,6-dichlorophenylhydrazine was complete. Crystallization from ethanol gave 30.5 g (67%) of pure N′-methyl-2,6-dichlorophenylhydrazine hydrochloride, melting at 181–182°. Calc. for $C_7H_8N_2Cl_3$: C, 36.95; H, 3.99; N, 12.31; Cl, 46.75. Found: C, 36.84; H, 3.89; N, 12.36; Cl, 46.61. The infrared spectrum

Can. J. Chem. Downloaded from www.nrcresearchpress.com by 210.87.254.40 on 09/05/12
For personal use only.

of this compound showed the following bands: 3220 cm^{-1} (NH), a broad peak centered at 2930 cm^{-1} (CH_3), 2690 cm^{-1} (NH_2^+) (28), and a peak at 1560 cm^{-1} (aromatic unsaturation). The n.m.r. spectrum in D_2O showed signals at 7.0 τ (singlet, N—CH_3), 5.3 τ (singlet for DOH), and an AB_2 pattern at 2.3 to 2.9 τ. The hydrazine could be preserved undecomposed if kept as the hydrochloride.

4-Chloro-3-nitrophenylhydrazine

The 4-chloro-3-nitroaniline (29) was converted to 4-chloro-3-nitrophenylhydrazine by the procedure of Plant and Rosser (22). However, after the solution had been left to stand overnight, the precipitated hydrazine hydrochloride was separated by filtration (rather than heated again as these authors advocated) and dissolved in 200 ml of boiling water. The resulting solution was then filtered free of insoluble material and the filtrate treated with saturated aqueous sodium acetate to precipitate the hydrazine. This product was *crystallized immediately from Skellysolve B.* If the crystallization was not done at once, decomposition resulted. Yield of 4-chloro-3-nitrophenylhydrazine was 45.3%, m.p. 108–109° (reported m.p. 109° (22)).

Preparation and Cyclization of Phenylhydrazones

Cyclohexanone o-Chlorophenylhydrazone

This compound was prepared in 91% yield according to published directions (12). This compound decomposed readily, hence had to be used soon after its preparation.

Cyclization was accomplished preferably by the boron trifluoride – etherate procedure described by Snyder and Smith (30), affording an 82% yield of 8-chloro-1,2,3,4-tetrahydrocarbazole, m.p. 55–56° (from benzene – Skellysolve B). Reported m.p. 56° (12). The product decomposed rapidly at room temperature.

Cyclohexanone 4-Chloro-3-nitrophenylhydrazone

This compound was prepared in 84% yield according to the procedure of Plant and Rosser (22) and cyclized with boron trifluoride – etherate (30). The solid obtained was repeatedly crystallized from ethanol yielding 6-chloro-7-nitro-1,2,3,4-tetrahydrocarbazole (44%) melting at 186–187°, reported m.p. 184° (22, 23). Removal of the ethanol from the filtrate gave a yellow solid which when crystallized from benzene gave 6-chloro-5-nitro-1,2,3,4-tetrahydrocarbazole (11%) having the reported melting point of 162–163° (22, 23).

6-Chloro-5-nitro-9-methyl-1,2,3,4-tetrahydrocarbazole

6-Chloro-5-nitro-1,2,3,4-tetrahydrocarbazole was converted to 6-chloro-5-nitro-9-methyl-1,2,3,4-tetrahydrocarbazole by use of methyl sulphate according to published procedure (31). Yield of pure material, 61%, m.p. 154–155° (from ethanol). Calc. for $C_{13}H_{13}N_2O_2Cl$: C, 58.98; H, 4.95; N, 10.59; Cl, 13.40. Found: C, 59.09; H, 5.19; N, 10.50; Cl, 13.21.

That the nitrogen atom at position 9 had been methylated was shown by the disappearance of the NH signal at 4.94 τ found in the n.m.r. spectrum of the starting material, and the appearance of the N—CH_3 signal at 6.65 τ in the spectrum of the product.

5-Amino-6-Chloro-9-methyl-1,2,3,4-tetrahydrocarbazole

The nitro group of 6-chloro-5-nitro-9-methyl-1,2,3,4-tetrahydrocarbazole was reduced with Raney nickel and hydrazine (24). The solid amine obtained after removal of the nickel and the solvent was crystallized from ethanol and yielded pure material (79%) melting at 90–91°. Calc. for $C_{13}H_{15}N_2Cl$: C, 66.51; H, 6.44; N, 11.94; Cl, 15.11. Found: C, 66.64; H, 6.57; N, 12.18; Cl, 14.98. The n.m.r. spectrum in $CDCl_3$ showed the following signals: an aromatic AB pattern at 3.0–3.8 τ, N—H at 5.9 τ, N—CH_3 at 6.75 τ, methylene at 7.24, 7.58, and 8.30 τ.

Treatment of the amine in a small amount of benzene with a slight excess of acetic anhydride heated on the steam bath for 10 min afforded colorless crystals (from ethanol) of the N-acetyl derivative, m.p. 245°. Calc. for $C_{15}H_{17}N_2ClO$: C, 65.09; H, 6.18; N, 10.11; Cl, 12.81. Found: C, 65.24; H, 5.96; N, 10.29; Cl, 13.09.

Condensation of Cyclohexanone with N'-Methyl-2,6-dichlorophenylhydrazine

A quantity (6.84 g, 0.03 mole) of N'-methyl-2,6-dichlorophenylhydrazine hydrochloride was dissolved in water. The resulting solution was basified with dilute sodium hydroxide and the oil which separated was extracted with two 25 ml portions of ether. The combined extracts were dried ($MgSO_4$) and freed from ether with a rotary evaporator. To the residue left in the evaporator was added 50 ml of benzene followed by 2.94 g (0.03 mole) of cyclohexanone and the resulting solution slowly reduced to half its original volume in the rotary evaporator (bath temperature ~20°). A colorless precipitate was removed by filtration and when crystallized from ethanol it melted at 222–225° (0.30 g, 14.8%). This precipitate was quite water soluble. Its aqueous solution gave an instantaneous precipitate with silver nitrate. The aqueous solution of this colorless precipitate, when made alkaline with sodium hydroxide, produced an ammoniacal odor. Mixed melting point, and n.m.r. spectrum showed it to be identical with methylamine hydrochloride.

The rest of the benzene solution, after removal of the methylamine hydrochloride, was freed from benzene and gave a yellow oil. By chromatography on neutral alumina with Skellysolve B as eluant, 0.86 g (14.0%) of a pale yellow solid melting at 55–56° was obtained. This compound was shown to be identical with 8-chloro-1,2,3,4-tetrahydrocarbazole by mixed melting point and by infrared and n.m.r. spectra comparison with an

Can. J. Chem. Downloaded from www.nrcresearchpress.com by 210.87.254.40 on 09/05/12
For personal use only.

authentic sample (12). The compound was too unstable to be sent away for elemental analysis. Its infrared spectrum showed bonded N—H at 3100 cm^{-1}. The n.m.r. spectrum showed methylene signals at 7.29 τ and 8.20 τ and an N—H signal at 1.39 τ.

Further elution of the remaining material on the column with a 1:1 mixture of Skellysolve B and benzene yielded a tan, crystalline solid, m.p. 87–90°. Crystallization from alcohol gave 1.48 g (21%) of a colorless material, m.p. 90–91°. Calc. for $C_{13}H_{15}N_2Cl$: C, 66.51; H, 6.44; N, 11.94; Cl, 15.11. Found: C, 66.59; H, 6.49; N, 11.75; Cl, 15.37. The n.m.r. spectrum in $CDCl_3$ showed an aromatic AB pattern in the region 3.0 to 3.8 τ, an $-NH_2$ signal at 5.9 τ, an N—CH_3 signal at 6.75 τ, and methylene signals at 7.24, 7.58, and 8.30 τ. The above data agreed with the structure 5-amino-6-chloro-9-methyl-1,2,3,4-tetrahydrocarbazole. This compound showed properties identical with those of an authentic sample of 5-amino-6-chloro-9-methyl-1,2,3,4-tetrahydrocarbazole prepared by another route described above.

ACKNOWLEDGMENT

We express our gratitude to the National Research Council of Canada for their generous financial support during this work.

REFERENCES

1. R. B. Carlin and E. E. Fisher. J. Am. Chem. Soc. **70**, 3421 (1948).
2. D. S. Tarbell. Organic reactions. Vol. 2. John Wiley and Sons, Inc., New York. 1944. p. 16.
3. D. J. Cram. Steric effects in organic chemistry. *Edited by* M. S. Newman. John Wiley and Sons, Inc., New York. 1956. p. 295.
4. G. M. Robinson and R. Robinson. J. Chem. Soc. 639 (1918).
5. B. Robinson. Chem. Rev. **63**, 373 (1963).
6. H. Conroy and R. A. Firestone. J. Am. Chem. Soc. **78**, 2290 (1956).
7. D. Y. Curtin and H. W. Johnson, Jr. J. Am. Chem. Soc. **78**, 2611 (1956).
8. D. Y. Curtin and R. J. Crawford. J. Am. Chem. Soc. **79**, 3156 (1957).
9. H. Plieninger. Ber. **83**, 273 (1950).
10. H. Plieninger and I. Nogradi. Ber. **88**, 1964 (1955).
11. N. N. Suvorov, N. P. Sorokina, and Yu. N. Sheinker. J. Gen. Chem. USSR Eng. Transl. **28**, 1058 (1958).
12. R. B. Carlin, J. G. Wallace, and E. E. Fisher. J. Am. Chem. Soc. **74**, 990 (1952).
13. R. B. Carlin and G. W. Larson. J. Am. Chem. Soc. **79**, 934 (1957).
14. R. B. Carlin and D. P. Carlson. J. Am. Chem. Soc. **81**, 4673 (1959).
15. R. B. Carlin, W. O. Henley, Jr., and D. P. Carlson. J. Am. Chem. Soc. **79**, 5712 (1957).
16. W. Baker, W. D. Ollis, and J. D. Poole. J. Chem. Soc. 3389 (1950).
17. P. W. Neber, G. Knoller, K. Herbst, and A. Trissler. Ann. **471**, 113 (1929).
18. F. P. Robinson and R. K. Brown. Can. J. Chem. **39**, 1171 (1961).
19. F. W. Heyl and M. E. Herr. J. Am. Chem. Soc. **75**, 1918 (1953).
20. E. W. Dean and D. D. Stark. Ind. Eng. Chem. **12**, 486 (1920).
21. C. F. Allen and C. V. Wilson. J. Am. Chem. Soc. **65**, 611 (1943).
22. S. G. P. Plant and R. J. Rosser. J. Chem. Soc. 2454 (1928).
23. R. C. G. Moggridge and S. G. P. Plant. J. Chem. Soc. 1125 (1937).
24. B. E. Leggetter and R. K. Brown. Can. J. Chem. **38**, 2363 (1960).
25. E. Piers and R. K. Brown. Can. J. Chem. **41**, 329 (1963).
26. W. C. Sumpter and F. M. Miller. Heterocylic compounds with indole and carbazole systems. Interscience Publishers, Inc., New York. 1954. p. 5.
27. N. N. Suvorov, N. P. Sorokina, and Yu. N. Sheinker. J. Gen. Chem. USSR Eng. Transl. **29**, 962 (1959).
28. L. J. Bellamy. The infrared spectra of complex molecules. 2nd ed. John Wiley and Sons, New York. 1958. p. 260.
29. E. Forneau, M. Trefouel, and A. Wancoola. Bull. Soc. Chim. France, **47**, 743 (1930); Chem. Abstr. **24**, 5300 (1930).
30. H. R. Snyder and C. W. Smith. J. Am. Chem. Soc. **65**, 2452 (1943).
31. S. G. P. Plant. J. Chem. Soc. 899 (1936).
32. K. Clusius and H. R. Weisser. Helv. Chim. Acta, **35**, 400 (1952).

Can. J. Chem. Downloaded from www.nrcresearchpress.com by 210.87.254.40 on 09/05/12
For personal use only.

Can. J. Chem. Downloaded from www.nrcresearchpress.com by 210.87.254.40 on 09/05/12
For personal use only.

THE RATE OF REACTION OF ACTIVE NITROGEN WITH ETHANE, PROPANE, AND NEOPENTANE[1]

W. E. JONES[2] AND C. A. WINKLER
Upper Atmosphere Chemistry Research Group, McGill University, Montreal, Quebec
Received August 2, 1963

ABSTRACT

The reactions of active nitrogen with ethane, propane, and neopentane have been studied over the temperature range 0 to 450 °C. A cobalt probe technique was used to stop the reactions after various reaction times. Second order rate constants have been calculated on the assumption that nitrogen atoms are the only reactive species in active nitrogen. Broken Arrhenius lines were obtained for both the ethane and neopentane reactions but this behavior was not observed with the propane reaction. The dual activation energies have been attributed to a mechanism involving initiation by both excited molecules and either nitrogen or hydrogen atoms. Methods are outlined by which an estimate has been made of the concentration of excited species assumed to be involved in the ethane reaction.

INTRODUCTION

In previous investigations of the reactions of ethane (1, 2), propane (3), and neopentane (4) with active nitrogen, approximate rate constants, activation energies, and steric factors were evaluated from hydrogen cyanide yields at various temperatures, on the assumption that the reactions were second order. While there appeared to be only one activation energy associated with the propane reaction over the whole temperature range studied, the data for each of the other two reactions were found to correspond to two activation energies, one at lower, the other at higher temperatures. The values for the three reactions were:

Reaction	Temp. range (°C)	Activation energy	Steric factor	Reference
Ethane	−100 to 150	3	10^{-4}	2
	150 to 475	6	10^{-2}	
Neopentane	−40 to 115	2	10^{-5}	4
	150 to 350	7	10^{-3}	
Propane	63 to 250	6	10^{-2} to 10^{-3}	3

It was suggested that the results for ethane (2) and neopentane (3) could be explained by the concomitant attack of the parent hydrocarbon by both nitrogen atoms and hydrogen atoms formed by the nitrogen atom reaction, or by the presence of two reactive species in active nitrogen. The nature of such a second species is open to question, but recent evidence (5, 6, 7) suggests that the excited nitrogen molecule $N_2(A^3\Sigma_u^+)$ is capable of initiating reactions (8) with saturated hydrocarbons such as methane and ethane.

Recently, methods (9) have been developed by which active nitrogen reactions can be quenched at various points downstream from the reactant jet, with the advantage that reaction time may be controlled and more reliable estimates of the rate constants obtained. In the present study, a cobalt target (10) has been used to quench the active

[1]*Financial assistance from the National Research Council.*
[2]*Holder of N.R.C. Studentship 1962–63. Present address: Department of Chemistry, Dalhousie University, Halifax, N.S.*

nitrogen reactions with ethane, propane, and neopentane, to check the validity of the earlier results for these reactions.

EXPERIMENTAL

Ethylene, ethane, propane, and neopentane (Matheson Co. of Canada) were purified by two bulb-to-bulb distillations, only the middle two-thirds from each distillation being retained. 'Bone dry' nitrogen (Linde Air Products) was passed over heated copper to remove traces of oxygen, and through a liquid air trap to remove traces of water and carbon dioxide.

The apparatus was essentially similar to that used in a previous investigation in this laboratory (10), but incorporated several minor changes. The nitrogen stream, after passing through the flowmeter, could be admitted to the reaction system after activation by either a condensed discharge or by a microwave generator (Raytheon, 2450 Mc/s, 125 W). The flow rate of molecular nitrogen at a pressure of 2.2 mm Hg was 216×10^{-6} mole/s. A controlled small amount of water vapor was added to the nitrogen stream before it entered either discharge. It was assumed that this acted only as an efficient wall poison, and had no significant effect on the active nitrogen reactions (5).

Hydrocarbon entered the gas stream through a bulb with six small holes spaced at equal distances around its circumference. A constriction in the 25 mm i.d. reaction tube, just above the reactant jet, prevented back diffusion of the reaction mixture and resulted in a sharply defined initiation of the reaction at the hydrocarbon inlet, from where the zero time of reaction was measured. Provision was made to heat or cool the reaction tube, to permit measurements over the temperature range from about 0 to 450 °C.

Reaction rates were determined by measuring the amount of hydrogen cyanide produced when the reaction was terminated at different positions downstream from the reactant jet, that is, after different reaction times. The hydrogen cyanide was trapped at liquid air temperature, and its amount estimated by titration, as outlined previously (10).

It was convenient to estimate the relative nitrogen atom concentrations, in the 'active nitrogen' produced both by microwave and condensed discharges, from the maximum yields of hydrogen cyanide obtained from the ethylene – active nitrogen reaction (5). They were found to be quite constant over a wide temperature range for the conditions of the present study. The values so obtained should be regarded, perhaps, as minima, since the concentrations determined by the familiar nitric oxide titration method would have been higher by a factor of about 1.5 (cf. ref. 5).

To avoid inaccuracies that might result from contamination of the walls of the reaction vessel by particles of catalyst from the target, measurements were made only for movement of the quenching target from the bottom to the top of the reaction tube, i.e., for successively shorter reaction times. When the target reached the position of closest approach to the reactant jet, it was removed and the reaction vessel was cleaned and dried thoroughly. The nitrogen atom concentration was determined before proceeding with the next series of measurements, and periodically throughout the experiments, to ensure that any change in its value would be known.

RESULTS AND DISCUSSION

To compare the present results with those of earlier work, second order rate constants for the three reactions were calculated on the assumption that the reaction of each molecule of hydrocarbon produced hydrogen cyanide equivalent to the number of carbon atoms in the reactant molecule, and that nitrogen atoms were the only reactive species present in the active nitrogen. The integrated rate equation for ethane has the form

$$k = \frac{2.303}{t(a - 2b)} \log \frac{b(a - 2x)}{a(b - x)}$$

where x is the amount of ethane consumed, approximately one-half the hydrogen cyanide produced; a is the initial concentration of nitrogen atoms; b is the initial concentration of ethane; t is the duration of the reaction. Integrated rate equations similar to this, but with suitable corrections for the number of hydrogen cyanide molecules produced per molecule of hydrocarbon, have also been used to calculate the second order rate constants for the reactions of nitrogen atoms with neopentane and propane. The reproducibility of the measurements is indicated by the typical values for the second order rate constants given in Table I.

Can. J. Chem. Downloaded from www.nrcresearchpress.com by 210.87.254.40 on 09/05/12
For personal use only.

TABLE I

Typical second order rate constants for the reactions of active nitrogen with the three reactants

Reactant	Temp. (°K)	N-atom flow (mole/s × 10^6)	Time (s × 10^3)	Reactant flow (mole/s × 10^6)	HCN yield (mole/s × 10^6)	k (cc/molecule^{-1} s^{-1} × 10^{15})
C_2H_6 (condensed discharge)	278	18.1	17.3	5.1	1.0	1.0
				15.5	1.4	0.4
			58.2	4.3	1.7	0.6
				14.1	2.5	0.3
			116.4	2.1	1.1	0.4
				15.1	2.7	0.1
			Complete reaction	14.9	2.8	
	403	18.0	40.1	2.0	1.1	1.9
				3.9	1.9	1.6
				6.8	2.9	1.4
				14.9	4.8	1.1
		15.6	40.1	2.4	0.9	1.7
				4.3	1.3	1.1
				7.4	3.0	1.6
				15.5	4.1	1.1
		18.0	80.1	2.5	1.2	0.8
				4.4	2.1	0.8
				8.0	2.7	0.6
				14.6	4.0	0.5
C_2H_6 (microwave discharge)	273	1.79	23.6	2.7	0.023	0.3
				4.8	0.041	0.3
			59.1	2.6	0.043	0.2
				4.8	0.070	0.2
	403	1.79	40.1	2.6	0.082	0.9
				4.7	0.138	0.9
			80.1	2.7	0.096	0.5
				4.7	0.182	0.7
C_5H_{12} (microwave discharge)	273	1.79	23.6	2.0	0.071	0.5
				4.7	0.126	0.4
			59.1	2.2	0.140	0.4
				5.9	0.227	0.2
	428	1.86	37.7	2.0	0.236	1.5
				4.8	0.428	1.3
			56.6	2.1	0.295	1.3
				4.6	0.464	0.9
C_3H_8 (microwave discharge)	273	1.79	59.1	2.9	0.125	0.4
				5.0	0.186	0.3
			78.7	2.9	0.158	0.4
				5.1	0.258	0.4
	435	1.86	14.9	2.6	0.39	9
				4.9	0.80	12
			37.1	2.7	0.67	7
				4.9	1.20	9

The reaction of ethane with active nitrogen produced by the condensed discharge was studied over the temperature range 5 to 430 °C, at approximately 50° intervals. The production of hydrogen cyanide was measured at each temperature, for several flow rates of ethane, at three different reaction times. Typical plots to illustrate the variation of hydrogen cyanide production with ethane flow rate are shown in Fig. 1. The plots show a behavior somewhat similar to the induction effect observed previously (2). Close inspection of these curves suggests that this induction effect involves a rapid initial production of hydrogen cyanide, followed by a tendency for the curve to level out, which is followed, in turn, by a second gradual increase in production of hydrogen cyanide to a plateau value. This behavior is well illustrated by the lowest curve of Fig. 1B. The reaction of ethane with active nitrogen produced by the microwave discharge was also

Can. J. Chem. Downloaded from www.nrcresearchpress.com by 210.87.254.40 on 09/05/12
For personal use only.

Can. J. Chem. Downloaded from www.nrcresearchpress.com by 210.87.254.40 on 09/05/12
For personal use only.

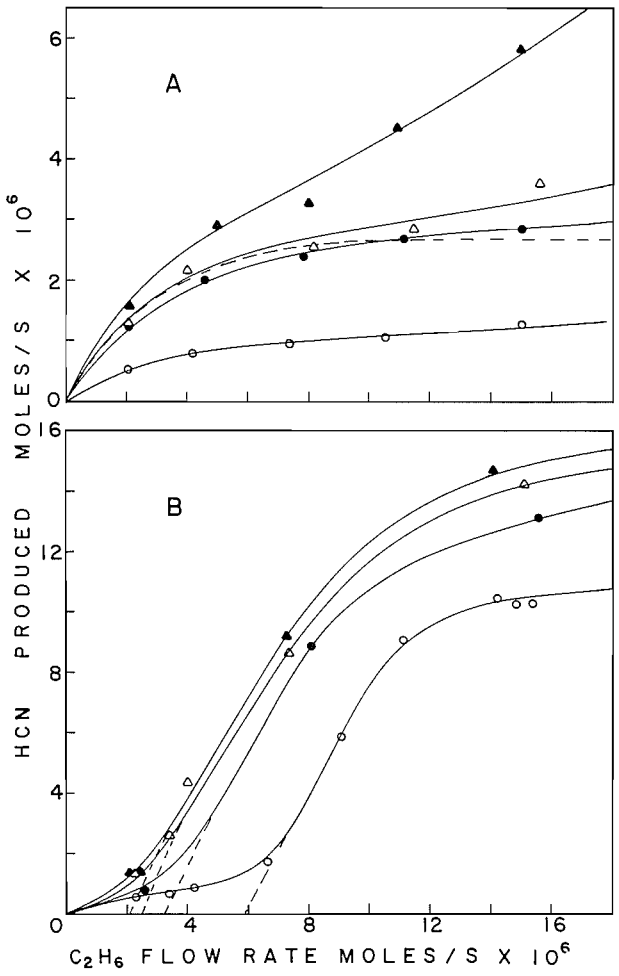

FIG. 1. Production of hydrogen cyanide at various reaction times from the reaction of ethane with active nitrogen produced by a condensed discharge: (A) temperature 80 °C, ○ 20.5 × 10^{-3} s, ● 51.2 × 10^{-3} s, △ 76.8 × 10^{-3} s, ▲ 102.4 × 10^{-3} s; (B) temperature 380 °C, ○ 10 × 10^{-3} s, ● 24.9 × 10^{-3} s, △ 37.4 × 10^{-3} s, ▲ 49.9 × 10^{-3} s.

studied over a wide temperature range (0 to 430 °C), but plots similar to those of Fig. 1 were not made, owing to the low yield.

The second order rate constants (averages of those found for several ethane flow rates at three or more different reaction times for each temperature) are given in Table II and shown graphically in the Arrhenius plot, Fig. 2A. The plot clearly confirms the earlier observation that different activation energies are associated with the reaction in the low and high temperature ranges. The results for the microwave and condensed discharges are in excellent agreement in the higher temperature range but do not agree as well for low temperatures. The differences, however, are of the same order as the experimental error.

The reaction of neopentane was studied only with active nitrogen produced by the microwave discharge. The average second order rate constants are given in Table II and shown graphically in Fig. 2B. Neopentane shows the same type of behavior as

TABLE II

Average second order rate constants for the three hydrocarbon – active nitrogen reactions

Temp. (°K)	Reaction time (s × 10^3)	k (cc/molecule^{-1} s^{-1} × 10^{15})	k_{av} (cc/molecule^{-1} s^{-1} × 10^{15})
	Ethane (condensed discharge)		
278	17.3	0.70	0.48
	58.2	0.43	
	116.4	0.28	
353	20.5	0.90	0.78
	51.2	0.89	
	76.8	0.66	
	102.4	0.66	
403	40.1	1.7	1.3
	80.1	0.78	
	40.1	1.4	
453	70.4	1.7	1.7
503	32.2	4.1	3.4
	64.4	2.9	
553	58.2	5.4	5.4
603	26.8	8.4	8.0
	53.6	7.7	
653	10.0	15.1	11.5
	24.9	10.9	
	37.4	8.3	
	49.9	9.5	
703	22.9	24.6	19.8
	45.8	16.0	
	Ethane (microwave discharge)		
273	23.6	0.28	0.22
	59.1	0.21	
	118.1	0.18	
318	10.2	0.59	0.49
	20.3	0.63	
	50.8	0.42	
	101.6	0.32	
334	19.4	0.93	0.62
	48.4	0.51	
	96.8	0.40	
353	45.8	0.48	0.44
	91.6	0.39	
403	40.1	0.88	0.72
	80.1	0.61	
503	12.9	3.2	2.6
	32.2	3.1	
	64.4	1.9	
603	26.8	13.5	10.5
	53.6	8.9	
703	4.6	26.2	38.5
	9.2	47.5	
	22.9	53.7	
	45.8	28.3	
	Neopentane (microwave discharge)		
273	23.6	0.41	0.33
	59.1	0.28	
	78.7	0.29	
328	19.7	0.66	0.49
	49.3	0.46	
	73.9	0.34	
388	16.7	1.1	0.77
	41.6	0.70	
	62.5	0.51	
428	15.1	2.0	1.5
	37.7	1.4	
	56.6	1.1	

Can. J. Chem. Downloaded from www.nrcresearchpress.com by 210.87.254.40 on 09/05/12
For personal use only.

TABLE II (*Concluded*)

Temp. (°K)	Reaction time (s × 10^3)	k (cc/molecule^{-1} s^{-1} × 10^{15})	k_{av} (cc/molecule^{-1} s^{-1} × 10^{15})
523	12.4	7.4	4.9
	30.9	4.1	
	46.3	3.4	
625	10.4	25.2	16.0
	25.8	12.0	
	38.8	10.8	
724	8.9	40.2	32.9
	22.3	33.6	
	33.5	22.5	
	Propane (microwave discharge)		
273	23.6	0.43	0.38
	59.1	0.36	
	78.7	0.37	
323	20.1	1.7	1.3
	50.2	1.4	
	75.3	1.1	
379	17.1	6.3	6.3
435	14.9	10.3	9.9
	37.1	7.8	
	55.7	11.7	
523	12.4	42.3	38.9
	30.9	38.1	
	46.3	33.8	
623	10.4	118	118

k represents the average of the rate constants found for at least three reactant flow rates at each time indicated.
k_{av} represents the average of all rate constants found at different reactant flow rates and different reaction times at the given temperature.

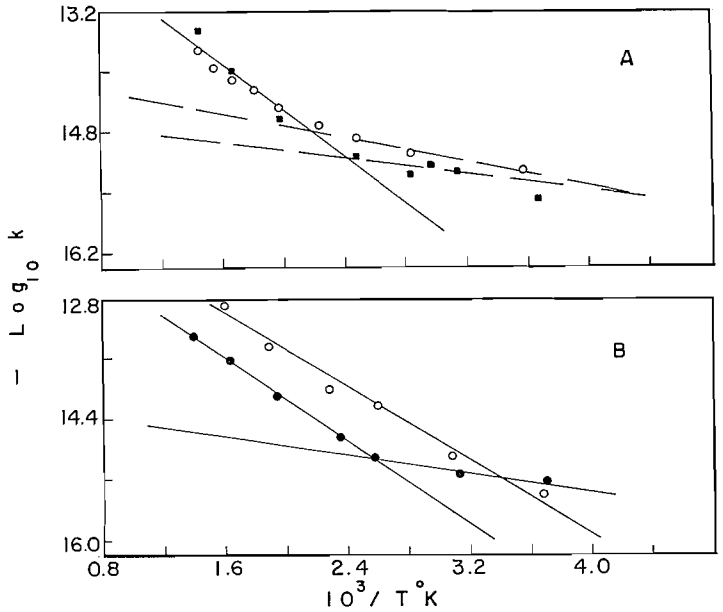

FIG. 2. Arrhenius plot of the reaction of active nitrogen with the three hydrocarbons: (A) ethane, ○ condensed discharge, ■ microwave discharge; (B) propane, ○ microwave discharge; neopentane, ● microwave discharge.

Can. J. Chem. Downloaded from www.nrcresearchpress.com by 210.87.254.40 on 09/05/12
For personal use only.

ethane, i.e., different activation energies for low and high temperature ranges, and the results are in agreement quantitatively with those of earlier work (4).

The reaction with propane was also studied only with the microwave system. Average values for the second order rate constants are given in Table II, and an Arrhenius plot of these in Fig. 2B.

The kinetic constants, inferred from the second order rate constants for the reactions of active nitrogen with all three of the hydrocarbons studied are summarized in Table III.

TABLE III

Summary of kinetic constants calculated from Arrhenius plots of the second order rate constants assuming atomic nitrogen as reactive species

	Activation energy (kcal mole^{-1})	A (cc molecule^{-1} s^{-1})	Z (cc molecule^{-1} s^{-1})	P
Ethane				
Low temp. range	1.7	8.7×10^{-15}	4.2×10^{-10}	2.0×10^{-5}
High temp. range	7.0	3.8×10^{-12}	6.2×10^{-10}	6×10^{-3}
Neopentane				
Low temp. range	1.5	4.8×10^{-15}	4.5×10^{-10}	1.0×10^{-5}
High temp. range	6.6	2.3×10^{-12}	6.7×10^{-10}	3.4×10^{-3}
Propane	5.5	8.7×10^{-12}	4.6×10^{-10}	1.9×10^{-2}

It will be noted that the activation energies and steric factors are quite similar for the ethane and neopentane reactions for both the low and high temperature ranges, and that the values differ considerably from the corresponding values for the propane reaction. It should be emphasized, perhaps, that these values are all based on the rate constants calculated on the assumption that nitrogen atoms are the only reactive species in active nitrogen. The values obtained are of the same order of magnitude as those obtained in earlier investigations.

The induction effect with concentration of reactant (Figs. 1A and 1B) was not observed for the shorter reaction times (20.5 and 51.2 ms) at low temperatures, over the range of reactant flow rates used, but it did become evident for the longer reaction times. This suggests that, in these two reactions, some initiating step is followed by other reactions leading to the formation of hydrogen cyanide. From the grouping of the curves for the ethane reaction in Fig. 1A, it appeared that a plateau to represent the amount of the initiating reaction with this reactant may be drawn as indicated by the dashed curve. This plateau value corresponds to about 2.8 μmoles/s of hydrogen cyanide, from which it might be tentatively concluded that the flow rate of the initiating species was about 1.4 μmoles/s.

If the minimum nitrogen atom flow rate is taken to be about 18 μmoles/s, from the maximum hydrogen cyanide production from ethylene, it is unlikely that nitrogen atoms should be responsible for initiating a reaction that attains a plateau in hydrogen cyanide production at only 2.8 μmoles/s. Accordingly, it is suggested that this low plateau corresponds to the flow rate of an excited molecular species, perhaps $N_2(A^3\Sigma_u^+)$. Such a species, by collision with the hydrocarbon, might bring about its excitation or decomposition, and thereby initiate subsequent reactions that lead to the formation of hydrogen cyanide.

The above argument would suggest that the maximum amount of hydrogen cyanide produced at sufficiently low temperatures, e.g. 0 °C, might be governed entirely by the

Can. J. Chem. Downloaded from www.nrcresearchpress.com by 210.87.254.40 on 09/05/12
For personal use only.

extent of the initiating reaction, i.e., by the flow rate of the initiating species. The maximum yield of hydrogen cyanide at this temperature was 2.8 μmoles/s (Table I), which might again be taken to correspond to a flow rate of 1.4 μmoles/s for the initiating species.

From Fig. 1B, the induction effect appears to be marked at higher temperatures. This behavior would be expected if the amount of reaction caused by an initiating species remained relatively unaltered, while subsequent reactions became pronounced as the temperature was increased. If the steeper portions of the curves, representing hydrogen cyanide production from the subsequent reactions, are extrapolated to the axis of ethane flow rate, the intercepts might be interpreted to be the flow rates of ethane necessary for the second reaction to become significant at the given reaction time. A plot of these intercepts against the reciprocal of the corresponding distance of the cobalt target from the reactant jet (i.e., 1/time of reaction) is shown in Fig. 3. If the line in Fig. 3 is extrapo-

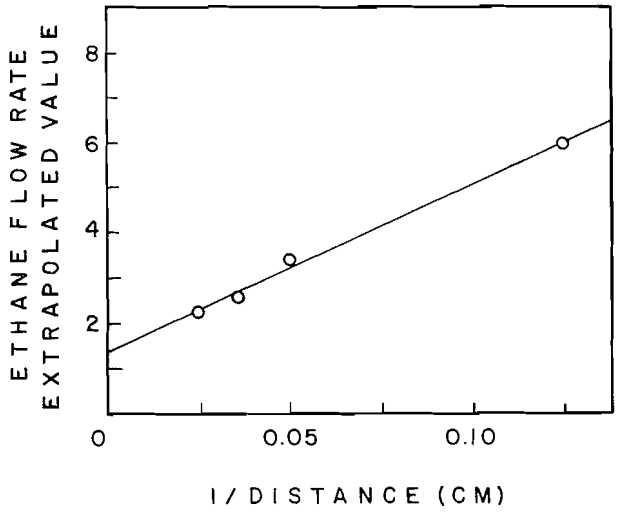

FIG. 3. Variation in the minimum amount of ethane necessary before the secondary atom reaction becomes noticeable.

lated to a value of zero for the reciprocal of distance, corresponding to infinite reaction time, a value of 1.4 μmoles/s is obtained for the minimum flow rate of ethane required for the subsequent reactions to become significant, i.e., the maximum amount of ethane that will react with the initiating species. This value is in good agreement with the previous estimates of concentration for the possible initiating species.

The accelerated production of hydrogen cyanide with increase of either reaction time or temperature might be due to increased extent of direct nitrogen atom reaction with the hydrocarbon under such conditions. However, it seems more likely, particularly in view of the long induction effect in the curve for the shortest reaction time at 380 °C, that the increased production of hydrogen cyanide results from fast nitrogen atom reactions with free radicals formed when the hydrocarbons are attacked by hydrogen atoms produced in the initiating step or in subsequent nitrogen atom reactions.

In summary, it would seem that the reaction scheme appropriate to lower temperatures and short reaction times might be represented by

$$N_2^* + RH \rightarrow N_2 + RH^*,$$

Can. J. Chem. Downloaded from www.nrcresearchpress.com by 210.87.254.40 on 09/05/12
For personal use only.

followed by fast reactions of nitrogen atoms with RH*, or free radicals derived from its decomposition, to produce hydrogen cyanide and other products, including hydrogen atoms. At higher temperatures, production of hydrogen cyanide is probably increased to some extent by direct nitrogen atom attack on the hydrocarbon, but mainly by a reaction sequence of a type exemplified by

$$C_2H_6 + H \rightarrow C_2H_5 + H_2$$
$$C_2H_5 + N \rightarrow HCN + CH_3 + H$$
$$CH_3 + N \rightarrow HCN + 2H.$$

The activation energies for the reactions of nitrogen atoms, or hydrogen atoms, with hydrocarbons are of comparable magnitude, and considerably higher than the activation energy that might be expected for the formation of hydrogen cyanide by the mechanism involving an energy transfer and subsequent nitrogen atom reactions, as outlined above. The observed increase in hydrogen cyanide production with increase of temperature, and the change in slope of the Arrhenius lines for the ethane and neopentane reactions, would therefore be in accord with the mechanisms proposed for the different experimental conditions.

Since the reaction with propane gave no indication of two activation energy values, it seems likely that it involves only direct nitrogen atom attack to produce hydrogen cyanide. It would seem, at least, that the direct nitrogen atom reaction masks any participation of excited molecules or hydrogen atoms that might be present in this reaction.

Although attempts have been made to resolve mathematically the kinetic behavior reflected in Figs. 1A and 1B, no satisfactory treatment has yet been developed.

REFERENCES

1. H. Blades and C. A. Winkler. Can. J. Chem. **29**, 1022 (1951).
2. P. A. Gartaganis and C. A. Winkler. Can. J. Chem. **34**, 1457 (1956).
3. M. Onyszchuk, L. Breitman, and C. A. Winkler. Can. J. Chem. **32**, 351 (1954).
4. M. Onyszchuk and C. A. Winkler. J. Phys. Chem. **59**, 368 (1955).
5. A. N. Wright, R. L. Nelson, and C. A. Winkler. Can. J. Chem. **40**, 1082 (1962).
6. G. R. Freeman and C. A. Winkler. J. Phys. Chem. **59**, 371 (1955).
7. K. D. Bayes. Can. J. Chem. **39**, 1074 (1961).
8. A. N. Wright and C. A. Winkler. Can. J. Chem. **40**, 1291 (1962).
9. A. Y. Ung. Ph.D. Thesis, McGill University, Montreal, Que. 1961.
10. E. M. Levy and C. A. Winkler. Can. J. Chem. **40**, 686 (1962).

Can. J. Chem. Downloaded from www.nrcresearchpress.com by 210.87.254.40 on 09/05/12
For personal use only.

Can. J. Chem. Downloaded from www.nrcresearchpress.com by 210.87.254.5 on 09/05/12
For personal use only.

THE IONIZATION BEHAVIOR OF AMIDES IN CONCENTRATED SULPHURIC ACIDS

I. A NEW ACIDITY FUNCTION BASED ON A SET OF PRIMARY AMIDE INDICATORS

KEITH YATES AND JOAN B. STEVENS
Department of Chemistry, University of Toronto, Toronto, Ontario

AND

A. R. KATRITZKY
School of Chemical Sciences, University of East Anglia, Norwich, England

Received April 6, 1964

ABSTRACT

A set of eight suitably substituted primary amides of progressively weaker basicity have been prepared. Their ionization curves have been determined in sulphuric acids by spectrophotometric methods. These show good overlap and parallelism for successive indicators, enabling the pK values of the indicators to be determined by direct stepwise comparison. Using these pK values and measured ionization ratios, values of a new acidity function, H_A, have been obtained for aqueous solutions up to 82% sulphuric acid. The H_A function decreases much less rapidly than H_0 in this range, being nearly 3 log units less negative at the highest acidity studied. The reasons for this large difference are discussed. The H_A function is shown to be applicable to other amides which have not been employed as indicators.

INTRODUCTION

The acidity function H_0 was originally conceived by Hammett and Deyrup (1) to describe the ionization behavior of weak organic bases in concentrated acid solutions. It has been assumed to be generally applicable to uncharged bases ionizing by simple proton addition, as in

$$B + H^+ \rightleftharpoons BH^+$$

for which $K_{BH^+} = a_B \cdot a_{H^+}/a_{BH^+}$ is the thermodynamic equilibrium constant defined in terms of molar activities. The acidity function is defined by

$$H_0 = -\log (a_{H^+} \cdot f_B/f_{BH^+}) = pK_{BH^+} - \log [BH^+]/[B].$$

The only well recognized exceptions of this charge type have been carbinol and olefin type bases which form carbonium ions on protonation. These have been found to follow the H_R (2) and H_R' (3) functions respectively.

Recently it has been recognized that the applicability of the H_0 function is considerably more limited than was at one time supposed. This question has been discussed in an excellent and comprehensive review by Arnett (4). The limited generality of the H_0 scale has been clearly demonstrated by the results of two recent investigations. Jorgenson and Hartter (5) have redetermined the H_0 scale using a set of structurally related indicators composed solely of primary anilines, unlike the original Hammett indicators, which although mainly of this type, included an N,N-disubstituted aniline as well as several oxygen type bases. Their new H_0 scale shows considerable divergence from that based on the old set of indicators (1). This demonstrates that acidity functions of the H_0 type are strongly dependent on structural changes in the indicators, even for simple bases of the same charge type. Previously (6) it has been shown that many amides are not Hammett bases, although they ionize by simple proton addition (7). This was shown by the fact that slopes of their log $[BH^+]/[B]$ values against H_0 were far from unity, as required by the

defining equation, and that these deviations were too large to be explained by medium effects on the absorption spectra used to obtain ionization ratios.

Thus the results of all previous pK determinations on amides, employing the H_0 scale, do not yield thermodynamic equilibrium constants, but "pK" values in the sense described by Arnett (4). These correspond numerically to the H_0 values of the acids in which the base is half-ionized.

Therefore in general structure pK correlations for weak bases must be interpreted with caution. In addition, rate–acidity function correlations such as those of Bunnett (8), and their interpretation in terms of hydration changes (9), lose much significance in cases where it can be shown that the acidity scale used is not applicable to the type of substrate being considered.

We have therefore investigated the possibility that primary amides are following some other "general" acidity function and wish to report values of a new acidity function, H_A. This function is based on a set of structurally related primary amide indicators and appears to be generally applicable to the ionization behavior of this class of base. It is considerably different numerically to the H_0 scale even in moderately concentrated acids.

EXPERIMENTAL

Indicators

The following commercially available indicators were recrystallized to constant melting point: 3,4,5-trimethoxybenzamide from methanol–water; m.p. 178.5–179.5 °C (lit. m.p. 176–177 °C (10)); 2,4-dichloro-3,4-dinitrobenzamide from aqueous ethanol; m.p. 262–263 °C. We are unable to find a reported melting point for this compound but analysis gave C, 30.18; H, 1.01; N, 14.96; Cl, 25.59. Calculated for $C_7H_3N_3Cl_2O_5$: C, 30.0; H, 1.07; N, 15.0; Cl, 25.35. Samples of *p*-methoxybenzamide, m.p. 166–167 °C (lit. m.p. 163 °C (11)) and *m*-nitrobenzamide, m.p. 140–141 °C (lit. m.p. 141–143 °C (11)) were kindly supplied to us by Professor J. T. Edward of McGill University. These were also recrystallized to constant melting point before use. The remaining indicators were prepared as follows from the corresponding carboxylic acids, which are all commercially available. The acid chloride was prepared by a standard method (12) and reacted with cold aqueous ammonia to give 3,5-dinitro-4-methylbenzamide, which was recrystallized from aqueous ethanol; m.p. 189.2–190.5 °C (lit. m.p. 187 °C (13)). Calculated for $C_8H_7N_3O_5$: C, 42.7; H, 3.18; N, 18.7. Found: C, 42.6; H, 3.06; N, 18.6. The same method was used for 2,3,6-trichlorobenzamide. This amide has apparently not been prepared previously; m.p. 170–171 °C. Calculated for $C_7H_4Cl_3NO$: C, 37.4; H, 1.78; Cl, 47.5; N, 6.24. Found: C, 37.3; H, 1.45; Cl, 47.48; N, 6.09. A modified method (14, 15) was used to prepare 2,4,6-trinitrobenzamide. This was recrystallized from benzene – acetone – petroleum ether; m.p. 267.5–268.5 °C (lit. m.p. 264 °C (15)). Calculated for $C_7H_4N_4O_7$: C, 32.8; H, 1.56; N, 21.87. Found: C, 32.75; H, 1.50; N, 22.0. Our 2-pyrrolecarboxamide was prepared by the method of Fischer and Van Slyke (16); the product being recrystallized from water; m.p. 174.5–175.5 °C (lit. m.p. 176.5 °C (16)). Calculated for $C_5H_6N_2O$: C, 54.55; H, 5.45; N, 25.45. Found: C, 54.13; H, 5.85; N, 25.25.

Sulphuric Acids

Sulphuric acid solutions ranging from 0.001 N to 90% by weight were prepared by diluting Fischer C. P. Reagent Grade sulphuric acid (95% min.). Concentrations were determined by titrating weighed samples with standard sodium hydroxide.

Measurement of Ultraviolet Spectra

All spectra were measured on a Bausch and Lomb Spectronic 505 Recording Spectrophotometer using 1 cm quartz cells and a thermostatically controlled cell-block at 25±0.05 °C. Solutions of indicators were prepared as described previously (17). It has been shown (18) that hydrolysis of the amides is negligible during the time required to measure spectra. Periodic checks of solutions of various acid concentrations confirmed this in the present work.

Treatment of Data

Since all compounds gave clearly defined absorption peaks in acid solutions strong enough to convert them essentially to their ionized forms, the wavelengths near this peak, $\lambda_{BH^+}{}^{max}$, were used to determine ionization ratios. Absorption spectra of the free base forms obtained in water or dilute acids showed some absorption at this wavelength but the change in ϵ at $\lambda_{BH^+}{}^{max}$ on going from essentially free base to conjugate acid was in every case large. Plots of ϵ against H_0 were examined for different λ in the region of $\lambda_{BH^+}{}^{max}$. Sigmoid type curves were obtained and that wavelength which gave the smoothest curve was chosen to calculate ionization ratios. These were obtained from the relation

$$I = [BH^+]/[B] = (\epsilon - \epsilon_B)/(\epsilon_{BH^+} - \epsilon)$$

Can. J. Chem. Downloaded from www.nrcresearchpress.com by 210.87.254.5 on 09/05/12
For personal use only.

where ϵ_B is the absorption at $\lambda_{BH^+}^{max}$ in a solution in which the base is completely un-ionized, ϵ_{BH^+} is the corresponding value in a solution where it is essentially completely ionized and is the value in a solution of intermediate acidity. Values of ϵ_B and ϵ_{BH^+} were obtained for individual compounds as follows. The H_0 value at the inflection point of the above sigmoid curve was assumed to correspond approximately to the point of 50% ionization ([B] = [BH$^+$]). Acid solutions having H_0 values 2 log units above and below this value were taken to be acids in which the base was completely unionized and fully ionized respectively, and their ϵ values taken as first approximate ϵ_B and ϵ_{BH^+} values. These were then used to obtain approximate log I values. Plots of these log I values against percent H_2SO_4 showed good parallelism and overlap for successive indicators. These were then used in the standard stepwise procedure to calculate a set of approximate pK values for the indicators and from these a first approximate set of amide acidity function values was obtained. Since this function decreased less steeply than the H_0 function, our original assumptions about the acids corresponding to ϵ_B and ϵ_{BH^+} were in error. This was particularly the case on the strongly acid side of the 50% ionization point. Next, acids of lower and higher acidities than before were chosen to obtain ϵ_B and ϵ_{BH^+} values respectively. These were chosen to correspond (on the first approximate amide acidity scale) to values ± 1.5 log units about the 50% ionization point. Thus it was hoped to minimize medium effects according to the method of Stewart and Granger (19). These new ϵ_B and ϵ_{BH^+} values were then used to obtain a further set of log I values and the whole calculation of pK and amide acidity function values repeated. It was again necessary to make small corrections in the acid concentrations used to obtain ϵ_B and ϵ_{BH^+}. These were very small in the less concentrated acids used to obtain ϵ_B. The whole procedure was reiterated until no further significant changes in the acidity function or pK values were produced and the acids used to obtain ϵ_B and ϵ_{BH^+} were at least 1.5 log units either side of the pK value. By using the method of Stewart and Granger (19) to select the 0% and 100% ionization acids, errors of about 3% in ϵ_B and ϵ_{BH^+} can be introduced by the arbitrary choice of ± 1.5 log units, if there are no spectral shifts produced by the solvent. However, since the arms of the sigmoid curve are in fact sloping because of spectral shifts, it is felt that introducing a possible error of known magnitude is far less serious than choosing extremely strong acids to obtain ϵ_{BH^+} and thereby introducing errors of unknown magnitude.

Plots of the final log I values against the final acidity function values give straight lines of unit slope. All the individual values of the amide acidity function lie closely on a smooth curve when plotted against acid concentration.

RESULTS AND DISCUSSION

Selection of Indicators and Measurement of Ionization Ratios

Guided by the same general criteria as Jorgenson and Hartter (5), we have prepared a set of structurally related primary amides of progressively weaker base strength. These are principally benzamides substituted in various positions of the benzene ring with methoxy, methyl, halogen, and nitro groups, chosen so that their measurable ionization ranges overlap as much as possible for successive indicators. The overall range of measurable ionization behavior for this set extends from 5–82% aqueous sulphuric acid. Individual indicators were chosen on the following basis. The slopes of plots of log I versus the H_0 function were obtained for 22 primary amides, using previously reported data (6, 17) as well as data obtained in the present study. Except for two widely deviating points (*o*-toluamide and *p*-nitrobenzamide) the values of these slopes fall in the range 0.49–0.78. (Redetermination of the slope (0.62) for *m*-toluamide showed that the previously reported (6) value of 1.00 is incorrect.) These values are not randomly scattered within this range but show a general trend, depending on the acidity region in which the amide undergoes extensive ionization. The most strongly basic amides studied have log I versus H_0 slopes of approximately 0.7–0.8, decreasing to slopes of 0.5–0.6 for the most weakly basic. It was this general trend of deviation from H_0 type behavior which suggested the possibility that an amide acidity function could be constructed. Eight amides were then chosen which had the most representative slopes and which gave the best overlap and parallelism of indicator ratio curves spanning the above acidity range.

Ionization ratios (I = [BH$^+$]/[B]) for all indicators were determined by spectrophotometric methods. The amides used have strong absorption maxima in the 215–260 mμ region. On protonation the spectra undergo changes in both λ_{max} and intensity as shown in Table I. In some cases both the neutral molecule and the cation give well-defined peaks

Can. J. Chem. Downloaded from www.nrcresearchpress.com by 210.87.254.5 on 09/05/12
For personal use only.

Can. J. Chem. Downloaded from www.nrcresearchpress.com by 210.87.254.5 on 09/05/12
For personal use only.

TABLE I

Absorption maxima and pK values of indicators

Indicator	λ_B^{max} (mμ)	log ϵ_B^{max}	% H_2SO_4* (w/w)	$\lambda_{BH^+}^{max}$†	log $\epsilon_{BH^+}^{max}$	% H_2SO_4‡ (w/w)	pK (average)	Mean deviation	n§
2-Pyrrolecarboxamide	263	2.92	0	288	4.32	55.6	−1.23	±0.04	20
4-Methoxybenzamide	253	3.21	0	283	4.22	58.7	−1.44	±0.03	5
3,4,5-Trimethoxy-	257	3.41	0	283	3.96	63.8	−1.82	±0.01	6
3-Nitro-	215	3.97	12.0	230	4.33	71.8	−2.42	±0.02	8
3,5-Dinitro-4-methyl-	217	4.21	24.0	235	4.36	75.5	−2.69	±0.02	10
2,3,6-Trichloro-	233 sh	3.00	33.5	258	3.87	81.5	−3.30	±0.01	6
2,4-Dichloro-3,5-dinitro-	216 sh	4.06	44.5	235	4.26	86.1	−3.73	±0.01	5
2,4,6-Trinitro-	224	4.36	52.0	224	4.45	88.2	−4.08	±0.03	6

*Solution used to determine absorption of free base.
†Wavelength near λ_{max} used to determine indicator ratio from log $(\epsilon_B - \epsilon)/(\epsilon - \epsilon_{BH^+}) = I$.
‡Solution used to determine absorption of conjugate acid.
§Number of experimental points used to calculate pK values.

Can. J. Chem. Downloaded from www.nrcresearchpress.com by 210.87.254.5 on 09/05/12
For personal use only.

which are separated by 25–30 mμ. In other cases this separation is less, notably for the nitro derivatives, and in two cases the absorption of the free base appears as a shoulder on the side of a more intense band occurring below 200 mμ. However, in more strongly acid solutions where protonation has occurred, all compounds give well-defined absorption maxima. In cases where the absorption maxima of the free base (λ_B) and of the conjugate acid (λ_{BH^+}) are well defined and separated, the method of Davis and Geissman (20) has been most frequently employed to obtain log I values. This involves using data obtained at both wavelengths. Since this was not in general the case in the present work, it was decided for uniformity to use data obtained at one wavelength only, namely λ_{BH^+}, to calculate I values. This method gives reliable ionization ratios if there is a large change in intensity at this wavelength in going from the neutral base to the conjugate acid. This was the case with every compound studied. The values obtained give smooth sigmoid curves when plotted against acid concentration. Varying the choice of λ_{BH^+} by 5 mμ resulted in only small changes (±1%) in the log I values obtained. As a check, the method of Davis and Geissman was used where possible. The ionization curves obtained by each method were identical within the experimental error. In one case only, that of 2,4,6-trinitrobenzamide, the position of the absorption maximum does not shift appreciably with increasing acidity. However, as the acidity is increased, the spectrum undergoes a large increase in intensity and a plot of intensity against acidity does give a titration-type curve. This is considered to be the least reliable of the indicators used. Fortunately it is the weakest indicator base in the set and has therefore not been used to determine any further pK values. Nonetheless its ionization behavior does parallel that of the preceding indicators, and the base strength determined for it on the basis of the I values is in good agreement with what would be predicted from substituent effects, as will be shown in the second part of this series of papers.

The ionization ratios for these amides in various acid concentrations are listed in Table II. The values for each indicator give smooth curves when plotted against percent acid as shown in Fig. 1, with the expected progressive steepening of slopes at higher acidities. These curves are almost linear, although linearity is not necessarily to be expected when log I is plotted against this concentration scale, as is customary (5). The parallelism between overlapping indicator curves is good and shows that Hammett's activity coefficient postulate (4) is valid for this set of structurally related indicators. This means that

$$\log (f_{A_iH^+} f_{A_j} / f_{A_i} \cdot f_{A_jH^+}) = 0$$

for two amide indicators A_i, A_j in any given solution where their log I values are both measurable. Thus the activity coefficient behavior of this set of amides is reasonably independent of changes in structure. The relationship

$$pK_{A_iH^+} - pK_{A_jH^+} = \log [A_iH^+]/[A_i] - \log [A_jH^+]/[A_j] - \log (f_{A_i} f_{A_jH^+} / f_{A_iH^+} f_{A_j})$$

which holds for any two indicators, can therefore be reduced to

$$[1] \qquad pK_{A_iH^+} - pK_{A_jH^+} = \log [A_iH^+]/[A_i] - \log [A_jH^+]/[A_j]$$

for use in solutions where the ionization ratios of each are measurable. Hence the pK_{AH^+} value of any of these amides can be determined by direct stepwise comparison providing the pK_{AH^+} value of the preceding indicator is known.

Consideration of Medium Effects on Indicator Curves

The values of ϵ^{max} and λ^{max} are both affected by changes in the medium, independently

TABLE II

Ionization ratios* of amide indicators

% H_2SO_4	Log I†	% H_2SO_4	Log I†
2-Pyrrolecarboxamide		*p*-Methoxybenzamide	
4.93	−1.235	10.0	−0.934
10.09	−0.824	14.5	−0.686
16.05	−0.450	20.35	−0.455
20.35	−0.239	23.6	−0.273
23.87	−0.044	28.8	−0.029
28.58	+0.225	33.3	+0.191
34.57	+0.514	33.9	+0.238
38.95	+0.750	38.3	+0.472
41.05	+0.898	39.4	+0.507
3,4,5-Trimethoxybenzamide		44.6	+0.788
16.07	−0.993	46.2	+0.966
20.35	−0.762	49.6	+1.072
28.58	−0.401	*m*-Nitrobenzamide	
34.57	−0.117	28.58	−1.000
38.92	+0.103	34.57	−0.697
41.05	+0.215	38.92	−0.491
43.20	+0.316	41.05	−0.402
45.28	+0.469	43.20	−0.287
49.04	+0.682	45.28	−0.197
51.69	+0.860	49.04	+0.011
3,5-Dinitro-4-methylbenzamide		51.69	+0.148
34.46	−0.913	55.11	+0.346
38.80	−0.748	57.5	+0.488
43.07	−0.575	61.53	+0.800
48.21	−0.277	2,3,6-Trichlorobenzamide	
51.55	−0.154	49.04	−0.947
55.02	+0.067	51.69	−0.818
57.5	+0.250	55.11	−0.506
61.32	+0.526	57.5	−0.356
64.10	+0.724	61.53	−0.109
68.82	+0.983	64.2	+0.051
2,4-Dichloro-3,5-dinitrobenzamide		66.48	+0.203
55.59	−0.857	69.98	+0.449
58.3	−0.658	73.27	+0.715
61.53	−0.547	2,4,6-Trinitrobenzamide	
64.21	−0.369	61.53	−1.004
66.48	−0.235	64.21	−0.749
69.98	+0.015	66.48	−0.612
73.27	+0.291	69.98	−0.381
76.11	+0.501	73.27	−0.077
77.83	+0.581	76.11	+0.193
79.59	+0.834	77.83	+0.277
81.82	+0.946	79.59	+0.502
		81.82	+0.713

*Values used to calculate pK and H_A values.
†Determined at $\lambda_{BH^+}^{max}$ given in Table I.

of the changes produced by protonation. These medium effects are of uncertain magnitude and extremely difficult to correct for adequately. Since these could substantially affect the slopes of ionization curves on which acidity functions are based, several methods of attempting to correct for these effects have been considered. Apart from the previously mentioned method of Davis and Geissman (20), which leads to a partial cancellation of medium effects on ϵ values, there are two other methods available. One is the well-known isobestic point method, which has been used by Hammett (21), and involves shifting absorption curves laterally until they all intersect at a common point, as they theoretically should in the absence of medium effects. Ionization ratios are then calculated from ϵ values based on these shifted curves. A second method has been described previously (6)

Can. J. Chem. Downloaded from www.nrcresearchpress.com by 210.87.254.5 on 09/05/12
For personal use only.

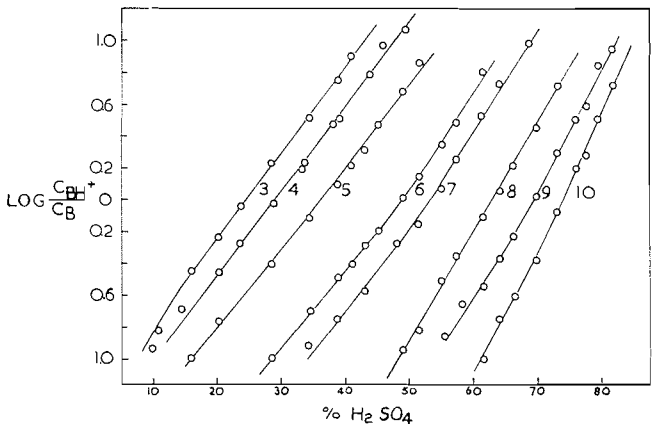

FIG. 1. Ionization curves for amide indicators in concentrated sulphuric acids (for indicator numbers see Table III).

and involves the assumption that medium effects are approximately linearly dependent on acidity. Corrected ϵ values are then obtained by an extrapolation procedure. Edward and Meacock (22) have reported substantial medium effects on the spectra of *p*-methoxybenzamide. We have analyzed our data for this compound by four different methods, using absorption spectra measured in 14 different solutions in the range 0–58% sulphuric acid. The log I values obtained have been treated by the method of least squares. The results are shown below.

Method	Slope vs. H_0	"pK"	Slope vs. H_A	pK_{BH^+}	Ref.
Davis and Geissman	0.67	−1.79	0.99	−1.50	(20)
Isobestic point	0.77	−1.77	1.08	−1.47	(21)
Linear extrapolation	0.75	−1.68	—	—	(6)
Present method	0.70	−1.71	1.00	−1.44	
Average	0.72	−1.74	1.02	−1.47	

Although there are some large differences in individual log I values, there is reasonable agreement between the slopes and intercepts of the ionization curves obtained by the different methods. Since the differences which result are not large none of these correction methods was applied to the data used to obtain ionization curves in the present study. All of these correction methods are at best inadequate for the following reasons. The Davis and Geissman method only gives good linear plots if λ_B^{max} and $\lambda_{BH^+}^{max}$ are well separated. This was not the case with several of the amides studied. The isobestic point method involves arbitrariness in deciding how to shift experimental absorption curves to produce an approximate isobestic point. Different isobestic points can be chosen, giving different indicator ratios. Further, the procedure is laborious and does not give good linear log I plots. Application of the linear extrapolation method requires knowledge of an acidity scale which itself is not subject to medium effects.

Since medium effects can not be eliminated satisfactorily it was decided to limit their seriousness by using the approach of Stewart and Granger (19) as described previously. It can easily be shown that if medium effects result in errors in individual ϵ values as large as 10%, fortuitous cancellation will result in errors of only about 2–3% in the slopes of indicator curves obtained using the method described in this paper. In addition most

Can. J. Chem. Downloaded from www.nrcresearchpress.com by 210.87.254.5 on 09/05/12
For personal use only.

of the spectral measurements were carried out in only moderately concentrated acids where medium effects are less serious than in the concentrated range (1).

Selection of Primary Indicator

In order to carry out the standard stepwise method of determining pK values, it is necessary to choose a primary indicator base whose ionization behavior can be studied in dilute aqueous solution, where

$$\mathrm{pH} = \mathrm{p}K_{\mathrm{HIn}^+} - \log [\mathrm{HIn}^+]/[\mathrm{In}] \quad .$$

and the activity coefficients of all species involved can be taken to be approximately unity. In this way potentiometric determination of pH and the observable indicator ratio will yield a respectable thermodynamic equilibrium constant. All pK values determined from this by direct comparison will also be thermodynamic equilibrium constants, referred back to ideal dilute aqueous solution as standard state, as will be any acidity function based on these values.

In the present work we are studying ionization equilibria of primary amides. Therefore it is evident that the primary indicator should if possible be an amide. The difficulty is

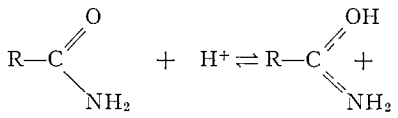

that amides as a class are considerably weaker bases than amines and it has so far proved impossible to find a primary amide which is strong enough to be measurably ionized in dilute aqueous solution. The strongest bases in this class that we have been able to find are acetamide, propionamide, 2-pyrrolecarboxamide, *p*-anisamide, and 2-hydroxyphenylurea, in order of decreasing basicity. None of these is measurably ionized in the region accessible to accurate measurements with the glass electrode. While it is true that the introduction of electron-donating substituents would produce stronger bases, it is unlikely that any of the derivatives would be appreciably ionized in dilute aqueous solution either. It is known that the ionization of amides is not very sensitive to substituent effects, particularly resonance effects (23). For example, *p*-methoxy substitution only changes the half ionization point of benzamide from 36% to 29% sulphuric acid. It is unlikely that even 2,4,6-trimethoxybenzamide would be sufficiently strong to ionize in the pH range. This is illustrated by considering that in the acid dissociation of benzoic acids, which has a similar ρ value to the basic ionization of amides (24), 2,4,6-trimethoxybenzoic acid has a pK_a only 0.63 log units different from that of benzoic acid itself (25).

We have therefore selected as primary indicator *p*-nitroaniline, which was used to establish the H_0 scale. In this case we have assumed that the variation of $f_{\mathrm{AH}^+}/f_{\mathrm{A}}$ for amide type bases will be very similar to the variation of $f_{\mathrm{BH}^+}/f_{\mathrm{B}}$ for the aniline type, over a limited region of acidity extending from 0–2 M sulphuric acid. This assumption is not strictly valid (6), but since the acidity region considered is narrow, it is reasonable that $f_{\mathrm{BH}^+}f_{\mathrm{A}}/f_{\mathrm{AH}^+}f_{\mathrm{B}}$ will not differ significantly from unity in this range. As a secondary indicator we have selected 2-pyrrolecarboxamide, for the following reasons. It is stable enough in dilute acids and its absorption characteristics are such that consistent and reliable log I values can be obtained. Its measurable ionization range overlaps considerably those of *p*-nitro- and *o*-nitro-aniline, as well as those of two of the more strongly basic amides, so that it can be used to bridge the pK gap between dilute solution and those acids where the

Can. J. Chem. Downloaded from www.nrcresearchpress.com by 210.87.254.5 on 09/05/12
For personal use only.

benzamides are appreciably ionized. The nuclear magnetic resonance (n.m.r.) spectrum of this compound in fluorosulphuric acid at low temperatures shows that it protonates on the carbonyl oxygen like the other amides studied (26).

The log I versus concentration curve for 2-pyrrolecarboxamide is reasonably parallel with those of the two nitroanilines as shown in Fig. 2. Thus the above assumption about

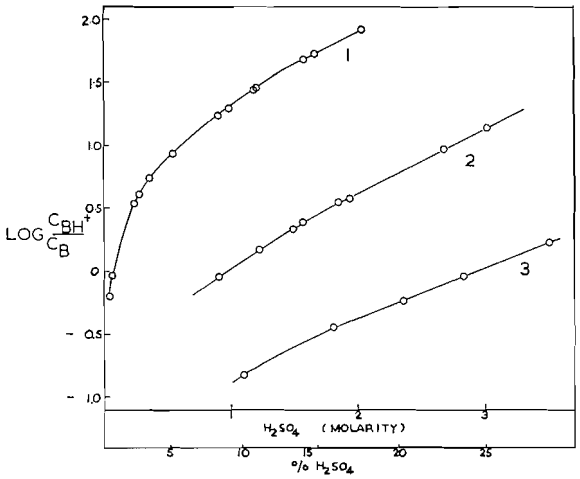

FIG. 2. Ionization curves for (1) *p*-nitroaniline, (2) *o*-nitroaniline, (3) 2-pyrrolecarboxamide in dilute sulphuric acid region.

activity coefficient behavior appears to be valid. Its curve is also closely parallel with those of *p*-methoxy and 3,4,5-trimethoxybenzamide as shown in Fig. 1. We have used the available data for *p*-nitro- and *o*-nitro-aniline (27) as well as our own data to establish the pK value for this secondary indicator using Equation [1]. The results are shown in Table I, the average pK value for 2-pyrrolecarboxamide calculated from a large number of measurements in several different acids. The agreement between the values is quite good, giving an average value of -1.23 ± 0.04 for the pK of this indicator. This value has been adopted as a standard for the determination of pK for the remaining amide indicators. It should be noted that any uncertainty introduced by the above treatment as to the absolute value of this pK will be carried through to any pK's or acidity function values determined from it.

Determination of pK Values of Indicators

The pK values of the other seven primary amides have been obtained by direct stepwise comparison using Equation [1] and the above pK of 2-pyrrolecarboxamide as a starting point. We have calculated successive pK values from ionization ratios for each overlapping pair of indicators, taking data directly from the experimental points where possible. In a few cases interpolations have been made from the best smooth curves through the experimental points. Only log I values in the range ±1.0 (corresponding to 10–90% protonation) were used, since the experimental uncertainty increases rapidly as the ionization ratio takes on very high or very low values. The individual values for a given indicator, obtained in each case from data in several different acids, show good agreement. These have been averaged and are given in Table I. The eight compounds listed constitute a structurally uniform set of amide indicators, suitable for obtaining acidity values for solutions up to 80% sulphuric acid.

Can. J. Chem. Downloaded from www.nrcresearchpress.com by 210.87.254.5 on 09/05/12
For personal use only.

The H_A Acidity Scale in Sulphuric Acid

We can now define a function, H_A, in an analogous manner to other acidity functions, such that

$$H_A = -\log (a_{H^+} f_A / f_{AH^+}) = pK_{AH^+} - \log [AH^+]/[A]$$

where pK_{AH^+} is the thermodynamic dissociation constant for an amide conjugate acid. Values of this function have been determined from the pK values and indicator ratios previously described. The individual H_A values for a given acid concentration were obtained using all indicators which were measurably protonated in that acid, again taking only log I values in the range ± 1.0. These H_A values are listed in Table III, along

TABLE III

Values of H_A in sulphuric acid solutions

% H_2SO_4 (w/w)	$-H_A$ (average)	Mean deviation*	Indicators used†
16.1‡	0.78	±0.02	1, 2, 3
20.4	0.99	—	3
23.9	1.18	—	3
28.6	1.43	±0.01	3, 4, 5
34.6	1.72	±0.02	3, 4, 5
38.9	1.95	±0.03	4, 5, 6
41.1	2.03	±0.01	4, 5, 6
43.2	2.14	±0.005	4, 5, 6
45.3	2.26	±0.02	4, 5, 6
49.0	2.47	±0.04	5, 6
51.7	2.57	—	6
55.1	2.78	±0.005	6, 7
57.5	2.92	0	6, 7
61.5	3.20	±0.01	6, 7, 8
64.2	3.32	±0.05	7, 8, 9
66.5	3.50	±0.01	7, 8, 9
70.0	3.74	±0.005	7, 8, 9
73.3	4.02	±0.005	8, 9
76.1	4.25	±0.02	9, 10
77.8	4.35	±0.04	9, 10
79.6	4.58	—	10
81.8	4.79	—	10

*Mean deviation between H_A values obtained using different indicators.

†H_A determined from the following indicators: 1, *p*-nitroaniline; 2, *o*-nitroaniline; 3, 2-pyrrolecarboxamide; 4, *p*-methoxybenzamide; 5, 3,4,5-trimethoxybenzamide; 6, *m*-nitrobenzamide; 7, 3,5-dinitro-4-methylbenzamide; 8, 2,3,6-trichlorobenzamide; 9, 2,4-dichloro-3,5-dinitrobenzamide; 10, 2,4,6-trinitrobenzamide.

‡H_A values for acids more dilute than this are assumed to be the same as the H_0 values of Bascombe and Bell (27).

with the particular indicators used for a given acid. Where more than one indicator was used, the H_A values were averaged. The agreement between the values obtained using different indicators is good. All values of H_A fall on a smooth curve when plotted against percent sulphuric acid. This curve is shown in Fig. 3 with the H_0 scale in the same acid range for comparison.

The difference between the two acidity functions is striking, even at moderate acid concentrations. For example, H_A is nearly 1 log unit less negative than H_0 even in 50% sulphuric acid, this difference becoming more than 3 log units at the highest acidities studied in the present work. This means that aqueous sulphuric acid can be up to 1000 times less effective in converting a primary amide to its conjugate acid than it is in the corresponding protonation of a primary amine of similar pK value. Thus the protonation behavior of the two types of base, although formally very similar, is considerably different

Can. J. Chem. Downloaded from www.nrcresearchpress.com by 210.87.254.5 on 09/05/12
For personal use only.

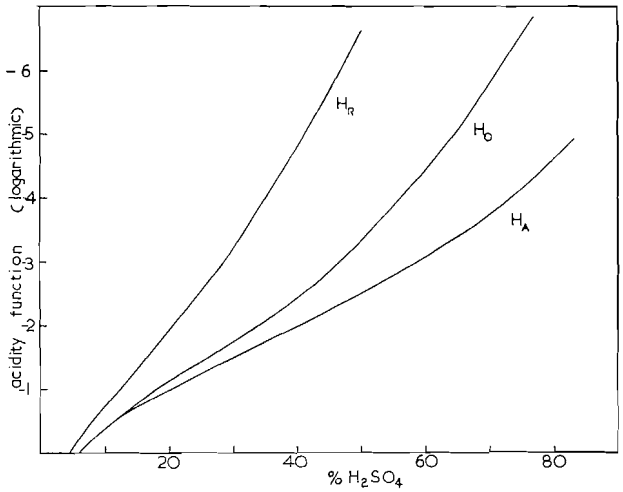

FIG. 3. Comparison of the H_A acidity function with H_0 and H_R. Values of H_0 taken from references 1, 5, and 27, and H_R from reference 2.

quantitatively. This again stresses the fact that acidity functions can be strongly dependent on indicator structure. The actual shape of the H_A curve is roughly similar to that for H_0 but is considerably less steep outside the dilute acid range and is approximately linear in the 10–60% acid region.

Comparison of the H_A and H_0 Functions

The reasons for the large observed differences in the ability of aqueous sulphuric acid to protonate primary amides as against primary amines are not immediately obvious. It is well recognized that the hydration requirements of the indicator species are important factors in determining the rate of rise of indicator acidity. This is especially true of the cations, rather than the neutral bases, as evidenced by the much more rapid rise of h_R with increasing acid concentration than that of h_0, carbonium ions being much less strongly hydrogen bonded to solvent molecules than anilinium ions. Just how this factor operates in the present case is not clear. If the two types of equilibria are written in terms of fully hydrated species, for the amides we have

$$AH^+(H_2O)_m + (a + p - m)H_2O \rightleftharpoons A(H_2O)_a + H^+(H_2O)_p$$

and for the anilines

$$BH^+(H_2O)_n + (b + p - n)H_2O \rightleftharpoons B(H_2O)_b + H^+(H_2O)_p.$$

We can now define the nonlogarithmic acidity functions in terms of fully hydrated species as

$$h_A = (a_{H^+(H_2O)_p} \cdot f_{A(H_2O)_a} / f_{AH^+(H_2O)_m} \cdot a_{H_2O}{}^{(a+p-m)})$$

$$h_0 = (a_{H^+(H_2O)_p} \cdot f_{B(H_2O)_b} / f_{BH^+(H_2O)_n} \cdot a_{H_2O}{}^{(b+p-n)})$$

The difference between the two functions can be expressed as the ratio

$$[2] \qquad h_A/h_0 = (f_{BH^+{}_h} \cdot f_{A_h} / f_{B_h} \cdot f_{AH^+{}_h})^{a_{H_2O}{}^{(m-a)-(n-b)}}$$

where the subscripts h refer to hydrated species. The less rapid increase of h_A with acidity

Can. J. Chem. Downloaded from www.nrcresearchpress.com by 210.87.254.5 on 09/05/12
For personal use only.

Can. J. Chem. Downloaded from www.nrcresearchpress.com by 210.87.254.5 on 09/05/12
For personal use only.

can be attributed to the hydration requirements of the amides in several ways. If the change in hydration on going from a neutral amide to a more strongly hydrated cation is greater than the corresponding hydration change on protonating an aniline, then $[(m - a) - (n - b)]$ will be positive. Hence, as the acid concentration is increased, and the water activity is decreased, h_A/h_0 will decrease, as is observed. If an amide conjugate acid is more strongly hydrated than the corresponding anilinium ion, f_{AH^+} will increase more rapidly with increasing acid than f_{BH^+}. Similarly, if a neutral amide is less strongly hydrated than the corresponding aniline, f_A will rise less rapidly than f_B. Each of these factors will contribute to a less rapid rise of h_A with acid concentration, when compared with h_0. Any or all of these factors may undergo significant variation with changes in the medium but their relative importance is difficult to predict. Assuming for the moment that the separation of terms in Equation [2] is valid, and that the net variation of the activity coefficient term is less important than that of the term in the water activity, we can write approximately

$$H_0 - H_A = [(m - a) - (n - b)] \log a_{H_2O} + \text{constant.}$$

Plotting $(H_0 - H_A)$ against $\log a_{H_2O}$ should then give a curve whose slope at any point can be related to the net hydration changes involved in the two types of equilibria. We have plotted $(H_0 - H_A)$ against available water activity data (28). The relationship is not linear, which is as expected, since even if the above assumptions are valid, the individual hydration numbers can take on different values in different regions of acidity, depending on the amount of "free" water available. The plot shows a steadily decreasing curvature as $\log a_{H_2O}$ is decreased. It is approximately linear over two wide regions, giving a slope of about 1.7 in the 30–60% acid range and about 0.75 in 70–85% range. This suggests that the net increase in hydration on protonation of an amide involves one or two more water molecules than the corresponding increase on protonation of an aniline. Taft (29) has suggested that a hydration number of 3 for an anilinium ion is reasonable in view of the fact that such an ion can hydrogen bond strongly to three water molecules through its acidic protons. However, considering only the numbers of such protons available for hydrogen bonding in the various indicator species, it is difficult to see how $[(m - a) - (n - b)]$ can differ very much from zero. One way around this difficulty is to postulate the following structure for the hydrated amide cation so that its hydration

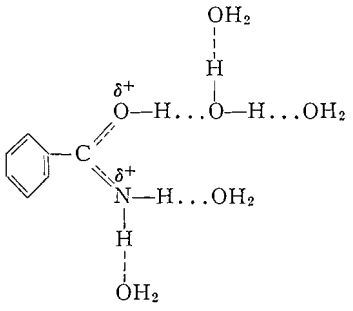

number can be 5 in solutions where there is sufficient water available. In support of this it is known that [O—H...O] bonds are on the average considerably stronger than the [N—H...O] type (30). Further, aldehydes (31) and ketones (32) whose conjugate acids have only one acidic proton, follow the H_0 function reasonably well. This suggests strongly that a protonated carbonyl group is hydrated by more than one water molecule.

This simple explanation of the difference between H_A and H_0 obviously leaves much to be desired except in a qualitative sense, since we have neglected possible variations in the $\log(f_{BH^+_h} \cdot f_{A_h}/f_{B_h} \cdot f_{AH^+_h})$ term of Equation [2]. However, this term would also have to decrease as the water activity is decreased, to account for the observed differences in h_A and h_0, and would require similar kinds of hydration changes on protonation of amides and anilines, i.e. that $(m - a) > (n - b)$.

A knowledge of the activity coefficients of amides and their conjugate acids is clearly desirable in order to be able to assess the importance of the various terms in Equation [2]. We are at present investigating the activity coefficient behavior of some typical amides and their salts. We hope by comparing these results with Boyd's values for typical aniline indicators (33) to be able to assess more quantitatively the importance of the various factors involved.

The Applicability of the H_A Scale

It is evident that the H_A function, like any other acidity function, will be of limited generality. It is, however, important that it be applicable at least to primary amides as a class, in order that it may be used to obtain thermodynamic pK's for other amides and also be useful in studying reaction mechanisms. We have therefore tested the generality of H_A in the following way. Using available experimental data we have plotted log I values against H_A for 12 primary amides not used as indicators in the present work. Ten of these gave least mean squares slopes between 0.95 and 1.05 which can be considered as being effectively unity as required by the defining equation for H_A. The mean value and deviation for all 12 was 0.97 ± 0.06. Thus within the experimental uncertainty caused by medium shifts on the spectra towards the red, which would result in slopes of less than unity, these amides appear to be following H_A reasonably well. It would be interesting to test the generality of the H_0 function in a similar way using representative anilines. This has apparently not been done.

The behavior of the individual amides and the significance of derived pK values will be discussed in detail in Part II of this series.

Estimated Accuracy of the H_A Values

It is impossible to estimate precisely the numerical accuracy of any particular H_A value, since individual errors in determined pK values may be cumulative. Also, as mentioned previously, any uncertainty in the pK of the secondary standard base will be carried through to all subsequently determined pK's, and hence to any H_A values determined from them. The usual estimate of the experimental uncertainty in any pK value obtained by the standard spectrophotometric technique is ± 0.05 log unit. Therefore the H_A values should not be considered as known to any better than ± 0.1 units in the lower acidity range and probably ± 0.2 units in the more concentrated region above 60% acid. Nonetheless the following considerations give confidence in the reliability of the values within these limits. The parallelism of the indicator curves is good. These curves are closely spaced enough so that considerable overlap has been achieved. Hence not too much weight has been placed on any one indicator. The several H_A values obtained for any given solution are consistent and all experimental points fall closely on a smooth curve when plotted against concentration.

ACKNOWLEDGMENTS

The financial assistance of the National Research Council of Canada is gratefully acknowledged. We are also grateful for the award of a Province of Ontario Graduate Fellowship to one of us (J. B. S.).

Can. J. Chem. Downloaded from www.nrcresearchpress.com by 210.87.254.5 on 09/05/12
For personal use only.

REFERENCES

1. L. P. HAMMETT and A. J. DEYRUP. J. Am. Chem. Soc. **54**, 2721 (1932).
2. N. C. DENO, J. J. JARUZELSKI, and A. SCHRIESHEIM. J. Am. Chem. Soc. **77**, 3044 (1955).
3. N. C. DENO, P. GROVES, J. J. JARUZELSKI, and M. LUGASCH. J. Am. Chem. Soc. **82**, 4719 (1960). N. C. DENO, P. GROVES, and G. SAINES. J. Am. Chem. Soc. **81**, 5790 (1959).
4. E. M. ARNETT. *In* Progress in physical organic chemistry. Vol. 1. *Edited by* S. G. Cohen, A. Streitwieser, Jr., and R. W. Taft. Interscience, New York. 1963. p. 223 ff.
5. M. J. JORGENSON and D. R. HARTTER. J. Am. Chem. Soc. **85**, 878 (1963).
6. A. R. KATRITZKY, A. J. WARING, and K. YATES. Tetrahedron, **19**, 465 (1963). J. T. EDWARD and I. C. WANG. Can. J. Chem. **40**, 966 (1962).
7. R. J. GILLESPIE and T. BIRCHALL. Can. J. Chem. **41**, 148 (1963).
8. J. F. BUNNETT. J. Am. Chem. Soc. **83**, 4956 (1961).
9. J. F. BUNNETT. J. Am. Chem. Soc. **83**, 4968, 4973, 4978 (1961).
10. M. MARX. Ann. **263**, 250 (1891).
11. I. HEILBRON and H. M. BUNBURY. Dictionary of organic compounds. Eyre and Spotteswood, London. 1946.
12. R. L. SHRINER and R. C. FUSON. Identification of organic compounds. 3rd ed. Wiley, New York. 1948. p.157.
13. I. K. BARBEN and H. SUSCHITZKY. J. Chem. Soc. 672 (1960).
14. V. MEYER. Ber. **27**, 3153 (1894).
15. P. J. MONTAGNE. Rec. Trav. Chim. **21**, 382 (1902).
16. E. FISCHER and D. D. VAN SLYKE. Ber. **44**, 3169 (1911).
17. K. YATES and B. F. SCOTT. Can. J. Chem. **41**, 2320 (1963).
18. J. T. EDWARD, H. S. CHANG, K. YATES, and R. STEWART. Can. J. Chem. **38**, 1518 (1960).
19. R. STEWART and M. R. GRANGER. Can. J. Chem. **39**, 2508 (1961).
20. C. T. DAVIS and T. A. GEISSMAN. J. Am. Chem. Soc. **76**, 3507 (1954).
21. L. A. FLEXSER, L. P. HAMMETT, and A. DINGWALL. J. Am. Chem. Soc. **57**, 2103 (1935).
22. J. T. EDWARD and S. C. R. MEACOCK. J. Chem. Soc. 2000 (1957).
23. R. B. HOMER and R. B. MOODIE. J. Chem. Soc. 4377 (1963).
24. K. YATES and J. B. STEVENS. Unpublished results.
25. R. A. ROBINSON and R. H. STOKES. Electrolyte solutions. Butterworth's, London. 1959. pp. 526, 530.
26. R. J. GILLESPIE. Personal communication. (See also Reference 7.)
27. K. N. BASCOMBE and R. P. BELL. J. Chem. Soc. 1096 (1959).
28. W. F. GIAUQUE, E. W. HORNUNG, J. E. KUNZLER, and T. R. RUBIN. J. Am. Chem. Soc. **82**, 62 (1960).
29. R. W. TAFT. J. Am. Chem. Soc. **82**, 2965 (1960).
30. L. N. FERGUSON. The modern structural theory of organic chemistry. Prentice-Hall, New Jersey. 1963. p. 128.
31. K. YATES and R. STEWART. Can. J. Chem. **37**, 664 (1959).
32. R. STEWART and K. YATES. J. Am. Chem. Soc. **80**, 6355 (1958).
33. R. H. BOYD. J. Am. Chem. Soc. **85**, 1555 (1963).

Can. J. Chem. Downloaded from www.nrcresearchpress.com by 210.87.254.5 on 09/05/12
For personal use only.

Can. J. Chem. Downloaded from www.nrcresearchpress.com by 210.87.254.42 on 09/05/12
For personal use only.

FRACTIONATION OF GERMANIUM ISOTOPES IN CHEMICAL REACTIONS

H. M. BROWN[1] AND H. R. KROUSE
Department of Physics, University of Alberta, Edmonton, Alberta
Received January 8, 1964

ABSTRACT

Isotopic vibrational frequencies and the corresponding partition-function ratios for several compounds containing Ge^{70} and Ge^{76} have been calculated at various temperatures. The theoretical equilibrium constants for germanium isotope-exchange reactions derived from these partition-function ratios indicate that noticeable germanium isotope fractionation might be effected with laboratory reactions. Calculated kinetic isotope effects in the breaking of diatomic bonds also predict observable alterations of the Ge^{70}/Ge^{76} ratio.

A kinetic isotope effect of 1.0% observed in the chemical reduction of GeO_2 to GeO is discussed.

INTRODUCTION

With the discovery of deuterium in 1932 by Urey, Brickwedde, and Murphy (1), it became apparent that the isotopes of an element differ noticeably in their physical and chemical behaviors. These differences are due to the dependence of many thermodynamic quantities upon the vibrational frequencies of the molecules, and the dependence in turn of these frequencies upon the masses of the constituent atoms. Lighter elements have received considerable study because of the large percentage mass differences between their isotopes. Heavy elements which possess a number of isotopes, however, may also have a significant percentage mass difference between their lightest and heaviest isotope, and therefore noticeable fractionation might be possible in natural and laboratory processes.

Element 32, germanium, is such an element, with five stable isotopes of mass numbers 70, 72, 73, 74, and 76 and approximate abundances of 20.5, 27.4, 7.8, 36.5, and 7.8% respectively. The percentage mass difference is about 8% between Ge^{70} and Ge^{76}. The isotopes of the element were first investigated mass spectrometrically by Aston in 1923 (2), and since then their abundances have been measured by a number of workers (Bainbridge (3), Dempster *et al.* (4), Hibbs *et al.* (5), Graham *et al.* (6), Reynolds (7), and Shima (8)).

Of these, Graham *et al.* (6) and Shima (8) investigated samples from various sources. Shima found no difference in the isotopic composition of germanium from eight meteorites and a terrestrial sample, outside of the error of his solid-source mass-spectrometric analyses. Graham *et al.* (6) had previously examined six samples from widely varying geographical and geological origins. Analyses were made with both $GeCl_4$ and GeF_4 in a gas-source mass spectrometer. Within the precision of their measurements, they found all but one of these samples to have the same isotope abundance. The sample which differed (0.7% in the Ge^{70}/Ge^{76} ratio) from the others had the lighter isotopes favored at the expense of the heavier ones, while the isotopes of intermediate mass were of about the same abundance as in the other samples. This is precisely the effect that one would expect in a natural isotope-fractionation process which is solely a function of mass.

The study reported here is a theoretical and experimental attempt to determine the extent to which the Ge^{70}/Ge^{76} ratio might be altered in laboratory and natural processes.

[1]*Present address: Research Council of Alberta, Edmonton, Alberta.*

Can. J. Chem. Downloaded from www.nrcresearchpress.com by 210.87.254.42 on 09/05/12
For personal use only.

THEORY

Equilibrium Isotope Effects

Urey and Rittenburg (9) were the first to apply statistical mechanics to the calculation of equilibrium isotope-exchange constants. Later simplification by Urey (10) and by Bigeleisen and Mayer (11) has made it possible to calculate these constants (except in the case of hydrogen) solely from a knowledge of the isotopic vibrational frequencies of the participating molecules.

An isotopic-exchange reaction may be written

$$[1] \qquad aA_1 + bB_2 \rightleftharpoons aA_2 + bB_1$$

where the subscripts 1 and 2 refer to the light and heavy isotopes respectively, and A and B are molecules having the element under consideration as common constituent. The equilibrium constant for this exchange is given by

$$[2] \qquad K = \left[\frac{Q_{A_2}}{Q_{A_1}}\right]^a \Big/ \left[\frac{Q_{B_2}}{Q_{B_1}}\right]^b,$$

where the Q's are the total partition functions of the molecules. Urey (10) and Bigeleisen and Mayer (11) have shown that this constant can be expressed in terms of isotopic partition-function ratios Q_2'/Q_1' which depend only on the vibrational frequencies of the isotopic molecules. In this work the simplification of Bigeleisen and Mayer, where the ratio is given by

$$[3] \qquad \frac{Q_2'}{Q_1'} = \frac{\sigma_1}{\sigma_2}\left[1 + \sum_i \left(\frac{1}{2} - \frac{1}{u_{2i}} + \frac{1}{e^{u_{2i}} - 1}\right)\Delta u_i\right],$$

has been used. Here $u_i = hcw_i/kT$ and w_i is the i'th vibrational frequency in cm^{-1}. The summation is over i fundamental frequencies, a d-fold degeneracy being counted d times. The ratio of symmetry numbers σ_1/σ_2 is unity if the molecule under consideration contains only one atom of the element being exchanged or if the molecule contains more than one such atom, but these atoms occupy indistinguishable positions in the molecule and are all exchanged. $\Delta u_i = u_{1i} - u_{2i}$ is always positive. The function

$$G(u_i) = \frac{1}{2} - \frac{1}{u_{2i}} + \frac{1}{e^{u_{2i}} - 1}$$

has been tabulated by Bigeleisen and Mayer (11) for values of $0 \leq u \leq 25$.

Kinetic Isotope Effects

The general problem of reaction rates has been developed from a statistical viewpoint by Eyring (12) and by Evans and Polanyi (13). Bigeleisen (14) has used their "theory of absolute rates" to develop an expression for the ratio of reaction rates for competing isotopic reactions. It is

$$[4] \qquad \frac{k_1}{k_2} = \frac{K_1}{K_2}\cdot\frac{\sigma_1}{\sigma_2}\cdot\frac{\sigma_2^{\ddagger}}{\sigma_1^{\ddagger}}\cdot\frac{\nu_{1L}^{\ddagger}}{\nu_{2L}^{\ddagger}}\left\{1 + \sum_i^{3n-6} G(u_i)\Delta u_i - \sum_i^{3n-7} G(u_i^{\ddagger})\Delta u_i^{\ddagger}\right\}.$$

Here $G(u_i)$ is the free-energy function previously defined, ‡ refers to the activated complex of absolute reaction rate theory, σ_i are symmetry numbers, 1 and 2 refer to the light and heavy isotopes respectively, and $\nu_L^{\ddagger}$ is the imaginary frequency of vibration along the reaction coordinate. The ratio of transmission coefficients, K_1/K_2, has been shown by Hirschfelder and Wigner (15) to be nearly unity at and above room temperature.

The ratio $\nu_{1L}^{\pm}/\nu_{2L}^{\pm}$ is generally given the value $(\mu_2^*/\mu_1^*)^{\frac{1}{2}}$, where μ^* denotes the reduced mass along the reaction coordinate. Previously this was taken to be the reduced mass of the two atoms joined by the bond being ruptured, in agreement with work on classical models by Slater (16). Bigeleisen and Wolfsberg (17) suggest, however, that because the molecule is being torn into two fragments μ^* should be considered as the reduced mass of the two fragments.

Equation [4] is difficult to apply because of our limited knowledge of the activated complex and hence our inability to calculate the term

$$\sum_i^{3n-7} G(u_i^{\pm})\Delta u_i^{\pm}.$$

In general, however, the activated complex will be intermediate in form between the reactants and products, enabling two limits to be calculated for the ratio of rate constants. One limit arises when it is assumed that the activated complex is like the reactant, i.e.

$$\sum_i^{3n-6} G(u_i)\Delta u_i = \sum_i^{3n-7} G(u_i^{\pm})\Delta u_i^{\pm}.$$

In this case the ratio of rate constants is the ratio of the reduced masses and is temperature independent. If the activated complex is like the product, then

$$\sum_i^{3n-7} G(u_i^{\pm})\Delta u_i^{\pm} = \left(\sum_i^{3n-6} G(u_i)\Delta u_i\right)_{\text{product}}.$$

For a diatomic reactant molecule, since there is no vibrational frequency,

$$(G(u_i)\Delta u_i)_{\text{product}} = 0.$$

An experimentally measured ratio of rate constants is expected to fall within these two extremes.

THEORETICAL CALCULATIONS

Using the above theory, the partition function ratios for various compounds containing Ge^{70} and Ge^{76} were calculated. The vibrational frequencies for these isotopic molecules were calculated by means of known "force equations" from the experimentally observed frequencies, which were assumed to apply to the most abundant Ge^{74} molecules. These known "force equations" relate the fundamental vibrational frequencies to force constants and atomic weights on the assumption of a particular model for the molecule under consideration.

TABLE I

Diatomic molecular frequencies (cm^{-1})

Molecular species	Frequency		
	Obs. for species containing Ge^{74}(26)	Calc. for species containing Ge^{70}	Calc. for species containing Ge^{76}
GeS^{32}	572.2	577.1	569.9
$GeSe^{80}$	404.4	411.6	401.6
$GeCl^{35}$	404.9	408.5	403.2
$GeTe^{130}$	321.4	327.2	318.7
GeF	659.6	663.5	657.9
GeBr*	294.8	299.1	292.8
GeO^{16}	977.1	982.0	974.8

*Bromine has two isotopes 79 and 81 which are each approximately 50% abundant. Therefore the atomic weight was used in the calculation.

Can. J. Chem. Downloaded from www.nrcresearchpress.com by 210.87.254.42 on 09/05/12
For personal use only.

TABLE II

Polyatomic molecular frequencies (cm^{-1})
w_2 and w_3 are triply degenerate; w_4 is doubly degenerate

Molecule	w_1	w_2	w_3	w_4	Reference
$Ge^{74}Cl_4$	397	451	171	132	Observed (27)
$Ge^{70}Cl_4$	397	455.8	171.9	132	Force equations used (27)
$Ge^{76}Cl_4$	397	448.5	169.8	132	"
$Ge^{74}Br_4$	234	328	111	78	Observed (27)
$Ge^{70}Br_4$	234	333.5	111.7	78	Force equations used (27)
$Ge^{76}Br_4$	234	325.1	110.6	78	"
$Ge^{74}F_4$	738	800	260	205	Observed (28)
$Ge^{70}F_4$	738	805.6	262.0	205	Force equations used (28)
$Ge^{76}F_4$	738	797.5	259.1	205	"
$Ge^{74}H_4$	2090	819.3	2113.6	930.9	Observed (29)
$Ge^{70}H_4$	2090	820.2	2114.1	930.9	Force equations used (30)
$Ge^{76}H_4$	2090	819.1	2112.6	930.9	"

Tables I and II summarize the vibrational frequencies calculated for some diatomic and polyatomic species containing Ge^{70} and Ge^{76}. References to the spectroscopic data used, the set of force equations employed, and the method of calculation are given. In Table III the partition-function ratios and the equilibrium constants for some possible $Ge^{70} \leftrightarrow Ge^{76}$ exchange reactions are summarized. The equilibrium constant for an exchange reaction between any two compounds listed is contained in the body of the table

TABLE III

Equilibrium constants for $Ge^{76} \rightleftharpoons Ge^{70}$ exchange reactions

	$\frac{Ge^{76}F_4}{Ge^{70}F_4}$	$\frac{Ge^{76}Cl_4}{Ge^{70}Cl_4}$	$\frac{Ge^{76}Br_4}{Ge^{70}Br_4}$	$\frac{Ge^{76}H_4}{Ge^{70}H_4}$	$\frac{Ge^{76}O^{16}}{Ge^{70}O^{16}}$	$\frac{Ge^{76}Se^{80}}{Ge^{70}Se^{80}}$	$\frac{Ge^{76}S^{32}}{Ge^{70}S^{32}}$	$\frac{Ge^{76}Te^{130}}{Ge^{70}Te^{130}}$	Temp. (°C)
$\frac{Q_3'}{Q_1'}$	1.041	1.023	1.019	1.015	1.012	1.009	1.008	1.006	0
	1.035	1.020	1.016	1.013	1.011	1.007	1.007	1.005	25
	1.024	1.013	1.010	1.009	1.007	1.005	1.005	1.003	100
	1.013	1.007	1.005	1.006	1.004	1.003	1.003	1.002	250
$\frac{Ge^{76}F_4}{Ge^{70}F_4}$	1.000	1.018	1.022	1.026	1.029	1.032	1.033	1.035	0
		1.015	1.019	1.022	1.024	1.028	1.028	1.030	25
		1.011	1.014	1.015	1.017	1.019	1.019	1.021	100
		1.006	1.008	1.007	1.009	1.010	1.010	1.011	250
$\frac{Ge^{76}Cl_4}{Ge^{70}Cl_4}$		1.000	1.004	1.008	1.011	1.014	1.015	1.017	0
			1.004	1.007	1.009	1.013	1.013	1.015	25
			1.003	1.004	1.006	1.008	1.008	1.010	100
			1.002	1.001	1.003	1.004	1.004	1.005	250
$\frac{Ge^{76}Br_4}{Ge^{70}Br_4}$			1.000	1.004	1.007	1.010	1.011	1.013	0
				1.003	1.005	1.009	1.009	1.011	25
				1.001	1.003	1.005	1.005	1.007	100
				0.999	1.001	1.002	1.002	1.003	250
$\frac{Ge^{76}H_4}{Ge^{70}H_4}$				1.000	1.003	1.006	1.007	1.009	0
					1.002	1.006	1.006	1.008	25
					1.002	1.004	1.004	1.006	100
					1.002	1.003	1.003	1.004	250
$\frac{Ge^{76}O^{16}}{Ge^{70}O^{16}}$					1.000	1.003	1.004	1.006	0
						1.004	1.004	1.006	25
						1.002	1.002	1.004	100
						1.001	1.001	1.002	250
$\frac{Ge^{76}Se^{80}}{Ge^{70}Se^{80}}$						1.000	1.001	1.003	0
							1.000	1.002	25
							1.000	1.002	100
							1.000	1.001	250
$\frac{Ge^{76}S^{32}}{Ge^{70}S^{32}}$							1.000	1.002	0
								1.002	25
								1.002	100
								1.001	250
$\frac{Ge^{76}Te^{130}}{Ge^{70}Te^{130}}$								1.000	0
									25
									100
									250

Can. J. Chem. Downloaded from www.nrcresearchpress.com by 210.87.254.42 on 09/05/12
For personal use only.

at the intersection of the appropriate row and column. An equilibrium constant greater than unity indicates that the heavier isotope will concentrate in the compound listed in the left column.

TABLE IV

Kinetic isotope effect: ratio of rate constants k_{70}/k_{76}

Temp. (°C)	GeS^{32}	$GeSe^{80}$	$GeCl^{35}$	$GeTe^{130}$	GeF^{19}	GeBr	GeO^{16}
Maximum value of k_{70}/k_{76}:							
0	1.021	1.031	1.018	1.033	1.016	1.026	1.020
25	1.020	1.029	1.017	1.032	1.015	1.025	1.018
100	1.015	1.028	1.016	1.030	1.013	1.024	1.015
250	1.015	1.025	1.015	1.028	1.011	1.023	1.011
Minimum value of k_{70}/k_{76}:							
	1.013	1.022	1.013	1.027	1.009	1.022	1.007

For diatomic species, Table IV shows the maximum and minimum values to be expected in the ratios of the rate constants in a kinetic isotope effect. These values indicate (for a particular molecular species and reaction temperature) how much faster the species with the lighter (Ge^{70}) isotope will react than that with the heavier (Ge^{76}) isotope in competitive reactions.

EXPERIMENTAL KINETIC ISOTOPE-EFFECT STUDY

Reduction of GeO_2

To see if the extent of isotope fractionation predicted theoretically could be verified experimentally, GeO_2 was partially reduced in an aqueous medium and a kinetic isotope effect was observed.

The reduction procedure was based upon the method of Dennis and Hulse (18) in which hypophosphorous acid was used as the reducing agent. Schenk (19) has represented this overall reaction by the following equation.

$$GeO_2 + H_3PO_2 = GeO + H_3PO_3$$

One gram of GeO_2 was dissolved in 500 ml of H_2O and the solution was made ~3 *N* with respect to HCl. This solution was heated to 100 °C, and 25 ml of 50% H_3PO_2 (also heated to 100 °C) were added with vigorous stirring. The reaction was stopped upon partial completion by neutralizing with NH_4OH. This neutralization precipitated hydrous GeO, which ranged in color from yellow to brown depending upon the extent of hydration. The times for various degrees of reduction were predetermined experimentally and found to be within the range of 1 to 2 minutes for 10% and 20% reductions at 100 °C. A 10% reduction at 80 °C with the above concentrations required 13 minutes. It would have been more convenient to have effected a partial reduction by adding the appropriate insufficiency of H_3PO_2, but all attempts to do this were unsuccessful. After precipitation, the hydrous GeO was separated from the solution by centrifuging and was then reoxidized to GeO_2 with H_2O_2. From this GeO_2 sample, GeF_4 gas was prepared by the method of Dennis and Laubengayer (20) and the Ge^{76}/Ge^{70} ratio was determined in a gas-source mass spectrometer. This ratio was compared to that of a standard GeF_4 sample prepared from "non-reduced" GeO_2.

Mass Spectrometry

Two different mass spectrometers were used during the course of the investigation. The first was a single collection 6 in. radius 60° magnetic analyzer with a strip-chart recorder to trace mass spectra "peaks". Normally the run procedure consisted of tracing 22 complete spectra of a sample and then similarly recording a "standard". Typically a run consisted of 3 or 4 such comparisons. To determine the relative abundances of the germanium isotopes, the relative peak heights were measured.

The second mass spectrometer was a 12 in. radius 90° magnetic-analyzer instrument employing simultaneous collection. A null method of recording was used where a measured portion of the voltage produced by one ion current is fed back inversely to cancel the voltage produced by the other ion current. A magnetic-valve system (21) enabled samples to be changed within about 5 minutes and allowed three continuous recordings of a sample and a standard to be made in 1 hour.

In both instruments, the most abundant ion spectrum GeF_3^+ was used. The sample-handling systems were of pyrex glass with metal Hoke valves, to eliminate contaminations from stopcock grease, and were designed to introduce both the standard and the sample into the mass spectrometer at the same pressure. Memory effects were present, but these were short time and did not cause much difficulty.

Can. J. Chem. Downloaded from www.nrcresearchpress.com by 210.87.254.42 on 09/05/12
For personal use only.

Contaminants included SiF_4 and HF, which were produced when $BaGeF_6$ was decomposed according to the Laubengayer method. It was felt that the HF was trapped when the crystals of $BaGeF_6$ were precipitated since heating the crystals below their decomposition temperature proved an effective means for HF removal. SiF_4 could be pumped away from the sample by using a solid–liquid ethyl alcohol bath. Another contamination was the presence of chloride species. This was believed to be due to the use of $BaCl_2$ in the preparation of $BaGeF_6$. This problem was most acute with small samples. Two difficulties arise: (*a*) the mass spectrometer cannot resolve the $Ge^{73}FCl^{35+}$ ion current from that of $Ge^{70}F_3^+$ and (*b*) germanium isotopes might exchange between the halide species and fractionate. Although corrections seem possible for contaminated samples, only the measurements from samples with negligible chloride content are reported here.

RESULTS AND DISCUSSION

Tables III and IV indicate that the Ge^{70}/Ge^{76} ratio might be altered by as much as 3% if mechanisms for such alterations existed.

The experimental results confirm the possibility of fractionating germanium isotopes. Measurements on five 10% reductions at 100 °C gave

$$R_{10} = \frac{(Ge^{70}/Ge^{76})_{\text{GeO product}}}{(Ge^{70}/Ge^{76})_{\text{unreduced GeO}_2}} = 1.010 \pm 0.002.$$

A 10% reduction at 80 °C gave a result slightly higher than the above average but within the standard deviation.

Four 20% reductions at 100 °C gave a much lower result,

$$R_{20} = \frac{(Ge^{70}/Ge^{76})_{\text{GeO product}}}{(Ge^{70}/Ge^{76})_{\text{unreduced GeO}_2}} = 1.004 \pm 0.001.$$

The mechanism and kinetics of this reduction have not been studied in detail. However, there is considerable agreement (22, 24) that GeO_2 is present as the un-ionized monomer in 3 *N* HCl (HCl does not start to complex with Ge^{IV} until >6 *N*). The reduced germanium is easily complexed by HCl and is likely present as $GeCl_3^-$ or $GeCl_4^=$ (24). It would appear that the oxygen in the product GeO is not that originally present in GeO_2. It seems desirable therefore to attribute the results to a kinetic isotope effect in the competitive reactions

$$^{70}GeO_2 \xrightarrow{k_{70}} {}^{70}Ge^{II}$$

$$^{76}GeO_2 \xrightarrow{k_{76}} {}^{76}Ge^{II}$$

where Ge^{II} simply refers to the various species with germanium present in the +2 valence state. Since in the reaction, oxygen atoms are being removed from the germanium, the simplest interpretation is that the observed isotope fractionation results during a germanium–oxygen bond breakage.

When R_{10} and R_{20} are corrected to zero reduction, they should of course give the same value. Using equations given by Bigeleisen and Wolfsberg (17), this was not found to be the case; R_{10} gave $k_{70}/k_{76} = 1.012 \pm 0.002$ while R_{20} gave $k_{70}/k_{76} = 1.006 \pm 0.001$. However, when the procedure is considered, this discrepancy is not surprising. Shenk (19) suggests that similarly prepared GeO usually contains a few percent of GeO_2. The presence of unreduced GeO_2 in the hydrous GeO precipitate would reduce the ratio *R*. Furthermore, since the solubilities of GeO_2 and GeO in neutral aqueous solution have been reported as

Can. J. Chem. Downloaded from www.nrcresearchpress.com by 210.87.254.42 on 09/05/12
For personal use only.

0.45 g/100 ml (25) and 0.04 g/100 ml (23) respectively at 25 °C, it is probable that some of the reduced product remained dissolved in the reaction medium.

In two 10% reductions, the abundances of the other germanium isotopes were also compared. On the basis of the above interpretation it was found that

$$\frac{k_{70}}{k_{72}} = \frac{k_{72}}{k_{74}} = \frac{k_{74}}{k_{76}} = 1.003 \pm 0.001,$$

which is consistent with the results of R_{10}. GeO_2 completely reduced to GeO and reoxidized was found to be identical with unreacted GeO_2 with less than 0.05% standard deviation, suggesting that the inconsistency noted is a result of the limitations on chemical control of the reduction rather than in instrumentation.

Vibrational frequencies could not be found for GeO_2 monomer in solution, and attempts to measure them under the reaction conditions were unsuccessful. If a simplified model of the reaction is assumed, namely the breaking of a Ge–O diatomic bond, Table IV predicts a maximum and minimum value for k_{70}/k_{76} at 100 °C of 1.015 and 1.007.

This theoretical result further suggests that the fractionation observed represents the isotope effect in the breaking of a germanium–oxygen bond.

It would be desirable to study the mechanism of this reaction thoroughly, so that a more exact interpretation could be made of the isotope effect noted. The measurements are significant, however, in that they demonstrate the feasibility of fractionating germanium isotopes in chemical reactions.

ACKNOWLEDGMENTS

The authors are indebted to G. L. Cumming of the Physics Department, University of Alberta, Edmonton, for his part in the mass spectrometry in the initial stages of this study and to D. A. Everest of the National Chemical Laboratory, Teddington, Middlesex, for correspondence regarding the behavior of germanium in solution.

Financial assistance from the National Research Council, Ottawa, is also gratefully acknowledged.

REFERENCES

1. H. C. Urey, F. G. Brickwedde, and G. M. Murphy. Phys. Rev. **39**, 164, 864 (1932).
2. F. W. Aston. Nature, **111**, 771 (1923); **122**, 167 (1928); Proc. Roy. Soc. London, Ser. A, **132**, 487 (1931).
3. A. J. Dempster, A. E. Shaw, M. G. Inghram, R. J. Hayden, and D. C. Hess, Jr. Plutonium Project Report ANL-4082. Nov. 1947.
4. K. T. Bainbridge. Phys. Rev. **43**, 1056 (1933).
5. R. F. Hibbs, J. W. Redmond, H. R. Gwinn, and W. D. Harmon. Phys. Rev. **75**, 533 (1949).
6. R. P. Graham, J. Macnamara, I. H. Crocker, and R. B. MacFarlane. Can. J. Chem. **29**, 89 (1951).
7. J. H. Reynolds. Phys. Rev. **90**, 1047 (1953).
8. M. Shima. J. Geophys. Res. **68**, 4289 (1963).
9. H. C. Urey and D. Rittenburg. J. Chem. Phys. **1**, 137 (1933); J. Am. Chem. Soc. **56**, 1885 (1934).
10. H. C. Urey. J. Chem. Soc. 562 (1947).
11. J. Bigeleisen and M. G. Mayer. J. Chem. Phys. **15**, 261 (1947).
12. H. Eyring. J. Chem. Phys. **3**, 107 (1935).
13. M. G. Evans and M. Polanyi. Trans. Faraday Soc. **31**, 875 (1935).
14. J. Bigeleisen. J. Chem. Phys. **17**, 675 (1949).
15. J. O. Hirschfelder and J. Wigner. J. Chem. Phys. **7**, 616 (1939).
16. N. B. Slater. Trans. Roy. Soc. London, Ser. A, **246**, 57 (1953).
17. J. Bigeleisen and M. Wolfsberg. Advances in chemical physics. Vol. 1. Interscience Publishers Inc., New York. 1958. p. 15.
18. L. M. Dennis and R. E. Hulse. J. Am. Chem. Soc. **52**, 3553 (1930).
19. P. W. Schenk. Handbook of preparative inorganic chemistry. Vol. 1. Academic Press Inc., New York. 1963. p. 711.
20. L. M. Dennis and A. W. Laubengayer. Z. Physik. Chem. **130**, 520 (1927).

Can. J. Chem. Downloaded from www.nrcresearchpress.com by 210.87.254.42 on 09/05/12
For personal use only.

21. R. K. WANLESS and H. G. THODE. J. Sci. Instr. **30**, 395 (1953).
22. R. L. BENOIT and P. CLERC. J. Phys. Chem. **65**, 676 (1961).
23. D. A. EVEREST and H. Terry. J. Chem. Soc. No. 476, 2282 (1950).
24. D. A. EVEREST. Private communication.
25. R. SCHWARZ and E. HUF. Z. Anorg. Chem. **203**, 188 (1931).
26. G. HERZBERG. Molecular spectra and molecular structure. Van Nostrand. 1957.
27. D. F. HEATH and J. W. LINNETT. Trans. Faraday Soc. **44**, 878 (1948).
28. A. D. CAUNT, L. N. SHORT, and L. A. WOODWARD. Trans. Faraday Soc. **48**, 873 (1952).
29. D. F. HEATH, J. W. LINNETT, and P. J. WHEATLEY. Trans. Faraday Soc. **46**, 137 (1950).
30. J. W. LINNETT and P. J. WHEATLEY. Trans. Faraday Soc. **45**, 39 (1949).

Can. J. Chem. Downloaded from www.nrcresearchpress.com by 210.87.254.42 on 09/05/12
For personal use only.

Can. J. Chem. Downloaded from www.nrcresearchpress.com by 210.87.254.6 on 09/05/12
For personal use only.

THE TRANSMISSION OF THE POLAR EFFECTS OF SUBSTITUENTS IN AROMATIC AND ARYLALIPHATIC CARBOXYLIC ACIDS

REACTIONS OF THE ACIDS WITH DIAZODIPHENYLMETHANE IN ETHANOL

K. Bowden, N. B. Chapman, and J. Shorter
Chemistry Department, The University, Hull, England

Received February 4, 1964

ABSTRACT

Rate coefficients have been determined for the reactions in ethanol at 30° of diazodiphenylmethane with several groups of carboxylic acids. Each group included the parent acid and three nuclear substituted acids. The parent acids were: benzoic, phenylacetic, β-phenylpropionic, phenoxyacetic, and *trans*-cinnamic acid. The reactions of 3-fluoro- (or chloro-) or 4-methyl-biphenyl-4′-carboxylic, and of 9-X-10-anthroic acids (X = Me, Cl, or Br) were also studied similarly. The Hammett polar susceptibility constant, ρ, has been calculated for each set of reactions. The values of ρ are discussed in terms of transmission of electronic effects through the side-chain by a field effect, and for side-chains conjugated with the ring, by a π-electron effect, both of which are inversely proportional to the first power of the distance of the carbonyl group from the ring.

INTRODUCTION

In a recent series of papers, Chapman and Shorter and their co-workers have discussed the separation of polar and steric effects in the reactions of aromatic and arylaliphatic carboxylic acids and their esters (1–5). The reactions of carboxylic acids with diazodiphenylmethane have received particular attention (1, 3, 5). We have obtained the Hammett polar susceptibility constant, ρ (6), for the reactions with diazodiphenylmethane in ethanol of a number of aromatic and arylaliphatic acids of the type Ar—Y—CO_2H. One of us (K. B.) has already used these values of ρ, in conjunction with other published data, to discuss the transmission of polar effects by aryl and alkyl systems (7). We now present the experimental results underlying the values of ρ, and discuss further the influence of Y on the transmission of the polar effects of substituents in the aryl group on the reactivity towards diazodiphenylmethane of the carboxyl group in Ar—Y—CO_2H.

The kinetics of the reactions of carboxylic acids with diazodiphenylmethane have been studied in recent years, by using a spectrophotometric technique to follow the consumption of diazodiphenylmethane (see ref. 5 for references). In ethanolic solution diazodiphenylmethane reacts with carboxylic acids to form diphenylmethyl carboxylates:

$$R\cdot CO_2H + Ph_2C{:}N_2 \rightarrow R\cdot CO_2\cdot CHPh_2 + N_2.$$

There is also a concurrent reaction between solvent ethanol and diazodiphenylmethane, catalyzed by the acid to give ethyl diphenylmethyl ether:

$$EtOH + Ph_2C{:}N_2 \rightarrow Et\cdot O\cdot CHPh_2 + N_2.$$

Roberts, Watanabe, and McMahon (8) investigated the mechanism of each of these reactions, and concluded that these were essentially independent. However, Bowden, Buckley, Chapman, and Shorter (5), and Miller and O'Ferrall (9) have concluded that the ester and ether formation proceed by way of a common intermediate, the distinction between ester formation and ether formation arising only in the breakdown of the intermediate to the products. The mechanism involves a rate-determining proton transfer from the acid to the diazodiphenylmethane.

Can. J. Chem. Downloaded from www.nrcresearchpress.com by 210.87.254.6 on 09/05/12
For personal use only.

RESULTS AND DISCUSSION

Second order rate coefficients for the reactions of the carboxylic acids with diazodiphenylmethane in ethanol at 30° are assembled in Table I. We give also the values of R,

TABLE I

Reactions of carboxylic acids with diazodiphenylmethane in ethanol at 30°

Acid series	Substituent k_2^a,* (R)†			
Benzoic‡	H	*m*-Me	*m*-Cl	*m*-NO_2
	0.991 (59.1)	0.830 (61.1)	2.42 (60.0)	4.45_5 (60.0)
Phenylacetic	H	*p*-Me	*p*-Br	*p*-NO_2
	1.08 (65.1)	0.983 (64.9)	1.40 (63.3)	2.26 (63.0)
β-Phenylpropionic	H	*p*-Me	*m*-Cl	*p*-NO_2
	0.735 (62.0)	0.722 (62.2)	0.904 (62.5)	1.12 (61.7)
Phenoxyacetic	H	*m*-Me	*p*-Cl	*m*-NO_2
	6.60 (61.4)	6.44 (61.6)	7.68 (60.4)	9.97 (61.0)
trans-Cinnamic	H	*p*-Me	*m*-Cl	*m*-NO_2
	0.972 (59.7)	0.834 (59.4)	1.38 (60.3)	1.88 (60.0)
3- or 4-Biphenyl-4′-carboxylic	H	4-Me	3-F	3-Cl
	1.00 (58.3)	0.962 (59.0)	1.20_5 (59.5)	1.24 (59.7)
9-X-10-Anthroic	H	9-Me	9-Cl	9-Br
	8.49 (65.9)	8.22 (65.3)	12.9 (66.0)	15.8 (65.0)

*The second order rate coefficients, k_2^a ($l\ mole^{-1}\ min^{-1}$) are reproducible to ±2% or better.
†Values of R (%; for significance see main text) are reproducible to ±0.2% (unit) or better.
‡Measurements by Mr. A. Buckley.

the ratio (%) of the amount of diazodiphenylmethane consumed in esterification to the total amount consumed (esterification plus etherification). In accordance with our view of the mechanism of the reaction (5), we do not correct the measured second order rate coefficient (k_2^a) to give the "true" rate coefficient (k) for the esterification (cf. refs. 1, 3, and 10); k_2^a is now understood to relate to the common rate-determining step. The values of R and of k_2^a for the various parent acids have been discussed elsewhere (5). Table I shows that the effect of substituents on R in each series is very small and no further comment is needed.

The choice of substituents in each series was partly governed by the accessibility of the acids and their solubility in ethanol. However, since the results were to be used to evaluate ρ-values, in accordance with the views of van Bekkum, Verkade, and Wepster (11), *meta* substituents were selected as far as possible, and *para* substituents capable of strong mesomeric interaction with the carboxyl group were avoided. In the correlation of log k_2^a with σ, the values of σ used for *meta* substituents were taken from ref. 11; for *para* substituents σ^n-values were used (11). The ρ-values for the reactions of the various series of acids listed in Table I are shown in Table II, together with ρ-values calculated from the results obtained by other authors for three related systems (12, 13, 14).

The correlation coefficients differ only slightly from unity except for reactions of the 9-X-10-anthroic acids. We therefore suggest that σ-values based on the behavior of benzene derivatives apply only in a limited way to the anthracene system, owing to the more extensive conjugation of the latter. (We have avoided substituents whose electronic effects might be influenced by steric interaction with the *peri*-hydrogen atoms.)

The values of ρ for the reactions of the various series of acids with diazodiphenylmethane in ethanol vary in parallel fashion with the ρ-values for the ionization of the acids (7) (a rho–rho relation; ref. 15). Such a relation is to be expected if, as we suggest, the mechanism of the diazodiphenylmethane reaction involves a rate-determining proton transfer (5, 9). Bowden tabulated ρ/ρ_0 values for several types of reaction of the various series of

TABLE II

Hammett polar susceptibility constants, ρ, for the reactions of carboxylic acids with diazodiphenylmethane in ethanol at 30°

Acid series	ρ	log k_0*	r†	ρ/ρ_0‡ (obs.)	ϕ§	ρ/ρ_0¶ (calc.)
Benzoic	0.944	−0.002	0.998	1.00	1.00	1.00
Phenylacetic	0.403	0.039	1.000	0.43	0.78	0.42
β-Phenylpropionic	0.218	−0.123	0.995	0.23	0.48‖	0.27‖
Phenoxyacetic	0.247	0.825	0.999	0.26	0.51‖	0.28‖
trans-Cinnamic	0.416	−0.018	0.999	0.44	0.48	0.39
3- or 4-Biphenyl-4′-carboxylic	0.224	0.007	0.995	0.24	0.30	0.26
9-X-10-Anthroic	0.697	0.973	0.952	0.74	—	—
Phenylpropiolic**	0.310	1.284	0.988	0.33	0.44	0.36
4- or 5-X-*o*-Toluic††	0.887	−0.017	1.000	0.94	—	—
4-X-2,6-Dimethyl-benzoic‡‡	0.642	0.549	0.993	0.68	—	—

*log k_0 is log k_2^{H} for the parent acid, as calculated by the least squares treatment.
†Correlation coefficient.
‡ρ_0 is the susceptibility constant for the benzoic acid series.
§See text and ref. 7.
¶See text.
‖For "*anti*"-conformer, see ref. 7.
**Ref. 12. Substituents: H, *m*-Cl, *p*-Cl, *m*-NO_2, *p*-NO_2.
††Ref. 13. Substituents: H, *m*-Me, *m*-Br, *m*-NO_2, *p*-NO_2. Calculation by van Bekkum, Verkade, and Wepster (11).
‡‡Ref. 14. Substituents: H, *p*-Me, *p*-CO_2Me, *p*-Br. σ^n for *p*-CO_2Me taken as 0.484; an incorrect value is given in ref. 11.

acids (7), (ρ_0 is the susceptibility constant for the benzoic acid series, taken as a reference system). Besides the diazodiphenylmethane reaction, the processes considered were ionization in water and in 50% ethanol, and alkaline hydrolysis of ethyl esters in aqueous ethanol. Each series was discussed in terms of the mean value of ρ/ρ_0; the part played by the direct field effect, and by σ- and π-inductive effects in the transmission of the polar effects of substituents was tentatively assessed.

Bowden (7) calculated the direct field effect along the lines proposed by Kirkwood and Westheimer (16), with slight modification. According to Kirkwood and Westheimer the transmission of the effect of a dipolar substituent is determined by the factor $\cos\theta/r^2D'$, where r is the distance between the center of the dipole and the reaction center, D' the effective dielectric constant, and θ the angle between the line joining the reaction center to the center of the dipole and the axis of the dipole. Bowden calculated $\cos\theta/r^2$ for the various systems on the basis of a simple model. The center of the dipole was considered to be situated at the "*para*"-carbon atom of the aromatic ring in Ar—*Y*—CO_2H. The direction of the dipole vector was then taken as the line generated by joining the "*para*"-carbon atom to the carbon atom linked to the functional group. The reaction center was sited on the extension of the bond joining the carboxyl carbon to the ring, at a distance of 0.89 Å beyond the carbon of the carboxyl group. For each system $\cos\theta/r^2$ divided by the related quantity for the reference system (benzoic acid) was denoted by ϕ.

Values of ϕ are given in Table II. For β-phenylpropionic acid and phenoxyacetic acid, ϕ refers to the sterically preferred "*anti*"-conformer. If D' is nearly the same for all the systems, then $\rho/\rho_0 \sim \phi$ *provided that the main influence of the substituent is the direct field effect.* Whether the mean values of ρ/ρ_0 given by Bowden or the values of ρ/ρ_0 based on the diazodiphenylmethane reaction are used, ϕ is not equal to ρ/ρ_0, but there are qualitative similarities. For *trans*-cinnamic acid ϕ and ρ/ρ_0 agree well, but for β-phenylpropionic acid, which has almost the same value for ϕ, only very poorly. The high value of ρ/ρ_0 for *trans*-cinnamic acid as compared with β-phenylpropionic acid indicates the importance of a π-electron effect in the former acid; the agreement between ρ/ρ_0 and ϕ for *trans*-cinnamic

Can. J. Chem. Downloaded from www.nrcresearchpress.com by 210.87.254.6 on 09/05/12
For personal use only.

acid must be largely fortuitous. This attempt to interpret ρ solely in terms of a direct field effect calculated as above is thus not very fruitful.

We therefore now present an interpretation of ρ/ρ_0, suggested by considering the way of calculating the direct field effect in benzene compounds recently developed by Dewar and Grisdale (17). These authors argue that the field effect on the 1-side-chain of a 3- or 4-dipolar substituent should be regarded as the effect at the 1-carbon atom of the charge induced at the 3- or 4-carbon atom by the attached substituent. Regarded in this way the field effect varies inversely with "distance", cf. the inverse dependence on ("distance")^2 in the Kirkwood–Westheimer approach (16). For the series of acids Ar—Y—CO_2H, we assume that the substituent effect which reaches the 1-carbon atom is transmitted from there to the reaction center (*a*) by a field effect which depends inversely on the distance between the 1-carbon atom and the carbon atom of the carboxyl group, and (*b*) if the carboxyl group, and Y, and Ar form a conjugated system, by a π-electron effect, also varying inversely with distance as above. The second effect will be present in the benzoic, *trans*-cinnamic, 3- or 4-X-biphenyl-4′-carboxylic, and phenylpropiolic acid series. We assume that the effective dielectric constant for (*a*) does not depend markedly on the nature of Y.

The π-electron effect for benzoic acid may be estimated from the results for 4-X-2,6-dimethylbenzoic acids, in which this effect is suppressed by the steric inhibition of conjugation caused by the *ortho*-methyl groups (5). The value of ρ/ρ_0 for 4-X-2,6-dimethylbenzoic acids is 0.68; we therefore take ρ/ρ_0 for 'unconjugated' benzoic acid as $\sim$0.70. (The results for the 9-X-10-anthroic acid series are also in accord with this; $\rho/\rho_0 = 0.74$. The 4- or 5-X-*o*-toluic acid system shows little suppression of conjugation; $\rho/\rho_0 = 0.94$; see ref. 1). Values of ρ/ρ_0 (calc.) for the phenylacetic, β-phenylpropionic, and phenoxyacetic acid series are given by the product of 0.70 and the distance between carbon atom 1 and the carboxyl-carbon in benzoic acid (1.48 Å), divided by the corresponding distance in the acid under consideration. (Distances were calculated from data in ref. 18). The "*anti*"-conformation was assumed for the β-phenylpropionic and phenoxyacetic acid series. The agreement between ρ/ρ_0 (calc.) and ρ/ρ_0 (obs.) is satisfactory, and far better than that between ϕ and ρ/ρ_0 (obs.).

For the conjugated acids we assume that the "distance ratio" should give ρ/ρ_0, i.e. the π-electron effect and field effect are treated together, and assumed to vary inversely with distance; the influence of any inherent differences in the degree of conjugation of the various systems is ignored. Again there is reasonable agreement between ρ/ρ_0 (calc.) and ρ/ρ_0 (obs.), although there are no doubt specific factors which our treatment neglects. For example the difference between the values of ρ/ρ_0 (calc.) for *trans*-cinnamic and phenylpropiolic acid is 0.03; the observed difference is 0.11. This suggests that the relatively inferior transmission of the triply bound system is not simply a matter of distance (7).

To sum up, it appears that a satisfactory, almost quantitative, account of the transmission of electronic effects through the side-chain in the systems we have studied can be given in terms of a direct field effect, and a π-electron effect, where appropriate, inversely dependent on distance.

EXPERIMENTAL

Materials

The acids were commercial samples or were prepared by standard methods. We thank Dr. G. W. Gray and Dr. R. C. Wilson for samples of substituted biphenylcarboxylic acids. The acids were recrystallized to constant m.p., and they had m.p. identical with, or very close to, those recorded in the literature. The equivalent weight of each acid was determined by titration, and found to be well within 1% of the calculated value. Where possible the purity of each acid was examined by vapor-phase chromatography of the methyl ester as described previously (5). No impurities were found.

Can. J. Chem. Downloaded from www.nrcresearchpress.com by 210.87.254.6 on 09/05/12
For personal use only.

Diazodiphenylmethane was prepared by the method of Schroeder and Katz (19). Solutions were stored in a refrigerator. Pure ethanol, b.p. 78.3°, n_D^{25} 1.3591 (lit. ref. 20, 78.3°, 1.35941), was prepared by Smith's method (21). Fischer titration (22) showed a water content < 0.02% by weight. The ethanol was stored and manipulated under dry nitrogen with very careful exclusion of atmospheric moisture.

Measurements

Values of k_2^a and R were determined as described previously (10).

One of us (K. B.) is indebted to the Department of Scientific and Industrial Research for a Research Studentship.

REFERENCES

1. N. B. CHAPMAN, J. SHORTER, and J. H. P. UTLEY. J. Chem. Soc. 1824 (1962).
2. N. B. CHAPMAN, J. SHORTER, and J. H. P. UTLEY. J. Chem. Soc. 1291 (1963).
3. K. BOWDEN, N. B. CHAPMAN, and J. SHORTER. J. Chem. Soc. 5239 (1963).
4. K. BOWDEN, N. B. CHAPMAN, and J. SHORTER. J. Chem. Soc. In press. (1964).
5. K. BOWDEN, A. BUCKLEY, N. B. CHAPMAN, and J. SHORTER. J. Chem. Soc. In press (1964).
6. L. P. HAMMETT. Physical organic chemistry. McGraw-Hill Book Co. Inc., New York. 1940. Chap. 7.
7. K. BOWDEN. Can. J. Chem. **41**, 2781 (1963).
8. J. D. ROBERTS, W. WATANABE, and R. E. MCMAHON. J. Am. Chem. Soc. **73**, 760 (1951).
9. S. I. MILLER and R. M. O'FERRALL. Abstracts of Papers, 145th Meeting of the American Chemical Society. 1963. p. 44T.
10. A. BUCKLEY, N. B. CHAPMAN, and J. SHORTER. J. Chem. Soc. 178 (1963).
11. H. VAN BEKKUM, P. E. VERKADE, and B. M. WEPSTER. Rec. Trav. Chim. **78**, 815 (1959).
12. J. D. ROBERTS and R. A. CARBONI. J. Am. Chem. Soc. **77**, 5554 (1955).
13. J. D. ROBERTS and J. A. YANCEY. J. Am. Chem. Soc. **73**, 1011 (1951).
14. J. D. ROBERTS and C. M. REGAN. J. Am. Chem. Soc. **76**, 939 (1954).
15. R. M. O'FERRALL and S. I. MILLER. J. Am. Chem. Soc. **85**, 2440 (1963).
16. J. G. KIRKWOOD and F. H. WESTHEIMER. J. Chem. Phys. **6**, 506 (1938).
17. M. J. S. DEWAR and P. J. GRISDALE. J. Am. Chem. Soc. **84**, 3548 (1962).
18. H. J. M. BOWEN *et al.* (*Compilers*). Tables of interatomic distances and configuration in molecules and ions. The Chemical Society, London. 1958. Special Publication No. 11.
19. W. SCHROEDER and L. KATZ. J. Org. Chem. **19**, 718 (1954).
20. A. WEISSBERGER. Technique of organic chemistry. 2nd ed. Vol. VII. Interscience Publ. Inc., New York. 1955.
21. A. I. VOGEL. Practical organic chemistry. 3rd ed. Longmans, London. 1957. p. 168.
22. W. SEAMAN, W. H. MCCOMAS, and G. A. ALLEN. Anal. Chem. **21**, 510 (1949).

Can. J. Chem. Downloaded from www.nrcresearchpress.com by 210.87.254.6 on 09/05/12
For personal use only.

Can. J. Chem. Downloaded from www.nrcresearchpress.com by 210.87.254.5 on 09/05/12
For personal use only.

STUDIES ON THE THERMODYNAMICS AND CONDUCTANCES OF MOLTEN SALTS AND THEIR MIXTURES

PART IV. THE ELECTRICAL CONDUCTANCES OF MOLTEN LITHIUM CHLORATE AND OF ITS MIXTURES WITH PROPYL ALCOHOL, LITHIUM NITRATE, WATER, METHYL ALCOHOL, AND LITHIUM HYDROXIDE

A. N. Campbell and D. F. Williams
Chemistry Department, University of Manitoba, Winnipeg, Manitoba

Received April 14, 1964

ABSTRACT

The electrical conductance and its temperature dependence of molten lithium chlorate have been determined. Similar results have been obtained for lithium chlorate melts containing small quantities of methyl alcohol, propyl alcohol, lithium nitrate, lithium hydroxide, and water.

The results obtained, taken in conjunction with the results of previous work, all indicate that the melt is complex. There is probably considerable association and this is especially evident slightly above the melting point: at temperatures in this region the temperature change of the properties of the lithium chlorate melt is greatest.

The activation energy of conductance is approximately the same as the activation energy of viscous flow, for pure lithium chlorate melt and for mixtures of lithium chlorate with lithium nitrate. From this it appears that the melt constituents are not principally the simple ions, but that some form of cohesion exists between the simple constituents of the melt.

The addition of water to the lithium chlorate melt causes the melt properties to alter considerably, especially the transport properties, viscosity and conductance. It is suggested that these changes may in part be due to a breakup of the structural entities of the pure melt, though the increase in electrical conductance cannot be completely explained in this way. A cryoscopic investigation seems to indicate that water is not present as such in the melt.

EXPERIMENTAL

Molten lithium chlorate does not attack pyrex glass and, therefore, a horizontal cell of conventional design was used. Since the specific conductances were high, it was necessary to make the central part of the cell of capillary glass, to increase the cell constant. The electrodes were widely separated to avoid the Parker effect. It was found by experiment that the apparent resistance varied by about 0.5%, as the frequency of the input signal was varied from 500 to 10 000 c s^{-1}. The resistance of the cell was measured at frequencies of 1000, 2000, 5000, and 10 000 c s^{-1}: the measured resistance was plotted against $1/\sqrt{\text{frequency}}$ and extrapolated to infinite frequency. A Jackson audio oscillator capable of delivering a low-power input at a frequency anywhere between 0 – 10 000 c s^{-1}, in conjunction with a Jones bridge and an amplifier coupled to an oscilloscope, were used. With this arrangement it was possible to detect a resistance change of 1 Ω in 10 000 Ω. The cell constants were determined with aqueous potassium chloride, at 25 °C, and corrected to the temperature of experiment by the method of Washburn (1).

A large double-jacketed thermostat was constructed. It contained Marcol G. X. oil, obtained from Imperial Oil Limited, and was heavily insulated with vermiculite. The oil polymerized and darkened rapidly but the loss of visibility was no great drawback here. A systematic probe of the oil bath showed that the temperature nowhere varied more than 0.05°. Our temperatures are correct to ±0.1°, and constant to ±0.05°.

The method of filling the cell with the extremely hygroscopic lithium chlorate should be obvious from the descriptions given in previous papers of this series (2). The cell was left in the thermostat for at least 2 h and the conductance then determined, using frequencies of 1000, 2000, 5000, and 10 000 c s^{-1}, followed by extrapolation to infinite frequency.

For experiments involving liquid additives, a calibrated syringe was filled with the necessary quantity, which was added to the melt through the cap of the cell. Solid lithium nitrate was added directly to the cell contents, but for lithium hydroxide a different technique was necessary. The mixture of lithium chlorate and lithium hydroxide was made up in the drybox, melted, and filtered through a coarse filter disc and then transferred to the conductance cell. This was necessary because unfiltered melts containing lithium hydroxide left a slight suspension in the melt.

For the study of freezing point depression a cryostat similar to that developed by Keenan (3) and by Janz (4) was used, but the very high viscosity of the medium caused considerable experimental difficulty.

Can. J. Chem. Downloaded from www.nrcresearchpress.com by 210.87.254.5 on 09/05/12
For personal use only.

RESULTS

The densities and specific and equivalent conductances, at 131.8 °C, of lithium chlorate and its mixtures containing small quantities of propyl alcohol, lithium nitrate, and water, are given in Table I. The equivalent conductances were calculated on two different

TABLE I

Densities and specific and equivalent conductances, at 131.8 °C, of lithium chlorate and of mixtures of lithium chlorate with propyl alcohol, with lithium nitrate, and with water

Mole fraction of additive	Density	Specific conductance	Equivalent conductance (λ_1 or λ_2)
Mixtures with propyl alcohol			
0.000		0.1150	
0.000		0.1149	
0.004		0.1145	
0.005		0.1140	
0.009		0.1132	
0.011		0.1127	
0.013		0.1127	
0.015		0.1125	
0.020		0.1115	
0.022		0.1113	
0.026		0.1108	
Mixtures with lithium nitrate			λ_2
0.000	2.0881	0.1150	4.979
0.067	2.0841	0.1163	4.961
0.098	2.0824	0.1167	4.959
0.124	2.0803	0.1176	4.960
0.156	2.0767	0.1182	4.969
0.181	2.0727	0.1188	4.958
0.207	2.0690	0.1206	5.010
Mixtures with water			λ_1
0.000	2.0881	0.1150	4.979
0.013	2.0831	0.1171	5.079
0.025	2.0784	0.1202	5.253
0.038	2.0731	0.1227	5.393
0.043	2.0708	0.1243	5.474
0.061	2.0628	0.1268	5.629
0.072	2.0579	0.1302	5.804
0.084	2.0523	0.1326	5.945
0.116	2.0360	0.1368	6.231
0.126	2.0306	0.1397	6.393
0.175	2.0022	0.1492	7.019
0.216	1.9761	0.1594	7.693
0.240	1.9599	0.1631	7.997
0.256	1.9490	0.1662	8.236

assumptions. The equivalent conductance of an aqueous solution is defined as the conductance of a volume of solution containing one gram equivalent of electrolyte, that is, the solvent is treated as an indifferent medium contributing nothing to the conductance. On the other hand, Bloom and Heymann (5) have determined the equivalent conductances of several salt mixtures, using as the equivalent weight the mean equivalent weight calculated by the mixture rule. Thus two different equivalent conductances result, one calculated on the assumption that lithium chlorate is the sole conducting body (λ_1) and one calculated by the method of Bloom and Heymann (λ_2). For mixtures containing water, λ_1 has been used, and λ_2 for the lithium chlorate – lithium nitrate mixtures. The analytical representation of the dependence of both specific and equivalent conductances on mole

TABLE II

Analytical representation of specific and equivalent conductances as functions of mole fraction of additive, at 131.8 °C

	General eq. K or $\lambda = A + Bn_2 + Cn_2^2$					
	Constants in eq. for specific conductance			Constants in eq. for equivalent conductance		
Additive	A	B	C	A	B	C
Water	0.1152	0.194	0.0238	4.99	9.92	10.87 (λ_1)
Lithium nitrate	0.1151	0.0095	0.0737	4.98	−0.57	3.09 (λ_2)

fractions of lithium nitrate and of water are given in Table II. These results were obtained from a least square fit of the results.

The temperature dependences of the specific conductances of pure lithium chlorate and its mixtures with water, lithium nitrate, and methyl alcohol have been determined experimentally and are given in Table III. The equivalent conductances have also been calculated for most mixtures, and these are also given in Table III. With these results for

TABLE III

Variation with temperature of the specific and equivalent conductances of pure lithium chlorate and of mixtures of lithium chlorate with lithium nitrate and with water

t (°C)	Density	Specific conductance	Equivalent conductance
	Pure lithium chlorate		λ_2
131.4	2.0883	0.1147	4.965
131.5	2.0883	0.1148	4.969
137.5	2.0834	0.1286	5.580
145.2	2.0772	0.1467	6.384
154.8	2.0692	0.1719	7.510
155.1	2.0690	0.1770	7.734
157.5	2.0672	0.1809	7.911
163.8	2.0621	0.1973	8.649
169.7	2.0574	0.2163	9.503
173.5	2.0544	0.2252	9.909
	Lithium chlorate – lithium nitrate mixture, mole fraction lithium nitrate = 0.156		
			λ_2
132.0	2.0763	0.1186	4.986
136.4	2.0728	0.1343	5.656
138.7	2.0716	0.1392	5.866
142.6	2.0697	0.1494	6.307
148.9	2.0629	0.1704	7.211
154.9	2.0581	0.1833	7.774
159.3	2.0547	0.1981	8.416
162.4	2.0531	0.2090	8.886
167.9	2.0481	0.2238	9.539
170.9	2.0457	0.2332	9.951
	Lithium chlorate – lithium nitrate mixture, mole fraction lithium nitrate = 0.181		
			λ_2
131.8	2.0727	0.1188	4.958
135.9	2.0692	0.1290	5.393
139.4	2.0666	0.1392	5.827
146.4	2.0611	0.1585	6.652
150.7	2.0577	0.1712	7.208
154.7	2.0547	0.1826	7.688
159.6	2.0508	0.1960	8.268

Can. J. Chem. Downloaded from www.nrcresearchpress.com by 210.87.254.5 on 09/05/12
For personal use only.

TABLE III (*Continued*)

t (°C)	Density	Specific conductance	Equivalent conductance
159.9	2.0506	0.1977	8.340
163.3	2.0477	0.2090	8.829
169.8	2.0427	0.2295	9.719
171.4	2.0413	0.2333	9.883
Lithium chlorate – lithium nitrate mixture, mole fraction lithium nitrate = 0.206			
			λ_2
131.8	2.0690	0.1205	5.006
134.3	2.0667	0.1274	5.298
137.6	2.0637	0.1360	5.664
142.0	2.0606	0.1479	6.169
146.0	2.0575	0.1591	6.646
151.3	2.0532	0.1757	7.355
156.3	2.0493	0.1908	8.002
160.0	2.0464	0.2026	8.509
166.6	2.0418	0.2228	9.379
171.4	2.0376	0.2324	9.803
Lithium chlorate – lithium nitrate mixture, mole fraction lithium nitrate = 0.255			
			λ_2
137.7	2.0564	0.1378	5.727
140.6	2.0542	0.1465	6.058
143.2	2.0522	0.1539	6.368
146.4	2.0496	0.1630	6.753
149.4	2.0474	0.1721	7.138
151.0	2.0458	0.1764	7.322
153.1	2.0447	0.1829	7.595
157.1	2.0415	0.1949	8.106
159.4	2.0398	0.2021	8.413
161.2	2.0386	0.2130	8.872
165.2	2.0325	0.2203	9.203
167.6	2.0336	0.2291	9.566
169.5	2.0322	0.2358	9.852
170.9	2.0308	0.2402	10.08
Lithium chlorate – lithium nitrate mixture, mole fraction lithium nitrate = 0.300			
			λ_2
150.1	2.0405	0.1648	6.780
151.1	2.0396	0.1805	7.430
152.4	2.0386	0.1846	7.602
155.7	2.0362	0.1959	8.077
158.4	2.0343	0.2037	8.406
163.4	2.0307	0.2201	9.099
164.3	2.0301	0.2227	9.209
166.6	2.0284	0.2298	9.511
170.9	2.0252	0.2451	10.160
173.0	2.0237	0.2545	10.558
Lithium chlorate – water mixture, mole fraction water = 0.098			
			λ_1
131.8	2.0457	0.1361	6.143
143.1	2.0366	0.1653	7.413
152.1	2.0299	0.1913	8.703
158.7	2.0248	0.2069	9.436
158.8	2.0248	0.2074	9.459
162.7	2.0215	0.2181	9.963
162.7	2.0215	0.2186	9.986
170.1	2.0156	0.2407	11.030
170.1	2.0156	0.2410	11.041
174.3	2.0122	0.2470	11.335
Lithium chlorate – water mixture, mole fraction water = 0.175			
			λ_1
131.8	2.0022	0.1562	7.350
139.1	1.9970	0.1704	8.042

Can. J. Chem. Downloaded from www.nrcresearchpress.com by 210.87.254.5 on 09/05/12
For personal use only.

TABLE III (*Concluded*)

t (°C)	Density	Specific conductance	Equivalent conductance
141.6	1.9951	0.1754	8.282
149.3	1.9895	0.1949	9.229
154.2	1.9859	0.2074	9.839
158.0	1.9831	0.2204	10.471
161.0	1.9809	0.2289	10.886
165.3	1.9776	0.2404	11.452
168.7	1.9752	0.2514	11.991
Lithium chlorate – water mixture, mole fraction water = 0.256			λ_1
131.8	1.9490	0.1662	8.236
139.0	1.9438	0.1855	9.217
143.9	1.9402	0.1987	9.891
150.1	1.9358	0.2135	10.652
155.9	1.9314	0.2263	11.316
160.5	1.9282	0.2413	12.086
165.5	1.9246	0.2550	12.796
169.8	1.9212	0.2675	13.447
175.7	1.9170	0.2928	14.247
Lithium chlorate – methyl alcohol mixture, mole fraction methyl alcohol = 0.030			
131.6		0.1139	
131.7		0.1141	
132.0		0.1147	
134.5		0.1197	
138.5		0.1284	

λ_1 and λ_2, the Arrhenius equations for the dependence of conductance on temperature have been calculated. These equations are given in Table IV, together with the respective activation energies of conductance. The specific conductances of a lithium chlorate – lithium hydroxide mixture, and of a lithium chlorate – lithium hydroxide – water mixture were determined over the temperature range 130–170 °C. The results are given in Table V. The Arrhenius equations and the activation energies of conductance are given in Table VI.

TABLE IV

Arrhenius equations expressing the temperature variation of specific and equivalent conductances of lithium chlorate and of mixtures of lithium chlorate with water and with lithium nitrate

Mole fraction additive	Arrhenius eq. type: K or $\lambda = B \exp(-\Delta E/RT)$			
	Specific conductance (K)		Equivalent conductance	
	B	ΔE	B	ΔE
	Pure lithium chlorate			
0.00	197.0	6022	10 200	6168
	Additive water			
0.098	76.64	5122	4360	5318 (λ_1)
0.175	48.21	4546	3086	4906
0.256	37.00	4368	2730	4506
	Additive lithium nitrate			
0.156	231.1	6132	11 437	6244 (λ_2)
0.181	249.7	6194	12 445	6330
0.206	231.6	6110	11 462	6252
0.255	219.4	6044	12 682	6324

Can. J. Chem. Downloaded from www.nrcresearchpress.com by 210.87.254.5 on 09/05/12
For personal use only.

TABLE V

Temperature variation of specific and equivalent conductances of mixtures of lithium chlorate with lithium hydroxide and with water and lithium hydroxide

t (°C)	Density	Specific conductance	Equivalent conductance (λ_1)
Mixture with lithium hydroxide, mole fraction lithium hydroxide = 0.076			
131.9	2.041	0.1040	4.694
133.4	2.040	0.1072	4.841
135.0	2.039	0.1112	5.024
135.2	2.039	0.1162	5.249
137.4	2.037	0.1165	5.268
139.8	2.035	0.1217	5.509
144.8	2.031	0.1333	6.045
154.0	2.024	0.1550	7.054
157.3	2.021	0.1625	7.406
159.5	2.019	0.1687	7.697
162.0	2.017	0.1752	8.001
167.3	2.013	0.1889	8.644
171.7	2.009	0.2012	9.225
Mixture with lithium hydroxide and water, mole fraction lithium hydroxide = 0.0691, mole fraction water = 0.071			
131.8	2.012	0.1158	5.397
132.0	2.012	0.1165	5.430
136.3	2.009	0.1265	5.904
140.4	2.007	0.1371	6.406
144.4	2.002	0.1455	6.815
147.6	2.000	0.1528	7.164
154.1	1.995	0.1687	7.930
159.9	1.990	0.1815	8.553
165.0	1.987	0.1953	9.217
166.8	1.986	0.2016	9.519
171.2	1.983	0.2126	10.054

TABLE VI

Analytical representation of the temperature variation of specific and equivalent conductances of lithium chlorate – lithium hydroxide and lithium chlorate – lithium hydroxide – water mixtures

Mole fractions			Arrhenius eq. K or $\lambda = A \exp(-\Delta E/RT)$			
			Specific conductance		Equivalent conductance (λ_1)	
Lithium chlorate	Lithium hydroxide	Water	A	ΔE	A	ΔE
0.924	0.076	—	115.8	5866	8182	6050
0.860	0.069	0.071	104.0	5494	5667	5640

DISCUSSION

The specific conductance of pure lithium chlorate, 0.1150 Ω^{-1} cm^{-1} at 131.8 °C compares favorably with the figure obtained by Patterson (6), 0.1180, but is lower than that of Klotschko and Grigorjew (7). Their higher value for the specific conductance, 0.1252 Ω^{-1} cm^{-1}, and lower density value both indicate the presence of water in their sample.

For most fused salts, the specific conductance and other transport parameters lie within the following limits: K = 1–5 Ω^{-1} cm^{-1}; Λ = 30–150 cm^2 Ω^{-1} equiv^{-1}; ΔE_K = 1–5 kcal mole^{-1}. The values of K and Λ for lithium chlorate are slightly lower than those of

Can. J. Chem. Downloaded from www.nrcresearchpress.com by 210.87.254.5 on 09/05/12
For personal use only.

Can. J. Chem. Downloaded from www.nrcresearchpress.com by 210.87.254.5 on 09/05/12
For personal use only.

other salts of polyatomic anions which have low melting points, but they are considerably larger than those of salts which form covalent melts, such as mercuric chloride.

The ratio of activation energy of viscosity to activation energy of conductance normally has a value between 2–4 for ionic melts. The deviation of this ratio from unity is said to indicate that viscous flow in molten salts of this kind involves a greater configurational change than does the ionic migration in an electric field. The value of the ratio for lithium chlorate is 1.26, (see Part 2 of this series (2)), and, since this value is below the lower limit given above, this is thought to be indicative of association of some kind in the melt. For the nitrates, ΔE_η and ΔE_Λ are frequently found to be equal, and this is interpreted as showing that in the nitrates the species are not the simple ions: a similar deduction would, therefore, appear to be applicable to lithium chlorate.

A method of calculating the degree of dissociation of molten electrolytes has been put forward by Greenwood and Martin (8), which is indeed little more than the old classical rule of Arrhenius, and involves gross approximations and untenable assumptions such as the validity of the Walden rule. Nevertheless, the method does sometimes appear to give results in rough agreement with accepted values. Thus, for the salts KBr, $AgNO_3$, $CdCl_2$, AgI, and KNO_3, the values of α calculated by this method vary between 1.71 ($AgNO_3$) and 0.79 (KNO_3): the value for $LiClO_3$ is 0.80. For this calculation we have used the viscosity data of our earlier work (2). In so far as this calculation is reliable, it appears, therefore, that the lithium chlorate melt is completely ionized, although this conclusion is not in agreement with some of our other conclusions.

A recent theoretical equation (9)

$$\Lambda = \sum AT^{-1} \exp(-\Delta H/RT)$$

has been applied satisfactorily to the conductance process of the alkali halides, whose melts consist of simple symmetrical anions and cations. According to this theory, the experimental heat of activation for conductance, ΔH_Λ^+, is identified with the enthalpy of hole formation and that of the ionic jump, so that

$$\Delta H_{\text{jump}} + \Delta H_{\text{hole}} = \Delta H_\Lambda^+ + RT.$$

The enthalpy of hole formation can be calculated from Furth's equation (10)

$$\Delta H_{\text{hole}} = 4\pi r^2(\gamma - T(d\gamma/dT)).$$

Making the usual assumption that ΔH_{jump} is equal to about 0.1 ΔH_{hole} the values obtained for lithium chlorate and lithium nitrate at corresponding temperatures are:

Ion	Crystallographic ionic radius (Å)	Free energy of hole formation (kcal mole^{-1})	$\Delta H_{\text{jump}} + \Delta H_{\text{hole}}$ (kcal mole^{-1})	$\Delta H_\Lambda^+ + RT$
Li^+	0.60	0.55	0.98	6.5
ClO_3^-	2.00	6.17	9.4	
Li^+	0.60	0.72	0.99	5.8
NO_3	2.3	10.6	13.3	

The value for the calculated activation enthalpy of conductance for the lithium ion is seen to be much lower than the experimental enthalpy, in both cases, while the calculated activation enthalpies of the anions are both larger than the experimental values. Duke and Owens (11) have determined the transport number of the lithium ion in the lithium

nitrate melt as 0.84 ± 0.06, indicating that the conductance is primarily uni-ionic. Nevertheless, if the simple ions (principally Li^+) constituted the conducting species, the experimental activation energy should be close to that calculated for the Li^+ ion. Since this is not so, the radius of the ionic species involved in ionic migration in the lithium chlorate melt is not the same as the crystallographic radius of the lithium ion, but much larger, despite the fact that the cation is the principal conducting species. This, together with the fact that the activation energies of conductance and of viscous flow are approximately equal, indicates that the conducting species is associated in some manner, despite the result of the Greenwood and Martin calculation.

The self-consistency of our results is shown, when they are substituted in the equation proposed by Martin (12)

$$\Delta E_\Lambda = \Delta E_K + RT^2\alpha$$

where ΔE_K is the activation energy of specific conductance and ΔE_Λ the activation energy of equivalent conductance and α the coefficient of thermal expansion. Thus

$$\Delta E_K\ (6.02) + \alpha RT^2\ (0.16) = 6.18$$

compared with the experimental value of 6.12 kcal $mole^{-1}$.

The specific conductance of a lithium chlorate melt increases rapidly with the addition of small quantities of water, increases slightly with addition of small quantities of lithium nitrate, and decreases with the addition of propyl alcohol, methyl alcohol, and nitrobenzene. The slight increase of conductance caused by the addition of lithium nitrate is presumably due to the higher specific conductance of the latter, while the decrease in conductance due to the addition of organic compounds may be explained as a dilution effect. The smaller decrease in conductance due to methyl alcohol as compared with that caused by an equimolar addition of propyl alcohol may be due to the larger size of the propyl alcohol molecule and possibly also to a breakdown of the cluster effect in the presence of methyl alcohol, owing to the higher dielectric constant of the latter. The rapid increase in conductance on addition of water, however, must have a more profound cause: in part, no doubt, it is due to the decrease in viscosity. We suggest, as a possibility, that the small amount of water in the lithium salt melts may not be in the molecular form and that it may even be in the form of ions and that these play a direct part in the conductance of the melt.

If the results of Table I are calculated as equivalent conductances (λ_2), at 131.8 °C, these are seen to be practically independent of the concentration of lithium nitrate, when calculated by the method of Bloom. This apparent constancy must be considered as a coincidence, the decrease in the conductance of lithium chlorate being balanced by the increase due to lithium nitrate. Since the viscosities of these mixtures are greater than that of a (supercooled) lithium nitrate melt at the same temperature, it is not possible to calculate the deviation from ideality. On the other hand, the equivalent conductances of the lithium chlorate – water mixtures increase considerably as the water content increases.

The temperature effect on the conductance of the lithium chlorate – water, lithium chlorate – lithium nitrate, and lithium chlorate – propyl alcohol mixtures, is considerable, the specific conductance being doubled for a 40° rise in temperature. The activation energy of specific conductance decreases as the water content of the mixture increases, whereas the lithium nitrate mixtures exhibit an activation energy comparable to that of pure lithium chlorate, though a slight increase is noted at mole fraction 0.3. The addition

Can. J. Chem. Downloaded from www.nrcresearchpress.com by 210.87.254.5 on 09/05/12
For personal use only.

of methyl alcohol causes a decrease of activation energy, probably because of a decrease of viscosity. The activation energies of specific and of equivalent conductance, for lithium nitrate and for water mixtures with lithium chlorate, are plotted against mole fraction of additive in Figs. 1 and 2.

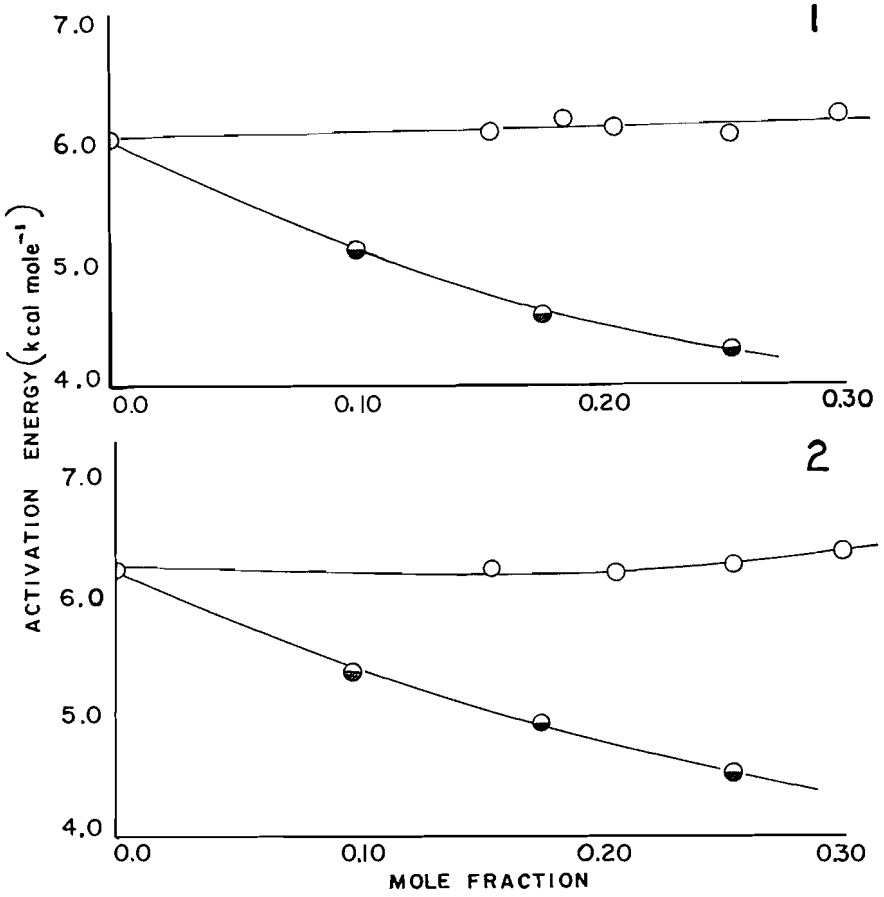

FIGS. 1 and 2. Activation energy of specific conductance vs. mole fraction: ◒ water mixtures, ○ lithium nitrate mixtures.

The question of the state of small amounts of water in molten salts is one of great importance but it is a question not easy to answer. We thought that the addition of lithium hydroxide to a lithium chlorate melt might, by adding free OH^- ions to the melt, increase the conductance. In fact, however, the conductance of a lithium chlorate – lithium hydroxide mixture (mole fraction = 0.076) is less than that of pure lithium chlorate, though the activation energy of conductance remains the same. This suggests that the average energy required for ionic migration in the lithium hydroxide mixture and in pure lithium chlorate is almost the same and, therefore, probably the OH^- ion plays only a small part in the conductance process, which is thus principally dependent on the Li^+ ion.

Since the addition of water increases the equivalent conductance considerably (λ_1), while the addition of lithium nitrate has little effect on λ_2, it is perhaps permissible to speculate whether under these circumstances water is not itself a conducting species. The

Can. J. Chem. Downloaded from www.nrcresearchpress.com by 210.87.254.5 on 09/05/12
For personal use only.

decrease in viscosity produced by the addition of water must, however, be taken into account in explaining the increased conductance and this has been done to some extent in Table VII, in which equimolar solutions of water and of lithium hydroxide are compared at temperatures at which their viscosities are the same. According to this table it would appear that the equivalent conductances are more or less the same, but this comparison, in turn, neglects the effect of temperature on ion velocity and this is not solely determined by viscosity. Thus, while λ_1 for the aqueous mixtures appears to be slightly less than that of pure lithium chlorate and the same as that of the lithium hydroxide mixture, the temperature of the aqueous mixture is 132° or 137° and those of pure lithium chlorate and of the lithium hydroxide mixtures are 13° higher. We suggest that, despite the Greenwood–Martin calculation, the addition of water may cause an increase of free ions (not necessarily from the lithium chlorate) available for conductance and even that water itself may take part in the conduction. The problem, therefore, becomes that of the determination of the state or molecular condition of small quantities of water in lithium chlorate melts.

TABLE VII

Equivalent conductances at temperatures of equal viscosity

	Viscosity = 0.235 P		Viscosity = 0.21 P	
Nature of melt	t (°C)	Equivalent conductance (λ_1)	t (°C)	Equivalent conductance (λ_1)
$LiClO_3$	145	6.4	150	6.9
$LiClO_3 + 0.07\ H_2O$	132	5.9	137	6.5
$LiClO_3 + 0.07$ LiOH	145	5.9	150	6.5

Though the Greenwood–Martin calculation implies that lithium chlorate is almost completely ionized in the molten state, the electrical conductivity is much lower than those of many salts formed either from salts having simple symmetrical anions and cations or salts having high melting points. Although there has been much controversy over methods for the experimental determination of transport numbers in a pure melt, there is general agreement that the result of Duke (11) for lithium nitrate ($t_{Li^+} = 0.9, t_{NO_3^-} = 0.1$) is of the correct order. Because of the similarity in size of the nitrate and chlorate ions, it is possible that lithium chlorate is also a uni-ionic conductor the current being carried practically entirely by the lithium ion. The experimental value of the activation energy of conductance, however, (6.1 kcal mole^{-1}) is not in agreement with that calculated for a lithium ion having its crystallographic radius, viz. 0.98 kcal mole^{-1}, and hence it is improbable that the simple Li^+ ion is the current-carrying unit: it is probably a much larger species. Indeed, since the ratio of the activation energy of viscous flow to that of electrical conductance is approximately unity, it would seem that the structural changes involved in viscous flow, which are dependent on the largest species present in the melt, are similar to those involved in conductance.

The viscosity of lithium chlorate is very high compared to those of other simple salts and this also indicates that the constituents of the melt are complex. Zinc chloride also has a high viscosity, because of the formation of large complex ions, but this type of association does not occur in the lithium chlorate melt, as is shown by the fact that the activation energy for viscous flow is independent of temperature, whereas for zinc chloride a considerable temperature dependence is found.

To summarize the work of this series of papers (2), it appears that the density, surface

Can. J. Chem. Downloaded from www.nrcresearchpress.com by 210.87.254.5 on 09/05/12
For personal use only.

tension, viscosity, and electrical conductance all indicate that the lithium chlorate melt has a considerably associated character. It is possible that the type of association which has been supposed to exist in a lithium nitrate melt is also present in molten lithium chlorate. From the properties we have investigated it is not possible to determine the actual constituents of the melt, nor the nature of the forces responsible for the presumed association, but we think it probable that the molten salt retains a considerable "liquid lattice" structure formed of large entities having a structure similar to that of the crystalline salt.

The large decrease in the viscosity of lithium chlorate, slightly above its melting point, produced by the addition of a small quantity of water, compared to the smaller decrease produced by the same addition at a higher temperature, indicates a strong interaction between water and the residual crystalline lattice, which is thought to exist in the melt just above its melting point. The addition of lithium hydroxide caused a slight decrease in the specific conductivity but no change in the activation energy of conductance, while addition of water caused a rapid increase in conductance and a decrease in activation energy. This suggests that the overall energy required for ionic conductance is unchanged by the addition of OH^- ion but that the addition of water causes a general increase in the ionic character of the melt. The decrease in the coefficient of expansion, as water is added, is also indicative of a decrease in association.

To understand further the nature of the water interaction, a cryoscopic investigation, with molten lithium chlorate as solvent, was undertaken: the additives were water and lithium nitrate respectively. The freezing point depression caused by lithium nitrate can only be due to the addition of one species foreign to the melt, viz. either molecular lithium nitrate or NO_3^- ion. At first glance, addition of water would be expected to have the same effect, per mole. However, our equilibrium studies of the lithium chlorate – water and lithium chlorate – lithium nitrate systems (13, 14) had indicated that the freezing point constants of the two systems were not the same. Using a cryostat similar to that developed by Keenan (3) and by Janz (4), we found the freezing point depression constant to be 6.9° per mole per 1000 g $LiClO_3$ considered as solvent, for lithium nitrate additions, and 12.4° for water. The latent heat of fusion of lithium chlorate calculated from the depression constant with lithium nitrate is 2.2 kcal per mole compared with the experimental value of Campbell and Nagarajan (2) of 2.47 kcal per mole. These results indicate that the addition of water forms more than one particle foreign to the lithium chlorate. To say that exactly twice as many particles originate from the water as from the lithium nitrate is too bold a statement since nothing is known about the activities of the two depressants in this unusual medium. If the above deduction is admitted on a qualitative basis, however, it follows that the water cannot retain its simple molecular character in the lithium chlorate melt. A nuclear magnetic resonance (n.m.r.) spectrum was taken of the proton resonance in a 0.15 *M* water mixture, at 131 °C, but only a single absorption peak was obtained. This may indicate that each proton of the water molecule was in the same environment within the melt but it is more likely that the rate of exchange of protons at this temperature is so great that the environment is averaged out in a n.m.r. spectrum.

REFERENCES

1. E. W. Washburn. J. Am. Chem. Soc. **38**, 2431 (1916).
2. A. N. Campbell and M. K. Nagarajan. Can. J. Chem. **42**, 1137 (1964); **42**, 1616 (1964). A. N. Campbell and D. A. Williams. Can. J. Chem. **42**, 1778 (1964).
3. A. G. Keenan. J. Phys. Chem. **61**, 780 (1958).
4. C. Solomons and G. J. Janz. Rev. Sci. Instr. **29**, 302 (1958).

Can. J. Chem. Downloaded from www.nrcresearchpress.com by 210.87.254.5 on 09/05/12
For personal use only.

5. H. BLOOM and E. HEYMANN. Proc. Roy. Soc. Ser. A, **188**, 392 (1946).
6. A. N. CAMPBELL, E. M. KARTZMARK and W. G. PATTERSON. Can. J. Chem. **36**, 1004 (1958).
7. M. A. KLOTSCHKO and J. C. GRIGORJEW. English translation of a paper in Akad. Wiss. USSR Nacht. Abt. Physik-Chem. Analyse, **21**, 288 (1950).
8. N. N. GREENWOOD and R. L. MARTIN. J. Chem. Soc. 1427 (1953).
9. J. O'M. BOCKRIS, E. H. CROOK, H. BLOOM, and N. E. RICHARDS. Proc. Roy. Soc. Ser. A, **255**, 588 (1960).
10. R. FURTH. Proc. Cambridge Phil. Soc. **37**, 352 (1941).
11. F. R. DUKE and B. OWENS. J. Electrochem. Soc. **105**, 548 (1958).
12. R. L. MARTIN. J. Chem. Soc. 3246 (1954).
13. A. N. CAMPBELL and J. E. GRIFFITHS. Can. J. Chem. **34**, 1647 (1956).
14. A. N. CAMPBELL, E. M. KARTZMARK, and M. K. NAGARAJAN. Can. J. Chem. **40**, 1258 (1962).

Can. J. Chem. Downloaded from www.nrcresearchpress.com by 210.87.254.5 on 09/05/12
For personal use only.

Can. J. Chem. Downloaded from www.nrcresearchpress.com by 210.87.254.105 on 09/05/12
For personal use only.

A THEORETICAL STUDY OF RING CLOSURE

APPLICATION TO THE CYCLIC–LINEAR DISTRIBUTION IN POLYDIMETHYLSILOXANE[1]

J. B. CARMICHAEL[2] AND J. B. KINSINGER
Kedzie Chemical Laboratory, Michigan State University, East Lansing, Michigan

Received December 30, 1963

ABSTRACT

The purpose of this work was to provide insight into the formation of cyclics from fundamental considerations of chain geometry. The structural variables which must be specified are the length(s) of the valence bond in the skeletal structure, bond angle(s) in the skeletal structure, and the energetics and positions of the allowed conformations in the system. A mathematical model involving only these structural variables has been developed which is valid for chains with any number of bonds.

This model is applied to the polydimethylsiloxane system in which cyclic molecules containing from six to eighteen atoms in their skeletal structures make up approximately 12 to 20% by weight of the equilibrated system. A three-rotational-state model is assumed for the polydimethylsiloxane chain. The relationship between cyclic formation and other features of polymer behavior and structure will be interpreted in terms of the model. A good correlation is shown between the experimental equilibrium constant for octamethylcylcotetrasiloxane and the theoretical equilibrium constant from the model calculation.

INTRODUCTION

A major unsolved problem in inorganic polymerization is understanding why, on a molecular basis, cyclic molecules are formed in significant amounts.

In 1950, Stockmayer and Jacobson published a theoretical paper in which they predicted the equilibrium molecular size distributions of linear and cyclic molecules for polymers (1). A major assumption of this work was that the distribution of end-to-end distances (r) of a randomly coiled chain, ($W(r)\mathrm{d}r$), is Maxwellian. That is, $W(r)\mathrm{d}r = \beta^3/\pi^{3/2} \exp(r^2\beta^2) 4\pi r^2 \mathrm{d}r$, where $\beta^2 = 3/(2<r_0^2>)$ and $<r_0^2>$ represents the unperturbed mean-square end-to-end distance of the polymer. From this, a formalism was developed for the chain–cyclic distribution. However, no calculations based on this formalism were undertaken for polydimethylsiloxane.

Calculations were performed on the ring–chain equilibrium in polydecamethylene adipate and compared with experimental results. More ring structures were predicted than actually observed.

The purpose of this work is to provide insight into the formation of cyclics in the polydimethylsiloxane ring–chain equilibrium from detailed considerations of chain structure and geometry. A theoretical equilibrium constant for cyclic formation which can be compared with the experimental equilibrium constant is obtained.

DISCUSSION OF EXPERIMENTAL BACKGROUND

1. Occurrence of Cyclics in Polydimethylsiloxane

Hartung and Camiolo (2) have studied the equilibrium between linear and cyclic polymers in the polydimethylsiloxane system by reacting octamethylcyclotetrasiloxane with KOH catalyst in 25 to 75% by weight of xylene and quantitatively reported the equilibrium weight fraction of cyclic species from trimer to nonamer. A summary of these data extrapolated by us to the bulk polymer is seen in Table I.

[1]*Presented at the Inorganic Polymer Symposium, London, Ontario, September 4–6, 1963.*
[2]*Present address: Dow Corning Corporation, Midland, Michigan.*

TABLE I

Weight fraction of cyclic species in equilibrated polydimethylsiloxane $((CH_3)_2SiO)_n$ (2)

n	Weight fraction	Standard deviation
3	0.0017	0.0004
4	0.100	0.014
5	0.0610	0.0076
6	0.0185	0.0042
7	0.0038	0.0013
8	0.0025	0.0004
9	0.0017	0.0003

The decrease in abundance of dimethylsiloxane rings was discussed earlier by Flory (3) who stated, on the basis of less complete data than that of Hartung, that the trend is that expected if the decrease is due solely to the statistical decrease in probability of ring closure with increasing chain length, specific steric factors being of minor importance. He concluded that "the greater length of the Si–O bond and the large SiOSi angle may alleviate the repulsions between substituents (in this case $-CH_3$), which in rings consisting of $-CH_2-$ have been suggested as being responsible for both the strong preference for five- and six-membered rings and for the severe difficulty of forming rings of eight- to twelve-members."

2. Preferred Conformations and Molecular Structure of the Lower Cyclic Dimethylsiloxanes

The planarity of the six-membered ring, hexamethyclyclotrisiloxane, has been demonstrated by X-ray (4, 5) and electron (6) diffraction. Results of these investigations are summarized in Table II.

Tanaka has measured heats of formation of several of the lower members of the dimethyl and methyl-isopropoxycyclopolysiloxanes (7). From this data, he concludes that the six-membered ring has strain energy of up to 9 kcal/mole and that the higher rings are strain free. The conclusion that strain exists in the six-membered ring agrees with the smaller value of $\angle$ SiOSi found for this molecule (130° as compared with 140° in octamethylcyclotetrasiloxane and the linear polymer (8)).

One possible interpretation of the planarity of this ring, in terms of the structure of the polymer chain, is to postulate the existence of a *cis* conformation in the chain (9). This postulate will be explored later in this paper.

The structure of octamethylcyclotetrasiloxane has been studied by Steinfink *et al.* (10) and Yokoi (11). These results are summarized in Table II.

Yokoi has constructed six models that give theoretical intensity curves which approximate closely the experimental curve. Figures 1 and 2 are diagrams of these structures and the intensity curves respectively.

Structure B, which gives the best fit to the experimental curve, has a cradle form with four silicon atoms in a plane, one set of opposite oxygen atoms being above this plane and the other set of opposite oxygen atoms below this plane.

THEORETICAL DEVELOPMENT

1. Mechanism of Cyclic Formation

For an n-membered ring to form, the magnitude of the end-to-end chain vector ($|\boldsymbol{r}|$) must approach zero at that value of n. In the case of a preformed chain with an active end, $|\boldsymbol{r}|$ is the distance from the active end to any other link in the chain n links away. The value

Can. J. Chem. Downloaded from www.nrcresearchpress.com by 210.87.254.105 on 09/05/12
For personal use only.

Can. J. Chem. Downloaded from www.nrcresearchpress.com by 210.87.254.105 on 09/05/12
For personal use only.

TABLE II

Structure of hexamethylcyclotrisiloxane and octamethylcyclotetrasiloxane

Compound	Si–O (Å)	∠OSiO	∠SiOSi	Ref.	Comments
Hexamethylcyclotrisiloxane: 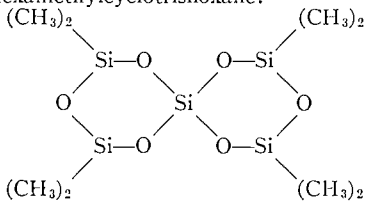	1.64±0.03	109±4°	130±4°	5	Reported the $(Si–O)_3$ ring to be planar
$((CH_3)_2SiO)_3$	1.61	104°	136°	4	Reported ring to be planar
$((CH_3)_2SiO)_3$	1.66±0.04	115±5°	125±5°	6	Reported ring to be planar
Octamethylcyclotetrasiloxane: $((CH_3)_2SiO)_4$	1.65	109°	142.5°	10	X-ray diffraction. Ring is puckered
$((CH_3)_2SiO)_4$	1.63	109.5° (assumed)	140±5°	11	Electron diffraction. Best fit to theoretical intensity curves was cradle form of the ring, B (See Fig. 1)

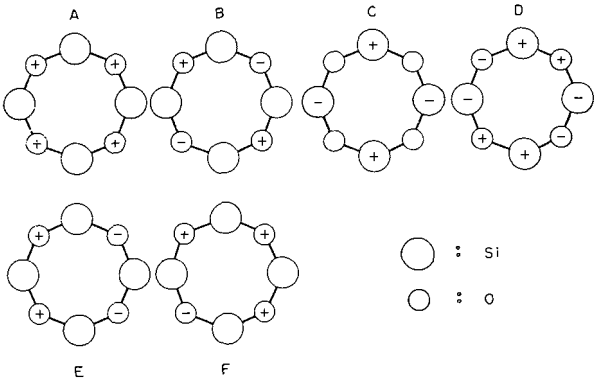

FIG. 1. Conceivable forms of octamethylcyclotetrasiloxane.

of $|r|$ is a function of the chain bond length (l), the bond angles in the chain (θ_1, θ_2), and the rotational states available to the chain (ϕ_i). Presently, we consider $|r|$ to be unperturbed by any solute species and dependent only on short-range intramolecular interactions. Also, we assume the condition for formation of a cyclic molecule is defined as $r < l$.

2. Assignment of Rotational States

From the X-ray diffraction study of the filled and vulcanized elastomer by Damaschun (8), calculation of the stable helical conformations of the structurally similar polyoxymethylene chain by Liquori *et al.* (12), and the measurement by Ciferri of the temperature coefficient of the polymer dimensions (13), the approximate plot of the potential energy vs. rotational angle in Fig. 3 was constructed for the polydimethylsiloxane chain where the

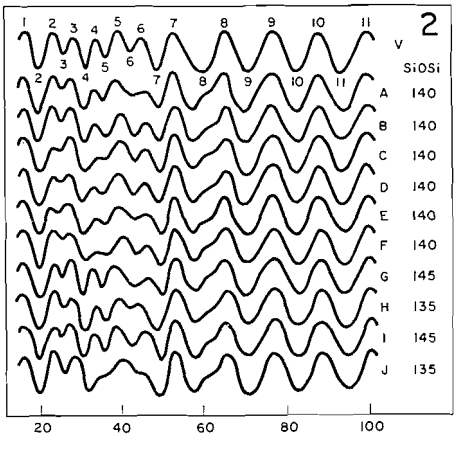

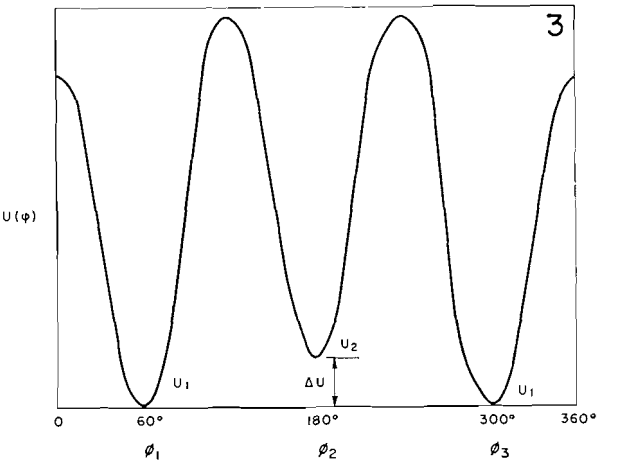

FIG. 2. Visual and theoretical intensity curves of octamethylcyclotetrasiloxane.
FIG. 3. Model for the polydimethylsiloxane chain.

chain conformations are considered to be statistically independent. Since each of the potential wells is symmetric about the minimum energy in the well, the continuous potential function can be well approximated by a point function. Thus, the chain is represented as an equilibrium mixture of discrete rotational conformations, G ($\phi = 60°$),

Can. J. Chem. Downloaded from www.nrcresearchpress.com by 210.87.254.105 on 09/05/12
For personal use only.

T ($\phi = 180°$), G' ($\phi = 300°$). The *cis* conformation, C ($\phi = 0°$), is explored as a possibility in Results, Part 1. The conformations are assumed to be equally probable for computational simplification.

3. Development of Equations for $|\boldsymbol{r}|$ for the Polydimethylsiloxane Chain

Consider now the polydimethylsiloxane chain, a representative segment of which is pictured in Fig. 4. Here $\theta_1' = \angle$ OSiO, $\theta_2' = \angle$ SiOSi.

The end-to-end distance vector $\boldsymbol{r}$ for a given total microscope conformation is

$$\boldsymbol{r} = \sum_{i=1}^{n} l_i,$$

where r is a function of the bond length, l, the supplements of the valence angles, θ_1 and θ_2, and the internal rotation angles, ϕ_i.

To each bond is attached an orthogonal coordinate system of its own. Then all of these coordinate systems can be transformed to a common system, here chosen to be the system attached to the bond l_1, by a series of successive elementary matrix transformations (14). The coordinate system attached to the first bond is chosen so that its z axis points in the direction of that bond, its y axis lies in the plane which passes through this bond and the bond preceding it, and its x axis points in the direction of the vector product $\boldsymbol{l}_1 \times \boldsymbol{l}_2$ of these two bond vectors (15).

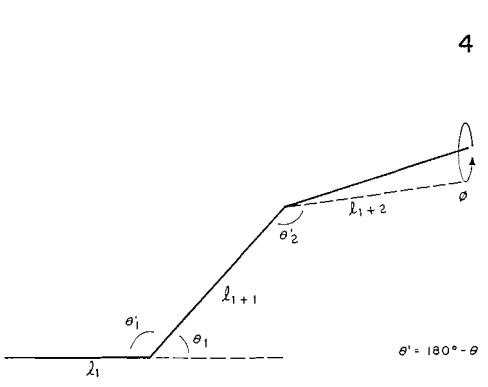

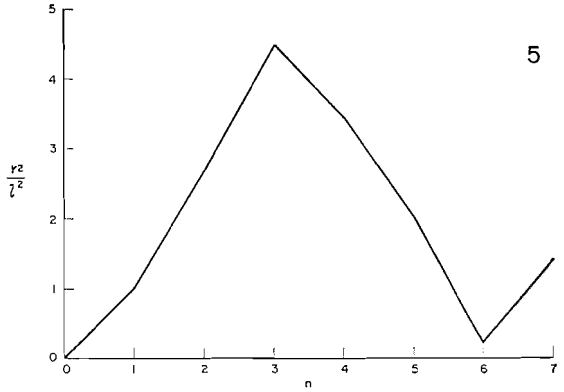

FIG. 4. Representation of siloxane chain segment.
FIG. 5. r^2/l^2 vs. n for all *cis* chain, $\angle$SiOSi = 140°, $\angle$OSiO = 109° 28′.

Consider now the transformation A which transforms the $(k + 1)$th coordinate system into the kth. It may be obtained by two successive elementary transformations. The first, θ, is a rotation of the $(k + 1)$th coordinate system by an angle θ around the x axis. This transformation leaves the x axis unchanged and rotates y and z in their own plane so that the z axis points in the direction of $\boldsymbol{l}_k$. This transformation is given by the matrix:

$$[\theta] = \begin{bmatrix} 1 & 0 & 0 \\ 0 & \cos\theta & \sin\theta \\ 0 & -\sin\theta & \cos\theta \end{bmatrix}.$$

Next the new coordinate system is rotated by an angle θ_k around the new z axis (i.e., around $\boldsymbol{l}_{k-1}$) until it will coincide with the kth coordinate system. Since this transformation

Can. J. Chem. Downloaded from www.nrcresearchpress.com by 210.87.254.105 on 09/05/12
For personal use only.

leaves z unchanged and rotates y and x in their plane, it is given by the matrix:

$$[\phi] = \begin{bmatrix} \cos\phi_k & \sin\phi_k & 0 \\ -\sin\phi_k & \cos\phi_k & 0 \\ 0 & 0 & 1 \end{bmatrix}.$$

These two successive transformations are represented by the matrix product:

$$A = [\theta]\,[\phi] \begin{bmatrix} \cos\phi_k & \sin\phi_k & 0 \\ -\cos\theta\sin\phi_k & \cos\theta\cos\phi_k & \sin\theta \\ \sin\theta\sin\phi_k & -\sin\theta\cos\phi_k & \cos\theta \end{bmatrix}$$

and transform the $(k+1)$th coordinate system into the kth coordinate system. The vector $\boldsymbol{l}_{k+1}$ which in its own coordinate system was given by $\boldsymbol{l}_{k+1} = (0,0,l)$ is therefore expressed in the kth system by $\boldsymbol{l}_k = (0,0,l)A$, whereas l_k is represented in this system by $\boldsymbol{l}_k = (0,0,l)$. This procedure of elementary transformations may be repeated, transforming the coordinate systems of all bond vectors into that of the first one, $\boldsymbol{l}_1$.

For the polydimethylsiloxane chain, there must be two transformation matrices, corresponding to the two bond angles in the chain. These matrices are designated A_1 and A_2 so $\boldsymbol{l}_{1+2} = \boldsymbol{l}_i A_2 A_1$.

Thus, the $\boldsymbol{l}_{i+k}$ bond vector can be expressed back in terms of the $\boldsymbol{l}_i$ vector by the relation: $\boldsymbol{l}_{i+k} = \boldsymbol{l}_i(A_2A_1)^{k/2}$, an even integer.

To avoid the troublesome situation of fractional powers of the matrix product A_2A_1, two different expressions for $\boldsymbol{r}$ will be written; one for the case of an odd number of links in the polymer chain and the other for the case of an even number of links in the polymer chain.

In the system of coordinates previously described, the end-to-end distance is thus given: for n odd

$$[1] \qquad \boldsymbol{r} = (0,0,l)\,(I + A_1 + A_2A_1 + \ldots (A_2A_1)^{(n-5)/2} + A_1(A_2A_1)^{(n-5)/2} + (A_2A_1)^{(n-3)/2} + A_1(A_2A_1)^{(n-3)/2} + (A_2A_1)^{(n-1)/2}),$$

for n even

$$[2] \qquad \boldsymbol{r} = (0,0,l)\,(I + A_1 + A_2A_1 + \ldots A_1(A_2A_1)^{(n-6)/2} + (A_2A_1)^{(n-4)/2} + A_1(A_2A_1)^{(n-4)/2} + (A_2A_1)^{(n-2)/2} + A_1(A_2A_1)^{(n-2)/2}).$$

Note that in both cases, for n links in the chain, the last term in the expression for $\boldsymbol{r}$ must be the product of $n-1$ matrices.

RESULTS

1. *The Distribution of $|\boldsymbol{r}|$'s for a Three-Rotational-State Chain*

We consider now the entire set of $|\boldsymbol{r}|$'s for the case of a growing three-rotational-state chain. The total number of chain conformations increases as 3^{n-1}, where n = number of links in the chain. Many of the $|\boldsymbol{r}|$'s thus produced are degenerate. The cases of $n = 6$ and $n = 8$ will be examined in detail.

Consider the interval tabulation for the 243 $|\boldsymbol{r}|$'s at $n = 6$ in Table III. Note that no $|\boldsymbol{r}|$ falls within the range of 0 to l. If the three-state model were an exact description of the potential-energy profile in the chain and if the requirement for ring closure were $|\boldsymbol{r}| < l$, no

Can. J. Chem. Downloaded from www.nrcresearchpress.com by 210.87.254.105 on 09/05/12
For personal use only.

Can. J. Chem. Downloaded from www.nrcresearchpress.com by 210.87.254.105 on 09/05/12
For personal use only.

TABLE III

Distribution of $|r|$'s

n	Range of $\|r\|$	No. of $\|r\|$'s in the interval	Fraction of $\|r\|$'s in the interval
6	0–$.5l$	0	0.
"	$.5l$–l	0	0.
"	l–$1.5l$	6	0.0247
"	$1.5l$–$2l$	6	0.0247
"	$2l$–$2.5l$	0	0.
"	$2.5l$–$3l$	42	0.1728
"	$3l$–$3.5l$	36	0.1481
"	$3.5l$–$4l$	60	0.2469
"	$4l$–$4.5l$	51	0.2099
"	$4.5l$–$5l$	42	0.1728
		243	0.9999
8	0–$.5l$	12	0.00548
"	$.5l$–l	0	0.0000
"	l–$1.5l$	58	0.0265
"	$1.5l$–$2l$	44	0.0201
"	$2l$–$2.5l$	84	0.0384
"	$2.5l$–$3l$	152	0.0695
"	$3l$–$3.5l$	102	0.0466
"	$3.5l$–$4l$	294	0.1344
"	$4l$–$4.5l$	320	0.1463
"	$4.5l$–$5l$	316	0.1445
"	$5l$–$5.5l$	367	0.1678
"	$5.5l$–$6l$	372	0.1701
"	$6l$–$6.5l$	66	0.0302
		2187	0.9999

TABLE IV

List of small values of $|r|/l$ and corresponding configurations for $n = 8$

$\|r\|/l$	Configurations	$\|r\|/l$	Configurations
0.3025	*TGG'G'GGG'* *GG'GGG'G'G* *GGG'G'GGG'* *TG'GGG'G'G* *G'GG'G'GGG'* *G'G'GGG'G'G*	1.2312	*GTGG'GG'G* *GTG'GG'GG'* *TTGG'GG'G* *G'TG'GG'GG'* *G'TGG'GG'G* *TTG'GG'GG'*
0.4639	*TGG'GG'GG'* *GG'GG'GG'G* *GGG'GG'GG'* *TG'GG'GG'G* *G'GG'GG'GG'* *G'G'GG'GG'G*	1.2380	*GGG'GG'G'G* *GGG'G'GG'G* *GG'GGG'GG'* *TGG'GG'G'G* *TGG'G'GG'G* *GG'GG'GGG'* *G'G'GG'GGG'* *G'G'GGG'GG'*
1.2309	*GGG'GG'GT* *GG'GG'GG'T* *TGG'GG'GT* *G'G'GG'GG'T* *G'GG'GG'GT* *TG'GG'GG'T*		*G'GG'G'GG'G* *TG'GG'GGG'* *TG'GGG'GG'* *G'GG'GG'G'G*

six-membered ring would form in the siloxane system. As pointed out, however, the six-membered ring does form and is planar. Two possible mechanisms for the formation of this ring are offered. Mechanism A: (1) A puckered six-membered ring is formed by a sequence of gauche rotational states, some or all of which are shifted from 60° and 300°

so that for this sequence $|\boldsymbol{r}| < l$. (2) The ring rearranges from the puckered form into the planar form. Since specific steric factors are thought not to influence ring configurations, due to the large SiOSi angle and the comparatively long SiO bond, a shift from a puckered to a planar ring form would probably require energy (since any puckered ring that could form would be expected to be rather stable). (3) In order to accommodate the geometrical requirements of the planar ring, the SiOSi bond angle shifts from 140° to 130°. This change in bond angle will require absorption of energy. Mechanism B: (1) A *cis* rotational state is available to the chain (probably with much lower probability of occupancy than the gauche and *trans* states). (2) The chain grows to a length of six links occupying all *cis* states. A graphical representation of this chain follows in Fig. 5. Plotted is r^2/l^2 vs. n where $r^2 = |\boldsymbol{r}|^2$. Calculation from the graph shows $|\boldsymbol{r}| = 0.49l$. Thus, the chain ends are slightly less than half a bond length apart at $n = 6$. For the ring to form, the bond angle SiOSi must compress from 140° to 130°.

The energy required to form the six-membered ring is probably least for mechanism B, so that if the *cis* state is available to the polymer chain, mechanism B may represent the most likely route to the formation of hexamethylcyclotrisiloxane.

Consider now the interval tabulation for the 2187 $|\boldsymbol{r}|$'s at $n = 8$ in Table III.

There are 12 $|\boldsymbol{r}|$'s in the range of 0 to $1l$. All of these are less than $0.5l$ and are probably within the range of cyclic-forming molecules. A list of all values of $|\boldsymbol{r}|/l < 1.3$ appears in Table IV. We recall that Yokoi postulated six reasonable structures for the eight-membered ring, octamethylcyclotetrasiloxane. Structure B, the structure which gives the best fit to the experimental radial distribution function, is formed by all the following sequences of configurations:

$G,G,G',G',G,G,G';$
$G',G',G,G,G',G',G;$
$G,G',G,G,G',G',G;$
$G',G,G',G',G,G,G';$
$T,G,G',G',G,G,G';$
$T,G',G,G,G',G',G.$

For structure B, $|\boldsymbol{r}| = 0.303l$.

Structure A has a crown form with the four silicon atoms in one plane and the four oxygen atoms lying in a plane above the silicons. This ring is formed by the sequences of configurations:

$G,G',G,G',G,G',G;$
$G',G,G',G,G',G,G';$
$G,G,G',G,G',G,G';$
$G',G',G,G',G,G',G;$
$T,G,G',G,G',G,G';$
$T,G',G,G',G,G',G.$

These 12 sets correspond to the 12 $|\boldsymbol{r}|$'s found to be less than $0.5l$ and are those most likely to form rings. These 12 $|\boldsymbol{r}|$'s represent 0.0548% of the total number of 2187 chains that are generated. The experimental evidence which must be reconciled is that 10% of an equilibrated polymer is octamethylcyclotetrasiloxane. The experimental data and theoretical calculation are compared through the equilibrium constant for the formation of octamethylcyclotetrasiloxane.

Can. J. Chem. Downloaded from www.nrcresearchpress.com by 210.87.254.105 on 09/05/12
For personal use only.

2. Equilibrium Constant for R_4 Formation

Following the treatment of Stockmayer and Jacobson (1), we consider a siloxane chain, C, of $(n + 4)$ –SiO– units in equilibrium with a chain of n units and a cyclic, R, of four units.

[3] $$C_{n+4} \rightleftharpoons C_n + R_4$$

[4] $$K = \frac{[C_n]\,[R_4]}{[C_{n+4}]}$$

Because the chains C_{n+4} and C_n lie very close to one another on the molecular weight distribution curve for the high polymer, $[C_{n+4}] \sim [C_n]$.

[5] $$\text{Therefore } K \sim [R_4]$$

A. Calculation of Experimental Equilibrium Constant

Density of $R_4 = 0.9558$ g/cm^3 at 20 °C
Density of polydimethylsiloxane = 0.9660 g/cm^3 at 25 °C (16)
Molal volume of $R_4 = 312$ cm^3/mole
Consider 1000 g of mixture: 100 g = R_4 and 900 g = C_n
Volume of $R_4 = 100$ g/0.9558 g cm^{-3} = 104.2 cm^3
Volume of $C_n = 900$ g/0.9660 g cm^{-3} = 931.0 cm^3

Total volume = 1035 cm^3, assuming volume additivity

[6] $K_{\text{exptl}} = 100$ g R_4/cm^3 = 100/74.13 moles of –SiO– units/cm^3
$K_{\text{exptl}} = 13.2 \times 10^{-4}$ moles of –SiO– units/cm^3

B. Calculation of Theoretical Equilibrium Constant

The general development here closely follows that of Stockmayer and Jacobson (1). Important departures are noted in the text.

Since reaction [3] involves no change in number of chemical bonds, we may assume it takes place with a negligible change of internal energy.* With this assumption, the prediction of K in [5] requires the calculation of the entropy change in the equilibrium reaction. For this purpose, reaction [3] is broken up into steps.

[7] $$C_{n+4} \rightleftharpoons C_n + C_4$$

[8] $$C_4 \rightleftharpoons R_4$$

For reaction [7], the entropy change is:

[9] $$S_7 = k \ln (V/2v_s)$$

where v_s is volume of the constrained skeletal atom under consideration, and V is the volume of the system as a whole which is available to this atom once the bond is broken. The symmetry number of a chain molecule is 2. In the Stockmayer–Jacobson development, v_s cancelled with the same term in the numerator of S_8, and calculation of v_s was unnecessary. In this development, v_s remains in the final expression for K and is calculated separately.

**For R_4 the assumption seems valid based on the freedom from bond angle strain in octamethylcyclotetrasiloxane. However, for R_3 where strained bond angles are present such an assumption would be invalid.*

Can. J. Chem. Downloaded from www.nrcresearchpress.com by 210.87.254.105 on 09/05/12
For personal use only.

The entropy change in reaction [8] is:

$$S_8 = k \ln (P/4) \quad [10]$$

where P is the fraction of chains which will close. The symmetry number of an n-membered ring is $2n$. (The fact that the symmetry number of a siloxane chain is 2 means that either end has an equivalent opportunity to close back on itself to form a ring. For a ring containing n siloxane units, a symmetry number of $2n$ means that there are $2n$ equivalent bonds that can be broken when the ring reacts with a chain to form a larger chain.)

Combining the results of equations [9] and [10], the equilibrium constant is:

$$K = PV/8v_s. \quad [11]$$

In the Stockmayer–Jacobson development, P was obtained by assuming a Gaussian distribution of end-to-end distances and integrating over the volume element v_s. Here P is obtained from the set of chains generated from the three-rotational-state model and found to be 0.00548.

Calculation of v_s will complete the specification of variables from which K can be calculated. The approach is that of Mayer and Mayer (17). The one-dimensional length available to an atom (along the reaction coordinate giving its distance) from another atom to which it is bound is twice the average amplitude, $\frac{1}{2}\xi$, of vibration. The value of ξ as a function of temperature is given to a good approximation by the empirical equation:

$$\xi = (RT/D)^{1/2} \text{ Å} \quad [12]$$

where D is the energy necessary to break the chemical bond.

The two-dimensional surface available to an atom rotating about another is:

$$A = 4\pi r_0^2 \quad [13]$$

where r_0 is the distance between the two atoms.

The constrained atom of the molecule (the chain of $n + 4$ segments) moves in a shell of radius r_0 and thickness ξ about the atom regarded as free. Therefore, the volume, v_s, is:

$$v_s = 4\pi r_0^2 \xi. \quad [14]$$

For the Si–O bond,

$$r_0 = 1.65 \text{ Å}$$
$$D = 93 \text{ kcal/mole (18)}$$

at 135 °C,

$$\xi = 0.094 \text{ Å}.$$

Inserting these data into [14],

$$v_s = 3.2 \text{ Å}^3. \quad [15]$$

Substituting the values of v_s and P into [11] and assuming a system volume, V, of 1 cm^3, we find:

$$K = 3.6 \times 10^{-4}. \quad [16]$$

Can. J. Chem. Downloaded from www.nrcresearchpress.com by 210.87.254.105 on 09/05/12
For personal use only.

DISCUSSION

This result is tabulated with two values of K calculated from the Stockmayer–Jacobson theory and the experimental K in Table V. In no case is there good agreement between

TABLE V

Comparison of experimental and theoretical calculations of the equilibrium constant for R_4

Reference	$K \times 10^{-4}$ (moles/cm^3)
Hartung and Camiolo (2)	13.2
Stockmayer–Jacobson[a] (1)	1.2
Stockmayer–Jacobson[b] (1)	0.42
This work[a]	3.6

[a]Calculated assuming equally probable rotational states. For the Stockmayer–Jacobson calculation, $\langle r_{0f}^2 \rangle / nl^2 = 3.2$, where r_{0f}^2 refers to the mean square dimensions of a freely rotating siloxane chain with three rotational states at 60°, 180°, and 300° (9).

[b]Calculated using experimentally determined $\langle r_0^2 \rangle / nl^2 = 6.3$ (19).

theory and experiment. However, K calculated in this work represents an improvement over the earlier Stockmayer–Jacobson result. The only difference between the two derivations is in obtaining P and v_s. Stockmayer and Jacobson assumed a Gaussian distribution with an effective link length parameter, b, and we obtain P from a conformation model with equally probable rotational states. Also, we find it necessary to calculate v_s, whereas Stockmayer and Jacobson found K independent of v_s.

We must remember that Hartung's data, upon which the calculation of K_{exptl} was based, is data extrapolated for the undiluted polymer from solvent polymerizations. Certainly, Hartung meant this extrapolation as a guide to be used for predicting cyclic contents at solvent concentrations beyond the limits of those he used. We are, no doubt, subjecting the extrapolated concentration of R_4 to undue scrutiny in Table V. Moreover, recent work being carried out for undiluted polymerizations indicates that the concentration of R_4 is an increasing function of the average degree of polymerization of the linear portion and for very high molecular weights (10^6 g/mole) has the value of 7.4×10^{-4} moles of –SiO– units/cm^3 (20, 21). By comparison with this data, the value of K obtained in this work is about 50% low.

Certainly the model developed here is a primitive beginning to the ring closure problem. Evaluating preferred conformations and relating these to ring formation in siloxanes with other organic side groups could help provide fundamental groundings in this hitherto undeveloped area. No mention has been made here of specific solvent effects which are, at present, impossible to evaluate theoretically. No published data is available on the effect of media viscosity on cyclic concentration. It is hoped that this reexamination of the ring-closure problem will lead to further critical experimental studies.

APPENDIX

Probability of Ring Closure for a Preferred-Rotational-State Model

Let ΔE be the energy difference between gauche and *trans* rotational states.

Consider now the twelve paths which lead to formation of R_4. There are eight sequences which consist of all G or G' (seven in each sequence). Order is unimportant since a statistically independent model is assumed. There are four sequences beginning with T followed by G and G' states.

Can. J. Chem. Downloaded from www.nrcresearchpress.com by 210.87.254.105 on 09/05/12
For personal use only.

[i] $$P = 8P_s(P_G)_7 + 4P_sP_T(P_G)_6$$

[ii] $$P = 8(1)\left(\frac{1}{2 + e^{\Delta E/RT}}\right)^7 + 4(1)\left(\frac{e^{\Delta E/RT}}{2 + e^{\Delta E/RT}}\right)\left(\frac{1}{2 + e^{\Delta E/RT}}\right)^6$$

Simplifying [ii] yields:

[iii] $$P = 4\left(\frac{1}{2 + e^{\Delta E/RT}}\right)^6.$$

The equation [iii] is easily checked for the case of equally probable rotational states. Then $\Delta E = 0$, and

[iv] $$P = 4(\tfrac{1}{3})^6 = 0.00548.$$

If ΔE is assumed to equal -500 cal/mole (thus increasing the probability of gauche states),

[v] $$P = 4\left(\frac{1}{2 + e^{-500/RT}}\right)^6.$$

At 298 °K, $P = 0.0218$. From eqn. [11] in the text, $K = 14.3 \times 10^{-4}$. The assumption of an energy difference of 500 cal/mole is arbitrary but reasonable.

ACKNOWLEDGMENTS

The authors wish to thank the Wright-Patterson Air Force Base for the partial support of this work.

We wish to thank Professor W. H. Stockmayer for pointing out the utility of the equilibrium constant for cyclic formation in comparing experimental results with the theoretical calculations.

REFERENCES

1. H. Jacobson and W. H. Stockmayer. J. Chem. Phys. **18**, 1600 (1950).
2. H. A. Hartung and S. M. Camiolo. Abstracts of Papers, Meeting of the American Chemical Society, Division of Polymer Science, Washington, D.C. 1961. pp. 268–72.
3. P. J. Flory. Principles of polymer chemistry. Cornell University Press, Ithaca. N.Y. 1953. Chap. 10.
4. W. L. Roth and D. Harper. Acta Cryst. **1**, 34 (1948).
5. G. Peyronel. Atti Accad. Naz. Lincei, Rend. Classe Sci. Fis. Mat. Nat. **15**, 402 (1953); **16**, 78, 231 (1954).
6. E. H. Aggarwal and S. H. Bauer. J. Chem. Phys. **18**, 420 (1950).
7. T. Tanaka. Bull. Chem. Soc. Japan, **33**, 282 (1959).
8. G. Damaschun. Kolloid-Z. **180**, 65 (1962).
9. J. B. Carmichael and J. B. Kinsinger. J. Polymer Sci. A, **1**, 2459 (1963).
10. H. Steinfink, B. Post, and I. Fankuchen. Acta Cryst. **5**, 802 (1954).
11. M. Yokoi. Bull. Chem. Soc. Japan, **30**, 100 (1957).
12. P. De Santis, F. Giglio, A. W. Liquori, and A. Ripamonti. J. Polymer Sci. A, **1**, 1383 (1963).
13. A. Ciferri. Trans. Faraday Soc. **57**, 846, 853 (1961).
14. H. Eyring. Phys. Rev. **39**, 746 (1932).
15. S. Lifson. J. Chem. Phys. **29**, 80 (1958).
16. R. C. Osthoff and W. T. Grubb. J. Am. Chem. Soc. **76**, 399 (1954).
17. J. E. Mayer and M. G. Mayer. Statistical mechanics. John Wiley and Sons, Inc., New York. 1940.
18. A. J. Barry and H. N. Beck. Inorganic polymers. Academic Press, New York. 1962. Chap. 5.
19. P. J. Flory, V. Crescenzi, and J. E. Mark. J. Am. Chem. Soc. **86**, 146 (1964).
20. P. L. Brown. Private communication.
21. J. B. Carmichael and R. E. Winger. To be published.

Can. J. Chem. Downloaded from www.nrcresearchpress.com by 210.87.254.105 on 09/05/12
For personal use only.

Can. J. Chem. Downloaded from www.nrcresearchpress.com by 210.87.254.105 on 09/05/12
For personal use only.

AN ELECTRON IMPACT STUDY OF METHYL PHENYL ETHERS

F. MEYER AND A. G. HARRISON[1]
Department of Chemistry, University of Toronto, Toronto, Ontario
Received April 15, 1964

ABSTRACT

The mass spectra of anisole, anisole-methoxy-d_3, meta and para methylanisole, meta and para methyl-d_3-anisole, and meta and para methylanisole-methoxy-d_3 have been recorded. From the deuterium labelling and appearance potential studies, the main fragmentation paths on electron impact have been elucidated. The energetics of formation of the $CH_3OC_7H_6^+$ ion from the methylanisoles, benzyl methyl ether, 7-methoxycycloheptatriene, and the ethylanisoles have been studied.

INTRODUCTION

The mass spectra of the isomeric meta and para methoxybenzyl chlorides show large differences which are consistent with the interpretation that the $CH_3OC_7H_6^+$ ions formed by loss of Cl retain the benzyl configuration and therefore have different energy contents for the two isomers (1). Such differences usually are not encountered in the mass spectra of isomeric benzyl derivatives presumably because of rearrangement to the symmetrical tropylium structure (2). These observations have prompted us to undertake a detailed study of the mass spectra and energetics of ion formation for methoxybenzyl derivatives. The present paper reports a study of anisole, meta and para methylanisole, and meta and para ethylanisole. Since this work was begun, both Barnes and Occolowitz (3) and Pelah *et al.* (4) have reported surveys of the mass spectra of methoxy substituted aromatic systems. The information obtained by deuterium labelling in the present work provides a more detailed picture of the fragmentation paths and in many cases suggests fragmentation paths not considered by the previous workers.

EXPERIMENTAL

All mass spectra were obtained with an A.E.I. MS-2 Mass Spectrometer which has been described previously (1). Mass spectra were recorded at 50 V electron energy, 20 μA ionizing current, and a repeller voltage of 3 V (7 V/cm). Appearance potentials were measured as described previously (5) using xenon to calibrate the voltage scale.

Anisole, *m*-methylanisole, *p*-methylanisole, *p*-ethylanisole, and benzyl methyl ether were commercial samples. The *m*-ethylanisole was prepared by reaction of *m*-ethylphenol with sodium and methyl bromide. The methoxy-d_3 anisoles were prepared by reaction of the appropriate phenol with sodium and methyl-d_3 bromide (6). The *m*-methyl-d_3 and *p*-methyl-d_3 anisoles were prepared from the corresponding bromoanisoles by reaction of the Grignard reagent with dimethyl-d_6 sulphate. The methyl-d_3 bromide and dimethyl-d_6 sulphate were obtained from Merck, Sharp and Dohme, Montreal. Final purification of all anisoles was by gas chromatography on a diisodecylphthalate column.

The sample of 7-methoxycycloheptatriene was very kindly supplied by Mr. R. B. Medz and Professor H. J. Dauben, Jr., of the University of Washington.

RESULTS AND DISCUSSION

Anisole

The mass spectra of anisole and anisole-methoxy-d_3 are presented in Table I. Both spectra have been corrected for naturally occurring ^{13}C and, in addition, the spectrum of the deuterated molecule has been corrected, in the parent region only, for 0.9% anisole-d_2 as determined by low-energy analysis. The spectra show a rather large H/D isotope

[1]*Alfred P. Sloan Fellow 1962–1964.*

TABLE I

Mass spectra of anisole and anisole-methoxy-d_3

Mass	Anisole	Anisole-d_3	Mass	Anisole	Anisole-d_3
111		100.0	78	56.71	3.36
110		0.49	77	16.22	6.43
109		1.10			
108	100.0		66	0.80	1.71
107	2.37		65	63.01	56.71
			64	4.26	4.54
94	0.51	1.23	63	8.49	8.53
93	15.21	13.35			
92	1.68	1.98	53	1.47	2.68
			52	3.23	2.14
83		0.97	51	15.57	8.69
82		4.80	50	8.57	5.97
81		4.28			
80	0.95	3.28	40	0.39	0.81
79	9.70	41.70	39	28.56	24.62
			38	6.27	6.12

Metastables

Anisole:

56.3: $108^+ \rightarrow 78^+$

45.4: $93^+ \rightarrow 65^+$

23.5: $65^+ \rightarrow 39^+$

Anisole-methoxy-d_3:

59.1: $111^+ \rightarrow 81^+$

57.7: $111^+ \rightarrow 80^+$

56.2: $111^+ \rightarrow 79^+$

45.4: $93^+ \rightarrow 65^+$

23.5: $65^+ \rightarrow 39^+$

effect amounting to 1.3 to 1.4 in those regions which involve C–H bond breaking or rearrangement. This is particularly evident in the parent-H region, the C_6 region, and the C_4 region, which is formed by decomposition of the C_6 ions. Such isotope effects make detailed calculations more difficult.

The ion of mass 93 in anisole remains practically completely at the same mass in the spectrum of the d_3 compound, although perhaps 6% of the total intensity appears at mass 94, suggesting a slight amount of exchange of the ring and methyl hydrogens in the parent ion. Similarly the mass spectrum of the deuterated compound shows little change in the C_5 region, providing confirmation for the fragmentation reaction [1] proposed by Barnes and Occolowitz (3).

[1] $$C_6H_5OCH_3^+ \rightarrow CH_3 + C_6H_5O^+ \rightarrow C_5H_5^+ + CO$$

The major differences in the two mass spectra occur in the C_6 region and in the C_4 region, which is formed by decomposition of the C_6 ions. The spectrum of anisole shows a peak of moderate intensity of mass 79 ($C_6H_7^+$) and, after isotope correction, a small peak at mass 80 which must correspond to the $C_6H_8^+$ ion. These ions have not been discussed by previous workers (3, 4). In the spectrum of the d_3 compound the ion of mass 80 has moved to mass 83, as expected, and an appreciable amount of the $C_6H_7^+$ intensity has moved to mass 82, indicating retention of all three methoxy hydrogens. The $C_6H_6^+$ ion has shifted predominantly to mass 79, indicating retention of one of the methyl hydrogens, while a rather large amount of the $C_6H_5^+$ intensity remains at mass 77, indicating that none of the methyl hydrogens have been retained.

If it is assumed that the H/D isotope effect applies equally to all ions in the C_6 region, a reasonable assignment of the ion contributions in the deuterated compound can be made. These assignments are shown in Table II. The data for the unlabelled anisole were obtained by multiplying the data of Table I by 1/1.3 to allow for the observed isotope effect. The following points are evident.

Can. J. Chem. Downloaded from www.nrcresearchpress.com by 210.87.254.105 on 09/05/12
For personal use only.

TABLE II

Mass spectra of anisole and anisole-methoxy-d_3 in C_6 region

Mass	Anisole	Ion contribution	Anisole-d_3	Ion contribution
83			0.98	$C_6H_5D_3^+$
82			4.80	$C_6H_4D_3^+$
81			4.28	$C_6H_5D_2^+ = 2.68$, $C_6H_3D_3^+ = 1.60$
80	0.73	$C_6H_8^+$	3.29	$C_6H_4D_2^+$
79	7.46	$C_6H_7^+$	41.70	$C_6H_5D^+ = 38.40$, $C_6H_3D_2^+ = 3.30$
78	43.74	$C_6H_6^+$	3.36	$C_6H_4D^+$
77	12.49	$C_6H_5^+$	6.43	$C_6H_5^+$

The ratio $C_6H_4D_3/C_6H_5D_2$ is equal to 5/3 within experimental error and thus indicates complete scrambling of the ring and methyl hydrogens in formation of $C_6H_7^+$. This suggests reaction [2] as the mechanism of formation.

[2] $$C_6H_5OCH_3^+ \rightarrow CO + C_6H_8^+ \rightarrow H + C_6H_7^+$$

The appearance potential of $C_6H_7^+$ was found to be 12.1 ± 0.1 eV which leads to ΔH_f $(C_6H_7^+) = 237$ kcal/mole assuming reaction [2]. This value is in good agreement with the value of 235 kcal/mole reported from the appearance potential of this ion from cyclohexadiene (7) and with the value of 233 kcal/mole from appearance potentials in methyl-substituted cyclopentadienes (8).

The calculations in Table II indicate that 88% of the $C_6H_6^+$ ion is formed with retention of one of the methyl hydrogens, the remainder being formed with retention of two and of all three methyl hydrogens. The mechanism appears to be by direct rearrangement of the parent ion since metastables are found at masses 56.2, 57.7, and 59.1 corresponding to reactions [3], [4], and [5].

[3] $$C_6H_5OCD_3^+ \rightarrow C_6H_5D^+ + CD_2O$$

[4] $$C_6H_5OCD_3^+ \rightarrow C_6H_4D_2^+ + CDHO$$

[5] $$C_6H_5OCD_3^+ \rightarrow C_6H_3D_3^+ + CH_2O$$

Reactions [4] and [5] must involve exchange of the ring and methyl hydrogens in the parent ion. Low-energy scans indicated the energy dependence of the three reactions were identical.

The large intensity for $C_6H_5^+$ in the deuterated anisole shows that the major portion of the $C_6H_5^+$ ion cannot arise by decomposition of the $C_6H_6^+$ ion as proposed by previous workers (3, 4) nor by decomposition of the $C_6H_7^+$ ion, since in both cases extensive deuterium retention would be expected. The decomposition of $C_6H_7^+$ is probably responsible for formation of the $C_6H_4D^+$ and $C_6H_3D_2^+$ ions. No changes in the $C_6H_4D^+/C_6H_5^+$ ratio with electron energy could be detected indicating mechanisms of similar energetics. We suggest formation of $C_6H_5^+$ by reactions [6] and [7].

[6] $$C_6H_5OCH_3^+ \rightarrow CO + H + C_6H_7^+ \rightarrow H_2 + C_6H_5^+$$

[7] $$C_6H_5OCH_3^+ \rightarrow H + C_6H_5OCH_2^+ \rightarrow CH_2O + C_6H_5^+$$

The loss of hydrogen from the parent ion involves predominantly the methyl hydrogens as shown by the relative intensities at masses 109 and 108 in the deuterated anisole. This fact is consistent with reaction [7]. The appearance potential of $C_6H_5^+$ in anisole-d_3 was 15.0 ± 0.2 eV which leads to $\Delta H_f(C_6H_5^+) = 305$ kcal/mole assuming reaction [7], in

Can. J. Chem. Downloaded from www.nrcresearchpress.com by 210.87.254.105 on 09/05/12
For personal use only.

agreement with the value of 305 kcal/mole reported by Momigny (9) from appearance potential studies in benzene and related compounds. Assumption of CD_3O as the neutral fragment leads to ΔH_f ($C_6H_5^+$) = 330 kcal/mole which appears unreasonably high.

Methylanisoles

The mass spectra of *m*-methylanisole, *p*-methylanisole, the methoxy-d_3 labelled molecules, and the methyl-d_3-anisoles are given in Table III. The important metastables

TABLE III

Mass spectra of methylanisoles

	p-Methylanisole			*m*-Methylanisole		
Mass	Unlabelled	Methoxy-d_3	Methyl-d_3	Unlabelled	Methoxy-d_3	Methyl-d_3
125		100	100		100	100
124		45.20	13.53		14.74	4.28
123			20.40			3.65
122	100			100		
121	45.40			13.50		
110			35.90			16.44
107	35.20	31.80		20.10	19.38	
96		0.48	1.15		0.89	5.02
95		0.57	8.77		2.45	22.15
94		1.32	18.75		1.95	32.10
93	1.26	6.66	5.80	5.13	16.58	14.20
92	7.65	8.67		21.60	25.50	
91	24.40	9.65		48.30	9.58	
82			35.30			29.27
81			4.80			4.65
80			20.30			16.34
79	32.00	31.80	26.80	33.20	31.04	22.16
78	10.86	12.35	7.87	9.25	10.53	6.16
77	45.10	38.20	2.10	41.00	35.08	2.52
68			2.67			2.73
67		0.52	5.20		0.69	5.63
66		2.06	2.80		3.04	3.46
65	8.44	4.23	2.68	9.90	5.63	7.86
64	1.75	2.12	3.23	2.21	2.58	6.23
63	7.03	6.05	3.97	7.64	6.68	6.45
56			4.41			4.30
55			4.90			4.71
54			5.95			4.37
53	7.98	8.30	7.56	7.20	7.50	6.86
52	8.05	9.52	6.10	6.82	7.80	5.27
51	14.40	15.41	5.08	12.44	12.93	4.76
50	6.25	6.84	3.10	5.39	5.82	3.22

observed in the mass spectra are assembled in Table IV. The spectra have been corrected for ^{13}C and, for the labelled molecules, for deuterium isotopic impurity in the parent mass region. Again comparison of the spectra shows a considerable deuterium effect where C–H bond breaking or hydrogen rearrangement is involved.

The $CH_3OC_7H_6^+$ ion (mass 121) moves to mass 124 in the methoxy labelled compounds, indicating negligible loss of the methoxy hydrogens. For the methyl-d_3 compounds both the methyl and ring hydrogens are lost as shown by the peaks at masses 124 and 123. Neglecting any isotope effects the relative intensities show that loss of the methyl hydrogens accounts for 60% of the total in the para case and 46% in the meta case, whereas complete scrambling of the ring and methyl hydrogens should lead to 43% loss of the

Can. J. Chem. Downloaded from www.nrcresearchpress.com by 210.87.254.105 on 09/05/12
For personal use only.

TABLE IV

Metastable transitions in methylanisoles

Metastable mass	Transition	Unlabelled	Methylanisole-methyl-d_3	Methylanisole-methoxy-d_3
96.8	$125^+ \rightarrow 110^+$		×	
93.8	$122^+ \rightarrow 107^+$	×		
91.6	$125^+ \rightarrow 107^+$			×
72.2	$125^+ \rightarrow 95^+$		×	
70.3	$123^+ \rightarrow 93^+$		×	
69.4	$122^+ \rightarrow 92^+$	×		
69.2	$125^+ \rightarrow 93^+$			×
68.4	$121^+ \rightarrow 91^+$	×		
68.2	$124^+ \rightarrow 92^+$			×
61.1	$110^+ \rightarrow 82^+$		×	
58.3	$107^+ \rightarrow 79^+$	×		×

methyl hydrogens. Since any isotope effect is likely to reduce the loss of the methyl deuteriums, it is quite evident that there is a pronounced preference for loss of the methyl hydrogens in the para case and a small preference in the meta case. The energetics of formation of the $CH_3OC_7H_6^+$ ions will be discussed in a later section.

The mass spectra of the labelled compounds are complex in the C_7 region, and it is not possible to define completely the reactions producing the $C_7H_9^+$, $C_7H_8^+$, and $C_7H_7^+$ ions. The methylanisoles show a significant intensity at mass 93 corresponding to $C_7H_9^+$, the ion being much more abundant in the meta isomer. In the methyl-d_3 compounds the ion shifts to mass 96, indicating retention of the ring methyl hydrogens, while in the methoxy-labelled compound the ion is found at masses 96, 95, and possibly 94, indicating interchange of the ring and methoxy hydrogens. The appearance potential from the meta isomer was 11.69 ± 0.1 eV yielding ΔH_f ($C_7H_9^+$) = 219 kcal/mole assuming H + CO as the neutral fragments, a fragmentation similar to that found for formation of $C_6H_7^+$ from anisole. This ionic heat of formation is in agreement with the value of 219 kcal/mole obtained by electron impact on methylcylopentadienes (8) but somewhat lower than the value of 231 kcal/mole obtained from appearance potentials in cycloheptadiene (10). The mechanism of formation would appear to be by reaction [8] although the details are not clear; there is no $C_7H_{10}^+$ intermediate similar to the intermediate in formation of $C_6H_8^+$ from anisole.

[8] $$CH_3C_6H_4OCH_3^+ \rightarrow H + CO + C_7H_9^+$$

Both the methylanisoles show a significant ion current at mass 92 ($C_7H_8^+$) formed by direct decomposition of the parent ion, as indicated by the metastable at mass 69.4 corresponding to reaction [9]. For the methyl-d_3 anisoles the ion current moves to mass 95 and the metastable to mass 72.0, indicating complete retention of the methyl hydrogens. In the methoxy-labelled compounds the metastable at 69.2 corresponds to reaction [10],

[9] $$CH_3OC_6H_4CH_3^+ \rightarrow CH_2O + C_7H_8^+$$

[10] $$CD_3OC_6H_4CH_3^+ \rightarrow CD_2O + C_7H_7D^+,$$

indicating transfer of one of the methoxy hydrogens to the ring. A portion of the ion current may have moved to mass 94, indicating some scrambling of the ring and methoxy hydrogens, similar to the formation of $C_6H_6^+$ in anisole.

The formation of $C_7H_7^+$ in the methylanisoles may occur by at least four reactions, indicated below.

Can. J. Chem. Downloaded from www.nrcresearchpress.com by 210.87.254.105 on 09/05/12
For personal use only.

[11] $CH_3OC_6H_4CH_3^+ \rightarrow H + CO + C_7H_9^+ \rightarrow H_2 + C_7H_7^+$

[12] $CH_3OC_6H_4CH_3^+ \rightarrow CH_2O + C_7H_8^+ \rightarrow H + C_7H_7^+$

[13] $CH_3OC_6H_4CH_3^+ \rightarrow H + CH_3OC_7H_6^+ \rightarrow CH_2O + C_7H_7^+$

[14] $CH_3OC_6H_4CH_3^+ \rightarrow CH_3O + C_7H_7^+$.

Reaction [11], involving decomposition of the $C_7H_9^+$ ion, is known from studies in methylcyclopentadienes (8) and other C_7H_{10} isomers (10, 11). Reaction [12] is a well-known decomposition of $C_7H_8^+$ ions (2), although the metastable observed previously (3) was not found in the present work. Reaction [13] is indicated by the metastable at mass 68.4 in the methylanisoles. For the methoxy-d_3 compounds reaction [13] should lead exclusively to $C_7H_6D^+$, while decomposition of the $C_7H_7D^+$ formed in reaction [12] should lead predominantly (88%) to $C_7H_6D^+$. The $C_7H_9^+$ intermediate of reaction [11] is found mainly as $C_7H_6D_3^+$ and $C_7H_7D_2^+$ and should lead to extensive deuterium retention in the $C_7H_7^+$ fragment. The large intensity at mass 91 ($C_7H_7^+$) in the methoxy-labelled compounds therefore cannot arise to a significant extent by these three reactions but must arise by a decomposition which involves complete loss of the methoxy group. The most logical reaction is [14] given above. Examination of the spectra suggests for both isomers a contribution to the $C_7H_7^+$ formation by reaction [14] amounting to a maximum of 9% of the parent ion intensity. The spectra are too complex to permit an assessment of the relative contributions of the other three reactions.

The $C_6H_7^+$ ion (mass 79) is formed by loss of CO from mass 107 as shown by the metastable at mass 58.3 corresponding to the last step of reaction [15].

[15] $CH_3OC_6H_4CH_3^+ \rightarrow CH_3 + CH_3C_6H_4O^+ \rightarrow CO + C_6H_7^+$

The mass spectra of the labelled compounds clearly show that the methoxy methyl is lost in this reaction sequence while the ring methyl is maintained. The remaining fragment ions in the C_6 region, predominantly $C_6H_6^+$ and $C_6H_5^+$, undoubtedly are formed by decomposition of the $C_6H_7^+$ ion. For the methyl-d_3-anisoles this ion becomes $C_6H_4D_3^+$ and provides an opportunity to examine the disposition of the hydrogens in these fragmentation processes. Table V compares the measured spectra with that calculated from the

TABLE V

Mass spectra of methyl-d_3-anisoles in C_6 region

	m-$CD_3C_6H_4OCH_3$		*p*-$CD_3C_6H_4OCH_3$	
Mass	Measured	Calculated	Measured	Calculated
82	29.27	29.27	35.30	35.30
81	4.65	4.66	4.80	6.73 (4.78)*
80	16.34	13.82	20.30	19.39 (21.24)*
79	22.16	20.77	26.80	28.47
78	6.16	5.72	7.87	7.75
77	2.51	0.98	2.10	1.25
76	1.00	0.98	1.14	1.47
75	1.15	0.21	0.70	0.32

*Calculated assuming 2:3 ratio for loss of H to loss of D.

spectra of the methylanisoles assuming statistical loss of the hydrogens and deuteriums in the $C_6H_4D_3^+$ ion. For the meta case satisfactory agreement is obtained indicating complete scrambling; for the para isomer, however, somewhat better agreement is obtained if it is assumed that the loss of H to loss of D is in the ratio 2:3 rather than the statistical

Can. J. Chem. Downloaded from www.nrcresearchpress.com by 210.87.254.105 on 09/05/12
For personal use only.

TABLE VI

Ionization and appearance potentials

Ionization process	Appearance potential, eV (±0.1)	ΔH_f (ion), kcal/mole (±3)
$C_6H_5CH_2OCH_3 \rightarrow C_6H_5CH_2OCH_3^+$	9.34	196
$C_7H_7OCH_3 \rightarrow C_7H_7OCH_3^+$	8.58	203
m-$CH_3C_6H_4OCH_3 \rightarrow m$-$CH_3C_6H_4OCH_3^+$	8.56	172
p-$CH_3C_6H_4OCH_3 \rightarrow p$-$CH_3C_6H_4OCH_3^+$	8.48	170
$C_6H_5CH_2OCH_3 \rightarrow CH_3OC_7H_6^+ + H$	10.65	174
$C_7H_7OCH_3 \rightarrow CH_3OC_7H_6^+ + H$	9.70	176
m-$CH_3C_6H_4OCH_3 \rightarrow CH_3OC_7H_6^+ + H$	12.13	202
m-$CD_3C_6H_4OCH_3 \rightarrow CH_3OC_7H_3D_3^+ + H$	12.10	201
m-$CD_3C_6H_4OCH_3 \rightarrow CH_3OC_7H_4D_2^+ + D$	12.10	201
p-$CH_3C_6H_4OCH_3 \rightarrow CH_3OC_7H_6^+ + H$	11.98	199
p-$CD_3C_6H_4OCH_3 \rightarrow CH_3OC_7H_3D_3^+ + H$	12.10	201
p-$CD_3C_6H_4OCH_3 \rightarrow CH_3OC_7H_4D_2^+ + D$	12.10	201
p-$CH_3OC_6H_4CH_2CH_3 \rightarrow CH_3OC_7H_6^+ + CH_3$	10.80	187
p-$CD_3OC_6H_4CH_2CH_3 \rightarrow CD_3OC_7H_6^+ + CH_3$	10.90	189
m-$CD_3OC_6H_4CH_2CH_3 \rightarrow CD_3OC_7H_6^+ + CH_3$	11.70	207

ratio of 4:3. It is interesting to note that decomposition of $C_6H_7^+$ by reaction [16] does

[16] $$C_6H_7^+ \rightarrow C_4H_5^+ + C_2H_2$$

not involve complete loss of hydrogen identity. This is shown by the large intensity at mass 56 ($C_4H_2D_3^+$) in the methyl-d_3 compounds. Comparison of the 56/55 ratio shows that the loss of C_2H_2 to loss of C_2HD is approximately 1:1 rather than the 1:2 expected for complete scrambling.

The mass spectra of the labelled methylanisoles show considerable deuterium retention in the C_5, C_4, and C_3 regions, but detailed calculations do not appear to be justified. The mass spectra of the methylanisoles are compared in Fig. 1 with the spectra of the isomeric compounds, benzyl methyl ether and 7-methoxycylcoheptatriene. All four spectra are quite similar, as might be expected. The base peak for the methylanisoles is the parent ion due to the increased stability of the disubstituted aromatic system. For the other two isomers the base peak is mass 91, presumably the tropylium ion, $C_7H_7^+$. This ion can be formed in these cases by simple bond fission or a simple rearrangement, compared to the extensive rearrangement required for the methylanisoles. To a considerable extent the differences in the mass spectra can be explained by the differences in the stability of the molecule ion, as indicated by the data in Table VI, which presents the ionization potentials and some appearance potentials for the four isomers. The activation energies for decomposition of the methoxycycloheptatriene ion appear to be less than for the other isomers.

Perhaps the most surprising feature is the difference in the mass spectra of the two methylanisoles. The ionization potentials of the two isomers are practically identical and the appearance potentials of most of the major fragment ions are identical, yet the spectra show considerable differences in the parent-H and the C_7 region. These differences cannot be attributed to differences in activation energies for the fragmentation processes and may be due to steric factors.

Energetics of Formation of $CH_3OC_7H_6^+$

In previous work (1) it was concluded from appearance potential differences that the $CH_3OC_7H_6^+$ ions from the meta and para methoxybenzyl chlorides retained the benzyl

Can. J. Chem. Downloaded from www.nrcresearchpress.com by 210.87.254.105 on 09/05/12
For personal use only.

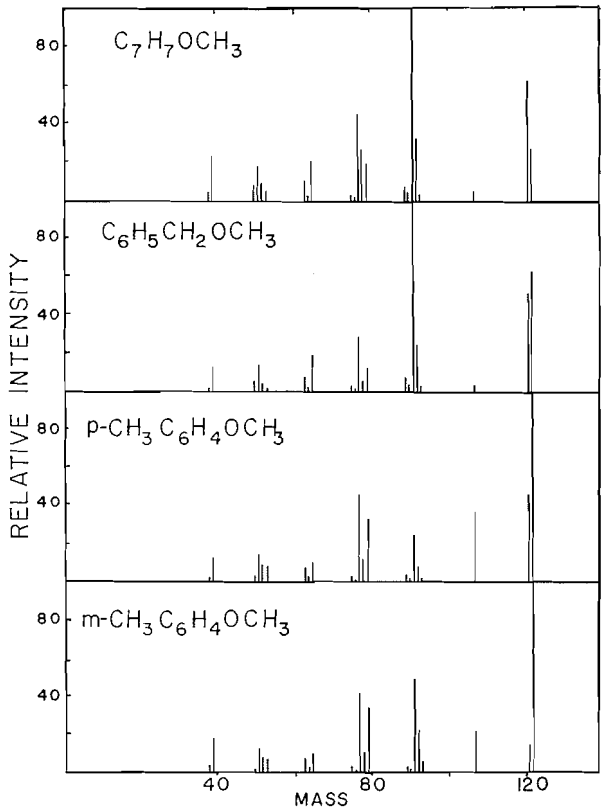

FIG. 1. Comparison of mass spectra of $C_7H_7OCH_3$ isomers.

configuration at the appearance potential threshold. One of the original objectives of the present work was to extend this investigation to other methoxybenzyl derivatives. To this end, a detailed study was made of the energetics of formation of the $CH_3OC_7H_6^+$ ion. Table VI records the data obtained for the methylanisoles, benzyl methyl ether, 7-methoxycycloheptatriene, and meta and para ethylanisole. In the latter compounds the methoxy group was labelled to distinguish the methyls lost in the dissociation process. The heats of formation of the methoxy compounds necessary for the calculations in Table VI were estimated by the bond-energy scheme due to Cox (12).

The appearance potentials of the $CH_3OC_7H_6^+$ ion from benzyl methyl ether and from methoxycycloheptatriene both lead to ΔH_f $(CH_3OC_7H_6^+) = 175 \pm 3$ kcal/mole. The mass spectra of these two compounds are practically identical, as discussed above, and it is probable that in both cases the $CH_3OC_7H_6^+$ ion has the tropylium structure. On the other hand, the data for the methylanisoles lead to ΔH_f $(CH_3OC_7H_6^+) = 201$ kcal/mole. The identity of the appearance potentials for both isomers indicates that the positional effect of the substituent has been lost. Furthermore, the extensive scrambling of the ring and methyl hydrogens (see above) in the dissociation process indicates a tropylium-like structure for the ion, by analogy with the behavior of toluene and related isomers (2). It should be noted that the appearance potentials for loss of the ring and methyl hydrogens are identical, as is shown by the data in Table VI. If this interpretation is correct for the methylanisoles, the appearance potential may only reflect the minimum energy required

Can. J. Chem. Downloaded from www.nrcresearchpress.com by 210.87.254.105 on 09/05/12
For personal use only.

to form the lowest excited state of the molecule ion capable of decomposition to the $CH_3OC_7H_6^+$ ion.

For the meta and para ethylanisoles the appearance potentials of the $CD_3OC_7H_6^+$ ion differ by 0.9 eV in agreement with the difference of 0.99 eV predicted (1) for the energies of formation of the respective methoxybenzyl ions from the correlation (13) of these energies with the σ^+ constant for the substituent. This would suggest that in these cases the $CH_3OC_7H_6^+$ ion retains the benzyl structure. It should be noted, however, that the heat of formation calculated from the para isomer is not greatly different from the value obtained from benzyl methyl ether and methoxycycloheptatriene, while the value from the meta isomer is only slightly greater than that obtained from the methylanisoles. Since the data for the other isomers probably refer to methoxytropylium ions of different excitational energies, one cannot disregard the possibility that the results for the ethylanisoles also indicate the formation of tropylium ions of different excitational energies. If such is the case, it would indicate that the excited energy levels of the molecule ion differ considerably for the two isomeric ethylanisoles.

The mass spectra of the ethylanisoles show differences which are to be expected from the difference in energy content of the $CH_3OC_7H_6^+$ ion. Partial mass spectra of the unlabelled and methoxy-d_3 ethylanisoles are given in Table VII. In all cases loss of CH_3

TABLE VII

Partial mass spectra of ethylanisoles

	p-Ethylanisole		*m*-Ethylanisole	
Mass	Unlabelled	Methoxy-d_3	Unlabelled	Methoxy-d_3
139		30.7		69.7
136	35.2		74.4	
124		100.0		100.0
121	100.0	1.20	100.0	4.29
94		1.74		2.72
93	1.28	3.24	5.00	8.80
92	2.00	5.70	5.54	25.78
91	10.67	7.89	36.67	21.10
66		2.08		5.05
65	5.34	7.18	12.05	13.67

forms the base peak of the spectra, the spectra of the labelled molecules showing that this methyl is lost predominantly from the ethyl side chain. The major fragmentation path for the $CH_3OC_7H_6^+$ ion is by reaction [17] to give the tropylium ion.

[17] $$CH_3OC_7H_6^+ \rightarrow CH_2O + C_7H_7^+$$

This is supported by observation of the appropriate metastables in all cases. For the $CD_3OC_7H_6^+$ ion this fragmentation should lead exclusively to $C_7H_6D^+$ (mass 92). The mass 91 ion current in the labelled compounds must be ascribed to the $C_7H_7^+$ ion and must arise by a different path, presumably by decomposition of the $C_7H_9^+$ ion which is found in the spectra. We would suggest that the $C_7H_9^+$ is formed by reaction [18], which involves loss of the labelled methoxy methyl.

[18] $$C_2H_5C_6H_4OCH_3^+ \rightarrow CH_3 + C_2H_5C_6H_4O^+ \rightarrow CO + C_7H_9^+$$

The mass 92 in the labelled ethylanisoles is thus a measure of the $C_7H_7^+$ formed by reaction [17]. It is obvious that in the meta case the abundance of the $CH_3OC_7H_6^+$ ion in comparison with the parent ion or the $C_7H_7^+$ fragment is greatly reduced compared to the

Can. J. Chem. Downloaded from www.nrcresearchpress.com by 210.87.254.105 on 09/05/12
For personal use only.

para isomer. For the meta isomer not only is more energy required for formation of the $CH_3OC_7H_6^+$ ion but also the activation energy for further decomposition is reduced.

ACKNOWLEDGMENTS

The authors are indebted to the National Research Council of Canada and to the Alfred P. Sloan Foundation for generous financial support of this work.

REFERENCES

1. J. M. S. TAIT, T. W. SHANNON, and A. G. HARRISON. J. Am. Chem. Soc. **84**, 4 (1962).
2. S. MEYERSON and H. M. GRUBB. Mass spectra of alkyl benzenes. *In* Mass spectrometry of organic ions. Academic Press, New York. 1963.
3. C. S. BARNES and J. L. OCCOLOWITZ. Australian J. Chem. **16**, 219 (1963).
4. Z. PELAH, J. M. WILSON, H. BUDZIKIEWICZ, and C. DJERRASI. Tetrahedron, **19**, 2233 (1963).
5. A. G. HARRISON and T. W. SHANNON. Can. J. Chem. **40**, 1730 (1962).
6. F. DALTON, R. D. HILL, and G. D. MEAKINS. J. Chem. Soc. 2927 (1960).
7. J. L. FRANKLIN, F. W. LAMPE, and H. E. LUMPKIN. J. Am. Chem. Soc. **81**, 3152 (1959).
8. F. MEYER, P. HAYNES, S. MCLEAN, and A. G. HARRISON. To be published.
9. J. MOMIGNY, L. BRAKIER, and L. D'OR. Bull. Acad. Roy. Belge, **48**, 1002 (1962).
10. C. LIFSHITZ and S. H. BAUER. J. Phys. Chem. **67**, 1629 (1963).
11. K. BIEMANN. Mass spectrometry. McGraw-Hill, New York. 1962. p. 138.
12. J. D. COX. Tetrahedron, **18**, 1337 (1962).
13. A. G. HARRISON, P. KEBARLE, and F. P. LOSSING. J. Am. Chem. Soc. **83**, 777 (1961).

Can. J. Chem. Downloaded from www.nrcresearchpress.com by 210.87.254.105 on 09/05/12
For personal use only.

Can. J. Chem. Downloaded from www.nrcresearchpress.com by 210.87.254.5 on 09/05/12
For personal use only.

NOTES

ASYMMETRIC SYNTHESIS BY THE REACTION OF MERCURIC ACETATE WITH OPTICALLY ACTIVE THIOACETALS

EDGAR PAGE PAINTER

Fischer (1) found that mercuric chloride removes —SR groups of thioacetals. The product in aqueous or alcohol solution with excess mercuric chloride is an aldehyde (or *gem*-diol) or an acetal formed by the overall reactions:

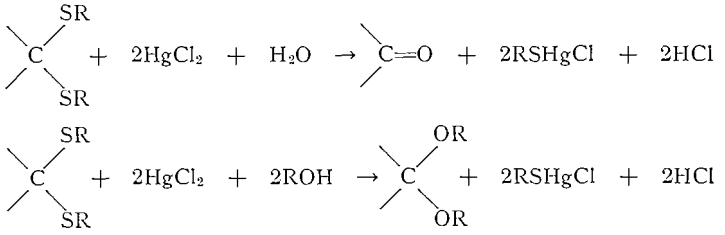

Unlike the above reactions where both thio groups are substituted, we find that acetoxy substitutes a single —SR group when thioacetals are dissolved in acetic acid – acetic anhydride mixtures with mercuric acetate (reaction 1).

[1] 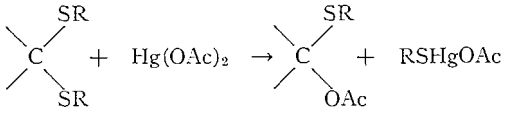

Thioacetals which contain an asymmetric carbon (C_α in I) bonded to the acetal carbon have structural requirements for asymmetric induction so that unequal amounts of the thiohemiacetal acetates produced in reaction 1 would be expected. This is indeed the experimental result as each of four optically active substrates (which differ by R in I) give unequal amounts of diastereomers.

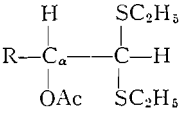

I

When one makes the reasonable assumption that substitution of thioacetals by the action of Lewis acids is in essence a process analogous to acid-catalyzed substitution of acetals (2, 3, 4), the reactive intermediate in the present case can be considered a carbonium (or sulphonium) ion.

By analogy to the cationic intermediate in the substitution of acetals (4), II may be considered planar. Bonding to C_1 (of II) is then similar to the many examples of asymmetric synthesis achieved by addition of nucleophiles to carbonyl compounds (5–9). In each case the new asymmetric center is the result of bonding to planar carbon adjacent

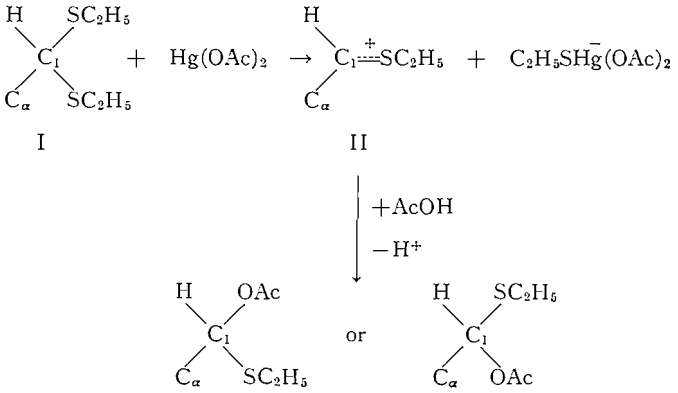

to an asymmetric carbon already in the molecule. Rules suggested by Cram and Abd Elhafez (7) to predict the major product by asymmetric induction in the carbonyl systems should then be applicable to our substrates.

Four substrates, the penta-O-acetyl diethyl dithioacetal of D-glucose (III), D-galactose (IV), D-mannose (V), and the tetra-O-acetyl diethyl dithioacetal of L-arabinose (VI), which have an asymmetric carbon bonded to the acetal carbon, are stable in solutions of acetic acid – acetic anhydride. Mercuric acetate reacts with each substrate. In each case a single ethylthio group is substituted by acetoxy to give 1-ethylthio-1-acetoxy products: III → VII; IV → VIII; V → IX; VI → X. Each of the crystalline products isolated (VII, VIII, and X) is one member of the pair of diastereomers expected. The product IX is a syrup which, presumably, is a mixture.

Measured rotations of the substrates, of the products in solution after the reaction with mercuric acetate, and of the isolated products are shown in Table I. Since the change

TABLE I

Measured rotation of 5% solutions of substrate and isolated products in equal volumes of acetic acid – acetic anhydride

Substrates		Rotation after reaction with $Hg(OAc)_2$	Products	
No.	Rotation		No.	Rotation
III	−0.33°	+0.39°	α-VII	+0.40°
IV	+0.34°	+1.45°	α-VIII	+1.72°
V	+1.21°	+0.61°	IX	+0.55°
VI	−1.40°	−0.17°	β-X	+0.18°

in mass in the substitution reaction is small (for the hexose derivative the molecular weight changes from 496 to 494), the rotations serve as a useful guide to product composition.

From the measured rotation and the yields of VII, it is seen that III is converted nearly quantitatively to α-VII. This example is then comparable to an addition to a carbonyl compound leading almost exclusively to a single isomer, as described by Benjamin, Schaeffer, and Collins (6). The high yields of α-VIII and β-X show that these are the major products in each case. The diastereomer from IV is designated α-VIII because we have isolated from the reaction mixture of IV crystalline products which are more levorotatory than the compound listed in Table I. The mother liquor from the crystallization of the diastereomer from VI gives a syrup more levorotatory than the reaction

Can. J. Chem. Downloaded from www.nrcresearchpress.com by 210.87.254.5 on 09/05/12
For personal use only.

products; therefore, the product described (a member of the L-series) is designated β-X.

Since the isolated products, α-VII, α-VIII, and β-X, are stable in acetic acid – acetic anhydride solutions containing mercuric acetate, the α/β ratio of each pair of diastereomers is given by irreversible bonding of acetoxy to II; i.e., II does not form from 1-ethylthio-1-acetoxy products. Both α-VII and α-VIII have been prepared by esterifying the parent 2,3,4,5,6-penta-0-acetyl-1-S-ethyl monothiohemiacetals of D-glucose and D-galactose with acetic anhydride (10). In one case the substrate was isolated as a solid; in the other case the mixture of thiohemiacetals formed in the equilibrium

[2] 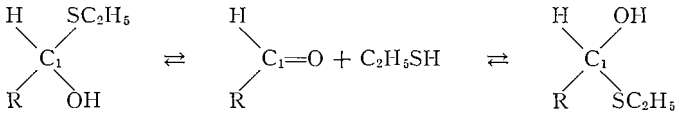

XII XI XIII

was esterified. The diastereomer isolated in the larger amount from the glucose derivative was α-VII; a single diastereomer (α-VIII) was isolated from the galactose derivative. It is tempting to conclude that the same steric forces influence the product distribution (XII and XIII) in equation 2 that control the steric course of direct substitution described by equation 1. We cannot, however, be sure the esterified product composition is a measure of the above equilibrium because XII and XIII may not esterify at equal rates.

Heptaacetate (10, 11) was also identified as one of the products formed by esterification of the mixture in equation 2. This is a product of XI as we find that *aldehydo* pentaacetates of hexoses are converted to C_1-*gem*-diacetates in nearly quantitative yields by acetic anhydride with a catalyst. We are unable to find evidence for the formation of *gem*-diacetates in the reaction of dithioacetals with mercuric salts.

An acetoxy group in the favored conformation of I is in a position to give anchimeric assistance (12) when a C–S bond is broken by the action of mercuric salt.

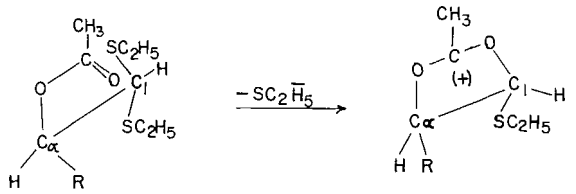

The intermediate II*a* can react with acetic acid at C_1 to give substituted product VII, or at the acetoxy carbon to give (when the substrate is III) 3,4,5,6-tetra-0-acetyl-1,2-0-(1-acetoxy-ethylidine)*aldehydo*-D-glucose S-ethyl monothioacetal. The two products are analytically identical. There is no reason to question the structures of VII and VIII but the possibility of orthoacid structures among our products is not eliminated. Acetoxy is in a better position to give anchimeric assistance in our acyclic systems than it is in the favored conformation in some cyclic forms which give orthoester products.

Preferential C–O cleavage of hemithioacetals and ketals of the type has been demonstrated by Eliel and co-workers (13, 14) with aluminum chloride as the catalyst. Leggetter

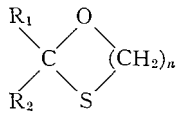

Can. J. Chem. Downloaded from www.nrcresearchpress.com by 210.87.254.5 on 09/05/12
For personal use only.

and Brown (15) recently applied the reaction to other substrates and found that aluminum chloride cleaved dioxolanes faster than oxathiolanes and dithiolanes not at all. Preferential bonding of Al^{3+} to oxygen to give C–O cleavage is expected; Hg^{2+} would be expected to preferentially bond to divalent sulphur but the C–S bond in our 1-ethylthio-1-acetoxy compounds was not cleaved. A question arises about why $C_2H_5S-\underset{|}{\overset{|}{C}}-SC_2H_5$ substitutes rapidly whereas $C_2H_5S-\underset{|}{\overset{|}{C}}-O\overset{O}{\overset{\|}{C}}CH_3$ does not in acetic acid solutions of mercuric acetate. The answer must lie in the cationic intermediate given by cleavage of a C–S bond. Whereas divalent sulphur is an electron donor to carbon giving the relatively stable intermediate,

$$\overset{+}{C}-SC_2H_5 \longleftrightarrow C=\overset{+}{S}C_2H_5$$

oxygen of the acetoxy group is such a poor electron donor that we are unable to detect substitution products of the unstable intermediate

$$\overset{+}{C}-O\overset{O}{\overset{\|}{C}}CH_3 \longleftrightarrow C=\overset{+}{O}\overset{O}{\overset{\|}{C}}CH_3.$$

EXPERIMENTAL

The O-acetyl derivatives of the diethyl dithioacetals were prepared by slow addition of the thioacetals (1 part) to acetic anhydride (8 parts) saturated with sodium acetate at 100–110°. After 2 h at this temperature the solution was allowed to cool to room temperature and the product was isolated and recrystallized by procedures described by Wolfrom (16).

Each of the four substrates was heated with from 1 to 3 moles of mercuric acetate in mixtures of acetic acid – acetic anhydride and the rotation (sodium D line) measured (in portions of the solutions cooled to room temperature) until there was no further change. In all cases the substitution reaction was essentially complete in a 1:1 mixture of acetic acid and acetic anhydride with excess mercuric acetate before the temperature reached 100°. Dissolved mercuric acetate does not significantly modify the rotation of isolated substitution products.

The following procedure was followed for the preparation of products. Five grams of substrate (III, IV, V or VI) plus 5 g of mercuric acetate were dissolved in 100 ml of acetic acid – acetic anhydride (equal volumes) and the flask heated in a water bath until the temperature in the reaction mixture reached 80°. When the reaction mixture had cooled to room temperature the volume of solvent was reduced under vacuum to about 20 ml. Twenty-five grams of sodium acetate and a quantity of crushed ice to give a final volume near 200 ml were added. The contents of the flask was frequently stirred until the acetic anhydride hydrolyzed (no separate phase evident) and kept at 0° or colder for an additional hour. The product from V was an oil; the other substrates gave a white crystalline mass. Each product was washed with several small portions of ice water and dried at room temperature.

*1,2,3,4,5,6-Hexa-O-acetyl-*D*-glucose S-ethyl Monothioacetal (α-VII)*

The crude product (above) from 5 g of III weighed 4.3 g and melted by 101°. Two crystallizations, by dissolving the product in hot 96% ethanol and cooling in the refrigerator, gave 3.3 g (66%) of pure α-VII, m.p. 104; α_D = +7.9 (acetic acid – acetic anhydride, C = 4, 29°), +12.6 (chloroform, C = 4, 26°), Calc. for $C_{20}H_{30}O_{12}S$: C, 48.57; H, 6.11; S, 6.48; acetoxy, 6 equiv./494 g. Found: C, 48.37; H, 6.10; S, 6.26; acetoxy, 6.02 equiv.

*1,2,3,4,5,6-Hexa-O-acetyl-*D*-galactose S-ethyl Monothioacetal (α-VIII)*

The crude product from 5 g of IV weighed 4.6 g and melted by 90°. This was dissolved in 20 ml of absolute methanol and the crystals, which formed overnight at −19°, were filtered and washed with methanol at −19°. A second recrystallization by the procedure just described gave 3.9 g (78%) of pure materials, m.p. 95–96°, α_D = +38.5 (chloroform, C = 4, 25°), +34.3 (acetic acid – acetic anhydride, C = 4, 25°). Calc. for $C_{20}H_{30}O_{12}S$: C, 48.57; H, 6.11; S, 6.48; acetoxy, 6 equiv./494 g. Found: C, 48.69; H, 6.03; S, 6.34; acetoxy, 6.08 equiv.

Can. J. Chem. Downloaded from www.nrcresearchpress.com by 210.87.254.5 on 09/05/12
For personal use only.

*1,2,3,4,5,6-Hexa-O-acetyl-*D*-mannose S-ethyl Monothioacetal (IX)*

This product has not been crystallized. Different preparations gave α_D = 10.7 to 11.5 (acetic acid – acetic anhydride C = 4, 25°). The product contains S and gives a reducing sugar after treatment with sodium methoxide in methanol. Saponification gave 6.08 equiv. acetoxy/494 g.

*1,2,3,4,5-Penta-O-acetyl-*L*-arabinose S-ethyl Monothioacetal (β-X)*

The crude product was dissolved in $CHCl_3$ and filtered, and the solvent was removed at reduced pressure. The solid residue was dissolved in ethyl acetate and the volume reduced until crystallization began at room temperature. Two volumes of hexane were then added and after allowing the solution to stand overnight in the refrigerator the crystals were filtered and washed with hexane. The product was dissolved in hot absolute methanol and the volume reduced until crystals formed at room temperature. After the product was left overnight in the refrigerator it was washed with ice cold methanol. Yield 2.8 g (56%), m.p. 120°, α_D = +3.5 (acetic acid – acetic anhydride, C = 4, 25°), +6.3 (chloroform, C = 4, 24°). Calc. for $C_{17}H_{26}O_{10}S$; C, 48.34; H, 6.16; S, 7.58; acetoxy, 5 equiv./422 g. Found: C, 48.37; H, 6.02; S, 7.60; acetoxy, 4.99 equiv.

The author is grateful to Mr. Norman Kurihara for the acetoxy determinations and assistance in the preparation of acetylated dithioacetals.

1. E. Fischer. Ber. **27**, 673 (1894).
2. J. M. O'Gorman and H. J. Lucas. J. Am. Chem. Soc. **72**, 5489 (1950).
3. M. M. Kreevoy and R. W. Taft, Jr. J. Am. Chem. Soc. **77**, 3146, 5590 (1955).
4. M. M. Kreevoy, C. R. Morgan, and R. W. Taft, Jr. J. Am. Chem. Soc. **82**, 3064 (1960).
5. J. H. Stocker, P. Sidisunthon, B. M. Benjamin, and C. J. Collins. J. Am. Chem. Soc. **82**, 3913 (1960).
6. B. M. Benjamin, H. J. Schaeffer, and C. J. Collins. J. Am. Chem. Soc. **79**, 6160 (1957).
7. D. J. Cram and F. A. Abd Elhafez. J. Am. Chem. Soc. **74**, 5828 (1952).
8. D. J. Cram and J. D. Knight. J. Am. Chem. Soc. **74**, 5835 (1952).
9. D. J. Cram and K. R. Kopecky. J. Am. Chem. Soc. **81**, 2748 (1959).
10. M. L. Wolfrom, D. I. Weisblat, and A. R. Hanze. J. Am. Chem. Soc. **62**, 3246 (1940).
11. N. W. Pirie. Biochem. J. **30**, 374 (1936).
12. S. Winstein and R. E. Buckles. J. Am. Chem. Soc. **64**, 2780 (1942).
13. E. L. Eliel and M. N. Rerick. J. Am. Chem. Soc. **81**, 6087 (1959).
14. E. L. Eliel, L. A. Pilato, and V. G. Badding. J. Am. Chem. Soc. **84**, 2377 (1962).
15. B. E. Leggetter and R. K. Brown. Can. J. Chem. **41**, 2671 (1963).
16. M. L. Wolfrom. J. Am. Chem. Soc. **52**, 2414 (1930).

Received January 31, 1964.
Department of Chemistry,
University of California,
Davis, California.

THE ELECTRON PARAMAGNETIC RESONANCE SPECTRA OF THE 2-CYANO-2-PROPYL RADICAL AND RELATED SPECIES*

J. T. Pearson, P. Smith,† and T. C. Smith

The 2-cyano-2-propyl radical, $(CH_3)_2\dot{C}(CN)$, is a commonly used radical chain initiator and a model radical similar to some involved in vinyl polymerization (1, 2). Nevertheless it does not appear that the e.p.r. spectrum of this radical has been reported despite the considerable extra interest (3–9) originating from the observation (10) that it can react as though the unpaired electron is appreciably delocalized

$$(CH_3)_2\dot{C}—C\equiv N \leftrightarrow (CH_3)_2C=C=N\bullet.$$

The aim of the present investigation was to obtain a well-resolved e.p.r. spectrum for the 2-cyano-2-propyl radical in solution by use of the new and simple flow technique of Dixon and Norman (11).

*Supported by a grant from the United States Public Health Service, Division of General Medical Sciences.
†To whom correspondence should be addressed.

Can. J. Chem. Downloaded from www.nrcresearchpress.com by 210.87.254.5 on 09/05/12
For personal use only.

*1,2,3,4,5,6-Hexa-O-acetyl-*D*-mannose S-ethyl Monothioacetal (IX)*

This product has not been crystallized. Different preparations gave α_D = 10.7 to 11.5 (acetic acid – acetic anhydride C = 4, 25°). The product contains S and gives a reducing sugar after treatment with sodium methoxide in methanol. Saponification gave 6.08 equiv. acetoxy/494 g.

*1,2,3,4,5-Penta-O-acetyl-*L*-arabinose S-ethyl Monothioacetal (β-X)*

The crude product was dissolved in $CHCl_3$ and filtered, and the solvent was removed at reduced pressure. The solid residue was dissolved in ethyl acetate and the volume reduced until crystallization began at room temperature. Two volumes of hexane were then added and after allowing the solution to stand overnight in the refrigerator the crystals were filtered and washed with hexane. The product was dissolved in hot absolute methanol and the volume reduced until crystals formed at room temperature. After the product was left overnight in the refrigerator it was washed with ice cold methanol. Yield 2.8 g (56%), m.p. 120°, α_D = +3.5 (acetic acid – acetic anhydride, C = 4, 25°), +6.3 (chloroform, C = 4, 24°). Calc. for $C_{17}H_{26}O_{10}S$; C, 48.34; H, 6.16; S, 7.58; acetoxy, 5 equiv./422 g. Found: C, 48.37; H, 6.02; S, 7.60; acetoxy, 4.99 equiv.

The author is grateful to Mr. Norman Kurihara for the acetoxy determinations and assistance in the preparation of acetylated dithioacetals.

1. E. Fischer. Ber. **27**, 673 (1894).
2. J. M. O'Gorman and H. J. Lucas. J. Am. Chem. Soc. **72**, 5489 (1950).
3. M. M. Kreevoy and R. W. Taft, Jr. J. Am. Chem. Soc. **77**, 3146, 5590 (1955).
4. M. M. Kreevoy, C. R. Morgan, and R. W. Taft, Jr. J. Am. Chem. Soc. **82**, 3064 (1960).
5. J. H. Stocker, P. Sidisunthon, B. M. Benjamin, and C. J. Collins. J. Am. Chem. Soc. **82**, 3913 (1960).
6. B. M. Benjamin, H. J. Schaeffer, and C. J. Collins. J. Am. Chem. Soc. **79**, 6160 (1957).
7. D. J. Cram and F. A. Abd Elhafez. J. Am. Chem. Soc. **74**, 5828 (1952).
8. D. J. Cram and J. D. Knight. J. Am. Chem. Soc. **74**, 5835 (1952).
9. D. J. Cram and K. R. Kopecky. J. Am. Chem. Soc. **81**, 2748 (1959).
10. M. L. Wolfrom, D. I. Weisblat, and A. R. Hanze. J. Am. Chem. Soc. **62**, 3246 (1940).
11. N. W. Pirie. Biochem. J. **30**, 374 (1936).
12. S. Winstein and R. E. Buckles. J. Am. Chem. Soc. **64**, 2780 (1942).
13. E. L. Eliel and M. N. Rerick. J. Am. Chem. Soc. **81**, 6087 (1959).
14. E. L. Eliel, L. A. Pilato, and V. G. Badding. J. Am. Chem. Soc. **84**, 2377 (1962).
15. B. E. Leggetter and R. K. Brown. Can. J. Chem. **41**, 2671 (1963).
16. M. L. Wolfrom. J. Am. Chem. Soc. **52**, 2414 (1930).

Received January 31, 1964.
Department of Chemistry,
University of California,
Davis, California.

THE ELECTRON PARAMAGNETIC RESONANCE SPECTRA OF THE 2-CYANO-2-PROPYL RADICAL AND RELATED SPECIES*

J. T. Pearson, P. Smith,† and T. C. Smith

The 2-cyano-2-propyl radical, $(CH_3)_2\dot{C}(CN)$, is a commonly used radical chain initiator and a model radical similar to some involved in vinyl polymerization (1, 2). Nevertheless it does not appear that the e.p.r. spectrum of this radical has been reported despite the considerable extra interest (3–9) originating from the observation (10) that it can react as though the unpaired electron is appreciably delocalized

$$(CH_3)_2\dot{C}—C\equiv N \leftrightarrow (CH_3)_2C=C=N\bullet.$$

The aim of the present investigation was to obtain a well-resolved e.p.r. spectrum for the 2-cyano-2-propyl radical in solution by use of the new and simple flow technique of Dixon and Norman (11).

*Supported by a grant from the United States Public Health Service, Division of General Medical Sciences.
†To whom correspondence should be addressed.

Can. J. Chem. Downloaded from www.nrcresearchpress.com by 210.87.254.42 on 09/05/12
For personal use only.

In this technique hydroxyl radicals are generated at room temperature within the cavity of an e.p.r. spectrometer by the reduction of hydrogen peroxide with titanous ions in acidified aqueous solution. When an organic substrate is present in the reactant streams it is attacked in secondary processes by the hydroxyl radicals and the products so formed can be detected by e.p.r. spectroscopy.

The substrate employed here was isobutyronitrile. This yielded the desired 2-cyano-2-propyl radical in sufficient concentration for a well-resolved e.p.r. spectrum to be successfully obtained. As expected this spectrum of the 2-cyano-2-propyl radical shows appreciable interaction of the unpaired electron with the nitrogen nucleus. Besides obtaining the e.p.r. spectrum of the 2-cyano-2-propyl radical another radical product from the reaction of hydroxyl radicals with isobutyronitrile was found and identified by its e.p.r. spectrum.

EXPERIMENTAL

A Varian (100 kc s^{-1}) V-4502-06 X-band e.p.r. spectrometer system was employed. It was equipped with the V-4548 aqueous solution sample cell accessory, the V-4532 dual-sample cavity attachment to the V-4531 multipurpose cavity, and the G-22A dual-channel graphic recorder. The flow system utilized the mixing arrangement of Dixon and Norman (11) and the aqueous solution cell accessory. The maximum total flowrate was 5 ml s^{-1}. The reactant streams were 0.1 *M* in sulphuric acid (Baker and Adamson, c. p.) and, respectively, 0.05 and 0.1 *M* in hydrogen peroxide (Becco, 98% w/w) and titanous chloride (Fisher, 20% w/w solution). The reaction temperature was 25 ± 1 °C. Isobutyronitrile (Eastman, yellow label) and acetonitrile (Fisher, certified reagent) were used without further purification, since no impurities were detected by vapor phase chromatography (v.p.c.) analysis. When the substrate was isobutyronitrile both reactant streams were made 0.3 *M* in nitrile. When acetonitrile was used in place of isobutyronitrile both reactant streams were 2 *M* in substrate. The hyperfine coupling constants were measured with peroxylamine disulphonate as the reference standard (12), with use of the dual-sample cavity, and on the assumption that the nitrogen hyperfine coupling constant is 13.0 ± 0.1 G (12).

RESULTS AND DISCUSSION

With isobutyronitrile as the substrate two superimposed spectra were observed as shown in Fig. 1. These are ascribed to the following radicals

I

II

These species are products of the abstraction by hydroxyl radicals of hydrogen atoms situated relative to the nitrile group on the 1- and 2-positions, respectively. Isotropic coupling constants for I and II are given in Table I.

TABLE I

Coupling constants for radicals formed by the reaction of hydroxyl radicals with isobutyronitrile

Radical	Spectral type	Coupling constants, G*		
		H_α	H_β	^{14}N
I	Septet (1:6:15:20:15:6:1) of triplets (1:1:1)	—	21.5 ±0.5	3.6 ±0.4
II	Triplet (1:2:1) of doublets (1:1)	23.2 ±0.4	25.1 ±0.5	—

*Each coupling constant given is the arithmetic mean of all measurements of that coupling constant taken from two consecutive field scans. The cited precision index is the maximum absolute deviation from the arithmetic mean. The designations α and β refer to the position relative to the carbon which bears the unpaired electron.

Can. J. Chem. Downloaded from www.nrcresearchpress.com by 210.87.254.42 on 09/05/12
For personal use only.

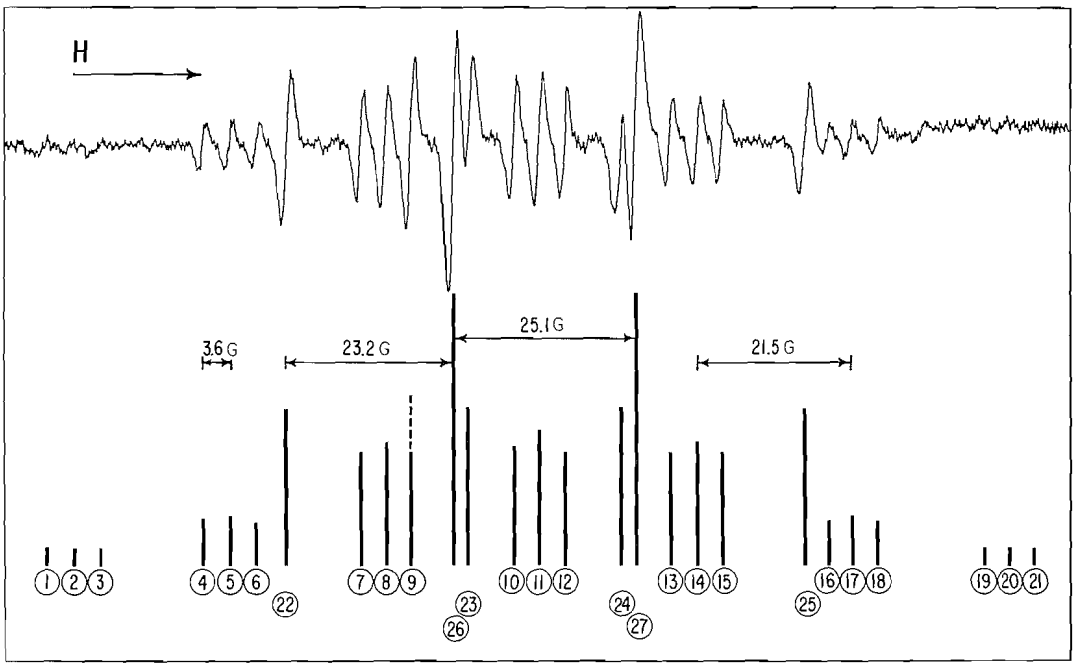

FIG. 1. The electron paramagnetic resonance spectrum for the reaction of hydroxyl radicals with isobutyronitrile; chart speed, 1 in. min^{-1}; time of scan, 25 min. Lines numbered 1 through 21 refer to radical I; lines 22 through 27, to radical II. Line 9 is abnormally intense because of the superimposed singlet signal from unreacted hydroxyl radicals.

The major splitting in the spectrum assigned to radical I is analogous to that reported (11) for the predominant radical formed by attack of hydroxyl radicals on isopropyl alcohol $(CH_3)_2\dot{C}(OH)$. The minor splitting because of coupling with the nitrogen is experimentally indistinguishable from the value of 3.53 ± 0.05 G recently claimed for the acrylonitrile monomer radical, $(HOCH_2)\dot{C}H(CN)$, by Fischer (13). The narrow six-line spectrum is ascribed to radical II. It consists of an overlapping triplet of doublets arising from successive coupling with the protons located with reference to the unpaired electron on the α- and β-position, respectively, i.e., the α- and β-proton couplings are non-equivalent, unlike those reported for the analogous radical $(\cdot CH_2)CH(OH)(CH_3)$ formed from isopropyl alcohol (11).

More nitriles are being studied under these conditions, e.g., acetonitrile. This substrate gives rise to two or more superimposed spectra. The most intense, a triplet (1:2:1) of triplets (1:1:1), has been assigned to the cyano-methyl radical $\cdot CH_2CN$. The rest of the spectrum consists of four (1:2:2:1) triplets (1:1:1) and may be a consequence of radical addition with, perhaps, accompanying polymerization. This feature has not been clearly settled but is receiving further attention along with the investigation of spectra from other nitriles.

1. J. C. BEVINGTON. Radical polymerization. Academic Press Inc., New York, N. Y. 1961.
2. M. TALÂT-ERBEN and S. BYWATER. Ric. Sci. A, **25**, 11 (1955).
3. P. SMITH and A. M. ROSENBERG. J. Am. Chem. Soc. **81**, 2037 (1959).
4. P. SMITH and S. CARBONE. J. Am. Chem. Soc. **81**, 6174 (1959).
5. P. SMITH, N. MULLER, and W. C. TOSCH. J. Polymer Sci. **57**, 823 (1962).
6. G. S. HAMMOND, O. D. TRAPP, R. T. KEYS, and D. L. NEFF. J. Am. Chem. Soc. **81**, 4878 (1959).

Can. J. Chem. Downloaded from www.nrcresearchpress.com by 210.87.254.42 on 09/05/12
For personal use only.

7. G. S. HAMMOND, C.-H. S. WU, O. D. TRAPP, J. WARKENTIN, and R. T. KEYS. J. Am. Chem. Soc. **82**, 5394 (1960).
8. M. TALÂT-ERBEN and A. N. ISFENDIYAROĞLU. Can. J. Chem. **36**, 1156 (1958).
9. M. TALÂT-ERBEN and A. N. ISFENDIYAROĞLU. Can. J. Chem. **37**, 1165 (1959).
10. M. TALÂT-ERBEN and S. BYWATER. J. Am. Chem. Soc. **77**, 3710, 3712 (1955).
11. W. T. DIXON and R. O. C. NORMAN. J. Chem. Soc. 3119 (1963).
12. J. S. HYDE. Personal communication. Sixth Annual NMR-EPR Workshop, Varian Associates, Palo Alto, California. 1962.
13. H. FISCHER. Z. Naturforsch. **18a**, 1142 (1963).

RECEIVED JANUARY 5, 1964.
DEPARTMENT OF CHEMISTRY,
DUKE UNIVERSITY,
DURHAM, NORTH CAROLINA.

Can. J. Chem. Downloaded from www.nrcresearchpress.com by 210.87.254.42 on 09/05/12
For personal use only.

THE REACTION OF UNSATURATED CARBOHYDRATES WITH CARBON MONOXIDE AND HYDROGEN. III. STRUCTURE AND STEREOCHEMISTRY OF THE HEXITOLS FROM 3,4-DI-*O*-ACETYL-D-ARABINAL

ALEX ROSENTHAL AND HANS J. KOCH

In Part II of this series (1) it was shown that 3,4-di-*O*-acetyl-D-xylal reacted with carbon monoxide and hydrogen at a temperature of about 130° and at a pressure of about 4000 p.s.i. in the presence of dicobalt octacarbonyl to yield two anhydrodeoxyhexitols. This paper reports the results of an investigation of the application of a similar reaction to 3,4-di-*O*-acetyl-D-arabinal. The oxo product, first freed of catalyst, was deacetylated with methanolic sodium methoxide to afford a mixture of two hexitols contaminated with traces of sugars. Treatment of the mixture with sodium borohydride in water reduced the sugars to hexitols. Cellulose chromatography of the mixture gave the hexitols (I) and (II).

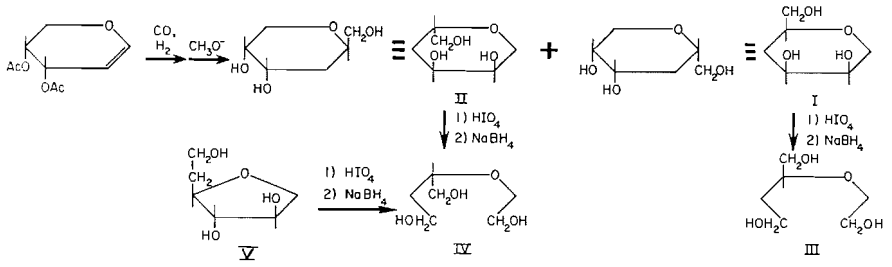

The structure and stereochemistry of the anhydrodeoxyhexitols (I) and (II) were determined in the same way as described in Part II of this series (1). Periodate oxidation of each hexitol (each consumed 1 molar equivalent of periodate) afforded sirupy dialdehydes. Sodium borohydride reduction of these dialdehydes yielded the triol ethers (III) and (IV), which had similar infrared spectra and equal but opposite optical rotations. Further confirmation that these triol ethers were enantiomers was provided by their characterization as crystalline *p*-nitrobenzoates with similar melting points. Direct comparison (m.p., mixed m.p., and infrared spectra) revealed that the *p*-nitrobenzoate of (IV) was identical with the *p*-nitrobenzoate of the triol ether obtained from 1,4-anhydro-5-deoxy-D-*arabino*-hexitol (V). Thus, the configuration of C-5 of the hexitol (II) is the same as that of C-4 of 1,4-anhydro-5-deoxy-D-*arabino*-hexitol (V), and compounds (I) and (II) are 1,5-anhydro-4-deoxy-D-*lyxo*-hexitol and 1,5-anhydro-4-deoxy-L-*ribo*-hexitol, respectively.

7. G. S. HAMMOND, C.-H. S. WU, O. D. TRAPP, J. WARKENTIN, and R. T. KEYS. J. Am. Chem. Soc. **82**, 5394 (1960).
8. M. TALÂT-ERBEN and A. N. ISFENDIYAROĞLU. Can. J. Chem. **36**, 1156 (1958).
9. M. TALÂT-ERBEN and A. N. ISFENDIYAROĞLU. Can. J. Chem. **37**, 1165 (1959).
10. M. TALÂT-ERBEN and S. BYWATER. J. Am. Chem. Soc. **77**, 3710, 3712 (1955).
11. W. T. DIXON and R. O. C. NORMAN. J. Chem. Soc. 3119 (1963).
12. J. S. HYDE. Personal communication. Sixth Annual NMR-EPR Workshop, Varian Associates, Palo Alto, California. 1962.
13. H. FISCHER. Z. Naturforsch. **18a**, 1142 (1963).

RECEIVED JANUARY 5, 1964.
DEPARTMENT OF CHEMISTRY,
DUKE UNIVERSITY,
DURHAM, NORTH CAROLINA.

Can. J. Chem. Downloaded from www.nrcresearchpress.com by 210.87.254.42 on 09/05/12
For personal use only.

THE REACTION OF UNSATURATED CARBOHYDRATES WITH CARBON MONOXIDE AND HYDROGEN. III. STRUCTURE AND STEREOCHEMISTRY OF THE HEXITOLS FROM 3,4-DI-*O*-ACETYL-D-ARABINAL

ALEX ROSENTHAL AND HANS J. KOCH

In Part II of this series (1) it was shown that 3,4-di-*O*-acetyl-D-xylal reacted with carbon monoxide and hydrogen at a temperature of about 130° and at a pressure of about 4000 p.s.i. in the presence of dicobalt octacarbonyl to yield two anhydrodeoxyhexitols. This paper reports the results of an investigation of the application of a similar reaction to 3,4-di-*O*-acetyl-D-arabinal. The oxo product, first freed of catalyst, was deacetylated with methanolic sodium methoxide to afford a mixture of two hexitols contaminated with traces of sugars. Treatment of the mixture with sodium borohydride in water reduced the sugars to hexitols. Cellulose chromatography of the mixture gave the hexitols (I) and (II).

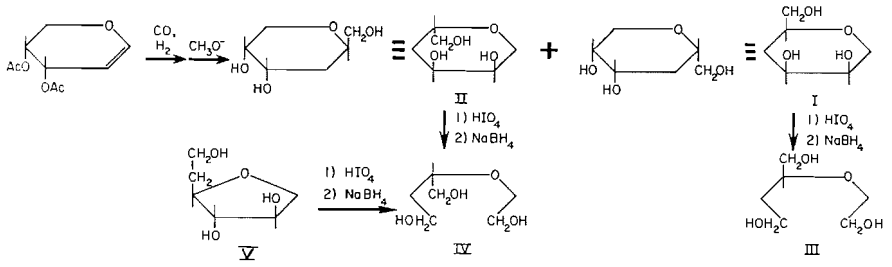

The structure and stereochemistry of the anhydrodeoxyhexitols (I) and (II) were determined in the same way as described in Part II of this series (1). Periodate oxidation of each hexitol (each consumed 1 molar equivalent of periodate) afforded sirupy dialdehydes. Sodium borohydride reduction of these dialdehydes yielded the triol ethers (III) and (IV), which had similar infrared spectra and equal but opposite optical rotations. Further confirmation that these triol ethers were enantiomers was provided by their characterization as crystalline *p*-nitrobenzoates with similar melting points. Direct comparison (m.p., mixed m.p., and infrared spectra) revealed that the *p*-nitrobenzoate of (IV) was identical with the *p*-nitrobenzoate of the triol ether obtained from 1,4-anhydro-5-deoxy-D-*arabino*-hexitol (V). Thus, the configuration of C-5 of the hexitol (II) is the same as that of C-4 of 1,4-anhydro-5-deoxy-D-*arabino*-hexitol (V), and compounds (I) and (II) are 1,5-anhydro-4-deoxy-D-*lyxo*-hexitol and 1,5-anhydro-4-deoxy-L-*ribo*-hexitol, respectively.

It is apparent that analysis of the nuclear magnetic resonance (n.m.r.) spectra (described in Experimental section) reveals the molecular structure of each of the anhydrodeoxyhexitols (I) and (II). Because each multiplet of peaks (equivalent to two hydrogens) occurs at about $\delta = 1.8$, it can be inferred from previous work (1) that each isomer possesses a methylene group on C-4. Thus, the two anhydrodeoxyhexitols must be linear and differ only in the configuration of C-5. The stereochemistry of C-5 of each of the anhydrodeoxyhexitols cannot be ascertained from the n.m.r. spectra because of overlapping peaks.

EXPERIMENTAL

General Considerations

These have been described previously (1).

*3,4-Di-O-acetyl-*D*-arabinal*

This was prepared following the procedure for the preparation of 3,4-di-*O*-acetyl-D-xylal (1).

*Reaction of 3,4-Di-O-acetyl-*D*-arabinal with Carbon Monoxide and Hydrogen to Yield 1,5-Anhydro-4-deoxy-*D*-lyxo-hexitol (I) and 1,5-Anhydro-4-deoxy-*L*-ribo-hexitol (II)*

The 3,4-Di-*O*-acetyl-D-arabinal (12 g) was allowed to react with 500 p.s.i. of carbon monoxide and 2500 p.s.i. of hydrogen in the presence of dicobalt octacarbonyl (2 g) for 1.5 h at 125°. The product (13 g), first freed of catalyst by filtration through Florisil, contained traces of reducing sugars. Reaction of the same substrate with carbon monoxide and hydrogen (1:8 by pressure) at 113° to 120° for 0.5 h yielded 33% reducing sugars and about 65% hexitols. The product was deacetylated with 0.1 *N* methanolic sodium methoxide. Sugars were reduced with sodium borohydride before separation of the hexitols by chromatography. Chromatography of 1.43 g of the deacetylated product on a powdered cellulose column (410 × 47 mm diam.) with water-saturated 1-butanol as developer yielded 0.80 g of fraction (I) and 0.55 g of fraction (II). Fractionation was also readily achieved using water-saturated 1-butanol containing 5% ethanol as developer.

Characterization of Fraction (I)

Fraction (I) (1,5-anhydro-4-deoxy-D-*lyxo*-hexitol) crystallized slowly when kept in a desiccator for several months over phosphorus pentoxide; m.p. 85–87°; $[\alpha]_D^{20}$ −50° (*c*, 1.7 water); $R_f = 0.26$. Attempts to crystallize (I) from methanol – isopropyl ether were unsuccessful. Anal. Calc. for $C_6H_{12}O_4$: C, 48.64; H, 8.17. Found: C, 48.38; H, 8.22. N.M.R. (deuterium oxide): multiplet of peaks, centered at $\delta = 1.68$ to 1.80, equal to 2 hydrogens. This spectrum was identical with that of a similar compound isolated by Gorin (2) from the hydrogenolysis of methyl-α-D-glucopyranoside.

Characterization of Fraction (II)

Fraction (II) (1,5-anhydro-4-deoxy-L-*ribo*-hexitol) solidified when kept in a desiccator over phosphorus pentoxide for several months. The substance was very hygroscopic. Attempts to crystallize (II) from various solvents were unsuccessful. $[\alpha]_D^{20}$ +29° (*c*, 2.5 water); $R_f = 0.36$. Anal. Calc. for $C_6H_{12}O_4$: C, 48.64; H, 8.17. Found: C, 48.49; H, 8.22. N.M.R. (deuterium oxide): multiplet of peaks, centered at $\delta = 1.60$ to 1.80, equal to 2 hydrogens.

*Preparation of 1,5-Anhydro-2,3,6-tri-O-benzoyl-4-deoxy-*D*-lyxo-hexitol*

Fraction (I) was benzoylated according to the procedure of Smith and Van Cleve (3) to yield sirupy 1,5-anhydro-2,3,6-tri-*O*-benzoyl-4-deoxy-D-*lyxo*-hexitol; $[\alpha]_D^{21}$ −63° (*c*, 3 ethanol). Anal. Calc. for $C_{27}H_{24}O_7$: C, 70.41; H, 5.25. Found: C, 70.60; H, 5.42.

*Preparation of 1,5-Anhydro-2,3,6-tri-O-benzoyl-4-deoxy-*L*-ribo-hexitol*

Fraction (II) was benzoylated in the usual way to yield 1,5-anhydro-2,3,6-tri-*O*-benzoyl-4-deoxy-L-*ribo*-hexitol, and the product was recrystallized from ethyl acetate – light petroleum ether, or methanol–water; m.p. 132–133°; $[\alpha]_D^{21}$ +79° (*c*, 1.58 chloroform). Anal. Calc. for $C_{27}H_{24}O_7$: C, 70.41; H, 5.25. Found: C, 70.75; H, 5.31.

Structure and Stereochemistry of Fractions (I) and (II)

Fraction (I) was oxidized, according to the procedure previously described (1), with 0.1 *M* periodic acid (1 molar equivalent consumed). The dialdehyde was immediately reduced with sodium borohydride to yield the triol ether (III); $[\alpha]_D^{21}$ −17° (*c*, 1 water). The triol ether was characterized as the *p*-nitrobenzoate; m.p. 102–102.5°; $[\alpha]_D^{22}$ −23° (*c*, 2 chloroform). Anal. Calc. for $C_{27}H_{23}N_3O_{13}$: C, 54.27; H, 3.88; N, 7.03. Found: C, 54.55; H, 3.96; N, 7.36.

Similarly fraction (II) was converted into the triol ether (IV); $[\alpha]_D^{24}$ +17° (*c*, 1 water). The infrared spectra of III and IV were similar. Reaction of the triol ether (IV) with *p*-nitrobenzoyl chloride in pyridine

Can. J. Chem. Downloaded from www.nrcresearchpress.com by 210.87.254.42 on 09/05/12
For personal use only.

yielded the tris-*p*-nitrobenzoate; m.p. 102–102.5°; $[\alpha]_D^{22}$ +22.3 (*c*, 3.6 chloroform). Anal. Calc. for $C_{27}H_{23}N_3O_{13}$: C, 54.27; H, 3.88; N, 7.03. Found: C, 54.39; H, 3.98; N, 7.29.

The infrared spectra of the two *p*-nitrobenzoate derivatives were identical. The mixed m.p. of the tris-*p*-nitrobenzoate of compound (IV) and the tris-*p*-nitrobenzoate of 2-deoxy-3-*O*-(2-hydroxyethyl)-L-*glycero*-tetritol (1) (obtained by sodium borohydride reduction of the periodate oxidation product of authentic 1,4-anhydro-5-deoxy-D-*arabino*-hexitol (V)) was 101–103°. The infrared spectra of the two *p*-nitrobenzoates were identical.

ACKNOWLEDGMENTS

The financial assistance of the National Cancer Institute of Canada and the National Research Council is gratefully acknowledged.

One of us (A. R.) spent the academic year 1963–64 as a guest of University Chemical Laboratory, Cambridge, England, in the laboratories of Professor Lord Todd where this manuscript was written, and wishes to thank the members of the Department of Chemistry for their hospitality.

1. A. Rosenthal and D. Abson. Can. J. Chem. In press.
2. P. A. J. Gorin. Can. J. Chem. **38**, 641 (1960).
3. F. Smith and J. W. Van Cleve. J. Am. Chem. Soc. **77**, 3091 (1955).

Received February 24, 1964.
Department of Chemistry,
University of British Columbia,
Vancouver 8, British Columbia.

Can. J. Chem. Downloaded from www.nrcresearchpress.com by 210.87.254.42 on 09/05/12
For personal use only.

PROPYLENE GAS HYDRATE STABILITY[1]

E. C. Clarke, R. W. Ford, and D. N. Glew

INTRODUCTION

Although the formation conditions for propane hydrate are well characterized (1, 2, 3), the comparable conditions for the formation of propylene hydrate from liquid water and propylene gas have been little studied and are known only approximately. From the three measurements available (3) it appears that the propylene hydrate is considerably less stable than the propane hydrate, in spite of the similar physical properties of the propylene and propane species. An experimental investigation of the propylene hydrate system has thus been made to better define the conditions for hydrate formation.

EXPERIMENTAL

The propylene was Matheson C.P. grade which was found by gas chromatography to contain 99.4 mole % propylene, 0.56 mole % propane, 127 p.p.m. ethane, and less than 10 p.p.m. of any other volatile impurity. The water was distilled and deionized by passage through a mixed ion exchange resin column, and subsequently outgassed in the hydrate cell prior to use.

The hydrate cell which was fabricated from stainless steel contained a stirrer operated by magnetic induction. The portion of the apparatus in which the hydrate was formed could be completely immersed in a large thermostat bath which could be regulated to ±0.001 °C. Pressure was measured using a 0–100 p.s.i., 10 in. diameter Heise gauge, which was calibrated by a dead-weight tester. The barometric pressure was recorded at each measurement. This procedure gave pressure accurate to ±0.1 p.s.i. or ±0.006 atm.

The temperature of the cell was measured relative to a block of stainless steel immersed in the same thermostat bath by means of a ten-junction copper–constantan thermocouple. The temperature of the block was measured by a platinum resistance thermometer which was calibrated at the triple point of water.

[1]*Contribution No. 122.*

yielded the tris-*p*-nitrobenzoate; m.p. 102–102.5°; $[\alpha]_D^{22}$ +22.3 (*c*, 3.6 chloroform). Anal. Calc. for $C_{27}H_{23}N_3O_{13}$: C, 54.27; H, 3.88; N, 7.03. Found: C, 54.39; H, 3.98; N, 7.29.

The infrared spectra of the two *p*-nitrobenzoate derivatives were identical. The mixed m.p. of the tris-*p*-nitrobenzoate of compound (IV) and the tris-*p*-nitrobenzoate of 2-deoxy-3-*O*-(2-hydroxyethyl)-L-*glycero*-tetritol (1) (obtained by sodium borohydride reduction of the periodate oxidation product of authentic 1,4-anhydro-5-deoxy-D-*arabino*-hexitol (V)) was 101–103°. The infrared spectra of the two *p*-nitrobenzoates were identical.

ACKNOWLEDGMENTS

The financial assistance of the National Cancer Institute of Canada and the National Research Council is gratefully acknowledged.

One of us (A. R.) spent the academic year 1963–64 as a guest of University Chemical Laboratory, Cambridge, England, in the laboratories of Professor Lord Todd where this manuscript was written, and wishes to thank the members of the Department of Chemistry for their hospitality.

1. A. Rosenthal and D. Abson. Can. J. Chem. In press.
2. P. A. J. Gorin. Can. J. Chem. **38**, 641 (1960).
3. F. Smith and J. W. Van Cleve. J. Am. Chem. Soc. **77**, 3091 (1955).

Received February 24, 1964.
Department of Chemistry,
University of British Columbia,
Vancouver 8, British Columbia.

Can. J. Chem. Downloaded from www.nrcresearchpress.com by 210.87.254.42 on 09/05/12
For personal use only.

PROPYLENE GAS HYDRATE STABILITY[1]

E. C. Clarke, R. W. Ford, and D. N. Glew

INTRODUCTION

Although the formation conditions for propane hydrate are well characterized (1, 2, 3), the comparable conditions for the formation of propylene hydrate from liquid water and propylene gas have been little studied and are known only approximately. From the three measurements available (3) it appears that the propylene hydrate is considerably less stable than the propane hydrate, in spite of the similar physical properties of the propylene and propane species. An experimental investigation of the propylene hydrate system has thus been made to better define the conditions for hydrate formation.

EXPERIMENTAL

The propylene was Matheson C.P. grade which was found by gas chromatography to contain 99.4 mole % propylene, 0.56 mole % propane, 127 p.p.m. ethane, and less than 10 p.p.m. of any other volatile impurity. The water was distilled and deionized by passage through a mixed ion exchange resin column, and subsequently outgassed in the hydrate cell prior to use.

The hydrate cell which was fabricated from stainless steel contained a stirrer operated by magnetic induction. The portion of the apparatus in which the hydrate was formed could be completely immersed in a large thermostat bath which could be regulated to ±0.001 °C. Pressure was measured using a 0–100 p.s.i., 10 in. diameter Heise gauge, which was calibrated by a dead-weight tester. The barometric pressure was recorded at each measurement. This procedure gave pressure accurate to ±0.1 p.s.i. or ±0.006 atm.

The temperature of the cell was measured relative to a block of stainless steel immersed in the same thermostat bath by means of a ten-junction copper–constantan thermocouple. The temperature of the block was measured by a platinum resistance thermometer which was calibrated at the triple point of water.

[1]*Contribution No. 122.*

Since this calibration has changed by less than the uncertainty in a single measurement during a period of six months, the accuracy of temperature measurement is ±0.0005 °C.

The vapor pressure of propylene was measured from −13 °C to +6 °C. Liquid propylene was condensed in the cell, the temperature of the thermostat adjusted, and the pressure measured when no further change occurred. The results are given in Table I. The data can be represented by the equation: $\log_{10} P = 4.30595 \pm 0.00006 - (968.4 \pm 0.8)1/T$; where T is in °K and P in atm. The standard deviation of the data from this equation is ±0.004 atm.

TABLE I

Vapor pressure of propylene

t(°C)	P(atm)	t(°C)	P(atm)
−12.856	3.850	0.102	5.782
−11.830	3.984	0.132	5.787
−10.854	4.112	0.582	5.858
−9.844	4.246	0.973	5.928
−8.846	4.386	1.571	6.034
−7.858	4.522	2.074	6.122
−6.872	4.667	2.590	6.220
−5.860	4.824	3.006	6.297
−4.896	4.971	3.494	6.385
−3.895	5.127	4.010	6.488
−2.906	5.286	4.514	6.585
−1.916	5.448	5.008	6.679
−0.936	5.610	5.401	6.757
−0.098	5.753	5.990	6.871
0.000	5.770		

For hydrate experiments, approximately 90 ml of distilled, deionized water was put in the cell and degassed by alternately evacuating and admitting propylene. This was repeated several times. The thermostat was adjusted to approximately 0 °C and sufficient propylene admitted to form a layer of liquid in the cell. While stirring the cell, some of the propylene was vented giving nuclei for hydrate formation. The system was then allowed to equilibrate by consuming the liquid propylene and forming more hydrate.

The values of the total pressure of the system $P(\mathrm{hl_lg})$ at a number of temperatures were determined, allowing at least 8 h for the system to attain equilibrium. The results are given in Table II. After subtracting the vapor pressure of water, and converting the pressure of propylene to fugacity by means of the extrapolated data of Farrington and Sage (4), the data were found to fit the equation: $\log_{10} f = 24.8309 \pm 0.0001 - (6610 \pm 20)1/T$. The standard deviation of the data about this line is ±0.004 atm. The value of ΔH for the decomposition $C_3H_6.nH_2O(h) \rightarrow C_3H_6(g) + nH_2O(l_1)$, is 30 230 ± 90 cal/mole. The accuracy

TABLE II

Propylene hydrate total pressure

t(°C)	$P(\mathrm{hl_lg})$(atm)
−0.161[c]	4.569
−0.134[a]	—
−0.113	4.622
−0.064	4.674
+0.006	4.746
0.217	4.988
0.325	5.114
0.442	5.253
0.493	5.330
0.558	5.404
0.594	5.452
0.798	5.709
0.897	5.851
0.943	5.913
0.958[b]	—

[a,b]Lower and upper quadruple limits of ($\mathrm{hl_lg}$) line.
[c]Metastable.

Can. J. Chem. Downloaded from www.nrcresearchpress.com by 210.87.254.42 on 09/05/12
For personal use only.

of this value is less than that indicated by the standard deviation given because of an estimated 10% uncertainty in the fugacities. It is estimated that this increases the uncertainty to ±300 cal/mole. This enthalpy-change value indicates that propylene forms a structure II gas hydrate of formula $C_3H_6.17H_2O$, isomorphous with the propane and bromochlorodifluoromethane hydrates (5).

The lower quadruple point was measured and found to be -0.134 ± 0.001 °C. The upper quadruple point, which was calculated as the point of intersection of the hydrate equilibrium line and the propylene vapor pressure line, was $+0.958 \pm 0.001$ °C.

1. W. M. Deaton and E. M. Frost, Jr. U.S. Bur. Mines, Monograph 8 (1946).
2. W. I. Wilcox, D. B. Carson, and D. L. Katz. Ind. Eng. Chem. **33**, 662 (1941).
3. H. H. Reamer, F. T. Selleck, and B. H. Sage. J. Petrol. Technol. **4**, No. 8, 197 (1952).
4. P. S. Farrington and B. H. Sage. Ind. Eng. Chem. **41**, 1734 (1949).
5. M. v. Stackelberg and H. R. Müller. Z. Elektrochem. **58**, 25 (1954).

Received April 23, 1964.
Exploratory Research Laboratory,
Dow Chemical of Canada, Limited,
Sarnia, Ontario.

THE FORMATION OF TRIBUTYLIODOAMMONIUM IODIDE IN THE URANYL PHOTOSENSITIZED REACTION WITH TETRABUTYLAMMONIUM IODIDE

J. K. S. Wan, E. A. Schuck,[1] J. K. Foote, and J. N. Pitts, Jr.[2]

Recently the photochemistry of the iodide ion in aqueous solution has been extensively studied (1–8). Absorption of light seems to produce an excited iodide ion which may then dissociate into an iodine atom and a solvated electron, or alternatively decay back to the ground state. Scavengers such as proton donors react with the solvated electron thus preventing the secondary cage recombination.

However, we have been unable to find previously published reports on the reactivity of aqueous iodide ions photosensitized by uranyl ion. Since the energy of binding the electron of the iodide ion in the first excited state is only about 35 kcal (9), it appears that photooxidation of the iodide ion might be brought about by photosensitization with uranyl ion in the longer wavelength region. We wish to report here the reaction of tetrabutylammonium iodide in aqueous solution sensitized by uranyl nitrate and to disclose a photochemical method for preparing tributyliodoammonium iodide.

When an aqueous solution of uranyl nitrate and tetrabutylammonium iodide (I) was irradiated at room temperature with the 3660 Å line from a mercury vapor lamp, a black precipitate was formed. In the absence of light, no precipitation was observed. The identity of the precipitate as tributyliodoammonium iodide, $(C_4H_9)_3IN^+I^-$ (II), was confirmed by elementary analysis, molecular weight determination, infrared and nuclear magnetic resonance (n.m.r.) analyses. The molecular weight was found experimentally to be 442: calculated for II is 439. The infrared spectrum taken in a KBr matrix was consistent with that expected for II. The n.m.r. spectrum exhibits three complex multiplets centered on τ values of A, 8.90; B, 8.40 and C, 6.75; with integrated areas being in the ratio 1.55:2:1. Peak A can be assigned to the methyl protons (9H), peak B to the methylene protons (12H), and peak C to the protons (6H) adjacent to the nitrogen atom. The ultraviolet spectrum taken in ethanol solution showed an absorption onset at 5000 Å with maxima at 3650 and 3200 Å.

[1]*Member Air Pollution Research Center, University of California, Riverside.*
[2]*Address reprint requests to this author.*

Can. J. Chem. Downloaded from www.nrcresearchpress.com by 210.87.254.42 on 09/05/12
For personal use only.

of this value is less than that indicated by the standard deviation given because of an estimated 10% uncertainty in the fugacities. It is estimated that this increases the uncertainty to ±300 cal/mole. This enthalpy-change value indicates that propylene forms a structure II gas hydrate of formula $C_3H_6.17H_2O$, isomorphous with the propane and bromochlorodifluoromethane hydrates (5).

The lower quadruple point was measured and found to be -0.134 ± 0.001 °C. The upper quadruple point, which was calculated as the point of intersection of the hydrate equilibrium line and the propylene vapor pressure line, was $+0.958 \pm 0.001$ °C.

1. W. M. Deaton and E. M. Frost, Jr. U.S. Bur. Mines, Monograph 8 (1946).
2. W. I. Wilcox, D. B. Carson, and D. L. Katz. Ind. Eng. Chem. **33**, 662 (1941).
3. H. H. Reamer, F. T. Selleck, and B. H. Sage. J. Petrol. Technol. **4**, No. 8, 197 (1952).
4. P. S. Farrington and B. H. Sage. Ind. Eng. Chem. **41**, 1734 (1949).
5. M. v. Stackelberg and H. R. Müller. Z. Elektrochem. **58**, 25 (1954).

Received April 23, 1964.
Exploratory Research Laboratory,
Dow Chemical of Canada, Limited,
Sarnia, Ontario.

THE FORMATION OF TRIBUTYLIODOAMMONIUM IODIDE IN THE URANYL PHOTOSENSITIZED REACTION WITH TETRABUTYLAMMONIUM IODIDE

J. K. S. Wan, E. A. Schuck,[1] J. K. Foote, and J. N. Pitts, Jr.[2]

Recently the photochemistry of the iodide ion in aqueous solution has been extensively studied (1–8). Absorption of light seems to produce an excited iodide ion which may then dissociate into an iodine atom and a solvated electron, or alternatively decay back to the ground state. Scavengers such as proton donors react with the solvated electron thus preventing the secondary cage recombination.

However, we have been unable to find previously published reports on the reactivity of aqueous iodide ions photosensitized by uranyl ion. Since the energy of binding the electron of the iodide ion in the first excited state is only about 35 kcal (9), it appears that photo-oxidation of the iodide ion might be brought about by photosensitization with uranyl ion in the longer wavelength region. We wish to report here the reaction of tetrabutyl-ammonium iodide in aqueous solution sensitized by uranyl nitrate and to disclose a photochemical method for preparing tributyliodoammonium iodide.

When an aqueous solution of uranyl nitrate and tetrabutylammonium iodide (I) was irradiated at room temperature with the 3660 Å line from a mercury vapor lamp, a black precipitate was formed. In the absence of light, no precipitation was observed. The identity of the precipitate as tributyliodoammonium iodide, $(C_4H_9)_3IN^+I^-$ (II), was confirmed by elementary analysis, molecular weight determination, infrared and nuclear magnetic resonance (n.m.r.) analyses. The molecular weight was found experimentally to be 442: calculated for II is 439. The infrared spectrum taken in a KBr matrix was consistent with that expected for II. The n.m.r. spectrum exhibits three complex multiplets centered on τ values of A, 8.90; B, 8.40 and C, 6.75; with integrated areas being in the ratio 1.55:2:1. Peak A can be assigned to the methyl protons (9H), peak B to the methylene protons (12H), and peak C to the protons (6H) adjacent to the nitrogen atom. The ultraviolet spectrum taken in ethanol solution showed an absorption onset at 5000 Å with maxima at 3650 and 3200 Å.

[1]*Member Air Pollution Research Center, University of California, Riverside.*
[2]*Address reprint requests to this author.*

Can. J. Chem. Downloaded from www.nrcresearchpress.com by 210.87.254.105 on 09/05/12
For personal use only.

Can. J. Chem. Downloaded from www.nrcresearchpress.com by 210.87.254.105 on 09/05/12
For personal use only.

The product II exists at room temperature as a black powder with a melting point of 65–68 °C. The compound is stable at least up to 135 °C, and exhibits a reversible thermochromic phenomenon (from black to yellow) when warmed to 88 °C or higher. The infrared spectra of both color forms do not show any drastic changes.

A 1:1 molecular complex between tributyl amine and iodine was considered as possible reaction product. To this end the complex was prepared (10) and various spectra and other properties were determined. The complex exists at room temperature as a brown-yellowish oil and comparison of other spectra permitted elimination of this isomer. In addition, irradiation of a solution of uranyl nitrate, KI, and tributyl amine failed to produce II.

The rate of the photochemical reaction was followed by measuring the % transmission of the incident monochromatic light as a function of time. The concentrations of uranyl ion before and after irradiation were measured spectrophotometrically at 4200 Å and found to remain practically unchanged. To study the effect of pH on the rate of reaction, the solution was adjusted to the desired pH with nitric acid. The reaction rate was higher in acid medium and was dependent on the pH of the solution, rising rapidly in the region between pH 3 and 4. On the other hand, at a constant pH the reaction rate was found to increase with decreasing concentration of I.

The experimental data obtained to date are insufficient to establish the entire reaction mechanism, but seem to suggest that oxidation of the iodide ion is sensitized by the photoexcited uranyl ions, leading to an iodine atom and a solvated electron. The overall reaction may be

$$UO_2^{++} + R_4N^+ + 2I^- + H^+ \xrightarrow{h\nu} UO_2^{++} + R_3IN^+I^- + RH$$

where R is a butyl group. The effect of pH on the reaction rate can be explained by the hydrogen ions scavenging the solvated electron thus preventing iodine atom from cage recombination. In fact, it was observed that as the reaction proceeded, pH of the solution slowly increased. The observation in which the rate of reaction increases with decreasing concentration of tetrabutylammonium iodide suggests the presence of kinetically inactive ion pairs (11, 12).

The direct photolysis of an aqueous solution of I also was carried out by light shorter than 3000 Å. A black precipitate of II was recovered together with some free iodine. The formation of iodine could be due to the much higher light intensity which generated a high concentration of iodine atoms in a small volume, and (or) due to secondary photodecomposition of the product II. Further studies are in progress to investigate the photosensitized oxidation of iodide ions in a flow system, in an attempt to gain some insight into the mechanism of the reaction and the quantum efficiency of the sensitization.

EXPERIMENTAL

Polarographic grade of tetrabutylammonium iodide and analytical grade of uranyl nitrate were used in all experiments. Melting points were determined in capillary tubings and are uncorrected. The analyses were performed by C. F. Geiger, Ontario, California. The ultraviolet spectra were recorded on Cary spectrophotometer; infrared spectra were recorded on a Perkin–Elmer 221 spectrophotometer. Nuclear magnetic resonance spectra were taken at 60 Mc/s on a Varian A60 instrument using $CDCl_3$ as solvent and tetramethylsilane as an internal standard ($\tau = 10.0$). A Leeds and Northrups pH meter with glass electrodes was used for pH measurement, the instrument was standardized before and after each run with 0.05 *M* potassium acid phthalate (pH 4.01 at 25 °C). Molecular weight determinations were made using mg quantities of solute and 2 ml of acetone. Measurements were taken with a Mechrolab vapor pressure osometer model 301a, to determine vapor pressure lowering at 37 °C. The instrument was calibrated with benzil and with benzophenone solutions over a similar concentration range. Photosensitized reactions were carried

out with solutions in a pyrex cell and a 100 W PEK high pressure mercury lamp equipped with a 3660 Å interference filter as light source. The % transmission of the incident light was measured with a RCA 935 phototube–galvanometer system. For direct photolysis experiments, a quartz cell was used with a Hanovia medium pressure mercury arc as light source.

Photosensitized Reaction of Tetrabutylammonium Iodide

In a typical experiment, an aqueous solution (200 ml) of uranyl nitrate and I, each with an initial concentration of 0.02 *M*, was irradiated. The solution was stirred magnetically at a constant speed. After every few hours the black precipitate was filtered and the filtrate was subjected to further irradiation until no precipitation was observed. The combined precipitate was then dried at 130 °C; yield 0.8179 g (theoretical yield 0.8911 g). The product was insoluble in water, aqueous solutions of KI, acid and alkaline, ether, benzene, and carbon tetrachloride, but moderately soluble in alcohol and readily in acetone and chloroform. Found: C, 32.10; H, 5.98; N, 2.84; I, 59.44; calc. for II: C, 32.80; H, 6.15; N, 3.19; I, 57.86%.

In a similar experiment with 0.5800 g of ammonium iodide added, 1.5116 g of II was recovered.

Reaction of II with Silver Nitrate

A 0.1286 g sample (0.29 mmole) of II was dissolved in 400 ml ethanol in which an excess of saturated silver nitrate ethanolic solution was added. A yellow precipitate (0.6100 g, 0.26 mmole) of silver iodide was recovered at room temperature. This indicates that only one iodine atom was removed from the molecule II.

Photolysis of Tetrabutylammonium Iodide

An aqueous solution of I (200 ml) with an initial concentration of 0.02 *M* was irradiated in a quartz cell. When wavelengths shorter than 3200 Å were cut off by a pyrex filter, no reaction was observed. However, in the presence of light shorter than 3000 Å, a heavy brownish-black precipitate resulted. The precipitate was a mixture of II and iodine, after the latter was washed away with KI solution. The product II thus recovered weighed 0.6854 g.

ACKNOWLEDGMENTS

This research was supported in part by Grant AP 00109 from the Division of Air Pollution, Bureau of State Services, Public Health Service. We are indebted to Mr. Charles McKinney of Consolidated Electrodynamics Corp. for a mass spectrometric analysis, and to Mr. Jerry Brem for some technical assistance. One of us (J. K. F.) also wishes to acknowledge a National Defense Educational Act Fellowship.

1. R. M. Noyes. J. Am. Chem. Soc. **77**, 2042 (1955); **78**, 546 (1956).
2. L. I. Grossweiner and M. S. Matheson. J. Phys. Chem. **61**, 1098 (1957).
3. F. H. C. Edgecombe and R. G. W. Norrish. Proc. Roy. Soc. London, Ser. A, **253**, 154 (1959).
4. F. S. Dainton and S. A. Sills. Nature, **186**, 879 (1960).
5. J. Jortner, M. Ottolenghi, R. Levine, and G. Stein. J. Phys. Chem. **65**, 1232 (1961).
6. J. Jortner, M. Ottolenghi, J. Rabani, and G. Stein. J. Chem. Phys. **37**, 2488 (1962).
7. J. Jortner, M. Ottolenghi, and G. Stein. J. Phys. Chem. **66**, 2029, 2037, 2042 (1962); **67**, 1271 (1963).
8. K. Butkow. Z. Physik. **62**, 71 (1930).
9. G. Stein and A. Terenin. Trans. Faraday Soc. **55**, 1087 (1959).
10. H. Yada, J. Tanaka, and S. Nagakura. Bull. Chem. Soc. Japan, **33**, 1660 (1960).
11. C. C. Evans and S. Sugden. J. Chem. Soc. 270 (1949).
12. E. M. Morimoto and M. Kahn. J. Phys. Chem. **68**, 201 (1964).

Received April 8, 1964.
Department of Chemistry,
University of California,
Riverside, California.

Can. J. Chem. Downloaded from www.nrcresearchpress.com by 210.87.254.105 on 09/05/12
For personal use only.

Can. J. Chem. Downloaded from www.nrcresearchpress.com by 210.87.254.6 on 09/05/12
For personal use only.

Canadian Journal of Chemistry

Issued by THE NATIONAL RESEARCH COUNCIL OF CANADA

VOLUME 42 SEPTEMBER 1964 NUMBER 9

THE RADIATION CHEMISTRY OF AQUEOUS SOLUTIONS OF CHLORAL HYDRATE AND OF BROMAL HYDRATE

R. G. MCINTOSH, R. L. EAGER, AND J. W. T. SPINKS

Department of Chemistry and Chemical Engineering, University of Saskatchewan, Saskatoon, Saskatchewan

Received March 23, 1964

ABSTRACT

The radiation chemistry of aqueous solutions of chloral hydrate and of bromal hydrate has been further investigated. The electrical conductivity method of Andrews and Shore (1) was used to follow the appearance of acid. The yield of acid was found to be dependent on the dose rate, contrary to the conclusion reached by Andrews and Shore but in agreement with the results of other workers. A reexamination of Andrews and Shore's paper indicates that an incorrect interpretation was made of their data and reveals that, in fact, their data also indicate a dose rate dependence for the yield of acid. A free radical mechanism is proposed which is in good agreement with the observed dependence of the rate of formation of acid upon the dose rate and upon the solute concentration in both the presence and in the absence of oxygen.

Several reports have been published on the radiation chemistry of aqueous solutions of chloral hydrate (1–6) and of bromal hydrate (6–11). There is general agreement that one of the main products is the corresponding hydrohalic acid. In the earliest reported work, that of Andrews and Shore (1) on aqueous chloral hydrate solutions, the appearance of hydrochloric acid was followed by measurement of the electrical conductivity of the solution. A similar method was used by Hilsenrod (4). In the other work referred to, the production of acid was followed by titration with standard base. Andrews and Shore (1) interpreted their results in a manner which indicated that the G value (number of molecules of product per 100 eV of energy absorbed) of HCl was independent of dose rate. Hilsenrod (4) did not investigate the dose rate dependence. In contrast, all of the other workers (2, 3, 5, 6) reported a dose rate dependence, the G value being approximately inversely proportional to the square root of the dose rate. A similar dose rate dependence was found for aqueous solutions of bromal (6–9).

No satisfactory explanation for this large discrepancy in the dose rate dependence has been offered. While it seems unlikely, a possible explanation is that the different behavior reported arises because of the methods used to follow the appearance of the hydrohalic acid. The electrical conductivity method is not very specific, since the appearance of any electrolyte will result in an increase in electrical conductivity. The titration method is more specific, since it will respond only to acidic products. It should be noted that Andrews and Shore (1) did do some chloride analysis and pH measurements which indicated that the electrical conductivity measured by them was due mainly to hydrochloric acid. By titration with a base, they found that the amount of total acid present was somewhat larger than that which would be expected if only hydrochloric acid was responsible for the electrical conductivity. Similarly, Woods and Spinks (7), and Heusinger *et al.* (8)

found for ^{60}Co γ-irradiated bromal hydrate solutions that the total acid content of the solutions was somewhat larger than that of the hydrobromic acid present. The above observations would suggest that the reported discrepancy in the dose rate dependence is not due to the different methods used in following the appearance of the hydrohalic acid. In an attempt to resolve this difference, we decided to do a further study on the irradiation of aqueous solutions of chloral hydrate and of bromal hydrate by using the electrical conductivity method.

The electrical conductivity method would be expected to have several advantages over the titration method for following the appearance of the hydrohalic acid. The precision should be greater and the results should be obtained with less effort. Also, if the solution is irradiated in the conductivity cell, it is possible to follow the course of the reaction almost continuously. Because samples do not need to be withdrawn for analysis, the volume of the solution being irradiated is not altered and the dosimetry is simplified.

It was also felt that it would be worth while to bring together the results of the various workers referred to above so that their results together with those obtained in the present work could all be considered at one time.

EXPERIMENTAL

Apparatus and Reagents

The irradiations were made with a 90 curie ^{60}Co source housed in a concrete cave (12). Samples were located at various distances from the source in order to obtain different radiation intensities.

The Fricke ferrous sulphate dosimeter, as described by Weiss *et al.* (13), was used for dose determinations. The molar extinction coefficient of ferric ions was taken to be 2243 at a wavelength of 304 mμ. The G value of the dosimeter was taken to be 15.5 ferric ions per 100 eV of energy absorbed. When calculating the dose received by a sample, we corrected for the difference in the electron densities of the sample and of the dosimeter.

The conductivity cell was of the Arrhenius–Ostwald type. A thermometer was built into the cell, hence the temperature of the solution whose electrical conductivity was being determined was known. The cell constant was found to be 0.318 cm^{-1} by the use of a 0.0200 N potassium chloride solution. Preliminary experiments indicated that chloral hydrate would decompose, in the absence of radiation, when "platinized" platinum electrodes were used. This observation is in agreement with that made by Andrews and Shore (1). These authors found that no appreciable decomposition occurred when tungsten electrodes were used. In the present work, bright platinum electrodes were found to give results of acceptable accuracy and at the same time did not cause decomposition of either chloral hydrate or bromal hydrate. Electrical leads were run from the conductivity cell to a Wheatstone bridge located outside the cave.

Chloral hydrate of U.S.P. grade was used without further purification. Solutions of chloral hydrate were stored in the dark and were used within 4 days of preparation. Bromal hydrate was prepared by adding bromal to water and recrystallizing the product from a small volume of water. The solutions were stored in the dark and kept for only 3 days (9). The water used for preparing solutions for irradiation was purified by starting with distilled water and distilling it further, first from an alkaline permanganate solution, and then from an acidic dichromate solution. The water was finally passed through a mixed bed ion exchange resin column. The product had a specific conductance of 5×10^{-6} Ω^{-1} cm^{-1}.

The sample temperature was that of the cave, between 20 °C and 25 °C. The observed rates of change of specific conductance with time of irradiation were corrected to 25 °C by use of a temperature coefficient of 2.5% per °C for chloral hydrate solutions (2), and of 3.5% per °C for bromal hydrate solutions (7). Except for the determination of the cell constant, no correction was made for the effect of temperature on the equivalent conductance. This was justified by the fact that during a given run the temperature of the cave did not vary appreciably. Hence, the value obtained for the rate of reaction would not be affected, since it was determined by plotting specific conductances against time and measuring the slope of the resulting line.

The specific conductances of the unirradiated solutions were substracted from the specific conductances measured for the irradiated samples. These corrected specific conductances were used to indicate the extent of the reaction caused by the irradiation. Similarly, when the samples were titrated with standard base, a blank correction was made. For these titrations, the indicator was bromophenol blue.

RESULTS AND DISCUSSION

The relation between the specific conductances of the irradiated samples and the acid concentrations was found as follows. Samples of 1 M chloral hydrate or of 0.1 M bromal

413783

Can. J. Chem. Downloaded from www.nrcresearchpress.com by 210.87.254.6 on 09/05/12
For personal use only.

hydrate solutions were irradiated for various lengths of time in glass-stoppered pyrex test tubes. The dose rate was 214 rad/min for the chloral hydrate solutions and 225 rad/min for the bromal hydrate solutions. After irradiation for known lengths of time, the samples were transferred to the conductivity cell and the specific conductances measured. The samples were then transferred back to the test tube in which they had been irradiated and titrated with standard alkali to determine the amount of acid present. Specific conductances were plotted against acid concentrations. The results for the chloral hydrate solutions are shown in Fig. 1, where the lower curve is for the irradiated samples. From the

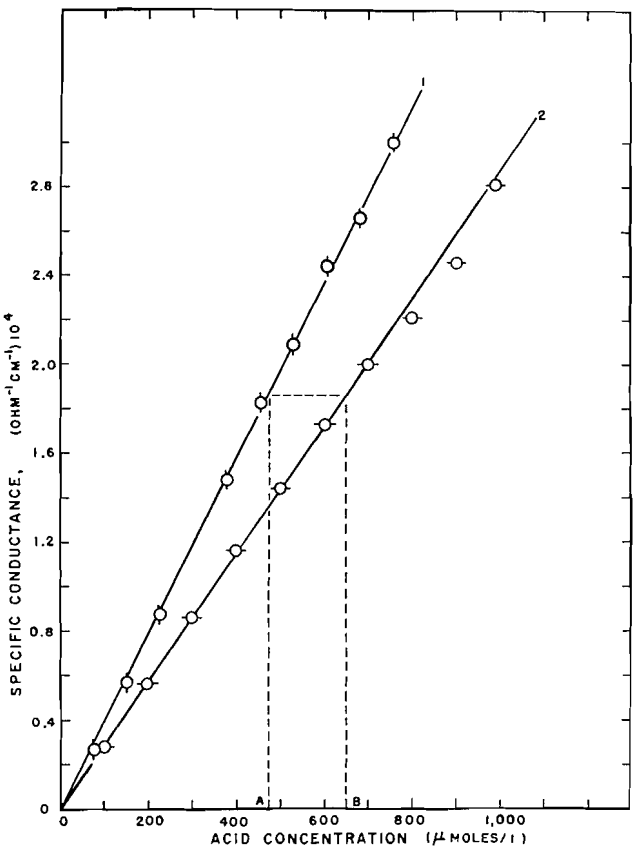

FIG. 1. Relation between specific conductance and acid concentration: ○ hydrochloric acid solutions; -○- irradiated 1 *M* chloral hydrate solutions.

slope of the straight line drawn through the experimental points, the conversion factor of 2.53 moles per l of acid per Ω^{-1} cm^{-1} was calculated. For bromal hydrate solutions the conversion factor was found to be 2.44 moles per l of acid per Ω^{-1} cm^{-1}.

The results from these experiments were also plotted in the form of specific conductance against total dose received. From the slopes of the resulting straight lines the *G* values may be calculated. These values are given later in Figs. 2 and 3. It is worth noting that these *G* values for irradiations done in the absence of platinum electrodes agree quite well with those obtained subsequently when the solutions were irradiated in the conductivity cell. Hence, it may be concluded that the presence of platinum electrodes did not affect the irradiation results.

Can. J. Chem. Downloaded from www.nrcresearchpress.com by 210.87.254.6 on 09/05/12
For personal use only.

Can. J. Chem. Downloaded from www.nrcresearchpress.com by 210.87.254.6 on 09/05/12
For personal use only.

The specific conductances of standard solutions of hydrochloric and of hydrobromic acid were also measured. The results of these measurements were plotted along with those for the irradiated solutions (see Fig. 1 for the hydrochloric acid results). If the only electrolyte produced in the irradiation was the haloform acid, and if this was also the only acid produced, then the specific conductances of the haloform acid solutions would be expected to fall on the same line as those of the irradiated samples, where both were plotted against acid concentration. This was found for the hydrobromic acid solutions and the irradiated bromal hydrate solutions. For the hydrochloric acid solutions and the irradiated chloral hydrate solutions, however, two distinct sets of results were found. In Fig. 1, the upper curve shows the results for the hydrochloric acid solutions. These results indicate that when chloral hydrate solutions are irradiated more alkali titratable acid is present than is indicated by the specific conductance if the latter were due solely to hydrochloric acid. For example, for an equivalent conductance of $1.86 \times 10^{-4}\ \Omega^{-1}\ cm^{-1}$ the hydrochloric acid concentration would be 471 μmoles per l (point A). However, in an irradiated chloral hydrate solution the total acid concentration is 650 μmoles per l (point B) for the same value of the equivalent conductance. Hence, the conclusion is reached that one or more weak acids are produced, as well as hydrochloric acid, when chloral hydrate solutions are irradiated. The results obtained for hydrobromic acid solutions and irradiated bromal hydrate solutions indicate that the only acid (and electrolyte) produced in the irradiation is hydrobromic acid.

The dependence of the reaction rate, expressed as μmoles of total acid (as a monoprotic acid) formed per l per min, and of the G value of total acid formed upon the dose rate was investigated. Both 1 M chloral hydrate solutions and 0.1 M bromal hydrate solutions were used. The results are given in Table I.

TABLE I

Dependence of the reaction rate and of the G value upon dose rate

1.0 M chloral hydrate solutions			0.1 M bromal hydrate solutions		
Dose rate (rad/min)	G_{acid}	Reaction rate (μmoles of acid l^{-1} min^{-1})	Dose rate (rad/min)	G_{acid}	Reaction rate (μmoles of acid l^{-1} min^{-1})
16.3	512	9.21	25.0	301	7.93
31.4	423	14.7	33.6	310	11.0
49.4	363	19.8	53.8	256	14.5
93.1	294	30.2	103	187	20.3
213*	203	47.0	115	189	22.8
221	209	51.2	191	123	24.7
250	192	52.4			
250	218	60.3	225*	131	29.7
404	177	78.5	429	98.3	44.4
655	142	103	831	67.9	59.5
1216	127	170			

*Sample irradiated in test tube.

The dependence of the reaction rate and of the G value on the concentration for chloral hydrate solutions and for bromal hydrate solutions was also investigated. The dose rate for the chloral hydrate solutions was 250.0 rad/min and for the bromal hydrate solutions it was 114.5 rad/min. The results are given in Table II.

The G values are shown plotted against the dose rate in Fig. 2 for 1.0 M chloral hydrate solutions and in Fig. 3 for 0.1 M bromal hydrate solutions. Also plotted in Figs. 2 and 3

TABLE II

Dependence of the reaction rate and of the G value upon concentration

Chloral hydrate solutions 250 rad/min			Bromal hydrate solutions 115 rad/min		
Conc. (M)	G_{acid}	Reaction rate (μmoles of acid l^{-1} min^{-1})	Conc. (M)	G_{acid}	Reaction rate (μmoles of acid l^{-1} min^{-1})
1.0	192	52.4	1.0	367	49.5
0.5	152	40.7	0.1	189	22.8
0.1	82.4	21.5	0.01	128	15.2
0.01	57.4	14.9	0.001	46.2	5.5

are the results of other workers. Where necessary, these latter results have been recalculated to express yields as G values and dose rates as rad/min. It is apparent that all the results are in good agreement.

It is of particular interest to note that for 1.0 M chloral hydrate solutions, the single value reported by Andrews and Shore (1) for the yield agrees very well with the data obtained by other workers (see Fig. 2). While Andrews and Shore had reported that the yield was independent of the dose rate, it seemed to be almost too much of a coincidence that their data should agree so well with other data which showed a dose rate dependence. A rereading of reference 1 revealed that the conclusion that the yield was independent of dose rate had not been directly determined, but rather that it had been inferred by a use of the Beatty equation (14). The equation formulated by Beatty relates the efficiency of an X-ray tube to the atomic number, Z, of the target material and to the tube voltage, V, as follows:

$$[1] \qquad \text{efficiency} = \frac{\text{X-ray energy}}{\text{cathode ray energy}} = 1.4 \times 10^{-9} ZV$$

where "X-ray energy" is the energy per unit time of the X rays produced and "cathode ray energy" is the energy imparted by the tube to the cathode ray per unit time. Andrews and Shore made only one direct determination of the yield, the value being one molecule of HCl per 0.42 eV absorbed. This value was tentatively assumed to be independent of the dose rate. For various tube voltages, the experimentally found rates of production of HCl were used to calculate values for the X-ray energy produced per unit time. It is important to note that these calculated values for the rate of production of X-ray energy will be correct only if the yield is independent of dose rate. Andrews and Shore plotted these calculated rates of production of X-ray energy against the tube voltage and found a straight line relation (their Fig. 3). This was taken to be consistent with the Beatty equation, and hence, a verification of their assumption that the yield was independent of dose rate.

We believe that the above treatment was a misuse of the Beatty equation. What is believed to be a correct use of the equation follows. The right hand side of [1] can be rearranged to give:

$$[2] \qquad \text{X-ray energy} = 1.4 \times 10^{-9} \text{ (cathode ray energy) } ZV.$$

The rate at which cathode ray energy is supplied is proportional to V_e, where e is the electronic charge, hence [2] becomes:

$$[3] \qquad \text{X-ray energy} = BV^2$$

Can. J. Chem. Downloaded from www.nrcresearchpress.com by 210.87.254.6 on 09/05/12
For personal use only.

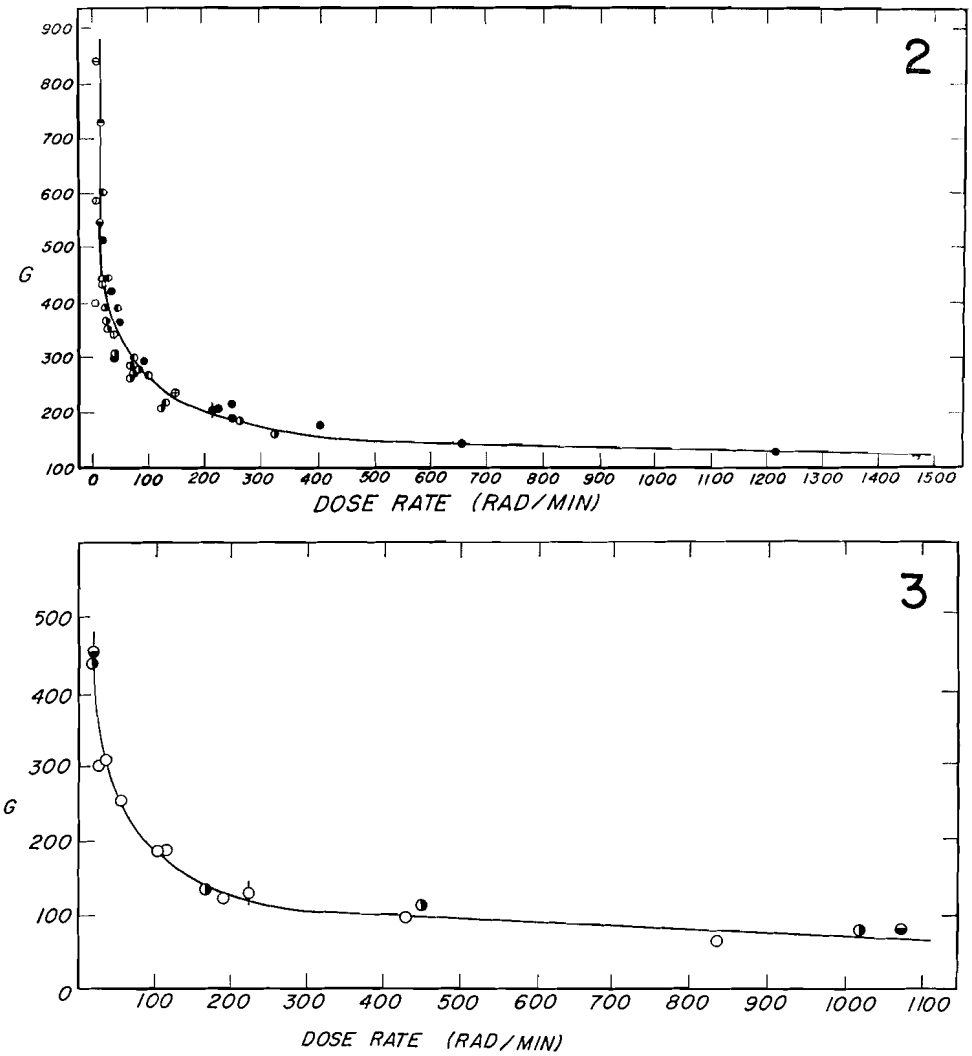

FIG. 2. Variation of G_{acid} with dose rate for 1 M chloral hydrate solutions: ● present work; ◖ present work, sample irradiated in a test tube; ◑ ^{60}Co γ-rays, Freeman *et al.* (2); ◑ betatron X rays, Freeman *et al.* (2); ◐ ^{90}Sr–^{90}Y β-particles using 1 ml samples, Platford and Spinks (5); ◒ ^{90}Sr–^{90}Y β-particles using 5 ml samples (5); ◓ ^{60}Co γ-rays, Platford (15); ⊖ internal ^{32}P β-particles (15); ⊕ X rays, Andrews and Shore (1).

FIG. 3. Variation of G_{acid} with dose rate for 0.1 M bromal hydrate solutions: ○ present work; ◌́ present work, sample irradiated in a test tube; ◒ ^{60}Co γ-rays, Heusinger *et al.* (8); ◑ ^{60}Co γ-rays, Woods and Spinks (6).

where B is a constant for a given target material. The dose rate, I, will be proportional to the rate at which X-ray energy is produced, and hence, from equation [3] we have:

$$I \alpha V^2 \text{ or } V \alpha I^{0.5}. \qquad [4]$$

Equation [4] may be used with the data given by Andrews and Shore as follows. Regardless of the correctness of their assumption that the yield is independent of the dose rate, the data presented in their Fig. 3 shows they found that the rate of production of HCl was proportional to the first power of the applied voltage of the X-ray tube. According to

Can. J. Chem. Downloaded from www.nrcresearchpress.com by 210.87.254.6 on 09/05/12
For personal use only.

equation [4], above, the rate, R, of production of HCl is then proportional to $I^{0.5}$. It would thus appear that the data of Andrews and Shore (1) are in agreement with those of other workers (i.e. that the yield, G, is proportional to $I^{-0.5}$).

Log–log plots were made of the data presented in Table I to see if they agreed with the equations:

$$G = KI^n \quad [5]$$

and

$$R = K'I^{n'}. \quad [6]$$

Here G has its usual significance, R is the reaction rate, expressed as μmoles of total acid (as a monoprotic acid) formed per l per min, and K, K', n, and n' are constants. Good linear relations were found. For the 1.0 M chloral hydrate solutions, the slopes of the straight lines drawn to give the best fit (by visual inspection) gave a value for n of -0.333 and a value for n' of 0.659. The values found for n and n' are consistent since it would be expected that

$$n' = 1 + n.$$

When values for the reaction rate from all sources (1, 2, 3, 5), together with those from the present work, for 1.0 M chloral hydrate solutions were similarly treated, a value of $n' = 0.660$ was obtained. This is a further indication of the good agreement between the results of the present work and those of other workers. Similarly, a value of 0.579 for n' was found for the 0.1 M bromal hydrate solutions. The difference between the values of n' for chloral hydrate and for bromal hydrate solutions may be partly due to the different concentrations used of the two compounds and, hence, not entirely because of a difference in the behavior of the two compounds.

Log–log plots were made of the data presented in Table II to see if they agreed with the equation:

$$R = K''[\text{solute}]^{n''}. \quad [7]$$

Good linear relations were found. For a dose rate of 250.0 rad/min, the value of n'' for chloral hydrate solutions was found to be 0.39. For bromal hydrate solutions, the value of n'' was found to be 0.34 at a dose rate of 114.5 rad/min.

The above results, in conjunction with those of other workers, lead to the following conclusions about the mechanism of the radiolysis of chloral and bromal hydrate solutions. They suggest that the reaction mechanisms are similar for both chloral hydrate and bromal hydrate solutions. The following points emphasize this similarity. The rate of production of acid is dependent to about the same extent upon both the dose rate and the solute concentration. For both compounds the presence of oxygen causes an increased rate of production of acid (2, 7, 8), the increase being about the same for both. The ratio of moles of hydrohalic acid produced per mole of oxygen originally present is essentially the same for both chloral hydrate and bromal hydrate solutions, the value being between 3 and 4 moles of hydrohalic acid per mole of oxygen (2, 6, 7, 8). It should be noted that the rate of production of acid remains constant at the higher rate while any oxygen is present in the solution and then falls abruptly with the exhaustion of the oxygen, i.e. apparently as long as any dissolved oxygen is present, the rate of production of acid is independent of the oxygen concentration. For both compounds the relatively large G values indicate a chain reaction mechanism.

Can. J. Chem. Downloaded from www.nrcresearchpress.com by 210.87.254.6 on 09/05/12
For personal use only.

Can. J. Chem. Downloaded from www.nrcresearchpress.com by 210.87.254.6 on 09/05/12
For personal use only.

The only significant difference between the radiolyses of the two compounds appears to be in the ratio of total acid to hydrohalic acid. The yield of total acid agrees closely with that found for hydrobromic acid, whereas for chloral hydrate solutions the yield of total acid is higher than that of hydrochloric acid. In the present work, the ratio of total acid to hydrochloric acid was found to be 1.38:1 for chloral hydrate solutions. Andrews and Shore (1) found a value of 1.29:1 and Platford (15) found a value of 1.30:1 for this ratio. For bromal hydrate solutions, the 1:1 value found for the ratio of total acid to hydrobromic acid is not in complete agreement with the value of 1.20:1 found by Woods and Spinks (6) or of 1.16:1 found by Heusinger *et al.* (8). Regardless of the exact value of this ratio for bromal hydrate solutions, it appears that the ratio of the yield of total acid per mole of hydrohalic acid is significantly greater for chloral hydrate solutions than for bromal hydrate solutions. It is thought that this difference is not due to a fundamentally different mechanism for the radiolysis of these two compounds but rather that it can be explained as a variation of one basic mechanism.

The following mechanism is proposed for the radiolysis of aqueous solutions of chloral hydrate or of bromal hydrate. In the following, I is the dose rate, S represents a molecule of chloral hydrate or of bromal hydrate, a dot over a symbol represents a free radical, and "acid" represents the appropriate hydrohalic acid.

$$(a) \qquad H_2O \xrightarrow{I} \dot{R}$$

$$(b) \qquad \dot{R} + S \xrightarrow{k_b} \dot{S} + R$$

$$(c) \qquad \dot{S} + O_2 \xrightarrow{k_c} \dot{S}O_2$$

$$(d) \qquad \dot{S}O_2 \xrightarrow[H_2O]{k_d} 3\ \text{acid} + \dot{R}$$

$$(e) \qquad \dot{R} + \dot{S} \xrightarrow{k_e} \text{stable product (or products)}$$

When the steady state treatment is used to solve for the $\dot{S}O_2$ concentration, a complicated expression is obtained. The expression may be greatly simplified by assuming that $(k_d k_e/k_c)([\dot{S}O_2]/[O_2])$ may be neglected in comparison with $k_b[S]$. This assumption appears plausible since [S] will certainly be much greater than $[\dot{S}O_2]$. With this assumption, the following expression is obtained for the rate of production of acid:

$$[8] \qquad \frac{d}{dt}[\text{acid}] = 3\frac{k_b k_c}{k_e}[S]^{1/2} I^{1/2}$$

The dependence of the rate of production of acid upon the oxygen and chloral hydrate or bromal hydrate concentrations and upon the dose rate as predicted by equation [8] is in good agreement with the experimental results. The primary interaction of the radiation with water in dilute aqueous solutions as postulated in (*a*) is generally accepted. Reactions (*b*), (*c*), and (*d*) form a chain reaction which is consistent with the large G values observed. This sequence of reactions is also in agreement with the observed ratio of acid produced to oxygen consumed and results in a rate expression which is independent of oxygen concentration. Reaction (*d*) is considered to be a composite reaction, consisting of a series of successive steps. Reaction (*e*) is postulated for the chain termination step as it gives the correct dependence on both [S] and I of the rate of acid production.

The results presented in the present paper indicate that the rate of acid production is

proportional to the dose rate raised to the 0.66 or 0.58 power for chloral hydrate or bromal hydrate solutions respectively, rather than to the 0.5 power as indicated by equation [8]. This would suggest that the chain termination step is not exclusively reaction (*c*) but that the following reaction also occurs to a certain extent:

$$(f) \qquad \dot{R} \xrightarrow[M]{k_f} \text{end of chain.}$$

This would result in the value for the exponent of the dose rate lying between 0.5 and 1.0.

So far the nature of the radicals $\dot{R}$ and $\dot{S}$ has not been considered. The radical $\dot{R}$ produced in reaction (*a*) is very likely H or OH, or even both. In the latter case, k_b would be a composite rate constant. Some deductions about the radical $\dot{S}$ may be made from a consideration of the overall activation energy for the production of acid. According to equation [8], the overall activation energy will be a composite one, and hence, any discussion involving it should include a consideration of the three reactions (*b*), (*c*), and (*e*). It may be speculated, however, since the overall activation energy for the chloral hydrate radiolysis is less than, or at the most, equal to that for bromal hydrate (2, 5, 7), that the free radical $\dot{S}$ has resulted from an attack on the aldehyde end of the chloral hydrate or bromal hydrate molecule by $\dot{R}$. If the attack was on the halogen end of the molecule, it would be expected that the activation energy for the production of acid would be higher for chloral hydrate solutions because the bond strength of the C—Cl bond is greater than that for the C—Br bond.

For bromal hydrate solutions Heusinger *et al.* (8) found for oxygen depleted solutions that the ratio of the amount of total acid formed to the amount of hydrobromic acid formed was the same as when oxygen was present in the solution. This would suggest that in the absence of oxygen the mechanism is still much the same as in the presence of oxygen, except that reaction (*c*) does not occur and that reaction (*d*) would become

$$\dot{S} \xrightarrow[H_2O]{k_{d'}} 3 \text{ acid} + \dot{R}.$$

The steady state treatment yields

$$[9] \qquad \frac{d}{dt}[\text{acid}] = 3\frac{k_b k_{d'}}{k_e}[S]^{1/2} I^{1/2}.$$

for the rate of production of acid. A comparison of equation [8] and [9] shows that, on the basis of the proposed mechanisms, the slower reaction resulting from the absence of oxygen is due to $k_{d'}$ being smaller than k_c. It is not unreasonable to postulate that $k_{d'}$ would be smaller than k_c. For both chloral hydrate and bromal hydrate solutions, the rate in oxygen free solutions is about one-fifth of that in solutions where oxygen is present (3, 7); this indicates that $k_{d'} = 0.04\ k_c$.

ACKNOWLEDGMENTS

Grateful acknowledgment is made to the Atomic Energy Control Board for financial support. One of us (R. G. M.) wishes to thank the National Research Council for a bursary.

REFERENCES

1. H. L. ANDREWS and P. A. SHORE. J. Chem. Phys. **18**, 1165 (1950).
2. G. R. FREEMAN, A. B. VAN CLEAVE, and J. W. T. SPINKS. Can. J. Chem. **31**, 1164 (1953).
3. G. R. FREEMAN, A. B. VAN CLEAVE, and J. W. T. SPINKS. Can. J. Chem. **32**, 322 (1954).
4. A. HILSENROD. J. Chem. Phys. **24**, 917 (1956).

Can. J. Chem. Downloaded from www.nrcresearchpress.com by 210.87.254.6 on 09/05/12
For personal use only.

5. R. F. PLATFORD and J. W. T. SPINKS. Can. J. Chem. **37**, 1022 (1959).
6. R. J. WOODS and J. W. T. SPINKS. Can. J. Chem. **38**, 77 (1960).
7. R. J. WOODS and J. W. T. SPINKS. Can. J. Chem. **35**, 1475 (1957).
8. H. HEUSINGER, R. J. WOODS, and J. W. T. SPINKS. Can. J. Chem. **37**, 1127 (1959).
9. A. C. BRICKNELL. Ph.D. Thesis, University of Saskatchewan, Saskatoon, Sask. 1959.
10. J. C. RUSSELL. Ph.D. Thesis, University of Saskatchewan, Saskatoon, Sask. 1962.
11. A. R. NORRIS. M.Sc. Thesis, University of Saskatchewan, Saskatoon, Sask. 1959.
12. A. L. RIEGERT and J. W. T. SPINKS. Proc. 7th Hot Laboratories Conference, Cleveland, Ohio. 1959. p. 315.
13. J. WEISS, A. O. ALLEN, and H. A. SCHWARZ. International Conference on Peaceful Uses of Atomic Energy. **14**, 179 (1956).
14. R. T. BEATTY. Proc. Roy. Soc., Ser. A, **89**, 314 (1913).
15. R. F. PLATFORD. Ph.D. Thesis, University of Saskatchewan, Saskatoon, Sask. 1958.

Can. J. Chem. Downloaded from www.nrcresearchpress.com by 210.87.254.6 on 09/05/12
For personal use only.

Can. J. Chem. Downloaded from www.nrcresearchpress.com by 210.87.254.105 on 09/05/12
For personal use only.

AMINO ACIDS AND PEPTIDES

II. SYNTHESIS OF ε-*N*-METHYL-L-LYSINE AND RELATED COMPOUNDS[1]

LEO BENOITON
Department of Biochemistry, Faculty of Medicine, University of Ottawa, Ottawa, Canada
Received March 20, 1964

ABSTRACT

ε-*N*-Methyl-L-lysine, ε-*N*-ethyl-L-lysine, and δ-*N*-methyl-L-ornithine have been synthesized by alkylation of the α-*N*-benzoyl-ω-*N*-*p*-toluenesulphonylamino acid. ε-*N*-Methyl-L-lysine was also prepared by the formaldehyde – formic acid methylation of α-*N*-carbobenzoxy-ε-*N*-benzyl-L-lysine, obtained by borohydride treatment of α-*N*-carbobenzoxy-L-lysine in the presence of benzaldehyde. ε-*N*,ε-*N*-Dimethyl-L-lysine, ε-*N*-benzyl-L-lysine, and ε-*N*-methyl-L-lysine ethyl ester were also prepared.

It has been shown that ε-*N*-methyl-lysine can replace lysine in the diet (2), is metabolized by rat kidney slices (2), and occurs in nature in flagellar proteins (3). We have recently reported the demethylation of ε-*N*-methyl-L-lysine by a rat kidney mitochondrial fraction (4) and have now carried out additional studies on the enzyme system involved (5). For these studies, optically active ε-*N*-methyl-lysine has been synthesized, together with several homologues. In this paper are described the synthesis of these compounds, namely, ε-*N*-methyl-, ε-*N*-ethyl-, ε-*N*-benzyl-, and ε-*N*,ε-*N*-dimethyl-L-lysine, and δ-*N*-methyl-L-ornithine, all of which are new compounds.

ε-*N*-Methyl-DL-lysine has previously been prepared (2, 6, 7) by methylation of ε-*N*-*p*-toluenesulphonylaminocaproic acid followed by α-amination by way of the bromo-derivative; and also by the action of methylamine on 5-δ-bromobutylhydantoin and subsequent saponification (8). However, neither of these procedures is adaptable to the synthesis of the optically active compounds which we desired for our studies.

There are two general classical methods for the preparation of *N*-monoalkylamino acids, namely, treatment of the arylsulphonylamino derivative with an alkyl iodide (9), or treatment of the appropriate halo derivative with an alkyl amine (10). Most of the optically active α-*N*-methylamino acids described have been prepared by the first of these (10), though it is now apparent that partial racemization has sometimes occurred (11). The second method leads to a racemate unless an optically active halide is used. If such is the case, a Walden inversion obtains (12). Since, in our case, we were concerned with the preparation of ω-*N*-alkylamino acids where no stereochemistry is involved, both of the above procedures could theoretically provide the desired compounds if the appropriate optically active α-amino acid were used as starting material.

Since α-*N*-methyl-L-lysine had already been prepared by alkylation of the α-*N*-arylsulphonyl-ε-*N*-benzoylamino acid (12), it was decided to investigate this approach for the synthesis of ε-*N*-methyl-L-lysine. ε-*N*-*p*-Toluenesulphonyl-L-lysine (I*a*) was benzoylated to the disubstituted derivative II*a*, which was treated with methyl iodide to give the ε-*N*-methyl derivative III*a*. Hydrolysis with fuming hydrobromic acid yielded the desired free *N*-methylamino acid IV*a*. Unfortunately, neither of the intermediates II*a* or III*a* could be crystallized. Extraction of III*a* into ether freed it of most of the unreacted II*a* but not completely, consequently the final product (IV*a*) was contaminated

[1]*For Part I, see reference 1.*

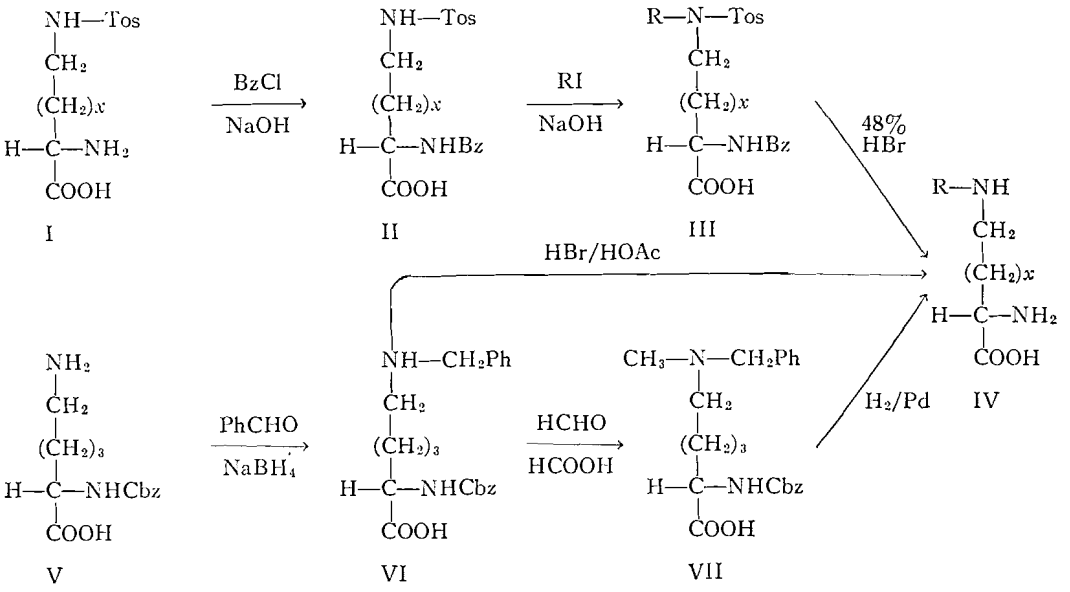

a: $x = 3$, R = CH_3
b: $x = 3$, R = C_2H_5
c: $x = 2$, R = CH_3
d: $x = 3$, R = $CH_2C_6H_5$

Abbreviations: Bz—benzoyl
Cbz—carbobenzoxy
Ph—phenyl
Tos—*p*-toluenesulphonyl

with L-lysine up to 10%. This was established by enzymatic assay, using lysine decarboxylase (13). For purification, it was found expedient to destroy the contaminant by incubation of the mixture with lysine decarboxylase until the increase in pH due to the formation of cadavarine had stopped. ϵ-*N*-Substituted lysine derivatives are inert to lysine decarboxylase (13, 14). Analytically pure ϵ-*N*-methyl-L-lysine, containing less than 0.5% lysine, was thus obtained in a yield of 30% based on ϵ-*N*-*p*-toluenesulphonyl-L-lysine.

ϵ-*N*-Ethyl-L-lysine was obtained in the same manner, in a yield of 19%. When the same reactions were applied to ornithine, the intermediates II*c* and III*c* crystallized readily. As a result, δ-*N*-methyl-L-ornithine (IV*c*) was obtained pure without having to be subjected to enzymic digestion.

When most of our work on the properties of the enzyme which demethylates IV*a* had been completed (5), there appeared in the literature a new procedure for the synthesis of optically active *N*-monomethylamino acids (11). This procedure was applied to the appropriately protected lysine derivative thus providing a second synthesis for ϵ-*N*-methyl-L-lysine. α-*N*-Carbobenzoxy-L-lysine (V) was converted to the ϵ-*N*-benzyl derivative VI by borohydride reduction of the benzylidene derivative. This was reductively methylated to VII which, without isolation, was hydrogenated to give chromatographically pure ϵ-*N*-methyl-L-lysine (IV*a*), in a 42% yield based on V. The intermediate VI, on treatment with hydrogen bromide in acetic acid, gave ϵ-*N*-benzyl-L-lysine (IV*d*).

Of the two procedures described for the synthesis of ϵ-*N*-methyl-L-lysine, the second seems more attractive. However, it suffers from a shortcoming encountered in the preparation of the starting material, α-*N*-carbobenzoxy-L-lysine (15). We were not able to obtain yields of over 45% (reported yield, 71%) for this compound. In view of this, attempts were made to prepare ϵ-*N*-benzyl-L-lysine directly from lysine with the hope of converting

Can. J. Chem. Downloaded from www.nrcresearchpress.com by 210.87.254.105 on 09/05/12
For personal use only.

Can. J. Chem. Downloaded from www.nrcresearchpress.com by 210.87.254.105 on 09/05/12
For personal use only.

it into VI. ϵ-*N*-Benzylidene-L-lysine (15) was submitted to both sodium borohydride and catalytic reduction, but in neither case could the reaction be induced to go to completion. No satisfactory procedure could be devised for purifying the derivative formed, which admittedly could have been a mixture of both α- and ϵ-isomers, so this approach was abandoned.

At first, attempts were made at preparing ϵ-*N*-,ϵ-*N*-dimethyl-L-lysine by catalytic hydrogenation of α-*N*-benzoyl-L-lysine in the presence of formaldehyde (16) as has been reported for the racemate (7), but subsequent acid hydrolysis of the α-*N*-benzoyl-ϵ-*N*,ϵ-*N*-dimethyl-L-lysine failed to give material of acceptable purity. The compound was finally successfully prepared from the acetyl derivative, despite the fact that crystallization of α-*N*-acetyl-ϵ-*N*,ϵ-*N*-dimethyl-L-lysine was much more difficult than for the corresponding benzoyl derivative.

Esterification of ϵ-*N*-methyl-L-lysine was effected by the thionyl chloride method of Brenner (17). Chromatographic data for all the compounds synthesized are presented in Table I.

TABLE I

Paper chromatography data

Compound (as HCl salt)	R_f	
	tert-Butanol – formic acid – water (70:15:15)	*m*-Cresol–phenol (1:1) saturated with 0.1 *N* pH 9.3 borate (3)
L-Lysine	0.24	0.34
ϵ-*N*-Methyl-L-lysine	0.30	0.46
ϵ-*N*-Ethyl-L-lysine	0.40	0.58
ϵ-*N*-Benzyl-L-lysine	0.51	0.68
ϵ-*N*,ϵ-*N*-Dimethyl-L-lysine	0.34	0.70
L-Ornithine	0.16	0.24
δ-*N*-Methyl-L-ornithine	0.22	0.46
ϵ-*N*-Methyl-L-lysine ethyl ester	0.55	0.89

EXPERIMENTAL

Melting points were determined with a Kofler Hotbench. Optical rotations were determined at 23 °C with a Rudolph Model 62 polarimeter using a 2-dm tube. Compounds were dried at 60° before analysis.

ϵ-N-Methyl-L-lysine Hydrochloride (IVa)

By Methylation of ϵ-N-p-Toluenesulphonyl-L-lysine

To a cooled, stirred solution of ϵ-*N*-*p*-toluenesulphonyl-L-lysine (18) (9.0 g; 0.03 mole) in 1 *N* sodium hydroxide (30 ml) were added dropwise benzoyl chloride (3.8 ml; 0.033 mole) and 2 *N* sodium hydroxide (17.5 ml) over a ½h period. The mixture was stirred an additional hour at 25°, and was then acidified (HCl) to Congo red. The gum which separated out was extracted into ethyl acetate, the extract was washed twice with water, dried (Na_2SO_4), and evaporated to dryness. The residue was extracted with hot ether (3 × 75 ml) and the ether was discarded.

The residue was transferred to a pressure bottle with the aid of 2 *N* sodium hydroxide (60 ml). The mixture was warmed (40°), methyl iodide (1.25 ml; 0.02 mole) was added, and the mixture was heated (70°) while being stirred magnetically for 1 h. The solution was cooled (40°), and the addition of methyl iodide and heating were repeated twice more. The cooled solution was then acidified (HCl) to Congo red, extracted with ether (3 × 100 ml), and the extract was dried (Na_2SO_4) and evaporated down.

The residue was refluxed in 48% hydrobromic acid (75 ml) for 2 h. The mixture was cooled, water (75 ml) was added, and the precipitate was filtered off and discarded. The filtrate was repeatedly evaporated to dryness, the residue was dissolved in water, the solution was treated with charcoal, and Dowex 50 (H^+ form; 50 ml) was added. After stirring for 1 h, the resin was filtered off, washed thoroughly with water, and then stirred for 15 min in 5 *N* ammonium hydroxide (50 ml). The mixture was filtered, and the filtrate was evaporated to dryness. The residue was dissolved in water, with the pH of the solution being adjusted to 5.8 with hydrochloric acid. The product can be obtained at this stage by evaporating the solution and triturating the residue with ethanol. It contains, however, up to 10% of lysine as estimated with lysine decarboxylase (13).

To the solution (about 100 ml) was added lysine decarboxylase (0.1 g) and the mixture was incubated at 37°. The pH was readjusted back to 6 several times during the first hours of digestion. After 24 h more enzyme was added. Next day, the pH was adjusted to 5.8, charcoal was added, and the mixture was boiled for 5 min. The mixture, after being cooled in ice, was filtered through kieselguhr, the filtrate was evaporated down, and the residue was crystallized from water–ethanol. Yield: 1.76 g (30%), $[\alpha]_D$ +9.9° (2, water), +23.1 (1, 6 *N* HCl). The material contained less than 0.5% lysine as determined manometrically with lysine decarboxylase (13). Found: C, 42.5; H, 8.7; N, 14.0; *N*-CH_3, 7.4. $C_7H_{17}ClN_2O_2$ (196.7) requires C, 42.7; H, 8.7; N, 14.2; *N*-CH_3, 7.6%.

The *picrate*, m.p. 230°, from water, was prepared by adding a hot ethanolic solution of picric acid to a concentrated aqueous solution of the amino acid, freed of chloride by resin treatment as described above. Found: C, 40.35; H, 5.0; N, 18.1. $C_{13}H_{19}N_5O_9$ (389.3) requires C, 40.1; H, 4.9; N, 18.0%.

By Reductive Methylation of ε-N-Benzyl-L-lysine

To a mixture of unrecrystallized α-*N*-carbobenzoxy-L-lysine (V) (15) (5.62 g; 0.02 mole) in 2 *N* sodium hydroxide (10 ml) was added freshly distilled benzaldehyde (2 ml; 0.02 mole). After stirring for 20 min, sodium borohydride (0.23 g; 0.006 mole) was added in portions (0.05 g) over a ½ h period, while the temperature of the reaction mixture was being kept below 15°. After 15 min, the benzaldehyde and borohydride treatments were repeated. The mixture was stirred for an additional 2 h, then extracted twice with ether, and acidified (HCl) to pH 6.0. The thick oil which separated out gradually crystallized when the mixture was cooled. (If required, a seed crystal can be obtained by repeatedly evaporating the oil in the presence of ethanol.) Next day, the crystals were collected, washed with water, and recrystallized, by suspending them in boiling water and adding acetic acid until all had dissolved, to give 4.75 g (64%) of *α-N-carbobenzoxy-ε-N-benzyl-L-lysine (VI)*, m.p. 210°, $[\alpha]_D$+4.8° (2, acetic acid). Found: C, 68.3; H, 7.2; N, 7.7. $C_{21}H_{26}N_2O_4$ (370.4) requires C, 68.1; H, 7.1; N, 7.6%.

To VI (3.7 g; 0.01 mole) in formic acid (5 ml) at 100° was added dropwise 38% aqueous formaldehyde (0.90 ml) while the solution was being stirred magnetically. After an additional 15 min, 90% acetic acid was added and the mixture was hydrogenated over palladium on charcoal for 48 h. The catalyst was filtered off, 1 *N* hydrochloric acid (10 ml) was added, and the acetic acid was removed by evaporation. The residue was taken up in water, brought to pH 5.8 with lithium hydroxide, and the solution was evaporated down again. Trituration of the residue in ethanol, followed by recrystallization of the product from water–ethanol gave 1.30 g (66%) of pure *ε-N-methyl-L-lysine hydrochloride (IVa)*, $[\alpha]_D$+21.9° (2, 6 *N* HCl). Found: C, 42.7; H, 8.65; N, 14.3. $C_7H_{17}ClN_2O_2$ (196.7) requires C, 42.7; H, 8.7; N, 14.2%.

ε-N-Ethyl-L-lysine Hydrochloride (IVb)

This compound was prepared by the action of ethyl iodide on ε-*N*-*p*-toluenesulphonyl-L-lysine as described for the corresponding methyl amino acid (IV*a*) except that after the methylation had been completed and the solution acidified, the mixture was extracted with ethyl acetate. The extract was then worked up in the same manner, including the incubation with lysine decarboxylase. The final product was obtained as the monohydrochloride at pH 5.8 from water–ethanol. Yield: 1.2 g (19%), $[\alpha]_D$ +3.4°(6 *N* HCl). Found: C, 45.3; H, 9.1; N, 13.0. $C_8H_{19}ClN_2O_2$ (210.7) requires C, 45.6; H, 9.1; N, 13.3%.

ε-N-Benzyl-L-lysine Hydrochloride (IVd)

To VI (0.74 g) in dry acetic acid (10 ml) was added 38% hydrogen bromide in acetic acid (10 ml) (19). After 30 min, the acetic acid was removed by evaporation and the residue was triturated with ether. Crystallization from ethanol–ether gave material whose analysis indicated a C:H:N:Br ratio of 1:1:1:1½. Therefore the product was freed of bromide by absorption on Dowex 50, subsequently eluted with ammonium hydroxide, and crystallized as the monohydrochloride at pH 5.8 from water–ethanol. Yield: 0.20 g (37%), $[\alpha]_D$ +13.4° (1, water). Found: C, 57.1; H, 7.75; N, 10.3. $C_{13}H_{21}ClN_2O_2$ (272.8) requires C, 57.2; H, 7.8; N, 10.3%.

δ-N-Methyl-L-ornithine Hydrochloride (IVc)

To a cold solution of *δ-N-p*-toluenesulphonyl-L-ornithine (I*c*) (20) (8.59 g; 0.03 mole) in 1 *N* sodium hydroxide (30 ml) were added dropwise benzoyl chloride (3.84 ml; 0.033 mole) and 2 *N* sodium hydroxide (17.5 ml) over a ½ h period. The mixture was stirred an additional hour at 25°, and was then acidified (HCl) to Congo red. Ethyl acetate was added, resulting in the formation of a precipitate floating between the two layers. The material was filtered off, and recrystallized by dissolving in 1 *N* sodium hydroxide and adding an equivalent of hydrochloric acid to give 7.35 g (62.4%) of *α-N-benzoyl-δ-N-p-toluenesulphonyl-L-ornithine (IIc)*, m.p. 188°, soluble in ethanol and tetrahydrofuran, insoluble in chloroform and ether. A sample recrystallized from ethyl acetate had m.p. 189°, $[\alpha]_D$ −3.0° (2, dimethylformamide). Found: C, 58.2; H, 5.6; N, 7.0. $C_{19}H_{22}N_2O_5S$ (390.9) requires C, 58.4; H, 5.7; N, 7.2%.

This compound (II*c*) (7.03 g; 0.018 mole) in 2 *N* sodium hydroxide (80 ml) was methylated with methyl iodide (3 ml total) as described for the corresponding lysine derivative (II*a*). After methylation, the cooled mixture was acidified to Congo red, and the oil which separated out was solidified by trituration in cold water. The material was recrystallized from ethanol–water to give 5.0 g (69%) of *α-N-benzoyl-δ-N-methyl-δ-N-p-toluenesulphonyl-L-ornithine (IIIc)*, m.p. 163°, $[\alpha]_D$ −3.0° (2, dimethylformamide), soluble in chloroform,

Can. J. Chem. Downloaded from www.nrcresearchpress.com by 210.87.254.105 on 09/05/12
For personal use only.

moderately in ether. Found: C, 59.7; H, 6.1; N, 6.7. $C_{20}H_{24}N_2O_5S$ (404.5) requires C, 59.4; H, 6.0; N, 6.9%.

This derivative (III*c*) (4.0 g) was refluxed in 48% hydrobromic acid (35 ml) for 2 h. Isolation of the amino acid by resin treatment as described for the corresponding lysine derivative and crystallization at pH 5.8 from water–ethanol afforded 1.1 g (55.8%) of *δ-N-methyl-L-ornithine hydrochloride (IV*c*)*, $[\alpha]_D$ +10.3° (2, water), +19.7° (2, 6 *N* HCl). Found: C, 39.7; H, 8.3; N, 15.0. $C_6H_{15}ClN_2O_2$ (182.7) requires C, 39.45; H, 8.3; N, 15.3%.

ε-N,ε-N-Dimethyl-L-lysine Hydrochloride

A mixture of *α-N*-acetyl-L-lysine (0.94 g; 0.005 mole) (21), 38% formaldehyde (3 ml), and palladium on charcoal catalyst (1 g) in a small volume of water was hydrogenated for 2 days. The filtered solution was repeatedly evaporated to dryness, and the residue was crystallized from ethanol–ether and finally ethanol, to give 0.63 g (50%) of *α-N-acetyl-ε-N,ε-N-dimethyl-L-lysine*, m.p. 196–198°, $[\alpha]_D$ +10.0° (2, water), slightly hygroscopic. A sample for analysis was dried at 80°. Found: C, 47.8; H, 9.6; N, 11.1. $C_{10}H_{20}N_2O_3.2H_2O$ (252.3) requires C, 47.6; H, 9.6; N, 11.1%.

In identical fashion, from *α-N*-benzoyl-L-lysine (5.0 g) (22), was obtained from ethanol–acetone, and finally acetone, 3.28 g (59%) of *α-N-benzoyl-ε-N,ε-N-dimethyl-L-lysine*, m.p. 209°, $[\alpha]_D$ +18.8° (1, water). Found: C, 64.9; H, 8.2; N, 9.9. $C_{15}H_{22}N_2O_3$ (278.3) requires C, 64.7; H, 8.0, N, 10.1%.

The acetyl derivative (1.62 g) was hydrolyzed by refluxing in 2 *N* hydrochloric acid (25 ml) for 1 h. Excess acid was removed by evaporation. The *ε-N,ε-N-dimethyl-L-lysine* was then converted to the monohydrochloride by the addition of Dowex 1 (OH^- form) to pH 6.0, and then obtained as a powder by precipitation from an ethanolic solution by the addition of ether. Yield: 0.81 g (60%), $[\alpha]_D$ +11.9° (1.8, water), slightly hygroscopic. A sample, reprecipitated, was dried at 80° for analysis. Found: C, 45.0; H, 9.0; N, 13.0. $C_8H_{19}ClN_2O_2$ (210.7) requires C, 45.6; H, 9.1; N, 13.3%.

ε-N-Methyl-L-lysine Ethyl Ester Dihydrochloride

ε-N-Methyl-L-lysine·HCl (0.59 g; 0.003 mole) was added to a solution of thionyl chloride (0.65 ml; 0.009 mole) in cold ethanol (5 ml) and the mixture was kept 24 h. Evaporation of the solvent, and reesterification gave a product still contaminated with starting material. The product was therefore dissolved in water, the solution was made alkaline with potassium carbonate, extracted with ether, and hydrogen chloride was bubbled through the solution. The ether was decanted off from the oil which separated out, and the product was crystallized from ethanol–ether. Yield: 0.51 g (66%), m.p. 145°, $[\alpha]_D$ +11.9° (2, water), hygroscopic. Found (dried at 80°): C, 41.7; H, 8.5; N, 10.8. $C_9H_{23}Cl_2N_2O_2$ (262.3) requires C, 41.2; H, 8.8; N, 10.7%.

ACKNOWLEDGMENTS

The technical assistance of Mrs. H. Williams and the financial support of the Medical Research Council are gratefully acknowledged.

REFERENCES

1. L. Benoiton. Can. J. Chem. **41**, 1718 (1963).
2. E. Neuberger and F. Sanger. Biochem. J. **38**, 125 (1944).
3. R. P. Amber and M. W. Rees. Nature, **184**, 56 (1959). R. J. Martinez. Biochem. Biophys. Res. Commun. **12**, 180 (1963).
4. S. Kim, L. Benoiton, and W. K. Paik. Biochim. Biophys. Acta, **71**, 745 (1963).
5. S. Kim, L. Benoiton, and W. K. Paik. J. Biol. Chem. In press.
6. R. Enger and H. Steib. Z. Physiol. Chem. **191**, 97 (1930).
7. K. Poduska. Collection Czech. Chem. Commun. **24**, 1025 (1959).
8. L. M. Babineau and L. Berlinguet. Can. J. Chem. **40**, 1626 (1962).
9. E. Fischer and W. Lipschitz. Ber. **48**, 360 (1915). W. Cocker. J. Chem. Soc. 1683 (1937).
10. J. P. Greenstein and M. Winitz. Chemistry of the amino acids. J. Wiley & Sons, Inc., New York, N.Y. 1961. p. 2750.
11. P. Quitt, J. Hellerbach, and K. Vogler. Helv. Chim. Acta, **46**, 327 (1963).
12. N. Izumiya and S. Ota. J. Chem. Soc. Japan, Pure Chem. Sect. **72**, 445 (1951).
13. W. K. Paik, L. Bloch-Frankenthal, S. M. Birnbaum, M. Winitz, and J. P. Greenstein. J. Biol. Chem. **209**, 485 (1954).
14. E. F. Gale and H. M. Epps. Biochem. J. **38**, 232 (1944).
15. B. Bezas and L. Zervas. J. Am. Chem. Soc. **83**, 719 (1961).
16. R. E. Bowman and H. H. Stroud. J. Chem. Soc. 1342 (1950).
17. M. Brenner and W. Huber. Helv. Chim. Acta, **36**, 1109 (1953).
18. R. Roeske, F. C. H. Steward, R. J. Stedman, and V. du Vigneaud. J. Am. Chem. Soc. **78**, 5883 (1956).
19. D. Ben-Ishai and A. Berger. J. Org. Chem. **17**, 1564 (1952).
20. B. F. Erlanger, H. Sachs, and E. Brand. J. Am. Chem. Soc. **76**, 1806 (1954).
21. A. Neuberger and F. Sanger. Biochem. J. **37**, 515 (1943).
22. W. F. Ross and L. S. Green. J. Biol. Chem. **137**, 105 (1941).

Can. J. Chem. Downloaded from www.nrcresearchpress.com by 210.87.254.105 on 09/05/12
For personal use only.

Can. J. Chem. Downloaded from www.nrcresearchpress.com by 210.87.254.5 on 09/05/12
For personal use only.

CONSTITUTION OF A SYNTHETIC GLUCAN

III. PERIODATE OXIDATION

G. G. S. DUTTON

Department of Chemistry, University of British Columbia, Vancouver, British Columbia

AND

A. M. UNRAU

Department of Plant Science, University of Manitoba, Winnipeg, Manitoba

Received March 24, 1964

ABSTRACT

A synthetic glucan known to contain D-glucofuranose and D-glucopyranose units was subjected to a Smith periodate degradation. After mild acid hydrolysis any aldehydic compounds were oxidized with bromine and the neutral fragments separated from the acidic by ion exchange resins. The acidic portion, after lactonization and reduction, gave glycerol and a series of oligosaccharides. The neutral portion was resolved into glycerol, erythritol, and a series of seven fractions containing glycosides with degrees of polymerization up to eight. Each fraction which was homogeneous by paper chromatography contained at least two components. Some of these individual components were separated as their trimethylsilyl derivatives by vapor phase chromatography and the following glycosides were identified: 1-*O*-(α-D-glucopyranosyl)-glycerol, 1-*O*-(β-D-glucopyranosyl)-glycerol, 2-*O*-(D-xylofuranosyl)-D-erythritol, 2-*O*-(α-D-glucopyranosyl)-D-erythritol, 2-*O*-(β-D-glucopyranosyl)-D-erythritol, 1-*O*-(D-glucopyranosyl)-erythritol. These results demonstrate for the first time the separation of Smith degradation products by vapor phase chromatography. The presence in the polysaccharide of α and β linkages and the existence of D-glucofuranose residues are confirmed. The highly branched nature of the polymer is shown by the fact that four successive periodate oxidations and mild hydrolyses were necessary to oxidize all the hexose units.

Previous papers (1, 2) have demonstrated that the synthetic glucan prepared by Mora and his associates (3) has a highly branched structure in which all possible linkages except $1 \rightarrow 5$ have been found. In contrast to synthetic polysaccharides formed by acid treatment of monosaccharides at room temperature the polymers prepared by Mora contain a high proportion of sugar residues in the furanose form. The general features of the synthetic glucan have already been reported (1) and these results confirmed by a detailed study of the fragments obtained by hydrolysis of the fully methylated polysaccharide (2).

In recent years the Smith degradation (4) has been useful as a means of investigating the fine structure of polysaccharides and has been applied to hemicelluloses (5, 6, 7, 8), gums (9), and a synthetic xylan (10). The present paper reports the application of Smith's method to this synthetic glucan and in addition to providing further evidence on the structure discusses some of the problems which may be encountered in the separation of the cleavage fragments obtained by this technique.

The glucan was oxidized with periodate, reduced with borohydride, and hydrolyzed at room temperature for 8 h with 0.2 *N* hydrochloric acid. The solution was neutralized with lead carbonate and oxidized with bromine for 24 h in the presence of barium carbonate, after which the acidic and neutral compounds were separated by ion exchange resins.

The Neutral Fraction

The neutral fraction was shown to contain glycerol and erythritol, characterized as their *p*-nitrobenzoates, and at least seven non-reducing fractions (Table I) which were resolved

TABLE I
Properties of the neutral fractions

Fraction	Wt., mg	$[\alpha]_D$	R_{xylose} Solvent A	R_{xylose} Solvent B	Analysis,* molar ratios† G:X:Gy:E
1	57	11°	1.04	1.02	1 1 / 1 1
2	29	15°	0.78	0.74	2 1 / 2 1
3	29	25°	0.72	0.59	2 1 / 2 1
			$R_{glucose}$		
4	90	25°	0.81	0.73	2 1 / 2 1
5	81	39°	0.63	0.58	4 1 / 1 1.5 A:S = 1:3
6	33	47°	0.45	0.41	2 1 / 1 1 A:S = 1:4–5
7	277	33°	0.24	0.28	2 1 A:S = 1:7

*G = glucose, X = xylose, Gy = glycerol, E = erythritol, A = total alcohols, S = total sugars.
†The data illustrate the relationship between G and Gy and between X and E. The ratio between G and X and Gy and E varied in different experiments depending on the exact hydrolysis conditions employed.

by paper chromatography. Several purifications were necessary and the losses were high, but the fractions eventually obtained were chromatographically homogeneous in several solvents. When these fractions were hydrolyzed and analyzed the presence of the four compounds glucose, xylose, glycerol, and erythritol strongly suggested that each fraction contained two components although they were not resolvable by paper chromatography or paper electrophoresis in borate buffer. Since the xylose must have arisen from the loss of C_6 from a glucofuranose unit it followed that if one of the compounds was a xylosyl erythritol it must be a xylofuranosyl erythritol. It should thus be possible to preferentially hydrolyze this furanoside. This was achieved by heating fraction 1 with 0.5 N H_2SO_4 at 50 °C for 4 h when chromatography showed the formation of xylose and erythritol in a 1:1 ratio and a component with an R_f identical with the original starting material. This latter was a glucopyranosyl glycerol, since on elution and hydrolysis it gave a 1:1 ratio of glucose and glycerol.

The hydrolysates of fractions 1, 2, and 3 were combined and the individual compounds separated by chromatography. Erythritol and glycerol were characterized as their *p*-nitrobenzoates while D-xylose and D-glucose were crystallized and converted to their phenylosazones.

For the higher fractions some estimate of their degree of polymerization (D.P.) was obtained by measuring the amount of formaldehyde (11) obtained by periodate oxidation (Table II). Formaldehyde will be obtained from glycosides terminated by glycerol substituted at position 1 and erythritol substituted at positions 1 or 2. Reduction and hydrolysis of the oxidized material gave some or all of ethylene glycol, glycerol, erythritol, glucose, and xylose as shown in Table II. By comparing the data for fractions 5 and 7 it will be noted that as the D.P. increases larger amounts of sugar survive the periodate oxidation indicating progressively complex structures for these fractions.

The hydrolysates of fractions 4–7 were combined and the individual compounds

Can. J. Chem. Downloaded from www.nrcresearchpress.com by 210.87.254.5 on 09/05/12
For personal use only.

TABLE II

Periodate oxidation of the neutral fractions

Fraction	D.P.	Products obtained by IO_4^-, BH_4^-, H^+ Molar ratios EG, Gy, E, G, X*
4	3	1 3 5 – –
5	4	1 6 2 10 1 A:S = 28:1
6	5	1 8 4 A:S = 30:1
7	7–8	5.5 19 8 2 1 A:S = 11:1

*EG = ethylene glycol, other abbreviations as Table I.

characterized as before. In a similar manner the degradation products, ethylene glycol, glycerol, and erythritol were characterized as their *p*-nitrobenzoates.

Further work on these fractions was hindered by lack of suitable methods for separating each component, a problem accentuated by the small amounts available. The recent publication of a successful application of silylation to carbohydrates and the resolution of these derivatives by vapor phase chromatography (12) suggested that this method might be suitable in the present case, particularly since it had been used for tetrasaccharides as well as compounds of lower molecular weight.

Figure 1A shows the elution pattern for the silyl derivatives of fraction 1. Compounds 1*a* and 1*b* were desilylated and gave on hydrolysis glucose and glycerol in a 1:1 ratio. Periodate oxidation gave one molecular proportion of formaldehyde and reduction followed by hydrolysis gave glycerol and ethylene glycol in a 1:1 ratio. These results together with the observation that α-anomers have a lower retention time than the β-forms (12, 13) show that compound 1*a* is 1-*O*-(α-D-glucopyranosyl)-glycerol and that compound 1*b* is 1-*O*-(β-D-glucopyranosyl)-glycerol. The observed rotation of the latter, $[\alpha]_D$ 12°, is consistent with this assignment and a sufficient amount of this compound was obtained to form a crystalline *p*-nitrobenzoate. Compound 1*c* gave xylose and erythritol in a 1:1 ratio and periodate oxidation gave 1 mole of formaldehyde. Reduction and hydrolysis of the oxidized product gave glycerol as the only product. These results show compound 1*c* to be 2-*O*-(D-xylofuranosyl)-D-erythritol. The available evidence does not permit a decision as to whether only one anomer was present or the column was incapable of separating the two anomers.

Figure 1B shows the elution pattern for the silyl derivatives of fraction 2 and Tables III and IV record the properties and periodate data on the desilylated components. It thus follows that component 2*a* was 2-*O*-(α-D-glucopyranosyl)-D-erythritol, and that

TABLE III

Properties of components isolated from fraction 2

Component*	$[\alpha]_D$ in water	Composition	*p*-Nitrobenzoate, m.p. °C
2*a*	+50°	Glucose and erythritol in 1:1 ratio	190–194
2*b*	−10°		215–218
2*c*	+35°		205–208

*Data refer to desilylated components shown in Fig. 1B.

Can. J. Chem. Downloaded from www.nrcresearchpress.com by 210.87.254.5 on 09/05/12
For personal use only.

TABLE IV

Periodate analysis of components isolated from fraction 2

Component*	Amount oxidized, mg	HCHO, mg	Mol. wt.	Hydrolysate of BH_4^- reduction product
2*a*	7	0.74	284	Glycerol
2*b*	10	1.05	286	Glycerol
2*c*	7	0.72	292	Ethylene glycol and glycerol 1:1

*See footnote Table III.

component 2*b* was the corresponding β-anomer. From the rotation component 2*c* was presumably 1-*O*-(α-D-glucopyranosyl)-erythritol. Although a small amount of xylosyl erythritol was known to be present in fraction 2, it was not detected.

Figure 1C shows an attempt to resolve the higher molecular weight material of fraction 3. Component 3*a*, appearing as two partially separated peaks, gave upon hydrolysis glucose, xylose, and glycerol in a 1:1:1 ratio. Periodate oxidation yielded an amount of formaldehyde corresponding to a molecular weight of 380 (calc. 390) and reduction followed by hydrolysis gave xylose, erythritol, glycerol, and ethylene glycol in a molar ratio of 1:1:2:2. These results indicate that at least two structurally different oligosaccharides were present. Some possible structures are (i) D-G_p(1 → 2 or 3)-D-Xyl_f(1 → 1)glycerol, (ii) D-Xyl_f(1 → 4)-D-G_p(1 → 1)glycerol, (iii) D-Xyl_f(1 → 6)-D-G_f(1 → 1)glycerol. Component 3*b* on hydrolysis gave glucose and erythritol in the ratio of 2:1 and the yield of formaldehyde obtained by periodate oxidation gave a molecular weight of 415 (calc. 446). Reduction and hydrolysis of the oxidized material gave glucose, erythritol, glycerol, and ethylene glycol in the ratio 1:2:8:1. The presence of some of the following structures could account for these results D-G_p(1 → 3 or 4 or 6)-D-G_p(1 → 1 or 2)-erythritol.

The Acidic Material

The acidic material from the bromine oxidation was eluted from the anion exchange resin with sodium hydroxide and passed through a cation exchange resin. The eluate was evaporated and heated *in vacuo* to effect lactonization. Reduction of this product with sodium borohydride gave glycerol together with several non-reducing oligosaccharides of which four were obtained in reasonable purity by several separations on paper. The analytical data of these fractions are shown in Table V. The presence of small amounts of

TABLE V

Periodate analysis of oligosaccharides from acidic portion

Fraction	Wt., mg	$[\alpha]_D$	$R_{glucose}$ solvent A	Products* obtained after IO_4^-, BH_4^-, H^+
A	56	15°	2.4	G:Gy 1:1 X:E 1:1 X:G 1:4
B	70	24°	2.0	G:Gy 2:1 X:E 2:1 X:G 1:4
C	55	33°	1.0	Gy:E:Glucitol 7:1:1 X:G 1:6 A:S 1:3
D	85	42°	0.65	Gy:E:Glucitol 2:3:2 X:G 1:4 A:S 1:5

*Abbreviations as in Table I.

Can. J. Chem. Downloaded from www.nrcresearchpress.com by 210.87.254.5 on 09/05/12
For personal use only.

glucitol is presumably due to hydrolysis of some furanoside bonds in the mild acid treatment of the original polyol.

Successive Periodate Oxidations

A fresh sample of the glucan was oxidized with periodic acid and the polyaldehyde reduced with sodium borohydride. A portion of the polyalcohol was completely hydrolyzed and analyzed for sugars and polyols. The bulk of the polyalcohol was hydrolyzed with 0.1 *N* hydrochloric acid at room temperature for 4 h and then reoxidized with periodate. This treatment was repeated and it required a total of four oxidations to completely degrade all the sugar units in the polysaccharide, thus providing further convincing evidence of its highly branched character. This data is given in Table VI.

TABLE VI

Successive periodate oxidations of glucan

Oxidation	Sugar remaining, %	G:X* ratio	Gy:E:EG ratio
1	6.5	5:1	5:1:0
2	2.1	3:1	10:3:2
3	0.3	10:7	8:1:3
4	—	—	18:1:6

*Abbreviations as in Tables I and II.

CONCLUSIONS

A striking feature of this work is that it has been possible to isolate oligosaccharides up to an apparent D.P. of 8. By the same token it is unfortunate that the complexity of these fractions has precluded the determination of their structure in detail. The glucan which has been examined is a highly artificial polysaccharide containing as it does both glucofuranose and glucopyranose units joined by a wide variety of linkages.

The combination of the Smith degradation with vapor phase chromatography is shown to be most useful in structural investigations as suggested earlier (10) and the preparation of silyl derivatives to achieve adequate volatility has the additional merit that the original compound may be readily recovered by mild hydrolysis.

The identification of the anomers of 1-*O*-(D-glucopyranosyl)-glycerol provides experimental proof for the existence of α and β linkages and the identification of 2-*O*-(D-xylofuranosyl)-D-erythritol further confirms the existence of D-glucofuranose units in the polysaccharide.

Attention should be drawn to the observation that hexose-triitol and pentose-tetritol compounds may have the same mobility on paper chromatograms and that certain of these glycosides have high R_f values.

The isolation of glycerol from the acidic fraction demonstrates the presence of $1 \rightarrow 2$ linkages in the polymer as previously described (1). The highly branched nature of the glucan is confirmed by the fact that four periodate oxidations are required to degrade all the sugar units.

The complex nature of this glucan makes the further elucidation of its structure a matter of interest. No doubt useful information could be obtained by graded hydrolysis, enzymic hydrolysis, and acetolysis but lack of material prevents this.

Can. J. Chem. Downloaded from www.nrcresearchpress.com by 210.87.254.5 on 09/05/12
For personal use only.

Can. J. Chem. Downloaded from www.nrcresearchpress.com by 210.87.254.5 on 09/05/12
For personal use only.

EXPERIMENTAL

Chromatographic separations were carried out by the descending technique using Whatman 1 paper for qualitative and quantitative analyses. Whatman 3MM paper was used for preparative separations. Solvent systems were A, ethyl acetate:acetic acid:water (8:2:2) and B, ethyl acetate:pyridine:water (9:2:2). Spray reagents were *p*-anisidine trichloroacetate and ammoniacal silver nitrate.

Reducing sugars were estimated by the phenol – sulphuric acid method (14) and polyols by chromotropic acid after oxidation with periodate (11). Periodate uptake was measured by the arsenite method (15).

For vapor phase chromatography an aerograph A90-P2 instrument was used (i) with a 4.5-ft column (0.25-in diameter) containing 60/80 mesh firebrick coated with 20% GESF-96 and purchased from Wilkens

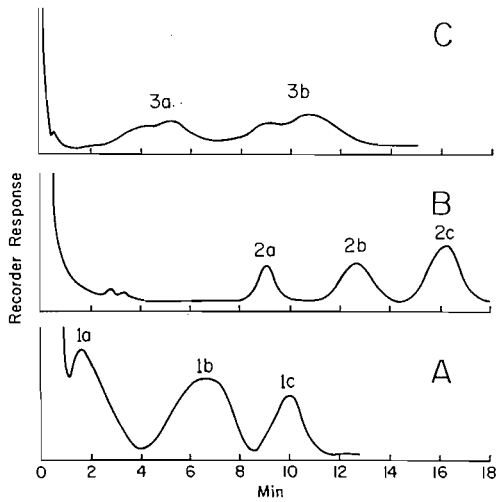

FIG. 1. Vapor phase chromatography of trimethysilylated fractions: (A) fraction 1, column temperature 165 °C, helium flow 120 ml/min; (B) fraction 2, column temperature 190 °C, helium flow 150 ml/min; (C) fraction 3, column temperature 265 °C, helium flow 180 ml/min.

Instrument and Research Inc. (column 1, Figs. 1A and 1B), (ii) with a 2-ft column packed with 10% S.E. 30 on Diatoport (column 2).

Evaporations were carried out *in vacuo* at 40 °C. Specific rotations are equilibrium values at 22 ± 2 °C. Melting points are uncorrected.

Smith Degradation

The oxidation (IO_4^-), reduction (BH_4^-), and mild hydrolysis (0.2 *N* HCl at 25 °C) has already been described (1) together with the bromine oxidation and the separation of the fragments into acidic and neutral portions.

Characterization of Components—Neutral Fraction

This fraction contained glycerol, erythritol, and seven non-reducing components (Table I). The former two have been characterized (1) and the experiments on the remainder are described here.

Fraction 1.—This fraction contained 56.6 mg, $[\alpha]_D$ 11° (*c*, 0.6 in H_2O). A portion was hydrolyzed for 8 h at 100 °C with H_2SO_4 (1 *N*) and after neutralization ($BaCO_3$), chromatographic examination (solvent A, 16 h) showed xylose, glucose, glycerol, and erythritol. The result of a typical analysis was: glucose 333 μg or 1.85 μmoles; xylose: 131 μg or 0.87 μmoles; glycerol: 177 μg or 1.92 μmoles; erythritol: 84 μg or 0.69 μmoles.

Fractions 2 and 3.—These fractions (Table I) were similarly analyzed and the hydrolysates of fractions 1, 2, and 3 were combined and separated on paper using solvent A. Glycerol and erythritol were converted to their tri- and tetra-*O*-*p*-nitrobenzoates, m.p. and mixed m.p. 189–192 °C and 252–254 °C respectively. D-Xylose was obtained crystalline, m.p. and mixed m.p. 142–144 °C, $[\alpha]_D$ 17° (*c*, 1.2 in H_2O); phenylosazone, m.p. 156–159 °C. D-Glucose crystallized spontaneously and had m.p. and mixed m.p. 144–145° C, $[\alpha]_D$ 51° (*c*, 1.1 in H_2O); phenylosazone, m.p. 203–206 °C.

Fraction 4.—This fraction contained 90 mg, $[\alpha]_D$ 25° (*c*, 0.9 in H_2O). (*a*) A portion (8.6 mg) was oxidized at 5 °C with periodic acid (12 ml, 0.1 *M*) and after 72 h 640 μg of formaldehyde had been produced (11). This indicated a D.P. of 3 on the assumption that each mole of glycoside gave one mole of formaldehyde.

Periodate and iodate were removed by the addition of barium carbonate, and sodium borohydride (15 mg) was added to the filtrate. The solution was left at room temperature for 24 h and then evaporated to dryness. Borate was removed (16) and the residue boiled with sulphuric acid (1 *N*) for 8 h. After neutralization and deionization, chromatography showed a glycerol to ethylene glycol ratio of 3:1. (*b*) A second portion (27 mg) was boiled with sulphuric acid (1 *N*) for 8 h and the hydrolysate shown to contain glucose, xylose, glycerol, and erythritol. These ratios and those for fractions 5, 6, and 7 are given in Tables I and II. The hydrolysates of fractions 4–7 were combined, resolved on paper, and identified as for fractions 1–3. Likewise the periodate degradation fragments of fractions 4–7 were combined and resolved on paper. Ethylene glycol was converted to the di-*p*-nitrobenzoate, m.p. 139–140 °C, and the glycerol, erythritol, D-glucose, and D-xylose characterized as before.

Vapor Phase Chromatography of Fractions 1, 2, and 3

Fraction 1.—A portion of this fraction was converted to the trimethylsilyl derivative (12) which was chromatographed without isolation using column 1 and the conditions shown in Fig. 1A. The components were condensed in 6-in lengths of glass tubing which were then immersed in 80% ethanol and refluxed for 24 h to effect desilylation. The structural determinations were carried out on the desilylated fractions. Component 1*a*, 1-*O*-(α-D-glucopyranosyl)-glycerol: a portion (7 mg) was hydrolyzed with 1 *N* H_2SO_4 and shown to contain glucose and glycerol in a 1:1 ratio. The remainder (12 mg) was oxidized with periodate and gave 1.45 mg of formaldehyde indicating a molecular weight of 250 (calc. 254). Periodate and iodate were removed by precipitation with barium carbonate and sodium borohydride (20 mg) added. After hydrolysis and deionization glycerol and ethylene glycol were identified chromatographically and shown to be present in a 1:1 molar ratio. Component 1*b*, 1-*O*-(β-D-glucopyranosyl)-glycerol: had $[\alpha]_D$ 12° (*c*, 2 in H_2O) and hydrolysis showed a 1:1 molar ratio of glucose and glycerol. Periodate oxidation and measurement of the formaldehyde (1.76 mg from 15 mg) gave a mol. wt. of 250 while reduction and hydrolysis gave ethylene glycol and glycerol in a 1:1 ratio. The remaining material (13 mg) formed a hexa-*p*-nitrobenzoate, m.p. 105–108 °C. Calc. for $C_{51}H_{36}O_{26}N_6$: N, 7.32%. Found: N, 7.30%. Component 1*c*, 2-*O*-(D-xylofuranosyl)-D-erythritol: (6 mg) gave on hydrolysis xylose and erythritol in a 1:1 ratio. A second portion (10 mg) gave 1.17 mg formaldehyde corresponding to a mol. wt. of 250 and hydrolysis of the reduced product showed only glycerol. An attempt to prepare a *p*-nitrobenzoate from the remaining material (8 mg) met with limited success. The yield was poor and the product melted at 165–174 °C.

Fraction 2.—This fraction was similarly resolved, using column 1, into three components (Fig. 1B) the properties of which are given in Table III and their analytical data in Table IV. Components 2*b* and 2*c* formed *p*-nitrobenzoates. Calc. for $C_{59}H_{41}O_{30}N_7$: N, 7.38%. For 2-*O*-(β-D-glucopyranosyl)-D-erythritol hepta-*O*-*p*-nitrobenzoate, found: N, 7.50%. For 1-*O*-(α-D-glucopyranosyl)-erythritol hepta-*O*-*p*-nitrobenzoate, found: N, 7.48%.

Fraction 3.—The resolution of this fraction was attempted using a 2-ft column (0.25-in diameter) packed with Diatoport* coated with 10% S.E. 30† with a helium flow rate of 180 ml/min at 260 °C. The results are shown in Fig. 1C. Component 3*a* was a mixture as seen by the incomplete separation of the peaks. Hydrolysis gave a glucose:xylose:glycerol ratio of 1:1:1. The formaldehyde produced on periodate oxidation indicated a mol. wt. of 380 while reduction and hydrolysis gave xylose:erythritol:glycerol:ethylene glycol as 1:1:2:2. Component 3*b* contained glucose and erythritol (2:1) and had an apparent mol. wt. of 380. Periodate oxidation, reduction, and hydrolysis gave glycerol:erythritol:glucose:ethylene glycol as 8:2:1:1.

Characterization of Components—Acid Fraction

The four non-reducing components with slower R_f values than glycerol (1) were hydrolyzed for 8 h with sulphuric acid (1 *N*) and the analytical data are presented in Table V.

Successive Periodate Oxidations of Glucan

The glucan (2.0 g) was oxidized with periodic acid, reduced with sodium borohydride, and the polyalcohol isolated. A small portion was completely hydrolyzed and the hydrolysate quantitatively analyzed. The bulk of the polyalcohol was hydrolyzed at room temperature with hydrochloric acid (0.1 *N*) for 4 h whereupon an excess of sodium periodate was added and the reaction sequence repeated. A total of four oxidations were performed and the results are summarized in Table VI.

ACKNOWLEDGMENTS

We are indebted to Miss Judith Hunter for skillful technical assistance and to the Public Health Service (U. S. A.) for financial support (RG 7652).

**F and M Scientific Corporation Inc.*
†Wilkens Instrument and Research Inc.

Can. J. Chem. Downloaded from www.nrcresearchpress.com by 210.87.254.5 on 09/05/12
For personal use only.

REFERENCES

1. G. G. S. DUTTON and A. M. UNRAU. Can. J. Chem. **40**, 1196 (1962).
2. G. G. S. DUTTON and A. M. UNRAU. Can. J. Chem. **41**, 2439 (1963).
3. P. T. MORA and J. W. WOOD. J. Am. Chem. Soc. **80**, 685 (1958).
4. I. J. GOLDSTEIN, G. W. HAY, B. A. LEWIS, and F. SMITH. Abstracts, 135th American Chemical Society Meeting, Boston. April, 1959. p. 3D.
5. D. V. MYHRE and F. SMITH. Abstracts, 135th American Chemical Society Meeting, Boston. April, 1959. p. 6D.
6. G. W. HAY and F. SMITH. Abstracts, 135th American Chemical Society Meeting, Boston. April, 1959. p. 6D.
7. G. G. S. DUTTON and A. M. UNRAU. Can. J. Chem. **40**, 348 (1962).
8. G. O. ASPINALL and K. M. ROSS. J. Chem. Soc. 1681 (1963).
9. G. G. S. DUTTON and A. M. UNRAU. Can. J. Chem. **41**, 1417 (1963).
10. G. G. S. DUTTON and A. M. UNRAU. Can. J. Chem. **40**, 2101 (1962).
11. A. M. UNRAU and F. SMITH. Chem. Ind. London, 330 (1957).
12. C. C. SWEELEY, R. BENTLEY, M. MAKITA, and W. W. WELLS. J. Am. Chem. Soc. **85**, 2497 (1963).
13. A. M. UNRAU. Unpublished results.
14. N. DUBOIS, J. K. HAMILTON, K. A. GILLES, P. A. REBERS, and F. SMITH. Anal. Chem. **28**, 350 (1956).
15. P. P. FLEURY and J. LANG. J. Pharm. Chim. **17**, 107 (1933).
16. D. R. BRIGGS, E. F. GARNER, R. MONTGOMERY, and F. SMITH. Anal. Chem. **28**, 1333 (1956).

Can. J. Chem. Downloaded from www.nrcresearchpress.com by 210.87.254.5 on 09/05/12
For personal use only.

Can. J. Chem. Downloaded from www.nrcresearchpress.com by 210.87.254.105 on 09/05/12
For personal use only.

PRIMARY PROCESS STUDIES BY MONOISOTOPIC PHOTOSENSITIZATION ON THE REACTIONS OF Hg $6(^3P_1)$ ATOMS WITH ALKYL CHLORIDES

J. K. S. WAN,[1] O. P. STRAUSZ, W. F. ALLEN, AND H. E. GUNNING
Department of Chemistry, University of Alberta, Edmonton, Alberta

Received April 3, 1964

ABSTRACT

The specific nature of the primary process in the reaction of ^{202}Hg $6(^3P_1)$ atoms, photoexcited in natural mercury vapor by a cool ^{202}Hg electrodeless discharge source, with CH_3Cl has been examined in detail. Primary C–Cl bond scission occurs with unit efficiency. Quantum yields (φ) for the two primary modes of decomposition

$$^{202}Hg + Cl + CH_3 \overset{b}{\leftarrow} [CH_3Cl + {}^{202}Hg^*] \overset{a}{\rightarrow} {}^{202}HgCl + CH_3$$

were found to have values of 0.71 (b) and 0.29 (a). The effect of various reaction parameters on the ^{202}Hg enrichment in the calomel product has been investigated and the importance of isotopic mercury depletion in the reaction zone demonstrated by the use of intermittent illumination.

A brief study of the reaction of ethyl, *n*-propyl, *i*-propyl, *t*-butyl, and *n*-amyl chlorides has revealed a relation between the molecular structure of the alkyl chloride and the efficiency of the monoisotopic route (a) to calomel formation. Thus, while the reactions of all the normal alkyl chlorides have φ_a values between 0.29 and 0.32, φ_a (isopropyl chloride) is only 0.22 and φ_a (*t*-butyl chloride) is 0.17.

INTRODUCTION

Among the alkyl halides only methyl chloride has been studied in detail by mercury photosensitization. Thus Le Roy (1) has shown calomel to be a major product of the reaction. Masson and Steacie (2) studied the reaction at elevated temperatures in a static system at high mercury vapor concentrations and found that C–Cl bond rupture is the sole primary step and that it proceeds with unit quantum efficiency. They attributed calomel formation exclusively to chlorine atom abstraction by mercury atoms from secondary CH_2Cl radicals. This hypothesis, however, appears to be rather doubtful on energetic grounds. In addition Osborn and Gunning (3) have shown, by ^{202}Hg monoisotopic sensitization, that at least a fraction of the calomel product arises in the primary interaction between the Hg $6(^3P_1)$ atoms and CH_3Cl. The isotopic analyses in this latter study were accomplished by resonance absorbiometry (4).

In the present study, recent refinements in the technique of monoisotopic photosensitization have been employed to explore in detail the primary processes in the CH_3Cl reaction. In addition the effect of the alkyl side chain on the primary processes has been studied by examining the ethyl, *n*-propyl, *i*-propyl, *t*-butyl, and *n*-amyl chloride reactions. By such means it was hoped to resolve discrepancies in previous studies on the CH_3Cl reaction and, of greater importance, to gain some insight into the specific nature of the energy-transfer process in the interaction between RCl molecules and Hg $6(^3P_1)$ atoms.

EXPERIMENTAL

A standard single-pass high vacuum system was used. An umbrella-type mercury diffusion pump, installed between the gas inlet and reaction zone, served as mercury saturator. The exit condenser of the diffusion pump was temperature-regulated at 30 °C. The gas-inlet system was constructed so that a single gas, or a mixture of two gases in variable proportions, could be introduced. Flow rates were regulated by a pair of Hoke model 318 needle valves and by the interchangeable capillaries of the Schilling-type flow meters, which were calibrated separately for each gas used. The reaction cell, a quartz tube 1.5 cm i.d. and 60 cm

[1]*Present address: Department of Chemistry, University of California, Riverside, California.*

in length, wound into five helical coils 2.5 cm i.d., was attached to the system by a pair of ground-glass joints. Provision was made for the trapping of the effluent reactants for analysis.

The light source consisted of a quartz electrodeless discharge tube containing mercury, 98.3 atom % in ^{202}Hg. It was axially mounted within the coils of the spiral cell. The discharge was maintained by a 2450 Mc oscillator (Baird Atomic), operating at 80% power output. Ionization in the discharge was initiated by a Tesla coil. The temperature of the lamp wall was controlled by flowing a thin sheath of distilled water along it, thermostated at 18–20 °C.

For the intermittent-illumination studies a simple rotating tubular sector was devised. A quartz tube, 17.5 mm i.d., was coated with black vinyl tape leaving a vertical slit of desired width and was placed concentrically between the lamp and spiral reaction cell. The bottom of the tubing was securely mounted to a Sargent hollow-spindle rotor. The speed of rotation was controlled by a powerstat, and the angular velocity of the rotation measured with a stroboscope. Constant speed of rotation within 10% could thus be maintained. The direction of rotation of the sector was opposite to that of the gas flow.

For the experiments in which the isotopic composition of the effluent mercury was studied, the mercury samples were collected in a small U-trap, inserted in the line downstream from the reaction cell. The trap was filled with fresh copper turnings and maintained at 0 °C. All the experiments reported here were performed at 30 ± 5 °C.

For the isotopic analyses, recovery of mercury from the calomel product was effected by dissolution in hot ca. 0.01 *M* EDTA solution, followed by plating out on a freshly cleaned copper wire immersed in the solution. After removal from the solution the wire was thoroughly washed with distilled water, rinsed with methanol, and allowed to dry at room temperature. The mercury was distilled *in vacuo* from the copper to a breakseal for analysis.

All the isotopic analyses of the mercury samples were made with a Metropolitan-Vickers model MS-2, mercury-free mass spectrometer. The instrument was equipped with a special inlet system, provided with a low pressure constriction-free inlet tube leading directly from the sample to the ion source. Between analyses the inlet system was heated to 150–200 °C for about 30 minutes while pumping through a liquid nitrogen trap to insure against memory effects. At least twenty scans were allowed, and the heights of the last five peaks were taken to calculate the mean values for each isotope. No effort was made to analyze ^{196}Hg. From time to time standard mercury samples of various isotopic compositions from Oak Ridge National Laboratory were analyzed to check on the accuracy of the instrument.

The quantitative determination of calomel was carried out by EDTA titration (5) with Eriochrome Black-T indicator. Check determinations on known samples in the range 10^{-4}–10^{-5} mole indicated a ±2% error limit.

Gaseous reaction products were identified by g.c. retention times and mass spectrometric analyses of the separated chromatographic effluents. In the CH_3Cl reaction, non-condensables, after low-temperature fractionation, were separated on a charcoal column and the dichloroethane fraction was separated on a silica-gel column with He as carrier gas.

Methyl and ethyl chlorides, C.P., and propane, instrument grade, were from the Matheson Company. The remaining alkyl chlorides studied, 1-chloropropane, 2-chloropropane, 2-chloro-2-methyl-propane, and 1-chloropentane, were all Eastman products. The natural mercury was triply distilled. Standard isotopic-mercury samples were obtained from the Oak Ridge National Laboratory.

RESULTS

The products of the CH_3Cl reaction were calomel, methane, 1,2-dichloroethane, hydrogen chloride, traces of ethane, and possibly some ethyl chloride. The calomel products were more or less enriched in ^{202}Hg, depending on experimental conditions. Through a systematic study, the relations between product enrichment and the various reaction parameters were investigated in detail.

First the effect of flow rate on the fractional abundance of ^{202}Hg (f_{202}) was examined. In continuous illumination with flow rates increasing from 1 to 7 millimoles/min at a CH_3Cl pressure of 15 mm and $I \sim 1$ μeinstein/min, f_{202} increased from the natural abundance value of 0.298 to 0.373. The f_{202} data obtained under the conditions of intermittent illumination are presented in Table I. With increasing flow rate f_{202} increases in both cases but levels off at different flow rates: at ca. 0.37 for continuous and 0.50 for intermittent illumination. In Table I the total isotopic analyses are given to illustrate that all isotopes other than 202 are present in their natural distribution ratio, indicating that no overlap of the emission line envelope on absorption hyperfine contours adjacent to that of ^{202}Hg is occurring in the present system.

Can. J. Chem. Downloaded from www.nrcresearchpress.com by 210.87.254.105 on 09/05/12
For personal use only.

TABLE I

Effect of flow rate on total isotopic composition of calomel product in the methyl chloride reaction under intermittent illumination*

Flow rate, millimole/min	Isotopic composition					
	202	198	199	200	201	204
—	0.298†	0.100†	0.168†	0.231†	0.132†	0.069†
0.0	0.311	0.097	0.167	0.232	0.130	0.064
0.2	0.406	0.078	0.136	0.198	0.118	0.063
0.4	0.423	0.067	0.119	0.188	0.143	0.060
0.9	0.444	0.077	0.133	0.185	0.107	0.055
1.7	0.481	0.072	0.124	0.171	0.099	0.052
2.1	0.487	0.072	0.123	0.169	0.098	0.051
2.7	0.509	0.067	0.117	0.164	0.095	0.048
4.0	0.492	0.070	0.122	0.173	0.097	0.047
4.9	0.505	0.069	0.118	0.163	0.095	0.050
6.0	0.494	0.069	0.120	0.169	0.099	0.050

*Sector speed = 290±10 r.p.m., slit width = 2 mm, CH_3Cl pressure = 15±1 mm, exp. time = 40 min.
†Natural abundance.

The effect of mode of mercury recovery from the calomel product on the f_{202} values was also examined. It was found that dissolution in (*a*) KI–$Na_2S_2O_3$ solution (0.2 *N* in KI and 0.01 *N* in $Na_2S_2O_3$), (*b*) 0.01 *M* EDTA solution,[2] and (*c*) hot concentrated ammonia, all gave identical f_{202} values regardless of whether or not the calomel had been freed from adsorbed mercury by pumping before dissolution. It was thus concluded that exchange reactions between product and adsorbed mercury, after the photochemical reaction, are unimportant (6).

To establish optimum conditions for intermittent illumination a series of experiments was performed measuring f_{202} as a function of sector rotation speed and slit width. The

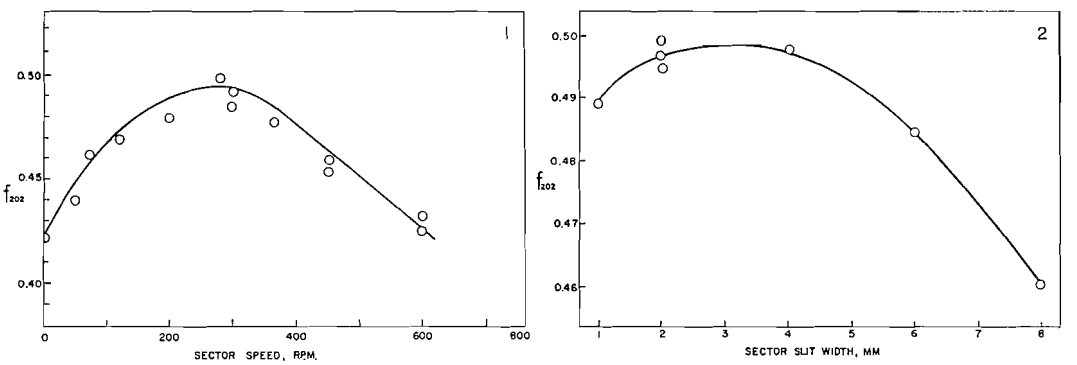

FIG. 1. Plot of f_{202} as a function of sector speed for the methyl chloride reaction at an exposure time of 40 min, sector slit width of 2 mm, and a pressure of 15 ± 1 mm.
FIG. 2. Plot of f_{202} as a function of sector slit width (sector speed = 280–300 r.p.m.) for the methyl chloride reaction at an exposure time of 40 min, flow rate of 6 millimoles/min, and a pressure of 15 ± 1 mm.

results are shown in Figs. 1 and 2. Maximum enrichments were obtained at a sector slit width of 2 mm and speed of rotation of 280–300 r.p.m.

A major problem in monoisotopic photosensitization studies is the effect of isotopic mercury depletion. Thus increasing flow rates lead to a more uniform distribution of

[2]*Solution of calomel in EDTA proceeds via the disproportionation of* Hg_2^{++} *to* Hg^{++} *and* Hg. *The absence of isotopic fractionation in this process was demonstrated experimentally.*

Can. J. Chem. Downloaded from www.nrcresearchpress.com by 210.87.254.105 on 09/05/12
For personal use only.

Can. J. Chem. Downloaded from www.nrcresearchpress.com by 210.87.254.105 on 09/05/12
For personal use only.

natural mercury throughout the entire cell, in contrast to the situation at low flow rates where a concentration gradient in ^{202}Hg exists along the linear length of the spiral cell. In the entrance coil ^{202}Hg will be present in natural abundance. However, during reaction, some ^{202}Hg is removed by $^{202}HgCl$ formation, and if the flow rate is insufficient to sweep this portion of substrate out of the illuminated zone immediately, accumulated depletion will lead to a continuous decrease of ^{202}Hg concentration as the gas stream traverses the remaining coils of the cell.

In order to determine the effect of depletion in the present study, a series of experiments was performed under optimum sector conditions and at various flow rates. The fractions of the calomel deposited along the cell axis were recovered in two separate portions, which are here labelled "entrance HgCl" and "exit HgCl", corresponding respectively to an individual recovery of mercury from calomel product from the first coil of the cell in which the gas flow entered, and the last two coils before the exit. In addition, the effluent mercury in the gas stream leaving the reaction cell was collected and analyzed for each run. The results are tabulated in Table II. It is of note that the "entrance HgCl" had the maximum

TABLE II

Effect of flow rate on fractional abundance of ^{202}Hg in calomel formed in effluent mercury and at entrance and exit of reaction cell*

Flow rate, millimole/min	f_{202}		
	Hg (effluent)	HgCl (entrance)	HgCl (exit)
0.2	0.016	0.501	0.301
0.4	0.033	0.501	0.342
0.9	0.101	0.504	0.403
2.1	0.224	0.504	0.437
2.9	0.300	0.510	0.506
5.0	0.301	—	—

*Sector speed = 290±10 r.p.m., slit width = 2 mm, CH_3Cl pressure = 15±1 mm, exp. time = 40 min.

TABLE III

Quantum yield of calomel formation in the methyl chloride reaction under various sector conditions*

Slit width, mm	Sector speed, r.p.m.	I_a, μeinstein/min	φ_{HgCl} mole/einstein
1	280	8.0	0.87
2	280	11.0	0.91
2	600	11.0	0.91
2	50	11.0	0.91
4	280	17.0	0.89
6	280	22.0	0.91
8	280	26.0	0.89

*Flow rate = 6.0 millimoles/min, CH_3Cl pressure = 15±1 mm, exp. time = 40 min.

enrichment at all flow rates while the enrichment in the "exit HgCl", as well as the 202 content of the effluent mercury, increased with flow. At flow rates exceeding 3 millimoles per minute, both fractions of calomel are seen to have the same maximum enrichment, and the effluent mercury had a natural isotopic composition.

In a subsequent experiment, performed in the same reaction system as above, the vertical length of the sector slit was varied in each run so that only a fraction of the cell length was irradiated. The effluent mercury in each run was collected and analyzed. The

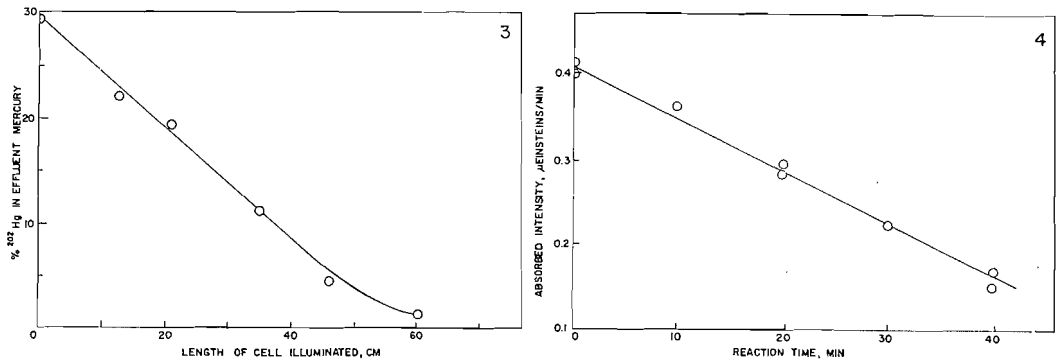

FIG. 3. Plot of percentage ^{202}Hg in the effluent mercury as a function of cell length illuminated in the methyl chloride reaction at an exposure time of 40 min, flow rate of 0.2 millimoles/min, sector slit width and speed of 2 mm and 280–300 r.p.m., and a pressure of 15 ± 1 mm.

FIG. 4. Plot of absorbed intensity as a function of reaction time for the methyl chloride reaction at a flow rate of 6 millimoles/min, sector slit width and speed of 2 mm and 600 r.p.m., and a pressure of 15 ± 1 mm.

plot of f_{202} versus irradiated cell length is given in Fig. 3. It is seen from the plot that for total cell-length illumination (60 cm), the ^{202}Hg concentration in the effluent mercury was only 1.6% and the mean concentration of ^{202}Hg present in the entire cell volume was only 16% instead of the natural abundance of 29.8%.

The quantum yield for calomel formation in continuous illumination was found to have a value of 0.86 mole/einstein at flow rates exceeding 4.8 millimole/min. φ_{HgCl} was also measured under intermittent illumination, and these values are reported in Table III. The determination of absorbed intensities by propane actinometry (7, 8) presented serious experimental difficulties, partly because of the complexity of the propane reaction itself and partly because of the decrease in the transparency of the cell wall in the course of an experiment, due to calomel deposition. For this transparency decrease a proper correction, based on the experimental curve shown in Fig. 4, was applied. This curve was obtained from light intensity measurements carried out in the reaction vessel, which was coated with calomel from the methyl chloride reaction performed previously for various times as shown on the abscissa of Fig. 4. It was assumed that the destruction of calomel, either by H-atoms or photolysis, is insignificant. The validity of this assumption was proven experimentally.

The rate and quantum yield data obtained for methane and 1,2-dichloroethane formation are given in Table IV.

From several check experiments it is estimated that maximum uncertainty in the

TABLE IV

Rate and quantum yield data for methane and dichloroethane formation*

Rate, μmole/min		φ, mole/einstein	
CH_4	$C_2H_4Cl_2$	CH_4	$C_2H_4Cl_2$
0.228	0.125	0.80	0.45
0.222	0.125	0.81	0.45
0.222	0.120	0.81	0.45

*Methyl chloride flow = 3.0 millimoles/min, I_a = 0.275 μeinstein/min, CH_3Cl pressure = 15±1 mm, exposure time = 40 min.

Can. J. Chem. Downloaded from www.nrcresearchpress.com by 210.87.254.105 on 09/05/12
For personal use only.

quantum yield measurements is ±10%, attributable largely to the uncertainty in the light intensity determinations.

The reactions of some of the higher alkyl chlorides were also examined. Product enrichment and quantum yield values as obtained under various experimental conditions for the ethyl, *n*-propyl, *i*-propyl, *t*-butyl, and *n*-amyl chloride reactions are shown graphically in Figs. 5–9 and the optimum values are summarized in Table V.

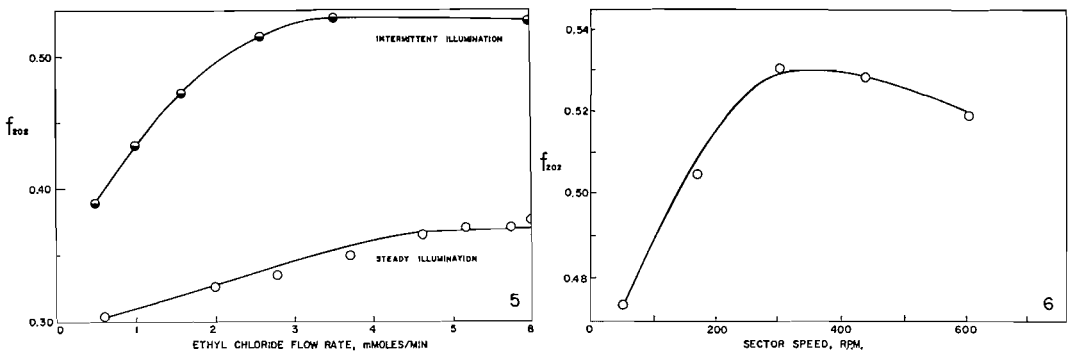

FIG. 5. Plot of f_{202} as a function of flow rate for 15 ± 1 mm ethyl chloride under steady illumination (exposure time = 45 min) and intermittent illumination (exposure time = 40 min), sector slit width and speed = 2 mm and 300 r.p.m.

FIG. 6. Plot of f_{202} as a function of sector speed for the ethyl chloride reaction at an exposure time of 40 min, flow rate of 6 millimoles/min, sector slit width of 2 mm, and a pressure of 15 ± 1 mm.

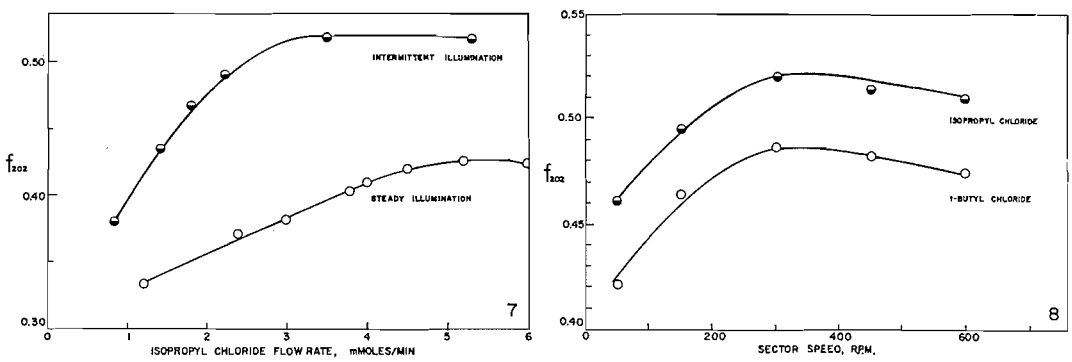

FIG. 7. Plot of f_{202} as a function of flow rate for 15 ± 1 mm isopropyl chloride under steady illumination (exposure time = 45 min) and intermittent illumination (exposure time = 40 min), sector slit width and speed = 2 mm and 300 r.p.m.

FIG. 8. Plot of f_{202} as a function of sector speed for 15 ± 1 mm isopropyl chloride and *t*-butyl chloride at an exposure time of 40 min, sector slit width of 2 mm, and flow rate of 5 millimoles/min.

In contrast to the HCl reaction (6, 9, 10), addition of 1,3-butadiene to the alkyl chloride systems was found to have no effect on the isotopic enrichment of the calomel products in agreement with previous studies (3). The inefficiency of butadiene in scavenging Cl atoms is probably associated with the formation of excited chlorobutenyl radicals, which at low pressures readily revert to butadiene and chlorine (11). Furthermore, it was observed that the calomel from all of the alkyl chloride reactions was free from desorbable mercury, indicating that no appreciable reduction of the solid calomel occurs during reaction. In this connection, since methyl radicals would be the most probable reducing

Can. J. Chem. Downloaded from www.nrcresearchpress.com by 210.87.254.105 on 09/05/12
For personal use only.

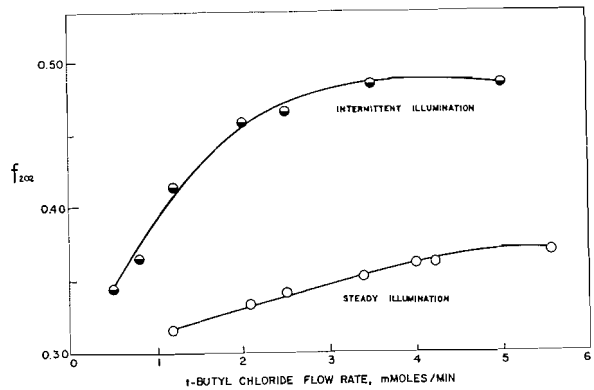

FIG. 9. Plot of f_{202} as a function of flow rate for 15 ± 1 mm *t*-butyl chloride at an exposure time of 40 min. Sector speed = 300 r.p.m. and slit width = 2 mm.

TABLE V

Quantum yield and product enrichment data for the alkyl chloride reactions

Substrate	φ_{HgCl}, mole/einstein		f_{202}, steady	Isotopic composition, intermittent					
	Steady	Intermittent		202	198	199	200	201	204
MeCl	0.86	0.91	0.375	0.509	0.067	0.117	0.164	0.095	0.048
EtCl	0.84	0.91	0.378	0.531	0.062	0.111	0.159	0.091	0.050
n-PrCl	n.d.*	0.90	n.d.*	0.541	0.063	0.110	0.154	0.088	0.046
n-AmCl	n.d.*	0.90	n.d.*	0.543	0.063	0.109	0.153	0.087	0.045
i-PrCl	0.63	0.70	0.427	0.518	0.065	0.115	0.161	0.094	0.047
t-BuCl	0.54	0.64	0.367	0.485	0.069	0.122	0.174	0.099	0.050
^{n}Hg	—	—	0.298	0.298	0.100	0.168	0.231	0.132	0.069

*n.d. = not determined.

agent present during reaction, separate experiments were performed in which acetone was photolyzed in the presence of a deposit of calomel in the reaction cell; no detectable amounts of methyl chloride could be found after irradiation.

DISCUSSION

The nature of the reaction products suggests, in partial agreement with the conclusion of the previous studies (2, 3), the following mechanism for the methyl chloride reaction, where ^{n}Hg is natural mercury.

[1] $$^{n}Hg + h\nu_{202} \rightarrow {}^{202}Hg^*$$

[2*a*] $$^{202}Hg^* + CH_3Cl \rightarrow {}^{202}HgCl + CH_3$$

[2*b*] $$\rightarrow {}^{202}Hg + Cl + CH_3$$

[3*a*] $$Cl + {}^{n}Hg + M \rightarrow {}^{n}HgCl + M$$

[3*b*] $$2HgCl + M \rightarrow (HgCl)_2 + M$$

[4] $$CH_3 + CH_3Cl \rightarrow CH_4 + CH_2Cl$$

[5] $$2CH_2Cl \rightarrow C_2H_4Cl_2$$

[6] $$CH_3 + CH_2Cl \rightarrow C_2H_5Cl$$

[7] $$2CH_3 \rightarrow C_2H_6$$

[8] $$Cl + CH_3Cl \rightarrow HCl + CH_2Cl$$

The measured value for the total quantum yield of calomel, φ_{HgCl}, was 0.91, which is the minimal value for $\varphi_{[2]}$. Since step [8] has a low activation energy (Arrhenius parameters

Can. J. Chem. Downloaded from www.nrcresearchpress.com by 210.87.254.105 on 09/05/12
For personal use only.

are: log A = 10.4 in l mole s units, and E_a = 3.1 kcal/mole (12)) some of the Cl atoms formed in step [2*b*] are consumed in reaction [8]. Indeed, HCl was detected among the reaction products, but it was not measured quantitatively. Its yield, however, can be estimated from that of methane and dichloroethane. From the stoichiometry of the reaction it follows that

$$\varphi_{HCl} = 2\varphi_{C_2H_4Cl_2} - \varphi_{CH_4} = 0.90 - 0.81 = 0.09 \text{ mole/einstein},$$

and the combined quantum yield for primary steps [2*a*] and [2*b*] will be

$$\varphi_{[2]} = \varphi_{HgCl} + \varphi_{HCl} = 0.91 + 0.09 = 1.00 \text{ mole/einstein}.$$

Since reaction [7] is relatively unimportant, $\varphi_{C_2H_5Cl}$ may be crudely estimated:

$$\varphi_{C_2H_5Cl} = 1 - \varphi_{CH_4} = 1 - 2\varphi_{C_2H_4Cl_2} + \varphi_{HCl} = 0.19 \text{ mole/einstein}.$$

Although product accountability is reasonably good, the possibility of primary C–H bond scission to a minor extent cannot be completely ruled out from the present data. However, the absence of hydrogen among the reaction products would support omission of this primary step (13). The probability of C–H vs. C–Cl bond rupture can be estimated from the relative quenching efficiencies of the two groups within the molecule.[3] If we take $\sigma_Q^2(CH_3) \simeq 0.05$ and $\sigma_Q^2(Cl) \simeq 24$ Å^2, for the relative probability of C–H/C–Cl bond cleavage we obtain a value of ca. 0.002.

The efficiency of the abstraction reaction [4] may appear to be improbably high in view of Masson and Steacie's finding that E_a = 9.4 kcal/mole and $P = 2.8 \times 10^{-3}$ (12). However, the conditions under which the present determinations were performed (spacially intermittent illumination at low incident intensities) strongly favor abstraction over recombination.

Before attempting to evaluate the $\varphi_{[2a]}$ and $\varphi_{[2b]}$ values separately, we have to examine the reaction parameters influencing the magnitude of product enrichments. The importance of eliminating isotopic mercury depletion was convincingly demonstrated by the data of the previous section (Table II). The significant increase in f_{202} brought about by the application of the rotating sector is an interesting, although not surprising, result, indicating the seriousness of the isotopic mercury depletion effect and possibly also the presence of secondary processes destructive of ^{202}HgCl. The effect of intermittent illumination is largely, although not entirely, due to the attenuation of the incident light intensities. It is evident from the data of Table II that the enrichment at the entrance is only very slightly dependent on flow rates, while the exit and effluent mercury compositions are strongly dependent. This result is not much altered by sector speed. Thus the main effect of the sector is to slow down the rate of mercury consumption, thereby allowing sufficient time for the flow- and diffusion-controlled replenishment of natural mercury. If the Cl atoms in reaction [3] react with mercury depleted in ^{202}Hg instead of natural mercury, a diminution of f_{202} in the recovered calomel will result.

In the course of the present study it was demonstrated that the destruction of solid ^{1}HgCl (where ^{1}Hg is isotopically specific mercury) by isotopic exchange reactions during dissolution or by secondary free-radical attack under illumination is unimportant. Now, since the isotopic energy exchange: $^{1}Hg^* + {}^{n}Hg \rightarrow {}^{n}Hg^* + {}^{1}Hg$, has been shown to be insignificant at high substrate pressures (10, 15), the only conceivable reaction whereby isotopic calomel could be consumed is the gas-phase isotopic-exchange reaction

[9] $$^{202}HgCl + {}^{n}Hg \rightarrow {}^{n}HgCl + {}^{202}Hg.$$

[3]*The pertinent* σ_Q^2 *data are:* $CH_4 = 0.06$, $C_2H_6 = 0.1$, *neo*-$C_5H_{12} = 1.5$, $HCl = 24$, *and* $CH_3Cl = 24$ Å^2 *(14).*

Can. J. Chem. Downloaded from www.nrcresearchpress.com by 210.87.254.105 on 09/05/12
For personal use only.

The existence of an optimum speed for sector rotation (cf. Figs. 1, 6, and 8) may be due to this or some other similar type of reaction, although this assumption is rather speculative at present.

Now, the value of $\varphi_{[2a]}$ is given by the expression

$$[10] \qquad \varphi_{HgCl}(f_{202}(\max) - 0.298)/0.702 f_{202}^*,$$

where f_{202}^* is the fractional isotopic abundance in the discharge source. From the nature of monoisotopic photosensitization, it follows that for the evaluation of $\varphi_{[2a]}$ the maximum measured value of f_1 has to be considered. Substituting the experimental values in [10], we obtain $\varphi_{[2a]} = 0.29$ and thus $\varphi_{[2b]} = 0.71$ mole/einstein.

The kinetic features of all the higher chlorides studied, with respect to such parameters as flow and sector conditions, closely resemble those of the methyl chloride system. The quantum yields of calomel formation for all the *n*-isomers have values of 0.90–0.91. This is somewhat surprising, since, at least in the amyl chloride case, some C–H bond scission would be expected to occur in the primary step. The $\varphi_{[2a]}$ values, 0.29, 0.31, 0.32, and 0.32 mole/einstein respectively for CH_3Cl, C_2H_5Cl, *n*-C_3H_7Cl, and *n*-$C_5H_{11}Cl$, may indicate a minor trend upward with increasing chain length.

Isopropyl and *t*-butyl chlorides were studied to determine the effect on the primary process of increasing alkyl substitution on the α-carbon atom. Whereas values of the quantum yields of total calomel (φ_{HgCl}) and isotopically specific calomel (φ_1) were almost constant over the series of primary alkyl chlorides studied, both φ_{HgCl} and φ_1 decreased for the secondary and decreased again for the tertiary alkyl chlorides.

It is not clear whether this results from separate effects on the isotopically specific and non-specific processes which by chance balance to give little change in the total isotopic composition of the product, or whether a competing primary process (or processes) operates to decrease φ_{HgCl} but leave $\varphi_{[2a]}$ and $\varphi_{[3a]}$ in the same ratio.

Further discussion of the mechanisms of energy transfer and the nature of the transition complex formed in these systems between excited mercury atoms and substrates molecules will be advanced in some forthcoming communications from this laboratory.

ACKNOWLEDGMENTS

The support of the National Research Council of Canada under N.R.C. Grant No. T-162 is gratefully acknowledged.

REFERENCES

1. D. J. Le Roy. Can. J. Res., B, **28**, 492 (1950).
2. C. R. Masson and E. W. R. Steacie. J. Chem. Phys. **19**, 183 (1951).
3. K. R. Osborn and H. E. Gunning. J. Chem. Phys. **37**, 1315 (1959).
4. K. R. Osborn and H. E. Gunning. J. Opt. Soc. Am. **45**, 552 (1955).
5. N. Tritani, T. Tanaka, and E. Sakai. J. Pharm. Soc. Japan, **76**, 1068 (1956).
6. J. A. Poole. Ph.D. Thesis, University of Alberta. 1961.
7. S. Bywater and E. W. R. Steacie. J. Chem. Phys. **19**, 319 (1951).
8. R. A. Back. Can. J. Chem. **37**, 1834 (1959).
9. H. E. Gunning. J. Chim. Phys. **60**, 197 (1963).
10. H. E. Gunning and O. P. Strausz. Advances in photochemistry. Vol. 1. *Edited by* W. A. Noyes, Jr., G. S. Hammond, and J. N. Pitts. Interscience. 1963.
11. M. G. Bellas, J. K. S. Wan, W. F. Allen, O. P. Strausz, and H. E. Gunning. J. Phys. Chem. In press.
12. P. Goldfinger. Pure Appl. Chem. **5**, 423 (1962).
13. G. L. Lee and D. J. Le Roy. Can. J. Res. B, **28**, 500 (1950). E. Cremer, J. Curry, and M. Polanyi. Z. Physik Chem., B, **23**, 445 (1933).
14. J. R. Bates. J. Am. Chem. Soc. **52**, 3825 (1930). B. deB. Darwent. J. Chem. Phys. **18**, 1532 (1950). M. G. Bellas, Y. Rousseau, O. P. Strausz, and H. E. Gunning. J. Chem. Phys. In press. (See also ref. 11.).
15. M. Desnoyer, G. Nief, and E. Roth. J. Chim. Phys. **60**, 209 (1963).

Can. J. Chem. Downloaded from www.nrcresearchpress.com by 210.87.254.105 on 09/05/12
For personal use only.

Can. J. Chem. Downloaded from www.nrcresearchpress.com by 210.87.254.105 on 09/05/12
For personal use only.

THE PHENYL EFFECT IN DISTORTION POLARIZATION

HELMUT HUBER AND GEORGE F WRIGHT
Department of Chemistry, University of Toronto, Toronto, Ontario
Received October 18, 1963

ABSTRACT

Diphenylmercury has been used as a model to show that the electron and atom parts of the distortion polarization cannot reliably be evaluated by optical methods. The measured electron polarization extrapolated to infinite wavelength is larger than the combined electron and atom polarization measured at radio frequency. The difference has been defined as the "phenyl effect" and has been attributed to the mobility at radio frequencies of electrons in the resonance-hybridized orbitals of the aromatic nucleus. It has been suggested that the effect is general for aromatic compounds.

The total electric polarization of diphenylmercury has been measured or discussed by a number of workers (1–8). There is a discrepancy between this total polarization and the calculated electron polarization. It has been postulated (2) that this discrepancy is due to an abnormally high atom polarization. This postulation has been proven to be false on the basis of a direct measurement of the combined electron and atom polarization (6). Therefore the discrepancy is still in question.

It has been shown (6) that the total polarization of diphenylmercury in a number of solvents is strongly temperature dependent. Any dependence of atom polarization on temperature is so slight (9) that the discrepancy cannot be explained in this way. The atom polarization of the mercury atom does not seem to be involved in any abnormality because for at least one substance, dicyclohexylmercury (10), the measured distortion polarization is not abnormal.

The direct method for measurement of distortion polarization from the dielectric constant of randomly oriented compressed solids has been developed (11) to give good precision and many substances have been examined (10, 12). Among these substances some give the expected values on the basis of a calculated electronic polarization (13, 14). Other substances give values which are higher than the calculated P_E and these are of two types. The structures of one type have features such as conjugated linkages which ought to give high polarizations due to exaltation of P_E which would not be predicted from atom or bond polarizabilities. The other type contains highly polar groups which would be expected to contribute to high P_A. Thus distortion polarizations (P_E and P_A) which are equal to or greater than the calculated electron polarizations are not unexpected. On the other hand, there is another type of substance for which the measured distortion polarization is lower than the calculated P_E according to Eisenlohr (13) or Vogel (the additive P_E). This is the type in which aromatic groups, especially phenyl groups, are present.

Diphenylmercury is one of the substances for which the distortion polarizations measured at 5 mc are lower than the additive P_E. Since this is one of the substances for which the postulations (2) of high atom polarization have been proven to be in error by actual experimental determination, it has seemed worthwhile to try to evaluate experimentally the parts (P_E and P_A) of the distortion polarization separately. By this procedure some insight toward the underlying discrepancy might be found, together with an explanation for low distortion polarization and its relation to substances containing aromatic groups.

Can. J. Chem. Downloaded from www.nrcresearchpress.com by 210.87.254.105 on 09/05/12
For personal use only.

In order to evaluate the apparent abnormality in the distortion polarization of diphenylmercury, one must first have an opinion about its electronic polarization. There have been several opinions about this and some confusion in respect of the refractivity of mercury. A value of 11.2 cc for mercury was established by Wilde (15) from a series of primary alkyl bis-mercurials (C_1 to C_8), in contradiction of the value of 12.3 to 13.4 reported by others (16) with the assumption that the Eisenlohr value for methylene was constant throughout the series. Wilde's claim on the basis of his extrapolation method that methylene was not constant through the series seems to be valid but his further claim that the extrapolated value (11.0 ± 0.1) is the constant at $\lambda = 5893$ Å for mercury does not seem warranted. Thus Jones *et al.* (16) report much higher values for secondary and tertiary bis-mercurials. To be sure, the refractivity value derived from our experimental refraction at 5893 Å for 2-butyl-bis-mercury at 40 °C is lower (13.4 cc) than the 14.3 cc reported by Jones *et al.* but is much higher than Wilde's supposedly universal value. However, its magnitude is supported by the mercury value of 12.8 cc which we found from the refraction at 5893 Å at 40° for 2-butylmercuric chloride and of 13.5 cc at 50° for 2-butylmercuric bromide.

Actually Wilde's constant would seem to be discrepant from his own determination of the molar refraction of diphenylmercury (64.7 cc at 5893 Å and 15 °C) but his determination was made in the polarizing solvent, pyridine, so the apparent discrepancy (3.1 cc) may be explainable. However Wilde's experimental value of 64.7 cc is closer to that of Bergmann and Shutz (7) (65.2 cc, which has been used by Hampson and others) than is Wilde's calculated value of 61.6. Nor is the situation altered appreciably by calculation from Vogel's bond refractivities because the $MR_D = 62.6$ cc from double and single bond values or $MR_D = 62.1$ cc from aromatic ring bond summation are based on a bond refractivity for mercury of C—Hg = 6.5 cc which was derived from Wilde's value.

On the other hand the value of Bergmann and Schutz may be questioned because of the small differences between the refractive indices of the dilute solutions that they employed. For this reason we have measured the refractive indices experimentally by use of concentrated solutions containing up to 50 weight percent of diphenylmercury in dioxane at 40°. The relations between density and molecular refraction versus mole fraction are shown for wavelength 5893 Å in Fig. 1 and are linear. The molecular refraction of pure diphenylmercury may be calculated from the mixture relation,

$$R_{\text{mixture}} = \frac{n^2 - 1}{n^2 + 2} \cdot \frac{X_1 M_1 + (1 - X_1) M_2}{d}$$

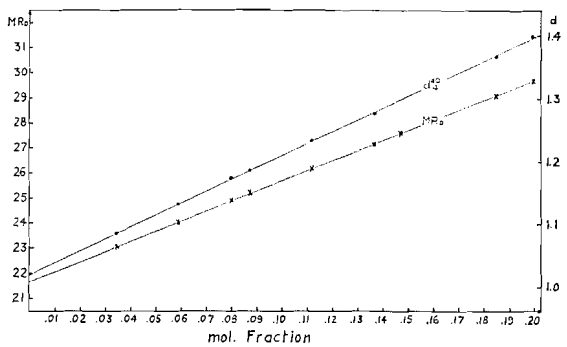

FIG. 1. Density and molecular refraction of diphenylmercury in dioxane.

where M_1 and M_2 are the molecular weights of diphenylmercury and dioxane respectively, X_1 is the mole fraction of the mercurial and d is the density for each solution of the series that was measured. This calculation leads to a molecular refraction at 5893 Å of 62.2 cc for diphenylmercury, surprisingly close to that of the additive values from atom or bond polarizabilities based on Wilde's constant but considerably lower than the extrapolated value obtained by Bergmann and Shutz with dilute solutions in benzene. We do not construe this apparent agreement as support for Wilde's constant when it is applied to groups which are not primary alkyl ones.

Of course the electronic polarization used in most electrical polarization studies is P_E at radio frequencies. Since this value cannot be determined directly, an approximation must be made by use of the Sellmeir extrapolation from linearly related optical dispersions to infinite wavelength. We have used the dioxane solutions at 40° for measurement at five wavelengths in the visible region. When the mixture relation is applied to these values, shown in Fig. 2, the following MR values are found: 64.1 cc at 4341 Å, 62.7 cc at 5460 Å, 62.3 cc at 5893 Å, and 61.8 cc at 6563 Å.

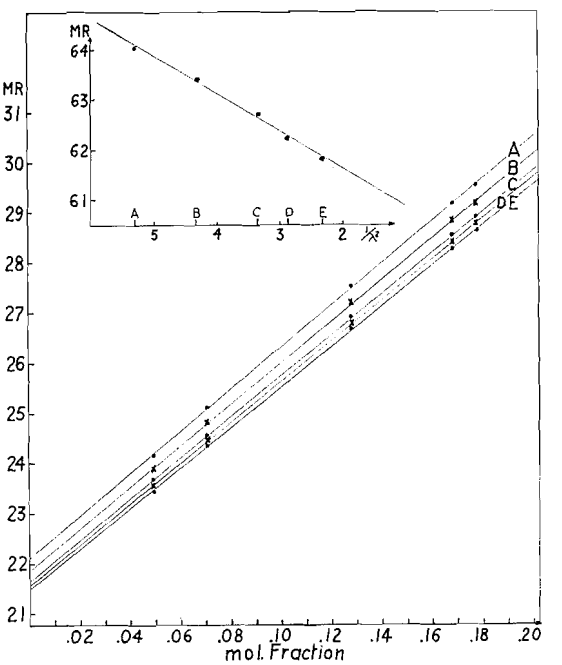

FIG. 2. Dispersion of diphenylmercury.

As may be seen from the insert of Fig. 2 these molecular refractions vary linearly with respect to the square of the wavelength and thus are applicable to the Sellmeir relation

$$R_\infty = \frac{\lambda_1^2 - \lambda_2^2}{(\lambda_1^2/R_1) - (\lambda_2^2/R_2)}$$

where R_1 and R_2 are any of the two molecular refractions at the appropriate wavelengths λ_1 and λ_2. The value of MR_∞ is found in this way to be 60.2 cc, which should be equal within experimental error to P_E at 10^6 c.p.s. The extrapolated value of 60.2 cc indicates that diphenylmercury is strongly dispersive of optical radiation to which it is exposed.

Can. J. Chem. Downloaded from www.nrcresearchpress.com by 210.87.254.105 on 09/05/12
For personal use only.

Can. J. Chem. Downloaded from www.nrcresearchpress.com by 210.87.254.105 on 09/05/12
For personal use only.

Among chemists who evaluate electric moments it is customary to arrive at the orientation polarization of substance by subtracting the molecular refraction for sodium D radiation (5892 Å) from the total polarization in the expectation that the difference between MR_D and MR_∞ will allow for the atom polarization of the substance.

Of course the assumption that this difference is approximate to the atom polarization is unwarranted and is justified only by the comparative difficulty in a separate evaluation of P_A. This evaluation may be done by the method of Whiffen (17) derived from the Kramers–Kronig relation. This may be expressed in terms of the contribution from each spectral absorption,

$$P_{A_j} = \frac{NC}{3\pi^2}\int \frac{\alpha(\nu)d\nu}{\nu^2 c},$$

where N is the Avogadro number, C is the velocity of the radiation, c is concentration, ν is the frequency of the jth absorption band, and α is the extinction coefficient integrated over the bandwidth $d\nu$. It may be seen that in the summation,

$$P_A = \sum P_{A_j},$$

the most important contributions will be those of low frequency, i.e. in the far infrared region. We have examined diphenylmercury in the region (300–50 cm^{-1}) as a dispersion in polyethylene wax (11) in the Perkin–Elmer 301 spectrometer.

The separate contributions to P_A are shown in Table I. The bands are found to be

TABLE I

Calculation of atom polarization for spectral absorption (900–50 cm^{-1}) by diphenylmercury

Sample No.	Freq. (cm^{-1})	Band envelope for	Baseline (% T)	Intensity (cm^2 $mole^{-1}$)	Band width (cm^{-1})	P_{A_j}
1[a]	100	Unsym.	80	38 474	29	12.99
1	207	Unsym.	75	50 599	102	8.26
1	253	Unsym.	75	10 346	51	1.38
1	100	Sym.	80	37 294	27	12.59
1	207	Sym.	75	5 246	21	0.86
1	253	Sym.	75	4 291	29	0.40
2	460	Unsym.[b]	95	5 265	38	0.40
2	705	Sym.[c]	93	1 585	21	0.08
2	735	Sym.[c]	93	1 895	38	0.09

[a]Examined in PE-301 as 15 w/w% in polyethylene wax.
[b]Examined in IR-4 with polyethylene wax in reference beam.
[c]The bands (IR-4) at 705 and 735 (from 10% solutions in benzene), unlike that at 460 cm^{-1} in benzene, are symmetrical.

unsymmetrical with "tailing" at the low-frequency side. This dissymmetry might be accounted as light scattering in the PE-301 at low frequencies: 100, 207, and 253 cm^{-1} but light scattering can not account for the unsymmetrical band at 460 cm^{-1} which has also been observed for benzene solutions by use of the IR-4 spectrophotometer. More likely the "tailing" is due to the so-called "hot bands" caused by transitions of order higher than $0 \rightarrow 1$ and is not due to instrumental error or to appreciable crystal lattice vibrations. Consequently integration over the entire band envelopes ought to be realistic and P_{A_j} values calculated in this way are shown in Table I as "unsym.". For the purpose of comparison P_{A_j} has also been calculated by exclusion of absorption outside of the symmetrical band expected from the contour on the high-frequency side of the bond. These values are listed in Table I as "sym.".

Can. J. Chem. Downloaded from www.nrcresearchpress.com by 210.87.254.105 on 09/05/12
For personal use only.

These results of Table I show that by either calculation the summation to P_A gives very large values. By inclusion of the entire bands (unsym.) the P_{A_j} is 23.2 cc. Limitation to symmetrical absorption still contributes 14.3 cc and neither value includes the minor contributions in the near infrared.

Because of the variation of total polarization for diphenylmercury with respect to temperature, a definite value does not exist. However, an approximate mean value of 69–70 cc may be specified. The difference between this P_T and our extrapolated P_E of 60.2 cc is less than the P_A values (23.2 cc or 14.4 cc) calculated from the spectral data. It would seem that the spectral data are quantitatively meaningless and cannot be used to support the postulation of abnormally high P_A for diphenylmercury. The situation remains unchanged in that not only is there no experimental basis for the postulation but there is experimental proof against it.

It remains to explain the discrepancy between our extrapolated P_E of 60.2 cc and our P_{E+A} of 57.1 cc with crystalline diphenylmercury at 10^6 c.p.s. This discrepancy is profound because P_E ought to be smaller, rather than 3.1 cc larger than P_{E+A}. Actually the discrepancy is not unexpected in view of our measurements of other substances containing phenyl groups (10, 12). Indeed a recent comparison of P_{E+A} for diphenylmercury and dicyclohexylmercury (10) shows that the difference is a property of the phenyl group.

The tendency for substances containing phenyl groups to show abnormal distortion polarization has been authenticated by a large number of examples in this laboratory. An additional and informative example is provided by comparison of P_D for N,N′-diphenyl-2,2,4,4-tetramethyl-1,3-cyclobutanediimine, B, with that of 6,6,12,12-tetramethyl-1,4,8,11-tetroxadispiro-[4,1-4,1]-dodecane, A. Both substances are solids, so their molecular refractions cannot conveniently be measured directly, but MR_D calculated by summation of atom polarizabilities (13) or bond polarizabilities (14) are 90.1 cc and 90.5 cc respectively (mean 90.3 cc) for B, whereas the distortion polarization calculated from measurement of

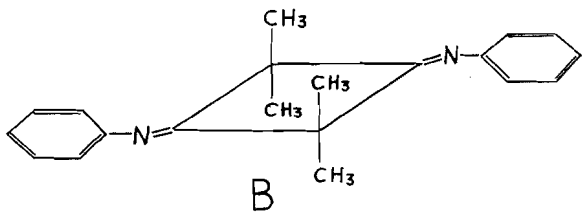

B

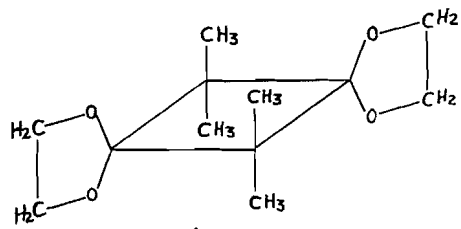

A

the dielectric constant of the compressed solid is 80.7 cc on the basis of a density of 1.098 determined by flotation. This large difference (−9.4 cc), which may be attributed to the presence of phenyl groups, is in marked contrast to the difference (+5.1 cc) between

MR_D (58.2 and 57.6 cc respectively, mean 57.9 cc) and P_D (63.0 cc based on flotation density of 1.20) for the dispirane, A. If the anil, B, has an atom polarization (unlikely) such as may be assigned to A it is hidden by the abnormally high diminution caused by the phenyl groups.

The appreciable number of phenyl substituted substances which have been shown (10) to have lower experimentally determined P_{E+A} values than would be expected from MR values leaves no doubt that a "phenyl effect" exists. One might expect that benzene itself would show the effect strongly but the only report of the dielectric constant of solid benzene (20) states that it leads to a higher rather than lower polarization than the MR_D. However the authors (21) have pointed out that their dielectric constants for solids "can be considered only as approximate" and, in experimental detail, that interspace between plates and dielectric is likely to be present in their apparatus. This interspace, which is not present in our apparatus, would lead to high results. Unfortunately our technique is not applicable to substances which melt below room temperature so a definitive P_{E+A} for benzene by our method is not now available.

If the "phenyl effect" was related to the electronic part of P_{E+A} then it ought to be observed from the refractive index of benzene at visible wavelengths. Actually a slight effect has been noted by Fajans and Bauer (22) and later by Syrkin *et al.* (23) as a small "negative exaltation". However the discrepancy of 0.17–0.3 cc between the Sellmeier extrapolation to MR_∞ of the refractive index of benzene and the MR_D calculated from bond or atom polarizabilities is smaller than we would expect in view of the approximate diminution (roughly 2 cc per phenyl group) which we have found from the dielectric constants of phenyl substituted compounds in the solid state. Of course the difference in spectral region must be considered. At radio frequencies, far from any absorption bands, the effect will not be complicated by anomalous dispersion, which may be expected to enhance the apparent polarization at frequencies slightly lower than those at which phenyl substituted compounds, and benzene itself, absorb in the ultraviolet region. On the basis of the "negative exaltation" of benzene at electronic frequencies the "phenyl effect" must involve the P_E part of the distortion polarization.

Actually the opposite effect, enhancement of reactance due to electron bonding, is the well-known phenomenon of positive exaltation in molecular refraction. This retardation of the speed of electromagnetic radiation at optical frequencies, (increased reactance) should also be observed at radio frequencies. A notable example is found (12) in P_{E+A} from the dielectric constant of crystalline β-carotene. This distortion polarization is 9–10 cc higher than would be calculated from bond or atom polarizabilities and may be attributed to the conjugated system in this substance.

In this sense the conjugation of double bonds, although it involves orbital hybridization, does not resemble benzenoid hybridization in that non-aromatic conjugation retards radiation at frequencies of 5 mc or more whereas benzenoid hybridization accelerates it relative to the equivalent non-conjugated and non-aromatic unsaturation. The two effects may thus be antagonistic as has been noted (10) by contrasting tetraphenylethylene and tetraphenylcyclobutane (12) (P_{E+A} are respectively 12 cc and 8 cc less than additive MR_D) with the tetraphenylated allene, butatriene, and hexyne (items 55–57) of Table I, ref. 10. Likewise the positive exaltation (P_{E+A} = 70.2 cc vs. MR_D = 67.4 cc) of 2.8 cc for 1,4-diphenylbutadiene (12) may be contrasted to a negative exaltation (P_{E+A} = 110.7 cc vs. MR_D = 116.6 cc) of −5.9 cc for 1,1,4,4-tetraphenylbutadiene. Of interest in this connection is 2,3,4,5-tetraphenylpyrrole. The exaltation of 3.5 cc is negative (P_{E+A} = 114.7 cc vs. MR_D = 118.2 cc) but one might have expected the negative value

Can. J. Chem. Downloaded from www.nrcresearchpress.com by 210.87.254.105 on 09/05/12
For personal use only.

to be larger in view of the known negative exaltation of pyrrole (22). However it is probable that pyrroles behave in the same manner as furans, where it has been found (24) that unsaturated substituents reverse the negative exaltation of furan itself to positive values in substituted furans. If the same effect is operative in 2,3,4,5-tetraphenylpyrrole the relatively small negative exaltation may be considered to be a consequence of counteraction between positive exaltation and the "phenyl effect".

We have used the term "phenyl effect" to describe less-than-expected reactance at 5 mc but the term is not limited to benzene and its substituents. The dielectric constants of an appreciable number of crystalline polynuclear aromatic substances have been measured and found to be low (10, 12) but definite correlation must await a larger number of such results as well as a precise method of measuring the concomitant electronic polarization of these solid substances. These studies are in progress.

EXPERIMENTAL

Spectral Studies

Both benzene solutions and polyethylene wax wafers containing diphenylmercury were used for studies with the Beckman IR-4 spectrometer but only the wafers were used in the Perkin–Elmer 301 spectrometer. These wafers were prepared according to the method already outlined (11) but reference wafers were made from the same weight rather than the same thickness of polyethylene wax in the sample wafer because of the relatively high percentage of candidate substance required for the low-frequency spectrometer.

The PE-301 spectrometer was maintained dry by a positive pressure of gas from a liquid nitrogen container. Samples were examined by use of both globar and mercury-arc energy sources with appropriate gratings and restrahlen filters and with scanning rates from 2.75 cm^{-1} per min (grating No. 20) to 1 cm^{-1} per min (grating No. 8).

The spectral intensities were obtained by summation of the 1 cm^{-1} increments on the chart and also by weight-integration of the graph paper.

Densities and Refractive Indices

The refractive indices of solutions of pure diphenylmercury, m.p. 124°, in pure, peroxide-free dioxane at 40 °C and at $\lambda = 5893$ mμ were measured in an Abbe refractometer of precision ± 0.00004. The densities of these solutions were determined by pycnometer in a bath constant to ± 0.02 °C. The experimental data are shown in Fig. 1.

The densities were determined in like manner for 2-butane-bis-mercury at 40° (1.779), 2-butylmercuric chloride at 40° (2.547), and 2-butylmercuric bromide at 50° (2.846). Also the refractive indices were determined at the respective temperatures and from them the molar refractions have been calculated for the several wavelengths and recorded in Table II.

TABLE II

	MR (cc) for wavelengths in Å							
Substance	4341	4360	4800	5460	5770	5893	6563	∞
2-Butane-bis-mercury		53.70		52.70	52.53	52.50		50.3
2-Butylmercuric chloride			38.42	38.33		38.30	38.21	37.9
2-Butylmercuric bromide				42.2	41.9			40.2

Substituted Tetramethylcyclobutanes

The three cyclobutanes used in the study were obtained from the Tennessee Eastman Company and were crystallized to constant melting point from ethanol. Pure A melted at 105–105.5 °C while pure B melted at 141–141.8 °C.

The apparent dielectric constant of various thicknesses of wafers made from N,N′-diphenyl-2,2,4,4-tetramethyl-1,3-cyclobutanediimine, B, and 6,6,12,12-tetramethyl-1,4,8,11-tetroxadispiro-[4,1-4,1]-dodecane, A, have been plotted against wafer thickness to give the extrapolated values 2.317 and 2.486 respectively, shown in Fig. 3. Densities of B and A have been found by flotation to be 1.089 and 1.200 respectively (20 °C). The maintenance of purity during the preparation and measurement of the compressed wafers of the dispirane, A, is shown by the measurement before and after the determination of the X-ray diffraction pattern using Cu (Ni filtered) radiation. The six largest d spacings in angstrom units at intensities I/I_1 for

Can. J. Chem. Downloaded from www.nrcresearchpress.com by 210.87.254.105 on 09/05/12
For personal use only.

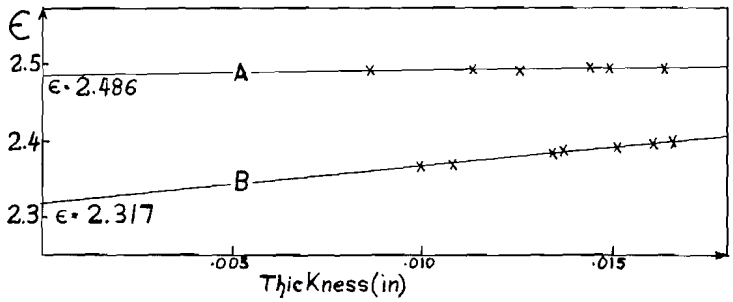

FIG. 3. Apparent dielectric constants vs. wafer thickness: (A) 6,6,12,12-tetramethyl-1,4,8,11-tetroxadispiro-[4,1-4,1]-dodecane, (B) N,N′-diphenyl-2,2,4,4-tetramethyl-1,3-cyclobutanediimine.

the dispirane, A, are: [10] 5.29, [9] 6.19, [8] 6.29, [7] 4.73, [6] 3.23, [5] 5.79, and are the same for both samples, before and after measurement of dielectric constant.

Conjugated Dienes

The melting points of the 1,1,4,4-tetraphenyl-1,3-butadiene and the 2,3,4,5-tetraphenylpyrrole used for determination of solid dielectric constant were 202.3–202.9 °C and 214.3–215.0 °C respectively. The density (flotation) of the tetraphenylbutadiene was 1.2386 at 20° and the extrapolated dielectric constant was 2.863 from which the distortion polarization is calculated to be 110.7 cc. The density (flotation) of the tetraphenylpyrrole at 20° was 1.247 and the extrapolated dielectric constant was 2.883 from which the distortion polarization is calculated as 114.7 cc. The extrapolation plots of apparent dielectric constant versus thickness were as linear as those shown in Fig. 3.

We are grateful to the Defence Research Board for financial support of this investigation and to the Tennessee Eastman Company for ample supplies of the cyclobutanes used in this study. Thanks are due to Drs. E. Whalley and J. Bertie of the National Research Council for use of the PE-301 spectrometer.

REFERENCES

1. G. C. HAMPSON. Trans. Faraday Soc. **30**, 877 (1934).
2. E. I. COOP and L. E. SUTTON. J. Chem. Soc. 1269 (1938).
3. R. S. ARMSTRONG, C. G. LEFEVRE, and R. J. W. LEFEVRE. J. Chem. Soc. 371, (1957).
4. E. N. DICARLO and C. P. SMYTH. J. Am. Chem. Soc. **84**, 1128 (1962).
5. E. CHARNEY. J. Am. Chem. Soc. **83**, 578 (1961).
6. H. SAWATZKY and G. F WRIGHT. Can. J. Chem. **36**, 1555 (1958).
7. E. BERGMANN and W. SCHUTZ. Z. Physik. Chem., B. **19**, 401 (1932).
8. C. C. MEREDITH, L. WESTLAND, and G. F WRIGHT. J. Am. Chem. Soc. **79**, 2385 (1957).
9. K. H. ILLINGER and C. P. SMYTH. J. Chem. Phys. **35**, 400 (1961).
10. W. C. HORNING, F. LAUTENSCHLAEGER, and G. F WRIGHT. Can. J. Chem. **41**, 1441 (1962).
11. M. BEDARD, H. HUBER, J. L. MYERS, and G. F WRIGHT. Can. J. Chem. **40**, 2278 (1962).
12. C. C. MEREDITH and G. F WRIGHT. Can. J. Chem. **38**, 1177 (1960).
13. F. EISENLOHR. Z. Physik. Chem. **75**, 585 (1910); **79**, 129 (1912).
14. A. I. VOGEL. J. Chem. Soc. 134, (1946); 654 (1948).
15. W. K. WILDE. J. Chem. Soc. 72, (1949).
16. W. J. JONES, D. P. EVANS, T. GULWELL, and D. E. GRIFFITHS. J. Chem. Soc. 39, (1935).
17. D. H. WHIFFEN. Trans. Faraday Soc. **54**, 327 (1958).
18. H. HUBER and G. F WRIGHT. Can. J. Chem. **42**, 1446 (1964).
19. R. W. WOOD. Physical optics. Macmillan and Co. 1934. p. 405.
20. C. P. SMYTH. Dielectric behavior and structure. McGraw-Hill, New York. 1955. p. 134.
21. S. O. MORGAN and H. H. LOWRY. J. Phys. Chem. **34**, 2385 (1930).
22. A. WEISSBERGER. Physical methods of organic chemists. Interscience Publishers, New York. 1934. p. 677. H. GILMAN. Organic chemistry. 2nd ed. Wiley, New York. 1943. p. 1752.
23. G. G. KIKINA, YA. K. SYRKIN, and E. A. SHOTT-LVOVA. Izv. Akad. Nauk SSSR, Otd. Khim. Nauk, 563 (1954). Chem. Abstr. **48**, 13316 (1954).
24. E. C. HUGHES and J. R. JOHNSON. J. Am. Chem. Soc. **53**, 737 (1931).

Can. J. Chem. Downloaded from www.nrcresearchpress.com by 210.87.254.105 on 09/05/12
For personal use only.

Can. J. Chem. Downloaded from www.nrcresearchpress.com by 210.87.254.6 on 09/05/12
For personal use only.

SUR LES ÉTHERS ÉNOLIQUES DÉRIVÉS DU FORMYL-3 CAMPHRE*

JEAN-CLAUDE RICHER ET REGINALD CLARKE
Département de Chimie, Université de Montréal, Montréal, Québec

Reçu le 5 mars 1964

RÉSUMÉ

Les spectres r.m.n. d'éthers énoliques dérivés du formyl-3 camphre (I) ont été examinés. L'isomérie *cis–trans* (formes *a* et *b*) autour de la double liaison hydroxyméthylénique a été observée. Des résultats expérimentaux indiquant la présence de la forme aldéhydo-énolique (forme I*c*) dans les solutions éthérées du formyl-3 camphre sont présentés.

INTRODUCTION

Au cours d'une étude récente des spectres de résonance magnétique nucléaire (r.m.n.) des formyl-2 cyclanones, Garbisch (1) a observé que le formyl-3 camphre (I) en solution existe à l'état d'équilibre entre les diverses formes I, I*a* et I*b*. La présence de la forme aldéhydo-énolique I*c* n'a toutefois pas été décelée.

L'examen des spectres r.m.n. des éthers *O*-méthyliques (II), *O*-éthyliques (III), *O*-butylique (IV) et *S*-butyliques (V) dérivés du formyl-3 camphre a permis de confirmer l'existence des isomères *trans* (forme *a*) et *cis* (forme *b*) dans ces éthers. Les travaux que nous rapportons ici ont aussi permis de mettre en évidence des éthers (forme *c*) dérivés de la forme aldéhydo-énolique (I*c*).

RÉSULTATS ET DISCUSSION

La réaction du formyl-3 camphre (I) avec le diazométhane, le diazoéthane, le méthanol, l'éthanol, le butanol-1 ou le butanethiol-1 (2) conduit aux éthers *O*-méthyliques (II), *O*-éthyliques (III), *O*-butylique (IV) ou *S*-butyliques (V) qui peuvent théoriquement exister sous les formes *a*, *b* ou *c*. La chromatographie de ces éthers sur plaques minces (3) montre d'ailleurs que les dérivés ne sont pas homogènes. Les résultats de ces chromatographies, rapportés dans le Tableau I, seront donc interprétés en fonction de la présence des formes *a*, *b* ou *c* dans les produits.

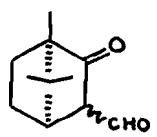

I

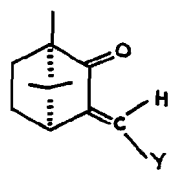

a

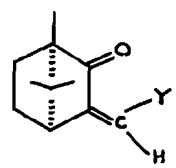

b

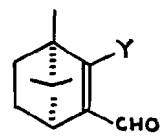

c

I*a*	Y = OH	I*b*	Y = OH	I*c*	Y = OH
II*a*	Y = OMe	II*b*	Y = OMe	II*c*	Y = OMe
III*a*	Y = OEt	III*b*	Y = OEt	III*c*	Y = OEt
IV*a*	Y = OBu	IV*b*	Y = OBu	IV*c*	Y = OBu
V*a*	Y = SBu	V*b*	Y = SBu	V*c*	Y = SBu

**Les résultats rapportés dans cette communication sont extraits du mémoire soumis par R. Clarke à la Faculté des Sciences de l'Université de Montréal en vue de l'obtention du grade de Maître ès Sciences. Ces travaux ont été présentés en partie devant le 31ème congrès annuel de l'Association Canadienne-Française pour l'Avancement des Sciences tenu à Québec, Québec, en novembre 1963.*

Afin de déterminer la nature des divers produits composant ces mélanges, les spectres r.m.n. de ces éthers ont été déterminés et les résultats les plus significatifs sont présentés dans le Tableau II.

TABLEAU I

Chromatographie sur plaques minces*

Éther	Mode de préparation	Nombre de taches	R_f
II	Méthanol	2	0.88 0.75
II	Diazométhane	3	0.88 0.75 0.25
III	Éthanol	1	0.88
III	Diazoéthane	3	0.88 0.75 0.25
IV	Butanol-1	1	0.63
V	Butanethiol-1	2	0.56 0.35

*Ces chromatographies sont réalisées à l'aide de couches de 250 microns de Silica Gel G. Les éthers examinés sont appliqués sous forme de solution dans l'éther de pétrole, et les chromatogrammes sont développés au moyen d'une solution méthanol et benzène 2:98. Les produits sont révélés sous forme de taches bleues sous l'action d'une solution à 2% de chlorure ferrique dans le *n*-butanol.

TABLEAU II

Spectres de résonance magnétique nucléaire*

Produits	Préparation	Protons oléfiniques		Aldéhydiques,	Groupes méthoxyles	
		Forme *a*	Forme *b*	forme *c*	Formes *a*, *b*	Forme *c*
I†	—	7.35 (50)	6.78 (41)	9.58 (6) 9.63 (3)		
II	Méthanol	6.75 (92)	6.57 (8)		3.70 (100)	
II	Diazométhane	6.73 (52)	6.58 (40)	9.42 (8)	3.70 (92)	4.00 (8)
III	Éthanol	6.83 (100)				
III	Diazoéthane	6.80 (80)	6.60 (10)	9.50 (10)		
IV	Butanol-1	6.80 (100)				
V	Butanethiol-1	6.85 (58)	6.27 (42)			

*Les spectres r.m.n. ont été mesurés à l'aide d'un appareil Varian A-60 pour des solutions dans CCl_4 à moins d'indications contraires. La position des bandes (échelle δ) en p.p.m. se réfère au tétraméthylsilane utilisé comme standard interne. Les valeurs entre parenthèses indiquent la proportion de chacune des formes dans le mélange considéré.
†Ce spectre a été mesuré à l'aide d'une solution à 10% dans l'éthoxyéthane.

SUR L'ISOMÉRIE *cis–trans* DANS LES DÉRIVÉS HYDROXYMÉTHYLÉNIQUES

Les résultats rapportés dans le présent travail nous permettent de constater que les produits isomères (I*a* et I*b*) dérivés du formyl-3 camphre (I) existent en solution dans l'éthoxyéthane dans la proportion 55/45. Ces résultats complémentent ceux de Garbisch (1) qui a observé que la proportion relative d'isomères *cis/trans* (I*b*/I*a*) varie de 95/5 pour une solution à 10% dans le CCl_4 jusqu'à 22/78 pour une solution à 14% dans du CCl_4 contenant 8% de diméthylsulfoxyde.

L'isomérie *cis–trans* autour de la double liaison hydroxyméthylénique est aussi observée dans les éthers énoliques préparés (II–V). La proportion de formes *cis* (*b*) et *trans* (*a*) dans ces éthers varie suivant le mode de préparation et le substituant introduit. Les résultats suivants montrent l'influence du mode de préparation: dans l'éther méthylique (II) préparé selon un procédé où le contrôle de la réaction est cinétique (réaction de I en solution dans l'éthoxyéthane avec le diazométhane) on note que la proportion d'isomères *cis/trans* (II*b*/II*a*) est de 56/44 alors que cette proportion est de 8/92 dans l'éther préparé dans des conditions où le contrôle de la réaction est thermodynamique. Dans le cas de l'éther éthylique (III) les proportions d'isomères *cis/trans* (III*b*/III*a*) sont respectivement de 11/89 et 0/100 pour des réactions où le contrôle est cinétique et thermodynamique.

Can. J. Chem. Downloaded from www.nrcresearchpress.com by 210.87.254.6 on 09/05/12
For personal use only.

Lorsque des conditions expérimentales favorisant un équilibre thermodynamique des produits sont employées pour préparer les éthers, on note chez les éthers *O*-alcoylés que les deux isomères stable (forme *a*) et instable (forme *b*) ne se forment que dans le cas des dérivés méthylés (II) où le substituant est peu volumineux. Seul l'isomère thermodynamiquement le plus stable (III*a* ou IV*a*) se forme lorsque le substituant devient plus volumineux. Le fait que les deux isomères *cis* (V*b*) et *trans* (V*a*) soient présents dans l'éther *S*-butylique (V) alors que seul l'isomère le plus stable (*trans*, IV *a*) est présent dans l'éther *O*-butylique, s'explique grâce à la différence de longueur des liens C–S (1.80 Å) et C–O (1.40 Å) (4). Le lien C–S plus long éloignerait le groupe butyle du carbonyle avec lequel il interfère et permettrait une accommodation plus facile de ce radical volumineux. Une explication de ce type est avancée par Eliel (5) pour rendre compte du fait que les dérivés sulfurés occupent plus facilement les configurations axiales que les dérivés oxygénés.

SUR LA PRÉSENCE DE LA FORME ALDEHYDO-ÉNOLIQUE (I*c*) DANS LES SOLUTIONS ÉTHÉRÉES DU FORMYL-3 CAMPHRE

Le traitement d'une solution éthérée de formyl-3 camphre (I) par un excès de diazométhane conduit à l'éther méthylique (II) dont le spectre r.m.n. montre une bande aldéhydique à 9.42 p.p.m. Ce résultat indique que l'éther II*c* est présent dans le produit et cette conclusion est confirmée grâce aux observations suivantes: l'éther méthylique (II) préparé par réaction du formyl-3 camphre (I) avec du méthanol consiste en un mélange de produits II*a* et II*b* (voir plus haut); alors que le spectre r.m.n. de ce produit ne montre qu'un pic à 3.70 p.p.m. dans la région des groupes méthoxyles celui de l'éther méthylique II obtenu par l'action du diazométhane montre en plus du pic à 3.70 p.p.m. une bande à 4.00 p.p.m. Cette dernière bande serait due au groupe méthoxyle présent dans la forme II*c*. La présence de cet éther aldéhydo-énolique (II*c*) dans le produit réactionnel implique que la forme aldéhydo-énolique I*c* est présente en quantité finie en solution éthérée. Les pics aldéhydiques dans le spectre r.m.n. du formyl-3 camphre (I) représentent un maximum de 9% du produit total; on peut donc conclure que cette valeur indique une limite supérieure à la quantité possible de la forme I*c* dans la solution.

Le spectre r.m.n. du formyl-3 camphre (I) en solution dans l'éthoxyéthane montre des bandes à 9.58 et 9.63 p.p.m. Ces pics correspondant à ceux (9.62 et 9.68 p.p.m.) observés par Garbisch (1) pour des solutions de I dans le CCl_4 indiquent la présence d'aldéhydes dans le milieu et ont été attribués (1) aux formes exo (I exo) et endo (I endo) du formyl-3 camphre non énolisé.

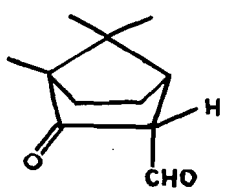

I endo

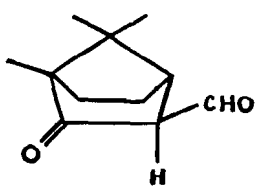

I exo

Deux explications alternatives à celle de Garbisch (1) pourraient être avancées pour rendre compte de la présence de deux bandes aldéhydiques dans le spectre r.m.n. du formyl-3 camphre (I) en solution:

(A) Une des bandes serait due au proton aldéhydique du formyl-3 camphre (I) non énolisé alors que l'autre serait due à la forme aldéhydo-énolique (I*c*).

Can. J. Chem. Downloaded from www.nrcresearchpress.com by 210.87.254.6 on 09/05/12
For personal use only.

(B) Les deux bandes pourraient être dues aux formes aldéhydo-énoliques libre (I*c* libre) et liée (I*c* liée).

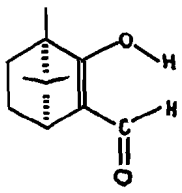

I*c* libre

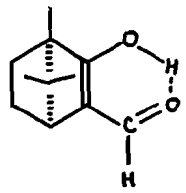

I*c* liée

Ces deux explications alternatives rendraient compte du fait que la forme aldéhydo-énolique (I*c*) est présente dans la solution et d'autre part que le pic aldéhydique de l'éther II*c* est unique. Les résultats récents de Anet (6) sur l'énergie d'activation nécessaire pour la rotation du groupe aldéhydique rendent l'alternative B moins plausible que l'alternative A; les faits connus actuellement ne nous permettent toutefois pas de faire un choix définitif entre ces diverses alternatives.

PARTIE EXPÉRIMENTALE

Les points de fusion ont été déterminés en tubes capillaires ouverts au moyen d'un thermomètre étalonné avec des substances pures de p.f. connus. Les spectres infrarouges ont été mesurés sur un appareil Perkin–Elmer modèle 21, prisme NaCl. Les indices de réfraction ont été déterminés à l'aide d'un réfractomètre Abbé 60. Les indices de rotation ont été mesurés au moyen d'un polarimètre Bellingham et Stanley, modèle A; à moins d'indication contraire, ces indices ont été déterminés pour des solutions à 4% dans de l'éthanol 95%. Les analyses élémentaires sont de C. Daesslé, Organic Microanalysis, Montréal. Les spectres ultraviolet ont été déterminés en solution éthanolique à l'aide d'un spectrophotomètre Perkin–Elmer, modèle 4000-A.

1. Synthèse du formyl-3 camphre

Le formyl-3 camphre, obtenu par réaction du formiate d'éthyle sur le sodio-3 camphre, fond à 78–80° (litt. (7) 80–81°) et présente un indice de rotation de +204.1° (litt. (7) +198°).

2. Préparation des dérivés du formyl-3 camphre

2.1. Éther méthylique dérivé du formyl-3 camphre

2.11. Action du méthanol.—Une solution de 3 g (17 moles) de formyl-3 camphre, 2 ml de méthanol et 50 mg d'acide *p*-toluènesulfonique dans 30 ml de benzène anhydre est chauffée à reflux sous atmosphère d'azote. L'eau formée au cours de la réaction est éliminée à l'aide d'un décanteur du type Dean–Stark. Lorsqu'il n'y a plus d'eau qui se forme le benzène est éliminé et le produit repris par de l'éther. La solution éthérée est lavée avec une solution aqueuse de soude 10%, lavée avec de l'eau jusqu'à neutralité, séchée sur du sulfate de sodium anhydre, et évaporée au travers d'une colonne Widmer (30 cm).

L'éther méthylique (II) purifié par distillation présente les caractéristiques suivantes: p.é. 86° à 0.6 mm Hg (litt. (8) 143.5° à 17 mm); $[\alpha]_D^{26}$ +201.6°; n_D^{26} 1.5082 (litt. (8) n_D^{25} 1.509). Spectre r.m.n.: protons éthyléniques à 6.75 p.p.m. et 6.57 p.p.m.; groupe méthoxyle à 3.70 p.p.m.

2.12. Action du diazométhane.—À 2 g de formyl-3 camphre en solution dans 10 ml d'éther anhydre, on ajoute une solution éthérée de diazométhane préparée selon Vogel (9). Le produit isolé à la manière habituelle est purifié par distillation et présente les caractéristiques suivantes: p.é. 90° à 1 mm; $[\alpha]_D^{26.5}$ +200.6°; n_D^{26} 1.5091. Spectre r.m.n.: proton aldéhydique à 9.42 p.p.m.; protons éthyléniques à 6.73 p.p.m. et 6.58 p.p.m.; groupes méthoxyles à 4.00 p.p.m. et 3.70 p.p.m.

2.2. Éther éthylique (III) dérivé du formyl-3 camphre

2.21. Action d'éthanol.—L'action de 2 ml d'éthanol sur 3.0 g de formyl-3 camphre dans les conditions décrites à la section 2.11 fournit l'éther éthylique III avec un rendement de 80%. Le produit purifié par distillation présente les caractéristiques suivantes: p.é. 91° à 0.6 mm (litt. (10) 147° à 17 mm); $[\alpha]_D^{26}$ +196.5°; n_D^{26} 1.5015 (litt. (10) n_D^{17} 1.5047). Spectre r.m.n.: proton éthylénique à 6.80 p.p.m.

2.22. Action du diazométhane.—La réaction du formyl-3 camphre avec une solution éthérée de diazoéthane préparée selon la méthode de Adamson (11) conduit à l'éther éthylique (III) qui, après purification par distillation, présente les caractéristiques suivantes: p.é. 95° à 1 mm; $[\alpha]_D^{26}$ +195.8°; n_D^{25} 1.5049. Spectre r.m.n.: proton aldéhydique à 9.50 p.p.m.; protons éthyléniques à 6.80 p.p.m. et 6.60 p.p.m.

Can. J. Chem. Downloaded from www.nrcresearchpress.com by 210.87.254.6 on 09/05/12
For personal use only.

2.3. Éther butylique (IV) dérivé du formyl-3 camphre

L'action de 5 ml de butanol-1 sur 6.0 g de formyl-3 camphre dans des conditions semblables à celles décrites à la section 2.11 conduit à l'éther butylique (IV) avec un rendement de 78%. Une fraction analytique présente les caractéristiques suivantes: p.é. 103° à 0.2 mm; $[\alpha]_D^{25}$ +173.2°; n_D^{26} 1.4942. Spectre ultraviolet: λ_{max} 268 mμ, log ε 4.14. Spectre r.m.n.: proton éthylénique à 6.80 p.p.m. Anal. Calc. pour $C_{15}H_{24}O_2$: C, 76.22; H, 10.23. Trouvé: C, 76.37; H, 10.08.

2.4. Éther thiobutylique (V) dérivé du formyl-3 camphre

L'action de 9.0 g (0.1 mole) de butanethiol-1 sur 10 g (0.056 mole) de formyl-3 camphre dans des conditions semblables à celles décrites par Ireland (2) a conduit à 9.5 g (67.5% du rendement théorique) de l'éther désiré (V). Une fraction analytique présente les caractéristiques suivantes: p.é. 127° à 1 mm; $[\alpha]_D^{26}$ +236.7°; n_D^{26} 1.5362. Spectre ultraviolet: λ_{max} 315 mμ, log ε 4.18. Spectre r.m.n.: protons éthyléniques à 6.85 et 6.27 p.p.m. Anal. Calc. pour $C_{15}H_{24}OS$: C, 71.38; H, 9.58; S, 12.70%. Trouvé: C, 71.22; H, 9.40; S, 12.82%.

REMERCIEMENTS

Les auteurs remercient le Conseil National de Recherches pour l'aide financière apportée sous forme d'octroi de recherches.

BIBLIOGRAPHIE

1. E. GARBISCH. J. Am. Chem. Soc. **85**, 1696 (1963).
2. R. IRELAND et J. MARSHALL. J. Org. Chem. **27**, 1615 (1962).
3. E. STAHL. Angew. Chem. **73**, 646 (1961).
4. G. W. WHELAND. Resonance in organic chemistry. John Wiley and Sons. 1955. p. 732.
5. E. L. ELIEL et L. A. PILATO. Tetrahedron Letters, 103 (1962).
6. F. A. L. ANET et M. AHMAD. J. Am. Chem. Soc. **86**, 119 (1964).
7. W. J. POPE et J. READ. J. Chem. Soc. **103**, 445 (1913).
8. K. VON AUWERS. Ann. **415**, 169 (1918).
9. A. VOGEL. Practical organic chemistry. Longmans, Green & Co., Inc., 1959. p. 969.
10. J. W. BRÜHL. J. Prakt. Chem. Ser. 2, **50**, 137 (1894).
11. D. W. ADAMSON et J. KENNER. J. Chem. Soc. 1551 (1937).

Can. J. Chem. Downloaded from www.nrcresearchpress.com by 210.87.254.6 on 09/05/12
For personal use only.

Can. J. Chem. Downloaded from www.nrcresearchpress.com by 210.87.254.42 on 09/05/12
For personal use only.

LA DÉTERMINATION DU RAYON DE GIRATION DES MACROMOLÉCULES EN CHAÎNES DANS LES BONS SOLVANTS PAR DIFFUSION DE LA LUMIÈRE[1]

JACQUES PRUD'HOMME ET YVON SICOTTE
Laboratoire de Chimie Physique, Université de Montréal, Montréal, Québec

Reçu le 20 avril 1964

RÉSUMÉ

L'approximation de Zimm pour la détermination des rayons de giration des macromolécules en chaînes en solution par diffusion de la lumière a des limites d'utilisation très étroites. D'une façon presque générale, il faut connaître à priori la forme de la distribution angulaire d'intensité de diffusion pour en tirer la valeur du rayon de giration. Dans le cas des bons solvants, la fonction approchée de Peterlin–Benoît–Ptitsyn semble très bien représenter les données expérimentales.

INTRODUCTION

Debye (1) et Zimm (2) ont montré comment on pouvait déterminer les dimensions des macromolécules en solution par l'étude de la fonction $P(\theta)$, c'est à dire la variation angulaire de l'intensité de diffusion. En particulier, on sait que près de l'origine la fonction $P(\theta)$ ne dépend que du rayon de giration S de la molécule par rapport à son centre de masse. Guinier (3) a montré en effet que l'éq. [1]:

$$P(\theta) = e^{-u/3} \qquad [1]$$

constitue une approximation excellente près de l'origine pour n'importe quelle forme de particules, où u représente $4\pi^2\sigma^2S^2$, σ est la quantité $(2/\lambda)\sin(\theta/2)$ et λ est la longueur d'onde de la lumière incidente mesurée dans le milieu. Zimm a utilisé (2) une expression analogue:

$$P^{-1}(\theta) = 1 + u/3 \qquad [2]$$

pour calculer le rayon de giration à partir de la pente à l'origine. L'équation [2] est contituée en fait des deux premiers termes du développement en série de n'importe quelle fonction $P(\theta)$. Cette approximation ne sera utilisable par conséquent que pour des valeurs relativement faibles de u. L'intervalle de la variable expérimentale σ qui est accessible à l'aide d'un appareil donné est fixé par la longueur d'onde de la radiation utilisée et par l'intervalle angulaire exploré. Par contre la région de u étudiée sera fonction du rayon de giration. Par conséquent si le rayon de giration est assez grand, la pente à l'origine ne sera pas accessible directement: c'est-là une chose connue depuis très longtemps. Par ailleurs la région d'utilisation de l'approximation de Zimm variera suivant la forme de la fonction $P(\theta)$. Pour chaque forme de particule, il faut donc étudier le domaine d'utilisation de cette approximation.

Lorsque la pente à l'origine n'est pas accessible directement, on doit choisir à priori une fonction $P(\theta)$ pour évaluer le rayon de giration. Pour un certain nombre de cas particuliers, la fonction $P(\theta)$ est connue. Par exemple on sait que pour une macromolécule en chaîne en solvant Θ, c'est à dire quand les interactions entre chaînons éloignés s'annulent, on obtient, comme loi de probabilité caractérisant la répartition des distances

[1]*Les résultats utilisés dans le présent travail sont tirés du mémoire de Maîtrise ès Sciences en Chimie présenté par l'un de nous (J. P.) à la Faculté des Sciences de l'Université de Montréal (1964).*

entre deux chaînons, une loi de Gauss. Debye (4) a calculé la fonction $P(\theta)$ pour cette chaîne gaussienne:

$$P(\theta) = 2(e^{-u} - 1 + u)/u^2. \quad [3]$$

En solvant non Θ, on sait que la chaîne n'est plus gaussienne, et pour obtenir le $P(\theta)$ dans ce cas, il faudrait tenir compte de la perturbation introduite par l'effet de solvant dans la configuration de la molécule. Cet effet de solvant, ou effet de volume exclu, a fait l'objet récemment d'un grand nombre de travaux théoriques: voir à ce sujet les revues de Ptitsyn (5) et de Kurata et Stockmayer (6). Malheureusement les résultats obtenus à date sont sous forme de séries à convergence très lente dont on n'a réussi à évaluer que les premiers termes (7), de sorte qu'on ne peut les utiliser que pour des solvants très voisins des solvants Θ. La fonction $P(\theta)$ a d'ailleurs été calculée rigoureusement dans ces conditions (8, 9) où elle se confond en pratique avec l'éq. [3].

Dans le cas des bons solvants, Peterlin (10) a donné une solution qui tient compte au moins partiellement du caractère non gaussien de la chaîne. Expérimentalement on sait que, quelque soit le solvant, la relation entre le carré moyen de la distance entre les bouts de la chaîne et la masse moléculaire peut s'écrire sous la forme:

$$\langle L^2 \rangle \simeq M^{\mu}. \quad [4]$$

Une des façons d'obtenir l'éq. [4] est de supposer que le carré moyen de la distance entre le chaînon i et le chaînon $i + p$ est donné par $p^{\mu}b^2$, quelque soit p; b et μ sont des paramètres caractérisant un système polymère—solvant donné. En solvant Θ, μ serait égal à l'unité. Si on admet que la loi de distribution des distances n'est pas sérieusement perturbée par l'effet de solvant et qu'on peut toujours la considérer comme gaussienne, on obtient la fonction approchée suivante (10–12):

$$P(\theta) = \frac{2}{N^2} \int_{p=0}^{N} (N - p) \exp\{-2\pi^2\sigma^2 b^2 p^{\mu}/3\} dp, \quad [5]$$

ce qui donne pour le rayon de giration:

$$\langle S^2 \rangle = \frac{b^2 N^{\mu}}{(1 + \mu)(2 + \mu)}. \quad [6]$$

N est le nombre de chaînons. Benoît (11) et Ptitsyn (12) ont montré comment évaluer par des séries l'intégrale [5]. Elle a d'ailleurs été calculée directement à l'aide d'un calculateur numérique (13). Cette fonction $P(\theta)$ approchée a été utilisée par de nombreux chercheurs (voir par exemple les références 10 à 19), mais en général la polydispersité des échantillons utilisés ne permettait pas de vérification critique de cette fonction, sauf aux grandes valeurs de u où l'effet de la polydispersité est beaucoup moins important.

Par ailleurs plusieurs études récentes du problème de volume exclu, faites à l'aide de calculateurs numériques (20–25) semblent indiquer clairement que la loi de distribution des distances est fortement perturbée par l'effet de volume exclu, contrairement à l'hypothèse sous laquelle l'éq. [5] a été obtenue. Cette perturbation, si vraiment elle est importante, devrait évidemment se faire sentir, au moins dans une région du $P(\theta)$, et une comparaison entre l'éq. [5] (obtenue sans tenir compte de cet effet) et les résultats expérimentaux devrait nous permettre d'évaluer l'importance de cette perturbation de la loi de distribution des distances.

Puisqu'il semble que pour les hautes valeurs de u l'éq. [5] représente très bien les

Can. J. Chem. Downloaded from www.nrcresearchpress.com by 210.87.254.42 on 09/05/12
For personal use only.

résultats expérimentaux, (13–16), nous avons voulu étendre cette vérification vers les basses valeurs de u, c'est à dire jusqu'à la région près de l'origine où l'éq. [2] devient valide. Pour cela nous avons entrepris l'étude d'une série de fractions de polystyrène les plus monodispersées possibles.

PARTIE EXPÉRIMENTALE

Le polymère brut a été obtenu de la maison Dow Corning (échantillon B-25). Les fractions ont été obtenues d'une solution à 1% dans la butanone par addition de quantités croissantes de méthanol. Les fractions ainsi obtenues ont été redissoutes par élévation de température puis reprécipitées par retour lent à la température initiale. Douze fractions ont ainsi été obtenues dont six ont été utilisées pour le présent travail. Les solvants utilisés étaient de qualité "Reagent" et ont été redistillés dans une colonne de 2 mètres de hauteur, garnie d'hélices de verre, sous un rapport de reflux de un à dix.

Pour chaque fraction, on a préparé une solution mère par pesée. Les autres solutions ont été préparées par dilution volumétrique. Les mesures ont été prises pour cinq concentrations dans chaque cas. Toutes les solutions ont été dépoussiérées par centrifugation dans un appareil Lourdes (LCA 1–37 000 g) durant 1 heure.

Les mesures de diffusion de la lumière ont été effectuées à l'aide du photogoniodiffusomètre de Wippler et Scheibling (26) fabriqué par SOFICA. Le benzène a été utilisé comme standard pour calibrer l'appareil en prenant comme valeur du rapport de Rayleigh pour ce liquide, à 5461 Å, 17.2×10^{-6} (27).

RÉSULTATS ET DISCUSSION

Pour chaque fraction, les résultats expérimentaux, $c/I(\theta)$, ont été extrapolés à concentration nulle pour chaque angle d'observation par la méthode des moindres carrés: c est la concentration en grammes de soluté par millilitre de solution, et $I(\theta)$ est l'intensité de diffusion normée. Pour retrouver le rayon de giration et la masse moléculaire, on trace alors une courbe de log $P(\theta)$ en fonction de log u et on superpose par translation $x - y$ la courbe log $[c/I(\theta)]_{c=0}$ en fonction de log σ^2. La superposition des abcisses expérimentales (en σ^2) et théoriques (en u) donne log $4\pi^2S^2$. La superposition des ordonnées donne log M. Cette méthode (28) donne évidemment les mêmes résultats que la méthode maintenant classique de Zimm (2) dans les cas où la pente à l'origine est directement accessible à l'expérience. Il importe cependant de noter que le fait que cette dernière condition ne soit pas remplie ne se traduit pas nécessairement par l'apparition d'une courbure évidente dans le diagramme de Zimm. En effet, sur un intervalle de u donné, les erreurs expérimentales normales peuvent noyer complètement l'effet de courbure, et si on prend alors la pente moyenne sur cet intervalle comme une mesure du rayon de giration, éq. [2], on fait une erreur qui peut être importante. La Fig. 1 montre un exemple de diagramme de Zimm obtenu. Aux erreurs d'expérience près, il n'y a pas de courbure évidente, et pourtant on n'est certainement pas dans la région où l'éq. [2] peut s'appliquer. La pente à l'origine obtenue par la méthode décrite plus haut est également tracée sur la Fig. 1: elle conduit à attribuer au rayon de giration une valeur de 530 Å, alors que la pente moyenne de la "droite" expérimentale conduirait à 575 Å. Zimm a d'ailleurs proposé une méthode (2) pour corriger point par point les résultats expérimentaux, dans le cas de la chaîne gaussienne, et les ramener sur la "tangente limite" équivalente, donnée par l'éq. [2].

Dans le cas qui nous intéresse de la chaîne en bon solvant, si on admet au moins à titre d'hypothèse de travail la validité de l'éq. [5], il n'est pas étonnant que les résultats expérimentaux semblent donner une droite. En effet nous avons tracé à la Fig. 2 le $P^{-1}(\theta)$ obtenu pour $\mu = 1.17$. La concavité de cette courbe dans la région étudiée est toujours très faible. Elle est nulle près de l'origine où l'éq. [2] s'applique pour donner la pente à l'origine (prolongée en pointillés). La concavité est ensuite dirigée vers le haut, puis repasse par zéro pour être ensuite dirigée vers le bas. Il en résulte qu'une droite peut constituer une excellente approximation à cette courbe si on admet une incertitude de

Can. J. Chem. Downloaded from www.nrcresearchpress.com by 210.87.254.42 on 09/05/12
For personal use only.

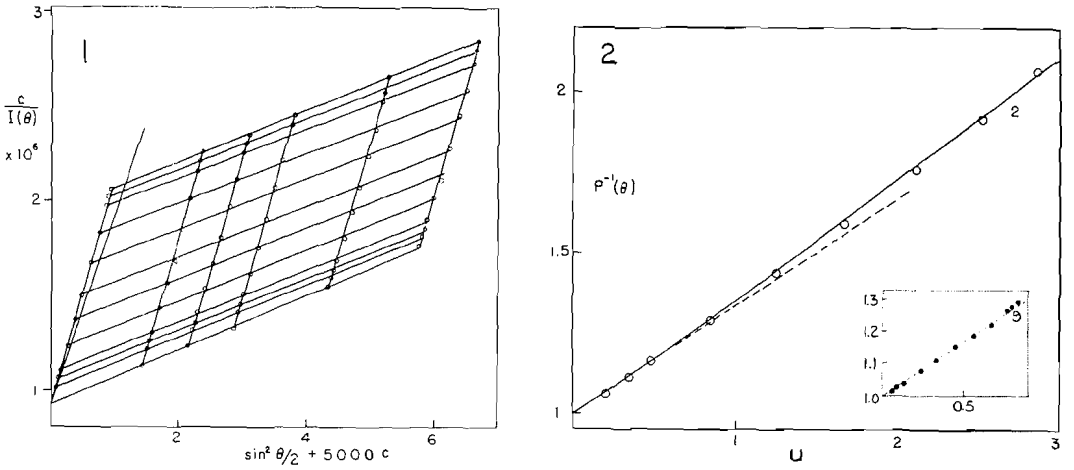

FIG. 1. Diagramme de Zimm pour la fraction B-25-2 en solution dans le toluène, à 25 °C, à 5461 Å.
FIG. 2. Comparaison des données de diffusion à dilution infinie de la fraction B-25-2 et de la courbe théorique (éq. [5] pour $\mu = 1.17$). En médaillon, la fraction B-25-9.

1 ou 2%. Et de fait, comme on le voit, les résultats expérimentaux se superposent aussi bien à la courbe de la Fig. 2 qu'à la droite de la Fig. 1. L'équation [2] a donc des limites d'utilisation assez étroites et nous avons préféré procéder systématiquement par superposition des données expérimentales aux courbes théoriques.

Il faut évidemment pour tracer la courbe théorique choisir une valeur pour le paramètre μ. Théoriquement on pourrait tirer la valeur de ce paramètre des données de diffusion de la lumière elles-mêmes. Particulièrement à haute valeur de u, le $P(\theta)$ est très sensible à la valeur de μ (13, 14). Par contre, puisque nous sommes dans la région des basses valeurs de u, région qui se prête moins bien à la détermination de μ, nous avons préféré suivre la suggestion de Loucheux, Weill et Benoît (14, 15) et tirer μ de la relation empirique entre viscosité intrinsèque et masse moléculaire:

$$[\eta] = KM^a. \qquad [7]$$

En effet, si on admet la relation de Flory (29):

$$[\eta] = \phi \frac{\langle L_0^2 \rangle^{3/2}}{M} \alpha^3, \qquad [8]$$

où ϕ est une constante universelle, $\langle L_0^2 \rangle$ est le carré moyen de la distance entre les bouts de la chaîne en solvant Θ, et $\alpha^2 = \langle L^2 \rangle / \langle L_0^2 \rangle$, on obtient:

$$\mu = [2(a + 1)]/3. \qquad [9]$$

Si on utilise plutôt la relation de Kurata et Yamakawa (30),

$$[\eta] = \phi \frac{\langle L_0^2 \rangle^{3/2}}{M} \alpha^{2.43}, \qquad [10]$$

on obtient:

$$\mu = [2(a + 0.715)]/2.43. \qquad [11]$$

En pratique les deux relations entre a et μ diffèrent très peu. En utilisant pour a la

Can. J. Chem. Downloaded from www.nrcresearchpress.com by 210.87.254.42 on 09/05/12
For personal use only.

valeur 0.72 (31), on obtient pour μ 1.15 ou 1.18. Puisque les $P(\theta)$ correspondant à ces deux valeurs seront très peu différents, nous avons choisis d'utiliser 1.17.

Sur la Fig. 3, nous avons représenté l'ensemble des points expérimentaux, superposés à la courbe tirée de l'éq. [5], pour les six fractions étudiées. Pour plus de clarté nous avons pour chaque fraction successivement décalé la courbe et les points expérimentaux vers le bas. Sur la Fig. 3, les différentes courbes sont identifiées par le numéro de la fraction.

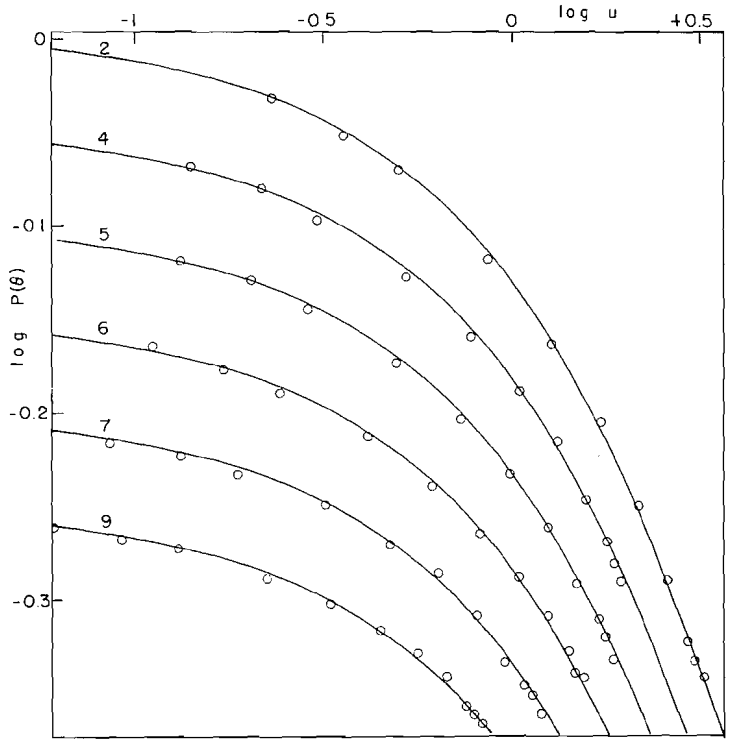

FIG. 3. Superposition de l'ensemble des résultats à la courbe théorique (éq. [5] pour μ = 1.17).

De la superposition des données expérimentales et de la courbe théorique, nous avons obtenu les valeurs de masses moléculaires et de rayons de giration rapportés au Tableau I. Nous avons également rapporté au Tableau I les valeurs de masses moléculaires et de rayons de giration obtenues à l'aide d'un diagramme de Zimm (éq. [2]).

TABLEAU I

Masses moléculaires et rayons de giration obtenus

	Masse moléculaire ($\times 10^{-5}$)		Rayon de giration (Å)		
Fraction	Éq. [5]	Éq. [2]	Éq. [5]	Éq. [2]	Éq. [3]
2	10.6	10.8	530	575	516
4	7.4	7.5	425	444	413
5	7.0	7.0	414	435	404
6	6.1	6.1	373	385	364
7	4.9	4.9	324	336	326
9	3.9	3.9	275	279	272

Can. J. Chem. Downloaded from www.nrcresearchpress.com by 210.87.254.42 on 09/05/12
For personal use only.

On voit donc, comme il fallait s'y attendre, que l'utilisation de l'éq. [2] peut amener des erreurs importantes pour les hautes valeurs de rayons de giration, erreurs par contre qui ne sont pas apparentes à l'examen du diagramme de Zimm. Evidemment lorsque le rayon de giration est assez petit, les deux méthodes, éq. [2] et éq. [5], donnent des résultats identiques. A titre d'exemple, nous avons tracé à la Fig. 2, en médaillon, les données correspondant à la fraction 9. On voit que dans ce cas, avec les mêmes angles d'observation, la pente à l'origine se dessine très nettement, contrairement au cas de la fraction 2.

Plusieurs des déterminations apparaissant au Tableau I ont été reprises deux ou trois fois. Les résultats de rayon de giration obtenus de cette façon, pour une même fraction, en utilisant une fonction $P(\theta)$ donnée, sont cohérents à 1 ou 2% près; mais ceci ne peut évidemment pas être interprété comme étant la précision des mesures, puisqu'il peut se produire des erreurs systématiques.

On voit également au Tableau I que les masses moléculaires obtenues à l'aide de l'éq. [2] ou de l'éq. [5] ne diffèrent pas d'une façon significative.

Pour fins de comparaison, nous avons également déterminé les rayons de giration par superposition des données expérimentales à la fonction $P(\theta)$ de Debye (éq. [3]). On voit que la différence entre les résultats obtenus à l'aide de l'éq. [3] et à l'aide de l'éq. [5] sont faibles dans la région de u où nous sommes: la différence maximum est de 3% (fraction 2) ce qui dépasse à peine la cohérence des mesures. Cette faible différence n'est pas surprenante. En effet Debye a montré récemment (32) que l'éq. [3] se superpose aux données de diffusion en bons solvants, aux erreurs d'expérience près (5% près dans son cas), dans cette région de u où nous sommes. Nous pouvons reprendre la même affirmation, avec cette fois une précision de l'ordre de 1% sur les intensités de diffusion. Cette affirmation, et il faut le souligner, ne vaut évidemment que pour la région de u où nous avons travaillé. Aux plus hautes valeurs de u (11–19), on sait que l'équation de Debye (éq. [3]) ne se superpose plus aux données expérimentales, alors que l'équation de Péterlin (éq. [5]) semble être valide jusqu'à des valeurs de u très élevées.

CONCLUSION

La région d'utilisation de l'approximation de Zimm (éq. [2]) apparait comme étant très étroite. Dans le cas des macromolécules en chaînes, dès que le rayon de giration atteint quelques centaines d'angstroms, la pente à l'origine de la distribution angulaire d'intensité de diffusion n'est plus accessible directement avec les appareils courants, et ceci se produit bien avant que n'apparaisse une courbure évidente dans le diagramme de Zimm. En effet, pour les macromolécules en chaînes, spécialement en bons solvants, il semble que la fonction $P(\theta)$ soit telle que, dans une région assez étendue de u, on obtienne pratiquement des droites dont la pente cependant n'est pas nécessairement celle de l'éq. [2]. En conséquence, sauf pour les molécules relativement petites, il faut se donner à priori une fonction $P(\theta)$ pour pouvoir déterminer la rayon de giration des macromolécules en chaînes.

Dans le cas des bons solvants, il semble, aux erreurs d'expérience près, que l'approximation de Peterlin pour cette fonction $P(\theta)$, développée par Benoît et Ptitsyn, soit superposable aux données expérimentales. Evidemment cette fonction n'est qu'approchée en ce sens qu'elle ne tient pas compte de la perturbation qu'amène l'effet de solvant dans la loi statistique de distribution des distances entre chaînons, bien qu'elle tienne compte évidemment, et suivant une loi qui semble correcte, de l'allongement des distances moyennes sous l'influence du solvant. Mais comme on peut le voir à la Fig. 3, les résultats expérimentaux se superposent très bien à cette fonction $P(\theta)$, et il faut conclure que la précision des résultats ne permet pas de mettre en évidence cette perturbation, pas plus

Can. J. Chem. Downloaded from www.nrcresearchpress.com by 210.87.254.42 on 09/05/12
For personal use only.

dans la région de u où nous sommes que pour des valeurs de u plus élevées où ceci avait déjà été vérifié (13–16). Par ailleurs, non seulement cette perturbation n'apparait pas, mais le caractère non gaussien de la chaîne lui-même, qui apparait nettement aux valeurs élevées de u, ne semble pas se refléter appréciablement dans la forme de la fonction $P(\theta)$ dans la région étudiée. En effet l'équation de Debye et l'équation de Peterlin donnent des résultats presqu'identiques, alors que l'équation de Debye suppose une chaîne gaussienne et que l'équation de Peterlin tient compte, au moins partiellement, de l'écart au comportement gaussien.

D'autre part puisque, dans le présent travail, nous n'avons exploré pour chaque fraction qu'une zone relativement étroite de valeurs de u, il ne faut pas éliminer la possibilité d'erreurs systématiques introduites par l'utilisation de l'une ou l'autre fonctions $P(\theta)$. Pour le vérifier, nous nous proposons d'effectuer des mesures encore plus fines de variation angulaire d'intensité de diffusion et ce dans des intervalles de u plus étendus. Nous nous proposons également d'étudier l'effet de la polydispersité résiduelle de nos fractions sur la fonction $P(\theta)$. Pour le présent travail, nous avons en effet pris pour acquis que cette polydispersité était assez faible pour ne pas modifier appréciablement la fonction $P(\theta)$. Il ne s'agissait évidemment-là que l'une première approximation que nous nous proposons maintenant de vérifier.

REMERCIEMENTS

Nous tenons à exprimer nos remerciements au Docteur H. W. McCormick et à la maison Dow Chemical pour nous avoir fourni des échantillons de polystyrène. Nous remercions également le Conseil National des Recherches du Canada pour l'octroi d'une subvention de recherche (Y. S.) et d'une bourse (J. P.).

BIBLIOGRAPHIE

1. P. DEBYE. J. Appl. Phys. **15**, 338 (1944).
2. B. ZIMM. J. Chem. Phys. **16**, 1093 (1948).
3. A. GUINIER. Ann. Phys. Paris, **12**, 161 (1939).
4. P. DEBYE. J. Phys. Chem. **51**, 18 (1947).
5. O. B. PTITSYN. Soviet Phys. Usp. **2**, 797 (1960).
6. M. KURATA et W. H. STOCKMAYER. Fortschr. Hochpolymer Forsch. **3**, 196 (1963).
7. J. A. SUBIRANA, A. MUNSTER, W. R. KRIGBAUM et H. BENOÎT. J. Chim. Phys. **59**, 1099 (1962).
8. M. KURATA, H. YAMAKAWA et E. TERAMOTO. J. Chem. Phys. **28**, 785 (1958).
9. O. B. PTITSYN et Y. E. EIZNER. Vysokomolekul. Soedin. **1**, 966 (1959).
10. A. PETERLIN. J. Chem. Phys. **23**, 2464 (1955).
11. H. BENOÎT. Compt. Rend. **245**, 2244 (1957).
12. O. B. PTITSYN. J. Phys. Chem. USSR. **31**, 1091 (1957).
13. A. J. HYDE, J. H. RYAN, F. T. WALL et T. F. SCHATZKI. J. Polymer Sci. **33**, 129 (1958).
14. C. LOUCHEUX, G. WEILL et H. BENOÎT. J. Chim. Phys. **55**, 540 (1958).
15. C. LOUCHEUX, G. WEILL et H. BENOÎT. J. Polymer Sci. **34**, 539 (1959).
16. A. J. HYDE. Trans. Faraday Soc. **56**, 591 (1960).
17. A. PETERLIN. Ann. N.Y. Acad. Sci. **89**, 593 (1961).
18. A. PETERLIN. Proc. of the Interdisciplinary Conference on Electromagnetic Scattering. 1962. Pergamon Press, Potsdam, N.Y. 1963. p. 357.
19. H. BENOÎT. Proc. of the Interdisciplinary Conference on Electromagnetic Scattering. 1962. Pergamon Press, Potsdam, N.Y. 1963. p. 285.
20. F. T. WALL, S. WINDWER et P. J. GANS. J. Chem. Phys. **38**, 2220 (1963).
21. F. T. WALL et J. J. ERPENBECK. J. Chem. Phys. **30**, 637 (1959).
22. F. T. WALL et J. MAZUR. Ann. N.Y. Acad. Sci. **89**, 608 (1961).
23. F. T. WALL et J. J. ERPENBECK. J. Chem. Phys. **30**, 634 (1959).
24. P. H. VERDIER et W. N. STOCKMAYER. J. Chem. Phys. **36**, 227 (1962).
25. T. F. SCHATZKI. J. Polymer Sci. **57**, 337 (1962).
26. C. WIPPLER et G. SCHEIBLING. J. Chim. Phys. **51**, 201 (1954).
27. Y. SICOTTE et M. RINFRET. Trans. Faraday Soc. **58**, 1090 (1962).
28. P. DEBYE et E. W. ANACKER. J. Phys. Colloid Chem. **55**, 644 (1951).
29. P. J. FLORY. Principles of polymer chemistry. Cornell. 1953.
30. M. KURATA et H. YAMAKAWA. J. Chem. Phys. **29**, 311 (1958).
31. U. BIANCHI et V. MAGNESCO. J. Polymer Sci. **41**, 177 (1959).
32. P. DEBYE, B. CHU et H. KAUFMANN. J. Polymer Sci. A**1**, 2387 (1963).

Can. J. Chem. Downloaded from www.nrcresearchpress.com by 210.87.254.42 on 09/05/12
For personal use only.

Can. J. Chem. Downloaded from www.nrcresearchpress.com by 210.87.254.5 on 09/05/12
For personal use only.

THE ANALYSIS OF THE VOLATILE OILS OF THE LEAVES OF ARTEMISIA MEXICANA AND ARTEMISIA KLOTZCHIANA[1]

A. MANJARREZ AND F. MEDINA
Instituto de Química, Universidad Nacional Autónoma de México, México, D.F.

Received March 23, 1964

ABSTRACT

The analysis of neutral and phenolic fractions of the essential oils from *A. mexicana* and *A. klotzchiana* by means of gas–liquid chromatography was attempted. The mixtures of neutral fractions were resolved using preparative g.l.c., and identification of components was made by chemical, spectrophotometric, and n.m.r. methods. The phenolic components were identified by means of relative retention ratios and addition methods. From *A. mexicana* (−) α-phellandrene, (+) limonene, (−) β-phellandrene, (−) camphor, (−) borneol, thymol, carvacrol, and eugenol were identified. From *A. klotzchiana* (−) α-phellandrene, (+) limonene, 1,8-cineole, (+) β-thujone, (−) camphor, (−) borneol, carvacrol, and eugenol were isolated.

INTRODUCTION

The study of the composition of the essential oils from numerous species of genus *Artemisia* have been described widely in the literature. So far as we are aware, the composition of essential oils from *A. mexicana* and *A. klotzchiana* has not yet been reported.

With the advent of preparative g.l.c. and its many attractive possibilities, we were provided with an analytical tool well suited to the separation and identification of the components of such essential oils.

It is difficult to resolve complex mixtures, as essential oils are, by direct analysis; therefore we separated the phenolic fraction (no acidic fraction was present) from the neutral portion for each oil and analyzed these fractions separately.

Successful separation of terpenoid compounds has been described in the literature. Among the most notable of these investigations were those of von Rudloff (1, 2, 3), Zubyk and Conner (4), Bernhard (5), and Cvrkal and Janák (6). From the data contained in the above communications and the nature of components isolated from another *Artemisia* species, it was concluded that for preparative g.l.c. of neutral fractions, the most promising stationary liquid phase would be ethyleneglycol adipate (APEG). Dimethyl polysiloxane has been reported by Navés and Grampoloff (7), as well as Janák and Komers (8) among others, to give good separation of phenolic mixtures. We choose Silicone D.C. 200 as the silicone type of stationary liquid phase for analysis of phenolic fractions of oils from both artemisias.

APPARATUS

An Aerograph Autoprep A-700 chromatograph (Wilkens Instrument and Research Inc.) was used in conjunction with a Leeds and Northrup, model H recorder (0–1 mV scale). The chart speed was 1.2 cm/min, and the flow rate of helium carrier gas was measured at the exit by the soap bubble method.

Samples of the neutral fractions were introduced on the column automatically without solvent, and phenolic samples were introduced on the column with a Walls liquid sampler (9). The column exhaust was at atmospheric pressure (750–752 mm), whereas the pressure at the column inlet was varied to give the desired flow rates.

[1]*Contribution No. 170 of Instituto de Química, Universidad Nacional de México.*
We are indebted to Dr. J. Valdéz Gutiérrez, from Jardín Botánico, U.N.A.M. for the classication of the Artemisia species.

Preparation of columns.—The solid support used in this work was Chromosorb W (Johns Manville Co.). This type of support is manufactured specifically for gas chromatography and was used without treatment except for removal of fines by water washing. Column packings were prepared by the usual method (4), using methylene chloride as solvent for both chemicals. Aluminum tubing 3/8 in. × 20 ft and 3/16 in. × 20 ft was filled with the dry, free-flowing packings (prepared as described above) by the vibrating-vacuum method (10). After the insertion of glass wool plugs in each end of the tubing, the columns were coiled to fit the Autoprep chromatograph. Conditioning was carried out by passing a stream of nitrogen through the columns while heating for several hours at 200 °C.

EXPERIMENTAL

Samples of *Artemisia* oils were obtained by steam distillation of the leaves and terminal branches of locally grown plants. Oils were dissolved in ether and extracted with 10% sodium bicarbonate solution and 10% sodium hydroxide solution to isolate the acidic and phenolic fractions respectively. The characteristics of essential oils are given in Table I.

TABLE I

Characteristics of essential oils

	A. mexicana	*A. klotzchiana*
Date of collection	Sept. 1963	Oct. 1963
Wt. of fresh plant	15 kg	15 kg
Yield of oil	68 g; 0.46% 67.2 g neutral 0.0 g acidic 0.560 g phenolic	37 g; 0.25% 36.2 g neutral 0.0 g acidic 0.520 g phenolic
d^{25}*	0.9362	0.8985
n_D^{25}†	1.4722	1.3645
$[\alpha]_D^{25}$‡	−16°	−7°

*Determined in a Fisher Davidson gravitometer using ethylbenzene as standard.
†Determined in an Abbé refractometer (Bausch and Lomb).
‡Determined in a Schmidt and Haensch polarimeter.

Analysis of Neutral Fractions

Samples of neutral fractions were chromatographed on APEG under the following conditions.

Column—20 ft × 3/8 in. aluminum.
Packing—30% APEG on 60/80 Chromosorb W.
Column temperature—180 °C.
Gas flow rate—200 ml/min.
Injection—on column.
Sample size—200 μl.

The Autoprep was automated to repeat the cycle every 30 minutes.

After a small sample (5 μl) of every component had been injected to prove its purity and whether or not it had suffered thermal decomposition, tentative identification of the components was made by infrared and n.m.r.[2] determinations and checked by chemical derivatives, following directions reported in the literature (see Table II.)

Analysis of Phenolic Fractions

Samples of phenolic fractions were chromatographed on Silicone 200 D.C. under the following conditions.

Column—20 ft × 3/16 in. aluminum.
Packing—30% Silicone 200 D.C. on 60/80 Chromosorb W.
Column temperature—190 °C.
Gas flow rate—200 ml/min.
Injection—on column.
Sample size—10 μl.

Components were identified tentatively by relative retention times. These were checked by adding a synthetic mixture of phenols of approximately the same composition (11); comparison of the recorder-tracing with that of the sample mixture showed identical peaks and retention times.

[2]*Infrared spectra were determined on film with a Perkin–Elmer model 21 spectrophotometer, and the n.m.r. spectra were determined with a Varian A-60 instrument.*

Can. J. Chem. Downloaded from www.nrcresearchpress.com by 210.87.254.5 on 09/05/12
For personal use only.

TABLE II

Analysis of neutral fraction from essential oils of *A. mexicana* and *A. klotzchiana*

Peak No.	Relative composition area, %	t_R*	Identification	Derivative
A. mexicana				
1	12.37	0.83	(−) α-Phellandrene	Maleic anhydride adduct m.p. 125–127° (14)
2	12.98	1.0	(+) Limonene	Tetrabromide m.p. 103–105° (15)
3	13.91	1.12	(−) β-Phellandrene	α-Nitrosite m.p. 102° (16)
4	53.60	1.36	(−) Camphor	2,4-Dinitrophenylhydrazone m.p. 174–175° (17)
5	7.08	1.50	(−) Borneol	*p*-Nitrobenzoate m.p. 136° (18)
A. klotzchiana				
1	5.12	0.83	(−) α-Phellandrene	Maleic anhydride adduct m.p. 125–127° (14)
2	6.11	1.0	(+) Limonene	Tetrabromide m.p. 103–105° (15)
3	16.59	1.09	1,8-Cineole	Resorcinol adduct m.p. 88–89° (19)
4	33.77	1.20	(+) β-Thujone	Semicarbazone m.p. 170–172° (20)
5	35.23	1.36	(−) Camphor	2,4-Dinitrophenylhydrazone m.p. 174–175° (17)
6	3.14	1.50	(−) Borneol	*p*-Nitrobenzoate m.p. 136° (18)

*Retention time of limonene = 1.

RESULTS AND DISCUSSION

Results obtained from the analysis of the neutral fractions are given in Table II and those obtained from phenolic portions in Table III.

However, most essential oils, including those from *Artemisia* species, include, in addition to monoterpenes, components such as lactones, coumarins, sesquiterpenes, etc. (12). It is possible that higher-boiling components have not eluted and therefore are not considered as part of neutral or phenolic portions of either oil. From these considerations it appears that the composition area percentages in the tables listed above are relative and not absolute quantitative values. The areas under each peak were determined with a planimeter and not by weighing the different components separated. The reason for this procedure is that in order to obtain pure components, regions near the base line were not collected ("heart cutting"). There is another possible source of error in the weighing method: since a certain amount of carrier gas passes through the collector bottle during sample collection, it is bound to sweep away some component vapors (13).

TABLE III

Analysis of phenolic fraction from essential oils of *A. mexicana* and *A. klotzchiana*

Peak No.	Relative composition area, %	Standard* relative t_R	Experimental relative t_R	Identification
A. mexicana				
1	6.8	1	1	Thymol
2	26.0	1.04	1.05	Carvacrol
3	67.5	1.42	1.39	Eugenol
A. klotzchiana				
1	65.21	1.04	1.06	Carvacrol
2	34.78	1.42	1.40	Eugenol

*Retention time of thymol = 1.

CONCLUSIONS

Using preparative g.l.c. the components of the neutral fractions of *A. mexicana* and *A. klotzchiana* have been identified. Isolation of individual components in more than

Can. J. Chem. Downloaded from www.nrcresearchpress.com by 210.87.254.5 on 09/05/12
For personal use only.

milligram amounts permitted chemical and spectroscopic identification. (−) Camphor was found to be the main constituent of both oils, but the oil of *A. klotzchiana* also contained substantial amounts of (+) β-thujone. Phenolic fractions were very small, and components were identified by means of relative retention times and addition methods.

REFERENCES

1. E. VON RUDLOFF. Can. J. Chem. **38**, 631 (1960).
2. E. VON RUDLOFF. Can. J. Chem. **39**, 1190 (1961).
3. E. VON RUDLOFF. Can. J. Chem. **39**, 1200 (1961).
4. W. J. ZUBYK and A. Z. CONNER. Anal. Chem. **32**, 912 (1960).
5. R. A. BERNHARD. Anal. Chem. **34**, 1576 (1962).
6. H. CVRKAL and J. JANÁK. Collection Czech. Chem. Commun. **24**, 1967 (1959).
7. Y. R. NAVÉS and A. V. GRAMPOLOFF. Bull. Soc. Chim. France, 1233 (1959).
8. J. JANÁK and R. KOMERS. Collection Czech. Chem. Commun. **24**, 1960 (1959).
9. F. WALLS and J. PADILLA. Bol. Inst. Quim. Univ. Nal. Auton. Mex. **15**, 32 (1963).
10. A. BLANCO and A. MANJARREZ. Bol. Inst. Quim. Univ. Nal. Auton. Mex. **15**, 34 (1963).
11. A. I. M. KEULEMANS. Gas chromatography. Reinhold Publishing Corporation, New York. 1957. Chap. 2. p. 26.
12. E. GUENTHER. The essential oils. Vol. V. D. Van Nostrand Company, Inc. 1949. p. 484.
13. WILKEN INSTRUMENT AND RESEARCH INC. Aerograph Previews and Reviews. Dec. 1962.
14. O. DIELS and K. ALDER. Ann. **460**, 98 (1928).
15. A. BAEYER. Ber. **27**, 448 (1894).
16. E. GUENTHER. The essential oils. Vol. II. D. Van Nostrand Company, Inc. 1949. p. 46.
17. O. L. BRADY. J. Chem. Soc. **133**, 756 (1931).
18. W. HÜCKEL. Ann. **549**, 186 (1941).
19. E. GUENTHER. The essential oils. Vol. II. D. Van Nostrand Company, Inc. 1949. p. 709.
20. J. SIMONSEN. The terpenes. Vol. II. Cambridge. 1949. p. 43.

Can. J. Chem. Downloaded from www.nrcresearchpress.com by 210.87.254.5 on 09/05/12
For personal use only.

SYNTHESIS OF 1-PHENYLPROPYNE-2,3-$^{13}C_2$[1]

R. N. RENAUD AND L. C. LEITCH
Division of Pure Chemistry, National Research Council, Ottawa, Canada
Received April 9, 1964

ABSTRACT

A method of preparing the title compound from methyl-^{13}C iodide through acetophenone-2-^{13}C, 1-phenylethanol-2-^{13}C, styrene-2-^{13}C, styrene-2-^{13}C dibromide, and 1-phenylacetylene-2-^{13}C is described. The overall yield based on methyl-^{13}C iodide was 24%.

In connection with the measurement of the spin–spin coupling constants of certain C–C linkages by Bernstein and Frei (1), 1-phenylpropyne-2,3-$^{13}C_2$ with an isotopic abundance of 55% above normal in the marked positions was synthesized.

In a review of the literature up to 1958, Hurd and Tockman (2) record no suitable method for the preparation of 1-phenylpropyne labelled as indicated above. The synthesis reported in that paper is also inconvenient because it would involve the preparation of 1-phenylacetone-2,3-$^{13}C_2$. The method of Tripett and Gough (3), employing the pyrolysis of α-phenylacetonylidenetriphenylphosphorane, gave 1-phenylpropyne which was very impure and difficult to purify on a small scale.

For these reasons, 1-phenylpropyne-2,3-$^{13}C_2$ was synthesized by the reactions shown below.

$$C_6H_5MgBr + {}^{13}CH_3CN \rightarrow C_6H_5CO{}^{13}CH_3 \rightarrow C_6H_5CH(OH){}^{13}CH_3$$
$$C_6H_5CH(OH){}^{13}CH_3 \rightarrow C_6H_5CH{=}{}^{13}CH_2 \rightarrow C_6H_5CHBr{}^{13}CH_2Br$$
$$C_6H_5CHBr{}^{13}CH_2Br \rightarrow C_6H_5C{\equiv}{}^{13}CH \rightarrow C_6H_5C{\equiv}{}^{13}C{}^{13}CH_3$$

The preparation of the intermediates up to and including styrene dibromide by methods already reported requires no special comment.

We attempted initially to prepare 1-phenylpropyne from styrene dibromide in one step, by dehydrobromination with lithium amide in liquid ammonia followed by methylation of the phenylacetylene formed. The product was, however, contaminated with an appreciable amount of styrene. When the reaction was carried out in boiling tetrahydrofuran with only a slight excess of lithium amide the product then contained bromostyrene. However, in the presence of excess lithium amide and only a catalytic amount of ammonia in boiling tetrahydrofuran, a 60% yield of 1-phenylpropyne (98.5% pure as determined by vapor phase chromatography) was obtained, provided an excess of methyl iodide was employed. While this is a satisfactory method of preparing 1-phenylpropyne in one step from styrene dibromide, a rather large amount of expensive methyl-^{13}C iodide would be required to prepare the labelled compound. In other words the yield based on methyl iodide is quite low. Consequently, attempts to prepare 1-phenylpropyne in one step were abandoned and attention was directed to the preparation of phenylacetylene.

According to Vaughn, Vogt, and Nieuwland (6) phenylacetylene is obtained in 64% yield by dehydrobromination of styrene dibromide with sodamide in liquid ammonia. Campbell and Campbell (7) report yields of 47–52% in this same preparation. We have repeated the experiments of the authors cited above and observe the formation of appreciable amounts of styrene in this reaction. The similarity in boiling point and refractive

[1]*National Research Council No. 8046.*

Can. J. Chem. Downloaded from www.nrcresearchpress.com by 210.87.254.5 on 09/05/12
For personal use only.

index of phenylacetylene and styrene prevents the use of these physical constants as criteria of the purity of the phenylacetylene. The presence of styrene in the product was established by vapor phase chromatography of a sample in a Perkin–Elmer Fractometer on a type "O" column at 147°; styrene and phenylacetylene had retention times of 3.5 and 4 min respectively, with good resolution. The formation of olefins in this type of reaction had in fact been reported by Vaughn, Vogt, and Nieuwland (6), who found that stilbene dibromide gave an 83% yield of stilbene rather than diphenylacetylene. It seemed that the preparation of phenylacetylene might best be achieved in good yield by dehydrobromination with excess sodamide in anhydrous ether (or tetrahydrofuran) in the presence of traces of ammonia as described earlier. Phenylacetylene of 96% purity was in fact isolated in 90% yield by this method.

The cobaltous chloride catalyzed reaction between phenylethynyl bromide and methylmagnesium bromide is reported by Kharasch, Lambert, and Urry (4) to give a 62% yield of 1-phenylpropyne, but Black, Horn, and Weedon (5) obtained at best only a 34% yield. Our results agreed with those of Weedon and co-workers and this method was therefore abandoned. The methylation was then carried out with lithium amide in liquid ammonia, and methyl iodide in anhydrous ether. An 80% yield of 1-phenylpropyne, 97% pure, was obtained.

1-Phenylacetylene-2-^{13}C and 1-phenylpropyne-2,3-$^{13}C_2$ were prepared in exactly the same way from styrene-2-^{13}C dibromide and methyl-^{13}C iodide.

DISCUSSION

Conventional elimination mechanisms readily explain the formation of phenylacetylene from styrene dibromide and sodium amide but, to our knowledge, the formation of styrene in this reaction has not been explained. To rationalize this with both sodium amide and ammonia as reagents we suggest the following reactions.

(1) Proton abstraction to yield a methylene (9):

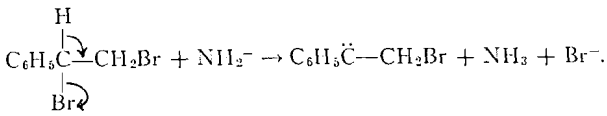

(2) In the absence of ammonia the methylene undergoes dehydrobromination to phenylacetylene, but in its presence addition of a hydride ion takes place and styrene is formed:

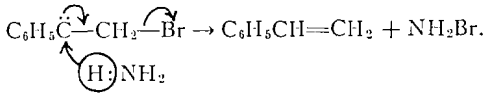

EXPERIMENTAL

Methyl-^{13}C Cyanide

The nitrile was prepared by the method of Cox, Warner, and Turner reported in *Organic Synthesis with Isotopes* (8, p. 40). Yield: 95%.

Acetophenone-2-^{13}C

The ketone was prepared as described by Brown, Cerwonka, and Anderson in *Organic Synthesis with Isotopes* (8, p. 664). Yield: 60%.

1-Phenylethanol-2-^{13}C

The alcohol was prepared by reducing the ketone with aluminum isopropoxide. Yield: 85%.

Can. J. Chem. Downloaded from www.nrcresearchpress.com by 210.87.254.5 on 09/05/12
For personal use only.

Styrene-2-^{13}C

The alcohol was dehydrated as described by Berstein, Bennett, and Fields (8, p. 1686). Yield: 75%.

Styrene-2-^{13}C Dibromide

Styrene-2-^{13}C (1.2 g; 0.011 mole) was dissolved in 25 ml of chloroform, and a solution of 1.95 g of bromine, also dissolved in chloroform, was added. The dibromide, 3.0 g (93%), was recovered by distilling off the solvent.

1-Phenylpropyne

1. From Styrene Dibromide and Excess $LiNH_2$ in Liquid Ammonia

Lithium amide was prepared in the usual manner from 0.295 g of lithium and 10 ml of liquid ammonia in a flask equipped with a cold finger condenser, which was packed with dry ice and protected from moisture by a drying tube filled with Drierite. After the mixture had been stirred for 15 min, a solution of 3.7 g (0.014 mole) of styrene dibromide in 20 ml of anhydrous ether was added dropwise. The reaction mixture, which turned dark brown, was stirred for 3 h. Methyl iodide (2.3 g; 0.016 mole) in 20 ml of dry ether was added dropwise and the reaction mixture was stirred 2 h under reflux and allowed to stand overnight. In the morning it was decomposed with water. The ether solution was separated, dried over $MgSO_4$, and evaporated. The residue was distilled on the vacuum line and analyzed by vapor phase chromatography. The yield of 1-phenylpropyne was 38%, that of styrene 40%, and that of phenylacetylene 22.

A run with a 5 mole excess of lithium amide on the same scale gave an oil which analyzed 22% styrene, 50% phenylacetylene, and only 16% 1-phenylpropyne.

2. From Styrene Dibromide with an Equivalent Amount of $LiNH_2$ in Tetrahydrofuran (THF)

Styrene dibromide (3.58 g; 0.013 mole) was added in portions to 1.1 g (0.05 mole) of lithium amide in tetrahydrofuran and the reaction mixture was heated overnight under reflux with stirring. Methyl iodide (0.5 mole excess) was added to the reaction mixture at ambient temperature. Stirring was continued for 12 h, and then for 1 h under reflux. The tetrahydrofuran was distilled off on the steam bath, and the residue was taken up in ether before adding water. The reaction product was isolated as described in the preceding experiment. The main fraction of material distilled on the vacuum line contained 28.6% monobromostyrene and 27.4% styrene in addition to 33.4% 1-phenylpropyne.

3. From Styrene Dibromide with Excess $LiNH_2$ in Tetrahydrofuran, Traces of Ammonia, and Excess CH_3I

Lithium amide (1.7 g; 0.074 mole), prepared in the usual manner from lithium and liquid ammonia, was freed of solvent, and 40 ml of dry tetrahydrofuran was added. A trace of dry ammonia was bubbled through the mixture. Styrene dibromide (3.9 g; 0.015 mole) was added in portions over a period of 3 min. The reaction mixture was heated with stirring under reflux overnight. Dry methyl iodide (6.3 g; 0.045 mole) in dry tetrahydrofuran was added, and the reaction mixture was stirred at room temperature for 2 days. The solvent was distilled off on the steam bath, the residue was taken up in ether and worked up as described before. The yield of product, 98.5% pure, was 1.1 g (65%).

Anal. Calc. for C_9H_8: C, 93.1; H, 6.85. Found: C, 92.99; H, 6.83. There were traces of styrene and phenylacetylene in the product.

Phenylacetylene

Sodamide was prepared in the usual manner from 1.3 g of sodium (0.06 mole). The ammonia was removed by pumping the flask on the vacuum line. Anhydrous ether (50 ml) was added, and a trace of dry ammonia was bubbled through the mixture followed by a solution of 3.7 g (0.012 mole) of styrene dibromide dissolved in 10 ml of ether. The reaction mixture became reddish, turned dark brown, and then turned light brown. White solid LiBr was formed. After the mixture had stood overnight, 4.0 g of ammonium chloride in water was added. The phenylacetylene was isolated in the usual manner. The yield was 1.3 g (90%) of phenylacetylene, which analyzed 96% by vapor phase chomatography. A small amount of styrene was present as an impurity.

1-Phenylacetylene-2-^{13}C was prepared in exactly the same way.

1-Phenylpropyne

Lithium amide was prepared from 0.16 g (0.023 mole) of lithium (100% excess), 10 ml of liquid ammonia, and a trace of ferric nitrate. After the mixture had been stirred for 30 min, a solution of 1.0 g of phenylacetylene in 50 ml of absolute ether was added with stirring. This was followed by 1.6 g (0.011 mole) of methyl iodide in 25 ml of ether. The ammonia was allowed to evaporate overnight, and the reaction mixture was worked up as before. The yield of 1-phenylpropyne, 97% pure as determined by vapor phase chromatography, was 1.1 ml (80%) after purification by distillation on the vacuum line.

1-Phenylpropyne-2,3-$^{13}C_2$ was prepared in exactly the same way from 1-phenylacetylene-2-^{13}C. The overall yield based on methyl-^{13}C iodide was 24%.

ACKNOWLEDGMENTS

The authors are indebted to Dr. O. E. Edwards of this Division for suggesting the mechanism mentioned in the discussion.

Can. J. Chem. Downloaded from www.nrcresearchpress.com by 210.87.254.5 on 09/05/12
For personal use only.

REFERENCES

1. K. FREI and H. J. BERNSTEIN. J. Chem. Phys. **38**, 1216 (1963).
2. C. D. HURD and A. TOCKMAN. J. Org. Chem. **23**, 1087 (1958).
3. S. TRIPETT and S. T. D. GOUGH. J. Chem. Soc. 2333 (1962).
4. M. S. KHARASCH, F. L. LAMBERT, and W. H. URRY. J. Org. Chem. **10**, 298 (1945).
5. H. K. BLACK, D. H. S. HORN, and B. C. L. WEEDON. J. Chem. Soc. 1954 (1706).
6. T. H. VAUGHN, R. R. VOGT, and J. A. NIEUWLAND. J. Am. Chem. Soc. **56**, 2120 (1934).
7. K. N. CAMPBELL and B. K. CAMPBELL. Org. Syn. **30**, 72 (1950).
8. A. MURRAY, III and D. L. WILLIAMS. Organic syntheses with isotopes. Interscience Publishers, N.Y. 1958.
9. L. FRIEDMAN and J. G. BERGER. J. Am. Chem. Soc. **83**, 492 (1961).

Can. J. Chem. Downloaded from www.nrcresearchpress.com by 210.87.254.5 on 09/05/12
For personal use only.

Can. J. Chem. Downloaded from www.nrcresearchpress.com by 210.87.254.42 on 09/05/12
For personal use only.

ISOLATION AND SOME STRUCTURAL FEATURES OF A POLYSACCHARIDE FROM BIRCH SAP[1]

B. URBAS,[2] G. A. ADAMS, AND C. T. BISHOP
Division of Biosciences, National Research Council, Ottawa, Canada

Received April 29, 1964

ABSTRACT

A polysaccharide, precipitated by cetyltrimethylammonium hydroxide from the non-dialyzable portion of birch xylem sap, contained D-galactose, D-mannose, and D-glucose in a molar ratio of 2:1.4:1 and small amounts of D-glucuronic acid. Periodate oxidation studies indicated that the polysaccharide was branched and contained a high proportion of periodate-resistant monosaccharides. This was confirmed by methylation and hydrolysis which yielded 2,3,4,6-tetra-*O*-methyl-D-glucose (2.0 moles); 2,4,6-tri-*O*-methyl-D-mannose (0.9 mole); 2,4,6-tri-*O*-methyl-D-galactose (3.8 moles); unidentified tri-*O*-methyl hexose (1.2 moles); and 3,5-di-*O*-methyl-D-mannose (1.8 moles). The latter, a new di-*O*-methyl-D-mannose, showed the presence of D-mannofuranose units in the polysaccharide. This, together with the $1 \rightarrow 3$ linked α-D-mannopyranose units, makes this polysaccharide unique among plant products. Immunochemical tests with antipneumococcal and antiparatyphoid B horse sera confirmed the presence of D-glucuronic acid and D-glucopyranose non-reducing end groups and supported the other structural conclusions by showing that there were few, if any, $1 \rightarrow 4$ and $1 \rightarrow 6$ linked D-mannopyranose units or D-galactopyranose non-reducing end groups.

Until recently very little was known about the chemistry of wood saps, apart from the sucrose content of maple sap and the glucose and fructose contents of birch sap (1). Interest in the other constituents of these saps arose because it seemed possible that wood sap might contain intermediates or precursors in the synthesis of wood polysaccharides. Previous papers from this laboratory have described the isolation and structural investigation of a polysaccharide from maple sap (2, 3), analyses of the oligosaccharides present in birch (1) and maple (4) saps, and a study of the glycoside hydrolase activity in the xylem saps of birch and maple (5).

The present paper reports the isolation and structural investigation of a polysaccharide from the xylem sap of white birch (*Betula papyrifera* Marsh).

The polysaccharides, isolated from the non-dialyzable sap constituents by precipitation with ethanol, showed several peaks on moving-boundary electrophoresis (6) and yielded galactose, glucose, mannose, xylose, arabinose, rhamnose, and a uronic acid on acid hydrolysis. A polysaccharide that was homogeneous by electrophoresis and ultracentrifugation was obtained from this mixture by precipitation with cetyltrimethylammonium hydroxide (7). This polysaccharide, which made up 27% of the non-dialyzable material, contained D-galactose, D-mannose, and D-glucose in a molar ratio of 2:1.4:1 and 20% of hexuronic acid as estimated by the carbazole method (8). The small amount of hexuronic acid obtained by hydrolysis of the polysaccharide was converted to its parent monosaccharide by successive reduction and hydrolysis of its methyl ester, methyl glycoside. The chromatographic identification of glucose from this procedure indicated that the hexuronic acid was D-glucuronic acid, and this was confirmed by the immunological tests discussed below. In a similar way an aldobio- and aldotrio-uronic acid were partially characterized as a glucuronosylgalactose and a glucuronosylgalactosylmannose. The low yields of these uronic acid derivatives precluded more definitive characterizations.

[1]*Issued as N.R.C. No. 8047.*
[2]*National Research Council Postdoctoral Fellow 1961–1963.*

When the polysaccharide was oxidized by periodate, the moles of oxidant consumed and of formic acid produced per mole of anhydrohexose were 0.818 and 0.365 respectively. The oxidized polysaccharide was reduced and hydrolyzed (9); the hydrolysis products were reduced again to yield a mixture of sugar alcohols which were analyzed by gas–liquid chromatography (10, 11). The results, given in Table I, provide some

TABLE I

Analysis of polyols derived from periodate-oxidized birch sap polysaccharide

	% composition	
	Column 1*	Column 2†
Glycerol	33.1	36.5
Erythritol	6.2	6.0
Glucitol	2.7	2.6
Galactitol }	58.0	33.4
Mannitol }		21.4

*Gas–liquid chromatography of acetates on 8 ft × 1/4 in. column, 10% DCQF-1 (a fluorosilicone polymer) on acid-washed Chromosorb W, 100–120 mesh, 200 °C, 80 ml He/min.

†Gas–liquid chromatography of acetates on 4 ft × 1/4 in. column, 10% of ethylene glycol isophthalate polyester on Gas-Chrom Z, 100–120 mesh, 190 °C, 60 ml A/min.

information about the structure of the polysaccharide. Thus glycerol could arise from non-reducing terminal units or 1 → 2 or 1 → 6 linked units within the polysaccharide chains. However, of these three possibilities, only the 1 → 2 linked units would yield glycerol without also producing a mole of formic acid. The excellent agreement between the glycerol (0.365 mole per mole) and formic acid produced (0.365 mole per mole) strongly suggests that the glycerol was formed by oxidation and reduction of non-reducing terminal units or 1 → 6 linked residues. The oxidation of each such unit requires 2 moles of periodate, and the oxidation of a 1 → 4 linked hexose to yield erythritol in this procedure would require 1 mole of periodate. The amount of oxidant required by the products in Table I is therefore 0.790 mole, a value in good agreement with the 0.818 mole found experimentally. The small amount of glucitol present in these products (Table I) indicated that most of the glucose in the polysaccharide was linked through positions that permitted its oxidation by periodate. The converse was true for galactose and mannose: the large amounts of galactitol and mannitol indicated that most, if not all, of the parent monosaccharides were linked in the polysaccharide through positions which made them resistant to attack by periodate. These conclusions were supported and amplified by the results of methylation and hydrolysis which yielded the following neutral sugars; no acidic derivatives could be isolated.

2,3,4,6-Tetra-*O*-methyl-D-glucose	(2.0 moles)
2,4,6-Tri-*O*-methyl-D-mannose	(0.9 mole)
2,4,6-Tri-*O*-methyl-D-galactose	(3.8 moles)
Unidentified tri-*O*-methyl hexoses	(1.2 moles)
3,5-Di-*O*-methyl-D-mannose	(1.8 moles)

The only derivative of glucose found was the tetramethyl ether; the amount (20.6 mole %) was not sufficient to account for all of the glycerol produced on periodate

Can. J. Chem. Downloaded from www.nrcresearchpress.com by 210.87.254.42 on 09/05/12
For personal use only.

Can. J. Chem. Downloaded from www.nrcresearchpress.com by 210.87.254.42 on 09/05/12
For personal use only.

oxidation and reduction, but some of the very volatile tetramethyl ether may have been lost during evaporation. Glucose was the only tetra-*O*-methyl sugar found, and hence this sugar formed all of the non-reducing terminal units in the polysaccharide. The small amounts of $1 \rightarrow 4$ linked hexoses indicated by erythritol in Table I and the small amount of unoxidized glucose, indicated by glucitol, may possibly be accounted for in the unidentified tri-*O*-methyl fraction. The remaining *O*-methyl hexoses were derived from units that would resist periodate oxidation, and the total amount of such units (70 mole %) is not greatly different from that found by periodate oxidation (55–58 mole %), particularly since the former value is probably high because of the loss of tetra-*O*-methyl-D-glucose. The 2,4,6-tri-*O*-methyl-D-mannose and 2,4,6-tri-*O*-methyl-D-galactose represented the unbranched portions of the polysaccharide. The polysaccharide therefore consisted largely of $1 \rightarrow 3$ linked D-manno- and D-galacto-pyranose units, probably in the α-configuration because of the high positive specific rotation of the polysaccharide (+173°). The 3,5-di-*O*-methyl-D-mannose represented a branch point with a D-mannose unit substituted in positions 1, 2, and 6, *in the furanose ring form*. As far as the authors are aware, this is the first time that mannose has been found in the furanose form in a polysaccharide. 3,5-Di-*O*-methyl-D-mannose also does not appear to have been reported before. It is a crystalline product having melting point 126–127 °C and $[\alpha]_D^{21}$ +14.5° (*c*, 1.50% in water) and was characterized by successive reduction and periodate oxidation to yield 2,4-di-*O*-methyl-D-arabinose, identified as its crystalline anilide.

The results of cross-reactions of the birch sap polysaccharide in antipneumococcal and antiparatyphoid B horse sera (12) fully supported the structural features given above. Thus, reactions in types II and V antipneumococcal sera provided further evidence for the identity of the hexuronic acid as D-glucuronic and indicated that these units were present as non-reducing end groups. Reaction in type I antipneumococcal serum indicated the presence of either D-galacturonic acid or D-galactose; the latter is preferred because there was no chemical evidence of D-galacturonic acid in the polysaccharide. The weak reaction in type XIV antipneumococcal serum indicated few if any non-reducing end groups of D-galactose, and the weak reaction in antiparatyphoid B sera showed that the D-mannose is probably not linked by $1 \rightarrow 4$ and $1 \rightarrow 6$ glycosidic bonds. In fact, no non-reducing end groups of D-galactose could be found, nor was there any chemical evidence for $1 \rightarrow 4$ or $1 \rightarrow 6$ linked D-mannose units.

The results of periodate oxidation, methylation studies, and immunochemical tests revealed the main structural features of the birch sap polysaccharide. It consists of basic chains of $1 \rightarrow 3$ linked α-D-manno- and α-D-galacto-pyranose units. Branch points occur at mannofuranose units by linkages through the C-1, C-2, and C-6 positions. Some chains are terminated at the non-reducing end by D-glucuronic acid units linked to galactose units which are in turn linked to mannose units. All other non-reducing terminal units consist of D-glucose residues. Several of these features are unique among plant polysaccharides; thus, while $1 \rightarrow 3$ linked D-galactopyranose units form the basic structure of a large number of plant gums (13), neither D-mannofuranose units nor $1 \rightarrow 3$ linked α-D-mannopyranose units have been found in polysaccharides from plants. It is apparent, therefore, that this polysaccharide bears no resemblance whatsoever to the polysaccharides of birch wood or bark (14–16). The only possible way in which it could serve as a precursor or intermediate in the synthesis of wood or bark polysaccharides would be as a donor of monosaccharide residues in a transferase system.

The glucuronoglucomannogalactan that has been described formed 27% of the non-dialyzable material in birch sap. The remaining 73% was a complex mixture from which a small amount of an arabinogalactan has been isolated; it is not yet known if this resembles the rhamnoarabinogalactan isolated from maple sap (3).

EXPERIMENTAL

Paper chromatograms were run by the descending method on Whatman No. 1 paper in the following solvent systems (v/v ratio).

(A) Butan-1-ol:ethanol:water = 40:11:19.
(B) Pyridine:ethyl acetate:water = 1:2.5:2.5.
(C) Ethyl acetate:acetic acid:formic acid:water = 18:3:1:4.
(D) Butanone saturated with water.
(E) Benzene:ethanol:water:ammonia = 200:47:14:1.
(F) Butan-1-ol:pyridine:water = 10:3:3.

Paper electrophoreses were done on Whatman 3MM paper in 0.1 *M* sodium tetraborate at a potential gradient of 25 V/cm for 2 h. Sugars were detected on papers by *p*-anisidine hydrochloride (17) or alkaline silver nitrate (18) spray reagents. Evaporations were done at 35 °C under diminished pressure, melting points are corrected, and specific rotations are equilibrium values unless otherwise stated.

Isolation of Polysaccharide

Sap (620 l) was collected from white birch trees (*Betula papyrifera* Marsh) by tapping the xylem and was concentrated to 20 l before being poured into ethanol (80 l) with vigorous stirring. The precipitate which formed was centrifuged, washed with 80% ethanol, redissolved in water, and dialyzed against tap water for 48 h. The solution of non-dialyzable material was freeze-dried to yield the crude sap polysaccharides as a cream-colored powder (30 g; ash, 39.6%; N, 0.57%). Chromatographic examination (solvents B, C, and F) of an acid hydrolysate of this material showed the presence of galactose, glucose, mannose, xylose, arabinose, rhamnose, and a uronic acid. The crude polysaccharide preparation, which showed several peaks on moving-boundary electrophoresis (6), was passed over Amberlite IR-120 (H^+) exchange resin. Cetyltrimethylammonium hydroxide was added to the acidic solution until precipitation was complete (7). The sticky precipitate was centrifuged, washed thrice with water, dissolved in 1 *M* sodium chloride, and dialyzed against tap water for 18 h. The solution of non-dialyzable material was concentrated to a small volume, and the polysaccharide was precipitated by the addition of ethanol to a concentration of 70%. The polysaccharide (4.86 g; ash, 0.34%; N, nil) showed $[\alpha]_D^{22}$ +173° (*c*, 1.34% in 1% sodium hydroxide) and gave a single, sharp peak on moving-boundary electrophoresis in 0.5 *M* sodium tetraborate and on ultracentrifugation in the same solution or in 0.5 *M* sodium acetate. Acid hydrolysis of the purified polysaccharide yielded galactose, glucose, mannose, and uronic acid as shown by paper chromatography in solvents B, C, and F.

Neutral Sugars

The polysaccharide (250 mg) was hydrolyzed by 1 *N* sulphuric acid in a sealed tube at 100 °C for 15 h. The hydrolysate was deionized by Amberlite IR-120 (H^+) and Duolite A-4 (OH^-) exchange resins, and neutral sugars in the solution were separated by preparative paper chromatography in solvent B.

(a) D-*Glucose.*—The sirup (35 mg) showed $[\alpha]_D^{22}$ +51° (*c*, 1.2% in water) and yielded crystalline *N*(*p*-nitrophenyl)α-D-glucopyranosylamine, m.p. 182–184 °C (19).

(b) D-*Mannose.*—The sirup (38 mg) showed $[\alpha]_D^{22}$ +12° (*c*, 1% in water) and was converted to crystalline D-mannose phenylhydrazone, m.p. 194–196 °C (20).

(c) D-*Galactose.*—The sirup (60 mg) crystallized and was recrystallized from 80% ethanol to yield a product with m.p. 164–166 °C and $[\alpha]_D^{22}$ +80° (*c*, 1.9% in water).

Mixtures of each of these crystalline compounds with corresponding authentic samples had melting points that were not depressed.

For quantitative estimation the polysaccharide was hydrolyzed as described above, and the neutral sugars in the deionized hydrolysate were separated by paper strip chromatography in solvent B. The separated sugars were eluted from the paper with water and estimated colorimetrically (21, 22). The polysaccharide (15 mg) yielded glucose (3.119 mg), mannose (4.182 mg), and galactose (6.102 mg).

Uronic Acids

The purified birch sap polysaccharide contained 20% of hexuronic acid as determined by the carbazole method (8). Preliminary experiments showed that hydrolysis of the polysaccharide for periods longer than 6 h gave only traces of oligouronides. Two sets of hydrolysis conditions were therefore selected for preparation of the uronic acid and of the oligouronides.

(1) Uronic acid.—Polysaccharide (200 mg) was heated with 1 *N* sulphuric acid (10 ml) in a sealed tube at 100 °C for 15 h.

Can. J. Chem. Downloaded from www.nrcresearchpress.com by 210.87.254.42 on 09/05/12
For personal use only.

(2) Oligouronides.—Polysaccharide (200 mg) was heated with 1 *N* sulphuric acid (10 ml) under reflux at 97 °C for 6 h.

Both hydrolysates were adjusted to pH 6.0 by additions first of barium hydroxide and then barium carbonate. Barium sulphate was removed by filtration, and cations in the filtrate were adsorbed on a column of Amberlite IR-120 (H^+) exchange resin. Uronic acids were then adsorbed on Dowex 1-X4 (OH^-) exchange resin after which the resin was washed with water until a negative anthrone test showed that all sugars had been removed. Uronic acids were then eluted from the resin by 1 *N* sodium hydroxide and converted to the free acid form by removal of sodium ions on Amberlite IR-120 (H^+) exchange resin. Paper chromatography in solvent C showed that both hydrolysates contained a mixture of the same three components but in different amounts.

Hydrolysate	Component 1 *R*(glucose) = 0.83	Component 2, *R*(glucose) = 0.68	Component 3, *R*(glucose) = 0.28
1	++++	+	+
2	Trace	+++	+++

The three components were isolated by preparative paper chromatography in solvent C.

Component 1

The acid (19 mg), which had the same *R*(glucose) value in solvent C as glucuronic acid, was converted to its parent monosaccharide by successive methanolysis, reduction with lithium aluminum hydride, and hydrolysis. This procedure yielded only glucose, which was identified by its chromatographic properties.

Component 2

This acid appeared to be an aldobiouronic acid on the basis of its paper electrophoretic mobility in 0.025 *N* sodium bicarbonate in comparison with known oligouronides. Hydrolysis with 2 *N* sulphuric acid at 100 °C for 15 h yielded a uronic acid and galactose as shown by paper chromatography (solvent C). The aldobiouronic acid (12 mg) was converted to its methyl ester, methyl glycoside, and reduced to the neutral disaccharide glycoside by lithium aluminum hydride. Hydrolysis with 1 *N* sulphuric acid yielded glucose and galactose as shown by paper chromatography in solvent B. The aldobiouronic acid must therefore have been a glucuronosylgalactose.

Component 3

Acid hydrolysis of this product yielded a uronic acid and approximately equal amounts of galactose and mannose. Paper electrophoretic mobility indicated that this component was an aldotriouronic acid. Reduction of the methyl ester, methyl glycoside, by lithium aluminum hydride yielded the glycoside of a neutral trisaccharide which on hydrolysis gave galactose, mannose, and glucose in equal amounts. Reduction of the original aldotriouronic with sodium borohydride followed by acid hydrolysis yielded mannitol, galactose, an aldobiouronic acid, and glucuronic acid. These results showed that component 3 was a glucuronosylgalactosylmannose.

Periodate Oxidation

The purified birch sap polysaccharide (100 mg) was oxidized by 0.33 *M* sodium metaperiodate (10 ml) at 5 °C in the dark. Aliquots were removed at intervals for estimation of periodate (23) and formic acid (24). The results are given below in moles per anhydrohexose unit.

Time (h)	24	48	72	96	120
Periodate	0.618	0.748	0.787	0.794	0.818
Formic acid	0.172	0.265	0.321	0.346	0.365

In a separate experiment a sample (100 mg) of the polysaccharide was oxidized as above, excess periodate was destroyed by ethylene glycol, and the mixture was dialyzed. The non-dialyzable material was then reduced with sodium borohydride and hydrolyzed by 1 *N* sulphuric acid (9). The neutralized hydrolysate was evaporated to a sirup which was again reduced with sodium borohydride. Examination of the reduced products by paper chromatography (solvent A) revealed the presence of galactitol, mannitol, erythritol, glycerol, and traces of glucitol and uronic acid. The mixture of alcohols was acetylated and examined by gas–liquid chromatography (10, 11) on two different liquid phases; the results are shown in Table I. Quantitative estimations were made from the areas under the peaks given by the individual components. The results from the two ion-exchange columns were in reasonable agreement, although column 1 failed to give a separation of galactitol from mannitol.

Methylation

The polysaccharide (4.0 g) was methylated eight times with dimethyl sulphate and 45% sodium hydroxide (25), then a further four times with the same reagents but in 80% dioxane solution. The product was recovered by extraction into chloroform, and the extract was dried (anhydrous sodium sulphate) and

Can. J. Chem. Downloaded from www.nrcresearchpress.com by 210.87.254.42 on 09/05/12
For personal use only.

evaporated. The oily residue was dissolved in methanol (100 ml), the solution was poured into an ethereal solution (150 ml) of diazomethane (prepared from 12 g of nitrosomethylurea), and the mixture was kept at 5 °C for 18 h. The precipitate which formed was filtered off, washed with ether, and dried (2.09 g). Anal. Calc. OCH_3: 45.6%. Found: 44.5%. The methylated polysaccharide had $[\alpha]_D^{24}$ +138° (*c*, 0.80% in chloroform) and showed no hydroxyl absorption in the infrared.

The methylated polysaccharide (2.0 g) was dissolved in 72% sulphuric acid (10 ml) and left for 1 h (26). The reaction mixture was diluted with water (90 ml) and heated for 20 h at 100 °C. The solution was neutralized with barium carbonate, filtered, and passed first through a column of Amberlite IR-120 (H^+) exchange resin and then through one of Duolite A-4 (OH^-). The eluate was evaporated to give the neutral *O*-methyl monosaccharides as a sirup (1.4 g).

Products recovered from the Duolite A-4 (OH^-) resin were shown to contain the same partially methylated sugars as were found in the neutral fraction, and no acidic components could be isolated or distinguished.

Hydrolysis Products from Methylated Polysaccharide

The mixture of *O*-methyl monosaccharides (1.4 g) was resolved by chromatography on a cellulose column (6 × 50 cm) with solvent D as eluant. Fractions (15 ml) were collected automatically every 15 min and were analyzed by paper strip chromatography; the results are shown in Table II.

TABLE II

Hydrolysis products from methylated polysaccharide

Fraction	Tube No.	Yield (mg)	Components identified
1	20–34	243.2	2,3,4,6-Tetra-*O*-methyl-D-glucose
2	39–59	250.2	2,4,6-Tri-*O*-methyl-D-mannose
3	67–91	417.1	2,4,6-Tri-*O*-methyl-D-galactose
4	102–134	184.7	3,5-Di-*O*-methyl-D-mannose

Fraction 1

This product (243.2 mg) crystallized spontaneously and had m.p. 88–92 °C and $[\alpha]_D^{23}$ +79° (*c*, 1.24% in water). Demethylation with boron trichloride (27) gave glucose. It was chromatographically identical, in solvents A, D, and E, with 2,3,4,6-tetra-*O*-methyl-D-glucose and after recrystallization from ether:light petroleum (1:1) had m.p. 92–95° and $[\alpha]_D^{23}$ +85° (*c*, 1.53% in water). The derived *N*-phenyl 2,3,4,6-tetra-*O*-methyl-D-glucosylamine had m.p. 136–137 °C in agreement with the reported value (28).

Fraction 2

This fraction (250.2 mg) yielded glucose and mannose with minor amounts of galactose when demethylated. Paper chromatography in solvent F revealed two components with R_f 0.64 and 0.55; these were separated by preparative paper chromatography in the same solvent. The first component (R_f 0.64, 132 mg) yielded glucose, mannose, and galactose on demethylation and attempts to resolve the mixture further by paper, thin-layer, or gas–liquid chromatography were unsuccessful.

The second component (R_f 0.55, 100 mg) had the same chromatographic properties in solvents A, D, and E as an authentic sample of 2,4,6-tri-*O*-methyl-D-mannose. The sirup crystallized spontaneously and after recrystallization from ether had m.p. 62–65 °C and $[\alpha]_D^{21}$ +17° (*c*, 1% in water). These values are the same as those reported (29), and the melting point of a mixture with an authentic sample was not depressed. Oxidation of the tri-*O*-methyl-D-mannose with bromine and distillation of the product yielded 2,4,6-tri-*O*-methyl-D-mannonolactone, m.p. 95–97 °C. This lactone, on successive treatments with methanolic hydrogen chloride and methanolic ammonia, gave crystalline 2,4,6-tri-*O*-methyl-D-mannonamide (30), m.p. 145 °C and $[\alpha]_D^{22}$ +6° (*c*, 1.0% in water).

Fraction 3

This product (417.1 mg) had the same chromatographic properties as an authentic sample of 2,4,6-tri-*O*-methyl-D-galactose in solvents A and D. Methyl glycosides of this component showed the same retention times as methyl 2,4,6-tri-*O*-methyl α,β-D-galactoside, and demethylation (27) yielded only galactose. The tri-*O*-methyl-D-galactose crystallized spontaneously, m.p. 90–98 °C, and recrystallization from ether yielded colorless needles of 2,4,6-tri-*O*-methyl-D-galactose (31), m.p. 102–104 °C, $[\alpha]_D^{23}$ +92.5° (*c*, 1.88% in water). The derived *N*-phenyl 2,4,6-tri-*O*-methyl-D-galactosylamine (32, 33) had m.p. 172–174 °C, undepressed on admixture with an authentic sample.

Fraction 4

This component (184.7 mg) yielded only mannose on demethylation. It was homogeneous by paper chromatography (solvents A, D, and E) and by paper electrophoresis in borate buffer (34), having an *M*(glucose) value in the latter of 0.56. The compound gave a reddish-brown color with the *p*-anisidine spray reagent. Anal. Calc. for a di-*O*-methyl hexose OCH_3: 29.8%. Found: 30.1%. The di-*O*-methyl-D-mannose crystallized and after recrystallization from ethyl acetate had m.p. 126–127 °C and $[\alpha]_D^{21}$ +14.5° (*c*, 1.58% in water).

Can. J. Chem. Downloaded from www.nrcresearchpress.com by 210.87.254.42 on 09/05/12
For personal use only.

The di-*O*-methyl mannose (30 mg) was reduced with sodium borohydride (35), and the sirupy di-*O*-methyl-D-mannitol was oxidized by sodium metaperiodate. The oxidation was complete after 6 h, with an oxidant consumption of 0.93 moles per mole di-*O*-methyl-D-mannitol. The mixture was deionized by exchange resins and evaporated to a sirup (16.8 mg) which showed the same chromatographic behavior in solvents A, D, and E as an authentic sample of 2,4-di-*O*-methyl-L-arabinose. The specific rotation of this product, −87.5° (*c*, 1.68% in methanol) was of the same magnitude, but of opposite sign, as that reported for 2,4-di-*O*-methyl-L-arabinose (36). The derived *N*-phenyl 2,4-di-*O*-methyl-D-arabinosylamine had m.p. 134–135 °C after recrystallization from ethanol. The reported melting points for the L-enantiomorph of this compound are 145 °C (36) and 126 °C (37). The X-ray diffraction pattern of the unknown was identical with that of an authentic specimen (38) of the L-enantiomorph having m.p. 142–144 °C.

Immunochemical Tests

The purified birch sap polysaccharide was tested for cross-reactions in antipneumococcal horse sera types I, II, V, and XIV and in antiparatyphoid B horse serum (12). Portions of sera (1 ml) were mixed in the cold with 0.05 mg of polysaccharide in 0.9% sodium chloride (1 mg of polysaccharide per ml of 0.9% sodium chloride). First readings were taken after 6–7 days; second readings were taken a further 6–7 days after addition of another 0.15 mg of polysaccharide. The results are shown in Table III.

TABLE III

Immunochemical tests on purified birch sap polysaccharide

	Horse sera†				
Reading*	I	II	V	XIV	Paratyphoid B
1	++	++++	+±	−	+
2	+±	++++	++±	+	±

*Arbitrary scale − to ++++, with ++ = 8.20 μg of antibody nitrogen precipitated and ++++ = 50 μg or more of antibody nitrogen precipitated. Results of duplicate tests are given.

†Antipneumococcal types.

ACKNOWLEDGMENTS

The authors wish to thank Dr. M. Heidelberger, Institute of Microbiology, Rutgers, the State University, New Brunswick, N.J., U.S.A., for performing and interpreting the immunochemical tests. We are grateful to Dr. R. A. Fraser, Petawawa Forest Experiment Station, Chalk River, Ontario, for a generous supply of birch sap, and to Dr. H. O. Bouveng, Swedish Forest Products Research Laboratory, Stockholm, Sweden, for a sample of *N*-phenyl 2,4-di-*O*-methyl-L-arabinosylamine. The technical assistance of F. P. Cooper and W. R. Rowsome is gratefully acknowledged.

REFERENCES

1. S. Haq and G. A. Adams. Can. J. Biochem. Physiol. **40**, 989 (1962).
2. G. A. Adams, C. T. Bishop, and I. J. McDonald. Can. J. Biochem. Physiol. **37**, 507 (1959).
3. G. A. Adams and C. T. Bishop. Can. J. Chem. **38**, 2380 (1960).
4. S. Haq and G. A. Adams. Can. J. Chem. **39**, 1165 (1961).
5. S. M. Martin and G. A. Adams. Can. J. Botany, **41**, 1605 (1963).
6. D. M. Northcote. Biochem. J. **58**, 353 (1954).
7. J. E. Scott. Chem. Ind. 168 (1955).
8. T. Bitter and H. M. Muir. Anal. Biochem. 4, 330 (1962).
9. M. Abdel-Akher, J. K. Hamilton, R. Montgomery, and F. Smith. J. Am. Chem. Soc. **74**, 4970 (1952).
10. C. T. Bishop. Methods Biochem. Analy. **10**, 1 (1962).
11. C. T. Bishop and F. P. Cooper. Can. J. Chem. **38**, 793 (1960).
12. M. Heidelberger. Progr. Chem. Org. Nat. Prod. **18**, 503 (1960).
13. F. Smith and R. Montgomery. Chemistry of plant gums and mucilages. Reinhold Publishing Corp., New York. 1959.
14. C. P. J. Glaudemans and T. E. Timell. J. Am. Chem. Soc. **80**, 1209 (1958).
15. A. J. Mian and T. E. Timell. Tappi, **43**, 775 (1960).
16. T. E. Timell. Tappi, **43**, 844 (1960).
17. L. Hough, J. K. N. Jones, and W. H. Wadman. J. Chem. Soc. 1702 (1950).
18. W. E. Trevelyan, D. P. Procter, and J. S. Harrison. Nature, **166**, 444 (1950).
19. E. Weygand, W. Perkow, and P. Kuhner. Ber. **84**, 594 (1951).
20. E. Fisher and J. Hirschberger. Ber. **21**, 1805 (1888).

Can. J. Chem. Downloaded from www.nrcresearchpress.com by 210.87.254.42 on 09/05/12
For personal use only.

21. M. SOMOGYI. J. Biol. Chem. **160**, 61 (1945).
22. N. NELSON. J. Biol. Chem. **153**, 375 (1944).
23. L. M. MALPRADE. Compt. Rend. **186**, 382 (1928).
24. A. JEANES and C. A. WILHAM. J. Am. Chem. Soc. **72**, 2657 (1950).
25. W. N. HAWORTH. J. Chem. Soc. **107**, 8 (1915).
26. I. CROON and B. LINDBERG. Acta Chem. Scand. **11**, 192 (1957).
27. S. ALLEN, T. G. BONNER, E. J. BOURNE, and N. M. SAVILLE. Chem. Ind. 630 (1958).
28. J. C. IRVINE and A. M. MOODIE. J. Chem. Soc. **93**, 95 (1908).
29. N. PRENTICE, L. S. CUENDET, and F. SMITH. J. Am. Chem. Soc. **78**, 4439 (1956).
30. W. N. HAWORTH, R. L. HEATH, and S. PEAT. J. Chem. Soc. 833 (1941).
31. D. J. BELL and S. WILLIAMSON. J. Chem. Soc. 1196 (1938).
32. A. L. CLINGMAN, J. R. NUNN, and A. M. STEPHEN. J. Chem. Soc. 197 (1957).
33. E. L. HIRST and J. K. N. JONES. J. Chem. Soc. 506 (1946).
34. A. B. FOSTER. Advan. Carbohydrate Chem. **12**, 81 (1957).
35. M. ABDEL-AKHER, J. K. HAMILTON, and F. SMITH. J. Am. Chem. Soc. **73**, 4691 (1951).
36. J. K. N. JONES. J. Chem. Soc. 1672 (1953).
37. P. ANDREWS, D. H. BALL, and J. K. N. JONES. J. Chem. Soc. 4090 (1953).
38. H. O. BOUVENG and B. LINDBERG. Acta Chem. Scand. **10**, 1515 (1956).

Can. J. Chem. Downloaded from www.nrcresearchpress.com by 210.87.254.42 on 09/05/12
For personal use only.

Can. J. Chem. Downloaded from www.nrcresearchpress.com by 210.87.254.6 on 09/05/12
For personal use only.

MAGNETIC SUSCEPTIBILITIES OF SOME COMPOUNDS OF SILICON

M. W. Lister and R. Marson
Department of Chemistry, University of Toronto, Toronto, Ontario
Received April 17, 1964

ABSTRACT

Magnetic susceptibility measurements are reported for a number of derivatives of silicon of general formula $SiR_aH_bX_c$, where R is an alkyl group and X is a halogen. The results are compared with earlier measurements on similar compounds of carbon and show deviations from additivity that can be interpreted in terms of bond interactions. The interactions, in general, are less for compounds of silicon than they are for compounds of carbon.

The magnetic susceptibilities of halogenated methanes have been examined in detail by Lacher, Scruby, and Park (1), who showed that the susceptibilities deviated somewhat from additivity in terms of the atoms contained in the compound. They obtained reasonable agreement with experiment if they included terms in their calculated susceptibilities arising from the interactions of various pairs of bonds. These terms were, in general, paramagnetic and they associated them with the paramagnetic term in Van Vleck's equation for diamagnetic susceptibility (2).

A more rigorous derivation of essentially the same equation as used by Lacher was given by Hameka (3). Hameka's equation may be most briefly written as follows:

$$\chi_M = \Sigma\chi(\text{atoms}) + \Sigma\chi(\text{bonds}) + \Sigma\chi(\text{bond interactions}).$$

Here χ_M is the molar susceptibility of the compound, and this is made up from terms for (i) each atom, (ii) each bond, and (iii) each interaction between any two bonds starting from the same atom. Of course, the sizes of the terms depend on the atoms involved. The interaction term is in general paramagnetic and, though introduced somewhat differently, is in effect the same as Lacher's paramagnetic term.

Lacher *et al.* observed that interactions between halogens increased with their size, as would be expected if large neighboring atoms modified each other's electron clouds. The present work is concerned with the susceptibilities of a similar series of compounds of silicon, the silicon being attached to various combinations of hydrogen, chlorine, bromine, iodine, or alkyl groups. Since silicon is a larger atom, it would be expected that the interactions would be less. However, it is well known that silicon–halogen distances are shorter than the sums of the covalent radii, to an extent not found in carbon compounds, the deviation being least for silicon–iodine bonds. If this is caused by partial double bonding, it should decrease the magnetic susceptibilities. The susceptibilities of the silicon compounds were compared with the carbon compounds to see whether such an effect could be detected.

As a knowledge of the molar volumes is required to convert the initially measured volume susceptibilities to molar susceptibilities, the densities of a number of silicon compounds were also measured.

EXPERIMENTAL

Preparation of Compounds

Silicon tetrachloride was fractionally distilled in a stream of nitrogen, and the middle fraction (20 ml out of an initial 150 ml) was used. This boiled at 57.3 °C, in agreement with previous values (4).

Silicon tetrabromide was prepared by passing a mixture of bromine vapor and nitrogen over heated ferrosilicon. The product was refluxed over mercury and then fractionally distilled to give a colorless middle fraction boiling at 152.5 °C. The freezing point, 5.6 °C, remained constant after recrystallization. Ferrosilicon was used, as it was found that pure silicon was not attacked under these conditions.

Silicon tetraiodide was similarly prepared by passing iodine vapor and nitrogen over ferrosilicon at a dull-red heat. The product was dissolved in carbon disulphide, shaken with mercury, and then fractionally distilled at low pressure. The middle fraction was very pale pink and melted at 122.5 °C, in agreement with earlier values (4) ranging from 120 to 123.8 °C.

Trichlorosilane, from the Anderson Chemical Co., was fractionally distilled in nitrogen, and the middle fraction (20 ml out of 300 ml) was used. It boiled at 32 °C. McKenzie, Mills, and Scott (5) give 31.8 °C.

Methyldichlorosilane, from the Anderson Chemical Co., was fractionated under vacuum, and the middle fraction (20 ml out of 300 ml) boiled at 40.9 °C. Gmelin (6) gives 40.7 °C.

Ethyldichlorosilane, from the Anderson Chemical Co., was fractionated under vacuum, and the middle fraction (20 ml out of 250 ml) boiled at 75.2 °C. McKenzie *et al.* (5) give 74.9 °C.

Dimethyldichlorosilane, from the Anderson Chemical Co., was fractionally distilled, and the middle fraction (20 ml out of 400 ml) boiled at 70 °C, in agreement with previous values (6).

Trimethylchlorosilane, from the Anderson Chemical Co., was fractionally distilled to give a middle fraction (20 ml out of 600 ml) boiling at 57.5 °C, in agreement with previous results (6).

Triethylchlorosilane was prepared by treating tetraethyl orthosilicate with ethyl magnesium bromide in ether in the molar ratio of 1 to 3. This was found to give a better yield than with excess Grignard reagent as recommended by di Giorgio *et al.* (7). The mixture was refluxed until it no longer gave the Gilman test for a Grignard reagent. The ether was distilled off, and the solid residue heated for 2 days on a steam bath.

$$Si(OC_2H_5)_4 + 3C_2H_5MgBr \rightarrow SiOC_2H_5(C_2H_5)_3 + 3C_2H_5OMgBr.$$

The residue is triethylethoxysilane, and it was added to dilute sulphuric acid at 0 °C to give hexaethyldisiloxane, $(C_2H_5)_3SiOSi(C_2H_5)_3$. This was extracted with ether, dried over calcium chloride, and fractionally distilled under vacuum. It was then dissolved in concentrated sulphuric acid, and ammonium chloride was added in the molar ratio of 1 to 2. The triethylchlorosilane so formed was extracted with hexane and distilled. It was finally distilled under vacuum to give a product boiling at 145 °C (Gmelin (6) gives 143 to 145 °C). This was fractionally distilled once more to give the final sample.

Trimethylbromosilane was prepared from trimethylchlorosilane, which was first hydrolyzed in boiling water under reflux. The hexamethyldisiloxane so formed was separated, dried over calcium chloride, and distilled. It was sealed into a wide pyrex tube with phosphorus tribromide in the molar ratio of 1 to 1.7, with 0.25 g of ferric chloride as catalyst (8). The mixture stood for 1 day and was then fractionally distilled under vacuum. The product boiled at 79.5 to 80 °C (Gmelin (6) gives 79.5 °C) and was used after one more fractional distillation.

Methyltribromosilane was prepared by McCusker and Reilly's method (9) from silicon tetrabromide and methyl magnesium iodide. The product was distilled several times to give a main fraction boiling at 132–134 °C (Gmelin (6) gives 133.5 °C), which, after one more fractionation, was used for magnetic measurements.

Ethyltribromosilane was prepared by the same method using ethyl magnesium bromide. Repeated fractional distillation gave a product with a constant boiling point of 157 °C.

Trimethyliodosilane. Attempts to prepare this from hexamethyldisiloxane, potassium iodide, and phosphoric acid were unsuccessful, though other halosilanes can be prepared by analogous reactions (10). The method used was a modification of that of Voronkov and Khudobin (11), who refluxed hexamethyldisiloxane with iodine and aluminum granules. It was found that amalgamated aluminum was much more effective, and that it was better to add the iodine gradually in small portions. The molar ratios used were 1.0 of disiloxane, 1.1 of aluminum and 1.5 of iodine. Reflux distillation was continued until the condensate was colorless, and the mixture was then distilled. The product was redistilled over copper filings, in the absence of light which caused decomposition.

Another method, similar to that of Eaborn (12) was also used. Tetramethylsilane and iodine in equimolar amounts were refluxed together for 10 h. Small amounts of amalgamated aluminum were added at intervals to produce aluminum iodide, which acts as a catalyst. Traces of unreacted iodine were then removed by copper filings, and the product was distilled.

The combined products of both methods were fractionally distilled under vacuum to give a colorless middle fraction, boiling at 107–108 °C (Gmelin (6) gives 107 °C).

Triethyliodosilane. Hexaethyldisiloxane, prepared by di Giorgio's method (7), was refluxed under nitrogen with iodine, in a molar ratio of 2 to 3. Freshly amalgamated aluminum was added in the ratio of 1.1 g-atom per g-mole of disiloxane, the method being a modification of that of Voronkov and Khudobin (11). After refluxing, the product was distilled off under vacuum and redistilled over copper filings to give a crude product boiling at 190–195 °C.

Since the yield was only moderate, a preparation similar to that of Eaborn (12), above, was carried out using silicon tetraethyl. The combined products were twice fractionally distilled to give a middle fraction boiling at 192–193 °C (Anderson (13) gives the b.p. as 193 ± 1 °C).

Can. J. Chem. Downloaded from www.nrcresearchpress.com by 210.87.254.6 on 09/05/12
For personal use only.

Dimethyldiiodosilane was prepared by refluxing trimethyliodosilane with equimolar amounts of iodine in an atmosphere of nitrogen (12).

$$(CH_3)_3SiI + I_2 \rightarrow (CH_3)_2SiI_2 + CH_3I.$$

Amalgamated aluminum was again added as a catalyst. The product was distilled, decolorized by copper filings, and redistilled under nitrogen in the absence of light. Redistillation gave a constant boiling product of b.p. 167 °C. This is a little lower than the previously reported value of 170–171 °C. A further vacuum distillation was carried out, and the middle fraction used.

Ethyltriiodosilane was prepared by Anderson's method (13) from ethyltrichlorosilane. The resulting solution was treated with copper filings and distilled under vacuum. The product was redistilled in a nitrogen atmosphere to give a middle fraction with a constant b.p. of 246 °C (Anderson gives 250 ± 1 °C). It was redistilled under vacuum and the middle fraction used.

Tetramethylsilane, from the Anderson Chemical Co., was distilled to give a middle fraction, b.p. 26 °C (Gmelin (6) gives 26.2 °C).

Tetraethylsilane was obtained similarly, and gave a middle fraction, b.p. 154.5 °C.

Density Measurements

These were made by weighing pycnometers of conventional design, with precautions against evaporation. The results are given in Table I. In other cases reliable values were available in the literature, as noted in Table I, and these were used.

TABLE I

Compound	Density, g/ml at 25 °C	Molar susceptibility[a] Obs.	Calc.
$SiCl_4$	1.4723[b]	87.4_5	87.4
$SiBr_4$	2.7715[c]	123.3_5	123.4
SiI_4	3.57	186.2	186.2
$SiHCl_3$	1.3313[d]	70.6_5	70.65
CH_3SiHCl_2	1.110	66.9_5	67.2
$C_2H_5SiHCl_2$	1.0872[d]	78.9_5	78.7
$(CH_3)_2SiCl_2$	1.057	81.3	83.3
$(CH_3)_3SiCl$	0.855	79.0	79.45
$(C_2H_5)_3SiCl$	0.8953	110.5_5	113.95
CH_3SiBr_3	2.213[f]	115.5	115.65
$C_2H_5SiBr_3$	2.0671[f]	127.5	127.45
$(CH_3)_3SiBr$	1.1727[f]	91.3	91.15
$C_2H_5SiI_3$	2.710	171.7	171.55
$(CH_3)_2SiI_2$	2.205	131.8	132.7
$(CH_3)_3SiI$	1.467	104.1_5	104.15
$(C_2H_5)_3SiI$	1.350	139.3	138.65
$(CH_3)_4Si$	0.6373[g]	74.9	74.4
$(C_2H_5)_4Si$	0.7620[h]	120.1	120.4

[a]Molar susceptibilities are in units of -10^{-6} e.m.u.
[b]Ref. 16.
[c]Ref. 17.
[d]Ref. 5.
[e]Ref. 6.
[f]Ref. 9.
[g]Ref. 18.
[h]Ref. 19.

Magnetic Susceptibility Measurements

These were made as outlined in a previous paper (14). The standard substance was benzene, carefully freed from oxygen. It was assumed to have a volume susceptibility of -0.6187×10^{-6} e.m.u. per ml, as determined by Eggleston, Evans, and Richards (15).

In every case the susceptibility tube was filled by vacuum distillation, and, when full, nitrogen was admitted up to 1 atm.

The results are given in Table I.

DISCUSSION OF RESULTS

Relevant values for other compounds in the literature are: $(C_2H_5)_2SiCl_2$, 105.8; CH_3SiCl_3, 87.45; $C_2H_5SiCl_3$, 98.84 (20); SiH_4, 20.4 (21).

Can. J. Chem. Downloaded from www.nrcresearchpress.com by 210.87.254.6 on 09/05/12
For personal use only.

The equation of Hameka (3) quoted above can be expressed in terms of the following parameters for a compound of formula $SiR_aH_bX_c$, where R is an alkyl group and X is a halogen.

$$\chi_M = aA + bB + cC + abU + acV + bcW.$$

Here a, b, and c are the numbers of the atoms or groups present, and A, B, C, U, V, and W are parameters related to Hameka's various terms as explained below.

The parameter A is given by:

$$A = 0.25\chi(\mathrm{Si}) + \chi(\mathrm{R}) + \chi(\mathrm{Si—R}) + 1.5\chi\left(\mathrm{Si}\begin{smallmatrix}\diagup\mathrm{R}\\ \diagdown\mathrm{R}\end{smallmatrix}\right)$$

where $\chi(\mathrm{Si})$ and $\chi(\mathrm{R})$ are the contributions of the silicon atom and the group R, $\chi(\mathrm{Si—R})$ is the contribution of the Si—R bond, and $\chi\left(\mathrm{Si}\begin{smallmatrix}\diagup\mathrm{R}\\ \diagdown\mathrm{R}\end{smallmatrix}\right)$ is the term due to the interactions of two Si—R bonds to the same silicon. In the same notation,

$$B = 0.25\chi(\mathrm{Si}) + \chi(\mathrm{H}) + \chi(\mathrm{Si—H}) + 1.5\chi\left(\mathrm{Si}\begin{smallmatrix}\diagup\mathrm{H}\\ \diagdown\mathrm{H}\end{smallmatrix}\right),$$

$$C = 0.25\chi(\mathrm{Si}) + \chi(\mathrm{X}) + \chi(\mathrm{Si—X}) + 1.5\chi\left(\mathrm{Si}\begin{smallmatrix}\diagup\mathrm{X}\\ \diagdown\mathrm{X}\end{smallmatrix}\right),$$

$$U = \chi\left(\mathrm{Si}\begin{smallmatrix}\diagup\mathrm{R}\\ \diagdown\mathrm{H}\end{smallmatrix}\right) - 0.5\chi\left(\mathrm{Si}\begin{smallmatrix}\diagup\mathrm{R}\\ \diagdown\mathrm{R}\end{smallmatrix}\right) - 0.5\chi\left(\mathrm{Si}\begin{smallmatrix}\diagup\mathrm{H}\\ \diagdown\mathrm{H}\end{smallmatrix}\right),$$

$$V = \chi\left(\mathrm{Si}\begin{smallmatrix}\diagup\mathrm{R}\\ \diagdown\mathrm{X}\end{smallmatrix}\right) - 0.5\chi\left(\mathrm{Si}\begin{smallmatrix}\diagup\mathrm{R}\\ \diagdown\mathrm{R}\end{smallmatrix}\right) - 0.5\chi\left(\mathrm{Si}\begin{smallmatrix}\diagup\mathrm{X}\\ \diagdown\mathrm{X}\end{smallmatrix}\right),$$

$$W = \chi\left(\mathrm{Si}\begin{smallmatrix}\diagup\mathrm{H}\\ \diagdown\mathrm{X}\end{smallmatrix}\right) - 0.5\chi\left(\mathrm{Si}\begin{smallmatrix}\diagup\mathrm{H}\\ \diagdown\mathrm{H}\end{smallmatrix}\right) - 0.5\chi\left(\mathrm{Si}\begin{smallmatrix}\diagup\mathrm{X}\\ \diagdown\mathrm{X}\end{smallmatrix}\right).$$

As regards the difference between methyl and ethyl compounds, the same treatment leads to the conclusion that there will be a certain increment in susceptibility on replacing a methyl by an ethyl group, but none of the other parameters will be altered. In effect A is increased, but U and V are unchanged.

The data in Table I give an average value of 11.5 for this increment from methyl to ethyl, and this makes $A = 18.6$ for methyl groups. The susceptibility of silane quoted above (21) makes $B = 5.1$, and if we take C from the various tetrahalides we can calculate average values for the other parameters. The results are:

Halogen	C	V
Cl	21.85	0.6
Br	30.85	1.5
I	46.55	0.6

In addition $SiHCl_3$ makes W for chlorine approximately zero, and the two compounds $SiRHCl_2$ make $U = -1.4$. These numbers are used to calculate the susceptibilities given in the last column of Table I; and for the compounds quoted above from the literature, the values are: $(C_2H_5)_2SiCl_2$ obs. 105.8, calc. 106.3; CH_3SiCl_3, obs. 87.45, calc. 86.0; $C_2H_5SiCl_3$ obs. 98.85, calc. 97.5. The average deviation between calculated and observed

Can. J. Chem. Downloaded from www.nrcresearchpress.com by 210.87.254.6 on 09/05/12
For personal use only.

values is 0.52 or 0.47%. It cannot be claimed that the results demonstrate that the silicon compounds follow Hameka's equation; but if they do, the various parameters have the value given above.

Corresponding measurements on carbon compounds (1, 21, 22) fit the following constants: $A = 15.75$, $B = 4.35$, $U = 0.50$, and values of C and W for various halogens are:

Halogen	C	W
F	9.8	−1.65
Cl	16.7	1.1
Br	23.4	2.4
I	33.9	3.8

These are larger interaction parameters than for silicon compounds, especially when it is borne in mind that W values are for interactions between hydrogen and halogen.

Lacher, Scruby, and Park (1) deduce the individual interaction terms by calculating atomic susceptibilities using Slater-type orbitals, with some correction for the effect of bonding. These, coupled with the observed susceptibilities, enable them to obtain values for the interaction terms, such as $\chi(C\langle^{H}_{H})$, and they note that these are all negative (or paramagnetic). Their results depend on a value of 12.7 for the susceptibility of methane and more recent work (21) has given a higher value of 17.4, which would considerably change the estimate of $\chi(C\langle^{H}_{H})$.

However, some comparison can be made. If we take the atomic susceptibility for carbon, 7.84, as calculated by Angus' method (23), and use Lacher, Scruby, and Park's values for halogens (with bond depressions), the interaction terms are found to be $\chi(C\langle^{Cl}_{Cl}) = -3.0$, $\chi(C\langle^{Br}_{Br}) = -6.0$, and $\chi(C\langle^{I}_{I}) = -8.9$, in the expected order. From the W values, if we assume $\chi(C\langle^{H}_{H})$ to be negligibly small, we get $\chi(C\langle^{H}_{Cl}) = -0.4$, $\chi(C\langle^{H}_{Br}) = -0.6$, and $\chi(C\langle^{H}_{I}) = -0.7$, again forming a reasonable sequence. Similarly for silicon, Angus' method gives an atomic susceptibility of 22.3, and using the same halogen values we get: $\chi(Si\langle^{Cl}_{Cl}) = -2.0$, $\chi(Si\langle^{Br}_{Br}) = -3.5$, and $\chi(Si\langle^{I}_{I}) = -2.9$. These are less than the carbon series but the iodine term seems unduly low. The V values only enable us to determine $\chi(Si\langle^{CH_3}_{X}) - \chi(Si\langle^{CH_3}_{CH_3})$, which for various halogens has the values: Cl, −0.4; Br, −0.3; I, −0.9. Presumably $\chi(Si\langle^{CH_3}_{CH_3})$ is less than $\chi(Si\langle^{Cl}_{Cl})$ as the atoms are smaller, and this would make the $\chi(Si\langle^{CH^3}_{X})$ values also fairly small. Consequently these comparisons support the idea that interactions are less if the central atom is relatively large. There is no indication of possible double bonding between a halogen and the central silicon atom, which presumably would lead to relatively large paramagnetic terms with chlorine.

Can. J. Chem. Downloaded from www.nrcresearchpress.com by 210.87.254.6 on 09/05/12
For personal use only.

REFERENCES

1. J. R. Lacher, R. E. Scruby, and J. D. Park. J. Am. Chem. Soc. **72**, 333 (1950).
2. J. H. Van Vleck. Theory of electric and magnetic susceptibilities. Oxford University Press. 1932. p. 275.
3. H. F. Hameka. J. Chem. Phys. **34**, 1996 (1961).
4. Gmelin's Handbuch der Anorganischen Chemie. System Nummer 13 (1954).
5. C. A. McKenzie, A. P. Mills, and J. M. Scott. J. Am. Chem. Soc. **72**, 2032 (1950).
6. Gmelin's Handbuch der Anorganischen Chemie. System Nummer 15, Teil C (1958).
7. P. A. Giorgio, W. A. Strong, L. H. Sommer, and F. C. Whitmore. J. Am. Chem. Soc. **68**, 1380 (1946).
8. W. F. Gilliam, R. N. Meals, and R. O. Sauer. J. Am. Chem. Soc. **68**, 1161 (1946).
9. P. A. McCusker and E. L. Reilly. J. Am. Chem. Soc. **75**, 1583 (1953).
10. E. A. Flood. J. Am. Chem. Soc. **55**, 1735 (1933).
11. M. G. Voronkov and Y. I. Khudobin. Izv. Akad. Nauk SSSR Otd. Khim. Nauk, 713 (1956).
12. C. Eaborn. J. Chem. Soc. 2755 (1949).
13. H. H. Anderson, D. L. Seaton, and R. P. T. Rudnicki. J. Am. Chem. Soc. **73**, 2144, 2351 (1951).
14. M. W. Lister and R. Marson. Can. J. Chem. **42**, 1817 (1964).
15. B. C. Eggleston, D. F. Evans, and R. E. Richards. J. Chem. Soc. 941 (1954).
16. J. H. Hildebrand. J. Chem. Phys. **15**, 727 (1947).
17. S. M. Kennard and P. A. McCusker. J. Am. Chem. Soc. **70**, 1039 (1948).
18. S. Tannenbaum, S. Kaye, and G. F. Lewenz. J. Am. Chem. Soc. **75**, 3753 (1953).
19. S. Sugden and M. Wilkins. J. Chem. Soc. 126 (1931).
20. R. M. Mathur. Trans. Faraday Soc. **54**, 1477 (1958).
21. C. Barter, R. G. Meisenheimer, and D. P. Stevenson. J. Phys. Chem. **64**, 1312 (1960).
22. J. Broersma. J. Chem. Phys. **17**, 873 (1949).
23. W. R. Angus. Proc. Roy. Soc. Ser. A, **136**, 569 (1932).

Can. J. Chem. Downloaded from www.nrcresearchpress.com by 210.87.254.6 on 09/05/12
For personal use only.

Can. J. Chem. Downloaded from www.nrcresearchpress.com by 210.87.254.6 on 09/05/12
For personal use only.

FAR INFRARED AND RAMAN SPECTRA AND STRUCTURE OF DITHIOPHOSGENE[1]

W. K. BUSFIELD,[2] M. J. TAYLOR,[3] AND E. WHALLEY
Division of Applied Chemistry, National Research Council, Ottawa, Canada

Received April 2, 1964

ABSTRACT

The infrared spectrum in the range 3000–50 cm^{-1} and the Raman spectrum of solutions of dithiophosgene have been obtained. There are no coincidences in the infrared and Raman spectra, and the only structure consistent with this and approximately tetrahedral carbon valencies is

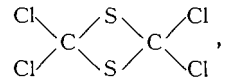

that is tetrachloro-1,3-dithietane, in which the ring is planar or nearly planar. A tentative assignment of the observed bands is given on the basis of D_{2h} symmetry.

1. INTRODUCTION

Carbon disulphide polymerizes under high pressure to a black substance (1) that has essentially the structure (2)

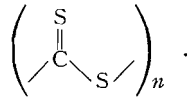

Thiophosgene Cl_2CS might be expected to form a similar polymer, and attempts have been made in this laboratory to polymerize it at pressures up to 20 kbar. No polymer was obtained, the thiophosgene being converted to the dimer, which had previously been made (3) by irradiation of thiophosgene with ultraviolet light. Although direct evidence was lacking, it was suggested (3) that the dimer had the structure

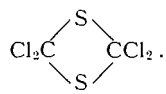

Silicon disulphide has a polymeric chain structure

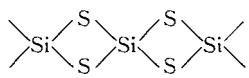

in which alternate four-membered rings are at right angles to one another. It seems likely that carbon disulphide can exist in a similar structure and might be converted to it by applying a high enough pressure. When the work reported in this paper was done, no unambiguous proof of structure of a ring 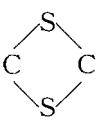 had been obtained, and only an incomplete investigation of the infrared spectrum of dithiophosgene (4) without a detailed discussion had been made. An attempt has been made therefore to verify the structure by

[1]*N.R.C. No. 8048.*
[2]*N.R.C. Postdoctoral Fellow 1960–62.*
[3]*N.R.C. Postdoctoral Fellow 1961–62.*

investigating the infrared and Raman spectra. Since this work was completed, the infrared and Raman spectra of the fluorinated analogue of dithiophosgene have been reported (5) and its structure confirmed.

2. EXPERIMENTAL METHODS AND RESULTS

Dithiophosgene was prepared as colorless crystals by the action of ultraviolet light on thiophosgene, and was purified by repeated vacuum sublimation.

The Raman spectrum was obtained by examination of approximately 5 ml samples of saturated solutions in carbon tetrachloride, chloroform, and benzene. By use of these three solvents the possibility of any additional lines being masked by solvent frequencies was eliminated. The exciting line was Hg 4358 Å from a Toronto-type mercury arc, isolated by a filter of saturated aqueous sodium nitrite solution. The spectra were recorded photographically by means of a Hilger E612 two-prism spectrograph with an E614 f/5.7 camera (dispersion about 95 cm^{-1}/mm in the region of 4358 Å). Kodak 103a-G plates were used, and the spectra were recorded with a wide range of exposure times. Frequencies were determined using the well-defined Raman lines of the solvents as reference, and the limits of error are about ± 2 cm^{-1}. States of polarization were measured qualitatively by the method of polarized incident light. The frequencies, polarizations, and rough relative intensities are summarized in Table I.

TABLE I

Raman spectrum of dithiophosgene in saturated solution in carbon tetrachloride, chloroform, and benzene

ν/cm^{-1}	Relative intensity	Polarization	Tentative assignment
876	vw	p?	A_g CCl_2 sym. stretching and ring breathing
755	vw	dp	B_{2g} CCl_2 antisym. stretching
714	w	dp	B_{1g} ring in-plane stretching
494	vs	p	A_g CCl_2 sym. stretching and ring breathing
366	s	p	A_g CCl_2 sym. bending and ring in-plane bending
321	w	dp	B_{1g} CCl_2 wagging
253	w	dp	B_{2g} CCl_2 rocking
199	m	p	A_g CCl_2 sym. bending and ring in-plane bending

Abbreviations: v, very; s, strong; m, medium; w, weak; p, polarized; dp, depolarized.

Infrared spectra of solutions of various concentrations in benzene, cyclohexane, carbon disulphide, carbon tetrachloride, and tetrachloroethylene were recorded between 3000 and 650 cm^{-1} using a Perkin–Elmer Model 21 spectrophotometer with a sodium chloride prism, between 800 and 250 cm^{-1} with a Beckman IR-7 prism-grating spectrophotometer, and between 320 and 50 cm^{-1} with a Perkin–Elmer Model 301 double-beam filter-grating spectrophotometer. For calibration, polystyrene (for the Model 21), carbon dioxide, and water vapor were employed. Above 800 cm^{-1} the accuracy is about ± 2 cm^{-1} and below 800 cm^{-1} about ± 1 cm^{-1}. The infrared spectrum is shown in Fig. 1 and summarized in Table II. The band shown at 220 cm^{-1} is the band of a mull of dithiophosgene in Nujol. In benzene solution the band is very broad.

Some dissociation of the dimer occurred in the solutions, particularly when the Raman spectrum was being taken, and the solution became brown. The strongest Raman line of thiophosgene (1140 cm^{-1} (6)) could then be observed faintly in the spectrum of the solution. When this occurred the solution was purified by distilling off the solvent and the thiophosgene in vacuum, and dissolving the dimer in fresh solvent.

Can. J. Chem. Downloaded from www.nrcresearchpress.com by 210.87.254.6 on 09/05/12
For personal use only.

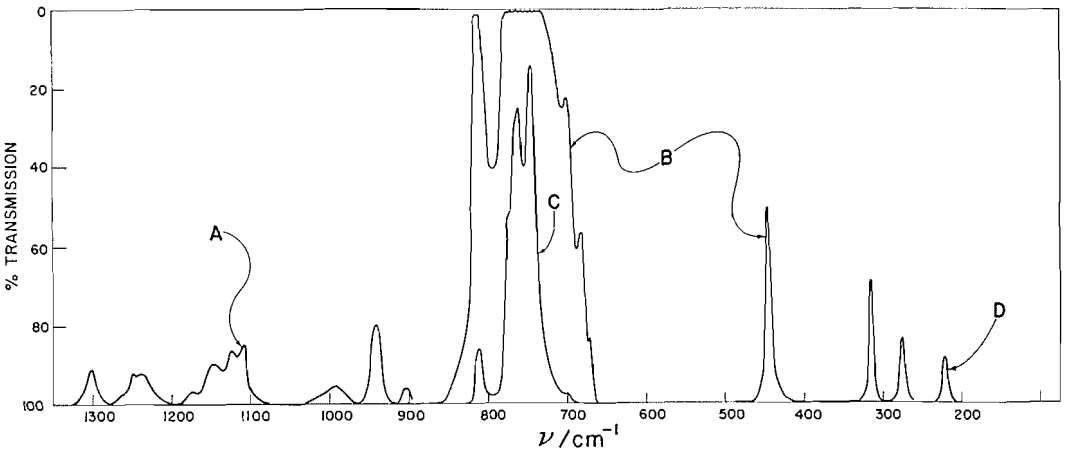

FIG. 1. Infrared spectrum of dithiophosgene in solution in benzene, cyclohexane, carbon disulphide, carbon tetrachloride, and tetrachloroethylene. Curve A, 0.4 *M* in 1.0 mm cell. Curve B, 0.4 *M* in 0.5 mm cell. Curve C, 0.025 *M* in 0.1 mm cell. Curve D, mull in Nujol.

TABLE II

Infrared spectrum of dithiophosgene as solution in benzene, cyclohexane, carbon disulphide, carbon tetrachloride, and tetrachloroethylene

ν/cm^{-1}	Relative intensity	Assignment
1303	w	811 + 494
1249	w	761 + 494
1234	w	745 + 494
1174	vvw	811 + 366
1147	w	Monomer
1122	m	761 + 366
1108	m	745 + 366
988	vw, b	274 + 714, 811 + 199, etc.
939	m	445 + 494
904	vw	?
811	vs	B_{3u} ring in-plane stretching
770	m, sh	274 + 494, 445 + 321
761	vvs	B_{1u} CCl_2 antisym. stretching
745	vvs	B_{3u} CCl_2 sym. stretching
699	s	B_{2u} ring in-plane stretching
680	m	314 + 366
668	vw	CO_2
445	s	B_{3u} CCl_2 sym. bending
314	s	B_{2u} CCl_2 wagging
274	m	B_{1u} CCl_2 rocking
220	m	B_{1u} ring out-of-plane bending

Abbreviations: w, weak; m, medium; s, strong; b, broad; sh, shoulder.

3. DISCUSSION

There are a number of possible structures of the dithiophosgene molecule which conform to the usual valencies. A structure containing a four-membered ring of alternate carbon and sulphur atoms has D_{2h} symmetry if the ring is planar, but only C_{2v} symmetry if it is bent about either the S—S or C—C axes. If the structure is

$$\begin{array}{ccc} & & Cl_2C\text{—}S \\ & & | \quad | \\ Cl_2C\text{—}S & & \end{array}$$

the symmetry is C_{2v}. The open-chain structures $Cl_3CSCCl{=}S$ and $Cl_2C{=}CClSSCl$, and all structures with three-membered rings, have a maximum symmetry C_s.

Can. J. Chem. Downloaded from www.nrcresearchpress.com by 210.87.254.6 on 09/05/12
For personal use only.

Can. J. Chem. Downloaded from www.nrcresearchpress.com by 210.87.254.6 on 09/05/12
For personal use only.

For D_{2h} symmetry, the 18 normal vibrations are divided into symmetry species as follows: $4A_g + 1A_u + 2B_{1g} + 3B_{1u} + 2B_{2g} + 2B_{2u} + 1B_{3g} + 3B_{3u}$. The nine vibrations symmetric to the center of symmetry are Raman active, with the four totally symmetric vibrations giving rise to polarized Raman lines. The vibrations of species B_{1u}, B_{2u}, and B_{3u} are infrared active. The one vibration of species A_u is inactive in both spectra. Under the lower symmetries C_{2v} or C_S all 18 normal vibrations are Raman active, and all are infrared active except for the few A_2 vibrations that occur under C_{2v} symmetry.

In the observed spectra (Tables I and II) there are no coincidences between infrared and Raman bands. There are only eight Raman lines, and only about eight infrared bands appear to be strong enough to be fundamentals. The number of polarized Raman lines is certainly three and possibly four. It appears therefore that the spectrum is close to that expected for D_{2h} symmetry, but is far too sparse for the lower symmetries mentioned, and we can conclude that the structure of dithiophosgene is 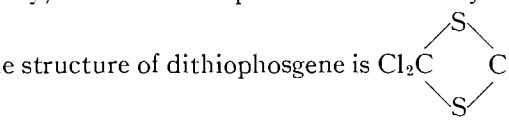 , that is tetrachloro-1,3-dithietane. The symmetry requires the ring to be planar but not rectangular; however, a small departure from planarity may not of course be detected spectroscopically.

A detailed unambiguous assignment of the fundamentals is not possible without more work. Nevertheless an attempt is expected and has been made, although the results are on much less firm ground than the conclusion in the preceding paragraph. For ease of reference, the vibrations are described in terms of localized vibrations. This is of course a very crude approximation, and because the chlorine and sulphur atoms have nearly the same mass there will be considerable coupling of their motions except as forbidden by symmetry. Drawings of the approximate forms of the vibrations are given in ref. 7. The assignment is attempted using internal evidence, the assignment of the Raman-active vibrations of the aluminum halides based on a vibrational analysis (7, 8), and the assignment of the vibrations of the fluoro analogue, tetrafluoro-1,3-dithietane (5), for which vapor infrared spectra were obtained and band contours used to determine the symmetry species.

The assignment of the frequencies is best started from the Raman spectrum. The three polarized lines 494, 366, and 199 cm^{-1} must be due to A_g vibrations, and the weak line of uncertain polarization at 876 cm^{-1} is a likely candidate for the fourth A_g vibration. Two of these lines are due to C—Cl and C—S stretching vibrations, and two to bending vibrations. Uncoupled C—Cl and C—S stretching frequencies are usually about 700 cm^{-1}. The A_g C—Cl stretching and ring breathing vibrations are therefore probably strongly coupled to give the 876 and 494 cm^{-1} bands. The A_g CCl_2 symmetric bending and ring in-plane bending vibrations are also probably coupled to give the 366 and 199 cm^{-1} bands. The two high-frequency depolarized bands at 755 cm^{-1} and 714 cm^{-1} are to be assigned to the two remaining Raman-active stretching vibrations, the B_{2g} CCl_2 antisymmetric stretching and the B_{1g} ring in-plane (C—S) stretching vibrations. The best guess at the present time is that the 755 cm^{-1} line is due to the B_{2g} vibration and the 714 cm^{-1} line is due to the B_{1g} vibration. Three Raman-active vibrations remain, the B_{1g} CCl_2 wagging, B_{2g} CCl_2 rocking, and B_{3g} CCl_2 twisting vibrations. One is missing which, by analogy with the aluminum halides (7), may be the B_{3g} vibration. The 321 and 253 cm^{-1} bands are to be assigned to the remaining two, and by analogy with the aluminum halides (7) are probably due to the B_{1g} and B_{2g} vibrations respectively.

We turn next to the infrared spectrum. Eight fundamental bands are expected. On the grounds of intensity the obvious choice is 811, 761, 745, 699, 445, 314, 274, and 220 cm^{-1}.

Can. J. Chem. Downloaded from www.nrcresearchpress.com by 210.87.254.6 on 09/05/12
For personal use only.

There are four infrared-active mainly stretching vibrations to be assigned. These are the B_{1u} CCl_2 antisymmetric stretching, the B_{3u} CCl_2 symmetric stretching, and the B_{2u} and B_{3u} ring in-plane stretching vibrations. Since C—Cl stretching vibrations are usually stronger in absorption than C—S stretching vibrations, the very strong pair 761 and 745 cm^{-1}, which are close to the Raman-active B_{2g} CCl_2 antisymmetric stretching vibration at 755 (or 714) cm^{-1}, are probably the B_{1u} antisymmetric and B_{3u} symmetric CCl_2 stretching vibrations, but it is not certain which is which. In the fluoro analogue the B_{1u} vibration has the higher frequency, and this may also be true for dithiophosgene. The 811 cm^{-1} band is probably due to either the B_{2u} or the B_{3u} ring in-plane stretching vibration, the B_{3u} vibration being perhaps more likely than the B_{2u}. The B_{2u} ring in-plane stretching must be of reasonably high frequency, and the band at 699 cm^{-1}, which is close to the Raman-active B_{1g} ring in-plane stretching frequency at 714 (or 755) cm^{-1}, is an obvious choice. In the fluoro analogue the B_{3u} vibration has the higher frequency, which provides some support for this choice.

The B_{1u} ring out-of-plane bending has only a small harmonic restoring force in simple rings (7, 9). However, in dithiophosgene, coupling with the B_{1u} CCl_2 rocking motion is expected because the sulphur and chlorine atoms have about the same mass. The lowest frequency vibration observed, 220 cm^{-1}, is the most likely candidate for this vibration. In the fluoro analogue the corresponding vibration was at 60 cm^{-1}. It is higher in dithiophosgene presumably because coupling with the rocking vibration is greater. The B_{1u} CCl_2 rocking vibration is probably at 274 cm^{-1}. If this assignment is correct, the similarity of the frequency of these two B_{1u} vibrations indicates that the motions are very mixed.

The infrared-active vibrations remaining to be assigned frequencies are the B_{2u} CCl_2 wagging and the B_{3u} CCl_2 symmetric bending. The remaining apparently fundamental frequencies are 445 and 314 cm^{-1}. The 314 cm^{-1} band is probably due to the bending and the 445 cm^{-1} to the wagging vibration. The assignment of the fundamental bands is summarized in Table III.

The infrared-active combination bands can be assigned satisfactorily on the basis of observed bands, except for the 988 and the 904 cm^{-1} bands. The 988 cm^{-1} band could be

TABLE III

Symmetry species, activity, approximate description, and tentative assignments of the fundamental frequencies of dithiophosgene under symmetry D_{2h}

Symmetry species	Activity	Approximate description	ν/cm^{-1}
A_g	R, p	CCl_2 symmetric stretching	876
		Ring breathing	494
		CCl_2 symmetric bending	366
		Ring in-plane bending	199
A_u	Inactive	CCl_2 twisting	—
B_{1g}	R, dp	Ring in-plane stretching	714
		CCl_2 wagging	321
B_{1u}	IR	CCl_2 antisymmetric stretching	761
		CCl_2 rocking	274
		Ring out-of-plane bending	220
B_{2g}	R, dp	CCl_2 antisymmetric stretching	755
		CCl_2 rocking	253
B_{2u}	IR	Ring in-plane stretching	699
		CCl_2 wagging	445
B_{3g}	R, dp	CCl_2 twisting	—
B_{3u}	IR	CCl_2 symmetric stretching	745
		Ring in-plane stretching	811
		CCl_2 symmetric bending	314

274 + 714, but, if it is, then the assignment of the fundamentals requires altering. It is, however, a broad band, and probably has several components. There are two unobserved fundamentals, the A_u CCl_2 twisting vibration which is inactive, and the B_{3g} CCl_2 twisting which is Raman active but was not observed. The unassigned combinations could involve these vibrations.

REFERENCES

1. P. W. BRIDGMAN. Proc. Am. Acad. Arts Sci. **74**, 399 (1941).
2. E. WHALLEY. Can. J. Chem. **38**, 2105 (1960).
3. A. SCHONBERG and A. STEPHENSON. Ber. **66B**, 567 (1933).
4. J. I. JONES, W. KYNASTON, and J. L. HALES. J. Chem. Soc. 614 (1957).
5. J. R. DURIG and R. C. LORD. Spectrochim. Acta, **19**, 769 (1963).
6. H. W. THOMSON. Trans. Faraday Soc. **37**, 251 (1941); J. Chem. Phys. **6**, 748 (1938). A. J. Downs. Spectrochim. Acta, **19**, 1165 (1963).
7. R. P. BELL and H. C. LONGUET-HIGGINS. Proc. Roy. Soc. Ser. A, **183**, 357 (1945).
8. H. GERDING and E. SMIT. Z. Physik. Chem. B, **50**, 171 (1941).
9. R. P. BELL. Proc. Roy. Soc. Ser. A, **183**, 328 (1944). A. Danti, W. T. Lafferty, and R. C. Lord. J. Chem. Phys. **33**, 294 (1960).

Can. J. Chem. Downloaded from www.nrcresearchpress.com by 210.87.254.6 on 09/05/12
For personal use only.

Can. J. Chem. Downloaded from www.nrcresearchpress.com by 210.87.254.105 on 09/05/12
For personal use only.

THE RELATIVE EASE OF REDUCTIVE CLEAVAGE OF 1,3-DIOXOLANES AND 1,3-DIOXANES IN ETHER SOLUTION BY $LiAlH_4$–$AlCl_3$[1]

B. E. Leggetter, U. E. Diner, and R. K. Brown
Department of Chemistry, University of Alberta, Edmonton, Alberta
Received April 27, 1964

ABSTRACT

In ether solution, 1,3-dioxolanes are hydrogenolyzed faster by $LiAlH_4$–$AlCl_3$ than are the corresponding 1,3-dioxanes. This difference is attributed to the relative ease of oxocarbonium ion formation in the rate-determining step of the reaction. The results obtained have been utilized to explain the selective cleavage of the five- and six-membered acetal structures found in the polyacetals of hexitols.

INTRODUCTION

It is known that, in general, acetals and ketals are stable to the action of lithium aluminum hydride and advantage has been taken of this fact to protect certain carbonyl groups from reduction by this hydride (1). However, in the presence of Lewis acids, these acetals and ketals are hydrogenolized by lithium aluminum hydride to the corresponding ethers. Cyclic acetals and ketals under these conditions yield hydroxy ethers (2, 3, 4).

Of the two mechanisms suggested for this reaction (2), hydride attack on the carbonium ion resulting from the complex formed between the Lewis acid and the acetal *or* reduction of an α-halo ether formed by reaction of the Lewis acid with the acetal, the former is preferred on the basis of results obtained from hydrogenolysis of 1,3-oxathiolanes by $LiAlH_4$–$AlCl_3$ (5). Additional evidence in support of a mechanism involving carbonium ion formation in the rate-determining step of the $LiAlH_4$–$AlCl_3$ hydrogenolysis of 1,3-dioxolanes has been given in a recent study of the influence of substituents on the ease and direction of ring-opening during hydride reductive cleavage of 1,3-dioxolanes (6). In this work it was found that electron donor substituents on C_2 enhance while electron-withdrawing groups retard the rate of hydrogenolysis, a situation quite similar to that found for the hydrolysis of acetals and ketals, which is believed to proceed via carbonium ion formation in the rate-determining step (7). A similar, but much less pronounced effect occurs because of substituents on C_4 of the 1,3-dioxolane system. However, in addition, C_4 substituents have a marked control on the *direction* of ring-opening during the reductive cleavage (6).

During work in this laboratory on the reductive cleavage of cyclic acetals and ketals, a marked difference was noted in the ease of reduction of the five-membered ring structures, the 1,3-dioxolanes, and the six-membered ring structures, the 1,3-dioxanes. This paper presents the results of comparative hydrogenolysis of these two types of compounds in ether solution by lithium aluminum hydride in the presence of aluminum chloride.

RESULTS AND DISCUSSION

Reductions and analyses of products were carried out according to the general procedure described previously (6). Care was taken to ensure that the reductions of each of

[1]*Taken in part from the thesis of B. E. Leggetter, submitted to the Faculty of Graduate Studies, University of Alberta, Edmonton, Alberta, in partial fulfillment of the requirements for the degree of Doctor of Philosophy.*

the pairs of compounds, the 1,3-dioxolane and the 1,3-dioxane, were carried out identically. The results of the experiments are shown in Table I.

TABLE I

Comparative ease of reduction of 1,3-dioxolanes and 1,3-dioxanes by $LiAlH_4$–$AlCl_3$ in ether solution

Expt. No.	Dioxane or dioxolane	Reduction* time	Total† recovery, %	Yield of‡ starting material, %	Yield of‡ reduction product, %
1	1,3-Dioxolane	24 h	55§	40	60
2	1,3-Dioxane	24 h	75	72	28
3	4-Methyl-1,3-dioxolane	1.5 h	85	8	92
4	4-Methyl-1,3-dioxane	48 h	86	66	34
5	2-Phenyl-1,3-dioxolane	1.0 h	70	0	100
6	2-Phenyl-1,3-dioxane	1.0 h	63	0	100
7	2-Phenyl-1,3-dioxolane	15 min	95	0	100
8	2-Phenyl-1,3-dioxane	15 min	98	7‖	93‖
9	2,2,4-Trimethyl-1,3-dioxolane	1.5 h	86	0	100
10	2,2,4-Trimethyl-1,3-dioxane	1.5 h	84	0	100
11	2,2,4-Trimethyl-1,3-dioxolane	15 min	93	0	100
12	2,2,4-Trimethyl-1,3-dioxane	15 min	96	0	100

*This includes the time taken for addition of the Lewis acid as well as the length of stirring following the addition of reagents.
†Includes both reduction products and starting material.
‡Based upon total recovery.
§Total recovery was low. From experience it was found that the reduction product rather than initial material was absorbed preferentially on the aluminum salts and required exhaustive extraction for removal. Here only two extractions were made, but further extraction would no doubt give more of the reduced product and intensify the differences found for expts. 1 and 2.
Exhaustive extraction was done for expts. 7, 8 and 11, 12 giving the high recovery noted.
‖This was measured using CH_3CH_2—O—CH_2—CH_2—O—CH_2—CH_2—O—CH_2CH_3 as internal standard.

It is clearly seen that 1,3-dioxanes reduce at a rate slower than that for the analogous 1,3-dioxolanes. For those pairs of compounds which possess a phenyl substituent on C_2 (expts. 5–8) or a methyl substituent (expts. 9–12), the usual reaction time of 1 h or more gave complete hydrogenolysis of both the five- and six-membered rings. However, the difference in rates for one of these did show up when the total time of reduction was reduced to 15 min.

The difference in rates of reduction can be explained on the basis of ease of formation of the intermediate oxocarbonium ion. Oxocarbonium ion formation requires that the atoms of the C_2—O_3—C_4 group attain coplanarity for optimum stabilization.* This is more readily achieved in the five-membered ring because it is more nearly coplanar initially (8) than is the 1,3-dioxane whose ideal conformation approaches that of the chair form of cyclohexane. In the six-membered ring there must first occur a distortion to the half chair form to allow the overlap of the *p*-orbital of the oxygen atom with the developing empty *p*-orbital of the C_2 atom (Fig. 1). The greater distortion required for the six-membered ring would thus retard oxocarbonium ion formation and hence reduction.

Recently Bishop and Cooper (9) have shown that the anomerization of five-membered ring glycosides is considerably faster than that of the six-membered ring glycosides and have suggested that the difference in rate is due to the more facile formation of the intermediate carbonium ion transition state of the five-membered ring.

**During the attainment of the transition state, before the ring is actually broken, there must occur an approximation to coplanarity to permit stabilization of the carbonium ion and thus allow further advance in the breaking of the* C_2—O_1 *bond. That the "greater strain of a five-membered ring" is not the controlling factor is shown by the much slower reductive cleavage of 2,2,4,4,5,5-hexamethyl-1,3-dioxolane versus either 2,2,4,4-tetramethyl-1,3-dioxolane or 2,4,4-trimethyl-1,3-dioxolane (B. E. Leggetter and R. K. Brown. Can. J. Chem. 42, 1005 (1964)).*

Can. J. Chem. Downloaded from www.nrcresearchpress.com by 210.87.254.105 on 09/05/12
For personal use only.

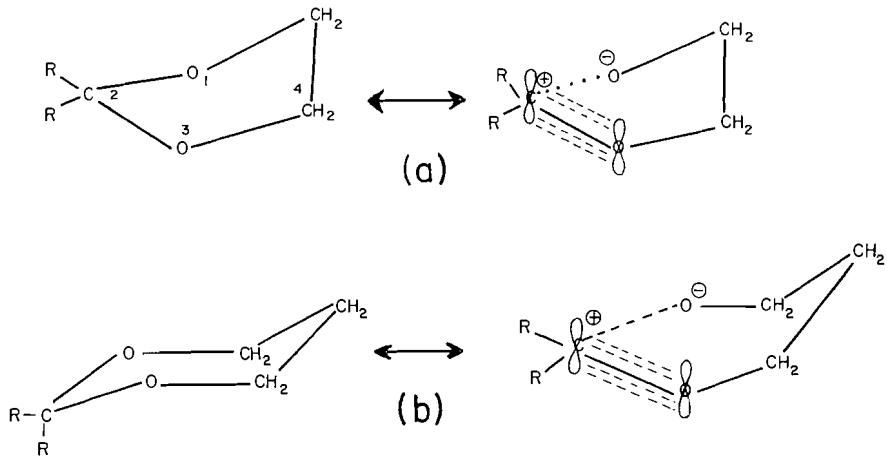

FIG. 1. (*a*) 1,3-Dioxolane—little distortion required; (*b*) 1,3-dioxane—more distortion required.

The discovery by Doukas and Fontaine (10) that when diosgenin was hydrogenolyzed by lithium aluminum hydride in the presence of acids, only the six-membered ring was cleaved (Fig. 2) while the five-membered ring remained intact can be explained on the same basis.

Carbonium ion formation by cleavage of the six-membered ring is preferred because of the more facile overlap of the *p*-orbital of the oxygen atom of the five-membered ring with the developing empty *p*-orbital of the carbon atom common to both rings (Fig. 3).

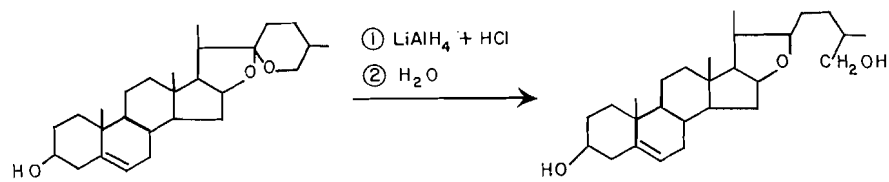

FIG. 2.

Because of the similarity between the acid-catalyzed hydrolysis of acetals and their Lewis acid catalyzed hydrogenolysis with lithium aluminum hydride, in that the rate-controlling step is the formation of the oxocarbonium ion, the results of this work and that describing the effects of substituents on the ease and direction of ring-opening (6) offer an explanation for the anomalous selective acid-catalyzed cleavage of the acetals of a number of hexitols.

The stability of the 2,4-O-methylene ring in 1,3:2,4:5,6-tri-*O*-methylene-D-sorbitol to aqueous acid (11), to acetolysis (12), to acetyl trifluoracetate (13), and to boron trifluoride in methylene chloride (14) can be due to (*a*) its six-membered ring structure, (*b*) the presence of hydroxymethyl groupings on each of the carbon atoms C_4 and C_6, whose *inductive effect* retards carbonium ion formation (6), and (*c*) the greater difficulty of attaining the necessary coplanarity for carbonium ion stabilization because of the large

Can. J. Chem. Downloaded from www.nrcresearchpress.com by 210.87.254.105 on 09/05/12
For personal use only.

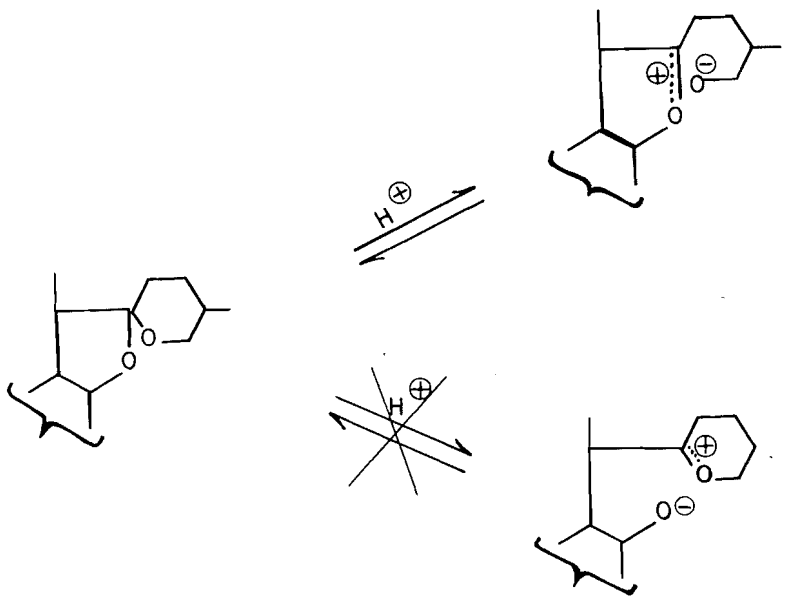

FIG. 3.

equatorial groups on C_4 and C_6 which in the transition state would tend towards the more restricted axial conformation (15).

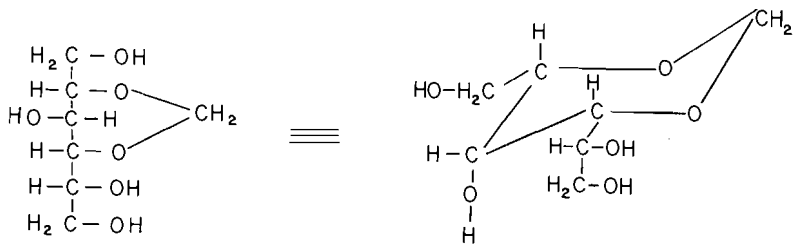

The 5,6-O-methylene ring of this compound, being a five-membered cyclic acetal, is expected to (and does) hydrolyze more readily than do either the 1,3 or the 2,5 rings (ref. 15, p. 186).

EXPERIMENTAL

Procedure for the Reduction of 1,3-Dioxolanes and 1,3-Dioxanes

Details of the procedure followed those previously described (6).

Preparation of Compounds

Synthesis of the *1,3-dioxolanes* and *their reduction products* has been reported elsewhere (6).

A. 1,3-Dioxanes

2-Phenyl-1,3-dioxane was prepared by a modification of Salmi's procedure (16). A mixture of benzaldehyde (60 g, 0.57 mole), 1,3-propanediol (38 g, 0.5 mole, Eastman Kodak Co.), *p*-toluenesulphonic acid (1 g), and toluene (150 ml) was heated under reflux in an apparatus equipped with a Dean–Stark water separator (17) until the requisite amount of water (9 ml) was removed. The cooled reaction mixture was poured into saturated aqueous sodium bicarbonate solution and the organic layer separated, washed with water, and

Can. J. Chem. Downloaded from www.nrcresearchpress.com by 210.87.254.105 on 09/05/12
For personal use only.

dried (Na_2CO_3). Fractional distillation afforded 55 g (67%) of material boiling at 95–96°/12 mm. This oil solidified when cooled, and after crystallization from Skellysolve B melted at 45–46°. Lit. m.p. 49–51° (18).

1,3-Dioxane was prepared by the directions used for the preparation of 1,3-dioxolane (6), starting with 1,3-propanediol. B.p. 101°/700 mm. Lit. b.p. 105°/755 mm (19).

2,2,4-Trimethyl-1,3-dioxane was prepared by the procedure of Fischer and Pfahler (20) modified as follows.

A mixture of 1,3-butanediol (1.09 mole, Eastman Kodak Co.), anhydrous magnesium sulphate (40 g), *p*-toluenesulphonic acid (1 g), and acetone (600 ml) stood at 25° for 60 h. The filtrate from this mixture was concentrated and the residue poured into saturated aqueous sodium carbonate. The ether extract from this was dried (magnesium sulphate), freed from solvent, and the residue distilled yielding the required dioxane. B.p. 125°/700 mm. Lit b.p. 131–132° (21).

4-Methyl-1,3-dioxane was prepared according to published directions (22).

B. Reduction Products

3-Methoxy-1-propanol was synthesized by a modification of the procedure described by Henze and Rogers (23).

Sodium (5.0 g, 0.22 mole) was dissolved in 120 ml of methanol and the resulting solution was stirred under reflux while 3-chloro-1-propanol (19.0 g, 0.2 mole, Eastman Kodak Co.) was added dropwise. The mixture was then stirred for 3 h, cooled, and poured into cold water. The ether extract was dried ($MgSO_4$), freed from solvent, and distilled affording 3.8 g (21%) of material boiling at 144–146°/700 mm. Lit. b.p. 148–149° (24).

3-Benzyloxy-1-propanol was prepared by modification of a published procedure (25). Sodium metal (2.7 g, 0.12 mole) was dissolved in 30 ml of hot 1,3-propanediol. To the resulting solution was added slowly 15.0 g (0.12 mole) of benzyl chloride. The mixture was heated at 120° for 2 h, then cooled, and poured into water. The dried ether extract ($MgSO_4$) was freed from solvent and the residue distilled giving 7.2 g (37%) of the alcohol boiling at 107°/1.5 mm. Lit. b.p. 155°/23 mm (25).

4-Isopropoxy-2-butanol was prepared by the procedure used for the synthesis of 3-benzyloxy-1-propanol above, starting with 1,3-butanediol and 2-bromopropane. B.p. 94°/45 mm; η_D^{25}, 1.4518. Calc. for $C_7H_{16}O_2$: C, 63.64; H, 12.12. Found: C, 63.96; H, 12.37.

4-Methoxy-2-butanol was prepared according to the above procedure, starting with 1,3-butanediol and methyl iodide. B.p. 85°/62 mm. Lit. b.p. 145° (26).

3-Methoxy-1-butanol was prepared according to the literature (27).

3-Isopropoxy-1-butanol was prepared by the reduction of isopropyl β-isopropoxybutyrate with lithium aluminum hydride according to standard procedure (28). B.p. 93°/35 mm; η_D^{25}, 1.4156. Calc. for $C_7H_{16}O_2$: C, 63.64; H, 12.12. Found: C, 64.04; H, 12.17.

The precursor, isopropyl β-isopropoxybutyrate, was prepared from isopropyl crotonate (29) and isopropyl alcohol by the procedure of Doering and Young (27). Yield, 43% of material boiling at 47°/1.5 mm. Calc. for $C_{10}H_{20}O_3$: C, 63.83; H, 10.64. Found: C, 63.45; H, 10.85.

ACKNOWLEDGMENT

The authors express their appreciation to the National Research Council of Canada whose financial assistance made this work possible.

REFERENCES

1. N. G. Gaylord. Reduction with complex metal hydrides. Interscience Publishers Inc., New York, N.Y. 1956. pp. 673–680.
2. E. L. Eliel and M. N. Rerick. J. Org. Chem. **23**, 1088 (1958).
3. E. L. Eliel. Record Chem. Progr. **23**, 129 (1961).
4. E. L. Eliel, V. G. Badding, and M. N. Rerick. J. Am. Chem. Soc. **84**, 2371 (1962).
5. B. E. Leggetter and R. K. Brown. Can. J. Chem. **41**, 2671 (1963).
6. B. E. Leggetter and R. K. Brown. Can. J. Chem. **42**, 990 (1964).
7. M. M. Kreevoy and R. W. Taft, Jr. J. Am. Chem. Soc. **77**, 5590 (1955).
8. R. U. Lemieux, J. D. Stevens, and R. R. Fraser. Can. J. Chem. **40**, 1955 (1962).
9. C. T. Bishop and F. P. Cooper. Can. J. Chem. **40**, 224 (1962).
10. H. M. Doukas and T. D. Fontaine. J. Am. Chem. Soc. **73**, 5917 (1951).
11. E. J. Bourne and L. F. Wiggins. J. Chem. Soc. 517 (1944).
12. A. T. Ness, R. M. Hann, and C. S. Hudson. J. Am. Chem. Soc. **66**, 665 (1944).
13. E. J. Bourne, J. Burden, and J. C. Tatlow. J. Chem. Soc. 1864 (1959).
14. T. G. Bonner and N. M. Saville. J. Chem. Soc. 2851 (1960).
15. S. A. Barker and E. J. Bourne. Advan. Carbohydrate Chem. **7**, 137 (1952).
16. E. J. Salmi. Ber. **71**, 1803 (1938).
17. E. W. Dean and D. D. Stark. Ind. Eng. Chem. **12**, 486 (1920).
18. E. Fischer. Ber. **27**, 1537 (1894).
19. H. T. Clarke. J. Chem. Soc. 1803 (1912).

Can. J. Chem. Downloaded from www.nrcresearchpress.com by 210.87.254.105 on 09/05/12
For personal use only.

20. E. FISCHER and E. PFAHLER. Ber. **63**, 1606 (1920).
21. E. J. SALMI and V. RANNIKKO. Ber. **72**, 600 (1939).
22. R. B. CARLIN and L. O. SMITH, JR. J. Am. Chem. Soc. **69**, 2007 (1947).
23. H. R. HENZE and B. F. ROGERS. J. Am. Chem. Soc. **61**. 433 (1939).
24. L. I. SMITH and J. A. SPRUNG. J. Am. Chem. Soc. **65**, 1276 (1943).
25. G. M. BENNETT and A. L. HOCK. J. Chem. Soc. 472 (1927).
26. Ger. pat. No. 962,787 (Apr. **25**, 1957); Chem. Abstr. **53**, 11235 (1959).
27. W. VON E. DOERING and R. W. YOUNG. J. Am. Chem. Soc. **74**, 2997 (1952).
28. Org. Reactions, **6**, 469 (1951).
29. O. BRUNNER and P. HANKE. Monatsh. **83**, 1485 (1952).

Can. J. Chem. Downloaded from www.nrcresearchpress.com by 210.87.254.105 on 09/05/12
For personal use only.

Can. J. Chem. Downloaded from www.nrcresearchpress.com by 210.87.254.40 on 09/05/12
For personal use only.

A STUDY OF HINDERED ROTATION IN SOME PROTONATED BENZYLAMINES

W. F. REYNOLDS* AND T. SCHAEFER
Department of Chemistry, University of Manitoba, Winnipeg, Manitoba

Received May 11, 1964

ABSTRACT

The effect of hindered rotation upon methylene and ammonio proton shifts and coupling constants of eight protonated benzylamines has been determined. It is shown that the necessary and sufficient condition for methylene proton asymmetry in protonated benzylamines is the absence of a plane of symmetry along the $C_6H_5CH_2$—N bond axis. It is established that the maximum value of the *gauche* H—C—N—H^+ coupling constant is 3.15 c/s and that the minimum value of the *trans* H—C—N—H^+ coupling constant is 9.45 c/s. From the relative values of the rotationally averaged coupling constants, it is established that the steric effect of the substituent decreases in the following order: isopropyl, phenyl > benzyl ≈ ethyl > methyl. It cannot be decided from the available evidence whether the phenyl group or the isopropyl group causes greater steric hindrance.

INTRODUCTION

Considerable work has been done on the problem of configurational isomerism of substituted ethanes with high resolution nuclear magnetic resonance (1–10). There was some misunderstanding in the early literature about the roles of asymmetry and conformational populations in producing magnetic non-equivalence of nuclei (4, 5). This confusion has lately been cleared up (11–13).

From the temperature dependence of coupling constants involved (7), or from an observed averaged coupling constant at one temperature and a value of energy differences between isomers obtained from vibrational spectra (8), values of vicinal coupling constants have been estimated as 10 to 18 c/s for *trans* coupling constants and 1 to 3.5 c/s for *gauche* coupling constants of protons attached to saturated carbon atoms in substituted ethanes.

While investigating a series of protonated anilines and related compounds, we noted that the methylene protons of certain protonated benzylamines were non-equivalent. Protonated benzylamines (ϕH_2C—$NHRS)^+$ are analogous to triply substituted ethanes (XH_2C—CHYX). We have investigated a series of substituted benzylamines and dibenzylamines in a protonating solvent in an attempt to determine the magnitudes of coupling constants, asymmetry shifts, and isomer population differences for this type of compound.

The equivalence or non-equivalence of rotamer population was established for the series of compounds studied. The predictions of Gutowsky (13) about the effect of substitution upon methylene proton asymmetry were confirmed. Maximum values of the *gauche* coupling constants and minimum values of the *trans* coupling constants were established. A qualitative estimate of the relative steric hindrance caused by several substituents was made. There were not sufficient data available to determine exact values of the vicinal coupling constants and the energy differences between the various isomers.

(A) Effect of Energy Levels upon Rotation Rates about Single Bonds and upon Relative Populations of Rotational Isomers

Steric hindrance of rotation about single bonds in saturated hydrocarbons has often been considered to be due to van der Waals' forces of repulsion between substituents (14).

**Holder of a National Research Council of Canada Studentship*, 1962–1963.

Since this repulsion will generally be greatest when substituents are in eclipsed positions, it is usually assumed that substituted ethanes exist in their three possible staggered configurations (rotamers). The relative populations of rotamers depend upon their relative energy levels. The relative populations are given by the Boltzmann factors. An increase in temperature will cause the relative populations to approach equality.

The rotation rate about a single bond depends upon the heights of the energy barriers and the temperature. If one of the energy barriers is very high, a rocking motion will occur instead of rotation. Since this normally will have the same effect upon the proton spectrum as rotation, further discussion will be based upon the assumption that rotation occurs about the single bond. If two of the barriers are much higher than the other barrier, then this assumption will no longer be justified.

(B) Effect of Rotation Rate and Rotamer Population upon Methylene Proton Asymmetry

Concerning the conditions which cause methylene proton asymmetry, Waugh and Cotton (11), and Bishop (12) pointed out a fundamental error in the reasoning of previous workers. Gutowsky has established the minimum substitution required to cause non-equivalence of methylene protons in compounds of the substituted ethane type (13). His treatment will be applied here to the methylene groups of protonated benzylamines.

(1) Type 1

Consider a compound of the general type $XH_2C—(NRSH_X)^+$. The possible rotational configurations are shown in Fig. 1. There are three more possible rotamers which are mirror images of the three shown.

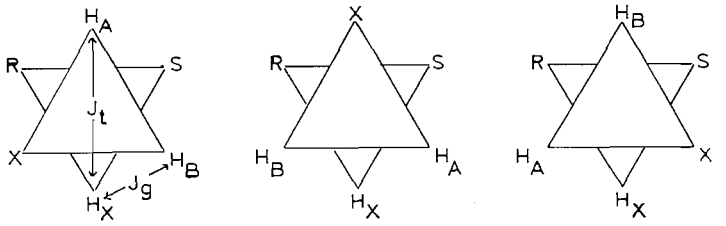

FIG. 1. The three possible rotamers for a protonated compound of the type $XCH_2—(NRSH)^+$ (type 1). The methylene carbon atom lies above the plane of the diagram and the nitrogen atom lies below this plane.

The rotationally averaged proton shifts are

[1] $$\bar{\nu}_A = \sum_n x_n \nu_n^A \quad \text{and} \quad \bar{\nu}_B = \sum_n x_n \nu_n^B$$

or in general,

[2] $$\bar{\nu}_i = \sum_n x_n \nu_n^i,$$

where x_n = mole fraction of rotamer n and ν_n^i = the chemical shift of the ith nucleus of rotamer n. The shift of proton H_X is not considered for reasons outlined in the section on results. It can be seen from the configuration diagrams that all three rotamers are identical if X = H. Therefore,

[3] $$\bar{\nu}_A = \bar{\nu}_B = \sum_n \tfrac{1}{3}\nu_n^A = \sum_n \tfrac{1}{3}\nu_n^B,$$

i.e., $$(\overline{\nu_A - \nu_B}) = 0.$$

Can. J. Chem. Downloaded from www.nrcresearchpress.com by 210.87.254.40 on 09/05/12
For personal use only.

All A and B protons are equivalent only if rapid rotation occurs about the C—N bond axis. Equation [3] is obtained by noting that $\nu_1^A = \nu_3^B$, etc. However, there is still an intrinsic asymmetry which would be observed if rotation were stopped, since $\nu_1^A \neq \nu_2^A \neq \nu_3^A$, etc.

If X ≠ H, then three different rotamers are present. The presence of X changes all six proton shifts ν_n^A and ν_n^B. The net result is a chemical shift between H_A and H_B

$$[4] \qquad \Delta\bar{\nu}_A = \sum_n x_n(\nu_n^A - \nu_n^B) = (\overline{\nu_A - \nu_B}).$$

This may be rewritten as

$$[5] \qquad \Delta\bar{\nu}_A = \sum_n x_n(\Delta\nu_n^0 + \delta\nu_n),$$

where $\Delta\nu_n^0$ = the shift between the protons of rotamer n of the parent compound (where X = H) and $\delta\nu_n$ = the change in $\Delta\nu_n^0$ caused by the substitution of X for H. But from eq. [3] we find that

$$[6] \qquad \sum_n \tfrac{1}{3}\Delta\nu_n^0 = 0.$$

Substitution of this result in eq. [5] yields

$$[7] \qquad \Delta\bar{\nu}_A = \sum_n (x_n - \tfrac{1}{3})\Delta\nu_n^0 + \sum_n [(x_n - \tfrac{1}{3})\delta\nu_n + \tfrac{1}{3}\delta\nu_n],$$

which was derived by Gutowsky (13).
Equation [7] can be rearranged in terms of eq. [4] to give

$$[8] \qquad \Delta\bar{\nu}_A = \sum_n (x_n - \tfrac{1}{3})(\nu_n^A - \nu_n^B) + \sum_n \tfrac{1}{3}\delta\nu_n.$$

The first term depends upon relative populations and upon differences in chemical shifts in the three rotamers. The second term depends solely upon the additional shifts caused by the substitution of X for H. This additional shift has been referred to as the asymmetry effect (13).

Equations [1] to [8] can be used to predict the types of spectra that would be expected for type 1 compounds for different populations of rotamers and for different rates of rotation about the C—N bond. There are three basic situations which must be considered. These are (1) no rotation – slow rotation, (2) rapid rotation with equal rotamer population, and (3) rapid rotation with unequal rotamer populations. If the compound does not rotate about the C—N bond, the spectra of the individual rotamers will be obtained, if they are sufficiently populated to be observed. As the rotation rate increases, the spectra of the individual rotamers collapse to a single, averaged spectrum. Collapse is complete when the rotation rate exceeds $2\pi(\nu_1^A - \nu_2^A)$ s^{-1}, etc. Since none of the compounds studied showed evidence of slow rotation about the C—N bond, there will be no further discussion of this possibility.

Equation [8] indicates that the methylene protons of type 1 compounds are non-equivalent even when rapid rotation occurs about the C—N bond. The averaged shift will alter with changing temperature until the populations of the three rotamers are equal. At this point a small shift will remain which will not alter with increasing temperature. This asymmetry shift is a second-order effect, which results from different interactions between the various substituent groups. It is very difficult, if not impossible, to

Can. J. Chem. Downloaded from www.nrcresearchpress.com by 210.87.254.40 on 09/05/12
For personal use only.

predict the expected value of the asymmetry effect. It is also difficult to obtain experimentally, because equalized populations normally are obtained only at very high temperatures.

(2) Type 2

Type 2 compounds are those with two identical groups bonded to the nitrogen (other than the benzyl group). There are two possibilities: $XH_2C—(NR_2H)^+$ (type 2*a*) and $XH_2C—(NRH_2)^+$ (type 2*b*). In terms of the asymmetry of the methylene group they are both of the general type $XH_2C—(NRS_2)^+$ and therefore may be considered together. The diagrams in Fig. 2 represent the type 2*a* rotamers. These can be considered as a *trans*

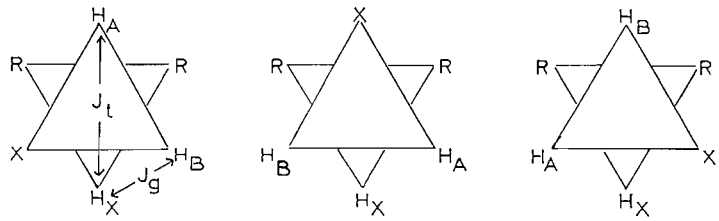

FIG. 2. The three possible rotamers for a protonated compound of the type $XCH_2—(NR_2H)^+$ (type 2*a*).

form (2), referring to X and H_X, and two *gauche* forms (1 and 3). It can be seen that $\nu_1^A = \nu_3^B$, $\nu_3^A = \nu_1^B$, $\nu_2^A = \nu_2^B$, and $x_1 = x_3$, since rotamers 1 and 3 are sterically equivalent. Substitution of the above relations into eq. [1] yields

$$\bar{\nu}_A = \bar{\nu}_B = x_2\nu_2^A + 2x_1(\nu_1^A + \nu_1^B) \quad [9]$$

or

$$\bar{\nu}_A = \bar{\nu}_B = x_t\nu_2^A + x_g(\nu_1^A + \nu_1^B) \quad [10]$$

where $x_g = x_1 + x_3$. Equations [9] and [10] predict that protons H_A and H_B are equivalent, regardless of the relative populations of the *trans* and *gauche* rotamers, if rotation is rapid enough to average chemical shifts. The averaged shifts will vary with temperature until rotamer populations are equal, and then will remain constant.

(3) Type 3

If the $(NRS_2)^+$group is changed to $(NH_3)^+$ (type 3), it can easily be shown that all rotamers are equivalent and that no shift differences will be found, regardless of the rate of rotation about the C—N bond.

From the above discussion it can be seen that only type 1 compounds show methylene proton asymmetry when rapid rotation occurs about the C—N bond. This asymmetry persists even for free rotation (equal populations). The methylene protons of type 2 and type 3 compounds are always equivalent when rotation is rapid enough to average the differences in shift of the individual rotamers. Therefore, methylene proton asymmetry occurs when three different groups, other than the benzyl group under observation, are bonded to the nitrogen atom. In other words, the necessary condition for methylene proton asymmetry is the absence of a plane of symmetry along the C—N bond axis. Complete nitrogen asymmetry is a sufficient but not a necessary condition since some substituted dibenzylamines should show methylene proton asymmetry. For example, protonated *N*-methyldibenzylamine should show methylene proton asymmetry because

Can. J. Chem. Downloaded from www.nrcresearchpress.com by 210.87.254.40 on 09/05/12
For personal use only.

Can. J. Chem. Downloaded from www.nrcresearchpress.com by 210.87.254.40 on 09/05/12
For personal use only.

it has three different groups, other than the benzyl group under consideration, bonded to the nitrogen: C_6H_5—CH_2—$N(CH_3)(C_6H_5CH_2)(H^+)$. There is no plane of symmetry along the $C_6H_5CH_2$—N bond. Thus the methylene protons will be asymmetric even though the nitrogen atom is not asymmetric.

(C) Effect of Rotamer Population and Rotation Rate upon Proton Coupling Constants

There are two basic types of coupling constants between methylene protons and ammonio protons of molecules in staggered configurations: J_{gauche} (J_g) and J_{trans} (J_t). The values of J_g and J_t will vary slightly for the different rotamers for the same reason that there is an asymmetry effect. It is normally assumed that all values of each type of coupling constants within a given molecule are equal (15). It is known that *trans* and *gauche* F–F coupling constants can vary by as much as 4 c/s within a given molecule (10, 16). The constancy of the different *trans* and *gauche* H–H coupling constants within a given ethane-type molecule has apparently never been proved. It has been suggested that F–C–C–F coupling constants are affected also by a "through space" mechanism which principally involves non-bonded F–F interactions (17, 18). On the other hand, H–H coupling constants are believed to depend upon the electron distribution in the intervening bonds (19). If these theories are correct, then vicinal H–H coupling constants should be altered by the electronegativity of the substituents while vicinal F–F coupling constants should be sensitive to steric effects which alter the separation of the fluorine atoms. Since steric factors probably cause different F–F distances in the various rotamers, it is quite possible that vicinal fluorine coupling constants vary more within a given molecule than the corresponding proton coupling constants. In any case, it will be assumed that the values of J_g and J_t are the same for all the rotamers of a given molecule. It is necessary to make this assumption, since without knowledge of the energy levels of the three rotamers, it is impossible to determine the constance of J_g and J_t (10)*.

From the previous equations and diagrams, it is possible to predict the effect of population changes upon proton coupling constants.

(1) Type 1

This type of compound is expected to give an ABX spectrum for the methylene protons and the ammonio proton with the methylene protons being A and B. The AB coupling constant is measurable. The possible values of J_{AX} and J_{BX} can be obtained from the rotamers illustrated in Fig. 1. For fast rotation, the averaged coupling constants are:

$$\bar{J}_{AX} = x_1\bar{J}_t + (x_2 + x_3)\bar{J}_g, \quad [11]$$

$$\bar{J}_{BX} = (x_1 + x_2)\bar{J}_g + x_3\bar{J}_t. \quad [12]$$

The difference between the two coupling constants depends only upon the mole fractions of rotamers 1 and 3 and the values of J_g and J_t. (We assume $J_t > J_g$.)

$$\bar{J}_{AX} - \bar{J}_{BX} = (x_1 - x_3)(\bar{J}_t - \bar{J}_g). \quad [13]$$

In general, $\bar{J}_{AX} \neq \bar{J}_{BX}$ except by coincidence (when $x_1 = x_3$). If it is assumed that J_g and J_t are constant, then it is possible to determine the relative populations and consequently the relative stability of the two rotamers. As populations approach equality, both $\bar{J}_{AX}$ and $\bar{J}_{BX}$ approach a limiting value of $(2/3\,J_g + 1/3\,J_t)$. Inequality of $\bar{J}_{AX}$ and $\bar{J}_{BX}$ definitely indicates unequal rotamer populations. Equality of $\bar{J}_{AX}$ and $\bar{J}_{BX}$ indicates

**A referee points out that, in principle, if the temperature dependence of $\bar{J}$ could be measured with sufficient accuracy, an experimental check could be made of the constancy of J_g and J_t without a priori knowledge of the rotational potential function.*

that $x_1 = x_3$ and that possibly all populations are equal. The situation where $x_1 = x_3 \neq x_2$ might exist if the steric effects due to R and S were approximately equal, because there would then be little energy difference between rotamers 1 and 3. This corresponds to type 2*a* discussed below.

(2) Type 2a

Compounds of this type should give A_2X spectra when rapid rotation occurs about the C—N bond axis. Since the methylene protons are equivalent, it is impossible to measure the geminal coupling constant (20).

The values of $\bar{J}_{AX}$ and $\bar{J}_{A'X}$ can be obtained from Fig. 2 ($H_{A'} \equiv H_B$ in Fig. 2). The rotationally averaged coupling constants are:

$$\bar{J}_{AX} = x_1 J_t + (x_1 + x_3) J_g = \frac{x_g}{2} J_t + \left(1 - \frac{x_g}{2}\right) J_g, \qquad [14]$$

$$\bar{J}_{BX} = x_3 J_t + (x_1 + x_2) J_g = \frac{x_g}{2} J_t + \left(1 - \frac{x_g}{2}\right) J_g. \qquad [15]$$

The averaged coupling constants are therefore equal. The magnitudes of $\bar{J}_{AX}$ and $\bar{J}_{A'X}$ will vary with relative populations up to a limiting value of $(2/3\, J_g + 1/3\, J_t)$.

(3) Type 2b

The rotamers for compounds of this type are shown in Fig. 3. It can be seen from the

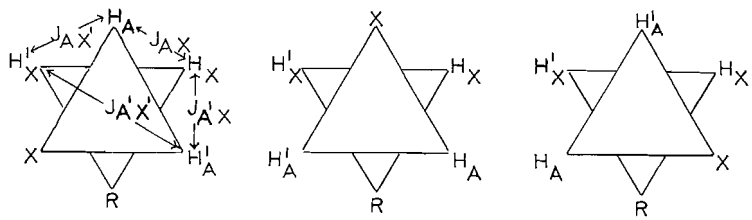

FIG. 3. The three possible rotamers for a compound of the type XCH_2—$(NRH_2)^+$ (type 2*b*).

diagram that $\bar{J}_{AX} \equiv \bar{J}_{A'X'}$ and $\bar{J}_{A'X} \equiv \bar{J}_{AX'}$ since rotamers 1 and 3 are sterically equivalent. If one takes into account that there are two coupling constants of each type per rotamer, the averaged values of the coupling constants are:

$$\bar{J}_{AX} = \frac{(1 + x_2) J_g + (x_1 + x_3) J_t}{2} = \frac{(1 + x_t) J_g + x_g J_t}{2}, \qquad [16]$$

$$\bar{J}_{A'X} = (x_1 + x_3) J_g + x_2 J_t = x_g J_g + x_t J_t. \qquad [17]$$

In general, $\bar{J}_{AX} \neq \bar{J}_{A'X}$. Both will alter with temperature up to a limiting value of $(2/3\, J_g + 1/3\, J_t)$ when populations are equal.

Experimentally, the sums and differences of $\bar{J}_{AX}$ and $\bar{J}_{A'X}$ are measured. These two variables have the following values:

$$\bar{J}_{AX} + \bar{J}_{A'X} = \left(1 + \frac{x_g}{2}\right) J_g + \left(1 - \frac{x_g}{2}\right) J_t, \qquad [18]$$

Can. J. Chem. Downloaded from www.nrcresearchpress.com by 210.87.254.40 on 09/05/12
For personal use only.

[19] $$\bar{J}_{AX} - \bar{J}_{A'X} = \left(x_t - \frac{x_g}{2}\right)(J_t - J_g).$$

If it is assumed that the *gauche* rotamers are sterically less favorable than the *trans* rotamer, then it is found that $(\bar{J}_{AX} - \bar{J}_{A'X})$ varies by $(J_t - J_g)$ when the relative rotamer populations change from $x_t = 1$ to $x_t = 1/2\, x_g$. For the same change in relative populations, $(\bar{J}_{AX} + \bar{J}_{A'X})$ varies by only $1/3(J_t - J_g)$. Consequently the measured difference in coupling constants should be more temperature dependent than the sum of the coupling constants for type 2*b* molecules. The limiting values for the two variables are 0 for $(\bar{J}_{AX} - \bar{J}_{A'X})$ and $(4/3\, J_g + 2/3\, J_t)$ for $(\bar{J}_{AX} + \bar{J}_{A'X})$.

(4) Type 3

Regardless of temperature, rotation rate, etc., a single, averaged value of $(2/3\, J_g + 1/3\, J_t)$ will be obtained for $\bar{J}_{AX}$.

The most notable feature of the effect of temperature upon coupling constants is the constancy of the limiting value of the average coupling constants obtained for the three types of molecules. In type 2 compounds the methylene protons are equivalent and changes in chemical shift can only be measured relative to a reference signal. However, definite values of coupling constants can always be obtained. Definite values of coupling constants are preferable to relative values of chemical shifts since there is always uncertainty whether the reference and (or) the methylene protons may show additional shifts due to factors other than changes in rotamer populations as the temperature changes.

(D) Effect of Proton Exchange upon Methylene Proton Asymmetry and Observed Coupling Constants

Exchange alters the shape of the observed methylene proton spectrum by two mechanisms. Firstly, exchange between the protonated and unprotonated forms of the substituted benzylamine produces an averaged methylene proton spectrum. Experimental evidence* shows that aniline in trifluoracetic acid (TFA) is almost completely protonated. Benzylamines are stronger bases and should be even more completely protonated in solution. Since the concentration of free base is much smaller than that of the protonated base, the observed spectrum should be little different from that of protonated benzylamine in the absence of exchange. Secondly, the exchange of a proton bonded to a nitrogen atom may be accompanied by an inversion of the nitrogen atom valences. This inversion effectively interchanges the A and B protons of the methylene group of a type 1 molecule and the AB spectrum collapses to an A_2 spectrum since the protons become indistinguishable. If the lifetime of unprotonated benzylamine in solution is long compared to the time taken for rearrangement of the nitrogen valences, then every second exchange on an average will invert the nitrogen atom valences.

Exchange will also alter the observed values of $\bar{J}_{AX}$ and $\bar{J}_{BX}$. As the X proton exchanges, there is an increasing uncertainty about the X proton spin alignment. Only every second exchange will result in an interchange of the X proton spin.

(E) Analysis of A_2X, ABX, and A_2X_2 Proton Spectra when the X Proton Spectra are Unmeasurable

The X (ammonio) proton spectra of protonated benzylamines do not yield any useful information, for reasons discussed later. Consequently, the amount of useful information which can be obtained is limited.

**To be published.*

Can. J. Chem. Downloaded from www.nrcresearchpress.com by 210.87.254.40 on 09/05/12
For personal use only.

(1) A_2X and A_3X Spectra

Only the AX coupling constant can be obtained. When the two protons are equivalent (20), J_{AA} is not observable.

(2) ABX Spectra

The AB part of an ABX spectrum consists of two quartets. The quartets are easily identified since they contain four spacings equal to J_{AB}. Since the X part of the spectrum cannot be measured, the information obtainable is limited. However, if it is assumed that $\bar{J}_{AX}$ and $\bar{J}_{BX}$ have the same sign, then it is possible to obtain the magnitudes of $\bar{J}_{AX}$, $\bar{J}_{BX}$, and the chemical shift. This is a reasonable assumption since it has been shown that the vicinal coupling constants in substituted ethanes have the same sign (7, 9, 21). The values of $1/2|\bar{J}_{AX} + \bar{J}_{BX}|$ and $1/2|\bar{J}_{AX} - \bar{J}_{BX}|$ can be obtained from the spectrum (22). There are two possible values of the latter term, depending upon whether the defined constants $D^+\cos 2\theta^+$ and $D^-\cos 2\theta^-$ (22) have the same or opposite signs. Only one of the two possible values will give $|\bar{J}_{AX} + \bar{J}_{BX}| > |\bar{J}_{AX} - \bar{J}_{BX}|$. This relation must hold if $\bar{J}_{AX}$ and $\bar{J}_{BX}$ have the same sign. The chemical shift can also be obtained from the expressions defining $D^+\cos 2\theta^+$ and $D^-\cos 2\theta^-$. The signs of J_{AB}, $\bar{J}_{AX}$, and $\bar{J}_{BX}$ cannot be obtained. It is also impossible to decide which coupling constant is $\bar{J}_{AX}$ and which is $\bar{J}_{BX}$.

(3) A_2X_2 Spectra

The theory of A_2X_2 spectra has been developed in general (23) and also for the specific case of disubstituted ethanes with unequal rotamer populations (9, 10). The coupling constants are defined as shown in Fig. 3. It is convenient to define the following quantities:

$$K = J_{AA'} + J_{XX'};\ L = \bar{J}_{AX} - \bar{J}_{A'X};\ M = J_{AA'} - J_{XX'};\ N = \bar{J}_{AX} + \bar{J}_{A'X}.$$

If $K \gg L$ and $M = 0$, then the methylene proton spectrum will consist of five peaks: an intense doublet with spacing equal to N and a triplet whose outside peaks are L c/s apart. Both spectral groupings have the same center of gravity. As L increases with respect to K, the central line of the triplet splits into a doublet. If $M \neq 0$, then the outside peaks of the triplet are split into doublets. The spacing from center to center of the two doublets is equal to $(M^2 + L^2)^{1/2}$ and the doublet splitting is equal to M. If L is small or M is large, the total spectrum collapses to a triplet. Only the value of N can definitely be obtained from an A_2X_2 spectrum.

EXPERIMENTAL

Eleven different protonated benzylamines were investigated. In three cases no useful results were obtained. All solutions contained 5 mole percent of the benzylamine being investigated and 2 mole percent of cyclohexane as an internal reference. Trifluoracetic acid was used as a protonating solvent. All chemicals were Eastman White Label grade and were used without further purification.

Proton resonance spectra were measured at 60 Mc/s on a Varian DP-60 spectrometer. Samples were degassed and sealed in thick-walled 5 mm glass sample tubes. Spectra were obtained at different temperatures with the aid of a variable temperature probe manufactured at N.R.C. (24). Sample temperatures were measured by a copper–constantan thermocouple attached to a Varian G-11 recording potentiometer. The temperature measurements are believed accurate to within 2 °K. Peak separations were measured by sideband techniques, using a Hewlett–Packard 521C frequency counter. All results are the average of at least six measurements. The temperature range was limited by the high freezing points of the solutions and by their high volatility.

RESULTS

The calculated chemical shifts and coupling constants are given in Table I. The measured shifts of the centers of gravity of the methylene groups relative to internal cyclohexane are given in Table II. These shifts do not vary in any meaningful manner as temperature changes, and will not be further discussed.

Can. J. Chem. Downloaded from www.nrcresearchpress.com by 210.87.254.40 on 09/05/12
For personal use only.

TABLE I

Coupling constants and internal chemical shifts of the methylene protons of substituted benzylamines in TFA

Compound	Temp. (°K)	Chem. shift (c/s)	Coupling constants (c/s)		
			J_{AB}	J_{AX},J_{BX}	$J_{H_X-CH_3}$
(A) Type 1 compounds					
N-Methyldibenzylamine	299±2	14.8±0.2	12.85±0.15	6.5, 4.4±0.2	5.2±0.1
	305	14.9	13.05	6.6, 4.4	5.3
	317	14.75	13.0	6.5, 4.45	5.2
	325	14.6	13.1	6.55,4.6	5.35
	339	14.4	13.1	6.55,4.55	5.3
	353	14.2	13.2	6.45,4.65	5.2
	379	14.25	13.1	6.4, 4.55	5.15
	393	14.2	13.1	6.3, 4.55	5.3
	407	14.3	12.9	6.05,4.55	5.2
N-Phenyldibenzylamine	298	12.1±0.2	12.95±0.1	7.85,3.75±0.2	—
N-Ethyl-*N*-phenylbenzylamine	298	13.5±0.2	12.75±0.1	7.6, 3.65±0.2	—
			J_{AX}	$J_{H_X-CH_3}$	
(B) Type 2*a* compounds					
N,*N*-Dimethylbenzylamine	299±2		5.57±0.1	5.14±0.1	
	309		5.58	5.30	
	321		5.52	5.23	
	335		5.50	5.28	
	347		5.50	5.28	
	372		5.48	5.26	
	388		5.47	5.36	
Tribenzylamine	298		5.3 ±0.1	—	
	323		5.22±0.1	—	
	353		5.24±0.1	—	
	382		5.19±0.1	—	
			$J_{AX}+J_{A'X}$	$M+(L^2+M^2)^{1/2}$	
(C) Type 2*b* compounds					
Dibenzylamine	298±2		11.99±0.15	—	
	323		11.86±0.1	—	
	353		11.80±0.2	—	
	384		11.62±0.1	—	
N-Isopropylbenzylamine	299		12.50±0.1	4.10±0.1	
	321		12.56±0.1	3.89±0.1	
	351		12.50±0.1	3.61±0.1	
2-Benzylamino-6-methylheptanol-6	324		12.05±0.15	—	
	351		12.12±0.2	—	
	383		11.88±0.15	—	

Rapid proton exchange between *N*,*N*-dibenzylethylenediamine and TFA collapsed the methylene proton spectrum below room temperature, preventing the observation of coupling constants. Proton exchange also collapsed the methylene proton spectra of *N*-ethyl-*N*-phenylbenzylamine and *N*-phenyldibenzylamine at temperatures above room temperature.

Separate peaks were observed for the benzyl and ethyl protons of *N*-ethyl-*N*-phenylbenzylamine and 2-benzylamino-6-methylheptanol-6. Presumably, the anisotropy of the phenyl groups caused a low field shift of the benzyl methylene protons relative to the ethyl methylene protons. However, in the spectra of *N*-benzylethanolamine and *N*-benzyldiethanolamine, the ethyl and benzyl methylene protons overlapped, rendering these compounds useless for investigation.

Can. J. Chem. Downloaded from www.nrcresearchpress.com by 210.87.254.40 on 09/05/12
For personal use only.

TABLE II

Chemical shift of methylene protons of benzylamines in TFA (relative to internal cyclohexane)

Compound	Temp. (°K)	Chem. shift (p.p.m.)
N-Methyldibenzylamine	299±0.2	−2.88±0.03
	328	−2.90
	376	−2.87
	403	−2.86
N-Phenyldibenzylamine	298	−2.85
N-Ethyl-*N*-phenylbenzylamine	298	−2.90
N,*N*-Dimethylbenzylamine	299	−2.93
	337	−2.92
	440	−2.88
Tribenzylamine	298	−3.13
	323	−3.12
	353	−3.12
	382	−3.04
Dibenzylamine	298	−2.87
	323	−2.89
	353	−2.91
	384	−2.88
N-Isopropylbenzylamine	299	−2.88
	321	−2.88
	351	−2.87
2-Benzylamino-6-methylheptanol-6	324	−2.90
	351	−2.92
	383	−2.88

Four main types of methylene proton – ammonio proton spectra were observed. Since the methylene protons resonated at more than 4 p.p.m. to high field of the ammonio protons, the spectra can be classified as A_2X, ABX, A_3X, and A_2X_2. Typical spectra are shown in Figs. 4–7. The analysis of the spectra was complicated by the fact that the ammonio proton spectra always consisted of single broad peaks. A combination of slow proton exchange and ^{14}N quadrupole relaxation effects presumably caused the collapse of the X proton spectra.

The estimated errors in measurements are given in Tables I and II. In the case of ABX spectra, the derived values of chemical shift and coupling constants are not as accurately known as other values of coupling constants since they are obtained by the differences of other derived values.

Two major factors limited the accuracy of the measurements. The individual peaks were quite broad because of the high viscosities of the solutions. Also, the thick-walled sample tubes and the temperature probe reduced the sensitivity of the spectrometer so much that it was difficult to obtain signals. (The sensitivity of the spectrometer has since been increased by a factor of 2 in the signal to noise ratio.) The benzylamine concentration used represented a compromise between too much viscosity broadening and too little signal amplitude. The solution of 2-benzylamino-6-methylheptanol-6 was so viscous that the spectrum could not be accurately measured at room temperature.

DISCUSSION OF RESULTS

(A) Effect of Proton Exchange

Since proton exchange alters the observed coupling constants and chemical shifts, it was considered necessary to determine whether or not appreciable ammonio proton exchange was occurring in the other solutions studied. Since benzylamines are stronger bases than aniline, the activation energies of proton exchange should exceed 25 kcal/mole.*

**To be published.*

Can. J. Chem. Downloaded from www.nrcresearchpress.com by 210.87.254.40 on 09/05/12
For personal use only.

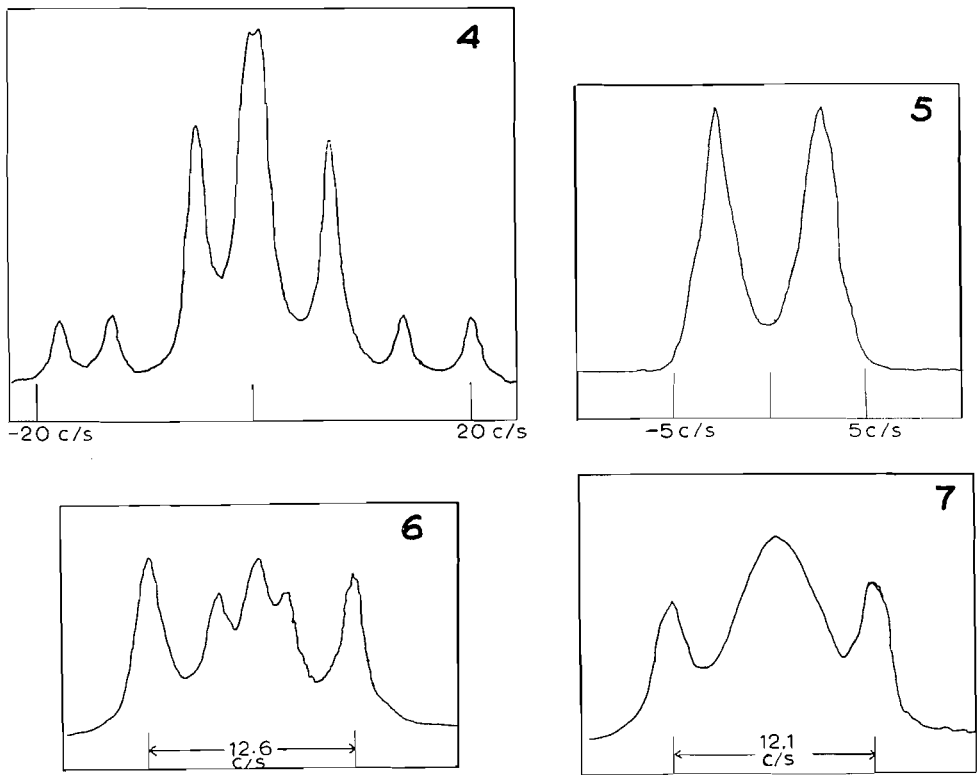

FIG. 4. Reproduction of the methylene proton spectrum of protonated *N*-methyldibenzylamine. This is the AB part of an ABX spectrum (type 1).
FIG. 5. Reproduction of the methylene proton spectrum of protonated *N,N*-dimethylbenzylamine. This is the A_2 part of an A_2X spectrum (type 2*a*).
FIG. 6. Reproduction of the methylene proton spectrum of protonated *N*-isopropylbenzylamine. This is the A_2 part of an A_2X_2 spectrum (type 2*b*).
FIG. 7. Reproduction of the methylene proton spectrum of protonated dibenzylamine. This is the A_2 part of an A_2X_2 spectrum (type 2*b*).

Therefore, the collapse of the methylene proton spectra should occur over a narrow temperature range. Depending upon the peak separations, the spectra will collapse over a temperature range of 15 to 30 °K. This can be shown in the following way: the rate of collapse of a doublet as a result of exchange is approximately given by (25)

$$[20] \qquad \frac{\text{separation of peaks}}{\text{separation of peaks for large } \tau} = \left[1 - \frac{1}{2\pi^2\tau^2(\nu_A - \nu_B)^2}\right]^{\frac{1}{2}}$$

where τ = lifetime of protonated molecule in s. For two peaks 10 c/s apart, the calculated separations are respectively 9.94, 9.75, 8.93, 4.26, and 0.00 c/s for exchange rates of 5.0, 10.0, 20.0, 40.0, and 44.4 exchanges/s. If the activation energy of exchange is 25 kcal/mole and if exchange takes place at a temperature of 330 °K, then the exchange rate will change from 4.4 to 44 exchanges/s over a temperature range of approximately 22 °K.

It is interesting to note that eq. [20] predicts that there is little change in measured peak separations at low exchange rates. Consequently, only the measurements at the highest temperatures are likely to be in error since if appreciable exchange was occurring at lower temperatures, the methylene proton spectra would be completely collapsed at higher temperatures.

Can. J. Chem. Downloaded from www.nrcresearchpress.com by 210.87.254.40 on 09/05/12
For personal use only.

Exchange causes a broadening of the spectral peaks as well as a decrease in peak separation. Such behavior was not noticed for any solutions other than the three mentioned, even at the highest temperatures. Additional evidence for the absence of appreciable exchange was provided by the two compounds containing *N*-methyl groups. These formed type 3 groupings because of rotation about the N—CH_3 bonds. In both cases the (H—N--C—H)$^+$ coupling constants were temperature independent, as would be expected for type 3 groupings in the absence of exchange.

Of all the monoamino compounds studied, only those with a phenyl group bonded directly to the nitrogen atom showed evidence of appreciable proton exchange. Presumably, the withdrawal of electrons from the nitrogen atom by the phenyl group increased the acid strength of the ammonio group to such an extent that appreciable proton exchange occurred at higher temperatures. The methylene proton spectra of *N*-ethyl-*N*-phenyldibenzylamine and *N*-phenylbenzylamine were only partly collapsed at 50 °C. Because the collapse occurred over a narrow temperature region and because no evidence of proton exchange at room temperature was noted for either of the two compounds, it is assumed that the room temperature results for protonated *N*-ethyl-*N*-phenylbenzylamine and *N*-phenyldibenzylamine are reliable.

(B) Type I Compounds

The spectra of all three compounds indicate non-equivalent methylene protons. Protonated *N*-phenyldibenzylamine and *N*-methyldibenzylamine contain symmetric nitrogen atoms while protonated *N*-ethyl-*N*-phenylbenzylamine does not. All lack a plane of symmetry along the benzyl–nitrogen bond. This confirms the statement in the introduction that the absence of a plane or axis of symmetry along the bond axis is the sufficient condition for methylene proton asymmetry.

The chemical shifts between the methylene protons are small in all three compounds. In the case of *N*-methyldibenzylamine, the shift decreases when the temperature is increased, but appears to level off at higher temperatures. However, this cannot be true. If rotamer populations are equal at 407 °K, then $\bar{J}_{AX}$ and $\bar{J}_{BX}$ should be equal (see eqs. [11] and [12]). The non-equivalence of $\bar{J}_{AX}$ and $\bar{J}_{BX}$ in all three compounds indicates that the rotamer populations are unequal in all three compounds. Presumably, the asymmetry shift would be found to be quite small if it could be determined. This is not surprising since the asymmetry shift arises from second order effects.

For *N*-ethyl-*N*-phenylbenzylamine, *N*-phenyldibenzylamine, and *N*-methyldibenzylamine, $|J_{AB}|$ has values of 12.75 ± 0.1, 12.95 ± 0.1, and 13.0 ± 0.2 c/s respectively. Thus J_{AB} is essentially constant for the three compounds. Karplus has calculated that $J_{AB} = +12.85$ for H—C—H bonds when the carbon valences are in a tetrahedral configuration (19), although his calculation is probably in error. It is probable that J_{AB} is negative and that $\bar{J}_{AX}$ and $\bar{J}_{BX}$ are positive, since the corresponding coupling constants in substituted ethanes have those signs (26).

As shown by eq. [13], the difference between $\bar{J}_{AX}$ and $\bar{J}_{BX}$ is determined by the difference in mole fractions of rotamers 1 and 3. If it is assumed that J_g and J_t are the same for all three compounds, then it is possible to estimate the relative amounts of steric hindrance caused by the various substituents. It has been shown that the size of vicinal proton coupling constants in polyhaloethanes depends upon the electronegativity of the substituents (10, 27, 28). Since in all three compounds three carbon atoms are bonded to a nitrogen atom, J_g and J_t probably do not alter appreciably from compound to compound. The bonding of a phenyl group to a nitrogen atom may cause some change in J_g and J_t since the bonding carbon atom is trigonally hybridized.

Can. J. Chem. Downloaded from www.nrcresearchpress.com by 210.87.254.40 on 09/05/12
For personal use only.

In all three compounds, rotamer 2 would be expected to be energetically least favored since in this rotamer a phenyl group (X) is adjacent to two other bulky substituents (see Fig. 1). The non-equivalence of $\bar{J}_{AX}$ and $\bar{J}_{BX}$ in *N*-methyldibenzylamine is presumably due to the fact that the benzyl groups are bulkier than the methyl group. The non-equivalence of the vicinal coupling constants in the other two type 1 compounds is most reasonably explained by assuming that the phenyl group causes more steric hindrance than either the ethyl or the benzyl group. If it is assumed that the phenyl group causes less steric hindrance than the other two groups, then one must conclude that it also causes less steric hindrance than the methyl group. This does not seem reasonable. Since the coupling constants of *N*-phenyldibenzylamine and *N*-ethyl-*N*-phenylbenzylamine are nearly identical, the ethyl and the benzyl groups must cause approximately the same amount of steric hindrance. Consequently one concludes from the differences between $\bar{J}_{AX}$ and $\bar{J}_{BX}$ for the three compounds that the steric hindrance of the substituents decreases in the following order: phenyl > benzyl ≈ ethyl > methyl. This order seems quite reasonable. This suggests that the assumption that J_g and J_t do not alter from compound to compound is at least approximately correct.

The value of the $H^+—N—CH_3$ coupling constant of *N*-methyldibenzylamine is 5.25 ± 0.15 c/s. The constancy of the coupling constant confirms that no appreciable proton exchange occurs in the temperature range used. Since this is a type 3 grouping, 5.25 c/s should represent the value of $|2/3\,J_g + 1/3\,J_t|$. If the value of another combination of J_g and J_t could be found, then the values of J_g and J_t could be obtained algebraically.

(C) Type 2a Compounds

The value of the vicinal coupling constant of protonated *N*,*N*-dimethylbenzylamine changes very little over a temperature range of 90 °K and is only slightly larger than the expected value when rotamer populations are equal. This indicates that the methyl groups have little effect on the ΔE values of the rotamers. The observed value of the $H^+—N—CH_3$ coupling constant is 5.25 c/s. It is independent of temperature. Therefore, no appreciable ammonio proton exchange can be occurring in the temperature range studied.

The results for tribenzylamine are curious. The vicinal coupling constant is almost temperature independent and is identical, within experimental error, with the two values obtained for $|2/3\,J_g + 1/3\,J_t|$. This indicates that all three rotamers have nearly equal energies and populations. It is difficult to visualize why a phenyl group situated between two benzyl groups should not be in a sterically less favorable position than a phenyl group adjacent to only one benzyl group. However, the results indicate that the two positions are equivalent.

The shifts of the methylene protons, relative to cyclohexane, do not change significantly as the temperature changes. Therefore, no conclusions can be drawn about the effect of changing rotamer population upon chemical shift.

The equivalence of the methylene protons in type 2 compounds confirms that the absence of an axis or plane of symmetry along the C—N bond axis is the necessary condition for methylene proton asymmetry.

(D) Type 2b Compounds

The methylene protons of the three compounds of this type give five line spectra corresponding to the A_2 parts of A_2X_2 spectra. The triplet splitting is measurable only in the spectrum of *N*-isopropylbenzylamine. In the spectra of dibenzylamine and 2-benzylamino-6-methylheptanol-6 the central peaks of the methylene proton spectra are

Can. J. Chem. Downloaded from www.nrcresearchpress.com by 210.87.254.40 on 09/05/12
For personal use only.

broadened rather than split into distinct triplets. The spacing of the outer peaks of the triplet is equal to $M + (M^2 + L^2)^{1/2}$. If $M = 0$, then values of $\bar{J}_{AX}$ and $\bar{J}_{A'X}$ can be obtained from the sums and differences of the two coupling constants. It is not known, but is unlikely, that $M = 0$ in the compounds studied. All that can be stated with certainty is that the value of the triplet splitting represents an upper limit of L. The value of the triplet splitting changes more rapidly with temperature than the value of the doublet splitting. It was shown in the introduction that L should change three times as fast as M as temperature changes.

The value of N for *N*-isopropylbenzylamine appears to be temperature independent. The value of N changes with temperature for dibenzylamine and is, in general, lower than N for *N*-isopropylbenzylamine. This implies that the isopropyl group causes more steric hindrance than the benzyl group. This is not surprising when one notes that the results for type 1 compounds indicated that the benzyl and ethyl groups cause approximately equal amounts of steric hindrance.

The value of N for 2-benzylamino-6-methylheptanol-6 is independent of temperature within the limits of experimental error. It is slightly lower than the corresponding value for *N*-isopropylbenzylamine.

In all cases the rotamer populations must be unequal since N is always smaller than the expected value for equal populations: $|4/3\, J_g + 2/3\, J_t| = 10.5$ c/s.

(E) Possible Values of J_g and J_t

If the energy difference between *trans* and *gauche* rotamers of a type 2*b* compound becomes very large, then most of the compound should exist as the *trans* rotamer (see Fig. 3). If one assumes that protonated *N*-isopropylbenzylamine exists solely as the *trans* rotamer at room temperature, then $|J_g + J_t| = 12.6$ c/s. With this value and the previously obtained value of $|2/3\, J_g + 1/3\, J_t|$, it follows that $|J_g| = 3.15$ c/s and $|J_t| = 9.45$ c/s. These values represent an upper limit of $|J_g|$ and a lower limit of $|J_t|$ since the actual value of $|J_g + J_t|$ may be larger than 12.6 c/s. The values of J_g have been found to be between 1.0 and 3.5 c/s in substituted ethanes, while J_t has values between 10 and 18 c/s (7, 9).

It is possible to use values of J_g and J_t to calculate energy and population differences for the various rotamers. We are presently studying these benzylamines in chlorosulphonic acid. This acid allows us to work over a temperature range of at least 250 °C and, as well, the solutions are much less viscous than the TFA solutions. We hope that the resulting increases in range and accuracy for the J values will allow us to apply the analysis described by Gutowsky (29) to obtain ΔE values and better values for J_g and J_t.

SUMMARY AND CONCLUSIONS

It has been shown that the necessary and sufficient condition for methylene proton asymmetry in protonated benzylamines is the absence of a plane of symmetry along the $C_6H_5CH_2$—N bond axis. Rotamer populations are unequal for all compounds except protonated tribenzylamine. The maximum value of $|J_g|$ in protonated benzylamines is 3.15 c/s. The minimum value of $|J_t|$ is 9.45 c/s. The steric hindrance caused by the various substituents decreases in the following order: isopropyl, phenyl > benzyl ≈ ethyl > methyl. It cannot be decided from the experimental evidence whether the phenyl group or the isopropyl group causes greater steric hindrance.

ACKNOWLEDGMENTS

We are grateful to the National Research Council for financial support.

Can. J. Chem. Downloaded from www.nrcresearchpress.com by 210.87.254.40 on 09/05/12
For personal use only.

REFERENCES

1. D. M. Graham and J. S. Waugh. J. Chem. Phys. **27**, 968 (1957).
2. J. N. Shoolery and B. L. Crawford, Jr. J. Mol. Spectry. **1**, 270 (1957).
3. J. A. Pople, W. G. Schneider, and H. J. Bernstein. Can. J. Chem. **35**, 1060 (1957).
4. J. J. Drysdale and W. D. Phillips. J. Am. Chem. Soc. **79**, 319 (1957).
5. P. M. Nair and J. D. Roberts. J. Am. Chem. Soc. **79**, 4565 (1957).
6. J. Shug, P. E. McMahon, and H. S. Gutowsky. J. Chem. Phys. **33**, 843 (1960).
7. H. S. Gutowsky, G. G. Belford, and P. E. McMahon. J. Chem. Phys. **36**, 3353 (1962).
8. R. W. Fessenden and J. S. Waugh. J. Chem. Phys. **37**, 1466 (1962).
9. N. Sheppard and J. J. Turner. Proc. Roy. Soc., Ser. A, **252**, 506 (1959).
10. R. K. Harris and N. Sheppard. Trans. Faraday Soc. **59**, 606 (1963).
11. J. S. Waugh and F. A. Cotton. J. Phys. Chem. **65**, 562 (1961).
12. E. O. Bishop. Ann. Rept. Progr. Chem. Chem. Soc. London, **58**, 67 (1961).
13. H. S. Gutowsky. J. Chem. Phys. **37**, 2196 (1962).
14. S. Mizushima. Structure of molecules and internal rotation. Academic Press Inc., New York. 1954. p. 64.
15. J. A. Pople, W. G. Schneider, and H. J. Bernstein. High resolution nuclear magnetic resonance. McGraw-Hill Book Co., Inc., New York. 1959. p. 378.
16. W. S. Brey and K. C. Ramey. J. Chem. Phys. **39**, 844 (1963).
17. L. Petrakis and C. H. Sederholm. J. Chem. Phys. **36**, 1087 (1962).
18. Soon Ng and C. H. Sederholm. J. Chem. Phys. **40**, 2090 (1964).
19. M. Karplus. J. Chem. Phys. **30**, 11 (1959).
20. J. A. Pople, W. G. Schneider, and H. J. Bernstein. High resolution nuclear magnetic resonance. McGraw-Hill Book Co., Inc., New York. 1959. p. 117.
21. R. R. Fraser, R. V. Lemieux, and J. D. Stevens. J. Am. Chem. Soc. **83**, 3901 (1961).
22. H. J. Bernstein, J. A. Pople, and W. G. Schneider. Can. J. Chem. **35**, 65 (1957).
23. H. M. McConnell, A. D. McLean, and C. A. Reilly. J. Chem. Phys. **23**, 1152 (1955).
24. J. A. Pople, W. G. Schneider, and H. J. Bernstein. High resolution nuclear magnetic resonance. McGraw-Hill Book Co., Inc., New York. 1959. p. 73.
25. H. S. Gutowsky and C. H. Holm. J. Chem. Phys. **25**, 1228 (1956).
26. P. C. Lauterbur and R. J. Kurland. J. Am. Chem. Soc. **84**, 3405 (1962).
27. R. E. Glick and A. A. Bothner-By. J. Chem. Phys. **25**, 362 (1956).
28. C. N. Banwell and N. Sheppard. Discussions Faraday Soc. No. **34**, 118 (1962).
29. H. S. Gutowsky. Pure Appl. Chem. **7**, 93 (1963).

Can. J. Chem. Downloaded from www.nrcresearchpress.com by 210.87.254.40 on 09/05/12
For personal use only.

Can. J. Chem. Downloaded from www.nrcresearchpress.com by 210.87.254.105 on 09/05/12
For personal use only.

NOTES

THE THERMAL UNIMOLECULAR DECOMPOSITION OF $\Delta^{2,5}$-BICYCLO[2.2.1]HEPTADIENE[1]

B. C. ROQUITTE[2]

The vapor phase thermal decomposition of $\Delta^{2,5}$-bicyclo[2.2.1]heptadiene, BCHD[2.2.1], has received some attention previously (1, 2); recently the kinetic parameters of the thermal decomposition of BCHD have been reported (3). It was found that acetylene, cyclopentadiene, cycloheptatriene, and toluene are the principal products of decomposition. The present investigation on BCHD was undertaken to see whether acetylene and cyclopentadiene could have been formed from the valence tautomer BCHD[3.2.0] as follows:

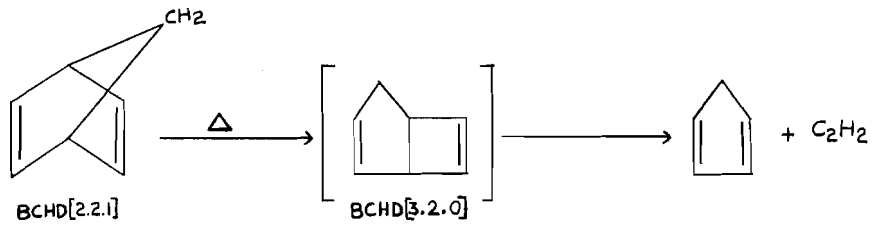

The decomposition of BCHD[3.2.0] to cycloheptatriene is known (4). However, BCHD[3.2.0] also could decompose to give cyclopentadiene and acetylene in the same fashion as cyclobutane compounds (5). It was hoped that this study would throw some light on the transition state involved in the decomposition of BCHD[2.2.1].

BCHD[2.2.1] supplied by Chemical Intermediate and Research Laboratories, Cuyahoga Falls, Ohio, was subjected to fractional distillation, and a middle cut was further purified by gas chromatography and found to be 99.9% pure. Cyclopentadiene used in the calibration of the gas chromatograph was prepared (6) from dicyclopentadiene (Eastman Kodak Co.) and subsequently purified by gas chromatography. Acetylene (Matheson 99.66%) was used without further purification, except trap-to-trap distillation, for gas chromatographic calibration. Nitric oxide (Matheson 98.7%) was purified by several distillations from −160 to −196°. Oxygen (Matheson 99.5%) was used directly from the cylinder.

The apparatus used and the experimental procedure were in part similar to that described previously (7). Two cylindrical reaction vessels made of pyrex were used in a vertical furnace: (*a*) unpacked vessel, (*b*) vessel packed with thin-walled pyrex tubings to increase the surface:volume ratio by a factor of 25.

After each run the reaction mixture was condensed out of the reaction zone into an

[1]*Issued as N.R.C. No. 8004.*

[2]*N.R.C. Postdoctoral Fellow, 1962–64. Present address: Radiation Research Laboratories, Mellon Institute, Pittsburgh 13, Pennsylvania.*

ampoule at liquid nitrogen temperature and sealed off under vacuum. The reaction mixture was then introduced into the inlet system of an F and M temperature-programmed gas chromatograph model 720 by means of a crushing device developed in this laboratory. The compounds present in the reaction mixture were initially identified by comparison of the retention times of the various products with those of the authentic samples. The individual compounds were separately trapped as they were eluted from the column and subsequently analyzed by a mass spectrometer. The amount of each product was estimated quantitatively by measuring the area under the peak on the chromatogram. The results of the quantitative determination of the products are summarized in Table I.

TABLE I

Decomposition of $\Delta^{2,5}$-bicyclo[2.2.1]heptadiene under various conditions

T, °C	P_0, mm	ΔP, mm	P_{CPD}, mm	P_{AC}, mm	Reaction condition	Tol/CHT	$k \times 10^4$ s^{-1}	k_a/k_b
320	15.77	1.93	1.93	1.92	—	0.074	1.35	2.04
330	18.75	5.62	5.60	5.61	—	—	2.81	2.04
340	13.39	2.74	2.74	2.76	—	0.073	4.97	2.05
350	23.87	4.92	4.92	4.93	Pkd.	0.174	10.13	2.11
350	16.90	4.39	4.37	4.37	—	0.079	10.36	2.06
350	24.76	5.37	5.37	—	NO	0.077	10.13	2.10
350	15.95	3.61	3.61	—	O_2	0.065	10.20	2.04
350	12.15	2.64	2.60	2.59	Pkd.	0.180	10.23	2.01
350	4.39	0.94	0.90	0.91	—	0.107	10.23	2.08
360	21.90	7.15	7.15	7.13	—	0.067	18.84	2.13

ΔP = increase in pressure corrected for dead space.
P_{CPD} = pressure of cyclopentadiene.
P_{AC} = pressure of acetylene.
Pkd. = packed reaction vessel.

On the basis of product identification, it appears that there are at least two simultaneous reactions occurring in the pyrolysis of BCHD[2.2.1]:

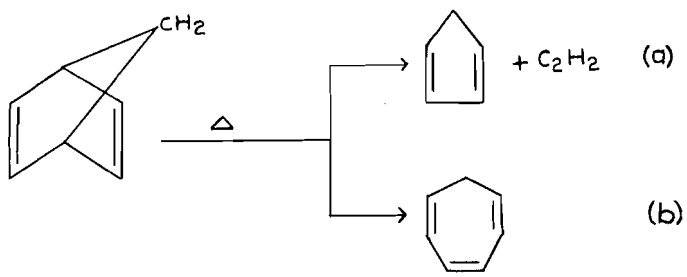

The major portion of toluene (if not all) most probably was produced by the reaction (8):

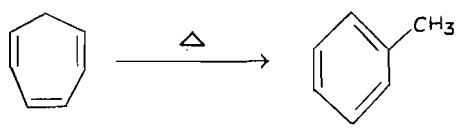

Three runs were carried out to 100% decomposition. It was observed that the ratio tol/CHT (toluene/cycloheptatriene) had increased in these runs. Moreover, the amount of toluene produced was negligible in experiments in which the decomposition was less

Can. J. Chem. Downloaded from www.nrcresearchpress.com by 210.87.254.105 on 09/05/12
For personal use only.

than 5% but the CHT formed was detected readily. The rate constants of the overall reaction in the pressure range 4–30 mm at temperature 320–360° were calculated from the slope of the straight line obtained from a plot of the left side of the following equation against time t:

$$\log \frac{P_0 L}{(1 - L)P_0 - P_t} = \frac{k}{2.303} t$$

where P_0 is the initial pressure, L is the fraction of BCHD decomposed by step (a), and P_t is the pressure measured at time t; $k = k_a + k_b$. A typical plot is shown in Fig. 1.

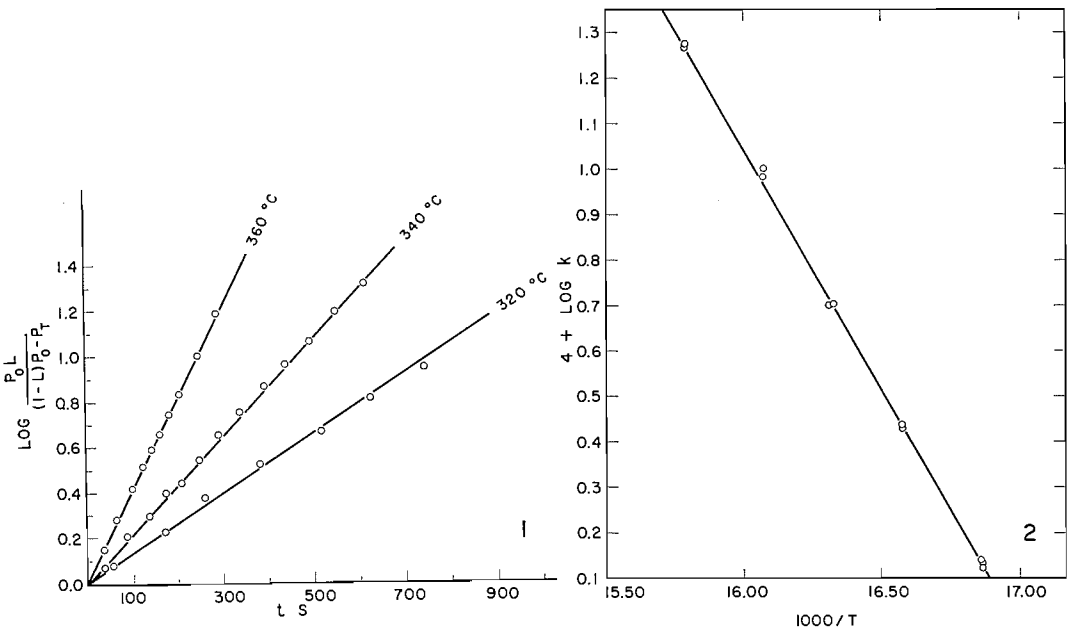

FIG. 1. Unimolecular plot; ordinate scale—for run at 360° to be increased by a factor of 2 and for run at 320° to be decreased by a factor of 2.
FIG. 2. Arrhenius plot for the decomposition of BCHD[2.2.1].

The pressure–time curve has the shape expected for an unimolecular reaction without an induction period. If the lifetime of BCHD[3.2.0] is longer than that of BCHD[2.2.1], then the absence of an induction period would seem to rule out the possibility that decomposition is taking place via an intermediate like BCHD[3.2.0]. This conclusion is further supported by the fact that BCHD[3.2.0] is not a product of the decomposition (confirmed by nuclear magnetic resonance analysis). Since oxygen and nitric oxide did not have an effect on the rate of the overall decomposition, it is safe to conclude that free radicals are not involved in the decomposition of BCHD[2.2.1]. In addition, the change of surface: volume ratio seems to have no effect on the rate of the reaction, which suggests that the decomposition of BCHD is an entirely homogeneous reaction.

The Arrhenius plot for the overall reaction is shown in Fig. 2 and is given by $k = 2.99 \times 10^{14} \exp(-49\,800/RT)\ s^{-1}$. A plot of the ratio of $2C_2H_2/(\text{tol} + \text{CHT})$ ($= k_a/k_b$) vs. temperature (not shown) has a slope of zero although there is some scatter in the plot. This corroborates the fact that there is little or no difference in activation energy between

Can. J. Chem. Downloaded from www.nrcresearchpress.com by 210.87.254.105 on 09/05/12
For personal use only.

the processes (*a*) and (*b*); the individual rate constants are, therefore, $k_a = 2.01 \times 10^{14} \exp(-49\,800/RT)\ s^{-1}$ and $k_b = 0.87 \times 10^{14} \exp(-49\,800/RT)\ s^{-1}$. The entropy of activation of the overall reaction was found to be −2.5 e.u. A small negative entropy usually indicates that the structure of the transition state involved does not differ greatly from that of the original molecule.

ACKNOWLEDGMENT

The author is indebted to Drs. K. O. Kutschke and R. A. Back for much advice and encouragement during the progress of this work.

1. W. G. Woods. J. Org. Chem. **23**, 110 (1958).
2. W. M. Halper, G. Gaertner, E. W. Swift, and G. E. Pollard. Ind. Eng. Chem. **50**, 1131 (1958).
3. J. H. Birely and J. P. Chesick. J. Phys. Chem. **66**, 568 (1962).
4. W. G. Dauben and R. L. Cargill. Tetrahedron, **12**, 186 (1961).
5. (*a*) C. T. Genaux, F. Kern, and W. D. Walters. J. Am. Chem. Soc. **75**, 6196 (1953).
   (*b*) M. N. Das and W. D. Walters. Z. Physik. Chem. Frankfurt, **15**, 22 (1958).
   (*c*) R. E. Wellman and W. D. Walters. J. Am. Chem. Soc. **79**, 1542 (1957).
6. Org. Syn. **32**, 41 (1952).
7. B. C. Roquitte and W. D. Walters. J. Am. Chem. Soc. **84**, 4049 (1962).
8. K. N. Klump and J. P. Chesick. J. Am. Chem. Soc. **85**, 130 (1963).

Received March 17, 1964.
Division of Pure Chemistry,
National Research Council,
Ottawa, Canada.

Can. J. Chem. Downloaded from www.nrcresearchpress.com by 210.87.254.105 on 09/05/12
For personal use only.

FURTHER INVERSE GAMMA-DEUTERIUM ISOTOPE EFFECTS IN SOLVOLYTIC REACTIONS[1]

M. J. Blandamer[2] and R. E. Robertson

The inverse secondary γ-deuterium isotope effect reported by Leffek *et al.* (1, 2) in the hydrolysis of *n*-propyl halides and sulphonates appeared to provide confirmation of the suggestion that there was a loss of torsional freedom coupled with lesser effects on bending and stretching frequencies as a consequence of the close juxtaposition of the terminal methyl group, the nucleophilic water, and the leaving group (3). By extension of this argument, the γ-deuterium isotope effect seemed to provide a means of exploring the arguments advanced by Dostrovsky, Hughes, and Ingold (4) about enhanced steric hindrance to nucleophilic displacement from isobutyl and neopentyl groups. It follows that in these examples the enhanced steric hindrance would lead to a corresponding increase in the inverse γ-deuterium isotope effect. This expectation was not supported by experiment (Table 1). The inverse γ-deuterium isotope effect for the hydrolysis of *n*-propyl halides was reduced for the isobutyl cases and was "normal" for the neopentyl methanesulphonate. The simplest explanation would seem to be that nucleophilic interaction is successively reduced here, as it is in the analogous displacement from the methyl and the isopropyl groups, with a corresponding shift in the α-deuterium isotope effect

[1]*N.R.C. No. 8059.*
[2]*National Research Council of Canada Postdoctoral Fellow, 1960–61. Present address: University of Leicester, Leicester, England.*

the processes (*a*) and (*b*); the individual rate constants are, therefore, $k_a = 2.01 \times 10^{14} \exp(-49\,800/RT)\ s^{-1}$ and $k_b = 0.87 \times 10^{14} \exp(-49\,800/RT)\ s^{-1}$. The entropy of activation of the overall reaction was found to be −2.5 e.u. A small negative entropy usually indicates that the structure of the transition state involved does not differ greatly from that of the original molecule.

ACKNOWLEDGMENT

The author is indebted to Drs. K. O. Kutschke and R. A. Back for much advice and encouragement during the progress of this work.

1. W. G. Woods. J. Org. Chem. **23**, 110 (1958).
2. W. M. Halper, G. Gaertner, E. W. Swift, and G. E. Pollard. Ind. Eng. Chem. **50**, 1131 (1958).
3. J. H. Birely and J. P. Chesick. J. Phys. Chem. **66**, 568 (1962).
4. W. G. Dauben and R. L. Cargill. Tetrahedron, **12**, 186 (1961).
5. (*a*) C. T. Genaux, F. Kern, and W. D. Walters. J. Am. Chem. Soc. **75**, 6196 (1953).
   (*b*) M. N. Das and W. D. Walters. Z. Physik. Chem. Frankfurt, **15**, 22 (1958).
   (*c*) R. E. Wellman and W. D. Walters. J. Am. Chem. Soc. **79**, 1542 (1957).
6. Org. Syn. **32**, 41 (1952).
7. B. C. Roquitte and W. D. Walters. J. Am. Chem. Soc. **84**, 4049 (1962).
8. K. N. Klump and J. P. Chesick. J. Am. Chem. Soc. **85**, 130 (1963).

Received March 17, 1964.
Division of Pure Chemistry,
National Research Council,
Ottawa, Canada.

Can. J. Chem. Downloaded from www.nrcresearchpress.com by 210.87.254.6 on 09/05/12
For personal use only.

FURTHER INVERSE GAMMA-DEUTERIUM ISOTOPE EFFECTS IN SOLVOLYTIC REACTIONS[1]

M. J. Blandamer[2] and R. E. Robertson

The inverse secondary γ-deuterium isotope effect reported by Leffek *et al.* (1, 2) in the hydrolysis of *n*-propyl halides and sulphonates appeared to provide confirmation of the suggestion that there was a loss of torsional freedom coupled with lesser effects on bending and stretching frequencies as a consequence of the close juxtaposition of the terminal methyl group, the nucleophilic water, and the leaving group (3). By extension of this argument, the γ-deuterium isotope effect seemed to provide a means of exploring the arguments advanced by Dostrovsky, Hughes, and Ingold (4) about enhanced steric hindrance to nucleophilic displacement from isobutyl and neopentyl groups. It follows that in these examples the enhanced steric hindrance would lead to a corresponding increase in the inverse γ-deuterium isotope effect. This expectation was not supported by experiment (Table 1). The inverse γ-deuterium isotope effect for the hydrolysis of *n*-propyl halides was reduced for the isobutyl cases and was "normal" for the neopentyl methanesulphonate. The simplest explanation would seem to be that nucleophilic interaction is successively reduced here, as it is in the analogous displacement from the methyl and the isopropyl groups, with a corresponding shift in the α-deuterium isotope effect

[1]*N.R.C. No. 8059.*
[2]*National Research Council of Canada Postdoctoral Fellow, 1960–61. Present address: University of Leicester, Leicester, England.*

TABLE I

Gamma isotope effects in hydrolysis

	T, °C*	$k_H \times 10^4$†	k_H/k_D		Reference
n-Propyl bromide	79.994	1.602±0.003	0.92_1	d_3	2
n-Propyl methanesulphonate	60.004	1.370±0.003	0.94_3	d_3	2
Isobutyl bromide	95.005	2.699±0.006	0.95_8	d_6	This work
Isobutyl methanesulphonate	90.004	7.973±0.007	0.96_8	d_6	This work
Neopentyl methanesulphonate	90.027	4.392 (calc.)‡	1.01_7	d_9	This work

*Since k_H/k_D, in every case, is close to unity, the difference in temperature will not alter our conclusion.
†Average of 3 to 4 replicate runs.
‡From three-constant equation.

from inverse to normal (5). However, this facile explanation must be tempered by the knowledge that even in nucleophilic displacement from the methyl group, the α-deuterium isotope effect has been shown to be "inverse" or "normal" depending on the nucleophile, the leaving group, and the medium. Thus Leffek has shown that displacement of the tosyl ion by a strong nucleophile ($S_2O_3^=$) leads to a "normal" α-deuterium isotope effect, whereas displacement in hydrolysis gives an "inverse" effect (6). These and similar results merely serve to underline the need for the development of a better understanding of the secondary deuterium isotope effects before we can utilize this probe in the exploration of detailed mechanism.

The isobutyl bromide-d_6 and neopentyl alcohol-d_9 were supplied by Merck, Sharp & Dohme and were isotopically better than 95% pure. The former was converted to the corresponding methanesulphonate by exchange with the silver salt (7). The neopentyl methanesulphonate was made by standard methods (7). All were purified to give good first order plots. Rate determinations and attending experimental considerations followed our standard practice (8).

1. K. T. Leffek, J. A. Llewellyn, and R. E. Robertson. Chem. Ind. 588 (1960).
2. K. T. Leffek, J. A. Llewellyn, and R. E. Robertson. J. Am. Chem. Soc. **82**, 6315 (1960).
3. P. W. C. Barnard and R. E. Robertson. Can. J. Chem. **39**, 881 (1961).
4. I. Dostrovsky, E. D. Hughes, and C. K. Ingold. J. Chem. Soc. 173 (1946).
5. K. T. Leffek, J. A. Llewellyn, and R. E. Robertson. Can. J. Chem. **38**, 1505 (1960).
6. K. T. Leffek. Can. J. Chem. **42**, 851 (1964).
7. R. S. Tipson. J. Org. Chem. **9**, 235 (1949).
8. R. L. Heppolette and R. E. Robertson. J. Am. Chem. Soc. **83**, 1834 (1961).

Received May 29, 1964.
Division of Pure Chemistry,
National Research Council,
Ottawa, Canada.

A SUBLIMATION PROCEDURE FOR THE PURIFICATION OF ORGANIC SUBSTANCES AT LOW TEMPERATURES[1]

Ralph H. Petrucci[2] and Barbara L. Edsall

We wish to report a novel method for purifying organic liquids. This method involves *freezing* the mixture of organic liquid and its impurity, subjecting the resulting solid to sublimation, and condensing a *liquid* phase rich in the impurity. In this sublimation

[1]*This work was supported by a grant from the American Cancer Society.*
[2]*Present address (to which all inquiries should be sent): California State College at San Bernardino, San Bernardino, California.*

Can. J. Chem. Downloaded from www.nrcresearchpress.com by 210.87.254.6 on 09/05/12
For personal use only.

TABLE I

Gamma isotope effects in hydrolysis

	T, °C*	$k_H \times 10^4$†	k_H/k_D		Reference
n-Propyl bromide	79.994	1.602±0.003	0.92_1	d_3	2
n-Propyl methanesulphonate	60.004	1.370±0.003	0.94_3	d_3	2
Isobutyl bromide	95.005	2.699±0.006	0.95_8	d_6	This work
Isobutyl methanesulphonate	90.004	7.973±0.007	0.96_8	d_6	This work
Neopentyl methanesulphonate	90.027	4.392 (calc.)‡	1.01_7	d_9	This work

*Since k_H/k_D, in every case, is close to unity, the difference in temperature will not alter our conclusion.
†Average of 3 to 4 replicate runs.
‡From three-constant equation.

from inverse to normal (5). However, this facile explanation must be tempered by the knowledge that even in nucleophilic displacement from the methyl group, the α-deuterium isotope effect has been shown to be "inverse" or "normal" depending on the nucleophile, the leaving group, and the medium. Thus Leffek has shown that displacement of the tosyl ion by a strong nucleophile ($S_2O_3^=$) leads to a "normal" α-deuterium isotope effect, whereas displacement in hydrolysis gives an "inverse" effect (6). These and similar results merely serve to underline the need for the development of a better understanding of the secondary deuterium isotope effects before we can utilize this probe in the exploration of detailed mechanism.

The isobutyl bromide-d_6 and neopentyl alcohol-d_9 were supplied by Merck, Sharp & Dohme and were isotopically better than 95% pure. The former was converted to the corresponding methanesulphonate by exchange with the silver salt (7). The neopentyl methanesulphonate was made by standard methods (7). All were purified to give good first order plots. Rate determinations and attending experimental considerations followed our standard practice (8).

1. K. T. Leffek, J. A. Llewellyn, and R. E. Robertson. Chem. Ind. 588 (1960).
2. K. T. Leffek, J. A. Llewellyn, and R. E. Robertson. J. Am. Chem. Soc. **82**, 6315 (1960).
3. P. W. C. Barnard and R. E. Robertson. Can. J. Chem. **39**, 881 (1961).
4. I. Dostrovsky, E. D. Hughes, and C. K. Ingold. J. Chem. Soc. 173 (1946).
5. K. T. Leffek, J. A. Llewellyn, and R. E. Robertson. Can. J. Chem. **38**, 1505 (1960).
6. K. T. Leffek. Can. J. Chem. **42**, 851 (1964).
7. R. S. Tipson. J. Org. Chem. **9**, 235 (1949).
8. R. L. Heppolette and R. E. Robertson. J. Am. Chem. Soc. **83**, 1834 (1961).

Received May 29, 1964.
Division of Pure Chemistry,
National Research Council,
Ottawa, Canada.

A SUBLIMATION PROCEDURE FOR THE PURIFICATION OF ORGANIC SUBSTANCES AT LOW TEMPERATURES[1]

Ralph H. Petrucci[2] and Barbara L. Edsall

We wish to report a novel method for purifying organic liquids. This method involves *freezing* the mixture of organic liquid and its impurity, subjecting the resulting solid to sublimation, and condensing a *liquid* phase rich in the impurity. In this sublimation

[1]*This work was supported by a grant from the American Cancer Society.*
[2]*Present address (to which all inquiries should be sent): California State College at San Bernardino, San Bernardino, California.*

Can. J. Chem. Downloaded from www.nrcresearchpress.com by 210.87.254.40 on 09/05/12
For personal use only.

procedure the solid mixture yields a vapor which condenses at or near the eutectic temperature to a liquid having approximately the eutectic composition, and, at least as a first approximation, this liquid composition is independent of the solid composition. Thus the method is especially effective for the removal of trace impurities.

This sublimation method, one in which the impurity is concentrated in a liquid sublimate and the unsublimed solid becomes more pure, has been applied previously to organic solids at temperatures above room temperature (1). However, the method seems especially promising for systems of organic liquids that are ordinarily difficult to separate by conventional means such as fractional distillation, for in essence what is done is to utilize the invariant equilibrium, solid–solid–vapor–liquid, instead of the more conventional liquid–vapor equilibrium. As an example consider some of the results obtained in working with mixtures of *p*-xylene (major component) – *o*-xylene (impurity).

EXPERIMENTAL

Mixtures of the components were prepared from the highest purity materials available from Eastman Kodak Co. The two compositions used were "99%" and "99.999%" *p*-xylene. These percentages, of course, represent only the nominal compositions of the mixtures since the individual components themselves were not absolutely pure.

These mixtures were frozen completely and the sublimation of the solid mixtures carried out over a ½ h period in a nitrogen atmosphere in a glass sublimation apparatus. The sublimation well was maintained at approximately −33.5° (by using a $Mg(NO_3)_2 \cdot 9H_2O$ – ice eutectic bath) and the condenser at approximately −36° (by using acetone cooled in a $K_2CO_3 \cdot 6H_2O$ – ice eutectic bath). The *p*-xylene – *o*-xylene eutectic temperature is −36.4° (2). The liquid condensates obtained in the sublimations were removed by dissolving in a small volume of 95% ethanol and the resulting solutions were analyzed by vapor phase chromatography.

The gas chromatographic analyses were performed with a Perkin–Elmer Model 154 using 7,8-benzoquinoline on Celite column at 80° and a thermal conductivity detector. An absolute calibration of the response of the column and detector to *p*-xylene – *o*-xylene mixtures was not made, but a standardization experiment was performed. In this experiment (experiment 1, Table I) a mixture of *p*-xylene – *o*-xylene of the eutectic composition was subjected to chromatographic analysis. The results of other experiments were compared to this standard.

TABLE I

Vapor phase chromatography data on *p*-xylene – *o*-xylene mixtures

Expt.	Solution analyzed	Relative peak areas (units)		Remarks
		p-Xylene	*o*-Xylene	
1	Standard eutectic mixture: 27.8% *p*-xylene – 72.2% *o*-xylene	6	15	1 μl of a 1.0% solution of the standard eutectic mixture in ethanol was taken for analysis
2	Liquid condensate from the sublimation of a "99%" *p*-xylene – "1%" *o*-xylene solid mixture	7	11	20 μl of a solution obtained by dissolving the liquid sublimate in 0.07 ml of ethanol
3	A repeat of expt. 2	9	16	Same sampling procedure as in expt. 2
4	Liquid condensate from the sublimation of a "99.999%" *p*-xylene – "0.001%" *o*-xylene solid mixture	5	2	Same sampling procedure as in expts. 2 and 3

Can. J. Chem. Downloaded from www.nrcresearchpress.com by 210.87.254.40 on 09/05/12
For personal use only.

RESULTS AND DISCUSSION

From the results in Table I it can be seen that considerable enrichment of the impurity in the liquid condensate was obtained by the sublimation procedure described here. That the condensates obtained did not possess exactly the eutectic composition perhaps can be attributed to the fact that the sublimation was not carried out exactly at the eutectic temperature and also to the fact that equilibrium conditions were probably not attained during the short sublimation period ($\frac{1}{2}$ h). The liquid condensed in experiment 4 contained a ratio of *p*-xylene to *o*-xylene considerably different from the eutectic value, and should have had an equilibrium freezing point of about 0 °C. Quite likely this was a supercooled solution. The formation of supercooled solutions by this sublimation method has been noted previously (3). Despite the fact that the conditions for achieving the maximum degree of separation of *o*-xylene impurity from *p*-xylene were not attained in the experiments described here, it is still quite clear that this sublimation technique can be used to effect the purification of organic substances at low temperatures.

1. R. H. PETRUCCI and J. C. WEYGANDT. Anal. Chem. **33**, 275 (1961).
2. J. TIMMERMANS. The physico-chemical constants of binary systems in concentrated solutions. Vol. I. Interscience, New York. 1959. p. 162.
3. R. H. PETRUCCI and C. H. SORUM. Can. J. Chem. **34**, 649 (1956).

RECEIVED APRIL 2, 1964.
DEPARTMENT OF CHEMISTRY,
WESTERN RESERVE UNIVERSITY,
CLEVELAND, OHIO, 44106.

Can. J. Chem. Downloaded from www.nrcresearchpress.com by 210.87.254.40 on 09/05/12
For personal use only.

HIGH PRIMARY QUANTUM EFFICIENCY IN THE REACTION OF NEOPENTANE WITH Hg 6($^3P_1$) ATOMS

R. J. NORSTROM, O. P. STRAUSZ, AND H. E. GUNNING

In the determination of the mechanism of energy transfer for collisions between alkane molecules and Hg 6($^3P_1$) atoms (1), the low quantum yield (0.0045) previously reported for the neopentane reaction (2) was thought to have provided important evidence for the role of molecular symmetry in the energy-transfer process. During primary process studies on reactions initiated by Hg 6($^3P_1$) atoms, we have reinvestigated the neopentane reaction and the results are reported below.

EXPERIMENTAL

The neopentane was Phillips Research Grade (stated purity, 99.98%) with *n*-butane the probable impurity. This material was further refined, after thorough degassing, by distillation from methanol slush (−98°) to liquid nitrogen, discarding head and tail fractions. Fractionation from toluene slush (−100°) to *n*-pentane slush (−130°) followed, with continuous pumping, and rejection of the lead fraction. Preliminary experiments indicated that the last traces of impurities could best be removed by photosensitization. After this pre-irradiation, noncondensables were pumped off, and the neopentane was recovered by distillation through a trap at −100°, which retained heavy products. The substrate thus obtained showed no impurities by gas chromatography (g.c.) (6 foot, medium-activity, silica gel column). For the runs reported here a rotating sector technique was used; this has been previously described (3). Absorbed light intensities (I_a) were measured by propane actinometry, taking $\Phi_{H_2} = 0.50$ in the constant $DH_2/\Delta t$ region at propane pressures of

RESULTS AND DISCUSSION

From the results in Table I it can be seen that considerable enrichment of the impurity in the liquid condensate was obtained by the sublimation procedure described here. That the condensates obtained did not possess exactly the eutectic composition perhaps can be attributed to the fact that the sublimation was not carried out exactly at the eutectic temperature and also to the fact that equilibrium conditions were probably not attained during the short sublimation period ($\frac{1}{2}$ h). The liquid condensed in experiment 4 contained a ratio of *p*-xylene to *o*-xylene considerably different from the eutectic value, and should have had an equilibrium freezing point of about 0 °C. Quite likely this was a supercooled solution. The formation of supercooled solutions by this sublimation method has been noted previously (3). Despite the fact that the conditions for achieving the maximum degree of separation of *o*-xylene impurity from *p*-xylene were not attained in the experiments described here, it is still quite clear that this sublimation technique can be used to effect the purification of organic substances at low temperatures.

1. R. H. PETRUCCI and J. C. WEYGANDT. Anal. Chem. **33**, 275 (1961).
2. J. TIMMERMANS. The physico-chemical constants of binary systems in concentrated solutions. Vol. I. Interscience, New York. 1959. p. 162.
3. R. H. PETRUCCI and C. H. SORUM. Can. J. Chem. **34**, 649 (1956).

RECEIVED APRIL 2, 1964.
DEPARTMENT OF CHEMISTRY,
WESTERN RESERVE UNIVERSITY,
CLEVELAND, OHIO, 44106.

Can. J. Chem. Downloaded from www.nrcresearchpress.com by 210.87.254.6 on 09/05/12
For personal use only.

HIGH PRIMARY QUANTUM EFFICIENCY IN THE REACTION OF NEOPENTANE WITH Hg 6($^3P_1$) ATOMS

R. J. NORSTROM, O. P. STRAUSZ, AND H. E. GUNNING

In the determination of the mechanism of energy transfer for collisions between alkane molecules and Hg 6($^3P_1$) atoms (1), the low quantum yield (0.0045) previously reported for the neopentane reaction (2) was thought to have provided important evidence for the role of molecular symmetry in the energy-transfer process. During primary process studies on reactions initiated by Hg 6($^3P_1$) atoms, we have reinvestigated the neopentane reaction and the results are reported below.

EXPERIMENTAL

The neopentane was Phillips Research Grade (stated purity, 99.98%) with *n*-butane the probable impurity. This material was further refined, after thorough degassing, by distillation from methanol slush (−98°) to liquid nitrogen, discarding head and tail fractions. Fractionation from toluene slush (−100°) to *n*-pentane slush (−130°) followed, with continuous pumping, and rejection of the lead fraction. Preliminary experiments indicated that the last traces of impurities could best be removed by photosensitization. After this pre-irradiation, noncondensables were pumped off, and the neopentane was recovered by distillation through a trap at −100°, which retained heavy products. The substrate thus obtained showed no impurities by gas chromatography (g.c.) (6 foot, medium-activity, silica gel column). For the runs reported here a rotating sector technique was used; this has been previously described (3). Absorbed light intensities (I_a) were measured by propane actinometry, taking $\Phi_{H_2} = 0.50$ in the constant $DH_2/\Delta t$ region at propane pressures of

1000 torr. The continuous I_a was 0.358 μeinstein/min, and the sector opening was 9°, resulting in a time-averaged I_a for the intermittent irradiation of 0.00895 μeinstein/min. Noncondensables were measured by gas burette, with analysis by g.l.c. on a molecular sieves column. For the heavy products a high-capacity capillary column was used (Perkin–Elmer, 505U (squalane)) with a helium flow of 45 ml/min. Product characterizations were by nuclear magnetic resonance (n.m.r.) and mass spectrometry.

RESULTS AND DISCUSSION

The major products of the reaction at 25° are hydrogen and a C-10 paraffin. The proton n.m.r. spectrum of the heavy product shows peaks at 8.87 and 9.13 τ in relative intensities of 1:4.4. Hence the product is 2,2,5,5-tetramethylhexane or dineopentyl (DN). The mass spectrum is also consistent with DN. At higher substrate pressures small quantities of a second C-10 product were detected by g.l.c. Quantities obtained by g.l.c. peak isolation were too minute for a complete n.m.r. analysis. However, two uncoupled peaks at 8.8 and 8.9 τ were found which, from intensity ratios, were not methylene protons. These results suggest that the minor heavy product is a mixture of the *cis* and *trans* forms of 2,2,5,5-tetramethylhexene-3.

Under steady illumination (I_a = 0.075 μeinstein/min) the quantum yield (Φ) for hydrogen was 0.60 at substrate pressures exceeding 800 mm. For the rotating sector runs the quantum yield data are given in Table I.

TABLE I

Product quantum yields as a function of substrate pressure and exposure time for the reaction of neopentane with Hg $6(^3P_1)$ atoms

Run No.	Neopentane pressure (torr)	Exposure time (min)	Φ_{H_2}	Φ_{DN}[a]	Δ[b]	Φ_X[c]
1	102	120	0.367	0.342	0.025	—
2	257	120	0.546	0.478	0.068	—
3	478	120	0.656	0.615	0.041	—
4	680	120	0.705	0.670	0.035	—
5	854	120	0.744	0.690	0.054	—
6	1012	61	0.762	0.695	0.067	0.02
7	1012	120	0.755	0.685	0.070	—
8	1012	120	0.760	0.690	0.070	0.03
9	1012	240	0.739	0.672	0.067	0.01
10	1012	360	0.722	0.661	0.061	0.01

[a]Quantum yield of dineopentyl formation.
[b]$\Delta = \Phi_{H_2} - \Phi_{DN}$.
[c]Quantum yield of minor C-10 product.

It should first be noted from Table I that Φ_{H_2} values under intermittent irradiation, at pressures exceeding 800 mm, are higher than that obtained under steady illumination (0.60). Furthermore (Table I) Φ_{H_2} rises with increasing substrate pressure (P_S) and appears to level off at 0.76 for P_S = 1012 torr. Runs 6–10 show that Φ_{H_2} falls off fairly linearly with exposure time (t). The relation between Φ_{H_2} and P_S can best be shown by plotting $1/\Phi_{H_2}$ vs. $1/P_S$ for the 120 min runs, as in Fig. 1. The function is linear, and yields an extrapolated value for Φ_{H_2} at $P_S = \infty$ of 0.87 ($\Phi_{H_2}^{\infty}$). Pertinently, Yang (4) has made some very careful, low-conversion measurements of Φ_{H_2} for a number of paraffins including propane and neopentane. For his actinometric standard he takes $\Phi_{H_2}^{\infty} = 1.00$ for propane from an analogous plot to Fig. 1. On this basis, Yang's data (4) give $\Phi_{H_2}^{\infty} = 0.86$ for neopentane, in excellent agreement with our findings. Of equal interest is the fact that the two actinometric reference values for the propane reaction appear equally valid.

Can. J. Chem. Downloaded from www.nrcresearchpress.com by 210.87.254.6 on 09/05/12
For personal use only.

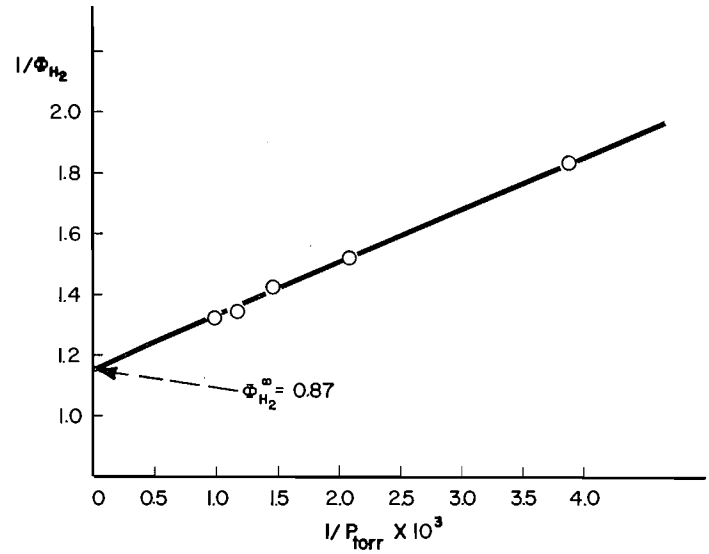

FIG. 1.

If we take R = *t*-butyl, the initial steps in the mechanism are clearly:

[1] $$RCH_3 + Hg\ 6(^3P_1) \rightarrow RCH_2 + H + Hg\ 6(^1S_0)$$

[2] $$H + RCH_3 \rightarrow H_2 + RCH_2$$

[3] $$2RCH_2 \rightarrow RCH_2CH_2R.$$

Since Φ_{H_2} rises with P_S in the complete quenching region, we must add the reaction

[4] $$H + RCH_2 \rightarrow RCH_3.$$

Increasing P_S would favor [2] over [4], and thus both Φ_{H_2} and Φ_{DN} should rise as observed (Table I). Since $\Phi_{H_2}^{\infty}$ is 0.86 and not unity, either [1] is inherently inefficient, or, at the mean I_a used, the linear extrapolation in Fig. 1 to $P_S = \infty$ fails to cancel out the effect of [4].

The above four-step sequence requires that $\Phi_{H_2} = \Phi_{DN}$, whereas, in fact, the difference, Δ, is finite (Table I) and rises with P_S (run 2 excepted) to at least 0.07 at P_S = 1012 torr. This suggests that the heavy DN product is suffering decomposition in the reaction zone, as further indicated by the presence of the minor C-10 olefin detected. Since Δ is constant with increasing t at fixed P_S (runs 6–10, Table I), a steady DN level in the reaction zone is indicated, in which rate of formation and loss by diffusion and reaction are balanced. At constant t the steady DN level would shift upward with P_S, and increased consumption of DN by reaction would result, causing Δ to rise as observed (Table I).

Consumption of DN could arise by three processes:

[5] $$H + RCH_2CH_2R \rightarrow H_2 + R\dot{C}HCH_2R$$

[6] $$RCH_2 + RCH_2CH_2R \rightarrow RCH_3 + R\dot{C}HCH_2R$$

[7] $$Hg\ 6(^3P_1) + RCH_2CH_2R \rightarrow R\dot{C}HCH_2R + H + Hg\ 6(^1S_0)$$

followed by

[8] $$RCH_2 + R\dot{C}HCH_2R \rightarrow RCH_3 + RCH{=}CHR$$

[9] $$RCH_2 + R\dot{C}HCH_2R \rightarrow (RCH_2)_2CHR.$$

Can. J. Chem. Downloaded from www.nrcresearchpress.com by 210.87.254.6 on 09/05/12
For personal use only.

The secondary C—H bonds in DN would render abstraction reactions more facile than in neopentane, and, in addition, markedly increase the quenching cross section. Through [9] DN is lost as a C-15 product which we would not detect. The minor C-10 olefin found likely forms through [8]. This latter product possibly explains why both Φ_{H_2} and Φ_{DN} decrease slowly with t at fixed P_S. By the scavenging reaction

[10] $$H + RCH{=}CHR \rightarrow R\dot{C}HCH_2R$$

competing with [5], Φ_{H_2} and Φ_{DN} would be reduced as found.

From the present study it can be concluded that the alkane, neopentane, shows no exceptional behavior in its primary reaction with Hg $6(^3P_1)$ atoms and closely resembles ethane, since the primary quantum yield is 0.87 and possibly unity.

1. H. E. Gunning and O. P. Strausz. Advan. Photochem. **I**, 209 (1963).
2. B. DeB. Darwent and E. W. R. Steacie. Can. J. Res. **27B**, 181 (1949).
3. A. R. Knight and H. E. Gunning. Can. J. Chem. **39**, 2251 (1961).
4. K. Yang. Private communication.

Received June 17, 1964.
Department of Chemistry,
University of Alberta,
Edmonton, Alberta.

OBSERVATIONS BY X-RAY DIFFRACTION ON DISCOLORED ZINC OXIDE AFTER HEATING

E. A. Secco

As part of a general program on solid state reactions at temperatures up to 1200 °C, we have studied the effect of temperature on discolored zinc oxide—the discoloration is associated with impurities lodged in the oxide matrix. The discolored zinc oxide was obtained from a melt of varying proportions of ZnO and ZnF_2.

The preparation procedure consisted simply of heating the mixture containing varying proportions of U.S.P. zinc oxide and Technical Grade zinc fluoride, in a graphite or alundum crucible, at 1000 °C for 2–5 hours followed by slow cooling in the furnace. That is, the crucible and contents remained in the cooling furnace until room temperature was attained. With an oxide-rich mixture a green residue was obtained, while with a fluoride-rich mixture a blue residue resulted.

The discolored residue was crushed to a powder in a mortar and prepared for the specimen stage of Model X-86-N high-temperature, high-vacuum attachment (1) to the Norelco wide range goniometer. The specimen stage supplied with the attachment was an elevated surface and the specimen, a suspension in a volatile liquid, was placed on the surface. With this arrangement only a very thin film was available for investigation and there existed the possibility of contamination with constituents other than the specimen. The stage was modified to overcome these potential difficulties by depressing the surface to a depth of 1 mm and enclosing the stage with retaining walls of platinum foil of 1 mm, as shown in Fig. 1. The powder sample was now placed on the stage with a spatula and pressed to

Can. J. Chem. Downloaded from www.nrcresearchpress.com by 210.87.254.6 on 09/05/12
For personal use only.

The secondary C—H bonds in DN would render abstraction reactions more facile than in neopentane, and, in addition, markedly increase the quenching cross section. Through [9] DN is lost as a C-15 product which we would not detect. The minor C-10 olefin found likely forms through [8]. This latter product possibly explains why both Φ_{H_2} and Φ_{DN} decrease slowly with t at fixed P_S. By the scavenging reaction

[10] $$H + RCH{=}CHR \rightarrow R\dot{C}HCH_2R$$

competing with [5], Φ_{H_2} and Φ_{DN} would be reduced as found.

From the present study it can be concluded that the alkane, neopentane, shows no exceptional behavior in its primary reaction with Hg $6(^3P_1)$ atoms and closely resembles ethane, since the primary quantum yield is 0.87 and possibly unity.

1. H. E. Gunning and O. P. Strausz. Advan. Photochem. **I**, 209 (1963).
2. B. DeB. Darwent and E. W. R. Steacie. Can. J. Res. **27B**, 181 (1949).
3. A. R. Knight and H. E. Gunning. Can. J. Chem. **39**, 2251 (1961).
4. K. Yang. Private communication.

Received June 17, 1964.
Department of Chemistry,
University of Alberta,
Edmonton, Alberta.

OBSERVATIONS BY X-RAY DIFFRACTION ON DISCOLORED ZINC OXIDE AFTER HEATING

E. A. Secco

As part of a general program on solid state reactions at temperatures up to 1200 °C, we have studied the effect of temperature on discolored zinc oxide—the discoloration is associated with impurities lodged in the oxide matrix. The discolored zinc oxide was obtained from a melt of varying proportions of ZnO and ZnF_2.

The preparation procedure consisted simply of heating the mixture containing varying proportions of U.S.P. zinc oxide and Technical Grade zinc fluoride, in a graphite or alundum crucible, at 1000 °C for 2–5 hours followed by slow cooling in the furnace. That is, the crucible and contents remained in the cooling furnace until room temperature was attained. With an oxide-rich mixture a green residue was obtained, while with a fluoride-rich mixture a blue residue resulted.

The discolored residue was crushed to a powder in a mortar and prepared for the specimen stage of Model X-86-N high-temperature, high-vacuum attachment (1) to the Norelco wide range goniometer. The specimen stage supplied with the attachment was an elevated surface and the specimen, a suspension in a volatile liquid, was placed on the surface. With this arrangement only a very thin film was available for investigation and there existed the possibility of contamination with constituents other than the specimen. The stage was modified to overcome these potential difficulties by depressing the surface to a depth of 1 mm and enclosing the stage with retaining walls of platinum foil of 1 mm, as shown in Fig. 1. The powder sample was now placed on the stage with a spatula and pressed to

Can. J. Chem. Downloaded from www.nrcresearchpress.com by 210.87.254.6 on 09/05/12
For personal use only.

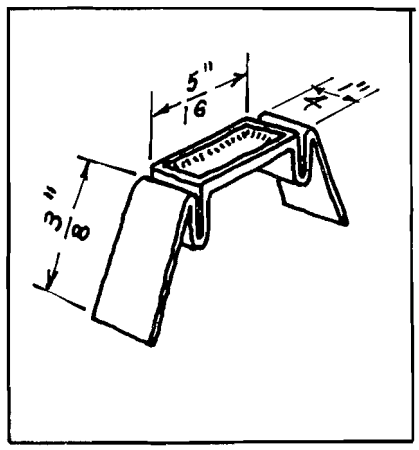

FIG. 1. Modified design of stage for powder specimen.

present a smooth surface to the incident X-ray beam. After the specimen had been positioned and aligned for maximum reflection, the powder was scanned. The diffracted radiation was detected by a Geiger counter and fed to the recorder for a trace of the pattern or diffractogram.

RESULTS AND DISCUSSION

Figure 2 shows a sequence of diffractograms obtained with grey–blue ZnO, I–IV, along with untreated U.S.P. Merck ZnO, V. These traces were obtained under identical operating conditions: angular aperture 1°; receiving slit 0.003 in.; X-radiation, CuK_α, at 45 kV and 15 mA; G.-M. tube voltage, 1550 V; scale factor 16, multiplier 1, time constant 2; scanning speed 1° (2 θ) per min; scan at room temperature (15–20 °C).

During the heating prior to trace II, fumes were observed through the window and a pungent odor was detectable. After the anneal prior to trace IV, the specimen had undergone a significant color change to grey–yellow. Similar annealing of the U.S.P. zinc oxide up to 720 °C did not alter the diffractogram but at 850–875 °C sublimation of the oxide occurred, which reduced all peak intensities proportionately.

No apparent correlation between temperature or time of anneal and the variation in peak intensities was evident, as shown in Fig. 3. Heating in nitrogen or air atmosphere produced the same effects. Similar observations were made on the intensities' variation of the characteristic peaks of crushed natural sphalerite, ZnS, after heating before the onset of oxidation, while such variation was absent with pure ZnS and on crushed natural "red" zincite, ZnO. The qualitative conclusion is that the peak intensity variations are associated with impurities in the host oxide rather than with particle size and (or) the amorphous character of the particles (2).

A possible interpretation of these results is based on impurities incorporated in the oxide. The exact nature of the impurity is not known but fluoride is suspected as the most probable. The radii of $O^=$ and F^- given as 1.40 Å and 1.36 Å respectively (3), suggest that the fluoride ion may be substituted for the oxide ion without distortion of the oxide lattice to yield an anionic substitution compound of composition ZnF_xO_{1-x}, with $x < 0.1$. Since $O^=$ and F^- are isoelectronic their X-ray scattering factors are the same and the supposed ZnF_xO_{1-x} would be expected to give a typical ZnO diffraction pattern. On

Can. J. Chem. Downloaded from www.nrcresearchpress.com by 210.87.254.6 on 09/05/12
For personal use only.

Can. J. Chem. Downloaded from www.nrcresearchpress.com by 210.87.254.6 on 09/05/12
For personal use only.

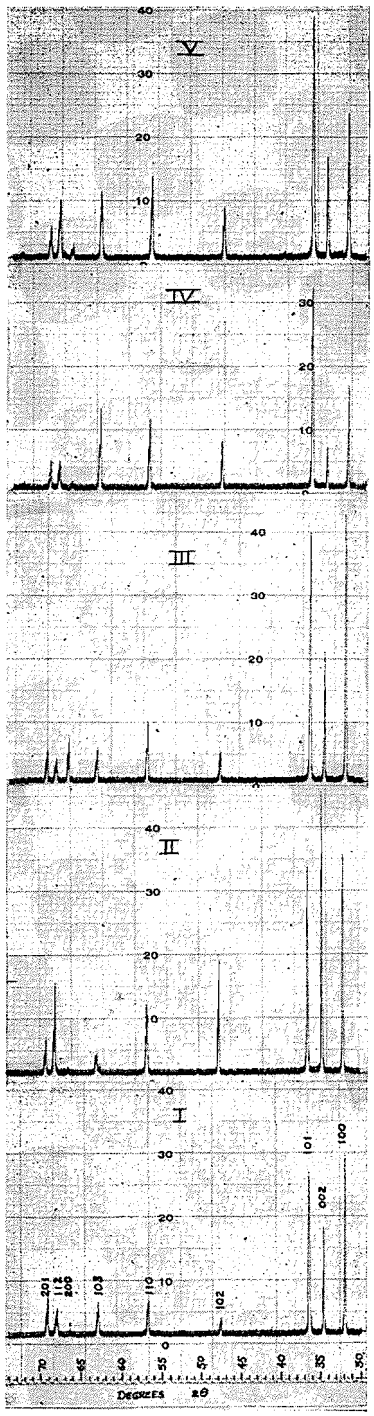

FIG. 2. I, Unannealed grey-blue ZnO; II, same specimen heated in air at 510 °C for 40 min; III, same specimen heated in air at 720 °C for 30 min; IV, same specimen heated in air at 850–875 °C for 183 min; V, Merck, U.S.P. ZnO.

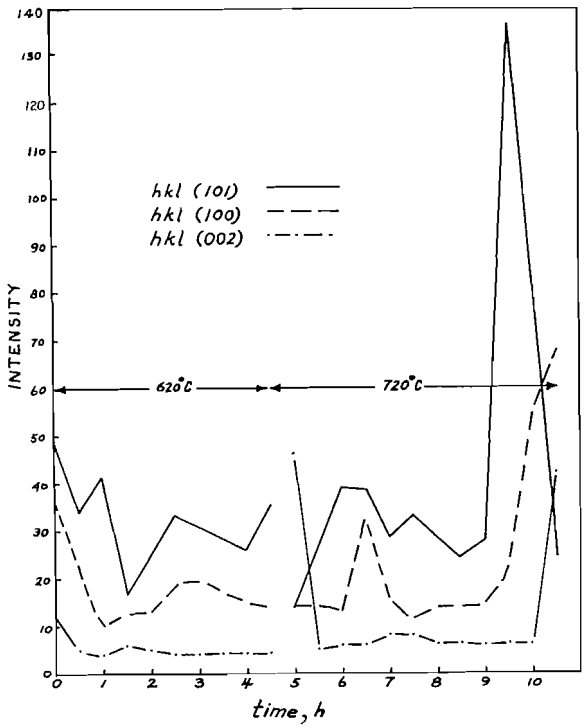

FIG. 3. Variation of peak intensities vs. time of anneal.

heating the presumed compound in air or in nitrogen atmospheres the volatile F^- is expected to move out of the lattice, causing a fractional collapse with subsequent rearrangement of the host ions. The diffractogram after heating would represent the rearranged lattice quenched in a random state of orientation after a loss of a certain fraction of F^-. With sufficient annealing or at sufficiently high temperature, all the effective F^- will have sublimed from the oxide and the diffractogram intensities approach those intensities recorded in A.S.T.M. index No. 5-0664.

A feature which militates against such an interpretation is that the elimination of F^- from the lattice would be expected to be progressive and that such a progression would be reflected in the peak intensities' variation, in contrast to Fig. 3. However, two processes are operative in each anneal, that is, the migration of F^- ions to the particle surface and redistribution of the F^- ions in the particle bulk. These two processes contributing to lattice disruptions and subsequent rearrangements after successive anneals would depend on such factors as F^- ion mobility rate, the stability of the various crystal faces (4), the relative composition of the particles, and the particle-size distribution. The interplay of these factors is beyond the scope of our present understanding.

ACKNOWLEDGMENT

Grateful acknowledgment is made to the National Research Council of Canada for generous support of this research.

Can. J. Chem. Downloaded from www.nrcresearchpress.com by 210.87.254.6 on 09/05/12
For personal use only.

1. J. INTRATER and S. HURWITT. Rev. Sci. Instr. **32**, 905 (1961).
2. F. SCHOSSBERGER. *In* Encyclopedia of X-rays and gamma rays. *Edited by* George L. Clark. Reinhold Publishing Corp., New York. 1963. pp. 728–33.
3. L. PAULING. Nature of chemical bond. 3rd ed. Cornell University Press. 1959. p. 514.
4. E. A. SECCO. J. Phys. Chem. Solids, **24**, 469 (1963).

RECEIVED FEBRUARY 13, 1964.
CHEMISTRY DEPARTMENT,
ST. FRANCIS XAVIER UNIVERSITY,
ANTIGONISH, NOVA SCOTIA.

Can. J. Chem. Downloaded from www.nrcresearchpress.com by 210.87.254.6 on 09/05/12
For personal use only.

THE REACTION OF DL-PROPYLENIMINE WITH MESO-1,2;3,4-DIEPOXYBUTANE

SANDRA L. HOLTON, JAMES E. CHRISTENSEN, OSBORNE P. CREWS, AND LEON GOODMAN

A previous paper (1) from these laboratories described the preparation of *meso*-1,4-bis(1-aziridinyl)-2,3-butanediol, an interesting anti-tumor agent, from the reaction of ethylenimine and *meso*-1,2;3,4-diepoxybutane. The conversion of that bis-aziridine to the potential anti-radiation drug, 1,4-bis-[(2-mercaptoethyl)amino]-*meso*-2,3-butanediol dihydrochloride, was described in a subsequent manuscript (2). The interesting biological activity of the bis-aziridine and the bis-thiol was the impetus for the preparation of some C-methyl substituted analogues of these compounds. This note reports these studies.

The reaction of DL-propylenimine with *meso*-1,2;3,4-diepoxybutane can give three possible diastereoisomeric products; these are represented as I*a*, I*b*, and I*cd* below. It is apparent that I*a* and I*b* are two optically compensated *meso*-forms and that I*c* and I*d*

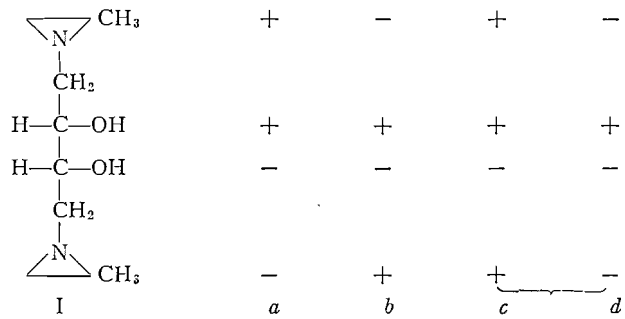

constitute a DL-racemate. In practice, reaction of the *meso*-diepoxide with excess DL-propylenimine gave three crystalline solids. The two higher melting materials were easy to obtain as sharply melting solids; the lowest melting material was obtained with some difficulty from the reaction residues. The reaction of D(+)-propylenimine with *meso*-1,2;3,4-diepoxybutane gave a sharply melting crystalline solid which obviously is isomer I*c*. The nuclear magnetic resonance (n.m.r.) spectra, run in deuterium oxide, of the three diastereoisomers from the DL-propylenimine reaction were distinctly different, the major differences appearing in the absorptions due to the six ring protons. The n.m.r. spectrum

1. J. INTRATER and S. HURWITT. Rev. Sci. Instr. **32**, 905 (1961).
2. F. SCHOSSBERGER. *In* Encyclopedia of X-rays and gamma rays. *Edited by* George L. Clark. Reinhold Publishing Corp., New York. 1963. pp. 728–33.
3. L. PAULING. Nature of chemical bond. 3rd ed. Cornell University Press. 1959. p. 514.
4. E. A. SECCO. J. Phys. Chem. Solids, **24**, 469 (1963).

RECEIVED FEBRUARY 13, 1964.
CHEMISTRY DEPARTMENT,
ST. FRANCIS XAVIER UNIVERSITY,
ANTIGONISH, NOVA SCOTIA.

Can. J. Chem. Downloaded from www.nrcresearchpress.com by 210.87.254.6 on 09/05/12
For personal use only.

THE REACTION OF DL-PROPYLENIMINE WITH MESO-1,2;3,4-DIEPOXYBUTANE

SANDRA L. HOLTON, JAMES E. CHRISTENSEN, OSBORNE P. CREWS, AND LEON GOODMAN

A previous paper (1) from these laboratories described the preparation of *meso*-1,4-bis(1-aziridinyl)-2,3-butanediol, an interesting anti-tumor agent, from the reaction of ethylenimine and *meso*-1,2;3,4-diepoxybutane. The conversion of that bis-aziridine to the potential anti-radiation drug, 1,4-bis-[(2-mercaptoethyl)amino]-*meso*-2,3-butanediol dihydrochloride, was described in a subsequent manuscript (2). The interesting biological activity of the bis-aziridine and the bis-thiol was the impetus for the preparation of some C-methyl substituted analogues of these compounds. This note reports these studies.

The reaction of DL-propylenimine with *meso*-1,2;3,4-diepoxybutane can give three possible diastereoisomeric products; these are represented as I*a*, I*b*, and I*cd* below. It is apparent that I*a* and I*b* are two optically compensated *meso*-forms and that I*c* and I*d*

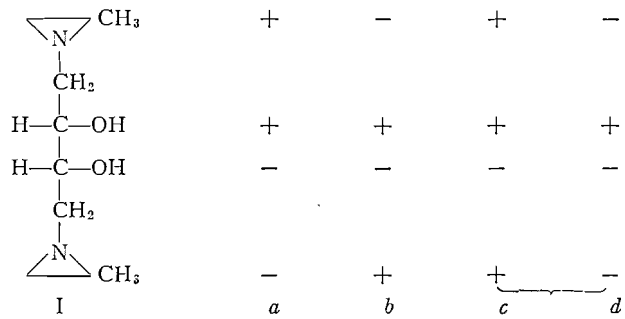

constitute a DL-racemate. In practice, reaction of the *meso*-diepoxide with excess DL-propylenimine gave three crystalline solids. The two higher melting materials were easy to obtain as sharply melting solids; the lowest melting material was obtained with some difficulty from the reaction residues. The reaction of D(+)-propylenimine with *meso*-1,2;3,4-diepoxybutane gave a sharply melting crystalline solid which obviously is isomer I*c*. The nuclear magnetic resonance (n.m.r.) spectra, run in deuterium oxide, of the three diastereoisomers from the DL-propylenimine reaction were distinctly different, the major differences appearing in the absorptions due to the six ring protons. The n.m.r. spectrum

of I*c* was essentially identical with that of the low melting diastereoisomer which is therefore the DL-racemate; the two higher melting isomers are therefore the *meso*-forms I*a* and I*b*.

The three diastereoisomers were converted to a series of potential anti-radiation drugs.

A series—from high melting *meso*-bis-aziridine.
B series—from low melting *meso*-bis-aziridine.
C series—from DL-racemate form of the bis-aziridine.

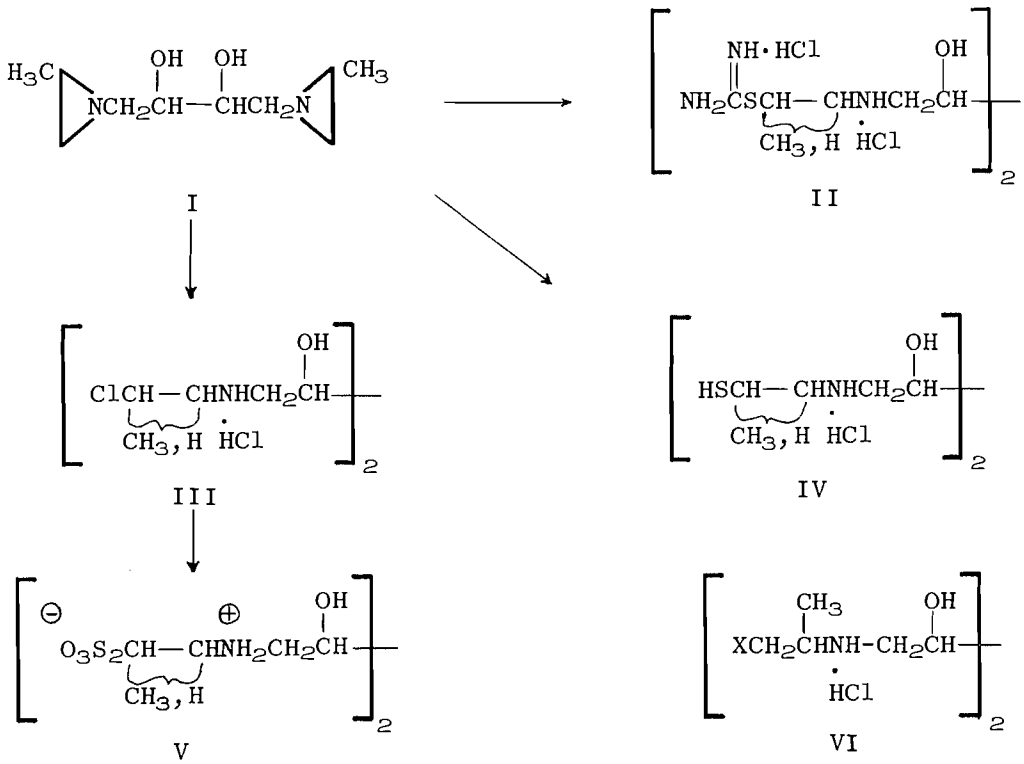

Thus reaction of the bis-aziridines (I) with hydrogen sulphide followed by reaction of the resulting thiols with hydrogen chloride afforded the bis-mercaptans (IV). Opening of the isomeric compounds I with hydrochloric acid yielded the chloroethylamines (III) that could be converted to the Bunte salts (V) with thallous thiosulphate (3) or, in the case of IIIB, with sodium thiosulphate. The reaction of IA and IB with thiourea and hydrochloric acid (4) gave the bis-isothiuronium salts (IIA and IIB). Compounds II, III, IV, and V are represented as mixtures which result from opening of the aziridine ring at C-2 or C-3; the predominant products would be expected to be those (VI) from attack at the secondary ring carbon.

EXPERIMENTAL

1,4-Bis-(2-methyl-1-aziridinyl)-meso-2,3-butanediol (I)

A stirred mixture of 20.0 g (0.232 mole) of *meso*-1,2;3,4-diepoxybutane, 52.9 g (0.928 mole) of DL-propylenimine and 75 ml of methylal was heated at reflux for 18 h, then cooled to room temperature, and filtered.

Can. J. Chem. Downloaded from www.nrcresearchpress.com by 210.87.254.6 on 09/05/12
For personal use only.

A crystalline precipitate, 8.5 g (18%), m.p. 167–169° (from IA) was isolated. From a previous run a sample of IA was obtained, m.p. 171–172°, and was analyzed. Anal. Calc. for $C_{10}H_{20}N_2O_2$: C, 60.0; H, 10.1; N, 14.0. Found: C, 59.9; H, 10.1; N, 14.3.

The filtrate from IA was chilled (0°) and the solid IB precipitated, 6.6 g (14%), m.p. 107–109°. Recrystallization from ethyl acetate of this solid gave 4.0 g, m.p. 110–113°. From a previous run an analytical sample of the *meso*-compound IB had been obtained by several recrystallizations from Skellysolve C (b.p. 88–99°), m.p. 113–115°. Anal. Found: C, 60.2; H, 10.0; N, 14.2.

The filtrate from IB was evaporated *in vacuo* and the residue recrystallized from ethyl acetate affording 7.9 g of the DL-racemate (IC), m.p. 75–77°. Anal. Found: C, 59.8; H, 10.2; N, 14.2.

The three forms IA, IB, and IC as Nujol mulls gave well-resolved infrared spectra, that were characteristic and reproducible for each compound. Compound IA had a band at 13.0 μ that was absent in the spectra of the other two isomers. Compounds IB and IC had distinctly different infrared spectra, but there were no strong bands in the spectrum of one that were free of absorption in the spectrum of the other. The n.m.r. spectra, determined in deuterium oxide for forms IA, IB, and IC were also different and distinctive for each form. The major differences were found in the patterns for the six aziridine ring protons.

1,4-Bis-[(D(+)-2-methyl-1-aziridinyl)]-meso-2,3-butanediol

A mixture of 0.40 g (4.64 mmoles) of *meso*-butadiene diepoxide, 1.4 g (24 mmoles) of D(+)-propylenimine,* and 1 ml of isopropanol was heated at 50° for 5.5 h then was allowed to stand at room temperature for 48 h. The mixture was evaporated *in vacuo* giving a colorless sirup which slowly crystallized when chilled under 2–3 ml of ether. The crystalline solid, 0.40 g (43%), m.p. 78–84°, was sublimed at 60–70° and 0.4 mm to give the analytical sample, m.p. 83–85°, $[\alpha]_D^{24}$ −56° (0.935% in water). Its n.m.r. spectrum in deuterium oxide was virtually superimposable on that of IC and was distinctly different than those of the two *meso*-forms (IA and IB). Anal. Calc. for $C_{10}H_{20}N_2O_2$: C, 60.0; H, 10.1; N, 14.0. Found: C, 59.7; H, 9.8; N, 14.1.

1,4-Bis-[(meso and DL-2-mercapto-(1)2-methylethyl)amino]-meso-2,3-butanediol (IV)

1. From IA

Hydrogen sulphide gas was bubbled through a suspension of 2.00 g (10.0 mmoles) of IA in 30 ml of methanol for 1 h at room temperature during which time the solid dissolved. Hydrogen chloride was then bubbled through the clear solution until it was distinctly acidic to pH paper (pH ~2). Ether was added to the cloud point and the mixture was chilled. The white, crystalline, nitroprusside-positive solid 1.74 g (57%) was collected, m.p. 170–190° dec. Anal. Calc. for $C_{10}H_{26}Cl_2N_2O_2S_2$: C, 35.2; H, 7.68; Cl, 20.8; N, 8.21; S, 18.8. Found: C, 35.2; H, 7.76; Cl, 20.6; N, 8.07; S, 18.4.

2. From IB

Using the above procedure, starting with 0.41 g of IB, there was obtained 0.20 g (32%) of product, m.p. 162–166° dec. Anal. Found: C, 35.1; H, 7.79; Cl, 21.2; N, 8.22; S, 18.5.

3. From IC

A solution of 0.73 g of IC in 120 ml of methanol was treated with hydrogen sulphide as described above. The solution, which contained undissolved solid, was filtered and treated with a 2% solution of hydrogen chloride in methanol to pH 2 (pH paper), then was evaporated *in vacuo* and the residue thoroughly triturated with ether. A solid formed when the residue was maintained in high vacuum for several hours. The very hygroscopic solid melted with decomposition over a wide range with decomposition more vigorous at 100°. Anal. Found: C, 35.2; H, 7.95; Cl, 20.7; N, 8.24; S, 18.6.

1,4-Bis-[(meso or DL-2-chloro-(1)2-methylethyl)amino]-meso-2,3-butanediol Dihydrochloride (III)

1. From IA

To 50 ml of chilled (0°), stirred, concentrated aqueous hydrochloric acid was added slowly 0.50 g (2.5 mmoles) of IA and the resulting solution was stirred at 0° for 1 h, then evaporated *in vacuo* at room temperature. The solid white residue was washed several times with ether giving 0.86 g (100%) of product. Recrystallization from 20 ml of 95% ethanol afforded 0.41 g (48%) of white crystals, m.p. 215–230° dec. A second crystallization from methanol–ether gave 0.36 g of solid, m.p. 220–228° dec. and a third recrystallization from methanol–ether gave 0.32 g of the analytical sample, m.p. 220–227° dec. Anal. Calc. for $C_{10}H_{24}Cl_4N_2O_2$: C, 34.7; H, 6.99; Cl, 41.0; N, 8.09. Found: C, 35.0; H, 6.95; Cl, 41.0; N, 8.16.

2. From IB

Using the same quantities and the same procedure with IB that was described for IA, there was obtained 0.55 g (64%) of the analytical sample, m.p. 223–229° dec. Anal. Found: C, 34.3; H, 7.38; Cl, 40.6; N, 7.92.

3. From the DL-Racemate, (IC)

Using the same procedure as described for IA, 0.63 g of IC gave 0.27 g (25%) of the analytical sample of III, m.p. 216–223° dec. Anal. Found: C, 34.7; H, 7.30; Cl, 41.0; N, 8.14.

**A generous supply of this compound was provided by Dr. Robert R. Engle, Riker Laboratories, Inc., Northridge, California.*

Can. J. Chem. Downloaded from www.nrcresearchpress.com by 210.87.254.6 on 09/05/12
For personal use only.

1,4-Bis-[(meso or DL-*2-mercapto-(1)2-methylethyl)amino]-meso-2,3-butanediol-S,S-disulphate (V)*

1. From IIIA

A suspension of 18.32 g (53 mmoles) of the bis-(2-chloroethyl) amine (IIIA), 57.6 g of thallous thiosulphate (0.247 mole), and 280 ml of water was heated with stirring at 70–80° for 1 h, then a second 57.6-g portion of thallous thiosulphate was added and heating was continued for 18 h. The suspension was cooled to room temperature and filtered, and the filtrate was chilled affording 13.5 g (58%) of white crystals, m.p. 209–213° dec. Recrystallization from 200 ml of boiling water yielded 11.5 g (49%) of the analytical solid, m.p. 211–216° dec. Anal. Calc. for $C_{10}H_{24}N_2O_8S_4 \cdot H_2O$: C, 26.9; H, 5.87; N, 6.27; S, 28.7. Found: C, 26.9; H, 5.46; N, 6.02; S, 28.4.

2. From IIIB

A solution of 2.56 g (7.40 mmoles) of IIIB, 3.66 g (11.5 mmoles) of sodium thiosulphate (pentahydrate), and 40 ml of water was stirred at 80° for 1.5 h, then a second 3.66-g portion of sodium thiosulphate was added and the mixture was heated for 13 h more, then chilled. The white crystalline precipitate, 2.55 g, was collected and recrystallized from 20 ml of hot water affording 2.35 g (74%) of crystals, m.p. 193–200° dec. Anal. Calc. for $C_{10}H_{24}N_2O_8S_4$: C, 28.0; H, 5.64; N, 6.54; S, 29.9. Found: C, 27.7; H, 6.05; N, 6.32; S, 29.9.

3. From IIIC

The reaction of 1.77 g (5.11 mmoles) of IIIC with thallous thiosulphate as described for the preparation of IIIA gave 1.28 g (58%) of the crude bis-Bunte salt. Recrystallization from 5 ml of hot water afforded 0.75 g (34%) of the analytical sample, m.p. 184–192° dec. Anal. Found: C, 27.7; H, 6.09; N, 6.50; S, 29.7.

1,4-Bis[meso-1(2)methyl-2-isothiuroniumethyl]amino-2,3-meso-dihydroxybutane Tetrahydrochloride (II)

1. From IA

To a stirred solution of 4.08 g (53.7 mmoles) of thiourea in 40 ml of methanol containing 9.1 ml of concentrated hydrochloric acid (0.107 mole) was added slowly 5.37 g (26.8 mmoles) of IA. After the addition, the mixture was stirred at room temperature for 0.5 h, then chilled. The white precipitate, 4.68 g (35%), m.p. 205–215° dec., was washed with methanol and ether. A second crop, 4.73 g (36%), m.p. 205–211° dec., was obtained by the addition of ether to the filtrate. Anal. Calc. for $C_{12}H_{32}Cl_4N_6O_2S_2$: C, 28.9; H, 6.48; Cl, 28.5; N, 16.9, S, 12.9. Found (for first crop): C, 29.0; H, 6.64; Cl, 28.4; N, 16.7; S, 12.7; (for second crop): C, 29.1; H, 6.87; Cl, 28.5; N, 16.8; S, 12.7.

2. From IB

The conversion of 0.51 g of IB by the procedure described above for the high melting *meso*-form (IA) gave a low yield of a white crystalline solid that was recrystallized from 1 ml of methanol yielding 0.26 g (20%) of product, m.p. 205–213° dec. Anal. Found: C, 29.1; H, 6.50; Cl, 28.2; N, 16.5; S, 13.2.

ACKNOWLEDGMENTS

This work was carried out under the joint auspices of the Medical Research and Development Command, Office of the Surgeon General, under Contract No. DA-49-193-MD-2068, and of the Cancer Chemotherapy National Service Center, National Cancer Institute, National Institutes of Health, Public Health Service, under Contract No. SA-43-ph-1892. The opinions expressed in this article are those of the authors and not necessarily those of either sponsoring agency.

The authors are indebted to Dr. Peter Lim and his group for the optical rotation and the n.m.r. spectra.

1. E. J. Reist, I. G. Junga, M. E. Wain, O. P. Crews, L. Goodman, and B. R. Baker. J. Org. Chem. **26**, 2139 (1961).
2. J. E. Christensen and L. Goodman. J. Org. Chem. **28**, 847 (1963).
3. H. Z. Lecher and E. M. Hardy. J. Org. Chem. **20**, 475 (1955).
4. S. J. Brois. P. B. Report 135447, from U. S. Govt. Research Repts. **31**, 133 (1959).

Received April 15, 1964.
Life Sciences Research,
Stanford Research Institute,
Menlo Park, California.

Can. J. Chem. Downloaded from www.nrcresearchpress.com by 210.87.254.6 on 09/05/12
For personal use only.

NEW PHENCYCLONE ADDUCTS FROM ETHYLENIC COMPOUNDS

C. F. H. Allen and R. Y. Ning

The formation of adducts from cyclopentadienones ("cyclones") and unsaturated compounds is now well known. Since the extensive literature has appeared in two reviews (1, 2), pertinent references will be given specifically only as needed. It has been reported that adducts are obtained most readily and retained the carbonyl bridge best with phencyclone (I) (3); such a behavior has been confirmed in this laboratory. Since a few investigators have successfully used (1, 2, 4) ethylenic compounds the possibility of using this reaction to identify styrenes and simple non-conjugated olefinic substances, by preparing solid derivatives, was undertaken.

Seven new adducts (II) of phencyclone were prepared. The latter are carbonyl-bridged derivatives of triphenylene, bearing substituents in the 2-position; for example, styrene gives 13-oxo-1,2,4-triphenyl-1,2,3,4-tetrahydro-1,4-methanotriphenylene (II, A = C_6H_5).

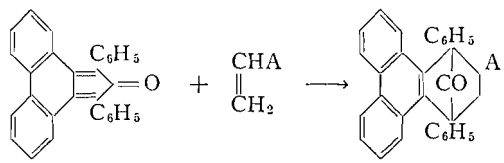

I II

The unsaturates employed were 1-hexene, 1-octene, styrene, allyl acetate, butyl acrylate, isopropyl methacrylate, and 2-β-phenethyl methacrylate. Hence, in the adducts, the groups in the 2-position are butyl, hexyl, phenyl, 2-acetoxymethyl, 2-butoxycarbonyl, 2-isopropoxycarbonyl-2-methyl, and 2-methyl-2-β-phenethoxycarbonyl respectively. Oils and gums resulted when vinyl ethers, 2-ethylhexyl acrylate, and 2-methyl- and 4-methylpentenes were employed.

From the limited examples described in this note it appears that phencyclone may be useful in giving solid adducts with styrenes, olefines having terminal unsaturation, allyl compounds, and acrylates, provided no large aliphatic groups are present. Unfortunately, the slow addition, even to the most reactive but difficultly accessible phencyclone, contamination by products of subsequent decarbonylation or other secondary reactions, and reluctance to crystallize, renders this objective discouraging. Active work was discontinued upon the announcement that adducts suitable for the same purpose of identification could be easily obtained by the use of 1,3-dipolar compounds (5); the yields are excellent, but reaction time of 90 hours is rather long. Our results are reported at this time as a contribution to the field of carbonyl bridge compounds.

EXPERIMENTAL

Phencyclone is not easy to prepare. In our hands the best yield (88%) was obtained by modifying the procedure (6) by using propyl alcohol as a solvent and "Triton B" as catalyst. A mixture of 25 g (0.12 mole) of phenanthrenequinone (Eastman Number 1269) and 26 g (0.12 mole) of dibenzyl ketone (Eastman Number P974) is stirred to a thin paste with a little propyl alcohol, and the rest of a total of 1 l of propyl alcohol added. The suspension is stirred and heated to boiling, so that partial solution takes place. The hot mixture is then cooled in ice water to about 60°. While the mixture is cooling, a solution of 5 ml of Triton B (a 40% aqueous solution of benzyltrimethylammonium hydroxide) in 10 ml of propyl alcohol is

Can. J. Chem. Downloaded from www.nrcresearchpress.com by 210.87.254.40 on 09/05/12
For personal use only.

added from a medicine dropper, in small squirts; with each addition, the mixture is vigorously stirred. The rate of addition is timed so that all the base has been added only when the temperature has dropped to 60°. (If too much of the base is admitted without efficient cooling, flocks of a white contaminant become visible.) The temperature is maintained at 60°, and stirring is continued until the orange color of the quinone disappears (5–10 min). The phencyclone is then collected on a filter, rinsed with ethyl alcohol, and dried at about 100°. The average yield was 88%, and the melting point, 245–255°.

Preparation of adducts.—Preliminary exploratory tests showed that addition was rapid (solution decolorized) at about 150° (b.p. of styrene or cumene), but to avoid decarbonylation the temperature must be kept lower. Boiling toluene or dimethylformamide at various temperatures were successfully used; the latter solvent was generally employed, though uniform conditions were not observed. Toluene was preferred with styrene and with butyl acrylate. In all instances a *trace* of concentrated sulphuric acid was added as a catalyst.

A mixture of 4 g of phencyclone and 6 ml of styrene in 60 ml of toluene, with a microtrace of sulphuric acid, was heated to boiling. The initial green color quickly changed to yellow. The solution was cooled in ice water and the adduct was precipitated by addition of an equal volume of hexane. It was recrystallized from toluene–hexane.

A mixture of 6 ml of isopropyl methacrylate and 4 g of phencyclone in 25 ml of dimethylformamide, with a trace of sulphuric acid, was warmed for 2 h at 40° with occasional shaking, and let stand 2 days. The adduct was precipitated by water, and recrystallized from acetone or benzene – petroleum ether. It is light sensitive.

The properties of the new adducts are collected in Table I. The presence of the carbonyl bridge was evident from the analytical figures, and was confirmed by the infrared spectra.

TABLE I

Properties of the adducts (II)

Addend	Group A in 2 position	M.p., °C	Mol. wt.	Analyses			
				Calc., %		Found, %	
				C	H	C	H
1-Hexene	Butyl	206–207	$C_{35}H_{30}O$	90.1	6.5	90.4	6.7
1-Octene	Hexyl	186–187	$C_{37}H_{34}O$	89.8	6.9	89.5	6.7
Styrene	Phenyl	264–267 dec.	$C_{37}H_{26}O$	91.4	5.4	91.2	5.6
Allyl acetate	2-Acetoxymethyl	219–220	$C_{34}H_{26}O_3$	84.6	5.4	84.0	5.3
Butyl acrylate	2-Butoxycarbonyl	201	$C_{36}H_{30}O_3$	84.7	5.9	84.6	6.1
Isopropyl methacrylate	2-Isopropoxycarbonyl-2-methyl	217	$C_{36}H_{36}O_3$	84.7	5.9	84.6	5.6
2-β-Phenethyl methacrylate	2-Methyl-2-β-phenethoxy-carbonyl	164–166 dec.	$C_{41}H_{32}O_3$	86.2	5.4	86.0	5.6

1. C. F. H. Allen. Chem. Rev. **37**, 209 (1945).
2. C. F. H. Allen. Chem. Rev. **62**, 653 (1962).
3. V. S. Abramov. Dokl. Akad. Nauk SSSR **63**, 637 (1948); Chem. Abstr. **43**, 2585 (1949).
4. L. A. Rothman and E. I. Becker. J. Org. Chem. **25**, 2203 (1960). B. A. Arbuzov, L. A. Shapshinskaya, and M. I. Kudryavtseva. Izv. Akad. Nauk SSSR Otd. Khim. Nauk, 2160 (1961); Chem. Abstr. **57**, 11223 (1962).
5. R. Huisgen. Centenary Lecture, Dec. 8, 1960; Proc. Chem. Soc. 357 (esp. p. 366) (1961).
6. W. Dilthey. Ger. Patent No. 575, 857; Chem. Abstr. **28**, 1356 (1934).

Received April 17, 1964.
Department of Chemistry,
Rochester Institute of Technology,
Rochester, New York.

Can. J. Chem. Downloaded from www.nrcresearchpress.com by 210.87.254.40 on 09/05/12
For personal use only.

Can. J. Chem. Downloaded from www.nrcresearchpress.com by 210.87.254.40 on 09/05/12
For personal use only.

Canadian Journal of Chemistry

Issued by THE NATIONAL RESEARCH COUNCIL OF CANADA

VOLUME 42 OCTOBER 1964 NUMBER 10

PHOTOCHEMICAL TRANSFORMATIONS OF DIENES[1]

II. THE PHOTOLYSIS OF 3-METHYLCHOLESTA-3,5-DIENE (V)[2]

G. JUST AND V. DI TULLIO[3,4]

Department of Chemistry, McGill University, Montreal, Quebec

Received December 27, 1963

ABSTRACT

Photolysis of 3-methylcholesta-3,5-diene (V) in ethanol gave 3-methylenecholest-5-ene (VI), 6β-ethoxy-3α-methyl-3β,5-cyclo-5β-cholestane (VII), 3β-ethoxy-3α-methylcholest-5-ene (VIII), and 3α-methylcholesterol (VIII*a*) as well as a number of unidentified hydrocarbons and alcohols. A similar photolysis in pentane, followed by reaction of the resulting 3β,5;4α,6α-bicyclo-5β-cholestane (II*a*) with ethanol, gave the cyclo ether VII as the only isolable product.

Recently, Dauben *et al.* (2) reported that the photolysis of cholesta-3,5-diene (I) in ethanol gave 6-ethoxy-3β,5-cyclo-5β-cholestane (III) accompanied by a minor amount of the A-nor ether IV. These two products were also obtained in identical yields by the reaction of ethanol with the bicyclobutane II, itself obtained by irradiation in pentane

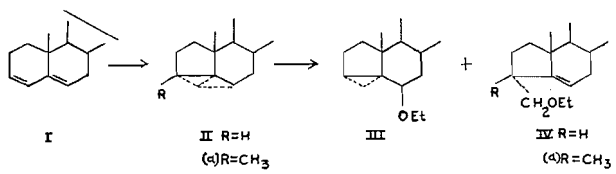

of diene I. Since we were interested in obtaining compounds of type III bearing an alkyl group at C_3, we decided to irradiate 3-methylcholesta-3,5-diene (V).

Cholest-4-en-3-one (3) was treated with methyl magnesium iodide (4). The resulting diene V absorbed in the ultraviolet at 232, 239, and 248 mμ (log ϵ 4.26, 4.29, 4.16).

A solution of diene V in ethanol–pentane (1:9)[5] was irradiated with a 450 W mercury arc lamp until the ultraviolet absorption of the reaction mixture between 220 and 400 mμ was negligible. The solvent was then evaporated and the residue chromatographed on silica gel.

1. Hexane eluted an oil (6.8%) which could not be crystallized. The nuclear magnetic resonance (n.m.r.)[6] indicated the presence of starting material, 3-methylenecholest-5-ene (VI), and other olefins which could not be separated.

[1]*For paper I, see reference 1.*
[2]*Presented in part at the A.C.F.A.S. meetings in Montreal (1962) and Quebec (1963).*
[3]*From part of the thesis presented by V.D.T. in partial fulfillment of the requirements for the Ph.D. degree.*
[4]*Holder of a National Research Council of Canada Studentship 1962–1963.*
[5]*Very similar results were obtained when absolute ethanol was used as solvent.*
[6]*Tetramethylsilane = 0.*

2. Further elution with hexane gave a crystalline diene, ν 3030, 1648, and 888 cm^{-1} ($C{=}CH_2$), δ 4.55 p.p.m. (2H, $C{=}CH_2$) and 5.29 p.p.m. (1H, C=CH—), in approximately 15% yield. The diene VI did not absorb in the ultraviolet between 220 and 400 mμ and was hence not conjugated. Catalytic hydrogenation with platinum oxide in acetic acid gave 3-methylcholestane (IX) (5). Treatment with perchloric acid in dioxane at 70° overnight gave a quantitative yield (by ultraviolet) of 3-methylcholesta-3,5-diene (V). Chemical and spectral properties of the diene were compatible with 3-methylene-cholest-5-ene (VI). However, all attempts to prove the proposed structure by degradation reactions or by synthesis were unsuccessful. An indirect proof of structure was therefore sought. Diene VI was treated with slightly less than one equivalent of diborane in diglyme for 1 h (6). Chromatography gave 3-hydroxymethylcholest-5-ene (X), identical in all respects with a sample prepared by reaction of the Grignard reagent from cholesteryl chloride (XI) in tetrahydrofuran with paraformaldehyde.

3. Elution with benzene and crystallization from hexane gave a compound, $C_{30}H_{52}O$,[7] in 20–30% yield. Its n.m.r. spectrum showed a pair of one proton doublets (J = 4.5 c.p.s.) at −0.47 and 0.45 p.p.m. characteristic for geminal protons (7) on a cyclopropane ring, and a three proton signal in the 3–3.5 p.p.m. region. This signal was very similar to that shown by photoether III. By analogy with Dauben's work (2) on cholesta-3,5-diene (I), this compound was assigned structure VII. Heating under reflux of photoether VII with perchloric acid in dioxane gave 5% (identified by ultraviolet analysis) of 3-methyl-cholesta-3,5-diene (V) and a mixture of alcohols which could not be separated.

Chromatography of the photoether VII on alumina (activity I) resulted in the loss of the elements of ethanol (2*a*) and the formation of olefin XIII, similar to that described by Dauben (2) in the 3-unsubstituted series. The signals for the C_4-cyclopropane protons were now at −0.08 and 0.59 p.p.m. (J = 5 c.p.s.). The olefinic protons at C_6 and C_7 were chemically equivalent and appeared as a singlet at 5.38 p.p.m. Comparison of the n.m.r. spectrum of this olefin with 3β,5-cyclo-5β-cholest-6-ene (XIII*a*) (2*a*) and 3α.5-cyclo-5α-cholest-6-ene (XV) (8, p. 318) supported quite conclusively the stereochemical assignment of the cyclopropane ring (see Table I). In the case of the Δ^6-3β,5-cyclo derivatives, the two olefinic protons appeared essentially as a singlet, whereas in the 3α,5-cyclo compound, the C_6 and C_7 olefinic protons appeared as an evenly spaced (J = 10 c.p.s.) four line system centered at 5.33 p.p.m. Heating olefin XIII under reflux with perchloric acid in aqueous dioxane gave a 24% yield of 3-methylcholestadiene (V). When ethanol was used as a solvent and the solution refluxed overnight, 21% diene V (identified by ultraviolet analysis) and variable yields (5–30%) of 3β-ethoxy-3α-methylcholest-5-ene (VIII) were obtained. Ether VIII was identical in all respects with the photoether described below. These experiments showed that the 3-methyl group influenced markedly the course of the acid-catalyzed reaction of both ether VII and olefin XIII, and probably stabilized a positive charge at C_3 in an intermediate carbonium ion (no formation of cholestadiene or cholesterol was detected in a similar reaction of photoether III).

Catalytic hydrogenation of olefin XIII with platinum oxide in acetic acid at 40° and 60 p.s.i. gave 3α-methyl-3β,5-cyclo-5β-cholestane (XIV), δ 0.44 p.p.m. (1H, doublet, J = 4.45 c.p.s.) and −0.35 p.p.m. (1H, triplet,[8] J = 4.5 c.p.s.).

4. Elution with benzene–ether (4:1) gave an olefinic ether, in 20–30% yield. The n.m.r. spectrum showed low-field signals at 3.45 p.p.m. (2H, quartet, J = 7 c.p.s., OCH_2CH_3) and 5.26 p.p.m. (1H, broad, C=C—H) only. Heating ether VIII under reflux with

[7]*This compound could also be obtained by direct crystallization of the crude photoylsis mixture.*
[8]*Due probably to long-range coupling, which will be discussed in a forthcoming paper.*

Can. J. Chem. Downloaded from www.nrcresearchpress.com by 210.87.254.40 on 09/05/12
For personal use only.

pyridine hydrochloride in acetic acid gave 3-methylcholesta-3,5-diene (V). Catalytic reduction at 60 p.s.i. and 40° in acetic acid gave 3-methylcholestane (IX) (5) (29%) and 3β-ethoxy-3α-methylcholestane (XII) (51%). The reduced photoether was obtained in 78% yield as the only crystalline product when sodium nitrite was added to the reaction mixture (9). All attempts to hydrolyze the ether function of either VIII or XII failed and resulted either in recovery of starting material or formation of olefins. The reduced photoether XII was oxidized with ruthenium tetroxide in carbon tetrachloride (10) to a

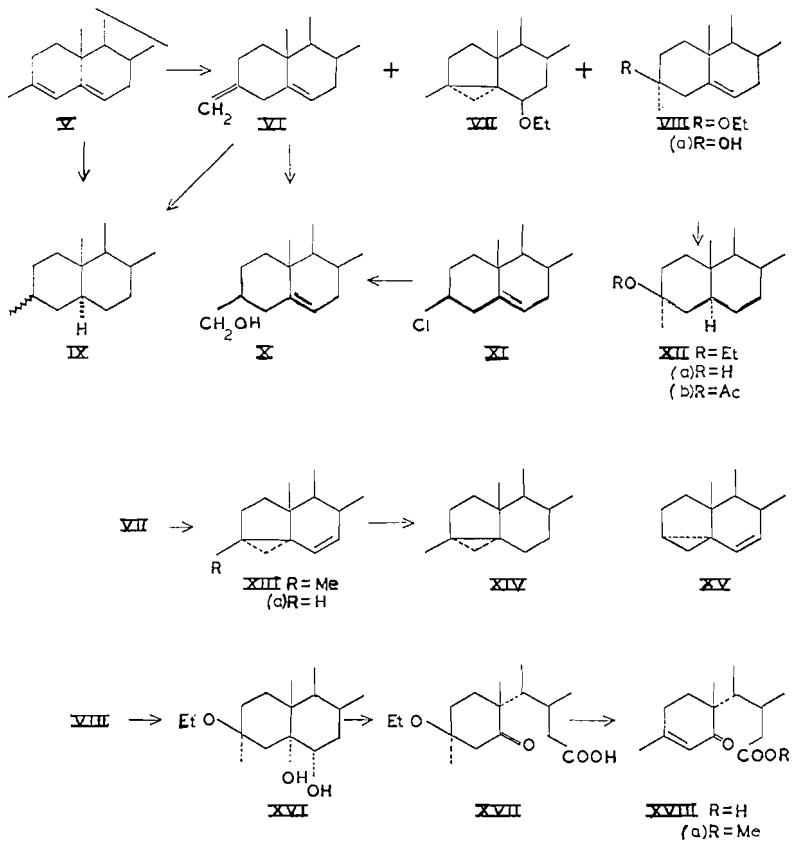

mixture of 3α-methylcholestan-3β-ol (XII*a*) and its acetate XII*b*. Both compounds were identified by comparison with an authentic sample (5*b*, 11), and were distinctly different from the C_3-epimers (5*b*). This proved the stereochemistry at the C_3-position.

Since the reduction of photoether VIII had resulted in hydrogenolysis, when no sodium nitrite had been added, and since molecular rotation increments upon hydrogenation of VIII to XII did not permit unambiguous assignment of the position of the double bond to either the 4- or the 5-position, it was determined in the following way. Reaction with osmium tetroxide gave diol XVI, which was further oxidized to keto acid XVII (3.37 p.p.m., 2H, quartet, $J = 7$ c.p.s.) by chromic acid in aqueous acetic acid at room temperature. When the chromic acid oxidation was carried out at a higher temperature, the dehydroethoxylated keto acid XVIII was obtained. Keto acid XVIII was also obtained by heating XVII with Fehling's solution or with pyridine hydrochloride in acetic acid. Keto acid XVIII, obtained from the three reactions, was amorphous. Its spectral properties were characteristic of an α,β-unsaturated ketone ($\lambda_{max}^{C_6H_{12}}$ 231 mμ, λ_{max}^{EtOH} 236 mμ,

Can. J. Chem. Downloaded from www.nrcresearchpress.com by 210.87.254.40 on 09/05/12
For personal use only.

ν_{CCl_4} 1675 cm^{-1}) and not of an α,β-unsaturated acid. When XVIII was treated with ethereal diazomethane, an amorphous methyl ester was obtained. It absorbed in the ultraviolet at 236 mμ (ethanol) and in the infrared at 1675 cm^{-1} and 1738 cm^{-1}, confirming the assignment of the functional groups in XVIII.

The identity of photoether VIII was further proved by comparison with the ethanolysis product of 3α-methylcholesteryl mesylate (5*b*).

5. Elution with ether gave, in 6.7% yield, an oil from which some 3α-methylcholesterol (5*b*) was isolated.

When the photolysis of 3-methylcholesta-3,5-diene (V) was carried out in pentane, and the solvent evaporated carefully, an oil, $[\alpha]_D$ −85°, δ −0.34 p.p.m. (J = 2.65 c.p.s.) was obtained (see Fig. 1). The high-field n.m.r. signal of the oil was most likely due to a

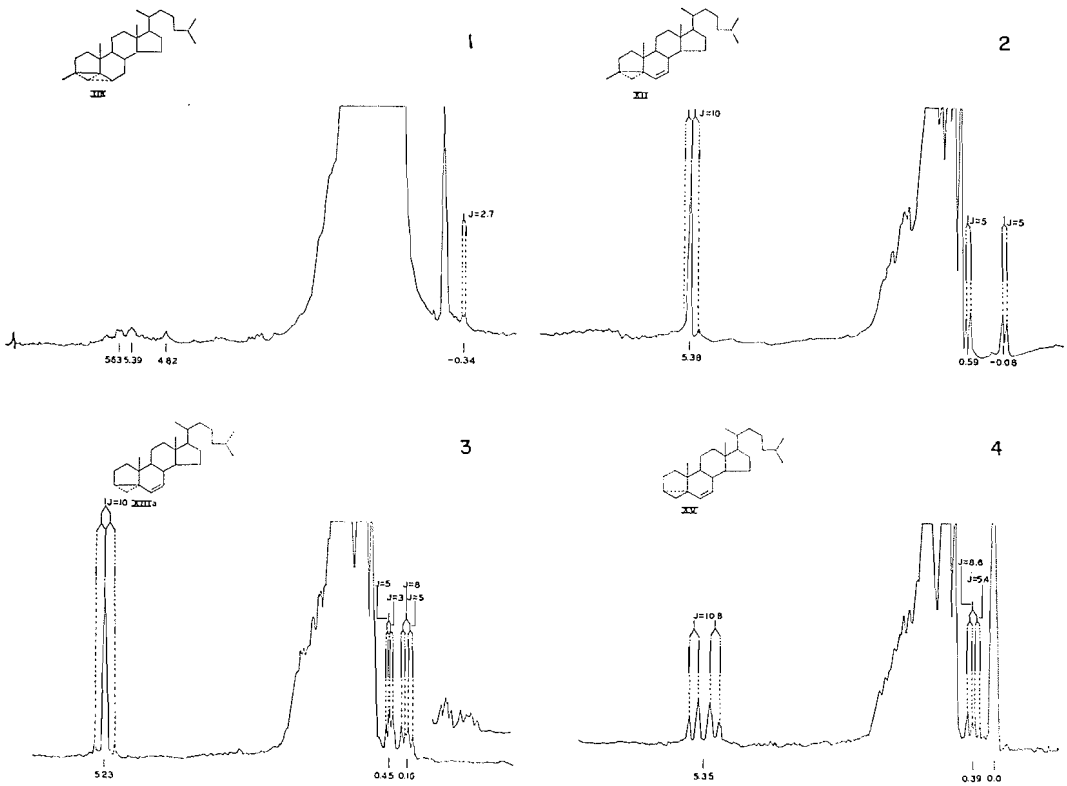

FIGS. 1–4. Fig. 1, taken in deuterochloroform; Figs. 2–4, taken in carbon tetrachloride.

proton attached to the bicyclobutane ring system in II*a*, which, judging from the intensity of the peak, was present in approximately 30%. Treatment of the oil with boiling ethanol gave photoether VII as the only crystalline product in 20–30% yield. The reaction was repeated a number of times. In no instance was it possible to detect even a trace of VIII either by thin-layer chromatography or by other chromatographic procedures.

The photolysis in ethanol hence gave a different product distribution than the photolysis in pentane, followed by a dark reaction in ethanol. This is in marked contrast to the results described by Dauben for the 3-unsubstituted cholestadiene (I), in which identical products had been obtained in both sets of reactions.

Can. J. Chem. Downloaded from www.nrcresearchpress.com by 210.87.254.40 on 09/05/12
For personal use only.

Further work is in progress to establish the mode of formation of some of the photoproducts described.

EXPERIMENTAL

All melting points were taken in a melting point tube and were uncorrected. Infrared spectra were taken on a Perkin–Elmer 21 spectrophotometer in carbon tetrachloride unless otherwise stated. Ultraviolet spectra were taken on a Bausch and Lomb Spectronic 505 or Beckman DK 1 spectrophotometer. Nuclear magnetic resonance spectra were taken on a Varian HR 60 spectrometer in carbon tetrachloride (tetramethylsilane = 0 p.p.m.). Optical rotations were measured on a C. Zeiss Photoelectric Precision polarimeter (0.005°) in chloroform. The adsorbents used for chromatography were Woelm neutral alumina and Grace No. 923 silica gel. The microanalyses were carried out by Mr. A. Bernhardt, and associates, Mulheim, Germany, and Dr. C. Daessle, 5757 Decelles St., Montreal.

Preparation of 3-Methylcholesta-3,5-diene (V)

Diene V was prepared by slowly adding 15 g of cholest-4-en-3-one, dissolved in 100 ml of absolute ether, to 20 ml of ethereal methyl magnesium iodide, prepared from 2.66 g of magnesium and 7.35 ml of methyl iodide, and the solution was gently refluxed overnight. Aqueous ammonium chloride was added to the cooled mixture. Ether was added and the organic solution was washed neutral with water. After evaporation of the ether, the oily residue was refluxed overnight in 200 ml of ethanol and 20 ml of concentrated hydrochloric acid, diluted with ether, and washed with aqueous sodium bicarbonate and water until neutral. The solvent was then evaporated until crystals began to form. A slow crystallization gave 11.683 g of diene V, m.p. 82–83° (80° (4*a*)); $[\alpha]_D$ −120.4° (*c* 1.4); δ 5.36 p.p.m. (C=C_6—H), 5.78 p.p.m. (C=C_4—H). Calc. for $C_{28}H_{46}$: C, 87.88; H, 12.12. Found: C, 87.80; H, 12.21.

Photolysis of Diene V in Ethanol – n-Pentane[9]

Diene V (10 g) was dissolved in 405 ml of spectrograde *n*-pentane. To the solution was added 45 ml of absolute ethanol. The solution was then irradiated with a 450 W high pressure mercury arc lamp,[10] until there was no absorption in the ultraviolet between 220 and 400 mμ (67 h). The pentane–ethanol was removed by distillation. The oily residue (14.821 g) was dissolved in 50 ml of warm hexane. After the mixture had cooled and had been allowed to stand at room temperature for a few hours, 1.1 g of 6β-ethoxy-3α-methyl-3β,5-cyclo-5β-cholestane (VII), m.p. 129°, was obtained. The mother liquors were chromatographed on 500 g of silica gel.

Elution with 300 ml of hexane gave 0.79 g of a hydrocarbon mixture containing trace amounts of starting material and non-conjugated diene VI, which could not be separated into its components by preparative thin-layer chromatography.

Further elution with 900 ml of hexane gave 1.754 g of crystalline 3-methylenecholest-5-ene (VI), m.p. 109°. Crystallization from ether–acetone raised the melting point to 109–110°; $[\alpha]_D$ −32.4° (*c* 0.344); ν 3030, 1648, 888 cm^{-1} (C=CH_2); δ 4.55 p.p.m. (2H, singlet, C=CH_2), 5.29 p.p.m. (1H, poorly resolved, C=C_6—H). Calc. for $C_{28}H_{46}$: C, 87.88; H, 12.12. Found: C, 87.81; H, 12.03.

Elution with hexane–benzene mixtures gave small amounts (0.138 g) of oil.

Benzene (600 ml) eluted 2.388 g of 6β-ethoxy-3α-methyl-3β,5-cyclo-5β-cholestane (VII), m.p. 120–123°. Two crystallizations from hexane gave 1.22 g of VII, m.p. 130–131°; $[\alpha]_D$ 26.1° (*c* 1.5); ν 3040 cm^{-1} (cyclopropane), 1092, 1102, 1128, 1162 cm^{-1} (C—O—C); δ −0.47 and 0.45 p.p.m. (1H each, doublet, J = 4.5 c.p.s., geminal protons on cyclopropane ring), 3–3.5 p.p.m. (3H, poorly resolved). Calc. for $C_{30}H_{52}O$: C, 84.04; H, 12.23. Found: C, 83.91; H, 12.13.

Further elution with 450 ml of benzene–ether (9:1) gave 0.572 g of a colorless oil.

Elution with 150 and 450 ml of benzene–ether (4:1 and 1:1 respectively) gave 3.111 g of VIII, m.p. 120–121°. Two crystallizations from acetone gave long fine needles, m.p. 125–126°; $[\alpha]_D$ −20.7° (*c*, 1.06); ν 1070, 1110, 1125 cm^{-1} (C—O—C); δ 3.45 p.p.m. (2H, quartet, J = 7 c.p.s. OEt), 5.26 p.p.m. (1H, poorly resolved, C=C_6—H). Calc. for $C_{30}H_{52}O$: C, 84.03; H, 12.22; OEt, 10.5%; molecular weight, 428.7. Found: C, 83.78; H, 11.97; OEt, 9.09%; molecular weight, 411 (Rast).

Elution with ether gave 1.8 g of a yellow oil, ν 3500, 1000–1100 cm^{-1} (broad bands, OH).

When the photolysis was carried out in *n*-pentane until the ultraviolet was clear between 220 and 400 mμ, and the pentane was removed by vacuum distillation at room temperature, an oily residue, $[\alpha]_D$ −85° (*c* 0.8 in $CDCl_3$) was obtained (see Fig. 1 for n.m.r.). The oily residue was refluxed with 100 ml of absolute ethanol for 1 h. The ethanol was distilled off and the semicrystalline residue taken up in hexane. Crystallization gave photoether VII, m.p. 127°. Chromatography of the mother liquors on silica gel gave additional amounts of photoether VII only.

Hydrogenation of 3-Methylenecholest-5-ene (VI)

An acetic acid solution of diene VI (0.196 g) was hydrogenated at room temperature for 20 h using

[9]*The yields obtained in several runs varied considerably.*

[10]*The lamp was cooled by running water in a quartz or vycor jacket, supplied by Hanovia Lamp Division, 100 Chestnut St., Newark, N.J., U.S.A.*

Can. J. Chem. Downloaded from www.nrcresearchpress.com by 210.87.254.40 on 09/05/12
For personal use only.

0.15 g of platinum oxide as catalyst. The platinum was filtered off and the filtrate diluted with water and ether. A saturated sodium bicarbonate solution (125 ml) was added slowly until the acetic acid was neutralized. The ether layer was then washed neutral, dried over magnesium sulphate, and evaporated. The crystalline residue, m.p. 91–94°, melted after two recrystallizations from ether–methanol at 100–101° (142 mg), $[\alpha]_D$ 24.8° (*c* 0.55). The melting point was not depressed upon admixture of an authentic sample of 3-methyl-cholestane (IX) (*5b*). Calc. for $C_{28}H_{50}$: C, 86.97; H, 13.03. Found: C, 87.01; H, 13.11.

3-Methylcholesta-3,5-diene from VI

Diene VI (0.18 mg) was dissolved in 10 ml of spectrograde dioxane. To this solution was added 1 drop of 72% perchloric acid. The ultraviolet (u.v.) spectrum was transparent between 220–400 mμ. Upon standing at 70° for 12 h, the solution absorbed at 232, 239, and 248 mμ (log ε 4.26, 4.29, and 4.16).

3-Hydroxymethylcholest-5-ene (X)

1. From 3-methylenecholest-5-ene (VI)

Sodium borohydride (18 mg) was added to 383 mg (1 mmole) of diene VI in 25 ml of diglyme. Boron trifluoride etherate (1 ml) was added to the solution. After the mixture was stirred for 1 h, 10 ml of 30% hydrogen peroxide was added slowly. The solution was diluted with 50 ml of ether and 50 ml of water. The ether layer was washed until neutral, dried over magnesium sulphate, and evaporated. The oily residue (350 mg) was chromatographed on 20 g of silica gel. Hexane eluted 63 mg of oil containing 3-methylcholesta-3,5-diene (V) (u.v.). Further elution with hexane–benzene and benzene–ether mixtures gave oils which were not investigated. Ether eluted 97 mg of 3-hydroxymethylcholest-5-ene (X) (8, p. 33), m.p. 120°. Recrystallizations from acetone gave pure X, m.p. 129–130°; $[\alpha]_D$ −38.4° (*c* 1.0); ν 3630, 975–1050 cm^{-1} (broad band, OH); δ 2.96 p.p.m. (1H, singlet, exchanged in D_2O, OH), 3.4 p.p.m. (2H, poorly resolved signal, CH—CH_2—O) and 5.33 p.p.m. (1H, poorly resolved signal, C=C_6—H). Calc. for $C_{28}H_{48}O$: C, 83.93; H, 12.08. Found: C, 83.72; H, 12.19.

2. From Cholesteryl Magnesium Chloride and Formaldehyde

Cholesteryl chloride (12) was prepared by dissolving cholesterol in thionyl chloride and destroying the excess thionyl chloride by addition to a large excess of water. The water-washed solid residue was recrystallized from ether to give pure cholesteryl chloride, m.p. 97°. Tetrahydrofuran (100 ml) was refluxed over lithium aluminum hydride and distilled directly into a flask containing 2.48 g of magnesium. Methyl iodide (3 ml) was then added and the mixture was heated under reflux for 48 h. After cooling of the mixture, 9.2 g of cholesteryl chloride was added, and the solution was heated under reflux for 48 h. Solid paraformaldehyde (4.6 g) was added to the refluxing solution and the heating continued for another 24 h. A cold aqueous ammonium chloride solution (8 g NH_4Cl in 50 ml of water) was added drop by drop to the cooled reaction mixture. The mixture was taken up in ether, washed neutral with water, dried over magnesium sulphate, and evaporated. The semicrystalline residue (6.4 g) was chromatographed on alumina (II–III, 200 g).

Elution with hexane gave 3.6 g of cholest-5-ene, m.p. 90–91°. Recrystallization from ether gave pure cholest-5-ene, m.p. 92–93°; $[\alpha]_D$ −70.5° (*c* 2.4); δ 5.09 p.p.m. (1H, broad signal, C=C_6—H). Calc. for $C_{27}H_{46}$: C, 87.49; H, 12.51. Found: C, 87.38; H, 12.48.

Cholest-5-ene, on hydrogenation in acetic acid with platinum oxide, gave cholestane, m.p. 78–79°, which was depressed upon admixture of 3-methylcholestane and not depressed upon admixture of authentic cholestane.

Further elution with benzene gave 2.153 g of 3-hydroxymethylcholest-5-ene (X), m.p. 110–115°, which, on two crystallizations from acetone, melted at 129–130°. The infrared spectrum of X was identical with that obtained from the hydroboration of 3-methylenecholest-5-ene (VI) described above.

Further elution with the same solvent gave 0.37 g of cholesterol, m.p. 146–148°, which was not depressed upon admixture of an authentic sample. The reaction was carried out in absolute tetrahydrofuran. Use of dioxane or tetrahydrofuran which was not meticulously dried gave only cholest-5-ene and cholesterol. In "absolute" ether, only cholesterol was isolated.

3α-Methyl-3β,5-cyclo-5β-cholest-6-ene (XIII)

Photoether VII (411 mg) was chromatographed on alumina (I, 20 g). Elution with hexane gave 252 mg of 3α-methyl-3β,5-cyclo-5β-cholest-6-ene (XIII), m.p. 56–61°. Two crystallizations from ethyl acetate raised the melting point to 67–68°, $[\alpha]_D$ 22.8° (*c* 1.0), δ −0.08 and 0.59 p.p.m. (1H each, J = 5 c.p.s., geminal protons on cyclopropane ring), and 5.38 p.p.m. (2H, "singlet"). Calc. for $C_{28}H_{46}$: C, 87.88; H, 12.12. Found: C, 87.78; H, 12.01.

3α-Methyl-3β,5-cyclo-5β-cholestane (XIV)

An acetic acid – ether (4:1, 5 ml) solution of 202 mg of XIII was hydrogenated at atmospheric pressure in the presence of 150 mg of platinum oxide. After 16 h, the platinum was filtered off. The filtrate was diluted with ether and water. The ether layer was washed until neutral, dried over magnesium sulphate, and evaporated. Chromatography of the oily residue on alumina (I, 10 g) gave 3α-methyl-3β,5-cyclo-5β-cholestane (XIV), m.p. 72–74°. Two crystallizations from acetic acid raised the melting point to 77–78°,

Can. J. Chem. Downloaded from www.nrcresearchpress.com by 210.87.254.40 on 09/05/12
For personal use only.

$[\alpha]_D$ 32.0° (*c* 1.1), δ 0.44 p.p.m. (1H, doublet, J = 4.45 c.p.s.), and −0.35 p.p.m. (1H, triplet, J = 4.5 c.p.s.). Calc. for $C_{28}H_{48}$: C, 87.42; H, 12.58. Found: C, 87.15; H, 12.75.

Treatment of 3α-Methyl-3β,5-cyclo-5β-cholest-6-ene (XIII) with Perchloric Acid and Ethanol

Perchloric acid (72%, 30 mg) was added to an ethanolic solution (30 ml) of 141 mg of XIII. The solution was heated under reflux overnight, cooled, and diluted with water and ether. The dried ether layer gave, upon evaporation, 155 mg of an oily residue, which had the characteristic ultraviolet absorption pattern of 3-methylcholesta-3,5-diene (V), λ_{max}^{EtOH} 239 mμ (log ε 3.61, i.e. 21% diene V). The oily residue was chromatographed on alumina (I, 10 g). Elution with hexane gave 43 mg of oils. Further elution gave 25 mg of 3-methylcholesta-3,5-diene (V), m.p. 79°. Benzene eluted 48 mg (34%) 3β-ethoxy-3α-methylcholest-5-ene (VIII), m.p. 119–123°. Recrystallization from acetone raised the melting point to 126°. Admixture of an authentic sample did not depress the melting point.

Treatment of 3α-Methyl-3β,5-cyclo-5β-cholest-6-ene (XIII) with Perchloric Acid in Aqueous Dioxane

The reaction described above was carried out in 50 ml of 10% aqueous dioxane containing 1 ml of 72% perchloric acid. Evaporation of the ether gave an oily residue which contained 24% of 3-methylcholesta-3,5-diene (V) (by u.v., λ_{max}^{EtOH} 239 mμ (log ε 3.65)). Chromatography on alumina (I) gave diene V, m.p. 78°, as the only crystalline compound.

3β-Ethoxy-3α-methylcholestane (XII)

Photoether VIII (153 mg) in 40 ml of acetic acid was hydrogenated for 14 h at 40° and 60 p.s.i. with 141 mg of platinum oxide catalyst in a Parr apparatus. The reaction mixture was worked up as described above. The oily residue (152 mg) was chromatographed on alumina (I, 5 g). Elution with hexane gave 44 mg of 3-methylcholestane (IX), m.p. 99°. Crystallization raised the melting point to 99–100°. Admixture of an authentic sample did not depress the melting point. Elution with hexane : benzene (1:1) gave 77 mg of 3β-ethoxy-3α-methylcholestane (XII), m.p. 81–83°. Crystallization from ether–methanol raised the melting point to 89–90°, $[\alpha]_D$ 2° (*c* 0.33), ν 1165, 1100 cm^{-1} (OEt). Calc. for $C_{30}H_{54}O$: C, 83.65; H, 12.64. Found: C, 83.84; H, 12.79.

As was found out later, the hydrogenolysis reaction could be suppressed by the addition of 10% (based on the weight of VIII) sodium nitrite (5*b*, 9). In this case, a 78% yield of XII, m.p. 89–90°, was obtained.

Oxidation of 3β-Ethoxy-3α-methylcholestane (XII) with Ruthenium Tetroxide

Ether XII (55 mg) in 10 ml of carbon tetrachloride was oxidized with 42 mg of ruthenium tetroxide at room temperature, according to the procedure of Bokowicz and Rylander (10). The oily reaction product (161 mg) was chromatographed on alumina (II–III, 2 g). Elution with hexane gave 16 mg of 3β-acetoxy-3α-methylcholestane (XII*b*), m.p. 85–95°. The infrared spectrum was identical with that of an authentic sample and different from that of 3α-acetoxy-3β-methylcholestane (5*b*). Elution with benzene gave 32 mg of 3α-methylcholestan-3β-ol (XII*a*), m.p. 148°. Crystallization from ether–methanol raised the melting point to 149° (150° (11)). Admixture of authentic sample did not depress the melting point. The infrared spectrum was identical with that of an authentic sample and markedly different from its epimer in the 1000–1250 cm^{-1} region (5*b*); $[\alpha]_D$ 36.9° (*c* 0.34), lit. 28° (*c* 1.68) (11). Calc. for $C_{28}H_{50}O$: C, 83.51; H, 12.52. Found: C, 83.38; H, 12.30.

Oxidation of 3β-Ethoxy-3α-methylcholest-5-ene (VIII) with Osmium Tetroxide

Photoether VIII (402 mg) was dissolved in 10 ml of dry ether and 2 ml of pyridine which contained 397 mg of osmium tetroxide (13). The oxidation was carried out in the dark at 33° for 7 days. The solution was worked up according to the procedure given by Woodward *et al.* (13). The oily residue (446 mg) was chromatographed on alumina (IV, 15 g). Elution with hexane gave 315 mg of diol XVI, m.p. 140–141°. Crystallization from hexane raised the melting point to 141–142°, $[\alpha]_D$ 21.6° (*c* 0.44), ν 3475, 3600, 1160 cm^{-1} (OH), δ 2.45 p.p.m. (1H, broad singlet, OH), 3.31 p.p.m. (2H, quartet, J = 6.6 c.p.s., OEt), 4.61 p.p.m. (1H, singlet, OH). It was found that at 18°, 25°, and 33°, the yields of diol XVI were 30, 70, and 74% respectively. Calc. for $C_{30}H_{54}O_3$: C, 77.86; H, 11.76. Found: C, 77.62; H, 11.60.

5,6-Seco-3β-ethoxy-3α-methylcholestan-5-on-6-oic Acid (XVII)

Chromium trioxide (120 mg) in 50% aqueous acetic acid (12 ml) was added slowly to 158 mg of diol XVI in 10 ml of acetic acid. The reaction mixture was kept at 50° overnight. (Under reflux, dehydroethoxylation occurred.) A few drops of methanol were added to destroy excess chromium trioxide. The solvent was removed at 40° under reduced pressure. The keto acid XVII was extracted with ether, and the organic solution washed until neutral, dried over magnesium sulphate, and evaporated. The oily residue (141 mg) was dissolved in a minimum amount of acetic acid, and a slow (3 days) crystallization was permitted to occur after a few drops of water had been added. Recrystallization of keto acid, m.p. 138–139°, gave 14 mg of keto acid XVII, m.p. 152°, $[\alpha]_D$ 66° (*c* 0.46), ν 3000 cm^{-1} and 1705 cm^{-1}, δ 2.26 p.p.m. (2H, poorly resolved peak, CH—CH_2—COOH), 2.67 p.p.m. (2H, singlet, O—C—CH_2—C=O), 3.37 p.p.m. (2H, quartet, J = 7 c.p.s., OEt), 10.63 p.p.m. (1H, poorly resolved singlet, COOH). Calc. for $C_{30}H_{52}O_4$: C, 75.60; H, 11.00. Found: C, 75.74; H, 10.86.

Can. J. Chem. Downloaded from www.nrcresearchpress.com by 210.87.254.40 on 09/05/12
For personal use only.

Dehydroethoxylation of Keto Acid XVII

A solution of 182 mg of keto acid XVII in 20 ml acetic acid containing 400 mg of pyridine hydrochloride was refluxed overnight. The solution was diluted with ether and water. The ether layer was washed until neutral, dried over magnesium sulphate, and evaporated. The oily residue was chromatographed on silica gel (7.5 g). Benzene–ether mixtures eluted an oil which could not be crystallized; ν 1705 cm^{-1} (COOH), 1675 cm^{-1} (C=C—C=O), $\lambda_{max}^{cyclohexane}$ 230.5 mμ, λ_{max}^{EtOH} 236 mμ.

In the presence of Fehling solution, the keto acid XVII was also dehydroethoxylated.

Methyl 5,6-seco-3-methylcholest-3-en-5-on-6-oate (XVIIIa)

Ethereal diazomethane was added to 126 mg of amorphous acid XVIII in cold ether containing a few drops of methanol. After 1 h, the excess diazomethane was destroyed by adding a few drops of acetic acid. The solvent was evaporated and the oily residue chromatographed on alumina (II–III, 5 g). Benzene and benzene–ether (95:5) eluted 66 mg of methylester XVIII*a*, which could not be crystallized. The spectral data of XVIII*a* were λ_{max}^{EtOH} 236 mμ (log ϵ 3.91), ν 1738 cm^{-1} ($COOCH_3$), 1675 cm^{-1} (C=C—C=O), δ 1.93 p.p.m. (3H, singlet, C=C—CH_3), 2.2 p.p.m. (2H, doublet, J = 4.1 c.p.s., CH—CH_2—COO), 3.57 p.p.m. (3H, singlet, $COOCH_3$), 5.57 p.p.m. (1H, singlet, C=CH—C=O).

ACKNOWLEDGMENTS

We thank the National Research Council of Canada and Messrs. Ayerst, McKenna and Harrison for financial support. We also thank Dr. C. Stammer of this Department for taking the n.m.r. spectra and Mr. J. Kastner of Ayerst, McKenna and Harrison for high pressure hydrogenations.

REFERENCES

1. G. Just and C. C. Leznoff. Can. J. Chem. **42**, 79 (1964).
2. (*a*) W. G. Dauben and J. A. Ross. J. Am. Chem. Soc. **81**, 6521 (1959).
   (*b*) W. G. Dauben and F. G. Willey. Tetrahedron Letters, 893 (1962).
3. T. L. Cairns. (*Editor*). Org. Syn. **35**, 39 (1955).
4. (*a*) Krekeler. Thesis, University of Göttingen, pp. 6, 9, 12, 17, 20, 21. *As quoted in* Elsevier's Encycl. of Org. Chem. Springer-Verlag, Heidelberg. 1959. Vol. 14. p. 2428s.
   (*b*) W. Bergmann and F. Hirshmann. J. Org. Chem. 4, 40, 47 (1939).
5. (*a*) S. N. Farmer and A. R. Kon. J. Chem. Soc. 414, 419 (1937).
   (*b*) G. Just and V. Di Tullio. Can. J. Chem. In Press.
6. H. C. Brown, K. J. Murray, J. A. Snover, and G. Zweifel. J. Am. Chem. Soc. **82**, 4233 (1960).
7. D. J. Patel, M. E. Howden, and J. D. Roberts. J. Am. Chem. Soc. **85**, 3218 (1963).
8. L. F. Fieser and M. Fieser. Steroids. Reinhold Publ. Corp., New York. 1959.
9. S. Nishimura and K. Mori. Bull. Soc. Chim. Japan, **36**, 318 (1963).
10. L. M. Bokowicz and P. N. Rylander. J. Am. Chem. Soc. **80**, 6682 (1958).
11. D. H. R. Barton, A. Da S. Campos-Neves, and R. C. Cookson. J. Chem. Soc. 3500 (1956).
12. I. M. Heilbron, K. M. Samart, and J. C. E. Simpson. J. Chem. Soc. 1410, 1412 (1933).
13. R. B. Woodward, F. Sondheimer, D. Taub, K. Heusler, and W. M. McLamore. J. Am. Chem. Soc. **74**, 4223 (1963).

Can. J. Chem. Downloaded from www.nrcresearchpress.com by 210.87.254.40 on 09/05/12
For personal use only.

Can. J. Chem. Downloaded from www.nrcresearchpress.com by 210.87.254.40 on 09/05/12
For personal use only.

COMPLEXES DU GERMANIUM (IV) AVEC LA DICHLORO-2,5 DIHYDROXY-3,6 *p*-BENZOQUINONE[1]

A. BEAUCHAMP[2] ET R. L. BENOIT
Département de Chimie, Université de Montréal, Montréal, Québec

Reçu le 20 mars 1964

RÉSUMÉ

La formation de complexes entre le germanium (IV) et le ligand dichloro-2,5 dihydroxy-3,6 *p*-benzoquinone (H_2R) a été étudiée en milieu de force ionique 0.49. On a montré par spectrophotométrie que les seuls complexes présents comportent 2 ligands par germanium et que la constante de stabilité apparente est $\beta_2 = 10^{6.16}$ en milieu d'acidité 0.49 *M*. Les constantes d'acidité du ligand, $k_1 = 10^{-0.66}$ et $k_2 = 10^{-2.37}$ ont été déterminées, et la constante de stabilité du complexe $Ge(OH)_2R_2^{2-}$ $\beta_2^0 = 10^{6.57}$ a été obtenue par potentiométrie. On a mis en évidence la présence de deux acidités sur $Ge(OH)_2R_2H_2$, l'une forte, l'autre de constante $\mathcal{K}_2 = 10^{-0.8}$. Des formules sont proposées pour les complexes. On compare la nature et la stabilité des complexes du germanium et du zirconium (IV) et relie leurs spectres d'absorption à ceux des différentes formes H_2R, HR^-, et R^{2-} du ligand.

Le germanium (IV) en solution aqueuse forme des complexes avec certains ligands organiques comportant plusieurs atomes d'oxygène donneurs, tels que des polyalcools (1) et polyphénols (2), des acides polycarboxyliques (3), des hydroxy-acides (4), des hydroxy-cétones (5). Des complexes de ce type ont été mis en évidence par des méthodes physico-chimiques et par isolation de composés solides. Toutefois on ne connaît qu'un nombre limité de constantes de stabilité, citons celle du complexe 1 germanium: 2 trihydroxy-2,3,7 phényl-9 fluorone-6 (6, 7), le nature des groupes coordinés dans ce chélate, soit

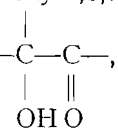

soit

, prêtant d'ailleurs à discussion (8).

Dans le cadre d'une étude quantitative de complexes du germanium (IV) avec une série de ligands "oxygénés" et "azotés" où l'on se propose de relier la stabilité des complexes à des propriétés des ligands, on présente les résultats obtenus avec la dichloro-2,5 dihydroxy-3,6 *p*-benzoquinone (acide chloranilique). L'acide chloranilique a été choisi pour plusieurs raisons: c'est un composé simple comportant le groupe

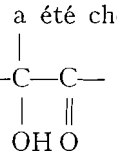

qui paraît donner lieu à une réaction avec le germanium (IV) (5), sa solubilité et celle du chélate permettent d'éviter l'emploi de solvant additionnel ou d'agent dispersif, l'utilisation de méthodes d'étude spectrophotométriques et potentiométriques semble a priori possible. Une revue des propriétés et réactions de l'acide chloranilique a été publiée (9) ainsi qu'une étude spectrophotométrique des complexes avec un autre élément du groupe IV, le zirconium (10). Au cours de notre travail Nazarenko & Flyantikova (11) ont fait paraître

[1]*Communication présentée au Congrès de l'A.C.F.A.S. à Québec, P.Q., 1–3 novembre 1963.*
[2]*Boursier du Conseil National de Recherches du Canada 1963–1964.*

un article sur ce même sujet. Certains résultats et l'interprétation de ces auteurs diffèrent essentiellement des nôtres et la critique en sera faite après l'exposé de nos résultats. Place (12) a récemment étudié les réactions de l'acide chloranilique avec le tétrachlorure de germanium en milieu non-aqueux et mis en évidence la formation de complexes comportant deux, trois, et quatre ligands par germanium.

PARTIE EXPÉRIMENTALE

Réactifs

Les solutions de germanium (IV) environ 4×10^{-2} *M* sont préparées par dissolution de dioxyde GeO_2 de haute pureté gracieusement fourni par le Germanium Research Center et dosées par titrage potentiométrique avec de la soude non carbonatée en présence de mannitol.

Les solutions mères d'acide chloranilique 1×10^{-2} *M* sont préparées par pesée du produit Fisher et conservées au maximum 4 jours durant lesquels l'absorption reste constante. Le titrage potentiométrique par NaOH du produit commercial a indiqué une pureté de 99.6 ± 0.3% et le même produit sublimé sous vide n'a donné aucune différence notable. Tous les autres produits chimiques utilisés sont des réactifs purs pour analyse.

Technique expérimentale

L'extinction des solutions est mesurée avec un spectrophotomètre Zeiss (modèle M4-Q11) comportant un chariot thermostaté, en employant une gamme de cuvettes d'épaisseur allant de 0.5 à 50.0 mm.

Une pH mètre Radiometer (modèle 4) est utilisé pour les mesures de pH, avec un système d'électrodes de verre et calomel – KCl saturé. Des solutions d'acide de concentration connue et de force ionique donnée servent à la standardisation, de façon à obtenir directement $-\log [H^+]$, la linéarité de réponse de l'électrode a été vérifiée dans l'intervalle $2 < -\log [H^+] < 4.5$.

L'extinction et l'acidité des solutions de complexes sont mesurées à température constante, 25.0 °C, ces mesures s'avérant sensibles aux variations de température.

RÉSULTATS EXPÉRIMENTAUX

I. Constantes d'acidité de l'acide chloranilique

L'acide chloranilique par ses deux fonctions —OH est un diacide et donne lieu aux équilibres suivants:

$$H_2R \rightleftarrows HR^- + H^+.$$

$$[1] \qquad k_1 = \frac{[H^+][HR^-]}{[H_2R]}.$$

$$HR^- \rightleftarrows R^{2-} + H^+.$$

$$[2] \qquad k_2 = \frac{[H^+][R^{2-}]}{[HR^-]}.$$

Les valeurs de pk_1 et pk_2 données par divers auteurs varient selon les méthodes et les milieux ioniques adoptés: Schwarzenbach (13) 0.85, 3.18; Voigt (14) 1.09, 2.42; Van Rysselberghe (15) 1.22, 3.01; Wallenfels (16) 0.73, 3.08. Ces valeurs concordant mal et ne correspondant pas au milieu de force ionique 0.5 adopté pour ces expériences, la détermination en a été faite en milieu HCl–NaCl 0.484 *M* par deux méthodes. Les constantes d'équilibre sont définies ici à partir des concentrations.

(a) Spectrophotométrie

L'acide chloranilique possède deux bandes d'absorption dans la région 220–800 mμ. Un premier maximum à 302 mμ en milieu acide, se déplace vers 330 mμ à pH > 4.5. Le second maximum à 450 mμ pour des solutions fortement acides ($[H^+] > 2$ *M*), passe à 520 mμ avec élévation du pH.

Définissons ϵ_0, ϵ_1 et ϵ_2 comme étant les coefficients d'extinction molaire de R^{2-}, HR^- et H_2R respectivement, et $\epsilon_L = A_s/C_L$, le coefficient d'extinction molaire moyen, A_s est

Can. J. Chem. Downloaded from www.nrcresearchpress.com by 210.87.254.40 on 09/05/12
For personal use only.

la densité optique correspondant à une épaisseur de 1.00 cm, et C_L la concentration totale d'acide chloranilique. La fonction $\epsilon_L = f(-\log [H^+])$ (Fig. 1) présentant un maxi-

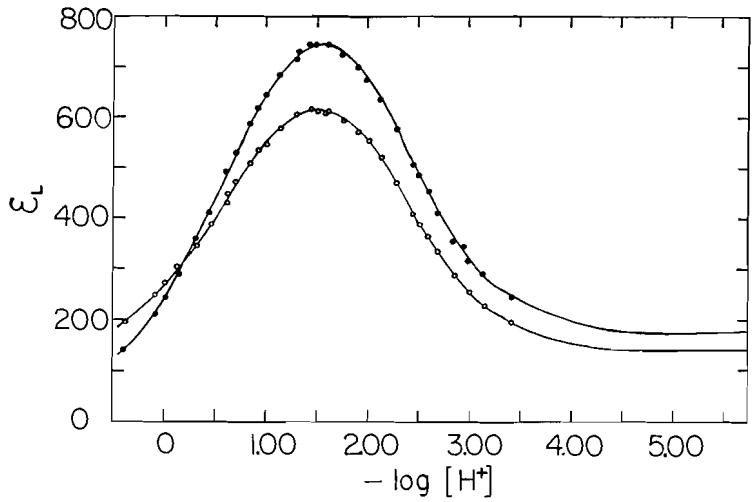

FIG. 1. Coefficient d'extinction molaire moyen ϵ_L de l'acide chloranilique en fonction de $-\log [H^+]$: HCl + NaCl = 0.484 M, T = 25 ± 1 °C, ● 520 mμ, ○ 490 mμ.

mum pour les longueurs d'onde 490 et 520 mμ, on peut appliquer la méthode de Ang (17) pour la détermination des constantes d'acidité.

c_1 et c_2 étant les deux concentrations de H^+ correspondant à une valeur donnée de ϵ_L, on montre que

$$[3] \qquad \epsilon_L = \epsilon_1 - k_2 P \quad \text{où} \quad P = \frac{(\epsilon_L - \epsilon_0)(c_1 + c_2)}{c_1 c_2}$$

$$[4] \qquad \epsilon_L = \epsilon_2 + k_1 Q \quad \text{où} \quad Q = \frac{\epsilon_1 - \epsilon_L}{c_1 + c_2}.$$

On a fait varier la concentration d'acide chloranilique entre 2.38×10^{-3} et 2.03×10^{-4} M; les valeurs de ϵ_0, déterminées dans NH_3 0.5 M (pH 9.97), sont à 490 mμ, 142 ± 2 et à 520 mμ, 177 ± 2. Les valeurs des constantes d'acidité et de ϵ_1 et ϵ_2, obtenues d'après les courbes donnant ϵ_L en fonction de P et Q, (Figs. 2 et 3) sont les suivantes: à 520 mμ: pk_1 0.66 ± 0.03; pk_2 2.37 ± 0.02; ϵ_1 915 ± 10; ϵ_2 94 ± 7; à 490 mμ: pk_1 0.66 ± 0.03; pk_2 2.37 ± 0.03; ϵ_1 755 ± 9; ϵ_2 158 ± 6.

(b) Potentiométrie

La courbe de titrage potentiométrique de l'acide chloranilique (Fig. 14) par NaOH a été utilisée pour déterminer la constante d'acidité k_2. Les relations suivantes sont vérifiées en tout point de la courbe, $[Na^+]$ étant la concentration de NaOH ajoutée,

$$[5] \qquad [H^+] + [Na^+] = [HR^-] + 2[R^{2-}]$$

$$[6] \qquad C_L = [H_2R] + [HR^-] + [R^{2-}].$$

Soit $\bar{n}' = ([HR^-] + 2[H_2R])/C_L$, le nombre moyen de H^+ non dissociés par molécule d'acide chloranilique, en portant dans cette expression les équations [1], [2], [5], et [6] et en réarrangeant, on obtient l'équation suivante de type $Y = 1/k_1k_2 + X/k_2$.

Can. J. Chem. Downloaded from www.nrcresearchpress.com by 210.87.254.40 on 09/05/12
For personal use only.

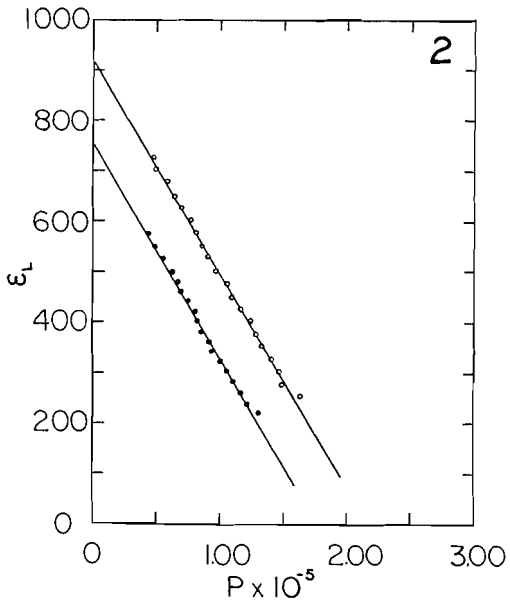

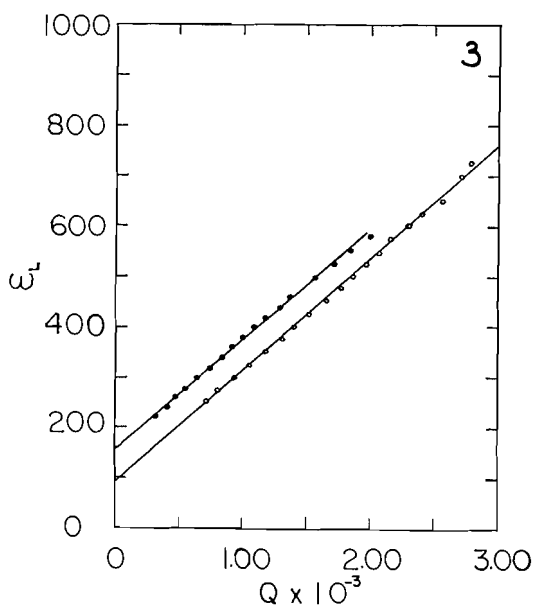

FIG. 2. Détermination de la constante d'acidité k_1 de l'acide chloranilique: ○ 520 mμ, ● 490 mμ.
FIG. 3. Détermination de la constante d'acidité k_2 de l'acide chloranilique: ○ 520 mμ, ● 490 mμ.

[7] $$\frac{\bar{n}'}{(2-\bar{n}')[H^+]^2} = \frac{1}{k_1k_2} + \frac{1}{k_2}\frac{(1-\bar{n}')}{(2-\bar{n}')[H^+]}.$$

La courbe donnant Y en fonction de X est représentée sur la Fig. 4, les valeurs correspondant au titrage de 100.0 ml d'acide chloranilique 1.002×10^{-2} M par NaOH 0.2352 M en milieu NaCl 0.484 M. La valeur pk_2 2.37 ± 0.03 calculée à partir de la pente de la droite concorde parfaitement avec les résultats des mesures spectrophotométriques. La valeur de l'ordonnée à l'origine $pk_1k_2 = 3.6 \pm 0.9$ est obtenue avec une mauvaise précision, la première dissociation de H_2R étant pratiquement complète au point initial du titrage ($\bar{n}' = 0.91$).

II. Constante de stabilité du complexe germanium (IV) – acide chloranilique

La formation de complexes entre l'acide chloranilique et le germanium (IV) est mise en évidence par un accroissement de la solubilité du ligand (18) ainsi que par une modification des bandes d'absorption du ligand. Les maxima à 450 mμ pour $[H^+] = 2$ M et 490 mμ pour $[H^+] = 0.50$ M passent à 520 mμ en présence de germanium (IV) et la densité optique augmente considérablement (Fig. 5); dans l'ultraviolet, le maximum est déplacé de 302 mμ à 315–320 mμ (Fig. 6). Les points isobestiques observés à 271 et 312 mμ suggèrent la présence de deux séries d'espèces absorbantes seulement. Le complexe a été étudié par plusieurs méthodes spectrophotométriques.

(a) Méthode de variations continues

La méthode de variations continues (19) permet dans les cas simples de déterminer la composition de complexes. Des expériences ont été effectuées à différentes acidités en utilisant des solutions de $HClO_4$ et des solutions-tampons chloracétate et acétate, les mesures d'absorption ont été faites à plusieurs longueurs d'onde. Les courbes donnant $A_s - \epsilon_L C_L$ en fonction de $C_L/(C_M + C_L)$ sont représentées sur la Fig. 7; C_M est la

Can. J. Chem. Downloaded from www.nrcresearchpress.com by 210.87.254.40 on 09/05/12
For personal use only.

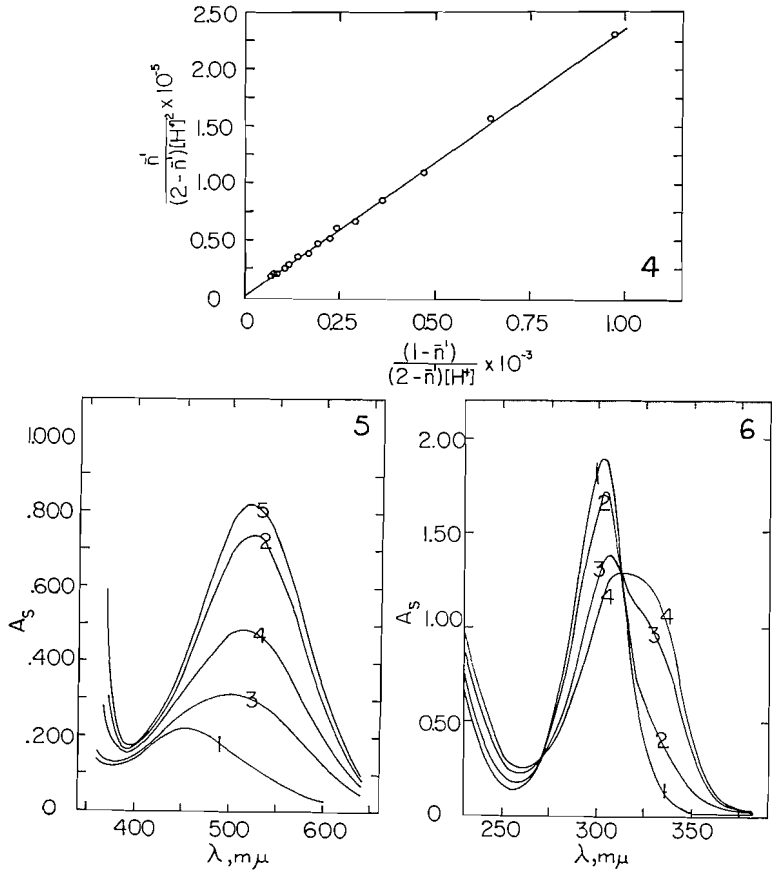

FIG. 4. Détermination des constantes d'acidité k_1 et k_2 de l'acide chloranilique: NaCl 0.484 M, $T = 25 \pm 0.5$ °C.

FIG. 5. Spectre visible de l'acide chloranilique 1.007×10^{-3} M en présence de germanium (IV): (1) $HClO_4$ 2.006 M, $C_M = 0$; (2) $HClO_4$ 2.006 M, $C_M = 2.96 \times 10^{-2}$ M; (3) $HClO_4$ 0.502 M, $C_M = 0$; (4) $HClO_4$ 0.502 M, $C_M = 3.15 \times 10^{-4}$ M; (5) $HClO_4$ 0.502 M, $C_M = 3.60 \times 10^{-2}$ M. Cuvette 1.00 cm.

FIG. 6. Spectre ultraviolet de l'acide chloranilique 1.006×10^{-4} M en présence de germanium (IV), HCl = 0.484 M: (1) $C_M = 0$, (2) $C_M = 1.043 \times 10^{-3}$ M, (3) $C_M = 1.043 \times 10^{-2}$ M, (4) $C_M = 3.55 \times 10^{-2}$ M. Cuvette 1.00 cm.

concentration totale du germanium (IV). Ces courbes présentent toutes un maximum pour un rapport $C_L/(C_M + C_L)$ voisin de 0.67, toutefois à pH 4.65 le maximum est mal défini. Ces résultats indiquent que l'acide chloranilique ne forme avec le germanium que des complexes de type M_mL_{2m} c'est-à-dire comportant 2 ligands par germanium.

(b) Détermination de la constante de stabilité du complexe

Deux méthodes indépendantes ont été utilisées pour montrer que les complexes M_mL_{2m} sont mononucléaires et déterminer la constante de stabilité β_2 du complexe ML_2 en milieu d'acidité 0.484 M. β_{2m} est une constante de stabilité apparente telle que

$$[8] \qquad \beta_{2m} = \frac{[M_mL_{2m}]}{[M]^m[L]^{2m}},$$

où [M] est la concentration du germanium (IV) libre, $[M_mL_{2m}]$ et [L] respectivement les concentrations du complexe et de l'acide chloranilique libre sous leurs différentes formes.

Can. J. Chem. Downloaded from www.nrcresearchpress.com by 210.87.254.40 on 09/05/12
For personal use only.

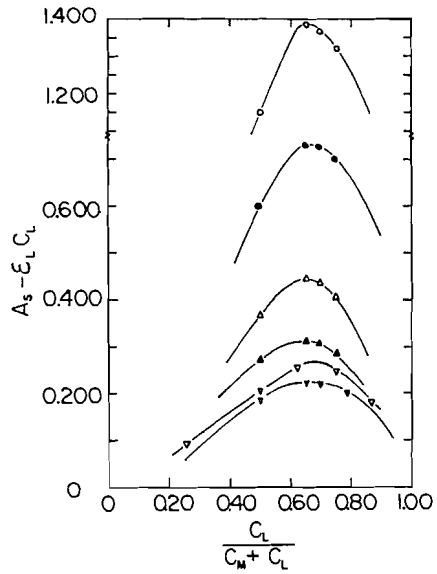

FIG. 7. Courbes de variations continues: ▽ $HClO_4$ 2.02 M, 520 mμ, $C_M + C_L = 2.03 \times 10^{-3}$ M, cuvette 1.00 cm; △ $HClO_4$ 0.502 M, 520 mμ, $C_M + C_L = 2.20 \times 10^{-3}$ M, cuvette 1.00 cm; ● $HClO_4$ 0.502 M, 350 mμ, $C_M + C_L = 2.20 \times 10^{-3}$ M, cuvette 0.200 cm; ○ $HClO_4$ 0.502 M, 340 mμ, $C_M + C_L = 2.20 \times 10^{-3}$ M, cuvette 0.200 cm; ▲ pH 2.64, 520 mμ, $C_M + C_L = 1.10 \times 10^{-2}$ M, cuvette 0.200 cm; ▼ pH 3.54, 520 mμ, $C_M + C_L = 1.10 \times 10^{-2}$ M, cuvette 0.200 cm.

1. Méthode de dilution.—Dans cette méthode on mesure l'extinction d'une série de solutions où les concentrations C_M et C_L sont maintenues dans le rapport stoechiométrique du complexe $C_M/C_L = 1/2$. On calcule $(A_s - \epsilon_L C_L)/C_M$ et on trace ensuite la courbe représentative de la fonction $\epsilon_c' = a - bx$ telle que:

$$[9] \qquad \epsilon_c' = \frac{A_s - \epsilon_L C_L}{C_M} = \frac{(\epsilon_c - 2m\epsilon_L)}{m} - \frac{(\epsilon_c - 2m\epsilon_L)^{(1-1/3m)}}{2^{2/3}(\beta_{2m})^{1/3m} m} \frac{(A_s - \epsilon_L C_L)^{1/3m}}{C_M},$$

où $x = (A_s - \epsilon_L C_L)^{1/3m}/C_M$, ϵ_c est le coefficient d'extinction molaire du complexe. La valeur de β_{2m} est calculable à partir des valeurs trouvées pour les coefficients a et b.

On a fait varier C_M entre 0.417×10^{-4} et 8.34×10^{-4} M. L'acidité a été maintenue à 0.484 M au moyen de HCl, à cette concentration d'acide il n'y a pas formation de complexes chlorogermaniques (20).

On a représenté sur la Fig. 8 les fonctions ϵ_c' pour $m = 1$, $m = 2$ et $m = 3$ à 345 mμ. On n'obtient une ligne droite que pour $m = 1$ ce qui démontre l'absence d'espèces polynucléaires. Les fonctions ϵ_c' pour $m = 1$ à 325 et 335 mμ sont aussi portées sur cette même figure. Les valeurs de β_2 obtenues pour les différentes longueurs d'onde sont résumées dans le Tableau I.

2. Méthode applicable aux complexes peu stables.—Cette méthode dérivée de celle de McConnell et Davidson (21) est applicable lorsque le complexe est relativement peu stable puisqu'elle repose sur l'approximation $[M] \sim C_M$. On mesure l'extinction d'une série de solutions où C_L est constant et C_M variable. On trace alors la courbe représentative de la fonction suivante dérivée pour le complexe ML_2

Can. J. Chem. Downloaded from www.nrcresearchpress.com by 210.87.254.40 on 09/05/12
For personal use only.

Can. J. Chem. Downloaded from www.nrcresearchpress.com by 210.87.254.40 on 09/05/12
For personal use only.

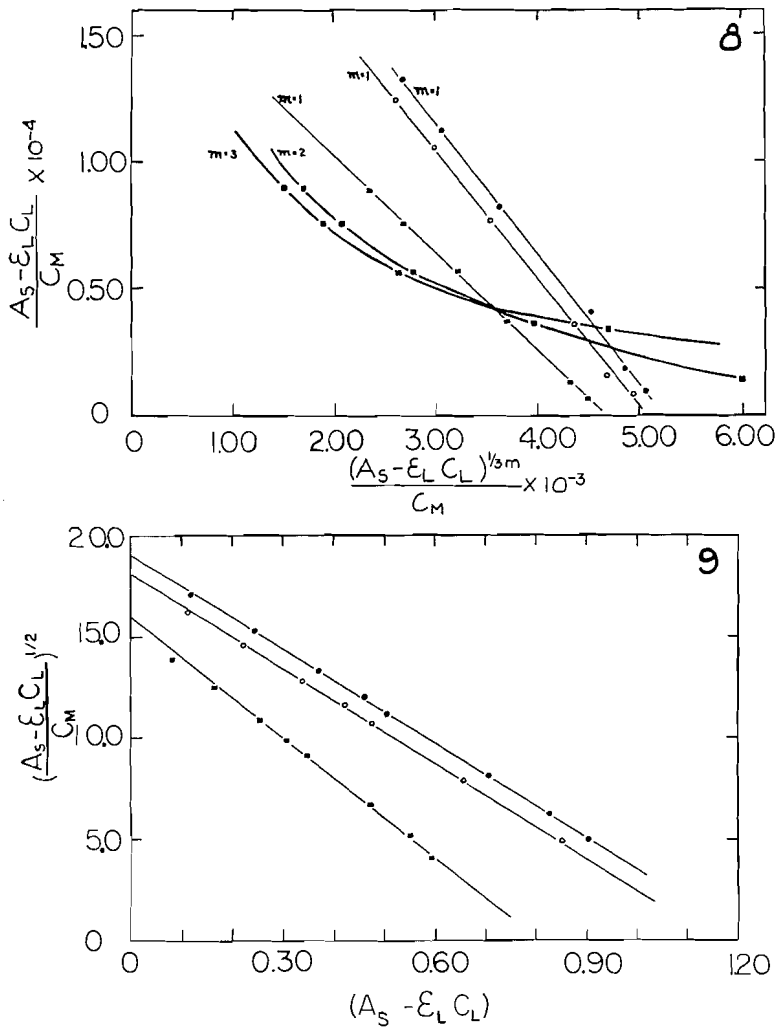

FIG. 8. Détermination de la constante de stabilité apparente β_2: $C_M/C_L = 1/2$, ● 335 mμ, ○ 325 mμ, ■ 345 mμ, $T = 25.0 \pm 0.2$ °C, HCl = 0.484 M.

FIG. 9. Détermination de la constante de stabilité apparente β_2: $C_L = 1.006 \times 10^{-4}$ M, ● 335 mμ, ○ 325 mμ, ■ 345 mμ, $T = 25.0 \pm 0.2$ °C, HCl = 0.484 M.

TABLEAU I

Méthode	λ, mμ	Concentration H^+ (M)	Log β_2	$\epsilon_c \times 10^{-4}$
b) 1	325	0.484	6.12±0.05	
b) 1	335	0.484	6.15±0.04	
b) 1	345	0.484	6.14±0.04	
b) 2	325	0.484	6.15±0.02	3.10±0.08
b) 2	335	0.484	6.16±0.02	2.72±0.07
b) 2	345	0.484	6.18±0.02	1.71±0.05
c)	520	0.502	6.16±0.03	

$$[10] \quad (\epsilon_c')^{1/2} = \left(\frac{A_s - \epsilon_L C_L}{C_M}\right)^{1/2} = \beta_2^{1/2} C_L(\epsilon_c - 2\epsilon_L)^{1/2} - \frac{2\beta_2^{1/2}}{(\epsilon_c - 2\epsilon_L)^{1/2}}(A_s - \epsilon_L C_L).$$

Cette fonction est du type $(\epsilon_c')^{1/2} = c - dx$ où $x = (A_s - \epsilon_L C_L)$. Les valeurs des coefficients c et d permettent d'obtenir β_2.

On a fixé la concentration d'acide chloranilique à 1.006×10^{-4} M et fait varier la concentration du germanium (IV) entre 4.17×10^{-4} et 3.56×10^{-2} M. Dans ces conditions, l'approximation $[M] \sim C_M$ est vérifiée à mieux de 99% pour $\beta_2 = 10^{6.2}$. L'acidité a été maintenue à 0.484 M avec HCl. La Fig. 9 reproduit les droites donnant $(\epsilon_c')^{1/2}$ aux différentes longueurs d'onde. Les valeurs de β_2 correspondantes sont portées dans le Tableau I. On a vérifié par ailleurs que les fonctions analogues correspondant aux complexes ML, ML_3 et $M_mL_{2m}(m > 1)$ conduisent à des courbes avec les données expérimentales obtenues.

(c) Méthode des solutions correspondantes

Les deux méthodes de calcul précédentes ne permettent toutefois pas de conclure à l'absence complète d'un complexe ML. Il convenait d'essayer de déterminer une limite pour la constante β_1 d'un tel complexe, c'est dans ce but que la méthode des solutions correspondantes a été utilisée. De plus afin de renforcer nos conclusions les mesures d'extinction ont été faites à 520 mμ au lieu de 325–345 mμ comme dans les méthodes précédentes.

ϵ_c' étant défini comme précédemment, Bjerrum (22) et Fronaeus (23) ont montré que pour une série de solutions ayant une même valeur de ϵ_c', ces solutions étant dites correspondantes, la concentration de ligand libre [L] et $\bar{n}$ le nombre moyen de ligands associés par atome de métal sont les mêmes. En portant ϵ_c' en fonction de C_L pour divers C_M, on détermine pour une valeur donnée de ϵ_c' les concentration C_L et C_M d'une série de solutions correspondantes. Les valeurs de [L] et $\bar{n}$ pour chaque série sont ensuite obtenues graphiquement en portant C_L en fonction de C_M, C_L et C_M étant reliés linéairement par l'équation $C_L = [L] + \bar{n}C_M$. La méthode de Rossotti (24) a ensuite été utilisée pour calculer β_1 et β_2 à partir des valeurs de [L] et $\bar{n}$. On a:

$$[11] \quad \bar{n} = \frac{C_L - [L]}{C_M} = \frac{[ML] + 2[ML_2]}{C_M} = \frac{\beta_1[L] + 2\beta_2[L]^2}{1 + \beta_1[L] + \beta_2[L]^2},$$

d'où

$$\frac{\bar{n}}{(1 - \bar{n})[L]} = \beta_1 + \beta_2 \frac{(\bar{n} - 2)}{(\bar{n} - 1)}[L],$$

une équation du type $y = \beta_1 + \beta_2 x$. Les β_1 et β_2 sont obtenus d'après la droite donnant y en fonction de x. On a fait varier la concentration de germanium (IV) entre 1.15×10^{-4} et 2.29×10^{-3} M et celle de l'acide chloranilique entre 2.09×10^{-4} et 2.00×10^{-3} M, cette dernière valeur étant la limite supérieure imposée par la solubilité; $HClO_4$ a été maintenu constant à 0.502 M. Les fonctions ϵ_c' sont représentées sur la Fig. 10 et les valeurs de $\bar{n}$ et [L] correspondant aux ϵ_c' sont rassemblées dans le Tableau II. Les points expérimentaux donnant $\bar{n}$ en fonction de $-\log [L]$ sont sur la Fig. 11. Les valeurs de $\bar{n}/((1 - \bar{n})[L])$ sont portées en fonction de $((\bar{n} - 2)/(\bar{n} - 1))[L]$ sur la Fig. 12. On trouve $\beta_2 = 10^{6.16 \pm 0.03}$ et $\beta_1 < 10^2$. Au moyen de la valeur de β_2 on a calculé $\bar{n}$ pour différentes valeurs de [L] et tracé la courbe de formation correspondante (Fig. 11). On note un bon accord entre la courbe calculée et les points expérimentaux.

Can. J. Chem. Downloaded from www.nrcresearchpress.com by 210.87.254.40 on 09/05/12
For personal use only.

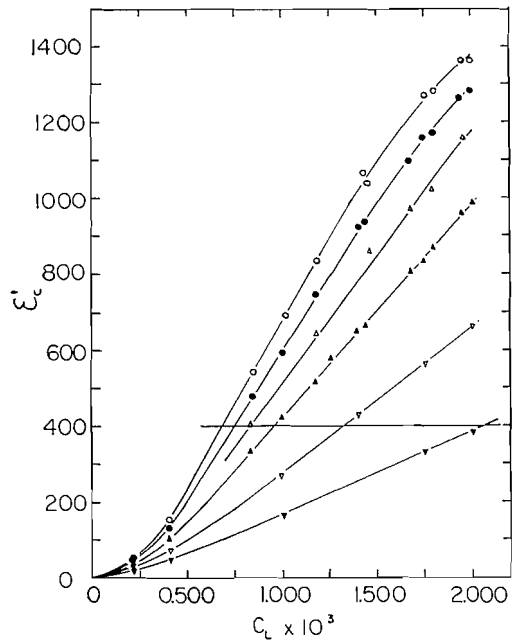

FIG. 10. Variations de $\epsilon_c' = (A_s - \epsilon_L C_L)/C_M$ en fonction de la concentration du ligand C_L: $HClO_4$ = 0.502 M, T = 25.0 ± 0.5 °C, ○ $C_M = 1.15 \times 10^{-4}$ M, ● $C_M = 2.29 \times 10^{-4}$ M, △ $C_M = 3.44 \times 10^{-4}$ M, ▲ $C_M = 5.73 \times 10^{-4}$ M, ▽ $C_M = 1.15 \times 10^{-3}$ M, ▼ $C_M = 2.29 \times 10^{-3}$ M.

TABLEAU II

ϵ_c'	$\bar{n}$	[L] × 10^3
50	0.09	0.22
75	0.12	0.26
100	0.17	0.30
200	0.32	0.42
300	0.47	0.51
400	0.62	0.61
500	0.77	0.70
600	0.90	0.79
700	1.04	0.90
800	1.17	1.00
900	1.30	1.10
1000	1.38	1.21
1100	1.45	1.34
1200	1.52	1.47

III. Propriétés acides–bases du complexe germanium (IV) – acide chloranilique

Comme les méthodes spectrophotométriques précédentes ne fournissent pour le complexe qu'une constante de stabilité apparente valable en milieu d'acidité 0.49 M, il convenait d'examiner l'influence de l'acidité. Les bandes d'absorption du ligand sont peu affectées par la présence de germanium aux faibles acidités, aussi a-t-on utilisé pour cette étude une méthode potentiométrique.

La courbe de neutralisation de 100.0 ml d'acide chloranilique 9.45 × 10^{-3} M par de la potasse 0.1939 N, représentée par la courbe 1 de la Fig. 13, est modifiée en présence de germanium (IV) 3.83 × 10^{-2} M (courbe 2). Sur cette dernière courbe, un premier point d'inflexion correspond à environ 1 milliéquivalent de base, c'est-à-dire à la neutralisation

Can. J. Chem. Downloaded from www.nrcresearchpress.com by 210.87.254.40 on 09/05/12
For personal use only.

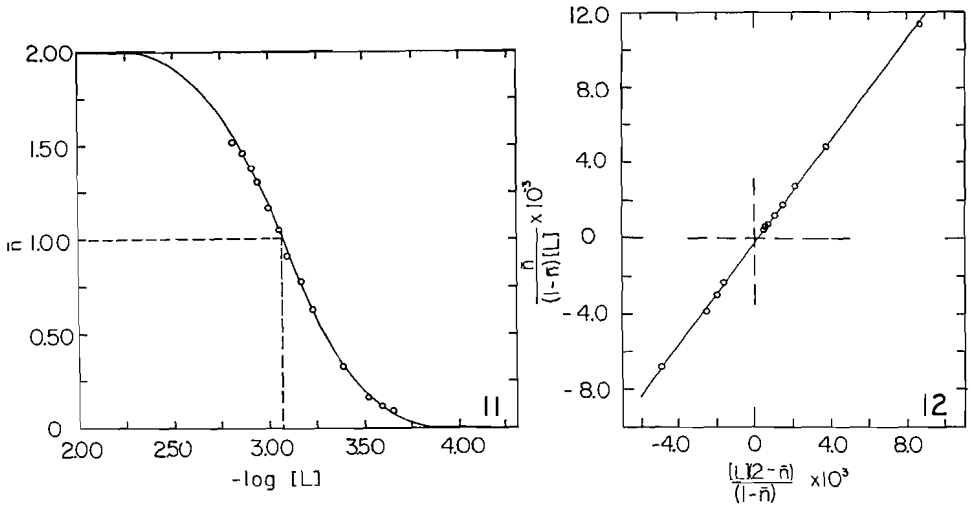

FIG. 11. Courbe de formation des complexes $\bar{n} = f[-\log [L]]$: $HClO_4$ 0.502 M, $T = 25.0 \pm 0.5$ °C.
FIG. 12. Détermination des constantes de stabilité apparentes β_1 et β_2: $HClO_4$ 0.502 M, $T = 25.0 \pm 0.5$ °C.

d'une acidité par ligand. Un deuxième point d'inflexion plus prononcé coincide avec le point équivalent de la courbe 1 et dénote la neutralisation des deux acidités du ligand.

Les réactions suivantes rendent compte qualitativement de l'allure de la courbe 2. Initialement le complexe 1:2 est formé quantitativement,

[a] $$Ge(OH)_4 + 2H_2R \rightarrow Ge(OH)_2R_2H_2 + 2H_2O,$$

jusqu'au premier point d'inflexion, les deux acidités du complexe sont neutralisées,

[b] $$Ge(OH)_2R_2H_2 + 2OH^- \rightarrow Ge(OH)_2R_2^{2-} + 2H_2O,$$

après le premier point d'inflexion le complexe est détruit,

[c] $$Ge(OH)_2R_2^{2-} + 2OH^- \rightarrow Ge(OH)_4 + 2R^{2-},$$

au delà du deuxième point d'inflexion, l'acide germanique de pK 9.2 (25) est neutralisé.

De plus, les positions relatives des débuts des courbes 1 et 2 permettent de conclure que les deux acidités de $Ge(OH)_2R_2H_2$ sont relativement fortes: ainsi initialement la solution environ 10^{-2} M en acide H_2R voit son pH passer de 2.03 à 2.06, en présence de Ge(IV) en excès, c'est-à-dire à une valeur correspondant à la dissociation quasi-totale de $2H^+$ pour le complexe à la concentration approximative 5×10^{-3} M.

La courbe de neutralisation de 150 ml d'une solution 6.52×10^{-3} M du ligand voisin, la dihydroxy-2,5 p-benzoquinone (Fig. 13, courbe 3) par de la potasse 0.2276 N est aussi modifiée en présence de germanium (IV) 6.83×10^{-3} M (courbe 4). L'analyse de cette dernière courbe confirme l'interprétation précédente. Le premier point d'inflexion est cette fois beaucoup plus net, ceci est dû en partie à ce que la dihydroxybenzoquinone est un acide plus faible, $k_1 = 10^{-2.71}$ et $k_2 = 10^{-5.18}$ (13). Pour cette même raison, la courbe 4 débute à des pH plus bas que la courbe 3, la valeur du pH initial sur la courbe 4 indique que les deux acidités du complexe sont aussi essentiellement fortes.

Sur la base de l'interprétation précédente, on a déterminé la deuxième constante d'acidité $\mathcal{K}_2$ du complexe $Ge(OH)_2R_2H_2$ correspondant à l'équilibre

Can. J. Chem. Downloaded from www.nrcresearchpress.com by 210.87.254.40 on 09/05/12
For personal use only.

$$Ge(OH)_2R_2H^- \rightleftarrows Ge(OH)_2R_2^{2-} + H^+$$

$$[12] \qquad \mathscr{K}_2 = \frac{[H^+][Ge(OH)_2R_2^{2-}]}{[Ge(OH)_2R_2H^-]},$$

$\mathscr{K}_2$ devant correspondre à une acidité relativement forte, la première acidité de $Ge(OH)_2R_2H_2$ étant elle-même forte.

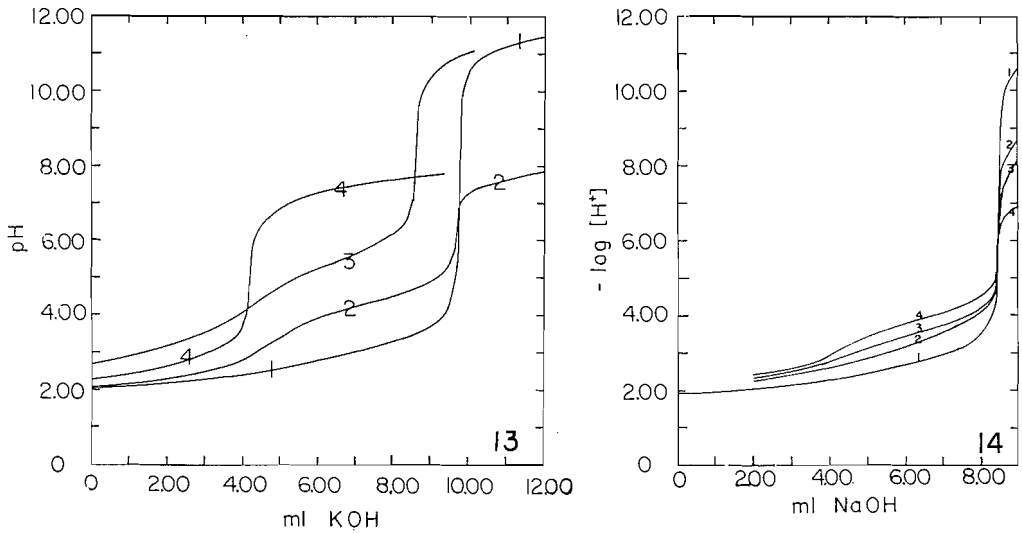

FIG. 13. Courbes de neutralisation de l'acide chloranilique et de la dihydroxy-2,5 *p*-benzoquinone par KOH: (1) acide chloranilique 9.45×10^{-3} *M*, KOH = 0.1939 *M*, $C_M = 0$; (2) acide chloranilique 9.45×10^{-3} *M*, KOH = 0.1939 *M*, $C_M = 3.83 \times 10^{-2}$ *M*; (3) dihydroxy-2,5 *p*-benzoquinone 6.52×10^{-3} *M*, KOH = 0.1138 *M*, $C_M = 0$; (4) D.H.Q. 6.52×10^{-3} *M*, KOH = 0.2276 *M*, $C_M = 6.83 \times 10^{-3}$ *M*.

FIG. 14. Courbes de neutralisation de l'acide chloranilique 1.002×10^{-2} *M* par NaOH 0.2352 *M* en présence de germanium (IV), NaCl = 0.484 *M*: (1) $C_M = 0$, (2) $C_M = 3.51 \times 10^{-3}$ *M*, (3) $C_M = 8.78 \times 10^{-3}$ *M*, (4) $C_M = 3.51 \times 10^{-2}$ *M*.

Dans une première étape, on a calculé la constante de formation du complexe $Ge(OH)_2R_2^{2-}$ telle que:

$$[13] \qquad \beta_2^0 = \frac{[Ge(OH)_2R_2^{2-}]}{[Ge(OH)_4][HR^-]^2}.$$

Pour cela, on a tracé les 3 courbes de neutralisation de 100 ml d'acide chloranilique 1.002×10^{-2} *M* en présence de germanium (IV) respectivement 3.51, 8.18 et 35.1×10^{-3} *M* et en milieu NaCl 0.48 *M* (Fig. 14). On a noté au début de la neutralisation la formation lente d'un précipité pourpre, avec augmentation correspondante du pH, le précipité se redissout quand on poursuit la neutralisation. On a utilisé pour le calcul les portions des courbes situées au delà du premier point équivalent, dans cette région l'espèce $Ge(OH)_2R_2^{2-}$ est la seule forme du complexe présente. Le β_2^0 est obtenu en résolvant le système d'équations [2], [14], [15] et [16].

$$[14] \qquad C_L = 2[Ge(OH)_2R_2^{2-}] + [HR^-] + [R^{2-}].$$

$$[15] \qquad C_M = [Ge(OH)_2R_2^{2-}] + [Ge(OH)_4].$$

$$[16] \qquad [Na^+] + [H^+] = 2[Ge(OH)_2R_2^{2-}] + [HR^-] + 2[R^{2-}].$$

Can. J. Chem. Downloaded from www.nrcresearchpress.com by 210.87.254.40 on 09/05/12
For personal use only.

Les valeurs de β_2^0 ont été calculées pour quelques 8 points de la courbe pour chaque concentration de germanium, les valeurs moyennes sont groupées dans le Tableau III.

TABLEAU III

C_M	Log β_2^0
3.51×10^{-2}	6.61 ± 0.05
8.18×10^{-3}	6.57 ± 0.04
3.51×10^{-3}	6.52 ± 0.07

Dans une deuxième étape, on a déterminé $\mathscr{K}_2$ en reliant β_2^0 à β_2, la constante apparente (équation [8]) dont la valeur est connue en milieu d'acidité 0.49 M.

$$[17]\quad \beta_2 = \frac{[ML_2]}{[M][L]^2} = \frac{[Ge(OH)_2R_2H^-] + [Ge(OH)_2R_2^{2-}]}{[Ge(OH)_4]([H_2R] + [HR^-] + [R^{2-}])^2}$$

$$= \beta_2^0 \frac{1 + ([H^+]/\mathscr{K}_2)}{(([H^+]/k_1) + 1 + (k_2/[H^+]))^2},$$

avec $\beta_2 = 10^{6.16}$ pour $[H^+] = 0.49$ et $\beta_2^0 = 10^{6.57}$, $k_1 = 10^{-0.66}$, $k_2 = 10^{-2.37}$.

La valeur obtenue pour $\mathscr{K}_2$, la deuxième constante d'acidité du complexe $Ge(OH)_2R_2H_2$ est $10^{-0.78\pm0.14}$.

DISCUSSION

La formation des seuls complexes comportant 2 acides chloraniliques par germanium, indiquée par la méthode de variations continues et la présence de points isobestiques a été confirmée par trois méthodes spectrophotométriques indépendantes, qui donnent en outre des valeurs concordantes $10^{6.16\pm0.02}$ pour β_2, la constante de formation apparente du complexe ML_2 en milieu d'acidité 0.49 M. Dans ces méthodes, on a utilisé des longueurs d'onde différentes et l'on a fait varier de façon appréciable le rapport des concentrations C_L/C_M: de 0.0028 à 17.3 ainsi que la concentration C_M: de 4×10^{-5} à 3.5×10^{-2} M. L'absence de complexes ML et ML_3 ainsi que d'espèces polynucléaires M_pL_n stables a été vérifiée.

Les conclusions de Nazarenko et Flyantikova dans leur récent article (11) quant à la présence des trois complexes ML, ML_2 et ML_3 sont donc mises en doute. Ces auteurs ont effectué des mesures spectrophotométriques à 530 mμ dans un domaine d'acidité allant de 1 à 4 M. Leurs courbes de variations continues ayant comme les nôtres, indiqué un complexe ML_2, les conclusions des auteurs reposent uniquement sur une interprétation de la méthode des rapports molaires. L'existence d'un complexe ML est déduite de la non linéarité initiale de la courbe donnant $A_s - \epsilon_L C_L$ en fonction de C_L/C_M. Nous avons confirmé cette courbure (Fig. 10) mais nous avons vérifié par le calcul que le complexe ML_2 suffisait à expliquer cette "anomalie". Quant au complexe ML_3 son existence n'est justifiée que par une cassure de la courbe reposant sur deux points expérimentaux à la seule acidité 1 M. Nos expériences ne nous ont pas conduits à observer de telles cassures comme l'indique la Fig. 10 où l'on a porté $\epsilon_c' = (A_s - \epsilon_L C_L)/C_M$ en fonction de C_L pour des valeurs données de C_M.

L'absence, ou la très faible stabilité, des complexes germanium – acide chloranilique ML et ML_3 est remarquable, d'autant plus que le zirconium (IV) donne avec ce même ligand des complexes ML et ML_2 stables (10). La nature et la stabilité des complexes du germanium (IV) et du zirconium (IV) sont comparées dans le Tableau IV, les constantes apparentes β_n sont calculées pour une acidité 1 M.

Can. J. Chem. Downloaded from www.nrcresearchpress.com by 210.87.254.40 on 09/05/12
For personal use only.

TABLEAU IV

	M	ML	ML_2	ML_3
M = Ge	$Ge(OH)_4$ aq.	$\beta_1 < 10^2$	$Ge(OH)_2R_2H^-$, $\beta_2 = 10^{5.9}$	—
M = Zr	Zr^{4+} aq.	ZrR^{2+} aq., $\beta_1 = 10^{5.7}$	ZrR_2 aq., $\beta_2 = 10^{9.5}$	

A l'encontre du complexe ZrR^{2+} aq. stable, l'espèce ML du germanium, soit $Ge(OH)_3R^-$ pentacoordinée, soit $Ge(OH)_3(OH_2)R^-$ ou $Ge(OH)_4R^{2-}$ hexacoordinée, est instable, par rapport à $Ge(OH)_2R_2H^-$ et $Ge(OH)_4$ aq. Le comportement anormal de ce complexe ML semble devoir être relié à la forte "hydratation" du germanium (IV) qui déplace l'équilibre de dismutation $2ML \rightleftarrows M + ML_2$ par stabilisation de M. On a d'ailleurs dans une étude en cours (26) sur les complexes du germanium avec la 8-hydroxyquinoléine, HOx, mis en évidence une seule espèce de composition ML_2, $Ge(OH)_2Ox_2$, en solution aqueuse, alors que la présence d'un complexe ML dans le chloroforme est indiquée. En ce qui concerne l'absence, ou la faible stabilité, du complexe ML_3, elle peut aussi être rapprochée de l'instabilité en solution aqueuse de l'ion complexe $GeOx_3^+$ apparemment présent dans le solide $GeOx_3FeCl_4$ et stable dans certains solvants non hydroxylés (27).

L'absence de polymères est aussi remarquable étant donné que l'acide chloranilique possède deux groupes *o*-hydroxycétones susceptibles de conduire à une chélation. La formation de solides polymériques avec certains ions métalliques, et avec $GeCl_4$ en milieu non-aqueux, a d'ailleurs été signalée (10, 12).

Les complexes du germanium étant nettement moins stables que ceux du zirconium, une méthode d'analyse spectrophotométrique basée sur la réaction avec l'acide chloranilique ne présenterait pas le même intérêt pour le germanium que pour le zirconium (10). D'ailleurs la phénylfluorone est un réactif analytique du germanium supérieur à l'acide chloranilique vue la beaucoup plus grande stabilité du complexe ML_2 correspondant $10^{12.9}$ (6), les valeurs des coefficients d'extinction ϵ_c étant aussi quelque peu favorables à la phénylfluorone, 8.7×10^4 au lieu de 3.3×10^4.

La méthode potentiométrique a permis de préciser les propriétés acides–bases du complexe ML_2, ce dernier possède deux acidités, l'une forte, l'autre de constante $\mathcal{K}_2 = 10^{-0.8}$ et la formule $Ge(OH)_2R_2H_2$ rend compte des propriétés observées. De plus, l'étude du complexe $Ge(OH)_2Ox_2$ précédemment cité, ayant indiqué que les —OH directement liés au germanium sont très faiblement acides (26) on peut conclure que les deux H^+ de $Ge(OH)_2R_2H_2$ proviennent des deux ligands. La formation du chélate a donc renforcé l'acidité du groupe —OH restant libre sur chaque ligand, par rapport aux acidités préexistantes du ligand, $k_1 = 10^{-0.66}$ et $k_2 = 10^{-2.37}$. Un tel effet de la chélation sur l'acidité de groupes libres sur le ligand a été récemment observée par Freiser (28) et Lions (29).

Voigt (10) a aussi montré que la chélation de Zr^{4+} par l'acide chloranilique se faisait avec libération d'environ $2H^+$ par ligand dans un domaine d'acidité allant de 1 à 2 *M*. Le nombre d'H^+ libérés étant d'ailleurs quelque peu inférieur à 2, il est possible que le chélate du zirconium possède des propriétés acides–bases similaires à celles du chélate du germanium.

Une formule, avec le germanium hexacoordiné, est donnée ici pour l'anion complexe $Ge(OH)_2R_2^{2-}$, cette formule est à rapprocher de celle suggérée par Place (12) pour le sel complexe $GeCl_2R_2$ $(pyH)_2 \cdot CH_3NO_2$ préparé à partir de $GeCl_4$ et H_2R en milieu non aqueux.

Can. J. Chem. Downloaded from www.nrcresearchpress.com by 210.87.254.40 on 09/05/12
For personal use only.

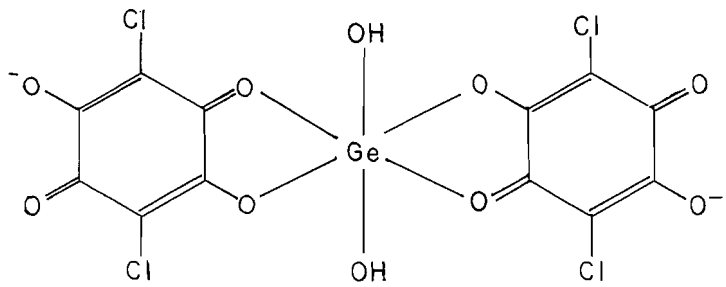

Cependant, en plus des deux formes résonantes correspondant à cette structure, on doit aussi considérer la possibilité de deux autres structures, où la chélation est effectuée soit par une forme diphénol, soit par une forme dicétone. On est ainsi conduit à envisager une délocalisation probable des électrons; la délocalisation des charges négatives de l'anion complexe pourrait dans une certaine mesure, être à l'origine des propriétés fortement acides de $Ge(OH)_2R_2H_2$.

Il semble probable que la phénylfluorone est coordinée au germanium dans le complexe ML_2 d'une façon analogue plutôt que par le groupe *o*-diphénol en position 2,3, ceci d'autant plus que les ligands comportant ce dernier groupe paraissent conduire à des complexes ML_3 avec le germanium (18). Kanno (5) après avoir étudié un certain nombre de ligands a conclu que ceux qui possèdent un groupe *o*-hydroxycétone réagissent avec le germanium en milieu acide; bien que ce point de vue se trouve confirmé par ce travail, on a observé que certains ligands de cette classe ne donnent pas de réaction (12). Il est ainsi nécessaire de considérer en plus des groupements fonctionnels d'autres propriétés du ligand pour prévoir si celui-ci réagit avec le germanium.

Les caractéristiques des spectres d'absorption des complexes et des différentes formes, H_2R, HR^- et R^{2-} du ligand sont comparées dans le Tableau V. Les valeurs correspondent

TABLEAU V

	λ, mμ	$\epsilon \times 10^{-4}$	λ, mμ	$\epsilon \times 10^{-3}$
ZrR^{2-} (10)	330	1.8	525	
$Ge(OH)_2R_2^{2-}$ et $Ge(OH)_2R_2H^-$	330	3.28	522	1.87
HR^-	307	1.65	525	0.92
H_2R	303	2.0	450	0.22
R^{2-}	334	3.0	525	0.18

aux maxima des deux bandes d'absorption. Les longueurs d'onde sont données à ±5 mμ près et les coefficients ϵ comportent une erreur maximum de ±5%. Les valeurs des coefficients d'extinction molaires du complexe ne sont pas affectées de façon notable par l'acidité entre 0.5 *M* et pH 3.3. On constate que le coefficient ϵ_c du complexe $Ge(OH)_2R_2^{2-}$ comportant 2 ligands R^{2-} est égal à environ 2 fois celui du ligand protoné HR^-, aux deux maxima. Une situation analogue prévaut dans le cas de ZrR^{2+}. On observe souvent des relations telles lorsque les bandes d'absorption des complexes proviennent de modifications des transitions internes des ligands (30) comme dans le cas présent. La bande de HR^- vraisemblablement due à la transition $\pi \rightarrow \pi^*$ (31) est déplacée de 306 à 327 mμ, lors de la chélation du germanium tandis que la bande due à la transition $n \rightarrow \pi^*$ du groupe carbonyle reste inchangée à 525 mμ.

Can. J. Chem. Downloaded from www.nrcresearchpress.com by 210.87.254.40 on 09/05/12
For personal use only.

REMERCIEMENTS

Nous exprimons nos remerciements au Conseil National de Recherches du Canada pour une bourse (A. B.) et un octroi de recherches (R. L. B.).

SUMMARY

Complex formation between germanium (IV) and 2,5-dichloro-3,6-dihydroxy-*p*-benzoquinone (H_2R) as ligand is studied at ionic strength 0.49. Spectrophotometric methods are used to show that only complexes with two ligands per germanium atom are present and to calculate the apparent stability constant $\beta_2 = 10^{6.16}$ in 0.49 *M* H^+. The values of the ligand acidity constants are $k_1 = 10^{-0.66}$ and $k_2 = 10^{-2.37}$. The stability constant of $Ge(OH)_2R_2^{2-}$ is found to be $\beta_2^0 = 10^{6.57}$ by potentiometry. The complex $Ge(OH)_2R_2H_2$ is a strong acid in its first dissociation, the constant of the second dissociation is $\mathcal{K}_2 = 10^{-0.8}$. Formulae are suggested for the complexes. The nature and stability of the germanium and zirconium complexes are compared and their absorption spectra are discussed in relation to those of the ligand species H_2R, HR^-, and R^{2-}.

BIBLIOGRAPHIE

1. P. J. Antikainen. Acta Chem. Scand. **13**, 312 (1959).
2. N. Konopik et G. Wimmer. Monatsh. Chem. **93**, 1404 (1962).
3. A. Tchakirian. Ann. Chim. Paris, **12**, 415 (1939).
4. E. R. Clark. J. Inorg. Nucl. Chem. **24**, 81 (1962).
5. T. Kanno. Sci. Rept. Tohoku Univ., First Ser. **12**, 175 (1960).
6. E. B. Sandell. Colorimetric determination of traces of metals. Interscience Publ., New York, N.Y. 1959. p. 485.
7. P. Stipanits et F. Hecht. Z. Anal. Chem. **152**, 185 (1956).
8. V. A. Nazarenko, N. V. Lebedeva, E. A. Biryuk et M. B. Shustova. Russ. J. Inorg. Chem. **7**, 1423 (1962).
9. K. Ueno. Bunseki Kagaku, **9**, 257 (1960).
10. B. J. Thamer et A. F. Voigt. J. Am. Chem. Soc. **73**, 3197 (1951).
11. V. A. Nazarenko et G. V. Flyantikova. Russ. J. Inorg. Chem. **7**, 1210 (1962).
12. J. Place. Thèse de Doctorat, Université de Montréal, Montréal, P.Q. 1964.
13. G. Schwarzenbach et H. Suter. Helv. Chim. Acta, **24**, 617 (1941).
14. B. J. Thamer et A. F. Voigt. J. Phys. Chem. **56**, 225 (1952).
15. J. Weissbart et P. Van Rysselberghe. J. Phys. Chem. **61**, 765 (1957).
16. K. Wallenfels et K. Friedrich. Chem. Ber. **93**, 3070 (1960).
17. K. P. Ang. J. Phys. Chem. **62**, 1109 (1958).
18. S. V. Rao. Travaux non publiés. 1963.
19. P. Job. Ann. Chim. Paris, **9**, 113 (1928).
20. R. L. Benoit et P. Clerc. J. Phys. Chem. **65**, 676 (1961).
21. H. McConnell et N. Davidson. J. Am. Chem. Soc. **72**, 3164 (1950).
22. J. Bjerrum. Kgl. Danske Videnskab. Selskab, Mat.-Fys. Medd. **21**, no. 4 (1944).
23. S. Fronaeus. Acta Chem. Scand. **5**, 139 (1951).
24. F. J. C. Rossotti et H. Rossotti. The determination of stability constants. McGraw-Hill Book Co., New York. 1960. p. 89.
25. N. Ingri. Acta Chem. Scand. **17**, 597 (1963).
26. R. L. Benoit et P. Clerc. Ann. Acfas, 29 (1963) (sous presse).
27. R. L. Benoit. Ann. Acfas, 27 (1961).
28. A. Corsini, Q. Fernando et H. Freiser. Inorg. Chem. **2**, 224 (1963).
29. R. W. Green, P. S. Hallman et F. Lions. Inorg. Chem. **3**, 376 (1964).
30. C. K. Jørgensen. Absorption spectra and chemical bonding in complexes. Pergamon Press, Oxford. 1962.
31. C. N. R. Rao. Ultra-violet and visible spectroscopy. Butterworths, London. 1961.

Can. J. Chem. Downloaded from www.nrcresearchpress.com by 210.87.254.40 on 09/05/12
For personal use only.

Can. J. Chem. Downloaded from www.nrcresearchpress.com by 210.87.254.42 on 09/05/12
For personal use only.

THE HYDROGEN–CHLORINE SYSTEM IN THE MM PRESSURE RANGE

I. ENERGY DISTRIBUTION AMONG VIBRATIONALLY EXCITED STATES

F. D. FINDLAY[1] AND J. C. POLANYI

Department of Chemistry, University of Toronto, Toronto, Ontario

Received April 27, 1964

ABSTRACT

When atomic plus molecular hydrogen coming from a Wood's discharge tube are mixed with molecular chlorine, infrared emission is observed (1). At low reagent pressures, $\sim 10^{-2}$ mm Hg, this emission can be related to the relative rate of the reaction $H + Cl_2 \rightarrow HCl\dagger_v + Cl$ proceeding to form HCl in vibrationally excited states $v = 1$–6, of the ground electronic state. In the present work this system has been investigated for the first time at $\sim 100\times$ the reagent pressure (~ 1 mm Hg). The reaction was shown to proceed by a chain mechanism. The translational–rotational temperature was 1300 ± 100 °K under the experimental conditions normally used. The vibrational distribution was notable for the presence of vibrators in levels $v = 7$ and 8, which are respectively 4 and 10 kcal higher in energy than the exothermicity of the $H + Cl_2$ reaction. The population in these levels appeared to be related to that in the levels with $v \leqslant 6$; it was proposed that vibrational–vibrational exchange among these lower levels was responsible for populating the higher ones. A simple model yielded a collision efficiency for $HCl\dagger_{v=1} + HCl\dagger_{v=6} \rightarrow HCl\dagger_{v=7} + HCl\dagger_{v=0}$, of $Z_{1,6}{}^t = 6 \times 10^3$ collisions per transfer. Addition of HCl to the reaction mixture brought about a redistribution among vibrationally excited states indicative of a fast vibrational transfer, $HCl_{v=0} + HCl\dagger_{v=2} \rightarrow 2\ HCl\dagger_{v=1}$.

At reduced pressure of HCl† the stationary-state distribution among higher vibrational states approximated closely to that observed at 10^{-2} mm Hg total pressure (where collisional deactivation is insignificant), suggesting that collisional deactivation was not of major importance even at the pressure used in the present work. In order to account for the high translational–rotational temperature, in the absence of substantial vibrational deactivation, it was necessary to suppose that the greater part of the energy liberated by the reaction $H + Cl_2$ went *directly* into translational and rotational motion of the products.

INTRODUCTION

When $H_2 + H$ coming from a discharge is mixed with Cl_2, infrared emission (but no visible emission) is observed. This emission (1.5–4.5 μ) was first recorded in experiments conducted at ca. 0.1 mm Hg reagent pressure (1). The objective was to obtain information concerning the vibrational energy distribution in the product of the primary reaction, $H + Cl_2 \rightarrow HCl\dagger + Cl$. The observation of a near-Boltzmann distribution among vibrational states led to the suspicion that the vibrators once formed might be randomizing their energy through rapid vibrational–vibrational transfer. Subsequent experiments (2) were conducted in the 0.01 mm Hg pressure range. At these pressures a markedly non-Boltzmann distribution was observed among the vibrational states of HCl. A steady-state analysis of this distribution led to a series of relative rate constants, k_v, for the $H + Cl_2$ reaction proceeding to form HCl† (vibrationally excited HCl in its ground electronic state) in specified states v.

In the present work we have set out to achieve a qualitative or semi-quantitative understanding of the complicating processes that occur at higher reagent pressure. For this purpose we have gone beyond the original 0.1 mm 'medium' reagent pressure, to a 'high' pressure region of 1–2 mm Hg.

[1]*Present address: National Physical Laboratory, Teddington, Middlesex, England.*

EXPERIMENTAL

A block diagram of the apparatus would be identical to Fig. 1 of ref. 1, with the exception of a second reagent supply running parallel to the first. Experiments were conducted under conditions of continuous flow. Materials (H_2, Cl_2, and HCl) were from the same sources as in ref. 1. However, in order to make possible the much greater flows used in the present work, the gases were delivered directly from cyclinders. Flowmeters consisted of lengths of capillary tubing across which the pressure drop could be measured. These meters were calibrated with the experimental gas at the experimental fore-pressure, either by condensing the material passed in a given time or (for H_2) by measuring a small pressure rise in a closed volume downstream. The pumping facilities consisted of a 2 in. butterfly valve (Edwards QSB-2) directly below the reaction vessel, a liquid-air trap (Edwards NTM-2A), a 4 in. oil booster diffusion pump (NRC QB-4), and a mechanical pump (Edwards ISC-450B; 8.1 liters per second capacity). Only the mechanical pump was used under running conditions, since the reaction vessel pressure was in the range 1–2 mm Hg. Following an experiment, chlorine and hydrogen chloride condensed in the liquid-air trap were distilled into a copper sidearm and removed.

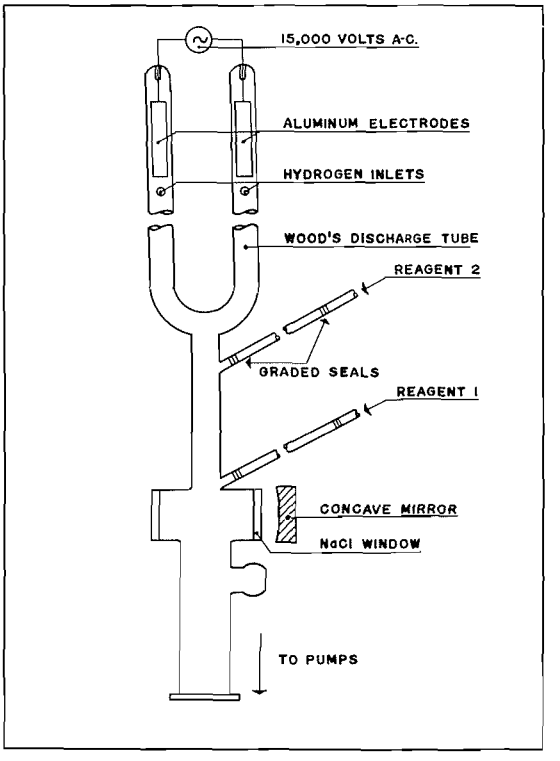

FIG. 1. Reaction vessel assembly.

The reaction vessel assembly (Fig. 1) consisted of a Wood's discharge tube, made from 30 mm pyrex 30 in. long, attached to a cylindrical reaction vessel, 10 cm long by 5 cm diameter, which in turn was attached to a 2 in. diameter by 6 in. long glass tube terminating in a flat flange. The flange was greased and made a vacuum seal either with a flat metal plate or with an O-ring set into a metal plate. In one version the reaction vessel was pyrex with NaCl windows held to either end by glyptal varnish, in another the vessel was made entirely of pyrex with pyrex windows sealed on, and in a third design the vessel was quartz with quartz windows sealed directly to either end. The Wood's tube was poisoned, following a cleaning with 10% hydrofluoric acid, with 30% orthophosphoric acid, to reduce the rate of atom recombination at the walls.

To determine the concentration of hydrogen atoms formed in the discharge, a tungsten-wire probe was inserted through the ball-and-socket joint directly beneath the reaction vessel. The filament (2 cm long by 0.01 cm diameter) formed one arm of an a-c. bridge; it was used as an isothermal calorimeter to measure the heat liberated on H-atom recombination (3). H-atom concentration was only measured in the absence of chlorine. It was found to be constant throughout the cell, to better than ±5%. As the variable transformer

Can. J. Chem. Downloaded from www.nrcresearchpress.com by 210.87.254.42 on 09/05/12
For personal use only.

in the primary of the Wood's tube transformer was increased from the 20 to the 100 V setting, the percentage dissociation of H_2 present in the reaction vessel rose almost linearly from 2 to 17%. In most experiments ('normal' conditions) the variable transformer was set at 45 V, resulting in ca. 8% dissociation in the vessel.

Chlorine was normally introduced through reagent inlet tube No. 1, directly above the vessel. The quartz insert between the graded seals on this sidearm was used in experiments where an r.f. discharge was applied to the Cl_2. In experiments where HCl was added, reagent inlet No. 2, located about 5 in. above the vessel, was used.

In normal operation the optics were aligned so that a beam emerging from the spectrometer gave rise to an image of the spectrometer slit (12 mm high) in the center of the front window of the cell; within the cell the beam diverged with a 15° angle. The pressure in the reaction vessel was measured at the ball-and-socket joint 2 in. below the vessel. The flexible metal vacuum tube leading from this joint to the McLeod gauges could be replaced by the tungsten-filament probe.

A spherical mirror with large radius of curvature was placed behind the reaction vessel, giving an increase in intensity of slightly less than a factor of two.

The spectrometer was a Perkin–Elmer 112G double-pass grating instrument, with KBr fore-prism. The detector was a liquid-air-cooled 'Infratron' lead sulphide cell. After an experiment, the spectrometer was calibrated for change in transmissivity with wavelength and, simultaneously, the detector was calibrated for change in sensitivity with wavelength. This was done by making a trace of the emission from a black-body source, recorded at the experimental spectrometer slit width. In correcting line areas for changing efficiency of the instrument, allowance was made for the fact that the dispersion of the grating changes slightly, even within a single order; this affects the signal from the black body used in calibration, but does not affect the areas under the spectral lines.

RESULTS

Infrared emission was recorded in the fundamental, first-overtone, and second-overtone regions of the HCl spectrum. No visible emission was detected.

In preliminary experiments, traces of the first-overtone spectrum were made under very similar flow conditions employing pumps similar to those described in ref. 1 (pressure in the reaction vessel 0.1–0.2 mm, contact time ca. 0.05 s). The gain in intensity on converting to the high-flow system used in the bulk of the present experiments was in the region of 10–100× (pressure in the reaction vessel 1–2 mm, contact time ca. 0.01 s). It may be remarked that Cashion and Polanyi (1) reported a *decrease* in intensity when reagent inflows were increased. In their case, however, an increase in reagent inflow meant a decrease in linear flow rate across the reaction vessel; it appears probable, considering both the gain in intensity referred to above and experiments to be described below (Section 3), that the diminution in intensity in their experiments was due to a displacement of the zone of most intense emission upwards out of the cone-of-sight of their spectrometer.

An actual chart record of a typical fundamental spectrum is shown in Fig. 2. Emission was observed from the $v(1–0)$, $v(2–1)$, $v(3–2)$, and $v(4–3)$ bands. The experimental conditions are recorded in the caption of the figure. A quartz reaction vessel cooled by air jets was used (the transmission of quartz is down to 65% by 3.8 μ). The entire spectrum is not reproduced. The band-head of $v(1–0)$ R-branch (not shown) was observed at $J = 25$.

Part of the first-overtone spectrum, consisting of 130 vibration–rotation lines of $v(2–0)$, $v(3–1)\ldots v(7–5)$, is shown in Fig. 3. The spectrum was recorded using an all-pyrex vessel (transmission 92% in this wavelength region). The reaction $H + Cl_2$ cannot form emitters in levels with $v > 6$; the source of the emission from $v = 7$ will be discussed later.

The second-overtone spectrum shown in Fig. 4 was recorded under the same flow conditions as Fig. 3, but with wide slits owing to the low intensity of the higher overtone. The $v(3–0)$, $v(4–1)\ldots v(8–5)$ can be picked out by their prominent R-branches. Because of the large difference between the rotational constants for the upper and lower vibrational states in these $\Delta v = 3$ transitions, the R-lines converge rapidly and reach a band-head at $J = 10$, giving this spectrum its characteristic appearance. The P-lines diverge rapidly so that the R-branch of any band is overlapped by only three P-lines from the neighboring

Can. J. Chem. Downloaded from www.nrcresearchpress.com by 210.87.254.42 on 09/05/12
For personal use only.

lower transition. The dotted line at the base of each R-branch indicates the level of intensity from the unresolved P-lines of the neighboring band.

DISCUSSION

In some experiments the Cl_2:HCl ratio in the product was obtained by measuring the pressure over the condensate at various temperatures, in a calibrated volume. It was found that in an experiment with H_2 inflow about 1300 μmoles/s, percentage dissociation about 8%, and Cl_2 inflow 480 μmoles/s, the Cl_2 was at least 90% converted to HCl. This indicates a chain of 4 or 5 links:

[1] $\quad H + Cl_2 \rightarrow HCl + Cl \qquad \Delta H = -45$ kcal/mole

[2] $\quad Cl + H_2 \rightarrow HCl + H \qquad \Delta H = 1$ kcal/mole

The activation energy for reaction [1] is about 2.5 kcal/mole (4), so that there is a total of 47.5 kcal to be distributed among the products. Evidence will be presented in Section 5 below which points to the fact that the major part of this energy is liberated as translation and rotation of the products. The Cl that collides with H_2 in reaction [2] could therefore have excess energy (H_2 is present in excess and is the most likely gas-phase 'coolant'). Even normal thermal collisions, however, would have a high collision efficiency. In Section 1, it will be shown that the translational–rotational temperature of the bulk of the gas is 1250 ± 50 °K. At this temperature reaction [2], which has an activation energy of ca. 6 kcal/mole, would occur every 10–100 collisions (assuming a steric factor of 1–0.1). Since the $v = 1$ level of HCl is 8.25 kcal above $v = 0$, [2] will form HCl primarily in $v = 0$.

The possibility of a chain was demonstrated in an experiment where the discharge through the hydrogen was at first switched off, thus cutting off the supply of atomic H while maintaining normal flows of H_2 and Cl_2 into the reaction vessel. The emission fell to zero. When, however, a radio frequency discharge was applied to the quartz inlet tube carrying the Cl_2, the emission was restored to full intensity, with the normal heating of the vessel walls.

The intensity of a vibration–rotation line in emission, $I_{vJ}^{v'J'}$, is related to the population, $N_{v'J'}$, in the upper state of the transition, by the expression

$$[3] \qquad I_{vJ}^{v'J'} = \frac{64\pi^4 c N_{v'J'}}{3(2J'+1)} \cdot (\omega_{vJ}^{v'J'})^4 \cdot |R_v^{v'}|^2 \cdot S_J \cdot F_{vJ}^{v'J'}$$

where $\omega_{vJ}^{v'J'}$ is the wave-number frequency of the line, $R_v^{v'}$ is the transition moment for the band, S_J is the line strength (J' for an R-branch line, $J' + 1$ for P-branch) and $F_{vJ}^{v'J'}$ is the vibration–rotation interaction factor (2, 5).

1. Rotational Distribution

In considering rotational distribution within a single band we can write,

$$[4] \qquad I_J \propto \frac{N_{J'} \cdot \omega_J{}^4 S_J F_J}{2J'+1}.$$

For a Boltzmann-type distribution

$$[5] \qquad N_{J'} \propto (2J'+1)e^{-J'(J'+1)Bhc/kT}$$

where B is the rotational constant. Substituting into the previous equation and rearranging,

$$[6] \qquad \log \frac{I_J}{\omega_J{}^4 S_J F_J} \propto -J'(J'+1) \cdot Bhc/kT.$$

Can. J. Chem. Downloaded from www.nrcresearchpress.com by 210.87.254.42 on 09/05/12
For personal use only.

Can. J. Chem. Downloaded from www.nrcresearchpress.com by 210.87.254.42 on 09/05/12
For personal use only.

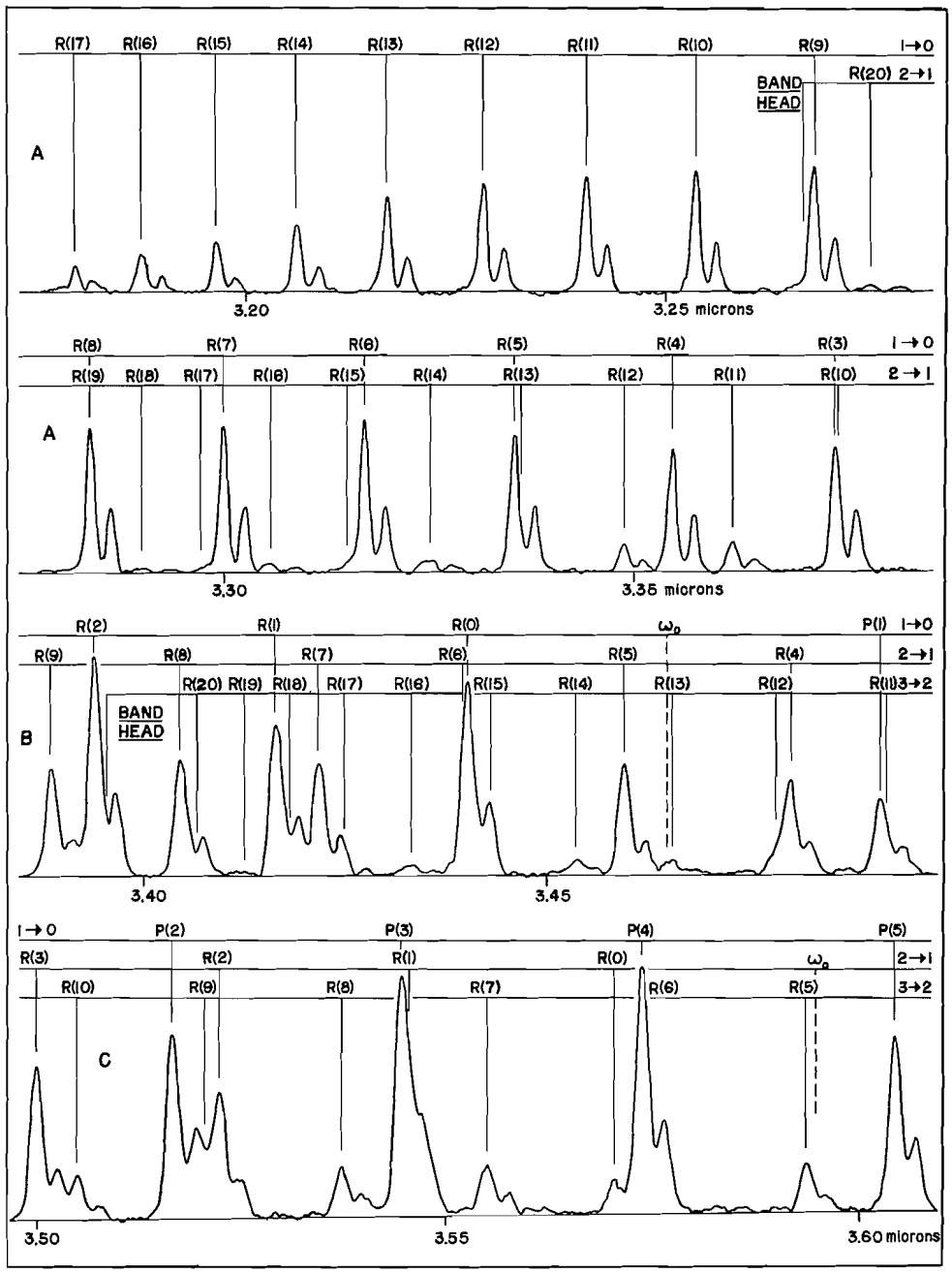

FIG. 2. Fundamental spectrum of HCl. Reagent inflows, 1150 μmoles/s of $H_2 + H$ (dissociation ca. 10%), 450 μmoles/s Cl_2. Total pressure in the reaction vessel 1.15 mm Hg. Contact time 0.0076 s. Grating 300 grooves/mm blazed at 3 μ, used in the first order. Grating monochromator slit widths: A, 0.150 mm; B, 0.250 mm; C, 0.300 mm. The lines are labelled $P(J)$ and $R(J)$ in the P- and R-branches.

Can. J. Chem. Downloaded from www.nrcresearchpress.com by 210.87.254.42 on 09/05/12
For personal use only.

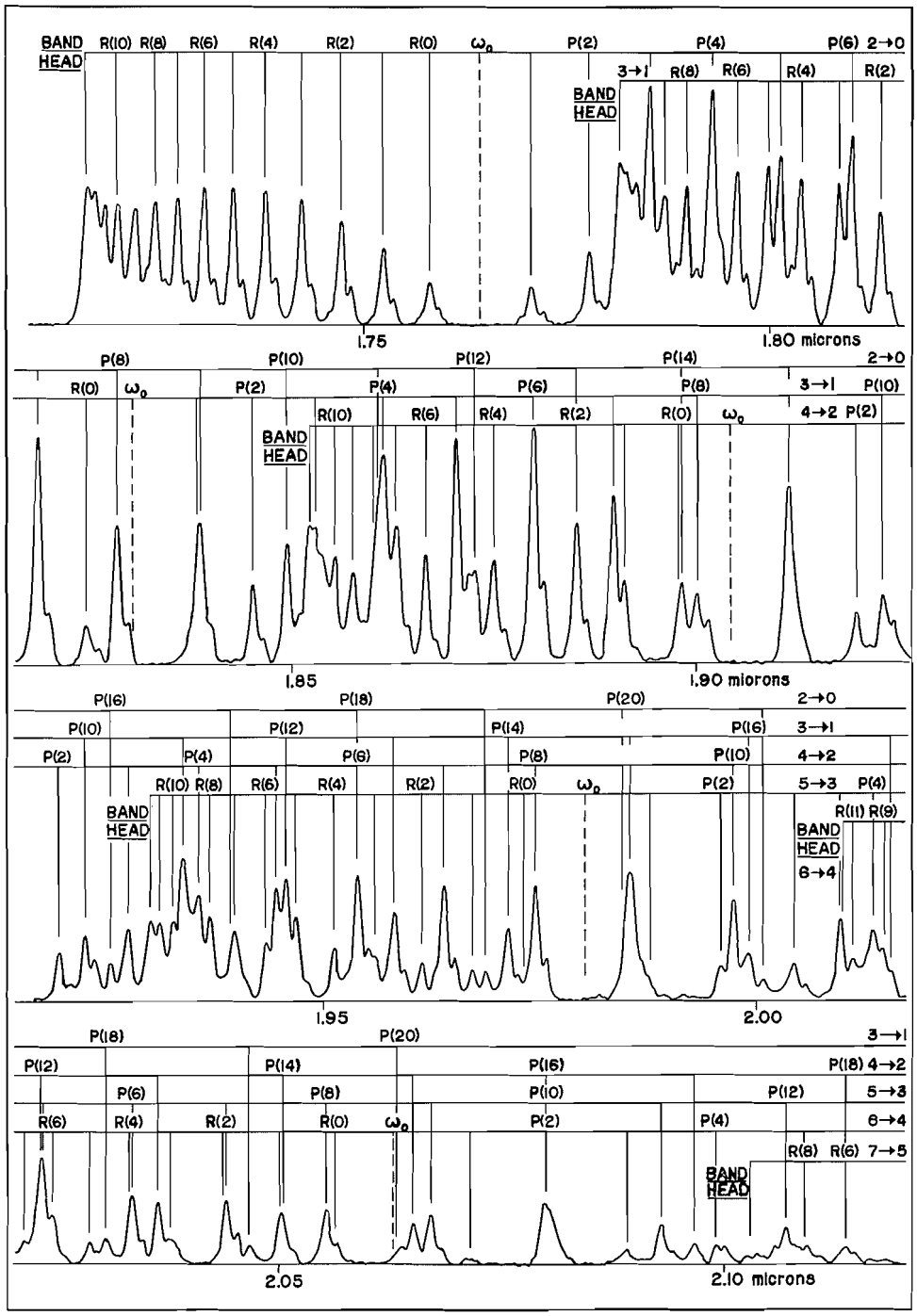

FIG. 3. First-overtone spectrum of HCl. Reagent inflows, 1380 μmoles/s of H_2 + H, 490 μmoles/s Cl_2. Total pressure 1.45 mm Hg. Contact time 0.0084 s. Grating 600 grooves/mm blazed at 1.6 μ, used in the first order. Grating monochromator slit width: 0.250 mm.

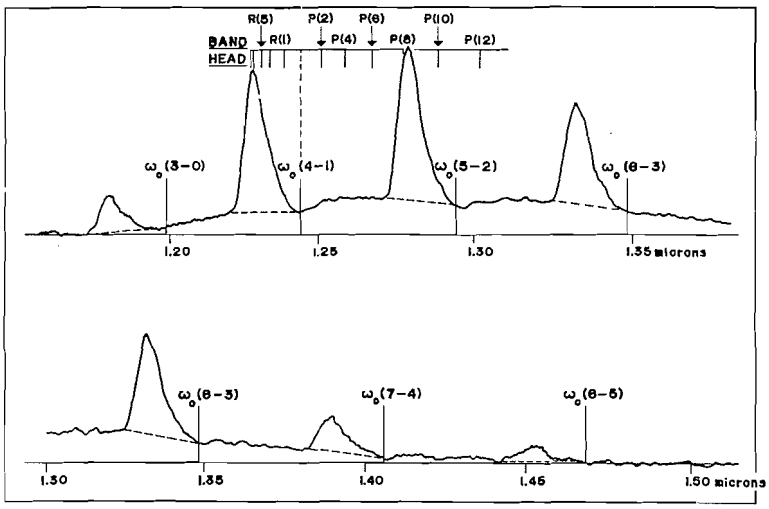

FIG. 4. Second-overtone spectrum of HCl. Reagent inflows, total pressure, and contact time as for Fig. 3. Grating as for Fig. 3, used in the first order. Grating monochromator slit width: 2.0 mm.

Figure 5 shows a plot of log $I_J/\omega_J{}^4 S_J F_J$ for levels $v = 1, 2, 3$, derived from the fundamental spectrum. The plots are linear over the greater part of their length, demonstrating that equilibrium exists within each vibrational state. The exceptions are the states of low J' in $v = 1$ and to a lesser extent $v = 2$, and a few states of very high J', $\geqslant 16$, in $v = 1$ and $v = 2$. The former anomaly will be shown in Part II to be apparent only,

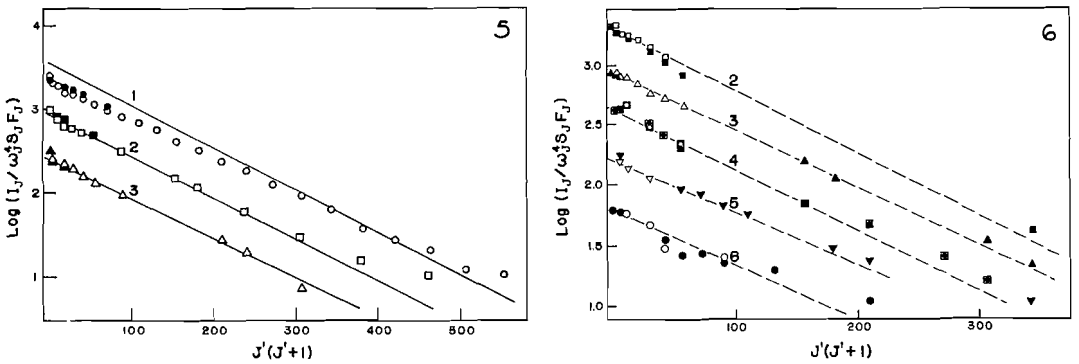

FIG. 5. Rotational distribution in $v = 1, 2, 3$, from the fundamental spectrum. Curve 1 refers to $v = 1$, for which T_{ROT} was *assumed* to be 1250 °K (see Part II); 2 refers to $v = 2$, for which $T_{ROT} = 1270$ °K; 3 refers to $v = 3$ for which $T_{ROT} = 1310$ °K. ● calculated from *P*-branch, ○ from *R*-branch lines.

FIG. 6. Rotational distribution in $v = 2, 3 \ldots 6$, from the first-overtone spectrum. The numbers above the curves give the vibrational quantum number of the level. $T_{ROT} = 1250 \pm 50$ °K for all levels.

being due to self-absorption of the $v(1–0)$ and $v(2–1)$ emissions. This apparent deviation from Boltzmann distribution will be shown to provide a useful clue to the relative and absolute pressures of HCl in the various rotational states of $v = 0$. The deviation among high J' will be discussed later in this section.

The rotational temperatures in $v = 2$ and 3 are the same, 1290 ± 20 °K, within experimental error.

Can. J. Chem. Downloaded from www.nrcresearchpress.com by 210.87.254.42 on 09/05/12
For personal use only.

Figure 6 shows rotational plots for the best lines (those not subject to appreciable overlap) in the $v(2–0)$, $v(3–1)\ldots v(6–4)$ bands. Once again, within experimental error there appears to be a Boltzmann rotational distribution within each vibrational state. The rotational temperature is roughly the same in all vibrational states: the dashed lines in the figure have slopes 1250 ± 50 °K.

The constancy of rotational temperature, 1300 ± 100 °K, in all vibrational states $v = 2$ to 6 (with 2 independent estimates for $v = 2$ and 3) can most easily be explained on the hypothesis that the rotators are in equilibrium with a translational heat bath at this temperature. (In Part II it will be shown that $v = 0$ is at a similar elevated rotational temperature.) Since the walls of the vessel are at about 400 °K (estimated from thermocouple measurement of the temperature of the outside surface) this implies the presence of a rotational temperature gradient across the vessel, and also indicates that the HCl has about 2 kcal/mole of rotational energy in excess of the thermal energy available at the wall.

Using a restricted cone-of-acceptance for the spectrometer, experiments were made in which only the R-branch of $v(2–0)$ was recorded, at various points in the reaction vessel. Spectra taken at either side of the vessel close to the wall gave a rotational temperature of about 600 °K. Spectra taken at the top and bottom of the vessel, though differing in intensity by a factor of $10\times$, gave roughly the same rotational temperature at normal H-atom concentration, ca. 1300 °K. It would appear that we are dealing here with rapid streaming flow from top to bottom of the vessel, combined with slower, perhaps diffusive, lateral flow to either side of the normal optical axis. The rapid top-to-bottom flow extended, in depth, along the major part of this optical axis, since the exit pipe, where it met the reaction vessel, encompassed more than half the length of the vessel. (Except for this, Figs. 5 and 6 would show curved rotational plots.)

It appears very probable that this rotational temperature is indicative of a similar translational temperature. Only on this assumption can we plausibly explain the observation of rotational Boltzmann distributions in all vibrational levels. It would be possible for HCl to be formed by the reaction in high states of rotation (9), but, except by far-fetched coincidence, this could not give rise directly to a Boltzmann distribution. If we suppose that rotational excitation is still present in excess of translational, it becomes necessary also to suppose that the non-Boltzmann rotational distributions in each vibrational level relaxed to Boltzmann distributions before losing their excess rotational energy to translation (presumed, for the sake of this argument, to be at 400 °K). It is quite contrary to what we know about energy transfer that (non-resonant) transfer in a quantized degree of freedom (rotation) should be faster than transfer into an unquantized degree of freedom (translation) (7). Moreover, it is hardly to be expected that this type of relaxation would lead by chance to the same rotational temperature in all levels $v = 1$ to 6.

We conclude that the rotational temperature of the excited HCl reflects the rotational and the translational temperature of all the gases in the central part of the reaction vessel. From the fact that the reaction, as evidenced by the emission, is almost complete by the time the vessel has been traversed, and yet the rotational temperature is maintained, we conclude that the loss of heat to the wall is slow. The following rough calculation confirms this.

For simplicity we shall assume a linear temperature gradient of 1000° from the faces of a 1 cm cube at the center of the cell, to the wall. The thermal conductivity of HCl is 3×10^{-5} cal/s deg cm (8), and it follows that 0.09 cal/s will flow from the cube for a 500°/cm gradient at its walls. If we assume, for this order-of-magnitude calculation, that

Can. J. Chem. Downloaded from www.nrcresearchpress.com by 210.87.254.42 on 09/05/12
For personal use only.

the entire heat of reaction is available for conduction to the wall and that all 450 μmoles of chlorine entering the reaction vessel per second is converted to HCl (see above) then we have 20 cal/s liberated in the reaction vessel. Reaction takes place more rapidly in a central core of the vessel; we shall suppose that the reaction is completed in 100 cc, one-half the volume of the vessel. Thus the heat liberated is 0.2 cal/s cc. This agrees within a factor of about 2× with the heat loss that must be offset in order to maintain temperatures in the 1000 to 2000° range. (Better agreement than this would be fortuitous, considering the crudity of the model.)

From Figs. 5 and 6, it can be seen that there is some evidence of rotators in excess of the Boltzmann proportion in high rotational states, $J' \geqslant$ ca. 17. In experiments at $10^{-2}\times$ these pressures (2), a similar anomaly was observed for $J' = 9$–18. (Very high rotational levels, $J' > 18$, lay below the limit of detection.) This could reflect a large excess of rotational energy, produced by the reaction $H + Cl_2 \rightarrow HCl + Cl$. Owing to the low moment of inertia of HCl, conservation of angular momentum would not be violated by the presence of large amounts of rotational energy in HCl (9). In the low-pressure experiments with lower collision frequency, some of this rotational excess may survive collisional deactivation even in levels with J' as low as 9. In the present high-pressure experiments the excess in these lower levels has presumably been erased by rotational–translational transfer, and only the residue of an excess in $J' \geqslant 17$ remains. Two reasons might be advanced to explain the greater persistence of the excess in very high J' levels; either the original excess is greater in these levels, or deactivation of the highly rotating molecules is more difficult, owing to wide spacing of the quantum levels.

However, the persistence of even the smallest degree of rotational disequilibrium, under conditions where an emitter suffers an average of 10^5 collisions in the course of a radiative lifetime, is sufficiently unexpected (7) to throw doubt on the reality of the observation. Futher experiments are required before the possibility of a systematic error can be discounted.

2. Vibrational Distribution

For the special case of a molecule having $\theta \approx 1$ ($\theta = M_0/M_1 r_e$, where M_0 and M_1 are the first two coefficients in the Taylor series expansion of the dipole moment) equation [3] reduced to (6)

$$[7] \qquad I_v^{v'} = \frac{64\pi^4 c N_{v'}}{3} \cdot [(\omega_0)_v^{v'}]^4 \cdot |R_v^{v'}|^2.$$

That is to say, the total intensity of a band bears the same relationship to the total number of molecules in the vibrational upper state, whatever the rotational distribution in that upper state. By making the substitution

$$[8] \qquad A_v^{v'} = \frac{64\pi^4[(\omega_0)_v^{v'}]^3}{3h} |R_v^{v'}|^2$$

equation [7] can be abbreviated and rearranged to

$$[9] \qquad N_{v'} = \frac{I_v^{v'}}{hc(\omega_0)_v^{v'} A_v^{v'}}.$$

The Einstein transition probability for HCl, $A_v^{v'}$, has been calculated on the basis of Morse-oscillator eigenfunctions and linear dependence of the dipole moment on internuclear separation and is available in the literature (10).

Can. J. Chem. Downloaded from www.nrcresearchpress.com by 210.87.254.42 on 09/05/12
For personal use only.

Can. J. Chem. Downloaded from www.nrcresearchpress.com by 210.87.254.42 on 09/05/12
For personal use only.

For the fundamental region of the spectrum, Figs. 2 and 5, $I_v^{v'}$ was calculated only for the R-branches of $v(1–0)$, $v(2–1)$, and $v(3–2)$, by summing line intensities. On the basis of the considerations presented in the preceding sections, the rotational temperature was assumed to be the same in all these levels, and hence $(I_v^{v'})_R$ represented the same fraction of the total $I_v^{v'}$, in each case, to within experimental accuracy. Relative $N_{v'}$ were therefore calculated from relative $(I_v^{v'})_R$. These are shown in Table I. $(I_0^1)_R$ and $(I_1^2)_R$ were corrected

TABLE I

Relative stationary-state populations in vibrational levels v', derived from fundamental (corrected for self-absorption), first-overtone, and second-overtone spectra; $\Delta v = 1, 2, 3$

		$N_2/N_{v'}$		$N_3/N_{v'}$	
v'	$N_1/N_{v'}$, $\Delta v = 1$	$\Delta v = 1$	$\Delta v = 2$	$\Delta v = 2$	$\Delta v = 3$
1	1				
2	4.85	1	1		
3	12.9	2.66	2.52	1	1
4			6.99	2.78	2.71
5			19.4	7.70	8.35
6			64.0	25.4	24.3
7			290	115	119
8					475

for self-absorption by the methods described in Part II. As a check on [9], $N_{v'J'}$, calculated individually from $I_{vJ}^{v'J'}$ and [3], were summed to give $N_{v'}$. The result agreed to within 1% with that obtained from [9].

In calculating relative stationary-state concentrations in vibrational levels $v = 2$ to 7 inclusive from the first-overtone data of Figs. 3 and 6, sufficient lines were available in both R- and P-branches so that it was unnecessary to resort to the device of comparing $(I_v^{v'})_R$ only. The few non-overlapped lines in $v(7–5)$, not plotted in Fig. 6, indicated $T_{\text{ROT}} = 1200$ °K; the remainder of the $v(7–5)$ lines were interpolated assuming a rotational Boltzmann distribution at this temperature. Populations relative to $N_{v=2}$, and also relative to $N_{v=3}$ for comparison with the second overtone, are listed in Table I.

Relative stationary-state concentrations $N_3/N_{v'}$ for $v' = 3–8$ were calculated from the second overtone, Fig. 4, and are listed in Table I. The procedure in this calculation was to measure the apparent $(I_v^{v'})_R$, correct for the contribution from $(I_v^{v'})_P$ of the next lower band, and then apply [9] to the R-branches only, as for the fundamental.

Examination of Table I shows five ratios of $N_{v'}$, each of which has been obtained from two different bands with different spectrometer transmissivity corrections, different corrections for overlapping lines, different $A_v^{v'}$, etc. The deviations appear to be random; they have a maximum value of 8%.

If the distribution of HCl among vibrational levels were of the Boltzmann type, then

$$[10] \qquad \frac{N_1}{N_{v'}} = \exp\left[-(G_0(1) - G_0(v'))hc/kT\right]$$

$$[11] \qquad \log\frac{N_1}{N_{v'}} = \frac{0.625}{T}\left[G_0(v') - G_0(1)\right]$$

where $G_0(v)$ is the term value, the vibrational energy in units of cm^{-1}. The factor $0.625 = hc/2.303\ k$. Figure 8 shows a plot of $\log N_1/N_{v'}$ versus $G_0(v') - G_0(1)$. Points indicated by open circles refer to an experiment made some months later than that recorded in

Table I. The experimental conditions were similar (rotational temperature was, however, 100° lower: 1200 °K) and are referred to as 'normal' conditions, to distinguish these experiments from others made at very low or high percentage dissociation of H_2 or with added HCl, unusual alignment of the spectrometer, etc.

The 'normal' curve of Fig. 8 was chosen for graphical presentation since it was recorded immediately before the second (added-HCl) curve in the figure. It showed the same main features as the data of Table I (with the exception of a slight upward displacement of N_1/N_2 in the Table I data, which will be discussed in Section 4). The distribution, though much closer to a Boltzmann distribution than in Charters and Polanyi's (2) experiments at 10^{-2} mm pressure, was nevertheless non-Boltzmann, decreasing in vibrational 'temperature' from about 4000 to 3000 °K; this curvature was particularly noticeable starting at about $v = 6$. In the 10^{-2} mm low-pressure experiments the curvature of the Boltzmann plot was in the same sense, but much more extreme; the vibrational temperature, initially 8000 °K, had fallen to 2930 °K by $v = 5$.

A second striking feature of the 'normal' vibrational distribution in these experiments was the presence of detectable concentrations of emitters in levels 7 and 8. Stationary-state concentrations in these levels must have been at least 10× greater here than in Charters and Polanyi's low-pressure experiments.

Levels with $v > 6$ cannot be populated by the reaction $H + Cl_2 \rightarrow HCl + Cl$, which yields 45 kcal/mole exothermicity plus 2.5 kcal activation energy. The most probable explanation of the presence of these vibrators in $v > 6$ is that vibrational–vibrational transfer among HCl molecules, which is of negligible significance when HCl is present at $\leqslant 10^{-2}\times$ the concentration, is promoting HCl from the lower vibrational levels in which it is originally formed to higher levels. Vibrational–vibrational exchange would ultimately randomize the energy in the vibrational degree of freedom producing a Boltzmann distribution characterized by a unique vibrational temperature (not necessarily the same temperature as the translational–rotational temperature). Vibrational–vibrational transfer would account not only for the presence of vibrators in $v = 7$ and 8, but also for the fact that the distribution in levels $v \leqslant 5$ is close to a Boltzmann distribution. Two factors favor vibrational–vibrational exchange in the present work as against that of Charters and Polanyi: increased pressure of vibrationally–excited HCl and increased ambient temperature.

An alternative mechanism for the population of $v = 7$ and 8 which should be considered is 'collisional transfer', that is to say translational-to-vibrational transfer. At 1300 °K, however, collisional excitation from $v = 6$ could only produce a stationary-state concentration in $v = 8$ with less than 0.7% of the population of $v = 6$. (The energy jump is 12.7 kcal, and the rate of removal from $v = 8$ is greater than from $v = 6$.) The observed fraction (Table I) was 8× as great as this upper limit. The same argument appears to rule out the possibility that $v = 8$ might be populated directly by a high-temperature reaction between $H + Cl_2$, for which the minimum activation energy would be 12.7 kcal. In addition it would be expected that the 'intrinsic' efficiency of transfer into $v = 8$ would be less than that into $v = 6$, in the same way as that into $v = 6$ is less than that into $v < 6$ (2), further decreasing the yield in $v = 8$ by this chemical route.

Two further mechanisms which, at the increased stationary-state pressures of H and Cl, might possibly also produce highly vibrating HCl ($v = 7$ and 8) are

$$H + Cl + M \rightarrow HCl\dagger + M, \qquad [12]$$

atomic combination in the gas, where M is some gaseous third body, or

Can. J. Chem. Downloaded from www.nrcresearchpress.com by 210.87.254.42 on 09/05/12
For personal use only.

Can. J. Chem. Downloaded from www.nrcresearchpress.com by 210.87.254.42 on 09/05/12
For personal use only.

[13] $$H + Cl + W \rightarrow HCl\dagger + W,$$

where W is the wall and HCl† is desorbed into the gas, as a vibrationally-excited species. However, if these were the principal sources of $HCl\dagger_{v=7,8}$, there would be no reason why N_7 and N_8 should always fall on a smooth continuation of the curve (Table I, Fig. 7, and Fig. 8) which passes through N_4, N_5, and N_6. If, however, the body of vibrators are approaching a Boltzmann distribution, some dependence of N_7 and N_8 on $N_{\leqslant 6}$ would be expected. It would, moreover, be predicted that at lower concentrations of $HCl\dagger_{v\leqslant 6}$ the proportion of $HCl\dagger_{v=7,8}$ would decrease. Two methods have been used to decrease $HCl\dagger_{v\leqslant 6}$ (i.e. to decrease the emission intensity, which is directly linked to the stationary-state concentrations of emitters through eq. [3] or [9]); one method is to decrease the percentage dissociation of H_2 (Section 3 below), the other is to add $HCl_{v=0}$ (Section 4). Both these alterations do have the effect of sharply decreasing the proportion of vibrators in $v = 7$ and 8 and, at the same time, increase the degree of disequilibrium among vibrators in the lower states.

The most probable mechanism for the production of $HCl\dagger_{v=7}$ by vibrational–vibrational exchange, both on concentration grounds and on the grounds that the change in vibrational quantum number is a minimum, is

[14] $$HCl\dagger_{v=1} + HCl\dagger_{v=6} \rightarrow HCl\dagger_{v=7} + HCl_{v=0}.$$

This reaction is exothermic by 1.78 kcal. The average number of collisions that $HCl\dagger_{v=6}$ suffers with an $HCl\dagger_{v=1}$ (total pressure in all rotational states, 0.06 mm Hg; see Part II) in the course of transit through the vessel is $\sim 5 \times 10^3$. We conclude that $\sim 5 \times 10^3$ collisions $HCl\dagger_{v=1} + HCl\dagger_{v=6}$ are capable of producing a detectable concentration of $HCl\dagger_{v=7}$. It would be much more valuable to have a figure for the collision efficiency of this process. In the following paragraphs the stationary-state equations which govern the (known) concentration of $HCl\dagger_{v=7}$ will be set up and solved for the rate constant and hence collision efficiency of the transfer process [14].

The general stationary-state equation governing N_v in this system can be written

[15] $$R_v + \sum_{uw} k_{uw}{}^t N_u N_w + \sum_{uu} k_{uu}{}^t N_u{}^2 + \sum_w A_v{}^w N_w + Z \sum_w P_{wv} N_w = [\sum_u k_{vu}{}^t N_u + \sum_w k_{vw}{}^t N_w + k_{vv}{}^t N_v + \sum_u A_u{}^v + Z \sum_u P_{vu} + \tau^{-1}] N_v$$

where $u < v < w$, k is a rate constant, P is probability of deactivation per collision, Z is the collision frequency, and τ is the mean contact time in the vessel. Terms on the left-hand side of [15] give rates of processes forming vibrators in v, while terms on the right-hand side give rates of processes removing vibrators from v. Those on the left, taken in sequence, give rate of chemical reaction directly into v; rates of the vibrational transfer processes $HCl_u + HCl_w \rightarrow HCl_v$ and transfer processes $2HCl_u \rightarrow HCl_{u+1} + HCl_{u-1}$; rates of radiation from all higher levels into v; and rates of collisional transfer from all higher levels into v. Terms on the right give rates of three categories of transfer process out of level v; rates of radiative and collisional transfer out of v; and rate of removal from the reaction vessel by pumping. Wall deactivation can probably be neglected in view of the slow rate of transfer to the wall. (Evidence has already been presented for a reactive 'core' of gas.)

In applying [15] to $v = 7$ we can write $R_7 = 0$. In the light of evidence to be presented in the following section, we shall neglect collisional transfer into and out of v. We shall

make two assumptions: (a) only transfer process [14] is important, since it is favored both by relatively high concentration in $v = 1$ and also by the fact that Δv is a minimum; (b) rates of processes terminating in, or originating from, $v \geqslant 9$ can be ignored. This assumption is acceptable in accounting for $N_{v=7}$ since $A_7^9 < A_7^8$ and $N_9 < N_8$. It will, however, introduce some error into $k_{17}{}^t$ (eq. 17). Fortunately $k_{17}{}^t$ only figures as a correction to $k_{16}{}^t$. From [17], $k_{17}{}^t$ is 2.5×10^{10} cc/mole s. If this is out by a factor of 2, then $k_{16}{}^t$ (eq. 16) is altered by 25%.

The stationary-state equations employed for $v = 7$ and 8 were,

$$[16] \qquad k_{16}{}^t N_1 N_6 + A_{87} N_8 = k_{17}{}^t N_1 N_7 + [\sum_u A_{7u} + \tau^{-1}] N_7$$

$$[17] \qquad k_{17}{}^t N_1 N_7 = [\sum_u A_{8u} + \tau^{-1}] N_8.$$

Using absolute values for N_1, N_6, N_7, and N_8 based on $N_1 = 0.06$ mm Hg, obtained in Part II, we calculated $k_{16}{}^t = 3.4 \times 10^{10}$ cc/mole s. The probability for vibrational transfer per collision is then

$$P_{uw}{}^t = k_{uw}{}^t / Z_{A,B},$$

where $Z_{A,B}$ is the bimolecular collision rate under the standard conditions of 1 mole/cc concentration. For $\sigma_{A,B}$ (mean collision diameter) = 3 Å, $T = 1300$ °K, $Z_{A,B} = 2 \times 10^{14}$ cc/mole s. It follows that $P_{16}{}^t = 1.7 \times 10^{-4}$. The collision efficiency, the average number of collisions per transfer, is therefore $Z_{1,6}{}^t = 5.9 \times 10^3$. Inclusion of collisional deactivation terms (vibration → translation in the collision partner) in [16] and [17], using an experimental upper limit for the deactivation probability (2), decreases $Z_{1,6}{}^t$ by a factor of about 2.5.

$Z_{1,6}{}^t \approx 6 \times 10^3$ obtained here may be compared with the value of 2.5×10^3 yielded by the theory of Schwartz, Slawsky, and Herzfeld (11, 7) for this energy discrepancy ($\Delta\nu = 1.78$ kcal or 620 cm^{-1} and temperature 1300 °K). The depth of the Lennard–Jones minimum in this calculation was, $\epsilon/k = 360$ °K (14). The orientation parameter, Z^0, was taken as 9, in conformity with Callear (11). The force constant in the exponential repulsion was $l = 0.2$ Å (11).

It is instructive to compare $Z_{1,6}{}^t$ calculated for two HCl molecules, with Z^t calculated by Callear for energy transfer between molecules BC, with atomic weights $M_B = M_C = 15$, $\epsilon/k = 90$ °K (14). For $\Delta\nu = 620$ cm^{-1}, Callear, using the Schwartz–Slawsky–Herzfeld (S.S.H.) theory, obtains $Z^t \approx 2 \times 10^6$, at $T = 300$ °K. $Z_{1,6}{}^t$ for transfer between HCl molecules calculated for this same temperature is 1.1×10^5: an order-of-magnitude fewer collisions are required for HCl–HCl vibrational transfer than for BC–BC transfer, despite the fact that the energy discrepancy is the same as in the HCl–HCl case. This apparent anomaly arises from a term $(M_B M_C / M_B{}^2 + M_C{}^2)^2$ in the S.S.H. equation for Z^t; a term which is small for $M_B \ll M_C$.

3. Variation in H-Atom Concentration

The method of measuring H-atom concentration, in the absence of chlorine, has already been described.

The experiments discussed in the two previous sections were performed at a setting of the discharge-tube primary voltage that resulted in approximately 8% dissociation of H_2, in the absence of chlorine. Spectra were also recorded at a number of H-atom concentrations equivalent to 3–17% dissociation of the incoming H_2. The effects of this

Can. J. Chem. Downloaded from www.nrcresearchpress.com by 210.87.254.42 on 09/05/12
For personal use only.

Can. J. Chem. Downloaded from www.nrcresearchpress.com by 210.87.254.42 on 09/05/12
For personal use only.

sixfold variation in percentage dissociation on total intensity, rotational temperature, and vibrational distribution were explored.

Total intensity from, and hence stationary-state population in, levels $v = 2$–6 rose to a maximum as the percentage dissociation of H_2 increased from 3 to 8%, then fell as the dissociation was further increased from 8 to 17%. These observations were made with the normal spectrometer alignment, viewing a cone in the center of the vessel. When a similar series of experiments were conducted viewing a narrower region close to the top of the vessel, the emission intensity from these same levels rose continuously as the percentage dissociation was increased from 3 to 17%. It appears that the decrease in intensity observed at the center of the vessel at the highest H-atom concentrations was merely due to an upward shift of the main reaction zone. This is in accord with the postulate of streaming flow through the vessel, with a vertical time axis.

Traces were made of the R-branch of $v(2–0)$ with normal optical alignment, over the whole range of H-atom concentrations. Rotational analysis yielded linear Boltzmann plots, with rotational temperatures rising from 590 to 2100 °K as the H-atom concentration was increased. It has already been noted that there existed a rotational-temperature gradient perpendicular to the flow axis. This gradient became steeper at higher H-atom concentrations. Apparently a greater proportion of the reaction was occurring away from the vessel walls.

The effect on vibrational distribution of reduced H-atom concentration, reduced emission intensity, and hence reduced HCl† stationary-state concentration was investigated since it was hoped by this means to decrease the effects of vibrational–vibrational transfer. The intention was to approach the conditions of the low-pressure experiments of Charters and Polanyi, with the single important difference that the low pressure of vibrators would, in the present case, be bathed in a 'high' pressure of gas (~1 mm as against $\sim 10^{-2}$ mm).

To save time in analysis, only second-overtone spectra were recorded over the full range of H-atom concentration. Figure 7 shows the results at the three lowest H-atom

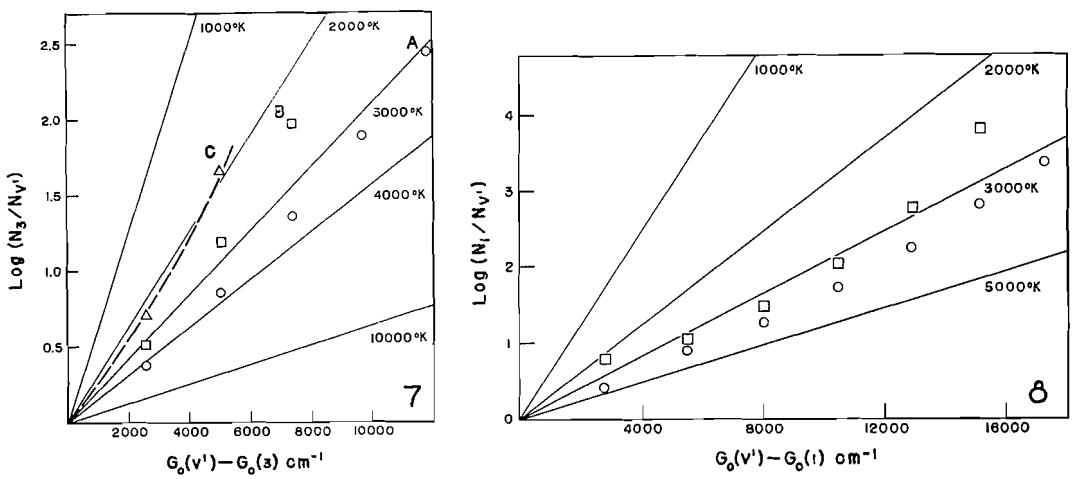

FIG. 7. Vibrational distribution in levels $v = 3, 4\ldots$: A with normal, B with 3/4 normal, and C with 1/2 normal percentage dissociation. Inflows, 1450 μmoles/s of H_2 + H, 520 μmoles/s of Cl_2. The broken curve is taken from the results of Charters and Polanyi (2) at $10^{-2}\times$ this total pressure.

FIG. 8. Vibrational distribution in levels $v = 1, 2\ldots 8$: ○ under normal experimental conditions; □ with added HCl.

concentrations used. The stationary-state distribution for the lowest H-atom concentration is very similar to that obtained in Charters and Polanyi's experiments (2).

The factors governing relative vibrational stationary-state concentrations in Charters and Polanyi's experiments were adjudged to be the rates of chemical reaction into each vibrational level, the rates of radiation into and out of each level, and the rate of removal from the vessel by pumping. These factors were almost the same in the present work (the only difference was a factor of about 2× in residence time in the vessel). Gas-phase collisional deactivation was believed to be unimportant in Charters and Polanyi's experiments, at $\sim 10^{-2}$ mm pressure. Since the low-concentration vibrational distribution in this work, curve C, agrees with Charters and Polanyi's, it would appear that collisional deactivation of the HCl vibrators is not of major importance even at ~1 mm pressure. At this total pressure the average number of collisions per vibrational radiative lifetime was $\sim 10^5$. The ambient temperature, curve C, was roughly 600 °K. A shock-tube study of pure HCl has yielded $Z_{10} \approx 1 \times 10^6$ for vibrational relaxation at this temperature (15).

4. Addition of $HCl_{v=0}$

Two fundamental spectra, $v' = 1, 2, 3$, and two second-overtone spectra, $v' = 3, 4 \ldots 8$, were recorded successively under normal conditions of hydrogen and chlorine flow (approximately 1100 μmoles/s and 450 μmoles/s respectively). In the second of the pair of experiments HCl was introduced, through the second-reagent inlet, at a flow of 600 μmoles/s.

Analysis showed that in the 'normal' spectrum the rotational temperature was ca. 1200 °K in $v = 1$, 2, and 3. (The second overtone could not be sufficiently well resolved to yield rotational temperatures). In the spectrum with added HCl the rotational temperature had dropped to 700–750 °K. This was probably due in part to a decrease in energy release per unit volume, caused by increased likelihood for the thermoneutral reaction

$$H + HCl \rightarrow H_2 + Cl$$

to carry the chain in place of the exothermic

$$H + Cl_2 \rightarrow HCl + Cl$$

reaction. In part it was due simply to the loss of rotational and translational energy from the products of reaction 1 to the room temperature HCl.

If the amount of reaction $H + Cl_2$ in the cone-of-sight decreases, a general decrease in emission intensity from all vibrationally excited states would be expected. Since some of the population observed under normal conditions in the higher vibrational levels appears to be due not to direct reaction into these levels but to vibrational–vibrational transfer, a more marked decrease in intensity and in N_v would be expected from successively higher vibrational levels.

The observed ratios of N_v' recorded in the presence of added HCl, to N_v without added HCl (both corrected for self-absorption, see Part II) were: for $v = 1$, 0.96; $v = 2$, 0.40; $v = 3$, 0.69; $v = 4$, 0.57; $v = 5$, 0.47; $v = 6$, 0.29; $v = 7$, 0.10; $v = 8$ was only detectable in the absence of added HCl. The figures conformed to the expected pattern, with the exception of $v = 2$ and $v = 1$; the decrease in population of $v = 2$ was anomolously large, *greater* than that in the next higher levels, and the decrease in population in $v = 1$ anomolously small. This anomaly can be seen clearly in Fig. 8, which shows a Boltzmann plot of vibrational populations under standard conditions, with added HCl (corrected for self-absorption). The higher vibrational states lie in an upward curve, similar to that

Can. J. Chem. Downloaded from www.nrcresearchpress.com by 210.87.254.42 on 09/05/12
For personal use only.

observed when HCl† concentration is reduced by a small decrease in H-atom concentration. However, N_1'/N_2' is anomolously high[2] in the presence of added $HCl_{v=0}$.

The anomaly provides evidence for a vibrational energy transfer process (12)

[18] $$HCl_{v=0} + HCl_{v=2} \rightarrow 2HCl_{v=1} \qquad -0.3 \text{ kcal/mole}$$

which must proceed more rapidly than the competing vibrational energy transfer processes which involve collisions $HCl_{v=0} + HCl_{v>2}$, for which the energy match is less good. An energy transfer of this type has been postulated in connection with the relaxation of vibrationally excited NO following flash photolysis (13).

5. Energy Distribution Among $H + Cl_2$ Reaction Products

It has been shown in Section 1 of this Discussion that the rotational temperature of the HCl must reflect the translational and rotational temperature of the gas present in the reaction vessel. The maximum rotational temperature recorded, at maximum H-atom concentration, Section 3, was 2100 °K. Under normal conditions $\geqslant 90\%$ of chlorine inflow was converted to HCl; we shall suppose that 100% of the chlorine inflow was converted to HCl under conditions of maximum H-atom concentration. (This supposition received qualitative confirmation from the marked falloff in intensity from the mixing point at the top of the vessel down the flow-axis). The molar inflow rate of hydrogen in this experiment was 900 μmoles/s, that of chlorine 450 μmoles/s; this would form 450 μmoles/s of HCl by way of reaction [1] of the chain, 450 μmoles/s of HCl by way of reaction [2]. 450 μmoles of hydrogen would remain unreacted every second. Thus in the formation of each mole of HCl by reaction [1] we must 'heat up' rotationally and translationally 2 moles of HCl and 1 mole of H_2. The energy required is

$$\Delta H = C_p \Delta T = 7/2\, R\Delta T, \qquad \text{where } \Delta T = 1800 \text{ °K};$$

Therefore $\Delta H = 12.5$ kcal/mole of mixture. If the reaction $H + Cl_2$, which produces only 0.33 of the mixture $2HCl + H_2$, is to cause this amount of heating, it must produce 38 kcal/mole of HCl formed in reaction 1. In addition it must supply 1 kcal to offset the endothermicity of [2], bringing the requirement to roughly 39 kcal/mole of HCl from [1]. (We can neglect the 0.22 kcal which we calculate leaves the system by radiation, for each mole of HCl formed in [1]). This figure is to be compared with $-\Delta H$ for reaction [1], which is 45 kcal/mole.

This crude calculation indicates that the major part of the heat liberated by the reaction [1] is present as translation and rotation in our reaction vessel. In Section 3 evidence was presented which indicated that there is little collisional deactivation of vibrators in this system. If this is correct, it follows that the major part of the heat of reaction [1],

$$H + Cl_2 \rightarrow HCl + Cl,$$

is liberated *directly* as translation and rotation, not as vibration.[3]

[2] *A much smaller effect of qualitatively the same type (i.e. N_1/N_2 high) was discernible in some traces made under optimum conditions without added* HCl. *A graphical record of the data in Table I would show the effect; the 'normal' trace of Fig. 8 does not. Whether or not this small effect is detectable will depend on the ambient temperature and the relative population in $v = 0$; $N_{v=0}$ is variable independently of $N_{v>0}$ since $N_{v=0}$ is populated in part by a different reaction, the reaction* $Cl + H_2$ *that governs chain length.*

[3] *It is instructive to consider the implications of the opposite model, in which the major part of Q would go initially into vibration, forming* $HCl_{v=6}$. *Under normal flow conditions 10–20 cal/s must have entered the rotational plus translational degrees of freedom to maintain the observed temperature (see Section 1). On the model under consideration, this would require that* $\sim 2 \times 10^{20}$ *molecules of* $HCl\dagger_{v=6}$ *are transferred to $v = 0$ per second. Considering the observed stationary-state concentration of* $HCl\dagger_{v=6}$ *and the low total pressure, this transfer would only be possible if about 1 in 20 collisions were successful in deactivating $v = 6 \rightarrow v = 0$. This is roughly $10^5\times$ the efficiency to be expected on the basis of recent experimental evidence (15).*

Can. J. Chem. Downloaded from www.nrcresearchpress.com by 210.87.254.42 on 09/05/12
For personal use only.

This qualitative conclusion is of interest in view of the lack of information on this topic. Such information as exists (2) is concerned with the relative rate of reaction directly into the various accessible vibrationally-excited states of the product, without reference to the question of how the sum of these rates compares with the total rate. (The method described in Part II of this paper will, however, permit the rate into $v = 0$ to be measured in future.)

ACKNOWLEDGMENTS

The authors are grateful to the National Research Council of Canada, the Imperial Oil Co. of Canada, and the United States Air Force Cambridge Research Laboratories for financial assistance. One of them (J. C. P.) thanks the Alfred P. Sloan Foundation for the award of a Fellowship.

REFERENCES

1. J. K. CASHION and J. C. POLANYI. J. Chem. Phys. **29**, 455 (1958); Proc. Roy. Soc. London, Ser. A, **258**, 529 (1960).
2. P. E. CHARTERS and J. C. POLANYI. Discussions Faraday Soc. **33**, 107 (1962).
3. E. L. TOLLEFSON and D. J. LE ROY. J. Chem. Phys. **16**, 1057 (1948).
4. A. F. TROTMAN-DICKENSON. Gas kinetics. Butterworths, London. 1955.
5. R. HERMAN and R. F. WALLIS. J. Chem. Phys. **23**, 637 (1955).
6. J. K. CASHION and J. C. POLANYI. Proc. Roy. Soc. London, Ser. A, **258**, 564 (1960).
7. K. F. HERZFELD and T. A. LITOVITZ. Absorption and dispersion of ultrasonic waves. Academic Press, N.Y. 1959. T. L. COTTRELL and J. C. MCCOUBREY. Molecular energy transfer in gases. Butterworths, London. 1961.
8. A. F. FARKAS and H. W. MELVILLE. Experimental methods in gas reactions. MacMillan and Co., London. 1939.
9. J. C. POLANYI. Discussions Faraday Soc. **33**, 279 (1962).
10. F. D. FINDLAY and J. C. POLANYI. To be published.
11. R. N. SCHWARTZ, Z. I. SLAWSKY, and K. F. HERZFELD. J. Chem. Phys. **20**, 1591 (1952). A. B. CALLEAR. Discussions Faraday Soc. **33**, 28 (1962).
12. F. D. FINDLAY and J. C. POLANYI. Discussions Faraday Soc. **33**, 274 (1962).
13. R. G. W. NORRISH. Discussions Faraday Soc. **33**, 273 (1962).
14. J. O. HIRSCHFELDER, C. F. CURTISS, and R. B. BIRD. Molecular theory of gases and liquids. J. Wiley and Sons, New York. 1954.
15. P. BORRELL and D. F. HORNIG. Private communication.

Can. J. Chem. Downloaded from www.nrcresearchpress.com by 210.87.254.42 on 09/05/12
For personal use only.

Can. J. Chem. Downloaded from www.nrcresearchpress.com by 210.87.254.6 on 09/05/12
For personal use only.

THE HYDROGEN–CHLORINE SYSTEM IN THE MM PRESSURE RANGE

II. THE VIBRATIONAL GROUND STATE STUDIED BY SELF-ABSORPTION

J. R. Airey, F. D. Findlay,[1] and J. C. Polanyi
Department of Chemistry, University of Toronto, Toronto, Ontario

Received April 27, 1964

ABSTRACT

Studies of energy distribution among reaction products, through the agency of infrared chemiluminescence, have previously only yielded information concerning the distribution among vibrationally excited states. In the work described here it was shown that self-absorption of the infrared emission could be used as a measure both of the relative and the absolute amount of product present in the vibrational ground state, $v = 0$. Two independent methods were used to measure the extent of self-absorption. The first method relied on measurements of an apparent deviation from Boltzmann-type rotational intensity distribution within the $v(1–0)$ and $v(2–1)$ bands. The second method depended on measurements of an apparent deviation of the relative intensity of corresponding $H^{35}Cl$ and $H^{37}Cl$ isotopic lines from the natural abundance ratio. (It was shown, at the same time, that the isotopic reactions $H + {}^{35}Cl_2 \rightarrow H^{35}Cl + {}^{35}Cl$ and $H + {}^{37}Cl_2 \rightarrow H^{37}Cl + {}^{37}Cl$ have the same rate constant, within $\pm 10\%$). A third method of measuring the extent of self-absorption, which depends on the detection of an anomaly in the relative intensity of *P*- and *R*-branch emission lines is discussed.

The self-absorption method was applied to the study of the hydrogen–chlorine system in the 1–2 mm Hg pressure range (see also Part I). Mean partial pressures of $HCl_{v=0} \sim 10^{-2}$ mm Hg were measured in individual rotational states to an accuracy of ca. $\pm 10\%$, using an optical path length of 20 cm. The rotational distribution in $v = 0$ corresponded to a temperature of 1150 ± 150 °K (the uncertainty in this figure encompasses two independent methods of estimating the self-absorption), as compared with 1300 ± 100 °K for all vibrationally excited states (Part I).

INTRODUCTION

In the preceding paper (Part I) an account was given of an investigation of the infrared emission arising from the hydrogen–chlorine reaction at 1–2 mm Hg total pressure. This work formed part of a wider study, conducted in this laboratory, of the infrared emission from the same reaction at 10^{-1} and 10^{-2} mm pressures.

An obvious and serious limitation of these infrared emission studies is that they fail to give information concerning the vibrational state, $v = 0$. Infrared absorption measurements would, in principle, eliminate this difficulty. With one exception, however, infrared absorption is impractical as a means of detecting very low pressures of absorbing species. The exception is the case where a sharp infrared line source is available that matches the sharp line spectrum of the absorber; under these circumstances very low pressures can be detected in absorption.

This naturally suggests the possibility of using the emitting material itself as the infrared source, that is to say, of studying the self-absorption. In the work described here a simple model for the self-absorption in this system is proposed and tested. The technique is used to measure 10^{-2} mm pressure of HCl absorber in a 20 cm path length and is capable of detecting 10^{-3} mm pressure. With the increased path lengths used in other experiments currently under way, it will be possible to measure 10^{-4} mm, and detect 10^{-5} mm, pressures of absorbing material.

[1]*Present address: National Physical Laboratory, Teddington, Middlesex, England.*

Can. J. Chem. Downloaded from www.nrcresearchpress.com by 210.87.254.6 on 09/05/12
For personal use only.

THEORY

An exothermic gas-phase chain reaction giving rise to visible luminescence is commonly termed a flame. We are dealing in this work (1–2 mm reagent pressure) with a low-pressure flame which is evidenced exclusively by infrared luminescence.[2] In the interpretation of self-absorption in low-pressure flames it is commonly assumed that the 'excitation ratio', n_e/n_a, the ratio of the number of emitters to the number of absorbers in each elementary volume, is a constant throughout the volume under observation (1). The same assumption will be made here. This does not require that the emission intensity shall be constant throughout the region observed. It does require that the processes which affect the concentration of emitters and the processes which affect the concentration of absorbers shall be closely coupled.

In the present case emitters ($HCl_{v=1,2}$ are the emitters relevant to the self-absorption studies) are formed by a chemical reaction involving one set of reagents ($H + Cl_2$), whereas the absorbers are partly formed by this same reaction and partly by a reaction involving a different set of reagents ($Cl + H_2$). One of the latter reagents (Cl) is, moreover, formed only as a product of the first reaction. As long, therefore, as we are operating under conditions of combined streaming and diffusive flow, we must expect some degree of spatial separation between the regions of maximum rate for the two reactions, $H + Cl_2$ and $Cl + H_2$, with a consequent spatial variation in n_e/n_a.

We have nonetheless used the 'uniform excitation' model (constant excitation ratio) as a first approximation. The model gives reasonable figures for relative and absolute pressures of HCl in the rotational levels of $v = 0$. (For both of these quantities we have approximate values obtained by means independent of self-absorption.) This result is particularly gratifying since we are anxious to use the self-absorption technique in experiments at total pressure two orders of magnitude lower (with correspondingly increased optical path length) where the complications arising from chain reaction in conjunction with streaming and diffusive flow will be insignificant in comparison with the present work.

In addition to a spatial distribution for absorbers and emitters, the model must establish a functional dependence of the transition probability on the frequency, ω (cm^{-1}), to either side of the center, ω_0, of each line. There is little question that a Doppler line shape of half-width

$$\delta = [\ln 2(2\,kT\omega_0^2/m)]^{1/2} \qquad [1]$$

(m is the mass of the molecule) is appropriate to the temperatures and pressures encountered in the present work.

Cowan and Dieke (1) have calculated the fractional transmission for a source with uniform excitation and Doppler line shape, to be

$$\frac{I}{I_0} = \sum_{n=0}^{\infty} \frac{(-2p)^n}{(n+1)!(n+1)^{1/2}} \qquad [2]$$

Here n is an integer, and p is the 'absorption parameter' which brings together:

B, the absolute Einstein transition probability of absorption or stimulated emission for the line as a whole;

$P(\omega_0)$, the relative transition probability for absorption at ω_0 ($P(\omega)$ is normalized to unity, $\int P(\omega).\mathrm{d}\omega = 1$);

[2] *In very low-pressure studies, $\sim 10^{-2}$ mm total pressure (6) the luminescence can be characterized as 'chemiluminescence'. In the present work, as in conventional flame studies, physical processes (energy transfer) also contribute to the excitation, and hence to the subsequent luminescence.*

and $\bar{N}_a.x$, the total number of absorbers in the optical path, where $\bar{N}_a$ is the mean density of absorbers and $\bar{N}_e$ that of emitters along the optical path, and x is the optical path length.

[3] $$p = h\omega_0 P(\omega_0)(B_a\bar{N}_a - B_e\bar{N}_e)x.$$

Since the line shape is known, $P(\omega_0)$ in [3] can be expressed in terms of the half-width (1)

[4] $$P(\omega_0) = \left[\frac{\ln 2}{\pi\delta^2}\right]^{1/2}.$$

Introducing [1],

[5] $$P(\omega_0) = \frac{1}{\omega_0}\left[\frac{m}{2\pi kT}\right]^{1/2}.$$

Substituting into [3],

[6] $$p = h(B_a\bar{N}_a - B_e\bar{N}_e)\left[\frac{m}{2\pi kT}\right]^{1/2}x.$$

Introducing quantum numbers appropriate to the present case, and recognizing that $B_a/B_e = (2J' + 1)/(2J + 1)$,

[7] $$p_{vJ}^{v'J'} = h(B_{vJ}^{v'J'})_a(2J + 1)\left(\frac{\bar{N}_{vJ}}{2J + 1} - \frac{\bar{N}_{v'J'}}{2J' + 1}\right)x\left[\frac{m}{2\pi kT}\right]^{1/2}.$$

Since (3)

[8] $$\left(B_{vJ}^{v'J'}\right)_a = \frac{8\pi^3}{3h^2}\frac{|R_v^{v'}|^2.S_J.F_{vJ}^{v'J'}}{(2J + 1)},$$

therefore

[9] $$\frac{\bar{N}_{vJ}}{(2J + 1)} - \frac{\bar{N}_{v'J'}}{(2J' + 1)} = \frac{3hp_{vJ}^{v'J'}}{8\pi^3 x}\frac{1}{|R_v^{v'}|^2.S_J.F_{vJ}^{v'J'}}.\left[\frac{2\pi kT}{m}\right]^{1/2}.$$

To calculate $\bar{N}_{vJ} - \bar{N}_{v'J'}$ from the observed fractional transmission, I/I_0, the right-hand side of [2] was summed for trial values of p, the best value of p being chosen and inserted into [9]. A sum of the form required for [2] has been tabulated by Ladenburg and Levy (2).

RESULTS AND DISCUSSION

In all the experiments reported here, the apparatus and materials were identical to those described in Part I.

Three methods for the estimation of the fractional transmission, I/I_0, will be discussed. They are based on three types of abnormality which may appear in vibrational–rotational bands subjected to self-absorption.

1. Anomalous Rotational Distribution

In Part I there was noted an apparent deviation of the rotational distribution in the low rotational states of $v = 1$, from a Boltzmann-type distribution (see Fig. 5 of Part I, recorded under normal flow conditions). This deviation was of a sort that would imply an underpopulation of the low rotational states in $v = 1$. Significantly this apparent underpopulation of $v = 1$ was most marked for those transitions within the v(1–0) band, that

Can. J. Chem. Downloaded from www.nrcresearchpress.com by 210.87.254.6 on 09/05/12
For personal use only.

terminated in the most highly populated rotational levels of $v = 0$. It seemed probable that this anomaly could be accounted for by self-absorption.

Qualitative support for this view came from experiments in which these lines were traced with and without a plane mirror behind the reaction vessel: the gain in intensity which resulted from the presence of the mirror was found to be consistently less for the low rotational lines of $v(1–0)$ than for lines in $v(2–0)$. The $v(2–0)$ band did not show evidence of the low-J anomaly (see Fig. 6 in Part I). All these findings are consistent with the postulate of self-absorption in $v(1–0)$, no self-absorption in $v(2–0)$ (in this frequency range the intrinsic probability of first-overtone absorption, $v(2 \leftarrow 0)$ is two orders of magnitude less than for fundamental absorption, $v(1 \leftarrow 0)$).

Additional confirmation came from experiments with added HCl. Fig. 1 of this paper shows the apparent rotational distribution of HCl in level $v = 1$ when HCl is injected through the second-reagent inlet with a flow-rate comparable to that of $H_2 + H$ and of Cl_2 (see caption). The uncorrected $v = 1$ points show a systematic deviation from the linear plot characteristic of a Boltzmann distribution. No such deviation is detectable in the $v = 2$ and 3 points; the lines passing through these points have slopes corresponding to rotational temperatures of 700 °K and 750 °K. A line joining the points of highest J in $v = 1$ has a slope corresponding to 760 °K. The fact that this rotational temperature agrees quite well with the rotational temperatures from the higher vibrational states is an indication that this is the true slope of the $v = 1$ plot, since there is good reason to suppose that the rotational temperature in every vibrational state is the same (see Part I). The line passes through the points of high J since these spectral lines terminate in J levels of $v = 0$ with negligible population. On this view I/I_0 for the self-absorbed lines of $v = 1$, can be obtained from Fig. 1 by taking the difference in height between an 'unabsorbed' intensity (corresponding to a point on the line) and the self-absorbed value.

This has been done for the small anomaly in the $v = 1$ curve recorded under normal flow conditions, without added HCl (Fig. 5 of Part I), since these are the conditions of greatest interest. The best line of slope corresponding to 1300 °K (mean rotational

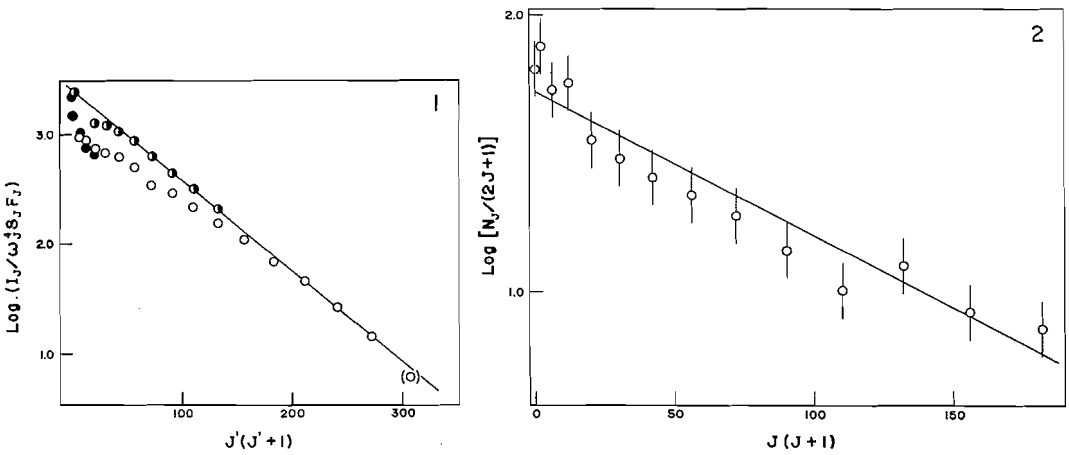

FIG. 1. Apparent rotational distribution of HCl among levels $v = 1$, taken from a fundamental spectrum with normal hydrogen and chlorine flows (1100 μmoles per sec and 450 μmoles per sec, respectively) with, in addition, 600 μmoles per sec of HCl entering through the second-reagent inlet. P-branch data, ●, R-branch data, ○, data corrected for self-absorption by the isotopic-ratio method, ◑.

FIG. 2. Rotational distribution in $v = 0$, calculated from the apparent deviation of the $v = 1$ rotational distribution from a Boltzmann curve. $T_{ROT} \approx 1300 \pm 100$ °K.

Can. J. Chem. Downloaded from www.nrcresearchpress.com by 210.87.254.6 on 09/05/12
For personal use only.

temperature in the higher vibrational states) was drawn through points of high J. The anomaly is detectable up to $J' = 14$ of the R-branch; that is to say, the self-absorption is appreciable up to $J = 13$. I/I_0 for each of these Js was converted into a value for N_J in $v = 0$. The anomaly in rotational distribution being very small, these $\bar{N}_J$ s are very approximate. However, they are sufficiently accurate to have some meaning, as evidenced by Fig. 2 of this paper, in which they are seen to conform to an approximately Boltzmann-like distribution for $v = 0$.

2. Anomalous Isotopic Ratios

The abundance ratio of $^{35}Cl_2$:$^{37}Cl_2$ in natural chlorine is 3.065:1. Provided that the H + Cl_2 reactions, which produces vibrationally-excited HCl, proceeds with the same rate whatever the isotope of chlorine, the relative stationary-state concentration of $H^{35}Cl$:$H^{37}Cl$ should also be 3.065:1. (Radiation, collisional deactivation, and flow are other processes which could in principle disturb this ratio of concentrations; in practice they are insufficiently selective to be significant here.) The expected intensity ratio I_{35}/I_{37} is very close to N_{35}/N_{37}, being given by

$$\frac{[I_{vJ}^{v'J'}]_{35}}{[I_{vJ}^{v'J'}]_{37}} = \frac{[N_{v'J'}\omega_{vJ}^{v'J'}|R_v^{v'}|^2 F_{vJ}^{v'J'}]_{35}}{[N_{v'J'}\omega_{vJ}^{v'J'}|R_v^{v'}|^2 F_{vJ}^{v'J'}]_{37}} \approx 1.004 \frac{[N_{v'J'}]_{35}}{[N_{v'J'}]_{37}}.$$

Twelve lines of the $v(2\text{–}0)$ and $v(3\text{–}1)$ overtone bands were recorded at 0.1 mm spectrometer slit width and slow tracing speed. Resolution of the isotopic lines was comparable to that shown in Fig. 3. The ratios I_{35}/I_{37} were found to fluctuate in a random fashion

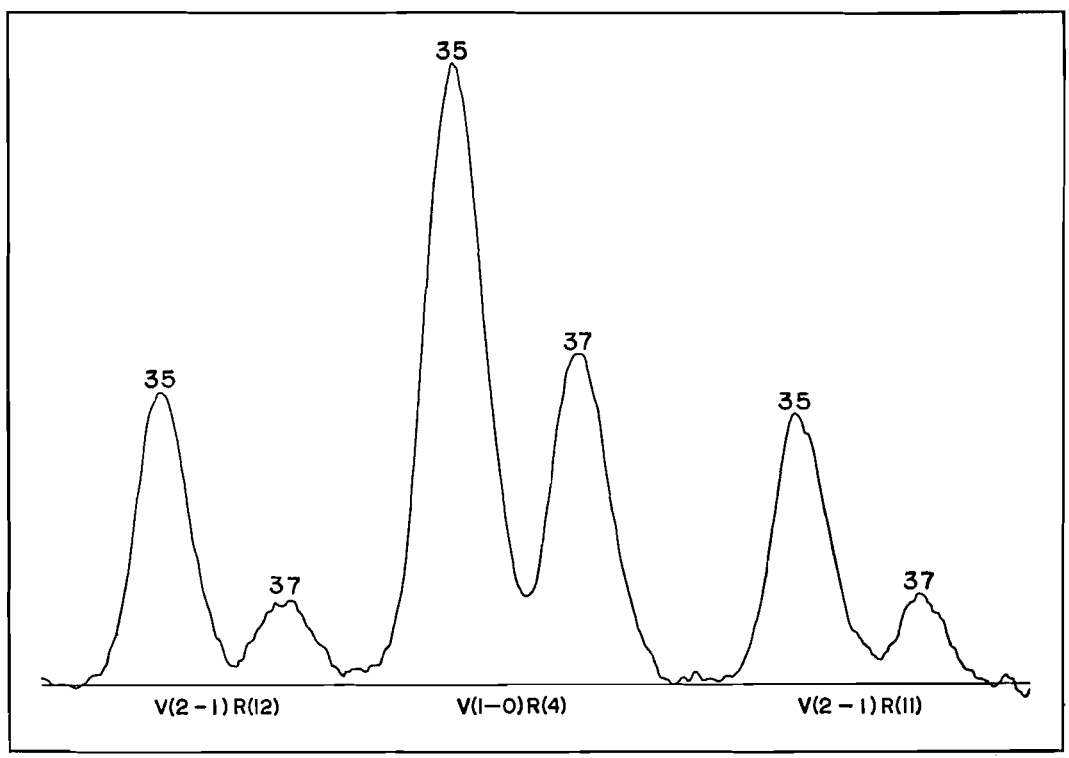

FIG. 3. Resolved isotopic lines in $v(1\text{–}0)$ and $v(2\text{–}1)$ of the fundamental. Actual trace recorded at 0.1 mm spectrometer slit width. The symbol $R(12)$ identifies an R-branch emission line terminating in $J = 12$.

Can. J. Chem. Downloaded from www.nrcresearchpress.com by 210.87.254.6 on 09/05/12
For personal use only.

in the range 3.02 ± 0.30. We conclude that the rate constants for the isotopic reactions

$$H + {}^{35}Cl_2 \rightarrow H^{35}Cl + {}^{35}Cl$$

and

$$H + {}^{37}Cl_2 \rightarrow H^{37}Cl + {}^{37}Cl$$

are the same, to within $\pm 10\%$.

Isotopic intensity ratios were recorded for six R-branch lines of $v(1\text{–}0)$ and three R-branch lines of $v(2\text{–}1)$, chosen for the fact that they were free from overlap by any other lines. Some of these lines are shown in Fig. 3. All are listed in Table I. It is apparent that

TABLE I

Partial pressures of HCl in some rotational levels of $v = 0$ and $v = 1$, as calculated from isotopic ratio data

Line	I_{35}/I_{37}	P_{37}	$[HCl]_{vJ}$ (mm Hg)
			$v = 0$
$v(1\text{–}0)$ $R(1)$*	2.37	0.211	0.017
" $R(4)$	1.86	0.535	0.060
" $R(10)$	2.36_5	0.214	0.035
" $R(11)$	2.56_5	0.140	0.025
" $R(12)$	2.74	0.086	0.016
" $R(13)$	2.80	0.069	0.013
			$v = 1$
$v(2\text{–}1)$ $R(5)$	2.80	0.069	0.0044
" $R(7)$	2.76	0.080	0.0058
" $R(8)$	2.84	0.058	0.0044

*$R(1)$ is the R-branch emission line terminating in $J = 1$.

for these lines the isotopic intensity ratio is significantly less than the theoretical ratio of 3.08. This we ascribe to self-absorption; the more abundant species being more self-absorbed than the less abundant, the intensity ratio I_{35}/I_{37} is reduced. In the language of the previous section we would say that the fractional transmission for $H^{35}Cl$ emission, I_{35}/I_{35_0}, is less than I_{37}/I_{37_0}, owing to the fact that the absorption parameter p_{35} is greater than p_{37}. To a good approximation $p_{35}/p_{37} = 2.98$. Representing the right-hand side of [2] as $f(2p)$ we have,

$$[10] \qquad \frac{I_{35}/I_{35_0}}{I_{37}/I_{37_0}} = \frac{f(5.96\, p_{37})}{f(2p_{37})}$$

$$[11] \qquad \frac{I_{35}}{I_{37}} = g(p_{37})$$

The function g includes a multiple, $I_{35_0}/I_{37_0} = 3.08$. I_{35}/I_{37} is the observed isotopic intensity ratio. Equation [11] was solved for a number of trial values of p_{37}, and the best value was chosen by interpolation (Table I). By equation [9], p_{37} yields $\bar{N}_{37}$; $\bar{N}_{37} + 3.065\, \bar{N}_{37} = \bar{N}_{vJ}$, which is listed as a partial pressure, $[HCl]_{vJ}$ mm Hg, in Table I. Figure 4 presents the derived populations in $v = 0$ and $v = 1$ in the form of Boltzmann plots.

The calculation from distorted isotopic ratios is more dependable than that from distortion in the Boltzmann plot, since it avoids the necessity for the advance assignment of a rotational temperature to the upper state of the transition and also the necessity of designating certain lines as 'unabsorbed'. (This designation is further complicated by the fact that at the highest J-numbers there is a second region of deviation from Boltzmann

Can. J. Chem. Downloaded from www.nrcresearchpress.com by 210.87.254.6 on 09/05/12
For personal use only.

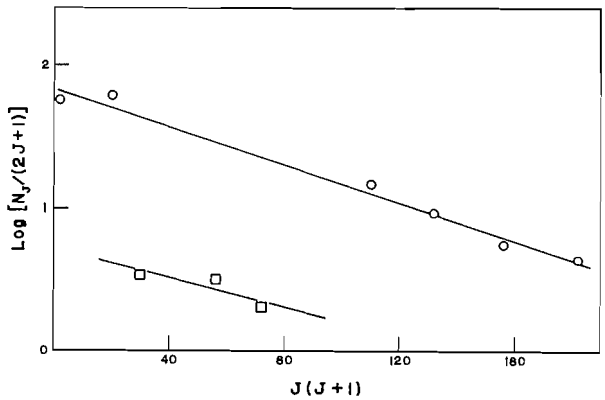

FIG. 4. Rotational distribution in $v = 0$, ○, and v = 1, □, calculated from the apparent deviation of the v (1–0) and v(2–1) isotopic ratios from the natural ratio. $T_{ROT} \approx 1000 \pm 100$ °K for $v = 0$; 1200 ± 200 °K for $v = 1$.

distribution—see Part I.) The method based on distortion of the Boltzmann distribution has, on the other hand, the advantage of versatility; it can be applied in cases where isotopic lines cannot be resolved, or are absent. (It would, however, be possible in such a case to add a known proportion of isotope, or other reagent whose competing reaction rate could be measured and which gave rise to product for which the constants of [9] were known.)

Strongly self-absorbed lines recorded in the presence of added HCl (Fig. 1) provided the best check on the degree of equivalence between methods 1 and 2. Pairs of isotopic lines were analyzed to yield I/I_0 for particular transitions, and this ratio was applied as a correction to the points in Fig. 1; the corrected points are seen to lie close to the line that describes the true Boltzmann curve, underlying method 1.

The rotational temperature of 1200 ± 200 °K for $v = 1$, calculated from v(2–1) self-absorption, is in fair agreement with the temperature of the 'heat bath' (translation + rotation) which is believed to be at 1300 ± 100 °K (Part I). The rotational temperature of 1000 ± 100 °K obtained by the isotopic-ratio method for $v = 0$ is somewhat lower than the temperature of the heat bath. This discrepancy could be caused by the fact that a greater proportion of $HCl_{v=0}$ than $HCl_{v>0}$ lies close to the vessel walls, in the path of the emitted radiation. (It may be permissible to draw this qualitative conclusion, even though the model used here is no longer strictly applicable once this complicating effect becomes significant.)

The partial pressures in the rotational states of $v = 0$ and $v = 1$ (Table I) were summed with the aid of the Boltzmann curves of Fig. 4 to give a pressure of 0.48 mm Hg for $v = 0$, 0.06 mm Hg for $v = 1$; $N_0/N_1 = 8.0$. This partial pressure of HCl (in all levels v) corresponds to about 80% conversion of Cl_2 to HCl. Since from an analysis of the products (Part I) we know that conversion is $\geqslant 90\%$, this is a reasonable result.

The absolute pressure of $HCl_{v=1}$, 6×10^{-2} mm, can be compared with an estimated pressure of roughly 10^{-3} mm $HCl_{v=1}$, based on absolute intensity measurements (4, 5) made under conditions of hydrogen and chlorine flow which would be expected to yield 10^{-1} to 10^{-2} times the intensity, i.e. 10^{-1} to 10^{-2} times the mean pressure of vibrationally excited HCl in the cone-of-sight (see Part I). In the light of this earlier estimate, the figure of 6×10^{-2} mm for $HCl_{v=1}$ appears reasonable.

Can. J. Chem. Downloaded from www.nrcresearchpress.com by 210.87.254.6 on 09/05/12
For personal use only.

3. Anomalous Intensity Ratio, I_P/I_R

A molecule in any upper state, $v'J'$, has a known relative probability of transfer by a P-branch transition to v, $J = J' + 1$, or by R-branch transition to v, $J = J' - 1$:

$$\frac{I_P}{I_R} = \frac{[(\omega_{vJ}^{v'J'})^4 . S_J . F_{vJ}^{v'J'}]_P}{[(\omega_{vJ}^{v'J'})^4 . S_J . F_{vJ}^{v'J'}]_R}$$

In the $v(1\text{–}0)$ band of HCl this ratio is 2.0 for $J' = 1$ decreasing to 1.2 for $J' = 5$. The effect of self-absorption will parallel that described under Section 2 above; there will be a reduction in I_P/I_R, since the P-branch emission will be more self-absorbed than the R. From the extent of the reduction in I_P/I_R, provided the rotational temperature in the lower vibrational level is known, it would be possible to calculate the absorption parameter for P (or for R) and hence the absolute concentration $\bar{N}_{vJ}$ for the appropriate lower state.

However, the closer I_P/I_R, before self-absorption, is to unity, the smaller will be the distortion in this ratio for any given value of $B_a\bar{N}_a . x$ (more precisely, $(B_a\bar{N}_a - B_e\bar{N}_e)x$). For HCl the effect is small and has not, until now, been detected with any degree of certainty.

ACKNOWLEDGMENTS

The authors are grateful to the National Research Council of Canada, the Imperial Oil Company of Canada, and the United States Air Force Cambridge Research Laboratories for financial assistance. One of them (J. C. P.) thanks the Alfred P. Sloan Foundation for the award of a Fellowship.

REFERENCES

1. R. D. COWAN and G. H. DIEKE. Rev. Mod. Phys. **20**, 418 (1948).
2. VON R. LADENBURG and S. LEVY. Z. Physik, **65**, 189 (1930). A. C. G. MITCHELL and M. W. ZEMANSKY. Resonance radiation and excited atoms. Cambridge University Press. 1961.
3. G. HERZBERG. Spectra of diatomic molecules. D. Van Nostrand Co., New York. 1950. p. 21.
4. J. K. CASHION and J. C. POLANYI. Proc. Roy. Soc., Ser. A, **258**, 529 (1960).
5. J. K. CASHION and J. C. POLANYI. J. Chem. Phys. **35**, 600 (1961).
6. P. E. CHARTERS and J. C. POLANYI. Discussions Faraday Soc. **33**, 107 (1962).

Can. J. Chem. Downloaded from www.nrcresearchpress.com by 210.87.254.6 on 09/05/12
For personal use only.

Can. J. Chem. Downloaded from www.nrcresearchpress.com by 210.87.254.105 on 09/05/12
For personal use only.

ORGANIC COMPLEXES OF URANIUM

PART I. THE SYNTHESIS AND SPECTRUM OF URANYL PHTHALOCYANINE

J. E. BLOOR,[1] J. SCHLABITZ, C. C. WALDEN, AND (IN PART) A. DEMERDACHE
British Columbia Research Council, Vancouver, British Columbia

Received March 13, 1964

ABSTRACT

The preparation of uranyl phthalocyanine from uranyl chloride and dilithium phthalocyanine is described. The infrared and electronic spectra of the complex are quite different from that previously reported for uranyl phthalocyanine and it is suggested that previous workers obtained mainly a mixture of phthalocyanine (PcH_2) and inorganic uranyl compounds. The infrared spectra of α- and β-PcH_2, β-PcCu, $PcLi_2$, and $PcUO_2$ from 4000 to 300 cm^{-1}; the far infrared spectra of β-PcH_2, β-PcCu, and $PcUO_2$ from 300 to 100 cm^{-1}; and the electronic spectrum from 3500 to 10 000 Å of $PcUO_2$ in 1-chloronaphthalene are recorded. A tentative assignment of a band at 278 cm^{-1} to the O—U—O bending frequency is made. The electronic spectrum of $PcUO_2$ differs from previous spectra of metal phthalocyanines in that it possesses no strong absorption in the 6000–7000 Å region. It does, however, have a strong band at 9145 Å, $\epsilon = 4.15 \times 10^4$.

INTRODUCTION

Although many metal porphyrins have been prepared (1) no record of a uranyl phthalocyanine could be found when this work was started (2). The properties of such a compound might be expected to provide information about the structure of the uranyl group and, because the U—O bonds are very sensitive to their environment (3), a study of their spectra may provide information about the interaction of uranium with the porphyrin ring. Recently, two reports of the synthesis of uranyl phthalocyanine have appeared (4, 5). Since, however, we have been unable to prepare uranyl phthalocyanine by either of the two methods previously described* (4, 5) and since the spectroscopic properties of our compound differ considerably from those reported by others (5, 6) we report here our work in some detail, together with a discussion of the previous work.

EXPERIMENTAL

Preparation of Uranyl Phthalocyanine

Anhydrous uranyl chloride (1.51 g) was added to dried dimethyl formamide (2 ml) and the mixture heated until the uranyl chloride had dissolved. To the hot solution, phthalonitrile (1.16 g) was added and the solution refluxed under nitrogen for 30 min. The dark solution then turned green and precipitation of a dark green solid occurred. The mixture was allowed to cool to room temperature and ethanol (30 ml) added. The precipitate was filtered off and washed with ethanol. The precipitate was a mixture of reddish crystals of phthalocyanine, deep blue–black feather-like crystals of uranyl phthalocyanine, and inorganic and organic by-products, total dry weight 0.676 g. Purification of the uranyl phthalocyanine was achieved by extracting the precipitate with 1,2,4-trichlorobenzene until the extracting solution turned from deep green to light blue. The trichlorobenzene was reduced in bulk to 2 ml by distillation. The uranyl phthalocyanine recrystallized as bluish green leaflets (yield 0.21 g) (11.6% theoretical on phthalonitrile). Further purification was carried out by vacuum sublimation below 0.01 mm pressure at 400–450 °C. Anal. Calc. for $C_{32}H_{16}N_8O_2U$: C, 49.11; H, 2.06; U, 30.42. Found: C, 49.6; H, 2.07; U, 28.3.

[1]*To whom all correspondence concerning this paper should be sent. Present address: Franklin Institute Research and Development Laboratories, Philadelphia, Pa., U.S.A.*

**Dr. Frigerio in private communication has informed us that to prepare uranyl phthalocyanine from uranyl nitrate dimethyl formamide complex and dilithium phthalocyanine in dimethyl formamide (DMF) solvent extreme precautions must be taken to remove the last traces of water from the solvent by repeated fractional distillation. In our attempts to prepare $PcUO_2$ by this method we dried our DMF over Linde's 5A molecular sieve and distilled until our gas chromatograph failed to detect water (less than 50 p.p.m.).*

Can. J. Chem. Downloaded from www.nrcresearchpress.com by 210.87.254.105 on 09/05/12
For personal use only.

INFRARED SPECTRA

(a) Phthalocyanine and Metal Phthalocyanines

The infrared spectra of the α- and β-polymorphic forms of the parent phthalocyanine (9) and many of their metal derivatives have previously been recorded between 4000 cm^{-1} and 400 cm^{-1} (8, and references cited therein, 9). In the extensive study of Sidorov and Kotlyar the spectra were measured on samples deposited directly on sodium chloride or potassium bromide plates. Our spectra (Fig. 1 and Table I) were recorded on a Perkin–

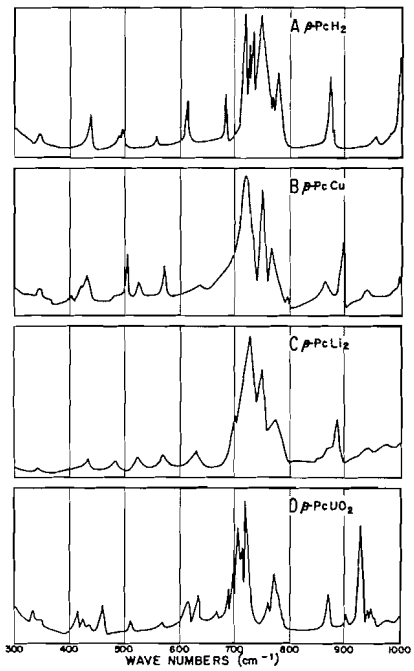

FIG. 1. Infrared spectra (Nujol mulls) of: A, β-phthalocyanine; B, β-copper phthalocyanine; C, lithium phthalocyanine; D, uranyl phthalocyanine.

Elmer 521 infrared spectrophotometer from 4000 cm^{-1} to 300 cm^{-1} using finely ground mulls of the relevant phthalocyanines. Comparison of our spectra of phthalocyanine and that in (9) shows only minor differences between the two spectra on changing from a thin film to a dispersed sample. The chief changes were in the relative intensities of different bands. We have therefore adopted the numbering system of (9) in Table I. We have also used an additional letter subscript, to introduce bands not numbered in the Table I of (9) although most are evident in the actual spectra (Fig. 2 of (9)). Our phthalocyanine (β-PcH_2) spectra differ from (9) mainly in: the resolution of band 32 into two quite sharp bands at 1615 and 1605 cm^{-1}; the presence of a band at 1530 cm^{-1}, which is present in the curve given in (9); the presence of a shoulder corresponding to band 19 in the metal derivatives at 1112 cm^{-1}; and the presence of weak bands at 1040 cm^{-1} and 480 cm^{-1}, probably due to the extra resolution of our grating instrument. We have also found a band at 340 cm^{-1} beyond the range of the spectrophotometer used in (9).

The spectra of the copper and magnesium phthalocyanine, PcCu and PcMg, are also very similar to those reported in (9). We do however find extra bands at 1312 cm^{-1} and

TABLE I

Infrared spectrum of phthalocyanine derivatives in Nujol mulls

Band No.	β-PcH_2	β-PcCu	PcMg	$PcLi_2$	$PcUO_2$ (this paper)	$PcUO_2$ of (6)	α-PcH_2* (a)	α-PcH_2* (b)
33	3280	—	—	—	—		3292	3280
				1635				
32	1615	1610	1606	1606	1605		1620	1615
31*a*	1605	1589	1586	1585	1575	1610	1610	1610
31*b*	1590				1520			
31*c*	1530					1530	1530	1535
30*a*					1510			
30*b*	1495	1504	1484	1484	1490		1503	1500
29	1478	1494 s	—	—			1478	
28	—	1448	1440	—	—		1461	1450
27*a*	1432	1420		—	—		1439	
27*b*	1400	1416	1408		1410			
27*c*	1342	1366	1370	—	1350			
26	1333	1334	1334	1336	1334	1325	1326	1340
25	1321	1312	—	—		1310	1321	1325
24	1302	—	—	—	1300 wk		1304	1308
23*a*	1280	1280	1280	1283	1285	1270	1277	1280
23*b*	1250	—	—	—				1250
	1195							
22*a*	1190	1192	—	—	—			1190
	1180							
22*b*	—	—	1170 s	—				
21	1155	1166	1165	1165	1050	1158	1160	1165
20*a*			1134					
20*b*	1120	1119	1118	1117	1120	1120	1119	1116
19	1112 s	1105	1198	—	—		—	—
18	1094	1094	1080	1090	1072	1095	1094	1092
17*a*	1070					1068 wk		1070 wk
17*b*	1040 vwk	1062	1058	1052	1030	1055 wk		1045 wk
16	1002	1004 wk	1002 wk	1002 wk	1020	1006 fs	1008	1008
15	955	—	952	945	950			
14	950	940	946	945	930	920	946	945
13	872	900	900		900		874	880
12	880	868	885	890	868	878	—	—
11	—	—	—		—		870	870
9	780	763	770	770	775		766	775
8	770	—			765		778	770
7	750	—			727		—	—
6*a*	735	756	750	750	720	732	730	735
6*b*	730			732	712	716	—	—
5	722	726	722		704		714	715
4*a*	683				675	680		690
4*b*					640			
4*c*	614	632	632	632	620	664 sh	—	620
3	560	572	572	572			557	—
2*a*	495	532	510	525			—	
2*b*	480	508	496	480	460		492	490
					435			
1*a*	432	436	430	432	415		434	438
1*b*	340	345	—	350	335			

ABBREVIATIONS: s—strong, fs—fairly strong, wk—weak, vwk—very weak.
*(*a*) α-PcH_2 spectra reported in (9) on sample sublimed directly on KBr plate.
(*b*) α-PcH_2 measured in Nujol mull, this work.

532 cm^{-1} in PcCu. We have labelled the first one as corresponding to band 25 although this is not listed in (9) as appearing in any of the other PcM spectra. The second one at 532 cm^{-1}, if not due to contamination, is probably due to one of the Cu—N vibrations which might be expected in this region (10). In the PcMg we find a new band at 1134 cm^{-1} not recorded in (9) and which appears to come from a splitting of band 20*b*. The spectrum of the dilithium phthalocyanine was not recorded in (9) and is reported here for the first

Can. J. Chem. Downloaded from www.nrcresearchpress.com by 210.87.254.105 on 09/05/12
For personal use only.

time. It is very similar to the other phthalocyanines except for an extra band at 1635 cm^{-1}.

The metal phthalocyanine spectra are in general very similar to those of the parent. The main differences are:

1. The disappearance on metal formation of the weak band at 3280 cm^{-1}, which is probably due to the N—H frequency (11). Our result and that given in (9) differ from those given by Frigerio (12) and Tyler and Ehrhardt (13) for PcCu. These workers report a band in the 3200 cm^{-1} region for PcCu and in (12) it is stated that the deuterated phthalocyanine also has a band at 3298 cm^{-1} but no N—D band in the 2000–2500 cm^{-1} region. This result differs from that reported in (9) where they report an N—D frequency at 2456 cm^{-1} for the (D_2) compound and at 2467 cm^{-1} for the mono deuterated (DH) compound. The Russian workers also claim to find the other expected changes on deuteration, whereas Frigerio (12) found no other changes. We are at the present time unable to explain these differences in experimental findings, therefore our assignment of the frequency at 3280 cm^{-1} to an N—H vibration must be regarded as tentative.

2. The spectra of the parent and the metal derivatives differ in that the 1250 cm^{-1} and 1321 cm^{-1} bands, 23*b* and 25, appear to be missing in the metal complexes except for the band found by us in PcCu.

3. A quite strong band 17*b* is found in the metal complexes in the 1060–1080 cm^{-1} region. It could however correspond to a weak one found by us in the parent. The strong band 16 appearing at 1002 cm^{-1} in the parent becomes either extremely weak or vanishes altogether in the metal complexes.

4. The major change in the infrared spectrum on substituting a metal into the phthalocyanine ring occurs in the 700–800 cm^{-1} region. In the β-PcH_2 this region has six clearly defined bands. These are reduced to three in all the metal phthalocyanines discussed in (9) and in the dilithium compound. Between 700–300 cm^{-1} little change occurs on metal formation although the frequency, at which band 2*b* appears, seems sensitive to the nature of the metal.

(b) Uranyl Phthalocyanine

The main evidence cited in (6) for the successful preparation of a uranyl phthalocyanine is the infrared spectrum of the sample. The spectra reported in (9) were taken as a standard in (6) although the spectra compared were not measured under the same conditions. If however we compare the spectrum reported in (6) with those of α-PcH_2 and β-PcH_2 measured under comparable conditions, i.e. in Nujol mulls, we find that most of the bands attributed to metal complex formation can be related, with some confidence, to bands in the parent phthalocyanine. This is demonstrated by comparison of the spectral data assembled in Table I. Our data for α- and β-PcH_2 are in columns 2 and 9 respectively and for the metal phthalocyanines in columns 3 to 6 inclusive. Data for the $PcUO_2$ reported by Lyalin and Kobyshev (6) are in column 7 and for α-PcH_2 (9) in column 8. Thus, for example, the band at 1530 cm^{-1} is found in the parent phthalocyanines. The fairly strong band at 1006 cm^{-1} reported by Lyalin for $PcUO_2$ clearly corresponds to band 16 observed in the parent molecules at 1002 cm^{-1} and found to be absent or extremely weak in other metal phthalocyanines. The very weak shoulders reported in (6) at 1055 and 1068 cm^{-1} can be related to weak bands observed in the parent phthalocyanine at 1040 cm^{-1} and 1070 cm^{-1}. The bands at 1095, 1120, and 1158 cm^{-1} reported in (6) can be related to bands 18, 20*b*, and 21 of the parent respectively. Between 700 cm^{-1} and 800 cm^{-1} the spectrum reported in (6) is most unusual since it has only one main peak at 732 cm^{-1} corresponding to band 6. If however we assume that either the resolution was poor in this region, or the sample

Can. J. Chem. Downloaded from www.nrcresearchpress.com by 210.87.254.105 on 09/05/12
For personal use only.

Can. J. Chem. Downloaded from www.nrcresearchpress.com by 210.87.254.105 on 09/05/12
For personal use only.

was not sufficiently well mulled to produce sharp bands,* we can match the shoulders to the peaks found in our spectrum of α-PcH_2. The remaining two bands are at 868 cm^{-1} and 920 cm^{-1}. The former can be related to band 11 or 12† whereas the latter is almost certainly due to the uranyl group. In the examination of 20 uranyl–organic complexes we have found in every case that the strong band in the 900–950 cm^{-1} region which is due to the O—U—O assymetric stretch is always extremely sharp. On the occasions where we have observed a broad band in this region similar to that shown in (6), we have always been able to trace it to a uranyl inorganic impurity. In particular in our early attempts to prepare uranyl phthalocyanine from phthalic anhydride and urea, we often obtained a blue solid giving a spectrum similar to that given in Fig. 1 of (6). On solvent extraction of the reaction product we isolated an inorganic insoluble residue and α-PcH_2.

From the above discussion of the properties of the substance reported in (6) we must conclude that it consists largely of unchanged α-phthalocyanine contaminated by inorganic uranyl substances.

Applying the method of preparation described in the experimental section we obtained a greenish-blue solid with a very different spectra from that reported in (6). This spectrum is compared with that of β-PcH_2 in Fig. 1 for the region 1000–300 cm^{-1}. All the observed bands from 4000–300 cm^{-1} are listed in Table I, column 6. No band could be found in the 3300 cm^{-1} region. Between 1650 and 1000 cm^{-1} the spectrum is very much like that of other metal phthalocyanines except that there was no trace of the weak band 19, and band 16 was about as strong as in the parent phthalocyanine but shifted from 1002 cm^{-1} to 1020 cm^{-1}. In the 800–700 cm^{-1} region the spectrum was more complicated than in other metal phthalocyanines but corresponded quite well to that of the parent with irregular shifts to lower frequencies of the order of 30 cm^{-1} for the six bands of the parent in this region. Below 700 cm^{-1} the uranyl phthalocyanine differs considerably from the parent phthalocyanine and other metal phthalocyanines. Thus band 1 appears as two bands, either of which could correspond to U—N stretching frequencies which are expected in this region.

In the 900–950 cm^{-1} region the very strong sharp peak which experience has led us to associate with organic uranyl chelates appears at 930 cm^{-1} together with a band of much lower intensity at 900 cm^{-1} which we have also found in many uranyl compounds. No trace of the O—U—O symmetric stretching frequency often assigned in the 800–900 cm^{-1} region could be found. This can be regarded as evidence that the UO_2 group is linear in $PcUO_2$ with very little distortion.

Thus we have prepared a compound possessing an infrared spectra considerably different from either the parent phthalocyanines or that of other metal phthalocyanines and which possesses the characteristics expected of a uranyl complex. That the phthalocyanine ring is present in the compound is clearly shown by the fact that on stirring the uranyl compound in concentrated sulphuric acid for 1 h at −4 °C, precipitating, and drying, we obtained a compound which gave an infrared spectrum identical with that of α-phthalocyanine (Table I, column 9).

FAR INFRARED SPECTRA (with A. Demerdache)

Metal–ligand stretching and bending frequencies are usually assumed to be low frequencies and very few, especially those below 300 cm^{-1}, have been assigned (14). In an

We occasionally experienced this phenomenon but achieved considerable sharpening on increasing the mulling time. Spectra measured in KBr *pellets also gave ill-defined spectra.*

†*There appears to be no justification for allotting two numbers 11 and 12 to the band appearing in this region, as in no compound studied in (9) do both occur simultaneously.*

attempt to identify the O—U—O bending frequency and possibly the frequencies due to the uranium–nitrogen bands we have recorded the infrared spectrum between polyethylene plates of finely ground Nujol mulls of β-PcH_2, β-PcCu, and $PcUO_2$ between 300 cm^{-1} and 100 cm^{-1}, using a Perkin–Elmer 301 instrument. The spectra, which are the first to be taken in this region for phthalocyanines, are given in Fig. 2 and tabulated in Table II.

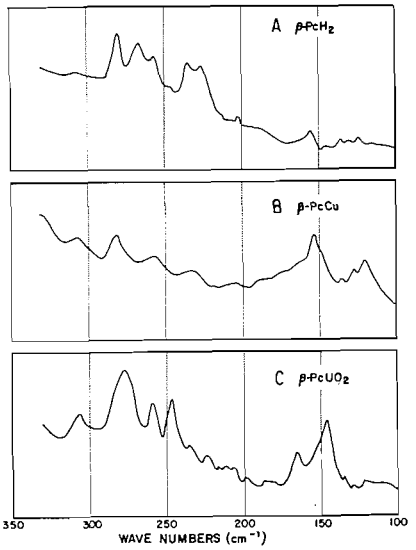

FIG. 2. Far infrared spectra (Nujol mulls between polyethylene plates) of: A, β-phthalocyanine; B, β-copper phthalocyanine; and C, uranyl phthalocyanine.

TABLE II

Far infrared spectra peaks of phthalocyanine derivatives in cm^{-1}

β-PcH_2	β-PcCu*	$PcUO_2$‡
	304	306
280	283	—
—	—	278 s (UO_2 band)
266	267	—
256 wk	258	258
233†	230	244
227†		
155 vwk	154	164 ms
	122	147 ms

ABBREVIATIONS: wk—weak, vwk—very weak, s—strong, ms—moderately strong.

*Peaks were weak and could not be sharpened by fine grinding or thickening the mull.

†This splitting could be false and due to difficulties in measuring spectra in this region.

‡The 280 cm^{-1} band is probably hidden by the UO_2 bending frequency.

The suggested correspondencies in this table are purely speculative. The only assignment we can make with any degree of certainty is to assign the band observed in uranyl phthalocyanine at 278 cm^{-1} to the O—U—O bending frequency.

The only previous direct observation of this bending frequency appears to be by Raman measurements of aqueous solutions of uranyl compounds where a band at 210 cm^{-1} was found, although the bending frequency should be Raman inactive (15, 16). In a study of the

Can. J. Chem. Downloaded from www.nrcresearchpress.com by 210.87.254.105 on 09/05/12
For personal use only.

far infrared of a number of inorganic and organic uranyl compounds we have always found a band in the 240–280 cm^{-1} region, but only rarely have we found a weak band in the 200–220 cm^{-1} region. Frequencies in the higher range have also been previously found in the vibrational fine structure of the electronic emission spectra of uranyl compounds (17, 18). We prefer therefore to assign the O—U—O bending frequency to the 240–280 cm^{-1} region since this bending frequency should be active only in the infrared and should not be observed by Raman measurements. The 210 cm^{-1} frequency may be due to either a lattice vibration (19) or to a splitting of the degenerate bending frequency of the linear UO_2 group by crystal field perturbations of the environment of the uranyl group.

ELECTRONIC SPECTRA

The electronic absorption spectrum of our $PcUO_2$ was measured in 1-chloronaphthalene solvent from 3500 Å to 11 000 Å, the result is shown in Fig. 3. The outstanding features

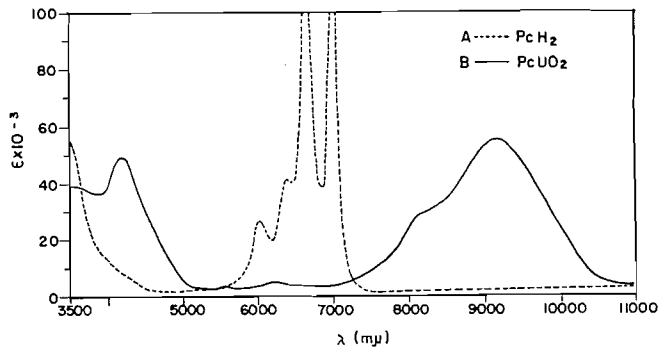

FIG. 3. Electronic spectra in 1-chloronaphthalene of: A, phthalocyanine - - - - and B, uranyl phthalocyanine ———.

of this spectrum are the absence of any strong bands in the 6000–7000 Å region and the presence of a strong band at 9145 Å ($\epsilon = 4.15 \times 10^4$) with a shoulder at 8100 Å. The spectra of many metal phthalocyanines and metal porphyrins have been recorded (20, and references cited therein, 21) and in no other case has it been found that there were no strong bands in the 6000–7000 Å. The only other example of a phthalocyanine with bands in the near infrared is that of manganese phthalocyanine (II) (22) which in pyridine solution has bands at 8800 Å and 8350 Å. The nature of the transitions responsible for these absorption bands is at the present a matter only of conjecture. In both cases the near infrared bands are unlikely to be due to localized transitions confined to the metal atoms. The intensity is too high and the frequency too low. Also we have not been able to observe such bands in other uranyl complexes, e.g. in UO_2 complexes of β-diketones and hydroxyarylazo compounds (23). We have also been unable to find any near infrared bands in either PcH_2 or PcCu. One must conclude therefore that the near infrared absorption bands in the Mn (II) and the UO_2 phthalocyanines must be due to interactions between the metal atomic orbitals and molecular orbitals of the Pc ring. In the former case the band is probably a charge transfer band in which in the ground state there is very little mixing of the Pc and manganese molecular orbitals. In the case of the uranyl phthalocyanine the considerable difference between the electronic spectra of the metal complex and the PcH_2 parent indicate considerable interaction between the UO_2 and Pc molecular orbitals. Since the absence of any band in the infrared spectra which can be assigned to the

Can. J. Chem. Downloaded from www.nrcresearchpress.com by 210.87.254.105 on 09/05/12
For personal use only.

symmetric stretching frequency of the UO_2 group implies that the UO_2 group has kept its linearity in the phthalocyanine, we can either consider $PcUO_2$ to be either an example of very strong perpendicular conjugation (24) of the oxygen atoms, with the Pc ring through the uranium, or a case of unusually strong interaction of the uranium atomic orbitals with the Pc ring. Both the asymmetric stretching frequency at 930 cm^{-1} and the bending frequency at 278 cm^{-1} are quite normal for uranyl chelates such as uranyl acetylacetonate and therefore do not support the first hypothesis that considerable ground state interaction exists between the oxygens and the Pc ring. The Pc ring is apparently still intact since on removing the UO_2 group with acid the resulting compound possesses the visible spectra characteristic of the parent phthalocyanine. The general problem of the nature of the bonding of the UO_2 group with organic ligands will be discussed in more detail elsewhere after we have reported the results (23) of our studies on other uranyl organic compounds.

ACKNOWLEDGMENTS

We wish to acknowledge gratefully the financial support of the Canadian Uranium Research Foundation, under whose auspices this work was undertaken. We wish to thank Dr. R. H. Wright for kind permission to measure far infrared spectra on the Perkin–Elmer 301 spectrophotometer (purchased under Contract No. DA-49-193-MD-2391 with the U.S. Army Medical R & D Commission).

REFERENCES

1. F. H. Moser and A. L. Thomas. Phthalocyanine compounds. Reinhold Corp., New York. 1963.
2. J. E. Bloor and J. Schlabitz. Canadian Uranium Research Foundation. Rept. Nos. CURF R-38, R-44 (1962); R-68 (1963).
3. S. P. McGlynn, J. K. Smith, and W. C. Neely. J. Chem. Phys. **35**, 105 (1961).
4. N. A. Frigerio. (to U.S.A. as represented by the U.S. Atomic Energy Commission), U.S. Patent 3 027 391 (March 27, 1962).
5. G. K. Kobyschev, G. N. Lyalin, and A. N. Terenin. Dokl. Akad. Nauk SSSR, **148**, 1053, 1294 (1963).
6. G. N. Lyalin and G. I. Kobyshev. Opt. Spectry. USSR (English Transl.), **15**, 253 (1963).
7. A. A. Ebert, Jr. and H. B. Gottlieb. J. Am. Chem. Soc. **74**, 2806 (1952).
8. G. P. Gurnovich, A. N. Sevchenko, and K. N. Solv'ev. Soviet Phys. Usp. (English Transl.), **6**, 173 (1963).
9. A. N. Sidorov and I. P. Kotlyar. Opt. Spectry. USSR (English Transl.), **XI**, 175, 1961.
10. R. G. Inskeep. J. Inorg. Nucl. Chem. **24**, 1763 (1962).
11. A. N. Terenin and A. N. Sidorov. Spectrochim. Acta Suppl. **9**, 574 (1957).
12. N. A. Frigerio. J. Org. Chem. **26**, 2115 (1961).
13. J. E. Tyler and S. A. Ehrhardt. Anal. Chem. **25**, 390 (1953).
14. K. Nakamoto. Infrared spectra of inorganic and coordination compounds. John Wiley and Sons, New York. 1963.
15. G. K. T. Conn and C. K. Wu. Trans. Faraday Soc. **34**, 1483 (1938).
16. J. C. Sutton. Nature, **169**, 235 (1952).
17. E. Rabinowitch. Argonne National Laboratory. Rept. Nos. ANL-5122, ANL-5173 (1953).
18. G. H. Dieke and A. B. F. Duncan. Spectroscopic properties of uranium compounds. McGraw-Hill, New York. 1949.
19. A. N. Sevchenko and B. I. Stepanov. Zh. Teoret. Fiz. **21**, 204, 212, (1951).
20. M. Gouterman. J. Mol. Spectry. **6**, 164 (1961).
21. R. P. Linstead. J. Chem. Soc. 2873 (1953).
22. G. Engelsma, Akio Yamamoto, E. Markham, and M. Calvin. J. Phys. Chem. **66**, 2517 (1962).
23. J. E. Bloor and J. Schlabitz. In preparation.
24. J. A. Elvidge and A. B. P. Lever. J. Chem. Soc. 1257 (1961).

Can. J. Chem. Downloaded from www.nrcresearchpress.com by 210.87.254.105 on 09/05/12
For personal use only.

MEASUREMENT OF ELECTRON SPIN RESONANCE DIFFERENCE SPECTRA AT 77 °K

APPLICATIONS OF THE METHOD IN LOW-TEMPERATURE RADIATION CHEMISTRY[1]

D. R. SMITH AND J. J. PIERONI

Research Chemistry Branch, Atomic Energy of Canada Limited, Chalk River, Ontario

Received May 29, 1964

ABSTRACT

The technique of measuring e.s.r. difference spectra has been extended to 77 °K. This enables elimination of the main signal due to irradiated silica sample tubes and of about 90% of the hydrogen atom signal from the same source. Under certain conditions, e.g. when the e.s.r. spectrum due to one species can be photochemically bleached, the method permits resolution of two superimposed spectra. This has been demonstrated by measurements which resolve the e.s.r. singlet due to trapped electrons in irradiated tetrahydro-2-methylfuran from the underlying septet. These developments have rendered the e.s.r. difference method very useful for the study of paramagnetic species formed in systems which have been γ-irradiated at 77 °K.

INTRODUCTION

Smith and Wilmshurst (1) have reported a method whereby, using a TE_{103} cavity containing two samples at room temperature, the difference between their electron spin resonance (e.s.r.) spectra was automatically obtained as the spectrometer output to a strip-chart recorder. The basis of the method is that the magnetic field modulation at one sample position be of equal frequency and amplitude but independent of, and 180° out of phase with respect to, the field modulation at the other sample position. The two samples (of identical dimensions) should be at equivalent positions (i.e. at antinodes) in the cavity and they should be subjected to identical d-c. magnetic fields.

We have extended the method by using a TE_{104} X-band cavity, Varian Associates dual cavity accessory (2), containing two Varian Associates liquid nitrogen dewars. A Varian 12 in. electromagnet enables both sample positions to be subjected to the same d-c. magnetic field without difficulty. This enables the e.s.r. difference spectrum of two samples at 77 °K to be obtained. Our modification of the method renders it useful to low-temperature radiation-chemical studies because it permits elimination of the e.s.r. signal due to irradiated silica sample tubes, it permits 90% elimination of the hydrogen atom signal due to adsorbed water in irradiated sample tubes, and in special cases it enables resolution of superimposed e.s.r. spectra due to irradiated samples. These applications and some results to illustrate them are discussed below.

EXPERIMENTAL

(a) The Electron Spin Resonance Difference Spectrum Technique

A Varian V-4502-04 X-band e.s.r. spectrometer with dual cavity and two liquid nitrogen dewar accessories was used. A field modulation of 100 kc/s was used, and it was first passed through a switch box so that the field could be modulated at either sample position separately or at both sample positions simultaneously, but 180° out of phase. First derivative spectra ($d\chi''H_1/dH$ vs. H) are shown in the figures.

Pairs of Spectrosil (British Thermal Syndicate) sample tubes, 0.100 in. I.D., whose I.D. and O.D. were equal within less than ± 0.00025 in. over the vertical dimension of the cavity were used. This accurate matching of the sample tubes reduces the difference (from this source of error) in the total number of unpaired spins in each tube to $\pm 0.5\%$.

[1]*Issued as AECL No. 2047.*

Can. J. Chem. Downloaded from www.nrcresearchpress.com by 210.87.254.40 on 09/05/12
For personal use only.

The following precautions were taken to ensure that the 100 kc magnetic field modulation at each sample position conformed to the requirements for this technique. A "pick-up" probe, consisting of an 80 turn (A.W.G. 38 copper wire) coil elongated to go into a sample tube, was placed first in one and then the other cavity sample position. By displaying the signal, induced by the 100 kc/s field modulation, on an oscilloscope it was verified that (*a*) the field modulation amplitudes were equal within 1% at both sample positions (a 240 mV signal was obtained when the amplitude was about 2.5 gauss); (*b*) at the back sample position field modulation due to the front pair of modulation coils was less than 0.5% of the detected amplitude at the front sample position, and vice versa; (*c*) at either sample position, for modulation amplitudes of 2.5 gauss or less, the modulation amplitude did not decrease by more than 1% when the modulation signal was fed to both pairs of modulation coils simultaneously, compared to feeding it to only one of the pairs of coils. Higher amplitudes were never used.

The relative phase of the magnetic field modulation at the two sample positions was determined by an oscilloscope. The X and Y inputs to the oscilloscope were obtained from "pick-up" probes located at the two sample positions. From the pattern observed it was concluded that the magnetic field modulations at the two sample positions were $180 \pm 3°$ out of phase with respect to each other. When phase sensitive detection is used, a 3° error in the relative phase of the field modulation at each position only introduces an error equal to $\pm(1 - \cos 3°) \times 100$ or $\pm 0.14\%$ in the subtraction of spectra.

It was observed that the phase of the field modulation depended on the load on the field modulation power supply. When there was a sample in one cavity position and the other position was empty, the intensity of the spectrum decreased by one-third when the modulation signal was fed to both pairs of modulation coils. The original intensity was restored by a simple adjustment of the phase of the 100 kc/s reference signal going to the phase sensitive detector. Consequently, the phase of the reference signal was always adjusted to maximize the intensity of the e.s.r. spectrum.

(b) Sample Preparation

Eastman tetrahydro-2-methylfuran was dried over a sodium mirror. After drying and degassing, samples were distilled into Spectrosil tubes (joined to quartz-to-pyrex graded seals) and sealed off, under vacuum, at a constriction. No grease or mercury was present in the vacuum system. Hoke TY440 valves (stainless steel with Teflon seats) and Edwards O-ring (Teflon) connectors were used instead of greased stopcocks, cones, and sockets (3).

RESULTS AND DISCUSSION

1. Subtraction of Identical Spectra

Figure 1A and B shows the room-temperature spectra of solutions of 2,2-diphenyl-1-picryl-hydrazyl (DPPH) in benzene (having identical concentrations) in tubes of inner diameter matched to $\pm 0.25\%$. Figure 1C, the measured difference between A and B, illustrates that about 98% accuracy in the subtraction can be achieved.

2a. Elimination of the Spectrum due to Irradiation of Silica Tubes

Samples are often irradiated and studied (at 77 °K) in Spectrosil silica tubes. Frequently, but not always, the e.s.r. spectrum due to the irradiated silica is negligible in intensity compared to the free radical spectrum. Silica tubes of lower purity (Suprasil) have been used (6), and the resultant e.s.r. spectrum was distorted by the sample tube signal.

There are techniques for avoiding the spectrum of the irradiated silica sample tube. Sometimes the sample is frozen on the bottom of the cavity (7). Other workers solidify a sample by dropping it into liquid nitrogen; the sample is then irradiated, and a few pieces are transferred at 77 °K into a dewar in the spectrometer cavity (8). However, these methods render it difficult to estimate free radical concentration because they do not facilitate reproduction of sample size and shape.

The subtraction technique described here eliminates the spectrum due to the irradiated silica tube. Consequently there is no objection to containing samples in these tubes. This reduces the problem of reproducing sample geometry to one of calibrating the inner diameter of the sample tube. The procedure is as follows: by placing an irradiated sample and tube in the dewar at one cavity position and an empty irradiated tube which has identical dimensions and which has received the same radiation dose in the dewar at the second cavity position, the e.s.r. difference spectrum automatically yields the spectrum of

Can. J. Chem. Downloaded from www.nrcresearchpress.com by 210.87.254.40 on 09/05/12
For personal use only.

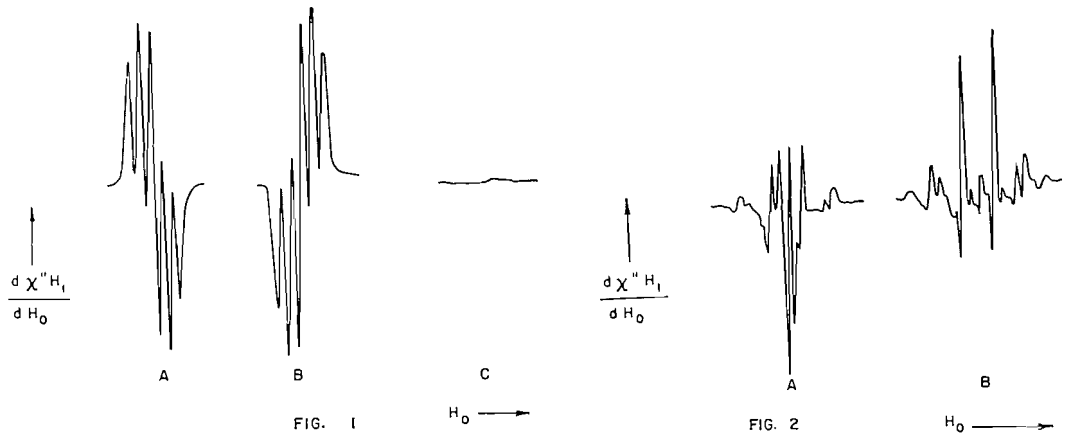

FIG. 1. A, DPPH solution in the front cavity position; B, DPPH solution in the rear cavity position; C, difference between A and B.

FIG. 2. A, Ethyl radical plus sample tube spectrum, ×100; B, difference between A and the spectrum of an empty irradiated tube, ×250.

the irradiated sample undistorted by a sample tube signal. The subtraction of the sample tube spectrum is illustrated in Fig. 2. An irradiated mixture of 15% ethane in krypton* in a Spectrosil tube at 77 °K was in one cavity position, and at the same time an empty irradiated Spectrosil sample tube was in the other position. Figure 2A was obtained by modulating the magnetic field at the sample position only. Figure 2B was obtained by modulating the magnetic field at both the sample and the empty irradiated tube simultaneously but in anti-phase. The spectrum in Fig. 2B is the same as that obtained for the ethyl radical by other workers (4, 5) in systems where the ethyl radical spectrum was intense enough to render the sample tube signal insignificant.

2b. Subtraction of the Sample Tube Hydrogen Atom Signals

The intensities of the hydrogen atom signals in two irradiated Spectrosil tubes, which had been previously flamed and sealed off under vacuum, differed by 10%. Thus the difference spectrum only achieved a 90% reduction in the hydrogen atom signal. To achieve this, narrow modulation amplitude (0.4 gauss) and extremely careful positioning of the cavity in the magnet gap were required, because the line widths are only 0.5 gauss between derivative maxima.

To study hydrogen atom formation in ice containing inorganic salts, Kevan *et al.* (9) made cylinders of ice 2 mm in diameter. They could not contain the ice in sample tubes because these develop hydrogen atom signals when irradiated. The large reduction in the intensity of the unwanted hydrogen atom signals, achieved by the subtraction technique, should enable the use of sample tubes in hydrogen atom studies such as the above-mentioned.

3. Resolution of Superimposed Spectra

Observations on trapped electrons in γ-irradiated systems have been complicated by the fact that their e.s.r. singlet is superimposed on the multiline spectrum due to another paramagnetic species (10–13). The technique of obtaining difference spectra enables the trapped electron singlet to be resolved. To demonstrate this, some results obtained in a

*Unpublished experiment with Dr. J. A. Stone.

Can. J. Chem. Downloaded from www.nrcresearchpress.com by 210.87.254.40 on 09/05/12
For personal use only.

study of irradiated tetrahydro-2-methylfuran (MTHF) are presented. These may be compared to those obtained by Salmon (13) using conventional methods.

To study MTHF a dimensionally matched pair of samples in Spectrosil tubes was prepared, slowly immersed in liquid nitrogen (MTHF forms a clear colorless glass), and ^{60}Co γ-irradiated at a dose rate of 6.46×10^{15} eV ml^{-1} s^{-1} for 2 hours. The samples developed a strong blue color. One member of the pair was then photochemically bleached by tungsten light transmitted by a Corning 2403 filter until the sample was again colorless. Both samples were then placed in the dual cavity at 77 °K, and their difference spectrum was recorded at 0.2 mW cavity input power and a modulation amplitude of 2.3 gauss. The e.s.r. spectra obtained are shown in Figs. 3 and 4. The results show that irradiation of

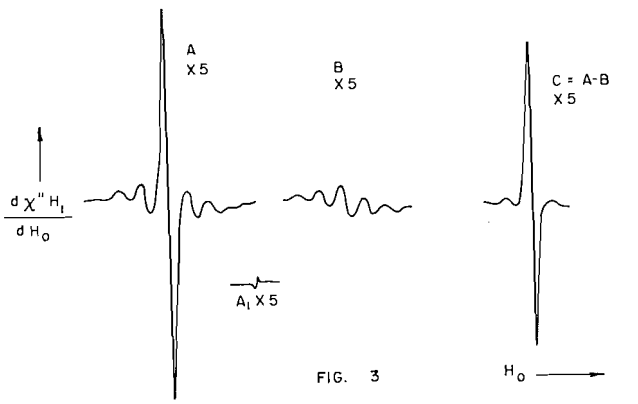

FIG. 3. A, Unbleached MTHF; A_1, difference between two unbleached MTHF samples; B, bleached MTHF; C, difference between unbleached and bleached MTHF.

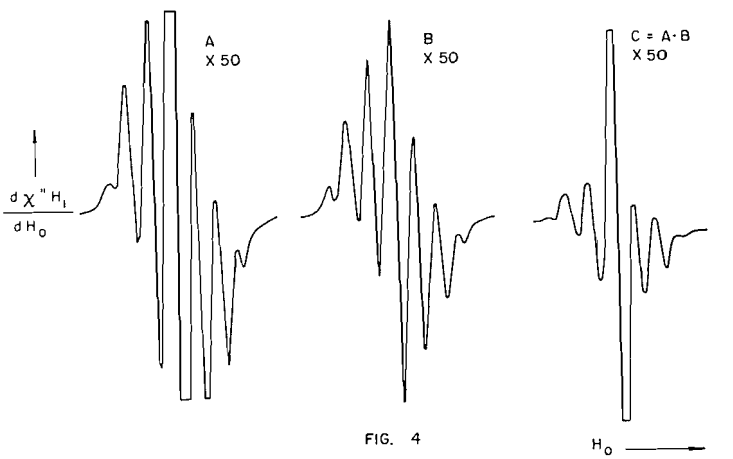

FIG. 4. A, B, and C are the same as A, B, and C in Fig. 3 except they are measured using a ten times greater sensitivity.

MTHF yields a narrow intense singlet superimposed on the center line of a septet spectrum. Bleaching causes the singlet and about 30% of the septet to disappear. These spectra do not give a true indication of the relative intensities of the singlet and septet. They are both saturated to a different extent at this power level. Their microwave satura-

Can. J. Chem. Downloaded from www.nrcresearchpress.com by 210.87.254.40 on 09/05/12
For personal use only.

tion curves differ such that, at a power level of 2.5 μW, the difference spectrum only reveals the electron singlet. Figure 5 shows the relative intensities of the singlet superimposed on the septet and of the resolved singlet at a power level of 2.5 μW. Neither of the spectra in Fig. 5 are saturated to a detectable extent.

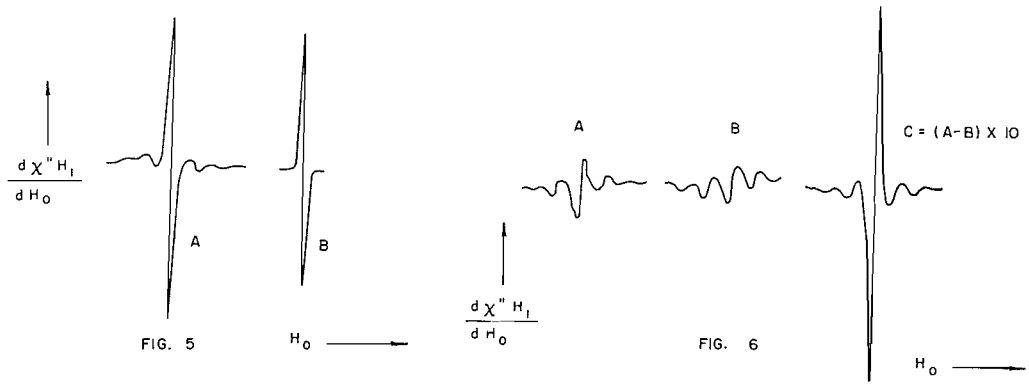

FIG. 5. Cavity input power 2.5 μW. A, unbleached MTHF; B, difference between unbleached and bleached MTHF.

FIG. 6. A, MTHF bleached until very pale blue; B, MTHF bleached until colorless; C, difference between A and B using a ten times greater sensitivity.

An experiment which illustrates the sensitivity of the technique is shown in Fig. 6. One irradiated MTHF sample was bleached until a very pale blue color remained, and the other was bleached until colorless. The spectrum of each and their difference spectrum (the latter at a sensitivity setting ten times greater than the former) was then recorded. Figure 6C clearly reveals the presence of trapped electrons while Fig. 6A only hints at their presence.

SUMMARY

The MTHF data have been presented to illustrate the difference technique. These data, together with data on trapped electrons in other systems, will be discussed in a subsequent paper. In particular, the technique is being used to measure the radiation-chemical *G*-values of trapped electrons with greater accuracy than is otherwise possible.

The technique could be used as a routine procedure to eliminate the central spectrum of the irradiated Spectrosil tube. This is valuable in systems where the radical yield is low and significant distortion of the free radical spectrum can occur.

In more specialized applications, the technique is limited to systems in which radiation-chemical yields can be reproduced fairly well. It is important to be able to produce pairs of samples having the same concentrations of the same paramagnetic species. Otherwise it is difficult to deduce, from the e.s.r. difference spectrum, chemical reactions resulting from an operation on one member of the pair, such as photochemical bleaching. We have encountered no trouble from this factor in several organic glasses studied. However, in polycrystalline systems, which may have a phase transition at a temperature above 77 °K, very careful annealing at the transition temperature will be necessary before one can even hope to succeed in reproducing radiation-induced yields of free radicals. This is because the free radical yield apparently depends on the structure of the crystal lattice. Plunging a sample rapidly into liquid nitrogen freezes a significant amount of the material in the form of the high-temperature phase. If the sample is first annealed at the phase transition tem-

Can. J. Chem. Downloaded from www.nrcresearchpress.com by 210.87.254.40 on 09/05/12
For personal use only.

perature and then cooled to 77 °K, the low-temperature phase structure is formed. In cyclohexane, Bensasson *et al.* (14) measured the yield of cyclohexyl radicals. The rapid-freezing procedure yielded $G(C_6H_{11}\cdot)$ equal to 3 or 4. Samples which were annealed at 193 °K (the phase transition temperature) for 15 hours before cooling to 77 °K yielded $G(C_6H_{11}\cdot)$ equal to about 1.2. Similar treatment of cyclopentane samples yielded $G(C_5H_9\cdot)$ equal to 2 and 0.3, respectively.

ACKNOWLEDGMENTS

We wish to thank Dr. J. S. Geiger for valuable advice and Mr. J. C. Tole for his assistance in checking the amplitude and phase of the 100 kc/s field modulation. Dr. R. H. Betts deserves thanks for his continuous encouragement and critical discussion.

REFERENCES

1. R. C. Smith and T. H. Wilmshurst. J. Sci. Instr. **40**, 371 (1963).
2. J. S. Hyde and H. W. Brown. J. Chem. Phys. **37**, 368 (1962).
3. P. J. Dyne, D. R. Smith, and J. Denhartog. Discussions Faraday Soc. **36**, 135 (1963).
4. P. B. Ayscough and C. Thomson. Trans. Faraday Soc. **58**, 1477 (1962).
5. B. Smaller and M. S. Matheson. J. Chem. Phys. **28**, 1169 (1958).
6. H. W. Fenrick, S. V. Filseth, A. L. Hanson, and J. E. Willard. J. Am. Chem. Soc. **85**, 3731 (1963).
7. H. S. Judeikis and J. M. Flournoy. J. Chem. Phys. **37**, 2272 (1962).
8. J. A. Staples, III. Nuclear Aerospace Research Facility Report NARF-63-4T. 1963.
9. L. Kevan, P. N. Moorthy, and J. J. Weiss. J. Am. Chem. Soc. **86**, 771 (1964).
10. C. Chachaty and E. Hayon. Nature, **200**, 59 (1963).
11. M. J. Blandamer, L. Shields, and M. C. R. Symons. Nature, **199**, 902 (1963).
12. D. Schulte-Frohlinde and K. Eiben. Z. Naturforsch. **17a**, 445 (1962).
13. A. Salmon. Discussions Faraday Soc. **36**, 286 (1963).
14. R. Bensasson, K. Leibler, R. Marx, and H. Szwarc. Bulletin Ampère, 9e année, fasc. spécial. 1960. p. 303.

Can. J. Chem. Downloaded from www.nrcresearchpress.com by 210.87.254.40 on 09/05/12
For personal use only.

THERMODYNAMICS OF TERNARY UNIVARIANT SYSTEMS OF THE TYPE: WATER – METAL SALT – ACID

J. W. LORIMER
Department of Chemistry, University of Western Ontario, London, Ontario
Received February 4, 1964

ABSTRACT

Thermodynamic equations for the variation of vapor pressure and composition with temperature along ternary univariant lines on phase diagrams of systems typified by H_2O–$ZnSO_4$–H_2SO_4 are developed. The usefulness of these equations in testing the consistency of experimental data, in estimating invariant points, and in obtaining thermodynamic data is discussed.

Quantitative thermodynamic treatments of phase diagrams are recognized as being valuable in "checking, extrapolation, interpolation, prediction" (1), and such treatments for binary systems and a number of types of ternary systems have been summarized (1, 2, 3). Ternary phase diagrams which describe, for example, the effect of addition of sulphuric acid on the solubility of a metal sulphate and its hydrates in water do not appear to have been subjected to systematic thermodynamic analysis. Ternary univariant lines are conspicuous features of diagrams of this type, and general equations for these lines are discussed in this paper.

Experimental data from the literature on the system H_2O–$ZnSO_4$–H_2SO_4 are used to illustrate the application of the theoretical analysis. Three hydrates, three incongruent binary transitions, and a ternary quintuple point are involved in the known equilibria in this system.

1. GENERAL EQUATIONS FOR THE TERNARY UNIVARIANT EQUILIBRIA

On the schematic isothermal ternary diagram shown in Fig. 1, A is a volatile component

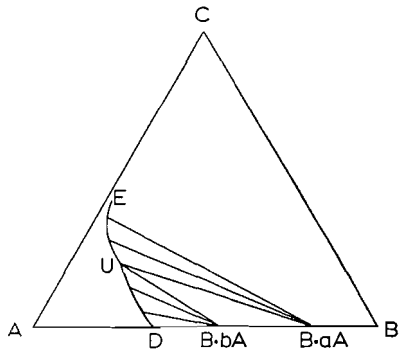

FIG. 1. Schematic isothermal ternary diagram (see text).

(e.g. H_2O) while B and C are nonvolatile (e.g. $ZnSO_4$, H_2SO_4, respectively). Components A and B form the binary compounds $B.aA$ and $B.bA$ ($b > a \geqslant 0$), which may melt either congruently or incongruently. The solubility curves UE, DU of these binary compounds intersect at the ternary univariant point U, at which the phases solid α (compound $B.aA$),

Can. J. Chem. Downloaded from www.nrcresearchpress.com by 210.87.254.105 on 09/05/12
For personal use only.

solid β (compound B.bA), solution saturated with respect to the two binary compounds, and vapor A are mutually in equilibrium. As the temperature is increased, point U moves towards the binary AB axis to become eventually a binary invariant point (either a eutectic or a transition point) or even a ternary invariant, or quintuple point.*

In principle, two cases must be distinguished in the analysis. (*a*) The total pressure P on the system is equal to the vapor pressure π of component A. This case is important for the comparison of the vapor pressure of the solution with the dissociation pressure of one solid phase. (*b*) The system is kept at a fixed total pressure P by addition of an indifferent gas; $dP = 0$, $d\pi \neq 0$. This is the condition under which most experimental composition–temperature data have been obtained. Strictly speaking, admission of air to the system introduces another component, and the system is divariant (cf. ref. 2, p. 148). The analysis is thus indeterminate unless the total pressure is kept constant.

At thermodynamic equilibrium, the conditions for chemical equilibrium are:

$$[1] \qquad d\mu^{\alpha} = a\, d\mu_1' + d\mu_2';\ d\mu^{\beta} = b\, d\mu_1' + d\mu_2';\ d\mu_1' = d\mu_1'',$$

where the superscripts α, β, $'$, $''$ refer to the two solid phases, solution, and vapor, respectively. Expansion of these equations as functions of temperature and pressure leads readily to the general vapor pressure equation:

$$[2] \qquad \Delta H_{tr}\, dT/T - \Delta V_{tr}\, dP = (b - a)(d\mu_1'')_{T,P}$$

and

$$[3] \qquad (d\mu_1')_{T,P} = RT\, d \ln f_i' x_i' = dk_i(T, P), \qquad i = 1, 2,$$

where

$$[4] \qquad \begin{cases} dk_1(T, P) = -\Delta H_v\, dT/T - v_1'\, dP + RT\, d \ln \pi, \\ dk_2(T, P) = (a\Delta H_v + \Delta H_s^{\alpha})\, dT/T - (a\Delta V_v + \Delta V_s^{\alpha})\, dP - aRT\, d \ln x_1'' \\ \qquad\qquad = (b\Delta H_v + \Delta H_s^{\beta})\, dT/T - (b\Delta V_v + \Delta V_s^{\beta})\, dP - bRT\, d \ln x_1'', \end{cases}$$

$$[5] \qquad x_3'(d\mu_3')_{T,P} = -x_1'(d\mu_1')_{T,P} - x_2'(d\mu_2')_{T,P}.$$

Subscripts 1, 2, 3 refer to compounds A, B, C, respectively. ΔH_{tr} is the enthalpy of dissociation of compound β into α plus A vapor, ΔH_v is the enthalpy of vaporization from the saturated solution, $\Delta H_s^{\alpha,\beta}$ are the enthalpies of solution of α and β, v_1' is the partial molal volume of A in solution, π is the partial pressure of A in the vapor, and f_i' is the mole fractional activity coefficient of i. The volume terms are in each case defined analogously to the enthalpies.

2. THE VAPOR PRESSURE CURVES

Case (a) $P = \pi$

Equation [2] gives rigorously

$$[6] \qquad d\pi/dT = \Delta H_{tr}/T\Delta V_{tr},$$

the ternary univariant Clapeyron equation, which has been deduced by other methods (3, 4). The volume term may be written

$$[7] \qquad \Delta V_{tr}/(b - a) = (V^{\alpha} - V^{\beta})/(b - a) + RT/\pi + B,$$

where $B \sim 31$ cm^3 mole^{-1} is the van der Waals' covolume for water vapor. The molal

**Univariant systems involving ternary compounds (such as the hydrate of a metal acid sulphate) do not always have a dissociation pressure and are excluded specifically from this analysis.*

Can. J. Chem. Downloaded from www.nrcresearchpress.com by 210.87.254.105 on 09/05/12
For personal use only.

volumes of the hydrates of zinc sulphate are (5): $7H_2O$, 146; $6H_2O$, 130; H_2O, 58 cm^3 $mole^{-1}$. The term $V^\alpha - V^\beta$ is thus negative, and partially cancels B, making the approximation

$$\Delta V_{tr} = (b - a)RT/\pi \quad [8]$$

good to at least 0.03% for vapor pressures of 0.5 atm and lower and temperatures between 0 and 90 °C. The approximation gives

$$d \ln \pi/d(1/T) = -\Delta H_{tr}/R(b - a). \quad [9]$$

Equation [9] can be deduced without any reference to the solution phase, and is therefore also valid for the binary univariant system with phases solid B.aA, solid B.bA, and A vapor. The vapor pressure of the volatile component is the "dissociation pressure" for B.bA. Dissociation pressures for the system $ZnSO_4$–H_2O have been reviewed recently (6, 7), and values of the heat of transition per mole of water are given in Table I as

TABLE I

Thermodynamic data for univariant equilibria in the system H_2O–$ZnSO_4$–H_2SO_4*

	Equilibrium solid phases		
	B.$7H_2O$–B.$6H_2O$	B.$7H_2O$–B.H_2O	B.$6H_2O$–B.H_2O
$\Delta H_{tr}/(b - a)$	14.7	12.2	11.8
$\Delta G_{tr}^0/(b - a)$ (298.16)	2.3	2.4	2.4
$\lambda_1 \equiv d \ln a_1'/d(1/T)$, deg	2.1×10^3	0.80×10^3	0.60×10^3
$\Delta H_{tr}'/(b - a)$	4.1	1.6	1.2
β_1, deg	214	92	100
$d \ln f_1'/d(1/T)$, deg	-1.9×10^3	-0.71×10^3	-0.50×10^3
β_2, deg	2.99×10^3	3.20×10^3	2.09×10^3

*All quantities are in kcal $mole^{-1}$, except where noted. B ≡ $ZnSO_4$.

$\Delta H_{tr}/(b - a)$. The variation of the heat of transition with temperature is negligibly small. For example, over the range of coexistence of the hepta- and hexa-hydrates (21–39 °C), heat capacity data (2, 7) indicate that ΔH_{tr} changes by only 30 cal $mole^{-1}$.

Case (b) P = Constant

Equation [2] again gives eq. [9]; i.e., the partial vapor pressure of A is essentially unaffected by addition of an indifferent gas to a total pressure of at least 1 atm. At a given temperature,

$$d \ln \pi/dP = (V^\beta - V^\alpha)/(b - a)RT \quad [10]$$

or, approximately

$$\Delta\pi/\pi_0 = (V^\beta - V^\alpha)(P - \pi_0)/(b - a)RT, \quad [11]$$

where π_0 is the vapor pressure with no indifferent gas present. At 0 °C and 1 atm, $\Delta\pi/\pi_0 \sim$ 0.06%, a negligible amount. The standard Gibbs' free energy of transition is

$$\Delta G_{tr}^0 = -\int_{1\text{ atm}}^{\pi\text{ atm}} \Delta V_{tr}\, dP = -(b - a)RT \ln \pi\text{ atm}, \quad [12]$$

values of which are given for 298 °K in Table I.

One further quantity may be calculated from the vapor pressures. If it is taken that

Can. J. Chem. Downloaded from www.nrcresearchpress.com by 210.87.254.105 on 09/05/12
For personal use only.

$a_1' = 1$ when $\pi = P_0$, the vapor pressure of pure component A at temperature T, the activity of component A in solution is, according to eqs. [1] and [3],

$$[13] \qquad (a_1')_{T,\pi} = \pi/P_0.$$

The quantity of interest here, however, is the variation of the activity of component A with temperature, which is discussed below.

3. THE COMPOSITION CURVES

Case (a) $P = \pi$

If, as in [8], the volume of the condensed phases is neglected in comparison with that of the vapor, and the vapor is ideal, eq. [4] becomes

$$[14] \qquad T\,\mathrm{d}k_1(T)/\mathrm{d}T = \Delta H_{tr}'/(b-a) \equiv R\lambda_1,$$

$$[15] \qquad \begin{aligned} T\,\mathrm{d}k_2(T)/\mathrm{d}T &= \Delta H_s^{\alpha} - a\Delta H_{tr}'/(b-a) \\ &= \Delta H_s^{\beta} - b\Delta H_{tr}'/(b-a) \\ &= (b\Delta H_s^{\alpha} - a\Delta H_s^{\beta})/(b-a) \equiv R\lambda_2, \end{aligned}$$

where

$$[16] \qquad \Delta H_{tr}' = \Delta H_{tr} - (b-a)\Delta H_v = \Delta H_s^{\beta} - \Delta H_s^{\alpha}$$

is the heat of transition (negative of the "enthalpy of hydration" (6)) for the process

$$\mathrm{B}.b\mathrm{A(s)} = \mathrm{B}.a\mathrm{A(s)} + (b-a)\mathrm{A(sat.\ soln.)}$$

and $R\lambda_1$, $R\lambda_2$ are abbreviations for the appropriate enthalpy terms. The heats of vaporization for the solution and for pure water differ by the relative partial molal heat content of water in the saturated solution, which in general is negligibly small compared to ΔH_v (see ref. 11, p. 541 for relevant data). Table I lists values of $\Delta H_{tr}'/(b-a)$ where average values of ΔH_v for pure water over the temperature range of stable existence of the various hydrates have been used (5). A substitution of [14] and [15] into [3] gives:

$$[17] \qquad \mathrm{d}\ln f_i' x_i'/\mathrm{d}(1/T) = -\lambda_i, \qquad i = 1, 2,$$

or

$$[18] \qquad \mathrm{d}\ln x_i'/\mathrm{d}(1/T) = -\mathrm{d}\ln f_i'/\mathrm{d}(1/T) - \lambda_i \equiv -\beta_i, \qquad i = 1, 2.$$

If the λ_i and β_i are independent of temperature, [37] and [38] integrate to

$$[19] \qquad f_i' x_i' = f_i'^{*} x_i'^{*} \exp\{\lambda_i(1/T^* - 1/T)\}, \qquad i = 1, 2,$$

and

$$[20] \qquad x_i' = x_i'^{*} \exp\{\beta_i(1/T^* - 1/T)\},$$

where $T = T^*$ at $x_i = x_i^*$, a reference temperature and mole fraction. Equations [18] and [5] give

$$[21] \qquad \begin{aligned} \mathrm{d}x_3'/\mathrm{d}(1/T) &= \beta_1 x_1' + \beta_2 x_2' \\ &= \lambda_1 x_1' + \lambda_2 x_2' - x_3'\,\mathrm{d}\ln f_3'/\mathrm{d}(1/T). \end{aligned}$$

Introduction of [20] into [21] and subsequent integration gives

$$[22] \qquad x_3' = x_3'^{*} + x_1'^{*}[1 - \exp\{\beta_1(1/T^* - 1/T)\}] + x_2'^{*}[1 - \exp\{\beta_2(1/T^* - 1/T)\}].$$

Can. J. Chem. Downloaded from www.nrcresearchpress.com by 210.87.254.105 on 09/05/12
For personal use only.

Case (b) P = Constant

Equation [4] again gives [14] and [15], if the volume of the condensed phases is neglected in comparison with that of the vapor; i.e., the composition curves are essentially unaffected by addition of an indifferent gas to a total pressure of, for example, 1 atm, the condition under which most solubility data have been obtained.

From eqs. [2] and [4], the explicit dependence of composition on pressure at a given temperature is

$$[23] \qquad \mathrm{d} \ln f_1' x_1' / \mathrm{d}P = -\Delta V_{tr} / RT(b - a),$$

$$[24] \qquad \mathrm{d} \ln f_2' x_2' / \mathrm{d}P = -(b\Delta V_s^{\alpha} - a\Delta V_s^{\beta}) / RT(b - a),$$

where $\Delta V_{tr}'$ is defined analogously to $\Delta H_{tr}'$. From the values for the molal volumes of the zinc sulphate hydrates, $v_1' \sim 18$ cm^3 mole^{-1} and $v_2' \sim 10$–20 cm^3 mole^{-1}, [23] and [24] indicate that the variation of activity with pressure will not exceed 0.1% per atm. Equations [17] through [22] may now be applied to experimental composition data. In systems such as H_2O–$ZnSO_4$–H_2SO_4, it is customary to analyze equilibrium systems for zinc and sulphate to obtain the number of moles of $ZnSO_4$ and H_2SO_4. The moles of H_2O are found by difference. Under these conditions,

$$\Delta n_i'/n_i' = \Delta x_i'/x_i', \qquad i = 2, 3,$$

that is, a relative error in the number of moles of $ZnSO_4$ or H_2SO_4 will give rise to the same relative error in the mole fractions of these two components. The mole fraction of H_2O, however, reflects errors in analyses of both of the other two components.

Figure 2 contains plots of log x_1' against $1/T$, which appear to be linear; that is, β_1 is

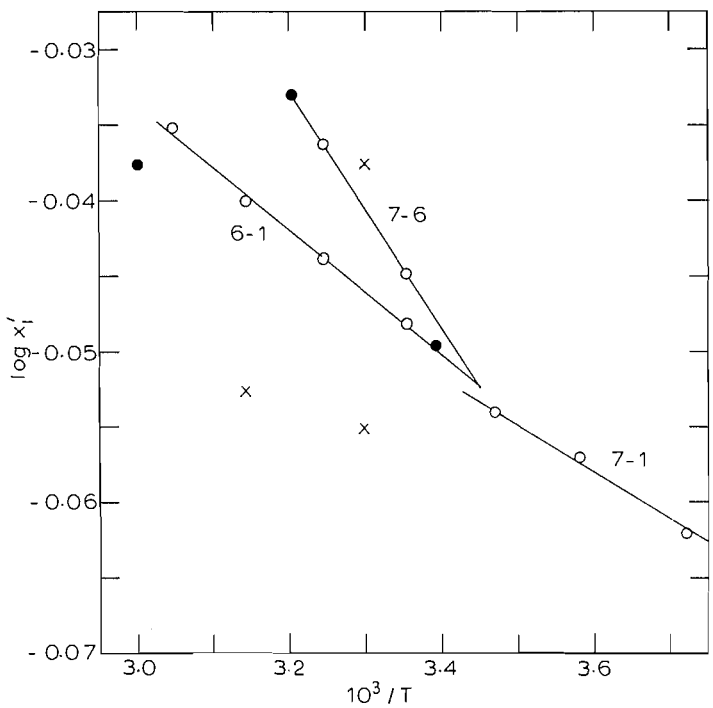

FIG. 2. Log (mole fraction of water) vs. reciprocal temperature plot for H_2O–$ZnSO_4$–H_2SO_4 ternary univariant solutions: ○ Copeland and Short (8); × Joshi and Devadatta (10); ● invariant points of Copeland and Short. The numbers 7–1, 7–6, 6–1 identify the solid hydrates present.

Can. J. Chem. Downloaded from www.nrcresearchpress.com by 210.87.254.105 on 09/05/12
For personal use only.

constant. Estimated invariant points (8) are also included on the plot. Since the vapor pressure data indicate that λ_1 is also constant, it follows that d ln f_1'/d$(1/T)$ is also constant to within experimental error. These plots are consistent with a quintuple point at 21 °C, $x_1' = 0.892$ (8), only if there is marked curvature of the 7–6 and 7–1 lines near this point, or if the experimental errors are large. The experimental data (8) indicate that the error in the mole fraction of H_2O can be as large as 3%. Since x_1' is close to unity, this error is magnified greatly on the logarithmic plot, and the plot is thus unsuitable for extrapolation or interpolation purposes. It is preferable, therefore, to note that x_1' is constant for any given transition to within 1%, and that eq. [18] may be written

$$[25] \qquad d(x_2' + x_3')/d(1/T) = \beta_1 x_1'.$$

Plots of $x_2' + x_3'$ against $1/T$ are shown in Fig. 3. While it is difficult to decide from the

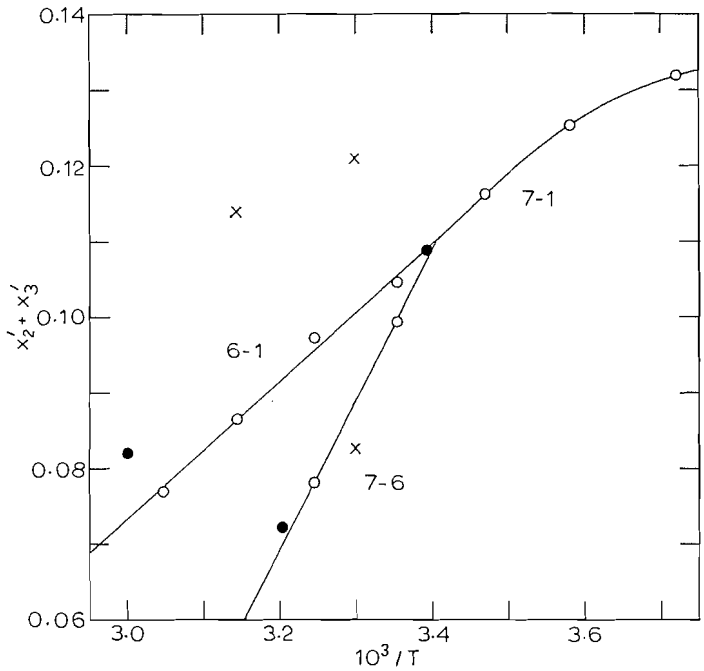

FIG. 3. Total mole fraction of $ZnSO_4$ and H_2SO_4 vs. reciprocal temperature plot for H_2O–$ZnSO_4$–H_2SO_4 ternary univariant solutions. The points correspond to those in Fig. 1.

available data whether or not these plots are curved (except for the low temperature portion of the $7H_2O$–H_2O transition line), best straight lines extrapolate to a quintuple point at 20 °C, $x_1' = 0.890$, in good agreement with other estimates (6, 8). The composition at the $7H_2O$–$6H_2O$ binary transition point appears to be slightly in error, since vapor pressure data (6) substantiate the transition temperature of 39 °C. There appears to be no support for the contention of Copeland and Short (8) that their data indicate a $6H_2O$–H_2O binary transition at 60 °C rather than at 70 °C (6). Table I lists the values of β_1 and d ln f_1'/d$(1/T)$ derived from these plots.

Figure 4 shows plots of log x_2' vs. $1/T$, including estimated invariant points (8). The plots are linear (with the exception of the high temperature portion of the $6H_2O$–H_2O transition line), and give a quintuple point at 21 °C, $x_2' = 0.0396$, in good agreement with

Can. J. Chem. Downloaded from www.nrcresearchpress.com by 210.87.254.105 on 09/05/12
For personal use only.

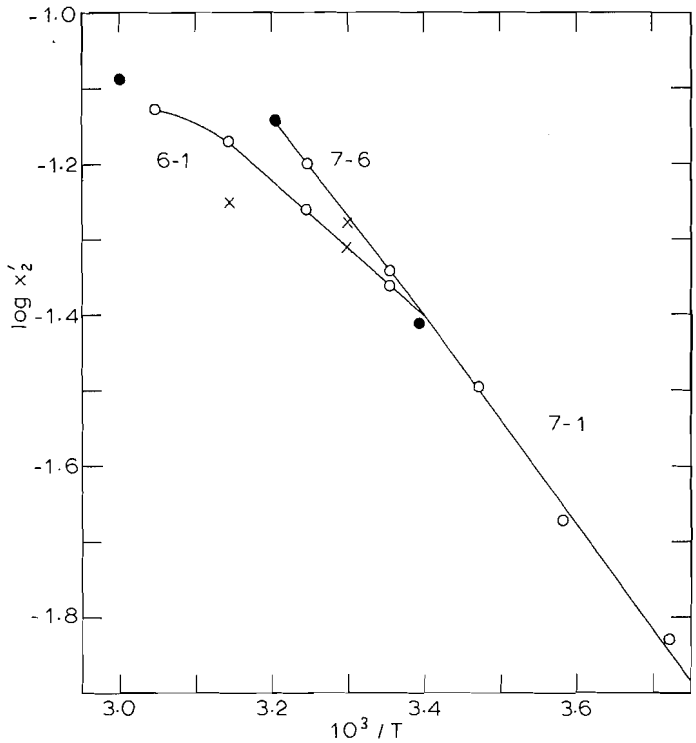

FIG. 4. Log (mole fraction of $ZnSO_4$) vs. reciprocal temperature plot for H_2O–$ZnSO_4$–H_2SO_4 ternary univariant solutions. The points correspond to those in Fig. 1.

other estimates ((6, 8) $x_2' = 0.0388$). Again, the composition at the $7H_2O$–$6H_2O$ binary transition appears to be slightly in error, and there is no support for a $6H_2O$–H_2O binary transition at 60 °C.

Unfortunately, no data are available which permit an estimate of the variation of the activity of $ZnSO_4$ along these univariant lines. However, it would appear that $d \ln f_2'/d(1/T)$ is constant along the linear portions of the plots in Fig. 4, since λ_2 should be almost independent of temperature. Values of β_2 from these plots are given in Table I.

Figure 5 shows plots of x_3' against $1/T$, including estimated invariant points (8). The solid lines in Fig. 5 have been calculated from eq. [22] using values of β_1 and β_2 from Table I and the quintuple point data from Figs. 3 and 4. ($10^3/T = 3.405$, $x_2' = 0.0395$, $x_3' = 0.0705$.) The broken lines are based on the same values of β_1 and β_2 and the quintuple point data estimated by Copeland and Short (8). From [18] and [21],

$$d^2x_3'/d(1/T)^2 = -(\beta_1^2 + \beta_2^2),$$

so that the x_3' vs. $1/T$ plots are always convex upwards.

The lines based on the quintuple point estimated by the above methods represent the experimental points better on the whole than the line based on the Copeland and Short quintuple point. The solid lines extrapolate to $x_3' = 0$ to give a $7H_2O$–$6H_2O$ binary transition at 38.9 °C, compared to the precisely known value 38.12 °C (7, 9). The $6H_2O$–H_2O transition point is, by extrapolation, 52.5 °C, in bad agreement with the value 70 °C from vapor pressure data (6). It is noteworthy that the $7H_2O$–H_2O binary transition from

Can. J. Chem. Downloaded from www.nrcresearchpress.com by 210.87.254.105 on 09/05/12
For personal use only.

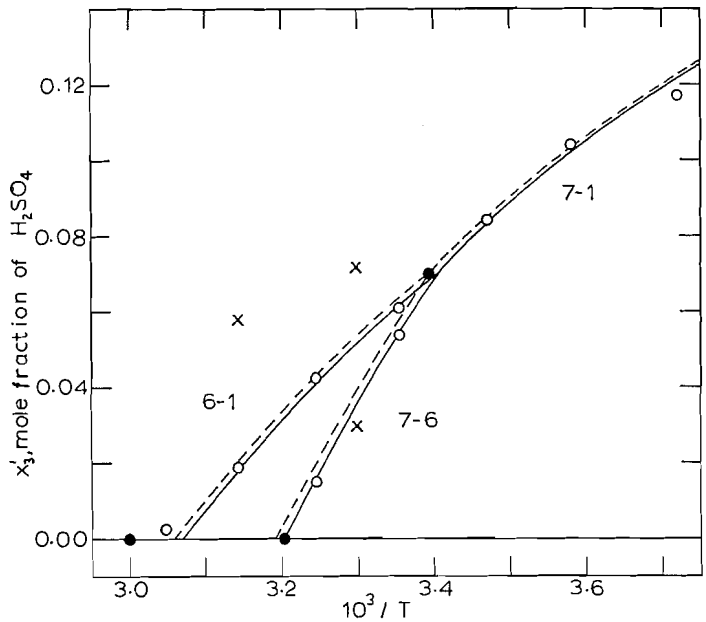

FIG. 5. Mole fraction of H_2SO_4 vs. reciprocal temperature plot for H_2O–$ZnSO_4$–H_2SO_4 ternary univariant solutions. The points correspond to those of Fig. 1; — and - - - are calculated lines based on quintuple points of this paper and of Copeland and Short (8), respectively.

vapor pressure data is 55 °C (6), which suggests that the higher temperature data for the $6H_2O$–H_2O equilibria may actually be for $7H_2O$–H_2O equilibria.

Two points for $6H_2O$–H_2O equilibria and one for $7H_2O$–$6H_2O$ determined by Joshi and Devadatta (10) are included in each of Figs. 2–5. The $7H_2O$–$6H_2O$ point agrees reasonably well with the Copeland and Short data, but the $6H_2O$–H_2O points are evidently greatly in error, except for one x_2' value.

Finally, the apparent insensitivity of the activity coefficients of H_2O and $ZnSO_4$ along the univariant lines must be considered. These activity coefficients are presumably determined by temperature, ionic strength, and total molality. It is difficult to estimate the ionic strength because of the significant ion-pair formation in $ZnSO_4$ solutions (11, p. 190) and the considerable variation of the second dissociation constant of H_2SO_4 with temperature (12). However, if it is assumed that the only ionic species present are H^+ and HSO_4^- (from H_2SO_4) and Zn^{2+} and SO_4^{2-} (from $ZnSO_4$), the ionic strength is simply

$$I = 55.5(2x_2' + x_3')/x_1'.$$

From the experimental data, it is found that this ionic strength varies less than 5% along the $7H_2O$–H_2O univariant lines and about 10% along the $7H_2O$–$6H_2O$ line. The total molality is given to a good approximation by $x_2' + x_3'$ (Fig. 3), and varies 30–40% along the univariant lines. Apparently the relatively small variation in ionic strength is the main reason that the variation of the activity coefficients with composition along the univariant lines is of little importance for the present analysis.

It should be noted that if the activity coefficients do vary with composition, the β_i in eq. [18] will in general no longer be constant, and the equations for the composition curves will take on a much more complex form.

Can. J. Chem. Downloaded from www.nrcresearchpress.com by 210.87.254.105 on 09/05/12
For personal use only.

REFERENCES

1. J. L. MEIJERING. National Physical Laboratory Symposium No. 9. Vol. II. Paper 5A. (1959).
2. I. PRIGOGINE and R. DEFAY. *Transl. by* D. H. Everett. Chemical thermodynamics. Longmans, Green and Co., London. 1954.
3. J. F. KIRKWOOD and I. OPPENHEIM. Chemical thermodynamics. McGraw-Hill Book Co. Inc., New York. 1961.
4. J. C. M. LI. J. Chem. Phys. **25**, 572 (1956).
5. International critical tables. 1st ed. McGraw-Hill Book Co., Inc., New York. 1929.
6. J. D'ANS, H.-E. FREUND, and E. KAUFMANN. Z. Elektrochem. **61**, 546 (1957).
7. R. E. BARIEAU and W. F. GIAUQUE. J. Am. Chem. Soc. **72**, 5276 (1950).
8. L. C. COPELAND and O. A. SHORT. J. Am. Chem. Soc. **62**, 3285 (1940).
9. E. COHEN, K. INOUYE, and C. EUWEN. Z. Physik. Chem. **75**, 1 (1910).
10. N. K. JOSHI and S. C. DEVADATTA. Proc. Indian Acad. Sci. Sect. A, **7**, 130 (1938).
11. H. S. HARNED and B. B. OWEN. The physical chemistry of electrolytic solutions. 2nd ed. Reinhold Publishing Corp., New York. 1950.
12. R. A. ROBINSON and R. H. STOKES. Electrolyte solutions. 2nd ed. Butterworths Scientific Publications, London. 1959. p. 387.

Can. J. Chem. Downloaded from www.nrcresearchpress.com by 210.87.254.105 on 09/05/12
For personal use only.

Can. J. Chem. Downloaded from www.nrcresearchpress.com by 210.87.254.40 on 09/05/12
For personal use only.

OCCURRENCE OF TRANS-3-HEXADECENOIC ACID IN A SEED OIL[1]

C. Y. Hopkins and Mary J. Chisholm
Division of Pure Chemistry, National Research Council, Ottawa, Canada

Received May 28, 1964

ABSTRACT

trans-3-Hexadecenoic acid was found to be a component of the glyceride oil of seeds of *Helenium bigelowii* A. Gr. It constituted about 10% of the total fatty acids. The acid was isolated and identified by oxidative cleavage and by its infrared and nuclear magnetic resonance (n.m.r.) spectra. Reaction with alkaline permanganate gave 3-hydroxypalmito-γ-lactone. Mild alkaline treatment of methyl *trans*-3-hexadecenoate caused a shift of the double bond to the 2-position. A sample of *Helenium hoopesii* seed oil did not contain any *trans*-unsaturated acid.

Glyceride acids with unsaturation in the 3-position were not known to occur in seed oils until very recently. Two such acids were reported in 1964, viz. a 3,9,12,15-tetraene acid, found by Hopkins and Chisholm in a species of *Tecoma* (Bignoniaceae) (1), and a 3,9,12-triene acid, found by Bagby and co-workers in a species of *Calea* (Compositae) (2). Both of these are C_{18} acids.

In the present work, the seed oil of *Helenium bigelowii* A. Gr. (family Compositae) was found to contain a substantial amount of a *trans*-monoene acid which proved to be *trans*-3-hexadecenoic acid. This species of *Helenium* is a herbaceous plant, native to North America, and is grown as a flowering perennial. A sample of a related species, *H. hoopesii* A. Gr., did not contain any *trans* fatty acid.

The seed oil of *H. bigelowii* had no conjugated unsaturation but its infrared spectrum revealed the presence of isolated *trans* olefinic unsaturation (υ_{max} = 960 cm^{-1}, C—H out-of-plane bending mode (3)). The oil was converted to methyl esters and submitted to gas–liquid chromatography (g.l.c.). The chromatogram indicated the presence of 12% of hexadecenoic acid.

The mixed acids were crystallized fractionally from acetone at low temperatures and the fractions were examined by g.l.c. and by infrared absorption. It was evident that the component responsible for *trans* absorption was in the hexadecenoic acid fraction. Repeated crystallization of this fraction from acetone at low temperatures gave a pure acid, m.p. 53–54°. Its methyl ester had an infrared maximum at 962 cm^{-1}, equal in intensity to the same peak in the spectrum of methyl elaidate, confirming the presence of one *trans* double bond.

Hydrogenation of the acid gave palmitic acid, establishing its structure as a straight chain, C_{16} acid. Oxidative cleavage gave tridecanoic acid, showing that the double bond is at the 3-position. The compound is therefore *trans*-3-hexadecenoic acid (I). The melting point is in agreement with recorded data (3). The structure was confirmed by the n.m.r. spectrum, which had the following bands (tetramethylsilane = 0):

Chem. shift, δ	Type of band	No. protons	Assignment
5.56	Quintuplet	2	CH=CH
3.07	Essentially doublet	2	=CHCH_2CO
2.04	Multiplet	2	CH_2CH=
0.89	Multiplet	3	CH_3

$CH_3(CH_2)_{11}CH{=}CHCH_2COOH$

[1]*Issued as N.R.C. No. 8065.*

The band at $\delta = 3.07$ is assigned to the methylene protons in the grouping $=CHCH_2CO$ on the basis of its chemical shift and its essentially doublet structure. This is supported by the absence of the band characteristic of the ordinary methylene group adjacent to carboxyl, which would appear at $\delta = 2.3$ (4). Furthermore, the band given by methylene protons adjacent to an isolated double bond ($\delta = 2.04$) represents only two protons.

Hydroxylation of the acid by alkaline permanganate gave a lactone, judged to be 3-hydroxypalmito-γ-lactone (II), because of the known ease of formation of γ-lactones from hydroxy acids. It had infrared maxima at 3540s (OH stretching) and 1763, 1785vs (C=O stretching in γ-lactone (5)).

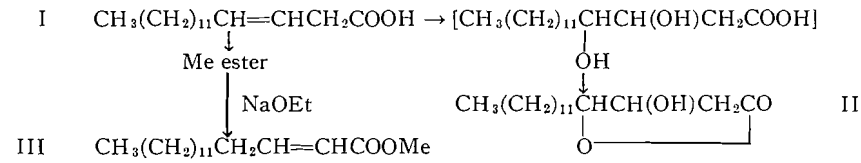

The ester of *trans*-3-hexadecenoic acid was heated with ethanol containing sodium ethoxide according to the procedure of Linstead and Noble (6). This caused a shift of the double bond to the 2-position (III), as shown by the infrared and n.m.r. spectra. A strong C=C stretching band appeared at 1653 cm^{-1} in the infrared (αβ-unsaturated ester (7)). This bond shift, produced under relatively mild conditions, is further proof that the original double bond is at Δ^3. The n.m.r. spectrum of the product had a typical ABX_2 pattern with multiplets centered at $\delta = 5.7$ and 7.0, representing the two olefinic protons. The coupling constant, J_{AB}, was 16 c.p.s., showing that the double bond is *trans* (8).

The amount of *trans*-3-hexadecenoic acid was about 10% of the total fatty acids of the oil. There was some evidence of a *trans* polyenoic acid.

EXPERIMENTAL

Infrared spectra were determined in carbon disulphide in a Perkin–Elmer model 21 spectrophotometer with sodium chloride prism. Nuclear magnetic resonance spectra were measured at 60 Mc/s on a Varian model A-60 spectrometer in deuterochloroform solution with tetramethylsilane as internal standard. Gas–liquid chromatography was carried out with a diethylene glycol – succinic acid polyester as liquid phase, on Celite, and a thermal conductivity detector. Petroleum ether refers to the fraction of b.p. 30–60°. Melting points were determined in capillary tubes and are corrected.

Helenium bigelowii Seed Oil

Seed of *Helenium bigelowii* A. Gr. was obtained from a reliable commercial source. Extraction of the ground seed with petroleum ether yielded 15% of oil. The oil had an infrared absorption peak at 960 cm^{-1} with intensity equivalent to a content of about 14% of *trans*-monoene fatty acid. There was no peak in the region 980–995 cm^{-1} (no conjugated unsaturation). A portion was converted to methyl esters. The mixed esters were analyzed by g.l.c. at 185°. The percentages of the various acids were (mean of three determinations): palmitic 10, hexadecenoic 12, octadecenoic 8, octadecadienoic 65, octadecatrienoic 5. There were no acids in the C_{20}–C_{22} region.

Isolation of the Acid

The oil was hydrolyzed by refluxing for 30 min with 6% ethanolic potassium hydroxide and the unsaponifiable matter was removed. The acids (31.2 g) were dissolved in 280 ml of acetone and the solution was cooled to −17° and then to −37°. Fatty acid crystals were filtered off at each stage and were examined by g.l.c. and by infrared absorption.

Fraction	Crystallizing temp., °C	Yield, g	Main component
F1	−17	3	Palmitic acid
F2	−37	4	*trans*-Hexadecenoic acid
F3	Filtrate	23	Octadecadienoic acid

Can. J. Chem. Downloaded from www.nrcresearchpress.com by 210.87.254.40 on 09/05/12
For personal use only.

Most of the *trans* acid was in fraction F2, which was solid. This fraction was crystallized from 30 ml of acetone at −20°. The crystals (2.55 g) consisted of 85% hexadecenoic acid and 15% palmitic acid, determined by g.l.c. One gram of this product, crystallized twice from acetone at −5°, yielded 118 mg of pure *trans*-3-hexadecenoic acid, m.p. 53–54° [lit. 53.5–55.0° (3)].

Anal. Calcd. for $C_{16}H_{30}O_2$: C, 75.5; H, 11.9. Found: C, 75.7; H, 12.25. Its n.m.r. spectrum is described above.

The methyl ester was prepared. It had υ_{max} = 962vs cm^{-1}, with intensity equivalent to one *trans* double bond.

Hydrogenation and Oxidative Cleavage

A portion of the acid (0.1 g) was hydrogenated in methanol with Adams platinum catalyst. It gave palmitic acid in quantitative yield, m.p. 62.0–62.5° alone and mixed with palmitic acid.

The monoenoic acid (0.06 g) was treated with permanganate–periodate by von Rudloff's procedure (9). On acidification, the reaction mixture gave a precipitate which was collected and crystallized once from acetone and once from pentane. It was tridecanoic acid, m.p. 38–39° alone and mixed with an authentic sample. The other products were extracted from the filtrate, esterified, and examined by g.l.c. There was no appreciable amount of any other monobasic acid.

3-Hydroxypalmito-γ-lactone

trans-3-Hexadecenoic acid (0.5 g) was dissolved in 500 ml of water containing 0.5 g of sodium hydroxide, mixed with 50 ml of 1% aqueous potassium permanganate, and allowed to stand at 20° for 6 min. The excess permanganate was destroyed, the solution was acidified and cooled in ice, and the precipitate was filtered off, dried, and washed with pentane to remove non-hydroxylic by-products. The residual product (0.14 g) was crystallized three times from ethanol at −20°, giving 3-hydroxypalmito-γ-lactone, m.p. 71–72°.

Anal. Calcd. for $C_{16}H_{30}O_3$: C, 71.1; H, 11.2. Found: C, 70.8; H, 11.0.

It formed glistening white flakes, moderately soluble in ethanol but insoluble in petroleum ether. It had υ_{max} = 3540s (OH), 1763, and 1785vs (γ-lactone). There was no peak in the region of acid carbonyl (ca. 1705 cm^{-1}).

Isomerization of the Ester

Methyl *trans*-3-hexadecenoate (0.3 g) was dissolved in 50 ml of absolute ethanol to which 0.035 g of sodium metal had been added. The solution was refluxed for 12 h, diluted with water, acidified, and extracted with petroleum ether. The extract contained some free acid. It was reesterified by methanol – hydrogen chloride. The liquid product (0.22 g) had υ_{max} 1653s (αβ-unsaturated ester). A model compound, methyl *trans*-2-octadecenoate, had a similar strong band at 1653 cm^{-1}.

Helenium hoopesii Seed Oil

Seed of *H. hoopesii* A. Gr. yielded 16% of oil, n_D^{25} 1.4753. Its ultraviolet spectrum had no maxima in the region 230–320 mμ (no conjugated diene or triene). The infrared spectrum showed much unsaturation (υ_{max} = 3000 cm^{-1}) but no *trans* double bonds (ca. 962 cm^{-1}). Analysis by g.l.c. showed the following percentages of fatty acids: palmitic 9; hexadecenoic, less than 1; octadecenoic 8; octadecadienoic 83.

DISCUSSION

Occurrence of a mono-unsaturated Δ^3 acid in seed oil fatty acids has not been observed previously. However, *trans*-3-hexadecenoic acid was detected by Debuch in 1961 in the leaves of two plant species (10) (not Compositae) and the same acid was isolated from an alga by Klenk and Knipprath in 1962 (3). Two polyenoic acids with unsaturation at Δ^3 are known to occur in seed oils (1, 2). The Δ^3 double bond in these three natural acids has the *trans* configuration. The 5-octadecenoic acid of *Thalictrum* seed oil is also *trans* (11). It is possible that ethylenic groupings near the carboxyl end of the chain tend to form in the *trans* configuration.

Natural monoenoic fatty acids include a group with various chain lengths in which the double bond is at position 3, 5, 9, 11, or 13, counting from the carboxyl end. This series, complete except for a Δ^7 acid, may be of significance in relation to the mechanism of biosynthesis. There is a strong likelihood that the longer chain monoenoic acids are formed by the addition of a 2-carbon unit at the carboxyl end of a shorter chain acid, e.g. 11-octadecenoic acid from 9-hexadecenoic acid (12), and 5-octadecenoic acid from 3-hexadecenoic acid.

Can. J. Chem. Downloaded from www.nrcresearchpress.com by 210.87.254.40 on 09/05/12
For personal use only.

ACKNOWLEDGMENTS

The authors are indebted to Mr. R. Lauzon for determining infrared spectra, to Mr. M. Lesage for n.m.r. spectra, and to Mr. H. Seguin for microanalyses.

REFERENCES

1. C. Y. HOPKINS and M. J. CHISHOLM. J. Chem. Soc. In press.
2. M. O. BAGBY, W. O. SIEGL, and I. A. WOLFF. *Presented before* the Am. Oil Chemists' Soc., New Orleans, U.S.A. April, 1964.
3. E. KLENK and W. KNIPPRATH. Hoppe-Seylers Z. Physiol. Chem. **327**, 283 (1962).
4. C. Y. HOPKINS. J. Am. Oil Chemists' Soc. **38**, 664 (1961).
5. A. D. CROSS. Introduction to practical infrared spectroscopy. Butterworth's, London. 1960. p. 64.
6. R. P. LINSTEAD and E. G. NOBLE. J. Chem. Soc. 610 (1934).
7. O. MERCURI, N. E. CARRAZONI, and R. R. BRENNER. J. Am. Oil Chemists' Soc. **41**, 89 (1964).
8. R. H. WILEY, T. H. CRAWFORD, and C. E. STAPLES. J. Org. Chem. **62**, 1535 (1962).
9. R. U. LEMIEUX and E. VON RUDLOFF. Can. J. Chem. **33**, 1701 (1955).
10. H. DEBUCH. Z. Naturforsch. **16**B, 561 (1961).
11. M. O. BAGBY, C. R. SMITH, JR., K. L. MIKOLAJCZAK, and I. A. WOLFF. Biochemistry, **1**, 632 (1962).
12. M. J. CHISHOLM and C. Y. HOPKINS. Can. J. Chem. **38**, 805 (1960).

Can. J. Chem. Downloaded from www.nrcresearchpress.com by 210.87.254.40 on 09/05/12
For personal use only.

Can. J. Chem. Downloaded from www.nrcresearchpress.com by 210.87.254.40 on 09/05/12
For personal use only.

THE REDISTRIBUTION REACTION OF BIS-MERCURIALS

W. E. French, N. Inamoto, and George F Wright
Department of Chemistry, University of Toronto, Toronto, Ontario
Received April 27, 1964

ABSTRACT

The demetalation of diorganosubstituted mercury compounds is catalyzed by peroxides. When organomercuric salts are present this demetalation leads to formation of mercurous salt plus mercury. This latter combination has been found to be a catalyst for the redistribution reaction of bis-mercurials. It is suggested that all previously reported catalysts for this reaction operate by formation of the mercurous salt – mercury combination. Equilibration studies with this combination as catalyst indicate that random exchange is not general for the redistribution reaction of mercury compounds.

The equilibration of organic substituent groups among mixtures of bis-organolead, organotin, and organomercurials has been summarized (1) by Calingaert, who coined the name "redistribution reaction" originally for the equilibration of tetraalkyllead compounds in which the substituents were homologous or structurally isomeric (2). He applied the name also to the simpler equilibration of bis-mercurials (3).

$$2R'—Hg—R \rightleftarrows R'—Hg—R' + R—Hg—R.$$

Obviously these reactions are, at most, "distributions"; the redundancy was unfortunate but at least it accentuated Calingaert's discovery that the "redistribution" was statistically random and unrelated to the structure of the substituent groups. Also, he demonstrated that the redistribution was catalyzed by metal halides and organometallic halides, including those related to the organometallic compounds that he was "redistributing".

Despite the mass of evidence relating to the redistribution reaction and its catalysis, we have found that for bis-mercurials it is quite erratic. For example, 4-cyclohexylmercuritoluene is recovered unchanged when it is treated in solvents such as methanol, petroleum ether, benzene, or dioxane with 1–5 mole % of the recommended (3) catalysts: boron fluoride etherate, aluminum chloride, magnesium bromide hydrate, zinc chloride, and cyclohexylmercuric chloride at room temperature. On the other hand, a moderately pure sample decomposes when heated without either solvent or any of the recommended catalysts, giving bis-4-tolylmercury. Likewise, for one operator, 2-butylmercuri-4-toluene in methanol or petroleum ether has been heated under reflux for 15 h without alteration in presence of mercuric bromide or 2-butylmercuric bromide. For another, a methanol solution of the substance has reacted in 8 h under reflux without added catalyst to give a 42% yield of bis-4-tolylmercury and a 47% yield of bis-2-butylmercury. Similar anomalies have been found for benzylmercuriethane.

Part of the reason for this lack of reliability has become evident during our attempts to isolate and preserve bis-cyclohexylmercury in a pure state for determination of its dielectric constant (4). The instability of this substance is apparent in its use (5) as a catalyst in the homopolar polymerization of vinyl acetate. We find that the recently crystallized white substance turns grey within an hour in air. If it is vacuum distilled immediately after crystallization, some decomposition occurs during the process, but the distillate is somewhat more stable than the crystalline material before distillation. However, it too begins to turn grey within a few hours. However, if the fresh distillate is

treated with alkali to decompose any contaminating mercurous salt and then is vacuum distilled, a product is obtained which is quite stable under vacuum or under pure nitrogen so long as it does not contain any peroxide.

It is evident that bis-cyclohexylmercury is very sensitive to oxygen. Indeed, we have been able to measure the dielectric constant in air only after addition of antioxidants. Among those tried the best is 2,5-di-*tert*-butylhydroquinone. Therefore, the oxygen seems to be acting as a source of organic peroxide.

In general, thermal stability of organomercurials (like other organometallic compounds) increases from tertiary to primary with respect to the substituent groups. Therefore, it is not unexpected that bis-benzylmercury, unlike bis-cyclohexylmercury, is stable in air at room temperature.

$$R—Hg—R' \rightleftarrows R—R' + Hg^0.$$

However, bis-benzylmercury without solvent decomposes slowly at 120–130° to metallic mercury and 1,2-diphenylethane. In benzene solution this decomposition is much slower but, as may be seen in Table I, it is accelerated by peroxidic catalysts.

TABLE I

Catalyzed decomposition of bis-benzylmercury in benzene (1:2 by weight)

Catalyst				
Name	Mole %	Temp., °C	Time, h	% Hg^0
None	0	85–105	9	1
t-Butylperoxide	5	Same	Same	6
t-Butylhydroperoxide	5	Same	Same	8
Ascaridole	5	Same	Same	40[a]
None	0	105–110	3	6
Mercurous chloride	5	Same	Same	8
Acetone peroxide	3	Same	Same	19
t-Butylperoxide	50	130	6	93[b]

[a]41% of 1,2-diphenylethane.
[b]69% of 1,2-diphenylethane, of preparative interest.

It would seem that a highly stable peroxide such as ascaridole is especially effective, as might be expected for a slow reaction such as this decomposition. It should be noted that mercurous chloride alone is relatively ineffective.

The catalysis demonstrated according to Table I explains why a comparatively stable unsymmetrical bis-mercurial, 2-butylmercuri-4-toluene, precipitates 55–60% of its mercury content as the metal during 4 h of reflux in the peroxidizable solvent dioxane. Similarly, a boiling methanol solution of the same mercurial to which 0.01% of conc. nitric acid has been added to generate peroxide (6) produces during 6 h *p*-bitolyl, of which 15% precipitates together with 88% of the original mercury in the form of the metal.

We knew that the bis-mercurials mentioned above contained traces of halogen, evidently as the organomercuric halides. Acting on the possibility that the redistribution proceeded via these salts, we have treated benzylmercuric chloride and cyclohexylmercuric chloride under the same conditions and with the same set of peroxidic catalysts as were used with the bis-mercurials. In every instance these salts have been recovered almost unchanged. However, a small amount (2–9%) of mercury and also of mercurous chloride is formed in presence of the peroxides. Thus the organomercuric salts are not catalytically redistributed by peroxides but their decomposition products might be involved.

Can. J. Chem. Downloaded from www.nrcresearchpress.com by 210.87.254.40 on 09/05/12
For personal use only.

Can. J. Chem. Downloaded from www.nrcresearchpress.com by 210.87.254.40 on 09/05/12
For personal use only.

With a knowledge of these contaminants in mind, we have now reviewed the redistribution reaction using 2-butylmercuri-4-toluene and benzylmercuriethane as typical disubstituted mercurials. The halogen-containing impurities have been removed from these mercurials by treating them with hydrazine hydrate at room temperature and then distilling them. No redistribution has been detected during distillation.

[1] $$4R—Hg—Cl + 5N_2H_4H_2O \rightarrow 2R—Hg—R + 4N_2H_5Cl + 5H_2O + N_2.$$

The examination of 2-butylmercuri-4-toluene has been made quantitatively with respect to the products, mercury and bis-4-tolylmercury, but only qualitatively with respect to the bis-2-butylmercury because of the tendency for this substance to decompose under some of the reaction conditions. The experiments (with magnetic stirring) have been carried out either in high boiling peroxide-free petroleum ether (S) or else neat (N, without solvent). Temperature, time, catalyst, and supernatant atmosphere (air or nitrogen) have been varied as shown in Table II.

It is evident from expts. 1 and 2 that the uncatalyzed reaction is impracticably slow. Moreover, substances like alkylmercuric halides (expts. 3, 5) are not effective catalysts, with or without peroxides, which themselves (expts. 4, 6, and 7) are of very low activity. In fact, the first substance which shows a significant effect is mercuric chloride (expt. 9), but the enhancement achieved by addition to it of metallic mercury (itself ineffective) shows (expt. 10) that a lower valence state is functioning. Involvement with mercurous chloride is indeed shown by the effectiveness of this substance with or without metallic mercury (expts. 11 and 12).

In fact, the effectiveness of these salts explains some of the erratic behavior characteristic of the redistribution reaction of bis-mercurials. Although Calingaert and his co-workers (3) do not mention any nonhomogeneity of their reacting systems, we have always observed that when redistribution occurs, a dirty second phase is present. Nor from the present findings would the system be expected to be clean. One may expect the following reactions to occur:

[2] $$RHgR \xrightarrow[\text{peroxide}]{\Delta} RR + Hg$$

[3] $$RHgX \rightarrow RX + Hg$$

[4] $$2RHgX \rightleftarrows R_2Hg + HgX_2$$

[5] $$HgX_2 + Hg \rightleftarrows Hg_2X_2.$$

Reaction [2] has been demonstrated in the present report (reaction [3] has been discovered, though not yet reported) from this laboratory. The equilibrium of reaction [4] will be strongly to the left, if RHgX is present only as a slight contaminant of R_2Hg. However, this equilibrium is a source of mercuric chloride which enters into the well-known equilibrium of reaction [5]. Thus, a proper combination of these four reactions will furnish some mercurous salt.

Because of a tendency for RHgCl to co-distill and co-crystallize with RHgR, it is very difficult to obtain halogen-free organodisubstituted mercury compounds. We believe that the seemingly spontaneous redistributions reported in the past were due to halogen contamination (and this belief includes our own work before we adopted the purification with hydrazine hydrate). Either because halogen is inadvertently present or else because it is introduced in ostensible catalysts such as Calingaert used, the presence of halogen will give rise to mercurous halide according to reactions [2]–[5]. Therefore, the actual catalyst may, in the past, have been synthesized *in situ*, more or less effectively. If, indeed,

Can. J. Chem. Downloaded from www.nrcresearchpress.com by 210.87.254.40 on 09/05/12
For personal use only.

TABLE II

Redistribution reaction of 2-butylmercuri-4-toluene (1.43 mmole) in 2 ml petroleum ether (S), b.p. 90–100 °C, or without solvent (N)

Expt. No.	Catalyst	Mole %	Gas phase	Solvent	Reaction time, h	Temp. °C	Products	
							Bis-*p*-tolyl-mercury, %	Hg^0, mg
1	None	0	Air	S	4.5	95	0.2	0
2	None	0	Air	N	3.5	95	3.6	1
3	2-Butylmercuric chloride	2	Air[a]	S	4	95	1.0	0
4	*tert*-Butylperoxide, (t-bu_2O_2)	4	Air	S	4.5	95	0.2	0
5	2-Butylmercuric chloride + t-bu_2O_2, 1:1	4	Air	S	4	95	1.0	0
6	Ascaridole	4	Air	S	4.5	95	0.1	1
7	Acetone peroxide	2	Air	S	4.5	95	2.0	1
8	Metallic mercury	2	Air	S	4.5	95	0.2	0
9	Mercuric chloride	2	Air	S	4	95	4.8	1
10	Mercuric chloride plus mercury 1:1	2	Air	S	4	95	9.8	4
11	Mercurous chloride	2	Air[a]	S	4	95	5.6	6
12	Mercurous chloride plus mercury 1:1	2	Air	S	4	95	11.7	11
13	Mercurous chloride plus t-bu_2O_2, 1:1	4	Air	S	4	95	1.8	5
14	Mercurous chloride	2	Air	N	3.5	95	56.2	18
15	Mercurous chloride	2	Air	N	1.5	95	25.5	—
16	Mercurous chloride	2	Air	N	2.5	90	17.2	—
17	Mercurous acetate	2	Air	N	2.5	90	12.9	—
18	Mercurous sulphate	2	N_2	S	4	95	66.5	18
19	Mercurous sulphate	2	N_2	S	2	80	40.2	9
20	Mercurous sulphate + mercury 1:1	2	N_2	S	2	80	68.0	9
21	Mercurous oxalate.H_2O	2	N_2	S	4	95	68.0	6
22	Mercurous oxalate.H_2O	2	N_2	S	2	80	24.9	6
23	Mercurous oxalate.H_2O + mercury, 1:1	2	N_2	S	2	80	31.5	6
24	Mercurous nitrate.$2H_2O$	2	Air[a]	N	2.5	90	68.6	—
25	Mercurous nitrate.$2H_2O$	2	Air	N	1.5	95	74.7	—
26	Mercurous nitrate.$2H_2O$	2	Air	S	4	95	74.1	36
27	Mercurous nitrate.$2H_2O$	2	N_2	S	4	95	69.4	7
28	Mercurous nitrate.$2H_2O$	2	N_2	S	2	80	49.2	6
29	Mercurous nitrate.$2H_2O$	2	N_2	S	4	40	20.8	6
30	Mercurous nitrate.$2H_2O$ + mercury, 1:1	2	N_2	S	2	80	42.8	6
31	Mercurous nitrite	2	N_2	S	2	80	64.3	11
32	Mercurous nitrite + mercury, 1:1	2	N_2	S	2	80	59.2	10

[a]The same results were obtained under nitrogen.

mercurous salt – mercury is the true catalyst, obviously it is better to add it deliberately.

Because of the reversibility of reactions [4]–[5], the effectiveness of additional mercurous salt as a redistribution reaction catalyst is not simply related. Thus, when diethylmercury is heated in acetone with 50 mole % of mercurous chloride, most of the latter is converted to metallic mercury, and ethylmercuric chloride is formed.

[6] $$R_2Hg + Hg_2Cl_2 \rightarrow 2RHgCl + Hg.$$

Similarly the reaction of benzylmercuri-2-butane with mercurous chloride yields mercury as well as benzylmercuric chloride and, qualitatively, 2-butylmercuric chloride. However, this heterogeneous reaction [6] is slower in the presence of a nonpolar solvent, or without solvent, than it is in acetone.

The participation of reactions [4]–[5] (i.e. reaction [6]) is quite apparent by the darkening of the surface of a white mercurous salt when it is added to a bis-mercurial either neat or in solvent. But this darkening does not proceed rapidly and only at the end of the reaction period may the mercurous salt largely or completely disappear. That is to say, the presence of mercury seems to retard reaction [4] when it is heterogeneous. This may be simply a mechanical inhibition or, more likely, it may involve a metal-rich intermediate.

[7] $$Hg + X—Hg—Hg—X \rightleftarrows X—Hg—(Hg)_n—HgX.$$

The enhancement of redistribution when metallic mercury is included initially by mortar-grinding with mercurous chloride, as shown by expt. 11 vs. 12 and elsewhere in Table II, seems to indicate this involvement. The same effect is observed when twice the amount of catalyst is treated with a half equivalent of hydrazine hydrate.

Among other mercurous salts the acetate (expt. 17) is less effective than mercurous chloride, but the sulphate (expts. 18–20) and the oxalate (expts. 21–23) are more active catalysts. The effect of either is enhanced by inclusion of metallic mercury.

The most effective catalyst is mercurous nitrate (expts. 24–30), but the rate is unaltered by inclusion of metallic mercury. Although mercurous nitrite is less effective than the nitrate, its effectiveness also is unaltered appreciably by added mercury metal which enhances the effect of the chloride, sulphate, and oxalate. This apparent contradiction is resolved by the observation that the nitrite and nitrate generate metal according to reaction [6] from the solution of bis-mercurial much more rapidly than does the chloride, sulphate, or oxalate. Thus sufficient mercury to satisfy eq. [7] is soon present and added metal is superfluous. The ready evolution of the metal may be due to the peroxide-forming tendency of nitrate (and nitrite) salts.

The catalysts that are mentioned in Table II are nominally heterogeneous. There is visual evidence of reaction at the catalyst surface in an unstirred system in which bis-4-tolylmercury or bis-benzylmercury appears as a crystalline solid because the crystals seem to be growing from the mass of darkened mercurous salt. Of course the catalysis might actually be homogeneous despite this appearance. We have found difficulty in making a firm decision because systems which are strictly homogeneous cause reaction alternative to redistribution. The inclusion of acid to bring about homogeneity causes demetalation.

Since mercurous nitrate is somewhat soluble in methanol, a solution has been refluxed containing 1 equivalent of 2-butylmercuri-4-toluene, 0.02 equivalent of mercurous nitrate, and a small amount of nitric acid sufficient to make a clear solution. After 6 h, 0.9 equivalent of the mercury precipitated as the metal and no bis-4-tolylmercury was isolable. Instead *p*-bitolyl was found. Elimination of the nitric acid from the system reduces metal formation markedly and a 19% yield of the symmetrical bis-4-tolylmercury was obtained, but the system was cloudy (heterogeneous) in absence of the nitric acid. A relatively

Can. J. Chem. Downloaded from www.nrcresearchpress.com by 210.87.254.40 on 09/05/12
For personal use only.

clearer solution is obtained without acid when the 2-butylmercuri-4-toluene and 0.02 equivalent of mercurous nitrate are refluxed 4 h in peroxide-free dioxane under nitrogen, but redistribution, as exemplified by bis-4-tolylmercury, occurs only by a few percent despite precipitation of about 0.02 equivalent of metallic mercury. In summation, the catalysis does not seem to be homogeneous but our proof is equivocal.

Likewise, it might be doubted whether our redistribution catalyst is alternative to those reported by Calingaert *et al.* or whether the substances that they used for catalysis actually generated mercury plus mercurous salt. They do not describe their reaction systems in sufficient detail to disclose whether a nondescript second phase is present. We have attempted to simulate their systems by comparing the effectiveness of mercurous chloride plus mercury on the one hand with aluminium chloride, and on the other at room temperature with four bis-mercurial combinations: benzylmercuriethane, bis-ethylmercury plus bis-*p*-tolylmercury, 2-butylmercuri-4-toluene and bis-2-butylmercury plus bis-4-tolylmercury. With either of the two catalysts the systems did not come to equilibrium even after 140 h, but they are about equally effective. Moreover, the two catalysts resemble each other in appearance while the reactions are proceeding. It is our opinion that aluminium chloride is effective as a catalyst for redistribution because it reacts with bis-mercurials that are present to give mercurous chloride and mercury.

The evidence for this opinion is the presence of metallic mercury among the final products. Although mercurous chloride could not be identified, its presence may be expected during the reaction if the following equations are valid.

$$R_2Hg + AlX_3 \leftrightarrows RHgX + RAlX_2 \quad [8]$$

$$RHgX + AlX_3 \leftrightarrows RHg^+(AlX_4)^- \quad [9]$$

$$RHg^+ \rightarrow R^+ + Hg^0 \quad [10]$$

$$R^+(AlX_4) \rightarrow RX + AlX_3. \quad [11]$$

Equation [8] is well known; indeed Calingaert invoked it (1) in his mechanism according to which he would consider RHgX to be the catalyst. Since the present study excludes this type as the direct catalyst, we suggest that metallic mercury is formed according to [9]–[11] because the RHg^+ cation will be unstable (7). Since mercuric halide is potentially available from the equilibrium [4], the initial presence of mercurous halide may be expected in view of [5]. Therefore the catalyst combination, mercurous salt plus mercury, can arise from aluminium chloride and bis-mercurial.

Of course, a reaction which is accelerated by a material catalyst should proceed satisfactorily without that catalyst, if the temperature is sufficiently raised, providing of course that the system (or part of it) is otherwise stable. Rausch has reported (8) that methylmercuribenzene, as well as bis-methylmercury plus bis-phenylmercury, undergoes the redistribution reaction cleanly and to almost the same equilibrium. Evidently, no metallic mercury is formed. This is a necessary condition since if one of the three bis-mercurials in the system were thermally more or less stable than the others a false equilibrium value might be observed, depending on the relative rates of the redistribution versus the demetalation reaction. The error would not necessarily be detected by the alternative directions of approach to equilibrium. Since Rausch did not report any metallic mercury in his redistribution reaction, it would seem that bis-methylmercury, bis-phenylmercury, and methylmercuribenzene all are equally stable at 150°. But this circumstance may not prevail with other substituent groups.

Can. J. Chem. Downloaded from www.nrcresearchpress.com by 210.87.254.40 on 09/05/12
For personal use only.

The error would easily be detectable if R—Hg—R or R′—Hg—R′ were much less stable than R—Hg—R′, especially if the redistribution rate were slow, i.e., if k_4 or $k_5 \gg k_2 > k_3$,

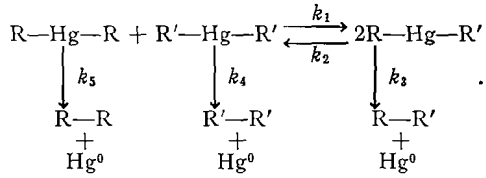

This circumstance is apparent in the following two examples. When 2-butylmercuri-4-toluene on the one hand, and an equimolar mixture of bis-2-butylmercury and bis-4-tolylmercury on the other, are heated at 140–150° under nitrogen for 4.5 h the amounts of mercury precipitated are 7% and 30% respectively. The system initially containing the mixed bis-mercurial yields 45% of the bis-4-tolylmercury expected if the distribution were random, while the system initially two-component yields 167% of the bis-4-tolylmercury expected upon random distribution. Clearly, in this case, the bis-2-butylmercury has demetalated at a rate faster than redistribution equilibrium can be established.

An extreme case where redistribution is impossible at high temperatures is shown by an initially equivalent mixture of bis-ethylmercury and bis-benzylmercury. When this mixture is heated to 140–150° for 4.5 h, 50% of the total mercury is precipitated as the metal. Except for traces, all that is left is bis-ethylmercury, the dibenzylmercury having been demetalated completely.

From these results it is apparent that thermal redistribution equilibration is impractical when secondary alkyl, aralkyl, and other electropositive substituents are involved.

It is apparent that if one disregards the obvious basis of error, i.e. appearance of metallic mercury, a false value for equilibrium will be obtained if $k_3 >$ or $= k_2 > k_4 = k_5$ because the equal amounts of bis-mercurials in the product will be misleading. Perhaps it is fortuitous that unsymmetrically disubstituted mercury is frequently more stable thermally than the bis-mercurials to which redistribution would convert it, so that this error will be unlikely. However, one cannot be certain that this rule is unequivocal and circumstances where k_1–k_5 are all of the same order of magnitude may exist and lead to erroneous conclusions. When secondary or tertiary alkyl, aralkyl, or other electropositive substituents are present, the precipitated metal may be expected during high-temperature redistribution. In this circumstance an equilibrium value is unreliable.

At lower temperatures in hydrocarbon solvent one may with some bis-mercurials get a meaningful value for equilibrium by use of catalyst such as mercurous nitrate. Table III shows how the value is chosen for the benzyl–ethyl–mercury system. Comparison of uncatalyzed expts. 1 and 5 of Table III shows that neither represents a state of equilibrium, but it does indicate that k_2 is larger than k_1. These magnitudes are reflected in the approximate constant k_1/k_2 of about 0.24 which may be derived from the data of expts. 2 and 3 where the region of equilibrium seems to be established. The value should be accepted with some reservation in view of the amount of metallic mercury which is evolved. However, it may be noted that expt. 4 at room temperature produces about the same amount of metal, although equilibrium seems not to have been attained. It would seem from expt. 4 that the production of metal is not due to a high-temperature demetalation.

Can. J. Chem. Downloaded from www.nrcresearchpress.com by 210.87.254.40 on 09/05/12
For personal use only.

TABLE III

Redistribution with stirring in 2 ml of petroleum ether (b.p. 90–100°) per mmole of R_2Hg where R = ethyl or benzyl, using 4 mole % of mercurous nitrate dihydrate as catalyst

Expt. No.	Disubstituted mercury, mmole			Catalyst, mole	Time, h	Temp., °C	Hg^0, mg	Final R_2Hg, mmoles
	Diethyl	Dibenzyl	Ethyl benzyl					
1 Initial	1.00	1.00		0	24	90–92	2	1.92
Final	0.80	0.82	0.30					
2 Initial	1.00	1.00		4	24	90–92	19	1.91
Final	0.74	0.77	0.40					
3 Initial			2.00	4	24	90–92	20	1.85
Final	0.74	0.78	0.33					
4 Initial			2.00	2+2[a]	385	25	17	1.66
Final	0.62	0.58	0.46					
5 Initial			2.00	0	24	90–92	1	1.88
Final	0.33	0.33	1.22					

[a]After 80 h the initial 2 mole % of catalyst was augmented by 2 mole % more.

TABLE IV

Redistribution under nitrogen in petroleum ether (b.p. 90–100°) of R_2Hg where R = 2-butyl and 4-tolyl using mercurous nitrate dihydrate as catalyst

Expt. No.	Disubstituted mercury, mmole			Catalyst, mole %	Solvent, ml per mmole	Temp., °C	Hg^0, mg	Time, h
	Di-2-butyl	Ditolyl	2-Butyl 4-Tolyl					
1 Initial			2.00	0	1	86–88	0	6
Final	0.08	0.09	1.68					
2 Initial	1.00	1.00		0	3	89–91	35	108
Final	0.67	0.96	0.04					
3 Initial			2.00	2	0.75	80–85	6	8
Final	0.48	0.67	0.50					
4 Initial			2.00	4	1	86–88	7	6
Final	0.48	0.63	0.68					
5 Initial			2.00[a]	4	1.7	90–92	12	24
Final	0.76	0.83	0.32					
6 Initial			2.00	4	1.7	25	5	330
Final	0.63	0.64	0.70					
7 Initial	1.00	1.00		2	1.2	80–85	17	8
Final	0.65	0.96	0.07					

[a]Magnetically stirred.

Attempts to find the redistribution equilibrium for the system bis-2-butylmercury plus bis-4-tolylmercury $\rightleftarrows$ 2-butylmercuri-4-toluene have not been so satisfactory according to Table IV. Evidently the difficulty is due to the instability of bis-2-butylmercury as may be seen by comparison of expts. 1 and 2 where a catalyst is not involved and of expts. 2 and 7 where bis-2-butylmercury is present initially. The same disparity between the unstable secondary bis-mercurial and the aromatic bis-mercurial is seen in expts. 3–4. As may be seen in expt. 6 the instability problem may be compensated by low temperature and long duration, but it is doubtful whether equilibrium has been reached. Actually expt. 5 in which the system is stirred gives values which may be close to equilibrium, in which case k_1/k_2 is about 0.17. Whether or not expts. 6 and 5 approach or reach equilibrium, the direction is such that the equilibrium constant cannot equal four.

Can. J. Chem. Downloaded from www.nrcresearchpress.com by 210.87.254.40 on 09/05/12
For personal use only.

If the redistribution reaction of organodisubstituted mercury were a random exchange process regardless of the polarity of the substituents as Calingaert *et al.* have tried to demonstrate, then the equilibrium constant ought to be four. As may be seen from the results of Tables IV and V, the observed equilibria, even if they are in error, could never conform to the Calingaert condition. We suggest that the small difference in polarity among the lower alkyl groups that form the basis for Calingaert's postulation are not sufficiently different in polarity to warrant a generalization about the redistribution reaction. If the term "redistribution" has become associated with randomization then this association ought to be discontinued.

TABLE V

Attempted equilibration by means of aluminium chloride

Expt. No.	Disubstituted mercury, mmole			Time, h	Hg^0, mg
	Bis-2-butyl	Bis-4-tolyl	2-Butyl, 4-tolyl		
1 Initial	3.92	3.92	None	137	30
Final	2.96	3.36	0.53		
	Bis-2-butyl	Bis-4-tolyl	2-Butyl, 4-tolyl		
2 Initial	None	None	4.33	139	50
Final	0.14	0.23	3.58		
	Bis-ethyl	Bis-benzyl	Ethyl, benzyl		
3 Initial	3.92	3.92	None	141	110
Final	2.08	3.30	0.73		
	Bis-ethyl	Bis-benzyl	Ethyl, benzyl		
4 Initial	None	None	3.90	117	45
Final	0.21	0.26	2.56		

It follows also that if randomization is not characteristic of the redistribution reaction then the correlative concept that redistribution occurs via free radical transfer likewise has no experimental basis.

EXPERIMENTAL*

Bis-cyclohexylmercury, Halogen and Peroxide Free

The stirred Grignard reagent prepared in 85% yield, 0.34 mole, from cyclohexyl bromide (9), b.p. 88° (76 mm), n_D^{14} 1.49572, m.p. −49 to −48, was treated slowly under nitrogen with 50.4 g (0.14 mole) of dry mercuric bromide during 9 h at 25° and then was poured onto crushed ice. After acidification of the system with 30 ml of acetic acid the nonaqueous layer, dried with magnesium sulphate, was evaporated, leaving 44 g (86%) melting above 70°. This crude product in 15 ml of diethyl ether was treated with 10 ml of 99–100% hydrazine hydrate in the dark during a minimum time of 20 h. After addition of 10 ml of water and separation of the aqueous phase the latter was twice extracted with ether which was added to the nonaqueous phase. The combined ether solution, washed once with water, was dried with magnesium sulphate, and distilled at 125° (1 mm). The distillate, m.p. 76–78°, which contained some mercury, was crystallized from absolute ethanol, m.p. 78–79°. This product will begin to decompose in air after several hours, but will remain white for long periods under nitrogen or in vacuum. It may be stabilized for 24 h in air, if it is dissolved in acetone containing 2% of 2,5-di-*tert*-butylhydroquinone and the resulting solution evaporated to dryness *in vacuo*. A portion heated to 170 °C *in vacuo* (2.43 mmole) liberated cyclohexene according to infrared absorption at 3.32 and 5.92 μ. The thermal stability of this bis-mercurial at 25° was not decreased by contamination with mercurous chloride.

Benzylmercuriethane, Halogen and Peroxide Free

The Grignard reagent from 0.09 g-atom of magnesium and 0.09 mole of ethyl bromide in 150 ml of diethyl ether was stirred under nitrogen at +4 °C while 11.7 g (35.8 mole) of benzylmercuric chloride, m.p. 105.5–106°, (10) was added in small portions during 15 min. After 30 min subsequent stirring the system was poured into a mixture of ice plus 1% aqueous sulphuric acid. The aqueous layer was twice extracted with peroxide-free diethyl ether and the entire nonaqueous portion, dried with magnesium sulphate, was distilled finally at 0.04 mm to give 10.9 g (70%) of benzylmercuriethane, b.p. 89–91°. The distillation residue yielded 0.6 g of bis-benzylmercury, m.p. 108–110.

**Melting points have been corrected against reliable standards.*

Can. J. Chem. Downloaded from www.nrcresearchpress.com by 210.87.254.40 on 09/05/12
For personal use only.

The crude product in 10 ml of diethyl ether was treated with 10 ml of 95–100% hydrazine hydrate. After the mixture was stirred for at least 24 h, 10 ml of water was added and the aqueous layer was extracted with peroxide-free ether. The combined ether solution, twice washed with water and dried with magnesium sulphate, was distilled at 0.01 mm, b.p. 85–90 °C, in 78% recovery.

2-Butylmercuri-4-toluene, Halogen and Peroxide Free

The Grignard reagent, from 0.156 g-atom of magnesium and 0.155 mole of *p*-bromotoluene, in 270 ml of diethyl ether was stirred at −11 °C while a solution of 31.15 g (0.092 mole) of 2-butylmercuric bromide (11), m.p. 42.5–43 °C, in 260 ml of diethyl ether was added during 35 min. After 30 min stirring at the same temperature the whole was poured into a mixture of ice and 1% aqueous sulphuric acid. The aqueous layer was extracted with peroxide-free ether. The combination of nonaqueous parts was washed with water and then was stirred with 20 ml of 99–100% hydrazine hydrate for 24 h. The nonaqueous layer was separated, dried with magnesium sulphate, and distilled finally at 95–100° (0.01 mm) to yield 30.1 g (94%).

When (+)2-butylmercuric bromide, $[\alpha]_D^{28} = +3.24°$ in acetone, was used in this preparation the resulting 2-butylmercuri-4-toluene gave 2-butylmercuric bromide, m.p. 34–35°, $[\alpha]_D^{28} = +2.80°$ in acetone, when it was treated with 1 equivalent of mercuric bromide in methanol.

Benzylmercuric Chloride with Peroxides

A solution of benzylmercuric chloride (0.5 g) in benzene containing 4.3 mole % of ascaridole, *tert*-butyl hydroperoxide, or di-*tert*-butyl peroxide in 2 ml of benzene was heated to 110° for 3.5 h. The rest was taken up in benzene to leave 10–15 mg of mercurous chloride (black with alkal, positive for chlorine upon elemental analyses). The benzene solution upon evaporation left 410 mg (82%) unchanged chloromercurial, m.p. 105.5–106°.

Preparation of Mercurous Salts

Mercurous oxalate monohydrate was prepared in 99% yield by treating (12) a solution of 1.12 g of mercurous nitrate dihydrate in 3 ml of water containing 10 mg of conc. nitric acid with 0.5 g of oxalic acid with shaking. The precipitate was filtered, washed with water, acetone, and ether, and dried *in vacuo*. The salt did not lose water at 60° *in vacuo* for 22 h.

Mercurous sulphate was prepared in 33% yield (13) by treatment of 1.12 g of mercurous nitrate dihydrate in 3 ml of water plus 10 mg of conc. nitric acid with 2 ml of 30% aqueous sulphuric acid. The precipitate was washed with water and vacuum dried.

Mercurous nitrite was prepared by treating a solution of 5 ml conc. nitric acid and 15 ml of water with 20 g of metallic mercury at 30–35° for 5 h and then at 25° for 3 days. The filtrate from this sytem when cooled gave white crystals instead of yellow ones (14). They gave a positive Liebermann test. According to the mercurous chloride obtained from 300 mg, this salt is the dihydrate of the monomeric species.

Redistribution with Aluminium Chloride

The experiments summarized in Table V were effected in petroleum ether (b.p. 40–60, 3 ml for the unsymmetrical and 6 ml for the symmetrical mercurials) at 20–25° and were processed after reaction by filtration; the filtrate was treated with water, then dried and distilled. The initial precipitate was extracted with benzene, leaving dirty metallic mercury. Evaporation of the benzene left the petroleum ether insoluble bis-mercurial.

Preparation of Mercurous Salt – Mercury Metal Systems

Generally the ingredients were ground in a mortar until the metal was no longer visible. In one instance 1.12 g of mercurous nitrate was suspended in 1 ml of water to which 39 mg of 100% hydrazine hydrate was added. The suspension was filtered after 10 min and washed with water and acetone, then vacuum dried.

Bis-ethylmercury with Mercurous Chloride

A system comprised of 1.61 g (3.42 mmole) of mercurous chloride and 1.77 g (6.84 mmole) of bis-ethylmercury in 30 ml of acetone was heated for 1 h. The mercurous chloride gradually was converted to metallic mercury. After 15 h the metal was filtered off, 0.675 g (97%). The filtrate was evaporated and the residue (1.95 g) was washed with petroleum ether, b.p. 40–60°, leaving 0.80 g (88%) of ethylmercuric chloride, m.p. 190–192°.

Redistribution Reaction, Heterogeneous Catalyst

Reactions were carried out in 25 ml Erlenmeyer flasks under a reflux condenser in a temperature-regulated bath. When stirring was desired a glass-covered Kovar bar was used with magnet drive. Some reactions were carried out under air and some under nitrogen. When petroleum ether (b.p. 90–100°) was used it was dry, free from unsaturated impurities, and peroxide free.

Upon completion, the insoluble part was filtered off and washed with petroleum ether (b.p. 40–60°), dried, and weighed. Then it was extracted with benzene if bis-4-tolylmercury was to be removed or with acetone if it contained bis-benzylmercury. The spent catalyst (principally metal) was then weighed to obtain by difference the yield of bis-benzylmercury or bis-4-tolylmercury. The extracts were vacuum evaporated at room temperature via a dry ice cooled trap, and the weighed residue was distilled. The boiling points of the

Can. J. Chem. Downloaded from www.nrcresearchpress.com by 210.87.254.40 on 09/05/12
For personal use only.

several products are: bis-ethylmercury, b.p. 72–74° (35 mm); bis-2-butylmercury, 45–48° (0.8 mm); benzylmercuriethane, b.p. 85–88° (0.01 mm); benzylmercuri-2-butane, b.p. 90–94° (0.02 mm); 2-butylmercuri-4-toluene, b.p. 105–110° (0.06 mm). Since the first two of these products tended to co-distill with the solvent the cold-trap content was treated with an amount of mercuric bromide in acetone, which was equivalent to the difference between the theoretical yield and the amount obtained by distillation. After 1 h this system was vacuum evaporated. From the increased weight the additional dialkylmercury could be calculated. The distilled dialkylmercury was also dissolved in acetone or methanol and treated with an equivalent amount of mercuric bromide, to identify the distillate by the melting point of the corresponding alkylmercuric bromide.

The residues in the flasks after distillation were dissolved in benzene or acetone, filtered, vacuum evaporated, washed with petroleum ether, b.p. 40–60, and dried before weighing as bis-4-tolylmercury (m.p. 243–245°) or bis-benzylmercury (m.p. 110–111°).

Redistribution Reaction, "Homogeneous Catalyst"

A cloudy system of 0.5 g (1.43 mmole) of 2-butylmercuri-4-toluene and 16 mg (0.029 mmole) of mercurous nitrate in 15 ml each of water and methanol plus 25 ml of acetone was heated for 6 h under reflux at a bath temperature of 83–90°. Subsequently 70 ml of water was added and the remaining precipitate was filtered off, weight 220 mg containing mercury. Extraction with benzene left 150 mg, largely mercury. Evaporation of the benzene solution left 70 mg (19%) of bis-4-tolylmercury, m.p. 241–243°. Similar results were obtained when the reaction medium was methanol alone, but the yield, m.p. 240–242°, was only 5 mg when dioxane was the medium.

When 5 mg of conc. nitric acid was included in the system where methanol alone was used, the precipitation of metal was very large (250 mg) and the isolable product was 4,4′-ditolyl, m.p. 115–118°. These products were the same in type and yield when mercurous nitrate was not included in the system.

ACKNOWLEDGMENTS

The authors are grateful for a grant in aid from the National Research Council which made this study possible.

REFERENCES

1. G. Calingaert and H. A. Beatty. Organic chemistry. *Edited by* H. Gilman. 2nd ed. John Wiley, New York. 1943. pp. 1806–1820.
2. G. Calingaert, H. A. Beatty, and H. Soroos. J. Am. Chem. Soc. **62**, 1099 (1940).
3. G. Calingaert, H. Soroos, and V. Hnizda. J. Am. Chem. Soc. **62**, 1107 (1940).
4. W. C. Horning. F. Lautenschlager, and G. F Wright. Can. J. Chem. **41**, 1441 (1962).
5. M. M. Koter. Dokl. Akad. Nauk SSSR **88**, 991 (1953); Chem. Abstr. **48**, 8727 (1954).
6. A. M. Birks and G. F Wright. J. Am. Chem. Soc. **62**, 2412 (1940).
7. J. H. Robson and G. F Wright. Can. J. Chem. **38**, 21 (1960).
8. M. D. Rausch. Symposium, Current Trends in Organometallic Chemistry, Cincinnati, Ohio. June 12–15, 1963.
9. E. Reid, J. R. Ruhoff, and R. E. Burnett. Org. Syn. **15**, 26 (1935).
10. F. C. Whitmore. Organic compounds of mercury. The Chemical Catalogue Co. Inc. 1921. p. 185.
11. H. B. Charman, E. D. Hughes, and C. K. Ingold. J. Chem. Soc. 2530 (1959).
12. G. Gantsh and E. Schuster. Monatsh **68**, 399 (1936).
13. H. Wackenroder. Ann. **41**, 319 (1842).
14. P. C. Ray. Z. Anorg. Chem. **12**, 365 (1896).

Can. J. Chem. Downloaded from www.nrcresearchpress.com by 210.87.254.40 on 09/05/12
For personal use only.

Can. J. Chem. Downloaded from www.nrcresearchpress.com by 210.87.254.105 on 09/05/12
For personal use only.

PHOTO-INITIATED REACTIONS OF THIOLS AND OLEFINS

I. THE THIYL RADICAL CATALYZED ISOMERIZATION OF BUTENE-2 AND 1,2-ETHYLENE-d_2

D. M. GRAHAM, R. L. MIEVILLE, AND C. SIVERTZ
Department of Chemistry, University of Western Ontario, London, Ontario

Received February 21, 1964

ABSTRACT

Kinetic studies have been made of the isomerization of butene-2 and 1,2-ethylene-d_2 catalyzed by thiyl radicals produced from the photolysis of methanethiol. The rate of isomerization was found to be first order with respect to both the olefin and $CH_3\dot{S}$ concentrations. The lack of influence of pressure on the reaction rate, at pressures above about 4 mm, leads to a simple mechanism in which isomerization is considered to occur as a result of thermal decomposition of the collisionally stabilized adduct radical produced in the reaction $CH_3\dot{S} + RCH{=}CHR + M \rightarrow CH_3SCH(R)\dot{C}HR + M$. The rate constants for this attack step were found to be 2×10^7 and 4.8×10^6 l mole^{-1} s^{-1} for butene-2 and ethylene-d_2, respectively. In both cases the activation energy for isomerization was found to be close to zero. From a kinetic study of the isomerization of *cis*-butene-2 in the presence of butadiene-1,3, which acts as a retarder, the attack constant for butadiene at 25 °C was found to be 4.5×10^8 l mole^{-1} s^{-1}.

INTRODUCTION

The addition of thiols to olefins has been extensively studied in solution. The reaction was found to be a comparatively fast chain reaction of considerable chain length. Because of this latter fact, a simple kinetic analysis of the system could be made and the rate constants for the individual steps in the chain sequence could be readily determined. These results have been summarized in a number of review articles (1, 2). When an attempt to extend the measurements to the gas phase was made, it was found that, for unconjugated olefins, the overall activation energy which was observed to be of the order of 3 kcal in solution became negative by about 8 kcal (3). In addition, it was observed that in the case of *cis*-butene-2, the addition reaction was accompanied by a much faster isomerization reaction (4). These results may be explained by assuming that the attack of the thiyl radical on a double bond is reversible.

The work reported here was undertaken to determine the detailed mechanism for this reverse reaction and its role in isomerization and addition, the latter to be discussed in Part II (5).

EXPERIMENTAL

Chemicals

All of the hydrocarbons used were Phillips "Pure Grade" and, with the exception of ethylene, were purified by gas chromatography on a 50 ft diethylformamide column. The compounds, *cis*- and *trans*-ethylene-d_2, were prepared by reduction of acetylene-d_2 with copper-activated zinc and chromous chloride, respectively (6). Sulphur hexafluoride (Matheson, 98.0%) and carbon dioxide (Matheson, 99.99%) were used after six successive trap-to-trap distillations at 10^{-6} mm. Methanethiol (Eastman Reagent Grade) was purified in a similar manner; no impurities could be detected by gas chromatography.

Apparatus

The reaction cell consisted of a cylindrical quartz vessel, 5 cm in diameter and 10 cm long, with plane windows, and was connected to a grease-free vacuum manifold by means of Springham diaphragm valves in such a way that the "dead volume" was restricted to less than 1% of the total. The cell was housed in an aluminium block thermostat with quartz windows which could be regulated to ±0.1 °C. The light source was a Hanovia SH 616A high-pressure mercury arc operated at 1.2 A and 127 V d-c. using a regulated power supply. A system of quartz lenses was used to focus and collimate the light. Most of the work was carried out using a 10 mm thick solution filter of 2,7-dimethyl-3,6-diazocyclohepta-1,6-diene iodide (10% in water) to isolate the 2537 Å region.

Analysis

The isomerization of *cis*- and *trans*-butene-2 was followed by gas chromatography using a 300 ft polypropylene glycol capillary column and a hydrogen flame ionization detector. The isomerization of *trans*-

ethylene-d_2 was determined using the bands at 842 cm^{-1} (*cis*) and 987 cm^{-1} (*trans*) by means of a Beckman IR-7 infrared spectrophotometer.

Rate of Initiation

Photolysis of methanethiol produces hydrogen and methyl disulphide with a quantum yield approaching 1 (7). In the presence of olefin both of the primary products, $CH_3\dot{S}$ and H, are very reactive and will be capable of initiating a chain. There will arise some uncertainty about the details of the initiating reaction under widely varying concentration conditions because of the competition for H between thiol and olefin. However, provided the chain length is sufficiently long, this information is not required and it is only necessary to know the number of initiating radicals produced in unit time. Therefore, since the chain lengths observed were about 100, the reasonable assumption has been made that the rate of initiation in the presence of olefin is twice the rate of hydrogen production in its absence.

The rate of formation of hydrogen was measured as a function of the thiol concentration by means of a mass spectrometer. A known amount of helium was added to the reaction cell initially and was used as an internal reference.

Since, even at low thiol pressures, an appreciable fraction of the total light is absorbed by the reacting mixture, the rate of primary radical production is not uniform throughout the cell. The mean rate of isomerization (or addition) is therefore proportional to the square root of the initiation rate averaged over the length of the cell, assuming biradical termination. A procedure by which $\overline{r_i^{1/2}}$ may be calculated has been developed by Burns and Dainton for a system in which monochromatic light is used to initiate reaction (8). Unfortunately it proved impossible to isolate one single active spectral line from the lamp used, and it was necessary to modify the averaging procedure to allow for the different absorption characteristics of the various wavelengths present.

The rate of initiation in a layer of depth dl, at a distance l from the illuminated face of the cell, will depend on the number of quanta absorbed in unit time, I_a, and the quantum yield for primary radical formation. Therefore, for polychromatic light,

$$[1] \qquad r_i\,(\text{local}) = \sum_\lambda (\phi I_a)_\lambda = \frac{d}{dl}\sum_\lambda (\phi I_0)_\lambda[1 - e^{-\epsilon_\lambda c l}] = \sum_\lambda (\phi I_0)_\lambda \epsilon_\lambda c\, e^{-\epsilon_\lambda c l},$$

where I_0 is the light intensity of wavelength λ entering the illuminated face of the cell and c is the concentration of absorbing substance whose extinction coefficient is ϵ_λ.

The mean rate of initiation in a cell of path length L is

$$[2] \qquad \overline{r_i} = \frac{1}{L}\int_0^L r_i\,(\text{local})\,dl = \frac{1}{L}\sum_\lambda (\phi I_0)_\lambda[1 - e^{-\epsilon_\lambda c L}].$$

The mean square root rate of initiation is

$$[3] \qquad \overline{r_i^{1/2}} = \frac{1}{L}\int_0^L r_i^{1/2}\,(\text{local})\,dl = (\phi I_0)_{\lambda_1}^{1/2} g,$$

where

$$g = \left(\frac{\epsilon_{\lambda_1} c}{L}\right)^{1/2}\int_0^L G^{1/2}(c, l)\,dl,$$

$$G(c, l) = \sum_\lambda \frac{(\phi I_0)_\lambda \epsilon_\lambda}{(\phi I_0)_{\lambda_1}\epsilon_{\lambda_1}} e^{-\epsilon_\lambda c l},$$

and ϕ_{λ_1}, $I_{0\lambda_1}$, and ϵ_{λ_1} are, respectively, the quantum efficiency, the incident light intensity, and the extinction coefficient for one specific wavelength.

These equations were readily applied since it was possible to attribute the initiation to three lines at 254, 257, and 265 mμ on the basis of the transmission characteristics of the filter and of methanethiol, and the spectral distribution of the lamp. Using the measured extinction coefficients of methanethiol at these wavelengths and the variation in rate of hydrogen production with thiol concentration in the absence of olefin, one can obtain an equation of the form of [2]. The relation obtained for the 10 cm cell was

Can. J. Chem. Downloaded from www.nrcresearchpress.com by 210.87.254.105 on 09/05/12
For personal use only.

$$[2'] \qquad r_i \times 10^{10} = 48.6(1 - e^{-1431c}) + 25.0(1 - e^{-699c}) + 143(1 - e^{-168c}).$$

A comparison of the initiation rate calculated from this equation with the experimentally observed rates is given in Fig. 1.

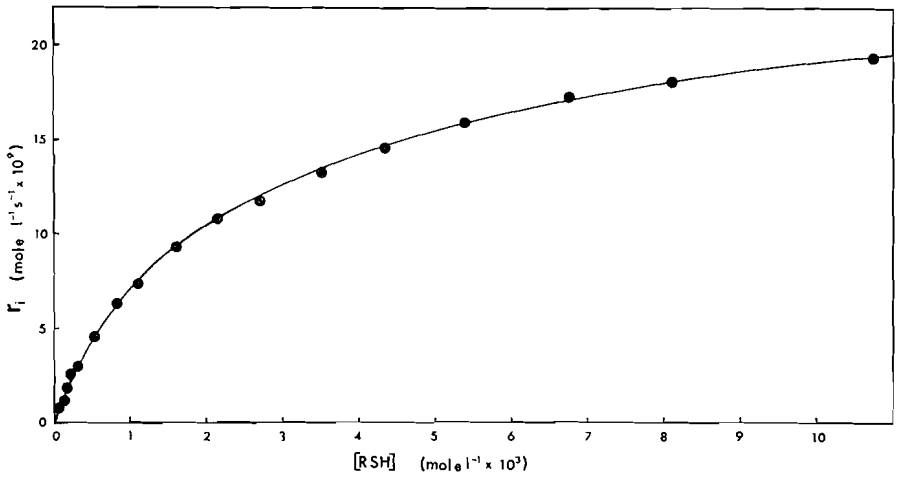

FIG. 1. Rate of initiation: the curve is calculated from eq. [2']; the points were obtained from the rates of hydrogen production in the absence of olefin.

$G(c, l)$ can therefore be determined as a function of path length and concentration; g may be evaluated for different thiol concentrations by numerical integration of $G^{1/2}(c, l)$; and the mean square root initiation evaluated.

The rate of isomerization of a standard mixture of reactants was determined several times during the course of the hydrogen evolution measurements. The isomerization rate of this mixture was used during the subsequent experimental work to correct for variations in light intensity. It has, however, been assumed that the relative intensities of the three spectral lines remained the same, i.e., that g remains constant. This assumption is not unreasonable since the transmission characteristics of the filter solution was found to be unchanged over the period in which this work was carried out and, since the operating conditions of the lamp were maintained constant, it is unlikely that the spectral distribution of the lamp should change appreciably.

RESULTS AND DISCUSSION

The Mechanism

The main features of the gas phase reaction may be explained in terms of the formation of an adduct radical, $\dot{X}^*$, which contains initially the exothermic heat of reaction. Dissociation of $\dot{X}^*$ to produce *cis* or *trans* olefin occurs after a short time interval which depends upon the way in which the energy is initially distributed. Competing with the reverse reaction is collisional de-energization to $\dot{X}$. This stabilized radical then may either dehydrogenate thiol or undergo collisional re-energization to the state $\dot{X}^0$, which may then dissociate to *cis* or *trans* olefin and $R\dot{S}$. The distinction between the species $\dot{X}^*$ and $\dot{X}^0$ is necessary since the former arises from chemical energization whereas the latter is produced thermally and will thus belong to a much broader energy distribution. For a large exothermic heat of reaction, all $\dot{X}^*$ will have approximately the same energy. The proposed mechanism is shown in Fig. 2.

Application of the steady state approximation to this mechanism yields the following expression for the initial rate of isomerization, R_1, in this case the initial rate of formation of *trans* from pure *cis* olefin.†

†*For consistency the probability factor* ρ_{-1}^0 *has been rewritten* ρ_3 *in eq. [4].*

Can. J. Chem. Downloaded from www.nrcresearchpress.com by 210.87.254.105 on 09/05/12
For personal use only.

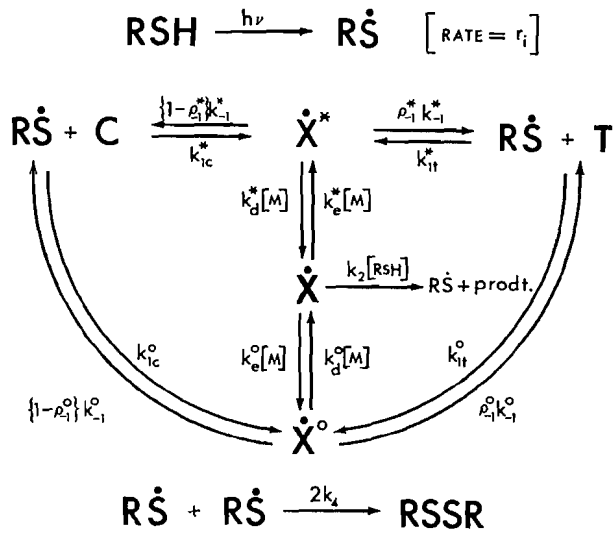

FIG. 2. The reaction mechanism: C and T represent the *cis* and *trans* forms of the olefin; $\dot{X}^*$, $\dot{X}$, $\dot{X}^0$ represent the chemically energized, the de-energized, and the re-energized adduct radicals, respectively; ρ is the probability that a decomposition reaction produces the *trans* isomer.

[4] $$R_1 = \left[\frac{d[T]}{dt}\right]_0 = \rho_{-1}{}^*k_{-1}{}^*[\dot{X}^*] + \rho_{-1}{}^0k_{-1}{}^0[\dot{X}^0]$$

$$= \left[\frac{r_i}{2k_4}\right]^{1/2} \phi^* k_{1c}[C]\left\{\frac{\rho_{-1}{}^*k_{-1}{}^*}{k_d{}^*[M]} + \frac{\rho_3 k_3}{k_3 + k_2[RSH]}\right\}.$$

where

$$\phi = k_d[M]/[k_d[M] + k_{-1}],$$

$$k_3 = \phi^0 k_{-1}{}^0 k_e{}^0[M]/k_d{}^0[M].$$

k_3 represents a mean effective rate constant for the thermal decomposition of $\dot{X}$, the stabilized intermediate. It will depend on pressure in the same way as the quenching coefficient ϕ^0, and at high pressures, as $\phi^0 \rightarrow 1$, k_3 will become independent of pressure.

Isomerization of Butene-2

According to eq. [4], if isomerization occurs by dissociation of $\dot{X}^*$, there will be an inverse relation between isomerization and pressure. On the other hand, the isomerization path through the thermal decomposition of $\dot{X}$ should be independent of pressure at sufficiently high pressures. To distinguish between these two paths, isomerization rates were measured as a function of total pressure in the presence of an inert gas. It was found that, below about 4 mm total pressure of reactants, addition of SF_6 or CO_2 increased the rate of isomerization. The increase was linearly dependent on the amount of gas added at low pressures, and at higher pressures of inert gas the rate approached a maximum value. This pressure effect is just the opposite of what might be expected on the basis of eq. [4]. It can be explained, however, in terms of wall termination. Whereas the high-pressure rate was found to be proportional to the square root of the incident light intensity, I_0, and of the initial thiol concentration (Fig. 3), the low-pressure rate was almost first order with respect to both of these variables. Since at low thiol concentrations $r_i = kI_0[RSH]$, these results indicate second order termination at high pressures and predominantly first

Can. J. Chem. Downloaded from www.nrcresearchpress.com by 210.87.254.105 on 09/05/12
For personal use only.

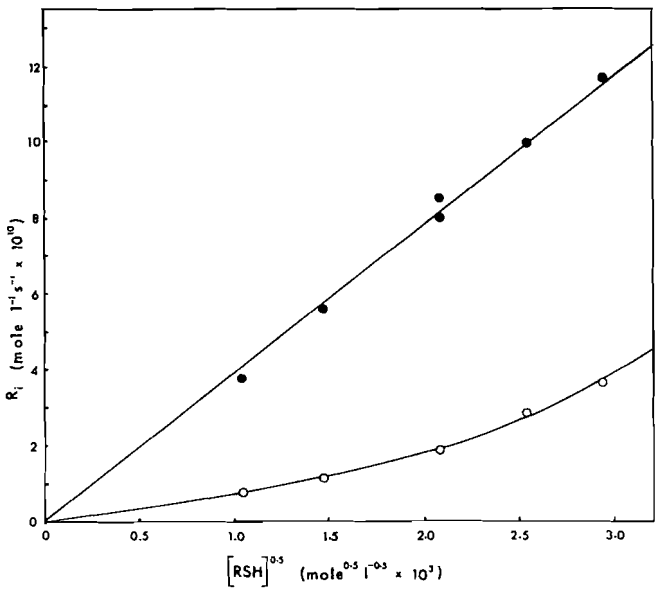

FIG. 3. Dependence of the initial rate of isomerization on thiol concentration at 25 °C, [C] = 5.38×10^{-6}: ● [SF_6] = 50 mm; ○ [SF_6] = 0.

order at low pressures. The dependence on inert gas pressure is also what might be expected for first order wall termination.

It may be concluded therefore that isomerization is due to thermal decomposition of the energized radical $\dot{X}$, and the rate becomes independent of pressure for homogeneous termination.

$$[5] \qquad R_1 = \left[\frac{d[T]}{dt}\right]_0 = \left[\frac{r_i}{2k_4}\right]^{1/2} \frac{\rho_3 k_3 k_{1c}[C]}{k_3 + k_2[RSH]}.$$

From the results given in Fig. 4 and Table I, it is seen that the initial rate of isomerization is first order with respect to olefin and zero order with respect to thiol. This is consistent with eq. [5] if, at 25 °C and [RSH] $< 3 \times 10^{-3}$ mole l^{-1}, $k_3 \gg k_2$ [RSH].

These conclusions are also consistent with the observations on the temperature dependence of the isomerization rate given in Fig. 5. At low thiol concentrations (2×10^{-4} mole l^{-1}) the isomerization rate is independent of temperature ($E_a = 0.050 \pm 0.046$ kcal), whereas at higher thiol concentrations a small positive activation energy of 1.9 ± 0.7 kcal (90% confidence limits) appears. The activation energy for the thermal decomposition of $\dot{X}$, E_3, should be of the same order of magnitude as the exothermic heat of reaction for the attack step. The heats of formation of the thiyl radical and the adduct radicals, $\dot{X}$, have been estimated according to Franklin's method (9), and from these the estimated heats of reaction are about 15 kcal for ethylene and 18 kcal for butene. At low [RSH], $k_3 \gg k_2$ [RSH] and the overall activation energy will be $E_{1c} + E_{\rho_3} - \frac{1}{2}E_4$. The second term might be expected to be small and negative and may to a certain extent compensate for the small activation energy possible in the attack step. At high thiol concentrations the term k_2[RSH] begins to contribute to the denominator and E_3 begins to contribute to the total activation energy.

Can. J. Chem. Downloaded from www.nrcresearchpress.com by 210.87.254.105 on 09/05/12
For personal use only.

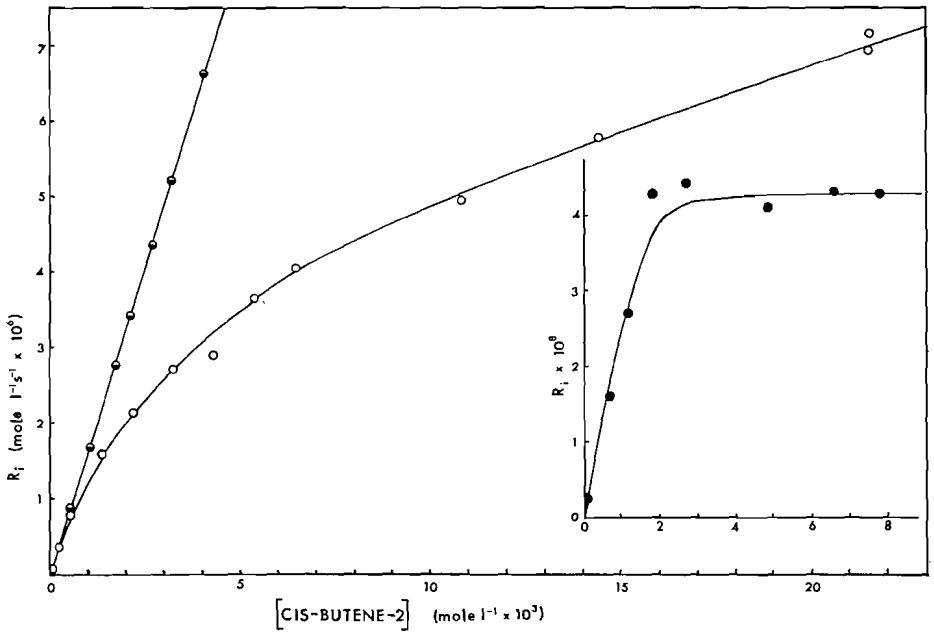

FIG. 4. Dependence of the isomerization rate on the initial *cis*-butene-2 concentration. The abscissa scale is the same for both plots: ○ unpurified, [RSH] = 5.38×10^{-4} mole l^{-1}; ● unpurified, [RSH] = 2.29×10^{-6} mole l^{-1}; ◒ purified, [RSH] = 5.38×10^{-4} mole l^{-1}.

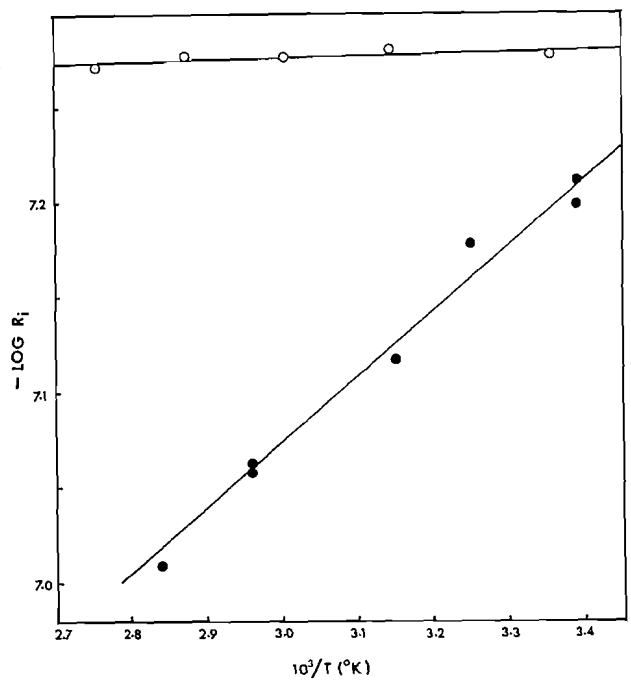

FIG. 5. Temperature dependence of the rate of isomerization: ● [C] = 1.73×10^{-5} mole l^{-1}, [RSH] = 2.79×10^{-3} mole l^{-1}; ○ [C] = 5.38×10^{-4} mole l^{-1}, [RSH] = 2.15×10^{-4} mole l^{-1}. (The ordinate scale in this case is $1 - \log R_i$.)

Can. J. Chem. Downloaded from www.nrcresearchpress.com by 210.87.254.105 on 09/05/12
For personal use only.

Thus far in the discussion it has been assumed that chain termination occurs primarily by combination of two thiyl radicals. It may be readily shown that if either $\dot{X} + R\dot{S}$ or $\dot{X} + \dot{X}$ termination predominated, the rate of isomerization would be either one-half or zero order, respectively, with respect to *cis*-olefin concentration. Since first order dependence on olefin was observed over a wide concentration range of both olefin and thiol it may be concluded that $R\dot{S} + R\dot{S}$ termination does indeed predominate. This is also confirmed by the kinetics of the addition reaction and by the fact that the termination rate constant, determined by applying the method of intermittent illumination to the addition reaction, was the same within experimental error for ethylene, propylene, butene-2, and isobutene (5, 10).

For the concentration region where $k_3 \gg k_2[\mathrm{RSH}]$ the rate equation may be integrated to give

$$[6] \qquad -\ln\left\{1 - \left(\frac{1+K}{K}\right)\alpha\right\} = \left(\frac{r_i}{2k_4}\right)^{1/2}\left(\frac{1+K}{K}\right)\rho_3 k_{1c} t,$$

where α is the fractional conversion of *cis* to *trans* and the equilibrium constant K is defined as

$$[7] \qquad K = \frac{[\mathrm{T}]_{eq}}{[\mathrm{C}]_{eq}} = \frac{k_{1c}\rho_3}{k_{1t}(1-\rho_3)}.$$

The rate constant $\rho_3 k_{1c}$ may be evaluated either from eq. [5] using initial rates or from eq. [6] if α is determined as a function of time. The results obtained by both methods from data of the form given in Fig. 4 and from integrated plots of the type shown in Fig. 6 were

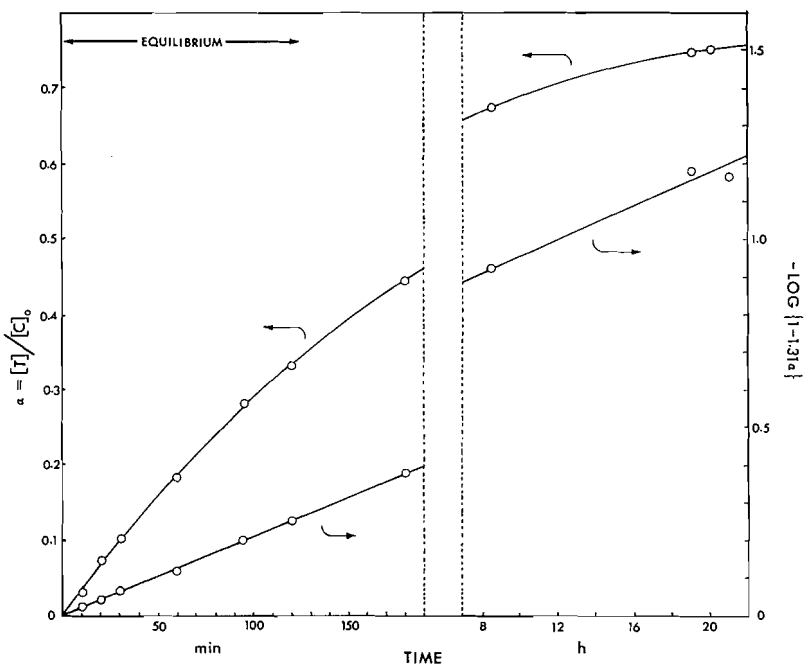

FIG. 6. Isomerization of *cis*-butene-2 at 25 °C: [RSH] = 2.15×10^{-4} mole l^{-1}, [C] = 3.29×10^{-4} mole l^{-1}, $\overline{r_i^{1/2}} = 8.35 \times 10^{-7}$ mole$^{1/2}$ $l^{-1/2}$ $s^{-1/2}$.

Can. J. Chem. Downloaded from www.nrcresearchpress.com by 210.87.254.105 on 09/05/12
For personal use only.

found to be in good agreement. Some of the former results are given in Table I. It is apparent from these that eq. [5] with $k_3 \gg k_2[RSH]$ is valid over a wide range of butene and thiol concentrations, and that the relation between $\overline{r_i^{1/2}}$ and thiol concentration determined from hydrogen evolution measurements is also valid over a wide concentration range.

TABLE I

Isomerization of *cis*-butene-2 at 25 °C

$[RSH]_0$ mole $l^{-1} \times 10^5$	g	$(\phi I_0)_{254}$ mole^{-1} l^{-1} $s^{-1} \times 10^{10}$	$[C]_0$ range mole $l^{-1} \times 10^5$	Slope R_i vs. $[C]_0$ $s^{-1} \times 10^3$	Slope $\overline{g(\phi I_0)_{254}^{1/2}}$
269	0.488	95.6	0.645–5.60	3.59	75.4
53.8	0.307	228	21.5–538	3.07	66.4
53.8	0.307	49.2	53.8	1.46*	67.9
0.229	0.0213	49.2	0.114–1.39	0.111*	74.2

*In the presence of 50 mm SF_6.

For $K = 3.2$ at 25 °C (11) and $k_4 = (2.5 \pm 0.7) \times 10^{10}$ l mole^{-1} s^{-1} (5), it is found that $\rho_3 k_{1c} = 1.6 \times 10^7$ l mole^{-1} s^{-1}. The corresponding rate constant for the isomerization of the *trans* form may be determined from equations equivalent to [5] and [6]. However, the experimental difficulties in measuring the very small conversions necessary do not permit precise estimates to be made in this way. Rather eq. [7] has been used to calculate $(1 - \rho_3)k_{1t} = 4.9 \times 10^6$ l mole^{-1} s^{-1}. The probability factor ρ_3 is likely greater than 0.5, thus making k_{1c} and k_{1t} approximately of the same magnitude and of the order of 2×10^7 l mole^{-1} s^{-1}.

Isomerization of trans-Ethylene-d_2

The rate of isomerization was determined both in the presence and the absence of 100 mm carbon dioxide; the results are plotted in the integrated form in Fig. 7. In spite of

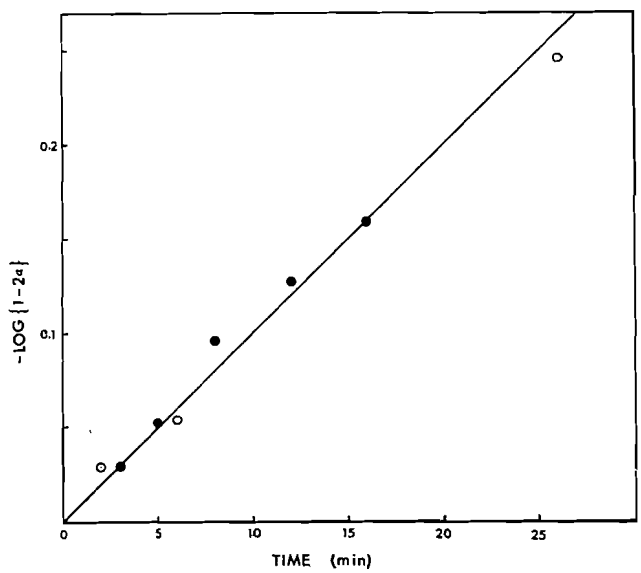

FIG. 7. Isomerization of *trans*-ethylene-d_2 at 25 °C: [RSH] = 1.07×10^{-4} mole l^{-1}, [T] = 3.96×10^{-4} mole l^{-1}, $\overline{r_i^{1/2}} = 2.15 \times 10^{-9}$ mole$^{1/2}$ $l^{-1/2}$ $s^{-1/2}$.

Can. J. Chem. Downloaded from www.nrcresearchpress.com by 210.87.254.105 on 09/05/12
For personal use only.

an appreciable amount of scatter, it may be concluded that the rate of isomerization is independent of pressure down to at least 10 mm. By means of eq. [6] with $K = 1$, $\rho_3 = 0.5$, $k_{1c} = k_{1t} = k_1$, the attack constant for ethylene is found to be $k_1 = 4.8 \times 10^6$ l mole^{-1} s^{-1} at 25 °C. No measurable change in rate was observed on increasing the temperature to 75 °C, and it would appear likely that, as with butene, the activation energy for isomerization is close to zero; although further work is necessary to establish this more rigorously.

Thus butene-2 is roughly four times as reactive as ethylene. This increase in reactivity on alkyl substitution of the double bond is consistent with the electrophilic nature of the thiyl radical and is similar to, although much smaller than, that observed for atomic oxygen which may also be considered an electrophilic reagent (12). Steric restrictions are undoubtedly more important for $CH_3\dot{S}$ than for O attack and these will tend to diminish the increase in rate resulting from the increase in p-character of the olefinic carbons brought about by alkyl substitution.

Isomerization of Butene-2 in the Presence of Butadiene

The results obtained in the early stages of this work exhibited complex kinetics which could not be reconciled with any reasonable mechanism. The observed variation of the rate of isomerization with *cis*-butene-2 concentration is shown in Fig. 4. Although simple first order kinetics were observed at low butene pressures, the initial rate fell off more rapidly at higher pressures, and in the limit became practically independent of the olefin concentration. This behavior is just what might be expected if the termination mechanism changes from $R\dot{S} + R\dot{S}$ at low olefin concentrations, through $R\dot{S} + \dot{X}$, to $\dot{X} + \dot{X}$ as the concentration of olefin is increased. The rate equations derived on this basis however were not consistent with the kinetics of the addition reaction. This explanation may also be eliminated by consideration of the dependence of the isomerization rate on the thiol concentration. At low thiol concentrations, the rate of initiation is directly proportional to the concentration and hence the rate of isomerization should be proportional to the square root of the thiol concentration provided mutual termination of thiyl radicals predominates. The results shown in Fig. 8 indicate however that the rate of isomerization is first order with respect to thiol and therefore linearly proportional to the rate of initiation. This can occur only if chain termination results from a first order reaction involving the chain carriers. Since wall termination should be negligible at these pressures, it appears likely that at high olefin concentrations chain termination occurs as a result of the reaction of $R\dot{S}$ with a reactive impurity which acts as a retarder.‡ The subsequent results, which were reported in the previous sections, obtained using butene-2 purified by gas chromatography, show none of these kinetic anomalies and tend to confirm the presence of a reactive contaminant.

Since conjugated olefins are known to act as efficient inhibitors for the addition of thiols to olefins in solution (1), it appeared likely that the observed retardation of isomerization was due to the presence of trace quantities of butadiene-1,3. This was further suggested by the fact that the retardation could be reduced (but not completely eliminated) by bubbling the *cis*-butene-2 through a refluxing solution of maleic anhydride in benzene. Confirmation of the presence of butadiene was obtained by gas chromatography. In order to reduce the tail of the *cis*-butene-2 peak which completely masked the butadiene, about 80% of the *cis*-butene-2 was first removed by fractionation on a dimethylsulpholane column (diameter 3/8 in., length 25 ft) at 0 °C. (The difference in retention times of *cis*-butene-2 and butadiene on this column was 26 min.) This sample was then analyzed

‡*Phillips "Research Grade" cis-butene-2 appeared to contain a slightly higher amount of the retarder.*

Can. J. Chem. Downloaded from www.nrcresearchpress.com by 210.87.254.105 on 09/05/12
For personal use only.

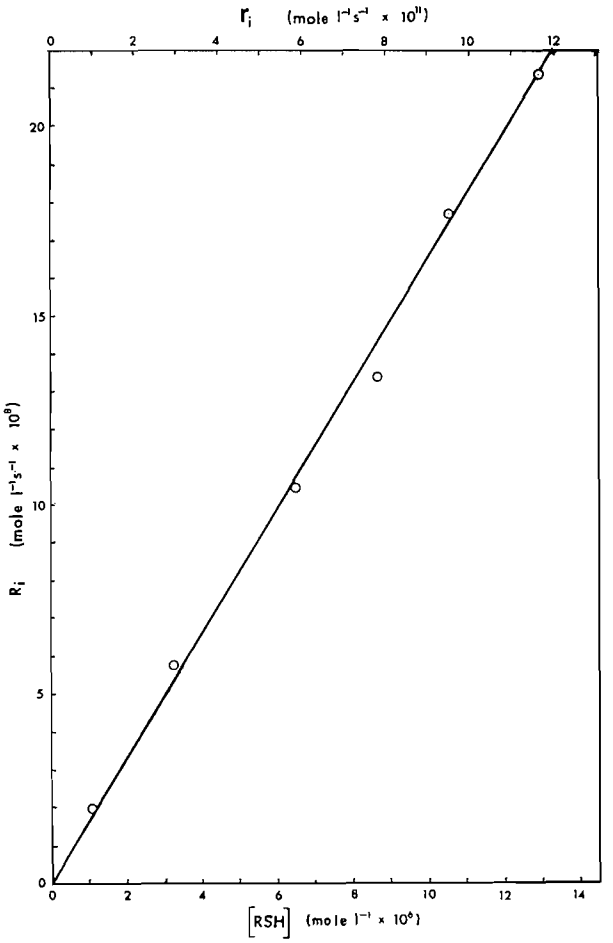

FIG. 8. Dependence of the isomerization rate on the thiol concentration or initiation rate at low pressures at 25 °C: [C] = 4.84×10^{-3} mole l^{-1}.

on a 200 ft dimethylsulpholane capillary column. Tailing of the remaining *cis*-butene interfered with the quantitative analysis but it could be estimated that there was 0.0019 ± 0.0009 mole % butadiene in the original sample. This agrees reasonably well with an estimate of 0.003% made spectrophotometrically at 220 mμ, assuming all of the absorption at this wavelength to be due to butadiene. That the retardation was due specifically to this impurity was shown by removing only the material with retention time in the immediate neighborhood of that of butadiene on the 3/8 in. diameter column. The resulting *cis*-butene-2 exhibited no retardation.

The addition of $\dot{RS}$ to butadiene (B) would produce a stable allylic radical ($\dot{Y}$) which would dehydrogenate thiol relatively slowly. It may therefore be assumed that, in the presence of butadiene, the termination reaction [4] (Fig. 2) may be replaced by

$$\dot{RS} + B \xrightarrow{k_7} \dot{Y},$$

$$\dot{Y} + \dot{RS} \xrightarrow{k_8} \text{product},$$

Can. J. Chem. Downloaded from www.nrcresearchpress.com by 210.87.254.105 on 09/05/12
For personal use only.

$$\dot{Y} + \dot{Y} \xrightarrow{k_9} \text{product.}$$

When $[\dot{Y}] \gg [R\dot{S}]$, termination reaction [8] will predominate and the initial rate of isomerization of *cis* will be

[8] $$R_1 = r_1\rho_3 k_{1c}[C]/k_7[B].$$

At lower concentrations of $\dot{Y}$, when reaction [8] becomes the main mode of termination, a factor of 2 will appear in the denominator of eq. [8].

Thus for a constant ratio of olefin to butadiene, the rate of isomerization should be independent of olefin concentration for high olefin and hence high butadiene concentrations, and at low rates of generation of $R\dot{S}$. This is consistent with the observations presented in Fig. 4. The rate constant k_7 (or $2k_7$) may be evaluated from the limiting rate of isomerization from Fig. 4 (4.3×10^8 l mole^{-1} s^{-1}) and from the slope of Fig. 8 (4.7×10^8 l mole^{-1} s^{-1}). The results are in good agreement and the average is k_7 (or $2k_7$) $= 4.5 \times 10^8$ l mole^{-1} s^{-1}. This result compares well with the result reported for styrene in solution where $k_1 = 8 \times 10^8$ l mole^{-1} s^{-1} (1).

Further work on butadiene is now in progress and this mechanism and result must be considered as tentative at present. It would appear perhaps surprising that butadiene, which is only about 15 times as reactive as butene-2 should have such a profound effect on the rate of isomerization at such a slow concentration. This behavior however must be due to the fact that attack of $R\dot{S}$ on butadiene is not reversible at 25 °C because of the formation of a stable allylic radical and because of the long chain length of the isomerization reaction, this irreversible removal of $R\dot{S}$ results in a large decrease in reaction rate.

ACKNOWLEDGMENTS

We are grateful to the National Research Council for the financial assistance received. We would also like to thank Polymer Corporation Ltd. for the use of a mass spectrometer.

REFERENCES

1. C. SIVERTZ. J. Phys. Chem. **63**, 34 (1959).
2. W. A. PRYOR. Mechanisms of sulfur reactions. McGraw-Hill, N.Y. 1962. Chap. 3.
3. C. SIVERTZ, W. ANDREWS, W. ELSDON, and K. GRAHAM. J. Polymer Sci. **19**, 587 (1956).
4. R. TOWNSHEND, R. PALLEN, and C. SIVERTZ. The Mechanisms of Radical Induced *cis–trans* Inversion. Presented at N.Y. meeting A.C.S. September 13, 1957.
5. D. M. GRAHAM, R. L. MIEVILLE, R. H. PALLEN, and C. SIVERTZ. Can. J. Chem. Part II. **42**, 2250 (1964).
6. B. S. RABINOVITCH and F. S. LOONEY. J. Am. Chem. Soc. **75**, 2652 (1953).
7. N. P. SKERRETT and H. W. THOMPSON. Trans. Faraday Soc. **37**, 81 (1941).
8. W. G. BURNS and F. S. DAINTON. Trans. Faraday Soc. **46**, 411 (1950).
9. J. L. FRANKLIN. J. Chem. Phys. **21**, 2029 (1953).
10. W. ANDREWS. M.Sc. Thesis, University of Western Ontario, London, Ontario, 1955.
11. N.B.S. Circular. Selected Properties of Hydrocarbons. A.P.I. Project 44.
12. R. J. CVETANOVIC. J. Chem. Phys. **30**, 19 (1959).

Can. J. Chem. Downloaded from www.nrcresearchpress.com by 210.87.254.105 on 09/05/12
For personal use only.

Can. J. Chem. Downloaded from www.nrcresearchpress.com by 210.87.254.5 on 09/05/12
For personal use only.

PHOTO-INITIATED REACTIONS OF THIOLS AND OLEFINS

II. THE ADDITION OF METHANETHIOL TO UNCONJUGATED OLEFINS

D. M. GRAHAM, R. L. MIEVILLE, R. H. PALLEN, AND C. SIVERTZ
Department of Chemistry, University of Western Ontario, London, Ontario

Received February 21, 1964

ABSTRACT

Kinetic studies have been made of the addition of methanethiol to ethylene, propylene, and butene-2. The results obtained are consistent with the mechanism postulated for the isomerization reaction (1). The overall activation energy was found to be negative and could be explained in terms of two competing reactions of the adduct radical: thermal decomposition leading to $CH_3\dot{S}$ and olefin and dehydrogenation of thiol yielding addition product. Only the ratio of the rate constants for these two reactions could be determined. The method of intermittent illumination was used to evaluate the termination rate constant for the combination of two $CH_3\dot{S}$ radicals which was found to be $(2.5 \pm 0.7) \times 10^{10}$ l mole^{-1} s^{-1}.

INTRODUCTION

In Part I(1) it was shown that the thiyl radical catalyzed isomerization of butene-2 and 1,2-ethylene-d_2 could be explained at pressures above 4 mm by the reaction sequence shown in Fig. 1. To investigate further the results of the reversibility of the attack step [1]

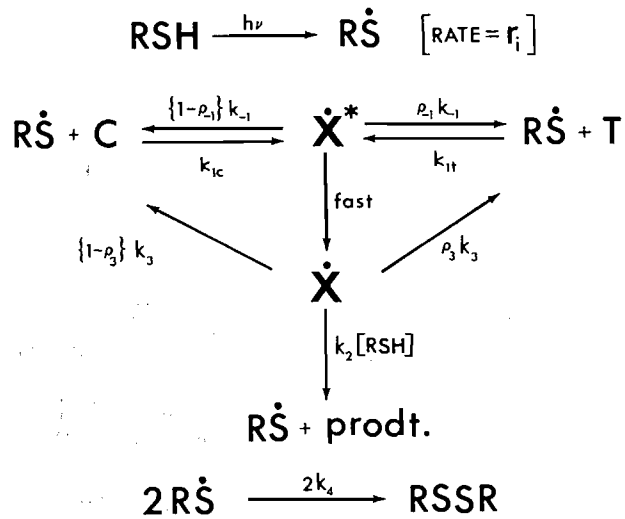

FIG. 1. The reaction mechanism. As was explained in Part I, because of the observed lack of pressure dependence of the rate of isomerization, decomposition of the adduct radical may be represented by a simple first order reaction (reaction [3]) which is the high-pressure limit of the more complicated unimolecular sequence given previously. Superscripts on the rate constants are no longer necessary to distinguish between the two possible decomposition paths, and have been dropped. C and T represent the *cis* and *trans* forms of the olefin; $\dot{X}^*$ and $\dot{X}$ represent the chemically energized and the de-energized adduct radicals, respectively; ρ is the probability that a decomposition reaction produces the *trans* isomer.

and to test the validity of the proposed mechanism, the kinetics of the addition reaction have been studied.

EXPERIMENTAL

Purification of the chemicals used and a description of the apparatus have been given in Part I. For the intermittent illumination experiments, the optical system was modified by the addition of a light stop with an opening of about 5 mm and a rotation sector at the focal point of one of the lenses. The sector motor was

operated from a thyratron-controlled d-c. power supply, and the ratio of light to dark period was 1:1. It was established using a photometer that the apparatus produced reasonably good square wave modulation.

The pressure change arising from the addition reaction was followed using a differential manometer. In the early stages of the work a wide-bore mercury manometer was used; reliable pressure measurements could be made to ±0.1 mm using a cathetometer. In the later stages a Wallace–Tiernan differential manometer in which the sensing element is a beryllium–copper capsule 2 cc in volume was used; this gauge permitted pressure measurements accurate to ±0.01 mm.

RESULTS AND DISCUSSION

The Termination Rate Constant

The isomerization kinetics discussed in Part I indicate that chain termination occurs exclusively by thiyl radical combination even at high olefin concentrations. The addition kinetics to be reported here confirm this. The method of intermittent illumination allows the mean lifetime of the chain carrier $CH_3\dot{S}$ to be determined. However the application of this technique was complicated by the experimental conditions under which addition rates could be measured. In order to obtain measurable rates, it was necessary to work at relatively high thiol pressures resulting in a large radical concentration gradient along the length of the cell because of strong absorption of light by the thiol. A procedure for applying the method of intermittent illumination in such cases has been developed by Burns and Dainton (2) for a system in which monochromatic light is used. With the system used to initiate the reactions of methanethiol, it proved impossible to isolate one single active spectral line and it was necessary to modify this procedure to account for the different absorption characteristics of the various wavelengths present.

On the basis of measurements of the rate of hydrogen production from the photochemical decomposition of methanethiol, it was shown in Part I that the rate of initiation in a layer of depth dl at a distance l from the illuminated face of the cell may be described by an equation of the form

$$[1] \qquad r_i\,(\text{local}) = \sum_{\lambda} (\phi I_0)_\lambda \epsilon_\lambda c\, e^{-\epsilon_\lambda c l}$$

The summation is taken over the three active wavelengths found to be present, 254, 257, and 265 mμ, with molar extinction coefficients ϵ_λ = 143, 69.9, and 16.8, respectively. ϕ_λ is the quantum efficiency for primary radical production and I_{0_λ} is the incident light intensity at wavelength λ; this product may be evaluated from the hydrogen production measurements. The concentration of thiol is c.

For a sector producing light and dark periods of the same duration the significant ratio is

$$[2] \qquad \rho = \sqrt{2}\,\frac{\text{sectored rate}}{\text{rate for continuous illumination}}.$$

Under conditions of non-uniform illumination this ratio must be averaged over the length of the cell, L, and it is readily shown that

$$[3] \qquad \bar{\rho} = \frac{\int_0^L r_i^{1/2}(\text{local}) f[t_l k_t^{1/2} r_i^{1/2}(\text{local})]\, dl}{\int_0^L r_i^{1/2}(\text{local})\, dl} = \frac{\int_0^L G^{1/2}(c, l) f[m' G^{1/2}(c, l)]\, dl}{\int_0^L G^{1/2}(c, l)\, dl},$$

Can. J. Chem. Downloaded from www.nrcresearchpress.com by 210.87.254.5 on 09/05/12
For personal use only.

where

$$G(c, l) = \sum_{\lambda} \frac{(\phi I_0)_\lambda \epsilon_\lambda}{(\phi I_0)_{\lambda_1} \epsilon_{\lambda_1}} e^{-\epsilon_\lambda c l}.$$

The subscript λ_1 refers to one specific wavelength; in this case the 254 mμ line was chosen. t_l is the duration of the flash and k_t is the rate constant for the termination reaction. The form of the function $f[m'G^{1/2}(c,l)]$ is identical with that obtained for $f(m)$ for the case of uniform illumination (3) and $\bar{\rho}$ may be evaluated by numerical integration for different values of the dimensionless parameter $m' = t_l[k_t(\phi I_0)_{\lambda_1} \epsilon_{\lambda_1} c]^{1/2}$. The curve calculated in this manner is then compared with the experimental curve obtained from [2] for $\bar{\rho}$ as a function of t_l and the termination constant determined in the usual way.

The experimental results and the theoretical curve are shown in Fig. 2. Although there

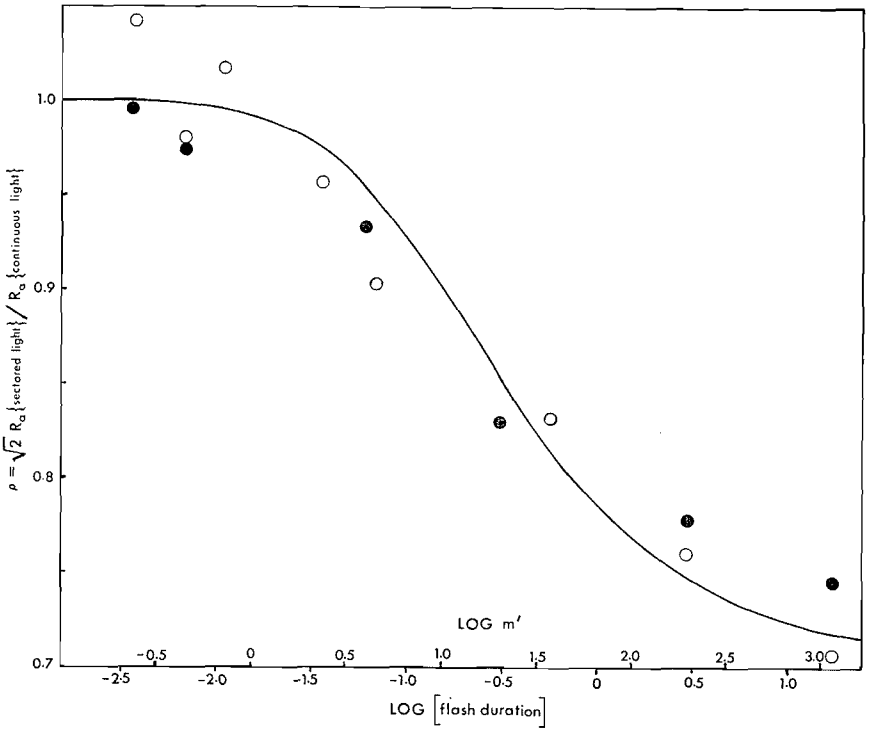

FIG. 2. Rotating sector curve: ● butene-2; ○ ethylene.

is an appreciable amount of scatter in the points, it is apparent that the termination constant is the same under these conditions for the butene-2 and ethylene systems. This is consistent with the kinetic evidence that termination occurs in both cases by combination of thiyl radicals. The rate constant for reaction [4] is found to be $k_4 = k_t/2 = (2.5 \pm 0.7) \times 10^{10}$ l mole^{-1} s^{-1}. The limits quoted indicate the maximum range over which the calculated and experimental curves may be fitted. It is hoped that a considerably better estimate of k_4 will be obtained by applying this technique to the isomerization rate. These measurements may be made more accurately and at very much lower thiol concentrations where the correction for non-uniform illumination will be small.

Can. J. Chem. Downloaded from www.nrcresearchpress.com by 210.87.254.5 on 09/05/12
For personal use only.

Kinetics of the Addition Reaction

The isomerization results indicated that, at pressures above 4 mm, collisional de-energization of the adduct radical $\dot{X}^*$, which contains the exothermic heat of reaction [1], is very fast and the rate of reaction should be independent of the total pressure. The rate of addition under these conditions is found to be

$$[4] \qquad R_a = -\frac{d[RSH]}{dt} = \left(\frac{r_i}{2k_4}\right)^{1/2} \frac{k_2[RSH](k_{1c}[C] + k_{1t}[T])}{k_3 + k_2[RSH]}.$$

Since isomerization is very much more rapid than addition, the isomers are in their equilibrium concentrations during the period in which addition rate measurements are made. It is therefore convenient to use a mean attack constant, k_1, which is averaged over the equilibrium concentrations, and to represent the total olefin concentration as [A]. Then [4] becomes

$$[5] \qquad R_a = \left(\frac{r_i}{2k_4}\right)^{1/2} \frac{k_1 k_2[RSH][A]}{k_3 + k_2[RSH]}$$

where

$$k_1 = \frac{k_{1c} + Kk_{1t}}{1 + K}$$

and

$$K = [T]_{eq}/[C]_{eq}.$$

The pressure–time plots for ethylene were linear over the range of conversion ($< 5\%$) used to determine R_a. For butene-2, however, a short non-reproducible inhibition period was observed, during which time almost no pressure decrease was observed. When the butene was purified by gas chromatography, the inhibition period disappeared and the rate of addition became greater. A similar effect was observed for the isomerization reaction and the retarder was identified as butadiene-1,3 (1). Because the chain length for addition is much less than that for isomerization, initial inhibition rather than retardation, as in the case of the isomerization reaction, occurs. The subsequent retardation of the addition rate is likely due to the products of the inhibition reaction. With unpurified butene the rate was less than first order with respect to olefin, which is consistent with the retardation mechanism postulated for the isomerization reaction.

Equation [5] predicts a first order dependence on olefin which is in agreement with the experimental observations for ethylene and butene-2 over the wide concentration ranges shown in Figs. 3 and 5. The results given in Figs. 4 and 5 show that after the rate is divided by $\overline{r_i^{1/2}}$, it is directly proportional to the thiol concentration. This will follow from eq. [4] only if $k_3 \gg k_2[RSH]$, which was also concluded from the observed isomerization kinetics.

The Rate Constants

It is possible therefore to obtain from these results the ratio $k_1k_2k_3^{-1}$ since k_4 has been determined. Some of the values obtained are given in Table I. The propylene results were calculated assuming identical kinetic behavior. The temperature dependence of the ratio is shown in Fig. 6, and from these results, $E_1 + E_2 - E_3$ may be evaluated assuming E_4 to be zero; these activation energies are also given in Table I. The estimated values of $k_2k_3^{-1}$ given were calculated using the attack constant (k_1) values obtained from the isomerization studies and assuming that $E_1 \simeq 0$ (1).

Unfortunately it is at present impossible to draw any general conclusions from the

Can. J. Chem. Downloaded from www.nrcresearchpress.com by 210.87.254.5 on 09/05/12
For personal use only.

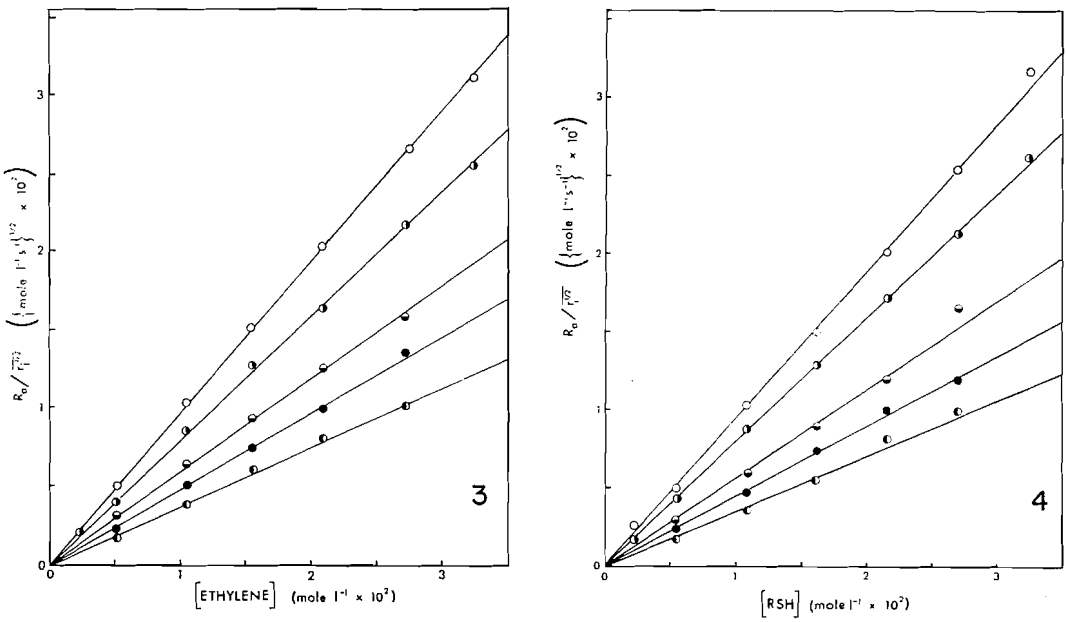

FIG. 3. Dependence of the rate of addition of methanethiol to ethylene on olefin concentration, [RSH] = 1.08×10^{-2} mole l^{-1}: ○ 25 °C; ◑ 30 °C; ◒ 40 °C; ● 50 °C; ◐ 60 °C.

FIG. 4. Dependence of the rate of addition to ethylene on the methanethiol concentration, [A] = 1.08×10^{-2} mole l^{-1}: ○ 25 °C; ◑ 30 °C; ◒ 40 °C; ● 50 °C; ◐ 60 °C.

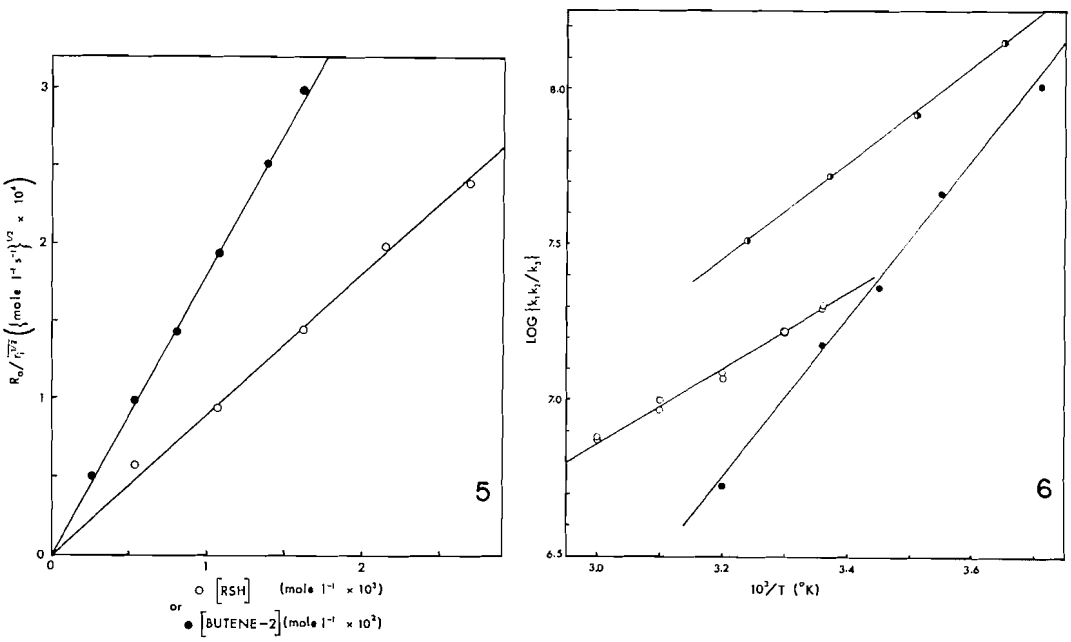

FIG. 5. Dependence of the rate of addition of methanethiol to butene-2 on the olefin and thiol concentrations at 25 °C: ● olefin varied, [RSH] = 2.69×10^{-3} mole l^{-1}; ○ thiol varied, [A] = 1.34×10^{-2} mole l^{-1}.

FIG. 6. Temperature dependence of the rate constant ratio k_1k_2/k_3: ○ ethylene; ◑ propylene; ● butene-2.

Can. J. Chem. Downloaded from www.nrcresearchpress.com by 210.87.254.5 on 09/05/12
For personal use only.

TABLE I

Addition rate constants. The propylene results are interpolated values from Fig. 6. For ethylene $k_1 = 4.8 \times 10^6$ l mole^{-1} s^{-1}, and it is assumed that for butene $k_{1c} = k_{1t} = k_1 = 2.1 \times 10^7$ l mole^{-1} s^{-1} (1)

Temp., °C	Ethylene		Propylene	Butene-2	
	$k_1k_2k_3^{-1} \times 10^{-6}$*	$k_2k_3^{-1}$†	$k_1k_2k_3^{-1} \times 10^{-6}$*	$k_1k_2k_3^{-1} \times 10^{-6}$*	$k_2k_3^{-1}$†
25	20	4.1	51	15	0.76
40	12	2.5	29	5.1	0.26
60	7.5	1.6	14	1.8	0.088
$E_1 + E_2 - E_3$ (kcal)	-5.3 ± 0.1		-7.0 ± 0.2	-11.7 ± 0.5	

*Units: l^2 mole^{-2} s^{-1}.
†Units: l mole^{-1}.

values obtained for the rate constant ratios or the activation energy differences. The rate constant at 30 °C and the activation energy for methyl radical dehydrogenation of methanethiol (corresponding to reaction [2]) have been roughly estimated to be 2×10^4 l mole^{-1} s^{-1} and 5 kcal. If it is assumed that k_2 and E_2 have approximately these values for all olefins, the results obtained are intuitively unreasonable. For example a greater k_3 value is obtained for butene than for ethylene even though the corresponding activation energies bear the opposite relation. It must be concluded therefore that the rates of both reactions [2] and [3] are dependent upon the structure of the adduct radical.

The rate constants k_2 and k_3 could be separated if rate measurements could be carried out at sufficiently high concentrations of $\dot{X}$ (i.e., at high olefin and low thiol concentrations and at low temperatures) that a termination reaction other than [4] would predominate. This appears to be beyond the technique reported here but further investigation of this possibility is planned.

The complexity of eq. [5] for the rate of addition emphasizes the danger inherent in obtaining "relative reactivities" from relative rates of addition (4). This procedure can be valid only for cases in which the attack step is not reversible or for reaction systems in which the thiol concentration is chosen such that $k_2[\mathrm{RSH}] \gg k_3$.

ACKNOWLEDGMENTS

We are grateful to the National Research Council for the financial assistance received.

REFERENCES

1. D. M. GRAHAM, R. L. MIEVILLE, and C. SIVERTZ. Can. J. Chem. **42**, 2239 (1964).
2. W. G. BURNS and F. S. DAINTON. Trans. Faraday Soc. **46**, 411 (1950).
3. G. M. BURNETT. Mechanism of polymer reactions. Interscience Inc., New York. 1954. p. 192.
4. C. WALLING and W. HELMREICH. J. Am. Chem. Soc. **81**, 1144 (1949).

Can. J. Chem. Downloaded from www.nrcresearchpress.com by 210.87.254.5 on 09/05/12
For personal use only.

Can. J. Chem. Downloaded from www.nrcresearchpress.com by 210.87.254.105 on 09/05/12
For personal use only.

IONIZATION POTENTIALS OF METHYL-SUBSTITUTED BENZENES AND CYCLOPENTADIENES

F. MEYER AND A. G. HARRISON[1]
Department of Chemistry, University of Toronto, Toronto, Ontario
Received June 4, 1964

ABSTRACT

The ionization potentials of a number of methyl-substituted benzenes and cyclopentadienes have been measured by electron impact. The experimental results are compared to calculations based on a group orbital method.

INTRODUCTION

The relation between structure and ionization potentials of organic compounds has been the subject of a considerable number of investigations, both experimental and theoretical. It has become evident that more series of related compounds are needed to test the semi-empirical methods of calculation and to widen the field of their applicability. We have recently measured the electron-impact ionization potentials of a number of methyl-substituted benzenes and cyclopentadienes. We have compared the results obtained for these two series with calculations based on a group orbital method.

The group orbital method is a simplification of the equivalent orbital method developed by Lennard-Jones and Hall (1, 2). They showed that the total wave function of a molecule can be considered either as a set of equivalent orbitals or as a set of molecular orbitals. The two sets can be derived from each other by a unitary transformation. The energy to remove an electron from a molecular orbital can be calculated starting from an equivalent orbital description which refers to bonds and lone pairs of electrons in the molecule. Hall (3) showed for planar molecules, in the case where the observed ionization potential is for removal of an electron from an orbital antisymmetric in the plane of the molecule, that only the antisymmetric combinations of the equivalent orbitals need to be considered.

In such a case the ionization potentials can be calculated from certain group parameters. The ionization potentials, E, are the roots of the secular equation

$$|e_{m,n} - E\delta_{m,n}| = 0, \qquad [1]$$

where m and n refer to the various groups in the molecule. To a good approximation, $e_{m,n}(m = n)$ can be taken as the ionization potential of the hydride of group m, and the interaction factors $e_{m,n}$ $(m \neq n)$ can be calculated from experimental data. For $m = n$, $\delta_{m,n} = 1$, and for $m \neq n$, $\delta_{m,n} = 0$. The group orbital method has been extensively applied in this form to the calculation of ionization potentials by Franklin (4).

EXPERIMENTAL

The ionization potentials were measured with an A.E.I. MS-2 mass spectrometer previously described (5). The ionization potentials were determined in the usual manner (6) using xenon to calibrate the voltage scale. The methylbenzenes were commercial samples, while the methylcyclopentadienes were very kindly supplied by Mr. P. Haynes and Professor S. McLean of this Department. Details of the synthesis and proof of structure of the cyclopentadienes will be published elsewhere (7) as will a detailed consideration of the mass spectra (8). The methylcyclopentadienes were purified by gas chromatography and kept at dry-ice temperature until used.

[1]*Alfred P. Sloan Fellow 1962–1964.*

RESULTS AND DISCUSSION

The measured ionization potentials for cyclopentadiene and a number of methyl-substituted cyclopentadienes are compared with calculations based on the group orbital method in Table I. The details of the calculations will be discussed below. Our value of

TABLE I

Ionization potentials of methylcyclopentadienes in electron volts

Substituents	Experimental (±0.05 eV)	Calculated $a = 1.53$ $b = 1.15$	Calculated $a = 1.53$ $b = 0$
H	8.93	(8.93)	(8.93)
1-Monomethyl	8.43	8.45	8.45
2-Monomethyl	8.46		
1,2-Dimethyl	8.1±0.1		
Mixture 1,2- and 2,3-dimethyl	8.17	8.18	8.05
5,5-Dimethyl	8.22		
1,2,3-Trimethyl	7.96	8.00	7.69
1,5,5-Trimethyl	8.00		
1,2,3,4-Tetramethyl	7.8±0.1	7.88	7.37
1,4,5,5-Tetramethyl	7.84		
Mixture 1,2,3,5,5- and 1,2,4,5,5-pentamethyl	7.77	7.78	7.07
Hexamethyl	7.74	7.70	6.79

8.93 eV for cyclopentadiene is in good agreement with previous electron-impact values of 9.00 eV (9) and 8.9 eV (10) and the calculated value of 8.91 eV (11). The ionization potentials of the methylcyclopentadienes have not been measured previously.

It is interesting to note that the ionization potentials of the positional isomers in the cyclopentadienes are identical, within experimental error, although the ring positions are not identical. This is even true for the 5,5-disubstituted cyclopentadienes where one might have expected the interaction between the methyl groups and the π-electron system to be reduced. It does not appear that this lack of structural effect can be due to thermal isomerization in the ion chamber prior to ionization. It has been reported (12) that 1,5,5-trimethylcyclopentadiene undergoes rearrangement to 1,2,3-trimethylcyclopentadiene when the compound at 400 °C is passed through a 60 cm tube partially filled with glass wool. However, the ion source temperature is only 20–30 °C above room temperature, as measured with a thermocouple under operating conditions, and any rearrangement of the 5,5-disubstituted compounds will be very slow at this temperature. The 1- and 2-methylcyclopentadienes do isomerize by an alpha hydrogen shift in the liquid phase giving an equilibrium mixture (13), but the rate is slow compared to the residence time in the ion source. Furthermore, no appreciable rearrangements of the compounds studied were observed on separation in a gas chromatograph with an inlet temperature of 200 °C and a column temperature of 75 °C. Significant differences were noted in the mass spectra of the 5,5-disubstituted compounds compared to the isomers with methyl groups in other positions (8). On the other hand, 5-monomethylcyclopentadiene rearranges very rapidly at room temperature and has not been included in this study.

The ionization potentials of a number of methyl-substituted benzenes are compared in Table II with calculations based on the group orbital method and with previous electron-impact results (14). The ionization potentials measured in the present work are in reasonable agreement with previous values, although the present values for the xylenes and

Can. J. Chem. Downloaded from www.nrcresearchpress.com by 210.87.254.105 on 09/05/12
For personal use only.

TABLE II

Ionization potentials of methylbenzenes in electron volts

Substituent	Experimental		Calculated		
	This work (±0.05 eV)	Literature (14)	$a = 1.32$ $b = 0.40$	$a = 1.09$ $b = 0$ (4)	$a_1 = 1.265$ $a_2 = 1.09$ $b = 0$
H	9.60	9.3–9.8	(9.60)	(9.52)	(9.60)
Methyl	9.23	9.15–9.23	9.18	9.23	9.22 (a_1)
1,2-Dimethyl	8.88	8.96			8.96 (a_1, a_2)
1,3-Dimethyl	8.88	9.01	8.88	8.96	8.96 (a_1, a_2)
1,4-Dimethyl	8.78	8.86			8.88 (a_1, a_1)
1,2,3-Trimethyl	8.67	8.75			8.74 (a_1, a_2, a_2)
1,2,4-Trimethyl	8.55	—	8.64	8.74	8.66 (a_1, a_1, a_2)
1,3,5-Trimethyl	8.64	8.75			8.74 (a_1, a_2, a_2)
1,2,3,5-Tetramethyl	8.47	—	8.45	8.53	8.46 (a_1, a_1, a_2, a_2)
1,2,4,5-Tetramethyl	8.50	—			8.46 (a_1, a_1, a_2, a_2)
Pentamethyl	8.30	—	8.29	8.27	8.27 (a_1, a_1, a_2, a_2, a_2)
Hexamethyl	—	—	8.14	8.15	8.08 (a_1, a_1, a_2, a_2, a_2, a_2)

trimethylbenzenes are slightly lower. The ionization potentials of the tetramethylbenzenes and pentamethylbenzene do not appear to have been measured previously by electron impact.

Calculation of Ionization Potentials

Franklin (4) calculated the ionization potential of cyclopentadiene using one methane and two ethene groups to build up the molecule. The interaction factor, a, between a methane and an ethene was calculated from the ionization potential of propene; the interaction factor, b, between two ethene groups was obtained from the ionization potential of butadiene. Both these factors can be obtained by solving equation [1]. The ionization potentials of methane and ethene were taken as 13.31 eV and 10.50 eV respectively. The secular equation for cyclopentadiene can be written as:

$$\begin{vmatrix} 13.31 - E & a & a \\ a & 10.50 - E & b \\ a & b & 10.50 - E \end{vmatrix} = 0$$

where the lowest root for E corresponds to the ionization potential which is measured experimentally. The determinant factorizes into

$$(10.50 - b - E)\{(13.31 - E)(10.50 + b - E) - 2a^2\} = 0,$$

which gives as the lowest root $E = 10.50 - b$. This is, however, identical with the ionization potential of butadiene since from the method of calculation of b,

$$10.50 - I(\text{butadiene}) = b.$$

This implies that there is no interaction between the methane part of the molecule and the butadiene part of the molecule as far as the lowest ionization potential is concerned and obviously leads to the conclusion that substitution in the 5 position will have no effect on the ionization potential. This is clearly not in agreement with the results for the 5,5-disubstituted compounds and indicates that this method of building up the cyclopentadiene molecule cannot be used[2].

[2]*In this regard it might be pointed out that if cyclopropane is built up from three methane groups with an interaction factor derived from the ionization potential of ethane, the calculated I(cyclopropane) is the same as I(ethane), expressing the fact that on this model no interaction is possible between the methane and ethane parts of the molecule. Similarly, if cyclopentane is built up from a methane and two ethane groups, I(cyclopentane) equals I(butane) since I(butane) is used to calculate the interaction between the two ethane groups.*

Can. J. Chem. Downloaded from www.nrcresearchpress.com by 210.87.254.105 on 09/05/12
For personal use only.

It seems justified, however, in these substituted ring compounds to consider the ring nucleus as one group and the substituents as separate groups. Calculation of the ionization potential for an n-methyl substituted ring compound then requires the solution of the following determinant, where H is the ionization potential of the unsubstituted ring compound, 13.31 eV is the ionization potential of methane[3], $a_1, a_2, a_3 \ldots a_n$ are the interaction factors of the methyl groups with the ring, and $b_1, b_2, b_3 \ldots b_n$ are the interaction factors between the methyl groups.

$$\begin{vmatrix} H-E & a_1 & a_2 & a_3 & \ldots \\ a_1 & 13.31-E & b_1 & b_2 & \ldots \\ a_2 & b_1 & 13.31-E & b_3 & \ldots \\ a_3 & b_2 & b_3 & 13.31-E & \ldots \\ \cdot & \cdot & \cdot & & \\ \cdot & \cdot & \cdot & & \\ \cdot & \cdot & \cdot & & \end{vmatrix} = 0$$

In the cyclopentadiene series there is no observable difference between the different methyl-substituted isomers; this suggests that all a factors are the same and also that all b factors are the same. For the case where $a_1 = a_2 = a_3$, etc. and $b_1 = b_2 = b_3$, etc. $\neq 0$ the determinant factorizes into

$$(H - a^2/b - E)(13.31 - b - E)^{n-1}(13.31 + (n-1)b - E) + a^2/b(13.31 - b - E)^n = 0.$$

It appears that $n - 1$ roots are equal to $13.31 - b$, and the lowest root can be calculated from the resulting quadratic equation.

For the cyclopentadiene series values of $a = 1.53$ eV and $b = 1.15$ eV yield calculated ionization potentials (column 3, Table I) in agreement with measured values within experimental error for the whole series. For comparison we give in the final column of Table I a set of values calculated assuming $a = 1.53$ eV but $b = 0$, that is, assuming no methyl–methyl interaction. In this case the discrepancies between measured and calculated values become very large for the polysubstituted members of the series. The introduction of the factor b has the effect of slowing down the decrease in ionization potential with increasing number of methyl substituents. Attempts were made to fit the series with $b = 0$ by adjusting the ring–methyl interaction factor, a, but no satisfactory agreement could be obtained for the whole series.

In the benzene series there are small differences in the ionization potentials of positional isomers, suggesting that all the interaction factors are not identical. If these small differences are neglected as a first approximation, one can calculate ionization potentials in reasonable agreement with the mean value for each group, using $a = 1.32$ eV and $b = 0.40$ eV as shown in column 4 of Table II. In this case the secondary interaction factor, b, has little effect, and agreement which is almost as good can be obtained using $b = 0$ and adjusting the other parameters. This is shown by the calculations due to Franklin (4) which are reproduced in column 5 of Table II.

The small differences between positional isomers such as that observed for the isomeric dimethyl and trimethyl compounds cannot be reproduced using only one set of interaction parameters. An explanation for the observed differences in ionization potentials for positional isomers has been presented in terms of simple molecular orbital theory by Bralsford *et al.* (15) and discussed with reference to the xylenes by Streitwieser (16). The

[3]*We have taken 13.31 eV as the ionization potential of ethane to correspond to the value used in previous calculations by Franklin (4).*

Can. J. Chem. Downloaded from www.nrcresearchpress.com by 210.87.254.105 on 09/05/12
For personal use only.

methyl substitution is considered as a perturbation of benzene. The two highest occupied molecular orbitals in benzene are shown schematically in Fig. 1, both orbitals having the

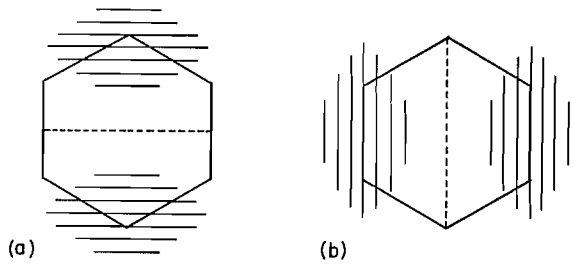

FIG. 1. Molecular orbitals of benzene.

same energy. The interaction of the methyl substituent is considered to depend on the magnitude of the wave function at the point of substitution and, since a methyl group has the highest possible interaction in the 1 position of the molecular orbital in Fig. 1(*a*), this orbital becomes the highest occupied orbital with the lowest ionization potential. The interaction in the 4 position is the same, while the interactions in the 2, 3, 5, and 6 positions are less. Thus paraxylene has two methyls capable of strong methyl–ring interaction and, therefore, a lower ionization potential than either the ortho- or meta-xylene, each of which only have one methyl in a position to interact strongly.

This model suggests that at least two methyl–ring interaction parameters should be used in the calculation of the ionization potentials of methylbenzenes by the group orbital methods. One of these parameters, a_1, should express the strong interaction possible in the 1 and 4 position of Fig. 1(*a*), while the second parameter, a_2, expresses the weaker interaction in the other positions. The final column of Table II shows the results obtained using $a_1 = 1.265$ eV and $a_2 = 1.09$ eV, with the combinations of a_1 and a_2 factors used for each molecule given in brackets after the calculated value. In these calculations the methyl–methyl interaction factor, b, was zero. The calculated values agree quite well with the experimental values and, in addition, correctly reproduce the differences between structural isomers. A better fit for the dimethyl and trimethyl cases would probably require the introduction of one or more methyl–methyl interaction factors.

It is clear from the present work that the group orbital method can be used satisfactorily to reproduce the ionization potentials of a homologous series of compounds. However, the fact that a second interaction parameter, b, must be introduced, as for the cyclopentadienes, seriously limits the usefulness of the method since this parameter cannot be estimated without a knowledge of the ionization potential of higher members of the series. In addition, to reproduce small differences among isomers, different substituent–ring interactions which cannot be estimated without experimental guides must be used.

ACKNOWLEDGMENTS

The authors are indebted to the National Research Council of Canada and to the Alfred P. Sloan Foundation for financial support.

REFERENCES

1. G. G. HALL. Proc. Roy. Soc. London, Ser. A, **205**, 541 (1951).
2. J. LENNARD-JONES and G. G. HALL. Discussions Faraday Soc. **10**, 18 (1951).
3. G. G. HALL. Proc. Roy. Soc. London, Ser. A, **213**, 102 (1952).

Can. J. Chem. Downloaded from www.nrcresearchpress.com by 210.87.254.105 on 09/05/12
For personal use only.

4. J. L. FRANKLIN. J. Chem. Phys. **22**, 1304 (1954).
5. J. M. S. TAIT, T. W. SHANNON, and A. G. HARRISON. J. Am. Chem. Soc. **84**, 4 (1962).
6. A. G. HARRISON and T. W. SHANNON. Can. J. Chem. **40**, 1730 (1962).
7. S. MCLEAN and P. HAYNES. To be published.
8. F. MEYER, P. HAYNES, S. MCLEAN, and A. G. HARRISON. To be published.
9. A. G. HARRISON, L. R. HONNEN, H. J. DAUBEN, Jr., and F. P. LOSSING. J. Am. Chem. Soc. **82**, 5593 (1960).
10. J. HISSEL. Bull. Soc. Roy. Sci. Liege, **21**, 457 (1952).
11. A. STREITWIESER, Jr. J. Am. Chem. Soc. **82**, 4123 (1960).
12. K. ALDER and R. MUDERS. Ber. **91**, 1083 (1958).
13. S. MCLEAN and P. HAYNES. Tetrahedron Letters. In press. 1964.
14. R. W. KISER. Tables of Ionization Potentials, U.S. Atomic Energy Commission, Report TID-6142. 1960.
15. R. P. BRALSFORD, P. V. HARRIS, and W. C. PRICE. Proc. Roy. Soc. London, Ser. A, **258**, 459 (1960).
16. A. STREITWIESER, Jr. Ionization potentials in organic chemistry. *In* Progress in physical organic chemistry. Vol. 1. Interscience. 1963.

Can. J. Chem. Downloaded from www.nrcresearchpress.com by 210.87.254.105 on 09/05/12
For personal use only.

Can. J. Chem. Downloaded from www.nrcresearchpress.com by 210.87.254.42 on 09/05/12
For personal use only.

PHOTOLYSE DE L'IODURE DE VINYLE EN SOLUTION DANS LE TETRACHLORURE DE CARBONE

PIERRE C. ROBERGE ET JAN A. HERMAN
Département de Chimie, Université Laval, Québec, Québec

Reçu le 29 avril 1964

ABSTRACT

The photolysis of vinyl iodide in carbon tetrachloride solutions gives several products among which the most important are: acetylene, hydrogen iodide, iodine, ethylene, and vinyl chloride. A mechanism based on diffusion-controlled disproportionation of geminate radicals, as first proposed by Hamill, agrees well with the observed phenomena. To explain the diminishing production of ethylene and iodine with increasing concentration of the monomer, it is necessary to postulate a telomerization of the vinyl iodide.

INTRODUCTION

La polymérisation photochimique (ou radiochimique) des halogénures de vinyle, liquides purs ou en solution, ne présente pas de difficultés à l'exception de celle de l'iodure de vinyle. Toutefois, nous avons réussi à le polymériser (1) par l'action des rayons X, en solution dans les solvants chlorés tels que CH_2Cl_2, $CHCl_3$ et CCl_4.

Les espèces primaires actives produites sous l'influence du rayonnement ionisant étant très nombreuses, l'étude du mécanisme de la radiolyse s'avère très complexe. C'est pourquoi nous avons décidé d'étudier le mécanisme photochimique, en espérant en tirer des indications utiles pour la radiolyse.

Emschwiller (2), dans une étude sur la photochimie de l'iodure de vinyle liquide, a trouvé de l'éthylène, de l'acétylène et de l'iode comme produits de décomposition. Son interprétation des résultats fait intervenir deux molécules d'iodure de vinyle: (*a*) celle qui a subi l'action de la lumière perd à la fois son atome d'iode et un atome d'hydrogène, le groupement restant se transpose en acétylène; (*b*) les atomes d'hydrogène et d'iode concourent alors avec une deuxième molécule de monomère à la production de l'éthylène et de l'iode moléculaire. Emschwiller trouve un rapport C_2H_2/C_2H_4 de 1.25 et un rapport gaz en C_2/atome d'iode de 1.55. Il explique ce déficit de l'éthylène par rapport à l'acétylène et de l'iode relativement aux gaz en C_2 par une fixation de l'iode sur l'acétylène et surtout sur l'éthylène. Le ΔH^0 de réaction (calculé) étant de -6.4 kcal/mole pour la fixation d'iode sur l'acétylène et de $+7.3$ kcal/mole pour la fixation sur l'éthylène, on voit immédiatement que cet argument ne saurait tenir.

A la suite des travaux plus récents de Hamill (3, 4) sur la photolyse des iodures et en particulier de l'iodure d'éthyle, il nous est permis d'imaginer une production d'acide iodhydrique dans le système et son importance pour les réactions secondaires. A la lumière de ces faits, nous avons entrepris l'étude de la photolyse de l'iodure de vinyle dans le tétrachlorure parce que, d'une part, la polymérisation radiochimique est maximum (1) et, d'autre part, en cas de réaction entre ce monomère et le solvant, les produits formés seraient marqués par les atomes de chlore.

PARTIE EXPÉRIMENTALE

Réactifs

L'iodure de vinyle est préparé par la méthode de Spence (5). On le distille sur une colonne à 30 plateaux théoriques, à un taux de reflux très grand. On recueille la fraction correspondant à une concentration en impureté inférieure à 0.01%, tel que vérifié par chromatographie en phase gazeuse. L'iodure ainsi obtenu est

finalement distillé plusieurs fois sous haut vide, de piège en piège maintenus à une température de −76 °C. Il est conservé sous haut vide à l'obscurité et dans ces conditions s'avère stable.

Le tétrachlorure de carbone "pour analyse" et l'acide chlorhydrique de Matheson Co. sont dégazéifiés par distillation de piège en piège à −185 °C. L'acide iodhydrique est préparé suivant la méthode usuelle de déshydratation d'une solution aqueuse de HI et est débarassé de l'iode par distillation à très basse température et est ensuite dégazéifié par les procédés habituels.

Dispositif d'irradiation

La source lumineuse utilisée est une lampe à mercure Hanovia à haute pression (Utility Model, No. 30600), dont l'intensité est beaucoup plus grande dans le visible et le proche ultraviolet que dans l'ultraviolet lointain. Le système optique est choisi de façon à obtenir un faisceau lumineux presque parallèle et d'intensité maximum. La cellule d'irradiation, en quartz à fenêtres optiquement polies, est soudée par l'intermédiaire d'un joint gradé à une cellule en pyrex s'adaptant directement à la place des cellules d'absorption des spectrophotomètres Beckman DU et DKA. La partie en pyrex de cette cellule d'irradiation est pourvue d'une pointe cassable sous vide. La cellule est nettoyée à l'acide sulfurique concentré, bouillant et dégazéifiée sous haut vide en chauffant à environ 300 °C avant chaque irradiation. L'espace occupé par la vapeur au-dessus du liquide est recouvert de papier d'aluminium de façon à éliminer la photolyse en phase gazeuse.

L'iodure de vinyle absorbe très fortement entre 2000 et 3500 Å (11) alors que le tétrachlorure de carbone n'absorbe practiquement plus au-dessus de 2400 Å (6, 7). Comme le système optique coupe environ 80% de l'intensité lumineuse sous 2500 Å et que l'intensité de la lampe, également sous 2500 Å, n'est que d'environ 15% de la lumière émise entre 2500 et 3500 Å (8), on peut assumer que la lumière n'est pratiquement absorbée que par l'iodure. La photolyse du solvant peut donc être considérée comme négligeable, si elle se produit.

Pour faire varier l'intensité d'irradiation, on emploie un filtre optique approprié qui réduit de 8.3 fois l'intensité du spectre de la lampe nue. Les irradiations sont faites à température ambiante, soit à 23° ± 2 °C.

Préparation des échantillons

Les solutions d'un volume total d'environ 5 ml sont préparées par distillation séparée de CCl_4 et de C_2H_3I à travers un mélange de chaux sodée et de sulfate de magnésium, de façon à sécher et à éliminer toute trace de chlore et d'acide iodhydrique ou d'iode suivant le cas; cette distillation est suivie de distillations successives de piège en piège à −80 °C, sous haut vide. Les poids du solvant et de l'iodure de vinyle sont obtenus par pesées successives. Finalement, les deux substances sont distillées ensemble dans la cellule qui est scellée sous vide. Ces cycles de dégazéification sont très longs mais absolument essentiels si l'on veut obtenir des résultats reproductibles. En effet, on doit éliminer avec grand soin toute trace d'oxygène dont l'influence sur la photolyse des iodures organiques (9, 10) est énorme.

Analyse

Dans chacune des irradiations, on suit la formation d'iode par la mesure de la densité optique à 500 mμ. Une calibration spectrophotométrique préalable d'iode dans des solutions de diverses concentrations en C_2H_3I et CCl_4 à 500 mμ permet de transposer les lectures des densités optiques en fractions molaires d'iode dans l'échantillon irradié. Après irradiation, la cellule est soudée à un dispositif d'extraction des gaz que nous avons mis au point (Fig. 1). La cellule est soudée en A et, lorsque le vide est bon dans l'appareil, on brise la pointe et l'on distille le contenu de la cellule en B. On ajoute alors environ 10 ml d'eau, préalablement dégazéifiée en C, de façon à retenir l'acide iodhydrique, le tout est congelé à l'air liquide. Le serpentin D est maintenu à 0 °C pour qu'il y ait le moins possible de distillation d'eau vers le diverticule E, froid et tenu à −80 °C. Une pompe Toepler pompe continuellement les gaz. Dans ces conditions, on peut recueillir très facilement et totalement C_2H_2 et C_2H_4, ainsi qu'une partie de C_2H_3Cl et C_4H_6 contenus dans la solution.

Une fois cette première fraction recueillie à −80 °C, on ramène la température du diverticule E à 0° et collecte une deuxième fraction contenant, cette fois, le reste de C_2H_3Cl et C_4H_6 et une bonne quantité d'iodure de vinyle, dont la tension de vapeur à cette température est d'environ 5 cm. Les gas ainsi collectés sont analysés par chromatographie à gaz. Une fois les gas recueillis, on récupère la solution en la congelant en B, dans l'azote liquide. Cette solution est décantée et la phase aqueuse contenant l'acide iodhydrique est lavée au cyclohexane pour extraire CCl_4 et l'iode demeurés en solution. L'analyse de HI est alors faite à partir de cette solution aqueuse en mesurant l'absorption de l'acide iodhydrique à 2260 Å. Lorsque la concentration de HI est suffisamment élevée, on peut vérifier les résultats spectrophotométriques par titrage avec une solution diluée de NaOH.

RÉSULTATS ET INTERPRETATION

Nous avons pu distinguer et analyser quantitativement les produits de photolyse suivants: C_2H_2, C_2H_4, HI, I_2, C_2H_3Cl et C_4H_6. Pour éviter l'intervention des réactions secondaires qui pourraient brouiller l'aspect cinétique du problème, nous n'avons jamais poussé la conversion au-delà de 1%, travaillant en général à un pourcentage de conversion de l'ordre de 0.1%.

Can. J. Chem. Downloaded from www.nrcresearchpress.com by 210.87.254.42 on 09/05/12
For personal use only.

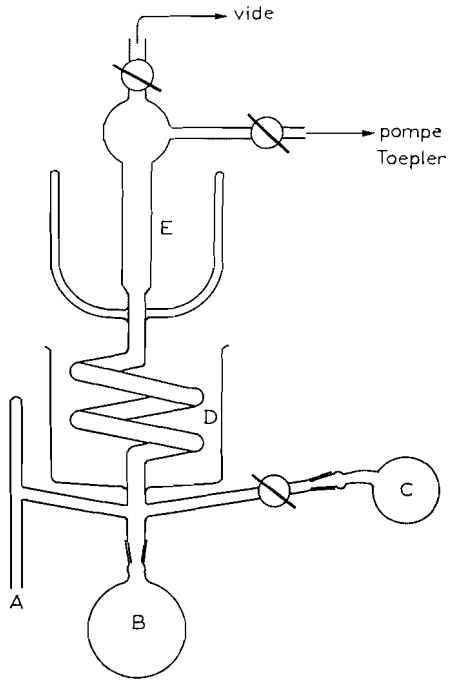

FIG. 1. Dispositif d'extraction des gaz des échantillons irradiés.

Formation de l'acétylène et de l'acide iodhydrique

En ce qui concerne la formation de l'acétylène, on trouve les faits suivants. (*a*) Sa formation est proportionnelle au temps d'irradiation (Fig. 2), du moins jusqu'à des conversion de l'ordre de 1%. (*b*) La production de C_2H_2 est indépendante de la concentration en monomère (Fig. 3). Dans les conditions de nos expériences, la vitesse de formation est de 6.6×10^{-9} mole ml^{-1} min^{-1}. (*c*) Il n'y a pas d'effet d'intensité de la lumière sur la vitesse de formation de C_2H_2, comme le montre le Tableau I où l'on voit que le rapport des productions pour un même temps d'irradiation est égal au rapport des intensités. Pour cette raison nous avons utilisé la production d'acétylène comme étalon interne pour les effets d'intensité des autres produits de photolyse. (*d*) L'addition de HI ou de HCl, jusqu'à des concentrations de 0.1 mole/l, n'affecte pas la quantité d'acétylène produite (Tableau II). Toutefois, l'addition d'oxygène en concentration de l'ordre de 0.03 mole/l entraîne une réduction d'environ 40% de la production de C_2H_2 (Tableau II). En présence d'oxygène, cette expérience doit être menée à basse concentration en C_2H_3I (environ 2% mole) car à plus haute concentration l'oxydation thermique est de loin trop rapide et, comme elle mène aussi à la formation d'acétylène (11), on ne peut guère en tirer de conclusions.

La formation de l'acide iodhydrique (Fig. 2) est caractérisée par les faits suivants. (*a*) Elle est proportionnelle à l'énergie absorbée jusqu'à des conversions de l'ordre de 1%. (*b*) Le taux de production est indépendant de la concentration en monomère, tout au moins jusqu'à des concentrations de l'ordre de 25% en C_2H_3I (Fig. 4), la vitesse de formation est d'environ 5.2×10^{-9} mole ml^{-1} min^{-1}. (*c*) Il n'y a pratiquement pas d'effet d'intensité sur la production de HI (Tableau I). On voit qu'à intensité réduite, la vitesse de formation de HI est 1.22 fois plus grande.

Can. J. Chem. Downloaded from www.nrcresearchpress.com by 210.87.254.42 on 09/05/12
For personal use only.

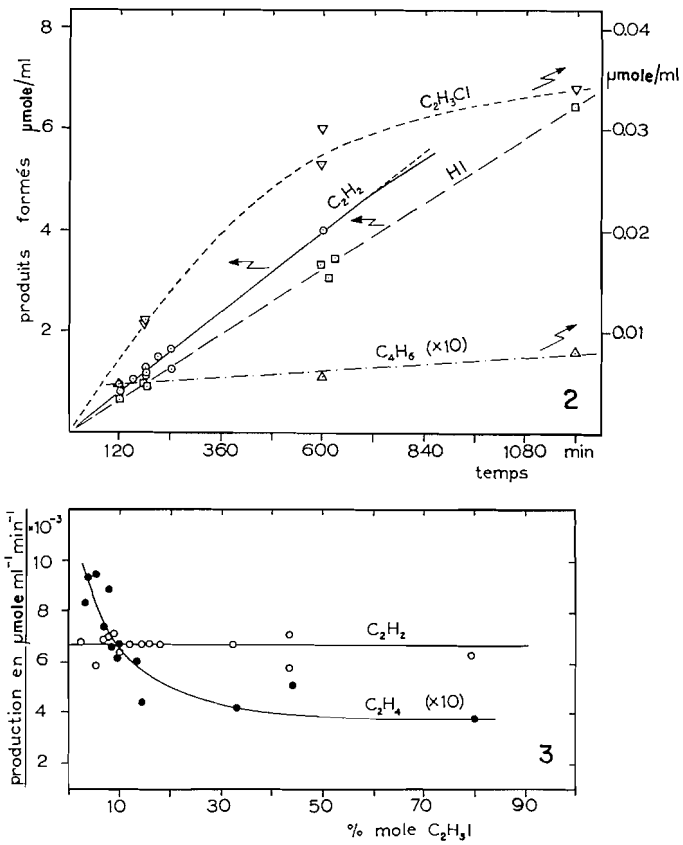

FIG. 2. Formation des produits en fonction du temps: acétylène (○), acide iodhydrique (□), chlorure de vinyle (▽), butadiène (△). Les courbes de formation du chlorure de vinyle et du butadiène sont pour une solution de 14% mole en monomère.

FIG. 3. Vitesse de formation de l'acétylène (○) et de l'éthylène (●) en fonction de la concentration en C_2H_3I. La courbe de l'éthylène est pour 180 min d'irradiation.

TABLEAU I

Influence de l'intensité, I, sur la production d'acétylène et de l'acide iodhydrique pour une même période d'irradiation

Vitesses (mole/min ml)	Intensités relatives 1.0	Intensités relatives 0.12	$I_{1.0}/I_{0.12}$	$R_{1.0}/R_{0.12}$
$R_{C_2H_2}$	6.6×10^{-3}	8.2×10^{-4}	8.3	8.0
R_{HI}	5.2×10^{-3}	7.5×10^{-4}	8.3	6.9

TABLEAU II

Influence de HI et de HCl sur la formation de l'acétylène et de l'éthylène ainsi que du chlorure de vinyle pour 180 min d'irradiation

C_2H_3I (% mole)	Additif	C_2H_2 (µmole/ml)	C_2H_4 (µmole/ml)	C_2H_3Cl (µmole/ml)
3.5	—	1.2	—	—
3.5	O_2 (0.03 mole/l)	0.7	—	—
10.2	—	1.2	0.12	—
10.2	HCl (0.05 mole/l)	1.12	0.12	—
16.2	—	1.2	0.099	1×10^{-2}
16.2	HI (0.1 mole/l)	1.2	0.75	2×10^{-4}

Can. J. Chem. Downloaded from www.nrcresearchpress.com by 210.87.254.42 on 09/05/12
For personal use only.

Il existe un parallèlisme frappant entre la formation de l'acétylène et de l'acide iodhydrique: dans les deux cas, l'influence du temps d'irradiation et de la concentration en iodure de vinyle est la même. De plus, les vitesses de formation de ces substances sont du même ordre de grandeur. Il faut, en outre, mentionner que l'on ne retrouve pas d'hydrogène, même pour des temps d'irradiation de l'ordre de 1200 min. Ces diverses constatations peuvent s'expliquer par le processus de "dismutation controlée par diffusion" tel que proposé d'abord par Hamill (3, 12) et repris par Willard (13) et Wijnen (14, 15) dans la photolyse de l'iodure d'éthyle liquide. L'absorption de photons dans l'acte primaire conduirait à une situation représentée symboliquement par la réaction [1],

$$[1] \qquad C_2H_3I \xrightarrow{h\nu} (C_2H_3 + I),$$

où les particules entre parenthèses, appelées radicaux jumelés (16), sont sujettes à une interaction par diffusion: soit la dismutation,

$$[2] \qquad (C_2H_3 + I) \rightarrow C_2H_2 + HI,$$

soit des réactions en compétition avec la dismutation,

$$[3] \qquad (C_2H_3 + I) \rightarrow C_2H_3\cdot + I\cdot$$

$$[1a] \qquad (C_2H_3 + I) \rightarrow C_2H_3I.$$

L'étape [3] représente la transition de la cinétique de diffusion à la cinétique en état stationnaire. L'effet cage, traditionnelement évoqué pour expliquer une décroissance du rendement photochimique en raison de la réaction du type [1*a*], peut expliquer ici un phénomène inverse en raison de la réaction [2]. Ce schéma a l'avantage d'expliquer, à partir d'un même acte primaire, la production de radicaux soumis à une cinétique en état stationnaire et la production directe de fragments moléculaires C_2H_2 et HI.

La formation de l'acétylène et de l'acide iodhydrique par la dismutation contrôlée par diffusion est formellement équivalente au processus de détachement moléculaire directe,

$$[A] \qquad C_2H_3I \xrightarrow{h\nu} C_2H_2 + HI,$$

sauf en ce qui concerne les effets d'intercepteurs de radicaux. Dans le cas de détachement moléculaire directe, l'effet d'intercepteurs devrait être nul, alors que dans le cas de la dismutation contrôlée par diffusion, l'effet sur la production de C_2H_2 devrait être assez important, à condition que la concentration des intercepteurs soit suffisamment grande pour qu'ils puissent s'introduire dans les cages. Or, nous l'avons vu, l'oxygène affecte très fortement la production de l'acétylène, ce qui plaide en faveur du mécanisme [1].

Formation de l'iode

La formation de l'iode donne des résultats peu reproductibles; nous soupçonnons que les traces d'impuretés et d'oxygène en sont la cause. De façon générale, nous avons constaté que la quantité d'iode formée croît avec le temps (mais non de façon linéaire). La Fig. 5 illustre cet effet; nous y avons présenté, choisies parmi les nombreux résultats, quelques courbes typiques de production d'iode en fonction du temps pour diverses concentrations en monomère. Par ailleurs, la vitesse de formation décroît avec l'augmentation de la concentration en iodure de vinyle. Cette diminution de vitesse (Fig. 4) est rapide pour les basses concentrations de C_2H_3I et devient lente à mesure que la solution est plus concentrée.

La réaction majeure qui conduit à l'apparition de l'iode moléculaire est la recombinaison des atomes d'iode:

$$[4] \qquad I\cdot + I\cdot \rightarrow I_2.$$

Can. J. Chem. Downloaded from www.nrcresearchpress.com by 210.87.254.42 on 09/05/12
For personal use only.

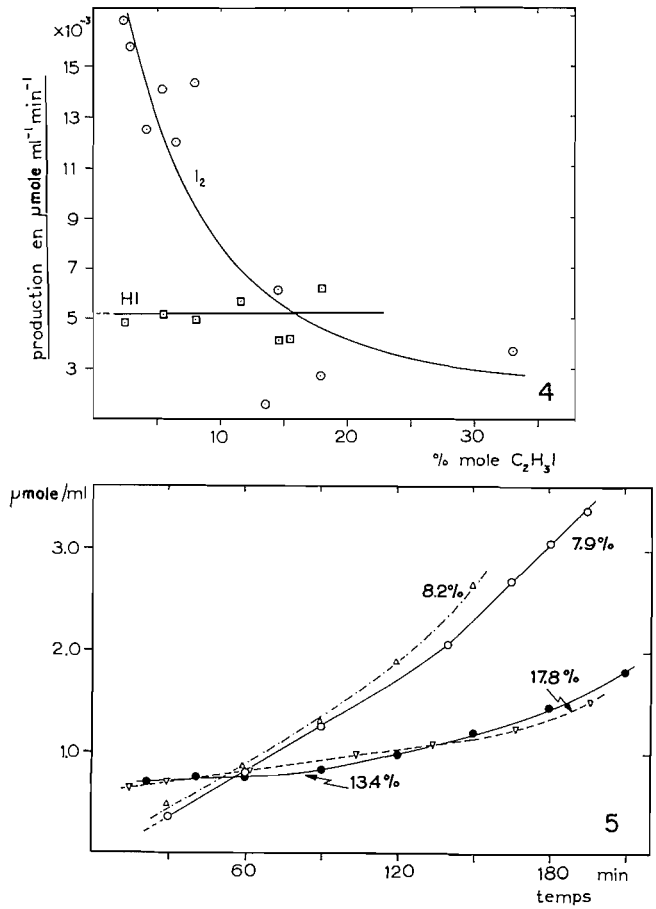

FIG. 4. Vitesse de formation de l'acide iodhydrique (□) et de l'iode (○) en fonction de la concentration en C_2H_3I. La courbe de l'iode est pour 180 min d'irradiation.

FIG. 5. Formation de l'iode en fonction du temps pour différentes concentrations (% mole) en iodure de vinyle.

La réaction de formation de l'iode moléculaire par l'action de l'iode atomique sur l'iodure de vinyle:

[4*a*] $$C_2H_3I + I\cdot \rightarrow C_2H_3\cdot + I_2$$

ne peut être importante, car elle conduirait à un accroissement de la production de C_2H_4 en fonction de la concentration en monomère, ce que l'on n'observe pas expérimentalement.

Formation de l'éthylène

La formation de l'éthylène suit des lois complexes. (*a*) Elle est fonction du carré du temps d'irradiation (Fig. 6) pour des périodes inférieures à 600 min. L'allure des courbes expérimentales peut être décrite par l'équation [B],

[B] $$[C_2H_4] = Kt^2,$$

où K est fonction de la concentration en iodure de vinyle. (*b*) La Fig. 3 montre la vitesse de formation de C_2H_4 en fonction de la concentration en monomère pour une même dose d'énergie absorbée. En comparant les valeurs des vitesses de production de l'éthylène et

Can. J. Chem. Downloaded from www.nrcresearchpress.com by 210.87.254.42 on 09/05/12
For personal use only.

celles de l'acétylène, on constate que les premières sont environ 10 fois plus faibles pour 180 min d'irradiation. (*c*) L'addition d'acide iodhydrique avant irradiation entraîne un accroissement de la formation d'éthylène, d'un facteur de huit, comme en témoigne les chiffres du Tableau II. (*d*) Le Tableau III indique qu'il y a un effet d'intensité très net sur la vitesse de formation de l'éthylène. Dans ce tableau les vitesses de production de l'éthylène sont rapportées à celles de l'acétylène que nous savons indépendantes de l'effet d'intensité. Les rapports sont calculés pour un même temps d'irradiation.

TABLEAU III

Effet de l'intensité sur la production de l'éthylène et du chlorure de vinyle

C_2H_3I (% mole)	Temps (min)	$R_{C_2H_2}/R_{C_2H_4}$ pour intensité relative de		$R_{C_2H_2}/R_{C_2H_3Cl}$ pour intensité relative de	
		1.0	0.12	1.0	0.12
2.0	420	2.2	16	—	—
8.3	300	4.3	40	—	—
11.7	480	3.3	35	—	—
13.5	1380	1.1	7.5	—	—
14.0	180	—	—	9.0	10.0
25.0	420	5.2	55	—	—

La production d'éthylène étant proportionnelle au carré du temps et au carré de l'intensité, ce gaz doit donc être produit à partir de deux produits de photolyse, dont l'un s'accumule avec le temps d'irradiation. Ce fait nous pousse à rejeter une réaction de type classique, c'est-à-dire l'abstraction par un radical vinyle d'un atome d'hydrogène sur une molécule de vinyle, réaction qui serait d'ailleurs défavorisée thermodynamiquement.

Un premier type de réaction conduisant à la formation de C_2H_4 et faisant intervenir deux produits de photolyse est la dismutation de deux radicaux vinyles. Ce mécanisme, déjà proposé par Tickner et Le Roy (17), a été évoqué par Herman et Hupin (18) pour interpréter la formation d'éthylène dans la radiolyse du chlorure de vinyle gazeux. Dans ce cas l'expression de la formation de l'éthylène devrait être une fonction linéaire du temps, ce qui n'est pas vérifié expérimentalement. Par conséquent, s'il y a participation de ce mécanisme à la formation d'éthylène, elle ne peut être importante. Exprimé en d'autres termes, cela revient à dire qu'en phase liquide le rapport dismutation–recombinaison des radicaux vinyles est très petit.

On doit donc penser à la réaction suivante:

[5] $$C_2H_3\cdot + HI \rightarrow C_2H_4 + I\cdot.$$

Ce genre de réaction entre un radical et l'acide iodhydrique a déjà été évoqué par Hamill (3), Willard (14) et Wijnen (15) dans la photolyse de divers iodures organiques. Une telle réaction serait très favorisée thermodynamiquement ($\Delta H^0 \sim -40$ kcal/mole). On peut voir, sur la Fig. 2, que la concentration en HI croît linéairement en fonction du temps d'irradiation. L'éthylène produit à partir de la réaction [5] devrait alors afficher une dépendance du carré du temps et une influence de l'intensité lumineuse d'ordre un, ce qui correspond bien aux résultats expérimentaux.

Ce mécanisme est aussi vérifié par le fait qu'une addition d'acide iodhydrique entraîne un accroissement de la quantité d'éthylène. Toutefois, cette quantité d'éthylène (Tableau II) est inférieure de 25% à la quantité calculée à partir de la concentration en acide (valeur calculée, 1.0×10^{-6} mole/ml). Mais on peut expliquer cet écart: (*a*) soit par le fait que

Can. J. Chem. Downloaded from www.nrcresearchpress.com by 210.87.254.42 on 09/05/12
For personal use only.

l'on atteint la limite de solubilité de HI dans CCl_4, (*b*) soit par le fait que tous les radicaux disponibles sont déjà captés à une plus faible concentration en acide iodhydrique.

La réaction [5] peut donc expliquer toute la production de l'éthylène et, si les deux autres réactions mentionnées y participent, leur participation ne serait que de l'ordre de quelques pourcents, soit la précision sur les mesures de l'éthylène.

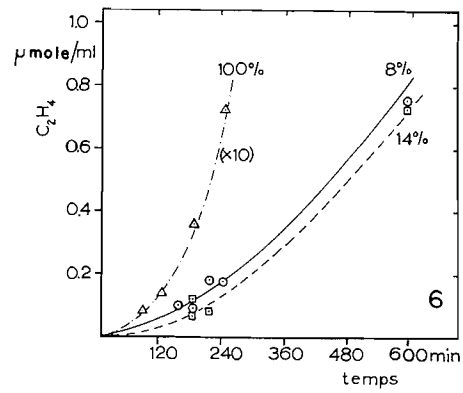

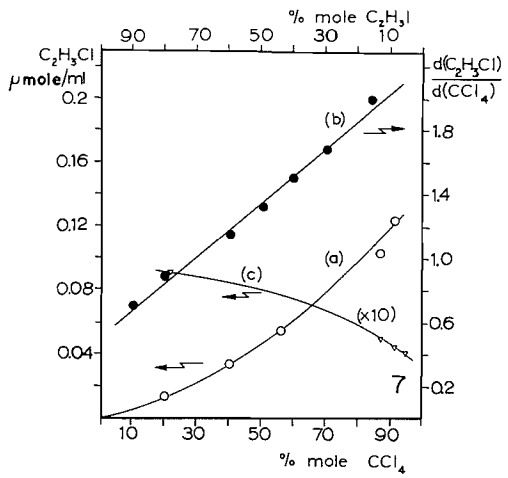

FIG. 6. Formation de l'éthylène en fonction du temps pour différentes concentrations (% mole) en iodure de vinyle.

FIG. 7. Formation du chlorure de vinyle (courbe *a*) et du butadiène (courbe *c*) en fonction de la concentration pour 180 min d'irradiation. La courbe *b* représente la dérivée, $d(C_2H_3Cl)/d(CCl_4)$, de la courbe *a*.

Formation du chlorure de vinyle

Dans le cas du chlorure de vinyle, nous constatons les faits expérimentaux suivants: (*a*) sa formation croît linéairement en fonction du temps, puis ralentit à mesure que le temps augmente (Fig. 2); (*b*) la formation de C_2H_3Cl est fonction du carré de la concentration en CCl_4 (Fig. 7, courbe *a*), comme en témoigne la linéarité de la dérivée (Fig. 7, courbe *b*); (*c*) l'addition de l'acide iodhydrique au système diminue la production de C_2H_3Cl mais ne l'inhibe pas complètement (Tableau II); (*d*) la vitesse de formation de C_2H_3Cl ne montre pas d'effet d'intensité (Tableau III).

La réaction suivante permet d'interpréter la formation du chlorure de vinyle:

[6] $$C_2H_3^{\cdot} + CCl_4 \rightarrow C_2H_3Cl + CCl_3^{\cdot}.$$

Can. J. Chem. Downloaded from www.nrcresearchpress.com by 210.87.254.42 on 09/05/12
For personal use only.

Cette réaction, favorisée thermodynamiquement ($\Delta H^0 \sim -17$ kcal/mole) en raison de la grande stabilité relative du radical $CCl_3^{\cdot}$, ne montre pas d'effet d'intensité, ce qui est conforme à l'expérience. L'effet du temps sur la formation de C_2H_3Cl se comprend aussi si l'on songe qu'avec l'accroissement du temps de photolyse il y a augmentation de la concentration en intercepteurs de radicaux, HI et I_2, et que leurs effets entrent en compétition avec la réaction [6]. Dans la discussion nous reviendrons sur l'effet de concentration.

Par contre, les réactions des atomes de chlore, formés à partir de CCl_4, avec les radicaux vinyles ou avec le monomère lui-même ne peuvent être prises en considération pour les raisons suivantes. Cette réaction d'atomes de chlore avec les radicaux vinyles devrait présenter une dépendance linéaire de l'intensité, ce qui n'est pas le cas; nous pouvons donc l'éliminer. D'autre part, la réaction d'échange atome de chlore–monomère, favorisée thermodynamiquement, ne devrait aucunement présenter une dépendance du carré de la concentration en CCl_4, elle peut donc être également éliminée. Comme nous l'avons vu au début de cet exposé, ces faits vérifient bien que le dispositif expérimental peut assurer une photolyse négligeable du solvant.

Formation du butadiene

La Fig. 2 montre que le butadiène se forme surtout au début de la photolyse; après 180 min, la production devient très faible. Mais il existe un léger accroissement dans la formation de C_4H_6 en fonction de la concentration en monomère (Fig. 7, courbe *c*). Signalons de plus que l'addition de l'acide iodhydrique inhibe complètement la production du butadiène.

Comme source majeure de formation du butadiène, on peut admettre une réaction de recombinaison des radicaux vinyles,

[7] $$C_2H_3^{\cdot} + C_2H_3^{\cdot} \rightarrow C_4H_6,$$

réaction qui permet d'expliquer l'effet du temps: au cours de la photolyse, la concentration en intercepteurs, HI et I_2, croît également et l'on doit s'attendre à un effet d'inhibition encore plus prononcé que dans le cas de la réaction [6]. L'effet de concentration peut aussi s'expliquer par le fait qu'au fur et à mesure que la concentration en iodure de vinyle augmente, l'absorption de la lumière se fait en couches de plus en plus minces, favorisant ainsi la recombinaison de deux radicaux vinyles par suite de leur grande concentration locale.

Si l'on considère néanmoins l'effet de concentration en monomère sur la formation du butadiène, on peut imaginer les réactions suivantes:

[8] $$C_2H_3^{\cdot} + C_2H_3I \rightarrow C_4H_6 + I^{\cdot}$$

ou (et)

[8*a*] $$C_2H_3I^* + C_2H_3I \rightarrow C_4H_6 + 2I^{\cdot}.$$

Une telle réaction a déjà été proposée par West et Fitelson (19, 20) dans la photolyse de l'iodure d'éthyle. Cependant, un tel mécanisme devrait conduire à une production de butadiène sensiblement proportionnelle au temps de photolyse, et l'on ne voit pas pourquoi il serait plus sensible à l'action des intercepteurs que la réaction de production du chlorure de vinyle [7].

Il semble donc que la formation du butadiène doit être attribuée surtout à la réaction [7], sans toutefois rejeter totalement une participation de la réaction [8] en raison de l'effet de concentration.

Can. J. Chem. Downloaded from www.nrcresearchpress.com by 210.87.254.42 on 09/05/12
For personal use only.

Can. J. Chem. Downloaded from www.nrcresearchpress.com by 210.87.254.42 on 09/05/12
For personal use only.

DISCUSSION

Avant d'établir un schéma cinétique qui rendrait compte dans les grandes lignes des phénomènes observés, nous devons porter notre attention sur deux faits expérimentaux qui n'ont pas reçu d'explication dans le chapitre précédent: les productions du chlorure de vinyle et de l'éthylène en fonction de la concentration en iodure de vinyle.

En admettant la réaction [6] pour la formation du chlorure de vinyle, on devrait trouver une dépendance linéaire de la concentration en CCl_4. En fait, on trouve une dépendance du carré de la concentration (Fig. 6). La seule manière d'expliquer ce fait est d'admettre une dépendance de la concentration des radicaux vinyles vis-à-vis de la concentration en CCl_4 ou, vice versa, vis-à-vis de la concentration en C_2H_3I.

Considérons maintenant la formation de l'éthylène. Si l'on admet que la concentration en HI ne varie pas sensiblement avec la concentration en C_2H_3I, ce qui semble être le cas du moins dans la région entre 0 et 25% (Fig. 4), la seule façon d'expliquer la diminution de formation de l'éthylène en fonction de la concentration en iodure de vinyle est de postuler une variation de la concentration des radicaux vinyles.

Or, une réaction d'amorçage de chaîne polymériques par les radicaux vinyles pourrait bien être l'explication des phénomènes observés.

[9] $$C_2H_3^{\cdot} + C_2H_3I \rightarrow C_4H_6I^{\cdot}.$$

On ne peut, ici, parler véritablement de polymérisation mais plutôt de télomérisation, la présence d'inhibiteurs dans le système, HI et I_2, limitant la propagation d'une chaîne probablement à deux ou trois unités de monomère:

[10] $$(C_2H_3I)_n^{\cdot} + HI \rightarrow (C_2H_3I)_n + I$$

[11] $$(C_2H_3I)_n^{\cdot} + I_2 \rightarrow (C_2H_3I)_n + I.$$

Cette réaction n'a rien de surprenant si l'on considère que les composés éthyléniques sont des intercepteurs de radicaux et que tous les halogénures de vinyle polymérisent facilement. La réaction d'amorçage [9] est en principe favorisée par la concentration croissante du monomère et ceci justifie, dans une certaine mesure, l'allure des courbes de formation du chlorure de vinyle et de l'éthylène.

Mais les réactions [6] et [9] sont compétitives; on peut alors expliquer que la formation du chlorure de vinyle dépende du carré de la concentration en iodure de vinyle. Dans le cas de l'éthylène, la dépendance de la concentration n'est pas aussi simple (Fig. 3); ce qui peut s'expliquer par le fait que la vitesse de formation de l'éthylène dépend à la fois des vitesses des réactions [6] et [9], alors que celle du chlorure de vinyle ne dépend que de la vitesse de la réaction [9].

Les réactions [5] et [10] sont fonction de l'intensité lumineuse et rendent compte de l'effet d'intensité sur la production de l'acide iodhydrique; la quantité produite par unité de dose absorbée est légèrement plus grande à plus faible intensité. En outre, par la nature même des réactions [5] et [10], on peut admettre que les constantes de vitesse k_5 et k_{10} sont du même ordre de grandeur. Or, le fait que la production d'acide iodhydrique est sensiblement constante quelle que soit la concentration en iodure de vinyle corrobore cette constatation car, si seule la réaction [5] existait, on devrait s'attendre à une variation de la quantité d'acide iodhydrique formée en fonction de la concentration. Puisque ce n'est pas, c'est—d'une certaine façon—une preuve de l'existence de la réaction [10] avec une constante de vitesse comparable à k_5.

Toutefois, les tentatives pour retrouver le télomère ont été vaines parce que la quantité formée est trop faible pour être détectée par les méthodes usuelles. Néanmoins, après des

irradiations prolongées, on constate la présence d'un résidu huileux qui distille plus lentement que le monomère, mais dans lequel on n'a pu identifier avec certitude des télomères.

La consommation d'acide iodhydrique par la réaction [5] n'est que de 3 à 4% de la quantité totale produite. Comme la précision du dosage de HI est d'environ 10%, on peut donc comprendre que, pour toute fin pratique, on ne puisse distinguer l'influence de la formation de l'éthylène sur la formation de l'acide iodhydrique. Par conséquent, le déficit en HI par rapport à C_2H_2 doit avoir une autre origine: soit l'addition de HI à la double liaison du monomère, soit l'absorption de HI sur les parois, soit, encore, une autre cause qui nous échappe actuellement.

L'ensemble des réactions [1] à [11] ainsi que la réaction [12] rendent compte des phénomènes observés.

[12] $$C_2H_3\cdot + I_2 \rightarrow C_2H_3I + I\cdot$$

En appliquant l'hypothèse de stationnarité et en négligeant la réaction [8] (dont la contribution est faible), les réactions de terminaison des télomères [10] et [11] (dont nous ne saurions tenir compte), ainsi que la réaction [7] (qui n'est importante qu'au tout début de l'irradiation), on trouve les expressions suivantes pour la production de l'éthylène et du chlorure de vinyle:

[C] $$\frac{d[C_2H_4]}{dt} = R_{C_2H_4} = \frac{\phi_3 k_5[HI]}{k_5[HI] + k_6[CCl_4] + k_9[C_2H_3I] + k_{12}[I_2]}$$

[D] $$\frac{d[C_2H_3Cl]}{dt} = R_{C_2H_3Cl} = \frac{\phi_3 k_6[CCl_4]}{k_5[HI] + k_6[CCl_4] + k_9[C_2H_3I] + k_{12}[I_2]}$$

où ϕ_3 est égal au rendement quantique de la réaction [3]. On voit que:

[E] $$R_{C_2H_4}/R_{C_2H_3Cl} = \frac{k_5[HI]}{k_6[CCl_4]}.$$

Cette expression devrait être vérifiée pour des périodes supérieures à 120 min, alors que la production du butadiène est déjà terminée; la Fig. 8 prouve qu'il en est bien ainsi. La pente de la droite donne un rapport $k_5/k_6 = 1.2 \times 10^4$.

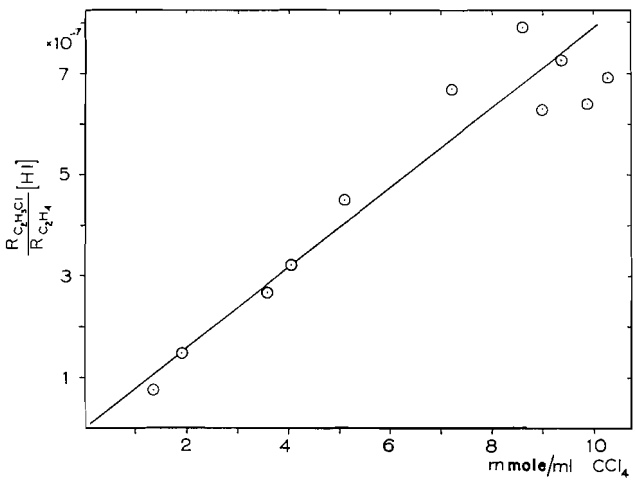

FIG. 8. $(R_{C_2H_3Cl}/R_{C_2H_4})[HI]$ en fonction de la concentration en CCl_4.

Can. J. Chem. Downloaded from www.nrcresearchpress.com by 210.87.254.42 on 09/05/12
For personal use only.

A partir de ces expressions cinétiques, on peut calculer le rapport des constantes de vitesses; on trouve $k_{12}/k_5 = 1.5 \pm 1$ et $k_9/k_6 = 5 \pm 3$. En ce qui concerne le rapport k_{12}/k_5, l'incertitude des résultats significatifs pour la formation de l'iode peut conférer une erreur importante à la valeur trouvée.

Si l'on compare les rapports de vitesse ainsi obtenus et si l'on tient compte de l'aptitude de la double liaison vinylique à intercepter les radicaux, nous voyons immédiatement que l'efficacité du radical $C_2H_3^{\cdot}$ dans l'amorçage des chaînes polymériques est réellement faible; conclusion à laquelle sont arrivés Melville (21) de même que Herman et Hupin (18), le premier en étudiant la photopolymérisation du chlorure de vinyle, les seconds en étudiant la radiolyse de ce même chlorure.

Le rapport des vitesses $R_{C_2H_2}/R_{C_2H_4}$ permet d'estimer celui des rendements quantiques ϕ_2/ϕ_3, qui à l'aide de l'hypothèse de l'état stationnaire peut s'exprimer par l'équation suivante:

[F] $$\frac{R_{C_2H_2}}{R_{C_2H_4}} = \frac{\phi_2}{\phi_3} + \left[\frac{\phi_2}{\phi_3}\frac{k_9}{k_5[HI]}\left(1 + \frac{k_6[CCl_4]}{k_9[C_2H_3I]} + \frac{k_{12}[I_2]}{k_9[C_2H_3I]}\right)\right][C_2H_3I].$$

Une extrapolation à concentration nulle en monomère devrait donner la valeur de ϕ_2/ϕ_3; on trouve ainsi $\phi_2/\phi_3 = 1.2 \pm 0.3$. Il est à remarquer que pour la photolyse de l'iodure d'éthyle dans le cyclohexane (3), le rapport des rendement quantiques des réaction correspondant aux réactions [2] et [3] est égal à 1.8. Si l'on admet une analogie entre la photolyse de C_2H_5I et celle de C_2H_3I, $\phi_2/\phi_3 > 1$ indiquerait que la réaction [6] peut se passer à l'intérieur de la cage soumise à la diffusion:

[6a] $$(C_2H_3 + I + CCl_4) \rightarrow C_2H_3Cl + (I + CCl_3).$$

Cette réaction devrait normalement diminuer le rendement ϕ_3. Il n'est toutefois pas exclus que ce type de réaction nécessite des radicaux chauds, comme il semble que ce soit le cas pour l'iodure d'éthyle en solution dans le cyclohexane (3). Mais, d'autre part, pour les conditions de nos expériences, la non-concurrence de réactions telles que:

[13] $$C_2H_3^{\cdot} + C_2H_3I \rightarrow C_2H_4 + C_2H_2I^{\cdot},$$

possibles à partir de radicaux chauds, laisse prévoir que peut de radicaux formés réagissent en tant que radicaux chauds. Ceci correspond d'ailleurs aux conclusions de Wijnen (14) sur la photolyse de l'iodure d'éthyle. Tout un problème reste donc à résoudre, qui fera l'objet d'une prochaine publication.

CONCLUSIONS

Les conclusions que nous pouvons tirer de ce travail sont les suivantes: (1) le mécanisme de la "dismutation contrôlée par diffusion" explique bien les phénomènes observés; (2) l'éthylène est principalement formé par la réaction de radicaux vinyliques thermalisés par HI; (3) nous devons postuler une réaction de télomérisation pour expliquer la diminution de la production d'éthylène et de l'iode avec l'augmentation de la concentration en iodure de vinyle; (4) l'efficacité d'amorçage des chaînes polymériques par le radical $C_2H_3^{\cdot}$ est faible comparée aux autres réactions compétitives de disparition de ce radical.

REMERCIEMENTS

Nous remercions le Dr. W. Forst pour les judicieux commentaires qu'il nous a faits durant ce travail. Nos remerciements vont également au Conseil National de Recherche du Canada pour une bourse accordée à l'un de nous (P. C. R.) et pour l'aide matérielle qui nous a permis de mener à bien cette étude.

Can. J. Chem. Downloaded from www.nrcresearchpress.com by 210.87.254.42 on 09/05/12
For personal use only.

BIBLIOGRAPHIE

1. J. A. HERMAN et P. ROBERGE. J. Polymer Sci. **62**, S 116 (1962).
2. G. EMSCHWILLER. Compt. Rend. **198**, 464 (1934).
3. D. L. BUNBURY, R. R. WILLIAMS, JR. et W. H. HAMILL. J. Am. Chem. Soc. **78**, 6228 (1956).
4. H. A. GILLIS, R. R. WILLIAMS, JR. et W. H. HAMILL. J. Am. Chem. Soc. **83**, 17 (1961).
5. J. SPENCE. J. Am. Chem. Soc. **55**, 1290 (1933).
6. B. C. ROQUITTE et M. H. J. WIJNEN. J. Chem. Phys. **38**, 4 (1963).
7. J. R. LACHER, L. E. HUMMEL, E. F. BONHNFALK et J. D. PARK. J. Am. Chem. Soc. **72**, 5486 (1960).
8. A. FARKAS et H. MELVILLE. Experimental methods in gas reactions. MacMillan and Co., London. 1939. p. 219.
9. T. IREDALE. J. Phys. Chem. **33**, 290 (1933).
10. S. HACOBIAN et T. IREDALE. Nature, **166**, 157 (1950).
11. P. ROBERGE. Résultats non publiés.
12. J. C. ROY, J. R. NASH, R. R. WILLIAMS, JR. et W. H. HAMILL. J. Am. Chem. Soc. **78**, 519 (1956).
13. R. H. LUEBBE, JR. et J. E. WILLARD. J. Am. Chem. Soc. **81**, 761 (1959).
14. R. SCHINDLER et M. H. J. WIJNEN. Z. Physik. Chem. **34**, 109 (1962).
15. J. A. GUERCIONE et M. H. J. WIJNEN. J. Chem. Phys. **38**, 1 (1963).
16. T. C. VOGT, JR. et W. H. HAMILL. J. Phys. Chem. **67**, 292 (1963).
17. A. W. TICKNER et D. J. LE ROY. J. Chem. Phys. **19**, 1247 (1951).
18. J. A. HERMAN et P. Hupin. Résultats non publiés.
19. W. WEST et J. FITELSON. J. Am. Chem. Soc. **62**, 3021 (1940).
20. E. W. R. STEACIE. Atomic and free radical reactions. Reinhold Publishing Corp., New York. 1954. p. 402.
21. H. MELVILLE. Proc. Roy. Soc. Ser. A, **187**, 45 (1946).

Can. J. Chem. Downloaded from www.nrcresearchpress.com by 210.87.254.42 on 09/05/12
For personal use only.

Can. J. Chem. Downloaded from www.nrcresearchpress.com by 210.87.254.42 on 09/05/12
For personal use only.

COMMENTS ON N.M.R. SPECTRA OF THE $X_nAA'X_n'$ TYPE

R. K. HARRIS[1]
Mellon Institute, Pittsburgh, Pennsylvania
Received May 15, 1964

ABSTRACT

General expressions are derived for line positions and relative intensities in the X spectrum for an $X_nAA'X_n'$ nuclear magnetic system in the case when $J_X = 0$. It is shown that in most cases it is possible to obtain the coupling constants involved by direct measurement of the spectrum using simple equations, but that this is not possible in certain limiting cases where the spectrum is deceptively simple.

I. INTRODUCTION

The development of nuclear magnetic resonance (n.m.r.) theory in the analysis of spectra has led to the extensive use of computers for the more complex nuclear magnetic systems. On the other hand, as the magnetic field strength has been increased in modern spectrometers, more spectra may be classified as first order (1), and the coupling constants and chemical shifts can be obtained by direct measurement. There exist, however, types of nuclear magnetic system for which the spectra are never first order but which yield the n.m.r. parameters by direct measurement, using appropriate formulae. This is so for all nuclear magnetic systems in which there are nuclei which are chemically (or structurally) equivalent but not magnetically equivalent (2). We shall distinguish such nuclei by a prime, as in the notation of Corio (3). The direct measurement of parameters from spectra is of course a more convenient and less costly procedure than the use of computers, but there have been few instances in the literature where the formulae have been presented. The XAA'X' system is, of course, well known (1), and several papers have dealt with cases of $X_2AA'X_2'$ (4) and $X_3AA'X_3'$ (5, 6) spectra. However, it is not generally realized that many of the formulae developed for these spectra are appropriate also for the more general $X_nAA'X_n'$ case. This paper presents these general formulae for the $X_nAA'X_n'$ system subject to three limitations: (i) only expressions for resonances of the X nucleus will be presented, (ii) it will be assumed that coupling J_X between nuclei of types X and X' is zero, and (iii) only nuclei of spin 1/2 will be considered. The theory was developed for the analysis of the proton spectra of $(CH_3)_2P(:S)P(:S)(CH_3)_2$ and $(CH_3)_2PP(CH_3)_2$, which are examples of $X_6AA'X_6'$ systems (7) for which these conditions are valid and for which the correspondingly high-resolution ^{31}P spectra were unobtainable in this laboratory. However, the formulae will be applicable to a range of symmetrical methyl compounds.

II. TRANSITION ENERGIES OF THE X NUCLEI

Since we are assuming that $J_X = 0$ and also that the chemical shift between the A and X nuclei is large with respect to all other coupling constants in the system (this assumption is implicit in the nomenclature (1, 3)), there are only three nuclear magnetic parameters that affect the spectrum (5, 6). These are the coupling constant J_A between the A and A' nuclei, and the two types of coupling constant between an A or A' nucleus and an X or X' nucleus, $J_{AX} = J_{A'X'}$ and $J_{AX'} = J_{A'X}$. These latter parameters will be written J_{AX} and $J_{AX'}$ respectively, and will be referred to as the short-range and long-range (A, X) coupling

[1]*Permanent address: School of Chemical Sciences, Wilberforce Road, Norwich, England.*

Can. J. Chem. Downloaded from www.nrcresearchpress.com by 210.87.254.42 on 09/05/12
For personal use only.

constants. It will, however, prove to be more convenient (1) to use combinations L and N of these coupling constants defined by $L = |J_{AX} - J_{AX}'|$ and $N = |J_{AX} + J_{AX}'|$. Since the n nuclei of type X are magnetically equivalent, coupling between them does not affect the spectrum and can be ignored (1). Similarly we can neglect coupling between the n nuclei of type X′. The basic spin functions, α and β, will be used to describe the spin states of the A and A′ nuclei, while the total spin (in the direction of the magnetic field) of the X_n and X_n' groups of nuclei will be given by $I_z(X_n) = p$ and $I_z(X_n') = m$, the overall spin state being denoted by (p, m).

Because of the assumptions listed above, there are no off-diagonal elements of the spin Hamiltonian between states differing in $I_z(A) + I_z(A')$. Therefore we may separate the total matrix representation of the Hamiltonian into three sub-matrices appropriate for (i) the $\alpha\alpha$, (ii) the $\beta\beta$, and (iii) the $\alpha\beta$ and $\beta\alpha$ spin states. There will be mixing between states differing only by an interchange of spins between the A and A′ nuclei (that is, in sub-matrix (iii)), due to J_A. However, sub-matrix (i) may be further divided into symmetric and antisymmetric parts (see ref. 1) and when $J_X = 0$, there are no off-diagonal elements in either part. Consequently, transitions within these parts all occur at the same frequency, namely $(\nu_X + \frac{1}{2}N)$, where ν_X is the unperturbed resonance frequency of the X and X′ nuclei. Similarly from sub-matrix (ii) a single line is obtained at $(\nu_X - \frac{1}{2}N)$. Here we have assumed for the sake of convenience that the absolute sign of $(J_{AX} + J_{AX}')$ is positive, but in fact this sign does not affect the final result that sub-matrices (i) and (ii) together give an intense doublet symmetrically disposed about ν_X, with a splitting of N.

The sub-matrix (iii) gives rise to a more complex series of lines. However, the only off-diagonal elements are those between $\alpha\beta$ and $\beta\alpha$ states of the AA′ nuclei, and these elements all have the value $\frac{1}{2}J_A$. The sub-matrix therefore reduces to a series of 2×2 sub-sub-matrices. The diagonal elements are given in general form for a single sub-sub-matrix as follows,

[1]
$$\begin{array}{ll} (p, m)\alpha\beta \text{ state} & \frac{1}{2}(p - m)L \\ (p, m)\beta\alpha \text{ state} & -\frac{1}{2}(p - m)L. \end{array}$$

In these expressions terms in ν_X have been omitted, since ν_X occurs in all the X and X′ transition energies. Diagonalization of the sub-sub-matrix results in eigenvalues ϵ given by

[2]
$$\epsilon(p, m) = \pm\tfrac{1}{2}[(p - m)^2L^2 + J_A^2]^{\frac{1}{2}},$$

where $(p - m)$ may take any integral value between n and $-n$ inclusive. Obviously these eigenvalues are independent of the sign of $(p - m)$, so that all allowed X transition energies may be expressed relative to ν_X by a single equation:

[3]
$$(\epsilon_\chi - \epsilon_{\chi-1}) = \pm\tfrac{1}{2}\{[\chi^2L^2 + J_A^2]^{\frac{1}{2}} \pm [(\chi - 1)^2L^2 + J_A^2]^{\frac{1}{2}}\},$$

where χ (which is $|p - m|$ for the upper state) may be any integer between 1 and n inclusive. These lines are symmetrically situated about ν_X and may be divided into two types. The pair with a plus sign between the square root terms, here referred to as the outer lines, has a separation $S_o(\chi)$ given by

[4]
$$S_o(\chi) = \{\chi^2L^2 + J_A^2\}^{\frac{1}{2}} + \{(\chi - 1)^2L^2 + J_A^2\}^{\frac{1}{2}},$$

whereas the lines with a minus sign between the square root terms (the inner lines) have a separation $S_i(\chi)$:

[5]
$$S_i(\chi) = \{\chi^2L^2 + J_A^2\}^{\frac{1}{2}} - \{(\chi - 1)^2L^2 + J_A^2\}^{\frac{1}{2}}.$$

Since X and X′ are chemically equivalent, the expressions [3] to [5] apply to both X transitions ($\Delta p = 1$) and X′ transitions ($\Delta m = 1$).

III. RELATIVE INTENSITIES

The values are initially calculated (before normalization) with unit intensity for an allowed transition between two of the basis states. Thus for a molecule with k magnetic nuclei the total intensity will be $k2^{k-1}$, while for an $X_nAA'X_n'$ system the sum of the intensity of the X and X′ transitions will be $2n2^{2n+1}$. The doublet of separation N will comprise half of this value, since it originates from half of the A and A′ spin states. The situation is again much more complex for sub-matrix (iii). Each sub-sub-matrix has a degeneracy of ${}^nC_{(n/2)+p} \times {}^nC_{(n/2)+m}$ for the number of ways of obtaining $I_z(X_n) = p$ and $I_z(X_n') = m$ from n nuclei of spin 1/2. When we consider the number of X transitions, we must multiply by $(n/2 + p)$ for the number of ways of changing p by $+1$ for a single wave function. For a given transition we must then sum over all possible values of p, keeping $p - m = \chi$ constant with $n/2 \geqslant m \geqslant -n/2$ and $n/2 \geqslant p \geqslant -n/2 + 1$. The limits set by these conditions for positive χ are $n/2$ and $\chi - n/2$, and expression [6] is obtained.

$$[6] \qquad \sum_{p=\chi-(n/2)}^{p=n/2} \left(\frac{n}{2} + p\right) {}^nC_{(n/2)+p}\, {}^nC_{(n/2)+p-\chi}.$$

However, the transition energy for $p - 1 \rightarrow p$ is the same as that for $-p \rightarrow -p - 1$, so [6] must be multiplied by 2 and two further factors of 2 are necessary to include (a) the X′ transitions and (b) both $\alpha\beta$ and $\beta\alpha$ AA′ spin states. This gives the total relative intensity for the four lines with energies given by [3] for a single value of X. In the absence of mixing between the $\alpha\beta$ and $\beta\alpha$ spin states (that is $J_A = 0$), the outer lines [4] are forbidden and thus have zero intensity while the inner lines [5] will each have intensity

$$4\sum_{r=\chi}^{n} r^nC_r\, {}^nC_{r-\chi},$$

where $r = n/2 + p$. For the weakest pair of inner lines ($\chi = n$), the above expression gives intensity $4n$, so that if we normalize to these lines, the relative intensities are given by [7]:

$$[7] \qquad \frac{1}{n}\sum_{r=\chi}^{n} r^nC_r\, {}^nC_{r-\chi}.$$

This will be referred to as the limiting intensity of each line. On this scale each line of the doublet of separation N will have intensity $2^{2(n-1)}$.

However, when J_A becomes appreciable, the outer lines acquire energy from the inner lines. The perturbations of intensities introduced may be calculated as in ref. 1. For the sub-sub-matrix [2] the parameter (1), $\tan 2\theta$, is $J_A/(p - m)L$ and the eigenstates are $\cos\theta|(p, m)\alpha\beta > +\sin\theta|(p, m)\beta\alpha) >$ and $-\sin\theta|(p, m)\alpha\beta > +\cos\theta|(p, m)\beta\alpha >$. The relative transition intensities for the outer and inner lines may be found by multiplying the appropriate coefficients $\sin\theta$ and $\cos\theta$, summing over allowed transitions between the basis functions, and taking the square of the result. Thus for the inner lines we must weight [7] by the factor $\frac{1}{2}(1 + g)$, where $g = [\chi(\chi - 1)L^2 + J_A^2]/\{[\chi^2L^2 + J_A^2][(\chi - 1)^2L^2 + J_A^2]\}^{\frac{1}{2}}$.

Therefore the inner lines each have intensity $Z_1(\chi)$ given by [8]:

$$[8] \qquad Z_1(\chi) = \frac{1}{2n}(1 + g)\sum_{r=\chi}^{n} r^nC_r\, {}^nC_{r-\chi}.$$

Can. J. Chem. Downloaded from www.nrcresearchpress.com by 210.87.254.42 on 09/05/12
For personal use only.

The outer lines will each have intensity $Z_0(\chi)$ given by [9]:

$$[9] \qquad Z_0(\chi) = \frac{1}{2n}(1 - g)\sum_{r=\chi}^{n} r^nC_r{}^nC_{r-\chi}.$$

The expression for g may easily be put in terms of $(L/J_A)^2$ alone (or, alternatively, in terms of $(J_A/L)^2$). The intensities then depend only on the relative magnitude of the two coupling constants L and J_A. It can be shown that g falls off as χ increases, and that for each value of χ there is a minimum in g (and therefore a maximum in $Z_0(\chi)$) when $(L/J_A)^2 = 1/\chi(\chi - 1)$. For $\chi = 2$ this minimum value of g is as large as 0.943, and it increases with χ. Consequently the outer lines for $\chi \geqslant 2$ are always very weak and will usually be unobservable (7).

IV. CHARACTERISTICS OF THE X SPECTRUM

There may be a total of $(2n + 1)$ pairs of lines symmetrically placed about ν_X. Half the total intensity (that is, relative intensity 2^{2n-1}) lies in the doublet of separation N, whereas the remaining intensity is spread over the $2n$ pairs of lines which are completely defined by eqs. [4], [5], [8], and [9]. The only nuclear magnetic parameters occurring in these equations are L and J_A, and the line positions and intensities (apart from a scaling factor) depend only on the ratio $L/|J_A|$. A typical spectrum, excluding the N doublet, is listed in Table I for $L/|J_A| = 1$ and values of χ up to 6. This shows several general features.

TABLE I

The X lines of an $X_6AA'X_6'$ nuclear magnetic system with $L/|J_A| = 1$

	Doublet separations[a]			
χ	Inner pair	Outer pair	Limiting intensity[b]	g
1	0.414	2.414	462	0.7073
2	0.822	3.650	330	0.9489
3	0.926	5.398	165	0.9898
4	0.961	7.285	55	0.9971
5	0.976	9.222	11	0.9992
6	0.984	11.182	1	0.9994

[a]In units of L.
[b]Given for each line by eq. [7]. Each line of the N doublet will have relative intensity 1024.

1. The doublet separations of the inner lines increase monotonically with χ, but they converge to the value L as $\chi \to \infty$. This fact can be used to obtain an approximate value of L by inspection of the spectrum. The doublet separation of the outer lines also increases with χ but diverges towards a constant increment of $2L$.

2. If any of the inner lines fall outside the N doublet, it immediately follows that J_{AX} and J_{AX}' are opposite in sign.

3. It can be anticipated that the inner pairs of lines will become difficult to resolve from one another for values of χ greater than about 3.

4. The limiting intensities fall off very rapidly as χ increases.

5. The value of g increases towards unity as χ increases. When considered together with feature 4, this fact means that it will usually not be possible to see outer lines with $\chi > 1$.

6. The inner and outer lines are usually well separated, for $S_i(\chi)$ must be less than L, as noted above, whereas the separation of a pair of outer lines $S_0(\chi)$ must be greater than L.

Can. J. Chem. Downloaded from www.nrcresearchpress.com by 210.87.254.42 on 09/05/12
For personal use only.

All three parameters, N, L, and $|J_A|$, may be obtained directly from the spectrum using only the separations of the three most intense lines. It is always easy to pick out the N doublet and this should then be mentally discarded from the spectrum. The separations of the first two pairs of inner lines (which are therefore the next most intense features of the spectrum) then give $S_1(1) = [L^2 + J_A^2]^{\frac{1}{2}} - |J_A|$ and $S_1(2) = [4L^2 + J_A^2]^{\frac{1}{2}} - [L^2+J_A^2]^{\frac{1}{2}}$. Equations [10] and [11] may then be used.

$$[10] \qquad |J_A| = [3S_1(1) + S_1(2)][S_1(1) - S_1(2)]/2[3S_1(1) - S_1(2)].$$

$$[11] \qquad L^2 = S_1(1)\cdot S_1(2)\cdot[S_1(1) + S_1(2)]/[3S_1(1) - S_1(2)].$$

However, if the first pair of *outer* lines is visible it becomes more convenient to measure the separation between one of these and the corresponding inner line, giving J_A directly (see Fig. 1). The separation $S_1(1)$ between the first pair of inner lines is then needed to

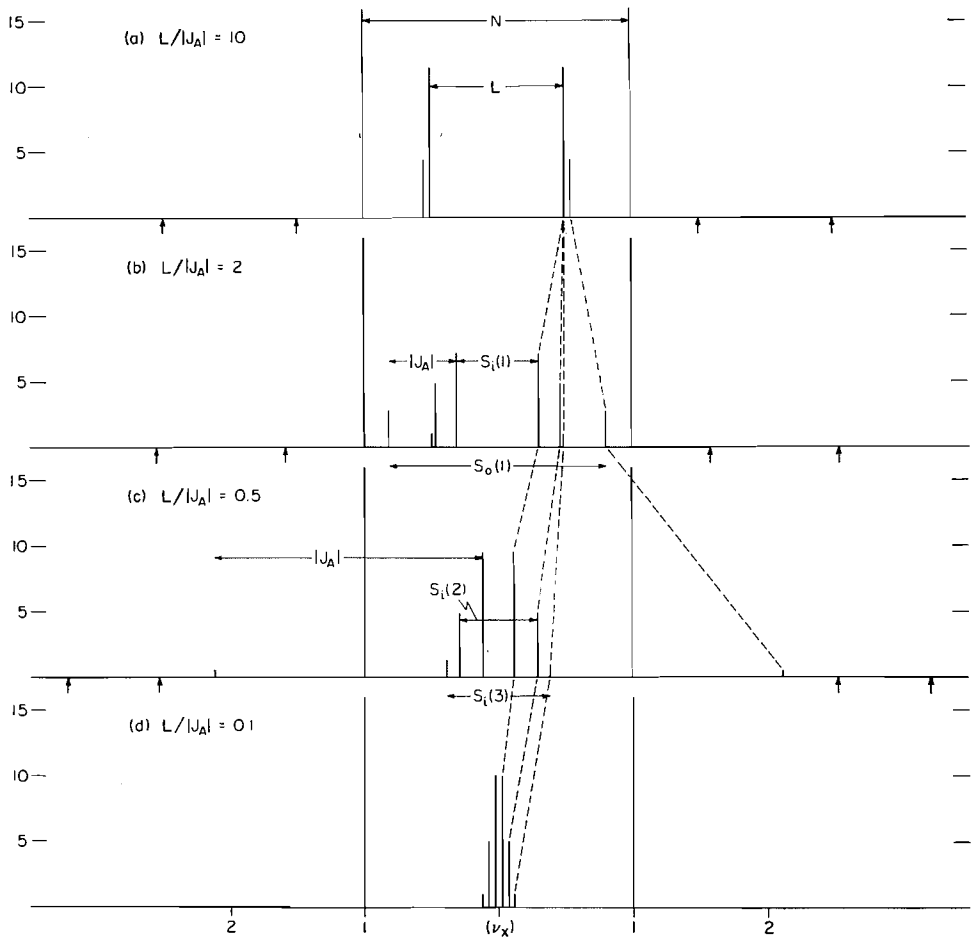

FIG. 1. Diagram to illustrate the variation of the X spectrum of $X_3AA'X_3'$ systems with changes in $L/|J_A|$. The relative intensities (as explained in the text) are plotted along the ordinates. The abscissae give line positions in units of L. The value of N is taken to be $2L$ (therefore J_{AX} and $J_{AX'}$ have the same sign). The small vertical arrows mark the positions of outer lines, which have negligible intensity (< 0.06), for $x = 2$ and 3. In (*d*) all three outer lines lie between 10 and 10.5 units of L from the center ($\simeq J_A$) and their total intensity is less than 0.04. Spectra (*a*) and (*d*) approach limiting cases B and A discussed in the text.

Can. J. Chem. Downloaded from www.nrcresearchpress.com by 210.87.254.42 on 09/05/12
For personal use only.

give L from the expression above. Since the spectrum in general yields L and N, it is usually possible to obtain the relative signs of J_{AX} and J_{AX}'. It is not possible, however, to determine the sign of J_A relative to these, nor is it possible to make any distinction between J_{AX} and J_{AX}', and so they cannot be assigned to actual couplings in the molecule (that is, we cannot tell which is the "long-range" coupling constant).

It is important to realize the relation between X spectra of systems of the $X_nAA'X_n'$ type. If the number of X and X′ nuclei are increased by 1 to $(n+1)$—while N, L, and J_A are left constant—the only spectral changes are (i) the addition of two very weak pairs of lines with $\chi = (n+1)$ and (ii) corresponding slight alterations in the relative intensities of other lines. Consequently it is usually possible to recognize the most intense lines as typical of a simple XAA′X′ system (with $J_X = 0$), or at any rate an $X_2AA'X'_2$ system. This type of relation also exists between spectra of the AB_{2n} type (8).

V. LIMITING CASES

The general description above may be considerably simplified in certain cases, giving rise to "deceptively simple" spectra (9). There are two possible extreme types, which are indicated in Fig. 1 for the $X_3AA'X_3'$ system.

(A) $|J_A| \gg L$, giving approximately an A_2X_{2n} spectrum (see Fig. 1d).—In this case the outer lines have negligible intensity ($g \approx 1$) and to a first approximation the separations $S_o(\chi)$ are all $2J_A$. The inner lines, with a total intensity of 2^{2n-1}, fall very close to ν_X, and therefore the whole X spectrum, including the N doublet, has the appearance of a 1:2:1 triplet. This is, of course, the spectrum that would be given if $J_{AX} = J_{AX}'$ but, as pointed out by Abraham and Bernstein (9), it is not necessary that L be identically zero (see also ref. 10). Only a single peak will be seen at ν_X if the separation of the first inner doublet is less than the effective resolution of the spectrometer, that is, the full width at half-height, $\Delta\nu_{\frac{1}{2}}$, of a single line. However, when $|J_A| \gg L$, then $S_1(1) = [L^2 + J_A^2]^{\frac{1}{2}} - J_A \approx \frac{1}{2}(L^2/|J_A|)$; therefore the condition for a deceptively simple spectrum reduces to [12]:

$$L^2 < 2|J_A|\Delta\nu_{\frac{1}{2}}. \qquad [12]$$

Such a spectrum may frequently be distinguished from that expected if A and A′ were magnetically equivalent by observation of peak heights (or widths). If L is small, but not zero, the central "line" of the triplet may appear broader than the two outer ones even when condition [12] is obeyed. Then the height of the central line will be less than twice that of the N doublet lines. The only information that may be derived from these deceptively simple spectra is the value N from the separation of the outer lines of the triplet and an upper limit to the value of $L^2/|J_A|$ from the width of the central line. It may be noted that the above discussion is only strictly valid for low values of χ (since the simplifying condition is really $|J_A| \gg \chi L$), but since these values give the most intense lines, they are the only ones that need to be considered. However, it is still true that for high values of χ (which necessitates high n), $S_1(\chi)$ tends to L, so the central line of the deceptively simple triplet may appear to tail off abnormally slowly on both sides.

In cases near the extreme discussed above, where $L < |J_A|$ but expression [12] is not obeyed, the separation of the inner pairs of lines simplifies to $S_1(\chi) = L^2(2\chi - 1)/2|J_A|$, except for high values of χ.

(B) $J_A \to 0$, giving approximately an X_nAM spectrum (see Fig. 1a).—Here $g = 0$ for $\chi = 1$, and consequently the inner and outer lines for this value of χ have the same intensity, and they also have the same separation, L. All the other inner lines also have separations $S_1(\chi) = L$, while the outer lines are separated by $S_o(\chi) = (2\chi - 1)L$ but have negligible

Can. J. Chem. Downloaded from www.nrcresearchpress.com by 210.87.254.42 on 09/05/12
For personal use only.

intensities because $g \simeq 1$. Thus the whole X spectrum consists of four lines with spacings N and L (see Fig. 1). An alternative choice of spacings for this case would be $|J_{AX}|$ and $|J_{AX}'|$, as expected for the X spectrum of an X_nAM system. Thus it is not possible to obtain J_A in this case nor is it possible to obtain the relative signs of the coupling constants. However, $|J_{AX}|$ and $|J_{AX}'|$ can be evaluated, in contrast to case A above. Also these conclusions are valid however large χ may become. This type of spectrum will frequently be encountered when the "long-range" coupling constant J_{AX}' is small, while the short-range one is large (coupling constants normally fall off rapidly as the number of bonds separating the coupled nuclei increases). In such cases it may become impossible to resolve the L doublet from the N doublet. We then have two effectively uncoupled X_nA systems giving a single doublet in the X spectrum.

When $L \gg |J_A|$ but $|J_A|$ is greater than the resolution of the instrument, the six lines of Fig. 1*a* may be seen. Whenever this is possible $|J_A|$ may be measured and the relative signs of J_{AX} and J_{AX}' obtained. When $L > |J_A|$ but more than six lines can still be resolved, the inner lines will have separations given approximately by the simplified formula $S_1(\chi) = L - (J_A^2/2\chi(\chi - 1)L)$.

REFERENCES

1. J. A. POPLE, W. G. SCHNEIDER, and H. J. BERNSTEIN. High-resolution nuclear magnetic resonance. McGraw-Hill, New York. 1959.
2. E. B. WILSON. J. Chem. Phys. **27**, 60 (1957). H. S. GUTOWSKY. Ann. N.Y. Acad. Sci. **70**, 786 (1958).
3. P. L. CORIO. Chem. Rev. **60**, 363 (1960).
4. C. NAAR-COLIN and A. A. BOTHNER-BY. Private communication.
5. F. A. L. ANET. J. Am. Chem. Soc. **84**, 747 (1962); Proc. Chem. Soc. 327 (1959).
6. A. A. BOTHNER-BY and C. NAAR-COLIN. J. Am. Chem. Soc. **84**, 743 (1962).
7. R. K. HARRIS and R. G. HAYTER. Can. J. Chem. **42**, 2282 (1964).
8. D. CHAPMAN and R. K. HARRIS. J. Chem. Soc. 237 (1963).
9. R. J. ABRAHAM and H. J. BERNSTEIN. Can. J. Chem. **39**, 216 (1961).
10. D. M. GRANT and H. S. GUTOWSKY. J. Chem. Phys. **34**, 699 (1961).

Can. J. Chem. Downloaded from www.nrcresearchpress.com by 210.87.254.42 on 09/05/12
For personal use only.

Can. J. Chem. Downloaded from www.nrcresearchpress.com by 210.87.254.5 on 09/05/12
For personal use only.

NUCLEAR MAGNETIC RESONANCE STUDIES OF COMPOUNDS RELATED TO TETRAMETHYLDIPHOSPHINE DISULPHIDE

R. K. HARRIS[1] AND R. G. HAYTER[2]
Mellon Institute, Pittsburgh, Pennsylvania

Received May 15, 1964

ABSTRACT

The proton n.m.r. spectra of tetramethyldiphosphine disulphide and a number of related compounds have been obtained, yielding values for the nuclear magnetic parameters. Brief comments are made on these parameters. Double resonance experiments yielded the relative signs of the coupling constants for tetramethyldiphosphine sulphide and spectral analysis provided similar information for the disulphide. Comparisons are made with published data.

INTRODUCTION

Although nuclear magnetic resonance (n.m.r.) studies have been carried out on quite a large number of phosphorus-containing compounds, many of these studies have consisted in obtaining chemical shifts for ^{31}P resonance. Consequently accurate values of (H, P) coupling constants were not obtained. Most of the proton resonance investigations of phosphorus-containing compounds have been carried out with acids, esters, and salts. The french group of Mavel, Martin, and their co-workers (1) have reported studies on a greater variety of compounds but much of their work is carried out at 25 Mc/s, which puts limitations on their results. Consequently there is a scarcity in the literature of accurate values for (P, H) coupling constants. Recently, relative signs have been reported (2–7) for a number of such coupling constants, but these signs have not been linked directly to that for the (^{13}C, H) coupling through one bond, which is commonly taken as a reference. Further investigations seemed warranted. This relative lack of data is much more pronounced for the case of (P, P) coupling. Only a few values have been reported (2, 8, 9), and of these only the results of Lynden-Bell (2) and Callis *et al.* (9) are for compounds with a direct P—P bond. On the other hand, there is, at the present time, a continued interest in the theoretical interpretation of coupling constants. For this purpose accurate experimental data are of great importance, and in particular there is need for values of coupling constants between directly bonded nuclei. Consequently it seemed worth while to study a series of substituted diphosphines and related compounds to obtain the nuclear magnetic parameters.

EXPERIMENTAL PROCEDURE

The proton spectra were taken using a Varian A60 spectrometer operating at 60 Mc/s and a sample temperature of 37 °C. Chloroform-*d* was used as a solvent for most of the compounds, with a small amount of tetramethylsilane added to serve as an internal reference. However, tetramethyldiphosphine, $(CH_3)_2P\cdot P(CH_3)_2$, (I), was examined as a neat liquid plus tetramethylsilane;* in particular because the ^{13}C satellites were observed. The sample tubes were 5 mm in outside diameter and were degassed and sealed under a vacuum before use. In some instances small peaks appeared in the proton resonance spectrum because of impurities, but these were always easily recognized as such.

The samples of tetramethyldiphosphine and dimethylchlorophosphine, $(CH_3)_2PCl$, (II), were prepared as

**We are very grateful to Dr. G. W. Parshall for informing us of his work on tetramethyldiphosphine and for sending his n.m.r. spectra of the compound.*

[1]*Permanent address: School of Chemical Sciences, Wilberforce Road, Norwich, England.*
[2]*Present address: Shell Development Co., Emeryville, California.*

described by Parshall in refs. 10 and 11 respectively. The method of Niebergall and Langenfeld (12) was used for tetramethyldiphosphine disulphide, $(CH_3)_2P(:S)P(:S)(CH_3)_2$, (III), and resulted in a product with melting point 233–235 °C (lit. 228–229).

The results of elemental analysis were C, 26.0; H, 6.55 (calculated values for $C_4H_{12}P_2S_2$ are C, 25.7; H, 6.5).

The n.m.r. spectrum was identical with that of a sample supplied by Dr. T. Shryne of Shell Development Co., Emeryville, California. Tetramethyldiphosphinesulphide, $(CH_3)_2P(:S)\cdot P(CH_3)_2$, (IV), was prepared by heating a 1:1 mixture of (III) with (I) in a sealed tube at ≈ 220 °C for 16 h (13). It was sublimed twice in a vacuum at 45–50 °C to obtain the analytical sample. The n.m.r. spectrum of the analytical sample was essentially identical with that taken directly with the reaction products. Consequently, since the compound is very air-sensitive, the ^{31}P spectra were obtained (using a nonspinning tube of 15 mm outside diameter) from the reaction products themselves.

Elemental analysis gave P, 37.8; S, 19.0; ratio P/S = 2.06/1 (calculated values for $C_4H_{12}P_2S$ are P, 40.2; S, 20.8).

Dimethyl(dimethylarsino)phosphine sulphide, $(CH_3)_2P(:S)As(CH_3)_2$, (V), was prepared in an analogous manner by heating a 1:1 mixture of (III) with cacodyl, tetramethyldiarsine, $(CH_3)_2As\cdot As(CH_3)_2$, (VI), in a sealed tube at ≈ 220 °C for 16 h. The reaction product was dissolved in $CDCl_3$ for the n.m.r. spectrum without analysis or purification. The method of Auger (14) was used to prepare (VI). Trimethylphosphine sulphide, $(CH_3)_3P:S$, (VII), was obtained from $PSCl_3$ and the Grignard reagent, CH_3MgBr (15).

Elemental analysis results were C, 32.1; H, 8.5; P, 28.5; S, 29.6 (calculated values for C_3H_9PS are C, 33.3; H, 8.4; P, 28.6; S, 29.65).

The double resonance experiments on (IV) were also performed on an A60 spectrometer, using the modifications and apparatus recently developed by N.M.R. Specialities Inc. Instabilities in the system could be attributed mainly to drift of the 5 kc/s signal of the spectrometer. The experiments reported here were not very sensitive to drifts of the order of 10 c/s and no difficulties were encountered during operation of the equipment. We are very grateful to N.M.R. Specialities Inc. for allowing us to perform these experiments at their New Kensington, Pa. laboratory.

ANALYSIS OF THE SPECTRA

The coupling constant notation of Musher and Corey (16) will be used here to designate by a numerical prefix the number of chemical bonds through which coupling occurs. In the compounds studied here, there are two such types of (H, P) coupling constants, coupling occurring through two and three chemical bonds. These two types of coupling constants will be written $^2J_{HP}$ and $^3J_{HP}$ and will be referred to as short-range and long-range (H, P) coupling respectively. A further division of the (H, P) coupling constants may be made since the phosphorus atom involved is trivalent or pentavalent. This will be indicated by a roman superscript as in $^2J_{HPIII}$. For the symmetrical molecules tetramethyldiphosphine and tetramethyldiphosphine disulphide, more convenient parameters than $^2J_{HP}$ and $^3J_{HP}$ can be shown to be $L = |^2J_{HP} - {}^3J_{HP}|$ and $N = |^2J_{HP} + {}^3J_{HP}|$, and so these latter will normally be used. The only (H, H) coupling between protons that are not magnetically equivalent occurs through five bonds and is negligibly small in the present instances. The only (P, P) coupling is between directly bonded phosphorus atoms, and will be designated simply J_{PP}. Further division into J_{PIIIPV}, $J_{PIIIPIII}$, and J_{PVPV} will occasionally be used.

The proton spectrum of cacodyl, (VI), consisted of a single, rather broad line. The samples of (II) and (VII) each gave rise to a doublet, as expected, and the nuclear magnetic parameters could be obtained directly. Two doublets were obtained from (V), $(CH_3)_2P(:S)As(CH_3)_2$, and these were assigned to the two types of methyl groups by comparing the chemical shifts and coupling constants with those for related compounds (see Table I).

The spectrum of tetramethyldiphosphine (I) was deceptively simple (17, 18), being a 1:2:1 triplet. Consequently only the sum of the two (P, H) coupling constants could be obtained, $N = 14.2$ c/s. However, the central line was distinctly broader than the outer lines (the ratio of line heights for the central:outer lines is 1.3:1 instead of the usual 2:1), showing that the methyl groups were not all magnetically equivalent. An estimate of $L^2/|J_{PP}|$

Can. J. Chem. Downloaded from www.nrcresearchpress.com by 210.87.254.5 on 09/05/12
For personal use only.

Can. J. Chem. Downloaded from www.nrcresearchpress.com by 210.87.254.5 on 09/05/12
For personal use only.

TABLE I

Magnitudes[d] of the n.m.r. parameters[c] for some phosphorus compounds

	Compound	Ref.	$^2J_{HP^{III}}$	$^3J_{HP^{III}}$	$^2J_{HP^{V}}$	$^3J_{HP^{V}}$	$^1J_{PP}$	$\tau(CH_3P^{III})$	$\tau(CH_3P^{V})$	$\tau(CH_3As^{III})$
I.	$(CH_3)_2P\cdot P(CH_3)_2$		6.9±0.2[a]	7.3±0.2[a]				8.94		
IV.	$(CH_3)_2P(:S)\cdot P(CH_3)_2$		4.09	5.84	12.02	17.61	220±5	8.79	8.24	
III.	$(CH_3)_2P(:S)\cdot P(:S)(CH_3)_2$				12.74[a,b]	7.26[a,b]	18.7		8.04	
V.	$(CH_3)_2P(:S)\cdot As(CH_3)_2$				11.83	15.55			8.19	8.81
VI.	$(CH_3)_2As\cdot As(CH_3)_2$									8.89
VII.	$(CH_3)_3PS$				13.10				8.22	
	$(CH_3)_3P$	4	2.7					9.06		
II.	$(CH_3)_2PCl$		8.31					8.35		
	$(CH_3CH_2)_3P$	6	0.5	13.7						
	$((CH_3)_2N)_3P$	1		8.9						
	$((CH_3)_2N)_3P{:}S$	1				11.1				
	$(CH_3)_3PCl_2$	34			13.8					

[a]Assignments uncertain—the two coupling constants may be interchanged.
[b]Further doubts about this assignment are introduced by lack of certainty about the structure of the molecule (see text).
[c]Coupling constants are in c/s.
[d]For relative signs of coupling constants see Table II.

Can. J. Chem. Downloaded from www.nrcresearchpress.com by 210.87.254.5 on 09/05/12
For personal use only.

can be made using eq. [12] of ref. 18. This equation is the condition for observation of a deceptively simple spectrum. If $J_{PP} \approx 100$ c/s (as in diphosphine) a value of $L < 11$ c/s is obtained, indicating that $^2J_{HP^{III}}$ and $^3J_{HP^{III}}$ have the same sign in this compound (see Table II for comparisons with other phosphorus-containing molecules). If L is appreciable, the satellites in the proton spectrum due to molecules containing a ^{13}C atom should appear as quartets (19). However, they still have triplet structure, although the height of the central line is but barely greater than the heights of the outer lines. It is concluded that $L \leqslant 0.8$ c/s, giving the coupling constants shown in Table I. It is not possible to distinguish the "long-range" value, $^3J_{HP}$, from the "short-range" coupling, $^2J_{HP}$.

The spectrum of (IV), $(CH_3)_2P(:S)P(CH_3)_2$, consists of four doublets which may be grouped into two pairs. By comparison of chemical shift values with the other compounds it can be seen that the two doublets at lower field are due to the protons of the methyl groups attached to the pentavalent phosphorus atom, whereas the high-field pair of doublets belong to the protons of the $P^{III}(CH_3)_2$ group. Consequently it is possible to distinguish $^2J_{HP^V}$ and $^3J_{HP^{III}}$ from $^2J_{HP^{III}}$ and $^3J_{HP^V}$. However, it is not possible by this evidence alone to distinguish $^2J_{HP^V}$ from $^3J_{HP^{III}}$ or $^2J_{HP^{III}}$ from $^3J_{HP^V}$. The ^{31}P spectrum of this compound at 15.1 Mc/s consists of four very broad bands in an AB type of pattern with a chemical shift between P_{III} and P_V of 94.5 ± 0.4 p.p.m. and a coupling constant $J_{PP} \approx 220$ c/s. The P_V resonance is considered to occur to low field of the P_{III} resonance (20). The breadth of the bands is due to unresolved coupling to the large number of methyl protons. It is noticeable that the two P_V bands are broader than the P_{III} lines, indicating that the average of the two (H, P^V) couplings is larger than the average of the (H, P^{III}) couplings.

A complete assignment was made and the relative signs of the coupling constants were obtained by double resonance techniques (21, 22). Because of the large band separations in the ^{31}P spectrum there was insufficient power available to decouple completely either of the phosphorus nuclei from the methyl protons. However, each of the four ^{31}P bands (that is, the centers of multiplets due to coupling with the methyl protons) were selectively irradiated at low power (23) in turn, and the effects on the proton spectrum noted (Fig. 1). In each case irradiation of the P^V bands caused the larger splittings in the proton spectrum to collapse, while irradiation of the P^{III} bands caused the collapse of the smaller splittings for both the $(CH_3)_2P^{III}$ quartet and the $(CH_3)_2P^V$ quartet. It was thus demonstrated that $^2J_{HP^V} > {}^3J_{HP^{III}}$ and $^3J_{HP^V} > {}^2J_{HP^{III}}$, and a complete assignment was established (Table I). Low-power irradiation (23) of the P^{III} band at highest field caused the *high*-field proton doublet of the $(CH_3)_2P^V$ group and the *low*-field doublet of the $(CH_3)_2P^{III}$ group to collapse (Fig. 1). This shows that J_{PP} and $^2J_{HP^V}$ have the same sign, while $^3J_{HP^V}$ is of the opposite sign (21, 33). Similar information regarding relative signs was obtained for the (H, P^{III}) coupling constants by irradiation of one of the P^V bands (Table II). In this case, however, collapse of two lines was not so marked, presumably because the (H, P^V) coupling constants are sufficiently large that the irradiating power necessary to cause selective collapse of lines in the proton spectrum also causes spectral side-effects to become noticeable (22, 23). However, it is clear (Fig. 1) that only two lines of the four for each type of methyl proton have been affected. Irradiation of the remaining ^{31}P bands confirmed the correctness of the deductions but provided no new information. In the above double-irradiation work it should be noted that the two types of methyl protons are treated completely independently, giving double resonance spectra typical for the X_6 nuclei of ABX_6 nuclear magnetic systems.

Can. J. Chem. Downloaded from www.nrcresearchpress.com by 210.87.254.5 on 09/05/12
For personal use only.

TABLE II

Relative signs of J_{PP} and J_{HP}

	Compound	Ref.	$^1J_{PP}$ Type	$^1J_{PP}$ Value[d]	$^1J_{HP}$ Type	$^1J_{HP}$ Value[d]	$^2J_{HXP}$ Type	$^2J_{HXP}$ Value[d]	$^3J_{HXYP}$ Type	$^3J_{HXYP}$ Value[d]	Notes
VIII.	$(CH_2{=}CH)_3P$	5					P^{III}, X = C	±11.74	P^{III}, X = Y = C(sp^2)	±13.62(*cis*) ±30.21(*trans*)	[a]
IX.	CH_3PH_2	3, 4			P^{III}	±186.4	P^{III}, X = C	±4.1			
X.	$(CH_3)_2PH$	3, 4			P^{III}	±191.6	P^{III}, X = C	±3.6			[b]
XI.	$(CH_3CH_2)_3P$	6					P^{III}, X = C	∓0.5	P^{III}, X = Y = C	±13.7	
XII.	$(CH_3)_2CHP(:O)Cl_2$	7					P^{V}, X = C	∓[h]	P^{V}, X = Y = C	±[h]	
XIII.	$(CH_3)_2CHP(:S)Cl_2$	7					P^{V}, X = C	∓[h]	P^{V}, X = Y = C	±[h]	
XIV.	$[O_3P{\cdot}PHO_2]^{3-}$	2, 9			P^{V}	±444	P^{V}, X = P^{V}	±94			
XV.	$H_2P{\cdot}PH_2$[e]	(i) 2	P^{III}, P^{III}	∓108.2							[c]
		(ii) 2			P^{III}	±186.5	P^{III}, X = P^{III}	±11.9			
I.	$(CH_3)_2PP(CH_3)_2$						P^{III}, X = C	±6.9	P^{III}, X = C, Y = P^{III}	±7.3	[f]
IV.	$(CH_3)_2P(:S)P(CH_3)_2$		P^{III}, P^{V}	∓220			P^{III}, X = C	±4.09	P^{III}, X = C, Y = P^{V}	±5.84	
							P^{V}, X = C	∓12.02	P^{V}, X = C, Y = P^{III}	±17.61	
III.	$(CH_3)_2P(:S)P(:S)(CH_3)_2$[g]						P^{V}, X = C	∓12.74	P^{V}, X = C, Y = P^{V}	±7.26	[f]

[a] $^2J_{HCH} = \pm 2.02$, $^3J_{HC=CH}{}^{cis} = \pm 11.76$, $^3J_{HC=CH}{}^{trans} = \pm 18.37$.
[b] $^3J_{HCPH} = \pm 7.61$.
[c] $^2J_{HPH} = \mp 12$, $^3J_{HPPH} = \pm 10.5$, ± 6.8 (*trans* and *cis*).
[d] All coupling constants are in c/s.
[e] It is not possible to determine the relative signs between groups (i) and (ii).
[f] The magnitudes may be interchanged.
[g] Assuming the accepted structure.
[h] Magnitudes not listed.

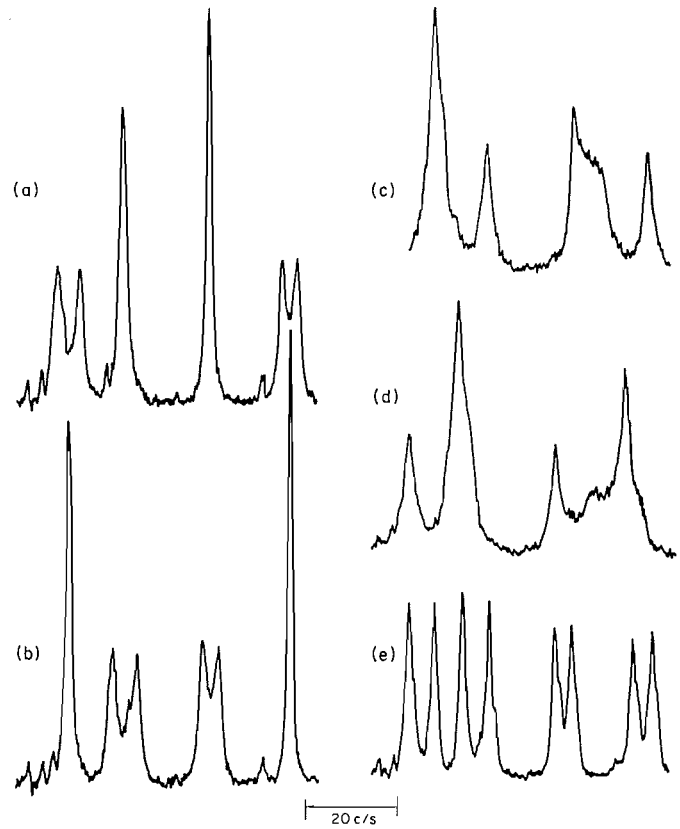

FIG. 1. Proton spectra of tetramethyldiphosphine sulphide, $(CH_3)_2P(:S)P(CH_3)_2$, in solution in chloroform-*d* during irradiation at low power in the region of the ^{31}P resonance. Spectra (*a*) to (*d*) correspond to irradiation of each of the four bands of the phosphorus spectrum in order of decreasing field-strength. Thus (*a*) and (*b*) are recorded for irradiation at P^{III} resonance frequencies, while for (*c*) and (*d*) irradiation is occurring at P^{V} frequencies. Trace (*e*) is the normal spectrum obtained while irradiating well to low field of any of the ^{31}P resonances of the compound. A few weak lines due to impurities may be seen in the spectra. The magnetic field strength increases from left to right for these spectra.

Tetramethyldiphosphine disulphide (III) was actually the first compound studied in this work (18). The structure of this molecule has been said to be $(CH_3)_2P(:S)P(:S)(CH_3)_2$ by Goubeau, Reinhardt, and Bianchi (24) and by Christen, Van der Linde, and Hooge (25). This compound gave a spectrum which is an excellent example of the $X_nAA'X_n'$ nuclear magnetic system, discussed in the previous paper (18), with $n = 6$. The two most intense lines are, as expected, those given by molecules with the $\alpha\alpha$ and $\beta\beta$ phosphorus spin states. The separation of this doublet immediately gives us $N = 5.48$ c/s. The fact that all the other lines lie outside this doublet is an indication that $^2J_{HP}$ and $^3J_{HP}$ are of opposite sign. The inner pairs of lines (see ref. 18) with $\chi = 1$ and $\chi = 2$ are resolved, but the pairs with $\chi = 3$, 4, 5, and 6 form two broad, weak bands. A calculation using the separations $S_1(1) = 8.49$ c/s and $S_1(2) = 16.73$ c/s with eq. [11] of ref. 18 gives the value $L = 20.24$ c/s. However, the first pair of *outer* lines ($\chi = 1$) are visible in the spectrum and this gives $|J_{PP}| = |J_A| = \frac{1}{2}[S_0(1) - S_1(1)] = 18.7 \pm 0.05$ c/s. A recalculation of L using this value of $|J_A|$ and the observed $S_1(1) = [L^2 + J_{PP}^2]^{1/2} - |J_{PP}|$ results in $L = 19.87$ c/s. This is considered good agreement with the value above since the lines are weak (the compound

Can. J. Chem. Downloaded from www.nrcresearchpress.com by 210.87.254.5 on 09/05/12
For personal use only.

is not highly soluble in $CDCl_3$), somewhat broad, and partly overlapped. The value of L which gives the best fit to the spectrum (Fig. 2) is 20.0 ± 0.15 c/s. The spectral charac-

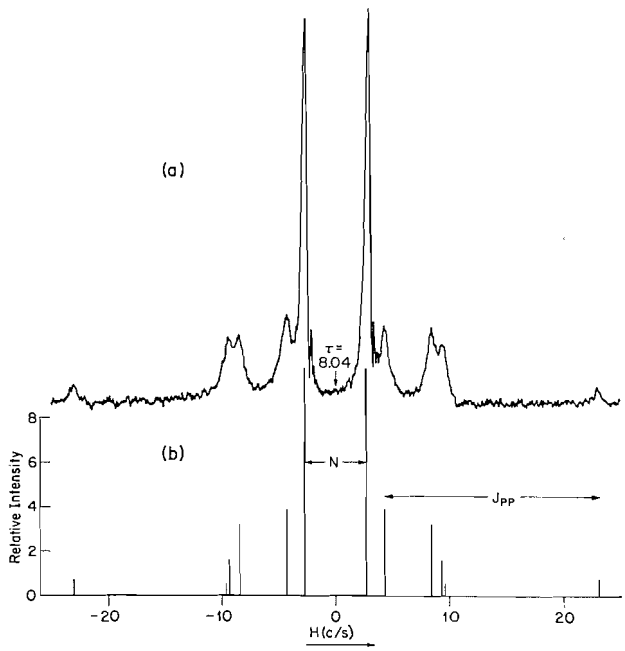

FIG. 2. Observed (*a*) and calculated (*b*) proton spectra of tetramethyldiphosphine disulphide, $(CH_3)_2P(:S)P(:S)(CH_3)_2$, in solution in chloroform-*d*. Spectrum (*b*) has been calculated using the parameters ${}^5J_{HH} = 0$, ${}^1J_{PP} = 18.7$, $L = |{}^2J_{HP} - {}^3J_{HP}| = 20.0$, and $N = |{}^2J_{HP} + {}^3J_{HP}| = 5.48$. Inner lines $S_i(5)$ and $S_i(6)$ are too weak and too close to $S_i(4)$ to be seen on this scale. Outer lines for $x > 1$ are too weak and too widely spaced to be observed. For nomenclature and the definition of the intensity scale see ref. 18.

teristics mentioned in ref. 18 are clearly shown by this example. It is not possible to obtain the sign of J_{PP} relative to the (H, P) coupling constants, nor is it possible to distinguish between ${}^2J_{HP}$ and ${}^3J_{HP}$. Table I therefore gives an arbitrary assignment—the other compounds listed are not sufficiently closely related to be of help here.

DISCUSSION

(a) The Nuclear Magnetic Parameters (Table I)

The pattern which emerges from the values of Table I is not simple. Moreover, it is complicated by the ambiguities in the assignment of the (P, H) coupling constants of (I) and (III). It is clear that (P, H) coupling constants across three bonds are of the same order of magnitude as those across two bonds, and indeed the former may be the larger. It seems that ${}^2J_{HP\,III}$ can be relatively small, but it has been reported as 24 c/s in methyl dibromophosphine (20). Consequently these coupling constants are of little use in structural determinations where decisions must be made between groupings of the type H—C—P^{III}, H—C—X—P^{III}, H—C—X—P^{V}, and H—C—P^{V} unless a very closely related series of molecules is considered. It seems from Table I that the chemical shift values may be of more diagnostic importance than the coupling constants, since the resonance of a methyl group attached to a trivalent phosphorus atom usually occurs approximately 0.6 p.p.m. to high field of that for a similar compound in which the phosphorus

Can. J. Chem. Downloaded from www.nrcresearchpress.com by 210.87.254.5 on 09/05/12
For personal use only.

atom is pentavalent. Replacement of P^{III} by As^{III} seems to cause only a very small shift in the resonance position. It is worth noting that proton resonances for methyl groups attached to arsenic have line widths ($\approx$ 1 c/s) greater than normal, presumably because of incomplete elimination of the effects of (As, H) coupling via the arsenic quadrupole moment.

(b) Tetramethyldiphosphine Disulphide, (III): J_{PP} and Structure

The value obtained for J_{PP} in (III) is very low in comparison to that of the monosulphide (IV) and diphosphine itself (2). This is probably not due to the absence of any trivalent phosphorus atoms in the disulphide, since the reported value (9) for the diphosphite ion $(P^{V}O_3P^{V}HO_2)^{3-}$ is much higher (480 c/s), whereas for anions containing the P^{V}—O—P^{V} linkage (9), it falls to $\approx$ 17 c/s, remarkably close to the present value. The contrast in values is so startling that it raises the question of whether the accepted structure (24, 25) is correct. The value of J_{PP} would be more reasonable if no direct bond existed between the two phosphorus atoms.* The evidence for the structure $(CH_3)_2P(:S)P(:S)(CH_3)_2$ seems to consist (24, 25) mainly in the observed mutual exclusion of infrared-active and Raman-active vibrational modes, which indicates that the molecule possesses a center of symmetry. Consequently the authors reject the structure $(CH_3)_2P$—S—S—$P(CH_3)_2$— although even in this case it is not impossible to pick a rotamer that has the desired symmetry. Moreover, the structure $(CH_3)_2P(:S)P(:S)(CH_3)_2$ is centrosymmetric only if the P=S bonds are in a transoid relation. The authors did not consider other possible structures. One possibility in accord both with the vibrational spectra and with the low value of J_{PP} is a four-membered P_2S_2 ring system. This is unlikely chemically, although four-membered ring systems containing two phosphorus atoms and two metal atoms are well known (26). Moreover, some support for the accepted structure $(CH_3)_2P(:S)P(:S)(CH_3)_2$, is provided by the fact that the two (H, P^{V}) coupling constants are of opposite sign, as they are for the analogous values in IV. It is interesting that recently the molecule $(CH_3)_4As_2S_2$ has been shown (27) to possess the structure $(CH_3)_2As(:S)$—S—$As(CH_3)_2$. The evidence of the vibrational spectra precludes such a possibility for (III). It must be noted that if (III) does not possess the accepted (24, 25) structure, then the nomenclature $^2J_{HP}$ and $^3J_{HP}$ used in Table I for this molecule is incorrect. On the other hand, if the accepted structure is correct the varying magnitudes of the (P, P) coupling constant for directly bonded phosphorus nuclei in the few known cases are rather puzzling. It must be concluded that it is not possible on the basis of present evidence to be certain of the structure of tetramethyldiphosphine disulphide. Further speculation should await the result of attempts to determine the structure by X-ray methods.

(c) The Relative Signs of the Coupling Constants (Table II)

Until very recently absolute signs of spin–spin coupling constants were unknown. Theoretical predictions are most likely to be accurate for coupling between directly bonded atoms, and Karplus (28) suggested that the sign of $^1J_{H^{13}C}$ be regarded as positive (in the sense that an antiparallel nuclear spin orientation corresponds to a more stable state than the parallel orientation) and that signs of other coupling constants should be related to that of $J_{H^{13}C}$. Recent work with the electric-field effect (29) has confirmed this hypothesis. Considerable progress has been made in placing the signs of (H, H) coupling constants on this scale (30, 31), but values for other situations are scarce. Consequently it is difficult to relate the signs of Table II unequivocally to the $^1J_{H^{13}C}$ scale. No measure-

**However, considerable variations in $^1J_{PP}$ have recently been reported (35) for some polyphosphine heterocycles.*

Can. J. Chem. Downloaded from www.nrcresearchpress.com by 210.87.254.5 on 09/05/12
For personal use only.

ments have been reported linking the signs of $^1J_{PP}$, $^1J_{HP}$, $^2J_{HP}$, or $^3J_{HP}$ directly to that of $^1J_{H^{13}C}$. However, it has been shown that the signs of coupling constants across two bonds, ^2J, are more variable than those for coupling across three bonds, ^3J (30). The latter are normally positive, certainly for the (H, H) case. Table II has been arranged as far as is possible so that the upper sign in each case is related to a positive sign for a ^3J in the same molecule. Thus the upper sign is considered the more reasonable, although the argument is not strong, especially when the comparison is to $^3J_{HCPH}$ or $^3J_{HPPH}$. The relation for trivinyl phosphine (VIII), that is all coupling constants positive (5), appears the most certain because the comparison is to the well-known vinyl $^3J_{HC=CH}$ values. The above procedure could not of course be followed for (IX), (XIV), and case (ii) for (XV) because there are no ^3J values for (XIV) and (XV) and the sign of ^3J for (IX) was not reported. However, (IX) and (X) are sufficiently similar that comparison is good in this case.

The assumption that ^3J values are all positive gives a fairly consistent picture, with the exception of the ambiguous (XIV) (2, 9). The values of $^2J_{HCPV}$ are then all negative (four cases) while $^2J_{HCPIII}$ is normally positive (five cases) except for the small negative value reported (6) for (XI). The single case of $^2J_{HPPIII}$ is also positive (2). The three values for $^1J_{HPIII}$ are all positive under these conditions. The results for compound (XIV) are anomalous whatever the absolute signs are, but it should be noted that both $^1J_{HP}$ and $^2J_{HXP}$ for this compound are of a unique type in the table. The most perturbing feature about this analysis is that both values for $^1J_{PP}$ appear to be negative, which is unexpected although this has already been proposed tentatively by Lynden-Bell (2) for XV. There is of course no fundamental reason why coupling between directly bonded nuclei should be positive; indeed it has been shown (32) that $^1J_{F^{13}C}$ is negative with respect to $^1J_{H^{13}C}$, but it is generally felt that fluorine may be unique in this respect. It is, of course, quite possible that the lower signs are correct for some of the compounds of Table II, that is that some ^3J values are negative. It therefore appears unprofitable to base too many conclusions on this table until more of the signs are directly related to that of $^1J_{H^{13}C}$. It should be noted that compound III gives relative signs consistent with the pattern of Table II when the accepted (24, 25) structure is assumed.

Finally it is perhaps instructive to convert the values of J_{PP} to the units proposed by Lynden-Bell and Sheppard (33) by dividing by the square of the magnetogyric ratio for phosphorus ($\gamma_P = 2.2610$). For tetramethyldiphosphine sulphide this yields the value $J_{PP} \approx 43$ coupling units. This compares with the value $J_{CC} = 17.54$ coupling units for ethane (33). The value for (III) is $J_{PP} = 3.7$ coupling units.

REFERENCES

1. R. BURGADA, G. MARTIN, and G. MAVEL. Bull. Soc. Chim. France, 2154 (1963) and earlier papers in this series.
2. R. M. LYNDEN-BELL. Trans. Faraday Soc. **57**, 888 (1961).
3. S. L. MANATT, G. L. JUVINALL, and D. D. ELLEMAN. J. Am. Chem. Soc. **85**, 2664 (1963).
4. G. M. WHITESIDES, J. L. BEAUCHAMP, and J. D. ROBERTS. J. Am. Chem. Soc. **85**, 2665 (1963).
5. W. A. ANDERSON, R. FREEMAN, and C. A. REILLY. J. Chem. Phys. **39**, 1518 (1963).
6. P. T. NARASIMHAN and M. T. ROGERS. J. Chem. Phys. **34**, 1049 (1961).
7. G. MARTIN and G. MAVEL. Proc. XI Colloque Ampère. *Reported in* Magnetic and electric resonance and relaxation. J. Smidt (*Editor*). 1962. p. 577.
8. M. L. NIELSEN and J. V. PUSTINGER, JR. J. Phys. Chem. **68**, 152 (1964). H. AGAHIGIAN, G. D. VICKERS, J. ROSCOE, and J. BISHOP. J. Chem. Phys. **39**, 1621 (1963). N. BODEN, J. W. EMSLEY, J. FEENEY, and L. H. SUTCLIFFE. Chem. Ind. 1909 (1962). M. L. HEFFERNAN and R. F. M. WHITE. J. Chem. Soc. 1382 (1961).
9. C. F. CALLIS, J. R. VAN WAZER, J. N. SHOOLERY, and W. A. ANDERSON. J. Am. Chem. Soc. **79**, 2719 (1957).
10. G. W. PARSHALL. J. Inorg. Nucl. Chem. **14**, 291 (1960).
11. G. W. PARSHALL. J. Inorg. Nucl. Chem. **12**, 372 (1960).
12. N. NIEBERGALL and B. LANGENFELD. Chem. Ber. **95**, 64 (1962).

Can. J. Chem. Downloaded from www.nrcresearchpress.com by 210.87.254.5 on 09/05/12
For personal use only.

13. L. MAIER. Helv. Chim. Acta, **45**, 281 (1962).
14. V. AUGER. Compt. Rend. **142**, 1153 (1906).
15. G. M. KOSOLOPOFF. Organophosphorus compounds. John Wiley and Sons, Inc., New York. 1958.
16. J. I. MUSHER and E. J. COREY. Tetrahedron, **18**, 791 (1962).
17. R. J. ABRAHAM and H. J. BERNSTEIN. Can. J. Chem. **39**, 216 (1961).
18. R. K. HARRIS. Can. J. Chem. **42**, 2275 (1964).
19. N. SHEPPARD and J. J. TURNER. Proc. Roy. Soc. Ser. A, **252**, 506 (1959).
20. K. MOEDRITZER, L. MAIER, and L. C. D. GROENWEGHE. J. Chem. Eng. Data, **7**, 307 (1962).
21. D. F. EVANS and J. P. MAHER. Proc. Chem. Soc. 208 (1961).
22. R. FREEMAN. Mol. Phys. **4**, 385 (1961).
23. J. D. BALDESCHWIELER and E. W. RANDALL. Chem. Rev. **63**, 81 (1963).
24. J. GOUBEAU, H. REINHARDT, and D. BIANCHI. Z. Physik. Chem. **12**, 387 (1957).
25. P. J. CHRISTEN, L. M. VAN DER LINDE, and F. N. HOOGE. Rec. Trav. Chim. **78**, 161 (1959).
26. R. G. HAYTER. Inorg. Chem. **2**, 1031 (1963) and references therein.
27. N. CAMERMAN and J. TROTTER. J. Chem. Soc. In press.
28. M. KARPLUS. J. Am. Chem. Soc. **84**, 2458 (1962).
29. A. D. BUCKINGHAM and K. A. MCLAUCHLAN. Proc. Chem. Soc. 144 (1963).
30. C. N. BANWELL and N. SHEPPARD. Discussions Faraday Soc. **34**, 115 (1962).
31. P. C. LAUTERBUR and R. J. KURLAND. J. Am. Chem. Soc. **84**, 3405 (1962).
32. G. V. D. TIERS. J. Am. Chem. Soc. **84**, 3972 (1962).
33. R. M. LYNDEN-BELL and N. SHEPPARD. Proc. Roy. Soc. Ser. A, **269**, 385 (1962).
34. J. B. HENDRICKSON, M. L. MADDOX, J. J. SIMS, and H. D. KAESZ. Tetrahedron, **20**, 449 (1964).
35. W. MAHLER. J. Am. Chem. Soc. **86**, 2306 (1964).

Can. J. Chem. Downloaded from www.nrcresearchpress.com by 210.87.254.5 on 09/05/12
For personal use only.

Can. J. Chem. Downloaded from www.nrcresearchpress.com by 210.87.254.42 on 09/05/12
For personal use only.

PROTONATION SITE IN ORGANIC BASES FROM INFRARED X—H DEFORMATION MODES[1,2]

DENYS COOK
Exploratory Research Laboratory, Dow Chemical of Canada, Limited, Sarnia, Ontario
Received June 1, 1964

ABSTRACT

The infrared absorption bands due to X—H stretching modes in protonated bases are diagnostically of little value in determining the protonation site. However, the deformation mode, δ_{XH}, shows promise of becoming a useful group frequency whose value is characteristic of the type of atom protonated. The following values, which have been confirmed by deuterium substitution of the sensitive hydrogen atom, are typical:

RNH_3^+	($\delta_{NH_3}^{as}$)	1580 cm^{-1};	($\delta_{NH_3}^{s}$)	1500 cm^{-1};	(ρ_{NH_3})	1155 cm^{-1}.	
$R_2NH_2^+$	(δ_{NH_2})	1585 cm^{-1};	(ω_{NH_2})	1415 cm^{-1}.			
R_3NH^+	(δ_{NH})	1402 cm^{-1}.		$R_2C{=}OH^+$	(δ_{OH})	1257 cm^{-1}.	
R_3NOH^+	(δ_{OH})	1463 cm^{-1}.		$R_2C{=}SH^+$	(δ_{SH})	968 cm^{-1}.	
$\rangle NH^+$	(δ_{NH})	1258 cm^{-1}.		R_2OH^+	(δ_{OH})	1072 cm^{-1}.	

Occasionally splittings occur so that two components of the bending mode are observed. These have been attributed in many cases to correlation field coupling in the solid state.

INTRODUCTION

The infrared spectra of protonated organic bases have one feature in common, a broad, strong band in the range 2000–3500 cm^{-1}, the position of which depends on the hydrogen-bonded distance $X^+—H \ldots Y^-$ and on the nature of the anion Y^- of the protonating acid.

It should be emphasized that, with the possible exception of primary and secondary amines, there is little in the shape or position of the X—H stretching absorption band for a particular acid HY which gives information on the nature of the atom protonated. The band contours will certainly vary slightly, but not in any pattern which can be related to the type of protonation site.

Some feature of the infrared spectrum of a protonated base which would give such information on the protonation site would obviously be valuable. Such information would have many applications including

(1) the determination of donor sites in a polyfunctional molecule where a choice of sites is possible;

(2) the ability to determine sites in stepwise protonation, and therefore to determine what functionality exists at different pH;

(3) the ability to determine whether a protonated function was capable of hydrogen bonding before protonation, and therefore whether protonation would disrupt such hydrogen bonding (of importance in biological systems);

(4) the ability to determine whether a particular site is protonated already (e.g. a zwitterion), and therefore not available for coordination (of importance in chelating systems).

Such a feature seems to be the X—H bending mode in protonated functional groups since it has been found to be quite characteristic of the type of atom protonated. This feature will be described below.

[1]*Contribution No. 105.*
[2]*Presented in part at the XIXth International Congress of Pure and Applied Chemistry, London, England, July 15, 1963.*

Previous literature references quoting substantiated values (i.e. those shown to shift on deuteration) of the deformation modes are extensive for primary amines (1–5), less so for secondary amines (3, 6, 7), and singular for tertiary amines (3). Until recently little information was available about XH deformation modes in other protonated bases.

RESULTS AND DISCUSSION

1. *Carbonyl Compounds*

The in-plane hydrogen-deformation mode, δ_{OH}, in compounds containing a protonated carbonyl group has been observed close to 1265 cm^{-1} (8–11). The slightly different values of δ_{OH} depending on the anion in these and other salts have been averaged. The out-of-plane hydrogen-bending mode, γ_{OH}, is near 750 cm^{-1}, but is much more variable in frequency, and in some compounds is not visible in the rock salt region. Some regularities have been

TABLE I

OH deformation frequencies in protonated carbonyl compounds

Compound	δ_{OH}	$\Delta\delta_{OH}$	δ_{OD}	$\Delta\delta_{OD}$	δ_{OH}/δ_{OD}
4-Pyrone (9)	1274	135	1025	59	1.24
2,6-Dimethyl-4-pyrone (9)	1253	92	971	57	1.29
1,2,6-Trimethyl-4-pyridone (10)	1245	48	959	73	1.30
1-Ethyl-2,6-dimethyl-4-pyridone (10)	1261	69	964	68	1.31
N,N-Dicyclohexylacetamide (10)	1282	0	1086	0	1.18
Antipyrine (11)	1265	94	1020	90	1.24
1,3-Dimethyluracil	1278	0	962	0	1.33
N,N-Dimethylacetamide	1253	147	1003	90	1.25
1-Methyl-2-pyrrolidone	1265	74	972	60	1.30
N-Acetylmorpholine	1243	0	955	0	1.30
N,N-Diacetylpiperazine	1238	0	956	0	1.30
1-Methyl-2-quinolone	1251	0	956	0	1.31
1-Methyl-2-pyridone	1228	0	955	0	1.29
Average	1257		983		

observed in this band and will be discussed elsewhere. Table I shows the experimental results obtained for many carbonyl compounds. They include straight-chain* and cyclic amides, $\alpha\beta,\alpha'\beta'$-unsaturated ketones ($\gamma$-pyrones and γ-pyridones), or other nitrogen heterocycles containing a carbonyl group. The value of δ_{OH} shown is, in many cases, an average value of two components, and the splitting between these two components is shown under the heading $\Delta\delta_{OH}$. This splitting of the deformation mode is attributed to correlation field coupling (12, 13); in one case where the crystallographic data is known, namely 2,6-dimethyl-4-pyrone·HBr (14), the doubling of the in-plane hydrogen-bending mode is quite in accord with the selection rules (9). To prove that the splitting is due to correlation field coupling, the technique of dilute isotopic solid solutions (15, 16) can be used. This requires replacement of the protonating H atom by randomly distributed D atoms. The force field around these D atoms is identical with that around the H atom, but because of the doubled mass, the vibration of the OD group is uncoupled from those of the OH groups. The OD group should, in this condition, have an absorption frequency which is the average of all the correlation field components. When the H_2SnBr_6 salt of 2,6-dimethyl-4-pyrone is exchanged with water containing 5% D_2O, a moderate enhancement of a very weak band at 962 cm^{-1} is observed. This is the uncoupled OD in-plane bending

**The n.m.r. spectra of amide salts first showed conclusively that the oxygen atom was the protonation site. Many details and references to earlier work can be found in the paper by R. J. Gillespie and T. Birchall. Can. J. Chem. 41, 148 (1963).*

Can. J. Chem. Downloaded from www.nrcresearchpress.com by 210.87.254.42 on 09/05/12
For personal use only.

mode, and is quite close to the average of the two coupled vibrations, 992 and 935 cm^{-1}, which were not observed in this spectrum. Similarly the uncoupled OH group deformation mode can be obtained as a weak band at 1251 cm^{-1} (close to the average of 1296 and 1202 cm^{-1}) in the solid derived from exchange with D_2O containing 5% H_2O.

2. Thiocarbonyl Compounds

Table II shows the values determined for the in-plane bending mode in thiocarbonyl compounds. The average value is near 968 cm^{-1}, and splittings are not observed.

TABLE II

SH deformation frequencies in protonated thiocarbonyl compounds

Compound	δ_{SH}	δ_{SD}	δ_{SH}/δ_{SD}
2,6-Dimethyl-4-thiopyrone	978	781	1.25
1,2,6-Trimethyl-4-thiopyridone	978	699	1.39
1-Methyl-4-thiopyridone	957	711	1.35
Thiourea (19)	981		
Thioacetamide (19)	948		
Average	968	730	

Protonation of thiocarbonyl groups has been described infrequently in the literature. Spinner (17) and Janssen (18) have made some assignments in some thioamide salts, but with insufficient detail to establish the absorptions of the SH bending modes. Kutzelnigg and Mecke (19) studied thiourea and thioacetamide salts, noting a band near 970 cm^{-1} as a likely candidate for δ_{SH}, but did not examine isotopically substituted salts. The reasons for preferring protonation of the C=S group in thiocarbonyl compounds are quite as valid for this group of compounds as they were for the carbonyl compounds shown in Table I. Thus the absence of a band near 1420 cm^{-1} in protonated 4-thiopyridones and thioamides rules out N protonation.

The much lower value of δ_{SH} for the protonated thiocarbonyl compounds (as well as the much lower value of ν_{SH}) compared with the OH values for carbonyl compounds has to do with the strength of the SH bond. In mercaptans the SH stretching frequency and bond energy are both lower than the corresponding OH compound.

3. Heterocyclic Nitrogen Compounds

Previously published work (20) has established that the in-plane hydrogen-bending mode in pyridinium salts gives rise to an absorption band near 1240 cm^{-1}. No splitting was observed in the HCl salt (or others), which is in accordance with the selection rules using the details of the crystal structure determined by Rérat (21). Spinner (22) assigned a band near 1250 cm^{-1} in the infrared spectra of the hydrochlorides of several 2-, 3-, and 4-substituted pyridines to the NH in-plane bending mode, though this assignment was not confirmed by deuterium substitution.

In the early stages of this work, 1240–1260 cm^{-1} seemed a reasonable range for δ_{NH}. As more salts were studied, however, it became obvious that this would have to be enlarged to about 1225–1300 cm^{-1}. This naturally raised the question of the correctness of the assignment. Correlation of all the bands having an isotopic shift showed no band to be more suited than the 1225–1300 cm^{-1} band, leading to the conclusion that there may be good reasons why there should be a wider variation in δ_{NH} in these bases than in other salts. This will be amplified in a later section.

Can. J. Chem. Downloaded from www.nrcresearchpress.com by 210.87.254.42 on 09/05/12
For personal use only.

TABLE III

NH deformation frequencies in protonated heterocyclic nitrogen compounds

Compound	δ_{NH}	δ_{ND}	δ_{NH}/δ_{ND}
Pyridine (20)	1242	932	1.33
11 Substituted pyridine HCl salts (22)	1248		
Benzothiazole	1240	991	1.25
N-Methylphthalazone	1261	897	1.40
Pyrazine	1250	916?	
2,6-Dimethylpyrazine	1250	980	1.28
N-Methylimidazole	1298	1082/852	
Caffeine	1295	935	1.38
Quinaldine	1298	950	1.36
2,2′-Bipyridyl	1228		
1,4,6-Trimethyl-2-oxopyrimidine	1231	953	1.30
Average	1258	944	

Other nitrogen heterocycles are listed in Table III. Benzothiazole is very similar to pyridine in that the deformation mode absorbs at 1240 cm^{-1}. N-Methylphthalazone shows two components in the bending mode, at 1300 and 1222 cm^{-1}. The splitting seems due to correlation field effects and dilute isotopic solid solutions studies are projected. In this compound O protonation can be discounted because of the following evidence. There is a rise in frequency of $\sim$ 38 cm^{-1} in the band which is found at 1640 cm^{-1} in the neutral compound and which is obviously associated with the carbonyl group. This seems about the right order of magnitude for the inductive effect of a positive charge on N_2. A positive charge on a nitrogen atom adjacent to a carbonyl group raises its frequency by over 140 cm^{-1} (8).

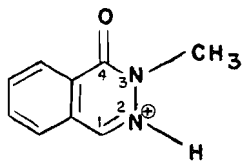

Generally, O protonation would result in the appearance of a new, fairly intense band near 1500 cm^{-1} associated with $\nu_{C=\overset{+}{O}H}$ (11), with little or no isotope shift. In fact, there is only a moderately strong band near 1529 cm^{-1} in the salt, which is not in the neutral base, and which moves to 1325 cm^{-1} on deuteration. This is strongly reminiscent of the behavior of pyridine salts and supports N protonation (20).

4. Tertiary sp^3 Amines

Protonated tertiary sp^3 amines occur widely. Since there is only one NH bond in an approximately tetrahedral arrangement with the other three NC bonds, there is only one non-degenerate NH deformation mode. Its average frequency is near 1402 cm^{-1}. Splitting is exceptional but no X-ray structures have been determined for any of the compounds listed in table IV, so that it is not possible to correlate splitting with structure. The spectra, apart from those of $(CH_3)_3NH^+$ salts, are quite complicated with several bands showing deuteration shifts. It is likely that some coupling of the ND mode with other modes occurs, the low δ_{NH}/δ_{ND} ratio of 1.19 in $(C_2H_5)_3NH^+$ salts being an indication of this.

Can. J. Chem. Downloaded from www.nrcresearchpress.com by 210.87.254.42 on 09/05/12
For personal use only.

TABLE IV

NH deformation frequencies in protonated tertiary sp^3 amines

Compound	δ_{NH}	$\Delta\delta_{NH}$	δ_{ND}	$\Delta\delta_{ND}$	δ_{NH}/δ_{ND}
$(CH_3)_3N$(3, 30)	1420	0		0	
$(C_2H_5)_3N$*	1420	0	1190	0	1.19
N-Methylpiperidine	1398	0		0	
Aminopyrine	1383	0	985	0	1.40
$(C_6H_5)_3N$†	1427	86	1093	140	1.31
Hexamethylenetetramine	1396	0	1085	0	1.29
Triethanolamine	1410	0	1118	0	1.26
1,4-Diazabicyclo[2.2.2]octane	1380	0	1045	0	1.32
Nicotine (mono H^+)	1390	0	975	0	1.42
Average	1402		1062		

*See also ref. 31.
†See also ref. 30.

An example of protonation of a tertiary sp^3 amine when two possible sites are present occurs in the case of nicotine. The spectrum of nicotine monohydrobromide in $CHBr_3$ solution shows clearly a band at 1390 cm^{-1} which is absent, but replaced by one at 975 cm^{-1}, in the monodeuterobromide. There is no evidence of a band near 1240 cm^{-1} which moves in the deuterated salt. This is adequate proof that in nicotine monoprotonated salts the pyrrolidine ring nitrogen atom is more basic than the pyridine ring.

5. Secondary Amines

Apart from the data of Heacock and Marion (6) and Stone *et al.* (7), information on secondary amines is sparse and needs augmenting. The figures shown in Table V seem to be consistent. A deformation (scissors) mode appears at about 1580 cm^{-1}, in roughly the same place as the asymmetric NH deformation in protonated primary amines. The wagging mode causes absorption near 1410 cm^{-1}, which is close to the deformation mode in tertiary (sp^3) amine salts. The rocking mode is not well characterized and may be subject to more perturbations than the scissors or wagging mode.

TABLE V

NH deformation frequencies in protonated secondary amines

Compound	δ_{NH_2}			ω_{NH_2}			ρ_{NH_2}		
$(CH_3)_2NH$(3)	1582	1157	1.37	1421	1035	1.35	878	689	1.27
Piperidine*	1580			1407			917		
21 Secondary amines† (6)	1594								
7 Secondary amines (7)	1585	1198	1.32						
Average	1585	1178		1415	1035		898	689	

*See also ref. 32.
†For some compounds where the presence of two absorptions suggested crystal splittings, the mean value of the two components was taken.

6. Primary Amines

The protonated primary amine group, RNH_3^+, should have an asymmetric and a symmetric deformation mode and a rocking mode. Table VI shows the asymmetric deformation to be near 1600 cm^{-1}. The symmetric deformation is not as well defined but is near 1500 cm^{-1}. Extensive observations of the NH deformation bands of this group in amino acids (2, 5) and in other primary amines (1, 3, 4) have been reported. Smaller cations with higher symmetry such as the methylammonium cation seem to have slightly non-typical values.

Can. J. Chem. Downloaded from www.nrcresearchpress.com by 210.87.254.42 on 09/05/12
For personal use only.

Two components seem to be present for the rocking mode. If there is a plane of symmetry in the molecule, then an in-plane and an out-of-plane rocking mode will be expected. Table VI shows average values for the two components. The $CH_3NH_3^+$ ion again seems to have a divergent value of the rocking modes.

TABLE VI

Deformation and rocking modes in protonated primary amines

Compound	$\delta_{NH_3}^{as}$			$\delta_{NH_3}^{s}$			ρ_{NH_3}		
CH_3NH_2(1, 2)	1580	1190	1.33	1538	1180	1.30	1265	1144*	1.11
$C_6H_5NH_2$†	1557	1212	1.29	1515 1465	1115		1187 1100	932 862	1.27 1.28
NH_2OH(4)	1569	1145	1.37	1473	1128	1.31	1163	857	1.36
18 Amino acids (5)	~1609	~1182	~1.36	~1514	~1118	~1.35	~1189 ~1119	~854 ~790	~1.39 ~1.42
Average	1580	1182		1500	1135		1201 1110		

*But see ref. 5 for different assignment.
†See also ref. 33.

7. Amine Oxides

Table VII shows the compounds for which adequate data are known. Two deformation modes should be observed for the protonated oxygen function, an in-plane and an out-of-plane hydrogen bending. In $(CH_3)_3NO$ salts the in-plane bending mode is split into two components near 1505 and 1425 cm^{-1}. This is quite in accordance (23) with the selection rules derived from the known structure of $(CH_3)_3NO \cdot HCl$ (24). In pyridine-1-oxide salts no splitting is observed, and one absorption near 1450 cm^{-1} on deuteration gives rise to a band at 1108 cm^{-1} having a normal isotopic shift. The analysis of the structure of pyridine-1-oxide hydrochloride (25, 26) seems to be in agreement with this behavior.

TABLE VII

OH deformation frequencies in protonated amine oxides

Compound	δ_{OH}	$\Delta\delta_{OH}$	δ_{OD}	$\Delta\delta_{OD}$	δ_{OH}/δ_{OD}
$(CH_3)_3NO$(23)	1465	80	1090	103	1.34
C_5H_5NO	1450	0	1108	0	1.31
4-Methoxypyridine-1-oxide	1496	0	1083	0	1.38
4-Benzyloxypyridine-1-oxide	1449	0	1056	0	1.37
2,6-Dimethylpyridine-1-oxide	1455	0	1083	0	1.34
Average	1463		1084		

8. Ethers

Protonation of ethers has been postulated in the very early chemical literature. Very few examples of solid salts from ethers and protonating acids have been substantiated. Cineole, a cyclic ether derived from menthol, forms salts with halogen acids (27) but their constitution is unknown. The HBr salt is tractable, though low melting, and as indicated in Table VIII there are two bands in the spectrum near 1140 and 1040 cm^{-1} which move to lower frequency on deuteration. These compare favorably with bands near 1150 and 1060 cm^{-1} in the spectrum of oxonium salts, attributed to the symmetric OH bending vibration (28) in H_3O^+. The cause of the doubling is not explained.

In the Raman and infrared spectra of ether solutions of HCl, Vidale and Taylor (29)

Can. J. Chem. Downloaded from www.nrcresearchpress.com by 210.87.254.42 on 09/05/12
For personal use only.

recorded a band near 1200 cm^{-1} and attributed this to the OH deformation mode of the protonated base. When DCl was used the band was observed near 800 cm^{-1}, the ratio of the two frequencies being close to $\sqrt{2}$.

TABLE VIII

OH deformation frequencies in protonated ethers

Compound	δ_{OH}	δ_{OD}	δ_{OH}/δ_{OD}
Cineole	1140 1038	900 792	1.27 1.31
H_3O^+(28)	1150 1060	785	1.35
Average	1072		

CONCLUSIONS

The average values quoted above for the deformation modes constitute useful group frequencies, helpful in the diagnosis of functional groups in organic molecules. The limits of variation are not wide at present but could possibly increase as more compounds are studied.

That there should be such constant values of δ_{XH} is to be expected. In the case of protonated carbonyl, thiocarbonyl, and N-oxide groups, at least two other atoms supervene between the proton and any other group which by an alteration in mass or electronic function could cause variation in the deformation mode. In amine and ether salts there is only one such supervening atom, but the stereochemical arrangement around it is constant and it is probably little affected by electronic influences. Compounds with heterocyclic (sp^2) nitrogen atoms would be expected to, and actually do, show the largest variation in δ_{XH}. In these compounds electronic influences are very easily transmitted through the π-electrons in the ring, and the effect of these and the size of the ring may have an effect on the σ-electrons in the X—H bond.

This is not to deny that systematic trends may be present within the boundaries of a group frequency. (The carbonyl frequency, a group frequency par excellence, has been the subject of countless efforts to correlate frequency with other parameters.) Not enough data have been collected at present to test this possibility, though Stone *et al.* have described a correlation between δ_{NH_2} and σ^*-values (7) for some secondary amines.

The existence of group frequencies for different X—H bonds must be due both to real variations in k_{XH}, the bending force constant, and non-bonded interactions between the X—H bond and its neighbors. While it is impossible to comment on the force constant aspect, two conclusions seem warranted about non-bonded interactions. Thus tetrahedrally arranged bonds have higher bending frequencies than those with a trigonal planar arrangement; and for the same spatial arrangement, δ_{XH} is lower when X is from a lower row of the periodic table.

Detailed assignments of the spectra of many of the salts described here will be published later.

EXPERIMENTAL

Materials

Organic compounds were purchased from commercial sources or synthesized in this laboratory. All were of high purity. Salts were made by standard methods previously described (8–11, 20, 23). Deuterium replacements were usually made with D_2O, though DBr and DCl were used occasionally to make some salts.

Can. J. Chem. Downloaded from www.nrcresearchpress.com by 210.87.254.42 on 09/05/12
For personal use only.

Spectra

The infrared spectra of emulsions of the finely ground solids in Nujol and Fluorolube were recorded on a Perkin–Elmer model 221 prism-grating spectrometer between 4000 and 650 cm^{-1}. Hygroscopic and deuterated salts were handled in a dry box.

ACKNOWLEDGMENT

The assistance of Mrs. R. H. Veach (C. D. Anderson) in preparing some of the materials and recording their spectra is gratefully acknowledged.

REFERENCES

1. R. D. WALDRON. J. Chem. Phys. **21**, 734 (1953).
2. M. TSUBOI, T. ONISHI, I. NAKAGAWA, and S. MIZUSHIMA. Spectrochim. Acta, **12**, 253 (1958).
3. E. A. V. EBSWORTH and N. SHEPPARD. Spectrochim. Acta, **13**, 261 (1959).
4. D. L. FRASCO and E. L. WAGNER. J. Chem. Phys. **30**, 1124 (1959).
5. M. TSUBOI, T. TAKENISHI, and A. NAKAMURA. Spectrochim. Acta, **19**, 271 (1963).
6. R. A. HEACOCK and L. MARION. Can. J. Chem. **34**, 1782 (1956).
7. P. J. STONE, J. CYMERMAN-CRAIG, and H. W. THOMPSON. J. Chem. Soc. 52 (1958).
8. D. COOK. Can. J. Chem. **40**, 2362 (1962).
9. D. COOK. Can. J. Chem. **41**, 505 (1963).
10. D. COOK. Can. J. Chem. **41**, 2575 (1963).
11. D. COOK. Can. J. Chem. **41**, 2794 (1963).
12. R. S. HALFORD. J. Chem. Phys. **14**, 8 (1946).
13. D. F. HORNIG. J. Chem. Phys. **16**, 1063 (1948).
14. H. HOPE. Acta Chem. Scand. **14**, 765 (1960).
15. H. J. HROWSTOWSKI and G. C. PIMENTEL. J. Chem. Phys. **19**, 661 (1951).
16. G. L. HIEBERT and D. F. HORNIG. J. Chem. Phys. **20**, 918 (1952).
17. E. SPINNER. Spectrochim. Acta, **15**, 95 (1959).
18. M. J. JANSSEN. Spectrochim. Acta, **17**, 475 (1961).
19. W. KUTZELNIGG and R. MECKE. Spectrochim. Acta, **17**, 530 (1961).
20. D. COOK. Can. J. Chem. **39**, 2009 (1961).
21. C. RÉRAT. Acta Cryst. **15**, 427 (1962).
22. E. SPINNER. J. Chem. Soc. 3860 (1963).
23. D. COOK. Can. J. Chem. **41**, 1127 (1963).
24. C. RÉRAT. Acta Cryst. **13**, 63 (1960).
25. Y. NAMBA, T. ODA, H. ITO, and T. WATANABE. Bull. Chem. Soc. Japan, **33**, 11 (1960).
26. G. TSOUCARIS. Acta Cryst. **14**, 914 (1961).
27. O. WALLACH. Ann. **246**, 281 (1888).
28. C. C. FERRISO and D. F. HORNIG. J. Chem. Phys. **23**, 1464 (1955).
29. G. L. VIDALE and R. C. TAYLOR. J. Am. Chem. Soc. **78**, 294 (1956).
30. R. H. NUTTALL, D. W. A. SHARP, and T. C. WADDINGTON. J. Chem. Soc. 4965 (1960).
31. P. SAUVAGEAU and C. SANDORFY. Can. J. Chem. **38**, 1901 (1960).
32. A. CABANA and C. SANDORFY. Can. J. Chem. **40**, 615 (1962).
33. A. CABANA and C. SANDORFY. Can. J. Chem. **40**, 622 (1962).

Can. J. Chem. Downloaded from www.nrcresearchpress.com by 210.87.254.42 on 09/05/12
For personal use only.

Can. J. Chem. Downloaded from www.nrcresearchpress.com by 210.87.254.6 on 09/05/12
For personal use only.

DIFFUSION COEFFICIENTS OF O AND N ATOMS IN INERT GASES*

J. E. MORGAN AND H. I. SCHIFF
Upper Atmosphere Chemistry Group, McGill University, Montreal, Quebec
Received April 23, 1964

ABSTRACT

The diffusion coefficients of atomic oxygen in O_2, N_2, Ar, and He, and of atomic nitrogen in N_2, have been measured as a function of pressure and temperature, using a previously described method.

The rigid sphere collision diameters of atomic oxygen and atomic nitrogen at 280 °K were calculated as 2.65 Å and 2.75 Å respectively. The temperature dependence of the diffusion coefficients of O in O_2 and N in N_2 yielded the following Lennard-Jones parameters:

$$\epsilon/k(O/O_2) = 154° \ (\sigma_O)_{L\text{-}J} = 2.33 \text{ Å},$$

$$\epsilon/k(N/N_2) = 78° \ (\sigma_N)_{L\text{-}J} = 2.94 \text{ Å}.$$

INTRODUCTION

In a previous communication from this laboratory (1), a method was described for determining the diffusion coefficients of atomic species in essentially inert atmospheres.

The basis of the method is to place an extremely efficient atom sink in a rapidly streaming, partially dissociated gas. If all of the atomic species can be removed without affecting the flow of inert carrier gas, a very steep concentration gradient will be produced in the vicinity of the sink. The slope of this concentration gradient will be governed almost entirely by the diffusion coefficient of the atomic species and the linear velocity of the carrier gas.

A simple analysis (1) shows that, in the absence of any localized sink, the concentration of the dilute atomic species as a function of distance, x, measured in the flow direction, is given by the following expression:

$$[1] \qquad C = C_0 \exp (V/2D - R)x,$$

where C_0 = atom concentration at an arbitrary origin ($x = 0$), V = linear velocity of carrier gas, D = binary diffusion coefficient, $R = (V^2 + 4kD)^{\frac{1}{2}}/2D$, k = composite first-order rate constant for homogeneous and heterogeneous recombination. This expression is valid for flow through an infinitely long reaction vessel under conditions of first-order atom removal. Implicit in the expression is the assumption of one-dimensional flow, i.e. negligible radial concentration gradients. Atoms are removed in such a system only by gas phase and wall recombination processes.

If a localized atom sink is now placed at $x = L$ with efficiency great enough to satisfy the condition that $C = 0$ at $x = L$, the expression becomes

$$[2] \qquad C' = \frac{[1 - \exp (-2R(L - x))]}{[1 - \exp (-2RL)]} C_0 \exp (V/2D - R)x,$$

where C' is now the *perturbed* atom concentration at any position $x(\leqslant L)$.

This work was supported in part by the U.S.A.F. Cambridge Research Laboratories and in part by the Defence Research Board of Canada.

Thus, at any given x in the flow stream, when the sink is situated downstream at L, the ratio of the perturbed to the unperturbed concentration will be given by

$$[3] \qquad C'/C = \frac{1 - \exp(-2R(L - x))}{1 - \exp(-2RL)}.$$

Provided the product $2RL$ is not too small (in the present experiments never less than 10), the denominator of [3] can be set equal to unity and the expression written as

$$\ln(1 - C'/C) = -2R(L - x).$$

A plot of $\ln(1 - C'/C)$ against $(L - x)$ should therefore yield a straight line of slope $-2R$.

The evaluation of the diffusion coefficient from R requires a knowledge of both k and the linear velocity V. However, if $V^2 \gg 4kD$, the influence of k will be small and it need not be known with great accuracy. For example, under typical operating conditions (V = 500–1000 cm s^{-1}, $k \simeq 5$ s^{-1}), the effect of neglecting the 'normal' recombination reactions completely ($k = 0$) and writing $D = V/2R$ is to introduce less than 1% error into the calculation of the diffusion coefficient.

This is the biggest single advantage of the method, since the accuracy of the diffusion coefficient measurement is governed almost completely by the accuracy of R and V, both of which can be measured with considerable precision. Also, provided $4D\ \mathrm{d}\ln C/\mathrm{d}x \ll V$, the restriction of overall first-order recombination can be removed, thus extending the applicability of the method.

EXPERIMENTAL

The procedure adopted to measure R has been outlined previously (1).

Essentially, a dilute atom stream is allowed to flow with relatively high velocity through a cylindrical reaction tube. Situated in the tube is a 0.4 mm thick disc of 40 mesh platinum gauze placed perpendicularly to the flow stream and with a diameter of 21 mm, only slightly less than that of the reaction vessel. For systems involving atomic oxygen, the disc was plated with silver which was rapidly converted to silver oxide on exposure to atoms. This disc acted as a very efficient localized atom sink.

It will be noted that R can be measured by two alternate procedures: (*a*) by measuring C' and C at varying x with L constant, and (*b*) by measuring C' and C at constant x as L is varied. In method *a* both C and C' are variable, although the variation of C with x is very much less than that of C' in the region of interest. Method *b* is considerably simpler and is preferable, since C at a given x is constant and only C' varies with L.

For atomic oxygen systems, the relative concentration at a fixed position in the reaction tube was measured by adding a trace of nitric oxide (2) through a fixed upstream inlet and viewing the resulting emission with a collimated 1P21 phototube. The net effect of the nitric oxide is to produce a catalyzed first-order recombination. This does not affect the diffusion coefficient measurement, provided the overall recombination rate satisfies the criterion given above.

With the atom sink sufficiently far downstream, the phototube output is proportional to the unperturbed concentration, C. The relative light intensity was then recorded on a Speedomax recorder as the atom sink was moved upstream in equal increments of 1.67 mm. From these data, C'/C at constant x was obtained as a function of $(L - x)$. Typical plots of the relative atom concentration and of $\ln(1 - C'/C)$ against $(L - x)$ were shown in the previous paper (1).

An approximate value of k was obtained for each experiment by withdrawing the sink and scanning the reaction vessel with the phototube.

For systems involving atomic nitrogen, the associated Lewis–Rayleigh afterglow provided the monitoring reaction. The atom sink in this case was plated with cobalt (3).

The following systems were studied: (1) atomic oxygen in O_2, (2) atomic oxygen in N_2, (3) atomic oxygen in Ar, (4) atomic oxygen in He, and (5) atomic nitrogen in N_2. System 1 was obtained by partially dissociating molecular oxygen, using a microwave generator. A trace of nitric oxide was added below the discharge to provide the monitoring emission. System 2 was obtained by slightly overtitrating discharged nitrogen with nitric oxide (4). The slight excess of nitric oxide again provided the monitoring emission. Systems 3 and 4 were obtained by dissociating a mixture of oxygen and inert gas (2–3% O_2, 97–98% inert gas), while system 5 was simply discharged nitrogen.

Diffusion coefficients of the atomic species in these systems were measured over a range of pressures (0.25–2.5 mm Hg) and temperatures (4–95 °C).

Can. J. Chem. Downloaded from www.nrcresearchpress.com by 210.87.254.6 on 09/05/12
For personal use only.

RESULTS AND DISCUSSION

Some of the diffusion coefficients are shown as a function of pressure at constant temperature (4–7 °C) in Fig. 1. The systems, O/N_2 and N/N_2, have not been reproduced in this figure, since they lie between those of O/Ar and O/O_2. The slopes, D^0, of these curves are shown in Table I.

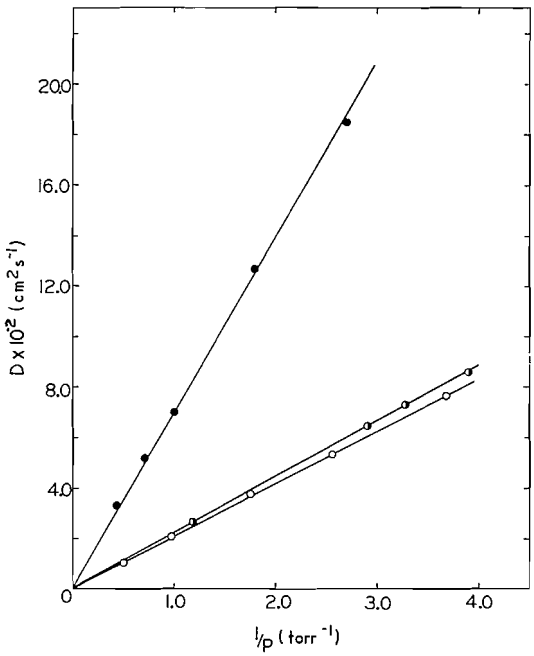

FIG. 1. Atom diffusion coefficients as a function of pressure at 280 °K: (●) O, He; (◑) O, O_2; (○) O, Ar.

TABLE I

Values of the diffusion coefficient, D^0, at 1 torr pressure and temperature 280 °K

System	$D^0 \times 10^{-2}$ (cm² s⁻¹)
O/He	7.0
O/Ar	2.09
O/N_2	2.18
O/O_2	2.22
N/N_2	2.21

It can be assumed that these diffusion coefficients are essentially those involving ground state atoms and molecules. Excited species, although undoubtedly present (5), will be in low concentration and will vary in amount depending upon the pressure conditions and the elapsed time to the point of measurement. Since constant values of $D \times P$ were obtained under a variety of flow conditions, it seems probable that the presence of excited species did not have any significant effect on the measured diffusion coefficients.

There are few published data for atomic diffusion coefficients with which the present results can be compared.

Can. J. Chem. Downloaded from www.nrcresearchpress.com by 210.87.254.6 on 09/05/12
For personal use only.

Can. J. Chem. Downloaded from www.nrcresearchpress.com by 210.87.254.6 on 09/05/12
For personal use only.

Krongelb and Strandberg (6) made two measurements of D_{O,O_2} at 1.0 and 1.5 mm Hg pressure. These were obtained by following the rate of change of atomic oxygen concentration in a closed sidearm when the concentration at the open end was suddenly reduced to zero. This time-dependent concentration is a complex function of both the diffusion coefficient and the recombination rate. The two isolated measurements yielded values of 2.40×10^2 and 2.25×10^2 cm^2 s^{-1} for D^0.

Young (7) measured D_{N,N_2} over a range of pressures by following the rate of decay of atomic nitrogen in a static system. In this method a long, closed sidearm was attached to a spherical reservoir. The time constant for the decay of atoms in the reservoir was measured as a function of the position of a catalyst situated in the sidearm. From these measurements both the diffusion coefficient and the recombination coefficient of the catalyst were obtained. The experimental data showed considerable scatter, yielding an average value of 5.6×10^2 cm^2 s^{-1} for $D_{N,N_2}{}^0$. Young indicates that this value could be reduced by as much as a factor of two if a reactive species is generated at the catalytic surface, but the argument appears unconvincing.

The method employed by Walker (8) makes use of eq. [1], D and k being evaluated by determining the exponent in this equation for two different values of V (V finite and zero respectively). This involves two separate experiments under markedly different flow conditions and any variation in the composite recombination rate constant will be reflected as an error in D. Over the pressure range 1.05–2.17 mm Hg, Walker obtained a value for $D_{O,O_2}{}^0$ at 298 °K of $2.3 \pm 0.1 \times 10^2$ cm^2 s^{-1}, in good agreement with the present work.

Collision Diameters from Diffusion Coefficients

Accurate diffusion coefficient data are useful in calculating collision parameters. If the colliding particles are regarded as incompressible rigid spheres, the binary diffusion coefficient is given by (9)

$$[4] \qquad D_{AB} = \frac{2.63 \times 10^{-3}}{P(\sigma_{AB})_{r.s.}{}^2}\left(\frac{T^3(M_A + M_B)}{2M_AM_B}\right)^{\frac{1}{2}},$$

where $(\sigma_{AB})_{r.s.}$ = rigid sphere collision diameter of particles A and B in Å, P = pressure in atm, and M_A, M_B = molecular weights of A and B.

The rigid sphere collision diameters of atomic oxygen and atomic nitrogen were calculated using this expression and are shown in Table II.

TABLE II

Rigid sphere collision diameters for atomic oxygen and nitrogen

A	B	$(\sigma_{AB})_{r.s.}{}^a$ (Å)	$(\sigma_B)_{r.s.}{}^b$ (Å)	$(\sigma_A)_{r.s.}$ (Å)
O	Ar	3.06_1	3.45	2.67
O	N_2	3.08_4	3.55	2.62
O	O_2	3.03_6	3.40	2.67
O	He	2.34_5	2.04	2.65
N	N_2	3.15_0	3.55	2.75

[a]Calculated from eq. [4] and the experimentally determined diffusion coefficient.
[b]Calculated from the Lennard-Jones parameters [tables IA and IM of ref. 9] using $(\sigma_B)_{r.s.}{}^2 = (\sigma_B)_{L\text{-}J}{}^2\Omega^{(1,1)*}$.

The consistent collision diameter of atomic oxygen in such diverse systems is rather surprising, and this could be regarded as a measure of the validity of the rigid sphere model. However, consistent measurements at a single temperature do not completely

justify this conclusion. The dependence of the collision diameter on temperature provides a more rigorous criterion since the inadequacy of the model will appear as a temperature-dependent collision cross section. The rigid sphere model requires the binary diffusion coefficient to be proportional to $T^{3/2}$. For the systems O/He, O/Ar, and O/N_2, a good linear dependence was found between $D_{AB}{}^0$ and $T^{3/2}$. This is illustrated by the data for $D_{O,He}{}^0$ shown in Fig. 2. For these systems the rigid sphere model appears to be an accurate description.

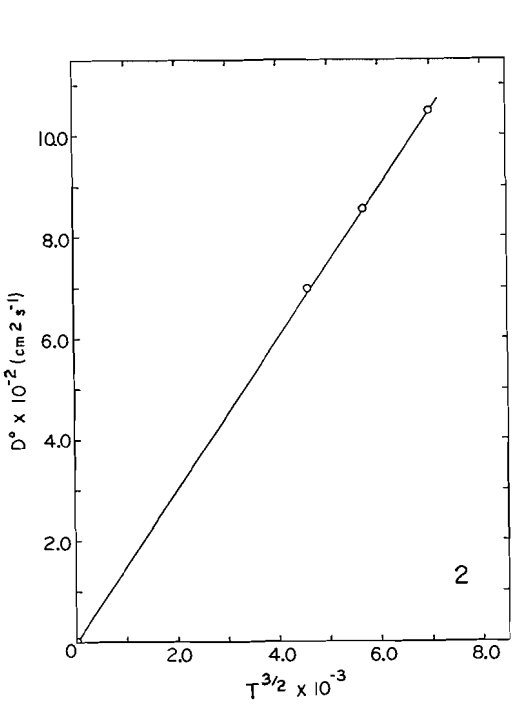

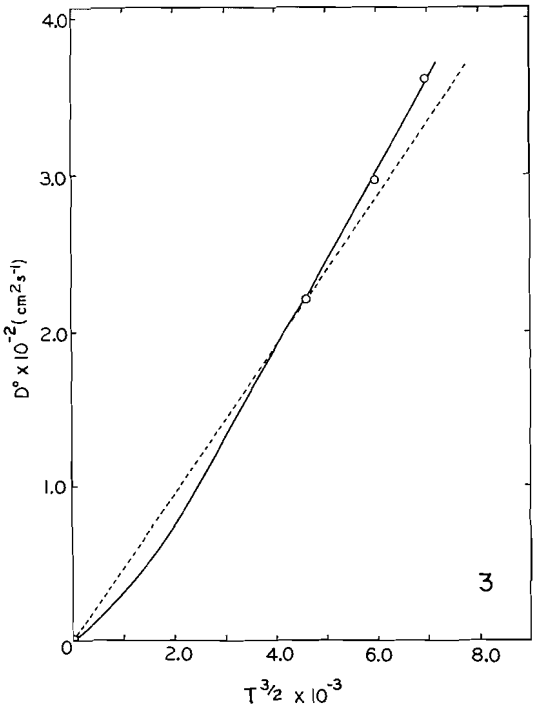

FIG. 2. Diffusion coefficient of atomic oxygen in helium as a function of temperature at 1 torr pressure.
FIG. 3. Diffusion coefficient of atomic oxygen in O_2 as a function of temperature at 1 torr pressure: O experimental results; – – – rigid sphere model; — Lennard-Jones model (ϵ/k = 154°).

However, the diffusion coefficient of O in O_2 showed a definite deviation from linearity and the rigid sphere model is inapplicable.

For more realistic potentials, such as the Lennard-Jones 12.6 potential, the binary diffusion coefficient can be written (9) in the form

$$[5] \qquad D_{AB} = \frac{2.63 \times 10^{-3}}{P(\sigma_{AB})_{L\text{-}J}{}^2\,\Omega^{(1,1)*}}\left(\frac{T^3(M_A + M_B)}{2M_AM_B}\right)^{\frac{1}{2}},$$

where $(\sigma_{AB})_{L\text{-}J}$ = temperature *independent* Lennard-Jones collision diameter and $\Omega^{(1,1)*}$ = temperature *dependent* collision integral.

The collision integral, $\Omega^{(1,1)*}$, can be calculated independently as a function of the reduced temperature T^* ($= kT/\epsilon$) where ϵ is the depth of the Lennard-Jones potential well.

From tabulated values of $\Omega^{(1,1)*}$ as a function of T^*, it should be possible to fit the experimental results by a suitable choice of ϵ. Thus the deviation of the experimentally determined diffusion coefficients from the $T^{3/2}$ dependence can be used to derive the Lennard-Jones parameters, ϵ and $(\sigma_{AB})_{L\text{-}J}$.

Can. J. Chem. Downloaded from www.nrcresearchpress.com by 210.87.254.6 on 09/05/12
For personal use only.

The data for $D_{O,O_2}{}^0$ as a function of temperature are shown in Fig. 3. The best Lennard-Jones fit to the experimental points (full line in Fig. 3) was obtained with $\epsilon/k = 154°$. If $(\sigma_{O_2})_{L\text{-}J}$ is taken equal to 3.43 Å (9), a value of 2.33 Å for $(\sigma_O)_{L\text{-}J}$ is obtained.

It should be pointed out that the shape of the Lennard-Jones plot is not very sensitive to changes in its parameters. For example, values of ϵ/k lying between 110° and 190° all give fits that are within the experimental uncertainty of the results. (The derived value of $(\sigma_O)_{L\text{-}J}$ of course will also change as ϵ/k is varied.)

A similar though slightly less pronounced deviation was obtained for N in N_2. For this system, a best fit was found with $\epsilon/k = 78°$, $(\sigma_{N_2})_{L\text{-}J} = 3.68$ Å (9) and $(\sigma_N)_{L\text{-}J} = 2.94$ Å.

An interesting comparison can be made between our experimental results and the theoretical considerations of Yun *et al.* (10), who have calculated the diffusion coefficients of partially dissociated oxygen and nitrogen as a function of temperature in the range 1000 – 10 000 °K. These authors point out that their calculated diffusion coefficients cannot be reliably extrapolated to room temperature since their force laws do not include the long-range dispersion forces which make an appreciable contribution at low temperature. However, they have calculated these dispersion forces independently and added them to their extrapolated short-range interactions and fitted the resulting potentials to a modified Buckingham (exp −6) potential of the form

$$\phi(r) = \frac{\epsilon}{1 - 6/\alpha}\left[\frac{6}{\alpha}\exp\left(\alpha[1 - r/r_m]\right) - (r_m/r)^6\right]$$

where ϵ, α, and r_m are adjustable constants.

From these parameters the diffusion coefficients at low temperature can be calculated and are shown in Table III.

TABLE III

Calculated diffusion coefficients for various intermolecular potentials

I T (°K)	II[a] $D_{N/N_2}{}^0 \times 10^{-2}$ (cm² s⁻¹)	III[b] $D_{N/N_2}{}^0 \times 10^{-2}$ (cm² s⁻¹)	IV[c] $D_{O/O_2}{}^0 \times 10^{-2}$ (cm² s⁻¹)	V[d] $D_{O/O_2}{}^0 \times 10^{-2}$ (cm² s⁻¹)	VI[e] $D_{O/O_2}{}^0 \times 10^{-2}$ (cm² s⁻¹)
200	1.20	1.19	1.16	1.16	1.24
250	1.79	1.75	1.78	1.77	1.80
300	2.46	2.37	2.50	2.50	2.44
350	3.21	3.09	3.31	3.32	3.19
400	4.03	3.88	4.23	4.23	3.95
500	5.88	5.68	6.28	6.31	5.74
600	7.99	7.78	8.63	8.70	7.80
700	10.33	10.13	11.25	11.36	10.10
800	12.91	12.70	14.12	14.30	12.61
900	15.60	15.56	17.24	17.44	15.37
1 000	18.54	18.64	20.60	20.92	18.33
1 000[f]	17.80	17.80	18.25	18.25	18.25

[a] Calculated using a Lennard-Jones potential $\phi(r) = 4\epsilon[(\sigma/r)^{12} - (\sigma/r)^6]$ with $\sigma = [(\sigma_N)_{L\text{-}J} + (\sigma_N)_{L\text{-}J}]/2 = 3.31$ Å and $\epsilon/k = 78°$.
[b] Calculated using exp −6 potential with $\alpha = 13$, $\epsilon/k = 12.3°$, and $r_m = 4.74$ Å (Yun *et al.* (10)).
[c] Calculated using a Lennard-Jones potential with $\epsilon/k = 154°$ and $\sigma = [(\sigma_O)_{L\text{-}J} + (\sigma_{O_2})_{L\text{-}J}]/2 = 2.88$ Å.
[d] Calculated using exp −6 potential with $\alpha = 15$, $\epsilon/k = 167°$, and $r_m = 3.19$ Å.
[e] Calculated using exp −6 potential with $\alpha = 15$, $\epsilon/k = 16.0$ °K, and $r_m = 4.20$ Å (Yun *et al.* (10)).
[f] Low-temperature limit of the high-temperature calculations of Yun *et al.* (10).

Columns II and IV in this table were calculated using the Lennard–Jones potentials which gave the best fit to the experimental results in the 280–365 °K range.

For the N–N_2 system (column II) this calculation grafts onto the high temperature calculated results quite satisfactorily. The exp −6 calculation, using Yun's parameters,

Can. J. Chem. Downloaded from www.nrcresearchpress.com by 210.87.254.6 on 09/05/12
For personal use only.

differs from the experimental results by only 3.5%, an agreement which is well within the combined uncertainty of the calculated and experimental values (column III).

The Lennard-Jones calculation for $D_{O,O_2}{}^0$ (column IV) does not match the high-temperature calculations as satisfactorily, being high by about 15% at 1000 °K. A fit of the experimental results with an exp -6 potential (column V) yields a similar discrepancy. It will be noted that both plots require values for ϵ/k which are much greater than predicted by Yun *et al.* The exp -6 calculation, using Yun's parameters, accurately predicts the experimental value at 280 °K, but the predicted rate of increase of D_{O,O_2} is less than that observed experimentally (column VI). This deviation (or alternatively the large value of ϵ/k) found for $D_{O,O_2}{}^0$ may possibly reflect the additional valence interaction between O and O_2. Further experimental work to extend the temperature range would be valuable in clarifying this point.

REFERENCES

1. J. E. MORGAN and H. I. SCHIFF. J. Chem. Phys. **38**, 2631 (1963).
2. F. KAUFMAN. Proc. Roy. Soc. Ser. A, **247**, 123 (1958).
3. J. E. MORGAN. Ph.D. Thesis, McGill University, Montreal, Que. 1962.
4. P. HARTECK, R. R. REEVES, and G. MANELLA. J. Chem. Phys. **29**, 608 (1958).
   J. E. MORGAN, L. ELIAS, and H. I. SCHIFF. J. Chem. Phys. **33**, 930 (1960).
5. F. KAUFMAN and J. R. KELSO. J. Chem. Phys. **28**, 510 (1958).
   J. T. HERRON and H. I. SCHIFF. J. Chem. Phys. **36**, 1159 (1958).
   S. N. FONER and R. L. HUDSON. J. Chem. Phys. **37**, 1662 (1962).
6. S. KRONGELB and M. W. P. STRANDBERG. J. Chem. Phys. **31**, 1196 (1959).
7. R. A. YOUNG. J. Chem. Phys. **34**, 1295 (1961).
8. R. E. WALKER, J. Chem. Phys. **34**, 2196 (1961).
9. J. O. HIRSCHFELDER, C. F. CURTISS, and R. B. BIRD. Molecular theory of gases and liquids. John Wiley and Sons, New York, N.Y. 1954.
10. K. S. YUN, S. WEISSMAN, and E. A. MASON. Phys. Fluids, **5**, 672 (1962).

Can. J. Chem. Downloaded from www.nrcresearchpress.com by 210.87.254.6 on 09/05/12
For personal use only.

Can. J. Chem. Downloaded from www.nrcresearchpress.com by 210.87.254.105 on 09/05/12
For personal use only.

THE SYNTHESIS OF β-GALACTO- AND β-GLUCO-PYRANOSYL DISACCHARIDES BY SPOROBOLOMYCES SINGULARIS[1]

P. A. J. GORIN, J. F. T. SPENCER, AND H. J. PHAFF[2]
National Research Council of Canada, Prairie Regional Laboratory, Saskatoon, Saskatchewan
Received June 1, 1964

ABSTRACT

Synthesis of β-D-galactopyranosyl disaccharides takes place in growing cultures of *Sporobolomyces singularis* containing lactose and a sugar acceptor. The products of galactosyl transfer using various acceptors arise mainly from substitution of secondary rather than primary hydroxyl groups. The minimal structural requirement for reaction with the acceptor appears to be a hydroxyl vicinal to the substituted hydroxyl group. A mechanism that accounts for the formation of secondary disaccharides is postulated.

The organism also contains a β-glucosidase which transfers *O*-β-D-glucopyranosyl groups from cellobiose to sugar acceptors. The positions of the glycosidic linkages in the disaccharide products are identical with those formed in the corresponding galactosyl transfer reaction.

INTRODUCTION

Sporobolomyces singularis, when grown on a medium containing lactose at an initial pH of 3.7, utilizes the glucose portion of the disaccharide as an energy source and transfers the galactose moiety to unused lactose to form a trisaccharide. This sugar has been characterized as *O*-β-D-galactopyranosyl-(1 → 4)-*O*-β-D-galactopyranosyl-(1 → 4)-D-glucose. By an additional galactosyl transfer reaction, part of the trisaccharide was converted to a tetrasaccharide containing three β-1,4 linkages (1). The yeast shows a high selectivity in carbohydrate utilization studies, and of 28 compounds examined it only utilized glucose, mannose, fructose, D-mannitol, D-sorbitol, cellobiose, and lactose (2). This small number of sugars utilized suggested that growth of the yeast on a medium containing lactose and an additional sugar would promote the transfer of galactose to the additive to give a β-galactosyl disaccharide.

A number of β-galactopyranosyl disaccharides of hexoses and pentoses were prepared by using this organism (Table I). Some experiments gave more than one disaccharide, but the major component could generally be isolated by crystallization after chromatography. The fractionation was necessary since the disaccharide(s) was generally contaminated with unused acceptor and trisaccharide formed by transfer of galactose to the synthesized disaccharide. For example, with L-arabinose as acceptor, trisaccharide was formed which contained an *O*-β-D-galactopyranosyl-(1 → 4)-*O*-β-D-galactopyranosyl unit attached to the 3-position of L-arabinose. Very little galactosyl lactose was obtained since L-arabinose competed successfully with lactose as an acceptor. The β-galactosidase responsible for the reaction was associated with the cells since culture filtrates had no detectable activity. In addition to this enzyme, a β-glucosidase was present, since β-glucopyranosyl disaccharides could be synthesized by growing *Sporobolomyces singularis* in a mixture of cellobiose and a carbohydrate acceptor.

Disaccharides synthesized by the growing organism were mostly formed by substitution of a secondary rather than a primary hydroxyl in the acceptor molecule. Most acceptors

[1]*Issued as N.R.C. No. 8098. Presented at the 47th Canadian Chemical Conference of the Chemical Institute of Canada, Kingston, Ontario, June, 1964.*
[2]*Department of Food Science and Technology, University of California, Davis, California.*

TABLE I

Products and yields of β-hexosyl transfer reactions

Acceptor	Glycosidic linkage in product	Disaccharide yield in β-galactopyranosyl series (based on acceptor), %	Disaccharide yield in β-glucopyranosyl series, %
1. L-Arabinose	3	25	21
	5	11	7
2. D-Arabinose	—	5	—
3. D-Xylose	2	9	4
	3	18	13[c]
4. D-Ribose	3 and 5	11	10
5. D-Galactose	3[a]	17	—
	4	2	—
6. D-Allose	4 (trace of 3)	55	—
7. 6-Deoxy-D-glucose	3	32	—
8. 6-Deoxy-D-galactose	3	38	52
9. 6-Deoxy-L-galactose	—	0	—
10. L-Rhamnose	2 and 3	18	—
11. *N*-Acetyl-D-glucosamine	4[b]	2	—
12. 1,2-*O*-Isopropylidene-D-glucofuranose	5	35	—
13. Methyl-α-D-glucopyranoside	4 (and 2?)	31	—
14. Benzyl-α-D-glucopyranoside	2	10	—
15. Methyl-3-deoxy-α-methyl-D-glucopyranoside	—	0	—
16. Methyl-α-D-galactopyranoside	4	43	—
17. Methyl-β-L-arabopyranoside	4	47	—
18. Methyl-α-D-mannopyranoside	?	5	—
19. D-Arabitol	4	5	—
20. Erythritol	2 (in D form)	19	—
21. Glucose	3[d]	14	—
	6[d]	8	—

[a]Synthesized by Pazur using yeast lactase enzyme from *o*-nitrophenyl-D-galactopyranoside and galactose (7).
[b]Synthesized by action of enzyme from *Lactobacillus bifidus* var. Penn on lactose and *N*-acetyl-D-glucosamine (20).
[c]Synthesized from cellobiose and D-xylose using cell free extracts of *Aspergillus niger* (21).
[d]Synthesized by disproportionation of lactose using an enzyme from *Saccharomyces fragilis* (22).

were substituted in only one position, thus rendering the method superior to conventional chemical synthetic methods which generally give secondary disaccharides in much lower yields.

Control of the substitution position could be achieved by modification of the acceptor molecule. For example, in the glucose series 2-, 4-, or 5-substituted β-galactopyranosyl glucose derivatives can be synthesized using benzyl-α-D-glucopyranoside, methyl-α-D-glucopyranoside, and 1,2-*O*-isopropylidene-D-glucofuranose, respectively, as starting materials. The enzyme system obtained by disintegration of cells of *Sporobolomyces singularis* could be used to obtain a mixture of 3-*O*- and 6-*O*-β-D-galactopyranosyl-D-glucose from lactose, the former (63%) being obtainable by crystallization. This system, unlike the growing organism, did not assimilate glucose.

Enzyme extracted from cells converted lactose and an acceptor to the same disaccharides as growing cells in the four instances examined. However, contamination with 3-*O*- and 6-*O*-β-D-galactopyranosyl-D-glucose always took place. These similarities in disaccharide structures suggest that sugar transport across the cell membrane is not a factor in determining the structures of the transglycosylation products.

Experiments with the cell extract showed that transglycosylation took place readily at pH values of 4.0 to 8.2 but was most rapid at pH 6.5.

Can. J. Chem. Downloaded from www.nrcresearchpress.com by 210.87.254.105 on 09/05/12
For personal use only.

Mechanism of Sugar Transfer

Wallenfels and co-workers (3) have studied extensively the β-galactosidases of *E. coli* and calf intestine, and have interpreted galactosyl transfer reactions in terms of active sites in the enzymes. The reaction is depicted in Fig. 1, substantially by the route visualized

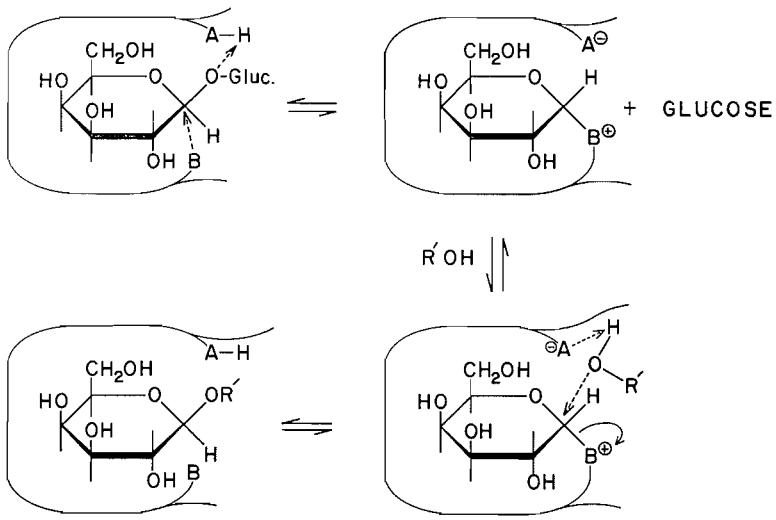

FIG. 1. Mechanism of β-galactosyl transfer.

by Wallenfels. After induction (4) of the β-galactosidase by the lactose molecule simultaneous protonation of the glycosidic oxygen by —A—H and nucleophilic attack by —B at C-1 takes place. The intermediate α-galactose–enzyme complex formed can react with a new alcohol to give a new β-galactoside. The intermediate complex in this reaction differs from that postulated by Wallenfels and Malhotra, who prefer a β-configuration (3). However, Koshland (5) has concluded that in an enzymic reaction in which a β-configuration is retained, the sugar–enzyme intermediate has an α-configuration. The latter theory appears to be more plausible on the basis of energy requirements in chemical replacement reactions at anomeric sugar centers.

A mechanistic description of disaccharide synthesis in the *Sporobolomyces singularis* system must answer two main questions. (*a*) Why are disaccharides formed in preference to galactose, which would arise by decomposition of the intermediate enzyme complex by the excess water present? (*b*) Why does the intermediate enzyme complex react with secondary rather than the more chemically active primary hydroxyl group of an acceptor?

Before these questions can be considered it is necessary to show that the relative rates of hydrolysis of the various products of β-galactosyl transfer are small. Hydrolysis rates have been shown to be important in the work of Wallenfels and Beck (6), who reported the transfer of *O*-α-L-arabopyranosyl residues from *o*-nitrophenyl-α-L-arabopyranoside to glucose using *E. coli* β-galactosidase. Over long periods of time this reaction gave mainly 6-*O*- and 4-*O*-α-L-arabopyranosyl-D-glucose. Although the 3-isomer was formed initially it eventually disappeared since it was hydrolyzed relatively rapidly. However, in growing cultures of *Sporobolomyces singularis* in two instances relatively little hydrolysis of disaccharides took place during disaccharide synthesis. For example, during the formation

Can. J. Chem. Downloaded from www.nrcresearchpress.com by 210.87.254.105 on 09/05/12
For personal use only.

of 3-*O*-β-D-galactopyranosyl-D-galactose from lactose and galactose only 1% of 6-*O*-β-D-galactopyranosyl-D-galactose (introduced in trace amounts labelled with ^{14}C in the reducing end unit) was hydrolyzed to galactose. Similarly, only 16% of 5-*O*-β-D-galactopyranosyl-L-arabinose-^{14}C was hydrolyzed in a culture containing lactose and arabinose, a reaction that gives mainly 3-*O*-β-D-galactopyranosyl-L-arabinose with smaller amounts of the 5-isomer. This figure compares with 20% hydrolysis noted when 3-*O*-β-D-galactopyranosyl-L-arabinose-^{14}C was introduced into a similar system.

Examination of the products of β-hexosyl transfer reactions listed in Table I shows that the substituted secondary hydroxyl group invariably has nearby hydroxyl groups. *N*-Acetyl-D-glucosamine and 1,2-*O*-isopropylidene-D-glucofuranose could be substituted on the 4- and 5-position respectively, whereas methyl-3-deoxy-α-D-glucopyranose did not function as an acceptor molecule. It appears that two vicinal hydroxyl groups are necessary for β-galactosyl transfer to take place. As an example the 6-position of 1,2-*O*-isopropylidene-D-glucofuranose should be bound to the galactose–enzyme complex prior to reaction of the 5-hydroxyl. This reaction is depicted in Fig. 2, in which the enzyme is represented as a

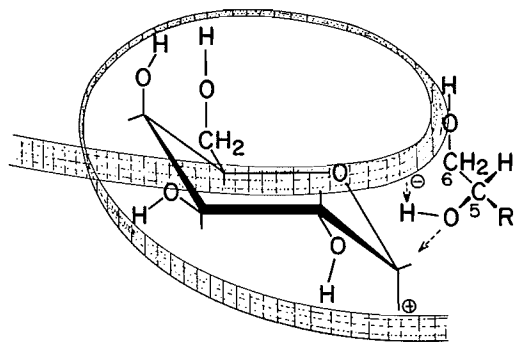

FIG. 2. Intermediate in transfer of galactose to 1,2-*O*-isopropylidene-D-glucofuranose.

spiral to which the sugar hydroxyl groups are bound, presumably by hydrogen bonds. This process would successfully explain the relative lack of reactivity of the monofunctional water hydroxyl group or the isolated primary hydroxyl group of a sugar.

In the acceptor molecule the presence of hydroxyl groups other than that vicinal to the reacting hydroxyl group may have a role in the reaction, since they also could be bound to the enzyme. This longer range effect is evident from the β-galactosyl transfer experiments carried out with L-arabinose, D-galactose, and their derived methyl pyranosides. Whereas the reducing sugars were substituted on the 3-position the glycosides gave 4-substituted disaccharides. It would be interesting to characterize the product from a similar experiment with methyl-α-D-galactopyranoside in the presence of *o*-nitrophenyl-D-galactopyranoside and the yeast lactase enzyme of Pazur (7) since the enzyme system from various yeasts may be similar. This author showed that when D-galactose was used as an acceptor substitution took place on the 3- or 6-position, and concluded that three vicinal secondary hydroxyl groups were necessary for substitution of the middle hydroxyl group.

Characterization of Transglycosylation Products

β-Galactopyranosyl and β-glucopyranosyl disaccharides with pentose reducing ends were characterized by following their lead tetraacetate oxidation kinetics (8) and by paper

Can. J. Chem. Downloaded from www.nrcresearchpress.com by 210.87.254.105 on 09/05/12
For personal use only.

chromatographic examination of the sodium borohydride reduction product of the oxidized sugars. These could be characterized by their R_F values on paper chromatograms depending on whether they were 2-*O*-β-hexopyranosyl pentitols, tetritols, or glycerol, derived from 2-, 3-, or 4-linked β-hexopyranosyl pentoses respectively. The products could in turn be distinguished from 1-*O*-β-hexopyranosyl glycerols, which would be formed from a 5-linked disaccharide.

The β-galactopyranosyl disaccharide fraction formed from L-arabinose contained a mixture of 3- and 5-links, the former predominating. Similarly linked disaccharides were obtained from D-ribose. The yields of the D-arabinose and D-ribose disaccharides were poor, but from L-arabinose 3-*O*-β-D-gluco- and 3-*O*-β-D-galactopyranosyl-L-arabinose could be readily prepared in crystalline form in good yield (21% and 25% respectively). The reaction of lactose with L-arabinose also gave a trisaccharide. This was shown to have a 3-linked reducing end by its lead tetraacetate oxidation characteristics. The oxidation product was reduced with sodium borohydride to give a galactobiosyl erythritol. This consumed 4 moles of sodium periodate with concomitant production of 1 mole of acid. The periodate oxidation product, when reduced with sodium borohydride and hydrolyzed, gave glycerol and erythritol thus characterizing the product as *O*-β-D-galactopyranosyl-(1 → 4)-*O*-β-D-galactopyranosyl-(1 → 2)-L-erythritol. The trisaccharide was, therefore, formed by transfer of D-galactose to the 4-position of the galactose portion of 3-*O*-β-D-galactopyranosyl-L-arabinose. By a similar procedure the characterization of a trisaccharide fraction from cellobiose and L-arabinose was attempted. This was unsuccessful since it appeared to contain two or more components.

Starting with D-xylose, 2-*O*- and 3-*O*-β-D-galactopyranosyl-D-xylose were prepared giving 9% and 18% yields respectively. The latter material crystallized, and the 2-linked disaccharide was isolated from the mother liquor after modification of the 3-linked disaccharide with lead tetraacetate. The 2- and 3-linked β-glucopyranosyl analogs could be synthesized from cellobiose and D-xylose.

O-β-D-Galactopyranosyl hexoses were characterized by techniques identical with those used for the pentose disaccharides. When grown on a mixture of lactose and galactose *Sporobolomyces singularis* provided a mixture, which was chromatographed to yield crystalline 3-*O*-β-D-galactopyranosyl-D-galactose and a lesser amount of the 4-linked disaccharide. Formation of the 3-linked disaccharide indicates that the corresponding 3-linked L-arabinose disaccharide arose from the pyranose and not the furanose form. D-Allose provided mainly crystalline 4-*O*-β-D-galactopyranosyl-D-allose and a smaller proportion of the 3-isomer.

It was shown that 6-deoxy-D-glucose and D-fucose (6-deoxy-D-galactose) were good acceptors in the hexosyl transfer reaction and were substituted in their 3-positions. On the other hand L-fucose could not participate as an acceptor in the reaction. This parallels the reactivity of arabinose, which reacted in the L-form, but not the D-form. Another methyl pentose, L-rhamnose, was substituted in the 2- and 3-positions.

2-Acetamido-2-deoxy-4-*O*-(β-galactopyranosyl)-D-glucose (*N*-acetyllactosamine) was synthesized from lactose and *N*-acetyl-D-glucosamine, giving a poor yield since glucosamine was utilized by the yeast. The disaccharide was identified by comparison with an authentic specimen. The 3-isomer was not obtained on seeding the mother liquor.

The product from lactose and 1,2-*O*-isopropylidene-D-glucose was shown to be substituted in the 5-position. Hydrolysis of the isopropylidene group yielded 5-*O*-β-D-galactopyranosyl-D-glucose, which was converted to 2-*O*-β-D-galactopyranosyl-L-erythritol by lead tetraacetate oxidation followed by sodium borohydride reduction. The product was identified

Can. J. Chem. Downloaded from www.nrcresearchpress.com by 210.87.254.105 on 09/05/12
For personal use only.

by its characteristics towards sodium periodate and by being distinguishable from 2-*O*-β-D-galactopyranosyl-D-erythritol (9).

Characterization of the products formed by transfer from lactose to methyl-α- and benzyl-α-D-glucopyranose and methyl-α-D-galactopyranoside was carried out by measurement of their sodium periodate uptakes. To distinguish between 2- and 4- linked disaccharide glycosides their oxidation products were reduced with sodium borohydride. Hydrolysis to erythritol and glycerol showed that the methyl-α-D-gluco- and galactopyranoside disaccharides were 4-linked. Since only glycerol was obtained from *O*-β-D-galactopyranosyl-(benzyl-α-D-glucopyranoside) it contained a 2-linkage. This method was not applicable in identification of the product from methyl-β-L-arabopyranoside. Instead it was methylated and the product then hydrolyzed. The mixture of methyl sugars was shown to be inert to lead tetraacetate, which indicated the presence of a 2-substituted dimethyl arabinose. The disaccharide consumed 3 moles of sodium periodate with formation of 1 mole of acid, and was therefore 4-*O*-β-D-galactopyranosyl-(methyl-β-L-arabopyranoside).

The β-galactosyl transfer reaction was highly specific when erythritol and D-arabitol were used as acceptors. The products were 2-*O*-β-D-galactopyranosyl-D-erythritol and 4-*O*-β-D-galactopyranosyl-D-arabitol respectively.

EXPERIMENTAL

Production of Oligosaccharides

The organism was grown on a medium containing 5% lactose (or cellobiose), 2.5% sugar acceptor, and 0.75% Difco yeast extract. Growth took place in 250 ml Erlenmeyer flasks containing 25 ml medium at 20 °C incubated on a New Brunswick shaker (240 r.p.m., 1 inch eccentricity). Other runs on varying scales were carried out in 125 ml Erlenmeyer flasks (12.5 ml medium) and 500 ml flasks (50 ml medium). Inoculation was directly from slants (yeast–nitrogen base agar containing 3% lactose). The mixture of lactose and yeast extract was adjusted to pH 3.7 and autoclaved. The acceptor solution was then sterilized by passage through a filter, pore size 0.45 μ, and added just before inoculation. The progress of the hexosyl transfer was followed by means of paper chromatography using ethyl acetate–acetic acid–water (9:2:2 v/v) as solvent and *p*-anisidine hydrochloride (10) as spray reagent in experiments in which the products were reducing di- or tri-saccharides. For nonreducing products *n*-butanol–ethanol–water (40:11:19 v/v) (solvent A) and the ammoniacal silver nitrate spray (11) were used. The lactose and cellobiose reactions were generally complete after 8 and 6 days respectively.

Isolation of Oligosaccharides

The products from the hexosyl transfer reactions were isolated using cellulose chromatography. The following abbreviations for column eluants are used in the text. Solvent B: acetone–water (10:1 v/v); solvent C: acetone–water (7:1 v/v); solvent D: acetone–water (5:1 v/v); solvent E: benzene–ethanol–water (500:50:1 v/v); solvent F: *n*-butanol, saturated with water; solvent G: *n*-butanol, one-half saturated with water.

Oligosaccharide Synthesis from Lactose and Acceptors Using the Intact Organism

(i) L-Arabinose Acceptor

The product from 25 ml of medium, when chromatographed on cellulose using solvent B, yielded L-arabinose (322 mg). Solvent C eluted the disaccharide fraction (752 mg) and solvent D the trisaccharide fraction (324 mg).

The disaccharide portion consumed 1.30, 1.33, and 1.34 moles of lead tetraacetate after 2, 5, and 15 min respectively. After addition of oxalic acid to remove excess oxidant, the oxidized sugar was reduced with sodium borohydride as described in the previous paper on galactosyl transfer reactions (1). The product was examined by paper chromatography in solvent A using the ammoniacal silver nitrate spray. It was shown to contain an *O*-β-galactopyranosyl erythritol and an *O*-β-galactopyranosyl glycerol. Since the consumption of lead tetraacetate oxidation did not increase appreciably with time, 1,4-linked disaccharides were absent (8). The data indicated that 3-*O*-β-D-galactopyranosyl-L-arabinose (70%) and the 5-linked disaccharide (30%) were present in the mixture.

The 3-linked disaccharide crystallized from 3 ml of methanol. The amorphous 5-isomer (12) remained in the mother liquor and had $[\alpha]_D$ +85° (*c*, 1.0, H_2O). A further recrystallization from methanol yielded 3-*O*-β-D-

Can. J. Chem. Downloaded from www.nrcresearchpress.com by 210.87.254.105 on 09/05/12
For personal use only.

galactopyranosyl-L-arabinose with m.p. 177–178 °C and $[\alpha]_D$ +30° → +45° (*c*, 1.0, H_2O). Aspinall, Auret, and Hirst (13) reported m.p. 202–203 °C and $[\alpha]_D$ +80° → +62° for the β-anomer.

Calcd. for $C_{11}H_{20}O_{10}$: C, 42.3; H, 6.5. Found: C, 42.1; H, 6.5.

When this experiment was repeated using 150 ml of medium, 1.42 g of the 3-linked and 1.35 g of the 5-linked disaccharides were isolated.

A portion (300 mg) of the trisaccharide fraction (1.20 g) was oxidized with 1 mole of lead tetraacetate and the oxidized sugar reduced with sodium borohydride. The product consisted of two materials and the major component (139 mg) ran on a paper chromatogram at the same speed as lactose in solvent D. The minor component (60 mg) had a slightly higher mobility. The former product was recrystallized twice from methanol to give material with m.p. 137–138 °C and $[\alpha]_D$ +4° (*c*, 1.0, H_2O). Acid hydrolysis yielded galactose and erythritol.

Calcd. for $C_{16}H_{30}O_{14}\cdot CH_3OH$: C, 42.7; H, 7.2. Found: C, 42.4; H, 7.05.

The material consumed 3.8 and 4.0 moles of sodium periodate after 6 and 25 h, yielding 0.9 and 1.0 moles of acid respectively. The resulting oxidation product was reduced with sodium borohydride and then hydrolyzed with acid. The presence of glycerol and erythritol in the hydrolysate and the lead tetraacetate and periodate data characterized the material as *O*-β-D-galactopyranosyl-(1 → 4)-*O*-β-D-galactopyranosyl-(1 → 2)-L-erythritol.

(ii) D-*Arabinose*

Procedures and amounts of reactants were identical with those used in section (*i*). The yield of β-galactopyranosyl-D-arabinose disaccharides was only 5% and characterization was not carried out.

(iii) D-*Xylose*

Identical isolation procedures as in the L-arabinose experiment were used. From 25 ml of medium xylose (219 mg), two disaccharide fractions, one (168 mg) being chromatographically pure and the other a mixture (181 mg), and a trisaccharide fraction (324 mg) were obtained. The chromatographically pure fraction consumed 0.90, 0.94, and 0.98 moles of lead tetraacetate after 2, 5, and 15 min respectively and was therefore 3-linked. It was recrystallized twice from methanol to give 3-*O*-β-D-galactopyranosyl-D-xylose with m.p. 196–200 °C and $[\alpha]_D$ +27° → +10° (*c*, 1.0, H_2O).

Calcd. for $C_{11}H_{20}O_{10}$: C, 42.3; H, 6.5. Found: C, 42.4; H, 6.7.

The mixed disaccharide fraction consumed 0.37, 0.40, and 0.46 moles of lead tetraacetate after 2, 5, and 15 min respectively. Oxidation of a portion (120 mg) with 0.40 moles of lead tetraacetate yielded a mixture which was fractionated on cellulose using solvent C. The resulting 2-*O*-β-D-galactopyranosyl-D-xylose was recrystallized twice from methanol to give material with m.p. 159–160 °C and $[\alpha]_D$ +25° (constant, *c*, 1.4, H_2O).

Calcd. for $C_{11}H_{20}O_{10}\cdot CH_3OH$: C, 41.9; H, 7.0. Found: C, 41.6; H, 6.9.

The results indicated that the β-galactosyl transfer product consisted of 66% of 3-*O*-β-D-galactopyranosyl-D-xylose and 34% of the 2-linked disaccharide.

(iv) D-*Ribose*

The mixture from 25 ml of medium yielded 420 mg of ribose and 138 mg of a disaccharide fraction after cellulose chromatography using solvent C. The latter consumed 0.85, 0.90, 0.95, and 1.02 moles of lead tetraacetate after 2, 5, 10, and 20 min respectively. The lead tetraacetate oxidation product, when reduced with sodium borohydride, was converted to galactopyranosyl erythritol and a smaller proportion of galactopyranosyl glycerol. The product therefore consisted of 3-*O*-β-galactopyranosyl-D-ribose and a smaller quantity of the 5-isomer.

(v) D-*Galactose*

The mixture obtained from 200 ml of medium was fractionated on cellulose using solvent C. The first disaccharide fraction (250 mg), which ran at a slightly faster rate than the main component on paper chromatograms, was twice recrystallized from methanol to give 4-*O*-β-D-galactopyranosyl-D-galactose (130 mg) with m.p. 195–198 °C and $[\alpha]_D$ + 85° → +67° (*c*, 1.0, H_2O). The disaccharide gave an X-ray diffraction pattern identical with an authentic specimen (14).

Calcd. for $C_{12}H_{22}O_{11}$: C, 42.1; H, 6.4. Found: C, 41.7; H, 6.45.

The second disaccharide fraction (1.57 g) was eluted and of this 1.32 g was recrystallized twice from methanol to yield 3-*O*-β-D-galactopyranosyl-D-galactose (7) (0.70 g) with m.p. 204–206 °C and $[\alpha]_D$ +56° (constant, *c*, 1.3, H_2O).

Calcd. for $C_{12}H_{22}O_{11}$: C, 42.1; H, 6.4. Found: C, 41.9; H, 6.5.

The remainder of the disaccharide fraction (0.25 g) was oxidized with lead tetraacetate and the product reduced with sodium periodate. Examination of the product on a paper chromatogram showed predominantly galactopyranosyl pentitol and two recrystallizations from methanol–ethanol yielded 4-*O*-β-D-galactopyranosyl-D-arabitol with m.p. 180–182 °C. It gave an X-ray diffraction pattern identical with an authentic specimen (15).

Calcd. for $C_{11}H_{22}O_{10}$: C, 42.0; H, 7.1. Found: C, 42.0; H, 7.0.

(vi) D-*Allose*

The product from 25 ml of medium was fractionated on a cellulose column using solvent C. The disaccharide fraction (0.53 g) consumed 1.40, 1.55, and 1.71 moles of lead tetraacetate after 2, 5, and 15 min respec-

Can. J. Chem. Downloaded from www.nrcresearchpress.com by 210.87.254.105 on 09/05/12
For personal use only.

tively. The oxidation product was reduced with sodium borohydride and examination of the reduction product on a paper chromatogram showed that a galactopyranosyl pentitol was the main product together with a smaller proportion of galactopyranosyl-erythritol. Two recrystallizations of the disaccharide fraction from methanol yielded 4-*O*-β-D-galactopyranosyl-D-allose with m.p. 112–113 °C and $[\alpha]_D$ +29° (constant, *c*, 1.0, H_2O). It consumed 1.09, 1.52, and 1.92 moles of lead tetraacetate after 2, 5, and 15 min respectively.

Calcd. for $C_{12}H_{22}O_{11}$: C, 42.1; H, 6.4. Found: C, 41.75; H, 6.8.

(vii) 6-Deoxy-D-glucose

Fractionation of the product, obtained from 25 ml of medium, on cellulose column using solvent C yielded a disaccharide fraction (0.40 g). Two recrystallizations from ethanol–methanol yielded 3-*O*-β-D-galactopyranosyl-6-deoxy-D-glucose (0.26 g), having m.p. 246–248 °C and $[\alpha]_D$ +25° (constant, *c*, 1.0, H_2O). It consumed 0.77, 0.97, and 1.05 moles of lead tetraacetate after 2, 5, and 15 min respectively.

Calcd. for $C_{12}H_{22}O_{10}$: C, 44.2; H, 6.8. Found: C, 44.0; H, 6.8.

(viii) D-Fucose

Cellulose column chromatography of the product from 25 ml of medium yielded, on elution with solvent B, D-fucose. A disaccharide fraction (0.38 g) was obtained using solvent C. One crystallization from methanol gave crystals (0.28 g) which on recrystallization from methanol had m.p. 245–246 °C and $[\alpha]_D$ +78° (constant, *c*, 1.0, H_2O).

Calcd. for $C_{12}H_{22}O_{10}$: C, 44.2; H, 6.8. Found: C, 44.25; H, 6.9.

The disaccharide was 3-linked since it consumed 1.00, 1.09, and 1.12 moles of lead tetraacetate after 2, 5, and 15 min respectively. The product obtained directly from the column consumed 0.91, 1.12, and 1.19 moles of oxidant after identical times and therefore consisted mainly of the 3-linked disaccharide.

(ix) L-Fucose

Only minute traces of disaccharide could be detected when the yeast was grown on a L-fucose–lactose mixture, using procedures and amounts identical with those described in section (*viii*).

(x) L-Rhamnose

Fractionation of the product from 25 ml of medium on a cellulose column gave rhamnose (518 mg) using solvent B. Solvent C eluted a disaccharide (227 mg), which appeared to contain 55% of 3-links and 45% of 2-links since 0.52, 0.57, and 0.68 moles of lead tetraacetate were consumed after 2, 5, and 15 min respectively.

(xi) N-Acetyl-D-glucosamine

From 75 ml of medium 220 mg of a disaccharide fraction was obtained by cellulose chromatography using solvent C. Crystallization from methanol gave 4-*O*-β-D-galactopyranosyl-*N*-acetyl-D-glucosamine (72 mg) with m.p. 176–178 °C. Its identity was established by comparison of its X-ray diffraction pattern with that of an authentic specimen (16).

(xii) 1,2-O-Isopropylidene-D-glucofuranose

The product from 25 ml of medium, by chromatography on cellulose using solvent E, yielded unchanged monoacetone glucose. Elution with solvent F gave a sirupy isopropylidene disaccharide (372 mg) which had $[\alpha]_D$ +15° (*c*, 1.2, MeOH). Partial hydrolysis on heating at 100 °C for 1 h in 0.01 *N* sulphuric acid gave the free disaccharide.The solution was then neutralized ($BaCO_3$), filtered, and evaporated. Oxidation of the product with 2.2 moles of lead tetraacetate followed by reduction with sodium borohydride gave a mixture of products. Chromatography on cellulose using solvent C yielded mainly a galactosyl erythritol with a smaller amount of a galactosyl glycerol. The erythritol derivative was recrystallized twice from ethanol and had m.p. 168–169 °C and $[\alpha]_D$ −6° (*c*, 1.0, H_2O).

Calcd. for $C_{10}H_{20}O_9$: C, 42.25; H, 7.1. Found: C, 42.15; H, 7.1.

It was characterized as 2-*O*-β-D-galactopyranosyl-L-erythritol, derived from 5-*O*-β-D-galactopyranosyl-D-glucose, since it consumed 3.0 moles of sodium periodate with production of 1.0 mole of acid after 25 h. The X-ray diffraction pattern differed from that of 2-*O*-β-D-galactopyranosyl-D-erythritol (9).

(xiii) Methyl-α-D-glucopyranoside

The product from 25 ml of medium was fractionated on a cellulose column using solvent G and unchanged glycoside (0.25 g) was eluted. The disaccharide glycoside (0.45 g) was obtained using solvent F. Crystallization from methanol–ethanol gave 0.36 g of crystals and a further crystallization from the same solvent yielded material which melted partly at 183 °C and partly at 220–230 °C and had $[\alpha]_D$ +102° (*c*, 1.0, H_2O). The product, which appeared to be a mixture, consumed 3.0 moles of sodium periodate with concomitant formation of 1.0 mole of acid after 6 to 25 h. The oxidized glycoside was reduced with sodium borohydride and the product hydrolyzed with acid. Formation of glycerol and erythritol indicated that the glycoside mixture contained 4-*O*-β-D-galactopyranosyl-methyl-α-D-glucopyranoside.

(xiv) Benzyl-α-D-glucopyranoside

Little galactosyl transfer took place on growth of the yeast in 16 ml of medium. Cellulose chromatography using solvent E eluted unchanged glycoside and solvent G provided the disaccharide glycoside (153 mg). Crystallization from ethyl acetate gave a product (68 mg) and a further crystallization from the same solvent yielded 2-*O*-β-D-galactopyranosyl-benzyl-α-D-glucopyranoside with m.p. 185–189 °C and $[\alpha]_D$ +78° (*c*, 0.9, H_2O).

Can. J. Chem. Downloaded from www.nrcresearchpress.com by 210.87.254.105 on 09/05/12
For personal use only.

Calcd. for $C_{19}H_{28}O_{11}$: C, 52.8; H, 6.5. Found: C, 52.9; H, 6.3.

It was characterized by sodium periodate oxidation which resulted in the consumption of 2.8 and 2.8 moles of oxidant with formation of 0.8 and 0.9 moles of acid after 6 and 25 h respectively. The oxidation product, on treatment with sodium borohydride followed by hydrolysis, gave glycerol, thus showing a 2-linkage.

(xv) Methyl-α-D-galactopyranoside

Using a procedure similar to that in the methyl-α-D-glucopyranoside experiment a methyl galactobioside (452 mg) was obtained. Recrystallization from methanol–ethanol gave crystals (0.36 g), which were recrystallized from the same solvent. The product had m.p. 207–208 °C and $[\alpha]_D$ +102° (*c*, 1.0, H_2O). Examination using the techniques described in section (*xiv*) characterized the product as 4-*O*-β-D-galactopyranosyl-methyl-α-D-galactopyranoside.

Calcd. for $C_{13}H_{24}O_{11}$: C, 43.8; H, 6.8. Found: C, 44.0; H, 6.7.

(xvi) Methyl-β-L-arabopyranoside

Chromatography of the contents of 25 ml of medium on cellulose using solvent F provided methyl-β-L-arabopyranoside (0.24 g) and a disaccharide glycoside (0.56 g). Recrystallization of the latter from ethanol gave material (0.37 g) which was recrystallized from the same solvent. The product had m.p. 216–218 °C and $[\alpha]_D$ +163° (*c*, 1.1, H_2O). The glycoside consumed 3.2 and 3.1 moles of sodium periodate releasing 1.0 and 1.1 moles of acid after 6 and 25 h respectively.

Calcd. for $C_{12}H_{22}O_{10}$: C, 44.2; H, 6.8. Found: C, 44.3; H, 6.7.

To ascertain whether the linkage was at the 2- or 4-position the glycoside was methylated by the aqueous sodium hydroxide–methyl sulphate method. Extraction of the neutralized solution with chloroform yielded a partially methylated material which was fully methylated by the silver oxide–methyl iodide method. The product was hydrolyzed in *N* hydrochloric acid at 100 °C for 18 h. Neutralization (Ag_2CO_3) and evaporation provided a sirup which contained 2,3,4,6-tetra-*O*-methyl-D-galactose and a di-*O*-methyl-L-arabinose. Paper chromatograms showed that the dimethyl sugar was not oxidized by lead tetraacetate indicating that it was substituted in the 2-position. These experiments characterized the glycoside as 4-*O*-β-D-galactopyranosyl-methyl-β-L-arabopyranoside.

(xvii) Methyl-α-D-mannopyranoside

Only 60 mg of disaccharide glycoside was obtained from 25 ml of medium using the same procedure as for methyl-α-D-glucopyranoside. Most of the mixture consisted of unchanged glycoside. The disaccharide glycoside was recrystallized twice from ethanol–methanol to give material (30 mg) with m.p. 168–170 °C and $[\alpha]_D$ +51° (*c*, 0.7, H_2O).

Calcd. for $C_{13}H_{24}O_{11}$: C, 43.8; H, 6.8. Found: C, 43.8; H, 6.9.

(xviii) D-Arabitol and D-Erythritol

The products from these polyols were fractionated on cellulose using solvent F.

From 50 ml of D-arabitol medium, galactosyl arabitol (125 mg) was obtained. Two recrystallizations from methanol gave 4-*O*-β-D-galactopyranosyl-D-arabitol with m.p. 178–181 °C. It gave an X-ray diffraction pattern identical with that of an authentic specimen (15).

Calcd. for $C_{11}H_{22}O_{10}$: C, 42.0; H, 7.1. Found: C, 42.0; H, 7.1.

Galactosyl erythritol (276 mg) was isolated from 25 ml of medium and was recrystallized twice from methanol–ethanol. It had m.p. 182–184 °C and gave an X-ray diffraction pattern corresponding to that of 2-*O*-β-D-galactopyranosyl-D-erythritol (9).

Calcd. for $C_{10}H_{20}O_9$: C, 42.25; H, 7.1. Found: C, 42.1; H, 6.9.

(xix) Methyl-3-deoxy-α-D-glucopyranoside

Cellulose fractionation of the mixture from 25 ml of medium using benzene–ethanol–water (200:50:1 v/v) eluted unchanged glycoside. No disaccharide glycoside was obtained on elution with solvent G.

Oligosaccharide Synthesis from Cellobiose and Acceptors Using the Intact Organism

The isolation procedures, column eluants, and characterization methods are similar to those using the corresponding acceptor in the lactose series.

(i) L-Arabinose Acceptor

The product from 150 ml medium contained disaccharides (2.16 g), trisaccharides (0.35 g), and a mixed fraction (0.50 g). The disaccharide contained 26% of 5-*O*-β-D-glucopyranosyl-L-arabinose and 74% of the 3-isomer. Fractional crystallization from methanol–ethanol gave the 3-linked disaccharide (0.81 g) and a further recrystallization provided material with m.p. 199–201 °C and $[\alpha]_D$ +70° (constant, *c*, 1.0, H_2O).

Calcd. for $C_{11}H_{20}O_{10}$: C, 42.3; H, 6.5. Found: C, 42.0; H, 6.6.

(ii) D-Xylose

The product (25 ml) provided di- (167 mg) and tri-saccharides (276 mg). The disaccharide fraction contained 76% 1,3- and 24% 1,2-links. From the mixture only 2-*O*-β-D-glucopyranosyl-D-xylose was obtained in crystalline form subsequent to oxidation of the 3-linked disaccharide with lead tetraacetate. It had m.p. 202–206 °C and $[\alpha]_D$ +7° (constant, *c*, 1.0, H_2O). Jones and Reid (17) report m.p. 200–202 °C and $[\alpha]_D$ 0° or this disaccharide.

Calcd. for $C_{11}H_{20}O_{10}$: C, 42.3; H, 6.5. Found: C, 42.6; H, 6.4.

Can. J. Chem. Downloaded from www.nrcresearchpress.com by 210.87.254.105 on 09/05/12
For personal use only.

(iii) D-*Ribose*

Only a small amount (136 mg) was obtainable from 25 ml of medium. The product appeared to contain mainly 1,3-links and a smaller proportion of 1,5-links.

(iv) D-*Fucose*

This substrate was efficiently converted to the disaccharide (0.65 g). It contained mainly 1,3-links since one recrystallization from methanol provided 3-*O*-β-D-glucopyranosyl-D-fucose (0.52 g). Recrystallization provided material with m.p. 250–252 °C and $[\alpha]_D$ +45° (constant, *c*, 1.0, H_2O).

Calcd. for $C_{12}H_{22}O_{10}$: C, 44.2; H, 6.8. Found: C, 44.0; H, 6.7.

Reaction Reversibility Studies Using ^{14}C*-Labelled Disaccharides*

(i) Lactose to L-*Arabinose Transfer Reaction*

3-*O*- and 5-*O*-β-D-galactopyranosyl-L-arabinose labelled with ^{14}C in the pentose portion were prepared by transglycosidation.

Two systems, each containing one of the labelled disaccharides (50 mg), L-arabinose (625 mg), lactose (1.25 g), and 0.75% Difco yeast extract in water (25 ml) were inoculated with *Sporobolomyces singularis*, which was allowed to grow for 8 days. The resulting L-arabinose was isolated by cellulose column chromatography using solvent F and its specific activity measured. During the course of the reaction 20% of the 3-*O*-β-D-galactopyranosyl-L-arabinose and 16% of the 5-isomer were hydrolyzed to arabinose.

(ii) Lactose to D-*Galactose Transfer Reaction*

A fermentation was carried out on a mixture containing 6-*O*-β-D-galactopyranosyl-D-galactose-^{14}C (18) (labelled in the reducing end-unit) (31.5 mg), lactose (625 mg), and D-galactose (312 mg). After 8 days D-galactose was isolated and its specific activity measured. The result indicated that only 1% of the radioactive disaccharide was hydrolyzed during the β-galactosyl transfer reaction.

Preparation of Cell Extracts

Sporobolomyces singularis (60–79) was grown in a medium containing 7.5% lactose and 0.75% Difco yeast extract. In a 500 ml Erlenmeyer flask 50 ml of medium was inoculated from a slant and incubated at 24 °C on a Gump rotary shaker (230 r.p.m., eccentricity 1 inch). The cells (15–20 g) from 10 flasks (500 ml of culture) were recovered by centrifugation and washed twice with cold water. The cells were disrupted in a modified Hughes press (19). The paste from the press was divided into four parts, mixed with buffers of the desired pH values, allowed to thaw, and centrifuged at high speed to remove cells and debris. The supernatant liquid, about 25 ml per portion, was returned and the pH determined and adjusted if necessary. The sugars, 0.25 g of L-arabinose and 0.5 g of lactose or cellobiose, were dissolved directly in about 12 ml of enzyme extract. The reaction was followed by chromatography on Whatman No. 1 paper, using as solvent ethyl acetate – acetic acid – water (8:2:2 v/v). The resulting glycosyl arabinoses were detected with the *p*-anisidine hydrochloride spray.

Effect of pH on β-Hexosyl Transfer Reactions

β-Hexosyl transfer took place readily at pH values 4.0, 6.5, and 8.2, the most rapid reaction occurring at about pH 6.5. The rate of reaction was greatly reduced at pH 2.5. The rate of glucose transfer to L-arabinose to give disaccharides, as shown on paper chromatograms, was appreciably greater than that of galactose transfer to the same acceptor.

(i) Oligosaccharides from Lactose Using Cell Extract

The product formed after 18 h incubation of lactose (1.50 g) with cell extract (25 ml) at pH 4.0 for 24 h was fractionated on a cellulose column using solvent C. Initially glucose (0.53 g) was eluted followed by a disaccharide fraction (172 mg) moving slightly faster than lactose on a paper chromatogram in the ethyl acetate – acetic acid – water (9:2:2 v/v) solvent. Two crystallizations from methanol gave 3-*O*-β-D-galactopyranosyl-D-glucose (54 mg) with m.p. 167–169 °C and $[\alpha]_D$ +37° (*c*, 0.8, H_2O).

Calcd. for $C_{12}H_{22}O_{11}$: C, 42.1; H, 6.5. Found: C, 40.8; H, 6.4.

It consumed 0.72, 0.98, and 1.05 moles of lead tetraacetate after 2, 5, and 15 min respectively. The product from the mother liquor consumed 1.34, 1.54, and 1.88 moles of oxidant after identical intervals. Reduction of the latter oxidized product with sodium borohydride gave products corresponding mainly to 4-*O*-β-D-galactopyranosyl-D-erythritol and 4-*O*-β-D-galactopyranosyl-D-arabitol on paper chromatograms. A trace of 6-*O*-β-D-galactopyranosyl-D-glucitol was also detected. These data indicated that 63% of 3-links, 37% of 6-links, and a trace of 2-links were present in the disaccharide fraction.

The next fractions consisted of the above disaccharides and lactose (227 mg) and lactose (251 mg). Two trisaccharides were eluted with solvent D, the first (0.12 g) was unidentified and the second (0.25 g) was characterized as *O*-β-D-galactopyranosyl-(1 → 4)-*O*-β-D-galactopyranosyl-(1 → 4)-D-glucose. After two recrystallizations from aqueous methanol it had a melting point and a mixed melting point of 225–228 °C.

(ii) Oligosaccharides from Lactose and Acceptors Using Cell Extract

The disaccharide fractions obtained on disproportionation of lactose (1.50 g) for 18 h in the presence of L-arabinose and D-galactose (0.75 g) and cell enzyme extract (25 ml) were isolated. Examination of the products was carried out by techniques described previously in the section on transglycosylation using intact cells. Other than 3-*O*- and 6-*O*-β-D-galactopyranosyl-D-glucose the disaccharide linkages formed by the cell

Can. J. Chem. Downloaded from www.nrcresearchpress.com by 210.87.254.105 on 09/05/12
For personal use only.

extract and intact cells were identical. The products were 3-*O*- and 5-*O*-β-D-galactopyranosyl-L-arabinose from L-arabinose and 4-*O*- (trace) and 3-*O*-β-D-galactopyranosyl-D-galactose from galactose.

(iii) Oligosaccharides from Cellobiose and L-*Arabinose Using Cell Extract*

The products obtained from cellobiose (1.50 g), L-arabinose (0.75 g), and enzyme extract (25 ml) were 3-*O*- and 5-*O*-β-D-glucopyranosyl-L-arabinose, as indicated by the lead tetraacetate oxidation characteristics and products obtained by sodium borohydride reduction of the oxidized material.

ACKNOWLEDGMENTS

The authors thank Mr. N. R. Gardner for technical asistance, and Mr. M. Mazurek for carrying out carbon and hydrogen microanalyses.

REFERENCES

1. P. A. J. GORIN, J. F. T. SPENCER, and H. J. PHAFF. Can. J. Chem. **42**, 1341 (1964).
2. H. J. PHAFF and L. DO CARMO-SOUSA. Antonie van Leeuwenhoek J. Microbiol. Serol. **28**, 193 (1962).
3. K. WALLENFELS and O. M. MALHOTRA. Advan. Carbohydrate Chem. **16**, 239 (1961).
4. D. E. KOSHLAND. *In* The enzymes. Vol. 1. 2nd ed. *Edited by* P. D. Boyer, H. Lardy, and K. Myrback. Academic Press, Inc., New York. 1959. p. 305.
5. D. E. KOSHLAND, JR. *In* The mechanism of enzyme action. *Edited by* W. D. McElroy and B. Glass. Johns Hopkins Press, Baltimore, Md. 1954. p. 608.
6. K. WALLENFELS and D. BECK. Ann. **630**, 46 (1960).
7. J. H. PAZUR, M. SHADAKSHARASWAMY, and A. CEPURE. Arch. Biochem. Biophys. **94**, 142 (1961).
8. A. J. CHARLSON and A. S. PERLIN. Can. J. Chem. **34**, 1200 (1956).
9. A. J. CHARLSON, P. A. J. GORIN, and A. S. PERLIN. Can. J. Chem. **34**, 1811 (1956).
10. L. HOUGH, J. K. N. JONES, and W. H. WADMAN. J. Chem. Soc. 1702 (1950).
11. S. M. PARTRIDGE. Nature, **158**, 270 (1946).
12. H. C. SRIVASTAVA and F. SMITH. J. Am. Chem. Soc. **79**, 982 (1957).
13. G. O. ASPINALL, B. J. AURET, and E. L. HIRST. J. Chem. Soc. 4408 (1958).
14. J. K. GILLHAM, A. S. PERLIN, and T. E. TIMELL. Can. J. Chem. **36**, 1741 (1958).
15. A. J. CHARLSON, P. A. J. GORIN, and A. S. PERLIN. Can. J. Chem. **35**, 365 (1957).
16. F. ZILLIKEN, P. N. SMITH, R. M. TOMARELLI, and P. GYORGY. Arch. Biochem. Biophys. **54**, 398 (1955).
17. J. K. N. JONES and R. E. REID. Can. J. Chem. **38**, 944 (1960).
18. K. FREUDENBERG, A. WOLF, E. KNOPF, and S. H. ZAHEER. Ber. **61**, 1743 (1928).
19. R. D. SAGERS. Appl. Microbiol. **10**, 37 (1962).
20. F. ZILLIKEN, P. N. SMITH, C. S. ROSE, and P. GYORGY. J. Biol. Chem. **208**, 299 (1954).
21. S. A. BARKER, E. J. BOURNE, G. C. HEWITT, and M. STACEY. J. Chem. Soc. 3541 (1957).
22. J. H. PAZUR, C. L. TIPTON, T. BUDOVICH, and J. M. MARSH. J. Am. Chem. Soc. **80**, 119 (1958).

Can. J. Chem. Downloaded from www.nrcresearchpress.com by 210.87.254.105 on 09/05/12
For personal use only.

Can. J. Chem. Downloaded from www.nrcresearchpress.com by 210.87.254.42 on 09/05/12
For personal use only.

AN APPLICATION OF SOME ELECTRON DENSITY, ELECTRIC DIPOLE, AND MAGNETIC DIPOLE MODELS TO THE GAS PHASE PROTON SHIFTS OF SOME SUBSTITUTED ETHYLENES

T. SCHAEFER AND T. YONEMOTO[1]
Department of Chemistry, University of Manitoba, Winnipeg, Manitoba
Received April 29, 1964

ABSTRACT

Measurements in the gas phase of the proton shifts relative to ethylene of methyl vinyl ether, of vinyl chloride, and of the three dichloroethylenes are reported. It is suggested that available molecular orbital calculations somewhat overestimate delocalization in the chloroethylenes. If this is so, then a model involving electrostatic fields arising from excess π-electron densities and from electric dipoles originating from the substituents, as well as magnetic fields from a point dipole representing the anisotropy of the substituents, predicts shifts in reasonable agreement with experiment for β-protons. The agreement for α-protons is not as good. The gas phase measurements are compared to measurements in the inert solvents, tetramethylsilane or cyclohexane.

INTRODUCTION

Considerable data exists supporting a linear correlation of proton magnetic resonance shifts with π-electron densities on neighboring carbon atoms in aromatic systems (1–8). In the empirical relation $\Delta\sigma_\pi = k\Delta q$, where Δq is the deviation from 1 of the π-electron density on the carbon atom and $\Delta\sigma_\pi$ is the corrected shift relative to benzene of the bonded proton, it appears that k has a value near 10 p.p.m./electron (5), although estimated values have a range from about 9–13 p.p.m./electron (9). It is known that simple molecular orbital calculations overemphasize the charge differences at various points in a molecule (5) and the measured shifts do suggest a more uniform distribution of π-electrons. Corrections to the experimental shifts have to be applied for the magnetic anisotropy of the substituents including ring current effects, ion association, and solvent effects (5), and for electric fields arising from bond dipoles due to substituents (6).

In an attempt to extend such a correlation to some simple aliphatic systems like substituted ethylenes, it became apparent that some of the available molecular orbital calculations are perhaps not reliable in their estimation of π-densities. We report some measurements here in support of this suggestion. We chose methyl vinyl ether, vinyl chloride, and the three dichloroethylenes. These could be measured in the gaseous phase without great difficulty, thus eliminating all sizeable corrections except those of magnetic anisotropy and electric dipole effects of the substituent. Also, these compounds were some of the few for which molecular orbital calculations were available. The reference substance in these cases is ethylene.

THE MODEL

We assume that replacement of a hydrogen atom in ethylene by oxygen or chlorine will affect the shielding of the remaining protons in three ways: (1) electrostatic fields from a delocalization of π-electrons into the double bond of ethylene polarize the C—H bonds and lead to changes in shielding; (2) electrostatic fields arising from the polar sigma bonds between carbon and oxygen or chlorine also polarize the C—H bonds; (3) the

[1]*N.R.C. Postdoctoral Fellow, 1963–64.*

C—O and C—Cl bonds introduce additional bond magnetic anisotropy leading to para- or dia-magnetic fields at the protons (10). Details of how these three effects were estimated are now described.

1. Effect of the π-Electrons

The π-electron densities of methyl vinyl ether were taken from the results of an improved LCAO–MO calculation by Julg and Bonnet (11). This calculation introduced a mutual deformation of the sigma orbitals between carbon and oxygen and gave excellent agreement with the experimental value of the first N → V transition. The π-densities for the chloroethylenes were derived from the calculations of Goldstein (12) and of Howe and Muirhead (13). These were simple MO approximations including overlap and the results were given in terms of a π-electron density matrix. To reduce these to the Coulson definition (14) we traced their calculations using Coulomb exchange and overlap integral values which they adopted as most adequate. Molecular orbitals and π-densities were then calculated in the usual way. Values of Δq are given in Table I.

TABLE I

Calculated values of charge densities, electric field shifts, and geometric factors for the magnetic anisotropy shifts in substituted ethylenes

Compound		Δq^a	u^b	$\Delta\sigma_E(1)^c$	$\Delta\sigma_E(2)^d$	$f_1(r,\theta)^e$	$f_2(r,\theta)^f$
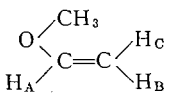	A	−0.11		−0.51	−0.73	0.075	0.046
	B	0.15	1.33	−0.12	−0.17	0.024	0.010
	C	0.15		−0.20	−0.28	−0.021	0.002
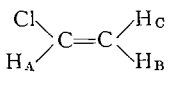	A	−0.03		−0.53	−0.75	0.067	0.043
	B	0.08	1.79	−0.13	−0.19	0.022	0.012
	C	0.08		−0.19	−0.28	−0.009	0.006
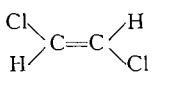		0.04	1.79	−0.66	−0.94	0.058	0.049
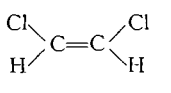		0.04	1.79	−0.72	−1.02	0.089	0.055
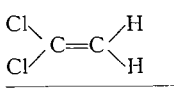		0.15	1.79	−0.32	−0.45	0.013	0.018

[a]Excess π-electron densities obtained as discussed in text.
[b]Group moment in Debyes obtained from ref. 17.
[c]Shift in p.p.m. using $a = -2.0 \times 10^{-12}$ and $b = 10^{-18}$ in eq. [1].
[d]Shift in p.p.m. using $a = -3.0 \times 10^{-12}$ and $b = 7.4 \times 10^{-19}$ in eq. [1].
[e]Geometrical factor of eq. [2] with the point dipole placed at the midpoints of the C—O and C—Cl bonds.
[f]As in footnote *e* with the point dipole placed at the oxygen or chlorine atoms.

We then use the relation $\Delta\sigma_\pi = k\Delta q$, with $k = 10$ p.p.m./electron to estimate values of $\Delta\sigma_\pi$. A more sophisticated treatment would take into account the polarization of the C—H bonds by excess charge densities on the other atoms (8), as well as including a term in the square of the field arising from the excess charges (8, 9). Buckingham's equation (15),

$$\Delta\sigma = aE_z - bE^2, \qquad [1]$$

where E_z is the electric field along the C—H bond direction and E is the field at the proton in question, can be rewritten in terms of Δq and interatomic distances, as has

Can. J. Chem. Downloaded from www.nrcresearchpress.com by 210.87.254.42 on 09/05/12
For personal use only.

been done by Schweizer *et al.* (8). However, in view of the uncertainties in Δq and of the range in accepted values of a and b in eq. [1], we retain the relation $\Delta\sigma_\pi = k\Delta q$.

2. Effect of the Electric Dipole from the C—O or C—Cl Bonds

The effect of the intramolecular electric field from the C—O or C—Cl dipoles was estimated using a point dipole model and eq. [1]. The question arose of the magnitude of the dipole and of where and in what direction to place it. One could use the experimental dipole moment of the molecule and place it on the midpoint of the line connecting the substituent to the midpoint of the C=C double bond, as has been suggested by some microwave studies (16). Or one could place it somewhere along the C—O or C—Cl bond and pointing along it.

We decided, however, to use a group moment and to place it on the Cl or O atom in the direction of the =C—X bond.* The magnitude of the group moment can be taken from the tables of Smyth (17). Goldstein *et al.* (18) had considerable success in correlating the chemical shifts of protons in substituted uracils using a group dipole moment and Musher (19) later showed that these correlations lead to reasonable values of a in eq. [1]. Values of the group dipole are given in Table I.

Another question concerns the values of the coefficients a and b in eq. [1]. Musher (9) quotes theoretical and experimental values ranging from -2 to -3.4×10^{-12} electrostatic units (e.s.u.) for a and suggests 7.38×10^{-19} e.s.u. for b, while Buckingham (15) estimated 1×10^{-18} e.s.u. for b. In Table I we have tabulated the values obtained for $\Delta\sigma_E$ using $a = -2 \times 10^{-12}$ and $b = 1 \times 10^{-18}$, as suggested originally by Buckingham (15); as well, $\Delta\sigma_E$ values using $a = -3.0 \times 10^{-12}$ and $b = 7.4 \times 10^{-19}$. It seems to us that these values of a and b give a reasonable estimate of the range of $\Delta\sigma_E$ values.

It must be remembered that the dipole model is a "long-range" model and that errors as large as about 50% may be expected in the calculations of $\Delta\sigma_E$ for protons on the α-carbon. For protons on the β-carbon the error should be considerably less.

3. Effect of the Magnetic Anisotropy of the C—O or C—Cl Bonds

The polar substituents are considered to be magnetically anisotropic. In the absence of a knowledge of the magnitude of this *neighbor anisotropy effect*, we assume (10) that the Cl or O susceptibility is axially symmetric about the C—Cl or C—O bond direction; and that, therefore, the neighbor anisotropy effect can be calculated by a point dipole approximation as

$$\Delta\sigma_M = \tfrac{1}{3}\Delta\chi(1-3\cos^2\theta)/|\boldsymbol{R}|^3, \qquad [2]$$

where $\boldsymbol{R}$ is the vector between the dipole and the proton, θ is the angle which $\boldsymbol{R}$ makes with the C—X bond, and $\Delta\chi = \chi_\parallel - \chi_\perp$. However, $\Delta\chi$ is unknown and must be different for each molecule, but it appears that in our compounds $\Delta\chi$ is such that a high-field shift will result for the α-protons (10, 20).

It must be decided where to place the point dipole. For the chloroethylenes we have placed it on the chlorine as well as midway along the C—Cl bond and have calculated the geometrical factors in eq. [2] for the two cases. These factors are given in Table I.

For methyl vinyl ether, the conformation of the molecule is important since there are two C—O bonds giving rise to magnetic anisotropy effects. Owen and Sheppard (24) have shown that in the gas phase the planar *cis* conformation is more stable by 1150 ± 250 cal/mole than a (probably) nonplanar *trans* form. Because of the approximate nature of our estimates we have considered the two forms I and II only.

**Placing the dipole at the midpoint of the C—X bond leads to much larger effects at the α-protons, as would be expected.*

Can. J. Chem. Downloaded from www.nrcresearchpress.com by 210.87.254.42 on 09/05/12
For personal use only.

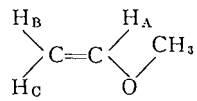

I
trans-planar

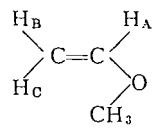

II
cis-planar

We assume that at 100 °C, where our measurements were carried out, it is sufficiently accurate to take the populations of isomers as 2/3 *cis* and 1/3 *trans*. The point dipole was placed at the oxygen as well as midway along the C—O bonds for the two conformations. The geometrical factors are given in Table I.

4. Geometry

For methyl vinyl ether we approximated bond angles about the double bond by 120°; the ∠ =C—O—CH_3 was taken as 105°; bond lengths: C=C 1.34 Å, C—O 1.4 Å, C—H 1.08 Å.

For vinyl chloride the more precise bond angle data in ref. 16 were used for the angles involving chlorine: ∠ Cl—C=C 122° 18′; ∠ Cl—C—H 113° 53′. All H—C=C angles were taken as 120°. These same values were taken for the dichloroethylenes. Bond lengths: C=C 1.32 Å, C—Cl 1.72 Å, C—H 1.08 Å.

EXPERIMENTAL

Samples were condensed into pyrex 5 mm outside diameter tubes on a vacuum line using liquid nitrogen. Each sample contained about 10% ethylene as a reference. The pressures at elevated temperatures were estimated on the basis of the ideal gas law and vapor pressure data. Temperatures and total pressures at which the spectra were taken ranged from 100 to 110 °C and 5 to 15 atm. The proton spectra were measured at 60 Mc.p.s. on a Varian DP60 spectrometer. The spectrum for *cis*-1,2-dichloroethylene was obtained by rapid passage techniques because the signal was very easily saturated. Signal-to-noise problems were not negligible for any compound but by repeated calibrations the reproducibility of the measured line positions was found to be ±0.4 c.p.s. for all except *gem*-dichloroethylene, for which it was ±1 c.p.s.

The spectra of the vinyl compounds were analyzed as ABC systems (14). The fit obtained was about ±0.3 c.p.s. or better and the shift values were estimated to be accurate to 0.3 c/s, which is sufficiently good for our purposes. The proton shifts relative to ethylene are given in Table II.

The proton shifts have been measured a number of times in solution. In Table II are given the shifts in solvents expected to be inert.

DISCUSSION

To predict the shifts we need values of $\Delta\chi$. For the C—C bond an average value* is about 5×10^{-30} cm^3 $molecule^{-1}$ (21). From Goldstein's estimate (20) of a 0.25 p.p.m. high-field shift due to magnetic anisotropy for proton A in vinyl chloride, we calculate $\Delta\chi = 4\text{–}6 \times 10^{-30}$ cm^3 $molecule^{-1}$ for the C—Cl bond. In the absence of a better value we will take $\Delta\chi = 5 \times 10^{-30}$ cm^3 $molecule^{-1}$ for both the C—O and C—Cl bonds. We realize that this value may be wrong by a factor of 2 or more.

1. Methyl Vinyl Ether

We calculate the various shifts in Table II. They represent the various combinations of the different estimates of $\Delta\sigma_E$ and $\Delta\sigma_M$ with 10 Δq. We cannot decide which calculated value is most reasonable but the simple average agrees reasonably well with experiment, when one considers the possible errors in the calculation of all three effects. It is interesting to note that the shift between protons B and C is predicted to be of the correct sign. Both $\Delta\sigma_E$ and $\Delta\sigma_M$ contribute to this shift. The largest error in our model would be expected for proton A, as is the case.

**Suggested values of $\Delta\chi$ range from about 2 to 8 $\times$ 10^{-30} cm^3 $molecule^{-1}$ (21–23).*

Can. J. Chem. Downloaded from www.nrcresearchpress.com by 210.87.254.42 on 09/05/12
For personal use only.

TABLE II

Comparison of experimental proton shifts with those calculated from π-electron density, electric dipole, and magnetic anisotropy model

Compound		Δq^a	$\Delta\sigma(1)^b$	$\Delta\sigma(2)^c$	$\Delta\sigma(3)^d$	$\Delta\sigma(4)^e$	Average^f	$\Delta\sigma_{expt}{}^g$	$\Delta\sigma s^h$
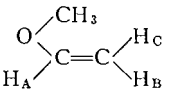	A	−0.11	−1.45	−1.39	−1.24	−1.60	−1.42	−1.13	−1.15
	B	0.15	1.45	1.43	1.50	1.38	1.44	1.45	1.41
	C	0.15	1.10	1.31	1.20	1.23	1.21	1.21	1.26
	CH_3	—	—	—	—	—	—	1.84	2.12
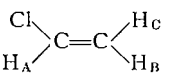	A	−0.015	−0.69	−0.35	−0.47	−0.57	−0.52	−0.93	−0.90
	B	0.02	0.07	0.18	0.13	0.12	0.13	0.11	0.01
	C	0.02	−0.05	−0.04	0.04	−0.13	−0.05	−0.09	−0.12
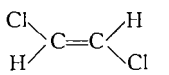		0.01	−0.60	−0.35	−0.42	−0.55	−0.48	−0.97	−0.95
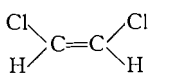		0.01	−0.65	−0.17	−0.35	−0.47	−0.42	−0.88	−0.99
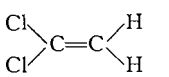		0.04	0.04	0.14	0.04	0.01	0.06	0.01	−0.10

[a]The value of Δq used in the equation $\Delta\sigma_\pi$ (p.p.m.) = 10 Δq.
[b]With $\Delta\sigma$ in p.p.m. calculated as 10 Δq + $\Delta\sigma_E(2)$ + $\Delta\sigma_M(2)$ from Table I. Note that we use $\Delta\chi = 5 \times 10^{-30}$ cm^3 molecule^{-1}.
[c]As in footnote *b* but taking 10 Δq + $\Delta\sigma_E(1)$ + $\Delta\sigma_M(1)$.
[d]As in footnote *b* but taking 10 Δq + $\Delta\sigma_E(1)$ + $\Delta\sigma_M(2)$.
[e]As in footnote *b* but taking 10 Δq + $\Delta\sigma_E(2)$ + $\Delta\sigma_M(1)$.
[f]Average of values of $\Delta\sigma$ calculated in footnotes *b*, *c*, *d*, and *e*.
[g]Experimental proton shift in gas phase relative to internal ethylene.
[h]Proton shifts in solution. The methyl ether shifts were taken in 10% volume solution in tetramethylsilane (25). The chloroethylene shifts were taken in tetramethylsilane or cyclohexane and extrapolated to infinite dilution (20). We have converted the shifts to values relative to ethylene by taking −5.29 p.p.m. as the shift of ethylene relative to tetramethylsilane (20).

2. *Vinyl Chloride*

It is clear from Table I that agreement of experimental with the calculated Δq values is not very good. If we arbitrarily reduce Δq values in Table I to −0.015 and 0.02 the calculated values in Table II agree well with experiment for protons B and C. For proton A, however, the agreement is worse, perhaps indicating an underestimation of the electric field from the C—Cl dipole and (or) that the point dipole approximation is poor for such a near proton. Moving the dipole down along the C—Cl bond would improve the agreement at proton A but not at protons B and C. Decreasing Δq at carbon A to −0.03 improves agreement with experiment. In view of the uncertainty in Δq values, our model may be considered reasonably successful.

3. *The Dichloroethylenes*

Even if we reduce the Δq values to 0.01 in the *cis* and *trans* compounds, agreement with experiment is not too good, as seen in Table II. This is expected in view of the results for proton A in vinyl chloride. It is very hard to say where the error lies since none of the three contributions is small. If $\Delta\sigma_M$ were set equal to zero for these two molecules the calculated average shifts become −0.70 and −0.84 p.p.m. respectively for the *trans* and *cis* compounds. This is very much closer to the experimental values. If we take Δq = 0.04 for the *gem*-dichloroethylene as indicated by the values of Δq taken for vinyl chloride, the calculated shift in Table II is in reasonable agreement with experiment. We might attribute this to the fact that the protons lie relatively far from the chlorines.

CONCLUSIONS

In view of the fair agreement between calculated and experimental shifts for protons farther removed from the substituent and in view of the poorer agreement for protons

Can. J. Chem. Downloaded from www.nrcresearchpress.com by 210.87.254.42 on 09/05/12
For personal use only.

attached to the same carbon as the substituents, we suggest that point dipole models have to be used with caution. We suggest also that the available molecular orbital calculations for the chloroethylenes somewhat overestimate the delocalization of electrons into the double bond, and that the values we have used for Δq are more reasonable, although arbitrary. We do not suggest that our results and calculations can be taken as supporting the value of $\Delta\chi$ we used for the C—O or C—Cl bonds.

Comparison of Proton Shifts in Gaseous Phase and in Solution

In the last column of Table II the proton shifts in the inert solvents, tetramethylsilane or cyclohexane, are presented. The differences between these and the gaseous shifts are not large in general. However, they are large enough to influence the consideration of small corrections like magnetic anisotropy effects appreciably in some cases. One large difference is the methyl proton shift in the methyl vinyl ether. The reason for the 0.36 p.p.m. shift to low field in the gas phase is not clear, but it may arise from a difference in conformation of the ether in the gas phase and in solvents. Owen and Sheppard (24) found that the stability of the planar *cis* form relative to the *trans* form decreased in polar solvents. In the planar *cis* form the CH_3 protons will be closer to the ethylenic double bond and may experience a greater low-field shift due to its anisotropy than in the *trans* form. Such an effect would explain the low-field shift in the gas phase, where a greater proportion of the molecules have the *cis* conformation.

ACKNOWLEDGMENTS

We are grateful to a referee for suggesting the additivity of the three effects we considered. We thank the National Research Council for financial assistance.

REFERENCES

1. G. Fraenkel, R. E. Carter, A. McLachlan, and J. H. Richards. J. Am. Chem. Soc. **82**, 5846 (1960).
2. H. Spiesecke and W. G. Schneider. Tetrahedron Letters, No. 14, 468 (1961).
3. C. MacLean and E. L. Mackor. Mol. Phys. 4, 241 (1961).
4. B. P. Dailey, A. Gower, and W. C. Neikam. Discussions Faraday Soc. **34**, 18 (1962).
5. T. Schaefer and W. G. Schneider. Can. J. Chem. **41**, 966 (1963).
6. J. C. Schug and J. C. Deck. J. Chem. Phys. **37**, 2618 (1962).
7. A. Zweig, J. E. Lehnsen, J. E. Lancaster, and N. T. Neglia. J. Am. Chem. Soc. **85**, 3940 (1963).
8. M. P. Schweizer, S. I. Chan, G. K. Helmkamp, and P. O. P. Ts'o. J. Am. Chem. Soc. **86**, 696 (1964).
9. J. I. Musher. J. Chem. Phys. **37**, 34 (1962).
10. H. M. McConnell. J. Chem. Phys. **27**, 226 (1957).
11. A. Julg and N. Bonnet. Theoret. Chim. Acta Berlin, **1**, 1 (1963).
12. J. H. Goldstein. J. Chem. Phys. **24**, 509 (1959).
13. J. A. Howe and J. S. Muirhead. J. Chem. Phys. **36**, 841 (1962).
14. B. H. Chirgwin and C. A. Coulson. Proc. Roy. Soc. Ser. A, **201**, 196 (1950).
15. A. D. Buckingham. Can. J. Chem. **38**, 300 (1960).
16. D. Kivelson and E. B. Wilson. J. Chem. Phys. **32**, 205 (1960).
17. C. P. Smyth. Dielectric behaviour and structure. McGraw-Hill Book Co., Inc., New York. 1955.
18. J. P. Kokko, L. Mandell, and J. H. Goldstein. J. Am. Chem. Soc. **84**, 1042 (1962).
19. J. I. Musher. Private communication.
20. J. H. Goldstein and G. S. Reddy. J. Chem. Phys. **36**, 2644 (1962).
21. J. I. Musher. J. Chem. Phys. **35**, 1159 (1961).
22. R. F. Zürcher. Helv. Chim. Acta, **44**, 1755 (1961).
23. R. F. Zürcher. J. Chim. Phys. **37**, 2421 (1962).
24. N. L. Owen and N. Sheppard. Trans. Faraday Soc. **60**, 634 (1964).
25. R. T. Hobgood, G. S. Reddy, and J. H. Goldstein. J. Phys. Chem. **67**, 110 (1963).

Can. J. Chem. Downloaded from www.nrcresearchpress.com by 210.87.254.42 on 09/05/12
For personal use only.

Can. J. Chem. Downloaded from www.nrcresearchpress.com by 210.87.254.6 on 09/05/12
For personal use only.

THE KINETICS OF THE INHIBITED AUTOXIDATION OF TETRALIN[1]

J. A. HOWARD AND K. U. INGOLD
Division of Applied Chemistry, National Research Council, Ottawa, Canada
Received May 22, 1964

ABSTRACT

The kinetics of the inhibition of the autoxidation of tetralin by 2,6-di-*t*-butyl-4-methylphenol, phenol, and 4-methoxyphenol have been investigated at 65 °C. The highly hindered 2,6-di-*t*-butyl-4-methylphenol follows simple first order kinetics and exhibits a normal deuterium isotope effect ($k_H/k_D = 10$). The kinetics with phenol are complicated by the fact that the phenoxy radical can abstract a hydrogen atom from both tetralin and its hydroperoxide. This leads to oxidation rates which are inversely proportional to the square root of the phenol concentration. The deuterium isotope effect has about the value to be expected in view of this square root relation. The kinetics with 4-methoxyphenol result from chain transfer and from chain termination by the coupling of 4-methoxyphenoxy radicals. The isotope effect varies between zero and a value that approaches the upper limit of about 10 at low inhibitor concentrations.

INTRODUCTION

The inhibition of the autoxidation of styrene by phenols has been described in considerable detail in a recent series of papers from this laboratory (1). The overall process can be represented by the following simplified reaction scheme:

[1] $$I_2 \rightarrow 2I\cdot$$

[2] $$R\cdot(I\cdot) + O_2 \rightarrow RO_2\cdot$$

[3] $$RO_2\cdot + RH \rightarrow ROOR\cdot H$$

[5] $$RO_2\cdot + RO_2\cdot \rightarrow \text{inactive products}$$

[6] $$RO_2\cdot + AH \rightarrow ROOH + A\cdot$$

[7] $$RO_2\cdot + A\cdot \rightarrow \text{inactive products.}$$

I_2 represents α,α'-azo-bis-isobutyronitrile (AIBN) which was used to initiate the oxidations. RH represents the styrene and AH the phenolic inhibitor. The radical R· in reaction [2] represents the poly(peroxy-styryl) radical. Our experimental conditions were such that chain termination occurred predominantly by reaction [7], so that the bimolecular self-termination reaction could be ignored. Under these conditions, the theoretical rate of oxidation of the styrene is given by

[I] $$P = \rho - (2e - 1)k_1[I_2] = \frac{ek_1k_3[RH][I_2]}{k_6[AH]},$$

where ρ is the measured inhibited rate and e is the efficiency with which the AIBN initiates reaction chains. The correction factor $(2e - 1)k_1[I_2]$ allows for oxygen absorption and nitrogen evolution by the AIBN. This equation describes the kinetics of the inhibition process with a variety of phenols at low concentrations where self-association of the phenol by hydrogen bonding and hydrogen bonding between the phenol and the initiator were unimportant.

These results in styrene differ in two important respects from the results reported by several other workers using basically the same technique but employing different hydrocarbon substrates. Firstly, a deuterium isotope effect $(k_6)_H/(k_6)_D \simeq 10.6$ at 65 °C was

[1]*Issued as N.R.C. No. 8097.*

obtained in styrene on deuterating the phenolic hydrogen of phenol, 4-*t*-amylphenol, 2,6-di-*t*-butylphenol, and 2,6-di-*t*-butyl-4-methylphenol (1). In contrast, previous workers did not observe an isotope effect in the N-methylaniline and diphenylamine inhibited oxidation of cumene and tetralin (2, 3) nor in the 2,6-di-*t*-butyl-4-methylphenol inhibited oxidation of 9,10-dihydroanthracene (4). The absence of an isotope effect with diphenylamine is reportedly not due to the loss of deuterium from the inhibitor by exchange since the addition of heavy water has no effect on the reaction rate (5).

Secondly, the simple kinetics which apply to the inhibition of the autoxidation of styrene by phenols are by no means universally obeyed.* Failure to follow these kinetics will occur when the self-termination process (reaction [5]) is not completely suppressed by the inhibitor (1). However, eq. [I] frequently fails to account for the kinetics even under conditions where reaction [5] can be neglected. Thus, Hammond *et al.* (3) have reported that the rate of the phenol and N-methylaniline inhibited oxidation of tetralin in chlorobenzene can be represented by

$$[II] \qquad P \propto \frac{[I_2]^{1/2}}{[AH]^{1/2}}.$$

Similar kinetics have also been found for the diphenylamine inhibited oxidation of cumene (9). Hammond *et al.* suggested that these kinetics resulted from the reversible formation of a peroxy radical – inhibitor complex, followed by decomposition of the complex by reaction with a second peroxy radical.

$$[6a] \qquad RO_2\cdot + AH \rightleftarrows (RO_2\cdot AH)$$

$$[7a] \qquad RO_2\cdot + (RO_2\cdot AH) \rightarrow \text{inactive products.}$$

Direct attempts to establish the existence of such complexes by electron spin resonance have been unsuccessful in themselves (9, 10), but they have led to three independent reinvestigations of the kinetics of these systems.† Two of these investigations provide simple alternative explanations for eq. [II].

Firstly, Thomas (11) has shown that cumene hydroperoxide increases the rate of the phenol-inhibited oxidation of cumene, the increase in rate being proportional to the square root of the initial peroxide concentration. This result is in contrast to a previous report that cumene hydroperoxide reduced the rate (5), and it implies that reaction [6] is reversible, i.e.,

$$[-6] \qquad A\cdot + ROOH \rightarrow AH + RO_2\cdot.$$

Hence,

$$[III] \qquad P = \frac{ek_1k_3[RH][I_2]}{2k_6[AH]}\left(1 + \left\{1 + \frac{4k_6k_{-6}[AH][ROOH]}{ek_1k_7[I_2]}\right\}^{1/2}\right),$$

which for large [ROOH] has the same form as eq. [II], but which calls for an inverse first order dependence of P on [AH] at zero initial hydroperoxide concentration. The fact that this was not observed was attributed to the hydroperoxide formed during the determination of the initial rate, but it can also be explained by chain transfer to the substrate (see below).

**Although previous workers have shown that these kinetics apply to the inhibition of the oxidation of ethyl linoleate by hydroquinone and other very active phenols (6) and to the inhibition of the oxidation of 9,10-dihydroanthracene by 2,6-di-t-butyl-4-methylphenol and 2,4,6-tri-t-butylphenol (7) and by N-phenyl-α- and N-phenyl-β-naphthylamine (8).*

†Incidentally, the effect of inert solvents on the rates of hydrocarbon autoxidation indicates that peroxy radicals do not complex very readily with aromatic hydrocarbons (1). This tends to argue against the formation of complexes by reaction [6a] but does not specifically preclude such an inhibition process.

Can. J. Chem. Downloaded from www.nrcresearchpress.com by 210.87.254.6 on 09/05/12
For personal use only.

Secondly, Mahoney and Ferris (12) showed that the rate of the phenol inhibited oxidation of tetralin and of 9,10-dihydroanthracene was 1.5 order with respect to hydrocarbon. This was explained by including the chain transfer reaction,

[8] $$A\cdot + RH \rightarrow AH + R\cdot,$$

instead of reaction [−6] in the kinetic analysis. With the assumptions (which are not necessarily justified) that $k_3[RH] \gg k_6[AH]$ and $k_8[RH] \gg k_7[RO_2\cdot]$, the following simplified expression was obtained.

[IV] $$P = k_3\left(\frac{ek_1k_8}{k_6k_7}\right)^{1/2}\frac{[RH]^{3/2}[I_2]^{1/2}}{[AH]^{1/2}}.$$

Another similar equation with $P \propto [RH]^{3/2}[I_2]^{1/2}[AH]^{-1/2}$ has been recently proposed by Lloyd and Lange (13). Their equation was derived as a limiting case for the condition that the phenol reacted solely with the radicals derived from the initiator (i.e., I· radicals, which were suggested to be 2-cyano-2-propoxy radicals)* with chain termination by reaction [5]. Because of the rapidity with which 2-cyano-2-propyl radicals react with oxygen to give the corresponding *peroxy* radicals,† it seems extremely unlikely that the low concentrations of phenol used in inhibition studies can seriously compete with oxygen for the propyl radicals.

By including both reactions [−6] and [8] in the kinetic analysis the following expression is obtained,

[V] $$P = \frac{ek_1k_3[RH][I_2]\alpha}{2k_6[AH]} + \frac{ek_1k_6k_8[RH][I_2][AH]\alpha}{2k_6[AH](k_{-6}[ROOH] + k_8[RH]) + ek_1k_7[I_2]\alpha},$$

where

$$\alpha = 1 + \left(1 + \frac{4k_6[AH](k_{-6}[ROOH] + k_8[RH])}{ek_1k_7[I_2]}\right)^{1/2}.$$

This equation would account for the dependence of P on $[AH]^{1/2}$ reported by Thomas (11) at zero initial hydroperoxide concentration.

Equation [IV] had been derived previously by Waters and Wickam-Jones (16) as a part of their broad theoretical treatment of inhibited oxidations. These authors point out that an inhibitor which undergoes a chain transfer reaction with the substrate will persist in a reaction medium for a longer time and may not reduce the rate to as great an extent as an equal concentration of an inhibitor which does not undergo chain transfer. When reactions [−6] or [8] are of any importance AH should be called a retarder rather than an inhibitor.

Equation [IV] had also been derived in a somewhat different form by Bickel and Kooyman (7), who showed that it accounted qualitatively for the inhibition of the oxidation of 9,10-dihydroanthracene by 2,4-di-*t*-butyl-6-methylphenol, 2,6-dimethyl-4-*t*-butylphenol (7), and N-methylaniline and aniline (8). These workers also tentatively identified the reaction,

[9] $$A\cdot + A\cdot \rightarrow A_2,$$

as the sole chain termination process with 4-*t*-butylphenol and 2-*t*-butyl-4-methylphenol

The existence of significant amounts of the propoxy radical in these systems, which contain a readily oxidizable substrate, would seem highly improbable.

†*This conclusion is drawn from the identification of 1-methyl-1-(2-cyano-2-propylperoxy)-3,5-di-t-butyl-2,5-cyclohexadienone-4 as the main product produced from 2,6-di-t-butyl-4-methylphenol by the decomposition of AIBN in the presence of oxygen (14, 15).*

Can. J. Chem. Downloaded from www.nrcresearchpress.com by 210.87.254.6 on 09/05/12
For personal use only.

(7). With this chain-terminating process and with chain transfer by reaction [8] the correct expression for the rate is

$$[VI] \qquad P = \frac{2ek_1k_3[RH][I_2]}{k_6[AH]}\left(1 + \frac{k_8[RH]}{2(ek_1k_9[I_2])^{1/2}}\right) + k_8[RH]\left(\frac{ek_1[I_2]}{k_9}\right)^{1/2}.$$

In the absence of chain transfer (i.e., $k_8 = 0$) this expression simplifies to its first term. It is therefore not possible to distinguish by means of rate measurements between termination by reaction [7] and [9] unless chain transfer is important. The distinction can, however, be made in the absence of chain transfer from the length of the induction period at low inhibitor concentrations.

A situation that probably occurs fairly commonly and which demonstrates the complexity of the kinetic expressions which are derived from quite simple elementary reactions arises when chain transfer by reaction [8] and chain termination by reactions [7] and [9] all take place. Equation [IV] is obtained if $k_7[RO_2\cdot] \gg 2k_9[A\cdot]$. The opposite condition that $k_7[RO_2\cdot] \ll 2k_9[A\cdot]$ leads to

$$[VII] \qquad P = k_3[RH][RO_2\cdot] + \frac{k_8[RH]}{4k_9}\left(4(ek_1k_9[I_2])^{1/2} - k_7[RO_2\cdot]\right),$$

where

$$[RO_2\cdot] = \frac{8ek_1k_9[I_2] + 4k_8[RH](ek_1k_9[I_2])^{1/2}}{4k_6k_9[AH] + k_7k_8[RH] + 4k_7(ek_1k_9[I_2])^{1/2}}.$$

Even more complicated expressions arise when additional elementary reactions are introduced into the kinetic scheme (see, for example, refs. 16, 17).

It is clear from the foregoing discussion that nonintegral and variable orders in [RH], [I_2], and [AH] will frequently be encountered in inhibited oxidation studies and that eq. [I] describes a highly idealized system. Because of the considerable differences between our data for phenolic inhibitors in styrene and much of the published literature, we decided to extend our study to a substrate containing a readily abstractable hydrogen atom. Tetralin was chosen as the substrate since it is readily oxidized and has been the substrate in many other inhibition studies. Three typical phenolic inhibitors were examined. (1) 2,6-Di-*t*-butyl-4-methylphenol as a representative highly hindered phenol; (2) phenol itself, in order to investigate the various theories as to the origin of eq. [II]; (3) 4-methoxyphenol as a representative very efficient but unhindered inhibitor.

EXPERIMENTAL

Fisher tetralin was purified by the usual procedure which involved washing with sulphuric acid and distillation. It was stored in the dark under nitrogen and the required amount was always passed through a 3 ft column of fresh chromatographic alumina immediately before each run to remove all traces of tetralin hydroperoxide. Samples as large as 150 ml were used for the very slow reactions. The reagents were preheated to 65 °C (the temperature at which all the present experiments were performed) before the addition of the AIBN initiator.

The rates of inhibited oxidations with 2,6-di-*t*-butyl-4-methylphenol, phenol, and 4-methoxyphenol are all independent of the oxygen pressure in the range 300–750 mm.

RESULTS AND DISCUSSION

The inhibition by 2,6-di-*t*-butyl-4-methylphenol (BMP) of the AIBN-initiated autoxidation of tetralin is accurately described by eq. [I]. That is, the inhibited rate is directly proportional to the tetralin concentration* and to the AIBN concentration and is inversely

**At concentrations below 3.0 mole/l upon further dilution with chlorobenzene or o-dichlorobenzene.*

Can. J. Chem. Downloaded from www.nrcresearchpress.com by 210.87.254.6 on 09/05/12
For personal use only.

proportional to the BMP concentration. If we take $e = 0.60$ and $k_1 = 1.8 \times 10^{-5}$ s^{-1} at 65 °C, then

$$k_3/k_6 = 6.66 \times 10^{-4}.$$

Therefore, if we take $k_3 = 13.6$ l/mole s (18), then $k_6 = 2.0 \times 10^4$ l/mole s. This value can be compared with the redetermined k_6 value of 2.7×10^4 l/mole s (18) for the reaction between styryl peroxy radicals and BMP at 65 °C. The fairly close agreement between the two values indicates that the rate of reaction [6] with a given phenol is, to a first approximation, independent of the nature of the peroxy radical.

The oxygen absorption curves show no evidence of autocatalysis, i.e., oxygen uptake is linear with time until a significant fraction of the initiator or BMP is consumed. The rate is almost unaffected by added hydroperoxide (see Fig. 1), which suggests that reaction [−6] is very slow with a hindered phenoxy radical (11, 19).

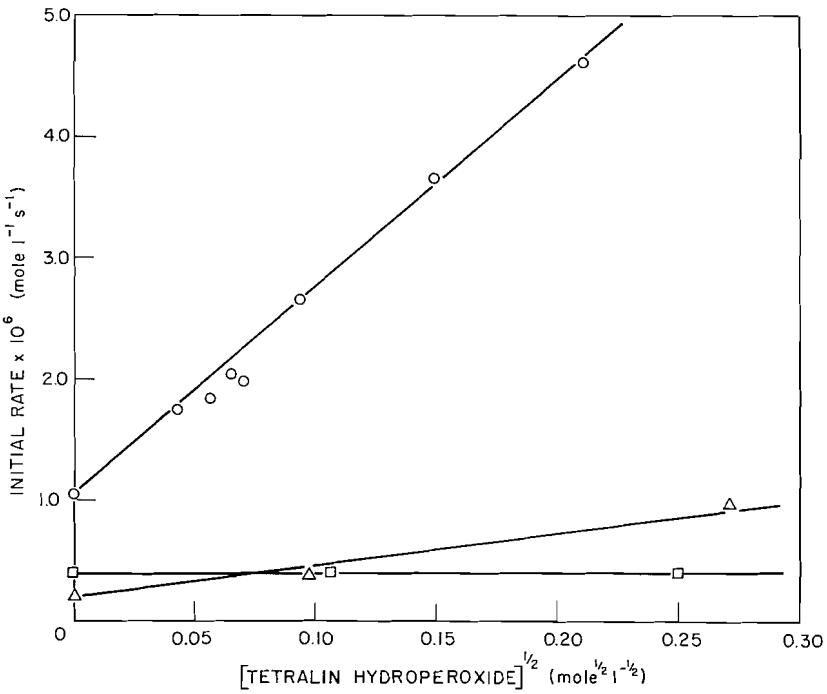

FIG. 1. The variation of the initial rate with the square root of the added tetralin hydroperoxide concentration. ○ Phenol (4.92×10^{-3} mole/l), AIBN (1.23×10^{-3} mole/l); □ BMP (4.98×10^{-5} mole/l), AIBN (4.92×10^{-4} mole/l); △ 4-methoxyphenol (1.73×10^{-4} mole/l), AIBN (9.76×10^{-4} mole/l).

The deuterium isotope effect in reaction [6] was measured by the technique we have previously employed in which the rates of inhibited oxidations in the presence of light and heavy water are compared (1). With BMP in tetralin the isotope effect was 9.7 at 65 °C, i.e., $(k_6)_H/(k_6)_D = 9.7$. This value is in good agreement with the value of 10.6 obtained previously with this inhibitor in styrene at 65 °C (1).

The oxygen absorption curves with phenol as the inhibitor show significant autocatalysis after the absorption of as little as 1×10^{-4} mole $[O_2]$ per liter of tetralin. The hydroperoxide formed in the oxidation is responsible for this autocatalysis since the same rate is obtained when the hydroperoxide is formed *in situ* during an oxidation as

Can. J. Chem. Downloaded from www.nrcresearchpress.com by 210.87.254.6 on 09/05/12
For personal use only.

when the same amount of hydroperoxide is added at the start of the reaction.* To obtain rates which are not affected by hydroperoxide it is necessary to work with large volumes of very pure tetralin and to measure only the initial rates. Figure 1 shows that the increase in the initial rate is proportional to the square root of the initial hydroperoxide concentration, a result which is the same as that reported by Thomas for the phenol-inhibited oxidation of cumene (11). Reaction [−6] is probably mainly responsible for this increase but hydrogen bonding between the phenol and the hydroperoxide may also contribute to the rate enhancement.

Figure 2 shows that, at a given phenol concentration, the rate is proportional to the square root of the initiator concentration. This relation is used in Fig. 3 to show that the rate is inversely proportional to the square root of the phenol concentration, provided the phenol concentration is below about 5×10^{-3} mole/l. That is, these two figures reconfirm the kinetics originally reported by Hammond *et al.* (3). At concentrations above 5×10^{-3} mole/l the order in [phenol] decreases. This is not entirely unexpected as the phenol will hydrogen bond with itself and with the initiator at these high concentrations, so that its activity decreases (1). Certain other factors which may also contribute to the decrease in kinetic order at high phenol concentrations are mentioned below.

In a recent paper from this laboratory we showed that apparently inert solvents can have a very pronounced influence on the rates of both uninhibited and inhibited oxidations (1). Their effect on inhibited oxidations seems to be related to the strength of the hydrogen bond between the inhibitor and the solvent, i.e., as the hydrogen bond strength increases the activity of the inhibitor decreases. This factor means that great care must be exercised in interpreting inhibited rates in solvents of varying composition such as must always be involved in any dilution experiments aimed at determining the kinetic order in [RH]. For this reason, two solvents were used in the dilution experiments with phenol as the inhibitor. One solvent, chlorobenzene, appears to depress the inhibited rate compared with its value in pure tetralin and the other, nitromethane, appears to enhance the rate (see Fig. 4). To minimize the effect of the changing solvent composition, the kinetic order in [RH] was determined from measurements at tetralin concentrations of 3.67 mole/l (50%) and less. In the absence of any initial hydroperoxide the measured orders in [RH] are 1.3 in chlorobenzene and 1.5 in nitromethane ([AH] = 2×10^{-3} mole/l, $[I_2] = 5.0 \times 10^{-4}$ mole/l). In the presence of 1×10^{-2} mole/l $[ROOH]_0$ the measured orders decreased to 1.0_4 and 1.0_8 respectively. The fact that the order is 1.5 in only one case tends to argue against the importance of reaction [8] as a general cause of the observed dependence of P on $[I_2]^{1/2}/[AH]^{1/2}$. Moreover, even if reaction [8] is of primary importance in the complete absence of hydroperoxide it is rapidly suppressed by the hydroperoxide formed in the reaction. That is, the lower kinetic orders observed in the presence of 10^{-2} mole/l $[ROOH]_0$ can be readily explained if reaction [−6] is much faster than reaction [8], i.e., this added peroxide reduces the phenoxy radical concentration sufficiently to reduce the rate of reaction [8] by a very large amount. Since it is impossible to be certain that any rate is completely uninfluenced by hydroperoxide, it is possible that the kinetic order of 1.3 in chlorobenzene in the *apparent* absence of hydroperoxide has been reduced from a somewhat higher value by traces of hydroperoxide.

On the whole, the phenol inhibition data can probably be best represented by eq. [V]. However, it must be remembered that reaction [8], although probably quite important in determining the kinetic orders for [RH], $[I_2]$, and [AH] in the absence of hydroperoxide, is

**Preliminary results with N-methylaniline suggest that its behavior in tetralin is very similar to the behavior of phenol.*

Can. J. Chem. Downloaded from www.nrcresearchpress.com by 210.87.254.6 on 09/05/12
For personal use only.

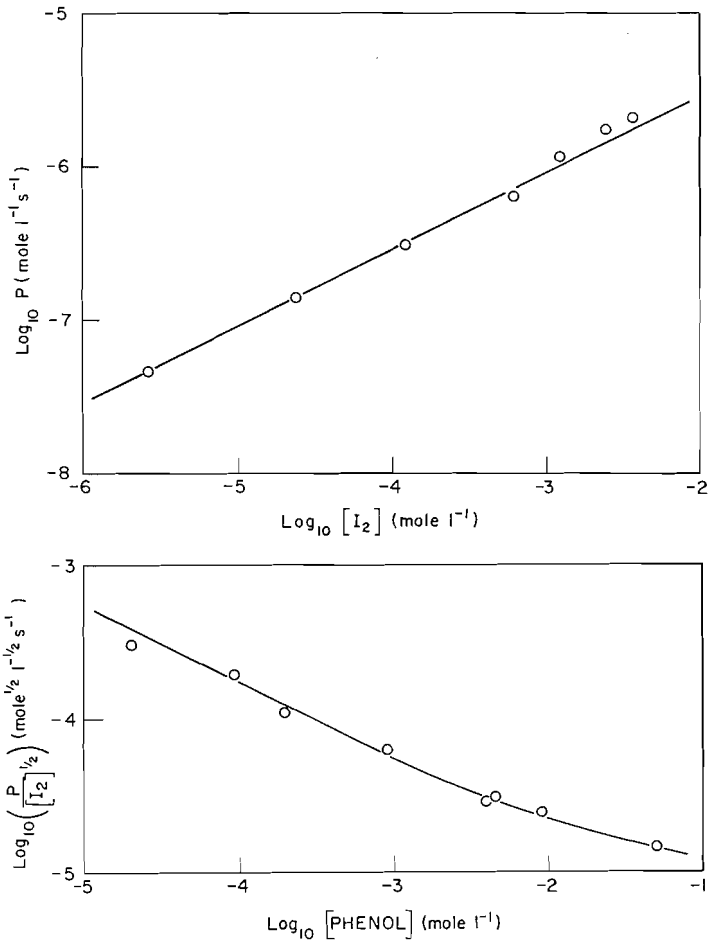

FIG. 2. Rate of oxidation of tetralin inhibited by 4.92×10^{-3} mole/l [phenol] as a function of AIBN concentration. The line in this figure has a slope of 0.5.

FIG. 3. $\text{Log}_{10}\ (P/[I_2]^{1/2})$ as a function of the phenol concentration. The linear region has a slope of 0.5.

rapidly suppressed by quite small concentrations of hydroperoxide and the data can then be represented by eq. [III]. Both equations predict that the rate will be proportional to $[I_2]^{1/2}/[AH]^{1/2}$ only over a comparatively small range of concentrations. At low [AH] or large $[I_2]$ both equations simplify to $P \propto [RH][I_2]/[AH]$ (i.e., eq. [I]). Such kinetics were not observed, but these particular limiting conditions were purposely avoided since self-termination between peroxy radicals (reaction [5]) also becomes important in this region. Equation [V] (but not eq. [III]) predicts that the rate will become proportional to $[RH]^{1/2}[I_2]^{1/2}[AH]^{1/2}$ as [AH] becomes very large. That is, this equation predicts that there will be a minimum in a plot of log P or of log $(P/[I_2]^{1/2})$ against log [AH], this minimum being followed by an increase in rate as [AH] is further increased. The slight curvature in Fig. 3 at high phenol concentrations may perhaps arise partly from this factor.

The deuterium isotope effect for the phenol-inhibited oxidation was measured at an AIBN concentration of 1.97×10^{-5} mole/l and a phenol concentration of 4.92×10^{-3} mole/l. In the absence of hydroperoxide the rate is 1.3×10^{-7} mole/l s (see Fig. 2). In

Can. J. Chem. Downloaded from www.nrcresearchpress.com by 210.87.254.6 on 09/05/12
For personal use only.

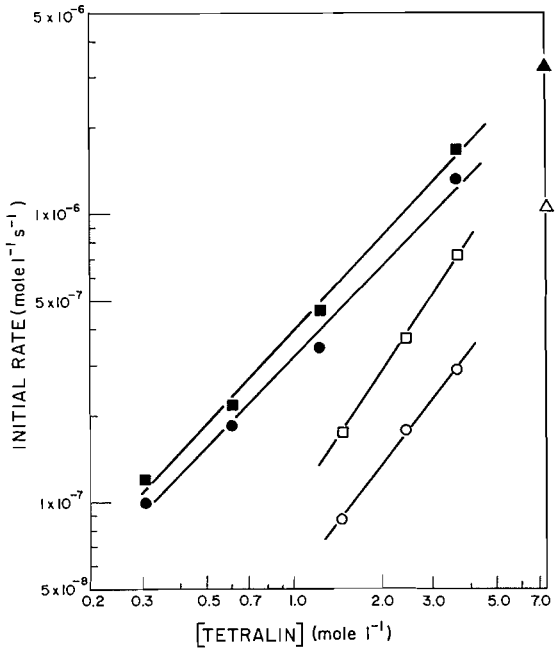

FIG. 4. The rate of oxidation of tetralin inhibited by 2.0×10^{-3} mole/l [phenol] and initiated by 5.0×10^{-4} mole/l [AIBN] as a function of the tetralin concentration. In the initial absence of hydroperoxide; ○ chlorobenzene as diluent, □ nitromethane as diluent, △ pure tetralin. In presence of 1×10^{-2} mole/l [tetralin hydroperoxide]; ● chlorobenzene as diluent, ■ nitromethane as diluent, ▲ pure tetralin.

the presence of H_2O and D_2O the rates were 2.2 and 6.8 $\times 10^{-7}$ mole/l s, respectively,* giving a directly measured isotope effect of 3.1. However, since the rate is proportional to $[AH]^{-1/2}$, the true isotope effect for the inhibition reaction is given by

$$(k_6)_H/(k_6)_D = (3.1)^2 = 9.6,$$

in excellent agreement with the value obtained with BMP.

The isotope effect was also measured under the same conditions of concentration but with the addition of 1×10^{-2} mole/l of hydroperoxide before the start of the reaction. Deuteration of the hydroperoxide would be expected to reduce the rate of reaction [−6]. This will tend to reduce the measured isotope effect since P will be decreased by a decrease in k_{-6} (see eq. [III]). In the absence of water the hydroperoxide increased the rate to 4.5×10^{-7} mole/l s. The addition of H_2O decreased the rate very slightly to 4.4×10^{-7} mole/l s† and the addition of D_2O raised the rate to only 7.2×10^{-7} mole/l s. These rates give an apparent isotope effect of 1.64, which is significantly less than the value in the absence of hydroperoxide.

4-Methoxyphenol appears to be a much more efficient inhibitor than phenol. The oxygen absorption curves show no evidence of autocatalysis and the comparative unimportance of reaction [−6] is further emphasized in Fig. 1. There is a very unusual relation between

*The higher rate in the presence of water is probably due to the loss of some of the added phenol into the aqueous phase. In the calculation of the isotope effect it is assumed that such physical effects of light and heavy water will be equal.

†The small effect of H_2O may be due to a compensation between the expected increase in rate produced by the loss of phenol into the aqueous phase and a decrease in rate resulting from a decrease in the rate of chain transfer because of hydrogen bonding between the hydroperoxide and H_2O.

Can. J. Chem. Downloaded from www.nrcresearchpress.com by 210.87.254.6 on 09/05/12
For personal use only.

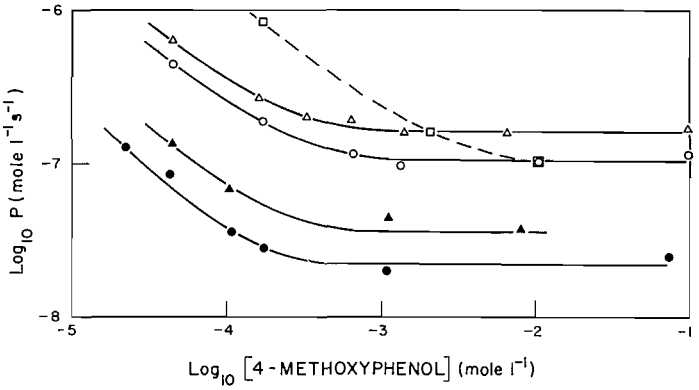

FIG. 5. The rate of oxidation of tetralin as a function of the 4-methoxyphenol concentration. △ 7.35 mole/l [RH], 1.95×10^{-3} mole/l [AIBN]; ○ 7.35 mole/l [RH], 9.76×10^{-4} mole/l [AIBN]; □ 7.35 mole/l [RH], 9.76×10^{-4} mole/l [AIBN] inhibited by 4-methoxyphenol O-*D*; ▲ 1.22 mole/l [RH] in chlorobenzene, 1.95×10^{-3} mole/l [AIBN]; ● 1.22 mole/l [RH] in chlorobenzene, 9.76×10^{-4} mole/l [AIBN].

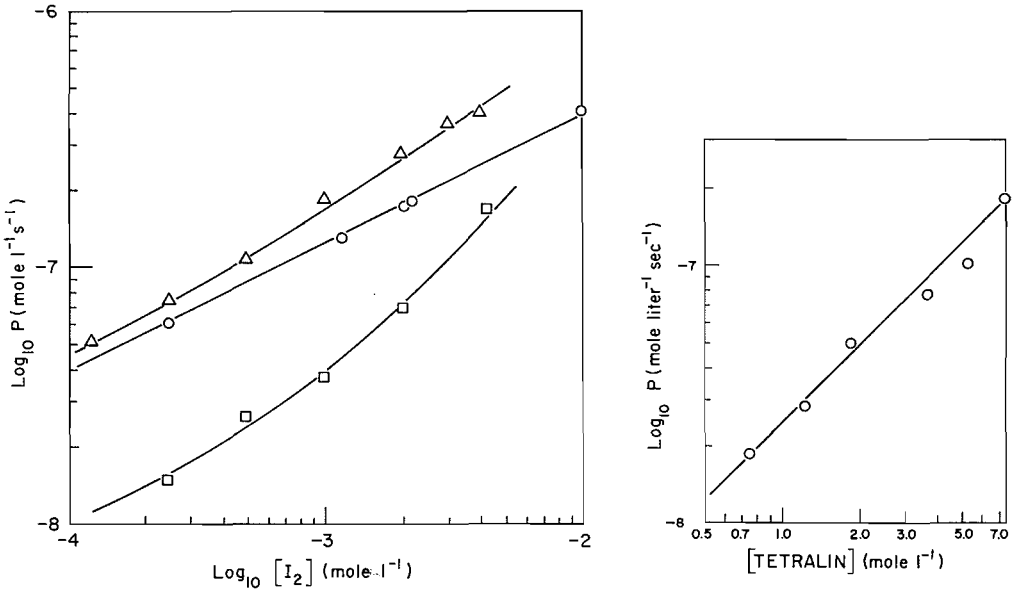

FIG. 6. The rate of oxidation of tetralin as a function of the AIBN concentration. ○ 7.35 mole/l [RH], 6.68×10^{-3} mole/l [4-methoxyphenol], this line has a slope of 0.5; △ 7.35 mole/l [RH], 1.66×10^{-4} mole/l [4-methoxyphenol]; □ 1.22 mole/l [RH] in chlorobenzene, 1.06×10^{-4} mole/l [4-methoxyphenol].

FIG. 7. Rate of oxidation of tetralin in chlorobenzene at an AIBN concentration of 9.76×10^{-4} mole/l and a 4-methoxyphenol concentration of 1.73×10^{-4} mole/l. The line has a slope of 1.0.

the rate and the 4-methoxyphenol concentration which is shown in Fig. 5. The data for this phenol can be most readily accounted for on the basis of eq. [VI]. At high phenol concentrations this equation predicts that only the last term will be important and therefore the rate will be independent of [AH] but will be proportional to $[RH][I_2]^{1/2}$. The limiting rate at high 4-methoxyphenol concentrations does indeed follow these predictions (see Figs. 5 and 6). At lower inhibitor concentrations the rate retains its direct proportionality to [RH] (Figs. 5 and 7) but the order in $[I_2]$ increases from 0.5 towards 1.0

Can. J. Chem. Downloaded from www.nrcresearchpress.com by 210.87.254.6 on 09/05/12
For personal use only.

as the initiator concentration is increased (see Fig. 6). Furthermore, at a given [AH], the order in $[I_2]$ increases as [RH] is reduced (Fig. 6). The order in [AH] increases from 0 to a value which definitely appears to exceed 0.5 and therefore, presumably, approaches 1.0 as the inhibitor concentration is reduced. All these changes in order are in agreement with the predictions of eq. [VI], which suggests that reaction[7] is relatively unimportant with 4-methoxyphenol.* Incidentally, some of the deviation of the phenol-inhibited rates at high phenol concentrations (Fig. 3) might also be connected with this limiting rate effect.

The most interesting feature of this type of inhibition is that the deuterium isotope effect varies from zero in the limiting rate region to a much larger value, which probably approaches a limit of about 10 at very low 4-methoxyphenol concentrations (see Fig. 5).

In conclusion, the different inhibition kinetics exhibited by the three phenols studied in this work provide an obvious explanation for the well-known empirical observation that the relative efficiencies of different phenols vary markedly from substrate to substrate.† The measured oxidation rates with different inhibitors can only be used to calculate relative k_6 values under ideal conditions where eq. [I] applies. More generally, the measured oxidation rates under a standard set of conditions reflect the individual values of so many different rate constants that comparisons of inhibitor efficiencies are almost meaningless when applied outside the actual substrate employed.

REFERENCES

1. J. A. Howard and K. U. Ingold. Can. J. Chem. **40**, 1851 (1962); **41**, 1744, 2800 (1963); **42**, 1044 (1964).
2. C. E. Boozer and G. S. Hammond. J. Am. Chem. Soc. **76**, 3861 (1954).
3. G. S. Hammond, C. E. Boozer, C. E. Hamilton, and J. N. Sen. J. Am. Chem. Soc. **77**, 3238 (1955).
4. A. F. Bickel and E. C. Kooyman. J. Chem. Soc. 2415 (1957).
5. G. S. Hammond and U. S. Nandi. J. Am. Chem. Soc. **83**, 1217 (1961).
6. J. L. Bolland and P. ten Haave. Trans. Faraday Soc. **43**, 201 (1947). Discussions Faraday Soc. **2**, 252 (1947).
7. A. F. Bickel and E. C. Kooyman. J. Chem. Soc. 2215 (1956).
8. A. F. Bickel and E. C. Kooyman. J. Chem. Soc. 2217 (1957).
9. J. R. Thomas and C. A. Tolman. J. Am. Chem. Soc. **84**, 2930 (1962).
10. J. R. Thomas. J. Am. Chem. Soc. **85**, 591, 593 (1963).
11. J. R. Thomas. J. Am. Chem. Soc. **85**, 2166 (1963).
12. L. R. Mahoney and F. C. Ferris. J. Am. Chem. Soc. **85**, 2345 (1963).
13. W. G. Lloyd and C. E. Lange. J. Am. Chem. Soc. **86**, 1491 (1964).
14. A. F. Bickel and E. C. Kooyman. J. Chem. Soc. 3211 (1953).
15. C. E. Boozer, G. S. Hammond, C. E. Hamilton, and J. N. Sen. J. Am. Chem. Soc. **77**, 3233 (1955).
16. W. A. Waters and C. Wickham-Jones. J. Chem. Soc. 812 (1951).
17. W. A. Waters and C. Wickham-Jones. J. Chem. Soc. 2420, 2427, 2432 (1952).
18. J. A. Howard and K. U. Ingold. Unpublished results.
19. J. C. McGowan and T. Powell. J. Chem. Soc. 238 (1960).

**There appears to be a very slight increase in the rate at very high 4-methoxyphenol concentrations. This would suggest that there may perhaps be a very slight contribution from reaction [7], i.e., from a term similar to the second term in eq. [V].*

†A secondary cause of this variation which is related to the strength of the hydrogen bond between the phenol and the substrate has been discussed in a previous publication from this laboratory (1).

Can. J. Chem. Downloaded from www.nrcresearchpress.com by 210.87.254.6 on 09/05/12
For personal use only.

Can. J. Chem. Downloaded from www.nrcresearchpress.com by 210.87.254.6 on 09/05/12
For personal use only.

GAS–SOLID EXCHANGE STUDIES BY THE FLOW METHOD: Zn–ZnS AND Zn–ZnO REACTIONS

ALLAN J. MACKINNON, RONALD R. MARTIN, AND E. A. SECCO
Chemistry Department, St. Francis Xavier University, Antigonish, Nova Scotia
Received May 4, 1964

ABSTRACT

The initial exchange of zinc vapor with polycrystalline zinc oxide and zinc sulphide has been studied by a flow method under different conditions of zinc vapor flow rates and temperature. The exchange rate was found to be independent of flow rate. Kinetic and mechanism interpretations of these results along with existing data from exchange studies by the static method are discussed.

INTRODUCTION

Recent studies (1, 2) on gas–solid exchange reactions by the static method have revealed two processes involved in the exchange reaction. The rapid initial rate interpreted as a simple exchange process was followed by a slower rate which appeared to be a diffusion-controlled process. The initial rate was not restricted to the surface but persisted to ca. one-half the particle radius, and the depth of penetration increased with temperature. The question now arises as to the exact nature of this initial exchange process. That is, the exchange rate may be determined by an adsorption or desorption step, by a direct exchange step, or by some partial combination of any two of these steps. The present investigation was undertaken to elucidate the initial exchange process in the Zn–ZnS and Zn–ZnO systems by studying their exchange rates by the flow method.

EXPERIMENTAL PROCEDURE

The polycrystalline ZnS and ZnO used in this work were from the sources previously reported (1, 2). The method of preparation of the zinc metal carrying the radioactive component, ^{65}Zn, and the counting technique have already been described (1).

The exchange runs were carried out by a flow method with use of the reaction chamber shown in Fig. 1. For each run, about 50 mg of the solid oxide or sulphide was placed on a fritted quartz disc holder fitted with a 18/9 ground-quartz ball joint. The fritted disc had to be of coarse porosity grade to permit passage of the vapor. The ball joint was fitted into a 18/9 ground-quartz socket joint of the quartz flow reactor. A weighed amount of radiozinc was placed in the quartz bucket suspended about 5 cm above the fritted disc holder. After installation of the holder and bucket with their contents in the flow reactor, the reactor was connected by a 24/40 ground taper to an oxygen-free nitrogen supply. The nitrogen (Matheson Prepurified Grade with a stated impurity of 0.003% oxygen and metered through a Fischer and Porter flowmeter), was allowed to flush the chamber for 25–45 min at room temperature, followed by flushing at 150 °C for an additional 20–25 min at the requisite flow rates to ensure complete purging. After the flushing was completed, the tubular furnace, set on tracks, was raised mechanically to a predetermined height to enclose the reactor. The furance thermocouple tip was located at the site of the ground socket joint.

The stream of nitrogen transported the radiozinc vapor through the fritted disc carrying the solid. The vapor was condensed and collected in a trap at the reactor's exhaust.

After the solid had been annealed for a definite time interval at a constant nitrogen flow rate, the furnace was lowered and the nitrogen flow was continued until the reactor attained room temperature, ca. 20 min. The bucket and holder were withdrawn, weighed, and counted. The amount of radiozinc metal used was determined by the loss in weight from the bucket and by the residual activity: these two measurements checked within limits of their operation errors. The activity uptake by the solid in the holder was a measure of the exchange reaction.

The positive pressure of the nitrogen above the fritted-disc holder ensured a leak-proof fit at the ball-and-socket joint. Tests made with water and with fritted discs of fine porosity grade confirmed a leak-proof fit during flow experiments.

Blank runs, i.e. without the solid component, were carried out with radiozinc and nitrogen passing through the fritted disc to check the possibility of trapped ^{65}Zn in the disc pores. No activity uptake by the disc was discernible.

The temperature profile of the tubular resistance furnace was determined using a platinum vs. platinum–rhodium thermocouple (Leeds and Northrup) calibrated at the National Bureau of Standards, Washington, D.C. (test No. 147033).

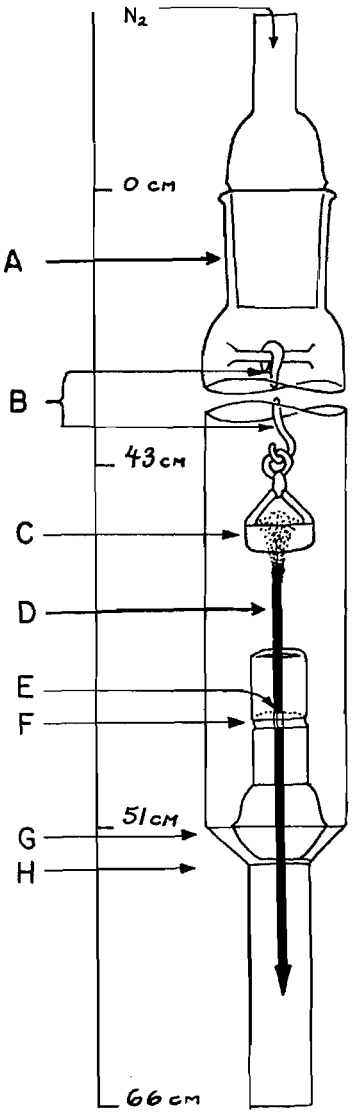

FIG. 1. Exchange reaction flow vessel. A, 24/40 ground joint; B, long slender (1 mm) quartz rod; C, zinc metal in bucket; D, zinc vapor; E, powder sample on disc; F, sintered-quartz disc; G, H, 18/9 ground ball-and-socket joint, where G is ball joint of bucket and H is socket joint of vessel.

RESULTS

Zn–ZnS Reaction

Figure 2 shows the reaction fraction as a function of time for 760 °C at the various nitrogen flow rates. The rate of exchange is independent of the flow rate within the limit

Can. J. Chem. Downloaded from www.nrcresearchpress.com by 210.87.254.6 on 09/05/12
For personal use only.

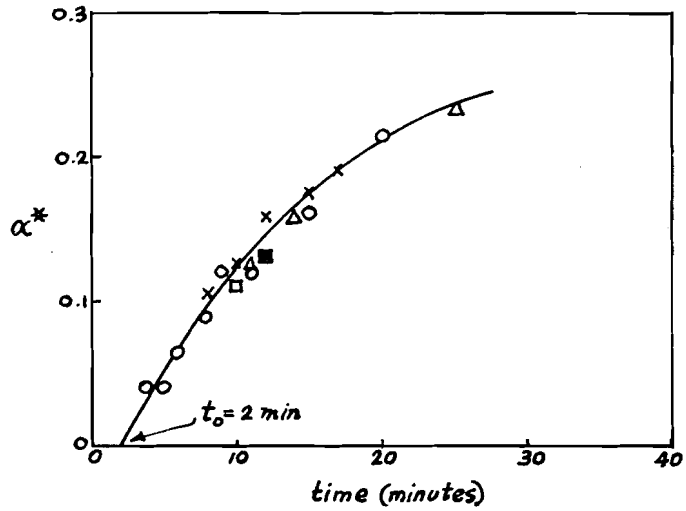

FIG. 2. Reaction fraction, α^*, vs. time for the Zn–ZnS reaction for △ 680, × 320, ○ 160, □ 80, and ■ 40 ml/min.

40–680 ml/min. The positive time intercept of 2 min is interpreted as the induction period for the evaporation of zinc metal.

The logarithms of the exchange rate constants are plotted against the reciprocals of the absolute temperature in Fig. 3. The exchange rate data are fitted to a first-order rate law with the Arrhenius expression given by

$$k_e = 1.7 \times 10^3 \exp(-30.5 \text{ kcal}/RT) \text{ s}^{-1}.$$

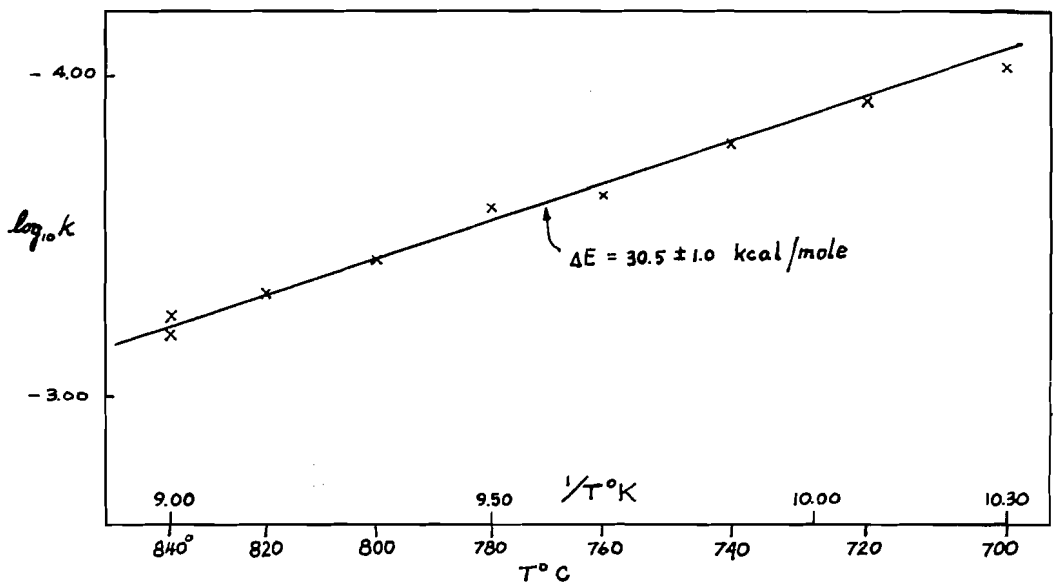

FIG. 3. Logarithm of exchange rate constant vs. reciprocal of absolute temperature.

Can. J. Chem. Downloaded from www.nrcresearchpress.com by 210.87.254.6 on 09/05/12
For personal use only.

It is evident that the rate constant obtained by the flow method is one-half the value obtained by the static method, i.e.

$$k_e \text{ (flow)} = \tfrac{1}{2} k_e \text{ (static)}.$$

Zn–ZnO Reaction

Figure 4 shows the reaction fraction as a function of time for 760 °C and 850 °C at a flow of 200 ml/min. The scatter of the exchange data in Fig. 4*a* is in striking contrast to

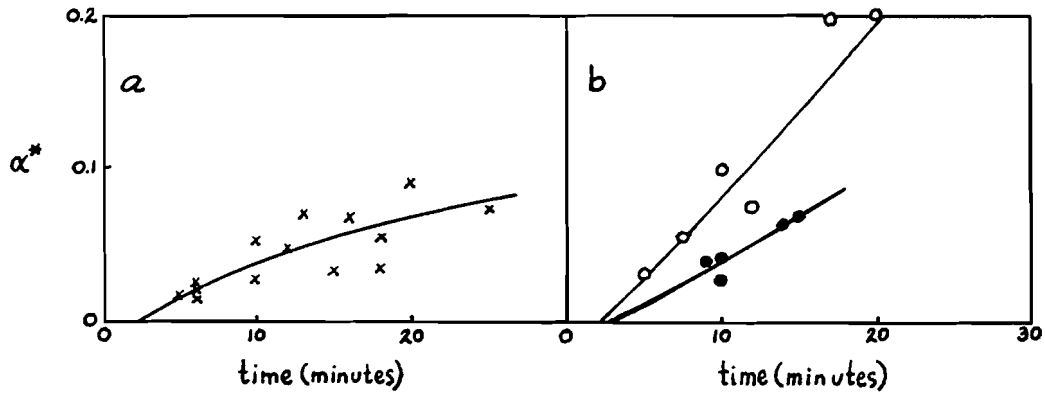

FIG. 4. Reaction fraction, α^*, vs. time for the Zn–ZnO reaction: (a) ZnO at 760 °C; (b) ZnO at 850 °C, ○ untreated, ● pretreated.

the high degree of reproducibility in the Zn–ZnS case. The more significant feature of Fig. 4*a* is the low reaction fraction, i.e. 0.07, as compared to that fraction, 0.60, observed in the static system at the same temperature. The constant value of ca. 0.07 corresponds very closely to the surface area of the oxide, 3.52 m^2/g, as determined by krypton adsorption measurements. The exchange data cannot be fitted to a first-order rate law with sufficient degree of confidence.

Figure 4*b* gives the exchange data at 850 °C for untreated oxide and for oxide pretreated in the flow reactor with inactive zinc vapor at the same temperature for 20 min at 200 ml/min nitrogen flow.

ANALYSIS OF DATA AND DISCUSSION

We consider the case of gas flowing through solid powder in the form of a porous wafer and assume that during the passage of a small increment of the gas the solid remains in a steady state. Let t_c be the time taken for the increment of gas to pass from the initial contact with the solid to a point at which the gas composition has changed from c_0 to c. Then, if the first-order kinetics obtain during the reaction,

$$[1] \qquad \frac{-dc}{dt} = kc.$$

If the constant term k is allowed to include parameters due to powder compactness and surface activity, eq. [1] may be integrated between the limits $t = 0$ and $t = t_c$, the "residence" time when the final composition is c_t, to yield

$$[2] \qquad \ln \frac{c_0}{c_t} = kt_c.$$

Can. J. Chem. Downloaded from www.nrcresearchpress.com by 210.87.254.6 on 09/05/12
For personal use only.

The rate equation for the uptake of radioactivity by a solid from the active vapor in a static system is given by

$$[3] \qquad \ln\left(1 - \frac{\alpha_t{}^s}{\alpha_\infty{}^s}\right) = -k_e t,$$

where k_e is the exchange rate constant. For a flow system with a fresh supply of vapor of specific activity $\alpha_0{}^g$ passing over the solid, the equilibrium specific activity of the solid, $\alpha_\infty{}^s$, will equal $\alpha_0{}^g$ so that eq. [3] reads,

$$[4] \qquad \ln\left(1 - \frac{\alpha_t{}^s}{\alpha_0{}^g}\right) = -k_e t,$$

which is the limiting case of the static system for the condition

$$n^g \gg n^s \text{ or } S = 0,$$

where

$$S = n^s/(n^s + n^g) \text{ and } \alpha_\infty{}^s = \alpha_0{}^g\,(1 - S);$$

α^g and α^s are activities of the gas and solid phases, while n^g and n^s are moles in the gas and solid phases respectively.

Replacing c_0/c_t by $1/(1 - \alpha^*)$, where α^* is the fraction of exchange $\alpha_t{}^s/\alpha_0{}^g$, we have

$$[5] \qquad k_e = \frac{2.303}{t_c} \log\,(1 - \alpha^*)\cdot$$

Theoretically, for a constant flow rate of vapor at a constant temperature, a plot of reaction fraction vs. the duration time of the experiment should be a plateau if direct exchange were the sole rate-determining step, since the flow rate determines the residence time. The longest residence time in these flow experiments was evaluated to be ca. 20 s, and for such a time interval the expected reaction fraction is ca. 1% as obtained from the static system. Furthermore, the exchange rate data were found to be independent of the gas flow rates.

In view of these facts and the zinc – zinc sulphide exchange data given in Fig. 2, we conclude that the direct exchange step is not the only step in the initial exchange process. The important step in the zinc – zinc sulphide exchange must be, therefore, the adsorption of zinc vapor on the sulphide surface. We visualize an adsorption–desorption equilibrium which precedes the actual exchange step of the type

$$Zn^*_{(g)} + ZnS_{(s)} \underset{k_1}{\overset{k_2}{\rightleftharpoons}} ZnS_{(s)} \ldots Zn^*_{(ads)} \xrightarrow{k_3} Zn^*S_{(s)} + Zn_{(g)}.$$

The observed exchange rate constant is then a product of an actual rate constant for the rate-determining process and the equilibrium constant of the preceding equilibrium. The difference in the exchange rate constant, i.e.

$$2k_e \text{ (flow)} = k_e \text{ (static)},$$

by the factor of 2 between the flow and static systems represents, therefore, the ratio of the adsorbed species $ZnS_{(s)} \ldots Zn^*_{(ads)}$ in the two systems.

The activation energy of 30.5 kcal as obtained from Fig. 3 is a composite quantity since it may include not only the true activation energy of the exchange reaction but also the heat of adsorption of zinc vapor.

Can. J. Chem. Downloaded from www.nrcresearchpress.com by 210.87.254.6 on 09/05/12
For personal use only.

The zinc – zinc oxide data from the flow system are in strong contrast to the exchange data obtained in the static system. The scatter of the exchange data indicates a sensitivity of the rate to the parameter suspected to be surface adsorption. The correspondence of the low exchange fraction with surface area does suggest a major role for adsorption in the exchange reaction. The reduction of the reaction fraction as a result of the pretreatment in zinc vapor at 850 °C, Fig. 4*b*, prior to exchange is consistent with the prominent role of the surface. Here again, the difference in the exchange rate constant, i.e.

$$10k_e \text{ (flow)} = k_e \text{ (static)},$$

by the factor of 10 represents the ratio of adsorbed species $ZnO_{(s)} \ldots Zn^*_{(ads)}$ in the two systems.

A very significant interpretation of these results is that the oxide and sulphide surfaces present adsorption sites of varying degrees of activity. The most active sites are occupied very readily, that is within the contact time of the flow method, whereas other sites require longer contact times which prevail in the static method. The fact that the exchange rate and adsorption was observed to be independent of the flow rates in the zinc – zinc sulphide militates against the above interpretation. However, if the adsorption sites show a discontinuous variation of adsorbing power, very strong and very weak, and if the flow conditions were varied within a particular band of activity, no effect on adsorption would be expected. We incline towards this discontinuous model for activity.

ADDENDUM: Since submitting the manuscript we tested our adsorption hypothesis by a fairly critical experiment. In addition to the contact time the dynamic method differs from the static method by the presence of the N_2 carrier gas. It was speculated that adsorbed N_2 can reduce the zinc adsorption and hence the exchange rate. Using the static method we injected sufficient N_2 to give 1 atm pressure at the exchange temperature. That is, the static study was followed in a manner similar to that previously described except that the solid was bathed in an ambient of zinc vapor and N_2 gas. The exchange results are given below.

	Static system		*Dynamic system*
Zn–ZnS reaction at 800 °C at constant time:			
	Zn, 39%	Zn + N_2, 41%	Zn + N_2, 20%
Zn–ZnO reaction at 760 °C at constant time:			
	Zn, 60%	Zn + N_2, 30%	Zn + N_2, 7%

We interpret these results as further support of our adsorption hypothesis.

ACKNOWLEDGMENTS

This work has received generous support from the National Research Council to whom the authors are indebted. The authors gratefully acknowledge the skilled assistance of Mr. George Ensell in constructing the prototype reaction chamber and the fritted-disc holder.

REFERENCES

1. E. A. SECCO. Can. J. Chem. **39**, 1544 (1961); Fourth International Symposium on the Reactivity of Solids. Elsevier Pub. Co., Inc., Amsterdam. 1960. p. 188.
2. E. A. SECCO. Can. J. Chem. **42**, 1396 (1964).

Can. J. Chem. Downloaded from www.nrcresearchpress.com by 210.87.254.6 on 09/05/12
For personal use only.

ADSORPTIVE AND GAS CHROMATOGRAPHIC PROPERTIES OF VARIOUS CATIONIC FORMS OF ZEOLITE X[1]

H. W. HABGOOD
Fuels Branch, Research Council of Alberta, Edmonton, Alberta

Received June 1, 1964

ABSTRACT

Gas chromatographic retention volumes for O_2, N_2, CH_4, C_2H_6, C_3H_8, C_4H_{10}, C_2H_4, and C_3H_6 have been measured over a range of temperatures between 25 and 400 °C, on columns of the following ion-exchanged forms of zeolite X: Li^+, Na^+, K^+, Mg^{++}, Ca^{++}, Ba^{++}, and Ag^+. In addition, for AgX zeolite, full isotherms have been determined for O_2, N_2, C_2H_6, and C_2H_4; and for NaX zeolite, isotherms for C_2H_6 and C_2H_4. The gas chromatographic retention volumes agree well with the isotherms in the case of NaX but are significantly low for AgX, presumably as the result of at least a portion of the adsorption process being slow. The heats of adsorption on NaX agree well with literature values for O_2, N_2, CH_4, and C_2H_6 but are low for C_3H_8 and C_4H_{10}; further indication of slow processes and hence of a limitation of the g.c. technique. The observations can be correlated qualitatively in terms of the interplay of the following effects: (*a*) cationic field increases with decreasing ionic radius; (*b*) shielding of smaller cations is greater—at least in the six-membered oxygen-ring sites; (*c*) divalent cations, while having greater fields, are only half the number of monovalent cations and tend to be found in less exposed sites; and (*d*) the polarizing power of silver ion, which also occupies all types of exposed sites, is very strong. The most intense interactions were found with AgX; with ethylene a much stronger complex is formed than has been reported for any other silver compound. The significance of molecular quadrupole interactions on these heteroionic surfaces is shown by the much weaker cationic effects observed with O_2 (which has negligible quadrupole moment) than with nitrogen.

INTRODUCTION

Following the earlier measurements of Barrer and Sutherland (1) and of Barrer Bultitude, and Sutherland (2) on the adsorption of various gases and vapors by NaX zeolite (synthetic near-faujasite), the important contribution of the exchangeable cations to the sorption process has been demonstrated by the measurements of Barrer and Stuart (3) on the adsorption of argon and of nitrogen by the Li, Na, and K forms of zeolite X (and of argon by the Ca, Sr, and Ba forms of the zeolite). The measurements with argon showed that the polarizing power of the cation contributed substantially to the energy of adsorption, and a comparison between argon and nitrogen showed a strong contribution, increasing from K^+ to Li^+, due to the interaction of the nitrogen electric quadrupole moment with the field gradient. The importance of quadrupole interactions to account for the greater adsorption of nitrogen than of either oxygen or argon was first pointed out in detail by Drain (4) and has also been analyzed by Kington and Macleod (5). Such interactions, which depend on the intensity of the electric field gradient, are expected to be particularly intense on the zeolite surfaces where the cations occupy positions of an unusually low degree of screening yet immediately adjacent to the oxygen anions of the alumino-silicate framework. The maximum effects, moreover, should be found at low adsorbate concentrations and, although Barrer and Sutherland found relatively little concentration dependence for NaX, Barrer and Stuart found that the heats of adsorption of nitrogen on LiX increased markedly at lower coverages. Their measurements, however, did not explore the region of lowest sorbate concentrations and for the most part involved concentrations greater than one molecule per cavity.

Gas chromatography offers a very convenient technique for the rapid measurement of

[1]*Contribution No. 269 from the Research Council of Alberta. Presented in part to the Western Regional Meeting of the Chemical Institute of Canada, Regina, 1960.*

the limiting low-pressure adsorption behavior. Kiselev, Khrapova, and Shcherbakova (6) have determined gas chromatographically the heats of adsorption of the lower hydrocarbons on type 5A (i.e. CaA) zeolites. Eberly (7), also using gas chromatography, has examined the adsorptive properties of cationic forms of zeolite X towards *n*-hexane and benzene. In general, the trends in cationic effects that he observed were more complex than those found by Barrer and Stuart; e.g., while the heats of adsorption on NaX were lower than on LiX, they were also lower than on KX, indicating an interplay of two opposing tendencies. However, there is also the question of whether, particularly with larger molecules, kinetic effects might become important so that the gas chromatographic values are low as compared with the equilibrium measurements.

The present work includes gas chromatographic measurements for O_2, N_2, CH_4, C_2H_6, C_3H_8, C_4H_{10}, C_2H_4, and C_3H_6 on the following cationic forms of zeolite X: Li^+, Na^+, K^+, Mg^{++}, Ca^{++}, Ba^{++}, and Ag^+. While oxygen has a small but finite quadrupole moment and therefore is less satisfactory than argon for comparison with nitrogen to indicate quadrupole energies, the difference between the adsorption of oxygen and of argon appears to be small. These observations therefore may be considered as extending the measurements of Barrer and Stuart to limiting low-pressure conditions as well as to a greater range of cations. They complement the gas chromatographic studies of Eberly by covering a greater range of adsorbates.

For the silver form of the zeolite a number of complete isotherms are also reported.

EXPERIMENTAL

For the gas chromatographic measurements, commercial zeolite in pellet form was used.[2] This contains approximately 20% clay binder which was assumed to have negligible adsorptive properties. From the parent sodium form, various cationic forms were prepared by ion exchange using 5% solutions of LiCl, KCl, $MgCl_2$, $CaCl_2$, and $BaCl_2$ percolated at 90 °C through 5 or 10 g samples of crushed pellets, 28–48 mesh. Two different samples of AgX pellets were prepared: AgX I by successive treatments with five portions of 1% $AgNO_3$ solution in the dark at room temperature and AgX II by treatments with 2% $AgNO_3$ followed by 3 treatments with 15% $AgNO_3$ solution at 60° also in the dark. The samples were washed with water to remove all salts, and the last washings were adjusted to pH 9.5 with the appropriate hydroxide to minimize any hydrolysis. The degree of exchange was confirmed by analysis to be over 90% in all cases. Except for AgX I for which no determination was made, the sorptive capacities of the various samples after activation in vacuum at 450° as measured by nitrogen adsorption at liquid nitrogen temperatures are included in Table I. These values indicate that there was negligible degradation of the material during preparation except for the magnesium species, which has an unusually low capacity and might on this basis be assumed to have lost some 35% of its crystallinity. The variations among the other forms are roughly consistent with the expected changes in cation volume.

The gas chromatographic measurements were carried out as previously described (8) but using this time a glass column 5 mm I.D. by 25 cm long which contained roughly 3.7 g (dry weight) of zeolite. The gas sample volume was 0.14 ml and the pressure of the sample could be varied as desired. The usual gas flow rate was 50 ml/min and retention volumes could be reproduced within ±1 ml, although the absolute accuracy was probably poorer than this. The columns were activated by heating in flowing helium up to 450°. The temperature range covered by the measurements was room temperature to 400°.

Helium was used as carrier gas and the dead space was determined with hydrogen. At room temperature it was necessary to extrapolate from higher temperatures since hydrogen itself is significantly retained. Because hydrogen reacts with the silver zeolite, dead space values for this column were estimated from the values for the other columns.

As pointed out previously (8) the numerical value of the net retention volume in ml of carrier gas per g of column packing expressed at 0 °C and in terms of effective mean column pressure approaches the value of the initial slope of the adsorption isotherm expressed in ml (s.t.p.) g^{-1}, atm^{-1}. A derivation of this relation has recently been presented by Gale and Beebe (9). This net retention volume per g may, in conformity with recommended nomenclature (10), be designated by V_g. The fact that V_g, which is called the specific retention volume, was originally defined to refer to 1 g of liquid phase in gas–liquid chromatography should cause no confusion when reference is to the adsorbent solid in gas–solid chromatography. For convenience in comparing the various cationic forms, all V_g's are further expressed in terms of 1 g of the parent dehydrated

[2] *Molecular Sieve 13X, 1/16 in. pellets, Linde Division, Union Carbide Corp.*

sodium pellet form. The actual retention volumes per g of the exchanged zeolite may be calculated with good approximation from the numbers given by applying a factor calculated on the basis of complete exchange and an initial sodium content of 12.5% in the anhydrous commercial material.

A sample of silver zeolite X in powder form was prepared by several successive treatments of pure NaX powder[3] with 5% $AgNO_3$ solution followed by the usual washings. Adsorption isotherms were determined for this material using a standard volumetric apparatus. Volumes of gas adsorbed are given in terms of 1 g of the pure NaX using the factor 1 g $AgX_{(anh)} \equiv 0.64$ g $NaX_{(anh)}$.

The oxygen used for isotherm measurements was chemically prepared by heating potassium permanganate; the nitrogen was commercial purified grade; and the hydrocarbons were either pure grade or research grade.

The silver form of the zeolite was somewhat unstable to light, and precautions were taken to shield it from bright light during transfer operations. In the dehydrated state it was found also to be reducible by hydrogen, turning black due to the formation of metallic silver. Separate experiments showed that the reduction could be carried quantitatively to completion, in some cases at room temperature, but the rate appeared to vary from one sample to another. This may have been due to variations in the amount of residual water but was not investigated further in detail.

Chromatographic measurements with the reduced silver pellet material gave retention volumes similar to those for NaX but only about one-third as great, indicating a partial loss of crystallinity. X-ray diffraction measurements on the reduced AgX powder confirmed this and also showed the presence of metallic silver. This latter observation indicates a significant migration of the atomic silver to form crystallites large enough to give coherent scattering of X rays.

RESULTS

Retention volumes were determined for each of the gases on the various columns over as wide a temperature range as possible between room temperature and an arbitrary upper temperature limit of 400°, chosen to minimize any possibilities for decomposition of the zeolite or cracking of the hydrocarbons. Within this range measurements were made at 8 to 10 separate temperatures in random order. With this particular choice of column size and flow rate it was possible to obtain conveniently measurements for ethane over nearly the whole temperature range. With oxygen, the most weakly retained adsorbate, the maximum convenient temperature was around 150°; above this the observed net retention volumes fell below 3 or 4 ml and the uncertainties became proportionately larger. For the most strongly retained gases the measurements were limited to temperatures above 250 or 300° to keep the observed retention volumes below around 1000 ml. Consequently the number of separate temperature points for each solute varied between 3 (occasionally only 2) and 6 or 8.

The elution peaks were all nearly symmetrical with only a slight tendency towards tailing. The peak widths, calculated in the recommended manner (10), corresponded to plate heights of approximately 1 mm, indicating efficient chromatographic processes. The variation of retention volume with sample pressure was small; two or three sample pressures between 0.5 and 15 cm (i.e. 0.4–12 μmoles) were usually used, and linear extrapolation to zero pressure involved at most a few tenths of a milliliter in V_g. Column AgX I was an exception to this and showed significantly more peak asymmetry, greater peak broadening, and greater dependence of retention volume on sample size. Some very extreme behavior of this sort was also observed in preliminary experiments with other species less completely exchanged than the ones described here. However, more extensive percolation of the hot exchanging solution and the final washings with the dilute hydroxide solution eliminated these features.

Plots of log V_g against reciprocal of the absolute temperature gave straight lines within the accuracy of the measurements, although there was sometimes a suggestion of a decrease in slope towards higher temperatures. Some curvature would be expected on theoretical grounds because of a temperature dependence of ΔH (11, 12), but most workers usually find similar linearity. The scatter of the experimental points about these lines led

[3]*Kindly provided by Dr. D. W. Breck of the Linde Division, Union Carbide Corp.*

to maximum uncertainties in the slope which varied with the solute. Expressed in terms of ΔH, these uncertainties ranged from ± 0.7 kcal/mole for O_2, where the relative scatter was quite high and the temperature range relatively short, down to ± 0.1 kcal/mole for C_2H_6, for which good measurements could be made over a wide temperature range, and increased again to as much as ± 1 kcal/mole for more strongly adsorbing gases such as butane and propylene, which could only be measured over short temperature ranges.

TABLE I

Gas chromatographic specific retention volumes* and heats of adsorption†

		LiX 145‡	NaX 154‡	KX 120‡	MgX 105‡	CaX 165‡	BaX 150‡	AgX I —	AgX II 158‡
O_2	V_g (50°)	1.3	1.2	1.2	0.7	3.2	2.0	1.2	2.3
	ΔH obs.	3.2	3.3	3.1	3.2	4.3	3.8	4.2	3.5
	" lit.§	3.2	2.9	3.0	—	4.7	3.3	—	—
N_2	V_g (50°)	11.8	4.1	2.3	9.6	33.3	6.0	42.0	89.2
	ΔH obs.	6.6	4.4	4.4	8.3	7.5	4.8	7.4	7.8
	" lit.‖	6.3	4.6	3.7	—	—	—	—	—
CH_4	V_g (50°)	12.7	7.2	6.7	6.1	50	14.1	155	261
	ΔH obs.	5.1	4.2	4.2	6.4	7.2	5.1	7.5	7.6
	" lit.¶	—	4.3	—	—	—	—	—	—
C_2H_6	V_g (150°)	11.4	9.0	9.4	4.0	27.8	23.3	120	182
	ΔH obs.	6.8	6.0	6.5	7.7	8.5	7.4	9.3	9.2
	" lit.¶	—	6.0	—	—	—	—	—	—
C_3H_8	V_g (150°)	62	50	58	11.5	154	160	1340	—
	ΔH obs.	8.4	7.8	8.4	6.6	10.6	9.1	10.9	12.6
	" lit.¶	—	11	—	—	—	—	—	—
n-C_4H_{10}	V_g (250°)	31	28	30	6.6	65	83	—	—
	ΔH obs.	9.5	9.2	10.2	7.4	13.9	11.2	—	—
	" lit.¶	—	14	—	—	—	—	—	—
C_2H_4	V_g (250°)	25.2	7.2	3.6	11.6	120	14.2	—	—
	ΔH obs.	8.4	8.4	7.6	14.1	(19)	9.6	—	—
C_3H_6	V_g (250°)	—	32	16	76	880	70	—	—
	ΔH obs.	—	10.9	10.0	15	(23)	(11)	—	—

*V_g is given in ml corrected to 0 °C and effective mean column pressure per g of dehydrated NaX pellets or equivalent.
†ΔH is given in kcal/mole.
‡Zeolite capacity given in ml N_2/g at 77 °K.
§Data for argon from Barrer and Stuart (3) extrapolated from 5 ml/g to zero coverage.
‖Estimated by extrapolation of curves of Barrer and Stuart (3) from 260 to 298 °K and from 10 ml/g to zero coverage.
¶Estimated by extrapolation of data of Barrer and Sutherland (1) to zero coverage.

The best fit straight lines to the measurements are summarized in Table I, which gives the value of V_g at a specified temperature and the heat of adsorption as obtained from the slope of the line. Values for the two separate AgX preparations are given, and it is interesting that although the V_g values differ by a factor of 2, the heats of adsorption are approximately the same. As noted above, AgX I did show evidence of slow adsorption and surface heterogeneity. Both preparations were shown by analyses to be nearly 100% exchanged, and while the low temperature sorptive capacity was not determined for AgX I, the value for AgX II as given in the table is normal. Even for AgX II, however, the V_g's are significantly lower than would be expected from the equilibrium isotherms, although here there was no excessive band broadening as might be expected for high transfer resistances. This puzzling behavior is further discussed later.

Table I also includes, for comparison, limiting isosteric heats of adsorption for argon and nitrogen on the alkali metal zeolites derived from Barrer and Stuart (3) and for the normal alkanes on NaX from Barrer and Sutherland (1). Argon and oxygen might reasonably be expected to show similar adsorptive behavior, and a few chromatographic measurements with argon gave V_g's close to those for oxygen. The agreement of the heats of adsorption and the isosteric heats is within experimental error. For nitrogen on NaX Barrer and Stuart found a 1 kcal/mole range in isosteric heats between 170 and 260 °K, whereas the chromatographic heats over the range 298–480 °K appear to be roughly constant and to agree with the estimated limiting isosteric value at 298°. A further comparison may be made between the observed initial slope of Barrer and Stuart's 273° isotherm for nitrogen on NaX and an extrapolated retention volume. The initial slope of the isotherm was estimated as 16 ml (s.t.p.) atm^{-1} g^{-1} hydrated zeolite or 21 ml (s.t.p.) atm^{-1} g^{-1} dehydrated zeolite; extrapolation of the retention volumes to 273 °K gives 16 ml/g of pelletized zeolite equivalent to approximately 20 ml/g of the binder-free material.

The initial heats of adsorption of the alkanes on NaX show good agreement with the estimated limiting isosteric values in the case of methane and ethane, but are significantly lower for propane and butane. There is some uncertainty concerning these last two comparisons because the isosteric values refer to coverages of 30 ml/g or higher. There is, however, no significant variation with coverage to suggest that the zero coverage limit should be much different, so that the discrepancy may well be real.

The gas chromatographic heats of adsorption reported by Kiselev *et al.* (6) for the adsorption of hydrocarbons on CaA zeolite are compared in Table II with the present

TABLE II

Gas chromatographic heats of adsorption on CaA and CaX zeolites

	Heat of adsorption, kcal/mole	
Adsorbate	CaA*	CaX
CH_4	4.0	7.2
C_2H_6	6.1	8.5
C_3H_8	8.4	10.6
C_4H_{10}	10.8	13.9
C_2H_4	9.0	(19)
C_3H_6	10.7	(23)

*Kiselev, Khrapova, and Shcherbakova (6).

results for CaX. Apart from the cases of ethylene and propylene where the present measurements are highly uncertain, the values for CaA are regularly 2–3 kcal/mole lower than those for CaX. There is, however, a suggestion from a comparison with a calorimetric result in Kiselev's work that their chromatographic values may be low by around 1 kcal/mole. Accessibility to the surface is more difficult through the smaller pores of CaA, and any temperature dependence here will give an apparently low heat of adsorption. Such a possibility is suggested by calculations of the plate heights from the chromatograms shown for ethane by Kiselev *et al.* which give values decreasing from around 3.6 mm at 30° to 1.5 mm at 100°. It would seem, therefore, that there is little conclusive evidence for any difference in heats of adsorption on X and on A zeolites, and from the similarities of their surfaces this is hardly surprising.

With further reference to the significance of quadrupole interactions as exemplified in

the comparison of nitrogen and oxygen, the ratio of the retention volumes of these two gases is of interest and is shown in Fig. 1 plotted against $1/T$. These values are, in effect,

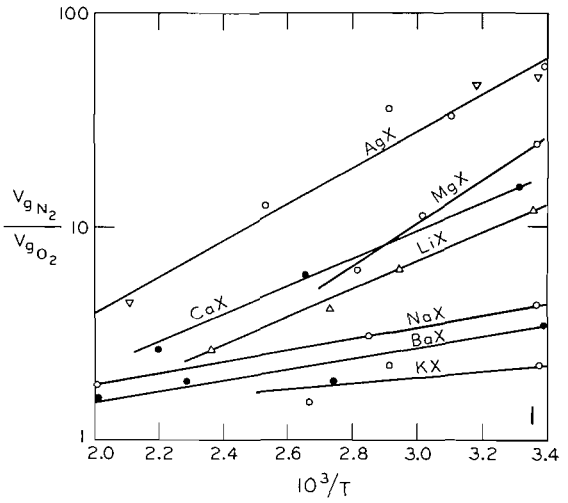

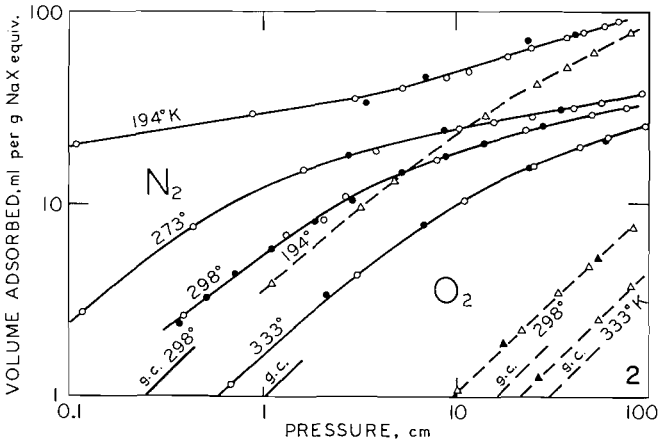

FIG. 1. Ratio of the specific retention volumes of nitrogen and oxygen as a function of temperature for various cationic forms of zeolite X. For AgX the circles refer to AgX I and the triangles to AgX II.

FIG. 2. Isotherm for the adsorption of nitrogen and oxygen by AgX powder. The lines labelled g.c. are the limiting isotherm slopes corresponding to the gas chromatographic results of AgX II.

the limiting separation factors that might be approached in the adsorption of nitrogen–oxygen mixtures at low coverage. The selectivity for nitrogen, particularly for the silver, calcium, and magnesium zeolites, approaches very high values—considerably larger than have been reported for other adsorbents at these temperatures. Such selectivity, of course, is also of interest from considerations of practical chromatography or of selective adsorption.

To investigate the extent of this high degree of preference for nitrogen, full isotherms were measured for nitrogen and oxygen on AgX, the species exhibiting the most extreme behavior. The results are shown in Fig. 2 and the corresponding isosteric heats in Fig. 3. Comparison is possible with the gas chromatographic measurements, and in Fig. 2 are

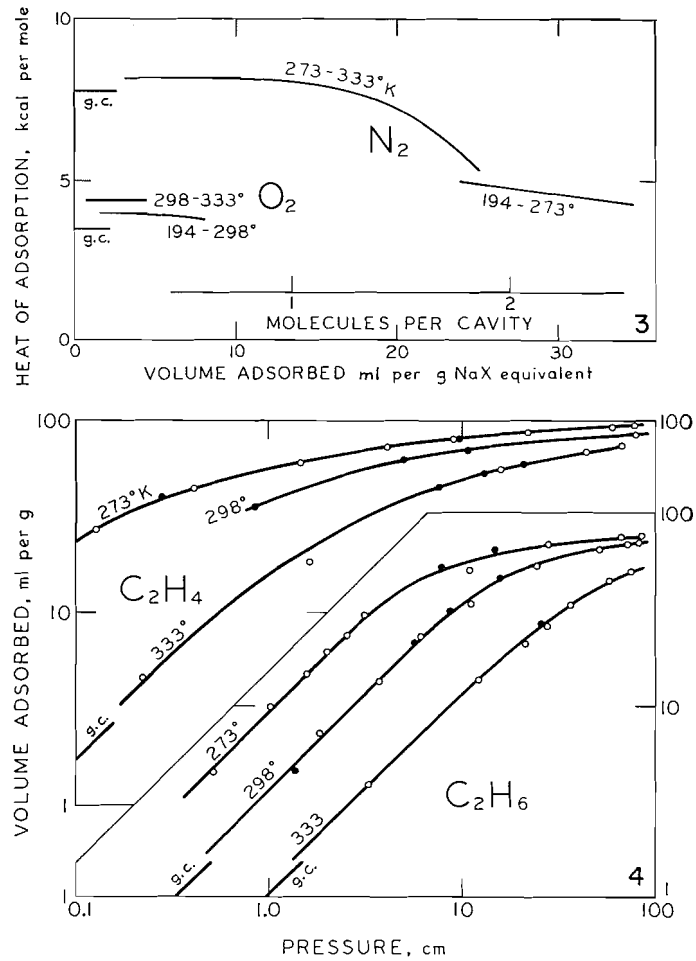

FIG. 3. Heats of adsorption of nitrogen and oxygen on AgX.
FIG. 4. Isotherms for the adsorption of ethane and ethylene on NaX powder.

shown the limiting portions of the isotherms at 25 and 60 °C (assumed linear) corresponding to the gas chromatographic retention volumes for AgX II increased by 25% to allow for the presence of binder in the pellets. Even these gas chromatographic values, the higher of the two columns measured, are only about two-thirds of the equilibrium isotherm measurements, although the heats of adsorption are in good agreement.

The data of Figs. 2 and 3 indicate clearly that the relatively strong adsorption of nitrogen is limited to low coverages—around 1 molecule per cavity or less. Such an effect was indicated by the work of Barrer and Stuart, but their measurements did not extend to the very lowest coverages and did not show any stepwise change in ΔH, as is indicated in Fig. 3.

Isotherms were also determined for ethane and ethylene on AgX and, for comparison, on NaX as well. These are shown in Figs. 4 and 5 and the isosteric heats of absorption in Fig. 6. The comparison with the limiting isotherms indicated by gas chromatography is seen to be fairly good for NaX, but the chromatographic values for AgX are significantly low, as was the case with the nitrogen and oxygen. It was very noticeable with AgX that

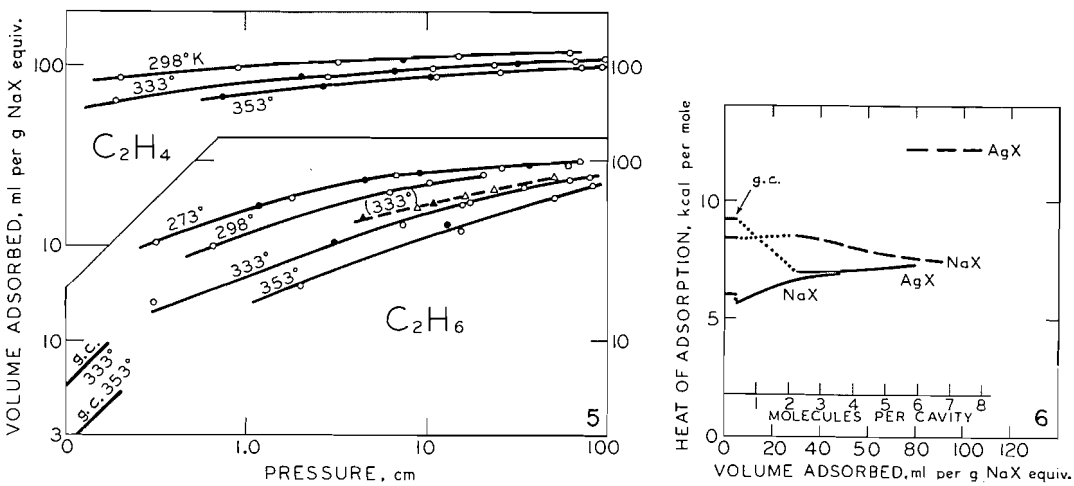

FIG. 5. Isotherms for the adsorption of ethane and ethylene on AgX powder. The broken line for ethane at 333° corresponds to the total ethane + ethylene when ethane is added to a sample containing 39 ml of ethylene/g NaX equivalent preadsorbed.

FIG. 6. Heats of adsorption of ethane (solid lines) and ethylene (broken lines) on NaX and AgX.

adsorption of all gases was much slower than for NaX, and with ethane and ethylene 2 to 3 h was necessary at every point to reach equilibrium. It would thus seem that while the total adsorptive capacity of the AgX pellets was not diminished as compared with the parent NaX, at least part of this capacity is only slowly accessible and not able to participate in the rapid adsorption and desorption processes involved in gas chromatography.

The behavior of ethylene on AgX requires additional comment. Ethylene was never eluted from the gas chromatographic columns, and during the isotherm measurements a portion of the ethylene resisted prolonged pumping into a liquid-nitrogen-cooled trap. This amount of residual ethylene varied from approximately 36 ml/g at 373 °K to 49 ml/g at 298 °K. Excessive heating led to some decomposition of the ethylene and apparently also some reduction of silver ion. This firmly held ethylene could, however, be completely displaced by water vapor.

The complexing of olefins with silver ions is well known and has been discussed by Dewar (13) in terms of combined d–π^* and s–π orbital interactions between Ag^+ and the double bond, but such complex formation is seldom very pronounced with the lower olefins and usually cannot be detected with ethylene. Quinn and Glew (14) recently reported studies of the complexing of olefins with anhydrous silver fluoborate to give the strongest complexes then reported for the lower olefins. Their 1:1 complex with ethylene, for example, had a vapor pressure at 25° of 12.75 mm. At least part of the ethylene adsorbed on AgX is much more strongly held; the 40 ml/g (approximately 3 molecules per cavity) which is not removable by pumping into a liquid-nitrogen-cooled trap must have a vapor pressure less than 2μ.

DISCUSSION

Because of some apparently real discrepancies between gas chromatographic and isotherm measurements, this work raises questions concerning the limitations of the gas chromatographic technique for studying the limiting low-pressure adsorption properties. The general validity and usefulness of the technique seems to have been clearly established

in previously reported studies (8, 9, 10) and is confirmed by at least a portion of the measurements reported here. However, in the case of systems involving either very active adsorbents such as AgX or relatively large adsorbate molecules such as propane and butane there is a clear suggestion that the gas chromatographic retention volumes and heats of adsorption may be low as compared with the equilibrium values. This would be expected if the adsorption processes are slow as compared to the time scale of the chromatographic process. The retention volumes would be smaller than the values corresponding to the initial slopes of the isotherms, and the discrepancy would be expected to be more serious the lower the temperature, thus giving too low a slope to the log V_g vs. $1/T$ plot and hence too low a value of ΔH. Such an effect might also just compensate for the expected curvature in the log V_g vs. $1/T$ plot to give the high degree of linearity often observed. Under these conditions the V_g's and ΔH's obtained by chromatography would tend to be minimum values, and this must be borne in mind in their application and interpretation.

It must be emphasized that except for column AgX I no *chromatographic* evidence of slow adsorption–desorption processes has been obtained in this work—such as excessively broad bands or an increase in retention volume with decrease in flow rate—but only limited attempts were made to look for such effects. Within the normal range of chromatographic conditions, however, processes slower by more than approximately two orders of magnitude than the dynamic transfer steps involved in elution simply would not be seen at all. For example, chromatography of carbon dioxide on NaX yielded reasonably symmetrical peaks corresponding to the rapid adsorption processes but showed no evidence of the slow chemisorption processes that have been demonstrated to occur (15). Such chemisorption processes are extreme examples. Slow adsorption such as observed for oxygen, nitrogen, or ethane on AgX may be the result of the presence of structural faults in the crystal which restrict access to some interior cavities. Alternatively, it may indicate merely slowness of redistribution after an initially high concentration is achieved in the outer cavities of a crystal. This redistribution process would be expected to have an activation energy comparable to the heat of adsorption and hence to vary significantly over the temperature range of the experiments. It should therefore result in heats of adsorption being too low and also be detectable chromatographically as a significant mass transfer resistance contribution to the plate height. Structural blockages might be relatively insensitive to temperature and therefore yield low V_g's but reasonably correct ΔH's, as appeared to be the case with the silver zeolite. It remains puzzling that there was so little evidence of band broadening in some of the other cases of low ΔH such as the measurements with propane and butane. Studies of mass transfer resistances in gas–solid chromatography of zeolites would be worthwhile.

In general, therefore, the gas chromatographic results must be considered as conservative, tending to be low rather than high both in retention volume and in heat of adsorption. Even with this degree of uncertainty, the present results clearly confirm the very pronounced contributions pointed out by Barrer and Stuart (3) of the exchangeable cations to the adsorptive properties of zeolite X. These authors discussed the various energy terms, dispersion, polarization, repulsion, and quadrupole interaction energies, contributing to the adsorption process, and in the light of their analyses it is pertinent to make some comments concerning the present results.

From the available knowledge of the crystal structure of zeolite X (16) it is clear that the exchangeable cations occupy positions of a very low degree of shielding. In each large cavity there are approximately eight univalent cations. Four of these have been located

in the six-membered oxygen rings which form the windows of the sodalite cages, and while a small cation such as lithium might be stable within the plane of the ring, the sodium and, even more so, potassium cations will probably project significantly into the adsorption cavity. This lower degree of screening of the larger cations in this site would tend to compensate for their weaker field. The other four cations have not been definitely located by crystallographic studies but probably occupy sites on the cavity surface, most probably adjacent to four-membered oxygen rings. These positions are much more exposed than the six-membered ring sites and would correspondingly have more intense fields and field gradients associated with them.

In the case of divalent cations it has not been demonstrated which sites are occupied, but it would be expected that the six-membered ring sites would be the more stable. Thus, the enhancement of adsorptive properties due to the higher charge density on the cations would not be as great as if these cations occupied the less shielded positions on the cavity surface.

A further factor relevant to the adsorption processes under discussion is the difference between silver ion and the others studied. The alkali and alkaline earth cations are all of a stable noble gas electronic configuration whereas the d orbitals of silver ion give it much more intense directional properties. Silver ion has a much stronger polarizing power than, say, sodium ion which is of the same total charge and very similar size. Furthermore, because Ag^+ is monovalent, half of these ions will be in the exposed positions on the cavity surface where this polarizing power can be most forcefully exerted.

As Barrer and Stuart have already shown, quadrupole interactions are the main reasons for the strong adsorption of nitrogen as compared with oxygen. From Fig. 1 it is seen that the selectivity increases in the order K, Na, Li and Ba, Ca, Mg, increasing with decreasing ionic size and hence with increasing charge density (charge density is used here in the sense that it applies to the individual ion and is proportional to the charge divided by the ionic radius squared). However, the difference between the two series is less marked than might be expected and this is probably because of the absence of the divalent cations from the exposed sites. The strongest effect of all is with silver ion which must occupy these sites. The limitation of the high selectivity in AgX to the first one or two molecules adsorbed per cavity suggests that the field around these exposed cationic sites is very sensitive to the perturbations of neighboring molecules.

Of the remaining adsorbates, only the olefins are likely to have significant quadrupole contributions to the energy of adsorption; methane has no quadrupole moment and the higher alkanes probably only have very small moments (17). With these substances it is more likely that polarization energies make significant contributions in addition to the usual dispersion and repulsion terms. Barrer and Stuart pointed out that adsorption on completely unscreened cations would yield ion-induced dipole polarization energies equal to or larger than the total observed heats of adsorption. Some screening must be present for the ions on any solid surface but, as already noted, it is probably minimal for the zeolites. Consequently it is considered probable that polarization effects are a major contributor to the increased heats of adsorption found with the more strongly polarizing cations.

Finally, one secondary effect should be mentioned. This is a tendency with larger adsorbate molecules for the adsorption on KX to be stronger than on NaX in opposition to the trend $Li^+ > Na^+ > K^+$. This same effect was evident in the measurements of Eberly (7) for the C_6 hydrocarbons. While this difference may be an accidental result of incomplete equilibration as mentioned earlier, it may also be explained as being due to the

greater ease with which a larger and somewhat more flexible molecule can fit against a large ion than against a small ion. In this way a greater total area of close adsorptive contact is obtained, even though the local field intensities are less. This enhancement of adsorption on KX relative to NaX is evident for ethane but not for the more rigid ethylene.

The observations reported herein have some practical significance for improved gas chromatographic resolutions through appropriate choice of the cationic species. These results are also felt to be relevant and useful in terms of conventional equilibrium adsorption processes, but kinetic limitations and the limitations of low coverage mean that great care must be taken in extending the conclusions of gas chromatography. Additional careful comparisons of gas chromatographic and equilibrium data would be worthwhile.

ACKNOWLEDGMENTS

The author thanks E. Dutcher and A. Vilonyay for carrying out most of the experimental work of the paper. Helpful discussions with Dr. F. Birss of the University of Alberta are gratefully acknowledged.

REFERENCES

1. R. M. Barrer and J. W. Sutherland. Proc. Roy. Soc., Ser. A, **237**, 439 (1956).
2. R. M. Barrer, F. W. Bultitude, and J. W. Sutherland. Trans. Faraday Soc. **53**, 1111 (1957).
3. R. M. Barrer and W. I. Stuart. Proc. Roy. Soc., Ser. A, **249**, 464 (1959).
4. L. E. Drain. Trans. Faraday Soc. **49**, 650 (1953).
5. G. L. Kington and A. C. Macleod. Trans. Faraday Soc. **55**, 1799 (1959).
6. A. V. Kiselev, Ye. V. Khrapova, and K. D. Shcherbakova. Neftekhimiya **2**, 877 (1962); Petrol. Chem. USSR, **2**, 558 (1963).
7. P. E. Eberly, Jr. J. Phys. Chem. **66**, 812 (1962).
8. H. W. Habgood and J. F. Hanlan. Can. J. Chem. **37**, 843 (1959).
9. R. L. Gale and R. A. Beebe. J. Phys. Chem. **68**, 555 (1964).
10. D. Ambrose, A. T. James, A. I. M. Keulemans, E. Kovats, H. Roeck, C. Rouit, and F. H. Stross. Pure Appl. Chem. **1**, 177 (1960).
11. S. Ross, J. K. Saelens, and J. P. Olivier. J. Phys. Chem. **66**, 696 (1962).
12. J. Hanlan and M. P. Freeman. Can. J. Chem. **37**, 1575 (1959).
13. M. J. S. Dewar. Bull. Soc. Chim. France, **18**, C79 (1951).
14. H. W. Quinn and D. N. Glew. Can. J. Chem. **40**, 1103 (1962).
15. L. Bertsch and H. W. Habgood. J. Phys. Chem. **67**, 1621 (1963).
16. K. Broussard and D. P. Shoemaker. J. Am. Chem. Soc. **82**, 1041 (1960).
17. B. Birnbaum and A. A. Maryott. J. Chem. Phys. **36**, 2032 (1962).

Can. J. Chem. Downloaded from www.nrcresearchpress.com by 210.87.254.5 on 09/05/12
For personal use only.

NOTES

ON THE EFFECT OF AN ATTRACTIVE MORSE POTENTIAL ON THE VIBRATIONAL ENERGY TRANSFER

H. SHIN

The effect of an attractive potential on the vibrational energy exchange, which has recently attracted considerable attention, is an important subject because of its significance in the general field of inelastic collisional processes (1–4). The importance is due to the argument that the attractive part is present in the true interaction in which the approaching molecules are "speeded up" in a potential well of depth D. Though such a physical argument is suggestive, there are some doubts regarding the exact forms of the D-dependent correction terms and their importance in the exponential part of the de-excitation probabilities per unit time (3–5).

In this note we shall point out that using the W.K.B. semiclassical approach (4, 6) we can formulate the D-dependent correction terms in different forms from the originally suggested form D/kT in the exponent of the de-excitation probability (1). For this study the assumed form of the interaction energy between an oscillator and an incident particle is the Morse type

$$w(x) = D(e^{-x/a} - 2e^{-x/2a}).$$

We also briefly discuss the de-excitation probability for a Lennard-Jones (L-J) potential.

If we omit the coefficient of the exponential factor, the de-excitation probability per unit time can be written in terms of the W.K.B. wave functions

$$[1] \quad P \sim \int_0^\infty \exp\left\{-\frac{2\sqrt{2\mu}}{\hbar}\left[\int_{x_2}^{x_0}\sqrt{w(x)-E'}\,dx - \int_{x_1}^{x_0}\sqrt{w(x)-E}\,dx\right] - \frac{E}{kT}\right\}dE,$$

where μ is the reduced mass of the collision partners, x_1, x_2 are the turning points, and $x_0 \to -\infty$, i.e., $w(x) \to \infty$, in the asymptotic limit. For the purely repulsive exponential interaction $w(x) = Ae^{-x/a}$, it has been shown that equation [1] gives (4)

$$P \sim \exp\left\{-\frac{3\chi}{kT} + \frac{\Delta}{2kT}\right\},$$

where

$$\chi = \left(\sqrt{\frac{\mu}{2}}\frac{\pi a \Delta kT}{\hbar}\right)^{2/3}$$

and $\Delta = E' - E$, the magnitude of the change in the oscillator's energy due to the collision.

Since the terms in the square brackets in equation [1] are proportional to the reciprocal of energy E, the integrand posesses a sharp maximum value at some energy E^*. An estimate of this energy which is the most probable value for energy transfer is obtained by minimizing the exponent of equation [1], i.e., the solution of

$$[2] \qquad \int_{x_2}^{x_0}\frac{dx}{\sqrt{w(x)-E'}} - \int_{x_1}^{x_0}\frac{dx}{\sqrt{w(x)-E}} = \frac{\hbar}{\sqrt{2\mu kT}}.$$

By changing $dx = (dx/dw)dw$ and by obtaining dx/dw in the region of strong repulsion as

$$\frac{dx}{dw} = -\frac{a}{w}\left[1 + \sqrt{\frac{D}{w}} - \frac{1}{2}\left(\frac{D}{w}\right)^{3/2} - \left(\frac{D}{w}\right)^{2} + \dots\right],$$

the l.h.s. of equation [2] can be expanded in a binomial series to obtain

$$[3] \qquad \sum_{i=0}^{\infty}\sum_{n=1}^{\infty}\left[(-1)^{n-1}\frac{\Gamma(n+i+\frac{1}{2})}{\Gamma(i+1)n!}\Delta^n a_i (E^*)^{-\frac{1}{2}-i-n}\right] = \frac{\hbar}{\sqrt{2\pi\mu kT}},$$

with $n = 1, 2, 3, \dots$

$i = 0, 1/2, 1, 3/2, 2, \dots$

$\alpha_0 = a$, $\alpha_{1/2} = a\sqrt{D}$, $\alpha_1 = 0$, $\alpha_{3/2} = -aD^{3/2}$. . . .

The solution of equation [3] is

$$[4] \qquad E^* = \chi + \frac{8\sqrt{D\chi}}{3\pi} - \frac{\Delta}{2}.$$

On the other hand, if the purely repulsive interaction $w(x) = Ae^{-x/a}$ is assumed, $E^* = \chi - \Delta/2$, so that the term $8\sqrt{D\chi}/3\pi$ characterizes the effect of the attractive part in $w(x)$.

In terms of the energy E^*, the de-excitation probability, equation [1] can now be written

$$[5] \qquad P \sim \exp\left\{\frac{\sqrt{2\pi\mu}}{\hbar}\sum_{i=0}^{\infty}\sum_{n=1}^{\infty}\left[(-1)^n\frac{\Gamma(n+i-\frac{1}{2})}{\Gamma(i+1)n!}\Delta^n a_i (E^*)^{\frac{1}{2}-n-i}\right] - \frac{E^*}{kT}\right\}.$$

When we calculate each term of the double-sum with respect to a set of i and n, the exponent in equation [5] becomes

$$[6] \qquad -\frac{\pi a\Delta}{\hbar}\sqrt{\frac{\mu}{2E^*}}\left[1 + \frac{8}{3\pi}\sqrt{\frac{D}{E^*}} - \frac{3}{4}\left(\frac{\Delta}{E^*}\right) - \frac{4}{3\pi}\frac{\Delta}{E^*}\sqrt{\frac{D}{E^*}} + 0\left(\frac{1}{E^{*2}}\right)\right] - \frac{E^*}{kT}.$$

By substituting equation [4] into [6], the final expression for the de-excitation probability, in the asymptotic limit, is

$$[7] \qquad P \sim \exp\left\{-\frac{3\chi}{kT} + \frac{4\sqrt{D\chi}}{\pi kT} + \frac{16D}{3\pi^2 kT} + \frac{\Delta}{2kT}\right\}.$$

The first term in the exponent is the leading term, the Landau–Teller term (7), and the same form also appears in the case of the purely repulsive interaction. The last term, $\Delta/2kT$, is a small correction which is quite independent of the exact form of $w(x)$, because symmetrization yielding this term affects only the leading term. The two intermediate (D-dependent) terms, which resulted from the i-summation in equations [3] and [5], are the corrections due to the presence of the attractive part $-2De^{-x/2a}$ in $w(x)$. Since both terms are positive, this additional part in $w(x)$ leads to more effective energy transfers, as it must.

Obviously, the presence of the first correction term $4\sqrt{D\chi}/\pi kT$, which is the geometric mean of the leading term and the second correction term $16D/3\pi^2 kT$, is important. In previous approaches, the existence of this term has not been reported (2, 8). Since at

Can. J. Chem. Downloaded from www.nrcresearchpress.com by 210.87.254.5 on 09/05/12
For personal use only.

ordinary temperatures χ/kT is 5–10 and D/kT is close to unity, the first correction significantly contributes to the overall value of P. The contribution of the second correction term is small, but it is important to note its existence, in view of Schwartz and Herzfeld's purely physical argument (1, 9), in obtaining a similar term D/kT. Numerically, therefore, the second correction is half of Schwartz and Herzfeld's term. While the latter workers have considered D/kT as the only term responsible for an attractive force between the collision partners, we have found an important D-dependent correction term $4\sqrt{D\chi}/\pi kT$ for a realistic Morse potential.

The present result may be compared to Nikitin's work (3) for a L-J potential. Using first-order perturbation theory he has obtained

$$P \sim \exp\,(-\,3\chi/kT + 4\sqrt{D\chi}/\pi kT + \Delta/2kT),$$

which is very similar to the expression obtained above. It should be noted, however, that he has neglected the attractive part of $w(x)$ in the formulation of dw/dq, where q is the vibrational coordinate, while he has included it in the calculation of the classical integral of motion. Therefore, it is not possible to compare the two results quantitatively, but the importance of the D-dependent correction terms is seen in both cases. Note that Nikitin's expression shows no term proportional to D/kT.

Since the nature of repulsive part in a L-J potential is somewhat different from that of the exponential case, its leading term in the exponent of P cannot be the Landau–Teller form for exponential interactions. In fact, for the 12–6 L-J potential,

$$w(x) = 4D[(a'/x)^{12} - (a'/x)^{6}],$$

the present method gives the leading term

$$\frac{19}{7}\left[7\frac{\Gamma(7/12)}{\Gamma(1/12)}\frac{\sqrt{2\pi\mu}a_0'\Delta kT}{\hbar}\right]^{12/19}\frac{1}{kT}$$

where $a_0' = a'(4D)^{1/12}/12$. This expression is entirely different from the Landau–Teller term given above for exponential interactions. However, this leading term can be closely related to the Landau–Teller term either by equating the leading terms of the double-sum in equation [5] for the two potentials, or by properly fitting the L-J potential to the Morse potential such that magnitudes are equal for $x = x_c$ and $x = x_1$, where x_c is the distance between molecular centers at the classical turning point and x_1 is the corresponding value for the energy zero of the L-J potential (1).

1. K. F. Herzfeld and T. A. Litovits. Dispersion and absorption of ultrasonic waves. Academic Press Inc., New York. 1959.
2. D. Rapp. J. Chem. Phys. **32**, 735 (1960). R. E. Turner and D. Rapp. J. Chem. Phys. **35**, 1076 (1961).
3. E. E. Nikitin. Opt. i Spektroskopiya, **6**, 141 (1959). (English transl.: Opt. Spectry. USSR, **6**, 93 (1959)).
4. B. Widom. Discussions Faraday Soc. **33**, 37 (1962). H. Shin and B. Widom. Bull. Am. Phys. Soc. **8**, 532 (1963). (Presented at the A.P.S. Autumn Meeting at Chicago.)
5. A. R. Blythe, T. L. Cottrell, and A. W. Read. J. Chem. Phys. **37**, 2733 (1962).
6. L. Landau and E. M. Lifshitz. Quantum mechanics. Pergamon Press, London. 1958. pp. 178–183.
7. L. Landau and E. Teller. Physik. Z. Sowjetunion, **10**, 34 (1936).
8. A. F. Devonshire. Proc. Roy. Soc. London, Ser. A, **158**, 269 (1937).
9. R. N. Schwartz and K. F. Herzfeld. J. Chem. Phys. **22**, 767 (1954).

Received April 20, 1964.
Department of Chemistry,
Cornell University,
Ithaca, New York.

Can. J. Chem. Downloaded from www.nrcresearchpress.com by 210.87.254.5 on 09/05/12
For personal use only.

QUANTITATIVE DECARBOXYLATIONS OF ELECTRONEGATIVELY SUBSTITUTED BENZOIC ACIDS VIA THE SCHMIDT REACTION

A. J. McNamara and J. B. Stothers

Can. J. Chem. Downloaded from www.nrcresearchpress.com by 210.87.254.105 on 09/05/12
For personal use only.

Reaction mechanism studies involving isotopic carbon frequently require the isolation, for isotopic analysis, of a particular carbon atom in a molecule. If the atom of interest is bonded to an aromatic ring, a common approach to its isolation involves an oxidation to the substituted aromatic carboxylic acid followed by decarboxylation to furnish carbon dioxide for mass spectrometric analysis or radio assay. While it is always desirable that this degradation to carbon dioxide be accomplished in high overall yield, for isotope effect studies it is essential. The most frequently employed methods for the decarboxylation step include the Schmidt reaction, the Hunsdiecker silver salt degradation, and the copper chromite – quinoline reaction. The relative merits of these methods have been discussed recently (1) and a thorough review of the Schmidt reaction has appeared (2). The major deficiency of the Schmidt reaction for this purpose was shown to be the poor yields obtained with aromatic acids bearing electronegative substituents (1), the presence of which so lowers the yield of carbon dioxide that the method is of little use for isotope effect studies. To our knowledge, however, most of the previous results have been obtained using *concentrated* sulphuric acid, either as the reaction medium or as a catalyst in a heterogeneous reaction mixture. While Newman and Gildenhorn (3) have reported the use of 100% sulphuric acid for the decarboxylation of 2,6-dimethyl substituted benzoic and terephthalic acids and Briggs, de Ath, and Ellis (4) noted the adverse effects of water on yields from this reaction, no studies of the Schmidt reaction on *m*- and *p*-substituted benzoic acids in anhydrous sulphuric acid appear in the literature. We have found that the yield of carbon dioxide from these acids is dramatically increased, if "100% sulphuric acid"* is used as the reaction medium.

Virtually quantitative yields of carbon dioxide, together with high yields of the appropriately substituted aniline, have been obtained for a series of meta- and para-substituted benzoic acids bearing a variety of electron-withdrawing groups. Typical data are listed in Table I in which the results for benzoic and *p*-anisic acids are included for comparison. The yields noted for the various anilines represent *lower* limits for the method, since these data represent the quantity of material actually isolated after recrystallization either as the aniline or as a derivative. The yields of carbon dioxide were obtained by precipitation as barium carbonate in the usual way (5). It is clear from these results that sulphonation is not an important side reaction for those acids having electron-withdrawing substituents although the presence of electron-releasing groups may lead to significant quantities of sulphonated products, as indicated by the reduced yields of the aniline from *p*-anisic and benzoic acids. No attempt was made to isolate sulphonated products from these reactions.

The reaction conditions (2 h at 40 °C) were chosen for convenience and to allow comparison with previous results using concentrated sulphuric acid (1, 6). These conditions are not particularly drastic and the reaction proceeds smoothly at even lower temperatures. Furthermore, Deno and his co-workers (7) have demonstrated that much more reactive species can be treated with, and recovered from, sulphuric acid solutions

**Prepared by the addition of the calculated amount of 95% H_2SO_4 to 20% oleum.*

TABLE I

Modified Schmidt reaction on benzoic acids

	Sulphuric acid concentration				
	96%	100%		20% oleum	
	% yield:				
Substituent	Barium carbonate	Barium carbonate	Aniline	Barium carbonate	Aniline
None	90.5	96.5	67*	—	—
4-OCH_3	91.8	96.5	0*	—	—
4-F	71.7	99.5	92	—	—
4-Cl	51.3	98.0	99	—	—
4-Br	50.3	97.5	96	—	—
4-CN	7.6	100.0	73†	—	—
4-CF_3	—	97.4	41‡	—	—
4-NO_2	8.1	99.0	99	—	—
3-NO_2	6.1	98.3	100	—	—
3,5-di-NO_2	—	3.2	—	97.6	82

*Sulphonation would be expected.
†As *p*-aminobenzamide.
‡As N-acetyl derivative.

without serious decomposition. While it would appear that the Schmidt reaction is complete in a shorter period of time, no quantitative kinetic data have been obtained to date. Each experiment was allowed to continue for 2 h to ensure that all of the evolved carbon dioxide was collected in the gas absorption trap.

Clearly the use of "100% sulphuric acid" in the Schmidt reaction affords sufficiently high yields of carbon dioxide for isotope work, but it is also interesting that the substituted aniline is formed in high yield. It appears, therefore, that this slight modification of the standard method may offer a straightforward route to certain substituted anilines which may be difficult and (or) tedious to prepare by other methods. All except one of those substituents in the present series are unaffected by the reagents. The lone exception, the cyano group, is hydrolyzed readily to the amido grouping in sulphuric acid producing a good yield of *p*-aminobenzamide. Our survey included 3,5-dinitrobenzoic acid to examine the effect of two strongly electron-withdrawing substituents on the yield of the reaction products. While reaction in "100% sulphuric acid" was negligible, the use of 20% oleum afforded a quantitative yield of carbon dioxide and an 82% yield of 3,5-dinitroaniline.

EXPERIMENTAL

The general procedure was similar to that described previously (6). An absorption train was set up, following the method of Phares (8), and to a cold (0°) solution of 1–2 mmole of the benzoic acid in 5 ml of sulphuric acid of the appropriate concentration was added sodium azide (15% excess over a 1:1 mole ratio, NaN_3:RCOOH). After connection to the absorption traps, the temperature of the reaction mixture was maintained at 40 ± 1° for 2 h while the evolved carbon dioxide was swept into 0.2 *M* carbonate free sodium hydroxide by a slow stream of purified nitrogen. The carbon dioxide was precipitated as barium carbonate in the usual way (5). Great care was taken in all operations to avoid contamination with extraneous carbon dioxide and suitable blanks were run at regular intervals to check the operations. To isolate the aniline, the reaction mixture was poured into cold water, sufficient alkali was added to make the solution definitely basic, and the product removed by ether extraction. Removal of the ether was followed by recrystallization of the residue in the case of the solid anilines; otherwise a suitable solid derivative was prepared and recrystallized. In the case of *p*-aminobenzamide (from *p*-cyanobenzoic acid), the reaction mixture was poured onto 15 g of ice and, with external cooling, was neutralized with concentrated NH_4OH (just basic to litmus); the insoluble amide was filtered off and recrystallized from $EtOH/H_2O$.

All of the starting materials, except *p*-trifluoromethylbenzoic acid which was kindly supplied by Prof.

Can. J. Chem. Downloaded from www.nrcresearchpress.com by 210.87.254.105 on 09/05/12
For personal use only.

A. N. Bourns, are commercially available and the purity of each was checked by a melting point determination. The compounds were purified by recrystallization before use if the melting point indicated the presence of impurities.

ACKNOWLEDGMENTS

We are grateful for the financial assistance of the National Research Council of Canada and we wish to thank Prof. A. N. Bourns for kindly providing a sample of *p*-trifluoromethylbenzoic acid.

1. F. B. FISHER and A. N. BOURNS. Can. J. Chem. **39**, 1736 (1961).
2. P. A. S. SMITH. *In* Molecular rearrangements. P. de Mayo, *editor*. Interscience Publishers, Inc., New York. 1964. Part I. Chap. 8.
3. M. S. NEWMAN and H. L. GILDENHORN. J. Am. Chem. Soc. **70**, 317 (1948).
4. L. H. BRIGGS, G. C. DE ATH, and S. R. ELLIS. J. Chem. Soc. 61 (1942).
5. M. CALVIN, C. HEIDELBERGER, J. C. REID, B. M. TOLBERT, and P. E. YANKWICH. Isotopic carbon. J. Wiley and Sons, Inc., New York. 1949. p. 83.
6. J. B. STOTHERS and A. N. BOURNS. Can. J. Chem. **38**, 923 (1960).
7. N. C. DENO, H. G. RICHEY, N. FRIEDMAN, J. D. HODGE, J. J. HOUSER, and C. U. PITTMAN. J. Am. Chem. Soc. **85**, 2991 (1963).
8. E. F. PHARES. Arch. Biochem. Biophys. **33**, 173 (1951).

RECEIVED MAY 25, 1964.
DEPARTMENT OF CHEMISTRY,
UNIVERSITY OF WESTERN ONTARIO,
LONDON, ONTARIO.

Can. J. Chem. Downloaded from www.nrcresearchpress.com by 210.87.254.105 on 09/05/12
For personal use only.

LA RÉACTION DU SULFURE DE BORE AVEC LES ALCOOLS

J. M. LALANCETTE

Moissan (1) rapporte que le sulfure de bore réagit avec certaines molécules organiques sans toutefois préciser le mode d'action du sulfure ou la nature des produits ainsi obtenus. Au cours d'une étude systématique de l'interaction de B_2S_3 avec différents types de composés organiques (2) la réaction de ce sulfure avec les alcools a été étudiée.

On a constaté que les alcools, tant aliphatiques qu'aromatiques, conduisent aux esters orthoboriques correspondants, avec de bons rendements, la réaction s'accompagnant d'un dégagement de H_2S.

$$6ROH + B_2S_3 \rightarrow 2(RO)_3B + 3H_2S,$$

où R = CH_3, C_2H_5, *n*-C_3H_7, *n*-C_6H_{13}, *n*-C_7H_{15}, C_6H_5, α-$C_{10}H_7$.

Cependant, certains phénols nitrés demeurent complètement inertes vis-à-vis le sulfure. Cette absence de réaction ne peut se justifier par une inhibition simple due au groupe nitro car le phénol donne une réaction avec B_2S_3 même en présence d'une quantité équimoléculaire de nitrobenzène. Cette réaction demeure à l'étude afin d'en préciser, si possible, le mécanisme.

PARTIE EXPÉRIMENTALE

Réaction du sulfure de bore avec les alcools

A une suspension de 12 g (0.10 mole) de sulfure de bore, préparé selon le mode usuel (2), dans le benzène anhydre, on ajoute 61 g (0.60 mole) d'hexanol normal redistillé. L'addition s'accompagne d'un échauffement prononcé et d'un fort dégagement de H_2S, ce gaz étant capté sous forme de sulfure de plomb. On isole ainsi 0.26 mole de gaz sulfhydrique. Après un reflux de 3 h, la masse réactionnelle est filtrée. Le résidu

A. N. Bourns, are commercially available and the purity of each was checked by a melting point determination. The compounds were purified by recrystallization before use if the melting point indicated the presence of impurities.

ACKNOWLEDGMENTS

We are grateful for the financial assistance of the National Research Council of Canada and we wish to thank Prof. A. N. Bourns for kindly providing a sample of *p*-trifluoromethylbenzoic acid.

1. F. B. FISHER and A. N. BOURNS. Can. J. Chem. **39**, 1736 (1961).
2. P. A. S. SMITH. *In* Molecular rearrangements. P. de Mayo, *editor*. Interscience Publishers, Inc., New York. 1964. Part I. Chap. 8.
3. M. S. NEWMAN and H. L. GILDENHORN. J. Am. Chem. Soc. **70**, 317 (1948).
4. L. H. BRIGGS, G. C. DE ATH, and S. R. ELLIS. J. Chem. Soc. 61 (1942).
5. M. CALVIN, C. HEIDELBERGER, J. C. REID, B. M. TOLBERT, and P. E. YANKWICH. Isotopic carbon. J. Wiley and Sons, Inc., New York. 1949. p. 83.
6. J. B. STOTHERS and A. N. BOURNS. Can. J. Chem. **38**, 923 (1960).
7. N. C. DENO, H. G. RICHEY, N. FRIEDMAN, J. D. HODGE, J. J. HOUSER, and C. U. PITTMAN. J. Am. Chem. Soc. **85**, 2991 (1963).
8. E. F. PHARES. Arch. Biochem. Biophys. **33**, 173 (1951).

RECEIVED MAY 25, 1964.
DEPARTMENT OF CHEMISTRY,
UNIVERSITY OF WESTERN ONTARIO,
LONDON, ONTARIO.

Can. J. Chem. Downloaded from www.nrcresearchpress.com by 210.87.254.5 on 09/05/12
For personal use only.

LA RÉACTION DU SULFURE DE BORE AVEC LES ALCOOLS

J. M. LALANCETTE

Moissan (1) rapporte que le sulfure de bore réagit avec certaines molécules organiques sans toutefois préciser le mode d'action du sulfure ou la nature des produits ainsi obtenus. Au cours d'une étude systématique de l'interaction de B_2S_3 avec différents types de composés organiques (2) la réaction de ce sulfure avec les alcools a été étudiée.

On a constaté que les alcools, tant aliphatiques qu'aromatiques, conduisent aux esters orthoboriques correspondants, avec de bons rendements, la réaction s'accompagnant d'un dégagement de H_2S.

$$6ROH + B_2S_3 \rightarrow 2(RO)_3B + 3H_2S,$$

où R = CH_3, C_2H_5, *n*-C_3H_7, *n*-C_6H_{13}, *n*-C_7H_{15}, C_6H_5, α-$C_{10}H_7$.

Cependant, certains phénols nitrés demeurent complètement inertes vis-à-vis le sulfure. Cette absence de réaction ne peut se justifier par une inhibition simple due au groupe nitro car le phénol donne une réaction avec B_2S_3 même en présence d'une quantité équimoléculaire de nitrobenzène. Cette réaction demeure à l'étude afin d'en préciser, si possible, le mécanisme.

PARTIE EXPÉRIMENTALE

Réaction du sulfure de bore avec les alcools

A une suspension de 12 g (0.10 mole) de sulfure de bore, préparé selon le mode usuel (2), dans le benzène anhydre, on ajoute 61 g (0.60 mole) d'hexanol normal redistillé. L'addition s'accompagne d'un échauffement prononcé et d'un fort dégagement de H_2S, ce gaz étant capté sous forme de sulfure de plomb. On isole ainsi 0.26 mole de gaz sulfhydrique. Après un reflux de 3 h, la masse réactionnelle est filtrée. Le résidu

solide ne renferme plus de sulfure de bore et la portion liquide est distillée après évaporation du benzène. On retrouve ainsi 52 g (0.16 mole) d'orthoborate de *n*-hexyle: p.éb. 182° à 12 mm; n_D^{25} 1.4250. Décrit (3): p.éb. 185° à 15 mm; n_D^{23} 1.4250. Spectre infrarouge: absence de bandes dans la région de 3500 cm^{-1}, bandes à 1470 cm^{-1} (moyenne), 1410 cm^{-1} (forte), 1335 cm^{-1} (très forte), 1080 cm^{-1} (moyenne). Ce spectre est identique à celui donné par un échantillon authentique d'orthoborate d'hexyle préparé à partir de l'alcool correspondant et de l'acide borique. En appliquant la même méthode avec l'alcool propylique normal et l'alcool heptylique normal, on retrouve les orthoborates correspondants.

Avec des alcools volatils (méthanol, éthanol), la réaction peut être réalisée sans diluant (benzène) et en utilisant un léger excès de sulfure de bore. De cette façon, les orthoborates correspondants sont produits et recueillis directement par distillation, sans nécessiter une séparation de l'azéotrope de l'ester borique d'un excès d'alcool ou de diluant. Les esters ainsi obtenus présentent les constantes suivantes, orthoborate de méthyle: p.éb. 67.5° à 750 mm; n_D^{25} 1.3612. Orthoborate d'éthyle: p.éb. 116° à 750 mm; n_D^{23} 1.3742. Décrit (3): orthoborate de méthyle: p.éb. 68.7° à 760 mm; n_D^{20} 1.3610. Orthoborate d'éthyle: p.éb. 117.3° à 760 mm; n_D^{20} 1.3741.

Le phénol et l'α-naphtol réagissent également bien. Utilisant le procédé décrit plus haut pour la préparation de l'orthoborate d'hexyle, on retrouve, à partir du phénol, l'orthoborate de phényle, p.f. 90–91°, avec un rendement de 76%. Par la même méthode l'orthoborate d'α-naphtyle est produit, p.f. 107°. En utilisant toujours la même technique mais portant la durée de reflux à 24 h, il s'est avéré impossible de faire réagir le *p*-nitrophénol dont on retrouve 96% de la quantité initialement mise en expérience. Le sulfure de bore est retrouvé également intact et de façon quantitative, par filtration de la masse réactionnelle, au terme du reflux. Un comportement similaire est noté avec le *m*-nitrophénol. Cependant le phénol (0.15 mole) en présence de nitrobenzène (0.15 mole) et de sulfure de bore (0.03 mole) donne, par la méthode usuelle, l'orthoborate de phényle, p.f. 90–91°, avec rendement de 72%.

REMERCIEMENTS

L'auteur remercie le Conseil National de Recherches du Canada de son aide financière.

1. H. Moissan. Ann. chim. et phys. **6**, 312 (1895).
2. S. Jerumanis et J. M. Lalancette. Can. J. Chem. **42**, 1928 (1964).
3. M. F. Lappert. Chem. Rev. **56**, 969 (1956).

Reçu le 22 avril 1964.
Faculté des Sciences,
Université de Sherbrooke,
Sherbrooke, Quebec.

PROTON MAGNETIC RESONANCE CHEMICAL SHIFTS OF THE S-METHYL GROUP

George R. Pettit, Irwin B. Douglass, and Ralph A. Hill

Among organosulphur compounds, the proton magnetic resonance (p.m.r.) signals exhibited by certain thiols (1), sulphides (2), hemithioketals (3), sulphonium salts (4), and sulphites (5) have received major study. Although a variety of other H—C—S group responses have been included in several useful collections of p.m.r. data (6) only a few examples (cf. refs. 6 and 7) of S-methyl proton resonance have been recorded. The need[1] for a more extensive p.m.r. survey of the methyl group influenced by an adjacent sulphur atom has led to the present investigation. In Table I we have summarized the p.m.r. chemical shifts of 17 S-methyl compounds containing divalent sulphur. Tables II and III contain an additional 12 substances bearing S-methyl sulphur atoms in higher valence states. A small number of related sulphur compounds have been included in each table.

[1]*Required as part of a general program (for example, see ref. 8) involving the chemistry of organosulphur compounds.*

Can. J. Chem. Downloaded from www.nrcresearchpress.com by 210.87.254.5 on 09/05/12
For personal use only.

solide ne renferme plus de sulfure de bore et la portion liquide est distillée après évaporation du benzène. On retrouve ainsi 52 g (0.16 mole) d'orthoborate de *n*-hexyle: p.éb. 182° à 12 mm; n_D^{25} 1.4250. Décrit (3): p.éb. 185° à 15 mm; n_D^{23} 1.4250. Spectre infrarouge: absence de bandes dans la région de 3500 cm^{-1}, bandes à 1470 cm^{-1} (moyenne), 1410 cm^{-1} (forte), 1335 cm^{-1} (très forte), 1080 cm^{-1} (moyenne). Ce spectre est identique à celui donné par un échantillon authentique d'orthoborate d'hexyle préparé à partir de l'alcool correspondant et de l'acide borique. En appliquant la même méthode avec l'alcool propylique normal et l'alcool heptylique normal, on retrouve les orthoborates correspondants.

Avec des alcools volatils (méthanol, éthanol), la réaction peut être réalisée sans diluant (benzène) et en utilisant un léger excès de sulfure de bore. De cette façon, les orthoborates correspondants sont produits et recueillis directement par distillation, sans nécessiter une séparation de l'azéotrope de l'ester borique d'un excès d'alcool ou de diluant. Les esters ainsi obtenus présentent les constantes suivantes, orthoborate de méthyle: p.éb. 67.5° à 750 mm; n_D^{25} 1.3612. Orthoborate d'éthyle: p.éb. 116° à 750 mm; n_D^{23} 1.3742. Décrit (3): orthoborate de méthyle: p.éb. 68.7° à 760 mm; n_D^{20} 1.3610. Orthoborate d'éthyle: p.éb. 117.3° à 760 mm; n_D^{20} 1.3741.

Le phénol et l'α-naphtol réagissent également bien. Utilisant le procédé décrit plus haut pour la préparation de l'orthoborate d'hexyle, on retrouve, à partir du phénol, l'orthoborate de phényle, p.f. 90–91°, avec un rendement de 76%. Par la même méthode l'orthoborate d'α-naphtyle est produit, p.f. 107°. En utilisant toujours la même technique mais portant la durée de reflux à 24 h, il s'est avéré impossible de faire réagir le *p*-nitrophénol dont on retrouve 96% de la quantité initialement mise en expérience. Le sulfure de bore est retrouvé également intact et de façon quantitative, par filtration de la masse réactionnelle, au terme du reflux. Un comportement similaire est noté avec le *m*-nitrophénol. Cependant le phénol (0.15 mole) en présence de nitrobenzène (0.15 mole) et de sulfure de bore (0.03 mole) donne, par la méthode usuelle, l'orthoborate de phényle, p.f. 90–91°, avec rendement de 72%.

REMERCIEMENTS

L'auteur remercie le Conseil National de Recherches du Canada de son aide financière.

1. H. Moissan. Ann. chim. et phys. **6**, 312 (1895).
2. S. Jerumanis et J. M. Lalancette. Can. J. Chem. **42**, 1928 (1964).
3. M. F. Lappert. Chem. Rev. **56**, 969 (1956).

Reçu le 22 avril 1964.
Faculté des Sciences,
Université de Sherbrooke,
Sherbrooke, Quebec.

PROTON MAGNETIC RESONANCE CHEMICAL SHIFTS OF THE S-METHYL GROUP

George R. Pettit, Irwin B. Douglass, and Ralph A. Hill

Among organosulphur compounds, the proton magnetic resonance (p.m.r.) signals exhibited by certain thiols (1), sulphides (2), hemithioketals (3), sulphonium salts (4), and sulphites (5) have received major study. Although a variety of other H—C—S group responses have been included in several useful collections of p.m.r. data (6) only a few examples (cf. refs. 6 and 7) of S-methyl proton resonance have been recorded. The need[1] for a more extensive p.m.r. survey of the methyl group influenced by an adjacent sulphur atom has led to the present investigation. In Table I we have summarized the p.m.r. chemical shifts of 17 S-methyl compounds containing divalent sulphur. Tables II and III contain an additional 12 substances bearing S-methyl sulphur atoms in higher valence states. A small number of related sulphur compounds have been included in each table.

[1]*Required as part of a general program (for example, see ref. 8) involving the chemistry of organosulphur compounds.*

Can. J. Chem. Downloaded from www.nrcresearchpress.com by 210.87.254.5 on 09/05/12
For personal use only.

Can. J. Chem. Downloaded from www.nrcresearchpress.com by 210.87.254.5 on 09/05/12
For personal use only.

TABLE I

Proton magnetic resonance chemical shifts (δ units) of divalent sulphur compounds[a]

Substance (ref.)	—C—H[e]	—C—CH_3	—SH	S —COCH$_3$	—SCH_3	—$SSCH_3$	S—CH_2—S	S—CH_2—O	S—CH_2—Cl
CH_3SH			0.91, 1.17[e] (J = 7.0 c.p.s.)		1.95, 2.05				
CH_3COSH		2.29	4.47						
CH_3SCH_3					2.0				
CH_3S—SCH_3					2.30				
CH_3S—S—SCH_3 (11)					2.43				
CH_3S—S—S—SCH_3 (12)[b]					2.55				
$CH_3CO_2CH_2SCH_3$ (13)		2.15			1.98			4.86	
$(CH_3)_2C(SCH_3)_2$ (14)		1.49			1.95				
$CH_3CH(SCH_3)_2$ (15)	3.50, 3.73 (J = 7.0 c.p.s.)	1.44, 1.55			2.0				
$CH_3SCH_2SCH_3$ (16)					2.05		3.45		
$CH_3\overset{O}{\overset{\|}{C}}SCH_3$		2.20			2.24				
$CH_3S\overset{O}{\overset{\|}{C}}$—NH⟨⟩[c] (17)					2.28				
$CH_3S\overset{O}{\overset{\|}{C}}SCH_3$ (18)					2.32				
$CH_3SS\overset{O}{\overset{\|}{C}}SCH_3$ (8*a*)					2.35	2.48			
$CH_3S\overset{O}{\overset{\|}{C}}Cl$[d]					2.40				
$CH_3O\overset{S}{\overset{\|}{C}}SCH_3$ (8*a*)				4.05	2.46				
CH_3SCN					2.50				
$CH_3S\overset{O}{\overset{\|}{S}}CH_3$ (19)					2.60				
$ClCH_2S\overset{O}{\overset{\|}{C}}CH_2Cl$ (20)									4.70

[a]Unless otherwise noted, the sample was studied in carbon tetrachloride solution.
[b]The specimen of tetrasulphide used here contained detectable (by p.m.r.) amounts of impurities which appeared to represent somewhat longer-chain sulphides.
[c]Acetonitrile as solvent.
[d]Stauffer Chemical Co.
[e]The chemical shifts presented correspond to quartets.

TABLE II

Proton magnetic resonance chemical shifts (δ units) of tricovalent sulphur compounds[a]

Substance (ref.)	O —SCH_3	O —$SOCH_3$
CH_3SCH_3[b]	2.43	
CH_3SOCH_3 (21)	2.46	3.56
CH_3SCl (22)	3.22	
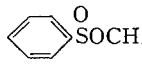 (13)		3.25
CH_3OSOCH_3 (23)		3.45

[a]Each substance was studied in carbon tetrachloride.
[b]Identical responses were observed when acetonitrile or carbon tetrachloride was used as solvent.

Several noteworthy observations were made during this study. First, a potentially useful property of multiple sulphur bonding was revealed while we were studying a series of methyl sulphides (Table I). Proton magnetic resonance signals exhibited by the methyl mono-, di-, tri-, and tetra-sulphides were separated by at least 0.1 p.p.m., and shielding of the methyl protons decreased at a decreasing rate with extension of the sulphur chain. The p.m.r. response arising from further lengthening of the sulphur chain will most probably reach a limiting value at ca. 6–8 sulphur units. However, the present results suggest that an appropriate p.m.r. study may provide a valuable method for rapidly assessing the length of relatively small sulphur chains in both symmetrical and unsymmetrical methyl sulphides.

The spectrum of N-bis(2-fluoroethyl)methanesulphonamide (Table III) also deserves comment. In addition to an S-methyl signal at 2.82δ, the spectrum exhibited a series of four triplets (J = 5.0 in each case), of nearly equal intensity, centered at 3.25, 3.65, 4.05, and 4.82δ. The two triplets at higher field most probably correspond to both protons adjacent to nitrogen, and the two at lower field to protons next to fluorine. Therefore, the triplets at 3.65 and 4.82δ provide an interesting example of spin–spin coupling involving fluorine (cf. ref. 9).

In general, the present data indicate that deshielding of the S-methyl protons increases in the order thiol $\cong$ sulphide < sulphoxide < sulphinate < sulphone < sulphonamide < sulphinyl halide < sulphonyl halide. As expected, the increasing chemical shift from tetramethylsilane appears related to the number and magnitude of electronegative atoms bonded to sulphur.

EXPERIMENTAL

The p.m.r. spectra were obtained by the use of a Varian Associates Model A-60 n.m.r. spectrometer. In each case, a 10% (by weight) solution of the specimen in spectro grade carbon tetrachloride or redistilled acetonitrile was prepared and diluted with enough tetramethylsilane to standardize the instrument. Scanning was performed from low to high field at a rate of 120 c.p.s./min. Measurements (at 20 °C) are reported (10) in terms of the frequency-independent unit δ (p.p.m.) with respect to tetramethylsilane.

Each (with exception of dimethyl sulphone from Crown Zellerbach Co.) of the organosulphur compounds studied was prepared and (or) purified in this laboratory.

Can. J. Chem. Downloaded from www.nrcresearchpress.com by 210.87.254.5 on 09/05/12
For personal use only.

Can. J. Chem. Downloaded from www.nrcresearchpress.com by 210.87.254.5 on 09/05/12
For personal use only.

TABLE III

Proton magnetic resonance chemical shifts (δ units) of tetracovalent sulphur compounds[a]

Substance (ref.)	C—CH_3	O —$SOCH_3$ O	O —$NSCH_3$ O	O —SCH_3 O	O —$SNCH_2$—[d] O	O —$SOCH_2$—[d] O	O —SCH_2 O
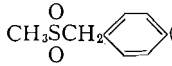 (24)				2.72			4.19
[b]				2.84			
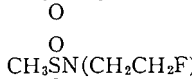 (25)			2.82				
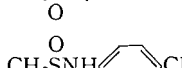	2.25		2.82				
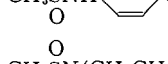 (25)			2.85	2.95	3.45 (J = 5.0 c.p.s.)	4.19 (J=5.0 c.p.s.)	
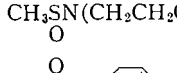			2.85				
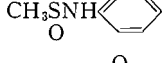 (25)	2.35			2.95	3.35 (J=6.0 c.p.s.)	4.19 (J=6.0 c.p.s.)	
			2.92				
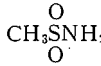 [b] (19)				3.17			

Can. J. Chem. Downloaded from www.nrcresearchpress.com by 210.87.254.5 on 09/05/12
For personal use only.

TABLE III (*Concluded*)

Proton magnetic resonance chemical shifts (δ units) of tetracovalent sulphur compounds[a] (*Concluded*)

Substance (ref.)	C—CH_3	O —$SOCH_3$ O	O —$NSCH_3$ O	O —SCH_3 O	O —$SNCH_2$—[d] O	O —$SOCH_2$—[d] O	O —SCH_2 O
$CH_3S(=O)Cl$[c]				3.52			
$CH_3OS(=O)OCH_3$[c]		3.80					
$CH_3OS(=O)Cl$[b] (26)		3.80					
$ClCH_2SN(CH_2CH_3)_2$ (27)							4.45
$ClCH_2SNH$–C$_6$H$_4$–CH_3 (27)	2.25						4.47
$ClCH_2SNH_2$ (27)							4.48
$ClCH_2SCH_2Cl$ (28)							4.71
$ClCH_2SCl$ (27)							4.75

[a]Each substance was studied in acetonitrile solution unless otherwise noted.
[b]Carbon tetrachloride as solvent.
[c]Identical responses were observed when acetonitrile or carbon tetrachloride was used as solvent.
[d]The value noted corresponds to the middle peak of a triplet.

ACKNOWLEDGMENTS

This investigation was supported in part by National Science Foundation Research Grant GB-249, American Cancer Society Grant T-79E, and a grant (to I. B. D.) from the Petroleum Research Fund, administered by the American Chemical Society.

1. G. E. McCasland, S. Furuta, A. Furst, L. F. Johnson, and J. N. Shoolery. J. Org. Chem. **28**, 456 (1963). E. L. Eliel and B. P. Thill. Chem. Ind. London, **88** (1963). S. Forsen. Acta Chem. Scand. **13**, 1472 (1959).
2. H. Hogeveen, G. Macagnani, F. Montanari, and F. Taddei. J. Chem. Soc. 628 (1964). K. Nukada, O. Yamamoto, T. Suzuki, M. Takeuchi, and M. Ohnishi. Anal. Chem. **35**, 1892 (1963).
3. E. L. Eliel, L. A. Pilato, and V. G. Badding. J. Am. Chem. Soc. **84**, 2377 (1962).
4. N. J. Leonard and C. R. Johnson. J. Am. Chem. Soc. **84**, 3701 (1962).
5. B. A. Arbouzov and Y. Y. Samitov. Tetrahedron Letters, 473 (1963). J. G. Pritchard and P. C. Lauterbur. J. Am. Chem. Soc. **83**, 2105 (1961).
6. M. W. Dietrich and R. E. Keller. Anal. Chem. **36**, 258 (1964). N. C. Bhacca, D. P. Hollis, L. F. Johnson, and E. A. Pier. NMR spectra catalog. Vol. 2. Varian Associates, Palo Alto, Cal. 1963. N. S. Bhacca, L. F. Johnson, and J. N. Shoolery. NMR spectra catalog. Varian Associates, Palo Alto, Cal. 1962. G. V. D. Tiers. Characteristic nuclear magnetic resonance shielding values for hydrogen in organic structures. Minnesota Mining and Manufacturing Co., St. Paul, Minn. 1958. Part I.
7. W. H. Nyberg and C. C. Cheng. J. Hetero. Chem. 1, 1 (1964). F. C. Stehling. Anal. Chem. **35**, 773 (1963). P. H. Todesco and P. Vivarelli. Boll. Sci. Fac. Chim. Ind. Bologna, **20**, 125 (1962); Chem. Abstr. **59**, 8562 (1963).
8. (*a*) I. B. Douglass and W. J. Evers. J. Org. Chem. **29**, 419 (1964). (*b*) G. R. Pettit and R. E. Kadunce. Can. J. Chem. **41**, 2695 (1963).
9. A. D. Cross and P. W. Landis. J. Am. Chem. Soc. **84**, 3784 (1962).
10. G. Slomp. J. Am. Chem. Soc. **84**, 673 (1962).
11. P. Klason. Chem. Ber. **20**, 3413 (1887).
12. H. Böhme and G. Zinner. Ann. Chem. **585**, 142 (1954).
13. S. Detoni and D. Hadzi. J. Chem. Soc. 3163 (1955).
14. B. P. Fedorov and I. S. Savel'eva. Izv. Akad. Nauk SSSR, Otd. Khim. Nauk, 223 (1950); Chem. Abstr. **45**, 1502 (1951).
15. M. L. Wolfrom and J. V. Karabenos. J. Am. Chem. Soc. **66**, 909 (1944).
16. W. Schneider. Ann. Chem. **386**, 349 (1911).
17. H. L. Wheeler and B. Barnes. J. Am. Chem. Soc. **24**, 60 (1900).
18. M. Delépine. Ann. Chim. Paris, **25**, 529 (1912).
19. I. B. Douglass and B. S. Farah. J. Org. Chem. **24**, 973 (1959).
20. I. Block and F. Höhn. Chem. Ber. **55B**, 53 (1922).
21. I. B. Douglass, D. A. Koop, and J. A. Stearns. J. Org. Chem. In press.
22. I. B. Douglass and D. R. Poole. J. Org. Chem. **22**, 536 (1957).
23. W. D. Harris, A. W. Feldman, and J. W. Zukel. U.S. Patent No. 2,802,727 (Aug. 13, 1957); Chem. Abstr. **52**, 432 (1958).
24. E. Fromm and J. D. Palma. Chem. Ber. **39**, 3315 (1906).
25. G. R. Pettit and R. L. Smith. Can. J. Chem. **42**, 572 (1964).
26. P. Behrend. J. Prakt. Chem. **15**, 32 (1877).
27. T. B. Johnson and I. B. Douglass. J. Am. Chem. Soc. **63**, 1571 (1941).
28. W. E. Truce, B. H. Birum, and E. T. McBee. J. Am. Chem. Soc. **74**, 3594 (1952).

Received May 4, 1964.
Department of Chemistry,
University of Maine,
Orono, Maine.

AN ALTERNATIVE SYNTHESIS OF 5-CARBOXYVANILLIN[1]

Hirokazu Morita

This report deals with the synthesis of 5-carboxyvanillin from commercially available materials and by a method which is more direct than those previously reported.

5-Carboxyvanillin has been prepared by a four-step synthesis starting from orthovanillic acid, the terminal conversion requiring an autoclave (1). The directions outlined

[1]*Soil Research Institute, Contribution No. 110.*

Can. J. Chem. Downloaded from www.nrcresearchpress.com by 210.87.254.5 on 09/05/12
For personal use only.

ACKNOWLEDGMENTS

This investigation was supported in part by National Science Foundation Research Grant GB-249, American Cancer Society Grant T-79E, and a grant (to I. B. D.) from the Petroleum Research Fund, administered by the American Chemical Society.

1. G. E. McCasland, S. Furuta, A. Furst, L. F. Johnson, and J. N. Shoolery. J. Org. Chem. **28**, 456 (1963). E. L. Eliel and B. P. Thill. Chem. Ind. London, **88** (1963). S. Forsen. Acta Chem. Scand. **13**, 1472 (1959).
2. H. Hogeveen, G. Macagnani, F. Montanari, and F. Taddei. J. Chem. Soc. 628 (1964). K. Nukada, O. Yamamoto, T. Suzuki, M. Takeuchi, and M. Ohnishi. Anal. Chem. **35**, 1892 (1963).
3. E. L. Eliel, L. A. Pilato, and V. G. Badding. J. Am. Chem. Soc. **84**, 2377 (1962).
4. N. J. Leonard and C. R. Johnson. J. Am. Chem. Soc. **84**, 3701 (1962).
5. B. A. Arbouzov and Y. Y. Samitov. Tetrahedron Letters, 473 (1963). J. G. Pritchard and P. C. Lauterbur. J. Am. Chem. Soc. **83**, 2105 (1961).
6. M. W. Dietrich and R. E. Keller. Anal. Chem. **36**, 258 (1964). N. C. Bhacca, D. P. Hollis, L. F. Johnson, and E. A. Pier. NMR spectra catalog. Vol. 2. Varian Associates, Palo Alto, Cal. 1963. N. S. Bhacca, L. F. Johnson, and J. N. Shoolery. NMR spectra catalog. Varian Associates, Palo Alto, Cal. 1962. G. V. D. Tiers. Characteristic nuclear magnetic resonance shielding values for hydrogen in organic structures. Minnesota Mining and Manufacturing Co., St. Paul, Minn. 1958. Part I.
7. W. H. Nyberg and C. C. Cheng. J. Hetero. Chem. 1, 1 (1964). F. C. Stehling. Anal. Chem. **35**, 773 (1963). P. H. Todesco and P. Vivarelli. Boll. Sci. Fac. Chim. Ind. Bologna, **20**, 125 (1962); Chem. Abstr. **59**, 8562 (1963).
8. (*a*) I. B. Douglass and W. J. Evers. J. Org. Chem. **29**, 419 (1964). (*b*) G. R. Pettit and R. E. Kadunce. Can. J. Chem. **41**, 2695 (1963).
9. A. D. Cross and P. W. Landis. J. Am. Chem. Soc. **84**, 3784 (1962).
10. G. Slomp. J. Am. Chem. Soc. **84**, 673 (1962).
11. P. Klason. Chem. Ber. **20**, 3413 (1887).
12. H. Böhme and G. Zinner. Ann. Chem. **585**, 142 (1954).
13. S. Detoni and D. Hadzi. J. Chem. Soc. 3163 (1955).
14. B. P. Fedorov and I. S. Savel'eva. Izv. Akad. Nauk SSSR, Otd. Khim. Nauk, 223 (1950); Chem. Abstr. **45**, 1502 (1951).
15. M. L. Wolfrom and J. V. Karabenos. J. Am. Chem. Soc. **66**, 909 (1944).
16. W. Schneider. Ann. Chem. **386**, 349 (1911).
17. H. L. Wheeler and B. Barnes. J. Am. Chem. Soc. **24**, 60 (1900).
18. M. Delépine. Ann. Chim. Paris, **25**, 529 (1912).
19. I. B. Douglass and B. S. Farah. J. Org. Chem. **24**, 973 (1959).
20. I. Block and F. Höhn. Chem. Ber. **55B**, 53 (1922).
21. I. B. Douglass, D. A. Koop, and J. A. Stearns. J. Org. Chem. In press.
22. I. B. Douglass and D. R. Poole. J. Org. Chem. **22**, 536 (1957).
23. W. D. Harris, A. W. Feldman, and J. W. Zukel. U.S. Patent No. 2,802,727 (Aug. 13, 1957); Chem. Abstr. **52**, 432 (1958).
24. E. Fromm and J. D. Palma. Chem. Ber. **39**, 3315 (1906).
25. G. R. Pettit and R. L. Smith. Can. J. Chem. **42**, 572 (1964).
26. P. Behrend. J. Prakt. Chem. **15**, 32 (1877).
27. T. B. Johnson and I. B. Douglass. J. Am. Chem. Soc. **63**, 1571 (1941).
28. W. E. Truce, B. H. Birum, and E. T. McBee. J. Am. Chem. Soc. **74**, 3594 (1952).

Received May 4, 1964.
Department of Chemistry,
University of Maine,
Orono, Maine.

AN ALTERNATIVE SYNTHESIS OF 5-CARBOXYVANILLIN[1]

Hirokazu Morita

This report deals with the synthesis of 5-carboxyvanillin from commercially available materials and by a method which is more direct than those previously reported.

5-Carboxyvanillin has been prepared by a four-step synthesis starting from orthovanillic acid, the terminal conversion requiring an autoclave (1). The directions outlined

[1]*Soil Research Institute, Contribution No. 110.*

Can. J. Chem. Downloaded from www.nrcresearchpress.com by 210.87.254.40 on 09/05/12
For personal use only.

below give somewhat poorer yields, but this is offset by the decided advantage in the simplicity of the procedure and by the easy accessibility of the reagents.

The experiment described here is based on the formylation of vanillic acid by hexamethylenetetramine in hot glacial acetic acid (2). The application of this reaction to orthovanillic acid readily affords 5-carboxyvanillin, which in turn can be oxidized cleanly to 5-carboxyvanillic acid. Oxidation of the 5-formylvanillic acid prepared according to Seshardi and Thiruvengadam (2) gave the identical acid.

EXPERIMENTAL

All melting points were determined on a calibrated Fischer–Johns apparatus.

X-ray powder diffraction patterns were obtained on a Norelco X-ray diffractometer unit using Cu Kα radiation. Line intensities were estimated visually from photographs of the Debye–Scherrer type.

5-Carboxyvanillin

Practical grade 2-hydroxy-3-methoxybenzaldehyde (Monsanto Chemical Company) was oxidized with silver oxide to orthovanillic acid (m.p. 147–148°) in 70% yield (3). Orthovanillic acid (10.1 g, 0.06 mole), hexamethylenetetramine (British Drug Houses; 42 g, 0.30 mole), and glacial acetic acid (80 ml) were heated on a boiling water bath for 7 h. Then hot (90°) 6 *N* hydrochloric acid (110 ml) was added, and the heating resumed for another 10 min. Upon cooling of the reaction mixture in the cold overnight, light cream-colored crystals of 5-carboxyvanillin were obtained. The crystals were collected by filtration, washed with water, and recrystallized from 40% ethanol in water (600 ml) to give colorless crystals, yield 3.5 g (26%), m.p. 256–258° (lit. 256–257°).

Analysis for $C_9H_8O_5$: Calcd.: C, 55.09; H, 4.11; CH_3O, 15.82. Found: C, 55.12; H, 4.10; CH_3O, 15.81.

The ultraviolet absorption spectrum in 95% ethanol showed maxima at 230 mμ (ϵ 18 000), 290 mμ (ϵ 10 700), and 320 mμ (ϵ 11 600). The X-ray powder diffraction pattern of the crystals showed prominent lines at *d*, 7.66 Å (I/I_1 70); *d*, 7.25 Å (I/I_1 80); *d*, 5.28 Å (I/I_1 70); *d*, 4.09 Å (I/I_1 80); *d*, 3.83 Å (I/I_1 50); *d*, 3.42 Å (I/I_1 80); *d*, 3.35 Å (I/I_1 100); *d*, 3.12 Å (I/I_1 60); *d*, 2.71 Å (I/I_1 50); *d*, 2.51 Å (I/I_1 50); *d*, 2.41 Å (I/I_1 50); *d*, 2.04 Å (I/I_1 50); *d*, 1.70 Å (I/I_1 50).

5-Carboxyvanillic Acid

Oxidation of 5-carboxyvanillin with silver oxide according to the procedure outlined by Pearl and Beyer (1) gave a product which, after repeated recrystallization from water, melted at 282.5–284°. This product was confirmed as 5-carboxyvanillic acid by comparison of its physical properties (mixed melting point, ultraviolet spectrum, and crystallographic features) with those observed for the dicarboxylic acid obtained from 5-formylvanillic acid.

5-Formylvanillic acid (m.p. 224–225°) was obtained in 25% yield by the formylation of vanillic acid as described by Seshardi and Thiruvengadam (2). Oxidation of this acid with alkaline silver oxide gave a quantitative yield of 5-carboxyvanillic acid, m.p. 283–284° (after repeated recrystallization from water) (lit. m.p. 276° (4); 283–284° (1), 271–272° (1)).

Analysis for $C_9H_8O_6$: Calcd.: C, 50.93; H, 3.80; CH_3O, 14.63. Found: C, 50.89; H, 4.02; CH_3O, 14.58.

The ultraviolet absorption spectrum in 95% ethanol showed maxima at 227 mμ (ϵ 27 400), 267 mμ (ϵ 7400), and 310 mμ (ϵ 3800). The X-ray powder diffraction pattern of the acid showed prominent lines at *d*, 10.66 Å (I/I_1 40); *d*, 9.03 Å (I/I_1 70); *d*, 6.97 Å (I/I_1 80); *d*, 4.61 Å (I/I_1 30); *d*, 4.51 Å (I/I_1 30); *d*, 4.03 Å (I/I_1 30); *d*, 3.86 Å (I/I_1 50); *d*, 3.23 Å (I/I_1 100); *d*, 3.14 Å (I/I_1 30).

ACKNOWLEDGMENT

The author is indebted to Dr. H. Kodama for the crystallographic data.

1. I. A. Pearl and D. L. Beyer. J. Am. Chem. Soc. **74**, 4263 (1952).
2. T. R. Seshardi and T. R. Thiruvengadam. Proc. Indian Acad. Sci. Sect. A, **32**, 25 (1950).
3. I. A. Pearl. Org. Syn. **30**, 101 (1950).
4. K. Freudenberg and F. Klink. Ber. B, **73**, 1369 (1940).

Received May 29, 1964.
Research Branch,
Canada Department of Agriculture,
Ottawa, Canada.

Can. J. Chem. Downloaded from www.nrcresearchpress.com by 210.87.254.40 on 09/05/12
For personal use only.

Can. J. Chem. Downloaded from www.nrcresearchpress.com by 210.87.254.6 on 09/05/12
For personal use only.

Canadian Journal of Chemistry

Issued by THE NATIONAL RESEARCH COUNCIL OF CANADA

VOLUME 42 NOVEMBER 1964 NUMBER 11

RING CONTRACTION DURING THE LEAD TETRAACETATE OXIDATION OF REDUCING SUGARS[1]

A. S. PERLIN

National Research Council of Canada, Prairie Regional Laboratory, Saskatoon, Saskatchewan

Received June 12, 1964

ABSTRACT

The rate of oxidation of D-glucose by lead tetraacetate in acetic acid is affected little by a large change in concentration of reactants, showing that the glycol cleavage step is not rate-controlling. Oxidation of 3-*O*-methyl-6-*O*-trityl-D-glucose yields 3-*O*-formyl-2-*O*-methyl-5-*O*-trityl-D-arabinose; the latter is not derived by production initially of a 4-*O*-formyl derivative that undergoes acyl migration. It is probable that the oxidation of D-glucose proceeds with conversion of the pyranose sugar into a furanose intermediate. By contrast, D-mannose appears to be oxidized mainly in the pyranose form, as shown by the oxidation patterns of D-mannose-1- and -2-^{14}C and 5-*O*-methyl-D-mannofuranose, and the effects of concentration change on the reaction of D-mannose and derivatives. The proximity of the ring oxygen atom to the 1,2-diol group may contribute to the unusually high reactivity of D-mannopyranose as compared with other types of monocyclic six-membered ring *vic*-diols.

Intermediate proportions of furanose and pyranose pathways characterize the lead tetraacetate oxidation of the other six aldohexoses. Similarities in the behavior of glucose and idose, gulose and mannose, and allose and talose may originate in steric similarities between these pairs of sugars.

The lead tetraacetate oxidation (1, 2) of reducing sugars in acetic acid involves primarily the cleavage of α-hydroxy hemiacetal glycol groups, and results in a stepwise shortening of the carbon chain (3, 4, 5). However, the uptake of oxidant in these reactions is lower than might be anticipated. For example, D-glucose (I) consumes only 2 moles of lead tetraacetate per mole rather than the 3 moles theoretically possible for the 1,2,3,4-tetrol grouping of the pyranose sugar (I), yielding a diformate ester of D-erythrose rather than of D-glycerose. A possible explanation for these results is to assume that a complex (6) between the tetravalent lead and the 1,2-diol group of α-D-glucofuranose (II) is an intermediate in the reaction. This complex could be formed directly from the pyranose sugar, by analogy with the formation of D-glucofuranose 1,2-acetals and borate complexes (7, 8), or from the furanose sugar if present in solution even as a minor constituent. Dissociation of the complex would give 3-*O*-formyl-D-arabinose, which, oxidized as a furanose sugar (III), would yield 2,3-di-*O*-formyl-D-erythrose (IV). Thus, involvement of a reactive structure such as II accounts for the high rate of the reaction (5, 9), as well as the consumption of only 2 moles of oxidant per mole. Consistent with these possibilities is the fact that derivatives of D-glucose that are prevented from going over to a furanose form by substituents at C-4 are oxidized much more slowly than D-glucose itself, whereas the rate is essentially unaltered by a substituent at C-3 or C-6 (10).

[1]*Issued as N.R.C. No. 8101.*

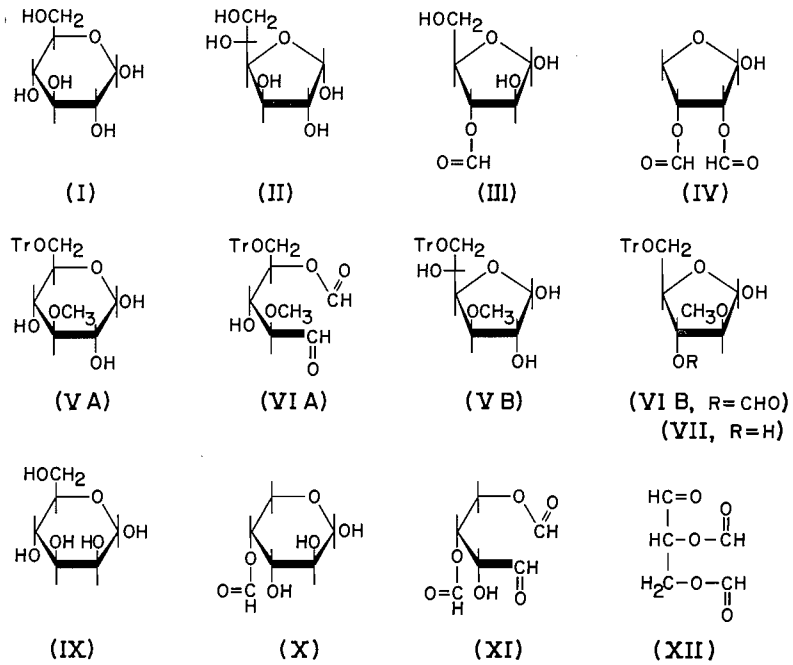

In the oxidation route depicted above, the initial product is a 3-, rather than a 4-, formate ester. Support for this step is provided by examining the oxidation of 3-*O*-methyl-6-*O*-trityl-D-glucose to mono-*O*-formyl-2-*O*-methyl-5-*O*-trityl-D-arabinose. If the pyranose sugar (VA) were to be degraded directly, the product should be a 4-formate of the *aldehydo*-pentose (VIA), whereas a furanose intermediate (involving VB) should yield a 3-formate of the pentofuranose (VIB). Nuclear magnetic resonance (n.m.r.) spectral evidence strongly favors the latter formulation for the oxidation product. Its spectrum (Fig. 1*a*) is affected little by deacylation (Fig. 1*b*), aside from the expected shift towards

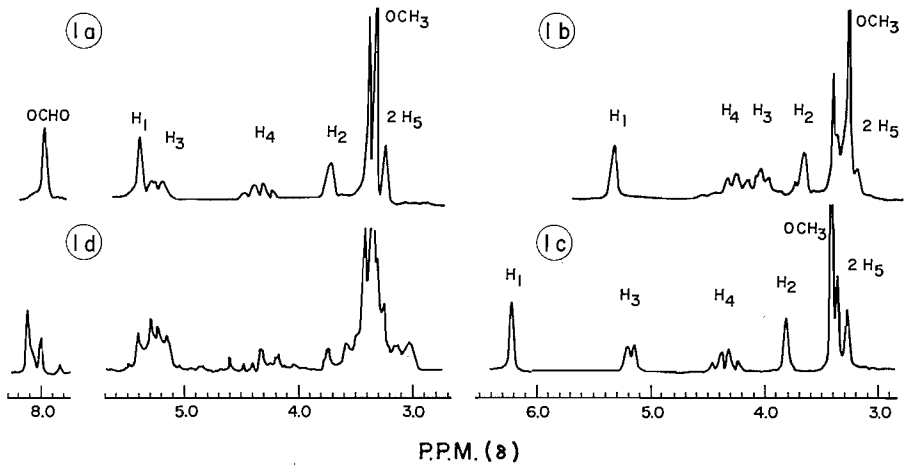

FIG. 1. The n.m.r. spectra of (*a*) 3-*O*-formyl-2-*O*-methyl-5-*O*-trityl-D-arabinose (VIB); (*b*) 2-*O*-methyl-5-*O*-trityl-D-arabinose (VII); (*c*) 1,3-di-*O*-acetyl-2-*O*-methyl-5-*O*-trityl-D-arabinose (signals for the acetyl protons are not shown); (*d*) the product (VIII) formed by oxidation with lead tetraacetate in benzene solution of 3-*O*-methyl-6-*O*-trityl-D-glucose.

Can. J. Chem. Downloaded from www.nrcresearchpress.com by 210.87.254.6 on 09/05/12
For personal use only.

higher field for the signal of the proton α to the formate group. If the oxidation product were acyclic (VIA), the gross conformational change inherent in its conversion into 2-*O*-methyl-5-*O*-trityl-D-arabinofuranose (VII) should surely be accompanied by greater differences than found between the spectra of these compounds. By contrast, the changes actually observed are those to be expected on simple deacylation of VI B to yield VII. Steric similarities between these latter two are emphasized further by acetylating VII. A n.m.r. spectrum is then obtained (Fig. 1*c*) that closely simulates the original spectrum (Fig. 1*a*), except that the H_1 signal has been shifted to lower field by the presence of the 1-acetoxy group.

Proton–proton coupling in Fig. 1*a* leads to the conclusion that H_3 of the oxidation product is located α to the formate group. The singlet at low field (5.4 p.p.m.) may be ascribed to H_1 (11)[2] and the singlet at 3.75 p.p.m. to its neighbor H_2, which appears at relatively high field because of the adjacent methoxyl group (12). Since H_2 is not coupled with H_3, the latter is undoubtedly the doublet at 5.25 p.p.m. which is split by coupling with H_4. Also, a proton situated at position-4 most readily accounts for the quartet at 4.40 p.p.m., since coupling is then permitted both with H_3 and the H_5 protons. Therefore, these data strongly support the conclusion that the product formed initially on oxidation of D-glucose is the 3-formate (III).

The oxidation of D-glucose to IV can be accounted for also by an alternative route whereby D-glucopyranose yields 4-*O*-formyl-D-arabinose, which then is converted into the 3-formate (III) by acyl migration (4).[3] This possibility could be favored even more with the trityl derivative (V), since migration of the formate from position-4 to position-3 (VIA $\rightarrow$ VIB) would permit ring closure. However, it is unlikely that such a transformation takes place, as shown by the following experiment in which V was treated with lead tetraacetate in benzene solution.

Since oxidations are much more rapid in benzene than in acetic acid (6), the pyranose form (VA) might itself be attacked in benzene with sufficient vigor to offset the displacement towards a furanose pathway, as presumably occurs in acetic acid. In fact, the product of oxidation in benzene (VIII) differs notably from the 3-formate (VIB), as seen in the contrast between its n.m.r. spectrum (Fig. 1*d*) and spectrum 1*a*. The major signal due to the formate proton is at slightly lower field in Fig. 1*d*; other signals are poorly resolved, with the broad multiplet at 3.3 p.p.m. accounting for about 7 of the remaining 10 protons. Relatively weak signals at 8.0, 5.4, 4.3, and 3.7 p.p.m., respectively (Fig. 1*d*), indicate that the 3-formate (VIB) is a minor constituent (about 25%) of this oxidation product. On deacylation, VIII yielded the same product as obtained from the 3-formate, i.e., VII (identified by chromatography and by the close identity of its n.m.r. spectrum with that shown in Fig. 1*b*). It is probable that VIII consists mainly of the 4-formate (VIA). Although VIII was not prepared in acetic acid, it was found to be quite stable in this solvent, showing that, if VIA had been produced by oxidation in acetic acid, it would not have rearranged readily to VIB. Therefore, a 3-formate must be derived from the D-glucose ether (V) and, undoubtedly, also from D-glucose itself by the initial cleavage of the α-hydroxy hemiacetal group in acetic acid.

Further evidence that D-glucose is oxidized in acetic acid via a reactive intermediate such as II is provided by examining the effect of dilution on the rates of cleavage of different *vic*-diols (Table I). The rate for the acyclic 3,4-diol group of 1,2:5,6-di-*O*-isopropylidene-D-mannitol is lowered by a factor of about 100 on dilution of the reaction mixture

[2]*This is supported by the effect of acetylation on the original (Fig. 1c) (12).*
[3]*This alternative has been regarded as highly likely (13).*

Can. J. Chem. Downloaded from www.nrcresearchpress.com by 210.87.254.6 on 09/05/12
For personal use only.

TABLE I

Influence of concentration on oxidation rate

	$T_{\frac{1}{2}}$(min)*		
	10^{-4} M†	10^{-2} M†	Ratio
1,2:5,6-Di-*O*-isopropylidene-D-mannitol	60	0.6	100
Cellobiose	450	9	50
Maltose	130	3	43
3-*O*-Methyl-D-glucose	2.5 (k_{27} 1 700)‡	0.7	3.5
3,5-Di-*O*-methyl-D-glucofuranose	— (k_{27} 100 000)‡	—	—
D-Glucose	2.5	0.5	5.0
4,6-*O*-Ethylidene-D-glucose	(very slow)	65	—
D-Mannose	3.5	0.1	35
4,6-*O*-Ethylidene-D-mannose	8.5	0.2	42

*Time required for uptake of 0.5 mole of lead tetraacetate per mole.
†Concentration of diol; the lead tetraacetate was present in 20% molar excess.
‡min^{-1} $mole^{-1}$ l; measured under the more dilute conditions.

100-fold. Similarly, a large decrease in rate is shown for D-glucopyranose when a change of ring size is prohibited, as with maltose or cellobiose (the reducing end-unit of which is oxidized preferentially (10)). By contrast, the rate of scission of the 1,2-diol group of 3-*O*-methyl-D-glucose is lowered by a factor of only 3.5 upon dilution.[4] This latter oxidation is controlled, not by the glycol cleavage step, but by the availability of some reactive species formed in an equilibrium displacement. That D-glucofuranose could function as such a species is suggested by the extreme reactivity of 3,5-di-*O*-methyl-D-glucofuranose compared with pyranose derivatives, its second-order rate constant being about 60 times that of even the 3-*O*-methyl derivative. With reactivity of this order, there need only be a small proportion of D-glucofuranose in the sugar solution to ensure its preferential oxidation in the presence of the dominant pyranose form. The ensuing equilibrium displacement step should be much less sensitive to a change in concentration than is the bimolecular oxidation step.

The reaction of D-mannose (IX) with lead tetraacetate contrasts sharply with that of D-glucose. Oxidation proceeds rapidly to a value of 2.8 moles per mole (4) and the product is chiefly di-*O*-formyl-D-glycerose (XII), with D-erythrose diformate (XI) being only a minor product. The oxidation is initiated primarily at the α-hydroxy hemiacetal group, as shown by the high yield of D-arabinose monoformate produced by limited oxidation (4). In addition, when D-mannose-1-^{14}C or -2-^{14}C is treated with 2.7 moles of lead tetraacetate per mole, products XI and XII account for almost all of the carbon-14, i.e.,

D-Mannose-1-^{14}C → products XI and XII,
(77 mμc/mmole CO_2) (76 mμc/mmole CO_2)

D-Mannose-2-^{14}C → products XI and XII.
(133 mμc/mmole CO_2) (126 mμc/mmole CO_2)

These results are readily explicable if the major reaction pathway proceeds in stepwise fashion, yielding at first 4-*O*-formyl-D-arabinose (X),[5] then 3,4-di-*O*-formyl-D-erythrose (XI), and finally the triose diformate (XII). Carbon-1 and carbon-2 of the original

[4]*Although not strictly comparable because of the overall greater uptake of oxidant involved, the reaction of* D-*glucose itself illustrates this same behavior. Thus, the time required for an uptake of 0.5 mole/mole is extended, on dilution, by a factor of only five.*

[5]*It was concluded earlier that 4-O-formyl-*D-*arabinose (X) cannot be the product formed initially in the oxidation of* D-*glucose. This is consistent with the oxidative behavior of* D-*mannose, for otherwise the two epimeric sugars should show the same overall reaction pattern.*

Can. J. Chem. Downloaded from www.nrcresearchpress.com by 210.87.254.6 on 09/05/12
For personal use only.

hexose are then retained in XII and carbon-3 is liberated.[6]

According to these data, a furanose pathway plays only a minor role in the oxidation of D-mannose. Nevertheless, D-mannofuranose should be highly reactive because it contains a *cis*-2,3-diol group on a five-membered ring, in addition to that potentially available at C-1 and C-2. As a model compound, 5-*O*-methyl-D-mannofuranose (14) was found to consume 1 mole of lead tetraacetate per mole very rapidly (k_{27} for this stage in dilute solution was estimated to be about 65 000) and additional oxidant much more slowly. Although acetal formation (15) and borate complexing (8) favor the 2,3- over the 1,2-diol group of D-mannofuranose, oxidation occurred chiefly at the 1,2-positions, since a pentose derivative was produced in 60% yield. Almost identical behavior was shown by 5-*O*-methyl-D-glucofuranose, in which the 2,3-diol group is *trans*. Clearly, then, the oxidation behavior of D-mannose itself cannot be reconciled with a high proportion of a furanose pathway, for the overall reaction should resemble more closely that of D-glucose.

Two other observations are consistent with a pyranose pathway predominantly for the D-mannose oxidation: the effect on reaction rates of (*a*) substitution at C-4, and (*b*) dilution. 4,6-*O*-Ethylidene-D-mannose[7] is oxidized at a rate comparable with that of the parent hexose both at low and high dilution, in marked contrast to the strong retarding effect of the same type of bicyclic system in the D-glucose series (Table I). In addition, a 100-fold dilution of the reaction mixture lowers the oxidation rate of D-mannose much more than that of D-glucose, showing that different types of pathways are operative for the two sugars.

The effect of a large change in concentration is seen in yet another way. The rapid uptake of 2.8 moles per mole by D-mannose (reported earlier) was measured at the higher concentration (ca. 10^{-2} *M*). Although this level of oxidation is reached with the more dilute reaction mixture (10^{-4} *M*), there is a marked decrease in rate after about 2 moles per mole have been taken up (Fig. 2). With the 4,6-*O*-ethylidene derivative there is also a sharp break in the curve, but this occurs at a level of 1 mole per mole. The 6-deoxy sugar (L-rhamnose) has been shown to consume rapidly about the same proportion of oxidant as does D-mannose (4). In dilute solution, its behavior is more akin to that of the *O*-ethylidene derivative. It is probable that the more rapid phases of these reactions involve cyclic forms of the sugars, and that the slower oxidations involve acyclic products (16). Thus, D-mannose and 4-*O*-formyl-D-arabinose (X) could together account for the rapid uptake of 2 moles per mole, whereas the resulting α-hydroxy aldehyde 3,4-di-*O*-formyl-D-erythrose (XI)[8] would be oxidized in the slow step. Similarly, *aldehydo* derivatives are produced by the initial degradation of 4,6-*O*-ethylidene-D-mannose to 3,5-*O*-ethylidene-4-*O*-formyl-D-arabinose (chromatographic evidence confirms a pentose product exclusively in this reaction) and of L-rhamnose to a 4-formate of 5-deoxy-L-lyxose. This could account for the rapid uptake of only 1 mole per mole by these latter sugars. By contrast, well-defined stages of this kind are not observed in the oxidation of D-glucose or of 6-substituted derivatives of it under the same conditions; however, no oxidizable acyclic products are expected in these reactions. D-Glucofuranose 5,6-carbonate, which initially should yield a 3,4,5-trisubstituted *aldehydo*-pentose,[9] is characterized by a two-

[6]*If the total reaction proceeds in this way, the product should actually be slightly more radioactive than the original hexose, since one unlabelled carbon atom would be lost as formic acid in the formation of XII.*

[7]*This derivative was kindly provided by Dr. D. M. Ball.*

[8]*At this stage, in fact, degradation has produced mainly tetrose formate, and very little triose formate has appeared. This was shown by chromatographic examination of the product formed on treating* D-*mannose with only 2 molar equivalents of lead tetraacetate under these dilute conditions.*

[9]*By oxidation of the hexose carbonate with 1 molar equivalent of lead tetraacetate,* D-*arabinose carbonate is obtained in high yield (17).*

Can. J. Chem. Downloaded from www.nrcresearchpress.com by 210.87.254.6 on 09/05/12
For personal use only.

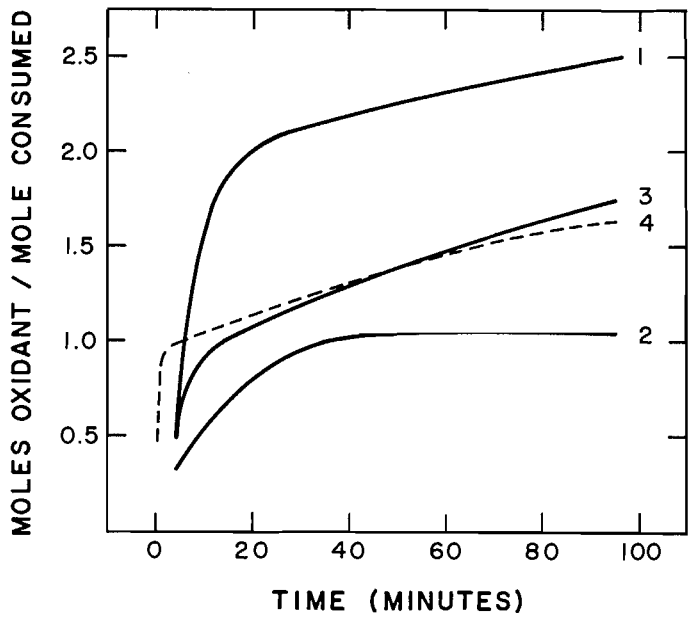

FIG. 2. Rates of lead tetraacetate consumption at high dilution (ca. 10^{-4} *M*) of (1) D-mannose; (2) 4,6-*O*-ethylidene-D-mannose; (3) 6-deoxy-L-mannose; (4) D-glucofuranose 5,6-carbonate (closely similar curves are given by D-erythrose and D-threose).

stage reaction. It is noteworthy that this latter curve is closely paralleled by those for D-erythrose and D-threose, each of which should afford an α-hydroxy aldehyde, viz. 3-*O*-formyl-D-glycerose.

The overall consistency of these different types of data leads to the conclusion that the oxidation of D-glucose in acetic acid involves preferential attack on D-glucofuranose or formation of a furanose intermediate, whereas, in the oxidation of D-mannose a pyranose form is involved chiefly. Apparently, the relative inertness of D-glucopyranose permits an equilibrium displacement in favor of the furanose pathway. However, even glucopyranose can be relatively reactive as compared with other kinds of monocyclic six-membered ring compounds; for example, the reducing unit of maltose or cellobiose is oxidized far more rapidly than is the nonreducing end-unit (10). D-Mannopyranose is a remarkably reactive monocyclic six-membered ring diol. This property of reducing sugars would not be predicted on steric grounds by comparing molecular models of pyranose forms with those of glycopyranosides and related cyclic polyhydric alcohols. In a free sugar, however, the unshared electron pair of the ring oxygen atom could aid materially in attracting the strongly electrophilic tetravalent lead atom towards the 1,2-diol group, increasing the effective concentration of oxidant about this region of the molecule. The models suggest that an orienting influence of this kind should be particularly noticeable with β-D-mannopyranose, the 1- and 2-oxygen atoms of which lie relatively close to the ring oxygen atom, but less so with α-D-glucopyranose (in accord with the higher reactivity of D-mannose).

Oxidation of Other Aldohexoses

The six other aldohexoses rapidly consume lead tetraacetate in proportions ranging between the values for D-glucose and D-mannose (4, 5) (Table II). Their oxidations have not been examined as extensively as those of the latter two sugars. A high yield of pentose

Can. J. Chem. Downloaded from www.nrcresearchpress.com by 210.87.254.6 on 09/05/12
For personal use only.

TABLE II

Lead tetraacetate uptake and configurational relations among the aldohexoses

	Furanose forms, ring configuration (19)	Pyranose forms						Lead tetraacetate uptake (moles/mole) (4, 5)
		Orientation of groups on:						
		C-1	C-2	C-3	C-4	C-5	Conformation	
α-D-Glucose	α-D-xylo-	*a*	*e*	*e*	*e*	*e*	*C 1*	2.0
β-D-Idose	α-L-xylo-	*a*	*e*	*e*	*e*	*a*	*1 C*	2.1
α-D-Galactose	α-D-arabino-	*a*	*e*	*e*	*a*	*e*	*C 1*	2.1
β-D-Altrose	α-L-arabino-	*a*	*e*	*e*	*a*	*a*	*1 C*	2.5
α-D-Allose	α-D-ribo-	*a*	*e*	*a*	*e*	*e*	*C 1*	2.3
β-D-Talose	α-L-ribo-	*a*	*e*	*a*	*e*	*a*	*1 C*	2.3
α-D-Gulose	α-D-lyxo-	*e*	*a*	*e*	*e*	*a*	*1 C*	2.7
β-D-Mannose	α-L-lyxo-	*e*	*a*	*e*	*e*	*e*	*C 1*	2.8

formate obtained by partial oxidation of D-galactose, D-allose, or D-altrose (4, 5) shows that these sugars are degraded preferentially in stepwise fashion from the reducing end. Di-*O*-formyl-D-threose is the major product obtained from D-galactose, consistent with a lead tetraacetate uptake of slightly over 2 moles per mole, whereas D-altrose, which consumes 2.5 moles per mole, affords about equimolar amounts of triose and tetrose formates.

The amounts of lead tetraacetate consumed in the oxidation of these aldohexoses may be interpreted in terms of the proportions of furanose and pyranose forms that have reacted. For example, D-idose consumes 2.1 moles of lead tetraacetate per mole, only slightly more than does D-glucose, so that its oxidation pathway probably involves chiefly a furanose form. It is noteworthy that the relative orientation of the 1-, 2-, and 3-hydroxyl groups and of C-5 in β-D-idofuranose is the same as in α-D-glucofuranose. This marked steric resemblance was emphasized by Isbell (19) in noting that these forms may be assigned the α-L-*xylo* and α-D-*xylo* configurations, respectively. Since there is little effective competition from a pyranose route in the oxidation of idose, the relative unreactivity of α-D-idopyranose is analogous to that of α-D-glucopyranose.[10] There are some notable steric similarities between these two forms. For example, in the two chair conformations (20) considered, the orientation of all substituents other than that of the C-6 carbinol groups is the same. On balance, free-energy changes accompanying the formation of the activated complexes could be lower by approximately the same amount for each furanose pathway than for each pyranose pathway, thus favoring the same oxidation pattern for the two aldohexoses.

This type of comparison, based on similar oxidation patterns and configurational resemblance, permits pairing of D-gulose with D-mannose. D-Allose and D-talose constitute a third pair for which there is good agreement, but the analogy does not hold as closely for the pair D-galactose and D-altrose.

The pyranose conformation listed for each sugar in Table II is chosen to emphasize similarities, and does not necessarily represent the most stable ground state of the individual compounds (20–24). Probably, this factor is not significant in some of the oxidations, since energy barriers separating conformers (23, 24) are small relative to, for example,

[10]*It is assumed that 1,2-cis-anomers of pyranose or furanose sugars are more likely to be attacked in these oxidations than are 1,2-trans-anomers.*

Can. J. Chem. Downloaded from www.nrcresearchpress.com by 210.87.254.6 on 09/05/12
For personal use only.

heats of reaction of lead tetraacetate oxidations (25, 26, 27). However, in an instance where both furanose and pyranose pathways are prominent (most notably, the oxidation of D-altrose), it could substantially affect the outcome, since this is dependent on the *difference* between overall free-energy changes for the competing pathways.

EXPERIMENTAL

Lead tetraacetate uptake was measured iodometrically (1, 2) with reaction mixtures in which the concentration of reactants was about 10^{-2} *M*, and spectrophotometrically (28) with reaction mixtures in which the concentration of reactants was about 10^{-4} *M*.

Proton magnetic resonance (n.m.r.) spectra were measured with a Varian A-60 high-resolution spectrometer, using chloroform or deuterochloroform as solvent and tetramethylsilane as internal standard. When the compound to be examined contained a free hydroxyl group, a preliminary deuterium exchange was carried out by shaking the chloroform solution twice with deuterium oxide.

Specific activity measurements were made by combustion analysis according to the procedure of Buchanan and Nakao (29).

Solutions were concentrated *in vacuo* at 40–45 °C.

*3-O-Methyl-6-O-trityl-*D*-glucose (V)*

3-*O*-Methyl-D-glucose (2.0 g) in pyridine (20 ml) was treated with chlorotriphenylmethane (3.4 g) at 3 °C for 18 h. Ice water was added, the syrupy deposit was extracted into chloroform, and the chloroform layer was washed well with water, dried, and concentrated. After being dried thoroughly in a high vacuum, the syrupy product was applied in chloroform solution (25 ml) to a column of dry silicic acid (4 cm × 40 cm). The column was developed with chloroform, fractions of the eluate being examined by thin-layer chromatography (solvent—benzene:methanol (9:1); spray—30% sulphuric acid; all products containing the trityl group gave a bright yellow color, whereas that also containing the sugar residue charred when the chromatogram was heated). Chromatographically pure material isolated was extracted into benzene, and the extract was concentrated, yielding a white solid (3.3 g); $[\alpha]_D$ 35° (*c*, 2, benzene).

Calcd. for $C_{26}H_{28}O_6$: C, 71.54; H, 6.47. Found: C, 71.81; H, 6.34.

*1,2,4-Tri-O-acetyl-3-O-methyl-6-O-trityl-β-*D*-glucose*

In a second preparation of V, on twice the scale above, additional pyridine (20 ml) and acetic anhydride (20 ml) were added to the reaction mixture at 48 h, and the solution was stored at 3 °C for a further 48 h. Ice water was added; the syrupy deposit was extracted into benzene; and the benzene extract was washed successively with cold sodium bicarbonate solution, cold tartaric acid solution, and water; then dried, and concentrated. The residue afforded crystalline material (2.8 g) from ethanol; m.p. 173–175 °C, $[\alpha]_D$ 18° (*c*, 2, chloroform.

Calcd. for $C_{32}H_{34}O_9$: C, 68.31; H, 6.09. Found: C, 68.57; H, 6.20.

*Lead Tetraacetate Oxidation of 3-O-Methyl-6-O-trityl-*D*-glucose (V)*

(*A*) To a solution of V in acetic acid (165 mg, 5 ml) was added an acetic acid solution of lead tetraacetate (7 ml; 160 mg (0.95 molar equivalents)). After 10 min reaction time, when a negative test was given for tetravalent lead, the solution was concentrated and the residue was extracted with benzene. The extract was washed three times with ice water, dried, and concentrated to a syrup (120 mg); $[\alpha]_D$ 20.6° (*c*, 3.3, methanol). The syrupy product (VI) absorbed strongly in the infrared region at 1725 and 1175 cm^{-1}, characteristic of a formate ester group; the n.m.r. spectrum is reproduced in Fig. 1*a*.

The oxidation product was taken up in methanol and treated with a slight excess of sodium methoxide; the calculated $[\alpha]_D$ of the deacylated product (VII) was 17.9°. Absorption bands in the infrared region due to a formate group were no longer detectable; otherwise, the spectra of VI and VII were virtually indistinguishable. The n.m.r. spectrum of VII is reproduced in Fig. 1*b*.

(*B*) A solution of V in dry benzene (100 mg; 5 ml) was treated with lead tetraacetate (92 mg) in dry benzene containing 2% of acetic acid (4 ml). A precipitate formed immediately, and a negative test for tetravalent lead was obtained within 30 s. The filtrate from the suspension was concentrated to yield a syrup (VIII) (80 mg), $[\alpha]_D$ − 4.0° (*c*, 3.7, chloroform), which was shown by infrared spectroscopy to contain a formate ester group; the n.m.r. spectrum is reproduced in Fig. 1*d*. After deacylation with sodium methoxide, the product gave an n.m.r. spectrum essentially the same as that shown in Fig. 1*b*. In another experiment, product VIII was stored for several hours as a solution in acetic acid. After removal of the solvent, the n.m.r. spectrum was indistinguishable from that shown in Fig. 1*d*.

*1,3-Di-O-acetyl-2-O-methyl-5-O-trityl-*D*-arabinose*

The deacylated oxidation product (VII) was taken up in a mixed solvent of pyridine and acetic anhydride (3 vol.:2 vol.), the solution was stored at 3 °C for 48 h and then poured into ice water. The syrupy deposit was extracted into benzene, the extract was washed with cold sodium bicarbonate solution, cold tartaric

Can. J. Chem. Downloaded from www.nrcresearchpress.com by 210.87.254.6 on 09/05/12
For personal use only.

acid solution, and ice water, and dried. Removal of the benzene afforded a colorless syrup, $[\alpha]_D$ 46° (*c*, 2.2, acetone).

Calcd. for $C_{29}H_{30}O_7$: C, 71.00; H, 6.16. Found: C, 71.19; H, 6.21.

*3,4-O-Isopropylidene-2-O-methyl-*D*-arabinose (30)*

2-*O*-Methyl-5-*O*-trityl-D-arabinose (VII) (120 mg; about one-half of this sample was derived from VIB and one-half from VIII) was taken up in acetone (5 ml), one drop of concentrated hydrochloric acid was added, and the solution was stored at 3 °C for 72 h. Excess lead carbonate was added, followed by water (10 ml); the neutral suspension was filtered, the filtrate was concentrated, and the residue was extracted with acetone. The acetone-soluble product (52 mg) solidified; m.p. 116–119 °C; $[\alpha]_D$ −107° (*c*, 2.5, methanol; no mutarotation observed).

D-*Mannose-2-*^{14}*C*

D-Mannose-2-^{14}C was prepared from D-mannono-1,4-lactone-2-^{14}C (kindly furnished by A. C. Neish) by reduction with sodium borohydride in the presence of Amberlite-IR-120 (H^+), according to the procedure of Frush and Isbell (31).

Lead Tetraacetate Oxidation of D-*Mannose or* D-*Mannose-*^{14}*C*

In a typical experiment, D-mannose (250 mg) in water (0.3 ml) was taken up in acetic acid (15 ml). A solution of lead tetraacetate (1.7 g; 2.7 molar equivalents) in acetic acid (50 ml) was added to the sugar solution over a period of 15 min, and this was followed 10 min later by a solution of oxalic acid (0.3 g) in acetic acid (5 ml). The precipitate of lead oxalate was filtered off through Celite, the filtrate was concentrated, and the residue was extracted with ethyl acetate. On being concentrated, the extract yielded a syrup which was purified by distillation (bath temp. 140 °C at 0.05 mm).

Samples of the syrup, after reduction with excess sodium borohydride, gave a mixture consisting mainly of erythritol and glyceritol (paper chromatographic evidence). These products were estimated, after elution from the chromatograms, by treatment with periodate, followed by analysis of the formaldehyde produced on oxidation (32). The ratio of erythritol to glyceritol was 6.8 to 3.2.

In experiments with D-mannose-^{14}C, the distilled oxidation product was used for the specific activity measurements.

*5-O-Methyl-*D*-glucose and 5-O-Methyl-*D*-mannose (2,5-dichlorophenyl) Hydrazones*

The 5-*O*-methyl sugars were prepared as chromatographically pure syrups by procedures described elsewhere (14, 33). By treatment with a methanolic solution of (2,5-dichlorophenyl) hydrazine (34), each sugar yielded a solid product that was recrystallized from ethyl acetate – benzene.

The substituted hydrazone of 5-*O*-methyl-D-glucose had m.p. 140–142 °C.

Calcd. for $C_{13}H_{18}Cl_3N_2O_5$: C, 44.20; H, 5.10. Found: C, 44.00; H, 5.31.

An attempt to prepare the dichlorophenylosazone by use of excess reagent and a longer reflux period, as with D-erythrose (35), was unsuccessful, only the substituted hydrazone being obtained in this experiment.

The substituted hydrazone of 5-*O*-methyl-D-mannose, m.p. 129–130 °C, contained benzene as solvent of crystallization (its presence being detected by gas–liquid chromatographic analysis of a concentrated solution of the hydrazone in methyl sulphoxide).

Calcd. for $C_{13}H_{18}Cl_2N_2O_5 \cdot O \cdot 5C_6H_6$: C, 48.99; H, 5.40; Cl, 18.08. Found: C, 49.00; H, 5.75; Cl, 18.47.

*Lead Tetraacetate Oxidation of 5-O-Methyl-*D*-glucose and -mannose*

The sugar derivative (10 mg) in acetic acid (1 ml) was treated with lead tetraacetate (22 mg) in acetic acid (1 ml) for 10 min; a negative test for tetravalent lead was given within this period. Water (5 ml) was added to the reaction mixture followed by excess of Amberlite-IR-120 (H^+), and the solution was warmed on the steam bath for 0.5 h, concentrated, and examined chromatographically. Three products were detected, the major component being indistinguishable from 4-*O* methyl-D-arabinose (unpublished preparation). Based on the intensity of color developed by the latter with the orcinol ferric chloride reagent for pentose (36), the yield of 4-*O*-methyl-D-arabinose produced in the oxidation of each 5-*O*-methyl hexose was estimated to be 57% (D-gluco isomer) and 60% (D-manno isomer).

When the sugar was treated at high dilution with 2 molar equivalents of lead tetraacetate, the uptake of oxidant (moles/mole) was as follows:

Time (min)	2	5	10	15	25
5-*O*-Methyl-D-glucose	0.83	1.00	1.18	1.27	1.36
5-*O*-Methyl-D-mannose	0.95	1.10	1.20	1.30	1.40

Measurement of lead tetraacetate uptake by 5-*O*-methyl-D-mannose at the outset of the reaction gave the following data, calculated as second-order rate constants (min^{-1} $mole^{-1}$ l) at 27 °C: 67 900 (0.20 min); 70 900 (0.25 min); 64 100 (0.30 min); 54 100 (0.40 min).

Can. J. Chem. Downloaded from www.nrcresearchpress.com by 210.87.254.6 on 09/05/12
For personal use only.

ACKNOWLEDGMENTS

The author gratefully acknowledges the able technical assistance of Mrs. J. Nuttall and Miss M. Gates. Microanalyses were performed by M. Mazurek, who, together with W. Haid, recorded n.m.r. and infrared absorption spectra. The n.m.r. spectra were measured in the Chemistry Department, University of Saskatchewan, Saskatoon, Saskatchewan.

REFERENCES

1. R. Criegee. Ber. **64**, 260 (1931).
2. R. Criegee. Ann. **495**, 211 (1932).
3. A. S. Perlin. J. Am. Chem. Soc. **76**, 2595 (1954).
4. A. S. Perlin and C. Brice. Can. J. Chem. **34**, 541 (1956).
5. A. S. Perlin. Advan. Carbohydrate Chem. **14**, 9 (1959).
6. R. Criegee, L. Kraft, and B. Rank. Ann. **507**, 159 (1933).
7. J. Böeseken. Advan. Carbohydrate Chem. **4**, 189 (1949).
8. M. Mazurek and A. S. Perlin. Can. J. Chem. **41**, 2403 (1963).
9. R. C. Hockett and M. Zief. J. Am. Chem. Soc. **72**, 2130 (1950).
10. A. J. Charlson and A. S. Perlin. Can. J. Chem. **34**, 1200 (1956).
11. R. U. Lemieux, R. K. Kullnig, H. J. Bernstein, and W. G. Schneider. J. Am. Chem. Soc. **80**, 6098 (1958).
12. L. M. Jackman. Applications of nuclear magnetic resonance spectroscopy in organic chemistry. Pergamon Press, Ltd., London. 1959. p. 55.
13. L. F. Fieser and M. Fieser. Advanced organic chemistry. Reinhold Publishing Corp., New York. 1961. p. 948.
14. A. S. Perlin. Can. J. Chem. **42**, 1365 (1964).
15. K. Freudenberg and R. M. Hixon. Ber. **56**, 2119 (1923).
16. R. C. Hockett, M. T. Dienes, and H. E. Ramsden. J. Am. Chem. Soc. **65**, 1474 (1943).
17. J. N. Baxter and A. S. Perlin. Unpublished results.
18. A. S. Perlin. Anal. Chem. **27**, 396 (1955).
19. H. S. Isbell. J. Res. Natl. Bur. Std. **57**, 171 (1956).
20. R. E. Reeves. Advan. Carbohydrate Chem. **6**, 107 (1951).
21. G. R. Barker and D. F. Shaw. J. Chem. Soc. 584 (1959).
22. R. S. Tipson and H. S. Isbell. J. Res. Natl. Bur. Std. A, **64**, 239 (1960).
23. R. U. Lemieux. Intern. Union Pure and Appl. Chem. Montreal. 1961. Abstr. p. 268.
24. S. J. Angyal. Intern. Union Pure and Appl. Chem. Montreal. 1961. Abstr. p. 275.
25. R. Criegee, E. Buchner, and W. Walther. Ber. **73**, 571 (1940).
26. J. P. Cordner and K. H. Pausacker. J. Chem. Soc. 102 (1953).
27. E. J. Moriconi, F. T. Wallenberger, and W. F. O'Connor. J. Am. Chem. Soc. **80**, 656 (1958).
28. A. S. Perlin and S. Suzuki. Can. J. Chem. **40**, 1226 (1962).
29. D. L. Buchanan and A. Nakao. J. Am. Chem. Soc. **74**, 2389 (1952).
30. G. R. Barker and D. C. C. Smith. Chem. Ind. London, 1035 (1952).
31. H. L. Frush and H. S. Isbell. J. Am. Chem. Soc. **78**, 2844 (1956).
32. M. Lambert and A. C. Neish. Can. J. Res. B, **28**, 83 (1950).
33. J. K. N. Jones. Can. J. Chem. **34**, 310 (1956).
34. I. Mandl and C. Neuberg. Arch. Biochem. Biophys. **35**, 326 (1952).
35. A. S. Perlin and C. Brice. Can. J. Chem. **33**, 1216 (1955).
36. W. Meijbaum. Z. Physiol. Chem. **258**, 117 (1939).

Can. J. Chem. Downloaded from www.nrcresearchpress.com by 210.87.254.6 on 09/05/12
For personal use only.

Can. J. Chem. Downloaded from www.nrcresearchpress.com by 210.87.254.5 on 09/05/12
For personal use only.

THE REARRANGEMENT OF 2,4-DIMETHYLTHIAZOLE 3-OXIDE WITH ACETIC ANHYDRIDE

HUGH J. ANDERSON, DOUGLAS J. BARNES, AND (IN PART) ZAHIR M. KHAN
Department of Chemistry, Memorial University of Newfoundland, St. John's, Newfoundland

Received May 28, 1964

ABSTRACT

The rearrangement in acetic anhydride of 2,4-dimethylthiazole 3-oxide has been found to produce 2-acetoxymethyl-4-methylthiazole and 4-acetoxymethyl-2-methylthiazole in the ratio of about 4.5 to 1. The same type of rearrangement with 4-methylthiazole 3-oxide gave both 4-acetoxymethylthiazole and 2-acetoxy-4-methylthiazole, but in poor yields. The structure of the sulphate salt of 2,4-dimethylthiazole 3-oxide has been established.

The rearrangement in acetic anhydride of 2- and 4-picoline 1-oxide (1) to the corresponding acetoxymethylpyridine has been used widely for the synthesis of oxygenated side chains. It has also been used extensively with more highly substituted pyridine 1-oxides as well as with the N-oxides of the other six-membered ring heterocycles (2). Rearrangements to form a heterocycle with an acetoxyl group in an open 2- or 3-position also take place readily with these heterocycles (2, 3).

Although several N-oxides have been prepared in the thiazole series (4), no previous investigation has been reported of their behavior in the acetic anhydride rearrangement. 2,4-Dimethylthiazole 3-oxide (I) rearranges with *p*-toluenesulphonyl chloride to give a good yield of 2-chloromethyl-4-methylthiazole (5). This agrees with other observations of the much greater activity of the 2-methyl than of the 4-methyl group in thiazoles. Bond fixation and variation of the degree of conjugation have been suggested as the cause (6).

While various 2-substituted thiazoles may be synthesized from available 2-aminothiazoles through diazonium and other reactions, none leads easily to compounds containing oxygenated side chains in the 2-position. It was hoped that the acetic anhydride rearrangement of the 3-oxide of the commercially available 2,4-dimethylthiazole might provide a satisfactory path to these compounds. The behavior of 4-methylthiazole 3-oxide under these conditions was also investigated.

By use of the standard preparative procedure (7) 2,4-dimethylthiazole 3-oxide (I) could be prepared in good yield and vacuum distilled to give a white, crystalline, but very hygroscopic solid of low melting point. If the crude product was left standing for some time a white solid of higher melting point could be obtained. This proved to be a sulphate salt of the N-oxide, whose structure is discussed below. Partial oxidative destruction of the ring must have produced a small amount of sulphuric acid to form this salt.

The crude N-oxide could be rearranged to give about the same overall yield of product as the distilled material. Distillation often gave extensive decomposition, so most rearrangements were carried out directly from the crude product. Vacuum distillation of the product gave a colorless oil which showed two peaks on gas–liquid partition chromatography of area ratio about 4.5 to 1. Similarly the nuclear magnetic resonance (n.m.r.) spectrum of the mixture, on integration, showed about 17% of the minor isomer to be present and no other impurities.

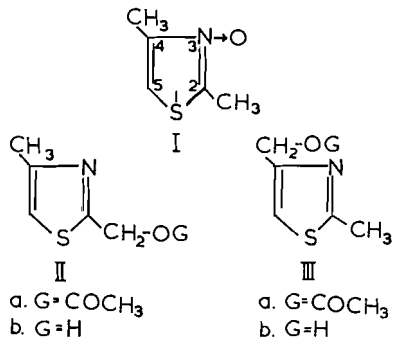

Chemical shifts (Table I) were consistent with the assignment of the structure of the major isomer as 2-acetoxymethyl-4-methylthiazole (II*a*) and the minor as 4-acetoxymethyl-2-methylthiazole (III*a*). It was possible to isolate the picrate of the major isomer directly from the mixture. Column chromatography on neutral alumina enabled concentration of the minor isomer. A second chromatography of the concentrate produced a small amount of the minor isomer showing less than 10% of the major isomer by gas chromatography and by n.m.r. Although a picrate was obtained, it could not be recrystallized without some decomposition, consequently its analysis was close, but unsatisfactory. Attempts to prepare other derivatives were also unsuccessful. Thus positive identification is based on the n.m.r. spectrum.

Hydrolysis of the acetoxymethyl mixture provided a good yield of a mixture of roughly the same proportions of the corresponding hydroxymethyl isomers II*b* and III*b*. Again n.m.r. supported the assigned structures. The picrate of the major isomer, the known 2-hydroxymethyl-4-methylthiazole (8), was prepared from the mixture. Oxidation of the mixture of hydroxymethyl isomers with alkaline permanganate gave a poor yield of the known 4-methyl-2-thiazolecarboxylic acid. Milder oxidation gave the corresponding 4-methyl-2-thiazolecarboxaldehyde, identified through its known thiosemicarbazone and *p*-nitrophenylhydrazone. A second N-oxidation followed by rearrangement has been found useful in the picoline series (1), but our attempts led to a complex mixture of compounds from which no recognizable pure substance could be isolated.

The usual as well as a wide variation of oxidation conditions gave a low yield of the known 4-methylthiazole 3-oxide (3). Rearrangement in acetic anhydride produced a mixture of products containing both 4-acetoxymethylthiazole and 2-acetoxy-4-methylthiazole. Gas–liquid partition chromatography showed only two peaks. Hydrolysis of the mixture produced a small amount of the known 2-hydroxy-4-methylthiazole, while careful oxidation of the residual hydrolysis product gave some of the known 4-thiazolecarboxylic acid. Because of the low yields throughout we abandoned further investigation.

The white solid by-product from the preparation of 2,4-dimethylthiazole 3-oxide analyzed correctly for $(C_5H_7NOS)_2.H_2SO_4$. It dissolved in water and gave a white precipitate with barium chloride solution in dilute nitric acid. The acetic anhydride rearrangement proceeded from this sulphate. It also gave the picrate of 2,4-dimethylthiazole 3-oxide.

N-Oxides in the pyridine series form two types of salts with monobasic acids, having structures which may be symbolized as

$$(\text{Het.}\overset{+}{\text{N}}\text{—O—H})\ \text{An}^- \qquad (\text{Het.N—O}\cdots\text{H}\cdots\text{O—NHet.})^+\ \text{An}^-$$

IV*a* IV*b*

Can. J. Chem. Downloaded from www.nrcresearchpress.com by 210.87.254.5 on 09/05/12
For personal use only.

Can. J. Chem. Downloaded from www.nrcresearchpress.com by 210.87.254.5 on 09/05/12
For personal use only.

TABLE I

Chemical shifts in carbon tetrachloride

Compound	2-	4-	5-	Other protons	Coupling
2,4-Dimethylthiazole	2.62 – CH_3	2.34 – CH_3	6.62		$J_{CH_3/5}$ = 1.12 c.p.s.
I	2.49 – CH_3	2.28 – CH_3	6.87		$J_{CH_3/5}$ = 1.10 c.p.s.
II*a*	5.24 – CH_2—O—	2.38 – CH_3	6.87	2.08 – CO—CH_3	
III*a*	2.66 – CH_3	5.06 – CH_2—O—	7.04	2.03 – CO—CH_3	
II*b*	4.75 – CH_2—O—	2.28 – CH_3	6.73	5.87 – OH*	$J_{CH_3/5}$ = 1.02 c.p.s.
III*b*	2.56 – CH_3	4.58 – CH_2—O—	6.97	5.87 – OH*	$J_{-CH_2-/5}$ = 0.98 c.p.s.

*Determined as a mixture, OH protons common.

TABLE II

Chemical shifts in dimethyl sulphoxide

Compound	2 – CH_3	4 – CH_3	5 – H
2,4-Dimethylthiazole	2.68	2.39	7.12
Sulphate salt	2.91	2.50	7.64
I	2.50	2.28	7.51
I sulphate salt	2.67	2.33	7.70

characterized by both infrared and n.m.r spectra (9, 10, 11). Although our sulphate is the salt of a dibasic acid and could form structures of either type:

$$(\mathrm{Thz.\overset{+}{N}—O—H)_2SO_4^{=}} \quad \text{or} \quad (\mathrm{Thz.N—O\cdots H\cdots O—NThz.)^{+}HSO_4^{-}},$$

Va Vb

it has been possible to assign to it structure V*a*. A very wide and intense band from 1800 to 2300 cm^{-1}, characteristic of the IV*a* type in the solid state (9, 10), was found in the infrared. This is the O—H stretching frequency found to be dependent on the anion of the salt. Although there are no recorded spectra of sulphate salts of N-oxides in the pyridine series the absorption pattern lies close to that of a bromide of the IV*a* type. The medium N—O band at 1249 cm^{-1} in the free 2,4-dimethylthiazole 3-oxide was diminished to a weak one at 1260 cm^{-1} in the sulphate salt.

In the pyridine series the strongest acids, such as perchloric and hydriodic, form salts of the IV*b* type while weaker acids, such as hydrochloric and hydrobromic, tend to form type IV*a*.

Infrared spectra indicate that type IV*b* salts are converted into IV*a* type in polar solvents. This is especially true for the strong proton acceptor dimethyl sulphoxide (DMSO) (10). The n.m.r. spectrum in $CDCl_3$ of a type IV*b* salt shows two different sets of signals for the picoline nuclear and methyl protons, indicating that the proton is not shared equally in this solvent. Because of the insolubility of the salt its n.m.r. spectrum was determined in DMSO (Table II). Only one set of signals was found where the acidic protons shifted strongly with dilution while the rest changed only slightly. For comparison, 2,4-dimethylthiazole 3-oxide was run in DMSO as well as 2,4-dimethylthiazole and its sulphate salt. Salt formation caused changes in chemical shifts qualitatively similar in the two compounds but about twice as large for the thiazole as for its N-oxide. Thus oxygen aids in dispersing the positive charge. There is a remarkably specific deshielding effect on the 5-proton in DMSO compared to carbon tetrachloride for both 2,4-dimethylthiazole and its 3-oxide. It has been pointed out before that the 5-proton of thiazole is the most susceptible to solvent effects (12).

EXPERIMENTAL

General

Melting points were determined on a Fisher–Johns apparatus and are uncorrected. Infrared spectra were recorded by a Unicam SP100 spectrophotometer using the potassium chloride disk technique (2 mg of sample in 200 mg KCl) or as capillary films.

The nuclear magnetic resonance spectra were determined at 60 Mc/s. The chemical shifts are in p.p.m. from tetramethylsilane as internal reference in carbon tetrachloride. In dimethyl sulphoxide the solvent peak was taken as 2.62 p.p.m. and used as internal reference.

Elemental analyses were determined by Alfred Bernhardt, Mulheim (Ruhr), Germany.

2,4-Dimethylthiazole 3-Oxide (I)

A mixture of 2,4-dimethylthiazole (22.5 g, 0.02 mole), 140 ml glacial acetic acid, and 25 ml hydrogen peroxide solution (30% w/v) was heated at 75–80° for 4 h in an oil bath. A further 20 ml of hydrogen

Can. J. Chem. Downloaded from www.nrcresearchpress.com by 210.87.254.5 on 09/05/12
For personal use only.

peroxide solution was added and heating continued for 17 h. The mixture was concentrated in a flash evaporator to about 50 ml, an equal volume of water was added, and the solution again was concentrated to a yellow syrup containing white crystalline material. This was taken up in 150 ml chloroform and was neutralized with a saturated aqueous solution of potassium carbonate. The chloroform layer was removed and dried with anhydrous sodium sulphate. The chloroform was then removed under vacuum. The residual oil was vacuum distilled, b.p. 104–105° at 1.0 mm; yield 14 g (55%) of oily, white solid with a melting point below 45° (from pentane) and very hygroscopic. Picrate (from ethanol); m.p. 151–152°, literature m.p. 149–152° (4).

Sulphate of I

A sample of crude N-oxide which had stood for some time contained a solid which was insoluble in dioxane and which could be recrystallized from isopropyl alcohol or pentane to colorless crystals, m.p. 124–125°. The solid was very soluble in water giving an acidic solution.

Anal. Calcd. for $C_{10}H_{16}N_2O_6S_3$: C, 33.70; H, 4.53; N, 7.87; S, 26.99. Found: C, 33.92; H, 4.35; N, 7.77; S, 27.04.

Rearrangement of 2,4-Dimethylthiazole 3-Oxide

The crude 2,4-dimethylthiazole 3-oxide (14.0 g) was added slowly to gently boiling acetic anhydride (40 ml). As soon as the reaction began, external heat was removed and the reaction proceeded vigorously. After addition was complete, the solution was refluxed for a further 20 min. Vacuum distillation gave a forerun of acetic anhydride followed by 15.0 g of a pale yellow oil, b.p. 80–82° at 1.5 mm. Gas–liquid partition chromatography of the product was carried out on a 30 in. column (Beckman No. 70 007) of Carbowax 4000 dioleate on firebrick operated at 190° with helium as the carrier gas at inlet pressure of 30 p.s.i.g. This showed two peaks in area ratio of 80–84% and 16–20%. The nuclear magnetic resonance spectrum showed, by integration, about 17% of the minor isomer present in the mixture. Chemical shifts were consistent with assignment of structures (see Table I). The major isomer was 2-acetoxymethyl-4-methylthiazole (II*a*). Picrate (from methanol): m.p. 84–85° was made from the mixed oil.

Anal. Calcd. for $C_{13}H_{12}N_4O_9S$: C, 39.10; H, 2.78; N, 14.03; S, 8.03. Found: C, 39.21; H, 2.96; N, 13.85; S, 8.09.

The minor isomer was 4-acetoxymethyl-2-methylthiazole (III*a*). It was concentrated by column chromatography of the mixture on neutral alumina (Woelm, activity grade I) to about 90% purity. From this mixture a picrate was obtained; m.p. 74–79° (from methanol), decomposed by recrystallization.

Hydrolysis of Rearrangement Product

The mixture of acetoxymethyl compounds (15 g) was dissolved in 100 ml 6 *N* hydrochloric acid, refluxed 1 h, cooled, and neutralized with 6 *N* sodium hydroxide solution. It was extracted with ether and the extract dried over sodium sulphate. After distillation of the ether, a pale yellow oil (8.0 g, 70%) was vacuum distilled at 92–93° and 1.0 mm. Literature boiling point for 2-hydroxymethyl-4-methylthiazole (II*b*) is 86° at 1 mm (8) and for 4-hydroxymethyl-2-methylthiazole (III*b*), 104° at 5 mm (13). Nuclear magnetic resonance spectrum (see Table I) showed, by integration, about 85% II*b* and 15% III*b*. Chemical shifts agreed with assigned structures. Picrate of the major isomer, 2-hydroxymethyl-4-methylthiazole, (from ethanol); m.p. 126–127°, literature m.p. 132° (11).

Anal. Calcd. for $C_{11}H_{10}N_4O_8S$: C, 36.98; H, 2.84; N, 15.69; S, 8.89. Found: C, 37.13; H, 2.78; N, 15.55; S, 8.82.

4-Methyl-2-thiazolecarboxylic Acid

To a suspension of the above mixture of hydroxymethyl isomers (II*b* and III*b*) in 20 ml 2.5% aqueous sodium carbonate solution was added slowly 40 ml 5% aqueous potassium permanganate solution during continuous shaking of the suspension at room temperature over 25 min. After a further 15 min the solution was filtered and the pH adjusted to 2 by addition of 10% hydrochloric acid (14). From a chloroform extract of the solution about 8% yield of 4-methyl-2-thiazolecarboxylic acid was obtained; m.p. 95–95.5° (pentane), literature m.p. 99° (15). The acid decarboxylated easily to an oil whose picrate was undepressed in mixed melting point with an authentic specimen of the picrate of 4-methylthiazole.

4-Methyl-2-thiazolecarboxaldehyde

Sodium dichromate (4 g) was dissolved in a solution of the mixture (5 g) of hydroxymethyl isomers (II*b* and III*b*) in 32 ml 6 *N* acetic acid. After 1 h at 75° the reaction mixture was cooled and, after addition of 10 g ice, neutralized with 10% aqueous sodium hydroxide. The solution was extracted with ether, the extract was dried, and the ether was removed. A liquid was vacuum distilled giving 2 g of oil; b.p. 64° at 17 mm, n_D^{25} 1.5018. Thiosemicarbazone of 4-methyl-2-thiazolecarboxaldehyde; m.p. 223° (decomp.), literature m.p. 224° (decomp.) (14). *p*-Nitrophenylhydrazone of 4-methyl-2-thiazolecarboxaldehyde (from ethanol); m.p. 195–196°, literature m.p. 195° (15).

Anal. Calcd. for $C_{11}H_{10}N_4O_2S$: C, 50.37; H, 3.81; S, 12.23. Found: C, 50.48; H, 3.78; S, 11.92.

4-Methylthiazole 3-Oxide

Following the procedure of Whitman (17) for pyridine N-oxide, 10 ml 35% hydrogen peroxide solution

Can. J. Chem. Downloaded from www.nrcresearchpress.com by 210.87.254.5 on 09/05/12
For personal use only.

was added to a vigorously stirred mixture of 4-methylthiazole (1g) (16), glacial acetic acid (35 ml), and tungstic acid (2.5 g) at a temperature of 55°. After the mixture was stirred for 5 h at 60–65°, the product was filtered and worked up. A yield of 2.5 g crude 4-methylthiazole N-oxide was obtained. Attempted vacuum distillation led to rapid decomposition. Picrate (from methanol); m.p. 127–129°, literature m.p. 130–132° (4).

Rearrangement of 4-Methylthiazole 3-Oxide

4-Methylthiazole 3-oxide (3.5 g) was refluxed in 18 ml acetic anhydride for 10 min. After removal of lower boiling material, an oil (2.7 g), b.p. 76° at 1 mm, was obtained. From this a picrate was obtained (from methanol), m.p. 123–124°. Literature m.p. for picrate of 4-acetoxymethylthiazole is 129–131° (18).

Anal. Calcd. for $C_{12}H_{10}N_4O_9S$: C, 37.31; H, 2.61; N, 14.50; S, 8.30. Found: C, 37.26; H, 2.89; N, 14.38; S, 8.15.

Hydrolysis of Rearrangement Product

The product from the above rearrangement (4 g) was refluxed in 10% hydrochloric acid (30 ml) for 1 h (much hydrogen sulphide evolved) cooled, neutralized with 6 *N* sodium hydroxide solution, and extracted with ether. On evaporation a small amount of crystalline solid, m.p. 99–100° (from hexane), was obtained. Literature melting point for 2-hydroxy-4-methylthiazole is 102° (19).

Anal. Calcd. for C_4H_5NOS: C, 41.72; H, 4.38; N, 12.16; S, 27.85. Found: C, 41.82; H, 4.61; N, 11.94; S, 27.45.

Oxidation of Hydrolysis Product

The residual oil from the above hydrolysis (about 1 g) was added to 5% potassium carbonate solution (20 ml). A 5% potassium permanganate solution (40 ml) was then added. The solution, shaken frequently, was allowed to stand 30 min at room temperature. A 10% hydrochloric acid solution was then added to lower the pH to 2. From the dried ether extract, crystals were obtained, m.p. 188° (decomp.). Literature m.p. from 4-thiazolecarboxylic acid is 194° (20).

ACKNOWLEDGMENTS

The authors are grateful to the Research Corporation for a Frederick Gardner Cottrell grant-in-aid which made this research project possible. They also thank professors F. A. L. Anet, L. Bauer, and E. Bullock for aid in the determination of n.m.r. spectra.

REFERENCES

1. V. Boekelheide and W. Linn. J. Am. Chem. Soc. **76**, 1286 (1954). O. H. Bullitt, Jr. and J. T. Maynard. J. Am. Chem. Soc. **76**, 1370 (1954).
2. D. V. Ioffe and L. S. Efros. Russ. Chem. Rev. English Transl. **30**, 569 (1961). E. N. Shaw. *In* Pyridine and its derivatives. Vol. II. *Edited by* E. Klingsberg. Interscience, New York. 1961. pp. 97–153.
3. M. Katada. Chem. Abstr. **45**, 9536 (1951). B. M. Bain and J. E. Saxton. J. Chem. Soc. 5216 (1961).
4. E. Ochiai and E. Hayashi. Chem. Abstr. **45**, 9533 (1951).
5. E. Matsumura, T. Hirooka, and K. Imagawa. Chem. Abstr. **57**, 12466 (1962).
6. A. R. Katritzky and J. M. Lagowski. Heterocyclic chemistry. Methuen & Co. Ltd., London. 1960. p. 229. A. Pullman and J. Metzger. Bull. Soc. Chim. France, 1021 (1948).
7. E. Ochiai. J. Org. Chem. **18**, 534 (1953).
8. D. J. Brown, A. H. Cook, and I. M. Heilbron. J. Chem. Soc. S106 (1949).
9. D. Hadži. J. Chem. Soc. 5128 (1962).
10. M. Szafran. Bull. Acad. Polon. Sci. Ser. Sci. Chim. **10**, 233 (1962); **11**, 111, 169 (1963).
11. J. F. Vozza. J. Org. Chem. **27**, 3856 (1962).
12. T. Schaefer and W. G. Schneider. J. Chem. Phys. **32**, 1224 (1960).
13. V. M. Zibarovskii and R. N. Moskaleva. Zh. Obshch. Khim. **32**, 570 (1962).
14. E. Campaigne, R. L. Thompson, and J. E. van Werth. J. Med. Pharm. Chem. **1**, 577 (1959).
15. H. Kondo and F. Nagasawa. Chem. Abstr. **32**, 1699 (1938). B. Prijs. Kartothek der thiazolverbindungen. S. Karger, Basle. 1952. pp. 117, 121.
16. R. P. Kurkjy and E. V. Brown. J. Am. Chem. Soc. **74**, 5778 (1952).
17. R. C. Whitman. U.S. Patent No. 3,047,579 (July, 1962): Chem. Abstr. **58**, 7916 (1963).
18. B. M. Mikhaĭlov and V. P. Bronovitskaya. Chem. Abstr. **51**, 16436 (1957).
19. A. Hantzsch. Ber. **61**, 1776 (1928).
20. H. Erlenmeyer, J. Junod, W. Guex, and M. Erne. Helv. Chim. Acta, **31**, 1342 (1948).

Can. J. Chem. Downloaded from www.nrcresearchpress.com by 210.87.254.5 on 09/05/12
For personal use only.

Can. J. Chem. Downloaded from www.nrcresearchpress.com by 210.87.254.105 on 09/05/12
For personal use only.

RING MIGRATION IN ALKYLATED FERROCENES

DONALD E. BUBLITZ
Western Division Research Laboratories, Dow Chemical Company, Walnut Creek, California
Received April 30, 1964

ABSTRACT

Alkylferrocenes have been found to undergo disproportionation to ferrocene and 1,1′-dialkylferrocenes in the presence of aluminium or gallium chloride. The mechanistic pathway has been shown to involve (π-ligand)–(π-ligand) exchange as opposed to the usual carbon–carbon cleavage found in benzene chemistry.

Aluminium chloride is the most widely used catalyst for Friedel–Crafts alkylation and acylation of ferrocene. The numerous compounds which have been prepared by these methods are, in part, the subjects of recent reviews (1, 2, 3). The stability of ferrocene under the conditions of these reactions has never been questioned, for the yields of acyl materials are generally quite good. The yield of any one particular alkylferrocene is generally low, however, since a complex mixture of mono- and isomeric di-, tri-, and polyalkylated materials is obtained. Recently various workers have reported that ferrocene undergoes decomposition after prolonged heating in different solvents in the presence of aluminium chloride to give various products (4–7).

In a study of the Friedel–Crafts acylation of *n*-propylferrocene in methylene chloride, we observed, by gas–liquid chromatography (g.l.c.) analysis of the products, the presence of two minor components identified as ferrocene and 1,1′-di-(*n*-propyl) ferrocene. Neither of these components was present in the starting material, as shown by g.l.c. analysis. It was subsequently shown that *n*-propylferrocene could be disproportionated to a mixture of ferrocene, *n*-propylferrocene, and 1,1′-di-(*n*-propyl)ferrocene in the presence of aluminium chloride in refluxing methylene chloride. The amount of isopropylated ferrocenes formed, if any, was less than 0.5%, as determined by the nuclear magnetic resonance (n.m.r.) spectrum of the reaction mixture. The lack of alkyl group isomerization was clearly demonstrated by the use of isobutylferrocene in the disproportionation reaction. The presence of less than 0.1%, if any, *t*-butylated ferrocenes was confirmed by n.m.r. analysis of the reaction products. This lack of alkyl group isomerization was a further indication that the reaction mechanism did not involve ring – alkyl group cleavage.

Proof that the mechanistic pathway proceeds via ring–metal scission has been obtained. When 1,1′,2-triethylferrocene was subjected to the conditions of the disproportionation, the only products present, as shown by g.l.c. of the mixture, were 1,1′-diethyl-, 1,1′-2-triethyl-, and 1,1′,2,2′-tetraethyl-ferrocene (eq. [1], R = CH_2CH_3). In addition, trace amounts of ethylferrocene formed by concomitant dealkylation were observed. Corresponding results were obtained when either 1,2-diethyl-, or 1,1′,3-triethyl-ferrocene was utilized (eq. [1], R = H; eq. 2). In both instances, trace amounts of ethylferrocene were again observed. A trace amount of 1,1′,2-triethylferrocene in the disproportionation products of 1,2-diethylferrocene was attributed to the dealkylation of the tetraalkylated product present. Dealkylation has been substantiated by treatment of 1,1′-diethylferrocene with aluminium chloride in refluxing methylene chloride. After 2 hours the reaction mixture was found to comprise 1,1′-diethylferrocene (93.4%), ethylferrocene (3.88%), and 1,1′,2-triethylferrocene (2.70%). The relative amounts of the last two products show realkylation occurs to an even lesser extent.

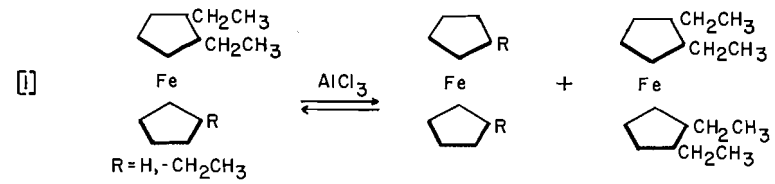

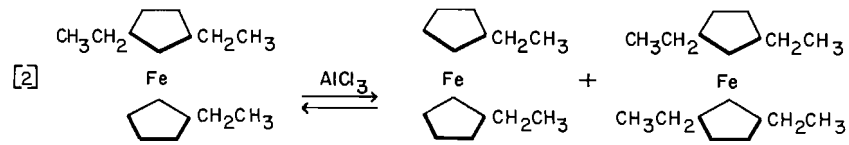

The structural assignments of 1,1′,2,2′- and 1,1′,3,3′-tetraethylferrocene were based on two facts. First, no 1,3-disubstitution products were generated from starting materials of a 1,2-disposition. Alternatively, when the substituents in the starting material were of a 1,3-nature, no 1,2-disubstitution products were observed. The conditions of the g.l.c. analysis permit such a distinction between these isomers if they are present. Thus, alkyl substituents do not migrate. Second, certain characteristic peaks in the infrared spectra of 1,3-diethyl-, and 1,1′,3-triethyl-ferrocene are present in 1,1′,3,3′-tetraethyl-ferrocene and are absent in their 1,2-counterparts. Similarly, certain characteristic infrared peaks common to the 1,2-family are absent in its 1,3-counterparts (8). Various workers have made similar observations with other 1,2- and 1,3-disubstituted ferrocene systems (9–11).

The equilibrium nature of the reaction has been shown by the appearance of ethyl-ferrocene in a mixture of ferrocene and 1,1′-diethylferrocene in the presence of aluminium chloride. A similar reaction of 1,1′-diethylferrocene with either ruthenocene (12) or methylcyclopentadienylmanganese tricarbonyl* was attempted but no synproportion-ation products were observed. The result for ruthenocene is parallel to earlier observations that its ring–metal bond is stronger than the ring–metal bond in ferrocene (13–16).

Aluminium chloride is not functionally unique in causing this disproportionation, gallium(III) chloride behaves in an identical fashion. No disproportionation is observed when antimony(III, V), arsenic(III), bismuth(III), indium(III), or tin(IV) chloride is used.

The recent observations of Nesmeyanov and co-workers (17, 18) concerning the exchange of a cyclopentadienyl or substituted cyclopentadienyl moiety for an aromatic moiety such as benzene or mesitylene, in the presence of aluminium chloride, agree with our observations of ring–metal cleavage. While the same mechanistic pathway is doubtless common to both reactions, the presence of excess benzene, or other solvents capable of forming π-complexes, evidently precludes the reverse combination of ferrocene fragments. In methylene chloride, a solvent not capable of such complex formation, the reverse reaction of recombination of ferrocene fragments is found to occur as we have shown.

Nesmeyanov *et al.* have shown acetylferrocene capable of cleavage by aluminium chloride in mesitylene. In agreement with the report of Rosenblum *et al.* (19), we found no evidence whatsoever for its disproportionation in refluxing methylene chloride. Analysis by g.l.c. demonstrated conclusively the absence of ferrocene even when 4 molar

**Purchased from Ethyl Corporation, New York, N.Y.*

Can. J. Chem. Downloaded from www.nrcresearchpress.com by 210.87.254.105 on 09/05/12
For personal use only.

equivalents of aluminium chloride were utilized. These results are in accord with the reported inhibitory effect of the acetyl group upon the ligand exchange reaction (17, 18).

EXPERIMENTAL

Gas–liquid chromatographic analyses were performed on an Aerograph Autoprep model A-700 equipped with a $\frac{3}{8}$ in. × 20 ft aluminium column packed with Apiezon L (20%) on 60/80 Chromasorb P. Nuclear magnetic resonance spectra of preparative g.l.c. samples were obtained on a Varian A-60 spectrometer. Boiling points were obtained for 1–2 mg samples on a DuPont model 900 differential thermal analyzer at 764.5 mm.

Preparation of 1,2-Diethylferrocene

A solution of 0.50 g 1-acetyl-2-ethylferrocene (9) in 20 ml ether was added dropwise to a stirred solution of 0.5 g lithium aluminium hydride and 1.5 g aluminium chloride in 100 ml ether at reflux (20). The solution was maintained at reflux temperature for 30 min and allowed to cool. The reaction mixture was then carefully hydrolyzed with water. The ether layer was separated, dried over anhydrous magnesium sulphate, and filtered. Evaporation of the ether left 0.48 g 1,2-diethylferrocene, n_D^{25} 1.5765, b.p. 287 °C.

Found: C, 69.27; H, 7.35. Calcd. for $C_{14}H_{18}Fe$: C, 69.43; H, 7.50.

Gas–liquid chromatographic analysis of this material showed it to be a single component, thus demonstrating the reducing reagent incapable of causing disproportionation.

Preparation of 1,1′,2- and 1,1′,3-Triethylferrocene

To a stirred solution of 5.5 g 1,1′-diethylferrocene (9) in 300 ml dry methylene chloride at reflux temperature was added dropwise under nitrogen a solution of 2.3 g acetic anhydride and 3.0 g aluminium chloride in 100 ml dry methylene chloride. The solution was maintained at reflux for a period of 4 h and then allowed to cool. The reaction mixture was then hydrolyzed with ice water. The organic layer was separated, dried over anhydrous magnesium sulphate, filtered, and evaporated to dryness. The residual oil was taken up in hexane and placed on a column of alumina (Alcoa Grade F-20) which had been deactivated to activity grade III (21).

Elution with hexane removed unchanged 1,1′-diethylferrocene (1.92 g) while 1% ether–hexane removed 1-acetyl-1′,2-diethylferrocene (0.57 g). When the eluent was changed to 10% ether–hexane, 1-acetyl-1′,3-diethylferrocene (1.48 g) was removed.

The structures of the clearly separated acetyl isomers, each a viscous liquid, were conclusively established by their n.m.r. spectra in carbon tetrachloride solution (22–24). In the ring proton region 1-acetyl-1′,2-diethylferrocene exhibits a single proton multiplet centered at 5.60 τ and a two proton multiplet centered at 5.85 τ. The spectrum of 1-acetyl-1′,3-diethylferrocene has a two proton multiplet centered at 5.53 τ and a single proton multiplet centered at 5.80 τ. In addition the spectrum of 1-acetyl-1′,2-diethylferrocene exhibits two quartets characteristic of ethyl group methylenes centered at 7.30 τ and 7.80 τ. The lower field group is assigned to the methylene of the 2-ethyl group and is attributed to magnetic anisotropy effects of the adjacent carbonyl group. This deshielding is not observed in the case of the 1,1′,3-disposed isomer.

Each of the pure acetyl-diethylferrocene isomers was reduced by means of lithium aluminium hydride/aluminium chloride in a manner identical with that given above for 1-acetyl-2-ethylferrocene. In each instance g.l.c. analysis demonstrated the reaction product to be a single component. The isomeric products were shown to be triethylated ferrocenes on the basis of their n.m.r. spectra and microanalytical data.

Found (1,1′,3-isomer): C, 70.99; H, 8.09; b.p. 299 °C. Found (1,1′,2-isomer): C, 71.24; H, 7.95; b.p. 302 °C. Calcd. for $C_{16}H_{22}Fe$: C, 71.12; H, 8.21.

Disproportionation of Ethylferrocene

A mixture of 1.00 g of ethylferrocene and 0.44 g of aluminium chloride in 150 ml of dry methylene chloride was stirred at reflux temperature for 2 h in an atmosphere of prepurified nitrogen. The mixture was then cooled and poured into ice water containing 0.1 g of ascorbic acid. The organic layer was separated, dried over anhydrous magnesium sulphate, filtered, and evaporated. The residue was analyzed by preparative g.l.c. and found to be a mixture composed of ferrocene, ethylferrocene (b.p. 263 °C), and 1,1′-diethylferrocene (b.p. 283 °C). The identities of the three components were proved by comparison of their infrared and n.m.r. spectra with those of authentic compounds.

Corresponding results were obtained without exception when methyl-, *n*-propyl-, *n*-butyl-, or *i*-butylferrocene was substituted for ethylferrocene in the reaction with aluminium chloride. The reaction product was composed of three components, as shown by g.l.c. analysis. The components were identified as ferrocene, starting alkylferrocene, and 1,1′-dialkylferrocene by their infrared and n.m.r. spectra. When acetylferrocene was substituted for ethylferrocene in the reaction with aluminium chloride, no disproportionation was observed.

The n.m.r. spectrum of *t*-butylferrocene has a sharp singlet at 8.80 τ in carbon tetrachloride solution while *i*-propylferrocene has a sharp doublet at 8.70 τ. Close examination of the n.m.r. spectra of the disproportionation products from *n*-propyl- and *i*-butyl-ferrocene failed to reveal any peaks in these locations, thus demonstrating the lack of alkyl group isomerization. The limits of detection were set at 0.1% for *t*-butyl groupings and 0.5% for *i*-propyl groupings.

Can. J. Chem. Downloaded from www.nrcresearchpress.com by 210.87.254.105 on 09/05/12
For personal use only.

Disproportionation of 1,1',2-Triethylferrocene

A solution of 0.30 g 1,1',2-triethylferrocene and 0.17 g aluminium chloride in 50 ml dry methylene chloride was stirred at reflux temperature in an atmosphere of prepurified nitrogen for 2 h. It was then cooled, poured into ice water containing 0.1 g ascorbic acid, and the organic phase was separated. The organic layer was dried over anhydrous magnesium sulphate, filtered, and evaporated to dryness. Analysis of the residue indicated the presence of three major components and a trace of a fourth. Two of the major components were identified as 1,1'-diethylferrocene and starting material by their infrared and n.m.r. spectra. The remaining major component was identified as a tetraethylated ferrocene (found: C, 72.04; H, 9.02; b.p. 319 °C; calcd. for $C_{18}H_{26}Fe$: C, 72.48; H, 8.79) and assigned the structure 1,1',2,2'-tetraethylferrocene. The trace material was identified as ethylferrocene by its infrared and n.m.r. spectra.

Similar treatment of 1,1',3-triethylferrocene gave correspondingly similar results. The tetraethylated product obtained in this latter reaction was assigned the structure 1,1',3,3'-tetraethylferrocene. (Found: C, 72.51; H, 8.52; b.p. 307 °C.)

When 1,2-diethylferrocene was utilized in place of 1,1',2-triethylferrocene, the major reaction products were ferrocene, starting material, and 1,1',2,2'-tetraethylferrocene. This tetraethylated derivative was identical in all respects with that obtained from the disproportionation of 1,1',2-triethylferrocene. In addition, traces of ethyl- and 1,1',2-triethylferrocene were detected.

The Synproportionation of Ferrocene and 1,1'-Diethylferrocene

A mixture of 0.42 g 1,1'-diethylferrocene, 0.32 g ferrocene, and 0.16 g aluminium chloride in 100 ml dry methylene chloride was stirred at reflux temperature in an atmosphere of dry argon for 2 h and worked up in the usual manner. Analysis of the reaction product indicated the presence of ethylferrocene in addition to the starting materials.

Similar reactions with ruthenocene (12) or methylcyclopentadienylmanganese tricarbonyl* in place of ferrocene were investigated. Analyses of the reaction products showed only the presence of starting materials.

REFERENCES

1. A. N. Nesmeyanov and E. G. Perevalova. Usp. Khim. **27**, 3 (1958).
2. M. D. Rausch. Can. J. Chem. **41**, 1289 (1963).
3. K. Plesske. Angew. Chem. Intern. Ed. Engl. **1**, 312, 394 (1962).
4. S. I. Goldberg. J. Am. Chem. Soc. **84**, 3022 (1962).
5. S. G. Cottis and H. Rosenberg. Chem. Ind. London, 860 (1963).
6. A. N. Nesmeyanov, N. S. Kochetkova, P. V. Petrovskii, and E. I. Fedin. Dokl. Akad. Nauk SSSR, **152**, 875 (1963).
7. S. G. Cottis and H. Rosenberg. J. Polymer Sci. B, **2**, 295 (1964).
8. D. E. Bublitz. In press.
9. M. Rosenblum and R. B. Woodward. J. Am. Chem. Soc. **80**, 5443 (1958).
10. M. Rosenblum. J. Am. Chem. Soc. **81**, 4530 (1959).
11. K. L. Rinehart, Jr., K. L. Motz, and S. Moon. J. Am. Chem. Soc. **79**, 2749 (1957).
12. D. E. Bublitz, W. E. McEwen, and J. Kleinberg. Org. Syn. **41**, 96 (1961).
13. E. R. Lippincott and R. D. Nelson. J. Chem. Phys. **21**, 1307 (1953). J. Am. Chem. Soc. **77**, 4990 (1955). Spectrochim. Acta, **10**, 307 (1958).
14. M. D. Rausch, E. O. Fischer, and H. Grubert. J. Am. Chem. Soc. **82**, 76 (1960).
15. E. O. Fischer and H. Grubert. Chem. Ber. **92**, 2302 (1959).
16. L. P. Friedman, A. P. Irsa, and G. Wilkinson. J. Am. Chem. Soc. **77**, 3689 (1955).
17. A. N. Nesmeyanov, N. A. Vol'kenau, and I. N. Bolesova. Dokl. Akad. Nauk SSSR, **149**, 615 (1963).
18. A. N. Nesmeyanov, N. A. Vol'kenau, and I. N. Bolesova. Tetrahedron Letters, 1725 (1963).
19. M. Rosenblum, J. O. Santer, and W. G. Howells. J. Am. Chem. Soc. **85**, 1450 (1963).
20. R. F. Nystrom and C. R. A. Berger. J. Am. Chem. Soc. **80**, 2896 (1958).
21. G. Hesse, I. Daniel, and G. Wohlleben. Angew. Chem. **64**, 103 (1952).
22. M. D. Rausch and V. Mark. J. Org. Chem. **28**, 3225 (1963).
23. R. A. Benkeser, Y. Nagai, and J. Hooz. Bull. Chem. Soc. Japan, **36**, 482 (1963).
24. K. L. Rinehart, Jr., D. E. Bublitz, and D. H. Gustafson. J. Am. Chem. Soc. **85**, 970 (1963).

**Purchased from Ethyl Corporation, New York, N.Y.*

Can. J. Chem. Downloaded from www.nrcresearchpress.com by 210.87.254.105 on 09/05/12
For personal use only.

Can. J. Chem. Downloaded from www.nrcresearchpress.com by 210.87.254.6 on 09/05/12
For personal use only.

ION–MOLECULE REACTIONS STUDIED BY TIME-OF-FLIGHT MASS SPECTROMETRY

II. REACTIONS IN CO–D_2 AND CH_4–D_2 MIXTURES[1]

CLIFFORD W. HAND[2] AND HANNS VON WEYSSENHOFF[3]

Jet Propulsion Laboratory, California Institute of Technology, Pasadena, California

Received April 20, 1964

ABSTRACT

The pulsed operation capability of the time-of-flight mass spectrometer has been used for the study of ion–molecule reaction kinetics. Reactions take place in a high-pressure (up to 0.08 Torr) region free from external electric fields, and time is used as a direct kinetic variable. The following reactions were studied.

$$CO^+ + D_2 \xrightarrow{k_3} DCO^+ + D,\ k_3 = 7.1_6 \times 10^{-10}\ cm^3/molecule\ s;$$

$$D_2^+ + CH_4 \xrightarrow{k_7} CH_4D^+ + D,\ k_7 \sim 2 \times 10^{-10}\ cm^3/molecule\ s.$$

In CH_4–D_2 mixtures a reaction in addition to $CH_4^+ + CH_4 \rightarrow CH_5^+ + CH_3$ leads to the formation of an ion of m/e 17. Various possibilities for this reaction are discussed.

INTRODUCTION

Gas phase reactions between ions and molecules have been studied in a variety of ways, usually involving more or less energetic ions as reactants. The most common technique has been the operation of a mass spectrometer at relatively high source pressures. The theory, experimental techniques, and results of such investigations have been reviewed (1, 2). The rate constants of ion–molecule reactions have been observed to depend on ion energy (velocity) and hence on the strength of the electric field in the reaction chamber; moreover, the form of the field dependence is not completely understood for all reactions (1). In view of the increasing interest in the role of ions in combustion processes (3), it is desirable to have available kinetic data which are obtained with ions reacting at thermal velocities in the absence of external electric fields. These conditions are met in a new method which has been briefly reported (4). An additional advantage of this method is that the measured kinetic variable is time, rather than the less direct variables of reservoir pressure or electric field.

EXPERIMENTAL

A description of the apparatus has been published (4), but for completeness will be summarized here. A Bendix Model 14 time-of-flight mass spectrometer (t.o.f.)* was modified to permit operation at relatively high pressures. The ion source region was enclosed in a stainless steel box with appropriate orifices provided for electron beam entrance and exit, ion exit, sample inlet, and pressure measurement. Source pressure was measured with a McLeod gauge and (or) a CEC micromanometer. The region around the source box was pumped by a 6″ CVC oil diffusion pump, and source pressures up to 0.080 torr could be attained without increasing the flight-tube pressure above 2×10^{-5} torr.

The gas temperature in the source was 15–20 deg above room temperature; an average value of 310 °K was used in all kinetic calculations. The gases were introduced into the vacuum rack through cold traps and had the following nominal purities: CO, Matheson C.P. (99.5%); CH_4, Phillips Research Grade (99.59%); D_2, Biorad (99.5%) or Matheson (99.5%). Semiquantitative mass spectral observation showed no significant impurities. Gas mixtures were prepared manometrically and allowed to stand at least 12 h before use.

[1]*This paper presents results of one phase of research carried out at the Jet Propulsion Laboratory, California Institute of Technology, under Contract No. NAS-7-100, sponsored by the National Aeronautics and Space Administration.*

[2]*Present address: Mellon Institute, Pittsburgh, Pa.*

[3]*Present address: Chemistry Department, Northwestern University, Evanston, Ill.*

**The operating principles of the t.o.f. are well described elsewhere. See, for example, D. B. Harrington. In Encyclopedia of spectroscopy. Editor, G. L. Clark. Reinhold, New York. 1960. p. 628.*

A time delay, variable and accurately known, was introduced between the ionizing electron beam pulse and the pulse which withdraws the ions for analysis. During this delay period the source region was free from external electric fields. Unless otherwise stated, the ionizing voltage was 70 V. The ionizing current was kept low to avoid overloading the detector and varied somewhat with pressure.

In a typical experiment a continuous flow of sample was introduced into the ion source through a Granville-Phillips variable leak. When observations of source pressure indicated that steady flow had been achieved, the intensities of the relevant mass peaks were measured as a function of delay time. These data were obtained for eight or nine different delay times in random sequence to minimize the effect of slow variations in operating parameters.

It was found necessary to keep the source and detector electrodes as clean and free from carbonaceous deposits as possible. Dirt on the electrodes showed up primarily as periodic fluctuations in the gain of the detector. Whenever this condition became intolerable the mass spectrometer was disassembled and cleaned.

RESULTS AND DISCUSSION

As a general check on the method we have reinvestigated (4) the reaction

[1] $$CH_4^+ + CH_4 \xrightarrow{k_1} CH_5^+ + CH_3.$$

With the usual assumptions of no important competing or consecutive reactions and equal ion collection efficiencies for all species, the kinetic equations may be integrated to yield

[2] $$\log_{10}\frac{I_{16} + I_{17}}{I_{16}} = \frac{k_1[CH_4]t}{2.303},$$

where I_N refers to the observed detector output due to the ions of m/e N. The plots of log $[(I_{16} + I_{17})/I_{16}]$ vs. delay time were linear up to approximately 75% reaction, and from them an average value of $k_1 = 12.6 \times 10^{-10}$ cm^3/molecule s was obtained.* This agreed well with the published (5, 6) values of 8.9×10^{-10} and 11.6×10^{-10} and confirmed that the method gave reliable results.

The System CO–D_2

It has been reported (7) that the species DCO^+ is a product of an ion–molecule reaction in a CO–D_2 mixture and suggested that CO^+ is the ionic reactant. Since the species D_2^+ is also a possible reactant, it was of interest to ascertain whether CO^+ or D_2^+ is the reactant and also to obtain an independent measure of the rate constant. A mixture of 1:1 CO–D_2 was used for all experiments. Preliminary experiments revealed a large peak at m/e 30, the intensity of which increased with pressure and delay time. Therefore the peak was identified as the secondary species DCO^+, arising from either of the ion–molecule reactions:

[3] $$CO^+ + D_2 \xrightarrow{k_3} DCO^+ + D$$

or

[4] $$CO + D_2^+ \xrightarrow{k_4} DCO^+ + D.$$

The only other species observed were D^+, D_2^+, D_3^+, C^+, O^+, and CO^+. The ionization efficiency curve of the species DCO^+ was found to be identical with that of CO^+; in particular there was no structure in the DCO^+ curve corresponding to the onset of D_2^+. Thus we conclude that under the conditions of our experiment the reactant ion is CO^+, and that [4] does not contribute appreciably to the formation of DCO^+. With the reaction system thus simplified, the kinetic equations may again be integrated to

[5] $$\log_{10}\left[\frac{I_{28} + I_{30}}{I_{28}}\right] = \frac{k_3[D_2]t}{2.303}.$$

**The value given in ref. 4 (11.1×10^{-10}) was not corrected for temperature. The true value is 12.6×10^{-10}, as above.*

Can. J. Chem. Downloaded from www.nrcresearchpress.com by 210.87.254.6 on 09/05/12
For personal use only.

The reaction was studied over a range of pressures and delay times, and the results are given in Table I. The data from two runs are presented in Fig. 1, where $\log_{10}[(I_{28} + I_{30})/I_{28}]$

TABLE I

Results of k_3 determination ($CO^+ + D_2 \xrightarrow{k_3} DCO^+ + D$)

P (torr $\times 10^3$)	k_3 (cm^3/molecule s $\times 10^{10}$)
3.1	5.5
3.4	9.1
4.4	7.0
5.3	6.6
5.4	6.6
5.4	7.2
5.6	5.9
6.0	10.2
6.1	7.2
6.2	6.9
6.4	7.2
6.5	7.2
7.8	7.2
8.0	6.2
10.7	6.3
18.0	7.0
27.0	8.5
Average: $7.16 \pm 0.117 \times 10^{-10}$ cm^3/molecule s	

is plotted vs. delay time. That the lines in Fig. 1 do not pass through the origin is a reflection of the arbitrary zero of time, due to the finite rise times and widths of the several electronic pulses, and the finite transit time of the ions emerging from the reaction chamber. The *differences* in delay times, hence the slopes and rate constants, are accurately known. Note that in Fig. 1 the lines produced meet at a common point on the time axis. In Table I each rate constant was obtained by a least squares treatment of the data. The least squares error in the slope was of the order of 3–4%, and did not vary widely from one run to the next. The average of the values in Table I is $7.1_6 \pm 0.12 \times 10^{-10}$ cm^3/molecule s, with a standard deviation of 1.6%. This may be compared with the published value (7) of 16.3×10^{-10} cm^3/molecule s. The difference between our value and the literature value cannot be explained, except to note that the latter is the result of a single determination at non-zero electric field in the reaction chamber.

The System CH_4–D_2

There are several recent papers (8–10) which mention the reaction

[6] $$[CH_4 + H_2]^+ \longrightarrow CH_5^+ + H$$

or its deuterated variations. The brackets indicate that either species may be the ionic reactant. Lampe and Field (8, 10) could not observe this reaction and were thus able to assign a rather low upper limit to the reaction rate, namely $k < 5 \times 10^{-12}$ cm^3/molecule s (10). On the other hand, Talrose and Frankevitch (9), although they did not measure its rate, observed the reaction without difficulty and used their results to calculate the proton affinity of methane.

We have investigated the charged species existing in an ionized mixture of methane and deuterium (5% methane). A small peak was observed at m/e 18, which, however, was significantly larger than the combined contributions of background and $^{13}CH_5^+$. This peak was identified as CH_4D^+, on the basis of the following evidence. The intensity of CH_4D^+ (relative to any of the primary ionic species) increased with delay time, as expected for a

Can. J. Chem. Downloaded from www.nrcresearchpress.com by 210.87.254.6 on 09/05/12
For personal use only.

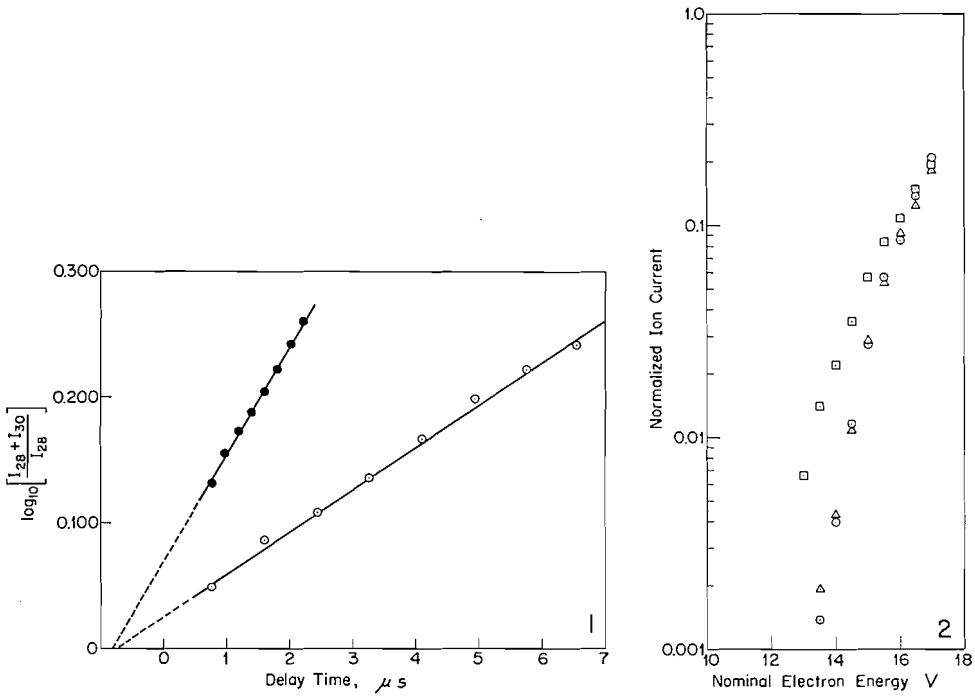

FIG. 1. Formation of DCO^+ vs. delay time in CO–D_2. (●) 0.018 torr, $k_3 = 7.0 \times 10^{-10}$ cm³/molecule s; (○) 0.008 torr, $k_3 = 6.2 \times 10^{-10}$ cm³/molecule s.

FIG. 2. Ionization efficiency in CH_4–D_2. (○) D_3^+, (△) CH_4D^+, (□) CH_5^+.

product ion. The ionization efficiency data for some of the species present in the mixture are shown in Fig. 2, where the detector signal (normalized to 40 V ionizing energy) is plotted vs. ionizing energy. For ease of comparison, all three species shown are secondary ions. It is seen that the ionization efficiency curve of CH_4D^+ very closely approximates that of D_3^+, and the conclusion may be drawn that both species are formed in reactions of the same precursor ion, namely D_2^+.* Thus in our system reaction [6] is readily observable; the ionization efficiency data allow us to identify the ionic reactant, and write

$$[7] \qquad CH_4 + D_2^+ \xrightarrow{k_7} CH_4D^+ + D.$$

Our own preliminary observations as well as the dispute in the literature indicated that the rate constant k_7 is quite low; its determination is complicated by competing reactions such as

$$[8] \qquad D_2^+ + D_2 \xrightarrow{k_8} D_3^+ + D.$$

This difficulty can be overcome by changing the experimental procedure to work only at low percent reaction. Under these conditions the exponential form of eq. [2] or [5] may be expanded and higher terms dropped to yield, in the case of reaction [7],

$$[9] \qquad \frac{I_{18}}{I_4} = k_7[CH_4]t.$$

**It is well established that D_3^+ is formed in the reaction $D_2^+ + D_2 \rightarrow D_3^+ + D$. See ref. 1, for example.*

Can. J. Chem. Downloaded from www.nrcresearchpress.com by 210.87.254.6 on 09/05/12
For personal use only.

Can. J. Chem. Downloaded from www.nrcresearchpress.com by 210.87.254.6 on 09/05/12
For personal use only.

It can be shown (1) that this form of the kinetic equations is valid even in the presence of competing reactions, so long as the percentage conversion is low.

Experimentally this technique is less accurate than the method used to obtain k_1 and k_3: the measurement of larger concentration ratios is inherently less accurate than smaller, and moreover, in our apparatus the measurement of small time delays is less accurate than large. The result of this experimental difficulty is illustrated in Fig. 3, where I_{18}/I_4 is plotted vs. delay time [arbitrary zero] for run C of Table II. It is seen that the scatter greatly exceeds that of Fig. 1 and that quantitative conclusions drawn from such plots must be regarded as estimates. The determination of the rate constant k_7 from the slope of the line in Fig. 3 is further complicated by a difficulty which does not arise in the case of reactions [1] or [3]. This difficulty is that the assumption of equal collection efficiencies for reactant and product ions is no longer valid when the species are as different as CH_4D^+ and D_2^+. The breakdown of this assumption has two causes. Firstly, the focussing properties of the t.o.f. mass spectrometer are not wholly mass independent, and secondly, the sensitivity of the electron multiplier detector is not the same for all ions. This latter effect is better known in terms of γ, the secondary electron emission coefficient. The variation of γ with experimental parameters has been discussed by many authors (11–16). Many of the experiments have yielded conflicting results, and the theoretical treatments (11–13) must be cautiously applied to real experiments. The results of Sternglass (12) may be used to predict that γ will increase with the square root of ionic mass in the t.o.f. spectrometer, but not all experiments support this. We do not feel confident in basing any rate constant corrections on either theoretical values of γ or on experimental values obtained under rather different conditions, but prefer to determine a correction factor of our own, as follows.

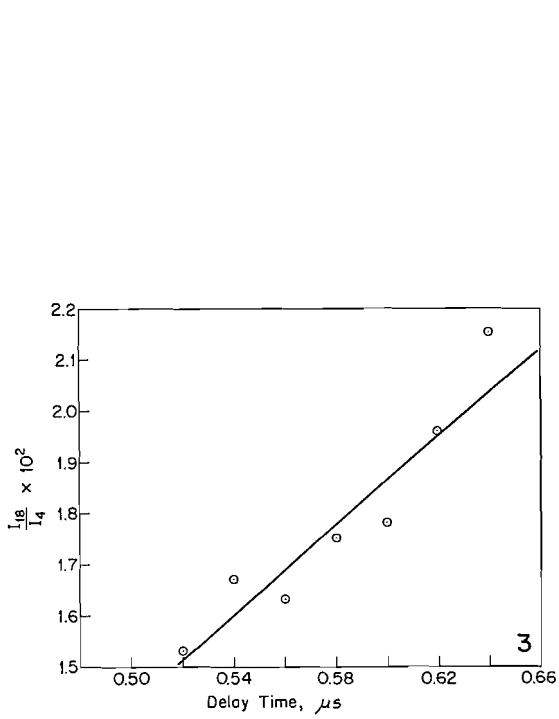

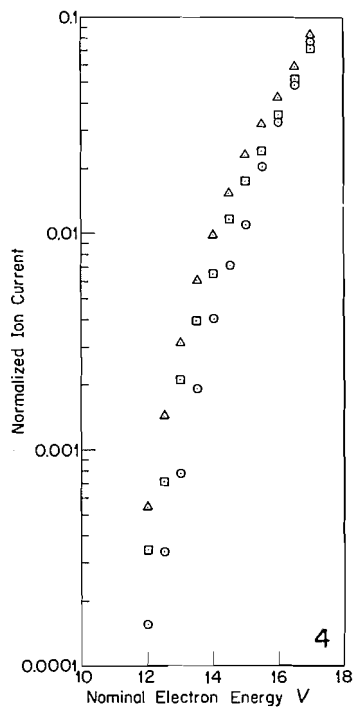

FIG. 3. Formation of CH_4D^+ vs. delay time in CH_4–D_2. 0.011_5 torr.
FIG. 4. Ionization efficiency in CH_4–D_2. (○) mass 15, (△) mass 16, (□) mass 17.

The results with reaction [1] indicate that the equal collection efficiency assumption is valid when applied to the species CH_4^+ and CH_5^+; CH_4D^+ may be expected to behave as CH_5^+, and hence the same as CH_4^+. Further the relative ionization efficiencies for D_2^+ from D_2 and CH_4^+ from CH_4 are known (17). Thus for a known mixture of CH_4 and D_2 one can calculate the relative concentrations of CH_4^+ and D_2^+ in the ion source immediately following ionization by 70 V electrons. Comparison of this calculated ratio with that obtained from the detector signals yields the relative collection efficiencies of CH_4^+ and D_2^+, hence those of CH_4D^+ and D_2^+. In our mixture of CH_4 (5%) and D_2 (95%) the experimental ratio D_2^+/CH_4^+ was 0.53, whereas the ratio calculated on the basis of known relative ionization efficiencies (17) is 9.56.* Thus in our mass spectrometer CH_4^+ and CH_4D^+ are collected 18 times as efficiently as D_2^+. Our experiments do not allow us to determine how much of this factor is due to difference in focussing efficiency and how much to difference in γ.

This correction was applied to the raw data of six runs in CH_4 (5%) – D_2 (95%) and the results are shown in Table II. The last column gives the corrected estimate of the rate constant. The average, $\sim 2 \times 10^{-10}$ cm^3/molecule s, may be compared to the upper limit of 5×10^{-12} set by Lampe and Field (8*b*).

TABLE II

Results of k_7 determination ($CH_4 + D_2^+ \xrightarrow{k_7} CH_4D^+ + D$)

Run	P (torr $\times 10^3$)	k_7 (cm^3/molecule s $\times 10^{10}$)
A	5.2	2.6
B	5.3	1.6
C*	11.5	1.2
D	10.1	2.7
E	19.8	3.0
F	14.7	3.1

*This run is the same as in Fig. 3.

Other Reactions in CH_4–D_2 Mixtures

During the course of preliminary experiments it was observed that the rate of reaction [1] measured in the CH_4–D_2 mixture considerably exceeded that measured in pure CH_4. This enhancement of k_1 was observed under conditions where the exponential approximation to eq. [2] was expected to hold, and was quite reproducible. A series of seven runs at varying pressures gave for the enhanced rate constant $k_1' = 59.7 \pm 7.1 \times 10^{-10}$ cm^3/molecule s. Compared to the pure methane value of $k_1 = 12.6 \times 10^{-10}$ cm^3/molecule s, this is an increase of a factor of almost 5.

A possible reason for this enhancement lies in some unspecified "mass effect" due to the high dilution with a low molecular weight species, perhaps related to differential effusion from the source chamber. This possibility was checked by measuring k_1 in mixtures of 5% CH_4 in He. If a "mass effect" is causing the enhancement, the substitution of He for D_2 in the mixture should have no effect. Five determinations in the CH_4–He mixture yielded $k_1'' = 27.6 \pm 3.6 \times 10^{-10}$ cm^3/molecule s, larger than the true value by a factor of 2.2. Thus a "mass effect" is not entirely responsible for the enhancement in D_2, and some other ion–molecule reaction producing a species of m/e 17 is taking place.

In the CH_4–D_2 system there are only two possibilities for increased intensity at m/e 17; these are CH_3D^+ and CHD_2^+. It might be expected that ionization efficiency data would

*This calculated ratio is itself subject to the errors of conventional mass spectrometry and may be in error by 50–100%.

Can. J. Chem. Downloaded from www.nrcresearchpress.com by 210.87.254.6 on 09/05/12
For personal use only.

provide a means of deciding between these two species, but further consideration shows this not to be the case. At least part of the intensity at m/e 17 is due to reaction [1]; if the other contributing reaction had the same precursor (CH_4^+), the ionization efficiency of m/e 17 would coincide with that of CH_4^+ and a positive identification could be made. If, however, the contributing reaction has some precursor X^+ different from CH_4^+, the ionization efficiency of m/e 17 will be intermediate between that of CH_4^+ and X^+, and no positive conclusion can be drawn. That the latter situation obtains is shown in Fig. 4, which shows the ionization efficiencies for m/e 15, 16, 17 in the CH_4–D_2 system. The curve for m/e 17 is *not* coincident with that of CH_4^+. From this, one can conclude that some other reaction is supplying part of m/e 17, and that this other ionic reactant has an appearance potential greater than that of CH_4^+. The curve for m/e 15, CH_3^+, is included in Fig. 4 for comparison.* There are several possible reactions in the CH_4–D_2 system which satisfy the requirements that they (i) be not endothermic, (ii) produce either CH_3D^+ or CHD_2^+, and (iii) involve an ionic reactant which has an appearance potential greater than that of CH_4^+.

TABLE III

Possible sources of m/e 17 from CH_4–D_2 mixtures

$CH_4 + D_2^+ \rightarrow CH_3D^+ + HD$
$CH_4 + D_2^+ \rightarrow CHD_2^+ + H_2 + H$
$CH_4 + D^+ \rightarrow CH_3D^+ + H$
$D_2 + CH_2^+ \rightarrow CHD_2^+ + H$
$D_2 + CH_3^+ \rightarrow CHD_2^+ + H_2$

Table III lists the possible reactions, but in the absence of further evidence we cannot draw any definite conclusions. However, if we assume that any one of these reactions is involved, an estimate of its rate constant can be made.

For example, if reaction [10]

[10] $$CH_4 + D^+ \xrightarrow{k_{10}} CH_3D^+ + H$$

is solely responsible,† a straightforward treatment of the kinetic equations leads to the expression

[11] $$k_1' = k_1 + \frac{[D^+]}{[CH_4^+]} k_{10},$$

where k_1 and k_{10} have their usual meanings, and k_1' is the enhanced rate constant measured in the presence of D_2 [for the moment we are ignoring the "mass effect" discussed above]. The ratio $[D^+]/[CH_4^+]$ can be obtained from the known mixture composition and the relative mass spectral sensitivities of D^+ and CH_4^+ given in the A.P.I. tables (17), and is equal to 0.16_5. Inserting this value and k_1', k_1 into eq. [11] we obtain $k_{10} = 280 \times 10^{-10}$ cm³/molecule s. This must be regarded as an upper limit to k_{10}, since it was obtained by ignoring the "mass effect".

**Some relevant appearance potentials from CH_4 and D_2 are CH_4^+, 13.1 V; CH_3^+, 14.4 V; CH_2^+, 20.1 V; D_2^+, 15.4 V; D^+, 18.2 V. Values taken from F. H. Field and J. L. Franklin. Electron impact phenomena. Academic Press, New York. 1957.*

†Reaction [10] is the simplest of the possibilities and therefore a likely secondary contributor to m/e 17. It may be regarded as either an S_E2 reaction or as a proton (deuteron) transfer reaction; the latter class of reaction is known for its high rate constants (1).

Can. J. Chem. Downloaded from www.nrcresearchpress.com by 210.87.254.6 on 09/05/12
For personal use only.

It will be recalled that the enhancement in the presence of helium yielded a rate constant k_1'' larger than k_1 by a factor of 2.2. If the enhancement in D_2 is regarded as a combination of "mass" and "chemical" effects, the value of k_1' must be adjusted by dividing it by 2.2. The new estimate of k_{10} can then be obtained as above, and is $k_{10} = 86 \times 10^{-10}$ cm^3/molecule s. The true value probably lies somewhere between these limits.

REFERENCES

1. F. W. LAMPE, J. L. FRANKLIN, and F. H. FIELD. *In* Progress in reaction kinetics. Vol. 1. *Edited by* G. Porter. Pergamon, London. 1959. p. 68.
2. V. L. TALROSE. Pure Appl. Chem. **5**, 455 (1962).
3. 9th Symposium (International) on Combustion. Academic Press, New York. 1963.
4. C. W. HAND and H. VON WEYSSENHOFF. Can. J. Chem. **42**, 195 (1964).
5. F. H. FIELD, J. L. FRANKLIN, and F. W. LAMPE. J. Am. Chem. Soc. **79**, 2419 (1957).
6. V. L. TALROSE. Izv. Akad. Nauk SSSR, Otd. Khim. Nauk, 1351 (1959); Chem. Abstr. **53**, 21184*e* (1959).
7. D. P. STEVENSON and D. O. SCHISSLER. J. Chem. Phys. **29**, 282 (1958).
8. F. W. LAMPE and F. H. FIELD. J. Am. Chem. Soc. **79**, 4244 (1957); **81**, 3242 (1959).
9. V. L. TALROSE and E. L. FRANKEVITCH. J. Am. Chem. Soc. **80**, 2344 (1958).
10. F. W. LAMPE and F. H. FIELD. Zh. Fiz. Khim. **33**, 732 (1959).
11. H. S. W. MASSEY and E. H. S. BURHOP. Electronic and ionic impact phenomena. Oxford. 1952. Chap. IX.
12. E. J. STERNGLASS. Phys. Rev. **108**, 1 (1957).
13. H. HAGSTRUM. Phys. Rev. **96**, 325 (1954).
14. M. HEALEA. Phys. Rev. **55**, 984 (1939).
15. B. AARSET, R. W. CLOUD, and J. G. TRUMP. J. Appl. Phys. **25**, 1365 (1954).
16. R. W. KISER. J. Chem. Phys. **36**, 2964 (1962).
17. American Petroleum Institute Research Project 44. Catalog of Mass Spectral Data. A & M Press, A & M College of Texas, College Station, Texas.

Can. J. Chem. Downloaded from www.nrcresearchpress.com by 210.87.254.6 on 09/05/12
For personal use only.

Can. J. Chem. Downloaded from www.nrcresearchpress.com by 210.87.254.40 on 09/05/12
For personal use only.

SYNTHESIS OF THIOHYDROXIMATES

THE ADDITION OF THIOLS TO NITRILE OXIDES

M. H. BENN
Department of Chemistry, University of Alberta, Calgary, Alberta
Received February 3, 1964

ABSTRACT

The addition of thiols to nitrile oxides is shown to constitute a general synthesis of thiohydroximates.

In a consideration of routes for the synthesis of mustard oil glucosides, the addition of thiols to nitrile oxides appeared to us to represent an attractively direct and simple method of constructing the thiohydroximate system characteristic of these compounds.

The only examples of the realization of this reaction which appear to be reported in the literature are the preparation by Alemagna and Bacchetti (1) of some benzothiohydroximates, e.g. IV (R′ = phenyl, R″ = benzyl).

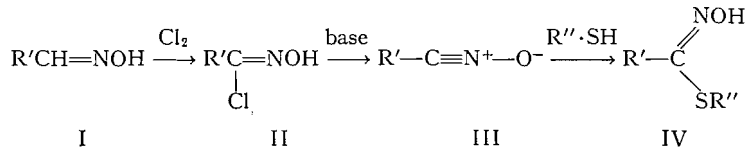

Before attempting the synthesis of a mustard oil glucoside, we carried out some model studies with aryl and alkyl nitrile oxides and thiols. We report here the results of these experiments, which demonstrate that the reaction is a general and excellent method for the synthesis of thiohydroximates.

Nitrile oxides are commonly prepared by treating a hydroxamoyl chloride (α-chlorooxime) (II) with base (2, 3, 4), the hydroxamoyl chloride having been prepared by chlorination of the corresponding aldoxime (I). The procedure which we usually followed was to generate the nitrile oxide *in situ* by treating a cold ethereal solution of the thiol and hydroxamoyl chloride with excess triethylamine. After about 30 minutes at room temperature the reaction was worked up to give the thiohydroximate, which usually crystallized spontaneously in a high state of purity. In this way we prepared a series of alkyl and aryl thiohydroximates (IV, R′ = alkyl or aryl, R″ = alkyl or aryl).

Proof that the products are indeed thiohydroximates with the structure IV includes comparison with thiohydroximates prepared by alternative routes (1, 5) and from their infrared and proton magnetic resonance (p.m.r.) spectra. The infrared spectra[1] show broad, strong intensity OH (stretch) absorption around 3300 cm^{-1} and a sharp, medium intensity band at 1625 $\pm$ 10 cm^{-1} corresponding to the C=N (stretch) absorption. The p.m.r. spectra[2] show a signal around $\tau = 0.3 \pm 0.2$, of intensity corresponding to one hydrogen, in the same position as the signal for hydrogen in the oxime function of ketoximes and aldoximes; the remaining features of the p.m.r. spectra are in accord with the structure IV.

Nitrile oxides formed *in situ* by the addition of triethylamine to an ethereal solution

[1]*Potassium bromide discs.*
[2]*Measured in chloroform and deuterochloroform at 60 Mc/s with tetramethylsilane as an internal standard.*

of the appropriate hydroxamoyl chloride have been trapped by addition to a variety of unsaturated compounds, reactions in which the nitrile oxide behaves as a 1,3-dipolar ion (4). Direct evidence that nitrile oxides are involved as intermediates[3] under our conditions for the thiohydroximate synthesis may be summarized as follows.

Thiols did not react with hydroxamoyl chlorides at an appreciable rate, under the conditions which we employed, if no triethylamine was added. Addition of triethylamine to a cold ethereal solution of hydroxamoyl chloride resulted in immediate precipitation of triethylamine hydrochloride and the filtered solution exhibited intense absorption at 2320 cm^{-1}, characteristic of nitrile oxides[4] (3). Addition of thiol to this solution resulted in extremely rapid disappearance of this absorption band, and evaporation of the solution yielded the thiohydroximate.

It is significant that, under the usual conditions which we employed for the thiohydroximate synthesis, *t*-butyl mercaptan gave a poor yield of benzothiohydroximate, the major product being the furoxan produced by dimerization of the initially formed benzonitrile oxide. Presumably here the rate of dimerization of benzonitrile oxide is competitive with the rate of reaction with the hindered thiol.

Various mechanisms can be written for the reaction of thiols with nitrile oxides which lead to either of the two possible configurations about the carbon–nitrogen double bond. Thus (*a*) attack of un-ionized thiol on the nitrile oxide leads to the *anti* (R, OH) configuration in a process reminiscent of the 1,3-dipolar addition of nitrile oxides to olefins (2, 4); (*b*) attack by thiolate anion leads to the same, *anti*, configuration; and (*c*) attack also by thiolate anion leads to the opposite, *syn*, configuration. Mechanism (*b*) represents a *trans* addition in which the lone pair of electrons develops on the nitrogen *trans* to the attacking thiolate anion, whilst in (*c*) the geometry of the transition state is such as to minimize repulsion between the formal charges on the thiolate nucleophile and the oxygen of the nitrile oxide.

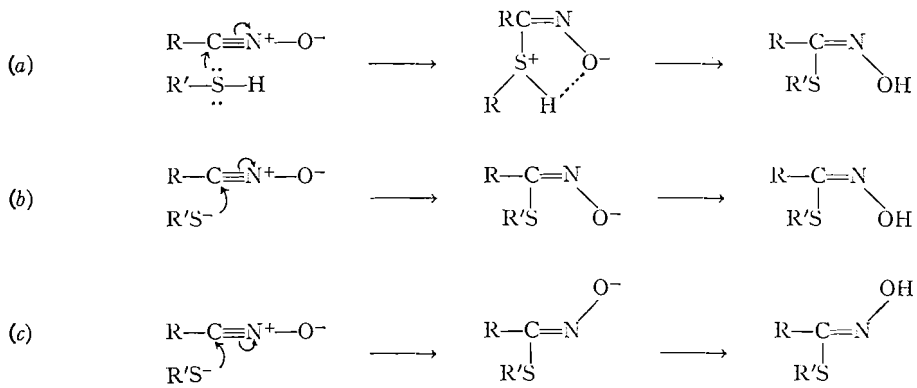

[3]*Ettlinger and Dateo have discovered (6) that O-sulphonated hydroxamoyl chlorides react with thiolate salts, forming thiohydroximates. In these cases nitrile oxide formation is blocked, and it appears that the thiolate species displace halide from these hydroxamoyl chlorides. However, the reaction may well proceed via an intermediate (V), closely related to a nitrile oxide.*

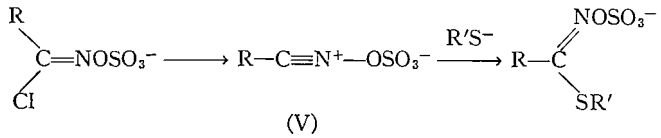

(V)

[4]*For spectroscopic purposes, it was more convenient to use carbon tetrachloride as solvent. The filtered solution then exhibited intense absorption at 2300 cm^{-1}, which as before disappeared upon addition of thiol.*

Can. J. Chem. Downloaded from www.nrcresearchpress.com by 210.87.254.40 on 09/05/12
For personal use only.

Whilst we do not have the rate data which would permit a definite decision, on the basis that yields of thiohydroximates appear to be higher when excess base is present, we favor a mechanism involving thiolate anion as the nucleophilic species. Discrimination between (*b*) and (*c*) is not possible on the basis of the results which we have obtained, but the stereochemistry about the carbon–nitrogen double bond may be deduced by the following argument.

The mustard oil sinigrin, a naturally occurring thiohydroximate, has been shown by X-ray crystallography (7) to have the *anti* configuration, and it is reasonable to assume that the other mustard oil glucosides have a similar configuration.

We have been able to use the addition of thiols to nitrile oxides in the synthesis of compounds identical with the natural mustard oil glucosides (5) under conditions which were most unlikely to result in change in configuration about the carbon–nitrogen double bond. We conclude therefore that the addition of thiols to nitrile oxides results in formation of thiohydroximates with the *anti* configuration.[5]

The thiohydroximates synthesized were stable, well crystallized solids and yields were, with the exception of the *S-t*-butyl thiohydroximate, good; in fact, the reaction of thiols with phenylacetonitrile oxide appears suitable for their characterization.

Selenols react analogously to yield selenohydroximates.

EXPERIMENTAL

Preparation of Hydroxamoyl Chlorides

Isobutyrohydroxamoyl Chloride

(II, R = isopropyl.) Isobutyraldoxime (3.0 g) was dissolved in chloroform (30 ml), the solution was cooled to 0° in an ice–salt bath, and a fairly slow stream of dry chlorine was bubbled through the solution for 30 minutes. The blue solution was concentrated under reduced pressure (bath $T \not> 40°$) to an almost colorless oil containing a little crystalline material, presumably a hydrochloride. The oil was dissolved in ether and the solvent again removed under reduced pressure (bath $T \not> 40°$). The residual oily isobutyrohydroxamoyl chloride was sufficiently pure for the subsequent reactions.

The following hydroxamoyl chlorides were obtained by the same procedure.

Acetohydroxamoyl Chloride

(II, R = methyl.) Oil. Lit. (8) oil.

Benzohydroxamoyl Chloride

(II, R = phenyl.) Cryst., m.p. 49° from petroleum ether. Lit. (9) m.p. 49°.

Phenylacetohydroxamoyl Chloride

(II, R = benzyl.) Cryst. m.p. 89–91° (5).

Preparation of Thiohydroximates by Method A

S-p-Tolyl Isobutyrothiohydroximate

(IV, R′ = isopropyl, R″ = *p*-tolyl.) Crude isobutyrohydroxamoyl chloride (1.50 g) and *p*-toluenethiol (1.20 g) were dissolved in ether (100 ml), and to the gently stirred solution was added triethylamine (2.5 g) in ether (10 ml) in one portion. There was an immediate copious precipitate of triethylamine hydrochloride. After 30 min at room temperature, the reaction mixture was poured into cold ca. 0.5 *N* aqueous sulphuric acid. The ether layer separated and the aqueous phase was re-extracted with ether (2 × 50 ml). The combined ether extracts were dried ($MgSO_4$) and evaporated to yield *S-p*-tolyl isobutyrothiohydroximate, which crystallized spontaneously from the concentrated ethereal solution in colorless laths; 1.33 g (66%), m.p. 155–159°, raised to 158–159° on recrystallization from ether – petroleum ether.

Anal. Calcd. for $C_{11}H_{15}NOS$: C, 63.12; H, 7.22; N, 6.69; S, 15.32. Found: C, 63.34; H, 7.46; N, 6.83; S, 15.03.

The following thiohydroximates were similarly prepared.

S-p-Tolyl Acetothiohydroximate

(IV, R′ = methyl, R″ = *p*-tolyl.) Colorless laths from ether – petroleum ether, m.p. 132–134° (61%).

Anal. Calcd. for $C_9H_{11}NOS$: C, 59.61; H, 6.11; N, 7.73; S, 17.68. Found: C, 59.37; H, 6.01; N, 8.35; S, 18.07.

[5]*This conclusion is opposite to the one which we gave initially (5). The structures given in these earlier communications should be amended to the anti configuration.*

Can. J. Chem. Downloaded from www.nrcresearchpress.com by 210.87.254.40 on 09/05/12
For personal use only.

S-Methyl Benzothiohydroximate

(IV, R′ = phenyl, R″ = methyl.) Colorless spars from ether – petroleum ether, m.p. 85° (50%).

Anal. Calcd. for C_8H_9NOS: C, 57.40; H, 5.43; N, 8.38; S, 19.18. Found: C, 57.60; H, 5.48; N, 8.20; S, 18.93.

S-Ethyl Benzothiohydroximate

(IV, R′ = phenyl, R″ = ethyl.) Colorless prisms from ether – petroleum ether, m.p. 90–91° (87%).

Anal. Calcd. for $C_9H_{11}NOS$: C, 59.63; H, 6.11; N, 7.73; S, 17.69. Found: C, 59.78; H, 6.26; N, 7.55; S, 17.72.

S-t-Butyl Benzothiohydroximate

(IV, R′ = phenyl, R″ = *t*-butyl.) Colorless spars from ether – light petroleum, m.p. 55–56° (12%).

Anal. Calcd. for $C_{11}H_{15}NOS$: C, 63.12; H, 7.22; N, 6.69; S, 15.32. Found: C, 63.36; H, 7.07; N, 6.83; S, 15.21.

In this preparation, the major product isolated was the furoxan (67%), formed by dimerization of the benzonitrile oxide, which crystallized first from ether – petroleum ether, m.p. 115–116°. Lit. (10) m.p. 114–115°.

S-(2-Carboxyethyl) Benzothiohydroximate

(IV, R′ = phenyl, R″ = CH_2CH_2COOH.) Prepared in ice-cold methanol solution and obtained as fine colorless prisms from ethanol, m.p. 146° (50%).

Anal. Calcd. for $C_{10}H_{11}NO_3S$: C, 53.30; H, 4.92; N, 6.22; S, 14.25. Found: C, 53.38; H, 5.10; N, 6.10; S, 14.24.

S-Benzyl Benzothiohydroximate

(IV, R′ = phenyl, R″ = benzyl.) Colorless laths from ether – petroleum ether, m.p. 121–122° (91%). Lit. (1) m.p. 121–122°.

S-Phenyl Benzothiohydroximate

(IV, R′ = phenyl, R″ = phenyl.) Colorless prisms from ethanol, m.p. 142–143° (91%).

Anal. Calcd. for $C_{13}H_{11}NOS$: C, 68.09; H, 4.84; N, 6.11; S, 13.99. Found: C, 68.04, H, 4.93; N, 6.34; S, 13.72.

S-p-Tolyl Benzothiohydroximate

(IV, R′ = phenyl, R″ = *p*-tolyl.) Colorless plates from ether – petroleum ether, m.p. 134–135° (84%).

Anal. Calcd. for $C_{15}N_{15}NOS$: C, 69.98; H, 5.87; N, 5.44; S, 12.46. Found: C, 70.25, H, 6.20; N, 5.78; S, 12.90.

S-Methyl Phenylacetothiohydroximate

(IV, R′ = benzyl, R″ = methyl.) Long spars from ether – petroleum ether, m.p. 85° (65%).

Anal. Calcd. for C_8H_9NOS: C, 57.40; H, 5.43; N, 8.38; S, 19.18. Found: C, 57.60; H, 5.48; N, 8.20; S, 18.93.

S-p-Tolyl Phenylacetothiohydroximate

(IV, R′ = benzyl, R″ = *p*-tolyl.) Colorless, flat plates from ether – petroleum ether, m.p. 134–135 (70%).

Anal. Calcd. for $C_{15}H_{15}NOS$: C, 69.98; H, 5.87; N, 5.44; S, 12.46. Found: C, 70.25; H, 6.20; N, 5.78; S, 12.90.

Se-Phenyl Benzoselenohydroximate

(IV, R′ = Ph, R″S = PhSe.) Colorless plates from ether – petroleum ether, m.p. 165–166° (35%).

Anal. Calcd. for $C_{13}H_{11}NOSe$: C, 56.53; H, 4.02; N, 5.07; Se, 28.59. Found: C, 56.45; H, 4.25; N, 5.17; Se, 28.44.

Preparation of Thiohydroximates by Method B

Isobutyrohydroxamoyl chloride (1.0 g) was dissolved in carbon tetrachloride (20 ml), and the solution was cooled to 0° and stirred whilst a solution of triethylamine (0.85 g) in carbon tetrachloride (5 ml) was added. The reaction mixture became pasty. The triethylamine hydrochloride was filtered off and washed with a little carbon tetrachloride, and the pale-yellow solution was refiltered. The solution exhibited intense absorption at 2300 cm^{-1}. Addition of *p*-toluenethiol (0.50 g) to this solution resulted in very rapid disappearance of this absorption band. (The band had completely disappeared by the time that the solution was reintroduced into the cell and the spectrum at 2300 cm^{-1} re-examined, ca. 1 min). Evaporation of the solution gave a yellow oil which crystallized from ether as the *thiohydroximate*, m.p. 156–158°, undepressed on admixture with the material prepared by method A. Better yields of the thiohydroximate were obtained by working with more dilute solutions of the hydroxamoyl chloride in ether.

The crystalline phenylacetohydroxamoyl and benzohydroxamoyl chlorides behaved similarly.

ACKNOWLEDGMENTS

We wish to thank Dr. M. G. Ettlinger of Rice University, Houston, Texas, for drawing our attention to the syntheses of mustard oil glucosides described in ref. 6 and for his helpful comments on the stereochemical aspects of the thiohydroximate synthesis.

We also wish to thank Evans Chemetics Inc., 250 East 43rd St., New York 17, N.Y.,

Can. J. Chem. Downloaded from www.nrcresearchpress.com by 210.87.254.40 on 09/05/12
For personal use only.

and Pitt-Consol Chemical Co., Newark 5, N.J., for gifts of thiols. Furthermore, we are grateful to the National Research Council for financial support of this research.

REFERENCES

1. T. BACCHETTI and A. ALEMAGNA. Rend. Ist. Lombardo Sci. Lettere, A, **91** (I), 30, 481 (1957).
2. A. QUILICO. Gazz. Chim. Ital. **67**, 589 (1937).
3. R. H. WILEY and B. J. WAKEFIELD. J. Org. Chem. **25**, 546 (1960) and references therein.
4. R. HUISGEN and W. MACK. Tetrahedron Letters, No. 17, 583 (1961).
5. M. H. BENN. Can. J. Chem. **41**, 2837 (1963); **42**, 163 (1964).
6. M. G. ETTLINGER and G. DATEO. Studies on Mustard Oil Glucosides. Final report to U.S. Army Quartermaster Research and Engineering Command on contract DA-19-129-QM-1059, Project 7-84-06-032. Simplified Food Logistics. 1961.
7. J. WASER and W. H. WATSON. Nature, **198**, 1297 (1963).
8. H. WIELAND. Ber. **40**, 1676 (1907).
9. H. RHEINBOLDT, M. DEWALD, F. JANSEN, and O. SCHMITZ-DUMONT. Ann. **451**, 161 (1926).
10. K. VON AUWERS and V. MEYER. Ber. **21**, 803 (1888).

Can. J. Chem. Downloaded from www.nrcresearchpress.com by 210.87.254.40 on 09/05/12
For personal use only.

Can. J. Chem. Downloaded from www.nrcresearchpress.com by 210.87.254.5 on 09/05/12
For personal use only.

PRÉPARATION DU *tert*-BUTYL-5 DIMÉTHYL-3,3 CYCLOHEXÈNE ET DE QUELQUES ISOMÈRES[1]

JEAN-CLAUDE RICHER ET PATRICE BÉLANGER[2]
Département de Chimie, Université de Montréal, Montréal, Québec
Reçu le 19 mai 1964

RÉSUMÉ

Les hydrocarbures isomères (III, X, XI, XII et XV) ont été préparés par des méthodes standards et ont été caractérisés grâce à leurs propriétés physiques et à leur temps de rétention en c.p.g.

Au cours d'une étude connexe sur la solvolyse des tosylates dérivés des *tert*-butyl-4 diméthyl-2,2 cyclohexanols (I), la formation des hydrocarbures III, X, XI, XII et XV comme produits réactionnels pouvait être envisagée. Le présent travail a été entrepris afin de réaliser la synthèse de ces hydrocarbures par des méthodes non ambigües. Les schémas réactionnels utilisés pour ces synthèses sont présentés dans le Diagramme I.

La pyrolyse du xanthogénate de méthyle (II) dérivé du *tert*-butyl-4 diméthyl-2,2 cyclohexanol-*trans* (I) selon la méthode de Tchougaeff (1) conduit à l'hydrocarbure III dont la pureté est confirmée par chromatographie en phase gazeuse (c.p.g.) analytique.

L'action du réactif de Grignard (iso-PrMgI) sur la *tert*-butyl-3 cyclopentanone (VII) conduit à un mélange de *tert*-butyl-3 isopropyl-1 cyclopentanols VIII et d'un solide dont la constitution n'a pas été établie mais qui est probablement la (*tert*-butyl-3 cyclopentylydène)-2 *tert*-butyl-4 cyclopentanone IX. La formation de composés semblables à ce dernier serait due à l'action aldolisante du dérivé magnésien (2) et a déjà été observée par plusieurs auteurs (3, 4, 5). Les acétates des alcools tertiaires isomères sont pyrolysées à 450° selon la méthode de DePuy (6). Les trois hydrocarbures (X, XI et XII), dont on peut théoriquement prévoir la formation, sont isolés à l'état pur par c.p.g. préparative. La structure X est assignée à l'hydrocarbure (n_D^{22}: 1.4640) qui donne naissance à la *tert*-butyl-3 cyclopentanone (VII) par ozonolyse oxydante. Les structures XI et XII sont attribuées respectivement aux hydrocarbures (n_D^{22} 1.4478 et 1.4522) dont le proton vinylique apparait dans le spectre r.m.n. sous forme de doublet (5.20 p.p.m.) et de triplet (5.28 p.p.m.).

Les *tert*-butyl-4 diméthyl-1,2 cyclohexanols isomères (XIV) obtenus par addition de l'iodure de méthylmagnésium sur la *tert*-butyl-4 méthyl-2 cyclohexanone (XIII) sont deshydratés à l'aide de l'iode selon les indications de Hammond et Nevitt (7). Une analyse du produit réactionnel par c.p.g. analytique indique la présence de cinq produits. Le produit majeur de la réaction (XV) est isolé à l'état pur par c.p.g. préparative. La structure XV attribuée à cet hydrocarbure est supportée par les spectres infrarouge et r.m.n. et est confirmée par ozonolyse oxydante du produit suivie d'une réaction haloformique qui conduit à de l'acide *tert*-butyl-3 adipique (VI*a*).

Les propriétés physiques des hydrocarbures obtenus ainsi que leurs temps de rétention en c.p.g. sont résumés dans le Tableau I. Il est à noter que par c.p.g. chacun de ces hydrocarbures présents dans un mélange peut être détecté.

[1]*Ce travail est extrait du mémoire soumis par P. Bélanger à la faculté des Sciences de l'Université de Montréal en vue de l'obtention du grade de maître ès sciences (août 1963).*
[2]*Détenteur d'une bourse de perfectionnement du Ministère de la Jeunesse de la province de Québec.*

Can. J. Chem. Downloaded from www.nrcresearchpress.com by 210.87.254.5 on 09/05/12
For personal use only.

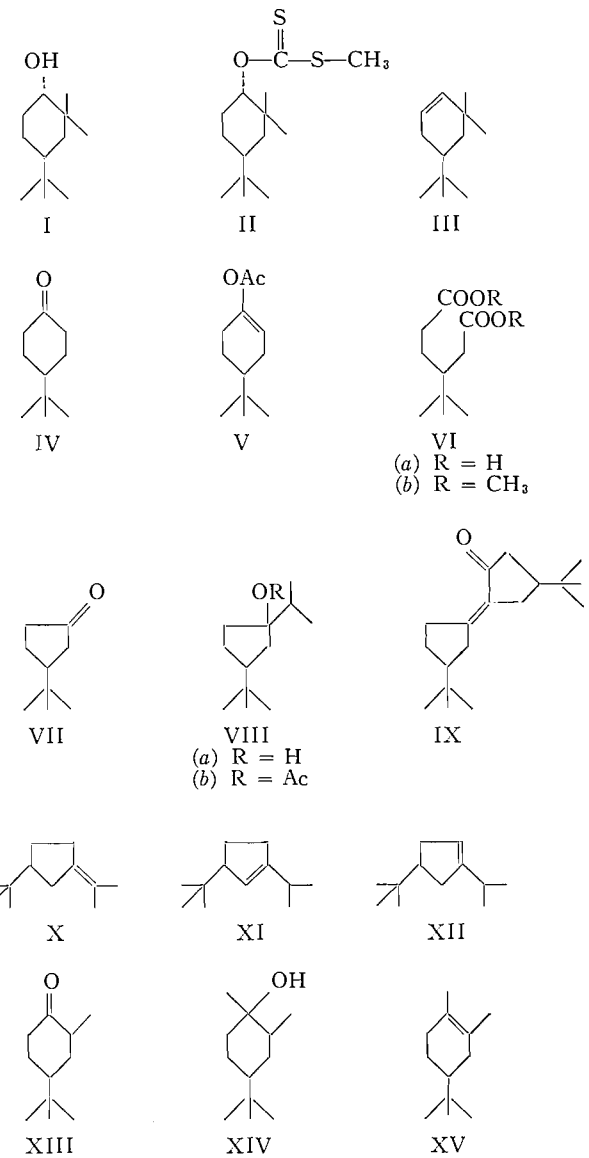

DIAGRAMME I

TABLEAU I

Proprietes physiques des hydrocarbures préparés

Hydrocarbure	Point d'ébullition	n_D^{22}	t_R*, min
III	69° à 41 mm	1.4452	4.5
X	67° à 32 mm	1.4640	14
XI	66° à 32 mm	1.4478	6.5
XII	65° à 32 mm	1.4532	7.5
XV	67° à 35 mm	1.4658	15

*Temps de rétention pour une colonne 2.5 m de Carbowax 20M sur Chromosorb P (20% p/p), température 120°, débit hélium 55 ml/min.

Can. J. Chem. Downloaded from www.nrcresearchpress.com by 210.87.254.5 on 09/05/12
For personal use only.

PARTIE EXPÉRIMENTALE

Les spectres infrarouge ont été mesurés à l'aide d'un spectrophotomètre "Perkin–Elmer" modèle 21 à double faisceau avec prismes de chlorure de sodium. Les analyses par c.p.g. sont effectués sur un appareil Kromo-Tog, modéle K-2 de la compagnie Burrell. Les points de fusion ont été déterminés dans des tubes capillaires dans un appareil dont le thermomètre avait été calibré avec des standards du Bureau des Standards de Washington. Les spectres de résonance magnétique nucléaire ont été enregistrés à l'aide d'un spectromètre modèle A-60 de Varian. Les déplacements chimiques, δ, sont exprimés en parties par million (p.p.m.) du champs total. Le tétraméthylsilane est utilisé comme standard interne. Les analyses élémentaires sont de C. Daesslé, Montréal.

Par extraction à la manière habituelle, on entend que le produit est extrait trois fois par de l'éther et que les solutions éthérées, lavées successivement par uns solution à 5% de bicarbonate de sodium et par de l'eau distillée jusqu'à neutralité, sont séchées sur du sulfate de sodium anhydre et évaporées au travers d'une colonne Widmer 30 cm.

1. Synthèse du tert-butyl-5 diméthyl-3,3 cyclohexène, III

1.1. Préparation du xanthogénate de méthyle (II) du tert-butyl-4 diméthyl-2,2 cyclohexanol trans, I

Une solution de 1 g de l'alcool I dans 15 ml de toluène anhydre est mise en contact avec 1 g de sodium et le tout est refluë durant 24 h. Après le reflux, l'excès de sodium est enlevé mécaniquement, 5 ml de sulfure de carbone est ajoutés et le mélange est agité à la température de la pièce durant 1 h. On ajoute alors 14 ml d'iodure de méthyle au mélange réactionnel qui est chauffé à reflux durant 4 h avant d'être laissé à la température de la pièce pour la nuit. Par extraction à la manière habituelle et distillation à 125–126° à 1 mm Hg, le xanthogénate désiré (II) est obtenu.

Un échantillon analytique, $n_D^{25} = 1.5262$, montre dans l'infrarouge des bandes caractéristiques à 1225 cm^{-1} et 1050 cm^{-1}.

Anal. Calc. pour $C_{14}H_{26}OS_2$: S, 10.71. Trouvé: S, 10.56.

1.2. Pyrolyse du xanthogénate, II

Dans un appareil à distillation contenant des morceaux de verre maintenus à une température de 300° à l'aide d'un bain de sable, on ajoute goutte à goutte 1 g de xanthogénate II. L'hydrocarbure brut distille au fur et à mesure de sa formation. Par redistillation, 0.54 g (90% du rendement théorique) de l'hydrocarbure désiré III sont obtenus. Un échantillon analytique du *tert*-butyl-5 diméthyl-3,3 cyclohexène (III) distille à 69–70° à 41 mm Hg, et son indice de réfraction est 1.4452 à 22°. La c.p.g. à l'aide d'une colonne de Carbowax 20% à 130° révèle la présence d'un seul produit. Le spectre infrarouge montre une bande à 1650 cm^{-1}.

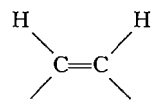

Les bandes principales apparaissant dans le spectre r.m.n. de cet hydrocarbure sont à 0.87 p.p.m. (9 protons dûs au groupe *tert*-butyle), 0.95 (6 protons, du groupe *gem*-diméthyle) at à 5.40 p.p.m. (2 protons dûs aux hydrogènes éthyléniques).

2. Synthèse des tert-butyl isopropyl cyclopentènes

2.1. Préparation de l'acide tert-butyl-3 adipique, VIa

2.11. Par l'intermédiaire de l'acétate énolique, V, de la tert-butyl-4 cyclohexanone

(a) Préparation de l'acétate énolique, V.—Dans un ballon à fond rond adéquat, 23 g de *tert*-butyl-4 cyclohexanone (IV) sont placés avec 72 ml d'acétate d'isopropényle et 0.5 ml d'acide sulfurique concentré. Sous une atmosphère d'azote, le mélange est maintenu à reflux durant 1 h puis 50 ml de solvant est distillé sous une pression réduite de 60 mm Hg. Le mélange réactionnel est alors extrait à la manière habituelle et le produit purifié par distillation à 112° à 25 mm Hg.

Une échantillon analytique, n_D^{25} 1.4638, montre dans l'infrarouge les bandes caractéristiques aux acétates énoliques à 1755 cm^{-1} et 1697 cm^{-1}.

Anal. Calc. pour $C_{12}H_{20}O_2$: C, 73.42; H, 10.27. Trouvé: C, 73.31; H, 10.50.

(b) Ozonolyse.—Une solution de 5 g de l'acétate énolique (V) en solution dans 100 ml d'éther de pétrole sans doubles liaisons est soumise à l'action d'un courant d'ozone dans l'oxygène. Lorsque la coloration bleue de l'ozone apparaît, l'éther de pétrole est évaporé sous un jet d'azote. On ajoute alors 50 ml d'acétate d'éthyle, 50 ml de peroxyde d'hydrogène 30% et 100 ml d'eau et on laisse le mélange réactionnel à la température de la pièce pour la nuit. Par extraction à la manière habituelle, l'acide *tert*-butyl-3 adipique, p.f. 117–118° (litt. (8) 118 °C), est obtenu.

L'estérification de cet acide par le diazométhane conduit au diesther méthylique (VI*b*), n_D^{23} 1.4425, ne montrant qu'un seul pic en c.p.g. analytique.

2.12. Oxydation de la tert-butyl-4 cyclohexanone, IV, par le permanganate de potassium

Dans un ballon de 5 l, on introduit 100 g de *tert*-butyl-4 cyclohexanone (IV), 80 g d'hydroxyde de potassium, 300 g de permanganate de potassium et 3000 ml d'eau. La température du mélange réactionnel est maintenue près de 50° grâce à un bain d'eau. Lorsque toute la cétone IV est passée en solution indiquant que la réaction est terminée, le mélange réactionnel est porté à son point d'ébullition pendant quelques instants. Après avoir refroidi le tout, le bioxyde de manganèse est éliminé par filtration et le filtrat est décoloré par addition de bisulfite de sodium. La solution est alors concentrée sous vide et acidifiée par de l'acide chlorhydrique concentré. L'acide *tert*-butyl-3 adipique se sépare sous forme de solide blanc que l'on récupère par filtration. Après recristallisation dans l'eau, l'acide VI*a* fond à 117–118° (litt. (8) 118°).

2.2. Tert-butyl-3 cyclopentanone, VII

Un mélange formé de 60 g d'acide *tert*-butyl-3 adipique (VI*a*) et de 200 ml d'anhydride acétique est chauffé à reflux dans un appareil à distiller du type Claisen; l'acide acétique distille au fur et à mesure de sa formation. Lorsque la réaction est terminée, l'anhydride acétique en excès est éliminé par distillation et l'anhydride de l'acide VI*a* est chauffé sur un bain de sable à une température de 300°; un liquide jaunâtre distillant à 208° est recueilli. Le produit brut est versé sur une solution d'hydroxyde de sodium 20%, laissé en contact pendant 15 min et finalement extrait à la manière habituelle. La *tert*-butyl-3 cyclopentanone (VII) purifiée par distillation à 74–75° à 15 mm Hg (litt. (8) 202° à 760 mm Hg) possède un indice de réfraction de 1.4482 (litt. (8) 1.4505 à 22°.

La semicarbazone de cette cétone fond à 203–204° (litt. (8) 194°) alors que sa dinitro-2,4 phénylhydrazone fond à 140° (litt. (8) 139°).

2.3. Tert-butyl-3 isopropyl-1 cyclopentanols et leurs acétates

2.31. Synthèse des tert-butyl-3 isopropyl-1 cyclopentanols, VIIIa

Dans un ballon adéquat, on place 15 g de magnésium et 25 ml d'éther anhydre. A cette suspension, 100 g d'iodure d'isopropyle dilués à l'aide de 200 ml d'éther anhydre sont ajoutés; le mélange réactionnel est porté à reflux durant 4 h puis refroidi. Une solution de 35 g de *tert*-butyl-3 cyclopentanone (VII) dans 50 ml d'éther anhydre est ajoutée lentement; lorsque l'addition est terminée, le mélange réactionnel est chauffé à reflux pour la nuit. De l'eau glacée est alors ajoutée lentement et la masse solide est dissoute par addition d'acide tartrique 1 *M*. La fraction éthérée est alors lavée à la manière habituelle et le produit brut est purifié par distillation sous vide.

La première fraction, de point d'ébullition 80° à 150 mm Hg, pèse 6.94 g (15% du rendement théorique). Un spectre infrarouge montre la présence d'une bande à 3400 cm^{-1} et une bande faible à 1745 cm^{-1}; cette dernière bande est attribuée à la cétone de départ qui n'a pas réagit et celle-ci est éliminée par des lavages à l'aide d'une solution saturée de bisulfite de sodium. Le produit obtenu (VIII*a*) ne montre alors qu'un seul pic par c.p.g. sur Carbowax 20%.

La seconde fraction, point d'ébullition 180° à 2.5 mm Hg, pèse 38.4 g (85% du rendement théorique) et se présente sous forme de liquide fortement coloré et très visqueux qui se solidifie après quelques semaines. Le spectre infrarouge montre de larges bandes carbonyles à 1735 et 1710 cm^{-1} et n'indique aucune bande dans le voisinage de 3400 cm^{-1}. Ce produit pour lequel la structure IX a été proposée n'a pas eté étudié plus à fond.

2.32. Acétylation des tert-butyl-3 isopropyl-1 cyclopentanols, VIIIa

Une solution formée de 5 g d'alcools VIII*a*, 5 g de chlorure d'acétyle et de 50 ml de diméthylaniline est portée à reflux pendant 2 h. Après refroidissement, le mélange est versé dans une solution glacée d'hydroxyde de sodium 20% et extrait à la manière habituelle. La redistillation du produit brut conduit aux acétates VIII*b*, p.é. 88° à 125 mm Hg n_D^{23} 1.4759, dont le spectre infrarouge montre une bande à 1740 cm^{-1}, caractéristique aux acétates.

2.4. Pyrolyse des acétates, VIIIb

Dans un appareil à distillation contenant des morceaux de verre dont la température est maintenue à 450°, on introduit 3 g des acétates VIII*b*. Le produit brut distille au fur et à mesure de sa formation et est ensuite extrait à la manière habituelle. Le produit obtenu est analysé par c.p.g. sur Carbowax 20% à 130°; cette méthode montre la présence de trois composants.

La c.p.g. est effectuée sur le mélange dans les conditions suivantes.

Appareil: Fisher Prep-partitionner.
Colonnes: 8 colonnes de Polyester de Craig 15%.
Températures: colonne 100 °C,
flash evaporator 290 °C,
cellule 200 °C.
Débit d'azote: 15 lbs/p.c.

De cette manière, le mélange est séparé en trois fractions. La première fraction, formée du *tert*-butyl-3 isopropyl-1 cyclopentène (XI), p.é. 66° à 32 mm Hg et n_D^{22} 1.4478, montre une bande à 1645 cm^{-1} dans l'infrarouge. Dans le spectre r.m.n. on note des bandes à 0.85 p.p.m. (9 protons du *tert*-butyle), 1.00 p.p.m. (doublet, $J = 7$ c.p.s.; 6 protons des méthyles du groupe isopropyle) et 5.20 p.p.m. (doublet mal défini; 1 proton éthylénique). La deuxième fraction, composée du *tert*-butyl-4 isopropyl-2 cyclopentène (XII),

Can. J. Chem. Downloaded from www.nrcresearchpress.com by 210.87.254.5 on 09/05/12
For personal use only.

p.é. 65° à 32 mm Hg et n_D^{22} = 1.4522, montre une bande à 1650 cm^{-1} dans l'infrarouge. Dans le spectre r.m.n. de cet hydrocarbure, on note des bandes à 0.85 p.p.m. (9 protons du *tert*-butyle), 1.04 p.p.m. (doublet, J = 7 c.p.s.; 6 protons des méthyles du groupe isopropyle) et 5.28 p.p.m. (triplet, J = 2.6 c.p.s.; 1 proton éthylénique). Pour des composés similaires à XI et XII Smith et Trotter (9) observent des pics à 5.13 et 5.23 p.p.m. respectivement. La troisième fraction, composé de *tert*-butyl-3 isopropylydènecyclopentane (X) p.é. 67° à 32 mm Hg et n_D^{22} 1.4640, ne montre aucune bande vers 1650 cm^{-1}, ce qui suggère une double liaison tétrasubstituée. Une ozonolyze oxydante de cet hydrocarbure (X), effectuée dans les conditions expérimentales décrites à la section 2.11, fournit de la *tert*-butyl-3 cyclopentanone (VII) décelée par c.p.g. sur une colonne de Carbowax 20% à 130°. Dans le spectre r.m.n. de cet hydrocarbure, aucune bande n'est notée dans la région de 5.25 p.p.m.; le groupe *tert*-butyle apparaît à 0.88 p.p.m. alors qu'un signal correspondant à 6 protons est noté à 1.57 p.p.m.

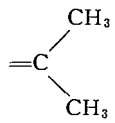

Il est à noter que la c.p.g. analytique de chacun des produits décrits ici ne montre qu'un pic.

3. Synthèse du tert-butyl-4 diméthyl-1,2 cyclohexène

3.1. Préparation des tert-butyl-4 diméthyl-1,2 cyclohexanols

Dans un ballon à fond rond de 500 ml surmonté d'un réfrigérant Vigreux, d'une ampoule à addition et d'un tube à chlorure de calcium on introduit 4.6 g de magnésium et 25 ml d'éther anhydre. A cette suspension, 25.4 g d'iodure de méthyle sont additionnés à une vitesse telle que l'éther reflue doucement. Après l'addition, le mélange est porté à reflux pendant 3 h puis refroidi. Au dérivé magnésien ainsi formé, 25 g de *tert*-butyl-4 méthyl-2 cyclohexanone (XIII, préparé suivant les indications de ref. 10) en solution dans 50 ml d'éther anhydre sont ajoutés lentement et le mélange réactionnel est laissé à la température de la pièce pour la nuit. Le dérivé magnésien en excès est détruit par addition d'eau glacée et la masse solide est dissoute par addition d'une solution d'acide chlorhydrique 10%. Après extractions à la manière habituelle, les alcools désirés (XIV) sont recueillis et purifiés par distillation.

Un échantillon analytique, p.é. 105° à 50 mm Hg et n_D^{22} = 1.4662, montre dan l'infrarouge une large bande hydroxyle à 3400 cm^{-1}. Par chromatographie en phase gazeuse analytique sur Carbowax 20%, on note la présence de deux produits différents du produit de départ.

Anal. Calc. pour $C_{12}H_{24}O$: C, 78.19; H, 13.13. Trouvé: C, 78.34; H, 12.97.

3.2. Deshydratation des tert-butyl-4 diméthyl-1,2 cyclohexanols, XIV

Dans un appareil à distillation Vigreux, la deshydratation est effectuée en chauffant 5 g de *tert*-butyl-4 diméthyl-1,2 cyclohexanols (XIV) en présence de 0.25 g d'iode à 170°. Un mélange d'eau et d'hydrocarbures distille à 140°. Le distillat ainsi formé est extrait à la manière habituelle et le produit brut obtenu, analysé par c.p.g. sur Carbowax 20% à 130°, est formé de cinq composants.

Par c.p.g. préparative dans des conditions semblables à celles décrites à la section 2.4, le *tert*-butyl-4 diméthyl-1,2 cyclohexène (XV) est obtenu à l'état pur. Le produit purifié, p.é. 67–68° à 35 mm et n_D^{22} 1.4658, ne montre aucune bande dans le voisinage de 1650 cm^{-1}. La structure de l'hydrocarbure est confirmée par son spectre r.m.n. qui montre des bandes à 0.86 p.p.m. (9 protons du *tert*-butyle) et 1.57 p.p.m. (6 protons des deux méthyles attachés à la double liaison).

3.3. Ozonolyse oxydante de tert-butyl-4 diméthyl-1,2 cyclohexène

Une solution de 500 mg de l'hydrocarbure XV dans 50 ml d'éther de pétrole libre de doubles liaisons est ozonolysée en suivant les indications décrites à la section 2.11. Après extraction à la manière habituelle, le produit obtenu est ajouté à une solution d'hypoiodite de sodium, formée par l'addition de 5 g d'iode à une solution d'hydroxyde de sodium 20%. Un précipité d'iodoforme se forme immédiatement et est éliminé par filtration. Le filtrat est acidifié par de l'acide chlorhydrique concentré et extrait à la manière habituelle. Après évaporation du solvant d'extraction, le résidu est dissous dans 50 ml d'éther anhydre et une solution de diazométhane est ajoutée jusqu'à persistance de la coloration jaune. L'éther est alors évaporé et le produit brut est chromatographié en phase gazeuse sur une colonne de Carbowax 20% à 150°. Un pic qui se superpose avec celui de l'ester méthylique (VI*b*) de l'acide *tert*-butyl-3 adipique est obtenu.

REMERCIEMENTS

Les auteurs remercient sincèrement le Conseil National de Recherches du Canada pour l'aide financière apportée sous forme de subvention de recherche (A-1295), le Ministère de la Jeunesse de la province de Québec pour la bourse de perfectionnement attribuée à P. Bélanger, la compagnie Dow Chemicals of Canada Ltd. pour un généreux échantillon de *tert*-butyl-4 cyclohexanone et la compagnie Pitt-Consol Chemical Company, Library, Pennsylvania, pour un généreux échantillon de *tert*-butyl-4 méthyl-2 phénol.

Can. J. Chem. Downloaded from www.nrcresearchpress.com by 210.87.254.5 on 09/05/12
For personal use only.

BIBLIOGRAPHIE

1. R. A. BENZECKER et J. J. HAZDRA. J. Am. Chem. Soc. **81**, 228 (1959).
2. D. IVANOFF et A. SPASSOFF. Bull. Soc. Chim. France, Ser. 5, **2**, 1435 (1935).
3. H. MEERWEIN. Ann. **405**, 155 (1914).
4. H. PINES et V. N. IPATIEFF. J. Am. Chem. Soc. **61**, 1076 (1939).
5. G. CRANE, C. BOORD et A. L. HENNE. J. Am. Chem. Soc. **67**, 1237 (1945).
6. C. H. DE PUY et R. W. KING. Chem. Rev. **60**, 431 (1960).
7. T. D. NEVITT et G. S. HAMMOND. J. Am. Chem. Soc. **76**, 4121 (1954).
8. H. PINES et V. N. IPATIEFF. J. Am. Chem. Soc. **61**, 3975 (1939).
9. G. V. SMITH et P. TROTTER. J. Org. Chem. **28**, 2450 (1963).
10. J. C. RICHER et G. PERRAULT. A paraître.

Can. J. Chem. Downloaded from www.nrcresearchpress.com by 210.87.254.5 on 09/05/12
For personal use only.

Can. J. Chem. Downloaded from www.nrcresearchpress.com by 210.87.254.105 on 09/05/12
For personal use only.

KINETICS OF THE CATALYZED HYDROLYSIS OF *p*-NITROPHENYL ACETATE

E. SACHER[1] AND K. J. LAIDLER
Department of Chemistry, University of Ottawa, Ottawa, Canada
Received May 28, 1964

ABSTRACT

Catalytic constants have been determined for the hydrolysis at 20 °C of *p*-nitrophenyl acetate in 9.56% (w/w) dioxane–water mixtures; catalysts used were hydroxide ions, imidazole and 2-methylimidazole, various substituted pyridines, serine, histidine and histidylhistidine. In the case of hydroxide ion catalysis, the rate constant falls off at high catalyst concentrations, and this is attributed to the establishment of an equilibrium involving the anion of the substrate. The results with the various catalysts indicate that there is no simple correlation between catalytic efficiency and pK or nucleophilicity. In the imidazole series there is evidence of steric hindrance when a group is present in a position next to the functional group. There is an indication of bifunctional catalysis in the hydrolysis by 2-(β-hydroxyethyl)pyridine and 4-(γ-hydroxypropyl)pyridine, both of which are much more effective than pyridine.

INTRODUCTION

The factors influencing the effectiveness of a catalyst are still by no means understood. The Brønsted relationships indicate that the ease with which a proton is transferred plays a very important role, but there are cases where there is serious interference by other effects. Because of these gaps in our knowledge the very high catalytic efficiencies of enzymes have still received no satisfactory explanation. Enzyme mechanisms involving bifunctional catalysis have been proposed for several systems (e.g. chymotrypsin (1, 2), acetylcholinesterase (3), the dehydrogenases (4), and ribonuclease (5)). Up to the present time, however, bifunctional catalysis has only been clearly established for the catalysis by 2-hydroxypyridine of mutarotation reactions (6). Since this work was done in benzene solution it does not offer a good analogy to an enzyme system.

The present work, carried out on *p*-nitrophenyl acetate with a series of catalysts, was done with the object of learning more about the factors influencing catalytic efficiency. It was also hoped to obtain clear-cut examples of bifunctional catalysis in aqueous solution, and it appears that these were found in the case of two hydroxyalkyl pyridines.

EXPERIMENTAL

Materials

All of the work was carried out in 9.56% (w/w) dioxane–water mixtures. The dioxane was purified by the method of Fieser (7) and was stored in pyrex and Teflon apparatus under nitrogen: precautions were taken to prevent the solvent from coming into contact with the atmosphere, so as to avoid the formation of peroxide impurities which are known to have a very strong catalytic effect.

The *p*-nitrophenyl acetate was prepared by the method of Chattaway (8), and was purified by several recrystallizations from an acetone–water mixture. The catalysts were pure commercial products which were carefully repurified either by vacuum sublimation or by fractional distillation.

The titrant used to follow the course of the reaction was 0.02 N sodium hydroxide solution, prepared from the Fisher Certified reagent.

Procedure

The reactions were followed using a pH-stat, the sodium hydroxide solution being continuously and automatically added so as to maintain a constant pH. The pH-stat equipment was that supplied by the Radiometer Company of Copenhagen (TTT1c titrator, TTA3 titration assembly, SBU1 burette and SBR2

[1]*Present address: Film Department, Research and Development Division, E. I. du Pont de Nemours and Company, Wilmington 98, Delaware, U.S.A.*

recorder). The pH values reported in this paper are those measured using this equipment; no solvent corrections have been made.

The reactions were carried out in 10 ml of 9.56% (w/w) dioxane–water mixture containing 2 meq of potassium chloride and maintained at 20.0 °C in a thermostatically controlled bath. Stock solutions of ester and catalysts were made up in dioxane, except for the amino acids and hystidylhistidine, for which water solvent was used. The concentration of the stock solutions was 0.2 *M*, or as close to 0.2 *M* as solubility allowed, and the reactions were carried out with the catalysts at a concentration of approximately 10^{-3} *M*.

The reactions were followed to about 5% completion, and rates were obtained from the initial slopes of the records.

RESULTS

Hydroxide Ion Catalysis

The catalysis by hydroxide ions was carried out from pH 8.4 to 10.7. A plot of rate against hydroxide ion concentration showed a marked deviation from linearity at high hydroxide ion concentrations, as shown in Fig. 1*a*. This behavior suggested that a law of the form

$$[1] \qquad v = \frac{a[\mathrm{S}][\mathrm{OH}^-]}{1 + b[\mathrm{OH}^-]}$$

was being obeyed. This was tested by making plots of $v/[\mathrm{OH}^-]$ against v (Fig. 1*b*) and of $1/v$ against $1/[\mathrm{OH}^-]$. From these plots the values obtained for the constants were

$$a = 21.5 \text{ l mole}^{-1} \text{ s}^{-1}$$

and

$$b = 6140 \text{ l mole}^{-1}.$$

The value of a, the second-order rate constant at low hydroxide ion concentrations, is consistent with the results of previous studies (9–12) carried out in different solvents. The previous investigations were not carried out over such a wide range of hydroxide ion concentrations, and did not reveal the falloff at high pH values.

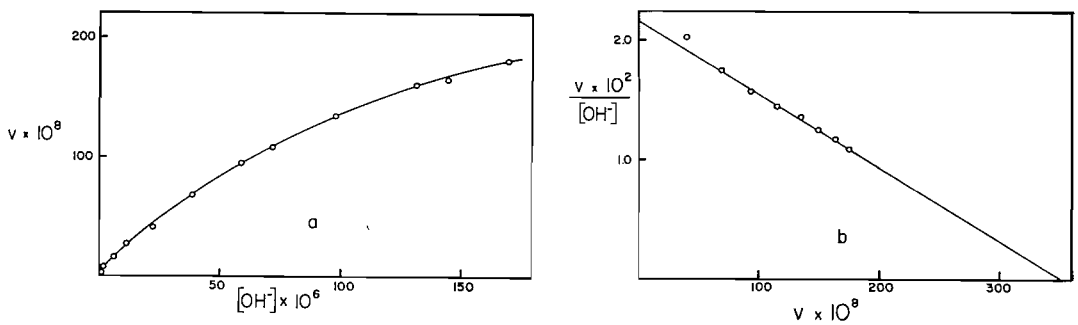

FIG. 1. Plot of v against $[\mathrm{OH}^-]$ (*a*) and of $v/[\mathrm{OH}^-]$ against v (*b*) for the alkaline hydrolysis of *p*-nitrophenyl acetate. The units of velocity are moles l^{-1} s^{-1}, while $[\mathrm{OH}^-]$ is in moles l^{-1}.

Catalysis by Imidazole and Its Derivatives

The hydrolysis of *p*-nitrophenyl acetate catalyzed by imidazole has previously been studied in various solvents (9, 12, 13), and the rate was found to be proportional to the concentrations of both substrate and catalyst. The same result was found in the present work, but the rate constant was significantly smaller, as shown in Table I. This difference is believed to be due to the presence in the previous work[2] of peroxides, as

[2]*This possibility is referred to in footnote 16 of ref. 13; unpurified dioxane has a marked catalytic effect on the reactions.*

Can. J. Chem. Downloaded from www.nrcresearchpress.com by 210.87.254.105 on 09/05/12
For personal use only.

contaminants in the dioxane solvent; peroxides are known to have a powerful catalytic effect. The previous study in dioxane (9) also showed excessive hydroxide ion catalysis, attributed to the same cause.

The hydrolysis catalyzed by 2-methylimidazole was also stated by previous investigators (14) to be first order in both catalyst and substrate, with a rate constant of 7.0×10^{-2} l mole^{-1} s^{-1}. The solvent was 28.5% (v/v) ethanol–water, and the temperature was 30.0 °C. No catalysis could be detected in the present investigation, from which it is concluded that the rate constant is less than 10^{-4} l mole^{-1} s^{-1}. The discrepancy is again attributed to peroxide catalysis in the previous investigation.

TABLE I

Rate constants for the catalysis of the hydrolysis of *p*-nitrophenyl acetate by imidazole

Solvent	Temperature (°C)	Rate constant (l mole^{-1} s^{-1})	Reference
Ethanol–water 1.90% (v/v)	25.0	0.425	Koltum *et al.* (11)
Dioxane–water 5.0% (v/v)	26.0	0.47*	Bender and Turnquest (13)
Ethanol–water 28.5% (v/v)	25.0	0.233	Bruice and Schmir (14)
Ethanol–water 28.5% (v/v)	30.0	0.355	Bruice and Schmir (14)
Dioxane–water 9.56% (w/w)	20.0	0.058±0.002	Present work

*This high value is suspect, as noted in footnote 16 of ref. 13; imidazole is reported to have a higher catalytic effect in 5% dioxane than in 1.9% ethanol, whereas the opposite is expected.

TABLE II

Rate constants for the catalysis of the hydrolysis of *p*-nitrophenyl acetate by pyridine and derivatives

Catalyst	Solvent	Temperature (°C)	Rate constant (l mole^{-1} s^{-1})	Reference
Pyridine	Water	25.0	16.7×10^{-4}	Jencks and Carriuolo (12)
Pyridine	Ethanol–water 28.5% (v/v)	30.0	14.7×10^{-4}	Bruice and Schmir (14)
Pyridine	Dioxane–water 5.0% (v/v)	26.0	5.3×10^{-4}	Bender and Turnquest (9)
Pyridine	Dioxane–water 9.56% (w/w)	20.0	0	Present work
2-Methylpyridine	Dioxane–water 9.56% (w/w)	20.0	0	Present work
4-Methylpyridine	Dioxane–water 5.0% (w/w)	26.0	7.95×10^{-3}	Bender and Turnquest (9)
4-Methylpyridine	Ethanol–water 28.5% (v/v)	30.0	8.2×10^{-3}	Bruice and Schmir (14)
4-Methylpyridine	Dioxane–water 9.56% (w/w)	20.0	$(4.6\pm0.15)\times10^{-3}$	Present work
2-Hydroxypyridine	Dioxane–water 9.56% (w/w)	20.0	$(1.7\pm0.16)\times10^{-3}$	Present work
2-(β-Hydroxyethyl)-pyridine	Dioxane–water 9.56% (w/w)	20.0	$(2.5\pm0.6)\times10^{-3}$	Present work
4-(γ-Hydroxypropyl)-pyridine	Dioxane–water 9.56% (w/w)	20.0	$(9.8\pm0.5)\times10^{-3}$	Present work

Can. J. Chem. Downloaded from www.nrcresearchpress.com by 210.87.254.105 on 09/05/12
For personal use only.

Catalysis by Pyridine and Its Derivatives

The results of the present work, and of previous investigations, are summarized in Table II. In all cases the reaction was first order in both substrate and catalyst.

Catalysis by Amino Acids

The rate law was again of the same form; the rate constants are summarized in Table III. It is to be noted that hystidylhistidine has about the same effectiveness as imidazole, when the presence of two groups is allowed for.

TABLE III

Rate constants for the catalysis of the hydrolysis of *p*-nitrophenyl acetate by amino acids

Catalyst	Solvent	Temperature (°C)	Rate constant (l mole^{-1} s^{-1})	Reference
Serine	Dioxane–water 9.56% (w/w)	20.0	$(2.4\pm0.1)\times10^{-2}$	Present work
Histidine	Dioxane–water 9.56% (w/w)	20.0	$(1.24\pm0.09)\times10^{-1}$	Present work
Histidylhistidine	Water	20.0	4.67×10^{-2}*	Jencks and Carriuolo (12)
Histidylhistidine	Dioxane–water 9.56% (w/w)	20.0	$(5.6\pm0.3)\times10^{-2}$*	Present work

*These rate constants have been divided by 2, to allow for the presence of two catalytic groups on each molecule.

TABLE IV

Catalytic constants for the hydrolysis of *p*-nitrophenyl acetate (solvent, 9.56% (w/w) dioxane–water; *T*, 25.0 °C)

Catalyst	Rate constant (l mole^{-1} s^{-1})	pK_a
Hydroxide ion	21.5	15.7
Imidazole	5.8×10^{-2}	7.04
2-Methylimidazole	0	7.75
Pyridine	0	5.34
2-Methylpyridine	0	6.18
4-Methylpyridine	4.6×10^{-3}	6.06
2-Hydroxypyridine	1.7×10^{-3}	1.28
2-(β-Hydroxyethyl)pyridine	2.5×10^{-3}	5.39
4-(γ-Hydroxypropyl)pyridine	9.8×10^{-3}	5.9
Serine	2.4×10^{-2}	2.21
Histidine	1.24×10^{-1}	6.04
Histidylhistidine	5.6×10^{-2}	6.8
Chymotrypsin	1.63×10^{2}*	—
Trypsin	71†	—

*At pH 8.0.
†In 20% (v/v) isopropyl alcohol, pH 7.0, 25 °C.

GENERAL DISCUSSION

The catalytic constants obtained in the present work, and the pK_a's of the acids conjugate to the basic catalysts, are summarized in Table IV. Included in addition are the second-order constants (at low substrate concentrations) for the hydrolysis by the enzymes chymotrypsin and trypsin. The value for chymotrypsin was obtained in these laboratories by Kaplan (15) using the same dioxane–water solvent and at pH 8.0; that for trypsin was obtained by Stewart and Ouellet (16) in 20% (v/v) isopropyl alcohol at 25 °C and pH 7.0.

It was found in the present work that the rate of the reaction catalyzed by hydroxide

Can. J. Chem. Downloaded from www.nrcresearchpress.com by 210.87.254.105 on 09/05/12
For personal use only.

ions rises to a limiting value as the catalyst concentration is increased. This result is of interest in connection with a study on anilide hydrolysis by Biechler and Taft (17), who found a similar dependence on hydroxide ion concentration in the case of trifluoroacetanilide, $C_6H_5CONHCF_3$. They attribute the fall off of rate constant at high hydroxide ion concentrations to the establishment of the equilibrium

$$C_6H_5CONHCF_3 + OH^- \rightleftarrows C_6H_5CON^-CF_3 + H_2O.$$

This proton extraction is favored by the strongly electron-attracting character of the CF_3 group. In *p*-nitrophenyl acetate the strongly electron-attracting power of the *p*-nitrophenyl group will similarly lead to the establishment of the equilibrium

$$CH_3\overset{\overset{O}{\|}}{C}OC_6H_4NO_2 + OH^- \rightleftarrows {}^-CH_2\overset{\overset{O}{\|}}{C}OC_6H_4NO_2 + H_2O,$$

and the ion will be stabilized by resonance involving the structure

$$CH_2{=}\overset{\overset{O^-}{|}}{C}OC_6H_4NO_2.$$

The kinetics of the hydrolysis by hydroxide ions may thus be formulated as follows:

$$SH + OH^- \underset{k_{-1}}{\overset{k_1}{\rightleftarrows}} S^- + H_2O$$

$$H_2O + S^- \xrightarrow{k_2} OH^- + \text{products.}$$

Application of the steady-state treatment gives

$$[2] \qquad k_1([SH]_0 - [S^-])[OH^-] - (k_{-1} + k_2)[S^-] = 0$$

where $[SH]_0$ is the total concentration of substrate: the water concentration is incorporated in the rate constants k_{-1} and k_2. The rate is then

$$[3] \qquad v = \frac{k_1k_2[SH]_0[OH^-]}{k_{-1} + k_2 + k_1[OH^-]},$$

which is of the same form as eq. [1]. If this interpretation is correct, it follows that

$$k_2 = a/b = 3.5 \times 10^{-3}\ s^{-1}.$$

The results obtained with the various catalysts are not capable of any simple interpretation. There is no apparent correlation between catalytic efficiency and either pK or nucleophilicity. There is evidence for steric hindrance, in that 2-methylimidazole is less effective than imidazole in spite of being more basic. Clear-cut evidence for steric hindrance in catalysis has been obtained by Butler and Gold (18) in the hydrolysis of acetic anhydride, for which pyridine is a catalyst whereas 2-methylpyridine and 2,6-lutidine are not. More recently Feather and Gold (19) have noted steric hindrance in the iodination of ketones, reactions in which the rate-determining step is a proton transfer; again there was hindrance when substituents were introduced into the 2 and 6 positions of pyridine.

At first sight it might appear that evidence for bifunctional catalysis was provided by the fact that 2-hydroxypyridine, although a weaker base than pyridine, is a more powerful catalyst. This conclusion is not, however, valid, since it is known (20–24) that 2-hydroxypyridine exists largely as the pyridone tautomer:

Can. J. Chem. Downloaded from www.nrcresearchpress.com by 210.87.254.105 on 09/05/12
For personal use only.

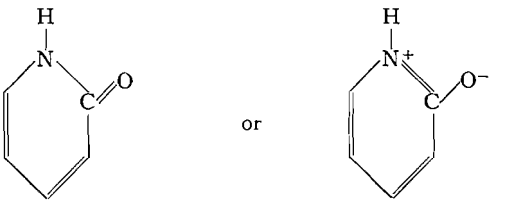

The nucleophilic group responsible for catalysis is therefore the carbonyl oxygen atom. An indication of bifunctional catalysis is, however, given by the fact that 2-(β-hydroxyethyl)pyridine and 4-(γ-hydroxypropyl)pyridine are much more effective than pyridine, in spite of the fact that they have approximately the same basicities. At the pH's of the present investigation these compounds exist in the forms in which the =N— and —OH groups are free. It therefore seems reasonable to suppose that catalysis is brought about by a nucleophilic attack by the nitrogen atom and a simultaneous proton transfer from the alcoholic hydroxyl group.

ACKNOWLEDGMENT

This work was supported by a grant from the National Cancer Institute of Canada.

REFERENCES

1. M. L. BARNARD and K. J. LAIDLER. J. Am. Chem. Soc. **74**, 6099 (1952).
2. M. L. BARNARD and K. J. LAIDLER. Trans. Faraday Soc. **52**, 497 (1956).
3. R. M. KRUPKA and K. J. LAIDLER. J. Am. Chem. Soc. **83**, 1458 (1961).
4. R. M. KRUPKA and K. J. LAIDLER. *In* Mechanism of action of steroid hormones. *Edited by* C. A. Villee and L. L. Engell. The Pergamon Press, Ltd., London. 1961. p. 235.
5. D. FINDLAY, D. G. HERRIES, A. D. MATHIAS, B. R. RABIN, and C. A. ROSS. Nature, **190**, 781 (1961).
6. C. G. SWAIN and J. F. BROWN. J. Am. Chem. Soc. **74**, 2538 (1952).
7. L. F. FIESER. Experiments in organic chemistry. D. C. Heath & Co., Boston. 1957. p. 284.
8. F. D. CHATTAWAY. J. Chem. Soc. 2495 (1931).
9. M. L. BENDER and B. TURNQUEST. J. Am. Chem. Soc. **79**, 1656 (1958).
10. T. C. BRUICE and R. LAPINSKI. J. Am. Chem. Soc. **80**, 2265 (1958).
11. W. L. KOLTUM, R. W. DEXTER, R. E. CLARK, and F. R. N. GURD. J. Am. Chem. Soc. **80**, 4188 (1958).
12. W. F. JENCKS and J. CARRIUOLO. J. Am. Chem. Soc. **82**, 1778 (1957).
13. M. L. BENDER and B. W. TURNQUEST. J. Am. Chem. Soc. **79**, 1652 (1957).
14. T. C. BRUICE and G. L. SCHMIR. J. Am. Chem. Soc. **80**, 148 (1958).
15. N. KAPLAN and K. J. LAIDLER. To be published.
16. J. A. STEWART and L. OUELLET. Can. J. Chem. **37**, 751 (1959).
17. S. S. BIECHLER and R. W. TAFT. J. Am. Chem. Soc. **79**, 6927 (1957).
18. A. R. BUTLER and V. GOLD. J. Chem. Soc. 4362 (1961).
19. J. A. FEATHER and V. GOLD. Proc. Chem. Soc. 306 (1963).
20. H. SPECKER and H. GAWROSH. Ber. **75**, 1338 (1942).
21. V. I. BLIZNUKOV and V. M. RESNIKOV. J. Gen. Chem. USSR, English Transl. **25**, 1735 (1955).
22. K. HOLGERLE and H. ERLENMEYER. Helv. Chim. Acta, **39**, 1203 (1956).
23. S. F. MASON. J. Chem. Soc. 4874, 5010 (1956); 674 (1958); 1253 (1959).
24. A. ALBERT and J. N. PHILLIPS. J. Chem. Soc. 1294 (1956).

Can. J. Chem. Downloaded from www.nrcresearchpress.com by 210.87.254.105 on 09/05/12
For personal use only.

Can. J. Chem. Downloaded from www.nrcresearchpress.com by 210.87.254.42 on 09/05/12
For personal use only.

AN ATTEMPT TO STUDY COMPLEX FORMATION BETWEEN 1,3,5-TRINITROBENZENE AND OLEFINS BY GAS CHROMATOGRAPHY[1]

R. J. CVETANOVIĆ, F. J. DUNCAN,[2] and W. E. FALCONER[3]
Division of Applied Chemistry, National Research Council, Ottawa, Canada
Received June 12, 1964

ABSTRACT

An attempt has been made to study complex formation between 1,3,5-trinitrobenzene (TNB) and olefins by a gas chromatographic technique. A particular interpretation of the data indicates that the TNB – olefin complexes exhibit progressive increases in stability with increasing double-bond substitution. Steric effects are less pronounced than for olefin complexes with silver nitrate or molecular iodine. Olefins are well separated by carbon number, and differences in retention times among the structural isomers of each molecular weight are sufficiently characteristic to provide a basis for assigning major structural features.

Molecular complexes, or electron donor–acceptor complexes, have received much attention during the past 15 years, and have been the subject of a recent book (1) and several reviews (2–5). The quantum mechanical description of the interaction of electron donors and electron acceptors developed by Mulliken and his co-workers (5, 6) has gained general acceptance and satisfactorily explains the observed features of charge-transfer spectra. The association constants of 1:1 molecular complexes have been most frequently determined by the spectrophotometric methods recently evaluated by Hayman (7), who compared their reliability with the more classical partition method. DeMaine (8) has pointed out the need for additional nonspectrophotometric methods for determining complex stabilities which can provide data for comparison with the copious spectrophotometric data. Gas chromatography can potentially provide one such method.

Gas chromatography has for some time exploited the phenomenon of electron donor–acceptor complex formation to separate olefins selectively using silver nitrate – ethylene glycol – firebrick mixtures (9). Specific retentions of individual olefins are affected by their solubility in the ethylene glycol solvent, as well as by the strength of their interaction with the Ag^+ ions. Muhs and Weiss (10), and independently Gil-Av and Herling (11), have proposed methods for separating the two effects. An extensive list of equilibrium constants for the reaction

$$\text{olefin} + AgNO_3 \rightleftarrows \text{olefin} \cdot AgNO_3,$$

with all species dissolved in ethylene glycol, has been published (10).

The chromatographic approach to determining the stability of electron donor–acceptor complexes has been extended to include interactions with the following electron acceptors: solid silver nitrate (12), some complexes of the transition metals (13, 14), iodine (15), and in this paper 1,3,5-trinitrobenzene (TNB). Although TNB is among the most-studied electron acceptors, data concerning its interactions with simple olefins are sparse, undoubtedly because these olefin complexes are much weaker than those with aromatic molecules which have commonly been the object of spectrophotometric investigations (16).

[1]*Issued as N.R.C. No. 8123.*
[2]*National Research Council of Canada Postdoctoral Fellow, 1961–1963.*
[3]*Bell Telephone Laboratories, Incorporated, Murray Hill, New Jersey, U.S.A.*

Can. J. Chem. Downloaded from www.nrcresearchpress.com by 210.87.254.42 on 09/05/12
For personal use only.

EXPERIMENTAL

Column packings were prepared in the following manner.

Packing 1.—8.0 g TNB (Eastman Organic Chemicals) dissolved in 100 ml benzene was mixed with 32.0 g 30–60 mesh firebrick (Johns–Manville Chromosorb P) and the benzene was slowly evaporated under reduced pressure.

Packing 2.—29.9 g of the same firebrick was precoated by first mixing the firebrick with 0.69 g NaOH dissolved in 100 ml water and then evaporating the water under reduced pressure. When dry, the pretreated firebrick was mixed with 5.2 g TNB dissolved in 75 ml acetone. The mixture immediately turned a deep purple–red color (cf. ref. 17), which persisted when the acetone was slowly evaporated under reduced pressure.

Packing 3.—30.0 g of the same firebrick was precoated by mixing the firebrick with 0.73 g H_3PO_4 dissolved in 50 ml water and then evaporating the water as before. When dry, the pretreated firebrick was mixed with 5.3 g TNB dissolved in 75 ml acetone. There was no evidence of chemical reaction. The acetone was slowly evaporated under reduced pressure.

Packing 4.—8.0 g of TNB dissolved in 75 ml benzene was mixed with 32.0 g 60–80 mesh celite (Johns–Manville Chromosorb W) and the benzene was slowly evaporated under reduced pressure.

All packings were dry, had a uniform appearance, and flowed easily. Columns were prepared in 16 ft lengths of 4 mm I.D. Pyrex tubing and maintained at 0 °C in an ice bath. Samples[4] were flushed onto the columns from a U-shaped bypass injector, volume ~2 cc. Helium was used as the carrier gas, and linear flows through the columns were ~4 cm s^{-1}. A 6:1 bypass system was inserted between the injection system and the column to reduce the effective injection time to a few tenths of a second. Detection was with a flame ionization detector (18) and recorder chart speeds of either 1 or 2 in. per min were used.

Most samples used were Phillips Petroleum Company pure grade or A.P.I. research hydrocarbons. The purity of any others was predetermined by gas chromatography.

Attempts to obtain retention data using a 400 ft length of 0.015 in. I.D. type 316 stainless steel capillary tubing coated with TNB at 0, −20, and −78 °C were unsuccessful. No attempt was made to use TNB solutions as liquid phases, as has been found successful in studying $AgNO_3$ complexes (9–11, 19).

RESULTS

The adjusted retentions (20) of all olefins and paraffins studied relative to 1-pentene are listed in Tables I and II, respectively. From these values, plus the retention data in Table III, actual retention times under typical experimental conditions can be obtained. The relative retentions in Tables I and II are reproducible to within the larger of ±0.01 units or ±2% for columns 1 and 2, but are somewhat less reproducible for columns 3 and 4 on which retention times were shorter.

Column efficiencies were measured for all peaks for columns 2, 3, and 4. On column 2 (TNB on firebrick pretreated with NaOH), efficiencies dropped from about 300 theoretical plates per foot for early peaks to less than 250 theoretical plates per foot for those compounds retained ~30 min. On column 3 (TNB on firebrick pretreated with H_3PO_4), a similar decline in efficiency with retention time was observed, the range being approximately 300–200 theoretical plates per foot. For column 4 (TNB on untreated celite), a variation in efficiency with compound type was superimposed upon the decrease observed with retention time. Efficiencies, which dropped from 300 to 15 theoretical plates per foot, were notably lower for cyclic olefins, cyclic paraffins, and nonterminal olefins. For column 1 (TNB on untreated firebrick), only a few random efficiencies were measured but their trend and order of magnitude appeared to be similar to columns 2 and 3.

Figure 1 shows that good linear plots of log r against number of carbon atoms present in the molecule are obtained for any given structural type using TNB on NaOH pretreated firebrick columns. Similar plots are obtained with the other three columns. Retention times increase fourfold with each additional carbon atom, and hence all compounds are well grouped by the carbon atom content of the molecules. Differences within each group

[4]*Small samples (~10^{-3} micromole) were used throughout this investigation to minimize peak asymmetry due to concentration effects. Larger samples can be used if necessary, subject to limitations similar to those for conventional packed columns.*

TABLE I

Relative retentions (r) of olefins on TNB columns at 0 °C
(1-pentene = 1.000)

Compound	Column* 1	2	3	4
Ethylene		0.00_6		
Propylene		0.05_5		0.12
1-Butene-d_8	0.26	0.24		
1-Butene	0.27	0.24_4	0.30	0.29
Isobutene	0.34	0.27	0.32	0.29
trans-2-Butene-d_8	0.34	0.28_8		
trans-2-Butene	0.35	0.29_3	0.35	0.37
cis-2-Butene-d_8	0.37	0.32		
cis-2-Butene	0.39	0.33	0.36	0.41
1,3-Butadiene-d_6	0.46	0.39_1		0.32
1,3-Butadiene	0.46	0.39_4	0.38	0.29
3-Methyl-1-butene	0.76	0.74	0.78	0.71
Cyclopentene	0.92	0.94	0.94	1.39
1-Pentene	1.00	1.00	1.00	1.00
2-Methyl-1-butene	1.25	1.11	1.19	1.00
trans-2-Pentene	1.26	1.16	1.15	
cis-2-Pentene	1.36	1.26	1.17	1.22
2-Methyl-2-butene	1.62	1.38	1.22	1.29
3-Methyl-1-pentene	2.44	2.67	2.32	2.34
4-Methyl-1-pentene	2.84	3.08	2.58	2.49
4-Methyl-2-pentene		3.09	2.64	2.73
1-Hexene	4.01	4.28	3.35	3.61
Cyclohexene	4.41	4.36	3.40	6.42
2-Ethyl-1-butene	4.61	4.27	3.68	3.68
trans-2-Hexene		4.60		
cis-2-Hexene	5.05	5.04	3.69	4.23
cis-3-Methyl-2-pentene	5.25	4.85	3.49	3.90
2-Methyl-2-pentene	5.33	4.77	3.53	4.00
2,3-Dimethyl-2-butene	6.66	5.68	4.05	4.90

*Columns 1, 2, 3, and 4 refer to columns prepared with packings 1, 2, 3, and 4, respectively.

TABLE II

Relative retentions (r) of paraffins on TNB columns at 0 °C
(1-pentene = 1.000)

Compound	Column* 1	2	3	4
Methane	0	0	0	0
Isobutane	0.13	0.15	0.23	0.27
n-Butane	0.17	0.19	0.27	0.37
Cyclopentane	0.51	0.73	0.87	1.54
Isopentane	0.52	0.67	0.80	0.88
n-Pentane	0.66	0.83	0.97	1.12
Cyclohexane	1.64	2.54	2.54	4.88
2,3-Dimethylbutane	1.68	2.33	2.23	2.68
3-Methylpentane	1.92	2.71	2.51	3.20
2-Methylpentane	1.96	2.67	2.48	3.10
n-Hexane	2.61	3.51	3.17	4.27

*Columns 1, 2, 3, and 4 refer to columns prepared with packings 1, 2, 3, and 4, respectively.

are determined by structural changes and are sufficiently characteristic and reproducible that major structural features could be assigned from a measurement of the retention time of an unknown olefin.

It is instructive to consider the numbers obtained when the retention times of olefins (t_{ol}) are normalized by dividing by the retention times of the structurally analogous

Can. J. Chem. Downloaded from www.nrcresearchpress.com by 210.87.254.42 on 09/05/12
For personal use only.

TABLE III

Retention times (t_R) for methane and 1-pentene

Column	t_R(methane), min	t_R(1-pentene), min
1	1.80±0.01	6.57±0.06
2	1.94	8.73±0.09
3	1.94	3.36±0.03
4	1.84	2.25±0.02

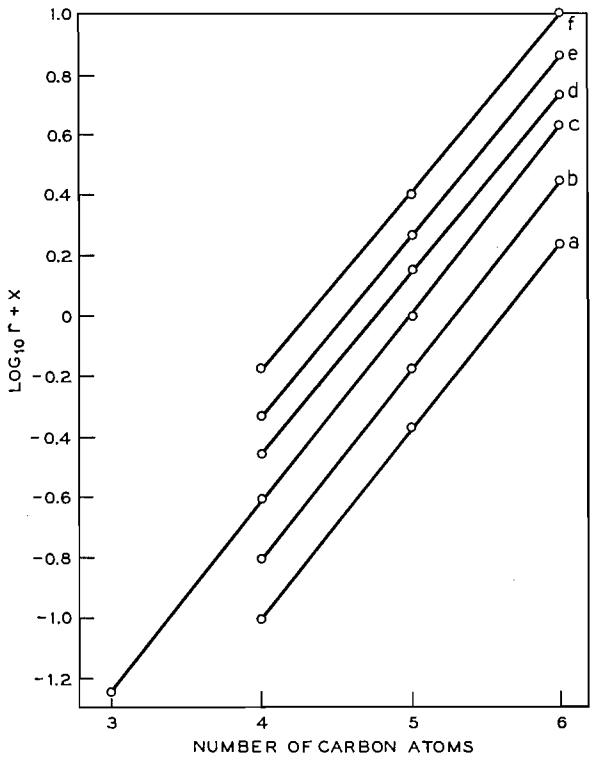

FIG. 1. Variation of $\log_{10} r$ with number of carbon atoms for column 2—(*a*) 2-methyl paraffins ($x = -0.2$), (*b*) *n*-paraffins ($x = -0.1$), (*c*) linear terminal olefins ($x = 0$), (*d*) 2-substituted terminal olefins ($x = 0.1$) (*e*) linear *trans*-2-olefins ($x = 0.2$), (*f*) linear *cis*-2-olefins ($x = 0.3$).

paraffins (t_p). Since paraffins do not complex and $RT \ln (t_{ol}/t_p) = -(\Delta F_{ol} - \Delta F_p)$, it can be assumed that, to a first approximation, this procedure removes the purely physical effect of surface condensation and the "normalized retention times" ($t_n = t_{ol}/t_p$) are determined by the free energies of complexing of olefins with TNB. Inasmuch as this assumption is correct, they should show the effects of increasing basicity of the double bond caused by electron donation from alkyl groups situated on the olefinic carbon atoms.[5]

Normalized retention times are listed in Table IV, grouped for each column by the number of carbon atoms in the olefin and the degree of double bond substitution. Mean

[5]*As might be expected, good correlations are also obtained by plotting log t_R against the boiling points. Distinct plots are obtained for different classes of compounds and these correlations are therefore of analytical value. However, they do not reveal the specific effect of complexing. For example, cycloolefins and cycloparaffins are retained very much less than might be expected from their boiling points. Nevertheless, the normalized retention times are close to those of other olefins. It appears that entropy requirements for surface condensation are similar for the structurally analogous olefins and paraffins, but differ from those for condensation into bulk liquids.*

Can. J. Chem. Downloaded from www.nrcresearchpress.com by 210.87.254.42 on 09/05/12
For personal use only.

TABLE IV

Variation of normalized retention times* with degree of double bond substitution for olefins containing 4, 5, or 6 carbon atoms

Degree of double bond substitution	Number of carbon atoms			
	4	5	6	Mean
Column 1				
Mono-	1.61	1.50±0.01	1.40±0.10	1.51
Di-	2.35±0.17	2.14±0.21	1.94	2.14
Tri-		3.18	2.72±0.01	2.95
Tetra-			3.95	3.95
Column 2				
Mono-	1.26	1.15±0.05	1.12±0.09	1.18
Di-	1.69±0.11	1.53±0.09	1.37±0.06	1.50
Tri-		2.07	1.79±0.01	1.93
Tetra-			2.43	2.43
Column 3				
Mono-	1.13	1.00±0.03	1.01±0.05	1.05
Di-	1.35±0.03	1.29±0.13	1.17	1.27
Tri-		1.53	1.41±0.02	1.47
Tetra-			1.82	1.82
Column 4				
Mono-	0.79	0.85±0.04	0.79±0.04	0.81
Di-	1.06±0.04	1.12±0.03	0.99	1.06
Tri-		1.47	1.26±0.04	1.36
Tetra-			1.83	1.83

*As defined in text.

deviations are given when more than one compound of a type has been studied. Only a relatively small decline is found with increasing carbon number. In the last column of Table IV average values for each degree of substitution are listed. Cyclic olefins have been omitted from these calculations, as their inclusion as disubstituted olefins increases the scatter. 2-Ethyl-1-butene has been omitted because the presence of an unsaturated group in the side chain is unique in the group of compounds studied, and a comparison with 3-methylpentane is not strictly analogous with the other normalizations. However, the inclusion of these compounds does not significantly affect the observed trends.

TABLE V

Ratios of mean normalized retention times* for unit increments in double bond substitution

Ratio	Column				Mean
	1	2	3	4	
Di-/mono-	1.42	1.27	1.21	1.31	1.30
Tri-/di-	1.38	1.29	1.15	1.28	1.27
Tetra-/tri-	1.34	1.26	1.25	1.34	1.30
					1.29

*As defined in text.

Effects of the increase in basicity of the double bond with alkyl substitution on the olefinic carbon atoms are reflected in the ratios of the mean normalized retention times for unit increments in the degree of substitution. Such ratios are listed in Table V; their mean value is about 1.3. (Very similar mean ratios are also obtained if the ratios for each carbon number first are evaluated and then are averaged for each of the four columns.) The results

Can. J. Chem. Downloaded from www.nrcresearchpress.com by 210.87.254.42 on 09/05/12
For personal use only.

in Table V show that the increase is independent of the extent of substitution, and depends only slightly on the column support. This provides strong evidence that the effect is due to complexing with TNB and that complications due to interaction with the solid support are largely eliminated in the ratios listed in Table V. These ratios are therefore believed to represent approximate ratios of the corresponding equilibrium constants for complex formation.[6]

Two major differences were observed in column behavior using different column packings. The absolute retention times were considerably greater in columns 1 and 2 than in columns 3 and 4. In addition, the difference in retention between olefins and paraffins decreased going from column 1 to column 4. These differences are probably caused by uneven covering of the solid support by TNB and perhaps also by variations in the basic properties of the different support materials used in the four columns.

DISCUSSION

The observed decrease in column efficiency with increasing retention time is contrary to the trend usually observed with packed columns (21). It is probably indicative of slower rates of complex formation and breakdown for the more strongly retained compounds. The low efficiencies observed with the TNB on celite support column for cyclic olefins, cyclic paraffins, and nonterminal olefins are probably also a result of slow equilibration processes. Pronounced differences in apparent efficiency have been observed in a parallel investigation of complex formation between iodine and olefins. The peak broadening effects of differences in the rates of equilibration will be discussed in greater detail separately (15).

In contrast to silver nitrate – olefin (19) and iodine–olefin (15) interactions, where the complexes are considerably strengthened by substitution of deuterium atoms for hydrogen atoms at the olefinic bond (22), deuterium substitution had no significant effect on the TNB – olefin complexes. The small effect that was observed showed a slight reduction in retention time, such as is observed in partition chromatography where separation is according to boiling point only (23). Furthermore, retention times generally increased with increasing substitution at the double bond, indicating that for TNB complexes the increase in basicity from double-bond substitution outweighs the opposing effect of steric hindrance which frequently predominates. Both these effects suggest that the role of steric changes in the olefins plays a lesser part in TNB – olefin complexes than in the other systems similarly investigated (9–12, 14, 15, 19, 22).[7]

The specific nature of the interactions of hydrocarbons with TNB may prove especially useful for specific analytical separations, complementing the usual columns for olefin separations and analyses (silver nitrate, etc.). The regular dependence on the carbon number (or the boiling point) within a structural group should prove a distinct advantage in some cases and may provide a method of characterizing the carbon content and structural features of unknown olefinic reaction products. Although quantitative values of the association constants for TNB complexes with individual olefins have not been obtained, the technique provides a rapid source of the relative strengths of these complexes. These results may be used to corroborate data acquired by conventional spectrophotometric techniques.

[6] *A mathematical treatment which is related to the case considered here will be given in ref. 15.*

[7] *Although steric effects do not appear to play too important a role in the olefin – TNB complexes, the gradual decline in t_n values with carbon number, shown in Table IV, suggests that they are not altogether negligible. Quantitative limitations of the data preclude any detailed conclusions in this respect.*

Can. J. Chem. Downloaded from www.nrcresearchpress.com by 210.87.254.42 on 09/05/12
For personal use only.

REFERENCES

1. G. BRIEGLEB. Elektronen-Donator-Acceptorkomplexe. Springer-Verlag, Heidelberg. 1961.
2. G. BRIEGLEB. Pure Appl. Chem. **4**, 105 (1962).
3. J. W. SMITH. Sci. Progr. London, **50**, 607 (1962).
4. V. P. PARINI. Russ. Chem. Rev. English Transl. **31**, 408 (1962).
5. R. S. MULLIKEN and W. B. PERSON. Ann. Rev. Phys. Chem. **13**, 107 (1962).
6. R. S. MULLIKEN. J. Am. Chem. Soc. **74**, 811 (1952).
7. H. J. G. HAYMAN. J. Chem. Phys. **37**, 2290 (1962).
8. P. A. D. DEMAINE. J. Miss. Acad. Sci. **8**, 241 (1962).
9. B. W. BRADFORD, D. HARVEY, and D. E. CHALKLEY. J. Inst. Petrol. **41**, 80 (1955). H. M. TENNEY. Anal. Chem. **30**, 3 (1958). M. E. BEDNAS and D. S. RUSSELL. Can. J. Chem. **36**, 1272 (1958).
10. M. A. MUHS and F. T. WEISS. J. Am. Chem. Soc. **84**, 4697 (1962).
11. E. GIL-AV and J. HERLING. J. Phys. Chem. **66**, 1208 (1962).
12. J. J. DUFFIELD and L. B. ROGERS. Anal. Chem. **34**, 1193 (1962).
13. D. W. BARBER, C. S. G. PHILLIPS, G. F. TUSA, and A. VERDIN. J. Chem. Soc. 18 (1959).
14. G. P. CARTONI, R. S. LOWRIE, C. S. G. PHILLIPS, and L. M. VENANZI. Gas chromatography 1960. *Edited by* R. P. W. Scott. Butterworths, London. 1960. p. 273.
15. R. J. CVETANOVIĆ, F. J. DUNCAN, and W. E. FALCONER. To be published.
16. L. N. FERGUSON and A. Y. GARNER. J. Am. Chem. Soc. **76**, 1167 (1954). G. BRIEGLEB and J. CZEKALLA. Z. Elektrochem. **59**, 184 (1955). C. C. THOMPSON, JR. and P. A. D. DEMAINE. J. Am. Chem. Soc. **85**, 3096 (1963). A. BIER and J. A. A. KETELAAR. Rec. Trav. Chim. **73**, 264 (1954).
17. A. BIER. Ph.D. Thesis, Amsterdam. 1954. *Quoted in* A. Bier and J. A. A. Ketelaar. Rec. Trav. Chim. **73**, 264 (1954).
18. L. L. G. BRADLEY and W. E. FALCONER. J. Sci. Instr. **40**, 606 (1963).
19. R. J. CVETANOVIĆ, F. J. DUNCAN, and W. E. FALCONER. Can. J. Chem. **41**, 2095 (1963).
20. D. AMBROSE, A. T. JAMES, A. I. M. KEULEMANS, E. KOVATS, H. ROCK, C. ROUIT, and F. H. STROSS. Gas chromatography 1960. *Edited by* R. P. W. Scott. Butterworths, London. 1960. p. 423.
21. S. DAL NOGARE and R. S. JUVET, JR. Gas chromatography. Interscience, New York. 1962.
22. R. J. CVETANOVIĆ, F. J. DUNCAN, W. E. FALCONER, and R. S. IRWIN. Unpublished data.
23. W. E. FALCONER and R. J. CVETANOVIĆ. Anal. Chem. **34**, 1064 (1962).

Can. J. Chem. Downloaded from www.nrcresearchpress.com by 210.87.254.42 on 09/05/12
For personal use only.

Can. J. Chem. Downloaded from www.nrcresearchpress.com by 210.87.254.5 on 09/05/12
For personal use only.

NEW NITROCHALCONES. VII[1,2]

T. SZELL[3] AND A. M. EASTHAM
Division of Applied Chemistry, National Research Council, Ottawa, Canada
AND
GY. SIPOS
University of Szeged, Szeged, Hungary
Received April 8, 1964

SUMMARY

A number of new nitrohydroxychalcones have been synthesized using sodium hydroxide and hydrogen chloride as catalysts. It has been found that with substituents which increase the acidity of acetophenones or the electrophilic character of benzaldehydes (e.g. NO_2, halogen, CN), sodium hydroxide is the better condensing agent, while with those substituents which increase the basic strength of the carbonyl, hydrogen chloride is satisfactory.

Since the pioneer work of Kostanecki (1), Wurtz (2), and Claisen (3) numerous examples in the literature have described the use of either sodium hydroxide or hydrogen chloride as the condensing agent in aldol condensations, without providing much guidance as to the choice of catalyst for any particular condensation. This work was undertaken to correlate the choice of catalyst with the structure of the reactants, using substituted benzaldehydes and acetophenones as the model compounds.

RESULTS

Table I lists the new chalcones and some of their properties; Table II records the results of experiments carried out with sodium hydroxide as the condensing agent and Table III the experiments carried out in the presence of hydrogen chloride. Reaction times are considered to be well below those required for the reactions to reach equilibrium but, nevertheless, all experiments in which precipitation of the product, its sodium salt, or its HCl adduct occurred have been excluded from the tables.

In alkaline catalysis, the substituents on the aldehyde component accelerate the rate of chalcone formation in aqueous ethanol in the following way: 2,4-dichloro- > 4-NO_2 > halogeno-* and 4-CN- > H ≈ 2-CH_3O- and 2-C_2H_5O- > α-naphthaldehyde > 3,4-methylenedioxy- > *p*-isopropyl- > 3,4-dimethoxy- and 3,4-diethoxy- > 4-hydroxy-3-methoxy- > 2-hydroxy- and 4-hydroxy-. In earlier work (4–7) the effect of benzaldehyde substituents was found to be 4-NO_2 > 4-Cl > 4-H and 3-OH > 4-OH; the acetophenone substituents were in the order 2-NO_2 > 4-NO_2 > 3-NO_2, 3-OH > 2- and 4-OH, 6-NO_2-3-OH > 4-NO_2-2-OH > 5-NO_2-2-OH > 3-NO_2-4-OH.

In acid catalysis the effect on the rate of substituents on the benzaldehyde component has been found to be in the following order: 4-hydroxy-3-methoxy- ⩾ 3,4-dimethoxy- ⩾ 4-hydroxy ≈ 4-methoxy- ⩾ H > halogeno- > 4-NO_2. Earlier work (8, 9) had shown the 4-hydroxy derivative to be more reactive than 4-nitro-benzaldehyde and had also shown

[1]*Part VI. T. Szell. J. Prakt. Chem. 17, 346 (1962).*
[2]*Issued as N.R.C. No. 8096.*
[3]*N.R.C. Postdoctoral Fellow, 1963–1964; present address: University of Szeged, Szeged, Hungary.*
**The order within the halogens (o-, p-, and m-; F, Cl, Br) is not clear. In part this is because some of the reaction mixtures were not homogeneous but it also appears that the order of reactivity of the o-, p-, and m-compounds is not the same for the different halogens. In general, the m-isomers seem more reactive than the p-isomers.*

Can. J. Chem. Downloaded from www.nrcresearchpress.com by 210.87.254.5 on 09/05/12
For personal use only.

TABLE I

No.	Chalcone	Formula	Nitrogen Calcd.	Nitrogen Found*	Melting point* (°C)	Shape and color
1	5′-NO_2-2′-OH-2-F-	$C_{15}H_{10}O_4NF$ (287.2)	4.88	4.8	154–155 (EtOAc)	Yellow needles
2	4′-NO_2-2′-OH-2-F-	"		4.7	180–181 (EtOAc)	"
3	3′-NO_2-4′-OH-2-F-	"		4.7	153–154 (EtOH)	"
4	6′-NO_2-3′-OH-2-F-	"		4.8	194–195 (EtOH–H_2O)	Pale yellow needles
5	5′-NO_2-2′-OH-3-F-	"		4.6	213–214 (EtOAc)	Yellow needles
6	4′-NO_2-2′-OH-3-F-	"		4.7	222–223 (EtOAc)	"
7	3′-NO_2-4′-OH-3-F-	"		4.7	190–191 (EtOH)	"
8	6′-NO_2-3′-OH-3-F-	"		4.8	184–185 (EtOH–H_2O)	Pale yellow needles
9	5′-NO_2-2′-OH-4-F-	"		4.6	232 (EtOAc)	Yellow needles
10	4′-NO_2-2′-OH-4-F-	"		4.8	192–193 (EtOAc)	"
11	3′-NO_2-4′-OH-4-F-	"		4.8	167–168 (EtOH)	"
12	6′-NO_2-3′-OH-4-F-	"		4.7	151–152 (EtOH–H_2O)	"
13	5′-NO_2-2′-OH-2-Cl-	$C_{15}H_{10}O_4NCl$ (303.7)	4.61	4.4	187–188 (EtOAc)	"
14	4′-NO_2-2′-OH-2-Cl-	"		4.4	191–192 (EtOAc)	Golden yellow needles
15	3′-NO_2-4′-OH-2-Cl	"		4.5	174–175 (EtOAc–EtOH)	Yellow needles
16	6′-NO_2-3′-OH-2-Cl	"		4.5	208–209 (EtOH–H_2O)	Pale yellow needles
17	5′-NO_2-2′-OH-3-Cl	"		4.4	199–200 (EtOH)	Yellow needles
18	4′-NO_2-2′-OH-3-Cl	"		4.6	223–224 (EtOAc)	"
19	3′-NO_2-4′-OH-3-Cl	"		4.5	154–155 (EtOH)	"
20	6′-NO_2-3′-OH-3-Cl	"		4.4	171–172 (EtOH–H_2O)	Pale yellow needles
21	5′-NO_2-2′-OH-2-Br-	$C_{15}H_{10}O_4NBr$ (348.2)	4.24	4.3	185–186 (EtOAc)	Yellow needles
22	4′-NO_2-2′-OH-2-Br-	"		4.2	195–196 (EtOAc)	Orange yellow needles
23	3′-NO_2-4′-OH-2-Br-	"		4.1	171–172 (EtOH)	Yellow needles
24	6′-NO_2-3′-OH-2-Br-	"		4.2	208–209 (EtOH–H_2O)	Pale yellow needles
25	5′-NO_2-2′-OH-3-Br-	"		4.0	177–178 (EtOAc)	Yellow needles
26	4′-NO_2-2′-OH-3-Br-	"		4.2	210–211 (EtOAc)	"
27	3′-NO_2-4′-OH-3-Br-	"		4.1	156–157 (EtOH)	"
28	6′-NO_2-3′-OH-3-Br-	"		4.1	162–163 (EtOH–H_2O)	Colorless needles
29	5′-NO_2-2′-OH-4-Br-	"		4.3	233–234 (EtOAc)	Yellow needles
30	4′-NO_2-2′-OH-4-Br-	"		4.2	203–204 (EtOAc)	"
31	3′-NO_2-4′-OH-4-Br-	"		4.2	198–199 (EtOAc–EtOH)	"
32	6′-NO_2-3′-OH-4-Br-	"		4.1	205 (EtOH–H_2O)	"
33	5′-NO_2-2′-OH-4-CN-	$C_{16}H_{10}O_4N_2$ (294.3)	9.5	9.1	228–229 (EtOAc)	"
34	4′-NO_2-2′-OH-4-CN-	"		9.3	211–212 (EtOAc)	"
35	3′-NO_2-4′-OH-4-CN-	"		9.3	233–234 (EtOAc–EtOH)	"
36	6′-NO_2-3′-OH-4-CN-	"		9.3	212–213 (EtOH–H_2O)	Pale yellow platelets
37	4′-NO_2-2′-OH-2,4-di-Cl-	$C_{15}H_9O_4NCl_2$ (338.1)	4.14	4.0	201–202 (EtOAc)	Orange yellow needles
38	3′-NO_2-4′-OH-2,4-di-Cl-	"		4.0	160–161 (EtOAc–EtOH)	Yellow needles

Can. J. Chem. Downloaded from www.nrcresearchpress.com by 210.87.254.5 on 09/05/12
For personal use only.

TABLE I (*Concluded*)

No.	Chalcone	Formula	Nitrogen		Melting point *(°C)	Shape and color
			Calcd.	Found*		
39	6′-NO_2-3′-OH-2,4-di-Cl-	$C_{15}H_9O_4NCl_2$ (338.1)	4.14	3.9	199–200 (EtOH–H_2O)	Pale yellow platelets
40	4′-NO_2-2′-OH-2-OCH_3-	$C_{16}H_{13}O_5N$ (299.3)	4.68	4.7	171–172 (EtOAc–EtOH)	Orange needles
41	3′-NO_2-4′-OH-2-OCH_3-	″		4.5	170–171 (EtOH)	Yellow needles
42	6′-NO_2-3′-OH-2-OCH_3-	″		4.6	171–172 (EtOH–H_2O)	Yellow platelets
43	5′-NO_2-2′-OH-2-OC_2H_5-	$C_{17}H_{15}O_5N$ (313.3)	4.47	4.4	175 (EtOAc)	Yellow needles
44	4′-NO_2-2′-OH-2-OC_2H_5-	″		4.3	165–166 (EtOAc–EtOH)	Orange needles
45	3′-NO_2-4′-OH-2-OC_2H_5-	″		4.2	194–195 (EtOAc–EtOH)	Yellow needles
46	6′-NO_2-3′-OH-2-OC_2H_5-	″		4.3	166–167 (EtOH–H_2O)	Pale yellow needles
47	4′-NO_2-2′-OH-3,4-di-OCH_3-	$C_{17}H_{15}O_6N$ (329.3)	4.25	4.2	180–181 (EtOAc–EtOH)	Red needles
48	3′-NO_2-4′-OH-3,4-di-OCH_3-	″		4.1	155–156 (EtOH)	Yellow needles
49	6′-NO_2-3′-OH-3,4-di-OCH_3-	″		4.1	201–202 (EtOH–H_2O)	Pale yellow platelets
50	5′-NO_2-2′-OH-3,4-di-OC_2H_5-	$C_{19}H_{19}O_6N$ (357.4)	3.92	3.8	160–161 (EtOAc)	Orange needles
51	4′-NO_2-2′-OH-3,4-di-OC_2H_5-	″		3.8	178–179 (EtOAc–EtOH)	Yellow needles
52	3′-NO_2-4′-OH-3,4-di-OC_2H_5-	″		3.7	140 (EtOH)	″
53	6′-NO_2-3′-OH-3,4-di-OC_2H_5-	″		3.8	155–156 (EtOH–H_2O)	Pale yellow platelets
54	5′-NO_2-2′-OH-4*i*-C_3H_7-	$C_{18}H_{17}O_4N$ (311.3)	4.50	4.3	156–157 (EtOAc)	Yellow needles
55	4′-NO_2-2′-OH-4*i*-C_3H_7-	″		4.3	170–171 (EtOAc)	″
56	3′-NO_2-4′-OH-4*i*-C_3H_7-	″		4.3	118–119 (EtOH–H_2O)	Pale yellow needles
57	4′-NO_2-2′-OH-3,4=OCH_2-	$C_{16}H_{11}O_6N$ (313.3)	4.47	4.4	245–246 (EtOAc)	Orange needles
58	3′-NO_2-4′-OH-3,4=OCH_2-	″		4.4	181–182 (EtOAc–EtOH)	Yellow needles
59	6′-NO_2-4′-OH-3,4=OCH_2-	″		4.2	165–166 (EtOH–H_2O)	Pale yellow platelets
60	3′-NO_2-4′,4-di-OH-3-OCH_3-	$C_{16}H_{13}O_6N$ (315.3)	4.44	4.1	224–225 (EtOAc)	Yellow needles
61	5-NO_2-2-OH-ω-(1-naphthylidene)-acetophenone	$C_{19}H_{13}O_4N$ (319.3)	4.39	4.2	242–243 (EtOAc)	″
62	4-NO_2-2-OH-ω-(1-naphthylidene)-acetophenone	″		4.2	225–226 (EtOAc)	″
63	3-NO_2-4-OH-ω-(1-naphthylidene)-acetophenone	″		4.1	209–210 (EtOH)	″
64	6-NO_2-3-OH-ω-(1-naphthylidene)-acetophenone	″		4.2	195–196 (EtOH–H_2O)	″
65	4′,3-di-NO_2-2′,2-di-OH-	$C_{15}H_{10}O_7N_2$ (330.2)	8.49	8.1	228–229 (EtOAc)	″
66	3′,3-di-NO_2-4′,2-di-OH-	″			194–195 (EtOH–AcOH)	″
67	6′,3-di-NO_2-3′,2-di-OH-	″			226–227 (EtOH–H_2O) (decomp)	Yellow platelets
68	6′-NO_2-3′-OH-4-CHO-	$C_{16}H_{11}O_6N$ (297.3)	4.7	4.6	>250 (EtOH–H_2O)	″
69	4′-NO_2-2′-OH-4-CHO-	″		4.3	>250 (EtOAc)	Yellow powder

*Yields are reported for crude products, melting points for the recrystallized materials. The melting points of the crude products were generally 1–4 °C below those of the purified materials.

TABLE II*

No.	Benzaldehyde	Acetophenone	Duration of run (min)	Concentration of NaOH (mole l^{-1})	Yield of chalcone (%)
1	2,4-di-Cl-	5-NO_2-2-OH-	135	0.24	85
2	4-NO_2-	"	"	"	75
3	2-Cl-	"	"	"	61
4	3-Cl-	"	"	"	58
5	4-Cl-	"	"	"	55
6	4-Br-	"	"	"	66
7	4-F	"	"	"	67
8	4-CN	"	"	"	37
9	H-	"	"	"	24
10	H-	"	"	0.48	35
11	H-	"	240	0.24	61
12	2-OCH_3-	"	"	0.80	50
13	3,4-CH_2(O-, O-)	"	"	"	35, 39
14	4-isopropyl-	"	"	"	33
15	3,4-di-OC_2H_5-	"	"	"	24
16	3-NO_2-2-OH-	"	"	"	13
17	4-OH-	"	"	"	1
18	3-OCH_3-4-OH-	"	"	"	1
19	4-F-	4-NO_2-2-OH-	135	0.24	83
20	4-CN-	"	"	"	74
21	H-	"	240	"	67
22	2-OCH_3	"	"	"	58
23	2,3-C_4H_4	"	"	"	58
24	3-Cl-	3-NO_2-4-OH-	135	"	47
25	2-OCH_3-	"	240	"	39
26	2,3-C_4H_4	"	"	"	36
27	3,4-di-OC_2H_5-	"	"	"	15
28	3-Cl-	6-NO_2-3-OH	135	"	69
29	4-CN	"	"	"	46
30	2-OCH_3	"	240	"	69

*Concentration of the reactant was 0.047 mole l^{-1} for runs 12–18. In all other runs it was 0.055 mole l^{-1}.

TABLE III*

No.	Benzaldehyde	Acetophenone	Duration of reaction (h)	Yield of new product (%)
1	4-NO_2	4-NO_2-2-OH-	4	3
2	2,4-di-Cl	"	20	13
3	4-Cl	"	4	11
4	H	"	4	25
5	4-OH	"	4	27
6	3,4-di-OCH_3	"	4	28, 32
7	3-OCH_3-4-OH	"	4	28
8	"	"	40	40
9	"	3-NO_2-4-OH-	5	69
10	"	5-NO_2-2-OH-	25	23
11	4-NO_2	4-NO_2	5	15 (9)
12	4-OCH_3	"	5	70 (9)
13	H	"	5	53 (9)
14	4-OCH_3	4-OH	5	68 (9)
15	4-OH	"	5	90 (9)

*Concentrations of the reactants were 0.07 mole l^{-1} for runs 1–10; and 0.1 mole l^{-1} for runs 11–15.

the following order for acetophenone substituents: 4-hydroxy-3-NO_2- > 2-hydroxy-4-NO_2- > 4-NO_2.

DISCUSSION

The pK_a values of substituted benzoic acids increase (10, 11), and the Hammett substituent constants decrease in the order 4-NO_2 > 3-NO_2 > 4-CN > halogeno >

Can. J. Chem. Downloaded from www.nrcresearchpress.com by 210.87.254.5 on 09/05/12
For personal use only.

H ≈ 3-OH > 3-CH_3 ≈ 4-CH_3 > 4-CH_3O > 4-OH > 3,4-dimethoxy. The pK_{BH+} values for a number of substituted benzaldehydes (12, 13) increase in the order 4-NO_2 > 3-Cl > 4-Cl > H > α-naphthaldehyde > 4-CH_3 > 4-CH_3O > trialkyl, while those for substituted acetophenones (14) increase in the order 4-NO_2 > 3-NO_2 > 3-hydroxy- > H > 4-hydroxy-. There is thus a close parallel between the effectiveness of the substituents in increasing the rate of the alkali-catalyzed condensation, in increasing the acidity of the benzoic acids, and in increasing the electrophilicity of the benzaldehyde (assuming that pK_{BH+} is directly related to electrophilicity). Such a correlation is not surprising, since the generally accepted mechanism for this condensation involves attack at the aldehyde carbon by a carbanion formed by removal of a proton from the acetophenone (15).

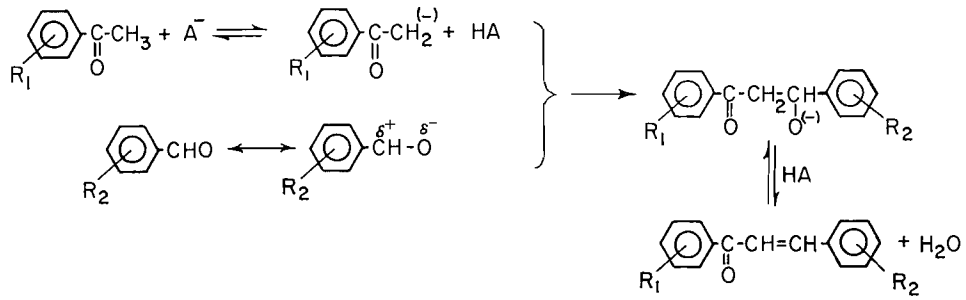

Since the mechanism of the acid-catalyzed condensation is less clear and more complex than the alkali-catalyzed, it is difficult to provide a satisfactory explanation for the effect of substituents on the rate (15). In general, the more basic the aldehyde the more rapid the rate, which suggests that the extent of protonation of the aldehyde is important, in accordance with the views of Noyce (15).

In general, the results suggest that for reactants having electron-withdrawing groups sodium hydroxide is the better condensing agent and that those containing electron-releasing groups can be satisfactorily condensed with hydrogen chloride. However, in many cases either catalyst seems effective and the choice may be governed by other factors. For example, ethanol–HCl is often particularly useful in preparing the 4′-nitrochalcones (9, 19) and, because the product precipitates, aqueous sodium hydroxide often gives good yields of the chalcones from mononitro-2- or mononitro-4-hydroxyacetophenones. On the other hand, a number of workers have reported difficulties in synthesizing hydroxychalcones in the presence of alkali (1, 7, 17). The alkaline condensation is simpler to use and can be applied even to those reactants having electron-releasing groups, if they will tolerate the longer reaction time; solvents of high dielectric constant such as water or aqueous alcohols are advantageous (4, 17). High concentrations of alkali should be avoided because of the possibility of Cannizzaro or other side reactions, especially with 2- or 4-nitro compounds (5, 7, 15, 16). Side reactions seem less important in acid solution but can occur (8, 16, 19).

Many specific deviations from these qualifications are known. Electron-withdrawing groups usually increase the yield in alkaline condensations (4, 6, 16, 20), but *p*-nitrobenzaldehyde does not always do so (9) and conversely, this same aldehyde sometimes improves the yields of acid-catalyzed condensations over those obtained with benzaldehyde (9, 19, 21, 22, 23). However, in some of these cases the improved yields may be due to precipitation and the poor yields due to the resinification of the product.

Can. J. Chem. Downloaded from www.nrcresearchpress.com by 210.87.254.5 on 09/05/12
For personal use only.

With *o*-hydroxybenzaldehyde in HCl, secondary or side reactions always occur; with the meta isomer and with *m*-hydroxyacetophenone they sometimes occur. Actually, *o*-hydroxybenzaldehyde condenses readily with acetophenones, but the products could not be identified (cf. Schraufstätter (16)). No difficulties were encountered in preparations with nitro-2- and nitro-4-hydroxyacetophenones but the preparation of 3′-hydroxychalcones in HCl was accompanied by considerable resinification. Many of these difficulties with phenolic compounds could probably be eliminated by acetylating or otherwise protecting the hydroxyl group (16, 22, 23). Perhaps for this reason as well as for its high electron-releasing power, the 4-methoxyl group gives satisfactory reactions in both acid and alkaline condensations and when present in either reactant (21); the duality of its reactivity is usually attributed to resonance effects (10, 12, 14, 24). Noyce has interpreted the effect of 4-methoxy and 4-nitro substituents as due to two counterbalancing factors, a change in basicity of the aldehyde and a change in the ease of bond formation between the reactants (15).

In acid solution the *p*-methyl group was found to give poorer yields than the ethyl, propyl, or butyl groups (19).

Under conditions of the present experiments 5-nitro-2-hydroxyacetophenone did not react with 4-hydroxybenzaldehyde, but reaction will occur under more drastic conditions (18); even 2,4-dihydroxyacetophenone will react, albeit in poor yield, with vanillin under sufficiently drastic conditions (7).

Clearly, with so many anomalies and because the experiments reported in the literature have been run under a wide variety of conditions, often with precipitation of the product and without correction for solubility of the product, sometimes in heterogeneous solution, and so on, any generalization other than the very broad one given above would be presumptuous.

EXPERIMENTAL

Materials

(a) Aldehydes

Halogeno- and cyano-benzaldehydes were obtained from Aldrich Chem. Co. Inc., the rest from Distillation Products, and all were used without further purification. A 13.58 mmole per 100 ml ethanolic solution was prepared from them.

(b) Acetophenones

5-Nitro-2-hydroxy-, 4-nitro-2-hydroxy, and 3-nitro-4-hydroxy-acetophenones were prepared by the Fries reaction from 4-, 3-, and 2-nitrophenylacetates, respectively (6, 25) and 6-nitro-3-hydroxyacetophenone was prepared according to Klinke's method (26), m.p. 103°, 65.5°, 133°, and 150°, respectively. A 4.92 g per 200 ml ethanolic solution was prepared from them.

(a) Synthesis of chalcones in the presence of *NaOH* was carried out as follows. To 4 ml of aldehyde solution 4 ml of ketone solution was added, the mixture was kept in a thermostat for 20 min at 30 °C then was mixed with 2 (or 4) ml of aqueous NaOH solution (96 g NaOH and 100 g H_2O). The reaction was stopped by acidifying the solution with 10 ml of an acetic acid solution. For 2-hydroxy ketones the acetic acid solution was prepared from 70 ml of acetic acid in 200 ml of water and 1800 ml of ethanol; for 3- and 4-hydroxy ketones the solution was prepared from 40 ml of acetic acid in 960 ml of water. On acidification, the chalcones precipitated and the starting materials remained in solution. Acidification was carried out in the same way even when the yellow or red sodium salt precipitated during the course of the run. After the mixture was cooled, the chalcones were filtered, washed with 2 ml of ethanol and 2 × 2 ml water, dried at 100°, and weighed. This weight was corrected for the solubility of chalcones which was determined for each run. In case of experiments 28 and 56 (Table I) oily material separated on acidifying the solution, but slowly solidified in the refrigerator.

(b) The syntheses in the presence of *HCl* were carried out by adding 4 ml of ketone solution to 4 ml of aldehyde solution and saturating the mixture with dry hydrogen chloride while cooling in ice. This was always accompanied by a change of color. Reactions were stopped by diluting the solutions with water and making them up to 20 ml, and the mixtures were then left overnight in the refrigerator. The chalcones were filtered off, weighed, and the weight corrected for the solubility. The product obtained from 4-isopropyl-benzaldehyde and 3-nitro-4-hydroxyacetophenone separated as an oil which could not be crystallized.

Can. J. Chem. Downloaded from www.nrcresearchpress.com by 210.87.254.5 on 09/05/12
For personal use only.

Recrystallization

Solvents used for recrystallization are given in Table I. Ethyl acetate – ethanol (EtOAc–EtOH), ethanol – acetic acid (EtOH–AcOH) were mixtures of 2:1 and 1:2, respectively. Recrystallization from ethanol–water was carried out by dissolving the raw products in as little boiling ethanol as possible, adding hot water until slightly turbid, and allowing the solution to cool slowly.

ACKNOWLEDGMENTS

We are grateful to Mrs. C. Lakos, Mrs. G. Bartok (University of Szeged, Hungary), and Mr. H. Seguin (N.R.C. Division of Pure Chemistry, Ottawa) for the microanalyses and to Mr. E. Gyurki and Mr. F. Kiszely (University of Szeged) for preparing the starting acetophenones.

REFERENCES

1. St. v. Kostanecki and H. Bablich. Ber. **29**, 233 (1896).
2. A. Wurtz. J. Prakt. Chem. Ser. 2, **5**, 457 (1872).
3. L. Claisen and A. Clapareda. Ber. **14**, 2460 (1881). L. Claisen. Ber. **20**, 646 (1887).
4. Gy. Sipos, A. Furka, and T. Szell. Monatsh. **91**, 643 (1960).
5. Gy. Sipos and T. Szell. Acta Phys. et Chem. Szeged, **6**, 109 (1960).
6. T. Szell. Ber. **91**, 2609 (1958).
7. D. N. Dhar. J. Org. Chem. **23**, 1159 (1958). J. Indian Chem. Soc. **37**, 799 (1960). J. Org. Chem. **25**, 1247 (1960).
8. T. Szell and R. E. M. Unyi. J. Org. Chem. **28**, 1146 (1963).
9. Gy. Sipos, I. Dobo, and B. Czukor. Acta Phys. et Chem. Szeged, **8**, 160 (1962).
10. R. Stewart and K. Yates. J. Am. Chem. Soc. **82**, 4059 (1960).
11. R. Stewart and M. R. Granger. Can. J. Chem. **39**, 2508 (1961).
12. K. Yates and R. Stewart. Can. J. Chem. **37**, 664 (1959).
13. G. Culbertson and R. Pettit. J. Am. Chem. Soc. **85**, 741 (1963).
14. R. Stewart and K. Yates. J. Am. Chem. Soc. **80**, 6355 (1958).
15. R. P. Bell. J. Chem. Soc. 1637 (1937). K. F. Bonhoeffer and W. D. Walters. Z. Physik. Chem. **181**, 441 (1938). L. P. Hammett. Physical organic chemistry. McGraw-Hill Book Co., Inc., New York. 1940. W. F. Luder and S. Zuffanti. The electronic theory of acids and bases. Dover Publications, New York. 1961. D. S. Noyce and W. A. Pryor. J. Am. Chem. Soc. **77**, 1397, 1402 (1955); **81**, 618 (1959). D. S. Noyce and W. L. Reed. J. Am. Chem. Soc. **80**, 5539 (1958).
16. E. Schraufstätter and S. Deutsch. Ber. **81**, 489 (1948).
17. L. Reichel, W. Burkart, and K. Müller. Ann. **550**, 146 (1940).
18. C. M. Cristian and G. C. Amin. Ber. **93**, 1064 (1960).
19. R. E. Lyle and L. P. Paradis. J. Am. Chem. Soc. **77**, 6667 (1955).
20. E. Coombs and D. P. Evans. J. Chem. Soc. 1295 (1940).
21. W. Davey and D. J. Tivey. J. Chem. Soc. 1230 (1958).
22. Z. Csürös and Gy. Deak. Acta Chim. Acad. Sci. Hung. **17**, 339 (1958).
23. J. F. Micquel. Bull. Soc. Chim. France, **61**, 1369 (1961).
24. H. H. Jaffe. Chem. Rev. **53**, 191 (1953). D. H. McDaniel and H. C. Brown. J. Org. Chem. **23**, 420 (1958).
25. A. Gerecs, T. Szell, and M. Windholz. Acta Chim. Acad. Sci. Hung. **3**, 459 (1953).
26. P. Klinke and H. Gibian. Ber. **94**, 26 (1961).

Can. J. Chem. Downloaded from www.nrcresearchpress.com by 210.87.254.5 on 09/05/12
For personal use only.

Can. J. Chem. Downloaded from www.nrcresearchpress.com by 210.87.254.40 on 09/05/12
For personal use only.

THE METAL-CATALYZED AUTOXIDATION OF TETRALIN

IV. THE EFFECT OF SOLVENT AND TEMPERATURE[1]

Y. KAMIYA[2] AND K. U. INGOLD

Division of Applied Chemistry, National Research Council, Ottawa, Canada

Received July 3, 1964

ABSTRACT

The limiting rate of oxidation of tetralin catalyzed by cobalt, manganese, and copper decanoates has been measured in 12 solvents at 65 °C. This rate is generally determined by the kinetic condition that the hydroperoxide reaches a steady-state concentration but the experimental rates are smaller than expected in some solvents. Both cobalt and manganese are able to terminate reaction chains and they therefore act as inhibitors of the oxidation at high concentrations. The ratio of the propagation rate constant (k_3) to the square root of the termination rate constant (k_6) for the oxidation of tetralin in acetic acid solution is given by

$$k_3/k_6^{1/2} = 300 \exp(-6\,900/RT) \text{ (l/mole s)}^{1/2}.$$

INTRODUCTION

In previous papers in this series it was shown that the rates of autoxidation of tetralin at 50 °C catalyzed by the acetates in acetic acid (1, 2) and the decanoates in pure tetralin (1, 3) of cobalt, manganese, copper, nickel, and iron tended to limiting values at high catalyst concentrations. In the case of cobalt, both in acetic acid (2) and, after applying a correction for tetralin consumption, in pure tetralin (3), it was shown that this limiting rate was in fairly good agreement with the theoretical predictions of Tobolsky (4). However, the rates for the other four metals were smaller than the theoretical limit both in acetic acid and in pure tetralin (1). These low rates were tentatively attributed to the low solubilities of the catalysts, since dilution with inert solvents gave rates that were in fairly close agreement with the theoretical value.

When the limiting rate is due to the production of a steady-state concentration of hydroperoxide (4), the kinetic scheme describing the overall reaction can be represented by (2, 5)

[1] $$\text{ROOH} + n\text{M} \xrightarrow{k_1'} \text{radical} \xrightarrow{\text{RH}} \text{R}\cdot$$

[2] $$\text{R}\cdot + \text{O}_2 \xrightarrow{k_2} \text{RO}_2\cdot$$

[3] $$\text{RO}_2\cdot + \text{RH} \xrightarrow{k_3} \text{ROOH} + \text{R}\cdot$$

[4] $$\text{RO}_2\cdot + \text{RO}_2\cdot \xrightarrow{k_6} \text{inactive products} + \text{O}_2.$$

When the rate of hydroperoxide decomposition is negligible compared with its rate of formation, the overall rate of oxidation is given by

[2] $$-\frac{\text{d}[\text{O}_2]}{\text{d}t} = k_3\left(\frac{k_1'}{2k_6}\right)^{1/2}[\text{RH}][\text{ROOH}]^{1/2}[\text{M}]^{n/2}.$$

[1] *Issued as N.R.C. No. 8118.*

[2] *N.R.C. Postdoctoral Fellow, 1962–1964. Present address: Department of Fuel, University of Tokyo, Tokyo, Japan.*

When the rate of hydroperoxide decomposition equals its rate of formation, this steady-state concentration is given by

$$[3] \qquad [\mathrm{ROOH}]_\infty = \frac{k_3^2[\mathrm{RH}]^2}{2k_1' k_6[\mathrm{M}]^n}$$

and, therefore, the limiting rate of oxidation is given by

$$[4] \qquad \left(-\frac{\mathrm{d}[\mathrm{O_2}]}{\mathrm{d}t}\right)_\infty = \frac{k_3^2[\mathrm{RH}]^2}{2k_6}.$$

A recent publication from this laboratory (6) lists values of $k_3/k_6^{1/2}$ at 65 °C for several hydrocarbons, including tetralin, in a variety of oxidation resistant solvents. These values were obtained from the oxidation of 1 ml of hydrocarbon in 20 ml of solvent initiated with 7×10^{-2} mole/l of α,α' azo-bis-isobutyronitrile (AIBN). They show a small but significant variation with the dielectric constant of the solvent. Now provided the limiting rate of a metal-catalyzed oxidation is controlled by the formation of a steady-state hydroperoxide concentration, it can be represented by eq. [4]. A comparison of the values of $k_3/k_6^{1/2}$ for tetralin derived from limiting rates in different solvents with the values obtained using AIBN as the initiator should provide a very sensitive test of Tobolsky's hydroperoxide steady-state theory, since the rate will be less sensitive to catalyst solubilities in dilute tetralin solutions. Moreover, the results should give some information as to whether or not peroxy radicals can complex with transition metal catalysts and still undergo the same propagation and termination reactions as uncomplexed "free" radicals. That is, it has been tentatively suggested by several authors (7, 8) that the formation of complexes between transition metal catalysts and peroxy radicals could affect metal-catalyzed oxidation rates by altering the rates of propagation and termination. A comparison of the $k_3/k_6^{1/2}$ values derived from metal-catalyzed limiting rates with the values obtained using AIBN should provide a fairly sensitive test for the existence of such complexes.

The present work describes the oxidation of tetralin in a variety of solvents at 65 °C catalyzed by the decanoates (or acetates in acetic acid solution) of cobalt, manganese, and copper since these three metals were the most active catalysts in pure tetralin (1). The effect of temperature on the limiting rates produced with these three metals, plus nickel and iron, has also been examined both in pure tetralin and in a 1:1 by volume solution of tetralin in acetic acid. The experimental technique has been described previously (2, 3).

RESULTS AND DISCUSSION

1. Solvent Effects

In a series of preliminary experiments the maximum rates of oxidation of 0.35 mole/l of tetralin (1 ml in 20 ml solvent) catalyzed by 5×10^{-2} mole/l of cobalt, manganese, and copper were measured in 12 solvents at 65 °C. The initial hydroperoxide concentration ($[\mathrm{ROOH}]_0$) was 5×10^{-2} mole/l in each experiment. This peroxide was added to eliminate the induction period which would otherwise be observed in the manganese-catalyzed oxidations because of the rapid chain-terminating process involving divalent manganese (1). It was also added to the cobalt- and copper-catalyzed reactions to keep all the experiments on a comparable basis. In nine experiments (noted in Table 1) no oxygen absorption took place in 3 000 – 5 000 s. In certain other experiments the rate

Can. J. Chem. Downloaded from www.nrcresearchpress.com by 210.87.254.40 on 09/05/12
For personal use only.

decreased very rapidly after achieving its maximum value right at the beginning of the reaction. Those cases where the rate fell to half its maximum value before 1 ml O_2 at s.t.p. had been absorbed are also noted in Table I. When the rate decreases this rapidly its maximum value can be obtained from only the first two or three readings and is therefore subject to considerable error. Moreover, a steady-state hydroperoxide concentration will not exist and therefore $k_3/k_6^{1/2}$ values cannot be derived from this rate.

The complete inhibition of oxidation with cobalt and manganese in several solvents led us to study one such system in considerable detail, namely, the cobalt decanoate catalyzed oxidation of tetralin in chlorobenzene. The measured maximum rates of oxidation at five tetralin concentrations (including pure tetralin) at 65 °C have been plotted against the cobalt concentration in Fig. 1. It is clear that at any particular tetralin concentration the rate tends to increase as the catalyst concentration is increased. This continues until the catalyst reaches a critical concentration ($[M]_c$) whereupon, with further small increases in catalyst concentration, the oxidation is inhibited and the rate (measured over the first few thousand seconds) suffers a catastrophic decline. That is, the cobalt functions as a catalyst below the critical concentration and as an inhibitor above it. Since the critical concentration decreases as the tetralin concentration is decreased the rate at any given catalyst concentration will drop to zero upon dilution of the tetralin past a certain critical point. That is, the curves in Fig. 1 show that at a given tetralin concentration there is a critical catalyst concentration and at a given catalyst concentration there is a critical tetralin concentration. The failure to obtain any oxidation with 0.35 mole/l tetralin catalyzed by 5×10^{-2} mole/l Co was obviously a specific aspect of a very general effect.

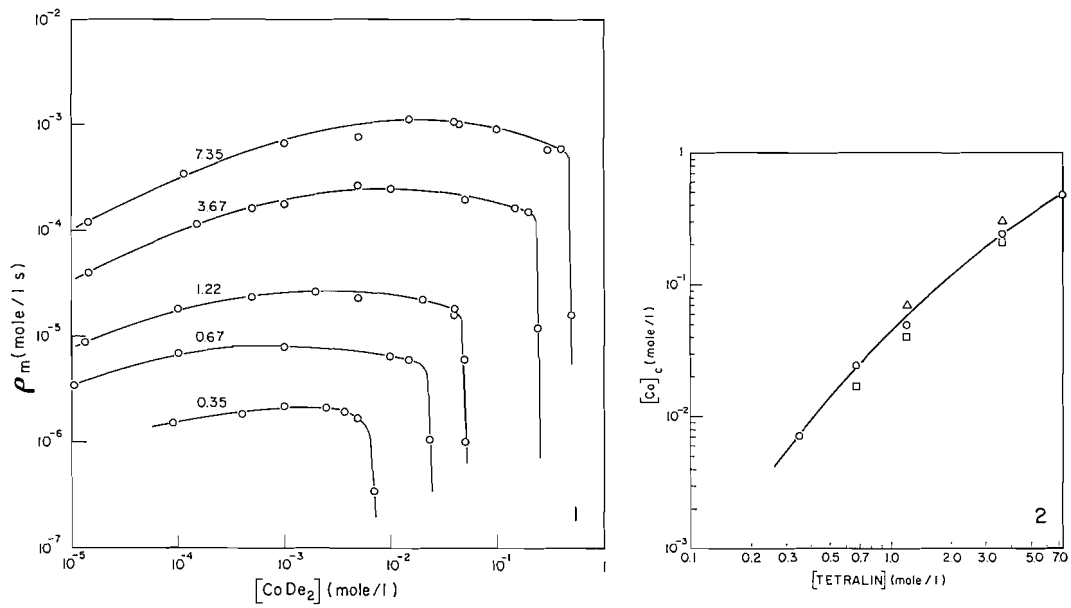

FIG. 1. The measured rate of oxidation of tetralin in chlorobenzene at 65 °C as a function of cobalt decanoate concentration. The numbers on the curves refer to the tetralin concentration in mole/l. The upper curve represents the rate in pure tetralin.

FIG. 2. Critical cobalt decanoate concentration as a function of tetralin concentration in chlorobenzene; ○ 65 °C, △ 95 °C, □ 35 °C.

Can. J. Chem. Downloaded from www.nrcresearchpress.com by 210.87.254.40 on 09/05/12
For personal use only.

TABLE I

Values of $k_3/k_6^{1/2}$ for tetralin in various solvents at 65 °C

Solvent	$k_3/k_6^{1/2} \times 10^3$ l$^{1/2}$ mole$^{-1/2}$ s$^{-1/2}$				[Co-decanoate]$_0$ mole/l $\times 10^{-2}$ in 1.22 mole/l tetralin
	AIBN (6)	Co	Mn	Cu	
None	9.8[a]	7.8	6.0	5.6	—
n-Decane	5.99	6.3[b]	6.0	8.6	3.5
Carbon tetrachloride	6.16	5.1[b]	6.4[b]	6.1[c]	3.5
t-Butylbenzene	6.50	6.3[b]	6.8[c]	7.1[c]	3.5
Benzene	10.1[a]	6.7[b]	8.1[c]	9.2	4.2
Acetic acid	10.2	10.3	10.2	3.6	>50
Chlorobenzene	11.5	6.5[b]	6.4[b]	11.7	5.0
t-Butanol	11.8	7.4[b]	7.3[c]	4.2	3.5
o-Dichlorobenzene	12.4	7.5[b]	8.8[c]	12.1	5.4
Nitrobenzene	13.5	8.9[c]	13.5	14.7	7.5
Dimethylphthalate	14.0[a]	13.8	14.2	9.0	>50
Nitromethane	22.3	12.4[c]	14.9	22.5	>50
Acetonitrile	28.3	29.0	15.0	28.0	>50

[a]Determined in this work.
[b]No oxidation in 3 000 – 5 000 s with 0.35 mole/l of tetralin catalyzed by 5×10^{-2} mole/l metal decanoate with $[ROOH]_0 = 5 \times 10^{-2}$ mole/l.
[c]The rate of oxygen absorption decreased to less than half its maximum value after the absorption of less than 1 cc O_2 at s.t.p. per cc tetralin with 0.35 mole/l tetralin catalyzed by 5×10^{-2} mole/l metal decanoate and with $[ROOH]_0 = 5 \times 10^{-2}$ mole/l.

Critical metal catalyst concentrations have occasionally been observed by other workers* and have been attributed to the chain termination process,

[8] $$RO_2\cdot + M \rightarrow RO_2M.$$

The limiting rate with this additional reaction is given by (1),

[4a] $$\left(-\frac{d[O_2]}{dt}\right)_\infty = \frac{k_3[RH]}{2k_6}(k_3[RH] - k_8[M]),$$

which predicts that the critical concentration should be directly proportional to [RH]. The values of $[M]_c$ from Fig. 1 (defined as the cobalt concentration at which the rate over the first few thousand seconds has declined to one tenth of its maximum value) have been plotted against [RH] in Fig. 2. The points appear to fall on a curve which shows the expected first-order dependence of $[M]_c$ on [RH] only at high [RH]. The apparent order in [RH] increases as [RH] decreases, the overall average order being about 1.5. This variable order suggests the occurrence of a third chain ending process which is first order in $[RO_2\cdot]$ and less than first order in [M] (i.e., probably zero or one-half order in [M]). If the chain ending step (11),

[10] $$RO_2\cdot \rightarrow \text{inactive products},$$

is introduced into the reaction scheme, the limiting rate is given by

[4b] $$\left(-\frac{d[O_2]}{dt}\right)_\infty = \frac{k_3[RH]}{2k_6}(k_3[RH] - k_8[M] - k_{10})$$

**For example, cupric stearate increases the maximum rate of oxidation of n-decane and causes small induction periods at concentrations below 0.06 mole %, but above this concentration the induction period is very greatly prolonged (9). In contrast, the sudden inhibition of the cobalt stearate catalyzed oxidation of butane upon dilution with benzene has been attributed to the chain terminating process (10):*

$$RO_2\cdot + C_6H_6 \rightarrow (RO_2\cdot C_6H_6) \rightarrow \text{inactive products}.$$

However, since the cobalt concentration was kept constant in these experiments, it seems more likely that chain termination by reaction [8] was responsible for the inhibition.

Can. J. Chem. Downloaded from www.nrcresearchpress.com by 210.87.254.40 on 09/05/12
For personal use only.

The experimental critical concentrations are in moderately good agreement with this equation, but the oxidation rates decrease more rapidly on approaching $[M]_c$ than is predicted. However, this may be due to the failure of the assumption that the occurrence of a steady-state hydroperoxide concentration still determines the kinetics when the catalyst concentration approaches $[M]_c$. Values of $[M]_c$ at 35 and 95° are also included in Fig. 2.

The measured rates of oxidation of 1.22 mole/l of tetralin in chlorobenzene at 65 °C are shown in Fig. 3 for catalysis by cobalt stearate and pivalate and by the decanoates of manganese and copper. The heavy line in this figure is the cobalt decanoate line from Fig. 1. Cobalt stearate and pivalate give a slightly larger maximum rate than was obtained with the decanoate but this rate is still well below the theoretical limit of 9.84×10^{-5} mole/l s calculated from the AIBN data. The critical catalyst concentration is greater for the stearate than for the decanoate (as was found previously in pure tetralin at 50 °C (3)) and is slightly greater again for the pivalate. The effect of the anion on $[M]_c$ probably results mainly from steric factors, i.e., the greater the steric protection of the coordination sites on the metal the slower will be reaction [8]. Solvent effects on $[M]_c$ (see Table I) may also be connected with steric factors resulting from the association of the solvent with the catalyst. However, the probable absence of critical concentrations in the more polar media which are good solvents for the catalyst suggests that this critical effect may be connected with some heterogeneous process on the surface of the undissolved catalyst. On the other hand, the critical cobalt decanoate concentration in chlorobenzene was unaffected by the addition of relatively large concentrations of cobalt phthalate or oxalate (both of which are very insoluble and are therefore very inactive catalysts). This rather argues against the importance of any surface reaction in determining $[M]_c$. The critical concentration was also unaffected by a threefold increase in the surface:volume ratio of the reaction vessel.

It can be seen from Fig. 3 that the cation has an even more profound effect on $[M]_c$

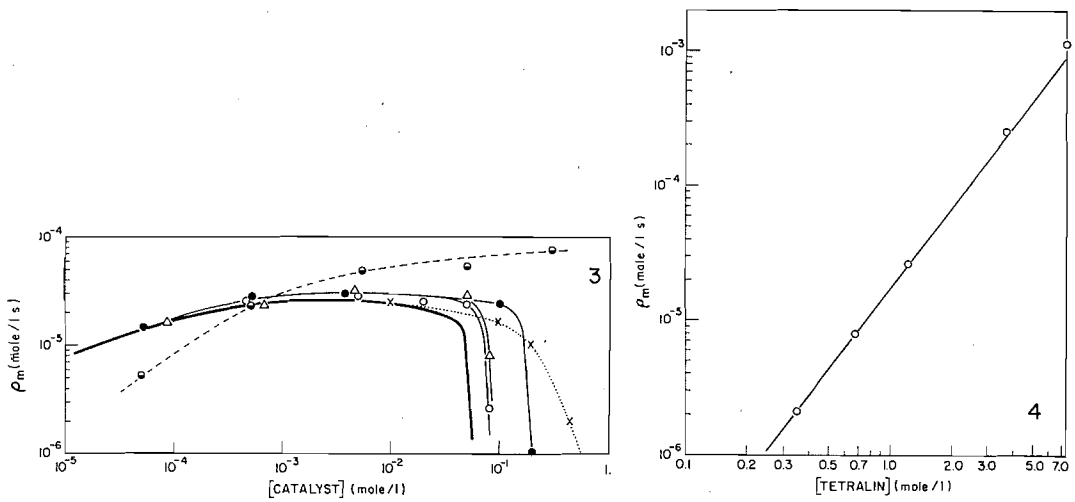

FIG. 3. The measured rate of oxidation of 1.22 mole/l of tetralin in chlorobenzene at 65 °C as a function of the catalyst concentration; ○ cobalt stearate, △ cobalt pivalate, ● manganese decanoate, ◒ copper decanoate, × cobalt decanoate together with 3×10^{-2} mole/l AIBN. The heavy line on the figure is the same as the line in Fig. 1 for the cobalt decanoate catalyzed oxidation of tetralin at this concentration. The theoretical limiting rate is 9.84×10^{-5} mole/l s.

FIG. 4. The measured maximum rate of oxidation of tetralin in chlorobenzene at 65 °C. The line on the figure has a slope of 2.0.

Can. J. Chem. Downloaded from www.nrcresearchpress.com by 210.87.254.40 on 09/05/12
For personal use only.

Can. J. Chem. Downloaded from www.nrcresearchpress.com by 210.87.254.40 on 09/05/12
For personal use only.

than the anion. That is, $[M]_c$ for manganese decanoate is four times as large as for cobalt decanoate although the limiting rates are about the same. The critical copper decanoate concentration must be quite large since the rate approaches the theoretical limit and this limit was easily reached at lower tetralin concentrations.

The fact that cobalt is a true inhibitor of the oxidation was further demonstrated by adding 3×10^{-2} mole/l AIBN to 1.22 molar tetralin in chlorobenzene. The critical cobalt decanoate concentration was increased and became less sharply defined (see Fig. 3), but at high cobalt concentrations the rate did decrease below the value found with AIBN alone (7.7×10^{-6} mole/l s). Incidentally, in the limiting rate region cobalt and AIBN appear to have an additive effect on the rate. For example, with 1.22 molar tetralin in chlorobenzene ρ_m is 2.4×10^{-5} mole/l s with 1×10^{-2} mole/l $CoDe_2$ or with 2×10^{-1} mole/l AIBN. Both catalysts together should therefore give a rate of $\sqrt{2} \times 2.4 \times 10^{-5} = 3.4 \times 10^{-5}$ mole/l s (bimolecular chain termination), which is in good agreement with the measured value of 3.3×10^{-5} mole/l s.

Values of $k_3/k_6^{1/2}$ at 65 °C calculated from the maximum rates of oxidation of dilute tetralin solutions (1.22 mole/l or less) catalyzed by the decanoates (or acetates in acetic acid) of cobalt, manganese, and copper at their optimum concentrations and with the optimum initial hydroperoxide concentrations* are given in Table I together with the values reported previously for the AIBN-initiated oxidation (6). The measured rates have been corrected for tetralin consumption where necessary. For example, the measured limiting rate with 0.35 molar tetralin in chlorobenzene is 2.15×10^{-6} mole/l s (Fig. 1) but this rate is not reached until a certain amount of oxygen has been absorbed. With the assumption that two molecules of oxygen oxidize three molecules of tetralin (2) the correction factor is found to be 1.2. Hence, $k_3/k_6^{1/2} = 6.5 \times 10^{-3}$ l$^{1/2}$mole$^{-1/2}$ s$^{-1/2}$. This value is considerably smaller than the value obtained previously with AIBN (6) (see Table I), i.e., the oxidation rate is smaller than would be predicted by eq. [4]. Similarly, in pure tetralin the corrected rate is 1.65×10^{-3} mole/l s (corresponding to $k_3/k_6^{1/2} = 7.8 \times 10^{-3}$ l$^{1/2}$ mole$^{-1/2}$ s$^{-1/2}$) which is considerably below the theoretical rate of 2.65×10^{-3} mole/l s obtained with AIBN.†

In many cases the agreement between AIBN and metal-catalyzed $k_3/k_6^{1/2}$ values is excellent. In these cases, it must be concluded that the metals have no significant effect on k_3 or k_6 and therefore metal-complexed peroxy radicals do not play any important role in the oxidation of tetralin in these solvents. This conclusion does not necessarily apply in those solvents where the $k_3/k_6^{1/2}$ values obtained from the metal-catalyzed oxidations are smaller than the values obtained with AIBN. However, these small values may also be due to the decomposition of some of the hydroperoxide to non-radical products or to radicals which are destroyed before they enter into reaction [3]. If the rate constant for all such processes is denoted by k_1^*, the limiting rate is reduced by the factor $k_1/(k_1 + k_1^*)$ but still has the correct dependence on $[RH]^2$, i.e.,

$$\left(-\frac{d[O_2]}{dt}\right)_\infty = \frac{k_3^2[RH]^2}{2k_6} \cdot \frac{k_1}{k_1 + k_1^*} \cdot \qquad [4c]$$

Only small amounts of peroxide were added to the copper-catalyzed oxidations since large amounts produced high initial rates which obviously did not correspond to the steady-state conditions from which values of $k_3/k_6^{1/2}$ could be derived.

†*The corrections for catalyst deactivation (3) and for the diluting effect of the catalyst are negligible. The correction factor of 1.45 for tetralin consumption is the same as at 50 °C (3). In our original work at 50 °C we included a correction for the diluting effect of the catalyst which gave a corrected rate approximately equal to the theoretical value (3). It now seems likely that this correction should not be applied since the catalyst is not completely soluble at high concentrations where this correction could become significant.*

On the other hand, the curves in Fig. 1 suggest that the limiting rates may be determined by the inhibiting action of the catalyst. That is, inhibition appears to become important at each tetralin concentration shortly before the limiting rate is reached. However, eq. [4*b*] does not account for the fact that these low limiting rates are often obtained over nearly a one hundredfold change in catalyst concentration nor will it account for the fact that these rates are exactly proportional to $[RH]^2$ (at tetralin concentrations below 1.22 mole/l where changes in the solvent composition cease to affect the rate (6), see Fig. 4). The chain terminating reactions

[8′] $$RO_2\cdot + M \rightleftarrows ROOM$$

[9] $$RO_2\cdot + ROOM \rightarrow \text{inactive products}$$

give

[4*d*] $$\left(-\frac{d[O_2]}{dt}\right)_\infty = \frac{k_3^2[RH]^2}{2k_6 + 2K_8' k_9[M]}$$

and might therefore contribute to the low limiting rates although they will not account for the detailed shape of the rate against catalyst concentration curves in Figs. 1 and 3. However, it must be remembered in relation to eqs. [4*a*], [4*b*], and [4*d*] that the basic assumption that there is a steady-state hydroperoxide concentration which determines the rate may not apply in the region where chain termination by the metal catalyst becomes important. At the present time, it does not seem possible to decide on the exact cause of the low $k_3/k_6^{1/2}$ values which are obtained with some metal catalysts in some solvents.

2. Temperature Effects

The rates of oxidation of pure tetralin and of 3.67 mole/l of tetralin in acetic acid were measured with all five metal catalysts over a temperature range from 26 to 95 °C. The rates in acetic acid were obtained with 5×10^{-1} mole/l of the metal acetate together with an equal initial concentration of tetralin hydroperoxide (see Fig. 5). Under these conditions the maximum rate occurs at or near the beginning of the reaction and there is no necessity to correct the measured rates for tetralin consumption. Furthermore, with the exception of the ferric acetate catalyzed reaction, the rates are fairly easily measured (except at 95 °C) since they decrease only as the tetralin is consumed, there being no deactivation of the catalyst (2, 3). The rates obtained with cobalt acetate at 35, 50, and 65 °C are equal, within the limits of experimental accuracy, to the theoretical rates derived from the AIBN-initiated oxidation of pure tetralin. Over the entire temperature range cobalt acetate gives an overall activation energy of 13.8 ± 0.4 kcal/mole. That is, from eq. [4]

$$E_3 - \tfrac{1}{2}E_6 = 6.9 \pm 0.2 \text{ kcal/mole}$$

and

$$k_3/k_6^{1/2} = 300 \exp(-6\,900/RT) \text{ (l/mole s)}^{1/2}.$$

These values are quite accurate because of the large temperature range that can be covered by this technique. The activation energy is smaller than the value of 8.2 ± 0.6 kcal/mole reported by Woodward and Mesrobian (5) from similar experiments over a smaller temperature range (50–81 °C). The difference almost certainly arises from the fact that Woodward and Mesrobian did not use a sufficiently large cobalt acetate concentration to reach the limiting rate at 50 °C (2). That is, E_1, the activation energy for the cobalt-catalyzed decomposition of tetralin hydroperoxide in acetic acid (21.2 ± 0.9 kcal/mole

Can. J. Chem. Downloaded from www.nrcresearchpress.com by 210.87.254.40 on 09/05/12
For personal use only.

(5)), is greater than E_3, the activation energy for the propagation reaction. Therefore, the rate of chain initiation by a given small concentration of cobalt acetate will increase more rapidly than the rate of the propagation reaction as the temperature is raised. This means that with insufficient catalyst the measured oxidation rate will approach the limiting rate as the temperature is raised, thus giving an anomalously high activation energy. The high temperature coefficients obtained in this work with manganese, nickel, and copper acetates arise from the same factor.

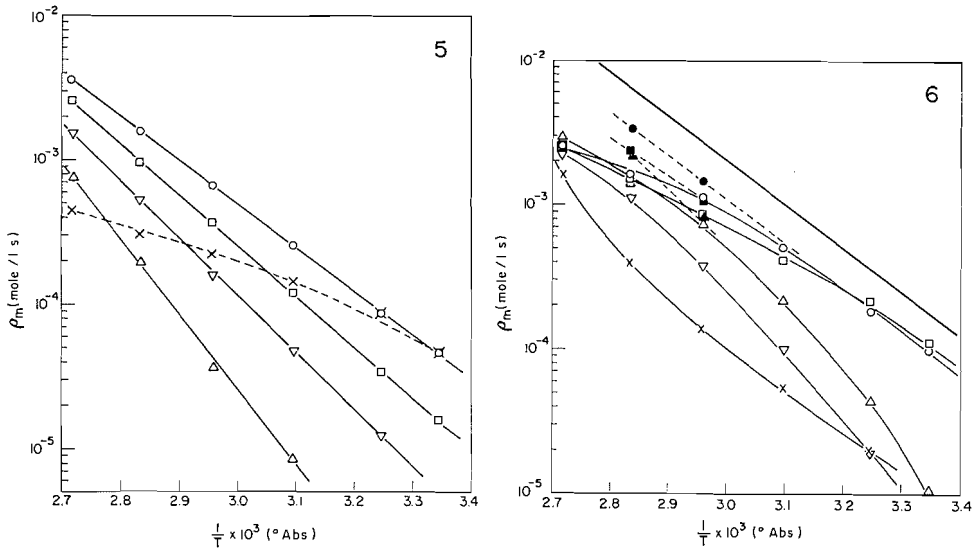

FIG. 5. Measured rates of oxidation of 3.67 mole/l of tetralin in acetic acid catalyzed by 5×10^{-1} mole/l of the following metal acetates; ○ cobalt, □ manganese, △ copper, ▽ nickel, and × iron. $[ROOH]_0 = 5 \times 10^{-1}$ mole/l.

FIG. 6. Measured rates of oxidation of pure tetralin catalyzed by 0.1 mole/l of manganese □, copper △, nickel ▽, and iron × decanoates. Maximum rates have been plotted for cobalt decanoate ○. The solid points represent the rates obtained with oxygen circulating continuously above the tetralin.

The rates obtained with ferric acetate are much less meaningful than the rates obtained with the other metal acetates. This is because oxidation only occurs to a very limited extent right at the beginning of the reaction, the rate quickly decreasing to a very small value as the iron is precipitated. As was pointed out above, such rates are not only difficult to measure but they also bear no relation to eq. [4] since a steady concentration of hydroperoxide is not set up.

The measured rates of oxidation of pure tetralin, catalyzed by 0.1 mole/l of manganese, copper, nickel, and iron decanoates, are shown in Fig. 6 as a function of the temperature. The initial hydroperoxide concentrations were 0.1 mole/l for manganese and 0.3 mole/l for the other three metals.* The points for cobalt decanoate represent the maximum rates obtained from curves of the rate against cobalt concentration at each temperature ($[ROOH]_0 \approx 10^{-3}$ mole/l). These rates are 10–20% larger than the rates obtained with 0.1 mole/l of cobalt (see Fig. 1). The heavy line in Fig. 6 represents the theoretical limiting rate of oxidation of pure tetralin.

The curvature and convergence at high temperatures of the Arrhenius plots for the

**For this reason, the rates with* Ni *and* Fe *at 50° differ from the values given previously with* $[ROOH_0] = 1.0$ *mole/l (Fig. 1, ref. 1).*

Can. J. Chem. Downloaded from www.nrcresearchpress.com by 210.87.254.40 on 09/05/12
For personal use only.

different metals is due to several factors. Firstly, the maximum rates are difficult to measure above 80 °C even with 1 ml samples, since the rate maintains its very high maximum value for only a short time at the beginning of the reaction. The tetralin in the reaction vessel therefore does not have time to come into temperature equilibrium with the surrounding oil bath. Secondly, the water formed in reaction [1] cannot be neglected at high temperatures. This water will produce a diminution in the apparent rate of oxygen absorption because one molecule of water vapor will be formed from two molecules of oxygen, i.e.,

$$2RH + 2O_2 \rightarrow 2ROOH \xrightarrow{M} RO\cdot + RO_2\cdot + H_2O\uparrow$$

and also because the oxygen will have increased difficulty in diffusing through this vapor into the tetralin. At high temperatures the measured oxidation rates therefore reflect the rate at which oxygen can diffuse into the tetralin rather than the rate at which it can react with the tetralin.* This was confirmed by a few experiments with Co, Mn, and Cu decanoate in which the oxygen was circulated continuously above the tetralin and through an air-cooled condenser to remove the water vapor as soon as it was formed. The rates obtained at 65 and 80 °C are increased (see solid points in Fig. 6) and the curvature of the Arrhenius plots is reduced or eliminated (dotted lines in Fig. 6). At 95 °C the rates were too great to measure. The correction to the measured maximum rate for tetralin consumption is about 40–45% for cobalt at all temperatures i.e., the corrected rate is smaller than the theoretical value by roughly the same amount at all temperatures. This correction is smaller for the other metals probably because of the higher initial peroxide concentrations that were used with these other metals (1). The small rates obtained with Cu, Ni, and Fe at the lower temperatures are probably due to the low solubilities of these rather inactive catalysts.

The present results illustrate the inherent dangers involved in assigning measured activation energies to specific elementary reactions unless independent evidence is available that the measured rates are related to the same elementary reactions over the entire temperature range. With the exception of the cobalt data in acetic acid, the temperature coefficients obtained from Figs. 5 and 6 cannot be assigned to any particular elementary reactions. That is, the measured rates are influenced to a different extent at each temperature by such factors as the catalyst concentration, the catalyst solubility, diffusion phenomena, the relative rates of hydroperoxide decomposition to radical and non-radical products, chain termination by the catalyst, etc. Many or all of these factors can influence the experimentally determined limiting rate at high metal-catalyst concentrations. However, Tobolsky's theory (4) that the steady-state hydroperoxide concentration determines the maximum possible value of the rate provides a unifying concept that clarifies the whole subject of metal-catalyzed oxidations.

REFERENCES

1. Y. Kamiya and K. U. Ingold. Can. J. Chem. **42**, 1027 (1964).
2. Y. Kamiya, S. Beaton, A. Lafortune, and K. U. Ingold. Can. J. Chem. **41**, 2020 (1963).
3. Y. Kamiya, S. Beaton, A. Lafortune, and K. U. Ingold. Can. J. Chem. **41**, 2034 (1963).

**The very low activation energy (6.5 kcal/mole) reported by George, Rideal, and Robertson (12) for the ferric stearate (4×10^{-3} mole/l) catalyzed oxidation of tetralin between 90 and 120° is also consistent with a reaction which is mainly diffusion-controlled at these high temperatures. These authors actually claimed that their reaction was not diffusion-controlled because the measured rate at 110 °C did not increase when the sample size was reduced from 2 ml to 0.5 ml. However, this test will be rather insensitive at temperatures where all the water produced in reaction [1] is evolved as steam. Incidentally, the rate obtained in our work with 0.1 mole/l of ferric decanoate at 95 °C falls on their Arrhenius plot but our value at 80° is very much less than would be expected from their data.*

Can. J. Chem. Downloaded from www.nrcresearchpress.com by 210.87.254.40 on 09/05/12
For personal use only.

4. A. V. TOBOLSKY. Rubber World, **118**, 363 (1948).
5. A. E. WOODWARD and R. B. MESROBIAN. J. Am. Chem. Soc. **75**, 6189 (1953).
6. J. A. HOWARD and K. U. INGOLD. Can. J. Chem. **42**, 1250 (1964).
7. H. S. BLANCHARD. J. Am. Chem. Soc. **82**, 2014 (1960).
8. K. U. INGOLD. Lipids and their oxidation. *Edited by* H. W. Schultz and E. A. Day. Avi Publishing Co., Inc., Westport, Conn. 1962. Chap. 5.
9. D. G. KNORRE, L. G. CHUCHUKINA, and N. M. EMANUEL. Zh. Fiz. Khim. **33**, 877 (1959).
10. E. A. BLYUMBERG, A. D. MALIEVSKII, and N. M. EMANUEL. Dokl. Akad. Nauk SSSR, **136**, 1130 (1961).
11. J. A. HOWARD and K. U. INGOLD. Can. J. Chem. **40**, 1851 (1962).
12. P. GEORGE, E. K. RIDEAL, and A. ROBERTSON. Proc. Roy. Soc. London, Ser. A, **185**, 288 (1946).

Can. J. Chem. Downloaded from www.nrcresearchpress.com by 210.87.254.40 on 09/05/12
For personal use only.

Can. J. Chem. Downloaded from www.nrcresearchpress.com by 210.87.254.40 on 09/05/12
For personal use only.

AMMONOLYSIS OF URONIC ESTER GROUPS IN BIRCH XYLAN[1]

PAUL Y. WANG, H. I. BOLKER,[2] AND C. B. PURVES

Wood Chemistry Division, Pulp and Paper Research Institute of Canada and Department of Chemistry, McGill University, Montreal, Quebec

Received June 10, 1964

ABSTRACT

Solvent-extracted white birch, kept near 20° in liquid ammonia under pressure for 72 h and then extracted with methanol to remove acetamide, retained 0.25% of amide nitrogen. Extraction of the very finely ground residual wood with hot water yielded 21% as a 4-O-methylglucuronoxylan containing 0.53% of amide nitrogen. Alkaline hydrolysis removed the amide absorption in the infrared and restored the normal xylan spectrum. These results, supported by various control experiments, showed that amide groups in the ammonia-treated wood were derived from lactone or ester groups in the original 4-O-methylglucuronoxylan. Some of the uronic acid groups in the native wood presumably existed as ester cross-links.

INTRODUCTION

It has long been known (1, 2) that the hardwoods in aqueous suspension are nearly neutral in reaction despite the 3–5% of uronic acid groups they contain (3). Yet, even if their ash content of 0.2–0.4% (3) is attributed entirely to calcium oxide, it is enough to neutralize only 25–80% of the uronic acid; the rest is presumably present as an ester or a lactone. Until now, the only ester linkages positively established in wood have been acetyl groups in the hemicellulose components (4) and possibly a few formyl groups (5). Nevertheless, some authors have inferred the presence of other esters from various experimental results (2), while others (1, 6) have particularly noted that non-extractable nitrogenous compounds analyzed as amides, remained in wood meals which had been immersed in liquid ammonia under pressure at room temperature. Ammonia, of course, yields ammonium salts from free carboxylic acid groups and only slowly cleaves esters at atmospheric pressure (−33°) (7). However, at room temperature ammonolysis of esters occurs in a reasonable time and produces acid amides. Such amides, other than acetamide, have never actually been recovered from the ammonolysis products of wood, and it was the object of the present research to isolate them from ammonia-treated birch wood meal.

By use of the procedure developed with other woods (1), birch wood meal was treated with a large excess of nearly anhydrous liquid ammonia under pressure (about 150 p.s.i.), washed several times with fresh liquid ammonia, and extracted with hot methanol in a Soxhlet apparatus to remove acetamide. As in the previous work, the quantitative differentiation of amide from ammonium nitrogen was based on the selective expulsion of ammonia from the latter by boiling with an aqueous suspension of magnesium oxide (8); control experiments with known mixtures of pure acetamide and ammonium acetate showed the method to be reliable. The Kjeldahl nitrogen content of the untreated wood was 0.06% and of this, 0.03% which responded as amide could probably be ascribed to nitrogen in the wood protein (9).

Table I shows that the amide nitrogen content of the wood increased with time of ammonolysis until a maximum value of 0.25% was reached after 24 h; a period of 72 h was chosen in subsequent experiments. Prior extraction of the wood with strong aqueous

[1]*From a thesis to be presented by P. Y. W. to McGill University in partial fulfillment of the requirements for the degree of Doctor of Philosophy; paper presented at the 47th Annual Conference of the Chemical Institute of Canada, Kingston, Ontario, June 2, 1964.*

[2]*To whom all correspondence should be addressed.*

TABLE I

Content of amide and ammonium nitrogen in samples treated near 20° with liquid ammonia under pressure (about 150 p.s.i.)

Sample		% nitrogen[a]		
		Ammonium	Amide	% soluble[b]
A. Birch wood meal				
(i) before ammonolysis[c]		0.01	0.03	—
(ii) after ammonolysis for	1 h	0.08	0.13	3.9
	2 h	0.14	0.16	—
	5 h	0.10	0.18	—
	10 h	0.14	0.22	—
	15 h	0.09	0.23	—
	25 h	0.10	0.25	—
	50 h	0.12	0.26	—
	100 h	0.12	0.25	4.6
B. "Xylan-poor" wood meal[d] after ammonolysis for 72 h		3.45	0.03	—
C. Extracted birch xylan[e] after ammonolysis for 72 h		0.23	0.01	—
D. Mixture (3:1) of (B) and (C) after ammonolysis for 72 h		2.03	0.03	—

[a]Calculated on oven-dry wood.
[b]Soluble in liquid ammonia.
[c]Kjeldahl N, 0.06%.
[d]After extraction of original meal with 24% potassium hydroxide under nitrogen.
[e]Recovered from the potassium hydroxide extract.

potassium hydroxide yielded a residual wood B and an extracted "xylan" C both of which were practically devoid of amide nitrogen, presumably because the potassium hydroxide had hydrolyzed all ester or lactone groups originally present. Ammonolysis caused the ammonium nitrogen content of the wood to attain its final, constant value of 0.11 ± 0.03% within an hour. The assumption that this value corresponded to carboxylic acid present originally as inorganic salt gave a salt:ester mole ratio (0.11:0.25) of about 3:7, and the sum of the ammonium and amide nitrogen, 0.36% was equivalent to 4.5% as uronic acid. Although birch wood was reported (3) to contain 4.6% of uronic acid, this excellent agreement was possibly fortuitous because the ammonium contents of the highly swollen wood residue B and of the extracted "xylan" C had no obvious connection with their content of uronic acid. The significance of the values for "ammonium" nitrogen after ammonolysis requires further study.

Confirmation of the presence of amides in ammonolyzed wood, freed of acetamide, was obtained by infrared spectroscopy. In earlier work (10) differential spectroscopy had been applied to determine the spectra of lignins in whole woods and pulps; in the present work the technique was altered, and the differential spectrum of holocellulose was determined by using wood in the sample beam and precisely calculated quantities of dioxane lignin, from the same wood, in the reference beam of the double-beam spectrometer. As shown in Fig. 1, the holocellulose differential spectrum (I) corresponds fairly well to the spectrum (against air) of isolated Tappi holocellulose (II). In the differential spectrum there are slight, but seemingly unavoidable, shifts of some of the principal bands, and also slight residues of the lignin spectrum, particularly at 1 500 and 1 600 cm^{-1}. However, these defects are not significant when the differential spectrum of the holocellulose in ammonia-treated wood (III) is observed. Here, as expected, the absorption bands at 1 730 cm^{-1} (C=O) and at 1 250 cm^{-1} (C—O), characteristic of acetyl groups, are absent, but a new, very strong band has appeared at 1 680 cm^{-1}. This band corresponds to the amide I band of α-D-glucuronamide (Fig. 2, V; IV is the spectrum of glucuronolactone for comparison), although the latter is found at a somewhat lower wave number (1 655 cm^{-1}). The amide II

Can. J. Chem. Downloaded from www.nrcresearchpress.com by 210.87.254.40 on 09/05/12
For personal use only.

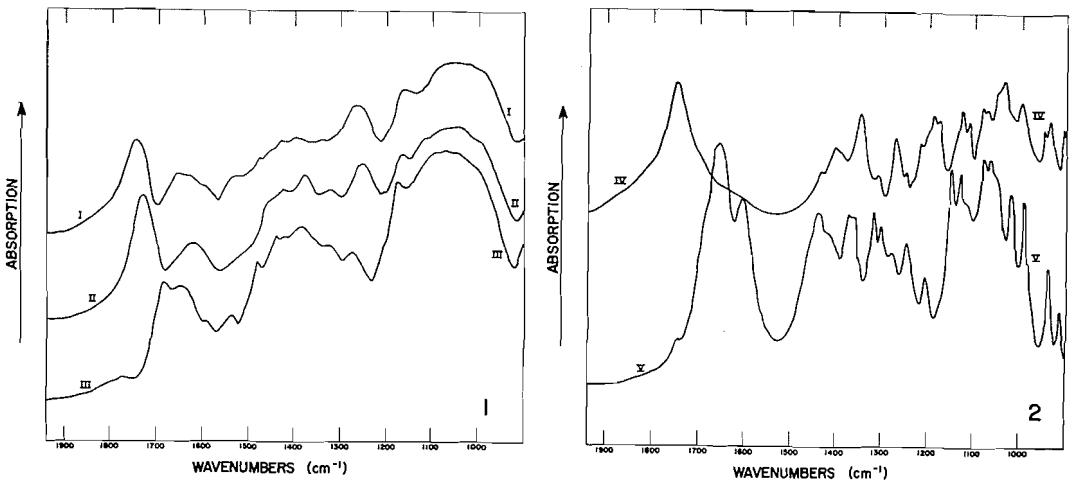

FIG. 1. Infrared spectra: (I) differential spectrum of holocellulose in untreated birch wood, (II) spectrum of birch (Tappi) holocellulose, (III) differential spectrum of holocellulose in ammonia-treated birch wood.
FIG. 2. Infrared spectra: (IV) glucuronolactone, (V) α-D-glucuronamide.

band at 1 608 cm^{-1} cannot be seen in the holocellulose spectrum, probably because of overlapping.

After the ammonia treatment and preliminary spectroscopic analysis, attempts were made to extract the "amide xylan" from the wood with dimethyl sulphoxide. Although the extraction was tried for 42 h under nitrogen, both at room temperature and at 80° with solids:liquor ratios varying from 1:15 to 1:100, and with the addition of up to 60% of water to the dimethyl sulphoxide, only about 1% of the wood substance was dissolved in each case. Pure water at room temperature yielded 1.5% of soluble material. Experiments then showed that if untreated wood meals of several species were first ground to almost colloidal size in a vibratory mill, hot water under neutral conditions extracted good yields of the hemicellulose fractions. When applied to the birch wood residue from ammonolysis, this procedure removed much of the hemicellulose and with it up to 75% of the original nitrogen. A larger scale preparation recovered 21% of the wood as a polysaccharide containing 0.53% of amide nitrogen (almost half the original amount) and only 1.7% of lignin. Acid hydrolysis followed by paper chromatography showed this polysaccharide to be nearly pure 4-O-methylglucuronoxylan.

The infrared spectrum of the above 4-O-methylglucuronoxylan (Fig. 3, VI) retained the prominent amide I absorption band near 1 680 cm^{-1} already noted in the differential spectrum of the ammonolyzed wood from which the xylan had been extracted (Fig. 1, III). Moreover, when this xylan was treated with 5% aqueous potassium hydroxide the amide band disappeared (VII) and the spectrum became identical with that of the xylan (VIII) extracted by 24% aqueous potassium hydroxide from untreated wood meal. These results showed that the 4-O-methylglucuronoxylan had been isolated from the ammonolyzed wood as an amide.

There is evidence that liquid ammonia yields amines from some reducing sugars (11), amides from acetylated disaccharides (12), and in appropriate conditions amides even from carboxylic acids (13). However, in the present research, control experiments produced no "aldose amide" from a fully acetylated cotton cellulose of DP_n, 395. When 4-O-methylglucuronoxylan plus added acetamide was immersed for 72 h in liquid ammonia

Can. J. Chem. Downloaded from www.nrcresearchpress.com by 210.87.254.40 on 09/05/12
For personal use only.

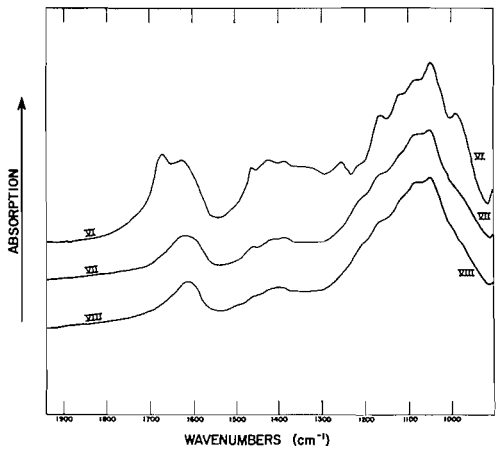

FIG. 3. Infrared spectra: (VI) "xylan amide" from ammonia-treated birch wood, (VII) "xylan amide" after hydrolysis in alkali, (VIII) alkali-extracted birch xylan.

under pressure at room temperature, the product was free of amide groups; hence a transfer reaction between acetamide and uronic acid or aldehyde groups in the xylan did not occur. These negative results minimized the possibility that the amide groups in the 4-O-methylglucuronoxylan from ammonolyzed birch wood originated in some unsuspected side reaction and strengthened the conclusion that many of the carboxyl groups in the untreated wood must have existed in the form of either lactone or ester groups, the latter as cross-links within the xylan itself or between xylan and other wood constituents.

EXPERIMENTAL

Materials

Wood meal, 60–80 mesh, from white birch (*Betula papyrifera*) was thoroughly extracted with ethanol–benzene, and was air-dried. After being screened again the meal was stored in screw-capped amber bottles. A published method (14) was used to extract 4-O-methylglucuronoxylan with 24% aqueous potassium hydroxide from some of the wood meal; yield: 24.3%. Acid hydrolysis followed by paper chromatography (15, 16) indicated the presence of much xylose and only traces of other sugars. The "xylan poor" wood residue (75.2%) was washed with distilled water until neutral to universal indicator paper, next with 0.02 *N* hydrochloric acid, then with distilled water again to neutrality, and, finally, air-dried.

Commercial liquid ammonia of 99.9% purity was used.

The acetylated raw Coastland cotton used in control experiments was described by Timell (17).

Analytical Methods

Klason lignin determinations were by TAPPI method (18).

A standard method (8) was adapted as follows for the determination, first of ammonium and then of amide nitrogen. An air dry, 1 g sample was placed in a 300 ml, 3-necked round-bottom flask equipped with 250 ml dropping funnel and a U-shaped splash-head connected to a condenser; the third neck was stoppered. The lower, distal end of the condenser was immersed in 25 ml of 1% aqueous boric acid containing 2 drops of a methyl purple indicator and just enough 0.02 *N* hydrochloric acid to make the solution purple. A suspension of 5 g of magnesium oxide (A.R. grade) in 150 ml of water was added through the dropping funnel, and the mixture was heated until about 80 ml, containing all of the liberated ammonia, had distilled into the boric acid solution. The latter was then titrated with 0.02 *N* hydrochloric acid, and the percentage of ammonium nitrogen was calculated. After providing a fresh 25 ml volume of the boric acid, with the indicator and of the proper pH, 150 ml of 60% aqueous potassium hydroxide was added through the dropping funnel and the third neck of the flask was equipped for a steam distillation; an ordinary distillation caused excessive "bumping". About 80 ml of distillate was collected in the boric acid solution which was then titrated as before. The result corresponded to the content of amide nitrogen, when correction was made for the small blank.

Found for pure acetamide, m.p. 81.5°: amide N, 23.2, 23.6; calcd.: 23.8. Found for pure ammonium acetate: ammonium N, 17.8, 17.8; calcd.: 18.2. Found for a mixture containing 0.30 g of acetamide and

Can. J. Chem. Downloaded from www.nrcresearchpress.com by 210.87.254.40 on 09/05/12
For personal use only.

0.63 g of ammonium acetate: amide N, 7.6; ammonium N, 11.6; calcd.: amide N, 7.7; ammonium N, 12.3. For a mixture containing 0.51 g of acetamide and 0.46 g of ammonium acetate, found: amide N, 11.9; ammonium N, 8.3; calcd.: amide N, 12.1; ammonium N, 8.4.

A Unicam S.P. 100 prism-grating spectrophotometer was used to determine infrared spectra, the finely ground samples being suspended in clear pressed discs of potassium bromide 16 mm in diameter. Differential spectra were determined on wood samples of known Klason lignin content which had been ball-milled in a stainless steel vial for 5 min. The method for incorporating a precise weight (about 5 mg) of sample into a 400 mg potassium bromide disc was described previously (10). An amount of birch dioxane lignin (19) corresponding to the Klason lignin content of the wood samples was incorporated in a similar disc for use in the reference beam.

Small-Scale Ammonolyses

In a typical experiment, 10 g samples of the solvent-extracted birch wood meal plus 15 ml of liquid ammonia for each 1 g of sample, were sealed in steel bombs equipped as described elsewhere (6). After being kept at room temperature for various times, the liquid ammonia was siphoned through a fine sintered-glass filter stick. The wood was then washed with more liquid ammonia, and the combined liquors on evaporation yielded a small residue. A 1 h ammonolysis extracted 3.9% of the wood, and a 100 h treatment removed only 4.6%.

The ammonia remaining in the wood was removed by keeping the sample under vacuum for 12 h. Then the wood was extracted in a Soxhlet apparatus with methanol for 2 h. After drying in air, the sample was analyzed. The results shown in Table I were the means of concordant duplicates.

Amide of 4-O-Methylglucuronoxylan

A larger steel bomb (6) made it possible to extract 300 g of the birch wood meal in 50 g batches for 72 h at room temperature by the method already described, but in this case the liquid ammonia:wood ratio was reduced to 5:1 (vol:wt.). The moisture in the wood amounted to about 1% of the volume of the liquid ammonia.

After the residual wood had been extracted with methanol and dried in the air, 20 g was ground, with no addition of liquid, in a vibrating ball mill (20) for 30 h at 4°. The extremely finely divided product was then boiled for 1 h under reflux with 2 l of water. Without cooling, the suspension was filtered through a medium porosity, sintered-glass funnel, and the residue was washed with three 500 ml volumes of boiling water, then with 500 ml of cold water. The combined liquors were concentrated at 50° under reduced pressure to about 70 ml, the concentrate was poured into 1 l of ethanol, and the mixture was kept overnight near 4°. The precipitate of hemicellulose was then recovered on a filter, solvent-exchanged through ethanol and petroleum ether (b.p. 30–60°), and dried *in vacuo*. Yield of the gray, white powder, 4.1 g (21%).

Found: amide N, 0.53; Klason lignin 1.7.

A small sample was hydrolyzed in acid (15) and the hydrolysate was chromatographed on paper with ethyl acetate – acetic acid – water (9:2:2 v/v) and with *n*-butanol–pyridine–water (10:3:3 v/v) as eluents (16). The R_f values of the major spots corresponded to those observed in control experiments with xylose, 4-O-methylglucuronic acid, and 2-O-[4-O-methyl-α-D-glucopyranosyluronic acid]-D-xylopyranose; only traces of galactose, glucose, mannose, and arabinose were found.

In a smaller-scale experiment, 1.0 g of the residual wood from the ammonolysis was extracted as before with hot water, the amide nitrogen contents of the extract and the residue were 0.15% and 0.05%, respectively, on the wood basis. That is, hot water had extracted 75% of the amide nitrogen from the wood, and it was in the xylan.

To hydrolyze the amide group in the above hemicellulose, 100 mg was boiled under reflux and in a nitrogen atmosphere for 3 h with 10 ml of 5% potassium hydroxide. Precipitation of the liquor in ethanol yielded 92 mg of the hemicellulose as the potassium salt.

α-D-Glucuronamide

In a modification of methods described in the literature (21, 22), 5 g α-D-glucuronamide was prepared in a crude yield of 48%. After purification by ion-exchange and five recrystallizations from water–isopropanol, yield 37%; m.p. 153–154° (decomp.); reported 150° and 158°; $[\alpha]_D^{20}$ (2% in water), +46° (10 min), +31° (90 min), +29.3° (22 h); reported (21) +78° (3 min), +31.6° (22 h).

Calcd. for $C_6H_{11}O_6N.H_2O$: N, 6.63. Found: N, 6.47, 6.51.

REFERENCES

1. L. G. NEUBAUER and C. B. PURVES. Can. J. Chem. **35**, 388 (1957).
2. J. W. T. MEREWETHER. *In* The chemistry of lignin. F. E. Brauns and D. Brauns. Suppl. Vol. Academic Press, New York. 1960. p. 630.
3. T. E. TIMELL. Tappi, **40**, 568 (1957).
4. T. E. TIMELL. Advan. Carbohydrate Chem. In press. 1964.
5. T. E. TIMELL. Svensk Papperstid. **60**, 762 (1957).
6. M. M. YAN and C. B. PURVES. Can. J. Chem. **34**, 1747 (1956).

Can. J. Chem. Downloaded from www.nrcresearchpress.com by 210.87.254.40 on 09/05/12
For personal use only.

7. K. J. BJÖRKVIST and L. JÖRGENSEN. Acta Chem. Scand. **5**, 978 (1951).
8. E. E. REID. Am. Chem. J. **21**, 284 (1899).
9. S. NICKEL. Holzforschung, **16**, 150 (1960).
10. H. I. BOLKER and N. G. SOMERVILLE. Pulp Paper Mag. Can. **64**, T-187 (1963).
11. I. E. MUSKAT. J. Am. Chem. Soc. **56**, 693 (1934).
12. J. O. DEFERRARI and R. A. CADENAS. J. Org. Chem. **28**, 1070 (1963).
13. W. J. HUND and L. ROSENSTEIN. Brit. Patent No. 445,148 (April 3, 1936); Fr. Patent No. 790,002 (Nov. 12, 1935). Chem. Abstr. **30**, 6389 (1936).
14. C. P. J. GLAUDEMANS and T. E. TIMELL. Svensk Papperstid. **60**, 869 (1957).
15. J. F. SAEMAN, W. E. MOORE, R. L. MITCHELL, and M. A. MILLETT. Tappi, **37**, 336 (1954).
16. T. E. TIMELL. J. Am. Chem. Soc. **82**, 5211 (1960).
17. T. E. TIMELL. J. Polymer Sci. Part C, Polymer symposia, **2**, 109 (1963).
18. Tappi Standard T-13M-54.
19. J. M. PEPPER, P. E. T. BAYLIS, and E. ADLER. Can. J. Chem. **37**, 1241 (1959).
20. F. H. FORZIATI, W. K. STONE, J. W. ROWEN, and W. D. APPEL. J. Res. Natl. Bur. Std. **45**, 109 (1950).
21. H. L. FRUSH and H. S. ISBELL. J. Res. Natl. Bur. Std. **41**, 609 (1946).
22. E. STUTZ and H. DEUEL. Helv. Chim. Acta, **41**, 1722 (1958).

Can. J. Chem. Downloaded from www.nrcresearchpress.com by 210.87.254.40 on 09/05/12
For personal use only.

Can. J. Chem. Downloaded from www.nrcresearchpress.com by 210.87.254.5 on 09/05/12
For personal use only.

CHEMICAL SCAVENGER PROBE STUDIES OF ATOM AND EXCITED MOLECULE REACTIVITY IN ACTIVE NITROGEN FROM A SUPERSONIC STREAM

A. FONTIJN, D. E. ROSNER, AND S. C. KURZIUS
AeroChem Research Laboratories, Inc., Princeton, New Jersey, U.S.A.

Received December 12, 1963

ABSTRACT

A quartz chemical scavenger probe has been developed to study the local composition of supersonic electrically discharged gas streams. The probe samples the central portion of a nonequilibrium jet and allows direct comparison with other local measurement techniques (e.g. differential catalytic detectors) for determining active species concentrations. Active nitrogen from a Mach 3 stream was sampled and reacted inside the probe with one of the scavenger gases NO, NH_3, or C_2H_4 at 18.8 mm Hg and at an average temperature of 500 °K. Limiting values of the NO destruction rate and the HCN production rate were observed; however, NH_3 destruction exhibited no plateau. The observed maximum rate of NO destruction was 2.1 times as large as the NO flow rate at the light titration end-point. This difference is attributed to a reaction of NO, added in excess of the titration end-point flow, with metastable electronically excited molecules formed within the discharge zone. The converging–diverging supersonic nozzle-glow discharge source used in these experiments apparently delivers metastable excited molecules to the reaction zone in a higher relative concentration than do the more conventional subsonic electrical discharge flow systems used for most previous active nitrogen studies.

INTRODUCTION

The chemistry of active nitrogen has received much attention in recent years and has been put on a sounder basis with the aid of spectroscopic and mass spectrometric techniques. While it is known that ground state, (^4S), nitrogen atoms are a major active component, interesting differences in the ratio of excited molecules to ground state atoms have been observed using active nitrogen from various sources. Thus a microwave discharge produces large quantities of vibrationally excited ground state, $X^1\sum_g^+$ (probably mainly $v = 1$), molecules (1–3), a species not observed in condensed (4) or radio-frequency (5) discharges. However, condensed discharges can apparently produce considerable amounts of electronically excited molecules (6). Since most of these observations have been made with nitrogen of similar purity under similar flow conditions, it appears that these differences are inherent to the type of discharge used, although the importance of other discharge parameters should be kept in mind.

Because of the advantages for certain experimental studies in nonequilibrium aerodynamics and chemical kinetics, a new type of high flow rate electrical discharge system has been in use in this laboratory for some time. In this apparatus (cf. Fig. 1) the products of a "high" pressure (usually above 20 mm Hg) continuous glow discharge are expanded through a converging–diverging nozzle-shaped electrode into an evacuated test section, resulting in a supersonic, activated gas jet at a translational static temperature of about 300 °K. The diameter of the jet is about equal to that of the nozzle exit diameter and its composition, in general, varies with radial position. To study active species concentrations in this environment, differential catalytic probes have been used (7). However, since every current technique for quantitative determination of the active species present in a discharged gas stream has its own inherent limitations, in practice it is necessary to apply fundamentally different techniques and to correlate the results. To this end a "chemical

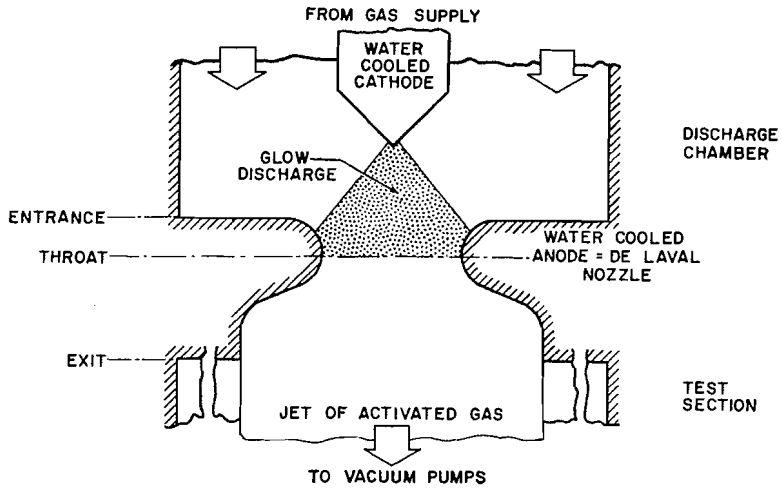

FIG. 1. Schematic of discharge apparatus.

scavenger probe" was developed which, like the catalytic probe methods used previously, allows measurement of *local* active species concentrations in the gas stream.

A chemical scavenger probe can be defined as a device which samples a gas stream containing active species (atoms, free radicals, excited species, or ions), and in which the sampled gas reacts rapidly with a "scavenger" gas to form stable products.[a] The concentration of the active species can be calculated from the amount of reaction.

This paper describes the scavenger probe and discusses the probe reactions of active nitrogen with NO, NH_3, and C_2H_4. The behavior of these reactants is relatively well known from previous studies[b] using subsonic Wood–Bonhoeffer type discharge flow systems (hereafter referred to as conventional flow systems) and they can be used to distinguish between atom and excited molecule reactivity. This work thus allows comparison of the reactivity of active nitrogen from the present electrical discharge source with that of more conventional discharges.

EXPERIMENTAL[c]

Chemical Scavenger Probe

It was undesirable to operate with high velocities within the probe, since this would have caused trapping difficulties and spatially extended reaction zones. A detached shock inlet probe (11), which consisted of a 30 mm outer diameter quartz tube (wall thickness 2 mm) with a 90° angle (cf. Fig. 2), was therefore designed. The end of the 8 cm long vertical section, the probe head, was partly blanked off, leaving an 8 mm diameter entrance orifice through which the active nitrogen jet was sampled. Immediately downstream of the probe entrance orifice was a 1 mm wide annular opening through which the secondary gas, consisting of a helium – scavenger gas mixture, was introduced. The helium served as a coolant and allowed measurement of the actual scavenger gas flow rate through the probe as described below. A thorough mixing of helium and titrant gas was obtained by passing the combined flow of these gases through a column packed with $\frac{1}{4}$ inch Berl saddles before introduction into the probe. The downstream portion of the 50 cm long horizontal section of the scavenger probe was brought outside the plasma jet test section through a vacuum tight O-ring connection. With an asbestos sleeve contained within a brass collar whose position could be closely controlled, it was possible to center the probe head with respect to the active nitrogen jet. The horizontal section of the probe ended in a 29/42 ground joint connected directly to a pyrex gas flow and analysis system.

The diameter of the supersonic jet (about 1.4 cm) was smaller than that of the flat face of the probe but

[a] *R. M. Fristrom has concurrently developed a scavenger probe of different design to study combustion flame intermediates, see refs. 8 and 9.*

[b] *For a summary of this field and its controversies see, e.g., refs. 4 and 10.*

[c] *For further details see ref. 10.*

Can. J. Chem. Downloaded from www.nrcresearchpress.com by 210.87.254.5 on 09/05/12
For personal use only.

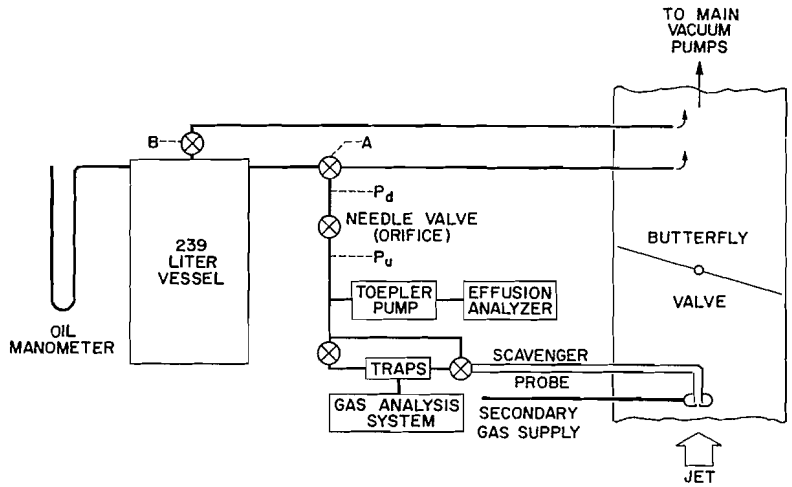

FIG. 2. Chemical scavenger probe flow system.

larger than that of the probe inlet orifice diameter by a factor of 1.7. The jet was thus stagnated by the probe and diffusely filled the test section downstream of the probe. Because of the deceleration of the gas behind the detached shock the actual region of the undisturbed jet sampled was smaller than the probe inlet opening (11) and corresponded to a central stream tube of about 2.4 mm diameter (i.e. some 3% of the jet). The probe was placed about 5 mm downstream of the nozzle exit and centered by visual observation of the nitrogen afterglow within the probe. The probe was considered properly centered when the afterglow filled the probe head. Small deviations from the centered position resulted in an unequal filling of the probe head, i.e. a beam of afterglow radiation was directed against a portion of the probe walls. During the centering operation the secondary gas used was helium without added titrant.

A 0.6 cm outside diameter stainless steel tube could be moved along the center of the scavenger probe downstream of the 90° bend through a vacuum tight O-ring packing. It contained the leads of a chromel–alumel thermocouple and was also connected to a pressure gauge. The tube was partially closed at the sensing end by a piece of quartz tubing which had a small hole, opening to the pressure tap, downstream from the thermocouple junction. The quartz served to hinder direct recombination or de-excitation on the junction. While the gas samples were taken this P,T probe was drawn out of the gas flow path.

Scavenger Probe Flow System

The scavenger probe flow system is shown schematically in Fig. 2. The effluent probe gases entering the analysis system consisted of N_2, He, unreacted scavenger gas, and reaction products. The condensables could be trapped by two consecutive cold traps and thence transferred in the conventional manner to a number of known volumes for PV measurement (using a silicone oil filled manometer) or to a demountable analysis flask. Liquid air traps were used which, for the NO experiments, were pumped down. A small coil of cobalt plated platinum wire was placed ahead of the traps to recombine O atoms formed in the reaction with NO. This procedure prevented ozone formation in the traps.

The flow rates of N_2 and He through the probe were calculated from the N_2/He ratio as determined by an effusion analyzer (see below) and the combined N_2 + He flow as determined by collection through a sonic orifice (see below) into a 239 l volume. The flow rate of scavenger gas through the probe before reaction in an active nitrogen experiment could then be calculated directly from the known scavenger–helium ratio. The difference between this flow rate and that determined by actual trapping gave the amount of scavenger destroyed by the active nitrogen. The scavenger–helium ratio was calculated from their individual metered flow rates and checked in blank experiments with the active nitrogen stream shut off.

The molecular effusion analyzer was submerged in a constant temperature water bath. It consisted of a fixed (≈250 cc) volume, out of which the gas mixture to be analyzed could effuse through a small hole into a continuously evacuated line. The pressure drop from a constant initial pressure (40 mm Hg) in the fixed volume after a certain time interval (30 min) was calibrated in terms of the N_2/He ratio. A Toepler pump was employed to fill the effusion analyzer. Gases analyzed by the effusion analyzer also contained uncondensable reaction products; however, these formed only a small fraction of the total flow and had an effect well within the limits of accuracy of the N_2/He ratio determinations (cf. Table I).

Upstream from the 239 l volume was a needle valve with which the flow rate through the probe could be adjusted (cf. Fig. 2). The pressure upstream, P_u, and downstream, P_d, from this "valve orifice" could be measured. With stopcock A open to the vacuum pump line the relation between P_u and P_d was such that

Can. J. Chem. Downloaded from www.nrcresearchpress.com by 210.87.254.5 on 09/05/12
For personal use only.

Can. J. Chem. Downloaded from www.nrcresearchpress.com by 210.87.254.5 on 09/05/12
For personal use only.

TABLE I

Scavenger probe observations: discharge potential 930 V; discharge current 630 mA; total system N_2 flow 7.74×10^{-3} mole s^{-1}; total system He flow 2.45×10^{-3} mole s^{-1}

N_2 flow 10^{-4} mole s^{-1}	He flow 10^{-4} mole s^{-1}	He flow / (He + N_2) flow	Probe pressure (mm Hg)	Probe temp. (°K)	Scavenger	Scavenger inlet flow 10^{-6} mole s^{-1}	Scavenger destruction 10^{-6} mole s^{-1}
2.57	4.45	0.634	18.10	498	NO	5.94	3.82
2.57	4.45	0.634	18.10	498	NO	3.07	3.07†
2.57	4.56	0.640	18.10	513	NO	8.80	4.70
2.60	4.63	0.641	18.25	502	NO	11.09	4.73
2.67	4.54	0.630	18.25	506	NO	6.92	3.62
2.68	4.79	0.609	18.50	499	NO	17.68	6.51
2.71	4.64	0.631	18.35	500	NO	11.71	5.42
2.74	4.67	0.631	18.40	491	NO	24.55	6.54
2.74	4.67	0.631	18.40	491	NO	3.01	3.01†
2.66	4.80	0.643	18.80	528	NO	34.4	6.70
2.66	4.80	0.643	18.80	528	NO	3.13	3.13†
2.74	4.47	0.620	18.28	523	NH_3	7.50	2.70
2.63	4.76	0.645	18.28	534	NH_3	11.15	3.26
2.55	4.56	0.641	18.07	498	NH_3	21.89	6.17
2.6*	4.6*	0.63*	18.42	497	NH_3	57.9	18.2
2.6*	4.6*	0.63*	18.45	534	NH_3	41.5	10.6
2.62	4.46	0.625	18.09	509	C_2H_4	3.40	0.969‡
2.51	4.48	0.641	18.05	499	C_2H_4	4.95	0.947‡
2.47	4.54	0.646	17.99	478	C_2H_4	8.35	0.933‡
Avg. 2.6	4.6	0.63	18.3	503			

*The He/(N_2 + He) ratio was not determined in these experiments. Instead, the average value over all other experiments was taken as a basis for the calculation of the individual N_2 and He flows.

†The values given are the light titration end-points, not actual destruction measurements.

‡The values given pertain to HCN production, not ethylene destruction.

the flow through the valve orifice was sonic. When stopcock A was turned so that the gas streamed into the previously evacuated calibrated 239 l volume, the flow rate through the valve orifice remained the same as before, as long as the flow through it was sonic. Before P_d reached a value for which this condition was no longer fulfilled, stopcock A was turned back again to the pump line. Measurement of the final pressure in the 239 l vessel and of the collection time gave the flow rate. At the flow rates used, the collection times were about 1 to 5 min. Stopcock B allowed the vessel to be re-evacuated for succeeding measurements.

General Apparatus

A Stokes model 1712 mechanical booster – vacuum pump combination of nominal capacity 2500 c.f.m. was used. Static pressures were measured with Bourdon type absolute pressure gauges. Flow rates of nitrogen and helium were measured with sonic orifice meters and titrant flows were measured by rotameters. The axisymmetric water-cooled copper nozzle, which served as the anode of the glow discharge, had an exit diameter of 1.36 cm and a throat diameter 0.657 cm (cf. Fig. 1). For a specific heat ratio $c_p/c_v = 1.4$ the design exit Mach number was about 3. The distance between the tip of the glow discharge cathode (a coaxial copper rod) and the nozzle entrance was 6.8 cm.

Materials

Airco prepurified nitrogen, U.S. welding helium, Matheson c.p. ethylene, and anhydrous ammonia were used without further purification. Matheson nitric oxide was freed of NO_2 by passage through a column of 8–20 mesh Fisher Caroxite. The oil manometers were filled with Dow-Corning 702 silicone oil. Reagent grade chemicals were used.

Experimental Conditions

The N_2 flow rate into the system was 7.74×10^{-3} mole s^{-1}; an electrical discharge through it was operated at a potential of 930 V and a current of 630 mA. The pressure in the discharge region was 38.5 ± 0.5 mm Hg and the test section pressure, which was approximately that of the undisturbed jet, was 1.00 ± 0.02 mm Hg. The He (secondary gas) flow into the probe was 2.45×10^{-3} mole s^{-1}. From Table I it may be seen that 3.4% of the total N_2 flow was sampled and that 18.8% of the premixed secondary gas – titrant flow went through the probe to the trapping system, the rest spilling out around the probe periphery, thereby minimizing any thermal problems which might have been associated with the direct impingement of the active nitrogen jet upon the otherwise uncooled probe. Possible errors associated with this spillage are discussed below. The interior probe walls were poisoned with phosphoric acid, and the whole flow system downstream from the sonic orifice meters in the N_2 and He lines was pumped out for periods of at least 16 h before an experiment. Measurements were made after discharge stabilization periods of at least 30 min.

Active nitrogen sucked in at the probe entrance orifice must initially have been at a temperature close to that of the shocked gas; i.e. $\approx$ 900 °K. The secondary gas entered the probe at a temperature somewhat above room temperature, since heat must have been absorbed from the inlet region heated by the shocked gas. Reaction occurred when primary and secondary gas mixed. The probe temperature given in Table I was measured at the 90° bend in the probe and thus represents an average temperature, which may be somewhat lower than the actual average reaction temperature since most of the reaction occurred in the probe head upstream from the 90° bend. Downstream from the 90° bend the gas temperature dropped to about 300 °K within a few cm. The average gas velocity in the probe at 503 °K was 2.4 m s^{-1}.

NO Destruction Experiments

To determine the total amount of undecomposed NO, present in the trapped products as NO and $NO_2 + N_2O_4$, a new method was developed. The trapped products of the NO reaction were transferred to a known volume V_1 and the pressure P_1 (< 10 mm Hg) was measured at room temperature, from which X, the number of moles in V_1, was calculated. The gas was then expanded into a second known volume, V_2, which included V_1 and was approximately $4V_1$. The pressure was now P_2 and Y moles of gas were present. From these data and the equilibrium constant $K_p = (P_{NO_2})^2/P_{N_2O_4}$, the amount of undecomposed NO was calculated in the following manner.[d] If a is the number of moles of NO and b the number of moles of $NO_2 + N_2O_4$, counted as NO_2, per mole of NO, then $a(1 + b)$ is the equivalent amount of undecomposed NO. Defining further α_1 and α_2 as the fraction of N_2O_4 dissociated in volume V_1 and V_2 respectively, and

$$Q \equiv \frac{4P_1}{K_p} \frac{Y - X}{X}$$

we obtain

$$[A] \qquad a(1 + b) = \frac{(1 - \alpha_1)Y + (1 - \alpha_2)X}{\alpha_2 - \alpha_1},$$

in which

$$[B] \qquad \alpha_2 = \alpha_1\{1 + [\alpha_1/(1 - \alpha_1)]Q\}$$

[d]*The equilibrium data of ref. 12 together with* $\Delta H(2NO_2 \rightarrow N_2O_4) = -13.9$ *kcal mole*$^{-1}$ *were used.*

Can. J. Chem. Downloaded from www.nrcresearchpress.com by 210.87.254.5 on 09/05/12
For personal use only.

and

$$[C] \qquad \frac{\alpha_1}{1-\alpha_1} = \frac{-1 + \{[V_2/(V_1Q)][Q + (V_2/V_1) - 1]\}^{1/2}}{Q + (V_2/V_1)}.$$

The method was checked by introducing known amounts of NO into the system followed by partial oxidation of the NO and agreement was found to be within 2%. The developed method involves, admittedly, considerable calculation but has the advantage of being experimentally faster than the conventional method of total oxidation of the trapped sample, followed by PV determination of the equivalent amount of NO as $NO_2 + N_2O_4$. For one experiment the equivalent amount of NO was determined both ways. The agreement was again better than 1% which also showed that less than 1 mole % of the condensables could have been substances other than NO and NO_2. The absence of N_2O in the reaction products is in agreement with the results of earlier workers (13, 14). The PV measurements also yield directly the amount of nonoxidized NO in the sample since

$$[D] \qquad a = \frac{(1+\alpha_2)X - (1+\alpha_1)Y}{\alpha_2 - \alpha_1},$$

which makes this method also applicable to the NO_2 titration of O atoms by the cleanup method (15).

NH_3 Experiments

The amount of undestroyed NH_3 was analyzed either by PV measurement or by dissolving into excess 0.1 N H_2SO_4 followed by back titration with 0.1 N KOH. Both methods agreed to within 2%. Hydrazine was analyzed by the method of Freier and Resch (16). Its production did not exceed 0.005% of the amount of NH_3 destroyed. These results confirm those of previous workers who showed that N_2 and H_2 were the only major reaction products (17, 18),

Ethylene Experiments

The trapped reaction products of the ethylene reaction were distilled at temperatures equal to or lower than 250 °K (the melting point of solid CCl_4, with which the traps were covered during the distillation) into a removable analysis flask containing about 25 cc of frozen 1 N KOH solution. This solution was next partially melted by submerging the bottom part of the flask in hot water and the still solid HCN was then dissolved in it.[e] In this way polymerization of HCN was prevented. The resulting KCN solution was then titrated by the Liebig–Deniges method (19) using standard 0.1 N $AgNO_3$.

RESULTS AND DISCUSSION

NO Light Titration and NO Decomposition

The results of the NO experiments are shown in Fig. 3, based on the data given in Table I. The NO light titration end-point, corresponding to complete consumption of the N atoms (20, 21)[f,g] by

$$[1] \qquad N + NO \rightarrow N_2 + O,$$

was seen as a series of blue and whitish-green flashes following each other in rapid succession through the full length of the probe. At NO flow rates slightly lower or higher (about ±1–2%) than that at the light titration end-point the blue or the whitish-green glow respectively, filled the probe. These glows were readily visible in a darkened room. Earlier work (5, 24) had shown that at the light titration end-point all the NO added is decomposed. It seems allowable therefore to include the results of the titration experiments in the NO destruction plot as corresponding to 100% destruction. As shown in Fig. 3 they fall on a straight line with the other NO destruction values below the destruction plateau but above the titration end-point, which in itself also indicates complete NO destruction at this point. The data show a limiting amount of NO destruction, i.e. a

[e] *This method was described to us by Dr. A. N. Wright of Dr. Winkler's laboratory at McGill University.*

[f] *See below for a discussion of the merits of the titration technique as a quantitative measure of N-atom flow.*

[g] *The long-lived metastables $N(^2P)$ and $N(^2D)$ like $N(^2S)$ may react with NO in a spin-allowed reaction and may be expected to have been consumed completely at the titration end-point. These atoms, located 2.38 and 3.58 eV, respectively, above the ^4S state, have been observed in active nitrogen (22, 23). Their relative concentration should, however, be small in pure nitrogen discharges (22).*

Can. J. Chem. Downloaded from www.nrcresearchpress.com by 210.87.254.5 on 09/05/12
For personal use only.

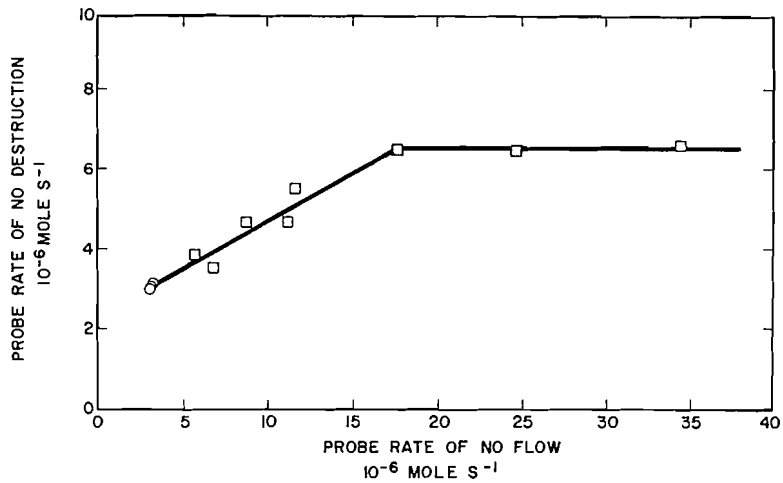

FIG. 3. NO experiments. Probe rate of N_2 flow: 2.6×10^{-4} mole s^{-1}; ○, NO light titration □, NO destruction.

plateau 2.1 times as high as the NO light titration end-point flow.[h] To explain this difference we postulate the presence of an excited molecule, N_2^*, which causes a reaction of the type

[2] $$NO + N_2^* \rightarrow \text{NO disappearance.}$$

Reaction [2] could result simply in the dissociation of NO followed by reaction [1], or be more complicated,[i] but in either case two NO molecules would ultimately disappear because of reaction [2]. From these scavenger probe data the N_2^* flow is thus 0.55 times the N-atom flow, as inferred from the NO light titration.

Reaction [2] has to be slow compared to [1] since $[N_2^*]$ is comparable to [N] and the reaction takes place with NO flows in excess of that at the titration end-point.[j] Had reaction [2] been of a rate comparable to that of [1] it would merely have increased the NO flow needed to obtain the titration end-point. It has been suggested (4, 13) that (i) large differences (factors of 1.4–2.4) observed in previous work between the NO titration end-point flow and the HCN formation plateau from ethylene are due to a reaction between excited molecules and NO and that (ii) the HCN formation plateau is a quantitative measure of the N-atom flow. Although further indirect evidence (27) in favor of this idea has been obtained, there are rather strong arguments[k] against it. However, even if the HCN production were a true measure of the N-atom flow, then to falsify the NO light titration appreciably an excited state of N_2 other than N_2^* must be involved, i.e. an N_2^{**} which reacts with NO much faster than N_2^*, the latter being responsible for the NO destruction beyond the light titration end-point.

[h] *In only one other case (4) has it been reported that under certain discharge conditions the limiting amount of* NO *destruction exceeded the light titration end-point flow. In that work the observed ratio was, at most, 1.25.*

[i] *Reactions of this nature have been discussed (25, 26). Although a reaction such as suggested by Wright and Winkler (25) or simple* NO *dissociation could not falsify the* NO *light titration (26), such reactions could be responsible for the destruction of* NO *added in excess of the light titration end-point flow with which the present discussion is concerned.*

[j] *Only at most a few percent of the* NO *added beyond the titration end-point is consumed (40) by* $O + NO + M \rightarrow NO_2 + M$ *since this reaction is followed by the much faster reaction* $O + NO_2 \rightarrow NO + O_2$.

[k] *For arguments against the* NO *titration indicating too high an atom concentration see refs. 1, 26, 28, 29.*

Can. J. Chem. Downloaded from www.nrcresearchpress.com by 210.87.254.5 on 09/05/12
For personal use only.

Can. J. Chem. Downloaded from www.nrcresearchpress.com by 210.87.254.5 on 09/05/12
For personal use only.

*Nature and Origin of N_2**

To obtain an idea of the nature of the N_2* postulated above the following residence and collision time calculations have to be considered. It took a given portion of the gas about 10^{-5} s to travel from the exit of the electrical discharge region (the nozzle throat) to the shock front, 10^{-4} s to pass from there through the probe entrance orifice during which time some initial reaction occurred, and 3×10^{-2} s from there to the 90° bend in the probe. An excited molecule would suffer, respectively, about 10^2, 10^4, and 3×10^6 collisions with N_2 during these periods. Mixing was judged complete within the probe head, since in the work with ethylene, discussed below, the characteristic blue reaction zone luminescence from the reaction $N + C_2H_4$, which is two to three orders of magnitude slower (e.g. ref. 30) than reaction [1] (28, 29, 31), did not extend beyond the 90° bend. The time required for most of the N_2* to react implies that it be a relatively long-lived, i.e. a metastable, molecule if it was formed inside the discharge region. The amount of N_2 formed by atom recombination between the nozzle throat and before complete atom consumption by reaction [1] was calculated [l] to be less than 10% of the initial atom concentration, and the heterogeneous recombination was estimated to be even smaller.[m] Both mechanisms are quite inadequate to explain the large N_2* concentration observed. It may thus be concluded that N_2* is predominantly or exclusively a metastable molecule (or a mixture of metastable molecules) formed in the electrical discharge region. No conclusion regarding the relative importance of possible mechanisms of N_2* formation in the discharge region (e.g. excitation by electron bombardment or atom recombination) can be made on the basis of the present results.

Several authors have recently discussed the various metastable states of nitrogen that could contribute to the chemical reactivity of active nitrogen (e.g. refs. 4 and 6). Our results do not make it possible to state definitely which excited state or states are involved in reaction [2] and such states as the $A^3\sum_u^+$, $^3\Delta_u$, and $a'^1\sum_u^-$ all have to be considered, as does $a^1\Pi_g$ state. The latter is too short-lived to have been of importance in previous conventional subsonic flow system studies (6)—where the average gas molecule typically was transported from the discharge to the reaction zone in times of the order of 10^{-2} s—but it may well cause considerable reaction in the present system. Such an assumption is not contradictory to reaction [2] being slow compared to [1] since the latter only requires about 10 collisions to occur. The high relative concentration of N_2* in the present system may be peculiar to the type of electrical discharge used—and the conditions under which it is operated—or to the faster delivery of discharge products to the reaction zone. For vibrationally excited $N_2(X^1\sum_g^+)$ to be involved in reaction [2], $v \geqslant 27$ would be required. It appears somewhat unlikely that many such highly vibrationally excited molecules would be present in the reaction zone but this possibility cannot be excluded entirely. Finally, it should be remarked that ion-initiated reactions, although highly energetic, can be discounted as major sources of NO destruction, since previous work (38, 39) at this laboratory had shown that the ion concentration in the free jet is less than 1% of the atom concentration.

[l] *A value for k in the expression* $-d[N]/dt = k[N]^2[M]$ *of* 3×10^{-32} *cc*^{2} *molecule*$^{-2}$ *s*$^{-1}$ *was used, which represents a reasonable upper limit. See, e.g., refs. 6, 32, 33, 34, 35.*

[m] *A wall recombination coefficient* $\gamma = 3 \times 10^{-4}$, *which represents an upper limit (33, 36, 37), was used in this calculation. In fact wall losses should have been considerably smaller than those calculated since, over most of the probe head, the regions near the probe walls were apt to be much richer in scavenger gas and helium than the central region of the flow. Reaction with the scavenger gas would thus have prevented most of the surviving* N *atoms from reaching the wall, since the rate of reaction [1] is* 10^3 *to* 10^4 *times the corresponding rate for wall reactions in the probe head.*

NH_3 Experiments

The addition of NH_3 did not extinguish the afterglow in the probe but diminished its intensity. The NH_3 reaction does not appear to involve N atoms (6, 17, 41). From Table I it may be seen that the amount of NH_3 reaction was much higher than that of any of the other reactants investigated and no destruction plateau could be observed for the NH_3 inlet flow rates used. Based on N_2^* concentrations estimated from the NO experiments, at least about 11 NH_3 molecules are destroyed for every N_2^* present. No reasonable chain mechanism seems to be capable of explaining these results on the basis of an N_2^* reaction alone, and it is therefore quite possible that an excited molecule $N_2^{\ddagger}$ incapable of NO destruction is responsible for most of the NH_3 decomposition observed. The same arguments as were given for N_2^* imply that $N_2^{\ddagger}$ molecules would be predominately metastables formed in the electrical discharge zone. Another explanation of these observations, suggested to us by the referee, is photodecomposition of NH_3 by light emitted from the discharge. Although this would clarify the apparent absence of a destruction plateau, there is no good precedent for it. A more definitive explanation of the ammonia destruction results must await further work.

HCN Formation

The results of Table I show that an ethylene flow – independent HCN production plateau is obtained. The observed flow rate ratio (NO light titration end-point)/(HCN production plateau) may be seen to be 3.2. This value should be compared to a ratio of 2.4 obtained in conventional flow system work at 16 mm Hg (13). The present result must be regarded as preliminary however, since it has been observed in conventional flow system studies that the height of the HCN production plateau can, depending upon flow conditions (4), increase with temperature up to about 520 °K (13). We have not established whether the observed HCN plateau was temperature-independent. In the absence of such data and because of the unresolved controversy between the HCN production plateau and the NO light titration technique as a measure for the atom concentration, the scavenger probe results reported here may be taken to indicate a mole fraction of nitrogen atoms in the sampled portion of the jet of from 0.37 to 1.18%, the higher value (inferred from the NO light titration) being the more likely one.

Absence of Diffusional Separation Effects

Two possible errors arising from the partial spillage of helium – scavenger gas mixture in the probe inlet region have to be considered in some detail. While the procedure used for calculating scavenger gas destruction was explicitly chosen because it allows for the possibility of such spillage, a basic assumption made here is that the helium/scavenger gas composition ratio in the reaction zone is negligibly different from the corresponding mixture ratio in the secondary gas supply system. This would not be the case if diffusional separation occurred in the probe inlet region because of the increased mobility of helium atoms through active nitrogen. Secondly, it has been assumed that the N_2^*/N ratio inferred from the nitric oxide experiments is negligibly different from that actually existing in the probe inlet region in the absence of scavenger gas flow and is not the result of preferential loss of N atoms from the system due to their higher mobility.

With regard to the first of these possibilities, the very fact that the nitric oxide data plotted in Fig. 3 exhibit a horizontal plateau constitutes experimental proof that helium – scavenger gas diffusional separation was negligible (10); i.e. if the concentration ratio in the reaction zone differed from that in the supply system in a manner consistent with the relative diffusion coefficients, then a horizontal plateau could never be observed. As

Can. J. Chem. Downloaded from www.nrcresearchpress.com by 210.87.254.5 on 09/05/12
For personal use only.

corollaries, it also follows that the difference between the NO titration end-point and NO peak destruction flow rates could not be the result of such a process; nor could the observed lack of an apparent NH_3 destruction plateau be the result of this process.

While the experimental data cannot be used directly to rule out a diffusional enrichment of the N_2^*/N ratio by a Fick mechanism, introduction of reasonable values for the fluid dynamic and transport parameters associated with the flow field in the inlet region of the probe revealed that the concentrations of either N atoms or N_2^* in the reaction zone could not possibly differ from their respective values behind the shock wave by more than a few parts per hundred (10). Order of magnitude estimates also led to the conclusion that N/N_2 separation by thermal and pressure diffusion was negligible under the experimental conditions investigated—thereby ruling out the sampling error recently discussed by Reis and Fenn (42), which can become significant for detached shock microprobes in supersonic streams.

CONCLUDING REMARKS

Our results show that the maximum rate of NO destruction by active nitrogen can be considerably larger than the NO flow rate at the light titration end-point. This is attributed to the presence of excited molecules, N_2^*, which react with NO too slowly to alter the light titration end-point measurably. It thus appears that the electrical discharge–supersonic nozzle source used in this work delivers active nitrogen to the reaction zone with a higher N_2^*/N ratio than observed in conventional subsonic discharge flow systems. The chemical scavenger probe method developed here is useful for quantitative studies of local concentrations of active species in nonequilibrium gas streams (43) and may also be employed to distinguish between various excited states of the same molecule.

ACKNOWLEDGMENTS

We thank the Propulsion Research Division of the Air Force Office of Scientific Research for their interest and support under Contract AF 49(638)-300. We also thank R. A. Ryan and G. R. Smith for their assistance with the laboratory work and the experimental design respectively, and Dr. H. F. Calcote for his helpful criticism.

REFERENCES

1. J. E. Morgan and H. I. Schiff. Can. J. Chem. **41**, 903 (1963).
2. F. Kaufman and J. R. Kelso. J. Chem. Phys. **28**, 510 (1958).
3. K. Dressler. J. Chem. Phys. **30**, 1621 (1959).
4. A. N. Wright, R. L. Nelson, and C. A. Winkler. Can. J. Chem. **40**, 1082 (1962).
5. M. A. A. Clyne and B. A. Thrush. Trans. Faraday Soc. **57**, 69 (1961).
6. H. B. Dunford. J. Phys. Chem. **67**, 258 (1963).
7. D. E. Rosner. A. S. M. E. J. Heat Transfer, **84**, 386 (1962).
8. R. M. Fristrom. Science, **140**, 297 (1963).
9. R. M. Fristrom. Ninth Symposium (International) on Combustion. Academic Press, Inc., New York. 1963. p. 560.
10. A. Fontijn, D. E. Rosner, and S. C. Kurzius. Chemical scavenger probe determinations of atom and excited molecule concentrations in nonequilibrium supersonic streams of active nitrogen. Aero-Chem TP-40; ASTIA AD 296 398; NASA N63-12804. August, 1962.
11. A. H. Shapiro. The dynamics and thermodynamics of compressible fluid flow. Vol. 1. The Ronald Press Co., New York. 1954. pp. 147–151.
12. B. N. Srivastava and A. K. Barua. J. Chem. Phys. **35**, 329 (1961).
13. G. J. Verbeke and C. A. Winkler. J. Phys. Chem. **64**, 319 (1960).
14. G. B. Kistiakowsky and G. G. Volpi. J. Chem. Phys. **27**, 1141 (1957).
15. L. Elias and H. I. Schiff. Can. J. Chem. **38**, 1657 (1960).
16. R. Freier and G. Resch. Z. Anal. Chem. **149**, 177 (1956).
17. G. R. Freeman and C. A. Winkler. J. Phys. Chem. **59**, 371 (1955).
18. J. K. Dixon and W. Steiner. Z. Physik. Chem. B, **17**, 327 (1932).
19. I. M. Kolthoff and E. B. Sandell. Textbook of quantitative inorganic analysis. The Macmillan Co., New York. 1952. pp. 458, 546.

Can. J. Chem. Downloaded from www.nrcresearchpress.com by 210.87.254.5 on 09/05/12
For personal use only.

20. F. KAUFMAN and J. KELSO. J. Chem. Phys. **27**, 1209 (1957).
21. P. HARTECK, R. R. REEVES, and G. MANNELLA. J. Chem. Phys. **29**, 608 (1958).
22. S. N. FONER and R. L. HUDSON. J. Chem. Phys. **37**, 1662 (1962).
23. J. F. NOXON. J. Chem. Phys. **36**, 926 (1962).
24. J. E. MORGAN, L. ELIAS, and H. I. SCHIFF. J. Chem. Phys. **33**, 930 (1960).
25. A. N. WRIGHT and C. A. WINKLER. J. Phys. Chem. **66**, 1747 (1962).
26. R. A. BACK and J. Y. P. MUI. J. Phys. Chem. **66**, 1362 (1962).
27. A. N. WRIGHT and C. A. WINKLER. J. Phys. Chem. **67**, 172 (1963).
28. J. T. HERRON. J. Chem. Phys. **35**, 1138 (1961).
29. L. F. PHILLIPS and H. I. SCHIFF. J. Chem. Phys. **36**, 1509 (1962).
30. E. M. LEVY and C. A. WINKLER. Can. J. Chem. **40**, 686 (1962).
31. M. A. A. CLYNE and B. A. THRUSH. Proc. Roy. Soc. Ser. A, **261**, 259 (1961).
32. C. MAVROYANNIS and C. A. WINKLER. Can. J. Chem. **39**, 1601 (1961).
33. R. A. BACK, W. DUTTON, and C. A. WINKLER. Can. J. Chem. **37**, 2059 (1959).
34. T. MARSHALL and R. A. KAWCYN. Phys. Fluids, **5**, 1657 (1962).
35. J. T. HERRON, J. L. FRANKLIN, P. BRADT, and V. M. DIBELER. J. Chem. Phys. **30**, 879 (1959).
36. R. A. YOUNG. J. Chem. Phys. **34**, 1292 (1961).
37. R. KELLY and C. A. WINKLER. Can. J. Chem. **37**, 62 (1959).
38. D. E. ROSNER. Diffusion, heat exchange and chemical surface catalysis in flow systems. Ph.D. Thesis, Princeton University, Princeton, N.J. 1960. University Microfilms, Ann Arbor, Michigan. Order 61-4825.
39. J. B. WILKINSON. Unpublished results.
40. J. T. HERRON and H. I. SCHIFF. Can. J. Chem. **36**, 1159 (1958).
41. A. N. WRIGHT and C. A. WINKLER. Can. J. Chem. **40**, 5 (1962).
42. V. H. REIS and J. B. FENN. J. Chem. Phys. **39**, 3240 (1963).
43. D. E. ROSNER, A. FONTIJN, and S. C. KURZIUS. AIAA J. **2**, 779 (1964).

Can. J. Chem. Downloaded from www.nrcresearchpress.com by 210.87.254.5 on 09/05/12
For personal use only.

Can. J. Chem. Downloaded from www.nrcresearchpress.com by 210.87.254.42 on 09/05/12
For personal use only.

THE PHOTOLYSIS OF FORMALDEHYDE, FORMALDEHYDE-d_2, AND THEIR MIXTURES[1,2]

M. VENUGOPALAN[3] AND K. O. KUTSCHKE
Division of Pure Chemistry, National Research Council, Ottawa, Canada

Received June 29, 1964

ABSTRACT

It has been verified that H atoms are formed when formaldehyde vapor at 300 °C is illuminated by the 3 655 Å group of the mercury arc. Isolation of the group of lines was achieved by a combination of glass and solution filters. This observation gives further support to the "high" value of D(H—CO).

It was found that D_2CO also is predissociated following absorption at this wavelength. This observation is not in agreement with predictions based on purely spectroscopic studies of these molecules.

INTRODUCTION

The technique used by Klein and Schoen (1) to locate the long wavelength limit for the predissociation of formaldehyde involved the photolysis at 300 °C of mixtures ($\sim$ 300 mm total pressure) of H_2CO and D_2CO at various wavelengths in the near ultraviolet. The detection of HD among the products at some wavelength indicated the formation of atoms in the primary process which then initiated the long chain reaction known (2) to occur for these conditions of temperature and concentration. It was found that the ratio $r = [HD]^2/[H_2][D_2]$ was near the equilibrium value of four and was independent of exciting wavelength in the region 3 100 to 3 700 Å. It was concluded that the quantum at 3 650 Å provided sufficient energy ($\sim$ 78 kcal/mole) to break the first C—H bond in H_2CO. This, together with the thermochemical datum (3), $H_2CO \rightarrow 2H + CO$, ΔH = 105.5 kcal/mole, provided a minimum value for D(H—CO) near 27 kcal/mole. The value of D(H—CO) has been in dispute for some time (1, 4–8).

The evidence of the predissociation limit has been questioned (4–6) on the basis that light of shorter wavelength might have been present in the output of the monochromator used (1). An attempt was made several years ago (9) to verify the existence of predissociation following absorption of the 3 655 Å group of the mercury arc spectrum; solution filters were used to isolate the 3 130 Å or 3 655 Å groups from the light source. Indeed, HD was observed in experiments similar to those described below when excitation was by the 3 655 Å group, but the value of r was near 1 at this wavelength and near 6 at 3 130 Å. Values of $r > 4$ are not compatible with the usual chain mechanism. It was thought that the low total pressures used in that work (9) (near 10 mm) favored unknown surface effects which led to the inconsistent value of r. Consequently the interpretation to be applied to that work is not straightforward and the present work was undertaken to obtain data at higher pressures where surface effects would be less favored.

EXPERIMENTAL

Monomeric formaldehyde was generated by the method of Spence and Wild (10) from well dried paraformaldehyde. Fully deuterated paraformaldehyde (Merck, Sharpe and Dohme, Montreal) was treated similarly. The individual species were stored at −80 °C, except when samples were taken for experiments;

[1]*Issued as N.R.C. No. 8116.*
[2]*Presented at the 47th Annual Conference, Chemical Institute of Canada, Kingston, Ontario, June 1–3, 1964.*
[3]*National Research Council Postdoctoral Fellow, 1961–1962. Present address: Department of Chemistry, Royal Military College, Kingston, Ontario.*

after storage for a few weeks, it was necessary to warm the storage ampoule above room temperature to generate sufficient vapor.

Those parts of the vacuum apparatus with which aldehyde made contact were maintained at ~ 115 °C. An air thermostat at that temperature contained a glass diaphragm pressure gauge, used as a null device, a glass impeller to circulate the mixed aldehydes through the reaction vessel, the quartz reaction vessel (10 cm long, 5 cm diameter) which was provided with additional heating to maintain it near 300 °C, and several metal valves (Hoke type 411 or 413). The mixture of carbon monoxide and the isotopes of hydrogen were separated at −196 °C, measured in a gas burette, and analyzed by mass spectrometry or gas chromatography (11).

The light source was a medium pressure mercury arc (Hanovia S-500) whose output was rendered nearly parallel. The 3 130 Å group was isolated with the combination recommended by Hunt and Davis (12) and the 3 655 Å group with the combination described by Kasha (13). Both in this work and that attempted earlier (9) the concentration of the "cn" dye in the Kasha filter (sometimes used as the perchlorate rather than the iodide) was increased to 1 g/l in order to decrease the transmission at 3 340 Å to values unobservable with a Cary recording spectrophotometer. An attempt was made to photolyze acetone (67 mm) with the light passed by the 3 655 Å filter. No absorption could be detected and the amount (~ 0.3 μmole) of noncondensable gases found after an exposure for 96 h at 141 °C was no larger than that produced by degassing from the walls of the vacuum system for a similar time.

Fractional absorptions were measured with an RCA 935 phototube coupled to a Keithley Electrometer (Model 210). Fractional absorptions less than 5% are subject to an instrumental error approaching 100% of the measured value. The output of the phototube was calibrated in absolute units of intensity by the photolysis of azomethane at 125 °C; Φ_{N_2} was taken as unity at both wavelengths (14). Photolysis of acetone at 125 °C provided an additional check at 3 130 Å; it agreed within 10%.

In most experiments with pure H_2CO, neutral density filters were used to adjust the incident intensity to values such that I_a was similar at 3 130 Å and 3 655 Å. Experiments with the mixtures also employed a similar adjustment but this was not done in experiments with pure D_2CO.

It was demonstrated that synthetic mixtures of H_2 and D_2 were unchanged after storage for several hours in the reaction system, that no equilibration of HD could be detected after similar treatment, and that mixtures of H_2 and CO could be recovered quantitatively.

RESULTS AND DISCUSSION

Data from several experiments are given in Tables I and II. The ratio of carbon monoxide to hydrogen is greater than unity as was also observed earlier with this system (1, 9). The cause of the deviation from unity is not known but, in view of the long chains involved for these conditions (2), it is not likely to be the result of the occurrence of another primary process which produces carbon monoxide but not hydrogen. The data on the photolysis of the mixtures at low pressure and on the thermal reaction demonstrate the difficulties encountered in attempts to reproduce and to interpret the data taken earlier (9).

The scatter in the observed fractional absorption of H_2CO at 3 655 Å presumably originates in instrumental error. Quantum yields calculated from these measurements are subject to similar uncertainties. An extinction coefficient near 0.1 $(\text{mole/l})^{-1}$ cm^{-1} (decadic logarithms) can be calculated; this is in reasonable agreement with 0.07 $(\text{mole/l})^{-1}$ cm^{-1} reported by Norrish and Kirkbride (15) at 100 °C. A somewhat larger value is expected at the higher temperature of this investigation since absorption at 3 655 Å is in the temperature-sensitive α-band of formaldehyde (16).

The much larger fractional absorption of D_2CO at 3 655 Å could be measured more precisely and presumably is a consequence of the near coincidence of the α-band of D_2CO, located by Brand (17) at 3 653 Å, with one of the components of the 3 655 Å group of the mercury arc. Moreover, the ν_4 and ν_6 frequencies in the $^1A_1$ ground state of D_2CO are lower than are the analogous frequencies of H_2CO (16). Enhancement of the absorption by the latter effect alone is insufficient to account for difference observed in the fractional absorption of the two species. It might also be noted that a band of the $^3A_1 \leftarrow {}^1A_1$ system of D_2CO lies nearby, 3 641 Å (8), but the absorption due to this transition is

Can. J. Chem. Downloaded from www.nrcresearchpress.com by 210.87.254.42 on 09/05/12
For personal use only.

TABLE I

Photolysis of formaldehyde or formaldehyde-d_2 at 300 ± 10 °C

$I_0 \times 10^{-11}$ (quanta/cc s)	Absorption (%)	Time (min)	P (mm)	H_2 or D_2* (μmole)	CO* (μmole)	Φ*,†
H_2CO, 3 130 Å						
22.0	52.1	15	312	21.1	24.6	62
				—	—	—
5.9	54.7	15	316	10.1	11.6	105
				8.9	—	92
8.7	47.3	15	252	12.3	17.5	100
				9.5	—	78
10.7	51.8	15	300	11.8	14.5	71
				10.6	—	64
6.6	52.4	15	305	9.2	12.9	89
				9.2	—	89
3.5	54.6	15	302	5.9	9.6	104
				5.9	—	104
H_2CO, 3 655 Å						
133	4.2	60	306	16.9	18.0	26
				—	—	—
210	2.6	60	321	17.3	18.3	26
				16.5	—	25
249	4.4	15	302	5.4	9.5	16
				5.2	—	16
233	2.4	15	302	5.3	8.9	32
				5.1	—	31
205	2.7	30	302	10.8	18.3	33
				10.4	—	32
D_2CO, 3 130 Å						
27.7	57.1	15	262	9.0	12.2	19
				9.4	—	20
3.0	71.1	15	300	2.8	4.7	48
				2.9	—	45
D_2CO, 3 655 Å						
277	22.0	15	288	11.2	17.6	$6._2$
				12.0	—	$6._8$
233	22.6	15	300	7.8	12.7	$5._4$
				9.5	—	$6._3$

*Two analyses are given for each experiment. The first analysis is that obtained by mass spectrometry in which the amount of each component could be estimated from the mass spectrum and measured sensitivities of each of the components. The second analysis was done by gas adsorption chromatography (11) which yielded only values for the amounts of the isotopes of hydrogen present in the mixture. For many of the experiments the results quoted are the average of two or more analyses by each of the two analytical methods. A value of Φ was calculated from the results of each kind of analysis.

† Φ represents the quantum yield for the formation of H_2 or D_2, as applicable.

so weak that it probably would not be detected by the present apparatus, nor is any such absorption likely to have given rise to a significant fraction of the photodecomposition.

The fractional absorption of the mixtures (Table II) is close to that expected from the amounts of the two components present.

The interpretation of the fractional absorption, and thus also of the quantum yields determined from them, is made more uncertain by the fact that the three somewhat broadened lines of the 3 655 Å group are absorbed in the relatively sharp rotational lines of the α-band. At lower temperature and pressure, these are resolvable at least to 0.1 cm^{-1} (8, 18, 19) and possibly show only Doppler broadening (0.03 cm^{-1} for H_2CO at 300 °C); of course, some further broadening is expected for the present experimental conditions. In calculating quantum yields, it has been assumed that none of the rotational lines show complete absorption. If complete, or very high, absorption is present in any of the lines, calculation of an effective reaction volume would be very difficult and consideration of the effect of longitudinal diffusion would be required.

Can. J. Chem. Downloaded from www.nrcresearchpress.com by 210.87.254.42 on 09/05/12
For personal use only.

TABLE II

Photolysis of the mixtures at 300 ± 6 °C

$I_0 \times 10^{-11}$ (quanta/cc s)	Absorption (%)	Time (min)	H_2CO (mm)	D_2CO (mm)	H_2 (μmole)*	HD (μmole)*	D_2 (μmole)*	CO (μmole)*	r*†	Φ‡
3 130 Å										
2.5	56.3	15	150	150	2.6	1.6	0.3_9	8.5	2.5	106
					2.7	1.4	0.2_8	—	2.4	102
2.5	56.1	15	151	151	2.2	1.6	0.4_0	7.3	2.9	99
					2.4	1.8	0.4_6	—	2.9	110
25.7	60.0	15	151	152	10.0	6.9	1.6	19.3	3.0	40
					9.2	6.6	1.6	—	3.0	38
25.8	60.7	15	150	150	9.4	5.5	1.2	16.5	2.7	34
					8.9	5.4	1.1	—	3.0	33
24.8	60.2	15	151	151	9.3	5.7	1.3	18.4	2.7	37
					8.9	5.0	0.7_7	—	3.6	36
23.6	7.4	60	10	10	0.7_2	0.4_7	0.1_5	1.6_2	2.0	$6._5$
					0.7_2	0.4_9	0.1_2	—	2.8	$6._4$
3 655 Å										
144	11.5	60	150	150	14.1	9.6	2.5	29.5	2.6	13
					12.7	8.1	2.6	—	2.0	12
144	11.5	30	151	151	8.0	5.0	1.2	16.1	2.6	14
					7.8	4.5	1.1	—	2.4	14
144	11.5	30	151	151	8.1	5.3	1.4	17.0	2.5	15
					8.2	5.4	1.4	—	2.5	15
138	4.0	240	10	10	0.4_7	0.2_3	0.4_5	1.3_8	0.2_5	0.4
					0.4_4	0.1_6	0.4_5	—	0.1_3	0.4
Thermal										
—	—	120	154	154	1.1_3	0.4_3	0.4_9	5.8	0.3_3	—
					1.0_4	0.3_4	0.3_9	—	0.2_8	—

See footnote of Table I. Values of r and of Φ were calculated from the results of each kind of analysis.
† $r = [HD]^2/[H_2][D_2]$.
‡ Φ represents the sum of the quantum yields for the formation of the isotopes of hydrogen.

Values of Φ in the tables refer to quantum yield for the formation of H_2, D_2, or $H_2 + HD + D_2$ from the photolyses of H_2CO, D_2CO, or the mixtures, respectively. Since all the Φ exceed unity at 3 655 Å a chain reaction must have occurred so that atoms were produced by excitation at this wavelength. Because Φ_{3130} exceeds Φ_{3655}, some inefficiency is present at the longer wavelength which does not occur at 3 130 Å. Fluorescence has been observed (20, 21) at lower temperature and pressure but no observations have been reported for the conditions employed here. A molecular process leading to carbon monoxide and hydrogen has been reported (1, 2) and another, giving rise to methanol and carbon monoxide, has been detected both in the photolysis at 3 130 Å and in the pyrolysis (1, 2, 22). However, it is not possible to present a quantitative description of the primary process at either wavelength.

It might be noted that Φ tends to decrease as I_a is increased in the photolysis of H_2CO at 3 130 Å. The present data at the lower intensities agree reasonably well with those from the experiments at the highest intensity reported by Calvert and Steacie (2). This observation suggests that the predominant termination process is changing in this region of I_a from one which is of the first order to a process which is of the second order in chain carriers. The data on the photolysis of D_2CO at both wavelengths are too limited in number and that on the photolysis of H_2CO at 3 655 Å too imprecise to permit any conclusion on this point for those systems.

HD was observed in the products of the photolyses of the mixtures at 3 655 Å. The value of r obtained, for which reasonable consistency was achieved by both analytical methods, is some 30% less than that obtained by Klein and Schoen (1); no explanation

Can. J. Chem. Downloaded from www.nrcresearchpress.com by 210.87.254.42 on 09/05/12
For personal use only.

can be offered for this discrepancy. The fractional absorptions of the components of the mixture suggest that most of the initiation occurred via the photodecomposition of D_2CO. Nevertheless, the quantum yield data discussed above supports the conclusion reached in earlier investigations (23, 24), in which scavengers were used, that H_2CO is predissociated at 3 655 Å. Absorption by H_2CO in this region is based on the ν_4(3.3 kcal/mole) or ν_6(3.6 kcal/mole) vibrations of the ground state (16). Thus D(H—CHO) $\leqslant$ 78.2 + 3.3(3.6) = 81.5 (81.8) kcal/mole and D(H—CO) $\geqslant \sim 24$ kcal/mole.

The absence of emission from the 1^+ level of the $^1A_2$ excited state of H_2CO has led to the conclusion that this level is predissociated (8, 17, 19); the 1^+ level lies 82.1 kcal/mole above the zero-point level of the ground state. This excellent agreement in the energetics might be purely fortuitous, however; the same type of spectroscopic evidence (19) suggests that no known levels of the $^1A_2$ state of D_2CO are predissociated. Values of Φ greater than unity in the photolysis of D_2CO at 3 655 Å obviously are at variance with this prediction.

ACKNOWLEDGMENT

The authors wish to thank Mr. R. J. Pilon for the mass spectrometric analyses. They also are grateful to Dr. D. A. Ramsay of these laboratories for most valuable discussions of the spectroscopy of formaldehyde.

REFERENCES

1. R. KLEIN and L. J. SCHOEN. J. Chem. Phys. **24**, 1094 (1956).
2. J. G. CALVERT and E. W. R. STEACIE. J. Chem. Phys. **19**, 176 (1951).
3. Natl. Bur. Std. U.S. Circ. No. 500.
4. J. G. CALVERT. J. Phys. Chem. **61**, 1206 (1957).
5. R. KLEIN and L. J. SCHOEN. J. Chem. Phys. **29**, 953 (1958).
6. J. G. CALVERT. J. Chem. Phys. **29**, 954 (1958).
7. T. W. SHANNON and A. G. HARRISON. Can. J. Chem. **39**, 1392 (1961).
8. G. W. ROBINSON and V. E. DiGIORGIO. Can. J. Chem. **36**, 21 (1958).
9. S. TOBY and K. O. KUTSCHKE. Unpublished work.
10. R. SPENCE and W. WILD. J. Chem. Soc. 338 (1935).
11. M. VENUGOPALAN and K. O. KUTSCHKE. Can. J. Chem. **41**, 548 (1963).
12. R. E. HUNT and W. DAVIS. J. Am. Chem. Soc. **69**, 1415 (1947).
13. M. KASHA. J. Opt. Soc. Am. **38**, 929 (1948).
14. M. H. JONES and E. W. R. STEACIE. J. Chem. Phys. **21**, 1018 (1953).
15. R. G. W. NORRISH and F. W. KIRKBRIDE. J. Chem. Soc. 1518 (1932).
16. D. A. RAMSAY. *In* Determination of organic structure by physical methods. Vol. 2. *Edited by* F. C. Nachod and W. D. Phillips. Academic Press, New York. 1962. Chap. 4. J. C. D. BRAND and D. G. WILLIAMSON. *In* Advances in physical organic chemistry. Vol. I. *Edited by* V. Gold. Academic Press, New York. 1963. Chap. 5.
17. J. C. D. BRAND. J. Chem. Soc. 858 (1956).
18. P. J. DYNE. J. Chem. Phys. **20**, 811 (1952).
19. J. C. D. BRAND and R. I. REED. J. Chem. Soc. 2386 (1957).
20. G. HERZBERG and K. FRANZ. Z. Physik, **76**, 720 (1932).
21. S. GRADSTEIN. Z. Physik. Chem. B, **22**, 384 (1933).
22. J. E. LONGFIELD and W. D. WALTERS. J. Am. Chem. Soc. **77**, 6098 (1955).
23. E. GORIN. J. Chem. Phys. **7**, 256 (1939).
24. L. J. SCHOEN. Fifth Symposium (International) on Combustion. Reinhold Publishing Corp., New York. 1955. p. 786.

Can. J. Chem. Downloaded from www.nrcresearchpress.com by 210.87.254.42 on 09/05/12
For personal use only.

Can. J. Chem. Downloaded from www.nrcresearchpress.com by 210.87.254.5 on 09/05/12
For personal use only.

LYCOPODIUM ALKALOIDS

XV. STRUCTURE AND MASS SPECTRA OF SOME MINOR ALKALOIDS OF L. FLABELLIFORME

S. N. ALAM, K. A. H. ADAMS, AND D. B. MACLEAN
Department of Chemistry, McMaster University, Hamilton, Ontario

Received July 7, 1964

ABSTRACT

Hydroxy-des-*N*-methyl-α-obscurine, $C_{16}H_{24}O_2N_2$, has been isolated from *L. flabelliforme* and a structure assigned to it on the basis of physical evidence. A structure is assigned to *Lycopodium* alkaloid L.5, which we have named flabellidine, on the basis of physical evidence and its chemical derivation from lycodine. The mass spectra of hydroxy-des-*N*-methyl-α-obscurine, flabellidine, and flabelline are discussed.

The alkaloids of *L. flabelliforme* were first investigated by Manske and Marion (1), who isolated lycopodine (the major alkaloid), nicotine, and six bases, which they designated by number only. Alkaloid L.1 is now known to be dihydrolycopodine (2), L.2 to be acetyldihydrolycopodine (3), and L.6 to be a mixture of α- and β-obscurine (4). The structures of lycopodine and its derivatives (2) and of α- and β-obscurine (5) are now known. The structure of alkaloid L.5, to which we have assigned the trivial name flabellidine, is discussed in this paper, leaving alkaloids L.3 and L.4 of the original six still uninvestigated.

By using chromatographic and countercurrent distribution methods, an additional seven alkaloids have been isolated from *L. flabelliforme* in this laboratory. Thus Young (6) has reported the isolation of two new alkaloids, flabelliformine and flabelline, to each of which a structure has been assigned (7, 8). Alam (9) has found four alkaloids of known structure (clavolonine, lycodine, annotinine, and des-*N*-methyl-α-obscurine) and a new base hydroxy-des-*N*-methyl-α-obscurine, the structure of which is discussed in this paper.

The structure assigned to hydroxy-des-*N*-methyl-α-obscurine I rests on physical evidence as insufficient material was available to investigate its chemistry.

The presence of a hydroxyl group in I is inferred from its infrared spectrum, which, in Nujol and in chloroform, shows a peak at 3510 cm^{-1}. The position of this peak in chloroform solution is not shifted upon dilution, thereby indicating that the hydroxyl group is intramolecularly hydrogen bonded. Aside from the peak in the hydroxyl region, the spectrum of this compound is remarkably similar to that of α-obscurine (II) and des-*N*-methyl-α-obscurine (III). The spectra of the three are reproduced in Fig. 1 for the region 3600–1500 cm^{-1}.

The ultraviolet spectrum of I ($\lambda_{max}^{CH_3OH}$ 255 mμ, log ε = 3.78) is almost identical with that of II ($\lambda_{max}^{CH_3OH}$ 255 mμ, log ε = 3.75) and III ($\lambda_{max}^{CH_3OH}$ 255 mμ, log ε = 3.81). From the spectral evidence it appears that I must have the same chromophoric system as II and III.

The mass spectrum of the hydroxy compound shows a molecular weight of 276, corresponding to the molecular formula $C_{16}H_{24}O_2N_2$. This formula differs in composition from III ($C_{16}H_{24}ON_2$) by one oxygen atom, suggesting that the new base may be a simple hydroxy derivative of the latter. The fragmentation pattern of I, discussed later, is in agreement with this proposition.

The nuclear magnetic resonance (n.m.r.) spectrum of I shows a three proton doublet

Can. J. Chem. Downloaded from www.nrcresearchpress.com by 210.87.254.5 on 09/05/12
For personal use only.

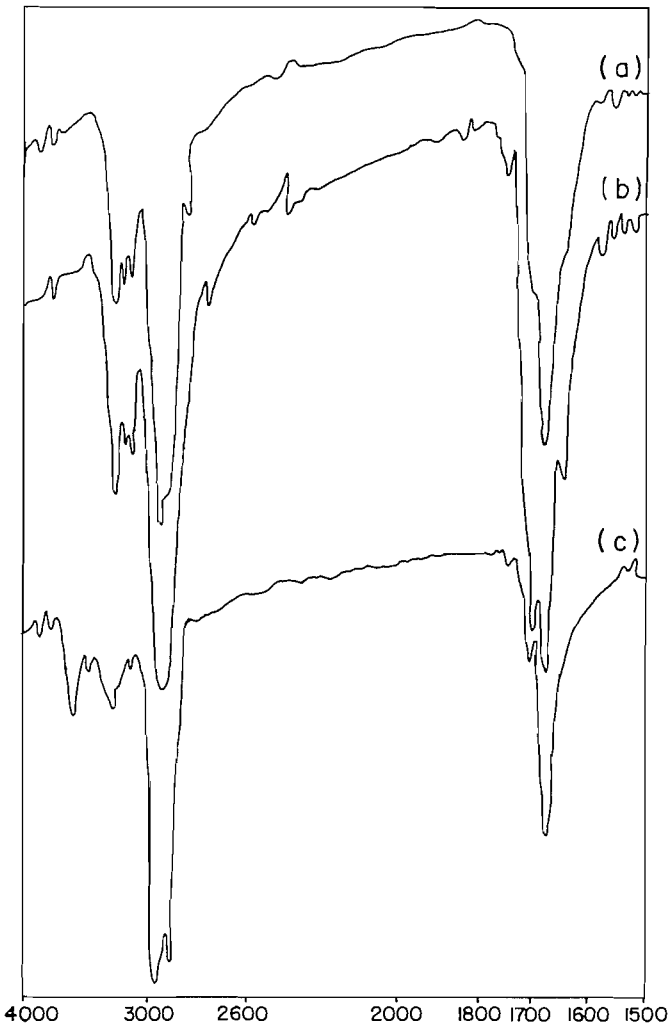

FIG. 1. Infrared spectra of (*a*) α-obscurine, (*b*) des-*N*-methyl-α-obscurine, and (*c*) hydroxy-des-*N*-methyl-α-obscurine.

at $\tau = 9.18$ corresponding to the presence of a $\diagup$CH—CH$_3$ group. In the low-field region the spectrum shows a signal at $\tau = 2.7$, which may be attributed to the hydrogen on the amide nitrogen atom, and a weak broad signal at $\tau = 2.3$, which may be due to the secondary amino proton. No signal corresponding to a $\diagup$N—CH$_3$ group is found in the spectrum, indicating that if the alkaloid conforms to the obscurine structure the second nitrogen atom is secondary in nature. Since there is no other signal in the low field region below $\tau = 6.5$, it may be concluded that the double bond is tetrasubstituted, as in II and III.

The data presented to this point suggest that I may be a hydroxy derivative of III. To locate the hydroxyl group within this framework, it is necessary to reexamine the n.m.r. and infrared data. The absence of a signal in the n.m.r. spectrum between $\tau = 2.7$ and

τ = 6.5 indicates that the hydroxyl group may be attached to a tertiary carbon atom. This observation, coupled with the fact that the hydroxyl group is intramolecularly hydrogen bonded, makes it possible to reduce the number of possible sites of attachment of the hydroxyl group in III. Attachment at C_{14} may be excluded on the basis of the n.m.r. spectrum, which shows a split peak at τ = 9.18 corresponding to a $\diagup\!\!\diagdown$CH—CH_3 group, and attachment at C_5 may be ruled out because intramolecular hydrogen bonding is forbidden on steric grounds. Thus it appears that the most likely position for the hydroxyl group is at C_4. The hydrogen bonding will then involve the lone pair of electrons of the amino nitrogen and is similar to that reported for the alkaloid lycodoline (10), which has the hydroxyl group in the same position—relative to the nitrogen atom. The location of the hydroxyl group at C_4 is further borne out by an examination of the fragmentation pattern of hydroxy-des-*N*-methyl-α-obscurine upon electron impact.

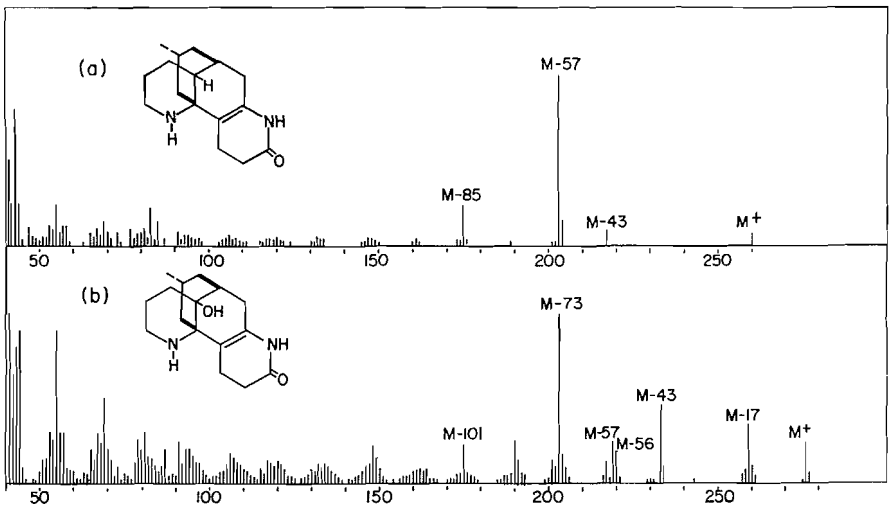

FIG. 2. Mass spectra of (*a*) des-*N*-methyl-α-obscurine and (*b*) hydroxy-des-*N*-methyl-α-obscurine.

In Fig. 2 the mass spectra of des-*N*-methyl-α-obscurine and hydroxy-des-*N*-methyl-α-obscurine are shown. The mass spectrum of des-*N*-methyl-α-obscurine (2*a*) is relatively simple with peaks appearing at M-43, M-57, and M-85, as in the case of lycopodine and of α-obscurine (11). A fragmentation mechanism compatible with the observed peaks in the mass spectrum of des-*N*-methyl-α-obscurine has been proposed previously (11). As in the case of many *Lycopodium* alkaloids, the loss of the bridge plus hydrogen (M-57) is the dominant feature in the spectrum.

The mass spectrum of hydroxy-des-*N*-methyl-α-obscurine (2*b*) shows a more complex pattern with more peaks in the high mass region. The M-73 peak (*m/e* 203) is now the most intense in the spectrum, while the M-57 peak (*m/e* 219), which is the most intense peak in the spectrum of des-*N*-methyl-α-obscurine, is now less intense than several other peaks. The spectrum also has intense peaks at M-17 (*m/e* 259), M-43 (*m/e* 233), and M-101 (*m/e* 175). A mechanism consistent with the formation of some of these ions is shown in Scheme I. The peak at M-43 is present in the spectrum of most *Lycopodium* alkaloids, although it is usually of low intensity, and it has been suggested that it arises by loss of three of the bridge carbon atoms and a hydrogen atom. It appears as a peak of

Can. J. Chem. Downloaded from www.nrcresearchpress.com by 210.87.254.5 on 09/05/12
For personal use only.

relatively high intensity only in those compounds which are substituted at C_4 (e.g. lycodoline and acrifoline) (11). The intensity of the molecular ion peak is also greatly increased relative to those of alkaloids unsubstituted at C_4.

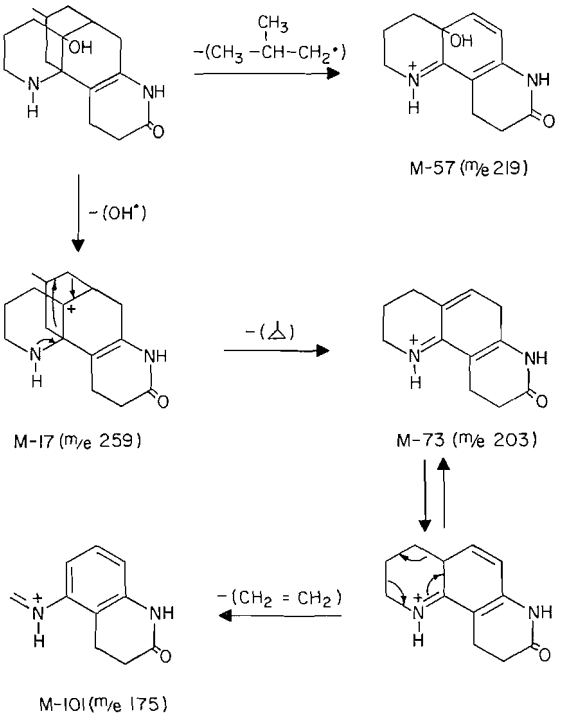

The spectrum of lycodoline IV, which carries a hydroxy group at C_4 differs from that of lycopodine (2) in much the same way as the spectrum of hydroxy-des-*N*-methyl-α-obscurine differs from that of des-*N*-methyl-α-obscurine. The spectrum of lycodoline has been discussed in detail elsewhere (11) and it is only necessary to indicate the points of similarity with the spectrum of hydroxy-des-*N*-methyl-α-obscurine. It has, for example, an intense M-17 peak and an intense M-73 peak. Its M^+ peak is more intense than that in lycopodine, just as the M^+ peak in I is more intense than in III, indicating that the hydroxylated molecules are less prone to fragment in each case. In both spectra the peak at M-57 is no longer the most intense peak in the spectrum and the M-56 peak is much stronger than a normal isotope peak. Furthermore, both spectra show relatively intense peaks at M-43.

The similarity in the spectra of hydroxy-des-*N*-methyl-α-obscurine and of lycodoline suggests that the hydroxyl group is situated in the same relative position in the two molecules. It was pointed out in an earlier paper that hydroxyl substitution at other sites in the lycopodine nucleus does not have such a profound effect on the fragmentation pattern (11). It is proposed, therefore, on the basis of the infrared, ultraviolet, n.m.r., and mass spectrometric examination, that hydroxy-des-*N*-methyl-α-obscurine has structure I.

The stereochemistry assigned is based solely on analogy with other *Lycopodium* alkaloids of known structure and stereochemistry. The properties of hydroxy-des-*N*-methyl-α-obscurine are very similar to those reported for base I, isolated by Burnell

Can. J. Chem. Downloaded from www.nrcresearchpress.com by 210.87.254.5 on 09/05/12
For personal use only.

et al. from *L. fawcettii* (12). It is possible that the two alkaloids may be identical but a direct comparison has not been made.

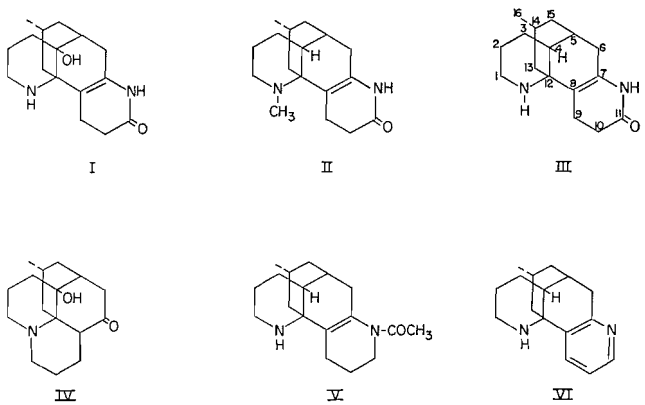

I II III IV V VI

The alkaloid, flabellidine V, was isolated as its perchlorate salt. The analysis of the perchlorate indicated that the alkaloid has the molecular formula $C_{18}H_{28}ON_2$. The melting point of flabellidine perchlorate (280–282°) is the same as that of alkaloid L.5 perchlorate (280–282°) and a comparison of flabellidine perchlorate with an authentic sample of L.5 perchlorate obtained from Dr. L. Marion showed that the two samples were identical. Although Manske and Marion (1) assigned the formula $C_{18}H_{28}O_2N_2$ to alkaloid L.5, the elemental composition reported by them can be better accommodated by the formula $C_{18}H_{28}ON_2$. The latter formula is consistent with the molecular weight of 288 found by mass spectrometry.

The presence of a secondary amino group in flabellidine is inferred from its infrared spectrum, which shows an absorption band at 3280 cm^{-1} (Nujol). This band may be assigned to a hydrogen-bonded N—H stretching absorption (13). In the infrared spectrum of flabellidine perchlorate, this band is very weak and, in addition, a series of bands between 2700–2625 cm^{-1} appear. This weakening of the normal N—H stretching band on salt formation and appearance of a complex series of absorption bands in the region 2700–2600 cm^{-1} ($\overset{+}{N}H_2$ stretching vibrations) has been shown (13) to be characteristic of the secondary amino group. The formation of an acetyl derivative of flabellidine, described later, substantiates the secondary nature of the basic nitrogen.

The infrared spectrum also shows bands at 1640 cm^{-1} (s) and 1680 cm^{-1} (m), which may be attributed to an amide carbonyl group and a carbon–carbon double bond respectively (13). The absence of amide II and III bands suggests that the amide function may be tertiary. This is further supported by the fact that the perchlorate salt of flabellidine does not show amide N—H stretching absorption. It has been found in the case of flabelline (8), which contains both a basic nitrogen and a secondary amide group, that the perchlorate salt has a medium intensity band in the N—H stretching region in the infrared spectrum.

The n.m.r. spectrum of flabellidine shows a split peak at $\tau = 9.12$ (3 protons) which indicates the presence of a $\rangle CHCH_3$ group, and a singlet at $\tau = 7.9$ (3 protons) which may be assigned to a $\rangle NCOCH_3$ group. In the low-field region, the spectrum has only a

Can. J. Chem. Downloaded from www.nrcresearchpress.com by 210.87.254.5 on 09/05/12
For personal use only.

very weak broad signal at $\tau = 2.84$ which may be due to the proton on the secondary nitrogen atom. Since there is no signal below $\tau = 6.10$ in the low-field region, other than that at $\tau = 2.84$, the double bond must be tetrasubstituted. The molecular weight 288 and the molecular formula $C_{18}H_{28}ON_2$, combined with the spectral evidence, indicate that flabellidine is tetracyclic.

The structural features deduced from the infrared and n.m.r. spectra of flabellidine may be accommodated within the framework of the known ring systems of the *Lycopodium* alkaloids in structure V for flabellidine. This structure is also compatible with the ultraviolet spectrum and the mass spectrum discussed below.

The ultraviolet spectrum of flabellidine shows an absorption at λ_{max}^{MeOH} 237 mμ (perchlorate, λ_{max}^{MeOH} 237, log $\epsilon = 3.84$). In contrast, flabelline (8), which is isomeric with flabellidine, shows no absorption above 220 mμ, while α-obscurine shows a band at λ_{max} 255 mμ (log $\epsilon = 3.75$). All three alkaloids have the chromophoric system $\diagdown$C=C—NCO—.
$\diagup$ R

In flabelline, only the double bond is incorporated in a ring system; in flabellidine, both the double bond and the nitrogen atom are incorporated in the ring system; while in α-obscurine, the double bond, nitrogen, and carbonyl are all present in a six-membered ring. One may explain the shift in the absorption maximum by the greater degree of planarity enforced upon the chromophoric system as one moves from flabelline to α-obscurine.

Confirmation of structure V for flabellidine was obtained by the conversion of lycodine VI into *N*-acetylflabellidine. Lycodine contains all the ring carbon atoms of the structure proposed by flabellidine. We considered that high pressure reduction of lycodine in the presence of acetic anhydride would lead to the formation of *N*-acetylflabellidine. It is known, for example, that a 7,8 double bond in the lycopodine system is highly resistant to saturation. Thus, anhydrodihydrolycopodine is not affected by hydrogen at 1050 p.s.i.g. and 110 °C (2). Similarly, it is known (8) that flabelline is formed upon high pressure reduction of lycopodine oxime in the presence of acetic anhydride. In the obscurine series it is found (5) that β-obscurine is converted to α-obscurine with lithium in ammonia, thereby showing that the 7,8 double bond is resistant to reduction. It seemed likely that the reduction of lycodine in the presence of acetic anhydride, hydrogen, and Raney nickel would stop at the tetrahydro stage and that the two nitrogen atoms would undergo acylation under the conditions employed.

Accordingly, lycodine was treated with acetic anhydride over Raney nickel and hydrogen at high pressure (1160 p.s.i.g.) and temperature (110°). The acidic reaction mixture, after decomposing with water, was extracted with chloroform, leaving basic material behind. The chloroform extract yielded a neutral crystalline compound melting at 150–152°.

The acetyl derivative of flabellidine was prepared by heating flabel dine with acetic anhydride and purifying the product by column chromatography. The crystalline compound obtained melted at 150–152°. The melting point of a mixture of this compound with the synthetic acetylflabellidine was undepressed. The infrared and ultraviolet spectra of the two, as well as the mass spectra (which are discussed in the next section), were identical.

Since the structure and the stereochemistry of lycodine is known (14), structure V is an adequate representation of the structure and stereochemistry of flabellidine.

The fragmentation pattern observed upon electron impact is consistent with the

Can. J. Chem. Downloaded from www.nrcresearchpress.com by 210.87.254.5 on 09/05/12
For personal use only.

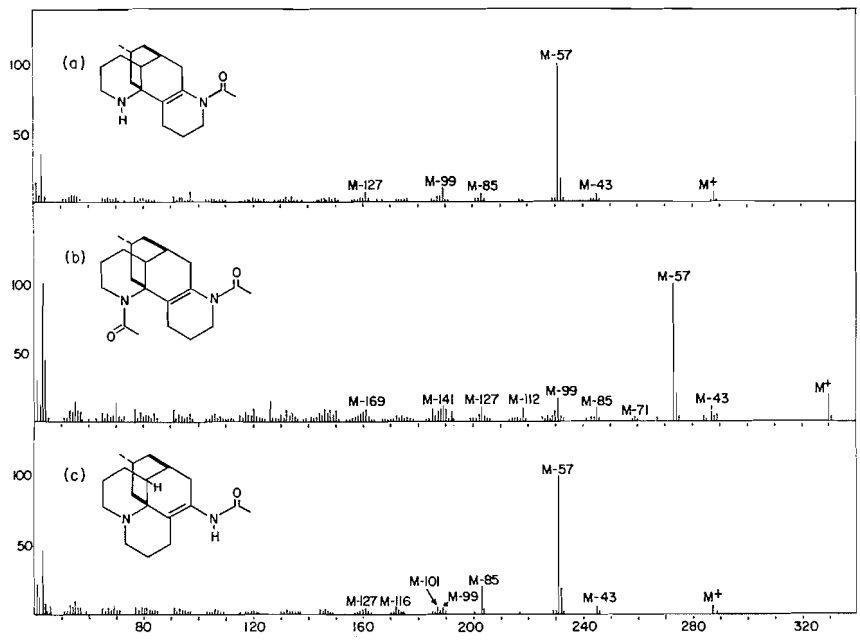

FIG. 3. Mass spectra of (*a*) flabellidine, (*b*) acetyl flabellidine, and (*c*) flabelline.

structure V for flabellidine. The mass spectrum of flabellidine (Fig. 3*a*) shows peaks in the high mass region at M-43, M-57, M-85, M-99, and M-127. The M-57 peak is by far the most intense peak in the spectrum. The origin of this peak is undoubtedly due to the loss of bridge plus hydrogen, a process common to *Lycopodium* alkaloids of the lycodine and lycopodine group. The M-85 peak, which may arise by the loss of 28 mass units from the M-57 fragment ion, and the M-43 peak are also common to alkaloids of both ring systems. The peaks characteristic of this alkaloid are at M-99 and M-127 and arise because of the presence of the *N*-acetyl group. It has been shown by Djerassi *et al.* (15) that amides readily lose ketene (CH_2=C=O) upon electron impact. The ions of M-99 and M-127 may arise by loss of ketene from the ions of M-57 and M-85 respectively. A mechanism consistent with the formation of these fragment ions is shown in Scheme II.

The mass spectrum of acetylflabellidine (Fig. 3*b*) and the mass spectrum of the acetylated product obtained from reduction of lycodine are identical. The fragmentation pattern is similar to that of flabellidine. Additional peaks are present, however, because of the presence of the second acetyl group. The peaks observed are at M-43, M-57, M-71, M-85, M-99, M-112, M-127, M-141, and M-169 mass units. The most intense peak in the spectrum is again the M-57 peak. Loss of 28 mass units from the fragment ion *m/e* 273 will give the peak at M-85 (*m/e* 245) mass units. On the other hand loss of 42 mass units (CH_2=C=O) from the fragment ion *m/e* 273 will give the M-99 peak (*m/e* 231). Loss of another ketene molecule from the ion of *m/e* 231 will result in the formation of the fragment ion *m/e* 189 (M-141), which then may lose another 28 mass units (CH_2=CH_2) forming the fragment ion *m/e* 161 (M-169). The peak at M-127 (*m/e* 203) may arise by the loss of 28 mass units from the fragment ion *m/e* 231 (M-99), which may lose 42 mass units giving rise to the M-169 peak (*m/e* 161).

The fragmentation pattern of flabellidine and acetylflabellidine upon electron impact

Can. J. Chem. Downloaded from www.nrcresearchpress.com by 210.87.254.5 on 09/05/12
For personal use only.

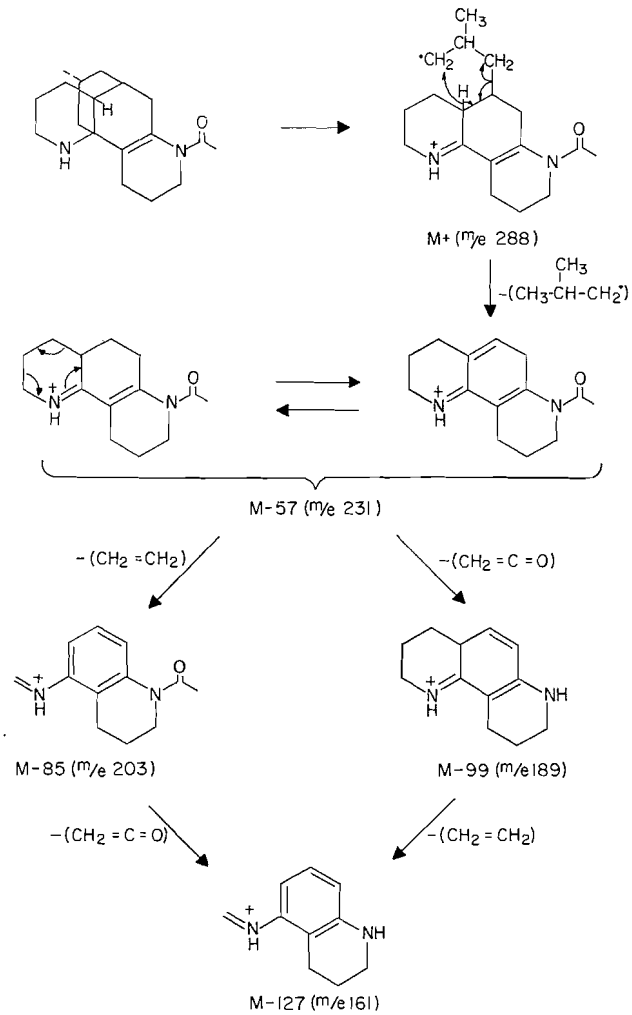

are in agreement with the proposed structure V and with the fragmentation patterns of other *Lycopodium* alkaloids.

A comparison of the mass spectrum of flabellidine with that of its isomer flabelline is made below. Flabellidine is a member of the lycodine group of *Lycopodium* alkaloids, while flabelline conforms in structural type to lycopodine (11). Flabelline is unique among the lycopodine group, however, inasmuch as it carries a nitrogenous substituent. It is of interest, therefore, to ascertain if the two structural types may be differentiated by the mass spectrometric method.

Although the mass spectra of flabelline and flabellidine are similar, a comparison shows that the presence of a secondary amide substituent in flabelline results in additional characteristic peaks in its spectrum. The spectrum (Fig. 3*c*) has peaks in the high mass region appearing at M-43, M-57, M-85, M-99, M-101, M-116, and M-127. The M-43, M-57, and M-85 peaks are again common to all *Lycopodium* alkaloids of the lycopodine and lycodine types. The peaks at M-99 and M-127 are present in the spectrum of both flabelline and flabellidine, confirming the assumption that they arise because of the

Can. J. Chem. Downloaded from www.nrcresearchpress.com by 210.87.254.5 on 09/05/12
For personal use only.

presence of an *N*-acetyl group. The peak at M-116 is absent in the spectrum of flabellidine and hence is characteristic of flabelline, although of relatively low intensity. A fragmentation mechanism accounting for the formation of these ions is postulated in scheme III.

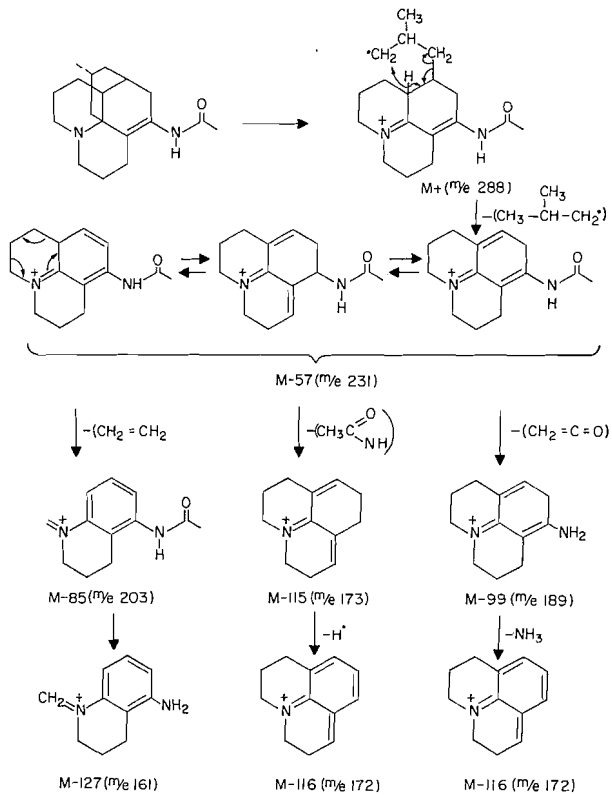

The peak at *m/e* 172 (M-116) corresponds to the loss of acetamide from the fragment of *m/e* 231 (M-57), and it appears that acetamide may be lost in more than one manner. In one stepwise process it is proposed that ketene is first eliminated to yield the ion of *m/e* 189 (M-99), which then loses ammonia. In support of this process there is a strong metastable peak in the spectrum at *m/e* 157.8, corresponding to loss of 17 mass units from the fragment of *m/e* 189 [$m^*(189 \rightarrow 172) = 156.8$]. Another stepwise process, the loss of $CH_3C(=O)NH$ followed by the loss of H, is suggested by the presence of metastable peaks at *m/e* 129.8 and 171.5, corresponding respectively to the transformations *m/e* 231 → 173 (m^* calcd. = 129.5) and *m/e* 173 → 172 (m^* calcd. = 171). A final possibility, the concerted elimination of acetamide, cannot be ruled out from the evidence at hand. To accommodate the formation of the fragments of *m/e* 203, 189, and 172, it is necessary to postulate that the double bonds and the hydrogen atoms in the fragment ions are mobile.

In the fragmentation of flabelline, the loss of one nitrogen atom in the transformation

Can. J. Chem. Downloaded from www.nrcresearchpress.com by 210.87.254.5 on 09/05/12
For personal use only.

m/e 189 → 172 is observed. The loss of one nitrogen atom as an ammonia molecule or as an amine fragment is less likely from a heterocylic system, and is not a discernible transformation in the spectra of lycodine or α-obscurine reported by MacLean (11) or that of flabellidine discussed above. It appears that the mass spectrometric method will differentiate between alkaloids with the lycopodine skeletal structure carrying a nitrogenous substituent and alkaloids with a lycodine skeleton where both nitrogens are incorporated into the ring system.

EXPERIMENTAL

Apparatus, Methods, Materials

Melting points were recorded on a Kofler micro hot stage melting point apparatus and are uncorrected.

The infrared spectra were recorded on a Beckman Model IR-5 recording spectrophotometer in Nujol mull, unless otherwise stated.

Ultraviolet spectra were measured in methanol on a Perkin–Elmer Model 4000 spectracord.

The mass spectra were determined on a C.E.C.-103 mass spectrometer at an ionizing potential of 70 eV and an ionizing current of 50 μA. Samples were introduced through a heated inlet system maintained at 140 °C. The samples were run through the courtesy of Professor K. Biemann, Massachusetts Institute of Technology, Cambridge, Massachusetts. All mass spectra are plotted in terms of relative abundance, with the most intense peak ("base peak") being taken as 100%.

The n.m.r. spectra were measured in deuterochloroform solutions, with tetramethylsilane as an internal standard, on a Varian V-4300 B high resolution spectrometer at a frequency of 60 Mc/s.

Isolation of Hydroxy-des-N-methyl-α-obscurine

The crude alkaloid from *L. flabelliforme* was worked up in the manner described by Young and MacLean (8). The fraction eluted by them with 2% methanol in chloroform was rechromatographed and the column eluted successively with chloroform, 1%, 1.5%, 2%, and 5% methanol in chloroform. The fraction eluted with 1.5% methanol in chloroform was subjected to a six funnel distribution between chloroform and citrate–phosphate buffer of pH 6. The base recovered from buffer fractions 1 and 2 crystallized from a methanol–acetone mixture. After recrystallization from the same solvent mixture, a compound melting at 237–238° was recovered. This compound was identified as clavolonine (16) by comparison with an authentic sample obtained from Dr. R. H. Burnell. The mother liquors from the original crystallization were taken to dryness and dissolved in chloroform. From the chloroform solution, 0.035 g of a crystalline base separated which, after recrystallization from methanol–acetone, melted at 300–305° with decomposition. The hydroxy-des-*N*-methyl-α-obscurine so obtained showed a molecular weight of 276 by mass spectrometry. Its ultraviolet, infrared, and n.m.r. spectra were discussed in the previous section.

Flabellidine (Alkaloid L.5)

This alkaloid was isolated as its perchlorate salt from *L. flabelliforme* by the procedure described by Alam (9). The perchlorate was purified by recrystallization from acetone and melted at 281–282°. A comparison of the ultraviolet and infrared spectrum of this compound with that of an authentic sample of L.5 perchlorate established the identity of the two.

Calcd. for $C_{18}H_{28}ON_2 \cdot HClO_4$: C, 55.52; H, 7.50; N, 7.20. Found: C, 55.49; H, 7.65; N, 7.37.

Preparation of Acetylflabellidine

Flabellidine (37 mg), regenerated from the perchlorate salt, was heated under reflux for 1¼ h with acetic anhydride (15 ml). The reaction mixture was cooled and poured on crushed ice (50 g) and the aqueous mixture was extracted with chloroform. The chloroform extract was washed with 10% aqueous sodium carbonate solution and water, and dried over anhydrous sodium sulphate. Removal of the solvent yielded a gummy substance which did not show a peak corresponding to flabellidine upon vapor phase chromatography but instead showed a new peak with higher retention time. The crude product was adsorbed on a non-basic alumina (Woelm) column and was eluted successively with petroleum ether, benzene, and chloroform. Most of the material was eluted with benzene. The residue from the benzene fraction, after removal of the solvent, crystallized from ether. After recrystallization from acetone–ether it melted at 150–152°. The ultraviolet spectrum of this compound showed an absorption at $\lambda_{max}^{CH_3OH}$ 237 mμ, log ε = 3.84. The infrared spectrum in chloroform solution showed an absorption peak at 1620 cm^{-1}, but no absorption in the N—H region. The mass spectrum showed a molecular weight of 330 for this compound.

Calcd. for $C_{20}H_{30}O_2N_2$: C, 72.70; H, 9.10; N, 8.48. Found: C, 72.25; H, 9.11; N, 8.06.

High Pressure Hydrogenation and Acetylation of Lycodine

Lycodine (0.095 g) was dissolved in freshly distilled acetic anhydride (30 ml) and Raney nickel (200–300 mg) added. The mixture was shaken with hydrogen (at 1160 p.s.i.g.) at 110 °C for 16 h. After removal of most of the acetic anhydride under reduced pressure, the reaction mixture was poured on crushed ice

Can. J. Chem. Downloaded from www.nrcresearchpress.com by 210.87.254.5 on 09/05/12
For personal use only.

and the aqueous mixture extracted with chloroform. The chloroform extract was washed with water, dried over anhydrous sodium sulphate, and the solvent removed. The residue crystallized from acetone–ether, and on recrystallization from the same solvent melted at 150–152°. A mixed melting point with acetylflabellidine was undepressed. The ultraviolet spectrum and the infrared spectrum were superimposable on those of acetylflabellidine. The mass spectrum (Fig. 3*b*) showed a molecular weight of 330 and was identical with that of acetyl flabellidine.

ACKNOWLEDGMENT

Financial assistance to S. N. Alam from the Canadian Commonwealth Scholarship Committee during the period 1960–1963 is gratefully acknowledged. This work was supported by a grant from the National Research Council of Canada.

Also, we wish to thank Dr. R. H. Burnell, who supplied an authentic sample of clavolonine.

REFERENCES

1. R. H. F. MANSKE and L. MARION. Can. J. Research, B, **20**, 87 (1942).
2. W. A. HARRISON, M. CURCUMELLI-RODOSTAMO, D. F. CARSON, L. R. C. BARCLAY, and D. B. MACLEAN. Can. J. Chem. **39**, 2086 (1961).
3. B. DOUGLAS, D. G. LEWIS, and L. MARION. Can. J. Chem. **31**, 272 (1953).
4. B. P. MOORE and L. MARION. Can. J. Chem. **31**, 952 (1953).
5. W. A. AYER, J. A. BEREZOWSKI, and G. G. IVERACH. Tetrahedron, **18**, 567 (1962).
6. J. C. F. YOUNG. M.Sc. Thesis, McMaster University, Hamilton, Ont. September, 1962.
7. M. CURCUMELLI-RODOSTAMO and D. B. MACLEAN. Can. J. Chem. **40**, 1068 (1962).
8. J. C. F. YOUNG and D. B. MACLEAN. Can. J. Chem. **41**, 2731 (1963).
9. S. N. ALAM. Ph.D. Thesis, McMaster University, Hamilton, Ont. May, 1964.
10. W. A. AYER and G. G. IVERACH. Tetrahedron Letters, No. 3, 87 (1962).
11. D. B. MACLEAN. Can. J. Chem. **41**, 2654 (1963).
12. R. H. BURNELL, B. S. MOOTOO, and D. R. TAYLOR. Can. J. Chem. **38**, 1927 (1960).
13. L. J. BELLAMY. The infrared spectra of complex molecules. 2nd ed. Methuen & Co. Ltd., London. 1960.
14. W. A. AYER and G. G. IVERACH. Can. J. Chem. **38**, 1823 (1960).
15. Z. PELAH, M. A. KIELCZEWSKI, J. M. WILSON, M. OHASHI, H. BUDZIKIEWICZ, and C. DJERASSI. J. Am. Chem. Soc. **85**, 2470 (1963).
16. R. H. BURNELL and D. R. TAYLOR. Tetrahedron, **15**, 173 (1961).

Can. J. Chem. Downloaded from www.nrcresearchpress.com by 210.87.254.5 on 09/05/12
For personal use only.

Can. J. Chem. Downloaded from www.nrcresearchpress.com by 210.87.254.40 on 09/05/12
For personal use only.

MECHANISM OF THERMAL DECOMPOSITION OF AMMONIUM METAVANADATE

M. TANIGUCHI[1] AND T. R. INGRAHAM[2]

Extraction Metallurgy Division, Mines Branch, Department of Mines and Technical Surveys, Ottawa, Canada

Received June 24, 1964

ABSTRACT

When ammonium metavanadate is roasted at 225 °C, ammonia and water are eliminated in the ratio 2:1 and an intermediate compound identified by weight loss and chemical analysis as $(NH_4)_2 \cdot O \cdot V_2O_5 \cdot$ is formed. An X-ray diffraction pattern for this material is reported. Transpiration experiments have been used to establish the free energy of this reaction. The second stage of the decomposition involves an endothermic and an exothermic process, both of which occur with the production of a gaseous product. The liberation of ammonia is not quantitative, and its oxidation on the vanadium pentoxide, in the last stage of decomposition, is suggested as a possible source of the exothermic heat.

INTRODUCTION

Ammonium metavanadate, which may be recovered from the hydrometallurgical treatment of some ores containing vanadium, is one of the major starting materials in the preparation of vanadium chemicals. Most vanadium pentoxide, for example, is produced by the roasting of ammonium metavanadate

[1] $$2NH_4VO_3 \rightleftharpoons V_2O_5 + 2NH_3 + H_2O.$$

Although there have been a number of investigations of the process of roasting ammonium metavanadate (1–5), there is no general agreement on the course of the reaction. It is agreed that a stable intermediate is formed, but it has not been positively identified. In Table I, some of the suggested intermediates are listed.

TABLE I

Weight losses accompanying formation of proposed intermediates

Proposed intermediate	% weight loss	Ratio NH_3:H_2O released
$(NH_4)_2 \cdot O \cdot (V_2O_5)_3$ (1, 2)	14.84	2:1
HVO_3*(3)	14.56	1:0
$NH_3 \cdot H_2O \cdot (V_2O_5)_2$ (4)	14.77	3:1

*Accepted by most current textbooks.

It will be apparent from Table I that since the weight losses involved in the production of the intermediate are almost identical, any technique based entirely on thermogravimetric methods would be likely to produce inconclusive results. When balanced chemical equations are written for the formation of each of these intermediates, it is evident from the wide variation in the ratio of ammonia to water, as shown in the third column of Table I, that analysis of the gaseous decomposition products should be helpful in resolving the reactions involved.

In this work chemical analyses have been made of the gaseous products of reaction.

[1]*National Research Council of Canada Postdoctoral Fellow. Present address: Department of Synthetic Chemistry, Tokyo Institute of Technology, Tokyo, Japan.*

[2]*Head, Research Section, Extraction Metallurgy Division, Mines Branch, Department of Mines and Technical Surveys, Ottawa.*

This information has been combined with the weight loss and chemical analysis to determine the composition of the intermediate. The transpiration method was used to estimate the free-energy change for the reaction to form the intermediate. Differential thermal analysis was used to detect the temperatures at which the most vigorous reaction was obtained, and to assess the complexity of the decomposition reactions.

EXPERIMENTAL METHODS AND RESULTS

Material

The ammonium metavanadate used in the experiments was "purified ammonium metavanadate" (14.56% NH_3, 44.48% V) supplied by Fisher Scientific Co. A few experiments were done using British Drug House reagent grade material, but, from the development of a yellow color on roasting, it was evident that the material was contaminated with a potassium salt.

Analytical Methods

Ammonia and Water

Two methods were used for the determination of ammonia. When only ammonia was required, it was absorbed from the gaseous decomposition products in 0.1 *N* H_2SO_4 and the excess back-titrated with standard alkali.

When both ammonia and water were required for determining the ratio in which they were produced during the decomposition, the products were passed through a known weight of concentrated sulphuric acid. The increase in weight was equivalent to the absorption of both water and ammonia. The amount of ammonia in the acid was determined by the Kjeldahl method.

Vanadium

Vanadium was determined by a redox titration, using *N*/30 $KMnO_4$, *N*/30 $Fe(NH_4)_2(SO_4)_2$, and a diphenylamine phosphoric acid indicator.

Differential Thermal Analysis and Effluent Gas Analysis Experiments

The first group of experiments on the thermal decomposition of ammonium metavanadate was done using a Robert L. Stone Co. differential thermal analysis apparatus equipped with a thermal conductivity cell for analyzing the effluent gas stream. During a run, a carrier gas was flushed through the powdered sample at the rate of 50 cc per min as the sample was heated at a rate of 3 °C per min. The carrier gases were nitrogen, oxygen, ammonia, and steam. The results of the thermal analysis and gas analysis were plotted simultaneously on a strip chart. Tracings of two typical charts are shown in Fig. 1.

It is evident, from the lines for a nitrogen carrier gas experiment shown at the bottom of Fig. 1, that the decomposition reaction is complex, involving several stages. The first stage of the reaction, which occurs in the temperature range 210–215 °C, may take place in two steps. A gaseous product is evolved, but the gas analysis trace does not differentiate the gas from each step. At the completion of the first stage of reaction, an intermediate product is formed that is stable up to a temperature of 260 °C. The material then undergoes an endothermic reaction, evolving a gaseous product at maximum rate at about 325 °C. The product from this second stage then undergoes additional reaction; an exotherm is developed at 375 °C and a gaseous product is evolved. The final product of this decomposition reaction in nitrogen was a dark-colored vanadium oxide in which the average vanadium valence was slightly less than 5.

When the same experiment was repeated using oxygen as a carrier gas, as shown at the top of Fig. 1, there was better differentiation of the doublet developed in the first

Can. J. Chem. Downloaded from www.nrcresearchpress.com by 210.87.254.40 on 09/05/12
For personal use only.

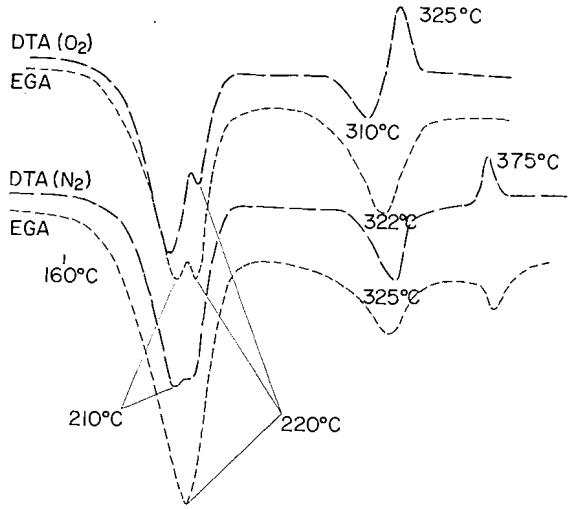

FIG. 1. Differential thermal analysis and effluent gas analysis traces of the reactions involved in the conversion of ammonium metavanadate to vanadium pentoxide, with oxygen and nitrogen sweep respectively.

stage of reaction. It was shown by both the thermal- and gas-analysis tracings. The first part of the second stage of decomposition was identical with that observed in nitrogen. However, because of the increased area under the gas analysis tracing and the occurrence of the exotherm at a temperature 50 deg less than that in the nitrogen experiment, it seems likely that both of the gases evolved in the second stage of the decomposition were released simultaneously. It also seems reasonable to expect that in an oxygen atmosphere, the intermediate is oxidized at a lower temperature than when vanadium pentoxide is the source of oxygen.

When the experiments were repeated using steam and ammonia as carrier gases, the effluent gas analysis tracings were erratic. In both instances, however, a single clearly defined peak was generated by the first stage of the reaction. The peak occurred at 225 °C in steam and at 240 °C in ammonia. The sharpness of the peaks indicated that some suppression of the reaction may have occurred.

Determination of the Composition of the Intermediate

In this group, three types of experiments were done. The first type consisted of heating a sample of ammonium metavanadate in an American Instrument Company recording thermogravimetric balance. The heating was done at a constant rate of 3 °C per min in a 50 cc per min stream of nitrogen gas. A tracing of the instrument-drawn chart is shown in Fig. 2, from which it is evident that the decomposition reaction takes place in two stages that are sufficiently well defined to warrant attempts to isolate the intermediate.

Isolation of the intermediate was done by heating 2 g samples of ammonium metavanadate in an open boat within a tube furnace in a slow stream of dry oxygen. Oxygen was used because the experiments shown in Fig. 1 indicated that the steps in the decomposition occur more sharply in it than in nitrogen. At a selected temperature, the boat was heated and then periodically cooled and weighed. It was found that at 225 °C a constant weight was attained after 2.5 h. The weight loss was 14.85%. At a temperature of 200 °C, equilibrium was not obtained after 4 h. At a temperature of 245 °C, there was no observable plateau in the weight loss curve.

Can. J. Chem. Downloaded from www.nrcresearchpress.com by 210.87.254.40 on 09/05/12
For personal use only.

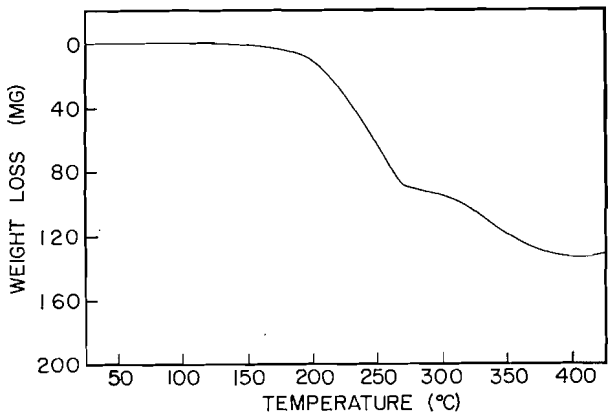

FIG. 2. Thermogravimetric analysis curve of the conversion of ammonium metavanadate to vanadium pentoxide – oxygen sweep at 3 deg per min increase in temperature.

When the conditions for achieving a constant composition had been established, the experiment was repeated and the product gases analyzed for ammonia and water. It was found that the weight loss was entirely accounted for by the combined loss of ammonia and water, and it was established that they are released in the ratio of 2.00 ± 0.02 ammonia to 1.00 water. Chemical analyses were done on the intermediate. The results are shown in Table II.

TABLE II

Percentage composition of intermediate

	NH_3	H_2O	V	O*	NH_3/V
Found	5.69	2.97	52.19	39.15	0.109
Calc'd.†	5.69	3.01	51.10	40.20	0.111

*By difference.
†Calculation was made on the assumption that the intermediate is of formula $(NH_4)_2 \cdot O \cdot (V_2O_5)_3$.

The weight loss, gas composition, and chemical analysis are in agreement with the following equation representing the first stage in the thermal decomposition of ammonium metavanadate:

[2] $$6NH_4VO_3 \rightleftharpoons (NH_4)_2 \cdot O \cdot (V_2O_5)_3 + 4NH_3 + 2H_2O.$$

X-ray powder diffraction patterns were made of the intermediate compound, and the results shown in Table III were obtained.

Transpiration Experiments

The object of the transpiration experiments (6) was to established the free-energy function for the formation of the intermediate compound from ammonium metavanadate. These experiments were done using the pyrex vessel shown schematically in Fig. 3. Preheated oxygen at a known flow rate was passed through a loosely fitted plug of pyrex glass wool into the saturation zone. This zone was about 7 cm in length in a 2.5 cm diameter pyrex glass tube. The ammonium metavanadate powder was piled in ridges to a depth of about 1 cm. The product-saturated oxygen stream was discharged through another plug of pyrex wool and a 2 cm length of 0.05 cm capillary. The exit gases were passed to

Can. J. Chem. Downloaded from www.nrcresearchpress.com by 210.87.254.40 on 09/05/12
For personal use only.

TABLE III

X-ray powder diffraction data for $(NH_4)_2 \cdot O \cdot (V_2O_5)_3$
(Cu K radiation, Ni filter)

d(Å)	I*	d(Å)	I*
8.2	vs	2.33	vw
6.2	vw	2.21	m
5.7	vw	2.04†	mw–b
4.1	m–b	1.93	vw
3.46	m	1.86	vw
3.34	m	1.80	s
3.17	s	1.76	mw
2.88†	vw–b	1.58	mw–b
2.71	w	1.54	mw–b
2.61	m	1.48	vw–b
2.42	mw	1.45	vw–b
		1.40	w–b
Plus additional weak lines			

*Abbreviations: vs(very strong), s(strong), m(medium), mw(medium weak), w(weak), vw(very weak), b(broad).
†Probably two unresolved lines.

absorbers for analysis. The gas saturation vessel was arranged in a fixed position and a movable 12 × 1 in. cylindrical tube furnace was used to heat the vessel. The temperature of the furnace was controlled to ±2 °C with a Kelvin and Hughes controller. Sample temperature was determined by a chromel–alumel thermocouple fitted in the central thermocouple well shown in Fig. 3.

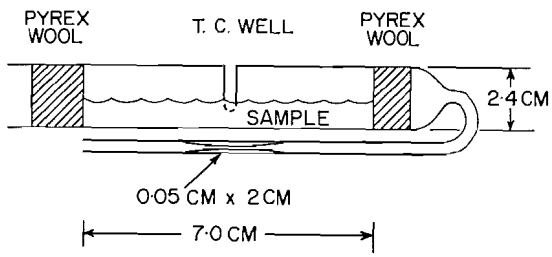

FIG. 3. Pyrex sample vessel used in transpiration experiments.

At a given temperature, experiments were done at a variety of flow rates with the object of establishing a gas composition over the sample such that the composition would be independent of changes in the gas flow rate and in which the partial pressures of ammonia and water would be identical with the decomposition pressures that the two gases would establish over the sample in an evacuated vessel at the same temperature. The results of this series of experiments are shown graphically in Fig. 4, from which it will be apparent that, for at least three of the experimental temperatures, there is a relatively wide range of gas flows for which the sample is in equilibrium with the gas flow.

From a chemical analysis of the ammonia in the oxygen stream, the partial pressure of ammonia in the equilibrium gas was calculated for each of the experimental temperatures. The calculations are shown in Table IV.

Regression analysis of the results in Table IV and Fig. 5 yielded the following equation for 1 mole of ammonium metavanadate

$$\text{Log } K = 10.148 - 5.052 \times 10^3/T$$

or

$$\Delta G^0 = 23\,115 - 46.4T.$$

Can. J. Chem. Downloaded from www.nrcresearchpress.com by 210.87.254.40 on 09/05/12
For personal use only.

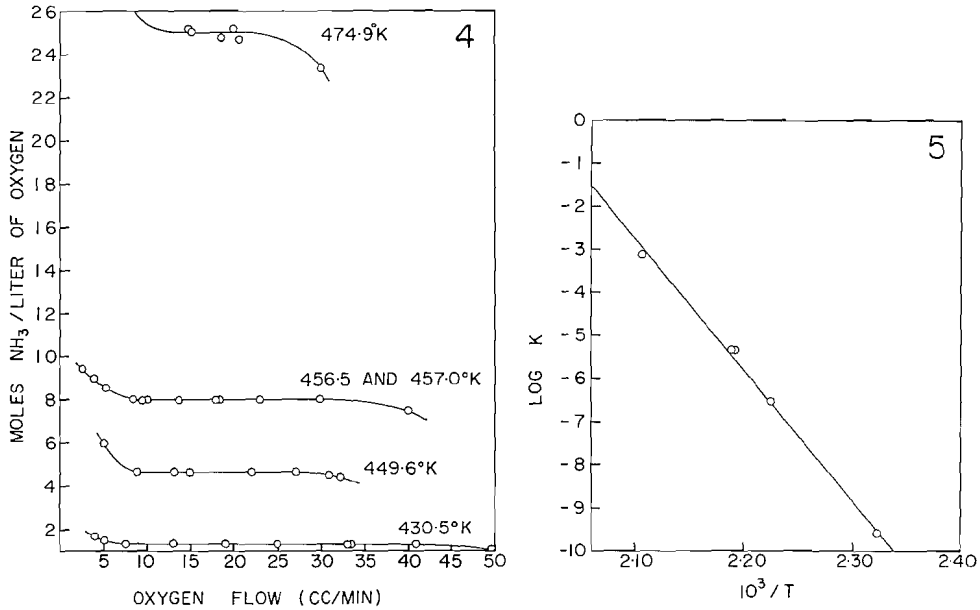

FIG. 4. Graph used to establish equilibrium ammonia pressure in transpiration experiments at 430.5, 449.6, 456.5, 457.0, and 474.9 °K.

FIG. 5. Log equilibrium constant vs. reciprocal temperature relation for the reaction to form $(NH_4)_2 \cdot O \cdot (V_2O_5)_3$ from NH_4VO_3.

TABLE IV

Decomposition pressures over ammonium metavanadate, calculated from a dynamic experiment ($p_{NH_3} + p_{H_2O} = 1.5\ p_{NH_3}$)

T (°K)	$10^3/T$	Moles NH_3 per l O_2 at 25 °C	$p^4_{NH_3}$	$p^4_{NH_3} \cdot p^2_{H_2O}$	Log K
430.5	2.323	13.18×10^{-4}	9.512×10^{-7}	2.319×10^{-10}	−9.634
449.6	2.225	4.66×10^{-3}	1.095×10^{-4}	2.865×10^{-7}	−6.543
456.5	2.191	8.02×10^{-3}	7.216×10^{-4}	4.846×10^{-6}	−5.315
457.0	2.188	7.77×10^{-3}	6.871×10^{-4}	4.503×10^{-6}	−5.346
474.9	2.106	25.1×10^{-3}	2.092×10^{-2}	7.564×10^{-4}	−3.121

Because a linear equation was used to fit the results in Table IV, the assumed ΔC_p for the reaction is 0; hence, $\Delta H^0_{298} = 23.1$ kcal/mole and $\Delta S^0_{298} = 46.4$ entropy units (e.u.). Because the heat of formation of ammonium netavanadate is not known, it is not possible to estimate the heat of formation of the intermediate compound. It is possible, however, to check the reasonableness of the entropy change. The principal change in entropy in reaction [2] is the evolution of 4 moles of ammonia and 2 moles of water for each 6 moles of ammonium metavanadate. Since the entropy of formation per mole of water at 298 °K is 45.11 e.u. and the entropy of formation of ammonia is 45.96 e.u., the combined entropy change per mole of ammonium metavanadate would be 45.7 e.u., which is in reasonable agreement with the experimental value of 46.4 e.u.

When both the transpiration technique and the analysis of the gas stream for the ratio of ammonia to water were applied to the reaction for the formation of vanadium pentoxide from the intermediate, the results were inconclusive. The ratio of ammonia to water in the decomposition gases was erratic, but always indicated that some of the ammonia was

Can. J. Chem. Downloaded from www.nrcresearchpress.com by 210.87.254.40 on 09/05/12
For personal use only.

being decomposed. In the experiments using a nitrogen carrier gas, the vanadium oxide product showed evidence of reduction. The vanadium oxide was its normal color only when oxygen was used. From these observations and from the evidence of differential thermal analysis and effluent gas analysis, it seems likely that the final stage of the decomposition reaction consists of the catalytic decomposition of ammonia on the surface of freshly formed vanadium pentoxide.

CONCLUSIONS

The production of vanadium pentoxide from ammonium metavanadate involves a series of chemical reactions. The first stage of the reaction is the almost simultaneous elimination of ammonia and water, in the molar ratio of 2:1, to produce an intermediate compound having the chemical composition $(NH_4)_2 \cdot O \cdot (V_2O_5)_3$. The second stage of the decomposition involves both an exothermic and an endothermic reaction. The endothermic reaction may be the liberation of water, and the exothermic reaction is consistent with the degradation of ammonia on the vanadium pentoxide surface.

ACKNOWLEDGMENT

The authors wish to express their thanks to P. Marier for the differential thermal analysis and effluent gas analysis experiments and to S. Kaiman for X-ray analyses.

REFERENCES

1. P. DUBOIS and P. BRETON. Compt. Rend. **206**, 1969 (1938).
2. K. TARAMA and S. TERANISHI. J. Chem. Soc. Japan, **55**, 68 (1952).
3. C. DUVAL. Inorganic thermogravimetric analysis. Elsevier Publ. Co., Inc., Amsterdam. 1963.
4. T. A. SESBES. Istanbul Univ. Fen Fak. Mecmuasi Seri C, **20**, 272 (1955).
5. J. TRAU. Roczniki Chem. **36**, 1365 (1962).
6. U. MERTEN and W. E. BELL. The transpiration method. U.S. Atomic Energy Commission Contract At(04-3)-164. Sept. 29, 1961.

Can. J. Chem. Downloaded from www.nrcresearchpress.com by 210.87.254.40 on 09/05/12
For personal use only.

Can. J. Chem. Downloaded from www.nrcresearchpress.com by 210.87.254.40 on 09/05/12
For personal use only.

THE SIGNIFICANCE OF HALIDE IN GRIGNARD REAGENTS

WARREN FRENCH AND GEORGE F WRIGHT
Department of Chemistry, University of Toronto, Toronto, Ontario
Received May 27, 1964

ABSTRACT

The optical activity of 1-phenylethanol from benzaldehyde and methyl chloride Grignard reagent coordinated with (+)2,3-dimethoxybutane is about one fourth of that found for the same product when bis-methylmagnesium is the reagent. The difference has been attributed to the relative coordinating power of magnesium chloride versus the optically active ether.

Grignard reagents usually contain bound halogen because they are commonly prepared by corrosion of magnesium by means of an organic halide. Indeed, this process historically defines the reagent. However, these reagents may be rendered halogen free by the dioxane precipitation technique of the Schlenks (1) and the resultant solution of bis-organomagnesium also has been considered to be a Grignard reagent. We adhere to this extended definition largely because the amount of magnesium halide in a Grignard reagent is dependent on the type of halide and upon the method of reagent preparation. Thus a reagent series may exist with bis-organomagnesium at one extreme and Grignard reagent saturated with magnesium halide at the other. Such a series would be important only if there is a difference in reactivity in time or type between the extremes. Interest in these differences has increased during recent years (2, 3, 4). In this report the difference in coordination of the organometallic compound with an ether has been investigated.

The method we used is the induction of optical activity in a product of Grignard reagent addition (5, 6, 7) by use of (+)2,3-dimethoxybutane to effect an asymmetric synthesis. We synthesized 1-phenylethanol from methyl Grignard reagent and benzaldehyde and compared yields and optical rotation when either bis-methylmagnesium or methyl chloride Grignard reagent is used.

For the comparison to be meaningful it is important that the first of these reagents be quite free from halide. Mosher (4) found it difficult to attain this condition. By contrast, our precipitate initially contains not only the halide *in toto* but also some of the halogen-free complex. To obtain a reasonable yield of bis-methylmagnesium we must wash the precipitate thoroughly. Subsequently a small amount of white precipitate tends to appear in the solution, presumably because of temperature variations. However, both the solution and the slight precipitate are halogen free by silver halide test. The difference between our results and those of Mosher may be due to our specific reagent or else to the dioxane–Grignard ratio or to our use of heat during the precipitation.

The halide-free solution contains bis-methylmagnesium dioxanate or dioxanate–etherate, so these ethers must be removed to ensure that the optically active ether will be fully effective. Most of the diethyl ether is removed easily at 50 °C under 1 atm of nitrogen, leaving a solid residue. Comparison of the weight of this residue with the basic magnesium equivalence, according to titration (8), indicates a composition of one-half dioxane per mole of bis-methylmagnesium.

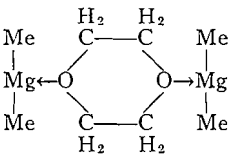

The removal of dioxane occurs under a pressure of 0.001 mm of mercury, slowly at 25 °C as is shown by the upper curve of Fig. 1 and more rapidly at 50 °C (lower curves). The weight loss does not reach the level of bis-methylmagnesium even when the final temperature is raised to 140°. This apparent retention of some dioxane even after 4 h is probably an analytical error caused by the necessity of releasing the systems to atmospheric pressure by means of nitrogen to make the intermediate weighings. An alternative possibility, splitting of the ether at elevated temperature, is unlikely because in preparative experiments involving only an initial and final weight (3), the loss conformed with complete removal of ether. Moreover, the amount of dioxane condensed in a dry ice trap during the experiments shown in Fig. 1 is exactly 0.5 mole.

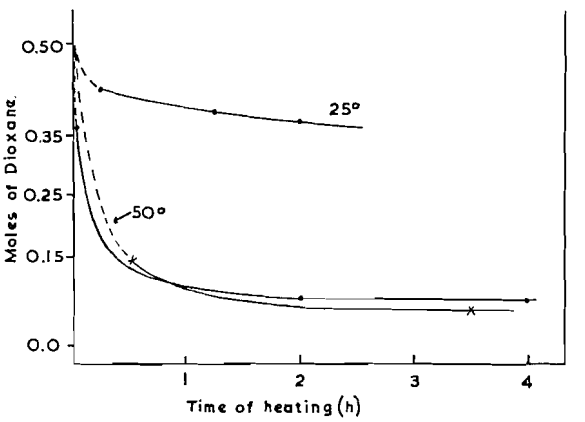

FIG. 1. Removal of ether from MeMg at < 0.001 mm pressure.

Ether-free bis-methylmagnesium is insoluble in benzene but the addition of a molar equivalent of (+)2,3-dimethoxybenzene to the benzene suspension causes immediate solution with heat evolution that is large in consideration of the ease with which dioxane removal is effected. Doubtless the strong coordinating power of the optically active ether is responsible for the ease with which methyl chloride reacts smoothly with magnesium in a solution of 1 molar equivalent of this ether in an equal volume of benzene to give the halide-containing Grignard reagent for our comparative reactions.

There are certain disadvantages in the reaction that we have chosen for demonstration. The chief disadvantage is a concomitant oxidation–reduction of the Meerwein type (9), because the benzyl alcohol so produced is difficult to separate from 1-phenylethanol by distillation or absorption chromatography on alumina. Moreover the by-product formation

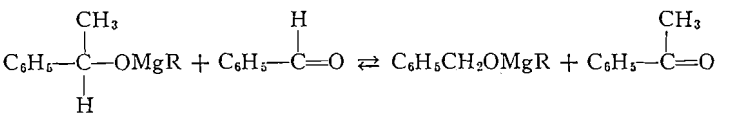

Can. J. Chem. Downloaded from www.nrcresearchpress.com by 210.87.254.40 on 09/05/12
For personal use only.

is greater in the system containing bis-methylmagnesium than in the halide-containing reagent, so the optical purity may appear to be lower than is warranted by its actual enantiomer content. Nor can it be purified by crystallization for closer evaluation because the racemic compound separates preferentially upon cooling. Against these disadvantages is the reliable knowledge of the specific rotation, +13.02°, of optically pure 1-phenylethanol (10, 11).

The two reactions were carried out with the same ratio of magnesium to carbonyl in order that only one C—Mg linkage would be involved in the comparative reactions. The results are shown in Table I where the halide-containing reagent is nominally described as "MeMgCl".

TABLE I

Asymmetric synthesis of 1-phenylethanol

Expt. No.	Grignard reagent	Yield of product (%)	n_D^{20}	$[\alpha]_D^{25}$ (neat)	Optical purity (%)
1	MeMgCl	74	1.5256	−0.72±0.02	5.5
2	MeMgCl	82	1.5251	−0.59±0.01	4.5
3	Me_2Mg	61	1.5283	−2.40±0.01	18.5+
4	Me_2Mg	67	1.5256	−2.61±0.01	20.0+

It may be seen from these experimental values that the extent of asymmetric synthesis is almost four times higher in absence of halide than in its presence. Actually the difference must be greater, because the product of expt. 3 when it was analyzed by gas–liquid chromatography was found to contain 10–15% of benzyl alcohol and acetophenone and therefore only 85% of the active alcohol, whereas the active alcohol of expt. 1 was essentially pure. Only traces of acetophenone and benzyl alcohol were found in the latter sample.

Thus it is the experimental fact that asymmetry is induced by an optically active ether much more when magnesium halide is absent than when it is present in the reaction between methyl Grignard reagent and benzaldehyde. Unfortunately, interpretation of this phenomenon depends upon a knowledge of the manner in which magnesium halide participates in Grignard system and this knowledge is largely lacking. For example there is still much controversy (ref. 2, p. 99), after 60 years, about the relative importance of the several constituent forms in the so-called Schlenk equilibrium.

$$2RMgX \rightleftarrows R_2Mg + MgX_2 \rightleftarrows R_2Mg \cdot MgX_2$$

However, none of the conclusions is entirely definitive. The demonstration by X-ray diffraction (12) that bromobenzene Grignard reagent yields crystals of structure $RMgX \cdot 2ET_2O$ tells nothing about the composition in solution, as is evident in the fact that diphenylmagnesium may be isolated in good yield from such a solution after the halide in the system is precipitated by dioxane. Actually these observations lead only to the conclusion that Grignard reagent systems are labile.

Morever there is evidence that any one system may be altered by the environment and perhaps by the temperature. Ashby and Becker (13) have shown that the state of complexity is dependent on the ether that is involved with the reagent. In tetrahydrofuran their ebullioscopic studies are interpreted to show that ethyl chloride and ethyl bromide Grignard reagents actually exist as RMgX, whereas the boiling point elevation in other ether media (14, 15) have indicated that RMgX is not predominant.

Actually even greater complexity is possible. After Jolibois (ref. 2, p. 109) showed that

Can. J. Chem. Downloaded from www.nrcresearchpress.com by 210.87.254.40 on 09/05/12
For personal use only.

Grignard reagents are electrically conducting it was found by electrolytic transport studies (16–19) that they show ionic properties where magnesium is both in the cation and the anion. In this circumstance ebullioscopic evidence for the monomeric form, RMgX, may also be interpreted in terms of an ionized dimer.

$$2RMgX \rightleftarrows R_2Mg_2X_2 \rightleftarrows Mg^{++} \text{ and } (MgR_2X_2^{--})$$

At the present time one cannot say whether monomer, dimer, ion pair, or ions predominate. Probably the predominance depends upon the specific reagent as well as the reaction medium. Each will serve for description, but the ionic formulation seems to be convenient to illustrate the effect of magnesium halide on our asymmetric synthesis.

An explanation is needed for the fact that although halogen-free Grignard reagents ordinarily are less reactive than those in which halide is present (20, 21) the presence of magnesium halide in the present reaction tends to reduce the extent of asymmetric induction due to an optically active solvent. The anomaly is resolved if magnesium halide is considered to be alternative to the ether as a coordinating agent. To the extent that it displaces (+)2,3-dimethoxybutane the tendency for enantiomeric preference cannot occur.

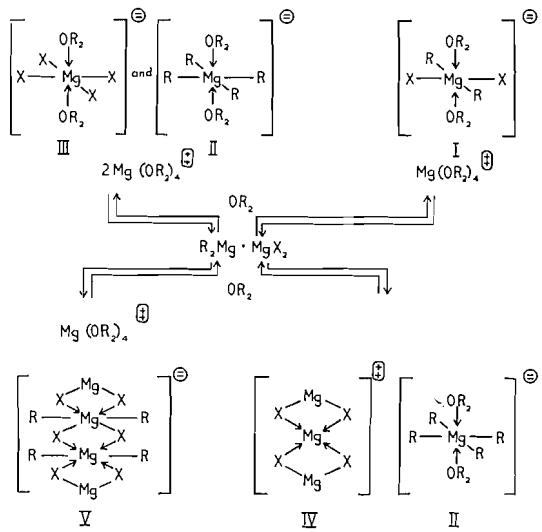

The deleterious effect of magnesium halide is not apparent in the ion pair I nor in ion pairs II and III because III would not enter into product formation with adducts like benzaldehyde. Likewise the asymmetry-inducing ether in the ion pair IV–II ought to be free to exert its influence on the entering adduct because the magnesium halide (even in excess over the composition $R_2Mg \cdot MgX_2$) is relegated to the cation. However, in the ion pair V the ether would be ineffective because it has been excluded from coordination by magnesium halide which occupies its place in the anion. Although the ether might (or might not) solvate the cation its effectiveness at this distance ought to be minimal, especially if the pair is dissociating in the medium. The existence of a complex species like V in significant amount cannot be excluded. Indeed it may be noted that its composition is such that it could be the source of the Et_2Mg plus $EtMg_2Cl_3 \cdot THF$ which was separated from solution by Ashby and Becker if, as seems likely, their R_2Mg was solvated.

Obviously there may be many variations of these five typical ions pairs, and it is

Can. J. Chem. Downloaded from www.nrcresearchpress.com by 210.87.254.40 on 09/05/12
For personal use only.

apparent that complexity and not necessarily charge separation is the significant factor. No matter how the Grignard reagent is described the effect of magnesium halide is best explained as a displacement at the reaction site of the asymmetry-inducing ether. No doubt the explanation is incomplete because the geometry of the complex must also be a factor. But this geometry is an additional attribute which will be discussed in a forthcoming extension of the present work.

EXPERIMENTAL

Methyl Chloride Grignard Reagent

Into a dry, nitrogen-filled flask fitted with a dry ice cold-finger condenser, mercury-sealed stirrer, and gas inlet tube leading near the bottom of the flask were placed 9.7 g (0.40 g-atom) of distilled magnesium and 30 ml of diethyl ether. Approximately 2 g of methyl chloride was introduced, and the mixture stirred until reaction started (ca. 10 min). When the reaction ceased the mixture was diluted with 200 ml of diethyl ether, and the rest of the methyl chloride (initially 15.7 g, 0.31 mole) was introduced during 15 h with occasional cooling of the mixture to control the rate of reaction. The reaction was accompanied by the formation of a thick, gray precipitate. The mixture was stirred 4 h longer at 25°, then poured under nitrogen into a centrifuge bottle. The clear colorless supernatant layer obtained by centrifuging at 1 500 r.p.m. for 20 min was transferred by syringe to a second three-necked flask, and the precipitate washed with four 30 ml portions of ether (Gilman test, negative). Titration of an aliquot of the ether solution indicated 0.272 equivalents (88%) of basic magnesium.

Solvent-Free Dimethylmagnesium

To the rapidly stirred methyl chloride Grignard reagent, described above, was added 27.3 g (0.31 mole) of dioxane during 15 min. The mixture was heated under gentle reflux with stirring for 30 min longer, then was poured under nitrogen into a centrifuge bottle. The supernatant layer formed on centrifugation was found to contain 0.118 equivalents (38%) of magnesium. Six washings of the precipitate with 25 ml portions of ether raised the yield to 0.130 equivalents (42%). A test of an aliquot was made in acidified silver nitrate. The chlorine-free ethereal solution of dimethylmagnesium slowly deposited a white solid on standing.

In order to obtain solvent-free dimethylmagnesium, the ether content of the dimethylmagnesium was determined at various temperatures in the following way.

Into a weighed nitrogen-filled 50 ml distilling flask, connected through an interchangeable joint to a liquid nitrogen trap and thence to a vacuum system, was placed 10 ml of a stock solution of dimethylmagnesium in ether (0.169 mmole/ml by titration, or gravimetrically as the oxinate). The ether was removed by distillation with an external bath at 50° leaving a white solid. The flask was then cooled in dry ice and evacuated to < 0.001 mm pressure. The dry ice was removed and the flask temperature returned to 25° during 20 min. At suitable intervals (ca. 1 h), the flask was filled with nitrogen, removed from the vacuum line, and weighed. The above procedure was repeated at various temperatures so that plots of weight vs. time were obtained. No magnesium was lost from the flask at high temperatures since the magnesium content of the residue was the same after heating as before. The magnesium content was determined by first dissolving the residue in dry ether, hydrolyzing with 15 ml of 0.5 *N* HCl, and precipitating the magnesium as the oxinate (22).

In another experiment, the solvent was removed from an ether solution containing 0.0514 mole (2.79 g) of dimethylmagnesium. Evaporation of the ether with an external bath at 50° left 5.36 g (corresponding to $Me_2Mg \cdot 0.57$ dioxane) of white solid. The flask was cooled in dry ice and evacuated to < 0.001 mm pressure, then warmed to 25° during 20 min. After 10 min at 25° (0.001 mm), the residue weighted 4.79 g (corresponding to $Me_2Mg \cdot 0.44$ dioxane). The cold trap between the sample and the vacuum system was cleaned and the apparatus reassembled. After evacuating the system to < 0.001 mm again, the dimethylmagnesium was heated to 75°. At the end of 4 h, the residue weighed 3.072 g (corresponding to $Me_2Mg \cdot 0.07$ dioxane). This weight is 10% higher than expected from the analysis of the starting solution by titration, but the preceding experiment (Fig. 1) also shows that a 10% weight excess exists even when the ether is removed at a higher temperature. The volatile material collected in the cold trap was distilled *in vacuo* into a weighed tube. The colorless liquid weighed 1.720 g (100%) and melted at 8.5–9.5°. A mixture melting point with dioxane was not lowered.

1-Phenylethanol

(a) From Dimethylmagnesium

To solvent-free dimethylmagnesium (0.0514 mole, 2.79 g) was added 50 ml of benzene, then 6.0 g (0.051 mole) of dextro-2,3-dimethoxybutane (5). Although the solid was insoluble in benzene, dissolution was rapid on addition of the ether and the system became very warm. The ether solution was cooled in an ice bath; then a solution of 6.05 g (0.057 mole) of freshly distilled benzaldehyde in 15 ml of benzene was added to it during 20 min. Fifty min after the addition was complete, the pale yellow solution was hydrolyzed with 50 ml of cold 15% aqueous ammonium chloride. The organic layer was separated, washed with water,

Can. J. Chem. Downloaded from www.nrcresearchpress.com by 210.87.254.40 on 09/05/12
For personal use only.

and dried over anhydrous potassium carbonate. The solvents were removed under reduced pressure and the pale yellow residual oil distilled at 12 mm pressure. The main fraction boiling at 85–86° (12 mm) weighed 4.20 g (67%). The before- and after-fractions, boiling two degrees on either side of this range, amounted to 0.76 g. The oil boiling at 85–86° (12 mm) had a melting range of 5.0–7.5°, $n_D^{20} = 1.5283$, and showed $[\alpha]_D^{25} = -2.43 \pm 0.04°$ in 95% ethanol ($c = 10.03$), $[\alpha]_D^{25} = -3.06 \pm 0.08°$ in chloroform ($c = 5.95$), and $[\alpha]_D^{25} = -2.40 \pm 0.01$ (neat). A portion (1%) of the product was analyzed by gas–liquid chromatography. It contained 15–20% of benzyl alcohol and acetophenone. The rest of the oil was dissolved in 15 ml of petroleum ether and cooled to −12°. The solid which separated was crystallized twice more by the same method to give 0.90 g of material melting at 15–17°. A small amount of material melting at 20.0–20.5° was obtained by further crystallization. The specific rotation of the material melting at 15–17° was −1.0° (neat), $n_D^{20} = 1.5233$. The material in the filtrate from the above purification procedure showed $[\alpha]_D^{25} = -2.75 \pm 0\ 01°$ (neat).

(b) From Methyl Chloride Grignard Reagent

To 2.43 g (0.10 g-atom) of sublimed magnesium under nitrogen was added 7.0 g (0.06 mole) of dextro-2,3-dimethoxybutane (5) in 25 ml of benzene. Methyl chloride was then slowly added to the stirred mixture through a gas inlet tube leading beneath the surface of the organic liquid (the reaction started within 10 min). The reaction mixture was stirred a further 1.5 h at 25° after the addition of methyl chloride (3.0 g, 0.06 mole) was complete, then was diluted with 25 ml of benzene. Titration of an aliquot of the clear, colorless supernatant layer (unchanged magnesium removed) indicated 0.047 equivalents (78%) of basic magnesium.

The stirred ice-cold Grignard solution was treated with 2.66 g (0.025 mole) of freshly purified and distilled benzaldehyde in 15 ml of benzene over a period of 15 min. A colorless oil separated from the reaction medium during the addition. Stirring was continued 20 min longer, then the mixture was hydrolyzed with 50 ml of cold 15% ammonium chloride solution. The organic layer was separated, washed with water, and dried over anhydrous sodium sulphate. Removal of the organic solvents by distillation left a colorless oil that was distilled under reduced pressure. The main fraction distilled at 79–80° (9 mm), weighed 2.5 g (82%), n_D^{20} 1.5251, and had a specific rotation of $[\alpha]_D^{25} = -0.59 + 0.01°$ (neat).

ACKNOWLEDGMENTS

The authors are grateful for financial support from the National Research Council during this investigation. Technical aid from M. Malaiyandi is acknowledged.

REFERENCES

1. W. Schlenk and W. Schlenk. Ber. B, **62**, 920 (1929).
2. M. S. Kharasch and O. Reinmuth. Grignard reactions of non-metallic substances. Prentice-Hall, Inc., New York. 1954. p. 967.
3. C. A. Guthrie, E. Y. Spencer, and G. F Wright. Can. J. Chem. **35**, 873 (1957).
4. D. O. Cowan and H. S. Mosher. J. Org. Chem. **27**, 1 (1962).
5. H. L. Cohen and G. F Wright. J. Org. Chem. **18**, 432 (1953).
6. N. Allentoff and G. F Wright. J. Org. Chem. **22**, 1 (1957).
7. N. Allentoff and G. F Wright. Can. J. Chem. **30**, 900 (1957).
8. H. Gilman, E. Zoellner, and J. B. Dickey. J. Am. Chem. Soc. **51**, 1576 (1929).
9. J. Marshall. J. Chem. Soc. 527 (1914); 509 (1915).
10. A. McKenzie and G. W. Clough. J. Chem. Soc. **103**, 687 (1913).
11. A. J. H. Houssa and J. Kenyon. J. Chem. Soc. 2260 (1930).
12. G. D. Stucky and R. E. Rundle. J. Am. Chem. Soc. **85**, 1002 (1963).
13. E. C. Ashby and W. E. Becker. J. Am. Chem. Soc. **85**, 118 (1963).
14. A. P. Terentiev. Z. Anorg. Chem. **156**, 73 (1926).
15. J. Meisenheimer and W. Schlichenmaier. Ber. B, **61**, 720 (1928).
16. L. W. Gaddum and H. E. French. J. Am. Chem. Soc. **49**, 1295 (1927).
17. J. Decombe and C. Duval. Compt. Rend. **206**, 1024 (1938).
18. W. V. Evans and R. Pearson. J. Am. Chem. Soc. **64**, 2865 (1942).
19. R. E. Dessy and G. S. Handler. J. Am. Chem. Soc. **80**, 5824 (1958).
20. H. Gilman and R. Brown. J. Am. Chem. Soc. **52**, 1181 (1930).
21. A. C. Cope. J. Am. Chem. Soc. **56**, 1578 (1934).
22. I. M. Kolthoff and E. B. Sandell. Textbook of quantitative inorganic analysis. 3rd ed. The Macmillan Co., New York. 1952. p. 362.

Can. J. Chem. Downloaded from www.nrcresearchpress.com by 210.87.254.40 on 09/05/12
For personal use only.

Can. J. Chem. Downloaded from www.nrcresearchpress.com by 210.87.254.42 on 09/05/12
For personal use only.

KINETICS OF THE REACTION $H + D_2 = HD + D$

W. R. SCHULZ AND D. J. LE ROY
Department of Chemistry, University of Toronto, Toronto, Ontario
Received July 6, 1964

ABSTRACT

The authors have measured the rate constant for the reaction $H + D_2 = HD + D$ in the temperature range 368–468° K. This was found to be given by the relation:
$k_4 = 4.3_7 \times 10^{12} \exp(-7.3_0 \times 10^3/RT)$ cm^3 mole^{-1} s^{-1}.
A comparison is made with previous experimental and theoretical work on the reaction.

During the past 30 years much attention has been directed to the possibility of calculating the kinetic parameters for chemical reactions from quantum mechanical principles. In this connection the major proving ground has been the experimental and theoretical study of the following reactions:

[1] $H + H_2 = H_2 + H$
[2] $D + D_2 = D_2 + D$
[3] $D + H_2 = DH + H$
[4] $H + D_2 = HD + D$
[5] $H + HD = H_2 + D$
[6] $D + DH = D_2 + H$
[7] $H + DH = HD + H$
[8] $D + HD = DH + D.$

On the theoretical side, the use of high-speed computers has made possible the calculation, with a considerable degree of sophistication, of the potential energy surfaces of the intermediate complexes (1–4). On the other hand, the available experimental data are far from adequate in providing a test for any theory. Indeed, many of the "experimental" data (e.g. ref. 5) are not experimental in the true sense. The present status of the experimental work has been critically reviewed by Shavitt (3) and need not be treated in detail here. It should be pointed out, however, that the high-temperature experiments (720–1 000 °K) consisted primarily in the determination of the kinetics of the overall reactions,

$$H_{2(p)} = H_{2(o)}$$
$$D_{2(o)} = D_{2(p)}$$
$$H_2 + D_2 = 2HD.$$

In addition to the purely experimental problems associated with the determination of the orders and rate constants for these overall reactions, the subsequent calculation of the rate constants for reactions [1]–[6] from these data (reactions [7] and [8] are unobservable even in this sense) involved a number of assumptions which can be questioned (3). The low-temperature experiments (283–373 °K) involved only a study of reaction [1]. In these experiments the atomic hydrogen was produced by an electrical discharge and its concentration measured with a Wrede gauge. While in principle the method was a good one, the experimental arrangement was such as to lead to uncertainties in the rate constant of a factor varying from 1.5 to 3.7.

Recent improvements in the method of Tollefson and Le Roy (6), and further refinements described here, have encouraged us to reinvestigate the kinetics of these reactions. In this paper we report the results of our investigation of reaction [4]. Because of the

importance of these results we will describe the experimental approach in reasonable detail.

EXPERIMENTAL

The reaction vessel consisted of a pyrex tube 2.54 cm internal diameter and 37 cm long. This was surrounded by a pyrex jacket through which fluid from a thermostat was circulated. The jacket was itself surrounded with glass wool insulation. The temperature of the reactor was maintained within ±0.01 °C; specially constructed tungsten resistance thermometers placed at the entrance and exit of the jacket were used to measure the temperature, subsequently defined as T_w, and the temperature gradient along the reactor. At the highest temperature used the gradient was 0.05 deg in the 37 cm tube.

To the top of the reactor was connected the dissociator chamber in which the atomic hydrogen was formed. This was approximately 30 cm long and 4.5 cm in internal diameter, except at the lower end where it tapered to the internal diameter of the reactor. The dissociator was surrounded by a jacket which was kept at 23 °C with the aid of an external thermostat and circulating system. The top of the dissociator was closed by a pyrex flange with an O-ring seal to which the lead-in wires and the H_2 inlet were attached. The hydrogen was partially dissociated by passage over an electrically heated tungsten spiral which extended over most of the length of the chamber. In the present experiments the concentration of atomic hydrogen produced in this way was varied from 2.5% to 3.5%. The dissociator filament was heated by direct current from a power supply with remote sensing leads which maintained the applied voltage constant to within ±0.025%.

The deuterium, mixed with the reference gas helium, entered the reactor through a capillary tube which passed through the wall of the tube joining the dissociator and reactor and then down the axis of the latter to a distance about 2.5 cm below the level of the jacket. The internal walls of the dissociator and reactor were coated with orthophosphoric acid applied in aqueous solution and subsequently baked under a stream of dry nitrogen.

The H-atom concentration in the reactor was measured with a detector, consisting of a flat spiral of 0.0125 in. diameter platinum wire which reached within about 1 mm of the wall of the reactor; it had a resistance of the order of 0.6 Ω under operating conditions. Two current and two potential leads were connected to the platinum and passed through glass-to-metal seals into a hollow ¼ in. stainless steel shaft. This shaft could be raised or lowered manually to determine the H-atom concentration throughout the reactor.

The bottom of the reactor was connected, through a flange and O ring, to a stainless steel block. This had a cylindrical hole coaxial with the reactor and of somewhat larger diameter which terminated in a flat surface containing a hole just large enough to permit the shaft of the detector to pass through. A Teflon gasket, in the shape of a hollow cone, at this point, and a similar one at the bottom of the block, permitted axial motion of the shaft. Compression of the gaskets was provided by adjustable metal washers. The space between the two gaskets was enlarged and connected to a separate pump to reduce the possibility of air leaking into the reactor, although no leak could be detected across either gasket with a pressure differential of 1 atm. The reaction products were removed through a ⅜ in. diameter hole leading into the side of the block immediately above the upper gasket.

The detector current was supplied by d-c. power supplies stable to ±0.01%. The actual current was measured in terms of the potential drop across a standard 1 Ω resistor in series; the potentials across this and the detector itself were measured with a Leeds and Northrup type K-2 potentiometer.

As in our previous work, the number of H atoms combining on the detector in unit time was measured in terms of W_H, the rate of heat liberation by H-atom combination, expressed as a wattage. Previously we determined W_H from the expression,

[i] $$W_H = R(I_0^2 - I^2),$$

in which I_0 is the current required to keep the detector at a constant temperature, corresponding to the resistance R, in the absence of H atoms, and I is the corresponding value when H atoms are present. The detector therefore acted as an isothermal calorimeter. This method had a number of disadvantages: very careful adjustment of I had to be made to maintain R constant (R was measured in a Wheatstone bridge type circuit); allowance had to be made for the lead resistance and its variation with temperature and with the position of the detector; a great deal of time was required to make the necessary measurements.

In this work the isothermal calorimeter method was given up in favor of determining W_H from the temperature rise (increase in R) brought about by H-atom combination. It was assumed that the rate of loss of energy from the detector was directly proportional to the difference in temperature between the detector and the wall.

[ii] $$W = \alpha(T_d - T_w).$$

It was also assumed that in the temperature range concerned in any particular measurement of W_H the resistance of the detector was a linear function of its temperature

[iii] $$R = R_0(1 + \beta T_d).$$

Can. J. Chem. Downloaded from www.nrcresearchpress.com by 210.87.254.42 on 09/05/12
For personal use only.

For any fixed position of the detector three measurements were made. (*a*) With the dissociator off, the resistance of the detector was measured using a current of 0.02 A. This current, while large enough to obtain four-figure accuracy in the determination of the resistance, was small enough to avoid heating the detector as much as 0.01 deg above its surroundings. This resistance was, therefore, defined as R_w, the resistance corresponding to the wall temperature. (*b*) With the same current, but with the dissociator on, the resistance of the detector was again determined and defined as R_H. (*c*) A calibration was then done by turning the dissociator off and measuring the resistance of the detector with a current of the order of 0.6–0.8 A flowing through it; this was defined as R_c, the corresponding wattage as W_c.

If [ii] and [iii] are valid, it follows that

$$[iv] \qquad W_H = W_c(R_H - R_w)/(R_c - R_w).$$

Equation [ii] was found to hold for any of the pressures and flow rates used in the present work. An example is shown in Fig. 1. The detector was placed in a fixed position and the value of T_w was varied while keeping

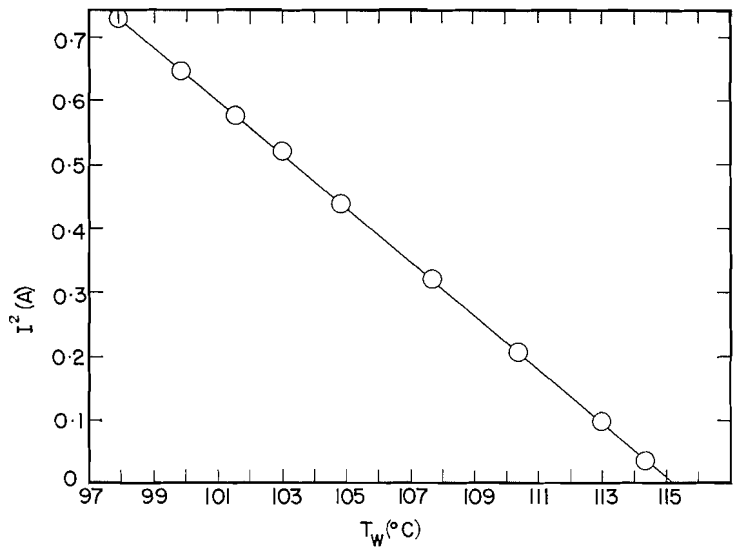

FIG. 1. Test of the relation $W = \alpha(T_d - T_w)$. I is the current required to maintain T_d at 115.2 °C.

the resistance of the detector, and hence its temperature T_d, constant by controlling the current. The wall temperature T_w was measured using the calibrated tungsten thermometers referred to previously. The strict linearity of Fig. 1 justifies the use of [ii]. Equation [iii] would be expected to hold if the temperature range were not too large; it was verified experimentally over the temperature range 90–195 °C.

A further check on the validity of [iv] was made in the presence of atomic hydrogen by measuring W_H by the original bridge method as well as by the new temperature-rise method. The average deviation from unity of the values of W_H determined by the two methods was ±3%. The new method is to be preferred because of its precision and speed.

The reagents were commercial electrolytic hydrogen, and deuterium and helium supplied by Matheson. The hydrogen was purified by passing it through a Deoxo catalytic unit, a trap at liquid nitrogen temperature, a water-cooled cylindrical vessel containing an electrically heated tungsten spiral, and a second trap cooled with liquid nitrogen. Its flow rate was determined in terms of the pressure drop across a calibrated capillary tube, as measured by a sensitive differential manometer. Slip and end corrections were applied to Poiseuille's equation. Immediately before entering the dissociator chamber the hydrogen pressure was reduced to the working value of ca. 3 mm by means of a needle valve.

The deuterium and helium were purified by passage over a hot tungsten filament and through a trap cooled with liquid nitrogen. The mixed gases were stored in a 10 l vessel at approximately 1 atm pressure. During an experiment they were admitted to the reactor through a fine uncalibrated capillary tube after having passed through a buffer volume. The pressure in this volume was kept within ±0.1 mm of a prearranged value in the range of 200 mm by means of an automatic device which controlled the rate of admission to the buffer volume from the storage vessel. The actual flow rate of the deuterium–helium mixture into the reactor could be measured by isolating the buffer volume from the storage vessel and measuring the time required for a calibrated portion of the buffer volume to be filled with mercury; the

Can. J. Chem. Downloaded from www.nrcresearchpress.com by 210.87.254.42 on 09/05/12
For personal use only.

rate of admission of the mercury was automatically controlled to maintain the same fixed pressure in the buffer volume.

The pressure in the reactor was measured with a McLeod gauge calibrated for use in the linear way. Most of the gas leaving from the bottom of the reactor was pumped off with a 40 c.f.m. Stokes Microvac pump. Fluctuations in pressure in the reactor were avoided by providing for sonic flow through a valve placed immediately before the pump. The remaining portion of the gas was removed upstream from this valve and compressed to 1 atm pressure by a Cenco Hyvac 2 pump. Sonic flow through the valve leading to this pump was also arranged. The compressed gas was allowed to flow continuously through a 25 cm^3 volume attached to the sampling valve of the gas chromatograph.

Preliminary experiments showed that under operating conditions there was no change in W_H when the deuterium–helium stream was turned on. Deuterium was therefore conserved by making the β_1 measurements in the absence of deuterium, setting the detector at the final value of x_0 to be used in the deuterium consumption measurements, and then turning on the deuterium–helium flow.

Separate experiments showed that no exchange took place in the sampling system. Hydrogen was used as the carrier gas in the gas chromatographic analysis, so the H_2 peak did not appear, except as indicated below. The column consisted of a 6 ft length of $\frac{1}{4}$ in. copper tubing filled with 80–100 mesh activated alumina; the separation was effected at the temperature of liquid nitrogen. The detector was of the two-thermistor bridge type and was specially constructed to be kept in an ice–water bath. A trace of an original chromatogram is shown in Fig. 2. It is evident that the column not only separates D_2, HD, and He but

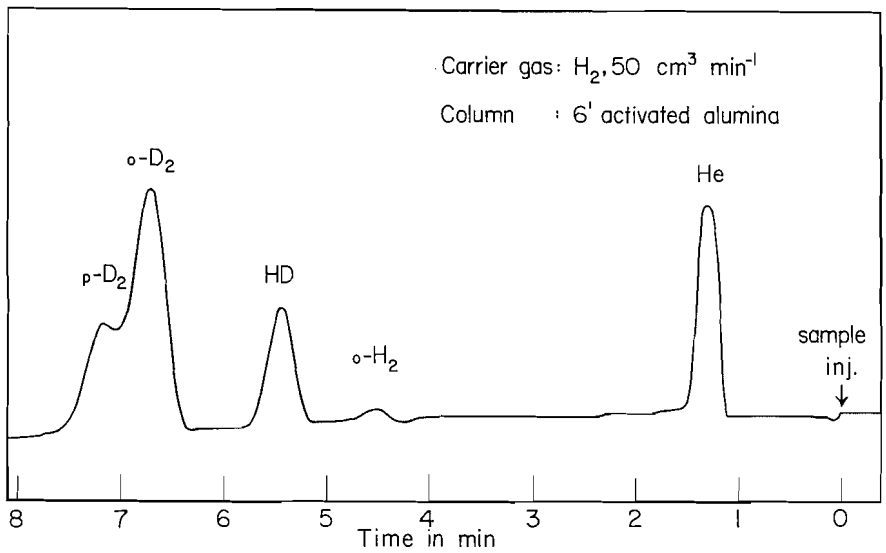

FIG. 2. Gas chromatographic analysis of D_2, HD, and He in the presence of H_2.

also achieves a partial separation of ortho and para deuterium. It also detects the excess ortho hydrogen in the sample; this arises because the ortho hydrogen content of the hydrogen in the sample is nearer to the high temperature equilibrium value of 75% than that of the carrier gas as the result of its passage through the dissociator chamber.

The ratio $[D_2]_0/[D_2]_{x_0}$ required in the calculation of k_4 was obtained from the relation,

$$[v] \qquad [D_2]_0/[D_2]_{x_0} = (A_{D_2}/A_{He})_0/(A_{D_2}/A_{He})_{x_0},$$

in which the A's are chromatographic peak areas (accurate to at least 1%) and the subscripts 0 and x_0 refer to the initial unreacted gas and to the gas leaving the reactor when the detector is at a distance x_0 from the deuterium inlet.

RESULTS AND DISCUSSION

The value of k_4 was obtained from the relation:

$$[vi] \qquad \ln \frac{[D_2]_0}{[D_2]_{x_0}} = \frac{k_4}{f} \int_0^{x_0} [H]\, dx = \frac{k_4 W_H}{4.184 \Delta HDAf(\beta_1 + \beta_2)} \left[\frac{e^{\beta_1 x_0}}{\beta_1} - \frac{1 - e^{-\beta_2 x_0}}{\beta_2} \right],$$

Can. J. Chem. Downloaded from www.nrcresearchpress.com by 210.87.254.42 on 09/05/12
For personal use only.

in which ΔH is the molar enthalpy of formation of atomic hydrogen at the temperature of the detector, D is the diffusion coefficient of atomic hydrogen, A is the cross-sectional area of the reactor, f is the linear flow rate in cm s^{-1}, $\beta_1 = (f/2D)[(1 + 4kD/f)^{1/2} - 1]$, and $\beta_2 = \beta_1 + f/D$; k is the first-order rate constant for the consumption of atomic hydrogen in the reactor.

Equation [vi] is based on the relation between [H] and W_H developed and confirmed experimentally by Schulz and Le Roy (6) and subsequently applied to the reaction between atomic hydrogen and propane (7). It takes into account the influence of the detector on the H-atom concentration in the reactor on the assumption that all H atoms reaching the level of the detector are combined thereon, and that H-atom consumption is first order in [H].

The values of β_1 were determined from plots of $-\ln W_H$ vs. x_0. These all showed some curvature as predicted (6). A smooth curve was drawn through the experimental points and the slope evaluated at a particular value of x_0. Assuming that the initial H-atom concentration is independent of x_0, the slope is equal to $\beta_1 + (\beta_1 + \beta_2)/(e^{(\beta_1+\beta_2)x_0} - 1)$. By setting β_1 equal to the slope in the first approximation, its actual value was obtained by successive approximations. A check on the validity of the values of β_1 obtained in this way was made in several instances by comparing the experimental values of $-\ln W_H$ with those predicted by the relation (6),

[vii] $$W_H = 4.184\Delta HDA[H]_0(\beta_1 + \beta_2)\, e^{-\beta_1 x_0}/(1 - e^{-(\beta_1+\beta_2)x_0}).$$

The value of $[H]_0$, the H-atom concentration at the inlet, was eliminated by arbitrarily making the curve pass through one of the experimental points, the one corresponding to the largest value of x_0. The experimental points fitted the theoretical curve quite well except at small values of x_0 where it was evident that the close proximity of the detector was reducing the value of $[H]_0$ at the inlet. A small error in β_1 could be tolerated, for a sample calculation showed that a change in β_1 of 18% led to a change in k_4 of only 3%.

It was necessary also to consider the effect of an error in D. Values calculated from Amdur's work (8) were used previously (6) and have also been used in the present work. However, if Schulz and Le Roy had taken the value of D at, for example, 1 mm pressure as the quantity to be determined their results (6) would indicate that the accepted value may be low by about 13%. To examine the influence of a possible error in D on the present results we evaluated k_4 using values of D 20% larger than those used in Table I. The effect was to decrease the Arrhenius activation energy by 0.08 kcal $mole^{-1}$ and the A factor by 3%, changes which are within the standard deviations of the present results.

In using eq. [vi] it is assumed that the heat liberated on the detector arises exclusively from the combination of H atoms, i.e. that the number of D atoms reaching the detector is negligible, even though they are produced in reaction [4]. We believe that this assumption can be justified as follows. Since wall recombination is a small effect in this work (β_1 is small), most of the D atoms formed in (4) would either have to undergo reaction (3) or combine on the detector. For a given H-atom concentration the rate of [3] relative to that of [4] will increase as the ratio $[D_2]/[H_2]$ is lowered, so that the correct value of k_4 could be obtained by plotting the experimental values against % D_2 and extrapolating to 0%. In a series of tests in which the bridge method was used to evaluate W_H the values of k_4 at a particular temperature were found to be in the ratio 1:1.04:0.96 for deuterium percentages of 1.81, 1.30, and 0.79, respectively. This would indicate that for these low percentages of D_2 the error is negligible. Actually, in the experiments reported in Table I the percentages of D_2 used were less than 0.5% in all cases. These experiments

Can. J. Chem. Downloaded from www.nrcresearchpress.com by 210.87.254.42 on 09/05/12
For personal use only.

TABLE I

Rate constants for the reaction H + D_2 = HD + D

Expt. No.	T (°K)	P (mm)	D ($cm^2\ s^{-1}$)	f ($cm\ s^{-1}$)	β_1 (cm^{-1})	β_2 (cm^{-1})	W_H (W)	$[D_2]_0$ $[D_2]_{x_0}$	k_4 ($cm^3\ mole^{-1}\ s^{-1} \times 10^8$)
37A	368.2	3.35	565.5	63.97	0.0195	0.1326	0.245	1.292	2.167
37B	368.0	3.44	550.4	60.70	0.0203	0.1306	0.249	1.322	2.101
37C	368.4	3.01	629.6	98.73	0.0195	0.1763	0.485	1.243	1.940
37D	368.8	3.01	631.4	99.77	0.0175	0.1755	0.486	1.245	2.019
43A	386.0	2.98	684.9	92.65	0.0202	0.1555	0.397	1.379	3.246
43B	386.2	2.98	685.3	90.89	0.0199	0.1525	0.398	1.400	3.293
38A	404.8	3.36	654.9	94.80	0.0165	0.1613	0.405	1.604	4.918
38B	404.4	3.38	649.8	93.54	0.0150	0.1590	0.399	1.590	4.833
42A	420.5	3.35	697.3	110.7	0.0184	0.1772	0.440	1.761	7.044
42B	421.0	3.35	698.5	111.2	0.0174	0.1766	0.446	1.746	6.966
39A	439.1	3.76	664.6	115.4	0.0148	0.1884	0.424	2.007	9.795
39B	439.7	3.79	660.7	114.3	0.0164	0.1894	0.405	2.034	10.13
41A	449.9	3.76	690.6	148.5	0.0174	0.2324	0.530	2.178	13.35
41B	449.1	3.77	686.9	147.4	0.0174	0.2320	0.536	2.070	12.16
40	467.7	3.33	829.0	140.6	0.0200	0.1896	0.243	1.635	17.28

Note: the value of x_0 was 27.7 cm in all experiments.

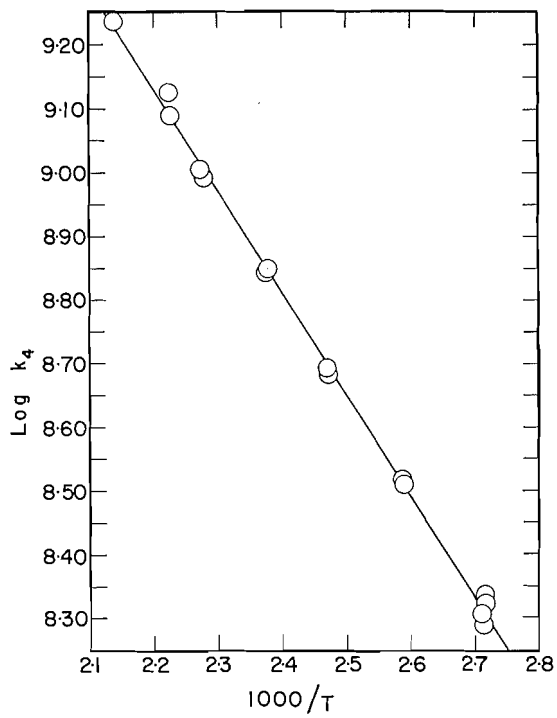

FIG. 3. Arrhenius plot of the rate constants for H + D_2 = HD + D.

support the generally accepted, but as yet experimentally unconfirmed assumption (3) that k_3 is considerably greater than k_4 in the temperature range of the present work.

The final results are given in Table I and are shown in the form of an Arrhenius plot in Fig. 3. A least-squares treatment yielded the relation:

$$k_4 = 4.3_7 \times 10^{12} \exp(-7.3_0 \times 10^3/RT)\ cm^3\ mole^{-1}\ s^{-1}.$$

The standard deviation of E_a was 0.1 kcal $mole^{-1}$, that of $\log_{10} A$ was 0.05.

Can. J. Chem. Downloaded from www.nrcresearchpress.com by 210.87.254.42 on 09/05/12
For personal use only.

The results obtained in the present experiments are not *directly* comparable with any of the previous experimental values. The temperature range used in the present experiments is well below that used in the high-temperature measurements on the rate of $H_2 + D_2$ made by Farkas, by Boato *et al.*, and by van Meersche, and which have been discussed by Shavitt (3). It is probably quite justifiable to extrapolate our results down to 300 °K and up to 500 °K; it may be less justifiable to extrapolate our results to the range 600 – 1 000 °K as the Arrhenius activation energy may increase with temperature (3). However, in Table II we have shown our own rounded and extrapolated results

TABLE II

Comparison of rate constants for $H + D_2 = HD + D$ (k_4 in $cm^3\ mole^{-1}\ s^{-1} \times 10^{-10}$)

T (°K)	This work	Previous expt.	Shavitt[a] I	Shavitt[a] II
300	0.00210		0.00506	0.00385
400	0.0448		0.101	0.0938
500	0.282		0.691	0.684
600	0.959		2.65	2.70
700	2.30	22.9[b]	7.25	7.49
800	4.43	43.6[b]	16.0	16.6
900	7.38	73.9[b]	30.2	31.5
1 000	11.10	120.0[c]	51.5	53.7
		61.0[d]		

[a]Taken directly from Shavitt's paper (3).
[b]van Meersche.
[c]Farkas and Farkas.
[d]Boata, Careri, Cimino, Molinari, and Volpi.

together with the other available experimental values and the calculated values of Shavitt (3). It should be realized that the latter are semi-empirical since Shavitt *assumed* a value of E_c, the classical activation energy without zero-point corrections (8.350 kcal $mole^{-1}$ in calculation I, 8.150 in calculation II). He had reason to believe that the imaginary force constant A_u used in calculation I (-7.32×10^4 dyn cm^{-1}) might be in error by as much as a factor of two, and in calculation II he used the value -3.58×10^4. Rapp and Weston (9) have pointed out that symmetry considerations require that Shavitt's values be multiplied by a factor of two.

In recent calculations on the H_3 system the values obtained for the potential energy barrier, e.g. 9.1 (4) and 9.7 kcal $mole^{-1}$ (10), have been closer to what one might guess the correct value to be than the value of 15.35 obtained by Boys and Shavitt (2). However, these values appear to be extremely sensitive to the triplet repulsions between the end atoms in the complex (10). In a recent interesting deviation from the usual statistical mechanical methods of deriving rate data from the properties of the activated complex, Karplus, Porter, and Sharma (11) have combined their interaction potential (4) with appropriate equations of motion to obtain reaction cross-sections as a function of the relative velocities of the reagents. An Arrhenius plot of the rate constants so obtained gave an activation energy of 7.49 kcal $mole^{-1}$, remarkably close to our value for reaction [4]. Their value of k_3 at 1 000 °K was greater than our extrapolated value of k_4 by a factor of 10.

ACKNOWLEDGMENTS

The authors are grateful to the National Research Council of Canada for generous financial support and for the award of a scholarship to one of us (W. R. S.). We would also like to thank Mr. F. Safian for his assistance.

Can. J. Chem. Downloaded from www.nrcresearchpress.com by 210.87.254.42 on 09/05/12
For personal use only.

REFERENCES

1. R. E. WESTON. J. Chem. Phys. **31**, 892 (1959).
2. S. F. BOYS and I. SHAVITT. University of Wisconsin Naval Research Laboratory Technical Report WIS-AF-13. 1959.
3. I. SHAVITT. J. Chem. Phys. **31**, 1359 (1959).
4. R. N. PORTER and M. KARPLUS. J. Chem. Phys. **40**, 1105 (1964).
5. S. GLASSTONE, K. J. LAIDLER, and H. EYRING. The theory of rate processes. McGraw-Hill Book Co., Inc., New York. 1941.
6. W. R. SCHULZ and D. J. LE ROY. Can. J. Chem. **40**, 2413 (1962).
7. H. A. KAZMI, R. J. DIEFENDORF, and D. J. LE ROY. Can. J. Chem. **41**, 690 (1963).
8. I. AMDUR. J. Chem. Phys. **4**, 339 (1936).
9. D. RAPP and R. E. WESTON. J. Chem. Phys. **36**, 2807 (1962).
10. J. K. CASHION and D. R. HERSCHBACH. J. Chem. Phys. **40**, 2358 (1964).
11. M. KARPLUS, R. N. PORTER, and R. D. SHARMA. J. Chem. Phys. **40**, 2033 (1964).

Can. J. Chem. Downloaded from www.nrcresearchpress.com by 210.87.254.42 on 09/05/12
For personal use only.

Can. J. Chem. Downloaded from www.nrcresearchpress.com by 210.87.254.40 on 09/05/12
For personal use only.

KINETIC STUDIES OF THE AgO/Ag_2O ELECTRODE IN ALKALINE SOLUTIONS

R. G. BARRADAS AND G. H. FRASER[1]
Department of Chemistry, University of Toronto, Toronto, Ontario
Received May 25, 1964

ABSTRACT

The anodic oxidation of Ag_2O to AgO in normal aqueous potassium hydroxide solution was investigated quantitatively under both galvanostatic and potentiostatic conditions at 25 °C. A few results for similar experiments in $N/40$ KOH are also reported. Tafel slopes and other parameters were determined. The experimental results show the dependence of current density as a hyperbolic function of overpotential, i.e. $i = 2i_0 \sinh(\lambda F\eta/2RT)$. The electron number λ was found to be 2 and the symmetry factor β was confirmed to be 1/2. It is proposed that the rate-determining step for the formation of AgO from Ag_2O occurs at the Ag_2O/AgO interface and involves the transfer of O^{-2} ions.

INTRODUCTION

Studies of anodic polarization of silver in aqueous alkaline solutions were extensively examined for many years and comprehensive reviews of this field have been carried out (1, 2). One of the most significant early works was that of Luther and Pokorny (3), who reported the conditions for formation of argentous and argentic oxides (Ag_2O and AgO respectively) when the silver electrode was polarized in normal sodium hydroxide solutions.

The increasing utility and importance of the silver–silver oxide electrodes in lightweight alkaline storage batteries capable of high discharge rates have been a strong incentive for considerable fundamental research activity (4–9). Despite the proliferation in the published literature, there appears to be disagreement concerning the actual thermodynamic and experimental values of potential for the AgO/Ag_2O and Ag_2O/Ag couples. In addition, considerable confusion exists about the kinetics of the reactions taking place on these electrodes. The anodic charging curve indicates that Ag_2O formation ceases in an abrupt manner in the transition region to the higher valent AgO. There does not appear to be any consistent explanation for this phenomenon. Furthermore, there is no agreement about whether the oxidation of silver proceeds via the penetration of the silver lattice by oxide ions (10) or by silver migrating through the oxide layer (11, 12).

The contradictory circumstances are not surprising in view of the inherent complexity of the system and of its associated experimental difficulties. Surface conditions of the electrode must be reproducible in order to obtain reliable current–potential relations, since it is well established that overpotential measurements vary with time as a result of changing surface characteristics.

Hitherto, the mechanisms proposed for the overall reactions,

$$[1] \qquad 2Ag + 2OH^- = Ag_2O + H_2O + 2e$$

$$[2] \qquad Ag_2O + 2OH^- = 2AgO + H_2O + 2e,$$

for the silver–silver oxide electrodes have been somewhat qualitative and speculative in nature owing in part to an absence of reliable kinetic data for diagnostic interpretations.

[1]*Holder of a Province of Ontario Government Fellowship, 1963–1964.*

Can. J. Chem. Downloaded from www.nrcresearchpress.com by 210.87.254.40 on 09/05/12
For personal use only.

EXPERIMENTAL

(a) Electrode Preparation

The anode and reference electrodes were constructed from commercially available silver plate (99.99% Ag and 0.03 in. supplied by Johnson, Matthey and Mallory, Ltd.). The silver was cleaned by washing in dilute nitric acid followed by distilled water. It was then subjected to either (i) mechanical polishing by successively finer grades of emery paper (final grade of 4/0), washed with acetone, and lastly with copious amounts of conductivity water or (ii) to electropolishing based on a modified* cyclic technique (13, 14) in a conventional cyanide bath, followed by repeated washing with liberal amounts of conductivity water. The latter method of polishing silver is slightly more satisfactory but there does not appear to be any significant difference on the course of experimental results obtained for the AgO/Ag_2O electrode. It may be possible, however, that polarization and kinetic studies of the Ag_2O/Ag electrode could depend more critically on the initial surface properties of the silver metal.

The counter and reference electrodes were composed of the Ag_2O/Ag couple and constructed in the same manner, but their thermodynamic properties were remarkably stable. Silver plate of suitable size was anodized at 1 mA/cm^2 until the potential began to rise from the first plateau in the oxidation curve. The electrode was partially reduced and then reoxidized. This procedure was repeated three times and resulted in a stable and satisfactory reference electrode. The potential of the Ag_2O/Ag reference electrode measured against a standard HgO/Hg couple was found to be 0.245 ± 0.002 V, which compares favorably with the value of 0.244 ± 0.005 V reported by Janz and Ives (15). Our experimental value corresponds to 0.343 ± 0.002 V, when calculated with respect to a standard hydrogen electrode as reported by other workers (16, 17, 18).

(b) Reagents and Solutions

The electrolyte was 1 *M* aqueous potassium hydroxide, and this solution was ascertained analytically in every run to contain less than 0.013 molar quantities of potassium carbonate. For some runs the electrolyte was diluted fortyfold. Conductivity water (1.0×10^{-6} mho/cm) was used throughout all the experiments and it was prepared by passing distilled water through an Illco-way research model deionizer or by redistillation in a tin-lined Barnstead Redistiller Model E.P.R. 1/2. The electropolishing bath contained 35 g silver cyanide, 37 g potassium cyanide, and 38 g potassium carbonate per liter.

(c) Electrolytic Cell

Standard two-compartment cells were used for all the experiments. These were constructed from pyrex glass and were capped with closed ground glass joints which had appropriate openings through the top for the insertion of the anode, cathode, and pre-electrolysis electrodes. The reference electrode was used in conjunction with a Luggin capillary probe. The ground glass joints were employed with close-fitting plastic sleeves and partly insulated with silicone grease to prevent "freezing" of the joints.

(d) Electrical Measurements

The galvanostatic and potentiostatic measurements were carried out at room temperature and corrected to 25 °C on a simple apparatus constructed in our laboratory, comprised of an electromechanical potentiostat and a constant current source. Details of this instrument will be published elsewhere.

(i) Galvanostatic Measurements

The anode was oxidized at a chosen constant current and after a predetermined amount of charge had passed, the driving applied potential was decreased. The new constant current was noted and the corresponding change in electrode potentials recorded. The potentials were recorded at each different constant current for periods of approximately 5 to 15 s. More rapid changes of constant current would lead to undesired voltage transients. On the other hand, any excessive polarization times would result in drastic changes of electrode surface conditions, giving kinetic data which would be almost impossible to resolve. The choice of intermediate time intervals of approximately 10 s duration tends to give reproducible Tafel behavior within reasonable limits of experimental error. On this basis one could assume that surface conditions of the electrode are moderately stable.

(ii) Potentiostatic Measurements

The electrode was polarized at several constant potentials for a few minutes at a time and the corresponding currents were determined. The polarization times were much longer than those used in the

**The cyclic technique means the attainment of oscillatory fluctuations in current during the electrolytic polishing process. Successful electropolishing depends on many factors, such as the composition of the bath, electrolytic cell geometry, history of the electrode, temperature, electrode separation and configuration, amount of applied current, cell voltage, and rate of stirring of the electrolyte. Quantitative changes of these and other parameters affect the nature of the finished surface. The cycling phenomenon results from repeated formation and destruction of the oxide films. Bright and smooth surfaces depend primarily on the achievement of cycling and at a rate of approximately 5–10 cycles per second under d-c. electrolysis. We have observed that the superimposition of an a-c. on the d-c. signal did not appreciably increase the rate of cycling, but it has led in several instances to an improved polish when viewed under a microscope. Further work in this area is presently being carried out and will be reported in detail elsewhere.*

galvanostatic studies reported above, but at considerably lower apparent current densities, which does not alter the surface conditions significantly.

RESULTS

(i) Galvanostatic Runs

Potential measurements were obtained at constant currents and plotted in a conventional Tafel manner (see Fig. 1). Average Tafel slopes ($2.3\ RT/\lambda\beta F$) for sets of runs

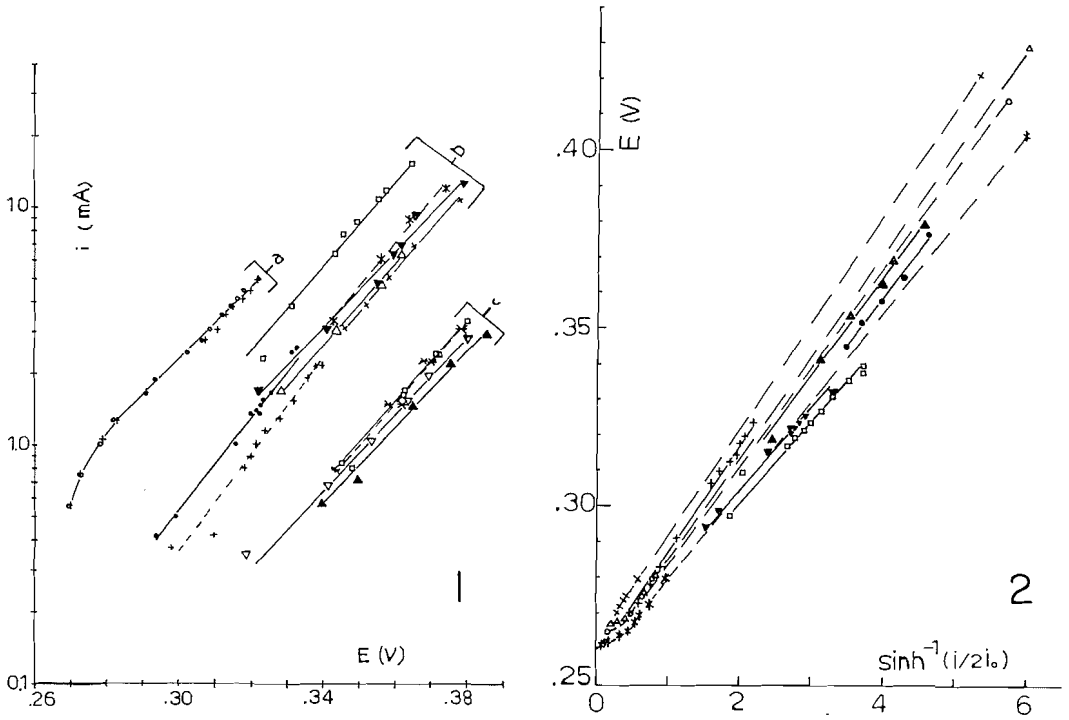

FIG. 1. Tafel plots for galvanostatic runs. Set *a*: two runs with mechanically polished electrodes in 1 *N* KOH. Set *b*: seven runs with electropolished electrodes in 1 *N* KOH. Set *c*: four runs with electropolished electrodes in *N*/40 KOH.

FIG. 2. Typical dependence of potential as hyperbolic function of current. Broken lines, potentiostatic data; solid lines, galvanostatic data.

marked *a*, *b*, and *c* were 0.0658 ± 0.0002, 0.0567 ± 0.0032, and 0.0595 ± 0.0007 respectively. They lead to respective calculated values of 0.90, 1.04 ± 0.06, and 0.99 ± 0.01 for the product $\lambda\beta$; λ, the stoichiometric number, is a small integer indicating the amount of charged passed in the rate-determining step and β is the usual symmetry factor. It is evident that if β is assumed to be 1/2 then we would obtain a value of approximately 2 for λ. For convenience the detailed information relating to Fig. 1 is summarized in Table I. Better reproducibility of potential measurements was obtained in the dilute electrolyte (*N*/40).

(ii) Potentiostatic Runs

In the low overpotential region (below 0.280 V) linear relations between current and potential have been obtained under potentiostatic conditions for mechanically polished electrodes. From these linear plots we have obtained values of $i_0\lambda$, according to the following equation:

$$i = i_0\lambda(F\eta/RT). \qquad [3]$$

Can. J. Chem. Downloaded from www.nrcresearchpress.com by 210.87.254.40 on 09/05/12
For personal use only.

TABLE I
Data for galvanostatic experiments

Run No.	Tafel slopes (2.3b)	"b" values (25 °C)	$\lambda\beta$	Experimental condition
1	0.0656	0.0285	0.90	
2	0.0660	0.0287	0.90	Set a*
3	0.0567	0.0246	1.04	
4	0.0578	0.0251	1.02	
5	0.0502	0.0218	1.17	
6	0.0525	0.0228	1.11	Set b†
7	0.0610	0.0265	0.97	
8	0.0567	0.0246	1.04	
9	0.0624	0.0271	0.94	
10	0.0590	0.0256	1.00	
11	0.0597	0.0259	0.99	
12	0.0607	0.0263	0.97	
13	0.0588	0.0256	1.00	Set c‡

*Set a: mechanically polished electrodes in 1 N KOH.
†Set b: electropolished electrodes in 1 N KOH.
‡Set c: electropolished electrodes in N/40 KOH.

At very low overpotentials (below 0.268 V)* some deviations from linearity were observed

DISCUSSION

The general equation for an activation-controlled anodic process can be written as

$$i = i_0 \exp(\beta\lambda F\eta/RT) - i_0 \exp[-(1-\beta)\lambda F\eta/RT]. \quad [4]$$

If the symmetry factor is equal to 1/2, one could write (19, 20)

$$i = 2i_0 \sinh(\lambda F\eta/2RT). \quad [5]$$

At high overpotentials eq. [4] reduces to the familiar Tafel relation

$$\eta = a + b \ln i. \quad 6]$$

However, at low overpotentials eq. [4] reduces to eq. [3], namely

$$i = i_0\lambda F\eta/RT. \quad [3]$$

Equation [5] can be written in the following form:

$$E/b = \sinh^{-1}(i/2i_0) + E_R/b, \quad [7]$$

where $E = \eta + E_R$ (E_R is the reversible potential of the AgO/Ag$_2$O couple) and

$$b = RT/\lambda F\beta \text{ or } 2RT/\lambda F. \quad [8]$$

From the Tafel plots (Fig. 1) for the galvanostatic results, i_0 values were obtained for each run by extrapolating the E vs. log i plot to the reversible potential of AgO/Ag$_2$O. Using these i_0 values in eq. [7] we obtain "b" values for the sets of runs a, b, and c of 0.0302 ± 0.0001, 0.0230 ± 0.0005, and 0.0262 ± 0.0002 respectively (listed in Table II), which are consistent with those derived from eq. [6] of 0.0286 ± 0.0001, 0.0246 ± 0.0014, and 0.0258 ± 0.0002. This treatment of the galvanostatic results was done to make comparison with the type of results obtained in the potentiostatic runs at lower fields. The overall results imply that the slope "b" remains relatively unchanged over the entire

*The observed reversible potential of the AgO/Ag$_2$O electrode vs. the Ag$_2$O/Ag electrode is in agreement with the value of 0.262 V reported by Bonk and Garrett (21).

Can. J. Chem. Downloaded from www.nrcresearchpress.com by 210.87.254.40 on 09/05/12
For personal use only.

TABLE II

Comparative potentiostatic and galvanostatic data derived from eq. [10]

Run No.	"b" Values (25 °C)	$\lambda\beta$	Experimental condition
1	0.0303	0.85	Galvanostatic set a*
2	0.0301	0.85	
3	0.0232	1.10	
4	0.0234	1.09	Galvanostatic set b†
5	0.0220	1.16	
6	0.0233	1.10	
11	0.0260	0.99	Galvanostatic set c‡
12	0.0264	0.98	
i	0.0278	0.92	
ii	0.0302	0.85	
iii	0.0290	0.89	Potentiostatic set a*
iv	0.0253	1.02	
v	0.0284	0.91	

*Set a: mechanically polished electrodes in 1 N KOH.
†Set b: electropolished electrodes in 1 N KOH.
‡Set c: electropolished electrodes in $N/40$ KOH.

range of overpotentials studied and also that the assumption of $\beta = 1/2$ is reasonably correct, otherwise eq. [7] would not be valid.

In the potentiostatic runs reported above, potential and current were in general linearly related but deviations were observed at very low overpotentials. The deviations from linearity may be due to either new kinetic processes or changes in surface conditions owing to the extended time of polarization. The latter explanation seems more acceptable when one considers that the potentials were decreased by manual control over a long period of time. One also notices that on reversing the procedure of measurement, i.e. from lower to higher potentials, somewhat smaller currents were observed. This gives in part some substance to the speculation that surface conditions may change, which may account for the variations in exchange currents experienced from run to run.

Since we have derived values of λi_0 from the potentiostatic runs, we can now choose suitable integral values of λ to calculate i_0. The computed values of i_0 were used to replot the results of each respective potentiostatic run according to eq. [7] (see Fig. 2). A hyperbolic relation between current and potential at conditions of low overpotentials (ca. 20 mV) is in itself not entirely significant, since eq. [7] readily reduces to eq. [3]. However, we have made corresponding measurements (i.e. within closely related time intervals and therefore similar electrode conditions) under galvanostatic control at considerably higher overpotentials (in excess of 140 mV). The latter results are linearly aligned with the plots obtained from eq. [7] at low overpotentials (see Fig. 2).

To derive "b" values from the potentiostatic data we had to make arbitrary choices for λ. The values of "b" were found to be relatively insensitive to choices of λ, e.g. when λ was changed from 2 to 4, the average value of "b" was decreased by only 8%. The choice of $\lambda = 2$ is justified from the observed slope of eq. [7].

The values of "b" and the corresponding values of $\lambda\beta$ for both galvanostatic and potentiostatic runs are summarized in Table II. Fairly good agreement within the limits of experimental error is reported. All the results are consistent with the conclusion that $\lambda = 2$ and $\beta = 1/2$, and hence the experimental Tafel slope for the formation of AgO from Ag_2O is $2.3RT/F$.

Recent stereochemical neutron diffraction studies (22) have confirmed that there are

Can. J. Chem. Downloaded from www.nrcresearchpress.com by 210.87.254.40 on 09/05/12
For personal use only.

two types of silver atoms in the AgO unit cell with bond lengths corresponding to the covalent bonding properties of $Ag^+(4\ d^{10})$ and $Ag^{3+}(4\ d^8)$. The two types of silver contained in the lattice explain the diamagnetic properties of AgO and exclude the presence in the lattice of $Ag^{2+}(4\ d^9)$. Hence one can write $2\ AgO \equiv Ag(I) - Ag(III)O_2$ and conversely one could write $Ag_2O \equiv Ag(I)_2O$.

We may consider the possibilities of a rate-determining reaction occurring at any of the three interfaces, i.e. the metal/Ag_2O, Ag_2O/AgO, and AgO/electrolyte (see Fig. 3). It

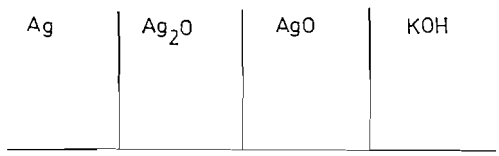

FIG. 3. Interfacial regions of the silver/silver oxide electrode in aqueous alkaline solution.

would be reasonable to eliminate reactions at the metal/Ag_2O interface, since only electron transfer could occur at this junction. For the other two interfaces one can propose mechanisms of the following type which would be consistent with the structural evidence cited above.

At the oxide/electrolyte interface we may write

[9] $$(OH^-)_{aq} = (OH^-)_s$$

followed by either [10], [11], or [12]

[10] $$(OH^-)_s + (OH^-)_{aq} = H_2O + (O^{-2})_s$$

[11] $$2(OH^-)_s = H_2O + (O^{-2})_s$$

[12] $$\begin{cases} (OH^-)_s = (H^+)_{aq} + (O^{-2})_s \\ \text{and} \\ (H^+)_{aq} + (OH^-)_{aq} = H_2O. \end{cases}$$

Reaction [12] represents a disproportionation of the adsorbed hydroxyl ion. The subscripts "s" and "aq" refer to the solid surface and the aqueous phases respectively.

At the Ag_2O/AgO interface we postulate the following reaction:

[13] $$Ag^+ = Ag^{3+} + 2e.$$

For reaction [13] we can write the following equations. For $\beta = 1/2$,

[14] $$v_1 = k_1[Ag^+] \exp(2\beta\eta F/RT) = k_1' \exp(\eta F/RT)$$

[15] $$v_{-1} = k_{-1}[Ag^{3+}] \exp(-2(1-\beta)\eta F/RT) = k_{-1}' \exp(-\eta F/RT);$$

$[Ag^+]$ and $[Ag^{3+}]$ may be assumed to be constant since both are solid-state concentration terms.

When $\eta = 0$,

[16] $$i_0 = i_1 = 2Fk_1[Ag^+] = i_{-1} = 2Fk_{-1}[Ag^{3+}].$$

From [14], [15], and [16] we obtain

[17] $$i = i_1 - i_{-1} = 2i_0 \sinh(\eta F/RT).$$

Hence $b = RT/F$.

We suggest that the rate-determining step may be given by eq. [13] and that the actual

Can. J. Chem. Downloaded from www.nrcresearchpress.com by 210.87.254.40 on 09/05/12
For personal use only.

mechanism of formation of AgO from Ag_2O involves [13] in conjunction with [9] and either [10], [11], or [12]. In essence we propose that O^{-2} ions can migrate by ionic conduction through the AgO layer to the mixed oxide interface where the slow step may take place. The migration process cannot be a rate-controlling step since there has been no dependence of the observed Tafel slope on the extent of conversion of Ag_2O to AgO, i.e. on the thickness of the AgO film. The two electrons shown in [13] may be presumed to enter the Ag_2O layer. Since Ag_2O has been suggested as a metal-deficit oxide (cf. Cu_2O) with cation vacancies (i.e. a p-type semiconductor (23)), the electrons may be expected to fill positive holes. Creation of new positive holes in the Ag_2O layer may occur by charge transfer across the Ag/Ag_2O interface.

There is also the possibility that the rate-controlling step could be the transfer of O^{-2} ions across the Ag_2O/AgO interface. If we consider that O^{-2} ions move over a symmetrical energy barrier, we would obtain a set of results comparable to that derived from [14], [15], and [16], namely forward and reverse slopes of RT/F and $-RT/F$ respectively. This mechanism, although equivalent in result to [13], is somewhat more attractive because there is no certainty that reaction [13] should lead to a one-step 2-electron liberation. One can allow for the possibility of two 1-electron steps. Furthermore, it is a simpler physical picture to visualize a mechanism involving the transfer of O^{-2}, followed by the coalescence of 2 p-holes and one Ag^+ ion in the Ag_2O layer to form the Ag^{3+} species.

Our theoretical analysis leads to results in good agreement with experimental evidence. This supports our contention that the rate-determining step for the formation of AgO from Ag_2O is probably the reaction involving the transfer of O^{-2} ions, which occurs at the mixed oxide interface. The small deviations in galvanostatic and potentiostatic measurements mentioned earlier in the experimental section may be adduced as additional evidence that this statement is correct. The Ag/Ag_2O and the AgO/electrolyte interfaces can conceivably be fairly stable in surface conditions. However, the suggested fluctuations of surface conditions referred to previously must be due to internal disruptions which originate at the Ag_2O/AgO interface. This must result in a departure from the idealized smooth "sandwich layers" of the two oxides as depicted in Fig. 3.

We have examined various other mechanisms involving the adsorption of *ionic* intermediates at the AgO/electrolyte interface and calculated the Tafel slopes using modifications of the theories proposed by Conway and his co-workers (24, 25). These predicted slopes were not in agreement with our experimental results for the silver oxide electrode. Our modified calculations and reaction schemes, showing dependence on Langmuir and Temkin conditions of surface coverage, which may be applicable to semiconductor oxide/solution interfaces other than AgO, will be presented in a future communication (26).

ACKNOWLEDGMENTS

The authors are indebted to the late Professor F. E. W. Wetmore, who initiated this project. Some experimental aspects described here are contained in an M.A. thesis by one of us (G. H. F.), who worked under his direction. After his untimely death in January 1963 the authors continued the work which led to the eventual conclusions reported in this paper. We are grateful to Professor M. J. Dignam for reading the manuscript and offering helpful discussions, and also to Mr. R. E. Barry for his assistance with the galvanostatic experiments performed on the mechanically polished electrodes. We wish to thank the National Research Council of Canada and the University of Toronto for generous financial support.

Can. J. Chem. Downloaded from www.nrcresearchpress.com by 210.87.254.40 on 09/05/12
For personal use only.

Can. J. Chem. Downloaded from www.nrcresearchpress.com by 210.87.254.40 on 09/05/12
For personal use only.

REFERENCES

1. T. P. DIRKSE. J. Electrochem. Soc. **106**, 453 (1959).
2. G. H. FRASER. M.A. Thesis, University of Toronto, Toronto, Ont. 1961.
3. R. LUTHER and F. POKORNY. Z. Anorg. Allgem. Chem. **57**, 290 (1908).
4. C. P. WALES and J. BURBANK. J. Electrochem. Soc. **106**, 885 (1959).
5. C. P. WALES. J. Electrochem. Soc. **108**, 395 (1961).
6. T. P. DIRKSE. J. Electrochem. Soc. **109**, 173 (1962).
7. C. P. WALES. J. Electrochem. Soc. **109**, 1119 (1962).
8. T. P. DIRKSE and G. J. WERKEMA. J. Electrochem. Soc. **106**, 88 (1959).
9. B. D. CAHAN, J. B. OCKERMAN, R. F. AMLIE, and P. RÜETSCHI. J. Electrochem. Soc. **107**, 725 (1960).
10. T. P. DIRKSE. J. Electrochem. Soc. **106**, 920 (1959).
11. H. GÖHR and E. LANGE. Z. Physik. Chem. Frankfurt, **17**, 100 (1958).
12. D. I. LEIKIS, G. L. VIDOVICH, L. L. KNOZ, and B. N. KABANOV. Z. Physik. Chem. Leipzig, A, **214**, 334 (1960).
13. L. I. GILBERTSON and O. W. FORTNER. Trans. Electrochem. Soc. **81**, 199 (1942).
14. H. T. FRANCIS and W. H. COLNER. J. Electrochem. Soc. **97**, 237 (1950).
15. D. J. G. IVES and G. J. JANZ. Reference electrodes, theory and practice. Academic Press, Inc., New York. 1961.
16. W. J. HAMER and D. N. CRAIG. J. Electrochem. Soc. **104**, 206 (1957).
17. G. CHARLOT. Selected constants : oxydo-reduction potentials. Pergamon Press, Ltd., London. 1958.
18. W. M. LATIMER. Oxidation potentials. 1st ed. Prentice-Hall, Inc., New York. 1938.
19. H. B. MORLEY and F. E. W. WETMORE. Can. J. Chem. **34**, 359 (1956).
20. A. A. ANTONIOU and F. E. W. WETMORE. Can. J. Chem. **37**, 222 (1959).
21. J. F. BONK and A. B. GARRETT. J. Electrochem. Soc. **106**, 612 (1959).
22. V. SCATTURIN, P. L. BELLON, and A. J. SALKIND. J. Electrochem. Soc. **108**, 819 (1961).
23. A. A. YAKOVLEVA, T. I. BORISOVA, V. I. VESELOVSKII. Russ. J. Phys. Chem. English Transl. **36**, 763 (1962).
24. B. E. CONWAY and E. GILEADI. Trans. Faraday Soc. **58**, 2493 (1962).
25. B. E. CONWAY and M. DZIECIUCH. Can. J. Chem. **41**, 21 (1963).
26. R. G. BARRADAS and G. H. FRASER. In preparation.

Can. J. Chem. Downloaded from www.nrcresearchpress.com by 210.87.254.40 on 09/05/12
For personal use only.

CHARACTERISTIC VIBRATIONAL FREQUENCIES OF COMPOUNDS CONTAINING Si—O—Si, P—O—P, S—O—S, AND Cl—O—Cl BRIDGING GROUPS

FORCE CONSTANTS AND BOND ORDERS FOR THE BRIDGE BONDS

R. J. GILLESPIE
Department of Chemistry, McMaster University, Hamilton, Ontario
AND
E. A. ROBINSON
Department of Chemistry, University of Toronto, Toronto, Ontario

Received May 22, 1964

ABSTRACT

The assignment of characteristic frequencies for the X—O—X group in compounds containing Si—O—Si, P—O—P, S—O—S, and Cl—O—Cl bonds is discussed with reference to the vibrational spectra of disiloxanes, diphosphoryl, and disulphuryl compounds and dichlorine heptoxide. The stretching force constants of the X—O—X bridging bonds have been obtained by treating the molecules as simple triatomic species X_2O. X—O bond orders and bond lengths have been calculated from the stretching force constants and the calculated and observed bond lengths are compared. The variation in the observed X—O—X angles is related to the bond orders and is discussed in terms of the electron-pair repulsion theory. It is shown that bond orders in the isoelectronic series $Si_2O_7^{6-}$, $P_2O_7^{4-}$, $S_2O_7^{2-}$, and Cl_2O_7 may be simply deduced from the empirical rule that the valency shell of a second-row element tends to be occupied by twelve electrons (the duodecet rule).

INTRODUCTION

We have recently proposed assignments for the characteristic vibrational frequencies of the S—O—S group in molecules such as the disulphuryl halides and SF_5OSF_5 (1). In this paper we discuss the characteristic vibrational frequencies of compounds containing the Si—O—Si group (e.g. the disiloxanes), the P—O—P group (e.g. diphosphoryl compounds), and the Cl—O—Cl group. From the frequencies and calculated force constants, information is obtained concerning the nature of Si—O—Si, P—O—P, S—O—S, and Cl—O—Cl bonds.

RESULTS

Compounds Containing the Si—O—Si Group

The occurrence of the asymmetric Si—O—Si stretch, ν_a, at approximately 1 050 cm^{-1} is well recognized and has been used previously as a diagnostic frequency for compounds containing Si—O—Si bonds (2), but the occurrence of the symmetric stretching frequency, ν_s, in the region 400–600 cm^{-1} has only recently been firmly established by Kriegsmann (3, 4, 5) although it had been recognized earlier by Lord and co-workers (6) as having frequencies of 606 and 555 cm^{-1} in the vibrational spectra of disiloxane and disiloxane-d_6 respectively. Table I shows the Si—O—Si frequencies (ν_s, ν_a, and ν_b, the bending mode) for a number of disiloxanes. Some of the data are taken from the work of Kriegsmann (3, 4, 5); in other cases we have reassigned the spectra observed by other workers. Lord and co-workers (6) find a frequency of 68 cm^{-1} for the bending vibrations of $[H_3Si]_2O$ and $[D_3Si]_2O$. They suggest that the Si—O—Si group is quasi-linear because of the large value of the Si—O—Si bond angle and that the Si—O—Si bending vibration may be highly anharmonic. For this particular molecule, therefore, the simple valence – force field

TABLE I

Characteristic Si—O—Si vibrational frequencies

Compound	State	Frequencies (cm^{-1}) ν_s	ν_a	ν_b	Ref.
$(H_3Si)_2O$	Gas	606	1 107	68	*a*
$(D_3Si)_2O$	Gas	555	1 094	—	*a*
$[H_2(CH_3)Si]_2O$	Gas	—	1 085	—	*b*
$[H(CH_3)_2Si]_2O$	Gas	552	1 073	188	*c*
	Liquid	550	1 058	—	*c*
$[(CH_3)_3Si]_2O$	Gas	—	1 073	180	*d*
	Liquid	522	1 055	—	*c*
$[HO(CH_3)_2Si]_2O$	Liquid	554	1 073	143*	*c*
$[Cl(CH_3)_2Si]_2O$	Liquid	488†	1 070	145*	*c*
$[C_6H_5(CH_3)_2Si]_2O$	Liquid	475†	1 063	191*	*c*
$[(C_6H_5)_3Si]_2O$	Liquid	393	1 075	99*	*e*
$(Cl_3Si)_2O$	Liquid	475	1 120	—	*c*
$[(C_2H_5)_3Si]_2O$	Liquid	493	1 010	141*	*c*
$Si_2O_7^{6-}$	Aqueous solution	503	1 029	169	*e*

*Lowest frequency observed.
†Reassignment.
[a]Lord *et al.*, ref. 6.
[b]E. A. V. Ebsworth, M. Onyszchuk, N. Sheppard, and J. T. Braunholtz. J. Chem. Soc. 1453 (1958).
[c]Kriegsmann, ref. 3.
[d]Kriegsmann, ref. 4.
[e]Kriegsmann and Schowta, ref. 5.

type of calculation of force constants is probably unreliable. Nevertheless we find that, in general, force constants obtained in this way are consistent with observed bond lengths. We have arbitrarily assigned ν_b, in compounds where no complete vibrational assignment is available, as the lowest frequency observable in the Raman spectrum. In the light of the results of Lord and co-workers (6) these arbitrarily assigned frequencies may all be too high, but we show later that this could give only a small error in the calculated values of the stretching force constants.

It is interesting to note that there appears to be a linear correlation between ν_s and $M^{\frac{1}{2}}$, where M is the mass of the group attached to silicon, as has been observed previously for the SOS group (Fig. 1). In this connection it is useful to examine the nature of $\nu_s(\nu_1)$ and

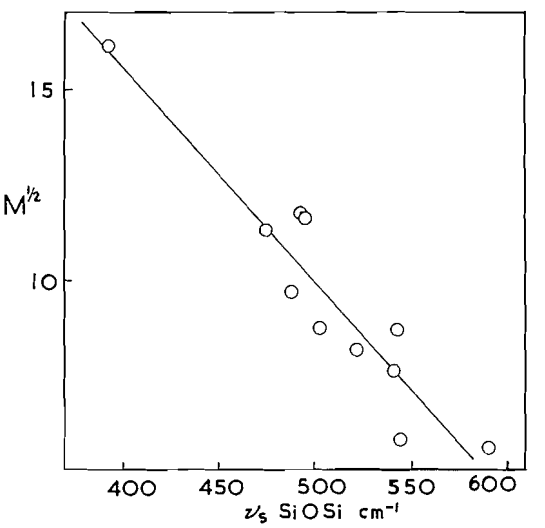

FIG. 1. Correlation between $\nu_{Si-O-Si}$ (sym.) and $M^{\frac{1}{2}}$.

Can. J. Chem. Downloaded from www.nrcresearchpress.com by 210.87.254.40 on 09/05/12
For personal use only.

$\nu_a(\nu_3)$ in a simple triatomic molecule YX_2. We assume that we can regard the compounds under discussion as triatomic molecules OX_2 where X is a group with a relatively large mass compared to that of oxygen. Herzberg (7) gives the vibrational frequencies and amplitudes of vibration for H_2O, F_2O, and Cl_2O, and as the mass of X becomes greater the asymmetric stretch (ν_3) can be reasonably described as a vibration in which only the oxygen atom moves. This is consistent with the observation that ν_a, in e.g. compounds containing the Si—O—Si group, occurs at a relatively constant frequency which is determined mainly by the character of the Si—O bonds and not by the mass of the group X. However, as the mass of X increases the symmetric stretch (ν_1) which in the case of H_2O involves essentially the motion of the H atoms only and has a frequency close to that of the asymmetric stretch, takes on much of the character of a bend involving movement of both the heavy X groups and the oxygen atom. It thus seems reasonable that the symmetric stretch becomes widely separated from the asymmetric stretch, and occurs at a much lower frequency as the mass of X increases.

Compounds Containing the P—O—P Group

Unfortunately there has been much less accurate work on compounds containing a P—O—P bridging group than on Si—O—Si or S—O—S compounds. The P—O—P asymmetric stretch is relatively well established at approximately 950 cm^{-1} (2, 8), but the frequencies of the P—O—P symmetric stretch and bend are less well known. Table II shows collected values of ν_s and ν_a for most of the diphosphoryl compounds that have been investigated. The only Raman or low-frequency infrared measurements that are available are those for the pyrophosphate ion (9, 10), the dihydrogen pyrophosphate ion (10), diphosphoryl tetrachloride (11, 12), and diphosphoryl tetrafluoride (13).

Compounds Containing the S—O—S Group

Assignments of the characteristic frequencies of the S—O—S bridging group have been discussed previously and are shown in Table III (1). Recently Walrafen, Irish, and Young (14) have discussed the vibrational spectra of S_2O_7 groups in the $S_2O_7^{2-}$ and $HS_2O_7^-$ ions and $H_2S_2O_7$. Without giving any detailed justification, they assign the symmetric stretching vibration of the S—O—S group of $S_2O_7^{2-}$, $HS_2O_7^-$, and $H_2S_2O_7$ at 730–738, 702–735, and 732–735 cm^{-1}, respectively and the asymmetric stretching vibrations at 790, 799, and 805–806 cm^{-1}, respectively. They assign the bending vibrations at 320–335, 316–325, and 325–326 cm^{-1}, respectively.

These assignments are in line with those of earlier workers, which we criticized previously (1).

Compounds Containing the Cl—O—Cl Group

The only known compound, apart from triatomic Cl_2O, which contains a Cl—O—Cl bridge is dichlorine heptoxide, Cl_2O_7. The vibrational spectrum has been investigated by Fonteyne (15) and recently by Savoie and Giguère (16). The latter authors assign lines in their spectra at 695, 429, and 280 cm^{-1} to ν_a, ν_s, and ν_b, respectively. They report all three lines to be polarized in the Raman spectrum. Although the line appears to be polarized in the Raman spectrum, the frequency of 695 cm^{-1} seems appropriate for the asymmetric stretch; moreover, there is no other line in the reported spectrum which could be reasonably assigned to this vibrational mode. In the light of the previous discussion of the characteristic frequencies of Si—O—Si, P—O—P, and S—O—S bonds a frequency of 429 cm^{-1} seems too high for ν_s in Cl_2O_7. The values of ν_a for Si—O—Si, P—O—P, S—O—S, and Cl—O—Cl bonds are approximately 1 050, 950, 800, and 695 cm^{-1}, respectively, and we have assigned

Can. J. Chem. Downloaded from www.nrcresearchpress.com by 210.87.254.40 on 09/05/12
For personal use only.

TABLE II

Characteristic P—O—P vibrational frequencies

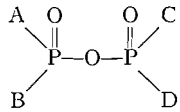

A	B	C	D	Frequencies (cm^{-1}) ν_s	ν_a	ν_b	Ref.
Cl	Cl	Cl	Cl	425	966	159	*a*
F	F	F	F	480	987	160	*b*
F	Cl	F	Cl	—	1 020 (?)	—	*c*
O^-	OH	O^-	OH	514(K^+) 507(Na^+)	954, 953	—	*d*
O^-	O^-	O^-	O^-	519(K^+)	966	—	*d*
C_2H_5O	CH_3	CH_3	C_2H_5O	—	943	—	*e*
i-C_3H_8O	CH_3	CH_3	*i*-C_3H_8O	—	945	—	*e*
sec-$C_4H_{11}O$	CH_3	CH_3	*sec*-$C_4H_{11}O$	—	947	—	*e*
C_2H_5O	C_2H_5	C_2H_5	C_2H_5O	—	922	—	*e*
i-C_3H_8	C_2H_5	C_2H_5	*i*-C_3H_8	—	922	—	*e*
sec-$C_4H_{11}O$	C_2H_5	C_2H_5	*sec*-$C_4H_{11}O$	—	928	—	*e*
C_2H_5O	C_2H_5O	C_2H_5O	C_2H_5O	—	940	—	*e*
$(CH_3)_2N$	$(CH_3)_2N$	$(CH_3)_2N$	$(CH_3)_2N$	—	925	—	*e*
$(CH_3)_2N$	$(CH_3)_2N$	C_2H_5O	$(CH_3)_2N$	—	926	—	*e*
$(CH_3)_2N$	C_2H_5O	$(CH_3)_2N$	C_2H_5O	—	938	—	*e*
$(CH_3)_2N$	$(CH_3)_2N$	C_2H_5O	C_2H_5O	—	940	—	*e*
CH_3O	CH_3O	CH_3O	CH_3O	—	980	—	*e*
$C_4H_{11}O$	$C_4H_{11}O$	$C_4H_{11}O$	$C_4H_{11}O$	—	953	—	*e*
$(CF_3)_2P—O—P(CF_3)_2$				—	925, 950	—	*f*
$(C_2H_5O)_2P(S)—O—P(S)(OC_2H_5)_2$				—	933	—	*g*

[a]Baudler *et al.*, ref. 11; Gerding *et al.*, ref. 12.
[b]Robinson, ref. 13.
[c]C. Stölzer and A. Simon. Ber. 94, 1976 (1961).
[d]T. J. Hanwick and P. O. Hoffmann. J. Chem. Phys. 19, 708 (1951).
[e]Harvey and Mayhood, ref. 8.
[f]J. E. Griffiths and A. B. Burg. J. Am. Chem. Soc. 82, 1507 (1960).
[g]R. A. McIvor, G. A. Grant, and C. E. Hubley. Can. J. Chem. 39, 1611 (1956).

TABLE III

Characteristic S—O—S vibrational frequencies

Compounds	Frequencies (cm^{-1}) ν_s	ν_a	ν_b
$S_2O_5F_2$	323	814	157
$S_2O_5Cl_2$	298	760	147
S_2O_5ClF	313	802	154
$H_2S_2O_7$	328	809	155
HS_2O_6F	325	794	140
HS_2O_6Cl	310	803	148
$K_2S_2O_7$	321	800	—
$Na_2S_2O_7$	346	805	—
$(CH_3)_2S_2O_5$	329	770	—
SF_5OSF_5	256	808	—

the symmetric stretches at approximately 500, 450, and 325 cm^{-1} for Si—O—Si, P—O—P, and S—O—S bonds, respectively. Thus the polarized line in the Raman spectrum of Cl_2O_7 at 280 cm^{-1} would seem more appropriate for the symmetric Cl—O—Cl stretching frequency since it fits an apparent trend in the values of ν_s for Si—O—Si, P—O—P, S—O—S, and Cl—O—Cl bonds which is similar to that for the asymmetric stretching frequency. No lines were reported in this spectrum below 280 cm^{-1} and it is likely that the bending mode occurs at a frequency below the limit of Savoie and Giguère's measurement.

Can. J. Chem. Downloaded from www.nrcresearchpress.com by 210.87.254.40 on 09/05/12
For personal use only.

Can. J. Chem. Downloaded from www.nrcresearchpress.com by 210.87.254.40 on 09/05/12
For personal use only.

DISCUSSION

We previously calculated (1) the stretching force constant k_{SO} and the bending force constant d_{SO} for the S—O—S bridge bonds in polysulphuryl compounds by treating the molecules as simple triatomic species X_2O and using a simple valency force field. The same method of calculation is used here for the force constants k and d of Si—O, P—O, and Cl—O bridge bonds. In these calculations the mass of the group X attached to the bridging oxygen atom has been used without modification. We have previously shown (1) that modification of the mass X, as e.g. Goubeau has suggested (17), makes very little difference to the value obtained for the force constant. Values for the stretching and bending force constants, k_1 and d, are given in Table IV. In the case of compounds containing Si—O—Si

TABLE IV

Force constants, bond orders, and calculated and observed bond lengths

	$k_1 \times 10^{-5}$		$d \times 10^{-5}$	n^*		r^*		r_{obs}
$(H_3Si)_2O$	5.1	(5.0)†	0.10	1.45	(1.45)	1.65	(1.65)	1.633
$(D_3Si)_2O$	5.0	(5.0)	0.09	1.45	(1.45)	1.65	(1.65)	—
$[H(CH_3)_2Si]_2O$	5.5	(5.4)	0.14	1.52	(1.51)	1.62	(1.63)	—
$[(CH_3)_3Si]_2O$	5.6	(5.4)	0.15	1.53	(1.51)	1.61	(1.63)	1.63±0.03
$[HO(CH_3)_2Si]_2O$	5.7	(5.6)	0.10	1.55	(1.53)	1.62	(1.61)	—
$[Cl(CH_3)_2Si]_2O$	5.6	(5.8)	0.11	1.53	(1.56)	1.61	(1.61)	—
$[C_6H_5(CH_3)_2Si]_2O$	5.9	(5.7)	0.12	1.57	(1.55)	1.60	(1.62)	—
$[(C_6H_5)_3Si]_2O$	5.9	(5.8)	0.09	1.57	(1.56)	1.60	(1.61)	—
$(Cl_3Si)_2O$	6.3	(6.3)	0.12	1.62	(1.62)	1.60	(1.60)	1.64±0.05
$[(C_2H_5)_3Si]_2O$	5.3	(5.1)	0.14	1.50	(1.47)	1.63	(1.64)	—
$Si_2O_7^{6-}$	5.2	(5.1)	0.13	1.49	(1.47)	1.63	(1.64)	1.607±0.007
$P_2O_3Cl_4$	4.7		0.14	1.30		1.60		—
$P_2O_3F_4$	4.9		0.13	1.33		1.59		—
$H_2P_2O_7^{2-}$	4.7		0.14	1.30		1.60		—
$P_2O_7^{4-}$	4.8		0.14	1.31		1.60		1.61±0.015
$S_2O_5Cl_2$	2.8		0.09	1.01		1.69		—
$S_2O_5F_2$	3.3		0.08	1.06		1.66		—
S_2O_5ClF	3.5		0.08	1.09		1.65		—
$H_2S_2O_7$	3.1		0.08	1.04		1.68		—
HS_2O_6F	3.0		0.07	1.03		1.68		—
HS_2O_6Cl	3.1		0.08	1.04		1.68		—
$S_2O_7^{2-}$ (K^+)	3.0		0.09	1.03		1.68		1.645±0.005
$S_2O_7^{2-}$ (Na^+)	3.1		0.10	1.04		1.68		—
$(CH_3)_2S_2O_5$	2.8		0.10	1.01		1.69		—
SF_5OSF_5	3.1		0.06	1.04		1.68		—
Cl_2O_7	3.2		0.10	1.00		1.72		1.725

*Calculated from force constants.
†The values in parenthesis have been calculated assuming $\nu_b = 0$.

bonds, values of the stretching force constant k_1 have been calculated from the vibrational frequencies given in Table I and also from the values of the symmetric and asymmetric stretches given in that table, assuming that the bending vibration has a very low frequency (approaching zero for relatively heavy groups X) as Lord and co-workers have suggested. Both sets of calculations give very comparable values and so it appears that even if the values of ν_b are unreliable the stretching force constants are close to the correct values.

We have recently obtained linear correlations between bond orders and stretching force constants of Si—O, P—O, S—O, and Cl—O bonds and also relations between their bond orders and bond lengths (18, 19). It is thus possible to calculate both the bond orders and bond lengths for the bridge bonds from the force constants, as is shown in Table IV. Experimental data for bond lengths are available for only a few species; these are also given in Table IV. The agreement between the observed and calculated values is reasonably good. Bond orders calculated from the observed bond lengths for these species and

TABLE V

Experimental bond lengths and bond angles* and calculated bond orders for compounds containing X—O—X bonds

	r_{X-O}(Å)	$\widehat{XOX}$	n§
$Si_2O_7^{6-}$†	1.607±0.007	—	1.50
$(SiH_3)_2O$	1.633±0.001	144±1°	1.43
$[(CH_3)_3Si]_2O$	1.63±0.03	130±10°	1.44
$(Cl_3Si)_2O$	1.64±0.05	130° (approx)	1.40
$(SiO_3^{2-})_n$	1.68	137.5°	1.29
$(SiO_2)_n$(α-quartz)	1.61	142°	1.50
$[(CH_3)_2SiO]_3$	1.68±0.04	115±5°	1.29
$[(CH_3)_2SiO]_4$	1.64–1.65	141.5°	1.40–1.37
$[(CH_3)_8Si_5O_6]$‡	1.61–1.67	129–134°	1.50–1.31
$P_2O_7^{4-}$	1.61±0.015	133.5°	1.28
P_4O_6	1.67±0.03	128.5±1.5°	1.14
	1.65±0.02	127.5±1°	1.18
P_4O_{10}	1.62±0.02	123.5±1°	1.25
	1.60	124.5°	1.30
$P_4O_6S_4$	1.61±0.02	128.5±1°	1.28
$P_4O_{12}^{4-}$	1.61	132°	1.28
(P_2O_5)	1.56±0.015	145°	1.42
$P_3O_9^{3-}$	1.61	—	1.28
$P_3O_{10}^{5-}$	1.61	—	1.28
	1.67	122°	1.14
$S_2O_7^{2-}$	1.645±0.005	124°	1.11
HS_2O_7	1.60	—	1.20
$(SO_3)_n$ (asbestos form)	1.59–1.63	121°	1.22–1.14
S_3O_9	1.60	114°	1.20
$S_3O_{10}^{2-}$	1.54	122°	1.34

*Data taken from L. Sutton "Interatomic distances", Chemical Society Special Publication No. 11, London (1958) and Cruickshank, ref. 21.
†Thortveitite, $Sc_2Si_2O_7$.
‡Octamethylspiro-5,5-pentasiloxane.
§Calculated from bond lengths.

for species containing X—O—X bridges in longer chains and rings are given in Table V. In each case the bond orders are greater than unity, confirming earlier suggestions (4, 20–23) that these bridge bonds have a certain amount of double-bond character and we see that the bond order increases in the series Cl—O—Cl, S—O—S, P—O—P, Si—O—Si. The general increase in the bond angle in this series indicates an increasing repulsion between the bonds and this is consistent with the increasing bond order.

Kriegsmann (4) gives values of $k_{Si-O} = 4.65 \times 10^5$ and $d_{Si-O} = 0.10 \times 10^5$ dyn cm^{-1} for the bridge bonds in hexamethyl disiloxane for which he estimates an Si—O bond order of approximately 1.25. An Si—O bond order of this magnitude would imply an Si—O bond length of about 1.72 Å, whereas the observed distance is 1.63 Å (Table V). The present treatment leads to a much greater bond order of 1.6, which is consistent with the observed bond length.

Cruickshank (21) has attributed the increasing bond angles in the series Cl—O—Cl, S—O—S, P—O—P, Si—O—Si to the increasing electrostatic repulsion between the two ends of the molecules and he considers that the amount of double-bond character is determined by the angle. Although this explanation could conceivably be correct in the series $Si_2O_7^{6-}$, $P_2O_7^{4-}$, $S_2O_7^{2-}$, and Cl_2O_7, it should be noted that very large bond angles are also found in uncharged molecules, such as $[(CH_3)_3Si]_2O$ and $[(CH_3)_2SiO]_4$, and electrostatic repulsion between the groups at the ends of the oxygen bridge hardly seems feasible in such cases. Our view is that there is delocalization of electrons onto the atom of the second-row element from the bridging oxygen atom. This occurs because there is space

Can. J. Chem. Downloaded from www.nrcresearchpress.com by 210.87.254.40 on 09/05/12
For personal use only.

(orbitals) available around the atom of the second-row element to accommodate the electrons which are delocalized because of strong repulsions between the electron pairs in the filled shell of oxygen (22). We consider that the resultant double bonding and the large repulsions between the double bonds leads to the large X—O—X bond angle rather than the double bonding being the consequence of a large bond angle caused by electrostatic repulsion between the ends of the molecule. For the isoelectronic series $Si_2O_7^{6-}$, $P_2O_7^{4-}$, $S_2O_7^{2-}$, and Cl_2O_7 the decreasing tendency of oxygen to delocalize its lone electron pairs into vacant orbitals on the adjacent second-row element (22) can perhaps be understood in the following manner.

If possible double bonding by the bridging oxygen is first ignored and if it is assumed that the most stable valence-bond structure will be that which has a minimum number of formal charges and in which any formal negative charges are localized on the most electronegative (oxygen) atoms, I, II, III, and IV will be the most stable structures:

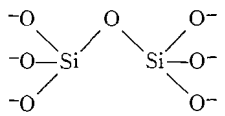

I

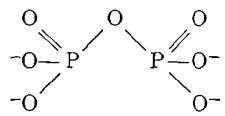

II

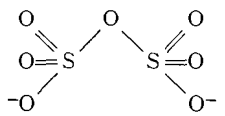

III

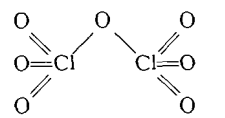

IV

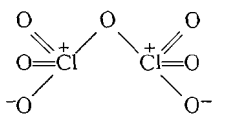

V

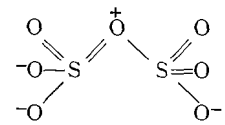

VI

If we also use a very useful empirical rule (the duodecet rule) (19), namely, that there is a tendency for the valency shell of a second-row element to contain twelve electrons (i.e. six pairs), which has been previously shown (18, 19) to be a realistic basis for describing the bonding in species such as e.g. SiO_4^{4-}, PO_4^{3-}, SO_4^{2-}, and ClO_4^-, and other molecules and ions containing highly electronegative ligands attached to Si, P, S, or Cl, then V rather than IV is a better representation of the bonding in Cl_2O_7. If the duodecet rule holds for all these compounds, there will be little tendency for delocalization of unshared electron pairs from the oxygen bridge atom into vacant orbitals on the second-row atom for Cl_2O_7 and $S_2O_7^{2-}$, but there will be an increasing tendency for this to occur in passing to $P_2O_7^{4-}$ and $Si_2O_7^{6-}$, because in II and I there are, respectively, only five and four electron pairs in the valency shell of the second-row atom. Because structures such as VI are expected to make a small contribution, some delocalization of the bridge oxygen lone pairs is to be expected even in the case of $S_2O_7^{2-}$ and the amount of double bonding by the bridging oxygen atom would therefore be expected to increase in the order Cl—O—Cl, S—O—S, P—O—P, Si—O—Si.

The sum of the experimental bond orders for the bonds formed by the second-row element in $Si_2O_7^{6-}$, $P_2O_7^{4-}$, $S_2O_7^{2-}$, and Cl_2O_7, as shown in Table VI, confirms the validity of the application of the duodecet rule in these cases. This rule also works well for species such as $(SiO_3^{2-})_n$, $(SiO_2)_n$(α-quartz), P_4O_{10}, $P_4O_{12}^{4-}$, $(P_2O_5)_\infty$, $(PO_3^-)_\infty$, $P_3O_{10}^{5-}$, $HS_2O_7^-$, $(SO_3)_n$, S_3O_9, and $S_3O_{10}^{2-}$ (Table VI), although the evidence comes from bond lengths alone, since the evaluation of force constants is not easily accomplished in these cases.

Can. J. Chem. Downloaded from www.nrcresearchpress.com by 210.87.254.40 on 09/05/12
For personal use only.

TABLE VI

Bond orders and the duodecet rule

		Bond order (n)*		
		Bridge bonds	Terminal bonds	Σn†
$Si_2O_7^{6-}$		1.52	1.51	6.1
$P_2O_7^{4-}$		1.28	1.61	6.1
$S_2O_7^{2-}$		1.13	1.71	6.2
Cl_2O_7		1.00	1.69	6.0
$(SiO_3^{2-})_\infty$		1.29	1.67	5.9
$(SiO_2)_\infty$		1.50	1.50	6.0
P_4O_{10}		1.30	2.18	6.1
$(P_2O_5)_\infty$		1.42	1.71	6.0
$P_3O_{10}^{5-}$	Terminal	1.28	1.65	6.2
	Center	1.28	1.71	6.0
$(PO_3^-)_\infty$		1.26	1.49	5.9
$P_4O_{12}^{4-}$		1.36	1.70	6.1
$(SO_3)_\infty$		1.17	1.93	6.2
$HS_2O_7^-$		1.20	1.62	6.1
S_3O_9		1.15	2.00	6.3
$S_3O_{10}^{2-}$	Terminal	1.00	1.95	5.9
	Center	1.54 (?)	2.00	7.1 (?)

*Calculated from bond lengths (Table V).
†Sum of the orders of the bonds formed by each Si, P, or S atom.

ACKNOWLEDGMENTS

We thank the National Research Council of Canada for generous financial support.

REFERENCES

1. R. J. GILLESPIE and E. A. ROBINSON. Spectrochim. Acta, **19**, 741 (1963).
2. L. J. BELLAMY. The infra-red spectra of complex molecules. 2nd ed. Wiley, New York. 1958. p. 338.
3. H. KRIEGSMANN. Z. Anorg. Chem. **299**, 79, 139 (1959).
4. H. KRIEGSMANN. Z. Elektrochem. **61**, 1088 (1957).
5. H. KRIEGSMANN and K. H. SCHOWTA. Z. Physik. Chem. Leipzig, **209**, 261 (1958).
6. R. C. LORD, D. W. ROBINSON, and W. C. SCHUMB. J. Am. Chem. Soc. **78**, 1327 (1956).
   D. W. ROBINSON, R. C. LORD, and J. R. ARONSON. J. Chem. Phys. **33**, 1004 (1960).
   D. W. ROBINSON, W. J. LAFFERTY, J. R. ARONSON, J. R. DURIG, and R. C. LORD. J. Chem. Phys. **35**, 2245 (1961).
7. G. HERZBERG. Molecular spectra and molecular structure. Vol. II. D. Van Nostrand Co., Inc., New York. 1945.
8. R. B. HARVEY and J. E. MAYHOOD. Can. J. Chem. **33**, 1552 (1955).
9. T. I. HANWICK and P. O. HOFMANN. J. Chem. Phys. **19**, 708 (1951).
10. A. SIMON and H. RICHTER. Z. Anorg. Chem. **301**, 154 (1960).
11. M. BAUDLER, R. KLEMENT, and E. ROTHER. Chem. Ber. **93**, 149 (1960).
12. H. GERDING, H. GIJBEN, B. NIEUWENHUIJSE, and J. G. RAAPHORST. Rec. Trav. Chim. **79**, 41 (1960).
13. E. A. ROBINSON. Can. J. Chem. **40**, 1725 (1962).
14. G. WALRAFEN, D. E. IRISH, and T. F. YOUNG. J. Chem. Phys. **37**, 662 (1962).
15. R. FONTEYNE. Ned. Tijdschr. Natuurk. Ghent, **20**, 112, 275 (1938).
16. R. SAVOIE and P. A. GIGUÈRE. Can. J. Chem. **40**, 991 (1962).
17. J. GOUBEAU. Anales Real Soc. Espan. Fis. Quim. Madrid, Ser. B, **45**, 807 (1949).
18. R. J. GILLESPIE and E. A. ROBINSON. Can. J. Chem. **41**, 2074 (1963).
19. E. A. ROBINSON. Can. J. Chem. **41**, 3021 (1963).
20. D. P. CRAIG, A. MACCOLL, R. S. NYHOLM, L. E. ORGEL, and L. E. SUTTON. J. Chem. Soc. 332 (1954).
21. D. W. J. CRUICKSHANK. J. Chem. Soc. 5486 (1961).
22. R. J. GILLESPIE. J. Am. Chem. Soc. **82**, 5978 (1960).
23. C. EABORN. Organo silicon compounds. Butterworths, London. 1960. p. 94.

Can. J. Chem. Downloaded from www.nrcresearchpress.com by 210.87.254.40 on 09/05/12
For personal use only.

Can. J. Chem. Downloaded from www.nrcresearchpress.com by 210.87.254.40 on 09/05/12
For personal use only.

THE PRESENCE OF EXCITED MOLECULES IN ACTIVE NITROGEN[1]

H. B. DUNFORD, E. R. V. MILTON,[2] AND D. L. WHALEN
Department of Chemistry, University of Alberta, Edmonton, Alberta

Received June 17, 1964

ABSTRACT

Spectra of active nitrogen have been photographed under conditions comparable to those used for most studies of reactions of active nitrogen with other molecules. Bands observed were identified as the first positive system of nitrogen and the β- and γ-bands of nitric oxide. No trace of Vegard–Kaplan emission was observed. The 2 537 line of mercury was detected under certain conditions.

The results are used to rationalize the large discrepancy which exists between estimates of the lifetime of $N_2(A^3\sum_u^+)$ by optical spectroscopy and reaction kinetics. In the former method, the measurements are performed in an oxygen-free system and are clearly related to a radiative lifetime. In the latter method, the measurements are performed in the presence of traces of oxygen and are believed to indicate a collisional lifetime. The reaction kinetic measurements are shown to be in complete agreement, both with regard to decay kinetics and lifetime, with electron spin resonance measurements on active nitrogen produced under near-identical conditions.

INTRODUCTION

Recent reviews have all agreed that the major reactive component in active nitrogen is $N(^4S)$ ground-state atoms (1–3). However, the possible concentrations of other species capable of causing chemical reaction remains a topic of controversy. In 1956, Evans and Winkler (1) postulated that $A^3\sum_u^+$ nitrogen molecules were spilling into highly excited metastable vibrational levels of the electronic ground-state, $X^1\sum_g^+$. It has since been shown that vibrationally excited nitrogen is indeed present, but only excited to the first vibrational level of the ground state, and this only in active nitrogen produced in a microwave discharge (4–7). A condensed discharge produces negligible concentrations of vibrationally excited ground-state nitrogen* (8, 9). Thus with both types of discharge, appreciable chemical reactions of highly vibrationally excited ground-state nitrogen appear to be ruled out.

Since 1956 Lichten's molecular-beam work (11) combined with the absorption spectroscopy experiments of Wilkinson and Mulliken (12) indicated that the lifetime of $A^3\sum_u^+$ molecules was 0.026 s. Oldenberg, Bills, and Carleton (13) actually detected the $B^3\pi_g \leftarrow A^3\sum_u^+$ system (first positive bands or Lewis–Rayleigh afterglow) in absorption in a discharge through nitrogen, a feat which had eluded many other competent spectroscopists. This provided the most direct proof that $A^3\sum_u^+$ molecules are present in detectable amounts in discharged nitrogen. Their work was extended to deduce that the radiative lifetime of the $A^3\sum_u^+$ state is 2 s for the $v = 0$ level (14, 15).

It seems well established that nitrogen atoms do not react with ammonia (16–19) and it has been suggested that the destruction of ammonia observed with active nitrogen produced in a condensed discharge is due to reaction with triplet A-state molecules (20, 21). In two recent studies an attempt was made to elucidate the kinetics of $A^3\sum_u^+$ molecule formation and decay from the reaction of active nitrogen with ammonia (8, 22). In the earlier work, by Wright, Nelson, and Winkler, it was assumed that $d[N_2^*]/dt = \frac{1}{2}ak_2[N]^2P$

[1]*Presented at the 47th Canadian Chemical Conference, Kingston, Ontario, June, 1964.*
[2]*Present address: Division of Natural Science, University of Saskatchewan, Regina, Saskatchewan.*
**Excitation by low-energy electrons through transient negative-ion formation (10), which would be favored in the microwave discharge, seems a likely explanation of these observations.*

$+ \frac{1}{2}bk_1[N] - k_3[N_2^*]$, where N_2^* represents $N_2(A^3\sum_u^+)$. The first term on the right represents formation of N_2^* by homogeneous atom combination, the second by heterogeneous combination, and the third term, decay of N_2^*. If it was assumed that $a = b = 1$, in other words that N_2^* is formed from all atom combinations, then a half-life of 0.08 s for N_2^* was obtained. If it was assumed that $a = 1$, $b = 0$, then a half-life of 0.07 s resulted. The assignment of unity to either a or b appears questionable. Recent theoretical work (23) indicates that atoms prefer to combine into the electronic ground-state of a molecule. The above equation is also incompatible with the plateaus observed in ammonia destruction in the presence of atomic nitrogen. If the equation were valid, then the plateau in ammonia destruction could only occur when all atoms are removed from the system. Values of k_3 are rather insensitive to the presence of the first two right-hand terms, however. In the later work, conducted in our laboratory, N_2^* was shown to decay by first-order kinetics, which indicates that its appreciable formation occurs in the discharge tube only. A half-life of 0.08 s was deduced from this study. In the present work, attempts are made to obtain more information on the properties of $N_2(A^3\sum_u^+)$.

EXPERIMENTAL

Active nitrogen was produced either by using a 4 μF condensed discharge or a Baird Atomic Hg 198 Microwave Exciter of 250 W output which was connected to a cylindrical cavity obtained from the Ophthos Instrument Company, Rockville, Maryland. The nitrogen of prepurified grade, obtained from the Canadian Liquid Air Company, Hamilton, was passed through a liquid nitrogen trap directly into the flow system, which was kept at a pressure of ~ 3 mm Hg. Flow rates of nitrogen were nearly identical with those of the earlier work conducted at 2.5 mm. The distance from discharge to viewing tube was 40 cm. A McLeod gauge was connected to the flow system but was kept isolated except for occasional pressure measurements. The viewing tube was made of Pyrex, 1 m long and 27 mm inside diameter. A quartz plate was attached to one end of the tube with sealing wax. The viewing tube was poisoned with water vapor and perhaps oxygen present in the atmosphere and then pumped down to a pressure of 10^{-4} mm before a series of experiments. Photographs of the spectrum were taken using a quartz medium Hilger instrument and either Kodak 1-O or 1-F plates. Exposure times ranged from 5 to 30 min. A low-pressure mercury arc was used to check the calibration scale of the Hilger instrument.

RESULTS

Band spectra were identified by comparison with plates published in Pearse and Gaydon (24) and Jevons (25). Bands identified were the β- and γ-systems of nitric oxide and the first positive system of nitrogen. In all cases a direct correlation was noted between the intensities of the nitric oxide bands and the nitrogen afterglow. In the first exposures obtained after pumping down the system, the NO and N_2 bands would appear brightly after 5 min exposure; these would then fade gradually and would become very weak when the discharge had been left running for many hours. Band intensities tended to be weaker for active nitrogen produced by the microwave method. When the condensed discharge was used and a trace of mercury was present, the 2 537 line was clearly apparent. In no cases were the 0-5 and 0-6 bands of the Vegard–Kaplan system present, although they would have been readily discernible despite the presence of the NO emission.

DISCUSSION

The estimate of a lifetime of 1 s or greater for $N_2(A^3\sum_u^+)$ (14, 15) has been supported by Noxon's study of active nitrogen at high pressure (26) and the recent work of Zipf (27). On the other hand, a great deal of evidence, much of it admittedly negative, points to the $A^3\sum_u^+$ state of nitrogen as the predominant species which reacts with ammonia, and studies of this reaction indicate that A-state molecules have a half-life of about 0.08 s, i.e. a lifetime of 0.12 s. If this conclusion is correct, it poses two serious problems. First,

Can. J. Chem. Downloaded from www.nrcresearchpress.com by 210.87.254.40 on 09/05/12
For personal use only.

there is a discrepancy in the spectroscopic and reaction kinetic estimates of the lifetime of $A^3\sum_u^+$ nitrogen, both of which appear to be well established, at least as to orders of magnitude. Second, estimates of the population of the $A^3\sum_u^+$ state by the two methods are also in disagreement. In the work of Carleton *et al.* (13–15, 28) the maximum estimate which they obtained was a population of 10^{11} A-state molecules per cc and this was right in the discharge tube, whereas in the work in this laboratory for example (22), a concentration of 4.5×10^{14} A-state molecules per cc is reported at a considerable distance from the discharge. Furthermore, these two discrepancies are operating in the wrong direction. Since for a given set of conditions the intensity of the Vegard–Kaplan emission is directly proportional to the population of the A state and inversely proportional to the lifetime of this state, then the greater the population, the longer the observed lifetime should be. Yet we have reported the greater population, the shorter lifetime, and furthermore observe no Vegard–Kaplan bands. It is the purpose of the following discussion to offer a rationalization of the above apparent conflict of evidence.

Conditions for observation of the Vegard–Kaplan bands are clearly established. The nitrogen must be exceptionally pure with particular care taken to remove the last traces of oxygen from the system. On the other hand, chemists, who are interested in studying atomic nitrogen reactions, find it necessary to operate under conditions where traces of oxygen, oxygen-containing materials, or other substances capable of performing the same role (29) are present. Although the ratio of the Lewis–Rayleigh afterglow intensity to the square of the nitrogen atom concentration is independent of oxygen concentration, the concentration of atomic nitrogen decreases with decreasing oxygen content (30). Furthermore, if the system is flamed out and carefully degassed, the afterglow intensity goes to zero (31). Our experiments have been conducted under conditions where a strong Lewis–Rayleigh afterglow is observed and so the absence of the Vegard–Kaplan bands might be expected.

The nitric oxide band emission is dependent upon the production of atomic oxygen, which could be formed by

[1] $$N_2(^3\Sigma) + O_2(^3\Sigma) \rightarrow N_2(^1\Sigma) + O_2(^5\Sigma)$$

[2] $$O_2(^5\Sigma) \rightarrow 2O(^3P).$$

The quintet state of molecular oxygen has not been observed but is postulated on grounds of spin conservation. It is equivalent to the case where there are no bonding electrons and hence would be a repulsive state. Rapid destruction of the nitric oxide, formed by atom combination, by atomic nitrogen reforms the atomic oxygen, so that only a trace of oxygen gives rise to strong nitric oxide emission. Although a precise kinetic study of the effect of traces of oxygen on Vegard–Kaplan emission remains to be carried out, it is difficult to envisage reaction [1] as the prime mechanism of quenching of the Vegard–Kaplan emission, since the trace of oxygen present would spend most of its time in its atomic state. The reaction

$$2O(^3P) + M \rightarrow O_2(^3\Sigma) + M$$

would not be able to compete with the reaction between atomic nitrogen and atomic oxygen because of the large excess of atomic nitrogen present. Whether oxygen plays a primary or secondary role, it would appear clear that the lifetime which we have measured, if it is indeed of the $A^3\sum_u^+$ state, is a collisional lifetime, whereas the work of Carleton *et al.* is definitely concerned with a radiative lifetime. In our work the A-state molecules are quenched before they have time to radiate and so the apparent discrepancy between the two lifetimes is removed.

Can. J. Chem. Downloaded from www.nrcresearchpress.com by 210.87.254.40 on 09/05/12
For personal use only.

In this connection, it is interesting to note that the magnetic resonance spectrum of active nitrogen produced in an electrode discharge in the presence of traces of oxygen has been studied by Anderson and Barry (32). They observed the presence of a species which was neither atomic nitrogen nor free electrons, and which decayed homogeneously by first-order kinetics with a half-life of 0.07 s at 4.4 mm pressure. The most logical candidate for such a paramagnetic substance would appear to be the $A^3\sum_u^+$ state of molecular nitrogen. If this assignment is correct, their work provides the first example of the detection of a diatomic free radical in the gas phase by conventional electron spin resonance (e.s.r.). Other radicals which have been detected have obeyed electric dipole rather than magnetic dipole selection rules (33, 34).

With regard to the apparent discrepancy in populations of the $A^3\sum_u^+$ state, if ammonia does indeed react with triplet-state nitrogen molecules, then the concentration of A-state molecules which it indicates should be correct. This could mean that (*a*) under our operating conditions, it is possible to produce a much higher population of A-state molecules than that obtained by Carleton *et al.*; (*b*) the latter workers actually produced a much higher concentration of A-state molecules than they at first believed. The latter statement if true would mean that the radiative lifetime of A-state molecules is considerably longer than 2 s and (or) one or more of the calculated quantities or experimental data which they had to use in order to deduce the population of the A state is in error (35, 36).

In summary, the reaction of ammonia with a non-atomic species, present to an appreciable extent in active nitrogen prepared in a condensed discharge, indicates that this species decays by first-order kinetics and that is has a half-life of 0.07–0.08 s. These observations are in complete agreement with results obtained by e.s.r. measurements on active nitrogen produced under near identical conditions, indicating that the non-atomic species is paramagnetic. A wide variety of evidence points to molecular nitrogen in its triplet A-state as the identity of this species. The absence of Vegard–Kaplan emission indicates that in the ammonia and e.s.r. work, the A-state molecules are being collisionally deactivated, which removes any necessary discrepancy with the much longer radiative lifetime which has been measured.

ACKNOWLEDGMENTS

We would like to acknowledge helpful comments from Drs. D. A. Armstrong, N. P. Carleton, and R. C. Millikan. At the same time we assume sole responsibility for any shortcomings of the present manuscript. We are grateful to the National Research Council for financial support for this research, and one of us (D. L. W.) is also indebted for the award of an N.R.C. Studentship.

REFERENCES

1. H. G. V. Evans and C. A. Winkler. Can. J. Chem. **34**, 1217 (1956).
2. K. R. Jennings and J. W. Linnett. Quart. Rev. London, **12**, 116 (1958).
3. G. G. Mannella. Chem. Rev. **63**, 1 (1963).
4. F. Kaufman and J. R. Kelso. J. Chem. Phys. **28**, 510 (1958).
5. K. Dressler. J. Chem. Phys. **30**, 1621 (1959).
6. J. E. Morgan, L. F. Phillips, and H. I. Schiff. Discussions Faraday Soc. **33**, 118 (1962).
7. J. E. Morgan and H. I. Schiff. Can. J. Chem. **41**, 903 (1963).
8. A. N. Wright, R. L. Nelson, and C. A. Winkler. Can. J. Chem. **40**, 1082 (1962).
9. H. B. Dunford. Unpublished results.
10. G. J. Schulz. Phys. Rev. **116**, 1141 (1959).
11. W. Lichten. J. Chem. Phys. **26**, 306 (1957).
12. P. G. Wilkinson and R. S. Mulliken. J. Chem. Phys. **31**, 674 (1959).
13. O. Oldenberg, D. G. Bills, and N. P. Carleton. J. Opt. Soc. Am. **51**, 526 (1961).
14. D. G. Bills, N. P. Carleton, and O. Oldenberg. Proc. Intern. Meeting Mol. Spectry. 4th Bologna 1959. Vol. 1. Macmillan, New York. 1962. p. 197.
15. N. P. Carleton and O. Oldenberg. J. Chem. Phys. **36**, 3460 (1962).

Can. J. Chem. Downloaded from www.nrcresearchpress.com by 210.87.254.40 on 09/05/12
For personal use only.

16. G. R. FREEMAN and C. A. WINKLER. J. Phys. Chem. **59**, 371 (1955).
17. G. B. KISTIAKOWSKY and G. G. VOLPI. J. Chem. Phys. **28**, 665 (1958).
18. K. D. BAYES and G. B. KISTIAKOWSKY. J. Chem. Phys. **29**, 949 (1958).
19. J. T. HERRON, J. L. FRANKLIN, P. BRADT, and V. H. DIBELER. J. Chem. Phys. **30**, 879 (1959).
20. R. KELLY and C. A. WINKLER. Can. J. Chem. **38**, 2514 (1960).
21. K. D. BAYES. Can. J. Chem. **39**, 1074 (1961).
22. H. B. DUNFORD. J. Phys. Chem. **67**, 258 (1963).
23. S. W. BENSON and I. FUENO. J. Chem. Phys. **36**, 1957 (1962).
24. R. W. B. PEARSE and A. G. GAYDON. The identification of molecular spectra. 2nd ed. John Wiley & Sons, Inc., New York. 1950.
25. W. JEVONS. Report on band spectra of diatomic molecules. Cambridge University Press, London. 1932.
26. J. F. NOXON. J. Chem. Phys. **36**, 926 (1962).
27. E. C. ZIPF, JR. J. Chem. Phys. **38**, 2034 (1963).
28. N. P. CARLETON. Private communication.
29. R. A. YOUNG, R. L. SHARPLESS, and R. STRINGHAM. J. Chem. Phys. **40**, 117 (1964).
30. J. BERKOWITZ, W. A. CHUPKA, and G. B. KISTIAKOWSKY. J. Chem. Phys. **25**, 457 (1956).
31. J. M. ANDERSON, A. D. KAVADAS, and R. W. MCKAY. Proc. Phys. Soc. London, A, **70**, 877 (1957).
32. J. M. ANDERSON and J. N. BARRY. Proc. Phys. Soc. London, **78**, 1227 (1961).
33. H. E. RADFORD. Phys. Rev. **122**, 114 (1961); **126**, 1035 (1962).
34. C. C. MCDONALD. J. Chem. Phys. **39**, 2587 (1963).
35. J. C. KECK, J. C. CAMM, B. KIVEL, and T. WENTINK, JR. Ann. Phys. N.Y. **7**, 1 (1959).
36. N. P. CARLETON and C. PAPALIOLIOS. J. Quant. Spectr. Radiative Transfer, **2**, 241 (1962).

Can. J. Chem. Downloaded from www.nrcresearchpress.com by 210.87.254.40 on 09/05/12
For personal use only.

Can. J. Chem. Downloaded from www.nrcresearchpress.com by 210.87.254.6 on 09/05/12
For personal use only.

A UNIFIED TREATMENT OF INTEGRALS FOR ONE-ELECTRON OPERATORS[1]

SERAFIN FRAGA
Department of Chemistry, University of Alberta, Edmonton, Alberta
Received June 4, 1964

ABSTRACT

A general formula has been developed to express, in terms of *C*-functions, the integrals appearing in the evaluation (when using Slater-type orbitals) of the expectation values of the most important one-electron operators.

INTRODUCTION

One of the goals of quantum-mechanical calculations is the theoretical evaluation of the physical and chemical properties of atomic and molecular systems. Since the introduction of high-speed, digital computers in recent years, the calculation of such quantities has received new emphasis.

The corresponding calculations could be simplified if one had a unified treatment for the integrals which are needed. It appears that the development of such a formulation should be based on the so-called *C*-functions (1, 2, 3), used in the evaluation of integrals required for the energy calculations.

The aim of this paper is the development of a simple formula which would enable one to express in terms of *C*-functions all the two-center integrals, using Slater-type orbitals (STO's), which appear (4, 5) when evaluating the expectation values of the one-electron operators corresponding to those properties.

GENERAL THEORY

In the present paper normalized STO's (in complex form), defined by

$$[1] \qquad \chi_{nlm}(r, \theta, \varphi) = (2\zeta)^{n+\frac{1}{2}}[(2n)!]^{-\frac{1}{2}} r^{n-1} e^{-\zeta r} Y_{lm}(\theta, \phi),$$

are used. In this equation r, θ, and ϕ are the polar coordinates; n, l, and m are the three quantum numbers; ζ is the orbital exponent, and $Y_{lm}(\theta, \phi)$ are the normalized spherical harmonics defined by

$$[2] \qquad Y_{lm}(\theta, \varphi) = \left[\frac{(l - |m|)!}{(l + |m|)!}\frac{2l + 1}{4\pi}\right]^{\frac{1}{2}} P_l^m(\cos\theta)\, e^{im\phi},$$

where $P_l^m(\cos\theta)$ is a Legendre function of the first kind. Expansion of eq. [2] leads to

$$[3] \qquad Y_{lm}(\theta, \phi) = \frac{1}{2^l \cdot l!}\frac{(2l)!}{(l - |m|)!}\left[\frac{(l - |m|)!}{(l + |m|)!}\frac{2l + 1}{4\pi}\right] (\sin\theta)^{|m|} e^{im\phi} \left\{(\cos\theta)^{l-|m|} - \frac{(l - |m|)(l - |m| - 1)}{2 \cdot (2l - 1)} (\cos\theta)^{l-|m|-2} + \frac{(l - |m|)(l - |m| - 1)(l - |m| - 2)(l - |m| - 3)}{2 \cdot 4 \cdot (2l - 1)(2l - 3)} (\cos\theta)^{l-|m|-4} - - - - -\right\},$$

which is the expression which will be used here.

[1]*This work has been supported in part by the National Research Council of Canada.*

Can. J. Chem. Downloaded from www.nrcresearchpress.com by 210.87.254.6 on 09/05/12
For personal use only.

The two centers are designated by the subscripts a and b; their mutual distance by R. The Cartesian coordinates at the centers a and b are chosen so that the z-axes lie along the internuclear axis, pointing toward each other.

Prolate spheroidal coordinates will be used. They are defined by

$$\xi = (r_a + r_b)/R,\ \eta = (r_a - r_b)/R,\ \phi = \phi_a = \phi_b;$$

the volume element is $(R^3/8)(\xi^2 - \eta^2)\,d\xi\,d\eta\,d\phi$, and the integration limits are 0 and 2π for ϕ, -1 and 1 for η, and 1 and ∞ for ξ. In the preceding expressions r is the distance of the electron to nucleus a or b.

Let us assume that the one-electron operator to be considered introduces a factor of the form

$$[4] \qquad P = (R/2)^{\omega}(\xi + \eta)^{\alpha'}(\xi - \eta)^{\beta'}(1 + \xi\eta)^{\gamma'}(1 - \xi\eta)^{\delta'}(\xi^2 - 1)^{\epsilon'}(1 - \eta^2)^{\epsilon'} f(\phi),$$

with

$$[5] \qquad \omega = \alpha' + \beta' + \gamma' + \delta' + 2\epsilon',$$

and where α', β', γ', and δ' are integers and ϵ' is integer or half-integer. For any two STO's, centered on nuclei a and b respectively, it can then be written

$$[6] \qquad \langle \chi_a | P | \chi_b \rangle \equiv \int \bar{\chi}_a P \chi_b \, d\tau$$

$$= k_a k_b (R/2)^{n_a + n_b + 1 + \omega} \zeta_a^{\,n_a + \frac{1}{2}} \zeta_b^{\,n_b + \frac{1}{2}} \pi^{-1} \left\{ \int_0^{2\pi} f(\phi)\, e^{-i(m_a - m_b)\phi}\, d\phi \right\}$$

$$\sum_p \sum_q c_{ap} c_{bq} \left\{ \int_1^{\infty} d\xi \int_{-1}^{1} e^{-(R/2)[(\xi+\eta)\zeta_a + (\xi-\eta)\zeta_b]} \right.$$

$$(\xi + \eta)^{n_a - l_a + 2p + \alpha'} (\xi - \eta)^{n_b - l_b + 2q + \beta'} (1 + \xi\eta)^{l_a - |m_a| - 2p + \gamma'} (1 - \xi\eta)^{l_b - |m_b| - 2q + \delta'}$$

$$\left. [(\xi^2 - 1)(1 - \eta^2)]^{\frac{1}{2}(|m_a| + |m_b|) + \epsilon'}\, d\eta \right\},$$

where

$$[7a] \qquad k = 2^{n - l - \frac{1}{2}} [(2n)!]^{-\frac{1}{2}} (l!)^{-1} (2l)! (2l + 1)^{\frac{1}{2}} [(l + |m|)!(l - |m|)!]^{-\frac{1}{2}},$$

$$[7b] \qquad c_0 = 1,$$

$$[7c] \qquad c_{\substack{p \\ (p>0)}} = (-1)^p \frac{(l - |m|)(l - |m| - 1) \ldots (l - |m| - 2p + 1)}{(2 \ldots 2^p)(2l - 1)(2l - 3) \ldots (2l - 2p + 1)}.$$

Making use of the C-functions,* defined by

$$[8] \qquad C\{\alpha, \beta, \gamma, \delta, \epsilon; \rho, \tau\} = (-1)^{\beta + \delta + \epsilon} (\rho_b/2)^{\alpha + \beta + \gamma + \delta + 2\epsilon + 1} \int_1^{\infty} d\xi$$

$$\int_{-1}^{1} e^{-\rho\xi - \tau\rho\eta} (\xi + \eta)^{\alpha} (\xi - \eta)^{\beta} (1 + \xi\eta)^{\gamma} (1 - \xi\eta)^{\delta} (\xi^2 - 1)^{\epsilon} (1 - \eta^2)^{\epsilon}\, d\eta,$$

with

$$[9a] \qquad \rho = \tfrac{1}{2}(\rho_a + \rho_b) = \tfrac{1}{2}(\zeta_a + \zeta_b)R,$$

$$[9b] \qquad \tau = (\rho_a - \rho_b)/(\rho_a + \rho_b) = (\zeta_a - \zeta_b)/(\zeta_a + \zeta_b),$$

**The definition used here for the C-functions is the one given in the technical report (see ref. 1); it differs from the one given in the published version of that report by the factor $(-1)^{\beta+\delta+\epsilon}$. In order to simplify the notation hereafter, the convention $C\{\alpha, \beta, \gamma, \delta, \epsilon; \rho, \tau\} = C_{\alpha\beta}{}^{\gamma\delta\epsilon}(\rho, \tau)$ will be adopted.*

eq. [6] yields

$$[10]\quad \langle\chi_a|P|\chi_b\rangle = (-1)^{-n_b-\frac{1}{2}(|m_a|-|m_b|)-\sigma} k_a k_b F(\phi) \zeta_a^{\,n_a+\frac{1}{2}} \zeta_b^{\,-(n_a+\frac{1}{2}+\omega)} \sum_p \sum_q c_{ap} c_{bq} C\{n_a - l_a + 2p + \alpha', n_b - l_b + 2q + \beta', l_a - |m_a| - 2p + \gamma', l_b - |m_b| - 2q + \delta', \tfrac{1}{2}(|m_a| + |m_b|) + \epsilon'; \rho, \tau\},$$

with

$$[11]\quad \sigma = \beta' + \delta' + \epsilon',$$

$$[12]\quad F(\phi) = \pi^{-1} \int_0^{2\pi} f(\phi)\, e^{-i(m_a - m_b)\phi}\, d\phi.$$

Equation [10] is completely general, subject only to the restrictions governing the C-functions, namely (1, 2, 3): (a) β, γ, δ, and ϵ are non-negative numbers; (b) the negative values of α are limited by the condition $\alpha + \gamma + 2\epsilon + 1 \geqslant 0$; ($c$) $\alpha + \beta + \gamma + \delta + 2\epsilon \geqslant 0$, if the C-function is to have a finite limit for $\rho \to 0$.

SUMMARY OF FORMULAE

In the following expressions the two STO's involved are designed by χ_i and χ_j, respectively. The operator P is supposed to be of the form

$$[13a]\quad P_a = (R/2)^{\omega}(\xi + \eta)^{\alpha'}(\xi - \eta)^{\beta'}(1 + \xi\eta)^{\gamma'}(1 - \xi\eta)^{\delta'}(\xi^2 - 1)^{\epsilon'}(1 - \eta^2)^{\epsilon'} f(\phi),$$

$$[13b]\quad P_b = (R/2)^{\omega}(\xi + \eta)^{\beta'}(\xi - \eta)^{\alpha'}(1 + \xi\eta)^{\delta'}(1 - \xi\eta)^{\gamma'}(\xi^2 - 1)^{\epsilon'}(1 - \eta^2)^{\epsilon'} f(\phi),$$

depending on whether it is referred to center a or b.

The integrals are then given by the following formulae:

$$[14]\quad \left.\begin{matrix}\langle\chi_{ia}|P_a|\chi_{jb}\rangle \\ \langle\chi_{ib}|P_b|\chi_{ja}\rangle\end{matrix}\right\} = (-1)^{-n_j-\frac{1}{2}(|m_i|-|m_j|)-\sigma} k_i k_j F(\phi) \left\{\begin{matrix}\zeta_i^{\,n_i+\frac{1}{2}} \zeta_j^{\,-n_i-\frac{1}{2}-\omega} \\ \zeta_j^{\,n_j+\frac{1}{2}} \zeta_i^{\,-n_j-\frac{1}{2}-\omega}\end{matrix}\right\}$$
$$\sum_p \sum_q c_{ip} c_{jq} C\{n_i - l_i + 2p + \alpha', n_j - l_j + 2q + \beta', l_i - |m_i| - 2p + \gamma', l_j - |m_j| - 2q + \delta', \tfrac{1}{2}(|m_i| + |m_j|) + \epsilon'; \rho, \tau\},$$

$$[15]\quad \left.\begin{matrix}\langle\chi_{ia}|P_b|\chi_{jb}\rangle \\ \langle\chi_{ib}|P_a|\chi_{ja}\rangle\end{matrix}\right\} = (-1)^{-n_j-\frac{1}{2}(|m_i|-|m_j|)-\sigma'} k_i k_j F(\phi) \left\{\begin{matrix}\zeta^{\,n_i+\frac{1}{2}} \zeta_j^{\,-n_i-\frac{1}{2}-\omega} \\ \zeta_j^{\,n_j+\frac{1}{2}} \zeta_i^{\,-n_j-\frac{1}{2}-\omega}\end{matrix}\right\}$$
$$\sum_p \sum_q c_{ip} c_{jq} C\{n_i - l_i + 2p + \beta', n_j - l_j + 2q + \alpha', l_i - |m_i| - 2p + \delta', l_j - |m_j| - 2q + \gamma', \tfrac{1}{2}(|m_i| + |m_j|) + \epsilon'; \rho, \tau\},$$

where ρ and τ are defined by eqs. [9a] and [9b], respectively, and with

$$[16]\quad \sigma' = \alpha' + \gamma' + \epsilon'.$$

Inspection of eqs. [14] and [15] shows that the relations

$$[17]\quad \langle\chi_{ib}|P_b|\chi_{ja}\rangle = (\zeta_j/\zeta_i)^{n_i+n_j+\omega+1} \langle\chi_{ia}|P_a|\chi_{jb}\rangle,$$

$$[18]\quad \langle\chi_{ib}\rangle P_a|\chi_{ja}\rangle = (\zeta_j/\zeta_i)^{n_i+n_j+\omega+1} \langle\chi_{ia}|P_b|\chi_{jb}\rangle$$

hold, assuming that the proper orbital exponents are used and taking into account that the C-functions which appear in the expression of the integral on the right-hand side are defined in terms of a τ with opposite sign to the one obtained when applying eq. [9b].

Can. J. Chem. Downloaded from www.nrcresearchpress.com by 210.87.254.6 on 09/05/12
For personal use only.

For the limiting cases the expressions of the integrals* are determined by the relations

$$[19] \qquad \langle \chi_{ib}|P_b|\chi_{jb}\rangle \equiv \langle \chi_{ia}|P_a|\chi_{ja}\rangle = \lim_{\rho\to 0}\langle \chi_{ia}|P_a|\chi_{jb}\rangle,$$

with

$$[20] \qquad \tau = (\zeta_i - \zeta_j)/(\zeta_i + \zeta_j)$$

(the limit is applied to the C-functions involved; there is a change of sign if $\chi_{jb} \to -\chi_{ja}$ when $\rho \to 0$), and

$$[21] \qquad \left.\begin{matrix}\langle \chi_{ib}|P_a|\chi_{jb}\rangle \\ \langle \chi_{ia}|P_b|\chi_{ja}\rangle\end{matrix}\right\} = (-1)^{1-(n_i+n_j)+\frac{1}{2}(|m_i|+|m_j|)-\sigma} k_i k_j F(\phi)\zeta_i^{n_i+\frac{1}{2}}\zeta_j^{n_j+\frac{1}{2}}(\zeta_i+\zeta_j)^{-(n_i+n_j+1+\omega)}$$

$$\sum_p \sum_q c_{ip}c_{jq} C\{1+\alpha', (n_i+n_j)-(l_i+l_j)+2(p+q)-1+\beta', \gamma',$$

$$(l_i+l_j)-(|m_i|+|m_j|)-2(p+q)+\delta', \tfrac{1}{2}(|m_i|+|m_j|)+\epsilon'; \rho, \tau\},$$

with

$$[22a] \qquad \rho = \tfrac{1}{2}(\zeta_i+\zeta_j)R,$$

$$[22b] \qquad \tau = -1.$$

In the case of the dipole-velocity operator† it can be written

$$[23] \qquad \left.\begin{matrix}\langle \chi_{ia}|\partial/\partial x|\chi_{jb}\rangle \\ \langle \chi_{ib}|\partial/\partial x|\chi_{ja}\rangle\end{matrix}\right\} = (-1)^{-n_j-\frac{1}{2}(|m_i|-|m_j|)} k_i k_j \left\{\begin{matrix}\zeta_i^{n_i+\frac{1}{2}}\zeta_j^{-n_i+\frac{1}{2}} \\ \zeta_j^{n_j+\frac{1}{2}}\zeta_i^{-n_j+\frac{1}{2}}\end{matrix}\right\} \Bigg(F(\cos\phi)\sum_p\sum_q c_{ip}c_{jq}$$

$$\Bigg[(-1)^{\frac{3}{2}}(n_j - l_j + 2q - 1)C\{n_i - l_i + 2p, n_j - l_j + 2q - 2,$$

$$l_i - |m_i| - 2p, l_j - |m_j| - 2q, \tfrac{1}{2}(|m_i|+|m_j|)+\tfrac{1}{2}; \rho, \tau\}$$

$$+ (-1)^{\frac{1}{2}}|m_j| C\{n_i - l_i + 2p, n_j - l_j + 2q, l_i - |m_i| - 2p, l_j - |m_j| - 2q,$$

$$\tfrac{1}{2}(|m_i|+|m_j|) - \tfrac{1}{2}; \rho, \tau\}$$

$$- (-1)^{\frac{1}{2}} \left\{\begin{matrix}1 \\ (\zeta_j/\zeta_i)\end{matrix}\right\} C\{n_i - l_i + 2p, n_j - l_j + 2q - 1, l_i - |m_i| - 2p,$$

$$l_j - |m_j| - 2q, \tfrac{1}{2}(|m_i|+|m_j|)+\tfrac{1}{2}; \rho, \tau\}\Bigg]$$

$$+ F(\sin\phi)\sum_p\sum_q c_{ip}c_{jq} C\{n_i - l_i + 2p, n_j - l_j + 2q, l_i - |m_i| - 2p,$$

$$l_j - |m_j| - 2q, \tfrac{1}{2}(|m_i|+|m_j|) - \tfrac{1}{2}; \rho, \tau\}\Bigg)$$

(a similar expression holds for $\partial/\partial y$, with $F(\cos\phi)$ and $F(\sin\phi)$ replaced with $F(\sin\phi)$ and $-F(\cos\phi)$, respectively; $F(\cos\phi)$ and $F(\sin\phi)$ are defined by eq. [12], with $f(\phi)$ being $\cos\phi$ or $\sin\phi$, respectively) and

$$[24] \qquad \left.\begin{matrix}\langle \chi_{ia}|\partial/\partial z|\chi_{jb}\rangle \\ \langle \chi_{ib}|\partial/\partial z|\chi_{ja}\rangle\end{matrix}\right\} = (-1)^{-n_j-\frac{1}{2}(|m_i|-|m_j|)} k_i k_j F(\phi) \left\{\begin{matrix}\zeta_i^{n_i+\frac{1}{2}}\zeta_j^{-n_i+\frac{1}{2}} \\ \zeta_j^{n_j+\frac{1}{2}}\zeta_i^{-n_j+\frac{1}{2}}\end{matrix}\right\} \sum_p\sum_q c_{ip}c_{jq}$$

$$[(n_j - l_j + 2q - 1)C\{n_i - l_i + 2p, n_j - l_j + 2q - 2, l_i - |m_i| - 2p,$$

$$l_j - |m_j| - 2q + 1, \tfrac{1}{2}(|m_i|+|m_j|); \rho, \tau\}$$

*The numerical values depend, of course, on the values of the orbital exponents of the orbitals involved.

†For this operator the Cartesian coordinate x, y and z are chosen in such a way that $\partial/\partial z = \partial/\partial z_a = -\partial/\partial z_b$; $\partial/\partial x = \partial/\partial x_a = \partial/\partial x_b$; $\partial/\partial y = \partial/\partial y_a = \partial/\partial y_b$.

Can. J. Chem. Downloaded from www.nrcresearchpress.com by 210.87.254.6 on 09/05/12
For personal use only.

$$+ (l_j - |m_j| - 2q)C\{n_i - l_i + 2p, n_j - l_j + 2q, l_i - |m_i| - 2p, l_j - |m_j| - 2q - 1, \tfrac{1}{2}(|m_i| + |m_j|); \rho, \tau\}$$

$$+ \begin{Bmatrix} 1 \\ (\zeta_j/\zeta_i) \end{Bmatrix} C\{n_i - l_i + 2p, n_j - l_j + 2q - 1, l_i - |m_i| - 2p, l_j - |m_j| - 2q + 1, \tfrac{1}{2}(|m_i| + |m_j|); \rho, \tau\}]$$

(where $F(\phi)$ is determined for $f(\phi) = 1$).

For the limiting cases the analytical expressions of the integrals are determined by the relations*

[25a] $$\langle \chi_{ib}|\partial/\partial x_b|\chi_{jb}\rangle = \langle \chi_{ia}|\partial/\partial x_a|\chi_{ja}\rangle = \lim_{\rho\to 0}\langle \chi_{ia}|\partial/\partial x|\chi_{jb}\rangle,$$

[25b] $$-\langle \chi_{ib}|\partial/\partial z_b|\chi_{jb}\rangle = \langle \chi_{ia}|\partial/\partial z_a|\chi_{ja}\rangle = \lim_{\rho\to 0}\langle \chi_{ia}|\partial/\partial z_a|\chi_{jb}\rangle$$

[in both cases the limit is taken for the C-functions involved; there is a change of sign if $\chi_{jb} \to -\chi_{ja}$ when $\rho \to 0$; $\tau = (\zeta_i - \zeta_j)/(\zeta_i + \zeta_j)$] and (5)

[26a] $$\langle \chi_{ib}|\partial/\partial x_a|\chi_{jb}\rangle = \langle \chi_{ia}|\partial/\partial x_a|\chi_{ja}\rangle,$$

[26b] $$\langle \chi_{ib}|\partial/\partial z_a|\chi_{jb}\rangle = \langle \chi_{ia}|\partial/\partial z_a|\chi_{ja}\rangle.$$

CONCLUSION

The preceding treatment has been applied to several one-electron operators: electronic charge cloud; electric potential, electric field, and electric field gradient produced by an electron at one of the nuclei; electric dipole (length, velocity, and acceleration) and quadrupole moments; electric polarizability; magnetic susceptibility; and nuclear magnetic shielding.

Tables† have been prepared (up to $n = 3$) for the basic operators involved in all those cases, using STO's.

REFERENCES

1. K. RUEDENBERG, C. C. J. ROOTHAAN, and W. JAUNZEMIS. Tech. Rept. Laboratory of Molecular Structure and Spectra, University of Chicago, Chicago, Illinois. 1952–1953. pp. 137–256.
2. K. RUEDENBERG, C. C. J. ROOTHAAN, and W. JAUNZEMIS. J. Chem. Phys. **24**, 201 (1956).
3. C. C. J. ROOTHAAN. J. Chem. Phys. **24**, 947 (1956).
4. W. C. HAMILTON. J. Chem. Phys. **26**, 1018 (1957).
5. S. EHRENSON and P. E. PHILLIPSON. J. Chem. Phys. **34**, 1224 (1961).

**The signs given are determined by the choice of axes, as indicated above.*

†These lables have been placed in The Depository of Unpublished Data, National Science Library, National Research Council, Ottawa 2, Canada, and photocopies may be obtained upon request to the Depository.

Can. J. Chem. Downloaded from www.nrcresearchpress.com by 210.87.254.6 on 09/05/12
For personal use only.

Can. J. Chem. Downloaded from www.nrcresearchpress.com by 210.87.254.5 on 09/05/12
For personal use only.

LYCOPODIUM ALKALOIDS

VII.[1] LYCODOLINE (ALKALOID L.8)[2,3]

W. A. AYER AND G. G. IVERACH
Department of Chemistry, University of Alberta, Edmonton, Alberta

Received July 15, 1964

ABSTRACT

Lycodoline (alkaloid L.8) is shown to have the structure and stereochemistry depicted in II. The transformation of lycodoline into lycopodine is described. The use of infrared spectroscopy in assigning the configuration at C-12 and the nitrogen in these and related alkaloids is described. The effect of the configuration at C-12 on the optical rotatory dispersion spectra and on the mass spectra of lycopodine (I) and 12-epilycopodine (X) is discussesd.

Lycopodium alkaloid L.8, for which we have chosen the name lycodoline, was first isolated by Manske and Marion in 1943 from *L. annotinum* Linn. (1). This substance is of particular interest since it is one of the most widely distributed of the minor alkaloids of the Lycopodiaceae, having also been isolated from *L. annotinum* var. *acrifolium* (2) (the substance as isolated from this species was originally designated alkaloid L.30, but it was later shown (3) that L.30 is identical with L.8), *L. selago* (4), *L. fawcettii* (5), *L. lucidulum* (6), *L. clavatum* (7, 8), and *L. prostratum* (9). The lycodoline used in this investigation was isolated from *L. annotinum* and was identical with an authentic sample of alkaloid L.8 provided by R. H. Manske.

Earlier workers had established that lycodoline has the molecular formula $C_{16}H_{25}O_2N$ (1, 2, 4, 5, 10), that the oxygens are present as a ketonic carbonyl group and a hydroxyl group (10), and that the nitrogen is tertiary (5, 10). Our analytical and spectroscopic data confirmed these conclusions and, in addition, revealed the presence of a secondary C–methyl group (0.68 mole of volatile acid on Kuhn–Roth oxidation, doublet at 9.14 τ in the nuclear magnetic resonance (n.m.r.) spectrum). Lack of olefinic absorption in the n.m.r. spectrum, coupled with the fact that lycodoline is recovered unchanged on attempted catalytic hydrogenation, leads to the conclusion that there are no carbon–carbon double bonds and that the molecule is tetracyclic.

The environment of the carbonyl group in lycodoline was defined in the following manner. The infrared spectrum, measured in CCl_4, showed absorption at 1703 cm^{-1}, accompanied by a band at 1410 cm^{-1}, indicative of the grouping —CO—CH_2— (11). Neither of these absorption bands was present in dihydrolycodoline ($C_{16}H_{27}O_2N$), the product obtained by lithium aluminum hydride reduction of the carbonyl group. Dehydration of dihydrolycodoline with thionyl chloride in methylene chloride at room temperature yielded anhydrodihydrolycodoline ($C_{16}H_{25}ON$), which showed a single olefinic proton at 4.56 τ (mult.) in its n.m.r. spectrum. Since it will be shown that the hydroxyl group lost in the dehydration is that one produced in the reduction of the keto group, then, provided that no rearrangement has occurred during the dehydration, the grouping —CH—CO—CH_2— must be present in lycodoline.

Concerning the environment of the nitrogen and hydroxyl group, it was found that

[1]*Part VI, W. A. Ayer, A. N. Hogg, and A. C. Soper. Can. J. Chem. 42, 949 (1964).*
[2]*A portion of this work was reported in a preliminary communication: W. A. Ayer and G. G. Iverach. Tetrahedron Letters, No. 3, 87 (1961).*
[3]*Taken in part from the Ph.D. thesis of G. G. Iverach, University of Alberta, 1963; presented at the XIXth International Congress of Pure and Applied Chemistry, London, July 10–17, 1963.*

Can. J. Chem. Downloaded from www.nrcresearchpress.com by 210.87.254.5 on 09/05/12
For personal use only.

lycodoline was resistant to both acetylation and mild oxidation (CrO_3–pyridine, CrO_3–acetic acid), suggesting that the hydroxyl as well as the nitrogen was tertiary. The position of the —OH stretching vibration in the infrared spectra of lycodoline and its derivations was especially informative. The infrared spectrum of lycodoline, measured in dilute carbon tetrachloride, showed a concentration-independent band at 3545 cm^{-1}. It is known (12) that intramolecular hydrogen bonding causes a concentration-independent shift of the —OH stretching vibration from the non-bonded 3615–3635 cm^{-1} region to lower frequency. In this case, we attribute the shift to intramolecular hydrogen bonding between the hydroxyl group and the tertiary nitrogen. The alternate possibility, that the association is between the hydroxyl group and the ketonic carbonyl group, was ruled out by the observation that dihydrodeoxylycodoline (in which the carbonyl group has been converted to a methylene group by Wolff–Kishner reduction) also shows H-bonded hydroxyl absorption (3545 cm^{-1}). Dihydrolycodoline showed —OH stretching vibrations at 3625 cm^{-1} (non-bonded) and 3550 cm^{-1} (H-bonded), while its dehydration product, anhydrodihydrolycodoline, displayed only the H-bonded absorption (3565 cm^{-1}), showing that it is the original hydroxyl group of lycodoline which is retained in the dehydration product. These studies indicate that the hydroxyl group and the nitrogen are in close proximity to one another. The fact that they are vicinal was shown in the following manner: reaction of lycodoline with ethyl bromoacetate gave a salt (A) which showed absorption in the infrared (Nujol) at 3240, 1753, and 1717 cm^{-1}, attributable to hydroxyl, ester carbonyl, and ketonic carbonyl stretching vibrations, respectively. Hydrolysis of the ester salt (A) with aqueous hydrobromic acid gave a lactone salt (B), which showed no hydroxyl absorption in the infrared, but showed carbonyl bands at 1756 (lactone) and 1705 (ketone) cm^{-1}. The lactone salt also formed to some extent when the ester was recrystallized from hot methanol. The ease of formation of the lactone, coupled with the fact that the lactonic carbonyl absorbs at essentially the same frequency as the ester carbonyl, strongly suggests that the lactone is six-membered. An analogous pair of salts was prepared from dihydrodeoxylycodoline. In this case the ester absorbed at 1747 cm^{-1} and the lactone at 1754 cm^{-1}, confirming the assignments made above.

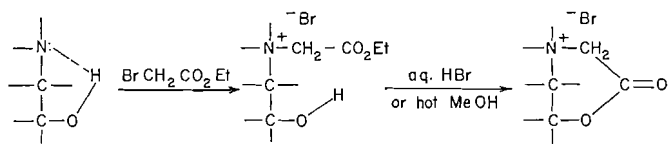

With these structural features established, it seemed possible that lycodoline might be very simply related to lycopodine (I), the most commonly occurring *Lycopodium* alkaloid. Replacement of the C-12 hydrogen in lycopodine by hydroxyl leads to a structure (II) which incorporates all of the features of lycodoline defined to this point. Structure III, the C-12 epimer of II, would also fit the evidence presented so far. The optical rotatory dispersion curve for lycodoline was positive and very similar to that of lycopodine (13). Since, however, the Octant Rule (14) states that substituents at C-4 of the carbonyl-containing ring have little or no effect on the dispersion curve, it was not possible to exclude structure III on this basis.

Evidence that lycodoline does indeed have the carbon–nitrogen skeleton shown in II and III was obtained in the following manner. Dihydrodeoxylycodoline, the product of

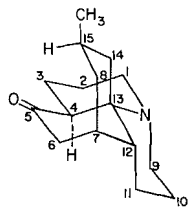

I.

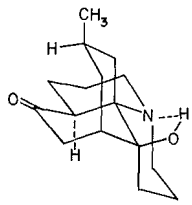

II.

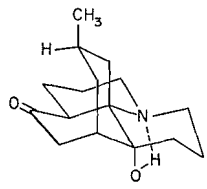

III.

Wolff–Kishner reduction of lycodoline, was dehydrated with phosphorus pentoxide in refluxing toluene. The product, anhydrodihydrodeoxylycodoline (IV), could not be obtained in crystalline form, but was conveniently isolated and characterized in the form of its hydrochloride. The free base showed no hydroxyl absorption in the infrared and a single olefinic proton at 4.64 τ (poorly resolved triplet) in its n.m.r. spectrum. Oppenauer oxidation of acrifoline (V) (15) gave the diketone VI, which was assigned the stereochemistry shown, since the transformation of C-5 from tetrahedral to trigonal should remove the non-bonded interaction which forces ring D into a boat conformation (16) and since the equilibrating conditions of the reaction should then favor the equatorial conformation for the methyl group. Wolff–Kishner reduction of the diketone VI yielded anhydrodihydrodeoxylycodoline (IV), confirming the proposed skeleton. Since the Wolff–Kishner reduction does not necessarily lead to the most stable of two possible epimers (17), this result does not establish the configuration at C-15.

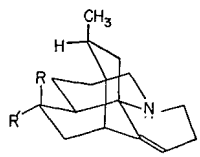

IV. R = R′ = H
IX. R = R′ = O

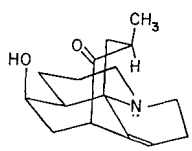

V.

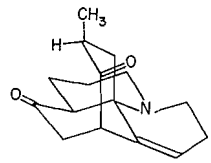

VI.

Catalytic hydrogenation of the olefin IV gave a mixture of the saturated amines VII (major product) and VIII, which was separable by chromatography. Compound VIII, in the form of its methiodide, was identical with dihydrodeoxylycopodine (13), the product of Wolff–Kishner reduction of lycopodine, thus rigorously establishing the carbon–nitrogen skeleton as well as the configuration at C-15. Compound VII, the major product of the reduction formed by addition of hydrogen from the less hindered side of the olefin IV, was also prepared from dihydroacrifoline (15, 16) by Oppenauer oxidation, followed by Wolff–Kishner reduction of the previously reported (16, 18) diketone.

The amines VII and VIII showed significant differences in their infrared spectra in the C—H stretching region. Bohlmann has pointed out (19, 20) that a series of absorption bands between 2700 and 2850 cm^{-1} are prominent in the infrared spectra of quinolizidine derivatives, in which at least two hydrogens *alpha* to the nitrogen are oriented *trans* diaxial to the electron pair on the nitrogen. In agreement with this generalization, amine VII shows well-developed bands in this region (Fig. 1) while the amine VIII does not. This observation provides us with a method for distinguishing between compounds which are epimeric at C-12 (and hence at the nitrogen), and thus between structures II and III for lycodoline. As shown in Fig. 2, lycodoline does not display these prominent bands and

Can. J. Chem. Downloaded from www.nrcresearchpress.com by 210.87.254.5 on 09/05/12
For personal use only.

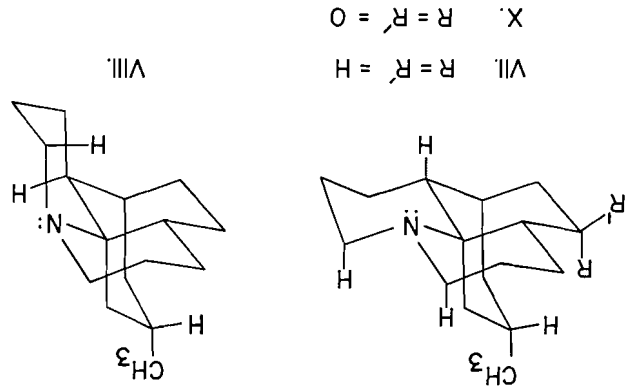

thus must possess structure II. Compounds with a double bond in the 11,12-position are free to take up either conformation about the nitrogen. Acrifoline (V) (Fig. 2), the olefin IV, and the diketone VI show prominent bands in the 2700–2850 cm^{-1} region, and hence must exist largely in the conformation shown. The formation of the epimers VII and VIII in the hydrogenation of anhydrodihydrodeoxylycodoline (IV) provides further evidence for the location of the double bond in IV, and thus the hydroxyl group in lycodoline.

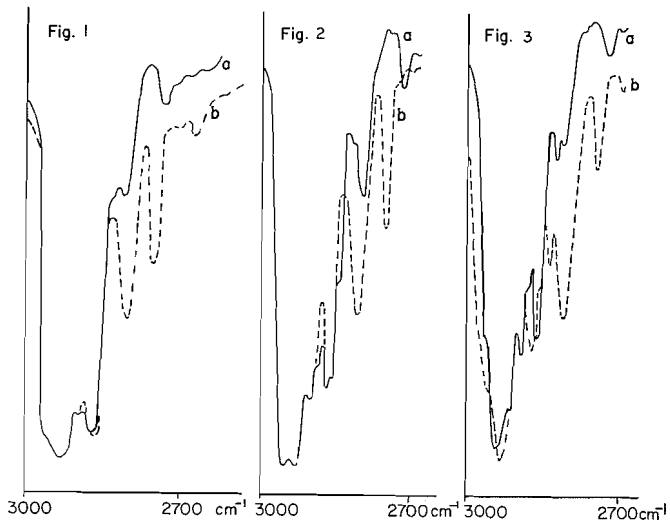

FIG. 1. Infrared spectrum of (*a*) the amine VIII, (*b*) the amine VII.
FIG. 2. Infrared spectrum of (*a*) lycodoline, (*b*) acrifoline.
FIG. 3. Infrared spectrum of (*a*) lycopodine, (*b*) 12-epilycopodine.

In order that we might more firmly establish the position of the carbonyl group in lycodoline, we now sought to transform lycodoline (II) directly into lycopodine (I). Dehydration of lycodoline with phenylphosphoric dichloride–pyridine gave anhydrolycodoline (IX) in 90% yield. Anhydrolycodoline was an unstable oil that was characterized by means of its mass spectrum (Fig. 4*a*). The n.m.r. spectrum showed a single olefinic proton at 4.44 τ (triplet, J = 3.5 c.p.s.) and the infrared spectrum (CCl_4) showed carbonyl absorption at 1698 cm^{-1} and C=C absorption at 1650 cm^{-1}. Catalytic hydrogenation of the perchlorate of IX, followed by liberation of the bases and chromatography over

Can. J. Chem. Downloaded from www.nrcresearchpress.com by 210.87.254.5 on 09/05/12
For personal use only.

alumina, gave a mixture of lycopodine (isolated in 10% yield) and 12-epilycopodine (isolated in 65% yield). 12-Epilycopodine (X) displayed well-developed bands in the 2700–2850 cm^{-1} region (see Fig. 3) as expected for the *trans*-quinolizidine system. The infrared spectrum of lycopodine is shown in Fig. 3 for comparison.

Unexpectedly, the optical rotatory dispersion curve for compound X showed a negative Cotton effect (extrema at 306 and 265 mμ, amplitude $-5100°$). Since the absolute configuration of lycopodine has been ascertained (6, 21), the cause of this anomoly is not readily apparent, but the fact that lycodoline shows a positive curve similar to that of lycopodine, whereas the C-12,N epimer X shows a negative Cotton curve, serves further to exclude structure III as a possibility for lycodoline.

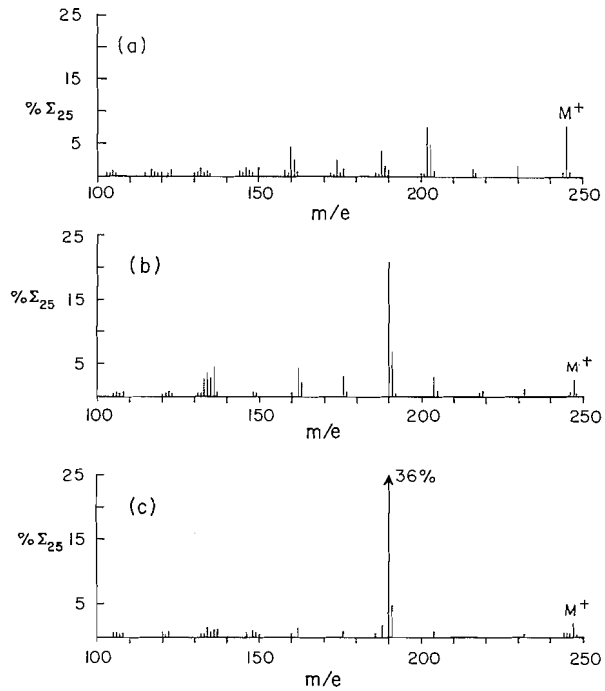

FIG. 4. Mass spectrum of (*a*) anhydrolycodoline, (*b*) 12-epilycopodine, (*c*) lycopodine.

The mass spectrum of 12-epilycopodine (X) (Fig. 4*b*) is worthy of comment. MacLean has suggested (22) that loss of ring D in lycopodine and related alkaloids, upon electron impact, may occur as shown in the following manner.

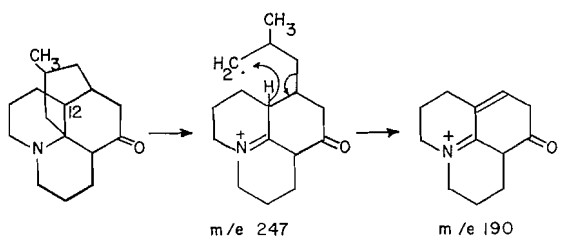

The base peak in the mass spectrum of 12-epilycopodine (Fig. 4*b*), like that of lycopodine (Fig. 4*c*), occurs at *m/e* 190. However, in the case of the epi compound X, the 190 peak

Can. J. Chem. Downloaded from www.nrcresearchpress.com by 210.87.254.5 on 09/05/12
For personal use only.

accounts for only 21% of $\sum_{25}$ (sum of the relative intensities of all peaks from mass 25 to the molecular weight (23)), whereas in lycopodine it accounts for 36%. This indicates that if a cyclic mechanism, such as that shown above, is operative, a *cis* arrangement of the C-12 hydrogen and the bridged ring facilitates, but is not necessary for, loss of the bridge. The mass spectrum of anhydrolycodoline (IX, Fig. 4*a*) again emphasizes the necessity of a hydrogen at C-12 for easy loss of the bridge (22), since in this case the parent peak is now the most intense peak in the spectrum, and the 188 peak (corresponding to loss of the bridge plus a hydrogen) is only 4% of $\sum_{25}$. In lycodoline (II), the mass spectrum of which has already been discussed (22), the parent peak is again the most intense peak in the spectrum.

EXPERIMENTAL

Ultraviolet spectra were measured in 95% ethanol and, unless otherwise specified, infrared spectra in carbon tetrachloride. For hydrogen-bonding studies, spectra were determined on 0.1, 0.05, and 0.01 *M* solutions in CCl_4 using a Perkin–Elmer Model 221 or 441 spectrophotometer. Nuclear magnetic resonance spectra were measured on ca. 5–10% w/v solutions in chloroform or deuterochloroform using a Varian Associates Model A-60 spectrometer. Internal tetramethylsilane was used as standard. Some of the optical rotatory dispersion curves were obtained by Dr. M. M. Marsh, Eli Lilly, Indianapolis; the others were determined by Mr. R. N. Swindlehurst of these laboratories using a Rudolph Automatic Recording Spectropolarimeter. The mass spectra were determined on an AEI MS2-H mass spectrometer. Samples were introduced through a heated inlet system maintained at 200°. Melting points were determined on a hot stage and are uncorrected. The alumina used for column chromatography, unless otherwise specified, was basic alumina of activity III–IV. Thin-layer chromatograms were carried out on 0.25 mm layers of Alumina G (Research Specialties Co., Richmond, California) and were developed with Dragendorff's reagent (24). Skellysolve B refers to Skelly Oil Company light petroleum, b.p. 62–70°. Microanalyses are by Pascher Mikroanalytisches Laboratorium, Bonn, West Germany, and C. Daessle, Montreal, Quebec.

Isolation of Lycodoline

Lycopodium annotinum L. was extracted as previously described (1) and most of the annotinine removed by crystallization (1). The resulting "annotinine-free" alkaloids were chromatographed over alumina. Lycodoline was eluted with ether and with ether – methylene chloride. Lycodoline has a characteristic sharp band at 960 cm^{-1} in the infrared which facilitates its detection. Suitable combination of fractions and crystallization from acetone gave lycodoline, m.p. 180–181°, identical with an authentic sample of alkaloid L.8 kindly furnished by R. H. Manske.

Infrared spectrum: ν_{max} 3545, 1703 cm^{-1}. Rotatory dispersion in methanol (*c*, 0.15): $[\alpha]_{308}$ +2660° (peak), $[\alpha]_{265}$ −6950° (trough).

Lithium Aluminum Hydride Reduction of Lycodoline

Lycodoline (148 mg) in ether (100 ml) was added to a slurry of $LiAlH_4$ (180 mg) in ether (75 ml) and the mixture refluxed for 18 h. Excess hydride was destroyed with wet ether and the solution extracted with dilute hydrochloric acid. The aqueous layer was made basic with aqueous ammonia and extracted with chloroform. Evaporation of the solvent and crystallization from acetone yielded dihydrolycodoline (0.10 g), m.p. 186–187°.

Calcd. for $C_{16}H_{27}O_2N$: C, 72.41; H, 10.26. Found: C, 72.16; H, 10.14.

Infrared spectrum: ν_{max} 3625, 3550 cm^{-1} (concentration independent).

Anhydrodihydrolycodoline

A solution of dihydrolycodoline (91 mg), methylene chloride (20 ml), and thionyl chloride (1.5 ml) was kept at room temperature for 2½ h. Then the solvents were removed at the pump. The oily residue was dissolved in dilute hydrochloric acid, washed with ether, and made basic with aqueous ammonia. Extraction with chloroform yielded a pale yellow oil (68 mg) which was chromatographed over alumina (2 g). Ether elution gave a colorless oil (62 mg) which was transformed to the hydrobromide in acetone solution. Recrystallization from acetone gave the analytical sample, m.p. 293–295°.

Calcd. for $C_{16}H_{25}ON \cdot HBr$: C, 58.55; H, 7.99. Found: C, 58.62; H, 8.11.

A sample of the free base was recovered from the hydrobromide and distilled at 130° at 0.5 mm. Infrared spectrum: ν_{max} 3565 (concentration independent), 1650 cm^{-1} (very weak). Nuclear magnetic resonance spectrum: 4.56 τ (1H, mult.), 9.08 τ (3H, poorly defined doublet).

Attempts to hydrogenate this olefin were not successful.

Dihydrodeoxylycodoline

Anhydrous hydrazine was added to a solution of sodium (0.5 g) in diethylene glycol (25 ml) until the solution refluxed at 190°. The solution was then cooled to 50° and lycodoline (200 mg) added, then the resulting

Can. J. Chem. Downloaded from www.nrcresearchpress.com by 210.87.254.5 on 09/05/12
For personal use only.

solution refluxed for 17½ h. The cooled reaction mixture was diluted with water, acidified with hydrochloric acid, continuously extracted with ether for 18 h (to remove diethylene glycol), made basic with aqueous ammonia, and extracted six times with chloroform. Evaporation of the chloroform left a solid which was recrystallized from acetone to give dihydrodeoxylycodoline (175 mg), m.p. 122.5–123.5°.

Calcd. for $C_{16}H_{27}ON$: C, 77.05; H, 10.91; O, 6.42; N, 5.62. Found: C, 76.51, 76.84; H, 10.65, 10.74; O, 6.82; N, 5.57.

Infrared spectrum: ν_{max} 3545 (concentration independent).

The perchlorate, recrystallized from acetone–ethyl acetate, melted at 273–275°.

Calcd. for $C_{16}H_{27}ON \cdot HClO_4$: C, 54.95; H, 8.07; N, 4.01. Found: C, 54.95; H, 8.07; N, 4.14.

Ester Salt (A) from Lycodoline

A solution of lycodoline (45 mg), ethyl bromoacetate (1.5 ml), and benzene (4 ml) was refluxed for 2 h. Filtration of the cooled reaction mixture gave the quaternary bromide (40 mg), m.p. above 340°, which was recrystallized from methanol–ether.

Calcd. for $C_{20}H_{32}O_4NBr$: C, 55.81; H, 7.50. Found: C, 55.51; H, 7.46.

Infrared spectrum: ν_{max}^{Nujol} 3240 (hydroxyl), 1753 (ester), 1717 cm^{-1} (ketone).

Ester Salt (A) from Dihydrodeoxylycodoline

The salt, prepared as above, melted at 212–213°.

Calcd. for $C_{20}H_{34}O_3NBr$: C, 57.69; H, 8.23; Br, 19.78. Found: C, 58.74; H, 8.53; Br, 19.78.

Infrared spectrum: ν_{max}^{Nujol} 3248 (hydroxyl), 1748 cm^{-1} (ester).

Lactone Salt (B) from Lycodoline

The ester salt from lycodoline (140 mg) was refluxed with 4 *N* HBr (10 ml) for 24 h. Then the solvent was evaporated and the residue recrystallized from methanol to give the lactone salt, m.p. above 340°.

Calcd. for $C_{18}H_{26}O_3NBr$: C, 56.26; H, 6.82; Br, 20.80. Found: C, 55.85; H, 6.64; Br, 21.50.

Infrared spectrum: ν_{max}^{Nujol} 1757 (lactone), 1710 cm^{-1} (ketone).

Lactone Salt (B) from Dihydrodeoxylycodoline

The lactone salt was prepared as described above for lycodoline and, after recrystallization from methanol–ether, melted at 325–326°.

Calcd. for $C_{18}H_{28}O_2NBr$: C, 58.38; H, 7.62. Found: C, 57.85; H, 7.35.

Infrared spectrum: ν_{max}^{Nujol} 1754 cm^{-1} (lactone).

Anhydrodihydrodeoxylycodoline (IV)

(A) From Dihydrodeoxylycodoline

A mixture of dihydrodeoxylycodoline (143 mg), phosphorus pentoxide (1 g), and toluene (100 ml) was heated under reflux for 3 h. Then the excess phosphorus pentoxide was decomposed with ice. The resulting two phase system was separated and the organic layer washed thoroughly with dilute hydrochloric acid. The combined acid solutions were washed with ether, made basic with aqueous ammonia, and extracted with chloroform. Evaporation of the chloroform left an oily residue (139 mg) which showed no hydroxyl absorption in its infrared spectrum. This product was dissolved in dilute hydrochloric acid and the hydrochloride extracted into chloroform. The hydrochloride hemihydrate obtained was recrystallized from acetone–ether, m.p. 232–233.5°.

Calcd. for $C_{16}H_{25}N \cdot HCl \cdot \frac{1}{2}H_2O$: C, 69.40; H, 9.83; Cl, 12.80. Found: C, 69.21, 69.60; H, 9.52, 9.65; Cl, 12.93.

The n.m.r. spectrum of the free base liberated from the purified hydrochloride showed signals at 4.64 τ (1H, poorly resolved triplet, J = 3 c.p.s.), and at 9.16 τ (3H, doublet, J = 5.5 c.p.s.).

(B) From Dehydroacrifoline (VI)

Dehydroacrifoline hydrobromide (210 mg, see below) was added to a solution of sodium, diethylene glycol, and hydrazine, made up as described for the preparation of dihydrodeoxylycodoline. The solution was refluxed for 14 h at 190°, then allowed to distil until the reflux temperature reached 215–220°. The solution was kept at this temperature for 11 h. Then the cooled solution was diluted with dilute hydrochloride acid and continuously extracted with ether for 1 day. The aqueous solution was made basic and extracted with chloroform to give a yellow oil, which was dissolved in dilute hydrochloric acid and the hydrochloride extracted into chloroform. Evaporation of the chloroform left a crystalline residue, which was recrystallized from acetone–ether to give anhydrodihydrodeoxylycodoline (IV) hydrochloride hemihydrate identical in melting point, mixed melting point, infrared spectrum ($CHCl_3$), and optical rotation ($[\alpha]_D^{23°}$ −28° (*c*, 1.9, ethanol)) with that prepared from lycodoline.

Hydrogenation of Anhydrodihydrodeoxylycodoline (IV)

The hydrochloride of IV (0.60 g) was shaken in methanol (100 ml) in the presence of platinum (from 300 mg of Adams' catalyst) and hydrogen (3 atm) for 3 h. Evaporation of the filtered reaction mixture left a crystalline residue (0.59 g) which was chromatographed on alumina (10 g). Elution with benzene (250 ml) removed the major component (0.50 g) (as evidenced by thin-layer chromatography of the fractions), and

Can. J. Chem. Downloaded from www.nrcresearchpress.com by 210.87.254.5 on 09/05/12
For personal use only.

elution with ether (200 ml) yielded the minor component (80 mg). The major component was dissolved in acetone and neutralized with 70% aqueous perchloric acid. Dilution of this solution with ethyl acetate yielded the crystalline perchlorate of the amine VII, which melted, after several recrystallizations from acetone – ethyl acetate, at 240–241°.

Calcd. for $C_{16}H_{27}N \cdot HClO_4$: C, 57.55; H, 8.45; N, 4.20. Found: C, 57.18; H, 8.51; N, 4.41.

The infrared spectrum of the free base showed prominent bands in the 2700–2850 cm^{-1} region (Fig. 1).

The minor component was shown to be dihydrodeoxylycopodine (VIII) in the following way. A portion (32 mg) of the material eluted with ether was dissolved in acetone (5 ml) and methyl iodide (1 ml) added. After 12 h at room temperature, the solvents were removed and the residue was recrystallized several times from acetone to give dihydrodeoxylycopodine methiodide, m.p. 290–291°, identical (mixed melting point, infrared spectrum) with an authentic sample (13).

Dehydroacrifoline (VI)

Acrifoline (V, 0.73 g) was dissolved in a solution of aluminum isopropoxide (0.8 g) in toluene (40 ml) and cyclohexanone (6 ml) added. The solution was refluxed for 3 h, diluted with benzene, and extracted with 1 *N* hydrochloric acid. The extract was washed with ether, made basic with aqueous ammonia, and extracted with chloroform to give a pale yellow oil (0.68 g) which was chromatographed over alumina (12 g). Elution with benzene (500 ml) gave an oily material (0.37 g) which was transformed to the hydrobromide in ethanol. Further elution with ether and chloroform gave unreacted acrifoline.

The ethanol solution of the hydrobromide was diluted with ethyl acetate. The resultant crystalline material was filtered off and recrystallized from ethanol – ethyl acetate to give dehydroacrifoline hydrobromide, m.p. 309–310° (sealed tube).

Calcd. for $C_{16}H_{21}O_2N \cdot HBr$: C, 56.56; H, 6.52; N, 4.12. Found: C, 56.21; H, 6.67; N, 3.76.

The infrared spectrum of the hydrobromide showed carbonyl absorption at 1728 and 1714 cm^{-1}, while the free base absorbed at 1712 and 1708 cm^{-1}.

Anhydrolycodoline (IX)

Lycodoline (II, 215 mg) was dissolved in a solution of phenylphosphonic dichloride (10 ml) and pyridine (10 ml) and the reaction mixture kept at 60–70° for 13 h. The excess phenylphosphonic dichloride was carefully decomposed with water. The resulting aqueous solution was made basic with 5% sodium hydroxide and extracted with chloroform to give, after evaporation of the chloroform, a deep red oil (0.20 g) which was chromatographed over alumina (6 g). Elution with benzene afforded a colorless oil (0.18 g) which showed a single spot on thin-layer chromatography but which rapidly colorized on standing. A portion was distilled (120° at 0.5 mm) and its mass spectrum recorded (see Fig. 4*a*). The infrared spectrum showed prominent bands in the 2700–2850 cm^{-1} region, no hydroxyl absorption, carbonyl absorption at 1698 cm^{-1}, and a weak band at 1655 cm^{-1} (C=C). Nuclear magnetic resonance spectrum: 4.44 τ (1H, triplet, J = 3.5 c.p.s.), 9.17 τ (3H, doublet, J = 5.5 c.p.s.). Rotatory dispersion in methanol (*c*, 0.08): $[\alpha]_{308}$ +1140° (peak), $[\alpha]_{264}$ −3900° (trough).

Hydrogenation of Anhydrolycodoline (IX)

A solution of anhydrolycodoline (170 mg) in methanol was acidified with perchloric acid and shaken with platinum (from 200 mg of Adams' catalyst) under hydrogen (3 atm). The catalyst was removed by filtration and the filtrate evaporated to a crystalline residue, which was dissolved in water, made basic with aqueous ammonia, and extracted with chloroform. The colorless oil (0.17 g), obtained when the chloroform was evaporated, showed two spots on thin-layer chromatography and was chromatographed over alumina (6 g), using pentane–ether, (400:1 to 9:1) as the eluant. Forty fractions (each 20 ml) were collected and each fraction was examined by thin-layer chromatography. Fractions 30–32 (17 mg) were homogeneous and showed an R_f identical with that of lycopodine. Crystallization from pentane–ether gave lycopodine, identical in melting point, mixed melting point, infrared spectrum, and optical rotation with an authentic sample.

Fractions 33–39 (0.15 g) were combined and rechromatographed over alumina (5 g). Elution with pentane (200 ml) removed only traces of material, while elution with benzene (50 ml) gave a crystalline fraction (0.11 g), which was recrystallized from pentane to give 12-epilycopodine (X), m.p. 89–90°.

Calcd. for $C_{16}H_{25}ON$: C, 77.67, H, 10.19; N, 5.66; molecular weight, 247. Found: C, 77.78; H, 9.99; N, 5.41; molecular weight, 247 (by mass spectrometry, see Fig. 4*b*).

Infrared spectrum: ν_{max} 2700–2850 cm^{-1} (see Fig. 3), 1698 cm^{-1}. Rotatory dispersion in methanol (*c*, 0.09): $[\alpha]_{306}$ −930° (trough), $[\alpha]_{265}$ +1130° (peak).

ACKNOWLEDGMENTS

We thank Dr. R. H. Manske for a sample of alkaloid L.8, Dr. P. Kebarle and Mr. A. N. Hogg for determining the mass spectra and for helpful discussion, Mr. R. N. Swindlehurst and Mrs. Gail Conway for determining the infrared and n.m.r. spectra, and Dr. M. M. Marsh for determining some of the optical rotatory dispersion curves. This research was

Can. J. Chem. Downloaded from www.nrcresearchpress.com by 210.87.254.5 on 09/05/12
For personal use only.

supported by grants from the National Research Council of Canada, to whom we express our thanks.

REFERENCES

1. R. H. MANSKE and L. MARION. Can. J. Res. B, **21**, 92 (1943).
2. R. H. MANSKE and L. MARION. J. Am. Chem. Soc. **69**, 212 (1947).
3. B. DOUGLAS, D. G. LEWIS, and L. MARION. Can. J. Chem. **31**, 272 (1953).
4. O. ACHMATOWICZ and W. RODEWALD. Roczniki Chem. **30**, 233 (1956).
5. R. H. BURNELL. J. Chem. Soc. 3091 (1959).
6. W. A. AYER, J. A. BEREZOWSKY, and D. A. LAW. Can. J. Chem. **41**, 649 (1963).
7. J. A. BEREZOWSKY. M.Sc. Thesis, University of Alberta, Edmonton, Alberta. 1962.
8. Y. INUBUSKI, Y. ISUDA, and T. SANO. Yakugaku Zasshi, **82**, 1083 (1962).
9. W. A. AYER and S. VALVERDE-LOPEZ. Unpublished.
10. G. S. PERRY and D. B. MACLEAN. Can. J. Chem. **34**, 1189 (1956).
11. R. N. JONES and C. SANDORFY. Technique of organic chemistry. Vol. IX. Interscience, New York. 1956. p. 498.
12. A. R. H. COLE. Technique of organic chemistry. Vol. XI. Part I. Interscience, New York. 1963. p. 148.
13. W. A. AYER and D. A. LAW. Can. J. Chem. **40**, 2088 (1962).
14. W. MOFFITT, R. B. WOODWARD, A. MOSCOWITZ, W. KLYNE, and C. DJERASSI. J. Am. Chem. Soc. **83**, 4013 (1961).
15. W. N. FRENCH and D. B. MACLEAN. Can. J. Chem. **39**, 2100 (1961).
16. F. A. L. ANET. Tetrahedron Letters, No. 20, 13 (1960).
17. C. DJERASSI, T. T. GROSSNICKLE, and L. B. HIGH. J. Am. Chem. Soc. **78**, 3166 (1956).
18. W. N. FRENCH and D. B. MACLEAN. Chem. Ind. London, 658 (1960).
19. F. BOHLMANN. Chem. Ber. **91**, 2157 (1958).
20. F. BOHLMANN and C. ARNDT. Chem. Ber. **91**, 2167 (1958).
21. K. WIESNER, J. E. FRANCIS, J. A. FINDLAY, and Z. VALENTA. Tetrahedron Letters, No. 5, 187 (1961).
22. D. B. MACLEAN. Can. J. Chem. **41**, 2654 (1963).
23. K. BIEMANN. Mass spectrometry: organic chemical applications. McGraw-Hill, New York. 1962. p. 44.
24. B. T. CROMWELL. *In* Modern methods of plant analysis. Vol. 4. *Edited by* K. Paech and M. W. Tracey. Springer-Verlag, Berlin. 1955. p. 373.

Can. J. Chem. Downloaded from www.nrcresearchpress.com by 210.87.254.5 on 09/05/12
For personal use only.

Can. J. Chem. Downloaded from www.nrcresearchpress.com by 210.87.254.5 on 09/05/12
For personal use only.

REGULARITIES IN THE INFRARED SPECTRA OF 4-PICOLINE COMPLEXES[1]

DENYS COOK
Exploratory Research Laboratory, Dow Chemical of Canada, Limited, Sarnia, Ontario
Received July 6, 1964

ABSTRACT

Complexes of 4-picoline with Lewis acids have been prepared and their infrared spectra from 4 000 to 650 cm^{-1} recorded. Regular trends in certain absorption bands in the aromatic molecule, particularly those due to vibrations of the CC and CN bonds, are similar to those in pyridine complexes.

INTRODUCTION

Complex formation of electron-deficient species with pyridine has been thoroughly investigated (1–12). The main result of infrared spectroscopic studies on such complexes has been the fact that fairly marked changes occur in the spectrum of the complex compared with the free base but that the complex spectra are quite similar. The fine details of the spectra reveal small trends in certain bands depending on the acceptor strength of the electron-deficient species.

While pyridine complexes have been studied exhaustively, very few other substituted pyridine complexes have been described (4). The present work was initiated to see if the behavior with pyridine was general.

RESULTS AND DISCUSSION

The absorption bands in the spectra are listed in Table I, and Fig. 1 shows schematically the trends in certain bands depending on the acceptor strength. To facilitate comparison,

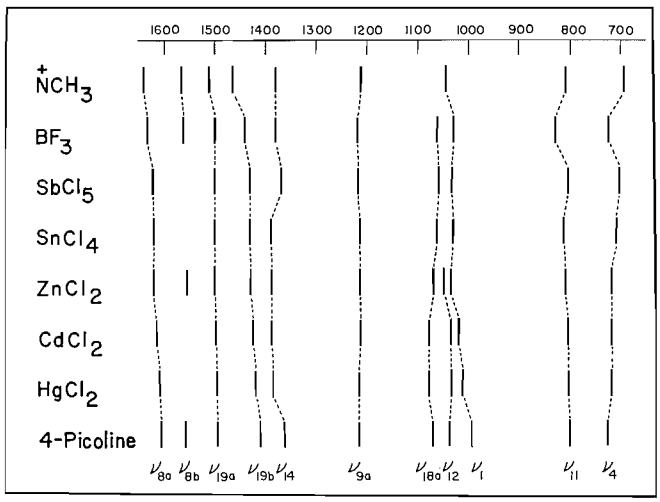

FIG. 1. Schematic representation of bands in 4-picoline complexes.

[1]*Contribution No. 125.*

Can. J. Chem. Downloaded from www.nrcresearchpress.com by 210.87.254.5 on 09/05/12
For personal use only.

TABLE I

Bands in 4-picoline complexes

	$HgCl_2$	$CdCl_2$	$CuCl_2$	$ZnCl_2$	$SnCl_4$	$SbCl_5$	BF_3	$^+NCH_3$
	3 045 w*	3 050 w, sh				3 106 w	3 120 w	
	3 030 w, sh	3 039 w		3 040 w			3 078 m	
				2 920 w				
		2 486 w		2 492 w	2 500 w			
	1 937 w	1 945 w		1 946 w	1 930 w	1 910 w		
				1 850 w	1 834 w			
	1 680 w			1 683 w	1 671 w			
	1 612 m, sh		1 620 s, sh					
ν_{8a}	1 610 s	1 614 s	1 615 vs	1 622 s	1 619 s	1 621 s	1 631 s	1 638 s
				1 619 s, sh			1 614 m, sh	1 618 m, sh
		1 610 m, sh		1 610 m, sh		1 615 m, sh		
	1 600 m, sh	1 598 w, sh	1 602 m, sh	1 600 m, sh	1 600 m, sh	1 602 m, sh	1 609 m, sh	
ν_{8b}			1 550 w	1 556 w			1 561 w	1 565 m
						1 504 w, sh		
ν_{19a}	1 496 m	1 499 w	1 501 m	1 498 m	1 499 m	1 498 m	1 500 m	1 512 m
			1 485 m, sh			1 492 w, sh	1 490 w	1 500 m, sh
ν_{19b}	1 421 m	1 427 m	1 426 m, sh	1 428 m	1 432 s	1 432 m	1 441 m	1 463 m
ν_{14}	1 386 m	1 390 m	1 387 m	1 389 w	1 388 m, sh	1 370 w?	1 380 w	1 382 w
	1 380 m, sh			1 368 w	1 374 m			
		1 350 w, sh				1 345 w	1 355 vw	1 346 vw
	1 336 w	1 340 w	1 342 w, sh	1 335 w	1 335 w, sh	1 337 w, sh		
				1 302 vw	1 311 w			
						1 260 vw		
	1 246 w	1 246 w, sh		1 250 w	1 235 m	1 235 w	1 248 w, sh	1 242 w
	1 229 w	1 232 m	1 231 m	1 232 m			1 230 s	

Can. J. Chem. Downloaded from www.nrcresearchpress.com by 210.87.254.5 on 09/05/12
For personal use only.

TABLE I *(Concluded)*

	$HgCl_2$	$CdCl_2$	$CuCl_2$	$ZnCl_2$	$SnCl_4$	$SbCl_5$	BF_3	$^+NCH_3$
ν_{9a}	1 218 m	1 215 m	1 213 m	1 215 m, sh	1 215 s	1 217 m	1 218 s	1 212 w
	1 210 w, sh			1 210 m		1 205 w, sh	1 208 s	
	1 205 w, sh			1 209 m, sh				1 194 m, sh
						1 170 w		1 186 m, sh
	1 120 w		1 122 vw			1 130 w		
	1 100 vw		1 105 w					
			1 075 m, sh					
ν_{18a}	1 078 m	1 078 m	1 071 m	1 070 m	1 064 s	1 062 s	1 064 s	
	1 073 w, sh							1 078 vw
	1 046 w, sh							
ν_{12}	1 036 w	1 038 w, sh	1 043 w, sh	1 050 w, sh				
	1 030 w, sh							
ν_1	1 014 s	1 021 s	1 030 s	1 037 s	1 031 s	1 034 s	1 028 s, sh	1 045 m
				1 032 s, sh				
			1 008 w					1 005 w
	970 w, sh							970 w
	968 w	972 w	965 w	972 w	986 w	974 vw	959 s	956 w
		878 w	873 vw		864 w			
			840 w					
		813 m, sh	818 s, sh	812 vs, sh		822 w		
ν_{11}	805 vs	805 vs	812 vs	810 vs	814 vs	805 vs	830 vs	810 s
			810 s, sh					
			792 w		796 m		788 m, sh	
					762 m			
ν_4	718 m	720 m	720 m	720 m	711 m	702 m	725 s	695 m
	668 w	662 w	660 w		660 w	664 w	672 vs	

*Abbreviations: s=strong, m=medium, w=weak, v=very.

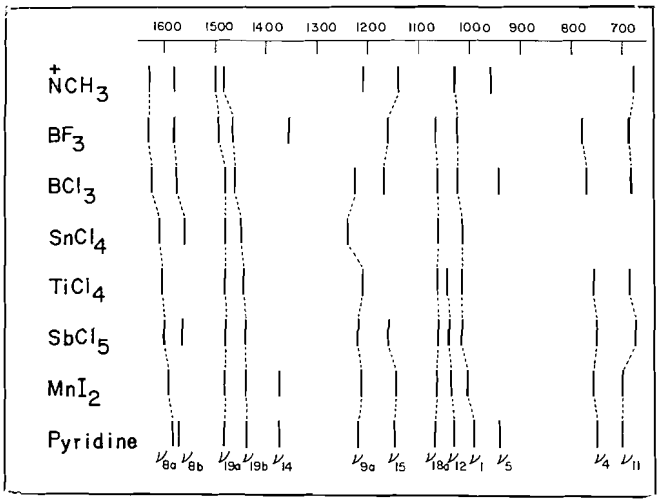

FIG. 2. Schematic representation of bands in pyridine complexes.

TABLE II

Trends* in certain bands in 4-picoline and pyridine complexes

	CC and CN vibrations†						
Compound	8*a* (A_1)	8*b* (B_1)	19*a* (A_1)	19*b* (B_1)	14 (B_1)	12 (A_1)	1 (A_1)
4-Picoline	T	C	t	t	C	C‡	T
Pyridine	T	C	t	T	C	C‡	T

	CH vibrations†					
Compound	9*a* (A_1)	15 (B_1)	18*a* (A_1)	10*b* (B_2)	4 (B_2)	11 (B_2)
4-Picoline	C	§‖	−t‖	C	C	§‖
Pyridine	C	C	C	§	C	C

*The sequence in the trends is base → base : weak complex → base : strong complex.
†Abbreviations: T, large trend; t, small trend; C, approximately constant.
‡Lack of information in the stronger complexes prevents an unequivocal decision (see text).
§No entry signifies insufficient data to make a choice.
‖Minus sign indicates a trend to lower frequency.

a similar diagram has been prepared for pyridine complexes in Fig. 2. Table II summarizes the activity of bands in the two series of complexes.

The assignments in 4-picoline have been considered by Spinner (13) on the basis of the infrared and Raman spectra of the pure liquid, and by Long and George (14) who also studied its vapor spectrum, and the infrared and Raman spectrum of the fully deuterated compound, 4-picoline-d_7. These results have been helpful in making the assignments in the complexes.

In considering the changes brought about by complex formation and the accompanying trends because of differences in acceptor properties, we will find it convenient to consider, in what follows, the sequence: base → base : weak acceptor → base : strong acceptor. A typical weak acceptor is $HgCl_2$, while the boron halides are examples of a strong acceptor.

Apart from bands due to the Lewis acid portion of the complexes, the spectra of all the complexes are rather similar. The differences between the spectra of the complexes

Can. J. Chem. Downloaded from www.nrcresearchpress.com by 210.87.254.5 on 09/05/12
For personal use only.

and the free base are smaller than in the pyridine series. Shifts in the individual band assignments and the trends in these bands will be considered in turn, beginning with CC (CN) vibrations.

Vibration ν_{8a}

In both the pyridine and 4-picoline series ν_{8a} shows an increase of 7–9 cm^{-1} on formation of a complex with a weak acceptor and a further 21–28 cm^{-1} increase in the strong complexes. At the head of the series with the largest shift is the quaternary compound 1,4-dimethylpyridinium iodide (I). The unique place occupied by this compound is due to the unit formal positive charge which exists on the nitrogen atom. This is thus similar to one of the limiting structural forms of the complexes where complete charge separation takes place. (See II and III.)

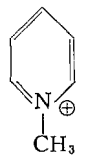

I

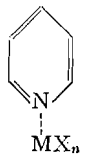

II

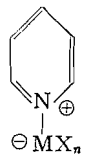

III

Vibration ν_{8b}

The assignments to this vibration must be viewed with reserve since the band is rather weak. Spinner (13) and Long and George (14) agree on the 1 561 cm^{-1} assignment to this vibration in the pure base, though neither comment on the shoulder at 1 600 cm^{-1}. This is probably the first overtone of the very strong 800 cm^{-1} band. The 1 561 cm^{-1} band is very difficult to follow in the complexes, and in some cases is not observed. In all of them the 1 600 cm^{-1} shoulder is present but may still be explained as above. In the pyridine series similar difficulties were experienced. If, in the BCl_3 complex, the Greenwood and Wade (5) assignment is preferred to that of Katritzky (4), then a fairly consistent set of figures between 1 565 and 1 585 cm^{-1} results with little trend. This would result in a similar situation in both the pyridine and 4-picoline series. If, on the other hand, a reversal of this preference is made, then a trend in ν_{8b} from 1 570 to 1 610 cm^{-1} would result, but without parallel in the 4-picoline series. Some Raman shifts of the 4-picoline complexes would be helpful to clear up this point.

Vibration ν_{19a}

The 1 495 cm^{-1} band assigned to this vibration shows no trend at all. This is almost the same behavior as in the pyridine series where the 1 482 cm^{-1} band is observed near 1 485 cm^{-1} with a scatter of a few reciprocal centimeters throughout the complexes.

Vibration ν_{19b}

The band assigned to this vibration in the free base is at 1 417 cm^{-1}. It moves about 3–4 cm^{-1} to higher frequency on complex formation, and as the acceptor becomes stronger a further rise of about 11–17 cm^{-1} is observed. Movements of the same size are seen in the pyridine series.

Vibration ν_{14}

Apart from an initial shift from 1 365 to 1 386 cm^{-1} on weak complex formation there is a random variation of no more than a few reciprocal centimeters in this absorption band. This situation cannot be compared to that in the pyridine series, since with the

Can. J. Chem. Downloaded from www.nrcresearchpress.com by 210.87.254.5 on 09/05/12
For personal use only.

exception of the weak complexes studied by Gill *et al.* (8), who quote a value near 1 375 cm^{-1} with no trend, the assignments to this vibration are quite sparse. From the available data a constant value of $\sim$ 1 375 cm^{-1} is indicated.

Vibration ν_{12}

The unsymmetrical ring breathing mode, ν_{12}, gives rise to an absorption band near 1 040 cm^{-1}, which is of variable, but chiefly weak, intensity. Assignments are therefore not complete, so that although it appears to be constant in position, the bands in the stronger complexes, where a trend would be most pronounced, are missing. A very similar situation exists in the pyridine series. The difficulty in discerning trends is compounded by the possibility of transposing assignments when three bands, ν_{18a}, ν_{12}, and ν_1, are close together.

Vibration ν_1

The totally symmetric ring breathing mode, giving an intense Raman line, and a moderately strong infrared absorption band, near 1 000 cm^{-1}, has been well characterized in the pyridine series. The band moves progressively to higher frequency in stronger complexes, as pointed out by Terenin *et al.* (2, 11) and Greenwood and Wade (5). 4-Picoline complexes show a similar trend of about 50 cm^{-1} magnitude, with no ambiguity in assignment. In both cases the quaternary salts give the largest shifts.

CH Vibrations

In most cases no systematic variations have been found for absorption bands due to CH vibrations. These are listed in Table II, the designation C meaning constant position. One band in the 4-picoline series, ν_{18a}, appears to shift to lower frequency in the stronger complexes by about 15 cm^{-1}, though comparable behavior in the pyridine series does not seem to be observed. No other regular trend to *lower* frequency has been found in any absorption band.

From the results presented it seems that the 4-picoline complexes duplicate rather closely the pyridine complexes in both the position of certain bands and their systematic variation with acceptor strength. This behavior is to be expected from such similar molecules.

The systematic variations are found only in bands due to vibrations involving CC and CN bonds, not in any bands due to CH vibrations. (There are some nonsystematic variations in γ_{CH}, the out-of-plane hydrogen-deformation vibrations, which will be taken up later.) This again seems reasonable since the primary effect on complex formation is at the nitrogen lone-pair electrons. These electrons in the complex are in the modified form of a coordinate bond which can be expected to have an influence on the other ring bonds. Nor would it be realistic to limit the modifications solely to σ-bonds, since some degree of interaction between the nitrogen sp^2 and $p\pi$ electron distribution must take place.

Such effects, being small in themselves, are either not transmitted to the CH bonds, or are so weakly transmitted that the methods of vibrational spectroscopy are too insensitive to detect them. Smith and Schneider (15) have suggested that protonation of pyridine results in large changes in the proton shielding in the α-, β-, and γ-sites, from the free base, and it may be that this more sensitive probe would reveal changes in the CH bonds in the 4-picoline complexes. This problem is being taken up.

Attempts have been made without success to relate a systematic variation in a band to the species, or symmetry type, of the vibration causing it. Table II clearly denies such a link. The mass of the acceptor molecule also plays little part in the vibrational behavior,

Can. J. Chem. Downloaded from www.nrcresearchpress.com by 210.87.254.5 on 09/05/12
For personal use only.

provided the molecular weight of the coordinated species is greater than about 15. Long and George (14), after calculating the frequencies of four-substituted pyridines with R = H, D, mass 15, and mass 99, concluded that little change in frequency in any of the bands listed in Table II occurred above mass 15, though large ones occurred below mass 15. Partly for this reason it has been deemed not a fair comparison to include the protonated bases or their N-deuterated analogues in these series.

Gill *et al.* (8), following a suggestion of Nyholm (16), believe that back-bonding of the metal d-electrons with the aromatic molecule is responsible for the similarity of the spectra of the compounds studied even though variations in ν_{16a} and ν_{16b} were related to the ionic radius of the metal. The acceptor strength of the inorganic molecules in the series was generally low, and the trends with ligands incapable of such back-bonding, such as BX_3, $\overset{+}{N}CH_3$, show that though this effect may be present, it is not the primary cause for the systematic variations.

It is believed that the systematic shifts are due primarily to the electron deficiency of the acceptor (2, 5, 11) for which relative orders have been proposed from spectroscopic evidence (17, 18). Superimposed on this effect is that of back-bonding which tends to counteract the effect of the Lewis acid. Thus the order in Fig. 1 which shows $SbCl_5$, believed to be a stronger Lewis acid than BF_3, in a position lower than BF_3, can be explained by the absence of back-bonding in the boron halide complexes. Similar anomalies are revealed in Fig. 2 and can be explained similarly. The anomalous position of $TiCl_4$ and $SbCl_5$ in Fig. 2 cannot be explained in the same way, and no satisfactory answer seems possible.*

A nonsystematic variation in the out-of-plane hydrogen deformation, ν_{11}, can perhaps best be accounted for by perturbations due to external forces rather than internal changes in the electronic structure of the base. Thus weak interactions of the C—H group with neighboring anions may slightly affect their out-of-plane vibrational characteristics.

EXPERIMENTAL

Spectra

Emulsions of the finely ground solid in Fluorolube or Nujol between sodium chloride plates were examined on a Perkin–Elmer model 221 prism-grating spectrometer between 4 000 and 650 cm^{-1}.

Complexes

$HgCl_2$.—Addition of 2.72 g $HgCl_2$ in 10 ml acetone to 0.93 g 4-picoline in 5 ml acetone gave an immediate white solid; m.p. 169–170°.

Anal. Calcd. for $C_6H_7N.HgCl_2$: N, 3.84. Found: N, 4.05.

$CdCl_2$.—On mixing 1.13 g 4-picoline in 10 ml ethanol with 2.22 g $CdCl_2$ in 125 ml hot ethanol a white precipitate; m.p. > 290°, was obtained.

Anal. Calcd. for $C_6H_7N.CdCl_2$: N, 5.07. Found: N, 5.08.

$CuCl_2$.—Slight warming of 1.70 g $CuCl_2$ and 1.86 g 4-picoline gave a blue solid. This was identical with the material prepared by boiling anhydrous $CuCl_2$ with excess 4-picoline; m.p. 163–164°.

Anal. Calcd. for $(C_6H_7N)_4.CuCl_2$: N, 11.05. Found: N, 10.73.

$ZnCl_2$.—Addition of 1.07 g 4-picoline to 1.57 g $ZnCl_2$ in 20 ml acetone gave a white solid on removal of the solvent; m.p. 152–154°.

Anal. Calcd. for $(C_6H_7N)_2.ZnCl_2$: N, 8.68. Found: N, 8.22.

$SnCl_4$.—On treating a CCl_4 solution of the base with $SnCl_4$ a pale yellow precipitate resulted; m.p. > 295°. This complex and those described below were handled in a dry box after preparation because of their very hygroscopic nature. For the same reason no analytical figures were obtained.

$SbCl_5$.—A Freon 113 solution of the base gave a light yellow solid when treated with $SbCl_5$; m.p. 103–105°.

**It may be mentioned here that these results for the pyridine complexes are from widely different sources and instrumental capability. Variations of a few cm^{-1} could displace a compound quite a few places in the overall order.*

Can. J. Chem. Downloaded from www.nrcresearchpress.com by 210.87.254.5 on 09/05/12
For personal use only.

BF_3.—The gas was passed into a solution of 4-picoline in Freon 113 giving a white solid; m.p. 65–68°.

1,4-Dimethylpyridinium iodide.—Excess methyl iodide was added to the free base with the usual exothermic reaction yielding the quaternary salt; m.p. 150–151°.

Anal. Calcd. for $C_7H_{10}NI$: N, 5.96. Found: N, 6.16.

ACKNOWLEDGMENTS

The assistance of Mrs. R. H. Veach (Miss C. D. Anderson) in preparing most of the compounds, and recording their spectra, is gratefully acknowledged. Mr. L. E. Swim and his associates (The Dow Chemical Company, Midland, Michigan, U.S.A.) are thanked for the microanalytical determinations.

REFERENCES

1. J. P. COLLMAN and H. F. HOLTZCLAW, JR. J. Am. Chem. Soc. **80**, 2054 (1958).
2. A. TERENIN, W. FILIMONOW, and D. BYSTROW. Z. Elektrochem. **62**, 180 (1958).
3. H. LUTHER, D. MOOTZ, and F. RADWITZ. J. Prakt. Chem. **5**, 242 (1958).
4. A. R. KATRITZKY. J. Chem. Soc. 2049 (1959).
5. N. N. GREENWOOD and K. WADE. J. Chem. Soc. 1130 (1960).
6. R. HULME, G. J. LEIGH, and I. R. BEATTIE. J. Chem. Soc. 366 (1960).
7. G. S. RAO. Z. Anorg. Allgem. Chem. **304**, 176 (1960).
8. N. S. GILL, R. H. NUTTALL, D. E. SCAIFE, and D. W. A. SHARP. J. Inorg. Nucl. Chem. **18**, 79 (1961).
9. K. DEHNICKE. Z. Anorg. Allgem. Chem. **308**, 72 (1961); **309**, 266 (1961).
10. P. C. H. MITCHELL. J. Inorg. Nucl. Chem. **21**, 382 (1961).
11. V. N. FILIMONOV and D. S. BYSTROV. Opt. Spectr. USSR English Transl. **12**, 31 (1962).
12. I. R. BEATTIE, G. P. MCQUILLAN, and R. HULME. Chem. Ind. London, 1429 (1962).
13. E. SPINNER. J. Chem. Soc. 3860 (1963).
14. D. A. LONG and W. O. GEORGE. Spectrochim. Acta, **19**, 1777 (1963).
15. I. C. SMITH and W. G. SCHNEIDER. Can. J. Chem. **39**, 1158 (1961).
16. R. S. NYHOLM. J. Chem. Soc. 3245 (1951).
17. M. F. LAPPERT. J. Chem. Soc. 542 (1961).
18. D. COOK. Can. J. Chem. **41**, 522 (1963).

Can. J. Chem. Downloaded from www.nrcresearchpress.com by 210.87.254.5 on 09/05/12
For personal use only.

Can. J. Chem. Downloaded from www.nrcresearchpress.com by 210.87.254.5 on 09/05/12
For personal use only.

^{19}F N.M.R. SPECTRA OF HEPTAVALENT FLUORIDES AND OXIDE PENTAFLUORIDES

N. BARTLETT,* S. BEATON, L. W. REEVES, AND E. J. WELLS
Department of Chemistry, University of British Columbia, Vancouver, British Columbia
Received June 8, 1964

ABSTRACT

The ^{19}F n.m.r. spectra of IF_7, ReF_7, IOF_5, $ReOF_5$, and $OsOF_5$ have been recorded. IF_7 gives rise to a broad symmetric doublet with a splitting of 4 100 ± 300 c.p.s. interpreted as partially collapsed and unresolved ^{19}F—^{127}I coupling. ReF_7 gives a single line of width 65 c.p.s. at low field. These spectra give no information about the molecular structure other than that there is a fast intramolecular process causing magnetic equivalence. IOF_5 and $ReOF_5$ both exhibit a quintet/doublet spectrum indicative of locked C_{4v} symmetry. The multiplet splittings in IOF_5 are not resolved in pure IOF_5 or in IOF_5/IF_7 mixtures, but can be seen for IOF_5 in solution in IF_5. The doublet lies to higher field than the quintet in IOF_5, but the reverse occurs in $ReOF_5$. In the paramagnetic molecule $OsOF_5$ only the resonance of the unique axial fluorine is observed, indicative of localization of the non-bonding d-electron in the equitorial plane of the molecule.

INTRODUCTION

The recent controversy (1, 2) over the molecular structure of IF_7 and the demonstration in these laboratories by infrared studies (3) that much of the earlier work on IF_7 was carried out on samples contaminated with IOF_5 have made a reinvestigation of the structure of these and related compounds desirable. We set out to characterize these molecules by their ^{19}F (n.m.r.) spectra. At the onset of our investigation of the heptafluoride the only previously reported n.m.r. study was from the early work of Gutowsky and Hoffman (4), who, using material of uncertain purity, reported a multiple ^{19}F spectrum which they ascribed to nonequivalent fluorine nuclei.

EXPERIMENTAL

Preparation of the Compounds

The fluorides or oxyfluorides were prepared in all-welded monel cans provided with Hoke A431 valves joined to them by monel solder tube fittings. The cans were joined to the fluorine line and the metal vacuum line by way of monel Swagelock fittings provided with Teflon front ferrules and nylon back ferrules.

Iodine pentafluoride was made by fluorinating iodine, the reaction being moderated by immersion of the can in cold water. The more volatile fluorides were removed by vacuum distillation.

Iodine heptafluoride was best made by fluorinating the distilled pentafluoride with a twofold excess of fluorine at 200° for an hour or so. Excess fluorine was removed under vacuum with the can held at −196°. Heptafluoride prepared in this way was shown by infrared spectroscopy to be oxyfluoride free.

Iodine oxide pentafluoride was most conveniently prepared by the addition of a quantity of water, calculated to satisfy the eq. $IF_7 + H_2O \rightarrow IOF_5 + 2HF$, to the heptafluoride which was measured out tensimetrically, then condensed in a KelF tube. This tube was joined to the vacuum system by a flare fitting. Hydrogen fluoride was removed by keeping the products of the reaction over sodium fluoride in a monel can. Indeed, hydrogen fluoride was conveniently removed from all of the fluorides in this way.

Rhenium oxide pentafluoride was prepared by the fluorination of rhenium dioxide as previously described (5), the reaction being done, however, in a monel can.

Rhenium heptafluoride was prepared according to the directions given by Malm and Selig (6).

Osmium oxide pentafluoride was prepared by the fluorination, at 200°, of osmium dioxide, the more volatile hexafluoride being removed by vacuum distillation at −20°. The purity of the material was checked by infrared spectroscopy.

Tungsten hexafluoride (high purity grade) was used as supplied by Allied Chemical Co.

**E. W. R. Steacie Memorial Fellow and Alfred P. Sloan Fellow.*

Preparation of the Samples

The sample tubes were generally of quartz or pyrex glass. Consequently the fluorides had to be hydrogen fluoride free to prevent the hydrolytic cycle: $4HF + SiO_2 \rightarrow SiF_4 + 2H_2O$, $H_2O + MF_x \rightarrow MOF_{x-2} + 2HF$, etc. The tubes of 3 mm internal diameter were joined by way of Swagelock compression fittings, with Teflon and nylon ferrules, to a monel vacuum system. This was provided with Hoke A431 valves and KelF traps. The system, including the sample tubes, was evacuated to better than 10^{-3} mm Hg and the tubes and lines heated. When all had been thoroughly dried the fluorides were separately distilled into the tubes and cooled in liquid nitrogen. The filled tubes were then drawn off under vacuum. Teflon containers were used for two samples of iodine heptafluoride. The cells each consisted of a flanged Teflon tube made by drilling and turning a rod. This was connected to a brass valve by compressing the Teflon flange against a brass counterpart on the valve. A brass collar in the throat of the tube and an external collar, which served as the connecting nut for the union, ensured a leak-tight joint.

Since rhenium and osmium oxide pentafluorides (m.p. 40.8 and 59.8° respectively) and rhenium heptafluoride (m.p. 48.3°) were considered to be too corrosive at their melting points to be kept in quartz, it was decided that solutions only would be examined. The convenient liquid range (m.p. 2.0°, b.p. 17.1°) (7) of tungsten hexafluoride, and its similarity to the materials in question, recommended it as a solvent. The simple n.m.r. spectrum, associated with the O_h symmetry, was an added advantage.

Nuclear Magnetic Resonance Spectra

The fluorine spectra were obtained at 40 or 56.4 Mc/s using a Varian HR machine. Chemical shifts and spin coupling constants were evaluated by standard techniques, either from sideband-calibrated charts, or in the case of sharp resonances, by superposition of the sidebands as observed visually on the oscilloscope. The sidebands were generated by a Hewlett-Packard audio oscillator and monitored by a Hewlett-Packard 522B frequency counter. Where possible, the sharp line of silicon tetrafluoride was used as an internal reference.

RESULTS

The data obtained are summarized in Table I. All of the compounds were studied in the liquid phase, either as pure liquids or as solutions in one another, or in IF_5 or WF_6.

The 40 Mc/s ^{19}F spectrum of IF_7 at 27 °C in a Teflon cell is reproduced in Fig. 1*a* and that of a fresh pure sample in flamed quartz is given in Fig. 1*b*. Comparison of the two spectra indicate rapid reaction of the IF_7 with the Teflon cell, yielding IF_5 as one of the reaction products. This product was identified by the shifts and splittings of the doublet and quintet impurity peaks which were found to correspond quite closely to those we have measured for pure IF_5 in pyrex at room temperature, against added silicon tetrafluoride as standard. These measurements are also quoted in Table I and correspond roughly to those given previously for this compound by Muetterties and Phillips (8). Figure 1*a* shows two other impurity peaks which evidently arise from the reaction of IF_7 and Teflon; one broad and centered in the IF_7 doublet, and the other sharp at +40 p.p.m. from SiF_4. It is suggested that these may be due to a reaction product $IF_6 \cdot CF_3$. On prolonged exposure of IF_7 to Teflon at room temperature extensive attack occurs (and rapidly at higher temperatures) with eventual perforation of the cell.

The course of the reaction of IF_7 in a silica cell is shown in Fig. 1*b*–1*e*, where the appearance of two broad peaks to high field of the IF_7 doublet, together with the reinforcement of the SiF_4 standard peak, is obvious. The assignment of the product giving rise to the broad doublet as IOF_5 follows from the data obtained for pure samples of this compound and displayed in Table I, and from infrared studies (3). We are evidently seeing here the net reaction:

$$2IF_7 + SiO_2 \rightarrow 2IOF_5 + SiF_4.$$

These results are in agreement with recent measurements of Muetterties (9), Alexakos, Cornwell, and Pierce (10),* and Gillespie and Quail (11).

**We thank both Dr. E. L. Muetterties and Dr. C. D. Cornwell for their courtesy in communicating their results in advance of publication.*

Can. J. Chem. Downloaded from www.nrcresearchpress.com by 210.87.254.5 on 09/05/12
For personal use only.

Can. J. Chem. Downloaded from www.nrcresearchpress.com by 210.87.254.5 on 09/05/12
For personal use only.

TABLE I

Compound	State (molar ratio given for solutions)	Chemical shifts (p.p.m. from SiF_4)		Coupling (c.p.s.)	Line width (c.p.s.)	
		Equatorial	Axial		Equatorial	Axial
IF_7	Pure liquid	-334 ± 3			4 100±300	
ReF_7	1:4 in WF_6	-510 ± 1			65±2	
IOF_5	Pure liquid	-236 ± 1	-272 ± 1		930±100	1 050±50
IOF_5	2:1 in IF_7	-236 ± 2	-271 ± 2		950±100	1 200±100
IOF_5	2:1 in IF_5	-234.5 ± 1	-272 ± 1	$J_{FF} = 280$	170±30	
$ReOF_5$	1:4 in WF_6	-361.9 ± 0.5	-159.6 ± 0.5	$J_{FF} = 68.6\pm1$	12±2	
$OsOF_5$	1:3 in WF_6	Not seen	-215 ± 2			1 100±200
IF_5	Pure liquid	-173.6 ± 0.5	-222.2 ± 0.5	$J_{FF}=85.0\pm0.8$	5±2	
WF_6	4:1 in ReF_7	-330.5 ± 0.5		$J_{^{183}W-F} = 43.8\pm0.5$		

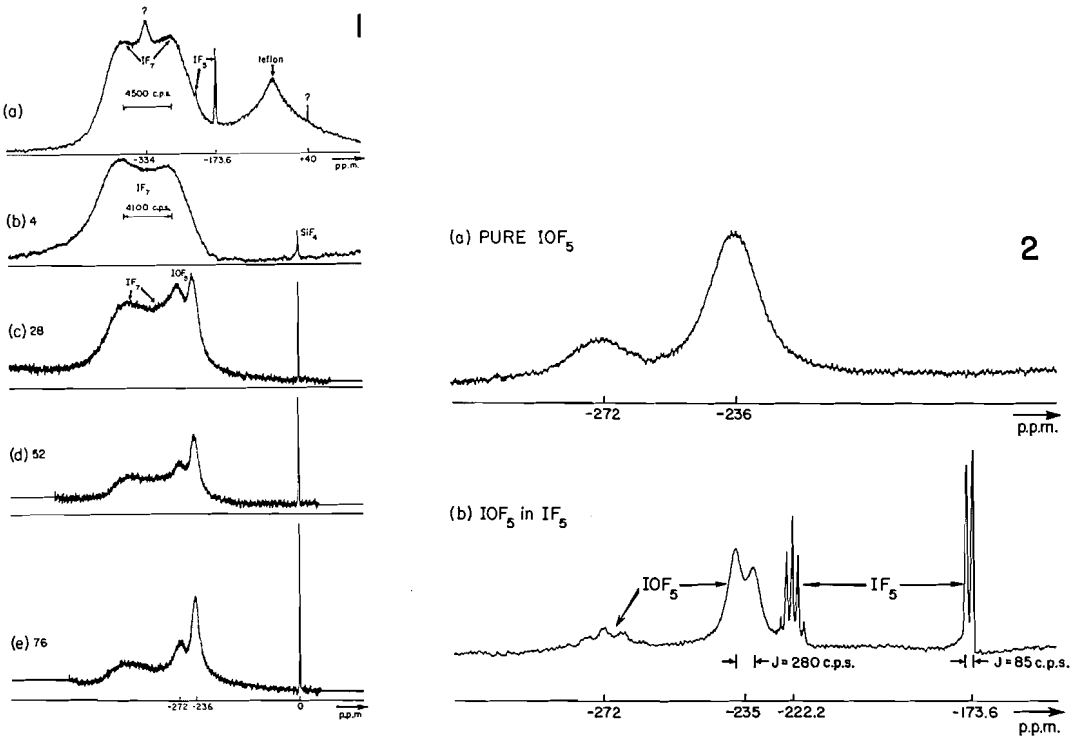

FIG. 1. ^{19}F spectra of IF_7 at 40 Mc/s. (*a*) In Teflon cell, showing the solid Teflon signal and reaction products of IF_7 with Teflon; (*b–e*) in flamed silica cell, showing the decomposition of IF_7 to IOF_5 and SiF_4 by prolonged reaction with silica.

FIG. 2. ^{19}F spectra of IOF_5 at 56.4 Mc/s. (*a*) Pure liquid; (*b*) 2:1 solution in IF_5, showing resolution into J_{F-F} multiplets, chemical shifts are relative to SiF_4 internal reference.

We have observed the two components of the IF_7 doublet to sharpen noticeably at elevated temperatures up to 70 °C. The IF_7 resonance at 28 °C for a 1:1 solution in IF_5 shows a doublet structure in a more complete stage of collapse, with a splitting of only 3 600 c.p.s. The IF_7 signal collapses to a single broad line on cooling this solution.

Solutions of rhenium heptafluoride in tungsten hexafluoride were used to obtain the room temperature ^{19}F spectrum of the heptafluoride. It is a single line of width 65 c.p.s., at −510 p.p.m. from internal silicon tetrafluoride. Its position and width in the liquid appear to be temperature independent. We have searched for a chemically shifted resonance without success.

The ^{19}F spectrum of pure iodine oxide pentafluoride at 56.4 Mc/s is given in Fig. 2*a* and is seen to consist of two broad resonances of intensity ratio near 1:4 and each of width at half-height of approximately 1 kc/s. This spectrum is to be compared with the 40 Mc/s ^{19}F resonance for IOF_5 in IF_7 shown in Fig. 1*b–1e*. The line widths are unchanged by the presence of sodium fluoride, which would remove hydrogen fluoride. Interestingly, when the IOF_5 is dissolved in IF_5 the absorption sharpens, as shown in Fig 2*b*, and a typical AB_4 type spectrum is seen with some second-order perturbation of intensities. The spin coupling here resolved is evidently fluorine–fluorine coupling between structurally non-equivalent nuclei, and is measured as 280 c.p.s. The spectrum indicates C_{4v} symmetry for the fluorine nuclei and thus a pseudo-octahedral structure for the molecule. These

Can. J. Chem. Downloaded from www.nrcresearchpress.com by 210.87.254.5 on 09/05/12
For personal use only.

Can. J. Chem. Downloaded from www.nrcresearchpress.com by 210.87.254.5 on 09/05/12
For personal use only.

results are in accord with very recent measurements on IOF_5 by Cornwell and his co-workers (10) and by Gillespie and Quail (11). The former authors note the resolution of the broad resonances into a doublet and quintet in the gas phase and the latter noted similar behavior in IF_5 solution.

Rhenium oxide pentafluoride in tungsten hexafluoride solution displays a sharp doublet and quintet with a shift large enough to produce a simple first-order spectrum. However, for this molecule the quintet from the apical fluorine nucleus occurs to much higher field than the doublet, which is the reverse situation observed for iodine oxide pentafluoride.

We have carried out a preliminary study of the ^{19}F resonance in the related paramagnetic species $OsOF_5$* also in WF_6. A single broad low-intensity peak was observed which, in the basis of its chemical shift at -215 p.p.m. from internal SiF_4 and its low intensity, is ascribed to the unresolved quintet of the axial fluorine. However, the anticipated stronger equatorial resonance was not observed.

DISCUSSION

The Heptafluorides

The ^{19}F spectrum of ReF_7 is a single sharp line and that of IF_7 a broad symmetrical doublet the splitting of which is field independent. These observations are most satisfactorily explained by a time-average magnetic equivalence of the seven fluorine nuclei in each molecule. Furthermore the experimental evidence indicates that the equivalence is due to a fast intramolecular rearrangement.

The central magnetic nuclei ^{127}I, ^{185}Re, and ^{187}Re all have spin 5/2, and for a spherically symmetric field gradient tensor at the central atom we should expect six equally spaced lines of equal intensity but not of equal half width for the resonance of the ^{19}F nuclei attached to the central quadrupolar nucleus, the sextet splitting being a measure of the X—F spin coupling. Appropriate patterns corresponding to this limiting case have been observed for species of O_h and T_d symmetry as in the $I = 9/2$ cases of $^{93}Nb\ F_6^-$ (12) and $^{73}Ge\ F_4$ (13), and for the $I = 3/2$ case of $^{11}BF_4^-$ (14, 15), $^{75}AsF_6^-$ (14), and SF_6 (16). However, when the field gradient symmetry at the quadrupolar nucleus is of low symmetry, as in the case of singly coordinated quadrupolar atoms, rapid relaxation of the quadrupolar nucleus occurs which results in a single sharp resonance absorption. If the heptafluoride molecules have the anticipated ligand close packing associated with the D_{5h} (2) model, the C_{2v} model (1), or other derivatives of an octahedral molecule, the field gradient symmetry will not deviate greatly from that in octahedral molecules. The heptafluorides are therefore expected to show an intermediate stage of collapse. The line shapes in the intermediate region have been calculated for spin 1 (17), spin 3/2 (15), and spin 9/2 (12) and have been estimated for spin 5/2 by Muetterties (9), who judges the ^{127}I—^{19}F coupling in IF_7 to be ~ 1 kc/s.†

**The electron spin resonance spectrum of this compound in tungsten hexafluoride solution has been recorded here by Dr. J. B. Farmer, who notes a signal centered approximately on the free electron value and some 200 gauss wide. No fine structure has been observed.*

†This value has recently been questioned by Gillespie and Quail, who have advised us, in advance of publication, that they disagree with the details of Muetterties and Packer's calculation, and prefer the value 2 100 c.p.s. for $J(^{127}I—^{19}F)$. They also point out that the fluoride ligands in IF_7 need not be equivalent but that small differences of no more than 2 p.p.m. in chemical shift would be detectable in the ^{19}F spectrum of IF_7. With such a small permitted chemical shift difference however, the fluorine ligands are still at least approximately equivalent. One would expect the ^{19}F chemical shifts difference for two sets of fluorine ligands as given by Burbank (1) for IF_7 in the crystal, with two I—F bonds at 1.97 Å and five at ~ 1.83 Å, to be of the order of 20–100 p.p.m. Thus our overall argument is not affected. However, Gillespie and Quail's value for $J(^{127}I—^{19}F)$ moves the point for IF_7 on Fig. 4 up to $(J/\gamma_X\gamma_F)^{\frac{1}{2}} = 19.2$, which is more in keeping with what we should expect for a group VII fluoride.

Interpretation of the spectra of IF_7 and ReF_7 in terms of very fast intramolecular averaging of the 7F nuclei together with unresolved spin coupling from the central nucleus to the surrounding fluorines is consistent with the following.

(*a*) The quadrupole moments of ^{185}Re, ^{187}Re (2.8, 2.6) are some four times larger than that of ^{127}I (0.75) and the Re—F coupling is expected to be an order of magnitude smaller than the I—F coupling (see later). It has been shown (15) that the inverse lifetime $\frac{1}{\tau}$ of a Zeeman level of a quadrupolar nucleus depends on the square of its quadrupole moment, and that the line shape is a function of $(J\tau)^2$, being a sharp multiplet for $J\tau$ large, and a collapsed single line for $J\tau$ small. Thus both above effects cause the ^{19}F signal in ReF_7 to show a much greater state of collapse than in IF_7, as is observed.

(*b*) The IF_7 doublet sharpens somewhat at high temperatures, and collapses at low, as required by the quadrupolar mechanism, and in contrast to the reverse behavior expected for an intermolecular exchange process. The IF_7 line width is independent of added NaF, which would abstract HF impurity. Intermolecular exchange via labile F atoms might be expected to be enhanced by hydrogen fluoride.

(*c*) Our picture of the quadrupolar mechanism means that the observed splitting of the IF_7 doublet is related to the I—F spin coupling, and leads to an estimated J of ~ 1 kc/s (9). This infers that all fluorine nuclei have a lifetime on a given ^{127}I nucleus of more than 1.5×10^{-4} s, and points to an *intra*-molecular averaging. A lower limit on the rate of this process is set by the absence of F—F coupling in the sharp ReF_7 signal. Assuming this to have a similar value to J_{F-F} in $ReOF_5$ (68 c.p.s.) sets the maximum lifetime of a given configuration of IF_7 or ReF_7 at $\sim 2.5 \times 10^{-3}$ s.

Bonding in the Oxide Pentafluorides

The ^{19}F n.m.r. spectra of IOF_5 and $ReOF_5$ are in accord with C_{4v} symmetry; a strong doublet, arising from four equivalent equatorial nuclei, and a weaker quintet from an axial nucleus is observed in each case. There is, however, marked difference in the two spectra. In $ReOF_5$ the quintet is greatly shifted to high field from the doublet, whereas in IOF_5 the quintet lies slightly to low field of the doublet.

In general the ^{19}F chemical shielding in the volatile transition metal fluorides is less than for nontransition element fluorides of related stoichiometry. For the fluorides under consideration the ^{19}F chemical shielding is also reduced when the oxidation state of the central atom increases, e.g. IF_7 resonates to lower field than IF_5, and ReF_7 to lower field than WF_6. Since oxygen does not have the electron-withdrawing power of fluorine, it is anticipated that the replacement of two fluorine ligands by one oxygen will reduce the positive charge on the central atom. Higher field ^{19}F resonance is therefore expected for the oxide pentafluorides than is observed in the heptafluorides. The equatorial ^{19}F resonance in $ReOF_5$ is to high field of ReF_7 and lower than WF_6, and the related resonance in IOF_5 is to high field of IF_7 but lower than the equatorial ^{19}F resonance in IF_5 (see Fig. 3). However, the axial fluorine in $ReOF_5$ is significantly affected by the *trans* oxygen ligand, since the ^{19}F resonance for this nucleus is far removed to high field from the ReF_7 or WF_6 resonances. Such is not the case in IOF_5, where axial and equatorial resonances are not widely separated.

These effects can be correlated with the availability of d-orbitals on the central atom for π-bonding with p-orbitals on the ligands. It may be supposed that in ReF_7 and WF_6, where vacant 5d-orbitals are available, the σ-bonding of the ligands is supplemented by $p\pi$–$d\pi$ bonding and that in the iodine fluorides there will be no such supplementation. The π-bonding will reduce the polarity of the fluorine-central atom bond and cause the

Can. J. Chem. Downloaded from www.nrcresearchpress.com by 210.87.254.5 on 09/05/12
For personal use only.

^{19}F resonance to be moved to lower field. Conversely if bonding is slight, or absent, a more polar bond will result and the ^{19}F resonance will appear at higher field.

Since an oxygen ligand is a better electron donor than a fluorine ligand the oxygen–rhenium $p\pi$–$d\pi$ bonds will be the strongest in $ReOF_5$ molecule. The oxygen will have two p-orbitals disposed for interaction with two d-orbitals of the rhenium. If the Re—O axis is taken as the z-axis, the latter orbitals will be d_{zy} and d_{zx}. Those are also the only d-orbitals which the axial fluorine ligand can use in bonding. The equatorial fluorine ligands, however, can interact with the d_{xy}-orbital, which is not available to the oxygen. Multiple bonding by the oxygen will therefore considerably diminish the possibility of $p\pi$–$d\pi$ bonding by the axial fluorine. The axial fluorine rhenium bond should, in consequence, be more polar than the equatorial bonds and the axial ^{19}F resonance should, therefore, be to high field of the equatorial resonance.

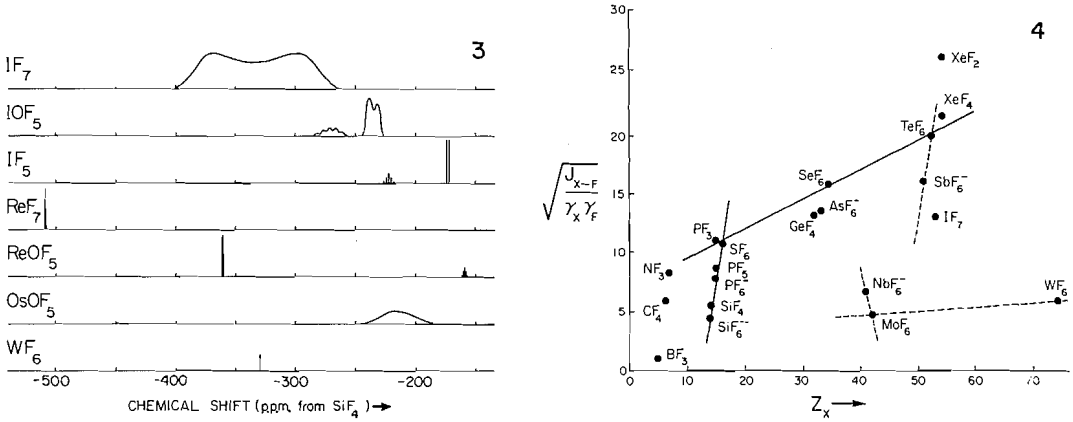

FIG. 3. Schematic diagram of 56.4 Mc/s ^{19}F spectra of heptavalent fluorides and oxide pentafluorides.
FIG. 4. Correlation plot of the reduced coupling constant $(J_{XF}/\gamma_X\gamma_F)^{\frac{1}{2}}$ against Z_x in a number of binary fluorides.

Since $OsOF_5$, which is paramagnetic (d^1), shows a single broad resonance to high field and in the region where, by analogy with $ReOF_5$, the quintet of the axial ^{19}F resonance should be observed (Fig. 3), it is presumed that this is a smeared quintet. If so, this is consistent with the model used to account for the $ReOF_5$ spectrum. Again assuming that the oxygen dominates as a π-bond donor and hence monopolizes the d_{zx}-orbitals and d_{zy}-orbitals, the non-bonding unpaired electron will be constrained to reside in the d_{xy}-orbital. Since this orbital can interact with the four equatorial fluorine ligands but not with the axial fluorine, the unpaired electron spin obscures only the equatorial fluorine resonance.

In IOF_5, where π-bonding is presumed to be absent, the σ-bonded O^- ligand will, as a consequence of its smaller nuclear charge, be larger than the isoelectronic σ-bonded F ligands. Because of the higher charge on the oxygen it will be the most strongly attracted ligand to the positive iodine but will have the most strongly repelling effect on the other ligands. The I—O bond will therefore be short, but the oxygen, equatorial-fluorine distances will be long. The length of each fluorine–iodine bond will be determined by the balance of the fluorine–iodine attraction and the fluorine – other ligand repulsion. The latter will be greater for the equatorial-fluorine ligands since the four ligands in close contact include the larger oxygen with its lower nuclear charge. The axial fluorine being

Can. J. Chem. Downloaded from www.nrcresearchpress.com by 210.87.254.5 on 09/05/12
For personal use only.

furthest from the oxygen will suffer less repulsion and experience the same attractive interaction as the other fluorines. Consequently the axial-fluorine – iodine bond should be slightly shorter (more covalent) than the equatorial.

Although the pattern of the ^{19}F resonance in IOF_5 is similar to that of IF_5, with the quintet slightly downfield of the doublet, the IOF_5 line widths are much greater than in IF_5. This indicates that the environment of the quadupolar iodine nucleus in IOF_5 cannot deviate too far from an O_h symmetry case, since the broadness of the lines must be attributed to unresolved I—F coupling.

It is reasonable to suppose the bonding in iodine fluorides to be analogous to that in the xenon fluorides, for which there are two distinct bonding schemes. One, which employs the molecular orbital approach, has been discussed by Pitzer (19, 20, 21) and Rundle (18). It utilizes only Xe 5p-orbitals and F 2p-orbitals for three center molecular orbitals of which the bonding and non-bonding are filled. The bonds represented by this model are semi-ionic in nature. The alternative valence bond approach supposes electron promotion to higher orbitals, followed by hybridization and the formation of normal, covalent, electron-pair bonds (22, 23). The high field ^{19}F shifts in XeF_2 and XeF_4 (20) and the small quadrupole splittings in ICl_2^- and ICl_4^- (24) favor the semi-ionic bonding model at least for the lower halides of iodine and xenon. However, the large values of $\{J_{XF}/\gamma_X\gamma_F\}^{\frac{1}{2}}$ in XeF_2 and XeF_4 (see Fig. 4 and later) indicate much more s-character in the XeF bonds than the molecular orbital model would suggest. The valence bond model may be a better approximation for the higher fluorides of iodine and xenon. Thus the molecular orbital model predicts an octahedral structure for XeF_6, whereas the valence bond model anticipates a distorted octahedron, all of the valence shell electrons being sterically active, as in IF_7. Some support for this expectation is given by the involvement of all eight valence electrons in xenon trioxide (25), the perxenates (26), and xenon tetroxide (27). It is interesting to note that if XeF_6 is distorted or undergoes intramolecular exchange as discovered in IF_7, then the ^{129}Xe—^{19}F coupling will appear sharply in the n.m.r. spectrum, whereas the ^{131}Xe—^{19}F coupling will show quadrupolar collapse. In octahedral XeF_6 both couplings will be sharp. Of all the bonding schemes so far advanced to describe the xenon fluorides, none has yet included the Xe 4f-orbitals which lie below the 5d-levels which are included. The energy considerations used by some authors to neglect even the 5d-contributions in XeF_6 do not appear valid, for such considerations should apply a fortiori to SF_6, long regarded as a normal sp^3d^2 octahedron.

IF_5 as a Solvent

Comparison of spectra of pure IF_7 and IOF_5 in the liquid and in the gas with those obtained in solution in IF_5 shows that IF_5 has the ability to raise the solute correlation time for molecular reorientation and thus yields spectra intermediate between the pure liquid solute spectrum and the pure solute in the gas. IF_5 is polar with a lone electron pair and the process could occur either through weak solute–solvent interaction via this lone pair, or perhaps through a solvent cage effect, by isolating a solute molecule from similar molecules for an appreciably longer time than a normal solvent.

Spin–Spin Coupling Constants

It was recently shown that proton spin–spin coupling constants correlate linearly with the atomic number of the conjugate nucleus in a series of compounds of similar hybridization (28, 29), and this correlation was interpreted in terms of the Fermi contact interaction of the nuclei and thus of the s-character of the bonds joining the nuclei. More recently fluorine couplings have been demonstrated to follow the same law (13), indicating

Can. J. Chem. Downloaded from www.nrcresearchpress.com by 210.87.254.5 on 09/05/12
For personal use only.

a similar coupling mechanism. We can now discuss the I—F coupling estimated in IF_7 (9) and the Xe—F coupling measured in XeF_2 and XeF_4 (20), along with many other X—F couplings previously reported (30, 12), for binary fluorides. An approximate parallelogram relation for $\{J_{XF}/\gamma_X\gamma_F\}^{\frac{1}{2}}$ vs. Z_X for octahedral nontransition metal species XF_6 is shown in Fig. 4. Deviations from the true parallelogram are probably due to variations in ionicity of the X—F bonds (31). A glance at the figure shows the transition metal fluorides MF_6 to have remarkably small couplings, presumably reflecting the use of outer s-bonding rather than inner s-bonding orbitals.

That fluorine couplings are transmitted through the s-electrons may be seen from the points for PF_3, PF_5, and PF_6^- in Fig. 4, for which the s-character of the P—F bond should be in the ratio 25%:20%:16.6%, and thus $J^{\frac{1}{2}}$ in the ratio 1.25:1.1:1. The measured ratio is 1.4:1.1:1.

The estimated value of 1 000 c.p.s. for J_{I-F} in IF_7 leads to the point shown in Fig. 4. The s-character of the I—F bonds in this molecule is probably smaller than in the XF_6 species, but the point lies within the region expected for nontransition metal fluorides. The large values of the reduced Xe—F couplings in XeF_2 and XeF_4 must then reflect high s-character bonding.

At the present time there appears to be no regularity in J_{F-X-F} couplings, apart from the fact that such couplings are small (< 100 c.p.s.) if X is a transition metal.

CONCLUSION

The ^{19}F n.m.r. spectra of IF_7 and ReF_7 indicate that both molecules are undergoing rapid intramolecular exchange causing magnetic equivalence of the seven F nuclei. The spectrum of IF_7 is complicated by quadrupolar broadened ^{127}I—^{19}F coupling, but there is no doubt that a single sharp ^{19}F signal analogous to that observed in ReF_7 would appear if the ^{127}I nuclei could be decoupled by double irradiation. The absence of F—F coupling in these molecules sets a minimum rate constant of about 4×10^2 s^{-1} on the intramolecular process. It is probably much faster.

A growing body of evidence points to rapid internal rearrangement of the ligands to be common in five and seven coordinate species. In $Fe(CO)_5$ all ^{13}C nuclei are equivalent down to -63 °C (32). Similarly PF_5 (33), RPF_4, and AsF_5 (30) and SOF_4 (34) all show equivalent ^{19}F nuclei in their n.m.r. spectra. The mechanism of this internal process may be thought of as an ammonia-like inversion or 'pseudo-rotation' occurring through a distorting vibration (35). In principle it should be possible to observe directly the tunnelling frequency in the radio or microwave region. However such an electric-dipole transition may be expected to be extremely weak owing to the combined effects of the near spherical symmetry, and low transition energy.

ACKNOWLEDGMENTS

Financial support from the National Research Council, The Research Corporation, and the Petroleum Research Fund of the American Chemical Society is gratefully acknowledged. One of us (S. B.) also thanks the National Research Council for a Scholarship.

REFERENCES

1. R. D. BURBANK. Acta Cryst. **15**, 1207 (1962).
2. R. C. LORD, M. A. LYNCH, W. C. SCHUMB, and E. J. SLOWINSKI. J. Am. Chem. Soc. **72**, 522 (1950).
3. N. BARTLETT and L. E. LEVCHUK. Proc. Chem. Soc. 342 (1963).
4. H. S. GUTOWSKY and C. J. HOFFMAN. J. Chem. Phys. **19**, 1259 (1951).
5. E. E. AYNSLEY, R. D. PEACOCK, and P. L. ROBINSON. J. Chem. Soc. 1622 (1950).
6. J. G. MALM and H. SELIG. J. Inorg. Nucl. Chem. **20**, 189 (1961).

Can. J. Chem. Downloaded from www.nrcresearchpress.com by 210.87.254.5 on 09/05/12
For personal use only.

7. G. H. CADY and G. B. HARGREAVES. J. Chem. Soc. 1565 (1961).
8. E. L. MUETTERTIES and W. D. PHILLIPS. J. Am. Chem. Soc. **79**, 322 (1957).
9. E. L. MUETTERTIES and K. J. PACKER. J. Am. Chem. Soc. **86**, 293 (1964).
10. L. G. ALEXAKOS, C. D. CORNWELL, and S. B. PIERCE. Proc. Chem. Soc. 341 (1963).
11. R. J. GILLESPIE and J. W. QUAIL. Proc. Chem. Soc. 278 (1963).
12. K. J. PACKER and E. L. MUETTERTIES. J. Am. Chem. Soc. **85**, 3035 (1963).
13. P. INGLEFIELD and L. W. REEVES. J. Chem. Phys. **40**, 2424, 2425 (1964).
14. R. HAQUE and L. W. REEVES. To be published.
15. J. BACON, R. J. GILLESPIE, and J. W. QUAIL. Can. J. Chem. **41**, 3063 (1963).
16. R. J. GILLESPIE and J. W. QUAIL. J. Chem. Phys. **39**, 2555 (1963).
17. J. POPLE. Mol. Phys. **1**, 168 (1958).
18. R. E. RUNDLE. J. Am. Chem. Soc. **85**, 112 (1963).
19. K. S. PITZER. Science, **139**, 414 (1963).
20. J. C. HINDMAN and A. SVIRMICKAS. *In* Noble gas compounds. *Edited by* H. H. Hyman. University of Chicago Press, Chicago. 1963. p. 257.
21. J. HINZE and K. S. PITZER. *In* Noble gas compounds. *Edited by* H. H. Hyman. University of Chicago Press, Chicago. 1963. p. 340.
22. L. D. ALLEN and W. DE W. HORROCKS. J. Am. Chem. Soc. **84**, 4344 (1963).
23. R. J. GILLESPIE. *In* Noble gas compounds. *Edited by* H. H. Hyman. University of Chicago Press, Chicago. 1963. p. 333.
24. C. D. CORNWELL and R. S. YAMASAKI. J. Chem. Phys. **27**, 1060 (1957); **30**, 1265 (1959).
25. D. H. TEMPLETON, A. ZALKIN, J. D. FORRESTER, and S. M. WILLIAMSON. J. Am. Chem. Soc. **85**, 817 (1963).
26. J. G. MALM, B. D. HOLT, and R. W. BANE. *In* Noble gas compounds. *Edited by* H. H. Hyman. University of Chicago Press, Chicago. 1963. p. 167.
27. H. SELIG, H. H. CLAASSEN, C. L. CHERNICK, J. G. MALM, and J. L. HUSTON. Science, **143**, 1322 (1964).
28. L. W. REEVES and E. J. WELLS. Can. J. Chem. **41**, 2698 (1963).
29. L. W. REEVES. J. Chem. Phys. **40**, 2423 (1964).
30. E. L. MUETTERTIES and W. D. PHILLIPS. J. Am. Chem. Soc. **81**, 1084 (1959).
31. D. P. SANTRY and J. A. POPLE. Private communication.
32. R. BRAMLEY, B. N. FIGGIS, and R. S. NYHOLM. Trans. Faraday Soc. **58**, 1893 (1962).
33. H. S. GUTOWSKY, D. W. MCCALL, and C. P. SLICHTER. J. Chem. Phys. **21**, 279 (1953).
34. F. B. DUDLEY, J. N. SCHOOLERY, and G. H. CADY. J. Am. Chem. Soc. **78**, 568 (1956).
35. R. S. BERRY. J. Chem. Phys. **32**, 933 (1960).

Can. J. Chem. Downloaded from www.nrcresearchpress.com by 210.87.254.5 on 09/05/12
For personal use only.

π-ELECTRON DENSITIES IN THE PYRIDINIUM CATION

THE EFFECT OF THE COUNTERION ON THE PROTON MAGNETIC RESONANCE SPECTRUM

G. KOTOWYCZ,* T. SCHAEFER, AND E. BOCK
Department of Chemistry, University of Manitoba, Winnipeg, Manitoba
Received June 30, 1964

ABSTRACT

Proton shifts relative to internal benzene of pyridine hydrochloride, hydrobromide, and hydriodide in methylene chloride, acetonitrile, nitromethane, and formic acid are reported. A model involving a hydrogen-bonded ion pair between the pyridinium cation and the counterion is discussed. It is assumed that the counterion reduces considerably the π-electron polarization in the pyridinium ion calculated for the isolated ion by the V.E.S.C.F. method. If the electric fields arising from the π-electrons, the counterion, and the positive charge in the N—H^+ sigma bond are taken into consideration, the observed order of the C—H proton shifts is predicted. The N—H^+ proton shifts are sensitive to the counterion, the solvent, and traces of water. In formic acid the N—H^+ proton shifts of the hydrochloride and hydrobromide are characteristic of the solvent only. In these two cases the N—H^+ proton does not exchange rapidly and an ^{14}N—H^+ coupling constant of 67.6 $\pm$ 0.5 c/s is found.

INTRODUCTION

The use of proton magnetic resonance shifts relative to benzene in the determination of π-electron densities of aromatic molecules and ions is by now well known (1–8). The presence of a heteroatom in the aromatic nucleus complicates the derivation of an electron density from the proton shift relative to benzene. For instance, in the case of pyridine, a low energy n–π^* transition causes a large low-field shift of the nitrogen resonance (9) as well as of the ortho proton resonance. Gil and Murrell (10) have very recently had considerable success in calculating the magnitude of these low-field shifts. In addition, they take into account the magnetic anisotropy contribution from the nitrogen to the proton shifts. They also estimate the effect on the proton shifts of the electric field from the lone pair on the nitrogen. The net result of these corrections is reasonable agreement of the corrected shifts with π-electron densities calculated by the V.E.S.C.F. method (11).

In the case of an ion, the simple linear relation (3) between the excess charge Δq on the carbon and the shift relative to benzene of the bonded proton $\Delta\sigma$, $\Delta\sigma = k\Delta q$, is perhaps a poor approximation (4, 7, 10, 12). In such a case, it is probably preferable to take into account the field from neighboring charges and to include a term in the square of the field arising from these charges (7, 12). Gil and Murrell (10) remark that this procedure results in poor agreement of the calculated π-densities (11) with experimental shifts (5) for the pyridinium cation. They surmise that the counterion is involved.

We shall present experimental evidence that this is indeed the case. Calculations based on various models involving the counterion suggest that the counterion is very important in determining the measured proton shifts. In this way we can understand why the shifts predicted by the π-densities calculated for an isolated pyridinium cation (11) do not fall in the same order as the experimental ones (5). The presence of the counterion appears to reduce the polarization of the π-cloud considerably, as might be expected.

Holder of a N.R.C. bursary, 1963–1964.

Can. J. Chem. Downloaded from www.nrcresearchpress.com by 210.87.254.105 on 09/05/12
For personal use only.

Can. J. Chem. Downloaded from www.nrcresearchpress.com by 210.87.254.105 on 09/05/12
For personal use only.

EXPERIMENTAL

(a) Preparation and Measurements

Pyridine hydrochloride, hydrobromide, and hydriodide were prepared by standard methods (13, 14). Because they are very hygroscopic they were kept in a desiccator. Their solubility in nonpolar solvents is very low and therefore proton magnetic resonance spectra were taken on 3 mole % solutions, whenever possible, in methylene chloride, acetonitrile, nitromethane, and formic acid. In some cases (see Table I)

TABLE I

Proton shifts in p.p.m. to low field from internal benzene for pyridine hydrohalides in four solvents

Salt	Concentration (Mole %)	Solvent	$\epsilon(25°)$*	$\Delta\sigma_{N—H^+}$	$\Delta\sigma_o$	$\Delta\sigma_m$	$\Delta\sigma_p$
Pyridine HCl	<3	CH_2Cl_2	8.9	8.74	1.58	0.70	1.18
Pyridine HBr	<3	CH_2Cl_2	8.9	5.20	1.61	0.72	1.20
Pyridine HI	Not sufficiently soluble in CH_2Cl_2						
Pyridine HCl	3	CH_3CN	36.7	8.17	1.43	0.66	1.19
Pyridine HBr	<3	CH_3CN	36.7	5.82	1.45	0.70	1.24
Pyridine HI	<3	CH_3CN	36.7	2.27	1.42	0.71	1.26
Pyridine HCl	3	CH_3NO_2	36.6	8.03	1.43	0.75	1.27
Pyridine HBr	3	CH_3NO_2	36.6	6.66	1.50	0.80	1.34
Pyridine HI	<3	CH_3NO_2	36.6	2.81	1.52	0.82	1.36
Pyridine HCl	3	H_2CO_2	80(65)†	6.75(t)‡	1.61	0.88	1.42
Pyridine HBr	3	H_2CO_2	80(65)	6.74(t)‡	1.65	0.89	1.43
Pyridine HI	<3	H_2CO_2	80(65)	—	1.62	0.90	1.44
Pyridine	3	H_2CO_2	80(65)	—	1.59	—	1.43

*Dielectric constant.
†Unpurified (purified).
‡Triplet center.

the solubility was considerably less than 3 mole %, in which case saturated solutions were used. The spectra were taken on a Varian DP-60 spectrometer and were calibrated relative to internal benzene.

The solvents were spectro grade and only formic acid was further purified. It was purified very thoroughly (15), and its dielectric constant was 65 as compared to $\approx$ 80 for the unpurified formic acid which contains some water. However, the proton spectra, including the $N—H^+$ proton spectrum, did not differ noticeably in the two cases.

(b) Determination of Shifts from Spectra

A proper analysis of the C—H proton spectra implies an A_2B_2C approach (16), not really feasible in our case. However, the shift between protons ortho to one another was not less than 0.5 p.p.m. An ortho coupling constant of about 8 c/s and much smaller meta and para constants (17) would therefore mean a reasonable approach to a first-order spectrum. We therefore determined the centers of gravity of the multiplets arising from the three types of protons and took these to be the shifts. In Fig. 2 a typical spectrum is shown and estimated shifts are indicated. We think that in this way the error in the shifts was reduced to 1 or perhaps 2 c/s. It is almost certain that the error introduced by this method of analysis is less than 0.03 p.p.m. For our purposes this is quite sufficient.

(c) The Effect of Water in Solvents

Experiments were done to determine the effect of water on the proton spectrum of the hydrochloride in methylene chloride. The C—H proton shifts were not much affected but the $N—H^+$ proton shifts were strongly shifted (the solubility of water in CH_2Cl_2 at room temperature is roughly 0.6 mole %, as determined by comparing the ^{13}C sideband intensities from the solvent with that of the water peak). In Fig. 1 a plot of the $N—H^+$ proton shift relative to internal benzene is given as a function of water concentration. Rapid exchange with water no doubt causes these shifts. Although we tried a number of techniques, we found none of them reliable in the determination of a really good value for the $N—H^+$ proton shift in the absence of water. This problem is not insoluble, of course. However, because the $N—H^+$ proton shift depends strongly on the counterion (see results) and because of ion-pair formation by hydrogen bonding (see discussion), we do not pursue this aspect further here. We are chiefly interested here in the C—H proton shifts, which are *not* sensitive to small amounts of water.

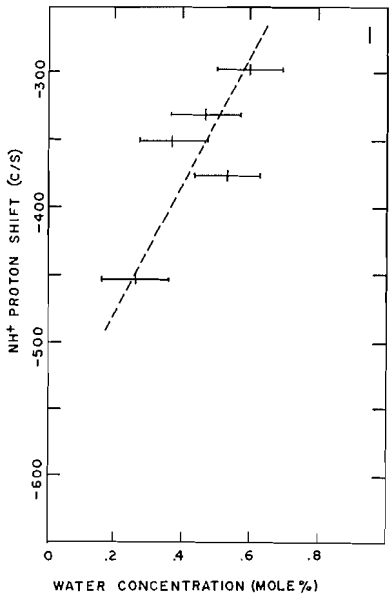

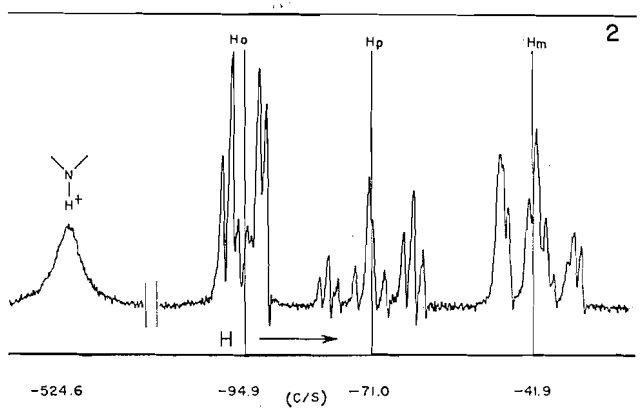

FIG. 1. A plot of the N—H+ proton shift relative to internal benzene of pyridine hydrochloride in methylene chloride as a function of water concentration, c/s at 60 Mc/s. Note the large uncertainty in the water concentration.

FIG. 2. The proton resonance spectrum of a saturated solution (< 3 mole %) of pyridine hydrochloride in methylene chloride. The calibration is in c/s at 60 Mc/s to low field of internal benzene. The vertical lines indicate the estimated shifts of the C—H protons.

RESULTS

In Table I the proton shifts of the ring protons are given relative to internal benzene. The average of all the C—H proton shifts is $\Delta\sigma_o = -1.53 \pm 0.13$, $\Delta\sigma_m = -0.78 \pm 0.13$, $\Delta\sigma_p = -1.30 \pm 0.13$, all in p.p.m. The value 0.13 p.p.m. is the maximum observed deviation for any salt in any solvent. In any individual case the order is $\Delta\sigma_o < \Delta\sigma_p < \Delta\sigma_m$. We found no rational trend in shift with respect to salt or solvent. Why this might be so is discussed below.

The N—H+ proton shifts are lowest for the hydrochloride and highest for the iodide in solvents other than formic acid. The broad single peaks (see Fig. 2) in these solvents indicate exchange, probably with small amounts of water. In formic acid (pure or impure) the N—H+ resonances for both the hydrochloride and the hydrobromide are triplets with the same shifts relative to benzene. The ^{14}N—H coupling constant is 67.6 ± 0.5 c/s. No N—H+ proton peaks were observed for the hydriodide or for pyridine dissolved in formic acid.

DISCUSSION

Before discussing the detailed calculations involving the counterion, we consider secondary contributions to the C—H proton shifts. The N—H+ proton shifts are discussed last.

(A) Secondary Contributions to the C—H Shifts

Since we measure our shifts relative to benzene, the replacement of a C—H by the N—H+ entity introduces a magnetic anisotropy contribution to the shifts. According to

Can. J. Chem. Downloaded from www.nrcresearchpress.com by 210.87.254.105 on 09/05/12
For personal use only.

Gil and Murrell (10) this amounts to not more than +0.03 p.p.m. at any position, small enough to be within our experimental error.

The low energy transition from the lone-pair orbital to the lowest vacant π-antibonding orbital lies at about 4.5 eV (18). It is no longer present in the protonated ion and this accounts for the small, low-field shift of the ortho proton signal on protonation relative to that of the meta and para protons (10). We will therefore ignore any contributions from this source, since the new $\sigma-\pi^*$ transition will be close to that for benzene and probably not lower than about 8 eV.

The proton shifts in Table I show no clear trend with dielectric constant of the solvent. Thus acetonitrile and nitromethane have the same dielectric constant and according to the reaction field theory (19, 20) the shifts should be the same in the two solvents (at least for the same salt). A plot of the shifts versus the dielectric function given by Buckingham (20) shows that some other effect masks the expected behavior.* It appears that the main function of the solvent, from our viewpoint, is as solvating agent for the counterion. If it forms a bulky solvated complex either with the counterion or with the pyridinium ion, thus removing the counterion sufficiently far from the cation, the effect on the proton shifts will be much larger than any reaction field shifts. The latter would not be expected to be larger than about 10% of the observed shifts. We will not consider them further.

(B) Ion-Pair Formation: Evidence from Other Work

Lord and Merrifield (21) found a shift of many hundreds of cm^{-1} in the N—H stretching frequency of solid pyridinium hydrochloride. This shift persists in solution and the stretching frequency itself is highly anharmonic. They attribute this to a very strong hydrogen bond interaction, perhaps even of a covalent character, of the $N—H^+$ entity with the counterion. For us it is important that the large shift is present also in solution, indicating ion-pair formation. Somewhat similar conclusions are reached by Chenon and Sandorfy (13) and by Spinner (22). Cook's infrared studies (22*a*) on the solid hydrohalides indicate a strong interaction between the $N—H^+$ hydrogen and the anion. The interaction is somewhat less for the hydriodide than for the hydrochloride but still very strong compared to the free state.

Rérat (23) has determined the crystal structure of the salt. The N—Cl distance is 2.95 Å, considerably less than the sum of the van der Waals' radii of 3.3 Å. The chloride ion lies 0.14 Å out of the plane of the ring. Together with the infrared data it seems probable that a solution model involving a counterion situated in the plane of the ring along the $N—H^+$ direction is reasonable.

The proton resonance measurements of Fraenkel (24) on solutions of anilinium salts strongly suggest ion-pair formation with, however, rapid exchange of counterions between pairs. If the time taken for transfer is very small on an n.m.r. time scale, as is usually assumed in rate studies (25), then the model mentioned above is still a good one. Reynolds and Schaefer (26) found that a similar ion-pair model predicted shifts of the ring protons of the anilinium ion in trifluoroacetic acid in reasonable agreement with experiment. We take these results as additional evidence in favor of ion-pair formation in our solutions.

There is evidence from electron spin resonance (e.s.r.) of aromatic ions in favor of ion-pair formation (27, 28).† Even at concentrations as low as 10^{-4} *M*, hydrocarbon anions form ion-pairs with alkali metal cations in solvents like acetonitrile or dimethoxyethane (28). Small cations like Li^+ or Na^+ are, however, highly solvated so that the effective

Also, for reasons of solubility, we could not use a solvent of very low dielectric constant, so that the range of values of the dielectric function is very small.

†*Reference 28 gives a good discussion of this evidence.*

Can. J. Chem. Downloaded from www.nrcresearchpress.com by 210.87.254.105 on 09/05/12
For personal use only.

counterion is a "bulky solvent complex which perturbs the state of the anion less strongly than the more weakly solvated larger cations like K^+" (28).† This conclusion does not apply to radical anions with functional groups, such as nitrobenzene anions, which appear to form stable complexes with the smaller counterions at the site of the functional group (29). In view of our much higher concentrations, the e.s.r. data support the assumption of ion-pair formation at the site of the N—H^+ group in our solutions.

Conductivity and ultraviolet spectra of solutions of aromatic hydrocarbon anions indicate one-to-one ion pairs between anion and alkali metal cation in ether solvents (30). The larger the radius of the counterion the smaller is the stability of the ion pair.

(C) The Counterion Models

a. The Various Models

We have considered a number of somewhat different models involving the counterion. The results of the calculations are given in Table II.

TABLE II

Average observed shifts (in p.p.m. to low field from internal benzene) and calculated shifts for the C—H proton in solutions of pyridine hydrohalides

Counterion distance (Å)	Δσ(expt.)			Δσ(1)*			Δσ(2a)			Δσ(2b)		
	ortho	meta	para	ortho	meta	para	ortho	meta	para	ortho	meta	para
2.0	1.53	0.78	1.30	0.06	1.04	2.15	1.16	1.84	2.91	1.64	1.99	3.03
2.5	±0.13	±0.13	±0.13	0.09	1.09	2.20	1.27	1.90	2.96	1.75	2.06	3.09
3.0				0.10	1.14	2.24	1.33	1.95	3.01	1.82	2.10	3.13
4.0				0.10	1.20	2.30	1.41	2.02	3.07	1.91	2.18	3.20
∞				0.01	1.39	2.53	1.51	2.24	3.32	2.03	2.41	3.44
	Δσ(3a)			Δσ(3b)			Δσ(4a)			Δσ(4b)		
	ortho	meta	para	ortho	meta	para	ortho	meta	para	ortho	meta	para
2.0	1.19	0.35	0.27	1.93	0.54	0.41	1.16	0.64	0.89	1.89	0.85	1.05
2.5	1.30	0.39	0.30	2.05	0.59	0.44	1.26	0.70	0.93	2.01	0.90	1.09
3.0	1.37	0.43	0.33	2.13	0.63	0.47	1.33	0.73	0.96	2.09	0.94	1.12
4.0	1.45	0.49	0.38	2.23	0.69	0.52	1.41	0.79	1.01	2.19	1.00	1.17
∞	1.56	0.66	0.55	2.37	0.86	0.70	1.52	0.97	1.21	2.33	1.19	1.37

*The shifts are calculated for the different models described in the text.

(1) This model uses the average of the four sets of π-electron densities calculated by the V.E.S.C.F. method (11) which are $\Delta q_o = -0.051$, $\Delta q_m = -0.097$, $\Delta q_p = -0.176$, and $\Delta q_N = 0.473$. The effect of the polar N—H^+ sigma bond is ignored. The counterion, approximated by a point charge of $\Delta q = 1.00$, is placed at various distances along the N—H^+ direction in the plane of the ring.

(2) This model differs from the first only in that it takes the N—H^+ bond into account by considering the additional contribution from a single positive charge of one electron unit placed (*a*) at the N—H^+ proton and (*b*) 0.34 Å along this bond from the proton.

(3) This model assumes that the π-electron density is unity on all the ring atoms. Otherwise it is the same as the second but the positive charge is placed (*a*) at the N—H^+ proton and (*b*) 0.515 Å (halfway) along the N—H^+ bond.

(4) Here we assume much smaller charges on the ring carbons arising from polarization of the π-electrons. These are $\Delta q_o = -0.01$, $\Delta q_m = -0.02$, $\Delta q_p = -0.05$, and $\Delta q_N = 0.11$.

†*It is probably for this reason that the proton shifts in the cyclopentadienyl, fluorenyl, indenyl, and other ions gave good agreement with the calculated π-electron densities in ref. 3. The counterions were* Li^+ *or* Na^+.

Can. J. Chem. Downloaded from www.nrcresearchpress.com by 210.87.254.105 on 09/05/12
For personal use only.

They run in the same order as those calculated for the isolated cation (11). It seems probable that the counterion will affect such a reduction in polarization. The positive charge is placed (*a*) at the N—H^+ proton and (*b*) 0.515 Å along the bond.

b. The Electric Field Calculations

We include the fields from the charges on all the atoms including the counterion on the shift of a particular C—H proton. We use the equation

$$\Delta\sigma \text{ (p.p.m.)} = 12.5 \times 10^{-6} \sum_i [(\Delta q_i \cos\theta_i)/R_i^2] - 17.0 \times 10^{-6}(\sum_i \Delta q_i/R_i^2)^2,$$

where Δq_i is the excess electron density at atom i, R_i is the distance in Å from that atom to the proton in question, and θ_i is the angle of the field vector with respect to the C—H bond axis. This equation was used by Schweizer *et al.* (7) and is obtained from the usual expression (20) for field calculations, $\Delta\sigma = -aE_z - bE^2$. The value of a is 2.60×10^{-12}, between the values of 2.0×10^{-12} suggested by Buckingham (20) and 2.9×10^{-12} found by Musher (12). Musher's value for b, as calculated by Marshall and Pople (31), was used.

The geometry of the pyridinium ion was taken as a regular hexagon with bond lengths of 1.39 Å and a C—H bond length of 1.08 Å. The N—H^+ bond length was taken as 1.03 Å, the same as in the ammonium ion (32, 33). The crystal structure data (23) indicate a distorted hexagon but their use would result in relatively small changes in calculated shifts, well within the approximations inherent in our models.

No doubt the interaction of the halide ion with the cation varies from ion to ion and from solvent to solvent. Our simple models cannot take this variation into account, except as a variation of the N—H^+. . .X^- distance. To a first approximation we therefore consider only the averages of the observed shifts. The calculated shifts are given in Table II.

c. Comparison of Observed and Calculated Shifts

From Table II it is clear that no model which assumes the V.E.S.C.F. π-densities of the free cation reproduces correctly the order of the observed shifts for the ortho, meta, and para protons (models 1, 2*a*, 2*b*). This is true also for the models (3*a*, 3*b*) which assume unit π-densities on the ring atoms. The models (4*a*, 4*b*) which assume a much lower polarization of the π-electrons do reproduce the observed order of the shifts. Only a slight adjustment of the π-electron densities, of the order of 0.01 units, together with a small shift of the positive charge along the N—H^+ bond would clearly produce complete agreement with observation for any counterion distance. Although the observed order is also predicted in the absence of the counterion, it would be hard to account for the reduced polarization of the π-electrons in that case. The agreement also depends on the positive charge in the N—H^+ sigma bond. Our model takes it into account in an admittedly naive way. Together with the other evidence discussed above, we feel that we have a fairly reasonable case for ion-pair formation in our solutions. We do not think that a refinement of our crude model would be very useful at present in accounting for the details of the shifts of individual salts in different solvents

(D) The N—H^+ Proton Shifts

We can make no definite statement about the isolated N—H^+ proton shift, of course, since it is affected by the field from the counterion and also by traces of water. Furthermore, the inclusion of a point positive charge very close to this proton in our models make them useless in calculating its shift. In the solvents other than formic acid the order of shifts (Table I) can be rationalized if one assumes incipient bond formation between

Can. J. Chem. Downloaded from www.nrcresearchpress.com by 210.87.254.105 on 09/05/12
For personal use only.

the proton and the halide ion. Thus HI has the highest proton shielding of the hydrogen halides due to magnetic anisotropy (34). The hydrochloride was the most hygroscopic of the three and if the shift had been completely determined by exchange with traces of water, the opposite order of N—H^+ shifts would have been expected.

In formic acid it appears that the shift is characteristic of the solvent, i.e. N—H^+. . .O instead of N—H^+. . X^-, where X^- is a halide ion. Chenon and Sandorfy (13) reached a similar conclusion from their infrared studies of these salts in water. The very similar shifts of the C—H protons for the three salts and pyridine in formic acid support this suggestion. However, we do not know why there is no proton exchange in the hydrochloride and hydrobromide, while for the hydriodide and pyridine no signal was observed at all. These matters merit further study.

CONCLUSIONS

Solutions of pyridine hydrohalides in methylene chloride, acetonitrile, and nitromethane contain hydrogen-bonded ion pairs. The presence of the counterion reduces considerably the π-electron polarization calculated for the isolated pyridinium ion. Models which take into account the effect of the counterion, the positive charge in the N—H^+ sigma bond, as well as the π-densities account for the observed order of the C—H proton shifts. In formic acid the shifts appear to be characteristic of a complex involving the solvent rather than the halide ion. The N—H^+ proton shifts are very sensitive to the solvent, counterion, and traces of water. In formic acid the N—H^+ protons do not exchange in the case of the hydrochloride and hydrobromide and the ^{14}N—H^+ coupling constant is 67.6 ± 0.5 c/s.

ACKNOWLEDGMENTS

We are grateful to B. Blackburn for a sample of pyridine hydrobromide. J. M. T. M. Gieskes kindly determined some dielectric constants. The financial support of the National Research Council is deeply appreciated.

REFERENCES

1. G. Fraenkel, R. E. Carter, A. McLachlan, and J. H. Richards. J. Am. Chem. Soc. **82**, 5846 (1960).
2. H. Spiesecke and W. G. Schneider. Tetrahedron Letters, No. 14, 468 (1961).
3. T. Schaefer and W. G. Schneider. Can. J. Chem. **41**, 966 (1963).
4. J. C. Schug and J. C. Deck. J. Chem. Phys. **37**, 2618 (1962).
5. I. C. Smith and W. G. Schneider. Can. J. Chem. **39**, 1158 (1961).
6. C. MacLean and E. L. Mackor. Mol. Phys. **4**, 241 (1961).
7. M. P. Schweizer, S. I. Chan, G. K. Helmkamp, and P. O. P. Ts'o. J. Am. Chem. Soc. **86**, 696 (1964).
8. A. Zweig, J. E. Lehnsen, J. E. Lancaster, and N. T. Neglia. J. Am. Chem. Soc. **85**, 3940 (1963).
9. J. D. Baldeschwieler and E. W. Randall. Proc. Chem. Soc. 303 (1961).
10. V. M. S. Gil and J. N. Murrell. Trans. Faraday Soc. **60**, 248 (1964).
11. R. D. Brown and M. L. Heffernan. Australian J. Chem. **12**, 554 (1959).
12. J. I. Musher. J. Chem. Phys. **37**, 34 (1962).
13. B. Chenon and C. Sandorfy. Can. J. Chem. **36**, 1181 (1958).
14. M. D. Taylor and L. R. Grant. J. Chem. Educ. **32**, 39 (1955).
15. J. M. T. M. Gieskes. Ph.D. Thesis, University of Manitoba, Winnipeg, Man. 1964.
16. J. A. Pople, W. G. Schneider, and H. J. Bernstein. High resolution nuclear magnetic resonance. McGraw-Hill Book Co., Inc., New York. 1959. Chap. 6.
17. J. A. Pople, W. G. Schneider, and H. J. Bernstein. High resolution nuclear magnetic resonance. McGraw-Hill Book Co., Inc., New York. 1959. p. 266.
18. S. F. Mason. J. Chem. Soc. 1240 (1959).
19. L. Onsager. J. Am. Chem. Soc. **58**, 1486 (1936).
20. A. D. Buckingham. Can. J. Chem. **38**, 301 (1960).
21. R. C. Lord and R. E. Merrifield. J. Chem. Phys. **21**, 166 (1953).
22. E. Spinner. J. Chem. Soc. 3860 (1963).
22*a*. D. Cook. Can. J. Chem. **39**, 2009 (1961).
23. C. Rérat. Acta Cryst. **15**, 427 (1962).

Can. J. Chem. Downloaded from www.nrcresearchpress.com by 210.87.254.105 on 09/05/12
For personal use only.

24. G. FRAENKEL. J. Chem. Phys. **39**, 1614 (1963).
25. H. S. GUTOWSKY and C. H. HOLM. J. Chem. Phys. **25**, 1228 (1956).
26. W. F. REYNOLDS and T. SCHAEFER. Can. J. Chem. **41**, 2339 (1963).
27. A. REDDOCH. Private communication.
28. J. R. BOLTON and G. K. FRAENKEL. J. Chem. Phys. **40**, 3307 (1964).
29. R. L. WARD. J. Chem. Phys. **30**, 852 (1959).
30. A. C. ATEN, J. Dieleman, and G. J. Hoijtink. Discussions Faraday Soc. **29**, 182 (1960).
31. T. W. MARSHALL and J. A. POPLE. Mol. Phys. **1**, 199 (1958).
32. H. S. GUTOWSKY, G. E. PAKE, and R. BERSOHN. J. Chem. Phys. **22**, 643 (1954).
33. H. A. LEVY and S. W. PETERSON. Phys. Rev. **86**, 766 (1952).
34. J. A. POPLE, W. G. SCHNEIDER, and H. J. BERNSTEIN. High resolution nuclear magnetic resonance. McGraw-Hill Book Co., Inc., New York. 1959. p. 179.

Can. J. Chem. Downloaded from www.nrcresearchpress.com by 210.87.254.105 on 09/05/12
For personal use only.

Can. J. Chem. Downloaded from www.nrcresearchpress.com by 210.87.254.5 on 09/05/12
For personal use only.

THE PRINCIPAL CONFORMATIONS OF SOME ORTHO-SUBSTITUTED DIPHENYL ETHERS[1]

W. D. CHANDLER, W. MACFARLANE SMITH, AND R. Y. MOIR
Department of Chemistry, Queen's University, Kingston, Ontario

Received July 13, 1964

ABSTRACT

A study of the nuclear magnetic resonance, infrared, and ultraviolet spectra showed that some doubly and triply ortho-substituted diphenyl ethers adopt, principally but not exclusively, the "H-inside" conformation, while the quadruply ortho-substituted 7-(4′-carbomethoxy-2′,6′-dinitrophenoxy)metameconine (V) adopts the "methoxy-inside" conformation. Interconversion of conformational isomers is extremely fast. Reduction of methyl 4-methoxy-3-nitrobenzoate with tin and hydrochloric acid gave methyl 3-amino-2-chloro-4-methoxybenzoate.

It has been well established[2] that the principal conformations of diphenyl ethers, in solution or in the gas phase, are asymmetric (Fig. 1),[3] one ring being in the C—O—C plane and able to accommodate the ethereal oxygen's p-electrons, the other ring lying in a plane approximately perpendicular to the first so that resonance with the ethereal oxygen is small or negligible.

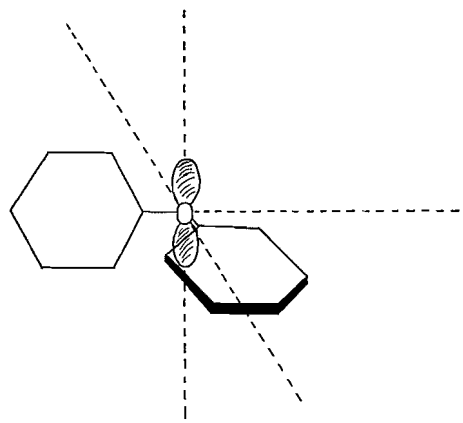

FIG. 1. Asymmetric diphenyl ether conformation.

Allen and Moir (17) pointed out that eight such conformations exist for a diphenyl ether bearing four different ortho-substituents, and that these conformations can be divided into two classes of four each. The members of each class are interconvertible by synchronous rotations which do not require ortho-groups to be forced past each other,

[1]*Most of the material of this paper was presented at the national meeting of the Chemical Institute of Canada, Toronto, June 8, 1963.*

[2]*The asymmetry of ethers of low steric hindrance has been shown by ultraviolet spectroscopy (1–3), dipole moments (4–7), electron and X-ray diffraction (8–10), microwave absorption, and relaxation times (11–14), and from theoretical calculations of ultraviolet spectra (15). For highly hindered diphenyl ethers, the fact has been assumed from a study of models (2, 16–18).*

[3]*For convenience and clarity, an unshared pair is represented as essentially in a p-orbital, the planes of the rings at right angles, and the* C—O—C *valence angle as near 90°. It will be understood that these are intended only as rough approximations suitable to the present qualitative discussion. Because the figure does not display the easy increase in the oxygen valence angle, some of the conclusions of the paper seem more obvious, a priori, than is justified.*

but a member of one class can be converted to a member of the other only by surmounting this barrier. (The same idea of synchronous rotation had been developed in considerable detail for diphenyl ether itself by Calderwood and Smyth (11), who used it to explain the abnormally low relaxation time of diphenyl ether in the absorption of microwaves.) It is the object of this paper to show which of the eight conformations are occupied preferentially. Since the eight conformations are divided into pairs of mirror images, and since in a symmetrical environment mirror-image conformations will be equally occupied (18), it is enough to distinguish among the four conformations[4] of a single class.

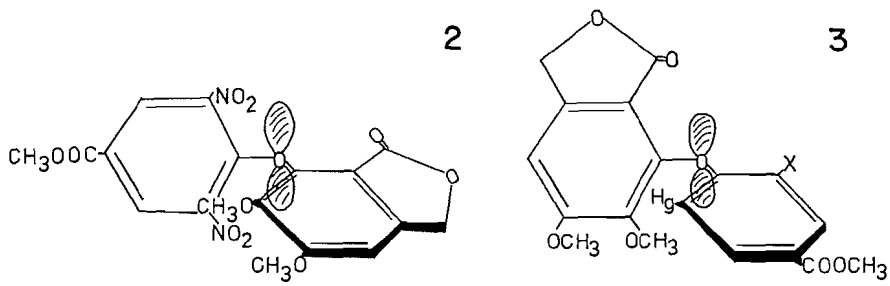

FIG. 2. "Methoxy-inside" conformation (V as example).
FIG. 3. "Hydrogen-inside" conformation (typical of I–IV).

The problem could be broken into two parts: to show (*i*) which ring lies in the C—O—C plane, and (*ii*) which ortho-substituent of this ring occupies the "inside" position (Figs. 1, 2, 3). Mangini and Passerini (1) were able to solve the first problem for some diphenyl sulphides by ultraviolet spectroscopy; the substances gave spectra typical of two almost independent chromophores, and the ring which included the sulphur in its chromophore must have been in the C—S—C plane. It will be shown later that this method can lead to erroneous conclusions if not carefully handled. The second problem does not seem to have been attempted previously. Our method is the straightforward one of comparing the proton magnetic resonance (n.m.r.), infrared, and ultraviolet spectra of a series of highly hindered diphenyl ethers with each other and with the spectra of the corresponding anisoles formed by replacing one or other of the phenyl groups with a methyl group.

Evidence from the N.M.R. Spectra

Although several factors determine the chemical shifts of aromatic protons, the relative shifts of H_a in a series such as I–VII depend mainly on inductive and resonance effects. Thus the electron-donating methoxy group would be expected to cause H_a to be more shielded in VI than in VII. The replacement of the 7-methoxy group in VI by aryloxy groups could have two opposite effects. (1) There would be a deshielding of H_a (relative to its environment in VI) by an increased inductive withdrawal of electrons which would become greater as the groups X and Y (in I–V) became more electronegative. The effect would be especially large if the lower ring were approximately in the plane of the C—O—C bonds. (2) A mesomeric electron donation, which would tend to offset the deshielding noted in (1), would occur if the upper ring were in the plane of the C—O—C bonds. The observed effects are noted in the second column of Table I. The shielding induced by the presence of methoxy at position-7 (VI), the lesser shielding by aryloxy groups in that

[4]*Each conformation is conveniently named by the ortho-group which occupies the "inside" position in that conformation (e.g. methoxy in Fig. 2, hydrogen in Fig. 3).*

Can. J. Chem. Downloaded from www.nrcresearchpress.com by 210.87.254.5 on 09/05/12
For personal use only.

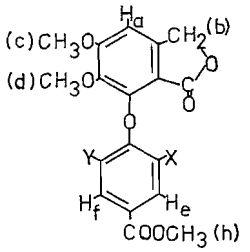

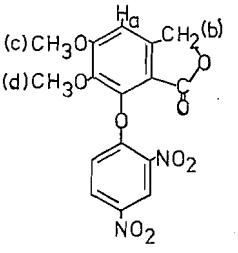

I : X = NH_2; Y = H_g
II : X = H_k ; Y = H_k
III : X = I ; Y = H_g
IV : X = NO_2; Y = H_g
V : X = NO_2; Y = NO_2

VIII

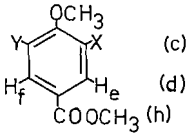

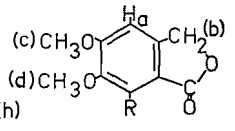

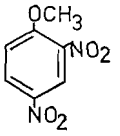

Ia : X = NH_2; Y = H_g
IIa : X = H_k ; Y = H_k
IIIa : X = I ; Y = H_g
IVa : X = NO_2; Y = H_g
Va : X = NO_2; Y = NO_2

VI : R = OCH_3
VII R = H

VIIIa

TABLE I

Chemical shifts* of hydrogens on the metameconine portion

Compound	Tau values			
	H_a	H_b†	H_c[5]	H_d[5]
VII	3.02	4.78	6.02	6.07
VI	3.25	4.82	6.03	6.12
I	3.13	4.82	6.02	6.23
II	3.10	4.80	6.03	6.23
III	3.07	4.82	6.03	6.20
IV	3.05	4.80	6.00	6.17
VIII	3.00	4.77	5.97	6.13
V	3.22	4.82	6.05	6.33

*In solution in chloroform or deuterochloroform, expressed as p.p.m. relative to an internal standard of tetramethylsilane set at $\tau = 10$.
†Split by about 0.5 c.p.s.[6] The values given are for band centers.

position (I–IV), and the uniformly declining shielding of H_a as the electronegativity of the groups X and Y increases, all are exactly as expected in the sequences I–IV and VI–VIII. However, there is a sharply increased shielding of H_a in going from IV to V, in

[5]*The assignment of the methoxy peaks was based on (a) their expected relative positions, and (b) the expected effects of changes in the group at position-7 and position-4, an ortho-methoxy being affected much more than a meta-methoxy. To some extent the conclusions have been checked with ethoxy analogues of substituted metameconines (7-ethoxymetameconine, 7-chloro-6-ethoxy-5-methoxyphthalide).*

[6]*These splittings of the phthalide hydrogens by a hydrogen ortho to them formed part of the evidence for the assignment of the configuration to the phthalide–isoquinoline alkaloids (19).*

Can. J. Chem. Downloaded from www.nrcresearchpress.com by 210.87.254.5 on 09/05/12
For personal use only.

spite of the much greater electron withdrawal of the groups in the latter. This can only mean that in V the two conformations corresponding to Fig. 2 are much more important than they are in I–IV or in VIII. In all these others, the two conformations corresponding to Fig. 3 must be more important than in V. It is most striking that the (inductively) electron-withdrawing aryloxy group produces almost the same shielding of H_a as does the methoxy group of VI.[7]

This argument cannot decide between the "methoxy-inside" conformation of Fig. 2 and the "carbonyl-inside" conformation for compound V. That the conformation of Fig. 2 is at least very important, and probably dominant,[7] is shown by an examination of the last column of Table I, where it is seen that the methoxy hydrogens H_d are much more shielded in V than in the other compounds, even though V possesses the most electron-withdrawing groups. Such shielding can only be due to the incursion of the methoxy into the shielding region of the other benzene ring (19–21). Since the effect is large,[7] the occupancy of the conformation of Fig. 2 must also be large in compound V, relative to that for the other compounds.[7]

A consideration of the chemical shifts of the hydrogens on the lower ring confirms and extends the previous conclusions. Examination of Figs. 4–9[8] shows that, except for compound I*a*, assignment of lines can be made by inspection, the ortho-coupling constants being much larger than the meta-coupling constants, and the para-coupling constants being unresolved. It will be seen that the signal for H_g in the triply ortho-substituted diphenyl ethers I, III, IV, and VIII lies at higher field by 16–23 c.p.s. than in the corresponding anisoles (I*a*, III*a*, IV*a*, and VIII*a*, respectively), the signal for H_f at higher field by 8–11 c.p.s., and the signal for H_e at lower field by 4–12 c.p.s. This variation for H_g and H_f is in a direction opposite to that actually observed for H_e (or for H_a in a similar situation in the upper ring). The increase in shielding of H_g and H_f can only be due to shielding by the other ring and the conformation of Fig. 3 must be important for these compounds.

The climax of our argument comes with the examination of the spectra of II and II*a* (Fig. 8). In the first place, the simple A_2B_2 pattern from II shows that the two "H-inside" conformations are exchanged at such a rate as to give each an average lifetime much shorter than the average lifetime of the proton spin states. In the second place, H_k is slightly less shielded in II than in the corresponding anisole II*a*; shielding by the other ring is not quite sufficient to compensate for inductive withdrawal, even though this is less than in III, IV, and VIII. Since the two "H-inside" states must be equally populated in II, the extra shielding of H_g in I, III, IV, and VIII shows that the "H_g-inside" conformation must be occupied much more than the "nitro-inside" conformation, and must be the dominant conformation.

The equivalence of the hydrogens H_e and H_f in V is less illuminating, since it could be due either to a predominantly "methoxy-inside" conformation (Fig. 2) or to a rapid averaging of the two "nitro-inside" conformations.

[7]*The fact that compounds I–IV, and VIII, have* H_a *either more shielded than, or about as shielded as, in metameconine (VII), and the fact that* H_d *is more shielded in them than in methoxymetameconine (VI), in spite of the electrical character of the lower rings, presumably mean that in them the conformation corresponding to Fig. 2 also must be occupied an appreciable part of the time, though much less than in V. In principle, the relative occupancies are calculable from both effects. This is now being attempted with more favorable examples.*

[8]*In all the spectra, except that for Ia, the lines reproduce the center and the approximate amplitude of the observed peaks. The spectrum for Ia is the result of an ABX calculation which agreed very closely indeed with the observed spectrum. ABX calculations were done for a few other compounds as well, but except for Ia, the changes incurred in band positions with respect to simple inspection were negligible.*

Can. J. Chem. Downloaded from www.nrcresearchpress.com by 210.87.254.5 on 09/05/12
For personal use only.

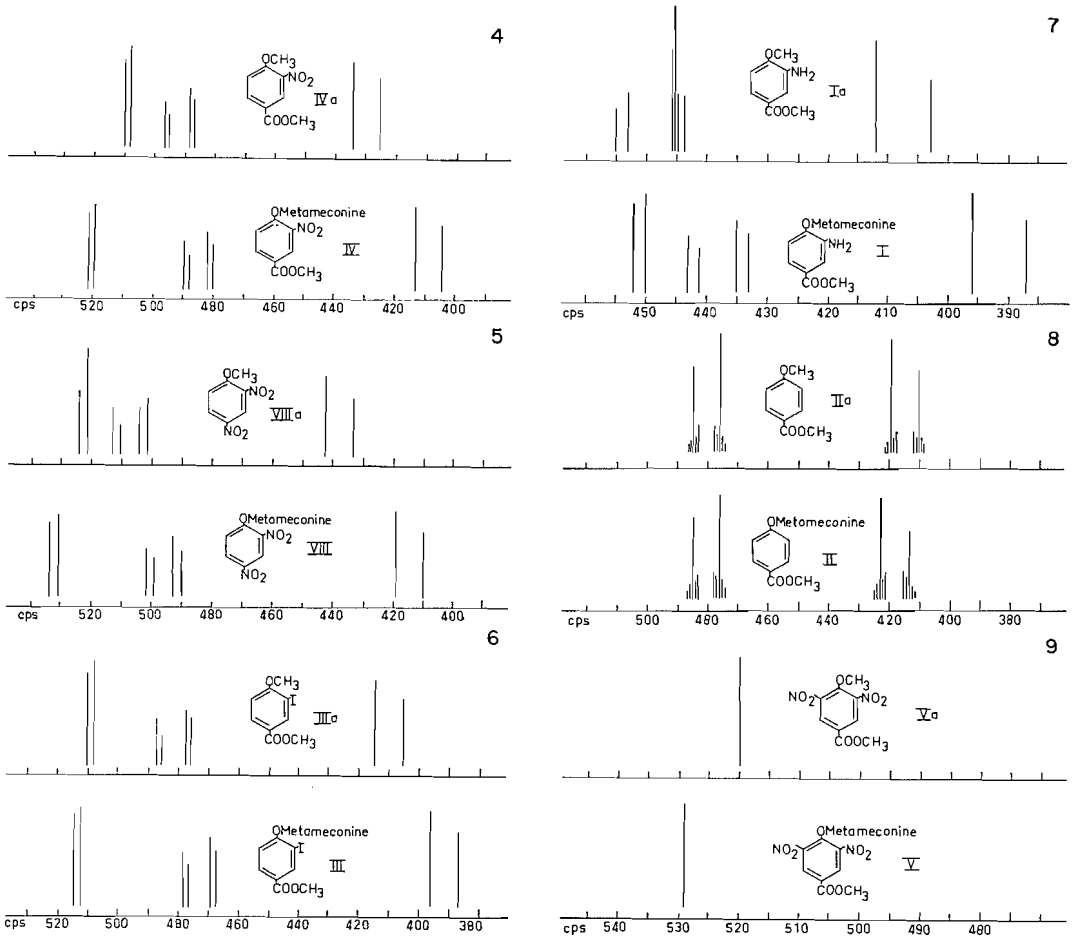

FIGS. 4–9. Schematic n.m.r. spectra of aromatic protons. C.p.s. down field from TMS in $CHCl_3$ or $CDCl_3$ solution, at 60 Mc.p.s.

General agreement with the geometry already proposed for the various ethers (and anisoles) can be deduced from Table II, in the manner already used for other groups.

TABLE II

Chemical shift of the carbomethoxy[9] protons H_h

Compound	Tau values	Compound	Tau values
I	6.15	IV	6.07
I*a*	6.15	IV*a*	6.07
II	6.13	V	5.98
II*a*	6.17	V*a*	5.98
III	6.13		
III*a*	6.13		

[9]*The signal was assigned on the basis of the expected chemical shift. It has been checked to some extent by comparing the spectrum of methyl 4-methoxy-3-nitrobenzoate (IVa) with that of the corresponding ethyl ester, and by comparing the spectrum of ester IV with that of the corresponding acid (in acetone).*

Can. J. Chem. Downloaded from www.nrcresearchpress.com by 210.87.254.5 on 09/05/12
For personal use only.

Evidence from Infrared Spectra

A plot of the stretching frequency of the phthalide carbonyl vs. the sum of the Hammett parameters σ_m for the ortho-groups of the lower ring of I, II, III, IV, and V (Fig. 10) shows a linear[10] variation for the first four ethers, but a sharp variation from the line for the fifth. The latter has a frequency lower than IV although it contains an extra nitro group. This evidence strongly indicates that the principal conformation of V must be that of Fig. 2, where the inductive effect is strongly opposed by electron donation from the ether oxygen to the carbonyl. Similarly, the high value of the asymmetric nitro stretching frequency (Table III), both for the quadruply ortho-substituted diphenyl ether V and the corresponding anisole V*a*, shows that in neither compound is the (lower) benzene ring coplanar with the C—O—C bond under study (Fig. 2). The lower values for IV and IV*a* are in agreement with the greater opportunities for resonance in the conformation similar to that of Fig. 3. The values for VIII and VIII*a*, though presumably they refer to the para-nitro group, also correspond to considerable resonance between the lower ring and the oxygen under study (Fig. 3).

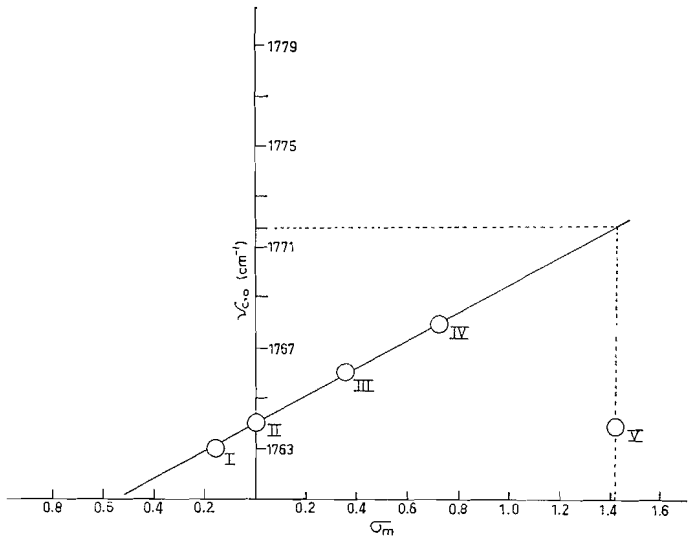

FIG. 10. Lactone carbonyl absorption vs. σ_m of ortho-substituent on other ring.

TABLE III

Asymmetric nitro absorption frequencies

Compound*	Frequency (cm^{-1})
V	1551
V*a*	1550
IV	1541
IV*a*	1539
VIII	1540†
VIII*a*	1531†

*In chloroform solution.
†With shoulder on the high-frequency side.

[10]*The linear variation is good evidence that the steric effects are the same in the four ethers concerned. The conformation of Fig. 3 also is strongly suggested, since otherwise the varying sizes of the ortho-groups would have a noticeable effect. However, it can be shown that the choice of σ_m, rather than some other, is not significant.*

Can. J. Chem. Downloaded from www.nrcresearchpress.com by 210.87.254.5 on 09/05/12
For personal use only.

The single sharp peak for the asymmetric nitro stretching vibration of V is noteworthy inasmuch as it is to be expected for the "methoxy-inside" conformation (Fig. 2), but would be surprising in the "nitro-inside" conformation because of the extremely short average lifetimes of vibration states. Conclusions from the ester carbonyl stretching frequency merely confirmed those made from the n.m.r. frequencies of the ester methyl.

Relation to the Ultraviolet Spectra

According to the method used by Mangini and Passerini (1) for diphenyl sulphides, the configuration of Fig. 2 (V) might be expected to show ultraviolet absorption approximately the same as the sum of the absorptions of methoxymetameconine (VI) and methyl 3,5-dinitrobenzoate, whereas the configuration of Fig. 3 should absorb the same as the sum of the absorptions of metameconine (VII) and the anisole corresponding to the other ring. In Figs. 11–16 are shown the absorption of several diphenyl ethers, together with the

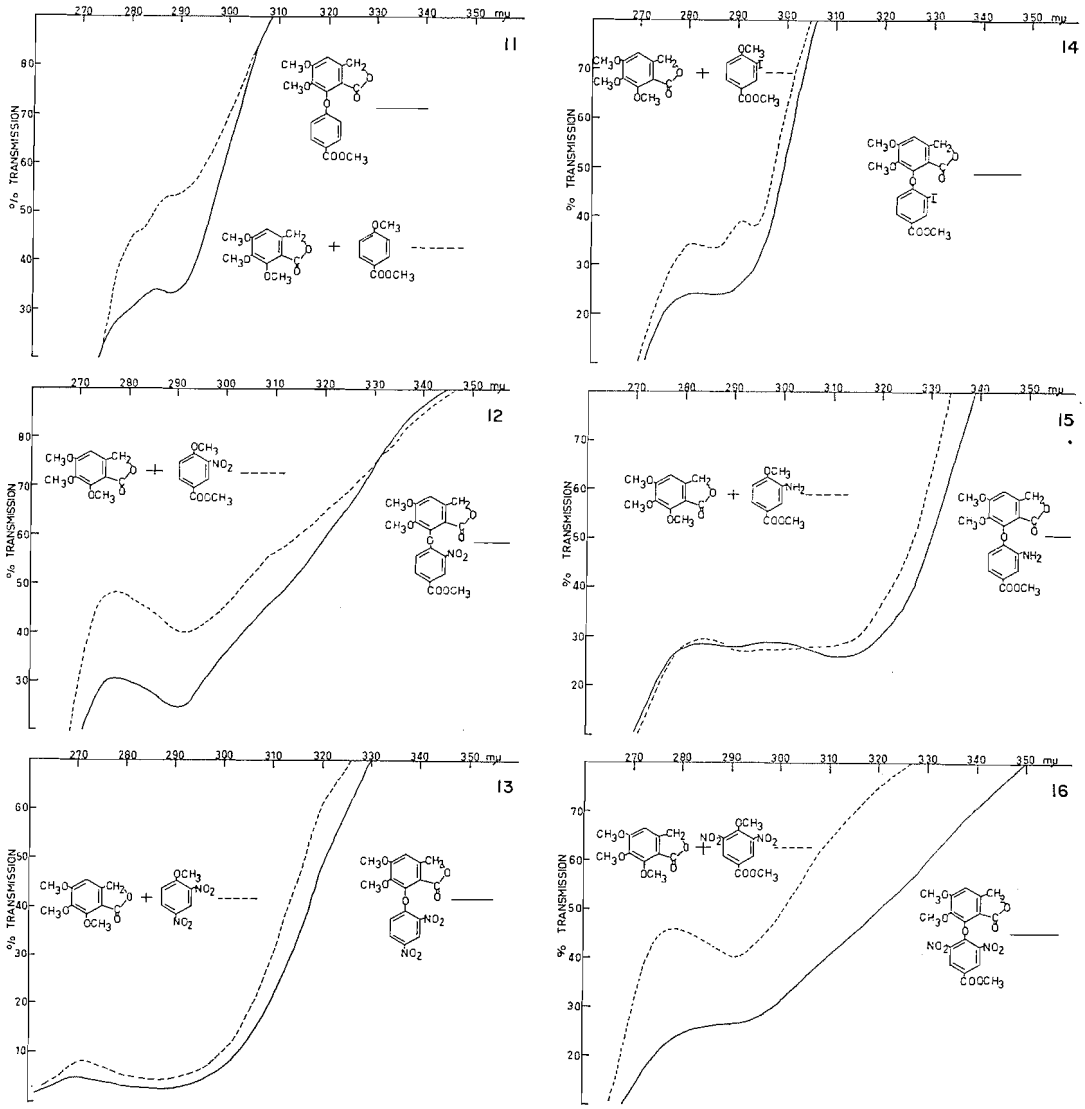

Can. J. Chem. Downloaded from www.nrcresearchpress.com by 210.87.254.5 on 09/05/12
For personal use only.

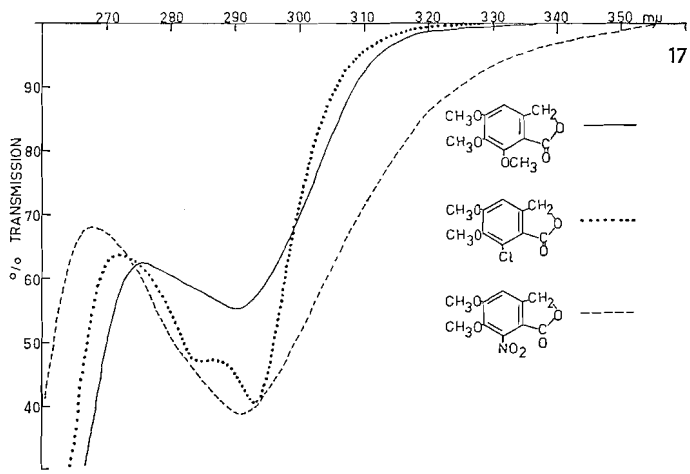

FIGS. 11–17. Ultraviolet spectra of diphenyl ethers and of corresponding anisoles. Concentrations are 1.00×10^{-4} *M* in CCl_4.

spectrum of a solution of a mixture of the two anisoles corresponding to the parts of the diphenyl ethers; each anisole is at the same molarity as its related diphenyl ether. It is at once evident that caution must be used in interpreting the curves. The absorption of each diphenyl ether is similar to, but greater than, the sum of the absorption of its two related anisoles, and therefore much greater than the absorption of the related anisole plus phenyl derivative considered by Mangini and Passerini. A first (naive) conclusion would be that the central ethereal oxygen is capable of resonance with both rings at once. The corrective to this conclusion is supplied by Fig. 17, where it is seen that an increasingly electron-withdrawing group at position-7 of metameconine results in an increasingly intense absorption. Therefore, the diphenyl ethers I–IV, and VIII, probably are acting simply as the summation spectra of the corresponding anisoles (I*a*–IV*a*, and VIII*a*, respectively) plus a metameconine substituted at position-7 with a group rather more electron-withdrawing than the methoxy group. In fact, the summation curve of IV*a* and either 7-nitrometameconine or 7-acetaminometameconine was found to be very close to that of the diphenyl ether IV. These results are therefore in agreement with the conformation of Fig. 3. We have not managed to obtain suitable monomers for comparison with V (expected to have the other configuration of Fig. 2), but at least it does differ empirically from all the other diphenyl ethers studied in the enormous difference in the long-wave absorption between the diphenyl ether (V) and its two related anisoles (VI and V*a*).

The practical utility of the determination of the principal conformations of diphenyl ethers was made apparent almost immediately by its use in the discovery of a new rearrangement reaction in the diphenyl ether series, and by the application of the method, based on the present work, to the determination of conformation and configuration in the phthalide–isoquinoline alkaloids (19). The present work is continuing in attempts to relate quantitatively the temperature, solvent, and the size and nature of the substituents to the principal variables of the system: the magnitude and area of the shielding current loops, the magnitude of the oxygen valence angle, and the percentage occupancy of each major conformation.

Can. J. Chem. Downloaded from www.nrcresearchpress.com by 210.87.254.5 on 09/05/12
For personal use only.

Can. J. Chem. Downloaded from www.nrcresearchpress.com by 210.87.254.5 on 09/05/12
For personal use only.

EXPERIMENTAL

Melting points below 215° were determined in a precision capillary apparatus; higher melting points were determined on a Kofler micro hot stage, and are uncorrected.

Solvents of spectral or analytical grade were used for ultraviolet and infrared spectroscopy. Ultraviolet spectra were determined on a Beckman model DK-1 recording spectrophotometer; calibration of the instrument with benzene (A.C.S. grade, 0.00788 *M* in heptane) showed that the corrections required were negligible (22). All spectra were obtained on solutions 1.00×10^{-4} *M* in carbon tetrachloride.

Infrared spectra were determined on a Perkin–Elmer model 21 spectrophotometer repeatedly calibrated with a polystyrene standard (23). With care, results were reproducible within 1 cm^{-1}. Spectra were determined on solutions in chloroform containing 6% of the substance investigated (w/v).

The n.m.r. spectra were determined on the Varian A-60 spectrometer at 60 Mc.p.s. At the end of the work, the same sweep width used to determine the reported frequencies was calibrated by a sideband method; the largest error was about 2 c.p.s. and was exceptional. The reproducibility of spectra taken several weeks apart ensured the stability of the calibration. Spectra for I*a*–VIII*a*, VI, and VII were determined on 75 mg of sample in 0.5 ml of chloroform or deuterochloroform. Minor variations in concentration were unimportant, as shown; IV*a* gave identical spectra in concentrations of 75 mg/0.5 ml and 30 mg/0.5 ml. The spectra of compounds II–V and VIII were determined using a concentration of 50 mg/0.5 ml chloroform or deuterochloroform. However, I, because of its low solubility, would dissolve only at a concentration of 20 mg/0.5 ml.

A few substances, mentioned in the introduction but not in the sections below, were available as analytical samples from previous work (16–18, 24).

The following substances were made by treatment of the appropriate phenol with ethereal diazomethane (the melting point after purification is also given): methyl 4-methoxybenzoate (II*a*) (25), 47.7–48.5°; methyl 4-methoxy-3-nitrobenzoate (IV*a*) (26), 109.1–109.4°; methyl 3,5-dinitro-4-methoxybenzoate (V*a*) (27, 28), 53.6–54.2°; 2,4-dinitroanisole (VIII*a*) (29), 87.2–88.1°.

Methyl 3-Amino-4-methoxybenzoate (Ia)

Methyl 4-methoxy-3-nitrobenzoate (IV*a*) (3.0 g, m.p. 107.5–108.5°) was covered with ethanol (95%, 150 ml) and water (100 ml) and stirred while amalgamated aluminium foil (10 pieces, 2 × 1 in.) was added. After 5–6 h, the heavy sludge was removed, the filtrate concentrated by evaporation, and then diluted with water to give needles, m.p. 69.3–69.6°, in a yield of 1.29 g. The needles were purified by solution in dilute hydrochloric acid and by reprecipitation with ammonia, and then by four recrystallizations from ligroin, to give the analytical sample, m.p. 70.1–70.8°, slightly yellow needles. The infrared spectrum showed the presence of N—H stretching bands and the absence of nitro-group stretching bands. The melting point differed considerably from the literature value of 85–86° (26).

Calcd. for $C_9H_{11}O_3N$: C, 59.66; H, 6.12; N, 7.73. Found: C, 59.71, 59.77; H, 6.06, 6.05; N, 7.66, 7.67.

Attempts to reduce the nitro ester with iron and acetic acid failed, though this reduction system worked well for the corresponding diphenyl ether (IV). Reduction of 4-hydroxy-3-nitrobenzoic acid with aluminium amalgam also failed. The course of reduction of IV*a* with tin and hydrochloric acid was unusual, as shown in the next section.

Methyl 3-Amino-2-chloro-4-methoxybenzoate

Methyl 4-methoxy-3-nitrobenzoate (IV*a*) (2.0 g, m.p. 107.5–108.5°) was stirred with concentrated hydrochloric acid (25 ml) and aqueous ethanol (5 ml) while mossy tin (six pieces the size of a pea) was added. Heat was applied until a green solution resulted. The solution was cooled, neutralized with aqueous sodium hydroxide (30%), and the heavy white precipitate (0.66 g) was collected. Two crystallizations from ligroin (the material insoluble in hot ligroin being discarded) gave the analytical sample, obtained as white plates, m.p. 91.7–92.2°. (Recrystallization from dilute ethanol gave needles.) The infrared spectrum showed two bands of medium intensity in the N—H stretching region, and the orientation of the compound followed from the n.m.r. spectrum, which showed an aromatic AB pattern with a coupling constant (8.4 c.p.s.) characteristic of ortho-protons.

Calcd. for $C_9H_{10}O_3NCl$: C, 50.13; H, 4.67; N, 6.50. Found: C, 50.30, 50.38; H, 4.84, 4.74; N, 6.32, 6.26.

Methyl 3-Iodo-4-methoxybenzoate (IIIa)

This compound was difficult to obtain. The iodination of methyl 4-hydroxybenzoate in aqueous potassium hydroxide and potassium iodide gave only the free acid corresponding to the starting material. Iodination of 4-hydroxybenzoic acid in ethanol with mercuric oxide and iodine by the method of Brenans and Prost (30) failed to give a recognizable product. Reduction of 3,5-diiodo-4-hydroxybenzoic acid with triphenylphosphine in boiling xylene (31), or with iron and acetic acid, gave only starting material. Small yields of 4-hydroxy-3-iodobenzoic acid were obtained by the reduction of the 3,5-diiodo-acid with zinc and aqueous sodium hydroxide.

Moderate yields of the desired acid were obtained by the method of Sanromá (32). Methyl 4-hydroxybenzoate (6.0 g) was dissolved in aqueous sodium hydroxide (2.85 g in 25 ml of water). Iodine (10.0 g) and sodium peroxide (1.8 g) were added in alternate portions over the course of 4 h, and the mixture kept a further 18 h. The product was then fractionally precipitated with hydrochloric acid, seven fractions being

obtained. The first six were united and recrystallized from a dilute aqueous solution of sodium bisulphite. The material insoluble in the hot solution was mainly the diido acid, while the cooled filtrate deposited crude 4-hydroxy-3-iodobenzoic acid, m.p. 160–175° (uncorrected), which gave a typical aromatic ABC pattern in the n.m.r. spectrum. (The seventh fraction seemed to be mainly 4-hydroxybenzoic acid.) The crude monoiodo acid was methylated with ethereal diazomethane and the product recrystallized once from ligroin, once from methanol, and once from absolute ethanol to give a fluffy white product, m.p. 94.6–95.2°. The lit. value (33) is 94–95°. Its aromatic spectrum showed a typical aromatic ABC pattern and two methoxy resonances; the infrared spectrum showed no bands due to hydroxyl or carboxyl.

7-(4′-Carbomethoxy-2′-nitrophenoxy)metameconine (IV) (16, 17), m.p. 155.6–156.6°, 7-(2′-amino-4′-carbomethoxyphenoxy)metameconine (I) (18), m.p. 197.1–197.8° (with slight softening at 195°), and 7-(4′-carbomethoxy-2′-iodophenoxy)metameconine (III) (18), m.p. 204.2–205.0°, were made as previously described.

4-Carbomethoxy-2-nitrophenyl Toluene-p-sulphonate

This compound, needed in the above syntheses, was made by a method giving a much purer product in better yield than obtained previously (16, 17). Methyl 4-hydroxy-3-nitrobenzoate (15 g) and *p*-toluenesulphonyl chloride (15 g tech.) were shaken with dry pyridine (25 ml) until the mass became almost solid (10–15 min). The solid was washed with water into a beaker containing dilute hydrochloric acid (500 ml) and ice, and the resulting lumps were thoroughly crushed under the acid solution. White crystals were recovered, washed, and dried, and without further purification had a m.p. of 93.4–94.2°, yield 26.65 g (100%).

7-(4′-Carbomethoxyphenoxy)-metameconine (II)

Sodium nitrite (0.124 g) was dissolved with slight heating in concentrated sulphuric acid (2.5 ml); the solution was cooled to 0° and treated with glacial acetic acid (2.5 ml). A second solution was prepared from 7-(2′-amino-4′-carbomethoxyphenoxy)-metameconine (I) (18) (0.5 g) in concentrated sulphuric acid (1.0 ml) and glacial acetic acid (2.5 ml). The second solution was slowly added to the first over a period of 0.5 h, the reaction temperature being kept slightly below 0°. A few milliliters of concentrated sulphuric acid were then added to make the mixture more fluid, and after a further 1.75 h, the mixture was poured onto ice (100 g) to which had been added a small amount of cupric sulphate. Hypophosphorous acid (12 ml, 50%) was added dropwise with stirring. The mixture was kept 42 h in the refrigerator, and the granular precipitate (0.45 g) recovered. Two recrystallizations from dilute ethanol gave yellowish-white crystals, m.p. 195.2–196.1°, more easily purified than those obtained by the previous method (18). The n.m.r. spectrum of the present sample was identical with that of the sample made in the previous work (18).

ACKNOWLEDGMENTS

The work was supported by the National Research Council with a grant and with a Scholarship awarded to one of us. The large amounts of vanillin needed were donated by Dr. G. H. Tomlinson, Howard Smith Paper Company, Cornwall, Ontario.

REFERENCES

1. A. Mangini and R. Passerini. J. Chem. Soc. 1168 (1952).
2. M. Dahlgard and R. Q. Brewster. J. Am. Chem. Soc. **80**, 5861 (1958).
3. H. E. Ungnade, E. E. Pickett, L. Rubin, and E. Youse. J. Org. Chem. **16**, 1318 (1951).
4. M. Gomel, H. Lumbroso, N. Marziano, and R. Passerini. Bull. Soc. Chim. France, 1908 (1959).
5. K. Higasi and S. Uyeo. Bull. Chem. Soc. Japan, **14**, 87 (1939).
6. G. C. Hampson and L. E. Sutton. Proc. Roy. Soc. Ser. A, **140**, 562 (1933).
7. N. J. Leonard and L. E. Sutton. J. Am. Chem. Soc. **70**, 1564 (1948).
8. K. Higasi, S. Uyeo, and N. Yamaguchi. Bull. Inst. Phys. Chem. Research Tokyo, **23**, 506 (1947). Chem. Abstr. **42**, 6768 (1948).
9. J. Toussaint. Mem. Soc. Roy. Sci. Liege Vol. Hors Ser. **12**, 1 (1952).
10. L. R. Maxwell, S. B. Hendricks, and V. M. Mosley. J. Chem. Phys. **3**, 699 (1935).
11. J. H. Calderwood and C. P. Smyth. J. Am. Chem. Soc. **78**, 1295 (1956).
12. K. Bergmann, D. M. Roberti, and C. P. Smyth. J. Phys. Chem. **64**, 665 (1960).
13. K. Higasi and C. P. Smyth. J. Am. Chem. Soc. **82**, 4759 (1960).
14. D. M. Roberti, D. F. Kalman, and C. P. Smyth. J. Am. Chem. Soc. **82**, 3523 (1960).
15. W. W. Robertson and F. A. Matsen. J. Am. Chem. Soc. **72**, 5250 (1950).
16. J. A. McRae, R. Y. Moir, J. J. Ursprung, and H. H. Gibbs. J. Org. Chem. **19**, 1500 (1954).
17. M. Allen and R. Y. Moir. Can. J. Chem. **37**, 1799 (1959).
18. M. Allen and R. Y. Moir. Can. J. Chem. **41**, 252 (1963).
19. S. Safe and R. Y. Moir. Can. J. Chem. **42**, 160 (1964).
20. J. A. Pople. J. Chem. Phys. **24**, 1111 (1956).
21. J. S. Waugh and R. W. Fessenden. J. Am. Chem. Soc. **79**, 846 (1957).
22. N. S. Bayliss and L. H. Hulme. Australian J. Chem. **6**, 257 (1953).
23. A. D. Cross. Introduction to practical infra-red spectroscopy. Butterworths, London. 1960. p. 39.

Can. J. Chem. Downloaded from www.nrcresearchpress.com by 210.87.254.5 on 09/05/12
For personal use only.

24. J. A. McRae, R. B. Van Order, F. H. Griffiths, and T. E. Habgood. Can. J. Chem. **29**, 482 (1951).
25. L. G. Radcliffe and W. H. Brindley. Perfumery Essent. Oil Record, **13**, 414 (1922). J. Chem. Soc. **124**, (i), 110 (1923).
26. K. Awers. Ber. **30**, 1475 (1897).
27. G. W. K. Cavill. J. Soc. Chem. Ind. London, **64**, 212 (1945).
28. J. Pollak and H. Feldsharek. Monatsh. **29**, 139 (1908).
29. J. Post and H. Mehrtens. Ber. **8**, 1552 (1875).
30. P. Brenans and C. Prost. Compt. Rend. **177**, 768 (1923).
31. H. Hoffmann, L. Horner, H. G. Wippel, and D. Michael. Ber. **95**, 523 (1962).
32. A. N. Sanromá. Spanish Patent No. 222,232 (Nov. 15, 1955). Chem. Abstr. **50**, 16858 (1956).
33. J. Seidel. J. Prakt. Chem. Ser. 2, **59**, 105 (1899).

Can. J. Chem. Downloaded from www.nrcresearchpress.com by 210.87.254.5 on 09/05/12
For personal use only.

Can. J. Chem. Downloaded from www.nrcresearchpress.com by 210.87.254.5 on 09/05/12
For personal use only.

THE SYNTHESIS OF 3-*O*-[(BENZYLTHIO)CARBONYL]-β-D-GLUCOPYRANOSE AND METHYL 2,4,6-TRI-*O*-BENZOYL-α AND β-D-GLUCOPYRANOSIDES

J. J. WILLARD,[1] J. S. BRIMACOMBE,[2] AND R. P. BRUETON[2]
Textile Research Institute, Princeton, New Jersey, U.S.A., and Chemistry Department, The University of Birmingham, England

Received May 26, 1964

ABSTRACT

The discovery that the (benzylthio)carbonyl group is stable in concentrated hydrochloric acid has permitted the removal in that medium of isopropylidene blocking groups from 3-*O*-[(benzylthio)carbonyl]-1,2;5,6-di-*O*-isopropylidene-α-D-glucofuranose to furnish crystalline 3-*O*-[(benzylthio)carbonyl]-β-D-glucopyranose. Benzoylation of the latter provided a derivative which has made possible the synthesis of methyl 2,4,6-tri-*O*-benzoyl-α and β-D-glucopyranosides.

INTRODUCTION

Two of the four possible anomeric pairs of the tribenzoate derivatives of the methyl glucopyranosides have been known for many years. The use of the specific triphenylmethyl ether group to block the primary (C-6) hydroxyl group permits the syntheses of methyl 2,3,4-tri-*O*-benzoyl-α and β-D-glucopyranosides (1). The 2,3-di-*O*-benzoate of each methyl glucopyranoside, prepared with the aid of the 4,6-*O*-benzylidene blocking group, was specifically benzoylated at C-6 to furnish the 2,3,6-tri-*O*-benzoyl derivatives (2). A recent paper (3) described the synthesis of methyl 2-*O*-[(benzylthio)carbonyl]-α-D-glucopyranoside, which served as a precursor to methyl 3,4,6-tri-*O*-benzoyl-α-D-glucopyranoside, by a specific substitution of the (benzylthio)carbonyl group at C-2 in methyl 4,6-*O*-benzylidene-α-D-glucopyranoside. The thiocarbonate ester, $C_6H_5—CH_2—S—CO—O—$, serves as a useful blocking group for the synthesis of partial esters of carbohydrates due to the ease with which it can be removed without cleavage of other ester groupings (4).

Attempts to duplicate this specific substitution reaction at C-2 with methyl 4,6-*O*-benzylidene-β-D-glucopyranoside resulted in the recovery of disproportionately high yields of the disubstituted product. This method does not serve, therefore, as a practical route to methyl 3,4,6-tri-*O*-benzoyl-β-D-glucopyranoside.

The synthesis of 3-*O*-[(benzylthio)carbonyl]-1,2;5,6-di-*O*-isopropylidene-α-D-glucofuranose has been described (4). Attempts to remove selectively the isopropylidene groups from this compound by treatment with acid under refluxing conditions resulted also in the hydrolysis of the (benzylthio)carbonyl group. A method of removing the isopropylidene groups has now been found which provides crystalline 3-*O*-[(benzylthio)carbonyl]-β-D-glucopyranose and, ultimately, methyl 2,4,6-tri-*O*-benzoyl-α and β-D-glucopyranosides. Thus, all of the isomeric tribenzoate derivatives of methyl-α-D-glucopyranoside have now been characterized and, in the β-series, only the 3,4,6-isomer remains unknown.

RESULTS AND DISCUSSION

When methyl 4,6-*O*-benzylidene-α-D-glucopyranoside (I) is treated with 1.1 moles of (benzylthio)carbonyl chloride (II) in pyridine solution, a 58% yield of the pure 2-*O*-

[1]*To whom inquiries should be directed. Present address: Textile Research Institute, Princeton, New Jersey, U.S.A.*
[2]*Present address: Chemistry Department, The University, Edgbaston, Birmingham 15, England.*

[(benzylthio)carbonyl] derivative of I is obtained, together with 10% of the 2,3-di-*O*-[(benzylthio)carbonyl] derivative (3). Repeated attempts to duplicate this experiment using methyl 4,6-*O*-benzylidene-β-D-glucopyranoside (III) and 1 mole of II resulted in the recovery of 40% of the disubstituted derivative (IV), previously described (4). From the remaining products, consisting necessarily of 40% of unreacted III, a monosubstituted product could be isolated only in very low yield.

It can be calculated[3] from considerations of chemical kinetics that 33.3% of the disubstituted product would be formed if it is assumed that the hydroxyl groups have equal reactivities which are not changed after substitution at the other position (see appendix). Substitution of the (benzylthio)carbonyl group at one of the hydroxyl groups would be expected to activate the remaining hydroxyl group (5). This activation can account for the high proportion (40%) of disubstituted product formed when the substitution is carried out on the β-glucoside. One explanation for the low yield (10%) of disubstituted product in the case of substitution in the α-glucoside is that the reactivity at C-2 is considerably greater than that at C-3 and substitution at C-2 does not increase the reactivity at C-3 sufficiently to enable it to compete with the more reactive C-2. This explanation is consistent with the observation (3) that all of the monosubstituted product isolatable in the case of the α-glucoside is that substituted at C-2. The radical difference in behavior of the α- and β-methyl glucosides encountered in these experiments was not expected.

Because of the low yield of mono-(benzylthio)carbonyl derivatives of III obtained, the synthesis of methyl 3,4,6-tri-*O*-benzoyl-β-D-glucopyranoside by this route is not practical. Another possible route to this compound was discarded, since repeated attempts to saponify preferentially one of the (benzylthio)carbonyl groups from the disubstituted product IV under mild conditions again resulted in the recovery of proportionately high yields of disubstituted and unsubstituted products.

Diethylmercaptal derivatives can be prepared directly from 1,2-*O*-isopropylidene derivatives by treatment with a mixture of concentrated hydrochloric acid and ethyl mercaptan (6). The behavior of 3-*O*-[(benzylthio)carbonyl]-1,2;5,6-di-*O*-isopropylidene-α-D-glucofuranose (V) in concentrated hydrochloric acid therefore was investigated. The optical rotation of a solution of V in concentrated hydrochloric acid at room temperature increased slightly and essentially was constant after 20 h. Evaporation of the acid *in vacuo* yielded a crystalline reducing product (VI) which was homogeneous, and readily distinguishable from D-glucose, on paper chromatograms. The pure product showed a mutarotation of $-4.3° \rightarrow +60.2°$ (in acetone), indicative of a β-configuration. Its elemental analysis agreed with that calculated for a mono-(benzylthio)carbonyl derivative of glucose.

The crystalline (benzylthio)carbonyl-D-glucose derivative VI was shown to have the β-pyranose configuration by the sequence of reactions shown in Fig. 1. Benzoylation in pyridine gave a tetrabenzoyl derivative (VII). Levene and Meyer (7) found that β-D-glucopyranose, under similar conditions, yielded the pentabenzoate derivative without any accompanying change in the configuration of the ring. Oxidative removal of the (benzylthio)carbonyl group from VII, followed by benzoylation of the regenerated hydroxyl group, gave a product (IX) having a melting point and optical rotation identical with those reported (7) for 1,2,3,4,6-penta-*O*-benzoyl-β-D-glucopyranose. The higher-melting crystalline form of this compound reported by Ness, Fletcher, and Hudson (8) was not encountered in this work. Migration of the (benzylthio)carbonate ester grouping

[3]*The authors would like to acknowledge the assistance of Dr. D. Prevorsek and Dr. S. Winchester, Textile Research Institute, in performing these calculations.*

Can. J. Chem. Downloaded from www.nrcresearchpress.com by 210.87.254.5 on 09/05/12
For personal use only.

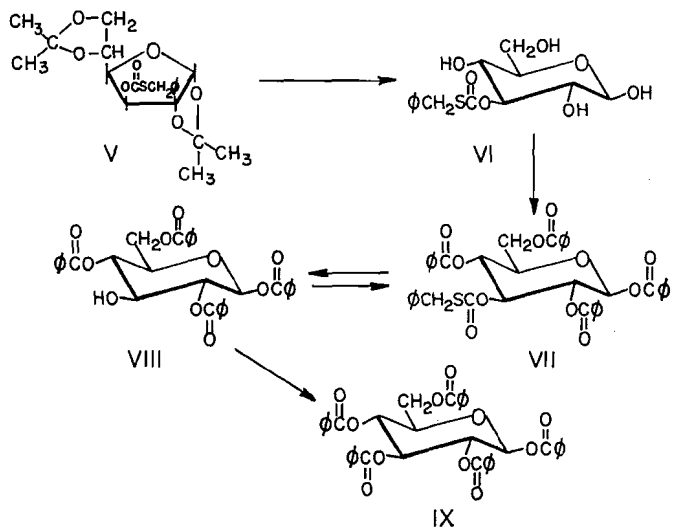

FIG. 1.

from C-3 under the acidic conditions used to remove the isopropylidene grouping is unlikely. The assignment of the (benzylthio)carbonate grouping to C-3 is confirmed by comparison of the physical properties of methyl 2,4,6-tri-*O*-benzoyl-α-D-glucopyranoside (XV) and its derivatives, subsequently synthesized, with those of the known 2,3,4-, 2,3,6-, and 3,4,6-derivatives.

When treated with (benzylthio)carbonyl chloride, VII was resynthesized from VIII, proving the absence of benzoyl migration during the removal of the (benzylthio)carbonyl group. The 3-*O*-acetyl and 3-*O*-(*p*-tolylsulphonyl) derivatives of VIII were prepared.

The 3-*O*-[(benzylthio)carbonyl]-tetra-*O*-benzoyl derivative (VII) was then used to synthesize methyl 2,4,6-tri-*O*-benzoyl-α and β-D-glucopyranosides, as shown in Fig. 2. Peracetylated hexoses are converted to the acetochlorohexose on treatment with titanium tetrachloride in chloroform (9). This method has been shown, more recently, to be applicable to perbenzoylated glucose derivatives (8, 10). The presence of the (benzylthio)-carbonyl group did not cause any anomalous behavior during the use of this reagent. The α-chloro derivative (X) was converted smoothly to methyl 2,4,6-tri-*O*-benzoyl-3-*O*-[(benzylthio)carbonyl]-β-D-glucopyranoside (XI) when treated with silver carbonate in boiling methanol. Oxidative removal of the (benzylthio)carbonyl group gave methyl 2,4,6-tri-*O*-benzoyl-β-D-glucopyranoside (XII), which on benzoylation gave the known (8, 11) methyl 2,3,4,6-tetra-*O*-benzoyl-β-D-glucopyranoside. The 3-*O*-(*p*-tolylsulphonyl) (XIII) and 3-*O*-acetyl derivatives of XII also were synthesized.

Anomerization of the β-glycosidic group in XI by a standard procedure (9) gave a sirupy product (XIV). Oxidative removal of the (benzylthio)carbonyl group gave a crystalline product, methyl 2,4,6-tri-*O*-benzoyl-α-D-glucopyranoside (XV), which on benzoylation gave the known (1, 8) methyl 2,3,4,6-tetra-*O*-benzoyl-α-D-glucopyranoside; its 3-*O*-(*p*-tolyl-sulphonyl) derivative (XVI) was prepared in the usual manner.

The structures of methyl 2,4,6-tri-*O*-benzoyl-α and β-D-glucopyranoside (XII and XV) were related unequivocally to that of 1,2,4,6-tetra-*O*-benzoyl-β-D-glucopyranose (VIII) by

Can. J. Chem. Downloaded from www.nrcresearchpress.com by 210.87.254.5 on 09/05/12
For personal use only.

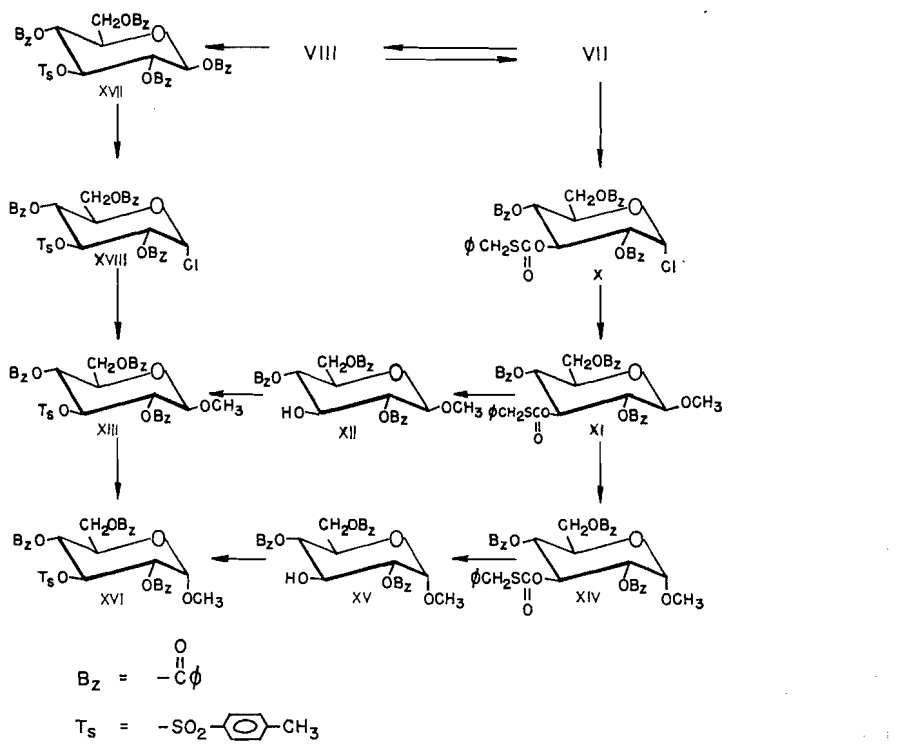

FIG. 2.

taking the *p*-tolylsulphonyl derivative (XVII) through the reaction sequence (XVII → XVIII → XIII → XVI) shown in Fig. 2. The *p*-tolylsulphonates (XIII and XVI) thus obtained were indistinguishable from those derivatives prepared from methyl 2,4,6-tri-*O*-benzoyl-α and β-D-glucopyranosides, respectively.

APPENDIX

The reaction of the methyl 4,6-*O*-benzylidene-α and β-D-glucopyranosides (I), containing two reactive hydroxyl groups, with 1 mole of (benzylthio)carbonyl chloride (II) falls into the class of competitive, consecutive (series) second-order reactions treated by Frost and Schwemer (11). The reactions are represented by:

$$A + B \xrightarrow{k_1} C,$$

and

$$A + C \xrightarrow{k_2} D,$$

where A, B, C, and D represent the molar concentrations of II, I, monosubstituted glucoside, and disubstituted glucoside, respectively. To apply the above reaction scheme, two assumptions must be made: (1) the two hydroxyl groups in the unsubstituted state have equal reactivities, and (2) substitution in one hydroxyl group produces the same change in reactivity as substitution in the other. The above authors solved the rate equations

Can. J. Chem. Downloaded from www.nrcresearchpress.com by 210.87.254.5 on 09/05/12
For personal use only.

$$[1] \qquad dA/dt = -k_1AB - k_2AC$$

$$[2] \qquad dB/dt = -k_1AB$$

$$[3] \qquad dC/dt = k_1AB - k_2AC$$

$$[4] \qquad dD/dt = k_2AC$$

for the case where initial concentrations were set at $A_0 = 2B_0$.

In the present study it was necessary to solve the above rate equations for the case where $A_0 = B_0$. From a material balance, summing eq. [1] $-$ 2 $\times$ eq. [2] $-$ eq. [3] and integrating gave

$$[5] \qquad A - 2B - C = A_0 - 2B_0.$$

Since $A_0 = B_0$,

$$[6] \qquad C = -2B + A + B_0,$$

and substituting in eq. [1],

$$[7] \qquad dA/dt = (2k_1 - k_2)AB - k_2A^2 - k_2AB_0.$$

If one chooses as dimensionless quantities:

$$[8] \qquad \alpha = A/A_0; \beta = B/B_0; \tau = B_0k_1t; \kappa = k_2/k_1,$$

then eqs. [2] and [7] can be solved to produce

$$[9] \qquad d\alpha/d\beta = (1 - 2\kappa) + \kappa(\alpha/\beta).$$

Integration of eq. [9] gives

$$[10] \qquad \alpha = \left(\frac{1 - 2\kappa}{1 - \kappa}\right)\beta + \left(\frac{1}{1 - \kappa}\right)\beta^\kappa - 1,$$

the constant of integration being determined at $\alpha = \beta = 1$.

Solutions of eq. [10] for β as a function of α at different κ values are shown plotted in Fig. 3. The case of particular interest in the present study is that in which the reactivities of the hydroxyl groups are not changed after substitution, that is, $k_1 = k_2$ or $\kappa = 1$. The solution was obtained for $\kappa = 0.99$, as an approximation for $\kappa = 1$ which is not readily solvable. At $\alpha = 0$, it is seen that $\beta = 0.333$; that is, at the end of the reaction one-third of the initial I remains unsubstituted. Another one-third of the initial I must therefore be disubstituted, since the unsubstituted and disubstituted products must be equal at the end of the reaction. By difference, the remaining one-third of the initial I would be present as monosubstituted product.

To obtain the 40% of disubstituted product in the present work with the β-glucoside, it can be calculated that $k_2 = 2.5k_1$. The 10% yield of disubstituted product obtained with the α-glucoside can be interpreted to mean that $k_1 = 13k_2$.

EXPERIMENTAL

3-O-[(Benzylthio)carbonyl]-β-D-glucopyranose (VI)

3-*O*-[(Benzylthio)carbonyl]-1,2;5,6-di-*O*-isopropylidene-α-D-glucofuranose (V) was synthesized as previously described (4). The pure form (recrystallized from ethanol–water) had m.p. 75–77° and $[\alpha]_D^{20}$ −24.6° (*c*,2, $CHCl_3$).

One gram of V was ground in a mortar and dissolved in 3 ml of concentrated (37%) hydrochloric acid. After standing at room temperature for 18 h, the solution was evaporated *in vacuo* with a bath temperature

Can. J. Chem. Downloaded from www.nrcresearchpress.com by 210.87.254.5 on 09/05/12
For personal use only.

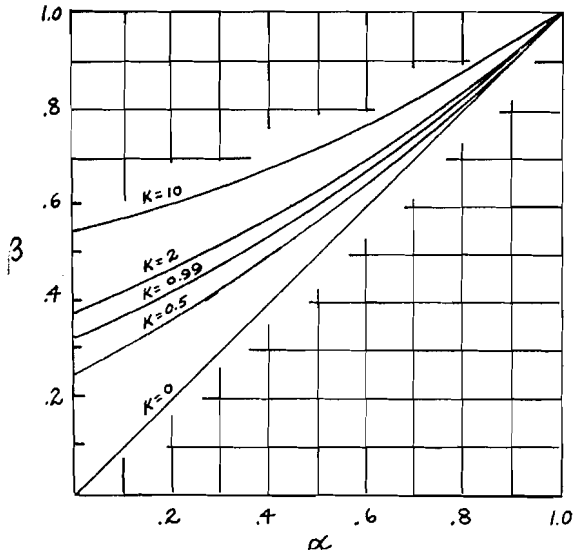

FIG. 3.

of 35–40°. The solid residue was washed with ice water until the washings were neutral and then dried *in vacuo* overnight over potassium hydroxide and phosphorus pentoxide. The product (0.78 g, 97%) reduced Fehling's solution and a paper chromatogram irrigated with butanol–ethanol–water (5:1:4, top layer) showed only one spot with R_f 0.87 (glucose R_f 0.17) when developed with alkaline silver nitrate. After recrystallization from boiling water, the product had m.p. 170–173° (decomp.), $[\alpha]_D^{21}$ −4.3° → +60.2° (*c*,1, acetone). The rotation reached a constant value after 26 h; it is seen that the acetone contained sufficient water to permit mutarotation.

Anal. Calcd. for $C_{14}H_{18}O_7S$: C, 50.91; H, 5.46; S, 9.70. Found: C, 50.64; H, 5.67; S, 9.59.

1,2,4,6-Tetra-O-benzoyl-3-O-[(benzylthio)carbonyl]-β-D-glucopyranose (VII)

To 2.0 g of VI in anhydrous pyridine (30 ml) was added benzoyl chloride (5.0 ml) with cooling in an ice bath. After standing overnight at room temperature, the solution was poured into ice water. The solid deposited was recovered by filtration and washed thoroughly with water. After drying, recrystallization from a mixture of acetone and ethanol gave the product (4.4 g, 98%) having m.p. 199–201°. Two further recrystallizations afforded the pure product having m.p. 200–202°, $[\alpha]_D^{24}$ −16.55° (*c*,1, $CHCl_3$).

Anal. Calcd. for $C_{42}H_{34}O_{11}S$: C, 67.57; H, 4.56; S, 4.28. Found: C, 67.46; H, 4.62; S, 4.11.

In a separate experiment, the solid product VI (50 g, m.p. 157–163°), obtained by evaporation of the hydrochloric acid but omitting the crystallization from water, was benzoylated in the same fashion and gave, after 1 crystallization, 100 g (89%) of VII, m.p. 190–194°. The pure product VII was obtained in 75% yield after 1 recrystallization.

1,2,4,6-Tetra-O-benzoyl-β-D-glucopyranose (VIII)

To a solution of VII (8.0 g) dissolved in chloroform (450 ml) and glacial acetic acid (550 ml) was added potassium acetate (2.0 g) and 30% hydrogen peroxide (150 ml). After standing for 7 days at room temperature, the solution was concentrated *in vacuo* (air-leak) to 150 ml, and water (30 ml) was added to turbidity. Cooling the mixture at 5° gave 6.3 g (98%) of product in 2 crops of crystals, m.p. 176–179°. Two recrystallizations from acetone–petroleum ether gave 5.6 g (89%) having m.p. 179–180° and $[\alpha]_D^{21}$ +8.7° (*c*,1, $CHCl_3$).

Anal. Calcd. for $C_{34}H_{28}O_{10}$: C, 68.46; H, 4.70. Found: C, 68.02; H, 4.82.

Derivatives of VIII

Derivatives of VIII were prepared from 0.5 g samples in pyridine solution by standard procedures. After 48 h reaction time at room temperature, each product was obtained as a solid by pouring the reaction mixture into ice water; filtration and recrystallization (twice) from acetone–petroleum ether afforded the pure compound.

1,2,3,4,6-Penta-O-benzoyl-β-D-glucopyranose (IX).—Yield: 0.45 g (77%); m.p. 156–158°; $[\alpha]_D^{19}$ +23.4° (*c*,1, $CHCl_3$). Reported (6): m.p. 157°; $[\alpha]_D$ +24° (*c*,3, $CHCl_3$).

Can. J. Chem. Downloaded from www.nrcresearchpress.com by 210.87.254.5 on 09/05/12
For personal use only.

3-O-Acetyl-1,2,4,6-tetra-O-benzoyl-β-D-glucopyranose.—Yield: 0.39 g (73%); m.p. 224–226°; $[\alpha]_D^{20}$ +9.4° (*c*,1, $CHCl_3$).

Anal. Calcd. for $C_{36}H_{30}O_{11}S$: C, 67.71; H, 4.70. Found: C, 67.39; H, 4.65.

1,2,4,6-Tetra-O-benzoyl-3-O-(p-tolysulphonyl)-β-D-glucopyranose (XVII).—Yield: 0.31 g (48%); m.p. 193° (decomp.); $[\alpha]_D^{20}$ +11.7° (*c*,1, $CHCl_3$). Another reaction using 4 days reaction time gave this product in 69% yield.

Anal. Calcd. for $C_{41}H_{34}O_{12}S$: C, 65.60; H, 4.54; S, 4.27. Found: C, 65.61; H, 4.59; S, 4.49.

2,4,6-Tri-O-benzoyl-3-O-[(benzylthio)carbonyl]-α-D-glucopyranosyl Chloride (X)

To a solution of VII (50 g) in pure, dry chloroform (1 500 ml) was added titanium tetrachloride (14.7 ml) and the solution was refluxed for 5 h with the exclusion of moisture. The product was isolated by pouring the solution on to ice pieces and by washing the separated chloroform layer with aqueous potassium bicarbonate and then 3 times with water. The dried ($MgSO_4$) chloroform solution was evaporated to dryness and the solid residue was recrystallized, first from acetone–ether and then from ethanol, to give the product (35 g, 78%), m.p. 139–141°. In purest form the product had m.p. 140.5–141° and $[\alpha]_D^{21}$ +122.8° (*c*,1, $CHCl_3$).

Anal. Calcd. for $C_{35}H_{29}O_9ClS$: C, 63.59; H, 4.39; Cl, 5.38; S, 4.84. Found: C, 63.33; H, 4.29; Cl, 6.14;[4] S, 4.97.

Methyl 2,4,6-Tri-O-benzoyl-3-O-[(benzylthio)carbonyl]-β-D-glucopyranoside (XI)

To a solution of X (6.3 g) in anhydrous methanol (600 ml) was added 15 g of freshly precipitated, dried silver carbonate and the mixture was refluxed (drying tube) for 5 h. The silver salts were removed by filtration of the reaction mixture prior to cooling. The product, which crystallized from the solution on addition of 50 ml of water, was dissolved in acetone and filtered through carbon to remove the last traces of silver salts. The acetone was evaporated and the residue recrystallized twice from ethanol to give the product (3.3 g, 53%), having m.p. 165–166° and $[\alpha]_D^{23}$ +24.9° (*c*,1, $CHCl_3$).

Anal. Calcd. for $C_{36}H_{32}O_{10}S$: C, 65.85; H, 4.88; S, 4.88. Found: C, 65.79; H, 5.08; S, 5.24.

Additional amounts of product could be obtained by further treatment with silver carbonate in methanol of the low-melting material obtained as final crops in the alcohol recrystallizations.

Methyl 2,4,6-Tri-O-benzoyl-β-D-glucopyranoside (XII)

The (benzylthio)carbonyl group was removed oxidatively from XI in the manner herein described for the synthesis of VIII. After 2 crystallizations from ethanol–water, the product (90%) had m.p. 152–154° and $[\alpha]_D^{21}$ +16.5° (*c*,1, $CHCl_3$).

Anal. Calcd. for $C_{28}H_{26}O_9$: C, 66.40; H, 5.14. Found: C, 66.16; H, 5.26.

Derivatives of XII

The following derivatives were prepared by standard procedures and were recrystallized twice from ethanol.

Methyl 3-O-Acetyl-2,4,6-tri-O-benzoyl-β-D-glucopyranoside.—Yield: 80%; m.p. 160–162°; $[\alpha]_D^{23}$ +28.4° (*c*,1, $CHCl_3$).

Anal. Calcd. for $C_{30}H_{28}O_{10}$: C, 65.69; H, 5.11. Found: C, 65.80; H, 5.26.

Methyl 2,4,6-Tri-O-benzoyl-3-O-(p-tolylsulphonyl)-β-D-glucopyranoside (XIII).—Yield: 78%; m.p. 191° (decomp.); $[\alpha]_D^{17}$ +33.9° (*c*,1, $CHCl_3$).

Anal. Calcd. for $C_{35}H_{32}O_{11}S$: C, 63.63; H, 4.85; S, 4.85. Found: C, 63.60; H, 4.94; S, 5.10.

Methyl 2,3,4,6-Tetra-O-benzoyl-β-D-glucopyranoside.—Yield: 66%; m.p. 158–160°; $[\alpha]_D^{19}$ +27.6° (*c*,1, $CHCl_3$). Reported (12): m.p. 160–162°; $[\alpha]_D$ +31° ($CHCl_3$).

Methyl 2,4,6-Tri-O-benzoyl-3-O-[(benzylthio)carbonyl]-α-D-glucopyranoside (XIV)

To a solution of XI (3.3 g) in pure, dry chloroform (300 ml) was added titanium tetrachloride (2.0 ml) and the solution was refluxed for 5 h. The product, isolated as described previously, could not be induced to crystallize and showed $[\alpha]_D^{21}$ +95.45° (*c*,2, $CHCl_3$).

Methyl 2,4,6-Tri-O-benzoyl-α-D-glucopyranoside (XV)

The product (XIV) from the foregoing experiment was treated in glacial acetic acid (100 ml) with potassium acetate (0.98 g) and 30% hydrogen peroxide (8.2 ml). The change in optical rotation was followed and attained a constant value after 9 days. The solution then was poured into 1 500 ml ice water and the solid product was recovered by filtration and was washed thoroughly. After drying, the product was crystallized twice from petroleum ether to give 1.82 g (72%), m.p. 74–76°, and $[\alpha]_D^{18}$ +94.9° (*c*,1, $CHCl_3$).

Anal. Calcd. for $C_{28}H_{26}O_9$: C, 66.40; H, 5.14. Found: C, 66.05; H, 5.02.

Derivatives of XV

Methyl 2,4,6-Tri-O-benzoyl-3-O-(p-tolylsulphonyl)-α-D-glucopyranoside (XVI).—This compound, prepared by the procedure previously described for XVII, had m.p. 163–165° and $[\alpha]_D^{18}$ +101.6° (*c*,0.8, $CHCl_3$).

[4]*The high value found in chlorine analysis can probably be attributed to interference from the sulphur present in the substance.*

Can. J. Chem. Downloaded from www.nrcresearchpress.com by 210.87.254.5 on 09/05/12
For personal use only.

Anal. Calcd. for $C_{35}H_{32}O_{11}$: C, 63.63; H, 4.85; S, 4.85. Found: C, 63.38; H, 4.75; S, 4.87.

Methyl 2,3,4,6-Tetra-O-benzoyl-α-D-glucopyranoside.—This compound, prepared as previously described, had m.p. 104–106° and $[\alpha]_D^{20}$ +84.2° (*c*,0.5, $CHCl_3$). Reported (7): m.p. 105–108° and $[\alpha]_D$ +84° (*c*,0.95, $CHCl_3$).

Synthesis of XIII and XVI from VIII. 2,4,6-Tri-O-benzoyl-3-O-(p-tolylsulphonyl)-α-D-glucopyranosyl Chloride (XVIII)

Compound XVII was treated in a manner identical with that for VII in the preparation of X. The product XVIII was crystallized twice from ethanol (yield 82%) and had m.p. 154–156°, $[\alpha]_D^{22}$ +123.8° (*c*,1, $CHCl_3$).

Anal. Calcd. for $C_{34}H_{29}O_{10}ClS$: C, 61.40; H, 4.36; Cl, 5.34; S, 4.82. Found: C, 61.45; H, 4.41; Cl, 6.36;[4] S, 5.04.

Compound XVIII was converted to XIII as described herein in the synthesis of XI from X. The product had m.p. 192° (decomp.) and $[\alpha]_D^{17}$ +32.8° (*c*,0.5, $CHCl_3$). A mixed melting point with XIII synthesized from XII was not depressed.

Anomerization of this product (XIII) to XVI, as described for the synthesis of XIV from XI, gave a product with m.p. 163–165° and $[\alpha]_D^{19}$ +102.4° (*c*,1, $CHCl_3$). Admixture with XVI, synthesized from XV, did not depress the melting point.

Resynthesis of VII from VIII

Compound VIII (0.15 g) was treated overnight in 2 ml pyridine with 0.15 g (benzylthio)carbonyl chloride and the solid obtained on pouring the reaction mixture into ice water was filtered off and recrystallized from acetone. The product (0.17 g), after 2 recrystallizations from ethanol, had m.p. 199–201° and did not depress the melting point of VII, obtained by benzoylation of VI.

ACKNOWLEDGMENTS

This investigation was carried out in part while one of us (J. J. W.) was supported by a Public Health Service Fellowship GPD-13,485-C1, from the Division of General Medical Sciences, Public Health Service. The same author would like to thank Professor M. Stacey for the use of his laboratories (1961–1963).

REFERENCES

1. B. Helferich and J. Becker. Ann. **440**, 1 (1924). K. Josephson. Ber. **62**, 313 (1929).
2. D. J. Bell. J. Chem. Soc. 1177 (1934). P. A. Levene and A. L. Raymond. J. Biol. Chem. **97**, 763 (1932).
3. J. J. Willard, J. Sadowski, and W. Vitale. Can. J. Chem. **41**, 1223 (1963).
4. J. J. Willard. Can. J. Chem. **40**, 2035 (1962).
5. A. K. Mitra, D. H. Ball, and L. Long, Jr. J. Org. Chem. **27**, 160 (1962).
6. M. L. Wolfrom, J. Bernsmann, and D. Horton. J. Org. Chem. **27**, 4505 (1962).
7. P. A. Levene and G. M. Meyer. J. Biol. Chem. **76**, 513 (1928).
8. R. K. Ness, H. G. Fletcher, and C. S. Hudson. J. Am. Chem. Soc. **72**, 2200 (1950).
9. E. Pacsu. Ber. **61**, 1508 (1928).
10. R. E. Reeves and L. W. Mazzeno. J. Am. Chem. Soc. **76**, 2219 (1954).
11. A. A. Frost and W. C. Schwemer. J. Am. Chem. Soc. **74**, 1268 (1952).
12. E. Fischer and B. Helferich. Ann. **383**, 68 (1911).

Can. J. Chem. Downloaded from www.nrcresearchpress.com by 210.87.254.5 on 09/05/12
For personal use only.

Can. J. Chem. Downloaded from www.nrcresearchpress.com by 210.87.254.40 on 09/05/12
For personal use only.

THE REACTIVITY OF THE CYCLIC POLYENES TOWARDS FREE RADICALS

I. COPOLYMERIZATION WITH ACRYLONITRILE

E. S. Ferdinandi, W. P. Garby, and D. G. L. James
Department of Chemistry, University of British Columbia, Vancouver, British Columbia

Received June 1, 1964

ABSTRACT

Cyclohexadiene-1,3 and bicyclo[2.2.1]heptadiene-2,5 each (B) copolymerize with acrylonitrile (A) in bulk at 60 °C in the presence of 0.01 *M* benzoyl peroxide. The copolymerization parameters for cyclohexadiene-1,3 are $r_A = 0.026 \pm 0.014$, $r_B = 0.20 \pm 0.01$, $Q_B = 1.76$, $e_B = -1.18$; for bicycloheptadiene the parameters are $r_A = 0.65 \pm 0.02$, $r_B = 0.47 \pm 0.08$, $Q_B = 0.27$, $e_B = 0.03$; limits of error are given at the 10% probability level. Cycloheptatriene and cyclooctatetraene inhibit the polymerization of acrylonitrile under similar conditions over a wide range of concentration. These results are discussed in terms of the general reactivity of the cyclic polyenes and of the behavior of structurally related monomers in polymerization, and a consistent pattern of reactivity emerges.

INTRODUCTION

The monocyclic polyenes have received little attention from investigators of free radical copolymerization and are not mentioned in Young's recent comprehensive review of copolymerization parameters (1). This neglect is surprising as the reactivity of the monocyclic polyenes toward the addition of free radicals is often of a high order. Table I includes some results from a recent kinetic study of the addition of the ethyl radical to various polyenes (2); both the rate constant at 60 °C, k_a, and the energy of activation, E_a, are given. In both respects each of the monocyclic polyenes is decidedly more reactive than the familiar monomer vinyl acetate (4).

TABLE I

Indices of reactivity among monomers

Monomer (B)	k_a at 60° (l mole^{-1} s^{-1})	Q_B	E_a (kcal/mole)	$1/r_A$	k_a/k_m at 60°
Cyclohexadiene-1,3	40 000	1.76	5.2±0.3	40.	4.7
Cycloheptatriene	15 000	—	6.4±0.2	—	4.2
Cyclooctatetraene	13 000	—	5.6±0.6	—	21.3
Bicycloheptadiene	5 200	0.27	7.0±0.1	1.5	>10.
Vinyl acetate	1 900	0.026	6.9±0.5	0.25	>10.

Constants k_a and k_m are respectively the rate constants for addition and metathesis of the ethyl radical with the monomers, and E_a the energy of activation for addition (2, 3); r_A is the reactivity ratio for copolymerization of the monomer (B) with acrylonitrile (A), and Q_B is the intrinsic reactivity of monomer B (this work and ref. 1), based upon the value $Q = 1.00$ for styrene.

Moreover the values of k_a are all greater than the propagation constants of typical vinyl monomers (5), which for vinyl acetate and acrylonitrile are 3 700 and 1 960 l mole^{-1} s^{-1} respectively at 60 °C. We suggest that the value of k_a provides an approximate index of the intrinsic reactivity of the monomer; certainly in Table I, k_a and Q are monotonically related.

It must be admitted that our present knowledge of the free radical polymerization of the monocyclic polyenes does not encourage us to regard these substances as reactive comonomers. Although cyclohexadiene-1,3, cycloheptatriene, and cyclooctatetraene all

homopolymerize under free radical conditions, the yields are generally poor and the reaction conditions severe. Cyclohexadiene-1,3 will polymerize thermally (6) in the range 100–155 °C but the yield of high polymer does not exceed 34%; azoisobutyronitrile seems to have almost no sensitizing action, and the degree of polymerization (7) does not exceed 15. The nature of the mechanism appears to be in dispute (8, 9). Cycloheptatriene requires rather severe conditions (10); a polymerization carried out in bulk with di-*tert*-butyl peroxide at 6 000 atm yielded only 3.6% of polymer in 6 h at 130 °C. Cyclooctatetraene can be polymerized by diluting the vapor heavily with steam, heating for a brief period above 500 °C, and quenching at a cool surface. A transparent film of polymer is deposited which does not soften at 250 °C and is resistant to solvents (11). Benzene is even more intractible; an attempt to copolymerize it with ethylene in the presence of di-*tert*-butyl peroxide under a pressure of 20 000 p.s.i. at 130 °C did indeed yield a copolymer containing a small proportion of benzene units, but it was established that these were incorporated entirely by a chain transfer process (12). As the polyethylene radical is probably the most reactive of the polymer radicals, it is likely that the free radical copolymerization of benzene by an addition mechanism is impossible.

Bicyclo[2.2.1]heptadiene-2,5 appears to stand in sharp contrast to the monocyclic polyenes in its reactivity towards free radical polymerization. Both the homopolymerization (13) and the copolymerization (14) of this monomer have been described, and neither requires other than mild conditions.

One purpose of this series is to question the apparent lack of reactivity of the monocyclic polyenes as monomers, and of this paper to demonstrate the reactivity of cyclohexadiene-1,3. Certainly cyclohexadiene-1,3, cycloheptatriene, and cyclooctatetraene are all reactive towards the addition of the ethyl radical. Relevant values of the rate constant, k_a, and the energy of activation, E_a, are given in Table I; in both respects each of the monocyclic polyenes is more reactive than bicycloheptadiene. However, in this study we are attempting to add the polyacrylonitrile radical to the polyene molecule and we must first establish whether values of k_a have any relevance. Certainly the ethyl radical should simulate the polyethylene radical quite well, accepting the usual assumption that the reactivity of a polymer radical is determined by the nature of the terminal unit. Denoting acrylonitrile by A and the polyene by B and the corresponding polymer radicals by A· and B· respectively we define the rate constants:

$$CH_3CH_2\cdot + B \rightarrow CH_3CH_2B\cdot \qquad (k_a)$$

$$2CH_3CH_2\cdot \rightarrow C_4H_{10} \qquad (k_c)$$

$$A\cdot + A \rightarrow A\cdot \qquad (k_{AA})$$

$$A\cdot + B \rightarrow B\cdot \qquad (k_{AB}) \qquad r_A = \frac{k_{AA}}{k_{AB}}$$

To discover whether the copropagation constant k_{AB} is simply related to k_a we have plotted log $(1/r_A)$ against 13 + log $(k_a/k_c^{\frac{1}{2}})$ for a series of monomers in Fig. 1. The values of r_A for the monomers named are taken from Young's tables (1); values of $k_a/k_c^{\frac{1}{2}}$ are given for the same or a closely related monomer (2, 4, 15, 16, 17), thus isoprene is represented by 2,3-dimethyl butadiene-1,3. A straight line of unit gradient has been drawn for reference. Correlation between k_{AB} and k_a is fairly good for the hydrocarbons, vinyl acetate and allyl alcohol; for those monomers polar effects are small and of similar magnitude for the two radicals. Wide deviations are observed for the two monomers with a nitrile substituent; electrostatic repulsion between the nitrile groups in the polyacrylonitrile radical and in the monomer molecule depresses $1/r_A$ in a manner not possible for

Can. J. Chem. Downloaded from www.nrcresearchpress.com by 210.87.254.40 on 09/05/12
For personal use only.

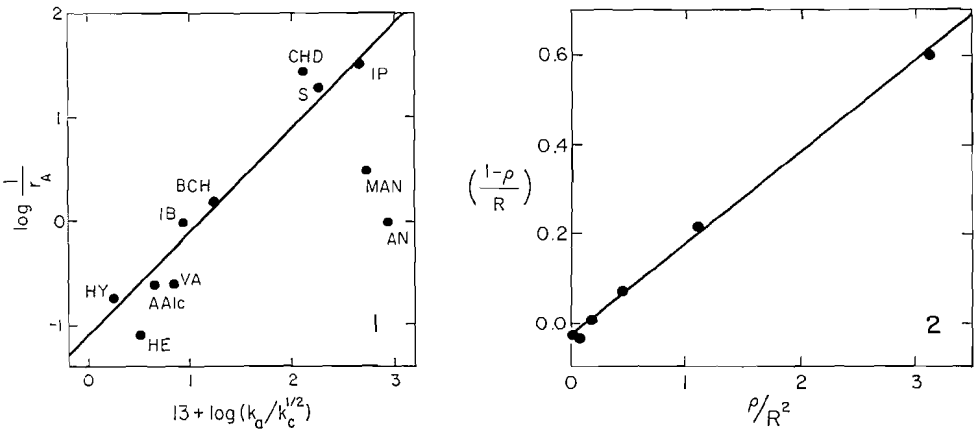

FIG. 1. Addition of the polyacrylonitrile radical (A·) and the ethyl radical to various monomers (B) at 60 °C; the reference line has unit gradient. Abbreviations: HY, hexyne-1; HE, hexene-1; AAlc, allyl alcohol; VA, vinyl acetate; IB, isobutene; BCH, bicycloheptadiene; CHD, cyclohexadiene-1,3; S, styrene; IP, isoprene; MAN, methacrylonitrile; AN, acrylonitrile.

FIG. 2. Fineman–Ross plot of $(1 - \rho)/R = r_B\rho/R^2 - r_A$ for acrylonitrile (A) and cyclohexadiene-1,3 (B) at 60°, yielding $r_A = 0.026 \pm 0.014$, $r_B = 0.20 \pm 0.01$.

the other monomers. Such deviations are to be expected from the difference in the electrostatic character of the two radicals, expressed by the values of e: acrylonitrile, 1.11 (18); ethylene, −0.21 (1), and should be observed with all monomers having a strongly electrophilic substituent in the vinyl group.

EXPERIMENTAL SECTION

All the monomers were commercial materials of the highest grade commonly obtainable. Each monomer was distilled through an efficient fractionating column in a stream of nitrogen; cyclooctatetraene was distilled at reduced pressure. The purity of fractions was tested by vapor phase chromatography; the monomers used were free from contaminants. Benzoyl peroxide, the White Label grade from the Eastman Co., was purified by three cycles of solution in chloroform and precipitation with methanol. The chloroform and methanol were of reagent grade.

All copolymerizations were attempted in the presence of 0.01 M benzoyl peroxide at 60.0 ± 0.5 °C (except where otherwise stated). The reaction vessels were pyrex tubes constricted for sealing off under vacuum. The sensitizer was introduced as an appropriate volume of 0.01 M benzoyl peroxide in chloroform, and the solvent removed under vacuum. The purified monomers were measured by using 5 ml graduated pipettes, and the mixture deaerated by five cycles of freezing, evacuating under vacuum, isolating, and melting. The reaction vessel was then sealed under vacuum, exposed to the reaction conditions for the required period, and quenched at −78 °C. The detailed procedure varied with the nature of the system, and will be described under the heading of the polyene, acrylonitrile being the comonomer unless explicitly stated.

Cyclohexadiene-1,3

The curvature of the copolymer composition line (Fig. 3) persuaded us to limit the yield of polymer to 1.5%; at this point the polymer usually began to precipitate. After the reaction the polymer was precipitated by methanol and proved to be almost insoluble in carbon tetrachloride, acetone, toluene, and petroleum ether. The only effective solvent found was N,N-dimethyl formamide, but this was unsuitable for purification as the copolymer composition was to be determined by nitrogen analysis. The polymer was washed exhaustively with methanol on a sintered glass filter crucible and dried for 3 days under vacuum over a 4-A molecular sieve. The composition of the polymer was determined with a Coleman Model 29 nitrogen analyzer. A 4% solution of the polymer in camphor ($K_f = 40$ deg kg/mole) did not depress the freezing point of camphor detectably; this and the general insolubility of the polymers indicate a fairly high degree of polymerization.

Bicycloheptadiene

The copolymer composition curve does not deviate much from the diagonal (Fig. 6), and conversions up to 5% were allowed; at this point the polymer usually began to precipitate. After the reaction, precipitation

Can. J. Chem. Downloaded from www.nrcresearchpress.com by 210.87.254.40 on 09/05/12
For personal use only.

was completed with methanol; the polymer was purified by solution in chloroform and reprecipitation with methanol, dried for 3 days under vacuum over a 4-A molecular sieve, and analyzed for nitrogen as above.

Cycloheptatriene and Cyclooctatetraene

Each of these polyenes inhibits the radical polymerization of acrylonitrile, and the details are more conveniently considered under the appropriate headings in the next section.

RESULTS AND DISCUSSION

The kinetics of the copolymerization of acrylonitrile (A) with the cyclic polyene (B) may be represented by four propagation steps and two reactivity ratios (19):

$$\begin{aligned} A\cdot + A &\rightarrow A\cdot \quad (k_{AA}) \qquad r_A = \frac{k_{AA}}{k_{AB}} \\ A\cdot + B &\rightarrow B\cdot \quad (k_{AB}) \\ B\cdot + B &\rightarrow B\cdot \quad (k_{BB}) \qquad r_B = \frac{k_{BB}}{k_{BA}} \\ B\cdot + A &\rightarrow A\cdot \quad (k_{BA}) \end{aligned}$$

The polymer radical is characterized by its terminal unit. Values of the reactivity ratios may be found from either of the conjugate plots of Fineman and Ross (20);

$$[1] \qquad (1 - \rho)/R = r_B\rho/R^2 - r_A$$

$$[2] \qquad R(\rho - 1)/\rho = r_A R^2/\rho - r_B,$$

where R is the molar ratio (A:B) of monomers in the feed and ρ is the molar ratio in the polymer. Such plots are shown in Figs. 2, 4, and 5. Alternatively, eqs. [1] and [2] may be

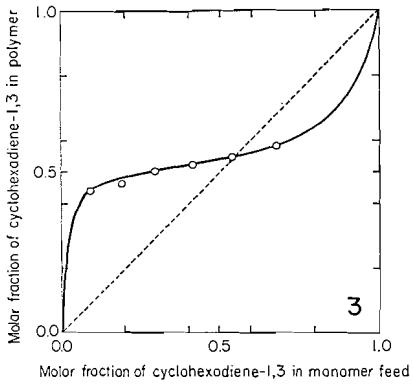

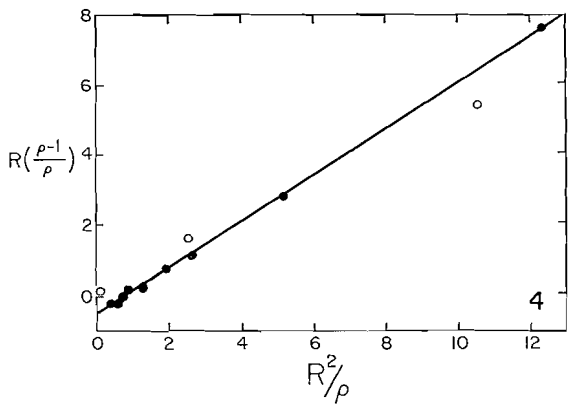

FIG. 3. Copolymer composition curve for acrylonitrile (A) and cyclohexadiene-1,3 (B) at 60°, drawn for $r_A = 0.026$, $r_B = 0.20$.

FIG. 4. Fineman–Ross plot of $R(\rho - 1)/\rho = r_A R^2/\rho - r_B$ for acrylonitrile (A) and bicycloheptadiene (B) at 60°, yielding $r_A = 0.65 \pm 0.02$, $r_B = 0.47 \pm 0.08$; ● this work, ○ ref. 14.

adapted to the method of Mayo and Lewis (21); concordant results were obtained in each case by the two methods. As each of the polyenes possesses a peculiar feature of interest, they will be discussed under separate headings.

Cyclohexadiene-1,3

Figure 2 shows the Fineman–Ross plot for the copolymerization of acrylonitrile (A) with cyclohexadiene-1,3 (B). The straight line drawn by the method of least squares yields the reactivity ratios:

$$r_A = 0.026 \pm 0.014; r_B = 0.205 \pm 0.011$$

Can. J. Chem. Downloaded from www.nrcresearchpress.com by 210.87.254.40 on 09/05/12
For personal use only.

(limits of error are given at the 10% probability level). The product $r_A r_B = 0.0053 \pm 0.0025$ indicates a considerable degree of alternation in this system. The parameters $Q_B = 1.76$ and $e_B = -1.18$ were calculated from $Q_A = 0.58$ and $e_A = 1.11$ for acrylonitrile (18). The value $r_A = 0.026$ reveals the high reactivity of cyclohexadiene-1,3 as a monomer in this system; this reactivity arises from the favorable conjunction of high values of Q_B and of $e_A - e_B$ (2.29). The positive deviation of the point for cyclohexadiene-1,3 from the reference line of Fig. 1 may be a natural result of the latter factor.

Cyclohexadiene-1,3 can homopolymerize by a radical mechanism (6–9) and this capacity is implicit in the value $r_B = 0.20$. Figure 3 gives the copolymer composition curve for this system; the experimental points fit the theoretical line drawn for $r_A = 0.026$, $r_B = 0.20$ quite well.

Barb (22) and Ham (23) have shown that in certain copolymerizations the reactivity of the polymer radical may be determined in part by nonterminal monomer units and that this phenomenon may be treated by characterizing a polymer radical by its terminal and its penultimate unit. This gives eight propagations steps and four reactivity ratios:

$$\begin{aligned}
&AA\cdot + A \rightarrow AA\cdot \quad (k_{AAA}) \qquad r_{AA} = \frac{k_{AAA}}{k_{AAB}}\\
&AA\cdot + B \rightarrow AB\cdot \quad (k_{AAB})\\
&BA\cdot + A \rightarrow AA\cdot \quad (k_{BAA}) \qquad r_{BA} = \frac{k_{BAA}}{k_{BAB}}\\
&BA\cdot + B \rightarrow AB\cdot \quad (k_{BAB})\\
&BB\cdot + B \rightarrow BB\cdot \quad (k_{BBB}) \qquad r_{BB} = \frac{k_{BBB}}{k_{BBA}}\\
&BB\cdot + A \rightarrow BA\cdot \quad (k_{BBA})\\
&AB\cdot + B \rightarrow BB\cdot \quad (k_{ABB}) \qquad r_{AB} = \frac{k_{ABB}}{k_{ABA}}\\
&AB\cdot + A \rightarrow BA\cdot \quad (k_{ABA})
\end{aligned}$$

This penultimate unit effect was observed (23) in the copolymerization of acrylonitrile (A) with styrene (B). Electrostatic repulsion between an acrylonitrile monomer molecule and an acrylonitrile unit in the penultimate position in the polymer radical is expected to make $r_{BA} > r_{AA}$ and $r_{AB} > r_{BB}$. Only the former of these inequalities will be detectable in a system for which the Fineman–Ross plot gives $r_B \gg r_A$; a good approximation is obtained by placing $r_{AB} = r_{BB} = r_B$. Moreover if r_A is very small it is reasonable to take r_{AA} as zero; then we obtain the relation:

$$[3] \qquad \rho = (1 + (1 + 1/r_{BA}R)^{-1})/(1 + r_B R).$$

To find whether a penultimate unit effect can be detected in the copolymerization of acrylonitrile with cyclohexadiene-1,3 we have compared the closeness of fit to the experimental points obtained from eq. [3] and a rearranged form of eq. [1]:

$$[1] \qquad \rho = (1 + r_A R)R/(r_B + R)$$

The values $r_A = 0.026$ and $r_B = 0.20$ were retained, and various values of r_{BA} tried. Crowding of the data was avoided by using axes of $(1/R, 1/\rho)$ and $(\log R, \log \rho)$. The curve drawn for the penultimate unit effect with $r_{BA} = 0.030$ (and $r_{AA} = 0$) gave the best fit; it was as good, but no better than, the fit obtained using eq. [1]. We conclude that there is no unequivocal evidence for a penultimate unit effect in this system.

Cycloheptatriene

Cycloheptatriene inhibited the radical polymerization of acrylonitrile, and thus stands

Can. J. Chem. Downloaded from www.nrcresearchpress.com by 210.87.254.40 on 09/05/12
For personal use only.

in complete contrast to cyclohexadiene-1,3. This is the more striking, since these two polyenes react very similarly towards the ethyl radical (k_a/k_m = 4.7 and 4.2 respectively at 60 °C) and should also possess similar values of *e*. The polymerization of acrylonitrile in the presence of 0.01 *M* benzoyl peroxide may be sensitized thermally at 60 °C, or photochemically at 0 °C; inhibition was observed in all such systems to which cycloheptatriene had been added, that is for the range from 2.3 to 74 mole % for the thermal sensitization, and from 2.3 to 22 mole % for the photochemical sensitization. Such systems did not become appreciably more viscous even after 24 h of reaction; this indicates a very efficient mode of inhibition able to prevent even the development of short chains. Evaporation yielded only a trace of white solid, which was identified as the sensitizer.

This evidence suggests rapid degradative chain transfer between the chain centers and cycloheptatriene. The mode of chain transfer must not form involatile materials, and so abstraction of a hydrogen atom from the cycloheptatriene molecule by the polyacrylonitrile radical or the benzoyloxy radical is indicated. Both radicals have a high electron affinity and the cycloheptatrienyl radical has the low ionization potential of 6.6 ± 0.1 eV (24); this conjunction should cause polar contributions to the transition state in metathesis to be particularly important and the transfer to be abnormally rapid. The low ionization potential of the cycloheptatrienyl radical is closely connected with the stability of the derived tropylium cation ($C_7H_7^+$) with its sextet of non-localized π-electrons; indeed both $C_7H_7^+ClO_4^-$ and $C_7H_7^+BF_4^-$ have been prepared in acetic acid solution by the action of oxygen on cycloheptatriene in the presence of the appropriate acid (25). The cyclohexadienyl radical does not yield a cation of comparable stability on ionization, and so there is no reason to suppose that cyclohexadiene-1,3 should share the peculiar reactivity of cycloheptatriene toward metathesis with the polyacrylonitrile or benzoyloxy radical.

Cyclooctatetraene

Cyclooctatetraene was found to inhibit the bulk polymerization of both acrylonitrile and 4-vinyl pyridine, sensitized by 0.02 *M* benzoyl peroxide at 60 °C. The induction period for acrylonitrile exceeded 45 h, whether cyclooctatetraene was present at a concentration of 14, 3.2, or 1.6 mole %, and during this period the color of the system changed gradually to deep amber. However, the induction period for 4-vinyl pyridine was only about 4 h in the presence of 4.5 or 2.2 mole % cyclooctatetraene; a similar but much more intense coloration developed, and the end of the induction period was marked by a sudden increase in viscosity. After a total period of 5 h polymer could be precipitated from this system with water, which, on drying, yielded a white, fibrous powder soluble in methanol. Analysis showed that all the cyclooctatetraene had been incorporated in this polymer.

Cyclooctatetraene has been shown to retard the γ-ray initiated polymerization (26) of vinyl acetate and of vinylpyrrolidone in bulk at 20 °C; even 0.1 mole % cyclooctatetraene lowered the yield of polymer very considerably. Similar retardation was observed with styrene and vinyl ethyl ether. The remarkable power of cyclooctatetraene to retard radiation-induced reactions parallels but exceeds that of benzene. Ellinger has suggested (26) that this power arises from the high electron affinity of the cyclooctatetraene molecule, which also governs the ease with which this substance captures thermal electrons in the vapor phase (27), undergoes reduction at the dropping mercury electrode (Table II and ref. 28), and polymerizes in the presence of sodium (29). Polar effects may well be expected to dominate the radical copolymerization of cyclooctatetraene.

Inhibition of the polymerization of acrylonitrile by cyclooctatetraene may proceed by

Can. J. Chem. Downloaded from www.nrcresearchpress.com by 210.87.254.40 on 09/05/12
For personal use only.

the addition of polyacrylonitrile radicals to cyclooctatetraene to form a radical which is unable to add to either acrylonitrile or cyclooctatetraene and which is terminated by mutual interaction. Certainly the structurally related α-cyanoisopropyl radical will add to cyclooctatetraene in bulk at 60 °C, and 1,4-radical addition then occurs to the exclusion of polymerization (30). A polymer radical terminated by a cyclooctatetraene unit would be highly electrophilic and would add extremely slowly to acrylonitrile ($e = 1.11$) but more rapidly to 4-vinyl pyridine ($e = -0.20$). Thus it is possible that some regeneration of chain centers occurs in the latter system, involving the incorporation of cyclooctatetraene units by a copropagation sequence and leading to a relatively short period of highly retarded polymerization rather than full induction.

The development of color during the induction period recalls the orange coloration observed when cyclooctatetraene is illuminated with 2 537 Å radiation, both in the vapor phase (31) and in solution in ether (32). The colored substance was provisionally identified as bicyclo[4.2.0]octatriene-2,4,7 (32), and appears to be the precursor of polycyclooctatetraene in the vapor-phase experiments (31). However the α-cyanoisopropyl radical adds to cyclooctatetraene yielding initially 5,8-bis-(α-cyanoisopropyl)-cyclooctatriene-1,3,6 without producing coloration, ring contraction, or polymerization (30). Possibly a substituted bicyclooctatriene is formed in our systems by a disproportionation reaction involving a polymer radical with a terminal cyclooctatetraene unit.

Bicyclo[2.2.1]heptadiene-2,5

Figures 4 and 5 are conjugate Fineman–Ross plots for the copolymerization of acrylonitrile (A) with bicycloheptadiene (B). Straight lines drawn by the method of least squares yield the reactivity ratios:

$$r_A = 0.65 \pm 0.02 \qquad r_B = 0.47 \pm 0.08 \qquad \text{(Fig. 4)}$$

$$r_A = 0.63 \pm 0.10 \qquad r_B = 0.44 \pm 0.08 \qquad \text{(Fig. 5)}$$

(limits of error are given at the 10% probability level).

From the first set we obtain $r_A r_B = 0.31 \pm 0.06$, which indicates only mild alternation in this system. The parameters $Q_B = 0.27$ and $e_B = 0.03$ were calculated from $Q_A = 0.58$ and $e_A = 1.11$ for acrylonitrile (18). Figure 6 gives the copolymer composition curve for this system; the experimental points fit the theoretical line drawn for $r_A = 0.65$, $r_B = 0.47$ quite well.

Our results are in partial agreement with those obtained at 50 °C by Zutty (14), from which he derived the ratios $r_A = 0.67$ and $r_B = 0.08$. His points are shown as open circles in Figs. 4, 5, and 6. From Fig. 6 it is apparent that only one of his analyses is in serious conflict with ours. Figures 4 and 5 show that Zutty's results complement our own, and therefore we prefer the values $r_A = 0.65$ and $r_B = 0.47$ obtained from Fig. 4.

CONCLUSIONS

The high intrinsic reactivity of cyclohexadiene-1,3 as a monomer is clear from the value $Q_B = 1.76$. However the labile nature of the α-methylenic hydrogen atoms leads to extensive chain transfer in the thermal homopolymerization (8, 9). A favorable polar effect is required to raise the ratio of propagation to transfer to produce high polymer in good yield and this is achieved in the system [acrylonitrile + cyclohexadiene-1,3] for which $e_A - e_B = 2.29$.

Cycloheptatriene and cyclooctatetraene also possess considerable intrinsic reactivity.

Can. J. Chem. Downloaded from www.nrcresearchpress.com by 210.87.254.40 on 09/05/12
For personal use only.

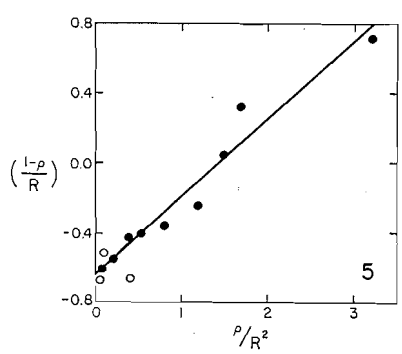

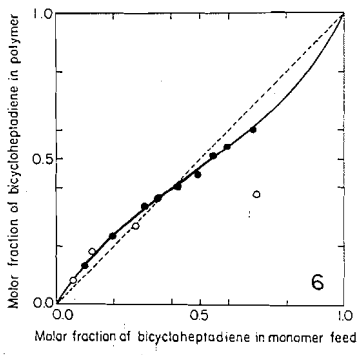

FIG. 5. Fineman–Ross plot of $(1 - \rho)/R = r_B\rho/R^2 - r_A$ for acrylonitrile (A) and bicycloheptadiene (B) at 60°, yielding $r_A = 0.63 \pm 0.10$, $r_B = 0.44 \pm 0.08$; ● this work, ○ ref. 14.

FIG. 6. Copolymer composition curve for acrylonitrile (A) and bicycloheptadiene (B) at 60°, drawn for $r_A = 0.65$, $r_B = 0.47$; ● this work, ○ ref. 14.

This is clear from the corresponding values of k_a and E_a in Table I, which are nearly as favorable as those for cyclohexadiene-1,3 and more favorable than those for bicycloheptadiene, a monomer which easily copolymerizes with acrylonitrile. The apparently anomalous behavior of cycloheptatriene and cyclooctatetraene towards acrylonitrile is due to the operation of an unfavorable polar effect in two distinct ways. This effect promotes degradative chain transfer in the case of cycloheptatriene and depresses the rates of the copropagation steps in the case of cyclooctatetraene. The slow copolymerization of cyclooctatetraene with 4-vinyl pyridine ($e = -0.20$) suggests the possibility of copolymerizing these polyenes with a monomer of high intrinsic reactivity and a low value of e, such as 2,3-dimethyl butadiene-1,3 ($Q = 5.86$, $e = -1.81$), and this is being pursued.

The values $Q = 1.76$, $e = -1.18$ for cyclohexadiene-1,3 seem reasonable when they are compared with the values $Q = 2.39$, $e = -1.05$ for butadiene-1,3 (Table II). The conjugated systems are closely similar, and the lack of terminal vinyl groups in cyclohexadiene-1,3 is likely to depress its intrinsic reactivity below that of butadiene-1,3. The values of e are consistent with the ready homopolymerization of both monomers with cationic initiators; indeed the homopolymerization of cyclohexadiene-1,3 is far more successful with boron trifluoride than with a radical sensitizer (33).

The values $Q = 0.27$, $e = 0.03$ for bicycloheptadiene are most appropriately compared with $Q = 0.019$, $e = -0.28$ for hexene-1. The enhanced intrinsic reactivity of bicycloheptadiene may arise from partial conjugation of the double bonds imposed by the geometry of the molecule.

TABLE II

Copolymerization parameters and some related characteristics

Monomer	Q	e	Half-wave potential (V)*	Most successful initiation
Cyclohexadiene-1,3	1.76	−1.18	No wave	Cationic
Cycloheptatriene	—	—	−1.96	?
Cyclooctatetraene	—	—	−1.28	Anionic
Bicycloheptadiene	0.27	+0.03	No wave	Radical
2,3-Dimethyl butadiene-1,3	5.86	−1.81	ca. −2.3	Cationic
Styrene	1.00	−0.80	−1.98	Cationic
Acrylonitrile	0.58	+1.11	−1.67	Anionic

*At 25 °C for 1 mM monomer in acetonitrile containing 0.1 M tetrabutyl ammonium iodide (2).

Can. J. Chem. Downloaded from www.nrcresearchpress.com by 210.87.254.40 on 09/05/12
For personal use only.

Table II reveals a pattern of reactivity among the monomers embracing values of e and of the polarographic half-wave potential and also the type of initiation to which the monomer responds best in homopolymerization.

ACKNOWLEDGMENT

The authors wish to thank the National Research Council of Canada for the financial support of this work.

REFERENCES

1. L. J. YOUNG. J. Polymer Sci. **54**, 411 (1961).
2. A. C. R. BROWN and D. G. L. JAMES. Proc. Chem. Soc. 81 (1962); and unpublished results.
3. A. C. R. BROWN and D. G. L. JAMES. Unpublished results.
4. D. G. L. JAMES and D. MACCALLUM. Proc. Chem. Soc. 259 (1961).
5. C. H. BAMFORD, W. G. BARB, A. D. JENKINS, and P. F. ONYON. The kinetics of vinyl polymerization by radical mechanisms. Butterworths, London. 1958. p. 92.
6. S. F. NAUMOVA and L. G. TSYKALO. Vyoskomolekul. Soedin. **3**, 1031 (1961).
7. B. V. EROFEEV, S. F. NAUMOVA, and L. G. TSYKALO. Sb. Nauchn. Rabot Akad. Nauk Belorussk. SSR Inst. Fiz. Organ. Khim. **9**, 71 (1961).
8. P. S. SHANTAROVICH and I. A. SHLYAPNIKOVA. Vysokomolekul. Soedin. **3**, 1364 (1961).
9. B. V. EROFEEV, S. F. NAUMOVA, and L. G. TSYKALO. Dokl. Akad. Nauk SSSR, **147**, 106 (1962).
10. A. M. POLYAKOVA, A. F. PLATE, M. A. PYRANISHNIKOVA, and N. A. LIPATNIKOV. Neftekhimiya, **1**, 521 (1961).
11. M. J. MAUE. U. S. Patent No. 2,758,989 (August 14, 1956).
12. G. A. MORTIMER and L. C. ARNOLD. J. Am. Chem. Soc. **84**, 4986 (1962).
13. R. H. WILEY, W. H. RIVERA, T. H. CRAWFORD, and N. F. BRAY. J. Polymer Sci. **61**, S38 (1962).
14. N. L. ZUTTY. J. Polymer Sci. Part A, **1**, 2231 (1963).
15. D. G. L. JAMES and E. W. R. STEACIE. Proc. Roy. Soc. Ser. A, **244**, 297 (1958).
16. A. C. R. BROWN and D. G. L. JAMES. Can. J. Chem. **40**, 796 (1962).
17. D. G. L. JAMES and TAKESHI OGAWA. Unpublished results.
18. B. R. THOMPSON and R. H. RAINES. J. Polymer Sci. **41**, 265 (1959).
19. C. H. BAMFORD, W. G. BARB, A. D. JENKINS, and P. F. ONYON. The kinetics of vinyl polymerization by radical mechanisms. Butterworths, London. 1958. p. 149.
20. M. A. FINEMAN and S. D. ROSS. J. Polymer Sci. **5**, 259 (1950).
21. F. R. MAYO and F. M. LEWIS. J. Am. Chem. Soc. **66**, 1594 (1944).
22. W. G. BARB. J. Polymer Sci. **11**, 117 (1953); **18**, 310 (1955).
23. G. E. HAM. J. Polymer Sci. **14**, 87 (1954).
24. A. G. HARRISON, L. R. HONNEN, H. J. DAUBEN, JR., and F. P. LOSSING. J. Am. Chem. Soc. **82**, 5593 (1960).
25. A. P. TER BORG, R. VAN HELDEN, and A. F. BICKEL. Rec. Trav. Chim. **81**, 164 (1962).
26. L. P. ELLINGER. J. Appl. Chem. London, **12**, 387 (1962).
27. L. E. LOVELOCK. Nature, **189**, 729 (1961).
28. T. J. KATZ, W. H. REINMUTH, and D. E. SMITH. J. Am. Chem. Soc. **84**, 802 (1962).
29. S. N. USHAKOV and O. F. SOLOMON. Zh. Prikl. Khim. **27**, 959 (1954).
30. J. L. KICE and T. S. CANTRELL. J. Am. Chem. Soc. **85**, 2298 (1963).
31. H. YAMAZAKI. Bull. Chem. Soc. Japan, **31**, 677 (1958).
32. G. J. FONKEN. Chem. Ind. London, 1625 (1963).
33. D. A. FREY, M. HASEGAWA, and C. S. MARVEL. J. Polymer Sci. Part A, **1**, 2057 (1963).

Can. J. Chem. Downloaded from www.nrcresearchpress.com by 210.87.254.40 on 09/05/12
For personal use only.

RAMAN SPECTRA AND VIBRATIONAL ASSIGNMENTS FOR TWO FORMS OF TETRAPHENYL CYCLOTETRAPHOSPHINE

R. L. AMSTER, W. A. HENDERSON, AND N. B. COLTHUP
Central Research Laboratories, American Cyanamid Company, Stamford, Connecticut
Received Aug. 23, 1963

ABSTRACT

Raman spectra have been obtained and vibrational assignments made for two isomeric compounds of tetraphenyl cyclotetraphosphine. The asymmetric P_4 ring stretch has been identified near 500 cm^{-1} while the symmetric ring-breathing vibration most probably mixes with other low-frequency motions and is not explicitly assigned.

There are reported in the literature two solid phosphorus compounds of the empirical formula C_6H_5P (1). Cryoscopic, mass spectrometric, and nuclear magnetic resonance (n.m.r.) data (1) have shown both compounds to be stereoisomeric forms of tetraphenyl cyclotetraphosphine, $(C_6H_5P)_4$. As part of an overall study of the vibrational frequencies of cyclotetraphosphines, Raman spectra of both compounds in the solid state were obtained and vibrational assignments made.

EXPERIMENTAL

Both compounds studied in this investigation were prepared as described by Henderson, Epstein, and Seichter (1). Compound A has a melting point of 153–155 °C while compound B melts at 195–199 °C. Each of the two crystalline compounds, approximately 1 g in quantity, was placed into a Raman tube which was then sealed under an atmosphere of dry nitrogen to prevent oxide formation.

Raman spectra, excited by Hg 4 358 Å were obtained using the instrument previously described (2). Spectra were recorded on Kodak IIa-O plates with exposure times ranging from 2 to 4 h. Tracings of the photographed spectra were made using a Leeds and Northrup microphotometer. Frequency values were obtained using helium calibration.

The observed frequencies for compounds A and B are listed in Table I along with relative intensities and vibrational assignments. Measured Raman shifts are estimated to be accurate within 5 cm^{-1}.

DISCUSSION

There is no literature available concerning the molecular symmetry of tetraphenyl cyclotetraphosphine. However, it is assumed in this study, as it was in the discussion of tetraalkyl cyclotetraphosphines (3), that the P_4 ring is puckered and by itself possesses D_{2d} symmetry. Addition of the four phenyl groups to the P_4 ring can yield a molecule of D_{2d} or lower symmetry depending upon the relative orientation of phenyl groups, and since several orientations appear reasonable, one might expect the existence of more than one form of tetraphenyl cyclotetraphosphine.

Interaction of the four phenyl groups attached to the P_4 ring can lead to the appearance of more than one Raman band corresponding to each vibration of a single monosubstituted phenyl group. However, since such band multiplicity does not occur for the alkyl vibrations in the tetraalkyl tetraphosphines (3) it is not expected to occur in the related phenyl compound. In addition to the often characterized modes of a monosubstituted benzene ring (4), there are in ϕ_4P_4 six vibrations corresponding to internal motions of the P_4 ring, and additional modes associated with deformations of the C—P—P angles. With respect to the six P_4 ring vibrations, the assumption of D_{2d} symmetry leads to a distribution of the motions as follows: a ring stretch and a ring deformation in class A_1, a class B_1 ring stretch and class B_2 ring deformation, a doubly degenerate ring deformation lying in

Can. J. Chem. Downloaded from www.nrcresearchpress.com by 210.87.254.5 on 09/05/12
For personal use only.

TABLE I

Vibrational frequencies and assignments for two forms of tetraphenyl cyclotetraphosphines

ϕ_4P_4 (A)	Relative intensity	Assignment*	ϕ_4P_4 (B)	Relative intensity
			3 192	1/2
			3 141	1/2
3 047	1	C—H stretch	3 052	1
1 578	8	C—C stretch (*k*, *l*)	1 581	9
1 479	1	C—C stretch (*m*)	1 480	1
1 431	1/2	C—C stretch (*n*)	1 436	1/2
			1 380	1/2
1 316	1/2	C—C stretch (*o*)	1 330	1/2
1 261	1/2	C—H in-plane bend (*e*)	1 266	1/2
1 190	1	C—H in-plane bend (*a*)	1 184	1
1 158	1	C—H in-plane bend (*c*)	1 160	1
1 087	5	X-sensitive (*q*)	1 095	5
1 073	Shoulder	C—H in-plane bend (*d*)	1 081	
1 024	5	C—H in-plane bend (*b*)	1 027	5
997	10	Ring (*p*)	1 001	10
		C—H out-of-plane bend (*j*)	988	Shoulder
		C—H out-of-plane bend (*h*)	965	1/2
946	1/2			
			936	1/2
925	1/2	C—H out-of-plane bend (*i*)	915	1/2
905	1/2			
		C—H out-of-plane bend (*g*)	867	1/2
736	1	C—H out-of-plane bend (*f*)	745	1
687	1	X-sensitive (*r*)	693	1
618	1	C—C—C bend (*s*)	620	1
510	1		512	Shoulder
488	3	Asymmetric P—P stretch	501	6
444	6	Symmetric P—P stretch + *t*	440	6
422	2	+ *y* phenyl vibrations	427	5
396	1		398	2
370	1		366	1/2
			329	1/2
304	1	P_4 ring + C—P—P deformations		
277	1	+ substituent-sensitive	289	1
		phenyl vibrations	253	1/2
215	1		219	4
178	1		197	1

*The description of the phenyl modes follows the notation of Whiffen (4).

class *E*. As mentioned previously, the overall molecular symmetry of ϕ_4P_4 may be lower than D_{2d}, thus necessitating a reclassification of these P_4 ring vibrations.

Reference to vibrational assignments for tetraalkyl cyclotetraphosphines (3) and ϕPH_2 (5) leads us to expect four substituent-sensitive phenyl vibrations and all P_4 ring vibrations to fall below 550 cm^{-1}; this region will also contain the low frequency C—P—P deformations (3). One would thus predict some mixing of the substituent-sensitive phenyl, P_4 ring, and C—P—P deformation vibrations in the low frequency normal modes. A simple characterization of most modes in this frequency range, therefore, cannot be made.

VIBRATIONAL ASSIGNMENTS

In the observed spectra, we have not been able to detect any splitting of vibrational bands as a result of crystal symmetry. Therefore, assignments for the crystalline state have been made on the basis of the normal vibrations of the isolated molecule. In the discussion below, the assignments are given together in the order A, B.

The substituent-insensitive phenyl modes are readily assigned for both A and B by comparison with vibrational assignments to ϕPH_2 (5) and other monosubstituted

Can. J. Chem. Downloaded from www.nrcresearchpress.com by 210.87.254.5 on 09/05/12
For personal use only.

benzenes (4). Raman bands at 1 087 and 1 095 cm^{-1} and 687 and 693 cm^{-1} are assigned, by comparison with ϕPH_2, to the substituent-sensitive phenyl modes *q* and *r*. The similarity in frequencies for *q* and *r* in ϕ_4P_4, *A* and *B*, and ϕPH_2 indicates that in the cyclotetraphosphines these normal modes receive little contribution from P_4 ring vibration. Furthermore, absence of more than one Raman band corresponding to each of these substituent-sensitive and substituent-insensitive vibrations points up a lack of significant interaction among phenyl groups.

Four bands are observed between 390 cm^{-1} and 505 cm^{-1}. In the tetraalkyl cyclotetraphosphines (2) the asymmetric P_4 ring stretch lies between 465 cm^{-1} and 490 cm^{-1} and the symmetric P_4 stretch lies between 390 cm^{-1} and 410 cm^{-1}. Furthermore, the substituent-sensitive modes *y* and *t* are observed in ϕPH_2 at 445 cm^{-1} and 392 cm^{-1}, respectively. The ϕ_4P_4 band at 488 and 501 cm^{-1} is, thus, most reasonably assigned to the asymmetric P_4 stretch. However, some mixing is expected to occur between the simple symmetric P_4 stretch and *y* and *t* vibrations. In addition, these modes most probably mix with the lower frequency P_4 ring and C—P—P deformations. Hence, it would be unrealistic to make an assignment to each of three bands between 390 cm^{-1} and 445 cm^{-1} in terms of a simple vibration. They are, therefore, ascribed as a group to the ν^s P—P, *t* and *y* vibrational modes. One might describe the (444, 440 cm^{-1}) band, the most intense of the group, as predominantly ν^s P—P since the P—P stretching vibrations give rise to the most intense bands in the 300–600 cm^{-1} region in the tetraalkyl cyclotetraphosphines.

The remaining bands below 400 cm^{-1} are assigned as a group to normal modes described as combinations of the simple substituent-sensitive phenyl vibrations and P_4 and C—P—P bending modes.

The similarity between the Raman spectra of compounds A and B, and their resemblance to the low-frequency Raman spectra of the tetraalkyl cyclotetraphosphines (3) support previous conclusions that both compounds are tetraphenyl cyclotetraphosphines.

REFERENCES

1. W. A. HENDERSON, M. EPSTEIN, and F. S. SEICHTER. J. Am. Chem. Soc. **85**, 2462 (1963).
2. M. C. TOBIN. J. Opt. Soc. Am. **49**, 850 (1959).
3. R. L. AMSTER, N. B. COLTHUP, and W. A. HENDERSON. Spectrochim. Acta, **19**, 1841 (1963).
4. D. H. WHIFFEN. J. Chem. Soc. 1350 (1956).
5. R. L. AMSTER and N. B. COLTHUP. Spectrochim. Acta, **19**, 1849 (1963).

Can. J. Chem. Downloaded from www.nrcresearchpress.com by 210.87.254.5 on 09/05/12
For personal use only.

Can. J. Chem. Downloaded from www.nrcresearchpress.com by 210.87.254.5 on 09/05/12
For personal use only.

ULTRAVIOLET ABSORPTION OF SUBSTITUTED PHENYL AND POLYCYCLIC ARYL CHALCONES

OWEN H. WHEELER, PETER H. GORE, MARCELINA SANTIAGO, AND ROSITA BAEZ
Department of Chemistry and Puerto Rico Nuclear Center, University of Puerto Rico, Mayaguez, Puerto Rico
Department of Chemistry, Brunel College, London

Received February 14, 1964

ABSTRACT

The ultraviolet and near-visible light absorption of a number of substituted *trans*-chalcones are reported.

Chalcones (I) possess a complex conjugate system since the carbonyl group is interposed between phenyl and styryl groups. *trans*-Chalcones generally show two main regions of selective ultraviolet absorption, one near 230 mμ (band II), the other beyond 300 mμ (band I) (see Table I). These two maxima were formerly attributed (1) to the partial benzoyl (PhCO—) and cinnamoyl (PhCH=CHCO—) chromophores, respectively, but the long wavelength band (band I) is now believed to involve the whole conjugate system (2). A third band, at 205 mμ, has been observed (3) and may be attributed to a modified E-band of the phenyl groups (cf. benzene λ_{max} 205 mμ, ε 6 300 (4)).

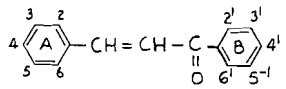

I

A so-called "middle" band, near 250 mμ, is shown by *cis*-chalcones (5) and by certain *trans*-chalcones (cf. compounds 5, 7, and 21, Table I) and this probably results from the partial (5) benzoyl (cf. PhCHO—, λ_{max} 248 mμ, ε 12 700 (6)) or benzoyl–vinyl (PhCOCH=CH—) chromophores (cf. PhCH=CHCOCH$_3$, λ_{max} 286 mμ, ε 25 000 (7)).

Szmant and Basso (2) have discussed the effect of para- and meta-substituents on the long wavelength band and have noted that a substituent produces a larger bathochromic displacement when it is located on ring A rather than on ring B (cf. Table II). In the case of band II, examination of the present data (Table I) and those reported in the literature (2, 3, 7–9) proved unsuccessful in arriving at general conclusions. The situation is complex since the singlet $\pi \rightarrow \pi^*$ transitions (K-bands) of most simple substituted aryl groups (contributing here as partial chromophores) fall within the region of absorption of band II (cf. styrene, λ_{max} 249 mμ, ε 10 000 (10); phenol, λ_{max} 270 mμ, ε 1 450 (11)).

ortho-Substituents are known to cause large hypsochromic effects in certain chalcones (2). Thus, negative values were shown for 2-chlorochalcones (8, 12) and for certain ortho-nitro (7) and mesityl derivatives (1*b*, 7). Similarly, 2-chloro-4′-methoxychalcone (compound 18) exhibits a $\Delta\lambda = -22$ mμ, compared to the calculated absorption (2). While one ortho-substituent in ring B may give a bathochromic displacement (e.g. 2′-hydroxychalcone, $\Delta\lambda = +17$ mμ), the introduction of a further ortho-substituent may give an overall hypsochromic effect (e.g. 2′-hydroxy-6′-methoxychalcone, $\Delta\lambda = -16$ mμ (9*b*)). A splitting of the K-band, with reduction of the intensity of absorption, has been observed in 2-methoxychalcone which exhibited λ_{max} 297 and 348 mμ, ε 15 400 and 14 800,

TABLE I

Absorption of substituted phenyl chalcones

No.	Substituents Ring A	Ring B	M.p.	Band II λ_{max} (ϵ_{max})	Band I[a] λ_{max} (ϵ_{max})	$\Delta\lambda$
1	—	—	56°	226(10 500)[c]	310(27 000)	+0
2	4-Me	4′-Br	104°	229(10 550)	320(28 200)	+10
3	4-Me	4′-OH	143°	230(7 700)	320(16 300) 386(6 400)	+10
4	4-Me	4′-OMe	95°	235(10 500)	298*(28 300) 316(31 300)	+6
5	4-OH	2′-OH	110°	222(15 200) 243(8 700)	285(19 600) 335(35 500)	+25
6	4-OMe	4′-Me	90°	236(11 100)	350(28 700)	+40
7	4-OMe	4′-Br	141°[d]	240(11 400)[d] 276(11 400)	291(10 200)[d] 344(28 400)	+34
8	4-OMe	4′-OMe	99°	236(13 000)[e]	350(32 000)	+40
9	4-OMe	3′-NO_2	167°[f]	244(23 400)[f]	352(23 000)[f]	+42
10	4-NO_2	4′-Me	133°	255(6 750)	318(31 700)[g]	+8
11	4-NMe_2	4′-Me	101°	266(16 100)	418(27 900)[h]	+108
12	4-NMe_2	4′-Br	153°	275(20 100)	326(3 100) 420(36 300)	+110
13	4-NMe_2	3′-OH	164°	268(26 900)	337(4 600) 420(31 400)	+110
14	3-OH	—	138°	246(11 300)	312(15 900)[i]	+2
15	3-OH	4′-Me	133°	260(8 000)	308(25 100)	−2
16	3-OH	4′-OMe	135°	282(11 800)	327(27 000)[j]	+17
17	3-OH	3′-OH	185°	252(11 700)	308(20 200)	−2
18	2-Cl	4′-OMe	72°	227(13 900)	299(15 300)	−11
19	2-OMe	4′-Br	62°	280(12 600)	293(13 950) 350(12 050)	+40
20	3,4-CH_2O_2	3′-OH	181°	258(13 800)	310(9 800) 357(23 900)	+47
21	3,4-CH_2O_2	2′-OH	134°	248(10 000) 284(5 700)	322(4 750)[k] 373(9 100)	+63
22	—	3′-OH	127°	227(10 950)	308(25 500)[l]	−2

[a]All data from the present work were obtained using 95% ethanol, unless otherwise stated. λ_{max} in mμ, asterisk denotes inflection; molar extinctions in parenthesis.
[b]$\Delta\lambda$ refers to K-band (band I).
[c]Reference 2 quotes 230(8 900), 312(26 700); ref. 6 quotes 205(15 800), 226(10 400), 308(25 400); ref. 9 quotes 228(9 800), 308(24 300).
[d]Reference 8 quotes m.p. 142.5°, and 265(15 500), 348.5(19 500).
[e]Reference 8 gives 231(14 400), 343(23 500).
[f]Reference 8 quotes m.p. 166–168°, and 242(26 600), 353(14 500).
[g]4-Nitrochalcone: 315.5(18 000) (ref. 8) or 316(28 000) (ref. 11).
[h]4-Dimethylaminochalcone: ~428(39 800) (ref. 12).
[i]Reference 2 reports maxima at 256 and 307 mμ.
[j]3,4′-Dihydroxychalcone: 242 and 321 mμ (ref. 8).
[k]2′-Hydroxy-3,4-dimethoxychalcone (ref. 9*a*) λ_{max} at 247, 264, and 371 mμ and inflection at 316 mμ.
[l]Reported λ_{max} at 315 mμ (ref. 9*b*).

TABLE II

Effects of para-substituents on the K-band of chalcone

Substituent	$\Delta\lambda$	Mean
Ring A		
—NMe_2	116 (12), 112,* 105 (1)	+111
—OMe	36 (7), 35,* 33 (8, 12)	+34
—NO_2	8 (8), 6 (12), 5.5 (7), 8*	+6.5
—Me	4,* 8*	+6
Ring B		
—NMe_2	84 (2), 74 (1)	+79
—OMe	17 (9*a*), 15,* 14 (9*a*) 11 (9*b*, 12)	+14
—NO_2	7 (7), 5 (2)	+6
—Me	−4,* 9,* 14 (9*a*)	+6

*Data from Table I.

Can. J. Chem. Downloaded from www.nrcresearchpress.com by 210.87.254.5 on 09/05/12
For personal use only.

respectively (8). A similar effect is noticed in 2-methoxy-4′-bromochalcone (compound 19) where three long wavelength bands are observed. Data recently obtained by Noyce and Jorgenson (8) on corresponding 2- and 4-substituted chalcones allow the calculation of the hypothetical angle of deformation, which may be responsible for the lowered intensity of the K-band of the 2-isomer. Assuming that the molar extinction of the K-band for the 2-isomer would be that of the 4-isomer (ϵ_0) in the absence of an angular deformation of one phenyl chromophore relative to the other, then the deformation angle (θ) in the 2-isomer may be calculated from the equation (13) $\cos^2\theta = \epsilon_a/\epsilon_0$, where ϵ_a is the value for the 2-isomer. The values so obtained are nearly equal for methyl-(35°), chloro-(36°), or methoxy-(39°) substituents, and are similar to those observed for 2,2′-disubstituted azoxybenzenes (14).

Polycyclic Chalcones

The K-bands of a series of chalcone derivatives with one of its aryl groups a naphthyl or phenanthryl residue are given in Table III. Substitution for phenyl in ring A results

TABLE III

Absorption of polycyclic aryl chalcones

Ar_1	Ar_2	Solvent	K-band	$\Delta\lambda$
Phenyl	Phenyl	EtOH	310(27 000)	—
1-Naphthyl	Phenyl	EtOH	352(14 700)	+42
2-Naphthyl	Phenyl	EtOH	328(24 300)	+18
1-Phenanthryl	Phenyl	EtOH	317[a](7 100)	+7
9-Phenanthryl	Phenyl	EtOH	352(13 200)	+42
Phenyl	2-Naphthyl	Dioxan	313(19 000)	+3
Phenyl	2-Phenanthryl	$CHCl_3$	316(20 600)	+6
Phenyl	3-Phenanthryl	$CHCl_3$	328(20 000)	+18

[a]Inflection.

in bathochromic shifts of the K-band maxima in increasing order of conjugating powers, phenyl < 1-phenanthryl < 2-naphthyl < 1-naphthyl < 9-phenanthryl, and in ring B, phenyl < 2-naphthyl < 2-phenanthryl < 3-phenanthryl. Significantly the effect is more pronounced in ring A than in ring B. Certain anthryl chalcones were also examined, but their K-bands correspond in wavelength with, and are submerged in, the absorption of the anthracene moiety.

EXPERIMENTAL

Chalcones

These were prepared by condensation of the appropriate acetophenones and benzaldehydes (15) and were recrystallized before use. Compounds 3, 13, 17, and 21 (Table I) were also purified by chromatography on alumina from benzene and hexane. Their melting points are recorded in Table I. The preparations of the polycyclic chalcones (Table III) will be published in connection with other work.

Spectra

The ultraviolet and near visible spectra were determined, unless otherwise stated, using solutions in 95% ethanol, which had been purified by refluxing with zinc dust and sodium hydroxide. The dioxan was purified by refluxing with, and distilling from, sodium, using only the center fraction. Chloroform was analytical grade. Measurements were made with a Bausch and Lomb spectronic 505 spectrophotometer with 1.0 cm cells. Concentrations were such as to give optical densities of 0.5–0.8. Several spectra were rechecked on a Beckman DU spectrophotometer.

ACKNOWLEDGMENTS

The authors are grateful to Dr. J. R. Gwilt for a gift of chalcones and the National Science Foundation for an Undergraduate Research Participant grant. The Puerto Rico

Can. J. Chem. Downloaded from www.nrcresearchpress.com by 210.87.254.5 on 09/05/12
For personal use only.

Nuclear Center is operated by the University of Puerto Rico for the U.S. Atomic Energy Commission.

REFERENCES

1. (*a*) E. R. KATZENELLENBOGEN and G. E. K. BRANCH. J. Am. Chem. Soc. **69**, 1615 (1947). (*b*) L. F. FERGUSON and R. P. BARNES. J. Am. Chem. Soc. **70**, 3907 (1948).
2. H. H. SZMANT and A. J. BASSO. J. Am. Chem. Soc. **74**, 4397 (1952).
3. P. KLINKE and H. GIBIAN. Ber. **94**, 26 (1961).
4. K. BOWDEN and E. A. BRAUDE. J. Chem. Soc. 1068 (1952).
5. W. B. BLACK and R. E. LUTZ. J. Am. Chem. Soc. **77**, 5134 (1955).
6. E. A. BRAUDE. *In* Determination of organic structures by physical methods. Vol. I. *Edited by* E. A. Braude and F. C. Nachod. Academic Press, Inc., New York. 1955. p. 153.
7. F. TIMURA. J. Chem. Soc. Japan, **22**, 1846 (1956).
8. D. S. NOYCE and M. J. JORGENSON. J. Am. Chem. Soc. **84**, 4312 (1962).
9. (*a*) L. JURD and R. M. HOROWITZ. J. Org. Chem. **26**, 2561 (1961). (*b*) L. JURD. *In* Chemistry of flavanoid compounds. *Edited by* T. A. Geissman. The Pergamon Press, Ltd., London. 1962. p. 141.
10. O. H. WHEELER and C. B. COVARRUBIAS. Can. J. Chem. **40**, 1224 (1962).
11. L. DOUB and J. M. VANDENBELT. J. Am. Chem. Soc. **69**, 2714 (1947); **71**, 2414 (1949).
12. V. ALEXA. Buletinul Societatea de Chimie din România, A, **18**, 93 (1936).
13. H. B. KLEVENS and J. R. PLATT. J. Am. Chem. Soc. **71**, 1714 (1949).
14. P. H. GORE and O. H. WHEELER. J. Am. Chem. Soc. **78**, 2160 (1956).
15. W. DAVEY and J. R. GWILT. J. Chem. Soc. 1008 (1957).

Can. J. Chem. Downloaded from www.nrcresearchpress.com by 210.87.254.5 on 09/05/12
For personal use only.

Can. J. Chem. Downloaded from www.nrcresearchpress.com by 210.87.254.6 on 09/05/12
For personal use only.

LYCOPODIUM ALKALOIDS

XVI. ANNOTINE

W. A. Szarek, K. A. H. Adams, M. Curcumelli-Rodostamo, and D. B. MacLean
Department of Chemistry, McMaster University, Hamilton, Ontario

Received July 13, 1964

ABSTRACT

Annotine, $C_{16}H_{21}O_3N$, is shown to be pentacyclic and to contain a tertiary hydroxyl group, a lactone function, a tertiary nitrogen atom, and a dialkylated double bond. The position of the double bond and the tertiary hydroxyl group relative to the nitrogen atom has been established by Emde degradation of annotine methiodide. The presence of a lactone function is inferred from the reduction of annotine to dihydroannotinol, a hemiacetal, which reacts with 1 mole of ethyl mercaptan. The reduction of the lactone to a diol in an annotine derivative has been carried out. The chemical studies and the examination of annotine and its derivatives by modern instrumental methods allow the assignment of a plausible structure to the alkaloid.

Annotine, $C_{16}H_{21}O_3N$ (I), was first isolated from *L. annotinum* of Canadian origin by Manske and Marion and designated alkaloid L.11 (1). It was subsequently found in European plant material by Bertho and Stoll (2), who assigned the name annotine to it, and by Achmatowicz and Rodewald (3). An examination of the functional groups of annotine was carried out by Perry and MacLean (4), who concluded that the alkaloid contained a tertiary nitrogen atom, a double bond, a hydroxyl group, a ketonic carbonyl group, and a third inert oxygen function, which they ascribed to an ether linkage other than an epoxide.

In this communication we wish to report further studies on annotine by chemical and modern instrumental methods. These studies have shown that annotine is a lactone and have thereby established the nature of the third inert oxygen function. They have also allowed an assignment of the position of the double bond and the hydroxyl group in the molecule relative to the nitrogen atom and have led to the development of a plausible structure for the molecule.

Nuclear magnetic resonance (n.m.r.) spectroscopy has been used extensively in this study and has provided useful information about the functional groups and their environment in annotine and its derivatives. The n.m.r. spectrum of annotine has a quartet centered at $\tau = 4.04$ ($J = 10$ c.p.s.) with an intensity corresponding to two protons. This band indicates the presence of the grouping $\begin{matrix} H \\ \diagdown \\ \quad C{=}C \\ \diagup \\ \quad \end{matrix}\!\!\begin{matrix} \quad \\ \diagup \\ H \\ \diagdown \\ \quad \end{matrix}$ and is an example of an intermediate case of an AB spectrum in which the chemical shift between the two nuclei is comparable to the coupling constant between them (5). It was possible to resolve each component of the quartet into a triplet in each of which the splitting was the same. These data indicate the presence of a methylene group adjacent to the double bond, as in the grouping $\begin{matrix} \quad \\ \diagup \\ C \\ \diagdown \\ \quad \end{matrix}\!\!-CH{=}CH-CH_2-$.

A singlet occurring at $\tau = 8.57$ with an intensity corresponding to three protons points to the presence of a methyl group attached to a quaternary carbon. The low τ value of the C—methyl group in this system can possibly be explained by the deshielding effect of a carbonyl group beta to the methyl protons. It has been postulated that the deshielding effect in such a system is due to the anisotropy of the carbonyl group and that the deshielding effect will be greatest if the methyl group lies in the plane of the carbonyl group (5).

The n.m.r. spectrum also shows a band at $\tau = 5.83$, corresponding in intensity to two protons. This band in more concentrated solution appears as two overlapping peaks, which are tentatively assigned to the groupings $>CH-O-C(=O)<$ and $>C-OH$. It should be pointed out at this stage that the hydroxyl group in annotine is believed to be tertiary, since the substance is recovered unchanged after treatment with chromic acid or by the Oppenauer method. Other peaks in the spectrum are more difficult to assign, but one might suggest that the peak at $\tau = 6.63$, corresponding to two protons, may be attributed to a methylene group sandwiched between the double bond and the nitrogen atom, while the peak at 7.32 is due to a second methylene group adjacent to nitrogen but attached to a saturated center.

In an effort to check the assignments above, we examined the n.m.r. spectrum of dihydroannotine (II). We found that the preparatory procedure reported previously (4) gave a product of uncertain composition, but that catalytic hydrogenation over platinum in the presence of a trace of hydrochloric acid gave a pure dihydroannotine in high yield. Its n.m.r. spectrum lacks the ethylenic absorption of annotine but retains the $>C-CH_3$ absorption at $\tau = 8.56$. The proton of the hydroxyl group probably gives rise to the sharp band observed in the spectrum at $\tau = 6.82$. A band of intensity equal to one proton at $\tau = 5.74$ has been assigned again to the grouping $>CH-O-C(=O)<$. The half-band width of 9.9 c.p.s. for this band indicates coupling to three or four protons.

The above n.m.r. data establish that the double bond is dialkylated and joined to a methylene group on one side and probably to a quaternary center on the other side. They show that the methyl group is attached to a quaternary carbon center and that it may be beta to a carbonyl function. The presence of the peak centered at 5.83 in annotine and 5.74 in the dihydro compound implies the presence of a hydrogen attached to a carbon carrying an ester function. This observation provided the first clue that annotine might be a lactone. The following structural sequences are suggested from the n.m.r. data:

$$>C-CH=CH-CH_2-N< \quad \text{and} \quad \begin{array}{l} \\ HC-O-C(=O)-C-CH_3 \\ \\ \end{array}$$

The experiments reported below support both of these structural assignments.

The sequence $>C-CH=CH-CH_2-N<$ suggested by the n.m.r. spectra of annotine and dihydroannotine has been confirmed and extended by degradation of annotine methiodide. Annotine readily forms a methiodide, and attempts were made to degrade it by several methods. An attempted elimination with potassium tertiary butoxide yielded an oil which resisted all attempts at crystallization. Attempts to prepare crystalline salts were also unsuccessful. Attention was therefore turned to the Emde degradation. Although annotine methiodide did not react with sodium amalgam, it readily reacted with hydrogen over Adams' catalyst to form a crystalline saturated compound III, $C_{17}H_{27}O_3N$.

The infrared spectrum of III shows absorption at 3485 cm^{-1} in the hydroxyl region and strong absorption at 1712 cm^{-1} in the carbonyl region. The n.m.r. spectrum of III shows that no ethylenic protons are present. It does indicate, however, the presence of two C—methyl groups in the compound with absorptions at $\tau = 8.55$ and $\tau = 8.98$. The signal at $\tau = 8.55$ is a single sharp peak and corresponds to the original $>C-CH_3$

Can. J. Chem. Downloaded from www.nrcresearchpress.com by 210.87.254.6 on 09/05/12
For personal use only.

group in the alkaloid. The band at $\tau = 8.98$ is quite broad, indicating coupling with neighboring protons. This band is assigned to a methyl group at the end of an alkyl chain formed by cleavage of a C—N bond in the hydrogenolysis reaction. A single sharp peak occurring at $\tau = 7.47$ with an intensity corresponding to three protons is assigned to the N—CH_3 group in the compound. A broad band at $\tau = 5.73$ is also present in the n.m.r. spectrum of compound III.

Significantly, dihydroannotine methiodide did not undergo an Emde degradation when treated with hydrogen over Adams' catalyst. The driving force for the Emde degradation of annotine must be the presence of the double bond, in a position β,γ to the nitrogen. In support of the latter hypothesis it should be noted that the pK_a values of annotine and dihydroannotine were found to be 7.5 and 8.61 respectively (4). These results substantiate the n.m.r. assignment.

The presence and the nature of an alkyl side chain in the Emde degradation product III were established by a modified Kuhn–Roth oxidation (6). The volatile carboxylic acids produced were separated and identified by gas chromatography of their methyl esters. Oxidation of the Emde degradation product III yielded acetic and propionic acids, a result that established the presence of an ethyl group in the compound. When the same oxidation procedure was applied to annotine itself, there was no carboxylic acid detected by gas chromatography. Considering the evidence for a $>C—CH_3$ group in the alkaloid, one would have expected acetic acid to have been produced by the oxidation—even if in low yield—because of the quaternary character of the $>C—CH_3$ group.

Detailed information on the structure of the ring opened in the Emde degradation was obtained from a study of the anhydro derivative of degradation product III. Attempts to dehydrate III with thionyl chloride or phosphoric acid were unsuccessful. It was dehydrated cleanly to compound IV, $C_{17}H_{23}O_2N$, by *p*-toluenesulphonic acid or 47% hydriodic acid. The infrared spectrum of compound IV shows carbonyl absorption at 1730 cm^{-1} but it does not show any hydroxyl absorption. The ultraviolet spectrum shows no absorption characteristic of an α,β-unsaturated carbonyl system.

Nuclear magnetic resonance spectroscopy provided key information about the anhydro compound IV. In the n.m.r. spectrum the $>N—CH_3$ group gives rise to a single sharp peak of intensity corresponding to three protons at $\tau = 7.79$, and a $>C—CH_3$ group appears as a singlet at $\tau = 8.76$. The band at $\tau = 8.96$, representing the methyl group at the end of the alkyl chain, appears as a distinct triplet, a result which establishes that the terminal methyl group is adjacent to a $—CH_2—$ group. This conclusion had been reached previously from the results of the modified Kuhn–Roth oxidation of the Emde product III. The n.m.r. spectrum also shows the ubiquitous broad band at $\tau = 5.63$. Of prime importance, however, is the triplet (splitting, 6.1 c.p.s.) of relative intensity 1:2:1 at $\tau = 4.77$ corresponding to one ethylenic proton. This band is assigned to the grouping $>C=CH—CH_2—$. Each component of the triplet could be resolved into a doublet (splitting, 0.9 c.p.s.). A grouping of the following type is compatible with this observation:

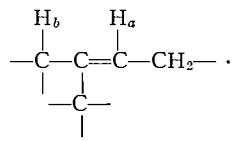

Can. J. Chem. Downloaded from www.nrcresearchpress.com by 210.87.254.6 on 09/05/12
For personal use only.

The doublet can be considered to arise from spin–spin coupling between H_a and H_b with coupling constant $J_{ab} = 0.9$ c.p.s. Usually, coupling only occurs across one, two, or three bonds, although it can and does extend further in systems with double bonds.

Catalytic reduction of the anhydro compound IV led to the formation of a non-crystalline compound V, $C_{17}H_{27}O_2N$. A modified Kuhn–Roth oxidation of compound IV yielded acetic and propionic acids, whereas the saturated compound V yielded butyric acid as well as propionic and acetic acids.

The results of the Kuhn–Roth oxidations in conjunction with information gleaned from the n.m.r. spectra of compounds derived from the Emde degradation indicate the presence of the system A in annotine:

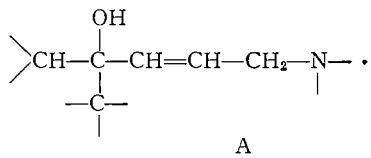

A

The results obtained by a study of the Emde degradation of annotine are summarized in Scheme I.

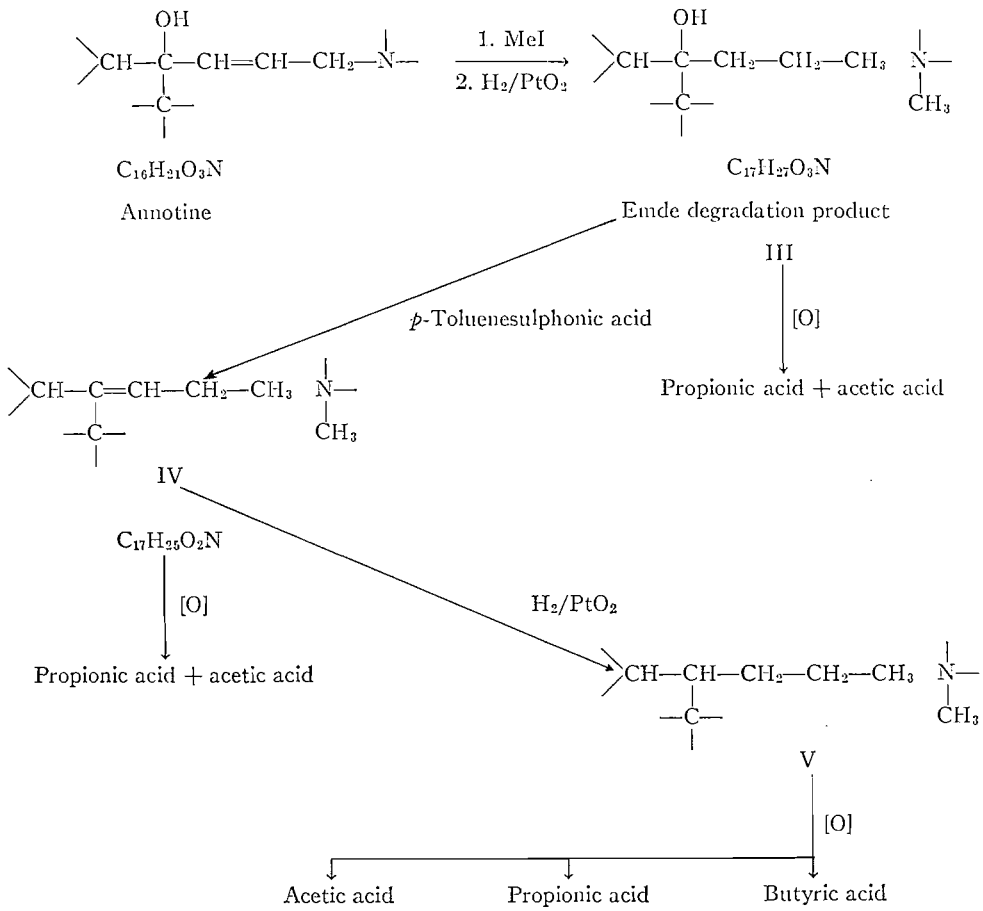

SCHEME I

Can. J. Chem. Downloaded from www.nrcresearchpress.com by 210.87.254.6 on 09/05/12
For personal use only.

Can. J. Chem. Downloaded from www.nrcresearchpress.com by 210.87.254.6 on 09/05/12
For personal use only.

It was intimated that annotine is a lactone and not a ketone, as Perry and MacLean believed (4). Their evidence for the ketonic character of the carbonyl group was based on two reactions. One of these was the treatment of annotine with sodium borohydride yielding annotinol, $C_{16}H_{23}O_3N$, which differs in composition from the starting compound by two hydrogens. Annotinol no longer had carbonyl absorption in its infrared spectrum and was converted to annotine by oxidation. The second reaction, with phenyl lithium, gave phenylannotine, $C_{22}H_{27}O_3N$. The analysis showed that a single phenyl group was incorporated and the compound showed no carbonyl absorption in its infrared spectrum. We have reexamined these two processes and have confirmed Perry and MacLean's observations. In addition, we independently established the molecular weight of phenylannotine by recording its mass spectrum, and have also examined its ultraviolet spectrum (which displayed only benzenoid absorption). There seemed little reason to doubt the presence of a ketonic carbonyl group.

There are a number of observations, however, at variance with their assignment. The n.m.r. spectra of annotine, dihydroannotine, and the products of Emde degradation all contain a peak at $\tau = 5.7 \pm 0.1$ of an intensity of one proton. This peak is lower than might be expected of a hydrogen in a cyclic ether, $\rangle CH—O—R$, but lies more in the region expected of a lactone or ester, $\rangle CH—O—C(=O)\langle$ (5). Secondly, we found that annotine was unreactive toward common carbonyl reagents. Thirdly, upon attempted Wolff–Kishner reduction, only a very small amount of annotine was recovered by chloroform extraction of the basic reaction mixture. It appears that annotine forms a water-soluble salt when it is heated at high temperatures with potassium hydroxide. In confirmation of this postulate, we found that annotine shows the same behavior when it is treated under conditions identical with those employed in the Wolff–Kishner reduction, but in the absence of hydrazine. Finally, a deuterium exchange study showed that there were no hydrogens in annotine that take part in enolate ion formation. At least one enolic hydrogen might be expected of a ketonic substance based on the structural framework common to the *Lycopodium* alkaloids of known structure. All the evidence noted above militates against the presence of a ketonic carbonyl group in annotine, but it does not directly support the presence of a lactone function.

There are two experiments which lend direct support to the lactone formulation for annotine. We found that dihydroannotinol, $C_{16}H_{25}O_3N$ (VI), formed by borohydride reduction of dihydroannotine, reacted with ethyl mercaptan in acid medium to form the substance $C_{18}H_{29}O_2NS$ (VII) in which a thioethyl group has apparently replaced a hydroxyl group of VI. A reaction of this nature can be readily interpreted on the basis of a lactone structure for annotine but not for a ketonic structure. Thus, the borohydride reduction of dihydroannotine would proceed to the hemiacetal, which, with ethyl mercaptan in the presence of acid, yields the product VII, as depicted by the partial formulae below:

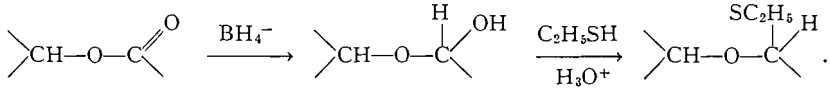

Dihydroannotinol reverted to dihydroannotine upon Oppenauer oxidation, indicating that the reaction was a simple reduction production.

In the n.m.r. spectrum of VII there is now a singlet at $\tau = 5.17$, presumably due to the hydrogen situated on the carbon carrying the thioethyl group. It is significant that the

peak present in other spectra at 5.7 ± 0.1 and assigned to the $>CH-OC<^{O}$ proton is no longer present; instead a broad peak corresponding to one proton is observed at $\tau = 6.19$. The methyl and methylene protons of the thioethyl group appear as a triplet at $\tau = 8.73$ and as a quartet centered at 7.35, respectively, but both underlie other absorption. The original C—methyl group has not altered appreciably in position, appearing at $\tau = 8.66$. Apparently the two electron-attracting groups attached to the beta carbon, —SR and —OR, have a deshielding effect equivalent to a carbonyl group in the beta position. The fact that two thioethyl groups were not introduced is another indication of the stability of this cyclic system. Other examples of its unreactivity toward ring opening are the resistance of the lactone to hydrolysis and the absence of carbonyl absorption in the infrared spectra of the hemiacetal, dihydroannotinol, and the hemiketal, phenylannotine.

In the second experiment, the lactone ring was successfully reduced to a diol with lithium aluminium hydride. Perry and MacLean reported that annotine was recovered unchanged upon treatment with $LiAlH_4$ in tetrahydrofuran and we have confirmed their findings. The failure of this reaction may be due to the formation, by interaction of $LiAlH_4$ with the hydroxyl group, of an insoluble salt which separates from the medium. Accordingly, we carried out the reaction on a derivative of annotine which no longer had the hydroxyl group. Compound IV was chosen because of its relative ease of preparation. Reaction of IV with $LiAlH_4$ yielded diol VIII, $C_{17}H_{29}O_2N$. The uptake of four hydrogen atoms in the conversion IV → VIII shows that the function which underwent reduction is a lactone rather than a ketone.

If the deductions regarding the position of the C—methyl group relative to the carbonyl carbon are correct, we may summarize these findings in expression B.

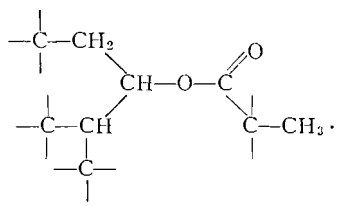

B

This formulation is compatible with the chemical and spectroscopic data presented before. Since the infrared absorption of the carbonyl group of annotine and its derivatives never appears above 1740 cm^{-1}, one must assume that the lactone is six-membered or larger.

All *Lycopodium* alkaloids of established structure with a single nitrogen atom conform in structure to lycopodine (6), with the exception of annotinine (7) and lyconnotine (8). The three alkaloids are closely related, having in common a hydrojulolidine system. In lyconnotine the hydrojulolidine system is not bridged as it is in annotinine and lycopodine. Since annotine occurs in the same plant as these alkaloids and since it may be deduced from its composition that it contains a combination of four carbocyclic and (or) heterocyclic rings other than its lactone ring, it seemed likely that it might conform in skeletal structure to either lycopodine or annotinine. However, attempted incorporation of expressions A or B into the skeletal framework of either alkaloid proved impossible. Other formulations based upon the hydrojulolidine framework were therefore considered, and

Can. J. Chem. Downloaded from www.nrcresearchpress.com by 210.87.254.6 on 09/05/12
For personal use only.

three of these (C, D, and E) are shown below along with the structures of annotinine, lycopodine, and lyconnotine.

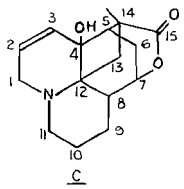

C

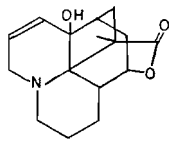

D

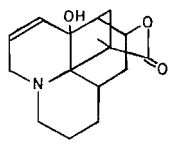

E

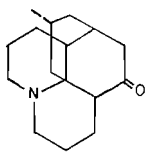

Lycopodine

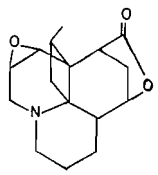

Annotinine

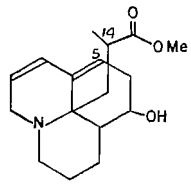

Lyconnotine X

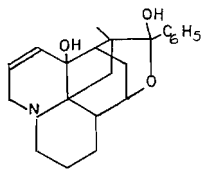

IX (a)

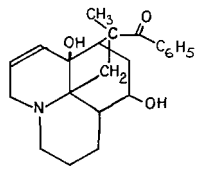

IX (b)

The placement of the bridge in C, D, and E follows from analogy to other alkaloids of this family. This placement is supported by the n.m.r. spectrum of IV which was discussed previously. The conclusions with respect to the structure of ring D are corroborated by investigation of the pyrolysis of phenylannotine. This compound, represented by structure IX*a* and IX*b*, was heated at 300° in the presence of zinc dust. The distillate collected during the pyrolysis was examined by gas–liquid partition chromatography. It was found to consist of two substances which, from their ultraviolet spectra, appeared to be phenones. The identity of the two compounds was established by comparison of their retention times with known phenones. They proved to be propiophenone and α-methylacrylophenone. In structure IX*b* the carbon atoms participating in the formation of α-methylacrylophenone are designated.

It is appropriate to consider here whether any of the structures C, D, or E proposed for annotine is favored over the others. The conclusion, discussed previously, that dihydroannotinol and phenylannotine exist in the hemiacetal and hemiketal forms, respectively, is evidence against structure E. Examination of molecular models, based on E, of dihydroannotinol and phenylannotine reveal that considerable strain is released by opening the hemiacetal and hemiketal rings, respectively. Thus if structure E were correct, one would expect dihydroannotinol to be a hydroxyaldehyde rather than a hemiacetal and phenylannotine to exist as the hydroxyketone, provided that reduction had ceased at this stage.

Structure C is favored over D and E on the basis of the following considerations. In all *Lycopodium* alkaloids of established structure there is a methylene group present at C_{13}. There is no recorded case of substitution at this site. Recently, structure X has been

Can. J. Chem. Downloaded from www.nrcresearchpress.com by 210.87.254.6 on 09/05/12
For personal use only.

proposed for lyconnotine, a new alkaloid isolated from *L. annotinum* (8). This structure bears a strikingly close relation to C. The carbon skeleton of annotine (as in C) is formally derived from X by formation of a bond between C_5 and C_{14}. Thus it may be that X and annotine are formed in the plant from a common precursor, or one may be the precursor of the other. The conversion of annotine to the carbon skeleton of X in vitro is readily visualized. Transformation of annotine to the hydroxymethyl ester (oxidation of the C_7 hydroxyl to the ketone followed by a β-elimination) leads to the carbon skeleton of X.

The configuration suggested for annotine in structure C is based upon the following considerations. Neither annotine itself nor dihydroannotine show the Bohlmann bands (9) characteristic of the *trans*-fused quinolizidine system in the 2900 cm^{-1} region of their infrared spectra. Anhydrotetrahydroannotine, obtained by dehydration of dihydroannotine over *p*-toluenesulfonic acid in xylene followed by reduction with hydrogen, does exhibit the Bohlmann bands. Reduction of the $\Delta^{3,4}$ double band would be expected to proceed from the least hindered side and to lead to the inverted configuration of C_4 and the *trans*-fused quinolizidine system. Unfortunately, neither the dehydration product nor the anhydrotetrahydroannotine were crystalline compounds and fully characterized, so that these conclusions must be accepted with some reservation. Furthermore, the hydroxyl group in dihydroannotine is intramolecularly hydrogen bonded, showing the hydroxyl absorption at 3545 cm^{-1} (which is not shifted upon dilution). This result is also compatible with the *cis*-fused quinolizidine system and is analogous to lycodoline (10), which carries a hydroxyl group in the same relative position in the hydrojulolidine system. The configuration at C_7 and C_8 follows from the stability of the lactone to hydrolysis and the stability of the hemiacetal and hemiketal forms of dihydroannotinol and phenylannotine, respectively.

EXPERIMENTAL

Apparatus and Methods

Melting points were recorded on a Kofler micro hot stage melting point apparatus and are uncorrected.

The infrared spectra were recorded on a Beckman Model IR-5 recording spectrophotometer in Nujol mull, unless otherwise stated.

Ultraviolet spectra were measured in methanol on a Perkin–Elmer Model 4000 spectracord.

The mass spectra were determined on a C.E.C.-103 mass spectrometer at an ionizing potential of 70 eV and an ionizing current of 50 μA. Samples were introduced through a heated inlet system maintained at 140 °C. The samples were run through the courtesy of Professor K. Biemann, Massachusetts Institute of Technology, Cambridge, Massachusetts.

The n.m.r. spectra were measured in deuterochloroform solutions with tetramethylsilane as an internal standard on a Varian V-4300 B high-resolution spectrometer at a frequency of 60 Mc/s.

Annotine (I)

Annotine was obtained from annotoxine which had crystallized from the mother liquors remaining after the separation of annotinine from the mixed alkaloids of *L. annotinum*. Annotoxine was readily separated into acrifoline and annotine by fractional crystallization of the hydrobromide salts.

Annotine was purified through the nitrate salt. The crude alkaloid was dissolved in the minimum volume of 2 *M* acetic acid and treated with a concentrated solution of sodium nitrate. The crystals of annotine nitrate were separated and dissolved in water, and the solution was basified with ammonia. Immediately after basification, the base precipitated in snowflake-like clusters. The base was separated by filtration and recrystallized from acetone, yielding rectangular plates which melted at 174.6–176 °C.

Calcd. for $C_{16}H_{21}O_3N$: C, 69.79; H, 7.69; N, 5.09. Found: C, 69.78; H, 7.83; N, 5.05.

The infrared spectrum in Nujol showed weak absorption at 3300 cm^{-1} in the hydroxyl region and a split peak at 1728 cm^{-1} and 1739 cm^{-1} in the carbonyl region. In chloroform solution there was absorption at 3500 cm^{-1} attributable to an intramolecularly bonded hydroxyl group, strong absorption at 1720–1730 cm^{-1} in the carbonyl region, and absorption at 1644 cm^{-1} which is assigned to unsaturation. There was also absorption at 1374 cm^{-1} attributable to a C—methyl group.

Preparation of Dihydroannotine (II)

A solution of annotine (0.050 g) in 30 ml of redistilled methanol containing 5 drops of concentrated

Can. J. Chem. Downloaded from www.nrcresearchpress.com by 210.87.254.6 on 09/05/12
For personal use only.

hydrochloric acid and 0.040 g of Adams' catalyst was subjected to a hydrogen pressure of 50 p.s.i.g. for 5 h. The solution was filtered free of catalyst and the organic solvent removed under reduced pressure. Water was added to the residue, and the resulting solution was basified with ammonia and extracted with chloroform. The chloroform extract was dried over anhydrous sodium sulphate and evaporated under reduced pressure to yield 0.050 g of product which crystallized immediately on contact with ether. Recrystallization from acetone–petroleum ether gave colorless crystals melting at 203–204 °C.

Calcd. for $C_{16}H_{23}O_3N$: C, 69.28; H, 8.36; N, 5.05; active H, 0.36 (1). Found: C, 69.55; H, 8.71; N, 5.23; active H, 0.37.

The infrared spectrum of this material in Nujol had hydroxyl absorption at 3510 cm^{-1}, carbonyl absorption at 1728 cm^{-1}, and strong absorption at 1118 cm^{-1}. In carbon disulphide solution there was hydroxyl absorption at 3545 cm^{-1} and carbonyl absorption at 1740 cm^{-1}.

Preparation of Annotine Methiodide

A solution of annotine (0.100 g) in 5 ml of acetone and 1 ml of methyl iodide was heated under reflux and within 5 min a crystalline methiodide began to separate. The mixture was heated under reflux for 15 min longer, cooled, and allowed to stand at room temperature for 1 h. Filtration gave 0.125 g (81%) of product melting at 235.5–237 °C (with decomposition). An additional 0.021 g (13%) of product was obtained from the filtrate on further treatment with methyl iodide in acetone. The methiodide was recrystallized first from methanol–acetone and then from water to yield colorless crystals melting at 236–237 °C (with darkening).

Calcd. for $C_{16}H_{21}O_3N \cdot CH_3I \cdot H_2O$: C, 46.90; H, 5.97; N, 3.22. Found: C, 47.24; H, 6.10; N, 3.74.

Achmatowicz and Rodewald (3) report a melting point of 317° (violent explosion) and Bertho and Stoll (2) a melting point of 236–237° for annotine methiodide.

Treatment of Annotine Methiodide with Hydrogen

A solution of annotine methiodide (0.200 g) in 50 ml of distilled water containing 0.200 g of Adams' catalyst was subjected to a hydrogen pressure of 50 p.s.i.g. for 5 h. The solution was filtered free of catalyst, basified with ammonia, and extracted several times with chloroform. The combined chloroform extract was dried over sodium sulphate and evaporated under reduced pressure to yield 0.111 g (79%) of product which crystallized on standing. Recrystallization from acetone–ether yielded rectangular plates melting at 221–222 °C.

Calcd. for $C_{17}H_{27}O_3N$: C, 69.59; H, 9.28; N, 4.77. Found: C, 69.10, 69.12; H, 9.24, 9.33; N, 4.77, 4.97.

The infrared spectrum of compound III showed absorption at 3485 cm^{-1} in the hydroxyl region and strong absorption at 1712 cm^{-1} in the carbonyl region.

Modified Kuhn–Roth Oxidation of Annotine

The oxidation procedure and analytical method described by Harrison *et al.* (6) were used. Oxidation of 0.057 g (0.21 mmole) of annotine did not yield any carboxylic acid detectable by vapor phase chromatography.

Modified Kuhn–Roth Oxidation of the Emde Degradation Product III

Oxidation of 0.018 g (0.062 mmole) of the Emde degradation product III yielded 0.079 meq (64%) of volatile carboxylic acids. Vapor phase chromatography of their methyl esters revealed the presence of methyl acetate and methyl propionate in the molar ratio of 78:22 respectively.

Dehydration of III

(a) With p-Toluenesulphonic Acid

Compound III (0.146 g) was heated under reflux with *p*-toluenesulphonic acid in *o*-xylene overnight. The reaction mixture was cooled, water added, and the *o*-xylene separated and washed with dilute acid. The combined aqueous layer and acid washings were washed with ether, basified with ammonia, and extracted several times with chloroform. The chloroform extract was dried over anhydrous sodium sulphate and evaporated under reduced pressure to yield a crystalline material (0.121 g). Recrystallization from acetone–petroleum ether gave crystals melting at 164 °C. The compound was purified for analysis by sublimation at 80° and 0.01 mm Hg, m.p. 164 °C.

Calcd. for $C_{17}H_{25}O_2N$: C, 74.14; H, 9.15. Found: C, 73.61; H, 9.12.

The infrared spectrum of compound IV showed carbonyl absorption at 1730 cm^{-1}, but no hydroxyl absorption. The ultraviolet spectrum showed no absorption characteristic of an α,β-unsaturated carbonyl system.

(b) With Hydriodic Acid

A solution of III (0.050 g) in 5 ml of 47% hydriodic acid was heated under reflux for 6 h. The reaction mixture was cooled and poured on ice. The aqueous solution was made alkaline with ammonia and extracted several times with chloroform. The combined chloroform extract was dried over anhydrous sodium sulphate and evaporated under reduced pressure to yield 0.040 g of a crystalline material whose infrared absorption spectrum was identical with that of the compound obtained from the treatment of compound III with *p*-toluenesulphonic acid.

Can. J. Chem. Downloaded from www.nrcresearchpress.com by 210.87.254.6 on 09/05/12
For personal use only.

Hydrogenation of IV

A solution of compound IV (0.110 g) in 40 ml of redistilled methanol containing 0.080 g of Adams' catalyst was subjected to a hydrogen pressure of 50 p.s.i.g. for 5 h. The solution was filtered free of catalyst and evaporated to dryness to yield a pale yellow oil which could not be induced to crystallize. This material was sublimed at 80 °C and 0.01 mm Hg to give a white amorphous solid.

Calcd. for $C_{17}H_{27}O_2N$: C, 73.60; H, 9.81; N, 5.05. Found: C, 73.45; H, 9.36; N, 5.22.

The infrared spectrum of compound V showed strong carbonyl absorption at 1730 cm^{-1}, but no hydroxyl absorption.

Modified Kuhn–Roth Oxidation of IV

Oxidation of 0.065 g (0.236 mmole) of IV yielded 0.40 meq (85%) of volatile carboxylic acids. Vapor phase chromatography of their methyl esters revealed the presence of methyl acetate and methyl propionate in the molar ratio of 66:34 respectively.

Modified Kuhn–Roth Oxidation of V

Oxidation of 0.060 g (0.216 mmole) of compound V yielded 0.31 meq (72%) of volatile carboxylic acids. Vapor phase chromatography of their methyl esters revealed the presence of methyl acetate, methyl propionate, and methyl butyrate in the molar ratio of 63:34:3 respectively.

Dihydroannotinol (VI)

A mixture of 0.060 g of sodium borohydride in 10 ml of ethanol and 0.200 g of dihydroannotine (II) in 10 ml of ethanol was refluxed for 4 h, cooled, and the excess borohydride destroyed by the addition of acetic acid. Most of the alcohol was removed by distillation, 50 ml of water was added, and the solution was basified with ammonia and extracted several times with chloroform. The combined chloroform extract was dried over anhydrous sodium sulphate and evaporated under reduced pressure to yield 0.190 g of a colorless oil which crystallized on standing. Recrystallization from chloroform gave crystals melting at 186–187 °C. The infrared spectrum of this compound (dihydroannotinol) showed hydroxyl absorption at 3526 cm^{-1}, but no carbonyl absorption. The mass spectrum showed a molecular ion peak at 279.

Calcd. for $C_{16}H_{25}O_3N$: active H, 0.72 (2). Found: active H, 0.74.

Oppenauer Oxidation of Dihydroannotinol

A solution of dihydroannotinol (0.050 g) and aluminium tertiary butoxide (0.300 g) in 5 ml of toluene and 1 ml of cyclohexanone was heated under reflux for 6 h, then poured into cold dilute hydrochloric acid, and the organic layer extracted several times with dilute acid. The aqueous extract was made alkaline with 10% sodium hydroxide solution and extracted several times with chloroform. The chloroform extract was dried over anhydrous sodium sulphate and evaporated under reduced pressure, leaving a white solid whose infrared spectrum was the same as that of dihydroannotine.

Treatment of Dihydroannotinol with Ethyl Mercaptan

Dihydroannotinol (0.030 g) in 1 ml of concentrated hydrochloric acid (density 1.19) was treated, at 0 °C and under mechanical stirring, with ethyl mercaptan (1 ml) for 10 h. The solution was poured on a mixture of sodium hydroxide solution (40%; 2 ml) and cracked ice. The basic solution was extracted several times with chloroform. The chloroform extract was dried over anhydrous sodium sulphate and evaporated under reduced pressure to yield a colorless oil (0.021 g) which crystallized on standing. This substance was recrystallized from acetone to yield rectangular plates melting at 130 °C.

Calcd. for $C_{18}H_{29}O_2NS$: C, 66.82; H, 9.03; S, 9.91. Found: C, 66.93; H, 9.09; S, 10.25.

The infrared spectrum of compound VII showed hydroxyl absorption at 3410 cm^{-1}, but no carbonyl absorption. Its molecular weight was found to be 323 by mass spectrometry.

Reduction of IV with Lithium Aluminium Hydride

Compound IV (190 mg) in dry ether was added dropwise to a suspension of excess lithium aluminium hydride in dry ether. The reaction mixture was stirred at room temperature overnight and the excess hydride decomposed with moist ether. The ether solution was decanted and evaporated to yield 160 mg of viscous oil. The oil was converted to its hydrobromide salt and the latter recrystallized from methanol–acetone. It melted at 301–305°. The infrared spectrum showed hydroxyl absorption, but no carbonyl absorption. The mass spectrum of the base liberated from the hydrobromide showed a molecular ion peak at 279 corresponding to the molecular formula $C_{17}H_{29}O_2N$.

Phenylannotine

This compound was prepared by the method of Perry and MacLean (4). It was recrystallized from acetone and melted at 215–217°. The mass spectrum showed a molecular ion peak at 353. The infrared spectrum has an intense band in the hydroxyl region at 3470 cm^{-1} and a weak band at 1640 cm^{-1} attributable to non-benzenoid unsaturation. There was no absorption in the carbonyl region. In the ultraviolet spectrum there was only benzenoid absorption.

Pyrolysis of Phenylannotine

A mixture of phenylannotine (0.02 g) and zinc dust (1 g) was placed in a pyrex tube and covered with

Can. J. Chem. Downloaded from www.nrcresearchpress.com by 210.87.254.6 on 09/05/12
For personal use only.

more zinc dust (1 g). The empty end of the tube was drawn to a capillary; the tube was then evacuated and the capillary sealed. The part of the tube carrying the mixture was placed in an oven and heated at about 300° for 1 h. The material which distilled in the capillary was studied by vapor phase chromatography. The following two columns were used: 5% SE-30 on Chromosorb W, 80–100 mesh, and 5% Carbowax 1500 on Chromosorb P, 60–80 mesh. The pyrolysis product consisted of two major components which had retention times identical with those of propiophenone and α-methacrylophenone, prepared by the method of Burckhalter and Fuson (11), on both columns.

The two components of the pyrolysis product mentioned above were collected together in methanol as they left the column and were thus separated from other minor constituents present in the pyrolysis mixture. The ultraviolet spectrum of the mixture of the two substances shows bands at 240 and 280 mμ.

ACKNOWLEDGMENTS

We are indebted to Dr. W. A. Ayer for a generous sample of annotine. The award of a National Research Council Bursary (1960–61) and Studentship (1961–62) to W. A. Szarek is gratefully acknowledged. This work was supported by the National Research Council of Canada.

REFERENCES

1. R. H. F. Manske and L. Marion. Can. J. Research, B, **21**, 92 (1943).
2. A. Bertho and A. Stoll. Chem. Ber. **85**, 663 (1952)
3. O. Achmatowicz and W. Rodewald. Roczniki Chem. **32**, 485 (1958)
4. G. S. Perry and D. B. MacLean. Can. J. Chem. **34**, 1189 (1956).
5. L. M. Jackman. Applications of nuclear magnetic resonance spectroscopy in organic chemistry. Pergamon Press, New York. 1959.
6. W. A. Harrison, M. Curcumelli-Rodostamo, D. F. Carson, L. R. C. Barclay, and D. B. MacLean. Can. J. Chem. **39**, 2086 (1961).
7. K. Wiesner, Z. Valenta, W. A. Ayer, L. R. Fowler, and J. E. Francis. Tetrahedron, 4, 87 (1958).
8. F. A. L. Anet *et al.* Tetrahedron Letters, No. 14, 751 (1964).
9. F. Bohlmann. Chem. Ber. **91**, 2157 (1958).
10. W. A. Ayer and G. G. Iverach. Tetrahedron Letters, No. 3, 87 (1962).
11. J. H. Burckhalter and R. C. Fuson. J. Am. Chem. Soc. **70**, 4184 (1948).

Can. J. Chem. Downloaded from www.nrcresearchpress.com by 210.87.254.6 on 09/05/12
For personal use only.

Can. J. Chem. Downloaded from www.nrcresearchpress.com by 210.87.254.6 on 09/05/12
For personal use only.

SOME CONSIDERATIONS ON THE STRUCTURE AND RADIATION CHEMISTRY OF WATER

ROBERT SCHILLER AND ISTVÁN KISS
Central Research Institute for Physics, Budapest, Hungary
Received March 31, 1964

ABSTRACT

The variation in the yields of products from the radiolysis of water at high solute concentrations and with increasing temperature are as yet unexplained by the diffusion theory. It is shown that by considering some structural features of water, both the temperature dependence of the yields and the concentration dependence of H_2 production in the entire range of solute concentration can be interpreted. The results predicted from the relations thus established agree within an order of magnitude with the measured temperature coefficients of the yields.

INTRODUCTION

The diffusion theory of aqueous radiation chemistry fails to account for some of the experimental observations. Thus, for example, the effect of temperature can be explained only by choosing values of parameters not fully justified by the physical conceptions of the theory. Similarly, the dependence of molecular H_2 yield on solute concentration is not satisfactorily explained. In the diffusion theory, liquid water is assumed to consist of disordered molecules without any preferential orientation or even any short-range order. Actually, however, water exhibits some definite structural properties which cannot be left out of consideration in establishing the mechanism of radiolytic processes. An attempt is made, using a semi-empirical treatment of the diffusion model, to consider the role played by the physical structure of water in its radiation chemistry.

Effect of the Structural Features of Water on Yields

Theories (e.g. refs. 1, 2) of the structure of water can be divided into two groups, namely the single state and the multistate models. In the former, the hydrogen bonds between the water molecules are assumed to extend over the whole system, and the partial disorder characterizing the liquid phase is assumed to be due to local distortions or ruptures of individual bonds. In the latter group, an almost ideal order is assumed within clusters consisting of a few or a few tens of water molecules. These clusters, held together by hydrogen bonds, are imbedded among water molecules interacting with one another and with the clusters by means of dipole forces. For simplicity, the multistate model will be used in present considerations.

Multistate models have been proposed recently by Wada (3), who assumed two states on the basis of phenomenological thermodynamics, and by Némethy and Scheraga (2), who proposed a five-state model derived by statistical mechanical methods. The former suggested only a "disordered" and an "ice-like" structure, while the latter distinguished between molecules in disordered arrangements and molecular species with from one to four hydrogen bonds. The hydrogen-bonded molecules are in rather large molecular clusters comprising 90 molecules at 0 °C and 20 molecules at 100 °C on the average. Without having precisely the structure of ice, they are ice-like in that the bonds are not distorted and contain the maximum possible number of molecules having coordination number four. The average lifetime of a cluster being about 10^{-10} s (4), there is a continuous interchange between clusters and disordered structures. The mole fraction of the hydrogen-bonded molecules monotonously decreases with increasing temperature.

Can. J. Chem. Downloaded from www.nrcresearchpress.com by 210.87.254.6 on 09/05/12
For personal use only.

Assuming two-state water, let us consider first the formation of radical spurs, which are known to form in close proximity to primary ionization acts. The ionization probability of a molecule bound in an "ice-like" cluster is equal to the mole fraction γ of water molecules in the "ice-state". Most radical reactions occur within about 10^{-10} s (the mean lifetime of a cluster (5)) after the primary act. Thus a cluster may be considered as stable with respect to the physicochemical steps of the radiolytic process which, in fact, determine the primary yields.

The substantial difference between the yields from ice and water (6) and, moreover, between the yields from crystalline and glassy ice (7), seems to indicate that the spur formation is not insensitive to the ordered or disordered structure of the water domain. It follows that at least two *average* spur types are expected in water, namely "ice-like" and "disordered" spurs. The radical yields should thus be considered as the weighted means of two yields, the weighting factor being the mole fraction of the water molecules having "ice-like" structure. Thus,

$$G_R = \gamma g_R^* + (1 - \gamma) g_R, \qquad [1]$$

where the contributions of the "ice-like" and "disordered" spurs to the measured average radiation chemical yield are g_R^* and g_R, respectively.

The combination of radicals results either in the formation of H_2 and H_2O_2 or in the re-formation of H_2O. Let us write the molecular yield G_M as the fraction $\sum$ of the combined radical yield G_c in the form

$$G_M = \Sigma G_c = \Sigma (G_p - G_R), \qquad [2]$$

where G_p is the yield of initially dissociated water molecules. Similarly, the molecular yields in "ice-like" and "disordered" domains are

$$g_M^* = \sigma^* g_c^* = \sigma^*(G_p - g_R^*)$$

$$g_M = \sigma g_c = \sigma(G_p - g_R)$$

respectively. The coefficient Σ is in fact again a weighted mean of the form

$$\Sigma = \gamma\sigma^* + (1 - \gamma)\sigma \qquad [3]$$

and G_c leads by definition to an expression similar to eq. [1], since G_p is taken to be the same for both structures.

From the measurements on crystalline ice, g_H^* and $g_{H_2}^*$ seem to be less than G_H and G_{H_2} respectively, i.e. $\sigma^* < \sigma$, $g_H^* < g_H$. If G_p is indeed independent of the structure, the only explanation of these facts is an increased probability of the H + OH reaction. In fact, primary recombination probability must be higher in the crystalline state because of the increased rigidity of the cage. Moreover, the diffusion is thought to proceed, at least in ordered structures, by a "valence transfer" mechanism as suggested by Semenoff (8) and represented for water molecules by the scheme

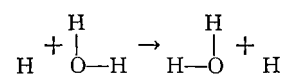

and

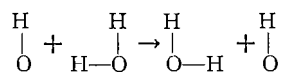

Thus diffusion paths are traced out by water molecules. Considering the structure of ice, the probability of geminate recombination is increased by "valence transfer diffusion" relative to that for "random diffusion", even after the radicals have traversed several water molecules.

If the presence of H_3O^+ ions is taken into consideration, the formulae for the yields become somewhat more complicated. In earlier papers (9, 10) the primary yields have been related to pH through the formula

$$\bar{G} = xG' + (1 - x)G, \qquad [4]$$

where x is the electron capture probability for H_3O^+ ions which increases from 0 to 1 with decreasing pH. G and G' are the yields in neutral and strongly acidic solutions, respectively. If the structure of water is also taken into account, G and G' each can be given by an equation of type [1]. Since the factor x is a function of spur structure, eqs. [1] and [4] combine to

$$\bar{G}_R = \gamma[x^* g_R^{*\prime} + (1 - x^*)g_R^*] + (1 - \gamma)[xg_R' + (1 - x)g_R], \qquad [5]$$

where the asterisks refer to "ice-like" spurs and the primed values to the strongly acidic system.

For the pH dependence of the molecular yields, one must take into consideration the dependence of both Σ and G_c, writing all the yields that contribute to Σ and G_c in the form of eq. [4]. Thus for strongly acidic solutions, where $x = x^* = 1$, the radical and molecular yields are

$$G_R' = \gamma g_R^{*\prime} + (1 - \gamma)g_R' \qquad [1']$$

$$G_M' = [\gamma\sigma^{*\prime} + (1 - \gamma)\sigma'][\gamma g_c^{*\prime} + (1 - \gamma)g_c'] \qquad [2', 3']$$

respectively.

Concentration Dependence of Molecular H_2 Yield

In a plot of $G(H_2)$ versus cube-root solute activity which is initially linear, Mahlman (11) observed a relatively abrupt break followed by a second linear portion with decreased slope. This second portion, when extrapolated to zero scavenger concentration, intersected the $G(H_2)$ axis at the value of $G(H_2)$ for crystalline ice. Only a simple linear cube-root dependence is expected from the diffusion model (12, 13). In the Ganguly–Magee (14) formulation used in these calculations (12, 13), however, the concentration never appears independently, but as a factor in the product $k_s t_0 c_s$ where k_s is the rate constant for reaction between radical and solute, c_s is the concentration and t_0 is a time characteristic of spur size. The numerical results calculated from the theory can be expressed in the form

$$G(H_2) = G_{H_2} - b(k_s t_0 c_s)^{1/3}. \qquad [6]$$

Thus if $G(H_2)$ is plotted against $c_s^{1/3}$, a straight line having a slope proportional to $(k_s t_0)^{1/3}$ will be obtained. The two different types of spur with different average radical concentrations appear in this formulation as two different values of k_s. Thus, $G(H_2)$ has to be expressed as the sum of two equations of the form [6] to take account of the two average spur types. Graphically, this can be done by superposition of two straight lines with different slopes. Numerical values could be obtained only by computing the differential equations of the diffusion theory with appropriate initial concentrations. Moreover, it follows from eq. [3], that for $\gamma = 1$, $G_{H_2} = g_{H_2}^*$, i.e. in a completely ordered structure like crystalline ice the total hydrogen yield is of the same magnitude as the contribution

Can. J. Chem. Downloaded from www.nrcresearchpress.com by 210.87.254.6 on 09/05/12
For personal use only.

of the "ice-like" spurs to the hydrogen yield in real water. Both results are in full agreement with Mahlman's observation.

The Temperature Effect

With increasing temperature the molecular yields of radiolysis are observed to decrease while the radical yields increase. The simple diffusion model predicts no such temperature effect since an increase in the diffusion constant with temperature is exactly balanced by an increase in the recombination rate constant (15). In solutions of moderate concentration the value of γ is independent of concentration and depends only on temperature. Values of g^* and g, on the other hand, as stated previously, are insensitive to temperature. The partial derivative with respect to temperature of the measured radical yield for neutral water is given by

$$[7] \qquad \left(\frac{\partial G_R}{\partial T}\right)_{c_s} = (g_R^* - g_R)\frac{d\gamma}{dT}$$

and that of the molecular yield by

$$[8] \qquad \left(\frac{\partial G_M}{\partial T}\right)_{c_s} = [(\sigma^* - \sigma)G_c + (g_c^* - g_c)\Sigma]\frac{d\gamma}{dT}.$$

For strongly acidic solutions the forms of eqs. [7] and [8] do not change, but the corresponding yields measured in acid systems are substituted.

The Dependence of Radical and Molecular Yields on Temperature

The validity of the present concept may be further checked by comparison of the temperature dependence of primary yields determined experimentally by Hochanadel and Ghormley (15) with relations [7] and [8]. In the present calculations it is assumed that (*a*) the radiation-chemical behavior of crystalline ice is similar to that of ice-like clusters in liquid water and (*b*) the stabilization process of radicals in the ice matrix competes as efficiently with recombination as ion-scavenging does in liquid water.

The terms on the right-hand sides of eqs. [7] and [8] are obtained as follows. The mole fraction of the "ice-like" water molecules is computed by means of a two-state water model. The value of γ is determined by Wada's theory at 1 deg intervals up to 10 °C and at 5 deg intervals from 10 to 20 °C. At higher temperatures the values given by Némethy and Scheraga (2) at 10 deg intervals in the range from 0 to 100 °C are used. Among the five species of the latter model the water molecules of coordination number three and four are regarded as bound in "ice-like" clusters. The combined use of the two approaches is thought to be justified by the agreement (to about 1%) between the temperature coefficients computed from the two models in the range from 0 to 20 °C. The absolute γ values determined from the two theories are much more different.

The characteristic paramagnetic resonance spectra of H atoms and OH radicals were measured in irradiated ice at 4.2 °K. In neutral ice the formation rate of the two radicals was found to be about the same, i.e., $g_H^* \cong g_{OH}^*$ (6). Above 4.2 °K the H atoms cease to be stable in neutral ice; in frozen acidic solutions however, they could be detected even at 77 °K. The H_2 yield from irradiated ice was also measured, after melting the sample (7). Since, to our knowledge, no measurements have yet been reported on frozen acidic solutions at 4.2 °K, in which the H atoms should be stable, no experimental data on $g^{*\prime}$ are available. The increase in $g^{*\prime}$ as compared with g^* is, however, attributed to the broader spatial distribution of H atoms in acidic solutions. The computations of Dyne and Kennedy

Can. J. Chem. Downloaded from www.nrcresearchpress.com by 210.87.254.6 on 09/05/12
For personal use only.

(5) show the yields to vary almost linearly with the distribution radius of the H atoms. Therefore, to a good approximation,

$$[9] \qquad g_R^{*\prime} = g_R^* + g_R' - g_R$$

and combining this equation with eqs. [1] and [1′] or with [2] and [2′] two simple sets of equations in three unknowns are obtained, one of them yielding $g_R^{*\prime}$, the other $g_M^{*\prime}$. The derivatives in eqs. [7] and [8] are approximated by the average rate of change in the temperature interval under investigation.

In Table I the data used in the present calculations are summarized, and in Table II the measured and calculated temperature coefficients of the yields are listed. A value of six was taken for G_p, the only quantity not measured (5).

TABLE I

Experimental data used in the present calculations

g_{OH}^*	G_{OH}	G_{OH}'
0.8[a]	2.28[b]	2.92[b]
g_H^*	G_H	G_H'
0.9[a]	2.78[b]	3.65[b]
$g_{H_2}^*$	G_{H_2}	G_{H_2}'
0.10[c]	0.45[b]	0.42[b]
$\gamma_{20°}$	$\left(\frac{\Delta\gamma}{\Delta T}\right)_{2-20°}$	$\left(\frac{\Delta\gamma}{\Delta T}\right)_{20-60°}$
0.35[d]	3.89×10^{-3} [e]	2.6×10^{-3} [e]

[a]Reference 6.
[b]Reference 16.
[c]Reference 7.
[d]Reference 3.
[e]Reference 2.

TABLE II

Measured and calculated temperature coefficients of the radical yields

	Calculated 2–20°	Measured (15) 2–23°	Calculated 20–60°	Measured (15) 23–65°
$\frac{\Delta G_{OH}'}{\Delta T} \times 10^3$	8.86	5.23	5.93	5.25
$\frac{\Delta G_H'}{\Delta T} \times 10^3$	11.2	3.82	7.50	3.58
$\frac{\Delta G_{H_2}'}{\Delta T} \times 10^3$	$\sim\pm0.2$	−0.52	$\sim\pm0.2$	−0.24

DISCUSSION

The agreement between the calculated and measured temperature coefficients is seen to be within an order of magnitude. A simple error-propagation law shows the error in the calculated values for radicals be about 20%, taking the relative error in g_R^* as high as 50% and neglecting that of other quantities. Considering the 30% error in the measured temperature coefficients, the agreement is fairly good for OH radicals. However, the difference between measured and calculated values for H atoms is considerably greater than the error limit. This may be due to the reducing agent appearing in two different forms, the H atom and the hydrated electron, the ratio of which may be sensitive to the temperature and the structural features of water.

Can. J. Chem. Downloaded from www.nrcresearchpress.com by 210.87.254.6 on 09/05/12
For personal use only.

The error in the calculated temperature dependence of the H_2 yield as determined as above is at least about 100%; moreover the error in g_{H_2}* (not reported) must be considerable. This and the 50% error of the measured value make it impossible to determine even the sign of the effect. The whole calculation involves, in addition to these factors, the uncertainty of γ values which depend strongly on the water model adopted.

REFERENCES

1. O. Y. Samoilov. Die Struktur wässriger Elektrolytlösungen und die Hydratation von Ionen. (German transl.) H. Hollandt. B. G. Teubner, Leipzig. 1961.
2. G. Némethy and H. A. Scheraga. J. Chem. Phys. **36**, 3382 (1962).
3. G. Wada. Bull. Chem. Soc. Japan, **34**, 955 (1961).
4. H. S. Frank and W. Y. Wen. Discussions Faraday Soc. **24**, 133 (1957).
5. P. J. Dyne and J. M. Kennedy. Can. J. Chem. **36**, 1518 (1958).
6. S. Siegel, J. M. Flournoy, and L. H. Baum. J. Chem. Phys. **34**, 1782 (1961).
7. R. Livingston and A. J. Weinberger. J. Chem. Phys. **33**, 499 (1960).
8. N. N. Semenoff. Chemical kinetics and chain reactions. Oxford, Clarendon Press, London. 1935. Chap. IV. Para. 4.
9. R. Schiller. J. Chim. Phys. **59**, 267 (1962).
10. R. Schiller, I. Kósa-Somogyi, and I. Kiss. Proc. Intern. Congr. Radiation Res. 2nd Harrogate Engl. 1962. North-Holland Pub. Co., Amsterdam. 1963.
11. H. A. Mahlman. J. Chem. Phys. **32**, 601 (1960).
12. K. Shinohara, R. Shida, and N. Saito. J. Chem. Phys. **35**, 1899 (1961).
13. M. Burton and K. C. Kurien. J. Phys. Chem. **63**, 899 (1959).
14. A. K. Ganguly and J. L. Magee. J. Chem. Phys. **25**, 129 (1956).
15. C. J. Hochanadel and J. A. Ghormley. Radiation Res. **16**, 653 (1962).
16. E. J. Hart and R. L. Platzman. Mechanisms in radiobiology. *Editors* M. Errera and A. Forssberg. Vol. I. Academic Press, New York. 1961. pp. 93–257.

Can. J. Chem. Downloaded from www.nrcresearchpress.com by 210.87.254.6 on 09/05/12
For personal use only.

Can. J. Chem. Downloaded from www.nrcresearchpress.com by 210.87.254.5 on 09/05/12
For personal use only.

SPECTRES ÉLECTRONIQUES DU FLUORANTHÈNE ET DE L'ACÉNAPHTYLÈNE EN SOLUTION A BASSE TEMPÉRATURE

L. PESTEIL, P. PESTEIL ET F. LAURENT
Laboratoire de Physique P.C.B.1; Faculté des Sciences de Marseille, Marseille, France
Reçu le 28 mai 1964

RÉSUMÉ

L'analyse de la structure vibrationnelle des spectres d'absorption et de fluorescence permet de déterminer les fréquences de vibrations actives; les résultats obtenus sont en accord avec les prévisions de la théorie des groupes; la structure de la bande 0–0 du fluoranthène obéit à une loi de forme quasi hydrogénoïde.

Ce mémoire a pour but d'appliquer aux molécules de fluoranthène $C_{16}H_{10}$ et d'acénaphtylène $C_{12}H_8$ la méthode d'analyse déjà décrite dans de nombreux articles (1–5). Nous rappellerons donc seulement le principe de ces recherches.

La molécule à étudier est mise en solution diluée dans le pentane *n*; la solution est refroidie à 20 °K, température d'ébullition de l'hydrogène. La fluorescence, excitée avec une lampe à vapeur de mercure et des filtres convenables, permet d'obtenir avec précision les vibrations de l'état fondamental qui interviennent dans la transition électronique; l'absorption, pour laquelle on utilise le spectre continu d'une lampe à xénon de 500 W, permet de connaitre les vibrations correspondantes de l'état excité. La fluorescence ne donne donc pas de résultats nouveaux, puisque les mêmes renseignements peuvent également être obtenus par diffusion Raman ou par absorption infrarouge; elle permet cependant de confirmer le cas échéant certains résultats. L'absorption, au contraire, qui permet d'atteindre l'état excité, ne peut être suppléée par aucune autre méthode.

Mais il y a encore un intérêt à ces recherches: la transition électronique pure (niveau non vibrationnel) est généralement séparée en de nombreux niveaux; il y a donc lieu d'étudier également la structure du niveau 0–0 du fluoranthène et de l'acénaphtylène, tant en absorption qu'en fluorescence, et de vérifier sur ces nouveaux exemples les résultats déjà obtenus pour d'autres molécules en solution (6, 7).

Les deux molécules dont il sera question dans le présent article ont déjà fait l'objet de recherches théoriques et expérimentales à la température ordinaire (8). Les auteurs ne recherchaient que la position de la transition électronique; l'élargissement des bandes ne leur permettant pas d'accéder aux structures vibrationnelle et électronique.

Les montages expérimentaux ne présentent rien d'exceptionnel; ils ont d'ailleurs été décrits dans des articles antérieurs (3, 4); nous n'en parlerons pas ici.

Dans l'exposé qui suit, nous observerons le plan suivant:

Aprés avoir effectué le dénombrement des vibrations prévisibles dans le cas des deux molécules, nous donnerons les résultats expérimentaux concernant la structure vibrationnelle; pour terminer, nous étudierons la structure de la bande 0–0 elle-même.

DÉNOMBREMENT DES VIBRATIONS

1. Fluoranthène (symétrie C_{2v})

Il y a 7 familles (*sets of equivalent atoms*) de carbones dans le plan *xz* et 2 familles sur l'axe *z*; il y a également 5 familles d'hydrogènes dans le plan *xz*. Les 26 atomes ont 78° de liberté qui donnent lieu à 72 vibrations internes. L'application simple de la théorie des

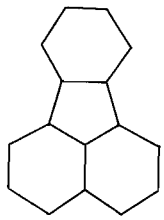

groupes permet de répartir les 72 vibrations de la façon suivante entre les divers types de symétrie:

25 vibrations A_1 (totalement symétriques),
11 vibrations A_2,
24 vibrations B_1,
12 vibrations B_2.

Il est bien évident que si les 72 vibrations apparaissaient dans les spectres de fluorescence et d'absorption, la structure, encore compliquée par l'éclatement de la transition électronique pure, serait inextricable. On admet généralement que, sauf cas exceptionnel, les seules vibrations actives sont celles qui sont totalement symétriques (ici les vibrations A_1); cela nous fait donc 25 vibrations à trouver.

On peut aussi, pour aider au dénombrement et à son interprétation, considérer la molécule de fluoranthène comme composée de deux groupes (un benzène et un naphtalène) liés par deux liaisons. La théorie justifie d'ailleurs cette hypothèse puisqu'elle indique des indices de liaison faibles (0.398) entre naphtalène et benzène (8). Nous essayerons donc, en première approximation, de considérer que les vibrations actives du fluoranthène sont la somme de vibrations du benzène et de vibrations du naphtalène qui deviennent totalement symétriques quand la symétrie diminue à C_{2v}; ces deux dernières molécules étant d'ailleurs substituées ont une symétrie différente de celle qui est la leur à l'état libre.

Il est alors facile de trouver les vibrations du benzène que l'on risque de voir dans les spectres du fluoranthène; ce sont les vibrations suivantes (9):

2 vibrations A_{1g}: 992 et 3062 cm^{-1},
4 vibrations E_g^+: 606, 1178, 1600 et 3060,
3 vibrations E_u^-: 1037, 1485 et 3080,
2 vibrations B_{2u}: 1110 et 1648.

Si l'on fait de même le dénombrement des vibrations actives du naphtalène, on peut s'attendre à trouver également les vibrations suivantes (4, 5):

9 vibrations A_{1g}: 512, 770, 941, 1026, 1237; 1390, 1638, 3028 et 3063,
8 vibrations B_{2u}: 362, 620, 1125, 1265, 1389, 1601; 2945 et 3014.

Il va sans dire que, tant pour le napthtalène que pour le benzène, l'alourdissement de la molécule conduit à une variation importante de ces fréquences dans le fluoranthène.

Les harmoniques et les combinaisons rendent la structure vibrationnelle extrèmement complexe vers les grandes fréquences; pour cette raison, nous avons arrété notre analyse vers 1700 cm^{-1}. Nous avons donc à trouver dans les spectres du fluoranthène 21 vibrations (sur 28) des deux molécules.

Can. J. Chem. Downloaded from www.nrcresearchpress.com by 210.87.254.5 on 09/05/12
For personal use only.

2. Acénaphtylène (symétrie C_{2v})

Il y a 5 familles de carbones et 4 familles d'hydrogènes dans le plan xz et 2 familles de

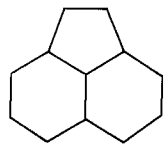

carbones sur l'axe z; les 20 atomes ont 54° de liberté de vibrations internes répartis de la manière suivante entre les 4 types de symétrie:

19 vibrations A_1,
8 vibrations A_2,
18 vibrations B_1,
9 vibrations B_2.

Comme pour le cas du fluoranthène, on peut aussi supposer que l'acénaphtylène dérive du naphtalène; on doit donc s'attendre à retrouver, dans ses spectres, les vibrations correspondant aux 17 oscillations du naphtalène considérées précédemment. Parmi ces vibrations, 4 sont de fréquences nettement supérieures à 1700 cm^{-1}; elles ne figureront donc pas dans nos résultats expérimentaux; par contre, on devra tenir compte de certaines vibrations du radical —CH=CH— (5 des vibrations des molécules $X_2Y_2Z_2$ sont de symétrie convenable).

RESULTATS EXPÉRIMENTAUX

1. Structures vibrationnelles

Nous avons réuni nos résultats dans deux figures; le premier est relatif à la fluorescence; le second à l'absorption.

A. Fluorescence

Nous n'avons pas obtenu le spectre de fluorescence de l'acénaphtylène qui est probablement trop faible pour impressionner la plaque photographique.

Nous avons réuni dans le Fig. 1 les fréquences de vibrations du fluoranthène, de l'acénaphtène (2, 4) et celles du benzène et du naphtalène. Nous avons bien trouvé les 21 vibrations prévues précédemment et nous avons essayé d'établir une correspondance entre les vibrations des diverses molécules; cette correspondance est indiquée par des flèches.

B. Absorption

Dans le Fig. 2, on trouvera, disposés de la même manière que dans le Fig. 1, les résultats relatifs aux structures vibrationnelles des spectres d'absorption correspondant à la même transition que les spectres de fluorescence. De plus, nous avons indiqué entre parenthèses les fréquences de vibrations correspondantes de l'état fondamental tirées du Fig. 1. Les points d'interrogation qui figurent sur la ligne du naphtalène indiquent des vibrations de symétrie B_{2u} dont on ignore la fréquence à l'état excité.

2. Structure des transitions électroniques

L'analyse vibrationnelle est toujours compliquée par la présence de nombreuses composantes de la bande électronique 0–0 qui sert d'origine. Récemment, il a été montré que les diverses raies sont liées entre elles par une loi en $1/n^2$ qui implique l'existence d'une quasi particule appelée *transféron* (10, 11).

Nous sommes parvenus à classer les raies 0–0 du fluoranthène et nous proposons la formule suivante:

$$\nu'(cm^{-1}) = 24\,857 - 3065/n^2.$$

Aprés les naphtalènes H_8 et D_8 (10) et les phénanthrènes H_{10} et D_{10} (11), c'est la cinquième molécule dont les spectres en solution présentent ce phénomène.

Dans le cas présent, nous avons trouvé (en absorption et en fluorescence) les niveaux $n = 3, 4, 5, 6, 7$ et 8; le niveau 7 est le plus intense à la concentration choisie (10^{-3} mole/l).

Nous n'avons pas trouvé le transféron de l'acénaphtylène; ce qui ne veut évidemment pas dire qu'il n'existe pas. Les principales raies qui servent d'origines au spectre de l'acénaphtylène sont les suivantes: 21 283, 21 301 et 21 322 cm^{-1}.

Can. J. Chem. Downloaded from www.nrcresearchpress.com by 210.87.254.5 on 09/05/12
For personal use only.

Can. J. Chem. Downloaded from www.nrcresearchpress.com by 210.87.254.5 on 09/05/12
For personal use only.

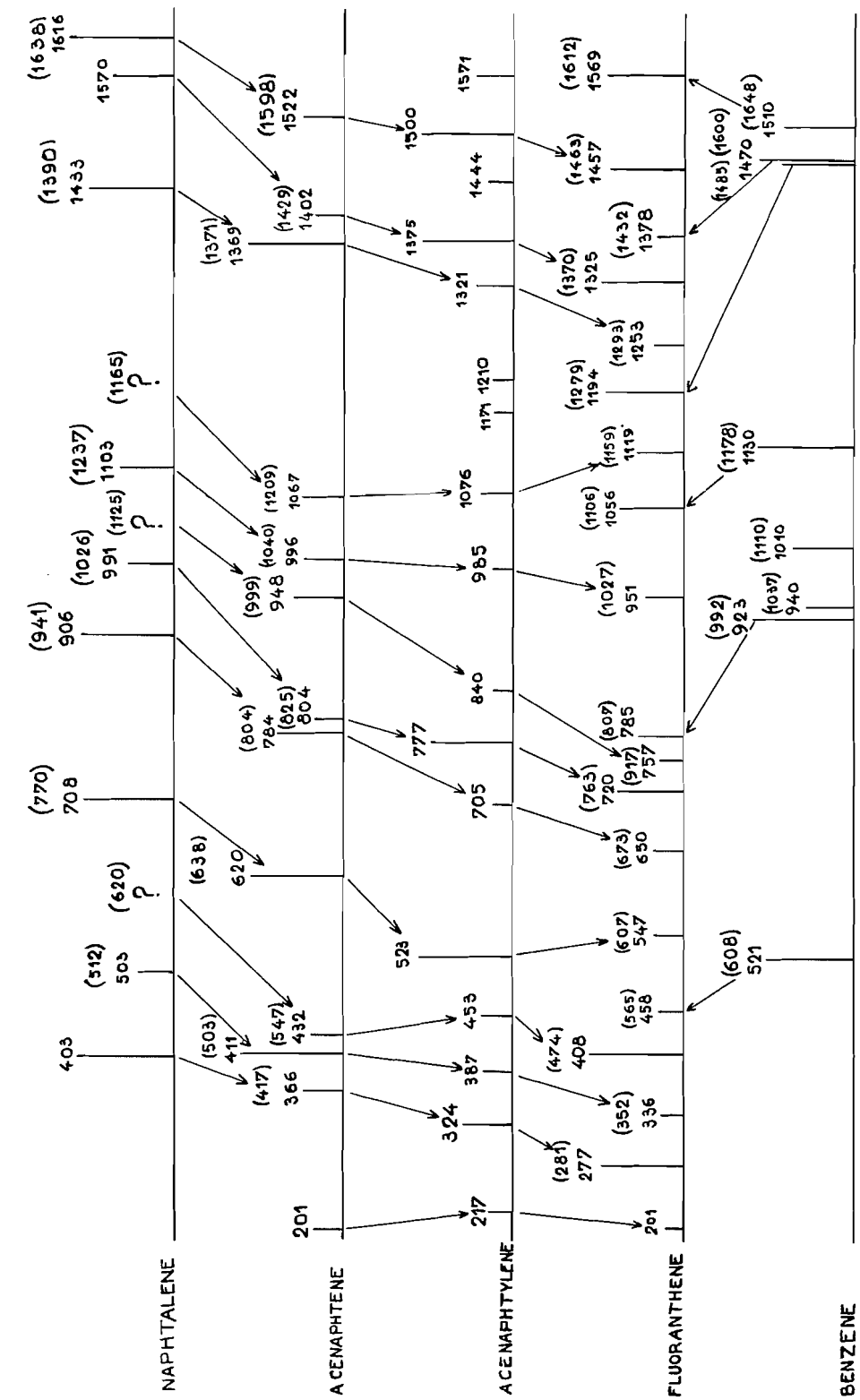

FIG. 1. Vibrations du premier état excité.

Can. J. Chem. Downloaded from www.nrcresearchpress.com by 210.87.254.5 on 09/05/12
For personal use only.

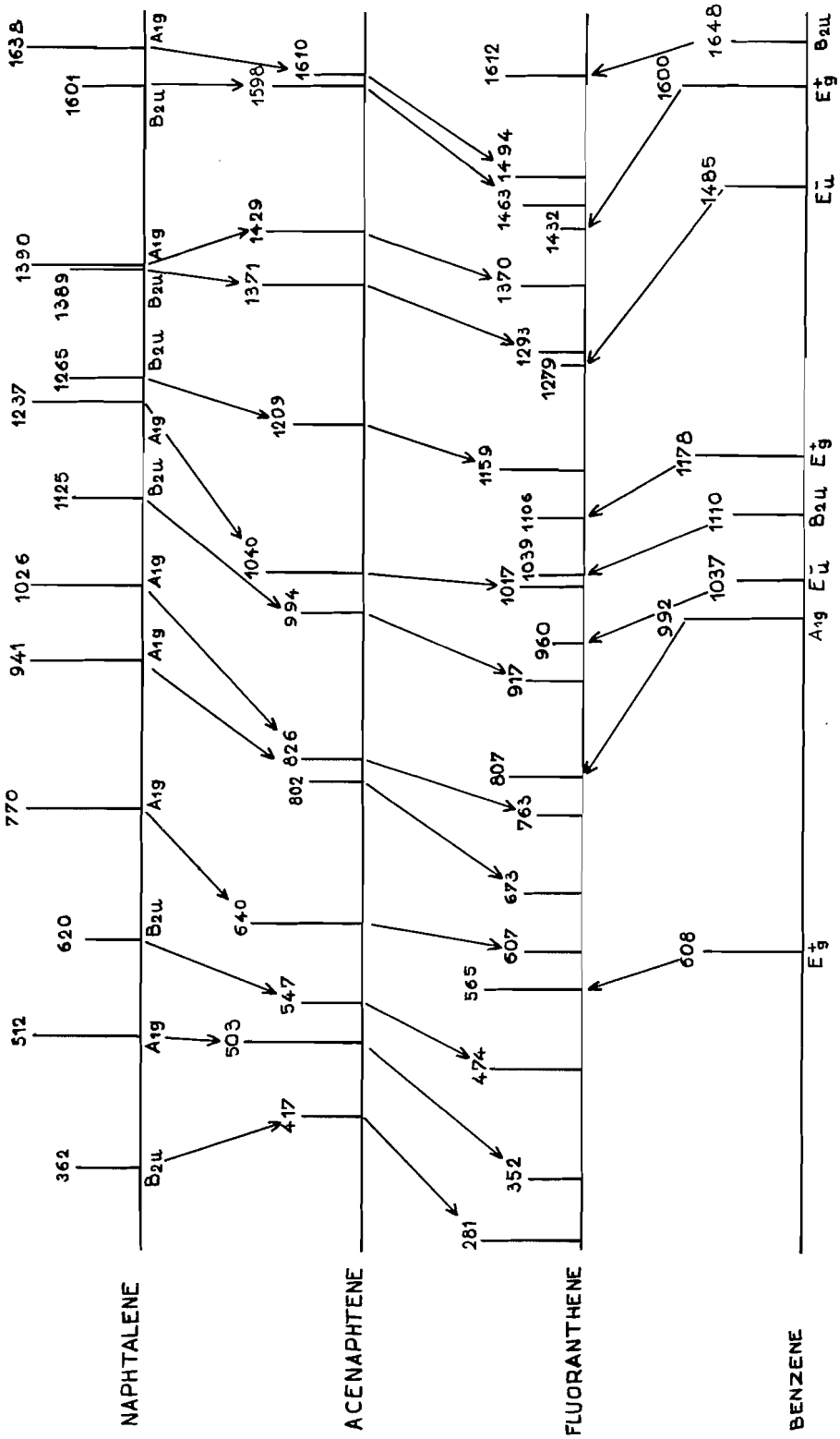

FIG. 2. Vibrations de l'état fondamental.

CONCLUSION

L'analyse vibrationnelle des spectres d'absorption et de fluorescence des deux molécules étudiées permet de retrouver d'une façon qui nous satisfait les prévisions théoriques concernant le nombre d'oscillations actives dans les transitions électroniques; les correspondances avec les molécules composantes (naphtalène et benzène) ne sont proposées qu'à titre indicatif.

La structure de la bande 0–0 du fluoranthène établit une fois de plus expérimentalement l'existence d'une loi de classement des raies de forme quasi hydrogénoïde.

BIBLIOGRAPHIE

1. L. PESTEIL. Compt. Rend. **250**, 497 (1960).
2. L. PESTEIL. J. Chim. Phys. **58**, 204 (1961).
3. L. PESTEIL et M. RABAUD. J. Chim. Phys. **59**, 167 (1962).
4. L. PESTEIL, J. VERGNES et P. PESTEIL. J. Chim. Phys. **60**, 492 (1963).
5. L. PESTEIL, R. TROISPLIS et P. PESTEIL. J. Chim. Phys. **60**, 1294 (1963).
6. E. V. SHPOL'SKII et A. A. IL'INA. Dokl. Akad. Nauk SSSR, **87**, 945 (1952).
7. A. CIAIS. J. Chim. Phys. **58**, 190 (1961).
8. A. PULLMAN, B. PULLMAN *et al.* J. Chim. Phys. **48**, 359 (1951).
9. C. K. INGOLD. J. Chem. Soc. 912 (1936); 222 (1946).
10. A. CIAIS et P. PESTEIL. Compt. Rend. **257**, 654 (1963).
11. P. PESTEIL, F. LAURENT, L. PESTEIL et J. P. DANOY. J. Chim. Phys. **61**, 953 (1964).

Can. J. Chem. Downloaded from www.nrcresearchpress.com by 210.87.254.5 on 09/05/12
For personal use only.

Can. J. Chem. Downloaded from www.nrcresearchpress.com by 210.87.254.42 on 09/05/12
For personal use only.

TRACER DIFFUSION OF THALLIUM IN THALLIUM AMALGAMS

WILLIAM T. FOLEY AND MICHAEL T. H. LIU
Department of Chemistry, St. Francis Xavier University, Antigonish, Nova Scotia
Received June 19, 1964

ABSTRACT

The tracer diffusion coefficient of thallium in thallium amalgams was measured at 25 °C by the capillary-reservoir technique. The values of 10^5D in $cm^2\ s^{-1}$ at 0.0075, 0.0713, 0.1610, 0.2004, 0.2858, 0.3460, 0.3868, 0.4158 mole fraction thallium were 0.98, 0.85, 0.71, 0.62, 0.47, 0.41, 0.38, 0.39 with an average standard deviation of $0.016 \times 10^{-5}\ cm^2\ s^{-1}$. The compound Tl_2Hg_5 plays a significant role in the tracer diffusion.

INTRODUCTION

This is a report on measurements, by the capillary method of Anderson and Saddington (1), of the tracer diffusion coefficient of thallium in thallium amalgams at 25 °C over the concentration range 0.76 to 42.04 weight % thallium. In the composition range studied, the amalgams are liquid at room temperature and, because of the presence of the compound Tl_2Hg_5, the two metals form a solution which is far from regular. Because the alloy is liquid over such a large concentration range and because of its nonideality, this liquid metal system constitutes an excellent system for diffusion studies.

Fick's second law of diffusion for a one-dimensional system states that

$$\frac{\partial C}{\partial t} = D\,\partial^2 C/\partial x^2, \qquad [1]$$

where C is the concentration of the diffusing species, t is the time, and D is the diffusion coefficient with dimensions of area per unit of time. Consider a capillary of length l with one end closed, having an initial concentration of C_i uniform throughout. Let the capillary be immersed in so large a volume of solution of composition C_∞ that at infinite time, when diffusion is complete and the composition within the capillary and outside the capillary is the same, the composition is still C_∞. The solution of eq. [1] for time t under these conditions is

$$\frac{C_{av} - C_\infty}{C_i - C_\infty} = \frac{8}{\pi^2} \sum_{n=0}^{n=\infty} \frac{1}{(2n+1)^2} \exp -\left(\frac{2n+1}{2l}\right)^2 \pi^2 Dt, \qquad [2]$$

where C_{av} is the average composition in the capillary at time t. The series on the right side of eq. [2] is rapidly convergent. Under the conditions of the experiment described here, the value of C_∞ is zero, so that a measurement of C_i, C_{av}, l, and t enable one to calculate D.

EXPERIMENTAL

Mercury was purified by making it the anode in an electrolysis cell using a platinum cathode and 1 N sulphuric acid as an electrolyte. The electrolysis was conducted at a current density of $5 \times 10^{-4}\ A/cm^2$ and the electrolysis was stopped when a film of mercurous sulphate appeared on the anode. The mercury was further purified by covering it with dilute nitric acid and then drawing air through the liquids. Finally the mercury was doubly distilled under reduced pressure.

The preparation of thallium amalgams, the apparatus, and the procedure for diffusion measurements were similar to those used by Foley and Reid (2) in the study of the interdiffusion of thallium in thallium amalgams. The apparatus consisted of a diffusion chamber, at the base of which a three-way stopcock was connected by spherical joints to two storage reservoirs holding amalgams of identical composition except that one of them contained ^{204}Tl. The two samples of the amalgam were made by an approximately

equal division of about 900 g of stock alloy, whose concentration had already been determined. The tagged amalgam was prepared under oxygen-free conditions by an exchange reaction between a solution of radioactive thallium nitrate and the thallium amalgam. The danger of thallium dissolving into the aqueous solution during the exchange was minimized by keeping the pH high by the addition of sodium acetate. After the exchange reaction had taken place, the metal was transferred to the reservoir. The activity of the amalgam corresponded to about three counts per min per mg.

In a run, the capillaries, which were 3 cm long by 1 mm in diameter, were first filled with radioactive amalgam and, after the diffusion chamber was emptied, the nonradioactive amalgam was run into the diffusion chamber until the capillaries were covered. The method of transferring the alloy was the same as that used in the above-mentioned work on the interdiffusion of thallium. The diffusion cell was left in the constant temperature bath, maintained at 25 °C, until it was judged that the concentration of radioactive thallium in the capillary had fallen to about 50% of its initial value. The radioactive amalgam was then transferred from the diffusion chamber and returned to the storage vessel. The duration of the diffusion run was recorded. The amalgam was withdrawn from the capillary and the activity of the amalgam was measured.

The concentration of ^{204}Tl could not be determined by direct measurement of the activity of the amalgam because of the rapidity with which thallium is oxidized by oxygen of the air. The procedure of Foley and Osyany (3) was used to separate the thallium in the form of the sulphate from the mercury. To this thallium sulphate sufficient inert thallium sulphate was added to bring the total weight of thallium sulphate to 400 mg. The thallium was precipitated as the chromate, dried, and counted.

RESULTS

The results are shown in Table I. The values of the diffusion coefficient are also plotted in curve *A* of Fig. 1.

TABLE I

Tracer diffusion of thallium at 25 °C

Mole fraction Tl	$D \times 10^5$ ($cm^2\ s^{-1}$)	Standard deviation $\times 10^5$ ($cm^2\ s^{-1}$)	Number of runs
0.0075	0.98	0.012	8
0.0713	0.85	0.021	6
0.1610	0.71	0.009	8
0.2004	0.62	0.020	9
0.2858	0.47	0.020	8
0.3460	0.41	—	2
0.3868	0.38	0.013	8
0.4158	0.39	0.013	8

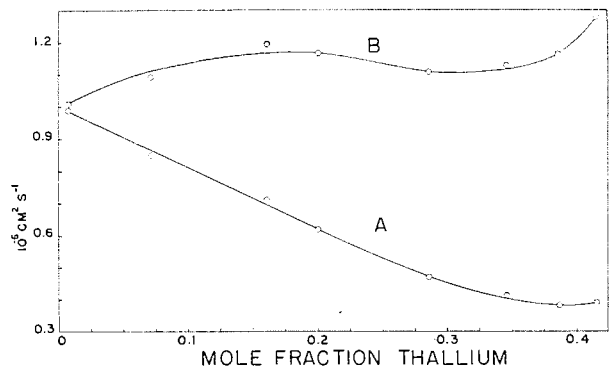

FIG. 1. Curve *A*, variation of tracer diffusion coefficient *D* with concentration; curve *B*, variation of $D\eta/\eta_{Hg}$ with concentration.

DISCUSSION

The results show that the diffusion coefficient suffers a steady decrease with increasing mole fraction of thallium until at mole fraction 0.2857, which corresponds to the com-

Can. J. Chem. Downloaded from www.nrcresearchpress.com by 210.87.254.42 on 09/05/12
For personal use only.

position of Tl_2Hg_5, there is a change in slope amounting almost to a halt. At the composition corresponding to the compound the forces of attraction between the constituents in the solution are at a maximum and as a result the tracer diffusion coefficient would be low. It is known (2) that the compound Tl_2Hg_5 exists in the liquid amalgam. At concentrations of thallium greater than that corresponding to the compound ($X_{Tl} = 0.2858$) the forces of attraction between the constituents of the liquid become smaller. Opposing this latter tendency for an increase in the tracer diffusion coefficient as X_{Tl} exceeds 0.2858 is the steady increase in viscosity with increase of thallium content. At about $X_{Tl} = 0.40$ a minimum occurs in D, and at this composition the opposing tendencies are equal. Curve B shows a plot of the product of the tracer diffusion coefficient and ratio of the viscosity (4) of the amalgam to the viscosity of mercury. Bearman (5) has shown that for regular solutions the value of the product of the tracer diffusion coefficient and the viscosity should be independent of the composition. Curve B confirms that the amalgam solutions are not regular.

ACKNOWLEDGMENT

Grateful acknowledgment is made by one of us, W. T. F., for a grant-in-aid of research from the National Research Council of Canada.

REFERENCES

1. J. S. Anderson and S. Saddington. J. Chem. Soc. S381 (1949).
2. W. T. Foley and L. E. Reid. Can. J. Chem. **41**, 1782 (1963).
3. W. T. Foley and J. M. Osyany. Anal. Chem. **33**, 1657 (1961).
4. W. T. Foley, A. K. Basak, and J. R. Delorey. Unpublished results.
5. R. J. Bearman. J. Phys. Chem. **65**, 1961 (1961).

Can. J. Chem. Downloaded from www.nrcresearchpress.com by 210.87.254.42 on 09/05/12
For personal use only.

Can. J. Chem. Downloaded from www.nrcresearchpress.com by 210.87.254.40 on 09/05/12
For personal use only.

ESSENTIAL OILS AND THEIR CONSTITUENTS[1]

XXII. DETECTION OF NEW TRACE COMPONENTS IN OIL OF GINGER

M. C. NIGAM,[2] ISHWAR C. NIGAM, AND LEO LEVI
Pharmaceutical Chemistry Division, Food and Drug Directorate, Ottawa, Canada
AND
K. L. HANDA
Regional Research Laboratory, Jammu-Tawi, India

Received June 22, 1964

ABSTRACT

Oil of ginger was found to contain the following, as yet unreported, constituents—cumene, β-pinene, myrcene, *p*-cymene, γ-selinene, β-elemene, 2-heptanol, 2-nonanol, and bornyl acetate. The presence of 2 alcohols, for which gas chromatographic and infrared criteria of identity were determined, was also demonstrated. These data are important for establishing the authenticity of the essential oil.

INTRODUCTION

Oil of ginger derived from *Zingiber officinale* Roscoe is an important raw material of the food, drug, and cosmetic industry. Its composition has been the subject of a number of studies reported since the beginning of this century. These established the presence of the following constituents—camphene, α-pinene, β-phellandrene, limonene, zingiberene, farnesene, *ar*-curcumene, bisabolene, *n*-decylaldehyde, *n*-nonyl aldehyde, citral, methyl heptenone, cineole, linalool, borneol, geraniol, and zingiberol (1–4). Specifications for ginger flavor, extract, and essence are given in the Canadian Food and Drugs Act. Ginger is, moreover, an official pharmacopoeial product used widely for masking objectionable tastes of medicinals. It is the purpose of this paper to describe the identification of some hitherto unreported compounds of this spice, achieved by detailed investigation of its essential oil. The data reported should prove of value for the recognition of genuine preparations and the detection of subtle product sophistication.

EXPERIMENTAL

Analytical Sample

The essential oil used in this study was made available by S. Kelkar and Co., Bombay, India. It was obtained by hydrodistillation of ginger roots grown in the state of Kerala (product yield 2.0%).

Physicochemical constants—d_{20}^{20} 0.9081; n_D^{20} 1.4950; $[\alpha]_D^{20}$ −46.40°; saponification value 1.8, after acetylation 46.9; carbonyl content ($C_{10}H_{16}O$) by oximation 2.7%.

Rectification of the Essential Oil

The oil was subjected to fractional distillation under reduced pressure through a Towers column. Four fractions were isolated, as shown in Table I.

TABLE I

Fractional distillation of oil of ginger

Fraction	Weight (g)	Pressure (mm)	Temp. (°C)	n_D^{20}	$[\alpha]_D^{20}$	% (w/w)
L	41.7	15	60–95	1.468	+34°	4.4
M	630.5	10	115–127	1.494	−55°	66.3
H	101.5	7	120–135	1.498	—	10.7
Residue	158.5	—	—	—	—	16.7

[1]*Paper XXI. J. Org. Chem. In press.*
[2]*National Research Council of Canada Postdoctoral Fellow, 1964.*

Refractionation of Fraction L

The isolate was rectified at atmospheric pressure and 10 subfractions (L-1 to L-10) weighing 3–3.5 g each were collected. They possessed the following physical characteristics—b.p. 156–178 °C; d_{20}^{20} 0.8660–0.8885; n_D^{20} 1.467–1.468; $[\alpha]_D^{20}$ +50.2 to +19.6°.

Refractionation of Fraction M

Rectification of this fraction was carried out at 15 mm pressure in a Towers column operated at a reflux ratio of 20:1. Twenty-three cuts were collected; b.p. 130–167 °C at 15 mm; d_{20}^{20} 0.895–0.874; n_D^{20} 1.479–1.497; $[\alpha]_D^{20}$ −20.6 to −49.0°.

Isolation of Carbonyls from Fraction M-1 to M-4

Infrared examination showed these fractions (71 g; 7.6% of the essential oil) to be rich in oxygenated compounds. They were combined and found to contain 36.0% of carbonyl constituents (oximation method). Treatment of a 36 g aliquot with Girard T reagent (5, 6) yielded 12.5 g carbonyl and 23.1 g non-carbonyl compounds.

Isolation of Total Hydrocarbons from the Essential Oil

The essential oil (2.0 g) was chromatographed over 50 g of basic grade 1 alumina and eluted with petroleum ether (b.p. 40–60 °C). Evaporation of the first 50 ml of effluent yielded 1.5 g of hydrocarbons.

Gas Chromatography of the Essential Oil and Isolated Fractions

Apparatus and general procedures have been described (7). Two stationary phases Reoplex 400 (20%) and Silicone Nitrile XE-60 (10%) deposited on acid washed Chromosorb W (60–80 mesh) were used. Columns and operating conditions are shown in Table II.

TABLE II

Experimental conditions for gas chromatographic analyses

Sample	Column	Temp. (°C)	Gas flow (ml/min)
Oil of ginger	Reoplex 400	170	75
Fraction L and subfractions	Reoplex 400	110	60
Fraction M and subfractions	Reoplex 400	170	75
Sesquiterpenes of fractions M and H	Silicone Nitrile	150	75

Identification and Determination of Constituents

Constituents were identified by the serial dilution technique and by comparison of infrared spectra of effluents—collected in carbon tetrachloride and purified by rechromatography under optimal conditions of temperature and carrier gas flow rate—with those of authenticated reference standards or published data (8). Percentages were calculated by the sigma method (9, 10).

RESULTS AND DISCUSSIONS

The gas chromatogram of the essential oil is reproduced in Fig. 1-A. In addition to its major constituents, sesquiterpenes, the presence of small amounts of a number of lower boiling compounds was also observed. Special attention was given to the characterization of minor and trace components detected. A quantity of 950 g of the oil was used in this investigation to obtain sufficient amounts of fractions which were enriched with these compounds. Preliminary rectification (Table I), which separated the distillate into low (L), middle (M), and high boiling (H) fractions, was halted when the sesquiterpene hydrocarbons appeared to have been distilled over completely.

Identification of Low-Boiling Constituents

All subfractions of fraction L were subjected to gas chromatographic analysis. The chromatogram of subfraction L-1 is reproduced in Fig. 1-B. The following constituents were identified by the techniques described.

Cumene.—The presence of trace amounts of this compound was detected in fraction L-1.

α-Pinene, β-pinene, camphene, and myrcene.—These constituents were readily detected in fractions L-1 to L-5 and trace amounts found to be present in later fractions also.

Can. J. Chem. Downloaded from www.nrcresearchpress.com by 210.87.254.40 on 09/05/12
For personal use only.

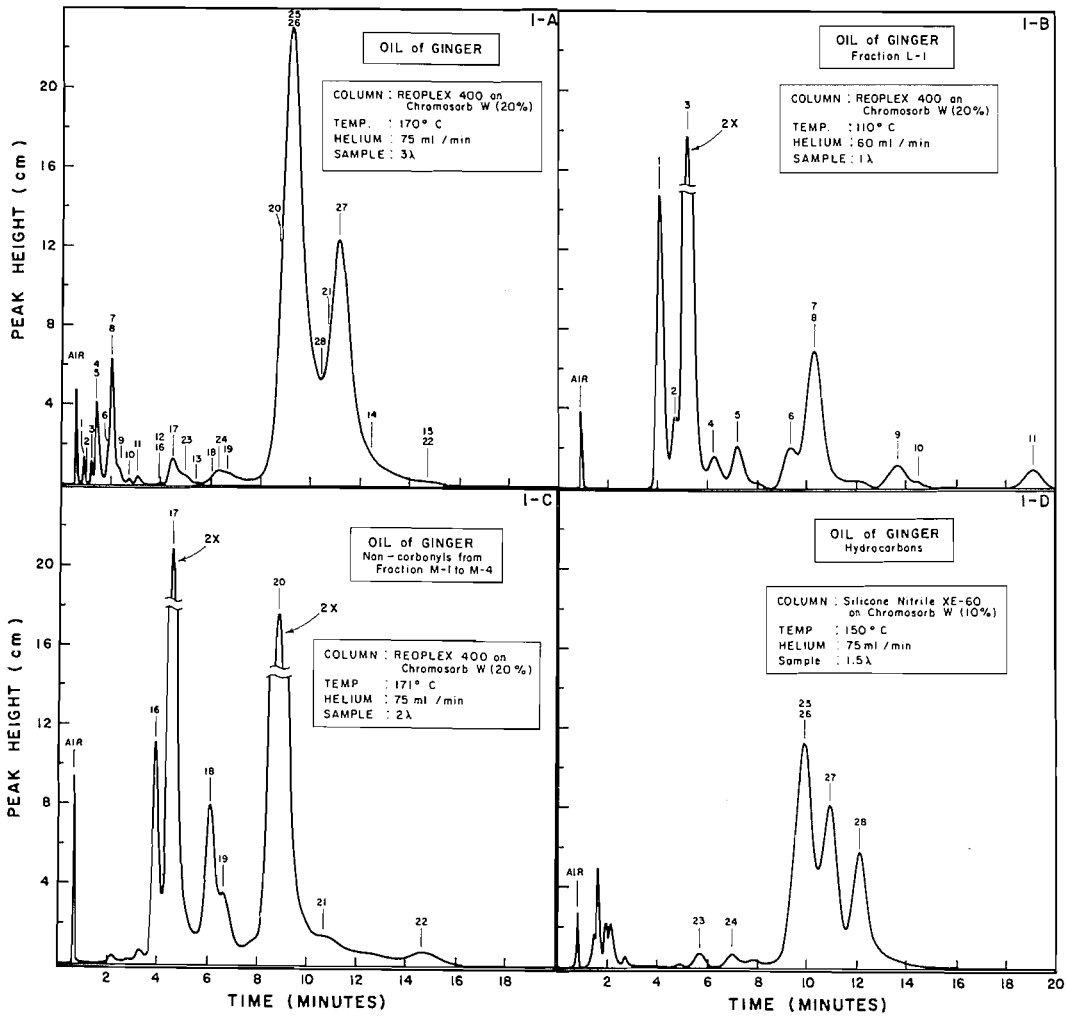

FIG. 1. Gas chromatographic examination of oil of ginger and its fractions.

Limonene.—This terpene was chiefly concentrated in fractions L-8 to L-10 but variable amounts were also found to occur in earlier fractions.

Cineole and β-phellandrene.—These two constituents formed a single peak when chromatographed on the Reoplex column. The presence of cineole in the oil was confirmed by isolation via its resorcinol complex, m.p. 81–82 °C (11). β-Phellandrene was identified in fraction L-9, which had been freed from cineole. Infrared analysis of g.l.c. effluent showed that the terpene obtained was almost free from admixture with cineole.

p-Cymene.—Small quantities of this compound were identified in fractions L-7 to L-9, and trace amounts found to be present in earlier fractions also.

2-Heptanol.—This alcohol appeared as a minor peak in the chromatograms of fractions L-1 to L-3 just before emergence of *p*-cymene.

Methyl heptenone.—A small peak appearing in the chromatograms of fractions L-8 to L-10 was found to be generated by this ketone.

Can. J. Chem. Downloaded from www.nrcresearchpress.com by 210.87.254.40 on 09/05/12
For personal use only.

Can. J. Chem. Downloaded from www.nrcresearchpress.com by 210.87.254.40 on 09/05/12
For personal use only.

Constituents of Fraction M

The first four of the 23 subfractions collected were rich in alcohols, esters, and carbonyls (infrared bands at 3 430, 1 730, 1 715, and 1 670 cm^{-1}), whereas succeeding ones (M-5 to M-23) were largely composed of sesquiterpene hydrocarbons.

Fractions M-1 to M-4 were combined, treated with Girard T reagent, and analyzed for carbonyl and non-carbonyl constituents.

Nonyl aldehyde, decyl aldehyde, and citral.—The presence of these constituents was confirmed in the isolate. Traces of methyl heptenone were also detected.

Linalool and borneol.—These alcohols were found to be the major constituents of the non-carbonyl fraction (30.1 and 51.8% respectively, see Fig. 1-C).

2-Nonanol, bornyl acetate, and geraniol.—These compounds gave rise to minor peaks in the chromatogram of the non-carbonyl fraction and were identified by infrared examination of effluents collected after repeated sample injections.

Alcohol A.—This constituent, emerging between linalool and bornyl acetate, was of semisolid consistency and had a musty odor. Its infrared spectrum displayed characteristic bands at 3 600, 3 400, 1 125, and 1 100 cm^{-1} (OH group) and at 3 020, 1 660, and 838 cm^{-1} (—C=CH— group). Additional absorptions were observed at 1 465, 1 445, 1 435, 1 375, 1 365, 1 312, 1 270, 1 213, 1 202, 1 170, 1 065, 1 037, 1 010, 988, 965, 950, 907, and 885 cm^{-1}. On catalytic hydrogenation, the alcohol yielded a product (m.p. 84–85 °C) showing absorptions at 3 600, 3 440, 2 950, 2 920, 2 870, 1 463, 1 455, 1 377, 1 370, 1 343, 1 307, 1 232, 1 207, 1 166, 1 142, 1 113, 1 088, 1 042, 1 030, 996, 963, 940, 930, 900, 870, and 853 cm^{-1}.

Alcohol B.—One of the peaks observed in Fig. 1-C was found to be generated by an aromatic hydroxy compound exhibiting distinct bands at 3 600, 3 480, and 1 095 cm^{-1} (OH group), 1 625 and 1 507 cm^{-1} (phenyl ring), and 1 645 and 900 cm^{-1} (—C(=CH_2)— group).

Sesquiterpene Hydrocarbons

Curcumene and Farnesene

Infrared and gas chromatographic analyses proved that fractions M-5 to M-23 were rich in sesquiterpene hydrocarbons which formed the bulk of fraction H. They were combined and separated by gas chromatography into three well-resolved fractions. Infrared examination identified the second and third of these isolates as curcumene and farnesene, respectively.

α- and β-Zingiberene and β-Bisabolene

The first of the three gas chromatographic fractions, which on the basis of its infrared analysis appeared to be a mixture of α- and β-zingiberene, was rechromatographed. Ascending and descending portions of the peak were collected separately and again purified by repeated gas chromatography at reduced temperature and flow rate (130 °C; 60 ml/min). The ascending portion was found to be composed of α-zingiberene and the descending portion further resolved into β-zingiberene and β-bisabolene.

γ-Selinene and β-Elemene

Gas chromatographic analysis of the hydrocarbon fraction isolated by column chromatography of the essential oil over alumina showed the presence of some minor constituents in the oil which emerged, following the elution of the monoterpenes and preceding the

elution of sesquiterpenes. Two of these constituents were identified as γ-selinene and β-elemene respectively (see Fig. 1-D).

High Boiling Sesquiterpene Alcohols

Infrared examination of the high-boiling residue obtained after fractional distillation of the oil showed that it consisted largely of hydroxy compounds. Gas chromatography could not be applied successfully, however, to the analysis of this isolate. Marked decomposition of some of the constituents to sesquiterpenes occurred at 250 °C. Thin-layer chromatography revealed a high degree of compositional complexity of the product and the presence of a number of alcohols.

Composition of Essential Oil

The composition of the oil as deduced from correlation of the distillation and gas chromatographic data is shown in Table III.

TABLE III

Composition of oil of ginger

Peak No.	Constituent	Retention time*				% (w/w)
		a	*b*	*c*	*d*	
1.	α-Pinene	0.44				0.4
2.	Cumene	0.50				Trace†
3.	Camphene	0.56				1.1
4.	β-Pinene	0.66				0.2
5.	Myrcene	0.77				0.1
6.	Limonene	1.00				1.2
7.	Cineole	1.11				1.3
8.	β-Phellandrene	1.11				1.3
9.	2-Heptanol	1.46				Trace†
10.	*p*-Cymene	1.55				0.1
11.	Methyl heptenone	2.05	0.56			0.1
12.	Nonyl aldehyde		0.67			0.1
13.	Decyl aldehyde		1.00			0.2
14.	Citral *b*		2.26			0.8
15.	Citral *a*		2.81			1.4
16.	2-Nonanol			0.88		0.2
17.	Linalool			1.00		1.3
18.	Alcohol A			1.35		0.2
19.	Bornyl acetate			1.49		0.1
20.	Borneol			1.95		2.2
21.	Geraniol			2.38		0.1
22.	Alcohol B			3.26		0.1
23.	γ-Selinene				0.52	1.4
24.	β-Elemene				0.65	1.0
25.	α- and β-Zingiberene				0.91	35.6
26.	β-Bisabolene				0.91	0.2
27.	*ar*-Curcumene				1.00	17.7
28.	Farnesene				1.11	9.8
	Sesquiterpene alcohols					16.7
	Unidentified				—	5.6

*Experimental conditions of gas chromatography given in Table II. Reference standards: (*a*) limonene, (*b*) decyl aldehyde, (*c*) linalool, and (*d*) *ar*-curcumene.
†Less than 0.01%.

ACKNOWLEDGMENTS

The authors express their appreciation to Dr. J. A. Campbell, Assistant Director, Research Laboratories, Food and Drug Directorate, Department of National Health and Welfare, Ottawa, Canada, and to Dr. I. C. Chopra, Director, Regional Research Laboratory, Jammu-Tawi, India, for their encouragement and support of this collaborative study.

Can. J. Chem. Downloaded from www.nrcresearchpress.com by 210.87.254.40 on 09/05/12
For personal use only.

REFERENCES

1. E. GUENTHER. The essential oils. Vol. V. D. Van Nostrand Co., Inc., New York. 1952. pp. 116–118.
2. V. HEROUT, V. BENESOVA, and J. PLIVA. Collection Czech. Chem. Commun. **18**, 248–256 (1953).
3. K. R. VARMA, T. C. JAIN, and S. C. BHATTACHARYYA. Perfumery Essent. Oil Record, **53**, 678–684 (1962).
4. K. R. VARMA, T. C. JAIN, and S. C. BHATTACHARYYA. Tetrahedron, **18**, 979–984 (1962).
5. C. L. TEITELBAUM. J. Org. Chem. **23**, 646 (1958).
6. I. C. NIGAM AND L. LEVI. Anal. Chem. **35**, 1087 (1963).
7. I. C. NIGAM and L. LEVI. Can. J. Chem. **40**, 2083 (1962).
8. J. PLIVA, M. HORÁK, V. HEROUT, and F. ŠORM. Die Terpene Sammlung der Spectren und Physikalischen Konstanten. Teil 1. Sesquiterpene. Akademi-Verlag, Berlin. 1960.
9. J. C. BARTLET and D. M. SMITH. Can. J. Chem. **38**, 2057 (1960).
10. D. M. SMITH and L. LEVI. J. Agr. Food Chem. **9**, 230 (1961).
11. E. GUENTHER. The essential oils. Vol. II. D. Van Nostrand Co., Inc., New York. 1949. p. 708.

Can. J. Chem. Downloaded from www.nrcresearchpress.com by 210.87.254.40 on 09/05/12
For personal use only.

Can. J. Chem. Downloaded from www.nrcresearchpress.com by 210.87.254.105 on 09/05/12
For personal use only.

THE THERMAL REVERSIBILITY OF THE MICHAEL REACTION

IV. THIOL ADDUCTS

C. F. H. ALLEN
Department of Chemistry, Rochester Institute of Technology, Rochester, New York

AND

J. O. FOURNIER AND W. J. HUMPHLETT
Research Laboratories, Eastman Kodak Co., Rochester, New York

Received June 8, 1964

ABSTRACT

The hydrochlorides of 27 Michael adducts, formed from alkylthiols and chalcones monosubstituted successively in each ring by nitro, chloro, and methoxy groups, were thermally cleaved by hot water. The amount of cleavage was readily determined iodimetrically.

A systematic study of the thermal reversibility of Michael adducts, formed by the addition of mercaptans to the conjugated system of double bonds present in ketones, esters, and the like, is believed to be new. The only instances on record are those described in one of our previous papers (1). The current account is limited to adducts which are formed from chalcones and which have β-alkylmercapto substituents. They comprise a new class that can be used for a study of thermal cleavage. A following paper will contain an account of similar adducts derived from unsaturated esters, nitriles, ketones with fewer substituents, and the like. It has been found that they are not sufficiently active to reverse thermally.

The extent of thermal cleavage is susceptible to quantitative estimation, since the mercapto addends regenerated can be titrated against standard iodine solutions. This operation is much more convenient than the use of gas chromatography, as previously employed (1). Since these adducts can give only normal cleavage, it makes possible an examination of the effect, if any, of substituents in different positions of both benzene rings on the extent of the reversal. The extent of cleavage of all the adducts is summarized in Table I.

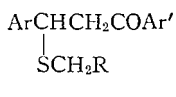

I

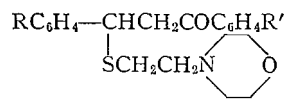

II

The adducts investigated were mainly those (II) formed from β-morpholinoethanethiol, because of its availability (2), because the hydrochloride salts are easily crystallized solids, because of their increased solubility, and because they give good cleavage rates. A few preliminary experiments showed that other thiols could be so used (Table I, Nos. 1, 2, 3, 7, 8), that the reversal was general, and that it was not confined to β-mercaptoethylamines. Three kinds of ring substituents were employed—nitro (strong electron-withdrawing), chloro (weak electron-withdrawing), and methoxy (electron-donating). These groups, one at a time, were located in ortho-, meta-, and para-positions in both rings.

The process may depend upon (*a*) the activity of the α-hydrogen atom of the adduct, (*b*) the resonance stabilization of the structure —C=C—C=O formed by cleavage, and

Can. J. Chem. Downloaded from www.nrcresearchpress.com by 210.87.254.105 on 09/05/12
For personal use only.

TABLE I

No.	Adduct	% yield	m.p., °C	Empirical formula	Analyses						% cleavage at 100° in H_2O	
					Calcd.			Found				
					C	H	N	C	H	N	2 min	30 min
1.	$C_6H_5CHCH_2COC_6H_5$ SCH_2CH_2OH	85[a]	68	$C_{17}H_{18}O_2S$	71.3	6.3	—	71.6	6.3	—	16.6	—
2.	$C_6H_5CHCH_2COC_6H_5$ SCH_2COOH	83	126[h]		—	—	—	—	—	—	6.8	57.5
3.	$C_6H_5CHCH_2COC_6H_5$ $SCH_2CH_2N(C_2H_5)_2\cdot HCl$	96[b] (crude)	110	$C_{21}H_{28}ClNOS$	66.7 (S, 8.7)	7.5		66.6 (S, 8.5)	7.7		69.2	—
	(*b*) ($HClO_4$ salt)	57[e]	92	$C_{21}H_{28}ClNO_5S$	57.1	6.4	3.2	57.3	6.5	3.2	—	—
4.	(*a*) $C_6H_5CHCH_2COC_6H_5$ SCH_2CH_2N O	92[c]	67	$C_{21}H_{23}NO_2S$	71.0	7.1	3.9	71.3	7.2	4.1	18.5, 18.0	43.5
	(*b*) (HCl salt)	87[d]	149	$C_{21}H_{26}ClNO_2S$	64.3	6.7	3.6	64.1	6.8	3.5	55.0, 59.0	—
5.	$C_6H_5CHCH_2COC_6H_4CH_3$-*p* SCH_2CH_2N O·HCl	80[d]	137	$C_{22}H_{28}ClNO_2S$	65.1	7.0	3.4	65.1	7.2	3.5	36.2, 36.2	—
6.	$C_6H_5CHCH_2COC_6H_4OH$-*p* (*a*) SCH_2CH_2N O	59[f]	127	$C_{21}H_{25}NO_3S$	68.0	6.8	3.8	68.0	6.8	3.9	—	—
	(*b*) (HCl salt)	—	201	$C_{21}H_{26}ClNO_3S$	61.8	6.4	3.4	61.4	6.6	3.4	38.9	—
7.	$C_6H_5CHCH_2COC_6H_4OCH_3$-*p* SCH_2COOH	82[a]	90	$C_{18}H_{18}O_4S$	65.4	5.5	—	65.5	5.8	—	—	39.8
8.	$C_6H_5CHCH_2COC_6H_4OH$-*p* SCH_2COOH	80[a]	130	$C_{17}H_{16}O_4S$	64.5	5.1	—	64.1	4.8	—	—	28.6

Can. J. Chem. Downloaded from www.nrcresearchpress.com by 210.87.254.105 on 09/05/12
For personal use only.

TABLE I *(Concluded)*

No.	Adduct	% yield	m.p., °C	Empirical formula	Analyses						% cleavage at 100° in H_2O	
					Calcd.			Found				
					C	H	N	C	H	N	2 min	30 min
9.	$C_6H_5CHCH_2COC_6H_4C_6H_5$-*p*	89[e]	116–7	$C_{27}H_{29}NO_2S$	75.2	6.8	3.2	75.2	7.0	3.2	0	40.8
	(*a*) SCH_2CH_2N O											
	(*b*) (HCl salt)	—	114–6	$C_{27}H_{30}ClNO_2S$	69.1	6.5	3.0	68.8	6.8	2.9	—	—
	m o O *o′ m′* *p* $CHCH_2C$ *p′* SCH_2CH_2N O·HCl											
10.	*p′*-NO_2	78[d]	154	$C_{21}H_{25}ClN_2O_4$	57.7	5.8	6.4	57.5	5.9	6.6	88.1, 88.4	—
11.	*o′*-NO_2	79[d]	135	$C_{21}H_{25}ClN_2O_4$	57.7	5.8	6.4	57.9	5.8	6.6	91.0, 91.4	—
12.	*m′*-NO_2	80[d]	141	$C_{21}H_{25}ClN_2O_4$	57.7	5.8	6.4	57.3	5.8	6.7	87.8, 87.7	—
13.	*p*-NO_2	81[d]	175	$C_{21}H_{25}ClN_2O_4$	57.7	5.8	6.4	57.9	5.6	6.1	77.4, 77.8	—
14.	*o*-NO_2	69[c]	191–2	$C_{21}H_{25}ClN_2O_4$	57.7	5.8	6.4	57.6	5.9	6.4	68.2, 68.2	—
15.	*m*-NO_2	85[e]	188	$C_{21}H_{25}ClN_2O_4$	57.7	5.8	6.4	57.5	5.9	6.3	63.8, 64.1	—
16.	*p′*-OCH_3	72[d]	147	$C_{22}H_{28}ClNO_3S$	62.6	6.7	3.3	62.5	6.6	3.3	34.0	—
17.	(*a*) *o′*-OCH_3	—	150	$C_{22}H_{28}ClNO_3S$	62.6	6.7	3.3	62.2	6.8	3.2	47.8, 49.6	—
	(*b*) *o′*-OCH_3·MeOH	74[d]	108	$C_{23}H_{32}ClNO_4S$	60.9	7.0	3.1	60.9	6.7	3.3	—	—
18.	*m′*-OCH_3	80[d]	161	$C_{22}H_{28}ClNO_3S$	62.6	6.7	3.3	62.4	6.8	3.3	60.8, 62.2	—
19.	*p*-OCH_3	72[d]	138	$C_{22}H_{28}ClNO_3S$	62.6	6.7	3.3	62.3	6.3	3.2	66.8[g]	—
20.	*o*-OCH_3	57[d]	67	$C_{22}H_{28}ClNO_3S$	62.6	6.7	3.3	62.2	6.9	3.3	53.3[g]	—
21.	*m*-OCH_3	83[d]	151	$C_{22}H_{28}ClNO_3S$	62.6	6.7	3.3	62.5	6.8	3.3	54.6[g]	—
22.	*p′*-Cl	81[d]	159	$C_{21}H_{25}Cl_2NO_2S$	59.1	5.9	3.3	58.9	6.2	3.2	51.4, 50.2	—
23.	*o′*-Cl	46[d]	114	$C_{21}H_{25}Cl_2NO_2S$	59.1	5.9	3.3	58.8	5.9	3.6	88.2, 88.2	—
24.	(*a*) *m′*-Cl	82[c]	124–6	$C_{21}H_{25}Cl_2NO_2S$	59.1	5.9	3.3	58.7	6.1	3.4	—	—
	(*b*) *m′*-Cl·MeOH	83[d]	69–70	$C_{22}H_{29}Cl_2NO_3S$	57.6	6.4	3.1	57.5	6.4	3.1	64.2, 64.3	—
25.	*p*-Cl	78[d]	179	$C_{21}H_{25}Cl_2NO_2S$	59.1	5.9	3.3	59.3	6.0	3.2	43.2, 46.2	—
26.	(*a*) *o*-Cl·MeOH	83[d]	75–77	$C_{22}H_{29}Cl_2NO_3S$	57.6	6.4	3.1	57.5	6.2	3.4	54.8, 54.0	—
	(*b*) *o*-Cl	—	133	$C_{21}H_{25}Cl_2NO_2S$	59.1	5.9	3.3	59.5	6.2	3.3	55.0	—
27.	*m*-Cl	79[d]	194–5	$C_{21}H_{25}Cl_2NO_2S$	59.1	5.9	3.3	59.1	6.2	3.7	47.2, 40.4	—

[a]From ether–ligroin (b.p. 35–60°).
[b]From ethyl acetate.
[c]From isopropanol.
[d]From methanol – ethyl acetate.
[e]From ethanol.
[f]From ether.
[g]Mean of four determinations.
[h]Reference 5.

(*c*) the anionic stability of RS^- (3). Different degrees of reactivity of adducts towards thermal reversal are observed to be dependent upon the kind of mercaptan added (Table II).

TABLE II

Adduct	Cleavage, % (2 min in H_2O at 100 °C)
$C_6H_5CHCH_2COC_6H_5$ SCH_2COOH	6.8
$C_6H_5CHCH_2COC_6H_5$ SCH_2CH_2OH	16.6
$C_6H_5CHCH_2COC_6H_5$ SCH_2CH_2N O	18.5, 18.0
$C_6H_5CHCH_2COC_6H_5$ SCH_2CH_2N O·HCl	55, 59
$C_6H_5CHCH_2COC_6H_5$ $SCH_2CH_2N(C_2H_5)_2$·HCl	69.2

The adducts (as their salts) were cleaved at 100 °C by a simple rapid procedure. The titration results suggest that the activity of the α-hydrogen atom of the adducts influences the extent of release of mercaptan.

Cleavage of adducts of chalcones to form a conjugated system, that is, a product having greater resonance, may be a predominant factor in heat-induced reversal. The adduct of methyl vinyl ketone with β-morpholinoethanethiol is incompletely reversed by alkali and only slightly affected by heat. However, the adduct of benzalacetone with this mercaptan is almost completely cleaved by alkali, as will be described in a forthcoming paper. All of the corresponding adducts of substituted chalcones are rapidly cleaved nearly quantitatively by alkali and, in addition, are reversed by heat.

The Conjugate Addition

Addition of β-morpholinoethanethiol to chalcones occurs rapidly in refluxing alcohol. The salts were formed by replacement of the solvent by ether and the addition of hydrogen chloride.

Addition of mercaptoethanol or mercaptoacetic acid by refluxing in acetic acid for 15 min forms adducts in 80–99% yield.

Sodium methoxide catalyzed addition of mercaptoacetic acid in alcohol produced the adduct in only a 17% yield (4). The data are included in Table I.

EXPERIMENTAL

Preparation of Starting Materials

3′-Methoxyacetophenone (5), b.p. 131° at 19 mm, n_D^{25} 1.5391; 2′-chloroacetophenone (6), b.p. 100° at 10 mm, n_D^{25} 1.5409; 3′-chloroacetophenone (7), b.p. 52–54° at 0.25 mm, n_D^{25} 1.5472; and β-morpholinoethanethiol, b.p. 97–98° at 15 mm, n_D^{25} 1.5020 (2) were prepared as described in the literature. All the chalcones were known: NO_2 and Cl (8), *o*-OCH_3 (9), *m*-OCH_3 (10), *p*-OCH_3 (11), *o*′-OCH_3 (12), *m*′-OCH_3 (13), *p*′-OCH_3 (14), *p*′-OH (15), *p*-CH_3 (16), and *p*′-C_6H_5 (17). The melting points agreed with the reported values except for the *o*′-chloro (9), which did not crystallize.

Anal. Calcd. for $C_{15}H_{11}ClO$: C, 74.2; H, 4.6; Cl, 14.6. Found: C, 74.5; H, 4.5; Cl, 14.4.

Can. J. Chem. Downloaded from www.nrcresearchpress.com by 210.87.254.105 on 09/05/12
For personal use only.

Preparation of Adducts

(a) From Chalcones and β-Morpholinoethanethiol or N,N-Diethylaminoethanethiol (2)

Equimolar amounts of the chalcone and the thiol were refluxed in absolute ethanol for 1 h and evaporated to dryness *in vacuo*. In some instances, the oils crystallized and the adduct was purified as the free base. The free base, oil or solid, was dissolved in ether and converted to the hydrochloride with hydrogen chloride. Perchlorates were prepared by treating the hydrochlorides with aqueous sodium perchlorate.

(b) From Chalcones and β-Mercaptoethanol or Mercaptoacetic Acid

A solution containing 1 mole of the chalcone and 1.5 moles of the mercaptan in glacial acetic acid was boiled for 15 min and allowed to cool. On addition of water an oil separated. The water was decanted and the oil rinsed with water two or three times, after which the oil crystallized. The products were recrystallized from ether–petroleum ether, b.p. 35–60°. The analyses are included in Table I.

Cleavage of Adduct and Titration of the Thiol

Approximately 1 meq of the adduct in a small aluminium foil "boat" was weighed exactly. The boat and the sample were then immersed for exactly 2 min in 100 ml of vigorously boiling water (in a 500-ml Erlenmeyer flask), at which time solution generally occurred, followed by formation of solids. Then 100 g of ice and water was added, the flask was set in an ice bath, and 50 ml of glacial acetic acid was added. These additions took 5–6 s. Ten milliliters of 0.25% starch indicator was then added and the mixture was titrated with a standard 0.1 *N* iodine solution to a blue end point.

REFERENCES

1. C. F. H. Allen and G. P. Happ. Can. J. Chem. **42**, 641 (1964).
2. D. D. Reynolds, D. L. Fields, and D. L. Johnson. J. Org. Chem. **26**, 5125 (1961).
3. D. S. Tarbell and D. P. Harnish. Chem. Rev. **49**, 1 (1951).
4. B. H. Nicolet. J. Am. Chem. Soc. **53**, 3066 (1931).
5. K. von Auwers. Ann. **408**, 246 (1915).
6. L. Thorp and E. R. Brunskill. J. Am. Chem. Soc. **37**, 1258 (1915).
7. D. E. Pearson, H. W. Pope, W. W. Hargrove, and W. E. Stamper. J. Org. Chem. **23**, 1412 (1961).
8. W. Davey and J. R. Gwilt. J. Chem. Soc. 1008 (1957).
9. P. Pfeiffer. Ann. **412**, 308 (1916).
10. H. Bauer and P. Vogel. J. Prakt. Chem. Ser. 2, **88**, 334 (1913).
11. E. P. Kohler and J. B. Conant. J. Am. Chem. Soc. **39**, 1702 (1917).
12. J. Jack, J. C. Watkins, and D. E. White. J. Chem. Soc. 3684 (1954).
13. K. von Auwers and H. Brink. Ann. **493**, 218 (1932).
14. H. Staudinger and N. Kon. Ann. **384**, 123 (1911).
15. S. V. Kostanecki and J. Tambor. Ber. **32**, 1924 (1899).
16. C. Weygand and A. Matthes. Ann. **444**, 57 (1926).
17. W. Dilthey. J. Prakt. Chem. Ser. 2, **101**, 196 (1920).

Can. J. Chem. Downloaded from www.nrcresearchpress.com by 210.87.254.105 on 09/05/12
For personal use only.

Can. J. Chem. Downloaded from www.nrcresearchpress.com by 210.87.254.5 on 09/05/12
For personal use only.

NOTES

RADIOLYSIS OF AQUEOUS BROMAL HYDRATE SOLUTIONS; DETECTION OF OXALIC AND GLYOXYLIC ACIDS

R. L. EAGER, R. W. O'DONNELL, AND L. J. TUSZ

Various workers have investigated the products from the irradiation of aqueous solutions of bromal hydrate with beta particles and gamma rays (1–5). All of these workers reported the formation of hydrobromic acid together with relatively small amounts of some additional acid. Woods and Spinks (1) also detected dibromoacetaldehyde and dibromoacetic acid. Heusinger, Woods, and Spinks (2) detected a small yield of carbon dioxide and carboxylic acids. Norris (3) detected dibromoacetaldehyde, tribromoacetic acid, and carbon dioxide. Norris' results indicated that various side reactions occur which yield very small quantities of products, thus making their identification by straightforward chemical means very difficult. Bricknell (4) made a tentative proposal of a mechanism for the radiolysis of aqueous bromal hydrate solutions. This mechanism predicts the formation of one molecule of oxalic acid for every three molecules of hydrobromic acid produced. The oxalic acid was postulated to be formed in the following reaction, which is one step of a chain reaction:

$$Br_2\dot{C}\cdot CH(OH)_2 + O_2 \rightarrow HBr + (COOH)_2 + Br\cdot$$

The present authors decided to look for oxalic acid in aqueous bromal hydrate solutions which had been irradiated with ^{60}Co gamma rays. Since it was possible that glyoxylic acid, CHO·COOH, might be an intermediate in the formation of oxalic acid we decided to look for it also.

EXPERIMENTAL

Samples of aqueous bromal hydrate solutions (0.05 *M* and 0.1085 *M*) were irradiated with ^{60}Co gamma rays. The temperature of the solutions was approximately 22 °C. During the radiolyses oxygen was bubbled through the solutions. To increase the sensitivity of detection of the two compounds, bromal hydrate labelled with ^{14}C in the aldehyde position was used.

Oxalic acid was determined as follows. A solution of inactive sodium oxalate, to serve as a carrier, was added to the irradiated solution. The solution was extracted with ether to remove bromal hydrate. An excess of calcium chloride, followed by sufficient ammonia water to bring the pH to a value of approximately 5.4, was added. Preliminary experiments had indicated that at this pH bromal hydrate did not tend to precipitate, and yet the recovery of calcium oxalate was good. The calcium oxalate precipitate was washed with cold water. A weighed sample of the precipitate was converted to carbon dioxide using the Van Slyke method. The radioactivity of the carbon dioxide was determined with a Dynacon vibrating-reed electrometer (supplied by Nuclear-Chicago Corporation). In control experiments, in which bromal hydrate solutions which had not been irradiated were treated in a similar fashion, the amount of radioactivity carried through to the counting step was found to be negligible.

From the specific activity of the calcium oxalate, the weight of carrier added, the specific activity of the bromal hydrate, and the dose absorbed by the sample, it is possible to calculate the *G* value for the production of oxalic acid. The results are summarized in Table I.

Glyoxylic acid was determined in the irradiated solutions by first adding inactive glyoxylic acid as carrier. Sodium bicarbonate was used to adjust the pH of the solution to the bromophenol blue end-point. The solution was extracted 10 times with chloroform. The aqueous layer was used to form the 2,4-dinitrophenylhydrazine derivative. The precipitate was washed with 5 *N* H_2SO_4 followed by a distilled water wash. The derivative was recrystallized twice from methanol. A weighed sample of the 2,4-dinitrophenylhydrazine derivative was converted to carbon dioxide and counted in a manner similar to that used for the calcium

TABLE I

Formation of oxalic acid

Dose rate (rads min^{-1})	Conc. (M)	Dose $\times 10^{-3}$ (rads)	G (oxalic acid)	Average G
1320	0.0534	256	0.14	
1320	0.0534	716	0.14	0.14
1320	0.0534	1030	0.14	
260	0.0534	371	0.14	
260	0.0534	609	0.14	0.14
260	0.0534	1810	0.14	
1140	0.1085	427	0.09	
1140	0.1085	755	0.13	0.11
1140	0.1085	1390	0.12	

oxalate precipitates. In control experiments the amount of radioactivity carried through to the counting step was found to be negligible. The G values for the production of glyoxylic acid were calculated and are given in Table II.

TABLE II

Formation of glyoxylic acid: dose rate 1140 rads min^{-1}

Conc. (M)	Dose $\times 10^{-3}$ (rads)	G (glyoxylic acid)
0.1085	1360	0.64
0.055	1500	2.6
0.055	1040	0.72

DISCUSSION

The results indicate that both oxalic acid and glyoxylic acid are formed when bromal hydrate solutions are irradiated with ^{60}Co gamma rays. For the dose rates and concentrations of bromal hydrate used in the present work the G value for the production of hydrobromic acid would be in the neighborhood of 100 (5).

The results presented in Table I should not be taken to indicate necessarily that the G value for the appearance of oxalic acid is independent of the dose rate. Over the range of dose rates investigated in the present work the effect of dose rate on the G value for the appearance of hydrobromic acid is also not very significant (5). The effect of concentration on the G value is similar to that for the appearance of hydrobromic acid (5), i.e. it is smaller for higher concentrations.

The much smaller G values found for the appearance of oxalic acid, compared to those for the appearance of hydrobromic acid, would indicate that it is not formed in the reactions by which most of the hydrobromic acid is produced. It is possible that the G value for the production of oxalic acid is actually higher than found in the present work because of radiolysis of oxalic acid itself. If the radiolysis of oxalic acid had been significant, the G values for its appearance would have been expected to decrease with an increase in the absorbed dose. Since the G values were constant over a wide range of absorbed doses it would appear that radiolysis of oxalic acid was not very singificant. Hence, the G values for the production of oxalic acid are probably close to the values reported here for the appearance of oxalic acid.

The results for glyoxylic acid production indicate that it, too, is not formed in the reactions by which most of the hydrobromic acid is produced in the radiolysis of bromal

Can. J. Chem. Downloaded from www.nrcresearchpress.com by 210.87.254.5 on 09/05/12
For personal use only.

hydrate solutions. From Table II it may be seen that there is some doubt about the *G* value for the appearance of glyoxylic acid. The value of 2.6 may, however, be in error since the amount of radioactivity being worked with was very small and hence, even a small amount of contamination would result in higher apparent *G* values. Thus, *G* values of 0.6 to 0.7 may be more nearly correct for the appearance of glyoxylic acid. It would appear that glyoxylic acid is not an intermediate in the formation of oxalic acid since, if it were, the *G* value for the appearance of oxalic acid might be expected to increase with increased absorbed dose.

ACKNOWLEDGMENTS

The authors thank Professor R. J. Woods for his helpful suggestions. Grateful acknowledgment is made to the Atomic Energy Control Board for financial support.

1. R. J. Woods and J. W. T. Spinks. Can. J. Chem. **35**, 1475 (1957).
2. H. Heusinger, R. J. Woods, and J. W. T. Spinks. Can. J. Chem. **37**, 1127 (1959).
3. A. R. Norris. M.Sc. Thesis, University of Saskatchewan, Saskatoon, Sask. 1959.
4. A. G. Bricknell. Ph.D. Thesis, University of Saskatchewan, Saskatoon, Sask. 1959.
5. R. G. McIntosh, R. L. Eager, and J. W. T. Spinks. Can. J. Chem. In press. 1964.

Received May 29, 1964.
Department of Chemistry and Chemical Engineering,
University of Saskatchewan,
Saskatoon, Saskatchewan.

SOME BASICALLY SUBSTITUTED CAMPHANES

Ling Wei and Edgar A. Steck[1]

There have been numerous indications (*inter alia*, refs. 1–6) that morpholine derivatives may exhibit valuable levels of pharmacological activity. For this reason, synthesis of I was undertaken. The route chosen for the preparation of the perhydro-5,8-methano-2*H*-1,4-benzoxazine type is indicated as II–IV to I. It was hoped that 3-bromo-*d*-camphor and ethanolamine would provide facile access to such a type. It was anticipated that these compounds would produce 3-(2-hydroxyethlyamino)camphor, III, however, *N*-(2-hydroxyethyl)camphanimine, V, was formed. This compound was obviously produced by a reductive debromination at the 3-position in I, followed by formation of the Schiff base. Such a fundamental reaction is well known (and not unexpected for such reducing agents) to occur when II is acted on by hydroxylamine (7–10) or phenylhydrazine (11). The structure assigned V was supported by infrared spectra, and also by synthesis from *d*-camphor and ethanolamine. Attempts were made to convert V to an oxazine type, but without success. These approaches included dehydration of V; conversion of V to VI, and dehydration of VI; transformation of V to VII, and of VI to VIII, followed by elimination of hydrogen chloride. No useful activity was uncovered when compounds V–VIII were subjected to broad pharmacological screening in rodents. All products were tested for effects on the central nervous system, and compounds VII and VIII were evaluated for possible actions on the autonomic nervous system. Neither antibacterial nor antifungal testing in vitro gave evidence of significant activity in this series.

[1]*Present address: Nalco Chemical Co., Chicago, Illinois 60638, U.S.A.*

Can. J. Chem. Downloaded from www.nrcresearchpress.com by 210.87.254.5 on 09/05/12
For personal use only.

hydrate solutions. From Table II it may be seen that there is some doubt about the *G* value for the appearance of glyoxylic acid. The value of 2.6 may, however, be in error since the amount of radioactivity being worked with was very small and hence, even a small amount of contamination would result in higher apparent *G* values. Thus, *G* values of 0.6 to 0.7 may be more nearly correct for the appearance of glyoxylic acid. It would appear that glyoxylic acid is not an intermediate in the formation of oxalic acid since, if it were, the *G* value for the appearance of oxalic acid might be expected to increase with increased absorbed dose.

ACKNOWLEDGMENTS

The authors thank Professor R. J. Woods for his helpful suggestions. Grateful acknowledgment is made to the Atomic Energy Control Board for financial support.

1. R. J. Woods and J. W. T. Spinks. Can. J. Chem. **35**, 1475 (1957).
2. H. Heusinger, R. J. Woods, and J. W. T. Spinks. Can. J. Chem. **37**, 1127 (1959).
3. A. R. Norris. M.Sc. Thesis, University of Saskatchewan, Saskatoon, Sask. 1959.
4. A. G. Bricknell. Ph.D. Thesis, University of Saskatchewan, Saskatoon, Sask. 1959.
5. R. G. McIntosh, R. L. Eager, and J. W. T. Spinks. Can. J. Chem. In press. 1964.

Received May 29, 1964.
Department of Chemistry and Chemical Engineering,
University of Saskatchewan,
Saskatoon, Saskatchewan.

SOME BASICALLY SUBSTITUTED CAMPHANES

Ling Wei and Edgar A. Steck[1]

There have been numerous indications (*inter alia*, refs. 1–6) that morpholine derivatives may exhibit valuable levels of pharmacological activity. For this reason, synthesis of I was undertaken. The route chosen for the preparation of the perhydro-5,8-methano-2*H*-1,4-benzoxazine type is indicated as II–IV to I. It was hoped that 3-bromo-*d*-camphor and ethanolamine would provide facile access to such a type. It was anticipated that these compounds would produce 3-(2-hydroxyethlyamino)camphor, III, however, *N*-(2-hydroxyethyl)camphanimine, V, was formed. This compound was obviously produced by a reductive debromination at the 3-position in I, followed by formation of the Schiff base. Such a fundamental reaction is well known (and not unexpected for such reducing agents) to occur when II is acted on by hydroxylamine (7–10) or phenylhydrazine (11). The structure assigned V was supported by infrared spectra, and also by synthesis from *d*-camphor and ethanolamine. Attempts were made to convert V to an oxazine type, but without success. These approaches included dehydration of V; conversion of V to VI, and dehydration of VI; transformation of V to VII, and of VI to VIII, followed by elimination of hydrogen chloride. No useful activity was uncovered when compounds V–VIII were subjected to broad pharmacological screening in rodents. All products were tested for effects on the central nervous system, and compounds VII and VIII were evaluated for possible actions on the autonomic nervous system. Neither antibacterial nor antifungal testing in vitro gave evidence of significant activity in this series.

[1]*Present address: Nalco Chemical Co., Chicago, Illinois 60638, U.S.A.*

Can. J. Chem. Downloaded from www.nrcresearchpress.com by 210.87.254.105 on 09/05/12
For personal use only.

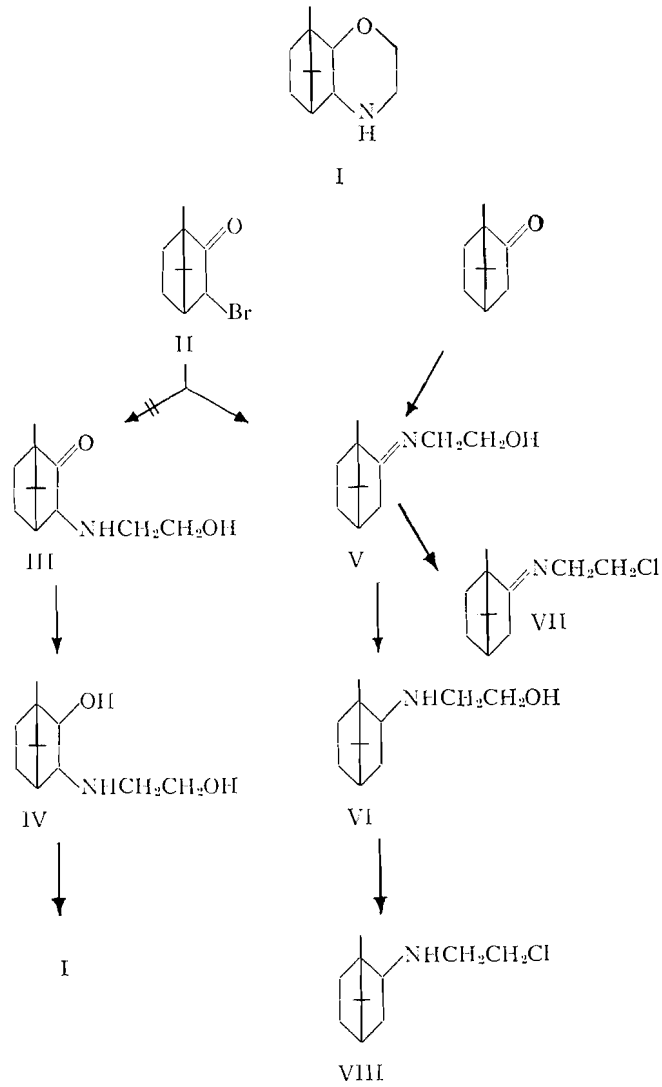

EXPERIMENTAL[2]

N-(2-Hydroxyethyl)camphanimine, V

(a) From 3-Bromo-d-camphor and Ethanolamine

A mixture of 23.1 g (0.1 mole) of 3-bromo-*d*-camphor, 30.5 g (0.5 mole) of ethanolamine, and 0.2 g of copper powder[3] was heated on the steam bath with vigorous stirring for 18 h. The cooled material was quenched on ice, filtered, and the solid was air-dried before dissolving in anhydrous ether, then filtered. Addition of dry hydrogen chloride to the ether solution gave a white precipitate of *N*-(2-hydroxyethyl)-camphanimine hydrochloride. It was crystallized from ethanol to obtain 14.5 g (61%) of prismatic needles which melted at 206° with decomposition; ν_{max} 3.10, 3.40, 3.65, 5.19, 5.86, 6.75, 6.90, 7.06, 9.26, 10.30 μ. The compound had a dull, somewhat camphoraceous odor.

Anal. Calcd. for $C_{12}H_{21}NO \cdot HCl$: C, 62.17; H, 9.57; N, 6.04. Found: C, 62.16; H, 9.58; N, 6.03.

A sample of the hydrochloride (5.0 g) was converted to the base with aqueous ammonia and crystallized

[2]*All melting points are uncorrected. Infrared spectra were determined with 2% potassium chloride pellets in a Perkin–Elmer Model 21 spectrophotometer. Messrs. J. Weinberger and P. D. Carp, of these laboratories, carried out the analytical determinations and spectral studies.*

[3]*The copper could be eliminated with no appreciable effect in yield of product.*

Can. J. Chem. Downloaded from www.nrcresearchpress.com by 210.87.254.105 on 09/05/12
For personal use only.

from ethanol. The creamy prisms (3.8 g) melted at 71–71.5°; ν_{max} 3.19, 3.42, 3.48 (shoulder), 5.94, 6.86, 7.56, 9.31, 11.04 μ. It had a musty, camphoraceous odor.

Anal. Calcd. for $C_{12}H_{21}NO$: C, 73.79; H, 10.83; N, 7.17. Found: C, 73.44; H, 10.82; N, 7.62.

(b) From d-Camphor and Ethanolamine

Interaction of *d*-camphor with an excess of ethanolamine was carried out on the steam bath with and without copper catalyst (cf. ref. 12). In all cases, *N*-(2-hydroxyethyl)camphanimine was formed, and was identified as V by comparison of infrared spectra and melting points of the base and hydrochloride with those produced in (*a*).

2-(2-Hydroxyethylamino)camphane VI

(a) Catalytic Hydrogenation of V

A solution of 19.5 g (0.1 mole) fo 2-(2-hydroxyethylimino)camphane in 50 ml of ethanol was reduced at 39 kg/cm^2 hydrogen pressure in the presence of 5 g of Raney nickel. The reaction required 3 h for completion, and then the filtered solution was treated with hydrogen chloride. A 96.1% yield (22.5 g) of hydrochloride resulted after crystallization of the crude product from ethanol. The microcrystalline solid, which melted at 271–272°, had a slight camphor-like odor; ν_{max} 3.10, 3.42, 6.51, 6.88, 6.95, 7.08, 9.30 μ.

Anal. Calcd. for $C_{12}H_{23}NO \cdot HCl$: C, 61.65; H, 10.35; N, 5.99. Found: C, 61.83; H, 10.56; N, 5.48.

(b) Sodium Borohydride Reduction of V

A solution of 9.8 g (0.05 mole) of *N*-(2-hydroxyethyl)camphanimine in 50 ml of ethanol was cooled to 0° and a solution of 2.0 g (0.05 mole) of sodium hydroxide in 10 ml of water was added. It was then treated with 4.7 g (0.125 mole) of sodium borohydride, portionwise, during 0.5 h. Then the mixture was stirred at room temperature for 1 h before heating on the steam bath for an hour. It was cooled and extracted with ether. The extracts were washed with water and then dried (sodium sulphate). The filtered extracts were treated with hydrogen chloride, and the precipitated salt collected, washed (acetone), and crystallized from methanol–ether. The product (9.5 g, 81% yield) melted at 271–272° and exhibited spectral characteristics identical with the compound prdouced by catalytic hydrogenation.

Anal. Calcd. for $C_{12}H_{23}NO \cdot HCl$: C, 61.65; H, 10.35. Found: C, 61.90; H, 10.30.

N-(2-Chloroethyl)camphanimine, VII

N-(2-Hydroxyethyl)camphanimine hydrochloride (11.6 g, 0.05 mole) was slowly treated, with stirring, with 22.8 g (0.2 mole) of thionyl chloride. The mixture was stirred at room temperature for 1 h, collected, and washed with acetone. It separated from benzene (12.0 g, 96% yield) in the form of platelets m.p. 226–227°, which had an odor resembling that of eucalyptol; ν_{max} 3.40, 3.84, 5.83, 6.80, 6.92, 7.08, 7.17, 8.28, 9.29 μ.

Anal. Calcd. for $C_{12}H_{20}ClN \cdot HCl$: C, 57.20; H, 8.46; N, 5.59. Found: C, 57.37; H, 8.58; N, 5.45.

2-(2-Chloroethylamino)camphane, VIII

This compound was prepared from VI in the manner employed for VII. It was obtained (92% yield; crystallized from benzene) as a cryptocrystalline solid which had a slight, dull, camphoraceous odor, m.p. 273° with decomposition; ν_{max} 3.40, 3.69, 6.25, 6.80, 6.88 (bifurcation), 7.02, 7.15 μ.

Anal. Calcd. for $C_{12}H_{22}ClN \cdot HCl$: C, 57.14; H, 9.15; N, 5.55. Found: C, 57.19; H, 9.30; N, 5.44.

ACKNOWLEDGMENTS

The authors have had the advantage of discussions with Dr. C. C. Cochrane and Dr. J. M. Sandri and express particular appreciation to them. We are pleased to acknowledge the efforts of the pharmacologists (under the direction of Dr. W. M. Govier) who tested the compounds at McNeil Laboratories.

1. O. Thomä. U. S. Patent No. 2,835,669 (May, 1958).
2. M. J. Kalm. U. S. Patent No. 2,832,777 (April, 1958).
3. Ravensberg G. m. b. H. Ger. Patent No. 1,109,175 (June, 1961).
4. A. Engelhardt, D. Jerchel, H. Weidmann, and H. Wick. Arch. Exptl. Pathol. Pharmakol. **235**, 10 (1958).
5. R. Haberl. Monatsh. **89**, 814 (1959).
6. B. Belleau. J. Med. Pharm. Chem. **2**, 553 (1960).
7. H. Goldschmidt and R. Koreff. Ber. **18**, 1632 (1885).
8. A. Angeli and E. Rimini. Gazz. Chim. Ital. **26**, II, 49 (1896).
9. F. Angelico and G. Montalbano. Gazz. Chim. Ital. **30**, 283 (1900).
10. F. Angelico. Atti Accad. Naz. Lincei Rec. **9**, 47 (1900).
11. L. Balbiano. Gazz. Chim. Ital. **16**, 132 (1886).
12. P. Saccardi. Ann. Chim. applicata, **20**, 489 (1930).

Received May 26, 1964.
Johnson and Johnson Research Center,
New Brunswick, New Jersey.

Can. J. Chem. Downloaded from www.nrcresearchpress.com by 210.87.254.105 on 09/05/12
For personal use only.

CORROBORATION THAT 3,3′-DIINDOLYL SULPHIDE IS THE COMPOUND OBTAINED FROM THE REACTION OF INDOLE MAGNESIUM BROMIDE WITH SULPHUR

R. V. Jardine and R. K. Brown

In an attempt to prepare 3-mercaptoindole by the reaction of indole magnesium bromide with sulphur, Madelung and Tencer obtained a compound which analyzed for a diindolyl sulphide (1). They found that this compound was unusually inert, being stable to oxidation by potassium permanganate, to boiling potassium hydroxide solution, and to acetic anhydride or nitrous acid. On this basis they suggested structure I as a possibility for this substance. Nevertheless, structure II (3,3′-diindolyl sulphide) was accepted, presumably because of the preference of indole magnesium bromide to react at the β-position (1–3).

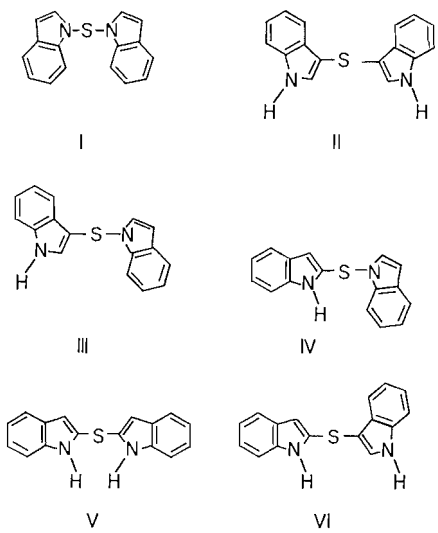

While seeking routes for the synthesis of 3-alkylthioindoles, we have obtained as one of the products from the reaction of indole magnesium bromide with ethanesulphenyl chloride a compound analyzing correctly for diindolyl sulphide and showing an infrared spectrum identical with that of the compound prepared according to Madelung and Tencer's procedure (1). We felt that the structure of this compound should be placed on a firmer basis before elucidation of the route to its formation could be investigated.

A clear choice of the appropriate structure from among I–VI could be made by the following infrared and nuclear magnetic resonance (n.m.r.) spectral examinations. Because of the general poor solubility of the diindolyl sulphide in suitable solvents, the infrared spectrum was obtained in a Nujol mull. A sharp doublet at 3395 cm^{-1} and 3410 cm^{-1}, in the region expected for indole N—H stretching (4), eliminated structure I and agreed with structures II–VI. Replacement of hydrogen on the nitrogen atom by deuterium, a reaction very easily accomplished for this compound by the usual procedure of repeated treatment of the sulphide with D_2O in pyridine or acetone, eliminated this doublet as well as doublets at 1405 and 1410 cm^{-1} and 1085 and 1095 cm^{-1} and also bands at 1105 cm^{-1} and 1118 cm^{-1}. A new band appeared at 2535 cm^{-1}, accompanied by a lesser band at 2522 cm^{-1} along with a new doublet at 910 and 915 cm^{-1}. This shift in

Can. J. Chem. Downloaded from www.nrcresearchpress.com by 210.87.254.40 on 09/05/12
For personal use only.

absorption of 3395 cm^{-1} to 2535 cm^{-1}, upon replacement of the hydrogen on nitrogen by deuterium, is approximately that predicted by Hooke's law (5).

The appearance of the doublets in the infrared spectrum indicated the possibility of structure VI, containing two slightly different N—H groups. However, n.m.r. evidence supported structure II. It has been shown (6) that in $CDCl_3$ solution, the C_2 and C_3 protons of indole absorb at $\tau = 3.32$ and 3.62 respectively (referred to tetramethylsilane). Because of the solubility limitations of the diindolyl sulphide, acetone was chosen as the solvent for n.m.r. analysis. In this solvent, the C_2 (or C_3) proton was shifted farther downfield because of the combined inductive effect of the sulphur and nitrogen atoms and appeared as a sharp doublet at $\tau = 2.43$ ($J = 2$ c.p.s.). The integrated area for this doublet corresponded to *two* protons. This assignment was made because replacement of the N—H by N—D caused the doublet to collapse to a sharp singlet, whose integrated area was equal to two protons. The disappearance of splitting provides evidence of coupling between the N—H and the C_2 (or C_3) proton and indicates that the protons (C_2 or C_3) are equivalent, thus eliminating structures III, IV, and VI and supporting structures II and V.

A decision between II and V could be made by determining the extent of the change in chemical shift of the signals for the C_2 (or C_3) proton of the indole structure as one changes from one solvent to another. It is known that the signal position of the C_2 proton of indoles is markedly affected by solvent, while that of the C_3 proton of indoles remains practically unchanged in various solvents (7). The poor solubility of the diindolyl sulphide limited the application of this technique but it was sufficiently useful to permit clear distinction between II and V.

The signals for the C_3 protons of indole, ethyl indole-2-carboxylate, and indole-2-carboxylic acid have been found to be nearly at the same positions in the three solvents dioxane, dimethyl sulphoxide, and acetone. However, the positions of the C_2 proton signals of the compounds indole, ethyl indole-3-carboxylate, and indole-3-carboxylic acid were found to vary considerably in these solvents (7). In any pair of the solvents used there was never more than a difference of 0.08 τ found for the C_3 proton signal position, but that of the C_2 proton changed as much as 0.18 to 0.24 τ.

The signal positions of the C_2 (or C_3) protons of the diindolyl sulphide are shown in Table I.

TABLE I

Signal positions of the C_2 (or C_3) proton of diindolyl sulphide

Solvent	Dioxane	Dimethyl sulphoxide	Acetone
Signal (doublet centered at)	2.66	2.40	2.43
J (c.p.s.)	2	2	2

Since the difference in the signal position in dioxane and dimethyl sulphoxide is 0.26 τ, this is strong evidence for the adoption of structure II rather than structure V.

The likelihood that the substance is a mixture of II and V is ruled out by the n.m.r. spectrum, which would show two doublets which are reduced upon deuteration to two singlets, one of which would shift in position more than the other upon solvent change. This has not been observed.

The doublet observed for the N—H stretching in the infrared spectrum of 3,3′-diindolyl sulphide (II) may be due to the interaction between neighboring molecules in the crystalline state (4, pp. 28 and 380). Hence, observation of multiplicity of N—H peaks in Nujol

Can. J. Chem. Downloaded from www.nrcresearchpress.com by 210.87.254.40 on 09/05/12
For personal use only.

can not be taken as evidence for the existence of *two different* N—H groups since each of the compounds II to VI could show this phenomenon. Therefore the appearance of absorption in this region indicates unequivocally only the *presence* of the N—H group.

Such band duplication disappears upon solvation of the substance, and, in fact, a solution of the sulphide in dioxane gave a single though somewhat broadened band whose maximum is at 3300 cm^{-1}. In methylene chloride, the infrared spectrum of II, measured at high resolution, showed a single peak at 3460 cm^{-1}.

EXPERIMENTAL

Infrared spectra were recorded on Perkin–Elmer Instruments models 21, 221G, and 421. Nuclear magnetic resonance spectra were recorded on a Varian Associates model A-60 instrument. Further details and spectra are available in the thesis of R. V. Jardine.*

Deuteration of 3,3'-Diindolyl Sulphide

About 120 mg of 3,3'-diindolyl sulphide (1) was dissolved in 8 ml of reagent acetone and then 2 ml of D_2O (99.7%) was added. The solution was stirred for 10 min and then freed of solvent in a rotary evaporator under vacuum. This treatment was repeated two or three more times. Final drying of the compound was carried out over P_2O_5 in a desiccator. Care was taken to protect all solutions from direct light.

The extent of deuteration was determined by infrared spectroscopy. Disappearance of the N—H peak between 3100 and 3500 cm^{-1} in the infrared and the appearance of a new peak due to N—D at a frequency of about 0.75 of the N—H stretching frequency gave a measure of the amount of deuterium exchange.

ACKNOWLEDGMENT

The authors express their gratitude to the National Research Council of Canada for financial assistance during this work.

1. W. Madelung and M. Tencer. Ber. **48**, 949 (1915).
2. B. Oddo and Q. Mingoia. Gazz. Chim. Ital. **62**, 299 (1932). Chem. Abstr. **26**, 4603 (1932).
3. W. C. Sumpter and F. M. Miller. The chemistry of heterocyclic compounds. Vol. 8. *Editor* A. Weisberger. Interscience Publishers, Inc., New York. 1954. p. 50.
4. R. J. Bellamy. The infra-red spectra of complex molecules. John Wiley & Sons, Inc., New York. 1958. p. 251.
5. A. D. Cross. Introduction to practical infra-red spectroscopy. Butterworth Scientific Publications, London. 1960. p. 2.
6. L. A. Cohen, J. W. Daly, H. Kny, and B. Witkop. J. Am. Chem. Soc. **82**, 2184 (1960).
7. R. V. Jardine and R. K. Brown. Can. J. Chem. **41**, 2067 (1963).

Received June 22, 1964.
Department of Chemistry,
University of Alberta,
Edmonton, Alberta.

**Entitled "The synthesis of some 3-diindolyl thioethers" and submitted to the Department of Chemistry, University of Alberta, Edmonton, Alberta, 1963.*

UNIT CELL DIMENSIONS AND SPACE GROUPS OF SYM-DIPHENYL THIOUREA AND SYM-DIPHENYL UREA

Roy Kari and N. R. Kunchur

A preliminary X-ray examination of *sym*-diphenyl urea and *sym*-diphenyl thiourea has been carried out as part of the program to study the crystal and molecular structures of the derivatives of urea and thiourea. These two derivatives are formed by a symmetrical substitution of one hydrogen by a benzene ring on each of the two nitrogen atoms of urea and thiourea. From the examination of the ultraviolet absorption spectra of the substituted ureas, Picard and McKay (2) pointed out that some double bond character

Can. J. Chem. Downloaded from www.nrcresearchpress.com by 210.87.254.40 on 09/05/12
For personal use only.

can not be taken as evidence for the existence of *two different* N—H groups since each of the compounds II to VI could show this phenomenon. Therefore the appearance of absorption in this region indicates unequivocally only the *presence* of the N—H group.

Such band duplication disappears upon solvation of the substance, and, in fact, a solution of the sulphide in dioxane gave a single though somewhat broadened band whose maximum is at 3300 cm^{-1}. In methylene chloride, the infrared spectrum of II, measured at high resolution, showed a single peak at 3460 cm^{-1}.

EXPERIMENTAL

Infrared spectra were recorded on Perkin–Elmer Instruments models 21, 221G, and 421. Nuclear magnetic resonance spectra were recorded on a Varian Associates model A-60 instrument. Further details and spectra are available in the thesis of R. V. Jardine.*

Deuteration of 3,3'-Diindolyl Sulphide

About 120 mg of 3,3'-diindolyl sulphide (1) was dissolved in 8 ml of reagent acetone and then 2 ml of D_2O (99.7%) was added. The solution was stirred for 10 min and then freed of solvent in a rotary evaporator under vacuum. This treatment was repeated two or three more times. Final drying of the compound was carried out over P_2O_5 in a desiccator. Care was taken to protect all solutions from direct light.

The extent of deuteration was determined by infrared spectroscopy. Disappearance of the N—H peak between 3100 and 3500 cm^{-1} in the infrared and the appearance of a new peak due to N—D at a frequency of about 0.75 of the N—H stretching frequency gave a measure of the amount of deuterium exchange.

ACKNOWLEDGMENT

The authors express their gratitude to the National Research Council of Canada for financial assistance during this work.

1. W. Madelung and M. Tencer. Ber. **48**, 949 (1915).
2. B. Oddo and Q. Mingoia. Gazz. Chim. Ital. **62**, 299 (1932). Chem. Abstr. **26**, 4603 (1932).
3. W. C. Sumpter and F. M. Miller. The chemistry of heterocyclic compounds. Vol. 8. *Editor* A. Weisberger. Interscience Publishers, Inc., New York. 1954. p. 50.
4. R. J. Bellamy. The infra-red spectra of complex molecules. John Wiley & Sons, Inc., New York. 1958. p. 251.
5. A. D. Cross. Introduction to practical infra-red spectroscopy. Butterworth Scientific Publications, London. 1960. p. 2.
6. L. A. Cohen, J. W. Daly, H. Kny, and B. Witkop. J. Am. Chem. Soc. **82**, 2184 (1960).
7. R. V. Jardine and R. K. Brown. Can. J. Chem. **41**, 2067 (1963).

Received June 22, 1964.
Department of Chemistry,
University of Alberta,
Edmonton, Alberta.

**Entitled "The synthesis of some 3-diindolyl thioethers" and submitted to the Department of Chemistry, University of Alberta, Edmonton, Alberta, 1963.*

UNIT CELL DIMENSIONS AND SPACE GROUPS OF SYM-DIPHENYL THIOUREA AND SYM-DIPHENYL UREA

Roy Kari and N. R. Kunchur

A preliminary X-ray examination of *sym*-diphenyl urea and *sym*-diphenyl thiourea has been carried out as part of the program to study the crystal and molecular structures of the derivatives of urea and thiourea. These two derivatives are formed by a symmetrical substitution of one hydrogen by a benzene ring on each of the two nitrogen atoms of urea and thiourea. From the examination of the ultraviolet absorption spectra of the substituted ureas, Picard and McKay (2) pointed out that some double bond character

Can. J. Chem. Downloaded from www.nrcresearchpress.com by 210.87.254.40 on 09/05/12
For personal use only.

exists between nitrogen of urea or thiourea and the phenyl group. Since urea and thiourea are known to have planar structures (2, 3), one can predict that their substituted compounds should have a similar configuration having a molecular symmetry identical with that of the parent molecules. The results of the preliminary work on *sym*-diphenyl thiourea shows that this compound has the same molecular symmetry as thiourea.

sym-Diphenyl Thiourea ($C_{13}H_{12}N_2S$)

Molecular weight 228.31. The crystals obtained by recrystallization from benzene are thin plates on (001) outlined by (100) and (010). The unit cell dimensions and space group were determined from various oscillation and Weissenberg photographs with Cu K_α radiation.

Crystal Data

Orthorhombic; $a = 8.15 \pm 0.03$ Å, $b = 26.17 \pm 0.05$ Å, $c = 5.63 \pm 0.02$ Å.

Volume of the unit cell is 1 200.8 Å^3.

Absorption coefficient for X rays; $\lambda = 1.542$ Å, $\mu = 21.8$ cm^{-1}.

Total number of electrons per unit cell $F(000) = 480$. The density, 1.25 g cm^{-1}, calculated on the assumption that the unit cell contains four molecules, agrees with the measured value (flotation method) of 1.24 g cm^{-3}. The systematic absences—$hk0$ for h odd and $0kl$ for $k + l$ odd—correspond to the space groups $Pnma$ and $Pn2_1a$. The ambiguity regarding the space group determination was resolved by doing the Wilson's statistical test which is consistent with the centrosymmetric space group $Pnma$. Since the symmetry of the general positions of this space group is eightfold and there are four molecules per unit cell, it follows that the molecule should occupy one of the special four-position 4*a*, 4*b*, or 4*c*. From chemical considerations, the molecule has a mirror plane of symmetry and so can be located at 4*c*, which also has a mirror plane point symmetry. The positions 4*a* and 4*b* can be ruled out since they require the molecule to posses a center of symmetry which it cannot have. A three-dimensional crystal structure analysis of this compound is in progress.

sym-Diphenyl Urea ($C_{13}H_{12}N_2O$)

Molecular weight 212.24. The crystals formed from ethanol are flat plates parallel to the '*b*' axis. The crystal data was obtained in a similar manner as described for the previous compound.

Crystal Data

Orthorhombic; $a = 9.07 \pm 0.03$ Å, $b = 11.70 \pm 0.03$ Å, $c = 10.60 \pm 0.03$ Å.

Volume of the unit cell is 1 124.8 Å^3.

Absorption coefficient for X rays; $\lambda = 1.542$ Å, $\mu = 7.5$ cm^{-1}.

Total number of electrons $F(000) = 448$.

The density 1.25 g cm^{-1} calculated on the assumption of four molecules in the unit cell, agrees with the experimental value (flotation method) of 1.24 g cm^{-3}. The systematic absences—$hk0$ for h odd and $0kl$ for $k + l$ odd—correspond to the space groups $Pnma$ and $Pn2_1a$.

No further work on this compound is planned.

1. J. P. Picard and A. F. McKay. Can. J. Chem. **31**, 896 (1953).
2. P. A. Vaughn and J. Donahue. Acta Cryst. **5**, 530 (1952).
3. N. R. Kunchur and M. R. Truter. J. Chem. Soc. 2551 (1958).

Received June 30, 1964.
Chemistry Department,
University of Western Ontario,
London, Ontario.

Can. J. Chem. Downloaded from www.nrcresearchpress.com by 210.87.254.40 on 09/05/12
For personal use only.

THE STRUCTURES AND ABSOLUTE CONFIGURATIONS OF ANHYDRODEOXYHEPTITOLS

A. CAMERMAN, H. J. KOCH, A. ROSENTHAL, AND J. TROTTER

Hydroformylation in the presence of dicobalt octacarbonyl (1) of tri-O-acetyl-D-glucal yielded two isomeric products, which then were deacetylated and the parent polyols separated by paper chromatography. The fast running fraction had m.p. 137–138°, $[\alpha]_D = 1°$ (*c*, 3.5, water), and the other isomer had m.p. 156°, $[\alpha]_D = +60°$ (*c*, 1.4, water). Proton magnetic resonance (p.m.r.) spectra of the individual deacetylated polyols indicated that the carbon skeletons were linear. Hence the compounds are isomeric anhydrodeoxyheptitols. Rotation rules (2) then suggested that the lower melting isomer is 2,6-anhydro-3-deoxy-D-*gluco*heptitol (I, $R_1 = R_2 = H$), and the higher melting isomer is 2,6-anhydro-3-deoxy-D-*manno*heptitol (II). However, since these rules are not of universal

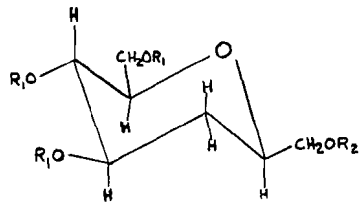

I

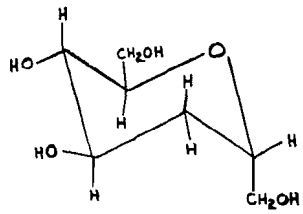

II

application and have not been applied to heptitols, further definite evidence for the structures was sought. The p.m.r. spectra of the polyols obtained by using deuterium in the hydroformylation gave further support to the tentative assignment of structure, but an X-ray investigation was undertaken to establish the structure conclusively.

For X-ray analysis the *p*-bromobenzenesulphonyl triacetyl derivative of the lower melting polyol was prepared by treatment of the mixture of triacetylanhydrodeoxyheptitols with *p*-bromobenzenesulphonyl chloride. The required derivative preferentially crystallized out of the reaction mixture, and subsequently was deacetylated and debrosylated by standard methods to yield a pure sample of the lower melting polyol. Crystals of the derivative (m.p. 104°, $[\alpha]_D = -10°$ (*c*, 3, chloroform)) are orthorhombic with four molecules in a unit cell of dimensions $a = 13.71$, $b = 29.37$, $c = 5.79$ Å, space group $P2_12_12$. The intensities of the reflexions were measured with a scintillation counter and Cu K_α radiation. The bromine and sulphur positions were determined from the three-dimensional Patterson function, the coordinates of the carbon and oxygen atoms were obtained from successive three-dimensional electron-density distributions, and all the parameters were refined by differential syntheses and the method of least squares; the final *R* factor was 0.09. A perspective drawing of the molecule is shown in Fig. 1 (the atom numbering is for convenience in the crystallographic investigation).

The structure is I($R_1 = CH_3 \cdot CO-$, $R_2 = Br \cdot C_6H_4 \cdot SO_2-$), in agreement with the indirect evidence. The ring has the chair form, and all the substituents are equatorial.

Can. J. Chem. Downloaded from www.nrcresearchpress.com by 210.87.254.105 on 09/05/12
For personal use only.

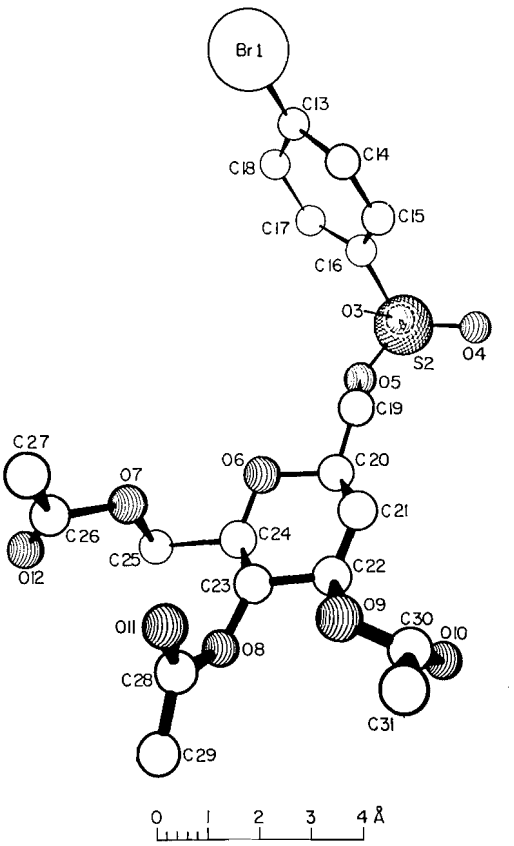

FIG. 1. Perspective drawing of the molecule.

1. A. ROSENTHAL and D. READ. Methods Carbohydrate Chem. **2**, 457 (1963).
2. C. S. HUDSON. J. Am. Chem. Soc. **31**, 66 (1909).

RECEIVED MARCH 12, 1964.
DEPARTMENT OF CHEMISTRY,
UNIVERSITY OF BRITISH COLUMBIA,
VANCOUVER 8, BRITISH COLUMBIA.

EFFECTS OF pH IN THE γ-RADIOLYSIS OF AQUEOUS SOLUTIONS OF CYSTEINE AND METHYL MERCAPTAN

D. A. ARMSTRONG AND V. G. WILKENING

Packer (1) has recently shown that the yield of peroxide, which accumulates in irradiated air-free acid solutions of cysteine, is consistent with the accepted molecular yield, $G_{H_2O_2}{}^M$. This observation confirms the earlier results of Whitcher, Rotheram, and Todd (2), and we may conclude that the molecular peroxide formed in acidified solutions does

Can. J. Chem. Downloaded from www.nrcresearchpress.com by 210.87.254.105 on 09/05/12
For personal use only.

Can. J. Chem. Downloaded from www.nrcresearchpress.com by 210.87.254.6 on 09/05/12
For personal use only.

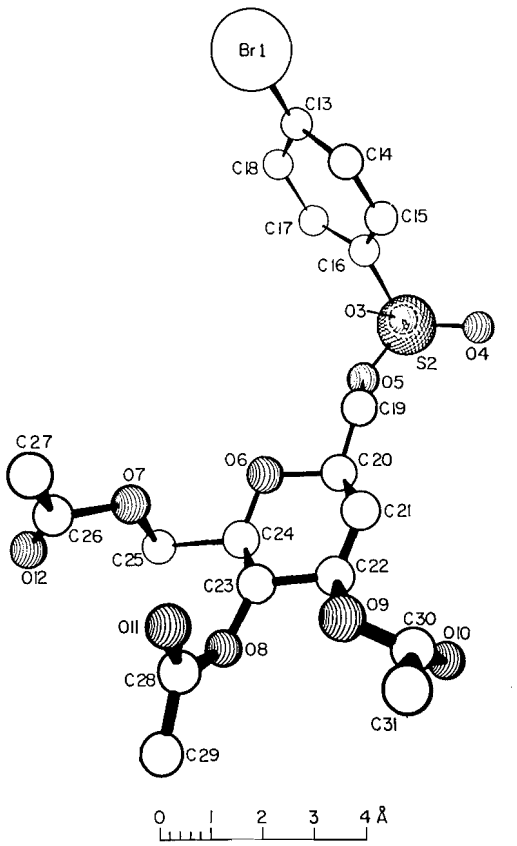

FIG. 1. Perspective drawing of the molecule.

1. A. ROSENTHAL and D. READ. Methods Carbohydrate Chem. **2**, 457 (1963).
2. C. S. HUDSON. J. Am. Chem. Soc. **31**, 66 (1909).

RECEIVED MARCH 12, 1964.
DEPARTMENT OF CHEMISTRY,
UNIVERSITY OF BRITISH COLUMBIA,
VANCOUVER 8, BRITISH COLUMBIA.

EFFECTS OF pH IN THE γ-RADIOLYSIS OF AQUEOUS SOLUTIONS OF CYSTEINE AND METHYL MERCAPTAN

D. A. ARMSTRONG AND V. G. WILKENING

Packer (1) has recently shown that the yield of peroxide, which accumulates in irradiated air-free acid solutions of cysteine, is consistent with the accepted molecular yield, $G_{H_2O_2}{}^M$. This observation confirms the earlier results of Whitcher, Rotheram, and Todd (2), and we may conclude that the molecular peroxide formed in acidified solutions does

not react with cysteine or affect its decomposition (provided the peroxide concentration never rises to such a level that it begins to compete for radical intermediates). Similar considerations should obviously apply for the molecular hydrogen.

It has generally been assumed (1, 3) that hydroxyl radicals will abstract hydrogen atoms from the thiol group,

[1] $$OH + RSH \rightarrow H_2O + RS,$$

and that in air-free solutions the resulting thiol radicals will dimerize,

[2] $$2RS \rightarrow RSSR.$$

These rather straightforward assumptions appear entirely reasonable to us. In contrast there is evidence that the reactions of the reducing radicals, e_{aq}^- and H, with cysteine are highly complex. Littman, Carr, and Brady (4) examined the products of reaction between hydrogen atoms from an electrical discharge and cysteine in aqueous solution. At pH's in the range 0–6 cystine was the major product, but smaller quantities of H_2S were also formed. These authors suggested that reaction [3],

[3] $$H + RSH \rightarrow RS + H_2,$$

predominated over [4],

[4] $$H + RSH \rightarrow R + H_2S,$$

and was followed by [2]. As the pH was increased above 7 the relative proportions of the two products began to be reversed until at a pH of 11 H_2S was by far the major product. This reversal was attributed to the ionization of the thiol group,

[5] $$RSH \rightleftharpoons RS^- + H^+$$

(pK = 8.36 (5)), and the replacement of reactions [3] and [4] by [6]:

[6] $$H + RS^- \rightarrow R + SH^-.$$

Earlier work by Dale and Davies (6) had shown that H_2S was an important product of the X-radiolysis of dilute aqueous cysteine solutions. The yield was appreciable in the region of pH 3 and passed through a maximum at pH 7. At pH's above 8, where Littman *et al.* had observed an enhancement of the H_2S yield from hydrogen-atom attack on cysteine, the radiolytic H_2S yield declined. The production of H_2S with a G value of the order of 3 from cysteine solutions at pH's lower than 7 was subsequently confirmed by Whitcher, Rotheram, and Todd (2) and by Markakis and Tappel (3). The results of these two groups are presented in Table I together with our own. The values of $G(H_2S)$ in parentheses were calculated from the data of the present study using the expression:

[i] $$G(H_2S) = \left\{G_H + G_e \frac{k_8[H^+]}{k_8[H^+] + k_7[RSH]}\right\} \frac{k_4}{k_3 + k_4} + G_e \frac{k_7[RSH]}{k_8[H^+] + k_7[RSH]}.$$

The rate constants in this expression are identified below and the values of G_H and G_e were taken from the current literature.

Clearly, if the work of Littman, Carr, and Brady is correct, it is rather difficult to reconcile the pH dependence of the radiolytic H_2S yields with hydrogen-atom attack on cysteine. It is necessary, therefore, to consider the possibility that reaction [7] produces H_2S,

[7] $$e_{aq}^- + RSH \rightarrow R + SH^-,$$

and competes with reaction [8],

[8] $$e_{aq}^- + RSH \rightarrow R + SH^-,$$

Can. J. Chem. Downloaded from www.nrcresearchpress.com by 210.87.254.6 on 09/05/12
For personal use only.

TABLE I

Products of X- or γ-radiolysis of aqueous cysteine solutions

Group	pH	[RSH], M	G(RSSR)	$G(H_2S)$	$G(H_2)$	G(RH)	$G(NH_3)$
Oxygen-free solutions							
W, R, and T†	8.0	4×10^{-4}		3.2 (3.1)			
W, R, and T	4.0	4×10^{-4}		2.4 (2.4)			
M and T‡	1.6	10^{-1}	3.7	2.9 (2.5)		2.9	(0.5)
This study	6.41	10^{-3}		2.96	1.03		
	5.51	10^{-3}		—	1.07		
	4.72	10^{-3}		2.80	1.17		
	4.28	10^{-3}		2.61	1.25		
	3.60	10^{-3}		—	1.57		
	3.48	10^{-3}		2.12	1.73		
	3.41	10^{-3}		—	1.80		
	3.32	10^{-3}		2.17	1.97		
	2.99	10^{-3}		—	2.26		
	2.59	10^{-3}		1.86	2.31		
	1.35	10^{-3}		1.46	2.48		
	0.72	10^{-3}		1.49	2.54		
Oxygenated solutions							
M and T‡	1.6	10^{-1}	(12.0)	2.6		3.9	1.8
W, R, and T†	1.6	4×10^{-4}	(12.0)	0.6		—	—

†See ref. 2.
‡See ref. 3.

which in acid solution converts e_{aq}^- to H. If k_7/k_8 is sufficiently large, the appearance of H_2S at pH's below those at which the thiol group is significantly ionized can then be explained. Such a competition for e_{aq}^- would be analogous to that already observed with the chloroacetic acids (7), and should manifest itself in drastic changes in the hydrogen and H_2S yields over the pH range in which [7] and [8] are competing.

Table I shows values of $G(H_2)$ and $G(H_2S)$ from experiments with air-free 10^{-3} M cysteine solutions in sulphuric acid at several different pH's between 0–8. Absorbed doses of ^{60}Co radiation were in the range 0.4–5 $\times$ 10^{18} eV/gm. The yields of H_2S in these solutions were measured by the molybdate method (8). Their downward trend over the pH range corresponding to the increase in the hydrogen yields provides strong support for a competition between reactions [7] and [8]. The hydrogen yields from 0.05 M methyl mercaptan solutions* showed a similar pH dependence with those obtained from cysteine, and the formation of H_2S in appreciable quantities at the higher pH's was confirmed colorimetrically.

For methyl mercaptan the R radical formed in reactions [4] and [7] would be a methyl radical. This should abstract a hydrogen atom from another thiol molecule to form methane, viz.

$$R + RSH \rightarrow RH + RS. \qquad [9]$$

In all the mercaptan experiments a second noncondensable gas remained after diffusion of the hydrogen through a palladium thimble. This was confirmed by mass spectrometric analysis to be methane. As shown in Fig. 1, $G(CH_4)$ followed the expected downward trend as the pH was decreased. In the case of cysteine, reaction [9] would yield alanine, and, in support of the proposed mechanism, we find $G(H_2S) \simeq G$(alanine) $\simeq 2.9$ from the data of Markakis and Tappel at pH 1.6 and a dose of 10^6 r. (Beyond this dose

These were prepared by admitting a known quantity of mercaptan to 5 ml of degassed acidic solvent in a cell of known total volume. After the contents of the cell were melted, the mercaptan was equilibrated at room temperature between the vapor and solution phases. Its concentration in solution was calculated using an experimentally measured solubility coefficient (3.8×10^{-3} moles per l per cm pressure of mercaptan).

Can. J. Chem. Downloaded from www.nrcresearchpress.com by 210.87.254.6 on 09/05/12
For personal use only.

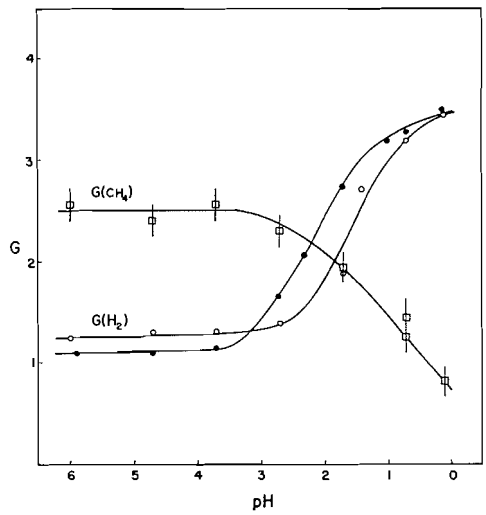

FIG. 1. Dependence of $G(CH_4)$ and $G(H_2)$ from γ-irradiated methyl mercaptan solutions on pH; (○) $G(H_2)$ from 0.04 to 0.06 M MeSH solutions, (□) $G(CH_4)$ from 0.04 to 0.06 M MeSH solutions, (●) $G(H_2)$ from 0.005 to 0.008 M MeSH solutions.

secondary reactions of the products become important.) If [1], [3] or [4], and [7] are the only important reactions of OH, H, and e_{aq} the total number of RS radicals from all sources would be equal to $G_{OH} + G_H + G_e$ (= 3.65 + 2.95, taken from ref. 9*a* for acid solutions; 3.65 = total $G_{reducing}$). Hence G(cystine) should be 3.30. Markakis and Tappel observed 3.7, in reasonable agreement.

Assuming $G_{H_2}^M = 0.3$ in 5×10^{-2} M mercaptan solutions, one may obtain $G_{reducing} = G(CH_4) + G(H_2) - G_{H_2}^M = 3.8$ at pH 0.72. This is consistent with other work (9) for acid solutions. Furthermore, since at this pH almost all e_{aq}^- appear to react via [8], k_3/k_4 should be equal to $(G(H_2) - G_{H_2}^M)/G(CH_4) = 6.4$. At pH's between 4 and 7 the data indicate values of $G_{reducing}$ and G_H slightly larger than those observed with most other scavengers. These results will be discussed in detail elsewhere. Similar calculations may be made for cysteine, for which k_3/k_4 has a value of about 1.5.

Application of the steady-state approximation leads to the expression:

$$[ii] \qquad \frac{1}{\Delta G(H_2)} = \frac{(k_3 + k_4)}{k_4 G_e}\left(1 + \frac{k_7[RSH]}{k_8[H^+]}\right),$$

in which $\Delta G(H_2)$ is the increase in hydrogen yield over that observed at higher pH's. Plots of $1/\Delta G(H_2)$ vs. $[RSH]/H^+]$ in accordance with [ii] gave $k_7/k_8 = 0.5 \pm 0.2$ and 0.8 ± 0.3 for cysteine and methyl mercaptan respectively. Since k_8 is known (10) it is possible to obtain $k_7 = 1.1 \pm 0.4 \times 10^{10}$ l mole^{-1}s^{-1} for cysteine. This large rate-constant means that careful consideration must be given to the possible importance of reaction [7] in radiation biological mechanisms. Also of significance is the fact that cysteine and other thiols will be able to compete with oxygen* at comparable concentrations for e_{aq}^-.

It must be remembered that, as well as influencing the rate of reaction [8], changes in pH and ionic strength will also alter the degree of ionization of the three acid groups of cysteine (5) and its conformation in solution. In this connection it is noteworthy that the

*$k_c + O_2 = 1.88 \times 10^{10}$ *l mole*$^{-1}$*s*$^{-1}$ *(10),* cf. *the appreciable formation of* H_2S *in the oxygenated solutions of Markakis and Tappel (Table I).*

Can. J. Chem. Downloaded from www.nrcresearchpress.com by 210.87.254.6 on 09/05/12
For personal use only.

decline in the radiolytic yield of H_2S observed by Dale and Davies (6) in the pH range 7–11 may be attributed to ionization of the thiol group* and the consequent replacement of reaction [7] by some other process which does not produce H_2S. Since the pK for the NH_3^+ group is slightly higher (pK of $NH_3^+ = 10.5$ (5)) than that for the SH group, reaction [10] is one such alternative process (ref. 11):

[10] $$e_{aq}^- + CH_2(S^-)—CH(NH_3^+)—C(=O)O^- \rightarrow CH_2(S^-)—\dot{C}H—C(=O)O^- + NH_3$$

in the pH range 10–11. It is clear, however, from the earlier work (3, 6) that ammonia is not an important product in the pH range 0–7.

ACKNOWLEDGMENTS

The authors acknowledge the financial assistance of the Defence Research Board. They are also indebted to Miss Meta Arends for assistance with the experimental work.

1. J. E. Packer. J. Chem. Soc. 2320 (1963). Nature, **194**, 81 (1962).
2. S. L. Whitcher, M. Rotherham, and N. Todd. Nucleonics, **11**, 30 (1953).
3. P. Markakis and A. L. Tappel. J. Am. Chem. Soc. **82**, 1613 (1960).
4. F. E. Littman, E. M. Carr, and A. P. Brady. Radiation Res. **7**, 107 (1957).
5. J. T. Edsall and J. Wyman. Biophysical chemistry. Academic Press, Inc., New York. 1958.
6. W. M. Dale and J. V. Davies. Biochem. J. **48**, 9 (1951).
7. E. Hayon and A. O. Allen. J. Phys. Chem. **65**, 2181 (1961).
8. W. Ando, K. Sugimoto, and S. Oae. Bull. Chem. Soc. Japan, **36**, 893 (1963).
9. (*a*) A. O. Allen. Radiation Res. Supplement, **4**, 54 (1964).
   (b) F. S. Dainton. Radiation Res. Supplement, **1**, 1 (1959).
10. M. S. Matheson. Radiation Res. Supplement, **4**, 1 (1964).
11. W. M. Garrison. Radiation Res. Supplement, **4**, 158 (1964).
12. E. J. Hart, J. K. Thomas, and S. Gordon. Radiation Res. Supplement, **4**, 74 (1964).
13. C. N. Trumbore *et al.* Radiation Res. **22**, 230 (1964). J. Am. Chem. Soc. **86**, 3175 (1964).

Received June 26, 1964.
Chemistry Department,
University of Alberta,
Calgary, Alberta.

**Note added in proof. This is also a possible reason for the fact that pulsed electron studies in "alkaline solutions" failed to reveal evidence of a rapid reaction between e_{aq}^- and cysteine (see ref. 12). More recent experiments in neutral solutions have provided evidence that k_8 is of the order of magnitude reported here (J. K. Thomas, private communication). El Samahy, White, and Trumbore have recently published conclusions which are similar to our own (see ref. 13).*

STABILITY CONSTANT OF THE BORON–DIAMINOCHRYSAZIN COMPLEX

R. S. Brown

One of the methods for the determination of boron in microgram amounts uses hydroxyanthraquinones (1) or substituted hydroxyanthraquinones (2, 3) as reagent and concentrated sulphuric acid as solvent. In some cases a formula for the complex has been suggested. For the formula the ratio of boron to reagent has been obtained from the continuous-variation method (4, 5) or the mole ratio method (6). A survey of the literature has shown that only in the case of 1,1′-dianthrimide has the stability constant of the boron

Can. J. Chem. Downloaded from www.nrcresearchpress.com by 210.87.254.6 on 09/05/12
For personal use only.

decline in the radiolytic yield of H_2S observed by Dale and Davies (6) in the pH range 7–11 may be attributed to ionization of the thiol group* and the consequent replacement of reaction [7] by some other process which does not produce H_2S. Since the pK for the NH_3^+ group is slightly higher (pK of $NH_3^+ = 10.5$ (5)) than that for the SH group, reaction [10] is one such alternative process (ref. 11):

[10] $$e_{aq}^- + CH_2(S^-)—CH(NH_3^+)—C(=O)(O^-) \rightarrow CH_2(S^-)—\dot{C}H—C(=O)(O^-) + NH_3$$

in the pH range 10–11. It is clear, however, from the earlier work (3, 6) that ammonia is not an important product in the pH range 0–7.

ACKNOWLEDGMENTS

The authors acknowledge the financial assistance of the Defence Research Board. They are also indebted to Miss Meta Arends for assistance with the experimental work.

1. J. E. Packer. J. Chem. Soc. 2320 (1963). Nature, **194**, 81 (1962).
2. S. L. Whitcher, M. Rotherham, and N. Todd. Nucleonics, **11**, 30 (1953).
3. P. Markakis and A. L. Tappel. J. Am. Chem. Soc. **82**, 1613 (1960).
4. F. E. Littman, E. M. Carr, and A. P. Brady. Radiation Res. **7**, 107 (1957).
5. J. T. Edsall and J. Wyman. Biophysical chemistry. Academic Press, Inc., New York. 1958.
6. W. M. Dale and J. V. Davies. Biochem. J. **48**, 9 (1951).
7. E. Hayon and A. O. Allen. J. Phys. Chem. **65**, 2181 (1961).
8. W. Ando, K. Sugimoto, and S. Oae. Bull. Chem. Soc. Japan, **36**, 893 (1963).
9. (*a*) A. O. Allen. Radiation Res. Supplement, **4**, 54 (1964).
   (b) F. S. Dainton. Radiation Res. Supplement, **1**, 1 (1959).
10. M. S. Matheson. Radiation Res. Supplement, **4**, 1 (1964).
11. W. M. Garrison. Radiation Res. Supplement, **4**, 158 (1964).
12. E. J. Hart, J. K. Thomas, and S. Gordon. Radiation Res. Supplement, **4**, 74 (1964).
13. C. N. Trumbore *et al.* Radiation Res. **22**, 230 (1964). J. Am. Chem. Soc. **86**, 3175 (1964).

Received June 26, 1964.
Chemistry Department,
University of Alberta,
Calgary, Alberta.

**Note added in proof. This is also a possible reason for the fact that pulsed electron studies in "alkaline solutions" failed to reveal evidence of a rapid reaction between e_{aq}^- and cysteine (see ref. 12). More recent experiments in neutral solutions have provided evidence that k_8 is of the order of magnitude reported here (J. K. Thomas, private communication). El Samahy, White, and Trumbore have recently published conclusions which are similar to our own (see ref. 13).*

STABILITY CONSTANT OF THE BORON–DIAMINOCHRYSAZIN COMPLEX

R. S. Brown

One of the methods for the determination of boron in microgram amounts uses hydroxyanthraquinones (1) or substituted hydroxyanthraquinones (2, 3) as reagent and concentrated sulphuric acid as solvent. In some cases a formula for the complex has been suggested. For the formula the ratio of boron to reagent has been obtained from the continuous-variation method (4, 5) or the mole ratio method (6). A survey of the literature has shown that only in the case of 1,1′-dianthrimide has the stability constant of the boron

Can. J. Chem. Downloaded from www.nrcresearchpress.com by 210.87.254.42 on 09/05/12
For personal use only.

complex been calculated (7). In the present investigation the reagent used was diaminochrysazin, and the stability constant of the boron complex has been determined spectrophotometrically.

METHODS

By analogy with metal–ligand complexes, it is assumed that boron is the central group and hydroxyanthraquinone is the ligand. The hydroxyanthraquinones are all highly colored in concentrated sulphuric acid, and in many cases the maximum absorbance of the boron complex is at a wavelength where the reagent has an appreciable absorbance. With a colored ligand the application of any method for calculation of a stability constant is limited to the small range of wavelengths where there is a sizeable difference between the absorbance of the complex and that of the ligand.

1. Continuous Variation

The method of continuous variation was originally proposed by Job (4) and extended by Vosburgh and Cooper (5). For the determination of compound formation, the continuous-variation method is least ambiguous when only one compound is formed. Application of the method at several wavelengths spread over the visible spectrum, all of which give a peak in the y function at the same mole fraction, can be taken as an indication that only one compound is formed. The use of several different total concentrations of boron plus reagent to give the same peak in y may be taken as additional evidence. To calculate the stability constant from the continuous-variation data it is necessary to know the molar absorbance of the complex. Since boron has no absorbance in the visible region, a large excess of boron may be added to the reagent. Under these conditions all the reagent should be in the form of the complex. The Beer–Lambert law may be checked and the molar absorbance of the complex obtained.

When the only complex formed is 1:1, the equation for the equilibrium is

$$B + Q \rightleftarrows BQ$$

and the equilibrium constant expression for the reaction is

$$K = \frac{C_C}{(C_B - C_C)(C_Q - C_C)},$$

where C_C is the concentration of the complex at equilibrium, C_B is the initial concentration of the boron, and C_Q is the initial concentration of the hydroxyanthraquinone.

Since only the complex and the reagent absorb in the visible range, then in the equilibrium system

$$A = (C_Q - C_C)\epsilon_Q + C_C\epsilon_C,$$

where A is the measured absorbance and the ϵ's are molar absorbancies. Thus, on rearranging,

$$C_C = \frac{A - C_Q\epsilon_Q}{\epsilon_C - \epsilon_Q},$$

where $A - C_Q\epsilon_Q$ is the y function of the method of continuous variation. From the y value, the stability constant, K, may be calculated at a series of concentrations used in the continuous-variation determination. For a 1:1 complex the value of K should be reproducible at any concentration and at any wavelength, provided it does not depend on a small difference between large numbers.

Can. J. Chem. Downloaded from www.nrcresearchpress.com by 210.87.254.42 on 09/05/12
For personal use only.

2. Corresponding Solutions

The method of corresponding solutions, originally formulated by Bjerrum (8), has been extensively used for the determination of stepwise formation constants. Woldbye (9) stated that the method is preferable to the continuous-variation method even when only one compound is formed. In the present work the method of corresponding solutions as outlined by Rossotti and Rossotti (10) has been used. The data obtained are a (free ligand concentration at equilibrium) and $\bar{n}$ (average number of ligands bound to a central group). When the only complex formed is 1:1, the stability constant can be obtained from the expression

$$K = \frac{\bar{n}}{(1 - \bar{n})a}.$$

The value of K obtained should be the same at any wavelength. However, since the calculations to obtain a and $\bar{n}$ depend on $A - C_Q\epsilon_Q$, the limitations are similar to those for the continuous-variation method with a ligand that absorbs in the same range as the complex.

3. Method of Rose and Drago

Rose and Drago (11) calculated the formation constant and the molar absorbance of molecular addition compounds of iodine. The molecular addition compound of iodine with benzene in carbon tetrachloride as solvent is a 1:1 complex. Their method assumes that ϵ_C is not known; by assigning a series of values to ϵ_C and by the use of the equation

$$K^{-1} = \frac{A - C_Q\epsilon_Q}{\epsilon_C - \epsilon_Q} - C_Q - C_B + \frac{C_Q C_B(\epsilon_C - \epsilon_Q)}{A - C_Q\epsilon_Q},$$

the corresponding values of K^{-1} are obtained. When K^{-1} values are plotted against ϵ_C, a straight line is obtained. Using a series of concentrations, all lines should intersect at the values of K^{-1} and ϵ_C. By this method it is possible to confirm the value of ϵ_C obtained by using a large excess of boron and also to check the value of K.

EXPERIMENTAL

The sulphuric acid used was commercial reagent grade and all solutions were made up in this solvent. The particular lot of acid used was analyzed 95.7% sulphuric acid by alkimetric titration.

Three samples of diaminochrysazin (trade name "boran") were purchased at different dates from the Lamotte Chemical Products Co. None of these samples had a lot number. The spectrum of each corresponded to that reported by Cogbill and Yoe (2) but the first sample obtained had a molar absorbance which was 20% below the other two. The second and third samples had identical melting points and were used without further purification. Before use, the samples were dried *in vacuo* at 60 °C overnight. A stock solution (2.22×10^{-3} M) was prepared by dissolving 600 mg in 1 l of concentrated sulphuric acid. The stock solution was stored in the dark. Solutions stored on open shelves showed some darkening after a few weeks, with a general increase in the absorbance above 450 mμ. Solutions ranging in concentration from (0.5 to 11.1) $\times 10^{-4}$ M were obtained by dilution of the stock solution.

Boric acid of reagent grade was dried *in vacuo* at 60 °C overnight. A stock solution (1 mg boron/ml) was prepared, and solutions in the range (1.0–40.0) $\times 10^{-4}$ M were prepared by dilution.

Absorption measurements were made in 1 cm matched Corex cells with a Beckman model DU spectrophotometer. For the higher concentrations, silica blocks 0.9 cm thickness were inserted in the 1 cm cells to give a light path of 0.1 cm of solution. The cell compartment was flanked by thermospacers through which water, maintained thermostatically at 25 °C, was circulated. When spectra over a wide range of wavelengths were desired, these were measured by a Bausch and Lomb model 505 spectrophotometer. Absorbances measured on the two instruments agreed with each other within 1%.

All glassware employed for volumetric purposes was of the "soft-glass" type (Kimble brand). For storage and ordinary handling of acid solutions, Corning alkali-resistant ("boron-free") glass No. 7280 was used.

Can. J. Chem. Downloaded from www.nrcresearchpress.com by 210.87.254.42 on 09/05/12
For personal use only.

Can. J. Chem. Downloaded from www.nrcresearchpress.com by 210.87.254.42 on 09/05/12
For personal use only.

RESULTS AND DISCUSSION

Results of the continuous-variation method at concentrations 1.11×10^{-4}, 2.22×10^{-4}, 5.55×10^{-4}, and 22.2×10^{-4} M and at wavelengths 372, 400, 440, 496, and 526 mμ all gave a maximum in the y function at a mole fraction of 0.5. The curves for the y function vs. mole fraction were similar to those given by Cogbill and Yoe (2). The continuous-variation method indicated that only the 1:1 complex is formed.

In an attempt to find the molar absorbance of the complex by adding an excess of boron, it was found that up to a 10-fold excess of boron gave consistent ϵ_C values which obey the Beer–Lambert law. When there was a 100-fold excess of boron, however, the ϵ_C value of the peaks at 496 and 526 mμ had decreased. The solution had changed color and a new peak had developed at 605 mμ. The molar absorbancies are listed in Table I. When a

TABLE I

Molar absorbancies $\times 10^{-3}$

Wavelength, mμ	ϵ_Q	ϵ_C 10-fold B excess	ϵ_C 100-fold B excess	ϵ_C Calcd. method 3
372	2.61	1.65	2.20	
400	4.32	2.14	1.84	
440	6.73	4.12	3.00	3.95
496	1.03	11.75	8.20	11.28
526	0.025	11.28	9.02	
605	0.012	0.46	8.76	

TABLE II

Stability constant of the boron–diaminochrysazin complex at 25 °C

Wavelength, mμ	Method 1 No. of points	Method 1 $K \times 10^{-3}$	Method 2 No. of points	Method 2 $K \times 10^{-3}$	Method 3 No. of points	Method 3 $K \times 10^{-3}$
400			9	3.52±0.28		
440	24	4.11±1.28	7	3.25±0.24		
496	24	3.50±0.36	13	3.47±0.15	43	3.70±0.22
526	24	3.51±0.37	15	3.63±0.15		

solution containing a 100-fold excess of boron was reduced to a 10-fold excess by addition of reagent and dilution, the peak at 605 mμ disappeared and the ϵ_C values at 496 and 526 mμ returned to the higher figures. Sillen *et al.* (12) have studied borates in water solution and have reported that above a concentration of 0.025 M there is polymerization of the borate. In the present work the new peak at 605 mμ was obtained with a reagent concentration of 1.0×10^{-3} M and a boron concentration ranging from 0.084 to 0.84 M. If there is comparable polymerization of borate in sulphuric acid solvent, this phenomenon would explain the decrease in molar absorbance at 496 and 526 mμ and would suggest that the peak at 605 mμ is due to some complex between the polymer and the reagent. Table II lists average values of the stability constant calculated by method 1 from ϵ_C values for a 10-fold boron excess.

The data a and $\bar{n}$ obtained by the corresponding solutions method are plotted in Fig. 1. The curve obtained for the four wavelengths is the same within the experimental error for each set. The stability constant has been calculated for each point and the average values are given in Table II.

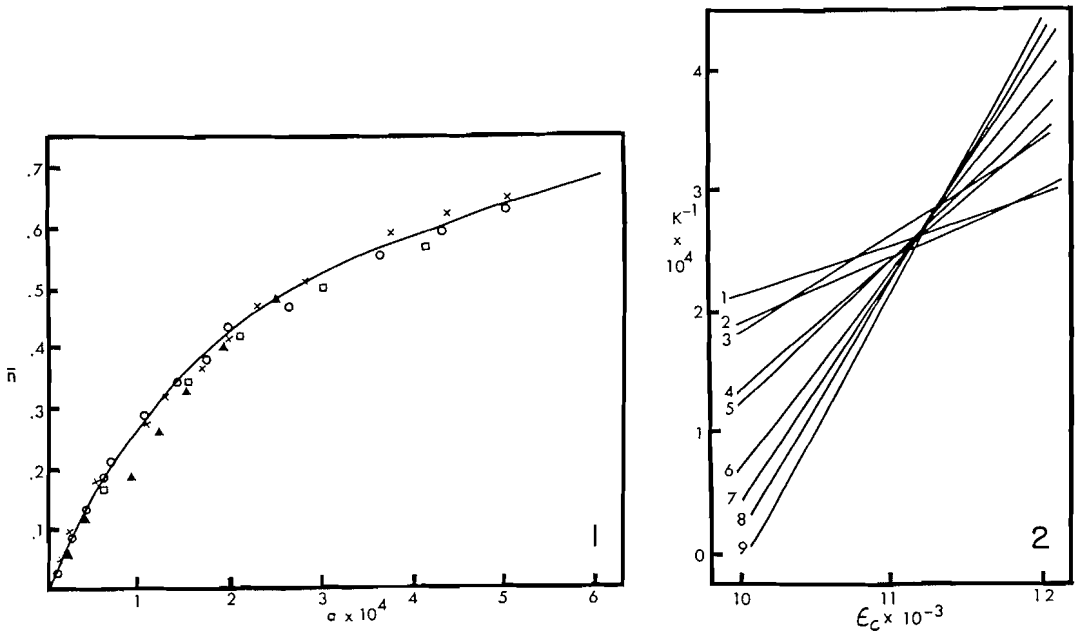

FIG. 1. Plot of n vs. a for the boron–diaminochrysazin complex: □ 400 mμ, ▲ 440 mμ, ○ 496 mμ, × 526 mμ.

FIG. 2. Plot of K^{-1} vs. ϵ_C for method 3.

Line	Molar concentration × 10^4 Diaminochrysazin	Boron
1	1.25	1.25
2	2.75	2.5
3	4.4	5.5
4	5.5	11.0
5	2.75	11.0
6	8.5	20.0
7	4.4	20.0
8	2.75	20.0
9	0.50	20.0

To check the above methods by that of Rose and Drago (11), 10 of the measured absorbancies at 496 mμ have been used to plot the K^{-1} vs. ϵ_C lines. The data chosen range from a solution 1.25B/1.25Q to 20B/8.5Q. A plot of these lines is given in Fig. 2. The 10 lines give 43 points of crossing, and the values of ϵ_C and K^{-1} were determined for each point. The value of K obtained by this method is given in Table II and that of ϵ_C in Table I.

If a 1:1 complex is assumed, each of the methods gives a comparable value for the stability constant. A possible structure for the complex is that outlined by Cogbill and Yoe (2).

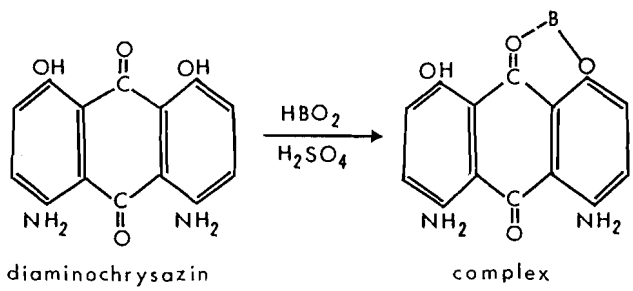

Can. J. Chem. Downloaded from www.nrcresearchpress.com by 210.87.254.42 on 09/05/12
For personal use only.

The average of all values by methods 1 and 2 (omitting those at 440 mμ by method 1) gives the stability constant of the boron–diaminochrysazin complex as $(3.50 \pm 0.22) \times 10^3$.

1. Assoc. Offic. Agr. Chemists. Official methods of analysis. 9th ed. 1960. p. 87.
2. E. C. Cogbill and J. H. Yoe. Anal. Chem. **29**, 1251 (1957).
3. J. H. Yoe and R. L. Grob. Anal. Chem. **26**, 1465 (1954).
4. P. Job. Ann. Chim. **9**, 113 (1928).
5. W. C. Vosburgh and G. R. Cooper. J. Am. Chem. Soc. **63**, 437 (1941).
6. J. H. Yoe and A. L. Jones. Ind. Eng. Chem. Anal. Ed., **16**, 111 (1941).
7. F. J. Langmyhr and O. B. Skaar. Acta Chem. Scand. **13**, 2107 (1959).
8. J. Bjerrum. Kgl. Danske Videnskab. Mat-fys. Medd. **21**, No. 4, (1944).
9. F. Woldbye. Acta Chem. Scand. **9**, 299 (1955).
10. F. J. C. Rossotti and H. Rossotti. The determination of stability constants. McGraw-Hill Book Co., Inc., New York. 1961. p. 282.
11. N. J. Rose and R. S. Drago. J. Am. Chem. Soc. **81**, 6138 (1959).
12. N. Ingri, G. Lagerstom, M. Frydman, and L. G. Sillen. Acta Chem. Scand. **11**, 1034 (1957).

Received May 6, 1964.
Department of Chemistry,
Ontario Agricultural College,
Guelph, Ontario.

Can. J. Chem. Downloaded from www.nrcresearchpress.com by 210.87.254.42 on 09/05/12
For personal use only.

Can. J. Chem. Downloaded from www.nrcresearchpress.com by 210.87.254.40 on 09/05/12
For personal use only.

Canadian Journal of Chemistry

Issued by THE NATIONAL RESEARCH COUNCIL OF CANADA

VOLUME 42 DECEMBER 1964 NUMBER 12

A STUDY OF PROTON EXCHANGE REACTIONS OF SUBSTITUTED ANILINES IN TRIFLUOROACETIC ACID

W. F. REYNOLDS* AND T. SCHAEFER

Department of Chemistry, University of Manitoba, Winnipeg, Manitoba

Received May 29, 1964

ABSTRACT

The acid proton exchange rates of solutions of some halo-substituted anilines in trifluoroacetic acid have been determined by measuring the acid proton signal width. In addition, the proton exchange rate of protonated N,N-dimethylaniline in trifluoroacetic acid is discussed. It is suggested that proton exchange occurs via the following reaction:

$$\phi NH_3^+ + A^- \rightleftharpoons (\phi NH_3^+ \ldots A^-) \rightleftharpoons \phi NH_2 + HA.$$

The reaction is believed to occur in two steps: the oppositely charged ions form ion pairs which then transfer protons internally. Experimental evidence indicates that the ion-pair dissociation constant is less than, or equal to, one.

The activation energies range from 10 to 24 kcal/mole. The rate constants at 25 °C for a possible bi-ionic reaction are calculated. Ionic activity coefficients are estimated by the Debye–Hückel equation. Another set of rate constants is calculated, assuming that the ions exist partly or completely as ion pairs.

The free energies, enthalpies, and entropies of activation are calculated for an ion-pair reaction and for an overall bi-ionic reaction. The free energies of activation range from 10 to 17 kcal/mole and for haloanilines are less than that of aniline. In the ortho- and para-substituted anilines, $\Delta F^{\ddagger}$, in general, decreases with decreasing halogen electronegativity. $\Delta F^{\ddagger}$ values for metasubstituted anilines decrease with increasing substituent electronegativity. $\Delta F^{\ddagger}$ values are largest for parahaloanilines and smallest for orthohaloanilines. The $\Delta F^{\ddagger}$ values for haloanilines can be rationalized by reasonable combinations of inductive and mesomeric effects. The values of entropies of activation are determined largely by the positions of the substituents. $\Delta S^{\ddagger}$ values range from 35 to −10 entropy units (e.u.) with aniline and para-substituted anilines having the largest positive values and orthosubstituted anilines having negative values. The value of $\Delta F^{\ddagger}$ for protonated N,N-dimethylaniline is larger than that for protonated aniline, as would be expected. $\Delta S^{\ddagger}$ is quite small. This is attributed to steric hindrance of solvation of the dimethylanilinium ion.

INTRODUCTION

The effect of chemical exchange upon nuclear magnetic resonance (n.m.r.) spectra was established several years ago (1–5). Since then, proton magnetic resonance (p.m.r.) spectroscopy has been used by various workers to study exchange reactions in aqueous and alcoholic solutions (6–23).

During the investigation of protonated anilines in trifluoroacetic acid (TFA) it was noted that the observed H^+—N—CH_3 coupling constant of protonated N,N-dimethylaniline was temperature dependent (24). The apparent temperature dependence of this coupling constant was measured, and the exchange rate and thermodynamic properties of exchange were calculated. It was originally intended to investigate the exchange reactions of a number of ring-substituted N-alkylanilines. This investigation would have

**Holder of a N.R.C. Studentship, 1962–1963.*

provided information about the effects of substituents upon exchange rates and thermodynamic variables. However, because of experimental difficulties in the measurements of small coupling constants, it was decided to try an alternative method. The TFA proton signal width depended upon the exchange rate of the protonated aniline in solution. The acid proton peak was intense and its width could be measured with minimum experimental difficulty. Therefore, the acid proton signal widths of a series of dilute solutions of haloanilines in TFA were measured at different temperatures. The haloanilines were chosen for study because there seemed to be some confusion about the nature of halogen substituent effects (25, 26).

The acid proton exchange rates of such solutions were measured, rate constants calculated from them for the postulated exchange reaction, and thermodynamic data estimated. Possible errors in the measurement of exchange rates are discussed.

EXPERIMENTAL

1. Materials and Preparation of Solutions

Most of the anilines used in this study were obtained from Distillation Products Ind. and were Eastman White Label grade. The *p*-fluoroaniline was Eastman Practical grade. *m*-Chloroaniline was obtained from K and K Laboratories, Inc. *m*-Fluoroaniline was obtained from Matheson, Coleman and Bell. *m*-Iodoaniline was obtained from Aldrich Chemicals. Solid anilines were used without purification. Liquid anilines were distilled under reduced pressure and small constant temperature fractions were collected for use in exchange studies. TFA was an Eastman White Label grade chemical. The aliquots of acid used in preparing the solutions were first treated with one or two drops of trifluoroacetic anhydride per aliquot to remove any water in the acid. TFA was not further purified. Cyclohexane was a Fisher Spectro-Analyzed reagent and was used without purification.

The TFA solutions were prepared by weighing. The solutions contained 3 mole % of cyclohexane and from 1 to 3 mole % of substituted aniline. Cyclohexane was chosen as an internal reference because it did not react with TFA or aniline and because it gave an intense signal, even when present in low molar concentration. Whenever possible, the aniline concentration was adjusted so that exchange-broadening of the acid proton signal occurred at temperatures just above room temperature. Solutions were placed in thick-walled 5 mm outside diameter sample tubes. The solutions were degassed and then the sample tubes were evacuated and sealed.

Originally, aniline concentrations of from 4 to 8 mole % were used. However, the plots of log (acid proton line width) vs. (absolute temperature)$^{-1}$ were always curved in the low-temperature regions (0–30 °C). In two extreme cases, the slope of the line actually changed sign. It was found that if aniline concentrations of from 1 to 3 mole % were used, the plots for all but one of the aniline solutions (*p*-fluoroaniline) were essentially linear in the region of slow exchange.

2. Acid Proton Line Width Measurements

Spectra were measured on a Varian DP-60 spectrometer. Experiments at different temperatures were carried out with the aid of an N.R.C. manufactured temperature device. The spinning air was heated by a nichrome wire heater. Temperature control was attained by variation of the air flow rate and by variation of the power supplied to the heater. Temperatures from 10 °C to room temperature were obtained by passing the spinning air through a copper coil immersed in an ice–salt mixture before it passed through the temperature device. To obtain lower temperatures it was necessary to use precooled nitrogen gas to spin the sample. The nitrogen gas was cooled by a dry ice – acetone mixture. Because the precooled nitrogen had to be heated approximately 80 deg and also because it was difficult to keep the nitrogen flow rate constant, it was impossible to maintain constant temperature in the temperature region below 10 °C. Therefore, line widths could not be accurately measured in this region. The exchange reactions of *o*-iodoaniline in TFA could not be studied, because rapid proton exchange occurred below 10 °C. One measurement of the line width of a *m*-chloroaniline solution was made at 0 °C. Since the line width was nearly constant at that temperature, temperature control was not very important.

Temperatures were measured with a copper–constantan thermocouple attached to a Varian G-11 recording potentiometer. The potentiometer was regularly recalibrated to insure that there was no error in the recorder readings. The temperature was usually changed by about 2–3 deg between runs. Solutions were allowed to equilibrate for at least 2 h at each temperature before the spectra were obtained. Usually solutions were heated slightly above the desired temperature and then allowed to cool to that temperature. It is estimated that temperature readings were accurate to within 0.5 °C.

The ammonio proton signals were broad and weak. Line widths of these signals could not be measured. However, the acid proton signal widths were easily measured. Because there were large concentrations

Can. J. Chem. Downloaded from www.nrcresearchpress.com by 210.87.254.40 on 09/05/12
For personal use only.

of acid protons in the solutions studied, low radiofrequency power could be used, even when the protons were exchanging rapidly. Therefore, signal saturation was not a problem. Signal widths between 1 and 15 c/s could be measured accurately. The possible error in measuring line widths of less than 1 c/s was quite large. If the signal was broader than 15 c/s, it was necessary to use high radiofrequency power and the signal sometimes appeared to be partially saturated.

The resolution was carefully controlled while acid proton signal widths were measured. Before each pair of measurements of the acid proton signal, the width of the cyclohexane signal was measured twice (forward and reverse) by placing sidebands of the signal 5 c/s on both sides of itself. The sideband frequency was measured with a Hewlett–Packard 521C electronic counter with an accuracy of 0.1 c/s. The sweep rate was approximately 10 c/s min. The width of the acid proton signal was then measured twice (forward and reverse). Sideband frequencies of 5–20 c/s were used for signals of different widths. The width of the cyclohexane signal was then remeasured. This procedure was repeated until 10 measurements of the acid proton line width were obtained. If the resolution changed appreciably while a pair of measurements of the acid proton line width were being made, those measurements were discarded. Occasionally, the acid proton line width at room temperature was remeasured at the finish of a series of measurements at higher temperatures to determine if chemical reaction or decomposition had altered the line width. In all cases, the two sets of measurements at room temperature agreed within experimental error.

Line widths were measured directly with a ruler calibrated in tenths of millimeters. In each spectrum the region to low field of the TFA proton signal was scanned because there were no peaks in that region and an accurate measurement of the base-line position could be obtained. The "half-height" of the peak was then determined and the width of the signal was measured at that point. This was compared to the peak-to-peak separation of the sidebands in order to calculate the line width in c/s.

3. Other Experiments

A number of specific experiments were carried out to determine points of interest. The line width of the acid proton signal of a solution containing only 2 mole % cyclohexane in TFA was measured at two temperatures. The width of the acid proton signal of a similar solution which contained 0.9 mole % of water was also measured.

The line width of the acid proton was also measured as a function of aniline concentration. Five solutions with aniline concentrations from 1 to 5 mole % were used. The samples were not degassed because it was felt that some of the TFA might evaporate. The cyclohexane line width was not larger than in other solutions. These experiments were carried out at 50 °C because viscosity effects seemed unimportant at this temperature and also because the 1 mole % solution did not exchange appreciably below this temperature. The chemical shifts of the acid and phenyl protons of the aniline solutions were measured relative to cyclohexane at different temperatures.

Trifluoroacetic anhydride was added to a series of solutions of aniline in TFA. The effect of changing anhydride concentration upon acid proton line widths at room temperature was investigated.

The ultraviolet spectrum of a 1 mole % solution of aniline in TFA was obtained to determine the amount of free aniline in solution. For purposes of comparison, a 20 mole % solution of aniline in TFA was prepared and diluted approximately 1:100 and 1:1000 in acetonitrile. A Beckmann DK spectrophotometer was used to obtain these spectra.

4. Calculation of Acid Proton Line Widths

For slow exchange between uncoupled protons in nonequivalent sites it can be shown (4) that the line width $\Delta\nu$ in c/s for a given proton site is $\pi\Delta\nu = 1/\tau + 1/T_2$. The line width is characterized by $1/T_2$ in the absence of exchange, and τ is the average lifetime in the site. For our solutions it was assumed that the line width of the cyclohexane peak, determined by field inhomogeneity, was equal to $1/\pi T_2$. The corrected line widths of the acid protons and their exchange rates (s^{-1}) were thus obtained.

RESULTS AND DISCUSSION

1. Line Widths in the Absence of Anilines; Effect of Water

The line widths of TFA and cyclohexane protons of two solutions of cyclohexane in TFA are given below. All results are the average of 10–12 measurements. The error limits are root mean square deviations. Since line widths are constant, T_2 must be the same for the protons of cyclohexane and TFA in the absence of aniline. T_2 for both types of protons appears to be independent of temperature in this range and is no doubt determined by the inhomogeneity of the magnetic field. Water apparently has little effect upon the acid proton line width. Luz and Meiboom have recently found that proton exchange between the carboxyl group of acetic acid and water is too rapid for direct measurement by our methods (30).

Can. J. Chem. Downloaded from www.nrcresearchpress.com by 210.87.254.40 on 09/05/12
For personal use only.

Concentration (mole %)			Line width (c/s)		Temperature (°C)
TFA	C_6H_{12}	H_2O	TFA	C_6H_{12}	
98.1	1.9	—	0.44±0.03	0.43±0.03	24.5±0.5
			0.45±0.04	0.46±0.06	42.5±0.5
97.0	2.1	0.9	0.45±0.05	0.44±0.05	24.7±0.5
			0.47±0.06	0.45±0.04	43.2±0.5

2. Line Widths of the Aniline Solutions

The corrected widths of the acid proton signals and acid proton exchange rates of various aniline solutions are given in Table I. The quoted error limits are the root mean square deviations. A least-squares plot of log (line width) vs. $1/T$ is given for a 4 mole % solution of aniline in Fig. 3. Figure 4 illustrates the unwanted behavior obtained for a *p*-fluoroaniline solution and will be discussed later. Figure 5 shows a typical plot of log (line width) vs. $1/T$ over the region from slow exchange to fast exchange.

TABLE I

Measured acid proton line width and acid proton exchange rates of solutions of substituted anilines in TFA

	Concentrations							
	Mole % as weighed			Moles/l assuming (1) ideal solutions and (2) complete protonation of aniline		Corrected acid proton line width (c/s)	Acid proton exchange rate (s^{-1})	Temperature (°C)
	TFA	ϕNH_2	C_6H_{12}	TFA	ϕNH_3^+			
Aniline	92.7	4.03	3.24	11.7	0.530	1.61±0.08	5.1±0.25	38.6±0.5
						2.67±0.10	8.4±0.3	42.5
						3.66±0.16	11.5±0.5	45.6
						4.93±0.11	15.5±0.3	48.1
						7.02±0.16	22.1±0.5	50.8
						9.50±0.17	29.8±0.5	53.6
						12.86±0.38	40.4±1.2	56.4
p-Fluoro-aniline (distilled)	95.0	2.00	3.03	12.2	0.265	0.65±0.06	2.05±0.2	25.5
						0.97±0.07	3.05±0.2	31.2
						1.45±0.12	4.55±0.4	36.8
						1.69±0.13	5.3±0.4	40.3
						1.98±0.08	6.2±0.25	43.3
						2.85±0.06	9.0±0.2	46.7
						3.33±0.13	10.5±0.4	48.6
						4.49±0.12	14.1±0.4	51.4
						6.12±0.17	19.2±0.5	54.2
						8.32±0.17	26.15±0.5	56.7
p-Fluoro-aniline (undistilled)	95.3	2.00	2.73	12.3	0.264	0.65±0.05	2.05±0.15	25.7
						1.13±0.08	3.55±0.25	34.8
						1.39±0.05	4.4±0.15	38.5
						1.87±0.09	5.9±0.3	42.2
						2.12±0.10	6.7±0.3	44.4
						3.81±0.06	12.0±0.2	49.8
						5.49±0.13	17.25±0.4	54.0
m-Chloroaniline	94.0	2.97	3.06	12.4	0.392	3.74±0.08	11.8±0.25	24.6
						4.69±0.12	14.7±0.4	27.6
						5.90±0.20	18.5±0.6	29.4
						7.12±0.12	22.4±0.4	31.8
						9.54±0.11	30.0±0.35	33.7
						10.33±0.25	32.45±0.8	35.4
						13.75±0.21	43.2±0.7	38.1
						16.93±0.32	53.2±1.0	40.6

Can. J. Chem. Downloaded from www.nrcresearchpress.com by 210.87.254.40 on 09/05/12
For personal use only.

TABLE I (*Concluded*)

	Concentrations							
	Mole % as weighed			Moles/l assuming (1) ideal solutions and (2) complete protonation of aniline		Corrected acid proton line width (c/s)	Acid proton exchange rate (s^{-1})	Temperature (°C)
	TFA	ϕNH_2	C_6H_{12}	TFA	ϕNH_3^+			
m-Bromo-aniline	95.0	1.95	3.05	12.3	0.258	1.71±0.08	5.4±0.25	22.0
						2.41±0.09	7.6±0.3	25.1
						3.91±0.09	12.6±0.3	28.6
						5.77±0.13	18.1±0.4	32.5
						7.50±0.11	23.6±0.35	34.8
						8.72±0.18	27.4±0.55	36.7
m-Iodoaniline	94.5	2.17	3.37	12.2	0.287	1.30±0.09	4.1±0.3	21.1
						2.02±0.11	6.35±0.35	25.0
						3.46±0.09	10.9±0.3	28.6
						5.02±0.14	15.8±0.4	31.3
						8.08±0.30	25.4±0.95	35.3
						9.16±0.15	28.8±0.5	37.2
o-Fluoroaniline	95.8	1.01	3.24	12.7	0.135	2.52±0.07	7.9±0.2	15.5
						3.00±0.12	9.4±0.4	18.0
						3.68±0.09	11.6±0.3	20.4
						4.35±0.14	13.7±0.4	23.8
						5.23±0.17	16.4±0.5	26.8
						4.46±0.16	—	33.3
						3.29±0.07	—	36.2
						2.41±0.06	—	39.1
						1.87±0.10	—	41.8
o-Chloroaniline	94.4	2.00	3.59	12.2	0.264	3.77±0.10	11.85±0.3	12.5
						4.18±0.10	13.1±0.3	14.8
						4.77±0.15	15.0±0.5	17.0
						6.35±0.15	19.95±0.5	19.9
						7.24±0.18	22.75±0.6	22.2
						10.11±0.27	—	27.7
						6.25±0.13	—	31.3
						4.60±0.16	—	33.8
						3.30±0.09	—	36.3
						2.47±0.08	—	39.3
						1.97±0.07	—	41.6
o-Bromo-aniline	95.9	1.02	3.13	12.3	0.135	3.57±0.10	11.2±0.3	9.7
						4.23±0.06	13.3±0.2	12.2
						4.72±0.17	14.8±0.5	14.0
						5.26±0.13	—	16.7
						5.30±0.29	—	19.8
						4.33±0.13	—	24.8
						3.36±0.16	—	27.4
						2.78±0.13	—	29.8
						2.10±0.06	—	32.2
						1.82±0.09	—	34.0

The corrected acid proton line widths of a series of aniline solutions of different concentrations are given in Table II. It was not possible to obtain the same temperature for each solution. The exchange rates have all been corrected to the expected rate at 50.2 °C from the measured activation energy for proton exchange of aniline in TFA (see below).

The chemical shifts of the acid protons and phenyl protons of the various solutions are given in Table III. The acid protons shift to high field with increasing temperature. The shifts seem to be nearly independent of aniline concentration. The phenyl proton shift is independent of aniline concentration and temperature in these solutions.

Can. J. Chem. Downloaded from www.nrcresearchpress.com by 210.87.254.40 on 09/05/12
For personal use only.

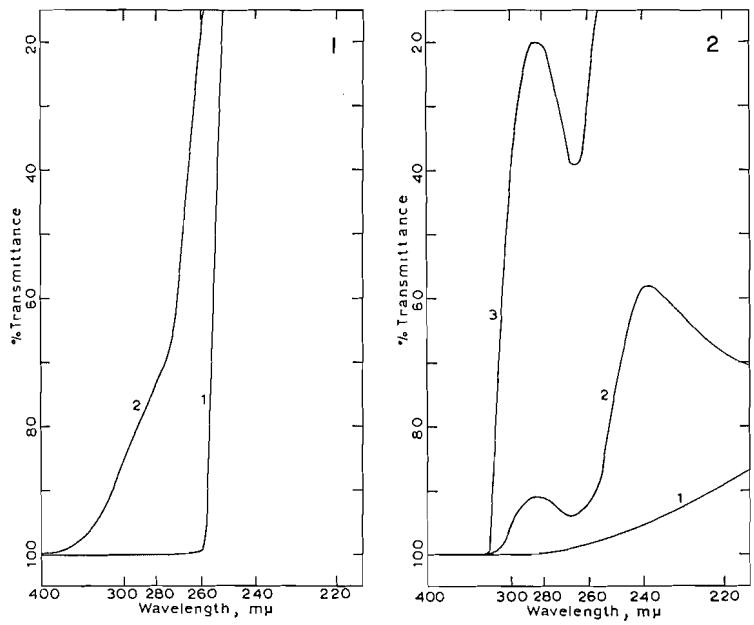

FIG. 1. Reproduction of the ultraviolet spectra of (1) pure TFA and (2) a 1 mole % solution of aniline in TFA.

FIG. 2. Reproduction of the ultraviolet spectra of a 20 mole % solution of aniline in TFA diluted (2) 1:1000 in acetonitrile and (3) 1:100 in acetonitrile. Line (1) represents the base line.

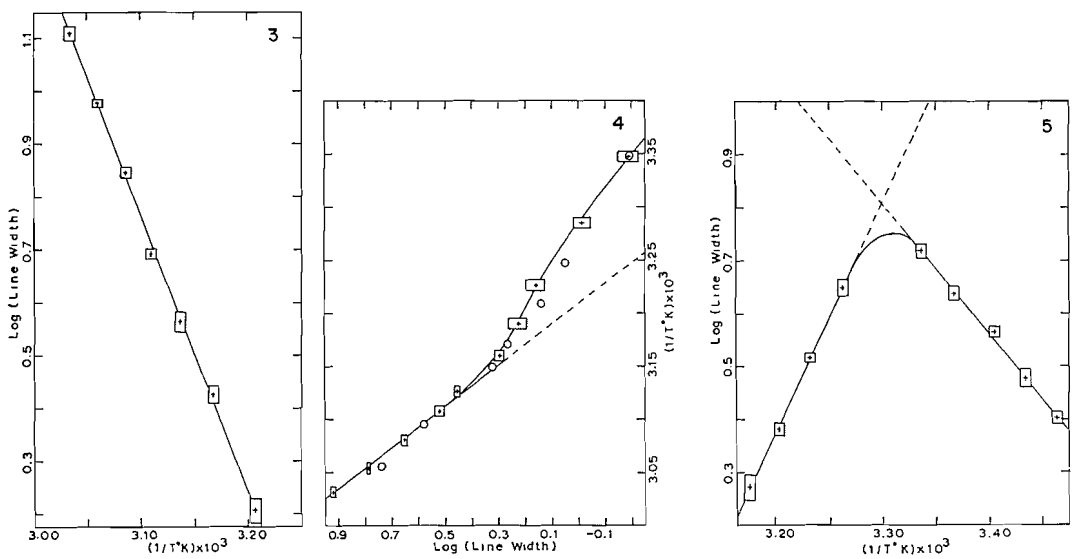

FIG. 3. Plot of log (TFA proton line width) vs. $1/T$ for a 4 mole % solution of aniline in TFA. The rectangles give the uncertainties in temperature and acid proton line width.

FIG. 4. Plot of log (TFA proton line width) vs. $1/T$ for a 2 mole % solution of *p*-fluoroaniline in TFA. Circles represent the proton line widths of the solution containing undistilled *p*-fluoroaniline.

FIG. 5. Plot of log (TFA proton line width) vs. $1/T$ for a 1 mole % solution of *o*-fluoroaniline in TFA.

Can. J. Chem. Downloaded from www.nrcresearchpress.com by 210.87.254.40 on 09/05/12
For personal use only.

TABLE II*a*

Acid proton exchange rates of different solutions of aniline in TFA

	Concentrations								
	Mole % as weighed			Moles/l assuming (1) ideal solutions and (2) complete protonation of aniline		Temperature (°C)	Line width (c/s)	Exchange rate (s^{-1})	Exchange rate at 50.2 °C
	TFA	ϕNH_2	C_6H_{12}	TFA	ϕNH_3				
(1)	95.9	1.01	3.09	12.6	0.1345	50.2±0.5	1.63±0.15	5.1±0.5	5.1±0.8
(2)	95.9	2.01	2.78	12.3	0.266	49.6	2.48±0.08	7.8±0.25	8.4±0.75
(3)	93.7	2.98	3.35	11.9	0.392	48.8	4.23±0.10	13.3±0.3	15.6±1.2
(4)	93.0	3.95	3.10	11.7	0.520	50.2	6.30±0.29	19.8±0.9	19.8±2.05
(5)	91.9	4.95	3.20	11.4	0.650	49.5	8.47±0.21	26.6±0.65	28.8±2.4

TABLE II*b*

Apparent and corrected rate constants* of proton exchange of solutions of aniline in TFA at 50.2 °C

	Apparent rate constants ($K_D = \infty$)		Corrected rate constants ($K_D = \infty$)		Corrected rate constants ($K_D = 1$) calculated from Fig. 6
	Calculated from measured acid proton line widths	Calculated from Fig. 6	Calculated from measured acid proton line widths	Calculated from Fig. 6	
(1)	3.58×10^3	2.83×10^3	1.86×10^4	1.47×10^4	1.69×10^4
(2)	1.46×10^3	1.56×10^3	1.14×10^4	1.22×10^4	—
(3)	1.21×10^3	1.15×10^3	1.25×10^4	1.19×10^4	—
(4)	8.57×10^2	9.10×10^2	1.09×10^4	1.16×10^4	—
(5)	7.77×10^2	7.65×10^2	1.18×10^4	1.17×10^4	1.72×10^4

*All rate constants have units of (l/mole s).

TABLE III

Chemical shifts of TFA protons and anilinium ion ring protons in different solutions of aniline in TFA at different temperatures

Concentration (mole % aniline as weighed)	Temperature (°C)	Chemical shift in c/s (relative to cyclohexane)	
		TFA protons	Anilinium ion ring protons
2.01	25.2±0.5	−602±1	−364±1
	49.8	−585.5	−365
2.98	24.5	−609.5	−363
	49.5	−593	−364
3.95	24.8	−611.5	−365
	50.2	−593	−365
4.95	26.8	−612.5	−365
	32.0	−609	−364
	38.4	−605	−365
	44.0	−600.5	−365
	49.5	−596	−365
	54.5	−591.5	−364
	60.2	−586	−364
	64.6	−579.5	−364
	69.4	−566.5	−364

Can. J. Chem. Downloaded from www.nrcresearchpress.com by 210.87.254.40 on 09/05/12
For personal use only.

The corrected line widths of solutions of aniline in TFA and trifluoroacetic anhydride are given in Table IV. The decrease in acid proton line width appears to be closely related to the ratio of aniline to trifluoroacetic anhydride.

TABLE IV

Acid proton line width of solutions of aniline and trifluoroacetic anhydride in TFA at 25 °C

Concentration (mole %)				Acid proton line width (c/s)	Change in line width when anhydride added	
ϕNH_2	C_6H_{12}	TFA anhydride	TFA		Anhydride / ϕNH_2	Original line width
5.1	2.0	0.0	93.0	3.70±0.17	—	—
5.9	2.1	0.0	90.8	4.79±0.14	—	—
7.0	2.2	0.0	90.8	6.40±0.19	—	—
5.0	2.3	0.2	92.5	3.55±0.12	—	—
5.8	2.2	0.2	91.8	4.67±0.06	—	—
6.9	1.9	0.3	90.9	6.30±0.13	—	—
5.1	2.1	2.0	90.9	2.52±0.11	0.4	0.3
5.8	2.0	2.1	90.1	3.12±0.09	0.35	0.35
7.0	2.2	2.1	88.7	4.29±0.14	0.3	0.3

3. The Ultraviolet Spectra

The ultraviolet spectra are given in Fig. 1 (aniline in TFA) and Fig. 2 (aniline and TFA in acetonitrile). There should be a secondary peak due to aniline at ≈ 280 mμ and one due to anilinium ions at ≈ 254 mμ. These values are for the two substances in water and may be slightly different in other solvents. The extinction coefficients are respectively 1 430 and 160. Consequently, the aniline peak should be relatively more intense. It can be seen in Fig. 1 that there is a large peak in the region of 270 mμ which partly overlaps with the solvent peak, starting at 252 mμ. The peak has a "tail" in the region 320–270 mμ which may or may not be due to aniline. In Fig. 2 there is a large peak at approximately 285 mμ which must be due to free aniline. The peak due to anilinium ions, if present, is obscured by the TFA peak. The aniline peak is quite broad and occurs in the same region as the "tail" of the anilinium ion in Fig. 1. Therefore, the tail probably represents a peak due to free aniline which partly overlaps with the anilinium ion peak. The ratio $[\phi NH_2]/[\phi NH_3^+]$ must be very small to give a spectrum of this type.

4. Activation Energies and Enthalpies of Activation

The experimental activation energies of acid proton exchange are given in Table V. The activation energies have been calculated from the least-squares plots of log (corrected acid proton line width) vs. $1/T$ by using the logarithmic form of the Arrhenius equation. The error limits are 95% confidence limits. There appears to be a general correlation with the position of ring substitution. The activation energy is greatest for parasubstituted anilines and least for orthosubstituted anilines. There is no specific correlation between types of substituents and activation energies, although the activation energies of the metasubstituted anilines do seem to be crudely related to substituent electronegativity. Enthalpies of activation at 25 °C are also given in Table V.

5. Calculation of Rate Constants for the Aniline Solutions at Various Concentrations at 50 °C

We consider that the acid proton exchange reactions are catalyzed by the anilinium ions. Of the many possible reactions which involve changes in the magnetic environments

Can. J. Chem. Downloaded from www.nrcresearchpress.com by 210.87.254.40 on 09/05/12
For personal use only.

TABLE V

Measured activation energies of proton transfer and calculated enthalpies of activation of proton transfer of solutions of aniline and substituted anilines in TFA

Substituent	Activation energy (kcal/mole)	Enthalpy of activation (kcal/mole) at 25 °C
H	23.85±0.75	23.25±0.75
p-F	>22.8	>22.2
p-Cl	21.7±1.55	21.1±1.55
p-Br	23.7±2.15	23.1±2.15
p-I	21.35±0.4	20.65±0.4
m-F	18.3±0.9	17.7±0.9
m-Cl	18.0±1.1	17.3±1.1
m-Br	20.3±1.15	19.6±1.15
m-I	22.5±2.1	21.9±2.1
o-F	11.3±1.5	10.7±1.5
o-Cl	11.7±3.9	11.1±3.9
o-Br	10.4±3.3	9.8±3.3
N,N-Di-Me	18.8±1.1	18.2±1.1

of protons, we assume the following to be predominant in determining the acid proton line width

$$[1] \qquad \phi NH_3^+ + A^- \underset{k_{-1}}{\overset{k_1}{\rightleftharpoons}} \phi NH_2 + HA.$$

The large excess of TFA alters equilibrium concentrations in favor of the ions. This is also indicated by the ultraviolet spectra discussed above.

The total acid proton exchange rate is $1/\tau[HA]$ and therefore

$$1/\tau = k_1[\phi NH_3^+]\,[A^-]/[HA] = k_{-1}[\phi NH_2],$$

where concentrations are in moles/l and the k's are apparent rate constants. We can also write the rate of reaction [1] in terms of the activities of the ions and the "true" second-order rate constant k_0,

$$1/\tau[HA] = k_0[\phi NH_3^+]\,[A^-]F = k_0[\phi NH_2^+]^2F,$$

where F is the activity coefficient term. Using the Debye–Hückel theory to estimate the activity coefficients (27, 28), we arrive at

$$\log k_0 = \log k_1 + [2.5\sqrt{\mu}/(1 + 0.89\sqrt{\mu})]$$

at 50 °C. We have taken the dielectric constant of TFA to be 39.5 and the parameter* a as 2 Å; μ is the ionic strength.

We have applied these equations to the exchange rates of the aniline solutions of various concentrations at 50 °C (Table II). First we plotted $[\phi NH_3^+]^n/[HA]$ vs. the lifetime of the acid protons and obtained the best fit for $n = 1.2$ (Fig. 6), although reasonable fits can be had with $n = 1.0$–1.4. In the first part of Table II*b* can be found the apparent rate constants, using experimental values of exchange rates and also "smoothed" values from Fig. 6. In the second part of Table II*b* are the corresponding "true" second-order rate constants, k_0. They do not vary as much as the apparent rate constants. In view of our crude model the values must be looked upon as a first approximation.

**a is often considered to be the distance of closest approach of charge centers in the extended Debye–Hückel theory. Other, perhaps more reasonable, values might be as high as 6 Å but the approximations involved in our case do not make this value critical.*

Can. J. Chem. Downloaded from www.nrcresearchpress.com by 210.87.254.40 on 09/05/12
For personal use only.

6. Effect of Ion-Pair Formation

We assume that the variation of the "true" second-order rate constants in Table II may be partly due to the formation of ion pairs.* In that case the activities of the ions in solution will be reduced. If a value of the ion-pair dissociation constant is known or assumed, the free-ion concentrations and their activity coefficients can be calculated. This results in a new set of rate constants. Thus, in the final column of Table II, the rate constants for an ion-pair dissociation constant of 1 are found to be nearly equal for the 1 and 5 mole % aniline solutions. Because the Debye–Hückel correction terms are probably too large, the actual dissociation constant is probably less than 1.

This crude approach allows us to rationalize the plot in Fig. 6. The exchange rate can be expressed in terms of the concentration of the ion pairs in solution. If the molar ion-pair dissociation constant (uncorrected for ionic activities) is

$$K_D = [\phi NH_3^+]\,[A^-]/[\phi NH_3^+ \ldots A^-],$$

we can write

$$1/\tau[HA] = k_1[\phi NH_3^+]\,[A^-] = k_1K_D[\phi NH_3^+ \ldots A^-].$$

Consider 0.25 M and 0.50 M solutions of aniline in TFA. Compare the ratios of $[\phi NH_3^+ \ldots A^-]$ and of [total ϕNH_3^+] for the two solutions. If $K_D = 10^{-1}$, we have

$$[\phi NH_3^+ \ldots A^-]_{0.5}/[\phi NH_3^+ \ldots A^-]_{0.25} = \{[\text{total } \phi NH_3^+]_{0.5}/[\text{total } \phi NH_3^+]_{0.25}\}^{n=1.3};$$

while if $K_D = 10^{-2}$ the exponent $n = 1.1$. Therefore, the plot of acid proton exchange rate vs. anilinium ion concentration in Fig. 6 is reasonable if the reaction is bi-ionic and the apparent molar ion-pair dissociation constant lies between 10^{-1} and 10^{-2}. Our results are too crude to justify any definite conclusions but an ion-pair dissociation constant of from 10^0 to 10^{-2} does appear reasonable from other work (27).

It seems to us that in terms of our (oversimplified) approach, the formation of an ion pair occurs as an intermediate step in the reaction, since ions must come together before they can react. At present we have no evidence concerning more sophisticated reaction mechanisms in our solutions, such as transfer of protons from cation to anion via intervening solvent molecules.

7. Calculation of Rate Constants, Free Energies, and Entropies of Activation at 25 °C

According to the theory of activated complexes (29) we have

$$k_{rate} = \kappa kTh^{-1} \exp(-\Delta F^{\ddagger}/RT).$$

We take κ, the transmission coefficient, as equal to 1. The specific rate constant, k_{rate}, must be expressed in terms of the activities of the reactants. We consider (*a*) an activated "bi-ionic" complex and (*b*) an activated "ion-pair" complex. (*a*) The free energy of activation, $\Delta F^{\ddagger}$, of an ionic reaction is the free energy change which occurs when the two ions are brought together plus the free energy required to activate the ion pair; (*b*) $\Delta F^{\ddagger}$ for a reaction of ion pairs does not include the free energy change which occurs when the ion pair is formed.

On this basis the specific rate constants for the two cases are to be obtained. The apparent rate constants for the bi-ionic reaction can be corrected by use of the Debye–Hückel term, as discussed before. For the ion-pair reaction we assume that the ion pair is a neutral group unaffected by the ionic strength of the solution. This approximation

**At the concentrations we are working this would seem to be a reasonable assumption (27).*

Can. J. Chem. Downloaded from www.nrcresearchpress.com by 210.87.254.40 on 09/05/12
For personal use only.

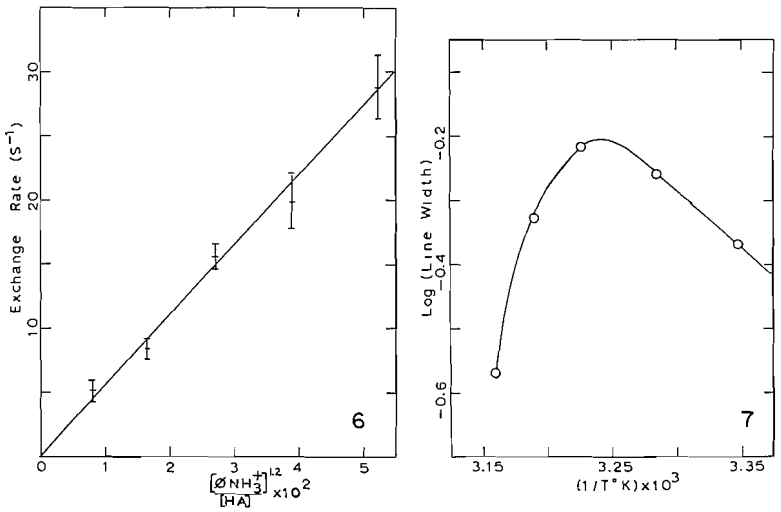

FIG. 6. Plot of TFA proton exchange rate vs. $([\phi NH_3^+]^{1.2}/[HA] \times 10^2)$. Concentrations are expressed in moles/l. It is assumed that the aniline is completely protonated.

FIG. 7. Plot of log (additional acid proton line width) vs. $1/T$ for a 1 mole % solution of *p*-fluoroaniline in TFA. The additional acid proton line width has been determined by extrapolating log (acid proton line width) in the high-temperature region to the low-temperature region (Fig. 4).

may not introduce drastic errors since the ion pair and the activated complex are both polar in character. From the last equation above it is clear that even if the activity coefficients differ by a factor of two the error will be only about 0.4 kcal/mole in the calculated free energies. The error should be similar for the different anilines.

Four different sets of rate constants have been calculated for the exchange reactions between substituted anilines and TFA at 25 °C. They are given in Table VI. The first set are the corrected second-order rate constants for the bi-ionic reaction, assuming that no ion pairs exist in solution. In column 3 the calculated rate constants for ion-pair reactions are given. These two sets of rate constants represent the limiting situations of our model. In addition, we have assumed $K_D = 1$. In this case the *apparent* rate constants of the bi-ionic reaction and the ion-pair reaction are the same because $[\phi NH_3^+][A^-]$

TABLE VI

Calculated rate constants for the overall reactions and the ion-pair reactions of solutions of aniline and substituted anilines in TFA at 25 °C

Substituent	Rate constant for overall reaction if $K_D = \infty$ (l/mole s)	Rate constant for ion-pair reaction if $K_D = 0$ (s^{-1})	Rate constant for ion-pair reaction if $K_D = 1$ (s^{-1})	Rate constant for overall reaction if $K_D = 1$ (l/mole s)
H	7.2×10^2	2.2×10^1	7.8×10^1	1.1×10^3
p-F	1.1×10^3	2.9×10^1	1.6×10^2	1.4×10^3
p-Cl	3.0×10^3	8.8×10^1	2.2×10^2	4.1×10^3
p-Br	8.5×10^3	2.3×10^2	1.2×10^3	1.0×10^4
p-I	9.3×10^3	2.5×10^2	1.4×10^3	1.2×10^4
m-F	2.0×10^4	4.6×10^2	4.4×10^3	2.0×10^4
m-Cl	1.3×10^4	3.7×10^2	1.6×10^3	1.8×10^4
m-Br	1.4×10^4	3.6×10^2	2.0×10^3	1.7×10^4
m-I	1.0×10^4	2.8×10^2	1.5×10^3	1.3×10^4
o-F	6.3×10^4	1.4×10^3	1.3×10^4	5.8×10^4
o-Cl	5.1×10^4	1.3×10^3	7.6×10^3	6.5×10^4
o-Br	1.1×10^5	2.6×10^3	2.4×10^4	1.1×10^5
N,N-Di-Me	—	1.1×10^0	2.7×10^0	—

Can. J. Chem. Downloaded from www.nrcresearchpress.com by 210.87.254.40 on 09/05/12
For personal use only.

$= [\phi NH_2 \ldots A^-]$. In column 4 the rate constants for the ion-pair reaction are given for $K_D = 1$ and in column 5 the corrected rate constants of the bi-ionic reaction for $K_D = 1$ are given.

From Table VI the $\Delta F^{\ddagger}$ values follow directly and are given in Table VII. The calculated values of $\Delta S^{\ddagger}$ for the ion-pair reactions are given in Table VIII. The error limits are determined by the estimated uncertainties in the values of enthalpies of activation. $\Delta S^{\ddagger}$ values for the bi-ionic reactions are not given. They are larger and show the same trend as the tabulated values.

TABLE VII

Calculated values of free energies of activation* for the overall reactions and the ion-pair reactions of solutions of aniline and substituted anilines in TFA at 25 °C

Substituent	$\Delta F^{\ddagger}$ for overall reaction if $K_D = \infty$	$\Delta F^{\ddagger}$ for ion-pair reaction if $K_D = 0$	$\Delta F^{\ddagger}$ for ion-pair reaction if $K_D = 1$	$\Delta F^{\ddagger}$ for overall reaction if $K_D = 1$
H	13.55	15.65	14.9	13.3
p-F	13.3	15.45	14.45	13.2
p-Cl	12.7	14.8	14.0	12.5
p-Br	12.1	14.25	13.25	12.05
p-I	12.05	14.2	13.15	11.9
m-F	11.6	13.8	12.5	11.6
m-Cl	11.85	13.95	13.1	11.65
m-Br	11.8	14.0	12.95	11.7
m-I	12.0	14.1	13.1	11.8
o-F	10.9	13.15	11.8	10.9
o-Cl	11.0	13.2	12.15	10.9
o-Br	10.55	12.8	11.45	10.6
N,N-Di-Me	—	17.4	16.9	—

*The units of $\Delta F^{\ddagger}$ are kcal/mole.

TABLE VIII

Calculated values of entropies of activation of the ion-pair reactions of solutions of aniline and substituted anilines at 25 °C

Substituent	$\Delta S^{\ddagger}$ (e.u.) if $K_D = 0$	$\Delta S^{\ddagger}$ (e.u.) if $K_D = 1$
H	25.5±2.5	33±2.5
p-F	21	26
p-Cl	21±5	29±5
p-Br	29.5±7	33±7
p-I	22±1	25±1
m-F	13±3	17.5±3
m-Cl	12±4	14±4
m-Br	19±4	22±4
m-I	26±7	29.5±7
o-F	−8±5	−4±5
o-Cl	−7±13	−3.5±13
o-Br	−10±11	−5.5±11
N,N-Di-Me	3±4	4±4

8. Discussion of $\Delta F^{\ddagger}$ and $\Delta S^{\ddagger}$ Values

The $\Delta F^{\ddagger}$ values are in general lowest for the orthosubstituted anilines and highest for parasubstituted anilines and always less than $\Delta F^{\ddagger}$ for aniline itself. The pattern is reasonable if the inductive effect of the halogens increases in the order I < Br < Cl < F and the mesomeric effect increases in the same order. In no case is an error larger than 0.3 kcal/mole necessary to fit the $\Delta F^{\ddagger}$ values into the postulated pattern. The results

Can. J. Chem. Downloaded from www.nrcresearchpress.com by 210.87.254.40 on 09/05/12
For personal use only.

in column 3 fit the pattern best. The overall consistency of $\Delta F^{\ddagger}$ values and their correlation with the inductive and mesomeric properties of the halogens suggests that our approach has at least some merit.

The $\Delta S^{\ddagger}$ values are too inaccurate to allow any reliable interpretations of the relative effects of the halogens upon entropies of activation.* However, there does seem to be a definite trend to lower $\Delta S^{\ddagger}$ as the substituent moves closer to the reaction center. This may be a result of a decrease in solvation of the substituent and the reaction center due to steric and electrostatic effects.

9. N,N-Dimethylaniline

For ring-substituted anilines, the rate constants were calculated from the acid proton exchange rates. The proton exchange rates of protonated N,N-dimethylaniline were measured directly (24). Perhaps, then, additional reactions were involved which do not affect the acid proton lifetimes. For example, the reaction

$$\phi N(CH_3)_2 + H^+(CH_3)_2N\phi \rightarrow \phi N(CH_3)_2H^+ + (CH_3)_2N\phi$$

would cause collapse of the methyl proton doublet but would not affect the acid proton line width.

The thermodynamic data in Tables V–VIII were obtained in the way discussed for the other anilines. Collapse of the methyl doublet was assumed to occur only as a result of reactions in which ammonio protons were replaced by protons which had spins opposite to that of the original protons. The proton exchange rate was assumed to be twice as large as the calculated spin exchange rate.

The activation parameters are consistent with those found for other anilines. This encourages us to think that the same reaction is involved when one measures the lifetime of acid protons as when one measures the lifetime of ammonio protons. The activation energy for proton transfer in N,N-dimethylanilinium ion is much lower than that of protonated aniline. $\Delta F^{\ddagger}$ is much larger, however, as would be expected since the former is a stronger base. The lower $\Delta S^{\ddagger}$ results in the smaller value of E_A for N,N-dimethylaniline. We suggest that steric hindrance to solvation by the methyl groups is involved.

10. Errors in Calculated Rate Constants and Parameters of Activation

These errors are in addition to those resulting from experimental uncertainties. They include the approximations in the correction factors for ionic activities. It is perhaps doubtful whether we are justified in using these correction factors for solutions as concentrated as ours. Furthermore, our estimates of ion-pair dissociation constants are at best approximate. They are presumably different for different compounds and change with temperature.

In this connection one may well ask what activation energy is being measured in our models. There is an activation energy for the overall bi-ionic reaction as well as for proton transfer by ion pairs. If ΔH^0 of dissociation of the ion pairs is zero, the ratio of free ions and ion pairs is independent of temperature and the experimental value of E_A is equal to the values of the activation energy for the overall reaction *and* for the ion-pair reaction. If ΔH^0 is positive, the concentration of ion pairs decreases with increase of temperature and thus the measured activation energy is smaller than the true activation energy for proton transfer by ion pairs. If ΔH^0 is negative, the measured activation energy

**The largest errors occur for the orthosubstituted anilines. A referee has suggested that this is because we used line width values very near the region of maximum line width. But the same objection could be used against some of the other anilines. We did have fewer points for the orthoanilines and, therefore, the 95% confidence units on the activation energies and, hence, enthalpies and entropies are relatively large.*

Can. J. Chem. Downloaded from www.nrcresearchpress.com by 210.87.254.40 on 09/05/12
For personal use only.

is larger than the activation energy of the overall bi-ionic reaction because the concentration of free ions decreases as the temperature increases. If anilines in solution exist almost entirely as ion pairs, then E_A is about equal to the activation energy for the reaction of ion pairs. If the anilines exist almost entirely as ions, then E_A is almost equal to the activation energy for the complete bi-ionic reaction. The difference in activation energies is equal to ΔH^0, which is usually less than 3 kcal/mole in magnitude (27). If this magnitude is less than 2 kcal/mole, our E_A will usually agree, within experimental error, with both values of the activation energies.

11. Effect of Impurities on the Experimental Line Widths

There probably were some impurities present in the compounds used to prepare the solutions. Only for the solution containing *p*-fluoroaniline was there any evidence that exchange was occurring between TFA and impurities. The plot of log (acid proton line width) vs. $1/T$ (Fig. 4) is nearly linear in the high-temperature region. If the straight line is extrapolated to lower temperatures (dotted line), then deviations from expected behavior can be plotted against $1/T$ (Fig. 7). The additional exchange rate increases, then decreases with increasing temperature. This is exactly the behavior expected for exchange between acid and an impurity. Distillation apparently concentrated the impurity since there were larger deviations from expected behavior in the solution containing redistilled *p*-fluoroaniline. Whatever the impurity was, it must have been present in appreciable quantities ($\simeq$ 10% of the total aniline concentration) since it broadened the acid proton peak by as much as 0.6 c/s. Since the exchange took place near room temperature, the impurity was quite probably some other substituted aniline.

The absence of proton exchange between TFA and impurities in other solutions is understandable, even though some impurities may have been present. Impurities will appreciably affect acid proton line widths only if they fulfill the following three conditions: (1) they must contain exchangeable protons or be able to accept protons, (2) they must be present in significant amounts, (3) they must exchange with acid at an intermediate rate at the same temperature at which the protonated aniline exchanges with TFA or else they must catalyze the anilinium ion exchange reaction. These three points can be dealt with in order. Firstly, any impurity which does not exchange protons with TFA will have no effect upon the acid proton line width since it will not alter the proton lifetime. Secondly, the maximum width of the acid proton signal depends upon the concentration of the substance with which it exchanges. For example, 3 mole % solutions of substituted anilines broadened the acid proton signal by as much as 15 c/s while the maximum line width of acid proton signals in 1 mole % solutions was about 6 c/s. If there is only a very low concentration of impurity in solution, then its relative exchange rate will be so much greater than that of the acid that the two signals will coalesce before the acid proton signal is appreciably broadened. Thirdly, there will normally be little broadening of the acid proton signal if the exchange rate of the reaction between the impurity and TFA is either very slow or very fast in the region of interest. However, this is not necessarily true if the impurity catalyzes the exchange reaction between anilinium ions and trifluoroacetate ions. For example, consider the effect of water in solution. It has been shown that water has little effect upon the acid proton line width. This probably indicates that water is rapidly exchanging protons with TFA (30). It is conceivable that unprotonated water molecules could accept protons from anilinium ions and donate them to trifluoroacetate ions. Such a transfer would introduce a proton with a different Larmor precession frequency into the system of acid and water molecules

Can. J. Chem. Downloaded from www.nrcresearchpress.com by 210.87.254.40 on 09/05/12
For personal use only.

and cause a broadening of the coalesced acid–water peak. There are three reasons why it is considered unlikely that catalysis reactions of this type occurred in the solutions studied. Firstly, it has been shown that the exchange reaction between ammonium ions and water has an activation energy of 12.2 kcal/mole (13). Since aniline is a weaker base, the corresponding exchange reaction between anilinium ions and water should have a lower activation energy. The experimental activation energy of proton transfer of the solution of aniline in TFA is 23.8 kcal/mole. Secondly, any water in the TFA was presumably almost completely protonated. Consequently, the concentration of free water molecules which could exchange with anilinium ions must have been small. Thirdly, if the measured exchange reactions had been catalyzed by water or other impurities, then there should have been no correlation between exchange rate and structure because the exchange rate would have depended upon the catalyst concentration.

Swarts showed that the reaction between aniline and TFA to form trifluoroacetanilide occurred after the reactants had been heated for 8 h at 120 °C (31). Therefore, it is unlikely that any appreciable reaction between aniline and TFA occurred at the temperatures used in this study. However, the decrease in acid proton line width observed when trifluoroacetic anhydride was added to solutions of aniline in TFA was probably due to formation of trifluoroacetanilide. This would explain the observed relation between the concentration ratio of aniline and trifluoroacetic anhydride and the acid proton line width. Less than 0.01 g of trifluoroacetic anhydride was added to each sample of TFA used to prepare a solution for exchange studies. It was added to the acid several minutes before the acid was added to the aniline. It possibly reacted with any water in the acid before the acid was added to the aniline. Because of the time interval and because only a very small amount of anhydride was added, it is considered unlikely that any appreciable reaction occurred between the anhydride and aniline.

12. Acid Proton Line Widths in the Collapsed Region

The line widths of the acid proton signals of 1 mole % solutions of anilines in TFA (Fig. 5) reach maximum values and then decrease with increasing temperature. The decreases must occur when the exchange rates are fast enough to coalesce the acid and ammonio proton signals. The acid proton exchange rate which causes this collapse depends upon the relative populations of acid and ammonio protons and upon the chemical shift between the two types of protons in the absence of exchange.

The slope and, therefore, E_A is higher in the collapsed region. The difference amounts to about 8 kcal/mole in all cases. Since the ammonio protons are present in much smaller concentrations than the acid protons, it is unlikely that incomplete collapse of the ammonio triplet or reactions which affect only the ammonio proton lifetimes are the reason. A probable explanation is suggested by the data in Table III. The acid proton resonance high-field shifts with temperature are large and nearly independent of aniline concentration. It is probable that the high-field shift results from a decrease in acid molecule hydrogen bonding. This would account for the increased slope of the line width plot in the collapsed region. The larger E_A is somehow related to the hydrogen bond breaking. There are possibilities here which merit further exploration.

ACKNOWLEDGMENTS

We are grateful to the referees for valuable criticisms. This work was supported by the National Research Council, Ottawa.

Can. J. Chem. Downloaded from www.nrcresearchpress.com by 210.87.254.40 on 09/05/12
For personal use only.

Can. J. Chem. Downloaded from www.nrcresearchpress.com by 210.87.254.40 on 09/05/12
For personal use only.

REFERENCES

1. H. S. GUTOWSKY and C. H. HOLM. J. Chem. Phys. **25**, 1228 (1956).
2. H. S. GUTOWSKY, D. MCCALL, and C. SLICHTER. J. Chem. Phys. **21**, 279 (1953).
3. H. S. GUTOWSKY and A. SAIKA. J. Chem. Phys. **21**, 1668 (1953).
4. H. M. MCCONNELL. J. Chem. Phys. **28**, 430 (1958).
5. M. TAKEDA and E. STEJSKAL. J. Am. Chem. Soc. **82**, 25 (1960).
6. R. A. OGG. Discussions Faraday Soc. **34**, 215 (1954).
7. R. A. OGG and J. D. RAY. J. Chem. Phys. **26**, 1339 (1957).
8. E. GRUNWALD, A. LOEWENSTEIN, and S. MEIBOOM. J. Chem. Phys. **27**, 630 (1957).
9. A. LOEWENSTEIN and S. MEIBOOM. J. Chem. Phys. **27**, 1067 (1957).
10. S. MEIBOOM, A. LOEWENSTEIN, and S. ALEXANDER. J. Chem. Phys. **29**, 969 (1958).
11. M. T. EMERSON, E. GRUNWALD, and R. KROMHOUT. J. Chem. Phys. **33**, 547 (1960).
12. E. GRUNWALD, P. J. KARABATSOS, R. KROMHOUT, and E. PURLEE. J. Chem. Phys. **33**, 556 (1960).
13. T. CONNOR and A. LOEWENSTEIN. J. Am. Chem. Soc. **83**, 560 (1961).
14. S. MEIBOOM. J. Chem. Phys. **34**, 375 (1961).
15. A. LOEWENSTEIN and A. SZOKE. J. Am. Chem. Soc. **84**, 1151 (1962).
16. M. ANBAR, A. LOEWENSTEIN, and S. MEIBOOM. J. Am. Chem. Soc. **80**, 2630 (1958).
17. E. GRUNWALD, C. JUMPER, and S. MEIBOOM. J. Am. Chem. Soc. **84**, 4664 (1962).
18. E. GRUNWALD, C. JUMPER, and S. MEIBOOM. J. Am. Chem. Soc. **85**, 522 (1963).
19. E. GRUNWALD and C. JUMPER. J. Am. Chem. Soc. **85**, 2051 (1963).
20. E. GRUNWALD and S. MEIBOOM. J. Am. Chem. Soc. **85**, 2047 (1963).
21. W. G. PATERSON. Can. J. Chem. **41**, 714 (1963).
22. W. G. PATERSON. Can. J. Chem. **41**, 2472 (1963).
23. W. G. PATERSON and H. SPEDDING. Can. J. Chem. **41**, 2477 (1963).
24. W. F. REYNOLDS and T. SCHAEFER. Can. J. Chem. **41**, 540 (1963).
25. J. N. MURRELL. Roy. Inst. Chem. London, Lectures, Monographs, Rept. **2**, 1 (1963).
26. R. O. C. NORMAN. Roy. Inst. Chem. London, Lectures, Monographs, Rept. **2**, 11 (1963).
27. C. W. DAVIES. Ion association. Butterworths, London. 1962.
28. K. J. LAIDLER. Chemical kinetics. McGraw-Hill Book Co., Inc., New York. 1950. Chap. 5.
29. K. J. LAIDLER. Chemical kinetics. McGraw-Hill Book Co., Inc., New York. 1950. Chap. 3.
30. Z. LUZ and S. MEIBOOM. J. Am. Chem. Soc. **85**, 3923 (1963).
31. F. SWARTS. Bull. Classe Sci. Acad. Roy. Belg. **8**, 343 (1922).

Can. J. Chem. Downloaded from www.nrcresearchpress.com by 210.87.254.42 on 09/05/12
For personal use only.

LOW-TEMPERATURE PYROLYSIS

I. THE PYROLYSIS OF HYDROGEN PHTHALATE ESTERS OF SOME TERTIARY ALCOHOLS

K. G. Rutherford and D. P. C. Fung
Department of Chemistry, University of Windsor, Windsor, Ontario
Received January 7, 1964

ABSTRACT

Some hydrogen phthalate esters of tertiary alcohols have been subjected to liquid phase pyrolysis. Olefinic mixtures and phthalic acid are the only products of the reaction. A study of the olefin distribution for each of the compounds pyrolyzed was made. Evidence of ionic character in liquid phase pyrolysis is presented.

INTRODUCTION

The vapor phase pyrolysis of esters of aliphatic and alicyclic alcohols has been the subject of intensive study by numerous investigators who were interested in olefin-producing reactions. In general, olefin-producing reactions fall into two classes: those which yield predominantly the most highly alkylated isomer (Saytzeff product) and those which yield predominantly the least alkylated isomer (Hofmann product). The vapor phase pyrolysis of esters (acetates and xanthates, etc.) of primary alcohols has been found by several workers to yield exclusively the Hofmann product while that of esters of secondary and tertiary alcohols yields a mixture of Hofmann and Saytzeff products (1). The mechanism of pyrolysis of acetate and xanthate esters has been well established in both cases and is known to involve a cyclic transition state of the nature

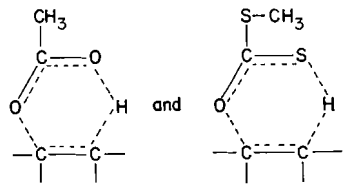

respectively. The appearance of both Hofmann and Saytzeff products in the vapor phase pyrolysis of acetates and xanthates of secondary and tertiary alcohols has been explained on the basis of statistical, steric, and thermodynamic effects. The high-temperature pyrolysis of *sec*-butyl acetate exemplifies the operation of statistical effects. The formation of 1-butene is favored statistically over 2-butenes by a factor of 3:2. The experimental values are in excellent agreement (57% 1-butene and 43% 2-butenes). Similar agreement between statistical and experimental results is obtained in the vapor phase pyrolysis of *tert*-amyl acetate. Steric effect appears to govern the proportion of the *cis*- and *trans*-2-butenes in the pyrolysis of *sec*-butyl acetate. Statistically they should be formed in equal amounts. However, the *trans* olefin predominates over the *cis* isomer by a factor of 2. De Puy and co-workers (2) suggest that the methyl–methyl repulsion in the transition state leading to the *cis* olefin is absent in the transition state leading to the *trans* olefin.

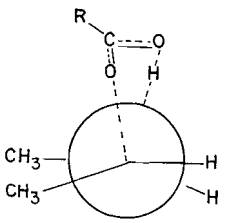

cis Olefin transition state

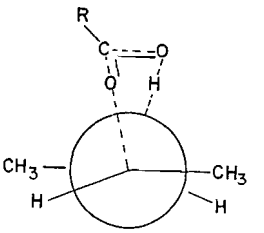

trans Olefin transition state

Hence, as a general rule, steric effects will favor the formation of primary and *trans* olefins and will hinder the formation of internal and *cis* olefins.

Thermodynamic considerations should favor the more stable isomer in pyrolytic elimination reactions. Voge and May (3) reported that at equilibrium at 500°, the butenes exist in the ratio 28% 1-butene, 41% *trans*-2-butene, and 31% *cis*-2-butene. However, the contact time in vapor phase pyrolysis is usually so small that thermodynamic effects should not be noticeable. Again, thermodynamic effects should be almost nonexistent in low-temperature pyrolysis in which the contact time is of the order of only a few seconds.

The pyrolysis of xanthates (Chugaev Reaction) can be carried out at much lower temperatures than required for corresponding acetates. While both pyrolytic reactions have been carried out with the same system, the product ratios have been found to compare favorably despite the great differences in temperature and conditions. For example, the acetate of 1-methylcyclohexanol yields, on pyrolysis at temperatures greater than 450°, 74% 1-methylcyclohexene and 26% methylenecyclohexane (2, 4). The xanthate yields, on pyrolysis at 200°, 79% of the former and 21% of the latter isomer (5). It is interesting to note, however, that liquid phase pyrolysis of the acetate of 1-methylcyclohexanol at 220° yields 83% 1-methylcyclohexene and 17% methylenecyclohexane. Bailey (4) concluded that liquid phase pyrolysis would be more apt to follow the Saytzeff rule than would vapor phase pyrolysis. Barton (6) had previously suggested, mostly on the basis of liquid phase pyrolyses, that the Saytzeff rule was followed quite generally. This involves two possibilities: the stability of the olefin may be a controlling factor or the mechanism of the elimination is shifting from a cyclic intermediate to one involving an ionic intermediate. Indeed Bailey has suggested both possibilities.

In the past six years some interesting cases of pyrolytic elimination reactions have appeared in the literature. Thus, Bordwell and Landis (7) have reported that *cis*-2-*p*-tolylsulfonylcyclohexyl-*s*-methyl xanthate (I) decomposes on heating to yield almost exclusively 1-*p*-tolylsulfonyl-1-cyclohexene (II) rather than the expected 3-cyclohexene isomer. This is interpreted mechanistically as a stepwise intramolecular "*trans*" elimination promoted by the high acidity of the beta hydrogen atom which undergoes elimination (Fig.1).

The same authors (8) also reported that pyrolytic decomposition of *cis*-2-*p*-tolylsulfonylcyclohexyl methyl sulfite yielded 1-*p*-tolylsulfonyl-1-cyclohexene, instead of the expected 3-cyclohexene derivative. Again the acidity of the beta hydrogen atom lost on pyrolysis presumably leads to a dipolar ion analogous to Fig. 1, thus accounting for the "*trans*" elimination product.

Kingsbury and Cram (9) reported that although the diastereomeric 1,2-diphenyl-1-propyl phenyl sulfoxides decomposed in a stereospecific manner at 80°, stereospecificity

Can. J. Chem. Downloaded from www.nrcresearchpress.com by 210.87.254.42 on 09/05/12
For personal use only.

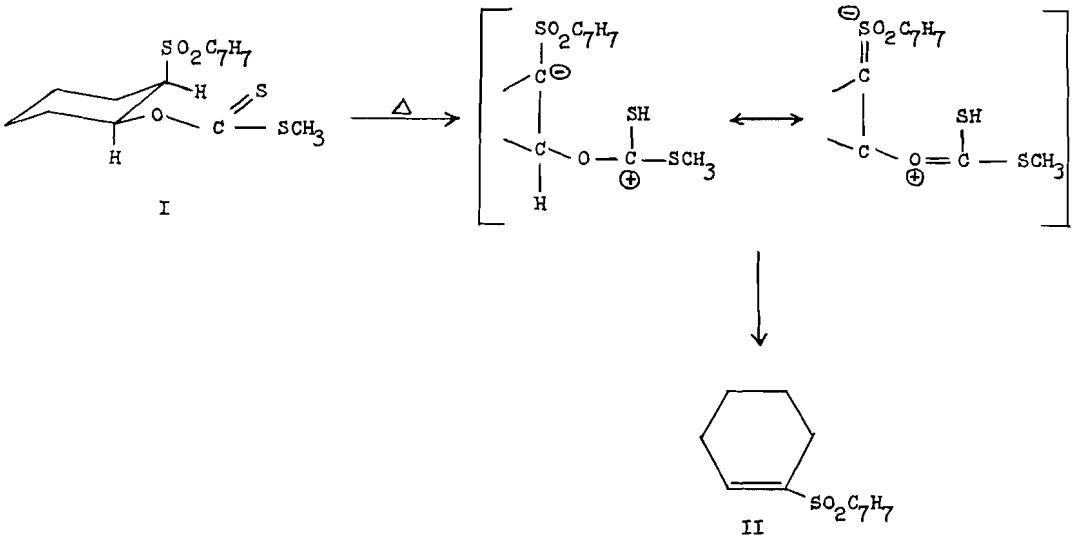

FIG. 1. Pyrolysis of *cis*-2-*p*-tolylsulfonylcyclohexyl-*s*-methyl xanthate.

was lost on decomposition at 120°. These authors proposed the formation of a radical pair to account for the loss of stereospecificity (Fig. 2).

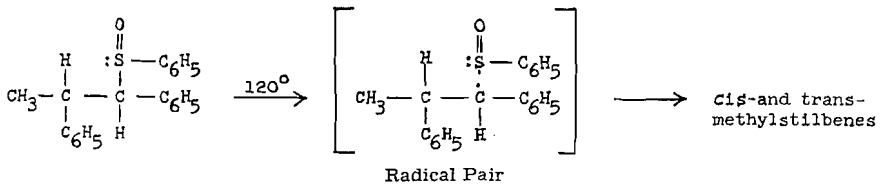

FIG. 2. Pyrolysis of diastereomeric 1,2-diphenyl-1-propyl phenyl sulfoxides at 120°.

Botteron and Shulman (10) found that the 2-methylcyclohexyl-*s*-methyl xanthates of *cis*- and *trans*-2-methylcyclohexanol did not decompose in a stereospecific manner. These authors suggest that the Chugaev reaction is not as stereospecific as once thought.

More recently Sixma and co-workers (11) have investigated the thermal decomposition of 27 aliphatic acetates. It was found that the rate of elimination was enhanced markedly as the degree of alkylation on the alpha carbon atom was increased. A tentative mechanism was proposed which was based on the reversible formation of an ion pair.

Our interest in low-temperature pyrolysis stemmed from a paper of Zeiss (12) who reported that the hydrogen phthalate derivative of 2-phenyl-2-butanol decomposed at its melting point (111°). Although no study was made of the decomposition products, it seemed reasonable to assume that an ordinary ester pyrolysis had occurred and at a very low temperature. The procedure for the preparation of the hydrogen phthalate derivative involved the conversion of the tertiary alcohol to its potassium salt in boiling benzene followed by the addition of phthalic anhydride. A more convenient procedure was developed in this laboratory for the preparation of hydrogen phthalate derivatives of tertiary alcohols and was reported in a previous paper (13). This procedure involves conversion of a tertiary alcohol to its sodium salt by means of the strong base triphenylmethyl sodium in ether solution, with subsequent addition of phthalic anhydride. Several

Can. J. Chem. Downloaded from www.nrcresearchpress.com by 210.87.254.42 on 09/05/12
For personal use only.

hydrogen phthalate esters of tertiary alcohols were characterized and reported. It is interesting to note that all the hydrogen phthalate esters prepared from the tertiary aliphatic and alicyclic alcohols are well-defined, sharp-melting solids and have decomposition points between 130–155°. The only products of decomposition are olefins and phthalic acid. It was logical, then, to study in detail the products of pyrolysis of a number of these esters since the low decomposition points suggest that a different mechanism may be operative in the decomposition of such internally strained systems.

The general procedure of pyrolysis consisted of heating an oil bath to the desired temperature and introducing into the bath a flask which contained the solid hydrogen phthalate ester. The flask was fitted with a Claisen head, thermometer, condenser, and receiving tube which was placed in a dry ice – acetone bath. Depending upon the boiling points of the olefins obtained, the system was subjected to reduced pressure. This eliminated excess contact of the olefinic mixtures with the phthalic acid generated and thus minimized possible isomerization. Later it was shown that the possibility of phthalic acid catalyzed isomerization of the olefinic mixtures was remote under the conditions employed.

RESULTS AND DISCUSSION

Table I summarizes the hydrogen phthalate esters under investigation in this work and indicates melting points, decomposition temperatures, and product distribution. Table II summarizes results of vapor phase pyrolysis of corresponding acetates. Wherever possible, low-temperature (liquid phase) pyrolysis results are given for comparison. It is to be noted that all the acetate esters are liquids.

In the low-temperature pyrolysis of both the acetate and hydrogen phthalate esters of tert-amyl alcohol, the Saytzeff product predominates. This is in sharp contrast to high-temperature (400°) acetate ester pyrolysis which yields 70% Hofmann isomer (2-methyl-1-butene). Low-temperature pyrolysis (155–160°) of the hydrogen phthalate and acetate esters of 1-methylcyclohexanol shows the same trend, with the hydrogen phthalate ester yielding 5% more Saytzeff product than the acetate ester. Pyrolysis of the hydrogen phthalate ester of 1-methylcyclopentanol at 150–160° yields an almost quantitative amount (97%) of the Saytzeff product in contrast to 84% obtained from high-temperature pyrolysis (450°) of the corresponding acetate. It is interesting to note that De Puy (2) claimed that no Hofmann product (methylenecyclopentane) could be obtained from the pyrolysis of the acetate of 1-methylcyclopentanol at 450°. However, the separation of methylenecyclopentane and 1-methylcyclopentene is extremely difficult. Bailey (14) separated the isomers effectively using a column containing silver nitrate in diethylene glycol absorbed on Johns–Manville Chromasorb (10–30 mesh, acid washed) in a "special" vapor phase chromatographic column. We were unsuccessful with this column packing in a 6 ft copper column (1/4 in. diameter) but managed to separate the isomers using a Golay "R" column (175 ft). The presence of the exo isomer could be detected by means of a small band at 11.2 μ in the infrared. This band disappeared when the olefinic mixture was boiled with *p*-toluenesulfonic acid for 3 h.

Of particular interest in this investigation are the products obtained from the pyrolysis of the hydrogen phthalate ester of *trans*-1,2-dimethylcyclohexanol, especially the appearance of 19% 1,2-dimethylcyclohexene. De Puy (2) had previously reported that this compound was not obtained on the pyrolysis of the corresponding acetate at 450° although a 28% yield was obtained from the *cis* isomer (Table II). The pyrolysis of the acetate of *trans*-1,2-dimethylcyclopentanol at 450° was reported to have yielded small amounts

Can. J. Chem. Downloaded from www.nrcresearchpress.com by 210.87.254.42 on 09/05/12
For personal use only.

Can. J. Chem. Downloaded from www.nrcresearchpress.com by 210.87.254.42 on 09/05/12
For personal use only.

TABLE I

Pyrolysis of hydrogen phthalate esters of tertiary alcohols

Hydrogen phthalate ester	Melting point	Oil bath temperature	Pressure	Product distribution	
				Saytzeff	Hofmann
tert-Amyl	62–63°	145–150°	Atmospheric	2-Methyl-2-butene (53%)	2-Methyl-1-butene (47%)
1-Methylcyclopentyl	68–69°	150–160°	Atmospheric	1-Methylcyclopentene (97%)	Methylenecyclopentane (3%)
1-Methylcyclohexyl	89–91°	155–160°	85 mm	1-Methylcyclohexene (88%)	Methylenecyclohexane (12%)
1-Methylcycloheptyl	90–91°	135–140°	100 mm	1-Methylcycloheptene (72%)	Methylenecycloheptane (28%)
trans-1,2-Dimethylcyclohexyl	124–125°	140–150°	24 mm	2,3-Dimethylcyclohexene (46%) 1,2-Dimethylcyclohexene (19%)	2-Methylmethylenecyclohexane (35%)

TABLE II

Pyrolysis of acetate esters of tertiary alcohols

Acetate ester	Decomposition temperature	Product distribution	
		Saytzeff	Hofmann
tert-Amyl	225° (4) 400°	2-Methyl-2-butene (58%) [30%]	2-Methyl-1-butene (42%) [70%]
1-Methylcyclopentyl	450° (9)	1-Methylcyclopentene (84%)	Methylenecyclopentane (16%)
1-Methylcyclohexyl	220° (4) 450°	1-Methylcyclohexene (83%) [74%]	Methylenecyclohexane (26%)
1-Methylcycloheptyl	440° (9)	1-Methylcycloheptene (76%)	Methylenecycloheptane (24%)
trans-1,2-Dimethylcyclohexyl	450° (2)	2,3-Dimethylcyclohexene (45%) 1,2-Dimethylcyclohexene (0)	2-Methylmethylenecyclohexane (55%)
cis-1,2-Dimethylcyclohexyl	450° (2)	2,3-Dimethylcyclohexene (26%) 1,2-Dimethylcyclohexene (28%)	2-Methylmethylenecyclohexane (46%)

(5–10%) of 1,2-dimethylcyclopentene as well as the other expected isomers but it was established that the olefin products isomerized under the conditions of pyrolysis. We find, however, in the case of the olefin mixture obtained from the cyclohexyl phthalate analogue that the olefin distribution obtained on pyrolysis does not change when redistilled from phthalic acid even at 180°. Thus it is inconceivable that isomerization occurs under the conditions employed. We suggest that carbonium-ion character is evident in the transition state in the pyrolysis of this hydrogen phthalate ester and that this elimination is kinetically controlled. This may well be extrapolated to the low-temperature pyrolysis of esters of the other tertiary systems studied. The fact that more of the 1,2-dimethylcyclohexene was not obtained may well be attributed to the "*cis* effect" which would be exhibited in the transition state of elimination. It is suggested then that in olefin formation involving initial ionization of the hydrogen phthalate ester, the amount of Saytzeff product is controlled by steric effects in the transition state as well as by statistical considerations. The possible elimination transition states for the 1,2-dimethylcyclohexyl carbonium ion are illustrated in Fig. 3. The steric effect of the *cis* methyl groups in transition state "A" would hinder the initial formation of 1,2-dimethylcyclohexene, the most stable isomer from hyperconjugative considerations. Pertinent to this, it has been observed (15) that iodine dehydration (an equilibrium process) of *trans*-1,2-dimethylcyclohexanol yields 73% 1,2-dimethylcyclohexene, 24% 2,3-dimethylcyclohexene, and 3% methylene-2-methylcyclohexene.

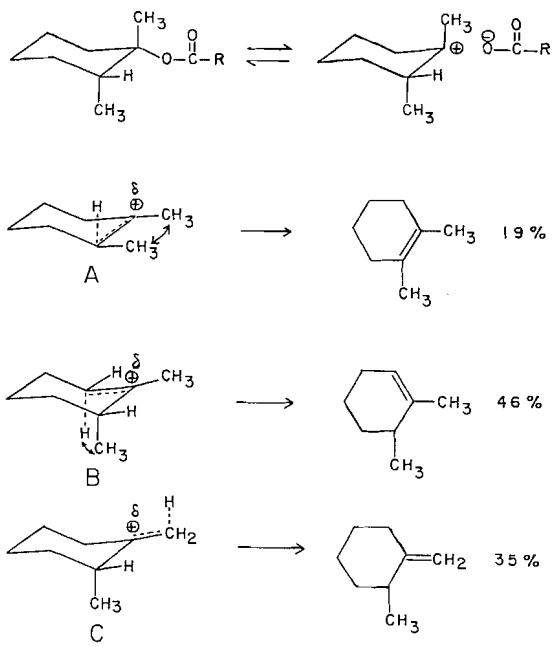

FIG. 3. Possible elimination transition states for 1,2-dimethylcyclohexyl carbonium ion.

There is much less "*cis* effect" in transition states "B" and "C". The former, however, would be more favorable from hyperconjugative influences. The abnormal amount of methylene-2-methylcyclohexane (35%) is indeed surprising when compared with the amount of methylenecyclohexane (12%) obtained from the low-temperature pyrolysis

Can. J. Chem. Downloaded from www.nrcresearchpress.com by 210.87.254.42 on 09/05/12
For personal use only.

of the hydrogen phthalate ester of 1-methylcyclohexanol. Again, this large amount of exo isomer would preclude the possibility of any isomerization reaction occurring during pyrolysis. It is possible that in transition state "B", 1,3-hydrogen – methyl interaction presents an adverse effect.

That the elimination reaction may in part occur by the usual cyclic mechanism cannot be completely excluded. Dreiding models show that the preferred orientation of the ring substituents is such that the methyl groups are axial and that if the ester carbonyl group occupies a position in the vicinity of the methyl hydrogen atoms on the same ring carbon atom then a maximum of free rotation of the benzene ring and the ortho carboxylic acid substituent is realized.

It is interesting to note that in the case of low-temperature pyrolysis of the hydrogen phthalate esters of methylcyclopentanol, methylcyclohexanol, and methylcycloheptanol, the amount of exo isomer (Hofmann product) increases markedly with increasing ring size (3%, 12%, and 28% respectively). One may conclude that the larger the ring size, the more favorable the ionic transition state since the ring bond angle can expand towards 120°.

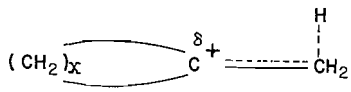

It is very difficult to draw a comparison with liquid phase pyrolysis of tertiary hydrogen phthalate esters and corresponding acetates. The former, because of much greater internal strain, may well lend themselves more readily to an ionic-type breakdown and thus decompose at much lower temperatures. Indeed, we have found that all aliphatic hydrogen phthalate esters of tertiary alcohols which contain one or two phenyl groups on the carbonyl carbon atom decompose at their melting points. Thus the hydrogen phthalate ester of 2-phenyl-2-propanol decomposes at 109–110° in mineral oil to yield on subsequent steam distillation 95% alpha-methylstyrene. Similarly, the hydrogen phthalate ester of 1,1-diphenylethanol yields 1,1-diphenylethylene at 110°. The presence of the phenyl grouping along with the low decomposition temperatures suggests added stability of the carbonium ion as well as increasing the internal strain of the molecule, thus enabling ion formation at even lower temperatures. With the limited amount of low-temperature experiments carried out with tertiary acetates, indications are that an increase in the ionic character of the elimination transition state is realized with a decrease in decomposition temperature.

The effect of benzenoid substituents which would increase or decrease carbonium-ion character in both acetate and hydrogen phthalate ester pyrolysis is presently under investigation.

EXPERIMENTAL

Melting points were taken on the Fisher–Johns melting point apparatus.

Preparation of Alcohols

1-Methylcyclopentanol, 1-methylcyclohexanol, and 1-methylcycloheptanol were prepared according to the procedure of Bailey and Hale (4). *trans*-1,2-Dimethylcyclohexanol was prepared according to the procedure of Hammond (16). Tertiary amyl alcohol was obtained commercially. The physical constants of all the alcohols agreed closely with reported values.

Hydrogen Phthalate Esters

All hydrogen phthalate esters were prepared according to the procedure developed in this laboratory

Can. J. Chem. Downloaded from www.nrcresearchpress.com by 210.87.254.42 on 09/05/12
For personal use only.

and reported in a previous paper (13). The esters of *t*-amyl alcohol, 1-methylcyclopentanol, and 1-methylcyclohexanol have been recorded in this previous work. The hydrogen phthalate esters of 1-methylcycloheptanol and *trans*-1,2-dimethylcyclohexanol were well-defined solids, m.p. 90–91° and 124–125° respectively, and were prepared in yields ranging from 85 to 90%.

Anal. Calcd. for $C_{16}H_{20}O_4$: C, 69.54; H, 7.30; neutralizing equivalent, 276.3. Found: C, 69.80; H, 7.56; neutralizing equivalent, 276.5.

Anal. Calcd. for $C_{16}H_{20}O_4$: C, 69.54; H, 7.30; neutralizing equivalent, 276.3. Found: C, 69.40; H, 7.43; neutralizing equivalent, 279.6.

Pyrolysis Studies

All the pyrolysis reactions were carried out essentially under the same conditions. An oil bath was preheated to desired temperature (see Table 1). A round-bottomed flask (100 ml) containing 10–15 g of hydrogen phthalate esters was fitted with a Claisen head, thermometer, Liebig condenser, and receiving tube and was immersed in the bath. The receiving tube was cooled in a dry ice – acetone bath. The olefins produced on pyrolysis of the esters of *t*-amyl alcohol and 1-methylcyclohexanol were collected at atmospheric pressure. The remaining pyrolyses were carried out under reduced pressure as indicated in Table I. In all cases the hydrogen phthalate esters melted sharply and then decomposed rapidly as the critical temperature was reached. The distillate was collected between 10 and 15 min, after which only traces of olefins distilled. As decomposition takes place, a deposit of phthalic acid accumulates rapidly in the reaction flask. This was found to trap some olefins, thus decreasing olefinic yields. Total olefinic yields obtained from the *t*-amyl, methylcyclopentyl, methylcyclohexyl, methylcycloheptyl, and *trans*-1,2-dimethylcyclohexyl systems were 70, 67, 67, 88, and 67% respectively. The olefinic mixtures obtained were subjected immediately to gas phase chromatographic analysis although no difference in isomer distribution was observed with any of the mixtures allowed to stand in the refrigerator for long periods of time. Separations of the olefinic mixtures from the *t*-amyl, methylcyclohexyl, and *trans*-1,2-dimethylcyclohexyl systems were effected with a Perkin–Elmer model 154 instrument using Column "A". Separations of the olefins obtained from the methylcyclopentyl and methylcycloheptyl systems were effected with a Perkin–Elmer model 800 using a Golay "R" column (175 ft).

Authentic samples of 2-methyl-1-butene, 2-methyl-2-butene, and 3-methyl-1-butene were obtained from the Phillips Petroleum Co., Bartlesville, Oklahoma. A mixture of 1-methylcyclopentene and methylenecyclopentane was obtained by the known iodine dehydration of 1-methylcyclopentanol (14). Similarly a mixture of 1-methylcyclohexene and methylene cyclohexane was obtained by the known iodine dehydration of 1-methylcyclohexanol (2). The thermal dehydration (14) of 1-methylcycloheptanol provided a mixture of 1-methylcycloheptene and methylenecycloheptane. Iodine dehydration (15) of *trans*-1,2-dimethylcyclohexanol provided 73% 1,2-dimethylcyclohexene, 24% 2,3-dimethylcyclohexene, and 3% methylene-2-methylcyclohexane. Retention times of all olefins obtained from low-temperature pyrolysis reactions were coincident with the known olefins. Authentic samples of 1-methylcyclopentene and 1-methylcycloheptene were obtained from the Aldrich Chemical Company.

ACKNOWLEDGMENTS

The authors would like to thank Dr. S. J. W. Price and Messrs. M. Jacko, M. Krech, and J. Kominar for able assistance with the gas phase chromatographic analysis and the National Research Council for financial support.

REFERENCES

1. C. H. De Puy and R. W. King. Chem. Rev. **60**, 431 (1960).
2. D. H. Froemsdorf, C. H. Collins, G. S. Hammond, and C. H. De Puy. J. Am. Chem. Soc. **81**, 643 (1959).
3. H. H. Voge and N. C. May. J. Am. Chem. Soc. **68**, 550 (1946).
4. W. J. Bailey and W. F. Hale. J. Am. Chem. Soc. **81**, 647 (1959).
5. R. A. Benkeser and J. J. Hazdra. J. Am. Chem. Soc. **81**, 228 (1959).
6. D. H. R. Barton. J. Chem. Soc. 2174 (1946).
7. F. G. Bordwell and P. S. Landis. J. Am. Chem. Soc. **80**, 2450 (1958).
8. F. G. Bordwell and P. S. Landis. J. Am. Chem. Soc. **80**, 6379 (1958).
9. C. A. Kingsbury and D. J. Cram. J. Am. Chem. Soc. **82**, 1810 (1960).
10. D. G. Botteron and G. P. Shulman. J. Org. Chem. **27**, 2007 (1962).
11. J. C. Scheer, E. C. Kooyman, and F. L. J. Sixma. Rec. Trav. Chim. **82**, 1123 (1963).
12. H. H. Zeiss. J. Am. Chem. Soc. **73**, 2391 (1951).
13. K. G. Rutherford, J. M. Prokipcak, and D. P. C. Fung. J. Org. Chem. **28**, 582 (1963).
14. W. J. Bailey and W. F. Hale. J. Am. Chem. Soc. **81**, 651 (1959).
15. M. Cardew and R. L. Burwell. J. Am. Chem. Soc. **82**, 6289 (1960).
16. T. D. Nevitt and G. S. Hammond. J. Am. Chem. Soc. **76**, 4124 (1954).

Can. J. Chem. Downloaded from www.nrcresearchpress.com by 210.87.254.42 on 09/05/12
For personal use only.

Can. J. Chem. Downloaded from www.nrcresearchpress.com by 210.87.254.5 on 09/05/12
For personal use only.

REACTIONS WITH DIAZOALKANES

III. 1,4-NAPHTHAQUINONE AND DIAZOALKANES*

WILLIAM IBRAHIM AWAD AND ALFRED BOULOS
Faculty of Science, A'in Shams University, Abbassia, Cairo, Egypt, U.A.R.

Received May 25, 1964

ABSTRACT

The addition of diazomethane to 1,4-naphthaquinone has been reexamined. Two products are isolated from this reaction, one of them (III*a*) has been previously reported. Similarly, diazoethane gives two products. The constitution of these products is discussed, particularly in the light of their ultraviolet and infrared spectra. The thermal stability of diazoalkane adducts to I is discussed.

A recent publication by Dean and Jones (1), which describes *inter alia* compounds derived from diazomethane and 1,4-naphthaquinone, prompts us to publish our related work on this topic. Dean *et al.* (1) suggested the following mechanism:

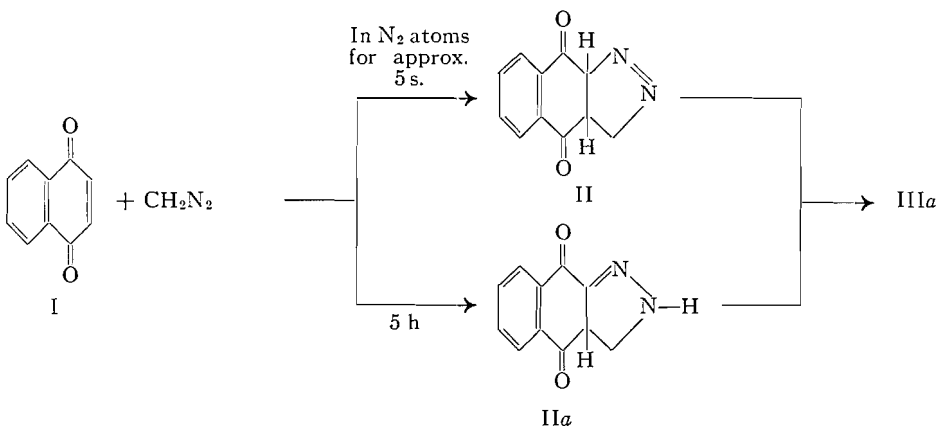

The elucidation of the structure of the immediately formed compound as 3*a*,4,9,9*a*-tetrahydro-3*H*-benz[*f*]indazole (II) may be uncertain. The band described for the azo linkage at 1548 cm^{-1} is unreliable, as similar bands appear in the case of III*a* at 1538 cm^{-1}. The lack of absorption close to 1620 cm^{-1}, from which it was concluded that the 2,3-double bond of the naphthaquinone nucleus has been removed, is actually a negative proof. In reality, this band is also absent in other compounds where it is expected, e.g. III*a*, III*b*, and VII.

It was found, however, in the present investigation that the reaction of diazomethane with I yields two products, one having a high melting point (345°) (III*a*) and the other a low melting point (172°) (IV*a*). These products are at a higher oxidation level than those described by Dean *et al.* (1). The latter compound has not been described either by early investigators (2, 3) or by recent ones (1). The fact that a mixture of compounds results from such a reaction may throw some doubt on the purity of the uncrystallized product used by Dean (1) for the analysis of the supposed II*a* (which, however, was at a lower level of oxidation than the compounds isolated in our work).

**Part II. W.I. Awad, S.M.A.R. Omran, and M. Sobhy, J. Chem. U.A.R. In press.*

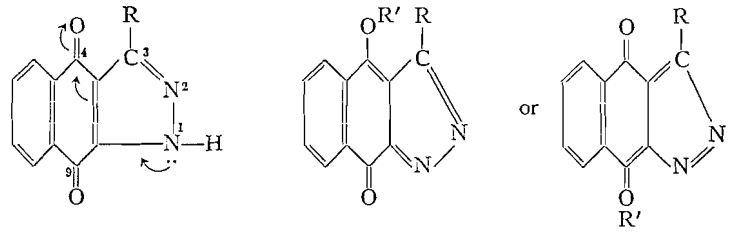

III

IV

III*a*; R = H
III*b*; R = CH_3

IV*a*; R = H, R′ = CH_3
IV*b*; R = CH_3, R′ = C_2H_5

The structure of IV*a* is based upon (i) absence of N—H stretching frequency near 3333 cm^{-1}, (ii) analytical data, (iii) presence of C=O stretching frequency of 1666 cm^{-1}, (iv) presence of a strong band at 1250 cm^{-1} (absent in IIIa and V) which is characteristic of enol–ether linkage (4), and (v) the fact that methylation of III*a* with dimethyl sulphate in alkaline medium gives two products—(*a*) a high melting compound (310°), which was previously isolated (1, 2, 3) and assigned the N–CH_3 structure (1) (V), and (*b*) a low melting compound (172°). The latter compound was identical with IV*a* isolated from the diazomethane experiment, as shown by mixed melting point determinations and infrared spectra.

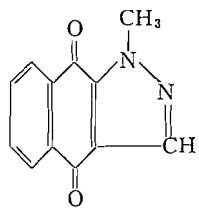

V

The ultraviolet spectra of III*a*, IV*a*, and V (Fig. 1) indicate that III*a* and V are of similar structure and that IV*a* is quite different. The action of diazomethane on III*a* gave mainly IV*a* together with a small quantity of V. Comparison of the ultraviolet spectra of III*a* in alcohol and in alkaline solution (Fig. 2) indicates that, in alkaline solution, there is only a slight bathochromic shift and a hyperchromic effect, and that the hybrid anion is fundamentally similar to III*a* (cf. curved arrows in III*a*).

Diazoethane has also been allowed to react with I. Two products have been isolated—a high melting compound to which structure III*b* is assigned and a low melting compound to which structure IV*b* is assigned. The structure III*b* is confirmed by (i) analytical data, (ii) infrared spectrum that shows N—H stretching frequency at 3333 cm^{-1} and a carbonyl stretching frequency at 1666 cm^{-1}, (iii) solubility in alkali, and (iv) its ultraviolet spectrum (Fig. 3), which shows its clear resemblance to that of III*a*. The structure of IV*b* is based upon (i) analytical data, (ii) the absence of a N—H stretching frequency near 3333 cm^{-1}, the presence of a carbonyl stretching frequency at 1665 cm^{-1} and the presence of a enol–ether stretching frequency at 1250 cm^{-1}, (iii) insolubility in alkali, and (iv) its ultraviolet spectrum (Fig. 3), which shows its resemblance to that of IV*a*.

The pyrolysis of diazoalkane derivatives from naphthaquinone is of interest. It is known (2, 5) that VI decomposes on pyrolysis with loss of nitrogen, that VII is stable

Can. J. Chem. Downloaded from www.nrcresearchpress.com by 210.87.254.5 on 09/05/12
For personal use only.

Can. J. Chem. Downloaded from www.nrcresearchpress.com by 210.87.254.5 on 09/05/12
For personal use only.

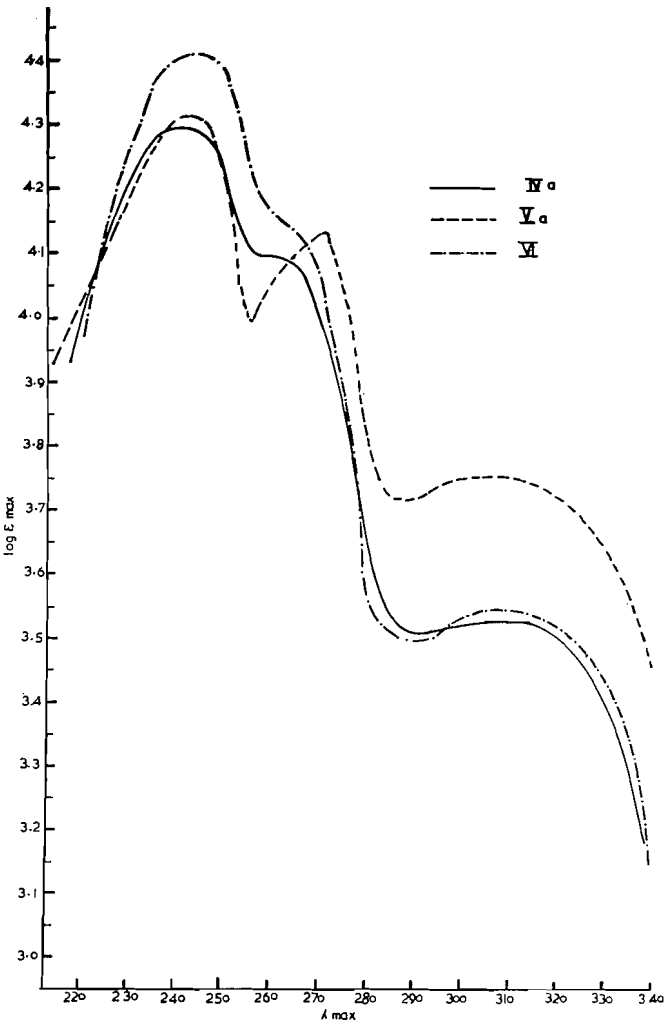

FIG. 1.

(2), that the corresponding acid can be decarboxylated (2), and that the oxidation product of VI, namely VIII, sublimes unchanged upon heating. We can conclude that

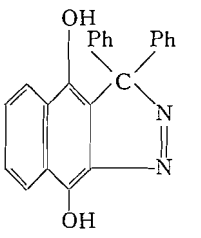

VI

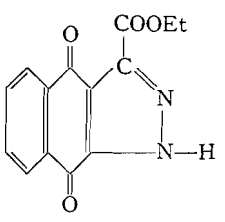

VII

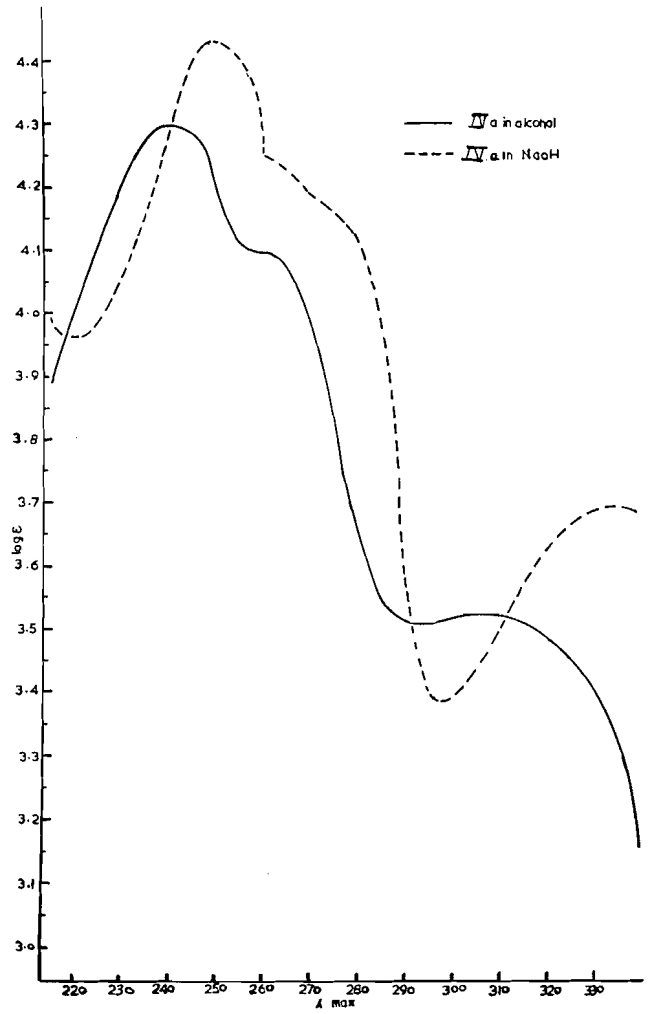

FIG. 2.

the heterocyclic ring is more stable when fused with quininoid rings rather than with benzenoid rings. Compounds III*a*, III*b*, VII, and VIII are thus thermally stable, and VI is thermally unstable.

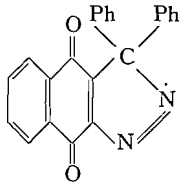

VIII

Can. J. Chem. Downloaded from www.nrcresearchpress.com by 210.87.254.5 on 09/05/12
For personal use only.

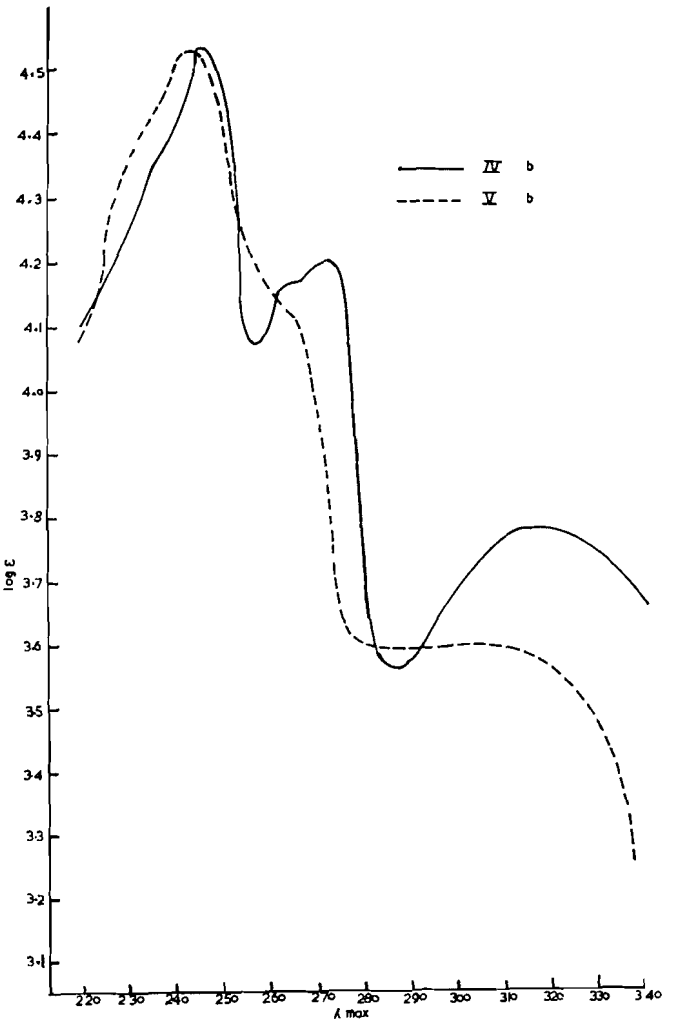

FIG. 3.

EXPERIMENTAL

Melting points are uncorrected. Analyses were carried out by Alfred Bernhardt, Max-Plank Institute, Mulheim, Germany. Infrared spectra were measured on a Perkin–Elmer Infracord Model 137 spectrophotometer, using the KBr Wafer technique. Ultraviolet spectra were measured on a Perkin–Elmer Spectracord Model 4000A spectrophotometer with ethyl alcohol solutions, except in case of III*a* (Fig. 2—the dotted curve) where it is carried out in 5% sodium hydroxide solution.

4,9-Dihydro-4,9-dioxo-1H-benz[f]indazol (IIIa) and its O-Methyl Derivative (IVa)

Naphthaquinone (1.0 g) and diazomethane (from nitrosomethyl urea, 4.0 g) were left for a couple of hours in ice-cooled ether (ca. 100 ml). The reaction began at once with the separation of a brownish precipitate. This precipitate was filtered off (0.65 g) and III*a* was crystallized from acetic acid as colorless crystals, m.p. ≈ 345°.

Calcd. for $C_{11}H_6O_2N_2$: C, 66.65; H, 3.05; N, 14.1. Found: C, 66.4; H, 3.3; N, 13.9.

III*a* sublimed unchanged *in vacuo*. The ethereal mother liquor was concentrated and cooled, at which

Can. J. Chem. Downloaded from www.nrcresearchpress.com by 210.87.254.5 on 09/05/12
For personal use only.

time IV*a* separated out (0.2 g). It was crystallized from light petroleum (80–100°) as colorless crystals, m.p. 172°. IV*a* was insoluble in alkali.

Calcd. for $C_{12}H_8O_2N_2$: C, 67.9; H, 3.8; N, 13.2. Found: C, 67.9; H, 3.7; N, 13.1.

Action of Dimethyl Sulphate on IIIa

Methyl sulphate (0.1 ml) was added to a filtered solution of III*a* (0.2 g) in 2 ml 5% NaOH. The mixture was shaken well and the precipitate formed was filtered off. The precipitate was boiled with light petroleum (80–100°). The fraction, which was soluble in light petroleum, crystallized out as colorless crystals (0.05 g), m.p. 172° (undepressed on admixture with IV*a* obtained previously). The insoluble fraction, 4,9-dihydro-1-methyl-4,9-dioxobenz[*f*]indazole, was crystallized from alcohol (0.05 g), m.p. 310° (2, 3, 4).

Action of Diazomethane on IIIa

An ice-cooled ethereal diazomethane solution (from methyl nitroso urea, 4 g) was added to III*a* (0.5 g) and left overnight. The insoluble part (0.1 g), which crystallized from EtOH, was proved to be V by means of mixed melting point determinations. The ethereal solution was concentrated to give IV*a* (0.40 g), crystallized from light petroleum (80–100°), and identified by melting points and mixed melting points.

4,9-Dihydro-4,9-dioxo-1H,3-methyl-benz[f]indazol (IIIb) and its O-Ethyl Derivative (IVb)

Naphthaquinone (7.00 g) and diazoethane (from ethyl nitroso urea, 20 g) were left in ice-cooled ether (ca. 350 ml) for a couple of hours. The reaction was similar to that described for diazomethane. The ether-insoluble product (4.0 g) was filtered off. III*b* was crystallized from ethyl alcohol as colorless crystals, m.p. 292°. Calcd. for $C_{12}H_8O_2N_2$: C, 67.9; H, 3.8; N, 13.8. Found: C, 68.1; H, 4.1; N, 13.6.

This product was soluble in 5% NaOH solution and sublimed unchanged *in vacuo*. The ethereal mother liquor was concentrated to give IV*b* (0.70 g), which was crystallized from light petroleum (80–100°) as colorless crystals, m.p. 119°. It was insoluble in alkali (cf. Fig. 3 for ultraviolet spectra).

Calcd. for $C_{14}H_{12}O_2N_2$: C, 69.99; H, 5.03; N, 11.66. Found: C, 70.5; H, 5.1; N, 11.5.

Action of Heat on VII and VIII

Both compounds (3) were heated under vacuum (2 mm/Hg), where they sublimed unchanged, as shown by melting points and mixed melting points.

REFERENCES

1. F. M. Dean and P. G. Jones. J. Chem. Soc. 5342 (1963).
2. L. F. Fieser and M. A. Peters. J. Am. Chem. Soc. **53**, 4080 (1931).
3. H. von Pechmann and E. Seel. Ber. **32**, 2292 (1899).
4. L. J. Bellamy. The infrared spectra of complex molecules. Methuen & Co. Ltd., London. 1960. p. 117.
5. A. R. Bader and M. G. Ettlinger. J. Am. Chem. Soc. **75**, 730 (1953).

Can. J. Chem. Downloaded from www.nrcresearchpress.com by 210.87.254.5 on 09/05/12
For personal use only.

Can. J. Chem. Downloaded from www.nrcresearchpress.com by 210.87.254.40 on 09/05/12
For personal use only.

THE ^{19}F N.M.R. SPECTRUM OF IF_7

R. J. GILLESPIE AND J. W. QUAIL[1]
Department of Chemistry, McMaster University, Hamilton, Ontario
Received July 8, 1964

ABSTRACT

It is shown that the line shape calculated for the n.m.r. spectrum of a magnetic nucleus attached to a nucleus of spin 5/2 undergoing quadrupole relaxation agrees well with the observed spectrum of iodine heptafluoride. The iodine–fluorine coupling constant was found to be $J_{IF} \simeq 2\,100$ c/s. The apparent magnetic equivalence of the fluorine atoms in IF_7 is discussed.

The ^{19}F nuclear magnetic resonance (n.m.r.) spectrum of IF_7 at room temperature is an extremely broad doublet (Fig. 1A). Our spectrum agrees closely with that reported previously (1–4). Muetterties and Packer (3) have suggested that the observed spectrum is a partially collapsed sextet arising from the coupling of seven spectroscopically equivalent fluorines to the iodine which is undergoing quadrupole relaxation. They did not, however, calculate the expected spectrum.

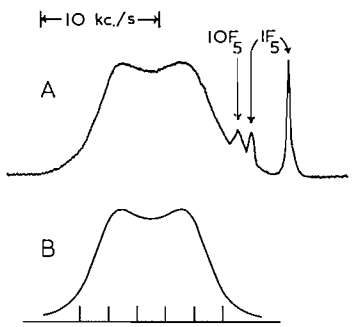

FIG. 1. (A) ^{19}F n.m.r. spectrum of IF_7 containing small amounts of IF_5 and IOF_5 and (B) theoretical line shape for the spectrum of a nucleus of spin 5/2 according to Suzuki and Kubo for a value of $\alpha = 55$. The vertical lines indicate the positions of the sextet in the absence of quadrupole relaxation.

Recently, Suzuki and Kubo (5) have given a general method for calculating multiplet line contours for the resonance of nuclei coupled to a high-spin nucleus which is undergoing quadrupole relaxation. Previous calculations of line shapes for nuclei coupled to nuclei having $I = 1$ (6, 7) and $I = 3/2$ (8) may be considered as limited applications of this more general theory. It has been pointed out that the theory involves some approximations (5, 6) but the agreement between calculated and experimental line shapes for $I = 3/2$ (8) indicates that the approximations do not lead to any serious error. Suzuki and Kubo calculate spectral shapes as a function of a parameter

$$\alpha = \left(\frac{e^2qQ}{\hbar}\right)^2 \frac{\tau_c}{2\pi J},$$

where e = the charge on an electron, eq = the electric field gradient at the nucleus, eQ = the quadrupole moment of the nucleus, τ_c = the correlation time for molecular

[1]*Present address: Department of Chemistry, University of Saskatchewan, Saskatoon, Saskatchewan.*

reorientation, and J = the coupling constant in c/s; $(e^2qQ/\hbar)$ = the quadrupole coupling constant in rad/s. For $I = 5/2$,

$$\alpha = \frac{1\,000}{24}\left(\frac{1}{T_1}\right)\frac{1}{2\pi J},$$

where T_1 = the relaxation time of the nucleus undergoing quadrupole relaxation.

We had already calculated line shapes for $I = 5/2$ by essentially the same method as that used by Suzuki and Kubo when their paper appeared. With these line shapes we are able to interpret the ^{19}F spectrum of IF_7.

The splitting between the peaks in the IF_7 spectrum (Fig. 1A) is $\sim 4\,000$ c/s, in agreement with the observation of Alexakos, Cornwell, and Pierce (2). Muetterties and Packer (3) report a value of 4 400 c/s for this splitting. The small discrepancy between the two values could be due to a higher viscosity in our sample and the sample of Alexakos *et al.* and thus a longer correlation time for the iodine nuclei. This higher viscosity could be the result of either the impurities in the samples or a lower sample temperature. The longer correlation time would result in more relaxation of the iodine nuclei and thus a more collapsed spectrum. Because of the extreme broadness of the lines the disagreement might, however, simply be due to the difficulty of determining the peak positions.

There are two peaks in our spectrum due to IF_5 (9) and a third peak due to IOF_5 (2, 10, 11). The other part of the IOF_5 spectrum is of too low an intensity to be observed. This absorption, which is one quarter as large as the observed IOF_5 line, is spread out on top of the high-field half of the IF_7 doublet (compare the spectrum in ref. 2).

A very good fit with the experimental spectrum is obtained for $\alpha \sim 55$ (Fig. 1B). This allows us to extract a coupling constant, $J_{IF} \sim 2\,100$ c/s, for this compound. An estimate of the relaxation time for the iodine nucleus can also be made ($T_1 \sim 5.7 \times 10^{-5}$ s). There is no reliable criterion of accuracy but errors in line-matching would introduce an error of less than 10%.

The discussion of the collapse of the spectrum arising from coupling to an $I = 5/2$ nucleus, given by Muetterties and Packer (3), is somewhat misleading. The description of the system as made up of six absorption signals, which are drawn together by transitions between the spin states of the $I = 5/2$ nucleus, is valid only for the very initial stages of the multiplet collapse (12). The theory shows that the spectral lines will merge, but they certainly cannot cross as supposed by Muetterties and Packer (3). Furthermore, by the time any appreciable movement of the absorption lines occurs, dispersion components have become appreciable in all of the lines, and thus the concept of individual absorption components loses its physical significance as the lines merge.

The relaxation of the iodine nucleus results from an interaction of the quadrupole moment of the iodine nucleus with the field gradient at the site of the nucleus through molecular reorientations characterized by the correlation time τ_c. In agreement with Muetterties and Packer we observed that the doublet sharpened at higher temperatures. The correlation time would then be shorter, resulting in a spectrum corresponding to a smaller value of α.

The field gradient at the iodine in IF_7 arises from the fact that although all the ligands are identical, no arrangement of seven ligands can have cubic symmetry. The structure of IF_7 is uncertain. Although the X-ray and spectroscopic data have generally been considered to indicate a pentagonal bipyramid structure, Burbank considered that the X-ray data in fact support a structure with C_{2v} symmetry which may be regarded as being derived from the 8-coordinated dodecahedral structure by merging two adjacent

Can. J. Chem. Downloaded from www.nrcresearchpress.com by 210.87.254.40 on 09/05/12
For personal use only.

positions (13). In any case there should be at least two groups of nonequivalent fluorines and therefore at least two peaks should be observed in the fluorine n.m.r. spectrum. To explain the apparent equivalence of the seven fluorine atoms Muetterties and Packer have proposed that intramolecular fluorine exchange provides a mechanism for time-averaging of the ligand environments. The same explanation has been proposed to explain the apparent magnetic equivalence of the fluorine atoms in PF_5 and other trigonal bipyramid molecules (14, 15). It should be noted, however, that in the case of IF_7 a chemical shift of 2 p.p.m. or less between nonequivalent fluorines and a variation in the coupling constant J_{IF} of as much as 10% would not appreciably affect the observed spectrum because of the extreme broadness of the lines. Such a small chemical shift is not unreasonable. For example, the chemical shift between the basal and equatorial fluorines in SF_5X compounds varies from over 80 p.p.m. in SF_5Br to nearly 0 p.p.m. in SF_5OOSF_5 (0.6 p.p.m.) and CF_3OOSF_5 (2 p.p.m.) and to negative values for other compounds such as CF_3SF_5 (~ -23 p.p.m.) (18). Thus, it cannot be concluded with certainty that there is a time-averaging of nonequivalent fluorines, although this seems very plausible.* We may note that there are at least four 7-coordinate structures of rather similar energies (13, 16, 17) and all except one of these could provide the close-lying vibronically excited states which it has been suggested (3) provide a mechanism for intramolecular fluorine exchange.

EXPERIMENTAL

Calculated spectra were obtained numerically using an IBM 7 040 computer. The ^{19}F n.m.r. spectrum of IF_7 was obtained using a Varian HR-56.4 n.m.r. system with a 15 mm insert and a 12 mm (outside diameter) sample tube. The oscilloscope trace of the spectrum was recorded photographically. IF_7 was prepared by the fluorination of iodine pentafluoride in a monel reaction tube at 250 °C. Purification was effected by trap-to-trap distillation.

ACKNOWLEDGMENTS

We thank the Directorate of Chemical Sciences of the United States Air Force Office of Scientific Research and the National Research Council of Canada for financial assistance. We also thank Dr. E. L. Muetterties for helpful comments on the manuscript.

REFERENCES

1. H. S. Gutowsky and C. J. Hoffman. J. Chem. Phys. **19**, 1259 (1951).
2. L. G. Alexakos, C. D. Cornwell, and S. B. Pierce. Proc. Chem. Soc. 341 (1963).
3. E. L. Muetterties and K. J. Packer. J. Am. Chem. Soc. **86**, 293 (1964).
4. L. W. Reeves, E. J. Wells, N. Bartlett, and S. Beaton. Private communication.
5. M. Suzuki and R. Kubo. Mol. Phys. **7**, 201 (1964).
6. J. A. Pople. Mol. Phys. **1**, 168 (1958).
7. A. Abragam. The principles of nuclear magnetism. Oxford University Press, London. 1961.
8. J. Bacon, R. J. Gillespie, and J. W. Quail. Can. J. Chem. **41**, 3063 (1963).
9. E. L. Muetterties and W. D. Phillips. J. Am. Chem. Soc. **79**, 322 (1957).
10. R. J. Gillespie and J. W. Quail. Proc. Chem. Soc. 278 (1963).
11. N. Bartlett and L. E. Levchuk. Proc. Chem. Soc. 342 (1963).
12. P. W. Anderson. J. Phys. Soc. Japan, **9**, 316 (1954).
13. R. D. Burbank. Acta Cryst. **15**, 1207 (1962).
14. S. Berry. J. Chem. Phys. **32**, 933 (1960).
15. E. L. Muetterties, W. Mahler, and R. Schmultzer. Inorg. Chem. **2**, 613 (1963).
16. R. J. Gillespie. Can. J. Chem. **38**, 818 (1960).
17. D. Britton. Can. J. Chem. **41**, 1632 (1963).
18. C. I. Merrill, S. M. Williams, G. H. Cady, and D. F. Eggers, Jr. Inorg. Chem. **1**, 215 (1962).

Dr. Muetterties (private communication) is in complete agreement with this statement. Muetterties and Packer (3) were suggesting the time-averaging situation as the most probable explanation of the spectroscopic equivalence.

Can. J. Chem. Downloaded from www.nrcresearchpress.com by 210.87.254.40 on 09/05/12
For personal use only.

Can. J. Chem. Downloaded from www.nrcresearchpress.com by 210.87.254.6 on 09/05/12
For personal use only.

THE STUDY OF HYDROGEN BONDING AND RELATED PHENOMENA BY SPECTROSCOPIC METHODS

PART VIII. THE ULTRAVIOLET AND INFRARED SPECTRA OF SOME 2,4-DINITRODIPHENYLAMINES[1]

A. Balasubramanian, J. B. Capindale, and W. F. Forbes
Chemistry Department, University of Waterloo, Waterloo, Ontario

Received April 14, 1964

ABSTRACT

The ultraviolet spectra of a number of 2,4-dinitrodiphenylamines suggest that these compounds are generally non-planar in a number of different solvents. The infrared and ultraviolet spectral data in different solvents also suggest that an intramolecular hydrogen bond is present in these molecules, at least in inert solvents. There is evidence that a *p*-nitro substituent is necessary to increase the positive charge on the amino group sufficiently to permit it to form this fairly strong type of hydrogen bond.

INTRODUCTION

2,4-Dinitrodiphenylamine (I) is of interest because compounds of this type are readily converted on irradiation to species containing unpaired electrons (unpublished information and cf. ref. 1). This suggests that such compounds may prove suitable as protective agents against various forms of radiation (cf. ref. 2). A series of substituted 2,4-dinitrodiphenylamines was prepared and their properties are being investigated. As part of these investigations, and since the geometry of substituted diphenylamines has not been investigated previously (cf. ref. 3), the ultraviolet and infrared spectra of these compounds have been determined.

EXPERIMENTAL

Ultraviolet Spectra

The ultraviolet spectra were determined by standard methods in matched 1 cm quartz cells, using both a Cary Model 14 spectrophotometer and a Beckman Model DU spectrophotometer, calibrated against a standard solution of potassium chromate. Wavelength readings obtained on the two instruments were found to be within 0.5 mμ of each other. The accuracy of λ_{max} values is estimated to be $\pm$ 1 mμ, and the precision of molar absorptivities $\pm 5\%$ or better. For each spectrum, at least two independent sets of observations were made and absorptivity values were generally found to be reproducible to $\pm 2\%$. Solute concentrations were usually between 1.5×10^{-5} and 7×10^{-5} molar, except that several spectra of more concentrated solutions were determined as previously described (4). 2′-Methyl-2,4-dinitrodiphenylamine, examined in this way, did not show any concentration dependence in the range 1.8×10^{-5} to 4.4×10^{-4} molar. The ultraviolet spectra of some of the reference compounds, but not of the substituted 2,4-dinitrodiphenylamines, have previously been determined by other workers. Our results are in good agreement with earlier data.

Infrared Spectra

The infrared spectra were determined on a Beckman Model IR9 spectrophotometer, calibrated against a polystyrene film using a KBr prism and diffraction gratings. The frequency accuracy in the 3400 cm^{-1} and 1400 cm^{-1} regions is believed to be ± 0.6 cm^{-1} and 0.4 cm^{-1} respectively and the frequency repeatability ± 0.1 cm^{-1}. Solutions were examined in matched 1 cm quartz cells (3400 cm^{-1} region) or in 0.5 mm, 0.2 mm, or variable path cells equipped with sodium chloride windows (1400 cm^{-1} region). The solute concentration was ca. 5×10^{-3} molar. The integrated absorption intensities (A_{RJ}) were calculated from the equation

$$A_{RJ} = K(1/cl) \log (T_0/T)_{max} \Delta\nu_{\frac{1}{2}} \times 2.303 \times 10^{-4},$$

where c is molar concentration, l the cell length in cm, $\log (T_0/T)_{max}$ the absorbance at the absorption maximum, and $\Delta\nu_{\frac{1}{2}}$ the band width in cm^{-1} at half maximum intensity (cf. ref. 5). K was determined from

[1]*Part VII. Can. J. Chem. 40, 1891 (1962).*

Ramsay's Tables (6). The intensities were also expressed in the new units, A_{IUPAC} (7). The accuracy of the A values are estimated to be ±5%. Two independent sets of observations were also carried out for the infrared data.

The solvents used, except the ethanol, were commercially available spectroanalyzed solvents (Fisher). The ethanol was best grade undenatured absolute ethanol (Consolidated Alcohol, Toronto).

The diphenylamines were prepared by heating together on the steam bath equimolar quantities of 2,4-dinitrochlorobenzene and the appropriate aniline until the mixture solidified. The solid was dissolved in hot benzene, the resulting solution was filtered, and the solid was reprecipitated by the addition of petroleum ether. The diphenylamines were recrystallized until the melting point indicated that the samples were pure. Most of the diphenylamines have been described in the literature with the exception of the following. 2,4-Dinitro-2′,6′-dimethyldiphenylamine, which crystallized from acetone–water in yellow prisms, m.p. 163.5–164.5 °C. (Calcd. for $C_{14}H_{13}N_3O_4$: C, 58.6; H, 4.55; N, 14.6. Found: C, 58.6; H, 4.65; N, 14.7.) 2,4-Dinitro-2′-fluorodiphenylamine, which crystallized from benzene – petroleum ether as orange needles, m.p. 132–134 °C. (Calcd. for $C_{12}H_8N_3O_4F$: C, 52.0; H, 2.9; N, 15.2; F, 6.9. Found: C, 52.1; H, 3.0; N, 15.0; F, 7.05.)

The remaining compounds were prepared by standard methods as described in the literature.

RESULTS AND DISCUSSION

Ultraviolet Spectra

The main ultraviolet absorption maxima of the diphenylamines and of suitable reference compounds are listed in Table I.

TABLE I

Main ultraviolet absorption maxima of 2,4-dinitrodiphenylamines and of suitable reference compounds in cyclohexane solution*

Compound	Long wavelength band		Short wavelength band	
	λ_{max} (mμ)	ϵ_{max}	λ_{max} (mμ)	ϵ_{max}
2,4-Dinitrodiphenylamine (I)	335.5	17 500	ca. *259*	*10 700*
2,4-Dinitro-4′-methyldiphenylamine	336	17 900	ca. *260*	*11 000*
2,4-Dinitro-3′-methyldiphenylamine	338	17 800	ca. *260*	*11 200*
2,4-Dinitro-2′-methyldiphenylamine	332	17 400	ca. *260*	*10 500*
2,4-Dinitro-2′-6′-dimethyldiphenylamine	328.5	18 500	ca. *256*	*11 200*
2,4-Dinitro-2′-bromodiphenylamine	331.5	16 600	ca. *260*	*10 500*
2,4-Dinitro-4′-chlorodiphenylamine	333	16 600	ca. *260*	*10 900*
2,4-Dinitro-2′-chlorodiphenylamine	331	15 100	ca. *250*	*11 300*
2,4-Dinitro-2′-fluorodiphenylamine	330	16 500	ca. *260*	*10 800*
2,4-Dinitro-4′-methoxydiphenylamine	337.5	16 500	ca. *258*	*12 600*
2,4,3′-Trinitrodiphenylamine	328	18 500	242.5	20 200
2,4,4′-Trinitrodiphenylamine	348‡	23 800‡	Inaccessible in CCl_4 solution	
2,4-Dinitro-2′-aminodiphenylamine	328.5	15 100	256.5	10 900
2,4-Dinitrocarbazole (II)	312†	15 750	251.5	17 800
	385.5	6 500	295	26 000
Diphenylamine (III)	282	17 200	ca. *240*	*4 800*
Carbazole (IV)	291	20 500	232	43 000
Tetrahydrocarbazole (V)	273	7 500	225	31 300
4-Nitroaniline	321	14 800	226	7 900
4-Nitrodiphenylamine	343	18 800	ca. *260*	*7 400*
2,4-Dinitroaniline‡	316‡	14 200‡	Inaccessible in CCl_4 solution	

*Values in italics represent inflections.
†Shoulder.
‡In CCl_4 solution; compound did not dissolve in cyclohexane.

Planarity of 2,4-Dinitrodiphenylamines

The existence of two separate band envelopes suggests absorption by two chromophores. This, in conjunction with the long wavelength band data, is consistent with the assumption that the 2,4-dinitrodiphenylamines in solution have a molecular conformation in which the two aromatic rings are as shown in structure I. Specifically, the following may be noted.

(*i*) All the 2,4-dinitrodiphenylamines listed in Table I absorb maximally at 338 ± 10 mμ whereas ring-substituted anilines show a wider variation in the location of the long

Can. J. Chem. Downloaded from www.nrcresearchpress.com by 210.87.254.6 on 09/05/12
For personal use only.

wavelength band as the substituent is altered. For example, in inert solvents 4-nitroaniline and aniline absorb at 321 mμ and 234 mμ respectively. Since the wavelength displacement between 2,4,4′-trinitrodiphenylamine and 2,4-dinitrodiphenylamine (I) is smaller, this indicates that the 4′-nitro substituent does not contribute as much to the long-wavelength band in the 2,4,4′-compound as in 4-nitroaniline.

(*ii*) Comparison of the spectra of 2,4-dinitro-2′,6′-dimethyldiphenylamine and 2,4-dinitro-4′-methyldiphenylamine shows that the two compounds have similar molar absorptivity values (see Table I). However, two ortho-methyl groups will almost certainly increase the non-planarity of a planar or nearly planar system, and such non-planarity would be expected to give rise to a pronounced hypochromic effect. Since no such effect is observed, it is probable that the 4′-methyl compound is already non-planar (as shown in structure I) and that for this reason the anticipated hypochromic effect is not observed in the di-ortho substituted diphenylamine.

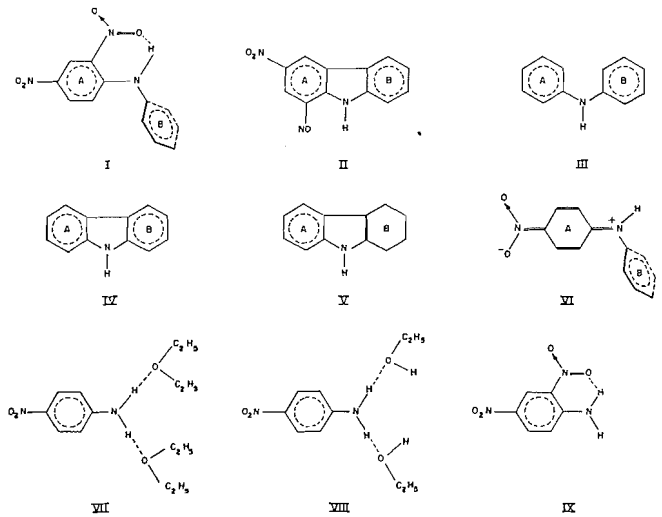

(*iii*) The main absorption maximum of aniline occurs at 234 mμ, whereas diphenylamine (III), in which both rings may be assumed to be perpendicular or nearly perpendicular to their C—N bond – unshared pair planes, absorbs maximally at 282 mμ. Hence introduction of a second benzene ring into the aniline system apparently affords a wavelength displacement of ca. 47.5 mμ, which corresponds to a frequency displacement of 7200 cm^{-1}. On the other hand, the wavelength displacement between 2,4-dinitroaniline and 2,4-dinitrodiphenylamine (I) in carbon tetrachloride solution is only 342.5 − 316 = ca. 26.5 mμ or 2450 cm^{-1}. This suggests that the main absorption maximum of I corresponds predominantly to the 2,4-dinitroaniline part of the molecule, which in turn can be rationalized by assuming that ring B is not coplanar with the unshared electron pair of the central nitrogen atom (structure I).

(*iv*) The 2,4-dinitrocarbazole (II), prepared by the method of Stárková *et al.* (8), absorbed at appreciably longer wavelength then 2,4-dinitrodiphenylamine (I). This again suggests that the rings in compound II are more nearly coplanar than in compound I (Table I). In contrast, the carbazole (IV) absorbs maximally at only slightly longer wavelength and with slightly greater absorption intensity than diphenylamine (III). This indicates that the effective length of the conjugated system which gives rise to the absorption band is greater for the carbazole (IV) than for the diphenylamine (III).

Can. J. Chem. Downloaded from www.nrcresearchpress.com by 210.87.254.6 on 09/05/12
For personal use only.

Appreciable conjugation must occur between the two benzene rings in diphenylamine (III), since the main absorption maximum of III occurs at longer wavelength than that of the tetrahydrocarbazole (V) (see Fig. 1 and Table I).

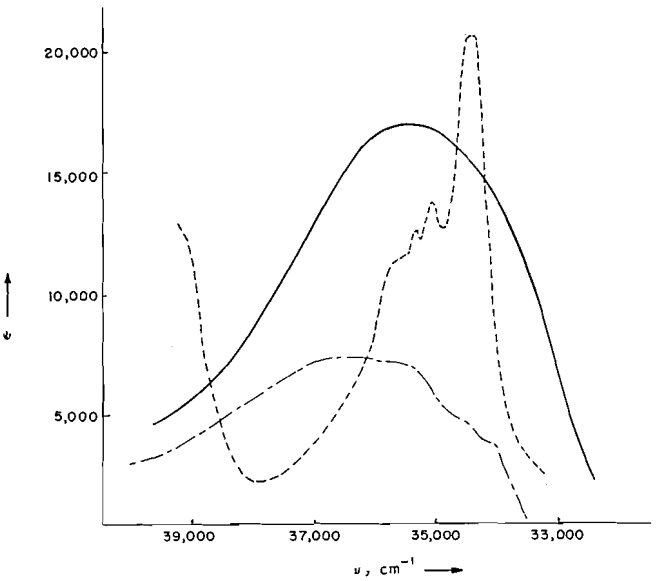

FIG. 1. Main ultraviolet absorption bands in cyclohexane solution of diphenylamine (III, —), carbazole (IV, - - -), and tetrahydrocarbazole (V, — - — -).

We therefore conclude that diphenylamine (III) is nearly planar, whereas 2,4-dinitrodiphenylamine is appreciably non-planar. This non-planarity may be caused by two factors. First, the *o*-substituents of ring A may displace the ring B as shown in structure I. Even in the absence of a large *o*-substituent, as in compounds like 4-nitrodiphenylamine, increased conjugation, which may be crudely represented by resonance forms of type VI, tends to change the bond configuration around the nitrogen atom from a tetrahedral configuration towards a trigonal structure. This would also decrease the N—C bond length because of the increased double bond character of the bond. This in turn may increase the steric interactions between the ortho groups and thus cause the B ring to be no longer perpendicular to the C—N bond – unshared pair plane. Such an explanation can account for the relatively small displacement observed between 4-nitroaniline and 4-nitrodiphenylamine (see Table I; cf. the wavelength displacement of ca. 48 mμ (7270 cm^{-1}) observed between aniline and diphenylamine).

Solvent Effects and Hydrogen Bonding in 2,4-Dinitrodiphenylamines

Table II lists the main absorption maxima of some of these compounds in different solvents. Comparison of the results in Table I and Table II shows that changing the solvent from cyclohexane to carbon tetrachloride gives rise to small spectral changes. For each compound the absorption maximum is displaced slightly to longer wavelength in carbon tetrachloride solution. This change may be associated partly with the red shift which increases approximately in proportion to the refractive index of the solvent, and with increased solute dipole – induced solvent dipole interactions (cf. refs. 9 and 10).

On changing the solvent from carbon tetrachloride to chloroform, slightly larger displacements are observed for 2,4-dinitro-*N*-methyldiphenylamine than for the other

Can. J. Chem. Downloaded from www.nrcresearchpress.com by 210.87.254.6 on 09/05/12
For personal use only.

2,4-dinitrodiphenylamines. Since other data (particularly the infrared N—H band data) suggest the presence of an intramolecular hydrogen bond, this difference may tentatively be associated with an intramolecular hydrogen bond. This implies that in carbon tetrachloride solution 2,4-dinitrodiphenylamines would absorb at slightly shorter wavelength in the absence of an intramolecular hydrogen bond. This bond may thus be responsible for a displacement of, approximately, 100 cm^{-1}. This is illustrated schematically in Fig. 2, which also indicates that the displacement ascribed to intramolecular hydrogen bonding is much smaller than that ascribed, partly, to intermolecular hydrogen bonding. The greater importance of intermolecular hydrogen bonding is not surprising since, for example, the non-intramolecularly bonded 4-nitro group can also interact with $CHCl_3$ molecules. The above rationalization is clearly not strong evidence for intramolecular hydrogen bonding in 2,4-dinitro substituted diphenylamines. However, it shows that the similar frequency displacements for 2,4-dinitro-*N*-methyldiphenylamine and other 2,4-dinitrodiphenylamines, observed on changing the solvent from cyclohexane or carbon tetrachloride to chloroform, are not inconsistent with the existence of an intramolecular hydrogen bond in the latter compounds.

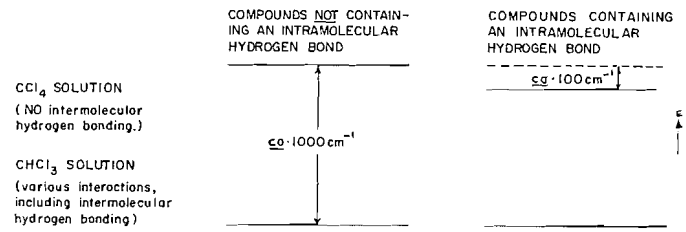

FIG. 2. Schematic representation of energy levels for compounds in the presence and in the absence of an intramolecular hydrogen bond.

In ether solution, the largest displacement is observed for 4-nitroaniline (see Table III), which may be associated with structures of type VII (cf. ref. 11). Strong intermolecular hydrogen bonding may be favored in this compound because of the presence of a *p*-nitro substituent and because of the absence of competitive intramolecular hydrogen bonding.

The spectral changes occurring on alteration of the solvent from chloroform to ethanol can also be rationalized in terms of available active hydrogen atoms. That is, for 4-nitroaniline the displacement of 1790 cm^{-1} (see Table II) may be associated with a number of interactions, including interactions of type VIII. For the 2,4-dinitro compounds this wavelength displacement is drastically reduced, presumably because in structures of type IX the nitrogen-bonded hydrogen atom is not as readily available for intermolecular (solvent–solute) hydrogen bonding.

Infrared Spectra

The discussion of the ultraviolet spectra in inert solution indicates that these spectra can be rationalized by assuming that the 2,4-dinitrodiphenylamines contain an intramolecular hydrogen bond (structure IX). If such bonding occurs, this should involve both the N—H and N—O vibrations. The observed infrared spectra of the N—H and N—O vibrational stretching frequencies are listed in Tables IV and V respectively.

The results in Table IV show that the N—H band in *o*-nitro-substituted diphenylamines, compared with the N—H band in diphenylamine, shows a pronounced frequency displacement of about 100 cm^{-1} to lower frequency (3). This displacement is much larger than is observed in the absence of intramolecular hydrogen bonding. For example, a

Can. J. Chem. Downloaded from www.nrcresearchpress.com by 210.87.254.6 on 09/05/12
For personal use only.

Can. J. Chem. Downloaded from www.nrcresearchpress.com by 210.87.254.6 on 09/05/12
For personal use only.

TABLE II

Main ultraviolet absorption maxima (long wavelength bands) of 2,4-dinitrodiphenylamines and of suitable reference compounds in different solvents

Compound	Carbon tetrachloride solution		Wavelength displacement (cm^{-1}) with respect to the absorption maximum in cyclohexane solution	Chloroform solution		Wavelength displacement (cm^{-1}) with respect to the absorption maximum in carbon tetrachloride solution	Ethanol solution		Wavelength displacement (cm^{-1}) with respect to the absorption maximum in chloroform solution
	λ_{max} ($m\mu$)	ϵ_{max}		λ_{max} ($m\mu$)	ϵ_{max}		λ_{max} ($m\mu$)	ϵ_{max}	
4-Nitroaniline	329	14 600	760	347	14 000	1 580	370	15 400	1 790
2,4-Dinitroaniline	316	14 200	—	327.5	14 300	1 110	334.5	14 700	640
2,4-Dinitro-4′-methyldiphenylamine	343	17 000	610	353	17 500	830	351	17 100	−170
2,4-Dinitro-2′-methyldiphenylamine	338	17 100	530	348	17 500	850	345	17 000	−250
2,4-Dinitro-2′,6′-dimethyldiphenylamine	333	18 600	410	344	18 400	960	342.5	17 500	−130
2,4-Dinitro-2′-aminodiphenylamine	332.5	14 400	370	343	15 400	920	346	15 200	+250
2,4-Dinitro-*N*-methyldiphenylamine*	362	14 000	310	376	15 200	1 030	373	14 400	−210
2,4,4′-Trinitrodiphenylamine	348	23 800	—	358	23 150	810	364	20 700	460
2,4-Dinitro-4′-methoxydiphenylamine	343	15 550	480	355	16 350	980	353	15 800	−160
2,4-Dinitrocarbazole	—	—	—	321	13 350		319.5	13 050	
				385†	7 200		385†	7 100	

*Main absorption maximum in cyclohexane solution: λ_{max} 358 $m\mu$, ϵ = 13 500.
†Shoulder.

TABLE III

Main ultraviolet absorption maxima of some anilines in cyclohexane and ether solution

Compound	Cyclohexane solution		Ether solution		Wavelength displacement (cm^{-1})
	λ_{max} (mμ)	ϵ_{max}	λ_{max} (mμ)	ϵ_{max}	
Aniline (10)	234.5	9 000	238	10 000	630
Diphenylamine	282	17 200	284	21 600	250
4-Nitroaniline	321	14 800	348	16 350	2 420
2,4-Dinitrodiphenylamine	335.5	17 500	342.5	18 400	610
2,4-Dinitro-4′-methyldiphenylamine	336	17 900	338	19 310	180
N-Methyl-2,4-dinitrodiphenylamine	358	13 520	367.5	11 960	720

frequency displacement of -4 cm^{-1} is observed between the N—H bands of diphenylamine and 4-nitrodiphenylamine and frequency displacements of 13 and 8 cm^{-1} are observed between the N—H bands of *p*-nitro- and *m*-nitro-*N*-methylanilines and *N*-methylaniline (12). Steric effects do not afford frequency displacements of such magnitude. For example, *p*-phenylaniline absorbs at 3483 and 3398 cm^{-1}, whereas *o*-phenylaniline absorbs at 3481 and 3393 cm^{-1}; 2,4,6-trichloroaniline absorbs at 3503 and 3404 cm^{-1} and 2,4,6-tribromoaniline absorbs at 3492 and 3394 cm^{-1}, whereas aniline absorbs at 3479 and 3396 cm^{-1} (12). The small frequency displacement of 5 cm^{-1} observed between 2,4-dinitro- and 2,4-dinitro-2′,6′-dimethyldiphenylamine may also be noted in this connection.

However, intramolecular hydrogen bonding does give rise to larger spectral displacements of the same order as are observed in *o*-nitro-substituted diphenylamines. For example, methyl-*N*-methylanthranilate absorbs at 3382 cm^{-1}, a frequency 71 cm^{-1} lower than does the methyl ester of *p*-aminobenzoic acid, and *o*-nitro-*N*-methylaniline absorbs at 3401 cm^{-1} compared with 3456 cm^{-1} for *p*-nitro-*N*-methylaniline (13). Incidentally, analogous observations may be made for the infrared carbonyl band data of compounds like acetophenones or benzophenones where again only hydrogen bonding causes pronounced displacements to lower frequency (cf. refs. 5, 14, 15). It is concluded that the explanation of the spectral change is to associate it with a strong intramolecular N—H - - - O—N hydrogen bond. It may further be noted from the data in Table IV that substituents in the second benzene ring (the B ring of structures I and VI) do not affect appreciably the ν_{max} or ϵ_{max} values of the N—H vibrational frequency. This suggests that the intramolecular hydrogen bond is not appreciably affected by that kind of substitution. This is consistent with structure I (see discussion of the ultraviolet spectra).

Three main bands might be expected to occur in the 1200–1550 cm^{-1} region. Actually, a more intense band, associated with the N—O symmetrical stretching band, is observed near 1340 cm^{-1} and a considerably weaker band occurs near 1315 cm^{-1} (see Table V). The displacement is of the order of 25 cm^{-1}, which is qualitatively similar to the displacement which has previously been noted for intermolecular hydrogen bonding (11). However, the aromatic C—N stretching band also occurs near 1310 cm^{-1}. Unfortunately, the N—O unsymmetrical stretching band could not be detected unequivocally because this band occurs at a similar frequency as the aromatic vibrations in that region.

ACKNOWLEDGMENTS

The authors thank Dr. J. C. Dearden for helpful discussions and Mrs. Carole T. Schmidt, Miss M. A. Shadbolt, Mr. J. F. Eix, and Mr. J. T. Miller for competent technical assistance. Financial assistance from the National Research Council is gratefully acknowledged.

Can. J. Chem. Downloaded from www.nrcresearchpress.com by 210.87.254.6 on 09/05/12
For personal use only.

Can. J. Chem. Downloaded from www.nrcresearchpress.com by 210.87.254.6 on 09/05/12
For personal use only.

TABLE IV

N—H Stretching vibrations of 2,4-dinitrodiphenylamines and of appropriate reference compounds

Compound	Solvent	ν_{max} (cm^{-1})	ϵ_{max}	Band widths, $\Delta\nu_{\frac{1}{2}}$	Integrated absorption intensity	
					A_{RJ} ($mole^{-1}\,l\,cm^{-2} \times 10^{-4}$)	A_{IUPAC} (practical)
Diphenylamine	CCl_4	3 434.5*	60	26	0.55	0.25
4-Nitrodiphenylamine	CCl_4	3 431	—	—	—	—
2,4-Dinitrodiphenylamine	CCl_4	3 338.5	135	34	1.70	0.75
	$CHCl_3$	3 343.5	175	33.0	2.10	0.91
2,4-Dinitro-4′-methyldiphenylamine	CCl_4	3 341*	170	33.0	2.10	0.90
2,4-Dinitro-2′-methyldiphenylamine	CCl_4	3 340.5	160	32.5	1.90	0.80
2,4-Dinitro-2′,6′-dimethyldiphenylamine	CCl_4	3 343	180	28.5	1.86	0.81
2,4-Dinitro-2′-aminodiphenylamine	CCl_4	3 345.0	125	28.0	1.25	0.55
		3 401.0 †				
		3 491.0 †				

*This band is slightly unsymmetrical. The reason for this is not known. The other N—H bands were found to be symmetrical.
†These bands correspond to the symmetrical and antisymmetrical N—H vibrations of the 2′-amino group.

Cain. J. Chem. Downloaded from www.nrcresearchpress.com by 210.87.254.6 on 09/05/12
For personal use only.

TABLE V

Main vibrations of 2,4-dinitrodiphenylamines and of appropriate reference compounds in the 1200–1550 cm^{-1} region

Compound	Solvent	ν_{max} (cm^{-1})	ϵ_{max}	Band widths, $\Delta\nu_{\frac{1}{2}}$	Integrated absorption intensity	
					A_{RJ} ($mole^{-1}$ l $cm^{-2} \times 10^{-4}$)	A_{IUPAC} (practical)
2,4-Dinitrodiphenylamine	CCl_4	1 338.0	1 390	9.0	4.50	1.95
		1 319	← weak →			
		1 525	(weak shoulder)			
2,4-Dinitro-4′-methyldiphenylamine	CCl_4	1 338.2	1 840	7.0	4.65	2.00
		1 317	← weak →			
		1 515.8	(band assignment doubtful)			
2,4-Dinitro-2′-methyldiphenylamine	CCl_4	1 338.5	1 770	9.0	5.75	2.50
		1 312	← weak →			
		1 512	(band assignment doubtful)			
2,4-Dinitro-2′,6′-dimethyldiphenylamine	CCl_4	1 339.0	2 200	6.0	4.80	2.10
		1 310	← weak →			
		1 513.5	(band assignment doubtful)			
2,4-Dinitro-2′-aminodiphenylamine	CCl_4	1 339.5	1 800	7.5	4.90	2.10
		1 313	← weak →			
		1 512	(band assignment doubtful)			

REFERENCES

1. K. H. GRELLMAN, G. M. SHERMAN, and H. LINSCHITZ. J. Am. Chem. Soc. **85**, 1881 (1963).
2. J. R. THOMAS and C. A. TOLMAN. J. Am. Chem. Soc. **84**, 2930 (1962).
3. H. MUSSO. Ber. **95**, 1714 (1962).
4. W. F. FORBES and A. R. KNIGHT. Can. J. Chem. **37**, 334 (1959).
5. R. N. JONES, W. F. FORBES, and W. A. MUELLER. Can. J. Chem. **35**, 504 (1957).
6. D. A. RAMSAY. J. Am. Chem. Soc. **74**, 72 (1952).
7. K. S. SESHADRI and R. N. JONES. Spectrochim. Acta, **19**, 1073 (1963).
8. B. STÁRKOVÁ, A. VYSTRČIL, and L. STÁRKA. Chem. listy, **51**, 536 (1957).
9. N. S. BAYLISS and E. G. MCRAE. J. Phys. Chem. **58**, 1002 (1954). E. G. MCRAE. J. Phys. Chem. **61**, 563 (1957).
10. J. C. DEARDEN and W. F. FORBES. Can. J. Chem. **38**, 896 (1960).
11. J. H. UTLEY. J. Chem. Soc. 3252 (1963).
12. P. J. KRUEGER and H. W. THOMPSON. Proc. Roy. Soc. London, Ser. A, **243**, 143 (1958).
13. P. J. KRUEGER. Can. J. Chem. **42**, 201 (1964).
14. J. C. DEARDEN and W. F. FORBES. Can. J. Chem. **38**, 1837 (1960).
15. W. F. FORBES, A R. KNIGHT, and D. L. COFFEN. Can. J. Chem. **38**, 728 (1960).

Can. J. Chem. Downloaded from www.nrcresearchpress.com by 210.87.254.6 on 09/05/12
For personal use only.

Can. J. Chem. Downloaded from www.nrcresearchpress.com by 210.87.254.40 on 09/05/12
For personal use only.

THE CHEMICAL FATE OF RECOIL IODINE ATOMS IN IODINE–METHYL IODIDE SOLUTIONS[1]

N. V. KLASSEN[2] AND A. P. BAERG
Division of Applied Physics, National Research Council, Ottawa, Canada

Received March 6, 1964

ABSTRACT

The organic yield of recoil ^{126}I, produced by the 14 MeV neutron irradiation of iodine–methyl iodide solutions, was examined over iodine concentrations from 0.34 mole fraction iodine to "pure" methyl iodide. By correcting for exchange between I_2 and methyl iodide, the initial organic yield at very low iodine concentrations was found to be 57%. The time for one-half of the I_2 to exchange with CH_3I was found to decrease with decreasing iodine concentration. At all iodine concentrations the organic products containing ^{126}I consisted mainly of CH_3I and CH_2I_2. The formation of products is discussed in terms of thermal reactions, diffusion-controlled reactions in the spurs, and hot reactions.

INTRODUCTION

Naturally occurring, monoisotopic ^{127}I can be converted into radioactive iodine by (n,γ), (n,2n), (d,p), and (γ,n) reactions. The radioactive iodine atoms are probably formed positively charged. Their average recoil energies are much greater than bond energies but are characteristic of the nuclear reaction involved. Most of these "hot" iodine atoms leave their parent compound and produce a track of ions and free radicals as they are slowed to thermal energies before entering into chemical combination. In methyl iodide and iodine – methyl iodide solutions the organic yield[3] is nearly independent of the nuclear reaction utilized despite large differences in the average recoil energies (1). However, the organic yield is strongly influenced by small quantities of molecular iodine which act as a scavenger for iodine atoms.

Conflicting results have been reported for the organic yield of the $^{127}I(n,\gamma)^{128}I$ reaction in pure methyl iodide. Levey and Willard (2) obtained a value of 56%. Brustad and Baarli (3) favored this result although they always obtained experimental values greater than 93%. Alimarin and Svoboda (4) found a value of 100%. A plausible explanation for such varied results has been provided by Behrens and Maddock (5, 6). They studied the iodine exchange reaction in dilute solutions of $^{131}I_2$ in methyl iodide to elucidate the scavenging effect of iodine and a time dependence of this effect found by others (7). The time for one-half of the I_2 to exchange was found to decrease with decreasing I_2 concentration. This suggested that the order of the exchange reaction is less than unity with respect to I_2. Thus, in very pure methyl iodide where the I_2 concentration is extremely low, the radioactive iodine present as I_2 should be rapidly and completely transferred to the methyl iodide, resulting in an apparent organic yield of 100%.

Svoboda (8, 9) has already recognized the influence of exchange reactions between separable inorganic iodine and the parent methyl iodide in the Szillard–Chalmers process. He suggested that an exchange of psuedo-monomolecular mechanism was responsible for raising organic yields. Recently (10) he has further reported organic yields of 50% for

[1]*Issued as N.R.C. No. 8148.*
[2]*National Research Council Postdoctoral Fellow 1961–1963. Present address: Radiation Research Laboratories, Mellon Institute, 4400 Fifth Avenue, Pittsburgh, Pa.*
[3]*The organic yield is defined as the fraction (expressed as a percentage) of the radioactive iodine which is not extractable by aqueous solutions of reducing agents such as sodium thiosulfate.*

methyl iodide stirred with sodium sulfite solutions during neutron irradiations and 100% organic yields for irradiations without simultaneous sodium sulfite extraction.

The present study was undertaken to investigate the exchange reaction directly in irradiated solutions, using 14 MeV neutrons which produce ^{126}I by the (n,2n) reaction. This was done to permit a further investigation of the distribution of radioactive organic products and the dependence on I_2 concentration, taking exchange effects into account.

EXPERIMENTAL

Purification of Materials

The alkyl iodides were obtained from Eastman Organic Chemicals. For most experiments methyl iodide was distilled slowly through a 130 cm column packed with glass beads. The middle fractions of methyl iodide were used to make up solutions with low iodine concentrations. Distillate, shown by gas chromatography to be less pure, was sometimes used to prepare concentrated iodine solutions after it was shown that this had no effect on the final product distribution. For some experiments the methyl iodide was dried overnight with phorphorus pentoxide and then carefully distilled at reduced pressures, the operation being carried out in a closed system. The purification of methyl iodide was carried out in semidarkness to reduce the possibility of photolytic formation of iodine.

Other alkyl iodides, used as carriers in the fractionation of the irradiation products, were not purified except when it was deemed advisable to remove the small amounts of iodine sometimes present by extraction with aqueous sodium thiosulfate. Analar brand iodine was used without purification.

Neutron Irradiations

Shortly before most irradiations the methyl iodide solutions were de-aerated by repeated evacuation of the frozen samples in a cyclic freezing–melting procedure. The solutions were then sealed in pyrex tubes. The irradiations were carried out in darkness at 25 °C. The neutrons, with an average energy of 14.6 MeV, were obtained from the T(d,n)^{4}He reaction using about 1 mA of 120 keV deuterons incident on a thick, tritium-loaded, titanium target.[4] The total flux of neutrons produced was about 10^{10} n s^{-1} and the samples were irradiated at a distance of 5 cm in front of the tritium target. A rough estimate of the maximum energy deposited in the methyl iodide by neutron scattering is 8×10^{15} eV per gram of methyl iodide per hour. Assuming that 100 eV produces 1.5 molecules of I_2 (11), the maximum rate of I_2 formation was 3×10^{-6} mole fraction per hour. The duration of the irradiations (3 min to 2 h) was chosen to avoid excessive alteration to the initial product distribution by exchange. A flux of slow neutrons sufficient to produce a useful ^{128}I activity could be achieved by surrounding the solutions and target with paraffin to moderate the neutrons.

Counting Radioactivity

The radioactivity of liquid samples was measured by counting their gamma activity with a 3 in. × 3 in. sodium iodide detector. The gamma spectrum and decay rate of irradiated methyl iodide indicated that the only radioactivity present was due to 25 min ^{128}I and 13 d ^{126}I. The two species were easily distinguished by decay curve analysis. In most instances 5 ml samples were counted. In activity measurements, differences in the self-absorption were found to be insignificant for methyl iodide, ethyl iodide, propyl iodide, and diiodomethane. The standard deviation in the activity measurements was usually less than 0.5%. However, for samples of lower activity such as those which contained only radioactive C_2H_5I, the standard deviation was about 2%.

Separation of Radioactive Products

The radioactive inorganic products (I_2 and HI) were extracted from the irradiated methyl iodide solutions into an aqueous solution of sodium thiosulfate and potassium iodide. The organic yield was determined by measuring the radioactivity of a solution before and after extraction. In some cases the inorganic activity was also measured to confirm that the techniques accounted for all of the activity. Before counting the inorganic activity, the aqueous solution into which it had been extracted was washed with inactive methyl iodide. Then the iodide ions were oxidized to I_2 with nitric acid and sodium nitrite, and the I_2 was extracted into methyl iodide for counting.

After the removal of inorganic products, the methyl iodide solutions were diluted with the carriers C_2H_5I, n-C_3H_7I, n-C_4H_9I, CH_2I_2, and CHI_3. Then a separation of some of the organic products was carried out by distillation. The specific activity of the distilled CH_3I, C_2H_5I, and CH_2I_2 each remained constant throughout its take-off interval. The removal, by distillation, of radioactive CH_3I was followed by the addition of inactive CH_3I to the residue to prevent radioactive contamination of the later, less active, fractions. The purity of each distillate fraction, except that of CH_2I_2, was checked by gas chromatography to permit small corrections due to impurities to be made to the observed specific activity. Most distillations were made at reduced pressures to prevent thermal decomposition. For example, CH_2I_2 was distilled at a pressure

[4] *A 150 kV Texas Nuclear Corporation neutron generator was used.*

Can. J. Chem. Downloaded from www.nrcresearchpress.com by 210.87.254.40 on 09/05/12
For personal use only.

of 8 mm Hg where its boiling temperature was 57 °C. Small amounts of I_2 accumulated in the residue during distillation, but the radioactivity present as I_2 was found to be insignificant.

Exchange Experiments

The exchange transfer of radioactive iodine from inorganic to organic products was measured after irradiation. The methyl iodide solution to be irradiated was divided and sealed, under vacuum, into several pyrex tubes. These tubes were kept in darkness during the irradiation and until they were opened, in semi-darkness, to extract the inorganic activity with aqueous sodium thiosulfate. The transfer of activity, by exchange, was followed by extraction of the samples in the separate tubes at various intervals of time. Exchange of ^{131}I (as I_2) with inactive methyl iodide was also examined. All exchange experiments were carried out at 25 °C.

RESULTS AND DISCUSSION

Most of the present results were obtained using ^{126}I (13 d half-life) from the (n,2n) reaction of 14.6 MeV neutrons. Some experiments were performed using the ^{128}I (25 min half-life) which could be formed simultaneously in the solution by the (n,γ) reaction of thermal neutrons. The longer half-life of ^{126}I permitted more time-consuming separations to be made and also permitted exchange to be studied over a wide range of I_2 concentrations. Unless otherwise specified, the radioactive isotope referred to is ^{126}I.

Exchange

It is important for the interpretation of observed product distributions to know whether the initial distribution was altered by exchange prior to separation. Behrens and Maddock (5, 6, 12) examined exchange in methyl iodide containing dilute $^{131}I_2$ and concluded that the transfer of ^{131}I from I_2 to CH_3I follows the usual unimolecular progress in time (i.e., the logarithm of the I_2 activity decreases linearly with time). Moreover, they found that the half-time for exchange decreases with decreasing I_2 concentration.

In the studies reported here the exchange of ^{126}I was examined, after irradiation, over I_2 concentrations from 7×10^{-5} mole fraction to "pure" methyl iodide (i.e., methyl iodide containing no added iodine but in which minute, unknown, amounts may have been present). Up to I_2 concentrations of 3.5×10^{-5} mole fraction the exchange could be followed essentially to equilibrium when the activity was all found to be in organic combination. In methyl iodide very rapid exchange is expected to take place between I_2 and HI (13), the most likely forms of inorganic iodine. The loss of inorganic activity due to exchange should then follow a simple exponential progress in time. The individual points in any one experiment at a given I_2 concentration were obtained by the analysis of separate samples irradiated simultaneously. The majority of the data in a single experiment were usually well represented in the simple exponential form. However, the reproducibility was poor and with a given experiment some individual samples showed large deviations from the average rate of exchange. In Fig. 1 the exchange half-times are shown as a function of I_2 concentration. The values in Fig. 1 are those graphically assessed to best fit the data, while the error bars indicate the maximum variations among all the samples of a given experiment.

There was no indication that the results were affected by the dim light to which the solutions were exposed during extraction of the inorganic products. The reasons for the poor reproducibility of the exchange experiments are not completely understood at present (cf. ref. 6), but heterogeneous effects have been suggested (12). Clearly, the samples in each experiment were not identical and, evidently, minute impurities can profoundly affect the exchange rate. Traces of water might lead to more rapid exchange. This contention seems to be supported by the relatively long half-times (cf. values 1 in Fig. 1) observed for the exchange in the methyl iodide which had been well dried over phosphorus

Can. J. Chem. Downloaded from www.nrcresearchpress.com by 210.87.254.40 on 09/05/12
For personal use only.

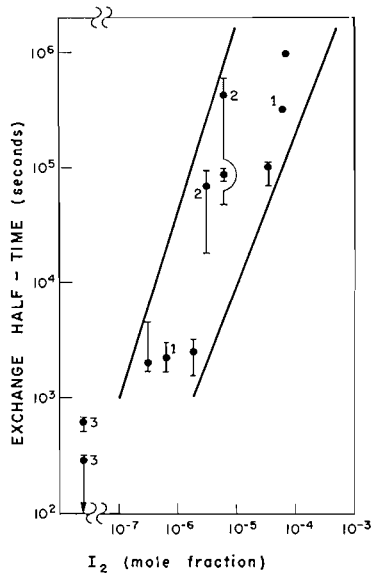

FIG. 1. The dependence of the I_2 – methyl iodide exchange half-time on I_2 concentration: (1) not done by irradiation but by adding $^{131}I_2$ to methyl iodide; (2) the methyl iodide was dried with phosphorus pentoxide; (3) "pure" methyl iodide, no I_2 added.

pentoxide. The larger degree of scatter of the data in these anhydrous solutions can reasonably be attributed to the greater role which traces of water would assume.

In Fig. 1 two lines have been drawn to form a band representing the range of observed exchange half-times. Included are the results of two experiments in which $^{131}I_2$ was used. The half-times observed here are in general agreement with those of Behrens and Maddock (6) for $^{131}I_2$ – methyl iodide exchange. The present results also support their contention that the apparent organic yield in dry, de-aerated, iodine-free methyl iodide must approach 100% due to rapid exchange. This can account for the high organic yield (3, 4) reported for the $^{127}I(n,\gamma)^{128}I$ reaction when irradiations were performed with little concomitant radiation damage. The value of 56% reported by Levey and Willard (2) suggests that irradiation may have produced sufficient iodine in their solutions to significantly increase the exchange half-times.

Organic Yield

The initial organic yield[5] of ^{126}I was determined in methyl iodide solutions containing from 3×10^{-7} to 0.34 mole fraction I_2. These results are given in Table 1 and illustrated in Fig. 2A. To determine the initial organic yields at the lower I_2 concentrations, it was necessary to follow the change in organic yield with time and to correct for exchange which had occurred during the irradiation and before analysis of the first sample. Between 3×10^{-5} and 3×10^{-7} mole fraction I_2 the initial organic yield remained essentially constant at 57%, even when the I_2 – methyl iodide solution, while being irradiated, was shaken with aqueous KI (see Table I, footnote *c*) in an attempt to convert the thermal, radioactive I atoms into the iodide form. This is in good agreement with the value of 56% reported by Levey and Willard (2) for the organic yield of ^{128}I in pure methyl iodide which may have acquired iodine during the irradiation (see preceding paragraph). The

[5]*The initial organic yield is that value which would have been observed if no exchange had occurred.*

Can. J. Chem. Downloaded from www.nrcresearchpress.com by 210.87.254.40 on 09/05/12
For personal use only.

TABLE I

Organic products of ^{126}I in methyl iodide at 25 °C

I_2, mole fraction	Organic yield,[a] %	$CH_3{}^{126}I$,[a] %	$C_2H_5{}^{126}I$,[a] %	Poliodomethanes (^{126}I),[a,b] %
2.5×10^{-7}	56.5[c]			
3.3×10^{-7}	57			
3.7×10^{-7}	56.6			
1.9×10^{-6}	56			
3.3×10^{-6}	57			
3.7×10^{-6}	57.5			
6.2×10^{-6}	57			
6.2×10^{-6}	56.7			
6.2×10^{-6}	58.0	43.9		11.8
6.2×10^{-6}	58			
3.4×10^{-5}	57.5			
3.6×10^{-5}	55			
6.2×10^{-5}	54.4			
6.7×10^{-5}	55.8			
6.9×10^{-5}	54.9	40.7	2.25	11.7
7.5×10^{-5}	51.5			
6.2×10^{-4}	50.5			
6.2×10^{-3}	46.9			
6.2×10^{-3}	46.0[d]	33.5	1.47	10.8[e]
6.2×10^{-3}	46.0[f]	33.7		10.6
6.3×10^{-3}	45.3			
1.2×10^{-1}	32.6	21.8	0.62	10.0
3.4×10^{-1}	25.7	16.31	0.25	9.1
3.4×10^{-1}	25.3	16.2	0.23	8.8
Experiments in which significant exchange preceded analysis				
None added	80.6	66.5		11.6
8×10^{-8}	95.1	80.1		12.5

[a]These values are the experimental determinations of the initial yields and have not been normalized.
[b]The yield of polyiodomethanes was calculated by subtracting the other organic products from the organic yield as described in the text.
[c]This solution was irradiated while shaking it with aqueous 0.01 *M* KI.
[d]This value of the organic yield was assumed to equal that marked [f].
[e]The activity in the *n*-C_3H_7I plus *n*-C_4H_9I distillate was 0.2%.
[f]See footnote [d].

decrease in organic yield which occurs as the mole fraction of I_2 is increased above 3×10^{-5} presumably arises from the very efficient scavenging of recoil atoms and free radicals by I_2.

Radioactive Organic Products

The analyses for some of the organic products of recoil ^{126}I in iodine – methyl iodide solutions are given in Table I. Obviously, the production of organic compounds must approach zero as the mole fraction of I_2 approaches unity. However, to a first approximation, the experimental yields of organic products can be corrected for that part of the decrease which is due solely to the dilution of methyl iodide by I_2 by simply dividing the yields by the mole fraction of methyl iodide. Results corrected in this manner will be designated as normalized yields, in the manner of Harris (14).

Methyl Iodide

In agreement with previous investigators (2, 3, 15) the most abundant organic product of ^{126}I was found to be $CH_3{}^{126}I$. In Fig. 2C the normalized yield of $CH_3{}^{126}I$ is plotted against the iodine concentration. Extrapolation of the curve suggests that the normalized yield of $CH_3{}^{126}I$ approaches 21% as the mole fraction of I_2 approaches unity.

Ethyl Iodide

The radioactivity which distilled with the ethyl iodide carrier probably represented only $C_2H_5{}^{126}I$ because no other unsaturated alkyl iodides boil within 16 °C of the boiling

Can. J. Chem. Downloaded from www.nrcresearchpress.com by 210.87.254.40 on 09/05/12
For personal use only.

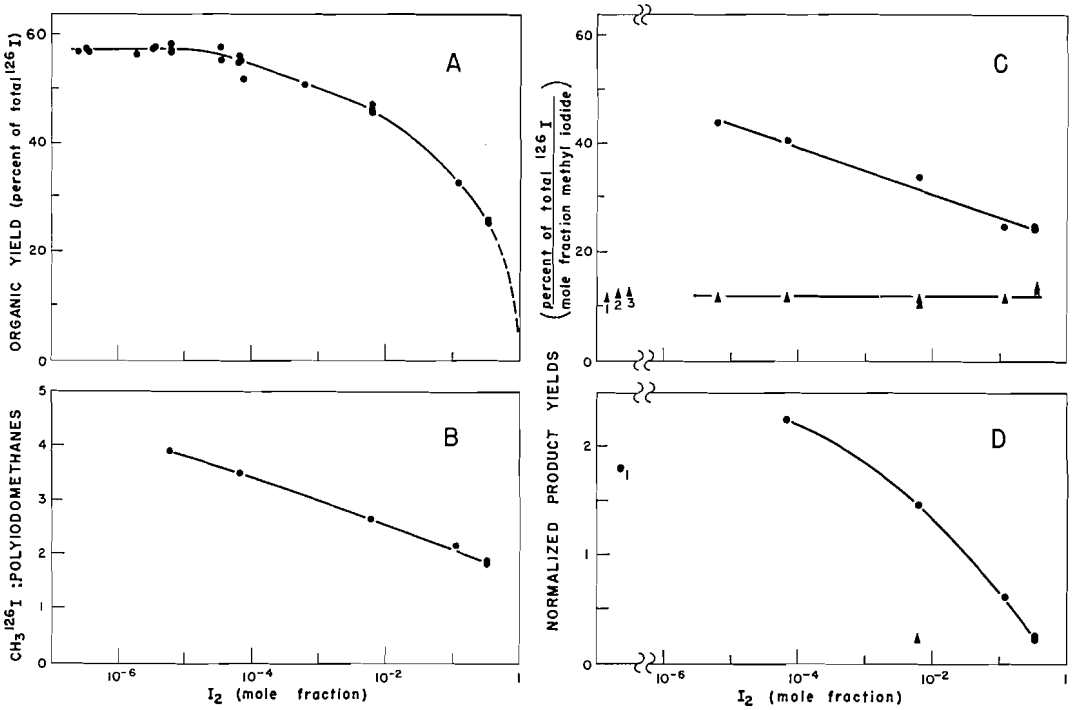

FIG. 2. The relation of products containing ^{126}I to the iodine concentration of the methyl iodide solution. In Fig. 2C ● $CH_3{}^{126}I$; ▲ ^{126}I in polyiodomethanes (in 1, 2, and 3 considerable exchange had occurred prior to analysis) (1) "pure" methyl iodide irradiated in the presence of solid potassium iodide, (2) 8×10^{-8} mole fraction I_2, (3) "pure" methyl iodide. In Fig. 2D ● $C_2H_5{}^{126}I$, (1) "pure" methyl iodide irradiated in the presence of solid potassium iodide; ▲ the activity which distilled with *n*-propyl iodide and *n*-butyl iodide.

point for ethyl iodide and because the specific activity of the distillate remained constant throughout its take-off interval. The normalized yield of $C_2H_5{}^{126}I$ (see Fig. 2D) approaches zero as the mole fraction of I_2 approaches unity. In one experiment in which "pure" methyl iodide was irradiated, the yield of $C_2H_5{}^{126}I$ was 1.8%. Thus, it appears that below 10^{-4} mole fraction I_2 the production of $C_2H_5{}^{126}I$ is about 2%.

Propyl and Butyl Iodide Fraction

A small amount of activity was found in the *n*-propyl iodide and *n*-butyl iodide distillate (see Fig. 2D). This activity, which could have been due to a number of products, represents less than 0.3% of the total activity. It appears that the fraction of ^{126}I in compounds containing more than two carbon atoms is very small indeed.

Polyiodomethanes

After distillation of *n*-butyl iodide from the organic products the undistilled residue still contained a significant fraction of the organic activity. This is believed to represent the higher boiling compounds $CH_2{}^{126}I_2$, $CH^{126}I_3$, and $C^{126}I_4$. This undistilled fraction will be referred to as the "polyiodomethanes". The production of polyiodomethanes bears a striking resemblance to the production of polybromomethanes by recoil Br atoms in bromine – methyl bromide, a system which has been examined in considerable detail by Harris (14). The activity of polyiodomethanes was not measured directly but was deduced by subtracting the activity of the $CH_3{}^{126}I$, the $C_2H_5{}^{126}I$, and the propyl butyl iodide fractions from the organic yield. In experiments where the relatively small contributions

Can. J. Chem. Downloaded from www.nrcresearchpress.com by 210.87.254.40 on 09/05/12
For personal use only.

of $C_2H_5{}^{126}I$ and of the propyl and butyl iodide fraction were not determined experimentally they were estimated from Fig. 2D. Three of the polyiodomethane estimates represent solutions in which considerable exchange had occurred prior to extraction of the inorganic products, and yet the normalized values of the polyiodomethane yields, as shown in Fig. 2C, remained constant at about 12% regardless of the iodine concentration or any exchange which may have occurred.

In an experiment with 0.34 mole fraction I_2 the polyiodomethane fraction was partially separated by distilling some of the diiodomethane. The experimental yield of $CH_2{}^{126}I_2$ was 6.3% and the activity due to undistilled, higher-boiling compounds was roughly 2.2% giving 8.5% as the total activity in the polyiodomethane fraction. By the subtraction method described above the total polyiodomethane activity was estimated to be 9.0%, a discrepancy which could be due to partial decomposition of $CH^{126}I_3$ and $C^{126}I_4$ during the distillation.

The Ratio $CH_3{}^{126}I$: Polyiodomethanes

The ratio $CH_3{}^{126}I$ activity : polyiodomethane activity vs. the mole fraction I_2 is shown in Fig. 2B for experiments in which no significant exchange occurred. The ratio appears to approach the value 1.6 as the mole fraction of I_2 approaches unity. The consistency of the data suggests that, independent of the organic yield, the experimental yields of $CH_3{}^{126}I$ and polyiodomethanes are quite accurate relative to one another.

Product Distribution at Low I_2 Concentrations

Below 10^{-5} mole fraction I_2, the $C_2H_5{}^{126}I$ and polyiodomethane yields remained essentially constant even in solutions which had experienced significant exchange. Since the initial organic yield was also constant at these concentrations it is evident that the initial yield of $CH_3{}^{126}I$ must also have been essentially constant.

The Exchange Reaction

In Fig. 3 the yield of $CH_3{}^{126}I$ is plotted against the observed organic yield. Organic yields above 57% represent experiments in which exchange occurred. By extrapolation it is seen that if exchange had been allowed to raise the organic yield to 100%, the apparent yield of $CH_3{}^{126}I$ would have been 85% leaving the other products essentially unaffected, at 12% polyiodomethanes, 2% $C_2H_5{}^{126}I$, and 1% other products. Therefore, within experimental error, exchange at low iodine concentrations serves only to increase the yield of $CH_3{}^{126}I$ and does not detectably affect the other organic products which are present in extremely low concentrations. These results may be compared with those of Behrens and Maddock (6) who found that 91% of the thermal exchange between $^{131}I_2$ and methyl iodide produced $CH_3{}^{131}I$. Badger, Chmiel, and Schuler (16) studied the exchange of $^{131}I_2$ with ethyl, *n*-propyl, and isopropyl iodides and found that $>98\%$ of the exchange transferred ^{131}I to the alkyl iodide comprising the solvent.

Reactions of Recoil Iodine Atoms

The thermal neutron (n,γ) reaction forms ^{128}I, with an estimated average recoil energy of the order of 100 eV (17) and with an average positive charge due to conversion and Auger electron emission. When gaseous ethyl iodide containing a little iodine is irradiated with thermal neutrons, the organic yield of ^{128}I is only 1% (18) indicating that almost every ^{128}I atom leaves the carbon atom which was the original partner. Formation of ^{126}I by the (n,2n) reaction gives ^{126}I atoms an estimated average recoil energy of 10^5 eV (17). The dissociation energy of the I—I bond in iodine is 1.5 eV and that of the C—I bond in methyl iodide is 2.4 eV. It may thus be safely assumed that an overwhelming

Can. J. Chem. Downloaded from www.nrcresearchpress.com by 210.87.254.40 on 09/05/12
For personal use only.

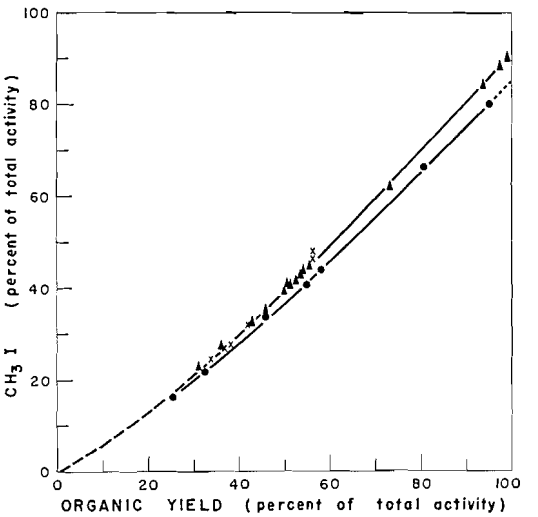

FIG. 3. The yield of radioactive CH_3I vs. the organic yield. × $CH_3{}^{128}I$ by Levey and Willard (2); ▲ $CH_3{}^{128}I$ by Brustad and Baarli (3); ● $CH_3{}^{126}I$ in present work.

proportion of the ^{126}I atoms formed will leave the atoms to which they were originally bound. If, as is likely, primary recombination is infrequent, then the reactions of all ^{126}I atoms, whether originating from I_2 or CH_3I, can be treated in the same manner.

It seems reasonable to attribute the products of ^{126}I in iodine – methyl iodide solutions to the three classes of reactions to which Harris (14) ascribed the products of recoil Br in the bromine – methyl bromide system. These are the reactions of thermalized recoil atoms, hot recoil atoms, and the diffusion-controlled reactions of recoil atoms in the spurs. The collisions which finally reduce the recoil atom to thermal energies leave it in a spur which contains a high local concentration of atoms and radicals. If the ^{126}I atom escapes combination with these atoms and radicals, it will diffuse freely in the solution. Its subsequent reactions are described as thermal. An iodine atom diffusing in the relatively unreactive solvent methyl iodide (19) will be very susceptible to scavenging by an exchange reaction with even minute concentrations of the extremely reactive iodine molecule (20). However, before escape from the spur can occur, the thermal ^{126}I atoms may undergo diffusion-controlled reactions with the reactive species in the spur. Only when the I_2 concentration is high enough to compete with, and for, these reactive species can I_2 significantly affect this class of diffusion-controlled reactions. On the other hand, reactions which are not influenced even by high concentrations of I_2, except to the extent of a simple dilution effect, are described as hot reactions. For example, the product of a hot reaction could be formed after a complete collisional transfer of energy from an energetic ^{126}I atom to a bound I atom if the thermalized ^{126}I atom, before diffusing, reacted with the fragments left by the departing I atom.

For each of the three classifications of reactions just described it is possible to predict the effect of allowing the mole fraction of I_2 to approach unity (as done by Harris (14) for the bromine – methyl bromide system). The normalized yields of organic products due solely to thermal reactions or diffusion-controlled reactions in the spurs must approach zero. The normalized yields of organic products due solely to hot reactions will, by definition, be unaffected by the I_2 concentration. If only a fraction of a product is formed by hot reactions, then its normalized yield will decrease with increasing I_2 concentration

Can. J. Chem. Downloaded from www.nrcresearchpress.com by 210.87.254.40 on 09/05/12
For personal use only.

and approach a finite value (equal to the extent of its formation by hot reactions) as the mole fraction of I_2 approaches unity. The unvarying value of the normalized yield of polyiodomethanes (Fig. 2C) indicates that normalization to the mole fraction of methyl iodide provides a satisfactory correction for the dilution effect up to at least 0.34 mole fraction I_2. However, it is possible that at still higher I_2 concentrations a more complicated normalization factor might be required. For example, in a solution comprised mainly of iodine, with which an I atom can be thermalized in a single collision, the energy distribution (and hence the reactions) of ^{126}I might be radically different from that in a solution of lower iodine content.

The preceding paragraph describes how it is possible to assess fairly unambiguously that fraction of a product which is formed by hot reactions. For thermal reactions and diffusion-controlled reactions in the spurs the assignment is less certain. It has been reported (21) that the rate constant for the exchange of I atoms with liquid methyl iodide is 20 ml $mole^{-1}$ s^{-1} at 25 °C, whereas that for the exchange of I atoms with I_2 in hexane (20) is 8×10^{10} ml $mole^{-1}$ s^{-1}. Hence, for all experiments in which the initial organic yields were determined, the I_2 concentrations were sufficient to insure that essentially all the thermal, freely-diffusing I atoms were scavenged by I_2; so even between 3×10^{-5} and 3×10^{-7} mole fraction I_2, where the organic yield is constant, all organic products result solely from hot reactions or diffusion-controlled reactions in the spurs. Roy, Williams, and Hamill (22) report that at low I_2 concentrations 5% of the inorganic yield is due to hot reactions. It is of interest that, if the remainder of the inorganic products resulted from freely-diffusing I atoms, the probability that recoil I atoms escape their spurs would be very similar to the 40–60% of I atoms, produced by the photolysis of I_2 in hexane at 25 °C (23), which excape recombination with their initial partners. The decrease of normalized organic yield with increasing I_2 concentration, above 3×10^{-5} mole fraction I_2, is believed to result solely from the scavenging by I_2 of thermalized I atoms in the spurs.

The value of the initial organic yield in absolutely pure methyl iodide would be difficult to determine. As the I_2 content of the liquid is decreased, the exchange reaction reaches equilibrium with increasing rapidity. Moreover, irradiations would have to be terminated before a significant amount of I_2 had been formed. The most enlightening approach seems to be to determine the extent to which organic and inorganic products are formed by hot reactions, by thermal reactions, and by diffusion-controlled reactions in the spurs.

The maximum observed yield of the predominant organic product, $CH_3{}^{126}I$, was 43%. The normalized yield of $CH_3{}^{126}I$ approaches 21% as the mole fraction of I_2 approaches unity. On the basis of the suggested model, 21% of the ^{126}I forms $CH_3{}^{126}I$ by hot reactions whereas a maximum of 22% forms $CH_3{}^{126}I$ by diffusion-controlled reactions in the spurs. The normalized yield of polyiodomethanes remains constant over the entire range of I_2 concentrations studied. Hence, polyiodomethanes must be produced predominantly by hot reactions. At present, it is difficult to suggest mechanisms to account for the quite significant formation of $CH_2{}^{126}I_2$ and $CH_2{}^{128}I_2$ in neutron-irradiated methyl iodide. However, it has been shown that ^{128}I formed in the presence of CH_4 can form $CH_3{}^{128}I$ by a hot reaction with the direct displacement of a hydrogen atom (18, 24). The normalized yield of $C_2H_5{}^{126}I$ approaches zero as the mole fraction of I_2 approaches unity. Probably $C_2H_5{}^{126}I$ is formed through diffusion-controlled reactions of two 1-carbon fragments within the spurs. If so, it is not surprising that products containing more than two carbon atoms are formed to an even lesser extent than $C_2H_5{}^{126}I$.

The particular reactions by which the products are formed are still largely speculative. The recoiling atom probably generates active species such as I, CH_3, CH_2, CH, etc. To

Can. J. Chem. Downloaded from www.nrcresearchpress.com by 210.87.254.40 on 09/05/12
For personal use only.

account for the relative insensitivity of product distribution to recoil energy, Willard (17) has suggested that charge neutralization near the end of the recoil track is an important factor in determining the course of reactions. Since charge neutralization is likely to be very rapid, the final reactions probably involve mainly neutral I atoms. More recently, Geissler and Willard (25) have proposed that a major portion of the organic yield in alkyl iodides is due to combination with radicals formed by the conversion and Auger electrons emitted by the atom itself. This hypothesis derives from their observation that high yields of the parent alkyl iodide occur even in dilute pentane solutions.

The mechanism by which methyl iodide and I_2 exchange in the absence of light is not yet understood. Estimates of exchange via I atoms which are present in thermal equilibrium with I_2 (19, 26) indicate exchange half-times many orders of magnitude longer than those observed. A mechanism involving a complex between I_2 and CH_3I (13) does not appear consistent with the observed decrease of exchange half-time with decreasing I_2 concentration. The possibility of heterogeneous effects has already been noted (12). Minute quantities of impurities appear to exert a profound influence on the observed exchange, and these may well obscure the exchange for the perfectly pure system.

Influence of Recoil Energy

The average recoil energy of ^{126}I produced by 14 MeV neutrons is about 10^5 eV compared to about 100 eV for ^{128}I from thermal neutrons. The effect of recoil energy on the fate of I atoms has been studied a number of times (1, 27–29). In alkyl iodides the organic yields of ^{126}I were almost identical to those of ^{128}I. This was confirmed in the present experiments where it was possible to produce ^{126}I and ^{128}I simultaneously in methyl iodide solutions with about 90% of the ^{128}I resulting from slow neutrons. At 6×10^{-5} mole fraction I_2 the organic yield of ^{126}I was 55.9% and of ^{128}I was 54.6% (an absolute difference of $2.4 \pm 1.6\%$). At 6×10^{-3} mole fraction I_2 the organic yield of ^{126}I was 46.1% and of ^{128}I was 45.5% (an absolute difference of $1.3 \pm 1.6\%$); whereas the yields of total organic products other than CH_3I (hence predominantly the "hot" polyiodomethanes) were 12.4% for ^{126}I and 11.2% for ^{128}I (an absolute difference of $10 \pm 4\%$). These results suggest that the yields of products which are formed predominantly by hot or by thermal reactions will be more sensitive than the total organic yield to differences in recoil energy. This arises because the yields of the products may be affected in opposing ways, resulting in a partial cancellation of the effect. In Fig. 3, $CH_3{}^{128}I$ yields determined by others (2, 3) are shown for comparison with the present $CH_3{}^{126}I$ yields.

REFERENCES

1. R. H. Schuler. J. Chem. Phys. **22**, 2026 (1954).
2. G. Levey and J. E. Willard. J. Am. Chem. Soc. **74**, 6161 (1952).
3. T. Brustad and J. Baarli. J. Chem. Phys. **22**, 1311 (1954).
4. I. P. Alimarin and K. F. Svoboda. Soviet J. At. Energy, English Transl. **5**, No. 1, 888 (1958).
5. H. Behrens and A. G. Maddock. J. Chem. Phys. **22**, 1139 (1954).
6. H. Behrens and A. G. Maddock. Proceedings of the Second Radioisotope Conference, Oxford. Butterworths Publications. 1954. pp. 33–39.
7. P. F. Shaw and C. H. Collie. J. Chem. Soc. 1217 (1949).
8. K. Svoboda. Proc. U.N. Intern. Conf. Peaceful Uses At. Energy, 2nd Geneva, **20**, 53 (1958).
9. K. Svoboda. Proc. Conf. Chem. Effects of Nuclear Transformations. Vol. I, I.A.E.A., Vienna. 1961.
10. K. Svoboda. Nature, **198**, 986 (1963).
11. R. H. Schuler and W. H. Hamill. J. Am. Chem. Soc. **74**, 6171 (1952).
12. A. G. Maddock. Private communication.
13. H. Schmied and R. W. Fink. J. Chem. Phys. **27**, 1034 (1957).
14. W. E. Harris. Can. J. Chem. **39**, 121 (1961).
15. E. Gluckauf and J. W. Fay. J. Am. Chem. Soc. 390 (1936).
16. R. G. Badger, C. T. Chmiel, and R. H. Schuler. J. Am. Chem. Soc. **75**, 2498 (1953).
17. J. E. Willard. Nucleonics, **19**, No. 10, 61 (1961).

Can. J. Chem. Downloaded from www.nrcresearchpress.com by 210.87.254.40 on 09/05/12
For personal use only.

18. J. F. HORNIG, G. LEVEY, and J. E. WILLARD. J. Chem. Phys. **20**, 1556 (1952).
19. M. B. NEIMAN, V. B. MILLER, and YU. M. SHAPOVALOV. Zh. Fiz. Khim. No. 3, 492 (1956).
20. R. M. NOYES and J. ZIMMERMAN. J. Chem. Phys. **18**, 656 (1950).
21. G. S. LAURENCE and D. R. STRANKS. International Atomic Energy Agency Conference on the Use of Radioisotopes in the Physical Sciences and Industry. Copenhagen. 1960. p. 483.
22. J. C. ROY, R. R. WILLIAMS, and W. H. HAMILL. J. Am. Chem. Soc. **76**, 3274 (1954).
23. J. ZIMMERMAN and R. M. NOYES. J. Chem. Phys. **18**, 658 (1950).
24. E. P. RACK and A. A. GORDUS. J. Chem. Phys. **34**, 1855 (1961).
25. P. R. GEISSLER and J. E. WILLARD. J. Phys. Chem. **67**, 1675 (1963).
26. M. C. FLOWERS and S. W. BENSON. J. Chem. Phys. **38**, 882 (1963).
27. C. E. MCCAULEY and R. H. SCHULER. J. Phys. Chem. **62**, 1364 (1958).
28. R. H. SCHULER and C. E. MCCAULEY. J. Chem. Phys. **25**, 1080 (1956).
29. C. E. MCCAULEY, G. J. HILSDORF, P. R. GEISSLER, and R. H. SCHULER. J. Am. Chem. Soc. **78**, 3246 (1956).

Can. J. Chem. Downloaded from www.nrcresearchpress.com by 210.87.254.40 on 09/05/12
For personal use only.

Can. J. Chem. Downloaded from www.nrcresearchpress.com by 210.87.254.40 on 09/05/12
For personal use only.

STEROIDS

VIII. SOME REACTIONS OF THE 3-METHYLCHOLEST-5-EN-3-OLS AND THEIR DERIVATIVES[1]

G. JUST AND V. DI TULLIO[2,3]
Department of Chemistry, McGill University, Montreal, Quebec
Received December 27, 1963

ABSTRACT

The preparation and ethanolysis of 3-methylcholesteryl derivatives is described. It was noticed that Δ^5-3-methyl-3-oxygenated steroids undergo hydrogenolysis, which can be suppressed by addition of sodium nitrite.

During the work described in the preceding paper (3), we required samples of the epimeric 3-methylcholest-5-en-3-ols II and III and their reduction products VI and VII, as well as their respective acetates and ethyl ethers.

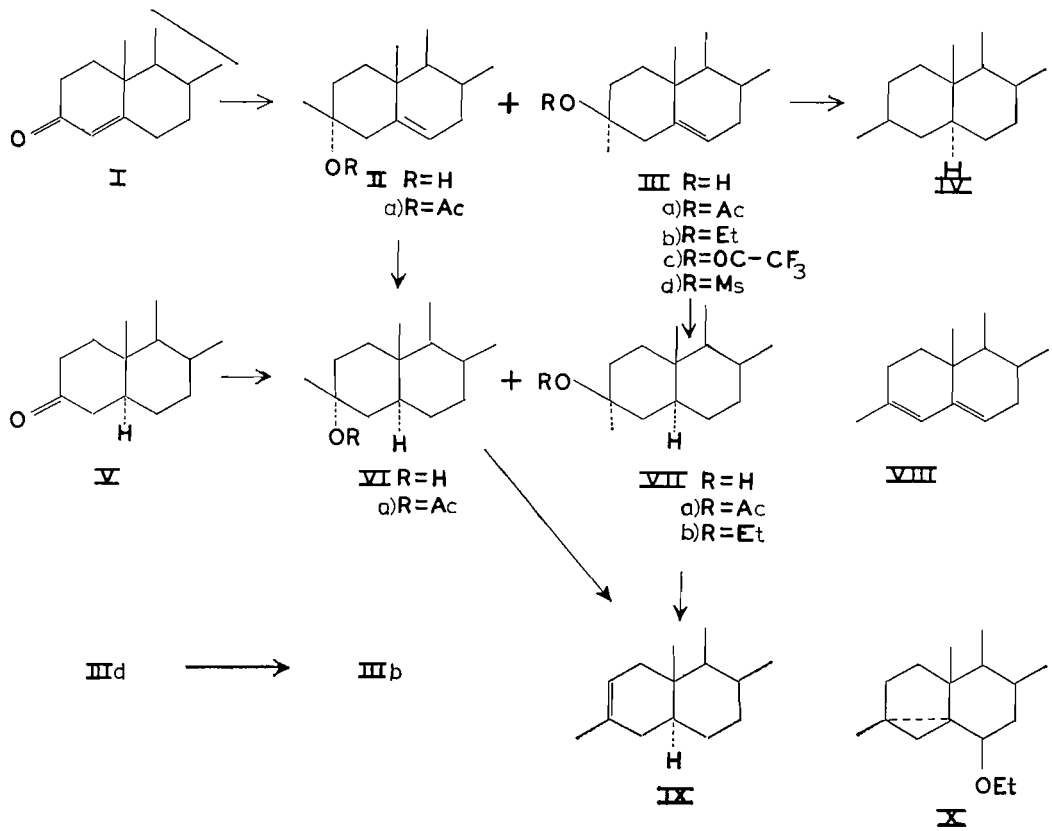

[1]*Part VII. See ref. 2.*
[2]*This work was supported by the National Research Council of Canada.*
[3]*Holder of a National Research Council of Canada Studentship, 1962–1963.*

Can. J. Chem. Downloaded from www.nrcresearchpress.com by 210.87.254.40 on 09/05/12
For personal use only.

Cholest-5-en-3-one (I) (4) was treated with methyl magnesium iodide. Chromatographic separation of the reaction product on alumina gave 3β-methylcholest-5-en-3α-ol (II), cholest-4-en-3-one, and 3α-methylcholest-5-en-3β-ol (III) in that order. The stereochemical assignments of the epimeric alcohols II and III were based on their relative ease of elution and the reactions described below. The possibility of the product being 4-en-3-ols can be excluded, since such allylic alcohols would have been dehydrated under the experimental conditions employed (5, 6).

The infrared spectrum of the 3α-alcohol II showed an absorption peak at 3 580 cm^{-1} (7). This band is shifted towards a lower frequency probably because of hydrogen bonding with the Δ^5-double bond, itself characterized by a nuclear magnetic resonance (n.m.r.) signal centered at 5.4 p.p.m. Attempted acetylation of alcohol II with acetic anhydride in pyridine at room temperature gave starting material. Treatment of the lithium salt of alcohol II with acetyl chloride (8) gave a good yield of acetate II*a*, ν 1 728, 1 274, and 1 239 cm^{-1}. Catalytic reduction of II in acetic acid, using Adam's catalyst, gave 3-methylcholestane (IV) (9). However, when sodium nitrite was added to the reducing mixture the hydrogenolysis reaction was suppressed (1) and a quantitative yield of the expected alcohol VI (8) was obtained.

3α-Methylcholest-5-en-3β-ol (III) showed, in the infrared, an unsymmetrical absorption band at 3 608 cm^{-1} and, in the n.m.r., a signal for a single proton centered at 5.45 p.p.m., which can be assigned to the C_6-olefinic hydrogen. Treatment of alcohol III with acetic anhydride in pyridine at room temperature gave starting material. At reflux temperature, a mixture of 3-methylcholesta-3,5-diene (VIII) and 3α-methylcholesteryl acetate (III*a*) was obtained. However, treatment of the lithium salt of III (8) with acetyl chloride gave a good yield of III*a*. Catalytic reduction of III resulted in the formation of 3-methylcholestane (IV) (9) and 3α-methylcholestan-3β-ol (VII) (8) in approximately 20 and 80% yield respectively. The hydrogenolysis could be eliminated by addition of sodium nitrite to the reducing mixture (1).

Since hydrogenolysis of homoallylic alcohols is somewhat unusual, we investigated this reaction to exclude the possibility of dehydration under the reaction conditions. 3β-Methylcholest-5-en-3α-ol (II), which had given hydrogenolysis products exclusively, was used as a model substance for more detailed work. A sample, dissolved in acetic acid containing prereduced platinum, was kept overnight under 60 p.s.i. of nitrogen at 40°. Only starting material was recovered. A similar reaction carried out at 100° and atmospheric pressure for 16 h, converted 19% of alcohol II to 3-methylcholesta-3,5-diene (VIII). These experiments prove that hydrogenolysis could have occurred by a dehydration–hydrogenation sequence to a small extent only, if at all.

The reaction of cholestan-3-one (V) with methyl magnesium iodide, described by Barton and co-workers (8), gave a 1:1 mixture of the epimeric 3-methylcholestanols VI and VII. In the reaction on cholest-5-en-3-one (I), we obtained the two alcohols II and III in 4 and 63% yield respectively. We proposed recently (10) that the ratio of axial to equatorial alcohols obtained in Grignard reactions depended on the degree of steric hindrance due mainly to 1,3-diaxial interactions. Removal of a hydrogen at the 5-position by introduction of a Δ^5-double bond should decrease the hindrance at C_3 and result in the formation of a large amount of 3β-alcohol. The yields of the alcohols obtained support the hypothesis. An electronic effect of the Δ^5-bond can be excluded since participation of the double bond during Grignard reaction would have favored the other epimer.

When alcohols VI and VII were treated with acetic anhydride or acetyl chloride in

pyridine at room temperature, only starting materials were recovered. When acetic anhydride, acetic acid, and *p*-toluene sulfonic acid (11) were used as an acetylating medium, 3-methylcholest-2-ene (IX), which appeared to be identical with IX described by Barton (8), was obtained in approximately 60% yield from either alcohol VI or VII. When the lithium salts of alcohols VI and VII (8) were treated with acetyl chloride, good yields of the acetate VI*a*, ν 1 730, 1 273, and 1 239 cm^{-1}, and VII*a*, ν 1 730 and 1 245 cm^{-1}, were obtained.

Attempts to form an ethyl ether of alcohol VII either by treatment of a lithium or sodium salt of VII with an ethyl halide (8, 12) or by reduction of acetate VII*a* with sodium borohydride and boron trifluoride etherate (13) failed. Hence it appeared necessary to find another reaction to transform a tertiary alcohol to its ethyl ether. Ethanolysis of a suitable derivative of 3α-methylcholesterol (III) should proceed through the homoallylic ion XI and give ethers III*b* and X. The methyl group at C_3 should stabilize a positive charge at the 3-position, and 3β-ethoxy-3α-methylcholest-5-ene (III*b*) should be formed as a major product.

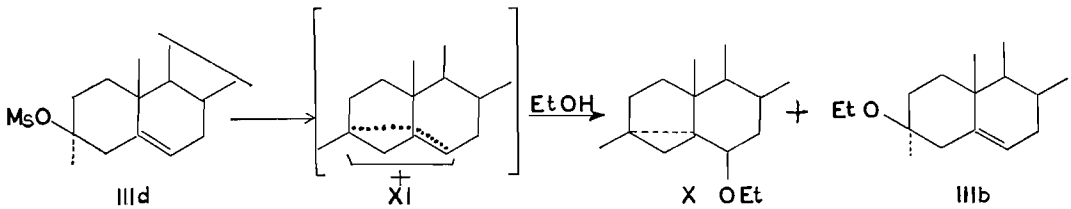

3α-Methylcholest-5-en-3β-ol (III) was converted to its trifluoroacetate III*c* by trifluoroacetic anhydride in pyridine at 0° (14). The trifluoroacetate III*c* was heated under reflux overnight in ethanol containing either potassium ethoxide or potassium acetate. Only starting alcohol III was obtained. Attempts to form the tosylate of the 3β-alcohol III failed. When 3α-methylcholest-5-en-3β-ol was reacted with methanesulfonyl chloride in pyridine at −5° overnight, 3-methylcholesta-3,5-diene (VIII) and starting material were isolated in 54 and 15% yields respectively. However, if the mesylation reaction was quenched with ethanol as soon as crystals of pyridine hydrochloride started to form and the mixture evaporated, there was obtained after chromatography on silica gel, 3-methylcholesta-3,5-diene (VIII) and 3β-ethoxy-3α-methylcholest-5-ene (III*b*), in 22 and 48% yields respectively. No trace of 6β-ethoxy-3β-methyl-3α,5-cyclo-5α-cholestane (X) could be detected. The ether III*b* was identical with 3β-ethoxy-3α-methylcholest-5-ene, obtained in the photolysis of 3-methylcholesta-3,5-diene (3).

EXPERIMENTAL[4]

Preparation of 3α-Methylcholesterol (III) and 3β-Methylcholest-5-en-3α-ol (II)

The alcohols II and III were prepared by adding 5 g of solid cholest-5-en-3-one (4) to 250 ml of an ethereal solution of an excess of methyl magnesium iodide. The solution was heated under reflux overnight. The excess reagent was destroyed by slowly adding 5 g of ammonium chloride in 25 ml of water. The ether layer was washed with water until neutral, dried over magnesium sulfate, and evaporated at 40° under reduced pressure. The oily residue was chromatographed on alumina (activity II–III, 150 g). Elution with benzene–ether (99:1) gave 3β-methylcholest-5-en-3α-ol (II) (214 mg, 4%), m.p. 112–115°. Three crystallizations from acetone raised the m.p. to 119–120°, $[\alpha]_D$ −28.6° (*c* 1.3), 3 580 cm^{-1}, δ 5.4 p.p.m. (1H, broadened singlet, C=C_6—H).

Anal. Calcd. for $C_{28}H_{48}O$: C, 83.93; H, 12.08. Found: C, 84.02; H, 12.00.

[4]*For details in instrumentation and general procedures, see ref. 3.*

Can. J. Chem. Downloaded from www.nrcresearchpress.com by 210.87.254.40 on 09/05/12
For personal use only.

Further elution with benzene–ether (9:1) gave cholest-4-en-3-one (1.2 g), identified by melting point, mixed melting point, and ultraviolet (λ_{max}^{EtOH} 239 mμ, $\lambda_{max}^{cyclohexane}$ 232 mμ).

Ether eluted 3α-methylcholesterol (III) (3.275 g, 63%), m.p. 161°. Three crystallizations from chloroform–ether raised the m.p. to 169–170°, $[\alpha]_D$ −27° (*c* 1.8), ν 3 608 cm^{-1}, δ 5.45 p.p.m. (1H, singlet, C=C_6—H).

Anal. Calcd. for $C_{28}H_{48}O$: C, 83.93; H, 12.08. Found: C, 83.77; H, 12.06.

3β-Methylcholestan-3α-ol (VI) and 3α-Methylcholestan-3β-ol (VII)

Using the condition described (8), 3β-methylcholestan-3α-ol (VI), m.p. 129° (lit. 126–127°), ν 3 610 cm^{-1}, and 3α-methylcholestan-3β-ol (VII), m.p. 150–151° (lit. 147–149°), ν 3 608 cm^{-1} were obtained in 51 and 45.5% yield respectively.

The Acetates of the 3-Methylcholest-5-ene-3-ols (IIa, IIIa) and 3-Methylcholestan-3-ols (VIa, VIIa)

1. An anhydrous ether solution (10 ml) of 3β-methylcholest-5-en-3α-ol (237 mg) was added to phenyl lithium (prepared from 261 mg of phenyl bromide and 190 mg of lithium in 50 ml of anhydrous ether) and stirred 4 h at room temperature (8). Acetyl chloride (2 ml) was added to the solution and the mixture stirred overnight. Methanol was added to the reaction mixture, which was then diluted with water. The ether extract was washed neutral, dried over magnesium sulfate, and evaporated under vacuum at 40°. The oily residue was chromatographed on alumina (activity II–III, 20 g). Elution with hexane gave 183 mg of 3β-methylcholest-5-en-3α-yl acetate (IIa) (70%), m.p. 70–71°. Recrystallization from acetone raised the m.p. to 75–76°, $[\alpha]_D$ −19.1° (*c* 1.3), ν 1 728, 1 274, and 1 239 cm^{-1}.

Anal. Calcd. for $C_{30}H_{50}O_2$: C, 81.39; H, 11.38. Found: C, 81.35; H, 11.67.

2. Similarly, alcohol III was transformed to 3α-methylcholesteryl acetate (IIIa) (61%), recrystallized from acetone, m.p. 129–130°. $[\alpha]_D$ −26.3° (*c* 1.2), ν 1 734 and 1 247 cm^{-1}.

Anal. Calcd. for $C_{30}H_{50}O_2$: C, 81.39; H, 11.38. Found: C, 81.73; H, 10.95.

3. Alcohol VI was transformed to its acetate VIa (85%), m.p. 87–89°, using the same conditions described above. Recrystallization from acetone raised the m.p. to 89–90°, $[\alpha]_D$ 26.4° (*c* 1.6), ν 1 730, 1 273, and 1 239 cm^{-1}.

Anal. Calcd. for $C_{30}H_{52}O_2$: C, 81.02; H, 11.79. Found: C, 81.21; H, 11.60.

4. Alcohol VII was also transformed to its acetate VIIa (67%), m.p. 110–114°. Recrystallization from acetone raised the m.p. to 114–115°, $[\alpha]_D$ 24.9° (*c* 0.9), ν 1 730 and 1 245 cm^{-1}.

Anal. Calcd. for $C_{30}H_{52}O_2$: C, 81.02; H, 11.79. Found: C, 81.19; H, 11.55.

3α-Methylcholest-5-en-3β-yl Trifluoroacetate (IIIc)

Alcohol III (105 mg, 0.21 mmole) was dissolved in 8 ml of pyridine (0 °C) followed by the addition of 3 ml of trifluoroacetic anhydride at −8° (14). The solution was kept at 0° for 5 min. As 25 ml of ice-cold water was added to the mixture, crystals began to form. The trifluoroacetate IIIc (107 mg), m.p. 132°, was washed free of trifluoroacetic acid and then crystallized from ether–methanol, m.p. 134–135°, $[\alpha]_D$ −22.6° (*c* 1.0), ν 1 780, 1 220, 1 168, and 1 095 cm^{-1}.

Anal. Calcd. for $C_{30}H_{47}O_2F_3$: C, 72.59; H, 9.46; F, 11.50. Found: C, 72.24; H, 9.59; F, 11.33.

Hydrogenation of 3-Methylcholest-5-en-3-ols (II, III) in the Presence and Absence of Sodium Nitrite

1. Platinum oxide (201 mg) and 255 mg of 3β-methylcholest-5-en-3α-ol (II) were added to 50 ml of acetic acid and hydrogenated in a Parr apparatus at 70° and 60 p.s.i. for 10 h. The platinum was filtered off and the filtrate diluted with 50 ml of concentrated aqueous sodium carbonate and ether. The ether layer was washed neutral, dried over magnesium sulfate, and evaporated under vacuum. The crystalline residue, m.p. 99°, was chromatographed on alumina (activity II–III, 10 g). The only crystalline compound eluted (by hexane) was 177 mg of 3-methyl-cholestane (IV), m.p. 99–100°. It was identified by mixed melting point and comparison of the infrared spectra with an authentic sample prepared below.

2. Under similar reaction conditions, 125 mg of 3α-ol II, dissolved in 25 ml of acetic acid, was hydrogenated in the presence of 95 mg of platinum oxide and 18 mg of sodium nitrite. The oily residue (138 mg) was chromatographed on alumina (activity II–III, 10 g). Elution with benzene gave 114 mg of 3β-methylcholestan-3α-ol (VI), m.p. 129°, identified by mixed melting point and comparison of its infrared spectrum with that of an authentic sample prepared above.

3. 3α-Methylcholesterol (III) (320 mg) in 30 ml of acetic acid was hydrogenated at room temperature and 60 p.s.i. in the presence of 200 mg of platinum oxide. The oily residue was chromatographed on alumina (activity II–III, 10 g). Elution with hexane gave 68 mg of 3-methylcholestane, m.p. 99°. Further elution with benzene gave 258 mg of 3α-methylcholestan-3β-ol (VII), m.p. 151°. The two compounds were identified by comparison with authentic samples (melting point, mixed melting point, and infrared) prepared above and below.

4. Alcohol III (230 mg) in 25 ml of acetic acid was hydrogenated in the presence of 210 mg of platinum oxide and 27 mg of sodium nitrite, using the same conditions described above. The crystalline residue, m.p. 120–122°, was chromatographed on alumina (activity II–III, 10 g). Benzene eluted 204 mg of 3α-methylcholestan-3β-ol (VII), m.p. 151–152°, identified by mixed melting point and comparison of its infrared spectrum with that of an authentic sample.

Can. J. Chem. Downloaded from www.nrcresearchpress.com by 210.87.254.40 on 09/05/12
For personal use only.

3-Methylcholestane (IV)

3-Methylcholesta-3,5-diene (VIII) (105 mg) in acetic acid was hydrogenated overnight in the presence of 140 mg of platinum oxide at 40° and 60 p.s.i. The crystalline reaction product, m.p. 93–95°, was recrystallized from hexane–acetone to give 81 mg of hydrocarbon IV, m.p. 99–100° (lit. 96–97° (6*b*)), $[\alpha]_D$ 23.3° (*c* 0.99).

Anal. Calcd. for $C_{28}H_{50}$: C, 86.97; H, 13.03. Found: C, 87.01; H, 13.11.

Treatment of 3β-Methylcholest-5-en-3α-ol (II) with Acetic Acid and Platinum

1. When alcohol II (83 mg) and 84 mg of platinum in 25 ml of acetic acid were heated at 40° in a 60 p.s.i. nitrogen atmosphere overnight, only starting material was recovered.

2. Repetition of the reaction using the recovered platinum (75 mg) from above along with 103 mg of alcohol II in 15 ml of acetic acid at 100° and atmospheric pressure for 16 h gave 96 mg of an oily residue. Chromatography on alumina (activity II–III, 8 g) and elution with hexane gave 19 mg of 3-methylcholesta-3,5-diene (VIII), m.p. 79°. Further elution with benzene gave 72 mg of starting material, m.p. 129°. Both samples were identified by comparison of their infrared spectra and by mixed melting point with authentic samples.

3-Methylcholest-2-ene (IX)

1. 3β-Methylcholestan-3α-ol (VI) (216 mg) was treated with an acetic anhydride – acetic acid – *p*-toluenesulfonic acid mixture as described by Turner (11) and 207 mg of crystalline 3-methylcholest-2-ene (IX), m.p. 82°, was obtained. The infrared spectrum showed no hydroxyl or carbonyl bands. Crystallization from ether–methanol raised the m.p. to 84–85°, $[\alpha]_D$ 71.6° (*c* 1.8), δ 1.63 p.p.m. (3H, singlet, C=C—CH_3), 5.27 p.p.m. (1H, poorly resolved doublet, C=CH—CH_2).

Anal. Calcd. for $C_{28}H_{48}$: C, 87.42; H, 12.58. Found: C, 87.51; H, 12.39.

2. When alcohol VII (107 mg) was treated under the same conditions, 100 mg of olefin IX, m.p. 84–85°, was obtained. There was no depression in melting point upon admixture of 3-methylcholest-2-ene (IX) obtained above.

3. 3α-Methylcholestan-3β-ol (VII) (141 mg) was heated under reflux overnight with 207 mg of sodium hydride and 5 ml of ethyl iodide in 20 ml of toluene (12). Work-up of the reaction mixture gave 114 mg of crystalline olefin IX, m.p. 78°. Recrystallization from ether–methanol raised the m.p. to 84–85°, which was not depressed upon admixture of 3-methylcholest-2-ene (IX).

Preparation and Ethanolysis of 3α-Methylcholest-5-en-3β-ol Mesylate (IIId)

To 3α-methylcholesterol (III) (169 mg) dissolved in 20 ml of pyridine at −5 °C, was added 10 ml of cold (−8°) methanesulfonyl chloride. The solution was kept at −5° for 1 h and then poured into 500 ml of absolute ethanol. The ethanol was evaporated. The oily residue was taken up in ether, washed neutral with water and then saturated sodium chloride solution, and evaporated. The oily residue (143 mg) was chromatographed on silica gel (10 g). Elution with hexane gave 36 mg of 3-methylcholesta-3,5-diene (VIII), m.p. 79–80°, λ_{max}^{EtOH} 232, 239, and 248 mμ (log ε 4.26, 4.29, and 4.16). Further elution gave 87 mg of 3β-ethoxy-3α-methylcholest-5-ene (III*b*), m.p. 124–125°. Recrystallization from acetone raised the m.p. to 125–126°. Ether III*b* was identified by comparison (mixed melting point and infrared and n.m.r. spectra) with a sample obtained elsewhere (3).

ACKNOWLEDGMENTS

We wish to thank Dr. C. Stammer of these laboratories for taking the n.m.r. spectra.

REFERENCES

1. S. NISHIMURA and K. MORI. Bull. Chem. Soc. Japan, **36**, 318 (1963).
2. G. JUST and F. E. SHORTLAND. Can. J. Chem. **42**, 470 (1964).
3. G. JUST and V. DI TULLIO. Can. J. Chem. In press.
4. L. F. FIESER. Org. Syn. **35**, 43 (1955).
5. W. BERGMANN and F. HIRSCHMAN. J. Org. Chem. **4**, 40 (1939).
6. (*a*) KREKLER. Thesis, University of Gottingen. pp. 6, 9, 12, 17, *et seq.*, 20, 21, as reported in ref. 6*b*.
   (*b*) F. RADT (*Editor*). Elsevier's encyclopaedia of organic chemistry. Springer-Verlag, Berlin. 1959. p. 2428s.
7. L. J. BELLAMY. The infrared spectra of complex molecules. Wiley, New York. 1959. p. 96.
8. D. H. R. BARTON, A. DA S. CAMPOS-NEVES, and R. C. COOKSON. J. Chem. Soc. 3500 (1956).
9. S. N. FARMER and A. R. KON. J. Chem. Soc. 415 (1937).
10. G. JUST and R. NAGARAJAN. Experientia, **18**, 402 (1962).
11. R. B. TURNER. J. Am. Chem. Soc. **75**, 3489 (1953).
12. J. H. FRIED and A. N. NUTILE. J. Org. Chem. **27**, 915 (1962).
13. G. R. PETTIT and D. M. PIATAK. J. Org. Chem. **27**, 2128 (1962).
14. P. E. PETERSON. J. Am. Chem. Soc. **82**, 5834 (1960).

Can. J. Chem. Downloaded from www.nrcresearchpress.com by 210.87.254.40 on 09/05/12
For personal use only.

Can. J. Chem. Downloaded from www.nrcresearchpress.com by 210.87.254.105 on 09/05/12
For personal use only.

THE STRUCTURE OF INDACONITINE[1]

ROBERT E. GILMAN[2] AND LÉO MARION
Division of Pure Chemistry, National Research Council, Ottawa, Canada
Received August 14, 1964

ABSTRACT

The alkaloid indaconitine has been converted into delphinine by replacement of a secondary hydroxyl by hydrogen and substitution of an imino-methyl for the imino-ethyl group originally present. This correlation rigorously establishes the structure of indaconitine and its absolute configuration. The product of the saponification of indaconitine, pseudaconine, is identical with the product of the saponification of pseudaconitine, and this last alkaloid has been correlated previously with aconitine. It follows that the secondary hydroxyl which was removed in the conversion of indaconitine to delphinine has the same configuration as in aconitine.

Indaconitine ($C_{34}H_{47}O_{10}N$) has been isolated from *Aconitum chasmanthum* Stapf by Dunstan and Andrews (1) nearly sixty years ago. According to these authors, it melts at 202–203°, has $[\alpha]_D$ +18.3° (EtOH), and forms crystalline salts. Further, on acid hydrolysis it yields acetic acid and benzoylpseudaconine, while on alkaline hydrolysis it produces acetic acid, benzoic acid, and pseudaconine ($C_{25}H_{41}O_8N$) which still contains the four methoxyl groups present in indaconitine. The alkamine, pseudaconine, is identical with that produced in the alkaline hydrolysis of pseudaconitine ($C_{36}H_{51}O_{12}N$). When heated above its melting point, indaconitine loses one mole of acetic acid and gives rise to pyroindaconitine ($C_{32}H_{43}O_8N$). It has also been established that indaconitine contains an imino-ethyl group (2).

In its behavior on hydrolysis and on pyrolysis indaconitine resembles aconitine I (R = Et; $R_1 = R_2 = OH$; $R_3 = C_6H_5CO$) and delphinine I (R = Me; $R_1 = R_2 = H$; $R_3 = C_6H_5CO$).

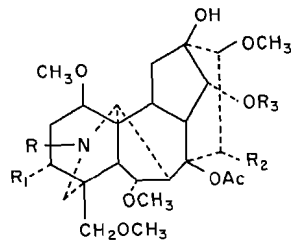

I

Since the empirical formula of indaconitine differs from that of aconitine only in containing one oxygen less, it has been assumed as a working hypothesis that indaconitine possessed the same carbon–nitrogen skeleton as aconitine (3, 4) and that it lacked one of the three hydroxyls present in the latter. The first step in the investigation, which has been the subject of a preliminary communication (5), was to determine which of the hydroxyls present in aconitine was absent in indaconitine.

[1]*Issued as N.R.C. No. 8140.*
[2]*National Research Council of Canada Postdoctoral Fellow.*

Aconitine is known to be oxidized by chromic oxide to the ketone, aconitinone (partial formula II), which readily loses the elements of methanol to form the $\alpha\beta$-unsaturated

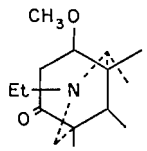

II

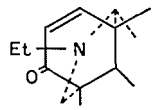

III

ketone, aconitoline III (6). Indaconitine has been found to undergo a similar oxidation with the formation of indaconitoline ($C_{33}H_{45}O_9N$), which is an $\alpha\beta$-unsaturated six-membered cyclic ketone as suggested by an absorption band at 1 675 cm^{-1} (CO) in its infrared spectrum and one at 710 cm^{-1} indicative of a double bond. Hence, like aconitine, indaconitine seems to contain a secondary hydroxyl group at R_1.

In the pyrolysis of aconitine (in which R_2 = OH) the acetoxy group is eliminated with a neighboring hydrogen, and there results the formation of an enol that tautomerizes to a ketone (7). On the other hand, in the pyrolysis of delphinine (in which R_2 = H) a similar elimination takes place resulting in the formation of an olefinic bond (8, 9). Pyroindaconitine, the product of the pyrolysis of indaconitine, was transesterified to pyropseudaconine, which showed no carbonyl absorption in the infrared but did show an absorption band at 1 620 cm^{-1} indicative of a double bond. It has been shown previously (10) that the double bond in pyropseudaconine can be isomerized and can be hydrogenated just like the double bond in pyrodelphonine. It can thus be concluded that it is the R_2 hydroxyl of aconitine that is absent in indaconitine, and that the structure of the latter must be represented by I (R = Et; R_1 = OH; R_2 = H; R_3 = C_6H_5CO). In order to prove or disprove this conclusion an attempt was made to convert indaconitine into delphinine by removal of the R_1 hydroxyl and replacement of the *N*-ethyl group by an *N*-methyl group.

Indaconitine when refluxed with thionyl chloride lost the elements of water and was converted into anhydroindaconitine, $C_{34}H_{45}O_9N$ (IV), which was purified as its perchlorate. Catalytic hydrogenation of anhydroindaconitine in absolute ethanol over platinic oxide gave rise to deoxyindaconitine (V) which, when refluxed in 3% acetic acid with

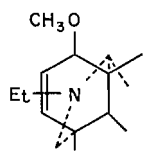

IV

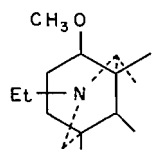

V

mercuric acetate, lost the imino-ethyl group. The amorphous secondary base, *N*-desethyl-deoxyindaconitine, thus produced had an n.m.r. spectrum that contained no ethyl group signal. That no other change had taken place in the course of the last reaction than the removal of the imino-ethyl group was ascertained by conversion of a small quantity of the product to deoxyindaconitine via the action of ethyl iodide.

Refluxing *N*-desethyl-deoxyindaconitine for 1 h with methyl iodide gave *N*-methyl-*N*-desethyl-deoxyindaconitine, m.p. 188–192°, $[\alpha]_D^{27}$ +26° (EtOH). The recorded physical

Can. J. Chem. Downloaded from www.nrcresearchpress.com by 210.87.254.105 on 09/05/12
For personal use only.

constants of delphinine are $[\alpha]_D^{25}$ +25° (EtOH) and m.p. 198–200°. The melting point was not altered by mixture of the product with an authentic sample of delphinine. The behavior of the product on a chromatoplate was identical with that of delphinine, and a mixture of the two gave only one spot. The infrared absorption spectra of both were superimposable, and the X-ray powder patterns were identical.

The conversion of indaconitine into delphinine confirms the correctness of the assumed structure of indaconitine I (R = Et; R_1 = OH; R_2 = H; R_3 = C_6H_5CO). Since the reactions involved in the conversion do not disturb the asymmetric centers of the molecule except for the removal of the R_1 hydroxyl, the stereochemical arrangement present in delphinine must also be present in indaconitine. Furthermore, since pseudaconitine has been correlated with aconitine (10), and the hydrolytic alkamine derived from indaconitine is identical with that derived from pseudaconitine, it follows that the stereochemistry of the R_1 hydroxyl of indaconitine is the same as that of the R_1 hydroxyl of aconitine.

Consequently, the conversion of indaconitine into delphinine not only proves the structure of indaconitine, but also establishes its absolute configuration to be the same as that of aconitine and delphinine. The relative positions and the configurations of the two ester groups in indaconitine which are derived from the correlation are also confirmed by the n.m.r. characteristics of the alkaloid (cf. ref. 11).

EXPERIMENTAL

In all column chromatographic separations, Woelm neutral alumina was used. Melting points were determined on a Kofler hot stage. The n.m.r. spectra were obtained on a Varian A-60 instrument.

Indaconitine

The indaconitine used in this investigation was isolated from the root of *Aconitum chasmanthum* Stapf.[3] It was purified by chromatography in ether solution over grade III alumina, and eluted with benzene–chloroform (4:1). The base recovered from the second fraction of the eluate was crystallized several times from ether, from which it separated as colorless hexagonal plates, m.p. 193–195° (decomp.), $[\alpha]_D^{25}$ +19.2° (*c*, 0.78 in EtOH).

Anal. Calcd. for $C_{34}H_{47}O_{10}N$: C, 64.86; H, 7.47. Found: C, 64.63; H, 7.40%.

The n.m.r. spectrum indicates the presence of four methoxyl groups, one *O*-acetyl, and one imino-ethyl.

Indaconitoline

Indaconitine (208 mg) was dissolved in acetone (10 ml). The solution was cooled to 5° and added to a solution of chromic oxide (210 mg) in acetone (10 ml) also previously cooled to 5°. The reaction mixture was set aside at room temperature for 2 d, by which time it had formed a bulky brown deposit. The mixture was evaporated to dryness, water was added to the residue, and a stream of sulfur dioxide was bubbled through until a clear solution was obtained (15 min). The solution was made basic (pH 8) with solid potassium carbonate and repeatedly extracted with chloroform. The combined extract was washed with water, dried over sodium sulfate, and evaporated to dryness. A residual colorless glass was left which was dissolved in ether; the solution was filtered and evaporated to dryness. The ether-soluble residue was dissolved in a 1:1 benzene–hexane mixture and chromatographed on grade III alumina. The chromatogram was eluted first with 1:1 benzene–hexane, then with benzene, and finally with chloroform. The chloroform eluate yielded the bulk of the material which was further purified by large scale thin-layer chromatography on silica gel, with benzene–cyclohexane–ethylamine (4.5:4.5:1) as developing solvent. The top main band was scraped off and extracted with chloroform, and the product left after evaporation of the chloroform was crystallized from ether – petroleum ether. The colorless indaconitoline (at a slow rate of heating) melted at 208–211° (decomp.).

Anal. Calcd. for $C_{33}H_{41}O_9N$: C, 66.54; H, 6.94; N, 2.35. Found: C, 66.41; H, 6.88; N, 2.43%.

Infrared spectrum analysis: ν, 1 725 cm^{-1} (ester carbonyl), 1 675 cm^{-1} ($\alpha\beta$-unsaturated six-membered cyclic ketone), 1 225 cm^{-1} (acetyl ester), 710 cm^{-1} (C=C).

Pyroindaconitine

Indaconitine (710 mg) was introduced into a distillation bulb which was then evacuated to 5 mm and heated in an air bath at 200–205° for 4 min. Evolution of gas took place. After cooling, the residue in the bulb was dissolved in ether, chromatographed in grade IV alumina, and eluted with ether. The residue (465 mg)

[3]*Obtained through the courtesy of Mr. K. L. Handa, Regional Research Laboratory, Jammu, India, to whom we express our gratitude.*

Can. J. Chem. Downloaded from www.nrcresearchpress.com by 210.87.254.105 on 09/05/12
For personal use only.

from the ether eluate was a colorless gum that could not be induced to crystallize. In the n.m.r. the acetyl protons signal was no longer present.

Pyroindaconitine (465 mg) was dissolved in absolute ethanol (30 ml) and a few mg of sodium was added to the solution which was left at room temperature for 2.5 h. The solution was evaporated to dryness, and the residue was dissolved in water and extracted with petroleum ether to remove the ethyl benzoate. The aqueous liquor was then extracted with chloroform, the extract was evaporated to dryness, and the residue was crystallized from ether. This product partially melted at 89–90°, resolidified, and melted at 157–167° (decomp.). In admixture with an authentic sample of pyropseudaconine (12), the behavior on melting was identical. The infrared spectrum contained a band at 1 620 cm^{-1} indicative of a double bond, but contained no carbonyl absorption. Pyropseudaconine readily forms a perchlorate which crystallizes from acetone–ether as colorless clusters, m.p. 215–225° (decomp.).

Anhydroindaconitine

Indaconitine (500 mg) was dissolved in thionyl chloride (previously distilled from quinoline) (5 ml), and the solution was refluxed for 4 h. The thionyl chloride was distilled off *in vacuo* and the residue (470 mg) was dissolved in methanol. The methanolic solution was evaporated to dryness, and the residue was dissolved in water, made basic (pH 8) with sodium carbonate, and extracted with three portions of chloroform. The combined extract was washed with water, dried over sodium sulfate, and evaporated to dryness. The residue from the extract was dissolved in benzene–chloroform (2:1), chromatographed over grade III alumina, and eluted with the same solvent. Fractions of 50 ml were collected. Fractions 2 to 11 were combined and the residue left after evaporation was crystallized from chloroform. The crystalline base was converted to the perchlorate, which crystallized from methanol–ether as colorless prisms, m.p. 190–203° (decomp.), $[\alpha]_D^{27}$ +31° (*c*, 0.5 in EtOH).

Anal. Calcd. for $C_{34}H_{45}O_9N \cdot HClO_4$: C, 57.45; H, 6.53. Found: C, 57.32; H, 6.51%.

Deoxyindaconitine

Anhydroindaconitine (720 mg) recovered from the perchlorate was dissolved in 95% ethanol and hydrogenated catalytically over platinum oxide. The product, worked up as usual, was dissolved in methylene chloride, chromatographed on grade III alumina, and eluted with methylene chloride. The eluate yielded 520 mg of benzene-soluble substance which was crystallized from hexane, m.p. 175–180° (decomp.), $[\alpha]_D^{27}$ +14° (*c*, 0.6 in EtOH).

Anal. Calcd. for $C_{34}H_{47}O_9N$: C, 66.54; H, 7.72; N, 2.28. Found: C, 66.69; H, 7.55; N, 2.40%.

The perchlorate of the base, which separated from methanol–ether as large colorless crystals, decomposed at 177–183°.

Anal. Calcd. for $C_{34}H_{47}O_9N \cdot HClO_4$: C, 57.18; H, 6.77. Found: C, 56.89; H, 6.52%.

N-Desethyl-deoxyindaconitine

Deoxyindaconitine (95 mg) was dissolved in 3% acetic acid (25 ml) and the solution warmed on the steam bath. Mercuric acetate (500 mg) was added, and the solution was kept on the steam bath for 8 h and allowed to stand overnight at room temperature. The reaction mixture was filtered and the filtrate extracted with three portions of chloroform. The combined extract was washed with aqueous sodium bicarbonate and with water, dried, and evaporated to dryness. The residue (56 mg) was dissolved in benzene–hexane (1:1) and chromatographed on grade III alumina. The column was eluted first with benzene–hexane, then in succession with benzene, 10% methylene chloride in benzene, 1:1 methylene chloride – benzene, and methylene chloride. The last fraction eluted with methylene chloride yielded only a trace of product, which no longer contained starting material. The elution was then continued with chloroform, which yielded 32 mg of product. This product, which could not be induced to crystallize, showed no signal indicative of the *N*-ethyl group in the n.m.r. A sample of *N*-desethyl-deoxyindaconitine, by treatment with ethyl iodide in methanol, was converted back to deoxyindaconitine, identical with the starting material.

N-Methyl-N-desethyl-deoxyindaconitine

N-Desethyl-deoxyindaconitine (50 mg) was dissolved in ether (5 ml) and a few drops of methyl iodide were added to the solution. A white precipitate formed immediately and more methyl iodide (3 ml) was added until the precipitate had dissolved. The solution was then refluxed on the steam bath for 1 h and subsequently evaporated to dryness. It left a residue which was dissolved in hot water. The filtered solution was cooled in ice, made alkaline with sodium carbonate, and extracted with three portions of chloroform. The combined extract was washed with water, dried over sodium sulfate, and evaporated to dryness *in vacuo*. The residue (50 mg) was dissolved in benzene–*n*-hexane (1:1) and chromatographed on grade III alumina. The column was eluted first with the same solvent, then with benzene, and finally with methylene chloride, and the eluate was collected in 30 ml fractions. The benzene eluate (fractions 5–7) yielded a crystalline product (14 mg) which after crystallization from *n*-hexane started to sinter at 180° and melted at 188–192°; $[\alpha]_D^{27}$ +26° (*c*, 0.6 in EtOH).

Anal. Calcd. for $C_{33}H_{45}O_9N$: C, 66.09; H, 7.56. Found: C, 66.30; H, 7.66%.

In admixture with an authentic sample of delphinine, it sintered at 184° and melted at 188–191°. The infrared spectra of the product and of delphinine were superimposable, and the X-ray powder patterns of the two bases were identical.

Can. J. Chem. Downloaded from www.nrcresearchpress.com by 210.87.254.105 on 09/05/12
For personal use only.

ACKNOWLEDGMENTS

We acknowledge with thanks our indebtedness to Dr. M. Przybylska for the X-ray powder patterns, to Mr. M. Lesage for the n.m.r. spectra, and to Mr. H. Seguin for the microanalyses.

REFERENCES

1. W. R. DUNSTAN and A. E. ANDREWS. J. Chem. Soc. **87**, 1620 (1905).
2. R. KONOWALOWA and A. OREKHOV. Bull. Soc. Chim. France, **7**, 95 (1940).
3. K. WIESNER, M. GÖTZ, D. L. SIMMONS, L. R. FOWLER, F. W. BACHELOR, R. F. C. BROWN, and G. BÜCHI. Tetrahedron Letters, No. 2, 15 (1959).
4. M. PRZYBYLSKA and L. MARION. Can. J. Chem. **37**, 1116 (1959).
5. R. E. GILMAN and L. MARION. Tetrahedron Letters, No. 20, 923 (1962).
6. H. MAYER and L. MARION. Can. J. Chem. **37**, 856 (1959).
7. D. J. MCCALDIN and L. MARION. Can. J. Chem. **37**, 1071 (1959).
8. K. WIESNER, F. BICKELHAUPT, D. R. BABIN, and M. GÖTZ. Tetrahedron Letters, No. 3, 11 (1959).
9. W. A. JACOBS and C. F. HUEBNER. J. Biol. Chem. **170**, 209 (1947).
10. Y. TSUDA and L. MARION. Can. J. Chem. **41**, 1485 (1963).
11. Y. TSUDA and L. MARION. Can. J. Chem. **41**, 1634 (1963).
12. L. MARION and O. E. EDWARDS. J. Am. Chem. Soc. **68**, 2565 (1946).

Can. J. Chem. Downloaded from www.nrcresearchpress.com by 210.87.254.105 on 09/05/12
For personal use only.

Can. J. Chem. Downloaded from www.nrcresearchpress.com by 210.87.254.5 on 09/05/12
For personal use only.

FURTHER ALKALOIDS RELATED TO ASPIDOALBINE AND LIMASPERMINE[1]

C. FERRARI[2] AND LÉO MARION
Division of Pure Chemistry, National Research Council, Ottawa, Canada

Received July 30, 1964

ABSTRACT

The stem bark of *Aspidosperma album* (Vahl) R. Ben. is shown to contain at least eight more alkaloids than had been reported previously. The new alkaloids have been separated from the extract by a combination of countercurrent distribution and preparative scale thin-layer chromatography. Of these eight alkaloids, five have been definitely characterized and their structure determined. They are the previously known aspidolimidine, together with N-propionyl-N-deacetylaspidolimidine, N-acetyl-N-depropionyllimaspermine, N-acetyl-N-depropionylaspidoalbinol, and aspidolimidinol. The natural occurrence of the last four alkaloids had not been reported previously.

The stem bark of *Aspidosperma album* (Vahl) R. Ben. already has been reported (1, 2) to contain the alkaloids aspidoalbine ($C_{24}H_{32}O_5N_2$), its N-acetyl-N-depropionyl homologue ($C_{23}H_{30}O_5N_2$), aspidocarpine ($C_{22}H_{30}O_3N_2$), and O-demethylaspidocarpine ($C_{21}H_{28}O_3N_2$). We now wish to report the isolation from this plant of eight more alkaloids which were separated through countercurrent distribution of the basic fraction of the crude plant extract and preparative scale thin-layer chromatography. Of these, three have not yet been identified and of the remaining five, one proved to be a known alkaloid and four were new.

From the countercurrent distribution four main fractions were obtained. Although all fractions contained more than one base, a different component was predominant in each of the first three. Fraction I contained mainly aspidoalbine; fraction II, mainly N-acetyl-N-depropionylaspidoalbine and alkaloid B; fraction III, mainly alkaloid A; while fraction IV yielded alkaloids C, D, and E.

Alkaloid A was obtained easily as colorless crystals, m.p. 192–195°, $[\alpha]_D$ +245° ($CHCl_3$). For aspidolimidine I, the literature (3) gives m.p. 196–199°, $[\alpha]_D$ +239° ($CHCl_3$). The infrared and nuclear magnetic resonance (n.m.r.) spectra of the base also suggested its identity with aspidolimidine, and a direct comparison with an authentic sample[3] confirmed the identity. The melting point of a mixture of the two bases was the same as that of alkaloid A. The X-ray powder patterns were identical and the behavior of alkaloid A in thin-layer chromatography was the same as that of authentic aspidolimidine.

Alkaloids B, C, D, and E failed to crystallize, but all formed crystalline salts. Alkaloid B gave a perchlorate that analyzed correctly for $C_{23}H_{30}O_4N_2.HClO_4$. The behavior of the free alkaloid B in countercurrent distribution and in thin-layer chromatography indicated that it might be N-propionyl-N-deacetylaspidolimidine II. Its n.m.r. spectrum was the same as that of aspidolimidine, except that it contained a triplet ($\delta \sim 1.26$) and a quartet($\delta \sim 2.57$) corresponding to an N-propionyl group instead of the N-acetyl signal ($\delta \sim 2.32$) present in the latter. Alkaloid B was hydrolyzed in the usual manner (2) to remove the imino-propionyl group and subsequently acetylated.

[1]*Issued as N.R.C. No. 8168.*
[2]*National Research Council of Canada Postdoctoral Fellow. Present address: Department of Chemistry, Queen's University, Kingston, Ontario.*
[3]*Kindly supplied by Dr. B. Gilbert, Instituto de Quimica Agricola, Ministerio da Agricultura, Rio de Janeiro, Brazil.*

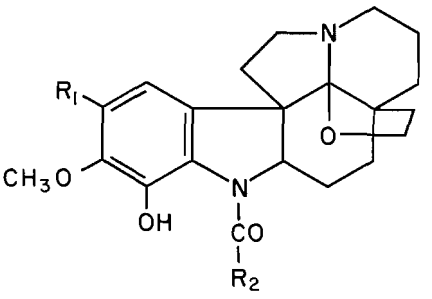

I ($R_1 = H$; $R_2 = CH_3$)
II ($R_1 = H$; $R_2 = C_2H_5$)
VI ($R_1 = CH_3O$; $R_2 = CH_3$)

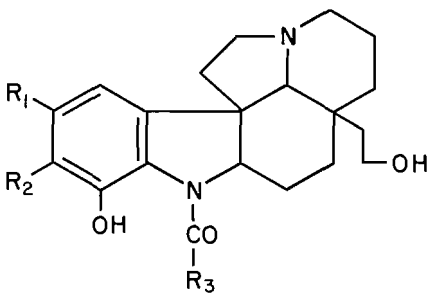

III ($R_1 = R_2 = H$; $R_3 = CH_3$)
IV ($R_1 = R_2 = CH_3O$; $R_3 = CH_3$)
V ($R_1 = H$; $R_2 = CH_3O$; $R_3 = CH_3$)

The N-acetyl-N-depropionyl alkaloid B thus produced was identical in every respect with aspidolimidine, thus confirming the structure (II) of the alkaloid.

After this work had been completed, Burnell, Medina, and Ayer in a short communication (4) reported the occurrence in *Aspidosperma fendleri* Woodson of fendlerine to which this same structure II has been assigned. Fendlerine is reported to melt at 179–181°, while alkaloid B could not be induced to crystallize. Since, however, fendlerine has been converted to aspidolimidine by the same method that we have used, it is highly probable that alkaloid B is identical with fendlerine.

The tubes 42–65 of the countercurrent distribution with pH 4 buffer (see experimental part) contained two main fractions that were separated by preparative scale thin-layer chromatography. The fraction with the higher R_f (alkaloid C) formed a crystalline perchlorate, m.p. 278–281°, $C_{21}H_{28}O_4N_2 . HClO_4$. The n.m.r. spectrum of the oily alkaloid C liberated from the perchlorate showed three aromatic protons, the typical hydrogen-bonded hydroxyl (δ 10.95), one acetyl group (δ 2.30), a triplet centered at δ 3.54 ($J = 7$ c.p.s.) indicative of —CH_2—CH_2OH, a multiplet at δ 4.09 corresponding to a C-2 hydrogen, and finally the peaks between δ 2.9–3.3 that have been considered characteristic of the aspidospermine carbon skeleton (3). No methoxyl or C-methyl signals were present. The infrared absorption spectrum showed a strongly hydrogen-bonded hydroxyl and contained the characteristic displaced and split carbonyl peak corresponding to the hydrogen-bonded amide (5). All this spectral evidence points to structure III for alkaloid C which would therefore be N-acetyl-N-depropionyllimaspermine. Comparison of the n.m.r. spectrum of the base with that published for limaspermine (6) revealed that the only difference between them was attributable to the different N-acyl groups. Replacement of the N-acetyl group in alkaloid C by an N-propionyl group via the usual procedure yielded a product that proved to be identical in every respect (melting point that of the mixture, X-ray patterns) with an authentic sample of limaspermine,[4] thus confirming structure III for alkaloid C.

The second main fraction obtained by preparative scale thin-layer chromatography of the contents of tubes 42–65 of the countercurrent distribution with pH 4 buffer—the fraction of lower R_f value—was a basic oil. In thin-layer chromatography it gave only one spot and seemed to be homogeneous, but it failed to crystallize or to form crystalline salts with either perchloric acid or picric acid. The n.m.r. spectrum of the basic oil, however, suggested that it probably consisted of a mixture of two alkaloids. It contained

[4]*Kindly sent by Dr. M. Pinar, Instituto de Quimica 'Alonso Barba', Madrid, Spain.*

Can. J. Chem. Downloaded from www.nrcresearchpress.com by 210.87.254.5 on 09/05/12
For personal use only.

two peaks of different intensities at low field (δ 10.96 and 11.36) corresponding to hydrogen-bonded aromatic hydroxyls and two peaks in the aromatic region (δ 6.32 and 6.58), also of different intensities. Since one peak in each region corresponded to less than one proton these peaks must be attributed to another alkaloid present in smaller quantity, so that the basic oil must be a mixture of two alkaloids which will be designated D and E. The larger peaks in each region (δ 11.36 and 6.32) were in a 1:1 relation suggesting partial structure (*a*). The two smaller peaks (δ 10.96 and 6.58) were in a 2:1 relation suggesting partial structure (*b*). The n.m.r. spectrum also contained a triplet at δ 3.56 (J = 7 c.p.s.) indicating the probable presence of a $-CH_2-CH_2OH$ group, together with signals attributable to methoxyl and N-acetyl groups. No C-methyl could be detected. All this evidence pointed to structures IV and V respectively for alkaloids D and E present in the mixture.

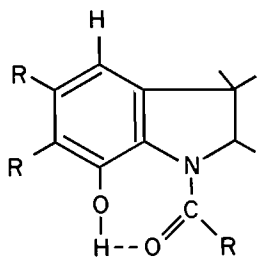

(a)

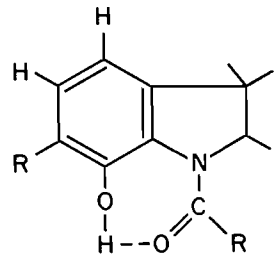

(b)

If these deductions be correct, then alkaloid D (structure IV) should be derivable from N-acetyl-N-depropionylaspidoalbine VI by reductive cleavage of its cyclic ether, and alkaloid E (structure V) should be derivable similarly from aspidolimidine I. Both N-acetyl-N-depropionylaspidoalbine VI and aspidolimidine were independently reduced with sodium borohydride. In thin-layer chromatography both products had the same R_f value as the mixture of alkaloids and the n.m.r. spectra of the products showed the correctness of the assignments previously made. It was found that synthetic N-acetyl-N-depropionylaspidoalbinol (IV) could be crystallized as its hydrochloride, while synthetic aspidolimidinol (V) formed a sparingly soluble crystalline hydrobromide. By making use of these properties it was possible to separate the mixture of alkaloids D and E into a hydrochloride and a hydrobromide that proved identical respectively with synthetic N-acetyl-N-depropionylaspidoalbinol hydrochloride and aspidolimidinol hydrobromide.

The alkaloids found and identified so far in *A. album* belong to three characteristic structures. They are the aspidospermine structure in which a C-ethyl side chain is present (aspidocarpine, O-demethylaspidocarpine), the limaspermine structure which contains a C-hydroxyethyl side chain (N-acetyl-N-depropionyllimaspermine, N-acetyl-N-depropionylaspidoalbinol, aspidolimidinol), and the aspidoalbine structure in which the side chain is involved in a cyclic ether (aspidoalbine, N-acetyl-N-depropionylaspidoalbine, aspidolimidine, N-propionyl-N-deacetylaspidolimidine).

EXPERIMENTAL

Unless otherwise specified, melting points were taken on a Kofler hot stage, and the analytical samples were dried at 100° *in vacuo* over phosphoric oxide. The n.m.r. spectra were obtained on a Varian A-60 instrument.

Can. J. Chem. Downloaded from www.nrcresearchpress.com by 210.87.254.5 on 09/05/12
For personal use only.

Separation of the Alkaloids

The basic fraction of the crude extract of *A. album* (1) was further separated into fractions containing one, two, or three main alkaloids by countercurrent distribution using chloroform as stationary phase and pH 3 buffer (citric acid – phosphate) as moving phase. After 100 transfers the main alkaloids were distributed as follows: fraction I (tubes 4–25) contained aspidoalbine; fraction II (tubes 30–50), N-acetyl-N-depropionylaspidoalbine and alkaloid B; fraction III (tubes 55–75), alkaloid A and two other components; fraction IV (tubes 76–99), mixture of several alkaloids. The fourth fraction was again subjected to countercurrent distribution, this time using pH 4 buffer; it yielded alkaloids C, D, and E.

Aspidolimidine (Alkaloid A)

Alkaloid A was obtained readily by direct crystallization from fraction III. It crystallized from methanol as colorless prisms, m.p. 192–195°, $(\alpha)_D$ +245° (*c*, 1.26 in $CHCl_3$). The literature (2) gives m.p. 196–199°, $[\alpha]_D$ +239° ($CHCl_3$) for aspidolimidine. In admixture with an authentic sample of aspidolimidine (m.p. 192–195°) obtained through the courtesy of Dr. B. Gilbert, alkaloid A melted at 191–195°. The X-ray powder patterns of the authentic sample and of alkaloid A were identical, and in thin-layer chromatography the behavior of both was the same.

N-Propionyl-N-deacetylaspidolimidine (Alkaloid B)

From the second fraction of the countercurrent distribution separation, alkaloid B was obtained by means of preparative scale thin-layer chromatography. The appropriate band was scraped off and extracted with ether. The extract was evaporated to dryness, the residue dissolved in methanol, and the solution adjusted to pH 4 by the addition of perchloric acid. Colorless crystals separated which were recrystallized from aqueous methanol, m.p. 209–211°.

Anal. Calcd. for $C_{23}H_{30}O_4N_2.HClO_4$: C, 55.35; H, 6.26; N, 5.61. Found: C, 55.51; H, 6.10; N, 5.79.

The free base liberated from the perchlorate failed to crystallize. After distillation *in vacuo*, it consisted of a colorless glass, $[\alpha]_D$ +226° (*c*, 1.08 in $CHCl_3$). The base was hydrolyzed and subsequently acetylated according to the usual procedure (1). This gave a product which after two crystallizations from methanol melted at 192–194° and, in admixture with an authentic sample of aspidolimidine,[3] at 190–195°. $[\alpha]_D$ +240° (*c*, 1.22 in $CHCl_3$). The infrared spectrum of the product was superimposable on that of aspidolimidine, and the behavior of the two bases in thin-layer chromatography was identical.

N-Acetyl-N-depropionyllimaspermine (Alkaloid C)

The fourth fraction obtained from the countercurrent distribution with pH 3 buffer as a moving phase was subjected to another countercurrent distribution, using pH 4 buffer. Tubes 42–65 collected in this second distribution contained two main components that could be separated either by preparative scale thin-layer chromatography or by chromatography on a grade III alumina column and elution with chloroform. The band with the higher R_f value was scraped off and extracted with ether. The extract yielded a base that formed a crystalline perchlorate, m.p. 278–281°, $[\alpha]_D$ +50° (*c*, 0.84 in 50% aqueous methanol).

Anal. Calcd. for $C_{21}H_{28}O_3N_2.HClO_4$: C, 55.21; H, 6.39; N, 6.13. Found (sample dried at 120°): C, 55.12; H, 6.39; N, 6.26.

The base (alkaloid C) liberated from the salt could not be induced to crystallize. After distillation *in vacuo*, it consisted of a colorless glass, $[\alpha]_D$ +127° (*c*, 0.52 in $CHCl_3$). According to its infrared absorption spectrum, alkaloid C contained an N-acetyl group. This group was hydrolyzed off and replaced by an N-propionyl group by the usual method (1). This substitution gave a product which, after two crystallizations from methanol, melted at 174–174.5°, $[\alpha]_D$ +113° (*c*, 0.54 in $CHCl_3$). For limaspermine the literature (4) reports m.p. 175–175.5° and $[\alpha]_D$ +108° ($CHCl_3$). In admixture with an authentic sample of limaspermine[4] (m.p. 172–174°) the product melted at 171–173°. The X-ray powder patterns of the two bases were different and the infrared spectra also showed some differences. Since these differences could be due to a difference in crystalline form, Dr. Pinar's sample was recrystallized from methanol. It then melted at 175–175.5° and in admixture with the product at 173–173.5°. The recrystallized sample had an infrared absorption spectrum superimposable on that of the product, and the X-ray powder patterns of the two were identical.

N-Acetyl-N-depropionylaspidoalbinol Hydrochloride

A sample of N-acetyl-N-depropionylaspidoalbine was reduced with sodium borohydride in the usual way. This cleaved the cyclic ether present in the alkaloid and gave rise to the primary alcohol, N-acetyl-N-depropionylaspidoalbinol. The product was purified by preparative scale thin-layer chromatography. It was subsequently dissolved in methanol and converted to the hydrochloride by the addition of methanolic hydrogen chloride. The solution was evaporated to dryness and the residue dissolved in a small volume of methanol. After the addition of ethyl acetate the salt crystallized out. The hydrochloride recrystallized once from methanol – ethyl acetate, melted at 267–269° (in a sealed evacuated capillary). For analysis it was dried at 120°.

Anal. Calcd. for $C_{23}H_{32}O_5N_2.HCl$: C, 60.98; H, 7.34; N, 6.18; Cl, 7.83. Found: C, 60.70; H, 7.50; N, 6,02; Cl, 7.85.

Aspidolimidinol

A sample of aspidolimidine was reduced with sodium borohydride by the usual procedure. The product was purified by preparative scale thin-layer chromatography, dissolved in methanol, and converted to

Can. J. Chem. Downloaded from www.nrcresearchpress.com by 210.87.254.5 on 09/05/12
For personal use only.

the hydrobromide by the addition of hydrobromic acid in methanol. The solution was evaporated to dryness and a few drops of methanol were added to the residue which immediately crystallized. The hydrobromide, after recrystallization from aqueous methanol, melted at 197–199°.

Anal. Calcd. for $C_{22}H_{30}O_4N_2.HBr$: C, 56.55; H, 6.70; N, 6.00; Br, 17.10. Found: C, 56.69; H, 6.82; N, 5.94; Br, 17.26.

Alkaloid E Hydrobromide

The mixture of alkaloids D and E was dissolved in methanol and the solution adjusted to pH 4 by the addition of hydrobromic acid diluted with methanol. The solution was evaporated to dryness and methanol was added to the residue. The hydrobromide crystallized immediately; it was recrystallized from aqueous methanol, m.p. 194–197°. After a second recrystallization from the same solvent, m.p. 197–200°, either alone or in admixture with aspidolimidinol hydrobromide, $[\alpha]_D$, +70° (*c*, 0.66 in H_2O). The infrared absorption spectra of the two salts were identical.

Alkaloid D Hydrochloride

The mother liquor from the initial crystallization of alkaloid E (aspidolimidinol) hydrobromide was diluted with water, and the solution neutralized with sodium bicarbonate. The liberated base was extracted with methylene chloride and the extract evaporated to dryness. The residue was dissolved in methanol and the solution adjusted to pH 4 by the cautious addition of methanolic hydrogen chloride. The acid solution was evaporated to dryness, the residue dissolved in a small volume of hot methanol, and ethyl acetate was added. This solution, on cooling, deposited the crystalline hydrochloride of alkaloid D. After two recrystallizations from methanol – ethyl acetate, m.p. (in sealed evacuated capillary) 267–269°, either alone or in admixture with N-acetyl-N-depropionylaspidoalbinol hydrochloride. The infrared absorption spectra of the hydrochloride of the product and of the synthetic N-acetyl-N-depropionylaspidoalbinol hydrochloride were superimposable. $[\alpha]_D$ +64° (*c*, 0.70 in CH_3OH).

ACKNOWLEDGMENTS

We acknowledge our indebtedness to Mr. M. Lesage for the n.m.r. spectra, to Mr. H. Séguin for the microanalyses, and to Mrs. Christine Mackey for the X-ray powder patterns. We also express our cordial thanks to Dr. B. Gilbert and to Dr. M. Pinar for the samples that they have so kindly supplied.

REFERENCES

1. C. Ferrari, S. McLean, L. Marion, and K. Palmer. Can. J. Chem. **41**, 1531 (1963).
2. C. Djerassi, L. D. Antonaccio, H. Budzikiewicz, J. M. Wilson, and B. Gilbert. Tetrahedron Letters, No. 22, 1001 (1962).
3. B. Gilbert, J. A. Brissolese, J. M. Wilson, H. Budzikiewicz, L. J. Durham, and C. Djerassi. Chem. Ind. 1949 (1962).
4. R. H. Burnell, J. D. Medina, and W. A. Ayer. Chem. Ind. 235 (1964).
5. S. McLean, K. Palmer, and L. Marion. Can. J. Chem. 1547 (1960).
6. M. Pinar, W. von Philipsborn, W. Vetter, and H. Schmid. Helv. Chim. Acta, **45**, 2260 (1962).

Can. J. Chem. Downloaded from www.nrcresearchpress.com by 210.87.254.5 on 09/05/12
For personal use only.

Can. J. Chem. Downloaded from www.nrcresearchpress.com by 210.87.254.42 on 09/05/12
For personal use only.

REACTION OF LOWER OLEFINS AND IODINE IN A LIQUID PHASE

NOVEL PREPARATION OF ALKENE IODOHYDRINS

GENE SUMRELL,[1] BERT M. WYMAN, RONALD G. HOWELL, AND MACK C. HARVEY
Research Department, El Paso Natural Gas Products Company, El Paso, Texas

Received June 29, 1964

ABSTRACT

A simplified procedure for preparing alkene iodohydrins has been developed utilizing olefin diiodide, aqueous acetone, and hydrogen peroxide. It was learned in this work that, contrary to general information in the literature, lower alkenes and iodine react quickly and essentially completely in a liquid phase at room temperature to give the diiodide.

Alkene iodohydrins are conventionally prepared either by the reaction of hydriodic acid with the appropriate epoxide (1) or by preparation of the appropriate chlorohydrin or bromohydrin followed by exchange of the halogen using sodium iodide and acetone (2). During an investigation in this laboratory involving the conversion of lower olefins to other materials of potentially greater economic value, attempts were made to develop a one-step procedure for converting these materials to their respective iodohydrins by carrying out the reaction of the olefin with iodine in a mixture of water and acetone or a variety of other water-miscible organic materials. For convenience the work was initiated with 1-pentene, since it is a liquid at room temperature. We quickly learned that in the presence of a liquid phase iodine rapidly undergoes a mildly exothermic reaction with 1-pentene at room temperature to go essentially completely to the right in the following equation:

$$CH_3CH_2CH_2CH{=}CH_2 + I_2 \rightleftarrows CH_3CH_2CH_2CHICH_2I.$$

This result is contrary to information commonly found in the literature (3, 4).[2] The pentene diiodide described above could not be prepared completely free of the olefin because of slow decomposition to iodine and 1-pentene even at room temperature and more rapidly at higher temperatures. The ratio of 1-pentene and diiodide could be readily determined by the use of nuclear magnetic resonance. When 1 mole of 1-pentene and a 0.5 mole of iodine were stirred together for a few minutes, the ratio of olefin to diiodide was 1:1. A trace of iodine remained as detected by its color, but the solution was transparent and titration with sodium thiosulfate indicated a negligible amount of free iodine present. The free iodine could be completely removed by stirring the mixture with aqueous sodium hydroxide. The decomposition was not hastened by the presence of aqueous caustic, however, and the major part of the diiodide was still present after many hours of stirring with 20% sodium hydroxide. No hydrolysis to iodohydrin or glycol occurred under these conditions.

When aqueous acetone was added to a mixture of 1-pentene and its diiodide, moderately rapid decomposition of the diiodide occurred, and within a few hours a layer composed

[1]*To whom inquiries should be directed. Present address: Southern Regional Research Laboratory, P.O. Box 19687, New Orleans, Louisiana, 70119.*

[2]*While our manuscript was in the hands of the referees, P. S. Skell and R. R. Paulis, J. Am. Chem. Soc., 86, 2956 (1964) reported the ready addition of iodine to the double bonds of the three butenes at −40° under illumination from a tungsten filament lamp. Our reactions were carried out without illumination other than the ordinary white fluorescent lighting of the laboratory, supplemented by diffuse daylight from a small window high up on one wall.*

Can. J. Chem. Downloaded from www.nrcresearchpress.com by 210.87.254.42 on 09/05/12
For personal use only.

mainly of 1-pentene and acetone had separated to the top. Some diiodide remained in the bottom aqueous acetone layer, and a large amount of iodoacetone was present. Slow hydrolysis of the diiodide occurred, and after three days of stirring at ambient temperature a 15% yield of pentene iodohydrin was present. The presence of hydrogen peroxide was found to increase the yield of the iodohydrin to 84% under the same conditions. The procedure is described in the experimental section.

The rapid reaction of iodine with propylene and 1- and 2-butene was confirmed by bubbling these gases into a slurry of iodine and water. In the case of propylene, the reaction was also carried out in numerous organic liquids (including carbon tetrachloride) and in all cases proceeded rapidly and essentially to completion, though enough free iodine always remained to color the solution. The recovery of the propylene and reuse of the iodine was investigated as a possible means of purifying propylene from small amounts of inert gases such as propane. Though the propylene could be recovered essentially quantitatively by heating the diiodide solution somewhat above 100°, after many recycles substantial amounts of isopropyl iodide began appearing in the off-gas and small amounts of iodine-containing tar became apparent in the pot, rendering the process uneconomical.

Propylene iodohydrin was prepared from the diiodide in 70% yield by the method described for pentene iodohydrin. The role of the hydrogen peroxide in these preparations is obscure, since, in the absence of acetone, no iodohydrin was detected even when stirring was carried out with hydrogen peroxide present.

EXPERIMENTAL

Boiling ranges are uncorrected. Fractionations were carried out using a 60 cm Podbielniak-type column with heated jacket and partial reflux head similar to that described by Cason and Rapoport (5). Gas chromatographic studies were done with an F & M Model 720 chromatograph using a 6 ft column packed with 20% Dow 9N9 nonionic surfactant on Chromasorb P of 30–60 mesh. The column was maintained at 200°, and helium used as the carrier. The n.m.r. spectra were obtained on a Varian A-60 spectrometer. Carbon tetrachloride was used as the solvent, and the chemical shift values are with respect to internal tetramethylsilane at 0 p.p.m.

Reaction of Iodine with 1-Pentene

When 1 mole of 1-pentene and 0.5 mole of iodine were stirred together at room temperature, the iodine dissolved within a few minutes, the temperature of the reaction mixture increased to the boiling point and 1-pentene refluxed (dry ice – acetone condenser) mildly for a time. After 1 h of stirring, the mixture was studied by gas chromatography and n.m.r. spectroscopy. The diiodide was not sufficiently stable to pass through the chromatographic column, decomposing to iodine and 1-pentene, and the latter passed through the column. The n.m.r. study revealed that the three vinyl hydrogens of 1-pentene give a series of lines from 4.8 to 6.2 p.p.m., while the three hydrogens on the first and second carbons of 1,2-diiodopentane give a series of sharp lines from 3.1 to 4.6 p.p.m. The chemical shifts and splitting of these latter lines are as would be expected for 1,2-diiodopentane, and this part of the spectrum is very similar to that shown for 1,2-dichloropropane (6). Assuming all the area under the lines at 3.1–4.6 p.p.m. as due to the three hydrogens on the first and second carbons of the diiodide and all the area under the lines at 4.8–6.2 p.p.m. as due to the three vinyl hydrogens of the olefin allowed determination of the mole ratio of these two materials in the mixture. The areas in these two parts of the n.m.r. spectrum of the reaction mixture described above were equal, indicating 50 mole % of 1-pentene and 50 mole % of 1,2-diiodopentane to be present. This mixture was colored with iodine, but titration for free iodine with sodium thiosulfate gave a negligible value. Similar results were obtained with another reaction mixture prepared using 1 mole of 1-pentene and 0.25 mole of iodine. For this mixture, the area under the lines at 4.8–6.2 p.p.m. and at 3.1–4.6 p.p.m. were in a ratio of 3:1, indicating the mixture to be composed of 75 mole % olefin and 25 mole % of the diiodide.

A number of attempts were made to bring about a chemical reaction with one or both iodines in the diiodide. The mixture composed of 50 mole % each of diiodide and 1-pentene was completely miscible with glacial acetic acid, but showed no reaction with it. When a similar mixture of the diiodide and 1-pentene was stirred with 20% aqueous sodium hydroxide, no reaction was observed except that the iodine color disappeared. The mole ratio of these components after stirring overnight was 45:55, indicating only a slow removal of iodine as the equilibrium shifted. The mixture was then warmed in the hope of speeding hydrolysis to form either the iodohydrin or glycol, but vigorous decomposition ensued, resulting in complete removal

of the iodine and formation of a colorless upper layer which gave a peak only for 1-pentene when passed through the chromatographic column.

Preparation of 1-Iodo-2-hydroxypentane

A 1 l, three-necked flask was fitted with a stirrer, thermometer, dropping funnel, and dry ice – acetone condenser, and a mixture of water (100 ml), iodine (0.5 mole), and 1-pentene (1 mole) was added to the flask. The mixture was stirred for 0.5 h to allow the diiodide to form, then was cooled to 10°. Acetone (250 ml) was added, followed by 30% hydrogen peroxide (56 ml, 0.55 mole). The cooling bath was removed and stirring continued for 3 days at ambient temperature. The mixture separated into two nearly equal phases (both somewhat discolored with iodine) when stirring was stopped. The lower phase contained most of the iodine-containing organic materials, while the upper phase consisted mainly of acetone and water. The two phases were separated and analyzed separately by gas chromatography. The data indicated the presence of 90.6 g (84.6% based on 0.5 mole of iodine) of the iodohydrin, 20.6 g (22.4%) of iodoacetone (*caution*: this material is extremely lachrymatory and is far more potent than chloroacetone), and 2.0 g (2%) of mixed iodopentanes. These various products were trapped by gas chromatography and identified by infrared and n.m.r. spectroscopy. Three iodopentanes were present, with the 2-isomer predominating. There was substantially less of the 3-isomer and a very small amount of 1-iodopentane. A portion of the organic phase was fractionally distilled, yielding a nearly colorless liquid at 68° (3 mm), n_D^{25} 1.5215.

Anal. Calcd. for $C_5H_{11}IO$: C, 28.07; H, 5.15; I, 59.31. Found: C, 28.30; H, 5.30; I, 59.40.

The above sample gave one peak when passed through the gas chromatographic column. Its n.m.r. spectrum was consistent for 1-iodo-2-hydroxypentane. A sextet centered at 3.55 p.p.m. (J = 6 c.p.s.) was assigned to the proton on the second carbon; a doublet centered at 3.25 p.p.m. (J = 6 c.p.s.) was assigned to the two protons on the first carbon; a singlet at 3.4 p.p.m. (which shifted upfield on dilution) was assigned to the hydroxy group; a mixture of a 5- and 7-line pattern centered at 1.4 p.p.m. was assigned to the four protons on the methylene groups of carbons 3 and 4; and a triplet centered at 0.95 p.p.m. (J = 7 c.p.s.) was assigned to the methyl group.

Another similar run was converted to the epoxide by the following procedure: The acetone was removed at water-pump pressure, and the residue was cooled to 0° and treated with 1 mole of 20% sodium hydroxide. The cooling bath was removed and stirring continued for 2 h as the mixture warmed to room temperature. The organic phase (31 g) was separated, and the aqueous layer extracted twice with 100 ml portions of diethyl ether. The extracts were added to the organic phase and the mixture was dried and fractionated, yielding 30.5 g (71% based on 0.5 mole of iodine) of 1,2-epoxypentane at 79–81° (665 mm), n_D^{25} 1.3930 (lit. (7) b.p. 89–90° (750 mm), n_D^{20} 1.3963).

Preparation of 1-Iodo-2-hydroxypropane

Propylene diiodide was prepared in a similar manner to that described for pentene diiodide except that propylene gas was bubbled into the iodine–water mixture until the gas was no longer absorbed (15–20 min). The reaction was mildly exothermic and the propylene was taken up quantitatively initially. Hydrogen peroxide was then added and the run carried out as described for pentene diiodide. Fractionation gave 65 g (70%) of the iodohydrin at 58–62° (9 mm), n_D^{25} 1.5340 (lit. (2) b.p. 59–63° (9 mm), n_D^{30} 1.5365).

REFERENCES

1. A. MICHAEL. Chem. Ber. **39**, 2785 (1906).
2. C. A. STEWART and C. A. VANDERWERF. J. Am. Chem. Soc. **76**, 1261 (1954).
3. L. F. FIESER and M. FIESER. Organic chemistry. 3rd ed. Reinhold Publishing Company, New York, N.Y. 1956. p. 59.
4. W. J. HICKENBOTTOM. Reactions of organic compounds. 2nd ed. Longmans, Green and Company, New York, N.Y. 1948. p. 24.
5. J. CASON and H. RAPOPORT. Laboratory text in organic chemistry. Prentice-Hall, Inc., New York, N.Y. 1950. p. 238.
6. N. S. BHACCA, L. F. JOHNSON, and J. N. SHOOLERY. NMR Spectra Catalog. National Press, Palo Alto, California. 1962. Spectrum No. 30.
7. W. D. EMMONS and A. S. PAGANO. J. Am. Chem. Soc. **77**, 90 (1955).

Can. J. Chem. Downloaded from www.nrcresearchpress.com by 210.87.254.42 on 09/05/12
For personal use only.

Can. J. Chem. Downloaded from www.nrcresearchpress.com by 210.87.254.40 on 09/05/12
For personal use only.

THE REACTIONS OF FREE RADICALS WITH NITROUS OXIDE[1]

T. N. BELL[2] AND K. O. KUTSCHKE
Division of Pure Chemistry, National Research Council, Ottawa, Canada
Received June 19, 1964

ABSTRACT

A study of the reactions of methyl, ethyl, and trifluoromethyl radicals with nitrous oxide has shown that each radical causes the formation of nitrogen at temperatures below 400°. It is believed that the oxygen abstraction reaction occurs.

$$R + N_2O \rightarrow RO + N_2.$$

A semiquantitative study of the reaction of trifluoromethyl with nitrous oxide has been made, and difficulties in studying this type of reaction quantitatively are discussed.

The interaction of free radicals with nitrous oxide is considered to be important, either as a chain transfer process in the oxidation of thermally stable molecules, such as methane (1), or as the initiation process in the oxidation of molecules which readily decompose into free radicals, such as ethane (2).

To elucidate fully the oxidation of ethane by nitrous oxide, Kenright, Robinson, and Trenwith (2) studied the reactions of ethyl and methyl radicals with nitrous oxide. They concluded that ethyl radicals produced during the pyrolysis of propionaldehyde and diethyl ether at 560° reacted with nitrous oxide to form ethoxy radicals and nitrogen. The results of similar experiments with methyl radicals from the pyrolysis of acetaldehyde gave no indication of a similar abstraction of oxygen atoms by the methyl radical.

Castellion and Noyes (3) studied the photochemical reaction between nitrous oxide and ethane at temperatures up to 105°. They concluded that ethyl radicals formed in the system do not undergo reaction with nitrous oxide at these temperatures.

Mandelcorn (4) photolyzed acetone in the presence of nitrous oxide at 360° and obtained no evidence for the formation of nitrogen in the products. He concluded that methyl radicals produced during the photolysis do not abstract oxygen.

Hydrogen atoms are produced in the ethane system through the decomposition of the ethyl radical. As a result of product analyses, Kenright, Robinson, and Trenwith concluded that in this system the hydrogen atom did not abstract oxygen. On the other hand, Melville (5) has demonstrated that the chain oxidation of hydrogen can be induced photochemically at 294°. One of the chain-propagating steps is undoubtedly

$$H + N_2O \rightarrow OH + N_2.$$

Kenright and Trenwith (6) measured the rate constant for the abstraction of oxygen from nitrous oxide by comparing the rate of formation of nitrogen to the rate of formation of ethylene in the nitrous oxide – ethane system. On the assumption that the ethylene results solely from the decomposition of the ethyl radical, the data leads to an evaluation of the rate constant for oxygen transfer by the ethyl radical compared with the rate constant for ethyl decomposition, as measured by Bywater and Steacie (7). The velocity constant for oxygen abstraction determined in this way gave $k = 10^{17} \exp -31\,000/RT$, cc mole^{-1} s^{-1}.

[1]*Issued as N.R.C. No. 8141.*
[2]*National Research Council of Canada Postdoctoral Fellow, 1963–1964. Permanent address: Department of Physical and Inorganic Chemistry, University of Adelaide, Adelaide, South Australia.*

In summarizing this previous work, we found that anomalies appear to exist and that an unusual marked difference in reactivity between the ethyl and methyl radical is apparent. To clarify this situation it seemed worthwhile to investigate the reactions of a number of free radicals with nitrous oxide.

Moreover, the very unusual A factor for oxygen abstraction by the ethyl radical would warrant a further quantitative study of the reaction,

$$R + N_2O \rightarrow RO + N_2.$$

The results obtained in this present study clearly show that methyl, ethyl, and trifluoromethyl radicals are capable of abstracting the oxygen atom from nitrous oxide at temperatures below 400°. It is considered that the earlier failure to observe this reaction of methyl radicals was due to the competing reactions which this radical could undergo under the conditions chosen in those experiments.

The photolysis of hexafluoroacetone is reasonably well understood (8) and is a convenient source of trifluoromethyl radicals. This system in the presence of nitrous oxide appeared to be ideally suited for an unambiguous quantitative study of the reaction,

$$CF_3 + N_2O \rightarrow CF_3O + N_2,$$

in comparison with the recombination step,

$$CF_3 + CF_3 \rightarrow C_2F_6.$$

In fact, the complexities of this system are such as to preclude an accurate determination of the rate constant. The present results cast some doubt on Kenright and Trenwith's value for the rate of the ethyl reaction.

EXPERIMENTAL

The source of methyl and ethyl radicals used was the pyrolysis of the corresponding mercury dialkyls, while the photolysis of hexafluoroacetone was used as the source of trifluoromethyl radicals.

The dialkyls, diethyl mercury from Eastman Kodak and dimethyl mercury from Chemical Procurement Laboratories, were thoroughly degassed before use, while the hexafluoroacetone from Allied Chemical Co. was fractionated and degassed thoroughly at −140° before use. This latter served to remove traces of fluoroform. The ketone was stored in a blackened bulb and kept at liquid nitrogen temperature.

The pyrolysis experiments were carried out in a silica reaction vessel (volume 156 ml). Known quantities of the reactants were condensed into a sidearm of the vessel and the vessel sealed from the storage system. The vessel was brought to temperature in a tubular furnace and the reaction initiated by rapid volatilization of the reactants from the external sidearm. After reaction, the noncondensable products were transferred via a break-seal on the reaction vessel to a gas burette, then to sample tubes for mass spectrometric and gas chromatographic analyses.

The latter employed a 3 ft column of 40/60 mesh activated charcoal at room temperature; hydrogen was used as a carrier gas at a flow rate of 72 ml/min. A Gow-Mac hot-wire detector was used as the sensing element.

Photolysis experiments were carried out in a quartz reaction vessel (volume 176 ml) fitted with plane parallel windows. This was suspended in the center of a tubular furnace in the path of a light beam from a Hanovia S-500 mercury lamp. The light beam was filtered with Corning filters, color specification 754 and 953, giving radiation in the range 2 600 – 4 000 Å. The single filter No. 754 transmitted sufficient radiation of low wavelength to cause decomposition of the nitrous oxide. The lamp was manually controlled and monitored with an R.C.A. 935 photocell in conjunction with a Keithley electrometer.

Temperature measurement was through chromel–alumel thermocouples taped to the cell walls.

The reaction vessel was connected directly through metal valves, Hoke 413, to the storage and analytical systems, the latter consisting of cold traps and a combined gas burette sampling system. Pressure measurements were made using a Pyrex spiral gauge as a null-point instrument.

In operation each reactant was admitted separately to the reaction vessel; the mixture was frozen into a small appendage protruding through the furnace and then pumped on for several minutes. After warming, mixing was allowed to occur for 55 min, in certain cases for 20 min.

Analysis of the noncondensable products was done using either a 40/60 mesh activated charcoal column (length 3 ft) at room temperature (helium carrier gas flow rate 50 ml/min) or a 30/60 mesh molecular

Can. J. Chem. Downloaded from www.nrcresearchpress.com by 210.87.254.40 on 09/05/12
For personal use only.

sieve, Linde 5A, column (length 18 in.) at room temperature (helium carrier gas flow rate 46 ml/min). The latter column was used only when checks for molecular oxygen were being made among the noncondensable products. In all cases these proved negative.

Analysis of the condensable products for hexafluoroethane from the hexafluoroacetone – nitrous oxide system proved troublesome because of the large excess of nitrous oxide; in general, the quantities involved were of the order: C_2F_6, 1 μmole; N_2O, 1 600 μmole. Conventional Ward Still separations proved impossible because of the similarity of the boiling points (N_2O −88°; C_2F_6 −78°).

Analysis by mass spectrometric means was attempted. The total condensable sample was scrubbed with water to remove hexafluoroacetone and other possible products by hydrate formation, followed by fractionation at −130°. To the volatile fraction was added a known amount of xenon (approximately 1 μmole) to act as an internal standard. The swamping effect of the large excess of nitrous oxide was too great to yield, even at the highest permissible input pressures, quantitatively measurable peaks at mass 69 and 132.

The infrared method (9) seemed possible and a spectrum of the volatile fraction after water scrubbing was recorded. Excellent C—F absorption bands were observed and this method gave indication of promise. Eventually the method described below was developed and used.

The analytical technique finally adopted involved "double gas chromatography". Here the total condensable sample including unreacted ketone, approximate volume 40 ml, was condensed into a U trap (volume 50 ml) through a sidearm, which was then sealed off; the vertical limbs of the U were fitted with break-seals. A bypass connected the limbs exterior to the break-seals.

One limb of the trap was connected to a helium carrier gas supply, the other to a 2 ft 6 in. column of molecular sieve, Linde 5A, mesh 40/60. The output from the column was sealed to a collecting U tube which was packed with glass wool and had a chromatographic sampling tube connected to it. The whole assemblage could be evacuated or opened to the atmosphere from a point after the collecting trap. No taps or valves were incorporated at any point between the sample trap and collecting trap.

In operation the whole assemblage was evacuated for several hours; the helium carrier was introduced and a flow rate of 30 ml/min was established with the collecting trap cooled in liquid nitrogen. The bypass connecting the limbs of the break-seal trap was sealed off, and the break-seals crushed. In this way the whole sample was swept onto the molecular sieve column, and any condensable effluent from the column collected for a period of 6 min. Periods of less than 6 min resulted in some of the hexafluoroethane being retained on the column.

After collection, the arm of the collecting trap adjacent to the column was sealed off and the trap then evacuated, followed by final sealing of the trap from the pump. Transfer of the sample collected to the chromatographic sample tube was achieved by condensation into this appendage and sealing off. The final sample contained all of the hexafluoroethane together with a small amount of nitrous oxide.

This sample, now in small bulk and highly enriched in hexafluoroethane, was analyzed on the 18 in. molecular sieve column described earlier. The peaks for nitrous oxide and hexafluoroethane were well separated.

RESULTS AND DISCUSSION

(a) Qualitative Results

N_2O–$(CH_3)_2Hg$ System

In a typical experiment, dimethyl mercury (90 μmole) and nitrous oxide (2 170 μmole), mole ratio 1/24, were heated for 75 min at 386°; the estimated total pressure in the reaction vessel was 560 mm. The noncondensable products (37 μmole) contained essentially equal amounts of nitrogen and carbon monoxide, ascertained from gas chromatography. Mass spectrometric analysis yielded N_2 + CO, 8%; CH_4, 91%; H_2, 1%.

N_2O–$(C_2H_5)_2Hg$ System

In a typical experiment, diethyl mercury (36 μmole) and nitrous oxide (882 μmole), mole ratio 1/24, were heated for 75 min at 390°; the estimated total pressure in the reaction vessel was 247 mm. The noncondensable products (6.7 μmole) contained similar amounts of carbon monoxide and nitrogen as determined by gas chromatography. Mass spectrometric analysis yielded N_2 + CO, 38%; CH_4, 58%; H_2, 4%. Blank experiments showed the absence of carbon monoxide and nitrogen from the reactants, when heated separately under conditions similar to those above.

N_2O–$(CF_3)_2CO$ System

A large number of experiments in which hexafluoroacetone – nitrous oxide mixtures were photolyzed were carried out between 193 and 375°. In all cases the noncondensable

Can. J. Chem. Downloaded from www.nrcresearchpress.com by 210.87.254.40 on 09/05/12
For personal use only.

products contained nitrogen and carbon monoxide; no oxygen was detected (vapor-phase chromatography and mass spectrometry). The amount of nitrogen formed increased with increasing temperature. Data is presented below where attempts to obtain quantitative information are discussed.

(b) Discussion of Qualitative Results

In all these experiments nitrogen is obtained in the presence of a free radical, and this is most simply explained by the occurrence of reaction [1].

[1] $$R + N_2O \rightarrow RO + N_2.$$

Strong competition to [1] will be encountered through reactions [2] in the case of methyl and through [3] and [4] in the corresponding ethyl case.

[2] $$CH_3 + (CH_3)_2Hg \rightarrow CH_4 + \text{other products.}$$

[3] $$C_2H_3 + (C_2H_5)_2Hg \rightarrow C_2H_6 + \text{other products.}$$

[4] $$C_2H_5 \rightarrow C_2H_4 + H.$$

The yield of nitrogen is thus governed by the competition among these reactions for the various radicals.

The alkoxy radical produced in [1] would be expected to react further, and the additional noncondensable products formed in the mercury dialkyl system lends support to the suggestion that the alkoxy radical is indeed formed. Decomposition of the alkoxy radical will in both cases lead to formaldehyde; carbon monoxide may be expected to arise by radical attack on the formaldehyde. In this sequence of reactions hydrogen will undoubtedly be formed. The methane produced in the ethyl – nitrous oxide system could well be produced through formation of the methyl radical from reaction [5].

[5] $$C_2H_5O \rightarrow CH_3 + CH_2O.$$

The photolysis of hexafluoroacetone under the experimental conditions is adequately described by the sequence,

[6] $$(CF_3)_2CO \xrightarrow{h\nu} 2CF_3 + CO,$$

[7] $$2CF_3 \rightarrow C_2F_6,$$

and in the presence of nitrous oxide the additional step [8] may be considered to occur.

[8] $$CF_3 + N_2O \rightarrow CF_3O + N_2.$$

If [8] is the only source of nitrogen and [7] the only source of hexafluoroethane, then

$$\frac{R_{N_2}}{R_{C_2F_6}^{1/2}[N_2O]} = \frac{k_8}{k_7^{1/2}}.$$

At first sight it would appear that the trifluoromethyl system would be an ideal one to determine the rate constant for the abstraction process by measuring the nitrogen and hexafluoroethane produced. Side reactions would be expected to be small compared with the ordinary alkyl systems, and a clean reference reaction is available. Experimentally this was not found to be so.

(c) Quantitative Results ($CF_3)_2CO$–N_2O System

A series of controlled experiments in which nitrous oxide (340 mm) and hexafluoroacetone (12 mm) were photolyzed for 60 min at temperatures between 316 and 375° were carried out. A constant mixing time was allowed in each case. The noncondensable products were analyzed for nitrogen and carbon monoxide.

Can. J. Chem. Downloaded from www.nrcresearchpress.com by 210.87.254.40 on 09/05/12
For personal use only.

In two separate experiments the hexafluoroethane was measured by the method outlined above to establish the material balance relation between the nitrogen, carbon monoxide, and hexafluoroethane formed.

375° CO 1.54 μmole, N_2 0.231 μmole, C_2F_6 1.45 μmole.

297° CO 1.57 μmole, N_2 0.055 μmole, C_2F_6 1.54 μmole.

Thus it appears that, to a first approximation, the stoichiometric relation holds.

$$CO = C_2F_6 + \tfrac{1}{2}N_2.$$

Because of the difficulty in measuring the hexafluoroethane formed each time, the relation $CO - \frac{1}{2}N_2$ was applied as a measure of the hexafluoroethane.

TABLE I

Quantitative data N_2O–$(CF_3)_2CO$ system, data in chronological order (mixing time constant = 55 min)

T (°C)	Photolysis time (min)	P (mm) $(CF_3)_2CO$	P (mm) N_2O	CO (μmole)	N_2 (μmole)	$C_2F_6 = CO - \frac{1}{2}N_2$	$\frac{k_9}{k_8^{1/2}} = \frac{R_{N_2}}{R_{C_2F_6}^{1/2}}[N_2O]$ (cc mole^{-1} s^{-1} × 10^3)
375	60	11.4	340	1.54	0.231	1.42	28.8
329	60	11.4	341	1.54	0.058	1.51	6.58
353	60	11.3	340	1.44	0.10	1.39	12.2
316	60	12.1	340	1.54	0.034	1.52	3.73
318	60	12.0	341	1.46	0.033	1.44	3.71
371	60	12.0	340	1.50	0.159	1.42	19.7
360	60	12.0	340	1.49	0.104	1.44	12.6
335	60	12.0	340	1.38	0.056	1.35	6.73

The results of a series of quantitative runs are given in Table I, and an Arrhenius plot of the $k_8/k_7^{1/2}$ values are shown in Fig. 1. A least-squares evaluation of the data yields

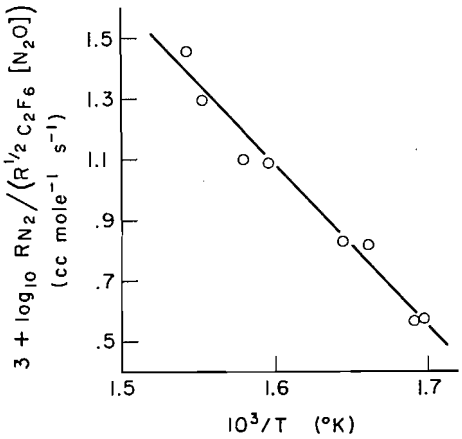

FIG. 1. Arrhenius plot of log $R_{N_2}/(R_{C_2F_6}^{1/2}[N_2O])$ against $1/T$.

$E_8 - \frac{1}{2}E_7 = 24 \pm 1$ kcal. If we use the value derived by Ayscough (10) for the recombination constant $k_7 = 2.3 \times 10^{13}$ cm^3 mole^{-1} s^{-1} and take $E_7 = 0$, k_8 may be derived. $k_8 = 1.4 \times 10^{13} \exp -24\,000/RT$ cc mole^{-1} s^{-1}. If we assume a collision diameter of 5 Å for CF_3 and N_2O species, the collision number for CF_3–N_2O collisions is 3×10^{14} cm^3 s^{-1} in concentration units appropriate to the rate constant above. Thus a steric factor of

Can. J. Chem. Downloaded from www.nrcresearchpress.com by 210.87.254.40 on 09/05/12
For personal use only.

10^{-1} is operative for the oxygen transfer process. This is comparable with a steric factor of 10^{-3} for hydrogen transfer processes involving similar radicals. In consideration of the more easily polarizable p-electrons on the oxygen atom and the strong polarizing power of the trifluoromethyl radical, longer range interactions would seem in order here.

Complicating Features

Hexafluoroacetone itself decomposes thermally under the experimental conditions; thus at 360° the carbon monoxide formed in the dark reaction is approximately 5% of that formed during the photolysis. However, this makes only a minor correction to the rates. Initially no thermal or photolytic decomposition of nitrous oxide was apparent; however, after a considerable number of runs it was noticed that a dark decomposition of nitrous oxide had intervened. Analysis of the noncondensable products showed only nitrogen to be formed. Nitrous oxide is thermally stable under the experimental conditions, and it must be concluded that the dark decomposition is caused by a heterogeneous process. Evidence that this is indeed the case arises through the fact that the extent of nitrous oxide decomposition is considerably reduced by baking the reaction vessel in oxygen at 550° for several hours. Thus at 360° it was found that the dark nitrogen contribution could be reduced by 75% after three such bakings.

The behavior observed is typical of carbon (11), which readily reduces nitrous oxide at these temperatures; alternatively, a fluorocarbon polymeric deposit on the walls of the reaction vessel could be responsible for the dark reaction involving nitrous oxide. Presumably this surface reaction arises through deposition from the thermal decomposition of hexafluoroacetone.

$$(CF_3)_2CO \xrightarrow{\Delta} CO + C \text{ or polymer.}$$

This would explain why initially the dark reaction was not detectable. Interestingly, mixtures of nitrous oxide and hexafluoroacetone gave the same amounts of nitrogen and carbon monoxide when heated together as each did separately. Thus a bimolecular reaction between the two reactants can be discounted.

The dark nitrous oxide decomposition was not noticed until a considerable number of runs had been made. Hence an unknown amount of heterogeneous nitrogen must be considered to be included in the quantitative data, and therefore the derived rate constants must be considered uncertain. It is, however, felt worthwhile to report these results in that the Arrhenius plot is reasonably consistent, and it is felt that if a large heterogeneous contribution were apparent, the nature of the reaction would be such as to destroy this consistency. Moreover the value derived for k_8 is not considered unreasonable for this type of reaction.

(d) Quantitative Discussion

A few comments are in order here with regard to previous findings.

Kenright, Robinson, and Trenwith failed to detect nitrogen in the system CH_3CHO–N_2O at 550° and concluded that methyl radicals did not undergo reaction [1]. In these experiments competition for methyl radicals is created by reaction [9].

[9] $$CH_3 + CH_3CHO \rightarrow CH_4 + CH_3CO$$

where $k_9 = 10^{12} \exp -7\,500/RT$ cc mole^{-1} s^{-1} (12*a*). In their system also the mole ratio $N_2O/CH_3CHO = 1$. Using the derived value for k_8 as a reasonable approximation to the truth, and assuming k_8 is, in value, similar to the general rate constant k_1, we have

$$\text{rate [9]/rate [1]} = 1\,700.$$

Can. J. Chem. Downloaded from www.nrcresearchpress.com by 210.87.254.40 on 09/05/12
For personal use only.

It is therefore not surprising that in this system the small quantity of nitrogen formed would not be detectable in the presence of the large amount of methane and carbon monoxide produced.

The same type of competition accounts for an early failure of Mandelcorn to detect nitrogen in the photolysis of acetone at 360° in the presence of equimolar amounts of nitrous oxide. In that system hydrogen abstraction by methyl [10] occurs some 1 600 times faster than oxygen abstraction.

[10] $$CH_3 + (CH_3)_2CO \rightarrow CH_4 + CH_2COCH_3.$$

In the system dimethyl mercury – nitrous oxide the strongest competition to oxygen abstraction is through [2] where k_2 is near $5 \times 10^{11} \exp -10\,800/RT$ cc mole^{-1} s^{-1} (12*b*). A similar calculation to that above allows the ratio, rate [2]/rate [1], to be determined. $R_{[2]}/R_{[1]} = 21$. Hence in this system reaction [1] proceeds at a measurable rate.

Similarly for the diethyl mercury – nitrous oxide system, rate [3]/rate [1] may be calculated taking $k_3 = 1.6 \times 10^{10} \exp -6\,200/RT$ cc mole^{-1} s^{-1} (12*c*). Here under the experimental conditions $R_{[3]}/R_{[1]} = 50$. Hence, as was indeed observed, nitrogen should be detectable in this system.

The only other quantitative measurement on reaction [1] is where R = ethyl (see introduction) (6). The value obtained for the velocity constant is vastly different from that obtained for trifluoromethyl in the present work. The A factor obtained is certainly abnormal; so much so that it appears impossible to account for except in terms of extremely improbable long range interactions between the ethyl radical and nitrous oxide, or that the parameters measured do not correspond exactly to reactions [1] and [11].

[11] $$C_2H_5 \rightarrow C_2H_4 + H$$

Some uncertainty is introduced into the calculated value of A_1 by the fact that A_{11} is not precisely determinable; Trotman-Dickenson (12*d*) discusses this point. The error involved, however, will not account for the large abnormality observed.

Other possible complicating factors include a contribution to the nitrogen formation through interaction of H atoms and CH_3 radicals with nitrous oxide. However the strong competition for these species through hydrogen abstraction from the ethane molecule might well be considered to make their contribution to nitrogen formation negligible. Thus the proposed overall mechanism for oxidation is not contravened by the present work.

If we note the complexities observed in the much simpler N_2O–$(CF_3)_2CO$ system, it appears probable that a heterogeneous contribution to nitrogen formation might be important in the N_2O–C_2H_6 system. The amounts of ethane present are much larger than the hexafluoroacetone used here, and at a temperature of 560° carbonation might well be expected to occur. Under these conditions, a heterogeneous contribution might well be large enough to account for the abnormalities in the observed rate constant.

In summation, it appears that the reaction between a free radical and nitrous oxide results in oxygen abstraction at temperatures below 400°; thus the reaction,

$$R + N_2O \rightarrow RO + N_2,$$

is quite general. The rate of this reaction, as measured by the nitrogen formed, is difficult to evaluate accurately owing to the existence of other reactions involving nitrogen formation.

Can. J. Chem. Downloaded from www.nrcresearchpress.com by 210.87.254.40 on 09/05/12
For personal use only.

ACKNOWLEDGMENTS

We thank Mr. R. Pilon for mass spectrometric analyses, and one of us, T. N. B., is grateful to the National Research Council for a Postdoctoral Fellowship.

REFERENCES

1. P. L. ROBINSON and E. J. SMITH. J. Chem. Soc. 3895 (1952).
2. R. KENRIGHT, P. L. ROBINSON, and A. B. TRENWITH. J. Chem. Soc. 660 (1958).
3. G. A. CASTELLION and W. A. NOYES. J. Am. Chem. Soc. **79**, 290 (1957).
4. L. MANDELCORN. Unpublished work.
5. H. W. MELVILLE. Proc. Roy. Soc. Ser. A, **146**, 737 (1934).
6. R. KENRIGHT and A. B. TRENWITH. J. Chem. Soc. 2079 (1959).
7. S. BYWATER and E. W. R. STEACIE. J. Chem. Phys. **19**, 326 (1951).
8. G. GIACOMMETTI, H. OKABE, and E. W. R. STEACIE. Proc. Roy. Soc. Ser. A, **250**, 287 (1959).
9. P. B. AYSCOUGH. Can. J. Chem. **33**, 1566 (1955).
10. P. B. AYSCOUGH. J. Chem. Phys. **24**, 944 (1956).
11. D. G. MADLEY and R. F. STRICKLAND-CONSTABLE. Trans. Faraday Soc. **49**, 1312 (1953). T. N. Bell. Unpublished work.
12. A. F. TROTMAN-DICKENSON. Gas kinetics. Butterworths. 1955. (*a*) p. 201; (*b*) p. 202; (*c*) p. 208; (*d*) p. 302.

Can. J. Chem. Downloaded from www.nrcresearchpress.com by 210.87.254.40 on 09/05/12
For personal use only.

Can. J. Chem. Downloaded from www.nrcresearchpress.com by 210.87.254.5 on 09/05/12
For personal use only.

PROTONATED CARBONYL GROUPS

IV. N,N-DIMETHYLACETAMIDE SALTS[1]

DENYS COOK
Exploratory Research Laboratory, Dow Chemical of Canada, Limited, Sarnia, Ontario

Received July 3, 1964

ABSTRACT

The infrared spectra of N,N-dimethylacetamide salts have been recorded and are consistent with protonation at the oxygen atom. ν_{OH} is between 2 095 and 3 360 cm^{-1} depending on the anion. The average value of the two components of the OH in-plane hydrogen-bending mode, δ_{OH}, is 1 253 cm^{-1} (splitting of about 147 cm^{-1} due to correlation field effects). The out-of-plane hydrogen-deformation mode occurs at 928 to 761 cm^{-1} depending on the salt. The 1 680 and 1 400 cm^{-1} bands which are present in all the salts are associated chiefly with stretching the CN and CO bonds respectively, in the OCN group, though it is likely that the vibrations are somewhat mixed.

Some salts of complex acids are of the 2 base : 1 acid variety with very strong broad absorption centered near 900 cm^{-1}, containing sharp transmission windows.

INTRODUCTION

Evidence now overwhelmingly favors the oxygen atom as the protonation site in the salts of carboxylic acid amides. The subject has recently been reviewed (1). Nuclear magnetic resonance (n.m.r.) spectroscopic results were instrumental in deciding this point, but infrared methods are becoming equally unequivocal (2). The central argument in the latter case is based on a fundamentally different absorption in the deformation mode between $\rangle N^+—H$ and $=O^+H$, the first corresponding to N protonation, the second to O protonation. Average frequencies for these modes are 1 420 and 1 265 cm^{-1} respectively (2).

The spectrum of N,N-dimethylacetamide.HCl has been examined once and several assignments were made (3). Unfortunately, only the HCl salt was described; had other salts been studied, the implausibility of some assignments would have been immediately apparent.

RESULTS AND DISCUSSION

The bands from the spectra have been collected in Table I. Bands due to the protonating H atom (and D atom) are summarized in Table II.

A comparison of the spectra of the HCl, HBr, and HI salts shows immediately that the band at 1 785 cm^{-1} in the HCl salt is not associated with an internal mode of the organic ion, but with the hydrogen bond, as it is not present in the other salts. This band is almost certainly some overtone or combination tone* and has been previously observed in salts of N,N-dicyclohexylacetamide (2*a*). A band similar to this is often present in salts of organic bases and, in some cases, can be more intense than the $X^+—H\cdots Y^-$ stretching fundamental, when the hydrogen bond is very strong. While the origin of the high intensity is not well understood, it is probable that the great breadth and rich structure of the X—H stretching vibration and this high intensity are related. Neither of these phenomena are observed in other systems with weaker hydrogen bonds, $X—H\cdots PF_6^-$, for example (2). It is also probable that other combination tones with low-lying lattice modes may be present in these salts with strong hydrogen bonds. Such salts may be expected to have the

[1]*Contribution No. 124.*
**For convenience this will be referred to as a Σ band.*

Can. J. Chem. Downloaded from www.nrcresearchpress.com by 210.87.254.5 on 09/05/12
For personal use only.

TABLE I

Absorption bands in the spectra of N,N-dimethylacetamide salts

	HCl	DCl	HBr	DBr	HI	DI	$HSbCl_6$	$DSbCl_6$	$HI.H_2O$	$DI.D_2O$	$HSbCl_6.H_2O$	$DSbCl_6.D_2O$
ν_{CH}	3046w											
			2685m									
	2260m,sh		2583m			2240w						
	2170m,b		2540m	2030s,b	2930m,b	2150m			2930w,b	2250w,b		
ν_{OH}	2095m,b		2460m,b	1972s	2720s,b	2115s	3360m,b	2485m,b	2780m,b	2115m,b	2515m,vb	2100m,b
	1955m		2288m	1960m,sh	2620m,b	1980m,sh			2470w,b	1855m,b		
				1901m	2470m,b	1888m						
				1862m	2350m,b	1855m						
Σ band	1785s	1311m	1646m	1180m	1480m,sh?	1072m,sh						
			1698m,sh		1696m,sh	1692m,sh		1695m,sh				
	1680s,sh	1670s,sh	1692s,sh	1680s,sh	1690s,sh	1680s,sh	1695s,sh	1690s,sh		1680m,sh	1690m,sh	1680m,sh
ν_{CN}	1670s	1662s	1688s	1668s	1685s	1672s	1690s	1674s	1684s	1664s	1680s	1664s
	1660s,sh	1650m,sh	1676s,sh	1660s,sh	1670m,sh	1665s,sh	1680m,sh	1663m,sh	1679s,sh	1659s,sh	1670m,sh	1647m,sh
	1650s,sh	1642m,sh	1650m,sh	1650s,sh	1665m,sh	1650m,sh	1670w,sh	1648m,sh	1648m,sh	1648m,sh	1664m,sh	1630m,sh
			1488m,sh									
δ_{CH}	1470s	1469m	1471m,sh	1470m,sh	1455m,sh	1455m,sh		1450m,sh	1460m,sh	1454m,sh	1458m,sh	1470m,sh
δ_{CH}	1454m,sh	1450m,sh	1465m	1450m	1432m	1430m	1426m	1420m	1435m	1430m	1442m	1438m
			1420m,sh						1402s,sh			
ν_{CO}	1402s	1402s	1402s	1398s	1391s	1392s	1401s	1396s	1395s	1399s	1403s	1406s
δ_{CH_3}	1370m,sh	1358m	1365m,sh	1362m	1358m,sh	1368m,sh	1380m,sh	1370m,sh	1368m,sh		1370m,sh	1368m
δ_{OH}	1352m	1050m	1342m	1048m	1310m	1048m	1300m	1045m,sh	1358m,sh	1047m	1360m,sh	1042m
				1315w					1320m			
ρ_{CH_3}	1248m	1250m	1240m	1252w	1226m	1251w	1211m	1211w	1243w	1252w	1231m	1232w
				1210w					1226m			
δ_{OH}	1188m	976m	1192m	974m	1182m	962m	1155m	922m	1184m	935m	1188m	975m
				1150w,sh					1140w,sh			
	1073w,sh	1072w,sh	1065m,sh	1067w,sh	1058w,sh	1058w,sh	1052w,sh				1055w,sh	1058w,sh
			1040m,sh									
ρ_{CH_3}	1035m	1032m,sh	1032m	1035m,sh	1031m	1032m	1035m	1035m	1030m	1030m,sh	1034m	1038m,sh
ν_{CC}	962m	960m	960m	952m	954m	938m	948m	945m	952m	952m	950m	948m
			952w,sh			955w,sh						
γ_{OH}	928m	662m	839m		761m				760m?			
		800w										
ν_{NCH_3}	752w		750w	742w	739w		734m	734w	739vw		735w,sh	742w
											718m	
											660w	660w
							H_2O bands	ν_{OH}	3288vs,b	2470s,b	3590m,b	2670m,b
								ν_{OH}	3210m,sh	2350m,b	3525m,b	2575m,b
								δ_{OH}	1630m,sh	1180w	1590m	1180m

TABLE II

OH and OD stretching and deformation bands in spectra of N,N-dimethylacetamide salts

	ν_{OH}	δ_{OH}	δ_{OH}	γ_{OH}	$2\gamma_{OH}$	$\sum$ band
HCl	2 095	1 352	1 188	928	1 856	1 785
DCl		1 050	976	662	1 324	1 311
Ratio		1.29	1.22	1.40	1.40	1.36
HBr	2 460	1 342	1 192	839	1 678	1 646
DBr	1 972	1 048	974			1 180
Ratio	1.25	1.28	1.22			1.39
HI	2 720	1 310	1 182	761	1 522	1 480
DI	2 115	1 048	962			1 072
Ratio	1.29	1.25	1.23			1.38
$HSbCl_6$	3 360	1 300	1 155			
$DSbCl_6$	2 485	1 045	922			
Ratio	1.35	1.24	1.25			

Average δ_{OH} 1 253 cm^{-1}: $\Delta\delta_{OH}$ 147 cm^{-1}
Average δ_{OD} 1 004 cm^{-1}: $\Delta\delta_{OD}$ 89 cm^{-1}

strongest coupling constants for vibrations involving any of the participants in the hydrogen bond and may give rise to stronger combinations and overtones than those with weak hydrogen bonds. In the sense that these bands unnecessarily complicate the vibrational spectrum, it is thought advisable to study salts with large complex anions or at least one other hydrogen halide as well as the HCl salt. Often, as is the present case, some of the salts of complex acids have a different stoichiometry than the 1:1 salts, for example 2 base : 1 acid (2*c*, 4). These are generally quite unsuited to a study of the protonated base, as they involve strong, possibly symmetrical, hydrogen bonds, which have totally different properties from those in the 1:1 salts.

X—H In-Plane Hydrogen-Deformation Modes

In the HCl salt two medium intensity bands near 1 352 and 1 188 cm^{-1} have been assigned to the in-plane hydrogen-deformation mode, δ_{OH}. These bands are not present in the deuterated salt but are replaced by two at 1 050 and 976 cm^{-1}. The ratio δ_{OH}/δ_{OD} for these two bands is 1.29 and 1.22 for the high-frequency and low-frequency pair respectively. The position of this bending mode is sufficient to exclude the possibility of N protonation, for as observed previously (2) a protonated sp^3-nitrogen atom has its deformation mode in the 1 420 cm^{-1} region.

Some difficulty was experienced in assigning the two components of the in-plane hydrogen-bending mode because of a complicating band at 1 250 cm^{-1}. This band diminishes markedly in intensity in the deuterated salt, but it is impossible to find three new bands in the deuterated salts. Its loss of intensity on deuteration may be simply because it is a shoulder of the 1 190 cm^{-1} band which does move on deuteration. This explanation receives some support from a consideration of the spectra of complexes of N,N-dimethylacetamide and Lewis acids (BCl_3 and BBr_3 (5), $HgCl_2$, $CdCl_2$, BF_3, $SbCl_5$, and BBr_3 (6)). In such complexes both the 1 350 and 1 190 cm^{-1} bands are absent (as are the bands due to ν_{OH} and γ_{OH}, of course), but the 1 250 cm^{-1} band is still present, though in a slightly shifted position, at 1 232 cm^{-1}.

The splitting of the bending mode is most plausibly explained by correlation field effects. These have been previously observed in many carbonyl compounds (2) and, in some cases, a knowledge of the crystal structure of the solid (2*b*) has permitted confirmation that the selection rules for the solid state demand such coupling. The splitting

Can. J. Chem. Downloaded from www.nrcresearchpress.com by 210.87.254.5 on 09/05/12
For personal use only.

in the present salts is the largest (147 cm^{-1}) that has been observed. From the theory underlying correlation field coupling in the unit cell (8) it results that the coupling constant is proportional to the splitting observed. Although lack of knowledge of the crystal structure of N,N-dimethylacetamide salts makes accurate calculation impossible, it seems reasonable to assume that those organic bases which give solid salts capable of forming the strongest hydrogen bonds should have the largest splitting. In this connection the available data show a rough parabolic relation between $\Delta\delta_{OH}$, the splitting, and ν_{OH} in various salts having a common anion, the largest splitting being associated with the lowest ν_{OH}. If it is assumed that ν_{OH} reflects the strength of the hydrogen bond (for the same base) then these data satisfy the assumption made above. This relation does not mean that those salts with strong hydrogen bonds *will* have large correlation field splittings. It means only that when the selection rules permit splitting, it should be large when the $X^+—H\cdots Y^-$ bond is strong.

A generalization seems to exist that stronger hydrogen bonds have lower X—H stretching frequencies and higher deformation frequencies (9). In compounds containing protonated carbonyl groups a very rough correlation between ν_{OH} and δ_{OH} exists, but the scatter is large (2). The rise in δ_{OH} associated with strengthening hydrogen bonds occurs chiefly in the HCl and HBr salts with little further movement in salts with more complex anions, even though there may still be a large shift in the stretching frequency. Table II shows a parallel behavior in the salts of N,N-dimethylacetamide in that those with the two smaller halide anions have δ_{OH} markedly higher than the other halide and the $SbCl_6^-$ salt, while a difference of over 600 cm^{-1} exists in the stretching frequency of the last two salts.

Further support for this generalization comes from an inspection of the infrared spectrum of the hydrate of the $HSbCl_6$ salt. This compound has bands at 3 590 and 3 523 cm^{-1} which are the asymmetric and symmetric OH stretching frequencies respectively of the water molecule. A deformation mode near 1 590 cm^{-1} is also observed. From these values it can be concluded that the OH groups form very weak hydrogen bonds. The other feature in the spectrum at 2 515 cm^{-1} is very broad and is assigned to the $O^+—H$ stretching vibration in the hydrogen bond $CO^+—H\cdots OH_2$. Its low frequency, compared with the anhydrous salt (3 360 cm^{-1}), arises from the much greater basicity of the water molecule than the $SbCl_6^-$ ion. The important fact about the hydrate is that since the $O^+—H\cdots OH_2$ bond has become stronger than the $O^+—H\cdots Cl_6Sb^-$ hydrogen bond in the anhydrous salt, the in-plane hydrogen-deformation mode now gives rise to the two split bands at a higher frequency, namely, 1 360 and 1 188 cm^{-1}.

X—H Out-of-Plane Hydrogen-Deformation Modes

Bands in the spectra at 928, 839, and 761 cm^{-1} are to be identified with the out-of-plane hydrogen-deformation (torsional) mode of the OH group in the HCl, HBr, and HI salts respectively. This band was not observed for the $HSbCl_6$ salt and is presumably below 650 cm^{-1}. These bands shift on deuteration but only in one case, that of the DCl salt, has it been possible to observe the torsional mode at 662 cm^{-1}. The ratio γ_{OH}/γ_{OD} is 1.40, indicating little interaction between this mode and others.

In contrast to the in-plane hydrogen-deformation mode, the out-of-plane hydrogen-deformation does show a marked dependence on the anion. A difference of over 150 cm^{-1} exists between the HCl and HI salts. Equally large variations have been observed in other amide and γ-pyridone salts, which, together with certain regularities in their position, will be reported elsewhere.

Can. J. Chem. Downloaded from www.nrcresearchpress.com by 210.87.254.5 on 09/05/12
For personal use only.

The calculated values of the first overtones of these out-of-plane deformation frequencies are at 1 856, 1 678, and 1 522 cm^{-1} (Table II) for the HCl, HBr, and HI salts respectively. Allowing for the effects of anharmonicity, these values are close to those of the Σ band discussed earlier, at 1 785 and 1 646 cm^{-1} in the HCl and HBr salts respectively. On this basis the HI salt would be expected to have a band near 1 480 cm^{-1} but, if present, it is not very pronounced. Nor could any band be found near 1 200 cm^{-1} in the $HSbCl_6$ salt which would be the first overtone of the torsional mode assumed to be near 620 cm^{-1}. The 1 155 cm^{-1} band is, however, broad and could be a doubled band. Information from the lower frequency region would be useful to solve this problem.

The intensity of the Σ bands varies rather markedly, that of the HCl salt being the greatest. It is in the HCl salt that the band comes closest to the OH stretching vibration at 2 095 cm^{-1}, and this proximity may be partly responsible for the high intensity. In salts of other bases this Σ band has been observed with greater intensity than the fundamental X—H stretching absorption. It is only in the more strongly hydrogen-bonded salts, however, that this occurs.

Vibrations Involving the Amide Skeleton

The reversal of the CN and CO stretching frequencies between the free base and the salts noted previously (2*a*) also occurs in the salts presently considered. Thus the 1 670 cm^{-1} band may be due chiefly to stretching the CN bond which now has acquired a larger bond order than in the free base and the 1 402 cm^{-1} band to the protonated carbonyl group stretching vibration. It is quite probable that some mixing of these two vibrational modes occurs as it does in the free amides (10). This idea is encouraged by comparison with values of ν_{CO} in other protonated heterocyclic carbonyl compounds where vibrational interaction seems less likely. These compounds show a fairly strong absorption near 1 500 cm^{-1} (2*b*, 2*c*, 2*d*).

Evidence derived from the infrared spectra of complexes of N,N-dimethylacetamide can also help in determining some of these assignments. In complexes of Lewis acids with compounds containing carbonyl groups, the decrease in ν_{CO} has been used frequently as a measure of the strength of the interaction (7). As the figures in Table III show, there is no

TABLE III

Bands in spectra of amide complexes

Lewis acid			
$HgCl_2$	1 591	1 409	1 264
$CdCl_2$	1 610	1 400	1 265
BF_3	1 630	1 404	1 260
$SbCl_5$	1 618	1 388	1 236
BBr_3	1 635	1 386	1 248

decrease in the 1 600 cm^{-1} band in the amide complex as the Lewis acid strength increases down the column, but rather an increase. The band at 1 400 cm^{-1} shows a small decrease down the column, but there is no correlation between the 1 600 and 1 250 cm^{-1} bands. These facts tend to confirm that the 1 600 cm^{-1} band should not be assigned to the carbonyl stretching mode, but, equally, the smallness of the shift to lower frequency in the 1 400 cm^{-1} band can only indicate that coupling exists between the CO and CN stretching modes. These assignments are different from those advanced previously (5). Other tentative assignments are indicated in Table I.

Can. J. Chem. Downloaded from www.nrcresearchpress.com by 210.87.254.5 on 09/05/12
For personal use only.

2 Base : 1 Acid Salts

Salts prepared from complex acids such as $HAsF_6$ are of the type 2 base : 1 acid, of which many examples are now known (2*c*, 4, 11–15). The spectrum of the $(C_4H_9NO)_2.HAsF_6$ salt shows the usual features associated with materials containing strong, possibly symmetrical hydrogen bonds, namely, strong, very broad absorption starting in the 1 500 cm^{-1} region reaching a maximum near 900 cm^{-1}. The characteristic transmission windows are also observed. These experimental findings are completely analogous to those described by Evans and Wright (16).

EXPERIMENTAL

Spectra

The spectra were determined under conditions described previously (2).

Materials

N,N-Dimethylacetamide was purchased from Distillation Products Industries and distilled before use. A fraction boiling at 164° and 760 mm Hg was used.

The HCl salt was prepared by saturating an ethereal solution of the amide with anhydrous HCl gas. The precipitated salt was handled in a dry box because of its hygroscopic nature; m.p. 121–2 °C.

Anal. Calcd. for $C_4H_9NO.HCl$: HCl, 29.5. Found: HCl, 29.4.

The DCl salt was prepared by exchange with a 100 fold excess of D_2O followed by removal of excess D_2O *in vacuo*.

The HBr salt precipitated when a Freon 113 solution of the amide was treated with anhydrous HBr gas. It was also handled in a dry box. m.p. 167–168 °C.

Anal. Calcd. for $C_4H_9NO.HBr$: HBr, 48.1. Found: HBr, 47.9.

The DBr salt was made by exchange with D_2O and by using DBr, both materials having identical spectra.

The HI salt was made by adding the stoichiometric amount of aqueous (57%) HI to the amide which gave the hydrate. The anhydrous salt was made by heating the hydrate *in vacuo*. m.p. 140–143° (decomp.).

Anal. Calcd. for $C_4H_9NO.HI$:HI, 59.4. Found: HI, 59.0.

Exchange with D_2O in a vacuum system gave the DI salt.

The $HSbCl_6$ salt was prepared by the method described by Klages and Zange (17); m.p. 158–161°. On exposure to atmospheric moisture it became hydrated; m.p. 104° (decomp.).

Anal. Calcd. for $C_4H_9NO.HSbCl_6.H_2O$: C, 10.90; H, 2.74; N, 3.18. Found: C, 10.86; H, 2.60; N, 3.24.

The deuterated analog was made by exchange with liquid DCl in a vacuum system. Signs of a 2:1 salt were evident, but this was not investigated further.

The HPF_6 salt crystallized about 24 h after mixing 4.03 g aqueous ($\sim$ 60%) HPF_6 and 1.56 g amide in a polyethylene vessel. The crystals were washed with methanol; m.p. 99–101°.

Anal. Calcd. for $(C_4H_9NO)_2.HPF_6$: C, 30.00; H, 5.98; N, 8.75. Found: C, 30.15; H, 6.22; N, 8.99.

Infrared (Nujol and fluorolube mull): 2 954 w, 1 658 m, 1 494 m, 1 452 m, 1 416 m, 1 378 m, 1 250 m, 1 195 m, 1 060 s, 835 vs (PF_6^-). The maximum in the very broad absorption seems to be near 900 cm^{-1}.

The $HAsF_6$ salt was made by adding 2.15 g aqueous ($\sim$ 60%) $HAsF_6$ to 0.67 g amide and allowing the water to evaporate. After about 24 h crystals of the 2:1 salt appeared; m.p. 121–122°.

Anal. Calcd. for $(C_4H_9NO)_2.HAsF_6$: C, 26.38; H, 5.26; N, 7.69. Found: C, 26.35; H, 5.22; N, 7.60.

Infrared (Nujol and fluorolube mull): 2 995 w, 2 951 m, 2 660 m, 1 503 m,sh, 1 496 m, 1 450 m, 1 418 m, 1 379 m, 1 254 m, 1 198 m, 1 062 s, 688 vs (AsF_6^-). The maximum in the broad absorption appears to be between 800 and 900 cm^{-1}.

ACKNOWLEDGMENTS

The author is indebted to Dr. J. C. Evans (The Dow Chemical Company, Midland, Michigan, U.S.A.) for discussion on the anomalous transmission in the 2:1 salts. The assistance of Mrs. R. H. Veach (Miss C. D. Anderson) in preparing some of the compounds and recording their spectra is gratefully acknowledged. Dr. L. E. Swim and his associates (The Dow Chemical Company, Midland, Michigan, U.S.A.) are thanked for the microanalyses.

REFERENCES

1. A. R. KATRITZKY and R. A. Y. JONES. Chem. Ind. London, 722 (1961).
2. D. COOK. Can. J. Chem. (*a*) **40**, 2362 (1962); (*b*) **41**, 505 (1963); (*c*) **41**, 2575 (1963); (*d*) **41**, 2794 (1963).
3. W. D. KUMLER. J. Am. Chem. Soc. **83**, 4983 (1961).

Can. J. Chem. Downloaded from www.nrcresearchpress.com by 210.87.254.5 on 09/05/12
For personal use only.

4. D. Cook. Chem. Ind. London, 607 (1963).
5. W. Gerrard, M. F. Lappert, H. Pyszora, and J. W. Wallis. J. Chem. Soc. 2144 (1960).
6. D. Cook. Unpublished results.
7. D. Cook. Can. J. Chem. **41**, 522 (1963).
8. R. S. Halford. J. Chem. Phys. **14**, 8 (1946). D. F. Hornig. J. Chem. Phys. **16**, 1063 (1948).
9. G. C. Pimentel and A. L. McClellan. The hydrogen bond. W. H. Freeman and Co., San Franscico, 1960. p. 118.
10. T. Miyazawa, T. Shimanouchi, and S. Mizushima. J. Chem. Phys. **29**, 611 (1958). I. Suzuki. Bull. Chem. Soc. Japan, **35**, 540 (1962).
11. N. Albert and R. M. Badger. J. Chem. Phys. **29**, 1193 (1958).
12. D. Hadži. J. Chem. Soc. 5128 (1962).
13. M. Szafran. Bull. Acad. Polon. Sci. Ser. Sci. Chim. **11**, 111, 169 (1963).
14. W. Takei. Ph.D. Thesis, California Institute of Technology, Pasadena, Calif. 1957.
15. H. H. Mills and J. C. Speakman. Proc. Chem. Soc. 216 (1963).
16. J. C. Evans and N. Wright. Spectrochim. Acta, **16**, 352 (1960). J. C. Evans. Spectrochim. Acta, **16**, 994 (1960); **17**, 129 (1961); **18**, 507 (1962).
17. F. Klages and E. Zange. Ann. **607**, 35 (1957).

Can. J. Chem. Downloaded from www.nrcresearchpress.com by 210.87.254.5 on 09/05/12
For personal use only.

Can. J. Chem. Downloaded from www.nrcresearchpress.com by 210.87.254.105 on 09/05/12
For personal use only.

ELECTROINITIATED POLYMERIZATION OF STYRENE

I. ELECTROLYSIS OF ALKALI METAL NITRATES IN DIMETHYLFORMAMIDE CONTAINING STYRENE MONOMER[1]

B. LIONEL FUNT AND SHARON WALKER LAURENT
Parker Chemistry Laboratory, University of Manitoba, Winnipeg, Manitoba

Received June 18, 1964

ABSTRACT

Electrolysis of alkali metal salts in dimethylformamide containing styrene monomer produced polymerization. The rate of reaction increased with increase in current and monomer concentration and varied dramatically with choice of initiating salt. The alkali metal nitrates from sodium to cesium produced polymer but lithium was ineffective. KNO_3 was the most efficient of the alkali metal salts tested.

The effects of inhibitors on the rates of polymerization together with analysis of copolymer composition established that polymerization proceeded by an anionic mechanism.

A detailed study with KNO_3 solution showed that relatively high electrical efficiencies were attained and that the number-average molecular weights ranged between 2 000 and 5 000.

Although there are now a number of reports of polymerization induced by electrolysis of solutions of monomer, most investigations have been confined to the polymerization of methyl methacrylate. Only fragmentary references to the polymerization of styrene have been made.

In 1952 Goldschmidt and Stockl (1) obtained polystyrene by electrolysis of solutions of monomer in anhydrous fatty acids containing the corresponding fatty acid salts. The major part of the product of the reaction consisted of dimer and trimer, and only 0.09 g of a "semi-colloid" of molecular weight 3 200 was obtained from the electrolysis of a solution containing 20 g of styrene. Das and Palit (2) reported a trace of polymer formed under similar conditions in propylene glycol.

A brief note by Yang, McEwen, and Kleinberg (3) reported on the initiation of styrene polymerization at a cathode. These workers electrolyzed a pyridine solution of NaI and monomer. An unstated quantity of polymer was obtained with molecular weight of 1 800. In the light of present knowledge it is probable that this was the first electrically initiated anionic polymerization. Kolthoff and Ferstandig were not successful in obtaining polystyrene with their redox systems, although acrylonitrile was polymerized with great efficiency. Failure to obtain polystyrene was also reported by Friedlander, Swann, and Marvel (4), and the field has recently been reviewed in excellent detail (5, 6, 7).

Exploratory experiments were conducted in our laboratories with the salt and solvent systems which we used for the anionic polymerization of acrylonitrile (8) and the free radical polymerization of methyl methacrylate (9). It became apparent that polystyrene can be formed by the electrolysis of anhydrous solutions in dimethylformamide if a suitable salt is employed. The present report represents an attempt to discover the effects of various parameters on the yield and configuration of the polymer formed by this method.

EXPERIMENTAL

The procedures and apparatus were based on those previously described by us.

Materials

Dimethylformamide (DMF), A.R. grade, was purified by mixing with 10% benzene previously dried

[1]*Presented at the Twelfth Canadian High Polymer Forum. Ste. Marguerite, Quebec. May 1964.*

over CaH_2. After standing 24 h the mixture was fractionally distilled, and the fraction boiling at 150–152 °C was collected over BaO, allowed to stand 24 h, and redistilled at reduced pressure (10).

Styrene monomer was passed through chromatographic alumina and then distilled at reduced pressure.

Salts were A.R. grade and were dried for 48 h before use.

Polymerizations

Electrically regulated constant current power supplies were employed. For voltages up to 40 V and currents to 100 mA the Power Designs type 4005 units were used. For high voltages and low currents to a maximum of 15 mA specially designed units from Mr. W. G. Hoyle of N.R.C. were employed. For some experiments manual adjustment of large dropping resistors powered by a 250 V d-c. regulated line proved satisfactory. In such instances the output was continually monitored by a pen recorder.

The polymerization cells were of a basic test tube type. Two platinum electrodes each of dimensions 1 in. × 1 in. and spaced 1 cm apart were sealed into a 34/45 inner joint and fitted into an outer joint test tube with a sidearm. The cells were purged with N_2 and sealed. A magnetic stirring bar agitated the solutions during electrolysis. A bank of four such cells was operated simultaneously in a constant temperature bath. One geared motor rotated a series of magnets which provided uniform, constant stirring for all cells. Samples were withdrawn with a hypodermic syringe through a serum cap fitted over the sidearm of each cell.

For kinetic analysis samples were precipitated in cold methanol, filtered, vacuum dried for 24 h, and weighed.

With all experimental runs blank experiments were performed, in which sample cells were allowed to stand for the full reaction time without passage of current. Precipitation of the contents showed that there was no detectable polymer formation in the absence of current.

Coloring of the reaction mixture during electrolysis of nitrate salts was noted previously and also occurred in this work. The characteristic color of the "living" styryl anion was not observed, and color formation is not attributed to this source.

RESULTS

With all parameters held constant except the nature of the salt, the maximum amount of polymer was formed in solutions saturated with KNO_3. The data are given in Table I together with the solubilities of salts in the system.

TABLE I

Relative yields of polystyrene with various salts at a current of 100 mA for 47 h

Salt	Solubility of salt, g/100 ml		% conversion of monomer
	In DMF	In solution	
$LiNO_3$	20		0
$NaNO_3$	16.4		0
KNO_3	1.05	0.28	33.4
$RbNO_3$	0.48	0.28	10.3
$CsNO_3$	0.48	0.15	10.2

The favored position of KNO_3 is puzzling. It is not the most soluble salt on either a molar basis or a weight basis, but its superiority to the other nitrates has been confirmed in a large number of experiments. On the other hand, all potassium salts will not give uniform polymer production at the cathode. This aspect of the polymerization mechanism deserves further investigation. Our attempts with polarographic measurements have not produced unequivocal results.

To determine the propagation mechanism, polymerizations were conducted in the presence of the free radical inhibitors *t*-butylcatechol and *p*-benzoquinone. Very high concentrations of inhibitor were used to insure that electrolytic destruction of the inhibitor would not invalidate the results. Even with 2.4% by weight of *t*-butylcatechol the degree of conversion was reduced only modestly in comparison with the uninhibited solution. The data are presented in Table II and indicate that the reaction occurs primarily by a non-radical mechanism.

Can. J. Chem. Downloaded from www.nrcresearchpress.com by 210.87.254.105 on 09/05/12
For personal use only.

TABLE II

The effect of inhibitors on the yield of polystyrene

Inhibitor	Concentration of inhibitor, %	Electrolysis time, h	Current, mA	Initial monomer concentration, %	% conversion
t-Butylcatechol	0	20	50	30	23.0
"	2.4	20	50	30	31.9
"	0	20	50	40	20.5
"	2.4	20	50	40	32.3
Benzoquinone	0	21	100	40	19
"	4.0	21	100	40	35
"	0	28	100	40	28
"	4.0	28	100	40	36.1

In an equimolar mixture of styrene and methyl methacrylate it is well known that the initial copolymer formed is approximately 50% polymethylmethacrylate in a radical copolymerization, but only 1% styrene in an anionic reaction (11).

A study of this point was made using ^{14}C-tagged monomer for ease of analysis. The data presented in Table III show that the free radical contribution is apparently confined to the first few % of polymerization, whereas at later stages the reaction is anionic. This is consistent with the inhibitor studies and may reflect some hydrogen atom initiation of the free radical reaction in the early stages.

TABLE III

The copolymerization of a mole-to-mole mixture of styrene and methyl methacrylate in a KNO_3–DMF system

Reaction time, h	% conversion	Activity of styrene monomer, counts/g min	Activity of copolymer, counts/g min	% free radical reaction
3	6.2	285 000	73 800	52.0
3	6.2	285 000	88 500	63.3
6	8.2	218 300	8 250	7.6
10	13.7	218 000	8 300	7.6
10	13.7	218 300	8 200	7.5

A systematic study was performed of the production of polymer at currents of 25, 50, and 100 mA for initial concentrations of 20, 30, and 40 volume % of monomer in dimethylformamide solutions saturated with KNO_3. The results are shown in Figs. 1 and 2 for the 30 and 40% systems.

Although the data show conclusively a dependence of polymerization rate on current and initial monomer concentration, it was not possible to assign a simple order dependence of the rate on these parameters. When the data are expressed in terms of the degree of conversion of the monomer initially present in the reaction mixture, they show an asymptotic approach to a maximum at about 50% conversion. This apparently reflects a wastage of some of the monomer in the formation of low molecular weight products which are not separated by our precipitation techniques. Hence the rate of monomer disappearance and the rate of polymer production are not equivalent in the present situation, and this fact results in a further complication in the kinetic analysis.

The molecular weights were measured on an absolute number-average basis with a Mechrolab vapor pressure instrument. The data in Table IV show no pronounced influence of the conditions of polymerization on the length of the polymer chain. The molecular weight is apparently increased by increase in monomer concentration and in temperature.

Can. J. Chem. Downloaded from www.nrcresearchpress.com by 210.87.254.105 on 09/05/12
For personal use only.

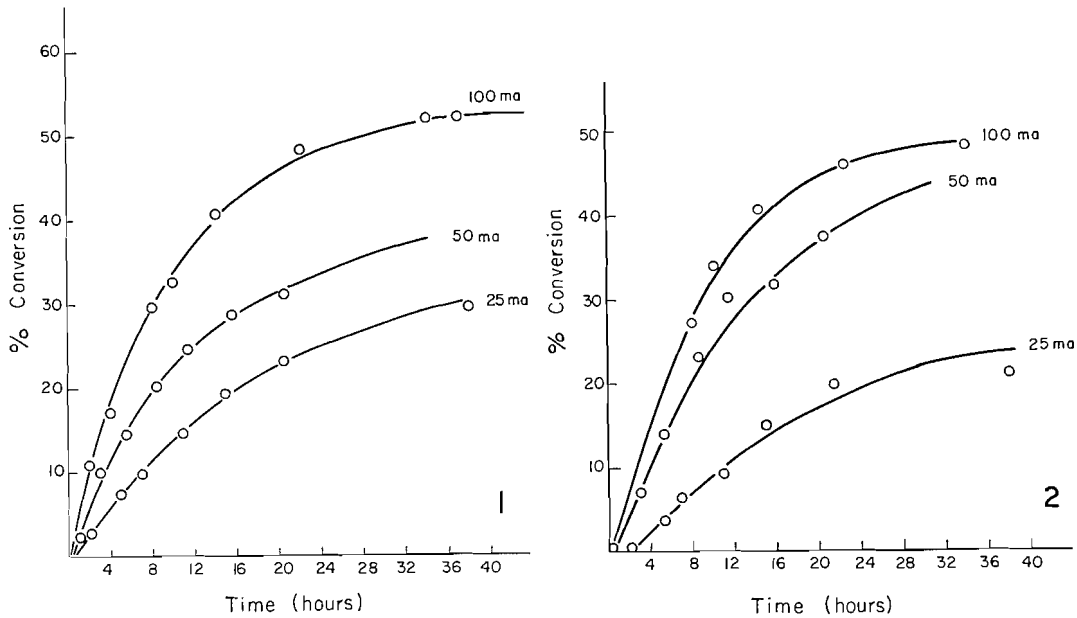

FIG. 1. Formation of polymer at inscribed currents for a 40 volume % solution of styrene in dimethylformamide containing KNO_3 as electrolyte.
FIG. 2. Formation of polymer for a 30 volume % solution of styrene in dimethylformamide containing KNO_3 as electrolyte.

However, changes in the initiating salt or the presence of free radical inhibitors exerted only a minor influence on the molecular weight.

TABLE IV
Molecular weight analysis

Styrene monomer concentration, volume %	Salt	Current, mA	Temperature, °C	Number-average molecular weight, g/mole
20	KNO_3	100	25	1 200
30	KNO_3	100	25	2 500
40	KNO_3	100	25	1 500
20	KNO_3	50	25	3 600
30	KNO_3	50	25	3 900
40	KNO_3	50	25	5 000
20	KNO_3	25	25	2 700
30	KNO_3	25	25	3 100
40	KNO_3	25	25	3 600
30	$RbNO_3$	100	25	3 700
30	$CsNO_3$	100	25	4 000
30	KNO_3	100	0	2 300
30	KNO_3	100	−30	900
30	KNO_3	100	25	2 800*
30	KNO_3	50	25	2 300†

*With benzoquinone as inhibitor.
†With *t*-butylcatechol as inhibitor.

The absolute electrical efficiency can be determined from Faraday's Laws, in terms of moles of polymer per faraday. The data are given in Table V and indicate a high electrical efficiency of approximately 20% of the theoretical maximum during the early stages of the reaction, although this percentage falls with time as the monomer becomes depleted.

Can. J. Chem. Downloaded from www.nrcresearchpress.com by 210.87.254.105 on 09/05/12
For personal use only.

TABLE V

The efficiency of electrolytic initiation in a 30 volume % solution

Current, mA	Electrolysis time, h	Molecular weight of polymer, g/mole	% efficiency
100	4.0	2 500	19.2
100	22.5	2 500	9.6
50	5.5	4 000	15.3
50	20.5	4 000	8.8
25	5.0	3 100	21.8
25	21.5	3 100	16.2

Infrared spectra were taken of samples of the electrically produced polymer. The data confirmed that the polymer thus produced was identical to that formed by conventional free radical polymerization.

It is evident that the KNO_3–dimethylformamide system represents the best medium thus far reported for the polymerization of styrene. Although the electrical efficiency is high, the system is not amenable to the type of kinetic analysis applied to our previous work on anionic polymerization of acrylonitrile (8). Nevertheless, we believe that the formation of a radical ion and its subsequent polymerization most probably represents the reaction path.

ACKNOWLEDGMENTS

The authors thank the National Research Council of Canada for a grant and the Camille and Henry Dreyfuss Foundation for financial assistance.

REFERENCES

1. S. GOLDSCHMIDT and E. STOCKL. Chem. Ber. **85**, 630 (1952).
2. M. N. DAS and A. R. PALIT. Sci. Cult. Calcutta, **16**, 34 (1950).
3. J. Y. YANG, W. E. MCEWEN, and J. KLEINBERG. J. Am. Chem. Soc. **79**, 5833 (1957).
4. H. Z. FRIEDLANDER, S. SWANN, and C. S. MARVEL. J. Electrochem. Soc. **100**, 408 (1953).
5. J. W. BREITENBACH and C. H. SRNA. Pure Appl. Chem. **4**, 245 (1962).
6. M. Y. FIOSHIN and A. P. TOMILOV. Plasticheskie Massy, **10**, 2 (1960).
7. A. P. TOMILOV and M. Y. FIOSHIN. Russ. Chem. Rev. **32**, 30 (1963).
8. B. L. FUNT and F. D. WILLIAMS. J. Polymer Sci. A, **2**, 865 (1964).
9. B. L. FUNT and K. C. YU. J. Polymer Sci. **62**, 359 (1962).
10. E. G. ROCHOW and A. B. THOMAS. J. Am. Chem. Soc. **79**, 1843 (1957).
11. C. WALLING, E. R. BRIGGS, W. CUMMINGS, and F. R. MAYO. J. Am. Chem. Soc. **72**, 48 (1950).

Can. J. Chem. Downloaded from www.nrcresearchpress.com by 210.87.254.105 on 09/05/12
For personal use only.

Can. J. Chem. Downloaded from www.nrcresearchpress.com by 210.87.254.5 on 09/05/12
For personal use only.

ELECTROINITIATED POLYMERIZATION OF STYRENE

II. KINETICS IN SOLUTIONS OF TETRAMETHYLAMMONIUM SALTS[1]

B. Lionel Funt and Suraj N. Bhadani
Parker Chemistry Laboratory, University of Manitoba, Winnipeg, Manitoba
Received June 18, 1964

ABSTRACT

The kinetics were studied of the electrically initiated polymerization of styrene in solutions of tetramethylammonium salts. The reaction was confined to the cathode and was found to proceed via an anionic mechanism. Free radical inhibitors had little influence on the yield of polymer, but the reaction was quenched by the addition of methanol.

The polymerization was investigated at six currents between 10 and 100 mA and at eight initial concentrations of monomer. Kinetic analysis of the data indicated a dependence on the first power of monomer concentration and of current.

The high electrical efficiencies and molecular weights of 15 000 to 50 000 contrast sharply with previous fruitless attempts to electroinitiate styrene polymerization. Some features of the mechanism are discussed.

Previous attempts to polymerize styrene by electrolytic means have not met with pronounced success. The work has been reviewed in an accompanying paper (1) in which the successful electroinitiated polymerization of this monomer in solutions of alkali metal nitrates was reported.

The possibility arose that the polymerization was merely a side effect due to the interaction of a deposit of the alkali metal with the monomer. Although this eventuality was eliminated by other observations, we nevertheless sought conclusive confirmation of our views. Therefore, we investigated the electrolysis of solutions of tetraalkylammonium salts. Breitenbach reported that with different anions these salts can result in either anionic or cationic polymerization (2). In these systems there is no possibility of depositing an active metal, and we found that satisfactory yields of polymer were obtained.

Further investigation proved that these systems were amenable to simple kinetic analysis, and a systematic study was undertaken of the rate of polymer formation as a function of monomer concentration, current, solvent, and salt.

EXPERIMENTAL

The experimental techniques and apparatus were similar to those described in an accompanying paper (1).

Tetramethylammonium chloride, 1.5 g, was added to 100 ml of monomer solution in dimethylformamide. This furnished a saturated solution with some excess salt present. During the course of the reaction samples were withdrawn periodically, and their polymer content was determined.

RESULTS AND DISCUSSION

Rates of Polymerization

The reaction profile as a function of current and time for a 40 volume % solution of styrene in dimethylformamide is shown in Fig. 1. A systematic increase of polymer formation with time and with impressed current is evident. Furthermore, there is no inhibition period for currents above 25 mA, and only a very small inhibition is noted for lower currents. With the small samples employed here, a correction of the volume change due to sample withdrawal did not appreciably alter the data (3) and is not presented here.

[1]*Presented at the Twelfth Canadian High Polymer Forum. Ste. Marguerite, Quebec. May 1964.*

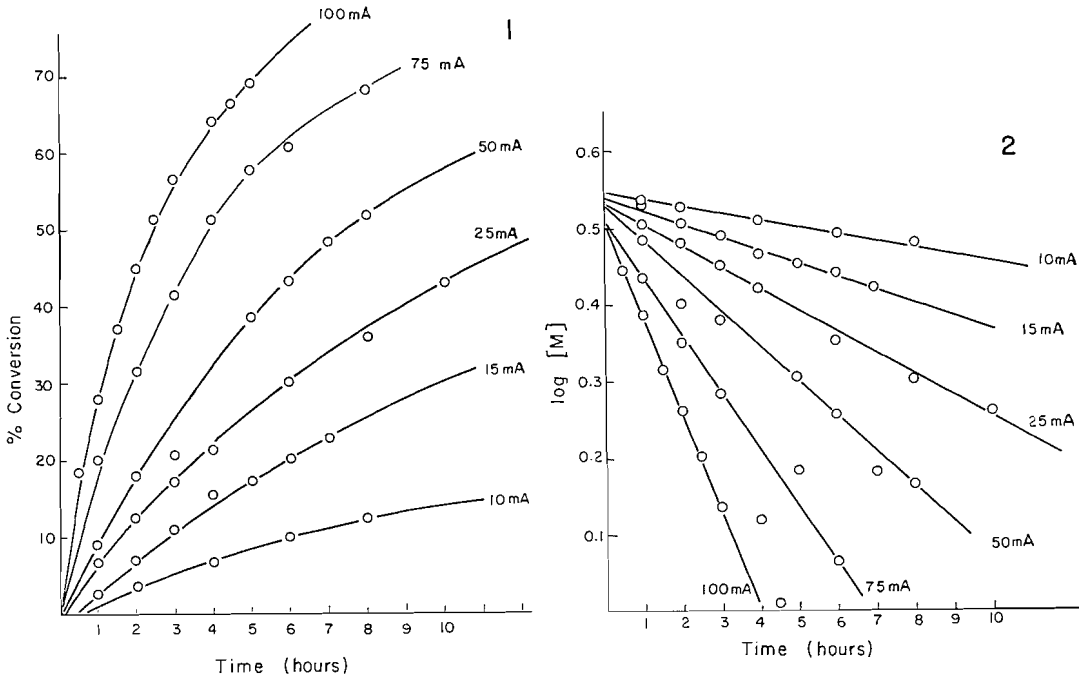

FIG. 1. Formation of polymer as a function of inscribed current and time for a 40 volume % solution of styrene in dimethylformamide containing 1.5 g of tetramethylammonium chloride.
FIG. 2. Logarithmic dependence of monomer concentration on time for a 40 volume % solution at the inscribed currents.

The results strongly suggested a first order dependence on monomer concentration. The data were expressed in terms of the logarithmic dependence of monomer concentration with time and are plotted in Fig. 2. Good linearity is observed. Similar data for 30% styrene are given in Table I.

TABLE I

Polymer formation (g/g sample) in solutions of styrene in dimethylformamide saturated with $(CH_3)_4NCl$

Time, h	Current					Time, h	Current, 100 mA
	10 mA	15 mA	25 mA	50 mA	75 mA		
40% styrene							
1	0.005	0.010	0.028	0.037	0.080	0.5	0.073
2	0.015	0.028	0.050	0.071	0.125	1.0	0.111
3	—	0.043	0.068	0.080	0.163	1.5	0.146
4	0.027	0.061	0.084	—	0.204	2.0	0.176
5	—	0.068	—	0.151	0.227	2.5	0.202
6	0.041	0.078	0.119	0.170	0.239	3.0	0.223
7	—	0.089	—	0.189	—	4.0	0.252
8	0.049	—	0.142	0.203	0.268	4.5	0.258
10	—	—	0.171	—	—	5.0	0.272
30% styrene							
1		0.008	0.021	0.040	0.053	0.5	0.059
2		0.021	0.039	0.064	0.082	1.0	0.089
3		0.035	0.060	0.084	0.111	1.5	0.107
4		0.042	0.079	0.097	0.124	2.0	0.126
5		—	—	0.109	0.127	2.5	0.140
6		0.064	0.095	0.119	0.139	3.0	0.151
7		0.070	—	0.128	0.151	4.0	0.169
8		0.074	0.110	0.137	0.154	4.5	0.173

Can. J. Chem. Downloaded from www.nrcresearchpress.com by 210.87.254.5 on 09/05/12
For personal use only.

The variation of yield of polymer with time at a constant current of 15 mA but with initial monomer concentrations of 20 to 70% by volume was investigated, and the data are shown in Fig. 3. A logarithmic dependence on time should be evidenced in a family of curves of the same slope and of differing intercepts, which correspond to the initial monomer concentration. The data are consistent with this point of view and are shown in Fig. 4. The slopes of the lines in Fig. 2 were determined. For a first-order reaction these would be proportional to the rate constants. In the present instance the slopes are dependent on current, and a plot of the slope against the impressed current was found to be linear.

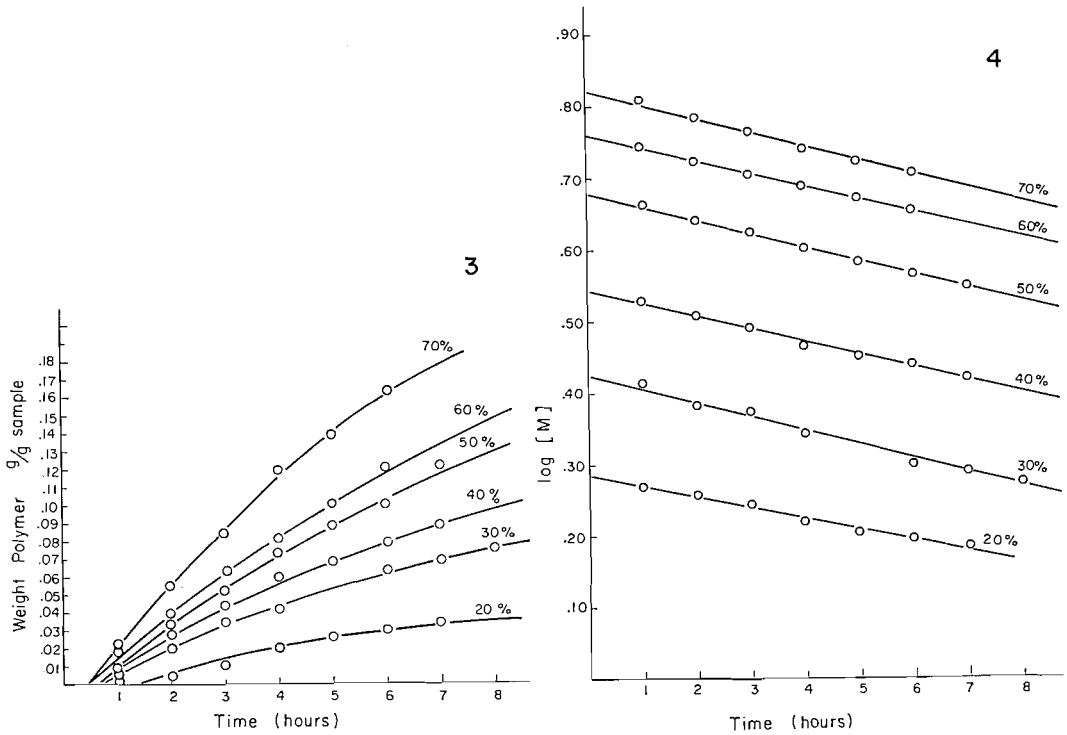

FIG. 3. Polymer formation at inscribed initial monomer concentrations with a current of 15 mA.
FIG. 4. Logarithmic dependence of polymer formation on time at the inscribed initial concentrations.

This suggested the possibility that all the data for different concentrations could be contained in a single unified expression. If the rate constant is a linear function of the impressed current, then

$$\ln (M/M_0) = - kIt,$$

where M and M_0 are instantaneous and initial monomer concentrations, I is the current, and t is the elapsed time. A plot of log $(M_0/M)/I$ versus t for all our data is shown in Fig. 5. A gratifying agreement is evident.

Locus of Polymerization

The locus of polymerization was determined to be the cathode. In an experiment with a divided cell in which the anode and cathode compartments were separated by a fritted disk, 1.29 g of polymer formed at the cathode during the first hour, but no polymer was

Can. J. Chem. Downloaded from www.nrcresearchpress.com by 210.87.254.5 on 09/05/12
For personal use only.

formed at the anode. Although polymer can be isolated from the anode compartment at later stages in the reaction, it is believed that this results from diffusion into rather than formation in this region. The same conclusion was reached for polymerizations with other anions. The data are given in Table II.

TABLE II

Polymer formation at anode and cathode compartments of a divided cell with 20 volume % of styrene in dimethylformamide and current of 15 mA

Salt	Electrolysis time, min	Wt. of cathodic polymer, g	Wt. of anodic polymer, g
$(CH_3)_4NCl$	30	0.503	<.002
$(CH_3)_4NCl$	58	1.293	<.002
$(CH_3)_4NCl$	90	1.300	.224
$(CH_3)_4NClO_4$	60	0.765	<.002
$(CH_3)_4NNO_3$	60	0.808	<.002

In this system there is little dependence of the yield of polymer or the electrical efficiency upon the anion employed. There is apparently some correlation between the yield of polymer and the solubility of the salt in the system. However, the data are too limited in range to consider this point established. This type of correlation was not found in the alkali metal systems (3).

Electrical Efficiency

The electrical efficiency, expressed in moles of monomer polymerized per faraday, increased with increase in monomer concentration to very high concentrations. In solutions of over 60 volume % of styrene, the conductance decreased to such an extent that lower currents had to be employed. The data are presented in Table III. Only at the very highest concentration of 80 volume % is there a notable decrease in electrical efficiency.

TABLE III

Yield and electrical efficiency at various initial monomer concentrations

Styrene concentration, volume %	Time of Electrolysis, h	Current, mA	Wt. polymer, g	Moles styrene polymerized per faraday
10	7	35	2.65	2.79
20	7	35	6.22	6.54
30	7	35	11.8	12.4
40	7	35	13.2	13.9
50	7	35	20.7	21.7
60	7.5	25	22.8	31.3
70	23	8	25.5	35.7
80	21	2	23.0	14.1

Molecular Weights

The molecular weights were determined on the basis of intrinsic viscosity measurements with values of $K = 1.12 \times 10^{-4}$ and $\alpha = 0.73$ (4). No notable change in molecular weight was found with variation of any of the controlled parameters. The data in Table IV show maximum possible changes from 14 000 to 19 000 molecular weight between 10 and 100 mA, but the scatter in the data indicates that this is the limit of variation. No intensive work was done with systems at low temperature, but an indication was obtained that the molecular weight increased for runs performed at 0 °C and −8 °C.

Can. J. Chem. Downloaded from www.nrcresearchpress.com by 210.87.254.5 on 09/05/12
For personal use only.

TABLE IV

Molecular weights of polymers formed at various currents and temperatures

Current, mA	Temperature, °C	Limiting viscosity number	Molecular weight
10	25	0.12	14 000
15	25	0.16	21 000
35	25	0.15	19 000
50	25	0.13	16 000
75	25	0.13	16 000
100	25	0.15	19 000
15	45	0.16	21 000
15	0	0.22	32 000
15	−8	0.29	47 000

Inhibitors

The kinetics were investigated in the presence of free radical inhibitors, *t*-butylcatechol and *p*-benzoquinone, and with methanol as a chain-stopping agent for anionic reactions. Approximately 0.4 to 0.5 weight % were used in each case, which corresponded to .036 *M* *p*-benzoquinone, 0.249 *M* *t*-butylcatechol, and 0.123 *M* methanol. The data are shown in Fig. 6. Little overall effect on the rate is exhibited by the free radical inhibitors. However, with 0.49 *M* methanol there is no sensible rate of reaction. The data strongly support the concept of anionic propagation as the dominant step in chain addition.

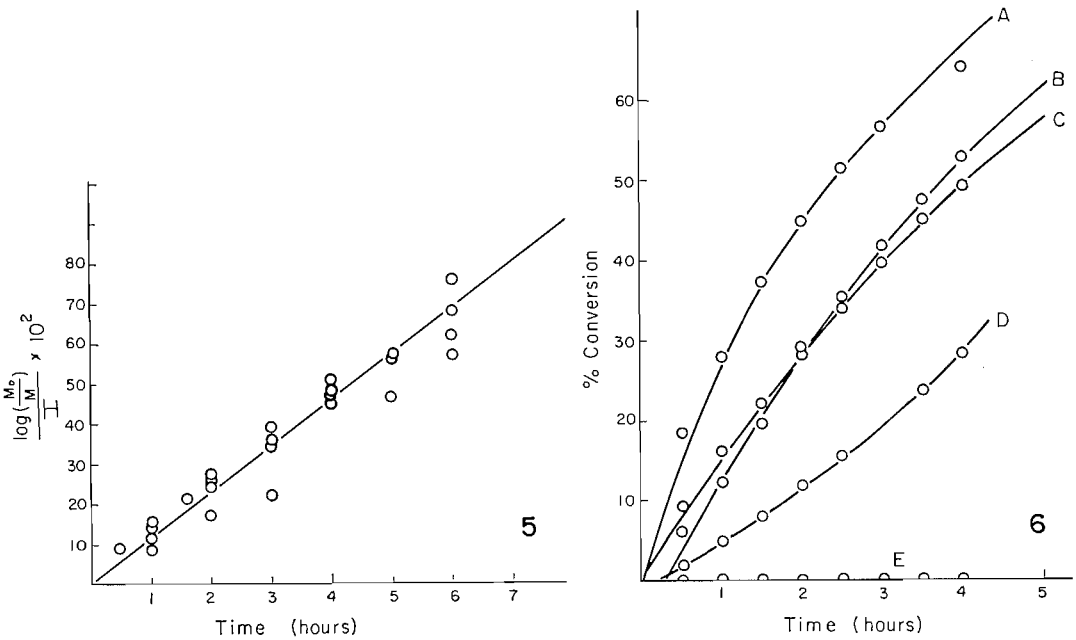

FIG. 5. Dependence of all the data on the proposed relationship with time and current.

FIG. 6. Effect of various free radical and ionic inhibitors of the rate of polymer formation at a current of 100 mA and an initial concentration of 40 volume % styrene. A, no inhibitor; B, 0.036 *M* *p*-benzoquinone; C, 0.0249 *M* *t*-butylcatechol; D, 0.123 *M* methanol; E, 0.493 *M* methanol.

Copolymerization

The propagation mechanism in electroinitiated polymerization has been determined from data on copolymerization. Thus from an equimolar mixture of styrene and methyl

Can. J. Chem. Downloaded from www.nrcresearchpress.com by 210.87.254.5 on 09/05/12
For personal use only.

methacrylate the initial polymer should be approximately 1% styrene for anionic polymerization but 50% styrene for free radical propagation. In replicate tracer experiments with ^{14}C-tagged styrene it was determined that the initial polymer contained 36% styrene. This result was confirmed by experiments at different currents. The experiments were repeated with tagged methyl methacrylate in order to eliminate any systematic error in analysis, but the data showed 64% by weight of methyl methacrylate, thus substantiating the previous results.

The bulk of the evidence is against these findings which are equivocal in the present instance. There is no other evidence to suggest a free radical contribution to the reaction. The formation of polymer solely at one electrode, the inhibitor studies, the smooth rate curves, and the constancy of molecular weight all point to an ionic mechanism and tend to eliminate a free radical mechanism. It is possible that the electrolysis is affecting the course of the copolymerization, but this, if it exists, must be considered a new effect.

The general kinetic features of the mechanism are similar to those exhibited in the acrylonitrile system which we investigated previously (3). One major difference in the present work is the smaller role of chain transfer to monomer. The lower electrical efficiency indicates a smaller degree of chain transfer than would be expected with styrene in contrast to acrylonitrile. However, the assumption, which we employed previously, that the rate-determining step is the dimerization of radical ions to form di-anions will explain the experimentally determined dependence of rate on current and on monomer concentration.

ACKNOWLEDGMENTS

The authors thank the National Research Council of Canada for a grant and the Camille and Henry Dreyfuss Foundation for financial assistance.

REFERENCES

1. B. L. Funt and S. W. Laurent. Can. J. Chem. **42**, 2728 (1964).
2. J. W. Breitenbach and C. H. Srna. Pure Appl. Chem. **4**, 245 (1962).
3. B. L. Funt and F. D. Williams. J. Polymer Sci. **A2**, 865 (1964).
4. J. H. S. Green. J. Polymer Sci. **34**, 514 (1959).

Can. J. Chem. Downloaded from www.nrcresearchpress.com by 210.87.254.5 on 09/05/12
For personal use only.

Can. J. Chem. Downloaded from www.nrcresearchpress.com by 210.87.254.6 on 09/05/12
For personal use only.

THE ALUMINIUM – ALUMINIUM BROMIDE AND ALUMINIUM – ALUMINIUM IODIDE SYSTEMS

JOMAR THONSTAD
Department of Metallurgical Engineering, University of Toronto, Toronto, Ontario
Received July 20, 1964

ABSTRACT

The Al–Al_2Br_6 and Al–Al_2I_6 binary systems have been investigated by cryoscopy and solubility measurements. Pure Al_2Br_6 melts at 98.01 ± 0.02 °C; the eutectic is found at 97.91 ± 0.02 °C and 0.017 wt. % Al; at 254 °C the solubility of aluminium increases to 0.0195 wt. %. Pure Al_2I_6 melts at 188.32 ± 0.02 °C; the eutectic is found at 188.17 ± 0.02 °C and 0.018 wt. % Al; at 320 °C the solubility increases to 0.021 wt. % Al. From the results it is concluded that dissolved aluminium is present in the melt either as Al_2^0 dimer species or as associated molecules of Al_4Br_6 and Al_4I_6.

INTRODUCTION

Aluminium bromide and aluminium iodide are white crystalline compounds that melt into colorless liquids. The melting points are given as 97.1 °C (1) to 97.5 °C (2) for the bromide and 191 °C (2) for the iodide. The boiling points are 255 and 381 °C (3) respectively.

The structure of aluminium bromide has been found (4) to consist of bromine in closest hexagonal packing, with the aluminium in adjacent tetrahedral holes. This corresponds to Al_2Br_6 molecules where aluminium is tetrehedrally surrounded by four bromine atoms, the two tetrehedra sharing an edge. A corresponding but somewhat distorted bimolecular structure is found (5) in the vapor phase of both bromide and iodide, although a certain dissociation takes place at high temperatures. Raman spectra (6) show that the bimolecular configuration is also maintained in the liquid phase for the bromide and the iodide. The covalent molecular state of the melts has been confirmed by measurements of specific conductivities (2) which were found to be extremely low.

The solubility of aluminium in aluminium iodide has been measured (7) and was found to be 0.6 mole % (Al in Al_2I_6) at 423 °C and 0.0 mole % at 380 °C. Apart from these measurements the solubilities of metals in metal halides of covalent molecular structure have not been studied. In view of this fact it was found to be of interest to investigate the solubility of aluminium in Al_2Br_6 and Al_2I_6 in some detail.

EXPERIMENTAL

Aluminium bromide and iodide were made by direct reaction of the component elements. The aluminium was of 99.998% purity (Refined ALCAN aluminium). The bromine and iodine were "Baker Analysed" reagents with the following analyses: bromine 99.8% Br, 0.01% non-volatile matter, 0.15% Cl, 0.05% I, 0.001% S0, .001% heavy metals; iodine 0.002% non-volatile matter, 0.001% Cl + Br.

Both compounds were extremely hyroscopic and had to be synthesized in evacuated pyrex tubes. The reactants were transferred to the reaction tubes in a dry-box under an inert nitrogen atmosphere.

The rates of reaction between the aluminium and the halide vapors were kept under control by maintaining the tubes at temperatures well below the boiling points of bromine and iodine respectively. The resulting compounds were distilled twice and could then be used directly for the solubility measurements. For the melting point determinations further purification was needed, as will be described subsequently.

Solubility Measurements

The distilled product was allowed to equilibrate with aluminium metal for 24 h in a furnace kept at constant temperature. At the end of this period the tube was tilted to separate the metal from the melt and was quenched in air. The quenched sample had a grayish tinge, probably because of its metal content.

The sample was then transferred to an analysis apparatus where it was dissolved in alcohol and water. To prevent the initially occurring violent reaction of the anhydrous salt with water, alcohol was added first. The excess metal content reacted with alcohol or water with the evolution of hydrogen

$$(\text{e.g. } Al + 3H_2O \rightarrow Al(OH)_3 + 3/2\,H_2),$$

which was determined by a combustion technique. To this purpose the evolved hydrogen, mixed with nitrogen as a carrier gas, was led through a liquid air trap to a heated tube containing CuO at 300 °C. The water vapor produced was absorbed in an absorption tube and weighed. The method was tested with blank runs and by using samples of different weights. The blanks gave no weight increase of the absorption tube, while the runs with samples of different weights showed a precision as given for the results.

Melting Point Determinations

The compounds were kept in capillary tubes immersed in a thermostatically heated oil bath. The temperature was measured with a Beckmann thermometer calibrated against an ERTCO precision thermometer, calibrated according to ASTM standards.

By manual control the temperature of the oil bath could easily be kept within ±0.005 °C. The melting points were determined by increasing the temperature in steps of 0.01 °C at intervals of 1–2 h, until the crystals in the capillary had melted.

The distilled samples did not melt at a definite temperature but over a range of 0.2–0.3 °C, either because of the influence of impurities or because of an excess of halogen or metal. For further purification the samples were kept within the observed solidus–liquidus range at gradually increasing temperatures, the molten phase being discarded each time. An alternative procedure was to let the compound crystallize out from the molten samples by keeping them within the corresponding liquidus–solidus range. The presence of seed crystals was necessary in this case because the melt had a strong tendency to undercooling. Undercooling was generally about 8 °C for Al_2Br_6 and about 12 °C for Al_2I_6.

Pure samples which melted completely at one definite temperature were finally obtained. Samples saturated with metal were made by equilibrating the pure samples with metal for 24 h before being transferred to the capillary. Intermediate compositions were obtained by adding the pure compound to the saturated mixtures. The samples were finally analyzed for their metal content.

Melting points could be determined with a precision better than ±0.01 °C. Thus freezing point depressions could be determined with a precision better than ±0.02 °C. Because of possible errors in the calibration of the thermometer, the accuracy of the melting points presented herein is given as ±0.02 °C.

RESULTS

From the combined results of the melting point and the solubility measurements, the liquidus curve for solutions of aluminium in aluminium bromide and aluminium iodide melts was determined.

The results for the Al–Al_2Br_6 system are given in Table I.

TABLE I

Melting points and solubilities in the Al–Al_2Br_6 system

	Temperature, °C	Composition, wt. % Al
From melting point determinations	98.01±0.02	0
	97.96±0.02	0.0084
	97.91±0.02	0.017
	105	0.017
From solubility measurements	145	0.018
	198	0.018
	241	0.019
	254	0.0195

The observed melting point for pure aluminium bromide is 98.01 ± 0.02 °C, which is 0.5–0.9 °C higher than the values given in the literature (1, 2). The results indicate a eutectic at 97.91 ± 0.02 °C and 0.017 wt. % Al. On a molar scale (atom % Al in Al_2Br_6) this composition corresponds to 0.34 mole % Al. Within the precision of the measurements, the freezing point depression of the eutectic is 0.10 ± 0.02 °C.

Can. J. Chem. Downloaded from www.nrcresearchpress.com by 210.87.254.6 on 09/05/12
For personal use only.

Five solubility determinations at 198 °C gave results between 0.0177 wt. % and 0.0188 wt. % Al. At higher temperatures the precision apparently was not so good.

The results for the Al–Al_2I_6 system are given in Table II.

TABLE II
Melting points and solubilities in the Al–Al_2I_6 system

	Temperature, °C	Composition, wt. % Al
From melting point determinations	188.32±0.02	0
	188.17±0.02	0.018
	190	0.018
From solubility measurements	202	0.0185
	265	0.020
	320	0.021

The observed melting point for pure aluminium iodide is 188.32 ± 0.02 °C, which is about 2.7 °C lower than the value given in the literature (2). The results indicate a eutectic at 188.17 ± 0.02 °C and 0.018 wt. % Al, corresponding to 0.54 mole % Al. The freezing point depression of the eutectic is 0.15 ± 0.02 °C. The precision of the solubility measurements was not as good as in the bromide system.

DISCUSSION

The measured melting points and the solubility data give the liquidus curves of the phase diagrams of the two systems, as shown in Figs. 1 and 2. The shape of the curves is similar to those available for some metal–salt systems (8), but the solubilities are in this case unusually low. This is probably due to the covalent molecular structure of the melts.

Extrapolation of the liquidus curve in Fig. 2 to 423 °C indicates that the solubility at that temperature is ~0.023 wt. % or ~0.7 mole % Al in Al_2I_6. This is in fair agreement with the measurement by Corbett and Winbush (7) giving a solublity of 0.6 mole % at 423 °C. The other measurement by these authors, indicating no solubility at 380 °C, is apparently in error.

From cryoscopic calculations some information can be obtained about the species that are present in the melt. Assuming ideal behavior and the absence of solid solubility, the simplified equation is:

$$\log N = -\frac{H_f}{R\,T_f^2}\,\Delta T,$$

where N, H_f, and T_f are the mole fraction, the heat of fusion, and the melting point respectively of the solvent (aluminium bromide or iodide), and ΔT is the corresponding freezing point depression.

The heats of fusion of the compounds are (9) 5.4 kcal/mole Al_2Br_6 and 7.6 kcal/mole Al_2I_6 respectively. The uncertainty of the data is estimated (9) to be ±0.4–0.6 kcal/mole.

Assuming different schemes of solution, corresponding values for N and ΔT can be calculated and the latter can be compared to the measured values. The following schemes are considered (X stands for Br or I, n is the number of moles).

1*a*. Free aluminium atoms:

$$Al \rightarrow Al^0$$

$$N_{Al_2X_6} = \frac{n_{Al_2X_6}}{n_{Al_2X_6} + n_{Al}}.$$

Can. J. Chem. Downloaded from www.nrcresearchpress.com by 210.87.254.6 on 09/05/12
For personal use only.

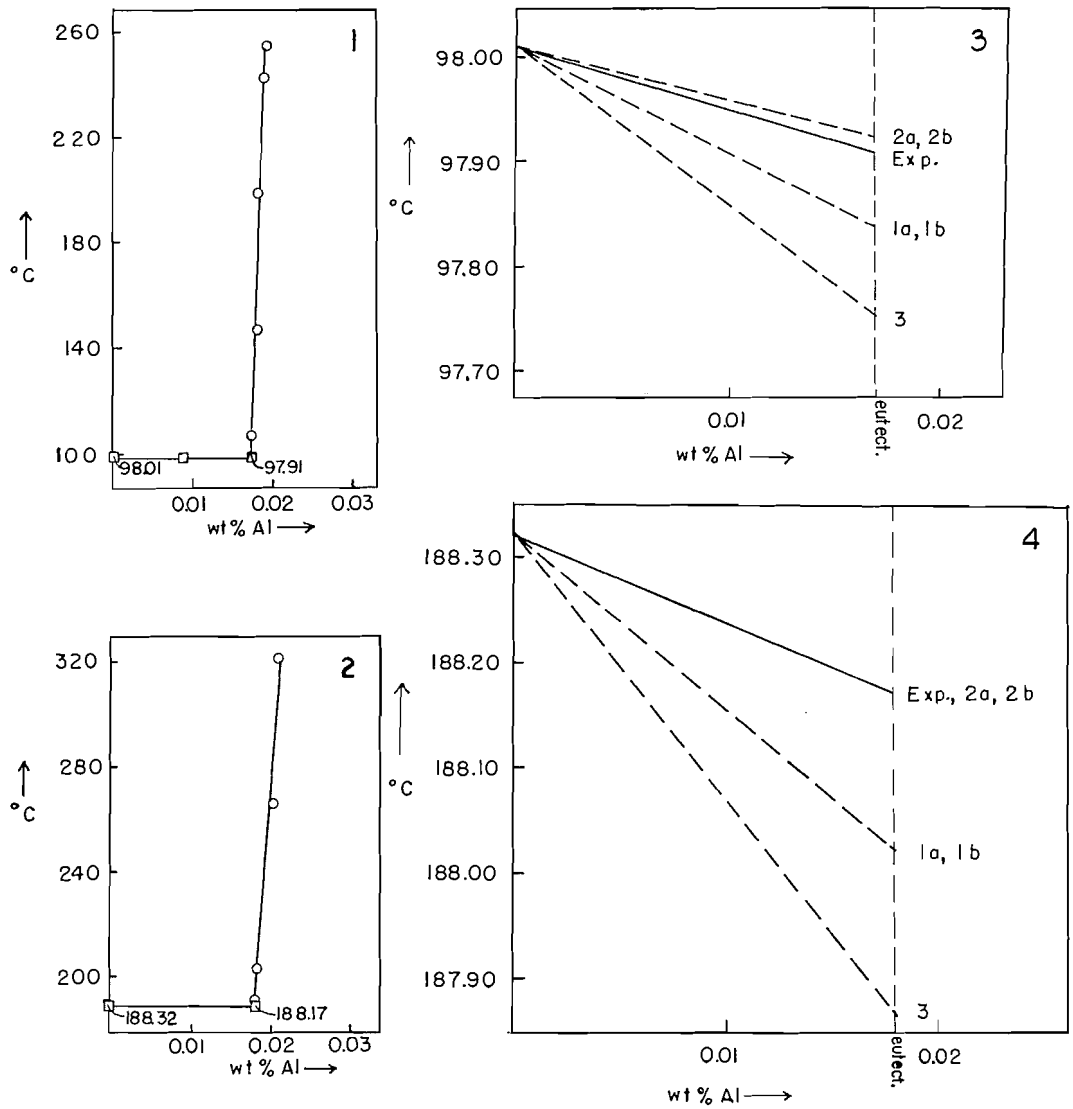

FIG. 1. Liquidus curve of the Al_2Br_6–Al system. □, From melting point determinations; ○, from solubility measurements.

FIG. 2. Liquidus curve of the Al_2I_6–Al system. □, From melting point determinations; ○, from solubility measurements.

FIG. 3. Measured and calculated freezing point depressions in the Al_2Br_6–Al system.

FIG. 4. Measured and calculated freezing point depressions in the Al_2I_6–Al system.

1*b*. Associated Al atoms:

$$Al + Al_2X_6 \rightarrow Al_3X_6$$

$$N_{Al_2X_6} = \frac{n_{Al_2X_6} - n_{Al}}{n_{Al_2X_6}}.$$

2*a*. Dimer aluminium atoms:

$$2Al \rightarrow Al_2^0$$

$$N_{Al_2X_6} = \frac{n_{Al_2X_6}}{n_{Al_2X_6} + \frac{1}{2}n_{Al}}.$$

Can. J. Chem. Downloaded from www.nrcresearchpress.com by 210.87.254.6 on 09/05/12
For personal use only.

2*b*. Associated dimers:

$$2Al + Al_2X_6 \rightarrow Al_4X_6$$

$$N_{Al_2X_6} = \frac{n_{Al_2X_6} - \frac{1}{2}n_{Al}}{n_{Al_2X_6}}.$$

3. Monovalent aluminium:

$$4Al + Al_2X_6 \rightarrow 6AlX$$

$$N_{Al_2X_6} = \frac{n_{Al_2X_6} - \frac{1}{4}n_{Al}}{n_{Al_2X_6} + \frac{5}{4}n_{Al}}.$$

The resulting liquidus curves calculated for the eutectic points are given in Figs. 3 and 4. Schemes 2*a* and 2*b* give almost identical results, and it may be seen that either scheme is in good agreement with the experimentally measured depressions of the freezing points. For the bromide system the calculated depression for the eutectic composition is 0.085 ± 0.006 °C as against the measured 0.10 ± 0.02 °C. For the iodide system the calculated depression is 0.15 ± 0.01 °C and the measured is 0.15 ± 0.02 °C. It should be noted that the same results are obtained if the bromides and iodides are taken as monomolecular ($AlBr_3$ and AlI_3). Testing of schemes other than those listed here confirms that 2*a* and 2*b* are the only conceivable models that agree with the experimental data.

From the preceding treatment it appears that the Al_2Br_6–Al and Al_2I_6–Al systems contain either neutral diatomic groups of aluminium or associated dimers like Al_4Br_6 and Al_4I_6.

ACKNOWLEDGMENT

The author wishes to thank Professor S. N. Flengas, University of Toronto, for helpful suggestions and for critically reading the manuscript.

REFERENCES

1. J. KENDALL, F. D. KRITTENDEN, and H. K. MILLER. J. Am. Chem. Soc. **45**, 963 (1923).
2. W. BILTZ and A. VOIGT. Z. Anorg. Allgem. Chem. **126**, 39 (1923).
3. W. FISCHER and O. RAHLFS. Z. Anorg. Allgem. Chem. **205**, 36 (1932).
4. P. A. RENES and C. H. GILLAVRY. Rec. Trav. Chim. **64**, 275 (1945).
5. K. J. PALMER and N. ELLIOTT. J. Am. Chem. Soc. **60**, 1852 (1938).
6. H. GERDING and E. SMIT. Z. Physik. Chem. B, **50**, 171 (1941).
7. J. D. CORBETT and S. VON WINBUSH. J. Am. Chem. Soc. **77**, 3964 (1955).
8. D. D. CUBICIOTTI and C. D. THURMOND. J. Am. Chem. Soc. **71**, 2149 (1949).
9. W. FISCHER. Z. Anorg. Allgem. Chem. **200**, 332 (1931).

Can. J. Chem. Downloaded from www.nrcresearchpress.com by 210.87.254.6 on 09/05/12
For personal use only.

Can. J. Chem. Downloaded from www.nrcresearchpress.com by 210.87.254.42 on 09/05/12
For personal use only.

RÉACTIONS AVEC LE DIFLUOROAMINO-PENTAFLUOROSULFURE[1]

JEAN L. BOIVIN
Centre Canadien de Recherches et de Perfectionnement des Armes, Département de Défense Nationale, Valcartier, Québec

Reçu le 29 mai 1964

ABSTRACT

Difluoroamino-sulphur pentafluoride was prepared in quantitative yield by heating tetrafluorohydrazine and disulphur decafluoride at 150° for a period of 12 h under autogenous pressure conditions. The reactions of the product with potassium iodide, oxygen, water, hydrogen chloride, sulphur dioxide, acetone, ethyl bromide, methyl iodide, ethyl nitrite, cyanogen bromide, and acetonitrile are reported.

INTRODUCTION

Le difluoroamino-pentafluorosulfure (DPS) a été synthétisé et utilisé dans ce laboratoire depuis quelques années (1), mais plusieurs méthodes de préparation ont été décrites dans la littérature par différents chercheurs (2, 3, 4).

Le produit a été préparé en faisant réagir la tétrafluorohydrazine sur le tétrafluorure de soufre, le pentafluoro-chlorosulfure ou le soufre avec des rendements n'excédant pas 30% (2). Une autre méthode consiste à faire réagir la tétrafluorohydrazine et le décafluorobisulfure; on a obtenu des rendements de 60% (3) et de 12% (4). La méthode que nous décrivons ici donne des rendements quantitatifs en difluoroamino-pentafluorosulfure.

Nous l'avons obtenu en chauffant la tétrafluorohydrazine et le décafluorobisulfure à une température de 150° durant 5 à 12 h sous pression autogène. Si l'on opère à des températures plus basses, on obtient aussi des rendements quantitatifs mais seulement après un temps de chauffage excessif. De plus, on ne peut chauffer le mélange à des températures dépassant 150°; le décafluorobisulfure commence à se décomposer d'une façon appréciable pour donner du tétrafluorure de soufre et de l'hexafluorure de soufre (5). Si l'on emploie un léger ou grand excès de décafluorobisulfure, on obtient un rendement quantitatif en DPS à partir de la tétrafluorohydrazine. Cependant, nous préférons employer le rapport stoichiométrique parce que le décafluorobisulfure est laborieux à préparer. Avec un excès de tétrafluorohydrazine, on a tendance à produire beaucoup d'hexafluorure de soufre grâce à l'oxydation de S_2F_{10} par l'action de N_2F_4.

Propriétés chimiques du difluoroamino-pentafluorosulfure

Quand on chauffe le DPS à des températures de 100 à 150°, on constate qu'il se décompose lentement suivant l'équation suivante:

$$2\ F_2N{-}SF_5 \rightarrow F_2N{-}NF_2 + F_5S{-}SF_5.$$

Lors de la détermination de la température critique du DPS, on a identifié du décafluorobisulfure dans les produits de décomposition. Cependant, à des températures supérieures (150–200°), on observe une décomposition importante du DPS en N_2F_4, SF_6 et SF_4 (2, 3, 4) suivant l'équation:

$$2\ F_2N{-}SF_5 \rightarrow F_2N{-}NF_2 + F_5S{-}SF_5 \downarrow SF_4 + SF_6.$$

[1]*Publié comme Mémoire Technique No. 436 et travail exécuté sous le numéro de projet: D46-10-28-34.*

A 200° et au-dessus, la décomposition de N_2F_4 continue jusqu'à NF_3 et N_2 (2, 3, 4).

Avec une solution aqueuse d'iodure de potassium, le DPS libère de l'iode, démontrant ainsi son pouvoir oxydant. Mais la réaction semble se produire en deux étapes; en premier lieu, le fluor de la partie NF_2 est libéré à température ordinaire, puis en chauffant la solution, il y a plus d'iode libéré lequel semble provenir de la partie SF_5.

Avec l'oxygène, le DPS se décompose en NO, N_2, NOF, SF_6 et SOF_2. La présence de NOF a été démontrée à partir de son spectre de masse et de son temps de rétention (6.2 min). Les pics de son spectre de masse se présentent à *m/e* 30 et 33 seulement, indiquant les groupements NO et NF. L'ion NF ne peut provinir de NF_3 ou N_2F_4 puisqu'ils n'ont pas le même temps de rétention dans le chromatogramme.

La réaction du DPS avec l'eau en léger excès donne naissance à N_2, NO, SF_6, SO_2 et HF comme produits principaux, démontrant ainsi que l'eau seule ne peut libérer complètement le fluor de la molécule.

Avec le chlorure d'hydrogène, le DPS donne N_2, SF_6, SF_4 et $ClSF_5$. Le produit principal de la réaction avec HCl dans des conditions optimum aurait été $ClSF_5$. Il serait formé suivant la réaction:

$$F_2N—SF_5 + HCl \rightarrow F_2NH + ClSF_5.$$

La difluoramine formée se décomposerait rapidement dans les conditions utilisées (150° pendant 10 h). La forte proportion de SF_6 obtenue indique que le fluor de la difluoramine a réagi avec les groupements SF_5.

La réaction du DPS avec l'acétone à une température de 100° donne plusieurs produits dont N_2, SF_6, SOF_2 et SO_2, tandis qu'à des températures plus élevées (150°) on obtient HF, SOF_2 et du carbone. Cela indique que le DPS enlève l'oxygène de la molécule d'acétone pour conduire à des produits du soufre et du fluor plus stables.

L'action du DPS sur le bromure d'éthyle produit du fluorure d'éthyle et du brome; avec l'iodure de méthyle, on obtient du fluorure de méthyle et de l'iode, et en plus SF_6 et SF_4. Le DPS décompose le nitrite d'éthyle en C_2H_5F, N_2O et SOF_2.

Le bromure de cyanogène et le DPS réagissent pour donner du cyanogène, du trifluorométhylimino-difluorosulfure, du trifluorosulfure d'azote et du brome. L'acétonitrile est décomposé par le DPS en tétrafluorométhane.

L'action de l'anhydride sulfureux sur le DPS donne naissance au difluoroamino-fluorure de sulfuryle (6) d'après l'équation suivante:

$$F_2N—SF_5 + SO_2 \rightarrow F_2N—SO_2F + SF_4.$$

PARTIE EXPERIMENTALE

Produits de départ

On a obtenu la tétrafluorohydrazine de Du Pont. Le produit était 95% pur et contenait des traces de NF_3, NO et de fluorocarbures. Le décafluorobisulfure nous a été donné par Defence Research Chemical Laboratories, Ottawa, et fut utilisé sans autre purification. Ce produit est très toxique.

Procédé général

La plupart de toutes les réactions ont été faites sous pression dans des autoclaves de 110 et 330 millilitres de capacité. Les liquides ou les gaz ont été distillés sous vide dans les autoclaves refroidis à −196°, −78° ou 0°, dépendant des propriétés des composés. Le mélange réactionnel a été chauffé par contrôle à distance dans un compartiment bien protégé contre les explosions. La réaction terminée, les gaz ont été analysés par chromatographie et spectrométrie de masse.

Pour l'identification et l'analyse des mélanges gazeux, on s'est servi d'un chromatographe en phase gazeuse accouplé à un spectrographe de masse à temps d'envol. Le chromatographe était un Perkin–Elmer modèle 154D dont la colonne mesurait 30 pieds. Elle consistait d'une longueur de 20 pieds faite de tube de cuivre de $\frac{1}{4}$ pouce de diamètre lequel avait été chargé de "Chromosorb P" contenant 33% d'huile Kel-F No. 10; l'autre partie, longue de 10 pieds, était chargée aussi de "Chromosorb P" contenant 10% de didodécyl

Can. J. Chem. Downloaded from www.nrcresearchpress.com by 210.87.254.42 on 09/05/12
For personal use only.

phtalate. Dans tous les cas, la colonne était maintenue à 35° et balayée par un courant d'hélium passant à un débit de 17 ml/min. Un intégrateur donnait le pourcentage de produit d'après l'aire relative occupée par les pics.

Une portion du gaz effluent du chromatographe était détournée pour alimenter un spectrographe de masse à temps d'envol Bendix. L'ionisation était maintenue constante à 50 V. Le spectre de masse était enregistré au moyen d'un Visicorder ou photographié sur l'écran d'un oscilloscope.

Difluoroamino-pentafluorosulfure

On a ajouté du décafluorobisulfure (20 g, 0.08 mole) dans un autoclave de 330 ml préalablement refroidi à la température de l'azote liquide et on a fait le vide sur le système jusqu'à 1 mm de Hg. Ensuite, on y a distillé sous vide de la tétrafluorohydrazine (8.3 g, 0.08 mole). On a chauffé le mélange sous pression autogène à 150° pour une période de 5 h et on l'a laissé refroidir à température ordinaire. Les produits gazeux de la réaction furent condensés dans un récipient refroidi dans l'azote liquide pour donner 28.0 g de produit brut. On a ensuite laissé le récipient à −30° pour se débarrasser de la tétrafluorohydrazine qui n'a pas réagi, de l'hexafluorure de soufre et du tétrafluorure de soufre. Lorsqu'on a laissé le mélange résiduel se réchauffer à température ordinaire, on a condensé le difluoroamino-pentafluorosulfure brut à −78° pour obtenir 23.0 g de produit, à peu près pur, p.e. −25° à −15°. En refractionnant ce produit, on a obtenu 22.5 g de DPS bouillant à −16.5° sous 750 mm de Hg. Rendement: 88%. On récupéra 2.5 g de S_2F_6. Le rendement est donc quantitatif si on le calcule à partir du S_2F_{10} utilisé dans la réaction.

Si l'on emploie un excès de décafluorobisulfure de 50% par rapport à la tétrafluorohydrazine et que l'on effectue la réaction dans les mêmes conditions que ci-haut, on obtient un rendement quantitatif de DPS à partir de N_2F_4.

La même réaction en présence d'un excès de 100% de tétrafluorohydrazine par rapport au décalfluorobisulfure conduit à un rendement faible en DPS. L'excès de N_2F_4 se décompose pour fluorer S_2F_{10} en SF_6.

Le DPS a donné un spectre de masse et infrarouge identiques aux données de la littérature (2, 3, 4).

La température critique du DPS fut déterminée par la méthode de Cailletet et Colardeau (7) comme étant 1 702° avec une pression critique d'environ 33 atm. La pression critique n'a pas pu être déterminée avec certitude parce que le DPS se décompose lentement à cette température.

On a mesuré aussi la pression de vapeur à 8, 21, 30 et 45° comme étant 48, 59, 72 et 100 lb/pouce^2 respectivement.

Le DPS avait un point d'ébullition de −16.5°, un point de fusion d'environ −110° et une densité à −78° de 2.0. On a déterminé le poids moléculaire par la méthode d'effusion des gaz et on a trouvé 174 au lieu de 179. Toutes ces constantes physiques concordent avec celles données dans la littérature (2, 3, 4).

Stabilité du DPS à température élevée

Dans un autoclave de 110 ml préalablement refroidi à la température de l'azote liquide et évacué à 1 mm de Hg, on a distillé du DPS pur (5.0 g, 0.028 mole) et on a chauffé le produit à 200° pendant 2 h. Après refroidissement de l'autoclave à température ordinaire, on a analysé les gaz par chromatographie et spectrométrie de masse pour obtenir les pics de temps de rétention suivants: 6.0 min, N_2 (0.1%); 7.2 min, SF_6 (4.0%); 7.6 min, N_2F_4 (3.8%); 10.2 min, SF_4 (24.7%); 12.8 min, DPS (67.4%).

Quand on a chauffé le même mélange pendant une période additionnelle de 10 h à 200°, on a obtenu les résultats suivants: 6.0 min, N_2 et NF_3 (traces); 7.2 min, SF_6 (13.0%); 7.6 min, N_2F_4 (10.6%); 10.2 min, SF_4 (46.7%); 12.8 min, DPS (29.7%).

On chauffa une autre quantité de DPS dans les mêmes conditions à 125° pendant 10 h. On obtint les résultats suivants: 7.2 min, SF_6 (traces); 7.6 min, N_2F_4 (5.0%); 12.8 min, DPS (90.0%); 28.7 min, S_2F_{10} (5.0%).

Comportement du DPS vis-à-vis l'iodure de potassium en solution aqueuse

En passant quelques millilitres de DPS à travers une solution aqueuse d'iodure de potassium, on obtint une libération instantanée d'iode. En chauffant légèrement la solution, une quantité plus grande d'iode est dégagée.

Réactions du DPS

1. Avec l'oxygène

Dans un autoclave de 110 ml refroidi à −196°, on a distillé du DPS (5.0 g, 0.028 mole) et de l'oxygène (1.0 g, 0.032 mole) sous un vide de 1 mm de Hg. Après chauffage d'une heure à 125°, l'analyse chromatographique des gaz donna les temps de rétention suivants: 6.0 min, N_2 et NO (10.5%); 6.2 min, NOF (2.4%); 7.2. min, SF_6 (5.0%); 7.6 min, N_2F_4 (0.7%); 8.8 min, SO_2F_2 (2.9%); 10.2 min, SOF_2 (10.1%); 12.8 min, DPS (68.4%). L'oxygène a complètement réagi.

La même réaction a été effectuée avec un grand excès d'oxygène (5.0 g) pour ne laisser aucune quantité de DPS n'ayant pas réagi, pendant que les autres produits étaient les mêmes que précédemment.

2. Avec l'eau

Dans un autoclave évacué à 1 mm de Hg, on a introduit de l'eau (2.0 g, 0.11 mole), puis on a refroidi l'autoclave à −196° pour condenser du DPS (5.0 g, 0.028 mole). On a chauffé le mélange à 125° pendant une

Can. J. Chem. Downloaded from www.nrcresearchpress.com by 210.87.254.42 on 09/05/12
For personal use only.

heure. L'analyse des gaz par chromatographie donna: 6.0 min, N_2 et NO (16.7%); 7.2 min, SF_6 (67.6%); 8.8 min, SO_2F_2 (10.8%); 19.2 min, SO_2 (5.9%). Le poids total des gaz étaient de 4.5 g. HF était aussi présent en grande quantité. L'analyse révèle que SF_6 est un des produits majeurs obtenus à partir de l'eau et du DPS.

3. Avec le chlorure d'hydrogène

Dans un autoclave de 110 ml refroidi à −196°, on a distillé du DPS (6.0 g, 0.033 mole) et HCl (1.0 g, 0.027 mole) sous un vide de 1 mm de Hg et on a chauffé le mélange à 100° pendant une heure. Il n'y eut aucune réaction. On le chauffa ensuite à 150° pour une période additionnelle de 10 h. On a obtenu le mélange de gaz suivants: 6.0 min, N_2 (14.8%); 7.2 min, SF_6 (22.8%); 7.6 min, N_2F_4 (0.1%); 10.2 min, SF_2 (52.1%); 12.8 min, DPS (8.4%); 14.8 min, $ClSF_5$ (1.8%).

4. Avec l'acétone

En employant la même méthode que précédemment, on a fait réagir de l'acétone (0.5 g, 0.008 mole) et du DPS (3. 0 g, 0.016 mole) à 125° durant 12 h. On a obtenu les pics chromatographiques suivants: 6.0 min, N_2 (32.5%); 7.2 min, SF_6 (3.9%); 8.8 min, SO_2F_2 (8.0%); 10.2 min, SOF_2 (7.3%); 19.2 min, SO_2 (48.3%).

Quand on a effectué la réaction à 150° pendant 10 h, le mélange se carbonisa et on obtint de l'acide fluorhydrique et du fluorure de thionyle.

5. Avec le bromure d'éthyle

On chargea l'autoclave de la façon habituelle avec du bromure d'éthyle (10.9 g, 0.1 mole) et du DPS (5.4 g, 0.03 mole) et on chauffa le mélange à 100° pendant 12 h, puis ensuite pour des périodes additionnelles identiques à 125° et à 150°. On obtint les résultats suivants: 6.0 min, N_2 (1.2%); 7.2 min, SF_6 (33.5%); 10.2 min, SF_4 (33.8%); 12.2 min, C_2H_5F (31.5%). L'autoclave contenait aussi du carbone et du brome (7.0 g, 0.043 mole).

6. Avec l'iodure de méthyle

La réaction fut faite de la façon habituelle avec l'iodure de méthyle (7.0 g, 0.05 mole) et le DPS (8.0 g, 0.044 mole). Le mélange fut chauffé à 125° pour une période de 5 h suivie d'une autre période de 5 h à 150°. La fraction gazeuse a donné les pics suivants: 6.0 min, N_2 (19.2%); 7.2 min, SF_6 (0.1%); 8.0 min, CH_3F (29.0%); 10.2 min, SF_4 (51.7%). Les autres produits qui restaient dans la bombe étaient du carbone et de l'iode (6.0 g, 0.024 mole).

7. Avec le nitrite d'éthyle

De la même façon, on a fait réagir du nitrite d'éthyle (7.5 g, 0.1 mole) et du DPS (4.5 g, 0.025 mole) en chauffant le mélange à 75° pendant 5 h, suivi d'une autre période de chauffage de 5 h à 100°. On obtint les pics chromatographiques suivants: 6.0 min, N_2 (40.9%); 7.2 min, SF_6 (0.2%); 7.8 min, N_2O (18.5%); 10.2 min, SOF_2 (34.4%); 12.2 min, C_5H_2F (3.0%); 19.2 min, SO_2 (traces). Il y avait aussi un liquide dans l'autoclave qui fut identifié comme du nitrite d'éthyle.

8. Avec le bromure de cyanogène

De la même façon que ci-haut, on a fait réagir du bromure de cyanogène (6.0 g, 0.056 mole) et du DPS (5.0 g, 0.028 mole) en chauffant le mélange pendant des périodes consécutives de 5 h à 75°, 100° et 125°. On a obtenu les résultats chromatographiques suivants: 6.0 min, N_2 (12.9%); 7.2–7.6 min, SF_6 et CO_2 et N_2F_4 (16.6% ensemble); 8.8 min, SiF_4 (1.3%); 10.2 min, SF_4 (3.6%); 13.3 min, $(CN)_2$ (12.0%); 14.0 min, NSF_3 (12.0%); 19.5 min, CF_3NSF_2 (8.7%); 28.7 min, S_2F_{10} (32.9%). Le décafluorobisulfure était présent dans le produit de départ comme impureté dans le DPS. Dans l'autoclave, il y avait du brome libre (3.5 g, 0.022 mole).

9. Avec l'acétonitrile

D'une façon semblable, on a fait réagir de l'acétonitrile (5.0 g, 0.12 mole) et du DPS (5.0 g, 0.028 mole) en chauffant le mélange pour des périodes consécutives de 5 h à 100° et 125°. Les produits suivants furent obtenus: 6.0 min, N_2 et CF_4 (17.7%); 7.2 min, SF_6 (13.9%); 10.2 min, SF_4 (7.9%); 12.8 min, DPS (52.0%); 14.0 min, NSF_3 (8.5%).

10. Avec l'anhydride sulfureux

Dans un autoclave de 110 ml refroidi à −78°, on a introduit de l'anhydride sulfureux (6.4 g, 0.1 mole) et du DPS (5.0 g, 0.028 mole). On a chauffé le mélange à 75° pendant 90 h et l'on obtint seulement des traces d'un produit qui correspondait, d'après le spectre de masse, au difluoroamino-fluorure de sulfuryle, $F_2N—SO_4F$. On chauffa alors le mélange de façon consécutive par périodes de 5 h à 100°, 125° et 150°. Après cette longue période de chauffage, tout le DPS avait été consumé. La fraction gazeuse consistait en gaz suivants: 6.0 min, N_2 (5.9%); 7.6 min, N_2F_4 (2.3%); 8.8 min, SiF_4 (traces); 8.8 min, SO_2F_2 (1.1%); 10.2 min, SF_4 (23.5%); 15.4 min, $F_2N—SO_2F$ (20.2%); 19.2 min, SO_2 (47.0%).

En chauffant le même mélange pendant 5 h à 150°, on a obtenu les résultats suivants: 6.0 min, N_2 (8.5%); 7.6 min, SF_6 (3.3%); 8.8 min, SO_2F_2 (1.4%); 10.2 min, SOF. (28.9%); 15.4 min, $F_2N—SO_2F$ (17.2%); 19.2 min, SO. (40.7%).

Le difluoroamino-fluorure de sulfuryle donna un spectre de masse dont les pics furent assignés aux ions positifs suivants: 102 (NFSOF), 97 (NSO_2F), 83 (SO_2F), 67 (SOF), 64 (SO_2), 52 (NF_2), 51 (SF), 48 (SO), 33 (NF). Ce spectre de masse est identique à celui rapporté dans la littérature (6).

Can. J. Chem. Downloaded from www.nrcresearchpress.com by 210.87.254.42 on 09/05/12
For personal use only.

RÉSUMÉ

Le difluoroamino-pentafluorosulfure a été préparé à partir de la tétrafluorohydrazine et du décafluorobisulfure avec un rendement quantitatif, en chauffant le mélange à une température de 150° durant une période de 12 h sous pression autogène. On a étudié le comportement du difluoroamino-pentafluorosulfure avec l'iodure de potassium, l'oxygène, l'eau, le chlorure d'hydrogène, l'anhydride sulfureux, l'acétone, le bromure d'éthyle, l'iodure de méthyle, le nitrite d'éthyle, le bromure de cyanogène et l'acétonitrile.

BIBLIOGRAPHIE

1. Can. Patent. No. 871,173 (mars 1963).
2. A. L. LOGOTHETIS, G. N. SAUSEN et R. J. SHOZDA. J. Inorg. Chem. **2**, 173 (1963).
3. G. F. CADY, D. F. EGGERS et B. TITTLE. Proc. Chem. Soc. 65 (1963).
4. E. C. STUMP, JR., C. D. PADGETT et W. S. BREY, JR. J. Inorg. Chem. **2**, 648 (1963).
5. W. R. TROST et R. L. MCINTOSH. Can. J. Chem. **29**, 508 (1951).
6. C. L. BUMGARDNER et M. LUSTIG. J. Inorg. Chem. **2**, 663 (1963).
7. S. GLASSTONE. Text-book of physical chemistry. D. Van Nostrand Co. Inc. N.Y. 1940. p. 422.

Can. J. Chem. Downloaded from www.nrcresearchpress.com by 210.87.254.42 on 09/05/12
For personal use only.

Can. J. Chem. Downloaded from www.nrcresearchpress.com by 210.87.254.105 on 09/05/12
For personal use only.

DENSITY AND VISCOSITY OF THALLIUM AMALGAMS

WILLIAM T. FOLEY, ARUN K. BASAK, AND JOHN R. DELOREY
Chemistry Department, Saint Francis Xavier University, Antigonish, Nova Scotia

Received June 29, 1964

ABSTRACT

The densities of thallium amalgams were measured at 25, 50, 70, 90, 105, 125, and 160 °C over the concentration range 0 to 42% thallium by weight and the results were fitted to equations of the form $d = a + bx + cx^2$, where d is the density in grams per ml, a, b, and c are constants and x is weight % thallium in the amalgam. The coefficient of expansion was calculated for the temperature range 25 to 90 °C. Viscosities relative to mercury were also determined over the same range of composition and at the same temperatures as were used in the density measurements. Equations were presented which show the variation of viscosity with composition and also the variation of viscosity with temperature.

INTRODUCTION

This is a report on the densities and viscosities of thallium amalgams over the concentration range of 0 to 42% thallium by weight and over a temperature range extending from 25 to 160 °C. T. W. Richards and J. H. Wilson (1) measured at 20 °C the densities of amalgams containing 0.793, 1.14, and 1.85% thallium by weight. T. W. Richards and F. Daniels (2) determined the densities at 20 and 30 °C of amalgams whose composition varied from 4.93 to 42.86% thallium by weight. Olsen and Johnson (3) reported the densities of amalgams at 25 °C over the range 0 to 42 weight % thallium. Feniger (4) reported the viscosity of 0.3, 0.5, and 0.8 weight % thallium amalgams at 18 °C.

EXPERIMENTAL

The pycnometer used in the present investigation was a modification of the type proposed by Robertson (5). It was constructed by sealing two micropipets to a pyrex bulb of 5 ml volume in such a manner that the bulb was in one arm of a U tube. The two micropipets, graduated to 0.001 ml, formed the upper limbs of the U tube and these two limbs were sealed to a glass tee. The pycnometer was calibrated with mercury which had been purified by a procedure to be described later. The calibration was such that the volume of the pycnometer was known at all readings of the graduated scales and at all temperatures selected.

The mercury was purified by electrolyzing it anodically in dilute sulfuric acid at a current density of 5×10^{-4} A/sq. cm until a precipitate of mercurous sulfate formed, and then the mercury was washed with dilute nitric acid while drawing air through it. The metal was distilled under reduced pressure three times. The source of thallium metal was thallium sulfate of 99.9% purity. The metal was plated into a mercury cathode from an electrolyte of thallium sulfate dissolved in 1 *N* sodium hydroxide. Hydrazine was used as an anodic depolarizer and the cathode potential was maintained at −0.50 V with respect to the normal hydrogen electrode. At this potential, lead, should it have been present, could not have been plated into the amalgam. The content of thallium in the amalgam was determined by the procedure of Foley and Osyany (6).

In an actual density determination the pycnometer was filled with metal under reduced pressure and then an atmosphere of nitrogen was admitted. The volume of the metal in the pycnometer was recorded at each temperature. For temperatures above 60° the liquid for the constant-temperature bath was Dow Corning 200 silicone fluid.

The modified Ostwald viscometer is shown in Fig. 1. The measuring bulb had an average diameter of 5 cm and the volume between fiducial marks was 35 ml. The capillary was 12 cm long and the diameter was 0.5 mm. The viscometer was maintained at 130° C under high vacuum for an hour before use and then it was cooled and filled through tube F with liquid metal under an atmosphere of purified nitrogen. The metal was transferred from the receiving bulb to the measuring bulb by closing the stopcock at the top of the viscometer and then lowering the pressure on the measuring-bulb side of the viscometer with the aid of a special pump attached at E. To make a measurement, the pressure in the two arms was equalized by opening the stopcock and then the time of transpiration was noted. The viscometer was held in the constant-temperature bath by a holder that ensured the same position of the viscometer every time it was used so that errors due to misalignment were avoided.

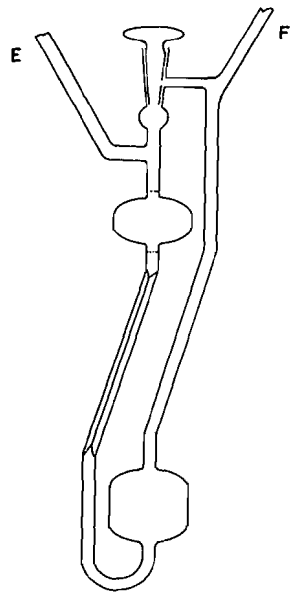

FIG. 1. Modified Ostwald viscometer.

For a viscometer used for relative measurements of viscosity, the equation which describes streamline flow is as follows

$$\eta = Apt - \frac{Bd}{t}, \qquad [1]$$

where η is the absolute viscosity, p is the average effective pressure, d is the density, t is the time, and A and B are constants for the viscometer (7). Mercury was used to calibrate the viscometer and the values of the viscosity coefficients used were those recommended by Erk (8). A calculation of Reynold's numbers showed that all flow rates were well below the turbulent region. Since the first portion of metal runs through the viscometer more rapidly than the last portion, the average pressure is not the mean of the initial and final pressure. To obtain the mean effective head, the difference in heights of the two mercury levels were observed with a cathethometer for successive positions of the menisci between the two extremes, together with the time required for each position to be reached as the liquid moved down under its own head. The values of the experimental pressures at various positions were plotted as ordinates against time as abscissae. The average pressure was determined by graphical integration. The viscometer was calibrated at eight temperatures between 5 and 95 °C. The values of the constants A and B were determined to be 4.209×10^{-10} and 1.272×10^{-1}, respectively, by the method of least squares. The values of the viscosity of mercury as calculated using these constants agreed with the values calculated from Erk's formula with an average deviation of 0.15% and a maximum deviation of 0.25%.

RESULTS AND DISCUSSION

Density

Densities were determined at 25, 50, 70, and 90 °C for amalgams having the following weight % thallium: 0.59, 4.98, 7.77, 14.09, 19.48, 24.89, 29.19, 33.54, 37.50, and 43.66. By the method of least squares, equations of the form,

$$d = a + bX + cX^2, \qquad [2]$$

were constructed, where d, is the density in grams per ml, X is the weight % thallium, and a, b, and c are the constants. The results are displayed in Table I. The last column

Can. J. Chem. Downloaded from www.nrcresearchpress.com by 210.87.254.105 on 09/05/12
For personal use only.

TABLE I

Constants for density–composition equations

T (°C)	a	$b \times 10^2$	$C \times 10^5$	Average deviation
25	13.532	−2.144	2.197	0.0038
50	13.470	−2.088	2.332	0.0048
70	13.422	−2.079	2.355	0.0046
90	13.375	−2.069	2.661	0.0037

in the table gives the average deviation of the experimental value for the density from the density calculated from the equation. There were also calculated for the temperature range 25 to 90 °C the volume coefficients for expansion, that is, the ratio of the change in volume per degree to unit volume at 25 °C and the results are shown in Table II. Density

TABLE II

Volume coefficient of expansion for 25 to 90 °C

Weight % Tl	5.00	10.00	15.00	20.00	25.00	30.00	35.00	40.00	43.66
Coefficient of expansion	179.3	177.7	175.6	173.4	170.8	167.7	164.5	160.7	157.9

measurements were also made at 105, 125, and 160 °C for amalgams having the following weight % thallium: 10.18, 19.06, 30.34, and 42.01. These densities were plotted against composition and the values given in Table III were read off from the curves.

TABLE III

Densities at 105, 125, and 160 °C

	Weight % Tl			
T (°C)	10.00	19.00	30.35	42.00
105	13.136	12.961	12.739	12.523
125	13.090	12.916	12.697	12.484
160	13.008	12.839	12.625	12.414

The estimated precision of the experimental values of the densities is 0.003 g per ml.

Viscosity

Viscosities of the amalgams were determined at 25, 50, 70, 90, 105, 125, and 160 °C. Equations of the form,

$$\eta = a + bx + cx^2, \quad [3]$$

where η is the viscosity in centipoise, a, b, and c are constants, and x is weight % thallium were obtained by the method of least squares. The constants for the temperatures chosen are given in Table IV. The last column in the table shows the average deviation of the measured viscosities from the viscosities calculated from eq. [3]. The plot of viscosity against temperature shows that as the temperature rises the viscosity–concentration curve tends to become a straight line. In fact, the curve for 160° is virtually a straight line. Because of the poorness of fit of eq. [3] at 25 and 50 °C the original data are offered in Table V.

Can. J. Chem. Downloaded from www.nrcresearchpress.com by 210.87.254.105 on 09/05/12
For personal use only.

TABLE IV

Constants for viscosity–concentration equations

T (°C)	a	$b \times 10^2$	$C \times 10^4$	Average deviation (cP)
25	1.546	4.789	8.224	0.0196
50	1.422	4.346	4.398	0.0103
70	1.342	3.943	2.796	0.0088
90	1.279	3.542	1.920	0.0093
105	1.230	3.440	1.107	0.0040
125	1.182	3.158	0.4913	0.0034
160	1.115	2.647	0.1634	0.0035

TABLE V

Viscosity in cP of thallium amalgams at 25 and 50 °C

Weight % Tl	8.29	10.73	16.05	21.01	22.00	28.38	35.70	42.19
25 °C	2.024	—	2.543	—	3.005	3.545	4.270	5.048
50 °C	1.829	1.951	2.233	2.533	2.588	2.998	3.518	4.055

Many workers have expressed the variation of viscosity with temperature in degrees Kelvin by means of the following equation:

[4] $$\eta = A\, e^{E_v/RT}.$$

The constants A and E_v are reported in Table VI. The last column in the table shows the

TABLE VI

Constants for eq. [4]

Weight % Tl	A	E_v (kcal/mole)	Average deviation (cP)
5	1.815	0.704	0.0007
10	1.835	0.802	0.0016
15	1.896	0.909	0.0025
20	1.988	1.022	0.0052
25	2.102	1.136	0.0090
30	2.233	1.249	0.0130
35	2.378	1.361	0.0187
40	2.534	1.469	0.0250

average deviation of the experimental viscosities from the viscosities calculated from eq. [4].

Viscosity measurements made on different samples of the same stock of amalgam agreed among themselves to better than 0.20% and measurements made on different stocks of amalgam having the same composition agreed to within 0.35%. If it is assumed that the viscosity of mercury is known to an accuracy of 0.3%, then it is estimated that the experimental results reported here have an accuracy of ±0.5%.

ACKNOWLEDGMENTS

Grateful acknowledgment is made by one of us, W. T. F., for a grant in aid of this research from the National Research Council of Canada and by one of us, A. K. B., to the Colombo Plan for a scholarship.

Can. J. Chem. Downloaded from www.nrcresearchpress.com by 210.87.254.105 on 09/05/12
For personal use only.

REFERENCES

1. T. W. RICHARDS and J. H. WILSON. Carnegie Inst. Wash. Publ. **118**, 9 (1909).
2. T. W. RICHARDS and F. DANIELS. J. Am. Chem. Soc. **41**, 1732 (1919).
3. D. A. OLSEN and D. C. JOHNSON. J. Phys. Chem. **67**, 2529 (1963).
4. H. FENNINGER. Ph.D. Thesis, Albert Ludwig University, Freiburg, Germany. 1914.
5. R. G. ROBERTSON. Ind. Eng. Chem. Anal. Ed. **11**, 464 (1939).
6. W. T. FOLEY and J. M. OSYANY. Anal. Chem. **33**, 1657 (1961).
7. R. C. HARDY. NBS Viscometer Calibrating Liquids and Capillary Tube Viscometer. NBS Monograph 55, U.S. Govt. Printing Office. 1962.
8. S. ERK. Z. Physik, **47**, 886–894 (1924).

Can. J. Chem. Downloaded from www.nrcresearchpress.com by 210.87.254.105 on 09/05/12
For personal use only.

Can. J. Chem. Downloaded from www.nrcresearchpress.com by 210.87.254.6 on 09/05/12
For personal use only.

THE INDUCED DECOMPOSITION OF *tert*-BUTYL HYDROPEROXIDE

R. HIATT,[1] JOHN CLIPSHAM, AND TEUNIS VISSER
Lash Miller Memorial Laboratory, University of Toronto, Toronto, Ontario

Received August 5, 1964

ABSTRACT

In a study of the "induced" decomposition of hydroperoxides by alkoxy radicals, *tert*-butyl hydroperoxide has been decomposed by the action of di-*tert*-butyl peroxyoxalate at 45°. The homolytic cleavage of peroxalate to *tert*-butoxy was unaffected by the presence of hydroperoxide and 7 to 10 molecules of hydroperoxide were destroyed for each radical thus produced. The kinetics have been analyzed and a mechanism developed which has significance for any system containing peroxy radicals.

INTRODUCTION

The thermal decomposition of hydroperoxides, while proceeding partially by unimolecular homolysis of the oxygen–oxygen bond, is usually complicated by a side reaction called "induced" decomposition arising from attack of radicals produced by the hydroperoxide on itself. This combination of unimolecular and induced decomposition may be analyzed by the method of Nozaki and Bartlett (1) devised for use in similar reactions of the diacyl peroxides. That hydroperoxides may be destroyed by a large variety of reagents, for example, acids, bases, phenols, and catalytic amounts of various metal ions (2) is well known. It has, however, remained to demonstrate the destruction of hydroperoxides by the radicals they themselves produce under conditions where the thermal decomposition is negligible. This we have done.

In an unreactive solvent *tert*-butyl hydroperoxide is suggested to decompose thermally according to the following scheme (3, 4):

[1] $$t\text{-BuOOH} \rightarrow t\text{-BuO}\cdot + \cdot\text{OH}, \qquad k_1.$$

[2] $$t\text{-BuO}\cdot + t\text{-BuOOH} \rightarrow t\text{-BuOH} + t\text{-BuOO}\cdot, \qquad k_2.$$

[3] $$2t\text{-BuOO}\cdot \rightarrow \text{O}_2 + 2t\text{-BuO}\cdot, \qquad k_3.$$

The hydroxy radical will presumably account for a molecule of hydroperoxide, but this is insignificant compared to the destruction caused by the regenerated alkoxy radical.

Di-*tert*-butyl peroxyoxalate decomposes thermally at low temperatures to *tert*-butoxy radicals and carbon dioxide (5). At 45 °C, where *tert*-butyl hydroperoxide is indefinitely stable, the peroxalate has a half-life of about 45 min. In the presence of the peroxalate at this temperature *tert*-butyl hydroperoxide could be subjected to attack by *tert*-butoxy radicals, the number and rate of production of which was subject to ready computation. The following is an account of the results of such experiments.

EXPERIMENTAL

tert-Butyl hydroperoxide was purchased from Lucidol Corporation, freed from gross amounts of water using a Dean-Stark apparatus, and distilled at reduced pressure to give material titrating iodometrically 99+%.

Di-tert-butyl peroxyoxalate was prepared by the method of Bartlett, Benzing, and Pincock (5).

Benzene was Fisher Reagent Grade used without further purification.

Kinetic runs involved dissolving weighed amounts of hydroperoxide and peroxalate in benzene, degassing the solution, decanting it into ampoules and sealing these off under vacuum. The ampoules were heated in a constant temperature bath, withdrawn at intervals, and the contents determined by iodometric titration. Since both the hydroperoxide and peroxalate liberate iodine, this gave a total peroxide concentration.

[1]*Present address: Stanford Research Institute, Menlo Park, California.*

To 1.00 ml of solution was added 15 ml of 20% acetic acid in isopropyl alcohol and approximately 300 mg of sodium iodide. After the mixture was refluxed for 20 min, the liberated iodine was titrated with aqueous sodium thiosulfate. This procedure gave quantitative results for *tert*-butyl hydroperoxide; it did not for the peroxalate, nor does any iodometric method. It did, however, give consistently a titer of 54 to 60% of theoretical depending on the concentration of the peroxalate in the benzene solution. Since the concentration of peroxalate could be calculated at any time from a knowledge of its rate of decomposition, the amount of iodine that would be liberated could be calculated and this subtracted from the total to give that corresponding to the *tert*-butyl hydroperoxide concentration.

Alternately di-*tert*-butyl peroxyoxalate was determined by its absorption at 1 783 cm^{-1} and *tert*-butyl hydroperoxide by its absorption at 1 327 cm^{-1}. This too had difficulties as *tert*-butyl alcohol, a product of the reaction, absorbs at 1 327 cm^{-1}, and it was necessary to assume a linear relation between hydroperoxide reacted and alcohol produced.

Both methods of analysis gave values of hydroperoxide concentration (subject to some uncertainty) relative to time of reaction that were consistent with each other and which were subjected to kinetic analysis.

Products in completely reacted solutions, containing no more titratable peroxides, were determined by gas-liquid chromatography (g.l.c.). The evolved noncondensable gas was measured quantitatively in a vacuum line and its constitution determined by mass spectrograph.

RESULTS AND DISCUSSION

Solutions in benzene of *tert*-butyl hydroperoxide, 0.05–0.8 *M*, and di-*tert*-butyl peroxyoxalate, 0.005–0.05 *M*, were heated at 45° *in vacuo*[2] and the rate of disappearance of hydroperoxide measured. The decomposition of the peroxalate was found to be unaffected by the presence of hydroperoxide. Rates measured with and without its addition were identical and compared well with those determined by Bartlett and co-workers (5).

The decomposition of one molecule of peroxalate was sufficient to destroy 12–20 molecules of hydroperoxide (or 6–10 molecules per *tert*-butoxy radical). This kinetic chain length was within experimental error, independent of initial concentration of either hydroperoxide or peroxalate (Table I) and did not vary much during the course of any run.

TABLE I

Decomposition of *tert*-butyl hydroperoxide by di-*tert*-butyl peroxyoxalate in benzene at 45 °C

$[ROOH]_0$	$[P]_0$	$\Delta[ROOH]/\Delta[P]$*
0.123	0.0059	12.5
0.145	0.0102	15.0
0.152	0.0194	12.3
0.140	0.050	12.6
0.156	0.0106	15.0
0.292	0.0087	13.9
0.502	0.0130	19.4
0.821	0.0071	14.6

*Average over 1 000 to 6 000 s depending on how far the run was carried.

Heating 2.034 mmoles of hydroperoxide and 0.207 mmoles of peroxalate, (in 20 ml of benzene for 12 h) gave 93 ± 5 mmoles oxygen, 2.046 mmoles of *tert*-butyl alcohol, 0.127 mmoles of di-*tert*-butyl peroxide, and 0.04 mmoles of acetone, thus accounting for 96.2% of the *tert*-butyl groups and almost all of the oxygen. Carbon dioxide was also produced from the peroxalate but was not measured quantitatively.

The rate of disappearance of *tert*-butyl hydroperoxide was not subject to ready analysis. The reaction is a chain one, depending on the regeneration of *tert*-butoxy radicals from

[2]*Since oxygen was produced almost quantitatively from the hydroperoxide, this might be regarded as a senseless precaution. However, it enabled comparison of initial rates of reaction where effects of oxygen would be minimal.*

Can. J. Chem. Downloaded from www.nrcresearchpress.com by 210.87.254.6 on 09/05/12
For personal use only.

tert-butyl peroxy radicals, and its kinetic form is dependent on a choice of radical formation. The amount of di-*tert*-butyl peroxide in the products suggests that this is the major termination product, and the reaction might be written

[4] $$2t\text{-BuO}\cdot \rightarrow t\text{-BuOO-}t\text{-Bu}, \qquad k_4.$$

Bartlett and Traylor, however, suggest that this is not a very probable reaction for tertiary alkoxy radicals (4). Alternately

[5] $$2t\text{-BuOO}\cdot \rightarrow t\text{-BuOO-}t\text{-Bu} + O_2, \qquad k_5.$$

Ignoring this mode of termination, using only eqs. [2]–[4] plus the initiation,

[6] $$t\text{-BuOO}\overset{\overset{O}{\|}}{\underset{\underset{O}{\|}}{C}}\!\!-\!\!\overset{\overset{O}{\|}}{\underset{\underset{O}{\|}}{C}}\text{-OO-}t\text{-Bu} \rightarrow 2t\text{-BuO}\cdot + 2CO_2, \qquad k_6,$$

and assuming steady states in oxy and peroxy radicals, the rate expression is

[7] $$-\frac{\partial[\text{ROOH}]}{\partial t} = k[\text{P}]^{1/2}[\text{ROOH}] \qquad \text{(where P = peroxalate).}$$

It was possible to fit some of the rate data to this expression but, at the extreme concentration ranges, the reaction seemed less responsive to hydroperoxide concentration and more to peroxalate concentration than predicted. Furthermore this expression predicts a chain length inversely proportional to $[\text{P}]^{\frac{1}{2}}$, which was contrary to the results.

The effect of discounting [4] and substituting [5] was not immediately obvious. However, setting up the steady state expressions:

[8] $$\frac{\partial[\text{RO}\cdot]}{\partial t} = 2k_6[\text{P}] - k_2[\text{RO}\cdot][\text{ROOH}] + 2k_3[\text{RO}_2\cdot]^2 = 0,$$

[9] $$\frac{\partial[\text{RO}_2\cdot]}{\partial t} = k_2[\text{RO}\cdot][\text{ROOH}] - 2(k_3 + k_5)[\text{RO}_2\cdot]^2 = 0.$$

Adding [9] to [8],

[10] $$k_6[\text{P}] = k_5[\text{RO}_2\cdot]^2.$$

If the chain length is reasonably long, the loss of RO· by attack on ROOH must be equalled by its regeneration from $\text{RO}_2\cdot$.

[11] $$k_2[\text{RO}\cdot][\text{ROOH}] = 2k_3[\text{RO}_2\cdot^2]$$

and

[12] $$[\text{RO}\cdot] = \frac{2k_6k_3[\text{P}]}{k_2k_5[\text{ROOH}]}.$$

Then since

[13] $$-\frac{\partial[\text{ROOH}]}{\partial t} = k_2[\text{RO}\cdot][\text{ROOH}],$$

[14] $$-\frac{\partial[\text{ROOH}]}{\partial t} = \frac{2k_3k_6[\text{P}]}{k_5}.$$

The invariance of chain length then results,

[15] $$+\frac{\partial[\text{ROOH}]}{\partial[\text{P}]} = \frac{2\,k_3}{k_5}.$$

Can. J. Chem. Downloaded from www.nrcresearchpress.com by 210.87.254.6 on 09/05/12
For personal use only.

Equation [14] can be integrated

$$-\frac{\partial[\mathrm{ROOH}]}{\partial t} = \frac{2k_3k_6}{k_5}[\mathrm{P}]_0\, e^{-k_6 t},$$

$$[\mathrm{ROOH}] = \frac{2k_3}{k_5}[\mathrm{P}]_0\, e^{-k_6 t} + [\mathrm{ROOH}]_0.$$

Using the published value of k_6 (6), plotting [ROOH] vs. $e^{-k_6 t}$ gives straight lines for all of the runs (Fig. 1) and the slopes are proportional to $[P]_0$, the initial concentration of peroxalate (Fig. 2).

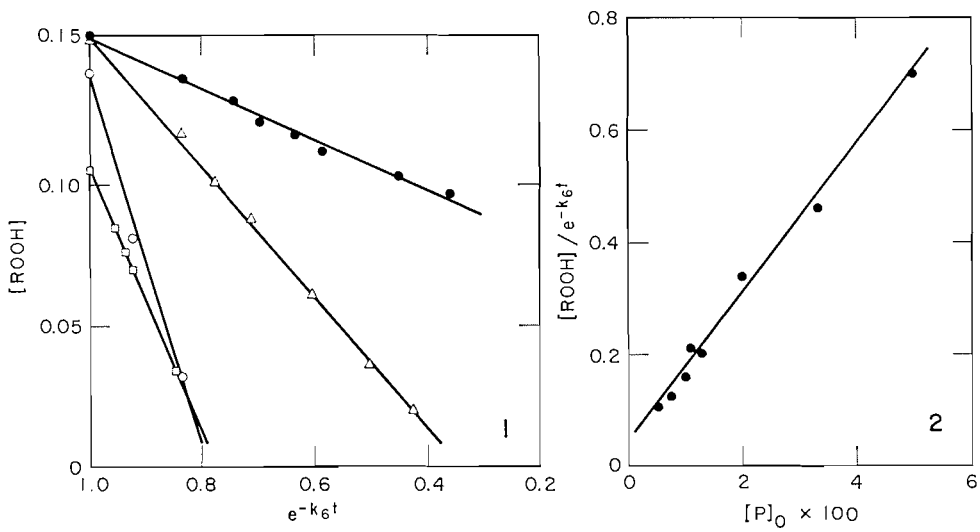

FIG. 1. [ROOH] vs. $e^{-k_6 t}$ at 45 °C in benzene.

FIG. 2. Slope of [ROOH] vs. $e^{-k_6 t}$ against $[P]_0$.

It was expected that this research would give some information regarding k_2, the rate constant for the induced decomposition. It seems to have been lost, however, in the steady state. The results do, on the other hand, offer confirmation of the general mechanism and constitute a proof of the probable termination reaction of alkoxy and peroxy radicals.

ACKNOWLEDGMENTS

We wish to thank Prof. A. Harrison for the mass spectrographic analyses, and the National Research Council of Canada for a grant under which this research was pursued.

REFERENCES

1. K. NOZAKI and P. D. BARTLETT. J. Am. Chem. Soc. **68**, 1686 (1946).
2. A. V. TOBOLSKY and R. B. MESROBIAN. Organic peroxides. Interscience, New York. 1954. Sections IV and V, pp. 95–122.
3. E. R. BELL, J. H. RALEY, F. F. RUST, F. H. SEUBOLD, and W. E. VAUGHAN. Discussions Faraday Soc. **10**, 242 (1951).
4. P. D. BARTLETT and T. G. TRAYLOR. J. Am. Chem. Soc. **85**, 2407 (1963).
5. P. D. BARTLETT, E. P. BENZING, and R. E. PINCOCK. J. Am. Chem. Soc. **82**, 1762 (1960).

Can. J. Chem. Downloaded from www.nrcresearchpress.com by 210.87.254.6 on 09/05/12
For personal use only.

Can. J. Chem. Downloaded from www.nrcresearchpress.com by 210.87.254.42 on 09/05/12
For personal use only.

THE CRYSTAL STRUCTURE OF K_2TeBr_6

I. D. BROWN
Department of Physics, Hamilton College, McMaster University, Hamilton, Ontario
Received May 27, 1964

ABSTRACT

Crystals of K_2TeBr_6 are monoclinic, space group $P2_1/n(C_{2h}^5)$ with $a = 7.521$, $b = 7.574$, and $c = 10.730$ Å; $\beta = 89° 40'$. Atomic positions have been found by three dimensional X-ray diffraction analysis (least squares $R = 0.12$). The crystals possess a K_2PtCl_6 structure which is distorted to allow a more efficient packing of the comparatively large anions than is possible with the undistorted cubic form. The stereochemistry of the octahedral $TeBr_6^=$ ion (Te—Br = 2.71 Å) is discussed.

INTRODUCTION

A few years ago, Gillespie and Nyholm (1) predicted that hexa-coordinated complexes of Te(IV) and Se(IV) should not possess a regular octahedral structure but rather one based on seven coordination with a lone pair of electrons occupying the seventh position. However, all structures so far reported, for example Cs_2TeCl_6 (2) and $(C_5H_5NH)_2TeCl_6$ (3), indicate that such complexes are in fact regular octahedra. A recent nuclear magnetic resonance (n.m.r.) and X-ray study by Nakamura *et al.* (4) indicated that K_2TeBr_6, while possessing a structure close to that of the cubic K_2PtCl_6, where the $PtCl_6^=$ ion is a regular octahedron, is distorted to orthorhombic or lower symmetry. The present work was undertaken to discover if the lower symmetry was caused by a deviation of the $TeBr_6^=$ ion from a regular octahedron.

EXPERIMENTAL

Bright red crystals of K_2TeBr_6 were prepared by the method described in Inorganic Syntheses (5). When rotated under a polarizing microscope, the crystals show the extinction pattern typical of non-cubic crystals, which indicates that they do not possess the regular cubic K_2PtCl_6 structure. Such an examination was used to select an untwinned crystal for X-ray measurements, but since twinning can be induced by a small uneven pressure on the crystal, particular care had to be taken in mounting it. The crystal which was finally chosen for the measurement of three-dimensional intensity data was an irregularly shaped plate, about 0.3 mm across and 0.05 mm thick, which was mounted on a precession camera with the plane $(10\bar{1})$ of the plate perpendicular to the X-ray beam. All X-ray diffraction measurements were made from precession photographs taken with Mo K_α radiation. The crystal data are summarized in Table I.

TABLE I
Crystal data for K_2TeBr_6

System	Monoclinic
Space group	$P2_1/n$ (C_{2h}^5)
a	7.521±0.003 Å
b	7.574±0.004
c	10.730±0.004
β	89°40′±4′

Number of formula units (K_2TeBr_6) per unit cell is 2.
Calculated density 3.72 g/ml.
Measured density 3.68 g/ml.
Systematic absences $\begin{cases} hOl & h + l = 2n + 1. \\ OkO & k = 2n + 1. \end{cases}$
Absorption coefficient for Mo K_α 96 cm^{-1}.
Relation between the axes chosen above and the axes of the cubic K_2PtCl_6 pseudo isomorph:
a is along the cubic $[1\bar{1}0]$ direction,
b is along the cubic [110] direction,
c is along the cubic [001] direction.

Intensity data were measured visually from films of the $hk0$, $h0l$, and h, k, $h + n$ layers, where n runs from 0 to 6 inclusive, and were corrected for Lorentz and polarization effects but not for absorption. The structure was initially refined on the assumption that it was a distortion of the K_2PtCl_6 structure belonging to the space group Pn and that the $TeBr_6^=$ ion was irregular and did not possess a center of symmetry. It soon became apparent that the true space group was $P2_1/n$ as indicated by the systematic absences. Difference electron density projections down [001] and [010] were used in the initial stages, and a full matrix least-squares refinement, using a Fortran program based on that of Busing, Martin, and Levy (6), was used later with three-dimensional data to produce a structure that gave a weighted agreement index $[(\sum\omega(|F_o| - |F_c|)^2/\sum\omega|F_o|^2)^{\frac{1}{2}}]$ of 0.122. The scattering factors used were taken from International Tables for X-ray Crystallography (7). The observed structure factors are given in Table II,* along with the final set of structure amplitudes calculated from the atomic parameters given in Table III.

DESCRIPTION OF THE STRUCTURE

Although it was assumed initially that the $TeBr_6^=$ ion was not a regular octahedron, it soon became clear that this assumption was wrong. The final parameters show that there is no significant difference in the three non-equivalent Te—Br distances and that the angles between them do not vary significantly from 90° (Table IV). The mean length of the Te—Br bond is 2.692 ± 0.006 Å before correction for the thermal motion of the atoms (8). The temperature factors (see Table V) of the bromine atoms show a marked anisotropy, indicating that their root-mean-square displacement perpendicular to the Te—Br bonds is about one and a half times as large as that (0.14 Å) along the bonds. A rigid $TeBr_6^=$ ion librating about the tellurium atom would give rise to an anisotropy of this sort and, if this were the case, the Te—Br bond length corrected for temperature effects would be 2.706 Å. However, it is possible that there is no correlation between the motions of the tellurium and bromine atoms, and that the anisotropy arises from the fact that the bending modes of vibration of the Te—Br bond have a larger amplitude than the stretching modes. If such were the case, the true Te—Br distance would be 2.724 Å. It is not possible to distinguish between these two cases, and the true situation probably lies somewhere between the two extremes.

The positions of the $TeBr_6^=$ ions in the crystal are the same as those of the $PtCl_6^=$ ions in the K_2PtCl_6 structure (Fig. 1*a*) to which K_2TeBr_6 is closely related. The large octahedral ions lie on a face-centered cubic lattice, with the alkali metal ions occupying the tetrahedral cavities between them. In K_2PtCl_6 the $PtCl_6^=$ ions are all equivalent and are arranged with the Pt—Cl bonds pointing along the directions of the three principal axes of the cubic cell. The K_2TeBr_6 structure is obtained from this by a reorientation of the $TeBr_6^=$ octahedra (Fig. 1*c*). Alternate octahedra, as viewed down the *c*-axis, which is the same in both the cubic K_2PtCl_6 and the monoclinic K_2TeBr_6 structures, are first twisted about the *c*-axis in opposite directions by 12°. They are then twisted about the monoclinic *b*-axis (cubic (110)) by 9°. Finally, the potassium atoms are displaced in the *b*-direction, and the axial lengths and angles are changed to accommodate these distortions.

Alternatively, the K_2PtCl_6 structure may be described as an approximately close-packed array of chlorine and potassium atoms with platinum atoms occupying octahedral holes. The chlorine and potassium atoms are arranged within the array so that every potassium atom has twelve chlorine nearest neighbors, and every chlorine atom is surrounded by four potassium atoms, four chlorine atoms belonging to its own $PtCl_6^=$ ion, and four chlorine atoms belonging to different $PtCl_6^=$ ions. In the K_2TeBr_6 structure the environment of the halogen atoms is only slightly altered but the environment of the potassium atom is markedly different (see Table IV and Fig. 2). It is still possible to pick out the twelve

**Table II has been placed in the Depository of Unpublished Data. Photocopies may be obtained upon request to: Depository of Unpublished Data, National Science Library, National Research Council, Ottawa 2, Canada.*

Can. J. Chem. Downloaded from www.nrcresearchpress.com by 210.87.254.42 on 09/05/12
For personal use only.

Can. J. Chem. Downloaded from www.nrcresearchpress.com by 210.87.254.42 on 09/05/12
For personal use only.

TABLE III

Parameters derived from the final least-squares refinement

Atom	Position coordinates			Standard error	Temperature factor*					
	x/a	y/b	z/c	Å	β_{11}	β_{22}	β_{33}	β_{12}	β_{13}	β_{23}
Te	0	0	0	—	1.07	0.71	0.31	0.09	−0.02	−0.24
Br(1)	0.0555	0.0022	−0.2473		2.08	2.60	0.13	−0.09	0.15	0.09
Br(2)	0.2875	−0.2082	0.0321	0.007	1.43	1.57	0.83	0.39	−0.18	0.14
Br(3)	0.2057	0.2889	0.0252		1.89	1.28	0.86	−0.31	−0.18	−0.32
K	0.012	−0.457	0.250	0.02	2.8	2.5	1.4	0.3	−0.7	0.2

*The temperature factors enter the structure factor calculation through the following expression:

$$\exp\left(-10^{-2}(\beta_{11}h^2 + \beta_{22}k^2 + \beta_{33}l^2 + 2\beta_{12}hk + 2\beta_{13}hl + 2\beta_{23}kl)\right).$$

TABLE IV

Interatomic distances and angles*

Atoms	Interatomic distance (Å) Uncorrected	Corrected for thermal motion	Mean corrected value	
$TeBr_6^=$ ion†				
1. Te—Br(1)	2.687	2.705		
2. —Br(2)	2.698	2.709	2.706	
3. —Br(3)	2.693	2.705		
4. Br(1)—Br(2)	3.82	3.83		
5. —Br(3)	3.81	3.83		
6. —Br(2)‡	3.80	3.81	3.82	
7. —Br(3)‡	3.79	3.81		
8. Br(2)—Br(3)	3.82	3.83		
9. —Br(3)‡	3.81	3.82		
The Br—Te—Br angles all lie within 0.3° of 90.0° and are not significantly different from it				
Environment of potassium ion				
10. K—Br(2)	3.37	3.40		
11. —Br(3)	3.41	3.44	3.46	
12. —Br(1)	3.45	3.48		
13. —Br(1)	3.48	3.51		
14. —Br(3)	3.61	3.64		
15. —Br(2)	3.68	3.71		
16. —Br(2)	3.65	3.68	3.69	3.84
17. —Br(3)	3.71	3.74		
18. —Br(1)	4.10	4.13	4.16	
19. —Br(1)	4.16	4.19		
20. —Br(3)	4.51	4.54	4.56	
21. —Br(2)	4.55	4.58		
Bromine—bromine contacts between anions				
22. Br(1)—Br(2)	3.82	3.85		
23. —Br(3)	3.84	3.86	3.86	
24. Br(2)—Br(3)	3.86	3.88		3.91
25. Br(1)—Br(2)	3.94	3.97		
26. —Br(3)	3.92	3.95	3.95	
27. Br(2)—Br(3)	3.91	3.93		

*The standard errors in bond distances indicated by the least-squares residual are: Te—Br, 0.006 Å; Br—Br, 0.01 Å; K—Br, 0.02 Å.

†The atoms defining the $TeBr_6^=$ ion have the coordinates listed in Table III. Those marked with a double dagger are related to these by inversion through the origin. The correction for thermal motion is made assuming that the $TeBr_6^=$ ion is librating.

nearest neighbors which are arranged symmetrically with respect to a mirror plane perpendicular to *c*, but they are no longer equally distant. There are four bromine atoms arranged almost tetrahedrally at a distance of 3.43 ± 0.04 Å. The next four are at a distance of 3.66 ± 0.04 Å, then there are two at a distance of 4.13 ± 0.03 Å and two at a distance of 4.53 ± 0.02 Å. These are arranged between the three non-equivalent bromine atoms in such a way that the mean distance between any one bromine atom and the four potassium atoms with which it is associated is 3.81 Å. The correction which should be applied to these lengths for thermal motion is about +0.03 Å if it is assumed that there is no correlation between the motions of the potassium and bromine atoms.

The van der Waals contacts between bromine atoms in different $TeBr_6^=$ ions are grouped into six short contacts of 3.83 Å and six long contacts of 3.93 Å, with an average contact of 3.88 Å between any one bromine and its four neighbors. These distances should be increased by about 0.025 Å if the thermal motions of the bromine atoms are uncorrelated.

Can. J. Chem. Downloaded from www.nrcresearchpress.com by 210.87.254.42 on 09/05/12
For personal use only.

TABLE V

Principal components of the temperature factors

Atom	B(Å^{-2})	Cosines of angles between the principal axes and a	b	c
Te	2.56	0.799	0.482	−0.360
	2.15	0.599	−0.577	0.555
	0.73	0.060	−0.659	−0.750
Br(1)	6.01	−0.133	0.990	0.043
	5.47	−0.984	−0.127	−0.123
	0.53	−0.117	−0.058	0.991
	Angle between the minor axis and the Te—Br(1) bond is 3.7°			
Br(2)	4.33	−0.643	−0.764	0.051
	4.13	0.280	−0.297	−0.913
	2.18	0.713	−0.572	0.405
	Angle between the minor axis and the Te—Br(2) bond is 16.7°			
Br(3)	4.73	0.696	0.134	−0.706
	4.49	0.619	−0.611	0.494
	1.93	−0.365	−0.780	−0.508
	Angle between the minor axis and the Te—Br(3) bond is 26.6°			
K	8.45	−0.714	−0.010	0.700
	6.28	−0.292	−0.904	−0.311
	3.76	0.636	−0.427	0.643

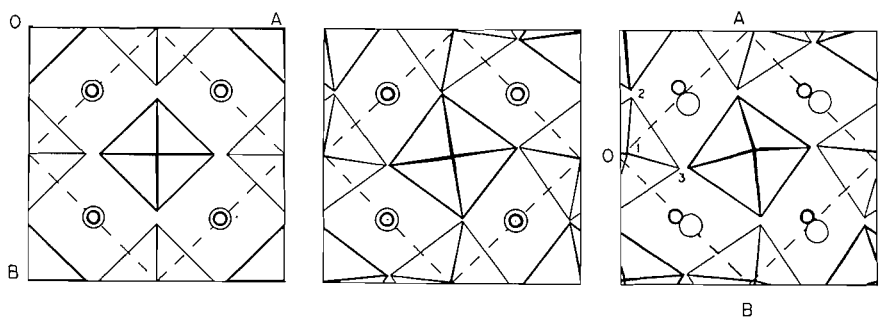

FIG. 1. The arrangement of cations (open circles) and anions (octahedra) in (*a*) K_2PtCl_6, (*b*) K_2SnBr_6, and (*c*) K_2TeBr_6 as viewed down the *c*-axis.

DISCUSSION OF THE $TeBr_6^=$ ION

The fact that the $TeBr_6^=$ ion has the configuration of a regular octahedron needs an explanation.

In four-coordinated complexes of Te (IV) the four ligands and the lone pair of electrons lie approximately at the apices of a trigonal bipyramid (for example $(C_6H_5)_2TeBr_2$ (9), $TeCl_4$ (11), and $(CH_3)_2TeCl_2$ (12)). Similarly, five-coordinated complexes have the five ligands and the lone pair at the apices of an octahedron (for example $CON_2H_5TeCl_5$ (3)). It has been suggested by Gillespie and Nyholm (1) that six-coordinated Te (IV) should have the six ligands and the lone pair arranged at the apices of a pentagonal bipyramid. However, in all the complexes of this sort which have so far been studied the ligands are arranged in a regular octahedron with the distance between the central atom and the ligands considerably longer than the covalent radius sums (2, 3, 10). It has been suggested by Beach (14) that in these complexes the lone pair occupies the s-orbital in the valence shell, leaving the p^3d^2s-orbitals for octahedral bonding. The reason why the lone pair

Can. J. Chem. Downloaded from www.nrcresearchpress.com by 210.87.254.42 on 09/05/12
For personal use only.

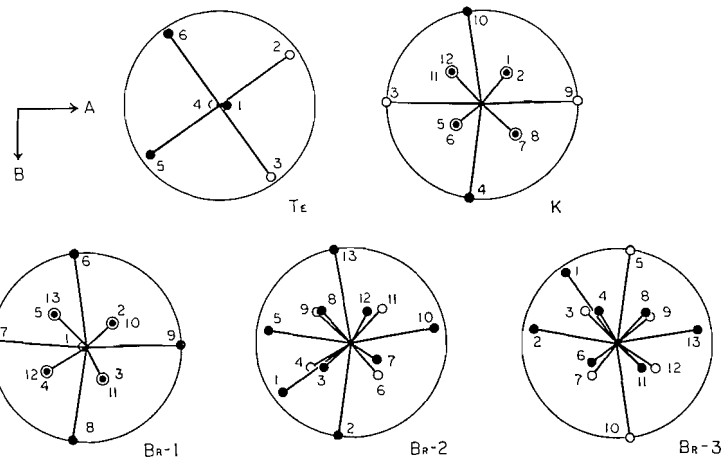

FIG. 2. Stereographic projections of the environment of atoms in K_2TeBr_6. The *c*-axis is the axis of projection. The numbering corresponds to that used in Table IV.

appears in the coordinating sphere when there are four or five ligands but not when there are six can be understood by considering the mutual repulsions between the ligands. If the distance between the ligands is greater than the van der Waals separation, the repulsion will be coulombic and relatively weak, but as the distance becomes shorter than the van der Waals separation, the stronger Pauli forces will dominate until a point is reached where further compression of the ligands can only be achieved at the expense of considerable energy. A $TeBr_6^=$ ion in the form of a seven coordinate pentagonal bipyramid with normal bonds would bring some of the bromine atoms to within 2.96 Å of each other, a distance which is only three-quarters of the normal van der Waals distance. An octahedral $TeBr_6^=$ ion with longer bonds, on the other hand, would have a Br—Br separation (3.82 Å) which is quite close to the van der Waals distance. The repulsions between the bromine atoms will thus tend to favor the octahedral form. In a tetrahedrally coordinated tellurium bromide ion, where the Br—Br distances will be greater than 4.0 Å, Pauli repulsion is absent and is only weak in ions with trigonal bipyramidal and octahedral coordination (Br—Br separation greater than 3.56 Å). Thus complexes with few ligands can accommodate the lone pair in the coordination sphere more conveniently than can those with many ligands. Similarly, complexes with a large central atom and small ligands will be able to accommodate the lone pair in the coordination sphere more easily than those with a small central atom and large ligands. Sevenfold coordination would be difficult for bromine atoms around tellurium, but several seven-coordinated fluoride complexes are known (15) and in these the fluorine–fluorine distances are, in general, not much shorter than the van der Waals distance.

DISCUSSION OF THE DISTORTION

The distortion of K_2TeBr_6 from the cubic K_2PtCl_6 structure is thus not related to a distortion of the $TeBr_6^=$ ion. It is rather the result of packing large anions with small cations. The anions form a face-centered array and are oriented in such a way that each halogen atom is in contact with four halogens on neighboring anions. This leaves cavities in the structure into which the cations fit. Each cavity is formed by twelve halogen atoms, three from each of the four anions which surround the cavity. Since the cations are usually

Can. J. Chem. Downloaded from www.nrcresearchpress.com by 210.87.254.42 on 09/05/12
For personal use only.

much smaller than the halogen atoms, the size of the cavity will be determined by the halogen–halogen contacts between anions, rather than the halogen–cation contacts. If the cation is very much smaller than the cavity into which it fits, it will be free to rattle inside the cavity unless the anions reorient themselves in such a way as to reduce the effective size of the cavity and thus lock the cation into place. Distortions which are probably due to this effect are found among many crystals with the K_2PtCl_6 structure where the quadrivalent metal is large (e.g. tellurium and tin) and in most of the iodide complexes in which the cation is potassium or ammonium. Some of these are listed in Table VI. An obvious criterion for deciding whether such a distortion will occur is the ratio of the

TABLE VI

Some crystals with the distorted K_2PtCl_6 structure

Compound	Radius ratio*	Structure	Reference
K_2TeI_6		Triclinic at 293 °K	†
K_2TeBr_6	0.83	Monoclinic at 293 °K	13
K_2PtI_6		Orthorhombic (?) at 293 °K	17
K_2SnBr_6	0.86	Tetragonal at 293 °K, cubic above 400 °K	18, 19
Rb_2SnI_6	0.88	Cubic at 293 °K	20
K_2TeCl_6	0.89	Monoclinic at 293 °K	2
$(NH_4)_2TeBr_6$	0.90	Cubic above 221 °K	4
K_2SnCl_6	0.92	Cubic above 262 °K	21, 2
K_2SeBr_6	0.93	Cubic above 240 °K	22, 23
K_2PtBr_6		Transforms to cubic between 63 and 200 °K	24, 17
K_2ReCl_6		Cubic above 111 °K	25, 26
K_2PtCl_6	0.98	Remains cubic below 4 °K	2, 27

*See Appendix.

†These crystals have been found in this laboratory to be triclinic with $a = 11.51$, $b = 11.51$, $c = 11.60$ Å, $\alpha = 90.0°$, $\beta = 90.5°$, $\gamma = 91.0°$.

size of the cation to the size of the cavity into which it must fit. The univalent ionic radii given by Pauling (16) are a suitable measure of the size of the cation, but a realistic measure of the size of the cavity is more difficult to obtain, since it involves a knowledge of the van der Waals radius of the halogen atom, and this is not as well defined as the ionic radius. Effective radii for the cavities in various complexes can be found empirically as described in the appendix, but these radii are not as reliable as could be desired. They have been used to calculate the cation–cavity radius ratios which are listed in Table VI, but because of their empirical nature, they may be in error by as much as 2%. However, even with this error certain trends are clear. Crystals with a radius ratio of less than about 0.89 are distorted at room temperature. Those crystals with radius ratios between about 0.89 and 0.98 are cubic at room temperature but distort at lower temperatures, while those with still larger radius ratios would not be expected to distort at any temperature. Unfortunately, the data for the low-temperature structures is far from complete, and it is not certain that all the phase transformations listed in Table VI correspond to a distortion of the kind discussed here. The only other crystal whose distortion has been studied in detail is K_2SnBr_6 (18) which has tetragonal symmetry (Fig. 1*b*). With a radius ratio of 0.86, this structure falls about midway between that of K_2TeBr_6 (radius ratio = 0.83) and an undistorted K_2PtCl_6 structure (radius ratio greater than 0.89). The distortion in the case of K_2SnBr_6 is of the same type as that in K_2TeBr_6 but is only about half as great. The rotation about the *c*-axis is only 7° and there is no rotation about the cubic [110] direction. It would be interesting to have more information about the distortions in other

Can. J. Chem. Downloaded from www.nrcresearchpress.com by 210.87.254.42 on 09/05/12
For personal use only.

crystals and in particular about the nature of the various phase transformations which have been reported.

ACKNOWLEDGMENTS

I wish to thank Dr. R. J. Gillespie for suggesting this problem and for helpful discussions, Mr. J. Vekris for preparing the crystals, Mr. R. C. Davidson for taking some of the X-ray photographs, and the National Research Council of Canada for financial support.

APPENDIX

Calculation of the Ratios of the Cation Radii to the Cavity Radii in K_2PtCl_6 Type Crystals

The cavity in which the cation in the K_2PtCl_6 structure fits is formed by 12 close-packed halogen atoms whose centers lie on a sphere with a radius (A) equal to the halogen–halogen contact distance. A section through this sphere is shown in Fig. 3. The space available to the cation is a smaller concentric sphere whose radius (B) is given by

$$B = A - C,$$

where C is the ionic radius of the halogen atom.

The radius ratio (R) is then given by

$$R = D/B = D/(A - C),$$

where D is the ionic radius of the cation.

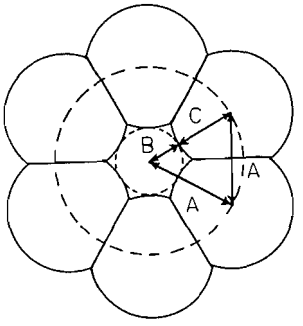

FIG. 3. A section through the environment of the cation site in a crystal with the K_2PtCl_6 structure.

The ionic radii, C and D, are conveniently chosen as the univalent ionic radii of Pauling (16), corrected for twelvefold coordination.

IONIC RADII	(Å)
K^+	1.45
NH_4^+	1.56
Rb^+	1.60
Cl^-	1.98
Br^-	2.10
I^-	2.30

The ionic radius given for NH_4^+ is an empirical one chosen to be consistent with the other radii.

The choice of the halogen–halogen distance (A) is a little more difficult, since the distance between halogen atoms in the same $MX_6^=$ ion and the distance between halogen atoms in different ions will in general not be the same. The former distance is influenced by the size

Can. J. Chem. Downloaded from www.nrcresearchpress.com by 210.87.254.42 on 09/05/12
For personal use only.

TABLE VII

Some observed halogen–halogen distances in crystals with the K_2PtCl_6 structure

Anion	Crystal	Interhalogen distance (Å) Within the anion	Between anions	Reference
$TeCl_6^=$	$(NH_4)_2TeCl_6$	3.60	3.60	2
	Rb_2TeCl_6	3.55	3.70	
	Cs_2TeCl_6	3.55	3.84†	
	Tl_2TeCl_6	3.52	3.66	
	$(C_5H_5NH)_2TeCl_6$*	3.62		3
	Mean	3.57	3.65	
	$A(TeCl_6^=)$	3.61		
$SeCl_6^=$	$(NH_4)_2SeCl_6$	3.37	3.66	2
	Rb_2SeCl_6	3.38	3.67	
	Cs_2SeCl_6	3.41	3.84†	
	Mean	3.39	3.66	
	$A(SeCl_6^=)$	3.52		
$SnCl_6^=$	K_2SnCl_6	3.46	3.60	2
	$(NH_4)_2SnCl_6$	3.41	3.69	
	Rb_2SnCl_6	3.43	3.72	
	Cs_2SnCl_6	3.44	3.88†	
	Tl_2SnCl_6	3.49	3.68	
	Mean	3.45	3.68	
	$A(SnCl_6^=)$	3.56		
$PtCl_6^=$	K_2PtCl_6	3.30	3.58	2
	$(NH_4)_2PtCl_6$	3.34	3.61	
	Rb_2PtCl_6	3.29	3.70	
	Cs_2PtCl_6	3.32	3.90†	
	Tl_2PtCl_6	3.25	3.66	
	Mean	3.30	3.64	
	$A(PtCl_6^=)$	3.46		
$TeBr_6^=$	K_2TeBr_6	3.81	3.88	13
	$A(TeBr_6^=)$	3.84		
$SeBr_6^=$	K_2SeBr_6	3.58	3.73	22
	$A(SeBr_6^=)$	3.66		
$SnBr_6^=$	$(NH_4)_2SnBr_6$	3.68	3.82	18
	Rb_2SnBr_6	3.69	3.85	
	Cs_2SnBr_6	3.75	3.90	
	Mean	3.71	3.86	
	$A(SnBr_6^=)$	3.78		
$SnI_6^=$	Rb_2SnI_6	4.03	4.18	20
	Cs_2SnI_6	4.05	4.20	
	Mean	4.04	4.19	
	$A(SnI_6^=)$	4.12		

Values of the cavity radii (Å) ($B = A - C$) are thus found to be

$TeCl_6^=$	1.63
$SeCl_6^=$	1.54
$SnCl_6^=$	1.58
$PtCl_6^=$	1.48
$TeBr_6^=$	1.74
$SeBr_6^=$	1.56
$SnBr_6^=$	1.68
$SnI_6^=$	1.82

*This crystal does not have the K_2PtCl_6 structure.
†See text.

Can. J. Chem. Downloaded from www.nrcresearchpress.com by 210.87.254.42 on 09/05/12
For personal use only.

of the central atom of the anion, while the latter ought to depend only on the van der Waals radius of the halogen atom. Some of the observed values for these two quantities are given in Table VII. The value that has been chosen for A for any one anion is the mean of several observations of the intraionic and inter-ionic X—X distances. It is apparent from the observations quoted in Table VII that the inter-ionic X—X distances representing van der Waals contacts, show a systematic increase with the cation size. For this reason the inter-ionic Cl—Cl distances observed in the caesium compounds were not used in the calculation of A. It was assumed in this case that the large caesium ion is affecting the size of the cavity, and that the observed Cl—Cl distances do not represent true van der Waals contacts. Because of the large standard error which is apparent in the observed value of the interhalogen distances, the estimates of the cavity radii will only be accurate to about 0.03 Å. This will result in the radius ratios (R) being accurate to about 2%.

REFERENCES

1. R. J. Gillespie and R. S. Nyholm. Quart. Rev. London, **11**, 339 (1957).
2. G. Engel. Z. Krist. **90**, 341 (1935).
3. E. E. Aynsley and A. C. Hazell. Chem. Ind. London, 611 (1963).
4. D. Nakamura, K. Ito, and M. Kubo. J. Am. Chem. Soc. **84**, 163 (1962).
5. Inorg. Syn. **2**, 189 (1946).
6. W. R. Busing, K. O. Martin, and H. A. Levy. Oak Ridge National Laboratory Report TM-305. 1962.
7. International Tables for X-ray Crystallography. Vol. 3. Tables 3.3.1A and 3.3.1B.
8. W. R. Busing and H. A. Levy. Acta Cryst. **17**, 142 (1964).
9. G. D. Christofferson and J. D. McCullough. Acta Cryst. **11**, 249 (1958).
10. L. Pauling. The nature of the chemical bond. 3rd ed. Cornell Univ. Press, Ithaca, New York. 1960. p. 224.
11. D. P. Stevenson and V. Schomaker. J. Am. Chem. Soc. **62**, 1267 (1940).
12. G. D. Christofferson, R. A. Sparks, and J. D. McCullough. Acta Cryst. **11**, 782 (1958).
13. I. D. Brown. Present work.
14. J. Y. Beach. *Quoted by* L. Pauling. *In* The nature of the chemical bond. 3rd ed. Cornell Univ. Press, Ithaca, New York. 1960. p. 251.
15. R. D. Burbank. Acta Cryst. **15**, 1207 (1962). W. H. Zachariasen. Acta Cryst. **7**, 792 (1954).
16. L. Pauling. The nature of the chemical bond. 3rd ed. Cornell Univ. Press, Ithaca, New York. 1960. p. 514.
17. D. Nakamura, Y. Kurita, K. Ito, and M. Kubo. J. Am. Chem. Soc. **82**, 5783 (1960).
18. G. Markstein and H. Nowotny. Z. Krist. **100**, 265 (1938).
19. E. E. Galloni, M. R. de Benyacar, and M. J. de Abeledo. Z. Krist. **117**, 470 (1962).
20. W. Werker. Rec. Trav. Chim. **58**, 257 (1939).
21. R. G. S. Morfee, L. A. K. Staveley, S. T. Walters, and D. L. Wigley. Phys. Chem. Solids, **13**, 132 (1960).
22. J. L. Hoard and B. N. Dickinson. Z. Krist. **84**, 436 (1933).
23. D. Nakamura, K. Ito, and M. Kubo. Inorg. Chem. **2**, 61 (1963).
24. A. G. Sharpe. J. Chem. Soc. 4177 (1953).
25. R. H. Busey, H. H. Dearman, and R. B. Bevan, Jr. J. Phys. Chem. **66**, 82 (1962).
26. B. Aminoff. Z. Krist. **94**, 246 (1936).
27. W. Low and P. M. Llewellyn. Phys. Rev. **110**, 842 (1958).

Can. J. Chem. Downloaded from www.nrcresearchpress.com by 210.87.254.42 on 09/05/12
For personal use only.

Can. J. Chem. Downloaded from www.nrcresearchpress.com by 210.87.254.105 on 09/05/12
For personal use only.

THE SYNTHESIS AND REACTIONS OF DIVINYL CARBONIUM IONS[1]

T. S. SORENSEN
Department of Chemistry, University of Alberta, Calgary, Alberta
Received July 7, 1964

ABSTRACT

A number of alkyl-substituted trienes have been protonated. In some cases, the existence of divinyl carbonium ions can be shown, while in others, a cyclization reaction leading to, cyclopentenyl carbonium ions takes place so rapidly that the presumed initially formed divinyl carbonium is never observed. Steric arguments are invoked to explain these differences. Complete n.m.r. and ultraviolet spectral data are presented in support of the assigned carbonium-ion structures. Some evidence has been obtained regarding the mechanism of the cyclization reaction. Finally, one of the cyclic carbonium ions is decomposed and the cyclic dienes which are produced are isolated and characterized.

INTRODUCTION

Recently, a number of stable carbonium ions have been prepared and characterized (1). In particular, the tricyclopropyl carbonium ion has been prepared (2) and found to be unusually stable. Our initial object was to prepare a trivinyl carbonium ion and to determine the stability and properties of this ion. The tetraene I was synthesized (3) and, by addition of a proton, might have been expected to yield the trivinyl carbonium ion II. The proton magnetic resonance (n.m.r.) spectrum of this ion would have been exceedingly

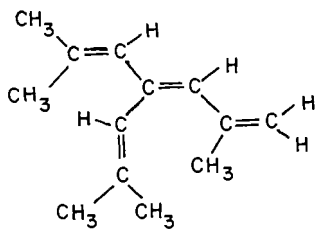

I

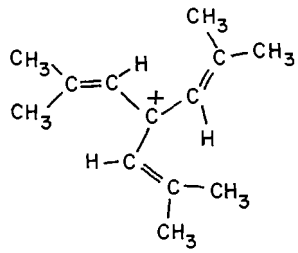

II

simple, one or perhaps two closely spaced peaks for the 18 methyl protons and a single broad peak for the 3 alkene protons. The spectrum which was obtained was much more complicated, however, suggesting that a rearrangement, probably a cyclization reaction, had occurred. To sort out this complex spectrum, we undertook the preparation of some divinyl carbonium ions. The cyclization products from these, if any, would be much simpler.

The only known analogs of divinyl carbonium ions* are protonated benzenoid compounds, of which a number have recently been reported (4). One might expect these two

[1]*Presented at the 47th Canadian Chemical Conference, Kingston, Ontario. Abstract of Paper, p. 34 of the Abstracts publication.*

**While this manuscript was in preparation, a communication appeared (14) describing the preparation of several divinyl carbonium ions including two of the systems which we describe in this paper. Our method of preparation is different, however, and we have made many added observations.*

systems to have similar ultraviolet spectra (taking appropriate account of the ring structure in the one case) and similar chemical shift positions, for similar types of protons in their n.m.r. spectra.

Interestingly, some of the carbonium ions reported in this work may have been previously prepared but not recognized as such. A Russian paper (5) has appeared describing compounds called "halochromic" alcohols, meaning that yellow and red colors are produced when these are dissolved in strong acids. Among the alcohols which they studied were several divinylcarbinols.

The carbonium ions discussed in this paper have been prepared by the protonation of conjugated trienes by 96% sulfuric acid. The problem, really, is getting the triene into the sulfuric acid in a very dilute form, so that polymerization is minimized or avoided. Deno *et al.* (6) have discussed this problem and were able to prepare reasonably pure cyclopentenyl cations by adding the organic compound through a capillary to the sulfuric acid, kept at 0 °C. Trienes, however, seem to be even more reactive and another method was necessary. We have added the trienes, in the gas phase at about 0.01 mm, to a sulfuric acid solution spread out over the bottom of a conical flask (Fig. 9) and vigorously stirred with a large magnetic stirring bar. Very clean n.m.r. spectra are obtained and this method has the advantage that the sulfuric acid can be kept at any particular temperature from −30 °C upwards, using a cooling bath. We have also used 87.5% sulfuric acid in the same procedure. Unless one is studying rates or the protonation equilibria involved, there is no advantage in using less than 96% acid.

RESULTS AND DISCUSSION

The first system studied was the hypothetical methyl divinyl carbonium ion (III). This should be obtained from the protonation of *cis-* or *trans*-2,4,6-trimethyl-1,3,5-heptatriene or 4-methylene-2,6-dimethyl-2,5-heptatriene. All of these compounds were available and each one was protonated. There was no detectable difference in the product of the protonation from each of these trienes, even though the carbonium ion, which was formed, was not III. The n.m.r. spectrum of these trienes in concentrated sulfuric acid is shown in Fig. 1. When the addition of the trienes to the sulfuric acid was carried out at 25 °C, a small peak was found at 2.32 τ which disappeared fairly rapidly giving the spectrum in Fig. 1B. Attempts to prepare the ion III by working at −30 °C resulted in a solution whose spectrum is shown in Fig. 1A; the peaks were considerably broadened by the viscosity of the acid. We were aided very much in the assignment of the peaks in our carbonium-ion spectra by the recent paper of Deno and co-workers (6) on cyclopentenyl and cyclohexenyl carbonium ions. In fact, the peaks in Fig. 1B agree perfectly with the spectrum Deno has published for the carbonium ion IV (our numbering system will be as shown in IV). The principal carbonium ion at −30 °C is V (about 65%) along with about 35% of IV. The rearrangement of V to IV has also been observed by Deno (7).

The second system studied was the divinyl carbonium ion VI. This should be obtained from the protonation of *trans*-2,6-dimethyl-1,3,5-heptatriene. The spectrum of the protonation product is shown in Fig. 2A. The position of the peaks are 7.33 and 7.38 τ, CH_3 on a carbonium-ion center; 2.79 and 3.01 τ, alkene protons at C3 and C5 split by a single proton at C4; 0.75, 0.96, and 1.18 τ, the proton at C4, is uniquely satisfied by the cation structure VI. The relative areas are 12:2.05:1; theory, 12:2:1. The magnitude of the coupling constant (J = 13.2 c.p.s.) between the protons at C3 and C5 and C4 can best be explained by assuming an s-*trans* conformation (about the 4,5 and 3,4 "single" bonds). At 25 °C, the carbonium ion VI has a half-life of about 3 days; at 76 °C, less than

Can. J. Chem. Downloaded from www.nrcresearchpress.com by 210.87.254.105 on 09/05/12
For personal use only.

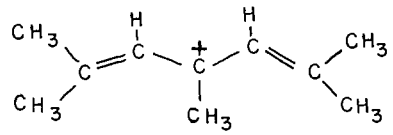

III

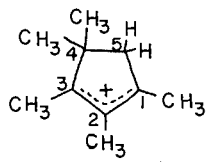

IV

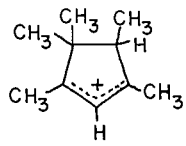

V

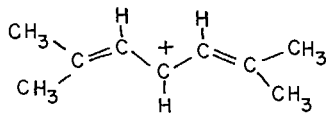

VI

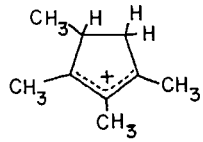

VII

10 min. This crude rate study indicates that this reaction rate is remarkably temperature dependent. The spectrum in Fig. 2C is that of the rearranged product and the spectrum in Fig. 2B shows that, in intermediate stages, only a mixture of the two carbonium ions of Figs. 2A and 2C is observed. The carbonium ion responsible for the spectrum in Fig. 2C can unambiguously be assigned the structure VII. Peaks at 8.53 and 8.66 τ, CH_3 not on a carbonium-ion center split by a single adjacent proton (J = 7.8 c.p.s.); 7.16 τ, CH_3 at C1 and C3; 6.46 and 6.75 τ, protons at C4 and C5. The relative areas are 3.1:3.3:6.3:2.7; theory, 3:3:6:3 (the methylene and methyl protons may overlap to some extent).

The triene, alloöcimene (VIII), was also protonated. Fig. 3A shows the n.m.r. spectrum of the resulting ion. A comparison with the ion VI, making allowance for an ethyl in place of a methyl group, indicates unambiguously that a divinyl carbonium-ion structure (IX) has been formed. Like VI, this ion also rearranges to a cyclic product. The spectrum of the rearrangement product is shown in Fig. 3B. One can see that, within experimental measurement, the ethyl group has ended up in, at most, only *three* of the four possible positions, viz. ions X, XI, and XII but not XIII. If ion XIII had been formed, one should have observed a quartet of peaks for the methylene protons in the 7–8 τ region. The cyclization reaction of IX proceeds at nearly the same rate as the ion VI.

The radically different behavior of the hypothetical carbonium ion III and the observed ion VI was rather baffling since it was assumed that, the more heavily alkyl-substituted (inductive, hyperconjugative effects) the carbonium ion, the more stable it would be. We considered that this conflicting behavior could be rationalized if one considered an argument based on steric effects. Studies of molecular models of the ion XIV indicated that the double bonds, needed for resonance delocalization of the positive charge, would have difficulty achieving coplanarity (carbons 2, 3, 4, 5, and 6 of XIV). Ion VI, on the other hand, is minus the worst offender, the methyl group at C4. Further support for a steric explanation is provided by an examination of the ultraviolet spectra of the trienes corresponding to these carbonium ions. The geometry of the trienes and their ions is not exactly the same but the analogy is fairly close. An analysis (7*a*) of this ultraviolet spectral data

Can. J. Chem. Downloaded from www.nrcresearchpress.com by 210.87.254.105 on 09/05/12
For personal use only.

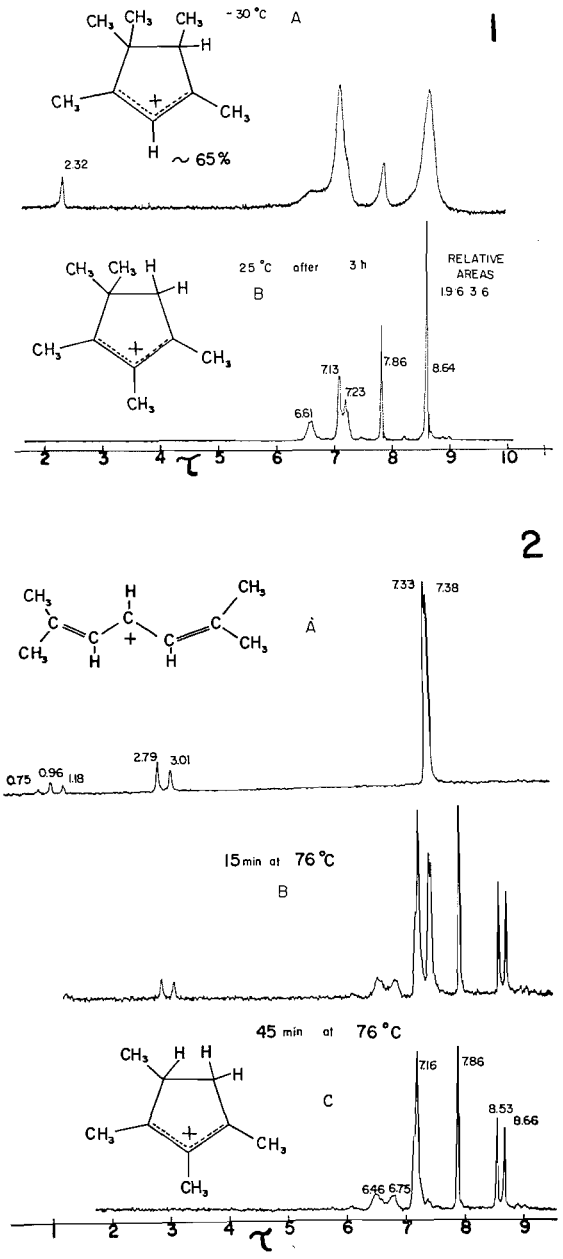

FIG. 1. Nuclear magnetic resonance spectra of IV and V.
FIG. 2. Nuclear magnetic resonance spectra of VI and VII.

has resulted in the conclusion that the trienes leading on protonation to XIV are not planar, while those leading to VI are planar. The stability of these divinyl carbonium ions is probably very much dependent upon the ability of the system to delocalize the positive charge. One would expect that progressive deviations from planarity, due to steric interactions, would be manifest in a steeply rising curve representing an energy loss of the

Can. J. Chem. Downloaded from www.nrcresearchpress.com by 210.87.254.105 on 09/05/12
For personal use only.

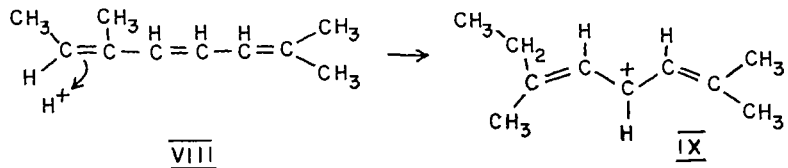

VIII IX

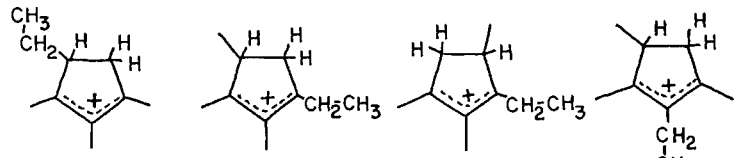

X XI XII XIII

ground state of the molecule. This could then result in a smaller activation energy for the conversion of III to IV as compared with VI to VII, other things being equal.

To test this hypothesis, we have studied systems where methyl groups are systematically removed from the ion XIV. Protonation of *trans*-4,6-dimethyl-1,3,5-heptatriene, which, if only normal protonation occurred, would correspond to the removal of one methyl group from the end position of XIV, gives a solution whose n.m.r. spectrum is shown in Fig. 4. This spectrum can be interpreted unambiguously in terms of the carbonium-ion structure XV. Peaks at 8.59 τ, CH_3 at C4; 7.03 and 7.13 τ, CH_3 at C1 and C3; 6.58 τ, CH_2; 2.50 τ, H at C2. The relative areas are 5.8:6.3:1.9:1; theory, 6:6:2:1. At −30 °C, the same spectrum was observed. We have previously shown that the triene used to make this carbonium ion exhibits ultraviolet spectral features rationalized as "steric hindrance to coplanarity" so it is perhaps not unexpected that a cyclization reaction also occurs in this system.

Attempts to prepare the carbonium ion resulting from the removal of two methyl groups from XIV, one at either end, viz. protonation of 4-methyl-1,3,5-heptatriene, result in a solution whose n.m.r. spectrum is shown in Fig. 5. This spectrum can be interpreted unambiguously in terms of the carbonium-ion structure XVI. Peaks at 8.50 and 8.62 τ, CH_3 on C4 split by a proton at C4 (J = 7.2 c.p.s.); 7.05 τ, CH_3 at C1 and C3; 6.40 and 6.58 τ, a complex pattern, protons at C4 and C5; and 2.43 τ, proton at C2. The relative areas are 3.0:6.2:2.7:1; theory, 3:6:3:1. When attempts were made to prepare this ion at −30 °C, polymerization took place to such an extent that the sulfuric acid became a solid mass. At 10 °C, however, little if any polymerization occurred. This behavior is unusual since these carbonium ions are normally more stable the lower the temperature. We suspect that the carbonium ion XVII may be formed at low temperatures and, being a very reactive species, polymerizes. Why this polymerization should disappear when the temperature is raised, we are not quite certain, since a large number of factors are involved (rates of the polymerization and the rearrangement reactions, diffusion rates of the ions formed on the surface of the acid, rate of addition of the trienes to the acid, etc.). Polymerization appeared to take place on the surface of the sulfuric acid, since each time the stirring bar exposed a new surface, a scum would immediately form over it.

This behavior points out the problem involved in attempting to substantiate our "steric interactions" argument discussed previously. Removing methyl groups from the ion XIV undoubtedly decreases the steric interactions but as the same time substantially decreases the stability of these ions by removing groups capable of providing inductive

Can. J. Chem. Downloaded from www.nrcresearchpress.com by 210.87.254.105 on 09/05/12
For personal use only.

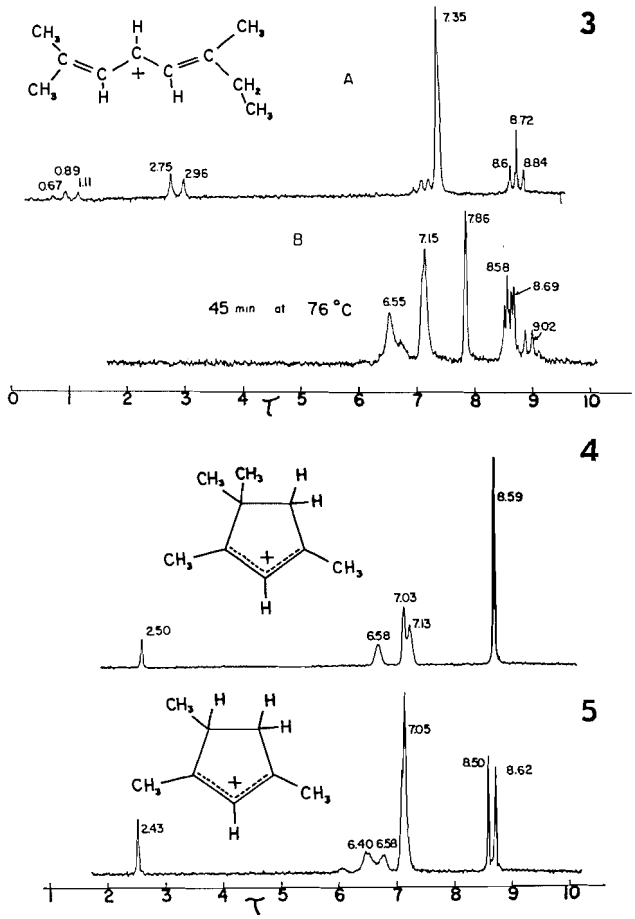

FIG. 3. Nuclear magnetic resonance spectra of IX and the resulting rearrangement products.
FIG. 4. Nuclear magnetic resonance spectrum of XV.
FIG. 5. Nuclear magnetic resonance spectrum of XVI.

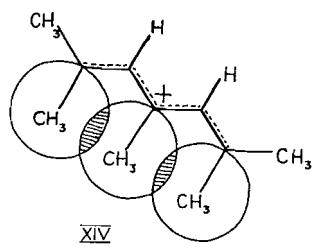

XIV

and hyperconjugative stability. This is shown very clearly in Fig. 6 where we present the spectrum of the solution obtained from the protonation of 2-methyl-1,3,5-heptatriene. If the normal carbonium ion were formed, it would correspond to the removal of one methyl group from the carbonium ion VI, previously shown be to relatively stable. At −30 °C, a spectrum, Fig. 6A, is obtained which can be readily assigned the carbonium-ion structure XVIII (compare with ion VI). Peaks at 7.27 τ, CH_3 on a carbonium-ion center; 2.59 and

Can. J. Chem. Downloaded from www.nrcresearchpress.com by 210.87.254.105 on 09/05/12
For personal use only.

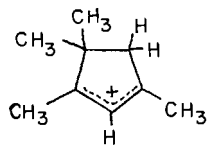

XV

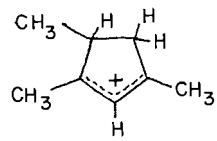

XVI

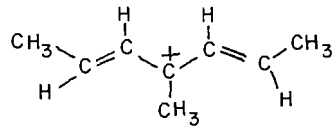

XVII

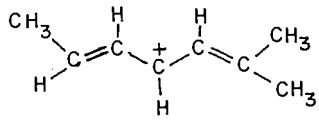

XVIII

2.81 τ, protons at C3 and C5; an unresolved peak about 1.70 τ, probably the proton at C6; a triplet of peaks 0.97, 1.17, and 1.37 τ, probably the proton C4. At −10 °C, a cyclization reaction begins and eventually results in an ion whose spectrum is shown in Fig. 6B. This spectrum can be readily assigned to the carbonium-ion structure XIX. Peaks at 8.55 τ, CH_3 group at C4, not connected to a carbonium-ion center; 6.91 τ, CH_3 at C3; 6.51 τ, protons at C5; 2.13 and 2.21 τ, proton at C2; −0.03 and 0.04 τ, proton at C1. The coupling constant of protons at C1 and C2 is 4.5 c.p.s. This ion is not very stable and after 1 h at 25° C, the spectrum shown in Fig. 6C is obtained. This spectrum is nondescript and probably represents a mixture of products, including polymers.

Attempts to prepare the carbonium ion resulting from the removal of two methyl groups from VI, one from each end, viz. addition of hepta-3,5-dien-2-ol to sulfuric acid at −10 °C, result in a solution whose spectrum is shown in Fig. 7. This spectrum can readily be interpreted in terms of the carbonium ion XX. Peaks at 7.72 τ, CH_3 at C2; 6.90 τ, CH_3 at C1; 6.23 and 6.50 τ, protons at C4 and C5; 0.23 τ, proton at C3. The relative areas are 3:2.9:3.7:1; theory, 3:3:4:1. This carbonium ion decomposes rapidly at 25 °C. Attempts to prepare this ion using 1,3,5-heptatriene resulted in extensive polymerization during the addition. The alcohol however is less volatile, thereby decreasing the gas-phase concentration (i.e. a more dilute addition), and is probably less reactive than the triene.

These final two systems demonstrate very clearly the decreased stability associated with the removal of methyl groups from the end positions of divinyl carbonium ions. We are therefore forced to conclude that we have neither proved nor disproved the original argument based on steric effects.

Ultraviolet Spectra

The ultraviolet spectral data for all of the carbonium ions which have been prepared in this work are shown in Table I. There seems to be a natural break in the absorption maxima for the cyclopentenyl cations depending upon whether a methyl group or a hydrogen is present as R_4. The positions of the observed absorption maxima are in good agreement with the results reported by Deno *et al.* (8) for similar cyclopentenyl ions; however, in the one case of duplication, our ϵ_{max} is somewhat higher. As expected, the divinyl carbonium ions absorb at much longer wavelengths than the allylic ions. The position of the maximum is similar to that found for protonated benzenes (9) but the intensities are higher, reflecting the open structure of the divinyl carbonium-ion system.

Can. J. Chem. Downloaded from www.nrcresearchpress.com by 210.87.254.105 on 09/05/12
For personal use only.

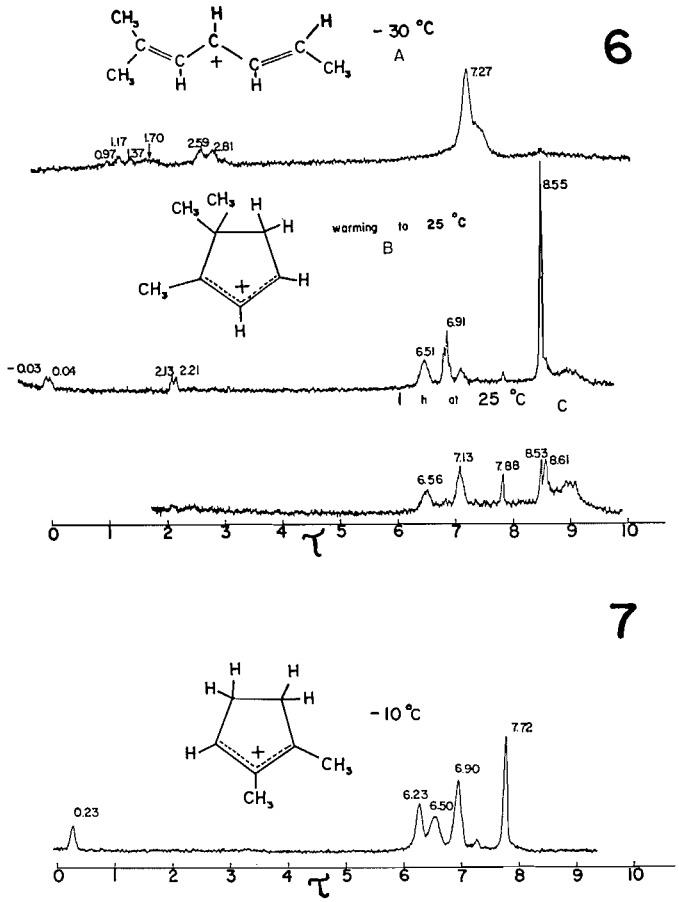

FIG. 6. Nuclear magnetic resonance spectra of XVIII and XIX.
FIG. 7. Nuclear magnetic resonance spectrum of XX.

TABLE I

Ultraviolet spectra

		λ_{max}	ϵ_{max}
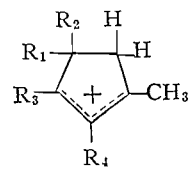	$R_1 = R_2 = R_3 = R_4 = CH_3$	297	14 200
	$R_1 = H$, $R_2 = R_3 = R_4 = CH_3$	294	13 300
	$R_1 = H$, $R_2 = R_4 = CH_3$, $R_3 = CH_3CH_2$ (a mixture)	294.5	12 500
	$R_1 = R_2 = R_3 = H$, $R_4 = CH_3$	288	>4 300
	$R_1 = R_2 = R_3 = CH_3$, $R_4 = H$	282.5	15 400
	$R_1 = R_3 = CH_3$, $R_2 = R_4 = H$	279.5	12 400
	$R_1 = R_2 = CH_3$, $R_3 = R_4 = H$	279	>9 600
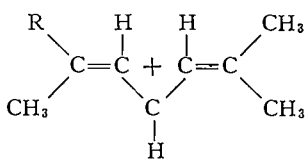	R = H (at −20 °C)	375	>60 000
	R = CH_3	396	50 000
	R = CH_3CH_2	399.5	38 000

Can. J. Chem. Downloaded from www.nrcresearchpress.com by 210.87.254.105 on 09/05/12
For personal use only.

Can. J. Chem. Downloaded from www.nrcresearchpress.com by 210.87.254.105 on 09/05/12
For personal use only.

Recovery Experiments

Using the high-dilution procedure employed by Deno *et al.* (6) (see experimental), we have recovered the dienes from the carbonium ion IV in 80% yield. These were separated by vapor-phase chromatography (g.l.c.) into the pure components: the low-retention product ca. 40% of the mixture, the middle one ca. 40%, and the highest-retention product ca. 20%. The low-retention product has an ultraviolet absorption maximum (in cyclohexane) at 258 mμ, ϵ_{max} = 3 600 and an n.m.r. spectrum (10% in carbon tetrachloride) as shown in Fig. 8A. The ultraviolet absorption (long wavelength, low intensity) is quite characteristic of cyclopentadienes and this assignment is backed by the n.m.r. spectral result which shows no methylene proton peaks and, on integration, only 1 alkene proton versus 15 methyl protons. On this basis, the structure of the low-retention product is 1,2,3,5,5-pentamethylcyclopentadiene, XXI. The presence of two sharp unequal peaks in the methyl region at 9.04 and 9.10 τ is an anomaly we are unable to explain. Analysis of this liquid on two different g.l.c. columns has failed to show the presence of significant amounts of impurity. The middle-retention product has an ultraviolet maximum (in cyclohexane) at 240.5 mμ, ϵ_{max} = 20 500; the high-retention product, 242 mμ, ϵ_{max} = 18 700. The n.m.r. spectra of these two dienes are shown in Figs. 8B and 8C. The other two

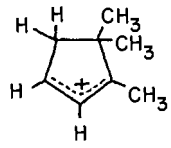

XIX

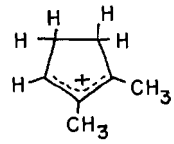

XX

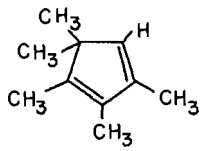

XXI

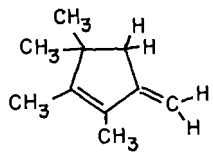

XXII

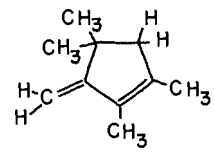

XXIII

possible products, besides XXI, from the de-protonation of the carbonium ion IV are dienes XXII and XXIII, for which the ultraviolet data (above) are in excellent accord (estimated from Woodward's rules, 242 mμ). The gross features shown in the n.m.r. spectra, two alkene protons, two methylene protons, two methyl groups on a double bond, and two not on a double bond, are also in excellent accord. In spite of their similarity in structure, their n.m.r. spectra are considerably different in detail. We have assigned to the high-retention product (n.m.r. in Fig. 8B) the structure XXII, based almost entirely on what appears to be coupling between the methylene group and the vinyl protons, such as appears possible only in XXII.

In addition to these monomers, about 10% of a product having a v.p.c. retention time of the right order of magnitude for a dimer was also recovered.

The triene, 2,6-dimethyl-1,3,5-heptatriene, has been recovered in over 80% yield using the same technique (as above). Attempts to recover monomers from the carbonium ion XX were less successful. Most of the recovered material appeared to be dimeric or trimeric (g.l.c. retention times).

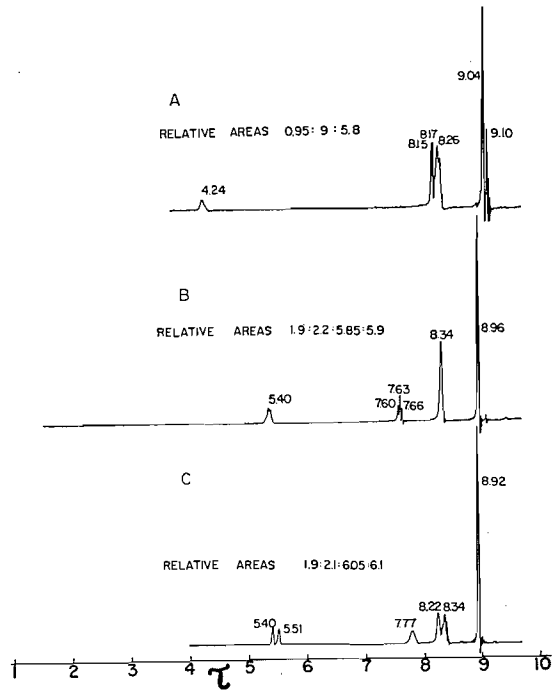

FIG. 8. A. Nuclear magnetic resonance spectrum of the low-retention product from the decomposition of IV. B. Nuclear magnetic resonance spectrum of the high-retention product from the decomposition of IV. C. Nuclear magnetic resonance spectrum of the middle-retention product from the decomposition of IV.

Mechanism

From the isomeric C_9H_{14} trienes, 4,6- and 2,6-dimethyl-1,3,5-heptatriene, one obtains finally the cyclopentenyl ions VII and XV. These are not interconverted one to the other under the same conditions under which these ions were formed originally. Thus there must be no common intermediate in these two rearrangement reactions. A postulated mechanism which accounts for the end products and the absence of a common intermediate is shown below. Note that concerted double methyl shifts are necessary if one is to proceed from one allylic system to another. In some cases this double shift is not possible; for example, the ion XIX is very unstable but, in spite of the fact that there is a stable isomeric ion, 1,2,3-trimethylcyclopentenyl cation (6) XXIV, the conversion of XIX to XXIV is not observed (or only in small amounts). All of the other products can also be explained using double methyl shifts and allylic proton rearrangements.

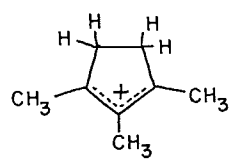

XXIV

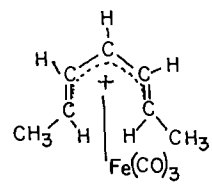

XXV

It is interesting to compare the stability of the divinyl carbonium ion – iron carbonyl complexes prepared by Mahler and Pettit (10) with those prepared in this work. The ion XXV is completely stable at ambient temperatures while the corresponding ion without

Can. J. Chem. Downloaded from www.nrcresearchpress.com by 210.87.254.105 on 09/05/12
For personal use only.

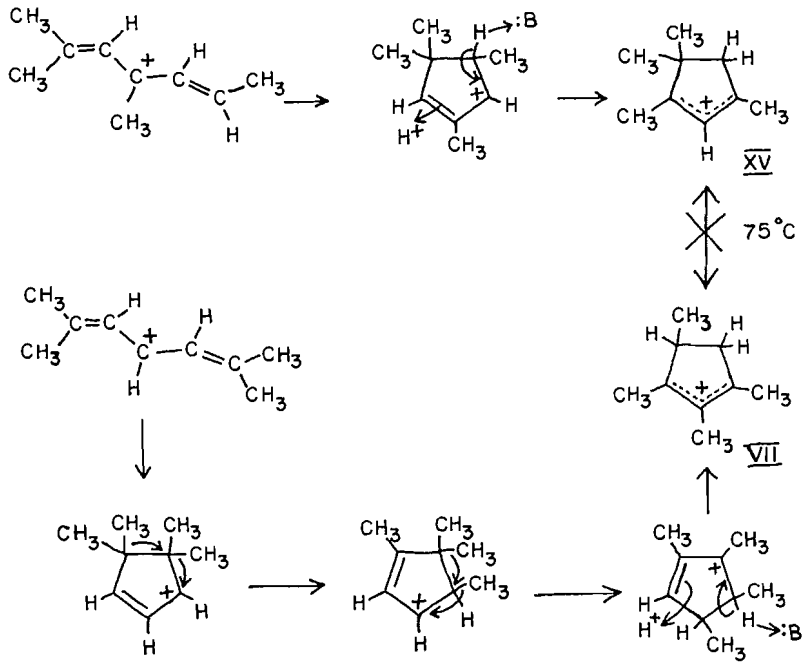

the iron carbonyl function undergoes a cyclization reaction very rapidly and has not been observed. The position of the n.m.r. proton signals of XXV also shows the increased electron density at all positions when compared with VI as a reference.

An interesting rate study could be made on S_N1 or S_N1' reactions leading to the transition states corresponding to III and VI. Would the former be significantly slower, due to a less stable carbonium ion being formed, or are the transition states in S_N1 reactions unrelated in structures to these "stable" carbonium ions?

EXPERIMENTAL

The preparation of all of the trienes used in this work has been described in a separate paper (7*a*), with the exception of alloöcimene and 1,3,5-heptatriene. Alloöcimene was kindly provided by the Hercules Powder Co. of Wilmington, Del. and was distilled before use, $n_D^{23} = 1.5421$, reported (11) $n_D^{20} = 1.5446$. Analysis by g.l.c. shows alloöcimene to be composed of two isomers in about equal amounts. This has previously been deduced (11) by spectral means although questioned in a later publication (12). Both isomers should (and do) protonate to give the same carbonium ion. A 96% yield of 3,5-heptadien-2-ol was obtained by the addition of methyl magnesium bromide to sorbaldehyde, b.p. 61.5–62 °C at 6 mm, $n_D^{20} = 1.4920$, reported (13) $n_D^{20} = 1.4882$. Heptatriene was prepared (13) by the dehydration of this alcohol.

The apparatus which was used to prepare these carbonium ions is shown in Fig. 9. The system was evacuated, with the flask containing the trienes cooled in liquid nitrogen. The system was then isolated by closing the stopcock and the flask containing the trienes allowed to warm up. Generally, about 200 mg of the triene was added to 2–3 ml of concentrated sulfuric acid, resulting in 4–5% carbonium-ion solutions. The addition of the trienes took anywhere from 10 min to an hour depending upon the pressure and the temperature differential between the acid and the trienes. The sulfuric acid could be kept at any temperature from 25 °C to −30 °C during the addition, in spite of the fact that the freezing point of the acid is − 15°C. It fortunately supercools quite easily. A number of the carbonium ions are stable for several weeks at 25 °C but many begin to darken noticeably after a few hours.

The n.m.r. spectra were obtained on a Varian Assoc. A-60 spectrophotometer equipped with a variable temperature probe. Tetramethylammonium cation was used as an internal reference for the sulfuric acid solutions (6) (set at 6.90 τ). Other compounds were measured as 10% solutions in carbon tetrachloride using tetramethylsilane (TMS) as the internal reference. Ultraviolet measurements were made using a Beckman DK-1 spectrophotometer with a variable temperature cell compartment.

Can. J. Chem. Downloaded from www.nrcresearchpress.com by 210.87.254.105 on 09/05/12
For personal use only.

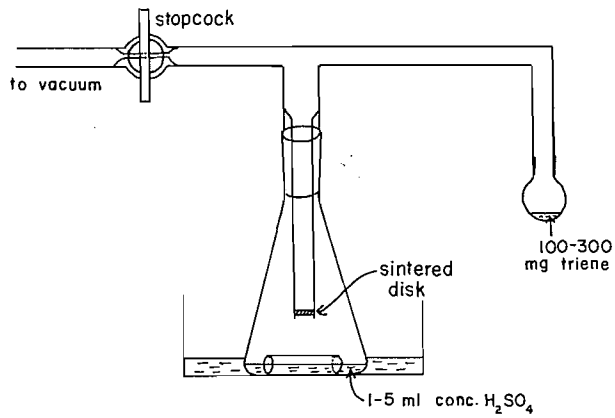

FIG. 9. Apparatus for preparing the carbonium ions.

Recovery of the dienes from the carbonium ion IV was accomplished by adding the sulfuric acid solution (from 2.75 g of triene and 30 ml concentrated sulfuric acid), from a 2 ml hypodermic syringe, to a vigorously stirred mixture of ice, dilute sodium hydroxide solution, and 50 ml of ether. The ether layer was separated and the aqueous solution extracted with two more 100 ml portions of ether. The combined ether extracts were dried over potassium carbonate. The ether was then carefully distilled off at atmospheric pressure. The residual dienes were then distilled at low pressure into a dry-ice cooled trap, 1.8 g (80% recovery). A small viscous residue remains in the distillation flask, 0.3 g (10% recovery). The volatile diene fraction consists of three components (analytical v.p.c.). These can be separated by preparative g.l.c. into the pure individual components (Aerograph "Autoprep", 12 ft. × ⅜ in. column of 30% carbowax 20 M on 60/80 Chromsorb W, HMDS treated, helium flow, 200 ml/min, column temperature, 90 °C, sample size, ca. 0.1 ml). The retention times and percentages of the total are low-retention product, 9.4 min, 40%, middle-retention product, 11.2 min, 40%, and high-retention product, 13.3 min, 20%.

Low-Retention Product, 1,2,3,5,5-Pentamethylcyclopentadiene(XXI)
Anal. Calcd. for C_9H_{16}: C, 88.16; H, 11.84. Found: C, 88.01; H, 12.12. n_D^{21} = 1.4610.

Middle-Retention Product, 1-Methylene-2,3,5,5-tetramethyl-2-cyclopentene(XXIII)
Anal. Calcd. for C_9H_{16}: C, 88.16; H, 11.84. Found: C, 87.74; H, 11.85. n_D^{21} = 1.4783.

High-Retention Product, 1-Methylene-2,3,4,4-tetramethyl-2-cyclopentene(XXII)
Anal. Calcd. for C_9H_{16}: C, 88.16; H, 11.84. Found: C, 88.10; H, 11.95. n_D^{25} = 1.4806.

The same procedure was used to recover the hydrocarbons from several other carbonium ions. A curious green-colored compound (azulenes?) was formed in some cases when the carbonium-ion solutions were decomposed (by adding water to them).

ACKNOWLEDGMENT

The author wishes to thank the National Research Council of Canada for financial support.

REFERENCES

1. T. J. KATZ and E. H. GOLD. J. Am. Chem. Soc. **86**, 1600 (1964) and references therein.
2. N. C. DENO, H. G. RICHEY, JR., J. S. LIU, J. D. HODGE, J. J. HOUSER, and M. J. WISOTSKY. J. Am. Chem. Soc. **84**, 2016 (1962).
3. T. S. SORENSEN. Unpublished results.
4. T. BIRCHALL and R. J. GILLESPIE. Can. J. Chem. **42**, 502 (1964). E. L. MACKOR, A. HOFSTRA, and J. H. VAN DER WAALS. Trans. Faraday Soc. **54**, 186 (1958). C. REID. J. Am. Chem. Soc. **76**, 3264 (1954).
5. B. N. DASHKEVICH, I. V. SMOLANKA, and YU. YU. Tsmur. Nauchn. Zap. Uzhgorodsk. Gos. Univ. **22**, 81 (1957).
6. N. C. DENO, H. G. RICHEY, JR., N. FRIEDMAN, J. D. HODGE, J. J. HOUSER, and C. U. PITTMAN, JR. J. Am. Chem. Soc. **85**, 2991 (1963).
7. N. C. DENO, N. FRIEDMAN, J. D. HODGE, and J. J. HOUSER. J. Am. Chem. Soc. **85**, 2995 (1963).
7*a*. T. S. SORENSEN. Can. J. Chem. This issue.

Can. J. Chem. Downloaded from www.nrcresearchpress.com by 210.87.254.105 on 09/05/12
For personal use only.

8. N. C. DENO, J. BOLLINGER, N. FRIEDMAN, K. HAFER, J. D. HODGE, and J. J. HOUSER. J. Am. Chem. Soc. **85**, 2998 (1963).
9. W. VON E. DOERING, M. SAUNDERS, H. G. BOYTON, H. W. EARHART, E. F. WADLEY, and W. R. EDWARDS. Tetrahedron, **4**, 178 (1958).
10. J. E. MAHLER and R. PETTIT. J. Am. Chem. Soc. **85**, 3955 (1963).
11. J. J. HOPFIELD, S. A. HALL, and L. A. GOLDBLATT, J. Am. Chem. Soc. **66**, 115 (1944).
12. P. DE MAYO. Mono- and sesquiterpenoids. Interscience Publishers, Inc., New York. 1959. p. 40.
13. K. ALDER, H. v. BRACHEL, and K. KAISER. Ann. **608**, 195 (1957).
14. N. C. DENO and C. U. PITTMAN, JR. J. Am. Chem. Soc. **86**, 1871 (1964).

Can. J. Chem. Downloaded from www.nrcresearchpress.com by 210.87.254.105 on 09/05/12
For personal use only.

Can. J. Chem. Downloaded from www.nrcresearchpress.com by 210.87.254.6 on 09/05/12
For personal use only.

THE PREPARATION AND PROPERTIES OF SOME METHYL-SUBSTITUTED HEPTATRIENES

T. S. SORENSEN
Department of Chemistry, University of Alberta, Calgary, Alberta
Received July 7, 1964

ABSTRACT

The synthesis and assignment of the geometry of a number of previously unknown methyl-substituted 1,3,5-heptatriens are described. A table of the ultraviolet spectral maxima of these and other trienes is included. Anomalies in the ultraviolet spectral curves of certain trienes are attributed to steric interactions affecting the coplanarity of the chromophore system.

INTRODUCTION

In connection with our studies of divinyl carbonium ions (1), we have had occasion to synthesize a number of aliphatic trienes. In particular, we were anxious to have pure geometric isomers available for this study. The assignment of the geometry to these isomers, however, is not always straightforward (2). We have used both proton magnetic resonance spectroscopy (n.m.r.) and ultraviolet spectroscopy and believe that the assigned structures are reasonably consistent with the facts. A table of the ultraviolet spectra of a large number of trienes is included, particularly to show that "steric hindrance to planarity" becomes serious in some highly substituted derivatives. This fact will be important in the related discussion of the carbonium ions.

The general synthetic method for preparing these trienes involves the addition of Grignard reagents to appropriate aldehydes and ketones, giving a diene-alcohol which is then dehydrated. Three of these triene systems have been prepared from an α,β-unsaturated carbonyl compound and an allylic Grignard reagent. The simultaneous addition (the allyl chloride and carbonyl compound) method of Nazarov (3) gave excellent yields of the unsaturated alcohols with no sign of products resulting from conjugate addition (4).

RESULTS AND DISCUSSION

2,4,6-Trimethyl-1,3,5-heptatriene

Dehydration of the alcohol I, obtained in good yield from the addition of methyl magnesium bromide to phorone (5), has been reported (6) to yield 4-methylene-2,6-dimethyl-2,5-heptadiene (II).

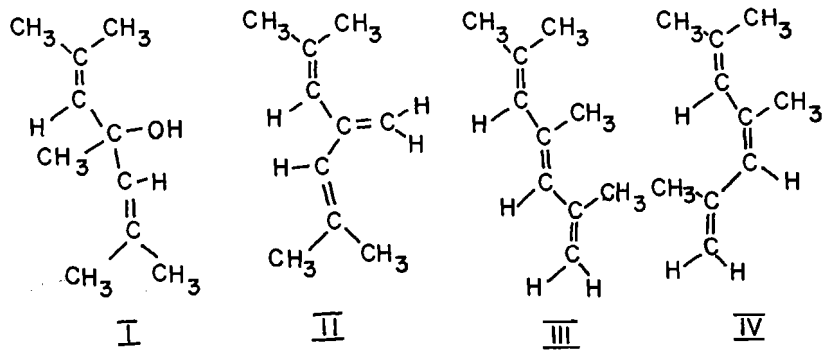

I II III IV

Can. J. Chem. Downloaded from www.nrcresearchpress.com by 210.87.254.6 on 09/05/12
For personal use only.

Using a catalytic amount of *p*-toluenesulfonic acid in benzene and removing the water formed in the dehydration by azeotropic distillation, we obtained three compounds, accounting for > 99% of the volatile dehydration products. This mixture of compounds was separated by preparative vapor-phase chromatography (g.l.c.) into the pure components. Their n.m.r. spectra show the absence of saturated methylene proton peaks in each case, so each isomer must be fully conjugated. There are only three possible conjugated products, viz. trienes II, III, and IV. Braude and co-workers (7) in a series of papers, have described the very facile allylic rearrangement of divinyl alcohols, including I, so the occurrence of trienes III and IV might be expected. The middle-retention product (24% of the total) can safely be assigned the structure II, on the basis of the exceedingly simple n.m.r. spectrum observed (and expected) for this symmetrical structure. The natural tendency might be to assign to the lowest-retention product the *cis*

TABLE I

Ultraviolet spectra of conjugated trienes

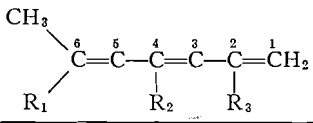

Compound	λ_{max} (mμ)	ϵ_{max}
$R_1 = R_2 = R_3 = CH_3$ (*cis*) IV	239.5	11 300
	209	8 800
(*trans*) III	258.5	9 900
$R_1 = R_2 = CH_3$, $R_3 = H$ (*cis*) VI	245.5	15 400
	207	13 300
(*trans*) VII	267	21 400
$R_1 = R_3 = CH_3$, $R_2 = H$ (*trans*)	262	27 700
	272	36 600
	282.5	28 700
$R_2 = CH_3$, $R_1 = R_3 = H$ (mixture of 3,4-*cis*-5,6-*trans* and 3,4-*trans*-5,6-*trans* XII	259	34 200
	268.5	45 700
	279.5	33 400
$R_1 = R_2 = H$, $R_3 = CH_3$ 3,4-*trans*-5,6-*trans* IX	253.5	31 800
	263.5	44 800
	274	35 600
$R_1 = R_2 = R_3 = H$* 3,4-*trans*-5,6-*cis*	263	46 900
	273	37 100
3,4-*trans*-5,6-*trans*	251	40 800
	260.5	53 200
	271.5	46 300
Hexatriene† (*cis*)	245	29 000
	255	41 000
	265	30 000
(*trans*)	245	36 000
	255	53 000
	265	44 000
Alloocimene‡	265 (shoulder)	32 000
	277	41 500
	287 (shoulder)	32 000
4-Methylene-2,6-dimethyl-2,5-heptadiene II	218	15 500
	240.5	11 600

*This datum was taken from ref. 10. However, these authors' assignment of the geometry of the two isomers may be open to question.

†This datum was taken from ref. 2.

‡Kindly provided by the Hercules Powder Co., Wilmington, Delaware. The g.l.c. analysis shows the presence of two isomers in nearly equal amounts. We thank a referee for pointing out the recent work of C. Cappas (Ph.D. Thesis, University of Florida, Gainesville, Florida. 1962. Dissertation Abstr. 23, 846 (1962)) in which these two isomers are separated and the ultraviolet absorption reported for the pure isomers. The two isomers are identified as 4,5-*trans*-6,7-*trans* and 4,5-*trans*-6,7-*cis*.

structure IV (41% of the total) and to the highest-retention product the *trans* structure III (35%). There seems to be no general justification for this, however (cf. the work of Hwa, de Benneville, and Sims (2) on hexatrienes).

The n.m.r. spectra of these two trienes are reasonably dissimilar and are shown in Fig. 1. The ultraviolet spectra are also dissimilar; the lower-retention product has a λ_{max} 239.5 and 209 mμ, ϵ_{max} 11 300 and 8 800, while the absorption of the high-retention product is λ_{max} 258.5 mμ, ϵ_{max} 9 900. A comparison of these with the complete ultraviolet spectral data in Table I for a number of trienes shows that both the intensity and the wavelength of the maxima are much smaller than would be expected. Similar effects have often been observed (8) in cases where steric repulsions prevent molecules from being completely planar. For each isomer there are four possible conformers, corresponding to rotation about the two single bonds of the backbone. For the *cis* isomer, two of these, the s-*cis-cis* and the s-*trans-cis*, are clearly very strained (repulsion by methyl groups at C2 and C6); the remaining two, IVA and IVB, are shown below.

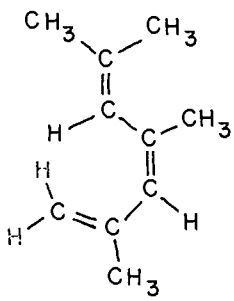

IV A

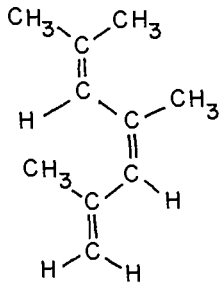

IV B

For the *trans* isomer, none of the four conformers is impossible; however, the s-*trans-trans* and the s-*cis-trans* appear to be the more impossible because of the accumulated repulsion of methyl groups on the one side of the backbone of the triene framework; the remaining two, IIIA and IIIB, are shown below.

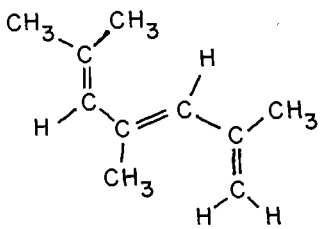

III A

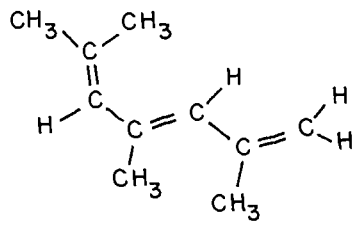

III B

The molecular models (Fisher–Hirschfelder–Taylor) of both the *cis* and *trans* isomer in all of the possible rotational states are never planar; however, the *trans* isomer in conformations IIIA or IIIB attains the greater coplanarity of the three double bonds. We, therefore, assign to the *trans* isomer the longer wavelength absorption maximum; this isomer also happens to be the higher g.l.c. retention product.

Can. J. Chem. Downloaded from www.nrcresearchpress.com by 210.87.254.6 on 09/05/12
For personal use only.

The interpretation of the n.m.r. spectra is fairly arbitrary. There is an abnormally shielded methyl group peak at 8.40 τ in the low-retention product. This same feature is also present in the n.m.r. spectrum of the low-retention product described below (Fig. 2),

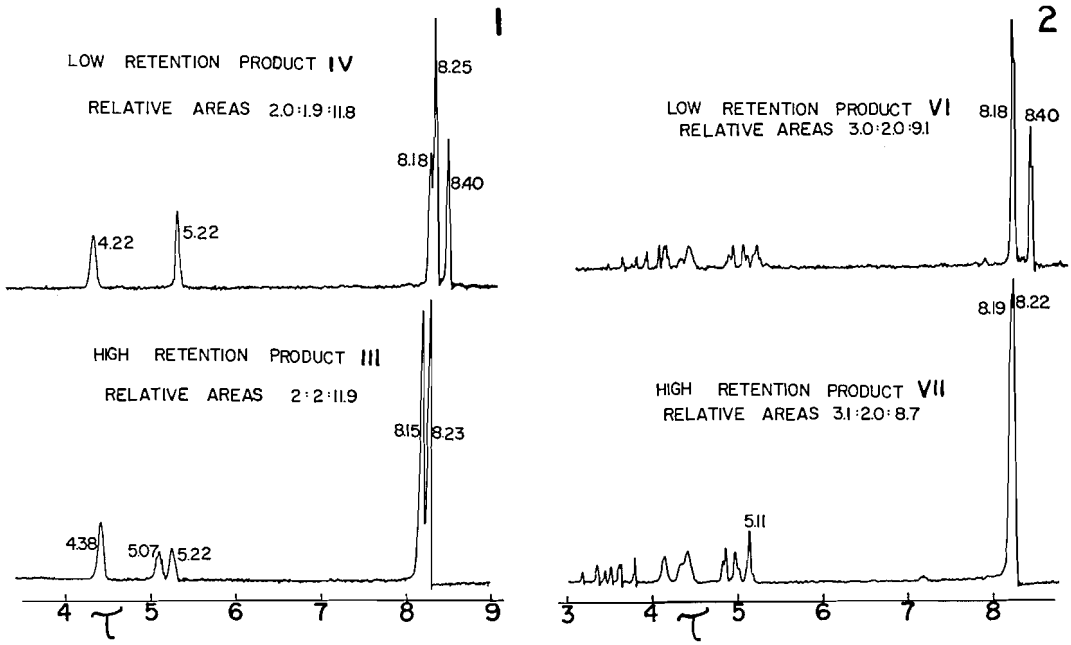

FIG. 1. Nuclear magnetic resonance spectra of *cis*- and *trans*-2,4,6-trimethyl-1,3,5-heptatriene.
FIG. 2. Nuclear magnetic resonance spectra of *cis*- and *trans*-4,6-dimethyl-1,3,5-heptatriene.

also assigned a *cis* geometry and having the same partial structure for carbon atoms 3 to 7. Methyl groups orientated near or in the π-electron cloud of double bonds have been observed to be abnormally shielded (9). This same situation can arise in both of the *cis* isomers referred to above, if one assumes (as the molecular models would indicate) that the 5,6-double bond is twisted about 90° from the plane of the remaining 1,2-3,4-planar diene system. This results in one of the terminal methyl groups being orientated above the diene π-electron system. We have no satisfactory explanation for the two peaks observed for the exocyclic methylene protons in the *trans* isomer as against the sharp single peak for this same structure in the *cis* compound. In a number of other compounds containing this partial structure, only one sharp peak has been observed.

4,6-Dimethyl-1,3,5-heptatriene

The reaction of allyl magnesium chloride and mesityl oxide produces the alcohol V, in excellent yield.

Dehydration (as above) yielded at least eight compounds, resolved or partially resolved by g.l.c. The two largest fractions, the lower-retention product about 25% of the total dehydration product and the higher about 35%, were separated by preparative g.l.c. and were identified as VI and VII respectively. The other compounds likely correspond to products formed from dehydration into the methyl group at C4 and from allylic rearrangement. The assignment of the structures of VI and VII was based upon (1) the absence of saturated methylene proton peaks in their n.m.r. spectra (Fig. 2), indicating completely

Can. J. Chem. Downloaded from www.nrcresearchpress.com by 210.87.254.6 on 09/05/12
For personal use only.

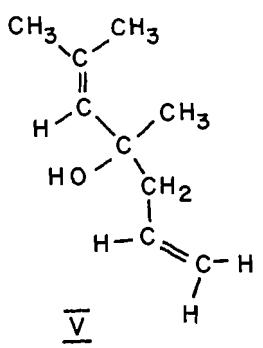

V

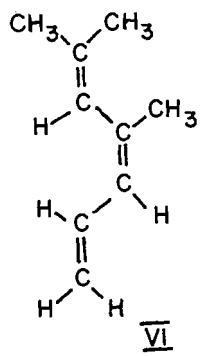

VI

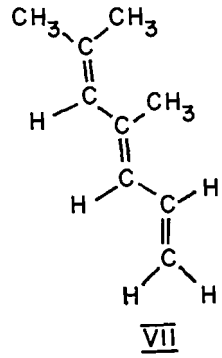

VII

conjugated compounds, and (2) absence of the partial structure in their n.m.r. spectra, indicating that these compounds are not of the isomeric 2,4-dimethyl-1,3,5-heptatriene system. The ultraviolet results (Table I) again show that the higher-retention product has the longest wavelength absorption. Molecular model studies again show that the *trans* isomer can attain better coplanarity of the chromophore system than the *cis* isomer and an analogous assignment to that previously discussed is made for the structures VI and VII. The decreased intensity of the ultraviolet absorption is again indicative of interference to the coplanarity of the system in both isomers.

2,6-Dimethyl-1,3,5-heptatriene

This compound was prepared by the reduction of phorone with lithium aluminium hydride (7). It shows a single peak when subjected to vapor-phase chromatography and although there are two possible geometric isomers, this one is in all likelihood the *trans* compound, in view of its relatively high melting point and normal ultraviolet spectrum. Molecular model studies of the two isomers indicate that the *cis* one would have serious steric interference to coplanarity of the double bonds, caused by the methyl group at C2 (or a hydrogen at C1) and the hydrogen at C5.

2-Methyl-1,3,5-heptatriene

The reaction of crotonaldehyde with methallyl magnesium chloride yields the alcohol VIII. This was dehydrated by adding it dropwise to powdered potassium acid sulfate at 150–160 °C. The crude mixture is resolved or partially resolved into nine peaks on g.l.c.; five of these (85% of the total mixture) come off the column with retention times expected for C_8 compounds. The two largest fractions were separated (pure) by preparative g.l.c.;

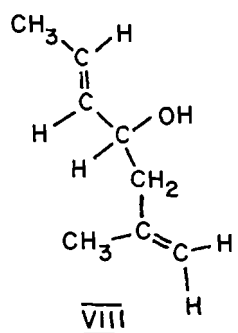

VIII

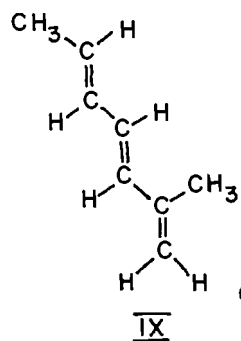

IX

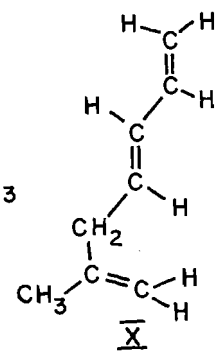

X

Can. J. Chem. Downloaded from www.nrcresearchpress.com by 210.87.254.6 on 09/05/12
For personal use only.

the higher retention product (30% of the total trienes) shows no saturated methylene proton peaks in its n.m.r. spectrum and is therefore conjugated. The partial structure 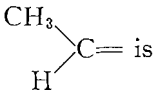 is still intact (n.m.r.), so this compound is not the isomeric 6-methyl-1,3,5-heptatriene. The steric arguments concerning this triene are very similar to those just discussed for 2-methyl-1,3,5-heptatriene. The *trans* isomer (the 3,4-double bond) can take up a planar structure, while the *cis* isomer has the same steric repulsions as previously discussed. In view of its normal ultraviolet absorption, we would assign to this compound the *trans-trans* structure. The geometry of the 5,6-double bond is *trans* in crotonaldehyde and presumably also in the dienol VIII. There would be no reason to expect that the major conjugated triene product would be the rearranged *cis*-5,6-triene. Some of the smaller peaks in the g.l.c. results may represent the *cis* isomers but the other major product collected (43% of the total trienes) shows saturated methylene proton peaks in its n.m.r. spectrum and must be the dehydration product X, corresponding to allylic rearrangement.

4-Methyl-1,3,5-heptatriene

The reaction of allyl magnesium chloride and 3-penten-2-one produced the alcohol XI, in excellent yield.

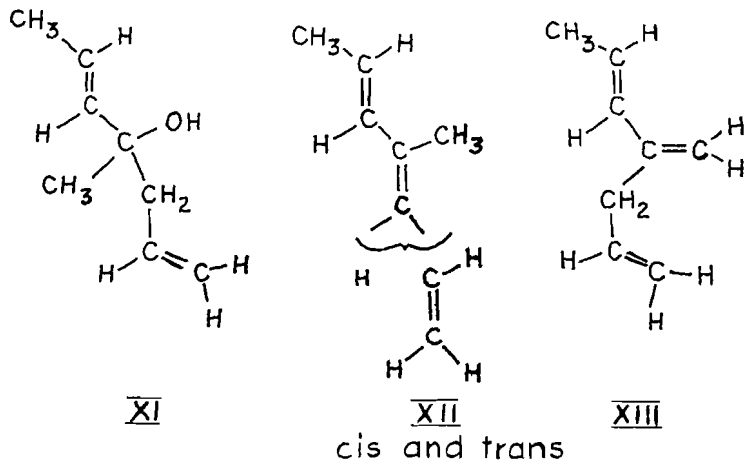

Dehydration again yielded a complex mixture of five or more compounds from which the two present in largest amounts were isolated by preparative g.l.c. The high-retention product, which was collected (70% of the mixture), is actually composed of two compounds with very close retention times, in the ratio of about 1:2. The n.m.r. spectrum of this mixture shows no saturated methylene proton peaks, so the trienes are fully conjugated. There are four geometric isomers of the title compound, however; it seems unlikely that the geometry of the 5,6-double bond will change from the expected *trans* position in the pentenone and the dienol XI, at least not to the extent that the major products have this geometry. These two compounds would then be the *cis* and *trans* isomers XII involving the 3,4-double bond. Molecular model studies show that neither of these isomers have significant steric interactions to distort the planarity of the chromophore system and, in agreement with this, normal ultraviolet absorption is observed for this triene-pair mixture. The lower-retention product (20% of the trienes)

Can. J. Chem. Downloaded from www.nrcresearchpress.com by 210.87.254.6 on 09/05/12
For personal use only.

shows saturated methylene proton peaks in its n.m.r. spectrum and presumably corresponds to a triene, XIII, resulting from dehydration into the 4-methyl group, since the partial structure $\begin{matrix} CH_3 \\ \diagdown \\ H \diagup \end{matrix}\!\!>C=$ is still present.

Ultraviolet Spectra

The significant feature of unhindered trienes is a triplet of peaks, the middle one being the highest, separated by about 10 mμ. The ultraviolet data in Table I also verify the bathochromic shift of the maxima expected when methyl groups are substituted on the basic triene system (except when steric effects become dominant).

EXPERIMENTAL

All melting points and boiling points are uncorrected. Ultraviolet spectra were measured in isoöctane or cyclohexane solution with a Beckman DK-1 spectrophotometer and are for the most part listed in Table I. Infrared spectra of all of the compounds described in this work were recorded by a Perkin–Elmer model 337 spectrophotometer and are available upon request. The n.m.r. spectra were obtained on a Varian Associates A-60 spectrophotometer using ca. 10% solutions in carbon tetrachloride and internal tetramethylsilane (TMS) as a reference. The n.m.r. results are often most useful in the negative sense that certain characteristic proton signals are not observed. No analysis of complex splitting patterns was attempted beyond ascertaining that this behavior was not unexpected; in addition, methyl group positions are reported as single peaks even in cases where they are actually doublets or multiplets with very small coupling constants (interaction with protons across a double bond). Gas chromatography separations were made using the Aerograph "Autoprep" model A-700. Analytical g.l.c. results were obtained with the above machine and an Aerograph "Hy-Fi", model 600. The purity of all of the compounds described here, whether separated in preparative amounts by g.l.c. or not, was finally checked by analytical g.l.c. and in most cases was 98% or better apparent homogeneity. All conjugated trienes are sensitive to air and subject to polymerization and were kept under nitrogen in a freezing compartment.

2,4,6-Trimethyl-hepta-2,5-dien-4-ol (I)

Phorone, recrystallized from diethyl ether, (40 g, 0.29 moles) in 200 ml of ether was added dropwise to a stirred solution of methyl magnesium bromide (ca. 0.36 moles) held at 0 °C. The solution was stirred an additional hour and then poured into ice and ammonium chloride. The ether layer was separated and the aqueous layer extracted with a further 100 ml of ether. The combined ether layers were dried over potassium carbonate. The ether was removed under vacuum to leave an oily solid. This was recrystallized from pentane to yield 25 g of the alcohol I (56%), m.p. 57 °C, reported (5) 57.5 °C. Peaks were observed in the n.m.r. spectrum at 8.69 τ, $O-\overset{|}{\underset{|}{C}}-CH_3$; 8.32 τ, CH_3; 8.12 τ, O—H; and a complex peak centered at 4.58 τ, $=CH$. The relative areas of the peaks were 3:12:1:2; theory 3:12:1:2.

Dehydration of I

A solution of 15 g I (0.097 moles) and 0.05 g of *p*-toluenesulfonic acid in 60 ml of dry benzene was heated to reflux, using a Dean-Stark trap to remove the water by azeotropic distillation. Ether was added to the remaining benzene and the resulting solution was washed with 5% sodium hydroxide solution and several times with water before drying over potassium carbonate. The solvent was removed by distillation and the residue distilled at 9 mm pressure to yield a fraction, b.p. 45–47 °C, n_D^{25} = 1.480, and another fraction b.p. 47–51 °C. Total yield of product, 10.7 g (81%). Analysis (g.l.c.) showed that neither fraction was a single compound and in subsequent runs only one triene fraction was collected. Analysis (g.l.c.) on the distilled and undistilled trienes yields the same number of peaks in the same relative area; low-retention product, 41% of the total, middle-retention product, 24%, and the high-retention product, 41%. The trienes were separated in preparative amounts using a 12 ft × 3/8 in. column of 30% carbowax 20 M on 60/80 Chromosorb W, HMDS treated. The column temperature was 110 °C, helium flow 150 ml/min, sample size ca. 0.1 ml, and the retention times 9, 11.25, and 12.75 min respectively.

Low-Retention Product, cis-2,4,6-Trimethyl-1,3,5-heptatriene (IV)

Nuclear magnetic resonance spectrum shown in Fig. 1, n_D^{23} = 1.4791.

Anal. Calcd. for $C_{10}H_{16}$: C, 88.16; H, 11.84. Found: C, 87.78; H, 11.93.

Middle-Retention Product, 4-Methylene-2,6-dimethyl-2,5-heptadiene (II)

Nuclear magnetic resonance peaks at 8.25 τ, CH_3; 5.14 τ, $=CH_2$, and 4.28 τ, $=CH$. The relative areas were 12.3:2.0:2.1; theory 12:2:2. n_D^{23} = 1.4799.

Anal. Calcd. for $C_{10}H_{16}$: C, 88.16; H, 11.84. Found: C, 87.75; H, 11.91.

Can. J. Chem. Downloaded from www.nrcresearchpress.com by 210.87.254.6 on 09/05/12
For personal use only.

High-Retention Product, trans-2,4,6-Trimethyl-1,3,5-heptatriene (III)
Nuclear magnetic resonance spectrum, Fig. 1. $n_D^{23} = 1.4897$.
Anal. Calcd. for $C_{10}H_{16}$: C, 88.16; H, 11.84. Found: C, 87.85; H, 12.13.

4,6-Dimethyl-hepta-1,5-dien-4-ol (V)
To a 1 l 3-necked flask equipped with a condenser and mechanical stirrer was added 100 ml of ether, 24.3 g (1.0 moles) of magnesium turnings, and a small crystal of iodine. A solution of 10 g of allyl chloride in 100 ml of ether was added to this stirred suspension; a small amount initially to start the reaction and the rest at such a rate that gentle refluxing was maintained. Then, a solution of 54 g (0.55 moles) of mesityl oxide and 66 g (0.87 moles) of allyl chloride in 300 ml of ether was added dropwise with stirring (maintaining moderate reflux) over a 2.5 h period, during which time magnesium chloride precipitates. This makes the solution very viscous but otherwise does not affect the reaction. The solution was allowed to stand at room temperature for 3 h and then decomposed by pouring it into 600 ml of ice – ammonium chloride solution. The ether layer was separated and the aqueous layer extracted with a further 150 ml portion of ether. The combined ether fractions were dried over anhydrous potassium carbonate. Removal of the ether by careful distillation at atmospheric pressure yielded an almost colorless liquid residue. This was distilled through a 1 m "Nester" spinning band column to yield essentially one fraction, b.p. 55–57 °C at 6–7 mm, $n_D^{26} = 1.4569$, reported (3) 1.462. Yield 70.0 g (90%).
Anal. Calcd. for $C_9H_{16}O$: C, 77.09; H, 11.50. Found: C, 77.28; H, 11.47.
Nuclear magnetic resonance peaks were found at 8.75 τ, O—C(—CH_3)—; 8.51 τ, O—H; 8.14 and 8.30 τ, two different CH_3 groups; 7.68 and 7.81 τ, $—CH_2—$ split by a single proton; and a very complex pattern of peaks from 4–5 τ, $=CH_2$ and $=C(—H)—$. The relative areas were 2.6:1:5.5:2:4; theory 3:1:6:2:4.

Dehydration of V
A solution of 32 g (0.23 moles) of the alcohol V and 0.1 g of *p*-toluenesulfonic acid in 200 ml of dry benzene was heated to reflux, using a Dean-Stark trap to remove the water. The benzene solution was then cooled, washed with 5% sodium hydroxide solution, and washed several times with water before being dried over potassium carbonate. The benzene was distilled at about 100 mm to leave a crude triene fraction. This was fractionated using a spinning band column; however, the individual fractions which were collected were each shown to be complex mixtures. In subsequent runs, only one fraction, b.p. 22–36 °C at 5–6 mm, was collected. Yield 20 g (70%), residue 3 g. The vapor-phase chromatogram of this triene mixture is shown in Fig. 3. The two largest peaks were collected using the preparative column previously described (sample size ca. 0.1 ml, helium flow 200 ml/min, column temperature 120 °C). The lower peak represents about 25% of the total trienes and the higher about 35%.

Low-Retention Product, cis-4,6-Dimethyl-1,3,5-heptatriene (VI)
Nuclear magnetic resonance spectrum, Fig. 2. $n_D^{26} = 1.4838$.
Anal. Calcd. for C_9H_{14}: C, 88.45; H, 11.55. Found: C, 88.08; H, 11.68.

High-Retention Product, trans-4,6-Dimethyl-1,3,5-heptatriene (VII)
Nuclear Magnetic resonance spectrum, Fig. 2, $n_D^{26} = 1.5128$.
Anal. Calcd. for C_9H_{14}: C, 88.45; H, 11.55. Found: C, 88.52; H, 11.53.

2,6-Dimethyl-1,3,5-heptatriene
This triene was prepared in 25% yield by the published procedure, b.p. 44.5–45.5 °C at 8–9 mm, $n_D^{21} = 1.5303$, reported (7) 1.5130–1.5190. The compound appeared to be completely homogenous (g.l.c.) and has a melting point of about −20 °C. Nuclear magnetic resonance peaks were found at 8.13 τ, CH_3; 8.21 τ, $2CH_3$ groups; 5.12 τ, $=CH_2$; and a complex series of peaks 3.4–4.3 τ, =C—H. The relative areas were 9.2:2.0:1.1:2.0; theory 9:2:1:2.
Anal. Calcd. for C_9H_{14}: C, 88.45; H, 11.55. Found: C, 87.94; H, 11.74.

4-Methyl-hepta-1,5-dien-4-ol (XI)
Using a procedure similar to that described for the preparation of V and starting with 7 g of allyl chloride in 75 ml of ether and 17.0 g (0.7 moles) of magnesium in 50 ml of ether and then adding a solution of 46.2 g (0.61 moles) of allyl chloride and 30.0 g (0.36 moles) of 3-penten-2-one (11) in 300 ml of ether, we obtained after removal of the ether, by careful distillation at atmospheric pressure, a liquid residue which was distilled through a spinning band column. Fractions, b.p. 44–46 °C at 5–6 mm, were collected and combined. Yield 28.3 g (78%), $n_D^{23} = 1.4528–1.4536$. Nuclear magnetic resonance peaks were found at 8.80 τ, O—C(—CH_3)—; 8.27 and 8.35 τ, $—CH_3$; 8.04 τ, O—H; 7.73 and 7.84 τ, $—CH_2—$ split by a single proton; and a complex

Can. J. Chem. Downloaded from www.nrcresearchpress.com by 210.87.254.6 on 09/05/12
For personal use only.

series of peaks from 3.8–5.2 τ, $=CH_2$ and $=C\begin{smallmatrix}H\\ \diagup\\ \diagdown\end{smallmatrix}$. The relative areas were 2.8:2.7:1.1:2.2:5; theory 3:3:1:2:5.

Anal. Calcd. for $C_8H_{14}O$: C, 76.14; H, 11.18. Found: C, 76.50; H, 11.31.

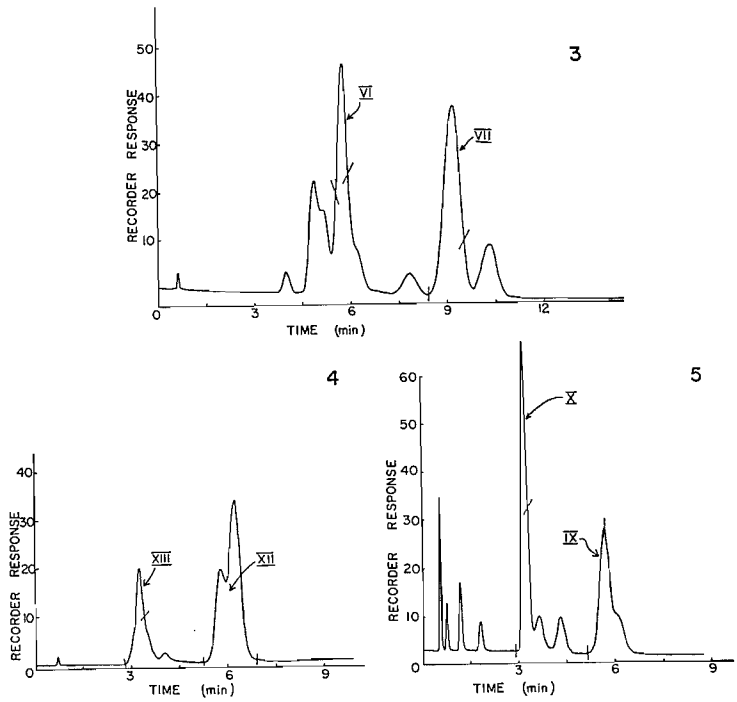

FIG. 3. Gas–liquid chromatography trace of dehydration products from V.
FIG. 4. Gas–liquid chromatography trace of dehydration products from XI.
FIG. 5. Gas–liquid chromatography trace of dehydration products from VIII.

Dehydration of XI

Dehydration of 20 g (0.16 moles) of the alcohol XI in a manner similar to that described for V gave, after distillation, a crude triene fraction, b.p. 25–35 °C at 35 mm. Yield 12 g (69%). The vapor-phase chromatogram of this triene mixture is shown in Fig. 4. The two largest peaks, the lower-retention product about 20% of the total trienes and the higher 70%, were collected using the same preparative column as previously (sample size ca. 0.1 ml, helium flow 200 ml/min, column temperature 120 °C). As can be seen from Fig. 4, the high-retention product which was collected is actually a mixture of two compounds in the ratio of about 1:2.

Low-Retention Product, 4-Methylene-1,5-heptadiene XIII

This compound was obtained in only about 90% purity (g.l.c.).

Nuclear magnetic resonance peaks for XIII were found at 8.19 and 8.28 τ, CH_3, split by a single proton; 7.08 and 7.17 τ, $—CH_2—$ split by a single proton; and a complex series of peaks 3.4–5.2 τ, $=CH_2$ and $=C\begin{smallmatrix}H\\ \diagup\\ \diagdown\end{smallmatrix}$. The relative areas were 3.2:1.7:7; theory 3:2:7.

High-Retention Products, cis-trans- and trans-trans-4-Methyl-1,3,5-heptatriene (XII)

Peaks in the n.m.r. spectrum were found at 8.26 τ, CH_3 split by a single proton and 8.18 τ, the other half of the split CH_3 and an unsplit CH_3, and a complex series of peaks from 2.9–5.2 τ, $=CH_2$ and $=C\begin{smallmatrix}H\\ \diagup\\ \diagdown\end{smallmatrix}$. The relative areas were 6:6; theory 6:6. $n_D^{25} = 1.5318$.

Anal. Calcd. for C_8H_{12}: C, 88.82; H, 11.18. Found: C, 88.72; H, 11.20.

Preparation of 2-Methyl-hepta-1,5-dien-4-ol (VIII)

Using a procedure similar to that described for the preparation of V and starting with 8 g of methallyl chloride in 50 ml of ether and 13.4 g (0.55 moles) of magnesium in 25 ml of ether and then adding a solution of 22 g (0.31 moles) of crotonaldehyde and 44 g (0.48 moles) of methallyl chloride in 300 ml of ether, we

Can. J. Chem. Downloaded from www.nrcresearchpress.com by 210.87.254.6 on 09/05/12
For personal use only.

obtained, after distillation through a spinning band column, essentially one fraction, 37.4 g (96%) of VIII, b.p. 56–57.5 °C at 6 mm, n_D^{25} = 1.4559.

Anal. Calcd. for $C_8H_{14}O$: C, 76.08; H, 11.17. Found: C, 76.14; H, 11.05.

Peaks were found in the n.m.r. spectrum at 8.35 τ, $-CH_3$ split by a proton and 8.27 τ, unsplit $-CH_3$ and the other half of the split peak; 8.11 τ, O—H; 7.80 and 7.91 τ, $-CH_2-$ split by a single proton; a complex band centered at 5.95 τ, H—C—O; 5.24 τ, $=CH_2$; and a complex pattern with the main peaks at 4.41, 4.48, and 4.55 τ, $=C\begin{smallmatrix}H\\ \diagup\\ \diagdown\end{smallmatrix}$. The relative areas were 6:1.2:2.4:1:2:2; theory 6:1:2:1:2:2.

Dehydration of VIII

The alcohol VIII, 5 g (0.04 moles), was added dropwise to 5 g of powdered potassium acid sulfate, contained in a 50 ml 2-necked round bottom flask immersed in an oil bath at 150–160 °C. The other outlet of the flask was connected to a condenser head, condenser, and a dry ice cooled receiver. As much of the round-bottomed flask as possible was immersed in the oil bath to decrease the amount of holdup. About 2 g (46%) of a hydrocarbon fraction and 0.3–0.4 ml of water were collected in the receiver. The hydrocarbon layer was separated from the lower water layer with a medicine dropper and dried over a small amount of anhydrous potassium carbonate. The vapor-phase chromatogram of this crude fraction is shown in Fig. 5. The two largest peaks, the lower-retention product about 43% of the total trienes and the higher 30%, were separated in gram quantities using the preparative column described previously (sample size 0.1–0.15 ml, helium flow 200 ml/min, column temperature 125 °C, retention times as shown in Fig. 5).

Low-Retention Product, 2-Methyl-1,4,6-heptatriene (X)

n_D^{25} = 1.4645, showing an ultraviolet maximum in cyclohexane at 226.5 mμ, ϵ_{max} 27 200, in reasonable agreement for a monosubstituted diene. Peaks were found in the n.m.r. spectrum at 8.45 τ, $-CH_3$; 7.35 and 7.45 τ, $-CH_2-$ split by a single proton; and a complex series of peaks 3.5–5.5 τ, $=CH_2$ and $=C\begin{smallmatrix}H\\ \diagup\\ \diagdown\end{smallmatrix}$. The relative areas were 3.1:2.0:7.2; theory 3:2:7.

Anal. Calcd. for C_8H_{12}: C, 88.82; H, 11.18. Found: C, 88.60; H, 11.13.

High-Retention Product, trans-trans-2-Methyl-1,3,5-heptatriene (IX)

n_D^{25} = 1.5232. Peaks were found in the n.m.r. spectrum at 8.33 τ, $-CH_3$ split by a proton and 8.24 τ, the second peak of this split CH_3 and an unsplit CH_3; 5.17 τ, $=CH_2$; and a complex series of peaks 3.6–4.7 τ. $=C\begin{smallmatrix}H\\ \diagup\\ \diagdown\end{smallmatrix}$. The relative areas were 6.1:2.1:4; theory 6:2:4.

Anal. Calcd. for C_8H_{12}: C, 88.82; H, 11.18. Found: C, 88.58; H, 11.54.

ACKNOWLEDGMENTS

The author wishes to thank the National Research Council of Canada for financial support.

REFERENCES

1. T. S. Sorensen. Can. J. Chem. This issue.
2. J. C. H. Hwa, P. L. de Benneville, and H. J. Sims. J. Am. Chem. Soc. **82**, 2537 (1960).
3. I. N. Nazarov and A. I. Kakhniashvili. Sb. Statei Obshcheĭ Khim. Akad. Nauk SSSR, **2**, 919 (1954).
4. E. R. Alexander and G. R. Coraor. J. Am. Chem. Soc. **73**, 2721 (1951).
5. T. von Fellenberg. Ber. **37**, 3578 (1904).
6. B. N. Dashkevich, I. V. Smolanka, and Yu. Yu. Tsmur. Nauchn. Zap. Uzhgorodsk. Gos. Univ. **22**, 81 (1957).
7. E. A. Braude and J. A. Coles. J. Chem. Soc. 1425 (1952).
8. G. W. Gray (*Editor*). Steric effects in conjugated systems. Butterworths, London. 1958.
9. W. A. Ayer, C. E. McDonald, and J. B. Stothers. Can. J. Chem. **41**, 1113 (1963).
10. K. Alder, H v. Brachel, and K. Kaiser. Ann. **608**, 195 (1957).
11. V. Grignard and M. Fluchaire. Ann. Chem. **9**, 5 (1928).

Can. J. Chem. Downloaded from www.nrcresearchpress.com by 210.87.254.6 on 09/05/12
For personal use only.

SELF-CONDENSATION OF *p*-CHLOROPHENACYL CHLORIDE IN THE PRESENCE OF GRIGNARD REAGENT

MARSHALL KULKA
Research Laboratories, Dominion Rubber Co. Ltd., Guelph, Ontario
Received May 12, 1964

ABSTRACT

A crystalline by-product, formed in the reaction of *p*-chlorophenacyl chloride (I) with ethylmagnesium chloride, has been identified as 1,3-dichloro-2,4-bis(*p*-chlorophenyl)-2,4-hexanediol (IV). Its formation has been attributed to aldolization of I followed by reaction with Grignard reagent at the carbonyl function. The dehydrochlorination of IV yielded one of two possible compounds to which the diepoxide structure VI was assigned on the basis of n.m.r. spectra. The dehydrochlorinated product (VI) was synthesized from 1-chloro-2,3-epoxy-2,4-bis(*p*-chlorophenyl)-4-butanone (VIII) by treatment with ethylmagnesium chloride followed by reaction of the resulting epoxy alcohol IX with alcoholic alkali. It is suggested that the epoxy alcohol IX did not dehydrochlorinate directly to the 3,4-epoxytetrahydrofuran derivative V but instead rearranged first by epoxide alcohol transposition to X and then dehydrochlorinated to 1,2,3,4-diepoxy-2,4-bis(*p*-chlorophenyl)hexane (VI).

The condensation of *p*-chlorophenacyl chloride (I) with ethylmagnesium chloride produced the normal compound, 1-chloro-2-*p*-chlorophenyl-2-butanol (II) (1) as well as a crystalline by-product. The latter was formed in higher yield when the order of addition was reversed and the Grignard reagent was added to I. This investigation describes the properties and identification of this crystalline by-product and provides evidence for the mechanism of its formation.

The infrared spectrum of this compound showed the presence of hydroxyl groups and the absence of carbonyl groups. The OH band appeared at 3.0 μ (3 333 cm^{-1}), a shift from the normal which indicated hydrogen bonding. The reluctance of the compound to react with phenyl isocyanate or with acetic anhydride suggested the presence of tertiary hydroxyl groups. Of the possible modes of formation of the hydroxyl group from the carbonyl group, aldolization appeared to be the most likely. Analysis of the unknown compound provided the formula $(C_9H_9Cl_2O)_n$ with half the chlorine not removable and the other half easily removable by dehydrochlorination with cold methanolic or ethanolic potassium hydroxide. The dehydrochlorination was accompanied by loss of the hydroxyl groups, as evidenced by infrared spectra, and this indicated epoxide formation from a chlorohydrin.

The molecular weight of the unknown compound could not be determined by the Rast method because it liberated hydrogen chloride on heating. The dehydrochlorinated compound, on the other hand, though sensitive to acids and bases, was more stable to heat and could be distilled *in vacuo*. Analysis and molecular weight determinations of the dehydrochlorinated compound gave the empirical formula $(C_9H_8ClO)_2$ from which the formula $(C_9H_9Cl_2O)_2$ could be deduced for the chlorohydrin. On the basis of the above evidence the structure IV was assigned to the by-product of the Grignard reaction and the structure V or VI to the dehydrochlorinated product. Degradation studies showed that IV could be cleaved by phosphorus pentoxide in boiling benzene to *p*-chlorophenacyl chloride (I) in 80% yield. This cleavage was attributed to retrograde aldolization.

The formation of 1,3-dichloro-2,4-bis(*p*-chlorophenyl)-2,4-hexanediol (IV) in the Grignard reaction can be explained by aldolization of two molecules of *p*-chlorophenacyl chloride (I) followed by attack of the intermediate hydroxyketone III by ethylmagnesium

Can. J. Chem. Downloaded from www.nrcresearchpress.com by 210.87.254.6 on 09/05/12
For personal use only.

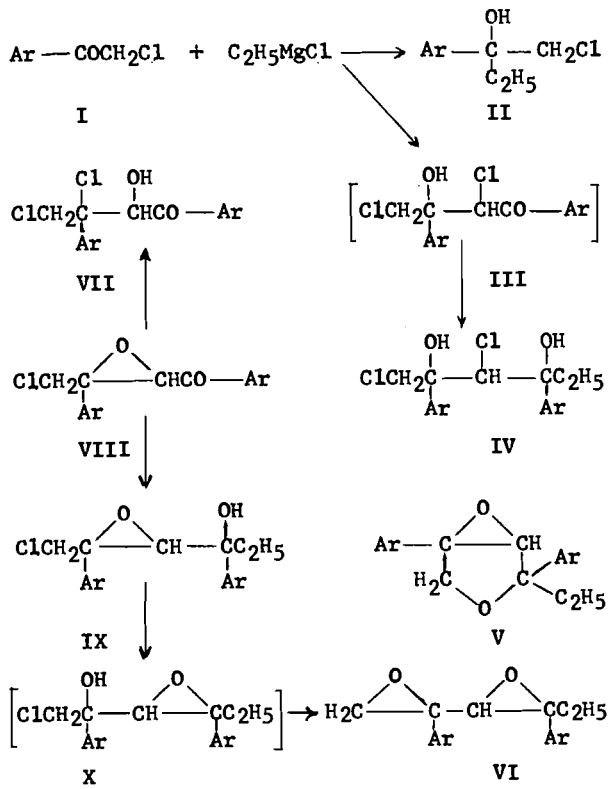

Ar = p-chlorophenyl

chloride at the carbonyl function. A similar aldolization occurs in the Darzens reaction but the intermediate halohydrin cannot survive the strong alkaline conditions and is converted into an epoxide by intramolecular displacement. The Darzens reaction (2, 3, 4) is illustrated by the self-condensation of phenacyl bromide (XI), catalyzed by alcoholic sodium alkoxides, to form the two geometrical isomers of 4-bromo-1,3-diphenyl-2,3-epoxy-1-butanone (XIII) (5–8).

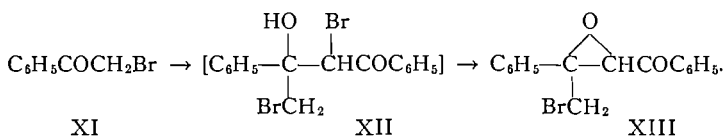

The intermediate bromohydrin XII has never been isolated. However there is one report (3) of the isolation of a fluorohydrin. In this investigation the isolation of the chlorohydrin IV was made possible through the stabilization of the aldolization product III by reaction with ethylmagnesium chloride.

The structure of 1,3-dichloro-2,4-bis(*p*-chlorophenyl)-2,4-hexanediol (IV) was confirmed by synthesis of its dehydrochlorination product. The starting material was 4-chloro-2,3-epoxy-1,3-bis(*p*-chlorophenyl)-1-butanone (VIII) which was obtained from *p*-chlorophenacyl chloride (I) by the Darzens method using sodium ethylate as catalyst. The

Can. J. Chem. Downloaded from www.nrcresearchpress.com by 210.87.254.6 on 09/05/12
For personal use only.

recent confirmation (5, 6) of the structure of the epoxyketone XIII obtained from phenacyl bromide under similar conditions validates the structure VIII. The first approach to IV failed because in the presence of hydrogen chloride the oxirane ring of VIII opened in the undesired direction to form 3,4-dichloro-2-hydroxy-1,3-bis(*p*-chlorophenyl)-1-butanone (VII) and not the required isomer III. That epoxyketone VIII yielded the secondary alcohol VII was established by infrared spectra and by the analogous behavior of 2,3-epoxy-1,3-diphenyl-1-butanone which yielded 3-chloro-2-hydroxy-1,3-diphenyl-1-butanone under similar conditions (9).

The second approach to IV consisted of the reaction of 4-chloro-2,3-epoxy-1,3-bis(*p*-chlorophenyl)-1-butanone (VIII) with ethylmagnesium bromide. In previously studied reactions of α,β-epoxyketones with Grignard reagents it had been observed that epoxyalcoholates are formed which undergo cleavage easily unless stabilized by very low temperatures or by introduction of an alpha substituent (10, 11). When the epoxyketone VIII was treated with ethylmagnesium bromide at $-10°$ followed by decomposition with dilute acid, the epoxyalcohol IX was formed. Since epoxyalcohols are labile compounds (12) no attempt to purify IX was made. Instead, the crude IX was treated with methanolic potassium hydroxide to form a crystalline compound which proved to be identical in all respects with the dehydrochlorinated product V or VI obtained from the unknown compound IV by a similar treatment.

The structure of the compound IV was thus established as 1,3-dichloro-2,4-bis(*p*-chlorophenyl-2,4-hexanediol by the deductive reasoning based on the fact that IV dehydrochlorinated to V or VI, the compound which also resulted from the reaction sequence VIII → IX → V or VI. There remained the task of assigning a structure to the product of dehydrochlorination, V or VI. A casual examination of the reaction sequence VIII → IX → V or VI would favor the assignment of the structure V. Such a structure would not be unreasonable because the 3,4-epoxytetrahydrofuran system is not very strained and has been prepared in the unsubstituted form (14, 15) as well as in the sugar series (16, 17). However, it is necessary to consider the remarkable ease of rearrangement of α,β-epoxyalcohols analogous to IX by transposition of hydroxyl and epoxide (β-oxanol rearrangement) (13). Thus 2,3-epoxy-1-chloro-2,4-bis(*p*-chlorophenyl)-4-hexanol (IX) on treatment with alcoholic alkali could first rearrange by alcohol epoxide transposition to 3,4-epoxy-1-chloro-2,4-bis(*p*-chlorophenyl)-2-hexanol (X) and then dehydrochlorinate to 1,2,3,4-diepoxy-2,4-bis(*p*-chlorophenyl)hexane (VI). Nuclear magnetic resonance (n.m.r.) spectra studies favor the assignment of structure VI to the dehydrochlorinated product of IV and this supports the suggestion that the rearrangement of IX to X does occur before the dehydrochlorination to VI.

The n.m.r. spectra of VI (or V) and of two model compounds are shown in Fig. 1. The peaks for the protons of epoxide methylenes in the spectra of VI (or V) and 2-*p*-chlorophenyl-2-ethyloxirane (XV) are upfield of where one would normally expect to find such resonances. This upfield shift is quite typical of strained three-membered systems which are pseudoaromatic because of some delocalization of electrons. The methylene proton peaks as shown in the spectra of the tetrahydrofuran model compound XIV (14, 15) are downfield and are more typical of protons on carbons directly bonded to oxygen. The geminal methylene protons of the epoxide VI (5.5 c.p.s.) as well as those of the model epoxide compound XV (5.5 c.p.s.) show small coupling constants as compared to those of the tetrahydrofuran model compound XIV (11 c.p.s.). On the basis of this evidence the diepoxide structure VI and not the epoxytetrahydrofuran structure (V) is assigned to the dehydrochlorinated product of IV.

Can. J. Chem. Downloaded from www.nrcresearchpress.com by 210.87.254.6 on 09/05/12
For personal use only.

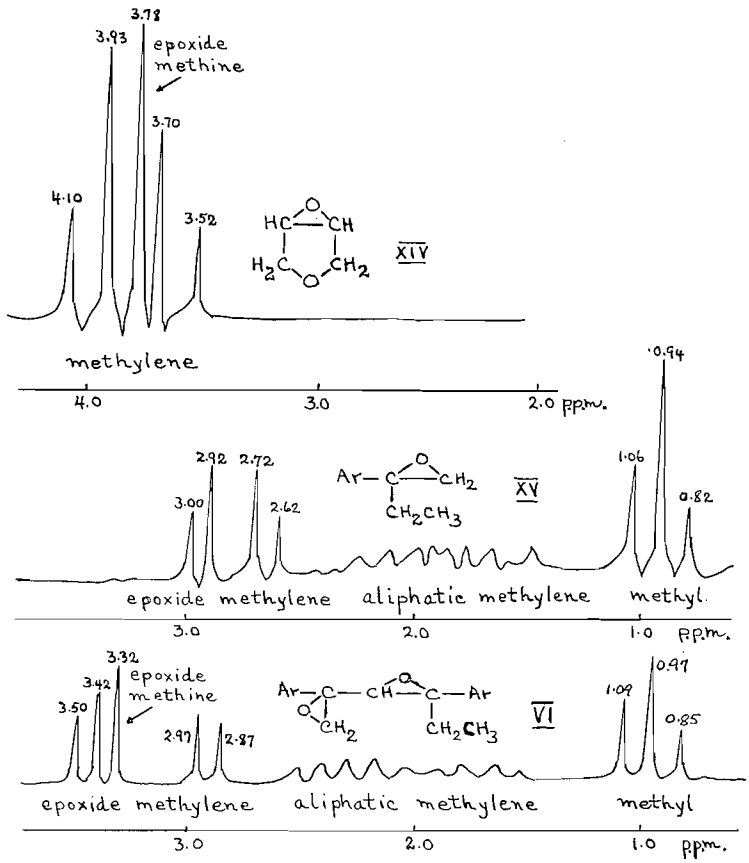

FIG. 1. Nuclear magnetic resonance spectra determined in deuterochloroform at 60 Mc referred to tetramethylsilane as standard.

EXPERIMENTAL

1,3-Dichloro-2,4-bis(p-chlorophenyl)-2,4-hexanediol (IV) and 1-Chloro-2-p-chlorophenyl-2-butanol (II)

A Grignard solution was prepared from magnesium turnings (30 g), dry ether (600 ml), and ethyl chloride (100 g) and decanted from the excess magnesium. Three quarters of this solution was added dropwise over 6 h to a cooled and stirred solution of *p*-chlorophenacyl chloride (I) (150 g) in dry benzene (850 ml). The temperature was kept at 10° by cooling on an ice bath. The reaction mixture was allowed to stand overnight and then treated at 10–15° with the other quarter of the Grignard solution. The resulting solution was decomposed with a cold solution of concentrated hydrochloric acid (120 ml) in water (200 ml) at 10–15°. The organic layer was separated, washed with water, concentrated *in vacuo* to about 200 ml, and allowed to cool. The white precipitate was removed by filtration, washed, and dried. The yield of IV from two crops was 46 g (28%), m.p. 180–182° with decomposition. Crystallization from benzene yielded white prisms melting at 185–186° with decomposition.

Anal. Calcd. for $C_{18}H_{18}Cl_4O_2$: C, 52.94; H, 4.41; Cl, 34.80. Found: C, 52.51, 52.82; H, 4.47, 4.63; Cl, 35.89.

The infrared spectrum of this compound showed the OH band at 3.0 μ (3 333 cm^{-1}). This is a shift from the free hydroxyl range and indicates hydrogen bonding.

The mother liquors from the above crystallizations were combined, taken to dryness *in vacuo*, and the residue distilled. The distillate of 1-chloro-2-*p*-chlorophenyl-2-butanol (II) (1) was a colorless liquid boiling at 92–95° (0.5 mm); n_D^{27} = 1.5465. The yield of II was 53 g or 30%.

Anal. Calcd. for $C_{10}H_{12}Cl_2O$: C, 54.80; H, 5.48. Found: C, 54.81, 55.00; H, 5.29, 5.40.

1,2,3,4-Diepoxy-2,4-bis(p-chlorophenyl)hexane (VI)

(a) From 1,3-Dichloro-2,4-bis(p-chlorophenyl)-2,4-hexanediol (IV)

To a solution of 1,3-dichloro-2,4-bis(*p*-chlorophenyl)-2,4-hexanediol (IV) (25 g) in methanol (500 ml) at 30° was added a solution of potassium hydroxide (10 g) in methanol (100 ml). Precipitation soon began.

Can. J. Chem. Downloaded from www.nrcresearchpress.com by 210.87.254.6 on 09/05/12
For personal use only.

After allowing the reaction mixture to stand for 3 h the precipitate was removed by filtration, washed well with water to wash out the potassium chloride, and dried, yielding 15 g of white crystals. The methanol filtrate on concentration gave a second crop weighing 2.5 g. The total yield of VI was 17.5 g or 85%, melting at 132–134°. Crystallization from methanol yielded sparkling white prisms melting at 133–134°.

Anal. Calcd. for $C_{18}H_{16}Cl_2O_2$: C, 64.48; H, 4.77; Cl, 21.19. Found: C, 64.70, 65.04; H, 4.86, 4.83; Cl, 21.27, 21.75.

(b) From 1-Chloro-2,3-epoxy-2,4-bis(p-chlorophenyl)-4-hexanol (IX)

To a solution of 1-chloro-2,3-epoxy-2,4-bis(*p*-chlorophenyl)-4-hexanol (IX) (see below) (2 g) in methanol (25 ml) was added a solution of potassium hydroxide (0.5 g) in methanol (5 ml). The resulting solution was allowed to stand overnight. The white crystals (1.2 g or 75%) were removed by filtration, washed with water and with methanol, and dried, m.p. 132–134°. Crystallization from methanol yielded white prisms melting at 132–134° alone or in admixture with the compound obtained in (*a*). The infrared spectra of the compounds obtained in (*a*) and (*b*) were identical. This compound could be easily distilled at 0.5 mm pressure at a bath temperature of 180°.

Anal. Calcd. for $C_{18}H_{16}Cl_2O_2$: C, 64.48; H, 4.77. Found: C, 64.83, 65.03; H, 4.63, 4.67.

1-Chloro-2,3-epoxy-2,4-bis(p-chlorophenyl)-4-butanone (VIII)

To a stirred solution of *p*-chlorophenacyl chloride (I) (40 g) in methanol (1 400 ml) cooled at 5 to 10° was added dropwise a solution of sodium (3 g) in methanol (150 ml) over 0.5 h. The resulting yellow solution was stirred at 10° for 2 h and then allowed to stand overnight. It was concentrated *in vacuo* to 500 ml and then poured into water. The sticky solid was extracted with benzene, washed with water, and the solvent removed. The residue on crystallization from methanol yielded white prisms (15 g or 42%), melting at 134–136°.

Anal. Calcd. for $C_{16}H_{11}Cl_3O_2$: C, 56.22; H, 3.22. Found: C, 56.62, 56.57; H, 3.21, 3.49.

The infrared spectrum of this compound showed a strong carbonyl band at 5.9 μ.

1-Chloro-2,3-epoxy-2,4-bis(p-chlorophenyl)-4-hexanol (IX)

A Grignard solution prepared from magnesium turnings (2 g), dry ether (100 ml), and ethyl chloride (6 g) was added dropwise over 0.5 h to a cooled and stirred solution of 2,4-bis(*p*-chlorophenyl)-1-chloro-2,3-epoxy-4-butanone (VIII) (4 g) in dry ether (100 ml). The temperature was kept at −8 to −10° by cooling on an ice–salt bath. The reaction mixture was stirred at −10° for 0.5 h and then decomposed at −10° first with wet ether and then with 1 *N* hydrochloric acid. The ether layer was washed with water and then the solvent was removed, the last traces *in vacuo*. The residual viscous liquid (4 g or 93%) would not crystallize.

Anal. Calcd. for $C_{18}H_{17}Cl_3O_2$: C, 58.14; H, 4.58. Found: C, 58.39, 58.44; H, 4.97, 4.82.

The infrared spectrum of this compound showed a strong band at 2.8 μ.

1,2,3,4-Diepoxy-2,4-bis(p-chlorophenyl)pentane

This was prepared in 1% yield by the condensation of *p*-chlorophenacyl chloride (I) with methylmagnesium bromide followed by treatment of the crude oily product with methanolic potassium hydroxide, following the method used for the preparation of 1,2,3,4-diepoxy-2,4-bis(*p*-chlorophenyl)hexane (VI) above. The intermediate 1,3-dichloro-2,4-bis(*p*-chlorophenyl)-2,4-pentanediol could not be isolated in pure form. The crude 1,2,3,4-diepoxy-2,4-bis(*p*-chlorophenyl)pentane distilled at 160–200° (0.5 mm) and the distillate when crystallized from methanol–benzene yielded white prisms melting at 153–154°.

Anal. Calcd. for $C_{17}H_{14}Cl_2O_2$: C, 63.55; H, 4.36; Cl, 22.1. Found: C, 63.46; H, 4.07; Cl, 23.82.

Degradation of 1,3-Dichloro-2,4-bis(p-chlorophenyl)-2,4-hexanediol (IV) to p-Chlorophenacyl Chloride (I)

To a stirred solution of 1,3-dichloro-2,4-bis(*p*-chlorophenyl)2,4-hexanediol (IV) (10 g) in dry benzene (500 ml) was added phosphorus pentoxide (25 g) and the resulting mixture was stirred and heated under reflux for 2 h. The benzene solution was decanted from the dark residue, washed with cold water, and the solvent removed. The residual semisolid was crystallized from carbon tetrachloride – petroleum ether (30–60°), yielding white prisms (3.5 g or 80%) melting at 99–100° alone or in admixture with *p*-chlorophenacyl chloride.

1,2-Dichloro-2,4-bis(p-chlorophenyl)-3-hydroxy-4-butanone (VII)

Into a solution of 1-chloro-2,3-epoxy-2,4-bis(*p*-chlorophenyl)-4-butanone (VIII) (10 g) in glacial acetic acid (150 ml) at 30° was passed hydrogen chloride until saturated and the solution was allowed to stand overnight. The solvent was removed *in vacuo* below 40° and the residue was crystallized from benzene – petroleum ether (30–60°). The white prisms (6.0 g or 55%) melted at 133–134° with decomposition. One recrystallization from the same solvent raised the melting point to 136–137° with decomposition.

Anal. Calcd. for $C_{16}H_{12}Cl_4O_2$: C, 50.79; H, 3.17. Found: C, 50.96, 50.68; H, 3.46, 3.29.

The infrared spectrum of this compound showed the ketone band at 5.95 μ and the secondary hydroxyl bands at 7.85 and 9.1 μ. This compound when treated with phosphorus pentoxide in benzene did not yield *p*-chlorophenacyl chloride. Also it did not react with ethyl magnesium bromide at 5°; at room temperature it reacted to give an intractable product.

Can. J. Chem. Downloaded from www.nrcresearchpress.com by 210.87.254.6 on 09/05/12
For personal use only.

ACKNOWLEDGMENTS

The author is indebted to Drs. Eugene A. Pier and J. L. Holcomb of Varian Associates, 611 Hasen Way, Palo Alto, California, and to Dr. D. B. MacLean, McMaster University, Hamilton, Ontario, for providing and interpreting the n.m.r. spectra.

REFERENCES

1. M. KULKA. Can. J. Chem. This issue.
2. M. BALLESTER and P. D. BARTLETT. J. Am. Chem. Soc. **75**, 2042 (1953).
3. L. FIELD and C. G. CARLILE. J. Org. Chem. **26**, 3170 (1961).
4. V. F. MARTYNOV and M. I. TITOV. Zhur Obshch. Khim. **30**, 4107 (1960); Chem. Abstr. **55**, 22223 (1961).
5. J. A. BERSON. J. Am. Chem. Soc. **74**, 5175 (1952).
6. H. H. WASSERMAN, N. E. AUBREY, and H. E. ZIMMERMAN. J. Am. Chem. Soc. **75**, 96 (1953).
7. W. MADELUNG and M. E. OBERWEGNER. Ann. **490**, 208 (1931).
8. O. WIDMAN. Ann. **400**, 86 (1913).
9. H. H. WASSERMAN and N. E. AUBREY. J. Am. Chem. Soc. **78**, 1726 (1956).
10. ST. F. DILGEN, C.S.J., and D. J. HENNESSY. J. Org. Chem. **27**, 1223 (1962).
11. E. P. KOHLER, N. K. RICHTMYER, and W. F. HESTER. J. Am. Chem. Soc. **53**, 205 (1931).
12. N. G. GAYLORD and E. I. BECKER. Chem. Rev. **49**, 509 (1951).
13. E. P. KOHLER and C. L. BICKEL. J. Am. Chem. Soc. **57**, 1099 (1935).
14. VON W. REPPE *et al.* Ann. **596**, 111, 138 (1955).
15. E. G. E. HAWKINS. J. Chem. Soc. 248 (1959).
16. C. D. ANDERSON, L. GOODMAN, and B. R. BAKER. J. Am. Chem. Soc. **81**, 3967 (1959).
17. A. BENITEZ, O. P. CREWS, L. GOODMAN, and B. R. BAKER. J. Org. Chem. **25**, 1946 (1960).

Can. J. Chem. Downloaded from www.nrcresearchpress.com by 210.87.254.6 on 09/05/12
For personal use only.

Can. J. Chem. Downloaded from www.nrcresearchpress.com by 210.87.254.6 on 09/05/12
For personal use only.

2-*p*-CHLOROPHENYLALKANOLS

MARSHALL KULKA
Research Laboratories, Dominion Rubber Co. Ltd., Guelph, Ontario
Received May 12, 1964

ABSTRACT

2-*p*-Chlorophenyl-1-butanol (V) has been synthesized by the condensation of *p*-chlorophenacyl chloride (I) with ethylmagnesium chloride and dehydrochlorination of the resulting 1-chloro-2-*p*-chlorophenyl-2-butanol (II) to 2-ethyl-2-*p*-chlorophenyloxirane (III), followed by reduction. It has been discovered that reduction of III with lithium aluminium hydride yielded the tertiary alcohol, 2-*p*-chlorophenyl-2-butanol (IV), while reduction of III with aluminium hydride yielded the primary alcohol V. The two alcohols IV and V were also prepared by unambiguous methods. Attempts to synthesize the higher homologues of the alcohol V were not very successful.

This paper describes the synthesis of some 2-*p*-chlorophenylalkanols which were required for evaluation as agricultural chemicals. The method devised for the synthesis of 2-*p*-chlorophenyl-1-butanol (V) comprised the condensation of *p*-chlorophenacyl chloride (I) with ethylmagnesium chloride, dehydrochlorination of the resulting 1-chloro-2-*p*-chlorophenyl-2-butanol (II) to 2-ethyl-2-*p*-chlorophenyl oxirane (III), and reduction of the oxirane (III) to V. In the condensation of ethylmagnesium chloride with I the order of addition was important. Best results were obtained when *p*-chlorophenacyl chloride (I) was added to the Grignard reagent. The reverse addition produced considerable amounts of a second component, a study of which is reported in another communication (1).

Theoretically the hydrogenation of the oxirane III could follow two reaction paths, one leading to the tertiary alcohol, 2-*p*-chlorophenyl-2-butanol (IV) and the other to the primary alcohol, 2-*p*-chlorophenyl-1-butanol (V). Actually it was found that catalytic hydrogenation of the oxirane III in the presence of Raney nickel catalyst gave a complex mixture from which the primary alcohol V was isolated in 30% yield. On the other hand, reduction with lithium aluminium hydride produced the tertiary alcohol IV in 80% yield. Finally reduction with a mixture of lithium aluminium hydride and aluminium chloride (3 to 1 ratio) which is in fact aluminium hydride gave the primary alcohol V in 80% yield. These results are in accord with those of Eliel and co-workers (2, 3) who have shown that reduction of 2,2,3-triphenyloxirane with lithium aluminium hydride alone led to diphenylbenzylcarbinol by attack at the least substituted carbon of the epoxide, whereas reduction with aluminium hydride produced phenylbenzhydrylcarbinol through ring opening and attack of hydride at the tertiary carbon atom.

The two reference compounds required in this investigation were synthesized by unambiguous methods. The tertiary alcohol IV was obtained through the condensation of *p*-chloroacetophenone with ethylmagnesium bromide. The primary alcohol, 2-*p*-chlorophenyl-1-butanol (V) was synthesized from *p*-chlorobenzyl cyanide by a number of steps which included ethylation with ethyl bromide in the presence of quaternary ammonium base, hydrolysis of the resulting 2-*p*-chlorophenylbutyronitrile (VII, R = ethyl) (4) to the acid VIII (R = ethyl), and reduction of the ester VI to V.

Attempts to prepare higher homologues of 2-*p*-chlorophenyl-1-butanol (V) by the Grignard method were not successful because alkylmagnesium halides higher than ethyl

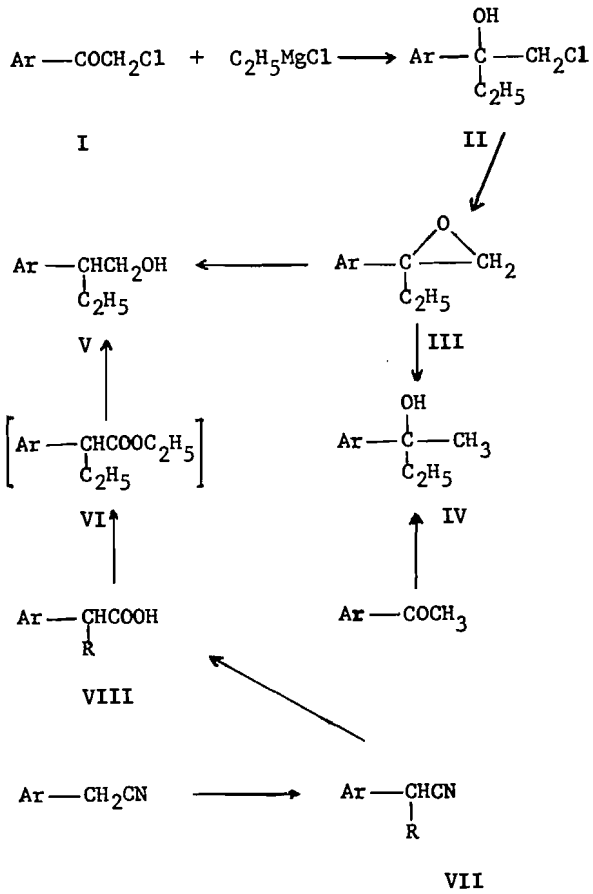

Ar = p-chlorophenyl

reacted with I to form complex mixtures. The abnormal behavior of long- or branched-chain alkylmagnesium halides in reactions with ketones has been observed by other workers (5–7). The cyanide method also found limitation because long chain substituted *p*-chlorobenzyl cyanides (VII, R = *n*-dodecyl and hexadecyl) could not be hydrolyzed to the corresponding acids even on prolonged heating with aqueous–alcoholic alkali. However 2-*p*-chlorophenylhexanoic acid (VIII, R = *n*-butyl) was obtained from the cyanide VII, (R = *n*-butyl) by prolonged hydrolysis. The reduction of its ester yielded 2-*p*-chlorophenyl hexanol.

EXPERIMENTAL

1-Chloro-2-p-chlorophenyl-2-butanol (II)

To a Grignard solution prepared from magnesium (10 g), dry ether (250 ml), and ethyl chloride (30 g) was added dropwise with stirring a solution of *p*-chlorophenacyl chloride (I) (50 g) in dry benzene (300 ml) over about 0.5 h. The temperature was kept at 10–15° by cooling. The reaction mixture was stirred for 5 h and then decomposed with dilute hydrochloric acid. The organic layer was separated, washed with water, and the solvent removed. The residue distilled at 92–95° (0.5 mm); n_D^{23} = 1.5472. The yield was 50 g or 86%.

Anal. Calcd. for $C_{10}H_{12}Cl_2O$: C, 54.80; H, 5.48. Found: C, 54.81, 55.00; H, 5.29, 5.40.

In another experiment when the Grignard reagent was added to the *p*-chlorophenacyl chloride the yield of II dropped and 1,3-dichloro-2,4-bis(*p*-chlorophenyl)-2,4-hexanediol formed (1).

Can. J. Chem. Downloaded from www.nrcresearchpress.com by 210.87.254.6 on 09/05/12
For personal use only.

1-Chloro-2-p-chlorophenyl-2-propanol

This was prepared in 30% yield as above from *p*-chlorophenacyl chloride (I) and methylmagnesium bromide. It boiled at 92–95° (1 mm); $n_D^{22} = 1.5576$.

Anal. Calcd. for $C_9H_{10}Cl_2O$: C, 52.68; H, 4.88; Cl, 34.61. Found: C, 52.85, 52.96; H, 4.82, 4.87; Cl, 34.35, 34.64.

2-Ethyl-2-p-chlorophenyloxirane (III)

To a stirred solution of 1-chloro-2-*p*-chlorophenyl-2-butanol (II) (62 g) in methanol (300 ml) was added dropwise at 15° a solution of potassium hydroxide (21 g) in methanol (150 ml). The reaction mixture was stirred 1 h at 15° and 1 h at room temperature. The solution was decanted from the precipitated potassium chloride, the solvent was removed, and the residue combined with the potassium chloride was treated with water. The precipitated oil was extracted with benzene, the extract washed with water, and the solvent removed. The residue distilled at 110–112° (11 mm) yielding 44 g or 88% of a colorless liquid; $n_D^{20} = 1.5315$.

Anal. Calcd. for $C_{10}H_{11}ClO$: C, 65.74; H, 6.03. Found: C, 65.94, 66.10; H, 5.93, 6.11.

2-Methyl-2-p-chlorophenyloxirane

This was prepared in 85% yield by the dehydrochlorination of 1-chloro-2-*p*-chlorophenyl-2-propanol as above, b.p. (11 mm) 106–108°; $n_D^{22} = 1.5390$.

Anal. Calcd. for C_9H_9ClO: C, 64.09; H, 5.34; Cl, 21.04. Found: C, 63.72, 64.06; H, 5.37, 5.47; Cl, 21.04, 21.18.

2-p-Chlorophenyl-1-butanol (V)

(a) By Catalytic Reduction of 2-p-Chlorophenyl-2-ethyloxirane

A mixture of 2-*p*-chlorophenyl-2-ethyloxirane (III) (30 g), methanol (100 ml), anhydrous sodium carbonate (0.5 g), and Raney nickel catalyst (ca. 0.5 g) was shaken under 50 lb of hydrogen pressure until there was a drop in pressure of 12 lb (ca. 5 h). The catalyst was filtered off and the filtrate distilled. The fraction distilling at 134–137° (11 mm) weighed 10 g (30%); $n_D^{21} = 1.5372$. This was identical with 2-*p*-chlorophenyl-1-butanol (V) obtained by an unambiguous method (see (*c*)).

Anal. Calcd. for $C_{10}H_{13}ClO$: C, 65.04; H, 7.05. Found: C, 64.87, 64.80; H, 7.02, 7.12.

(b) By reduction of 2-p-Chlorophenyl-2-ethyloxirane (III) with Aluminium Hydride

To a stirred suspension of pulverized lithium aluminium hydride (5 g) in dry ether (100 ml) was added, with cooling, aluminium chloride (7 g). This reaction mixture was stirred for about 15 min and then a solution of 2-*p*-chlorophenyl-2-ethyloxirane (III) (15 g) in dry ether (50 ml) was added dropwise with cooling on a water bath. After heating under reflux for 0.5 h the reaction mixture was cooled, and decomposed first with wet ether and then with dilute acid. The ether layer was washed, the solvent removed, and the residue distilled. The main fraction boiled at 140–142° (13 mm) yielding a colorless liquid (12 g or 80%): $n_D^{25} = 1.5350$, which gave an infrared spectrum identical with that given by the product of catalytic hydrogenation (*a*).

(c) By Reduction of Ethyl 2-p-Chlorophenylbutyrate (VI) with Lithium Aluminium Hydride

To a stirred suspension of pulverized lithium aluminium hydride (3 g) in dry ether (100 ml) was added dropwise a solution of ethyl 2-*p*-chlorophenylbutyrate (VI) (prepared from the nitrile VII (R = ethyl) by alkaline hydrolysis followed by esterification (4)) (12 g) in dry ether over about 15 min. The reaction mixture was heated under reflux for 30 min, cooled, and decomposed by addition of wet ether followed by dilute hydrochloric acid. The ether solution was washed with water, the solvent removed, and the residue distilled, b.p. 140–141° (13 mm); $n_D^{23} = 1.5342$. The yield of colorless liquid was 9.5 g or 85%. The infrared spectrum of this alcohol was identical with that of the alcohol obtained in (*a*).

2-p-Chlorophenyl-2-butanol (IV)

(a) By reduction of 2-p-Chlorophenyl-2-ethyloxirane (III)

To a suspension of powdered lithium aluminium hydride (6 g) in dry ether (150 ml) was added dropwise with stirring a solution of 2-*p*-chlorophenyl-2-ethyloxirane (III) (15 g) in dry ether (50 ml). After heating under reflux for 1 h the reaction mixture was decomposed in the usual manner and the product distilled. It boiled at 120–121° (10 mm) and weighed 12 g (80%); $n_D^{25} = 1.5330$. That this was the tertiary alcohol IV and not the primary alcohol V was shown by comparison of its properties and infrared spectra with those of IV prepared unambiguously (see (*b*) below).

(b) By the Reaction of Ethylmagnesium Bromide with p-Chloroacetophenone

To a Grignard solution prepared from magnesium (16 g), ethyl bromide (25 g), and dry ether (200 ml) was added dropwise with stirring and cooling a solution of *p*-chloroacetophenone (30 g) in dry ether (50 ml). The reaction mixture was decomposed with dilute sulfuric acid, the ether layer washed with water, and the solvent removed. The residue distilled at 120–121° (10 mm); $n_D^{25} = 1.5318$. The yield was 31 g or 80%.

Anal. Calcd. for $C_{10}H_{13}ClO$: C, 65.04; H, 7.05. Found: C, 64.90, 65.08; H, 7.30, 7.08.

2-p-Chlorophenylcapronitrile (VII, R = n-Butyl)

To a stirred solution of potassium hydroxide (100 g) in water (60 ml) was added benzyl triethylammonium chloride (5 g) followed by *p*-chlorobenzyl cyanide (100 g). This was cooled to 10° and *n*-butyl chloride (90 g) was added. The resulting reaction mixture was stirred at 12 to 15° for 24 h, diluted with water, and extracted

Can. J. Chem. Downloaded from www.nrcresearchpress.com by 210.87.254.6 on 09/05/12
For personal use only.

with benzene. The benzene extract was washed with water, the solvent removed, and the residue distilled. The distillate which boiled at 142–170° (11 mm) was dissolved in a solution of sodium (7 g) in methanol (200 ml) and treated with benzaldehyde (40 ml). After standing overnight the reaction mixture was filtered to separate the precipitated α-*p*-chlorophenyl-β-phenylacrylonitrile. The filtrate was diluted with water and extracted with benzene; the benzene solution was washed with water, with aqueous sodium bisulfite, and with water. The solvent was removed and the residue distilled yielding 42 g (32%) of nitrile boiling at 158–164° (12 mm); $n_D^{22} = 1.5192$.

Anal. Calcd. for $C_{12}H_{14}NCl$: C, 69.40; H, 6.75. Found: C, 69.03, 69.32; H, 6.92, 6.78.

The known compounds 2-phenylbutyronitrile (8, 9) (54%), 2-*p*-chlorophenylbutyronitrile (4) (60%), and 2-phenylcapronitrile (10) (41%) were prepared in the same manner as was VII (R = *n*-butyl).

α-n-Dodecyl-p-chlorobenzyl Cyanide (VII, R = n-Dodecyl)

This was prepared in 56% yield by the alkylation of *p*-chlorobenzyl cyanide with *n*-dodecyl bromid as above. The crude product distilled at 180–185° (0.5 mm); $n_D^{27} = 1.4959$.

Anal. Calcd. for $C_{20}H_{30}ClN$: C, 75.12; H, 9.39. Found: C, 75.30, 74.94; H, 9.09, 9.17.

The residue from the distillation of the above product was crystallized from benzene–methanol to yield (15%) white prisms of α,α-di-*n*-dodecyl-*p*-chlorobenzyl cyanide melting at 56–58°.

Anal. Calcd. for $C_{32}H_{54}ClN$: C, 78.77; H, 11.08. Found: C, 78.20, 78.79; H, 10.79, 10.99.

α-n-Hexadecyl-p-chlorobenzyl Cyanide (VII, R = n-Hexadecyl)

This was prepared in 49% yield by the alkylation of *p*-chlorobenzyl cyanide with *n*-hexadecyl bromide as above. It distilled at 211–215° (0.5 mm) and the distillate on crystallization from petroleum ether (30–60°) melted at 38–40°.

Anal. Calcd. for $C_{24}H_{38}ClN$: C, 76.70; H, 10.12. Found: C, 76.53, 76.45; H, 9.91, 9.90.

The residue from the above distillation on crystallization from methanol–benzene yielded (12%) almost white prisms of α,α-di-*n*-hexadecyl-*p*-chlorobenzyl cyanide melting at 56–58°.

Anal. Calcd. for $C_{40}H_{70}ClN$: C, 80.07; H, 11.68. Found: C, 79.63, 80.19; H, 11.54, 11.42.

2-p-Chlorophenylcaproic Acid (VIII, R = n-Butyl)

To a solution of sodium hydroxide (20 g) in water (200 ml) and ethanol (15 ml) was added 2-*p*-chlorophenylcapronitrile (VII, R = *n*-butyl) (30 g), and the reaction mixture was heated under reflux for 5 days. The resulting solution was acidified and extracted with benzene; the benzene solution was washed with water and the solvent removed. The residue distilled at 135–137° (0.5 mm) as a colorless liquid (29 g or 90%) which soon solidified; $n_D^{25} = 1.5215$. A small portion when crystallized from petroleum ether (30–60°) yielded white prisms which melted at 63–65°.

Anal. Calcd. for $C_{12}H_{15}ClO_2$: C, 63.72; H, 6.64. Found: C, 63.80, 63.95; H, 6.94, 6.69.

2-p-Chlorophenylmyristic Acid Amide

When α-*n*-dodecyl-*p*-chlorobenzyl cyanide (VII, R = *n*-dodecyl) was subjected to alkaline hydrolysis as above, no acid was obtained. Instead the amide was formed. It crystallized from methanol as white prisms melting at 90–92°.

Anal. Calcd. for $C_{20}H_{32}NClO$: C, 71.11; H, 9.48. Found: C, 71.31, 71.37; H, 9.31, 9.25.

2-Phenyl-1-hexanol

The ethyl ester of 2-phenylcaproic acid (prepared from 2-phenylcapronitrile, but not purified) (10, 11) was reduced with lithium aluminium hydride to form a colorless liquid boiling at 134–135° (11 mm); $n_D^{26} = 1.5085$. The yield was 90%.

Anal. Calcd. for $C_{12}H_{18}O$: C, 80.90; H, 10.11. Found: C, 80.23, 80.36; H, 9.68, 9.67.

2-p-Chlorophenyl-1-hexanol

This was prepared in 80% yield by the reduction of ethyl 2-*p*-chlorophenylcaproate with lithium aluminium hydride. It boiled at 158–160° (11 mm); $n_D^{22} = 1.5235$.

Anal. Calcd. for $C_{12}H_{17}ClO$: C, 67.76; H, 8.00. Found: C, 68.01, 68.13; H, 7.98, 8.00.

REFERENCES

1. M. KULKA. Can. J. Chem. This issue.
2. E. L. ELIEL and D. W. DELMONTE. J. Am. Chem. Soc. **80**, 1744 (1958).
3. M. N. RERICK and E. L. ELIEL. J. Am. Chem. Soc. **84**, 2356 (1962).
4. M. A. SPIELMAN, A. O. GEISZLER, and W. J. CLOSE. J. Am. Chem. Soc. **70**, 4189 (1948).
5. J. B. CONANT and A. H. BLATT. J. Am. Chem. Soc. **51**, 1227 (1929).
6. A. H. BLATT and J. F. STONE. J. Am. Chem. Soc. **54**, 1495 (1932).
7. M. S. KHARASCH and S. WEINHOUSE. J. Org. Chem. **1**, 209 (1936).
8. J. JARROUSSE. Compt. Rend. **232**, 1424 (1951); Chem. Abstr. **46**, 3973 (1952).
9. B. CHECHELSKA, B. MORAWSKI, and A. ZUPANSKI. Polish Patent No. 43,552 (1960); Chem. Abstr. **55**, 9351 (1961).
10. K. MISLOW and C. L. HARMERMESH. J. Am. Chem. Soc. **77**, 1590 (1955).
11. K. PETTERSSON and G. WILLDECK. Arkiv Kemi, **9**, 333 (1956); Chem Abstr. **50**, 9329 (1956).

Can. J. Chem. Downloaded from www.nrcresearchpress.com by 210.87.254.6 on 09/05/12
For personal use only.

Can. J. Chem. Downloaded from www.nrcresearchpress.com by 210.87.254.5 on 09/05/12
For personal use only.

PHOTOCHEMICAL TRANSFORMATIONS OF DIENES

IV. THE STEREOCHEMISTRY OF THE PHOTO-INDUCED ETHANOL ADDITION TO 3-METHOXYCHOLESTA-3,5-DIENE

CLIFFORD C. LEZNOFF[1,2] AND GEORGE JUST
Department of Chemistry, McGill University, Montreal, Quebec

Received May 15, 1964

ABSTRACT

The photolysis of 3-methoxycholesta-3,5-diene in ethanol-*d* resulted in a 1:1 mixture of 4α- and 4β-deuterio-3β-ethoxy-3α-methoxycholest-5-ene (II, II*a*). A stereospecific synthesis of 4β-deuterio-3α,5-cyclo-5α-cholestan-6β-ol is described.

Recently we have shown that the photo-induced addition of alcohols to 3-alkoxycholesta-3,5-dienes gave in reasonably good yield 3,3-dialkoxycholest-5-enes (1) (e.g. I $\rightarrow$ II). The addition of the alkoxy moiety seemed to be quite stereospecific (3β) (1). In this paper we wish to report on the stereochemistry of protonation of the diene system, and to propose a reaction scheme accounting for the products of these and related reactions (2, 3).

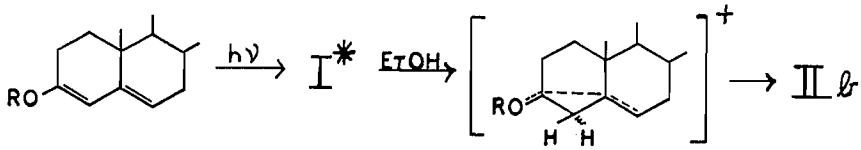

I A

The geminal protons at C-4 are clearly shifted away from most signals in the nuclear magnetic resonance (n.m.r.) spectrum of 3,3-dialkoxycholest-5-enes (1), but seem to be equivalent and hence give rise to a single two-proton peak. In order to determine the stereochemistry of the proton addition at C-4, it was necessary to devise a means of making the two protons at C-4 non-equivalent. In principle, this could be achieved by incorporating them into a cyclopropane ring. The C-4 deuterated product could then be compared by n.m.r. to 4β-deuterio-3α,5-cyclocholestan-6β-ol (VIII), stereospecifically synthesized by an independent route.

Cholest-4-en-3β-yl acetate (4) was treated with monoperphthalic acid (5) in ether and the resulting 4α,5α-epoxycholestan-3β-yl acetate (V) (6) reduced with lithium aluminium deuteride to give 4β-deuteriocholestan-3β,5α-diol (VI). These reductions are known to result in a *trans* diaxial opening of oxide rings (6, 7, 8). Monoacetylation and dehydration with thionyl chloride gave 4β-deuteriocholesteryl acetate (VII*a*), which, after hydrolysis, was transformed into 4β-deuteriocholesteryl tosylate (VII*b*). The n.m.r. spectrum of VII*b* in benzene showed a one-proton signal at 2.45 p.p.m. (doublet, J = 4.5 c.p.s.) corresponding to the C-4 α proton. Pure cholesterol tosylate shows a two-proton signal at

[1]*From a thesis to be presented to the Graduate Faculty, McGill University in partial fulfillment of the requirements for the Ph.D. degree.*

[2]*Holder of a National Research Council of Canada Bursary, 1961–1962, and National Research Council of Canada Studentships, 1962–1964.*

2.45 p.p.m. (doublet, J = 8.8 c.p.s.) due to the C-4 protons. Solvolysis of VII*b* yielded 4β-deuterio-3α,5-cyclocholestan-6β-ol (VIII) (9). Whereas 3α,5-cyclocholestan-6β-ol shows complex signals between 0.2 and 0.7 p.p.m. due to the cyclopropane protons, its 4β-deutero analogue showed in the high field region a one-proton doublet at 0.23 p.p.m. (J = 8.5 c.p.s.) only. The 4α-hydrogen is coupled with the hydrogen at C-3 and the coupling constant is that expected for *cis*-hydrogens on a cyclopropane ring (10, 11).

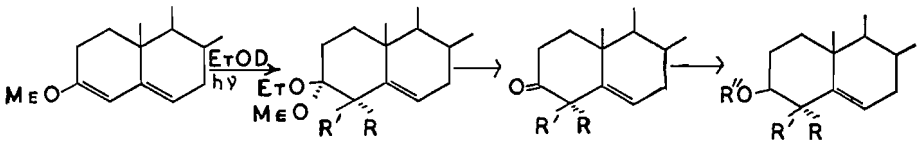

I

II R=H, R′=D
IIa R=D, R′=H
IIb R=H, R′=H

III R=H, R′=D
IIIa R=D, R′=H

IV R″=H, R=H, R′=D
IVa R″=H, R=D, R′=H
IVb R″=OTs, R=H, R′=D
IVc R″=OTs, R=D, R′=H

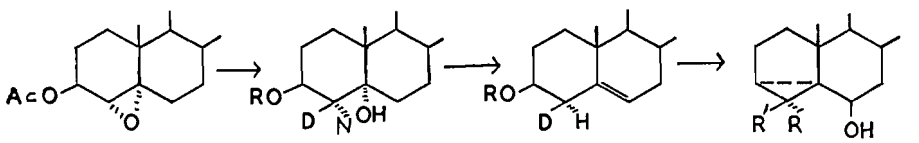

V

VI R=H
VIa R=OAc

VII R=OAc
VIIa R=H
VIIb R=OTs

VIII R=H, R′=D
VIIIa R=D, R′=H

Whereas the photolysis of 3-alkoxycholesta-3,5-dienes in methanol or ethanol proceeded without any difficulty, this was not the case for the corresponding reaction in deuterioethanol, prepared by decomposition of diethyl sulfite in heavy water (12). It seemed that in spite of all precautions taken in its preparation, a small amount of acidic material was present in the deuterated solvent. The reaction was hence carried out in deuterioethanol containing a small amount of pyridine. Mono-4-deuterio-3β-ethoxy-3α-methoxycholest-5-ene (II, II*a*) (1) was isolated in approximately 50% yield by chromatography. Its n.m.r. spectrum showed a one-proton peak at 2.56 p.p.m. (benzene), indicating that one deuterium atom had been taken up per molecule of diene. The ketal was hydrolyzed with malonic acid in acetone to 4-deuteriocholest-5-en-3-one (III, III*a*), which showed a signal at 2.80 p.p.m. (benzene) due to one proton at C-4. No exchange with solvent could have taken place to any large extent at this stage, since any resulting non-deuterated cholest-5-en-3-one would have given (*vide infra*) non-deuterated 3α,5-cyclocholestan-6β-ol (9), which has a very characteristic n.m.r. spectrum in the 0.2–0.7 p.p.m. region. Lithium aluminium hydride reduction of III and treatment of the resulting alcohol with *p*-toluenesulfonyl chloride in pyridine overnight yielded 4-deuteriocholesteryl tosylate (IV*b*, IV*c*).

Can. J. Chem. Downloaded from www.nrcresearchpress.com by 210.87.254.5 on 09/05/12
For personal use only.

Can. J. Chem. Downloaded from www.nrcresearchpress.com by 210.87.254.5 on 09/05/12
For personal use only.

Solvolysis of (IV*b*, IV*c*) in buffered aqueous acetone gave 4-deuterio-3α,5-cyclocholestan-6β-ol (VIII, VIII*a*). Its n.m.r. spectrum showed two signals (approximately 0.5 protons each) in the region characteristic of cyclopropane protons. The signal at 0.23 p.p.m. (doublet, J = 8.5 c.p.s.) was identical to that of 4β-deuterio-3α,5-cyclocholestan-6β-ol. The low-field signal, centered at 0.48 p.p.m., showed up as a triplet. There is little doubt that this signal can be assigned to the 4β-hydrogen, and that this proton is spin–spin coupled with the hydrogen at C_3. In addition, some long range coupling similar to that observed in 3α-methyl-3β,5-cyclocholestane (2) must also be present. The results can only be interpreted by assuming that the deuteration at C-4 was non-specific and that an approximately 1:1 mixture of 4α- and 4β-deuterio-3β-ethoxy-3α-methoxycholest-5-ene (II, II*a*) was obtained in the photo-induced reactions. This is in contrast with the stereochemistry of protonation of the 3β,5-cyclosteroids obtained in the photolysis of cholestadiene and its 3-methyl homologue, in which one deuterium atom was introduced stereospecifically at C-4β (2, 3). It seems therefore quite likely that no bicyclobutane intermediate was formed as a primary photoproduct, since a 3-ethoxybicyclobutane intermediate should be protonated by ethanol as specifically as the analogous 3-methyl and 3-unsubstituted bicyclobutanes.

In order to gain further insight into the reaction, the photolysis of 3-ethoxycholesta-3,5-diene was carried out in the presence of oxygen, which is known to react as a rule rapidly with triplets (13, 14, 15), although exceptions are known (16). The yield of 3,3-diethoxycholest-5-ene was identical to that obtained in the absence of oxygen.

Since benzophenone is known to induce photoreactions to go through the triplet state (17, 18), 3-ethoxycholesta-3,5-diene was photolyzed in the presence of benzophenone, using a "pyrex" tube to filter out wavelengths below 330 mμ. This reaction led to a rapid disappearance of the chromophore. No ketal, however, was formed under these reaction conditions.[3]

The photolyses of cholesta-3,5-diene and 3-alkoxycholesta-3,5-dienes can be summarized as follows: the former is sensitive to oxygen (3), proceeds through a bicyclobutane which can be isolated (19), and the intermediate bicyclobutane is protonated stereospecifically by deuterioethanol (2, 3) to give 4β-deuterio-6β-ethoxy-3β,5-cyclo-5β-cholestane. The products of photolysis in ethanol are identical to those obtained when the photolysis is carried out in pentane, and the intermediate bicyclobutane (19) reacted with ethanol. In contrast, the photolysis of 3-alkoxycholestadienes is insensitive to oxygen. No intermediate bicyclobutane can be isolated, when the enol ether is photolyzed in pentane, and reaction of that photoproduct with ethanol does not give ketals (1). The protonation at C-4 is not stereospecific. Based on the evidence presented, it is not unreasonable to assume that these two reactions proceed through different pathways, in particular since the photolysis of 3-methylcholesta-3,5-diene cannot be explained in terms of only one reaction path (2).

Too little information is available at the present time to give a more detailed interpretation of reaction course of these photolyses.[4]

EXPERIMENTAL[5]

4β-Deuteriocholestan-3β,5α-diol-3β-acetate (VIa)

To 0.300 g of lithium aluminium deuteride in 20 ml of anhydrous ether was added 2.0 g of solid V (6). Anhydrous ether (20 ml) was then added and the mixture stirred for 2 h. After careful addition of water, the

[3]*The same reaction, in the absence of benzophenone, resulted in the recovery of most of the starting material.*
[4]*See, however, ref. 21.*
[5]*General procedures and instrumentation as in ref. 1.*

solution was washed neutral, dried over sodium sulfate, and evaporated to dryness to give 1.9 g of crystals, m.p. 198–218°. Recrystallization from ethyl acetate gave 1.2 g of 4β-deuteriocholestan-3β,5α-diol (VI), m.p. 221° (lit. m.p. 224.5–225.5° (22)).

About 1.2 g of VI in 40 ml pyridine and 15 ml of acetic anhydride were left standing overnight at room temperature. After the usual work-up, recrystallization from acetone–methanol gave 1.2 g of 4β-deuteriocholestan-3β,5α-diol-3β-acetate (VI*a*), m.p. 184–185° (lit. 184.6–185.6° (23)).

4β-Deuteriocholesteryl Acetate (VII)

To a solution of 1.15 g of VI*a* in 20 ml of pyridine at 0 °C, 3 ml of thionyl chloride was added and the solution stirred for 20 min. Ice water was added and after the usual work-up, the oily crystals were crystallized twice from acetone–methanol to give 500 mg of VII, m.p. 105–109°.

4β-Deuterio-3α,5-cyclocholestan-6β-ol (VIII) (9)

About 425 mg of VII was hydrolyzed (6) and 300 mg of 4β-deuteriocholesterol (VII*a*), m.p. 146–148°, was obtained after crystallization from acetone–methanol.

Tosylation of 260 mg of VII*a* gave 290 mg of 4β-deuteriocholesteryl tosylate (VII*b*), m.p. 131–132° (9).

A solution of VII*b* (238 mg) in 12 ml of acetone and 3 ml of water was refluxed with 200 mg of sodium acetate for 15 h. Ether extraction, and chromatography of the resulting oil on 4 g of alumina, gave 60 mg of crystals, eluted by hexane–benzene mixtures. Recrystallization from acetone afforded 50 mg of VIII, m.p. 61–63° (identified by melting point and mixed melting point with an authentic sample (9)).

Irradiation of 3-Methoxycholesta-3,5-diene (I) in Ethanol-d

A solution of 2.1 g of I in 475 ml of dry pentane, 55 ml of ethanol-*d* (C_2H_5OD), and 0.25 ml pyridine was irradiated (Hanovia lamp, 450 W) for 3.5 h until little absorption could be detected in the ultraviolet After evaporation, the crude photolysis product was chromatographed on alumina. Elution with hexane gave 1.1 g of oily 4-deuterio-3β-ethoxy-3α-methoxycholest-5-ene (II, II*a*). Crystallization from ethanol gave 500 mg of (II, II*a*), m.p. 92–93° (1).

4-Deuteriocholest-5-en-3-one (III, IIIa)

A solution of 500 mg of 4-deuterio-3β-ethoxy-3α-methoxycholest-5-ene (II, II*a*) in 30 ml acetone and 3 ml of water containing 100 mg malonic acid was allowed to evaporate slowly at room temperature. After 66 h, 350 mg of 4-deuteriocholest-5-en-3-one (III, III*a*), m.p. 127–128°, was obtained by filtration. Its m.p. was not depressed upon admixture of cholest-5-en-3-one (24*a*).

4-Deuterio-3α,5-cyclocholestan-6β-ol (VIII, VIIIa)

To 350 mg of lithium aluminium hydride in 25 ml ether was added 350 mg of the 3-ketone (III, III*a*) obtained above. After stirring for 2 h, the reaction mixture was worked up and 355 mg of crystals were obtained. Recrystallization from acetone–methanol gave 210 mg of 4-deuteriocholesterol (IV, IV*a*), m.p. 138–140°. Its m.p. was not depressed upon admixture of cholesterol.

Tosylation of 4β-deuteriocholesterol obtained above gave 230 mg of 4-deuteriocholesteryl tosylate (IV*b*, IV*c*). The n.m.r. spectra of compounds (IV, IV*a*) and (IV*b*, IV*c*) were consistent with the structures assigned.

Solvolysis of 230 mg (see above) (9) of the tosylate gave 130 mg of (VIII, VIII*a*). Crystallization from acetone yielded 38 mg of (VIII, VIII*a*), m.p. 64–66°. Its melting point was not depressed upon admixture of an authentic sample (lit. m.p. 63–65° (9)).

Irradiation of 3-Ethoxycholesta-3,5-diene (IX) in Ethanol Saturated with Oxygen

A solution of 0.8 g of IX in 565 ml ethanol, through which oxygen had been bubbling for 40 min, was irradiated until the absorption maximum of IX had decreased to 2% of its original intensity (1 h). Chromatography on alumina gave, in the hexane fractions, 525 mg of 3,3-diethoxycholest-5-ene, m.p. 48–49°. Its melting point and infrared spectrum were identical to those of an authentic sample (1). Elution with ether yielded 75 mg of cholest-4-en-3-on-6β-ol, m.p. 182–183°, identified by mixed melting point with an authentic sample (24*b*). Both products had been formed in similar yields when oxygen had been excluded from the photolysis reaction (1).

Irradiation of 3-Ethoxycholesta-3,5-diene (IX) in Ethanol Using Benzophenone as a Photosensitizer

Irradiation (utilizing a pyrex sleeve to eliminate radiation below 330 mμ) of 0.5 g of IX in ethanol (525 ml), containing 0.5 g of benzophenone, for 2.5 h resulted in a decrease of the absorption maximum to less than 20% of the original absorbance. Evaporation of the solvent gave 0.2 g of benzpinacol as crystals. The remaining oil (0.6 g) was chromatographed on alumina. Elution with hexane gave 90 mg of IX. Further elution with hexane–benzene mixtures gave fractions which seemed to contain benzophenone, benzpinacol, and cholest-4-en-3-one. Elution with ether gave 190 mg crude cholest-4-en-3-on-6β-ol (X), from which 60 mg of X, m.p. 186–187°, was obtained by crystallization from hexane.

ACKNOWLEDGMENTS

We wish to thank the National Research Council of Canada and Bristol Laboratories, Syracuse, N.Y., for financial support, and Dr. C. Stammer, Department of Chemistry, McGill University, for taking the n.m.r. spectra.

Can. J. Chem. Downloaded from www.nrcresearchpress.com by 210.87.254.5 on 09/05/12
For personal use only.

REFERENCES

1. G. JUST and C. C. LEZNOFF. Can. J. Chem. **42**, 79 (1964).
2. G. JUST and V. DITULLIO. Can. J. Chem. **42**, 2153 (1964).
3. G. JUST, G. BAUSLAUGH, and V. DITULLIO. To be published.
4. PL. A. PLATTNER, H. HEUSSER, and A. B. KULKARNI. Helv. Chim. Acta, **32**, 265 (1949).
5. E. E. ROYALS and L. L. HARRELL. J. Am. Chem. Soc. **77**, 3405 (1955).
6. S. JULIA and J. P. LAVAUX. Bull. Soc. Chim. 1223 (1963).
7. A. FURST and PL. A. PLATTNER. Abstracts of Papers, 12th International Congress of Pure and Applied Chemistry, New York. 1951. p. 405.
8. D. H. R. BARTON. J. Chem. Soc. 1027 (1953).
9. E. M. KOSOWER and S. WINSTEIN. J. Am. Chem. Soc. **78**, 4347 (1956).
10. K. WIBERG and B. J. NIST. J. Am. Chem. Soc. **85**, 2788 (1963).
11. D. J. PATEL, M. E. H. HOWDEN, and J. D. ROBERTS. J. Am. Chem. Soc. **85**, 3218 (1963).
12. H. J. SHINE. J. Am. Chem. Soc. **78**, 4807 (1956).
13. G. S. HAMMOND and N. J. TURRO. Science, **142**, 1541 (1963).
14. R. SRINIVASAN. J. Am. Chem. Soc. **84**, 4141 (1962).
15. B. C. ROQUITTE. J. Am. Chem. Soc. **85**, 3700 (1963).
16. H. E. ZIMMERMAN and J. S. SWENTON. J. Am. Chem. Soc. **86**, 1436 (1964).
17. G. S. HAMMOND, N. J. TURRO, and R. S. H. LIU. J. Org. Chem. **28**, 3297 (1963).
18. J. S. BRADSHAW and G. S. HAMMOND. J. Am. Chem. Soc. **85**, 3953 (1963).
19. W. G. DAUBEN and F. G. WILLEY. Tetrahedron Letters, 893 (1962).
20. W. G. DAUBEN and J. A. ROSS. J. Am. Chem. Soc. **81**, 6521 (1959).
21. C. LEZNOFF. Ph.D. Thesis, McGill University, Montreal, Quebec. 1964.
22. PL. A. PLATTNER, H. HEUSSER, and M. FEURER. Helv. Chim. Acta, **32**, 587 (1949).
23. L. C. KING and J. A. CAMPBELL. J. Am. Chem. Soc. **71**, 3556 (1949).
24. L. F. FIESER and M. FIESER. Steroids. Reinhold Publishing Corp., New York, N.Y. 1959. (*a*) p. 50; (*b*) pp. 204–205.

Can. J. Chem. Downloaded from www.nrcresearchpress.com by 210.87.254.5 on 09/05/12
For personal use only.

Can. J. Chem. Downloaded from www.nrcresearchpress.com by 210.87.254.42 on 09/05/12
For personal use only.

LITHIUM CHLORIDE CATALYZED DECARBOXYLATION OF OXALACETIC ACID IN ETHANOL

G. W. Kosicki, S. N. Lipovac, and R. G. Annett
Department of Chemistry, University of Windsor, Windsor, Ontario
Received July 20, 1964

ABSTRACT

The monovalent metal salt lithium chloride promotes the decarboxylation of oxalacetic acid in ethanol. The absorption peak which appears at 230 mμ during the reaction is interpreted to be the enol form of pyruvic acid. Hydrogen chloride has a similar effect on the decarboxylation.

INTRODUCTION

Oxalacetic acid (OAA) decarboxylates spontaneously to pyruvic acid and CO_2 in water (1, 2, 3), and nonaqueous solvents (4). This reaction has been shown to be promoted by metal ions, but only by the di- and tri-valent metal salts (1, 5–10). The rates are dependent on the solvent, pH, and ionic strength (11, 12, 13). The addition of the di- and trivalent metal salts to ethanolic OAA solution causes a shift of the absorption maximum to higher wavelengths and an increase in the integral absorption, indicating formation of a chelate (14). The keto form of the acid has been shown to be the decarboxylating species (15) by using the α,α-dimethyl substituted oxalacetic acid, in which only the keto form can exist.

In this paper, using an ethanolic system, we present evidence for the decarboxylation of OAA promoted by the monovalent metal salt, lithium chloride. Ethanolic hydrogen chloride has a similar behavior on the promotion of decarboxylation. Addition of lithium chloride to ethanolic OAA does not show the characteristic absorption shift to higher wavelengths of the polyvalent metal salts.

EXPERIMENTAL

The following materials were commercial preparations: oxalacetic acid (Sigma Chemical Co.), lithium chloride (Fisher Reagent). Absolute ethanol was used as the solvent.

Absorption spectra were measured with a Bausch and Lomb Spectronic 505 Spectrophotometer. The rate of CO_2 production was followed with a Warburg Respirometer, using a modified flask enabling introduction of the solid acid into the CO_2 saturated ethanol system. Readings were taken at constant pressure, measuring increase of volume. The bath temperature was maintained at 25.0 ± 0.1 °C.

Kinetic experiments were performed spectrophotometrically using a Beckman monochromator and a Gilford Instrument Model 2000 Absorbance Recorder. One centimeter light path cuvettes of 3 ml volume were used. The temperature of the system was maintained at 25.0 ± 0.2 °C by means of a thermostated water circulation system. All solutions were prepared by quantitative volumetric dilution of a weighed OAA sample, followed by appropriate addition of a stock solution of ethanolic lithium chloride. The observed rate constants were calculated from the slopes of first-order rate plots.

RESULTS

(1) Spectral Changes

Oxalacetic acid in ethanol has a maximum of absorption at 260 mμ attributed to the enol form of the acid. Addition of LiCl to the ethanolic OAA increases the absorption in the region of 230 mμ as shown in Fig. 1. On the other hand, the addition of polyvalent cations increases the absorption with a shift of the maximum to 280–300 mμ, indicative of chelate formation (14). In ethanol freshly distilled pyruvic acid, probably all in the keto

form, has a negligible absorption (Fig. 1). Addition of LiCl and HCl to the pyruvic acid system increases the absorption in the region of 230–280 mμ.

(2) Rate of Reaction

The spectral pattern observed with LiCl and OAA in ethanol changes with time (Fig. 2). The absorption decreases at 260 mμ but at 230 mμ it initially increases then decreases, a behavior which is indicative of a consecutive reaction. Increasing the concentration of LiCl and consequently the LiCl/OAA ratio, increased the rate of absorption decrease when followed at 260 mμ, but a saturating ratio could only be approached (Fig. 3) because of the limited solubility of LiCl in ethanol. The rate constants used for the graph were calculated from the slopes of first-order plots of the absorption changes at 260 mμ. At the lower ratios of LiCl/OAA two phases appeared, where only the second phase of the

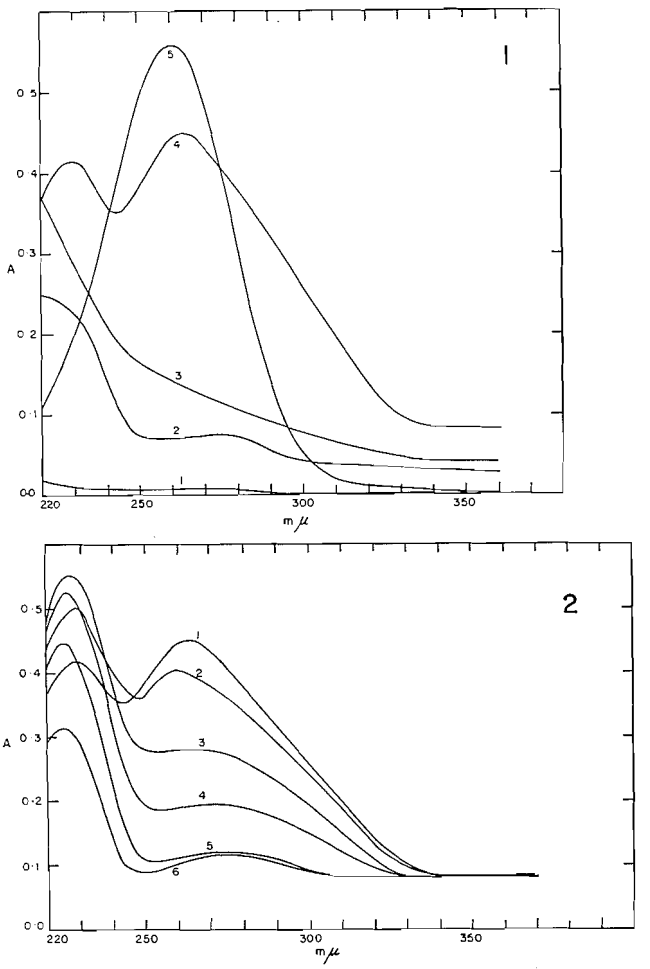

FIG. 1. The effect of LiCl on the spectra of OAA and pyruvic acid in ethanol. All samples were dissolved in absolute ethanol and measured in a 1 cm light path cell. The cuvettes contained (1) 1.0×10^{-4} *M* freshly distilled pyruvic acid, (2) 1.0×10^{-4} *M* pyruvic acid and 0.618 *M* LiCl, (3) 1.0×10^{-4} *M* pyruvic acid and 2.16 *M* HCl, (4) 1.0×10^{-4} *M* OAA and 0.618 *M* LiCl, and (5) 1.0×10^{-4} *M* OAA.

FIG. 2. Absorption spectra for OAA–LiCl–ethanol system as a function of time. The cuvette (1.0 cm light path) contained 1.0×10^{-4} *M* OAA and 0.618 *M* LiCl. The curves represent the change in the absorption of the acid at the following times after mixing; (1) 4 min, (2) 10 min, (3) 20 min, (4) 30 min, (5) 40 min, (6) 99 min, and (7) the same as curve six at 135 min.

Can. J. Chem. Downloaded from www.nrcresearchpress.com by 210.87.254.42 on 09/05/12
For personal use only.

reaction was linear. At higher concentrations of LiCl, those approaching saturation, the linearity of the second phase of the curve increased to over 85% of the reaction.

In Fig. 4 the absorption changes as a function of time are compared at three wavelengths (230 mμ, 243 mμ, and 260 mμ) for the spontaneous reaction and for the LiCl and HCl promoted reactions. These wavelengths were chosen because the difference in their behavior indicated that different species were being followed. At 243 mμ in the spontaneous system an isosbestic point was approached where there was no change in absorption during the first phase of the reaction, since the decrease of the absorption of the reactant was cancelled by the increase of the absorption of the product.

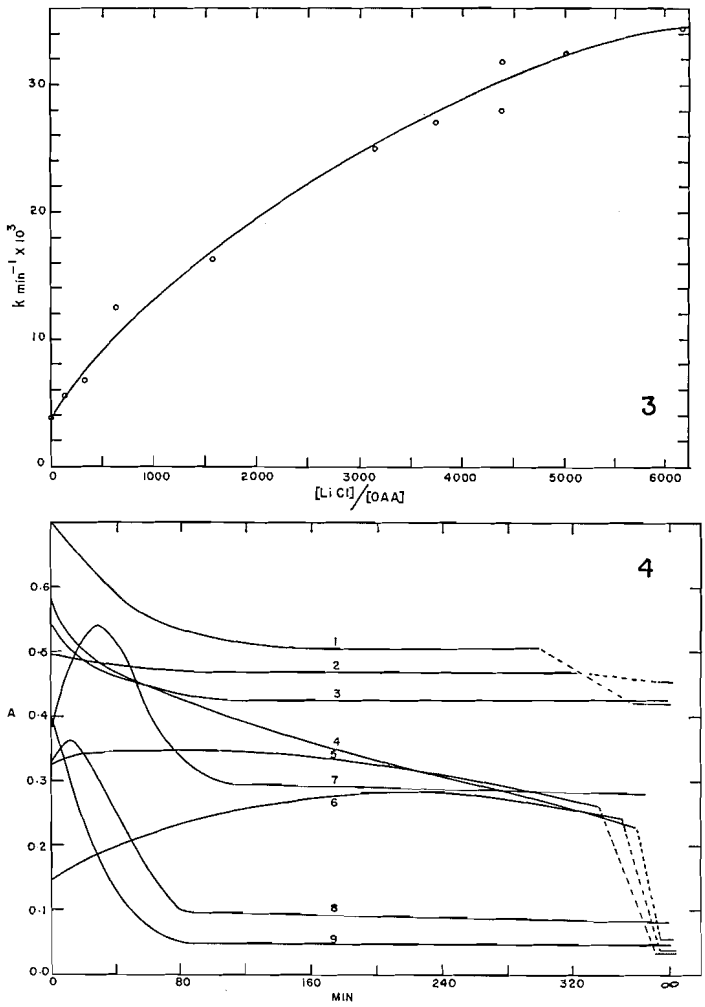

FIG. 3. Observed first-order rate constants as a function of the [LiCl]/[OAA] (260 mμ). Each cuvette contained 1.0×10^{-4} *M* OAA and LiCl of the appropriate concentration to give the indicated molar ratios.

FIG. 4. The rate of reaction for the catalyzed and the uncatalyzed decarboxylation of OAA in ethanol. The changes of absorption with time are shown for the uncatalyzed system, for the LiCl catalyzed system where the molar ratio of LiCl/OAA is 6 180, and for the HCl catalyzed system where the molar ratio is 21 600, at each of the wavelengths indicated. The OAA concentration is 1.0×10^{-4} *M*. The curves represent the system: (1) HCl catalyzed at 260 mμ, (2) HCl catalyzed at 230 mμ, (3) HCl catalyzed at 243 mμ, (4) uncatalyzed at 260 mμ, (5) uncatalyzed at 243 mμ, (6) uncatalyzed at 230 mμ, (7) LiCl catalyzed at 230 mμ, (8) LiCl catalyzed at 243 mμ, (9) LiCl catalyzed at 260 mμ.

Can. J. Chem. Downloaded from www.nrcresearchpress.com by 210.87.254.42 on 09/05/12
For personal use only.

TABLE I

The observed first-order rate constants

	260 mμ absorption decrease (1.0×10^{-4} *M* OAA)	CO_2 production (3.0×10^{-2} *M* OAA)
	$10^3 \times k_{obs}$ (min^{-1})	$10^3 \times k_{obs}$ (min^{-1})
OAA in ethanol	3.80	0.42
OAA + 2.16 *M* HCl	9.44	
OAA + 0.618 *M* HCl	5.98	
OAA + 0.618 *M* LiCl	34.6	
OAA + 0.625 *M* HCl		0.97
OAA + 0.625 *M* LiCl		2.52

Evolution of gas was measured during the reaction of OAA in ethanol in the presence and absence of KOH to confirm that CO_2 was one of the expected products. The observed first-order rate constant in the case of the spontaneous system (Table I) is lower than that measured spectrophotometrically at 260 mμ, probably because of the lower degree of dissociation of OAA in the manometric system. This situation arises because a much higher concentration (300×) of OAA is needed to follow the reaction. Pyruvic acid was confirmed to be the other expected product by assay with lactic dehydrogenase and reduced nicotinamide-adenine dinucleotide (16). The additions of LiCl (and HCl) increased the spontaneous rate of decarboxylation (Table I), but the high ratios of LiCl/OAA needed for saturation of the rate could not be reached in the manometric system because of the higher concentrations of OAA needed to observe the decarboxylation.

DISCUSSION

Oxalacetic acid undergoes a decarboxylation in ethanol. The reaction is promoted by the presence of lithium chloride and HCl. From the nature of the absorption changes at 260 mμ and 230 mμ an equilibrium system can be used to describe the reaction where each of the steps are catalyzed by LiCl and HCl.

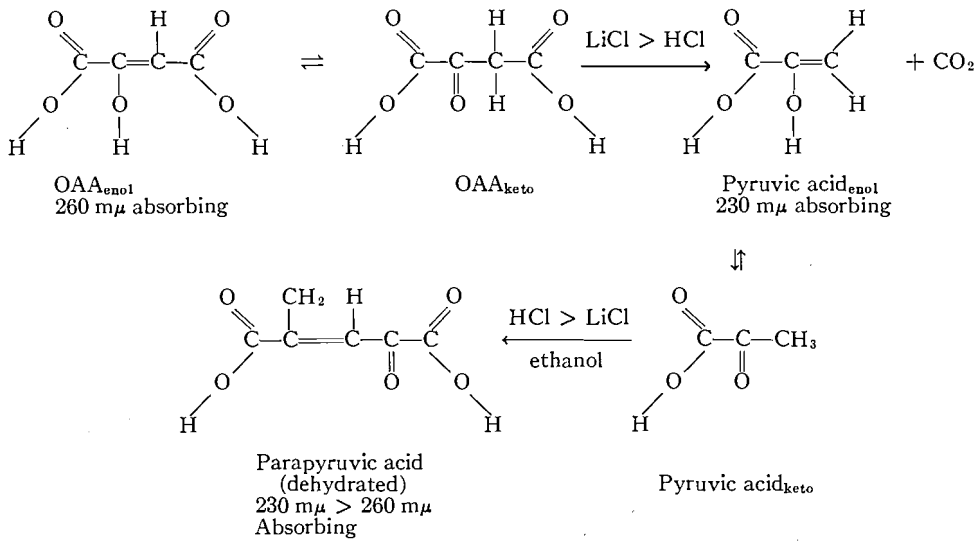

Can. J. Chem. Downloaded from www.nrcresearchpress.com by 210.87.254.42 on 09/05/12
For personal use only.

The active species that decarboxylates in ethanol is postulated to be the keto form of OAA, as in the aqueous system. The presence of LiCl (and HCl) which partially dissociated in ethanol to Li^+ would favor decarboxylation by coordination with the negative end of the polarized β-carbonyl group. The presence of LiCl and HCl would also catalyze the keto–enol tautomerization (17).

The successive appearance of the various species with their major contributions to the observed absorptions at the indicated wavelengths can account for the consecutive reactions observed in the uncatalyzed and LiCl catalyzed systems. The reaction begins with the rapid ketonization of OAA as the solid enol dissolves in ethanol, a rapid reaction too fast to measure at 25 °C in our system (4, 18, 19). As the keto form of OAA decarboxylates, the concentration of the intermediate enol of pyruvic acid increases as observed by the increase of absorption at 230 mμ. The principal assumption is that the enol form of pyruvic acid absorbs at 230 mμ in ethanol, an assumption that is supported by the approach to an isosbestic behavior at 243 mμ for the uncatalyzed system, at which wavelength the enol forms of OAA and pyruvic acid have approximately the same absorbancy index (cf. Fig. 4). The catalyzed formation of the dimer parapyruvic acid (20) causes a further increase in the absorption as shown in Fig. 1 so that the equilibrium absorption is greater than in the uncatalyzed reaction. The parapyruvic acid could dehydrate in the ethanolic system to form a conjugated acid with this greater absorption. The lack of an observed consecutive reaction at 230 mμ in the HCl–OAA system may be accounted for by the masking of the absorption with the fast formation of parapyruvic acid or its conjugated derivative.

The monovalent metal salt lithium chloride does promote decarboxylation of OAA in ethanol (Table I) but a high molar ratio of LiCl/OAA is required to reach a saturating rate effect. The effects of NaCl and KCl could not be compared in this system because of the insolubility of these salts in ethanol. Comparison of the effects in ethanol–water mixtures also presents difficulties arising from change in the degree of dissociation of both the OAA and the metal salts.

ACKNOWLEDGMENTS

The authors wish to thank the National Research Council of Canada for financial support of this project.

REFERENCES

1. H. A. KREBS. Biochem. J. **36**, 303 (1942).
2. S. OCHOA. J. Biol. Chem. **174**, 115 (1948).
3. F. LYNEN and H. SCHERER. Ann. Chem. **560**, 163 (1948).
4. G. W. KOSICKI and S. N. LIPOVAC. XI Colloq. Spectrog. Intern. Belgrad, 1963.
5. J. F. SPECK. J. Biol. Chem. **178**, 315 (1949).
6. P. M. NOSSAL. Australian J. Exptl. Biol. Med. Sci. **27**, 312 (1949).
7. A. KORNBERG, S. OCHOA, and A. MEHLER. J. Biol. Chem. **174**, 159 (1948).
8. E. GELLES. J. Inorg. Nucl. Chem. **8**, 625 (1958).
9. E. GELLES and J. CLYTON. Trans. Faraday Soc. **52**, 353 (1956).
10. E. GELLES and R. W. HAY. Part (I). J. Chem. Soc. 3673 (1958). E. GELLES and A. SALAMA. Part (II). J. Chem. Soc. 3685 (1958).
11. K. J. PEDERSEN. Acta Chem. Scand. **6**, 285 (1952).
12. E. GELLES. J. Chem. Soc. 4736 (1956).
13. G. W. KOSICKI and S. N. LIPOVAC. Can. J. Chem. **42**, 403 (1964).
14. G. W. KOSICKI and S. N. LIPOVAC. Nature, **200**, 359 (1963).
15. R. STEINBERGER and F. H. WESTHEIMER. J. Am. Chem. Soc. **71**, 4158 (1949); **73**, 429 (1951).
16. A. KORNBERG. *In* Methods in enzymology. Vol. I. *Edited by* S. P. Colowick and N.O. Kaplan. Academic Press Inc., N.Y. 1955. p. 441.
17. G. W. KOSICKI. Can. J. Chem. **40**, 1280 (1962).
18. B. BANKS. Part (I). J. Chem. Soc. 5043 (1961).
19. B. BANKS. Part (II). J. Chem. Soc. 63 (1962).
20. A. W. K. DEJANG. Rec. Trav. Chim. **20**, 81 (1901).

Can. J. Chem. Downloaded from www.nrcresearchpress.com by 210.87.254.42 on 09/05/12
For personal use only.

Can. J. Chem. Downloaded from www.nrcresearchpress.com by 210.87.254.105 on 09/05/12
For personal use only.

STRUCTURE OF MAGNESIUM ALUMINIOSILICATE LIQUIDS AT 1 700 °C[1]

E. F. RIEBLING

Research and Development Laboratory, Corning Glass Works, Corning, New York

Received August 6, 1964

ABSTRACT

An improved counterbalanced sphere viscometer–densitometer was used to obtain precise viscosity and density data for melts on (*a*) the silica·cordierite ($2MgO \cdot 2Al_2O_3 \cdot 5SiO_2$)·spinel ($MgO \cdot Al_2O_3$) join and (*b*) the 50 mole % SiO_2 line at temperatures between 1 500 and 1 720 °C. The viscosity, activation energy for viscous flow, and expansion data are indicative of a general tightening of melt flow parameters and structure as either the silica or the alumina content is increased.

The density-derived data have been interpreted in terms of a model that involves no significant change of the partial molar volume of SiO_2 (V_{SiO_2}). Crystalline coordination number information was used to develop a liquid molar volume model that agrees rather closely with the experimental information. This model involves AlO_4 tetrahedra as the major aluminium (III) species for all melts studied with Al_2O_3/MgO ratios equal to or less than unity. The gradual formation of MgO_6 octahedra from MgO_4 tetrahedra appears to accompany the substitution of MgO for Al_2O_3 in melts containing 50 mole % SiO_2.

It has been demonstrated that a reasonable correlation can exist between the coordination number of a given cation in the crystalline state and in high-temperature liquids of similar composition.

I. INTRODUCTION

The $MgO \cdot Al_2O_3 \cdot SiO_2$ ternary system is of current scientific and technological importance. Magnesium aluminiosilicate slags are encountered in steel manufacturing (1, 2, 3). Compounds such as forsterite ($2MgO \cdot SiO_2$), mullite ($3Al_2O_3 \cdot 2SiO_2$), periclase (MgO), spinel ($MgO \cdot Al_2O_3$), and corundum (Al_2O_3) make useful ceramic bodies. Corning Code 9606 glass–ceramic material contains crystals of cordierite ($2MgO \cdot 2Al_2O_3 \cdot 5SiO_2$).

This system is also of geophysical significance. It has been suggested that the structural state of natural cordierites can be used as a qualitative geologic timer for the crystallization history of the enclosing rock (4).

Schreyer and Shairer (4) have also shown that a series of metastable β-quartz solid solutions can be formed along the silica–spinel join. The Al^{+3} substitution for Si^{+4} is accompanied by Mg^{+2} "stuffing" or buttressing of the β-quartz structure. One Mg^{+2}, located in a β-quartz interstitial vacancy, and two Al^{+3} can substitute for two Si^{+4} species. Some low-temperature phases can possess the open high-temperature β-quartz structure because of this lattice buttressing.

It would be expected that the Si—O—Si bond angles and lengths for the low-temperature phases would be similar to those reported for pure SiO_2 at higher temperatures. The basic SiO_2 structure should be preserved, even for relatively large equimolar substitutions of MgO and Al_2O_3 for SiO_2. The present study is an attempt to relate the structure of specific high-temperature magnesium aluminiosilicate liquids to their low-temperature crystalline and glass analogues, some of which possess the open β-quartz structure.

The answers to two specific questions were sought:

1. Does molten SiO_2 in the presence of Al_2O_3 and MgO behave as it does in the presence of just MgO?

2. What coordination number changes occur and how are they related to the variation of composition?

[1]*Presented before a Symposium on High-Temperature Inorganic Chemistry, sponsored by The Chemical Institute of Canada, at Carleton University, Ottawa, Ontario, on September 2–4, 1964.*

Of additional interest was the effect of one network-forming species on another network-forming species. This is of importance with respect to the formation and structure of glasses, since more than one network-forming species is usually included in a given batch formulation.

An improved counterbalanced sphere viscometer–densitometer (5) was used to obtain precise viscosity and density data for melts on the silica·cordierite·spinel join and the 50 mole % SiO_2 system at temperatures between 1 500 and 1 720 °C. The structure of these ternary melts will be compared with those that have been postulated for binary alkaline earth silicate melts (6, 7).

II. EXPERIMENTAL

The MgO and Al_2O_3 powders used to prepare the glass samples were Baker reagent grade analyzed materials. The SiO_2 was 200 mesh Pennsylvania Glass Sand Company ceramic grade sand. Spectrographic analysis of the sand indicated 0.05 to 0.5 wt. % Al_2O_3, 0.01 to 0.1 % CaO, 0.005 to 0.05 % MgO and TiO_2, 0.001 to 0.01 % B_2O_3, Fe_2O_3, ZrO_2, and K_2O, 0.0005 to 0.005 % BaO and Na_2O, and lesser amounts of other oxides.

The powders were mixed and air-dried overnight at 800 °C. The 50 cc sample slugs were individually prepared to ensure close adherence to the desired compositions. The 600 to 1 200 g batches were melted for 6 to 8 h at 1 650 °C in Pt·20% Rh crucibles to allow time for complete reaction and fining. The more viscous liquids were mechanically stirred. Rapid cooling of the 50 cc samples, which were poured directly into the Pt·40% Rh crucibles, gave clear glasses. The samples were stored in dessicators.

The Al_2O_3 contents of the glasses were determined complexometrically with ethylenediaminetetraacetic acid (EDTA). After heating the solutions (at pH 4.6) to ensure complete reaction of the aluminium(III) and EDTA, the excess EDTA was backtitrated with standard zinc solution.

Silica was determined in these glasses by a procedure developed in this laboratory (8). The method is based on the precipitation of the silicomolybdate complex with 8-quinolinol. Excess standard 8-quinolinol solution is added to a solution of the silicomolybdate complex. The excess 8-quinolinol is backtitrated with coulometrically generated bromine.

The chemical analyses were generally within 1% of the attempted batch formulations. Therefore, it was assumed that the MgO contents could be determined by difference.

The improved high-temperature counterbalanced sphere viscometer–densitometer and its operation have been described previously (5, 9). No changes in design or operating procedure were instituted for the present study.

Portions of the ternary phase diagram for the $MgO·Al_2O_3·SiO_2$ system have been recently redetermined (4). One of the binary systems was the silica·spinel join. This information and the available viscosity data were used to decide the best composition and temperature range to be studied. All of the viscosity and density data were obtained at temperatures between 1 500 and 1 720 °C at viscosities that were under 10^3 P. This viscosity range allows a high sensitivity for density determinations with the counterbalanced sphere viscometer–densitometer instrument.

III. RESULTS

The experimental mole % compositions are depicted on the ternary diagram in Fig. 1.

The least squares viscosity and density equations, calculated from the experimental data, are presented in Tables I and II. The analyzed SiO_2 and Al_2O_3 contents are expressed in terms of mole %. Viscosity isotherms for the two systems are shown in Figs. 2 and 3 while the corresponding activation energy vs. composition plots are depicted in Figs. 4 and 5.

Machin and Yee (10) reported some viscosity results for seven high-silica melts in this ternary system. However, they were primarily interested in the quaternary system $CaO·MgO·Al_2O_3·SiO_2$. Bobkova (1) subsequently examined the viscosity of 45 melts, all but 5 of which contained additions of CaO, FeO, and Cr_2O_3. Shilo (2) also examined the viscosity of melts in this ternary system. The compositions corresponded to those of slags encountered in the production of silicochromium alloys. Liutikov and Tsylev recently studied the viscosity and electrical conductance of 50 melts (3) in the same general composition area that was covered by Shilo.

Can. J. Chem. Downloaded from www.nrcresearchpress.com by 210.87.254.105 on 09/05/12
For personal use only.

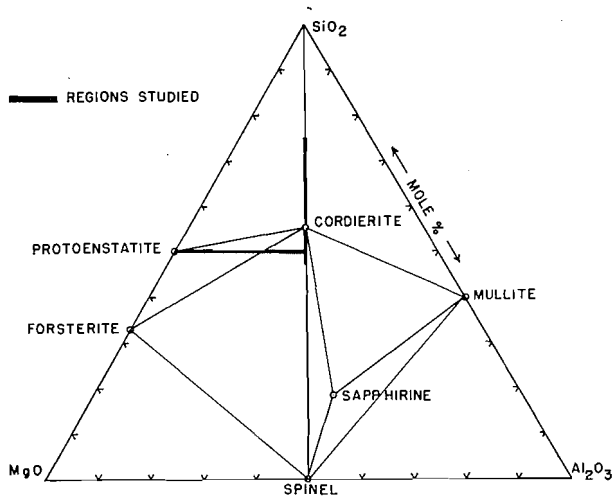

FIG. 1. Ternary mole % diagram of the $MgO \cdot Al_2O_3 \cdot SiO_2$ system showing the regions studied (heavy lines).

TABLE I

Viscosity equations for $MgO \cdot Al_2O_3 \cdot SiO_2$ melts
$\log \eta = -a + b \times 10^4/T(°K)$

Mole % SiO_2	Mole % Al_2O_3	a	b	T(°C) range
47.58	25.62	5.8729	1.3131	1580–1720
51.98	23.49	4.6915	1.1205	1570–1700
55.00	21.63	5.5007	1.3059	1580–1710
59.55	19.49	5.8184	1.4153	1570–1710
63.88	17.45	5.6374	1.4337	1550–1700
67.83	15.10	5.7845	1.5064	1540–1700
70.94	13.90	5.9598	1.5930	1520–1690
74.59	11.92	6.0999	1.6901	1550–1700
49.81	19.98	3.9451	0.9442	1550–1630
49.96	12.95	4.4972	1.0266	1500–1700
50.24	6.09	4.1395	0.9085	1570–1680

TABLE II

Density equations for $MgO \cdot Al_2O_3 \cdot SiO_2$ melts
$\rho(g/cc) = a - b \times T(°K)$

Mole % SiO_2	a	$b \times 10^3$
47.58	2.722	0.05599
51.98	2.669	0.06495
55.00	2.643	0.06531
59.55	2.576	0.05065
63.88	2.554	0.05549
67.83	2.410	—
70.94	2.397	—
74.59	2.221	—
49.81	2.692	0.07498
49.96	2.736	0.1016
50.24	2.742	0.1037

Can. J. Chem. Downloaded from www.nrcresearchpress.com by 210.87.254.105 on 09/05/12
For personal use only.

A comparison of the above studies with the present viscosity data for the 50 mole % SiO_2 system reveals absolute differences for individual points. However, the general trends with composition are similar. For example, the present 1 700 °C viscosity isotherm for the 50 mole % series (Fig. 3) falls between the values given by Shilo and those given by Liutikov and Tsylev. In some cases, the literature compositions do not exactly match each other or the ones presented herein. In addition, the purity of the literature samples apparently differed. Thus, Shilo cited previous experimental errors while Liutikov and Tsylev criticized Shilo's use of graphite crucibles. A complete quantitative comparison of the present viscosity data with the literature values is therefore difficult to justify.

Molar volume isotherms for 1 700 °C are presented in Figs. 6 and 7 while the corresponding molar volume expansion coefficients $(\Delta V/\Delta T)_P$ are given as functions of composition in Figs. 8 and 9. No previous literature values for these ternary melts are available for comparison. However, the binary magnesium silicate results of Bockris *et al.* (11) have been presented in Figs. 7 and 9.

IV. DISCUSSION

A. Viscosity

The viscosity isotherm presented in Fig. 2 shows that most of the structural alteration that occurs with the addition of equimolar amounts of MgO and Al_2O_3 requires less than 25 mole % SiO_2 substitution. The viscosity at 1 700 °C drops by a factor of about 10^4 in this composition region. Substitution of an additional 25 mole % SiO_2 only decreases the viscosity by a factor of 30. Figure 4 shows that the flow mechanism undergoes a similar transition. The activation energy for viscous flow decreases from the 120–160 kcal level to about 75 kcal with the substitution of the first 25 mole % SiO_2. The activation energy change for the substitution of an additional 25 mole % SiO_2 amounts to only about 25 kcal. It appears that not all of these equimolar magnesium aluminate liquids completely retain the rigid three dimensional SiO_2 array.

The experimental results are in general agreement with the discrete anion theory developed by Bockris and co-workers for binary silicate melts (6). The absence of ΔE_η^* maxima in the 75 to 50 mole % SiO_2 region supports the formation of anionic aggregates that are smaller than either infinitely long chains (at 50 mole % SiO_2) or infinite two dimensional sheets (at 67 mole % SiO_2).

A degree of inflexibility accompanies the substitution of Al_2O_3 for MgO in the 50 mole % SiO_2 melts (Figs. 3 and 5). The substitution of Al_2O_3 for 50% of the MgO in a binary 50 mole % magnesium silicate melt causes a fourfold viscosity increase (from about 2 to 8 P) that is accompanied by a 50% increase (about 16 kcal) in the activation energy for viscous flow. The binary data is that of Bockris *et al.* (12). It would appear that the aluminium(III) is entering into "network formation" in the form of AlO_4 tetrahedra.

If AlO_4 tetrahedra can take the place of SiO_4 tetrahedra in the discrete anions postulated for these 50 mole % SiO_2 melts, then one could regard a 25 mole % MgO·25 mole % Al_2O_3 melt as having general structure and flow properties similar to those postulated for a binary 25 mole % MgO silicate melt. Indeed, if the lower curve of Fig. 4 is extrapolated to 25 mole % MgO, the resultant ΔE_η^* is close to the value for the 50 mole % SiO_2 melt of the ternary system.

The recent viscosity studies of Rossin, Bersan, and Urbain (13) and also of Kozakevitch (14) in the binary aluminiosilicate system are of related interest. Their results for an equimolar binary aluminiosilicate melt composition are included in Figs. 3 and 5. The viscosity and activation energy increases reported herein are continuous and gradual with

Can. J. Chem. Downloaded from www.nrcresearchpress.com by 210.87.254.105 on 09/05/12
For personal use only.

Can. J. Chem. Downloaded from www.nrcresearchpress.com by 210.87.254.105 on 09/05/12
For personal use only.

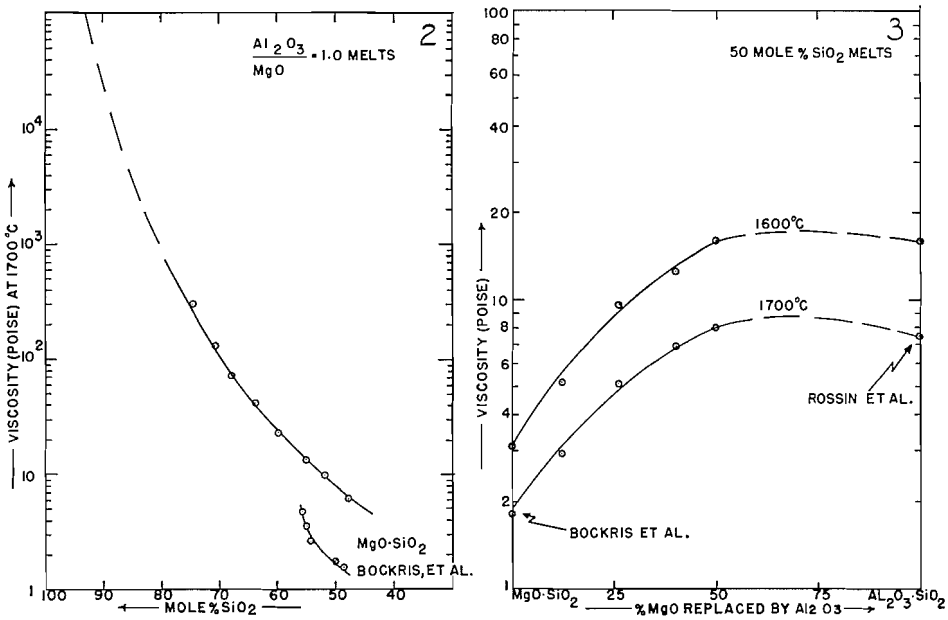

FIG. 2. Viscosity of melts studied on the silica–spinel join. Binary data of Bockris *et al.* shown for comparison.

FIG. 3. Viscosity of melts studied on the 50 mole % SiO_2 line. Binary data of Bockris *et al.* and Rossin *et al.* shown for comparison.

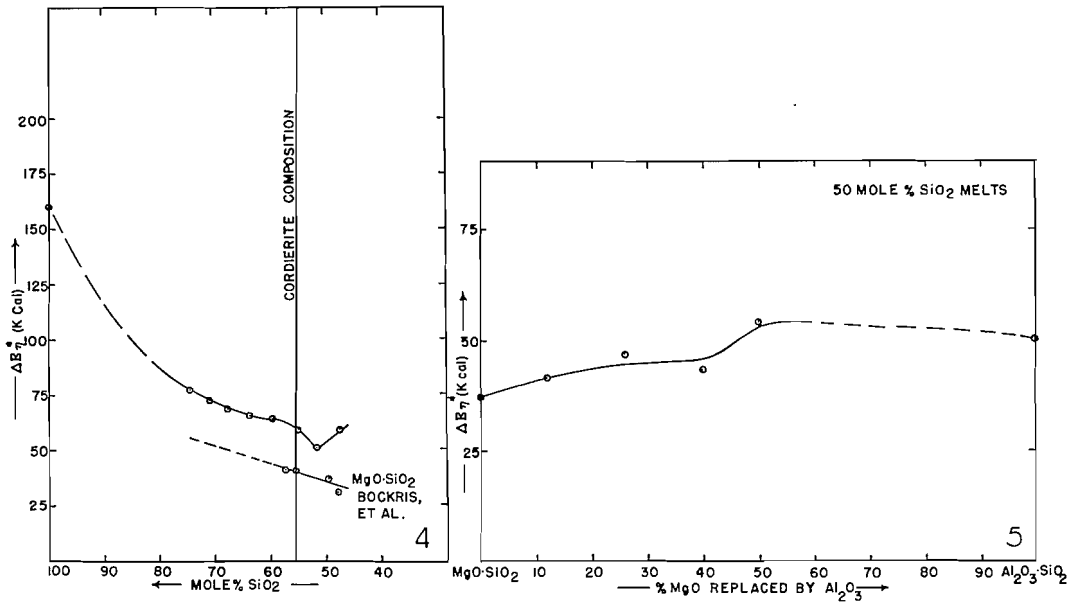

FIG. 4. Activation energy for viscous flow as a function of composition for the silica–spinel join.

FIG. 5. Activation energy for viscous flow as a function of composition for the 50 mole % SiO_2 melts.

the substitution of Al_2O_3 for MgO. Both functions appear to level off for Al_2O_3 substitutions of more than 50% (actual ternary compositions containing less than 25 mole % MgO). Thus, the presence of AlO_4 groups in the predominantly SiO_4 containing discrete anions does not significantly alter the flow mechanism in these 50 mole % SiO_2 liquids.

A change from octahedral to tetrahedral coordination for the Mg^{+2} ions could also influence the viscosity properties as the Al_2O_3 content was increased. Although the oxygen packing is less efficient in the tetrahedral configuration, the Mg—O distances would be slightly less than in the octahedral configuration. Thus, a more tightly bound liquid structure could occur.

It would appear that AlO_6 octahedra (which could form when $Al_2O_3/MgO > 1.0$)[2] do not radically alter the flow properties of these 50 mole % SiO_2 liquids. As pointed out by Rossin *et al.* (13) the low ΔE_η^* ($\sim$27 kcal) of molten Al_2O_3 is characteristic of other octahedral oxides such as CaO, FeO, etc. The addition of 50 mole % SiO_2 to molten Al_2O_3 only increases the ΔE_η^* to about 50 kcal. There must be a fair number of AlO_6 octahedra at the 50 mole % SiO_2 binary composition because most of the ΔE_η^* increase occurs with the addition of more SiO_2 in the form of SiO_4 tetrahedra. A similar behavior has been observed for binary borogermanate and borosilicate liquids (15).

The ΔE_η^* vs. composition trend observed for the 50 mole % SiO_2 melts (Fig. 5) is generally similar to the sequence reported by Kozakevitch (13) for melts in the $CaO \cdot Al_2O_3 \cdot SiO_2$ ternary system. He observed a steady increase of ΔE_η^* for melts with an O/Si ratio of 7/2. These compositions fall between the $CaO \cdot SiO_2$ binary (40 mole % SiO_2) and the Al_2O_3/CaO = unity line. The activation energy remained relatively constant between the Al_2O_3/CaO = unity line and the $Al_2O_3 \cdot SiO_2$ binary (67 mole % SiO_2). Kozakevitch postulated the formation of AlO_6 octahedra for $Al_2O_3/CaO >$ unity.

B. Density-Derived Information

1. Molar Volumes

An advantage of binary systems is that established procedures can be used to obtain partial molar quantities. The graphical method of intercepts (16) and a mirror technique (17), applied to a plot of ΔV (the deviation from ideality) vs. composition, allow a complete exploitation of the Gibbs–Duhem equation (18). This equation explains the interrelationships between the partial molar quantities for the components in a binary system.

The above advantage can be lost in a ternary system. However, it is possible to calculate partial molar quantities such as V_n in a ternary system if V_1 is known as a function of composition for a series of constant values of M_2/M_3 (where M_2 and M_3 are mole fractions) (19). This is usually a rather stringent requirement for the elevated temperatures encountered in molten oxide research.

Bockris *et al.* (20, 11) found that V_{SiO_2} differed very little from $V^0_{SiO_2}$ for alkali and alkaline earth contents of 0 to 50 mole %. This was especially true of the magnesium silicate melts where the difference was rather small. Riebling (21) has recently found that assumption of a constant V_{SiO_2} (equal to $V^0_{SiO_2}$) allowed the formulation of a reasonable model for melts in the system

$$0.25Na_2O \cdot (0.75 - x)GeO_2 \cdot xSiO_2.$$

[2]*D. E. Day and G. E. Rindone have recently obtained evidence for the formation of* AlO_6 *octahedra in alkali aluminiosilicate glasses when* $Al_2O_3/Na_2O > 1.0$. *Refractive index, density, and infrared results (J. Am. Ceram. Soc. 45, 489 (1962)), internal friction results (J. Am. Ceram. Soc. 45, 496 (1962)), and X-ray fluorescence data (J. Am. Ceram. Soc. 45, 579 (1962)) were cited. E. D. Lacy (Phys. Chem. Glasses 4, 234 (1963)) favors the formation of* AlO_4 *triclusters for similar compositions.*

Can. J. Chem. Downloaded from www.nrcresearchpress.com by 210.87.254.105 on 09/05/12
For personal use only.

Finally, a plot of ΔV vs. mole % SiO_2 for melts in the SiO_2–spinel join indicated that V_{SiO_2} was close (0.0–0.5 cc difference) to $V^0_{SiO_2}$ (27.22 cc). It was concluded that a constant value of 27.22 cc could be assumed for V_{SiO_2} for all melts on the SiO_2–spinel join as well as the 50 mole % SiO_2 series.

With V_{SiO_2} fixed, the number of unknowns in eq. 1 is reduced to two (V_{MgO} and $V_{Al_2O_3}$):

$$[1] \qquad V_{obs} = M_{MgO} \cdot V_{MgO} + M_{Al_2O_3} \cdot V_{Al_2O_3} + M_{SiO_2} \cdot V_{SiO_2}.$$

At 1 700 °C V_{MgO} is known for melts in the 40 to 55 mole % MgO region of the $MgO \cdot SiO_2$ system. Bockris *et al.* (11) give a value of 12.5 cc for V_{MgO} at 50 mole % SiO_2 in the binary system. This is relatively close to the molar volume of crystalline periclase (MgO) at 1 700 °C, the value of which is 12.20 cc as calculated from density (22) and expansion coefficient information (23). It would appear that magnesium(II) remains in octahedral coordination with the addition of SiO_2 to form the molten protoenstatite composition.

The coordination of magnesium(II) in spinel ($MgO \cdot Al_2O_3$) is known to be tetrahedral while the coordination of aluminium(III) is octahedral (24). The molar volume of the crystalline material at 1 700 °C, as calculated from density (25) and expansion coefficient information (23), is 41.57 cc.

The molar volume of corundum (Al_2O_3 with the aluminium(III) octahedrally coordinated) is 26.88 cc at 1 700 °C. This was also calculated from density (26) and expansion coefficient information (23). When this volume is combined with the molar volume of MgO (with MgO_6 octahedra (27)), a combined ideal volume of 39.08 cc is obtained for spinel. This ideal high-temperature molar volume for spinel is 2.49 cc less than the observed value (previous paragraph). It has been assumed that this difference of 2.49 cc is primarily due to the greater volume occupied by magnesium(II) in tetrahedral coordination. The molar volume of MgO has therefore been taken as 12.5 + 2.5 = 15.0 cc at 1 700 °C for the tetrahedral packing of oxygens around magnesium(II).

An additional problem concerns the volume increase accompanying the octahedral to tetrahedral coordination change for the aluminium(III) species. The low-temperature form of cordierite ($Al_3Mg_2(Si_5Al)O_{18}$) has a beryl ($Be_3Al_2Si_6O_{18}$) structure with cyclic $(SiO_3)_n^{-2n}$ ions (28). All of the Mg^{+2} ions occupy octahedral holes compared to only 75% of the Al^{+3} ions. Schreyer and Schairer (4) have stated that the X-ray derived density of cordierite is less than that observed for a glass of the same composition at room temperature (2.51 vs. 2.62 g/cc). However, they thought that the low thermal expansion of cordierite raised doubt as to whether the anomalous density behavior held at liquidus temperatures.[3] Thus, the evidence is not clear-cut in favor of three AlO_6 per AlO_4 in a liquid of the cordierite composition.

The feldspars (1–1–6 compounds) are known to possess the three dimensional network structure of SiO_2 with all of the aluminium(III) in the form of AlO_4 tetrahedra (29). They generally contain the larger cations such as Na^+, K^+, and Ca^{+2}. Although one crystalline modification of the $2MgO \cdot 2Al_2O_3 \cdot 5SiO_2$ composition (which is close to a typical feldspar composition) will tolerate only 25% of the aluminium(III) in the form of AlO_4 tetrahedra, the less restrictive liquid state could contain most of the aluminium(III) in the form of AlO_4 tetrahedra. There follows an attempt to determine (*a*) the volume occupied by Al_2O_3 in these liquids, (*b*) the molar volume associated with AlO_4 tetrahedra, and (*c*) the coordination numbers of the aluminium(III) and magnesium(II) species.

[3]*The thermal expansion of cordierite is only about one-half of the value for a 1–1–4 glass over the range 25–700 °C.*

Can. J. Chem. Downloaded from www.nrcresearchpress.com by 210.87.254.105 on 09/05/12
For personal use only.

(*a*) For a 50 mole % SiO_2 melt on the Al_2O_3/MgO = unity join, with MgO_4 tetrahedra assumed,

$$[2] \qquad V_{obs} = 25.35 = 0.50(27.22) + 0.25(15.0) + 0.25(V_{Al_2O_3}).$$

The calculated value of $V_{Al_2O_3}$ at 1 700 °C is 31.44 cc. This is 4.5 cc greater than the value previously calculated for pure corundum at the same temperature. It amounts to a 17% volume increase at 1 700 °C and compares favorably to the percentage increase observed at elevated temperatures for the same coordination change in GeO_2 (5.5 cc and 20%) (9). Similar values have been observed for SiO_2 (~6 cc and 32% for the stishovite to coesite change) (30) and MgO (2.5 cc and 20% as calculated above).[4] It would appear that the above 4.5 cc difference is associated with the octahedral to tetrahedral transformation for aluminium(III) in these magnesium aluminiosilicate liquids.

(*b*) It is possible to qualitatively check the previous conclusion for aluminium(III) by examining a compound in which AlO_4 tetrahedra are known to occur. $AlPO_4$ possesses a low cristobalite structure (AlO_4 and PO_4 tetrahedra) with an $\diagdown O \diagup$ angle of 145° (31). The molar volume of this compound is 47.53 cc at room temperature (32). If $AlPO_4$ consists of one-half mole of Al_2O_3 and one-half mole of P_2O_5, the calculated molar volume is 12.84 cc (one half V_M of corundum, with AlO_6 octahedra) plus 29.72 cc (one-half V_M of P_2O_5; P_4O_{10} consists of PO_4 tetrahedra) (33). This value of 42.56 cc is 4.97 cc less than the observed value at room temperature. The difference can be ascribed to the use of an Al_2O_3 volume that is associated with AlO_6 octahedra. The 4.97 cc difference agrees fairly well with the previous value of 4.5 cc that was calculated in an independent fashion.

(*c*) Figure 6 depicts the experimentally observed molar volume isotherm for 1 700 °C as a function of melt composition in the silica–spinel join. The lowest line represents the isotherm obtained if the assumed structural model for these melts consists of AlO_6 and MgO_6 octahedra. The line just below the experimental isotherm corresponds to a model that involves AlO_4 and MgO_4 tetrahedra. The second model gives much better agreement with experiment (to within 0.3–0.4 cc). This strengthens the concept that liquids on this join contain silica-like anionic species. It can be concluded that the aluminium(III) species are AlO_4 tetrahedra and that they occur within the silica-like anion aggregates rather than as individual ions. The main effect of adding 45% or more SiO_2 to spinel is apparently to create AlO_4 tetrahedra from AlO_6 octahedra, while retaining tetrahedrally coordinated Mg^{+2} ions.

Figure 7 depicts the experimentally observed molar volume isotherm for 1 700 °C as a function of composition for the 50 mole % SiO_2 system. The lowest line represents the isotherm obtained if the assumed structural model consists of AlO_4 tetrahedra and MgO_6 octahedra.[5] The line just below the experimental isotherm corresponds to a model that involves AlO_4 tetrahedra with the gradual formation of MgO_6 octahedra from MgO_4 tetrahedra as the MgO content is increased. The second model gives slightly better agreement with experiment. This strengthens the previously postulated occurrence of MgO_4 tetrahedra in melts on the silica–spinel join.[6] It would also appear that the AlO_4 tetrahedra are the major aluminium(III) species for melts with Al_2O_3/MgO ratios equal to or less than unity.

[4]*The smaller absolute difference for the coordination change in* MgO *is probably associated with the larger size of the* Mg^{+2} *ion as well as the stoichiometry involved. The octahedral configuration does not represent as efficient a method of packing, with respect to the tetrahedral configuration, for* Mg^{+2} *as it does for the smaller* Al^{+3} *and* Ge^{+4} *ions. Also, there are twice as many oxygens per metal atom in* GeO_2 *and* SiO_2 *and one and one-half as many oxygens per metal atom in* Al_2O_3 *as there are in* MgO.

[5]*Any model involving* AlO_6 *octahedra would give worse agreement.*

[6]*A distorted* MgO_6 *octahedra would be another possibility.*

Can. J. Chem. Downloaded from www.nrcresearchpress.com by 210.87.254.105 on 09/05/12
For personal use only.

A significant aspect of the complete liquid model is that within the composition limits studied in the silica–cordierite–protoenstate sub-ternary system, the Mg^{+2} ions, not the Al^{+3} ions, appear to be the cations involved in a coordination change.

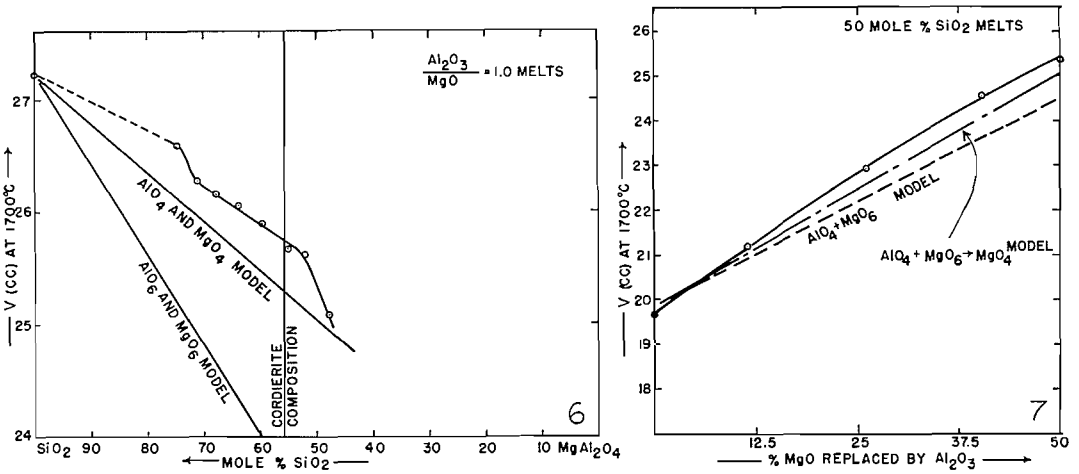

FIG. 6. Experimental molar volume isotherm compared to model isotherms for melts on the silica–spinel join.

FIG. 7. Experimental molar volume isotherm compared to model isotherms for melts on the 50 mole % SiO_2 line.

2. Expansion Coefficients

The absolute values of the expansion coefficients and their variations with composition can be relatively small for melts in the $MgO \cdot Al_2O_3 \cdot SiO_2$ ternary system. The addition of equimolar amounts of MgO and Al_2O_3 to molten silica at 1 700 °C produces no significant increase of $(\Delta V/\Delta T)_P$ until the amount of SiO_2 decreases below 65% (Fig. 8). This represents an MgO content of more than 18 mole %. Subsequent additions of MgO and Al_2O_3 only increase $(\Delta V/\Delta T)_P$ from zero to the 7×10^{-4} level. These results generally agree with the available information and model for melts in the binary alkaline earth silicate systems (11).

It would appear that the presence of Al_2O_3 serves to increase the amount of MgO required to break up the "disturbed SiO_2 network" postulated by Bockris *et al.* (11). About 18 mole % MgO is required to reach the same structural point in the ternary system that only 12 mole % MgO took in the binary system.

Figure 9 shows the marked effect of substituting 50% of the MgO with Al_2O_3 at a constant SiO_2 content of 50 mole %. The net result of the substitution of two Al^{+3} ions for one of two Mg^{+2} ions is to reduce the melt expansion coefficient by a factor of one-half. However, most of this change occurs for low Al_2O_3 contents. The higher field strength of Al^{+3}, compared to Mg^{+2}, is probably responsible for most of this reduction.

V. CONCLUSIONS

A synthetic liquid model had been previously shown to fit the experimental data for a portion of the $Na_2O \cdot GeO_2 \cdot SiO_2$ ternary system (21). This paper takes an additional step. The available crystalline information has been extensively used, in conjunction with a limited amount of previously known information on molar volumes of molten silicates, to construct a liquid model that agrees with the present experimental results. It is concluded

Can. J. Chem. Downloaded from www.nrcresearchpress.com by 210.87.254.105 on 09/05/12
For personal use only.

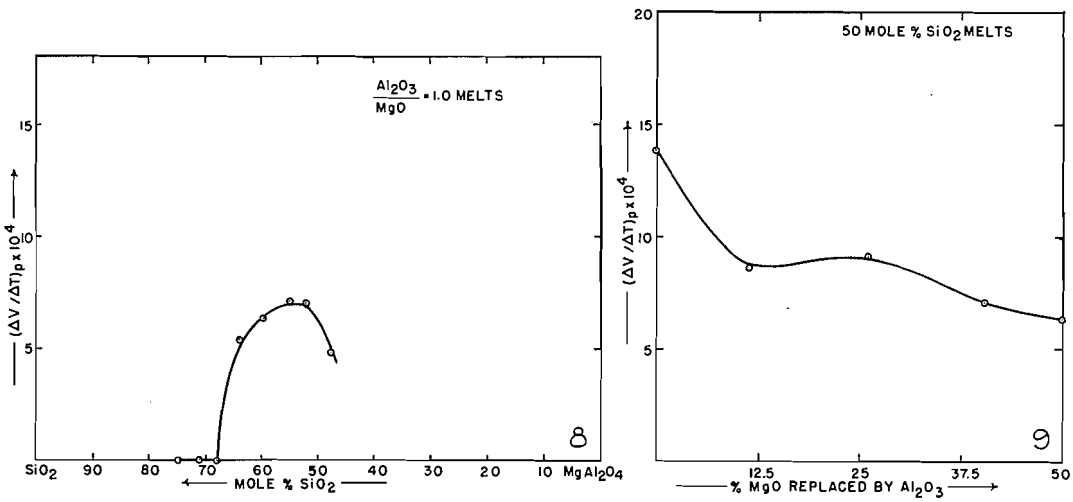

FIG. 8. Expansion coefficient as a function of composition for melts studied on the silica–spinel line.
FIG. 9. Expansion coefficient as a function of composition for melts on the 50 mole % SiO_2 line.

that crystalline information concerning oxide structure changes can be used to interpret the observed high-temperature density data for the corresponding ternary liquids.

It has been demonstrated that a reasonable correlation can exist between the coordination number of a given cation in the crystalline state and in high-temperature ternary liquids of similar composition. This could represent a useful concept for understanding and predicting the structure of more complex high-temperature oxide liquids. The extension of these concepts from liquids to their corresponding glasses awaits further attention.

ACKNOWLEDGMENTS

The author would like to thank Dr. S. D. Stookey for his interest, Dr. D. E. Campbell for his cooperation with the chemical analyses, and Dr. G. H. Beall for discussions concerning this system. I would also like to acknowledge the cooperation of Dr. A. A. Erickson who provided the melting facilities for sample preparation. Mr. P. C. Logel and Mr. P. E. Blaszyk assisted with the experimental work.

REFERENCES

1. O. S. BOBKOVA. Fiz. Khim. Osnovy Proizv. Stali, Akad. Nauk SSSR Inst. Met. Tr. 3-oi Konf. 488–496 (1955) (Publ. 1957). Chem. Abstr. **54**, 7474g (1960).
2. N. L. SHILO. Izv. Akad. Nauk SSSR Otd. Tekhn. Nauk Met. i Toplivo, 17–24 (1961). Chem. Abstr. **55**, 22014f (1961).
3. R. A. LIUTIKOV and L. M. TSYLEV. Izv. Akad. Nauk SSSR Otd. Tekhn. Nauk Met. i Gorn Delo, No. 1, 41–52 (1963). Chem. Abstr. **58**, 11010c (1963).
4. W. SCHREYER and J. F. SCHAIRER. J. Petrol. **2**, 324 (1961).
5. E. F. RIEBLING. Rev. Sci. Instr. **34**, 568 (1963).
6. H. BLOOM and J. O'M. BOCKRIS. *In* Modern aspects of electrochemistry. Vol. 2. *Edited by* J. O'M. Bockris. Academic Press, Inc., New York. 1959.
7. J. D. MACKENZIE. *In* Modern aspects of the vitreous state. *Edited by* J. D. Mackenzie. Butterworth and Company, Ltd., Washington, D.C. 1960.
8. Y. SU, D. E. CAMPBELL, and J. P. WILLIAMS. To be published.
9. E. F. RIEBLING. J. Chem. Phys. **39**, 3022 (1963).
10. I. S. MACHIN and T. B. YEE. J. Am. Ceram. Soc. **37**, 177 (1954).
11. J. W. TOMLINSON, M. S. R. HEYNES, and J. O'M. BOCKRIS. Trans. Faraday Soc. **54**, 1822 (1958).
12. J. O'M. BOCKRIS, J. D. MACKENZIE, and J. A. KITCHENER. Trans. Faraday Soc. **51**, 1734 (1955).
13. R. ROSSIN, J. BERSAN, and G. URBAIN. Compt. Rend. **258**, 562 (1964).

Can. J. Chem. Downloaded from www.nrcresearchpress.com by 210.87.254.105 on 09/05/12
For personal use only.

14. P. KOZAKEVITCH. Rev. Met. Paris, **57**, 147 (1960).
15. E. F. RIEBLING. J. Am. Ceram. Soc. In press. 1964.
16. G. N. LEWIS and M. RANDALL. Thermodynamics. 2nd ed. *Revised by* K. S. Pitzer and L. Brewer. McGraw-Hill Book Company, Inc., New York. 1961. pp. 207–208.
17. M. LATSHAW. J. Am. Chem. Soc. **47**, 793 (1925).
18. I. M. KLOTZ. Chemical thermodynamics. Prentice-Hall, Inc., New York. 1950. p. 191.
19. G. N. LEWIS and M. RANDALL. Thermodynamics. 2nd ed. *Revised by* K. S. Pitzer and L. Brewer. McGraw-Hill Book Company, Inc., New York. 1961. pp. 552–562.
20. J. O'M. BOCKRIS, J. W. TOMLINSON, and J. L. WHITE. Trans. Faraday Soc. **52**, 299 (1956).
21. E. F. RIEBLING. J. Chem. Phys. **41**, 451 (1964).
22. C. D. HODGMAN *et al.* (*Editors*). Handbook of chemistry and physics. 4th ed. Chemical Rubber Publishing Company, Cleveland, Ohio. 1962. p. 602.
23. J. L. WHITE. *In* Physiochemical measurements at high temperatures. *Edited by* J. O'M. Bockris, J. L. White, and J. D. Mackenzie. Academic Press, Inc., New York. 1959. p. 350.
24. A. F. WELLS. Structural inorganic chemistry. 3rd ed. Oxford University Press, London. 1962. p. 487.
25. C. D. HODGMAN *et al.* (*Editors*). Handbook of chemistry and physics. 44th ed. Chemical Rubber Publishing Company, Cleveland, Ohio. 1962. p. 598.
26. C. D. HODGMAN *et al.* (*Editors*). Handbook of chemistry and physics. 44th ed. Chemical Rubber Publishing Company, Cleveland, Ohio. 1962. p. 526.
27. A. F. WELLS. Structural inorganic chemistry. 3rd ed. Oxford University Press, London. 1962. p. 457.
28. A. F. WELLS. Structural inorganic chemistry. 3rd ed. Oxford University Press, London. 1962. p. 798.
29. A. F. WELLS. Structural inorganic chemistry. 3rd ed. Oxford University Press, London. 1962. p. 808.
30. D. H. LINDSLEY, B. T. C. DAVIS, and I. D. MACGREGOR. Science, **144**, 73 (1964).
31. A. F. WELLS. Structural inorganic chemistry. 3rd ed. Oxford University Press, London. 1962. pp. 407, 651–652.
32. C. D. HODGMAN *et al.* (*Editors*). Handbook of chemistry and physics. 44th ed. Chemical Rubber Publishing Company, Cleveland, Ohio. 1962. p. 528.
33. A. F. WELLS. Structural inorganic chemistry. 3rd ed. Oxford University Press, London. 1962. p. 646.

Can. J. Chem. Downloaded from www.nrcresearchpress.com by 210.87.254.105 on 09/05/12
For personal use only.

Can. J. Chem. Downloaded from www.nrcresearchpress.com by 210.87.254.5 on 09/05/12
For personal use only.

PHOTOCHEMICAL SYNTHESES

9. THE CONVERSION OF DIBENZOYLMETHANE TO TRIBENZOYLETHANE

G. KORNIS AND P. DE MAYO
Department of Chemistry, University of Western Ontario, London, Ontario
Received July 13, 1964

ABSTRACT

Irradiation of dibenzoylmethane in benzene gives tribenzoylethane. In more concentrated solution a solid dimer (II) separates which, on solution, is converted by dealdolization into an isomer. This isomer (I, R = H) on irradiation, gives tribenzoylethane in a photolytic reaction which has been shown to have some generality. The overall conversion of dibenzoylmethane to tribenzoylethane therefore involves two photochemical and one chemical reactions.

Some time ago, as part of our studies on photochemical cyclo-addition, we reported the reaction between acetylacetone and a number of alkenes and cycloalkenes (1). The main products derived from the process are indicated below.

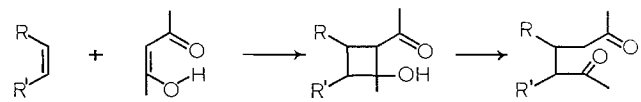

To ascertain whether the process was general for all enolized β-diketones, we studied the reaction between dibenzoylmethane and cyclohexene. This diketone is largely enolized in hydrocarbon solvents and the reaction could be conveniently followed by observing the formation of the non-enolized benzoyl grouping in the carbonyl region.

The products proved difficult to crystallize and the first substance obtained in crystalline form, from a study of its spectra, evidently did not contain a cyclohexyl residue. This conclusion was confirmed when it was found that the yield was greatly increased (to 37%) by irradiation of dibenzoylmethane in benzene solution.*

The substance showed only benzoyl carbonyl in the infrared spectrum, and the ultraviolet absorption was typical of acetophenones. The nuclear magnetic resonance (n.m.r.) spectrum showed the presence of only three protons other than aromatic hydrogen. These were a doublet (two protons) at τ 6.23 and a triplet (one hydrogen) at τ 3.85. These protons were coupled with $J = 7$ c.p.s. The two protons of the doublet were evidently identical. This required the part structure $-CH_2-CH\langle$.

Alkaline hydrolysis of the substance under mild condition gave diphenacyl and benzoic acid (1 mole) as the only isolable products. The substance was therefore identified as tribenzoylethane. The remarkably low-field position of the methine proton is noteworthy.

The mode of genesis of the tribenzoylethane was not immediately obvious, but since two molecules of dibenzoylmethane, at least, were required to participate in its formation the possibility of dimerization at some stage appeared reasonable. Accordingly, the irradiation was performed with a higher concentration of dibenzoylmethane.

Under these conditions the reaction proceeded differently. Although the infrared spectrum of the *solution* appeared to be showing the expected changes, a white crystalline solid separated during the irradiation. This material was separated by filtration and

**We are indebted to Mr. R. W. Yip for this observation.*

Can. J. Chem. Downloaded from www.nrcresearchpress.com by 210.87.254.5 on 09/05/12
For personal use only.

although it initially appeared insoluble in chloroform, it dissolved in a large volume of this solvent from which, after considerable concentration, it could be crystallized on the addition of light petroleum.

This substance was not tribenzoylethane, but a new substance. Again, the ultraviolet spectrum indicated essentially acetophenone-type absorption. The infrared spectrum showed absorption at 3 400 (hydroxyl), 1 680, and 1 645 cm^{-1}. From this it seemed probable that the absorption at 1 645 cm^{-1} was due to benzoyl carbonyl lowered by hydrogen bonding with the hydroxyl group. The n.m.r. spectrum showed the presence of three protons attached to carbon. These were present as three quartets centered at τ 6.29, 6.17, and 4.57. All three protons were therefore coupled together. This again suggested the $-CH_2-CH\langle$ system, where now the methylene protons were not identical.

The n.m.r. spectrum further indicated that the ratio of the ortho hydrogens to meta and para hydrogens (near τ 2.0 and 2.5 respectively) was not that (2:3) expected of benzoyl groups. It appeared to be rather greater than 1:2 which suggested that an isolated phenyl group might be present. Combination of these facts led to the consideration of (I, R = H) as a structure for this new substance.

Chemical attempts to confirm this by dealdolization to benzil and diphenacyl were unsuccessful. The desired object was achieved by heating at 195°, when both these substances sublimed away and were obtained in high yield.

In an earlier attempt to dehydrate (I) or to induce dealdolization, the substance was allowed to stand at room temperature in methanol in the presence of a small amount of sulfuric acid. A crystalline product separated which now lacked the hydroxyl group in the infrared spectrum, but which still showed only acetophenone absorption in the ultraviolet.

Six protons attached to carbon, other than aromatic protons, were visible in the n.m.r. spectrum. Of these one appeared near τ 4.0 as an apparent triplet and two in the τ 7.0–6.3 region as two quartets centered at τ 7.20 and 7.29. In addition a singlet (three protons) appeared at τ 7.62. No acetyl group or vinyl methyl was possible, and a methoxyl group, despite the impressively high position, seemed inevitable. This was confirmed by the analysis which revealed the presence of one methoxyl group. The structure (I, R = Me) or an alternative, cyclic, structure (IA, R = Me) is possible (and the equivalent IA, R = H may contribute to I) for this molecule; the latter formulation is supported by the ultraviolet extinction.*

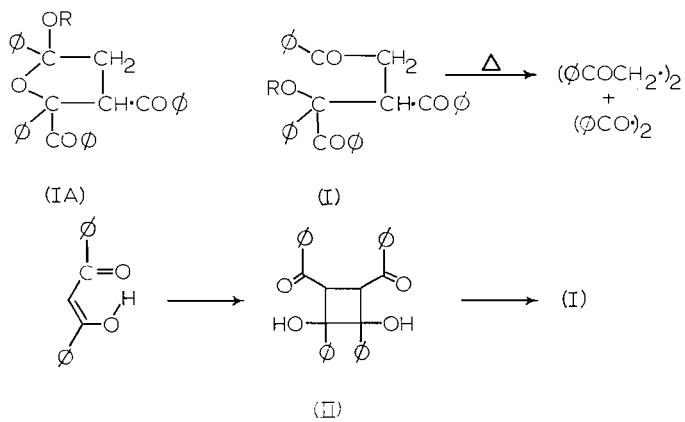

We are grateful to Dr. R. E. Lutz for informing us of his own relevant observations in similar systems and stressing the likelihood of the cyclic structure.

The structure (I, R = H) could be reasonably derived from a dimer (II) by dealdolization accelerated by relief of strain from the opening cyclobutane ring. At this point the original crystalline precipitate from the irradiation was subjected to closer scrutiny.

As originally obtained it was completely different from (I) in solubility in all solvents. However, once having been dissolved only (I) could be recovered. Hence the wish to examine its properties appeared necessarily subject to a degree of frustration. Its infrared spectrum in Nujol was significantly different from that of (I, R = H) (Fig. 1) and is at least compatible with the formulation (II).

The final step in the sequence was the required conversion of (I, R = H) into tribenzoylethane. In fact, irradiation of (I, R = H) in benzene gave the triketone in 48% yield. The formation of tribenzoylethane from dibenzoylmethane can thus be rationalized.

The photolysis of (I, R = H) was of general interest and was investigated briefly. Since the dibenzoylethyl group attached to the carbon bearing the hydroxyl group should be without special significance, similar cleavage could be expected when this grouping was replaced by some other function.

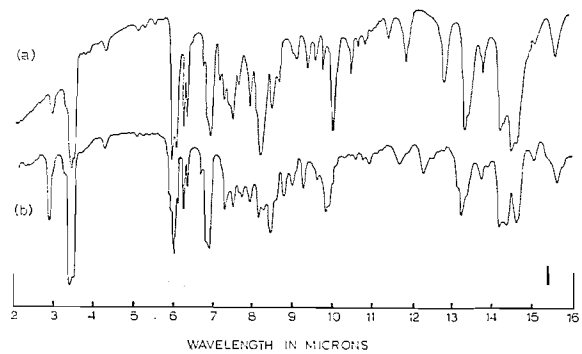

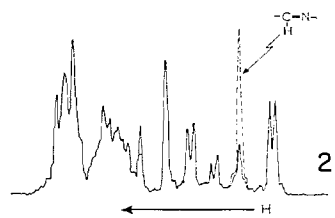

FIG. 1. Infrared spectrum (Nujol mull) of (*a*) alcohol (I) and (*b*) diol (II).
FIG. 2. Nuclear magnetic resonance spectrum of aromatic protons and azomethine proton in benzaldehyde 2,4-dinitrophenylhydrazone and the partially deuterated derivative. Solvent: dimethyl sulfoxide at 103°.

The substituted benzoin (III), itself having been prepared photochemically, was available in these laboratories from other studies (2). Irradiation of this in benzene solution gave benzoylacenaphthene (IV) (2), though in poor yield, and no benzaldehyde. Similar irradiation of benzoin (V, R = H) itself gave benzaldehyde. Irradiation of deuteriobenzoin (V, R = D) gave a mixture of benzaldehyde and (VI) deuteriobenzaldehyde. The location of the aldehydic deuteron was accomplished by a determination of the n.m.r. spectrum (in dimethylsulfoxide at 103°) of the 2,4-dinitrophenylhydrazone when, in the deuterated compound, the azomethine proton (see Fig. 2) was reduced by about 50%. This was confirmed by deuterium analysis. That the deuterium was not lost by exchange through hydrogen abstraction prior to photolysis was shown by brief irradiation, with partial conversion of the deuteriobenzoin. No methine proton was detected in the recovered benzoin.

The presence of the hydroxyl proton is necessary for benzaldehyde formation, but its absence, as in the phenyl ether (3), does not significantly affect the rate of destruction of the benzoin as measured by the disappearance of the methine proton. Hence, assuming the photolytic step is the same in both cases, it is not preceded by hydrogen abstraction

Can. J. Chem. Downloaded from www.nrcresearchpress.com by 210.87.254.5 on 09/05/12
For personal use only.

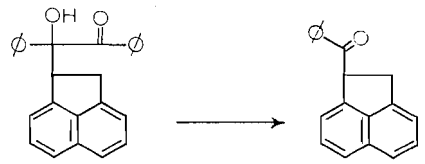

(III) (IV)

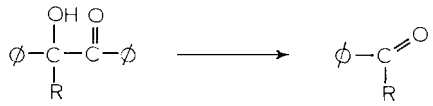

(V) (VI)

of the hydroxyl proton. Abstraction of the methine proton is unlikely since this proton is not present in the substituted benzoins already discussed. Furthermore the methine proton, as indicated by deuteration, appears in the same position in the resultant benzaldehyde.

No benzaldehyde in appreciable amount is produced in the substituted benzoins, so it seems likely that after photolysis, the benzyl radicals, by hydrogen transfer, act as

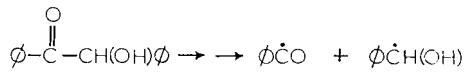

the only source of benzaldehyde. Such exchange as does occur probably occurs after the initial photolysis.

EXPERIMENTAL

Melting points were determined on the Kofler hot stage and are uncorrected. The term 'petrol' refers to petroleum ether of b.p. 60–80°. The benzene used (thiophene free) was percolated through a column of alumina before use. Infrared spectra were determined in chloroform solution and n.m.r. spectra in deuteriochloroform, unless otherwise stated.

Irradiations were conducted in a water-cooled vycor immersion apparatus of capacity ca. 250 ml under oxygen-free nitrogen, and with magnetic stirring. The light source was a Hanovia 450 W mercury arc and was encased in a pyrex cylinder.

Irradiation of Dibenzoylmethane

(a) A solution of dibenzoylmethane (5 g) in benzene (250 ml) was irradiated for 75 h (until the carbonyl absorption near 6 μ did not appear to be increasing). After evaporation of the solvent the residue was extracted with petrol until the extract was colorless. Evaporation of the petrol extract gave an oil which was dissolved in ethanol, and a solution (0.25 *M*) of 2,4-dinitrophenylhydrazine added until no more precipitate formed. Crystallization from ethyl acetate – petrol gave the 2,4-dinitrophenylhydrazone of benzaldehyde (36 mg, 11%) identical in every respect with an authentic specimen.

The residue remaining after petrol extraction was crystallized from ethyl alcohol to give tribenzoylethane (1.4 g, 37%), m.p. 153–155°, raised to 154–156° on recrystallization. (Lit. (4) 156–157°.) λ_{max} 248 mμ (log ϵ 4.7).

Anal. Calcd. for $C_{23}H_{18}O_3$: C, 80.68; H, 5.30. Found: C, 80.81; H, 5.72.

A solution of tribenzoylethane (0.21 g) in aqueous sodium hydroxide (0.1 *N*, 50 ml) and ethanol (100 ml) was allowed to stand at room temperature for 17 h. Concentration of the solution gave a precipitate of diphenacyl which on crystallization from methanol (0.11 g, 76%) had m.p. 145–146°. (Lit. (5) 145°, λ_{max} 244 mμ (log ϵ 4.42).)

Anal. Calcd. for $C_{16}H_{14}O_2$: C, 80.64; H, 6.92. Found: C, 80.59; H, 5.78.

Acidification of the aqueous filtrate gave, after isolation with ether and crystallization from water, benzoic acid, m.p. 120–122°, identical in every respect with an authentic specimen.

Can. J. Chem. Downloaded from www.nrcresearchpress.com by 210.87.254.5 on 09/05/12
For personal use only.

In a separate experiment titration of the hydrolyzed tribenzoylethane showed the generation of 1 equivalent of acid.

(b) A solution of dibenzoylmethane (30 g) in benzene (250 ml) was irradiated. After 45 h a heavy precipitate (6.3 g) was collected. Irradiation for 24 h more gave a further 4.9 g and prolonged irradiation (67 h) produced 0.9 g. The combined precipitates were washed with petrol and dried *in vacuo* to give a total of 12.1 g (40%), of (II), m.p. 140–141°.

Anal. Calcd. for $C_{30}H_{24}O_4$: C, 80.33; H, 5.39. Found: C, 79.57; H, 5.44.

1-Phenyl-1,2,3-tribenzoylpropan-1-ol (I, R = H)

A solution of (II) (12.1 g) in chloroform (500 ml) was heated under reflux for 1 h. Evaporation to dryness and crystallization from petrol gave the alcohol (I, R = H) (3.6 g), m.p. 138–140°. Admixture with (II) gave a depression of 20°. λ_{max} 250 mμ (log ϵ 4.46).

Anal. Calcd. for $C_{30}H_{24}O_4$: C, 80.33; H, 5.39. Found: C, 80.64; H, 5.10.

A solution of the alcohol (I, R = H) (45 mg) in acetone (5 ml) and 0.1 *N* sodium hydroxide (20 ml) was heated under reflux for 30 min. Concentration, collection of the precipitate, and crystallization from methanol gave diphenacyl (13 mg, 55%) identical in every respect with the material described above.

Sublimation of the alcohol (I, R = H) (40 mg) at 195° and 1.5 mm gave a yellow oil. Separation by thin-layer chromatography using silicic acid and eluting with chloroform gave diphenacyl (20 mg, 95%), m.p. 145–146°, and benzil (17 mg, 90%), melting point and mixed melting point 93–95°.

1-Methoxy-1-phenyl-1,2,3-tribenzoylpropane (I, R = Me or IA, R = Me)

To a solution of the alcohol (I, R = H) (0.1 g) in methanol (10 ml) concentrated sulfuric acid (2 drops) was added and the mixture allowed to stand. Crystallization occurred within 5 min, but the solution was left for 14 h. Collection of the crystalline precipitate and recrystallization from methanol gave the ether (I, R = Me) (48 mg, 47%), m.p. 189–191°, λ_{max} 252 mμ (log ϵ 4.32).

Anal. Calcd. for $C_{31}H_{26}O_4$: C, 80.56; H, 5.67; OMe (1), 6.7. Found: C, 80.88; H, 5.84; OMe, 6.21.

Irradiation of 1-Phenyl-1,2,3-tribenzoylpropan-1-ol (I, R = H)

The alcohol (0.114 g) in benzene (250 ml) was irradiated for 12 min. Evaporation of the solution and crystallization from ethanol gave tribenzoylethane (42 mg, 48%), m.p. 153–155°.

Irradiation of α-1-Acenaphthenylbenzoin (III)

A solution of (III) (0.2 g) in benzene (250 ml) was irradiated for 1 h. After evaporation of the solvent the brown residual oil was crystallized twice from methanol (charcoal) to give 1-benzoylacenaphthene (IV) (20 mg, 14%), m.p. 133–135°, identical in every respect with an authentic specimen.

Irradiation of Benzoin

A solution of benzoin (0.5 g) in benzene (250 ml) was irradiated for 70 min. The solvent was evaporated and the residue extracted with petrol. Conversion of the material extracted by the petrol to the 2,4-dinitrophenylhydrazone in the usual way gave the derivative of benzaldehyde (0.13 g, 20%) identical with an authentic specimen in every respect. The residue from the extraction contained material with the same retention time as benzyl alcohol on a 20% Carbowax 20M 6 ft × ¼ in. column at 150°. Calibration of response indicated that it was present to the extent of 4%.

Similar irradiation of α-deuteriobenzoin (0.53 g) gave the 2,4-dinitrophenylhydrazone containing 5.94% excess deuterium.

α-Deuteriobenzoin

Sodium (0.1 g) was added to a mixture of D_2O (99.6%, 3 ml) and dioxan (50 ml), followed by benzoin (2.2 g). The mixture was heated under reflux for 1 h under nitrogen, the solvent evaporated, and the residue redissolved in dioxan (50 ml) and D_2O (3 ml) and again refluxed for 1 h. The cycle of operation was repeated twice more, the mixture being protected from outside moisture throughout. After the final evaporation D_2O (8 ml) was added and the mixture acidified with *N* hydrochloric acid. The benzoin was collected and crystallized from benzene–petrol, m.p. 134–136°. No methine proton could be detected in the n.m.r. spectrum.

Irradiation of α-Deuteriobenzoin

The deuterated benzoin (0.13 g) was irradiated in benzene (250 ml) for 5 min. Evaporation of the solvent and crystallization from petrol gave recovered deuteriobenzoin (0.05 g, 39%). Irradiation of benzoin phenyl ether and benzoin in comparable concentrations (100 mg, 250 ml) in benzene showed approximately the same rate of disappearance of the methine hydrogen, as followed by n.m.r. Disappearance was complete in about 30 min.

ACKNOWLEDGMENTS

The authors are indebted to the A.F.O.S.R. for support of this research under grant AF-AFOSR-61-6. They thank Mr. R. E. Klinck and Mr. D. Ross for the n.m.r. spectra.

Can. J. Chem. Downloaded from www.nrcresearchpress.com by 210.87.254.5 on 09/05/12
For personal use only.

REFERENCES

1. P. DE MAYO and H. TAKESHITA. Can. J. Chem. **41**, 440 (1963).
2. P. DE MAYO and A. STOESSL. Can. J. Chem. **40**, 57 (1962).
3. C. K. BRADSER and R. ROSHER. J. Am. Chem. Soc. **61**, 1524 (1939).
4. H. KLEINFELLER and H. TROMMSDORFF. Ber. **71**, B, 2448 (1938).
5. I. HEILBRON and H. M. BUNBURY. Dictionary of organic compounds. Vol. II. Eyre and Spottiswoode, London. 1953. p. 400.

Can. J. Chem. Downloaded from www.nrcresearchpress.com by 210.87.254.5 on 09/05/12
For personal use only.

Can. J. Chem. Downloaded from www.nrcresearchpress.com by 210.87.254.6 on 09/05/12
For personal use only.

PHOTOCHEMICAL SYNTHESES

10. ADDITION OF MALEIC ESTER TO CYCLOALKENES: THE PRODUCTS

P. DE MAYO, S. T. REID, AND R. W. YIP
Department of Chemistry, University of Western Ontario, London, Ontario
Received July 13, 1964

ABSTRACT

The intermolecular photochemical cycloaddition of maleic ester to cyclopentene and to cyclohexene has been observed. The saturated products were diesters of the (3:2:0) and (4:2:0) bicycloheptane and octane series, respectively. The stereochemistry of these products was studied and, in the latter series, derivatives of the *trans*-fused (4:2:0) bicyclooctane system identified.

In addition to the saturated esters, cyclohex-2-enyl succinic ester and cyclopent-2-enyl succinic ester, produced by addition of the cycloalkenyl radical to maleic ester, also were formed.

At the outset of these investigations* only one example of intermolecular photochemically induced cycloaddition to an isolated ethylenic linkage had been reported (2, 3). In that instance (the addition of the enol of acetylacetone to cyclohexene), the intermediate cyclo-addition product (I) was not isolated because of its facile conversion, by dealdolization, to the pentane dione (II). It was, therefore, desirable to investigate a system in which

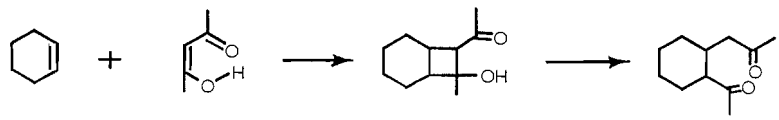

(I) (II)

the cyclobutane ring would be retained intact. As a result of an earlier observation made in these laboratories we noted that diethyl maleate added to cyclohexene. The present paper reports the structure and stereochemistry of the products—discussion of the mechanism will be deferred until a following paper in this series, wherein a more detailed study of the irradiation is reported.

While this work was in progress Eaton reported (4) the addition of cyclopentenone to cyclopentene. Simultaneously with our first publication (1),† Corey (5, 6) reported the addition of cyclohexenone to isobutene, and very shortly thereafter Barltrop (7) reported the addition of cyclohexene to maleic anhydride and maleic ester.

Irradiation of dimethyl maleate‡ in cyclopentene, followed by distillation, gave a mixture of esters which was separated by gas–liquid chromatography to give the unsaturated ester (III, R = Me), which was then hydrolyzed to the corresponding dicarboxylic acid, m.p. 127–129°.

Although no maximum in the ultraviolet spectrum was observed, the absorption at 200 mμ (ϵ, 4 870) clearly indicated unsaturation. Further, the n.m.r. spectrum of the ester showed a multiplet, centered at τ 4.33, of two protons, indicating the presence of two vinyl protons. In addition, another multiplet (two protons) was centered at about τ 8.33, there being no protons other than these above $\sim \tau$ 7.9. These protons are the only ones

Part of the material here presented formed a preliminary communication (1).
†*These results were first presented at the C.I.C. Organic Symposium, Hamilton, August, 1962.*
‡*Under the conditions of the reaction very little fumarate is produced. This will be discussed in a following paper.*

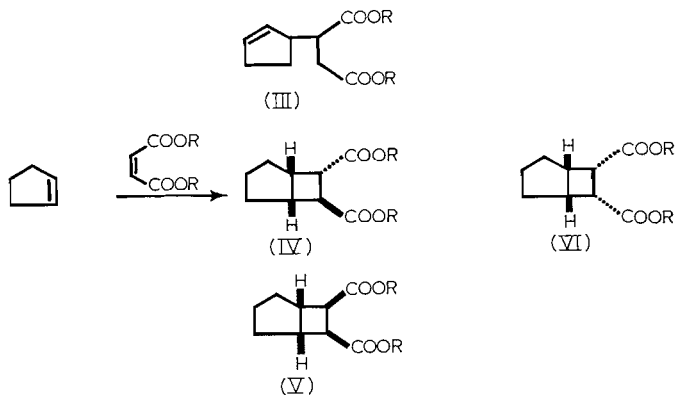

in the molecule not moved from the normal cycloalkyl methylene position by substitution. These two facts are sufficient to exclude the cyclopent-1- (one vinyl proton) and cyclopent-3-enyl (four high field protons) isomers. The nature of the carbon skeleton itself follows from mechanistic considerations and from analogy with the cyclohexene system to be described. Photochemically induced radical addition to maleic ester has been recorded, for instance, by Pitts (8) and by Schenck (9).

To facilitate the separation of the saturated products (effected by g.l.c. on Carbowax 20M) the unsaturated products were first destroyed by ozonolysis. Although three saturated esters were obtained, corresponding to the three possible *cis*-fused products, on hydrolysis one of the esters (VI, R = Me), obtained in very minor amount, was converted, by epimerization under the hydrolytic conditions, into the same decarboxylic acid (IV, R = H) that was obtained by hydrolysis of the largest saturated fraction. The remaining fraction, on hydrolysis, gave a new acid (V) m.p. 178–179.5°. By calibration, the percentage composition of the ester mixture was obtained.

Both acids were transparent in the ultraviolet, both showed absorption in the τ 7.0–7.3 region (2H) expected for the protons at the ring junction, and both showed complex multiplets (6H) in the τ 8.35 region for the cyclopentane protons. This evidence for the structure is persuasive and, when coupled with the more strictly defined analogy with the cyclohexene series, may be regarded as compelling.

By heating with acetic anhydride, the acid (V, R = H) was converted into an anhydride (showing bands in the infrared spectrum at 1 775 and 1 850 cm^{-1}) which was hydrolyzed by warming with water to regenerate the selfsame acid. In contrast, on similar treatment the acid (IV, R = H) was converted into acid (V, R = H). On this basis it must be concluded that in (IV) the carboxyls are *trans* and that in (V) they are *cis*. The minor ester, which is converted into (IV, R = H), must be that of the acid (VI, R = H) in which there are significant non-bonded interactions.

The allocated stereochemistry of the carboxyl groups was supported by pK measurements. Although the specific values for the pK's are without immediate significance, the difference in the pK_1 and pK_2 would be expected to be so. Thus, for instance, *cis*-caronic acid has ΔpK 5.7 and *trans*-caronic acid has ΔpK 1.5. (For a succinct summary, see ref. 10.) In agreement with our expectations, the *trans* diacid showed a smaller ΔpK (1.3) than the *cis* diacid (ΔpK, 2.3).

The irradiation of maleic ester with cyclohexene gave a mixture of products which was, however, more complex than that obtained from the use of cyclopentene as substrate.

Can. J. Chem. Downloaded from www.nrcresearchpress.com by 210.87.254.6 on 09/05/12
For personal use only.

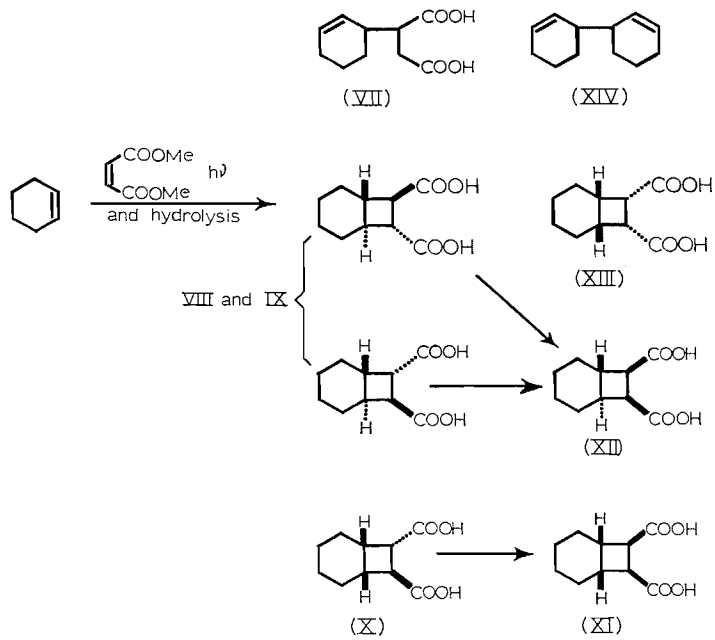

In this instance the unsaturated hydrocarbon, bicyclohexenyl (XIV), was isolated from the lower boiling material. By g.l.c. chromatographic separation of the ester mixture, the ester corresponding to VII was isolated and hydrolyzed to give the free dicarboxylic acid, m.p. 141–143°. The presence of unsaturation was shown by the extinction (3 500) at 200 mμ and by the presence of a multiplet near τ 4.4 for two protons in the n.m.r. spectrum. This, by analogy with the cyclopentene equivalent, places the ethylenic linkage. The carbon skeleton was established by hydrogenation to give cyclohexylsuccinic acid which was compared with an authentic specimen.

Ozonolysis of the ester mixture, followed by distillation, removed the unsaturated material. The remaining saturated esters were separated by g.l.c. on Carbowax 20M. After hydrolysis the separated acids were further purified, where necessary, by chromatography on silica gel. This was necessary since the preparative separation was not as efficient as the analytical procedure. Four acids were obtained: VIII, m.p. 181–182°; IX, m.p. 201–202°; X, m.p. 199–200°;* XI, m.p. 174–176°.

By treatment with acetic anhydride and hydrolysis the acid (VIII) was converted into XII, m.p. 153–155°; a similar observation was made for the diacid (IX). On the other hand acid (X) was converted into acid (XI). As expected, therefore, XI was recovered when subjected to this treatment.

All four acids were optically transparent down to 200 mμ, and all showed four protons in the τ 6.5–7.5 region for the methine protons adjacent to the ester functions and for the bridgehead methines. It seemed very likely, therefore, that all these acids, together with acid (XII), were bicyclo(4:2:0)octane derivatives. Further, because two acids (VIII and IX) could be converted into the same, necessarily *cis*-, dicarboxylic acid (XII) and were probably, therefore, both *trans*-dicarboxylic acids, the presence of a *trans*-fused bicyclo (4:2:0)octane system was most likely for this set. Only in the *trans*-fused system can there be two *trans*-dicarboxylic acids.

**This acid has also been reported by Barltrop (7).*

Can. J. Chem. Downloaded from www.nrcresearchpress.com by 210.87.254.6 on 09/05/12
For personal use only.

On this basis acids (X) and (XI) most probably belonged to the *cis*-fused bicyclooctane system. The gross structure of X was demonstrated by pyrolysis at 405–410°, when dimethyl fumarate was obtained. Dimethyl succinate was also formed (and at higher temperatures became the only C_4 acid derivative) and, in a separate experiment, it was shown that dimethyl fumarate is converted into succinate by heating at 410–415° with an equimolar amount of cyclohexene. Traces of cyclohexene were also detected.

Confirmation that the fusion of the ring system was *cis* in X was obtained by the oxidation of this substance with potassium permanganate. *cis*-Cyclohexane-1,2-dicarboxylic acid was obtained (isolated by g.l.c. as the ester) with no trace of the more stable *trans* acid. Less than one-fifth of 1% of the amount of *cis* acid actually obtained could have been detected of the *trans* acid, had it been formed. Accordingly, the stereochemistry indicated is assigned to acids X and XI. The all-*cis* alternative for XI—compound XIII—is not considered probable because of the more severe non-bonding interaction as compared with XI. The configurational assignments were supported by the pK measurements, ΔpK for X being smaller (1.7) than that for XI (2.3).

Confirmation of the gross structure of the *trans*-fused group of acids was sought in the pyrolysis of VIII (as the dimethyl ester). After hydrogenation of the pyrolyzate, over palladized charcoal in ethyl acetate, material having the same retention time and infrared spectrum as dimethyl sebacate was isolated, by chromatography, and characterized by conversion to sebacic acid. It appears that, in the *trans*-fused series, the additional strain induces preferential cleavage in the opposite sense to that of the *cis* series. The additional strain was reflected, also, in the fact that pyrolysis could be effected at as low a temperature as 340–350°. No trace of dimethyl fumarate or succinate could be detected.

Scheme

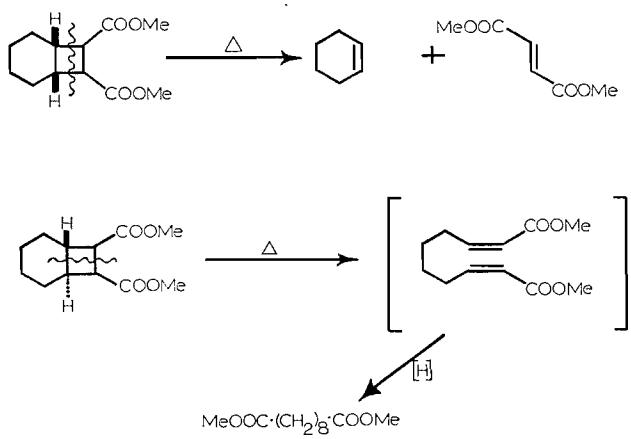

With the exception of the distinction between VIII and IX, the structure and stereochemistry of all the cycloaddition products is thus defined.

The reactions described provide a *direct* synthesis of the *trans*-fused (4:2:0) bicyclooctane system, which previously had been obtained only by ring contraction (11, 12).

EXPERIMENTAL

Materials

Cyclohexene (supplied by Matheson, Coleman, and Bell) and cyclopentene (Phillips Petroleum) gave single peaks on chromatography on Carbowax 20M (20 ft × 1/4 in.; 10% on 80–100M Chromosorb P at

Can. J. Chem. Downloaded from www.nrcresearchpress.com by 210.87.254.6 on 09/05/12
For personal use only.

63°, helium flow 120 ml/min). Cyclohexene was shaken repeatedly with saturated ferrous sulphate solution, washed, dried, and distilled. Cyclopentene was refluxed over zinc dust and distilled. Immediately prior to use the cycloalkenes were filtered through a column of alumina. Dimethyl maleate was prepared according to the method of Clemo and Graham (13). It gave a single peak on the above column (at 180°) under conditions adequate to resolve a mixture of maleate and fumarate.

Apparatus

(*a*) An apparatus previously described (14) was used, modified by replacing the nitrogen bubbler with a magnetic stirrer. An inlet for oxygen-free nitrogen was provided. An 80 W Hanovia CH-3 medium pressure arc was the source, the capacity of the container being about 200 ml. The immersion well was quartz.

(*b*) A similar apparatus was used in which the light source was a 450 W Hanovia medium pressure arc in a water-cooled Vycor immersion well (Engelhard Hanovia Inc.).

Nuclear magnetic resonance spectra were recorded on a Varian D.P.60. Melting points are uncorrected and were determined on a Kofler block.

Irradiation of Cyclopentene and Dimethyl Maleate

A solution of dimethyl maleate (25 ml) in cyclopentene (155 ml) was irradiated in apparatus (*a*) for 30 h. The adducts (b.p. 100–120° at 2 mm; 18 g) were separated from unreacted maleate, fumarate, and polymer by simple distillation. A portion of the mixture was chromatographed (20% Carbowax 20M at 205°, column 10 ft × 1/4 in., He flow 25 ml/min, retention time 43 min) to obtain the unsaturated isomer.

The mixture (23 g) in methylene chloride (100 ml) was ozonized at −70° until excess ozone was present. After removal of the solvent the residue was digested for 3 h with 15% hydrogen peroxide at 80°. The neutral material then was isolated in the usual way and distilled to give a mixture of saturated adducts (5.9 g). These were separated by repeated gas–liquid chromatography on 30% Carbowax 20M at 200°.

The estimated percentages of products (by calibration and integration) in the mixture are as follows (retention times in parentheses): (1) 64–65% (40 min); (2) 29–34% (45 min); (3) 2–5% (55 min); (4) 0.1–0.7% (59.5 min).

Hydrolysis and Characterization of the Cyclopentene Adducts

The unsaturated diacid (III) was obtained by refluxing the corresponding ester (I) (119 mg) in 5% aqueous KOH (1.5 ml) for 1 h 20 min. The hydrolysate was acidified with concentrated HCl and repeatedly extracted with chloroform. Evaporation of the dried solution gave 100 mg of crude acid. The residue was recrystallized 3 times from ethyl acetate – petrol giving material melting at 127–129°.

Calcd. for $C_9H_{12}O_4$: C, 58.69; H, 6.57. Found: C, 58.99; H, 6.59.

The diacid had no absorption maximum in the quartz ultraviolet, ϵ_{200}^{EtOH}, 4 870. The n.m.r. spectrum of the dimethyl ester (5% in CCl_4) showed the following bands: τ 8.32 (multiplet), τ 7.61 (multiplet), τ 7.15 (multiplet), τ 6.38 (singlet), and τ 4.33 (multiplet).

Diacid (IV) was obtained by heating the corresponding ester (2) (2.10 g) in 3 *N* NaOH (15 ml) under reflux for approximately 1 h. Acidification of the hydrolysate with concentrated HCl, followed by repeated extractions (approximately 20 times) with chloroform, yielded, after 1 recrystallization, an acid, m.p. 174.5–177° (1.26 g), which was raised to 175–177° on further recrystallization. Reesterification (diazomethane) gave an ester with identical retention time with the starting material, indicating that no inversion had taken place on hydrolysis.

Found: C, 59.16; H, 6.70.

The acid had no absorption maximum in the quartz ultraviolet, ϵ_{200}^{EtOH}, 140. The n.m.r. spectrum of the dimethyl ester (5% in CCl_4) showed the following bands: τ 8.35 (multiplet), τ 7.10 (multiplet), and τ 6.38 (singlet). Titration in carbon dioxide free water with *N*/10 sodium hydroxide gave pK_1 4.4, pK_2 5.7.

Diacid (V) was obtained by heating the corresponding ester (3) (357 mg) in aqueous 3 *N* NaOH (3.5 ml) under reflux for approximately 1 h. The hydrolysate was treated as previously and an acid (194 mg), m.p. 178–179.5°, was obtained after several recrystallizations.

Found: C, 58.80; H, 6.73.

The acid had no absorption maximum in the quartz ultraviolet (ϵ_{200}^{EtOH}, 167). The n.m.r. spectrum of the dimethyl ester (5% in CCl_4) showed the following bands: τ 8.35 (multiplet), τ 7.25 (multiplet), τ 7.01 (multiplet), and τ 6.44 (singlet). Titration in carbon dioxide free water with *N*/10 sodium hydroxide gave pK_1 4.6, pK_2 6.9.

Diacid (IV) also was obtained by heating the ester (4) (18 mg) in aqueous 3 *N* NaOH (0.5 ml) under reflux for 3 h. The hydrolysate was treated as previously and an acid (13 mg), m.p. 173–175°, was obtained after 4 recrystallizations from ethyl acetate – petrol. It was undepressed on admixture with the acid obtained from the hydrolysis of ester (2).

Treatment of Diacids IV and V with Acetic Anhydride

Diacid V (8.5 mg) was heated in redistilled acetic anhydride at 140° for 1 h in an 8 mm diameter pyrex tube equipped with a drying tube filled with anhydrous calcium chloride. Excess anhydride was removed under 1 to 4 mm pressure and the residue distilled for 1/2 h under water suction (cold trap, drying tube).

Can. J. Chem. Downloaded from www.nrcresearchpress.com by 210.87.254.6 on 09/05/12
For personal use only.

Can. J. Chem. Downloaded from www.nrcresearchpress.com by 210.87.254.6 on 09/05/12
For personal use only.

The white, crystalline distillate, m.p. 122.0–122.5°, possessed bands in the infrared (CCl_4) at 1 775 and 1 850 cm^{-1}. Hydrolysis of the anhydride by heating with a few drops of water yielded, after 1 recrystallization, a diacid (3.8 mg) with m.p. 174–176°, undepressed when mixed with V.

Diacid IV (9.6 mg), similarly treated with acetic anhydride, gave an anhydride with an infrared spectrum identical with that possessed by the anhydride from diacid V. Hydrolysis gave a diacid (2.9 mg), m.p. 172–174°, undepressed when mixed with compound V but depressed when mixed with diacid IV.

Irradiation of Cyclohexene and Diethyl Maleate

Diethyl maleate (25 ml) and cyclohexene (175 ml) were irradiated in apparatus (*b*) for 9 h. Cyclohexene was removed under reduced pressure and the residue distilled. The fraction boiling at 110–111° at 0.4 mm (12 g) was collected. The liquid was chromatographed on a 10 ft × 1/2 in., 20% diethylene glycol succinate (DEGS) column at 175° (He, 300 ml/min) and the following fractions were collected (retention times in parentheses): (1) (59 min); (2) (82 min); (3) (89 min); (4) (97 min).

In another experiment the fraction with b.p. 100–105° at 0.8 mm was collected and the fraction with retention time 21 min (15 ft × 3/8 in., 30% DEGS at 170°) was identified as bicyclohexenyl (n_D^{24} 1.5045). It had an infrared spectrum identical with that of an authentic specimen.

The unsaturated diacid (VII) was obtained by refluxing the ester (88 mg) corresponding to fraction 3 on the g.l.c. in 5% aqueous KOH (1 ml) for 4 h. The hydrolysate was acidified with concentrated HCl and extracted 10 times with chloroform. Evaporation of the dried chloroform extract yielded an acid (46 mg), m.p. 141–143° after 4 recrystallizations.

Calcd. for $C_{10}H_{14}O_4$: C, 60.59; H, 7.12. Found: C, 61.41; H, 7.01.

The acid had no absorption maximum in the quartz ultraviolet, ϵ_{200}^{EtOH}, 3 500. The n.m.r. of the diethyl ester (10% in CCl_4) showed bands at τ 8.75 (triplet), τ 8.4 (broad multiplet), τ 7.5 (multiplet), τ 5.88 (2 quartets), and τ 4.40 (multiplet).

Hydrogenation of the diacid (VII) (18 mg) over 10% PtO_2 (63 mg) in glacial acetic acid (5 ml) for 35 min (uptake of 1.06 moles H_2) gave cyclohexylsuccinic acid (13 mg), m.p. 143–145.5° after 1 recrystallization. The melting point was undepressed on admixture with an authentic specimen of m.p. 143–144° (15).

Irradiation of Cyclohexene and Dimethyl Maleate

Dimethyl maleate (n_D^{25} 1.4409) (25 ml) and cyclohexene (190 ml) were irradiated in apparatus (*b*) for 34 h. Cyclohexene was removed under reduced pressure and the residue distilled. The fraction boiling at 100–130° at 0.7 mm (16 g) was dissolved in CH_2Cl_2 (75 ml), and the solution ozonized at −70° (dry ice–acetone temperature) until a blue color due to excess ozone appeared and a negative test to tetranitromethane was obtained. The solvent was removed *in vacuo* and the residue was heated in a water bath at 90° in 15% aqueous H_2O_2 for 10 min. Extraction with $CHCl_3$, followed by distillation, gave 8 g of oil b.p. 106–118° at 0.7–0.8 mm. The n.m.r. spectrum of the oil (18% in CCl_4) showed no signal at τ 4.40. The adducts were separated preparatively by repeated g.l.c. (8 ft × 3/8 in., 30% Carbowax 20M and 10 ft × 3/8 in., 17% DEGS).

The estimated percentages of products and their retention times in parentheses are: (1) 14%, (63 min); (2) 5%, (66.5 min); (3) 70%, (77 min); (4) 10%, (85 min).

Hydrolysis of the Dimethyl Esters from Irradiation of Cyclohexene and Dimethyl Maleate

Diacid (VIII) was obtained by hydrolysis of a mixture of esters in fractions (1) and (2). Preparative g.l.c. poorly resolved the esters. By collecting only the first portion of the peak due the ester of acid VIII, a mixture, which was shown by analytical g.l.c. to contain 90% of the ester of VIII and 10% of the ester of IX, was obtained. The mixture (420 mg) was stirred overnight with 3 *N* NaOH (5 ml) at 35°. The hydrolysate was acidified with concentrated HCl and extracted repeatedly with chloroform. Evaporation of the dried chloroform extract and 2 recrystallizations from ethyl acetate–petrol yielded 174 mg of acid, m.p. 177–181°, raised to 181–182° on further crystallization.

Calcd. for $C_{10}H_{14}O_4$: C, 60.59; H, 7.12. Found: C, 60.93; H, 6.96.

The acid had no absorption maximum in the quartz ultraviolet, ϵ_{200}^{EtOH}, 154. The n.m.r. of the dimethyl ester (5% in CCl_4), showed bands at τ 8.35 (broad multiplet), τ 7.03 (broad multiplet), and τ 6.34 (singlet). Titration in carbon dioxide free water with 0.1 *N* NaOH gave pK_1 3.9, pK_2 5.8.

Diacid (IX) was obtained by chromatographing a mixture comprising acids VIII and IX over BDH silica gel. A mixture of the esters of acids VIII and IX (fractions (1) and (2)) was collected as a single peak on a DEGS column. The mixture (192 mg) was refluxed with 3 *N* aqueous NaOH (1.5 ml) for 1 h. Acidification of the hydrolysate, followed by the usual procedural steps, gave 130 mg of crude acid. The crude acid was chromatographed on 1 g of BDH silica gel. Elution with 85 ml benzene and 20 ml 2% ether–benzene gave, after 1 recrystallization from EtOAc–petrol, acid IX (14 mg), m.p. 198–201°, which was raised to 201–202° on further crystallization.

Found: C, 61.03, 7.14.

Diacid IX had no absorption maximum in the quartz ultraviolet, ϵ_{200}^{EtOH}, 280. Titration in carbon dioxide free water with 0.1 *N* NaOH gave pK_1 4.4, pK_2 5.9.

Diacid (X) was obtained by hydrolysis of the corresponding ester (fraction 3). The ester (580 mg) was

refluxed with 10% KOH for 2 h. Acidification of the hydrolysate, followed by the usual procedural steps, gave, after 2 recrystallizations, 164 mg of acid, m.p. 199–200°.

Found: C, 60.86; H, 7.41.

The melting point was depressed on admixture with acid IX. It had no absorption maximum in the quartz ultraviolet, ϵ_{200}^{EtOH}, 340. Titration in carbon dioxide free water with 0.1 *N* NaOH gave pK_1 3.6, pK_2 5.3. The n.m.r. of the dimethyl ester (5% in CCl_4) showed bands at τ 8.48 (multiplet), τ 7.53 (multiplet), τ 6.72 (approximate doublet), and τ 6.38 (singlet).

Diacid (XI) was obtained by refluxing the ester (200 mg) (fraction 4) with 3 *N* aqueous NaOH for 1 h. The usual procedure, followed by two recrystallizations, gave 84 mg of acid, m.p. 174–176°.

Found: C, 60.90; H, 7.10.

It had no absorption maximum in the quartz ultraviolet, ϵ_{200}^{EtOH}, 330. The n.m.r. showed bands at τ 8.57 (multiplet), τ 7.30 (multiplet), τ 7.04 (multiplet), and τ 6.40 (singlet). Titration in carbon dioxide free water with 0.1 *N* NaOH gave pK_1 4.7, pK_2 7.0.

Treatment of Diacids (VIII), (IX), (X), and (XI) with Acetic Anhydride

Diacid (VIII) (5.6 mg) was heated in redistilled acetic anhydride (0.3 ml) at 140° for 1 h in an 8 mm diameter tube equipped with a drying tube. Excess anhydride was removed under about 1 to 4 mm pressure and the residue distilled for 1/2 h under water suction (cold trap, drying tube). Hydrolysis of the oil (infrared bands at 1 775, 1 850 cm^{-1}) by heating with a few drops of water yielded after 2 recrystallizations, a diacid (XII), m.p. 150–155° (4.0 mg), whose m.p. was depressed when mixed with VIII. XII had end-absorption only in the quartz ultraviolet, ϵ_{200}^{EtOH}, 360. Titration in carbon dioxide free water with 0.1 *N* NaOH gave pK_1 4.2, pK_2 6.7.

Diacid (IX) (4.8 mg), similarly treated with acetic anhydride (0.3 ml), gave an anhydride with an infrared spectrum identical with that of the anhydride from diacid (VIII). Hydrolysis followed by 2 recrystallizations gave a diacid (1.0 mg), m.p. 153–155°. Its melting point was undepressed when mixed with XII, but was depressed when mixed with VIII and IX.

Diacid (X) (28 mg) on treatment with acetic anhydride (0.5 ml) gave an oil with infrared bands at 1 775 and 1 855 cm^{-1}. Hydrolysis of the oil, followed by 3 recrystallizations of the solid, yielded material melting at 172–173° (3.7 mg). The melting point was undepressed when mixed with XI but was depressed when mixed with X, the starting acid.

Diacid (XI) (6.5 mg) and acetic anhydride (0.3 ml) gave an anhydride with an infrared spectrum identical with that of the anhydride from X. Hydrolysis followed by 1 recrystallization afforded a diacid with m.p. 174–175°, identical with the melting point of XI, the starting acid.

Pyrolysis of the Dimethyl Esters of X and VIII

The dimethyl ester of X (22 mg), prepared by diazomethane esterification of the purified diacid, was sealed in a 10 mm diameter pyrex tube under a reduced pressure of between 1 to 4 mm. The sealed tube was heated in a sand bath at 400–410° for 10 min, cooled, and centrifuged. The products were estimated by g.l.c. (on 18 ft × 1/4 in., 10% DEGS column) and by the calibration of the response of the chromatographic apparatus with the following authentic compounds: dimethyl succinate (0.1 mg), dimethyl fumarate (0.1 mg), unchanged dimethyl ester of X (8.3 mg). Cyclohexene also was detected and identified by retention time (g.l.c.) and infrared spectrum. In a separate experiment starting with 68 mg of the dimethyl ester of X, dimethyl fumarate and succinate were isolated by g.l.c. and identified by comparison of their infrared spectra with authentic specimens. At higher temperatures 410–420° (17 min) of pyrolysis, only succinate is observed and no fumarate was detected.

Cyclohexene (24 mg) and dimethyl fumarate (31 mg) were heated in a sealed tube at 410–415° for 10 min, the tube having been sealed at −70° *in vacuo*. Chromatography of the product (25 ft × 1/4 in., 10% DEGS at 167°, He, 40 p.s.i.) permitted the isolation of dimethyl fumarate and dimethyl succinate (identified by retention time and infrared spectra).

The dimethyl ester of VIII (51 mg), prepared by repeated g.l.c. (8 ft × 3/8 in., 30% Carbowax 20M at 200°), was sealed in a 10 mm diameter pyrex tubing under a reduced pressure of between 1 to 4 mm. The sealed tube was heated at 400–410° for 10 min. The pyrolysis was repeated using 53 mg of ester. The combined pyrolyzates were distilled at 0.1 mm to separate the liquid pyrolyzates from tar. The distillate (62 mg) was hydrogenated overnight in ethyl acetate using 5% palladium on charcoal (32 mg) as catalyst. A liquid (3 mg) having the same retention time (35 min on 5 ft × 1/4 in., 20% Ucon Polar, 200°, He flow 67 ml per min) and infrared spectrum as that of dimethyl sebacate was isolated by g.l.c. The refluxing of the ester with 12% aqueous NaOH (0.4 ml) for 1 h, followed by repeated extraction with chloroform, the drying of the chloroform layer, and the evaporation of the solvent afforded, after 2 recrystallizations from ethyl acetate – benzene – petrol, a diacid (1.5 mg, m.p. 129–132°) whose melting point was undepressed when mixed with sebacic acid. Pyrolysis of the dimethyl ester of VIII was observed to occur as low as 340–350°.

Permanganate Oxidation of X

X (726 mg) was stirred overnight at room temperature with $KMnO_4$ (1.5 g), water (4 ml), and acetone (4 ml) in a flask equipped with a reflux condenser to prevent evaporation of solvent. Solvent was removed

Can. J. Chem. Downloaded from www.nrcresearchpress.com by 210.87.254.6 on 09/05/12
For personal use only.

under reduced pressures and the residue esterified with diazomethane. Chromatography of the esterified residue (on 18 ft × 1/4 in., 10% DEGS at 200°) revealed a peak which corresponded to *cis*-cyclohexane-1,2-dicarboxylate and revealed no trace of the *trans* isomer which preceded, and was clearly resolved from, the *cis* isomer. The peak corresponding to the *cis* isomer was isolated by g.l.c. and possessed an infrared spectrum indentical with that of an authentic specimen of the ester. Hydrolysis of the oil (3.5 mg) in 5% KOH (0.2 ml) at room temperature overnight, followed by the usual procedure, yielded a small quantity of crystals melting at 189–189.5°. The melting point was undepressed when mixed with an authentic sample of *cis*-1,2-cyclohexane dicarboxylic acid. The products were analyzed by g.l.c. by calibrating the response with each ester: dimethyl ester of X (204 mg), dimethyl *cis*-cyclohexane-1,2-dicarboxylate (3.5 mg), dimethyl adipate (approximately 10 mg), dimethyl glutarate (4 mg), and dimethyl succinate (4 mg). As little as 0.005 mg of the *trans* ester would have been detectable.

ACKNOWLEDGMENTS

The authors thank the Petroleum Fund of the American Chemical Society and the National Research Council of Canada for financial support. They are indebted to Dr. J. B. Stothers and Mr. R. E. Klinck for the n.m.r. spectra.

REFERENCES

1. P. DE MAYO, R. W. YIP, and S. T. REID. Proc. Chem. Soc. 54 (1963).
2. P. DE MAYO, H. TAKESHITA, and A. B. M. A. SATTAR. Proc. Chem. Soc. 119 (1962).
3. P. DE MAYO and H. TAKESHITA. Can. J. Chem. **41**, 440 (1963).
4. P. EATON. J. Am. Chem. Soc. **84**, 2454 (1962).
5. E. J. COREY, R. B. MITRA, and H. UDA. J. Am. Chem. Soc. **85**, 362 (1963).
6. E. J. COREY, R. B. MITRA, and H. UDA. J. Am. Chem. Soc. **86**, 485 (1964).
7. J. A. BARLTROP and R. ROBSON. Tetrahedron Letters, No. 9, 597 (1963).
8. J. N. PITTS, R. L. LETSINGER, R. P. TAYLOR, J. M. PATTERSON, G. RECKTENWALD, and R. B. MARTIN. J. Am. Chem. Soc. **81**, 1068 (1959).
9. G. O. SCHENCK, G. KOLTZENBURG, and H. GROSSMANN. Angew. Chem. **69**, 177 (1957).
10. J. F. KING. *In* The elucidation of structures by physical and chemical methods. *Editor* K. W. Bentley. Interscience Publishers, Inc., New York. 1963. p. 333.
11. M. P. CAVA and E. MOROZ. J. Am. Chem. Soc. **84**, 115 (1962).
12. J. MEINWALD, G. G. CURTIS, and P. G. GASSMAN. J. Am. Chem. Soc. **84**, 116 (1962).
13. G. R. CLEMO and S. B. GRAHAM. J. Chem. Soc. 213 (1930).
14. P. DE MAYO. *In* Advan. Org. Chem. Vol. 2. R. A. Raphael, E. C. Taylor, and H. Wynberg (*Editors*). Interscience Publishers, Inc., New York. 1960. p. 370.
15. W. S. JOHNSON, C. E. DAVIS, R. H. HUNT, and G. STORK. J. Am. Chem. Soc. **70**, 3021 (1948).

Can. J. Chem. Downloaded from www.nrcresearchpress.com by 210.87.254.6 on 09/05/12
For personal use only.

Can. J. Chem. Downloaded from www.nrcresearchpress.com by 210.87.254.105 on 09/05/12
For personal use only.

CONTRIBUTION A L'ÉTUDE STRUCTURALE DU CÉDRÉLANOL (δ-CADINOL), ALCOOL SESQUITERPÉNIQUE $C_{15}H_{26}O$ DE L'HUILE ESSENTIELLE CEDRELA ODORATA BRASILIENSIS

R. R. SMOLDERS

Service de Chimie Organique Générale et Analytique, Institut des Industries de Fermentation, Institut Meurice Chimie (CERIA), Bruxelles, Belgique

Reçu le 16 juin 1964

RÉSUMÉ

Le cédrélanol, alcool sesquiterpénique $C_{15}H_{26}O$ de l'huile essentielle *Cedrela odorata brasiliensis*, est identique aux (−)-δ-cadinol, pilgérol, albicaulol et alga cadinol. Il est, en outre, l'antipode optique du (+)-δ-cadinol, du sesquigoyol et du torreyol. Dans le présent travail, la structure proposée pour l'albicaulol par Dauben, Weinstein, Lim et Anderson, celle du Δ³-2,8-diméthyl-5-isopropyl-bicyclo-[0,4,4]-décèn-8-ol, est confirmée, mais la configuration de l'hydroxyle s'avère équatoriale plutôt qu'axiale. Dès lors, la configuration absolue du cédrélanol est celle indiquée par IV*b*.

Le cédrélanol, alcool sesquiterpénique $C_{15}H_{26}O$, p.f. 139–140°, $[\alpha]_D^{23}$ −106 ($CHCl_3$), a été isolé de l'huile essentielle *Cedrela odorata brasiliensis* et décrit depuis 1961 (1). Il est identique aux (−)-δ-cadinol, pilgérol, albicaulol et alga cadinol (1–4). D'autre part, (+)-δ-cadinol, torreyol et sesquigoyol sont trois noms désignant l'antipode optique du précédent (4, 5, 6).

La structure I du cédrélanol fut proposée sur la base d'une étude hâtive en résonance magnétique nucléaire (7) et de la conversion du composé (1) en cadalène II et en (−)-dichlorhydrate du cadinène dont la configuration absolue III est désormais connue (8).

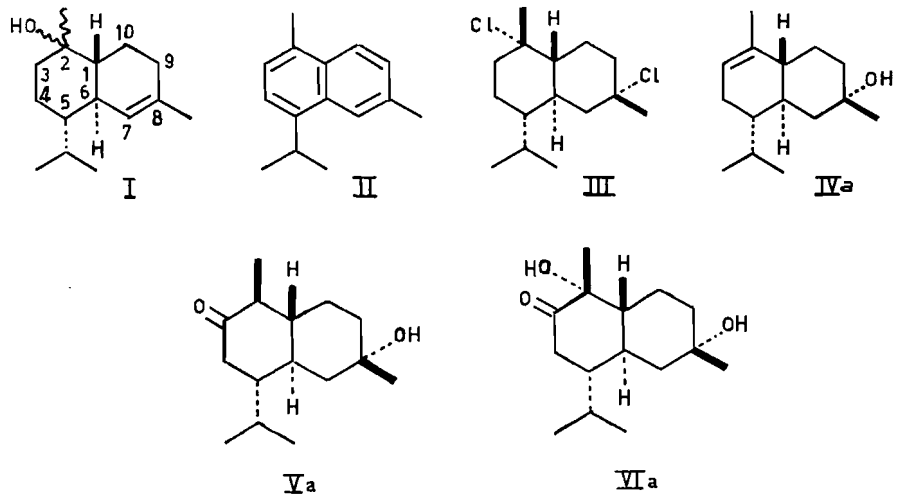

Dauben, Weinstein, Lim et Anderson (3) formulèrent IV*a* pour l'albicaulol au travers d'une étude attentive du spectre de résonance magnétique nucléaire du cadinol et de l'attribution, par dispersion rotatoire, des structures V*a* et VI*a* aux cétones dérivant du produit naturel par la transformation adéquate de la double liaison. Dans les formules IV*a*, V*a* et VI*a*, la configuration axiale de l'hydroxyle en C_8 était déduite de la résistance de IV*a* à l'estérification, tout comme l'avaient suggéré les chercheurs tchèques (2).

Quelques transformations chimiques du cédrélanol confirment la localisation de la double liaison en Δ^2 et, partant, celle de la fonction alcool en C_8 mais infirment le caractère axial de l'hydroxyle.

Une tentative de méthylation du carbone tertiaire de la double liaison du cédrélanol (désormais IV*b*), par action de l'iodure de méthylmagnésium sur l'époxycédrélanol, ayant échoué (9), nous nous sommes tourné vers la dihydroxycétone VI*b*, p.f. 140–141° (VI*a*, p.f. 143–144° selon (3)), $\nu_{C=O}$ 1 689 cm^{-1}. Il est surprenant d'observer, d'une part, que le spectre infrarouge de VI*b* est dépourvu de la bande d'absorption caractéristique des méthylènes voisins du carbonyle (10) dans la région sise entre 1 435 et 1 405 cm^{-1} et, d'autre part, que ce cétodiol présente un test de Zimmermann (11, 12) (cétone méthylénique, *m*-dinitrobenzène, alcali) négatif, encore que des exceptions notoires à ce test coloré soient connues, les 6-, 7- et 12-oxostéroides notamment (cf. (12) et les références y citées). Ces faits eussent plaidé en faveur de la structure I du cédrélanol.

L'action du méthyllithium sur VI*b*, suivie d'hydrolyse, conduit au méthylcédrélanetriol VII $C_{16}H_{30}O_3$, p.f. 180°, qui, déshydraté par le couple d'acides acétique et perchlorique, puis déshydrogéné par le soufre, fournit le méthylcadalène VIII (picrate, p.f. 140°; lit. p.f. 142.5–143° (13), 140–140.5°, 143–144° (14)).

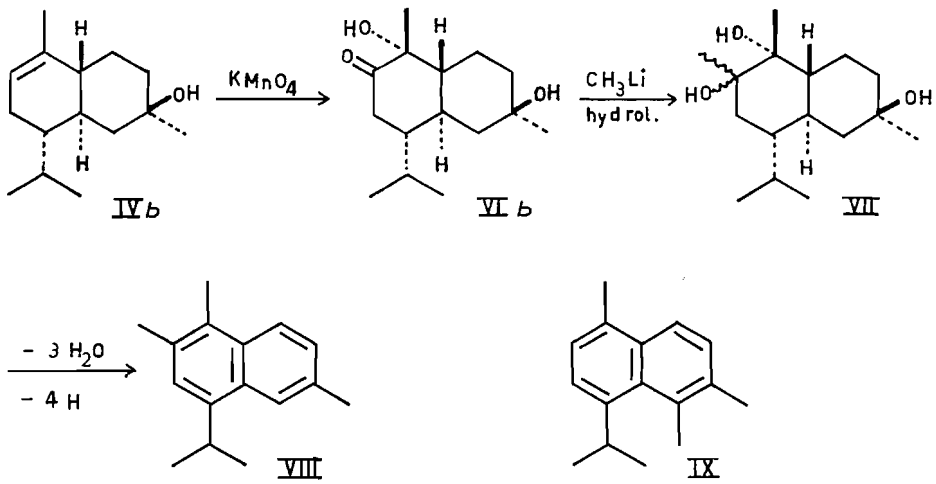

Un dérivé de référence du picrate de VIII ne nous a malheureusement pas été accessible pour effectuer l'épreuve de mélange. L'ensemble de ces résultats permet cependant de localiser, sans ambiguité, la double liaison en Δ^2 puisque I, au cours de la transformation effectuée, aurait conduit à l'aromatique IX dont le picrate (p.f. 102.5–103.5° (15), 103–104° (16)) est nettement distinct de celui de VIII.

D'autres expériences montrent le caractère équatorial de l'hydroxyle en C_8 et sont en accord avec IV*b*.

Le dihydrocédrélanol X (mélange des épimères en C_2), p.f. 65–68.5° $[\alpha]_D^{23}$ −38.1 (pyridine), est déshydraté ($SOCl_2$) en l'oléfine méthénique XI $C_{15}H_{26}$, $[\alpha]_D^{23}$ −14.3 (*n*-hexane), infrarouge 890, 1 646 et 3 080 cm^{-1}. Sachant qu'un tel comportement est l'apanage des 1-méthylcyclanols tertiaires dont l'hydroxyle est équatorial (17), la configuration absolue du cédrélanol est celle indiquée par IV*b*.

XI, après osmylation et traitement à l'hydrogène sulfuré, fournit le diol XII $C_{15}H_{26}O_2$, p.f. 110–120°, qui, via l'oxydation periodique, conduit à la cétone liquide XIII $C_{14}H_{24}O$,

Can. J. Chem. Downloaded from www.nrcresearchpress.com by 210.87.254.105 on 09/05/12
For personal use only.

$[\alpha]_D^{22}$ −29.6 (éther isopropylique), infrarouge $\nu_{C=O}$ 1 715 cm^{-1}. Cette cétone renferme quatre hydrogènes en α et α' du carbonyle comme le montre l'expérience de bromuration comparative suivante.

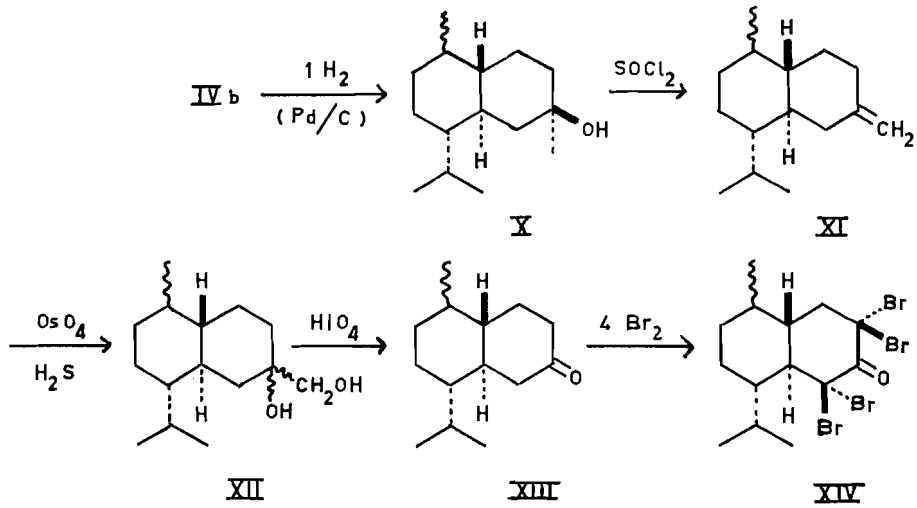

On a mis à réagir, séparément et à l'obscurité, la cétone XIII, la cyclohexanone, la cycloheptanone et la 2-méthylcyclohexanone à raison de 3.6×10^{-2} mole/l, dans un mélange de brome (4.5×10^{-1} mole/l) et d'une solution quasi-saturée d'acide trichloracétique dans le tétrachlorure de carbone. La bromuration, initiée à 40°, a été poursuivie à 50°. Le brome non consommé a été dosé, blanc à l'appui, à des intervalles de temps appropriés. La consommation de 4 équivalents de brome par mole de cétone est compatible avec la structure XIV et permet, une fois de plus, le rejet formel de I. Le déroulement de la bromuration est résumé dans le Tableau I. Une confirmation de la structure XIII par la conversion de cette cétone en 1-méthyl-4-isopropylnaphtalène sera rapportée ultérieurement.

TABLEAU I

Bromuration des carbones voisins du carbonyle

	Equivalents de brome consommés, par mole de cétone, au cours du temps:			
Cétone mise en oeuvre	20 h à 40°	70 h à 40°	70 h à 40° + 65 h à 50°	70 h à 40° +130 h à 50°
Cyclohexanone	3.59	3.61	3.81	3.91
XIII	2.22	2.78	3.49	3.82
Cycloheptanone	3.16	3.29	3.47	3.83
2-méthyl cyclohexanone	2.78	2.82	2.90	2.93

PARTIE EXPÉRIMENTALE

L'huile essentielle *Cedrela odorata brasiliensis* utilisée dans le présent travail provient de la Dierberger Oleos Essencias, Sao-Paulo, Brésil.

Les températures de fusion (F) ne sont pas corrigées.

Les spectres infrarouges de la quasi-totalité des produits manipulés ont été relevés en film mince pour les liquides et en pastille de bromure de potassium pour les solides, à l'aide d'un spectrographe Hilger H800 et (ou) d'un infracord Perkin–Elmer à double réseau, modèle 237B. Dans tous les cas, les valeurs des fréquences observées étaient en accord avec celles tabulées en (10) et (18).

Can. J. Chem. Downloaded from www.nrcresearchpress.com by 210.87.254.105 on 09/05/12
For personal use only.

Isolement du cédrélanol

L'huile brute (1 310 g) est tout d'abord débarassée de ses acides par la voie habituelle puis, par la distillation, démunie de ses matières les plus volatiles. Le résidu (171 g), à point d'ébullition supérieur à 70° sous 0.05 mm Hg, est une huile visqueuse et brunâtre que l'on chromatographie sur alumine neutre d'activité II (2 700 g). Après l'élution préliminaire à la ligroine et au tétrachlorure de carbone, le trichloréthylène, le benzène et l'éther, purs ou en mélange, ont désorbé une série de fractions cristallines qui, recristallisées dans l'isooctane ou, mieux, dans l'acétonitrile, fournissent le cédrélanol pur (5.5 g), aisément sublimable sous dépression; pf.. 139–140°, $[\alpha]_D^{23}$ −106 ($CHCl_3$).

Anal. Calc. pour $C_{15}H_{26}O$: C, 81.04; H, 11.73. Trouvé: C, 80.84; H, 11.68.

Méthylcédrélanetriol VII à partir de la dihydroxycétone VIb

Sous atmosphère d'azote, on met en présence le lithium (200 mg), coupé en parcelles menues, et l'éther éthylique anhydre (20 ml). A −10°, on y fait barboter du bromure de méthyle sec entraîné par un courant d'azote. Après 1 h de ce traitement, le lithium disparait et fait place à une suspension laiteuse à laquelle on ajoute, toujours sous refroidissement, une solution de VI*b* (525 mg) dans l'éther éthylique anhydre (20 ml). Successivement, on abandonne la préparation à la température ambiante durant 4 h 30 min, chauffe à reflux d'éther durant 2 h 30 min puis laisse séjourner le milieu réactionnel à la température ordinaire pendant 9 h. On additionne ensuite de l'éther saturé d'eau, de la glace puis de l'acide chlorhydrique dilué à 5% et glacé. La phase organique, séchée sur carbonate de potasse anhydre, est filtrée, portée à l'ébullition en présence d'une pincée de charbon actif et filtrée une seconde fois. Le filtrat, après évaporation, fournit le triol VII (551 mg), p.f. 180°, dépourvu d'absorption du carbonyle dans l'infrarouge.

Anal. Calc. pour $C_{16}H_{30}O_3$: C, 71.06; H, 11.18; O, 17.75. Trouvé: C, 71.05; H, 11.16; O, 17.79.

Déshydratation du triol VII et déshydrogénation subséquente

Le triol VII (535 mg) est dissout dans l'acide acétique glacial (6.2 ml) puis additionné de 5 gouttes d'acide perchlorique à 70%. La solution est chauffée au bain-marie bouillant durant 2 h 30 min, refroidie, diluée par l'eau (80 ml) et extraite par l'éther. La phase éthérée est lavée au bicarbonate dilué, séchée sur carbonate de potassium anhydre, filtrée et évaporée Il reste alors une huile jaune (423 mg) dont l'infrarouge montre la nature hydrocarbonée. Ce matériau brut est déshydrogéné durant 6 h 30 min entre 240 et 250°, par le soufre (143 mg). Le produit de réaction, mélangé à de l'alumine standard (1 g), est chromatographié sur le même adsorbant (8 g). En éluant par le *n*-hexane, on obtient 3 fractions: f(i) 16 mg (40 ml); f(ii) 14.5 mg (42 ml); f(iii) 3.2 mg (47 ml). Le picrate brut de f(ii) (EtOH, 1 ml; acide picrique 15 mg) fond entre 134 et 137°. Une recristallisation dans l'alcool absolu amène ce dérivé (16.5 mg) à fondre à 139°. Une deuxième recristallisation identique laisse un magma d'aiguilles oranges (12 mg) fondant à 140°.

Oléfine méthénique XI à partir du dihydrocédrélanol X

Le dihydrocédrélanol (3.20 g), p.f. 65–68.5°, $[\alpha]_D^{22}$ −38.1 (pyridine), est dissout dans la pyridine anhydre (26 ml) et refroidi à −15°. Une solution de chlorure de thionyle (4.2 ml) dans la pyridine anhydre (16 ml), refroidie à −10°, lui est ajoutée, par portions, de façon à maintenir le milieu entre −10 et −15°. L'ensemble maintenu d'abord durant 50 min dans cette zone de température, est progressivement réchauffé à 0° (50 min) avant d'être versé sur la glace et extrait par l'éther. La solution organique, lavée plusieurs fois à l'acide tartrique dilué (6%), est séchée sur du sulfate de magnésium anhydre et évaporée. Le résidu, chromatographié sur de l'alumine neutre d'activité II (60 g), fournit, par élution au *n*-hexane, l'oléfine liquide XI (2.94 g) $C_{15}H_{26}$, $[\alpha]_D^{23}$ −14.3 (*n*-hexane).

Anal. Calc. pour $C_{15}H_{26}$: C, 87.30; H, 12.70. Trouvé: C, 87.0; H, 13.0.

Diol XII à partir de l'oléfine XI (inspiré de (19))

A une solution de XI (2.80 g) dans le dioxanne sec (5 ml), on ajoute de la pyridine anhydre (0.5 ml) et une solution de tétroxyde d'osmium (5.20 g) dans le même éther (75 ml). Le milieu réactionnel séjourne 75 h à l'obscurité puis est traité par l'hydrogène sulfuré, filtré et évaporé. Les cristaux bruts obtenus (3.37 g) sont recristallisés, par deux fois, dans l'acétonitrile. Il reste alors 1.67 g de diol XII, p.f. 110–120°.

Anal. Calc. pour $C_{15}H_{26}O_2$: C, 74.95; H, 11.74; O, 13.31. Trouvé: C, 75.18; H, 11.60; O, 13.16.

Cétone XIII à partir du glycol XII (inspiré de (19))

A XII (0.254 g), dissout dans le dioxanne (21.5 ml), on additionne une solution aqueuse (5.2 ml) d'acide paraperiodique (0.648 g). Après un contact de 20 h, une large part du solvant est éliminé à 0°, sous dépression. Le reliquat, dilué par l'eau, est extrait à l'éther. L'extrait est séché au sulfate de magnésium anhydre, filtré puis évaporé. Le résidu, repris dans le *n*-pentane (4 ml), est chromatographié sur alumine standard (5.4 g) et livre, par élution au même solvant (70 ml), la cétone XIII (0.158 g), $[\alpha]_D^{23}$ −29.6 (éther isopropylique).

Anal. Calc. pour $C_{14}H_{24}O$: C, 80.71; H, 11.61; O, 7.68. Trouvé: C, 80.10; H, 12.10; O, 7.73.

Bromuration comparative de la cétone XIII

On dilue, jusqu'à 100 ml, 7.5 g de brome par une solution quasi-saturée d'acide trichloroacétique dans le tétrachlorure de carbone. A l'aide de ce mélange, on porte à 10 ml les quatre cétones suivantes: XIII (74.37 mg), cyclohexanone (35.32 mg), cycloheptanone (40.40 mg) et 2-méthylcyclohexanone (40.37 mg).

Can. J. Chem. Downloaded from www.nrcresearchpress.com by 210.87.254.105 on 09/05/12
For personal use only.

En plus d'un blanc, on chauffe ces échantillons, à l'obscurité, durant 70 h à 40° et 130 h à 50°. A des intervalles de temps appropriés, on effectue, au sein de prises de 1 ml, le dosage iodométrique du brome non consommé. Les résultats observés ont été consignés dans le Tableau I.

REMERCIEMENTS

L'auteur est heureux d'exprimer sa profonde gratitude à Messieurs G. Chiltz et J. M. Piérard, Directeur et Sous-Directeur de l'Institut des Industries de Fermentation – Institut Meurice Chimie, des larges facilités de recherches qu'ils n'ont cessé de lui accorder tout au long de ce travail.

Il remercie également le Docteur A. Toussaint des discussions fructueuses échangées durant le présent mémoire.

BIBLIOGRAPHIE

1. G. Chiurdoglu, R. R. Smolders et A. Soquet. Bull. Soc. Chim. Belges, **70**, 468 (1961).
2. O. Motl, V. Sykora, V. Herout et F. Sorm. Collection Czech. Chem. Commun. **23**, 1297 (1958).
3. W. G. Dauben, B. Weinstein, P. Lim et A. B. Anderson. Tetrahedron, **15**, 217 (1961).
4. K. T. Wang et B. Weinstein. Experientia, **19**, 519 (1963).
5. V. A. Pentegova, O. Motl et V. Herout. Dokl. Acad. Nauk USSR, **138**, 850 (1961).
6. T. Sakai, K. Nishimura, H. Chikamatsu et H. Hirose. Bull. Chem. Soc. Japan, **36**, 1261 (1963).
7. F. Alderweireldt, G. Chiurdoglu, R. R. Smolders, A. Soquet et M. Verzele. Bull. Soc. Chim. Belges, **70**, 470 (1961).
8. V. Sykora, V. Herout et F. Šorm. Collection Czech. Chem. Commun. **23**, 2181 (1958).
9. Communication au Symposium International de Chimie Organique conascré à l'Etude des Produits Nautrels (Bruxelles, juin 1962). (*a*) 1ère partie: R. R. Smolders, F. Alderweireldt, G. Chiurdoglu, A. Soquet et M. Verzele; (*b*) 2e partie: R. R. Smolders et G. Chiurdoglu.
10. R. N. Jones et C. Sandorfy. *Dans* Technique of organic chemistry. Arnold Weissberger (*Editor*). Vol. IX. Interscience Publishers, Inc., New York. 1956. p. 499.
11. W. Zimmermann. Z. Physiol. Chem. **233**, 257 (1935); **245**, 47 (1936). O. Neunhoeffer, K. Thewalt et W. Zimmermann. Z. Physiol. Chem. **323**, 116 (1961).
12. T. J. King et C. E. Newall. J. Chem. Soc. 367 (1962).
13. W. P. Campbell et M. D. Soffer. J. Am. Chem. Soc. **64**, 417 (1942).
14. J. Gripenberg et R. G. Lindahl. Acta Chem. Scand. **3**, 256 (1949).
15. S. Dev. Current Sci. India, **16**, 377 (1947). Chem. Abstr. **42**, 5890 (1948).
16. M. D. Soffer, M. Brey et J. Fournier. J. Am. Chem. Soc. **81**, 1678 (1959).
17. D. H. R. Barton, A. da S. Campos-Neves et R. C. Cookson. J. Chem. Soc. 3500 (1956).
18. L. J. Bellamy. The infra-red spectra of complex molecules. Methuen & Co., Ltd., London. 1958.
19. Y. Mazur, A. Weizmann et F. Sondheimer. J. Am. Chem. Soc. **80**, 6293 (1958).

Can. J. Chem. Downloaded from www.nrcresearchpress.com by 210.87.254.105 on 09/05/12
For personal use only.

Can. J. Chem. Downloaded from www.nrcresearchpress.com by 210.87.254.42 on 09/05/12
For personal use only.

SUBSTITUTED METHANES

PART XXXVI. CALCULATED WAVE NUMBERS, ASSIGNMENTS, AND THERMODYNAMIC PROPERTIES FOR CH_2DI AND CD_2HI, AND CALCULATED ROTATIONAL DISTORTION CONSTANTS AND MEAN AMPLITUDES FOR CH_3I AND CD_3I[1]

EARLE F. DITZEL,[2] ARNOLD G. MEISTER,[3] EDWARD A. PIOTROWSKI, FORREST F. CLEVELAND, Y. ANANTARAMA SARMA, AND S. SUNDARAM

Spectroscopy Laboratory,[4] Department of Physics, Illinois Institute of Technology, Chicago, Illinois

Received July 13, 1964

ABSTRACT

A set of potential energy constants has been obtained for CH_3I and CD_3I from their vibrational spectral data. From these constants, the rotational distortion constants and the mean amplitudes have been calculated for these two molecules. The rotational distortion constants D_J, D_{JK}, and D_K were, respectively, CH_3I, 6.34, 59.36, and 3 542.30; CD_3I, 3.90, 33.08, and 866.43 kc/s. The principal mean amplitudes of vibration in pm (pm = picometer = 10^{-12} meter = 10^{-2} Å) at 298.16 °K are CH_3I, 5.25 (C—I), 7.71 (C—H), 12.37 (H · · · H), and 12.00 (H · · · I); CD_3I, 5.14 (C—I), 6.63 (C—D), 10.85 (D · · · D), and 10.65 (D · · · I). The potential energy constants were used to obtain the wave numbers of CH_2DI and CD_2HI. A complete assignment of the observed wave numbers for the molecules CH_2DI and CD_2HI has been made. The fundamental wave numbers for the gaseous state of CH_2DI are a', 2 980, 2 235, 1 418, 1 170, 723, and 519; a'', 3 091, 1 266, and 871 cycles/cm. For CD_2HI, the corresponding values are a', 3 017, 2 174, 1 185, 1 009, 757, and 508; a'', 2 273, 1 279, and 676. With these wave numbers, the thermodynamic functions have been calculated for the two molecules for 12 temperatures from 100 to 1 000 °K for 1 atm pressure. The values of $(H^0 - E_0^0)/T$, $-(F^0 - E_0^0)/T$, S^0, and C_p^0 at 298.16 °K are, respectively, CH_2DI, 8.82, 54.66, 63.48, and 10.98; CD_2HI, 9.00, 55.20, 64.19, and 11.53 cal deg^{-1} mole^{-1}.

INTRODUCTION

Fenlon *et al.* (1) determined the potential energy constants of CH_3I from observed vibrational spectral data. The set of F's thus obtained when transferred to the isotopic molecule CD_3I gives an agreement between the observed and calculated wave numbers to within 2.24%. Transferability of the potential energy constants to isotopic molecules is one of the most important criteria for establishing the validity of the potential energy constants. Therefore it was necessary to redetermine the potential energy constants for CH_3I to satisfy the above criterion better than in the previous study (1).

The purpose of the present investigation is to obtain a set of potential energy constants for CH_3I and CD_3I which will not only reproduce the observed wave numbers, but also yield rotational distortion constants and mean amplitudes of vibration that agree with experimental values for these quantities. This is a better procedure, since the set of F's thus obtained would then have satisfied these additional criteria also.

Courtoy (2) and De Hemptinne and Doehaerd (3) have obtained the spectra for CH_2DI and CD_2HI, the other isotopic molecules in this series of iodomethanes. It was therefore the other main aim of this study to calculate the f's from the F's for CH_3I and CD_3I by the systematic procedure of Gold *et al.* (4) and to use these f's to calculate the wave numbers of the isotopic molecules CH_2DI and CD_2HI to facilitate the assignments of their spectral data (2, 3). This procedure made possible not only a complete analysis of

[1] *For previous papers in this series, see Spectroscopia Mol. 13, 56 (1964).*
[2] *Present address: Naval Research Laboratory, Code 5210, Washington 25, D.C.*
[3] *Present address: Physics Department, Arizona State University, Tempe, Arizona.*
[4] *Publication No. 183.*

the spectral data for CH_2DI and CD_2HI but also the establishment of the fundamentals and hence of the numerical values of the thermodynamic properties for these two molecules.

MOLECULAR CONSTANTS FOR CH_3I AND CD_3I

Using the previously tabulated values of the observed wave numbers (1), and the Wilson **FG** matrix method, the symmetrized F's were redetermined for CH_3I and CD_3I. The maximum difference between the calculated and observed wave numbers is 0.97% for CH_3I and 1.40% for CD_3I. The internuclear distances used in the calculations are 109.3 pm (1.093 Å) for C—H and C—D and 213.9 pm for C—I.

The set of F's thus obtained were then used to calculate the rotational distortion constants D_J, D_{JK}, and D_K by the method given by Dowling *et al.* (5). Previously, Chang (6) had calculated the constants D_J and D_{JK} for CH_3I, and observed values had been obtained by several investigators (7–9) for CH_3I and by Simmons (10) for CD_3I. The calculated and observed values are compared in Table I.

TABLE I

Rotational distortion constants for CH_3I and CD_3I*†

	CH_3I					CD_3I	
	Calculated		Observed			Calculated	Observed
D	P	C	J	SA	O-T	P	S
D_J	6.34	6.39	7.95	7.95	6.28	3.90	3.57
D_{JK}	59.36	88.70	99.40	99.40	98.50	33.08	48.30
D_K	3 542.30	—	—	—	—	866.43	—

*D = rotational distortion constant; P = present results; C = Chang, ref. 6; J = Johnson *et al.*, ref. 8; SA = Simmons and Anderson, ref. 7; O-T = Orville-Thomas *et al.*, ref. 9; and S = Simmons, ref. 10.
†All of the rotational distortion constants are in kc/s.

While the calculated values of D_J are in reasonable agreement with the observed values, the values of D_{JK} are somewhat smaller than the observed values. These differences may perhaps be due to the neglect of the anharmonicity, which would be rather large for these molecules and which would be different for the two molecules. Since the F's were adjusted to give the best agreement between the observed and calculated wave numbers of both molecules, the effect of differing anharmonicities could have produced some deviation of the calculated distortion constants from the observed values for each of the molecules. Further, the magnitudes of these quantities are such that maximum accuracy is not possible in evaluating them from experimental measurements.

The F's were then used to determine the mean square amplitudes of vibration for CH_3I and CD_3I. In terms of the potential energy matrix **F**, the mean square amplitude matrix **Σ** is given by (11)

$$|\mathbf{\Sigma F} - \mathbf{E\Delta\lambda}| = 0,$$

where **E** is the unit matrix and **Δ** and **λ** are related to the wave number σ by the expressions

$$\Delta_i = (h/8\pi^2 c\sigma_i) \coth (hc\sigma_i/2kT)$$

and

$$\lambda_i = 4\pi^2 c^2 \sigma_i^2,$$

where Δ_i and λ_i are the matrix elements corresponding to the ith fundamental vibrational mode, h is Planck's constant, k is Boltzmann's constant, and T is the temperature in degrees Kelvin.

Can. J. Chem. Downloaded from www.nrcresearchpress.com by 210.87.254.42 on 09/05/12
For personal use only.

By means of the potential energy constants, the matrix elements $\sum_{ij}$ and therefore the principal mean amplitude quantities for the various internuclear distances were computed for CH_3I and CD_3I. The calculations were made for 298.16 °K and the results are summarized in Table II. There are at present no experimental values for comparison. However, the values reported here should be useful in the analysis of future electron diffraction investigations on these molecules.

TABLE II

Mean amplitudes of vibrations in pm*

CH_3I		CD_3I	
C—H	7.71	C—D	6.63
C—I	5.25	C—I	5.14
H · · · H	12.37	D · · · D	10.85
H · · · I	12.00	D · · · I	10.65

*These calculated values correspond to 298.16 °K; pm = picometer = 10^{-12} meter = 10^{-2} Å.

A consistent set of f's was then obtained from the relation $\mathbf{f} = \tilde{\mathbf{U}}\mathbf{F}\mathbf{U}$ (4) and the values are listed in Table III, and the observed and calculated wave numbers for CH_3I and CD_3I are given in Table IV.

TABLE III

Potential energy constants for CH_3I, CH_2DI, CD_2HI, and CD_3I*

md/Å		md/rad		md Å/rad²	
f_i	2.27665†	f_i^{hh}	−0.06464	f_{hh}	0.45151
f_h	5.07113	f_i^{hi}	0.06464	f_{hi}	0.45672
f_h^h	−0.05060	f_h^{hh}	0.03792	f_{hh}^{hi}	−0.07609
f_h^i	0.06351	$f_h^{hh'}$	−0.28414	$f_{hh}^{h'i}$	−0.09076
		f_h^{hi}	0.21563	$f_{hh}^{hh'}$	−0.10429
		$f_h^{h'i}$	−0.00367	$f_{hi}^{h'i}$	−0.10689

*The potential energy constants are expressed in the descriptive notation of Davis, Cleveland, and Meister (J. Chem. Phys. 20, 454 (1952)): i = C—I, h = C—H or C—D, hh = H—C—H or D—C—D or H—C—D, hi = H—C—I or D—C—I, and h and h' represent different C—H or C—D bonds; md = millidyne; rad = radian.

†This number of significant figures is not justifiable by the accuracy of the experimental data but is needed to obtain the best reproduction of the observed wave numbers and to secure internal consistency in calculations.

TABLE IV

Calculated and observed wave numbers for fundamentals of CH_3I and CD_3I

	CH_3I		CD_3I	
	Calculated	Observed	Calculated	Observed
a_1	2 966	2 975	2 146	2 135*
	1 241	1 252	955	948
	536	533	486	493*
e	3 074	3 061	2 263	2 285*
	1 454	1 440	1 057	1 070
	888	882	664	665

*Observed value for the liquid state. All the other observed values and all of the calculated values are for the gaseous state.

ASSIGNMENTS AND FUNDAMENTALS FOR CH_2DI AND CD_2HI

The values of the f's obtained for CH_3I and CD_3I were then used to calculate the wave numbers for the fundamentals of CH_2DI and CD_2HI. The infrared spectrum of a mixture of CH_2DI and CD_2HI had been obtained previously by Courtoy (2) and the Raman

Can. J. Chem. Downloaded from www.nrcresearchpress.com by 210.87.254.42 on 09/05/12
For personal use only.

spectrum of a similar mixture had been observed by De Hemptinne and Doehaerd (3). The calculated wave numbers were compared with the observed ones and a complete analysis of the spectra of CH_2DI and CD_2HI was made. The assignments were made

TABLE V

Spectral data and assignments for CH_2DI and CD_2HI*

Infrared		Raman		Assignment			
σ_g	I_e	$\Delta\sigma_1$	I_e	σ_c	CH_2DI	CD_2HI	Type
—	—	501	8	*498*	—	σ_6	a'
—	—	511	8	*513*	σ_6	—	a'
—	—	—	—	*669*	—	σ_9	a''
714†	w	706	3	*724*	σ_5	—	a'
739	w	751	6	*765*	—	σ_5	a'
766	w						
~876	w	—	—	*863*	σ_9	—	a''
938	s	—	—	—	CD_3I	σ_2	a_1
957	s						
1 009	s	1 006	6	*1 012*	—	σ_4	a'
1 031	m, sh	—	—	1 016	—	$2\sigma_6$	A'
1 079	w, sh	—	—	1 038	$2\sigma_6$	—	A'
1 170	m, sh			*1 161*	σ_4	—	a'
1 185	vs	1 161	8	*1 183*	—	σ_3	a'
1 245	m	—	—	—	CH_3I	σ_2	a_1
—	—	—	—	*1 258*	σ_8	—	a''
1 263	m	—	—	—	CH_3I	σ_2	a_1
—	—	1 272	0	*1 297*	—	σ_8	a''
1 328	w, sh	—	—	1 352	—	$2\sigma_9$	A'
1 410	m	1 408	0	*1 427*	σ_3	—	a'
1 426	m						
1 443	m	—	—	1 446	$2\sigma_5$	—	A'
1 520	vw	—	—	1 514	—	$2\sigma_5$	A'
1 704	vw	—	—	1 716	$\sigma_2 - \sigma_6$	—	A'
1 880	vw	—	—	1 893	$\sigma_4 + \sigma_5$	—	A'
2 049	w, sh	—	—	2 041	$\sigma_4 + \sigma_9$	—	A''
2 174	m	2 178	8	*2 185*	—	σ_2	a'
—	—	2 227	6	*2 228*	σ_2	—	a'
—	—	—	—	*2 266*	—	σ_7	a''
—	—	2 312	3	2 322	$2\sigma_4$	$2\sigma_3$	A'
2 525	vw	—	—	2 558	—	$2\sigma_8$	A'
2 967	m	—	—	*3 004*	σ_1	—	a'
2 833‡	vw, sh	—	—	2 850	—	$\sigma_2 + \sigma_9$	A''
2 861	m	—	—	2 836	$2\sigma_3$	—	A'
2 954	w, sh	—	—	2 958	$\sigma_2 + \sigma_5$	—	A'
2 980	vs	2 982	3	*3 004*	σ_1	—	a'
3 017	w, sh	3 013	1	*3 037*	—	σ_1	a'
3 091	vw, sh	—	—	*3 095*	σ_7	—	a''
3 200	vw, sh	—	—	3 183	—	$\sigma_2 + \sigma_4$	A'
3 252	vw	—	—	3 282	—	$\sigma_4 + \sigma_7$	A''
3 350	vw	—	—	3 359	—	$\sigma_2 + \sigma_3$	A'
3 630	vw, sh	—	—	3 653	$\sigma_2 + \sigma_3$	—	A'
3 685	vw	—	—	3 693	—	$\sigma_1 + \sigma_9$	A''
3 725	vw	—	—	3 703	$\sigma_1 + \sigma_5$	—	A'
3 800	vw	—	—	3 814	$\sigma_5 + \sigma_7$	—	A''
3 900	vw	—	—	3 851	$\sigma_1 + \sigma_9$	—	A''
4 235	w	—	—	4 246	$\sigma_1 + \sigma_8$	—	A''
4 495	vw, sh	—	—	4 509	$\sigma_3 + \sigma_7$	—	A''
4 565	w	—	—	4 546	—	$2\sigma_7$	A'
5 115	vw	—	—	5 215§	$\sigma_1 + \sigma_2$	—	A'
5 990	w	—	—	5 960‖	$2\sigma_1$	—	A'

*σ_g = wave number in cycles/cm (c/cm) for the gas; I_e = estimated intensity (w = weak, m = medium, s = strong, v = very, sh = shoulder); $\Delta\sigma_1$ = Raman displacement in c/cm for the liquid; σ_c = calculated wave number.

†The 714 to 2 967 c/cm bands were obtained with a NaCl prism.

‡The 2 833 to 5 990 c/cm bands were obtained with a quartz prism.

§Five ternary summation bands also are allowed in this region.

‖The overtone and combination bands were calculated from the observed wave numbers given in Table VI.

Can. J. Chem. Downloaded from www.nrcresearchpress.com by 210.87.254.42 on 09/05/12
For personal use only.

not only for the fundamentals but also for the overtones and combinations of both the molecules. These results are given in Table V, and the observed and calculated wave numbers for the fundamentals extracted from Table V are listed in Table VI.

TABLE VI

The fundamentals of CH_2DI and CD_2HI*

	CH_2DI				CD_2HI			
ν	σ_g	σ_l	D	σ_c	σ_g	σ_l	D	σ_c
$\nu_1(a')$	2 980	2 982	−2	3 004	3 017	3 013	4	3 037
$\nu_2(a')$	2 235†	2 227	—	2 228	2 174	2 178	−4	2 185
$\nu_3(a')$	1 418	1 408	10	1 427	1 185	1 161	24	1 183
$\nu_4(a')$	1 170	1 161	9	1 161	1 009	1 006	3	1 012
$\nu_5(a')$	723	706	17	724	757	751	6	765
$\nu_6(a')$	519†	511	—	513	508†	501	—	498
$\nu_7(a'')$	3 091	3 083‡	—	3 095	2 273†	2 266§	—	2 266
$\nu_8(a'')$	1 266†	1 258§	—	1 258	1 279†	1 272	—	1 297
$\nu_9(a'')$	871†	863§	—	863	676†	669§	—	669

*ν is the frequency; σ_g, σ_l, and σ_c are respectively the gaseous, liquid, and calculated wave numbers in cycles/cm; and $D = \sigma_g - \sigma_l$.
†Estimated value: σ_l + the average value of D.
‡Estimated value: σ_g − the average value of D.
§The value calculated in the normal coordinate treatment; not observed directly.

THERMODYNAMIC PROPERTIES FOR CH_2DI AND CD_2HI

By means of the observed wave numbers for the gaseous state given in columns 2 and 6 of Table VI in the place of the ω's in the rigid-rotor harmonic-oscillator equations for the thermodynamic functions, the heat content function, free energy function, entropy, and heat capacity for CH_2DI and CD_2HI were calculated for 1 mole of ideal gas at 1 atm pressure for 12 temperatures from 100 to 1 000 °K. The results are given in Table VII.

TABLE VII

Heat content and free energy functions, entropy, and heat capacity of CH_2DI and CD_2HI for the ideal gaseous state at 1 atm pressure*

	$(H^0 - E_0^0)/T$		$-(F^0 - E_0^0)/T$		S^0		C_p^0	
T	CH_2DI	CD_2HI	CH_2DI	CD_2HI	CH_2DI	CD_2HI	CH_2DI	CD_2HI
100	7.96	7.96	45.71	46.18	53.66	54.14	8.02	8.04
200	8.22	8.28	51.28	51.76	59.50	60.04	9.15	9.42
273.16	8.64	8.79	53.90	54.42	62.54	63.21	10.49	10.99
298.16	8.82	9.00	54.66	55.20	63.48	64.19	10.98	11.53
300	8.83	9.01	54.72	55.25	63.55	64.26	11.01	11.57
400	9.62	9.91	57.36	57.97	66.98	67.88	12.89	13.59
500	10.44	10.82	59.60	60.28	70.04	71.10	14.54	15.29
600	11.24	11.69	61.57	62.33	72.81	74.02	15.93	16.72
700	12.00	12.50	63.36	64.19	75.36	76.69	17.12	17.92
800	12.71	13.24	65.01	65.91	77.72	79.15	18.15	18.94
900	13.36	13.92	66.55	67.51	79.91	81.43	19.04	19.81
1 000	13.97	14.55	67.99	69.01	81.96	83.56	19.81	20.54

*T is in degrees Kelvin and the other quantities are in cal deg^{-1} $mole^{-1}$.

ACKNOWLEDGMENT

This work was part of a research program which has been aided by grants from the National Science Foundation. The authors are grateful for this assistance.

Can. J. Chem. Downloaded from www.nrcresearchpress.com by 210.87.254.42 on 09/05/12
For personal use only.

REFERENCES

1. P. F. FENLON, F. F. CLEVELAND, and A. G. MEISTER. J. Chem. Phys. **19**, 1561 (1951).
2. CH. COURTOY. Ann. Soc. Sci. Bruxelles, Ser. I, **60**, 122 (1946); **61**, 55 (1947).
3. M. DE HEMPTINNE and TH. DOEHAERD. Acad. Roy. Belg. Bull. Classe Sci. Ser. V, **30**, 497 (1944).
4. R. GOLD, J. M. DOWLING, and A. G. MEISTER. J. Mol. Spectry. **2**, 9 (1958).
5. J. M. DOWLING, R. GOLD, and A. G. MEISTER. J. Mol. Spectry. **1**, 265 (1957).
6. T-S. CHANG. Thesis, University of Michigan, Ann. Arbor, Michigan. 1954.
7. J. SIMMONS and W. ANDERSON. Phys. Rev. **80**, 338 (1950).
8. C. M. JOHNSON, R. TRAMBARULO, and W. GORDY. Phys. Rev. **84**, 1178 (1951).
9. W. J. ORVILLE-THOMAS, J. T. COX, and W. GORDY. J. Chem. Phys. **22**, 1718 (1954).
10. J. SIMMONS. Private communication. 1958.
11. S. J. CYVIN. Acta Chem. Scand. **13**, 2135 (1959).

Can. J. Chem. Downloaded from www.nrcresearchpress.com by 210.87.254.42 on 09/05/12
For personal use only.

THE INHIBITION OF AUTOXIDATION BY 2,4,6-TRI-*tert*-BUTYL SUBSTITUTED PHENOL, ANILINE, AND THIOPHENOL[1]

D. V. GARDNER,[2] J. A. HOWARD, AND K. U. INGOLD
Division of Applied Chemistry, National Research Council, Ottawa, Canada
Received August 11, 1964

ABSTRACT

The reactions of peroxy radicals with 2,4,6-tri-*t*-butyl substituted phenol, aniline, and thiophenol have been examined by a kinetic method. The primary process involves abstraction of the hydrogen atom attached to the functional group, since all three compounds show fairly large isotope effects when this hydrogen is replaced by deuterium. The phenol and aniline react with about two peroxy radicals per molecule. In contrast, the thiophenol reacts with only a single peroxy radical.

The present work was undertaken because of the absence of reliable data on the rates and mechanism of the reaction of peroxy radicals with anilines and thiophenols. The reaction of phenols with peroxy radicals, i.e.,

[6]* $$RO_2\cdot + AH \rightarrow ROOH + A\cdot$$

[7] $$RO_2\cdot + A\cdot \rightarrow ROOA,$$

is now fairly well understood (1, 2, 3), but there is no comparable information regarding anilines and thiophenols. In particular, there is still disagreement in the literature as to whether or not amine-inhibited oxidations show any deuterium isotope effect when the amino hydrogen is replaced by deuterium. That is, there is disagreement as to whether or not the rate-controlling step for inhibition by amines involves reaction [6] (see refs. 1 and 4 for a discussion of the literature on amine inhibition). The reaction of thiophenols with peroxy radicals has not been studied previously.

The 2,4,6-tri-*t*-butyl derivatives of phenol, aniline, and thiophenol were chosen for study with the hope that steric protection of the reaction center would prevent chain transfer reactions between the inhibitor radical (A·) and the substrate,

[8] $$A\cdot + RH \rightarrow AH + R\cdot$$

or its oxidation product,

[−6] $$A\cdot + ROOH \rightarrow AH + RO_2\cdot.$$

Suppression of these reactions when A· is a phenoxy radical by a suitable choice of substrate (1, 2) or by steric protection of the hydroxyl group (3) greatly simplifies the kinetics of the inhibition process (3). Unfortunately, it was found that oxidations inhibited by the hindered amine and thiophenol did not follow the same simple kinetics as oxidations inhibited by the phenol.

The experimental technique has been described previously (1, 2, 3). α,α' Azo-bis-isobutyronitrile (AIBN) was used as the initiator, with styrene, tetralin, and cumene as the oxidizable substrates. The 2,4,6-tri-*t*-butylaniline was a gift from the E. I. du Pont Company and the 2,4,6-tri-*t*-butylthiophenol was prepared by the method of Rundel (5). Deuterium isotope effects were obtained from the ratio of the inhibited rates in the presence

[1]*Issued as N.R.C. No. 8178.*
[2]*National Research Council Summer Student, 1964.*
**All reactions have been numbered in the same way as in refs. 1, 2, and 3.*

Can. J. Chem. Downloaded from www.nrcresearchpress.com by 210.87.254.6 on 09/05/12
For personal use only.

of H_2O and D_2O (1, 2, 3). In no case did the added H_2O have any significant effect on the inhibited rate. All the work reported here was done at 65 °C.

The inhibited rates under standard conditions are given in Table I. These rates were not affected by a change in the oxygen pressure from 760 to 400 mm.

TABLE I

Oxidation rates at 65 °C in mole/l s $\times 10^7$ with 4.9×10^{-4} mole/l [AIBN]

Inhibitor	Styrene	Tetralin
None	135	44
Tri-*t*-butylphenol (1×10^{-4} mole/l)	62	2.2
Tri-*t*-butylaniline (1×10^{-3} mole/l)	46	14.5
Tri-*t*-butylthiophenol (1×10^{-4} mole/l)	145	6.2

Styrene

The kinetics for the inhibition of styrene autoxidation by 2,4,6-tri-*t*-butylphenol have been described previously (2). Over a wide range of reactant concentrations, the rate of the inhibited oxidation can be represented by (2)

$$[1] \qquad P\alpha \frac{[RH][I_2]}{[AH]},$$

where RH represents the styrene, I_2 the initiator, and AH the phenol. The inhibited rates in the presence of H_2O and D_2O gave a deuterium isotope effect $P_{D_2O}/P_{H_2O} = 10.5$, i.e., $(k_6)_{AH}/(k_6)_{AD} = 10.5$.

The rate for inhibition by the hindered aniline can be represented by

$$P\alpha \frac{[RH]^{1.28}[I_2]^{0.59}}{[AH]^{0.64}}$$

over a concentration range for I_2 of 10^{-4} to 10^{-2} mole/l and for AH of 10^{-3} to 2×10^{-2} mole/l. The kinetic order in styrene was determined by its dilution from 50% to 10% by volume with *o*-dichlorobenzene. Although the oxygen absorption curves do show a very slight auto-acceleration, the rate under the standard conditions was unaffected by the addition of 6×10^{-2} mole/l of styrene polyperoxide. Within the limits of experimental error, the above expression is equivalent to

$$P\alpha \frac{[RH]^{1.5}[I_2]^{0.5}}{[AH]^{0.5}},$$

which is the simplified kinetic relation describing inhibition with extensive chain transfer to the substrate (reaction [8] (3, 6)). Unfortunately, the relative rates of hydrogen-atom abstraction from the aniline and the phenol (i.e. the k_6's) cannot be compared because of the different kinetics exhibited by these two compounds. The measured deuterium isotope effect was 117/38 = 3.08 (see Fig. 1). Assuming that P is proportional to [aniline]$^{-1/2}$ then $(k_6)_{AH}/(k_6)_{AD} = (3.08)^2 = 9.5$ (3). The magnitude of the isotope effect for reaction [6] has almost certainly been overestimated since the measured order in [AH] was actually -0.64. Using this order rather than -0.5, we obtain $(k_6)_{AH}/(k_6)_{AD} = 5.8$.

The hindered thiophenol catalyzes the oxidation of styrene both in the presence and

Can. J. Chem. Downloaded from www.nrcresearchpress.com by 210.87.254.6 on 09/05/12
For personal use only.

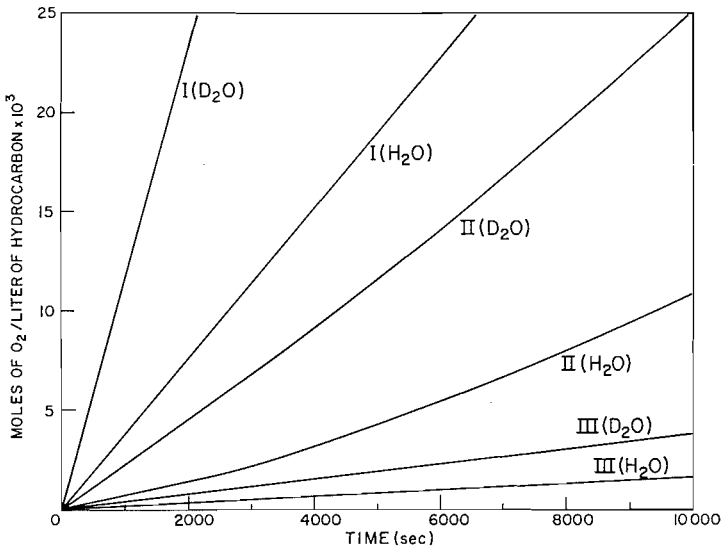

FIG. 1. Oxygen absorption curves at 65 °C. Key: (I) styrene with 4.9×10^{-3} mole/l [AIBN] and 1.4×10^{-2} mole/l [tri-*t*-butylaniline]; (II) tetralin with 9.8×10^{-4} mole/l [AIBN] and 8.2×10^{-3} mole/l [tri-*t*-butylaniline]; (III) tetralin with 4.9×10^{-4} mole/l [AIBN] and 5.6×10^{-4} mole/l [tri-*t*-butylthiophenol].

absence of AIBN. It has roughly half the efficiency of AIBN as an initiator. This behavior is similar to that reported for equimolar mixtures of styrene and 4-methoxythiophenol in heptane at room temperature (7). However, in the present case oxidation did not cease after the absorption of less than 1 molar equivalent of oxygen based on the amount of thiophenol (7). Instead, the rate showed no decrease until more than 10 equivalents of oxygen had been absorbed. This difference may be due either to the higher temperatures or to the lower concentrations of thiophenol relative to styrene which were employed in this work. It is also possible that the steric protection of the SH group by the adjacent *t*-butyl groups influenced the amount of oxygen absorbed. Since the thiophenol inhibits the oxidation of cumene and tetralin (see below), its catalysis of the oxidation of styrene can probably be best represented by

$$[1'] \qquad AH \xrightarrow{RH} A\cdot$$

$$[2'] \qquad A\cdot + RH \rightarrow AR\cdot H$$

$$[3] \qquad AR\cdot H + O_2 \rightarrow \text{normal chain propagation}$$

$$[5] \qquad RO_2\cdot + RO_2\cdot \rightarrow \text{non-radical products}$$

$$[6] \qquad AH + RO_2\cdot \rightarrow A\cdot + ROOH,$$

where reaction [1′] is slow and reaction [2′] is very fast (cf. ref. 8). Reaction [6] does not lead to chain termination since the A· radical is consumed in reaction [2′].

Tetralin

Equation [1] describes the kinetics of the tri-*t*-butylphenol inhibited oxidation. The rate was not affected by the addition of tetralin hydroperoxide, i.e., reaction [−6] does not occur. The measured deuterium isotope effect, $(k_6)_{AH}/(k_6)_{AD}$, was 10.0.

The oxygen absorption curves with the aniline show a strong autocatalysis. This is due to the hydroperoxide formed during the reaction, since the initial rate increases linearly

Can. J. Chem. Downloaded from www.nrcresearchpress.com by 210.87.254.6 on 09/05/12
For personal use only.

with the square root of the initial hydroperoxide concentration (3, 9). In this respect and in the overall kinetics, this compound shows a behavior which is very similar to that of phenol itself in tetralin (3). The sensitivity of the initial inhibited rate to added hydroperoxide is only slightly less than that of phenol itself. Reaction [−6] is therefore fairly rapid in spite of the hindering action of the two ortho-*t*-butyl groups. In the presence of an effective hydroperoxide concentration of about 2×10^{-3} mole/l,* the rate could be represented by

$$P\alpha \frac{[RH]^{1.0}[I_2]^{0.5}}{[AH]^{0.5}}$$

over a range of [RH] from 2% to 10% by volume in *o*-dichlorobenzene, a range of $[I_2]$ from 5×10^{-5} to 5×10^{-3} mole/l, and a range of [AH] from 2×10^{-4} to 10^{-2} mole/l. This expression describes the kinetics for inhibition when reaction [−6] is fast (3, 9). Reducing the effective initial hydroperoxide concentration to about 1×10^{-4} mole/l by increasing the reactant volume gave

$$P\alpha \frac{[RH]^{1.03}[I_2]^{0.71}}{[AH]^{0.66}}$$

over the same range in reactant concentrations. The fact that the order in [RH] did not increase significantly whereas the orders in $[I_2]$ and [AH] both did increase indicates that chain transfer with the tetralin (reaction [8]) is relatively unimportant in this system (3, 6). The deuterium isotope effect, measured at an oxygen absorption of 2×10^{-3} mole/l, was 23/7.5 = 3.0 (Fig. 1). This gives a maximum possible isotope effect for $(k_6)_{AH}/(k_6)_{AD}$ of 9.0.

The oxygen absorption curves with the hindered thiophenol were only very slightly autocatalytic and the inhibited rate was not significantly affected by the addition of 4×10^{-2} mole/l of hydroperoxide. These results indicate that reaction [−6] is relatively unimportant. The kinetics are described by

$$P\alpha \frac{[RH]^{1.06}[I_2]^{0.70}}{[AH]^{0.78}}$$

over a range in $[I_2]$ from 2×10^{-4} to 2×10^{-3} mole/l and in [AH] from 4×10^{-5} to 10^{-3} mole/l. The order in tetralin was obtained by its dilution to 20% by volume with *o*-dichlorobenzene. These kinetics can probably be most readily accounted for by the complex expression which describes inhibition with chain transfer by reaction [8] when this reaction is relatively slow (3). The fact that the thiophenoxy radicals disappear by dimerization (see below) suggests that at sufficiently high concentrations the thiophenol should show the same unusual kinetics that are exhibited by 4-methoxyphenol. That is, the rate should become independent of the thiophenol concentration when this is very large (3). This was not observed up to 3×10^{-2} mole/l [thiophenol]. That is, with 2×10^{-3} mole/l $[I_2]$, the order in [thiophenol] was found to have decreased only to −0.5 in the concentration range of 1×10^{-3} to 3×10^{-2} mole/l. Reaction [8] is therefore probably quite slow (cf. 4-methoxyphenol in tetralin (3)). The deuterium isotope effect was 3.8/1.65 = 2.3 (see Fig. 1). The measured order of −0.78 in thiophenol gives $(k_6)_{AH}/(k_6)_{AD}$ = 2.9.

**This was the average amount of hydroperoxide formed in the oxidation of a 5 ml sample at the point where the rate was measured.*

Can. J. Chem. Downloaded from www.nrcresearchpress.com by 210.87.254.6 on 09/05/12
For personal use only.

Cumene

This substrate was used only to determine the average number of radicals, n, trapped by the three inhibitors. The induction periods produced by these compounds were compared under the same experimental conditions with the induction period produced by 2,6-di-*t*-butyl-4-methylphenol, an inhibitor which is known to stop two oxidation chains per molecule (10). Cumene is an excellent substrate for induction period determinations because even weak inhibitors produce quite sharp breaks in the oxygen absorption curves. With 2.8×10^{-2} mole/l [AIBN] and 1.3×10^{-3} mole/l [AH] only tri-*t*-butylaniline had a significant initial rate (3.0×10^{-6} mole/l s). Under these conditions the induction periods were 4 200 s for 2,6-di-*t*-butyl-4-methylphenol* and 3 800 s for tri-*t*-butylphenol and tri-*t*-butylaniline ($n = 1.8$). In each case the final rate equalled the rate in the absence of inhibitor (i.e., 2.37×10^{-5} mole/l s). With tri-*t*-butylthiophenol, on the other hand, the induction period was only 2 000 s ($n = 0.95$) and the rate at the end of this induction period was only about one-third of the uninhibited rate. This rate very slowly increased and reached the uninhibited value after about 9 000 s. This suggests that the thiophenol reacts rapidly with only one peroxy radical per molecule (reaction [6]) and that the thiophenoxy radicals disappear by dimerization (presumably to the disulfide (5, 11) which must itself be a very weak inhibitor) rather than by reaction with a peroxy radical (reaction [7]).

In conclusion, the deuterium isotope effects observed in this work indicate that inhibition by these three compounds involves abstraction of the active hydrogen atom by a peroxy radical in the slow rate-determining step. The anilino and thiophenoxy radicals formed in this process undergo secondary reactions which complicate the kinetics and prevent a comparison of the rates of hydrogen atom abstraction from the phenol, aniline, and thiophenol.

REFERENCES

1. J. A. HOWARD and K. U. INGOLD. Can. J. Chem. **40**, 1951 (1962).
2. J. A. HOWARD and K. U. INGOLD. Can. J. Chem. **41**, 1744, 2800 (1963).
3. J. A. HOWARD and K. U. INGOLD. Can. J. Chem. **42**, 2324 (1964).
4. J. R. SHELTON and D. N. VINCENT. J. Am. Chem. Soc. **85**, 2433 (1963).
5. V. W. RUNDEL. Z. Naturforsch. **15b**, 546 (1960).
6. L. R. MAHONEY and F. C. FERRIS. J. Am. Chem. Soc. **85**, 2345 (1963).
7. M. S. KHARASCH, W. NUDENBERG, and G. J. MANTELL. J. Org. Chem. **16**, 524 (1951).
8. S. C. BARTON, R. A. BIRD, and K. E. RUSSELL. Can. J. Chem. **41**, 2737 (1963).
9. J. R. THOMAS. J. Am. Chem. Soc. **85**, 2166 (1963).
10. C. E. BOOZER, G. S. HAMMOND, C. E. HAMILTON, and J. N. SEN. J. Am. Chem. Soc. **77**, 3233 (1955).
11. W. RUNDEL and K. SCHEFFLER. Z. Naturforsch. **18b**, 984 (1963).

**We assumed n to be equal to 2.0. This induction period therefore corresponds to a chain initiation efficiency of 0.61.*

Can. J. Chem. Downloaded from www.nrcresearchpress.com by 210.87.254.6 on 09/05/12
For personal use only.

Can. J. Chem. Downloaded from www.nrcresearchpress.com by 210.87.254.5 on 09/05/12
For personal use only.

AGENTS AFFECTING LIPID METABOLISM

XIII. THE SYNTHESIS OF 1,4-DISUBSTITUTED BICYCLO[2.2.2]OCTANE DERIVATIVES[1]

L. G. HUMBER, G. MYERS, L. HAWKINS, C. SCHMIDT, AND M. BOULERICE
Ayerst Research Laboratories, Montreal, Quebec

Received March 25, 1964

ABSTRACT

Several routes to the synthesis of 1,4-disubstituted bicyclo[2.2.2]octanes have been explored and the syntheses of several such derivatives are reported. The 1,4-disubstituted bicyclo[2.2.2]-octane nucleus could not be prepared through an elimination reaction on a corresponding 2,5-disubstituted derivative or by the Diels–Alder reaction of various dienophiles with dimethyl 1,3-cyclohexadiene-1,4-dicarboxylate.

Unusual products are obtained from the reaction of tetracyanoethylene with dimethyl terephthalate and with 1,3-cyclohexadienes containing electron-attracting groups in the 1,4-positions. Some spectral properties of these compounds are described.

In connection with the synthesis of potential cholesterol-lowering agents related to *trans*-1,4-bis-(2-chlorobenzylaminomethyl)-cyclohexane (AY-9944) (1), it was of interest to obtain, as an intermediate, bicyclo[2.2.2]octane-1,4-dicarboxylic acid or a corresponding diester (I).

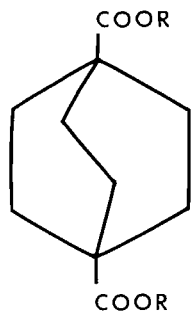

I (a) R= H
(b) R= C_2H_5
(c) R= CH_3

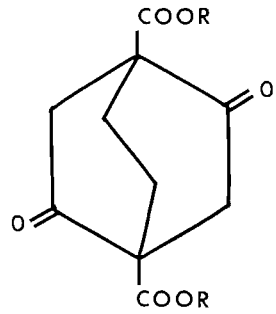

II (a) R= H
(b) R= C_2H_5

We have prepared I*b* in high yield by desulphurization of the bis-ethylenethioketal derivative of the diketo–diester II*b*, as described by Roberts *et al.* (2). II*b*, in turn, has been previously prepared (2, 3) by bridging diethyl 2,5-diketocyclohexane-1,4-dicarboxylate with ethylene dibromide, using a sodium alkoxide as the base. This bridging procedure gave low yields of impure material. We found that the bridging can be executed in consistently high yield (80–85%) by using sodium hydride as base and 1,2-dimethoxyethane as solvent.

A route was available, therefore, for the synthesis of the desired bicyclooctane derivatives I, but it required the use of large quantities of ethanedithiol and of Raney nickel.

[1]*For Part XII of this series, see ref. 1b.*

Thus we investigated alternate procedures not requiring the use of these reagents. The Clemmensen reduction of II*b* using anhydrous conditions (4) gave low yields of I*b*, and attempted desulphurization of the bis-ethylenethioketal derivative of II*b* with sodium and liquid ammonia (5) or with hydrazine and potassium hydroxide (6) was unsuccessful.

We next envisaged a bis-elimination on a suitable 2,5-disubstituted bicyclo[2.2.2]-octane-1,4-dicarboxylate (III) to yield a 2,5-bicyclooctadiene, which then would be reduced to the desired bicyclooctane I. The configurations of the 2,5-substituents in III are unknown. However, whether one or both of these substituents are exo or *endo* to the ring to which they are both attached, they will have identical environments with respect to the hydrogens in the alpha-positions, in that each substituent is eclipsed by one of these hydrogens. Elimination reactions resulting in bicyclooctene derivatives have been observed previously in such systems (7). Thus, the diketo–diester II*b* and the diketo–diacid II*a* (3) were reduced, in high yields, with ruthenium dioxide catalyst at high pressure in ethanol and water respectively, to give diethyl 2,5-dihydroxybicyclo[2.2.2]octane-1,4-dicarboxylate (III*a*) and the corresponding diacid, III*b*, which was characterized as its dimethyl ester.

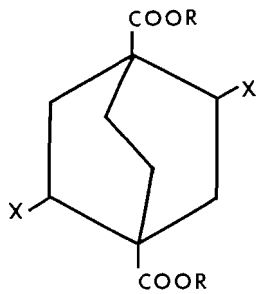

III

(a) R= C_2H_5 X= OH
(b) R= H X= OH
(c) R= C_2H_5 X= SO_3CH_3
(d) R= C_2H_5 X= p-$CH_3C_6H_4SO_3$
(e) R= C_2H_5 X= $OCOCH_3$
(f) R= C_2H_5 X= Br

The dihydroxy–diester (III*a*) was converted to a number of derivatives, viz. dimethanesulphonate (III*c*), di-(*p*-toluene)sulphonate (III*d*), diacetate (III*e*), and dibromide (III*f*).[2] When the dimethanesulphonate–diethyl ester (III*c*) was refluxed for 5 h with alcoholic sodium hydroxide, only the corresponding diacid was obtained; when the reflux period was extended to 30 h, terephthalic acid was obtained in 70% yield, as indicated by the ultraviolet spectrum. When the diacetoxy–diethyl ester (III*e*) was pyrolyzed at 350–400° for 30 min, a mixture of 20% diethyl terephthalate and starting material was obtained. When the dibromo–diester (III*f*) was refluxed in toluene with potassium *tert*-butoxide, a quantitative yield of diethyl terephthalate was obtained. The recovery of only starting materials or terephthalic acid derivatives in the above elimination experiments must be due to the instability of the initially formed 1,4-disubstituted bicyclo[2.2.2]-2,5-octadiene, which contains two electron-attracting groups in the 1,4-positions and probably undergoes a reverse Diels–Alder reaction with ease. Bicyclo[2.2.2]-2,5-octadiene itself (8) is reported to undergo a reverse Diels–Alder reaction on pyrolysis to yield benzene.

We have investigated also the susceptibility of diethyl 2,5-disubstituted bicyclo[2.2.2]-octane-1,4-dicarboxylates to substitution reactions. The dimethanesulphonate (III*c*), the di-(*p*-toluene)sulphonate (III*d*), and the dibromide (III*f*) were treated with sodium cyanide, with lithium fluoride, and with sodium iodide (in acetone solutions). In all cases only starting materials were recovered. Because of the symmetrical nature of the

[2]*This dibromo derivative was characterized as the corresponding diacid (see experimental).*

Can. J. Chem. Downloaded from www.nrcresearchpress.com by 210.87.254.5 on 09/05/12
For personal use only.

bicyclo[2.2.2]octane system, the accessibility of substituents, in the 2,5-positions, to rear end attack by a nucleophilic agent is identical, if the substituents are di-exo or di-*endo* with respect to the ring to which they are both attached. If they are exo–*endo*, then the exo-substituent would be expected to be subject to additional rear end shielding by the *endo*-substituent. However, the exo-substituent should react as readily as those in the di-exo and di-*endo* derivatives. Thus, the failure of the above displacement reactions with SN_2-type reagents is interpreted as indicating that, in a bicyclo[2.2.2]octane system, the non-bridgehead positions are inaccessible to rear end attack, as are the bridgehead positions. On the other hand, the dibromide (III*f*) readily undergoes acetolysis on treatment with silver acetate in acetic acid, yielding the diacetoxy derivative (III*e*).

The diketo–diacid (II*a*) was converted to the corresponding 1,4-dibromo derivative by a Hunsdiecker reaction on the silver salt. Bromination of this product yielded a compound $C_8H_6Br_4O_2$, $\nu_{max}^{CHCl_3}$ 1 768 cm^{-1} (probably 1,3,4,5-tetrabromo-2,5-diketobicyclo[2.2.2]-octane). Bromination of the diketo–diester (II*b*), gave a compound $C_{14}H_{16}Br_2O_6$, $\nu_{max}^{CHCl_3}$ 1 750 cm^{-1} (most likely the 3,6-dibromo derivative).

We next turned our attention to preparing the desired bicyclo[2.2.2]octane-1,4-dicarboxylate (I*c*) by a Diels–Alder reaction of dimethyl 1,3-cyclohexadiene-1,4-dicarboxylate (IV) and a suitable dienophile.

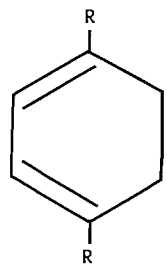

IV R= $COOCH_3$

V R= $CONH_2$

VI R= CN

VII R= CONH-CYCLOHEXYL

VIII R= $CONHCH_2$-CYCLOHEXYL

IX R= COCl

The diene–diester (IV) was prepared from cyclohexane-1,4-dicarboxylic acid in 70% overall yield, as described previously (8). IV has been described before by Baeyer (10) and by Burnell and Taylor (11), the latter authors reporting λ_{max} 309 mμ (ϵ = 27 300). In our hands a carefully purified sample had λ_{max} 309 mμ (ϵ = 13 100) and the nuclear magnetic resonance spectrum exhibited three sharp peaks at 2.91 (2 vinyl hydrogens), 6.20 (6 carbomethoxy hydrogens), and 7.44 τ(4 allylic hydrogens).

The Diels–Alder reaction between the diene–diester (IV) and the following dienophiles was investigated: ethylene, *cis*-dichloroethylene, vinyl chloride, maleic anhydride, and tetracyanoethylene (TCNE). Only starting materials were recovered with the first three dienophiles.

With maleic anhydride, 1,4-dicarbomethoxybicyclo[2.2.2]oct-2-ene-*endo*-5,6-dicarboxylic anhydride (X), m.p. 183–185°, was obtained in high yield. After this work was completed, this compound was reported by Smith *et al.* (12) and by Kauer (13) to have m.p.'s 191.5° and 188–188.6° respectively. Catalytic hydrogenation, followed by hydrolysis of the anhydride function of X, yielded the corresponding saturated diacid.

Attempts to convert this to a 1,4-disubstituted bicyclooctene (related to I*c*) by oxidative bis-decarboxylation (14) under various conditions were unsuccessful. The inability to effect this bis-decarboxylation has also been reported by Smith *et al.* (12).

Can. J. Chem. Downloaded from www.nrcresearchpress.com by 210.87.254.5 on 09/05/12
For personal use only.

Can. J. Chem. Downloaded from www.nrcresearchpress.com by 210.87.254.5 on 09/05/12
For personal use only.

The Diels–Alder reaction between TCNE and IV in tetrahydrofuran solution yielded a bright yellow crystalline compound, $C_{16}H_{12}N_4O_2$, m.p. 112–114° (XI), which did not exhibit the spectral properties expected for a Diels–Alder adduct. Smith *et al.* (12) have apparently obtained the same compound from this reaction. They report m.p. 120–140° and consider it to be a π-complex. Initially, we also had considered that XI was a stable molecular π-complex of the type proposed as an intermediate in Diels–Alder reactions with TCNE (15), and that it might be convertible to a normal Diels–Alder adduct; however, prolonged refluxing in benzene or toluene led only to recovery of XI. The appearance of the report of Smith *et al.* (12) prompted us to investigate further the spectroscopic properties of XI. π-Complexes between TCNE and various aromatic compounds have been described previously (16); they exhibit characteristic absorption bands in the visible or near ultraviolet. We have examined XI spectroscopically in these regions, both in tetrahydrofuran and in methylene chloride solutions, and, in contrast to the findings of Smith *et al.* (12), we are unable to detect any π-complex absorption, the spectra corresponding essentially to a summation of those of TCNE and the diene–diester IV (see Table I, *a* and *b*). Similar complexes with TCNE have been obtained with the diene–dinitrile VI and with dimethyl terephthalate, and they show spectral properties, in solution, analogous to those of XI.

TABLE I

Comparison of optical densities of the TCNE-adduct XI and components thereof*

(*a*) Diene–diester IV, TCNE, and their adduct in CH_2Cl_2 (concentration = 10^{-4} *M*)

λ	265 mμ	276 mμ	283 mμ	310 mμ
IV	0.22	0.46	0.65	1.34
TCNE	1.44	1.30	0.65	0.0
Total	1.66	1.76	1.30	1.34
TCNE–IV(XI)	1.77	1.82	1.27	1.34

(*b*) Diene–diester IV, TCNE, and their adduct in tetrahydrofuran (concentration = 10^{-4} *M*)

λ	262 mμ	270 mμ	310 mμ
IV	0.20	0.33	1.21
TCNE	0.74	0.67	0.15
Total	0.94	1.00	1.36
TCNE–IV(XI)	0.95	0.97	1.13

*In all cases, the adduct shows maxima at the same wavelengths as those of the components and no other maxima or inflections are discernible.

We considered that it might be possible to demonstrate π-complex character with XI in the solid state; however, examination of the visible and near ultraviolet spectra of XI and of its components in potassium bromide pellets does not show any characteristic π-complex absorption. When XI is dissolved in glacial acid, a pink color is observed and a visible spectrum of this solution (10^{-2} *M*) immediately after its preparation shows a weak absorption maximum at 525 mμ, which gradually reduces in intensity and is absent after 20 min. A spectrophotofluorimetric determination on this freshly prepared solution shows an activation wavelength at 395 mμ, and a fluorescence wavelength at 460 mμ.* Neither of these properties of XI in acetic acid are shown by either TCNE of the diene–diester IV at equivalent concentrations in the same solvent. Thus, it appears that XI is a weak

**Measured on an Aminco–Bowman spectrophotofluorimeter.*

molecular π-complex, whose existence can be demonstrated not by an examination of the absorption spectrum, but by a study of the fluorescence spectrum.

The failure of the dienes IV and VI to form Diels–Alder adducts with TCNE, whereas 1,3-cyclohexadiene itself forms such an adduct (15) and IV forms an adduct with maleic anhydride in high yield, can be attributed to the high electron-demand of TCNE, which is not met by the dienes IV and VI due to the strong electron-attracting groups attached to the ends of the diene system. Similarly, with dimethyl terephthalate, the presence of such groups attached to the benzene ring prevents the formation of a strong π-complex with TCNE, similar to the type formed with other benzene derivatives (16*a*, 16*c*).

A number of derivatives of 1,3-cyclohexadiene-1,4-dicarboxylic acid were prepared. The diacid chloride IX was converted to the substituted diamides VII and VIII by reaction with cyclohexylamine and cyclohexylmethylamine respectively. These diamides, as well as the dinitrile VI and the unsubstituted diamide V, could not be reduced to diamines with lithium aluminium hydride.

The reactions summarized in Chart I were carried out to obtain compounds XII–XVII for testing as cholesterol-lowering agents. Compounds XII–XIV were obtained by the condensation of 1,4-bisaminomethylbicyclo[2.2.2]octane with the appropriate aldehyde or ketone, followed by reduction of the resultant Schiff base with sodium borohydride. Compounds XV and XVI were obtained by lithium aluminium hydride reduction of the diamides obtained from condensation of bicyclo[2.2.2]octane-1,4-dicarboxyl chloride with the appropriate amines. Compound XVII was prepared from 2-chlorobenzaldehyde and 1,4-diaminobicyclo[2.2.2]octane, which was obtained in high yield by a Hofmann reaction on the corresponding diamide followed by hydrolysis of the intermediate dicarbamate.

EXPERIMENTAL[3]

Diethyl 2,5-Dioxobicyclo[2.2.2]octane-1,4-dicarboxylate (IIb)

A 49% dispersion of sodium hydride in mineral oil (60.0 g, 1.18 mole) and diethyl succinylsuccinate (17) (111.1 g, 0.394 mole) were added, alternately in 10.0 g portions, to 1,2-dimethoxyethane (400 ml) over 15 min with stirring to yield the disodium salt as a pink suspension. The mixture was distilled until 200 ml of 1,2-dimethoxyethane were removed. Ethylene dibromide (666 g) was added and the distillation was continued until an additional 150 ml of 1,2-dimethoxyethane had been removed. The mixture then was stirred and heated at 110–120° until the pink color had disappeared (ca. 20 h). The mixture was filtered while still hot and the solids washed with 3 × 25 ml of chloroform. Hexane (300 ml) was added to the filtrate and, on cooling, 70 g of product was obtained, m.p. 109–111°. The filtrate from the first crop was evaporated to dryness *in vacuo*. Trituration with methanol, filtration, and washing with hexane yielded an additional 23 g of product, m.p. 108–111°. Total yield: 83.7%. Lit. m.p. 108–110.5° (2).

The above diketo–diester (2.8 g) was dissolved in carbon tetrachloride (50 ml) and allowed to stand overnight at room temperature with bromine (3.5 g). Evaporation of the solvent and crystallization from an ether–hexane mixture yielded the dibromo derivative (2.6 g), m.p. 142–145°, $\nu_{max}^{CHCl_3}$ 1 750 cm^{-1}.

Anal. Calcd. for $C_{14}H_{16}Br_2O_6$: Br, 36.33. Found: Br, 36.31.

Bisethylenethioketal of Diethyl 2,5-Dioxobicyclo[2.2.2]octane-1,4-dicarboxylate

A solution of diethyl 2,5-dioxobicyclo[2.2.2]octane-1,4-dicarboxylate (II*b*) (70 g, 0.248 mole), boron trifluoride etherate (70 ml, 0.55 mole), and ethanedithiol (71.0 g, 0.75 mole) in glacial acetic acid (300 ml) was kept at room temperature for 17 h. Chloroform (200 ml) was added and the mixture washed with water (3 × 50 ml), 5% aqueous sodium hydroxide (2 × 200 ml), and water (2 × 100 ml), followed by drying and concentration *in vacuo*. Crystallization from methanol yielded the product (95.5 g, 88.9%), m.p. 82–85°. Lit. m.p. 91.8–92.7° (2).

Clemmensen Reduction of Diethyl 2,5-Dioxobicyclo[2.2.2]octane-1,4-dicarboxylate

Amalgamated zinc (prepared from mossy zinc (190 g)), mercuric chloride (9.5 g), and concentrated hydrochloric acid (45 ml)) was washed with absolute ethanol (4 × 100 ml). Then absolute ethanol (500 ml) was added, followed by diethyl 2,5-dioxobicyclo[2.2.2]octane-1,4-dicarboxylate (II*b*) (9.65 g). The mixture was refluxed for 60 h, during which it was saturated with hydrogen chloride 4 times. The ethanol solution was

[3]*All melting points are corrected and were recorded on a Thomas–Hoover apparatus.*

Can. J. Chem. Downloaded from www.nrcresearchpress.com by 210.87.254.5 on 09/05/12
For personal use only.

CHART I

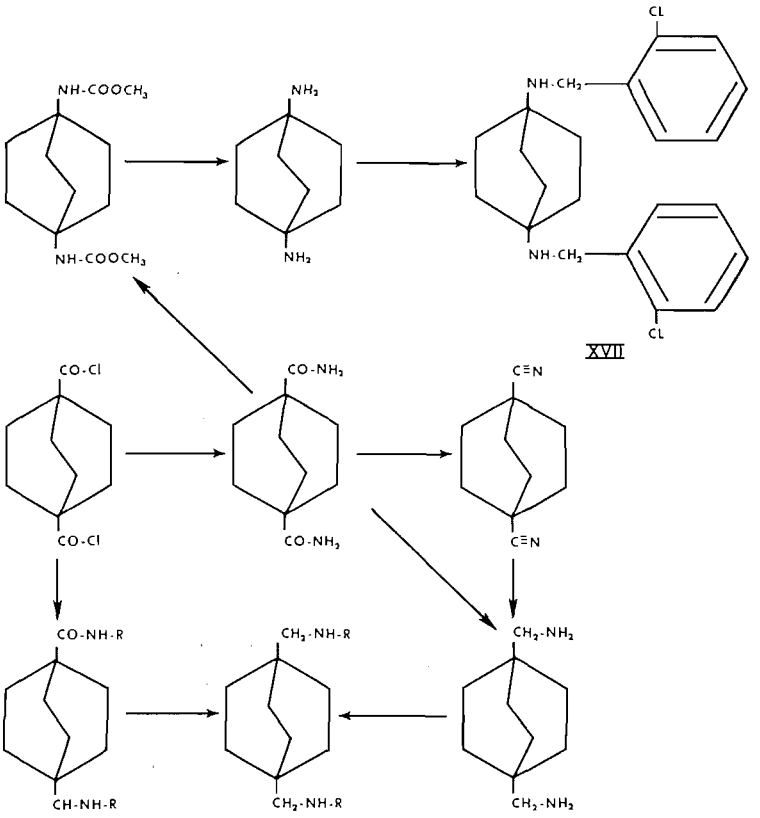

XII R= 2-ClC$_6$H$_4$CH$_2$

XIII R= 2-CF$_3$C$_6$H$_4$CH$_2$

XIV R= CYCLOHEXYL

XV R= CH$_2$-CYCLOHEXYL

XVI R= 1-INDANYL

decanted from the zinc, the ethanol removed *in vacuo*, and the residue distributed between ether and water. The ether phase was washed with water and dilute sodium bicarbonate solution, and then dried and fractionated to yield diethyl bicyclo[2.2.2]octane-1,4-dicarboxylate (I*b*) (3.5 g, 40%), b.p. 118–126° at 0.3 mm, n_D^{26} 1.4683. Roberts *et al.* (2) report b.p. 113–115° at 0.3 mm and n_D^{25} 1.4660.

Dimethyl 2,5-Dihydroxybicyclo[2.2.2]octane-1,4-dicarboxylate

To 2,5-dioxobicyclo[2.2.2]octane-1,4-dicarboxylic acid (3) (100 g), dissolved in water (500 ml), was added 5% ruthenium dioxide on Norite (5 g). The mixture was hydrogenated at 170 kg/cm² for 10 h at 150°, during which time the theoretical hydrogen uptake was observed. After removal of the catalyst, the solution was evaporated to dryness *in vacuo* to yield the diacid, which did not crystallize readily. It was converted to the dimethyl ester with diazomethane in methanol–ether solution. The diester was crystallized from benzene–ether to yield 97 g of product (95%), m.p. 129–130°, $\nu_{max}^{CHCl_3}$ 3 560, 1 706 cm^{-1}.

Anal. Calcd. for $C_{12}H_{18}O_6$: C, 55.80; H, 7.03. Found: C, 55.98; H, 7.30.

Diethyl 2,5-Dihydroxybicyclo[2.2.2]octane-1,4-dicarboxylate (IIIa)

Diethyl 2,5-dioxobicyclo[2.2.2]octane-1,4-dicarboxylate (II*b*) (100 g) was hydrogenated in absolute ethanol solution, under the same conditions as used for the corresponding diacid (*vide supra*). Removal of the catalyst and then the solvent *in vacuo* yielded an oil, which on trituration with ether yielded the title compound (60 g), m.p. 91°, $\nu_{max}^{CHCl_3}$ 3 560, 1 710 cm^{-1}.

Can. J. Chem. Downloaded from www.nrcresearchpress.com by 210.87.254.5 on 09/05/12
For personal use only.

Anal. Calcd. for $C_{14}H_{22}O_6$: C, 58.73; H, 7.75. Found: C, 58.40; H, 7.62.

The dimesylate (III*c*) had m.p. 107° (ethanol).

Anal. Calcd. for $C_{16}H_{26}O_{10}S_2$: C, 43.52; H, 5.93; S, 14.52. Found: C, 43.50; H, 6.11; S, 14.60.

The ditosylate (III*d*) had m.p. 122° (ethanol).

Anal. Calcd. for $C_{28}H_{34}O_{10}S_2$: S, 10.82. Found: S, 10.37.

The diacetate (III*e*) had m.p. 112° (ethanol).

Anal. Calcd. for $C_{18}H_{26}O_8$: C, 58.37; H, 7.08. Found: C, 58.08; H, 7.08.

2,5-Dibromobicyclo[2.2.2]octane-1,4-dicarboxylic acid

Diethyl 2,5-dihydroxybicyclo[2.2.2]octane-1,4-dicarboxylate, m.p. 91°, (143 g, 0.5 mole) was treated with triphenylphosphite (310 g, 1.0 mole) and hydrogen bromide at 20° (18) for 80 min. The mixture was poured onto cracked ice and extracted with ether. The ether solution was washed with dilute sodium hydroxide solution, dried, and fractionated to yield an oil (90 g), b.p. 175–180° at 1 mm. It was freed of traces of phosphorus by passing it through a column of alumina (2 700 g), using benzene as eluant. Fractionation yielded the diethyl ester of the title compound (III*f*), 70 g, b.p. 145–150° at 0.5 mm, $\nu_{max}^{CHCl_3}$, 1 710 cm^{-1}. Hydrolysis of the diethyl ester with glacial acetic acid and 47% hydrobromic acid yielded the diacid, which was obtained as a dihydrate on crystallization from ethanol–water (1:1), m.p. 285°.

Anal. Calcd. for $C_{10}H_{12}Br_2O_4 \cdot 2H_2O$: Br, 40.80; H_2O, 9.19. Found: Br, 40.75; H_2O, 9.1.

Elimination Reactions on Dibromo, Dimesyloxy, and Acetoxy Derivatives

(*a*) Diethyl 2,5-dibromobicyclo[2.2.2]octane-1,4-dicarboxylate (III*f*) (412 mg), dissolved in toluene (3 ml), was refluxed with potassium *t*-butoxide (448 mg) for 2 h. The mixture was poured into ice water. Acidification of the aqueous phase yielded terephthalic acid (100 mg), m.p. > 300°, λ_{max}^{EtOH} 240 mμ (ϵ = 20 000).

(*b*) Diethyl 2,5-dimesyloxybicyclo[2.2.2]octane-1,4-dicarboxylate (III*c*) (2 g), dissolved in ethanol (8 ml) and water (2 ml), was refluxed with sodium hydroxide (2.0 g) for 5 h. Removal of the alcohol *in vacuo*, dilution with water, and acidification yielded 2,5-dimesyloxybicyclo[2.2.2]octane-1,4-dicarboxylic acid (1.0 g), m.p. 202° (ethanol).

Anal. Calcd. for $C_{12}H_{18}O_{10}S_2$: C, 37.20; H, 4.71; S, 16.55. Found: C, 37.54; H, 4.87; S, 16.58.

When the above mixture was refluxed for 30 h, terephthalic acid was isolated in 70% yield.

(*c*) Diethyl 2,5-diacetoxybicyclo[2.2.2]octane-1,4-dicarboxylate (III*e*) (25 g) was pyrolyzed at 350–400° for 0.5 h. Only slight charring occurred. The mixture was distilled to yield diethyl terephthalate (5 g), b.p. 120° at 1 mm, m.p. 44°, λ_{max}^{EtOH} 240 mμ (ϵ = 20 450). The residue was identified as starting material.

1,4-Dibromo-2,5-dioxobicyclo[2.2.2]octane

The silver salt of 2,5-dioxobicyclo[2.2.2]octane-1,4-dicarboxylic acid (38.45 g, 0.087 mole), prepared by treatment of the corresponding diacid in potassium hydroxide solution with silver nitrate, was refluxed in carbon tetrachloride (200 ml) with bromine (27.9 g, 0.17 mole) for 8 h. Filtration of the mixture and evaporation of the filtrate yielded a residue which, on crystallization from chloroform, yielded the product (4.8 g, 18.5%), m.p. 169–170°, $\nu_{max}^{CHCl_3}$ 1 748 cm^{-1}.

Anal. Calcd. for $C_8H_8Br_2O_2$: Br, 54.02, C, 32.43, H, 2.72. Found: Br, 53.96, C, 32.09, H, 2.48.

The above 1,4-dibromo-2,5-dioxobicyclo[2.2.2]octane (2.96 g, 0.01 mole) was dissolved in 30 ml of acetic acid and 3.4 g of bromine and refluxed for 2 h. The solvents were removed, the residue dissolved in chloroform, and the resulting solution washed with dilute sodium bicarbonate solution. The chloroform was removed *in vacuo* and the residue crystallized from a chloroform–ether mixture. It had m.p. 210–211° and $\nu_{max}^{CHCl_3}$ 1 768 cm^{-1}.

Anal. Calcd. for $C_8H_6Br_4O_2$: Br, 70.1. Found: Br, 70.9.

Dimethyl 1,3-Cyclohexadiene-1,4-dicarboxylate (IV)

The title compound was prepared from dimethyl 1,4-dibromo-cyclohexane-1,4-dicarboxylate as described by Guha and Hazra (9). It was crystallized from a chloroform–hexane mixture and had m.p. 83–84.5°, λ_{max}^{EtOH} 309 mμ (ϵ = 13 100), $\nu_{max}^{CHCl_3}$ 1 640 and 1700 cm^{-1}, τ_{max} 2.91, 6.20, 7.44.[4]

Anal. Calcd. for $C_{10}H_{12}O_4$: C, 61.21; H, 6.17. Found: C, 61.31; H, 6.27; 6.31.

A tetracyanoethylene adduct was prepared by refluxing the diene–diester (0.68 g, 0.003 mole) with tetracyanoethylene (0.44 g, 0.003 mole) in tetrahydrofuran (20 ml) for 30 min. The solution was evaporated to dryness *in vacuo* and the residue crystallized from an ether–hexane (2:1) mixture to yield the adduct (0.87 g, 89.4%) as yellow crystals, m.p. 112–114°.

Anal. Calcd. for $C_{16}H_{12}N_4O_4$: C, 59.25; H, 3.73; N, 17.28. Found: C, 59.14; H, 3.78; N, 17.58, 17.68.

1,3-Cyclohexadiene-1,4-dicarbonylchloride (IX)

1,3-Cyclohexadiene-1,4-dicarboxylic acid (9), λ_{max} 309 mμ (ϵ = 13 000), (84 g, 0.5 mole) and thionyl chloride (500 ml) were refluxed for 3 h in the presence of a catalytic amount of dimethylformamide (19) (0.5 ml). The excess of thionyl chloride was removed *in vacuo* and the residue crystallized from an ether–hexane mixture to yield the product (85.6 g, 83%), m.p. 54–56°. A sample sublimed in high vacuum had m.p. 56–58°, λ_{max}^{ether} 329 mμ (ϵ = 16 500), $\nu_{max}^{CHCl_3}$ 1 740 and 1 630 cm^{-1}.

Anal. Calcd. for $C_8H_8Cl_2O_2$: Cl, 34.59. Found: Cl: 34.39, 34.44.

[4]*Run at 60 Mc/s using tetramethylsilane as standard.*

Can. J. Chem. Downloaded from www.nrcresearchpress.com by 210.87.254.5 on 09/05/12
For personal use only.

Can. J. Chem. Downloaded from www.nrcresearchpress.com by 210.87.254.5 on 09/05/12
For personal use only.

1,3-Cyclohexadiene-1,4-dicarboxamide (V)

The diacid chloride (20.5 g) was added in portions to concentrated aqueous ammonia (200 ml) at 0°. The mixture was warmed at 80° for 60 min. Filtration yielded the product, m.p. 300–310° (decomp.) (13.0 g, 78.4%). A sample, crystallized twice from methanol, had m.p. 312–314° (decomp.), ν_{max}^{Nujol} 3 160, 3 360, and 1 650 cm^{-1}, λ_{max}^{EtOH} 305 mμ (ε = 11 830).

Anal. Calcd. for $C_8H_{10}N_2O_2$: C, 57.81; H, 6.07; N, 16.86. Found: C, 57.22; H, 6.35; N, 16.74.

1,3-Cyclohexadiene-1,4-dicarbonitrile (VI)

The diamide (5.0 g) was refluxed in thionyl chloride (30 ml) for 18 h in a nitrogen atmosphere. The excess thionyl chloride was removed *in vacuo* and the residue was triturated with petroleum ether to yield the product, m.p. 163–165° (3.5 g, 89.8%). A sample was crystallized twice from a benzene – petroleum ether mixture. It had m.p. 170–172°, λ_{max}^{EtOH} 295 mμ (ε = 11 600) and 311 mμ (ε = 10 700).

Anal. Calcd. for $C_8H_6N_2$: C, 73.83; H, 4.65; N, 21.53. Found: C, 73.84; H, 4.68; N, 21.40.

A tetracyanoethylene adduct was prepared as described above. It had m.p. 127–130° (ether–hexane); $\lambda_{max}^{CH_2Cl_2}$ 247 mμ (ε = 14 700), 266 mμ (ε = 17 600), 277 mμ (ε = 18 700), 295 mμ (ε = 11 600), 307 mμ (ε = 11 400), 320 mμ (ε = 6 600).

Anal. Calcd. for $C_{14}H_6N_6$: C, 65.1; H, 2.39; N, 32.55. Found: C, 65.42; H, 2.78; N, 32.66.

TCNE Adduct with Dimethyl Terephthalate

The adduct was prepared from equimolar quantities of TCNE and dimethyl terephthalate and had m.p. 138–140°; $\lambda_{max}^{CH_2Cl_2}$ 242 mμ (ε = 30 200), 266 mμ (ε = 17 200), 276 mμ (ε = 14 600), 295 mμ (ε = 2 000).

Anal. Calcd. for $C_{16}H_{10}N_4O$: C, 59.63; H, 3.13. Found: C, 59.30; H, 3.12.

1,4-Dicarbomethoxybicyclo[2.2.2]oct-2-ene-endo-5,6-dicarboxylic Anhydride (X)

Dimethyl 1,3-cyclohexadiene-1,4-dicarboxylate (42.6 g, 0.22 mole) and maleic anhydride (23 g, 0.23 mole) were mixed together and heated at 90–100° under a nitrogen atmosphere in a sealed tube for 17 h. The reaction mixture was triturated with hot hexane and the residue was crystallized from chloroform to yield the product (36.5 g). The mother liquors were retreated with maleic anhydride (as described above) to yield an additional 12.5 g of product. The total yield was 49 g, 76.8%. It had m.p. 183–185°, $\nu_{max}^{CHCl_3}$ 1 735 and 1 780 cm^{-1}.

Anal. Calcd. for $C_{14}H_{14}O_7$: C, 57.16; H, 4.80. Found: C, 56.94; H, 4.81.

1,4-Dicarbomethoxybicyclo[2.2.2]octane-5,6-dicarboxylic Anhydride

The unsaturated anhydride (36.5 g) was hydrogenated in tetrahydrofuran (500 ml) in the presence of platinum oxide (0.5 g) at 50° and at a slight positive hydrogen pressure. Hydrogen uptake was complete in 1 h, and the product was isolated in the conventional manner. It had m.p. 163–165° ($CHCl_3$ – petroleum ether), (32.5 g, 88.4%).

Anal. Calcd. for $C_{14}H_{16}O_7$: C, 56.75; H, 5.44. Found: C, 57.07; H, 5.54.

1,4-Dicarbomethoxybicyclo[2.2.2]octane-5,6-dicarboxylic Acid

The saturated anhydride (11.9 g) was refluxed with water (150 ml) for 3 h. The solution was evaporated to dryness *in vacuo* and the residue crystallized from an ether–hexane mixture to yield the product (10.3 g), m.p. 190–192°.

Anal. Calcd. for $C_{14}H_{18}O_8$: C, 53.50; H, 5.77. Found: C, 53.58; H, 5.78.

N,N'-Dicyclohexyl-1,3-cyclohexadiene-1,4-dicarboxamide (VII)

The diacid chloride (1.03 g, 0.005 mole) and cyclohexylamine (1.98 g, 0.02 mole) were refluxed in benzene for 20 min. The solvent was removed, the residue was washed with water, and the solid was crystallized then from methanol to yield the product (1.0 g, 60.1%), m.p. > 310°, λ_{max}^{EtOH} 308 mμ (ε = 14 000), ν_{max}^{Nujol} 1 625 cm^{-1}.

Anal. Calcd. for $C_{20}H_{30}N_2O_2$: C, 72.68; H, 9.15; N, 8.48. Found: C, 72.41; H, 8.98; N, 8.34.

N,N'-Di-(cyclohexylmethyl)-1,3-cyclohexadiene-1,4-dicarboxamide (VIII)

The diacid chloride (4.1 g, 0.02 mole) and cyclohexylmethylamine (9.06 g, 0.08 mole) were reacted in benzene, as described above, to yield the title product (5.8 g, 81%), m.p. > 310° (methanol), λ_{max}^{EtOH} 307 mμ (ε = 14 700), ν_{max}^{Nujol} 1 625 cm^{-1}.

Anal. Calcd. for $C_{22}H_{34}N_2O_2$: C, 73.70; H, 9.56. Found: C, 73.70; H, 9.56.

1,4-Bisaminomethylbicyclo[2.2.2]octane

(*a*) Bicyclo[2.2.2]octane-1,4-dicarboxamide (20) (6.2 g) was refluxed in tetrahydrofuran (200 ml) with lithium aluminium hydride (5.0 g) for 30 h. The reaction was treated in the conventional manner to yield the product (4.4 g, 83%), b.p. 90° at 0.02 mm. The dihydrochloride salt had m.p. > 360°.

Anal. Calcd. for $C_{10}H_{22}Cl_2N_2$: N, 11.61; Cl, 29.3. Found: N, 11.63; Cl, 28.7.

(*b*) Reduction of bicyclo[2.2.2]octane-1,4-dicarbonitrile (20), using conditions similar to those described above for the diamide, gave a 90% yield of the bisaminomethyl derivative.

1,4-Bis-(2-chlorobenzylaminomethyl)-bicyclo[2.2.2]octane

1,4-Bisaminomethylbicyclo[2.2.2]octane (4.4 g, 0.026 mole) and 2-chlorobenzaldehyde (7.3 g, 0.052 mole) were refluxed in benzene (80 ml) for 6 h with removal of water through a Dean-Starke trap. The resultant Schiff base, $\nu_{max}^{CHCl_3}$ 1 640 cm^{-1}, λ_{max}^{EtOH} 250 mμ (ϵ = 28 000), a semisolid (10.7 g), was refluxed in methanol (100 ml) with sodium borohydride (1.9 g) for 10 h. The methanol was removed *in vacuo* and the residue distributed between water and benzene. The benzene phase yielded the product (8.0 g), m.p. 82–84° (ether–petroleum ether), λ_{max}^{EtOH} 263 mμ (ϵ = 468). The dihydrochloride salt had m.p. 289–290° (ethanol).

Anal. Calcd. for $C_{24}H_{32}Cl_4N_2$: N, 5.71; Cl, 28.92. Found: N, 5.71; Cl, 28.73.

1,4-Bis-(2-trifluoromethylbenzylaminomethyl)-bicyclo[2.2.2]octane

2-Trifluoromethylbenzaldehyde (1.74 g, 0.01 mole), b.p. 28–38° at 0.3–0.6 mm, prepared by lithium tri-(*t*-butoxy)-hydride reduction (21) of the corresponding acid chloride, and 1,4-bisaminomethylbicyclo-[2.2.2]octane (0.84 g, 0.005 mole) were converted to the Schiff base as described above. It was reduced with sodium borohydride (4.0 g) in methanol to yield the product as an oil, λ_{max}^{EtOH} 265 mμ (ϵ = 2 030), 272 mμ (ϵ = 1 710). The dihydrochloride salt had m.p. 284–286.5° (methanol–ether) (1.4 g, 50%).

Anal. Calcd. for $C_{26}H_{32}Cl_2F_6N_2$: Cl, 12.72; N, 5.03. Found: Cl, 12.65; N, 4.90, 5.28.

1,4-Bis-(cyclohexylaminomethyl)-bicyclo[2.2.2]octane

1,4-Bisaminomethylbicyclo[2.2.2]octane (1.54 g) and cyclohexanone (1.8 g) were converted to the Schiff base as described above. It had $\nu_{max}^{CHCl_3}$ 1 643 cm^{-1} and was reduced with sodium borohydride (4 g) in methanol to yield the title product as an oil. The dihydrochloride salt (2.3 g, 62%) had m.p. > 310° (methanol–ether).

Anal. Calcd. for $C_{22}H_{42}Cl_2N_2$: Cl, 17.49; N, 6.91. Found: Cl, 17.17; N, 6.94, 7.18.

N,N'-Dicyclohexylmethylbicyclo[2.2.2]octane-1,4-dicarboxamide

Bicyclo[2.2.2]octane-1,4-dicarbonyl chloride (7.05 g) was added to a benzene solution (100 ml) of cyclohexylmethylamine (13.5 g) (prepared by catalytic hydrogenation of benzylamine). The mixture was refluxed for 20 min and then the solvent was removed *in vacuo*. The residue was washed well with water and crystallized from methanol. It had m.p. 248–250°.

Anal. Calcd. for $C_{24}H_{40}N_2O_2$: C, 74.17; H, 10.38; N, 7.21. Found: C, 73.81; H, 10.64; N, 7.12, 7.16.

N,N'-Di-(d,l-1-indanyl)-bicyclo[2.2.2]octane-1,4-dicarboxamide

Bicyclo[2.2.2]octane-1,4-dicarbonyl chloride (3.5 g) and *d,l*-1-aminoindane (8 g) were reacted together as described above to yield the title diamide, m.p. 250–252° (methanol).

Anal. Calcd. for $C_{28}H_{32}N_2O_2$: C, 78.46; H, 7.53; N, 6.54. Found: C, 77.98; H, 7.80; N, 6.63.

1,4-Bis-(cyclohexylmethylaminomethyl)-bicyclo[2.2.2]octane

N,N'-Dicyclohexylmethylbicyclo[2.2.2]octane-1,4-dicarboxamide (9.8 g) and lithium aluminium hydride (10 g) were refluxed in tetrahydrofuran (500 ml) for 24 h. The reaction was treated in the conventional manner to yield the title product as an oil. The dihydrochloride salt had m.p. > 310° (ethanol).

Anal. Calcd. for $C_{24}H_{46}Cl_2N_2$: Cl, 16.35; N, 6.46. Found: Cl, 16.10; 16.34; N, 6.50.

1,4-Bis-(d,l-1-indanylaminomethyl)-bicyclo[2.2.2]octane

N,N'-Di-(*d,l*-1-indanyl)-bicyclo[2.2.2]octane-1,4-dicarboxamide (6.1 g) was reduced with lithium aluminium hydride (10 g), as described above, to yield the title compound as a semisolid. The dihydrochloride salt had m.p. 308–310° (ethanol–ether).

Anal. Calcd. for $C_{28}H_{38}Cl_2N_2$: Cl, 14.97; N, 5.92. Found: Cl, 14.44; N, 5.87.

Dimethyl Bicyclo[2.2.2.]octane-1,4-dicarbamate

A solution of sodium methoxide in methanol (600 ml), prepared from 22.5 g of sodium (0.97 mole), and bromine (30 ml, 0.58 mole) were added alternately, in small portions, to a refluxing mixture of bicyclo[2.2.2]-octane-1,4-dicarboxamide (10 g, 0.05 mole) in methanol (100 ml). The addition took 3 h. Then the hot reaction mixture was filtered and evaporated to dryness *in vacuo* and the residue triturated with water. The remaining solid was crystallized from methanol to yield the product (8.5 g, 65%), m.p. 166–168°,

Anal. Calcd. for $C_{12}H_{20}N_2O_4$: C, 56.33; H, 7.87; N, 10.93. Found: C, 56.74; H, 7.65; N, 10.88.

1,4-Bis-(2-chlorobenzylamino)-bicyclo[2.2.2]octane

The above dicarbamate (8.5 g) was refluxed with concentrated hydrochloric acid (100 ml) for 17 h. The acid was removed *in vacuo* and the residue crystallized from a methanol–ether mixture to yield the dihydrochloride of 1,4-diaminobicyclo[2.2.2]octane, m.p. > 310°.

Anal. Calcd. for $C_8H_{18}Cl_2N_2$: N, 13.15. Found: N, 12.76.

The free base obtained from the dihydrochloride salt (2.5 g, m.p. 83–85°) and 2-chlorobenzaldehyde (5.0 g) were converted to the bis-Schiff base by refluxing in benzene (100 ml) for 2 h. It was obtained in a crystalline form from a benzene–hexane mixture and had m.p. 170–175° (5.1 g). The Schiff base was reduced with sodium borohydride (8.0 g) in methanol (50 ml) to yield the product as a solid, m.p. 95–97°. The dihydrochloride salt (4.6 g) had m.p. > 310° (MeOH–ether).

Anal. Calcd. for $C_{22}H_{28}Cl_4N_2$: Cl, 30.68; N, 6.06. Found: Cl, 30.82; N, 6.07.

Can. J. Chem. Downloaded from www.nrcresearchpress.com by 210.87.254.5 on 09/05/12
For personal use only.

REFERENCES

1. (*a*) L. G. HUMBER. Belgian Patent No. 627,610 (1963). Derwent Belgian Patent Rept. 30 (1963).
   (*b*) L. G. HUMBER. J. Med. Chem. In press.
   (*c*) C. CHAPPEL, J. DUBUC, D. DVORNIK, M. GIVNER, L. HUMBER, M. KRAML, K. VOITH, and R. GAUDRY. Nature, **201** 497 (1964).
2. J. D. ROBERTS, W. T. MORELAND, and W. FRAZER. J. Am. Chem. Soc. **75**, 637 (1953).
3. P. C. GUHA. Ber. **72**, 1359 (1939).
4. A. K. SCHNEIDER and M. A. SPIELMAN. J. Biol. Chem. **142**, 345 (1942).
5. R. E. IRELAND, T. I. WRIGLEY, and W. G. YOUNG. J. Am. Chem. Soc. **80**, 4605 (1958).
6. V. GEORGIAN, R. HARRISON, and N. GUBISCH. J. Am. Chem. Soc. **81**, 5834 (1959).
7. (*a*) R. SEKA and O. TRAMPOSCH. Ber. B, **75**, 1379 (1942).
   (*b*) S. J. CRISTOL and N. L. HAUSE. J. Am. Chem. Soc. **74**, 2193 (1952).
8. C. A. GROB, H. KNY, and A. GAGNEUX. Helv. Chim. Acta, **40**, 130 (1957).
9. P. C. GUHA and G. D. HAZRA. J. Ind. Inst. Sci. A, **22**, 271 (1939). Chem. Abstr. **34**, 2822 (1940).
10. A. BAEYER. Ann. **251**, 280 (1889).
11. R. BURNELL and W. I. TAYLOR. J. Chem. Soc. 3636 (1954).
12. G. SMITH, C. L. WARREN, and W. R. VAUGHAN. J. Org. Chem. **28**, 3323 (1963).
13. J. C. KAUER. U.S. Patent No. 3,071,597 (January 1, 1963).
14. W. VON E. DOERING, M. FARBER, and A. SAYIGH. J. Am. Chem. Soc. **74**, 4370 (1952).
15. W. J. MIDDLETON, R. E. HECKERT, E. L. LITTLE, and C. G. KRESPAN. J. Am. Chem. Soc. **80**, 2783 (1958).
16. (*a*) R. E. MERRIFIELD and W. D. PHILLIPS. J. Am. Chem. Soc. **80**, 2778 (1958).
   (*b*) D. J. CRAM and R. H. BAUER. J. Am. Chem. Soc. **81**, 5971 (1959).
   (*c*) A. ZWEIG. Tetrahedron Letters, No. 2, 89 (1964).
   (*d*) M. J. S. DEWAR and H. ROGERS. J. Am. Chem. Soc. **84**, 395 (1962).
   (*e*) K. HAFNER and K. L. MORITZ. Ann. Chem. **650**, 92 (1961).
17. C. R. HAUSER and B. E. HUDSON. Org. Reactions, **1**, 283 (1942).
18. S. R. LANDOWER and H. N. RYDON. J. Chem. Soc. 2227 (1953).
19. H. H. BOSSHARD, R. MORY, M. SCHMID, and H. ZOLLINGER. Helv. Chim. Acta, **42**, 1653 (1959).
20. R. LUKES and J. LANGTHALER. Collection Czech. Chem. Commun. **24**, 2109 (1959).
21. H. C. BROWN and B. C. SUBBA RAO. J. Am. Chem. Soc. **80**, 5377 (1958).

Can. J. Chem. Downloaded from www.nrcresearchpress.com by 210.87.254.5 on 09/05/12
For personal use only.

Can. J. Chem. Downloaded from www.nrcresearchpress.com by 210.87.254.105 on 09/05/12
For personal use only.

THE WATER-SOLUBLE POLYSACCHARIDES OF DERMATOPHYTES

III. A GALACTOMANNAN FROM TRICHOPHYTON INTERDIGITALE[1,2]

F. BLANK

The Skin and Cancer Hospital, Department of Dermatology, Temple University School of Medicine, Philadelphia, Pennsylvania

AND

M. B. PERRY

Division of Biosciences, National Research Council, Ottawa, Canada

Received March 24, 1964

ABSTRACT

The water-soluble polysaccharide preparation from *Trichophyton interdigitale* was fractionated to give two distinct galactomannans and a glucan. A galactomannan isolated via its insoluble copper complex had $[\alpha]_D$ +75° (water) and was composed of D-galactose (12%) and D-mannose (88%). On periodate oxidation, the galactomannan consumed 1.73 mole periodate and released 0.67 mole formic acid and 0.12 mole formaldehyde per anhydrohexose unit. Hydrolysis of the methylated galactomannan gave 2,3,5,6-tetra-*O*-methyl-D-galactose (1 part), 2,3,4,6-tetra-*O*-methyl-D-mannose (1 part), 2,3,4-tri-*O*-methyl-D-mannose (4 parts), and 3,4-di-*O*-methyl-D-mannose (2 parts). Mild acid hydrolysis of the galactomannan removed all the galactose residues, leaving a mannan having $[\alpha]_D$ +84° (water) whose structure was analyzed by periodate oxidation and methylation techniques.

Previous papers in this series have described the structural features of polysaccharides isolated from *Trichophyton granulosum* (1) and *Microsporum quinckeanum* (2). The water-soluble polysaccharides of dermatophytes form a part of the antigenic materials of these organisms (3) and as part of a program directed towards a study of the immunological properties of a group of related dermatophytes, the water-soluble polysaccharides isolated from *Trichophyton interdigitale* Priestly, 1917, have now been investigated. This paper records the structural analysis of a galactomannan isolated via its insoluble copper complex from the crude polysaccharide preparation obtained on extraction of *T. interdigitale* with 3% sodium hydroxide solution.

The polysaccharides were extracted in about 6% yield from the powdered cells of *T. interdigitale* in the way described previously for *T. granulosum* (1). The product was a light-brown powder containing 0.6% nitrogen and 5.1% ash and on hydrolysis gave mannose, glucose, and galactose in the approximate ratio of 5:1:1. Moving boundary electrophoresis of the polysaccharides in 0.05 *M* sodium tetraborate solution showed it to be composed of at least three components having the mobilities 8.43×10^{-5}, 8.19×10^{-5}, and 3.83×10^{-5} cm²/V s. The preparation was fractionated according to the scheme outlined in Fig. 1.

The polysaccharide obtained via its insoluble copper complex (galactomannan I) on moving boundary electrophoresis in 0.05 *M* sodium tetraborate gave a single sharp symmetrical peak (Fig. 2) having the same mobility as the fastest moving component in the original polysaccharide mixture. The non-copper complexing polysaccharides were recovered by ethanol precipitation from the deionized Fehling solution and were then resolved by chromatography on diethylaminoethyl (DEAE) cellulose (4). A glucan, which had $[\alpha]_D^{21}$ −16° (water) and on moving boundary electrophoresis in 0.05 *M* sodium

[1]*Presented before the Division of Carbohydrate Chemistry at the 145th National Meeting of the American Chemical Society, New York City, September, 1963.*

[2]*Issued as N.R.C. No. 8150.*

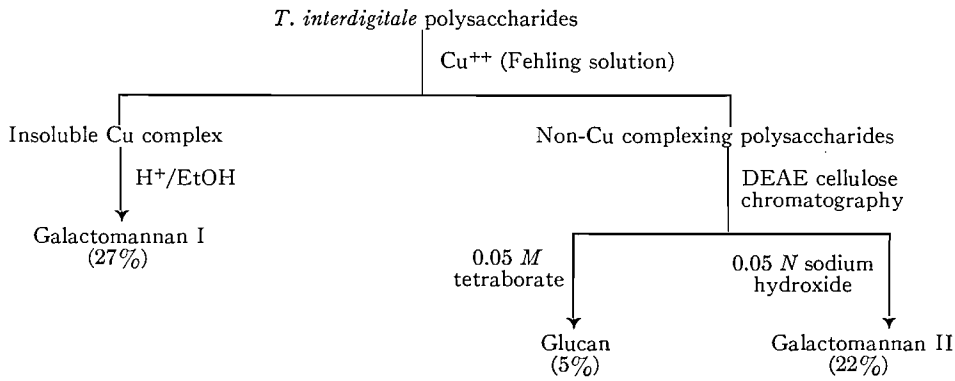

FIG. 1.

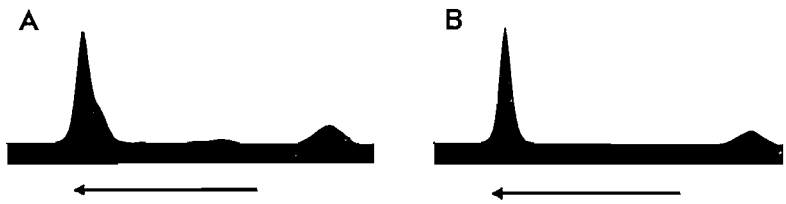

FIG. 2. Moving boundary electrophoresis of polysaccharides from *T. interdigitale*. (A) Crude polysaccharide mixture, (B) purified galactomannan I. Buffer, 0.05 *M* sodium tetraborate.

tetraborate had the same mobility as the slowest component of the original polysaccharide mixture, was eluted from the DEAE cellulose column by 0.05 *M* sodium tetraborate solution. A second galactomannan (galactomannan II) eluted from the column by 0.05 *N* sodium hydroxide solution had $[\alpha]_D^{20}$ +20.6° (water) and a mobility on moving boundary electrophoresis almost identical with that of the component in the original mixture which moved slightly slower than galactomannan I. The structures of the glucan and galactomannan II will be discussed in a future communication.

Galactomannan I was a white powder having $[\alpha]_D^{20}$ +75° (water), was readily soluble in water, and did not give a color with iodine or reduce Fehling solution. Acid hydrolysis of the polysaccharide followed by paper chromatographic examination of the hydrolysate showed it to be composed only of galactose and mannose. The component glycoses were separated chromatographically and were identified as D-galactose and D-mannose. Quantitative determinations of the component glycoses by the gas–liquid partition chromatographic (g.l.p.c.) method (5) and by the colorimetric phenol – sulfuric acid method (6) showed D-galactose and D-mannose to be present in a ratio 1:8.2. The change in the specific optical rotation of the polysaccharide on hydrolysis from +75° to +20.8° (constant value) is that expected of a glycan having the above composition.

Hydrolysis of galactomannan I with 0.02 *N* sulfuric acid at 100° was found to release all the galactose residues from the polysaccharide, leaving a polymer (mannan I) which had $[\alpha]_D$ +84° (water) and gave only mannose on hydrolysis. The above conditions have been shown (7) to effect the selective hydrolysis of galactofuranose residues without affecting the considerably more stable mannopyranose residues. It is considered that the mannan I retains the main structural features of galactomannan I.

Methylated galactomannan I was hydrolyzed, the mixture of products was analyzed by paper chromatography, and the individual components identified after isolation by

Can. J. Chem. Downloaded from www.nrcresearchpress.com by 210.87.254.105 on 09/05/12
For personal use only.

cellulose column chromatography (9). In addition, the methyl glycosides of the sugar ethers, prepared from a portion of the hydrolysate, were analyzed by gas–liquid partition chromatography (8). The overall data obtained by fragmentation analysis of the methylated polysaccharide are given in Table I.

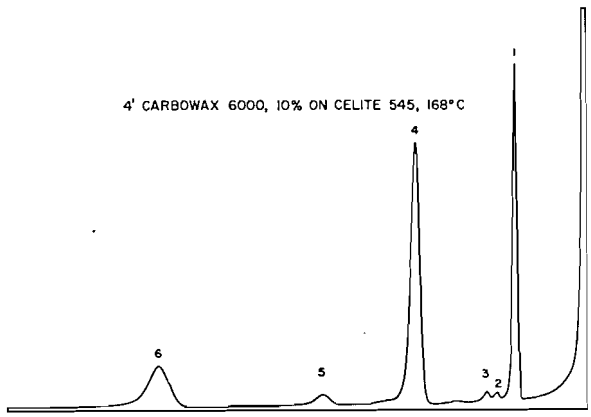

FIG. 3. Gas–liquid chromatogram of methyl *O*-methyl glycosides from the methylated galactomannan I of *T. interdigitale*. (1) Methyl 2,3,5,6-tetra-*O*-methyl-α-D-galactoside and methyl 2,3,4,6-tetra-*O*-methyl-α-D-mannoside (T_G 1.01), (2) methyl 2,3,5,6-tetra-*O*-methyl-β-D-galactoside (T_G 1.26), (3) methyl 2,3,4,6-tetra-*O*-methyl-β-D-mannoside (T_G 1.40), (4) methyl 2,3,4-tri-*O*-methyl-α-D-mannoside (T_G 2.37), (5) methyl 2,3,4-tri-*O*-methyl-β-D-mannoside (T_G 3.68), (6) methyl 3,4-di-*O*-methyl-α-D-mannoside (T_G 5.95).

Since the presence of even minor amounts of a particular type of glycosidic linkage in a polysaccharide is revealed in the immunological and serological properties of the material (10, 11), the tri-*O*-methyl and di-*O*-methyl glycose fractions were carefully examined to establish the absence of glycoses other than the identified components. The tri-*O*-methyl fraction gave only mannose on demethylation (12) and g.l.p.c. of the methanolysis product gave two peaks corresponding to methyl 2,3,4-tri-*O*-methyl-α- and 2,3,4-tri-*O*-methyl-β-D-mannoside (peaks 4 and 5, Fig. 3). All the other possible tri-*O*-methylmannopyranose derivatives, with the exception of 3,4,6-tri-*O*-methylmannose, give methyl glycosides having higher relative retention times. The absence of 3,4,6-tri-*O*-methylmannose was shown by the fact that paper electrophoresis of the fraction in borate buffer (13) did not reveal a mobile component. The purity of the fraction was further established by the fact that periodate oxidation of the glycitol produced by borohydride reduction of a portion of the fraction consumed 1 mole periodate and released 1.01 mole formaldehyde per mole of glycitol and the oxidation product contained only 2,3,4-tri-*O*-methylarabinose which was identified by paper chromatography and g.l.p.c. analysis; the only tri-*O*-methylmannose derivative which could give this result is 2,3,4-tri-*O*-methylmannose.

The di-*O*-methyl fraction gave only mannose on demethylation, and g.l.p.c. analysis of the product obtained on methanolysis of the fraction gave a single peak having the same relative retention time as authentic methyl 3,4-di-*O*-methyl-α-D-mannopyranoside. Thin-layer chromatography of the di-*O*-methyl fraction indicated the presence of trace amounts of a derivative having the chromatographic properties corresponding to 3,5-di-*O*-methyl-D-mannose.

The molecular ratios of the *O*-methyl glycoses were determined by quantitative paper chromatography, phenol – sulfuric acid being used for their colorimetric assay (6), and by quantitative analysis of the g.l.p. chromatogram. The results are in good agreement with those from the yields obtained in the cellulose column separation (Table I).

Can. J. Chem. Downloaded from www.nrcresearchpress.com by 210.87.254.105 on 09/05/12
For personal use only.

Can. J. Chem. Downloaded from www.nrcresearchpress.com by 210.87.254.105 on 09/05/12
For personal use only.

TABLE I

Molecular ratios of the methylated glycoses obtained from methylated galactomannan I

	2,3,5,6-Tetra-*O*-methyl-D-galactose	2,3,4,6-Tetra-*O*-methyl-D-mannose	2,3,4-Tri-*O*-methyl-D-mannose	3,4-Di-*O*-methyl-D-mannose
Quantitative paper chromatography	1	1.12	4.02	1.97
Gas–liquid partition chromatographic analysis of methyl glycosides	← 2 →		3.90	1.80
Cellulose column (weight of fraction)	1	1.02	4.22	2.13

The fission of methylated mannan I gave 2,3,4,6-tetra-*O*-methyl-D-mannose, 2,3,4-tri-*O*-methyl-D-mannose, and 3,4-di-*O*-methyl-D-mannose. The absence of any other glycoses in the tri-*O*- and di-*O*-methyl fractions isolated by preparative paper chromatography was established in the same way as that described above in the analysis of the methylated galactomannan I. Quantitative g.l.p.c. of the methyl glycosides prepared from the hydrolysate of the methylated mannan showed the tetra-*O*-, tri-*O*-, and di-*O*-methyl glycoses to be present in the molecular ratios 1:5:1.

The galactomannan I was oxidized with metaperiodate under unbuffered conditions. Extrapolation of the 'overoxidation' part of the periodate curve to zero time gave a value for the periodate uptake corresponding to 1.73 mole of periodate per anhydrohexose unit and a release of 0.67 mole of formic acid per anhydrohexose unit. Periodate oxidation of the polysaccharide also released 0.12 mole of formaldehyde (50 min constant value) per anhydrohexose unit, which probably all arises from the cleavage of the C_5-C_6 glycol system in the galactofuranose residues. Hydrolysis of the reduced, periodate-oxidized galactomannan I gave glycerol and no detectable amounts of tetritols or aldohexoses, which is the result expected from the polysaccharide having the proposed structure (II).

Periodate oxidation of the mannan I showed an uptake of 1.86 mole of periodate and a release of 0.76 mole of formic acid per anhydromannose unit. Hydrolysis of the reduced, periodate-oxidized mannan I, gave only glycerol and no mannose.

The methylation and periodate oxidation results are in agreement with a structure such as I for mannan I, although several other types of arrangement are clearly possible. As a means of limiting these possibilities, selective oxidation (14) of the side units to D-mannuronic acid residues has been attempted. So far this oxidation step has not been carried out successfully, but the formation of such residues should clearly permit aldobiuronic acids to be isolated from the oxidized polysaccharide and the type of linkage binding the end units to be established directly.

$$-\left[-(\text{D-Man}p)-(1\rightarrow 2 \text{ or } 6)-(\text{D-Man}p)-[-(1\rightarrow 6)-(\text{D-Man}p)]_4-\right]_n-.$$
$$\begin{array}{c} \\ \\ \\ 2 \text{ or } 6 \\ \uparrow \\ 1 \\ \text{D-Man}p \end{array}$$

(I)

The fact that the tri-*O*-methyl fraction obtained from the hydrolysate of the methylated mannan I contained only 2,3,4-tri-*O*-methyl-D-mannose and no 3,4,6-tri-*O*-methyl-D-mannose and the hydrolysate of the methylated galactomannan I contained 3,4-di-*O*-methyl-D-mannose as the di-*O*-methyl glycose leads to the conclusion that the D-galactofuranose residues in the original polysaccharide are linked $1\rightarrow 2$ to mannose units. One of the several possible structures for the galactomannan I, consistent with the methylation and periodate oxidation data, is given below (II). The indicated presence of a small

$$-\left[-(1\rightarrow 6)-(\text{D-Man}p)-(1\rightarrow 6)-[(\text{D-Man}p)-(1\rightarrow 6)]_2-(\text{D-Man}p)-(1\rightarrow 6)-[\text{D-Man}p)-(1\rightarrow 6)]_2-\right]_n-$$
$$\begin{array}{cc} 2 & 2 \\ \uparrow & \uparrow \\ 1 & 1 \\ \text{D-Gal}f & \text{D-Man}p \end{array}$$

(II)

Can. J. Chem. Downloaded from www.nrcresearchpress.com by 210.87.254.105 on 09/05/12
For personal use only.

proportion of 3,5-di-*O*-methyl-D-mannose in the di-*O*-methyl fraction obtained from the fission products of the methylated galactomannan I suggests the presence of 2-*O*- and 6-*O*-substituted D-mannofuranose residues in the original polysaccharide; this unusual possibility has not been unequivocally proved at this time. In view of the high positive specific optical rotation of the polysaccharide it is probable that most of the linkages have the α-D-configuration.

It appears that the galactomannan I from *T. interdigitale* bears a remarkable similarity in many of its structural features to the galactomannan from *T. granulosum* (1), which, to our knowledge, was the first galactomannan to be isolated from a microorganism. Both galactomannans are unusual in having all of the galactose units present as terminal nonreducing furanoside residues.

EXPERIMENTAL

Paper chromatography was performed by the descending method (15) on Whatman No. 1 filter paper using the following solvent systems: (A) pyridine : ethyl acetate : water (2:5:5 v/v, upper phase) and (B) butanone saturated with water. Paper electrophoreses were done on Whatman 3MM paper in 0.1 *M* sodium tetraborate at 700 V (potential gradient ca. 25 V/cm) and 25–35 mA for 2–3 h. The glycoses were detected on the paper chromatograms and electrophoretograms by (*a*) spraying with a solution of 2% (w/v) *p*-anisidine hydrochloride in butan-1-ol (16) or (*b*) with a solution of 2% (w/v) silver nitrate in acetone followed by 3% (w/v) ethanolic sodium hydroxide solution (17). The rates of movement of the glycoses on the paper chromatograms are quoted relative to that of D-galactose (R_{Gal}) or 2,3,4,6-tetra-*O*-methyl-D-glucose (R_G), and relative to D-glucose (M_G) on the paper electrophoretograms.

Gas–liquid partition chromatography was done with a Pye Argon Chromatograph fitted with an ionization detector (^{90}Sr, 80 μcuries) using straight glass columns (120 × 0.5 cm inside diameter) which were packed with 10% (w/w) Carbowax 6 000 on 80–100 mesh acid-washed Chromosorb W (Johns-Manville). The retention times of the glycoses are quoted relative to methyl 2,3,4,6-tetra-*O*-methyl-α-D-glucoside (T_G).

Solutions were concentrated under reduced pressure below 35°. Melting points were determined on a Fisher-Johns Apparatus and are corrected.

Preparation of Water-Soluble Polysaccharides

Trichophyton interdigitale was grown in 500 ml Erlenmeyer flasks containing 250–300 ml each of an agar medium containing the following nutrients: 4% (w/v) unpurified glucose (cerelose), 1% (w/v) neopeptone "Difco", 0.05% (w/v) yeast extract "Difco", 0.001% (w/v) thiamine, 0.005% (w/v) inositol, made up in tap water. The polysaccharides were extracted from the autoclaved, washed, freeze-dried, and milled mycelium as described previously for *T. granulosum* (1). The polysaccharides were obtained as a light-brown powder which contained 0.6% N and 5.1% ash and amounted to 5.9% of the dry mycelium. A sample of the preparation (10 mg) after hydrolysis with 2 *N* sulfuric acid for 5 h at 100 °C was found by paper chromatography (solvent A) to give spots corresponding to galactose, glucose, and mannose in the visual ratio 1:1:5. Moving boundary electrophoresis showed that at least three components were present.

Isolation of Galactomannan I

The polysaccharide preparation from *T. interdigitale* (50 g) was dissolved in water (350 ml) and Fehling solution A (500 ml). Fehling solution B (500 ml) was added dropwise over a 30 min interval to the vigorously stirred solution and after a further 30 min the precipitated complex was collected by centrifugation. The complex was washed twice with water (500 ml) by gentle mixing in a Waring Blendor and the product was then suspended in ice water (60 ml) and decomposed by the addition of just sufficient dilute acetic acid to bring the material into solution. The clear-blue solution was poured into 10 volumes of absolute ethanol and the precipitated polysaccharide was collected by centrifugation, deionized by passing its aqueous solution (70 ml) through columns of Amberlite IR120(H^+) and Amberlite IR45(OH^-) ion-exchange resins, and the neutral effluent and washings, after concentration to about 100 ml, was poured into absolute ethanol (1.2 l). The precipitated polysaccharide was collected by centrifugation, washed with ethanol, and dried under vacuum. The yield of polysaccharide (galactomannan I) was 13.5 g (27%). The non-copper complexing polysaccharides were recovered from the solution containing the excess Fehling solution by precipitation with ethanol.

Properties of Galactomannan I

Galactomannan I was a white powder, readily soluble in water, and had $[\alpha]_D^{22}$ +75° (*c*, 2 water).

Anal. Calcd. for hexosan $(C_6H_{10}O_5)_n$: C, 44.44; H, 6.22. Found: C, 44.0; H, 6.40; N, nil; ash, 0.03. The polysaccharide was neutral, gave no color with iodine, and did not reduce Fehling solution.

Moving boundary electrophoresis of galactomannan I in 0.05 *M* sodium tetraborate showed a single

Can. J. Chem. Downloaded from www.nrcresearchpress.com by 210.87.254.105 on 09/05/12
For personal use only.

sharp symmetrical peak having the mobility of the fastest component in the original polysaccharide preparation ($\mu = 8.43 \times 10^{-5}$ cm²/V s).

Component Glycoses of Galactomannan I

Galactomannan I (0.4 g) was hydrolyzed by 2 *N* sulfuric acid (50 ml) at 100° for 5 h, and, after neutralization ($BaCO_3$) and filtration, the filtrate was concentrated to a syrup. The syrup was fractionated on sheets of Whatman 3MM paper using solvent system A. Sections of the paper containing the glycoses were extracted with water. The solutions were deionized by passage through mixed Amberlite IR120(H^+) and Amberlite IR45(OH^-) ion-exchange resins and concentrated to dryness. The glycoses were identified as (A) D-galactose (the syrup (34 mg) had $[\alpha]_D^{22}$ +80° (*c*, 1 water) and gave a 1-methyl-1-phenylhydrazone derivative having m.p. and mixed m.p. 163°) and (B) D-mannose (the syrup (310 mg) had $[\alpha]_D^{20}$ +14° (*c*, 2 water) and gave a phenylhydrazone derivative having m.p. and mixed m.p. 186–187°).

Quantitative Estimation of the Component Glycoses of Galactomannan I

Samples of the galactomannan I (40–50 mg) were hydrolyzed for 6 h with 2 *N* sulfuric acid at 100°. The neutralized ($BaCO_3$) hydrolysates were concentrated and, after paper chromatographic fractionation with solvent A, the glycoses were estimated colorimetrically by the phenol – sulfuric acid method (6). The results indicate that the D-galactose and D-mannose are present in the ratio 1:8.6.

Found: D-galactose: 11.3, 12.1, 11.7. D-Mannose: 88.7, 87.9, 88.3%.

Quantitative analysis of reduced acetylated products of samples of the hydrolyzed galactomannan I (c. 5–6 mg) by gas–liquid partition chromatography using the procedure described by Gunner *et al.* (5) indicated the D-galactose : D-mannose ratio to be 1:7.4. On hydrolysis of a sample of the galactomannan I with 2 *N* hydrochloric acid at 100° the specific optical rotation of the solution was found to change from $[\alpha]_D^{20}$ +74° (*c*, 2) to $[\alpha]_D^{20}$ +20.8° (*c*, 1.2).

Partial Hydrolysis of Galactomannan I to Give Mannan I

Galactomannan I (1.5 g) was heated with 0.02 *N* sulfuric acid (100 ml) at 100 °C for 4 h and then deionized by passage through a column of Amberlite IR45(OH^-) ion-exchange resin. The neutral effluent was concentrated to about 12 ml and the solution was poured into absolute alcohol (200 ml). The precipitated polysaccharide (mannan I) was collected, washed with ethanol, and dried *in vacuo* (1.14 g, 76%). The polysaccharide had $[\alpha]_D^{20}$ +84° (*c*, 2 water). Paper chromatographic examination in solvent system A of a sample (5 mg) of the polysaccharide hydrolyzed for 6 h with 2 *N* sulphuric acid (3 ml) at 100° showed only mannose to be present. The ethanol solution was concentrated and on paper chromatographic analysis (solvent A) it showed a single spot, corresponding to galactose.

Methylation of Galactomannan I

To the galactomannan I (5 g) in water (50 ml) were added simultaneously and dropwise with stirring, 30% (w/v) sodium hydroxide solution (150 ml) and dimethyl sulfate (64 ml), at a rate such that the mixture remained slightly alkaline throughout. After 6 h, 30% (w/v) sodium hydroxide solution (160 ml) and dimethyl sulfate (50 ml) were added dropwise during 8 h and stirring was continued for 20 h. The mixture was then heated on a boiling water bath for 30 min to destroy any excess dimethyl sulfate and the cooled solution was very carefully neutralized in the cold with 2 *N* sulfuric acid. The partially methylated product was extracted with chloroform (6 × 100 ml) and the dried (Na_2SO_4) extract was concentrated to a syrup (5.42 g). The syrup (5.2 g) was further methylated (18) by treating its vigorously stirred solution in dimethylformamide (60 ml) and methyl iodide (50 ml) with finely powdered barium oxide (60 g). Water (0.2 ml) was added to the mixture and after 2 h the pasty reaction mixture was diluted with chloroform (300 ml). The reaction mixture was filtered and the filtrate was extracted with water (5 × 150 ml). The dried (Na_2SO_4) chloroform solution was concentrated to yield a syrup (5.1 g). The syrup, dissolved in ethanol (10 ml), was poured into light petroleum (b.p. 30–60°) (300 ml) and the precipitated methylated polysaccharide was collected (4.51 g). The final product was a cream-colored powder having $[\alpha]_D^{21}$ +80° (*c*, 2.1 chloroform) and OMe 44.5% (calcd. OMe 45.6%) which could not be raised by re-methylation.

Fission of Methylated Galactomannan I

The methylated galactomannan I (3.5 g) was dissolved in cold 72% (v/v) sulfuric acid (20 ml). After 30 min at room temperature, the solution was diluted with water (140 ml) and the hydrolysis was continued by heating the mixture on a boiling water bath for 5 h. The cooled solution was neutralized by passage down a column of Amberlite IR45(OH^-) ion-exchange resin and the effluent washings were evaporated in a stream of dry air to a syrup (3.7 g). Paper chromatographic examination of samples of the hydrolysate using solvent system A showed three spots having R_G 0.99, 0.87, and 0.72, respectively; four components having R_G 1.05, 0.98, 0.72, and 0.39 were detected, using solvent system B. A portion of the hydrolysate (60 mg) was heated in a sealed tube at 95° with 2% methanolic hydrogen chloride solution (5 ml) for 5 h. The cooled solution was neutralized (Ag_2CO_3), filtered, and the filtrate was concentrated to a thin syrup in a stream of dry air. The methyl glycosides were examined by gas–liquid partition chromatography to give the separation shown in Fig. 3.

The *O*-methyl glycoses (2.1 g) were separated chromatographically on a column of powdered cellulose (3 × 58 cm), using solvent system B, to yield the following fractions.

Can. J. Chem. Downloaded from www.nrcresearchpress.com by 210.87.254.105 on 09/05/12
For personal use only.

Can. J. Chem. Downloaded from www.nrcresearchpress.com by 210.87.254.105 on 09/05/12
For personal use only.

Fraction 1, 2,3,5,6-Tetra-O-methyl-D-galactose

Fraction 1 (141 mg) on paper chromatography gave a single spot having R_G 1.02 (solvent B) corresponding to authentic 2,3,5,6-tetra-*O*-methyl-D-galactose. Oxidation of a portion of the fraction (60 mg) with bromine gave a lactone which was converted to its amide (32 mg) which had $[\alpha]_D$ +8° (*c*, 2 water) and m.p. 158° which was undepressed on admixture with 2,3,5,6-tetra-*O*-methyl-D-galactonamide.

Fraction 2, 2,3,5,6-Tetra-O-methyl-D-galactose and 2,3,4,6-Tetra-O-methyl-D-mannose

The syrup (208 mg) contained two components with R_G 1.02 and 0.97 (solvent B) corresponding to 2,3,5,6-tetra-*O*-methylgalactose and 2,3,4,6-tetra-*O*-methylmannose respectively. Further fractionation of the syrup by filter paper chromatography gave pure 2,3,5,6-tetra-*O*-methyl-D-galactose (107 mg) and 2,3,4,6-tetra-*O*-methyl-D-mannose. The latter compound was combined with fraction 3.

Fraction 3, 2,3,4,6-Tetra-O-methyl-D-mannose

Fraction 3 (253 mg) was chromatographically pure giving a single spot corresponding to 2,3,4,6-tetra-*O*-methylmannose. It had $[\alpha]_D$ +3° (*c*, 1 water) and a portion of the syrup (60 mg) after heating under reflux with aniline (32 mg) in ethanol (2 ml) gave crystalline 2,3,4,6-tetra-*O*-methyl-*N*-phenyl-D-mannosylamine, which on recrystallization from ethanol had m.p. and mixed m.p. 142° and $[\alpha]_D$ −75° to −7° (*c*, 0.04 MeOH).

Fraction 4, 2,3,4-Tri-O-methyl-D-mannose

The fraction (982 mg) was shown by paper chromatography and electrophoresis to consist of one component. Bromine oxidation converted the material to a lactone from which 2,3,4-tri-*O*-methyl-D-mannanamide was prepared; when recrystallized from ethyl acetate, the amide had m.p. 142–143°, undepressed; $[\alpha]_D$ +5 (*c*, 1 water).

A portion of fraction 4 (60 mg) was reduced with excess of sodium borohydride. The derived glycitol consumed 1.0 moles of periodate and released 1.0 moles of formaldehyde per mole. The sugar formed in this oxidation, as shown by paper chromatography and by g.l.p.c. analysis of its methyl glycoside, appeared to consist entirely of 2,3,4-tri-*O*-methyl-L-arabinose.

Fraction 5, 3,4-Di-O-methyl-D-mannose

The fraction (465 mg) having R_G 0.72 (solvent A) and 0.72 (solvent B) and M_G 0.34 showed $[\alpha]_D^{22}$ +35.7° (*c*, 1.6 methanol) and corresponded in the above properties to 3,4-di-*O*-methyl-D-mannose. On standing, the fraction crystallized and the material after recrystallization from ethyl acetate solution had m.p. and mixed m.p. 78–79° and $[\alpha]_D^{20}$ +5.5° (*c*, 2 water). A sample of the original fraction, before crystallization, was refluxed with 2% (w/v) methanolic hydrogen chloride (4 ml) for 6 h and the product on g.l.p.c. examination was found to give a single peak corresponding to methyl 3,4-di-*O*-methyl-α-D-mannoside. Demethylation with BCl_3 of a portion of the fraction and paper chromatographic examination of the product showed only one spot corresponding to mannose. A portion of the di-*O*-methyl fraction examined by thin-layer chromatography on a silica gel G using benzene : acetone (1:1) as the developing solvent revealed a major component having the same mobility as 3,4-di-*O*-methyl-D-mannose and a minor component (ca. 4%) having a slightly greater mobility. The minor component isolated by preparative thin-layer chromatography had M_G 0.56 and R_G 0.67 (solvent A) and was indistinguishable chromatographically from 3,5-di-*O*-methyl-D-mannose.

Periodate Oxidation of Galactomannan I

The galactomannan I (0.210 g) was dissolved in water (200 ml), 0.3 *M* sodium metaperiodate solution (25 ml) was added, and the total volume adjusted to 250 ml with water. A blank solution containing no polysaccharide was prepared at the same time. Oxidation was allowed to proceed in the dark at 22°. At intervals, the periodate uptake was determined by transferring samples (10 ml) from the oxidation mixture and the blank to a fresh mixture of *M*/15 sodium phosphate buffer (pH 6.99) (100 ml) and 20% (w/v) potassium iodide solution (10 ml), and the liberated iodine was titrated with 0.025 *N* sodium thiosulfate solution, using starch as an indicator. Formic acid liberation was followed by titration of samples (10 ml) of the oxidation mixture, treated for 5 min with ethylene glycol to destroy the excess periodate, with 0.01 *N* sodium hydroxide solution using methyl red screened with methylene blue as the indicator. The results are recorded below (Table II).

The formaldehyde released from the galactomannan I on periodate oxidation was determined by treating the polysaccharide (32.8 mg) in water (20 ml) containing 0.05% *p*-hydroxybenzaldehyde with 0.3 *M*

TABLE II

Periodate oxidation of galactomannan I

Time of oxidation (h)	18	42	66	89	116	140	171
Mole of IO_4 consumed per 162 g galactomannan	1.60	1.85	1.92	1.97	2.07	2.12	2.20
Mole HCO_2H released per 162 g galactomannan	0.55	0.75	0.82	0.91	0.93	1.06	1.17

Can. J. Chem. Downloaded from www.nrcresearchpress.com by 210.87.254.105 on 09/05/12
For personal use only.

sodium metaperiodate solution (3 ml). The total volume of the reaction mixture was adjusted to 25 ml with water and the oxidation was allowed to proceed in the dark at 22°. Samples (1 ml) were withdrawn from the mixture at intervals and were neutralized with 20% (w/v) lead dithionate solution (1 ml) and, after removal of the precipitated lead salts by centrifugation, the formaldehyde contents of the clear supernatant liquids were determined by the chromotropic acid method (19). The moles of formaldehyde released per anhydrohexose unit were found to be 0.074 (3 min), 0.088 (10 min), 0.119 (25 min), 0.120 (50 min, constant value).

A sample of the galactomannan I (50 mg) in water (10 ml) was oxidized by the addition of 0.3 *M* sodium metaperiodate solution (5 ml) and after the reaction had been allowed to proceed in the dark at 22° for 50 h, the mixture was deionized by passage through a bed of mixed Amberlite IR120(H^+) and Duolite A4(OH^-) ion-exchange resins. The neutral solution was reduced by the addition of sodium borohydride (50 mg) and after 5 h the solution was treated with Amberlite IR120(H^+) ion-exchange resin to destroy the excess borohydride and remove sodium ions. The solution was filtered and the concentrated filtrate was hydrolyzed with 2 *N* sulfuric acid (4 ml) at 100° for 4 h. The neutralized solution ($BaCO_3$) was filtered and the filtrate was concentrated in a stream of dry air. Paper chromatographic examination of the residue using solvent system A showed a single spot whose chromatographic behavior was identical with glycerol, and no spots corresponding to tetritols or hexoses were observed.

Methylation of Mannan I

Mannan I (0.5 g) was methylated in the same way as that described for galactomannan I to give a product (0.38 g) having $[\alpha]_D^{20}$ +90° (*c*, 1 chloroform) and OMe 44.2%, which could not be raised by further methylation using silver oxide and methyl iodide.

Fission of Methylated Mannan I

Methylated mannan I (0.3 g) was dissolved in cold 75% sulfuric acid (3.6 ml) and after the addition of water (22 ml) the solution was heated on a boiling water bath for 7 h. The cooled reaction mixture was neutralized by passage down a column of Amberlite IR45(OH^-) ion-exchange resin and the solution containing the *O*-methyl glycoses was concentrated to a syrup by evaporation in a stream of dry air. Paper chromatography of the concentrate in solvent system A indicated the presence of 2,3,4,6-tetra-*O*-methylmannose, 2,3,4-tri-*O*-methylmannose, and 3,4-di-*O*-methylmannose having R_G 0.99, 0.86, and 0.71, respectively. A portion (30 mg) of the *O*-methyl glycoses was heated in a sealed tube with 2% methanolic hydrogen chloride (5 ml) for 7 h and after neutralization (Ag_2CO_3) and concentration of the solution, the methyl glycosides were examined by g.l.p.c. The gas–liquid partition chromatogram showed the same peaks as those obtained on methanolysis of the products obtained from the methylated galactomannan I. Quantitative analysis of the g.l.p.c. chromatogram indicated the glycoses to be present in the tetra-*O*- : tri-*O*- : di-*O*-methyl glycose ratios of 1 : 4.8 : 0.97.

The *O*-methyl glycoses were fractionated (solvent A) on two large sheets of Whatman 3MM filter paper to give (A) 2,3,4,6-tetra-*O*-methyl-D-mannose (32 mg), which gave a derivative 2,3,4,6-tetra-*O*-methyl-*N*-phenyl-D-mannosamine having m.p. and mixed m.p. 141°, (B) 2,3,4-tri-*O*-methyl-D-mannose (170 mg), which gave an amide having m.p. 141–143°, undepressed on admixture with authentic 2,3,4-tri-*O*-methyl-D-mannonamide, and (C) 3,4-di-*O*-methyl-D-mannose (28 mg), which had m.p. and mixed m.p. 78–79°. An examination of the tri-*O*-methyl fraction by paper electrophoresis in borate buffer showed only a single spot having M_G 0.00, and periodate oxidation of a portion of the reduced fraction gave a single product, identified by paper chromatography, and by g.l.p.c. analysis of its methyl glycoside preparation, as 2,3,4-tri-*O*-methylarabinose.

Periodate Oxidation of Mannan I

Mannan I (125 mg) was dissolved in water (200 ml) and after the addition of 0.3 *M* sodium metaperiodate the volume of the solution was adjusted to 250 ml. A blank solution containing no polysaccharide was prepared at the same time. Oxidation was allowed to proceed in the dark at 22° and at intervals samples were withdrawn for the determination of periodate uptake and formic acid release. The results are recorded below (Table III).

A sample of mannan I (60 mg) was dissolved in water (50 ml) and was oxidized by the addition of 0.3 *M* sodium metaperiodate. After oxidation had been allowed to proceed at 20° for 78 h, the reaction mixture was deionized by passing it through a bed of mixed Amberlite IR120(H^+) and Amberlite IR45(OH^-)

TABLE III

Periodate oxidation of mannan I

Time of oxidation (h)	20	26	45	72	96	118	150
Mole of IO_4 consumed per 162 g mannan I	1.78	1.87	1.98	2.01	2.07	2.14	2.20
Mole of HCO_2H released per 162 g mannan I	0.61	0.69	0.81	0.87	0.90	0.93	1.00

ion-exchange resins, and sodium borohydride (100 mg) was added. After 12 h the excess borohydride was destroyed with IR120(H^+) resin and the solution was evaporated to dryness. The residue was hydrolyzed with 2 *N* sulfuric acid (4 ml) at 100° for 4 h, neutralized ($BaCO_3$), and the filtered solution was evaporated to dryness. Paper chromatographic examination (solvent A) of the hydrolysate showed a single spot corresponding to glycerol. No mannose could be detected, even on heavily spotted chromatograms.

ACKNOWLEDGMENT

This work was, in part, supported by a grant from the John A. Hartford Foundation, Inc., New York.

REFERENCES

1. C. T. Bishop, F. Blank, and M. Hranisavljevic-Jakovljevic. Can. J. Chem. **40**, 1816 (1962).
2. H. Alfes, C. T. Bishop, and F. Blank. Can. J. Chem. **41**, 2621 (1963).
3. B. Bloch, A. Labouchere, and F. Schaaf. Arch. Dermatol. Syphilol. **148**, 413 (1925).
4. H. Neukom, H. Deuel, W. J. Heri, and W. Kündig. Helv. Chim. Acta, **43**, 64 (1960).
5. S. W. Gunner, J. K. N. Jones, and M. B. Perry. Chem. Ind. London, 255 (1961).
6. M. Dubois, K. A. Gilles, J. K. Hamilton, P. A. Rebers, and F. Smith. Anal. Chem. **28**, 350 (1956).
7. L. Hough and M. B. Perry. J. Chem. Soc. 2801 (1962).
8. C. T. Bishop. Methods Biochem. Analy. **10**, 1 (1962).
9. L. Hough, J. K. N. Jones, and W. H. Wadman. J. Chem. Soc. 2511 (1949).
10. M. Heidelberger. Progr. Chem. Org. Nat. Prod. **18**, 503 (1960).
11. M. Heidelberger, Z. Dische, W. B. Neeley, and M. L. Wolfrom. J. Am. Chem. Soc. **77**, 3511 (1955).
12. S. Allen, T. G. Bonner, E. J. Bourne, and N. M. Saville. Chem. Ind. London, 630 (1958).
13. A. B. Foster. Advan. Carbohydrate Chem. **12**, 81 (1955).
14. G. O. Aspinall and A. Nicolson. J. Chem. Soc. 2503 (1960).
15. S. M. Partridge. Biochem. J. London, **42**, 238 (1948).
16. L. Hough, J. K. N. Jones, and W. H. Wadman. J. Chem. Soc. 1702 (1950).
17. W. E. Trevelyan, D. P. Procter, and J. S. Harrison. Nature, **166**, 444 (1950).
18. R. Kühn, H. Trischmann, and I. Löw. Angew. Chem. **67**, 32 (1955).
19. J. F. O'Dea and R. A. Gibbons. Biochem. J. London, **55**, 580 (1953).

Can. J. Chem. Downloaded from www.nrcresearchpress.com by 210.87.254.105 on 09/05/12
For personal use only.

Can. J. Chem. Downloaded from www.nrcresearchpress.com by 210.87.254.42 on 09/05/12
For personal use only.

ENERGY TRANSFER IN THE RADIOLYSIS OF CYCLOPENTANE–CYCLOHEXANE MIXTURES[1]

J. A. STONE
Research Chemistry Branch, Atomic Energy of Canada Limited, Chalk River, Ontario

Received July 20, 1964

ABSTRACT

Energy transfer in the radiolysis of cyclopentane–cyclohexane mixtures has been studied by observing the yields of HD and D_2 obtained when small amounts of cyclohexane-d_{12} are added. Energy migration occurs from cyclopentane to cyclohexane but this transfer can be prevented by the addition of carbon tetrachloride or iodine. The relative yields of the dimers $(C_6H_{11})_2$, $C_5H_9C_6H_{11}$, and $(C_5H_9)_2$ show that the $\cdot C_6H_{11}$ and $\cdot C_5H_9$ radicals, which are the precursors of the dimers, can abstract hydrogen atoms from the solvent and may thus change their identity. Added iodine or carbon tetrachloride removes the diffusing radicals, and the residual dimer yield, which is unaffected by solute, has a composition determined solely by the composition of the mixtures. The yields of cyclohexene and cyclopentene show evidence of both energy transfer and radical change of identity.

INTRODUCTION

The lowering of the yields of hydrogen from the radiolysis of binary mixtures of hydrocarbons below those expected from a simple mixing of the two species has been interpreted in terms of energy transfer processes. This latter term includes any process, e.g. charge transfer, excitation transfer, or electron capture, which can be described as a physical process as opposed to chemical processes represented by, for example, radical scavenging. Most examples of energy transfer have resulted from studies on mixtures of a saturated and an aromatic hydrocarbon (1–4). Departures from ideality in the radiolysis of binary mixtures of saturated hydrocarbons are not so pronounced and hence not so readily observable. Fewer examples have been recorded.

Dyne and Denhartog (5) using isotopically labelled hydrocarbons have shown that different alkane solvents can influence the yield of hydrogen from a given hydrocarbon solute to widely differing extents. From a study of the products formed in the radiolysis of dilute solutions of cyclohexane in cyclopentane, they showed that an increase in cyclohexene yield above that expected from the electron fraction of the parent hydrocarbon occurred, but that the yield of dimers containing cyclohexyl groupings was reduced (6). The increased olefin yield was attributed to a transfer of energy initially absorbed in the cyclopentane to the cyclohexane. The decreased yield of dimeric products containing cyclohexyl groups was in agreement with earlier work of Muccini and Schuler (7). These authors found over the whole range of cyclohexane–cyclopentane mixtures a greater proportion of dimeric products containing cyclopentyl groupings than would be expected from the electron fraction of the parent hydrocarbon. This was explained in terms of a change in identity of the radicals which, they assumed, were formed initially according to the electron fraction of the parent hydrocarbons.

[1] $$\cdot C_5H_9 + C_6H_{12} \rightarrow \cdot C_6H_{11} + C_5H_{10}$$

[2] $$\cdot C_6H_{11} + C_5H_{10} \rightarrow \cdot C_5H_9 + C_6H_{12}$$

If the rate of reaction [2] is greater than that of [1], then the steady-state concentration of cyclopentyl radicals will be increased at the expense of the cyclohexyl radicals. The

[1]*Issued as A.E.C.L. No. 2081.*

saturated dimeric products (bicyclohexyl, bicyclopentyl, and cyclopentylcyclohexane) formed by radical dimerization should therefore show a bias towards cyclopentyl groups.

Previous work with cyclohexane – carbon tetrachloride mixtures (8) has shown that, at the lowest carbon tetrachloride concentration that it is practical to work with ($\sim 0.04\ M$), all cyclohexyl radicals are scavenged. However, although at this concentration the yield of the dimeric product bicyclohexyl has been reduced to a very low limiting value, the cyclohexene yield is still high and is not reduced to its limiting value until much higher solute concentrations. This demonstrates that cyclohexene is formed in at least two ways, one of which involves disproportionation of cyclohexyl radicals. The same conclusion will probably apply to the formation of cyclopentene from cyclopentane.

The present work was undertaken to study the cyclopentane–cyclohexane system in detail, and in particular the energy transfer process and its relationship to the yields of the major products.

EXPERIMENTAL PROCEDURES

Materials

Cyclopentane (Phillips Research Grade) was shaken with sulfuric acid to remove cyclopentene and was then fractionally distilled. Cyclohexane (Fisher Spectrograde), iodine (Anachemia), carbon tetrachloride (Fisher Certified Reagent), and cyclohexane-d_{12} (Merck) were used as received. As the cyclohexane was free of cyclohexene it was not further purified.

Sample Preparation and Irradiation

All samples were of 2 ml volume contained in pyrex tubes fitted with break seals. Samples were made up individually and were then degassed by the freeze-thaw-pump technique. ^{60}Co-γ-irradiations were carried out at dose rates of 1.66×10^{22} eV/l h and 1.43×10^{21} eV/l h to total doses of $\sim 3.3 \times 10^{22}$ eV/l.

Product Analysis

The measurement of the hydrogen yield has been described previously (9). The isotopic composition of the hydrogen was determined on a C.E.C. 21-610 mass spectrometer.

Liquid products, olefins and dimers, were determined by gas–liquid chromatography using the following columns and column conditions: for cyclohexene, 1/4 in. × 10 ft, 30% 1,2,3-tris(2-cyanoethoxy)propane at 65 °C; for cyclopentene, 1/4 in. × 12 ft, 10% squalane at 80 °C; for bicyclohexyl, either a 1/4 in. × 12 ft, 20% Xe-60 (General Electric) column at 170 °C or a 1/8 in. × 9 ft, 12% OS-124 (Monsanto) column at 145 °C. Identical results were obtained with the last two columns. Bicyclopentyl and cyclopentylcyclohexane were determined by temperature programming the OS-124 column from 60 to 160 °C. Standard solutions were run alternately with the irradiated samples. No standards were available for the dimers containing cyclopentyl groups and so these were determined from a comparison of the chromatographic peak areas with those of standard bicyclohexyl solutions, corrections being applied for the different carbon numbers since a hydrogen flame detector was used.

RESULTS AND DISCUSSION

A major advantage in choosing cyclohexane and cyclopentane for a study of the radiolysis of a binary hydrocarbon mixture lies in their relatively small range of major products. In the case of the pure compounds the major gaseous product is hydrogen whilst the main liquid products are the olefins, cyclohexene and cyclopentene, of the same carbon number as the parent hydrocarbon and the dimers bicyclohexyl and bicyclopentyl. In mixtures of the two hydrocarbons the only other major product is the mixed dimer cyclopentylcyclohexane.

(a) Hydrogen

For a total dose of 3.3×10^{22} eV/l, $G(H_2)$ for pure cyclohexane was 5.37 while that for pure cyclopentane was 4.97. Within experimental error $G(H_2)$ from mixtures of the two was a linear function of composition. It does not follow, however, that energy transfer does not occur. Hardwick (10) has shown that departures from ideal behavior do occur

Can. J. Chem. Downloaded from www.nrcresearchpress.com by 210.87.254.42 on 09/05/12
For personal use only.

in the hydrogen yield from binary mixtures of saturated hydrocarbons. Such deviations were, however, readily observable only in mixtures of hydrocarbons having markedly different $G(H_2)$ values, i.e. mixtures of normal and highly branched hydrocarbons. In the case of cyclohexane–cyclopentane mixtures the $G(H_2)$ values of the individual compounds are very similar. An energy exchange would therefore result in a decrease in $G(H_2)$ for one compound which might well be balanced by an almost equal increase in $G(H_2)$ for the other. A deviation from ideality in the hydrogen yield would not therefore be observed.

Deviations from ideal behavior can be readily observed in systems containing small quantities (2–5%) of a deuterated hydrocarbon (5). Figure 1 shows the yields of H_2, HD, and D_2 obtained from various mixtures of cyclohexane and cyclopentane each containing 5% by volume of cyclohexane-d_{12}. Although $G(H_2)$ is linear with composition,

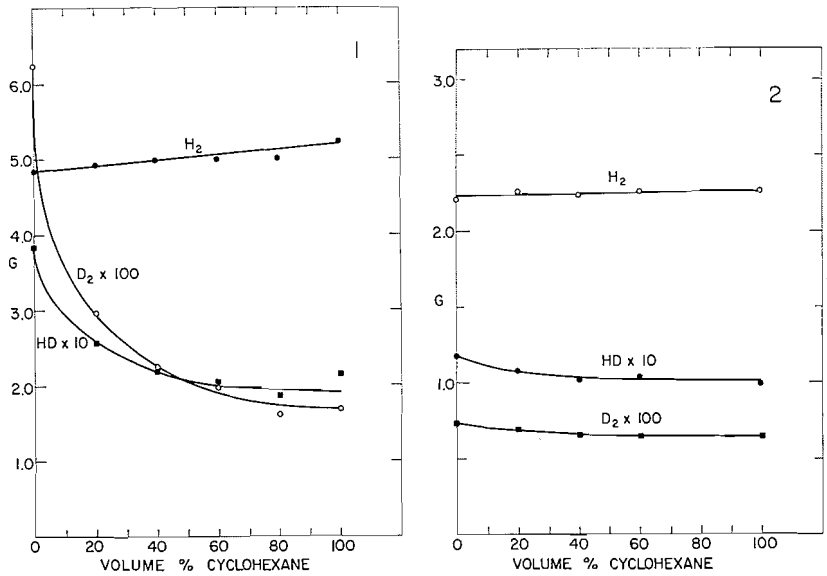

FIG. 1. The yields of H_2, HD, and D_2 from cyclopentane–cyclohexane mixtures each containing 5% by volume of cyclohexane-d_{12}.

FIG. 2. The yields of H_2, HD, and D_2 from cyclopentane–cyclohexane mixtures each containing 5% by volume of cyclohexane-d_{12} and 2% by volume of carbon tetrachloride.

both $G(HD)$ and $G(D_2)$ depart markedly from the behavior expected for a constant electron fraction of cyclohexane-d_{12}. The departure from ideality is not a linear function of solvent composition, but shows a rapid variation at low cyclohexane concentrations. The yields of HD and D_2 depend strongly on environment. The relative contributions to the total hydrogen yield from cyclohexane and cyclopentane must also be dependent on mixture composition. The same effect has been demonstrated in *n*-hexane – cyclohexane mixtures (11).

The value of $G(D_2) + G(HD)$ from 99.6% isotopically pure cyclohexane-d_{12} is 4.1 (12) so that it would be expected that the hydrogen evolved from mixtures of hydrocarbons containing 5% of this compound would be ~ 4 atom % in deuterium. This is not the case. As shown in Table I for cyclohexane we find 2.3 atom %, while for cyclopentane it is 5.1 atom %. Much of the deuterium is present as HD with about 20% present as D_2. This large difference in deuterium content cannot be attributed to a kinetic isotope effect on HD formation since (i) this would require too great a difference in the C—H bond

Can. J. Chem. Downloaded from www.nrcresearchpress.com by 210.87.254.42 on 09/05/12
For personal use only.

TABLE I

The deuterium content (HD + D_2) of the hydrogen evolved from cyclohexane and cyclopentane containing 5% by volume of cyclohexane-d_{12}

	Atom % deuterium	
Solvent	No solute	2% CCl_4
Cyclopentane	5.1	2.8
Cyclohexane	2.3	2.4

dissociation energy between cyclohexane and cyclopentane and (ii) the yield of D_2, which is formed in a unimolecular decomposition (13), shows a similar variation in going from one solvent to the other. The effect must be attributed to a migration of energy, presumably initially partitioned according to electron fraction, amongst the components.

Certain solutes in low concentration reduce the yields of hydrogen from saturated hydrocarbons to less than 50% of their initial values (14). Further addition of solute has little effect. Figure 2 shows the effect of the addition of 2.5% by volume of carbon tetrachloride on $G(H_2)$, $G(HD)$, and $G(D_2)$ for mixtures of cyclohexane and cyclopentane containing 5% by volume of cyclohexane-d_{12}. Similar results were obtained using iodine instead of carbon tetrachloride. Once again $G(H_2)$ is a linear function of mixture composition. However, $G(HD)$ and $G(D_2)$ do not now show the marked solvent effect, i.e. the yields are practically independent of whether cyclopentane or cyclohexane forms the environment of the cyclohexane-d_{12} molecules. The hydrogen evolved from pure cyclohexane containing 5% cyclohexane-d_{12} is 2.4 atom % in deuterium (Table I), while for cyclopentane the corresponding figure is 2.8 atom %. Carbon tetrachloride or iodine have no effect on the deuterium content in the case of cyclohexane but cause a large decrease in the case of cyclopentane. While there is considerable energy transfer in cyclohexane-d_{12}–cyclopentane mixtures which can be suppressed by the addition of solute little or no energy transfer occurs in cyclohexane–cyclohexane-d_{12} mixtures.

The direction of the energy migration is consistent with the charge transfer reaction suggested by Hardwick (10) which takes place whilst the molecules are in the ionized state, i.e. between the time of ionization and that of charge neutralization.

[3] $$C_5H_{10} \rightsquigarrow C_5H_{10}^+ + e$$

[4] $$C_5H_{10}^+ + C_6D_{12} \rightarrow C_5H_{10} + C_6D_{12}^+$$

[5] $$C_6D_{12}^+ + e \rightarrow C_6D_{12}^* \rightarrow D_2, HD \ldots$$

The first ionization potentials of cyclohexane and cyclopentane are different in the correct direction by about 0.5 eV, but since this is an effect observed so far with only one indicator molecule, cyclohexane-d_{12}, judgment must be reserved.

From a study of the effect of iodine and benzene on the H_2, HD, and D_2 yields from cyclohexane containing small amounts of cyclohexane-d_{12}, Dyne and Jenkinson (15) showed that no sharp distinction could be drawn between the residual hydrogen yield and the inhibitable hydrogen yield. Table I shows that although the addition of solute prevents energy transfer, the deuterium content (D_2 + HD) of the hydrogen evolved from pure cyclohexane containing 5% cyclohexane-d_{12} does not change. In particular, the yield of HD is still high, signifying that bimolecular hydrogen formation still occurs. This would be the case if the residual yield were due to reactions occurring in spurs.

If no energy transfer occurs in cyclohexane–cyclohexane-d_{12} mixtures, then the low deuterium content (D_2 + HD) of the hydrogen evolved is due to an isotope effect. Most

Can. J. Chem. Downloaded from www.nrcresearchpress.com by 210.87.254.42 on 09/05/12
For personal use only.

of the deuterium is present as HD which must be formed in a second-order process. We can therefore postulate two intermediate species, X_H and X_D, which are formed from cyclohexane and cyclohexane-d_{12} respectively and which react in second-order processes to yield H_2, HD, and D_2.

[6] $$X_H + C_6H_{12} \rightarrow H_2 + \ldots$$

[7] $$X_H + C_6D_{12} \rightarrow HD + \ldots$$

[8] $$X_D + C_6H_{12} \rightarrow HD + \ldots$$

[9] $$X_D + C_6D_{12} \rightarrow D_2 + \ldots$$

The species X could be atoms, excited molecules, or ions, the only qualification being that they take part in a bimolecular reaction to yield H_2, HD, or D_2. At the low concentrations of cyclohexane-d_{12} used, reaction [9] can be neglected. Every X_D formed must therefore react as in [8], i.e. HD will be formed in reaction [8] in proportion to the electron fraction of cyclohexane-d_{12} present in the mixture. The formation of HD via X_D will therefore not be susceptible to an isotope effect. HD can also be formed via [7] which is competing with [6]. An isotope effect will favor [6] over [7] resulting in HD yields lower than expected from the mixture composition. The low HD yield observed in cyclopentane–cyclohexane-d_{12} containing small amounts of carbon tetrachloride is similarly explained.

(b) Dimeric Products

Figure 3 shows the yields of the three main dimers, bicyclohexyl, bicyclopentyl, and cyclopentylcyclohexane, at a dose rate of 1.66×10^{22} eV/l h. In agreement with Muccini

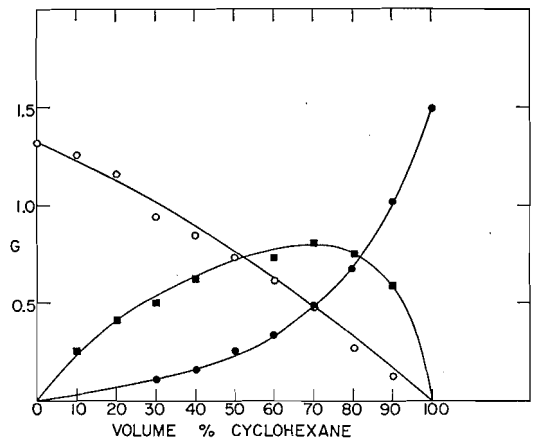

FIG. 3. The yields of bicyclohexyl, ●, bicyclopentyl, ○, and cyclopentylcyclohexane, ■, in cyclopentane–cyclohexane mixtures.

and Schuler (7) the yields are not as expected from the composition of the mixtures. More cyclopentyl groups are present than would be expected if the dimers were formed by a statistical mixing of radicals produced in the ratio of the electron fractions of the parent hydrocarbons. If radicals are produced according to the hydrocarbon electron fractions then the results are qualitatively in agreement with the radical transfer mechanism of reactions [1] and [2]. If [2] has a slightly greater rate constant than [1], then over the course of many such reactions before dimerization the concentration of cyclopentyl radicals will build up at the expense of the cyclohexyl radicals. If no radical transfer occurred, the yield of the mixed dimer, cyclopentylcyclohexane, would show a

Can. J. Chem. Downloaded from www.nrcresearchpress.com by 210.87.254.42 on 09/05/12
For personal use only.

maximum yield at very nearly equimolar hydrocarbon concentrations. In fact the maximum occurs in a mixture containing $\sim 70\%$ cyclohexane. This radical transfer mechanism is supported by dimer yields determined at the lower dose rate (1.43×10^{21} eV/l h). The cyclopentyl content of the dimer increases still further while the cyclohexyl content is correspondingly depleted. The maximum yield of the mixed dimer moves to even higher cyclohexane concentrations. A lowering of dose rate increases the time between formation of radicals and final dimerization, i.e. affords a greater time for change-of-identity reactions to occur.

The addition of iodine or carbon tetrachloride reduces the yield of dimers. In a previous paper we showed that at the solute concentrations used this reduction was probably due to a reaction with some precursor of the radicals rather than with the radicals themselves (8). The residual yields are of interest here. Figure 4 shows the measured dimer yields

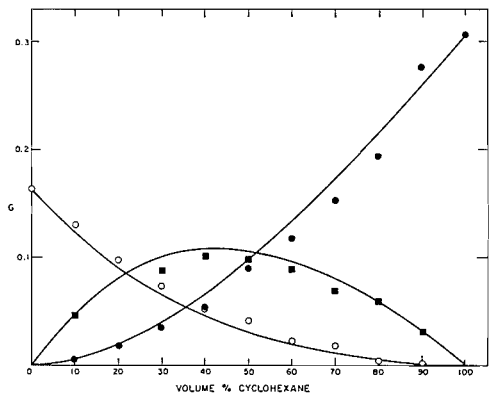

FIG. 4. The yields of bicyclohexyl, ●, bicyclopentyl, ○, and cyclopentylcyclohexane, ■, in cyclopentane–cyclohexane mixtures 0.0038 *M* in iodine. The solid lines are the "expected" values.

(points) together with the yields calculated by assuming a statistical combination of radicals (curves). These residual yields were obtained in the presence of 0.004 *M* iodine. The concentrations of the cyclohexyl and cyclopentyl radicals were calculated by assuming that they were proportional to the electron fractions of the parent hydrocarbons multiplied by the respective residual dimer yield in the pure hydrocarbons. The agreement between experiment and calculation is good. The mixed dimer yield in particular shows no evidence of radical transfer reactions. The residual yields are therefore formed according to the relative electron fractions (which are much the same as the relative mole fractions in this particular case) of the two hydrocarbons. The residual yields need not be formed by radical dimerization, but they cannot be due to freely diffusing species susceptible to solute attack. As in the case of the residual hydrogen yields the results are consistent with reactions occurring in spurs.

(c) Olefins

The precise mechanism of olefin formation in irradiated cyclohexane is not known. Evidence has been presented to show that there are at least two different processes, one which involves the disproportionation of cyclohexyl radicals (8) and one which involves the molecular detachment of hydrogen (13). The relative contributions of these two processes are not known, and other mechanisms of olefin formation may also be important. Cyclopentene would similarly be expected to be formed in more than one process. The

Can. J. Chem. Downloaded from www.nrcresearchpress.com by 210.87.254.42 on 09/05/12
For personal use only.

olefin yields in mixtures of these two hydrocarbons cannot therefore be expected to show a simple behavior. Such is the case as shown in Fig. 5 for cyclohexene and in Fig. 6 for cyclopentene. The broken lines show the yields expected if the system behaved

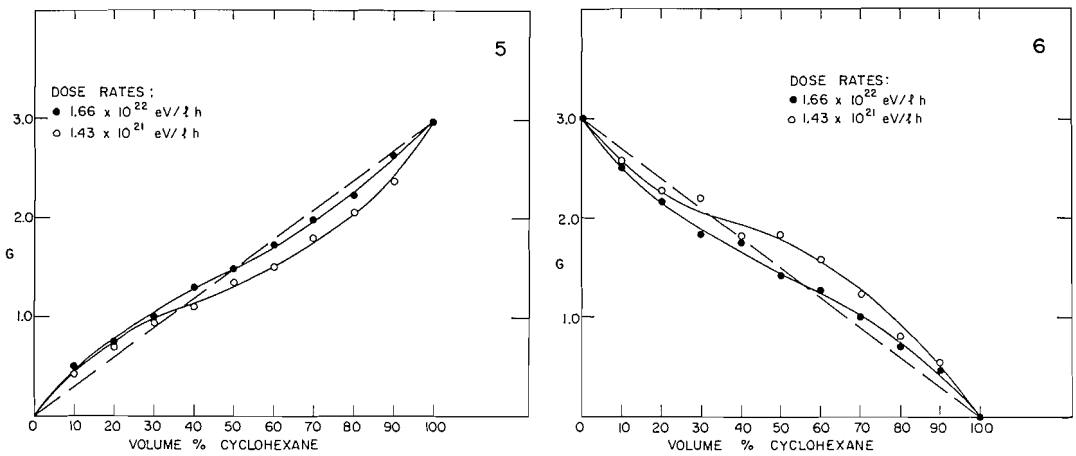

FIG. 5. The yields of cyclohexene in cyclopentane–cyclohexane mixtures.
FIG. 6. The yields of cyclopentene in cyclopentane–cyclohexane mixtures.

ideally. The cyclohexene yields are reduced at high cyclohexane concentrations but increased at low concentrations. The reverse is the case for cyclopentene.

The reduced cyclohexene yields and the increased cyclopentene yields at high cyclohexane concentrations are explicable in terms of the radical transfer reactions [1] and [2]. Since part of the olefin yield results from radical disproportionation, formation of cyclopentene will be favored at the expense of cyclohexene. With a decrease in dose rate an even greater deviation from the expected yields is found in accordance with this theory.

The enhanced yield of cyclohexene at low cyclohexane concentrations shows only a small dose-rate effect. Since the yield of cyclopentene is depressed in this region below the expected value, a mechanism other than one involving radical transfer must be responsible. Preferential formation of cyclohexene in disproportionation reactions cannot account for the effect since it would be dose-rate dependent. The effect can be correlated with the energy transfer process which accounted for the increased HD and D_2 yields described earlier. The energy which can be transferred must therefore result in cyclopentene or cyclohexene production without the prior formation of freely diffusing radicals.

ACKNOWLEDGMENTS

It is a pleasure to acknowledge the helpful advice and comments received from Dr. P. J. Dyne throughout this work and the critical comments of Dr. R. H. Betts on the contents of this paper.

REFERENCES

1. J. P. MANION and M. BURTON. J. Phys. Chem. **56**, 560 (1952).
2. M. BURTON and W. N. PATRICK. J. Phys. Chem. **58**, 421 (1954).
3. G. R. FREEMAN. J. Chem. Phys. **33**, 71 (1960).
4. J. A. STONE and P. J. DYNE. Radiation Res. **3**, 353 (1962).
5. P. J. DYNE and J. DENHARTOG. Can. J. Chem. **40**, 1616 (1962).
6. P. J. DYNE and J. DENHARTOG. Can. J. Chem. **41**, 1794 (1963).

Can. J. Chem. Downloaded from www.nrcresearchpress.com by 210.87.254.42 on 09/05/12
For personal use only.

7. G. A. MUCCINI and R. H. SCHULER. J. Phys. Chem. **64**, 1436 (1960).
8. J. A. STONE and P. J. DYNE. Can. J. Chem. **42**, 669 (1964).
9. P. J. DYNE and J. A. STONE. Can. J. Chem. **39**, 2381 (1961).
10. T. J. HARDWICK. J. Phys. Chem. **66**, 2132 (1962).
11. P. J. DYNE, J. DENHARTOG, and D. R. SMITH. Discussions Faraday Soc. **36**, 135 (1963).
12. J. R. NASH and W. H. HAMILL. J. Phys. Chem. **66**, 1097 (1962).
13. P. J. DYNE. J. Phys. Chem. **66**, 767 (1962).
14. W. H. HAMILL. *In* Comparative effects of radiation. *Edited by* M. Burton, J. S. Kirby Smith, and J. L. Magee. John Wiley & Sons, Inc., New York. 1960. p. 190.
15. P. J. DYNE and W. M. JENKINSON. Can. J. Chem. **38**, 539 (1960).

Can. J. Chem. Downloaded from www.nrcresearchpress.com by 210.87.254.42 on 09/05/12
For personal use only.

Can. J. Chem. Downloaded from www.nrcresearchpress.com by 210.87.254.40 on 09/05/12
For personal use only.

THE REACTION OF METHOXIDE ION WITH PERFLUOROCYCLOPENTENE

RICHARD F. STOCKEL, MICHAEL T. BEACHEM, AND FREDERIC H. MEGSON
American Cyanamid Co., Bound Brook, New Jersey

Received June 16, 1964

ABSTRACT

The reaction of methoxide ion with perfluorocyclopentene gave two major components. These have been identified as 1-fluoro-2-methoxyhexafluorocyclopentene (II*f*) and 1,2-dimethoxyhexafluorocyclopentene (II*e*).

A third component (3-methoxy-2,4,4,5,5-pentafluoro-2-cyclopenten-1-one (VII)) was isolated and a structure is proposed based on n.m.r. evidence.

A list of carbon–carbon double bond stretch frequencies is given for a number of 1,2-disubstituted perfluorocyclopentenes which follow the electronegativities of the atoms adjacent to the double bond.

INTRODUCTION

While the four- (1) and five-membered (2) 1,2-dichlorofluorocycloalkenes (I*a*, I*b*) gave the mono- (II*a*, II*b*) and tri-substituted (III*a*, III*b*) unsaturated ethers on treatment with methoxide ion, perfluorocyclobutene (3) (I*c*) yielded unexpectedly the 1,2-dimethoxy (II*d*) and the mono derivative (II*c*). For the latter procedure no trimethoxy compound was detected. Recently, a low yield of the dimethoxy derivative (4) (IV*a*) was obtained by

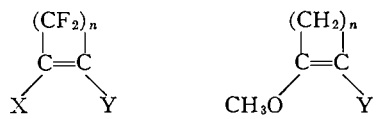

I*a*. $n = 2$, X = Y = Cl
I*b*. $n = 3$, X = Y = Cl
I*c*. $n = 2$, X = Y = F
I*d*. $n = 3$, X = Y = F

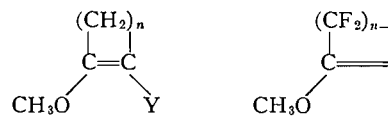

II*a*. $n = 2$, Y = Cl
II*b*. $n = 3$, Y = Cl
II*c*. $n = 2$, Y = F
II*d*. $n = 2$, Y = OCH_3
II*e*. $n = 3$, Y = OCH_3
II*f*. $n = 3$, Y = F

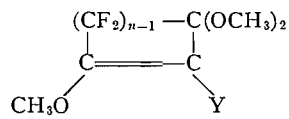

III*a*. $n = 2$, Y = Cl
III*b*. $n = 3$, Y = Cl
III*c*. $n = 3$, Y = F

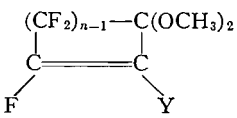

IV*a*. $n = 3$, Y = Cl

treating 1,2-dichlorohexafluorocyclopentene-1 (I*b*) with methoxide ion. This was found to be an extremely reactive intermediate because of the vinyl fluoride structure and it was easily converted to the more stable trimethoxy compound (III*b*).

DISCUSSION

To determine whether perfluorocyclobutene (I*c*) behaved anomalously with methoxide ion in comparison with the 1,2-dichlorofluorocycloalkenes, the reaction was studied with perfluorocyclopentene (I*d*) as the substrate. By the consecutive addition of two equivalents of methoxide ion to one equivalent of olefin at low temperature, a mono- and a di-alkoxide derivative were found to be the major components. These were (II*f*) and (II*e*), respectively, determined by analysis and infrared spectroscopy.

Thus both the perfluoro and 1,2-dichloro alicyclic olefins undergo a similar S_N2 for the first step by what is believed to be an addition–elimination mechanism (1, 5). The second methoxide ion must go via another addition–elimination with the perfluorocyclic olefin, while it is known that the 1,2-dichloro derivative undergoes an S_N2' (6) as the second step. The difference is that a vinyl fluoride is much more reactive towards nucleophilic dis-

placement than a vinyl chloride (5). Another factor is steric hindrance. Chlorine is much more bulky than fluorine, and this also contributes to the difference in mechanism.

From the experimental data it is obvious that the 1,2-dialkoxy derivative is stable towards further nucleophilic displacement under these conditions because the theoretical amount of base is not completely consumed.

From the second fraction a minor component ($\cong 4\%$) was obtained by a vapor-phase chromatographic (v.p.c.) Autoprep.* While analysis was inconclusive, both the infrared and n.m.r. spectra† were obtained and a structure was rationalized.

From the physical data three structures were possible, V, VI, or VII. The infrared

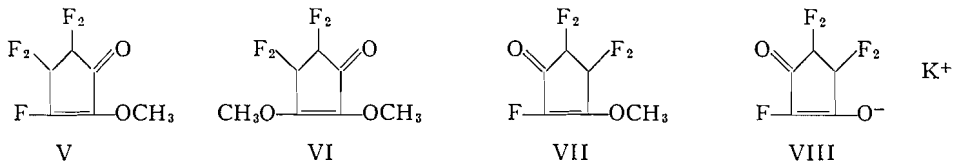

spectrum showed 3 H—C stretch bands at 3.35, 3.42, and 3.55 μ; a C—O—C stretch at 8.82–8.93 μ; a $\rangle C{=}O$ at 5.68 μ; and a $\rangle C{=}C\langle$ stretch at 5.98 μ. This information can fit any of the above structures; however, the fluorine n.m.r. of this component led to a more concrete decision. The spectrum showed a doublet (splitting $\cong$ 13.8 c.p.s.) at 121.0 ϕ, a doublet (splitting $\cong$ 5.4 c.p.s.) at 127.2 ϕ, and a complex band at 140.6 ϕ. Intensity ratio was 2:2:1. Therefore, VI was ruled out. A decision between V and VII was difficult, but it was significant that the average of the two F to F_2 couplings was about the same as that for compound VIII.‡ On this basis structure VII was favored. It should be noted that very little coupling occurred between the two F_2's and that the single F coupled appreciably to the OCH_3.

It is proposed that during the reaction, work-up, or distillation the allylic fluorines were hydrolyzed to a carbonyl group by the presence of water, which was not rigorously excluded. Alternately, structure VII could have come from the hydrolysis of the tri-substituted unsaturated ether (III*c*). This is the same type of product observed with the reaction of methoxide ion with the 1,2-dichlorofluorocycloalkenes (I*a*, I*b*). This would mean that two separate reaction paths are operating at the same time, with the latter resulting in the minor product. More studies are contemplated on this point in subsequent work.

Finally, a list of double bond absorptions for symmetrical and unsymmetrical 1,2-disubstituted hexafluorocyclopentene-1 is given. It is apparent from Table I that the 1,2-dimethoxy derivative is intermediate in relation to the 1,2-dichloro and 1,2-difluoro double bond position. The frequency of the double bond absorption follows the electronegativity (7) of the adjacent atoms, i.e., the order of increasing frequency is F > O > Cl. The magnitude of $\Delta\nu$ is also in this order. It is interesting to note that the 1,2-dichloro compound has approximately the same carbon–carbon double bond stretch as found in cyclopentene (10), so that the double bond order is not reduced to any degree by resonance effects involving chlorine.

**An Aerograph Autoprep was used with the following conditions: nonlinear program 70–135°, oven setting 40, on column injection, $\frac{1}{4}$ cc sample, 20 × $\frac{3}{8}$ in. SE 30 Silicon on 45/60 Chromosorb P column, flow rate 200 cc/min, retention time 6.84 min.*

†A Varian HR 60 operating at 56.4 mc run as a 10% solution using $CFCl_3$ *as an internal standard.*

‡The fluorine n.m.r. spectrum of this salt will be reported in another paper.

Can. J. Chem. Downloaded from www.nrcresearchpress.com by 210.87.254.40 on 09/05/12
For personal use only.

TABLE I

Compound	Infrared	Reference
	6.19 μ*	—
	6.00 μ	4
	5.85 μ	8
	5.70 μ	9
	5.80 μ	—
	5.90 μ	—

*A value of 6.13 was reported by C. O. Parker, J. Am. Chem. Soc. 81, 2183 (1950). However, a value of 6.19 μ was consistently obtained on a Perkin-Elmer Model 317 spectrophotometer. All spectra were run as films (neat).

EXPERIMENTAL

Reaction of Methoxide Ion and Perfluorocyclopentene

To 100 ml of methanol was added 4.6 g (0.2 mole) sodium with stirring. When all of the sodium reacted, the solution was cooled with dry ice. Then 42.4 g (0.2 mole) of olefin was added over a 10 min period. After stirring for 1 h at approximately −40°, another equivalent of methoxide ion, 4.6 g (0.2 mole) sodium in 50 ml of methanol, was added. The solution was then allowed to stir for 5 h. The solution was then poured into water (≅ 400 ml) and the organic layer (lower) was isolated and washed twice with 50 ml water and dried over magnesium sulfate. The crude weight was 40.5 g, excluding volatile starting material.

Distillation, at atmospheric pressure, of the crude in a microapparatus gave two fractions: (1) 99–102°, (2) 144–151°. Neither fraction was found to be homogeneous by an F&M Model 500 VPC equipped with an automatic integrator. On a 10 ft 10% Silicon Gum Rubber on Chromosorb P column run as an isotherm at 125°, a total of three peaks was obtained in both fractions with the following retention times in minutes, II*f*, 2.04; VII, 2.48; II*e*, 2.70. The combined integrated peak areas of both fractions were 34.36, 4.14, 61.50%, respectively.

The two major components were easily separated by redistillation of their respective fractions. From fraction one, II*f* was obtained in analytical purity. It was identified as 1-methoxyheptafluorocyclopentene-1 by analysis and infrared spectroscopy. Its boiling point was 100–101° (uncorrected). η_D^{27} = 1.3323. The infrared spectrum gave the following bands: three C—H stretches at 3.30, 3.36, and 3.48 μ; C=C stretch at 5.80 μ; C—O—C stretch, broad 8.70–8.80 μ with other bands at 6.83, 7.30, 7.50, 7.71, 8.29, 9.63, 10.15, 10.74, and 11.44 μ.

Anal. Calcd. for $C_6H_3F_7O$: C, 32.15; H, 1.34. Found: C, 31.76; H, 1.75.

Component II*e* was similarly identified by redistillation of the second fraction. Its boiling point was 148–149° (uncorrected). η_D^{27} = 1.3658. The infrared spectrum gave the following bands: three C—H stretches at 3.30, 3.35, and 3.49 μ; C=C stretch 5.90 μ; C—O—C stretch, broad 8.80–8.90 μ with other bands at 6.80, 7.40, 7.51, 7.73, 8.27, 8.34, 9.50, 10.00, 10.65, and 11.52 μ.

Anal. Calcd. for $C_7H_6F_6O_2$: C, 35.60; H, 2.56. Found: C, 35.70; H, 2.73.

ACKNOWLEDGMENTS

We are obliged to Dr. J. E. Lancaster for running and interpreting the n.m.r. fluorine spectrum and Dr. Richard A. Parent for the isolation of the minor component.

Can. J. Chem. Downloaded from www.nrcresearchpress.com by 210.87.254.40 on 09/05/12
For personal use only.

REFERENCES

1. J. D. PARK, C. M. SNOW, and J. R. LACHER. J. Am. Chem. Soc. **73**, 2342 (1951).
2. A. L. HENNE and K. A. LATIF. J. Indian Chem. Soc. **30**, 809 (1953).
3. J. D. PARK, M. L. SHARRAH, and J. R. LACHER. J. Am. Chem. Soc. **71**, 2337 (1949).
4. E. T. MCBEE, D. L. CRAIN, R. D. CRAIN, L. R. BELOHLOV, and H. P. BRAENDLIN. J. Am. Chem. Soc. **84**, 3557 (1962).
5. E. F. SILVERSMITH and D. SMITH. J. Org. Chem. **23**, 427 (1958).
6. J. D. PARK, J. R. DICK, and J. R. LACHER. J. Org. Chem. **28**, 1154 (1963).
7. L. N. FERGUSON. The modern structural theory of organic chemistry. Prentice-Hall, Inc., New York. 1963. p. 541.
8. J. A. SEDLAK. Ph.D. Thesis, Ohio State University, Columbus, Ohio. 1960. p. 63.
9. A. L. HENNE and K. A. LATIF. J. Am. Chem. Soc. **76**, 610 (1954).
10. H. B. HENBEST, G. D. MEAKINS, B. NICKOLIS, and R. A. L. WILSON. J. Chem. Soc. 997 (1957).

Can. J. Chem. Downloaded from www.nrcresearchpress.com by 210.87.254.40 on 09/05/12
For personal use only.

Can. J. Chem. Downloaded from www.nrcresearchpress.com by 210.87.254.42 on 09/05/12
For personal use only.

ANIONIC POLYMERIZATION OF ISOPRENE[1]

D. J. WORSFOLD AND S. BYWATER
Applied Chemistry Division, National Research Council, Ottawa, Canada
Received April 8, 1964

ABSTRACT

The polymerization of isoprene with butyllithium in cyclohexane has been studied. The initiation reaction was found to be complex; plots of conversion of butyllithium against time are sigmoidal. The order with respect to the initiator was found to be between one-half and one. The order of the isolated propagation reaction in polyisoprenyllithium was found to be one-quarter and was correlated with a fourfold association of active chain ends determined by dilute solution light-scattering measurements.

The major effect of tetrahydrofuran on the reaction was the great increase of the initiation rate. The kinetic order changes slowly with the addition of small amounts of tetrahydrofuran, suggesting that the aggregates are broken down with difficulty. The microstructure of the polymer has been determined by n.m.r. measurements and shows a steady transition from a largely 1:4 to a largely 3:4 structure as the polarity of the solvent is increased by the addition of tetrahydrofuran.

Very little attention has been paid to the initiation reaction in the polymerization of isoprene by *n*-butyllithium. Most studies of this system have been concerned with the structure of the polymer formed (1, 2) or with the kinetics of the propagation reaction (3, 4, 5) and the effect on both of additives. The reaction of *n*-butyllithium with both styrene (6) and 1,1-diphenylethylene (7) has been investigated in aromatic hydrocarbon solvents. It is found that when the solvent is cyclohexane, the kinetic behavior is considerably different for isoprene and also for styrene and butadiene (8).

The several published investigations of the propagation reaction have mostly acknowledged the difficulty of ascertaining whether the slow initiation reaction has gone to completion. By use of spectrophotometric measurements it is possible to determine more certainly when chain initiation is complete and hence to ensure that a true propagation rate can be measured. It is possible, also, to see the effect of only partial initiation on the propagation rate.

The microstructure of polyisoprene has been investigated, in the past, by infrared spectroscopy (9, 10) but the method is not always satisfactory, especially with anionic polymers. It is now possible to determine these structures by nuclear magnetic resonance n.m.r. (11) and, although this method still has some shortcomings, it supplements the infrared method. From these measurements, it seems necessary to modify previous ideas on these structures.

EXPERIMENTAL

The methods used to measure the reaction rates of *n*-butyllithium with isoprene were similar to those used in the past for other systems (6). The absorption band of polyisoprenyllithium in cyclohexane has a maximum at 270 mμ, ϵ 6 900, but to measure its concentration a wavelength of 275 mμ was used to avoid as far as possible the absorption of isoprene. Beers law was tested over the range 10^{-4}–10^{-2} *M*, the results showed a random scatter of ±5%. The isoprene concentration was measured at suitable lower wavelengths.

Cyclohexane was clarified by two passages through silica gel columns and stored in vacuum over calcium hydride. Before use it was transferred on the vacuum system to a flask containing butyllithium and from there to the reaction vessel.

[1]*Issued as N.R.C. No. 8135.*

Isoprene was fractionally distilled under nitrogen. Then, after it was degassed, it was distilled in the vacuum system onto butyllithium and allowed to stand for 15 min at room temperature. This was repeated three times. Distillation into a storage flask containing calcium hydride followed.

The *n*-butyllithium was supplied as a 15% hexane solution by the Foote Mineral Company.

Infrared spectra were measured on polymer films with a Perkin–Elmer model 21 spectrometer. The n.m.r. spectra were measured on a Varian Associates spectrometer at 56.4 mc/s with the polymer dissolved in either carbon tetrachloride or benzene.

The light-scattering measurements were made partly in a Brice-Phoenix instrument, and partly in a Sofica instrument in which angular scattering was also measured. The polymer concentrations were in the 0.1–0.6% range, and the carbanion concentration in the 10^{-5}–10^{-4} M range.

All reactions were made at 30 °C, and all reaction rates are in units of liters, moles, and minutes.

RESULTS AND DISCUSSION

Initiation

The increase of optical density at 275 mμ when isoprene and butyllithium are mixed together in cyclohexane can be used to measure the rate of formation of polyisoprenyllithium, as this has an absorption maximum at 270 mμ. It was found that the increase in optical density is not linear with time at the start of the reaction, but the rate of formation of the carbanion seems at first to gradually increase (Fig. 1). This initial stage is followed by a period where the concentration–time curve is linear. This could be artificial and may be caused by compensation of the apparent increase in active butyllithium by a decrease in isoprene concentration. Finally the rate decreases because of a decrease in butyllithium and isoprene concentrations. The curve is in fact sigmoidal.

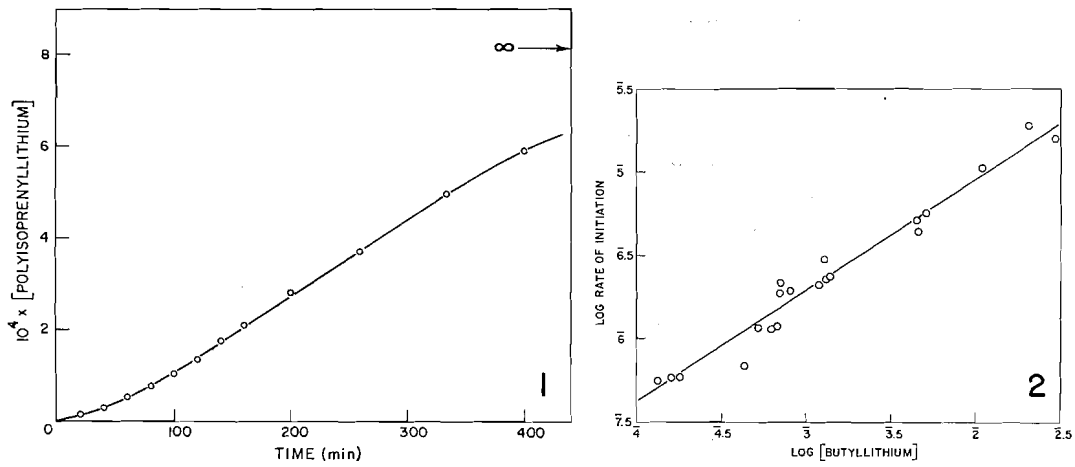

FIG. 1. Typical initiation reaction curve. [Butyllithium] = 1.18×10^{-3} M; [isoprene] = 0.60 M, at 30°. At ∞ not all the butyllithium had been consumed; a further addition of isoprene increased the polyisoprenyllithium concentration.

FIG. 2. Dependence of the linear part of the initiation reaction on the butyllithium concentration, at 30°.

Attempts were made to reduce this induction period by adopting even more rigorous techniques. For example, distilling the solvent and remaining monomer, from an already polymerizing mixture, onto fresh butyllithium in another part of the reaction vessel. But such methods did not remove the initial slow reaction. It was found that the slow reaction could be eliminated by breaking a bulb of air in the reaction vessel at the start of the reaction, sufficient oxygen being released to react with half the butyllithium. It is supposed that the lithium butoxide formed acts as a catalyst, the reaction in the absence of salts being very slow. The polyisoprenyllithium formed could itself act as a catalyst.

Can. J. Chem. Downloaded from www.nrcresearchpress.com by 210.87.254.42 on 09/05/12
For personal use only.

The reaction would then be autocatalytic and thus account for the initial increasing rate. It does, however, appear that the induction period is not caused by impurities and is a characteristic of initiation in cyclohexane.

If the apparently linear portion of the reaction curve is taken to be the rate of initiation, it is found that the reaction is close to first order in monomer and about 0.7 order in butyllithium (Fig. 2). There is considerable scatter in the points, and presumably the reaction is very sensitive to quite small amounts of adventitious salt-like impurities. In view of the complex nature of the reaction curve, these kinetic orders have no simple significance and give no clue to the mechanism of the reaction. The reaction is likely to be first order in monomer, but the order in butyllithium is unexpected.*

For the corresponding reaction in benzene solution of styrene and butyllithium the order in butyllithium is about one-sixth and can be correlated with the sixfold association of *n*-alkyllithiums in hydrocarbon solvents (12, 13, 14). With styrene in benzene no induction period in the initiation reaction is observable and the reaction must be less complex. In cyclohexane, however, styrene also exhibits an induction period similar to that for isoprene in the initiation. The apparent order in butyllithium, as determined by the apparently linear portion of the reaction curve, is also similar. Moreover, even the maximum rate is nearly two powers of ten lower than in benzene solution, indicating the reluctance of the reaction to take place in such a poor solvent for ionic species. Thus the presence of added salts or the increasing concentration of the polymer – lithium salt could well be thought of as providing centers of sufficient polarity to promote the conversion of the less polar butyllithium to the ionic polymer – lithium salt.

Propagation

The kinetics of the propagation reaction are far simpler. After all the butyllithium has reacted, the optical density at 275 mμ remains constant and it is then possible to follow the isolated propagation reaction by the decrease in the ultraviolet absorption of the residual isoprene or of a further addition of isoprene. It is found that the consumption of isoprene follows a first-order plot over at least three half-life times (Fig. 3).*

The order with respect to the initial concentration of butyllithium and, hence, the concentration of active chain ends is close to one-fourth. The rates are considerably more reproducible than those of the initiation reaction. The literature on this subject contains several values for this reaction order, which vary from one-half to one-sixth. A number of propagation rate constants from several authors have been plotted in Fig. 4 together with those from this work. The values of Sinn (4) were calculated from his 20° figures using his activation energy. Similarly the figures of Morton (15) were corrected to 30°. Only rates whose numerical values were given are used; both Sinn and Spirin *et al.* (3) have diagrams containing far more points which concur with the quoted values. There is a remarkable concordance among the various sets of results, particularly as the solvents differ, although all are hydrocarbons. The same kinetic behavior could be expected in different aliphatic hydrocarbons, but in toluene the rate might be expected to differ appreciably. The rates found by Morton are about 25% lower than the others, with the exception of one point. But this is not unexpected because reactions involving ions are very sensitive to solvents. The range of concentrations taken by Morton, however, really does not seem wide enough to allow us to say that the reaction order is appreciably different in hexane from that in the other solvents.

**The detailed rate data have been placed in the Unpublished Data Depository. Photocopies may be obtained upon request to Depository of Unpublished Data, National Science Library, National Research Council, Ottawa, Canada.*

Can. J. Chem. Downloaded from www.nrcresearchpress.com by 210.87.254.42 on 09/05/12
For personal use only.

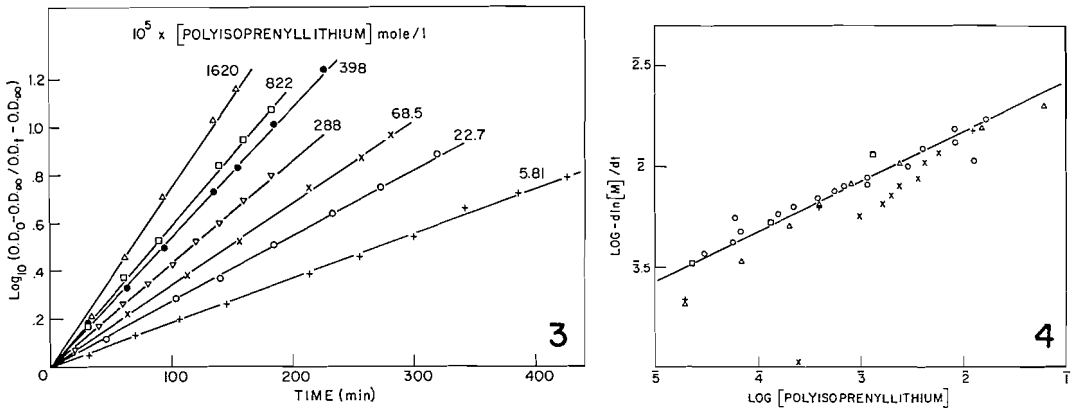

FIG. 3. First-order plots of the propagation reaction at various polyisoprenyllithium concentrations, at 30°.

FIG. 4. Dependence of the propagation rate on the polyisoprenyllithium concentration, at 30°. (△) Sinn *et al.* (4), in heptane solution; (×) Morton *et al.* (15), in hexane solution; (+) Spirin *et al.* (3), in heptane solution; (□) Spirin *et al.* (3), in toluene solution; (○) this work, in cyclohexane solution.

It was found that in the presence of an excess of butyllithium the propagation rate was depressed by appreciable amounts. When half the butyllithium was converted to polyisoprenyllithium, the propagation rate was half that expected from that concentration of polyisoprenyllithium. This suggests that there is some cross association of the butyllithium and the isoprenyllithium, which would also add to the complications in the initiation reaction. Morton has noted this cross association before (16) and V. Sinn has made a quantitative study of its effect on the propagation rate (17).

From the ratio of the rates of propagation and initiation, a several hundredfold excess of monomer would be required to complete initiation. The criterion for complete initiation of satisfactory first-order rate curves is of little value when the order in chain ends is so low, unless the reaction is followed for several half-life times. It is probably true to say that all reaction rates measured when the butyllithium concentration is greater than 10^{-2} M are suspect in the present work and that of others. Sinn (18) has also commented on this fact.

In all these studies the fractional order in polyisoprenyllithium has been attributed to polymer association caused by interaction of the ion-pair chain ends. Morton has made viscosity measurements on the 'living' and 'dead' polymerization solutions and from an extension of the bulk viscosity relation showed that the apparent degree of association was twofold (5), in agreement with his stated kinetic order. Unfortunately, this method can only give a ratio of weight average molecular weights, not the number averages which are really required, although the ratio of the two was probably quite close to one in Morton's work.

It is possible to use other methods of molecular weight determination to find the degree of association. Light-scattering measurements were made on several diluted polymerization solutions before and after the addition of methanol. The dilutions were effected by distillation of the solvent from one part of a complex all glass light-scattering cell to another. The whole process was carried out under vacuum with the apparatus first washed out by butyllithium solutions and rinsed as described for the vessels for the kinetic experiments. The results are shown in Table I. The calculated molecular weight is that derived from the monomer–catalyst ratio. In the second and third examples it was

Can. J. Chem. Downloaded from www.nrcresearchpress.com by 210.87.254.42 on 09/05/12
For personal use only.

checked against the polyisoprenyllithium concentration as measured spectrophotometrically. In the first experiment the conditions were such that chain initiation was incomplete. The observed molecular weights are much too high for this reason. Even in the last two experiments the molecular weight found for the terminated polymer is still somewhat higher than that calculated. Even under the most favorable conditions, which were chosen, chain initiation is barely completed before the monomer is consumed. This will lead to an $\bar{M}_W/\bar{M}_N$ ratio of about 1.3 in the polymer produced, which largely explains the results.

TABLE I

Molecular weights of 'living' and 'dead' polyisoprenes found by light scattering

Molecular weights		
Calculated	Killed	Living
27 000	89 000	142 000
48 000	77 000	188 000
58 000	70 000	257 000

The experiments show that the degree of association based on the calculated molecular weight of unassociated polymer is about four even at 10^{-5} M polyisoprenyllithium concentrations. This should be close to a ratio of number average molecular weights as the $\bar{M}_W/\bar{M}_N$ ratio will be less than 1.3 in the fourfold associated form. It is also clear from the first experiment that if chain initiation was incomplete, the polymer solution would show a low degree of association if based on measured molecular weights, presumably because butyllithium has taken the place of some polymer molecules in the associated species.

Effect of Tetrahydrofuran

The presence of ethers has been found to have a marked effect on the microstructure of the polymer produced with lithium based initiation. Also the polymerization rate has been reported greatly increased. The great increases in rate reported are undoubtedly due to the increased initiation rate, as is also suggested by the work of Kropacheva *et al.* (19). Normally initiation in cyclohexane at 30° will take hours but in the presence of ten molecules of tetrahydrofuran for every one of butyllithium, initiation is essentially complete in 15 min with 0.3 M monomer. At this level, however, tetrahydrofuran has only increased the propagation rate by 25%, at a 10^{-3} M concentration of chain ends, and a hundredfold excess is necessary to double the rate. This is the same order of magnitude as found by Morton (5) in hexane solution. It is found that at a tetrahydrofuran concentration of 7×10^{-3} M the kinetic order in chain ends is still low, about one-third or less, and even at 0.1 M tetrahydrofuran the order is still less than one, and averages about one-half over the range covered here (Table II). This indicates that the aggregates are not separated completely into ion-pairs until even greater concentrations are used. Thus it appears that the energy from ion-pair aggregation is very much greater than the solvation energy obtained from tetrahydrofuran.

Because of the small changes in rate it is not possible to carry out a full kinetic analysis of this system, as was done for the similar polymerization of styrene in benzene solution (24). Also the large amount of tetrahydrofuran necessary to complete the breakdown of aggregates would cause too large a change in the dielectric constant to be ignored. What

Can. J. Chem. Downloaded from www.nrcresearchpress.com by 210.87.254.42 on 09/05/12
For personal use only.

TABLE II

Propagation rates in the presence of tetrahydrofuran

[Polyisoprenyllithium] (moles/l × 10^4)	[THF] (moles/l × 10^4)	Rate (min^{-1} × 10^3)
2.94	7	7.95
11.3	7	9.86
1.23	70	4.84
2.44	70	5.83
3.56	70	7.26
9.11	70	9.90
15.5	70	12.7
31.2	70	14.6
62.2	70	15.0
0.151	1 000	1.66
0.155	1 000	1.75
1.41	1 000	7.05
2.10	1 000	8.5
4.53	1 000	17.7
6.54	1 000	18.4
15.8	1 000	21.2
110	1 000	61.0
127	1 000	53.2

evidence there is, however, does support Morton's contention that only a monoetherate is formed (5).

It has been shown (20) that in the presence of tetrahydrofuran the polyisoprenyl carbanion undergoes an isomerization. This takes about a day to complete when 1% tetrahydrofuran is present. Under these circumstances, measurements of the degree of association of reaction mixtures left to go to completion have little value when compared with kinetic studies.

Polymer Microstructure

The structure of the polymer formed from isoprene in hydrocarbon solvents by lithium based anionic initiators has been reported several times. Although the reported structures have always been high in *cis* 1:4 content and low in 3:4, the amount of *trans* 1:4 structures reported has varied. The normal method of determining structure has been by infrared analysis, but this presents considerable difficulties, both theoretical and practical, when determining a small amount of *trans* 1:4 structures in a predominantly *cis* 1:4 polymer, or any 1:4 in a highly 3:4 polymer. This is because the shape of the absorption peak is likely to be a function of the block length. Chen has shown (11) how n.m.r. measurements may be used to determine polyisoprene structures, and this method appears to be far more suitable for determining 1:4 structures. A complete analysis of the polymer structure may, in theory, be carried out but in practice this presents some difficulties with present equipment and a combination of infrared and n.m.r. studies is probably best. Nevertheless it still would be unrealistic to claim any great accuracy for the methods. All methods of analysis will fail to some extent for polymers made by some catalyst systems because of the presence of extraneous structures not included in the normal 1:4, 1:2, and 3:4 structures expected. This is particularly true for sodium and potassium initiated polymers (9, 20).

The structures found for variously prepared polyisoprenes are shown in Table III, using primarily the n.m.r. methods of Chen and supplementing them with infrared measurements. Several of the spectra are shown in Figs. 5 and 6. When the polymer had a low 3:4 content this was measured from the infrared spectrum and the ratio of the 1:4

Can. J. Chem. Downloaded from www.nrcresearchpress.com by 210.87.254.42 on 09/05/12
For personal use only.

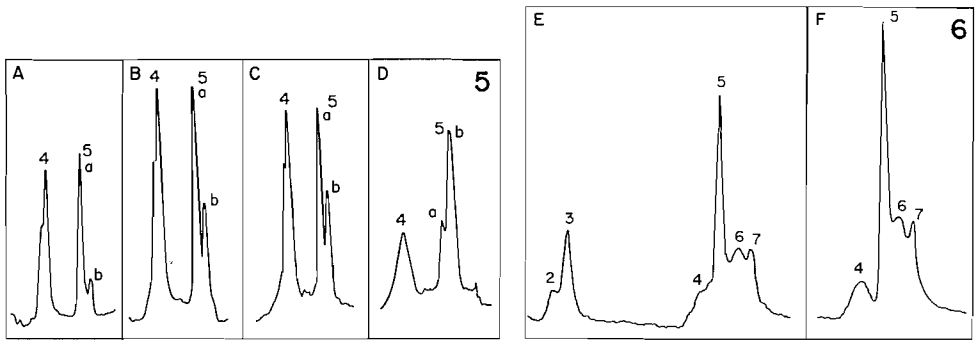

FIG. 5. The n.m.r. spectra of polyisoprenes dissolved in benzene. (A) Butyllithium in cyclohexane initiated, (B) butyllithium + lithium hydroxide initiated, (C) butyllithium + 2 moles THF initiated, (D) sodium in cyclohexane initiated.

FIG. 6. The n.m.r. spectra of polyisoprene initiated by butyllithium in THF. Polymer dissolved (E) in CCl_4, (F) in benzene.

structures estimated from the n.m.r. spectrum in benzene solution (Fig. 5). The peak assignments and numbers are those used by Chen (11). Peak 5 is resolved in benzene solution into 5*a* and 5*b* corresponding to the methyl group in *cis* 1:4 and the combined methyl groups of the *trans* 1:4 and 3:4 structures respectively. The polymers with low 1:4 content or mixed structures were analyzed entirely by the n.m.r. method. The peaks are seldom completely resolved, and sometimes considerable judgment is required to estimate the desired peak area. Nevertheless, where large differences from the infrared analyses occur the evidence for these differences is strong.

TABLE III

Polyisoprene microstructures

Initiator*	Solvent	Structure (%)			
		cis 1:4	*trans* 1:4	3:4	1:2
Butyllithium	Cyclohexane	80	15	5	—
Butyllithium + 2 moles THF	Cyclohexane	68	19	13	
Butyllithium + 15 moles THF	Cyclohexane	69		31	—
Butyllithium	Cyclohexane + 10% THF	—	26	66	9
Butyllithium	THF	—	—	74	26
Butyllithium + lithium hydroxide	Cyclohexane	68	27	5	—
Butyllithium + lithium butoxide	Cyclohexane	69	26	5	—
Sodium	Cyclohexane	29	29	42	—
Sodium	THF	—	—	82	18
Emulsion	Water (50°)	30	65	5	—

*Butyllithium concentration ca. 3×10^{-4} *M*.

The amount of *trans* 1:4 structures in the polymer formed in cyclohexane by butyllithium is rather higher than that usually found by infrared methods, which are weak at this point. The amount of 3:4 structures is in good agreement with that normally found. The effect of small amounts of tetrahydrofuran on the structure is seen to be less marked than normally found, the 3:4 content increasing less rapidly than found by Tobolsky and Rogers (2). This is partly because the more dilute solutions used in this investigation would cause less of the etherate to form. Also, in pure tetrahydrofuran it is seen that n.m.r. measurements show no 1:4 structures, although previous infrared studies have

Can. J. Chem. Downloaded from www.nrcresearchpress.com by 210.87.254.42 on 09/05/12
For personal use only.

shown considerable amounts. But infrared measurements are again unreliable in determining the low absorbance of the 1:4 bands compared with the strong 3:4 band. Chen also found very little 1:4 structure in a polymer formed in ether solution, so the absence of it in the even more polar tetrahydrofuran is not unexpected.

The sodium initiated polymer in tetrahydrofuran is even higher in 3:4 content than usually reported. This polymer is more stereospecific than is the Li/hydrocarbon polyisoprene, although it is the latter which is normally considered stereospecific because of its desirable structure. The polymer formed by sodium in cyclohexane shows a far more mixed *cis–trans* 1:4 structure than previously reported by infrared methods, but undoubtedly in this polymer extraneous structures are formed which interfere with the infrared measurements.

The structure found for the emulsion polymer was similar to that reported by other authors. The small amount of 1:2 structure probably present is not shown by the n.m.r. method.

From the structures found here, it is seen that the transition of structure from one anionic system to another, although large, is far less abrupt than previously thought. The Li/hydrocarbon polyisoprene is not overwhelmingly stereospecific and this initiator system with the addition of small amounts of tetrahydrofuran gives a more mixed structure, similar to the polymers formed in cyclohexane by sodium. The further transition to a solvent that is richer in tetrahydrofuran causes the polymer to become progressively enriched in 3:4 structures for both lithium and sodium initiation until the extreme ones formed in pure tetrahydrofuran have no 1:4 structures. Tobolsky has, however, reported before that little change in microstructure occurred after the abrupt change caused by the first small addition of tetrahydrofuran. The smoother change above is more in accord with the finding from ultraviolet studies of the polyisoprenyl carbanion formed in these systems (20). There appears to be very little change in the ionic nature of the carbon metal bond as the solvent and the alkali metal are changed, and little reason to expect abrupt changes in microstructure.

Why certain initiator systems should give certain structures is still not clear. Suggesting that the lithium/hydrocarbon system gives an intermediate of specific structure to explain the high *cis* 1:4 content, while the others do not, does not seem too satisfactory. It would appear that the equally high 3:4 content in the sodium/tetrahydrofuran system would deserve the formulation of a similar specific intermediate structure. The in-between ranges would then also need their intermediates, since their polymer microstructures are also quite well defined.

Both butadiene and isoprene give, with lithium-based initiators, polymers which are composed largely of 1:4 structures. Both monomers, when the solvent is made more polar, give polymers richer in pendant vinyl groups to the point where the polymers formed in tetrahydrofuran are almost entirely these structures. Similarly a change from lithium to sodium decreases the 1:4 structures. The effect must be caused by the increase in the effective cation size, because of solvation and the change from lithium to sodium. The high *cis* content in the largely 1:4 polyisoprene formed in hydrocarbon solvents by lithium-based reagents must be a function of the presence of the methyl group which distinguishes it from butadiene. The methyl group will modify the configuration of either the anion or the approaching monomer molecule.

Of interest is the effect of the presence of lithium compounds on the microstructure of the polymer formed by butyllithium in cyclohexane, as shown in Table III. A similar effect has been shown before for both butadiene and isoprene (21, 22). This suggests that

Can. J. Chem. Downloaded from www.nrcresearchpress.com by 210.87.254.42 on 09/05/12
For personal use only.

a complex of the polyisoprenyllithium and the lithium compound is an active polymerization agent in much the same way as the etherate is. But it also raises the question whether the free ion pair does in fact normally carry all the polymerization. Sinn has suggested, from very low-concentration studies (23), that the reaction is in fact more complex at least in that concentration range. But at such considerable dilutions as 10^{-7} M, the concentration of adventitious salts inevitably becomes significant and must affect the reaction.

ACKNOWLEDGMENTS

The authors wish to acknowledge the assistance of Dr. S. Brownstein in the interpretation of the n.m.r. spectra, and also for measuring these spectra.

REFERENCES

1. R. S. Stearns and L. E. Forman. J. Polymer Sci. **41**, 381 (1959).
2. A. V. Tobolsky and C. E. Rogers. J. Polymer Sci. **40**, 73 (1959).
3. Yu. L. Spirin, A. R. Gantmakher, and S. S. Medvedev. Dokl. Akad. Nauk SSSR, **146**, 368 (1962).
4. H. Sinn and F. Patat. Angew. Chem. **75**, 805 (1963).
5. M. Morton, L. J. Fetters, and E. E. Bostick. J. Polymer Sci. C, **1**, 311 (1963).
6. D. J. Worsfold and S. Bywater. Can. J. Chem. **38**, 1891 (1960).
7. A. G. Evans and D. B. George. J. Chem. Soc. 4653 (1961).
8. A. F. Johnson and D. J. Worsfold. To be published.
9. J. L. Binder and H. C. Ranshaw. Anal. Chem. **29**, 503 (1957).
10. W. S. Richardson and A. Sacher. J. Polymer Sci. **10**, 353 (1953).
11. H. Yu Chen. Anal. Chem. **34**, 1134, 1793 (1962).
12. T. L. Brown and M. T. Rogers. **79**, 1859 (1957).
13. F. Hein and H. Schram. Z. Physik. Chem. **151**, 234 (1930).
14. D. Margerison and J. P. Newport. Trans. Faraday Soc. **59**, 2058 (1963).
15. M. Morton, E. E. Bostick, R. A. Livigni, and L. J. Fetters. J. Polymer Sci. A, **1**, 1735 (1963).
16. M. Morton, E. E. Bostick, and R. Livigni. Rubber Plastics Age, **42**, 397 (1961).
17. V. Sinn and J. Minoux. Compt. Rend. **251**, 2020 (1960).
18. H. Sinn and W. Hofmann. Makromol. Chem. **56**, 234 (1962).
19. E. N. Kropacheva, B. A. Dolgoplosk, and E. M. Kuznetsova. Dokl. Akad. Nauk SSSR, **130**, 1253 (1960).
20. S. Bywater, A. F. Johnson, and D. J. Worsfold. Can. J. Chem. **42**, 1255 (1964).
21. V. A. Kropachev, B. A. Dolgoplosk, and N. I. Nikolaev. Dokl. Akad. Nauk SSSR, **115**, 516 (1957).
22. H. Sinn, C. Lundberg, and K. Kirchner. Angew. Chem. **70**, 744 (1958).
23. H. Sinn and O. T. Onsager. Makromol. Chem. **55**, 167 (1962).
24. S. Bywater and D. J. Worsfold. Can. J. Chem. **40**, 1564 (1962).

Can. J. Chem. Downloaded from www.nrcresearchpress.com by 210.87.254.42 on 09/05/12
For personal use only.

Can. J. Chem. Downloaded from www.nrcresearchpress.com by 210.87.254.40 on 09/05/12
For personal use only.

CARBONYL AND THIOCARBONYL COMPOUNDS

VIII.[1] SYNTHESIS OF FLUORENE ETHERS BY THE ACTION OF TETRAHALO-*o*-BENZOQUINONES

N. LATIF AND N. MISHRIKY
National Research Centre, Dokki, Cairo, U.A.R.

Received February 7, 1964

ABSTRACT

The halogenated fluorene ethers I*c*–I*f* are directly produced by the action of tetrachloro- and tetrabromo-*o*-benzoquinone on the corresponding halofluorene in boiling dry benzene. The preparation of the fluorene ethers by the action of tetrahalo-*o*-benzoquinones on 2-chloro- and 2,7-dichloro-fluorenone hydrazone is described. The ketohydrazones are readily oxidized by mercuric oxide to the corresponding 9-diazofluorenes which react readily with the haloquinones yielding the methylene ethers.

Cyclic ethers have become important commercial materials for use both as synthetic intermediates and as solvents and this has directed the attention of various authors to study the chemistry of this group of compounds in more detail. The chemistry of halogenated cyclic ethers was the object of various investigators in this laboratory. It has been shown (1) that the fluorene ethers, I*a* and I*b*, can be directly synthesized by the action of tetrachloro- and tetrabromo-*o*-benzoquinone, respectively, on fluorene. In an attempt to generalize this reaction which provides a new and simple method for the direct synthesis of fluorenylidene cyclic ethers, the action of tetrahalo-*o*-benzoquinones on 2-chloro- and 2,7-dichloro-fluorene was investigated. It was found that the methylene ethers I*c* and I*e* are readily produced when tetrachloro-*o*-benzoquinone is allowed to react with the corresponding halofluorene in boiling dry benzene. The bromo analogues, I*d* and I*f*, are obtained similarly when using tetrabromo-*o*-benzoquinone. The constitution of the fluorene ethers is based on their lack of color, on analytical data, and on their

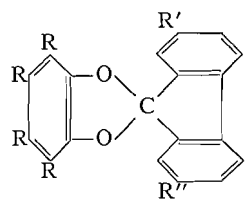

I*a*. R = Cl, R′ = R″ = H.
I*b*. R = Br, R′ = R″ = H.
I*c*. R = R′ = Cl, R″ = H.
I*d*. R = Br, R′ = Cl, R″ = H.
I*e*. R = R′ = R″ = Cl.
I*f*. R = Br, R′ = R″ = Cl.

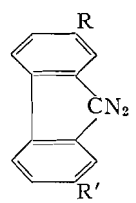

II*a*. R = Cl, R′ = H.
II*b*. R = R′ = Cl.

formation from either the halofluorene itself or its corresponding 9-diazo derivative. Thus, I*c*–I*f* are produced in excellent yield by the action of 2-chloro- (II*a*) and 2,7-dichloro-9-diazofluorene (II*b*) on the corresponding tetrahalo-*o*-benzoquinone. The formation of methylene ethers by the action of diazoalkanes on tetrahalo-*o*-benzoquinones is well established (2). The 9-diazofluorenes are readily produced by oxidizing the corresponding

[1]*For Part VII of this series see N. Latif and I. Fathy, J. Org. Chem. 27, 1633 (1962).*

fluorenone hydrazone with yellow mercuric oxide. The hydrazones are prepared by the action of hydrazine hydrate on the corresponding fluorenone in *n*-butanol. The 2-chlorofluorenone hydrazone obtained is different from the product, described by Warren (3), which was obtained when the reaction was carried out in ethanol. However, both compounds give the same diazofluorene upon oxidation. It has been shown (3) that some 2-substituted fluorenones, such as 2-iodo- and 2-cyano-fluorenone, yield two different hydrazones when they are allowed to react with hydrazine hydrate in ethanol. In each case, both hydrazones yielded the same diazofluorene upon oxidation.

In a previous report (4) it has been shown that methylene ethers are directly produced by the action of tetrahalo-*o*-benzoquinones on ketohydrazones. In the present investigation it is found that 2-chloro- and 2,7-dichloro-fluorenone hydrazone react readily with tetrachloro- and tetrabromo-*o*-benzoquinone to give directly I*c*–I*f*, respectively, according to the scheme below. The production of the corresponding tetrahalocatechol in this reaction together with evolution of gas supports the suggested mechanism.

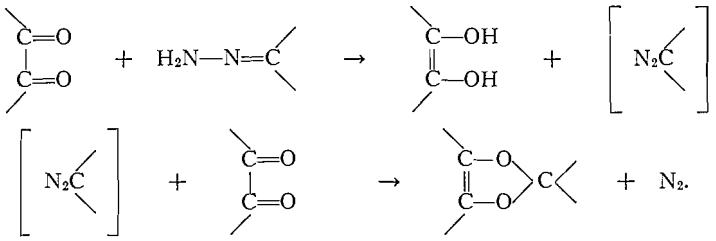

EXPERIMENTAL

Melting points were not corrected. Microanalyses were performed by A. Bernhardt, Germany, and by the microanalysis unit, National Research Centre, Cairo.

Preparation of 2-Chlorofluorenone Hydrazone

A solution of hydrazine hydrate (98–99%, 1.5 ml) and 2-chlorofluorenone (5) (2 g) in the least amount of *n*-butanol, was refluxed for 3 h, filtered while hot, concentrated, and left to cool. The product obtained was filtered off, washed with a few milliliters of methanol, and recrystallized from the same solvent to give 2-chlorofluorenone hydrazone (1.7 g) as yellow crystals, m.p. 145–146 °C.

Anal. Calcd. for $C_{13}H_9N_2Cl$: C, 68.42; H, 3.94; N, 12.28; Cl, 15.35. Found: C, 68.48; H, 4.11; N, 12.92; Cl, 14.53.

Preparation of 2,7-Dichlorofluorenone Hydrazone

This was obtained from 2,7-dichlorofluorenone (6) as yellow crystals, m.p. 175–176 °C.

Anal. Calcd. for $C_{13}H_8N_2Cl_2$: C, 59.31; H, 3.04; N, 10.64; Cl, 26.99. Found: C, 59.75; H, 3.26; N, 10.05; Cl, 26.06.

Preparation of 2-Chloro-9-diazofluorene (IIa)

2-Chlorofluorenone hydrazone (2 g) was oxidized with yellow mercuric oxide in the presence of ethanolic potassium hydroxide, according to the method described by Schönberg *et al.* (7). The diazo compound was obtained (1.6 g) as red crystals (from ether) which melted with vigorous decomposition at about 120 °C. The diazo compound is identical with that obtained by Warren (3).

Preparation of 2-Chloro-9-(tetrachloro-o-phenylenedioxy)fluorene (Ic)

Tetrachloro-*o*-benzoquinone (8) (1.2 g) was added in portions to a solution of 2-chloro-9-diazofluorene (1.1 g) in dry benzene (15 ml). A vigorous reaction with evolution of gas occurred after each addition. When all the quinone had been added, a solid crystalline product separated after a few minutes. This was filtered off, washed with acetone, and recrystallized from the same solvent to give I*c* (1.5 g) as colorless crystals, m.p. 281–282 °C.

Anal. Calcd. for $C_{19}H_7O_2Cl_5$: C, 51.35; H, 1.57; Cl, 39.98. Found: C, 51.83; H, 1.81; Cl, 38.87.

Preparation of 2-Chloro-9-(tetrabromo-o-phenylenedioxy)fluorene (Id)

Tetrabromo-*o*-benzoquinone (9) (2.1 g) was added to an ethereal solution of 2-chloro-9-diazofluorene (1.11 g) as above. The separated product was washed with acetone and crystallized from benzene to give I*d* as colorless crystals, m.p. 325-326 °C.

Can. J. Chem. Downloaded from www.nrcresearchpress.com by 210.87.254.40 on 09/05/12
For personal use only.

Anal. Calcd. for $C_{19}H_7O_2ClBr_4$: C, 36.65; H, 1.12; Cl, 5.62; Br, 51.44. Found: C, 37.38; H, 1.18; Cl, 5.66; Br, 51.29.

Reaction of Tetrachloro-o-benzoquinone with 2-Chlorofluorene

A solution of the quinone (2.4 g) and 2-chlorofluorene (10) (2.1 g) in dry benzene (30 ml) was refluxed (protected from moisture) for 6 h. The benzene was then evaporated to dryness under reduced pressure and a few ml of ether was added to the oily residue. The solid which separated was washed with acetone and crystallized from the same solvent to give I*c* (1.1 g). The infrared spectrum of the substance is identical with that obtained by the action of 2-chloro-9-diazofluorene on the quinone.

The bromo analogue I*d* was obtained in a similar manner by the action of tetrabromo-*o*-benzoquinone.

Reaction of Tetrachloro-o-benzoquinone with 2-Chlorofluorenone Hydrazone

The hydrazone (1.2 g) was added in small portions to a solution of the quinone (2.4 g) in dry ether (20 ml). When all the quinone had been added, the reaction mixture was refluxed for 10 min. The solid which separated (0.8 g) was crystallized from acetone and proved to be I*c*.

When tetrabromo-*o*-benzoquinone was used instead of the chloroquinone, I*d* was similarly obtained.

Preparation of 2,7-Dichloro-9-diazofluorene (IIb)

This was prepared as usual by oxidizing 2,7-dichlorofluorenone hydrazone with yellow mercuric oxide in benzene. It was obtained as light-red crystals (from ether) which melted with decomposition at about 160 °C.

Anal. Calcd. for $C_{13}H_6N_2Cl_2$: C, 59.77; H, 2.29; N, 10.72; Cl, 27.20. Found: C, 60.35; H, 2.62; N, 11.03; Cl, 26.02.

Preparation of 2,7-Dichloro-9-(tetrachloro-o-phenylenedioxy)fluorene (Ie)

Tetrachloro-*o*-benzoquinone (1.2 g) was added to a solution of II*b* (1.3 g) in dry benzene (15 ml), as in the case of the monochloro derivative. The reaction mixture was then warmed on a water bath for 15 min. The crystalline solid which separated on cooling was recrystallized from acetone to give I*e* (1.7 g) as colorless crystals which melted above 360 °C.

Anal. Calcd. for $C_{19}H_6O_2Cl_6$: C, 47.59; H, 1.25; Cl, 44.46. Found: C, 47.94; H, 1.53; Cl, 43.68.

Preparation of 2,7-Dichloro-9-(tetrabromo-o-phenylenedioxy)fluorene (If)

This was prepared from tetrabromo-*o*-benzoquinone (2.1 g) and II*b* (1.3 g), as in the case of I*e*. It was obtained as colorless crystals (2.4 g) from benzene, m.p. 355–357 °C.

Anal. Calcd. for $C_{19}H_6O_2Cl_2Br_4$: C, 34.7; H, 0.91; total halogen, 59.50. Found: C, 35.29; H, 1.09; total halogen, 58.42.

Reaction of Tetrachloro-o-benzoquinone with 2,7-Dichlorofluorene

A solution of the quinone (2.4 g) and the fluorene (11) (2.3 g) in dry benzene (30 ml) was refluxed for 6 h and worked up, as in the case of monochlorofluorene. The product which separated was crystallized from acetone to give I*e* (1.3 g). The infrared spectrum of the product is identical with that of the product obtained by the action of II*b* on the quinone.

When using tetrabromo-*o*-benzoquinone instead of the chloro derivative, the bromo analogue I*f* was obtained.

Reaction of Tetrachloro-o-benzoquinone with 2,7-Dichlorofluorenone Hydrazone

The quinone (2.4 g) and the hydrazone (1.3 g) were allowed to react together, as described in the case of the monochloro derivative. The product (0.85 g) was crystallized from acetone and proved to be I*e*.

When tetrabromo-*o*-benzoquinone was used in this experiment, the bromo analogue I*f* was similarly produced.

REFERENCES

1. N. LATIF, I. FATHY, N. MISHRIKY, and A. ATALLAH. J. Org. Chem. **25**, 1618 (1960).
2. A. SCHÖNBERG and N. LATIF. J. Chem. Soc. 446 (1952). N. Latif and I. Fathy. Can. J. Chem. **37**, 863 (1959).
3. K. D. WARREN. J. Chem. Soc. 1412 (1961).
4. N. LATIF and I. FATHY. J. Org. Chem. **24**, 1883 (1959).
5. P. CHANUSSOT. Anales Asoc. Quim. Arg. **15**, 216 (1927); Chem. Abstr. **22**, 776 (1928).
6. J. SCHMIDT and H. WAGNER. Ann. **387**, 161 (1912).
7. A. SCHÖNBERG, I. W. AWAD, and N. LATIF. J. Chem. Soc. 1368 (1951).
8. C. L. JACKSON and R. D. MACLAUREN. Am. Chem. J. **37**, 7 (1907).
9. TH. ZINCKE. Ber. **20**, 1777 (1887).
10. CH. COURTOT and C. VAGNATI. Compt. Rend. **184**, 1179 (1927); Chem. Abstr. **21**, 3616 (1927).
11. W. R. HODGKINSON and F. E. MATTHEWS. J. Chem. Soc. **43**, 170 (1883).

Can. J. Chem. Downloaded from www.nrcresearchpress.com by 210.87.254.40 on 09/05/12
For personal use only.

Can. J. Chem. Downloaded from www.nrcresearchpress.com by 210.87.254.42 on 09/05/12
For personal use only.

A STUDY OF THE HYPOCHLORINATION OF STYRENE

PREPARATION OF CHLOROHYDRINS IN AQUEOUS ACETONE

GENE SUMRELL,[1] BERT M. WYMAN, RONALD G. HOWELL, AND MACK C. HARVEY
Research Department, El Paso Natural Gas Products Company, El Paso, Texas

Received June 29, 1964

ABSTRACT

A study has been made of the hypochlorination of styrene and of the by-products which accompany the formation of styrene chlorohydrin. A process was developed utilizing hypochlorination in aqueous acetone which gave a yield of 72% of the chlorohydrin. Application of this procedure was extended to several other olefins with good results.

Because of a need for substantial quantities of styrene chlorohydrin for use as an intermediate in other work, we have investigated in some detail its preparation from styrene. Frisch (1) claims the production of approximately equal quantities of the chlorohydrin and dichloride of styrene by the passage of chlorine into an aqueous suspension of styrene in the presence of sodium bicarbonate. The yield of chlorohydrin was determined indirectly by conversion to styrene oxide and fractionation to separate the oxide from accompanying styrene dichloride. Since the dichloride and chlorohydrin of styrene are readily separable by fractionation (1) and since the former may, in turn, be hydrolyzed to the chlorohydrin, the simple method of Frisch for converting styrene to the chlorohydrin was attractive to us and served as a starting point in our work.

We were disappointed to learn early in this work that a large percentage of the material reported as styrene oxide by Frisch was actually β-chlorostyrene, which distills at essentially the same temperature as styrene oxide, and that the yield of chlorohydrin was far less than reported by Frisch. A typical run gave the following yields of products: β-chlorostyrene, 20%; styrene dichloride, 59%; and styrene chlorohydrin, 6%.

The possibility occurred to us that better results in hypochlorinating styrene by directly adding chlorine in the presence of water might be achieved if we also had present an inert water-miscible organic material which would keep the styrene and water in one phase or, at least, greatly increase the amount of water present in the same phase with the styrene. A number of such solvents were investigated and all gave improved yields of styrene chlorohydrin. However, acetone proved to be far superior to the others. The yields of products from a typical run, described in the experimental section, were styrene chlorohydrin, 72%; styrene dichloride, 13%; and β-chlorostyrene, 7%.

Similar work with cyclohexene gave a yield of 69% (isolated as the epoxide) of the chlorohydrin and 15% of the dichloride. Application of the aqueous acetone method to 1-pentene resulted in a yield of 66% of the mixed chlorohydrins (isolated as the epoxide) and 27% of the dichloride.

Investigation of the higher boiling residue from the cyclohexene chlorohydrin preparation showed it to be composed primarily of bis(2-chlorocyclohexyl) ether (II). This material undoubtedly results from the reaction of chlorohydrin already present with the chloronium intermediate, I, resulting from the initial reaction of olefin and chlorine (3) to give the ether, instead of the normal reaction with water to give the the chlorohydrin.

[1]*To whom inquiries should be directed. Present address: Southern Regional Research Laboratory, P.O. Box 19687, New Orleans, Louisiana, 70119.*

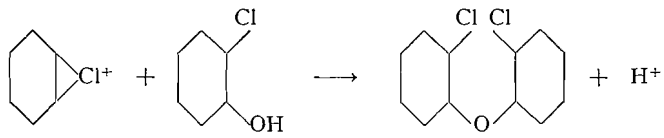

I II

Attempts were not made in our work to isolate ethers analogous to II from the higher boiling residues obtained with 1-pentene and styrene. However, cursory investigation by infrared spectroscopy indicated the presence of ether linkages, suggesting that analogs of II were in all likelihood present.

A cursory investigation was made of the conversion of gaseous olefins to their chlorohydrins by the aqueous acetone technique described in this paper. Such chlorohydrins are conventionally prepared from the olefin and chlorine in sufficient water to give a 5% solution of the resulting chlorohydrin, with yields of 60–70% for the C_4-alkenes and 80% for propylene. We found that in the presence of acetone the volume of water could be greatly reduced without sacrifice of yield. For example, an 80% yield of the chlorohydrin was obtained when 1 mole each of propylene and chlorine were passed into a mixture of 200 ml of water and 300 ml of acetone, a combined volume of only a quarter that required for a similar yield of chlorohydrin with water alone.

During our work with styrene, we learned that the styrene chlorohydrin, produced either by direct chlorination of styrene in the presence of water (1) or by hypochlorination using an alkali hypochlorite (4, 5), usually analyzed high in chlorine. We were able to isolate varying amounts of (1,2,2-trichloroethyl)-benzene from such material by treatment of the mixture with aqueous caustic which converted the chlorohydrin to the oxide while leaving the trichloroethylbenzene unchanged. These products were then easily separated by fractionation. The trichlorinated compound and styrene chlorohydrin distill at essentially the same temperature and cannot be separated by fractionation, which explains the fact that previous investigators have failed to observe the presence of (1,2,2-trichloroethyl)-benzene in their product. This material undoubtedly arises from addition of chlorine to the double bond of β-chlorostyrene. The latter appears to be invariably formed in varying amounts in preparations of styrene chlorohydrin. We found the ratio of styrene dichloride to β-chlorostyrene formed on a variety of preparations of styrene chlorohydrin to be of the order of 3:1 on a weight basis. This is the same ratio of dichloride and β-chlorostyrene as was reported by Emerson and Agnew (6) on the addition of chlorine to styrene in carbon tetrachloride solution at 40–50°. We also investigated the preparation of styrene dichloride by chlorinating styrene at 0–10° in a variety of solvents and at varying concentrations without greatly changing the ratio of addition to substitution from that reported by Emerson and Agnew.

EXPERIMENTAL

Melting and boiling ranges are uncorrected. Fractionations were carried out using a 60 cm Podbielniak-type column with heated jacket and partial reflux head similar to that described by Cason and Rapoport (7). Gas chromatographic studies were done with an F & M Model 720 chromatograph using a 6 ft column packed with 20% Dow 9N9 nonionic surfactant on Chromasorb P of 30–60 mesh.

Hypochlorination of Styrene in Aqueous Acetone

A mixture of styrene (1.25 moles), sodium carbonate (0.5 mole), acetone (1 000 ml), and water (250 ml) was placed in a 2 l, three-necked flask which was fitted with a mechanical stirrer, thermometer, and inlet

Can. J. Chem. Downloaded from www.nrcresearchpress.com by 210.87.254.42 on 09/05/12
For personal use only.

tube for chlorine gas. One mole of chlorine was allowed to vaporize during approximately 4 h from a cold trap and pass into the mixture. No cooling or heating was resorted to, and the temperature of the reaction mixture rose to 41° during this time. The mixture was present as one phase initially (with the carbonate out of the solution), but a lower aqueous phase separated soon after the chlorine addition was started. The aqueous layer grew in size during the addition and, at the end, contained most of the water in the reaction mixture as a nearly saturated sodium chloride solution. The latter was separated and acetone was removed from the organic layer by distillation. Fractionation of the residue gave a recovery of 24 g of styrene, followed by 9.8 g (7% based on the styrene consumed) of β-chlorostyrene at 69–70° (5 mm), n_D^{25} 1.5744 (lit. (8) b.p. 89–90° (15 mm), n_D^{13} 1.5781), 23 g (13%) of styrene dichloride at 93–95° (4 mm), n_D^{25} 1.5492 (lit. (2) b.p. 90° (4 mm), n_D^{15} 1.5544); and 113 g (72%) of styrene chlorohydrin at 108–109° (4 mm), n_D^{25} 1.5506 (lit. (4, 9) b.p. 110–111° (6 mm), n_D^{20} 1.5525).

Chlorination of Styrene in Aqueous Suspension

Chlorine (1 mole) was added as described in the preceding paragraph to an agitated mixture of water (500 ml), styrene (1 mole), and sodium bicarbonate (1 mole) with cooling to maintain the reaction mixture at approximately 10°. The heavy oil layer was separated, dried, and fractionated, yielding 28 g (20%) of β-chlorostyrene at 68–70° (5 mm), 103 g (59%) of styrene dichloride at 93–95° (4 mm), and 10 g (6%) of impure styrene chlorohydrin at 105–110° (4 mm), n_D^{25} 1.5520. The polymeric residue amounted to 19 g.

Separation of (1,2,2-Trichloroethyl)-benzene from the Styrene Chlorohydrin Runs

A sample of 150 g of impure styrene chlorohydrin was accumulated from a number of runs similar to that described in the preceding paragraph. This material was carefully fractionated and a cut of 109 g taken at 107–109° (3.5 mm), n_D^{25} 1.5522. The latter material analyzed 27.20% chlorine (theory for styrene chlorohydrin, 22.64%). A sample of 100 g of this cut was treated with 20% aqueous sodium hydroxide (0.6 mole), with stirring at room temperature, and then maintained at 50° for 1 h. The organic phase was separated, dried, and fractionated. After a very small forerun, 57 g of styrene oxide was taken at 67° (5 mm), n_D^{25} 1.5329 (lit. (2) b.p. 70° (5 mm)). After an intermediate cut of 3.5 g of material, n_D^{25} 1.5526, there was obtained 10 g of (1,2,2-trichloroethyl)-benzene at 108–110° (3 mm), n_D^{25} 1.5592 (lit. (8) b.p. 130° (17 mm)).

Anal. Calcd. for $C_8H_7Cl_3$: C, 45.86; H, 3.37; Cl, 50.77. Found: C, 45.70; H, 3.30; Cl, 50.50.

Chlorination of Styrene in Solution

Chlorine (1 mole) was added during 4 h to a solution of styrene (1 mole) in carbon tetrachloride (1 035 ml), with cooling to maintain the temperature at 0–10°. The mixture was stirred for 1 h after the addition was complete. Then the solvent was flashed off under a column and the residue was fractionated, yielding 39 g (28%) of β-chlorostyrene at 68–70° (5 mm), 119 g (68%) of styrene dichloride at 93–95° (4 mm), and 4.2 g (2%) of (1,2,2-trichloroethyl)-benzene at 107–110° (3 mm).

Cyclohexene Oxide

A mixture of acetone (250 ml), water (125 ml), and sodium carbonate (0.5 mole) was placed in a 1 l, three-necked flask which was fitted with a mechanical stirrer, dry ice – acetone condenser, dropping funnel, thermometer, and gas inlet tube extending below the surface. Chlorine (1 mole) was added through the inlet tube during 3 h while cyclohexene (1 mole) was concurrently added through the dropping funnel. Cooling was used to maintain the reaction mixture at 40–45°. After the additions were complete, the reaction mixture was filtered to remove precipitated salt. Then the acetone was removed at water-pump pressure under the column, and the two-phase residue was stirred for 1 h at room temperature with 20% aqueous sodium hydroxide (1 mole). The two phases were separated, and the organic phase was dried over sodium sulfate. Fractionation gave 68 g (69%) of cyclohexene oxide at 54–55° (50 mm), n_D^{25} 1.4492 (lit. (10) b.p. 54–55° (50 mm), n_D^{30} 1.4462), and 23 g (15%) of *trans*-1,2-dichlorocyclohexane at 52–53° (5 mm), n_D^{25} 1.4875 (lit. (11), b.p. 88–89° (30 mm), n_D^{20} 1.4904). After removal of an intermediate cut of 10 g of material at 53–137° (5–3.5 mm), n_D^{25} 1.5050, without any indication of a stable boiling point, there followed 9 g (7%) of bis(2-chlorocyclohexyl) ether at 137–139° (3.5 mm), n_D^{25} 1.5019. This material crystallized on standing and after recrystallization from acetone melted at 71–72° (lit. (12) m.p. 70–71°).

1,2-Epoxypentane

1-Pentene was converted to the epoxide in the same manner described above for cyclohexene, with the exception that the sodium carbonate was added portionwise to the reaction mixture after the additions of chlorine and olefin were complete.[2] Fractionation gave 57 g (66%) of 1,2-epoxypentane at 80–81° (665 mm), n_D^{25} 1.3932 (lit. (13) b.p. 89–90° (750 mm), n_D^{20} 1.3963). After a small intermediate fraction, 38 g (27%) of 1,2-dichloropentane was obtained at 55–57° (30 mm), n_D^{25} 1.4439 (lit. (14) b.p. 146° (739 mm), n_D^{25} 1.4448), leaving 9 g of higher boiling residue.

[2]*This procedure was used to avoid loss of the more volatile 1-pentene in the evolving carbon dioxide. In the case of cyclohexene it was found that the yields of products were essentially identical whether the sodium carbonate was present initially or added to the acidic mixture after the chlorination. Under acidic conditions, however, there was some slight attack on the acetone by chlorine, yielding chloroacetone and a slightly lachrymatory reaction mixture.*

Can. J. Chem. Downloaded from www.nrcresearchpress.com by 210.87.254.42 on 09/05/12
For personal use only.

REFERENCES

1. H. R. FRISCH. U. S. Patent No. 2,582,114; Chem. Abstr. **46**, 7590 (1952).
2. M. F. HANDLEY. U. S. Patent No. 2,776,982; Chem. Abstr. **51**, 8143 (1957).
3. H. J. LUCAS and C. W. GOULD, JR. J. Am. Chem. Soc. **63**, 2541 (1941).
4. W. E. HANBY and H. N. RYDON. J. Chem. Soc. 114 (1946).
5. W. S. EMERSON. J. Am. Chem. Soc. **77**, 516 (1945).
6. W. S. EMERSON and E. P. AGNEW. J. Am. Chem. Soc. **67**, 519 (1945).
7. J. CASON and H. RAPOPORT. Laboratory text in organic chemistry. Prentice-Hall, Inc., New York. 1950. p. 238.
8. F. BERGMANN, A. KALMUS, and E. BREUER. J. Am. Chem. Soc. **80**, 4543 (1958).
9. H. BODOT, E. DIEUZEIDE, and J. JULLIEN. Bull. Soc. Chim. France, 1086 (1960); Chem. Abstr. **55**, 18649 (1961).
10. F. C. FROSTICK, JR., B. PHILLIPS, and P. S. STARCHER. J. Am. Chem. Soc. **81**, 3355 (1959).
11. H. C. STEVENS and O. GRUMMITT. J. Am. Chem. Soc. **74**, 4876 (1952).
12. K. WIESNER, F. H. CLARKE, and S. KAIRYS. Can. J. Res. B, **28**, 234 (1950).
13. W. D. EMMONS and A. S. PAGANO. J. Am. Chem. Soc. **77**, 90 (1955).
14. C. F. KOELSCH and S. M. MCELVAIN. J. Am. Chem. Soc. **51**, 3393 (1929).

Can. J. Chem. Downloaded from www.nrcresearchpress.com by 210.87.254.42 on 09/05/12
For personal use only.

Can. J. Chem. Downloaded from www.nrcresearchpress.com by 210.87.254.105 on 09/05/12
For personal use only.

NOTES

THE NON-CATALYTIC FISCHER INDOLIZATION OF HEXANE-2,5-DIONE BISPHENYLHYDRAZONE

B. ROBINSON

It has recently been found that Fischer indolization of cyclohexane-1,4-dione bisphenylhydrazone leads to the formation of indolo (3′,2′;2,3) carbazole, I (1, 2), 3-phenylhydrazinocarbazole, II (1), and 1,2,3,4-tetrahydro-3-oxocarbazole (2), no formation of indolo (2′,3′;3,4) carbazole, III, being detected.

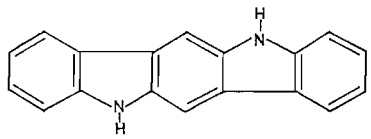

I

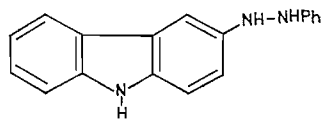

II

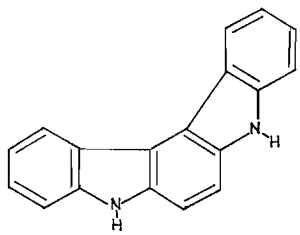

III

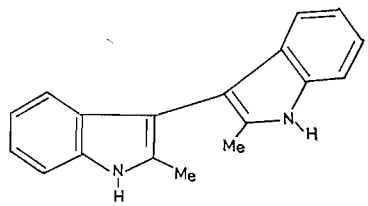

IV

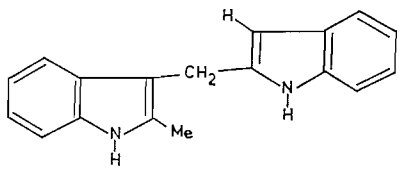

V

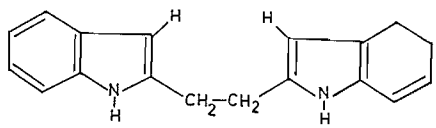

VI

The Fischer indolization of the acyclic analog of cyclohexane-1,4-dione bisphenylhydrazone, hexane-2,5-dione bisphenylhydrazone (3), has now been investigated. Since it has previously been shown (4) that hexane-2,5-dione bisphenylhydrazone under acidic conditions is converted into 1-anilino-2,5-dimethylpyrrole, the Fischer indolization was effected by the non-catalytic technique using refluxing monoethylene glycol (5) to prevent (or lessen) formation of the undesired pyrrole. The indolization could theoretically lead

to one or more of three compounds having structures IV, V, and VI. However, only one indolic product of molecular formula $C_{18}H_{16}N_2$ has been obtained from the reaction [although proton magnetic resonance data suggested the formation of traces of a further indolic product(s), possibly V and (or) VI (see experimental section)]. This product has been distinguished from V and VI and shown to have structure IV from the following evidence.

(i) The infrared spectrum (in Nujol) shows a single N—H stretching band at 3 350 ± 10 cm^{-1} [cf. the single N—H stretching band of 3,3′-diindole (prepared by the method of Gabriel, Gerhard, and Wolter (6)) (in Nujol) at 3 360 ± 10 cm^{-1}]. (Compound V might be expected to show two N—H stretching bands in its infrared spectrum since it contains two N—H groups in different environments.)

(ii) The compound was recovered unchanged after boiling under reflux for 24 h with acetic anhydride (compounds V and VI under these conditions would be expected to give mono- and di-acetyl derivatives respectively, since indoles having unsubstituted 2- and (or) 3-positions are known (7) to be acetylated at these positions in refluxing acetic anhydride).

(iii) The proton magnetic resonance spectrum (in pyridine and in dimethylsulfoxide) had no absorption band between 3.3 and 4.5 τ, and therefore indolic 3-protons (present in structures V and VI) are absent (8). The spectrum in pyridine, however, did have a strong singlet at 7.60 τ, indicative of the two equivalent methyl groups substituted at the 2- and 2′-positions of IV.

(iv) The mass spectrum shows, apart from a strong molecular ion peak at m/e = 260, only minor fragmentation with a weak peak at m/e = 130 (cf. the mass spectrum of 3,3′-diindole (6) which shows an abundant molecular ion peak with little fragmentation to an ion at m/e = 116 and a slightly more abundant ion at m/e = 115). This eliminates structure VI which would be expected to give an intense peak in its mass spectrum at m/e = 130.

(v) The ultraviolet spectrum was almost identical to that of 3,3′-diindole (6) (see experimental section).

Preferential or exclusive formation of IV in the above indolization may be explained by consideration of the direction of bisenehydrazine formation (the first stage in the mechanism of the indolization (9) and the one which ultimately controls the direction of cyclization), for whereas the bisenehydrazine intermediate which leads to compound IV is the fully conjugated bisenehydrazine system VII, the analogous intermediates which

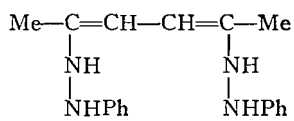

VII

would lead to structures V and VI would consist of two nonconjugated monoene-hydrazines and would therefore be less favorable (similar reasoning can be applied if one of the phenylhydrazone moieties indolizes before the other undergoes hydrazone–ene-hydrazine tautomerization). However, since one of the indolization products from cyclohexane-1,4-dione bisphenylhydrazone is the indolocarbazole I (1, 2), it is likely that bisenehydrazine formation in hexane-2,5-dione bisphenylhydrazone does not occur exclusively in favor of the fully conjugated system VII and the above discussion would not

Can. J. Chem. Downloaded from www.nrcresearchpress.com by 210.87.254.105 on 09/05/12
For personal use only.

therefore explain the sole formation of IV, although it could explain its formation as the major indolic product. It is known (10), however, that indolization of methyl alkyl ketone phenylhydrazones yields only the corresponding 2-methylindoles (with one exception) and therefore, by analogy, compound IV would be expected as the only indolic product in the indolization of hexane-2,5-dione bisphenylhydrazone.

EXPERIMENTAL

Infrared spectra were recorded on a Unicam SP 200 spectrophotometer, ultraviolet spectra were measured on a Beckmann DB spectrophotometer, and proton magnetic resonance spectra were recorded on a Varian A 60 spectrometer using tetramethylsilane as internal standard.

The Non-Catalytic Fischer Indolization of Hexane-2,5-dione Bisphenylhydrazone

Hexane-2,5-dione bisphenylhydrazone (3) (20 g) was added to redistilled monoethylene glycol (200 ml). The mixture was warmed to effect solution and then gently refluxed (a copious evolution of ammonia began after about 5 min) for 6 h, after which time the ammonia evolution had ceased and the initially pale-yellow solution had become dark brown. The reaction mixture was cooled to room temperature and water (1 l) was added, followed by extraction of the liberated oil with ether (8 × 150 ml). The combined ether extracts were washed with water (2 × 250 ml), extracted with 3 *N* hydrochloric acid (3 × 150 ml), washed with water (250 ml), and dried (magnesium sulfate) and the ether removed under reduced pressure (11 mm) to leave a dark-brown gum (A) (4.18 g) which, on cooling to 5° and trituration with ether, partially crystallized. After filtration and washing with a little ether, a white crystalline solid (1.17 g, 6.5%) was obtained which was sublimed [200–210° (bath temperature) at 0.4 mm] to give pure 2,2′-dimethyl-3,3′-diindole, IV, as a pale-yellow crystalline solid (0.90 g, 5%). Recrystallization from aqueous ethanol afforded white needles, m.p. 226–228° (uncorrected).

Anal. Calcd. for $C_{18}H_{16}N_2$: C, 83.04; H, 6.20; N, 10.76. mol. wt. 260. Found: C, 83.33; H, 6.31; N, 10.67; mol. wt. (mass spectrum) 260. λ_{max}^{EtOH} 232 mμ, log ε 4.64; 283 mμ, log ε 4.10; 291 mμ, log ε 4.08. λ_{min}^{EtOH} 260 mμ, log ε 3.79; 288 mμ, log ε 4.07. (Confer 3,3′-diindole (6). λ_{max}^{EtOH} 233 mμ, log ε 4.60; 282 mμ, log ε 3.91; 291 mμ, log ε 3.92. λ_{min}^{EtOH} 264 mμ, log ε 3.76; 286 mμ, log ε 3.90.)

The proton magnetic resonance spectrum (in dimethylsulfoxide) of the mother liquors remaining after the removal of compound IV from (A) shows a weak signal at 3.70 τ, suggesting the possible presence of traces of a 3-unsubstituted indole(s) (8) (i.e. V and (or) VI), but attempts to isolate such compounds or any other crystalline product(s) failed.

The combined dark-brown acidic extracts from above were carefully basified with sodium hydroxide pellets (with cooling by the addition of ice) and the liberated oil was extracted with ether (3 × 250 ml). The combined ether extracts, after drying (magnesium sulfate) and evaporation of the solvent, afforded a dark-brown oil (4.33 g) which could not be induced to crystallize or made to form a picrate with picric acid in ethanol or in benzene and was therefore not examined further.

ACKNOWLEDGMENT

I wish to thank Drs. G. Spiteller and H. Eggers of the University of Vienna for determination of the mass spectra of 3,3′-diindole and compound IV.

1. B. Robinson. J. Chem. Soc. 3097 (1963).
2. J. Harley-Mason and E. H. Pavri. J. Chem. Soc. 2504 (1963).
3. C. Paal. Ber. **18**, 58 (1885).
4. A. Smith. Ann. **289**, 310 (1896). A. Smith and H. N. McCoy. Ber. **35**, 2169 (1902).
5. J. T. FitzPatrick and R. D. Hiser. J. Org. Chem. **22**, 1703 (1957).
6. S. Gabriel, W. Gerhard, and R. Wolter. Ber. **56**, 1024 (1923). B. Oddo and L. Raffa. Gazz. Chim. Ital. **69**, 562 (1939). W. Carpenter, M. S. Grant, and H. R. Snyder. J. Am. Chem. Soc. **82**, 2739 (1960).
7. W. Borsche and H. Groth. Ann. **549**, 238 (1941).
8. R. V. Jardine and R. K. Brown. Can. J. Chem. **41**, 2067 (1963).
9. B. Robinson. Chem. Rev. **63**, 373 (1963).
10. B. Robinson. Chem. Rev. **63**, 387 (1963).

Received July 20, 1964.
Department of Pharmacy,
The University,
Manchester, England.

Can. J. Chem. Downloaded from www.nrcresearchpress.com by 210.87.254.105 on 09/05/12
For personal use only.

Can. J. Chem. Downloaded from www.nrcresearchpress.com by 210.87.254.5 on 09/05/12
For personal use only.

PRÉPARATION D'ESTERS ORTHOTHIOBORIQUES A PARTIR DU SULFURE DE BORE

J. BRAULT ET J. M. LALANCETTE

La première mention d'un ester orthothioborique $B(SR)_3$ est due à Goubeau et Wittmeier qui rapportent la préparation de l'homologue méthylé à partir du sel d'argent du méthanethiol et du tribromure de bore (1). Plus récemment, Brotherton et Petterson ont breveté une méthode de préparation de certains orthothioborates faisant appel à l'action d'un mercaptan sur un aminoborane en milieu acide (2) et Mikhailov a obtenu ces esters à partir du trichlorure de bore ou du diborane et des mercaptans (3).

Une nouvelle méthode permettant d'accéder à cette classe de composés a été mise au point en étudiant l'action des mercaptans sur le sulfure de bore. En effet nous avons noté que ce sulfure donne avec des mercaptans une réaction modérée, s'accompagnant d'un dégagement de H_2S et conduisant à l'ester orthothioborique correspondant avec de bons rendements.

$$6RSH + B_2S_3 \rightarrow 2B(SR)_3 + 3H_2S.$$

La réaction semble générale pour tous les mercaptans (voir le Tableau I) et offre un accès facile aux orthothioborates.

TABLEAU I

Esters orthothioboriques $(RS)_3B$

R	Point d'ébullition		n_D		%B	
	Trouvé	Décrit (6)	Trouvé (à 25°)	Décrit (à 20°)(6)	Calculé	Trouvé
CH_3	125° à 37 mm	93–96° à 14 mm	1.5819	1.5790	7.11	7.26*
C_2H_5	88° à 0.70 mm	72–73° à 1 mm	1.5481	1.5473	5.57	5.60
n-C_3H_7	116° à 0.68 mm	100–102° à 1 mm	1.5346	1.5324	4.58	4.49
i-C_3H_7	84° à 0.75 mm	80–80.5° à 1.5 mm	1.5263	1.5265	4.58	4.57
n-C_4H_9	142° à 0.70 mm	156–158° à 3 mm	1.5226	1.5228	3.89	3.78
n-C_5H_{11}	180° à 0.60 mm	—	1.5115	—	3.38	2.23
n-C_6H_{13}	194–196° à 0.18 mm	—	1.5096	—	2.99	2.57
n-C_7H_{15}	210–212° à 0.30 mm	—	1.5043	—	2.67	2.24
C_6H_5	Point de fusion 143–144°	—	—	—	3.20	3.78

*Déterminé sous forme de H_3BO_3 par une lente hydrolyse en présence d'air humide.

PARTIE EXPÉRIMENTALE

Préparation d'esters orthothioboriques

A une suspension de 23.0 g (0.20 mole) de sulfure de bore (4) dans l'éther de pétrole sec, p.éb. 40–50°, on ajoute 74.0 g (1.2 mole) d'éthanethiol Eastman Kodak, White Label. Suit un reflux de 36 h, sous bonne agitation. Au terme de cette période, le dégagement de H_2S a cessé et la filtration de la masse réactionnelle donne un filtrat que l'on concentre à pression atmosphérique et fractionne sous vide. Ces opérations, exécutées en milieu rigoureusement anhydre et sous atmosphère d'azote, conduisent à 57 g (0.29 mole) d'un liquide incolore, p.éb. 88° à 0.70 mm.

Anal. Calc. pour $BC_6H_{15}S_3$: C, 37.11; H, 7.78; S, 49.53; B, 5.57. Trouvé: C, 36.81; H, 7.60; S, 49.17; B, 5.60.

Le spectre infrarouge montre de nouvelles bandes dans la région de 900 cm^{-1} attribuables vraisemblablement à la liaison B—S.*

Un mode opératoire similaire permet d'accéder aux orthothioborates homologues supérieurs (voir le Tableau I). Avec le méthanethiol, les espèces sont mises en contact à froid (0 °C) et une pression de 0.3 atm est établie à l'intérieur du système. On porte alors le diluant à la température de reflux et procède selon le mode décrit plus haut.

**Les spectres infrarouges d'une série d'esters orthothioboriques feront l'objet d'une prochaine communication.*

Analyses élémentaires des esters orthothioboriques

Les orthothioborates s'avèrent des substances extrêmement hygroscopiques, la réaction des premiers termes avec l'eau étant quasi explosive. Cette sensibilité a rendu les analyses C—H—S très difficiles et n'ont été effectuées que pour le dérivé éthyle. Les déterminations de bore ont été effectuées en utilisant la méthode spectrométrique à flamme décrite par Yoshizaki (5). Les solutions standards d'acide borique servant à établir une courbe de calibration renfermait de l'éthanethiol dans le rapport molaire H_3BO_3/EtSH = 1/3. Des échantillons des esters orthothioboriques (≈1.0 g) ont été pesés exactement dans des ballons jaugés de 100 ml et hydrolysés par simple addition d'eau. Les mesures ont été effectuées à l'aide d'un spectromètre Beckman DU avec une flamme d'hydrogène, à une longueur d'onde de 519 mμ.

Avec l'orthothioborate de méthyle, un échantillon (1.0028 g) de l'ester a été placé dans un dessicateur contenant une solution à 20% de NaOH. Après 48 h sous un léger vide, l'ester est transformé en un solide dont le poids demeure constant; l'acide borique, 0.4162 g, p.f. 178°; soit 7.26% de bore dans l'ester initial.

Anal. Calc. pour $B(SCH_3)_3$: 7.11.

REMERCIEMENTS

Un des auteurs (J. M. L.) remercie le Defence Research Board de son aide financière (octroi No. 9530-30).

1. J. Goubeau et H. W. Wittmeier. Z. Anorg. Allgem. Chem. **270**, 16 (1952).
2. R. J. Brotherton et L. L. Petterson. Chem. Abstr. **55**, 9345 (1961).
3. B. M. Mikhailov, T. A. Shchegoleva, E. M. Shashkova et V. D. Sheludyakov. Bull. Acad. Sci. USSR, **7**, 1143 (1962).
4. S. Jerumanis et J. M. Lalancette. Can. J. Chem. **42**, 1928 (1964).
5. T. Yoshizaki. Anal. Chem. **35**, 2177 (1963).
6. B. M. Mikhailov et Yu. N. Bubnov. Bull. Acad. Sci. USSR, **8**, 1294 (1962).

Reçu le 31 juillet 1964.
Département de Chimie,
Université de Sherbrooke,
Sherbrooke, Québec.

THE SYNTHESIS OF 5-MERCAPTOTRYPTAMINE, THE THIOL ANALOG OF SEROTONIN

J. Kenneth Horner and W. A. Skinner

The antimetabolite concept of drug development is, of course, well known and widely utilized. Wooley (1) has discussed the use of antimetabolites of serotonin in the treatment of hypertension and certain other diseases. Serotonin (5-hydroxytryptamine) was first isolated from beef serum and its structure proved in 1948 (2). We report the synthesis of the thiol analog of serotonin, 5-mercaptotryptamine (V).[1]

The route to V was via 2,3-piperidione-3-(4′-benzylthio)phenylhydrazone (I). Compound I was prepared in 35% yield by a Japp-Klingemann reaction (3) from 4-benzylthiobenzene diazonium chloride and potassium 2-oxopiperidine-3-carboxylate at 0° by a general, published procedure (4, 5). The hydrazone I was cyclized smoothly with hydrogen chloride in glacial acetic acid (6) to 6-benzylthio-1,2,3,4-tetrahydro-1-oxo-β-carboline (II) in 73% yield. Recent experiments in the same field have shown that refluxing hydrazone I in 90% formic acid for 1 h also gave good yields of II. The β-carboline II was cleaved with aqueous-ethanolic potassium hydroxide (4) by refluxing overnight to afford 3-(2′-aminoethyl)-5-benzylthio-2-indole carboxylic acid (III) in quantitative

[1]*C. J. Peake, F. L. Benton, and C. E. Brambel, Abstracts of Papers, 140th A.C.S. Meeting, Chicago, September, 1961, p. 6-O, reported the synthesis of V in 1961. The meeting abstracts give no physical properties nor experimental details and no further reference to this compound is found in the later literature.*

Can. J. Chem. Downloaded from www.nrcresearchpress.com by 210.87.254.5 on 09/05/12
For personal use only.

Analyses élémentaires des esters orthothioboriques

Les orthothioborates s'avèrent des substances extrêmement hygroscopiques, la réaction des premiers termes avec l'eau étant quasi explosive. Cette sensibilité a rendu les analyses C—H—S très difficiles et n'ont été effectuées que pour le dérivé éthyle. Les déterminations de bore ont été effectuées en utilisant la méthode spectrométrique à flamme décrite par Yoshizaki (5). Les solutions standards d'acide borique servant à établir une courbe de calibration renfermait de l'éthanethiol dans le rapport molaire H_3BO_3/EtSH = 1/3. Des échantillons des esters orthothioboriques (≈1.0 g) ont été pesés exactement dans des ballons jaugés de 100 ml et hydrolysés par simple addition d'eau. Les mesures ont été effectuées à l'aide d'un spectromètre Beckman DU avec une flamme d'hydrogène, à une longueur d'onde de 519 mμ.

Avec l'orthothioborate de méthyle, un échantillon (1.0028 g) de l'ester a été placé dans un dessicateur contenant une solution à 20% de NaOH. Après 48 h sous un léger vide, l'ester est transformé en un solide dont le poids demeure constant; l'acide borique, 0.4162 g, p.f. 178°; soit 7.26% de bore dans l'ester initial.

Anal. Calc. pour $B(SCH_3)_3$: 7.11.

REMERCIEMENTS

Un des auteurs (J. M. L.) remercie le Defence Research Board de son aide financière (octroi No. 9530-30).

1. J. Goubeau et H. W. Wittmeier. Z. Anorg. Allgem. Chem. **270**, 16 (1952).
2. R. J. Brotherton et L. L. Petterson. Chem. Abstr. **55**, 9345 (1961).
3. B. M. Mikhailov, T. A. Shchegoleva, E. M. Shashkova et V. D. Sheludyakov. Bull. Acad. Sci. USSR, **7**, 1143 (1962).
4. S. Jerumanis et J. M. Lalancette. Can. J. Chem. **42**, 1928 (1964).
5. T. Yoshizaki. Anal. Chem. **35**, 2177 (1963).
6. B. M. Mikhailov et Yu. N. Bubnov. Bull. Acad. Sci. USSR, **8**, 1294 (1962).

Reçu le 31 juillet 1964.
Département de Chimie,
Université de Sherbrooke,
Sherbrooke, Québec.

THE SYNTHESIS OF 5-MERCAPTOTRYPTAMINE, THE THIOL ANALOG OF SEROTONIN

J. Kenneth Horner and W. A. Skinner

The antimetabolite concept of drug development is, of course, well known and widely utilized. Wooley (1) has discussed the use of antimetabolites of serotonin in the treatment of hypertension and certain other diseases. Serotonin (5-hydroxytryptamine) was first isolated from beef serum and its structure proved in 1948 (2). We report the synthesis of the thiol analog of serotonin, 5-mercaptotryptamine (V).[1]

The route to V was via 2,3-piperidione-3-(4′-benzylthio)phenylhydrazone (I). Compound I was prepared in 35% yield by a Japp-Klingemann reaction (3) from 4-benzylthiobenzene diazonium chloride and potassium 2-oxopiperidine-3-carboxylate at 0° by a general, published procedure (4, 5). The hydrazone I was cyclized smoothly with hydrogen chloride in glacial acetic acid (6) to 6-benzylthio-1,2,3,4-tetrahydro-1-oxo-β-carboline (II) in 73% yield. Recent experiments in the same field have shown that refluxing hydrazone I in 90% formic acid for 1 h also gave good yields of II. The β-carboline II was cleaved with aqueous-ethanolic potassium hydroxide (4) by refluxing overnight to afford 3-(2′-aminoethyl)-5-benzylthio-2-indole carboxylic acid (III) in quantitative

[1]*C. J. Peake, F. L. Benton, and C. E. Brambel, Abstracts of Papers, 140th A.C.S. Meeting, Chicago, September, 1961, p. 6-O, reported the synthesis of V in 1961. The meeting abstracts give no physical properties nor experimental details and no further reference to this compound is found in the later literature.*

Can. J. Chem. Downloaded from www.nrcresearchpress.com by 210.87.254.6 on 09/05/12
For personal use only.

yield. The decarboxylation of III was achieved with a mixture of 2 *N* hydrochloric acid and acetic acid (3:2, v/v) giving 5-benzylthiotryptamine (IV) in 70% yield. This facile decarboxylation during overnight refluxing was somewhat unexpected because of the published report (4) that 3-(2′-aminoethyl)-5-benzyloxy-2-indole carboxylic acid could not be decarboxylated under a variety of conditions. The thio ether IV was debenzylated with sodium in liquid ammonia under a nitrogen atmosphere and 5-mercaptotryptamine (V) was isolated as the picrate in 67% yield. The thiol V in dilute ammonia gave the characteristic aromatic thiol test with nitroprusside. Quantitative determination of the SH function of thiol V hydrochloride by ultraviolet spectrophotometry according to the method of Ellman (7) showed the absence of appreciable disulfide.

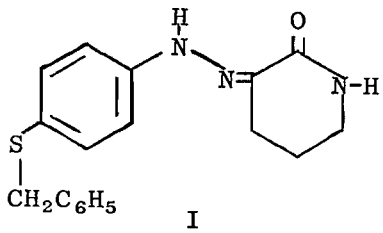

I

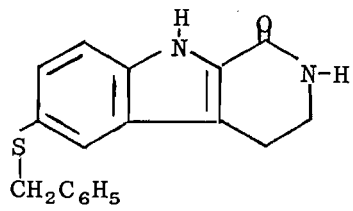

II

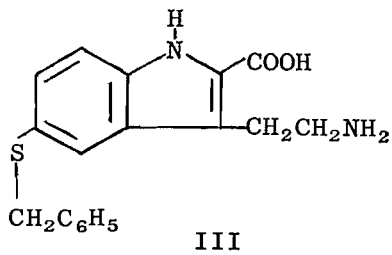

III

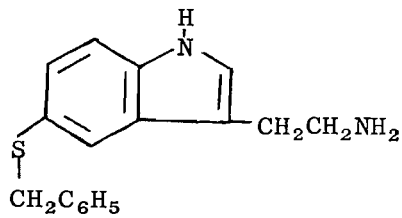

IV

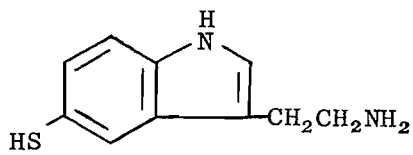

V

EXPERIMENTAL[2]

2,3-Piperidione-3-(4′-benzylthio)phenylhydrazone (I)

Ethyl 2-oxopiperidine-3-carboxylate (23.3 g, 0.136 mole) was dissolved in 60 ml of warm ethyl alcohol, cooled to 0° and diluted with a solution of 9.29 g (0.139 mole) of potassium hydroxide in 50 ml of water. This clear solution was cooled overnight, diluted with 500 g of ice water, and stirred while adding a suspension of 4-benzylthiobenzene diazonium chloride (prepared from 0.13 mole of 4-benzylthioaniline and 0.13 mole of sodium nitrite in 100 ml of 4 *N* hydrochloric acid). Immediately after the addition was complete, 20 g of sodium acetate was added. The tan mixture was stirred at 0° for 5 h then left at 25° overnight. The solid product was collected, washed with water, and recrystallized from dilute ethyl alcohol or methyl ethyl ketone to give 14.8 g deep-yellow rosettas, m.p. 203–205°. The analytical sample prepared by further recrystallizations from the same solvents melted at 207–208°. $\lambda_{max(\mu)}^{Nujol}$ 3.10, 3.15 (NH); 6.00 (amide C=O); 6.23 (aryl); 6.44 (amide II); 12.1 (1,4-disubstituted benzene).

Anal. Calcd. for $C_{18}H_{19}N_3OS$: C, 66.4; H, 5.89; N, 12.9. Found: C, 66.2; H, 5.99; N, 13.0.

[2]*All melting points are uncorrected and were taken with a Fisher–Johns melting block.*

Can. J. Chem. Downloaded from www.nrcresearchpress.com by 210.87.254.6 on 09/05/12
For personal use only.

6-Benzylthio-1,2,3,4-tetrahydro-1-oxo-β-carboline (II)

Dry hydrogen chloride was passed into a solution of 6.2 g (0.019 mole) of 2,3-piperidione-3-(4′-benzylthio)phenyl hydrazone (I) in 120 ml of warm acetic acid for 15 min. The resulting suspension was refluxed 15 min, reduced to half volume *in vacuo*, and poured over cracked ice. The resulting grey solid was collected and recrystallized from isopropyl alcohol to give 4.3 g of β-carboline II, m.p. 194–195°. Additional purification by recrystallization gave m.p. 197–198° $\lambda_{max(\mu)}^{CHCl_3}$ 2.89, 3.07 (NH); 5.97 (amide C=O); absence of 1,4-disubstituted benzene band at 12.1.

Anal. Calcd. for $C_{18}H_{16}N_2OS$: C, 70.1; H, 5.23; N, 9.09. Found: C, 70.3; H, 5.45; N, 9.26.

3-(2′-Aminoethyl)-5-benzylthio-2-indole Carboxylic Acid (III)

6–Benzylthio-1,2,3,4-tetrahydro-1-oxo-β-carboline (II) (4.0 g, 0.013 mole) was refluxed overnight with a solution of 8.6 g (0.13 mole) of potassium hydroxide, 48 ml of ethyl alcohol, and 32 ml of water. The red solution was concentrated to half volume and adjusted to pH 5 with acetic acid. The white solid was collected, washed with water, and dried to give a quantitative yield of product III, m.p. 224–227°. The analytical sample (dilute ethyl alcohol) decomposed at 237°. $\lambda_{max(\mu)}^{Nujol}$ 2.94 (NH); 3.10 (NH, OH); 5.90 (acid C=O); 6.20 (aryl); 13.0, 14.3 (monosubstituted benzene).

Anal. Calcd. for $C_{18}H_{18}N_2O_2S$: C, 66.2; H, 5.56; N, 8.58. Found: C, 66.0; H, 5.57; N, 8.70.

5-Benzylthiotryptamine (IV)

A solution of 3.0 g (0.009 mole) of 3-(2′-aminoethyl)-5-benzylthio-2-indole carboxylic acid (III) in 45 ml of 2 *N* hydrochloric acid and 30 ml of acetic acid was refluxed overnight. The clear, red solution was concentrated to half volume and cooled to yield 2.0 g of 5-benzylthiotryptamine hydrochloride, m.p. 207–210°. Recrystallization from isopropyl alcohol – ether produced the analytical sample, m.p. 213–214°. $\lambda_{max(\mu)}^{Nujol}$ 3.00 (indole NH); absence of acid C=O at 5.90; 6.20, 6.25 (NH_2, aryl); 12.9, 14.2 (monosubstituted benzene).

Anal. Calcd. for $C_{18}H_{18}N_2O_2S$: C, 64.0; H, 6.01; N, 8.79. Found: C, 63.9; H, 6.02; N, 8.90.

5-Mercaptotryptamine (V)

Dry 5-benzylthiotryptamine hydrochloride (0.5 g, 1.58 mmoles) in a dried 50 ml flask was finely powdered and covered with 15 ml of anhydrous ammonia. The reaction was immersed in a dry ice – acetone bath and protected from moisture with a drying tube packed with dried cotton. The mixture was stirred magnetically and 0.2 g of sodium in small pieces was added in one portion. The blue reaction mixture was stirred for 0.5 h. Then 0.002 mole of ammonium iodide was added and the ammonia removed at 25° under a dense stream of dry nitrogen. A prepared solution of 0.002 mole of hydroquinone, 0.002 mole of acetic acid, and 0.002 mole of picric acid in 33 ml water and 2 ml ethyl alcohol was quickly added. The solution was adjusted to pH 5 with 5 ml of acetic acid and the orange precipitate was stirred under nitrogen for 0.5 h, then left at 25° overnight. The picrate was collected and washed with water and dried to give 0.45 g, m.p. 220° (decomp.). The picrate (150 mg) was recrystallized from ethyl alcohol – water.

Anal. Calcd. for $C_{10}H_{12}N_2S \cdot C_6H_3N_3O_7$: C, 45.6; H, 3.59; N, 16.6. Found: C, 45.7; H, 3.55; N, 16.7.

5-Mercaptotryptamine picrate (0.4 g) was suspended in 50 ml of boiled ethyl alcohol and stirred under nitrogen overnight with 5 g of Dowex chloride resin. The mixture was filtered and the filtrate concentrated to give 5-mercaptotryptamine hydrochloride as an oil which was stored in a cold, dark place under nitrogen. $\lambda_{max(\mu)}^{film}$ 2.95, 3.05 (NH); 6.18 (aryl); absence of benzene monosubstitution bands at 12.9, 14.2. A solution of mercuric chloride was added to 0.043 mmoles of the thiol V hydrochloride in water to give 21.6 mg of the salt; theoretical weight for RSHgCl·HCl is 21.4 mg.

ACKNOWLEDGMENT

This work was supported by the U.S. Army Chemical Research and Development Laboratories under Contract No. DA-18-108-CML-7077.

1. D. W. Wooley. Progr. Drug Res. **2**, 627 (1960).
2. M. M. Rapport, A. A. Green, and I. H. Page. J. Biol. Chem. **176**, 1237 (1948); Science, **108**, 329 (1948); J. Biol. Chem. **176**, 1243 (1948). M. M. Rapport. J. Biol. Chem. **180**, 961 (1949).
3. Organic Reactions. Vol. X. John Wiley and Sons, Inc., New York. 1959. p. 159.
4. R. A. Abramovitch and D. Shapiro. J. Chem. Soc. 4589 (1956).
5. M. von Strandtmann, M. P. Cohen, and J. Shavel, Jr. J. Med. Pharm. Chem. **6**, 719 (1963).
6. A. Allais. Fr. Patent No. 1,186,258 (August 19, 1959); Chem. Abstr. **55**, 23562 (1961).
7. G. L. Ellman. Arch. Biochem. Biophys. **82**, 70 (1959).

Received July 24, 1964.
Department of Pharmaceutical Chemistry,
Stanford Research Institute,
Menlo Park, California.

Can. J. Chem. Downloaded from www.nrcresearchpress.com by 210.87.254.6 on 09/05/12
For personal use only.

HYDROGEN SORPTION BY CADMIUM OXIDE

M. J. D. Low and A. M. Kamel

In general, little is known of the surface properties of CdO and the knowledge of the interaction of CdO with hydrogen seems to be limited to reports that the reduction of CdO begins at 95° (1) or at 221° (2). Because of the possibility of comparison with the plentiful data on hydrogen sorption by ZnO, an attempt was made to study the surface properties of CdO. The simultaneous effects of surface "activation" and of changes in surface areas by thermal sintering and hydrogen reduction precluded quantitative study, but permitted quantitative observations to be made.

EXPERIMENTAL DETAILS

A conventional high-vacuum apparatus (3) suitable for the determination of nitrogen B.E.T. surface areas (4) and also for the measurement of hydrogen take up was used. Hydrogen was purified by diffusion through hot palladium. Nitrogen and helium were purified by passage through glass wool filled traps at the temperature of liquid nitrogen. Baker A. R. or Coleman C. P. CdO of equivalent purity and identical surface areas was used. The initial hydrogen pressure for all sorption experiments was 1.83 cm Hg.

EXPERIMENTS, RESULTS, AND DISCUSSION

The plots of Fig. 1 show that a rapid decline in surface areas of CdO occurred even at relatively low temperatures. The first point of each curve was obtained after heating at the various temperatures for 3 min. At 400 and 500° a cadmium mirror formed on the cool portion of the tubing leading from the sample chamber to the pumping system and the samples lost weight. Because of this the specific surface area was calculated on the basis of the final sample weight for the points shown as filled circles in Fig. 1. The single datum indicated by a filled triangle at zero time represents the surface area of the unsintered material after degassing at 22° for 12 h. That point is considerably lower than the 3 min points that mark the beginning of each sintering curve except that at 200°. However, it seems unlikely that the development of a new surface was involved by the mild heat treatment. A more reasonable explanation is that the solid had a network of pores that was made accessible to N_2 molecules after the 3 min degassing.

Numerous measurements of the uptake of hydrogen by CdO were made in an attempt to establish the conditions that would permit reproducible measurements to be made. In general, these experiments showed the surfaces to be unstable. Figures 2 and 3 illustrate such "activation" effects, which may plausibly be ascribed to a change in stoichiometry of the surface. Figure 4 illustrates the type of data obtained with arbitrarily selected "standard" degassing conditions. The characteristics of the sorption at 22° and 100° are like those generally observed for a chemisorption process. At the higher temperatures, however, the uptake process was not "normal." At the points R the decline in pressure ceased and the pressure within the adsorption system increased. Such increases were generally found at 200° and above and occasionally at 150°. On one occasion, a sample degassed for 12 h at 100° was exposed to hydrogen at 100°. The pressure initially decreased as hydrogen was taken up, but increased after about 15 min. When the temperature was raised to 200°, water condensed on the cold portions of tubing. In some cases, the surface area of the CdO was measured before and after exposure to hydrogen. The surface area of a CdO sample was 8.8 m^2/g after 30 min degassing at 200°. The hydrogen was then removed and after pumping for 15 min at room temperature, the surface area was again

Can. J. Chem. Downloaded from www.nrcresearchpress.com by 210.87.254.105 on 09/05/12
For personal use only.

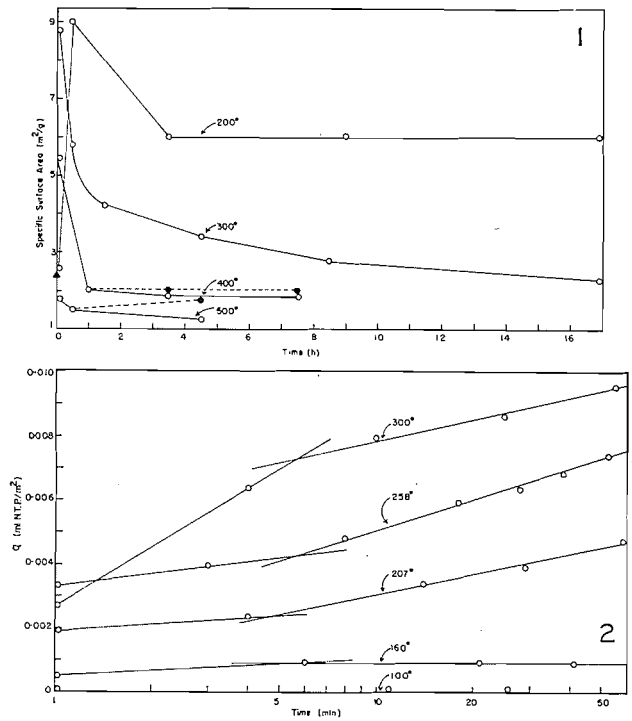

FIG. 1. Sintering of CdO in vacuum. A fresh CdO powder sample was used at each temperature. The sample was heated *in vacuo* for a predetermined time and the quenched and the B.E.T. surface area was measured. Heating then continued.

FIG. 2. Effect of degassing temperature on hydrogen sorption at 22°. A separate CdO sample was used for each experiment and was degassed by pumping at about 10^{-6} mm Hg for 12 h at each temperature indicated.

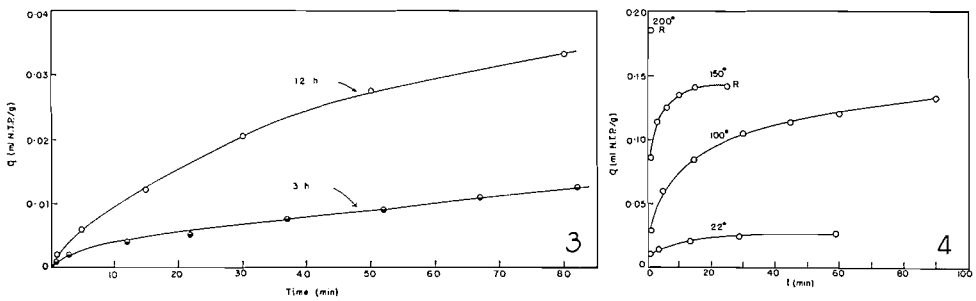

FIG. 3. Effect of degassing time on hydrogen sorption at 100°. Individual CdO samples were degassed at 150° for 3 or 12 h.

FIG. 4. Effect of temperature on hydrogen sorption. A fresh CdO sample was degassed at 200° for 12 h before each sorption experiment.

8.8 m²/g. The same sample was then re-exposed to hydrogen for 3 h at 200°. An increase of pressure within the system occurred. It was found that the surface area had declined to 2.5 m²/g. After a further degassing at 200° for 1 h, the surface area was 2.5 m²/g.

The various effects suggest that reduction of CdO occurred at and above about 100°. The observed pressure increases and the decrease in surface area with hydrogen treatment lend some support to the suggestion that some reduction occurred even below 100° and

Can. J. Chem. Downloaded from www.nrcresearchpress.com by 210.87.254.105 on 09/05/12
For personal use only.

that some or all of the water that was formed was retained by the surface. Desorption of appreciable amounts of water then would not occur until the surface had become fully covered with adsorbed water, the attainment of that saturated state being helped by the decline of the surface by the reduction process.

ACKNOWLEDGMENTS

Support for this work by the Government of the United Arab Republic and the Petroleum Research Fund of the American Chemical Society is gratefully acknowledged.

1. G. GALLO and M. DEL GUERRA. Ann. Chim. Rome, **41**, 51 (1951).
2. V. A. ROMANOV, V. M. DROZDOVA, and G. A. SHIF. Uch. Zap. Leningr. Gos. Univ. Ser. Khim. Nauk, No. 10, 79 (1951).
3. P. FAETH. Adsorption and Vacuum Technique. Rept. No. 66100-2-X, Univ. Michigan. 1962.
4. S. BRUNAUER, P. H. EMMETT, and E. TELLER. J. Am. Chem. Soc. **60**, 309 (1938).

RECEIVED JULY 13, 1964.
SCHOOL OF CHEMISTRY,
RUTGERS, THE STATE UNIVERSITY,
NEW BRUNSWICK, NEW JERSEY.

SUBSTITUTED HYDANTOINS AND OROTIC ACIDS

R. U. LEMIEUX AND I. PUSKAS

The structure of 5-(carbethoxymethylidene)-hydantoin (1) was established by Mitchell and Nyc (2, 3), who showed that treatment of the compound with aqueous base produced first the salt of 5-(carboxymethylidene)-hydantoin which was subsequently isomerized to the salt of orotic acid. That the rearrangement occurred before acidification was demonstrated by following the change in the ultraviolet spectrum of the basic solution (3). Direct evidence that the ring of the orotic acid was in fact established in the alkaline medium was obtained in the present investigation through the observation that potassium orotate precipitated directly from the reaction mixture.

Clerk-Bory and Mentzer (4) extended the method to the preparation of mono- and di-substituted orotic acids. The hydantoin acid could not be isolated as an intermediate when there was present a substituent at the 3-position of the starting material. We also failed to isolate the hydantoin-acid intermediate expected on the treatment of 3-methyl-5-(carbethoxybenzylidene)-hydantoin with base. The acid, was however, obtained by acid-catalyzed hydrolysis of the ethyl ester.

The main purpose of this communication is to report the hydantoin derivatives listed in Tables I and II and the substituted orotic acids shown in Table III. The methods used were virtually the same as those previously reported (2–4). Except for 3-phenyl-5-(carboxymethylidene)-hydantoin, as previously shown (4), the ultraviolet absorption maxima using 95% aqueous ethanolic solutions for the hydantoin derivatives, 296–309 mμ (ϵ_{max} = 10 000 – 14 500), were to higher wavelength than those for the substituted orotic acids, 280–283 mμ (ϵ_{max} = 7 000 – 9 500). For the 3-phenyl compound, the maximum absorption was at 280 mμ (ϵ_{max} = 14 500).

The infrared absorption frequencies observed in the carbonyl region are reported in Tables I–III. As seen, the hydantoin derivatives, as Nujol mulls, showed characteristic absorption in the region 1 758 – 1 803 cm^{-1}. The multiple strong absorptions in the carbonyl region displayed by substituted orotic acids are also present in the spectrum of

Can. J. Chem. Downloaded from www.nrcresearchpress.com by 210.87.254.105 on 09/05/12
For personal use only.

that some or all of the water that was formed was retained by the surface. Desorption of appreciable amounts of water then would not occur until the surface had become fully covered with adsorbed water, the attainment of that saturated state being helped by the decline of the surface by the reduction process.

ACKNOWLEDGMENTS

Support for this work by the Government of the United Arab Republic and the Petroleum Research Fund of the American Chemical Society is gratefully acknowledged.

1. G. GALLO and M. DEL GUERRA. Ann. Chim. Rome, **41**, 51 (1951).
2. V. A. ROMANOV, V. M. DROZDOVA, and G. A. SHIF. Uch. Zap. Leningr. Gos. Univ. Ser. Khim. Nauk, No. 10, 79 (1951).
3. P. FAETH. Adsorption and Vacuum Technique. Rept. No. 66100-2-X, Univ. Michigan. 1962.
4. S. BRUNAUER, P. H. EMMETT, and E. TELLER. J. Am. Chem. Soc. **60**, 309 (1938).

RECEIVED JULY 13, 1964.
SCHOOL OF CHEMISTRY,
RUTGERS, THE STATE UNIVERSITY,
NEW BRUNSWICK, NEW JERSEY.

SUBSTITUTED HYDANTOINS AND OROTIC ACIDS

R. U. LEMIEUX AND I. PUSKAS

The structure of 5-(carbethoxymethylidene)-hydantoin (1) was established by Mitchell and Nyc (2, 3), who showed that treatment of the compound with aqueous base produced first the salt of 5-(carboxymethylidene)-hydantoin which was subsequently isomerized to the salt of orotic acid. That the rearrangement occurred before acidification was demonstrated by following the change in the ultraviolet spectrum of the basic solution (3). Direct evidence that the ring of the orotic acid was in fact established in the alkaline medium was obtained in the present investigation through the observation that potassium orotate precipitated directly from the reaction mixture.

Clerk-Bory and Mentzer (4) extended the method to the preparation of mono- and di-substituted orotic acids. The hydantoin acid could not be isolated as an intermediate when there was present a substituent at the 3-position of the starting material. We also failed to isolate the hydantoin-acid intermediate expected on the treatment of 3-methyl-5-(carbethoxybenzylidene)-hydantoin with base. The acid, was however, obtained by acid-catalyzed hydrolysis of the ethyl ester.

The main purpose of this communication is to report the hydantoin derivatives listed in Tables I and II and the substituted orotic acids shown in Table III. The methods used were virtually the same as those previously reported (2–4). Except for 3-phenyl-5-(carboxymethylidene)-hydantoin, as previously shown (4), the ultraviolet absorption maxima using 95% aqueous ethanolic solutions for the hydantoin derivatives, 296–309 mμ (ϵ_{max} = 10 000 – 14 500), were to higher wavelength than those for the substituted orotic acids, 280–283 mμ (ϵ_{max} = 7 000 – 9 500). For the 3-phenyl compound, the maximum absorption was at 280 mμ (ϵ_{max} = 14 500).

The infrared absorption frequencies observed in the carbonyl region are reported in Tables I–III. As seen, the hydantoin derivatives, as Nujol mulls, showed characteristic absorption in the region 1 758 – 1 803 cm^{-1}. The multiple strong absorptions in the carbonyl region displayed by substituted orotic acids are also present in the spectrum of

Can. J. Chem. Downloaded from www.nrcresearchpress.com by 210.87.254.40 on 09/05/12
For personal use only.

Can. J. Chem. Downloaded from www.nrcresearchpress.com by 210.87.254.40 on 09/05/12
For personal use only.

TABLE I

Substituted hydantoin esters

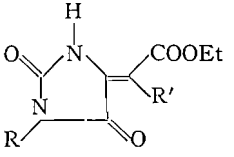

Compound			Elemental analysis				Melting point, °C	Yield, %	Infrared absorption,* cm^{-1} (Nujol mull)			
R	R'	Formula		% C	% H	% N						
CH_3	H	$C_8H_{10}N_2O_4$	Calcd.	48.48	5.09	14.14	141	75	1 795 (m)	1 740 (s)	1 695 (w)	1 665 (s)
			Found	48.34	4.95	14.64						
C_6H_5	H	$C_{13}H_{12}N_2O_4$	Calcd.	60.00	4.65	10.76	191	63	1 772 (m)	1 723 (s)	1 706 (w)	1 665 (s)
			Found	60.44	4.60	10.68					1 689 (s)	
H	C_6H_5	$C_{13}H_{12}N_2O_4$	Calcd.	60.00	4.65	10.76	183–184	15	1 780 (s)	1 735 (s)	1 666 (s)	
			Found	59.79	4.84	10.74						
CH_3	CH_3	$C_9H_{12}N_2O_4$	Calcd.	50.93	5.70	13.20	108–109	62	1 770 (s)	1 715 (s)	1 682 (s)	1 640 (s)
			Found	51.22	5.75	12.99						
CH_3	n-C_4H_9	$C_{12}H_{18}N_2O_4$	Calcd.	56.68	7.13	11.02	118–119	28	1 775 (s)	1 718 (s)	1 680 (s)	1 636 (s)
			Found	56.55	7.30	10.96						
CH_3	C_6H_5	$C_{14}H_{14}N_2O_4$	Calcd.	61.31	5.15	10.21	138–139	29	1 773 (s)	1 720 (s)	1 678 (s)	1 620 (m)
			Found	61.55	5.23	10.34						

*Letters in parentheses indicate the intensity of absorption; vs = very strong; s = strong; m = medium; w = weak.

Can. J. Chem. Downloaded from www.nrcresearchpress.com by 210.87.254.40 on 09/05/12
For personal use only.

TABLE II

Substituted hydantoin acids

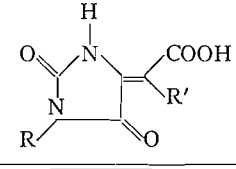

Compound				Elemental analysis			Melting point, °C	Yield, %	Infrared absorption,* cm^{-1} (Nujol mull)			
R	R′	Formula		% C	% H	% N						
H	*n*-C_4H_9	$C_9H_{12}N_2O_4$	Calcd.	50.93	5.70	13.20	231–233	—	1 803 (s)	1 720 (s)	1 688 (m)	1 635 (w)
			Found	51.51	5.82	13.11	(decomp.)					
H	C_6H_5	$C_{11}H_8N_2O_4$	Calcd.	56.90	3.47	12.07						
			Found†	56.92	3.69	12.21	220–240	86	1 757 (m)	1 710 (s)	1 675 (s)	1 630 (m)
			Found‡	57.00	3.44	11.91	220–240		1 785 (w)	1 718 (s)	1 680 (s)	1 628 (m)
									1 760 (s)			
CH_3	C_6H_5	$C_{12}H_{10}N_2O_4$	Calcd.	58.54	4.09	11.38	227–240	21	1 773 (s)	1 730 (s)	1 674 (s)	1 620 (m)
			Found	58.34	4.20	11.47						

*See footnote * in Table I.
†Colorless crystals from ethanol–benzene.
‡Yellowish crystals from water; see Hahn and Endicott (7) for similar phenomena.

Can. J. Chem. Downloaded from www.nrcresearchpress.com by 210.87.254.40 on 09/05/12
For personal use only.

TABLE III

Substituted orotic acids

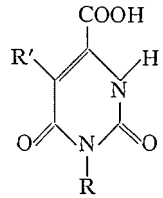

Compound			Elemental analysis				Melting point, °C	Yield, %	Infrared absorption,* cm^{-1} (Nujol mull)			
R	R′	Formula		% C	% H	% N						
H	*n*-C_4H_9†	$C_9H_{12}N_2O_4$	Calcd.	50.93	5.70	13.20	314	68	1 740 (s)	1 690 (m)	1 612 (m)	1 583 (w)
			Found	51.51	5.87	13.26	(decomp.)					
H	C_6H_5	$C_{11}H_8N_2O_4$	Calcd.	56.90	3.47	12.07	330–340	—	1 736 (s)	1 692 (s)	1 620 (s)	1 592 (m)
			Found	57.01	3.55	12.19	(decomp.)					
C_6H_5	H‡	$C_{11}H_8N_2O_4 \cdot H_2O$	Calcd.	52.80	4.03		278–280	98	1 725 (w)	1 705 (s)	1 655 (vs)	1 640 (vs)
			Found	52.97	4.05							
CH_3	H§	$C_6H_6N_2O_4$					325	90	1 734 (s)	1 709 (s)	1 635 (vs)	1 593 (vs)
							(decomp.)					
CH_3	CH_3	$C_7H_8N_2O_4$	Calcd.	45.66	4.38		286–289	88	1 709 (s)	1 681 (s)	1 640 (vs)	
			Found	45.92	4.63		(decomp.)					
CH_3	*n*-C_4H_9	$C_{10}H_{14}N_2O_4$	Calcd.	53.10	6.20	12.39	240–242	85	1 706 (s)	1 679 (m)	1 643 (vs)	1 610 (vs)
			Found	53.05	6.36	12.48						
CH_3	C_6H_5	$C_{12}H_{10}N_2O_4$	Calcd.	58.54	4.09		267–270	37	1 724 (s)	1 682 (m)	1 635 (vs)	
			Found	58.52	4.17							

*See footnote * in Table I.
†Previously reported (4), m.p. 281 °C.
‡Previously prepared by different route (8), m.p. 280 °C.
§Previously prepared by direct methylation of orotic acid (9), m.p. 306–311° (decomp.). The n.m.r. spectrum of the sodium salt in deuterium oxide showed, as expected, signals at 6.72 τ (3 protons) and 3.81 τ (1 proton).

orotic acid [1 695 (s), 1 645 (s), and 1 605 (w) cm^{-1}] and seem to require that these compounds exist in the keto forms rather than in the pyrimidine form sometimes inferred (5, 6) for orotic acid. The proton magnetic resonance spectra of the compounds and the neutral equivalents of the acids were in agreement with those expected for the structures indicated. Several of the compounds listed, especially the orotic acids, showed crystalline transitions in the course of the melting-point determinations.

EXPERIMENTAL

Substituted Hydantoins Esters (Table I)

Diethyl ketosuccinate or the appropriately 3-substituted diethyl ketosuccinate was condensed with either urea or the monosubstituted area following the directions reported by Clerk-Bory and Mentzer (4). When the product did not crystallize directly from the reaction mixture, it was isolated by solvent removal *in vacuo* for crystallization.

Substituted Hydantoin Acids (Table II)

Mild alkaline hydrolysis followed by acidification and recrystallization of the precipitate from aqueous ethanol (4) provided the desired acid except for 3-methyl-5-(carboxybenzylidene)-hydantoin. This compound was obtained by refluxing a solution of the ester (12 g) in 400 ml of a 1:1 mixture of ethanol and 1% aqueous perchloric acid for 9 days. The acid was isolated from the incompletely hydrolyzed product in the usual manner and purified by recrystallization from ethanol–benzene.

Substituted Orotic Acids (Table III)

Except as described below, the ethyl esters reported in Table I were heated for about 4 h in refluxing 2 *N* aqueous potassium hydroxide (4). In order to achieve homogeneous conditions, ethanol was added at the beginning of the heating period until solution was complete. The ethanol was then removed during the course of the reaction. In each case, when the reaction was stopped, the ultraviolet absorption spectrum of the solution no longer showed the maximum absorption above 290 mμ originally present for the hydantoin derivative. In the preparation of the 3-methyl- and 3-phenyl-orotic acids, the reaction mixture was stirred at 50° and the ethanol was not removed.

ACKNOWLEDGMENTS

We acknowledge, with thanks, financial support from Bristol Laboratories, Inc. and the technical assistance of Mr. Werner Merlo.

1. R. Müller. J. Prakt. Chem. **56**, 475 (1897).
2. H. K. Mitchell and J. F. Nyc. J. Am. Chem. Soc. **69**, 674 (1947).
3. J. F. Nyc and H. M. Mitchell. J. Am. Chem. Soc. **69**, 1383 (1947).
4. C. Clerk-Bory and C. Mentzer. Bull. Soc. Chim. France, 436 (1958).
5. H. Gershon. J. Org. Chem. **27**, 3507 (1962).
6. G. D. Daves, F. Baiocchi, R. K. Robins, and C. C. Chang. J. Org. Chem. **26**, 2755 (1961).
7. D. A. Hahn and M. M. Endicott. J. Am. Chem. Soc. **59**, 2741 (1937).
8. M. R. Atkinson, M. H. Maguire, R. K. Ralph, G. Shaw, and R. N. Warrener. J. Chem. Soc. 2363 (1957).
9. J. J. Fox, N. Yung, and I. Wempen. Biochim. Biophys. Acta, **23**, 295 (1957).

Received August 25, 1964.
Department of Chemistry,
University of Alberta,
Edmonton, Alberta.

RADIATION CHEMISTRY OF POTASSIUM PEROXYDISULFATE

R. L. Eager and J. F. Norris

This note gives the results obtained in a study of the radiation chemistry of potassium peroxydisulfate. Samples of the solid compound were irradiated with ^{60}Co γ-rays after which they were dissolved in water and the resulting solutions analyzed.

Can. J. Chem. Downloaded from www.nrcresearchpress.com by 210.87.254.40 on 09/05/12
For personal use only.

orotic acid [1 695 (s), 1 645 (s), and 1 605 (w) cm^{-1}] and seem to require that these compounds exist in the keto forms rather than in the pyrimidine form sometimes inferred (5, 6) for orotic acid. The proton magnetic resonance spectra of the compounds and the neutral equivalents of the acids were in agreement with those expected for the structures indicated. Several of the compounds listed, especially the orotic acids, showed crystalline transitions in the course of the melting-point determinations.

EXPERIMENTAL

Substituted Hydantoins Esters (Table I)

Diethyl ketosuccinate or the appropriately 3-substituted diethyl ketosuccinate was condensed with either urea or the monosubstituted area following the directions reported by Clerk-Bory and Mentzer (4). When the product did not crystallize directly from the reaction mixture, it was isolated by solvent removal *in vacuo* for crystallization.

Substituted Hydantoin Acids (Table II)

Mild alkaline hydrolysis followed by acidification and recrystallization of the precipitate from aqueous ethanol (4) provided the desired acid except for 3-methyl-5-(carboxybenzylidene)-hydantoin. This compound was obtained by refluxing a solution of the ester (12 g) in 400 ml of a 1:1 mixture of ethanol and 1% aqueous perchloric acid for 9 days. The acid was isolated from the incompletely hydrolyzed product in the usual manner and purified by recrystallization from ethanol–benzene.

Substituted Orotic Acids (Table III)

Except as described below, the ethyl esters reported in Table I were heated for about 4 h in refluxing 2 *N* aqueous potassium hydroxide (4). In order to achieve homogeneous conditions, ethanol was added at the beginning of the heating period until solution was complete. The ethanol was then removed during the course of the reaction. In each case, when the reaction was stopped, the ultraviolet absorption spectrum of the solution no longer showed the maximum absorption above 290 mμ originally present for the hydantoin derivative. In the preparation of the 3-methyl- and 3-phenyl-orotic acids, the reaction mixture was stirred at 50° and the ethanol was not removed.

ACKNOWLEDGMENTS

We acknowledge, with thanks, financial support from Bristol Laboratories, Inc. and the technical assistance of Mr. Werner Merlo.

1. R. Müller. J. Prakt. Chem. **56**, 475 (1897).
2. H. K. Mitchell and J. F. Nyc. J. Am. Chem. Soc. **69**, 674 (1947).
3. J. F. Nyc and H. M. Mitchell. J. Am. Chem. Soc. **69**, 1383 (1947).
4. C. Clerk-Bory and C. Mentzer. Bull. Soc. Chim. France, 436 (1958).
5. H. Gershon. J. Org. Chem. **27**, 3507 (1962).
6. G. D. Daves, F. Baiocchi, R. K. Robins, and C. C. Chang. J. Org. Chem. **26**, 2755 (1961).
7. D. A. Hahn and M. M. Endicott. J. Am. Chem. Soc. **59**, 2741 (1937).
8. M. R. Atkinson, M. H. Maguire, R. K. Ralph, G. Shaw, and R. N. Warrener. J. Chem. Soc. 2363 (1957).
9. J. J. Fox, N. Yung, and I. Wempen. Biochim. Biophys. Acta, **23**, 295 (1957).

Received August 25, 1964.
Department of Chemistry,
University of Alberta,
Edmonton, Alberta.

RADIATION CHEMISTRY OF POTASSIUM PEROXYDISULFATE

R. L. Eager and J. F. Norris

This note gives the results obtained in a study of the radiation chemistry of potassium peroxydisulfate. Samples of the solid compound were irradiated with ^{60}Co γ-rays after which they were dissolved in water and the resulting solutions analyzed.

Can. J. Chem. Downloaded from www.nrcresearchpress.com by 210.87.254.105 on 09/05/12
For personal use only.

Can. J. Chem. Downloaded from www.nrcresearchpress.com by 210.87.254.105 on 09/05/12
For personal use only.

EXPERIMENTAL

Reagent grade potassium peroxydisulfate which was further purified by recrystallization from water was used. The recrystallization step was found effective for removing traces of sulfate ions present in the reagent grade material.

The irradiation source was a Gamma Cell 220 ^{60}Co Irradiation Unit manufactured by Atomic Energy of Canada Ltd. Ferrous sulfate dosimetry was used, and the difference in the electron densities of the sample and the dosimeter was considered in calculating the absorbed dose. The samples were irradiated in 9 ml glass vials, each of which was closed with a plastic cap fitted with an aluminium foil washer.

The yield of acid was determined by microtitration with standard base using methyl red as an indicator. It was found necessary to add the indicator as close as possible to the end point to prevent it from being destroyed by the potassium peroxydisulfate before the end point was reached. With this technique very satisfactory end points were obtained.

The yield of sulfate ions was determined by a nephelometric method (1) using a Fisher Nefluoro-Photometer. The amount of sulfite ions present was determined by adding hydrogen peroxide to the solution before addition of $BaCl_2$.

Oxygen was determined by gas chromatography using a column packed with Linde 5A molecular sieve. The sample was dissolved in oxygen-free water kept under an atmosphere of helium. After solution of the sample was complete, the gas phase above the solution was pushed, by helium pressure, into the helium stream flowing through the column. For complete recovery of the oxygen it was necessary that all of the oxygen should diffuse from the solution into the helium stream in a short interval of time. Failure for this to occur may have been responsible, in part at least, for the low results obtained.

RESULTS AND DISCUSSION

Analysis of the aqueous solutions showed the presence of acid and of sulfate ions. Oxygen was detected by the use of gas chromatography. Figure 1 shows the variation of the yields of sulfate ions and of acid with the absorbed dose. The dose rate was 1 450 rads min^{-1}. The yield of acid was linear with respect to absorbed dose over the entire range of doses investigated, namely up to 78×10^6 rads. At this point approximately 4% of the peroxydisulfate ions had been decomposed, based on the yield of acid. From the slope of the line for the yield of acid vs. dose, it was calculated that $G_{acid} = 3.41$. Up to a dose of approximately 13×10^6 rads the yield of sulfate ions was also linear with respect to dose and is, within experimental error, equal to the yield of acid. This latter fact is in agreement with the equation:

$$[1] \qquad S_2O_8^{=} + H_2O \rightarrow 2SO_4^{=} + 2H^+ + \tfrac{1}{2}O_2.$$

At doses higher than 13×10^6 rads the yields of sulfate ions become increasingly lower than those of acid. That sulfite ions are also present is indicated by the increased amount of $BaSO_4$ formed when hydrogen peroxide is added to the solution before addition of $BaCl_2$. From the curves in Fig. 1 and the yield of sulfite ions for a dose of 47.9×10^6 rads, it follows that at this dose the yield of sulfate ions is 22% lower than the yield of acid, whereas the yield of sulfate ions plus sulfite ions is only 10% lower than the yield of acid.

Preliminary determinations of the yield of oxygen indicated that the yield may be in agreement with eq. [1]. The results were somewhat scattered and, based on the yields of acid, the observed yields of oxygen were somewhat lower than those predicted by eq. [1]. The low yields observed for oxygen may have been due to incomplete recovery of the oxygen liberated in the solution of the sample. The yields of oxygen became less as the particle size of the potassium peroxydisulfate was decreased. This may indicate that some of the oxygen was being lost from the sample before analysis either by diffusion from the solid or by reaction of the radiolysis products with adsorbed water.

Atkins *et al.* (2) have obtained the electron spin resonance (e.s.r.) spectra of alkali metal peroxydisulfates which had been irradiated either with γ-rays or with ultraviolet radiation. They reached the conclusion that γ-ray irradiation produces at least three

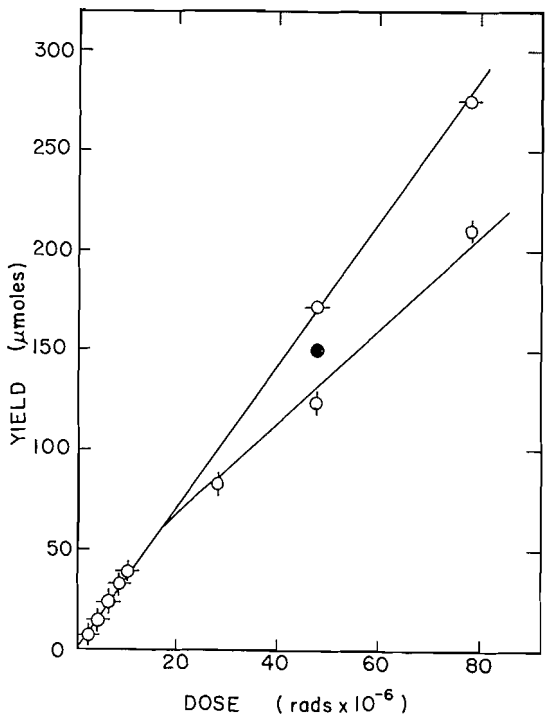

FIG. 1. Yield of products as a function of absorbed dose for γ-irradiated potassium peroxydisulfate; -O- acid; ○ sulfate ions; ● sulfate plus sulfite ions.

different radicals. Two of these were tentatively identified as SO_4^- and $S_2O_8^-$, the authors' types 2 and 1, respectively. It might be expected that SO_4^- radicals would react with water in an overall reaction as follows

[2] $$2SO_4^- + H_2O \rightarrow 2SO_4^{=} + 2H^+ + O$$

If it is assumed that the SO_4^- radicals were formed by a breaking of the peroxide bond in the peroxydisulfate ion,

[3] $$S_2O_8^{=} \rightsquigarrow 2SO_4^-,$$

then the stoichiometry suggested by eq. [1] would hold. A possible mechanism involving the $S_2O_8^-$ radical is given below.

[4] $$S_2O_8^{=} \rightsquigarrow e + S_2O_8^-.$$

Upon solution of the sample in water

[5] $$e + H_2O \rightarrow H + OH^-$$

[6] $$S_2O_8^- + H_2O + H \rightarrow SO_4^{=} + SO_3^{=} + O_2 + 3H^+.$$

The sum of eqs. [4], [5], and [6] is

[7] $$S_2O_8^{=} + H_2O \rightarrow SO_4^{=} + SO_3^{=} + O_2 + 2H^+.$$

Equation [7] together with eq. [1] predicts that the sum of the yields of sulfate and sulfite should be equal to the yield of acid, whereas the yield of oxygen should be higher than that given by eq. [1]. Since the sum of the yields of sulfate and sulfite has been found to be smaller than the yield of acid, the presence of some other sulfur containing species is

Can. J. Chem. Downloaded from www.nrcresearchpress.com by 210.87.254.105 on 09/05/12
For personal use only.

suggested. Since the yield of sulfite ions was smaller than the yield of sulfate ions, then, on the basis of the above mechanism, the number of SO_4^- radicals present in the irradiated salt must be several times larger than the number of $S_2O_8^-$ radicals. Using the smoothed curve in Fig. 1 for the yield of sulfate, we calculated, on the basis of the above mechanisms, for a dose of 47.9×10^6 rads, that the number of SO_4^- radicals is approximately seven times the number of $S_2O_8^-$ radicals. Atkins *et al.* give no estimate of the relative number of the two radicals, nor of the doses received by their samples. However, it would appear on the basis of their Fig. 1 that the number of SO_4^- radicals is several times larger than the number of $S_2O_8^-$ radicals.

ACKNOWLEDGMENTS

The authors are grateful to the National Research Council for financial assistance. The help given in the oxygen analysis by Dr. J. M. Roxburgh of the Prairie Regional Laboratory of the National Research Council is gratefully acknowledged.

1. G. W. EWING. Instrumental methods of chemical analysis. McGraw-Hill Book Company, Inc., New York. 1954. pp. 195, 395.
2. P. W. ATKINS, J. A. BRIVATI, A. HORSFIELD, M. C. R. SYMONS, and P. A. TREVALION. Sixth International Symposium on Free Radicals. University of Cambridge. 1963.

RECEIVED JUNE 29, 1964.
DEPARTMENT OF CHEMISTRY AND CHEMICAL ENGINEERING,
UNIVERSITY OF SASKATCHEWAN,
SASKATOON, SASKATCHEWAN.

MANIFESTATIONS OF CHANGES WITH AGE IN SILICA HYDROGELS[1]

A. F. SIRIANNI, F. W. MEADUS, AND I. E. PUDDINGTON

INTRODUCTION

Hydrocarbon oil dispersions of finely divided silica that has been prepared from aqueous solutions of sodium silicate by electrodialysis exhibit well-defined maximum yield values and sedimentation rates when the aquagels from which the silica was separated were prepared at about pH 5.5. A minimal electrophoretic mobility of the silica dispersed in oil and a pronounced minimum in the gelation time of the aquasols are also observed here (1). These maximal and minimal effects are presumably associated with the isoelectric point of the silica which is observed to be in the vicinity of pH 5 (2, 3). It was found by Plank and Drake (4) that the surface area of silica gels increased as the aquagels from which they were prepared were aged in a closed system. It was therefore of interest to look for changes in other properties of silica that might depend on the age of their aquagels. In particular, properties that depend on interaction between suspended silica particles have been examined.

EXPERIMENTAL

Solutions containing about 760 g of N grade sodium silicate produced by Philadelphia Quartz Co. dissolved in 5 l of distilled water were electrodialyzed to pH values ranging from 4.9 to about 6.0. A 6-l capacity lucite cell fitted with a screen platinum anode and a perforated copper cathode was used. A tightly woven cotton fabric which was resistant to alkali was found to be a very satisfactory membrane. The cathode compartment

[1]*Issued as N.R.C. No. 8167.*

Can. J. Chem. Downloaded from www.nrcresearchpress.com by 210.87.254.105 on 09/05/12
For personal use only.

suggested. Since the yield of sulfite ions was smaller than the yield of sulfate ions, then, on the basis of the above mechanism, the number of SO_4^- radicals present in the irradiated salt must be several times larger than the number of $S_2O_8^-$ radicals. Using the smoothed curve in Fig. 1 for the yield of sulfate, we calculated, on the basis of the above mechanisms, for a dose of 47.9×10^6 rads, that the number of SO_4^- radicals is approximately seven times the number of $S_2O_8^-$ radicals. Atkins *et al.* give no estimate of the relative number of the two radicals, nor of the doses received by their samples. However, it would appear on the basis of their Fig. 1 that the number of SO_4^- radicals is several times larger than the number of $S_2O_8^-$ radicals.

ACKNOWLEDGMENTS

The authors are grateful to the National Research Council for financial assistance. The help given in the oxygen analysis by Dr. J. M. Roxburgh of the Prairie Regional Laboratory of the National Research Council is gratefully acknowledged.

1. G. W. EWING. Instrumental methods of chemical analysis. McGraw-Hill Book Company, Inc., New York. 1954. pp. 195, 395.
2. P. W. ATKINS, J. A. BRIVATI, A. HORSFIELD, M. C. R. SYMONS, and P. A. TREVALION. Sixth International Symposium on Free Radicals. University of Cambridge. 1963.

RECEIVED JUNE 29, 1964.
DEPARTMENT OF CHEMISTRY AND CHEMICAL ENGINEERING,
UNIVERSITY OF SASKATCHEWAN,
SASKATOON, SASKATCHEWAN.

MANIFESTATIONS OF CHANGES WITH AGE IN SILICA HYDROGELS[1]

A. F. SIRIANNI, F. W. MEADUS, AND I. E. PUDDINGTON

INTRODUCTION

Hydrocarbon oil dispersions of finely divided silica that has been prepared from aqueous solutions of sodium silicate by electrodialysis exhibit well-defined maximum yield values and sedimentation rates when the aquagels from which the silica was separated were prepared at about pH 5.5. A minimal electrophoretic mobility of the silica dispersed in oil and a pronounced minimum in the gelation time of the aquasols are also observed here (1). These maximal and minimal effects are presumably associated with the isoelectric point of the silica which is observed to be in the vicinity of pH 5 (2, 3). It was found by Plank and Drake (4) that the surface area of silica gels increased as the aquagels from which they were prepared were aged in a closed system. It was therefore of interest to look for changes in other properties of silica that might depend on the age of their aquagels. In particular, properties that depend on interaction between suspended silica particles have been examined.

EXPERIMENTAL

Solutions containing about 760 g of N grade sodium silicate produced by Philadelphia Quartz Co. dissolved in 5 l of distilled water were electrodialyzed to pH values ranging from 4.9 to about 6.0. A 6-l capacity lucite cell fitted with a screen platinum anode and a perforated copper cathode was used. A tightly woven cotton fabric which was resistant to alkali was found to be a very satisfactory membrane. The cathode compartment

[1]*Issued as N.R.C. No. 8167.*

Can. J. Chem. Downloaded from www.nrcresearchpress.com by 210.87.254.5 on 09/05/12
For personal use only.

was kept short to reduce the electrical resistance of the cell and to allow the alkali produced in this compartment to be removed easily with a continuous stream of water. When a desired pH was obtained, measured with a Beckman pH meter, the sols were drained into clean 4 l pyrex beakers before shutting off the power and were tightly covered with saran wrap. These sols, which set with time to aquagels, were aged up to a period of about 2 years.

Dispersions of the silica aquagels in 1 P viscosity hydrocarbon oil and in stanolax ca. 0.4 P in viscosity contained 5% silica by weight. The removal of water from the suspensions by azeotropic distillation with *n*-propyl alcohol, homogenization of the pastes, and viscosity measurements were as previously described (1).

RESULTS AND DISCUSSION

The flow properties of the silica suspensions in the two hydrocarbon oils are indicated by Fig. 1 and Fig. 2. These show the change in yield value (Bingham yield value in arbitrary units) of the pastes as a function of the pH at which the silica sols were prepared.

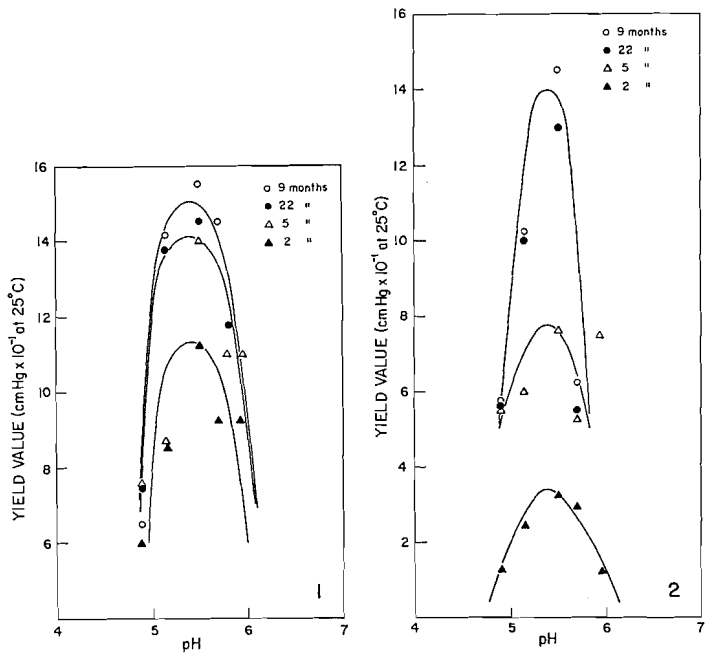

FIG. 1. Flow properties of silica suspensions in hydrocarbon oil ca. 1 P in viscosity.
FIG. 2. Flow properties of silica suspensions in Stanolax ca. 0.4 P in viscosity.

The maximum yield value at about pH 5.5 remained virtually constant over the aging period in both oils. The magnitude of the yield values increased with aging time reaching a maximum value after about 9 months.

Although the pastes made with stanolax using silica aged for short periods were considerably softer than the corresponding dispersions in the lubricating oil the differences disappeared with prolonged aging of the aquagels. No aging effects were detected after the water of the aquagels was replaced with oil. The pastes of maximum yield value prepared in stanolax were diluted to 1% silica by weight with reagent grade toluene. These suspensions were held in 1.5 cm diameter pyrex tubes filled to a height of 16 cm. After equilibrating for about 3 days, the sealed suspensions were homogenized by ultrasonic irradiation for about 5 min using a 40 kc Circo Ultrasonic Generator and their settling behavior is indicated by Fig. 3. The settling rates of the dispersions decreased and the sediment volume increased regularly as the yield value of the pastes increased.

Can. J. Chem. Downloaded from www.nrcresearchpress.com by 210.87.254.5 on 09/05/12
For personal use only.

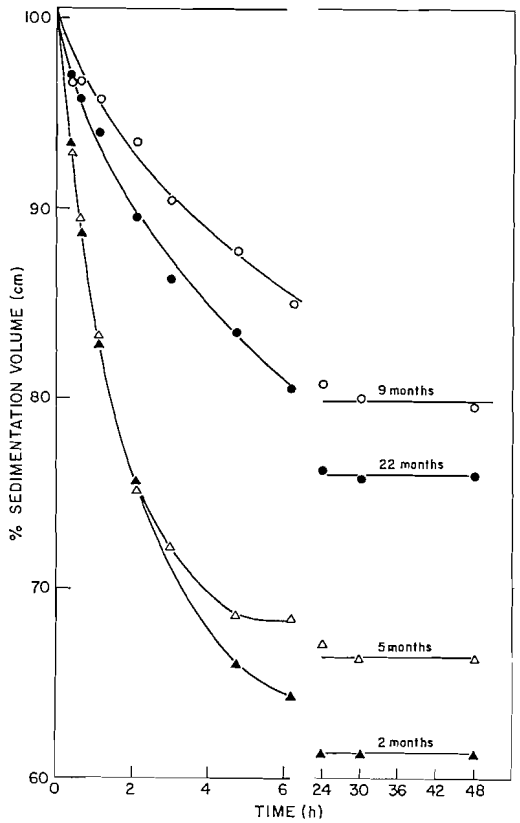

FIG. 3. The settling behavior of silica suspensions in toluene.

These observations suggest that the freshly prepared aquagels contain clusters of hydrous silica particles that are bonded sufficiently strongly to resist dispersion under the conditions of shear imposed during the preparation of the oil pastes. It is probable that the area of the junctions at the points of contact between the primary particles is an appreciable fraction of the area of the spheres. This fraction becomes larger with more dense forms of the packing on the clusters. Reinforcement of these junctions by the polymerization of added silica sol following initial gelation has been described by Iler (5) and it is possible that a similar phenomenon takes place to a degree during normal gelation. This form of aggregation is consistent with the relatively lower observed yield values of the pastes, the higher rates of settling, and the lower sedimentation volumes of the toluene-diluted pastes prepared from the fresher silica aquagel. To explain the subsequent behavior, the aging process would have to involve the reduction of the sizes and strengths of the contacting areas to a significant degree. This might come about through a ripening process that involved the preferential depolymerization of polysilicic acid at the junctions and its migration and deposition elsewhere. The repolymerization could take place either on new nuclei to form new primary particles or on established surfaces of different curvature. Changes of this kind would lead to an increased specific surface area of the separated gel following aging as reported by Plank and Drake (4). They would also explain the observations in the present work, since the bonds forming the clusters would be weakened

Can. J. Chem. Downloaded from www.nrcresearchpress.com by 210.87.254.5 on 09/05/12
For personal use only.

to the point where they would be broken by the shearing action applied during the preparation of the pastes. The increased number of separate primary particles would flocculate to less efficiently packed clusters giving higher equilibrium sedimentations volumes and lower sedimentation rates than the more densely packed material. The increased number of junctions would also lead to the higher observed yield values of the pastes made with fresh silica, and oils of two different viscosities may well reflect different amounts of shearing force transmitted to clusters during the preparation of the pastes. Since the oil viscosities differ by a factor of 2.5, this implies a rather critical shear strength of the bonds between the primary particles that was barely exceeded during the milling operation when the lower viscosity oil was used as the suspending medium. This seems a more attractive explanation, however, than the differences being ascribed to different surface activities of the two oils. The aging process can possibly be facilitated at an elevated temperature. A portion of freshly prepared gel pH 5.4 was aged at room temperature and a similar amount at 90 °C for 7 days and an additional 10 days at about 35 °C in tightly sealed pyrex beakers. Pastes in Stanolax "medium" and suspensions in toluene were prepared as described. A stiffer paste was obtained with the heated gel. The sedimentation volumes were of the order of 93.5 and 84.5% for the heated and the unheated aquagels respectively, after standing 48 h at room temperature. This is in good qualitative agreement with the behavior observed with the aquagels aged at room temperature for a long time. X-ray examination of the pastes revealed no differences in the silica particles from the fresh and from the aged aquagels. Both patterns consisted of equally broad halos of the type expected from the particles of this size range.

ACKNOWLEDGMENT

The authors wish to thank Dr. L. D. Calvert for the X-ray measurements.

1. A. F. Sirianni, F. W. Meadus, and I. E. Puddington. Can. J. Chem. **38**, 535 (1960).
2. H. W. Batchelor. J. Phys. Chem. **42**, 575 (1938).
3. R. K. Iler. The colloid chemistry of silica and silicates. Cornell Univ. Press, Ithaca, N.Y. 1955. p. 47.
4. C. J. Plank and L. C. Drake. J. Colloid Sci. **2**, 399 (1947).
5. R. K. Iler. The colloid chemistry of silica and silicates. Cornell Univ. Press, Ithaca, N.Y. 1955. p. 133.

Received July 10, 1964.
Division of Applied Chemistry,
National Research Council,
Ottawa, Canada.

PHOTOCHEMICAL TRANSFORMATIONS OF DIENES. III. THE PHOTOLYSIS OF 3- AND 3,6-SUBSTITUTED CHOLESTA-3,5-DIENES[1]

Clifford C. Leznoff[2] and George Just

As part of a study of the influence of substituents on the photolysis of cholesta-3,5-dienes (1, 2), we wish to report on the photo-induced reactions of the cholesta-3,5-dienes listed in Table I.

1. 6-Substituted-3-methoxycholesta-3,5-dienes

A 0.05% methanolic solution of 3-methoxy-6-methylcholesta-3,5-diene (II*a*)[3] was

[1]*This work was supported by the National Research Council of Canada and by Bristol Laboratories Ltd.*
[2]*Holder of a National Research Council of Canada Bursary 1961–1962 and Studentships 1962–1964.*
[3]*For preparation of starting materials, see Experimental.*

Can. J. Chem. Downloaded from www.nrcresearchpress.com by 210.87.254.5 on 09/05/12
For personal use only.

to the point where they would be broken by the shearing action applied during the preparation of the pastes. The increased number of separate primary particles would flocculate to less efficiently packed clusters giving higher equilibrium sedimentations volumes and lower sedimentation rates than the more densely packed material. The increased number of junctions would also lead to the higher observed yield values of the pastes made with fresh silica, and oils of two different viscosities may well reflect different amounts of shearing force transmitted to clusters during the preparation of the pastes. Since the oil viscosities differ by a factor of 2.5, this implies a rather critical shear strength of the bonds between the primary particles that was barely exceeded during the milling operation when the lower viscosity oil was used as the suspending medium. This seems a more attractive explanation, however, than the differences being ascribed to different surface activities of the two oils. The aging process can possibly be facilitated at an elevated temperature. A portion of freshly prepared gel pH 5.4 was aged at room temperature and a similar amount at 90 °C for 7 days and an additional 10 days at about 35 °C in tightly sealed pyrex beakers. Pastes in Stanolax "medium" and suspensions in toluene were prepared as described. A stiffer paste was obtained with the heated gel. The sedimentation volumes were of the order of 93.5 and 84.5% for the heated and the unheated aquagels respectively, after standing 48 h at room temperature. This is in good qualitative agreement with the behavior observed with the aquagels aged at room temperature for a long time. X-ray examination of the pastes revealed no differences in the silica particles from the fresh and from the aged aquagels. Both patterns consisted of equally broad halos of the type expected from the particles of this size range.

ACKNOWLEDGMENT

The authors wish to thank Dr. L. D. Calvert for the X-ray measurements.

1. A. F. Sirianni, F. W. Meadus, and I. E. Puddington. Can. J. Chem. **38**, 535 (1960).
2. H. W. Batchelor. J. Phys. Chem. **42**, 575 (1938).
3. R. K. Iler. The colloid chemistry of silica and silicates. Cornell Univ. Press, Ithaca, N.Y. 1955. p. 47.
4. C. J. Plank and L. C. Drake. J. Colloid Sci. **2**, 399 (1947).
5. R. K. Iler. The colloid chemistry of silica and silicates. Cornell Univ. Press, Ithaca, N.Y. 1955. p. 133.

Received July 10, 1964.
Division of Applied Chemistry,
National Research Council,
Ottawa, Canada.

PHOTOCHEMICAL TRANSFORMATIONS OF DIENES. III. THE PHOTOLYSIS OF 3- AND 3,6-SUBSTITUTED CHOLESTA-3,5-DIENES[1]

Clifford C. Leznoff[2] and George Just

As part of a study of the influence of substituents on the photolysis of cholesta-3,5-dienes (1, 2), we wish to report on the photo-induced reactions of the cholesta-3,5-dienes listed in Table I.

1. 6-Substituted-3-methoxycholesta-3,5-dienes

A 0.05% methanolic solution of 3-methoxy-6-methylcholesta-3,5-diene (II*a*)[3] was

[1]*This work was supported by the National Research Council of Canada and by Bristol Laboratories Ltd.*
[2]*Holder of a National Research Council of Canada Bursary 1961–1962 and Studentships 1962–1964.*
[3]*For preparation of starting materials, see Experimental.*

Can. J. Chem. Downloaded from www.nrcresearchpress.com by 210.87.254.6 on 09/05/12
For personal use only.

irradiated for 0.5 h. 3,3-Dimethoxy-6-methylcholest-5-ene (III*a*) was obtained in 75% yield by direct crystallization. Its n.m.r. spectrum showed the presence of two methoxy groups at 3.12_5 and 3.23 p.p.m. and a methyl group attached to a double bond (1.66 p.p.m.). The infrared spectrum of III*a* showed strong absorption in the ether region that was practically identical with that of 3,3-dimethoxy-cholest-5-ene (III), obtained in the photolysis of 3-methoxycholesta-3,5-diene (II) in methanol (1). Evaporation of the filtrate from the photolysis reaction product III*a* gave an oil, whose infrared spectrum showed the presence of III*a*, 6-methylcholest-5-en-3-one, and 6-methylcholest-4-en-3-one. Hydrolysis of III*a* with malonic acid in aqueous acetone for 3 days gave a mixture of 6-methylcholest-5-en-3-one (ν 1 720 cm^{-1}) and 6-methylcholest-4-en-3-one (I*a*) (ν 1 685 cm^{-1}).

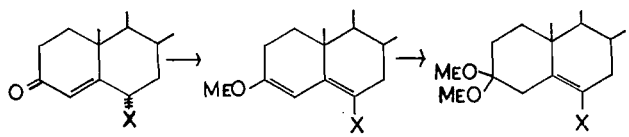

I	X = H	II	X = H	III	X = H
I*a*	X = CH_3	II*a*	X = CH_3	III*a*	X = CH_3
I*b*	X = F	II*b*	X = F	III*b*	X = F
I*c*	X = NO_2	II*c*	X = NO_2		

Similarly, 6-fluoro-3-methoxycholesta-3,5-diene (II*b*) was irradiated in methanol for 0.33 h and 3,3-dimethoxy-6-fluorocholest-5-ene (III*b*) was obtained in 85% yield, by direct crystallization. Its n.m.r. spectrum shows signals at 3.07 and 3.16 p.p.m. corresponding to the two methoxy groups. The infrared spectrum of III*b* showed strong absorption between 1 000 and 1 200 cm^{-1} due to the C—O and C—F stretching frequencies (3). Evaporating a solution of III*b* in carbon tetrachloride on the steam bath (1) resulted in hydrolysis of III*b*. The infrared spectrum of the oil showed the presence of an α,β-unsaturated ketone (ν 1 695 cm^{-1}) and a saturated ketone (ν 1 725 cm^{-1}). These peaks no doubt arise from the hydrolysis products of III*b*, i.e. 6-fluorocholest-4-en-3-one (I*b*) and 6-fluorocholest-5-en-3-one.

In the two photolysis reactions described, hydrolysis accounted for approximately 10% of the total reaction products, compared to 40% for 3-methoxycholesta-3,5-diene (II) (1).

When a solution of 3-methoxy-6-nitrocholesta-3,5-diene (II*c*) was irradiated in methanol, an oil was obtained from which no crystalline material could be isolated.

2. 3-Substituted Cholesta-3,5-dienes

A 0.2% ethanolic solution of 3-chlorocholesta-3,5-diene (IV) (5, 6) was irradiated until the absorption maximum of the solution had decreased to less than 5% of the original absorption (4 h). When the solvent was evaporated and a n.m.r. spectrum of the crude photolysis mixture taken, the presence of cyclopropyl protons was detected at 0.25 p.p.m. and at 0.5 p.p.m. Chromatography on silica gel or aluminium oxide gave in the hexane fraction about 50% of oily crystals from which was obtained by successive crystallizations 3–4% of impure V, m.p. 111–113°. Since no pure product could be obtained by a combination of column chromatography and crystallizations, the crude photolysate was purified by thin-layer chromatography (t.l.c.). Thin-layer chromatography revealed the presence of 18 products, 7 of them in trace amounts.

Can. J. Chem. Downloaded from www.nrcresearchpress.com by 210.87.254.6 on 09/05/12
For personal use only.

Fraction 9 (designated according to decreasing R_f values) yielded a saturated chloroether V, m.p. 131–133°. Its n.m.r. spectrum showed signals at 0.25 p.p.m. (one proton, $J = 4.0$ c.p.s.) and 0.5 p.p.m. (shoulder) characteristic of geminal protons attached to a cyclopropane ring (7, 8), and a complex, poorly resolved signal between 3.20 and 3.80 p.p.m. due to the three protons alpha to the oxygen function. The latter absorption was virtually identical to that observed for 6β-ethoxy-3β, 5-cyclocholestane (9, 10) and its 3-methyl analogue (2) and provides further evidence for the formulation of V as 3-chloro-6β-ethoxy-3β, 5-cyclocholestane. The infrared spectra of fractions 15–18 indicated that they were mixtures of saturated ketones, α,β-unsaturated ketones, and hydroxy ketones.

Photolysis of IV in spectrograde pentane yielded an inseparable mixture.

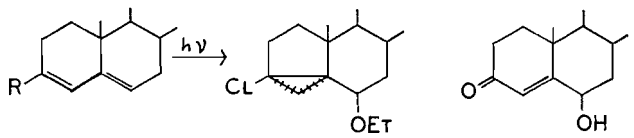

IV R = Cl
IV*a* R = OAc
IV*b* R = Ph
IV*c* R = p-OEtPh
IV*d* R = SEt
IV*e* R-N(CH$_2$)$_4$

V VI

When a 0.2% solution of 3-acetoxycholesta-3,5-diene (IV*a*) (II) was photolyzed in ethanol, methanol, or pentane, the absorption maximum at 234 mμ decreased rapidly (1 h). The only product which could be isolated from the complex reaction mixture in approximately 10% yield was cholest-4-en-3-on-6β-ol (VI), identified by comparison with an authentic sample (12*a*).

Irradiation of IV*b*, IV*c*, IV*d*, and IV*e* in various solvents gave intractable mixtures.

3. Chemical Shifts of the C-4 and C-6 Protons of Cholesta-3,5-dienes

In the course of studying these photolyses, it was observed that the chemical shifts of the C-4 proton of the cholesta-3,5-dienes varied by as much as 2 p.p.m. In order to compare them, it was necessary to provide a standard. The n.m.r. spectrum of cholesta-3,5-diene exhibits unresolved peaks between 5.20 and 5.90 p.p.m. By introducing deuterium at C-3, it was hoped to simplify the n.m.r. spectrum of this compound.

Cholest-4-en-3-one was reacted with lithium aluminium deuteride, and the resulting 3-deuteriocholest-4-en-3-ol was dehydrated directly by refluxing with hydrochloric acid in ethanol to give 3-deuteriocholesta-3,5-diene. The 3-deuteriocholesta-3,5-diene showed signals at 5.79 and 5.22 p.p.m. due to the C-4 and C-6 protons respectively.[4]

The chemical shifts of the C-4 and C-6 protons of the dienes are recorded in Table I.

Deshielding due to a negative inductive effect cannot be important except perhaps for 3-chlorocholesta-3,5-diene (14) in which the C-4 proton is deshielded compared to cholesta-3,5-diene by 0.28 p.p.m. The deshielding of the C-4 protons in 3-phenyl and 3-(*p*-ethoxyphenyl) cholesta-3,5-dienes is due to the paramagnetic effect of the benzene rings, which are probably coplanar with the diene system (13*b*).

When an oxygen or nitrogen atom is attached at C-3, the C-4 proton is strongly shielded.

[4]*The C-4 proton appears in all 3-substituted cholesta-3,5-dienes as a singlet, and the C-6 proton as a broad signal due to coupling with the C-7 protons.*

Can. J. Chem. Downloaded from www.nrcresearchpress.com by 210.87.254.6 on 09/05/12
For personal use only.

TABLE I

Nuclear magnetic resonance and irradiation data of some cholesta-3,5-dienes (T.M.S. = 0, chemical shifts in p.p.m.)

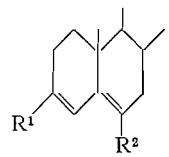

R^1	R^2	δ C_4-H	δ C_6-H	Irradiation time[f] (h)	Product Formula No.
$N(CH_2)_4$	H	4.53	4.79	6	Mixture
MeO	H	5.13	5.25	0.5	(1)
EtO	H	5.26	5.37	1.5	(1)
MeO	CH_3	5.28	—	0.5[b]	III[a]
MeO	F	5.39	—	0.33[b]	III[b]
AcO	H	5.61	5.315	1[a,b,c]	VI
Me	H	5.66	5.25	6	(2)
EtS	H	5.67	5.20	1[b,d]	Mixture
H	H	5.78[g]	5.22	6	(9,10)
D	H	5.79	5.22	—	—
Cl	H	6.06	5.40	4[a,c]	V
p-OEtPh	H	6.10	5.35	4[c],7[e]	Mixture
Ph	H	6.24	5.40	24[c]	Mixture
MeO	NO_2	6.26	—	0.2[b]	Mixture

Solvents in which irradiations were carried out: [a]pentane, [b]methanol–pentane, [c]ethanol, [d]ethanol and 0.25 ml pyridine, [e]acetic acid – pentane. [f]Time required for nearly complete disappearance of chromophore. [g]Doublet, J = 10 c.p.s. (13*a*).

This shielding must be due to the effect of the π-electrons of the oxygen or nitrogen atom (15, 16, 17).

The large deshielding effect of the 6-nitro group (1.13 p.p.m.) is not unusual (18) and overrides the shielding effect of the methoxy group in 3-methoxy-6-nitrocholesta-3,5-diene.

The chemical shifts of the C-6 protons of cholesta-3,5-dienes are only slightly affected by the substituent at C-3.

EXPERIMENTAL[5]

3-Methoxy-6-methylcholesta-3,5-diene (IIa)

To 0.55 g of 6α-methylcholest-4-en-3-one (I*a*) (19, 20) in 5 ml of dioxane and 0.5 ml of trimethylorthoformate was added one drop of concentrated sulfuric acid in 0.5 ml of dioxane and the solution was refluxed for 2 min. Pyridine (0.25 ml) was added and the solvent evaporated *in vacuo*. The resulting oil was covered with methanol and allowed to crystallize overnight. Recrystallization from methanol gave 0.47 g of II*a*, m.p. 89.5–91°, λ_{max}^{EtOH} 247 mμ (ε 24 800), (21), $[\alpha]_D$ −127° (*c*, 1.0 in pyridine). Calcd. for $C_{29}H_{48}O$: C, 84.40; H, 11.72. Found: C, 84.24; H, 11.73.

Irradiation of 3-Methoxy-6-methylcholesta-3,5-diene (IIa) in Methanol

Irradiation of 0.4 g of II*a* in 70 ml of pentane and 450 ml of methanol for 30 min gave directly by concentration of the solution and filtration about 0.32 g of 3,3-dimethoxy-6-methylcholest-5-ene (III*a*), m.p. 118–119°. Recrystallization from ether–methanol gave III*a*, m.p. 119–121°, $[\alpha]_D$ −43.5° (*c*, 1.14 in chloroform). Calcd. for $C_{30}H_{52}O_2$: C, 81.02; H, 11.79. Found: C, 81.55; H, 11.82.

Evaporation of the mother liquors left 110 mg of an oil whose infrared spectrum indicated the presence of ketal III*a*, an α,β-unsaturated ketone (ν 1 685 cm^{-1}), and a saturated ketone (ν 1 720 cm^{-1}).

A solution of 125 mg of III*a*, 50 mg of malonic acid, 10 ml of acetone, and 1 ml of water was allowed to stand for 4 days at room temperature. An infrared spectrum of the product, obtained after the usual work-up, showed that complete hydrolysis had occurred to give an α,β-unsaturated ketone (ν 1 685 cm^{-1}), and a saturated ketone (ν 1 720 cm^{-1}).

6-Fluoro-3-methoxycholesta-3,5-diene (IIb)

To a solution of 0.375 g of 6-fluorocholest-4-en-3-one (I*b*) (22) in 5 ml of dioxane and 0.5 ml of trimethylorthoformate was added one drop of concentrated sulfuric acid in 0.5 ml of dioxane and the solution was

[5]*See (1) for general procedures.*

Can. J. Chem. Downloaded from www.nrcresearchpress.com by 210.87.254.6 on 09/05/12
For personal use only.

refluxed for 2 min. Pyridine (0.25 ml) was added and the solvent was evaporated *in vacuo*. The oil obtained was covered with methanol to induce crystallization. Recrystallization from ether–methanol (containing one drop of pyridine) afforded 0.30 g of II*b*, m.p. 90.5–91.5°, $[\alpha]_D$ −107.5° (*c*, 0.93 in pyridine), λ_{max}^{EtOH} 239 mμ (ε 22 600). Calcd. for $C_{28}H_{45}OF$: C, 80.71; H, 10.89; F, 4.56. Found: C, 80.18; H, 10.26; F, 4.65.

Irradiation of 6-Fluoro-3-methoxycholesta-3,5-diene (IIb) in Methanol

Irradiation of 0.20 g of II*b* in 50 ml of pentane and 475 ml of methanol for 20 min gave directly by concentration of the solution and filtration 0.172 g of 3,3-dimethoxy-6-fluorocholest-5-ene (III*b*). Recrystallization from ether–methanol gave III*b*, m.p. 104–104.5°, $[\alpha]_D$ −31.4° (*c* 1.0 in chloroform). Calcd. for $C_{29}H_{49}O_2F$: C, 77.63; H, 11.01; F, 4.23. Found: C, 77.29; H, 10.28; F, 4.67.

Evaporation of the mother liquors gave 35 mg of oil whose infrared spectrum indicated the presence of ketal III*b*, an α,β-unsaturated ketone (ν 1 695 cm^{-1}), and a saturated ketone (ν 1 730 cm^{-1}).

A solution of 25 mg of III*b* in 5 ml of carbon tetrachloride was evaporated on the steam bath (1). The resulting oil showed absorption in the infrared spectrum at 1 730 cm^{-1} and 1 695 cm^{-1} indicating the formation of saturated and α,β-unsaturated ketones respectively.

6β-Nitrocholest-4-en-3β-ol (VII)

A solution of 5.0 g of 3β-acetoxy-6-nitrocholest-5-ene (4, 23) in 300 ml of methanol, containing 3.0 g of potassium hydroxide, was heated under reflux for 1.5 h. Acidification with acetic acid, addition of water, and filtration gave a product which was crystallized from aqueous methanol to yield 1.83 g of 6β-nitrocholest-4-en-3β-ol. Recrystallization from methanol gave VII, m.p. 141–142°, $[\alpha]_D$ −98.9° (*c* 0.89 in chloroform). Calcd. for $C_{27}H_{45}O_3N$: C, 75.13; H, 10.51; N, 3.25. Found: C, 75.01; H, 10.74; N, 3.70.

Its n.m.r. spectrum showed signals at 5.72_5, 4.50, 4.04, and 3.31 p.p.m. due to the C-4 olefinic, C-6α, C-3α, and hydroxy protons respectively. The position of the hydroxy proton was proved by exchange with heavy water.

6β-Nitrocholest-4-en-3-one (VIII)

To a solution of 1.0 g of VII in 60 ml of acetone at 0° was added an excess of Jones reagent (24, 25, 26) and the solution was stirred for 2 min. Addition of water and filtration of the resulting precipitate gave 1.0 g of VIII. Recrystallization from ether–methanol gave 0.8 g of VIII, m.p. 118–119°, $[\alpha]_D$ −98.8° (*c* 0.87 in chloroform), λ_{max}^{EtOH} 233 mμ (ε 12 600). Calcd. for $C_{27}H_{43}O_3N$: C, 75.48; H, 10.09; N, 3.26. Found: C, 75.44; H, 10.47 N, 3.29.

Its n.m.r. spectrum showed absorption bands at 6.02 p.p.m. and 4.83 p.p.m. corresponding to the C-4 olefinic and the C-6α protons respectively. The infrared spectrum of VIII showed the presence of a nitro group at 1 540 cm^{-1} and an α,β-unsaturated ketone at 1 670 cm^{-1}.

6α-Nitrocholest-4-en-3-one (Ic)

A solution of 0.6 g of VIII in 5 ml of methanol, containing 25 mg of potassium hydroxide was kept at room temperature for 2 min. After acidification with acetic acid, addition of water gave 0.6 g of I*c*. Recrystallization from methanol gave pure I*c*, m.p. 136–137°, $[\alpha]_D$ +78.0° (*c* 0.91 in chloroform), λ_{max}^{EtOH} 232 mμ (ε 15 800). Calcd. for $C_{27}H_{43}O_3N$: C, 75.48; H, 10.09; N, 3.26. Found: C, 75.55; H, 9.99; N, 2.47.

Its n.m.r. spectrum showed signals at 5.28 p.p.m. (doublet, J = 1.8 c.p.s.) and at 5.14 p.p.m. (multiplet) corresponding to the C-4 olefinic and C-6β protons respectively. The C-4 proton which appears as a doublet is apparently coupled with the C-6 hydrogen (27). The infrared spectrum of I*c* showed the typical nitro absorption at 1 543 cm^{-1} and an α,β-unsaturated ketone peak at 1 672 cm^{-1}.

3-Methoxy-6-nitrocholesta-3,5-diene (IIc)

To a solution of 0.35 g of I*c* in 5 ml of dioxane and 0.5 ml of trimethylorthoformate was added one drop of concentrated sulfuric acid in 0.5 ml of dioxane and the solution was refluxed for 2 min. Pyridine (0.25 ml) was added and the solvent removed *in vacuo* at 80°. The oil was covered with methanol and after standing in the cold overnight, 0.25 g of II*c*, m.p. 135–136°, was obtained. Recrystallization from ether–methanol (containing one drop of pyridine) decreased the m.p. of I*c* to 129–136°, $[\alpha]_D$ −8.3 (*c* 1.27 in pyridine), λ_{max}^{EtOH} 233 mμ (ε 14 000). Calcd. for $C_{28}H_{45}O_3N$: C, 75.80; H, 10.22; N, 3.16. Found: C, 76.01; H, 10.20; N, 2.58.

Irradiation of 3-Methoxy-6-nitrocholesta-3,5-diene (Ic) in Methanol

Irradiation of 0.2 g of I*c* in 10 ml of pentane and 515 ml of methanol for 10 min gave upon evaporation of the solvent 0.23 g of oil. Its n.m.r. spectrum showed broad absorption peaks indicative of a complex mixture of compounds.

Irradiation of 3-Chlorocholesta-3,5-diene (IV) in Ethanol

A solution of 1.8 g of IV (5, 6), λ_{max}^{EtO} 242 (ε 22 400), 250 (ε 20 400), and 230 (ε 15 300) mμ in 450 ml ethanol and 50 ml of pentane was irradiated until no ultraviolet absorption could be detected (4 h). After evaporation of the solvent, the photolysis mixture was separated by t.l.c. (silica gel). Using hexane as solvent, two fast (A and B) and two slow moving bands (C and C) were evident. Desorption of bands A and B with ether gave 200 mg of oil, which on rechromatography gave six fractions.

Can. J. Chem. Downloaded from www.nrcresearchpress.com by 210.87.254.6 on 09/05/12
For personal use only.

Desorption of band C with ether and rechromatography (t.l.c., hexane–benzene 4:1) yielded fractions 7–14. Fraction 9 gave 53 mg of crystals, m.p. 125–129°. Recrystallization from hexane gave 16 mg of pure 3-chloro-6β-ethoxy-3β,5-cyclocholestane (V), m.p. 131–133°, $[\alpha]_D$ +6.8 (*c* 1.5 in chloroform). Calcd. for $C_{29}H_{49}OCl$: C, 77.56; H, 11.00; Cl, 7.90. Found: C, 77.54; H, 10.57; Cl, 8.01.

Fractions 7, 8, 10, 11, 12, 13, and 14 could not be sufficiently purified for structural studies.

Band D, after extraction with ether, was rechromatographed (t.l.c., benzene–ether 19:1). Fractions 15–18, accounting for 65% of the photolysis products, were obtained but could not be characterized.

Irradiation of 3-Acetoxycholesta-3,5-diene (IVa)

A solution of 1.1 g of IV*a* (11), λ_{max}^{EtOH} 234 mμ (ε 16 000) in 1 700 ml of ethanol, methanol, or methanol containing a few drops of pyridine was irradiated until the absorption maximum had decreased to less than 5% of the original absorption (1 h). Chromatography on alumina yielded in the ether fractions 100 mg of cholest-4-en-6β-ol-3-one (VI), m.p. 160–165°. Recrystallization from hexane gave VI, m.p. 181–184° (mixed melting point with an authentic sample; 181–184°).

Irradiation of IV*a* in pentane yielded intractable mixtures.

3-(p-Ethoxyphenyl)cholesta-3,5-diene (IVc)

p-Bromophenetole (9 ml) in 40 ml of anhydrous ether was added slowly to 2.75 g of magnesium, activated by a few crystals of iodine. After completion of the reaction (3 h), 10 g of cholest-4-en-3-one was added to the Grignard reagent and the reaction mixture was stirred under reflux overnight. A 20% solution of hydrochloric acid in ethanol was added slowly to the reaction mixture to destroy excess Grignard reagent and the mixture was refluxed for 4 h to ensure dehydration of the reaction product.

About 8.0 g of IV*c*, m.p. 120–121°, λ_{max}^{EtOH} 288 mμ (ε 25 900), 227 (10 300), 234 (shoulder), was obtained. Calcd. for $C_{35}H_{52}O$: C, 86.00; H, 10.72. Found: C, 86.00; H, 10.38.

The n.m.r. spectrum of IV*c* showed signals at 6.84 p.p.m. (quartet, corresponding to the four aromatic protons), 6.10 p.p.m. (sharp singlet, C-4 proton), 5.35 p.p.m. (broad peak, C-6 proton), and 3.84 p.p.m. (a quartet, CH_3—CH_2—O protons).

Irradiation of 3-(p-Ethoxyphenyl)cholesta-3,5-diene (IVc)

Irradiation of 1.3 g of IV*c* in 1 800 ml of ethanol for 4 h gave some starting material and 0.74 g of oil. Chromatography on alumina did not result in isolation of pure product.

Irradiation of 1.3 g of IV*c* in 1 370 ml of pentane and 230 ml of acetic acid for 7 h yielded 1.45 g of product. Thin-layer chromatography of 1.45 g on silica gel revealed at least 12 major and over 20 minor bands.

Irradiation of 3-Phenylcholesta-3,5-diene (IVb) (28) in Ethanol

Irradiation of 1.2 g of IV*b* in 1 300 ml of ethanol and 400 ml of pentane for 24 h gave 2.8 g of product. Chromatography on alumina gave a total of 1.6 g of oily fractions. The n.m.r. spectrum of the major fraction indicated mixtures.

Irradiation of 3-Ethylthiocholesta-3,5-diene (IVd) (29) in Ethanol

Irradiation of 0.37 g of IV*d* in 425 ml of ethanol, 100 ml of pentane, and 0.25 ml of pyridine for 0.5 h yielded 0.5 g of a brown, smelly oil. Chromatography on alumina did not result in isolation of pure material.

Irradiation of 3-N-Pyrrolidinylcholesta-3,5-diene (IVe) (30, 31) in Pentane

Irradiation of 0.5 g of IV*e* in 525 ml of pentane for 1 h gave, upon evaporation of the pentane *in vacuo* at room temperature, 0.5 g of a clear oil. The n.m.r. spectrum of the oil showed very broad absorption characteristic of a mixture. Despite considerable effort to purify the material, no homogeneous fractions were obtained.

3-Deuteriocholesta-3,5-diene

To a solution of 0.2 g of lithium aluminium deuteride in 20 ml of ether was added as a solid 0.5 g of cholest-4-en-3-one and the solution was stirred for 1 h. A solution of 2 ml of concentrated hydrochloric acid in 10 ml of ethanol was added and the reaction mixture allowed to reflux for 1 h. After the usual work-up, 0.3 g of pure 3-deuteriocholesta-3,5-diene, m.p. 81°, was obtained. Its melting point was not depressed on admixture of authentic cholesta-3,5-diene (12*b*).

ACKNOWLEDGMENT

We should like to thank Dr. C. Stammer for taking the n.m.r. spectra.

1. G. Just and C. C. Leznoff. Can. J. Chem. **42**, 79 (1964).
2. G. Just and V. DiTullio. Can. J. Chem. **42**, 2153 (1964).
3. L. J. Bellamy. The infra-red spectra of complex molecules. Methuen and Co. Ltd., London. 1959 pp. 115, 329.
4. A. Bowers, M. B. Sanchez, and H. J. Ringold. J. Am. Chem. Soc. **81**, 3702 (1959).
5. R. Deghengi and R. Gaudry. Can. J. Chem. **40**, 818 (1962).

Can. J. Chem. Downloaded from www.nrcresearchpress.com by 210.87.254.6 on 09/05/12
For personal use only.

6. G. W. MOERSCH and W. A. NEUKLIS. Can. J. Chem. **41**, 1627 (1963).
7. K. B. WIBERG and B. J. NIST. J. Am. Chem. Soc. **85**, 2788 (1963).
8. D. J. PATEL, M. E. HOWDEN, and J. D. ROBERTS. J. Am. Chem. Soc. **85**, 3218 (1963).
9. W. G. DAUBEN and J. A. Ross. J. Am. Chem. Soc. **81**, 6521 (1959).
10. W. G. DAUBEN and F. G. WILLEY. Tetrahedron Letters, **20**, 893 (1962).
11. U. WESTPHAL. Ber. **70**, 2128 (1937).
12. L. F. FIESER and M. FIESER. Steroids. Reinhold Publishing Corp., New York, N.Y. 1959. *a*. pp. 204–205. *b*. p. 265.
13. L. M. JACKMAN. Nuclear magnetic resonance spectroscopy. Pergamon Press, London. 1959. *a*. p. 85. *b*. pp. 112–115.
14. E. B. WHIPPLE, W. E. STEWART, G. S. REDDY, and J. H. GOLDSTEIN. J. Chem. Phys. **34**, 2136 (1961).
15. C. N. BANWELL and N. SHEPPARD. Mol. Phys. **3**, 351 (1960).
16. J. FEENEY, A. LEDWITH, and L. H. SUTCLIFFE. J. Chem. Soc. 2021 (1962).
17. R. T. HOBGOOD, JR., G. S. REDDY, and J. H. GOLDSTEIN. J. Phys. Chem. **67**, 110 (1963).
18. R. R. FRASER. Can. J. Chem. **38**, 2226 (1960).
19. M. I. USHAKOV and O. S. MADAEVA. J. Gen. Chem. USSR. **9**, 436 (1939).
20. R. B. TURNER. J. Am. Chem. Soc. **74**, 5362 (1952).
21. D. BURN, B. ELLIS, P. FEATHER, D. N. KIRK, and V. PETROW. Chem. Ind. 1907 (1962).
22. A. BOWERS and H. J. RINGOLD. Tetrahedron, **3**, 14 (1958).
23. C. W. SHOPPEE and G. H. R. SUMMERS. J. Chem. Soc. 3361 (1952).
24. K. BOWDEN, I. M. HEILBRON, E. R. H. JONES, and B. C. L. WEEDON. J. Chem. Soc. 39 (1946).
25. R. G. CURTIS, I. M. HEILBRON, E. R. H. JONES, and G. F. WOODS. J. Chem. Soc. 461 (1953).
26. H. HEUSSER, M. ROTH, O. ROHR, and R. ANLIKER. Helv. Chim. Acta, **38**, 1178 (1955).
27. D. J. COLLINS, J. J. HOBBS, and S. STERNHELL. Tetrahedron Letters, 197 (1963).
28. Y. URUSHIBARA, T. ANDRO, H. ARAKI, and A. AZAWA. Bull. Chem. Soc. Japan, **12**, 353 (1937).
29. R. W. RALLS. J. Am. Chem. Soc. **71**, 3320 (1949).
30. F. W. HEYL and M. E. HERR. J. Am. Chem. Soc. **75**, 1918 (1953).
31. J. L. JOHNSON, M. E. HERR, J. C. BABCOCK, A. E. FONKEN, J. E. STAFFORD, and F. W. HEYL. J. Am. Chem. Soc. **78**, 430 (1956).

RECEIVED MAY 15, 1964.
DEPARTMENT OF CHEMISTRY,
MCGILL UNIVERSITY,
MONTREAL, QUEBEC.

COMPLEX METAL HYDRIDE REDUCTION OF A KETIMINE AND A THIOKETONE

M. R. V. SAHYUN

During a current investigation, 4,4′-bis(dimethylamino)benzhydrylamine (I*a*) and the corresponding thiol (I*b*) were desired. Both these compounds are well known and thoroughly characterized (1, 2). The reported routes for their synthesis are, however, relatively inconvenient, and more recent advances in organic synthesis commend other approaches.

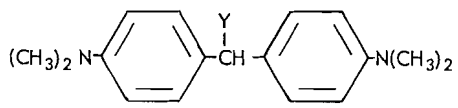

I(a, Y = NH_2; b, Y = SH; c, Y = OH)

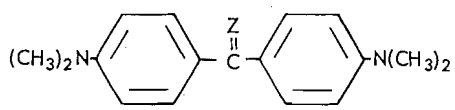

II(a, Z = NH; b, Z = S; c, Z = O)

The available starting materials were the ketimine (II*a*), commonly called "auramine," and the thioketone (II*b*), "Michler's" thioketone, respectively. Lithium aluminium hydride was expected to reduce II*a*, as the reduction of N-substituted aldimines to the secondary amines is known (3). The literature apparently contains no specific precedent for the lithium aluminium hydride reduction of ketimines which bear no substituent on the imino nitrogen atom. Sodium borohydride also reduces N-substituted aldimines (4).

Can. J. Chem. Downloaded from www.nrcresearchpress.com by 210.87.254.6 on 09/05/12
For personal use only.

6. G. W. MOERSCH and W. A. NEUKLIS. Can. J. Chem. **41**, 1627 (1963).
7. K. B. WIBERG and B. J. NIST. J. Am. Chem. Soc. **85**, 2788 (1963).
8. D. J. PATEL, M. E. HOWDEN, and J. D. ROBERTS. J. Am. Chem. Soc. **85**, 3218 (1963).
9. W. G. DAUBEN and J. A. Ross. J. Am. Chem. Soc. **81**, 6521 (1959).
10. W. G. DAUBEN and F. G. WILLEY. Tetrahedron Letters, **20**, 893 (1962).
11. U. WESTPHAL. Ber. **70**, 2128 (1937).
12. L. F. FIESER and M. FIESER. Steroids. Reinhold Publishing Corp., New York, N.Y. 1959. *a*. pp. 204–205. *b*. p. 265.
13. L. M. JACKMAN. Nuclear magnetic resonance spectroscopy. Pergamon Press, London. 1959. *a*. p. 85. *b*. pp. 112–115.
14. E. B. WHIPPLE, W. E. STEWART, G. S. REDDY, and J. H. GOLDSTEIN. J. Chem. Phys. **34**, 2136 (1961).
15. C. N. BANWELL and N. SHEPPARD. Mol. Phys. **3**, 351 (1960).
16. J. FEENEY, A. LEDWITH, and L. H. SUTCLIFFE. J. Chem. Soc. 2021 (1962).
17. R. T. HOBGOOD, JR., G. S. REDDY, and J. H. GOLDSTEIN. J. Phys. Chem. **67**, 110 (1963).
18. R. R. FRASER. Can. J. Chem. **38**, 2226 (1960).
19. M. I. USHAKOV and O. S. MADAEVA. J. Gen. Chem. USSR. **9**, 436 (1939).
20. R. B. TURNER. J. Am. Chem. Soc. **74**, 5362 (1952).
21. D. BURN, B. ELLIS, P. FEATHER, D. N. KIRK, and V. PETROW. Chem. Ind. 1907 (1962).
22. A. BOWERS and H. J. RINGOLD. Tetrahedron, **3**, 14 (1958).
23. C. W. SHOPPEE and G. H. R. SUMMERS. J. Chem. Soc. 3361 (1952).
24. K. BOWDEN, I. M. HEILBRON, E. R. H. JONES, and B. C. L. WEEDON. J. Chem. Soc. 39 (1946).
25. R. G. CURTIS, I. M. HEILBRON, E. R. H. JONES, and G. F. WOODS. J. Chem. Soc. 461 (1953).
26. H. HEUSSER, M. ROTH, O. ROHR, and R. ANLIKER. Helv. Chim. Acta, **38**, 1178 (1955).
27. D. J. COLLINS, J. J. HOBBS, and S. STERNHELL. Tetrahedron Letters, 197 (1963).
28. Y. URUSHIBARA, T. ANDRO, H. ARAKI, and A. AZAWA. Bull. Chem. Soc. Japan, **12**, 353 (1937).
29. R. W. RALLS. J. Am. Chem. Soc. **71**, 3320 (1949).
30. F. W. HEYL and M. E. HERR. J. Am. Chem. Soc. **75**, 1918 (1953).
31. J. L. JOHNSON, M. E. HERR, J. C. BABCOCK, A. E. FONKEN, J. E. STAFFORD, and F. W. HEYL. J. Am. Chem. Soc. **78**, 430 (1956).

RECEIVED MAY 15, 1964.
DEPARTMENT OF CHEMISTRY,
MCGILL UNIVERSITY,
MONTREAL, QUEBEC.

COMPLEX METAL HYDRIDE REDUCTION OF A KETIMINE AND A THIOKETONE

M. R. V. SAHYUN

During a current investigation, 4,4′-bis(dimethylamino)benzhydrylamine (I*a*) and the corresponding thiol (I*b*) were desired. Both these compounds are well known and thoroughly characterized (1, 2). The reported routes for their synthesis are, however, relatively inconvenient, and more recent advances in organic synthesis commend other approaches.

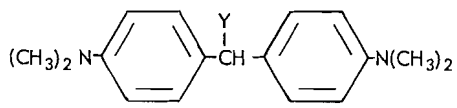

I(a, Y = NH_2; b, Y = SH; c, Y = OH)

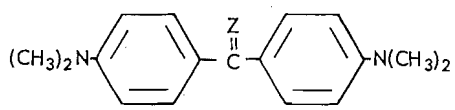

II(a, Z = NH; b, Z = S; c, Z = O)

The available starting materials were the ketimine (II*a*), commonly called "auramine," and the thioketone (II*b*), "Michler's" thioketone, respectively. Lithium aluminium hydride was expected to reduce II*a*, as the reduction of N-substituted aldimines to the secondary amines is known (3). The literature apparently contains no specific precedent for the lithium aluminium hydride reduction of ketimines which bear no substituent on the imino nitrogen atom. Sodium borohydride also reduces N-substituted aldimines (4).

Can. J. Chem. Downloaded from www.nrcresearchpress.com by 210.87.254.105 on 09/05/12
For personal use only.

Until now, the reduction of thioketones with sodium borohydride appears to be unknown.

Conover and Tarbell (5) found that aromatic amines with a carbonyl group para to the amino group underwent hydrogenolysis with lithium aluminium hydride, converting the carbonyl group into a methylene linkage. Mustafa and Hilmy (6) extended this observation to the thioketone (II*b*). Gaylord (7) interprets the above results by considering the compounds studied to be "vinylogs" of amides. As sodium borohydride does not ordinarily reduce amides (8), II*b* might thus be inert towards this reagent. The mechanism advanced for the hydrogenolysis of the carbonyl compounds studied by Conover and Tarbell (5) involves essentially an S_N1 nucleophilic displacement of the hydroxy group of the initially formed carbinol, e.g. I*c* from II*c*, by hydride ion. The ionization of the carbon–oxygen bond required by this mechanism is driven by the stabilization of the resulting carbonium-ion intermediate by the electron-releasing amino group (5, 7). The analogous ionization step would not, however, be expected with the amine (I*a*) under the reduction conditions. Hence, II*a* should not undergo hydrogenolysis with lithium aluminium hydride.

The reduction of II*a* with lithium aluminium hydride was tried first in tetrahydrofuran. It yielded 82% of the theoretical quantity of I*a*. The product formed the reported (1) blue color in glacial acetic acid (λ_{max} 610 mμ, log ϵ 5.11); this absorption is characteristic of the carbonium ion (III) (9). The spectral data further agree with the reported data for the carbonium ion generated by spontaneous ionization of the corresponding carbinol (I*c*) in nitromethane (λ_{max} 610 mμ, log ϵ 5.12)(9). A satisfactory analysis for I*a* was obtained. When the lithium aluminium hydride reduction was carried out in dimethoxyethane, the crystalline product differed from I*a* in melting point. In glacial acetic acid solution this product showed the absorption maximum at 610 mμ (log ϵ 5.14) and one at 433 mμ (log ϵ 4.35), suggestive of the starting material (II*a*) (λ_{max} 433 mμ, log ϵ 4.48). The compound analyzed for $C_{34}H_{41}N_5$; therefore, structure IV adequately represents this product. The visible spectrum in glacial acetic acid arises as follows.

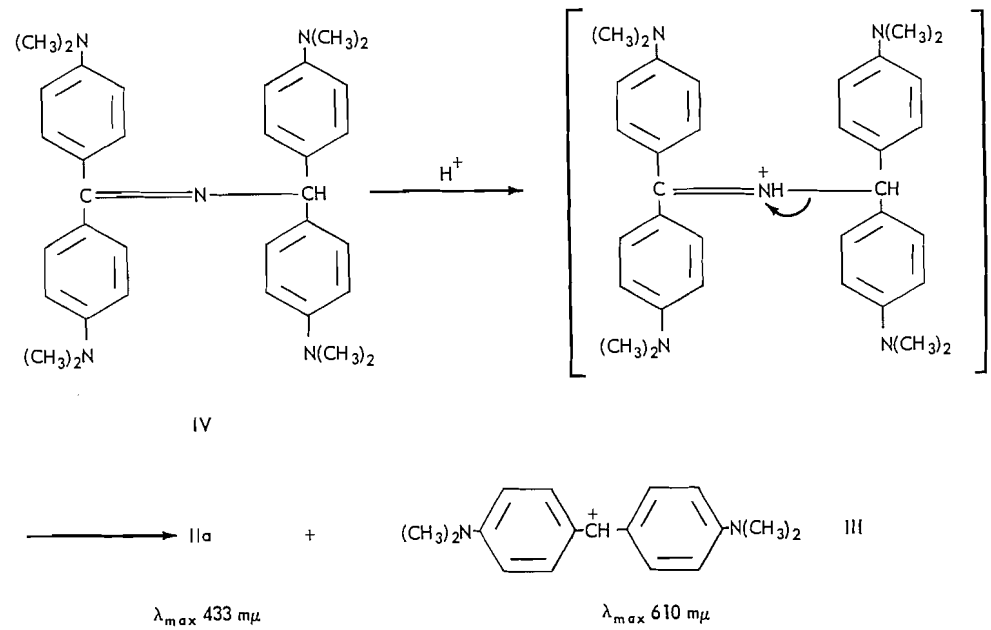

Can. J. Chem. Downloaded from www.nrcresearchpress.com by 210.87.254.105 on 09/05/12
For personal use only.

Sodium borohydride in 2-propanol also reduced II*a* smoothly and gave an optimal yield of 43% of the theoretical quantity of I*a*. As lithium aluminium hydride is unsatisfactory for the reduction of II*b* to I*b* (6), sodium borohydride was the only reducing agent used with II*b*. In 2-propanol, no reaction occurred below reflux temperature. After 20 min of refluxing, the only product isolated exhibited the characteristic absorption maximum at 610 mμ (log ϵ 5.38; two carbonium ions per molecule) in glacial acetic acid. The melting point was close to that reported for the sulfide (V), which reportedly also absorbs at 610 mμ in acetic acid (2).

V 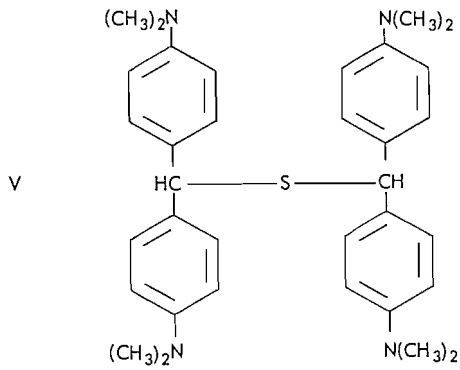

A strong odor of hydrogen sulfide had been noticed as soon as the reaction was quenched and indicated that V arose during the course of the reaction and not from I*b* in the process of isolating the product. Clearly compounds II*a* and II*b* cannot be considered analogous to amides in terms of their behavior with sodium borohydride (*vide supra*).

EXPERIMENTAL

Melting points (corrected) were determined on a Fisher-Johns melting point apparatus. The visible spectra were determined in glacial acetic acid with a Cary model 11 spectrophotometer. All the compounds obeyed Beer's law. All reactions were carried out under Seaford grade dry nitrogen.

*Reduction of 4,4′-bis(Dimethylamino)benzophenone Imine (II*a*)*

Tetrahydrofuran was redistilled from lithium aluminium hydride. In 100 ml of this dry solvent was placed 3.8 g (0.1 mole) of lithium aluminium hydride. In another 100 ml portion was dissolved 4.6 g (0.017 mole) of dry 4,4′-bis(dimethylamino)benzophenone imine (II*a*), obtained from the commercially available* hydrochloride. After the mixture of the above two solutions was refluxed 0.5 h the yellow color of the imine had disappeared. The excess lithium aluminium hydride was decomposed with water. The reaction mixture was then partitioned between methylene chloride and water. The organic phase was dried over magnesium sulfate and filtered. The solvent was removed under reduced pressure at room temperature. The solid residue was recrystallized from ethanol to give 3.7 g (0.014 mole) of the primary amine (I*a*) (82% yield), m.p. 130.5–131.5°, close to the published value of 135° (1). Analysis confirmed the formula $C_{17}H_{23}N_3$.

Anal. Calcd.: C, 75.78; H, 8.63; N, 15.59. Found: C, 75.84, H, 8.56, N, 15.30.

An undried sample (2.5 g, 8.7 mmole) of the imine (assumed to be the monohydrate) was dissolved in approximately 200 ml of 2-propanol which had been redistilled from sodium borohydride. To this solution was added 1.0 g (26 mmole) of sodium borohydride. After this solution was heated at reflux for 20 min, the solution became colorless. The resulting mixture was treated analogously to the lithium aluminium hydride reaction mixture to yield 1.0 g (3.9 mmole, 43% yield) of I*a*, m.p. 129–131°.

The reduction with lithium aluminium hydride in dimethoxyethane was conducted in the same manner as those described above. The only crystalline product isolated was that to which structure IV has been assigned (7% yield), m.p. 167–168°. The compound analyzed for $C_{34}H_{41}N_5$.

Anal. Calcd.: C, 78.57; H, 7.94; N, 13.49; molecular weight, 519. Found: C, 78.73; H, 8.16; N, 13.30; molecular weight, 520.

**"Auramine O" (IIa hydrochloride) was manufactured by Chroma Gesellschaft, Germany, and supplied by Roboz Surgical Instrument Co., Inc., 818 18th Street, N.W., Washington 6, D.C.*

Can. J. Chem. Downloaded from www.nrcresearchpress.com by 210.87.254.105 on 09/05/12
For personal use only.

Reduction of 4,4'-bis(Dimethylamino)thiobenzophenone (IIb)

In 500 ml of redistilled 2-propanol, 3.8 g (0.1 mole) of sodium borohydride and 2.8 g (9.8 mmole) of the commercially available* thioketone (II*b*) were dissolved. After the solution was refluxed for 20 min, the red color of the thioketone had disappeared. The product was isolated in the same manner as the amine above. After recrystallization from ethanol, the product weighed 1.7 g, m.p. 169–171°. The analysis suggested $C_{34}H_{42}N_4S$.

Anal. Calcd.: C, 75.77; H, 7.86; N, 10.40; S, 5.97; molecular weight, 538. Found: C, 76.05; H, 7.57; N, 10.34; S, 5.94; molecular weight, 520.

These data indicated that the compound was bis[4,4'-bis(dimethylamino)benzhydryl] sulfide (V), reported m.p. 172° (2).

ACKNOWLEDGMENTS

The author appreciates the cooperation of Dr. W. C. Hueper, Chief, Environmental Cancer Section, National Cancer Institute, in whose laboratory this work was carried out. The analyses and molecular weight determinations were performed by the Microanalytical Laboratory of the National Institute of Arthritis and Metabolic Diseases.

1. C. GRAEBE. Ber. **20**, 3265 (1887).
2. R. MOHLAU, M. HEINZE, and R. ZIMMERMAN. Ber. **35**, 375 (1902).
3. A. H. SOMMERS and S. E. AALAND. J. Org. Chem. **21**, 484 (1956). J. H. BILLMAN and K. M. TAI. J. Org. Chem. **23**, 535 (1958).
4. J. H. BILLMAN and R. C. DIESING. J. Org. Chem. **22**, 1068 (1957).
5. L. H. CONOVER and D. S. TARBELL. J. Am. Chem. Soc. **72**, 3586 (1950).
6. A. MUSTAFA and M. K. HILMY. J. Chem. Soc. 1343 (1952).
7. N. G. GAYLORD. Reduction with complex metal hydrides. Interscience Publishers, Inc., New York, N.Y. 1956. pp. 980–985.
8. N. G. GAYLORD. Reduction with complex metal hydrides. Interscience Publishers, Inc., New York, N.Y. 1956. p. 592.
9. L. G. S. BROOKER and R. H. SPRAGUE. J. Am. Chem. Soc. **63**, 3203 (1941).

RECEIVED MAY 5, 1964.
NATIONAL CANCER INSTITUTE,
BETHESDA, MARYLAND.

**The 4,4'-bis(dimethylamino)thiobenzophenone (IIb) was obtained from K and K Laboratories, New York, N.Y.*

PHOTOMETRIC OBSERVATIONS ON THE REACTIONS OF ACTIVE NITROGEN WITH CHLORINE AND BROMINE

K. S. RAXWORTHY AND L. F. PHILLIPS

In an earlier publication (1) evidence was presented for the formation of metastable $A(^3\Sigma_u^+)$ nitrogen molecules during the reaction of iodine with active nitrogen. Previous work on the reactions of active nitrogen with chlorine and bromine would probably not have revealed the production of metastable species and these reactions have therefore been reinvestigated with this possibility in mind.

Our observations with chlorine and bromine have substantially confirmed those of previous workers (2–6). The chlorine reaction gave rise to almost no emission other than the weakened nitrogen afterglow, while the main feature of the bromine reaction was bright orange NBr emission from a layer on or very close to the walls of the reaction vessel. (This was particularly apparent during the present experiments because the reaction vessel was of square cross section.) Emission from excited halogen molecules was in both cases extremely weak and decayed with time in a manner which paralleled the decay of the nitrogen afterglow. There was usually a net decrease in the intensity of radiation at the

Can. J. Chem. Downloaded from www.nrcresearchpress.com by 210.87.254.105 on 09/05/12
For personal use only.

Reduction of 4,4'-bis(Dimethylamino)thiobenzophenone (IIb)

In 500 ml of redistilled 2-propanol, 3.8 g (0.1 mole) of sodium borohydride and 2.8 g (9.8 mmole) of the commercially available* thioketone (II*b*) were dissolved. After the solution was refluxed for 20 min, the red color of the thioketone had disappeared. The product was isolated in the same manner as the amine above. After recrystallization from ethanol, the product weighed 1.7 g, m.p. 169–171°. The analysis suggested $C_{34}H_{42}N_4S$.

Anal. Calcd.: C, 75.77; H, 7.86; N, 10.40; S, 5.97; molecular weight, 538. Found: C, 76.05; H, 7.57; N, 10.34; S, 5.94; molecular weight, 520.

These data indicated that the compound was bis[4,4'-bis(dimethylamino)benzhydryl] sulfide (V), reported m.p. 172° (2).

ACKNOWLEDGMENTS

The author appreciates the cooperation of Dr. W. C. Hueper, Chief, Environmental Cancer Section, National Cancer Institute, in whose laboratory this work was carried out. The analyses and molecular weight determinations were performed by the Microanalytical Laboratory of the National Institute of Arthritis and Metabolic Diseases.

1. C. GRAEBE. Ber. **20**, 3265 (1887).
2. R. MOHLAU, M. HEINZE, and R. ZIMMERMAN. Ber. **35**, 375 (1902).
3. A. H. SOMMERS and S. E. AALAND. J. Org. Chem. **21**, 484 (1956). J. H. BILLMAN and K. M. TAI. J. Org. Chem. **23**, 535 (1958).
4. J. H. BILLMAN and R. C. DIESING. J. Org. Chem. **22**, 1068 (1957).
5. L. H. CONOVER and D. S. TARBELL. J. Am. Chem. Soc. **72**, 3586 (1950).
6. A. MUSTAFA and M. K. HILMY. J. Chem. Soc. 1343 (1952).
7. N. G. GAYLORD. Reduction with complex metal hydrides. Interscience Publishers, Inc., New York, N.Y. 1956. pp. 980–985.
8. N. G. GAYLORD. Reduction with complex metal hydrides. Interscience Publishers, Inc., New York, N.Y. 1956. p. 592.
9. L. G. S. BROOKER and R. H. SPRAGUE. J. Am. Chem. Soc. **63**, 3203 (1941).

RECEIVED MAY 5, 1964.
NATIONAL CANCER INSTITUTE,
BETHESDA, MARYLAND.

**The 4,4'-bis(dimethylamino)thiobenzophenone (IIb) was obtained from K and K Laboratories, New York, N.Y.*

PHOTOMETRIC OBSERVATIONS ON THE REACTIONS OF ACTIVE NITROGEN WITH CHLORINE AND BROMINE

K. S. RAXWORTHY AND L. F. PHILLIPS

In an earlier publication (1) evidence was presented for the formation of metastable $A(^3\Sigma_u^+)$ nitrogen molecules during the reaction of iodine with active nitrogen. Previous work on the reactions of active nitrogen with chlorine and bromine would probably not have revealed the production of metastable species and these reactions have therefore been reinvestigated with this possibility in mind.

Our observations with chlorine and bromine have substantially confirmed those of previous workers (2–6). The chlorine reaction gave rise to almost no emission other than the weakened nitrogen afterglow, while the main feature of the bromine reaction was bright orange NBr emission from a layer on or very close to the walls of the reaction vessel. (This was particularly apparent during the present experiments because the reaction vessel was of square cross section.) Emission from excited halogen molecules was in both cases extremely weak and decayed with time in a manner which paralleled the decay of the nitrogen afterglow. There was usually a net decrease in the intensity of radiation at the

Can. J. Chem. Downloaded from www.nrcresearchpress.com by 210.87.254.5 on 09/05/12
For personal use only.

wavelength of the halogen emission bands when halogen was added, but this decrease was appreciably less than that shown by the nitrogen afterglow at other wavelengths.

These results are in marked contrast to those for iodine, where intense emission in the blue and ultraviolet from excited I_2 is the most prominent feature of the reaction. Since the iodine emission is believed to be mainly due to energy transfer from A-state nitrogen molecules, the lack of similar emission with chlorine and bromine suggests either that A-state molecules are not produced or that the energy is not readily transferred. When bromine was added to the flow system at a point upstream from a jet through which iodine vapor was being introduced into active nitrogen, the blue iodine emission was quenched simultaneously with the nitrogen afterglow. This shows that the bromine reaction does not produce appreciable quantities of metastable species.

The essential steps of the mechanism which has been proposed (1, 6) for the reaction of a halogen with active nitrogen are

$$N(^4S) + X_2(^1\Sigma) \rightarrow NX(^3\Sigma) + X(^2P) \quad [1]$$

$$N(^4S) + NX(^3\Sigma) \rightarrow N_2 + X(^2P), \quad [2]$$

where the nitrogen molecule produced by reaction [2] is in the ground state unless X is iodine. There are actually two long-lived states of N_2 which could be produced in the iodine case, namely $A(^3\Sigma_u^+)$ and the predicted $^3\Delta_u$ state (7). There would probably not be sufficient energy available to produce the $^3\Delta_u$ state from NBr or NCl, since the dissociation energy of NBr is 58 kcal/mole (6), which leaves only 167 kcal/mole to be taken up by N_2, and the dissociation energy of NCl is likely to be still higher. The available evidence suggests that the energy of the $^3\Delta_u$ state is nearer to 175 kcal/mole (8). This would provide an explanation for the lack of metastable species from the bromine and chlorine reactions. No such explanation is available if it is the A-state that is involved. Experiments to decide between these two possibilities are in progress.

Halogen atoms are able to recombine very efficiently on the walls of the reaction vessel (9) so that halogens are expected to be present almost entirely as undissociated molecules. Graphs of log(afterglow intensity) vs. time have been found to be linear in the presence of halogens, and from the slopes of the lines and the partial pressures of the halogens the rate constants for reaction [1] at 20 °C have been calculated on the assumption that this reaction leads to the immediate removal of two nitrogen atoms. The results (in cm^3 $molecule^{-1}$ s^{-1}) are $k_1 = 2 \times 10^{-15}$ for chlorine and $k_1 = 2 \times 10^{-14}$ for bromine. The main source of error in these values is likely to be the neglect of the possibility of destruction of NBr and NCl at the walls, which could cause the values to be too low by up to a factor of two. In view of the apparent stability of NBr on the walls and the large volume-to-surface ratio of the reaction tube this neglect appears to be justified. The estimated error arising from the measurements is $\pm 30\%$ in each case.

EXPERIMENTAL

The apparatus was similar to that described previously (1) except that the reaction vessel consisted of a 38 cm length of square cross section quartz tubing, 3.5 cm wide, through which the gases were pumped at velocities of between 1 and 2 m/s at pressures between 1 and 4 torr. Analytical reagent grade bromine and fractionally distilled chlorine were carried to a spherical inlet jet by a stream of argon from saturators immersed in an ice bath and a solid CO_2/acetone bath respectively. Saturator temperatures were monitored with thermocouples. Halogen flows were calculated from the vapor pressure (10, 11), the measured argon flow, and the measured pressure drop across the saturator. Nitrogen, nitric oxide, and iodine were as described previously (1). Light intensities were measured with a 1P28 photomultiplier in combination with various filters. Spectrolab type P interference filters of 16 Å half-width at 6 250 Å and 5 590 Å were used for the nitrogen afterglow and the bromine emission respectively (12). For the chlorine emission a Baird-Atomic type A11 interference filter of 100 Å half-width at 2 600 Å was used (2).

Can. J. Chem. Downloaded from www.nrcresearchpress.com by 210.87.254.5 on 09/05/12
For personal use only.

ACKNOWLEDGMENTS

This work was supported by grants from the New Zealand Universities Research Committee and the United States Air Force Office of Scientific Research.

1. C. G. FREEMAN and L. F. PHILLIPS. J. Phys. Chem. **68**, 362 (1964).
2. W. H. B. CAMERON and A. ELLIOTT. Proc. Roy. Soc. London, Ser. A. **169**, 463 (1939).
3. A. ELLIOTT. Proc. Roy. Soc. London, Ser. A, **169**, 469 (1939).
4. H. B. DUNFORD and B. E. MELANSON. Can. J. Chem. **37**, 641 (1959).
5. E. R. V. MILTON and H. B. DUNFORD. J. Chem. Phys. **34**, 51 (1961).
6. E. R. V. MILTON, H. B. DUNFORD, and A. E. DOUGLAS. J. Chem. Phys. **35**, 1202 (1961).
7. R. S. MULLIKEN. The threshold of space. *Edited by* M. Zelikoff. Pergamon Press, New York. 1957. p. 169.
8. C. KENTY. J. Chem. Phys. **35**, 2267 (1961); **37**, 1567 (1962).
9. E. A. OGRYZLO. Can. J. Chem. **39**, 2556 (1961).
10. INTERNATIONAL CRITICAL TABLES. National Research Council, U.S.A. 1926.
11. W. F. GIAUQUE and T. M. POWELL. J. Am. Chem. Soc. **61**, 1970 (1939).
12. R. W. B. PEARSE and A. G. GAYDON. The identification of molecular spectra. 2nd ed. Chapman and Hall, London. 1950.

RECEIVED JULY 15, 1964.
DEPARTMENT OF CHEMISTRY,
UNIVERSITY OF CANTERBURY,
CHRISTCHURCH, NEW ZEALAND.

Can. J. Chem. Downloaded from www.nrcresearchpress.com by 210.87.254.5 on 09/05/12
For personal use only.

THE DENSITIES AND SURFACE TENSIONS OF LIQUID ETHANE AND NITROUS OXIDE

A. J. LEADBETTER, D. J. TAYLOR, AND B. VINCENT

The densities and surface tensions of ethane and nitrous oxide have been measured in the normal liquid ranges, using experimental techniques which have been fully described elsewhere (1). The ethane used was of 99.9% purity, as supplied by the National Chemical Laboratory. The nitrous oxide was medicinal grade (99.96%) supplied by the British Oxygen Company Limited.

The density was determined by condensing a known mass of gas into a volume-calibrated glass capillary tube. The mass of gas was determined by measuring its pressure, volume, and temperature and using, for ethane, the second virial coefficients of Michels *et al.* (2), and, for nitrous oxide, the data quoted by Blue and Giauque (3). The surface tension was measured by the method of capillary rise, using three interconnected capillaries. These were Veridia precision bore tubing, with nominal bores 0.2, 0.4, and 2.0 mm.

The cryostat consisted of a dewar vessel containing CF_2Cl_2 (Arcton 12, I.C.I. Limited). The temperature was controlled by a vapor pressure thermometer, containing nitrous oxide or ethane, which was used to regulate the flow of cold nitrogen through a cooling coil. The temperature was derived from the measured vapor pressures, using the data given in the A.P.I. tables for ethane (4) and that of Blue and Giauque (3) for nitrous oxide. In all cases, the overall uncertainty in the temperature was less than 0.1 °K.

RESULTS

A detailed discussion of the accuracy of the present experimental methods has been given previously (1). The probable error in the densities is estimated to be about $\pm 0.1\%$. The surface tension values calculated from the differences in height of the menisci in the three tubes were internally consistent to better than 0.5%. The results given below are

ACKNOWLEDGMENTS

This work was supported by grants from the New Zealand Universities Research Committee and the United States Air Force Office of Scientific Research.

1. C. G. FREEMAN and L. F. PHILLIPS. J. Phys. Chem. **68**, 362 (1964).
2. W. H. B. CAMERON and A. ELLIOTT. Proc. Roy. Soc. London, Ser. A. **169**, 463 (1939).
3. A. ELLIOTT. Proc. Roy. Soc. London, Ser. A, **169**, 469 (1939).
4. H. B. DUNFORD and B. E. MELANSON. Can. J. Chem. **37**, 641 (1959).
5. E. R. V. MILTON and H. B. DUNFORD. J. Chem. Phys. **34**, 51 (1961).
6. E. R. V. MILTON, H. B. DUNFORD, and A. E. DOUGLAS. J. Chem. Phys. **35**, 1202 (1961).
7. R. S. MULLIKEN. The threshold of space. *Edited by* M. Zelikoff. Pergamon Press, New York. 1957. p. 169.
8. C. KENTY. J. Chem. Phys. **35**, 2267 (1961); **37**, 1567 (1962).
9. E. A. OGRYZLO. Can. J. Chem. **39**, 2556 (1961).
10. INTERNATIONAL CRITICAL TABLES. National Research Council, U.S.A. 1926.
11. W. F. GIAUQUE and T. M. POWELL. J. Am. Chem. Soc. **61**, 1970 (1939).
12. R. W. B. PEARSE and A. G. GAYDON. The identification of molecular spectra. 2nd ed. Chapman and Hall, London. 1950.

RECEIVED JULY 15, 1964.
DEPARTMENT OF CHEMISTRY,
UNIVERSITY OF CANTERBURY,
CHRISTCHURCH, NEW ZEALAND.

Can. J. Chem. Downloaded from www.nrcresearchpress.com by 210.87.254.105 on 09/05/12
For personal use only.

THE DENSITIES AND SURFACE TENSIONS OF LIQUID ETHANE AND NITROUS OXIDE

A. J. LEADBETTER, D. J. TAYLOR, AND B. VINCENT

The densities and surface tensions of ethane and nitrous oxide have been measured in the normal liquid ranges, using experimental techniques which have been fully described elsewhere (1). The ethane used was of 99.9% purity, as supplied by the National Chemical Laboratory. The nitrous oxide was medicinal grade (99.96%) supplied by the British Oxygen Company Limited.

The density was determined by condensing a known mass of gas into a volume-calibrated glass capillary tube. The mass of gas was determined by measuring its pressure, volume, and temperature and using, for ethane, the second virial coefficients of Michels *et al.* (2), and, for nitrous oxide, the data quoted by Blue and Giauque (3). The surface tension was measured by the method of capillary rise, using three interconnected capillaries. These were Veridia precision bore tubing, with nominal bores 0.2, 0.4, and 2.0 mm.

The cryostat consisted of a dewar vessel containing CF_2Cl_2 (Arcton 12, I.C.I. Limited). The temperature was controlled by a vapor pressure thermometer, containing nitrous oxide or ethane, which was used to regulate the flow of cold nitrogen through a cooling coil. The temperature was derived from the measured vapor pressures, using the data given in the A.P.I. tables for ethane (4) and that of Blue and Giauque (3) for nitrous oxide. In all cases, the overall uncertainty in the temperature was less than 0.1 °K.

RESULTS

A detailed discussion of the accuracy of the present experimental methods has been given previously (1). The probable error in the densities is estimated to be about $\pm 0.1\%$. The surface tension values calculated from the differences in height of the menisci in the three tubes were internally consistent to better than 0.5%. The results given below are

weighted averages of the individual values, and are probably accurate to ±0.5%. The contact angle was assumed to be zero for both ethane and nitrous oxide.

Ethane

TABLE I

The density and surface tension of ethane

T (°K)	ρ (g cm^{-3})	T (°K)	γ (dyn cm^{-1})
126.9	0.6081	129.2	25.00
133.3	0.6017	133.2	24.54
135.0	0.5997	137.1	23.72
138.8	0.5951	149.1	21.75
141.6	0.5934	150.6	21.68
143.9	0.5906	155.9	20.71
148.1	0.5860	157.5	20.46
149.9	0.5831	161.3	19.86
157.6	0.5752	164.4	19.28
164.8	0.5677	170.3	18.31
167.2	0.5651	180.6	16.63
169.1	0.5630		
171.9	0.5599		
174.6	0.5572		
176.4	0.5551		
178.1	0.5527		
179.2	0.5516		
183.4	0.5478		

The present results for the density agree within experimental error over the whole temperature range with those of Barkelew *et al.* (5) and of Tester (6). The older results of Maass and co-workers (7, 8) in the temperature range 165–200 °K are about 1% higher. The surface tension of ethane has previously been measured by Maass and Wright (8) in the range 165–185 °K using the method of capillary rise. Their results, calculated using their own density data, are 0.5% higher than the present values.

Nitrous Oxide

TABLE II

The density and surface tension of nitrous oxide

T (°K)	ρ (g cm^{-3})	T (°K)	γ (dyn cm^{-1})
182.4	1.241	182.5	24.26
182.7	1.241	182.5	24.25
182.6	1.241	182.6	24.23
182.8	1.240	182.8	24.18
183.0	1.239	182.9	24.11
183.1	1.239	183.2	24.07
183.2	1.239	183.4	24.04
183.3	1.237	183.7	24.00
183.4	1.237	183.9	23.95
183.6	1.238	184.0	23.87
183.7	1.238	184.2	23.86
183.9	1.237	184.4	23.85
184.1	1.238		
184.2	1.236		
184.3	1.236		
184.3	1.236		
184.5	1.235		

The only previous work reported for the density and surface tension of nitrous oxide in the normal liquid region is that of Grunmach (9), who made measurements at the boiling point. He obtained values of 1.226 g cm^{-3} and 26.3 dyn cm^{-1}.

Can. J. Chem. Downloaded from www.nrcresearchpress.com by 210.87.254.105 on 09/05/12
For personal use only.

1. A. J. LEADBETTER and H. E. THOMAS. Trans. Faraday Soc. To be published.
2. A. MICHELS, W. VAN STRAATEN, and J. DAWSON. Physica, **20**, 17 (1954).
3. R. W. BLUE and W. F. GIAUQUE. J. Am. Chem. Soc. **57**, 991 (1935).
4. F. ROSSINI (*Editor*). Selected values of properties of hydrocarbons. American Petroleum Institute 1953. p. 336.
5. C. H. BARKELEW, J. C. VALENTINE, and C. O. HURD. Trans. Am. Inst. Chem. Engrs. **43**, 25 (1947).
6. H. E. TESTER. Thermodynamic functions of gases. Vol. III. *Edited by* F. Din. Butterworths, London. 1961.
7. O. MAASS and D. MCINTOSH. J. Am. Chem. Soc. **36**, 737 (1914).
8. O. MAASS and C. H. WRIGHT. J. Am. Chem. Soc **48**, 1098 (1921).
9. L. GRUNMACH. Ann. **3**, 660 (1900); **9**, 1261 (1902); **15**, 401 (1904).

RECEIVED AUGUST 11, 1964.
DEPARTMENT OF PHYSICAL CHEMISTRY,
UNIVERSITY OF BRISTOL,
BRISTOL, ENGLAND.

Can. J. Chem. Downloaded from www.nrcresearchpress.com by 210.87.254.105 on 09/05/12
For personal use only.

THE DETERMINATION OF MONOMER–DIMER SELF-ASSOCIATION EQUILIBRIUM CONSTANTS IN DILUTE SOLUTIONS

S. N. VINOGRADOV[1]

A compound containing an A—H group or an A—H and a B group (A, B = O, N, S etc.) is capable of self-association through hydrogen bonding (1) to open (linear) and (or) closed (cyclic) polymers, as shown below for the simplest case, that of a dimer.

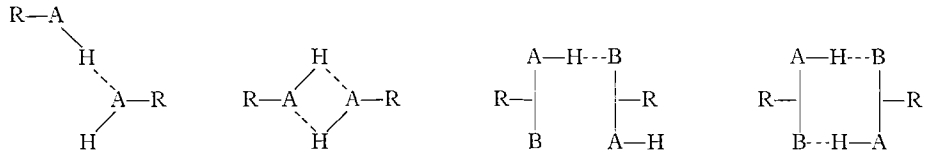

I*a* I*b* II*a* II*b*

The variation in intensity of a monomer absorption band as a function of concentration can be calculated from infrared spectroscopic data. From these data it is relatively simple to evaluate the mode of self-association for dilute solutions in inert solvents when only closed polymers are present. Methods for calculating the stepwise self-association equilibrium constants have been proposed (2).

Evidence has been accumulating that the contribution of "end" A—H groups from open polymers (as in I*a* and II*a*) to the absorption of "free" A—H groups must be taken into consideration (3). Coexistence of open and closed dimers was indicated in the cases of caprolactam (4) and cyclohexanol (5) in CCl_4, and the predominance of linear self-association has been established in the cases of imidazole, 1,2,4-triazole, benzotriazole, and 1,2,3-triazole (6, 7) in CCl_4 and C_6H_6. No treatment of infrared absorption intensity data has been proposed for any case of coexistence of open and closed polymers. Masschelein has used an empirical method in the specific case of the monomer – open dimer and monomer – closed dimer self-association of cyclohexanol (5), and several methods have been used in the determination of the overall monomer–dimer equilibrium constant (8, 9).

The concentration of the "free" A—H groups obtained from infrared absorption measurements is the sum of the "monomer" and "end" A—H group concentrations if the

[1]*Present address: Department of Biochemistry, Yale University, New Haven, Connecticut.*

1. A. J. LEADBETTER and H. E. THOMAS. Trans. Faraday Soc. To be published.
2. A. MICHELS, W. VAN STRAATEN, and J. DAWSON. Physica, **20**, 17 (1954).
3. R. W. BLUE and W. F. GIAUQUE. J. Am. Chem. Soc. **57**, 991 (1935).
4. F. ROSSINI (*Editor*). Selected values of properties of hydrocarbons. American Petroleum Institute 1953. p. 336.
5. C. H. BARKELEW, J. C. VALENTINE, and C. O. HURD. Trans. Am. Inst. Chem. Engrs. **43**, 25 (1947).
6. H. E. TESTER. Thermodynamic functions of gases. Vol. III. *Edited by* F. Din. Butterworths, London. 1961.
7. O. MAASS and D. MCINTOSH. J. Am. Chem. Soc. **36**, 737 (1914).
8. O. MAASS and C. H. WRIGHT. J. Am. Chem. Soc **48**, 1098 (1921).
9. L. GRUNMACH. Ann. **3**, 660 (1900); **9**, 1261 (1902); **15**, 401 (1904).

RECEIVED AUGUST 11, 1964.
DEPARTMENT OF PHYSICAL CHEMISTRY,
UNIVERSITY OF BRISTOL,
BRISTOL, ENGLAND.

Can. J. Chem. Downloaded from www.nrcresearchpress.com by 210.87.254.105 on 09/05/12
For personal use only.

THE DETERMINATION OF MONOMER–DIMER SELF-ASSOCIATION EQUILIBRIUM CONSTANTS IN DILUTE SOLUTIONS

S. N. VINOGRADOV[1]

A compound containing an A—H group or an A—H and a B group (A, B = O, N, S etc.) is capable of self-association through hydrogen bonding (1) to open (linear) and (or) closed (cyclic) polymers, as shown below for the simplest case, that of a dimer.

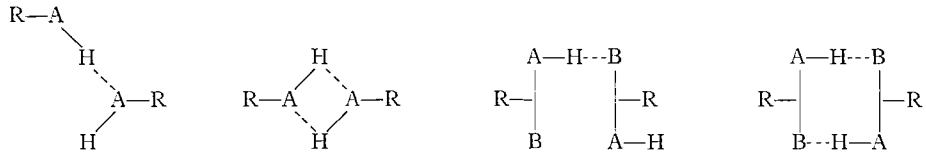

I*a* I*b* II*a* II*b*

The variation in intensity of a monomer absorption band as a function of concentration can be calculated from infrared spectroscopic data. From these data it is relatively simple to evaluate the mode of self-association for dilute solutions in inert solvents when only closed polymers are present. Methods for calculating the stepwise self-association equilibrium constants have been proposed (2).

Evidence has been accumulating that the contribution of "end" A—H groups from open polymers (as in I*a* and II*a*) to the absorption of "free" A—H groups must be taken into consideration (3). Coexistence of open and closed dimers was indicated in the cases of caprolactam (4) and cyclohexanol (5) in CCl_4, and the predominance of linear self-association has been established in the cases of imidazole, 1,2,4-triazole, benzotriazole, and 1,2,3-triazole (6, 7) in CCl_4 and C_6H_6. No treatment of infrared absorption intensity data has been proposed for any case of coexistence of open and closed polymers. Masschelein has used an empirical method in the specific case of the monomer – open dimer and monomer – closed dimer self-association of cyclohexanol (5), and several methods have been used in the determination of the overall monomer–dimer equilibrium constant (8, 9).

The concentration of the "free" A—H groups obtained from infrared absorption measurements is the sum of the "monomer" and "end" A—H group concentrations if the

[1]*Present address: Department of Biochemistry, Yale University, New Haven, Connecticut.*

self-association is partly or wholly linear and if the frequencies of the two types of A—H groups overlap. Thus the sum of the "free" A—H group concentrations, E, obtained from infrared absorption measurements is

$$E = \epsilon B/\epsilon_1^{m} = b_1 + \sum_{2}^{Q} \gamma\beta_{q0}{}^{o} b_1{}^{q},$$

where B is the stoichiometric concentration, ϵB is the total measured absorbance at the monomer peak, b_1 is the monomer concentration, $\beta_{q0}{}^{o}$ are the stepwise monomer – open Q-mer association equilibrium constants, and γ is the ratio $\epsilon_1{}^{e}/\epsilon_1{}^{m}$ of the absorptivities of the "end" and "monomer" A—H groups.

The simultaneous determination of the monomer – open dimer and monomer – closed dimer equilibrium constants from infrared absorption data is possible, based on the following assumptions: only the monomer–dimer equilibria exist in the solution, the dilute solution is ideal, Beer's law applies, and the absorptivity of the "monomer" A—H group is the absorptivity of the monomer peak at infinite dilution. Let $\beta_{20}{}^{c}$ and $\beta_{20}{}^{o}$ be the monomer – closed dimer and monomer – open dimer association equilibrium constants, respectively; assuming that $\epsilon_1{}^{m} = \epsilon_1{}^{e}$, the "free" A—H group concentration will be

$$E = b_1 + \beta_{20}{}^{o} b_1{}^{2}. \qquad [1]$$

Substitution of the relation,

$$B - E = (\beta_{20}{}^{o} + 2\beta_{20}{}^{c}) b_1{}^{2}, \qquad [2]$$

into the appropriate expression for B and into [1] yields

$$B/(B - E)^{1/2} = 1/[\beta_{20}{}^{o} + 2\beta_{20}{}^{c}]^{1/2} + (2(\beta_{20}{}^{o} + \beta_{20}{}^{c})/[\beta_{20}{}^{o} + 2\beta_{20}{}^{c}])(B - E)^{1/2} \qquad [3]$$

and a similar relation for $E/(B - E)^{1/2}$. Plots of $B/(B - E)^{1/2}$ and $E/(B - E)^{1/2}$ versus $(B - E)^{1/2}$ must be straight lines with a common intercept A and slopes A_1 and A_2 respectively ($A_1 = A_2 + 1$); either of the two equations can be solved for $\beta_{20}{}^{c}$ and $\beta_{20}{}^{o}$.

The plots for the self-association of caprolactam in CCl_4 (4) are shown in Fig. 1A. The results of the least-squares treatment of the data with standard deviations obtained in the usual manner (10) are: $A = 0.0693 \pm 0.0016$, $A_1 = 1.0679 \pm 0.0063$, $A_2 = 0.0677 \pm 0.0063$, giving $\beta_{20}{}^{o} = 14.2 \pm 2.1$ moles^{-1} l and $\beta_{20}{}^{c} = 97.3 \pm 5.4$ moles^{-1} l; the latter figure can be compared with the published value, which is calculated on the assumption that only closed dimers exist and which varies from 95 to 115 moles^{-1} l depending on the concentration range (4). Thus the magnitude of $\beta_{20}{}^{o}$, while only about a tenth of $\beta_{20}{}^{c}$, seems to be real. An investigation of the self-association of valerolactam (11) used a band assigned to the dimer, while closed-dimer association was assumed in a more recent study of caprolactam in various solvents (12).

The self-associations of *N*-methylmethanesulfonamide (13) and *N*-phenylmethanesulfonamide (14) in CCl_4, shown in Fig. 1B, illustrate the case of the coexistence of monomers and closed dimers only: $A_1 = 1$, $A = \beta_{20}{}^{o} = 0$, within the experimental error of the data.

The self-association of cyclohexanol in CCl_4 (5) shown in Fig. 1C, where the E function has a negative slope, is a case where one or more of the underlying assumptions probably do not hold, in agreement with the conclusions of Masschelein who found that $\epsilon_1{}^{m} \neq \epsilon_1{}^{e}$ and that $\beta_{20}{}^{c}$ and $\beta_{20}{}^{o}$ were not constants. Similar plots were obtained with the available data on the self-association of oximes in CCl_4 (15), which also is not simple (16).

Can. J. Chem. Downloaded from www.nrcresearchpress.com by 210.87.254.105 on 09/05/12
For personal use only.

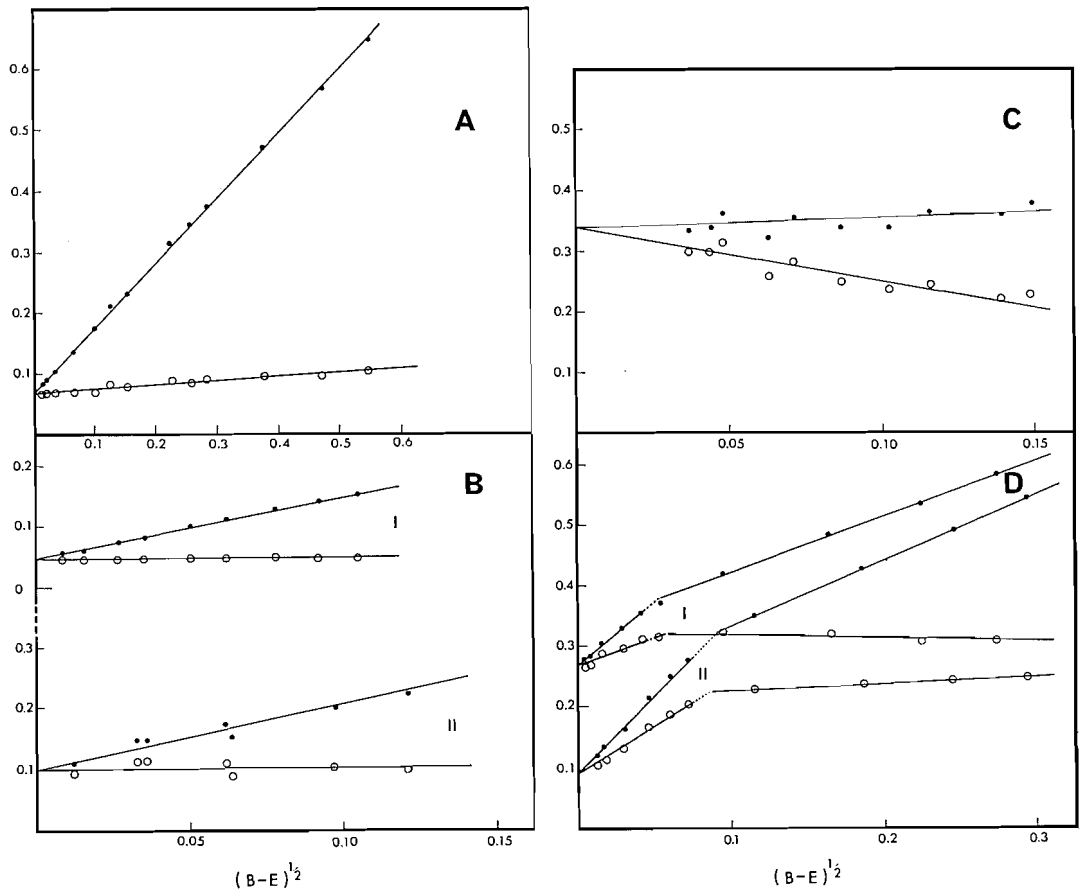

FIG. 1. Plots of $B/(B-E)^{1/2}$ (●) and $E/(B-E)^{1/2}$ (○) versus $(B-E)^{1/2}$: A, caprolactam in CCl_4 (4); B, I, *N*-methylmethanesulfonamide (13) and II, *N*-phenylmethanesulfonamide (14) in CCl_4; C, cyclohexanol in CCl_4 (5); D, *N*-phenylmethanesulfonamide in $CHCl_3$ (I, $\epsilon_1^m = 112$; II, $\epsilon_1^m = 130$) (14).

The plots for *N*-phenylmethanesulfonamide in $CHCl_3$ ($\epsilon_1^m = 130$ and $\epsilon_1^m = 112$) (14) shown in Fig. 1D illustrate the following important points which are strongly pertinent to any infrared spectroscopic investigation of self-association: ϵ_1^m must be known accurately, preferably measured directly, not obtained by extrapolation; a sufficient number of experimental points must be available over a given concentration range in order to avoid ambiguity in the determination of the mode of self-association; the possibility always exists that in some cases the mode of self-association may change with concentration.

In general it seems likely that in self-association of type I*a*, such as perhaps in the case of alcohols, and also in that of type II*a* where the groups A and B are adjacent, as in oximes, $\epsilon_1^m \neq \epsilon_1^e$. If $\epsilon_1^m \gg \epsilon_1^e$ then the usual discussion of the equilibria will be satisfactory, but in cases of possible coexistence of open and closed polymers it would be better to start with a treatment that does not neglect ϵ_1^e, the absorptivity of the "end" A—H groups.

An interesting relation for ϵ_1^e can be derived from $d\epsilon/dB$ at $B = 0$. Let $X = 1 - (\epsilon/\epsilon_1^m)$, then eq. [2] can be rewritten as $BX = b_1^2/A^2$, from which

$$B = A(BX)^{1/2} + A_1BX. \qquad [4]$$

Can. J. Chem. Downloaded from www.nrcresearchpress.com by 210.87.254.105 on 09/05/12
For personal use only.

Manipulation of [4] yields

$$B = A^2X(1 - A_1X)^2. \quad [5]$$

Differentiation and application of the condition $(X = 0)_{B=0}$ to [5] gives

$$(d\epsilon/dB)_{B=0} = -\epsilon_1{}^m/A^2 \quad [6]$$

whence

$$\epsilon_1{}^e = (1/\beta_{20}{}^o)(d\epsilon/dB)_{B=0} + (2\epsilon_1{}^m/\beta_{20}{}^o)(\beta_{20}{}^o + \beta_{20}{}^c). \quad [7]$$

Also, eq. [3] is transformed into

$$B/(B - E)^{1/2} = 1/[(2 - \gamma)\beta_{20}{}^o + 2\beta_{20}{}^c]^{1/2} + (2(\beta_{20}{}^o + \beta_{20}{}^c)/[(2 - \gamma)\beta_{20}{}^o + 2\beta_{20}{}^c])(B - E)^{1/2}. \quad [8]$$

If the plots of $B/(B - E)^{1/2}$ and $E/(B - E)^{1/2}$ as a function of $(B - E)^{1/2}$ are linear and have positive slopes A_1 and A_2 respectively, then

$$\gamma\beta_{20}{}^o = A_2/A^2 \quad \text{and} \quad \beta_{20}{}^o + \beta_{20}{}^c = A_1/2A^2 = -(A_1/2\epsilon_1{}^m)(d\epsilon/dB)_{B=0}. \quad [9]$$

Equations [6] and [8] are related and hence no unique set of values for γ, $\beta_{20}{}^o$, and $\beta_{20}{}^c$ can be calculated a priori. A physically valid set of values can perhaps be selected from the possible solutions in a specific case. No sufficiently precise set of measurements is available in the literature for a case of coexistence of open and closed polymers which could be used in a trial calculation.

Cases where the E function has a negative slope merit further attention and careful investigation using more than one physical method, particularly in the region of low concentrations.

ACKNOWLEDGMENTS

The data on the self-association of caprolactam was very kindly provided by Mr. T. J. Porro of the Perkin–Elmer Corporation.

1. G. C. Pimentel and A. L. McClellan. The hydrogen bond. Freeman & Co., San Francisco. 1960. Chap. 6.
2. F. J. C. Rossotti and H. Rossotti. J. Phys. Chem. **65**, 926, 930 (1961). G. Geiseler and E. Stockel. Spectrochim. Acta, **17**, 1185 (1961). S. N. Vinogradov. Can. J. Chem. **41**, 2719 (1963).
3. H. E. Hallam. *In* Infrared spectroscopy and molecular structure. *Edited by* M. Davies. Elsevier Publishing Co., Amsterdam. 1963. pp. 405–440.
4. R. C. Lord and T. J. Porro. Z. Elektrochem., **64**, 672 (1960). T. J. Porro. M.Sc. Thesis, Massachusetts Institute of Technology. 1958.
5. W. Masschelein. Spectrochim. Acta, **18**, 1557 (1962).
6. D. M. W. Anderson, J. L. Duncan, and F. J. C. Rossotti. J. Chem. Soc., 2165 (1961).
7. E. Borello and Z. Zecchina. Atti Accad. Sci. Torino, **96**, 332 (1961–1962); **97**, 1 (1963); Ann. Chim. Rome, **52**, 1302 (1962).
8. J. Kreuzer and R. Mecke. Z. phys. Chem. 1349, 309 (1941). E. G. Hoffman. Z. phys. Chem. **533**, 179 (1943). N. Coggeshall and E. Saier. J. Am. Chem. Soc. **73**, 5414 (1951). D. Bono. Compt. Rend. **242**, 637 (1956).
9. U. Liddel and E. D. Becker. Spectrochim. Acta, **10**, 70 (1957).
10. P. G. Guest. Numerical methods of curve fitting. Cambridge University Press. 1961. pp. 96–101.
11. M. Tsuboi. Bull. Chem. Soc. Japan, **24**, 75 (1951).
12. J. S. Franzen and R. E. Stephens. Biochem. **2**, 1321 (1963).
13. A. N. Hambly and R. H. Laby. Austr. J. Chem. **14**, 318 (1961).
14. J. N. Baxter, J. Cymerman-Craig, and J. B. Willis. J. Chem. Soc. 669 (1955).
15. S. Califano and J. Luttke. Z. Physik. Chem. **5**, 240 (1955).
16. W. Luck. Z. Electrochem. **65**, 355 (1961). G. Geiseler and S. Fruwert. Z. Physik. Chem. **26**, 111 (1960).

Received June 16, 1964.
Department of Chemistry,
University of Alberta,
Edmonton, Alberta.

Can. J. Chem. Downloaded from www.nrcresearchpress.com by 210.87.254.105 on 09/05/12
For personal use only.

BIOSYNTHESIS OF ERGOT ALKALOIDS. THE ORIGIN OF THE N-METHYL GROUP[1]

ROSS M. BAXTER, S. I. KANDEL, A. OKANY, AND R. G. PYKE

The origin of the N-methyl group of alkaloids has been the subject of a number of investigations (1). Two general types of mechanism could account for the N-methylation: (*a*) direct methylation by an active one carbon fragment such as formate, and (*b*) transmethylation by the transfer of the intact methyl group of methionine. In this work the origin of the N-methyl group of the ergot alkaloids has been investigated to ascertain via which of the two general mechanisms the N-methyl group arises. The following compounds were administered separately to growing cultures of *Claviceps purpurea*, ^{14}C-formate, L-methionine-methyl-^{14}C, and L-methionine-methyl-^{14}C,^{3}H.

TABLE I

Incorporation of methionine and formate into festuclavine and pyroclavine

Substance added	Total alkaloid, mg	Mixture of festuclavine and pyroclavine		
		Specific activity		Specific incorporation, %
		c.p.m.*/mmole	μc*/mmole	
Na-formate-^{14}C: 5.5 μc (0.224 mg) s.a. = 1.67 mc/mmole	2.4	8.72×10^{6}	6.18	0.37
L-Methionine-methyl-^{14}C: 5.6 μc (0.526 mg) s.a. = 1.099 mc/mmole	5.3	20.82×10^{6}	14.78	1.35

*Abbreviations: counts/min = c.p.m.; μcurie = μc.

It will be observed from Table I that although the specific activity (s.a.) (1.670 millicurie (mc)/mmole) of the added formate is higher than the specific activity (1.099 mc/mmole) of the added methionine, the specific percentage incorporation [(s.a. product/s.a. precursor) $\times$ 100] of the ^{14}C-labelled methionine is more than three times that of the ^{14}C-labelled formate. These data indicate that transmethylation is the preferred mechanism. The direct comparison of the percentage incorporation of the two supposed precursors assumes, however, that the rate of alkaloid formation before administration of the label is the same in all the experimental cultures. The variations in the alkaloid concentration (2) indicate that this assumption cannot be made. These difficulties were circumvented by the subsequent use of L-methionine-methyl-^{14}C,^{3}H as a substrate. The results in Table II show that the ^{3}H to ^{14}C ratio in methionine and in the total and individual alkaloids, purified by paper chromatography and crystallization, are essentially the same, indicating that the S-methyl of methionine is transferred as a unit into the alkaloids. Any significant incorporation of radioactivity as a result of direct methylation from formate would result in the drastic change in the ^{3}H to ^{14}C ratio in the alkaloids as compared to that of methionine. The finding that all of the incorporated radioactivity from ^{14}C formate and L-methionine-methyl-^{14}C resides in the N-methyl group of festuclavine-^{14}C rules out the earlier postulated role of formate (3, 4).

[1]*A preliminary report of part of this work appeared in Chem. Ind. 1453 (1961).*

Can. J. Chem. Downloaded from www.nrcresearchpress.com by 210.87.254.40 on 09/05/12
For personal use only.

TABLE II

^3H, ^{14}C ratio in the added methionine and in the recovered alkaloid

	^{14}C, d.p.m.*	^3H, d.p.m.*	$^3H/^{14}C$
L-Methionine	10.76×10^6	36.08×10^6	3.35
Total alkaloid	9.07×10^5	3.43×10^6	3.78
Chanoclavine, eluted from the paper chromatogram	1 705	5 920	3.47
Chanoclavine recrystallized	853	3 075	3.60
Festu- and pyro-clavine eluted from the paper chromatogram	5 962	20 090	3.37

*Abbreviation: disintegrations/min = d.p.m.

EXPERIMENTAL

Separation, Identification, and Estimation of the Alkaloids

The total alkaloids were obtained from a clavine-producing strain of *Claviceps purpurea* by utilizing the procedure as previously published (5). The purified and dried ether extract (total alkaloids) was chromatographed at room temperature on formamide-impregnated Whatman No. 1 paper with the solvent system composed of methylene chloride saturated with formamide (6). The following alkaloids were separated in order of increasing R_f. Chanoclavine, unknown I (M_I), unknown II (M_2), festuclavine, pyroclavine, agroclavine, and setoclavine. The identification of the individual spots is based on the comparison of their R_f values with that of the reference alkaloids, as compared under ultraviolet light and on development of the chromatograms with van Urk's reagent (1% paradimethylaminobenzaldehyde in 10% hydrochloric acid). The radioactive festuclavine and chanoclavine were also identified by co-crystallization of the eluted alkaloids with the respective authentic reference carrier alkaloids.

The concentration of the alkaloids was determined by the method of Allport and Cocking (7), at 590 mμ, using agroclavine as a standard.

Isolation of the Alkaloids

Chanoclavine, festuclavine, and the mixture of festuclavine and pyroclavine were eluted from the dried paper with ammoniacal peroxide-free ether (2 × 10 ml each spot). An aliquot of the eluate of the above-mentioned alkaloids was transferred into the counting vial, evaporated to dryness by a stream of nitrogen, and dissolved in 10 ml of anhydrous methanol. A volume of 2–5 ml of this methanolic solution was utilized for the quantitative estimation; the residue was evaporated and counted (Tables I and II).

An aliquot of the ether solution of chanoclavine (derived from L-methionine-methyl-^{14}C,^3H) was evaporated and unlabelled chanoclavine (30 mg) was added. The chanoclavine was dissolved in 2 ml of acetone, filtered, and evaporated. Aliquots of the ether solutions of the two festuclavines (derived from ^{14}C-formate, and L-methionine-methyl-^{14}C respectively) were treated similarly, except that unlabelled festuclavine (50 mg) prepared from agroclavine by catalytic hydrogenation, m.p. 239–242 (8), was added in each case. Chanoclavine was recrystallized from methanol and festuclavine from acetone. The specific activities of the crystalline samples remained constant after three recrystallizations. The two festuclavine samples so obtained were used for the degradation (Table III) and the chanoclavine sample for the determination of the ratio of ^3H to ^{14}C (Table II).

TABLE III

Radioactivities of festuclavine and its degradation product (s.a. d.p.m./mmole × 10^{-6})

Tracer	Festuclavine	Triethylmethyl-ammonium iodide	Recovery, %
Formate-^{14}C: 225 μc s.a. = 9.5 mc/mmole	2.29	2.27	99
L-Methionine-methyl-^{14}C: 7.5 μc s.a. = 4.96 mc/mmole	1.47	1.47	100

Preparation of Samples and Counting Procedures

Festuclavine from ^{14}C-labelled methionine and ^{14}C-labelled formate was degraded by the Herzig and Meyer technique, as modified by Brown and Byerrum (9), to obtain a crystalline derivative of the N-methyl

Can. J. Chem. Downloaded from www.nrcresearchpress.com by 210.87.254.40 on 09/05/12
For personal use only.

group of festuclavine. The slightly yellowish, crystalline trimethylammonium iodide so obtained was purified by recrystallization from dry acetone and petroleum ether (b.p. 60–80°). Yield 36–40%.

Crystalline samples of the ^{14}C-labelled compounds were combusted by the method of Van Slyke *et al.* (10). The carbon dioxide was collected in an ionization chamber and assayed with a Dynacon electrometer (Nuclear Chicago Corp.). Other ^{14}C-containing and all of the ^{3}H-containing samples and samples containing both ^{3}H and ^{14}C were counted with a Packard liquid scintillation spectrometer (Model 314E). The samples of the alkaloids were dissolved in 1 ml of anhydrous ethanol and the methionine samples in 1 ml of a 1 *M* solution of hyamine hydroxide 10-X in methanol (11) before addition of the fluor. The effect of quenching was determined in each sample by the use of an internal standard.

ACKNOWLEDGMENTS

This work was supported by a grant A-686 from the National Research Council of Canada. We wish to express our appreciation to Dr. A. Hofmann, Sandoz Ltd., Basel, and to Dr. M. Abe, Takeda Pharmaceutical Company, Osaka, Japan, for the samples of pure alkaloids and the sclerotia of the clavine-alkaloid-producing strain of *C. purpurea*, respectively.

1. K. Mothes. Symp. Soc. Exptl. Biol. **13**, 258 (1959).
2. D. Groger, K. Mothes, H. Simon, H. G. Floss, and F. Weygand. Z. Naturforsch. **156**, 141 (1960).
3. R. Robinson. The structural relations of natural products. Clarendon Press, Oxford. 1955. p. 107.
4. R. M. Baxter, S. I. Kandel, and A. Okany. Paper presented at the Symposium on Biochemistry and Physiology of Alkaloids, Halle, 1960. (*Published in* Abhandl. Deut. Akad. Wiss. Berlin, No. **4**, 335–341 (1963).)
5. R. M. Baxter, S. I. Kandel, and A. Okany. J. Am. Chem. Soc. **54**, 2997 (1962).
6. D. Groger. Arch. Pharm. **292**, 649 (1959).
7. N. L. Allport and T. T. Cocking. J. Pharm. Pharmacol. **5**, 341 (1932).
8. M. Abe and S. Yamatodani. J. Agr. Chem. Soc. Japan, **28**, 501 (1954).
9. S. A. Brown and S. V. Byerrum. J. Am. Chem. Soc. **74**, 1523 (1952).
10. D. D. Van Slyke, J. Plasin, and J. R. Weisiger. J. Biol. Chem. **191**, 259 (1951).
11. M. Vaughan, D. Steinberg, and J. Logan. Science, **126**, 446 (1957).

Received December 14, 1962.
Faculty of Pharmacy,
University of Toronto,
Toronto, Ontario.

Can. J. Chem. Downloaded from www.nrcresearchpress.com by 210.87.254.40 on 09/05/12
For personal use only.